TRANSACTIONS
OF THE
AMERICAN INSTITUTE
OF
ELECTRICAL ENGINEERS

VOLUME 74
1955

PART III. POWER APPARATUS AND SYSTEMS

PUBLISHED BY THE
AMERICAN INSTITUTE OF ELECTRICAL ENGINEERS
33 WEST 39TH STREET
NEW YORK 18, N. Y., U. S. A.

Copyright 1955 by the American Institute of Electrical Engineers
Printed in U. S. A. by The Mack Printing Company, Easton, Pa.

Preface

The AIEE *Transactions* for 1955 (volume 74) is published in three parts: Part I. Communication and Electronics; Part II. Applications and Industry; and Part III. Power Apparatus and Systems. The papers in each of the three parts are classified according to subject matter as follows:

Part I. Communication and Electronics

- Communication Switching Systems
- Communication Theory
- Radio Communications Systems
- Special Communications Applications
- Telegraph Systems
- Television and Aural Broadcasting Systems
- Wire Communications Systems
- Basic Sciences
- Computing Devices
- Dielectrics
- Electrical Techniques in Medicine and Biology
- Electronics
- Instruments and Measurements
- Magnetic Amplifiers
- Metallic Rectifiers
- Nucleonics
- Solid State Devices

Part II. Applications and Industry

- Air Transportation
- Domestic and Commercial Applications
- Land Transportation
- Marine Transportation
- Production and Application of Light
- Chemical Industry
- Electric Heating
- Electric Welding
- Feedback Control Systems
- General Industry Applications
- Industrial Control
- Industrial Power Rectifiers
- Industrial Power Systems
- Mining and Metal Industry
- Petroleum Industry

Part III. Power Apparatus and Systems

- Carrier Current
- Insulated Conductors
- Power Generation
- Protective Devices
- Relays
- Rotating Machinery
- Substations
- Switchgear
- System Engineering
- Transformers
- Transmission and Distribution

- Education
- Safety
- Research

Each part has been indexed separately in the back of that particular part. The three parts are not cross-referenced; hence the user should determine first whether the subject matter of the paper desired is in the field of communication and electronics, applications and industry, or power apparatus and systems. Papers are listed in the subject index under several key words in the titles. The original numbers assigned to the papers are given in the author index. Volume 74 contains the technical papers and related discussions presented at these meetings:

1. Winter General Meeting, New York, N. Y., January 31–February 4, 1955.
2. Southern District Meeting, St. Petersburg, Fla., April 13–15, 1955.
3. Middle Eastern District Meeting, Columbus Ohio, May 4–6, 1955.
4. Summer General Meeting, Swampscott, Mass., June 27–July 1, 1955.
5. Pacific General Meeting, Butte, Mont., August 15–17, 1955.
6. Fall General Meeting, Chicago, Ill., October 3–7, 1955.

Statements and opinions given in the papers and discussions published in *Transactions* are the expressions of the contributors for which the American Institute of Electrical Engineers assumes no responsibility.

Power Apparatus and Systems Index for 1955

1. Technical Subject Index

A-C Generators for Improved Performance, Rewinding. Seline........472–4; disc. 474
A-C Motor Windings, Measurement of Resistance of Energized. Waldschmidt.....1303–04; disc. 1305
A-C Network Analyzers, Combination Load-Flow and Stability Equivalent for Power System Representation on. Brown, Cloues..........782–6; disc. 786
A-C Resistance of Conventional Strand Power Cables in Nonmetallic Duct and in Iron Conduit. Burrell, Morris........1014–21; disc. 1021
A-C Test Circuits, Testing of D-C Interrupters on. Chen, Boehne........1073–9; disc. 1079
ACSR Conductor Sizes for Distribution Systems, A Method for Determining Economical. Funkhouser, Huber........479–83; disc. 483
ACSR, Measurement of Resistance and Reactance of Expanded. Tompkins, Jones, Tuttle........368–73; disc. 373
Air-Break Disconnect Switch, Power Auto-transformer Current Interruption with an. Anderson........1157–63
Air Circuit Breaker, A New High-Capacity Anode. Bottonari, Sprow..........1297–1302; disc. 1302
Air Circuit Breaker for 5,000,000 Kva, A 69-Kv Compressed. Kane, Walker........705–09; disc. 709
Air Circuit Breaker Interrupters, Flux Measurements in Magnetic. Carter..........1062–5; disc. 1065
Air-Disconnect Switches, High-Current Testing of. Gostin........21–5
Air Gap—A Novel Asynchronous Frequency Changer, Double-Energy Conversion in an. LaPierre, Louis........1373–5; disc. 1376
Air Magnetic Circuit Breaker of Simplified Design, A New 500-Megavolt-Ampere. Reilly, Weston........1093–8; disc. 1098
Alignment of Vertical-Shaft Hydroelectric Units as Practiced by Tennessee Valley Authority, Mechanical. Norris........586–9, disc. 589
Alternators, Design Principles of Flux-Switch. Rauch, Johnson........1261–8; disc. 1268
Aluminum Bus for Substations, Development of a Welded. Asbury, Hartman.......834–8; disc. 838
Aluminum Conductor on Transmission Lines, The Use of All-. Wright, Lambert.......849–53; disc. 853
Aluminum Connectors, Nontension. Boyer, Korges........844–7; disc. 847
Aluminum Distribution Conductors in the Philadelphia Electric Company, Design Problems and Operating Experience with. Nelson, Garrett........825–8; disc. 828...
Aluminum Distribution Systems, Eight Years' Experience With All-. Carpenter, Thornton........828–32; disc. 832
Aluminum in Heavy Current Conductors. Deans........1192–8; disc. 1198
Aluminum in Windings for Dry-Type Power Transformers, Experiences With the Use of. Tipton........1201–04
Aluminum-Sheathed Control Cable. McIlveen........1377–84; disc. 1384
Aluminum-Sheathed Power Cable. Del Mar, Merrell........292–8; disc. 298
Aluminum Squirrel Cage Rotors for Induction Motors, The Transient Stalled Temperature Rise of Cast. Rosenberry........819–24; disc. 824
Aluminum Widely Used in Power Switchgear. Talento........839–43; disc. 843
Amplifier, A Circuit Approach to the Analysis of a 2-Stage Dynamoelectric. Burtness........440–9; disc. 449
Analogue Solution of Cable Heat Flow Problems, An. deHaas, Sandiford, Cameron.....315–18; disc. 318
Analysis of a 2-Stage Dynamoelectric Amplifier, A Circuit Approach to the. Burtness........440–9; disc. 449
Analysis of Fault Currents for High-Voltage Circuit-Breaker Interruption. Lantz........41–5
Analyzers, Combination Load-Flow and Stability Equivalent for Power System Representation on A-C Network. Brown, Cloues....782–6; disc. 786
Analyzing Electric Machines, Two-Axis Method. Tang, Cosgriff........1449–55
Anechoic Chamber for Noise Tests on Large Power Transformers, An. Benoit, Hemmes, Schulz..50–6
Anode Air Circuit Breaker, A New High-Capacity. Bottonari, Sprow..........1297–1302; disc. 1302
Apparatus Noise Measurement. Wells........1170–3
Application of a New Nontracking Butyl to High-Voltage Instrument Transformers, The. Pfuntner, Norman, Wilterdink........1173–6
Application of Business Machines to Electrical Utility Load Forecasting, The. Gruetter........854–8
Application of Statistics to Motor Testing. Oldenkamp........815–18; disc. 818
Application of Volume Theory of Dielectric Strength to Oil Circuit Breakers. Wilson, Streater, Tuohy........677–84; disc. 684.
Approach to the Calculation of Synchronous Machine Reactances, A New. Talaat. Part I........176–82; disc. 182
Approach to the Definition of Excitation System Response, An. Bliss..........1008–12; disc. 1012
Arc Erosion of Electric Contact Materials, High-Current. Wilson........657–64; disc. 664
Arc Furnace Loads, Voltage Dip and Synchronous Condenser Swings Caused by. Concordia...951–6
Arc Furnaces—Electrical Characteristics and Corrective Equipment, Two Large Electric. Luther, Ghesquiere, Quick........1401–05; disc. 1406
Area Supply Methods, General Study of. Casazza, Rankin........1328–34; disc. 1334–5
Armature End Iron of Large Turbine Generators, Stray Losses in the. Winchester........381–9; disc. 389
Armature Windings, Some Factors Influencing the Temperature Rise of. Liwschitz-Garik......752–9
Armatures, Correlation of Temperature Measurements on D-C. Gerbetz, Ewing........391–4; disc. 395
Asynchronous Frequency Changer, Double-Energy Conversion in an Air Gap—A Novel. LaPierre, Louis........1373–5; disc. 1376
Attenuation in Power Cables, Surge. Valentine, Dillard, Clayton........1115–21; disc. 1122
Audible Noise Control, Recent Contributions to Transformer. Conover, Ringlee........77–90; disc. 90
Automatic Load Frequency Control System for Central Station Power. Ehrenberg........787–95
Automatic Load Shedding. (Committee Report)........1143–5; disc. 1145
Automatically Switched Capacitors in Steps on a Single Distribution Feeder. Fowler, Thomas........311–14; disc. 314
Autotransformer Current Interruption with an Air-Break Disconnect Switch, Power. Anderson........1157–63
Autotransformers, Thyrite Protection for Series Windings of. Albright........150–4; disc. 154
Auxiliary Busses, Transfer of Steam-Electric Generating-Station. Lewis, Marsh........322–30; disc. 330
Auxiliary Busses, Transfer Tests on Station. Backer, Barth, Huse, Taylor........1441–5; disc. 1446
Auxiliary Drive Motors in Power Plants, Economic Selection of. Gross, Bobrowicz........1237–46; disc. 1246
Axis Method of Analyzing Electric Machines, Two-. Tang, Cosgriff........1449–55

B

Balancing Double-Wye High-Voltage Capacitor Banks. Compton........573–8; disc. 578
Bank Relaying Systems, Line and Transformer. Blackburn, Rockefeller........334–9; disc. 339
Banks, Balancing Double-Wye High-Voltage Capacitor. Compton........573–8; disc. 578
Banks, Intermittently Increased Kilovar Output of Large Capacitor. Minder.......749–51; disc. 751
Bars of Squirrel-Cage Rotors, Computation of Skin Effect in. Liwschitz-Garik.....768–70; disc. 771
Basic Functions in Network Distribution Systems, The Limiter—Its. Xenis........913–15; disc. 944, 1463
Basic Sequence Networks. Kirschbaum........771–4
Behavior of High Voltage Busses and Insulators During Short Circuits. Milton, Chambers........742–6; disc. 746
Bibliography and Summary of Fault Location Methods. (Committee Report)........1423–7; disc. 1427
Bibliography of Relay Literature—1950–52. Gross........45–8
Blondel Theory, Current Loci of Salient-Pole Synchronous Motors: An Extension of. Douglas........1080–2; disc. 1082
Breakdown of Fully Impregnated Paper Insulation for High-Voltage Cables, Research on the Electric. Gazzana Priaroggia, Palandri..1343–57; disc. 1357
Bureau of Reclamation 230-Kv Transmission Lines in North Dakota. Austin........1147–51
Bus for Substations, Development of a Welded Aluminum. Asbury, Hartman........834–8; disc. 838
Business Machines to Electrical Utility Load Forecasting, The Application of. Gruetter........854–8
Busses and Insulators During Short Circuits, Behavior of High Voltage. Milton, Chambers........742–6; disc. 746
Busses, Transfer of Steam-Electric Generating-Station Auxiliary. Lewis, Marsh........322–30; disc. 330
Busses, Transfer Tests on Station Auxiliary. Backer, Barth, Huse, Taylor........1441–5; disc. 1446
Butyl-Rubber-Insulated Power Cable, Design and Evaluation of. Carroll, Lee, McKinley........1204–12; disc. 1212
Butyl to High-Voltage Instrument Transformers, The Application of a New Nontracking. Pfuntner, Norman, Wilterdink........1173–6

C

Cable, Aluminum-Sheathed Control. McIlveen........1377–84; disc. 1384
Cable, Aluminum-Sheathed Power. Del Mar, Merrell........292–8; disc. 298
Cable at High Frequency, Characteristics of Single-Conductor Electric. Sabol.....1280–5; disc. 1285
Cable by Oven Heating Tests, High Temperature Classification of Rubber and Rubberlike Insulation of Network. Couch, Crowdes........930–4; disc. 944, 1463
Cable Characteristics, The Co-ordination of Power and Communication. Short........281–7; disc. 287
Cable, Design and Evaluation of Butyl-Rubber-Insulated Power. Carroll, Lee, McKinley........1204–12; disc. 1212
Cable Heat Flow Problems, An Analogue Solution of. deHaas, Sandiford, Cameron.....315–18; disc. 318
Cable in Duct, Time-Current Damage Characteristics. Porter........919–21; disc. 944, 1463
Cable Systems, Oil Flow and Pressure Calculations for Pipe Type. (Committee Report)........251–9; disc. 259
Cable Temperature Transients, An Improved Approximate Technique for Calculating. Van Wormer........277–80; disc. 280
Cables, A Mathematical Method for Determining Insulation Damage Curves for Network. Kolks........934–8; disc. 944, 1463
Cables, A Method of Measurement of Carrier Characteristics of Power. Sparlin, Moynihan........31–3
Cables, Characteristic Properties of Secondary Network. Rosch........939–44; disc. 944, 1463
Cables, Freezing Oil-Type Pipe. Merrell........1023–31; disc. 1031
Cables in Nonmetallic Duct and in Iron Conduit, A-C Resistance of Conventional Strand Power. Burrell, Morris........1014–21; disc. 1021
Cables in Ontario, Gas-Pressurized 120-Kv and 161-Kv Pipe Type. Kozak, Prescott.....184–92; disc. 192
Cables, Mineral-Insulated Metallic-Sheathed. Jordan, Eager........198–212; disc. 212

Cables, Overload Classifications for Secondary Network. Graham..........916–19; disc. 944, 1463
Cables, Research on the Electric Breakdown of Fully Impregnated Paper Insulation for High-Voltage. Gazzana Priaroggia, Palandri..1343–57; disc. 1357
Cables, Some Performance Characteristics of High-Voltage Rubber-Insulated. Rosch..........1219–24; disc. 1224
Cables, Surge Attenuation in Power. Valentine, Dillard, Clayton..........1115–21; disc. 1122
Cage Winding Protective Relay for Synchronous Machines, Improved Fast-Acting Thermal Relay and Its Application as a. Baude.....349–53; disc. 353
Calculating Cable Temperature Transients, An Improved Approximate Technique for. Van Wormer..........277–80; disc. 280
Calculating Voltage Regulation Using Unit Impedance Power Reactive Diagrams, A Simplified Method of. Butler..........304–10; disc. 310
Calculation of Network Impedances, Digital. Glimn, Habermann, Henderson, Kirchmayer..........1285–95; disc. 1295
Calculation of Synchronous Machine Reactances, A New Approach to the. Talaat:
  Part I..........176–82; disc. 182
Calculation of the Complete Time/Current Characteristics of Cartridge Fuses With Single Wire Element, The. Guile........1108–15; disc. 1115
Calculations and Test Results, D-C Machines—Short-Circuit. O'Connor, Cybulski....222–30; disc. 230
Calculations, D-C Machines—Method for Short-Circuit. Cybulski, O'Connor..........214–21
Calculations for Pipe-Type Cable Systems, Oil Flow and Pressure. (Committee Report)...251–9; disc. 259
Calculations in Power System Transient Stability Studies, A Rational Method for the Step-by-Step. Norinder..........1087–91; disc. 1091
Calculations to Transmission Line Design, Practical Application of Sag and Tension. Lummis, Fischer..........402–13; disc. 413
Capacitance Switching Devices, Test Circuits for. Darrow, Phillips, Schultz, Shores.....624–34; disc. 634
Capacitance-Switching Facilities at the Switchgear Development Laboratory. Williams, Mankoff, Schneider..........375–80; disc. 380
Capacitance Switching, Some Fundamentals on. Johnson, Schultz, Schultz, Shores..........727–36; disc. 736
Capacitors in Steps on a Single Distribution Feeder Automatically Switched. Fowler, Thomas..........311–14; disc. 314
Capacitor Banks, Balancing Double-Wye High-Voltage. Compton..........573–8; disc. 578
Capacitor Banks, Intermittently Increased Kilovar Output of Large. Minder.......749–51; disc. 751
Capacitors, Report on the Operation of Switched. (Committee Report)..........1255–60; disc. 1260
Capture Effect in a Narrow-Band Frequency Modulated System, An Investigation of the. Hedges..........289–91; disc. 292
Carrier Characteristics on Power Cables, A Method of Measurement of. Sparlin, Moynihan........31–3
Carrier Coupling—An Analysis, Power-Line. Bienhoff..........1163–70
(Carrier Current) An Investigation of the Capture Effect in a Narrow-Band Frequency Modulated System. Hedges..........289–91; disc. 292
(Carrier Current) Design of the Adjustable Lin-O-Phase Filter. Lee..........273–7; disc. 277
(Carrier Current) Microwave System Parameters for Reliable Communications. Alvira, Corbell..........1100–07; disc. 1107
(Carrier Current) Quadriphase—A New Approach to Time Division Multiplexing. Evans, Lowe..........900–03
(Carrier Current) Recommendations for Improving Reliability of Stand-by Engine Generators for Microwave Communications Systems. Tharp..........261–6; disc. 266
Carrier-Frequency Noise on Power Lines, A Study of. Moynihan, Sparlin:
  Part IV. Conclusion of Field Measurements..........795–800
Carrier Pilot Relaying, Future Application Needs of. Cramer, Kringa..........1233–5; disc. 1235
Cartridge Fuses With Single Wire Element, The Calculation of the Complete Time/Current Characteristics of. Guile..........1108–15; disc. 1115
Casting of Dry-Type Current Transformers, Epoxy Resin. Farneth, Gallousis.......194–7; disc. 197
Central Station Power, Automatic Load Frequency Control System for. Ehrenberg..........787–95
Chamber for Noise Tests on Large Power Transformers, An Anechoic. Benoit, Hemmes, Schulz......50–6
Changer, Double-Energy Conversion in an Air Gap—A Novel Asynchronous Frequency. LaPierre, Louis..........1373–5; disc. 1376
Characteristic Properties of Secondary Network Cables. Rosch..........939–44; disc. 944, 1463
Characteristics and Application, Limiters, Their Design. Heller, Matthysse..........924–30; disc. 944
Characteristics and Corrective Equipment, Two Large Electric Arc Furnaces—Electrical. Luther, Ghesquiere, Quick..........1401–05; disc. 1406
Characteristics of Cartridge Fuses With Single Wire Element, The Calculation of the Complete Time/Current. Guile..........1108–15; disc. 1115
Characteristics of High-Voltage Rubber-Insulated Cables, Some Performance. Rosch..........1219–24; disc. 1224
Characteristics of Single-Conductor Electric Cable at High Frequency. Sabol.......1280–5; disc. 1285
Characteristics of Wood and Suspension Insulators in Series, Insulation. Clayton, Shankle..........1305–11; disc. 1312
Characteristics on Power Cables, A Method of Measurement of Carrier. Sparlin, Moynihan.......31–3
Characteristics, The Co-ordination of Power and Communication Cable. Short........281–7; disc. 287
Circuit Approach to the Analysis of a 2-Stage Dynamoelectric Amplifier, A. Burtness..........440–9; disc. 449
Circuit Breaker, A New High-Capacity Anode Air. Bottonari, Sprow..........1297–1302; disc. 1302
Circuit Breaker at Philip Sporn Power Plant, Field Tests on a 138-Kv High-Speed Oil. Naef, Hambrick..........710–24; disc. 724
Circuit Breaker for 5,000,000 Kva, A 69-Kv Compressed Air. Kane, Walker......705–09; disc. 709
Circuit Breaker Interrupters, Flux Measurements in Magnetic Air. Carter..........1062–5; disc. 1065
Circuit-Breaker Interruption, Analysis of Fault Currents for High-Voltage. Lantz..........41–5
Circuit Breaker of Simplified Design, A New 500-Megavolt-Ampere Air Magnetic. Reilly, Weston..........1093–8; disc. 1098
Circuit Breaker Recovery Voltages Associated with 2-Phase-to-Ground Short Circuits, Short-Circuit Currents and. Skeats..........688–93; disc. 693
Circuit Breakers, Application of Volume Theory of Dielectric Strength to Oil. Wilson, Streater, Tuohy..........677–84; disc. 684
Circuit Breakers, Dynamics of High-Capacity Outdoor Oil. Barkan..........671–6; disc. 676
Circuit Breakers for Switching Long 230-Kv Lines, Design Problems and Field Tests Concerning. Umphrey, Marsden..........693–701; disc. 701
Circuit Breakers, The Results of 7 Years' Experience with High-Capacity Outdoor Oil. Balentine, Darrow..........665–70; disc. 671
Circuit for the Concatenation of Induction Motors, Equivalent. Ku..........1214–18; disc. 1219
Circuit Transient Recovery Voltage Characteristics of Electric Power Systems, A Method for Studying. Kotheimer..........1083–6; disc. 1086
Circuit, Weighted Mutual Reactances for a Triple-Cage Motor. Martin..........765–8
Circuitry for Remotely Operated Electric Utility Substations, Control. Derr, Metz....450–9; disc. 459
Circuits, A Power Class Recloser for Higher Speed Clearing of Distribution. Field, Leatherberry..........986–91; disc. 991
Circuits for Capacitance Switching Devices, Test. Darrow, Phillips, Schultz, Shores..........624–34; disc. 634
Circuits for Single-Phase Motors, Equivalent. Siemon..........1335–42; disc. 1342
Circuits, Testing of D-C Interrupters on A-C Test. Chen, Boehne..........1073–9; disc. 1079
Clearing of Distribution Circuits, A Power Class Recloser for Higher Speed. Field, Leatherberry..........986–91; disc. 991
Coincident-Outage Probability in Secondary Network Vaults. Reps..........580–5; disc. 585
Combination Load-Flow and Stability Equivalent for Power System Representation on A-C Network Analyzers. Brown, Cloues.......782–6; disc. 786
Commercial Areas, Economics of Higher Primary and Secondary Voltages for. Lawrence, Reps..........1034–45; disc. 1945
(Committee Report) Automatic Load Shedding. (55-615)..........1143–5; disc. 1145
(Committee Report) Bibliography and Summary of Fault Location Methods. (55-709)..........1423–7; disc. 1427
(Committee Report) Effect of Shock and Vibration on Relays. (55-97)..........398–400; disc. 400
(Committee Report) Oil Flow and Pressure Calculations for Pipe-Type Cable Systems. (55-32)..........251–9; disc. 259
(Committee Report) Proposed Test Code for Functional Temperature Endurance Tests of Ventilated Dry Type Power and Distribution Transformers. (55-435)..........971–5; disc. 975
(Committee Report) Report on the Operation of Switched Capacitors. (55-710)..........1255–60; disc. 1260
(Committee Report) Review of the Factors Concerned with the Use of Protective Devices Shunting Reactors. (55-557)..........903–13
(Committee Report) Supervisory Control and Associated Telemetering Equipment—A Survey of Current Practice. (55-128)..........36–8
(Committee Report) System Planning Practices. (55-529)..........896–900
Communication Cable Characteristics, The Co-ordination of Power and. Short........281–7; disc. 287
Communications Equipment, Protection of Personnel Against Electrical Shock Hazards in Central Office. Jones..........893–6
Communications, Microwave System Parameters for Reliable. Alvira, Corbell.....1100–07; disc. 1107
Communications Systems, Recommendations for Improving Reliability of Stand-by Engine Generators for Microwave. Tharp....261–6; disc. 266
Compounds in Transformer Oil, Interpretation and Significance of Tests Indicating the Concentration of Polar. Johnson..........774–80; disc. 780
Compressed Air Circuit Breaker for 5,000,000 Kva, A 69-Kv. Kane, Walker.......705–09; disc. 709
Computation of Skin Effect in Bars of Squirrel-Cage Rotors. Liwschitz-Garik.......768–70; disc. 771
Computer, An Incremental Cost of Power-Delivered. Early, Phillips, Shreve..........529–34; disc. 534
Computer for Economic Scheduling and Control of Power Systems, A. Morrill, Blake..........1136–41; disc. 1141
Concatenation of Induction Motors, Equivalent Circuit for the. Ku..........1214–18; disc. 1219
Concentration of Polar Compounds in Transformer Oil, Interpretation and Significance of Tests Indicating the. Johnson..........774–80; disc. 780
Condenser Swings Caused by Arc Furnace Loads, Voltage Dip and Synchronous. Concordia..........951–6
Conductor Materials for Turbine Generators, Improved Field. Holley, Savidge..........72–6
Conductor on Transmission Lines, The Use of All Aluminum. Wright, Lambert...849–53; disc. 853
Conductor Sizes for Distribution Systems, A Method for Determining Economical ACSR. Funkhouser, Huber..........479–83; disc. 483
Conductors, Aluminum in Heavy Current. Deans..........1192–8; disc. 1198
Conductors in the Philadelphia Electric Company, Design Problems and Operating Experience with Aluminum Distribution. Nelson, Garrett..........825–8; disc. 828
Conduit, A-C Resistance of Conventional Strand Power Cables in Nonmetallic Duct and in Iron. Burrell, Morris..........1014–21; disc. 1021
Connectors, Nontension Aluminum. Boyer, Korges..........844–7; disc. 847
Constants for the General Transmission Loss Equation, A New Method of Determining. Early, Watson..........1417–21; disc. 1421
Constants With Tensors, ORACLE Computes Line. Shipley, Hochdorf, Watson......1052–6; disc. 1056
Contact Life of Voltage-Regulating Relays. Schoendube, Elliott..........1398–1400; disc. 1401
Contact Materials, High-Current Arc Erosion of Electric. Wilson..........657–64; disc. 664
Control and Associated Telemetering Equipment—A Survey of Current Practice, Supervisory. (Committee Report)..........36–8
Control Cable, Aluminum-Sheathed. McIlveen..........1377–84; disc. 1384
Control Circuitry for Remotely Operated Electric Utility Substations. Derr, Metz..........450–9; disc. 459
Control of Electrostatic Voltage Distribution in Power Transformer Design. Bennon, Cossaart..........1122–5; disc. 1125
Control System for Central Station Power, Automatic Load Frequency. Ehrenberg..........787–95
Controls for Step Voltage Regulators. Lennox..........1407–09; disc. 1410
Conventional Strand Power Cables in Nonmetallic Duct and in Iron Conduit, A-C Resistance of. Burrell, Morris..........1014–21; disc. 1021
Conversion in an Air Gap—A Novel Asynchronous Frequency Changer, Double-Energy. LaPierre, Louis..........1373–5; disc. 1376
Co-ordination of Hydro and Steam Generation. Watchorn..........142–8; disc. 148
Co-ordination of Power and Communication Cable Characteristics, The. Short.......281–7; disc. 287
Co-ordination of Secondary Network Protection. Leinbach, Brookes..........922–4; disc. 944, 1463
Cores During Impulse Testing, Magnetization of Transformer. Beavers, Holcomb, Leoni..........118–23; disc. 123
Corona on Traveling Waves, Effects of. Wagner, Lloyd..........858–72
Corona Studies—In Relation to Insulation. Liao, Nye, Brustle, Anderson.......1046–50; disc. 1050
Corrective Equipment, Two Large Electric Arc Furnaces—Electrical Characteristics. Luther, Ghesquiere, Quick..........1401–05; disc. 1406
Correlation of Temperature Measurements on D-C Armatures. Gerbetz, Ewing......391–4; disc. 395
Cost of Power-Delivered Computer, An Incremental. Early, Phillips, Shreve..........529–34; disc. 534

Coupled Windings, Oscillations of. Abetti, Adams, Maginnis..........12–21
Coupling—An Analysis, Power-Line Carrier. Bischoff..........1163–70
Current Conductors, Aluminum in Heavy. Deans..........1192–8; disc. 1198
Current Interruption with an Air-Break Disconnect Switch, Power Autotransformer. Anderson..........1157–63
Current-Limiting Fuses, Ribbon Elements for High-Voltage. Powell, Schuck..........635–41; disc. 641
Current Loci of Salient-Pole Synchronous Motors: An Extension of Blondel Theory. Douglas..........1080–2; disc. 1082
Current Ratings for Step Regulators, Increased. Sealey..........737–42; disc. 742
Current Sources for Electric Defibrillation, Field. Betz..........33–6
Current Transformers, Epoxy Resin Casting of Dry-Type. Farneth, Gallousis..........194–7; disc. 197
Currents and Circuit-Breaker Recovery Voltages Associated with 2-Phase-to-Ground Short Circuits, Short-Circuit. Skeats..........688–93; disc. 693
Currents for High-Voltage Circuit-Breaker Interruption, Analysis of Fault. Lantz..........41–5
Currents in Turbine Generators, Eccentricity, Vibration and Shaft. Rosenberg..........38–41
Curves for Network Cables, A Mathematical Method for Determining Insulation Damage. Kolks..........934–8; disc. 944
Curves for Small Motors from Motor Tests, Developing Iron Loss. Shaneman..........1176–9

D

D-C Armatures, Correlation of Temperature Measurements on. Gerbetz, Ewing..........391–4; disc. 395
D-C Interrupters on A-C Test Circuits, Testing of. Chen, Boehne..........1073–9; disc. 1079
D-C Machines—Method for Short-Circuit Calculations. Cybulski, O'Connor..........214–21
D–C Machines: Response to Impact Excitation. Brockman, Linkous..........500–03; disc. 503
D-C Machines—Short Circuit Calculations and Test Results. O'Connor, Cybulski...222–30; disc. 230
Damage Characteristics, Cable in Duct, Time-Current. Porter..........919–21; disc. 944, 1463
Damage Curves for Network Cables, A Mathematical Method for Determining Insulation. Kolks..........934–8; disc. 944, 1463
Defibrillation, Electric. Kouwenhoven, Milnor..........561–4; disc. 564
Defibrillation, Field Current Sources for Electric. Betz..........33–6
Definition of Excitation System Response, An Approach to the. Bliss..........1008–12; disc. 1012
Design and Evaluation of Butyl-Rubber-Insulated Power Cable. Carroll, Lee, McKinley..........1204–12; disc. 1212
Design and Operation of Secondary Network Systems, The Use of Probability in the. Neagle, Nelson..........567–72; disc. 572
Design Characteristics and Application, Limiters, Their. Heller, Matthysse..........924–30; disc. 944, 1463
Design, Investigation of European Practices in Power Line. Fritz..........505–09; disc. 509
Design of Induction Torque Motors and Servomotors, Optimum. Weiss..........809–15
Design of Large Induction Motors, Sonance. Wall..........1189–92
Design of the Adjustable Lin-O-Phase Filter. Lee..........273–7; disc. 277
Design Principles of Flux-Switch Alternators. Rauch, Johnson..........1261–8; disc. 1268
Design Problems and Field Tests Concerning Circuit Breakers for Switching Long 230-Kv Lines. Umphrey, Marsden..........693–701; disc. 701
Design Problems and Operating Experience With Aluminum Distribution Conductors in the Philadelphia Electric Company. Nelson, Garrett..........825–8; disc. 828
Detection of Grounds in Generator Field Windings. Barkle, Sterrett, Fountain..........467–70; disc. 470
Detector for Synchronous Generators, A Transductor Type Field Ripple. McConnell..........476–9; disc. 479
Determination of Incremental and Total Loss Formulas from Functions of Voltage Phase Angles, The. Cahn..........161–71; disc. 171
Determining Constants for the General Transmission Loss Equation, A New Method of. Early, Watson..........1417–21; disc. 1421
Developing Iron Loss Curves for Small Motors from Motor Tests. Shaneman..........1176–9
Development of a Welded Aluminum Bus for Substations. Asbury, Hartman..........834–8; disc. 838
Development of Small Hydroelectric Sites in Western North Carolina. Gnuse..........65–8
Devices, Test Circuits for Capacitance Switching. Darrow, Phillips, Schultz, Shores..........624–34; disc. 634
Diagrams, A Simplified Method of Calculating Voltage Regulation Using Unit Impedance Power Reactive. Butler..........304–10; disc. 310
Dielectric Strength to Oil Circuit Breakers, Application of Volume Theory of. Wilson, Streater, Tuohy..........677–84; disc. 684
Digital Calculation of Network Impedances. Glimn, Habermann, Henderson, Kirchmayer..........1285–95; disc. 1295
Direct-Stroke Protection of High-Voltage Switching Stations and Transformers. Griscom, Dillard, Hileman..........354–65; disc. 365
Disconnecting Switches, Results of High-Current Tests on 161-Kv. McNerney..........104–08; disc. 108
Dissymmetry Harmonics, Single-Phase Induction Motor Noise Due to. Muster, Wolfert..........1365–72; disc. 1372
Distribution Circuits, A Power Class Recloser for Higher Speed Clearing of. Field, Leatherberry..........986–91; disc. 991,
Distribution Conductors in the Philadelphia Electric Company, Design Problems and Operating Experience with Aluminum. Nelson, Garrett..........825–8; disc. 828
Distribution Feeder, Automatically Switched Capacitors in Steps on a Single. Fowler, Thomas..........311–14; disc. 314
Distribution in Power Transformer Design, Control of Electrostatic Voltage. Bennon, Cossaart..........1122–5; disc. 1125
(Distribution) Measurement of Resistance and Reactance of Expanded ACSR. Tompkins, Jones, Tuttle..........368–73; disc. 373
Distribution-Substation and Primary Feeder Planning. Denton, Reps..........484–97; disc. 497
Distribution System Parameters, Power. Kidder, Neher..........125–40; disc. 140
Distribution Systems, A Method for Determining Economical ACSR Conductor Sizes for. Funkhouser, Huber..........479–83; disc. 483
Distribution Systems, Eight Years' Experience with All-Aluminum. Carpenter, Thornton..........828–32; disc. 832
Distribution Systems, The Limiter—Its Basic Functions in Network. Xenis..........913–15; disc. 944, 1463
Distribution Transformers, Functional Life Expectancy Tests for Liquid Filled. Lockie..........977–82; disc. 982
Distribution Transformers, Impulse Tests on Low-Voltage Windings of. Holcomb..........1152–5; disc. 1155
Division Multiplexing, Quadriphase—A New Approach to Time. Evans, Lowe..........900–03
Double-Energy Conversion in an Air Gap—A Novel Asynchronous Frequency Changer. LaPierre, Louis..........1373–5; disc. 1376
Double-Wye High-Voltage Capacitor Banks, Balancing. Compton..........573–8; disc. 578
Dry-Type Current Transformers, Epoxy Resin Casting of. Farneth, Gallousis..........194–7; disc. 197
Dry-Type Power and Distribution Transformers, Proposed Test Code for Functional Temperature Endurance Tests of Ventilated. (Committee Report)..........971–5; disc. 975.
Dry-Type Power Transformers, Experiences With the Use of Aluminum in Windings for. Tipton..........1201–04
Dry-Type Power Transformers, Functional Life Evaluation of Group-2. Zambell..........956–70
Dry-Type Transformer Insulation, Evaluation and Application of Silicone-Organic Resin Combinations for. Simmons, Scheideler..........155–60; disc. 160
Dry-Type Transformers, Functional Life Tests of Insulation Systems for. Narbut..........1057–61; disc. 1061
Dry-Type Transformers, Functional Temperature Endurance Tests on a Silicone Glass Fiber Insulation System for. Manning..........91–8; disc. 98
Duct and in Iron Conduit, A-C Resistance of Conventional Strand Power Cables in Nonmetallic. Burrell, Morris..........1014–21; disc. 1021
Duct, Time-Current Damage Characteristics, Cable in. Porter..........919–21; disc. 944, 1463
Durability Testing of Valve Type Lightning Arresters, Transient. Kalb, Yost..........521–6; disc. 526
Dynamics of High-Capacity Outdoor Oil Circuit Breakers. Barkan..........671–6; disc. 676
Dynamoelectric Amplifier, A Circuit Approach to the Analysis of a 2-Stage. Burtness..........440–9; disc. 449

E

Eccentricity, Vibration, and Shaft Currents in Turbine Generators. Rosenberg..........38–41
Economic Scheduling and Control of Power Systems, A Computer for. Morrill, Blake..........1136–41; disc. 1141
Economic Selection of Auxiliary Drive Motors in Power Plants. Gross, Bobrowicz..........1237–46; disc. 1246
Economic Size of Steam-Electric Generating Units, An Investigation of the. Kirchmayer, Mellor, O'Mara, Stevenson..........600–09; disc. 609
Economical ACSR Conductor Sizes for Distribution Systems, A Method for Determining. Funkhouser, Huber..........479–83; disc. 483
Economics of Higher Primary and Secondary Voltages for Commercial Areas. Lawrence, Reps..........1034–45; disc. 1045
Effect of Shock and Vibration on Relays. (Committee Report)..........398–400; disc. 400
Effect of Skew on Induction Motor Magnetic Fields. Linkous..........760–5; disc. 765
Effect of Synchronous-Machine Transient Rotor Saliency on Changes in Terminal Voltage. Concordia..........25–31
Effects of Corona on Traveling Waves. Wagner, Lloyd..........858–72
Efficiency of Grounding Grids with Nonuniform Soil. Zaborszky..........1230–3
Eight Years' Experience with All-Aluminum Distribution Systems. Carpenter, Thornton..........828–32; disc. 832
Electric Arc Furnaces—Electrical Characteristics and Corrective Equipment, Two Large. Luther, Ghesquiere, Quick..........1401–05; disc. 1406
Electric Breakdown of Fully Impregnated Paper Insulation for High-Voltage Cables, Research on the. Gazzana Priaroggia, Palandri..1343–57; disc. 1357
Electric Cable at High Frequency, Characteristics of Single-Conductor. Sabol..........1280–5; disc. 1285
Electric Contact Materials, High-Current Arc Erosion of. Wilson..........657–64; disc. 664
Electric Defibrillation. Kouwenhoven, Milnor..........561–4; disc. 564
Electric Defibrillation, Field Current Sources for. Betz..........33–6
Electric Machines, Two-Axis Method of Analyzing. Tang, Cosgriff..........1449–55
Electric Power Industry, Research in the. Gaty..........553–6; disc. 556
Electric System Planning, Rural. Rixse..........1410–16; disc. 1416
Electric Utility Industry, Implementation of a Research Program for the. Hobson, Lewis, Oldacre..........545–50; disc. 550
Electric Utility Load Forecasting. Godard...1428–40
Electric Utility Substations, Control Circuitry for Remotely Operated. Derr, Metz..........450–9; disc. 459
Electrical Shock Hazards in Central Office Communications Equipment, Protection of Personnel Against. Jones..........893–6
Electrical Utilities, Manufacturer's Research in Relation to. Parker, Baird..........557–60
Electrical Utility Load Forecasting, The Application of Business Machines to. Gruetter..........854–8.
Electricity, Forecasting the Demand for. Hooke..........993–1005; disc. 1005
Electromagnetic Unbalance of Untransposed Transmission Lines. Gross, Nelson. Part II..........887–93
Electrostatic Voltage Distribution in Power Transformer Design, Control of. Bennon, Cossaart..........1122–5; disc. 1125
Elements for High-Voltage Current-Limiting Fuses, Ribbon. Powell, Schuck..........635–41; disc. 641
End Iron of Large Turbine Generators, Stray Losses in the Armature. Winchester..........381–9; disc. 389
Endurance Tests of Ventilated Dry-Type Power and Distribution Transformers, Proposed Test Code for Functional Temperature. (Committee Report)..........971–5; disc. 975
Energized A-C Motor Windings, Measurement of Resistance of. Waldschmidt..........1303–04; disc. 1305
Energy Control of Interconnected Power Systems, Load-Phase Tie-Line. Cahen..........1–5
Energy Conversion in an Air Gap—A Novel Asynchronous Frequency Changer, Double-. LaPierre, Louis..........1373–5; disc. 1376
Engine Generators for Microwave Communications Systems, Recommendations for Improving Reliability of Stand-by. Tharp..........261–6; disc. 266
Epoxy Resin Casting of Dry-Type Current Transformers. Farneth, Gallousis..........194–7; disc. 197
Equation, A General Transmission Loss. Early, Watson, Smith..........510–16; disc. 516
Equation, A New Method of Determining Constants for the General Transmission Loss. Early, Watson..........1417–21; disc. 1421
Equipment, Two Large. Electric Arc Furnaces—Electrical Characteristics and Corrective. Luther, Ghesquiere, Quick..........1401–05; disc. 1406
Equivalent Circuit for the Concatenation of Induction Motors. Ku..........1214–18; disc. 1219
Equivalent Circuits for Single-Phase Motors. Slemon..........1335–42; disc. 1342
Erosion of Electric Contact Materials, High-Current. Wilson..........657–64; disc. 664
European Practices in Power Line Design, Investigation of. Fritz..........505–09; disc. 509

Evaluation and Application of Silicone-Organic Resin Combinations for Dry-Type Transformer Insulation. Simmons, Scheideler......155–60; disc. 160
Excitation, D-C Machines: Response to Impact. Brockman, Linkous......500–03; disc. 503
Excitation System Response, An Approach to the Definition of. Bliss......1008–12; disc. 1012
Expanded ACSR, Measurement of Resistance and Reactance of. Tompkins, Jones, Tuttle......368–73; disc. 373
Experiences With the Use of Aluminum in Windings for Dry-Type Power Transformers. Tipton......1201–04
Experimental Gas-Insulated 138-Kv Current Transformer, An. Camilli......100–03; disc. 103

F

Factors Concerned with the Use of Protective Devices Shunting Reactors, Review of the. (Committee Report)......903–13
Fault Currents for High-Voltage Circuit-Breaker Interruption, Analysis of. Lantz......41–5
Fault Location Methods, Bibliography and Summary of. (Committee Report)......1423–7; disc. 1427
Feeder, Automatically Switched Capacitors in Steps on a Single Distribution. Fowler, Thomas......311–14; disc. 314
Feeder Planning, Distribution-Substation and Primary. Denton, Reps......484–97; disc. 497
Field Conductor Materials for Turbine Generators, Improved. Holley, Savidge......72–6
Field Current Sources for Electric Defibrillation. Betz......33–6
Field Ripple Detector for Synchronous Generators, A Transductor Type. McConnell...476–9; disc. 479
Field Tests Concerning Circuit Breakers for Switching Long 230-Kv Lines, Design Problems and. Umphrey, Marsden......693–701; disc. 701
Field Tests on a 138-Kv High-Speed Oil Circuit Breaker at Philip Sporn Power Plant. Naef, Hambrick......710–24; disc. 724
Field Windings, Detection of Grounds in Generator. Barkle, Sterrett, Fountain......467–70; disc. 470
Fields, Effect of Skew on Induction Motor Magnetic. Linkous......760–5; disc. 765
Filter, Design of the Adjustable Lin-O-Phase. Lee......273–7; disc. 277
500-Megavolt-Ampere Air Magnetic Circuit Breaker of Simplified Design, A New. Reilly, Weston......1093–8; disc. 1098
5,000,000 Kva, A 69-Kv Compressed Air Circuit Breaker for. Kane, Walker......705–09; disc. 709
Flatiron Power Plant, Pumped Storage and Hydro Generation at. Denton, Britt....614–18; disc. 618
Flowmeter, Principles and Application of the Ultrasonic. Swengel, Hess, Waldorf..112–17; disc. 117
Flux Measurements in Magnetic Air Circuit Breaker Interrupters. Carter......1062–5; disc. 1065
Flux-Switch Alternators, Design Principles of. Rauch, Johnson......1261–8; disc. 1268
Forced Oil Cooled Rotary Welding Transformer, The. Shenk......873–80
Forecasting, Electric Utility Load. Godard....1428–40
Forecasting the Demand for Electricity. Hooke......993–1005; disc. 1005
Formulas from Functions of Voltage Phase Angles, The Determination of Incremental and Total Loss. Cahn......161–71; disc. 171
Foundations, Maximum Short Circuit and Faulty Synchronizing Torques on Generator. Ruskin......618–23; disc. 623
4-Pole Induction Motor, Ten Part-Winding Arrangements in Sample. Courtin....1248–53; disc. 1253
Freezing Oil-Type Pipe Cables. Merrell......1023–31; disc. 1031
Frequency Changer, Double-Energy Conversion in an Air Gap—A Novel Asynchronous. LaPierre, Louis......1373–5; disc. 1376
Frequency Control System for Central Station Power Automatic Load. Ehrenberg......787–95
Frequency Modulated System, An Investigation of the Capture Effect in a Narrow-Band. Hedges......289–91; disc. 292
Frequency Noise on Power Lines, A Study of Carrier-. Moynihan, Sparlin:
  Part IV. Conclusion of Field Measurements......795–800
Frequency, Vibration in 2-Pole Induction Motors Related to Slip. Summers......69–72
Functional Life Evaluation of Group-2 Dry-Type Power Transformers. Zambell......956–70
Functional Life Expectancy Tests for Liquid-Filled Distribution Transformers. Lockie..977–82; disc. 982
Functional Life Tests of Insulation Systems for Dry Type Transformers. Narbut..1057–61; disc. 1061
Functional Temperature Endurance Tests of Ventilated Dry Type Power and Distribution Transformers, Proposed Test Code for. (Committee Report)......971–5; disc. 975
Functional Temperature Endurance Tests on a Silicone Glass Fiber Insulation System for Dry-Type Transformers. Manning......91–8; disc. 98
Functions of Voltage Phase Angles, The Determination of Incremental and Total Loss Formulas from. Cahn......161–71; disc. 171
Fundamental Relations of System Voltage Drop and System Loads. Miller, Robbins......267–72; disc. 272
Fundamentals on Capacitance Switching, Some. Johnson, Schultz, Schultz, Shores......727–36; disc. 736
Furnace Loads, Voltage Dip and Synchronous Condenser Swings Caused by Arc. Concordia......951–6
Fuses, Ribbon Elements for High-Voltage Current-Limiting. Powell, Schuck......635–41; disc. 641
Fuses With Single Wire Element, The Calculation of the Complete Time/Current Characteristics of Cartridge. Guile......1108–15; disc. 1115
Future Application Needs of Carrier Pilot Relaying. Cramer, Kringa......1233–5; disc. 1235

G

Gas-Insulated 138-Kv Current Transformer, An experimental. Camilli......100–03; disc. 103
Gas-Pressurized 120-Kv and 161-Kv Pipe-Type Cables in Ontario. Kozak, Prescott....184–92; disc. 192
General Study of Area Supply Methods. Casazza, Rankin......1328–34; disc. 1334–5
General Transmission Loss Equation, A. Early, Watson, Smith......510–16; disc. 516
Generating Station Auxiliary Busses, Transfer of Steam-Electric. Lewis, Marsh......322–30; disc. 330
Generating Units, An Investigation of the Economic Size of Steam-Electric. Kirchmayer, Mellor, O'Mara, Stevenson......600–09; disc 609.
Generation at Flatiron Power Plant, Pumped Storage and Hydro. Denton, Britt......614–18; disc. 618
Generation, Co-ordination of Hydro and Steam. Watchorn......142–8; disc. 148
Generator Field Windings, Detection of Grounds in. Barkle, Sterrett, Fountain......467–70; disc. 470
Generator Foundations, Maximum Short Circuit and Faulty Synchronizing Torques on. Ruskin......618–23; disc. 623
Generator Operating and Maintenance Methods of the Southern California Edison Company, Steam Turbine. Sidway, Clevenger......60–5
Generator Operation and Maintenance Practice of Philadelphia Electric Company, Turbine. Gallagher......48–9
Generator, Operation of Hydrogen-Cooled Turbine. Sterrett, Towne......433–8; disc. 439
Generator Stator Winding Temperatures at Various Hydrogen Pressures, Turbine. Alger, Kilbourne, Snell......232–50; disc. 250
Generator, Test Report on a Fully Supercharged. Beckwith, Koetting, Rosenberg, Staats......56–9
Generators, A Transductor Type Field Ripple Detector for Synchronous. McConnell......476–9; disc. 479
Generators During Off-Peak High Power Factor Periods—Practices of One Utility in a Metropolitan area Operation of Turbine. Roberts, Webb......461–5; disc. 466
Generators, Eccentricity, Vibration, and Shaft Currents in Turbine. Rosenberg......38–41
Generators for Improved Performance, Rewinding A-C. Seline......472–4; disc. 474
Generators for Microwave Communications Systems Recommendations for Improving Reliability of Stand-by Engine. Tharp......261–6; disc. 266
Generators, Production and Installation of Vertical Water Wheel. Houser, Hindle, Tyerman......536–43; disc. 543
Generators, Stray Losses in the Armature End Iron of Large Turbine. Winchester......381–9; disc. 389
Glass Fiber Insulation System for Dry-Type Transformers, Functional Temperature Endurance Tests on a Silicone. Manning......91–8; disc. 98
Gradients on High-Voltage Transmission Lines, Voltage. Adams......5–11
Grids for High-Voltage Stations, Grounding. Gross, Wise.
  Part II. Resistance of Large Rectangular Plates......801–09; disc. 809
Grids with Nonuniform Soil, Efficiency of Grounding. Zaborszky......1230–3
Ground-Relay Problems, Some Utility. Barnes, McConnell......417–28; disc. 428
Grounding Grids for High-Voltage Stations. Gross, Wise.
  Part II. Resistance of Large Rectangular Plates......801–09; disc. 809
Grounding Grids with Nonuniform Soil, Efficiency of. Zaborszky......1230–3
Grounds in Generator Field Windings, Detection of. Barkle, Sterrett, Fountain......467–70; disc. 470
Group-2 Dry-Type Power Transformers, Functional Life Evaluation of. Zambell......956–70

H

Harmonics, Single-Phase Induction Motor Noise Due to Dissymmetry. Muster, Wolfert......1365–72; disc. 1372
Hazards in Central Office Communications Equipment, Protection of Personnel Against Electrical Shock. Jones......893–6.
Heat Flow Problems, An Analogue Solution of Cable. deHaas, Sandiford, Cameron......315–18; disc. 318
High-Capacity Anode Air Circuit Breaker, A New. Bottonari, Sprow......1297–1302; disc. 1302
High-Capacity Outdoor Oil Circuit Breakers, Dynamics of. Barkan......671–6; disc. 676
High-Capacity Outdoor Oil Circuit Breakers, The Results of 7 Years' Experience With. Balentine, Darrow......665–70; disc. 671
High-Current Arc Erosion of Electric Contact Materials. Wilson......657–64; disc. 664
High-Current Testing of Air-Disconnect Switches. Gostin......21–5
High-Temperature Classification of Rubber and Rubberlike Insulation of Network Cable by Oven Heating Tests. Couch, Crowdes......930–4; disc. 944, 1463
High Voltage Busses and Insulators During Short Circuits, Behavior of. Milton, Chambers......742–6; disc. 746
High-Voltage Circuit-Breaker Interruption, Analysis of Fault Currents for. Lantz......41–5
High-Voltage Current-Limiting Fuses, Ribbon Elements for. Powell, Schuck......635–41; disc. 641
High-Voltage Instrument Transformers, The Application of a New Nontracking Butyl to. Pfuntner, Norman, Wilterdink......1173–6
High-Voltage Rubber-Insulated Cables, Some Performance Characteristics of. Rosch......1219–24; disc. 1224
High-Voltage Rubber Insulation, Modern. Couch, Hunt, Kenney, Ware......1387–97; disc. 1398
High-Voltage Stations, Grounding Grids for. Gross, Wise.
  Part II. Resistance of Large Rectangular Plates......801–09; disc. 809
High-Voltage Switching Stations and Transformers, Direct-Stroke Protection of. Griscom, Dillard, Hileman......354–65; disc. 365
High-Voltage Transmission Lines, Voltage Gradients on. Adams......5–11
Hydro and Steam Generation, Co-ordination of. Watchorn......142–8; disc. 148
Hydro Generation at Flatiron Power Plant, Pumped Storage and. Denton, Britt......614–18; disc. 618
Hydroelectric Sites in Western North Carolina, Development of Small. Gnuse......65–8
Hydroelectric Units as Practiced by Tennessee Valley Authority, Mechanical Alignment of Vertical-Shaft. Norris......586–9; disc. 589
Hydrogen-Cooled Turbine Generator, Operation of. Sterrett, Towne......433–8; disc. 439
Hydrogen Pressures, Turbine Generator Stator Winding Temperatures at Various. Alger, Kilbourne, Snell......232–50; disc. 250

I

(Ice) Relay Protection for Lines Being Sleet-Melted by the Short-Circuit Method. Hogan, Pebler......1067–71; disc. 1072
Impact Excitation, D-C Machines: Response to. Brockman, Linkous......500–03; disc. 503
Impedance Power Reactive Diagrams, A Simplified Method of Calculating Voltage Regulation Using Unit. Butler......304–10; disc. 310
Impedances, Digital Calculation of Network. Glimn, Habermann, Henderson, Kirchmayer......1285–95; disc. 1295
Impedances of Symmetrical 3-Phase Transformer Connections, Sequence. Cogbill......1313–23
Implementation of a Research Program for the Electric Utility Industry. Hobson, Lewis, Oldacre......545–50; disc. 550
Impregnated Paper Insulation for High-Voltage Cables, Research on the Electric Breakdown of Fully. Gazzana Priaroggia, Palandri..1343–57; disc. 1357
Improved Approximate Technique for Calculating Cable Temperature Transients, An. Van Wormer......277–80; disc. 280..
Improved Fast-Acting Thermal Relay and Its Application as a Cage Winding Protective Relay for Synchronous Machines. Baude......349–53; disc. 353
Improved Field Conductor Materials for Turbine Generators. Holley, Savidge......72–6
Impulse Testing, Magnetization of Transformer Cores During. Beavers, Holcomb, Leoni......118–23; disc. 123
Impulse Tests on Low-Voltage Windings of Distribution Transformers. Holcomb......1152–5; disc. 1155
Increased Current Ratings for Step Regulators. Sealey......737–42; disc. 742

Incremental and Total Loss Formulas from Functions of Voltage Phase Angles, The Determination of. Cahn....161–71; disc. 171
Incremental Cost of Power-Delivered Computer, An. Early, Phillips, Shreve....529–34; disc. 534
Induction Machine with Solid Iron Rotor, The. McConnell, Sverdrup....343–8; disc. 348
Induction Motor Magnetic Fields, Effect of Skew on. Linkous....760–5; disc. 765
Induction Motor Noise Due to Dissymmetry Harmonics, Single-Phase. Muster, Wolfert....1365–72; disc. 1372
Induction Motor, Ten Part-Winding Arrangements in Sample 4-Pole. Courtin....1248–53; disc. 1253
Induction Motors, Equivalent Circuit for the Concatenation of. Ku....1214–18; disc. 1219
Induction Motors, Predetermination of Sound Pressure Levels of Magnetic Noise of Polyphase. Erdelyi....1269–80; disc. 1280
Induction Motors Related to Slip Frequency, Vibration in 2-Pole. Summers....69–72
Induction Motors, Sonance Design of Large. Wall....1189–92
Induction Motors, The Transient Stalled Temperature Rise of Cast Aluminum Squirrel-Cage Rotors for. Rosenberry....819–24; disc. 824
Induction Torque Motors and Servomotors, Optimum Design of. Weiss....809–15
Industry, Implementation of a Research Program for the Electric Utility. Hobson, Lewis, Oldacre....545–50; disc. 550
Industry, Research in the Electric Power. Gaty....553–6; disc. 556
Installation of Vertical Water-Wheel Generators, Production and. Houser, Hindle, Tyerman....536–43; disc. 543
Instrument Transformers, The Application of a New Nontracking Butyl to High-Voltage. Pfuntner, Norman, Wilterdink....1173–6
(Instruments) Principles and Application of the Ultrasonic Flowmeter. Swengel, Hess, Waldorf....112–17; disc. 117
(Insulated Cables) Freezing Oil-Type Pipe Cables. Merrell....1023–31; disc. 1031
Insulated Cables, Some Performance Characteristics of High-Voltage Rubber-. Rosch....1219–24; disc. 1224
(Insulated Conductors) Aluminum-Sheathed Control Cable. McIlveen....1377–84; disc. 1384
(Insulated Conductors) Aluminum-Sheathed Power Cable. Del Mar, Merrell....292–8; disc. 298
(Insulated Conductors) An Analogue Solution of Cable Heat Flow Problems. deHaas, Sandiford, Cameron....315–18; disc. 318
(Insulated Conductors) An Improved Approximate Technique for Calculating Cable Temperature Transients. Van Wormer....277–80; disc. 280
(Insulated Conductors) Characteristic Properties of Secondary Network Cables. Rosch....939–44; disc. 944, 1463
(Insulated Conductors) Characteristics of Single-Conductor Electric Cable at High Frequency. Sabol....1280–5; disc. 1285
(Insulated Conductors) Co-ordination of Secondary Network Protection. Leinbach, Brookes....922–4; disc. 944, 1463
(Insulated Conductors) Gas-Pressurized 120-Kv and 161-Kv Pipe-Type Cables in Ontario. Kozak, Prescott....184–92; disc. 192
(Insulated Conductors) Limiters, Their Design Characteristics and Application. Heller, Matthysse....924–30; disc. 944, 1463
(Insulated Conductors) Oil Flow and Pressure Calculations for Pipe-Type Cable Systems. (Committee Report)....251–9; disc. 259
(Insulated Conductors) Overload Classifications for Secondary Network Cables. Graham....916–19; disc. 944, 1463
(Insulated Conductors) The Co-ordination of Power and Communication Cable Characteristics. Short....281–7; disc. 287
(Insulated Conductors) The Limiter—Its Basic Functions in Network Distribution Systems. Xenis....913–15; disc. 944, 1463
(Insulated Conductors) Time Current Damage Characteristics, Cable in Duct. Porter....919–21; disc. 944, 1463
Insulated Metallic-Sheathed Cables, Mineral. Jordan, Eager....198–212; disc. 212
Insulated Power Cable, Design and Evaluation of Butyl-Rubber-. Carroll, Lee, McKinley....1204–12; disc. 1212
Insulation Characteristics of Wood and Suspension Insulators in Series. Clayton, Shankle....1305–11; disc. 1312
Insulation, Corona Studies—In Relation to. Liao, Nye, Brustle, Anderson....1046–50; disc. 1050
Insulation Damage Curves for Network Cables, A Mathematical Method for Determining. Kolks....934–8; disc. 944, 1463
Insulation, Evaluation and Application of Silicone-Organic Resin Combinations for Dry-Type Transformer. Simmons, Scheideler....155–60; disc. 160
Insulation for High-Voltage Cables, Research on the Electric Breakdown of Fully Impregnated Paper. Gazzana Priaroggia, Palandri....1343–57; disc. 1357
Insulation, Modern High-Voltage Rubber. Couch, Hunt, Kenney, Ware....1387–97; disc. 1398
Insulation of Network Cable by Oven-Heating Tests, High-Temperature Classification of Rubber and Rubberlike. Couch, Crowdes....930–4; disc. 944, 1463
Insulation System for Dry-Type Transformers, Functional Temperature Endurance Tests on a Silicone Glass Fiber. Manning....91–8; disc. 98
Insulation Systems for Dry-Type Transformers, Functional Life Tests of. Narbut....1057–61; disc. 1061
Insulators During Short Circuits, Behavior of High-Voltage Busses and. Milton, Chambers....742–6; disc. 746
Insulators in Series, Insulation Characteristics of Wood and Suspension. Clayton, Shankle....1305–11; disc. 1312
Interconnected Power Systems, Load-Phase Tie-Line Energy Control of. Cahen....1–5
Intermittently Increased Kilovar Output of Large Capacitor Banks. Minder....749–51; disc. 751
Interpretation and Significance of Tests Indicating the Concentration of Polar Compounds in Transformer Oil. Johnson....774–80; disc. 780
Interrupters, Flux Measurements in Magnetic Air Circuit Breaker. Carter....1062–5; disc. 1065
Interrupters on A-C Test Circuits, Testing of D-C. Chen, Boehne....1073–9; disc. 1079
Interruption, Analysis of Fault Currents for High-Voltage Circuit-Breaker. Lantz....41–5
Interruption with an Air-Break Disconnect Switch, Power Autotransformer Current. Anderson....1157–63
Investigation of European Practices in Power Line Design. Fritz....505–09; disc. 509
Investigation of the Capture Effect in a Narrow-Band Frequency-Modulated System, An. Hedges....289–91; disc. 292
Investigation of the Economic Size of Steam-Electric Generating Units, An. Kirchmayer, Mellor O'Mara, Stevenson....600–09; disc. 609
Iron Conduit, A-C Resistance of Conventional Strand Power Cables in Nonmetallic Duct and in. Burrell, Morris....1014–21; disc. 1021
Iron Loss Curves for Small Motors from Motor Tests, Developing. Shaneman....1176–9
Iron of Large Turbine Generators, Stray Losses in the Armature End. Winchester....381–9; disc. 389
Iron Rotor, The Induction Machine with Solid. McConnell, Sverdrup....343–8; disc. 348

K

Kilovar Output of Large Capacitor Banks, Intermittently Increased. Minder....749–51; disc. 751

L

Laboratory, Capacitance-Switching Facilities at the Switchgear Development. Williams, Mankoff, Schneider....375–80; disc. 380
Levels of Magnetic Noise of Polyphase Induction Motors, Predetermination of Sound Pressure. Erdelyi....1269–80; disc. 1280
Life Evaluation of Group-2 Dry-Type Power Transformers, Functional. Zambell....956–70
Life Expectancy Tests for Liquid-Filled Distribution Transformers, Functional. Lockie....977–82; disc. 982
Life of Voltage-Regulating Relays, Contact. Schoendube, Elliott....1398–1400; disc. 1401
Life Tests of Insulation Systems for Dry-Type Transformers, Functional. Narbut....1057–61; disc. 1061
Lightning Arresters, Transient Durability Testing of Valve Type. Kalb, Yost....521–6; disc. 526
(Lightning) Direct-Strome Protection of High-Voltage Switching Stations and Transformers. Griscom, Dillard, Hileman....354–65; disc. 365
Lightning Protection in a 24-Kv Station—Field and Laboratory Studies. Armstrong, Ferguson, Hileman....1127–35; disc. 1135
(Limiter) A Mathematical Method for Determining Insulation Damage Curves for Network Cables. Kolks....934–8; disc. 944
(Limiter) Characteristic Properties of Secondary Network Cables. Rosch....939–44; disc. 944
(Limiter) Co-ordination of Secondary Network Protection. Leinbach, Brookes....922–4; disc. 944
(Limiter) High-Temperature Classification of Rubber and Rubberlike Insulation of Network Cable by Oven-Heating Tests. Couch, Crowdes....930–4; disc. 944
Limiter—Its Basic Functions in Network Distribution Systems, The. Xenis....913–15; disc. 944, 1463
(Limiter) Overload Classifications for Secondary Network Cables. Graham....916–19; disc. 944
(Limiter) Time Current Damage Characteristics, Cable in Duct. Porter....919–21; disc. 944
Limiters, Their Design Characteristics and Application. Heller, Matthysse....924–30; disc. 944, 1463
Lin-O-Phase Filter, Design of the Adjustable. Lee....273–7; disc. 277
Line and Transformer Bank Relaying Systems. Blackburn, Rockefeller....334–9; disc. 339
Line Constants With Tensors, ORACLE Computes. Shipley, Hochdorf, Watson....1052–6; disc. 1056
Lines Being Sleet-Melted by the Short-Circuit Method, Relay Protection for. Hogan, Pebler....1067–71; disc. 1072
Lines, Electromagnetic Unbalance of Untransposed Transmission. Gross, Nelson:
Part II....887–93
Liquid-Filled Distribution Transformers, Functional-Life Expectancy Tests for. Lockie....977–82; disc. 982
Load-Flow and Stability Equivalent for Power System Representation on A-C Network Analyzers, Combination. Brown, Cloues....782–6; disc. 786
Load Forecasting, Electric Utility. Godard....1428–40
Load Forecasting, The Application of Business Machines to Electrical Utility. Gruetter....854–8
Load Frequency Control System for Central Station Power, Automatic. Ehrenberg....787–95
Load-Phase Tie-Line Energy Control of Interconnected Power Systems. Cahen....1–5
Load Shedding, Automatic. (Committee Report)....1143–5; disc. 1145
Loads, Fundamental Relations of System Voltage Drop and System. Miller, Robbins....267–72; disc. 272
Location Methods, Bibliography and Summary of Fault. (Committee Report)....1423–7; disc. 1427
Loci of Salient-Pole Synchronous Motors: An Extension of Blondel Theory, Current. Douglas....1080–2; disc. 1082
Look to the Future of Power Transmission in the West, A. Hunkins....591–7; disc. 598
Loss Curves for Small Motors from Motor Tests, Developing Iron. Shaneman....1176–9
Loss Equation, A General Transmission. Early, Watson, Smith....510–16; disc. 516
Loss Equation, A New Method of Determining Constants for General Transmission. Early, Watson....1417–21; disc. 1421
Loss Formulas from Functions of Voltage Phase Angles, The Determination of Incremental and Total. Cahn....161–71; disc. 171
Losses in the Armature End Iron of Large Turbine Generators, Stray. Winchester....381–9; disc. 389
Low-Voltage Windings of Distribution Transformers, Impulse Tests on. Holcomb....1152–5; disc. 1155

M

Machine Transient Rotor Saliency on Changes in Terminal Voltage, Effect of Synchronous-. Concordia....25–31
Machine with Solid Iron Rotor, The Induction. McConnell, Sverdrup....343–8; disc. 348
Machines—Method for Short-Circuit Calculations, D-C. Cybulski, O'Connor....214–21
Machines: Response to Impact Excitation, D-C. Brockman, Linkous....500–03; disc. 503
Machines—Short-Circuit Calculations and Test Results, D-C. O'Connor, Cybulski....222–30; disc. 230
Machines to Electrical Utility Load Forecasting, The Application of Business. Gruetter....854–8
Machines, Two-Axis Method of Analyzing Electric. Tang, Cosgriff....1449–55
Magnetic Air Circuit Breaker Interrupters, Flux Measurements in. Carter....1062–5; disc. 1065
Magnetic Circuit Breaker of Simplified Design, A New 500-Megavolt-Ampere Air. Reilly, Weston....1093–8; disc. 1098
Magnetic Fields, Effect of Skew on Induction Motor. Linkous....760–5; disc. 765
Magnetic Noise of Polyphase Induction Motors, Predetermination of Sound Pressure Levels of. Erdelyi....1269–80; disc. 1280
Magnetization of Transformer Cores During Impulse Testing. Beavers, Holcomb, Leoni....118–23; disc. 123
Maintenance Practice of Philadelphia Electric Company, Turbine Generator Operation and. Gallagher....48–9
Manufacturer's Research in Relation to Electrical Utilities. Parker, Baird....557–06

Materials for Turbine Generators, Improved Field Conductor. Holley, Savidge..........72–6
Materials, High-Current Arc Erosion of Electric Contact. Wilson..........657–64; disc. 664
Mathematical Method for Determining Insulation Damage Curves for Network Cables, A. Kolks..........934–8; disc. 944, 1463
Maximum Short Circuit and Faulty Synchronizing Torques on Generator Foundations. Ruskin..........618–23; disc. 623
Measurement, Apparatus Noise. Wells..........1170–3
Measurement of Carrier Characteristics on Power Cables, A Method of. Sparlin, Moynihan...31–3
Measurement of Resistance and Reactance of Expanded ACSR. Tompkins, Jones, Tuttle..........368–73; disc. 373
Measurement of Resistance of Energized A-C Motor Windings. Waldschmidt......1303–04; disc. 1305
Measurements in Magnetic Air Circuit Breaker Interrupters, Flux. Carter.......1062–5; disc. 1065
Measurements on D-C Armatures, Correlation of Temperature. Gerbetz, Ewing...391–4; disc. 395
Mechanical Alignment of Vertical-Shaft Hydroelectric Units as Practiced by Tennessee Valley Authority. Norris..........586–9; disc. 589
Megavolt-Ampere Air Magnetic Circuit Breaker of Simplified Design, A New 500-. Reilly, Weston..........1093–8; disc. 1098
Metadyne Transients. Fegley..........1179–88
Metallic-Sheathed Cables, Mineral-Insulated. Jordan, Eager..........198–212; disc. 212
Method for Determining Economical ACSR Conductor Sizes for Distribution Systems, A. Funkhouser, Huber..........479–83; disc. 483
Method for Part-Winding Starting of Polyphase Motors, A New. Alger, Agacinsky.....1455–62; disc. 1462
Method for Short-Circuit Calculations, D-C Machines—. Cybulski, O'Connor..........214–21
Method for Studying Circuit Transient Recovery Voltage Characteristics of Electric Power Systems, A. Kotheimer..........1083–6; disc. 1086
Method for the Step-by-Step Calculations in Power System Transient Stability Studies, A Rational. Norinder..........1087–91; disc. 1091
Method of Analyzing Electric Machines, Two-Axis. Tang, Cosgriff..........1449–55
Method of Calculating Voltage Regulation Using Unit Impedance Power Reactive Diagrams, A Simplified. Butler..........304–10; disc. 310
Method of Determining Constants for the General Transmission Loss Equation, A New. Early, Watson..........1417–21; disc. 1421
Method of Measurement of Carrier Characteristics on Power Cables, A. Sparlin, Moynihan......31–3
Methods, Bibliography and Summary of Fault Location. (Committee Report).......... 1423–7; disc. 1427
Metropolitan Area, Operation of Turbine Generators During Off-Peak High Power Factor Periods—Practices of One Utility in a. Roberts, Webb..........461–5; disc. 466
Microwave Communications Systems, Recommendations for Improving Reliability of Stand-by Engine Generators for. Tharp..........261–6; disc. 266
Microwave System Parameters for Reliable Communications. Alvira, Corbell.......1100–07; disc. 1107
Mineral-Insulated Metallic-Sheathed Cables. Jordan, Eager..........198–212; disc. 212
Modern High-Voltage Rubber Insulation. Couch, Hunt, Kenney, Ware..........1387–97; disc. 1398
Motor Circuit, Weighted Mutual Reactances for a Triple-Cage. Martin..........765–8
Motor Magnetic Fields, Effect of Skew on Induction. Linkous..........760–5; disc. 765
Motor Noise Due to Dissymmetry Harmonics, Single-Phase Induction. Muster, Wolfert..........1365–72; disc. 1372
Motor, Ten Part-Winding Arrangements in Sample 4-Pole Induction. Courtin......1248–53; disc. 1253
Motor Testing, Application of Statistics to. Oldenkamp..........815–18; disc. 818
Motor Windings, Measurement of Resistance of Energized A-C. Waldschmidt.....1303–04; disc. 1305
Motors, A New Method for Part-Winding Starting of Polyphase Motors. Alger, Agacinsky..........1455–62; disc. 1462
Motors and Servomotors, Optimum Design of Induction Torque. Weiss..........809–15
Motors, Equivalent Circuit for the Concatenation of Induction. Ku..........1214–18; disc. 1219
Motors, Equivalent Circuits for Single-Phase. Slemon..........1335–42; disc. 1342
Motors from Motor Tests, Developing Iron Loss Curves for Small. Shaneman..........1176–9
Motors in Power Plants, Economic Selection of Auxiliary Drive. Gross, Bobrowicz.....1237–46; disc. 1246
Motors, Predetermination of Sound Pressure Levels of Magnetic Noise of Polyphase Induction. Erdelyi..........1269–80; disc. 1280
Motors Related to Slip Frequency, Vibration in 2-Pole Induction. Summers..........69–72
Motors, Sonance Design of Large Induction. Wall..........1189–92
Motors, The Transient Stalled Temperature Rise of Cast Aluminum Squirrel Cage Rotors for Induction. Rosenberry..........819–24, disc. 824
Multiplexing, Quadriphase—A New Approach to Time Division. Evans, Lowe..........900–03

N

Narrow-Band Frequency Modulated System, An Investigation of the Capture Effect in a. Hedges..........289–91; disc. 292
Network Analyzers, Combination Load-Flow and Stability Equivalent for Power System Representation on A-C. Brown, Cloues.....782–6; disc. 786
Network Cable by Oven Heating Tests, High Temperature Classification of Rubber and Rubberlike Insulation of. Couch, Crowdes..........930–4; disc. 944, 1463
Network Cables, A Mathematical Method for Determining Insulation Damage Curves for. Kolks..........934–8; disc. 944, 1463
Network Cables, Characteristic Properties of Secondary. Rosch..........939–44; disc. 944, 1463
Network Cables, Overload Classifications for Secondary. Graham..........916–19; disc. 944, 1463
Network Distribution Systems, The Limiter—Its Basic Functions in. Xenis......913–15; disc. 944, 1463
Network Impedances, Digital Calculation of. Glimn, Habermann, Henderson, Kirchmayer..........1285–95; disc. 1295
Network Protection, Co-ordination of Secondary. Leinbach, Brookes..........922-4; disc. 944, 1463
Network Systems, The Use of Probability in the Design and Operation of Secondary. Neagle, Nelson..........567–72; disc. 572
Network Vaults, Coincident-Outage Probability in Secondary-. Reps..........580–5; disc. 585
Networks, Basic Sequence. Kirschbaum.......771–4
New Method for Part-Winding Starting of Polyphase Motors, A. Alger, Agacinsky..1455–62; disc. 1462
New Method of Determining Constants for the General Transmission Loss Equation, A. Early, Watson..........1417–21; disc. 1421
Noise Control, Recent Contributions to Transformer Audible. Conover, Ringlee.......77–90; disc. 90
Noise Due to Dissymmetry Harmonics, Single-Phase Induction Motor. Muster, Wolfert..........1365–72; disc. 1372
Noise Measurement, Apparatus. Wells.......1170–3
Noise of Polyphase Induction Motors, Predetermination of Sound Pressure Levels of Magnetic. Erdelyi..........1269–80; disc. 1280
Noise on Power Lines, A Study of Carrier-Frequency. Moynihan, Sparlin:
  Part IV. Conclusion of Field Measurements..........795–800
Noise Tests on Large Power Transformers, An Anechoic Chamber for. Benoit, Hemmes, Schulz.....50–6
Nontension Aluminum Connectors. Boyer, Korges..........844–7; disc. 847
North Carolina, Development of Small Hydroelectric Sites in Western. Gnuse..........65–8
North Dakota, Bureau of Reclamation 230-Kv Transmission Lines in. Austin..........1147–51

O

Oil Circuit Breaker at Philip Sporn Power Plant, Field Tests on a 138-Kv High-Speed. Naef, Hambrick..........710–24; disc. 724
Oil Circuit Breakers, Application of Volume Theory of Dielectric Strength to. Wilson, Streater, Tuohy.......... 677–84; disc. 684
Oil Circuit Breakers, Dynamics of High-Capacity Outdoor. Barkan..........671–6; disc. 676
Oil Circuit Breakers, The Results of 7 Years' Experience With High-Capacity Outdoor. Balentine, Darrow..........665–70; disc. 671
Oil Cooled Rotary Welding Transformer, The Forced. Shenk..........873–80
Oil Flow and Pressure Calculations for Pipe Type Cable Systems. (Committee Report)...251–9; disc. 259
Oil, Interpretation and Significance of Tests Indicating the Concentration of Polar Compounds in Transformer. Johnson..........774–80; disc. 780
Oil-Type Pipe Cables, Freezing. Merrell..........1023–31; disc. 1031
161-Kv Disconnecting Switches, Results of High-Current Tests on. McNerney..........104–08; disc. 108
161-Kv Pipe Type Cables in Ontario, Gas Pressurized 120-Kv and. Kozak, Prescott...184–92; disc. 192
138-Kv Current Transformer, An Experimental Gas-Insulated. Camilli..........100–03; disc. 103
138-Kv High Speed Oil Circuit Breaker at Philip Sporn Power Plant, Field Tests on a. Naef, Hambrick..........710–24; disc. 724
120-Kv and 161-Kv Pipe-Type Cables in Ontario, Gas-Pressurized. Kozak, Prescott....184–92; disc. 192
Ontario, Gas-Pressurized 120-Kv and 161-Kv Pipe-Type Cables in. Kozak, Prescott..........184–92; disc. 192
Operating Experience With Aluminum Distribution Conductors in the Philadelphia Electric Company, Design Problems and. Nelson, Garrett..........825–8; disc. 828
Operation of Hydrogen-Cooled Turbine Generator. Sterrett, Towne..........433–8; disc. 439
Operation of Turbine Generators During Off-Peak High Power Factor Periods—Practices of One Utility in a Metropolitan Area. Roberts, Webb..........461–5; disc. 466
Optimum Design of Induction Torque Motors and Servomotors. Weiss..........809–15
ORACLE Computes Line Constants With Tensors. Shipley, Hochdorf, Watson......1052–6; disc. 1056
Organic Resin Combinations for Dry-Type Transformer Insulation, Evaluation and Application of Silicone-. Simmons, Scheideler..........155–60; disc. 160
Oscillations of Coupled Windings. Abetti, Adams, Maginniss..........12–21
Outage Probability in Secondary-Network Vaults, Coincident-. Reps..........580–5; disc. 585
Outdoor Oil Circuit Breakers, Dynamics of High-Capacity. Barkan..........671–6; disc. 676
Outdoor Oil Circuit Breakers, The Results of 7 Years' Experience with High-Capacity. Balentine, Darrow..........665–70; disc. 671
Oven-Heating Tests, High Temperature Classification of Rubber and Rubberlike Insulation of Network Cable by. Couch, Crowdes.930–4; disc. 944, 1463
Overload Classifications for Secondary Network Cables. Graham..........916–19; disc. 944, 1463

P

Paper Insulation for High-Voltage Cables, Research on the Electric Breakdown of Fully Impregnated. Gazzana Priaroggia, Palandri..1343–57; disc. 1357
Parameters for Reliable Communications, Microwave System. Alvira, Corbell.... .1100–07; disc. 1107
Parameters, Power Distribution System. Kidder, Neher..........125–40; disc. 140
Part-Winding Arrangements in Sample 4-Pole Induction Motor, Ten. Courtin.....1248–53; disc. 1253
Performance Characteristics of High-Voltage Rubber-Insulated Cables, Some. Rosch..........1219–24; disc. 1224
Performance, Rewinding A-C Generators for Improved. Seline..........472–4; disc. 474
Personnel Against Electrical Shock Hazards in Central Office Communications Equipment, Protection of. Jones..........893–6
Phase Angles, The Determination of Incremental and Total Loss Formulas from Functions of Voltage. Cahn..........161–71; disc. 171
Philadelphia Electric Company, Design Problems and Operating Experience With Aluminum Distribution Conductors in the. Nelson, Garrett..........825–8; disc. 828
Philadelphia Electric Company, Turbine Generator Operation and Maintenance Practice of. Gallagher..........48–9
Philip Sporn Power Plant, Field Tests on a 138-Kv High-Speed Oil Circuit Breaker at. Naef, Hambrick..........710–24; disc. 724
Pilot Relaying, Future Application Needs of Carrier. Cramer, Krings..........1233–5; disc. 1235
Pipe Cables, Freezing Oil-Type. Merrell..........1023–31; disc. 1031
Pipe-Type Cable Systems, Oil Flow and Pressure Calculations for. (Committee Report) 251–9; disc. 259
Pipe-Type Cables in Ontario, Gas-Pressurized 120-Kv and 161-Kv. Kozak, Prescott.. ..184–92; disc. 192
Pittsburgh Downtown 69-Kv Power Supply:
  Part I. Planning. Hill..........643–7; disc. 647
  Part II. Substation. Gue..........648–52; disc. 652
  Part III. Switchgear Development. Pierson..........653–6; disc. 656
Planning, Distribution-Substation and Primary Feeder. Denton, Reps..........484–97; disc. 497
Planning Practices, System. (Committee Report)..........896–900
Planning, Principles and Practices of Modern System. Fugill..........1323–26; disc. 1327
Planning, Rural Electric System. Rixse..........1410–16; disc. 1416
Polar Compounds in Transformer Oil, Interpretation and Significance of Tests Indicating the Concentration of. Johnson.......... 774–80; disc. 780
Polyphase Induction Motors, Predetermination of Sound Pressure Levels of Magnetic Noise of. Erdelyi..........1269–80; disc. 1280
Polyphase Motors, A New Method for Part-Winding Starting of. Alger, Agacinsky.1455–62; disc. 1462
Power and Communication Cable Characteristics, The Co-ordination of. Short..........281–7; disc. 287
Power and Distribution Transformers, Proposed Test Code for Functional Temperature Endurance Tests of Ventilated Dry-Type. (Committee Report)..........971–5; disc. 975

Power, Automatic Load Frequency Control System for Central Station. Ehrenberg..............787–95
Power Autotransformer Current Interruption with an Air-Break Disconnect Switch. Anderson..1157–63
Power Cable, Aluminum-Sheathed. Del Mar, Merrell..............................292–8; disc. 298
Power Cable, Design and Evaluation of Butyl-Rubber-Insulated. Carroll, Lee, McKinley..............1204–12; disc. 1212
Power Cables, A Method of Measurement of Carrier Characteristics on. Sparlin, Moynihan......31–3
Power Cables in Nonmetallic Duct and in Iron Conduit, A-C Resistance of Conventional Strand. Burrell, Morris....................1014–21; disc. 1021
Power Cables, Surge Attenuation in. Valentine, Dillard, Clayton. ....1115–21; disc. 1122
Power Class Recloser for Higher Speed Clearing of Distribution Circuits, A. Field, Leatherberry..............................986–91; disc. 991
Power-Delivered Computer, An Incremental Cost of. Early, Phillips, Shreve..........529–34; disc. 534
Power Distribution System Parameters. Kidder, Neher..............................125–40; disc. 140
Power Factor Periods—Practices of One Utility in a Metropolitan Area, Operation of Turbine Generators During Off-Peak High. Roberts, Webb..............................461–5; disc. 466
(Power Generation) An Approach to the Definition of Excitation System Response. Bliss..............................1008–12; disc. 1012
(Power Generation) An Investigation of the Economic Size of Steam-Electric Generating Units. Kirchmayer, Mellor, O'Mara, Stevenson..............................600–09; disc. 609
(Power Generation) Development of Small Hydroelectric Sites in Western North Carolina. Gnuse.....65–8
(Power Generation) Mechanical Alignment of Vertical-Shaft Hydroelectric Units as Practiced by Tennessee Valley Authority. Norris.........586–9; disc. 589
(Power Generation) Production and Installation of Vertical Water Wheel Generators. Houser, Hindle, Tyerman..............536–43; disc. 543
(Power Generation) Transfer of Steam-Electric Generating-Station Auxiliary Busses. Lewis, Marsh..............................322–30; disc. 330
(Power Generation) Transfer Tests on Station Auxiliary Busses. Backer, Barth, Huse, Taylor..............................1441–5; disc. 1446
Power Industry, Research in the Electric. Gaty..............................553–6; disc. 556
Power-Line Carrier Coupling—An Analysis. Bienhoff..............................1163–70
Power Line Design, Investigation of European Practices in. Fritz....................505–09; disc. 509
Power Lines, A Study of Carrier-Frequency Noise on. Moynihan, Sparlin:
  Part IV. Conclusion of Field Measurements..............................795–800
Power Plant, Field Tests on a 138-Kv High Speed Oil Circuit Breaker at Philip Sporn. Naef, Hambrick..............................710–24; disc. 724
Power Plant, Pumped Storage and Hydro Generation at Flatiron. Denton, Britt.........614–18; disc. 618
Power Plants, Economic Selection of Auxiliary Drive Motors in. Gross, Bobrowicz. 1237–46; disc. 1246
Power Reactive Diagrams, A Simplified Method of Calculating Voltage Regulation Using Unit Impedance. Butler...............304–10; disc. 310
Power Supply, Pittsburgh Downtown 69-Kv:
  Part I. Planning. Hill...........643–7; disc. 647
  Part II. Substation. Gue........648–52; disc. 652
  Part III. Switchgear Development. Pierson..............................653–6; disc. 656
Power Switchgear, Aluminum Widely Used in. Talento..............................839–43; disc. 843
Power System Representation on A-C Network Analyzers, Combination Load-Flow and Stability Equivalent for. Brown, Cloues..782–6; disc. 786
Power System Transient Stability Studies, A Rational Method for the Step-by-Step Calculations in. Norinder.................... 1087–91; disc. 1091
Power Systems, A Computer for Economic Scheduling and Control of. Morrill, Blake..............................1136–41; disc. 1141
Power Systems, A Method for Studying Circuit Transient Recovery Voltage Characteristics of Electric. Kotheimer..................1083–6; disc. 1086
Power Systems, Load-Phase Tie-Line Energy Control of Interconnected. Cahen....................1–5
Power Transformer Design, Control of Electrostatic Voltage Distribution in. Bennon, Cossaart..............................1122–5; disc. 1125
Power Transformers, Experiences With the Use of Aluminum in Windings for Dry-Type. Tipton..1201–04
Power Transformers, Functional Life Evaluation of Group-2 Dry-Type. Zambell.............956–70
Power Transmission in the West, A Look to the Future of. Hunkins. ....591–7; disc. 598
Practical Application of Sag and Tension Calculations to Transmission Line Design. Lummis, Fischer..............................402–13; disc. 413
Practices, System Planning. (Committee Report)..............................896–900
Predetermination of Sound Pressure Levels of Magnetic Noise of Polyphase Induction Motors. Erdelyi..............................1269–80; disc. 1280
Pressure Calculations for Pipe-Type Cable Systems, Oil Flow and. (Committee Report)..............................251–9; disc. 259
Pressurized 120-Kv and 161-Kv Pipe-Type Cables in Ontario, Gas. Kozak, Prescott...184–92; disc. 192
Primary and Secondary Voltages for Commercial Areas, Economics of Higher. Lawrence, Reps..............................1034–45; disc. 1045
Primary Feeder Planning, Distribution Substation and. Denton, Reps..................484–97; disc. 497
Principles and Application of the Ultrasonic Flowmeter. Swengel, Hess, Waldorf..........112–17; disc. 117
Principles and Practices of Modern System Planning. Fugill......................1323–26; disc. 1327
Probability in the Design and Operation of Secondary Network Systems, The Use of. Neagle, Nelson..............................567–72; disc. 572
Problems, An Analogue Solution of Cable Heat Flow. deHaas, Sandiford, Cameron.....315–18; disc. 318
Problems and Operating Experience with Aluminum Distribution Conductors in the Philadelphia Electric Company, Design. Nelson, Garrett..............................825–8; disc. 828
Problems, Traveling Wave Protection. Boehne:
  Part II..............................880–7
Production and Installation of Vertical Water-Wheel Generators. Houser, Hindle, Tyerman..............................536–43; disc. 543
Proposed Test Code for Functional Temperature Endurance Tests of Ventilated Dry-Type Power and Distribution Transformers. (Committee Report)..............................971–5; disc. 975
Protection, Co-ordination of Secondary Network. Leinbach, Brookes.........922–4; disc. 944, 1463
Protection for Lines Being Sleet-Melted by the Short-Circuit Method, Relay. Hogan, Pebler..............................1067–71; disc. 1072
Protection in a 24-Kv Station—Field and Laboratory Studies, Lightning. Armstrong, Ferguson, Hileman.......................1127–35; disc. 1135
Protection of High-Voltage Switching Stations and Transformers, Direct-Stroke. Griscom, Dillard, Hileman.................. 354–65; disc. 365
Protection of Personnel Against Electrical Shock Hazards in Central Office Communications Equipment. Jones..............................893–6
Protection Problems, Traveling Wave. Boehne.......
  Part II..............................880–7
Protective Devices Shunting Reactors, Review of the Factors Concerned with the Use of. (Committee Report)..............................903–13
(Protective Devices) Surge Attenuation in Power Cables. Valentine, Dillard, Clayton....1115–21; disc. 1122
(Protective Devices) Transient Durability Testing of Valve Type Lightning Arresters. Kalb, Yost..............................521–6; disc. 526
Pumped Storage and Hydro Generation at Flatiron Power Plant. Denton, Britt.... 614–18; disc. 618

Q

Quadriphase—A New Approach to Time Division Multiplexing. Evans, Lowe........... 900–03

R

Ratings for Step Regulators, Increased Current. Sealey..............................737–42; disc. 742
Rational Method for the Step-by-Step Calculations in Power System Transient Stability Studies, A. Norinder....................1087–91; disc. 1091
Reactance of Expanded ACSR, Measurement of Resistance and. Tompkins, Jones, Tuttle..............................368–73; disc. 373
Reactances, A New Approach to the Calculation of Synchronous Machine. Talaat:
  Part I..............................176–82; disc. 182
Reactances for a Triple-Cage Motor Circuit, Weighted Mutual. Martin..............................765–8
Reactors, Review of the Factors Concerned with the Use of Protective Devices Shunting. (Committee Report)..............................903–13
Recent Contributions to Transformer Audible Noise Control. Conover, Ringlee........77–90; disc. 90
Recloser for Higher Speed Clearing of Distribution Circuits, A Power Class. Field, Leatherberry..............................986–91; disc. 991
Recommendations for Improving Reliability of Stand-by Engine Generators for Microwave Communications Systems. Tharp...........261–6; disc. 266
Recovery Voltage Characteristics of Electric Power Systems, A Method for Studying Circuit Transient. Kotheimer....................1083–6; disc. 1086
Recovery Voltages Associated with 2-Phase to-Ground Short Circuits, Short-Circuit Currents and Circuit Breaker. Skeats................688–93; disc. 693
Regulating Relays, Contact Life of Voltage. Schoendube, Elliott................1398–1400; disc. 1401
Regulators, Controls for Step Voltage. Lennox..............................1407–09; disc. 1410
Regulators, Increased Current Ratings for Step. Sealey..............................737–42; disc. 742
Relay and Its Application as a Cage Winding Protective Relay for Synchronous Machines, Improved Fast-Acting Thermal. Baude........349–53; disc. 353
Relay Literature 1950-52, Bibliography of. Gross..45–8
Relay Problems, Some Utility Ground. Barnes, McConnell........................417–28; disc. 428
Relay Protection for Lines Being Sleet-Melted by the Short-Circuit Method. Hogan, Pebler..............................1067–71; disc. 1072
Relaying, Future Application Needs of Carrier Pilot. Cramer, Krings...............1233–5; disc. 1235
Relaying Systems, Line and Transformer Bank. Blackburn, Rockefeller.................334–9; disc. 339
(Relays) A Transductor-Type Field Ripple Detector for Synchronous Generators. McConnell..............................476–9; disc. 479
(Relays) Automatic Load Shedding. (Committee Report....................1143–5; disc. 1145
Relays, Contact Life of Voltage-Regulating. Schoendube, Elliott................1398–1400; disc. 1401
(Relays) Controls for Step Voltage Regulators. Lennox..............................1407–09
(Relays) Detection of Grounds in Generator Field Windings. Barkle, Sterrett, Fountain..............................467–70; disc. 470
Relays, Effect of Shock and Vibration on. (Committee Report)................398–400; disc. 400
Remotely Operated Electric Utility Substations, Control Circuitry for. Derr, Metz....450–9; disc. 459
Report on a Fully Supercharged Generator, Test. Beckwith, Koetting, Rosenberg, Staats......56–9
Report on the Operation of Switched Capacitors. (Committee Report)..........1255–60; disc. 1260
Research in the Electric Power Industry. Gaty..............................553–6; disc. 556
Research Program for the Electric Utility Industry, Implementation of a. Hobson, Lewis, Oldacre..............................545–50; disc. 550
Research in Relation to Electrical Utilities, Manufacturer's. Parker, Baird..................557–60
Research on the Electric Breakdown of Fully Impregnated Paper Insulation for High-Voltage Cables. Gazzana Priaroggia, Palandri..1343–57; disc. 1357
Resin Casting of Dry-Type Current Transformers, Epoxy. Farneth, Gallousis........194–7; disc. 197
Resin Combinations for Dry-Type Transformer Insulation, Evaluation and Application of Silicone-Organic. Simmons, Scheideler.....155–60; disc. 160
Resistance and Reactance of Expanded ACSR, Measurement of. Tompkins, Jones, Tuttle..............................368–73; disc. 373
Resistance of Conventional Strand Power Cables in Nonmetallic Duct and in Iron Conduit, A-C. Burrell, Morris................1014–21; disc. 1021
Resistance of Energized A-C Motor Windings, Measurement of. Waldschmidt........1303–04; disc. 1305
Response, An Approach to the Definition of Excitation System. Bliss................1008–12; disc. 1012
Results of High-Current Tests on 161-Kv Disconnecting Switches. McNerney...........104–08; disc. 108
Results of 7 Years' Experience with High-Capacity Outdoor Oil Circuit Breakers, The. Balentine, Darrow......................665–70; disc. 671
Review of the Factors Concerned with the Use of Protective Devices Shunting Reactors. (Committee Report)..............................903–13
Rewinding A-C Generators for Improved Performance. Seline..............................472–4; disc. 474
Ribbon Elements for High-Voltage Current-Limiting Fuses. Powell, Schuck......... 635–41; disc. 641
Rotary Welding Transformer, The Forced Oil Cooled. Shenk..............................873–80
(Rotating Machinery) A Circuit Approach to the Analysis of a 2-Stage Dynamoelectric Amplifier. Burtness..........................440–9; disc. 449
(Rotating Machinery) A New Approach to the Calculation of Synchronous Machine Reactances. Talaat:
  Part I..............................176–82; disc. 182
(Rotating Machinery) A New Method for Part-Winding Starting of Polyphase Motors. Alger, Agacinsky..............................1455–62; disc. 1462
(Rotating Machinery) Apparatus Noise Measurement. Wells..............................1170–3
(Rotating Machinery) Computation of Skin Effect in Bars of Squirrel-Cage Rotors. Liwschitz-Garik..............................768–70; disc. 771
(Rotating Machinery) Correlation of Temperature Measurements on D-C Armatures. Gerbetz, Ewing..............................391–4; disc. 395
(Rotating Machinery) Current Loci of Salient-Pole Synchronous Motors: An Extension of Blondel Theory. Douglas.............1080–2; disc. 1082
(Rotating Machinery) D-C Machines: Response to Impact Excitation. Brockman, Linkous..............................500–03; disc. 503

(Rotating Machinery) Design Principles of Flux-Switch Alternators. Rauch, Johnson..1261–8; disc. 1268
(Rotating Machinery) Double-Energy Conversion in an Air Gap—A Novel Asynchronous Frequency Changer. LaPierre, Louis.....1373–5; disc. 1376
(Rotating Machinery) Eccentricity, Vibration, and Shaft Currents in Turbine Generators. Rosenberg.......................38–41
(Rotating Machinery) Equivalent Circuits for Single-Phase Motors. Slemon.......1335–42; disc. 1342
(Rotating Machinery) Improved Field Conductor Materials for Turbine Generators. Holley, Savidge.......................72–6
(Rotating Machinery) Metadyne Transients. Fegley.......................1179–88
(Rotating Machinery) Operation of Hydrogen-Cooled Turbine Generator. Sterrett, Towne.......................433–8; disc. 439
(Rotating Machinery) Rewinding A-C Generators for Improved Performance Seline.....472–4; disc. 474
(Rotating Machinery) Single-Phase Induction Motor Noise Due to Dissymmetry Harmonics. Muster Wolfert.......................1365–72; disc. 1372
(Rotating Machinery) Some Factors Influencing the Temperature Rise of Armature Windings. Liwschitz-Garik.......................752–9
(Rotating Machinery) Steam Turbine Generator Operating and Maintenance Methods of the Southern California Edison Company. Sidway, Clevenger.......................60–5
(Rotating Machinery) Stray Losses in the Armature End Iron of Large Turbine Generators. Winchester.......................381–9; disc. 389
(Rotating Machinery) Test Report on a Fully Supercharged Generator. Beckwith, Koetting, Rosenberg, Staats.......................56–9
(Rotating Machinery) Turbine Generator Operation and Maintenance Practice of Philadelphia Electric Company. Gallagher.......................48–9
(Rotating Machinery) Two-Axis Method of Analyzing Electric Machines. Tang, Cosgriff......1449–55
Rotor Saliency on Changes in Terminal Voltage, Effect of Synchronous-Machine Transient. Concordia.......................25–31
Rotor, The Induction Machine with Solid Iron. McConnell, Sverdrup.......................343–8; disc. 348
Rotors, Computation of Skin Effect in Bars of Squirrel-Cage. Liwschitz-Garik.........768–70; disc. 771
Rotors for Induction Motors, The Transient Stalled Temperature Rise of Cast Aluminum Squirrel Cage. Rosenberry.............819–24; disc. 824
Rubber and Rubberlike Insulation of Network Cable by Oven Heating Tests, High Temperature Classification of. Couch, Crowdes...930–4; disc. 944, 1463
Rubber-Insulated Cables, Some Performance Characteristics of High-Voltage. Rosch.......................1219–24; disc. 1224
Rubber-Insulated Power Cable, Design and Evaluation of Butyl-. Carroll, Lee, McKinley.......................1204–12; disc. 1212
Rubber Insulation, Modern High-Voltage. Couch, Hunt, Kenney, Ware.........1387–97; disc. 1398
Rural Electric System Planning. Rixse.......................1410–16; disc. 1416

S

(Safety) Electric Defibrillation. Kouwenhoven, Milnor.......................561–4; disc. 564
(Safety) Field Current Sources for Electric Defibrillation. Bets.......................33–6
(Safety) Protection of Personnel Against Electrical Shock Hazards in Central Office Communications Equipment. Jones.......................893–6
Sag and Tension Calculations to Transmission Line Design, Practical Application of. Lummis, Fischer.......................402–13; disc. 413
Saliency on Changes in Terminal Voltage, Effect of Synchronous-Machine Transient Rotor. Concordia.......................25–31
Salient-Pole Synchronous Motors: An Extension of Blondel Theory, Current Loci of. Douglas.......................1062–2; disc. 1082
Scheduling and Control of Power Systems, A Computer for Economic. Morrill, Blake .1136–41; disc. 1141
Secondary Network Cables, Characteristic Properties of. Rosch.................939–44; disc. 944, 1463
Secondary Network Cables, Overload Classifications for. Graham.................916–19; disc. 944, 1463
Secondary Network Protection, Co-ordination of. Leinbach, Brookes.........922–4; disc. 944, 1463
Secondary Network Systems, The Use of Probability in the Design and Operation of. Neagle, Nelson.......................567–72; disc. 572
Secondary-Network Vaults, Coincident-Outage Probability in. Reps.................580–5; disc. 585
Secondary Voltages for Commercial Areas, Economics of Higher Primary and. Lawrence, Reps.......................1034–45; disc. 1045
Sequence Impedances of Symmetrical 3-Phase Transformer Connections. Cogbill............1313–23
Sequence Networks, Basic. Kirschbaum.......771–4
Series Windings of Autotransformers, Thyrite Protection for. Albright.................150–4; disc. 154
Servomotors, Optimum Design of Induction Torque Motors and. Weiss.......................809–15
Seven Years' Experience with High-Capacity Outdoor Oil Circuit Breakers, The Results of. Balentine, Darrow.......................665–70; disc. 671
Shaft Currents in Turbine Generators, Eccentricity, Vibration and. Rosenberg.................38–41
Sheathed Cables, Mineral-Insulated Metallic-. Jordan, Eager.......................198–212; disc. 212
Sheathed Power Cable, Aluminum. Del Mar, Merrell.......................292–8; disc. 298
Shedding, Automatic Load. (Committee Report).......................1143–5; disc. 1145
Shock and Vibration on Relays, Effect of. (Committee Report)................398–400; disc. 400
Shock Hazards in Central Office Communications Equipment, Protection of Personnel Against Electrical. Jones.......................893–6
Short Circuit and Faulty Synchronizing Torques on Generator Foundations, Maximum. Ruskin.......................618–23; disc. 623
Short-Circuit Calculations and Test Results, D-C Machines—. O'Connor, Cybulski.......................222–30; disc. 230
Short-Circuit Calculations, D-C Machines—Method for. Cybulski, O'Connor.......................214–21
Short-Circuit Currents and Circuit Breaker Recovery Voltages Associated with 2-Phase-to-Ground Short Circuits. Skeats.................688–93; disc. 693
Short-Circuit Method, Relay Protection for Lines Being Sleet-Melted by the. Hogan, Pebler.......................1067–71; disc. 1072
Short Circuit, Transformer Temperatures on. Sealey.......................1225–9; disc. 1229
Short Circuits, Behavior of High Voltage Busses and Insulators During. Milton, Chambers.......................742–6; disc. 746
Shunting Reactors, Review of the Factors Concerned with the Use of Protective Devices. (Committee Report).......................903–13
Silicone Glass Fiber Insulation System for Dry-Type Transformers, Functional Temperature Endurance Tests on a. Manning.................91–8; disc. 98
Silicone-Organic Resin Combinations for Dry-Type Transformer Insulation, Evaluation and Application of. Simmons, Scheideler....155–60; disc. 160
Simplified Method of Calculating Voltage Regulation Using Unit Impedance Power Reactive Diagrams, A. Butler.................304–10; disc. 310
Single-Conductor Electric Cable at High Frequency, Characteristics of. Sabol......1280–5; disc. 1285
Single Distribution Feeder, Automatically Switched Capacitors in Steps on a. Fowler, Thomas.......................311–14; disc. 314
Single-Phase Induction Motor Noise Due to Dissymmetry Harmonics. Muster, Wolfert.......................1365–72; disc. 1372
Single-Phase Motors, Equivalent Circuits for. Slemon.......................1335–42; disc. 1342
Single Wire Element, The Calculation of the Complete Time/Current Characteristics of Cartridge Fuses With. Guile................ 1108–15; disc. 1115
69-Kv Compressed Air Circuit Breaker for 5,000,000 Kva, A. Kane, Walker....... 705–09; disc. 709
69-Kv Power Supply, Pittsburgh Downtown:
  Part I. Planning. Hill...........643–7; disc. 647
  Part II. Substation. Gue........648–52; disc. 652
  Part III. Switchgear Development. Pierson.......................653–6; disc. 656
Skew on Induction Motor Magnetic Fields, Effect of. Linkous.......................760–5; disc. 765
Skin Effect in Bars of Squirrel-Cage Rotors, Computation of. Liwschitz-Garik........768–70; disc. 771
Sleet-Melted by the Short-Circuit Method, Relay Protection for Lines Being. Hogan, Pebler.......................1067–71; disc. 1072
Slip Frequency, Vibration in 2-Pole Induction Motors Related to. Summers.......................69–72
Soil, Efficiency of Grounding Grids with Nonuniform. Zaborszky.......................1230–3
Solid Iron Rotor, The Induction Machine with. McConnell, Sverdrup.................343–8; disc. 348
Solution of Cable Heat Flow Problems, An Analogue. deHaas, Sandiford, Cameron.....315–18; disc. 318
Some Factors Influencing the Temperature Rise of Armature Windings. Liwschitz-Garik.....752–9
Some Fundamentals on Capacitance Switching. Johnson, Schultz, Schultz, Shores......727–36; disc. 736
Some Performance Characteristics of High-Voltage Rubber-Insulated Cables. Rosch.......................1219–24; disc. 1224
Some Utility Ground-Relay Problems. Barnes, McConnell.......................417–28; disc. 428
Sonance Design of Large Induction Motors. Wall.......................1189–92
Sound Pressure Levels of Magnetic Noise of Polyphase Induction Motors, Predetermination of. Erdelyi.......................1269–80; disc. 1280
Sources for Electric Defibrillation, Field Current. Bets.......................33–6
Southern California Edison Company, Steam Turbine Generator Operating and Maintenance Methods of the. Sidway, Clevenger.......................60–5
Squirrel-Cage Rotors, Computation of Skin Effect in Bars of. Liwschitz-Garik........768–70; disc. 771
Squirrel Cage Rotors for Induction Motors, The Transient Stalled Temperature Rise of Cast Aluminum. Rosenberry.......................819–24; disc. 824
Stability Equivalent for Power System Representation on A-C Network Analyzers, Combination Load-Flow and. Brown, Cloues.......782–6; disc. 786
Stability Studies, A Rational Method for the Step-by-Step Calculations in Power System Transient. Norinder.......................1087–91; disc. 1091
Stand-by Engine Generators for Microwave Communications Systems, Recommendations for Improving Reliability of. Tharp....261–6; disc. 266
Starting of Polyphase Motors, A New Method for Part-Winding. Alger, Agacinsky...1455–62; disc. 1462
Station Auxiliary Busses, Transfer Tests on. Bacher, Barth, Huse, Taylor...........1441–5; disc. 1446
Stations, Grounding Grids for High-Voltage. Gross, Wise:
  Part II. Resistance of Large Rectangular Plates.......................801–09; disc. 809
Statistics to Motor Testing, Application of. Oldenkamp.......................815–18; disc. 818
Stator Winding Temperatures at Various Hydrogen Pressures, Turbine Generator. Alger, Kilbourne, Snell.......................232–50; disc. 250
Steam-Electric Generating-Station Auxiliary Busses, Transfer of. Lewis, Marsh......322–30; disc. 330
Steam-Electric Generating Units, An Investigation of the Economic Size of. Kirchmayer, Mellor, O'Mara, Stevenson.............600–09; disc. 609
Steam Generation, Co-ordination of Hydro and. Watchorn.......................142–8; disc. 148
Steam Turbine Generator Operating and Maintenance Methods of the Southern California Edison Company. Sidway, Clevenger.......................60–5
Step-by-Step Calculations in Power System Transient Stability Studies, A Rational Method for the. Norinder.......................1087–91; disc. 1091
Step Regulators, Increased Current Ratings for. Sealey.......................737–42; disc. 742
Step Voltage Regulators, Controls for. Lennox.......................1407–09; disc. 1410
Storage and Hydro Generation at Flatiron Power Plant, Pumped. Denton, Britt.........614–18; disc. 618
Stray Losses in the Armature End Iron of Large Turbine Generators. Winchester.........381–9; disc. 389
Studies—In Relation to Insulation, Corona. Liao, Nye, Brustle, Anderson........1046–50; disc. 1050
Study of Carrier-Frequency Noise on Power Lines, A. Moynihan, Sparlin:
  Part IV. Conclusion of Field Measurements..795–800
Substation and Primary Feeder Planning, Distribution. Denton, Reps.................484–97; disc. 497
Substations, Control Circuitry for Remotely Operated Electric Utility. Derr, Metz......450–9; disc. 459
Substations, Development of a Welded Aluminum Bus for. Asbury, Hartman...........834–8; disc. 838
(Substations) Grounding Grids for High-Voltage Stations. Gross, Wise:
  Part II. Resistance of Large Rectangular Plates.......................801–09; disc. 809
(Substations) Supervisory Control and Associated Telemetering Equipment—A Survey of Current Practice. (Committee Report).............36–8
Summary of Fault Location Methods, Bibliography and. (Committee Report).....1423–7; disc. 1427
Supercharged Generator, Test Report on a Fully. Beckwith, Koetting, Rosenberg, Staats......56–9
Supervisory Control and Associate Telemetering Equipment—A Survey of Current Practice. (Committee Report).......................36–8
Supply Methods, General Study of Area. Casazza, Rankin.......................1328–34; disc. 1334–5
Surge Attenuation in Power Cables. Valentine, Dillard, Clayton.................1115–21; disc. 1122
Survey of Current Practice, Supervisory Control and Associated Telemetering Equipment—A. (Committee Report).......................36–8
Suspension Insulators in Series, Insulation Characteristics of Wood and. Clayton, Shankle.......................1305–11; disc. 1312
Swings Caused by Arc Furnace Loads, Voltage Dip and Synchronous Condenser. Concordia.......951–6
Switch Alternators, Design Principles of Flux-. Rauch, Johnson.......................1261–8; disc. 1268
Switch, Power Autotransformer Current Interruption with an Air-Break Disconnect. Anderson..1157–63
Switched Capacitors in Steps on a Single Distribution Feeder, Automatically. Fowler, Thomas.......................311–14; disc. 314
Switched Capacitors, Report on the Operation of. (Committee Report)..........1255–60; disc. 1260
Switches, High-Current Testing of Air-Disconnect. Gostin.......................21–5
Switches, Results of High-Current Tests on 161-Kv Disconnecting. McNerney........104–08; disc. 108

(Switchgear) A New 500-Megavolt-Ampere Air Magnetic Circuit Breaker of Simplified Design. Reilly, Weston.........1093–8; disc. 1098
(Switchgear) A New High-Capacity Anode Air Circuit Breaker. Bottonari, Sprow..1297–1302; disc. 1302
(Switchgear) A Power Class Recloser for Higher Speed Clearing of Distribution Circuits. Field, Leatherberry.........986–91; disc. 991
(Switchgear) Aluminum in Heavy Current Conductors. Deans.........1192–8; disc. 1198
Switchgear, Aluminum Widely Used in Power. Talento.........839–43; disc. 843
(Switchgear) Analysis of Fault Currents for High-Voltage Circuit-Breaker Interruption. Lantz.........41–5
(Switchgear) Application of Volume Theory of Dielectric Strength to Oil Circuit Breakers. Wilson, Streater, Tuohy.........677–84; disc. 684
(Switchgear) Behavior of High-Voltage Busses and Insulators During Short Circuits. Milton, Chambers.........742–6; disc. 746
Switchgear Development Laboratory, Capacitance-Switching Facilities at the. Williams, Mankoff, Schneider.........375–80; disc. 380
(Switchgear) Development of a Welded Aluminum Bus for Substations. Asbury, Hartman.........834–8; disc. 838
Switchgear) Dynamics of High-Capacity Outdoor Oil Circuit Breakers. Barkan.........671–6; disc. 676
(Switchgear) Field Tests on a 138-Kv High Speed Oil Circuit Breaker at Philip Sporn Power Plant. Naef, Hambrick.........710–24; disc. 724
(Switchgear) Flux Measurements in Magnetic Air Circuit Breaker Interrupters. Carter.........1062–5; disc. 1065
(Switchgear) High-Current Arc Erosion of Electric Contact Materials. Wilson.........657–64; disc. 664
(Switchgear) Pittsburgh Downtown 69-Kv Power Supply:
  Part I. Planning. Hill.........643–7; disc. 647
  Part II. Substation. Gue.........648–52; disc. 652
  Part III. Switchgear Development. Pierson.........653–6; disc. 656
(Switchgear) Testing of D-C Interrupters on A-C Test Circuits. Chen, Boehne.........1073–9; disc. 1079
(Switchgear) The Calculation of the Complete Time/Current Characteristics of Cartridge Fuses With Single Wire Element. Guile...1108–15; disc. 1115
(Switchgear) The Results of 7 Years' Experience with High-Capacity Outdoor Oil Circuit Breakers. Balentine, Darrow.........665–70; disc. 671
(Switchgear) Short Circuit Currents and Circuit Breaker Recovery Voltages Associated with 2-Phase-to-Ground Short Circuits. Skeats.........688–93; disc. 693
(Switchgear) Ribbon Elements for High-Voltage Current-Limiting Fuses. Powell, Schuck.........635–41; disc. 641
(Switchgear) A 69-Kv Compressed Air Circuit Breaker for 5,000,000 Kva. Kane, Walker.........705–09; disc. 709
Switching, Some Fundamentals on Capacitance. Johnson, Schultz, Schultz, Shores.........727–36; disc. 736
Switching Stations and Transformers, Direct-Stroke Protection of High-Voltage. Griscom, Dillard, Hileman.........354–65; disc. 365
Switching Devices, Test Circuits for Capacitance. Darrow, Phillips, Schultz, Shores.........624–34; disc. 634
Switching Long 230-Kv Lines, Design Problems and Field Tests Concerning Circuit Breakers for. Umphrey, Marsden.........693–701; disc. 701
Symmetrical 3-Phase Transformer Connections, Sequence Impedances of. Cogbill.........1313–23
Symposium: How Can the Utilities Best Make Use of Modern Science?.........545–60
Synchronizing Torques on Generator Foundations, Maximum Short Circuit and Faulty. Ruskin.........618–23; disc. 623
Synchronous Condenser Swings Caused by Arc Furnace Loads, Voltage Dip and. Concordia.........951–6
Synchronous Generators, A Transductor-Type Field Ripple Detector for. McConnell.476–9; disc. 479
Synchronous Machine Reactances, A New Approach to the Calculation of. Talaat:
  Part I.........176–82; disc. 182
Synchronous-Machine Transient Rotor Saliency on Changes in Terminal Voltage, Effect of. Concordia.........25–31
Synchronous Machines, Improved Fast-Acting Thermal Relay and Its Application as a Cage Winding Protective Relay for. Baude.........349–53; disc. 353
Synchronous Motors: An Extension of Blondel Theory, Current Loci of Salient-Pole. Douglas.........1080–2; disc. 1082
(System Engineering) A General Transmission Loss Equation. Early, Watson, Smith.........510–16; disc. 516
(System Engineering) A Look to the Future of Power Transmission in the West. Hunkins.........591–7; disc. 598
(System Engineering) A New Method of Determining Constants for the General Transmission Loss Equation. Early, Watson...1417–21; disc. 1421
(System Engineering) An Incremental Cost of Power-Delivered Computer. Early, Phillips, Shreve.........529–34; disc. 534
(System Engineering) Co-ordination of Hydro and Steam Generation. Watchorn...142–9; disc. 148
(System Engineering) Digital Calculation of Network Impedances. Glimn, Habermann, Henderson, Kirchmayer.........1285–95; disc. 1295
(System Engineering) Electric Utility Load Forecasting. Godard.........1428–40
(System Engineering) Forecasting the Demand for Electricity. Hooke.........993–1005; disc. 1005
(System Engineering) General Study of Area Supply Methods. Casazza, Rankin...1328–34; disc. 1334
(System Engineering) Two Large Electric Arc Furnaces—Electrical Characteristics and Corrective Equipment. Luther, Ghesquiere, Quick.........1401–05; disc. 1406
System Parameters, Power Distribution. Kidder, Neher.........125–40; disc. 140
System Planning Practices. (Committee Report).........896–900
System Planning, Principles and Practice of Modern. Fugill.........1323–26; disc. 1327
System Planning, Rural Electric. Rizse.........1410–16; disc. 1416
System Response, An Approach to the Definition of Excitation. Bliss.........1008–12; disc. 1012
System Voltage Drop and System Loads, Fundamental Relations of. Miller, Robbins...267–72; disc. 272

T

Technique for Calculating Cable Temperature Transients, An Improved Approximate. Van Wormer.........277–80; disc. 280
Telemetering Equipment—A Survey of Current Practice, Supervisory Control and Associated. (Committee Report).........36–8
Temperature Classification of Rubber and Rubberlike Insulation of Network Cable by Oven Heating Tests, High. Couch, Crowdes.........930–4; disc. 944, 1463
Temperature Endurance Tests of Ventilated Dry-Type Power and Distribution Transformers, Proposed Test Code for Functional. (Committee Report).........971–5; disc. 975
Temperature Endurance Tests on a Silicone Glass Fiber Insulation System for Dry-Type Transformers, Functional. Manning.........91–8; disc. 98
Temperature Measurements on D-C Armatures, Correlation of. Gerbetz, Ewing.........391–4; disc. 395
Temperature Rise of Armature Windings, Some Factors Influencing the. Liwschitz-Garik.........752–9
Temperature Rise of Cast Aluminum Squirrel Cage Rotors for Induction Motors, The Transient Stalled. Rosenberry.........819–24; disc. 824
Temperature Transients, An Improved Approximate Technique for Calculating Cable. Van Wormer.........277–80; disc. 280
Temperatures at Various Hydrogen Pressures, Turbine Generator Stator Winding. Alger, Kilbourne, Snell.........232–50; disc. 250
Temperatures on Short Circuit, Transformer. Sealey.........1225–9; disc. 1229
Ten Part-Winding Arrangements in Sample 4-Pole Induction Motor. Courtin...1248–53; disc. 1253
Tennessee Valley Authority, Mechanical Alignment of Vertical-Shaft Hydroelectric Units as Practiced by. Norris.........586–9; disc. 589
Tension Calculations to Transmission Line Design, Practical Application of Sag and. Lummis, Fischer.........402–13; disc. 413
Tensors, ORACLE Computes Line Constants With. Shipley, Hochdorf, Watson.........1052–6; disc. 1056
Terminal Voltage, Effect of Synchronous-Machine Transient Rotor Saliency on Changes in. Concordia.........25–31
Test Circuits for Capacitance Switching Devices. Darrow, Phillips, Schultz, Shores.........624–34; disc. 634
Test Circuits, Testing of D-C Interrupters on A-C. Chen, Boehne.........1073–9; disc. 1079
Test Code for Functional Temperature Endurance Tests of Ventilated Dry-Type Power and Distribution Transformers, Proposed. (Committee Report).........971–5; disc. 975
Test Report on a Fully Supercharged Generator. Beckwith, Koetting, Rosenberg, Staats.........56–9
Testing, Application of Statistics to Motor. Oldenkamp.........815–18; disc. 818
Testing, Magnetization of Transformer Cores During Impulse. Beavers, Holcomb, Leoni.........118–23; disc. 123
Testing of Air-Disconnect Switches, High-Current. Gostin.........21–5
Testing of D-C Interrupters on A-C Test Circuits. Chen, Boehne.........1073–9; disc. 1079
Testing of Valve-Type Lightning Arresters, Transient Durability. Kalb, Yost.........521–6; disc. 526
Tests Concerning Circuit Breakers for Switching Long 230-Kv Lines, Design Problems and Field. Umphrey, Marsden.........693–701; disc. 701
Tests for Liquid Filled Distribution Transformers, Functional Life Expectancy. Lockie. 977–82; disc. 982
Tests Indicating the Concentration of Polar Compounds in Transformer Oil, Interpretation and Significance of. Johnson.........774–80; disc. 780
Tests of Insulation Systems for Dry-Type Transformers, Functional Life. Narbut.........1057–61; disc. 1061
Tests on a Silicone Glass Fiber Insulation System for Dry-Type Transformers, Functional Temperature Endurance. Manning.........91–8; disc. 98
Tests on Low-Voltage Windings of Distribution Transformers, Impulse. Holcomb.........1152–5; disc. 1155
Tests on 161-Kv Disconnecting Switches, Results of High-Current. McNerney.........104–08; disc. 108
Tests on Station Auxiliary Busses, Transfer. Backer, Barth, Huse, Taylor.........1441–5; disc. 1446
Theory of Dielectric Strength to Oil Circuit Breakers, Application of Volume. Wilson, Streater, Tuohy.........677–84; disc. 684
Thermal Relay and Its Application as a Cage Winding Protective Relay for Synchronous Machines, Improved Fast-Acting. Baude.........349–53; disc. 353
Thyrite Protection for Series Windings of Autotransformers. Albright.........150–4; disc. 154
Tie-Line Energy Control of Interconnected Power Systems, Load-Phase. Cahen.........1–5
Time/Current Characteristics of Cartridge Fuses With Single Wire Element, The Calculation of the Complete. Guile.........1108–15; disc. 1115
Time-Current Damage Characteristics, Cable in Duct. Porter.........919–21; disc. 944, 1463
Time Division Multiplexing, Quadriphase—A New Approach to. Evans, Lowe.........900–03
Torque Motors and Servomotors, Optimum Design of Induction. Weiss.........809–15
Torques on Generator Foundations, Maximum Short Circuit and Faulty Synchronizing. Ruskin.........618–23; disc. 623
Transductor-Type Field Ripple Detector for Synchronous Generators, A. McConnell.........476–9; disc. 479
Transfer of Steam-Electric Generating-Station Auxiliary Busses. Lewis, Marsh.........322–30; disc. 330
Transfer Tests on Station Auxiliary Busses. Backer, Barth, Huse, Taylor.........1441–5; disc. 1446
Transformer, An Experimental Gas-Insulated 138-Kv Current. Camilli.........100–03; disc. 103
Transformer Audible Noise Control, Recent Contributions to. Conover, Ringlee.........77–90; disc. 90
Transformer Bank Relaying Systems, Line and. Blackburn, Rockefeller.........334–9; disc. 339
Transformer Connections, Sequence Impedances of Symmetrical 3-Phase. Cogbill.........1313–23
Transformer Cores During Impulse Testing, Magnetization of. Beavers, Holcomb, Leoni.........118–23; disc. 123
Transformer Design, Control of Electrostatic Voltage Distribution in Power. Bennon, Cossaart.........1122–5; disc. 1125
Transformer Insulation, Evaluation and Application of Silicone-Organic Resin Combinations for Dry-Type. Simmons, Scheideler....155–60; disc. 160
Transformer Oil, Interpretation and Significance of Tests Indicating the Concentration of Polar Compounds in. Johnson.........774–80; disc. 780
Transformer Temperatures on Short Circuit. Sealey.........1225–9; disc. 1229
Transformer, The Forced Oil Cooled Rotary Welding. Shenk......... 873–80
Transformers, An Anechoic Chamber for Noise Tests on Large Power Power. Benoit, Hemmes, Schulz.50–6
Transformers, Direct-Stroke Protection of High-Voltage Switching Stations and. Griscom, Dillard, Hileman.........354–65; disc. 365
Transformers, Epoxy Resin Casting of Dry-Type Current. Farneth, Gallousis.........194–7; disc. 197
Transformers, Experiences With the Use of Aluminum in Windings for Dry-Type Power. Tipton...1201–04
Transformers, Functional Life Evaluation of Group-2 Dry-Type Power. Zambell.........956–70
Transformers, Functional Life Expectancy Tests for Liquid-Filled Distribution. Lockie.........977–82; disc. 982
Transformers, Functional Life Tests of Insulation Systems for Dry-Type. Narbut...1057–61; disc. 1061
Transformers, Functional Temperature Endurance Tests on a Silicone Glass Fiber Insulation System for Dry-Type. Manning.........91–8; disc. 98
Transformers, Impulse Tests on Low-Voltage Windings of Distribution. Holcomb.........1152–5; disc. 1155
(Transformers) Increased Current Ratings for Step Regulators. Sealey.........737–42; disc. 742
(Transformers) Oscillations of Coupled Windings. Abetti, Adams, Maginniss.........12–21

Transformers, Proposed Test Code for Functional Temperature Endurance Tests of Ventilated Dry-Type Power and Distribution. (Committee Report)..........971–5; disc. 975
Transformers, The Application of a New Nontracking Butyl to High-Voltage Instrument. Pfuntner, Norman, Wilterdink..........1173–6
(Transformers) Thyrite Protection for Series Windings of Autotransformers. Albright....150–4; disc. 154
Transient Durability Testing of Valve Type Lightning Arresters. Kalb, Yost..........521–6; disc. 526
Transient Recovery Voltage Characteristics of Electric Power Systems, A Method for Studying Circuit. Kotheimer..........1083–6; disc. 1086
Transient Rotor Saliency on Changes in Terminal Voltage, Effect of Synchronous-Machine. Concordia..........25–31
Transient Stability Studies, A Rational Method for the Step-by-Step Calculations in Power System. Norinder..........1087–91; disc. 1091
Transient Stalled Temperature Rise of Cast Aluminum Squirrel Cage Rotors for Induction Motors, The. Rosenberry..........819–24; disc. 824
Transients, An Improved Approximate Technique for Calculating Cable Temperature. Van Wormer..........277–80; disc. 280
Transients, Metadyne. Fegley..........1179–88
(Transmission) A Method for Studying Circuit Transient Recovery Voltage Characterisitcs of Electric Power Systems. Kotheimer..........1083–6; disc. 1086
(Transmission) A Rational Method for the Step-by-Step Calculations in Power System Transient Stability Studies. Norinder..........1087–91; disc. 1091
(Transmission) A Simplified Method of Calculating Voltage Regulation Using Unit Impedance Power Reactive Diagrams. Butler.....304–10; disc. 310
(Transmission) Balancing Double-Wye High-Voltage Capacitor Banks. Compton......573–8; disc. 578
(Transmission) Basic Sequence Networks. Kirschbaum..........771–4
(Transmission) Bibliography and Summary of Fault Location Methods. (Committee Report).......... 1423–7; disc. 1427
(Transmission) Coincident-Outage Probability in Secondary-Network Vaults. Reps..580–5; disc. 585
(Transmission) Combination Load-Flow and Stability Equivalent for Power System Representation on A-C Network Analyzers. Brown, Cloues..........782–6; disc. 786
(Transmission) Corona Studies—In Relation to Insulation. Liao, Nye, Brustle, Anderson..........1046–50; disc. 1050
(Transmission) Direct-Stroke Protection of High-Voltage Switching Stations and Transformers. Griscom, Dillard, Hileman......354–65; disc. 365
Transmission) Economics of Higher Primary and Secondary Voltage for Commercial Areas. Lawrence, Reps..........1034–45; disc 1045
(Transmission) Effects of Corona on Traveling Waves. Wagner, Lloyd..........858–72
(Transmission) Efficiency of Grounding Grids with Nonuniform Soil. Zaborszky..........1230–3
(Transmission) Fundamental Relations of System Voltage Drop and System Loads. Miller, Robbins..........267–72; disc. 272
Transmission in the West, A Look to the Future of Power. Hunkins..........591–7; disc. 598
(Transmission) Insulation Characteristics of Wood and Suspension Insulators in Series. Clayton, Shankle..........1305–11; disc. 1312
(Transmission) Intermittently Increased Kilovar Output of Large Capacitor Banks. Minder..........749–51; disc. 751
(Transmission) Investigation of European Practices in Power Line Design. Fritz.......505–09; disc. 509
Transmission Line Design, Practical Application of Sag and Tension Calculations to. Lummis, Fischer..........402–13; disc. 413
Transmission Lines, Electromagnetic Unbalance of Untransposed. Gross, Nelson:
  Part II..........887–93
Transmission Lines in North Dakota, Bureau of Reclamation 230-Kv. Austin..........1147–51
Transmission Lines, The Use of All-Aluminum Conductor on. Wright, Lambert....849–53; disc. 853
Transmission Lines, Voltage Gradients on High-Voltage. Adams..........5–11
Transmission Loss Equation, A General. Early, Watson, Smith..........510–16; disc. 516
Transmission Loss Equation, A New Method of Determining Constants for the General. Early, Watson..........1417–21; disc. 1421
(Transmission) ORACLE Computes Line Constants With Tensors. Shipley, Hochdorf, Watson..........1052–[illegible]; disc. 1056
(Transmission) Power Autotransformer C[illegible] Interruption with an Air-Break Discon[illegible] Switch. Anderson..........1157–63
(Transmission) Report on the Operation of Switched Capacitors. (Committee Report)..........1255–60; disc. 1260
(Transmission) The Use of Probability in the Design and Operation of Secondary Network Systems. Neagle, Nelson..........567–72; disc. 572
(Transmission) Traveling Wave Protection Problems. Boehne:
  Part II..........890–7
(Transmission) Voltage Dip and Synchronous-Condenser Swings Caused by Arc Furnace Loads. Concordia..........951–6
Traveling Wave Protection Problems. Part II. Boehne..........880–7
Traveling Waves, Effects of Corona on. Wagner, Lloyd..........858–72
Triple-Cage Motor Circuit, Weighted Mutual Reactances for a. Martin..........765–8
Turbine Generator Operating and Maintenance Methods of the Southern California Edison Company, Steam. Sidway, Clevenger..........60–5
Turbine Generator Operation and Maintenance Practice of Philadelphia Electric Company. Gallagher..........48–9
Turbine Generator, Operation of Hydrogen-Cooled. Sterrett, Towne..........433–8; disc. 439
Turbine Generator Stator Winding Temperatures at Various Hydrogen Pressures. Alger, Kilbourne, Snell..........232–50; disc. 250
Turbine Generators During Off-Peak High Power Factor Periods—Practices of One Utility in a Metropolitan Area, Operation of. Roberts, Webb..........461–5; disc. 466
Turbine Generators, Eccentricity, Vibration, and Shaft Currents in. Rosenberg..........38–41
Turbine Generators, Improved Field Conductor Materials for. Holley, Savidge..........72–6
Turbine Generators, Stray Losses in the Armature End Iron of Large. Winchester.......381–9; disc. 389
Two-Axis Method of Analyzing Electric Machines. Tang, Cosgriff..........1449–55
Two Large Electric Arc Furances—Electrical Characteristics and Corrective Equipment. Luther, Ghesquiere, Quick..........1401–05; disc. 1406
Two-Phase-to-Ground Short Circuits, Short-Circuit Currents and Circuit-Breaker Recovery Voltages Associated with. Skeats........688–93; disc. 693
Two-Pole Induction Motors Related to Slip Frequency, Vibration in. Summers..........69–72
24-Kv Station—Field and Laboratory Studies, Lightning Protection in a. Armstrong, Ferguson, Hileman..........1127–35; disc. 1135
230-Kv Lines, Design Problems and Field Tests Concerning Circuit Breakers for Switching Long. Umphrey, Marsden..........693–701; disc. 701
230-Kv Transmission Lines in North Dakota, Bureau of Reclamation. Austin..........1147–51

U

Ultrasonic Flowmeter, Principles and Application of the. Swengel, Hess, Waldorf..........112–17; disc. 117
Unbalance of Untransposed Transmission Lines, Electromagnetic. Gross, Nelson:
  Part II.......... 887–93
Unit Impedance Power-Reactive Diagrams, A Simplified Method of Calculating Voltage Regulation Using. Butler..........304–10; disc. 310
Use of All-Aluminum Conductor on Transmission Lines, The. Wright, Lambert..........849–53; disc. 853
Use of Probability in the Design and Operation of Secondary Network Systems, The. Neagle, Nelson..........567–72; disc. 572
Utilities, Manufacturer's Research in Relation to Electrical. Parker, Baird..........557–60
(Utilities) Research in the Electric Power Industry. Gaty..........553–6; disc. 566
Utility Ground-Relay Problems, Some. Barnes, McConnell..........417–28; disc. 428
Utility Industry, Implementation of a Research Program for the Electric. Hobson, Lewis, Oldacre..........545–50; disc. 550
Utility Load Forecasting, Electric. Godard....1428–40
Utility Load Forecasting, The Application of Business Machines to Electrical. Gruetter..........854–8
Utility Substations, Control Circuitry for Remotely Operated Electric. Derr, Metz...450–9; disc. 459

V

Valve-Type Lightning Arresters, Transient Durability Testing of. Kalb, Yost..........521–6; disc. 526
Vaults, Coincident-Outage Probability in Secondary-Network. Reps..........580–5; disc. 585
Vertical-Shaft Hydroelectric Units as Practiced by Tennessee Valley Authority, Mechanical Alignment of. Norris..........586–9; disc. 589
Vertical Water Wheel Generaturs, Production and Installation of. Houser, Hindle, Tyerman..........536–43; disc. 543
Vibration and Shaft Currents in Turbine Generators, Eccentricity. Rosenberg..........38–41
Vibration in 2-Pole Induction Motors Related to Slip Frequency. Summers..........69–72
Vibration on Relays, Effect of Shock and. (Committee Report)..........398–400; disc. 400
Voltage Cables, Research on the Electric Breakdown of Fully Impregnated Paper Insulation for High-. Gazzana Priaroggia, Palandri..1343–57; disc. 1357
Voltage Characteristics of Electric Power Systems, A Method for Studying Circuit Transient Recovery. Kotheimer..........1083–6; disc. 1086
Voltage Dip and Synchronous-Condenser Swings Caused by Arc Furnace Loads. Concordia...951–6
Voltage Distribution in Power Transformer Design, Control of Electrostatic. Bennon, Cossaart..........1122–5; disc. 1125
Voltage Drop and System Loads, Fundamental Relations of System. Miller, Robbins..........267–72; disc. 272
Voltage, Effect of Synchronous-Machine Transient Rotor Saliency on Changes in Terminal. Concordia..........25–31
Voltage Gradients on High-Voltage Transmission Lines. Adams..........5–11
Voltage Phase Angles, The Determination of Incremental and Total Loss Formulas from Functions of. Cahn..........161–71; disc. 171
Voltage-Regulating Relays, Contact Life of. Schoendube, Elliott..........1398–1400; disc. 1401
Voltage Regulation Using Unit Impedance Power Reactive Diagrams, A Simplified Method of Calculating. Butler..........304–10; disc. 310
Voltage Regulators, Controls for Step. Lennox..........1407–09; Disc. 1410
Voltages Associated with 2-Phase-to-Ground Short Circuits, Short-Circuit Currents and Circuit Breaker Recovery. Skeats..........688–93; disc. 693
Voltages for Commercial Areas, Economics of Higher Primary and Secondary. Lawrence, Reps..........1034–45; disc. 1045
Volume Theory of Dielectric Strength to Oil Circuit Breakers, Application of. Wilson, Streater, Tuohy..........677–84; disc. 684

W

Water Wheel Generators, Production and Installation of Vertical. Houser, Hindle, Tyerman..........536–43; disc. 543
Wave Protection Problems, Traveling. Part II. Boehne..........880–7
Waves, Effects of Corona on Traveling. Wagner, Lloyd..........858–72
Weighted Mutual Reactances for a Triple-Cage Motor Circuit. Martin..........765–8
Welded Aluminum Bus for Substations, Development of a. Asbury, Hartman..........834–8; disc. 838
Welding Transformer, The Forced Oil-Cooled Rotary. Shenk..........873–80
West, A Look to the Future of Power Transmission in the. Hunkins..........591–7; disc. 598
Winding Arrangements in Sample 4-Pole Induction Motor, Ten Part-. Courtin....1248–53; disc. 1253
Winding Protective Relay for Synchronous Machines, Improved Fast-Acting Thermal Relay and Its Application as a Cage. Baude...349–53; disc. 353
Winding Starting of Polyphase Motors, A New Method for Part-. Alger, Agacinsky....1455–62; disc. 1462
Windings, Detection of Grounds in Generator Field. Barkle, Sterrett, Fountain........467–70; disc. 470
Windings for Dry-Type Power Transformers, Experiences With the Use of Aluminum in. Tipton..........1201–04
Windings, Measurement of Resistance of Energized A-C Motor. Waldschmidt....1303–04; disc. 1305
Windings of Autotransformers, Thyrite Protection for Series. Albright..........150–4; disc. 154
Windings of Distribution Transformers, Impulse Tests on Low-Voltage. Holcomb....1152–5; disc. 1155
Windings, Oscillations of Coupled. Abetti, Adams, Maginniss..........12–21
Windings, Some Factors Influencing the Temperature Rise of Armature. Liwschitz-Garik.........752–9
Wood and Suspension Insulators in Series, Insulation Characteristics of. Clayton, Shankle..........1305–11; disc. 1312
Wye High-Voltage Capacitor Banks, Balancing Double-. Compton..........573–8; disc. 578

2. Author Index

Abbott, H. F. Disc.........543
Abetti, P. A. Disc.........123, 1125
Abetti, P. A.; G. E. Adams, F. J. Maginniss. Oscillations of Coupled Windings. (55-29)....12–21
Achtenberg, Donn C. Disc.........401, 429
Adams, C. G. Disc.........747
Adams, G. E. Voltage Gradients on High-Voltage Transmission Lines. (55-22).........5–11
Adams, G. E.; P. A. Abetti, F. J. Maginniss. Oscillations of Coupled Windings. (55-29).......12–21
Agacinsky, Lorraine M.; P. L. Alger. A New Method for Part-Winding Starting of Polyphase Motors (55-846).........1455–62; disc. 1462
Albright, J. W. Thyrite Protection for Series Windings of Autotransformers (55-52).....150–4; disc. 154
Aldridge, F. J.; P. A. Raine. Disc.........298
Alger, J. R. M.; C. E. Kilbourne, D. S. Snell. Turbine Generator Stator Winding Temperatures at Various Hydrogen Pressures. (55-118).........232–50; disc. 251
Alger, P. L. Disc.........765, 771, 818, 1219, 1253, 1342, 1372, 1376
Alger, P. L.; Lorraine M. Agacinsky. A New Method for Part-Winding Starting of Polyphase Motors. (55-846).........1455–62; disc. 1462
Alvira, A.; I. T. Corbell. Microwave System Parameters for Reliable Communications. (55-516).........1100–07; disc. 1107
Anderson, J. G.; T. W. Liao, J. R. Nye, H. H. Brustle. Corona Studies—In Relation to Insulation....... (55-437).........1046–50; disc. 1050
Anderson, M. W. Power Autotransformer Current Interruption with an Air-Break Disconnect Switch (55-623).........1157–63
Andrews, F. E.; R. W. Caswell. Disc.........1312
Arapakis, G H. Disc.........572, 585
Arman, A. N. Disc.........299
Armstrong, H. R.; R. W. Ferguson, A. R. Hileman. Lightning Protection in a 24-Kv Station—Field and Laboratory Studies. (55-556).........1127–35; disc. 1135
Asbury, C. E.; C. J. Hartman. Development of a Welded Aluminum Bus for Substations. (55-257).........834–8; disc. 839
Ashdown, K. T. Disc.........656
Ashdown, K. T.; N. Swerdlow. Disc.........1198
Atkinson, R. W. Disc.......192, 288, 321, 1122, 1359
Atkinson, R. W.; E. H. Kirkham. Disc.........259
Austin, Thomas M. Bureau of Reclamation 230-Kv Transmission Lines in North Dakota. (55-622).........1147–51

B

Backer, L. E.; Paul Barth, R. A. Huse, D. W. Taylor. Transfer Tests on Station Auxiliary Busses. (55-92).........1441–5
Baird, J.; E. E. Parker. Manufacturer's Research in Relation to Electrical Utilities. (55-245)...557–60
Baird, L. L. Disc.........1302
Baker, M. A. Disc.........395
Balentine, C. J. Disc.........724
Balentine, C. J.; K. G. Darrow. The Results of 7 Years' Experience With High Capacity Outdoor Oil Circuit Breakers. (55-213)..665–70; disc. 671
Baptist, J. V.; S. M. Denton. Disc.........1012
Barkan, Philip. Dynamics of High-Capacity Outdoor Oil Circuit Breakers. (55-216)...671–6; disc. 676
Barkle, J. E.; C. C. Sterrett, L. L. Fountain. Detection of Grounds in Generator Field Windings. (55-125).........467–70; disc. 471
Barnes, C. C. Disc.........299
Barnes, H. C. Disc.........353, 400, 470
Barnes, H. C.; S. H. Horowitz. Disc.........330
Barnes, H. C.; A. J. McConnell. Some Utility Ground Relay Problems. (55-99).......417–28; disc. 431
Barth, Paul; R. A. Huse, D. W. Taylor, L. E. Backer Transfer Tests on Station Auxiliary Busses. (55-92).........1441–5; disc. 1448
Bartlett, S. C. Disc.........1235
Bary, Constantine W. Disc.........140
Baude, John. Improved Fast-Acting Thermal Relay and Its Application as a Cage Winding Protective Relay for Synchronous Machines. (55-100).........349–53; disc. 354
Baudry, R. A. Disc.........590
Baumeister, Theodore. Disc.........550
Beavers, M. F. Disc.........983
Beavers, M. F.; J. E. Holcomb, L. C. Leoni. Magnetization of Transformer Cores During Impulse Testing. (55-30).........118–23; disc. 123
Beck, E. Disc.........365, 527
Beckwith, R. W. Disc.........277
Beckwith, Sterling; B. M. Koetting, L. T. Rosenberg, G. W. Staats. Test Report on a Fully Supercharged Generator. (55-123).........56–9
Bennon, Saul; R. J. Cossaart. Control of Electrostatic Voltage Distribution in Power Transformer Design. (55-521).........1122–5; disc. 1126
Benoit, A. W.; R. T. Hemmes, M. W. Schulz, Jr. An Anechoic Chamber for Noise Tests on Large Power Transformers. (55-26).........50–6
Bergseth, F. R. Disc.........401
Betz, Paul L. Field Current Sources for Electric Defibrillation. (55-87).........33–6
Bewley, Donald T. Disc.........230
Bienhoff, M. G. Power-Line Carrier Coupling—An Analysis. (55-698).........1163–70
Bigelow, R. O.; H. R. Tomlinson. Disc.........272
Black, K. G. Disc.........503
Blackburn, J. L.; G. D. Rockefeller. Line and Transformer Bank Relaying Systems. (55-88).........334–9; disc. 342
Blackburn, J. L.; G. D. Rockefeller. Disc.........428
Blake, J. A.; C. D. Morrill. A Computer for Economic Scheduling and Control of Power Systems......... (55-528).........1136–41; disc. 1142
Bliss, T. J. An Approach to the Definition of Excitation System Response. (55-459)...1008–12; disc. 1013
Bobrowicz, V. F.; E. T. B. Gross. Economic Selection of Auxiliary Drive Motors in Power Plants......... (55-681).........1237–46; disc. 1248
Bodicky, A. Disc.........945, 948
Boehne, E. W. Traveling Wave Protection Problems Part II. (55-475).........880–7
Boehne, E. W. Disc.........634
Boehne, E. W.; K. Chen. Testing of D-C Interrupters on A-C Test Circuits. (55-508).1073–9; disc. 1079
Bostwick, M. A. Disc.........400
Bottonari, S. A.; J. H. Sprow. A New High-Capacity Anode Air Circuit Breaker. (55-722).........1297–1302; disc. 1302
Boyer, O. A.; E. Korges. Nontension Aluminum Connectors. (55-248).........844–7; disc. 848
Brem, H. C. Disc.........1410
Bretch, Edward. Disc.........1342
Britt, H. O.; S. M. Denton. Pumped Storage and Hydro Generation at Flatiron Power Plant......... (55-164).........614–18; disc. 618
Brockman, J. J.; C. E. Linkous. D-C Machines: Response to Impact Excitation. (55-109).........500–03; disc. 504
Brookes, A. S.; E. L. Leinbach. Co-ordination of Secondary Network Protection. (55-445).........922–4; disc. 944
Brown, H. H. Disc.........552
Brown, W. T.; W. J. Cloues. Combination Load-Flow and Stability Equivalent for Power System Representation on A-C Power System Representation on A-C Network Analyzers. (55-282).........782–6; disc. 786
Browne, T. E., Jr. Disc.........1065
Brownlee, W. R. Disc.........171, 516
Bruncke, H. P. Disc.........339
Brustle, H. H.; T. W. Liao, J. R. Nye, J. G. Anderson. Corona Studies—In Relation to Insulation......... (55-437).........1046–50; disc. 1050
Bulkley, O. R. Disc.........609
Bullard, W. R. Disc.........1464
Buller, F. H. Disc.........280, 287, 319
Burdeshaw, T. A. Disc.........110
Burdick, E. J.; H. T. Seeley. Disc.........471
Burrell, R. W.; M. Morris. A-C Resistance of Conventional Strand Power Cables in Nonmetallic Duct and in Iron Conduit. (55-468).........1014–21 disc.; 1023
Burtness, R. W. A Circuit Approach to the Analysis of a 2-Stage Dynamoelectric Amplifier. (55-107).........440–9; disc. 450
Butler, R. M. A Simplified Method of Calculating Voltage Regulation Using Unit Impedance Power Reactive Diagrams. (55-89)....304–10; disc. 310

C

Cahen, Francois. Load-Phase Tie-Line Energy Control of Interconnected Power Systems. (55-24)....1–5
Cahn, C. R. The Determination of Incremental and Total Loss Formulas from Functions of Voltage Phase Angles. (55-25).........161–71; disc. 171
Cahn, Charles R. Disc.........516
Cameron, A. W. W.; E. de Haas, P. J. Sandiford. An Analogue Solution of Cable Heat Flow Problems. (55-55).........315–18; disc. 321
Cameron, A. W. W.; K. R. Knights. Disc.........475
Camilli, G. An Experimental Gas-Insulated 138-Kv Current Transformer. (55-12)...100–03; disc. 104
Cantwell, J. L. Disc.........976
Carothers, B. M. Disc.........1006
Carpenter, H. E.; R. E. Thornton. Eight Years' Experience With All-Aluminum Distribution Systems. (55-256).........828–32; disc. 833
Carroll, J. C.; A. R. Lee, R. B. McKinley. Design and Evaluation of Butyl-Rubber-Insulated Power Cable. (55-668).........1204–12; disc. 1213
Carter, J. G. Disc.........1236
Carter, W. A. Flux Measurements in Magnetic Air Circuit Breaker Interrupters. (55-460).........1062–5; disc. 1067
Casazza, J. A.; J. R. Rankin. General Study of Area Supply Methods. (55-669)....1328–34; disc. 1335
Caswell, R. W.; F. E. Andrews. Disc.........1312
Chambers, Fred; R. M. Milton. Behavior of High Voltage Busses and Insulators During Short Circuits. (55-11).........742–6; disc. 748
Chandler, W. G.; P. L. Dandeno. Disc.........149
Chen, K.; E. W. Boehne. Testing of D-C Interrupters on A-C Test Circuits. (55-508).........1073–9; disc. 1079
Clark, C. N.; B. M. Jones. Disc.........497
Clarke, D. D. Disc.........1406
Clayton, J. M.; D. F. Shankle. Insulation Characteristics of Wood and Suspension Insulators in Series. (55-712).........1305–11; disc. 1312
Clayton, J. M.; W. W. Valentine, J. K. Dillard. Surge Attenuation in Power Cables. (55-558).........1115–21; disc. 1122
Clevenger, C. M.; C. L. Sidway. Steam Turbine Generator Operating and Maintenance Methods of the Southern California Edison Company......... (55-119).........60–5
Cloues, W. J.; W. T. Brown. Combination Load-Flow and Stability Equivalent for Power System Representation on A-C Network Analyzers. (55-282).........782–6; disc. 786
Cobine, J. D. Disc.........664
Cogbill, B. A. Sequence Impedances of Symmetrical 3-Phase Transformer Connections. (55-671).........1313–23
Compton, O. R. Balancing Double-Wye High-Voltage Capacitor Banks. (55-146).........573–8; disc. 578
Concordia, C. Effect of Synchronous-Machine Transient Rotor Saliency on Changes in Terminal Voltage. (55-3).........25–31
Concordia, C. Voltage Dip and Synchronous Condenser Swings Caused by Arc-Furnace Loads. (55-448).........951–6
Conner, J. E. Disc.........703, 725
Conover, William B.; R. J. Ringlee. Recent Contributions to Transformer Audible Noise Control. (55-31).........77–90; disc. 90
Cope, R. R. Disc.........1199
Corbell, I. T.; A. Alvira. Microwave System Parameters for Reliable Communications. (55-516).........1100–07; disc. 1107
Cornelius, H. A. Disc.........365, 528, 1312
Cornwell, Fred E. Disc.........117
Cosgriff, Robert L.; K. Y. Tang. Two-Axis Method of Analyzing Electric Machines. (55-276)...1449–55
Cossaart, R. J.; S. Bennon. Control of Electrostatic Voltage Distribution in Power Transformer Design (55-521).........1122–5; disc. 1126
Couch, W. H.; G. J. Crowdes. High Temperature Classification of Rubber and Rubberlike Insulation of Network Cable by Oven Heating Tests......... (55-432).........930–4; disc. 944
Couch, W. H.; G. H. Hunt, N. D. Kenney, P. H. Ware. Modern High-Voltage Rubber Insulation......... (55-693).........1387–97; disc. 1398
Courtin, J. J. Ten Part-Winding Arrangements in Sample 4-Pole Induction Motor. (55-732).........1248–53; disc. 1254
Courtin, J. J. Disc.........1462
Coxe, E. H. Disc.........1050
Cramer, T. A.; F. C. Krings. Future Application Needs of Carrier Pilot Relaying. (55-695).........1233–5; disc 1236
Crandall, E. L.; Lee, A. R. Disc.........1384–5
Croft, Philip J. Disc.........300, 1224, 1385
Crowdes, G. J.; W. H. Couch. High Temperature Classification of Rubber and Rubberlike Insulation of Network Cable by Oven Heating Tests......... (55-432).........930–4; disc. 944
Curdts, E. B. Disc.........1224, 1427
Curtin, J. R. Disc.........310
Curtis, T. E. Disc.........108
Cushing, G. B. Disc.........703
Cuttino, W. H. Disc.........315
Cybulski, John. Disc.........397, 504
Cybulski, J.; J. P. O'Connor. D-C Machines—Short-Circuit Calculations and Test Results......... (55-114).........222–30; disc. 230
Cybulski, John; J. P. O'Connor. D-C Machines—Method for Short Circuit Calculations. (55-112).........214–21

D

Dakin, T. W. Disc. 1051
Dalziel, Charles F. Disc. 564
Dandeno, P. L.; W. G. Chandler. Disc. 149
Dandeno, P. L.; K. R. Knights. Disc. 623
Dandeno, P. L.; K. R. McClymont. Disc. 1012
Darrow, K. G. Disc. 703
Darrow, K. G.; G. J. Balentine. The Results of 7 Years' Experience with High Capacity Outdoor Oil Circuit Breakers. (55-213) .... 665–70; disc. 671
Darrow, K. G.; V. E. Phillips, A. J. Schultz, R. B. Shores. Test Circuits for Capacitance Switching Devices. (55-212) .... 624–34; disc. 635
Davies, E. G. Disc. 213
Dean, John E. Disc. 847
Deans, William. Aluminum in Heavy Current Conductors. (55-261) .... 1192–8; disc. 1200
Deans, William. Disc. 843
DeBaene, E. C. Disc. 945
deBellis, A. M. Disc. 647, 652, 657
Defoe, A. A. Disc. 374
deHaas, E.; P. J. Sandiford, A. W. W. Cameron. An Analogue Solution of Cable Heat Flow Problems (55-55) .... 315–18; disc. 321
Del Mar, William A. Disc. 321, 1212, 1361
Del Mar, W. A.; E. J. Merrell. Aluminum-Sheathed Power Cable. (55-53) .... 292–8; disc. 302
Denison, Clark. Disc. 314
Denton, S. M.; J. V. Baptist. Disc. 1012
Denton, S. M.; H. O. Britt. Pumped Storage and Hydro Generation at Flatiron Power Plant. .... (55-164) .... 614–18; disc. 618
Denton, W. J.; D. N. Reps. Distribution-Substation and Primary Feeder Planning. (55-158) .... 484–97; disc. 498
Derr, W. A.; W. L. Metz. Control Circuitry for Remotely Operated Electric Utility Substations. .... (55-127) .... 450–9; disc. 460
DeSieno, C. F. Disc. 373
Dewar, Harry. Disc. 1416
Dillard, J. K. Disc. 1421
Dillard, J. K.; S. B. Griscom, A. R. Hileman. Direct-Stroke Protection of High-Voltage Switching Stations and Transformers. (55-101) .... 354–65; disc. 367
Dillard, J. K.; W. W. Valentine, J. M. Clayton. Surge Attenuation in Power Cables. (55-558) .... 1115–21; disc. 1122
Doble, C. Disc. 550
Douglas, John F. H. Current Loci of Salient-Pole Synchronous Motors: An Extension of Blondel Theory. (55-507) .... 1080–2; disc. 1083
Driscoll, E. G. Disc. 1398
Duffy, F. H. Disc. 543
Dunaiski, R. M. Disc. 504
Dupre, H. P. Disc. 848
Dwight, H. B. Disc. 373

E

Eager, G. S., Jr. Disc. 945, 948, 1213
Eager, G. S., Jr.; C. A. Jordan. Mineral-Insulated Metallic-Sheathed Cables. (55-54) .... 198–212; disc. 213
Early, E. D.; W. E. Phillips, W. T. Shreve. An Incremental Cost of Power-Delivered Computer. .... (55-141) .... 529–34; disc. 535
Early, E. D.; R. E. Watson. A New Method of Determining Constants for the General Transmission Loss Equation. (55-720) .... 1417–21; disc. 1422
Early, E. D.; R. E. Watson, G. L. Smith. A General Transmission Loss Equation. (55-90) .... 510–16; disc. 518
Eason, W. E. Disc. 526
Ehrenberg, Gustave. Automatic Load-Frequency Control System for Central Station Power. (55-496) 787–95
Elliott, R. L.; C. W. Schoendube. Contact Life of Voltage-Regulating Relays. (55-718) .... 1398–1400; disc. 1401
Ellis, H. M. Disc. 365
Erdelyi, E. Predetermination of Sound Pressure Levels of Magnetic Noise of Polyphase Induction Motors. (55-726) .... 1269–80; disc. 1280
Erdelyi, Edward. Disc. 1219, 1372
Erdman, Herbert G., Jr. Disc. 431
Ernst, A.; P. Wildi. Disc. 197
Evans, W. E.; R. F. Lowe. Quadriphase—A New Approach to Time Division Multiplexing. .... (55-517) 900–03
Everhart, E. W. Disc. 848
Ewing, J. S.; D. D. Gerbetz. Correlation of Temperature Measurements on D-C Armatures. (55-106) .... 391–4; disc. 397

F

Fagerlund, A. C.; G. D. Stevens. Disc. 992
Farmer, G. E. Disc. 1107
Farneth, W. C.; G. Gallousis. Epoxy Resin Casting of Dry-Type Current Transformers. (55-34) .... 194–7; disc. 198
Fegley, K. A. Metadyne Transients. (55-108) 1179–88
Ferguson, R. W. Disc. 1013
Ferguson, R. W.; H. R. Armstrong, A. R. Hileman. Lightning Protection in a 24-Kv Station—Field and Laboratory Studies. (55-556) .... 1127–35; disc. 1135
Ferri, L. F. Disc. 401
Ferris, Livingston P. Disc. 565
Fett, G. H. Disc. 449
Field, E. J.; D. L. Leatherberry. A Power Class Recloser for Higher Speed Clearing of Distribution Circuits. (55-510) .... 986–91; disc. 992
Fink, L. H. Disc. 319
Fisch, J. Disc. 589
Fischer, H. D., Jr.; J. Lummis. Practical Application of Sag and Tension Calculations to Transmission Line Design. (54-501) .... 402–13; disc. 416
Flink, A. E. Disc. 400
Floyd, G. D. Disc. 709
Forbes, Sherman Guy, Jr. Disc. 266
Foti, Arem; J. B. Owens. Disc. 110
Fountain, L. L.; J. E. Barkle, C. C. Sterrett. Detection of Grounds in Generator Field Windings. (55-125) .... 467–70; disc. 471
Fowler, W. C.; C. W. Thomas. Automatically Switched Capacitors in Steps on a Single Distribution Feeder. (55-91) .... 311–14; disc. 315
Fox, George W. Disc. 1236
Freeman, W. C. Disc. 416
Friedrich, R. E. Disc. 671, 725
Frink, Russell. Disc. 1079, 1098
Fritz, Eduard. Investigation of European Practices in Power Line Design. (55-149) ... 505–09; disc. 510
Fritz, Eduard, Jr. Disc. 853
Fugill, A. P. Principles and Practices of Modern System Planning. (55-673) ..... 1323–26; disc. 1328
Funkhouser, A. W.; R. P. Huber. A Method for Determining Economical ACSR Conductor Sizes for Distribution Systems. (55-159) .... 479–83; disc. 483

G

Gallagher, E. I. Turbine Generator Operation and Maintenance Practice of Philadelphia Electric Company. (55-117) 48–9
Gallousis, George; W. C. Farneth. Epoxy Resin Casting of Dry-Type Current Transformers (55-34) .... 194–7; disc. 198
Garrett, K. S. Disc. 833
Garrett, K. S.; C. E. Nelson. Design Problems and Operating Experience with Aluminum Distribution Conductors in the Philadelphia Electric Company. (55-249) 825–8
Gaskill, W. A. Disc. 641
Gaty, L. R. Research in the Electric Power Industry. (55-145) .... 553–6; disc. 557
Gazzana Priaroggia, P.; G. Palandri. Research on the Electric Breakdown of Fully Impregnated Paper Insulation for High-Voltage Cables. (55-692) .... 1343–57; disc. 1362
George, E. E. Disc. 1296
Gerbetz, D. D.; J. S. Ewing. Correlation of Temperature Measurements on D-C Armatures. (55-106) .... 391–4; disc. 397
Getty, A. H.; K. M. Smith. Disc. 1334–5
Ghesquiere, J. D.; C. E. Quick, S. W. Luther. Two Large Electric Arc Furnaces—Electrical Characteristics and Corrective Equipment. (55-743) .... 1401–05; disc. 1406
Gibbs, W. J. Disc. 348
Gibson, J. W. Disc. 1115
Glimn, A. F.; R. Habermann, Jr., J. M. Henderson, L. K. Kirchmayer. Digital Calculation of Network Impedances. (55-680) ... 1285–95; disc. 1295
Glimn, A. F.; L. K. Kirchmayer. Disc. 172
Glimn, A. F.; L. K. Kirchmayer, R. D. Wood. Disc. 1421
Gnuse, H. H., Jr. Development of Small Hydroelectric Sites in Western North Carolina. (55-165) ... 65–8
Godard, W. Wallace. Electric Utility Load Forecasting. (55-531) 1428–40
Goldberg, Yale. Disc. 98
Goodrich, R. D. Disc. 310
Gossman, H. G. Disc. 847
Gostin, Belgrave F. High-Current Testing of Air-Disconnect Switches. (55-13) 21–5
Graham, R. C. Overload Classifications for Secondary Network Cables. (55-444) ..... 916–19; disc. 944
Graham, R. C. Disc. 946, 948, 949, 1212
Greenfield, E. W. Disc. 848
Griffard, W. F. Disc. 1135
Griscom, S. B. Disc. 1448
Griscom, S. B.; J. K. Dillard, A. R. Hileman. Direct-Stroke Protection of High-Voltage Switching Stations and Transformers. (55-101) .... 354–65; disc. 367
Gross, Eric T. B. Bibliography of Relay Literature—1950–52. (55-93) 45–8
Gross, Eric T. B. Disc. 479
Gross, E. T. B.; V. F. Bobrowicz. Economic Selection of Auxiliary Drive Motors in Power Plants. .... (55-681) .... 1237–46; disc. 1248
Gross, Eric T. B.; S. W. Nelson. Electromagnetic Unbalance of Untransposed Transmission Lines. Part II. (55-477) 887–93
Gross, Eric T. B.; R. B. Wise. Grounding Grids for High Voltage Stations.
Part II. Resistance of Large Rectangular Plates. (55-281) .... 801–09; disc. 809
Grosser, E. H.; R. L. Rowan. Disc. 260
Gruetter, James G. The Application of Business Machines to Electrical Utility Load Forecasting. .... (55-450) 854–8
Gue, E. M. Pittsburgh Downtown 69-Kv Power Supply Part II. Substation. (55-226) .... 648–52; disc. 653
Guess, L. T. Disc. 413
Guess, L. T.; J. S. Tompkins. Disc. 746
Guile, A. E. The Calculation of the Complete Time/Current Characteristics of Cartridge Fuses With Single Wire Element. (55-514). 1108–15; disc. 1115

H

Habermann, R., Jr.; A. F. Glimn, J. M. Henderson, L. K. Kirchmayer. Digital Calculation of Network Impedances. (55-680) .. 1285–95; disc. 1295
Hagenguth, J. H. Disc. 123, 366
Halacsy, A. A. Disc. 99, 160, 197
Hale, H. W.; J. B. Ward. Disc. 517, 1296
Halperin, Herman. Disc. 250, 300, 439, 609, 982
Hambrick, R. D.; O. Naef. Field Tests on a 138-Kv High Speed Oil Circuit Breaker at Philip Sporn Power Plant. (55-222) .... 710–24; disc. 726
Hampe, G. W. Disc. 341, 430, 1072
Hansson, Bror. Disc. 1357
Haralampu, George S. Disc. 1021
Harder, E. L. Disc. 1091
Harms, H. B. Disc. 1061
Harrington, Dean 182
Harrington, E. J. Disc. 736
Harrington, E. J.; E. C. Starr. Disc. 701
Hart, Lester C. Disc. 110
Hartman, C. J. Disc. 1200
Hartman, C. J.; C. E. Asbury. Development of a Welded Aluminum Bus for Substations. (55-257) .... 834–8; disc. 839
Hatcher, C. T. Disc. 300, 833
Hauch, W. J. Disc. 1416
Haupt, L. M., Jr. Disc. 1141
Heberlein, G. B. Disc. 1199
Hodges, C. D. An Investigation of the Capture Effect in a Narrow-Band Frequency Modulated System. (55-79) .... 289–91; disc. 292
Heller, F.; I. Matthysse. Limiters, Their Design Characteristics and Applications. (55-473) .... 924–30; disc. 944
Hemmes, R. T.; A. W. Benoit, M. W. Schulz, Jr. An Anechoic Chamber for Noise Tests on Large Power Transformers. (55-26) 50–6
Henderson, J. M.; A. F. Glimn, R. Habermann, Jr. L. K. Kirchmayer. Digital Calculation of Network Impedances. (55-680) ... 1285–95; disc. 1295
Henderson, J. R. Disc. 1334
Hess, W. B.; R. C. Swengel, S. K. Waldorf. Principles and Application of the Ultrasonic Flowmeter. (55-28) .... 112–17; disc. 117
Hicks, R. L. Disc. 1463
Higgins, Thomas J. Disc. 847, 1219, 1285, 1305
Hileman, A. R.; H. R. Armstrong, R. W. Ferguson. Lightning Protection in a 24-Kv Station—Field and Laboratory Studies. (55-556) .... 1127–35; disc. 1135
Hileman, A. R.; S. B. Griscom, J. K. Dillard. Direct-Stroke Protection of High-Voltage Switching Stations and Transformers. (55-101) .... 354–65; disc. 367
Hill, V. E. Pittsburgh Downtown 69-Kv Power Supply. Part I. Planning. (55-225) .... 643–7; disc. 647
Hill, V. E.; F. M. Kenney. Disc. 1006
Hindle, W. Disc. 475
Hindle, W.; W. D. Houser, J. A. Tyerman. Production and Installation of Vertical Water Wheel Generators. (55-162) .... 536–43; disc. 544
Hobson, J. E.; W. A. Lewis, M. S. Oldacre. Implementation of a Research Program for the Electric Utility Industry. (55-144) ...... 545–50; disc. 552

Hochdorf, Martin; R. B. Shipley, M. Watson. ORACLE Computes Line Constants With Tensors. (55-478)....1052–6; disc. 1056
Hoffman, C. H. Disc....786
Hogan, J. C.; C. G. Pebler. Relay Protection for Lines Being Sleet-Melted by the Short-Circuit Method. (55-469)....1067–71; disc. 1072
Holcomb, H. E.; M. F. Beavers, L. C. Leoni. Magnetization of Transformer Cores During Impulse Testing. (55-30)....118–23; disc. 123
Holcomb, J. E. Impulse Tests on Low-Voltage Windings of Distribution Transformers. (55-27)....1152–5; disc. 1155
Holley, C. H.; R. E. Savidge. Improved Field Conductor Materials for Turbine Generators. (55-131)....72–6
Hollingsworth, P. M. Disc....300
Hooke, R. G. Forecasting the Demand for Electricity. (55-530)....993–1005; disc. 1007
Hooke, R. G. Disc....1327
Horowitz, S. H.; H. C. Barnes. Disc....330
Horrell, R. F. Disc....1280
Horrell, R. F.; D. C. Martin. Disc....1254
Houser, W. D.; W. Hindle, J. A. Tyerman. Production and Installation of Vertical Water Wheel Generators. (55-162)....536–43; disc. 544
Hoyt, J. Curtis. Disc....1446
Hubbard, D. C. Disc....847
Huber, R. P.; A. W. Funkhouser. A Method for Determining Economical ACSR Conductor Sizes for Distribution Systems. (55-159)....479–83; disc. 483
Hunkins, H. D. A Look to the Future of Power Transmission in the West. (55-184)....591–7; disc. 599
Hunt, G. H.; N. D. Kenney, P. H. Ware, W. H. Couch. Modern High-Voltage Rubber Insulation. (55-693)....1387–97; disc. 1398
Huse, R. A.; D. W. Taylor, L. E. Backer, Paul Barth. Transfer Tests on Station Auxiliary Busses. (55-92)....1441–5

J

Jansen, M. A.; C. Morrison. Disc....340
Jeynes, Paul H. Disc....599
Johnson, I. B.; A. J. Schultz, N. R. Schultz, R. B. Shores. Some Fundamentals on Capacitance Switching. (55-224)....727–36; disc. 736
Johnson, J. Stuart. Disc....551
Johnson, L. J.; S. E. Rauch. Design Principles of Flux-Switch Alternators. (55-730)....1261–8; disc. 1268
Johnson, R. W. Interpretation and Significance of Tests Indicating the Concentration of Polar Compounds in Transformer Oil. (55-279)....774–80; disc. 780
Johnson, W. R. Disc....599
Johrde, P. S. Disc....590
Jones, B. L.; J. Tompkins, P. D. Tuttle. Measurement of Resistance and Reactance of Expanded ACSR. (55-98)....368–73; disc. 375
Jones, B. M.; C. N. Clark. Disc....497
Jones, B. M.; C. M. Stearns. Disc....1405–6
Jones, Byron M. Disc....1376
Jones, Ray V. Protection of Personnel Against Electrical Shock Hazards in Central Office Communications Equipment. (55-426)....893–6
Jordan, C. A.; G. S. Eager, Jr. Mineral-Insulated Metallic-Sheathed Cables. (55-54)....198–212; disc. 213

K

Kalb, J. W.; A. G. Yost. Transient Durability Testing of Valve Type Lightning Arresters. (55-136)....521–6; disc. 528
Kane, R. E.; J. K. Walker. A 69-Kv Compressed Air Circuit Breaker for 5,000,000 Kva. (55-218)....705–09; disc. 710
Kelly, Arnold R. Disc....1448
Kenney, F. M.; V. E. Hill. Disc....1006
Kenney, N. D.; P. H. Ware, W. H. Couch, G. H. Hunt. Modern High-Voltage Rubber Insulation. (55-693)....1387–97; disc. 1398
Kidder, A. H. Disc....318
Kidder, A. H.; J. H. Neher. Power Distribution System Parameters. (55-19)....125–40; disc. 140
Kilbourne, C. E.; J. R. M. Alger, D. S. Snell. Turbine Generator Stator Winding Temperatures at Various Hydrogen Pressures. (55-118)....232–50; disc. 251
Kilgore, Lee A. Disc....182, 390
Kilgour, A. E. Disc....380, 704, 709, 724
Killian, S. C. Disc....747
Kinghorn, J. H. Disc....1447
Kirchmayer, L. K.; A. F. Glimn. Disc....172
Kirchmayer, L. K.; A. F. Glimn, R. Habermann, Jr., J. M. Henderson. Digital Calculation of Network Impedances. (55-680)....1285–95; disc. 1295
Kirchmayer, L. K.; A. F. Glimn, R. D. Wood. Disc....1421
Kirchmayer, L. K.; A. G. Mellor, J. F. O'Mara, J. R. Stevenson. An Investigation of the Economic Size of Steam-Electric Generating Units. (55-183)....600–09; disc. 613
Kirkham, E. H.; R. W. Atkinson. Disc....259
Kirschbaum, H. S. Basic Sequence Networks. (55-278)....771–4
Klapper, D. B. Disc....148
Klein, N. Disc....1358
Knights, K. R. Disc....544
Knights, K. R.; A. W. W. Cameron. Disc....475
Knights, K. R.; P. L. Dandeno. Disc....623
Knutz, W. H. Disc....1312
Koenig, H. E. Disc....449
Koetting, B. M.; S. Beckwith, L. T. Rosenberg, G. W. Staats. Test Report on a Fully Supercharged Generator. (55-123)....56–9
Kolks, R. H. A Mathematical Method for Determining Insulation Damage Curves for Network Cables. (55-474)....934–8; disc. 944
Komives, L. I. Disc....192, 1362
Korges, Emerson; O. A. Boyer. Nontension Aluminum Connectors. (55-248)....844–7; disc. 848
Kotheimer, W. C. A Method for Studying Circuit Transient Recovery Voltage Characteristics of Electric Power Systems. (55-476)....1083–6; disc. 1087
Kouwenhoven, W. B.; W. R. Milnor. Electric Defibrillation. (55-95)....561–4; disc. 566
Kozak, S.; C. Prescott. Gas-Pressurized 120-Kv and 161-Kv Pipe-Type Cables in Ontario. (55-50)....184–92; disc. 193
Kozak, S.; H. D. Short. Disc....301
Krings, F. C. Disc....292
Krings, F. C.; T. A. Cramer. Future Application Needs of Carrier Pilot Relaying. (55-695)....1233–5; disc. 1236
Ku, Y. H. Equivalent Circuit for the Concatenation of Induction Motors. (55-675)..1214–18; disc. 1219
Ku, Y. H. Disc....1092

L

Lambert, E. G.; E. M. Wright. The Use of All-Aluminum Conductor on Transmission Lines. (55-250)....849–53; disc. 854
Lamborn, R. Disc....397
Landeau, Maurice. Disc....416
Langford, J. A. Disc....475
Lantz, Martin J. Analysis of Fault Currents for High-Voltage Circuit Breaker Interruption. (55-102)....41–5
LaPierre, W.; J. Y. Louis. Double-Energy Conversion in an Air Gap—A Novel Asynchronous Frequency Changer (55-676)....1373–5; disc. 1377
Larson, Robert E. Disc....828
Lawrence, R. F.; D. N. Reps. Economics of Higher Primary and Secondary Voltages for Commercial Areas. (55-481)....1034–45; disc. 1045
Lawton, F. L. Disc....117, 148, 543
Leatherberry, D. L.; E. J. Field. A Power Class Recloser for Higher Speed Clearing of Distribution Circuits. (55-510)....986–91; disc. 992
Lebens, J. C. Disc....1115
Lee, A. R.; J. C. Carroll, R. B. McKinley. Design and Evaluation of Butyl-Rubber-Insulated Power Cable. (55-668)....1204–12; disc. 1213
Lee, A. R.; E. L. Crandall. Disc....1384
Lee, Reuben. Design of the Adjustable Lin-O-Phase Filter. (55-78)....273–7; disc. 277
Lee, Tsai H. Disc....1296
Leeds, W. M. Disc....684
Leinbach, E. L.; A. S. Brookes. Co-ordination of Secondary Network Protection. (55-445)....922–4; disc. 944
Lemens, D. J. Disc....1086
Lennox, T. C. Controls for Step Voltage Regulators. (55-717)....1407–09; disc. 1410
Lentz, O. A. Disc....947
Leoni, L. C.; M. F. Beavers, J. E. Holcomb. Magnetization of Transformer Cores During Impulse Testing. (55-30)....118–23; disc. 123
Leslie, J. R. Disc....117
Lewis, D. G.; W. D. Marsh. Transfer of Steam-Electric Generating-Station Auxiliary Busses. (55-96)....322–30; disc. 333
Lewis, W. A. Disc....374
Lewis, W. A.; J. E. Hobson, M. S. Oldacre. Implementation of a Research Program for the Electric Utility Industry. (55-144)....545–50; disc. 552
Liao, T. W.; J. R. Nye, H. H. Brustle, J. G. Anderson. Corona Studies—In Relation to Insulation. (55-437)....1046–50; disc. 1050
Linders, J. R. Disc....340, 430
Lindquist, O. J. Disc....1406, 1410
Linkous, C. E. Effect of Skew on Induction Motor Magnetic Fields. (55-270)....760–5; disc. 765
Linkous, C. E.; J. J. Brockman. D-C Machines: Response to Impact Excitation. (55-109)....500–03; disc. 504
Liwschitz-Garik, M. M. Computation of Skin Effect in Bars of Squirrel-Cage Rotors. (55-271)....768–70; disc. 771
Liwschitz-Garik, M. M. Some Factors Influencing the Temperature Rise of Armature Windings. (55-275)....752–9
Lloyd, B. L.; C. F. Wagner. Effects of Corona on Traveling Waves. (55-453)....858–72
Lockie, A. M. Functional Life Expectancy Tests for Liquid-Filled Distribution Transformers. (55-520)....977–82; disc. 982
Lockie, A. M. Disc....975
Logan, James T. Disc....1145
Lokay, H. E.; D. N. Reps. Disc....140
Long, R. W.; R. H. Travers....173
Louis, J. Y.; W. LaPierre. Double-Energy Conversion in an Air Gap—A Novel Asynchronous Frequency Changer. (55-676)....1373–5; disc. 1377
Lowe, R. F.; W. E. Evans. Quadriphase—A New Approach to Time Division Multiplexing. (55-517)....900–03
Lucas, H. R. Disc....103
Lummis, J.; H. D. Fischer, Jr. Practical Application of Sag and Tension Calculations to Transmission Line Design. (54-501)....402–13; disc. 416
Lummis, Jordan. Disc....853
Luther, S. W.; J. D. Ghesquiere, C. E. Quick. Two Large Electric Arc Furnaces—Electrical Characteristics and Corrective Equipment. (55-743)....1401–05; disc. 1406
Lytle, C. M. Disc....1261

M

Mackenzie, W. F. Disc....330, 1446
Maginniss, F. J.; P. A. Abetti, G. E. Adams. Oscillations of Coupled Windings. (55-29)....12–21
Mankoff, L. L.; R. L. Williams, H. N. Schneider. Capacitance-Switching Facilities at the Switchgear Development Laboratory. (55-220)....375–80; disc. 381
Manning, M. L. Functional Temperature Endurance Tests on a Silicone Glass Fiber Insulation System for Dry-Type Transformers. (55-44)....91–8; disc. 98
Manning, M. L. Disc....160, 976
Marsden, D. J.; D. M. Umphrey. Design Problems and Field Tests Concerning Circuit Breakers for Switching Long 230-Kv Lines. (55-223)....693–701; disc. 705
Marsh, W. D.; D. G. Lewis. Transfer of Steam-Electric Generating-Station Auxiliary Busses. (55-96)....322–30; disc. 333
Marter, W. E. Disc....429
Martin, D. C.; R. F. Horrell. Disc....1254
Martin, E. R. Weighted Mutual Reactances for a Triple-Cage Motor Circuit. (55-273)....765–8
Matthysse, I. Disc....946
Matthysse, I.; F. Heller. Limiters, Their Design Characteristics and Application. (55-473)....924–30; disc. 944
McClymont, K. R.; P. L. Dandeno. Disc....1012
McConnell, A. J. Disc....1146
McConnell, A. J.; H. C. Barnes. Some Utility Ground Relay Problems. (55-99)....417–28; disc. 431
McConnell, H. M. A Transductor Type Field Ripple Detector for Synchronous Generators. (55-124)....476–9; disc. 479
McConnell, H. M.; E. F. Sverdrup. The Induction Machine with Solid Iron Rotor. (55-115)....343–8; disc. 349
McCoy, R. L. Disc....747
McGrath, M. H. Disc....1032
McIlveen, E. E. Aluminum-Sheathed Control Cable. (55-691)....1377–84; disc. 1386
McKean, A. L. Disc....288
McKeeby, R. B. Disc....589
McKinley, R. B.; J. C. Carroll, A. R. Lee. Design and Evaluation of Butyl-Rubber-Insulated Power Cable. (55-668)....1204–12; disc. 1213
McNerney, A. M. Results of High-Current Tests on 161-Kv Disconnecting Switches. (55-9)....104–08; disc. 111
Mellor, A. G.; L. K. Kirchmayer, J. F. O'Mara, J. R Stevenson. An Investigation of the Economic Size of Steam-Electric Generating Units. (55-183)....600–09; disc. 613
Merrell, Edwin J. Freezing Oil-Type Pipe Cables. (55-446)....1023–31; disc. 1033
Merrell, E. J.; W. A. Del Mar. Aluminum-Sheathed Power Cable. (55-53)....292–8; disc. 302
Merritt, M. Stephens. Disc....428
Metz, W. L.; W. A. Derr. Control Circuitry for Remotely Operated Electric Utility Substations. (55-127)....450–9; disc. 460
Meyerhoff, L. Disc....193, 1022, 1359
Meyers, E. H. Disc....395

Mickley, A. S. Disc.....746
Miller, G. M.; L. W. Robbins. Fundamental Relations of System Voltage Drop and System Loads. (55-41).....267–72; disc. 272
Miller, R. H. Disc.....149
Milnor, W. R.; W. B. Kouwenhoven. Electric Defibrillation. (55-95).....561–4; disc. 566
Milton, R. M.; F. Chambers. Behavior of High Voltage Busses and Insulators During Short Circuits. (55-11).....742–6; disc. 748
Minder, P. M. Intermittently Increased Kilovar Output of Larger Capacitor Banks. (55-356).....749–51; disc. 751
Mitchell, C. F. Disc.....984
Monfort, Charles E., Jr. Disc.....652
Moody, W. M. Disc.....460
Morrill, C. D.; J. A. Blake. A Computer for Economic Scheduling and Control of Power Systems. (55-528).....1136–41; disc. 1142
Morris, M.; R. W. Burrell. A-C Resistance of Conventional Strand Power Cables in Nonmetallic Duct and in Iron Conduit. (55-468).....1014–21; disc. 1023
Morrison, Charles; M. A. Jansen. Disc.....340
Morrison, Charles; C. C. Wolf. Disc.....497
Morton, Walter B. Disc.....556
Moses, Graham Lee. Disc.....975
Moses, Graham Lee; E. C. Whitney. Disc.....474
Moynihan, J. D.; B. J. Sparlin. A Method of Measurement of Carrier Characteristics on Power Cables. (55-77).....31–3
Moynihan, J. D.; B. J. Sparlin. A Study of Carrier-Frequency Noise on Power Lines.....
  Part IV. Conclusion of Field Measurements..... (55-458).....795–800
Munson, W. A. Disc.....742
Muster, D. F.; G. L. Wolfert. Single-Phase Induction Motor Noise Due to Dissymmetry Harmonics. (55-729).....1365–72; disc. 1372

N

Naef, Otto. Disc.....693, 704
Naef, Otto; R. D. Hambrick. Field Tests on a 138-Kv High Speed Oil Circuit Breaker at Philip Sporn Power Plant. (55-222).....710–24; disc. 726
Narbut, Paul. Functional Life Tests of Insulation Systems for Dry-Type Transformers. (55-449).....1057–61; disc. 1061
Neagle, N. M.; D. R. Nelson. The Use of Probability in the Design and Operation of Secondary Network Systems. (55-160).....567–72; disc. 572
Neher, J. H. Disc.....260, 280
Neher, J. H.; A. H. Kidder. Power Distribution System Parameters. (55-19).....125–40; disc. 140
Nelson, C. E.; K. S. Garrett. Design Problems and Operating Experience with Aluminum Distribution Conductors in the Philadelphia Electric Company. (55-249).....825–8
Nelson, D. R.; N. M. Neagle. The Use of Probability in the Design and Operation of Secondary Network Systems. (55-160).....567–72; disc. 572
Nelson, S. W.; E. T. B. Gross. Electromagnetic Unbalance of Untransposed Transmission Lines.
  Part II. (55-477).....887–93
Niebauer, K. L. Disc.....992
Niessink, T. Disc.....946
Nilsson, Einar. Disc.....331
Norinder, E. O. A Rational Method for the Step-by-Step Calculations in Power System Transient Stability Studies. (55-479).....1087–91; disc. 1092
Norman, R. S.; R. A. Pfuntner, B. W. Wilterdink. The Application of a New Nontracking Butyl to High Voltage Instrument Transformers. (55-715).....1173–6
Norris, C. L. Mechanical Alignment of Vertical Shaft Hydroelectric Units as Practiced by Tennessee Valley Authority. (55-163).....586–9; disc. 589
Nye, J. R.; T. W. Liao, H. H. Brustle, J. G. Anderson. Corona Studies—In Relation to Insulation..... (55-437).....1046–50; disc. 1050

O

Oberholtzer, J. R. Disc.....483, 498
O'Connor, J. P.; J. Cybulski. D-C Machines—Short-Circuit Calculations and Test Results. (55-114).....222–30; disc. 230
O'Connor, John P.; J. Cybulski. D-C Machines—Method for Short Circuit Calculations. (55-112).....214–21
Oldacre, M. S. Disc.....598
Oldacre, M. S.; J. E. Hobson, W. A. Lewis. Implementation of a Research Program for the Electric Utility Industry. (55-144).....545–50; disc. 552
Oldenkamp, J. L. Application of Statistics to Motor Testing. (55-286).....815–18; disc. 818
Oldenkamp, J. L. Disc.....1372
Oliver, F. S. Disc.....1051
O'Mara, J. F.; L. K. Kirchmayer, A. G. Mellor, J. R. Stevenson. An Investigation of the Economic Size of Steam-Electric Generating Units. (55-183).....600–09; disc. 613
Opsahl, A. M. Disc.....527
Osterle, W. H. Disc.....535
Ottinger, Brent. Disc.....1312
Owens, J. B.; A. Foti. Disc.....110

P

Padgett, J. D., Disc.....832
Palandri, G.; P. Gazzana Priarogga. Research on the Electric Breakdown of Fully Impregnated Paper Insulation for High-Voltage Cables. (55-692).....1343–57; disc. 1362
Parker, E. E.; J. Baird. Manufacturer's Research in Relation to Electrical Utilities. (55-245).....557–60
Parker, John C. Disc.....1031
Paulus, C. F. Disc.....332, 610
Pebler, C. G.; J. C. Hogan. Relay Protection for Lines Being Sleet-Melted by the Short-Circuit Method. (55-469).....1067–71; disc. 1072
Peirce, W. T.; V. Siegfried. Disc.....946
Perry, Irving D. Disc.....1107
Pfuntner, R. A.; R. S. Norman, B. W. Wilterdink. The Application of a New Nontracking Butyl to High-Voltage Instrument Transformers. (55-715).....1173–6
Phillips, A. F. Disc.....99
Phillips, H. W. Disc.....610
Phillips, V. E.; K. G. Darrow, A. J. Schultz, R. B. Shores. Test Circuits for Capacitance Switching Devices. (55-212).....624–34; disc. 635
Phillips, W. E.; E. D. Early, W. T. Shreve. An Incremental Cost of Power-Delivered Computer. (55-141).....529–34; disc. 535
Picken, Donald A. Disc.....566
Pierson, P. R. Pittsburgh Downtown 69-Kv Power Supply.....
  Part III. Switchgear Development. (55-214).....653–6; disc. 657
Pollard, E. I. Disc.....389
Porter, L. F. Time Current Damage Characteristics, Cable in Duct. (55-434).....919–21; disc. 944
Potter, C. P. Disc.....1462
Powell, A. H. Disc.....109
Powell, A. H.; C. L. Schuck. Ribbon Elements for High-Voltage Current-Limiting Fuses. (55-217).....635–41; disc. 642
Prescott, C.; S. Kozak. Gas-Pressurized 120-Kv and 161-Kv Pipe-Type Cables in Ontario. (55-50).....184–92; disc. 193
Price, W. S. Disc.....365, 527

Q

Quick, C. E.; S. W. Luther, J. D. Ghesquiere. Two Large Electric Arc Furnaces—Electrical Characteristics and Corrective Equipment. (55-743).....1401–05; disc. 1406
Quinn, Bayard E. Disc.....676

R

Rademacher, L. B.; W. L. Teague. Disc.....154, 1155
Radley, G. R. Disc.....564
Raine, P. A.; F. J. Aldridge. Disc.....298
Ramm, E. E. Disc.....838
Rankin, J. R.; J. A. Casazza. General Study of Area Supply Methods. (55-669).....1328–34; disc. 1335
Rauch, S. E.; L. J. Johnson. Design Principles of Flux-Switch Alternators. (55-730).....1261–8; disc. 1268
Reed, Myril B. Disc.....450
Reilly, M. J.; D. E. Weston. A New 500-Megavolt Ampere Air Magnetic Circuit Breaker of Simplified Design. (55-509).....1093–8; disc. 1045
Reinhard, J. W. Disc.....1005
Rembusch, J. E.; H. E. Smith. Disc.....1260
Render, T. J. Disc.....642
Reps, David N. Coincident-Outage Probability in Secondary-Network Vaults. (55-161).....580–5; disc. 586
Reps, D. N.; W. J. Denton. Distribution-Substation and Primary Feeder Planning. (55-158).....484–97; disc. 498
Reps, D. N.; R. F. Lawrence. Economics of Higher Primary and Secondary Voltages for Commercial Areas. (55-481).....1034–45; disc. 1045
Reps, D. N.; H. E. Lokay. Disc.....140
Retherford, R. W. Disc.....1416
Rheingans, William J. Disc.....589
Ribe, Marshall L. Disc.....1107
Richardson, P. E. Disc.....702
Richter, Henry. Disc.....212
Ringlee, Robert J.; W. B. Conover. Recent Contributions to Transformer Audible Noise Control..... (55-31).....77–90; disc. 90
Ringstad, Erling. Disc.....510
Risser, J. H., Jr. Rural Electric System Planning..... (55-746).....1410–16; disc. 1416
Robbins, L. W. Disc.....751
Robbins, L. W.; G. M. Miller. Fundamental Relations of System Voltage Drop and System Loads..... (55-41).....267–72; disc. 272
Roberts, J. F. Disc.....589
Roberts, W. J.; R. L. Webb. Operation of Turbine Generators During Off-Peak High Power Factor Periods—Practices of One Utility in a Metropolitan Area. (55-120).....461–5; disc. 467
Rockefeller, G. D.; J. L. Blackburn. Line and Transformer Bank Relaying Systems. (55-88).....334–9; disc. 342
Rockefeller, G. D.; J. L. Blackburn. Disc.....428
Rodee, H. H. Disc.....413, 854
Rosch, S. J. Characteristic Properties of Secondary Network Cables. (55-441).....939–44; disc. 944
Rosch, S. J. Some Performance Characteristics of High-Voltage Rubber-Insulated Cables. (55-678).....1219–24; disc. 1224
Rosch, S. J. Disc.....212, 301, 1386
Rosenberg, L. T. Eccentricity, Vibration, and Shaft Currents in Turbine Generators. (55-121).....38–41
Rosenberg, L. T. Disc.....1082
Rosenberg, L. T.; S. Beckwith, B. M. Koetting, G. W. Staats. Test Report on a Fully Supercharged Generator. (55-123).....56–9
Rosenberry, G. M., Jr. The Transient Stalled Temperature Rise of Cast-Aluminum Squirrel-Cage Rotors for Induction Motors. (55-255).....819–24; disc. 824
Ross, M. D. Disc.....250
Rowan, R. L.; E. H. Grosser. Disc.....260
Ruskin, Vernon W. Maximum Short Circuit and Faulty Synchronizing Torques on Generator Foundations. (55-173).....618–23; disc. 624

S

Sabol, J. T. Characteristics of Single-Conductor Electric Cable at High Frequency. (55-679).....1280–5; disc. 1285
Salin, J. A. Disc.....483
Sandell, D. H. Disc.....839
Sandiford, P. J.; E. deHaas, A. W. W. Cameron. An Analogue Solution of Cable Heat Flow Problems. (55-55).....315–18; disc. 321
Sanford, Frank E. Disc.....551
Satterlee, W. W. Disc.....99
Saunders, Rober M. Disc.....449, 1268
Savidge, R. E.; C. H. Holley. Improved Field Conductor Materials for Turbine Generators. (55-131).....72–6
Scheideler, A. L.; G. F. Simmons. Evaluation and Application of Silicone-Organic Resin Combinations for Dry-Type Transformer Insulation..... (55-43).....155–60; disc. 160
Schmidt, M. L. Disc.....396
Schneider, H. N.; R. L. Williams, L. L. Mankoff. Capacitance-Switching Facilities at the Switchgear Development Laboratory. (55-220).....375–80; disc. 381
Schneider, M. S. Disc.....439
Schoendube, C. W.; R. L. Elliott. Contact Life of Voltage-Regulating Relays. (55-718).....1398–1400; disc. 1401
Schofer, Carl. Disc.....509
Schuck, C. L.; A. H. Powell. Ribbon Elements for High-Voltage Current-Limiting Fuses. (55-217).....635–41; disc. 642
Schultz, A. J.; K. G. Darrow, V. E. Phillips, R. B. Shores. Test Circuits for Capacitance Switching Devices. (55-212).....624–34; disc. 635
Schultz, A. J.; I. B. Johnson, N. R. Schultz, R. B. Shores. Some Fundamentals on Capacitance Switching. (55-224).....727–36; disc. 736
Schultz, B. H. Disc.....1261
Schultz, N. R.; I. B. Johnson, A. J. Schultz, R. B. Shores. Some Fundamentals on Capacitance Switching. (55-224).....727–36; disc. 736
Schulz, M. W., Jr.; A. W. Benoit, R. T. Hemmes. An Anechoic Chamber for Noise Tests on Large Power Transformers. (55-26).....50–6
Schwarz, S. J. Disc.....809
Sealey, William C. Increased Current Ratings for Step Regulators. (55-353).....737–42
Sealey, W. C. Transformer Temperatures on Short Circuit. (55-714).....1225–9; disc. 1229
Seeley, H. T.; E. J. Burdick. Disc.....471
Seely, R. E. Disc.....1305
Seelye, Howard P. Disc.....551, 611
Sefine, W. G. Rewinding A-C Generators for Improved Performance. (55-132).....472–4; disc. 475
Sellers, L. R. Disc.....618
Shaneman, V. C. Developing Iron Loss Curves for Small Motors from Motor Tests. (55-728).....1176–9

Shankle, D. F.; J. M. Clayton. Insulation Characteristics of Wood and Suspension Insulators in Series. (55-712)..........1305–11; disc. 1312
Sharbaugh, Dr. Amandus H. Disc..........685
Sheadel, J. M. Disc..........748
Shenk, W. E. The Forced Oil Cooled Rotary Welding Transformer. (55-523)..........873–80
Sheppard, N. Rex. Disc..........578
Shipley, R. Bruce. Disc..........1295
Shipley, R. Bruce; M. Hochdorf, M. Watson. ORACLE Computes Line Constants With Tensors. (55-478)..........1052–6; disc. 1056
Shores, R. B. Disc..........709
Shores, R. B.; K. G. Darrow, V. E. Phillips, A. J. Schultz. Test Circuits for Capacitance Switching Devices. (55-212)..........624–34; disc. 635
Shores, R. B.; I. B. Johnson, A. J. Schultz, N. R. Schultz. Some Fundamentals on Capacitance Switching. (55-224)..........727–36; disc. 736
Short, H. D. The Co-ordination of Power and Communication Cable Characteristics. (55-56)..........281–7; disc. 287
Short, H. D.; S. Kozak. Disc..........301
Shreve, W. T.; E. D. Early, W. E. Phillips. An Incremental Cost of Power-Delivered Computer. (55-141)..........529–34; disc. 535
Skeats, W. F. Short-Circuit Currents and Circuit-Breaker Recovery Voltages Associated with 2-Phase-to-Ground Short Circuits.' (55-221)..........688–93; disc. 693
Sidway, C. L.; C. M. Clevenger. Steam Turbine Generator Operating and Maintenance Methods of the Southern California Edison Company.......... (55-119)..........60–5
Siegfried, Victor; W. T. Peirce. Disc..........946
Sills, H. R.. Disc..........475
Simmons, G. F.; A. L. Scheideler. Evaluation and Application of Silicone-Organic Resin Combinations for Dry-Type Transformer Insulation.......... (55-43)..........155–60; disc. 160
Simmons, H. O., Jr.; C. A. Woodrow. Disc..........466
Sinclair, W. A. Disc..........319
Slemon, G. R. Equivalent Circuits for Single-Phase Motors. (55-684)..........1335–42; disc. 1343
Smith, Frank V. Disc..........1246
Smith, G. L.; E. D. Early, R. E. Watson. A General Transmission Loss Equation. (55-90)..........510–16; disc. 518
Smith, H. E.; J. E. Rembusch. Disc..........1260
Smith, K. M. Disc..........1006
Smith, K. M.; A. H. Getty. Disc..........1334
Smith, Richard T. Disc..........389
Snell, D. S.; J. R. M. Alger, C. E. Kilbourne. Turbine Generator Stator Winding Temperatures at Various Hydrogen Pressures. (55-118)...232–50; disc. 251
Sommerman, G. M. L. Disc..........684, 780
Sparlin, B. J.; J. D. Moynihan. A Method of Measurement of Carrier Characteristics on Power Cables. (55-77)..........31–3
Sparlin, B. J.; J. D. Moynihan. A Study of Carrier Frequency Noise on Power Lines..........
  Part IV. Conclusion of Field Measurements.......... (55-458)..........795–800
Specht, T. R. Disc..........90
Sprow, J. H.; S. A. Bottonari. A New High-Capacity Anode Air Circuit Breaker. (55-722)..........1297–1302; disc. 1302
Staats, G. W. Disc..........390
Staats, G. W.; S. Beckwith, B. M. Koetting, L. T. Rosenberg. Test Report on a Fully Supercharged Generator. (55-123)..........56–9
Starr, E. C. Disc..........578
Starr, E. C.; E. J. Harrington. Disc..........701
Stearns, C. M.; B. M. Jones. Disc..........1405–06
Steinberg, M. J. Disc..........611
Sterrett, C. C.; J. E. Barkle, L. L. Fountain. Detection of Grounds in Generator Field Windings. (55-125)..........467–70; disc. 471
Sterrett, C. C.; R. A. Towne. Operation of Hydrogen-Cooled Turbine Generator. (55-116)..........433–8; disc. 439
Stevens, G. D.; A. C. Fagerlund. Disc..........992
Stevenson, J. R.; L. K. Kirchmayer, A. G. Mellor, J. F. O'Mara. An Investigation of the Economic Size of Steam-Electric Generating Units. (55-183)..........600–09; disc. 61
Streater, A. L.; W. R. Wilson, E. J. Tuohy. Application of Volume Theory of Dielectric Strength to Oil Circuit Breakers. (55-219)...677–84; disc. 685
Summers, Ernest W. Vibration in 2-Pole Induction Motors Related to Slip Frequency. (55-133)..........69–72
Sverdrup, E. F.; H. M. McConnell. The Induction Machine with Solid Iron Rotor. (55-115)..........343–8; disc. 349
Swengel, R. C.; W. B. Hess, S. K. Waldorf. Principles and Application of the Ultrasonic Flowmeter (55-28)..........112–17; disc. 117
Swerdlow, N.; K. T. Ashdown. Disc..........1198

T

Talaat, M. E. A New Approach to the Calculation of Synchronous Machine Reactances..........
  Part I. (55-6)..........176–82; disc. 182
Talento, J. L. Aluminum Widely Used in Power Switchgear. (55-264)..........839–43; disc. 844
Tang, K. Y.; Robert L. Cosgriff. Two-Axis Method of Analyzing Electric Machines. (55-276)...1449–55
Tarboux, J. G. Disc..........1405
Taylor, D. W.; L. E. Backer, Paul Barth, R. A. Huse. Transfer Tests on Station Auxiliary Busses. (55-92)..........1441–5; disc. 1449
Teague, W. L.; L. B. Rademacher. Disc....154, 1155
Tebo, G. B. Disc..........551
Tharp, Nelson B. Recommendations for Improving Reliability of Stand-by Engine Generators for Microwave Communications Systems. (55-42)..........261–6; disc. 266
Thomas, C. W.; W. C. Fowler. Automatically Switched Capacitors in Steps on a Single Distribution Feeder. (55-91)..........311–14; disc. 315
Thornton, R. E.; H. E. Carpenter. Eight Years' Experience With All-Aluminum Distribution Systems. (55-256)..........828–32; disc. 833
Tietze, H. Watson. Disc..........1405
Tipton, E. W. Experiences With the Use of Aluminum in Windings for Dry-Type Power Transformers. (55-686)..........1201–04
Tomlinson, H. R. Disc..........1072
Tomlinson, H. R.; R. O. Bigelow. Disc..........272
Tompkins, Joel S.; L. T. Guess. Disc..........746
Tompkins, Joel; B. L. Jones, P. D. Tuttle. Measurement of Resistance and Reactance of Expanded ACSR. (55-98)..........368–73; disc. 375
Towne, R. A.; C. C. Sterrett. Operation of Hydrogen-Cooled Turbine Generator. (55-116)..........433–8; disc. 439
Tracy, G. F. Disc..........1083
Travers, R. H. Disc..........1141
Travers, R. H.; R. W. Long. Disc..........173
Tuohy, E. J.; W. R. Wilson, A. L. Streater. Application of Volume Theory of Dielectric Strength to Oil Circuit Breakers. (55-219)..........677–84; disc. 685
Tuttle, P. D. Disc..........947
Tuttle, P. D.; J. Tompkins, B. L. Jones. Measurement of Resistance and Reactance of Expanded ACSR. (55-98)..........368–73; disc. 375
Tyerman, J. A.; W. D. Houser, W. Hindle. Production and Installation of Vertical Water Wheel Generators. (55-162)..........536–43; disc. 544

U

Umphrey, D. M.; D. J. Marsden. Design Problems and Field Tests Concerning Circuit Breakers for Switching Long 230-Kv Lines. (55-223)..........693–701; disc. 705

V

Valentine, W. W.; J. K. Dillard, J. M. Clayton. Surge Attenuation in Power Cables. (55-558)..........1115–21; disc. 1122
Van Wormer, F. C. An Improved Approximate Technique for Calculating Cable Temperature Transients. (55-51)..........277–80; disc. 280
Van Wormer, F. C. Disc..........498, 1045
Vaughan, D. C. Disc..........647
Veinott, C. G. Disc..........824
Vencill, G. J. Disc..........149
Vogel, F. J. Disc..........984, 1155, 1229
Vokac, Charles W. Disc..........1405

W

Wagner, C. F.; B. L. Lloyd. Effects of Corona on Travelling Waves. (55-453)..........858–72
Wagner, Robert N. Disc..........1302
Waldorf, S. K.; R. C. Swengel, W. B. Hess. Principles and Application of the Ultrasonic Flowmeter. (55-28)..........112–17; disc. 117
Waldschmidt, K. J. Measurement of Resistance of Energized A-C Motor Windings. (55-731)..........1303–04; disc. 1305
Walker, Eric A. Disc..........557
Walker, J. K.; R. E. Kane. A 69-Kv Compressed Air Circuit Breaker for 5,000,000 Kva. (55-218)..........705–09; disc. 710
Wall, R. L. Sonance Design of Large Induction Motors. (55-724)..........1189–92
Ward, J. B.; H. W. Hale. Disc..........517, 1296
Ware, P. H.; W. H. Couch, G. H. Hunt, N. D. Kenney. Modern High-Voltage Rubber Insulation.... (55-693)..........1387–97; disc. 1398
Watchorn, C. W. Co-ordination of Hydro and Steam Generation. (55-33)..........142–8; disc. 149
Watchorn, C. W. Disc..........118, 534, 550, 598, 612, 1006
Watkins, S. S. Disc..........459
Watson, E. C. Disc..........395
Watson, Marjorie; R. B. Shipley, M. Hochdorf. ORACLE Computes Line Constants With Tensors. (55-478)..........1052–6; disc. 1056
Watson, R. E.; E. D. Early. A New Method of Determining Constants for the General Transmission Loss Equation. (55-720).....1417–21; disc. 1422
Watson, R. E.; E. D. Early, G. L. Smith. A General Transmission Loss Equation. (55-90)..........510–16; disc. 518
Watts, Raymond S. Disc..........466
Webb, R. L. Disc..........709
Webb, R. L.; W. J. Roberts. Operation of Turbine Generators During Off-Peak High Power Factor Periods—Practices of One Utility in a Metropolitan Area. (55-120)..........461–5; disc. 467
Weed, L. J. Disc..........944
Weinfurt, William J. Disc..........991
Weiss, Gerald. Optimum Design of Induction Torque Motors and Servomotors. (55-506)..........809–15
Wells, R. J. Apparatus Noise Measurement. (55-725)..........1170–3
Wentz, E. C. Disc..........366
Weston, D. E.; M. J. Reilly. A New 500-Megavolt Ampere Air Magnetic Circuit Breaker of Simplified Design. (55-509)..........1093–8; disc. 1099
White, C. L. Disc..........509
Whitney, E. C.; G. L. Moses. Disc..........474
Wildi, Paul; A. Ernst. Disc..........197
Williams, R. L.; L. L. Mankoff, H. N. Schneider. Capacitance-Switching Facilities at the Switchgear Development Laboratory. (55-220)..........375–80; disc. 381
Williams, W. A. Disc..........154
Wilson, Robert E. Disc..........1384
Wilson, W. R. High-Current Arc Erosion of Electric Contact Materials. (55-215)....657–64; disc. 664
Wilson, W. R.; A. L. Streater, E. J. Tuohy. Application of Volume Theory of Dielectric Strength to Oil Circuit Breakers. (55-219)..........677–84; disc. 685
Wilterdink, B. W.; R. A. Pfuntner, R. S. Norman. The Application of a New Nontracking Butyl to High-Voltage Instrument Transformers. (55-715)..........1173–6
Winchester, R. L. Stray Losses in the Armature End Iron of Large Turbine Generators. (55-130)..........381–9; disc. 390
Winkelman, Paul F. Disc..........415
Wise, Richard B.; E. T. B. Gross. Grounding Grids for High Voltage Stations..........
  Part II. Resistance of Large Rectangular Plates.... (55-281)..........801–09; disc. 809
Wiseman, R. J. Disc..........320, 945, 947, 1022, 1032
Wolf, C. C.; C. Morrison. Disc..........497
Wolfert, G. L.; D. F. Muster. Single-Phase Induction Motor Noise Due to Dissymmetry Harmonics. (55-729)..........1365–72; disc. 1372
Wollaston, F. O. Disc..........260
Wood, A. J. Disc..........1327–28
Wood, G. D. Disc..........1098
Wood, J. D. Disc..........1066
Wood, R. D.; A. F. Glimn, L. K. Kirchmayer. Disc..........1421
Woodrow, C. A.; H. O. Simmons, Jr. Disc..........466
Wright, E. M. Disc..........416
Wright, E. M.; E. G. Lambert. The Use of All-Aluminum Conductor on Transmission Lines (55-250)..........849–53; disc. 854
Wyatt, Kenneth S. Disc..........1358

X

Xenis, C. P. The Limiter—Its Basic Functions in Network Distribution Systems. (55-443)..........913–15; disc. 944
Xenis, C. P. Disc..........1199

Y

Yost, A. G.; J. W. Kalb. Transient Durability Testing of Valve Type Lightning Arresters. (55-136)..........521–6; disc. 528
Young, C. C. Disc..........786, 1092

Z

Zaborszky, J. Efficiency of Grounding Grids with Nonuniform Soil. (55-713)..........1230–3
Zambell, H. G. Functional Life Evaluation of Group-2 Dry-Type Power Transformers. (55-452)..956–70

Load-Phase Tie-Line Energy Control of Interconnected Power Systems

FRANCOIS CAHEN
MEMBER AIEE

IN A previous paper[1] the author described the principle of an automatic control method based on the measurement of the integral of the deviation of the controlled quantity and upon the subjection to this integral of the load of the plants in control of the system. The method was more particularly applied in the case of a system which, although comprising a great number of generating stations, constitutes a single operation unit not interconnected to any other similar units. In this case, the quantity to be regulated is the frequency; the integral of the frequency deviation is a phase difference; the application of the method leads to subjecting the load of all the regulating machines to the value of this phase difference, hence the name load-phase control.

The advantages of this method permit an important decentralization of the control by utilizing several independent regulators distributed through the system and installed close to the power stations submitted to their action; the possibility of simultaneously operating several regulators quite independent of one another depends, as was shown, on the use of very accurate and very steady reference frequency generators. The regulators required for the application of this method have been studied and designed by Éléctricité de France and a certain number of tests carried out on the French system have shown, as stated in the previous paper, that this control process permitted both a very steady frequency maintained within a band of ±0.05 cycle per second and a very good distribution of the load among regulating plants without any manual intervention.

The author then pointed out that this control method could be extended to the case of several interconnected systems, each of which constitutes an operation unit; in such a case, however, the quantity to be regulated is no longer the frequency only but a combination of both the frequency and the power transferred between each system and all its neighbors according to the conventional frequency control with tie-line load-bias principle. It is then necessary to measure a linear combination of the frequency deviation and the tie-line load deviation in relation to the program, to integrate this combination which is transformed into a linear combination of a phase difference and tie-line energy difference, and then to subject the load of all the regulating machines to the value of this integral. That is why this process has been called load-phase tie-line energy control. Since that paper was presented, application tests of this method for those two cases have been and are being pursued on the French system; the aim of the present paper is to give a concise account of these tests.

New Tests and Industrial Application of the Load-Phase Control

New control tests have been made repeatedly on the French system in 1953 and 1954; they have confirmed results previously obtained, emphasizing the precision and flexibility of this control process. At the same time, the number of plants likely to take part in the control has been increased so as to make it possible to widen the control band. At the present time two independent integrating regulators are installed: one, in Paris, controls the steam plants of the Paris area and the other, in Brive, controls the hydroelectric plants of the Truyère and the Dordogne rivers in the Massif Central. The maximum capacity of the steam plants controlled by the first regulator is 875 megawatts (mw) (control band 250 mw); the maximum capacity of the hydroelectric plants controlled by the second regulator is 750 mw. A third regulator will be installed to control some hydroelectric plants in the Alps (maximum capacity 700 mw). As an indication, the maximum power supplied to the system by its power stations as a whole reached 8,000 mw in January 1954. In the periods when the French system can be isolated from the German system with which it is frequently interconnected, long deviation control tests are often being carried out.

Reminder of the Load-Phase Tie-Line Energy-Control Principle

The principle of this control method applicable to the case of several interconnected international systems has been mentioned in the foregoing. It is equivalent, in an integrated form, as stated in the previous paper,[1] to the conventional tie-line power and frequency control, the equation of which is

$$(P_t-P_0)+\lambda(f-f_0)=0$$

where

P_t = total power effectively transferred between the system and the other systems, mw
P_0 = transfer program, mw
f = effective value of frequency, cycles per second (cps)
f_0 = rated frequency, cps
λ = controlling energy of regulator

λ is expressed in mw per cycle or in an abridged form

$$\Delta f+\frac{\Delta P_t}{\lambda}=0 \tag{1}$$

where

$$\Delta f=f-f_0$$

$$\Delta P_t=P-P_0$$

The corresponding equation of the new method is

$$\alpha\int_0^t\left(\Delta f+\frac{\Delta P_t}{\lambda}\right)dt+\Delta p=0$$

or

$$\alpha\left(\Delta\varphi+\frac{\Delta W_t}{\lambda}\right)+\Delta p=0 \tag{2}$$

with

$$\Delta\varphi=\varphi-\varphi_0=\int_0^t \Delta f dt$$

where

φ = phase angle, revolutions
φ_0 = reference phase angle, revolutions

$$\Delta W_t=W_t-W_0=\int_0^t \Delta P_t dt$$

Paper 55-24, recommended by the AIEE System Engineering Committee and approved by the AIEE Committee on Technical Operations for presentation at the AIEE Winter General Meeting, New York, N. Y., January 31–February 4, 1955. Manuscript submitted October 13, 1954; made available for printing November 15, 1954.

FRANCOIS CAHEN is with Éléctricité de France, Paris, France.

The author wishes to thank Louis de Heem, Director of C.P.T.E., and the Belgian companies who own the power stations utilized for the tests for taking part in the load-phase tie-line energy-control tests and carrying out the necessary installations in Belgium. He also thanks Mr. Denis, Chief Engineer of the C.P.T.E., for the major part taken in carrying out these installations and in particular the control boards of the central dispatching office and of the power stations in control. Thanks are also due to André Chevallier, Éléctricité de France, who was mainly responsible for the creation and development of the automatic control methods based upon the measurement of the phase difference and the subjection to this difference of the load of the stations in control.

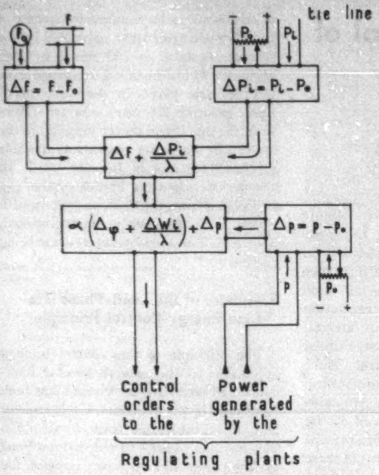
tie line
F
F_0
P_0
P_i
$\Delta F = F - F_0$
$\Delta P_i = P_i - P_0$
$\Delta F + \frac{\Delta P_i}{\lambda}$
$\alpha\left(\Delta\varphi + \frac{\Delta W_i}{\lambda}\right) + \Delta p$
$\Delta p = p - p_0$
p
p_0
Control orders to the
Power generated by the
Regulating plants

Fig. 1 (above). Basic diagram of load-phase tie-line energy controller

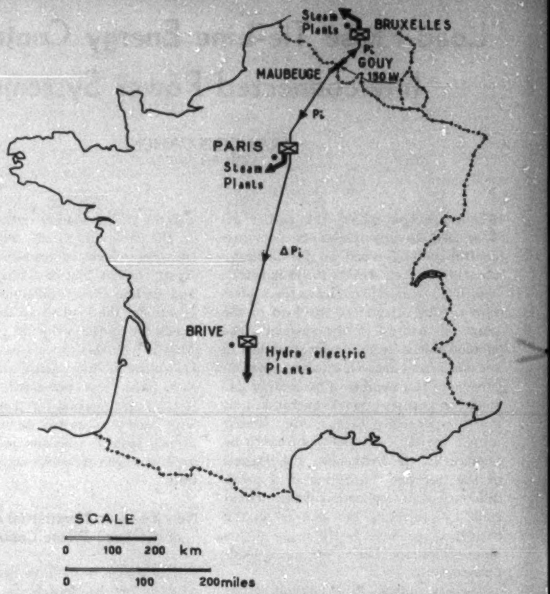
Steam Plants
BRUXELLES
P_i
GOUY
150 W
MAUBEUGE
P_i
PARIS
Steam Plants
ΔP_i
BRIVE
Hydro electric Plants
SCALE
0
100
200
km
0
100
200miles

Fig. 3 (right). Load-phase tie-line energy-control tests on August 26, 1954; geographic location of the regulators and the telemetering channels

where

W_t = transferred energy, mw-seconds
W_0 = reference transferred energy, mw-seconds

$\Delta p_m = p_m - p_0$

where

p_m = effective power output of the plants in control, mw
p_0 = basic load of the plants in control, mw

φ_0, W_0, and p_0 are chosen so that

$$p_m = p_0 \text{ for } \left(\varphi + \frac{W_t}{\lambda}\right) = \left(\varphi_0 + \frac{W_0}{\lambda}\right)$$

or

$$\Delta\varphi + \frac{\Delta W_t}{\lambda} = 0$$

Fig. 1 shows the basic diagram of the regulator.

Of course, if several independent integrating regulators operating simultaneously in the same system are utilized, the power deviation ΔP_t measured at a central point must be transmitted by telemetering to all the regulators.

Load-Phase Tie-Line Energy-Control Tests

A certain number of tests have been made in the past year to develop this control method and study its efficiency. Its working may be considered at present to be quite satisfactory; it makes possible the simultaneous control both of the frequency common to two interconnected systems and the power transferred between those two systems with a precision

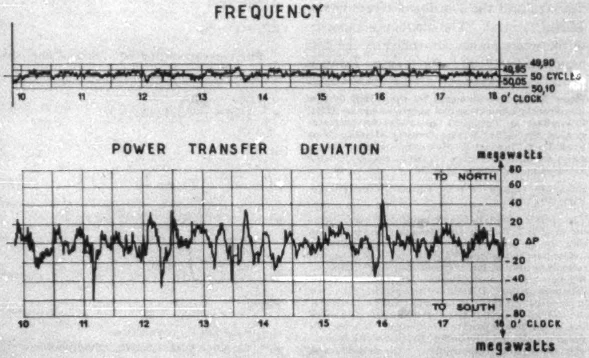

Fig. 2. Load-phase tie-line energy-control tests on June 29, 1954; frequency and power transfer deviation records

Table I. Test of June 29, 1954

	Southern System Division	Northern System Division
Production	mostly hydro-electric	thermal
Maximum power of the system during the test, mw	4,500	2,000
Available control band, mw	220—hydro-electric	170—thermal
Controlling power of the integrating regulator, mw per revolution	9	4
Controlling energy of the integrating regulator, mw per cycle	500	500

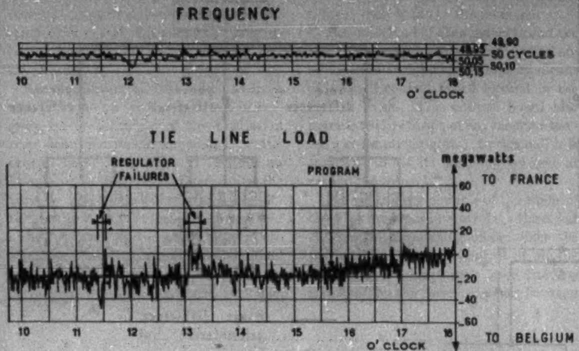

Fig. 4. Control tests on August 26, 1954; frequency and tie line load records

at least equal to that of the best conventional methods which do not utilize integrators. Moreover, within each of the systems, for the simultaneous putting under control of several power stations, advantages are offered for the balancing of their loads by the subjection of these stations to the integral of the deviation of the controlled quantity.

The essential aim of the first series of tests was the development of the load-frequency control device without paying too much attention to the problem of load distribution among the power stations in control, which the previous load-phase control tests permitted to consider as being solved. To this end, the French system has been divided into two parts, linked together by one or several 225-kv lines; on either side of the sham frontier, an integrating regulator acted upon several plants in control. The southern regulator controlled hydroelectric plants in the Massif Central, the northern regulator controlled steam plants located either in the north of France or in the Paris area. In the case when several 225-kv lines were utilized for interconnection, their loads were added together and the total compared with the program. The most recent test of this kind was made on June 29, 1954; the characteristics of this test are shown in Table I.

The test lasted from 10 a.m. to 6 p.m. Fig. 2 shows the recordings made of the frequency and of the deviation of the power transferred between the two systems in relation to the program.

The upper curve is that of the frequency; the latter was maintained throughout the test within the 49.95 to 50.05-cps band. The lower curve is that of the power deviation. Apart from extreme peaks (11:10 a.m., 12:05, 12:15, 12:25, 1:25, 1:45, 2:05, 3:50 and 4:00 p.m.) which result from modifications brought suddenly to the transfer program, it may be said that the power deviation in relation to the program has remained within a band having a width smaller than ±20 mw.

The aim of a second series of tests was to verify the smooth working of the control method, the latter being applied simultaneously to two interconnected systems, one of which utilized two distinct integrating regulators acting independently upon two groups of plants in control. For these tests, one of the systems was the Belgian system in which three distinct steam plants were controlled by a single integrator installed in Brussels at the central dispatching office of the Société pour la Coordination de la Production et du Transport de 'Élnergie Éléctrique. The other was the French system in which the two independent integrating regulators of Paris, controlling the Paris area steam plants, and of Brive, controlling the hydroelectric plants in the Massif Central, were operated simultaneously. A single 150-kv line was the interconnection link between the two systems; the load of this line was measured at the frontier and simultaneously transmitted by telemetering to Brussels and Paris. In Paris, this power was compared with the program and the measured deviation transmitted direct to the Paris regulator and telemetered to the Brive regulator. Fig. 3 shows schematically the geographic location of the regulators and the telemetering channels. The most recent test of this kind was made on August 26, 1954; the characteristics of this test are shown in Table II.

The test lasted from 9:46 a.m. to 5:42 p.m. Fig. 4 shows the recordings made of the frequency and of the power transferred between the two systems. Fig. 5 shows the load curves of the Belgian and French systems during the day of August 26. The upper curve is that of the frequency; the latter was maintained, for the duration of the test, within the 49.95 to 50.05-cps band, except about 12 o'clock when the deviation reached 0.1 cps because the control band of the French system, owing to unforeseen circum-

Table II. Test of August 26, 1954

	Belgian System	French System
Production	thermal	half-thermal half-hydroelectric
Maximum power of the system during the test, mw	1,500	6,400
Available, control band, mw	63 to 43 from three power stations	Paris: 225—thermal Brive: 390—hydroelectric 615
Controlling power of integrating regulators, mw per revolution	Brussels: 3, then 5	Paris: 4.6 Brive: 8 12.6
Controlling energy of the integrating regulator, mw per cycle	150 to 350	infinite, no load bias

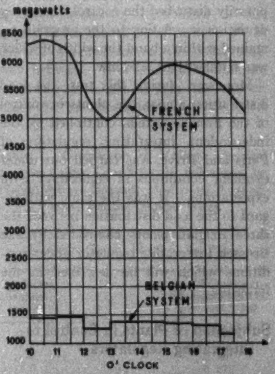

Fig. 5. Control tests on August 26, 1954; load curves of the Belgian and French systems

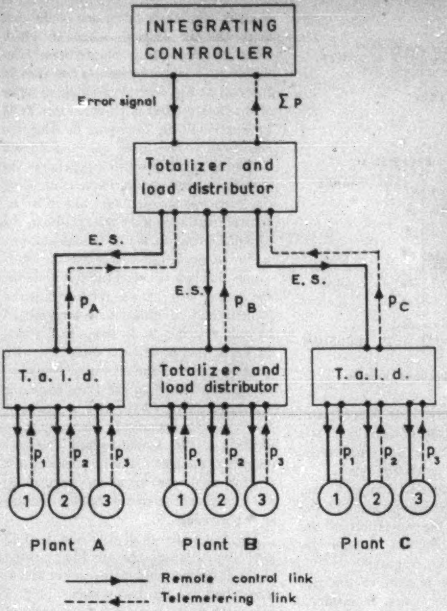

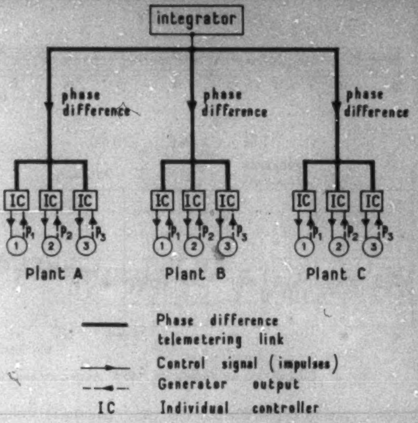

Fig. 6 (left). Utilization of a central integrating regulator for one group of generating plants; conventional load division

Fig. 7 (above). Utilization of a central integrator for one group of generating plants; direct subjection of the output of each machine to the phase difference, level control

stances, proved to be slightly insufficient.

The lower curve is that of the transferred power. The transfer program is shown by a thicker line; the difference of the ordinates of the two curves represents the power deviation. Apart from two short periods, at 11:30 a.m. and about 1:05 p.m., when a relay out of order temporarily disturbed the control, the power deviation in relation to the program remained within a band the width of which was smaller than ±20 mw.

Moreover, during this test, the load distribution among the plants in control of the French system, controlled by the independent integrating regulators of Paris and Brive, was carried out under excellent conditions in conformity with expectations. It was the same with regard to the load distribution between the three Belgian plants controlled by the Brussels integrating regulator under conditions which will be described in the following.

Subjection of Plants in Control to Integrating Regulators

As was stated in the previous paper,[1] the subjection of the output of the power stations in control to the integral of the difference of the controlled quantity, i.e., to the phase difference [$\Delta\varphi$ or $\Delta\varphi + (\Delta W_t)/\lambda$], may be achieved in different ways depending on the difference transmitted from the integrator near, more or less, to the regulating machines. Figs. 8, 9, and 10 of the previous report show schematically several instances of the working out of this subjection.

In the French system, the solution adopted so far consists in utilizing a central integrating regulator for each group of plants in control and in subjecting, on the spot, the total power supplied by these plants to the phase difference. This arrangement is schematically represented by Fig. 6. The regulator compares the total power of the plants with the phase difference and verifies whether these two values conform with the control characteristic sought. If agreement has not been reached, the regulator emits a signal proportional to the error it has measured; this signal is transmitted to the plants and, inside the latter, to the machines through distribution systems of a conventional type, securing the desired load distribution among the machines taking part in the control operations. This method has been utilized in the French system to take advantage of the existing installations of control signal transmission, of power totalization, and of signal distribution to the plants and machines. It has the disadvantage of requiring between the central regulator and the plants a double-link system transmitting in one direction the control signal and in the opposite direction the loads; moreover it makes it compulsory for the totalization of the latter to be made first at the plant, then at the central control station.

It is possible to eliminate any return power telemetering, any totalization, and any distribution devices by sending the value of the phase differences measured by a central integrator to all the plants in control and inside each of these to all the machines, and by subjecting separately the output of each of the machines to the phase difference by means of an individual regulator. This solution is schematically represented by Fig. 7. The individual regulator is a very simple device which makes the comparison between a voltage proportional to the phase difference and a voltage proportional to the difference between the power output of the machine and its basic load. When the law of subjection is fulfilled, the residual voltage is nil; when the law of subjection is no longer fulfilled, impulses of a duration proportional to the residual voltage drive the turbine speed-changing motor in the correct direction. This method has been called level control. The level is a current proportional to the phase difference; it is transmitted to all the regulating machines, the loads of which are subjected to it.

An installation of this kind has been experimented on for the first time in Belgium on the occasion of the regulation tests described in the foregoing. At the central dispatching office in Brussels an integrator is installed which emits the current, the intensity of which characterizes the level; the latter is transmitted either by wire, or by carrier current, to the three plants in control; the individual regulators of the machines, designed according to the aforementioned principle, subject their loads to the level.

The basic load of each machine and the rate of its participation in the control are adjusted in each power station by means of a small control board located in the control room. This control board also permits the operation of any machine having a constant program; to this end it is sufficient to set its participation rate at zero in the control.

The controlling power α of the whole of the power stations in control is adjusted at the central dispatching office; once the participation rates in control of all the regulating machines have been fixed, α is defined by the correspondence between the intensity of the current characterizing the level and the phase difference measured by the integrator. The tests of this method of subjecting the load of the power stations in control to the phase difference have been very satisfactory; its simple design and flexibility of utilization have been emphasized. Its application to the power stations in control of the French system is being contemplated.

Reference

1. Load-Phase Control—Method of Automatic Frequency Control of a Multiple Generating-Plant System, Francois Cahen. *AIEE Transactions*, vol. 73, pt. III, June 1954, pp. 571–77.

Voltage Gradients on High-Voltage Transmission Lines

G. E. ADAMS
ASSOCIATE MEMBER AIEE

A KNOWLEDGE of the voltage gradient which exists at the surface of a transmission-line conductor is necessary in many instances. This knowledge is especially important in studies regarding corona losses and radio interference.[1-3] The dimensions of laboratory models of transmission lines are often chosen so as to reproduce the voltage gradient which is to be actually encountered in practice.[4] An indication of the electrostatic unbalance of a transmission line can also be gained from a knowledge of the voltage gradients. Results of such calculations of voltage gradients are presented here for several cases in the form of curves which make calculations unnecessary. These results are in agreement with the pertinent portions of two other papers which have appeared upon this subject.[5,6]

The arrangements for which data are included are: single conductor above ground, single circuit horizontal, single circuit vertical, and double circuit vertical. The effect of conductor diameter, conductor spacing, conductor height above ground, ground wires, and conductor stranding upon the voltage gradients can be determined from the curves presented.

The information is presented in the form of curves from which the gradient factor of a particular transmission-line arrangement can be obtained. This factor when multiplied by the voltage applied to the line yields the voltage gradient at the conductor surface. A wide range of the pertinent variables has been investigated and the voltage gradients of existing and proposed lines can be easily obtained from the curves.

Method of Analysis

The voltage gradient at the conductor surface was calculated in two steps. The gradient was calculated first of all as though the conductors were infinitely long, were suspended above a perfectly conducting flat ground plane, and had smooth cylindrical surfaces over which the charges were uniformly distributed. The interconductor and conductor to earth spacings were assumed to be constant and the effect of supporting structures, near-by objects, etc., was neglected. The details of this calculation are presented in the Appendix.

The results of this calculation are presented in terms of a gradient factor F_1 which is the ratio of voltage gradient to applied voltage. F_1 has the units of volts per centimeter (cm) per kilovolt of applied voltage. Since the voltage applied to the line varies sinusoidally with time, the charges and the voltage gradient also vary sinusoidally with time. F_1 has been expressed as the ratio of the peak volts per cm to the applied rms voltage. This applied voltage is to be taken as line to ground for a single conductor and line to line for 3-phase conductors.

The second step in the calculation was the determination of the ratio of the maximum voltage gradient at the conductor surface for a stranded conductor to the voltage gradient of a smooth conductor having the same outside diameter and the same charge. This ratio is expressed as a a strand factor F_2. The voltage gradient, of course, varies along the surface of a stranded conductor from zero at the points where the adjacent strands are in contact to a maximum at the points midway between. If it is assumed that the stranding does not change the capacitance[7] of the conductor appreciably, the

Table I. Comparison of Voltage Gradient on the Center Conductor as Influenced by Height Above Ground, Horizontal Arrangement Without Ground Wires

d = 20 Feet. Base is Gradient for h = 60 Feet (h = 100 Gives Higher Gradient)

Conductor Diameter, Inches	% Difference in Gradient Between h-60 and h-100
0.8	0.146
1.2	0.151
1.6	0.167
2.0	0.175
2.4	0.181
2.8	0.186
3.2	0.194

Paper 55-22, recommended by the AIEE Transmission and Distribution Committee and approved by the AIEE Committee on Technical Operations for presentation at the AIEE Winter General Meeting, New York, N. Y., January 31–February 4, 1955. Manuscript submitted October 21, 1954; made available for printing November 10, 1954.

G. E. Adams is with the General Electric Company, Schenectady, N. Y.

The writer wishes to acknowledge the many helpful suggestions and comments made by S. B. Crary and C. Concordia and the preparation of many of the calculating machine programs used in this study by Mrs. M. S. Dyrkacz, all of the General Electric Company, Schenectady, N. Y.

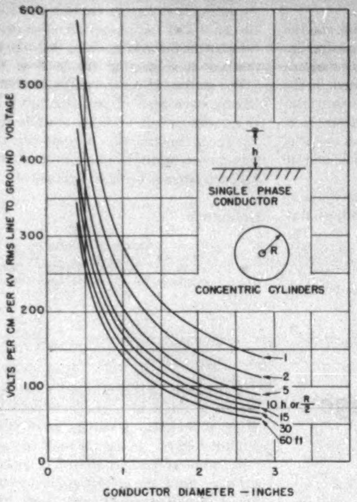

Fig. 1. Variation of gradient factor F_1 of a single-phase conductor with conductor diameter for various heights above ground

Table II. Percentage Difference Between Voltage Gradient of Center and Outer Conductor, Horizontal Arrangement Without Ground Wires

h=60 Feet Base is Gradient on Center Conductor

Conductor Diameter, Inches	% Difference, Where d =		
	10 Feet	20 Feet	40 Feet
0.8	− 7.92	−6.36	−4.58
1.2	− 8.53	−6.81	−4.88
1.6	− 9.03	−7.16	−5.11
2.0	− 9.45	−7.47	−5.31
2.4	− 9.82	−7.73	−5.48
2.8	−10.15	−7.97	−5.63
3.2	−10.46	−8.19	−5.77

Table III. Comparison of Voltage Gradient on the Center Conductor as Influenced by Height Above Ground, Vertical Arrangement Without Ground Wires

d = 20 Feet. Base is Gradient for h = 60 Feet (h = 100 Gives Higher Gradient)

Conductor Diameter, Inches	% Difference in Gradient Between h-60 and h-100
0.8	0.290
1.2	0.307
1.6	0.320
2.0	0.334
2.4	0.348
3.2	0.365

maximum gradient factor of a stranded conductor is given by $F = F_1 F_2$.

Results

Figs. 1, 2, and 3 and Tables I through VII show the dependence of the voltage gradient upon line arrangement. The gradient factor F_1 for a single conductor suspended at a height h feet above ground is given by Fig. 1 for a range of conductor diameters. This configuration is the one which is normally used for laboratory tests of conductors. This curve also gives the gradient factor for a conductor which is the inner member of a concentric cylinder arrangement. This latter configuration has also been used in laboratory tests of conductors.[6]

The charge, and consequently the voltage gradient, is uniformly distributed along the circumference of the conductor in the concentric cylinder arrangement. When the conductor is suspended above a flat ground plane, the charge becomes nonuniformly distributed over the surface. However, for values of h usually encountered in practice, this distortion of or deviation from a uniform distribution is less than 0.1 per cent (%) and may be neglected for all practical purposes.

Fig. 2 gives F_1 as a function of conductor diameter and spacing for the center conductor of a horizontal arrangement without ground wires. This set of curves was plotted for the particular case of height above ground h being equal to 60 feet. Table I shows a comparison of

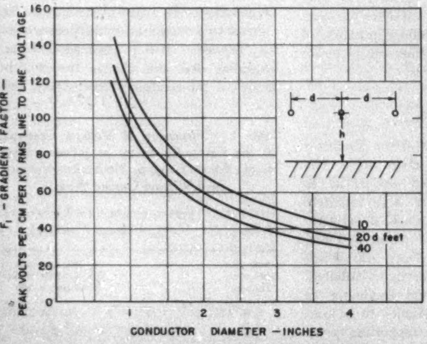

Fig. 2. Variation of gradient factor F_1 for the center conductor of a horizontal arrangement without ground wires with conductor diameter and spacing for a height above ground of 60 feet

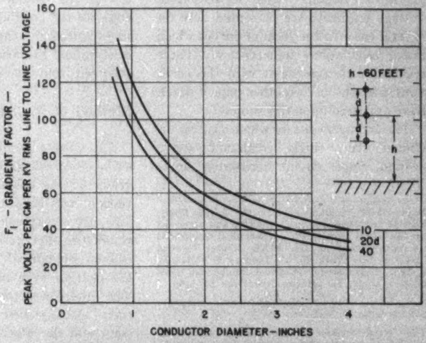

Fig. 3. Variation of gradient factor F_1 for the center conductor of a vertical arrangement without ground wires for a height above ground of 60 feet

Table IV. Percentage Difference Between Voltage Gradient of Center and Upper and Center and Lower Conductors; Vertical Arrangement Without Ground Wires

h=60 Feet. Base is Gradient on Center Conductor

Conductor Diameter, Inches	d=10 Feet		d=20 Feet		d=40 Feet	
	Lower	Upper	Lower	Upper	Lower	Upper
0.8	−6.88	− 8.70	−3.57	−7.98	6.03	−7.64
1.2	−7.48	− 9.34	−3.91	−8.47	6.28	−8.03
1.6	−7.95	− 9.85	−4.19	−8.86	6.48	−8.33
2.0	−8.36	−10.28	−4.43	−9.19	6.63	−8.58
2.4	−8.71	−10.66	−4.64	−9.47	6.77	−8.79
2.8	−9.03	−11.00	−4.83	−9.73	6.90	−8.98
3.2	−9.33	−11.31	−5.01	−9.96	7.01	−9.15

Table V. Comparison of Horizontal and Vertical Arrangements Having the Same Average Height Above Ground and the Same Spacing

h=60 Feet, d=20 Feet. Percentage Based on Horizontal Arrangement (Horizontal Arrangement Gives Higher Gradient on the Center Conductor) (Vertical Arrangement Gives Higher Average Gradient)

Conductor Diameter, Inches	% Difference in Gradient Factor on Center Conductor	% Difference in Average Gradient Factor of Three Conductors
0.8	0.219	0.188
1.2	0.219	0.207
1.6	0.222	0.219
2.0	0.225	0.228
2.4	0.231	0.237
2.8	0.240	0.246
3.2	0.243	0.257

values obtained for $h=60$ feet and $h=100$ feet. (See also Fig. 7(A) of reference 5.) Since the difference is very small, it can be concluded that Fig. 2 can be used for all values of h encountered in high-voltage practice. The height above ground becomes important only for abnormally small values of h. The voltage gradient is higher on the center than on the outer conductors. Table II gives the percentage difference between center and outer conductors as a function of conductor diameter and spacing. This difference varies as the ratio of conductor spacing to conductor dameter varies. The larger this ratio becomes, the smaller the difference.

Fig. 3 gives F_1 as a function of conductor diameter and spacing for the center conductor of a vertical arrangement without ground wires. The height of the center conductor or the average height of the conductors is taken as 60 feet. Table III shows a comparison between values for $h=60$ and $h=100$ feet. The difference is approximately twice as large as for the horizontal arrangement but still is very small and can be neglected for practical purposes for values of h and d encountered in practice. Since the upper and lower conductors are not at the same height above ground, the corresponding voltage gradients will not be equal. The voltage gradient on the bottom conductor will be larger than on the top conductor since it is closer to the ground. The center conductor, however, will have the largest voltage gradient except for extreme cases not usually encountered in practice when the lower conductor is very close to the ground. Table IV gives the percentage difference between center and upper and center and lower conductors. The minus signs indicate a gradient less than that of the center conductor.

Table V gives a comparison of horizontal and vertical arrangements without ground wires having the same average height above ground and the same spacing. The difference between gradient factors on the center conductors and between the average gradient factor of the three conductors is seen to be very small.

Table VI gives the gradient factor for the horizontal arrangement with ground wires as shown in Fig. 4. The radius of the ground wires r, the distance between ground wires $2l$, and the vertical distance between the plane of the ground wires and the plane of the conductors g was varied over a wide range. However, it is seen that the ground wire has little effect upon the gradient except when placed abnormally close to a conductor. In general, the ground wire increases the charge residing on and the voltage gradient of the nearest conductors and reduces the charge and gradient of conductors located further away. Hence ground wires placed near the outer conductors will tend to reduce the electrostatic unbalance of the line.[9] This reduction, however, is very small for practical spacings as is shown in Table VI.

Table VII gives the gradient factor F_1 of the ground wire itself for the horizontal arrangement. It is seen that the ground wire gradient factor is very small compared with that of the conductor unless the ground wire radius is unusually small and the ground wires are placed unusually close to the conductor.

Fig. 5 shows the strand factor F_2 as a function of the number of strands. This curve decreases from a value of $\pi/2$ for $n=2$ and approaches 1.40 as a close approximation as n becomes infinite.[10,11] Several intermediate values of n were investigated with the aid of a d-c board and yielded values close to 1.40. F_2 depends only upon the number of strands and not upon the diameter of the conductor. It can be seen from this curve that $F_2=1.40$ for nearly all conductors used in practice. Hence the maximum voltage gradient which exists at the surface of the conductor will be approximately 40% larger than the value calculated assuming a smooth conductor of the same outside diameter.

The voltage gradients of double-circuit transmission lines have also been con-

Table VI. Conductor Gradient Factor F_1. Horizontal Arrangement with Ground Wires; See Fig. 4

r=Ground Wire Radius in Inches

Conductor Diameter, Inches	g, Feet	Conductor	Gradient Factor Without Ground Wires	Gradient Factor with Ground Wires								
				l=5 Feet			l=10 Feet			l=20 Feet		
				r=0.25	r=0.50	r=1.0	r=0.25	r=0.50	r=1.0	r=0.25	r=0.50	r=1.0
1.6	10	Center	72.04	74.27	74.45	74.67	73.05	73.13	73.24	71.46	71.41	71.35
	10	Outer	66.88	66.30	66.26	66.21	67.09	67.13	67.18	69.16	69.39	69.68
	20	Center	72.04	72.59	72.63	72.67	72.38	72.41	72.44	71.93	71.92	71.91
	20	Outer	66.88	66.70	66.69	66.68	66.93	66.94	66.96	67.51	67.58	67.66
	40	Center	72.04	72.08	72.08	72.08	72.06	72.06	72.06	72.01	72.01	72.00
	40	Outer	66.88	66.88	66.88	66.88	66.91	66.91	66.91	67.00	67.01	67.02
2	10	Center	60.06	60.53	60.56	60.60	60.35	60.37	60.40	59.96	59.95	59.94
	10	Outer	55.58	55.43	55.42	55.41	55.63	55.64	55.65	56.13	56.18	56.25
	20	Center	60.06	61.97	62.13	62.31	60.92	61.00	61.08	59.57	59.51	59.46
	20	Outer	55.58	55.08	55.05	55.01	55.76	55.79	55.84	57.54	57.74	57.93
	40	Center	60.06	60.09	60.09	60.09	60.08	60.08	60.08	60.03	60.03	60.00
	40	Outer	55.58	55.58	55.58	55.58	55.60	55.61	55.61	55.68	55.69	55.79

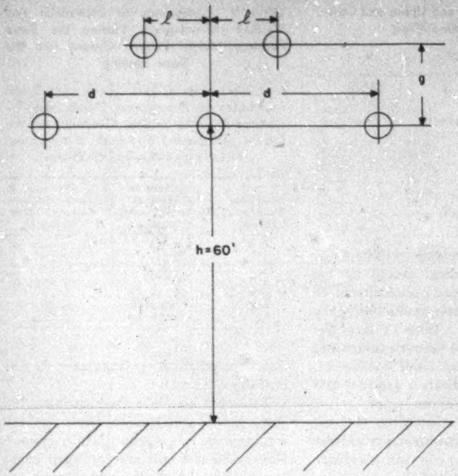

Fig. 4. Horizontal arrangement with ground wires

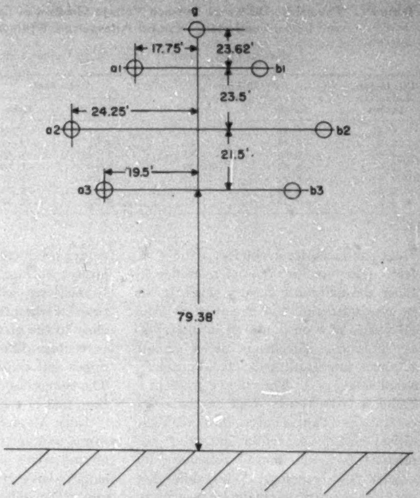

Fig. 6. Double-circuit arrangement, conductor diameter 1.6 inches

sidered. The equations to be solved are more complex than for single circuits although the method is the same. In addition, the gradients are affected by the choice of the conductor phasing. Different phasing arrangements result in appreciably different voltage gradients. If the exact voltage gradient on each conductor is desired, it is necessary to make a detailed analysis. However, for practical spacings a very close approximation to the gradient on the center conductors can be obtained by using either Figs. 2 or 3. The gradients on the upper and lower conductors are affected by the relative conductor phasing to a much larger degree than are those of the center conductors. Thus a calculation using Table IV might be a poor approximation. In general, the gradient is lower on the upper and lower conductors than on the center conductor.

The details of the calculations for the particular double-circuit arrangement shown in Fig. 6 are given in the Appendix. The voltage gradients of all seven conductors are given there for one particular set of instantaneous conductor voltages. If the voltage gradients are calculated for a range of values of time, the peak gradient on each conductor can be determined. This peak value of gradient, of course, occurs at a different time for each conductor.

The consideration of two particular phasing arrangements will serve to illustrate the general remarks made in the foregoing. Assume that balanced 3-phase voltages are applied to the double-circuit arrangement as given in Table VIII. The peak voltage gradients which result for $E=300$ kv line to line are also given. The gradients on the center conductors (*a2* and *b2*) differ from one another by less than 1/2 of 1%. Conductor phasing has little effect on the gradients of the center conductors. The average spacing *d* of this configuration is about 25 feet. The peak gradient factor as obtained from Fig. 2 for a 1.6-inch conductor is 70. For 300 kv, the peak voltage gradient thus obtained is 21,000 volts per cm as compared with the values in Table VIII. The double-circuit configuration affects the gradient of the center conductor by less than 1%. It is easily seen that the conductor phasing does effect the gradients of the upper and lower conductors considerably. The largest and smallest values of gradient shown differ by nearly 10%. The conductor phasing has a marked effect upon the ground wire gradient. However, even though the ground wire radius is small compared with the conductor radius, the ground wire gradient is very small compared with the conductor gradients.

Practical Applications

Fig. 7 gives the peak surface voltage gradient as a function of conductor diameter for various line-to-line voltages. The average height above ground was assumed to be 60 feet and the spacing 20 feet. While it is somewhat unrealistic to assume that the spacing does not vary with voltage, the curves shown were plotted from the preceding curves and serve to illustrate their use. The gradient was calculated using only the factor F_1.

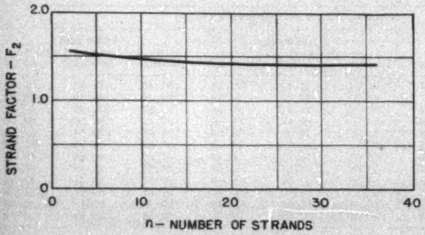

Fig. 5. Variation of the strand factor F_2 with the number of strands

Table VII. Ground Wire Gradient Factor F_1. Horizontal Arrangement, See Fig. 4

r = Ground Wire Radius in Inches

Conductor Diameter, Inches	g, Feet	l=5 Feet r=0.25	l=5 Feet r=0.50	l=5 Feet r=1.0	l=10 Feet r=0.25	l=10 Feet r=0.50	l=10 Feet r=1.0	l=20 Feet r=0.25	l=20 Feet r=0.50	l=20 Feet r=1.0
1.6	10	17.82	9.80	5.47	21.48	11.98	6.75	33.90	18.75	10.48
	20	8.28	4.53	2.56	14.92	7.85	4.17	18.08	9.94	5.54
	40		1.46	0.81	4.48	2.47	1.42	7.31	4.07	2.25
2.0	10	18.57	10.22	5.68	22.35	12.45	7.01	35.22	19.47	10.89
	20	8.54	4.68	2.65	15.13	7.95	4.26	18.72	10.33	5.76
	40	2.65	1.51	0.86	4.63	2.59	1.48	7.59	4.21	2.33

Table VIII. Applied Voltages and Peak Voltage Gradients for Double-Circuit Arrangement Example, See Fig. 6

Conductor Diameter 1.6 Inches

	Applied Voltage		Peak Voltage Gradient (300 Kv)	
Conductor	Arrangement 1	Arrangement 2	Arrangement 1	Arrangement 2
$a1$	$E \cos \omega t$	$E \cos \omega t$	19,879	18,621
$a2$	$E \cos (\omega t-120)$	$E \cos (\omega t-120)$	20,948	20,947
$a3$	$E \cos (\omega t+120)$	$E \cos (\omega t+120)$	20,615	20,207
$b1$	$E \cos (\omega t+120)$	$E \cos \omega t$	20,541	18,621
$b2$	$E \cos \omega t$	$E \cos (\omega t+120)$	20,847	20,947
$b3$	$E \cos (\omega t-120)$	$E \cos (\omega t-120)$	20,066	20,207
g	0.0000	0.0000	4,879	9,484

If the maximum peak voltage gradient for a stranded conductor is desired, the values of gradient obtained from the curve should be multiplied by 1.40.

Fig. 8 gives for stranded conductors the values of rms line-to-line voltage which result in a maximum peak voltage gradient of 30,000 volts per cm on the center conductor as a function of conductor diameter and spacing. According to Peek,[12] when this "disruptive critical voltage" is reached corona losses occur. This voltage results in a "disruptive critical gradient" which is constant at about 30 kv per cm for wires and cables having radii larger than 0.20 cm. This curve shows that large single conductors are necessary for high-voltage operation if the maximum gradients are to be kept below 30,000 volts per cm.

Of course, the maximum voltage gradient is not the only important factor which influences corona discharges. The characteristics of the electric field in the space surrounding the conductor must be considered and are greatly influenced by the nature of the conductor surface. The nature of the conductor surface also affects the emission of electrons from the surface and secondary processes which are essential to the discharge. It should be remembered that, on the one hand, no conductor can be absolutely smooth, so that small sharp projections can increase the gradient beyond that calculated for either a smooth or stranded conductor, and therefore some discharge may exist at values of calculated gradient below the critical, and that, on the other hand, this discharge will itself affect the gradient, and will moreover contribute to the aging of the conductor. These factors tend to reduce the abrupt change which might otherwise be expected when the disruptive critical gradient is approached or exceeded.

Conclusions

1. The diameter of the conductor has the most significant effect upon the surface voltage gradient for practical arrangements. An increase of conductor diameter decreases the voltage gradient. Since the charge for a given voltage increases with increasing diameter, the per-cent decrease in gradient will be somewhat smaller than the per-cent increase in diameter. The gradient will decrease about 0.8% for every 1% increase in conductor diameter.

2. The conductor spacing has the second largest effect upon the voltage gradient. The gradient increases as the spacing is reduced.

3. The height above ground has very

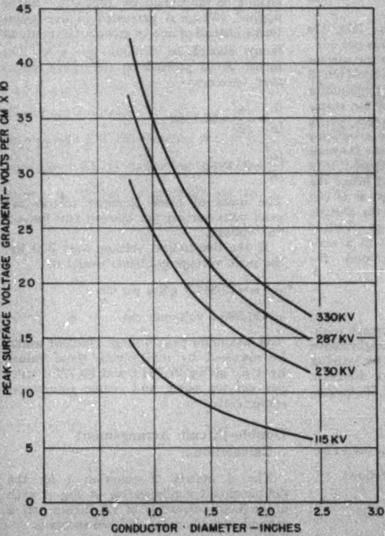

Fig. 7 (left). Variation of the peak surface voltage gradient on the center conductor of a horizontal arrangement with line-to-line applied voltage for a height above ground of 60 feet and a spacing of 20 feet

Fig. 8 (right). Variation of the disruptive critical voltage with conductor diameter and spacing for a stranded-conductor, single-circuit horizontal or vertical arrangement

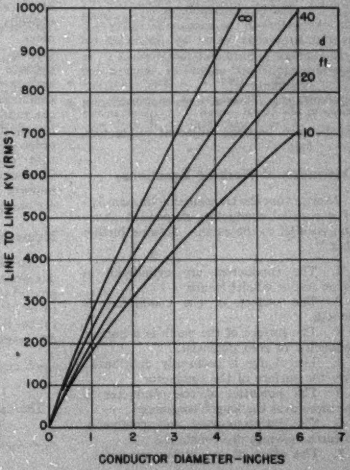

little effect upon the voltage gradient for practical arrangements.

4. Ground wires have very little effect upon the voltage gradient for conventional spacings.

5. For the stranded conductors in use today (having 20 or more outer strands), the maximum surface voltage gradient is approximately 40% larger than that calculated on the basis of a smooth conductor of the same outside diameter.

6. For the same conductor spacing and radius, the voltage gradient of the center conductor and the average voltage gradient for a horizontal configuration is only slightly different from the respective gradient of a vertical configuration of the same average height above ground.

7. The center conductor has the largest voltage gradient for all commonly used configurations.

8. For spacings and diameters of ground wires in common use, the ground wire gradients are very low as compared with those of the phase conductors.

9. The curves contained herein can also be used to obtain the voltage gradient on the center conductor of a double-circuit arrangement to a close approximation.

10. The electrostatic unbalance of a transmission line becomes less as the conductor spacing is increased. For practical spacings, ground wires reduce the unbalance very slightly.

Appendix. Calculation of Voltage Gradient

Nomenclature

h_n = height of conductor n above ground, feet
R_n = radius of conductor n, feet
r_{nm} = distance between actual conductors n and m
r_{nm}' = distance between actual conductor n and image conductor m'
Ln = logarithm to the base $\epsilon = 2.71828$
e_n = instantaneous value of potential between ground and conductor n
q_n = instantaneous value of charge on conductor n
ϵ_n = voltage gradient at surface of conductor n
d = distance between adjacent conductors, feet

Derivation of Working Equations

Assume that the transmission line consists of n parallel conductors suspended above and parallel to the earth. Assume further that:[13]

1. The conductors are cylindrical in shape and of infinite length.
2. The surface of the conductors is smooth.
3. The surface of the earth is a perfect conductor of zero potential.
4. The charge is uniformly distributed over the surface of the conductor.
5. The potential of the conductor is the same over the length considered.
6. The interconductor and conductor to earth spacings are constant.
7. The effect of supporting structures, near-by objects, and the character of the soil is neglected.

It is well known[14] that this system of conductors and ground can be replaced by an equivalent system composed of the actual conductors plus image conductors all of which are suspended in free space.

The voltages from ground to the conductors are related to the charges on the conductors by Maxwell's coefficients of capacitance.[14] The equations are then

$$\begin{aligned} e_1 &= A_{11}q_1 + A_{12}q_2 + \ldots + A_{1n}q_n \\ e_2 &= A_{21}q_1 + A_{22}q_2 + \ldots + A_{2n}q_n \\ e_n &= A_{n1}q_1 + A_{n2}q_2 + \ldots + A_{nn}q_n \end{aligned} \qquad (1)$$

where

$$A_{nn} = 2\text{Ln}\,\frac{2h_d}{R_n}$$

$$A_{nm} = 2\text{Ln}\,\frac{r_{nm}'}{r_{nm}}$$

When these equations are inverted, the charges are obtained as functions of the applied voltages. The equations become

$$\begin{aligned} q_1 &= B_{11}e_1 + B_{12}e_2 + \ldots + B_{1n}e_n \\ q_2 &= B_{21}e_1 + B_{22}e_2 + \ldots + B_{2n}e_n \\ q_n &= B_{n1}e_1 + B_{n2}e_2 + \ldots + B_{nn}e_n \end{aligned} \qquad (2)$$

Equations 2 are expressed in centimeter-gram-second units. If the applied voltages are expressed in statvolts, the charges obtained from equation 2 will be expressed in statcoulombs per cm of conductor length. If the charge is assumed to be uniformly distributed around the conductor, the electric flux leaving the conductor will be in a radial direction and $4\pi q$ lines per cm of conductor length in magnitude. The electric field intensity perpendicular to the conductor surface or voltage gradient is then given by

$$\epsilon_R = 2\frac{q}{R} \text{ statvolts per cm} \qquad (3)$$

If equation 3 is multiplied by 300, the gradient will be expressed in volts per cm.

The electric field intensity at the surface of a conductor as given by equation 3 depends upon the charge on that conductor alone. The other conductors of the transmission system also have charges which produce an electric field at the conductor surface. However, the distances between conductors are very large compared with the radius of the conductor and hence the electric field of the other charges is of the order of 1/2 of 1% or less of the electric field of the conductor charge itself.[5,6] This second-order effect results in a nonuniform electric intensity around the periphery of the conductor.

Numerical Example

Consider a horizontal arrangement without ground wires. Assume the height above ground to be 30 feet, the conductor spacing to be 16 feet, and the conductor diameter to be 0.1466 foot or about 1.76 inches. Also assume that

$$e_1 = E\cos\omega t,\; e_2 = E\cos(\omega t - 120),\; e_3 = E\cos(\omega t + 120)$$

The calculations proceed as follows

$$A_{11} = A_{22} = A_{33} = 2\text{Ln}\,\frac{60}{0.0733} = 13.4105$$

$$A_{12} = 2\text{Ln}\,\sqrt{1 + 4\left(\frac{30}{16}\right)^2} = 2.71216$$

$$A_{13} = 2\text{Ln}\,\sqrt{1 + \left(\frac{30}{16}\right)^2} = 1.50753$$

$$B_{11} = B_{33} = 0.0781541$$

$$B_{22} = 0.0804556$$

$$B_{12} = B_{23} = -0.0146227$$

$$B_{13} = -0.00582631$$

$$\frac{q_1}{E} = 0.0883786\cos\omega t - 0.00761788\sin\omega t$$

$$\frac{q_2}{E} = -0.0475392\cos\omega t + 0.0823402\sin\omega t$$

$$\frac{q_3}{E} = -0.0375920\cos\omega t - 0.0803470\sin\omega t$$

$$\left|\frac{q_1}{E}\right| = 0.0887010 \text{ statcoulomb per statvolt}$$

$$\left|\frac{q_2}{E}\right| = 0.0950730 \text{ statcoulomb per statvolt}$$

$$\left|\frac{q_3}{E}\right| = 0.0887010 \text{ statcoulomb per statvolt}$$

$$\left|\frac{\epsilon_1}{E}\right| = \left|\frac{\epsilon_3}{E}\right| = 0.0810135 \text{ statvolt per cm per statvolt}$$

$$\left|\frac{\epsilon_2}{E}\right| = 0.0868332 \text{ statvolt per cm per statvolt}$$

The units of the latter two quantities are obviously also volts per cm per volt. If the peak voltage gradient factor is desired, but it is more convenient to use rms values of applied voltage expressed in kilovolts, the gradient factors just given should be multiplied by $1000\sqrt{2}$. If the applied voltage is expressed in line-to-line terms instead of line to ground, the gradient factor should be divided by $\sqrt{3}$. The factor F_1 as plotted on the curve sheets then becomes

$$\left|\frac{\epsilon_1}{E}\right| = \left|\frac{\epsilon_3}{E}\right| = 66.1468$$

$$\left|\frac{\epsilon_2}{E}\right| = 70.8986$$

The units of these gradient factors are peak volts per cm per kilovolt rms line-to-line voltage.

If the line-to-line voltage were 300 kv, the peak voltage gradients would be

$\epsilon_1 = \epsilon_3 = 19{,}844.0$ volts per cm

$\epsilon_2 = 21{,}269.6$ volts per cm

The maximum peak voltage gradient would be obtained by multiplying these values by 1.40, giving 27,781.6 and 29,777.4 volts per cm for outer and center conductors respectively.

Double-Circuit Arrangement Calculations

The A matrix of equation 1 for the double-circuit configuration of Fig. 6 with a conductor diameter of 1.6 inches and a ground wire diameter of 0.576 inches is

	$a1$	$a2$	$a3$	$b1$	$b2$	$b3$	g
$a1$	16.449	4.4476	3.0195	3.9141	3.1210	2.5365	4.4467
$a2$	4.4476	16.030	4.2008	3.1210	2.9072	2.6813	3.1030
$a3$	3.0195	4.2008	15.551	2.5365	2.6813	2.8906	2.3273
$A=b1$	3.9141	3.1210	2.5365	16.449	4.4476	3.0195	4.4467
$b2$	3.1210	2.9072	2.6813	4.4476	16.030	4.2008	3.1210
$b3$	2.5365	2.6813	2.8906	3.0195	4.2008	15.551	2.3273
g	4.4467	3.1030	2.3273	4.4467	3.1210	2.3273	18.839

The inverse of the A or the B matrix of equation 2 is

	$a1$	$a2$	$a3$	$b1$	$b2$	$b3$	g
$a1$	0.071939	−0.013096	−0.0058169	−0.0087569	−0.0051853	−0.0036882	−0.010728
$a2$	−0.013096	0.073272	−0.013975	−0.0051853	−0.0047792	−0.0049088	−0.0046336
$a3$	−0.0058169	−0.013975	0.072481	−0.0036882	−0.0049088	−0.0076756	−0.0026521
$B=b1$	−0.0087569	−0.0051853	−0.0036882	0.071939	−0.013096	−0.0058169	−0.010728
$b2$	−0.0051853	−0.0047792	−0.0049088	−0.013096	0.073272	−0.013975	−0.0046336
$b3$	−0.0036882	−0.0049088	−0.0076756	−0.0058169	−0.013975	0.072481	−0.0026521
g	−0.010728	−0.0046336	−0.0026521	−0.010728	−0.0046336	−0.0026521	0.060328

As an example take:

$e_{a1}=e_{b1}=E\cos\omega t$

$e_{a2}=e_{b2}=E\cos(\omega t-120)$

$e_{a3}=e_{b3}=E\cos(\omega t+120)$

$e_g=0$

For 300-kv rms line-to-line voltage

$$E=\frac{300{,}000\sqrt{2}}{\sqrt{3}}=244{,}950 \text{ volts}=816.50 \text{ statvolts}$$

For $\omega t=0$

$a1$	816.50
$a2$	−408.25
$a3$	−408.25
$e=b1$	816.50
$b2$	−408.25
$b3$	−408.25
g	0.0000

Then from $q=Be$

$q_{a1}=q_{b1}=62.932$ statcoulombs per cm

$q_{a2}=q_{b2}=-35.180$ statcoulombs per cm

$q_{a3}=q_{b3}=-26.509$ statcoulombs per cm

$q_g=-11.570$ statcoulombs per cm

From $\epsilon=2(q/R)$, the electric intensities are

$\epsilon_{a1}=\epsilon_{b1}=62.002$ statvolts per cm $=$ 18,600 volts per cm

$\epsilon_{a2}=\epsilon_{b2}=-34.660$ statvolts per cm $=$ −10,398 volts per cm

$\epsilon_{a3}=\epsilon_{b3}=-26.117$ statvolts per cm $=$ −9,484 volts per cm

The calculations were carried out with the aid of an International Business Machines card programmed calculator. The availability of this machine made the collection of the foregoing results practical since it can solve the number of equations involved in a reasonable length of time.

References

1. Corona Considerations on High Voltage Lines and Design Features of Tidd 500 Kv Test Lines, C. F. Wagner, Anthony Wagner, E. L. Peterson, I. W. Gross. *AIEE Transactions*, vol. 66, 1947, pp. 1583–89.

2. Progress Report on Tidd 500-Kv Test Project of the American Gas and Electric Company—Corona, Radio Influence, and Other Factors. Philip Sporn, A. C. Monteith. *Ibid.*, vol. 69, pt. II, 1950, pp. 891–99.

3. Radio Influence Tests in Field and Laboratory—500-Kv Test Project of the American Gas and Electric Company, G. D. Lippert, W. E. Pakala, S. C. Bartlett, C. D. Fahrnkopf. *Ibid.*, vol. 70, pt. I, 1951, pp. 251–69.

4. Insulators and Line Hardware for Tidd 500 Kv Test Lines, I. W. Gross, R. L. McCoy, J. M. Sheadel. *Ibid.*, vol. 66, 1947, pp. 1592–1602.

5. Relative Surface Voltage Gradients of Grouped Conductors, M. Temoshok. *Ibid.*, vol. 67, pt. II, 1948, pp. 1583–89.

6. Capacitance and Surface Voltage Gradient of Transmission Lines, H. B. Dwight, F. E. Scheidler. *Ibid.*, vol. 71, pt. III, Apr. 1952, pp. 563–66.

7. Influence, Upon the Effect of Corona, of the Diameter and Profile of Very High Voltage Aerial Lines, F. Cahen, R. Pelissier. *Revue Generale de l'Electricite*, Paris, France, July 1949, pp. 279–90.

8 The Mechanism of Corona on A-C Transmission Lines, R. Pelissier, D. Renaudin. *Bulletin*, Societe Francaise des Electriciens, Paris, France, vol. 9, 1949, pp. 53–71.

9. Transposition of High-Voltage Overhead Lines and Elimination of Electrostatic Unbalance to Ground, Eric T. B. Gross, Andrew H. Weston. *AIEE Transactions*, vol. 70, pt. II, 1951, pp. 1837–44.

10. *Discussion* by Hillel Poritsky of Double Conductors for Transmission Lines, H. B. Dwight, E. B. Farmer, and Three-Phase Multiple Conductor Circuits, E. Clarke. *Ibid.*, vol. 51, 1932, pp. 821–22.

11. The Two Dimensional Magnetic or Electric Field Above and Below an Infinite Corrugated Sheet, N. H. Langton, N. Davy. *British Journal of Applied Physics*, London, England, vol. 4, no. 5, May 1952, pp. 134–37.

12. Dielectric Phenomena in High Voltage Engineering (book), F. W. Peek, Jr. McGraw-Hill Book Company, Inc., New York, N. Y., 3rd ed., 1929, p. 192.

13. Circuit Analysis of A-C Power Systems, Vol. I (book), E. Clarke. John Wiley and Sons, Inc. New York, N. Y., 1943, p. 434.

14. Principles of Electric and Magnetic Fields (book), W. B. Boast Harper and Brothers, New York, N. Y., 1948, chap. 7 and 8.

Oscillations of Coupled Windings

P. A. ABETTI
ASSOCIATE MEMBER AIEE

G. E. ADAMS
ASSOCIATE MEMBER AIEE

F. J. MAGINNISS
MEMBER AIEE

Synopsis: The oscillations of a single winding have been extensively investigated, but actually the most important practical case, the oscillations of coupled windings, has received but scant attention. The wave shapes and natural frequencies are determined in this paper for two coupled windings of any turn ratio and with the same or opposite winding direction, in air or on an iron core. The integral equation and the equivalent circuit methods, previously developed for single windings, are extended to introduce the effect of the secondary on the primary, and then to investigate various winding combinations of turns ratio varying from 1 to 1 to 1 to 9. Good agreement is found between computed and measured values of the natural frequencies and wave shapes.

EXTENSIVE theoretical and experimental investigations of the oscillations of single windings, in air or on an iron core, have been made in the past. To take into account completely and rigorously all mutual inductance linkages between all the turns, previously neglected, two of the authors have developed the equivalent circuit method[1] and the integral equation method.[2] The first method yielded all the natural frequencies of practical importance, but not the wave shapes; while the second gave both wave shapes and natural frequencies, but only for the fundamental oscillation. In both cases excellent agreement was obtained between calculations and measurements made on an experimental coil with air core or iron core, whose parameters could be varied over a wide range.

Knowledge of the normal functions of single windings is of fundamental importance for the determination of the response to impulse voltages and switching surges of air coils, iron-core coils, reactors, and generator windings. The most important practical application, however, concerns the behavior of transformer windings subjected to lightning, commercial impulse tests, and switching surges. Since transformers have at least two windings, and often more, it is astonishing that so little attention has been given in the literature to the oscillations of coupled windings. Bewley[3] investigated more than 20 years ago the transient oscillations of mutually coupled windings, and later Boyajian[4] and Vitins[5] the special case of an oscillating high-voltage secondary. All these authors assume that the wave shapes of the normal functions (or standing waves) are sinusoidal. It has been shown recently[2] from the solution of the integral equation, and confirmed by an extensive series of tests, that the normal functions of a single winding are not sinusoidal, and there is no reason to believe that the presence of another winding would alter this conclusion. Furthermore, Boyajian and Vitins neglected altogether the capacitances of the low-voltage winding and its oscillations.

Results obtained for single windings are generally used for transformers, and the mutual effect of the two windings is neglected altogether. In many practical cases this approximation yields astonishingly satisfactory results, but a theoretical justification is lacking, as well as the establishment of the limits within which it is valid. For these reasons, methods used for the analysis of oscillating single windings were extended, first to study the effect of the secondary winding on the primary oscillations and neglecting the less important secondary oscillations and, second, to analyze the oscillations of a system of two coupled windings, wherein both windings are considered on the same basis.

Effect of the Secondary on the Mutual Inductance Function of the Primary

First consider only the effect of the secondary winding on the fundamental oscillation of the primary. It will be assumed that:

1. Both windings are uniform.
2. The number of turns in the primary is much greater than the number of turns of the secondary.
3. The capacitance from secondary to ground is much larger than the sum of the capacitances from primary to secondary and from primary to ground, in parallel.
4. Primary and secondary series capacitances can be neglected.

The last assumption follows from the fact that we are considering only the fundamental oscillation of the primary and that series capacitance affects appreciably only the higher harmonics.[2-4] Assumptions 2 and 3 allow the conclusion that while the primary winding is oscillating there will not be any appreciable voltage transferred by electromagnetic or electrostatic induction to the secondary which, therefore, will always remain at ground potential.

Let $M(x,s)dxds$ be the mutual inductance of two elements of the primary winding located at points of abscissas x and s from one end of the winding, referred to the length of the winding taken as unity. If there is no secondary winding, this mutual inductance function[1] $M(x,s)$ can be assumed both for air-core and iron-core coils to be a function only of the distance $|x-s|$ between the two elements, and not of x and s separately. This leads to a discussion of the secondary winding and the study of its effects on the mutual inductance function. As long as the secondary is open-circuited no current can flow in it, and the function

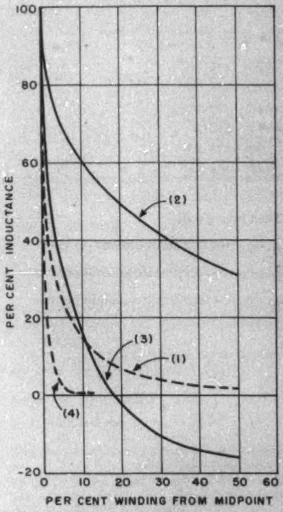

Fig. 1. Mutual inductance functions at center of an experimental coil

1—Air core, no secondary
2—Iron core, no secondary
3—Iron-core, short-circuited secondary
4—Air or iron-core, copper screen

Paper 55-29, recommended by the AIEE Transformers Committee and approved by the AIEE Committee on Technical Operations for presentation at the AIEE Winter General Meeting, New York, N. Y., January 31–February 4, 1955. Manuscript submitted October 19, 1954; made available for printing November 16, 1954.

P. A. ABETTI is with the General Electric Company, Pittsfield, Mass., and G. E. ADAMS and F. J. MAGINNISS are with the General Electric Company, Schenectady, N. Y.

All measurements were made by the staff of the High Voltage Engineering Laboratory of the General Electric Company, Pittsfield, Mass.

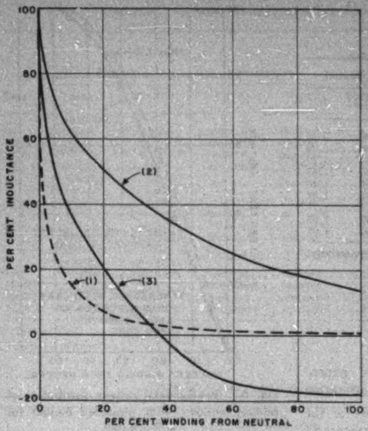

Fig. 2 (left). Mutual inductance function at ends of an experimental coil. Same designations as for Fig. 1

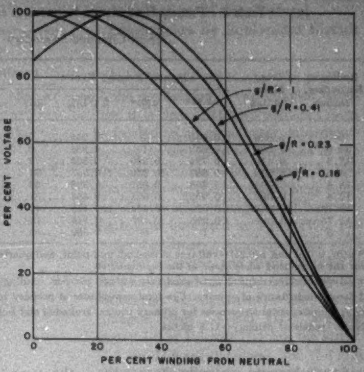

Fig. 4 (right). Fundamental voltage distributions of primary winding with isolated neutral for large values of g/R = (gap/average radius), short-circuited secondary

$M(x,s)$ is not affected. However, if the secondary is short-circuited the current flowing in it will completely change the flux pattern and thus the function $M(x,s)$. Furthermore, it is clear that now the mutual inductance between two primary turns will depend not only upon their distance, but also upon their location. Thus $M(x,s)$ is a function of both coordinates x and s. It is interesting to note that within certain regions the function $M(x,s)$ will take negative values. Figs. 1 and 2 show the function $M(x,s)$ at the center and at either end respectively of an experimental coil[1,2] for the following conditions: 1. With air core, secondary absent or open-circuited. 2. With iron core, secondary absent or open-circuited. 3. With short-circuited secondary, with iron core. These curves were computed from Grover's tables[6] and found to agree well with measurements. Similar results have been obtained by Karasev and Sklyanin.[7] It is seen that corresponding curves in Figs. 1 and 2 have different shape only for case 3, since both windings are uniform. To facilitate comparison, the maximum value, which is the self-inductance of a single turn, is taken as unity for all cases, and the actual values are given in Table I.

Table I. Self-Inductance of Single Turn of Experimental Coil

Case	Inductance, Microhenrys	
	At Center	At Ends
1, Open-circuited secondary, air core	2.66	2.66
2, Open-circuited secondary, iron core	3.50	3.61
3, Short-circuited secondary, iron core	1.83	2.84
4, Copper screen, air core and iron core	1.80	1.80

It should be mentioned at this point that when a metal screen such as a copper cylinder is substituted for the secondary winding, the mutual inductance function is not the same as with short-circuited secondary. In fact Fig. 1 shows that the function $M(x,s)$ with a screen, curve 4, decays much faster than for any other case and does not take negative values. The presence of the screen reduces the amount of mutual flux below the air-core value. Thus a coil with a short-circuited screen, with air core or iron core, behaves just as an air-core coil of much larger equivalent length to diameter ratio.[1] Therefore, in general, it is not permissible to substitute a metal screen for the secondary in the theoretical and experimental investigation of transformer transients. This confirms the results of a previous investigation by field theory.[8]

It may be concluded that when the secondary is short-circuited and the stated assumptions are valid, the primary winding can be treated as a single nonuniform winding with a self-inductance function[1]

$$L_0(x, s) = \int_0^x \int_0^s M(\xi, \sigma) d\xi d\sigma \qquad (1)$$

The integral equation method previously used[2] for nonuniform windings without secondary may also be used for uniform windings with short-circuited secondary.

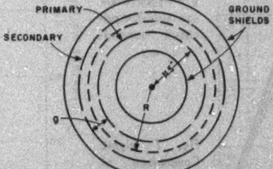

Fig. 3. Concentric windings. R = average radius, g = gap. Both windings 48 inches high

Effect of the Short-Circuited Secondary on the Fundamental Oscillations of the Primary

For the calculation of the fundamental oscillations, the 1,800-turn winding previously described[2] was considered to be the primary. Various secondaries were assumed to be located concentrically outside the primary (Fig. 3) and the ratio g/R of the gap g between primary and secondary to their average radius R was varied between wide limits, encompassing the geometry of 2-winding transformers with concentric windings. Calculations were made of the fundamental wave shapes and frequencies for the two most important primary terminal conditions: for 1. both ends grounded, and 2. line end grounded, neutral end isolated (obviously the role of the two ends is interchangeable because of symmetry). The results are summarized in Table II and in Figs. 4, 5, and 7 for isolated neutral; in Fig. 6 for grounded neutral. When the secondary winding has a much greater radius than the primary, its effect is negligible and the same results are obtained as for the primary alone in air (case 1 in Table I of reference 1).

First, consider the case of primary neutral isolated. As the short-circuited sec-

Table II. Primary Fundamental Frequencies and Wave Shapes

Short-Circuited Secondary

Radius of Secondary, Inches	Gap/ Mean Radius	Isolated Primary Neutral				Grounded Primary Neutral			
		u(0.5)*	u(0)*	$f_i\sqrt{LC_g}$	x_m†	u(0.25)*	x_m†	$f_g\sqrt{LC_g}$‡	f_g/f_i
∞	2.000	0.646	1	0.255	0	0.667	50	0.589	2.31
34.5	1.000	0.652	1	0.256	0	0.659	50	0.580	2.26
17.5	0.410	0.724	0.999	0.308	2	0.660	50	0.580	1.89
14.5	0.230	0.835	0.939	0.357	21	0.660	50	0.580	1.63
13.5	0.160	0.888	0.847	0.398	28	0.660	50	0.580	1.46
12.5	0.083	0.962	0.621	0.459	39	0.659	50	0.580	1.27
12.125	0.051	0.982	0.446	0.496	44	0.660	50	0.581	1.17
11.75	0.021	0.995	0.197	0.545	48	0.662	50	0.583	1.07
11.5	0	1	0	0.580	50	0.660	50	0.580	1.00

* u(0), u(0.5) and u(0.25) = voltages at neutral, mid-point, and quarter-points of the winding respectively, for the normalized wave shape of the fundamental.

† x_m = abscissa corresponding to maximum voltage, per-cent winding from neutral.

‡ L = self-inductance of primary; C_g = total capacitance of primary to ground.

f_g, f_i = fundamental frequencies for primary neutral grounded and isolated respectively.

Note: radius of primary = 11.5 inches.

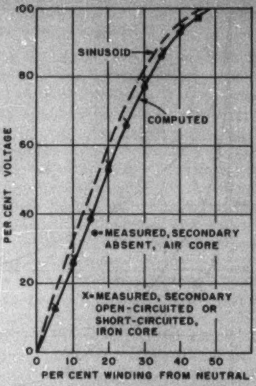

Fig. 6. Fundamental voltage distribution of primary winding with grounded neutral for g/R = 0.083

ondary is brought gradually closer to the primary, its effects are felt more and more. The voltage distribution becomes more peaked, the maximum voltage is found no more at the neutral end and the abscissa of the point with maximum voltage gradually approaches the mid-point of the winding (Figs. 4 and 5). At the same time the fundamental frequency with isolated neutral increases over a range equal to 2.31, the ratio of the fundamental frequencies with grounded and isolated neutral when the secondary is absent. These results are independent of turn ratio and relative winding directions. Usual values of the ratio g/R in power transformers vary between 0.2 and 0.04, so that the voltage distribution is by no means cosinusoidal, as generally assumed in the literature. As the gap is reduced to zero and the short-circuited secondary coincides with the primary, the fundamental voltage distribution is the same as if the primary neutral were grounded, because of the perfect coupling between the two windings. (This limiting case is the same as case 1 of Vitins' paper,[5] where the value 0.5 is obtained rather than 0.580 for $f_i\sqrt{L\ C_g}$ because of the simplifying assumptions with respect to the mutual inductance function.)

Now, in the case of primary neutral grounded, it is noted from Table II and Fig. 6 the surprising fact that when our initial assumptions are valid the secondary has no effect whatever on the fundamental oscillation of the primary. The minute differences in the values of $u(0.25)$ and of $f_g\sqrt{L\ C_g}$ are probably the result of slight inaccuracies in the evaluation of the kernels of the integral equation and in the iterative solution of this equation by means of digital computers. The physical explanation of this interesting fact is that, because of the symmetry with respect to the mid-point of the current distribution along the primary winding grounded at both ends, the sum of the ampere turns is always zero. Thus the sum of the flux linkages of the secondary winding is zero and no voltage can be measured between its open-circuited terminals. It will make no difference therefore whether these terminals are isolated or connected together. Since almost all high-voltage power transformers have the primary neutral grounded, and our initial assumptions are at least approximately valid for the majority of cases, this explains the hitherto unexplained fact that a circuit which "ignores the presence of the secondary circuits...strangely enough proves quite adequate to describe the internal high-frequency transients of the winding under consideration, not only qualitatively, but quantitatively as well."[3]

With secondary absent or open-circuited, or with a metallic screen, the ratio of f_g/f_i of the fundamental frequencies with grounded and isolated neutral can vary between 2 and very large values.[2] Values of about 2 are usually ob-

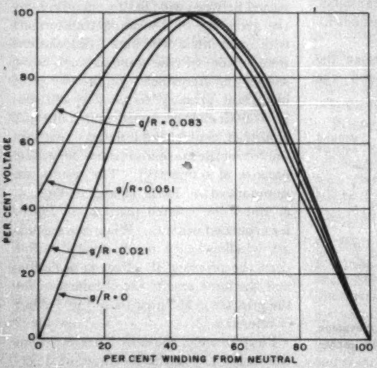

Fig. 5 (left). Fundamental voltage distributions of primary winding with isolated neutral for small values of g/R = (gap/average radius), short-circuit secondary

Fig. 7 (right). Comparison of computed and measured wave shapes for g/R = 0.083

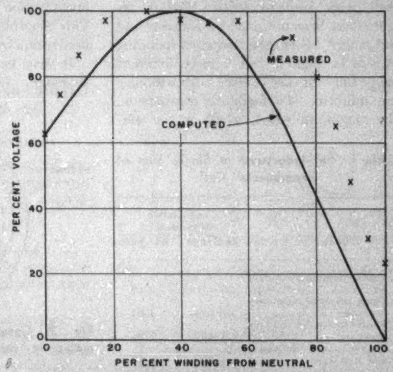

Table III. Terminal Conditions for Two Coupled Windings

Case	Primary		Secondary		Equation Number					
					2-Element			5-Element		
	Line	Neutral	Line	Neutral	Total	S*	A†	Total	S*	A†
I-1	isolated	isolated	isolated	isolated	6	4	2	12	6	6
I-2 I-3	isolated	isolated	grounded isolated	isolated grounded	5			11		
I-4	isolated	isolated	grounded	grounded	4	3	1	10	5	5
II-1	grounded isolated	isolated grounded	isolated	isolated	5			11		
II-2	grounded isolated	isolated grounded	grounded isolated	isolated grounded	4			10		
II-3	grounded isolated	isolated grounded	isolated grounded	grounded isolated	4			10		
II-4	grounded isolated	isolated grounded	grounded	grounded	3			9		
III-1	grounded	grounded	isolated	isolated	4	3	1	10	5	5
III-2 III-3	grounded	grounded	grounded isolated	isolated grounded	3			9		
III-4	grounded	grounded	grounded	grounded	2	2	0	8	4	4

* Symmetrical.

† Antisymmetrical.

Table IV. Description of Secondary Windings

TC No.	Core	Secondary Turns	Turn Ratio	Self-inductance, Microhenrys		Capacitance Values, Micromicrofarads, 5-Element Representation				
				L_{pp}	L_{ss}	C_{pp}	C_{ss}	C_{pg}	C_{ps}	C_{sg}
6	Air	200	9.00	86.8	1.32	5.0	23.5	32.0	248	236
7	Air	704	2.56	86.8	15.0	5.0	6.3	32.0	248	250
8	Air	1800	1.00	86.8	99.7	5.0	5.0	32.0	248	236
9	Iron	210	8.57	305.0	4.16	5.0	23.5	32.0	248	236
10	Iron	1800	1.00	305.0	317.5	5.0	5.0	32.0	248	236

tained with a screen, values of 2.2 to 2.9 for air coils, of 5 to 12 for power and distribution transformers. It is found that when the secondary is short-circuited this ratio will always be less than when the secondary is absent or open-circuited, and that for power transformers it will vary between 1.1 to 1.6. Since the leakage flux is essentially in air, it will make no difference whether both windings are in air or on an iron core. The self-inductance function was computed for the two windings in air, and Fig. 6 shows that the computed distribution for $g/R=0.083$ and primary neutral grounded is in excellent agreement with the distribution measured on the same windings (1,800-turn primary, 210-turn secondary), first in air and then on an iron core. The computed values of f_g, f_i (in KC) and f_g/f_i for this case are 19.0, 15.0, and 1.27 respectively; and the measured values 19.5, 15.5, 1.26 respectively. Measured and computed distributions with primary neutral isolated for the same ratio of g to R, but with an 1,800-turn secondary and iron core, are compared in Fig. 7. There is a general agreement in the wave shapes and in the neutral voltages (computed and measured values both 62 per cent (%) of maximum) and the differences result from the 1-to-1 turn ratio, which does not agree with the initial assumptions. The general conclusions obtained here concerning the ratio of the fundamental frequencies agree well with tests made on eight power transformers, ranging from 500 to 20,000 kva per phase. The measured frequency ratio f_g/f_i varied between 5.7 and 10.5 when the secondary was open-circuited, and between 1.11 and 1.62 when the secondary was short-circuited. Similar experimental results have been obtained by Karasev and Sklyanin[7] with two windings on an iron core. The measured frequency ratios were 7.3, 1.26, and 2.15 respectively for open-circuited secondary, short-circuited secondary, and secondary replaced by a copper screen. These values also agree very well with the theory presented here.

Determination of the Natural Frequencies by Equivalent Circuit

For a general solution of the problem of the oscillations of two coupled windings, it is clear that both windings must be treated on an equal basis, subordinating one to the other as was done in the previous section. The problem is also complicated by the fact that a large number of terminal conditions must be investigated, as indicated in Table III. Because of symmetry some conditions yield identical solutions, and when the roles of the primary and secondary (arbitrary but convenient designations) are interchanged, cases I-4 and III-1, are the same; I-2 or I-3 and II-1 are the same; II-2 and II-3 are the same; and II-4 and III-2 or III-3 are the same, so that six different conditions must be investigated analytically. This number should be doubled since the two windings can be wound in the same or in the opposite direction, but it will be sufficient to define all mutual inductances as numbers with their own signs, which will all be positive or negative depending on the relative winding directions. It will be shown that another terminal condition, that of secondary short-circuited but isolated from ground, can be derived from two of the six conditions just discussed.

The equivalent circuit method[1] has been extended to determine the natural frequencies of an arbitrary number of coupled windings, and will be explained for the case of transformers with two concentric windings. First, each winding must be subdivided into a number of elements, and the degree of accuracy of the natural frequencies will depend upon the number of elements used. For this investigation it was desired to calculate the fundamental frequency with at least 10% accuracy, and the second and third harmonic frequencies with at least 20% accuracy, and thus five elements were

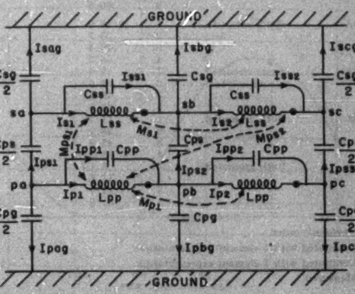

Fig. 8. Two-element representation of two coupled windings

Table V. Computed and Measured Natural Frequencies

Both Ends of Primary Grounded

			Frequency, Kilocycles			Ratio f_n/f_1	
TC No.	Secondary Terminals	n*	c(5)†	c(2)‡	m§	c(5)†	m§
6, 7, 8	Absent	1			27.5		1
		2			62.0		2.25
		3			101.0		3.67
		4			143.0		5.19
6A	Both isolated	1	22.1	19.5	24.2	1	1
		2	43.2		46.4	1.95	1.92
		3	69.6		79.8	3.15	3.29
6A	Both grounded	1	19.6	18.4	20.7	1	1
		2	43.2		46.5	2.20	2.24
		3	68.9		77.7	3.51	3.75
		4	91.0		112.6	4.65	5.44
6B	Both grounded	1	16.3		18.4	1	1
		2	36.4		41.7	2.23	2.26
		3	58.6		70.3	3.59	3.81
		4	76.9		102.0	4.71	5.55
7B	Both isolated	1	17.3		19.0	1	1
		2	27.9		28.7	1.61	1.51
		3	48.7		57.8	2.82	3.04
		4	58.5		66.9	3.38	3.52
7B	Both grounded	1	12.9		13.2	1	1
		2	29.1		30.4	2.25	2.29
		3	47.3		52.4	3.65	3.96
		4	62.5		78.4	4.82	5.91
8A	Both isolated	1	20.5	16.3	23.5	1	1
		2	21.2		24.7	1.04	1.05
		3	43.5		52.0	2.12	2.21
		4	46.7		54.5	2.28	2.32
8A	Both grounded	1	17.1	15.8	17.8	1	1
		2	36.6		39.8	2.14	2.23
		3	37.9		40.5	2.22	2.27
		4	60.5		81.0	3.54	4.55
8A	One grounded, one isolated	1	11.1	9.96	12.2	1	1
		2	21.1		24.0	1.91	1.96
		3	27.5		40.2	3.39	3.28
		4	45.0		53.0	4.06	4.32
8B	Both isolated	1	12.4	9.34	15.0	1	1
		2	16.2		17.4	1.30	1.16
		3	28.7		37.5	2.30	2.50
		4	38.8		40.5	3.12	2.70
8B	Both grounded	1	8.38	7.8	8.70	1	1
		2	19.0		20.0	2.26	2.30
		3	31.0		39.3	3.69	3.94
8B	One grounded, one isolated	1	7.55	7.29	7.80	1	1
		2	15.2		17.0	2.02	2.16
		3	22.4		26.8	2.97	3.44
		4	32.2		39.0	4.21	5.00
9, 10	Absent	1			17.0		1
		2			48.5		2.85
		3			90.0		5.30
		4			134.0		7.88
9A	Both grounded	1	12.2			1	
		2	32.2			2.64	
		3	50.9			4.17	
		4	73.3			7.01	
9B	Both isolated	1	13.1		17.4	1	1
		2	26.4		37.5	2.01	2.15
		3	43.3		71.0	3.30	4.07
		4	60.8		107.5	4.64	6.17
9B	Short circuited and isolated	1	13.1		19.5	1	1
		2	26.5		41.0	2.02	2.10
		3	43.3		75.0	2.30	3.84
		4	60.8		110.0	4.64	5.63
9B	Both grounded	1	9.98			1	
		2	26.5			2.65	
		3	42.3			4.23	
		4	60.8			6.08	
10A	Both isolated	1	13.6		14.5	1	1
		2	23.7		23.5	1.74	1.62
		3	46.3		43.3	3.40	2.99
		4	66.2		52.5	4.86	3.62
10A	Short circuited and isolated	1	13.6		15.2	1	1
		2	28.9			2.12	
		3	46.3		52.0	3.40	3.42
		4	65.5			4.81	
10A	Both grounded	1	11.1			1	
		2	28.9			2.60	
		3	45.8			4.12	
		4	65.5			5.89	
10B	Both grounded	1	5.19			1	
		2	13.8			2.65	
		3	22.1			4.26	
		4	31.8			6.12	

* Harmonic order.

† Computed with 5-element representation.

‡ Computed with 2-element representation.

§ Measured.

chosen to represent each winding. As previously, mutual inductances were included between each element and every other element, as well as the series and shunt capacitances of both windings.

For simplicity, the equations will be set up for a 2-element representation of each winding, as in Fig. 8. Subscript *p* refers to the primary, *s* to the secondary and *g* to ground, represented by the core and the tank. The equations describing the circuit of Fig. 8 can be written more simply on the nodal basis than on the loop basis. In fact, the system consists of 7 nodes, 17 elements, and 1 separate part: hence the number of independent node pairs if 6, while the number of independent loops is 11. The nodal equations for the system of Fig. 2 are derived in the Appendix and are easily adapted to the various terminal conditions. If a terminal is grounded, the corresponding voltage is set equal to zero and the corresponding nodal equation is no longer valid and hence is disregarded. For instance, if terminal *pa* is grounded, V_{pa} is zero and the first column and first row in the impedance matrix 11 of the Appendix are eliminated. Therefore the number of required equations depends upon the terminal conditions and is listed in Table III.

During the free oscillations of this system of coupled windings, a finite set of voltages will satisfy the equations only if the determinant of the impedance matrix is zero. This will happen for discrete values of the frequency ω, which are the natural frequencies of the system. Since the order of the determinant is equal to the number of equations, 2 to 6 for this simplest case, and 8 to 12 for the 5-element representation, the calculations can be done only with modern digital computers. Even so, the calculations become quite laborious as the order of the determinant increases and it is important to reduce the system of equations to be solved to the lowest order possible. This can be done by taking full advantage of the symmetry in some configurations of the boundary conditions. The equations (11) of the system are of such form that they group naturally into combinations having the sums and differences of the voltages as variables. As shown in the Appendix, the set of six equations is now broken into two independent sets of lower order which will yield the same natural frequencies as the original set and also the same wave shapes, if these are symmetrical with respect to the mid-points of the windings. The set of equations obtained by addition yields the symmetrical harmonics for which

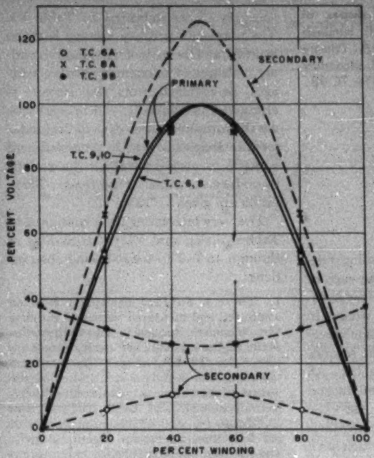

Fig. 9 (left). Wave shapes of first harmonic. All terminals grounded for TC 6A and 8A. Primary terminals grounded, secondary terminals isolated for TC 9B

Fig. 11 (right). Wave shapes of second harmonic. All terminals grounded for TC 6A. Primary terminals grounded, secondary terminals isolated for TC 9B

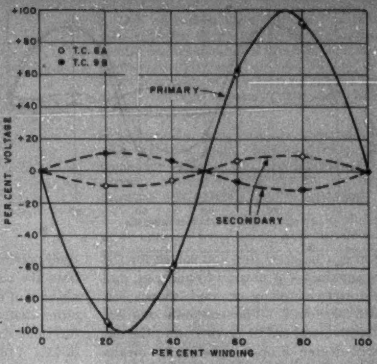

$V_{pa}=V_{pc}$ and $V_{sa}=V_{sc}$ (2)

The set obtained by subtraction yields the antisymmetrical harmonics for which

$V_{pa}=-V_{pc}$ and $V_{sa}=-V_{sc}$ (3)

The calculation of the natural frequencies and wave shapes is greatly simplified by this artifice, and Table III shows the cases when this is possible and the manner into which the equations are divided. The unequal distribution of equations into the two sets (symmetrical and antisymmetrical) is due to the fact that an even number of elements has been used to represent the windings. If an odd number of elements is used the two resulting sets will have the same number of equations.

The method described here for a 2-element representation is easily extended to the 5-element representation to be used for the computations. There are now 13 nodes, 38 elements and 1 separate part, so that the number of independent node pairs is 12. A total of 15 different self- and mutual inductances must be considered, the 2 self-inductances of each element of the primary and secondary, 4 mutual inductances between primary elements and 4 between secondary elements, and finally the 5 mutual inductances between primary and secondary elements. The number of equations, to be solved for the various terminal conditions, is given in Table III. The number of natural frequencies is equal to the order of the determinant, and they can be found by two different methods. The roots of the determinant can be determined by well-known numerical methods, or else a cut-and-try procedure can be used. In the latter case, several frequencies are assumed and the corresponding values of the determinant are calculated: then the frequencies are varied until the values of the determinant become zero.

Determination of the Wave Shapes by Equivalent Circuit

In addition to the natural frequencies of the first three harmonics, it was desired to calculate the wave shapes (or standing waves, or natural modes, or eigenfunctions) corresponding to these oscillations in order to gain a better understanding of the physical phenomena. Lanczos' method,[9,10] which yields both the eigenvalues and eigenvectors, corresponding to the natural frequencies and wave shapes respectively, was used for this purpose. It was first necessary to reduce the circuit equations to a form in which only the terms on the main diagonal contain a constant minus the square of the angular frequency, while all other terms are constant. This form is obtained by multiplying the equations through by the negative of the inverse of the terms in $\lambda=\omega^2$, which are the capacitance terms. The result is an unsymmetrical matrix of the form

$$\|(A-1\lambda)y=0\| \qquad (4)$$

The characteristic equation of this sys-

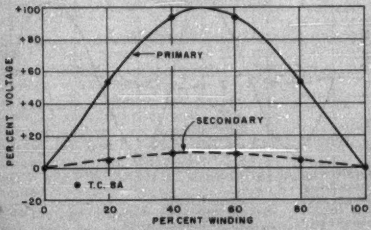

Fig. 10 (left). Wave shape of second harmonic, TC 8A. All terminals grounded

Fig. 12 (left). Wave shape of third harmonic, TC 8A. All terminals grounded

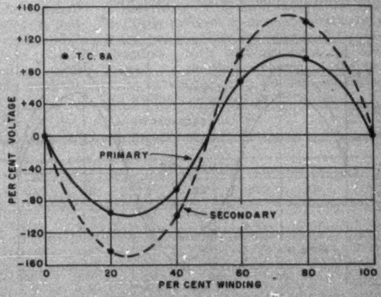

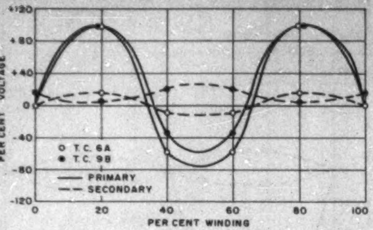

Fig. 13. Wave shapes of third harmonic; all terminals grounded for TC 6A. Primary terminals grounded, secondary terminals isolated for TC 9B

tem can be generated and solved for the eigenvalues λ or natural frequencies, and the eigenvectors y or wave shapes can also be found. The computations are iterative and can be carried on to the desired degree of approximation by means of digital computers. In the calculation of the wave shapes, relative voltage values are obtained only for the five nodal points of each winding. While it is convenient to connect these points with continuous curves for visualization purposes, it must be realized that these curves are necessarily arbitrary.

Example: Natural Frequencies of Coupled Windings in Air or on Iron Core

The equivalent circuit method was used to compute the first three or four natural frequencies of various combinations of two coupled windings in air or on an iron core. The primary winding, 23 inches in diameter and 48 inches long, has 1,800 turns and has been described previously.[1] Various secondary windings, 25 inches in diameter and 48 inches long, were located concentrically to the primary.

Two grounded concentric electrostatic shields represented the core and tank ground planes; see Fig. 3. The different winding combinations are designated as test conditions (TC). Each TC is referred to by a number and by a letter. The numbers from 6 to 10 (1 to 5 were used previously[1,3] for single windings) denote the turn ratio and the presence or absence of the iron core; the letter A denotes that both windings are wound in the same direction; B in opposite directions. A brief description of the secondary windings is given in Table IV. All the capacitances, and the self- and mutual inductances were computed for the various test conditions, using equivalent air-core coils[1] for TC 9 and 10, which have an iron core.

Since almost all high-voltage power systems in the country operate with grounded neutral, all computations were done for this case which corresponds to both primary terminals grounded. Various secondary conditions were investigated: 1. both terminals isolated; 2. both grounded; 3. terminals short-circuited but isolated from ground; 4. one terminal grounded, one isolated. The natural frequencies and their ratios, computed with the 5-element representation as well as the measured frequencies and ratios, are tabulated in Table V. This table includes also a few fundamental frequencies computed with the 2-element representation. To have a complete picture of the effect of the secondary, the measured frequencies are included with secondary absent for air core (corresponding to TC 6,7, and 8) and for iron core (corresponding to TC 9 and 10). The computed wave shapes are shown on Figs. 9 through 15, as indicated in Table VI. The maximum primary voltage is taken as unity, and the ratio of maximum secondary voltages to maximum primary voltages, as obtained from the curves, is also given in Table VI. Of interest also are the measured ratios[1] f_g/f_i of the fundamental frequencies with grounded and isolated primary neutral for the various secondary terminal conditions. These ratios are given in Table VII.

The very interesting data contained in Tables V, VI, and VII and in Figs. 9 through 15 lead to the following observations:

1. There is excellent agreement between computed and measured values of the first three harmonic frequencies and of the ratios of the higher harmonics to the fundamental, except for TC 9B. For TC 6, 7, and 8 (air-core) the standard deviations of the measured and computed values of the fundamental, second, and third harmonic are 10.4%, 10.1% and 16.9% respectively, of the first three harmonics together 12.8%. The standard deviation of the computed and measured frequency ratios is 9.7%. The agreement of the frequency ratios is more significant than the agreement of the frequency values, since the former are less affected by possible errors in the calculation of the coil capacitances. In accordance with theoretical considerations, the computed frequencies are less than the measured frequencies and the difference increases with the harmonic order.[1]

2. There is good agreement between computed and measured wave shapes for TC 9B, for which the first and second harmonic were measured. For the second harmonic, computed relative voltages at 20 and 40% winding from the neutral end were 100 and 69% for the primary, 12 and 8% for the secondary. Corresponding measured values were 100 and 68.8% for the primary, 11.8 and 8.1% for the secondary.

3. In considering the effect of the secondary winding the absolute values and the ratios of the natural frequencies should be discussed separately. Presence of the secondary reduces the natural frequencies with respect to the values with secondary absent. This effect is felt more and more

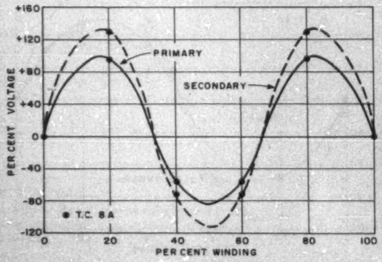

Fig. 14 (left). Wave shape of fourth harmonic, TC 8A. All terminals grounded

Fig. 15 (right). Wave shapes of fourth harmonic. All terminals grounded for TC 6A. Primary terminals grounded, secondary terminals isolated for TC 9B

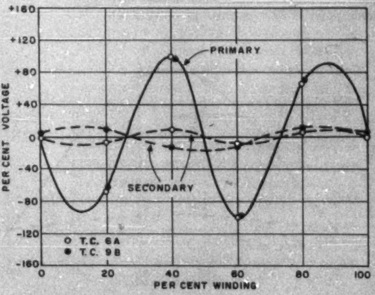

Table VI. Ratios of Maximum Secondary and Primary Voltages

Both Primary Terminals Grounded

TC	Secondary Terminals	n	Figure	Ratio Calculated	Ratio Measured
6A, turn ratio 1/9	Both grounded	1	9	1:9	
		2	11	1:10	
		3	13	1:7	
		4	15	1:10	
8A, turn ratio 1/1	Both grounded	1	9	5:4	
		2	10	1:11	
		3	12	3:2	
		4	14	4:3	
9B, turn ratio 1/8.57	Both isolated	1	9	1:2.67	1:2.6
		2	11	1:8.57	1:7.6
		3	13	1:3.5	
		4	15	1:6.7	

as the turn ratio approaches unity. It increases when the secondary terminal conditions change as follows: 1. both isolated; 2. short-circuited and isolated; 3. both grounded; 4. one grounded, one isolated. The effect of the secondary is also more important when the secondary is wound in the opposite direction to the primary than when it is wound in the same direction. For instance, the novel and interesting fact is revealed that the fundamental frequency for TC 8B is half the value for TC 8A, when both secondary terminals are grounded.

4. The ratios of the natural frequencies show less variation than the absolute values. For instance, the ratio of the second harmonic to the fundamental is the same whether the secondary is absent or present with both terminals grounded, despite variations of the order of 2.5 to 1 in the frequency values. This is because the sum of the primary ampere turns is zero for these modes of oscillation. The ratio of the second to the first harmonic is reduced by the presence of the secondary with isolated terminals, and this effect increases as the turn ratio approaches unity. For unity turn ratio the value of the second harmonic is only slightly greater than the value of the first harmonic.

5. If we look at the voltage distributions for TC 8A with both secondary terminals grounded (Figs. 9 and 10) it is seen that both first and second harmonics have the same wave shapes, and correspond approximately to half a sine wave encompassing each winding. However, the secondary amplitude is 5/4 of the primary amplitude for the first harmonic, but only 1/11 for the second. The third-harmonic frequency is a little larger than the second, but its wave shape, Fig. 12, shows that approximately two half sine waves encompass each winding.

6. For taansmission lines the harmonic order is equal to the number of half sine waves "standing" on the winding. This concept is incorrect for single windings with mutual inductance, but may be still used for visualization purposes. For two coupled windings the harmonic order is simply the order in which the natural frequencies appear and cannot be correlated with the number of standing sine waves.

7. The set of symmetrical equations is the same for both secondary terminals isolated or short-circuited and isolated. Also the set of antisymmetrical equations is the same for both terminals grounded or short-circuited and isolated. Thus the natural frequencies for the case of the secondary short-circuited and isolated are obtained from the values computed for the other two conditions.

8. The ratio f_g/f_i of the fundamental frequencies with grounded and isolated neutral is in agreement with the conclusions obtained in the preceding sections of this paper. This ratio is about the same (about 2.4 for air core, 3.4 for iron core) for secondary absent or isolated at both ends, with the exception of TC 8A (unity turn ratio). This ratio becomes considerably less (1.01 to 1.37) when the secondary is short-circuited, and it makes little difference whether the connected terminals are grounded or isolated. When one secondary terminal is isolated and one grounded, this ratio varies between 0.56 and 2.69 and thus in some cases is less than unity. This ratio also depends upon which terminal is grounded, either the terminal adjacent to the primary line end or to the primary neutral end. It is difficult to obtain a physical picture of these extensive variations.

Conclusions

The following conclusions can be drawn from the theoretical and experimental investigation of the oscillations of two coupled windings presented.

1. A method is presented for the determination of the fundamental frequencies and wave shapes of a primary winding with short-circuited secondary. This method is applicable to windings in air and iron core, if the turn ratio is considerably different from unity.

2. An equivalent circuit method is presented for the determination of the fundamental oscillation and of several successive harmonics, valid for two windings in air or on iron core, of any turn ratio, and for many different primary and secondary terminal conditions.

3. When the turn ratio is considerably different from unity, short-circuiting the secondary affects the frequencies with primary neutral isolated, but not the frequencies with primary neutral grounded.

4. In power transformers the ratio of the first natural frequencies with grounded and isolated neutral usually varies between 5 and 12, if the secondary is absent or open-circuited. If the secondary is short-circuited this ratio depends mainly upon the gap between primary and secondary, and usually varies between 1.1 to 1.6, as verified by measurements.

5. The values of the frequencies of two coupled windings with primary neutral isolated decrease gradually as the secondary terminal conditions change as follows: both terminals isolated; short-circuited and isolated; both grounded; one grounded and one isolated.

6. Measured and computed values of the first three harmonics of two coupled windings in air, with turn ratios varying from 1-to-1 to 1-to-9 and for various secondary terminal conditions, were in excellent agreement. The standard deviation of 33 pairs of computed and measured values was 12.8%, of 22 ratios of the second and third harmonic to the fundamental, 9.7%. Satisfactory agreement was obtained for frequencies and wave shapes of two windings with iron core.

7. As the turn ratio approaches unity, the effect of the secondary is more pronounced when the two windings are wound in opposite directions than when they are wound in the same direction.

8. The computation of impulse voltages in a power transformer may be done with good approximation as heretofore, considering only the impulsed winding, provided that the neutral of the impulsed winding is grounded and the turn ratio differs considerably from unity; for instance, is greater than 4 to 1. These conditions hold for most, but not all, practical cases.

9. If the neutral of the impulsed winding is isolated, or if the turn ratio is not substantially different from unity (particularly if the two windings are wound in opposite directions) both windings must be considered for the determination of the impulse voltages in either winding, employing the methods advanced in this paper.

Table VII. Ratio of Fundamental Frequencies with Primary Neutral Grounded and Isolated

Secondary Terminals	Test Condition 6A	6B	7B	8A	8B	9B	10A
Absent	2.38	2.38	2.38	2.38	2.38	3.43	3.43
Both isolated	2.38	2.47	2.33	3.00	2.38	3.22	3.45
Short-circuited and isolated	1.30	1.25	1.16	1.34	1.03	1.26	1.12
Both grounded	1.37	1.28	1.14	1.01	1.04	1.26	
Neutral grounded, line isolated	2.69	2.21	1.56	2.91	1.37		
Line grounded, neutral isolated	2.01	2.50	2.31	0.66	2.14		0.56

Appendix. Two-Element Representation

The voltage drops across the inductances in the circuit of Fig. 8 can be expressed in terms of the winding currents since all inductance elements are assumed to be coupled magnetically.

$$\begin{Vmatrix} V_{pba} \\ V_{pcb} \\ V_{sba} \\ V_{scb} \end{Vmatrix} = \begin{Vmatrix} V_{pa}-V_{pb} \\ V_{pb}-V_{pc} \\ V_{sa}-V_{sb} \\ V_{sb}-V_{sc} \end{Vmatrix} = j\omega \begin{Vmatrix} L_{pp} & M_{p1} & M_{ps1} & M_{ps2} \\ M_{p1} & L_{pp} & M_{ps2} & M_{ps1} \\ M_{ps1} & M_{ps2} & L_{ss} & M_{s1} \\ M_{ps2} & M_{ps1} & M_{s1} & M_{ss} \end{Vmatrix} \times \begin{Vmatrix} I_{p1} \\ I_{p2} \\ I_{s1} \\ I_{s2} \end{Vmatrix} \tag{5}$$

These equations can be inverted to obtain the currents in term of the voltages

$$\begin{Vmatrix} I_{p1} \\ I_{p2} \\ I_{s1} \\ I_{s2} \end{Vmatrix} = \frac{1}{j\omega} \begin{Vmatrix} \Gamma_{pp} & \Gamma_{p1} & \Gamma_{ps1} & \Gamma_{ps2} \\ \Gamma_{p1} & \Gamma_{pp} & \Gamma_{ps2} & \Gamma_{ps1} \\ \Gamma_{ps1} & \Gamma_{ps2} & \Gamma_{ss} & \Gamma_{s1} \\ \Gamma_{ps2} & \Gamma_{ps1} & \Gamma_{s1} & \Gamma_{ss} \end{Vmatrix} \times \begin{Vmatrix} V_{pba} \\ V_{pcb} \\ V_{sba} \\ V_{scb} \end{Vmatrix} \tag{6}$$

To write the nodal equations, the total current flowing away from each node, and associated with an inductive element, must be found in terms of the node voltages

$$\begin{Vmatrix} I_{pal} \\ I_{pbl} \\ I_{pcl} \\ I_{sal} \\ I_{sbl} \\ I_{scl} \end{Vmatrix} = \begin{Vmatrix} I_{p1} \\ I_{p2}-I_{p1} \\ -I_{p2} \\ I_{s1} \\ I_{s2}-I_{s1} \\ -I_{s2} \end{Vmatrix} = \frac{1}{j\omega} \begin{Vmatrix} \Gamma_{pp} & \Gamma_{p1}-\Gamma_{pp} & -\Gamma_{p1} & \Gamma_{ps1} & \Gamma_{ps2}-\Gamma_{ps1} & -\Gamma_{ps2} \\ \Gamma_{p1}-\Gamma_{pp} & 2(\Gamma_{pp}-\Gamma_{p1}) & \Gamma_{p1}-\Gamma_{pp} & \Gamma_{ps2}-\Gamma_{ps1} & 2(\Gamma_{ps1}-\Gamma_{ps2}) & \Gamma_{ps2}-\Gamma_{ps1} \\ -\Gamma_{p1} & \Gamma_{p1}-\Gamma_{pp} & \Gamma_{pp} & -\Gamma_{ps2} & \Gamma_{ps2}-\Gamma_{ps1} & \Gamma_{ps1} \\ \Gamma_{ps1} & \Gamma_{ps2}-\Gamma_{ps1} & -\Gamma_{ps2} & \Gamma_{ss} & \Gamma_{s1}-\Gamma_{ss} & -\Gamma_{s1} \\ \Gamma_{ps2}-\Gamma_{ps1} & 2(\Gamma_{ps1}-\Gamma_{ps2}) & \Gamma_{ps2}-\Gamma_{ps1} & \Gamma_{s1}-\Gamma_{ss} & 2(\Gamma_{ss}-\Gamma_{s1}) & \Gamma_{s1}-\Gamma_{ss} \\ -\Gamma_{ps2} & \Gamma_{ps2}-\Gamma_{ps1} & \Gamma_{ps1} & -\Gamma_{s1} & \Gamma_{s1}-\Gamma_{ss} & \Gamma_{ss} \end{Vmatrix} \times \begin{Vmatrix} V_{pa} \\ V_{pb} \\ V_{pc} \\ V_{sa} \\ V_{sb} \\ V_{sc} \end{Vmatrix} \tag{7}$$

The capacitive currents associated with the various nodes are also (by inspection from Fig. 8)

$$\begin{aligned}
I_{pac} &= I_{pp1}+I_{pag}+I_{ps1} = j\omega\left(\frac{C_{pg}+C_{ps}}{2}+C_{pp}\right)V_{pa}-j\omega C_{pp}V_{pb}-j\omega\frac{C_{ps}}{2}V_{sa} \\
I_{pbc} &= I_{pp2}-I_{pp1}+I_{pbg}+I_{ps2} = j\omega(C_{pg}+C_{ps}+2C_{pp})V_{pb}-j\omega C_{pp}V_{pa}-j\omega C_{pp}V_{pc}-j\omega C_{ps}V_{sb} \\
I_{pcc} &= -I_{pp2}+I_{pcg}+I_{ps3} = j\omega\left(\frac{C_{pg}+C_{ps}}{2}+C_{pp}\right)V_{pc}-j\omega C_{pp}V_{pb}-j\omega\frac{C_{ps}}{2}V_{sc} \\
I_{sac} &= I_{ss1}+I_{sag}-I_{ps1} = j\omega\left(\frac{C_{sg}+C_{ps}}{2}+C_{ss}\right)V_{sa}-j\omega C_{ss}V_{sb}-j\omega\frac{C_{ps}}{2}V_{pa} \\
I_{sbc} &= I_{ss2}-I_{ss1}-I_{ps2}+I_{sbg} = j\omega(C_{sg}+C_{ps}+2C_{ss})V_{sb}-j\omega C_{ss}V_{sa}-j\omega C_{ss}V_{sc}-j\omega C_{ps}V_{pb} \\
I_{scc} &= -I_{ss2}+I_{scg}-I_{ps3} = j\omega\left(\frac{C_{sg}+C_{ps}}{2}+C_{ss}\right)V_{sc}-j\omega C_{ss}V_{sb}-j\omega\frac{C_{ps}}{2}V_{pc}
\end{aligned} \tag{8}$$

The nodal equations are formed by simply stating that the sum of the currents flowing away from any node is zero

$$I_{pal}+I_{pac}=0 \qquad I_{pbl}+I_{pbc}=0 \qquad I_{pcl}+I_{pcc}=0 \qquad I_{sal}+I_{sac}=0 \qquad I_{sbl}+I_{sbc}=0 \qquad I_{scl}+I_{scc}=0 \tag{9}$$

Since each inductive term contains a factor $1/j\omega$, the equations can be simplified by multiplying both members by $j\omega$. All capacitive terms will have a factor $\lambda=\omega^2$. If the following abbreviations are used

$$\begin{aligned}
C_{p1} &= \frac{C_{pg}+C_{ps}}{2}+C_{pp}; \quad C_{p2}=C_{pg}+C_{ps}+2C_{pp} \\
C_{s1} &= \frac{C_{sg}+C_{ps}}{2}+C_{ss}; \quad C_{s2}=C_{sg}+C_{ps}+2C_{ss}
\end{aligned} \tag{10}$$

then there is the following system of equations

$$\begin{Vmatrix} 0 \\ 0 \\ 0 \\ 0 \\ 0 \\ 0 \end{Vmatrix} = \begin{Vmatrix} \Gamma_{pp}-C_{p1}\lambda & \begin{matrix}\Gamma_{p1}-\Gamma_{pp} \\ +C_{pp}\lambda\end{matrix} & -\Gamma_{p1} & \Gamma_{ps1}+\frac{C_{ps}}{2}\lambda & \Gamma_{ps2}-\Gamma_{ps1} & -\Gamma_{ps2} \\ \begin{matrix}\Gamma_{p1}-\Gamma_{pp} \\ +C_{pp}\lambda\end{matrix} & \begin{matrix}2(\Gamma_{pp}-\Gamma_{p1}) \\ -C_{p2}\lambda\end{matrix} & \begin{matrix}\Gamma_{p1}-\Gamma_{pp} \\ +C_{pp}\lambda\end{matrix} & \Gamma_{ps2}-\Gamma_{ps1} & \begin{matrix}2(\Gamma_{ps1}-\Gamma_{ps2}) \\ +C_{ps}\lambda\end{matrix} & \Gamma_{ps2}-\Gamma_{ps1} \\ -\Gamma_{p1} & \begin{matrix}\Gamma_{p1}-\Gamma_{pp} \\ +C_{pp}\lambda\end{matrix} & \Gamma_{pp}-C_{p1}\lambda & -\Gamma_{ps2} & \Gamma_{ps2}-\Gamma_{ps1} & \Gamma_{ps1}+\frac{C_{ps}}{2}\lambda \\ \Gamma_{ps1}+\frac{C_{ps}}{2}\lambda & \Gamma_{ps2}-\Gamma_{ps1} & -\Gamma_{ps2} & \Gamma_{ss}-C_{s1}\lambda & \begin{matrix}\Gamma_{s1}-\Gamma_{ss} \\ +C_{ss}\lambda\end{matrix} & -\Gamma_{s1} \\ \Gamma_{ps2}-\Gamma_{ps1} & \begin{matrix}2(\Gamma_{ps1}-\Gamma_{ps2}) \\ +C_{ps}\lambda\end{matrix} & \Gamma_{ps2}-\Gamma_{ps1} & \begin{matrix}\Gamma_{s1}-\Gamma_{ss} \\ +C_{ss}\lambda\end{matrix} & \begin{matrix}2(\Gamma_{ss}-\Gamma_{s1}) \\ -C_{s2}\lambda\end{matrix} & \begin{matrix}\Gamma_{s1}-\Gamma_{ss} \\ +C_{ss}\lambda\end{matrix} \\ -\Gamma_{ps2} & \Gamma_{ps2}-\Gamma_{ps1} & \Gamma_{ps1}+\frac{C_{ps}}{2}\lambda & -\Gamma_{s1} & \begin{matrix}\Gamma_{s1}-\Gamma_{ss} \\ +C_{ss}\lambda\end{matrix} & \Gamma_{ss}-C_{s1}\lambda \end{Vmatrix} \times \begin{Vmatrix} V_{pa} \\ V_{pb} \\ V_{pc} \\ V_{sa} \\ V_{sb} \\ V_{sc} \end{Vmatrix} \tag{11}$$

Two new sets of equations can be formed from these by adding or subtracting equations in *pa* and *pc*, *sa*, and *sc* and by multiplying the equations in *pb* and *sb* by two in order to retain symmetry

$$\left\| \begin{array}{c} 0 \\ 0 \\ 0 \\ 0 \\ 0 \\ 0 \end{array} \right\| = \left\| \begin{array}{cccccc} \Gamma_{pp}-\Gamma_{p1}-C_{p1}\lambda & 2(\Gamma_{p1}-\Gamma_{pp})+2C_{pp}\lambda & \Gamma_{ps1}-\Gamma_{ps2}+\frac{C_{ps}}{2}\lambda & 2(\Gamma_{ps2}-\Gamma_{ps1}) & & \\ 2(\Gamma_{p1}-\Gamma_{pp})+2C_{pp}\lambda & 4(\Gamma_{pp}-\Gamma_{p1})-2C_{p2}\lambda & 2(\Gamma_{ps2}-\Gamma_{ps1}) & 4(\Gamma_{ps1}-\Gamma_{ps2})+2C_{ps}\lambda & & \\ \Gamma_{ps1}-\Gamma_{ps2}+\frac{C_{ps}}{2}\lambda & 2(\Gamma_{ps2}-\Gamma_{ps1}) & \Gamma_{ss}-\Gamma_{s1}-C_{s1}\lambda & 2(\Gamma_{s1}-\Gamma_{ss})+2C_{ss}\lambda & & \\ 2(\Gamma_{ps2}-\Gamma_{ps1}) & 4(\Gamma_{ps1}-\Gamma_{ps2})+2C_{ps}\lambda & 2(\Gamma_{s1}-\Gamma_{ss})+2C_{ss}\lambda & 4(\Gamma_{ss}-\Gamma_{s1})-2C_{s2}\lambda & & \\ & & & & \Gamma_{pp}+\Gamma_{p1}-C_{p1}\lambda & \Gamma_{ps1}+\Gamma_{ps2}+\frac{C_{ps}}{2}\lambda \\ & & & & \Gamma_{ps1}+\Gamma_{ps2}+\frac{C_{ps}}{2}\lambda & \Gamma_{ss}+\Gamma_{s1}-C_{s1}\lambda \end{array} \right\| \times \left\| \begin{array}{c} V_{pa}+V_{pc} \\ V_{pb} \\ V_{sa}+V_{sc} \\ V_{sb} \\ V_{pa}-V_{pc} \\ V_{sa}-V_{sc} \end{array} \right\| \qquad (12)$$

References

1. Natural Frequencies of Coils and Windings Determined by Equivalent Circuit, P. A. Abetti, F. J. Maginniss. *AIEE Transactions*, vol. 72, pt. III, June 1953, pp. 495–504.

2. Fundamental Oscillations of Coils and Windings, P. A. Abetti, F. J. Maginniss. *AIEE Transactions*, vol. 73, pt. III, Feb. 1954, pp. 1–10.

3. Transient Oscillations of Mutually Coupled Windings, L. V. Bewley. *AIEE Transactions*, vol. 51, June 1932, pp. 299–308; discussion pp. 321–28.

4. Oscillations of a High-Voltage Secondary Winding, A. Boyajian. *AIEE Transactions*, vol. 65, 1946, pp. 1010–20.

5. Oscillatory Transient in Unloaded High-Voltage Windings of Transformers When Voltage Is Applied Suddenly on the Low-Voltage Side, J. Vitins. *Archiv für Elektrotechnik*, Berlin, Germany, vol. 41, 1954, pp. 196–209.

6. Inductance Calculations (book), F. W. Grover. D. Van Nostrand and Company, Inc., New York, N. Y., 1946.

7. On the Calculation of Overvoltages in Transformer Windings, V. A. Karasev, A. V. Sklyanin. *Elektrichestvo*, Moscow, USSR, no. 11, 1952, pp. 46–50.

8. Field Theory of Wave Propagation Along Coils, H. Poritsky, P. A. Abetti, R. P. Jerrard. *AIEE Transactions*, vol. 72, pt. III, Oct. 1953, pp. 930–39.

9. Solution of Systems of Linear Equations by Minimized Iterations, C. Lanczos. *Journal of Research*, National Bureau of Standards, Washington, D. C., vol. 49, 1952, pp. 33–53.

10. An Iteration Method for the Solution of the Eigenvalue Problem of Linear Differential and Integral Operators, C. Lanczos. *Journal of Research*, National Bureau of Standards, Washington, D. C., vol. 45, 1950, pp. 255–82.

High-Current Testing of Air-Disconnect Switches

BELGRAVE F. GOSTIN
MEMBER AIEE

TENNESSEE VALLEY Authority's rapidly expanding power system and the construction of several large-capacity steam plants have increased the incidence of short-circuit currents to an extent considerably greater than formerly experienced at the Authority or elsewhere. This requires new features in the design and performance of air-disconnect switches which are used to isolate breakers, bus sections, and transmission lines.

The possible magnitude of the fault current caused by a close-in fault to one of the new steam plants has reached a value that is impossible for at least some switch manufacturers to duplicate in their test laboratories. They find it more and more difficult to design a switch on paper that will successfully meet the rigorous requirements.

Since manufacturers could not always supply the information required for application to Tennessee Valley Authority's system, it was decided that a high-current test laboratory should be built and a series of tests undertaken on a number of various makes of disconnect switches in order to obtain the desired data under actual physical conditions.

Scope of Tests

A number of manufacturers were informed of the proposed tests and invited to submit three groups of switches for test purposes as follows:

Group 1, consisting of standard 161-kv switches, rated at 1,200 and 1,600 amperes.

Group 2, consisting of standard 69-kv switches, rated at 600 amperes.

Group 3, consisting of standard 46-kv switches, rated at 600 amperes.

In each group an alternate design switch, if desired, could be submitted.

The proposed tests were planned as follows:

1. In all cases there would be applied to the switch under test a magnetic force equivalent to that which would occur at normal phase spacing.
2. In all cases the test current applied to the switches would be a fully offset wave (maximum transient).
3. All 161-kv switches would be subjected to an initial test current equivalent to a short-circuit fault on a 10,000-mva system.
4. A temperature test would then be made on the switch to determine the extent of damage and the adequacy of design.
5. The switch would then be retested at a value of current equivalent to a short-circuit fault on a 15,000-mva system or it might be tested to destruction in order to determine its ultimate capacity.
6. All 69-kv and 46-kv switches would be tested at values of current recommended by National Electrical Manufacturers Association standards.

Since it was necessary to build the complete high-current laboratory from existing or readily obtainable material, it seemed advisable first to make such laboratory tests as would be required to determine the configuration of a single-

Paper 55-13, recommended by the AIEE Switchgear Committee and approved by the AIEE Committee on Technical Operations for presentation at the AIEE Winter General Meeting, New York, N. Y., January 31–February 4, 1955. Manuscript submitted September 20, 1954; made available for printing October 29, 1954.

Belgrave F. Gostin is with the Tennessee Valley Authority, Chattanooga, Tenn.

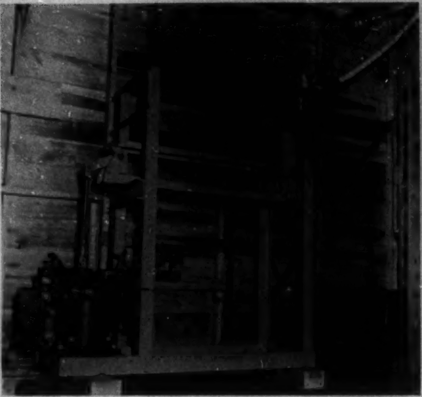

Fig. 1 (left). High-speed closing switch. Spring-operated, solenoid reset switch is capable of closing its contacts in 5 cycles, ±10 degrees, after initiating the closing operation

Fig. 3 (above). General view of high-current bus and supporting structure. All three busses are adjustable in length and separation

phase high-current bus to meet the test specifications.

Preliminary Design

The first requirement to be considered was that of providing for the fully offset test current. This could be obtained only by closing the power supply circuit at zero voltage on the rising half-cycle. Investigation disclosed that this requirement could be met by a spring-operated solenoid-reset air switch of special design. This switch, Fig. 1, was rated 12 kv at 1,200 amperes, it would close in 5 cycles ±10 degrees, and would reset in 20 cycles. The development laboratory then built an electronic timer and sequence operator which would close this switch at the proper instant and provide for reclosing automatically any desired number of times.

The next consideration was to design a bus structure which would act as a current limiter and at the same time provide the required magnetic forces. The dimensions of this bus structure were worked out from laboratory tests on a scale model operated at greatly reduced current. It was determined that this structure should consist of three parallel busses arranged so that the center bus would be fixed and the two outside busses could be varied in spacing from a 1-foot minimum to a 5-foot maximum. Also, there would be provided a short-circuiting bar which could be placed anywhere between 33 feet and 51 feet from the transformer end of the bus.

A 12-foot test section, Fig. 2, was provided in the center bus, within the 33-foot minimum length, in which would be installed the disconnect switches under test. By varying the length of bus and the spacing, the loop impedance could be set to limit the current at any desired value. Also, by setting the two outside busses at different distances from the center bus, any desired resultant force could be applied on the center bus and hence to the disconnect switch under test; see Figs. 3 and 4.

There were available two furnace transformers each rated 2,775 kva at 12 kv to 190-volt 17,000-ampere continuous duty. These transformers could be connected in series on the low-voltage side and, on a momentary basis, would supply a test current of 150,000-amperes rms into the bus structure. It remained then to clear the fault, once it had been established by the high-speed air switch. This was ac-

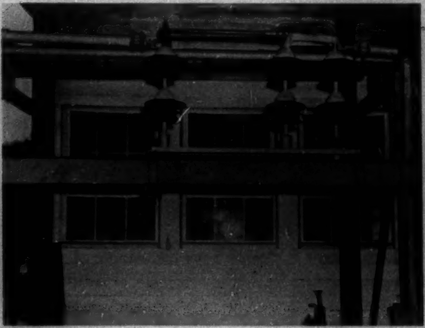

Fig. 2. Test section of bus showing a 46-kv 600-ampere disconnect switch installed and ready for test. Test controls are located in the room directly behind the switch

Fig. 4. Closeup of high-current bus. Note short-circuiting bar in center and backup supports on the two outside busses. Center bus is supported only at the extreme ends

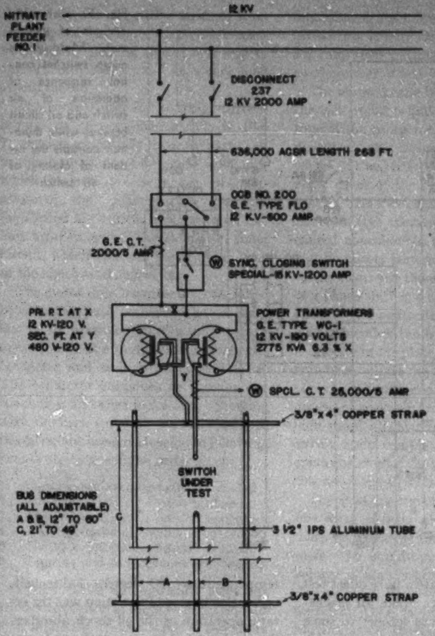
12 KV
NITRATE PLANT FEEDER NO. 1
DISCONNECT 237 12 KV 2000 AMP
636,000 ACSR LENGTH 268 FT.
OCB NO. 200 G.E. TYPE FLO 12 K.V-600 AMP.
G.E. C.T. 2000/5 AMP.
Ⓦ SYNC. CLOSING SWITCH SPECIAL-15 KV-1200 AMP
PRI. P.T. AT X 12 KV-120 V.
SEC. P.T. AT Y 480 V-120 V.
X
POWER TRANSFORMERS G.E. TYPE WC-1 12 KV-190 VOLTS 2775 KVA 6.3 % X
Y
Ⓦ SPCL. C.T. 25,000/5 AMP
3/8"x4" COPPER STRAP
SWITCH UNDER TEST
BUS DIMENSIONS (ALL ADJUSTABLE) A & B, 12" TO 60" C, 21' TO 49'
C
3 1/2" IPS ALUMINUM TUBE
A
B
3/8"x4" COPPER STRAP

Fig. 5 (left). Schematic diagram of test bus and power supply. All testing was done on single-phase basis. Maximum momentary current approached 200,000 - ampere peak

Fig. 6 (right). Circuit impedance curves for high-current bus. From these curves bus configuration could be determined to give any desired short-circuit current, and resultant magnetic forces could be calculated quickly

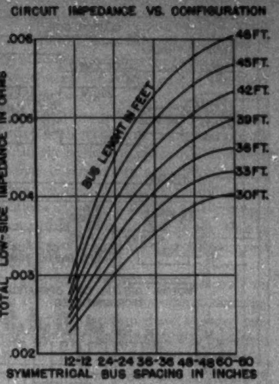

complished by the use of a 15-kv 600-ampere oil circuit breaker which had a momentary rating of 10,000 amperes.

Finally, it was necessary to provide suitable instrumentation to accomplish two things. First, a positive indication was needed of the point on the 60-cycle voltage wave at which the high-speed air switch closed. This was attained by using a double-channel direct-writing Brush oscillograph with one pen recording the transformer low-side fault current, and the other the transformer low-side voltage.

Second, there had to be accurate measurement of the fault current, the power transformer high and low voltages, and the air switch trip voltage. These measurements were attained with the use of a *PM-13* photographic-type oscillograph connected to a 25,000/5-ampere current transformer for recording the fault current, and to suitable potential transformers for recording the power transformer voltages. Later it was found that valuable additional information could have been obtained from a single-phase watt galvanometer connected to record the total power into the test bus. However, such a galvanometer was not available.

In addition to this instrumentation, two Bell and Howell type-*GSAP* 16-millimeter automatic cameras were mounted in the test bay of the bus structure and were set to photograph the hinge and break ends of the disconnects under test. These cameras operated successfully at their maximum speed of 62 frames per second. However, a higher speed, such as 180 or 240 frames per second, would have been quite an advantage.

Test Bus Structure

The test bus shown schematically in Fig. 5 and described briefly in the foregoing was constructed of $3^1/_2$ -inch aluminum tubing with 3/8 by 4-inch copper used for the short-circuiting bar and the transformer-end jumper.

The force equation for this double loop arrangement, operating single-phase, is

$$F=\frac{43.2(I_cI_1)}{D_1(10^7)}-\frac{43.2(I_cI_2)}{D_2(10^7)}\text{ pounds-per-foot length}\quad(1)$$

where

I = rms current of first half-cycle
D = spacing of bus, inches
F = force developed in pounds-per-foot length of bus

The effective impedance of this double loop, including transformer connections, was measured at reduced current and plotted as shown in Fig. 6. From this family of curves the configuration could be determined to provide a given fault current. Also, the data obtained during impedance measurements gave the division of current through the two outside busses for all symmetrical the nonsymmetrical spacings. Some of these data are reproduced in Table I.

Existing disconnect switches installed on the 161-kv system were designed for a

Table I. Part of Test Data Obtained During Original Calibration of High-Current Bus

Length, Feet	Spacing, Inches	North Bus, Amperes	Center Bus, Amperes	South Bus, Amperes	Bus, Volts	Bus, Impedance
45	36-36	1,098.5	2,146	1,098.4	10.60	0.00494
42	36-36	1,142.0	2,292	1,143.8	10.36	0.00452
39	36-36	1,168.9	2,342	1,172.7	9.96	0.00425
36	36-36	1,130.5	2,462	1,232.7	9.95	0.00404
33	36-36	1,280.5	2,577	1,260.0	9.89	0.00384
30	36-36	1,378.0	2,757	1,370.8	9.37	0.00340
30	36-32	1,355.6	2,802	1,440.4	9.30	0.00332
30	36-28	1,316.9	2,842	1,515.5	9.18	0.00323
30	36-24	1,269.0	2,892	1,609.5	9.00	0.00311
30	24-24	1,521.0	3,037	1,500.0	8.79	0.00289

These tests were made at greatly reduced current to simplify instrumentation.

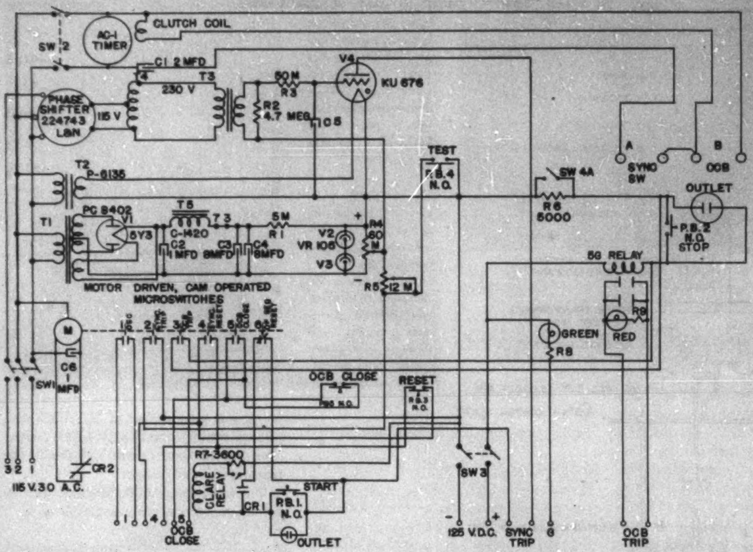
CLUTCH COIL
AC-1 TIMER
SW 2
C1 2 MFD
4
T3
230 V
50 M
R3
V4
KU 676
PHASE SHIFTER 224743 L&N
115 V
R2 4.7 MEG
1 0 5
T2
P-6135
TEST
P.B.4 N.O.
SW 4A
R6 5000
A
SYNC SW
B
OCB
OUTLET
T1
PC 8402
V1
5Y3
T5
C-1420
7 3
C2 1 MFD
C3 8MFD
C4 8MFD
5M
R1
+
V2
VR 105
V3
R4 60 M
−
R5 12 M
P.B.2 N.O. STOP
56 RELAY
MOTOR DRIVEN, CAM OPERATED MICROSWITCHES
M
1
2
3
4
5
6
GREEN
R8
RED
R9
C6 1 MFD
SW1
OCB CLOSE
P.B. N.O.
RESET
P.B.3 N.O.
3 2 1
CR2
115 V. 3Φ A.C.
R7-3600
CLARE RELAY
CR1
START
P.B.1. N.O.
OUTLET
SW 3
1
4
5
OCB CLOSE
−
+
125 V.D.C.
SYNC TRIP
G
OCB TRIP

Fig. 7. Schematic diagram of control unit. Motor-driven micro switches control sequence of operation of air switch and oil circuit breaker while thyratron controls the instant of closing of air switch

momentary fault current of 40,000 amperes rms, and assuming a symmetrical 3-phase fault, the magnetic force developed is 55 pounds per foot of length of bus or switch blade. When this value of force, the desired fault current, and the division of current corresponding to an arbitrary selection of bus spacing were substituted back into force equation 1, it was determined that the bus configuration for a 60,000-ampere momentary test would be: length, 33 feet; spacing, 36/27 inches.

For momentary tests on the 46- and 69-kv disconnect switches it was found that by disconnecting one of the outside busses and moving the other to 5-foot spacing (standard for this operating voltage) the available transformers would supply wthout difficulty the desired current into this relatively large loop. Thus, all tests on these two groups of switches were made at standard phase-spacing and National Electrical Manufacturing Association current values. In the final analysis, the exact value of current reached on each test shot was calculated from the *PM-13* oscillograph films according to the AIEE standard No. *22.*[1]

Controls and Instrumentation

The design of all control equipment was based on the premise that the high-speed air switch would be consistent in its operation and would initiate a fully offset test current on every shot. Like all mechanisms, this switch was subject to some variations and required considerable maintenance to keep it in top condition.

It was subject to variation caused by ambient temperature changes and in cold weather (30 to 40 degrees Fahrenheit) would vary as much as 1/2 cycle in its closing times. This variation was finally eliminated by enclosing the switch in a plywood housing and maintaining its temperature at 90 degrees Fahrenheit.

Another source of variation was the erratic operation of the oil shock absorber. On single test shots spaced several minutes apart, the oil shock absorber is satisfactory. However, for quick reclosing shots, spaced 2 or 3 seconds apart, this type of shock absorber is very erratic because of the presence of air bubbles in the oil. An air-damped type of shock absorber would be very much better for this mode of operation.

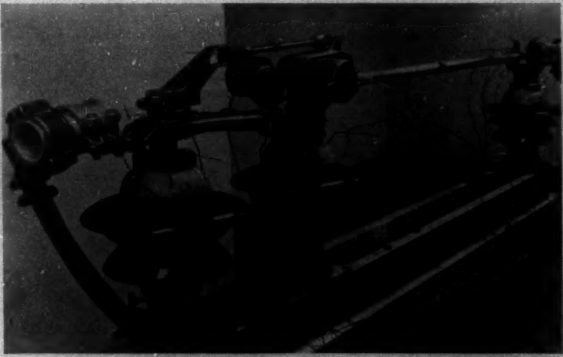

Fig. 8. Temperature test on a 161-kv 1,200-ampere disconnect switch showing placement of thermocouples. Current regulator and test instruments located outside test room

However, for the entire series of tests covering 560 test shots the average transient factor (ratio of rms of first loop to rms of steady state) was 1.48, a very good record indeed.

The control unit for the high-current laboratory, shown schematically in Fig. 7, consists essentially of two parts: 1. a synchronous motor-driven contactor which controls the sequence of operation of the oscillographs, cameras, high-speed air switch, and 12-kv oil circuit breaker, and 2. the thyratron timer circuit, which controls the tripping time of the high-speed air switch.

The motor driven contactor, controlled by a starting push button and a lock-in relay is so arranged that a momentary operation of the push button starts the contactor and seals in its control relay. The contactor continues to run for one revolution and then locks out. Starting with the high-speed air switch open and the oil circuit breaker closed, the following events take place in the order given:

1. Cameras and oscillographs are started.
2. The high-speed air switch is closed.
3. The 12-kv oil circuit breaker is opened.
4. The high-speed air switch is opened.
5. The 12-kv oil circuit breaker is closed.
6. Cameras and oscillographs are stopped.

The contactor automatically locks out at the completion of these events. Should it be desired to make a series of test shots representing the automatic reclosing of a breaker, it is only necessary to hold the starting push button closed for the desired number of test shots.

The elapsed time between reclosings of the test circuit is limited to the operating time of the contactor. In the equipment described, this operating time was 80 cycles. It was based on the over-all operating times of the high-speed air switch and the 12-kv oil circuit breaker. Any decrease in this operating time would have caused considerable difficulty in obtaining the proper sequence of events.

The electronic timer consists essentially of a phase shifter, a peaking transformer, and a grid-controlled thyratron tube. The trip coil of the high-speed air switch is directly in the plate circuit of the thyratron tube. Since the thyratron plate supply is obtained from a station battery, it is necessary to use an auxiliary switch on the high-speed air switch to open the plate circuit upon completion of the tripping operation so that the grid bias may regain control of the thyratron.

The peaking transformer converts the sine wave grid signal voltage to a single sharp pulse for each half-cycle of the sine wave. In stand-by operation the bias voltage is always greater than the positive pulse of signal voltage and thus the thyratron tube is blocked. When the starting push button is depressed, the grid bias voltage is reduced to a value which is less than the positive pulse of signal voltage and thus the thyratron tube fires, closing the trip circuit to the high-speed air switch.

The positive pulse of signal voltage is shifted with respect to the sine wave 12-kv supply by means of the phase shifter, making it possible to adjust the over-all circuit so that the high-speed air switch contacts close just as the 12-kv supply goes through zero. This is the setting which gives maximum transient current into the test bus.

Temperature tests were made only on the 161-kv group of disconnect switches. The switches were operated at rated current, and the temperature was measured at from 15 to 20 points on the current-carrying parts of the switch by means of copper-constantan thermocouples and a portable potentiometer. The test current applied to the disconnect switch was supplied through an induction regulator and a loading transformer having a low-voltage winding rated 5 volts at 2,000 amperes. Fig. 8 shows one of the disconnect switches set up on temperature test. Some of the results of these tests will be discussed in a subsequent article.

Reference

1. AIR SWITCHES, INSULATOR UNITS, AND BUS SUPPORTS. *AIEE Standard No. 22*, July 1952.

Effect of Synchronous-Machine Transient Rotor Saliency on Changes in Terminal Voltage

C. CONCORDIA
FELLOW AIEE

Synopsis: This paper presents the results of calculations made to determine the magnitude of the error in measurements of changes in bus voltages resulting from the assumption of a symmetric-rotor synchronous machine as usually made in transient stability studies on the a-c network analyzer. It is found that in some cases the effect of transient rotor saliency is important. (See the Appendix for explanation of terms.) In such cases the curves of this paper may be used to help estimate the magnitude of the error involved.

IN MOST studies of power system disturbances made on the a-c network analyzer, the transient rotor saliency of the synchronous machines is neglected. The validity of this assumption is well established. However, in some cases it has been desirable to measure the variations in several of the bus voltages during the disturbance. When the bus is electrically near to a synchronous machine (in the limit, when the voltage in question is at the terminals of one of the synchronous machines) the validity of neglecting saliency may be questioned. The paper presents curves of voltage variation at the terminals of a synchronous machine both including and neglecting machine saliency. From these curves, an estimate of the error involved in particular cases may be obtained.

System Considered

The system analyzed consists of a synchronous machine, tied through reactance to an infinite bus. Three initial load conditions on the synchronous machine were considered:

1. Full load, unit terminal voltage, 0.8 power factor (pf).
2. Full load, unit terminal voltage, 1.0 pf.
3. Zero load, unit terminal voltage, zero current.

Paper 55-3, recommended by the AIEE Rotating Machinery Committee and approved by the AIEE Committee on Technical Operations for presentation at the AIEE Winter General Meeting, New York, N. Y., January 31-February 4, 1955. Manuscript submitted March 24, 1954; made available for printing October 27, 1954.

C. CONCORDIA is with the General Electric Company, Schenectady, N. Y.

The calculations upon which this paper is based were made by Mrs. M. S. Dyrkacz of the General Electric Company.

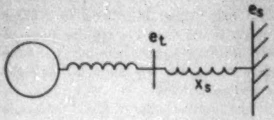

Fig. 1. System diagram

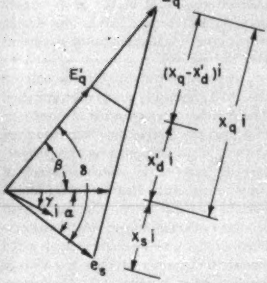

Fig. 2. Voltage phasor diagram

The initial tie-line reactance was taken as 0, 0.2, 0.4, and 0.8 per unit on the machine base. The direct-axis reactance x_d' of the machine is 0.3 per unit. (This will almost always be interpreted as the transient reactance.) The quadrature-axis reactance x_q of the machine was given three values: 0.3 (no saliency, to correspond to the usual assumption made in transient stability studies), 0.6, and 1.2. These three values of x_q should cover the range found in most applications. The value of x_d' is larger than may be found at the terminals of a turbine-generator, but is taken as being possibly the most nearly representative value for a range of cases. A schematic diagram of the system is shown in Fig. 1. In this figure, e_t is the machine terminal voltage and e_s is the equivalent voltage back of the system reactance x_s.

The voltage phasor diagram of this system is shown in Fig. 2. From this diagram the initial values of system voltage e_s and machine field flux E_q' may be determined. Both e_s and E_q' are assumed constant during the subsequent disturbance, and the resulting value of terminal voltage e_t calculated. Two kinds of disturbances are considered:

1. The angle δ of the machine relative to the system is varied, corresponding to a swing of the machine.
2. The system reactance x_s is varied, corresponding to the switching out or in of some line or other part of the system.

Method of Calculation

The initial conditions are calculated from the phasor diagram of Fig. 2 by the relations

$$e_s^2=(e_t-x_si\sin\gamma)^2+(x_si\cos\gamma)^2 \tag{1}$$

$$E_q^2=(e_t+x_qi\sin\gamma)^2+(x_qi\cos\gamma)^2 \tag{2}$$

where γ = initial power factor angle.

$$\alpha=\tan^{-1}\frac{x_si\cos\gamma}{e_t-x_si\sin\gamma} \tag{3}$$

$$\beta=\tan^{-1}\frac{x_qi\cos\gamma}{e_t+x_qi\sin\gamma} \tag{4}$$

$$\delta=\alpha+\beta \tag{5}$$

$$i_d=i\sin(\beta+\gamma) \tag{6}$$

$$E_q'=E_q-i_d(x_q-x_d') \tag{7}$$

The terminal voltage e_t following the disturbance is calculated, with E_q' and e_s as previously determined, from the relations

$$i_d=\frac{E_q'-e_s\cos\delta}{x_d'+x_s} \tag{8}$$

$$i_q=\frac{e_s\sin\delta}{x_q+x_s} \tag{9}$$

$$i^2=i_d^2+i_q^2 \tag{10}$$

$$\epsilon=\tan^{-1}\frac{i_d}{i_q} \tag{11}$$

$$\phi=\delta-\epsilon=\text{angle between } i \text{ and } e_s \tag{12}$$

$$e_t^2=(e_s-x_si\sin\phi)^2+(x_si\cos\phi)^2 \tag{13}$$

where either x_s or δ is changed from the initial conditions.

Also, the power is

$$e_si\cos\phi \tag{14}$$

Results

The principal results are shown in Figs. 3 through 19.

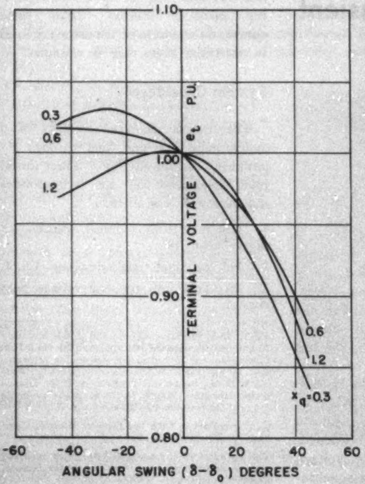

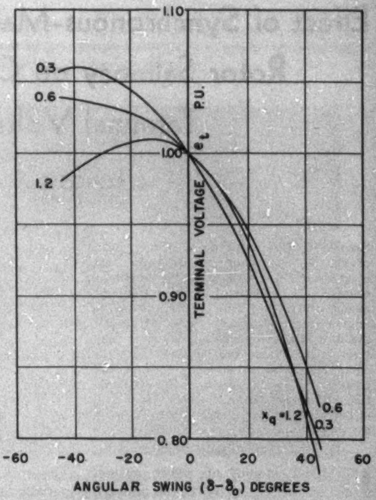

Fig. 3 (left) and Fig. 4 (right). Effect of synchronous-machine transient saliency on variation of terminal voltage with angle

Initial conditions: e_t=1.0; pf=1.0; i=1.0

In Fig. 3, x_s=0.2; for x_q=0.3, δ_0=28.0 degrees (°); for x_q=0.6, δ_0=42.3°; for x_q=1.2, δ_0=61.5°

In Fig. 4, x_s=0.4; for x_q=0.3, δ_0=38.5°; for x_q=0.6, δ_0=52.8°; for x_q=1.2, δ_0=72.0°

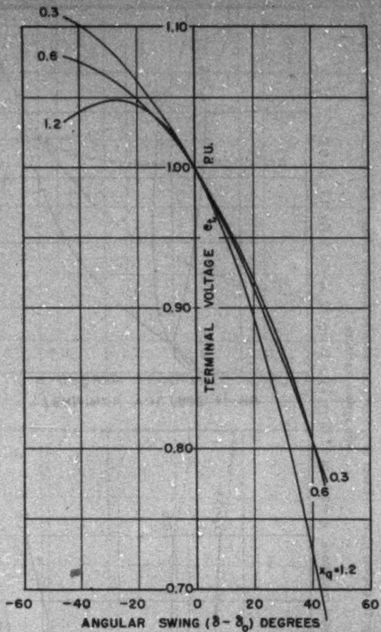

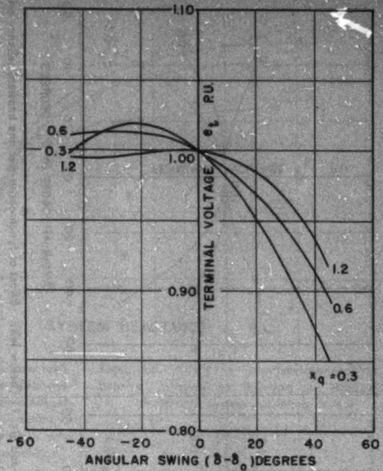

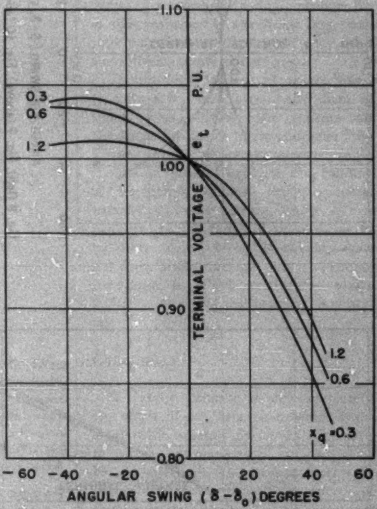

Fig. 5 (above left), Fig. 6 (above right), and Fig. 7 right). Effect of synchronous-machine transient saliency on variation of terminal voltage with angle

Initial conditions for Fig. 5: $e_t=1.0$, pf=1.0, $i=1.0$
In Fig. 5, $x_s=0.8$; for $x_q=0.3$, $\delta_0=55.4°$; for $x_q=0.6$, $\delta_0=69.6°$; for $x_q=1.2$, $\delta_0=88.9°$

Initial conditions for Figs. 6 and 7: $e_t=1.0$; pf=0.8; $i=1.0$
In Fig. 6, $x_s=0.2$; for $x_q=0.3$, $\delta_0=21.8°$; for $x_q=0.6$, $\delta_0=29.7°$; for $x_q=1.2$, $\delta_0=39.5°$
In Fig. 7, $x_s=0.4$; for $x_q=0.3$, $\delta_0=34.3°$; for $x=_q0.6$, $\delta_0=42.3°$; for $x_q=1.2$, $\delta_0=52.0°$

Figs. 3 through 11 show transient terminal voltage e_t as a function of angular swing $\delta-\delta_0$ (from the initial value δ_0) for various degrees of saliency.

Figs. 3 through 5, for unity terminal pf before the disturbance, indicate that the actual transient change of terminal voltage for a salient-pole machine is somewhat smaller than that obtained neglecting saliency when the system reactance is fairly small ($x_s=0.2$, Fig. 3), but may be slightly greater for positive angular swings when the system reactance is large ($x_s=0.8$, Fig. 5).

Figs. 6 through 8, for 0.8 terminal pf (overexcited) before the disturbance, show that the system behaves qualitatively just the same as for unity pf.

Figs. 9 through 11 for zero initial load and current show, first, that for small angular changes the voltage changes are negligible and, second, that for larger angular changes consideration of rotor saliency actually may cause the voltage to increase rather than decrease. Thus, neglect of saliency may in this case actually cause the indicated voltage change to be of the wrong sign.

Figs. 12 through 19 show the transient terminal voltage e_t as a function of system reactance x_s (with the angle δ fixed), as the system reactance is changed (presumably by switching in the network) to various values. The point on each curve corresponding to the initial reactance (before switching) is circled for convenient identification. Note that the case is now included of system reactance $x_s=0$. This was, of course, not necessary when the angular swing was being considered, since then $e_t=e_s$ always. On the other hand, the case of zero initial load and current is now left out, since then a sudden change of system reactance does not produce any change in terminal voltage.

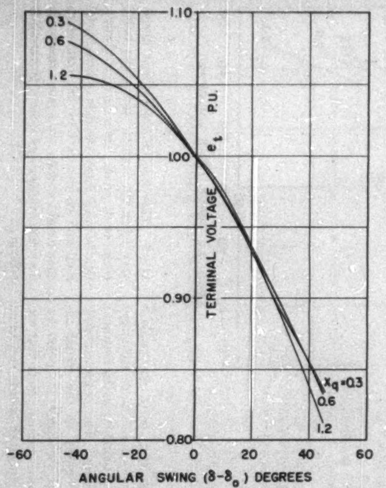

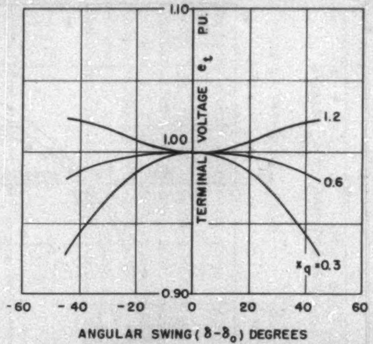

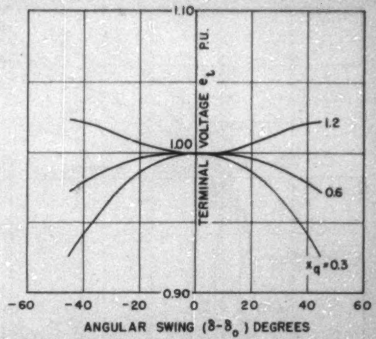

Fig. 8 (left), Fig. 9 (above), Fig. 10 (above right), and Fig. 11 (below left). Effect of synchronous-machine transient saliency on variation of terminal voltage with angle

Initial conditions for Fig. 8: $e_t=1.0$; pf=0.8; i=1.0. Initial conditions for Figs. 9, 10, and 11: $e_t=1.0$; $\delta_0=0$; i=0. Initial conditions for Fig. 8, $x_e=0.8$; for $x_q=0.3$, $\delta_0=62.4°$; for $x_q=0.6$, $\delta_0=70.3°$; for $x_q=1.2$, $\delta_0=80.1°$. In Fig. 9, $x_e=0.2$; in Fig. 10, $x_e=0.4$; in Fig. 11, $x_e=0.8$

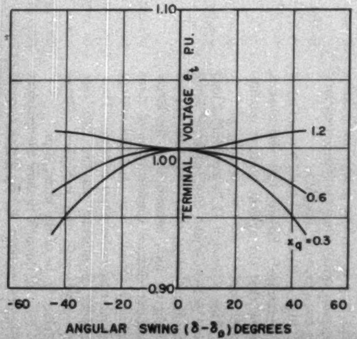

Fig. 12 (below) and Fig. 13 (below right). Effect of synchronous-machine transient saliency on variation of terminal voltage with system reactance

Initial conditions: $e_t=1.0$; pf=1.0; i=1.0. In Fig. 12, $x_e=0$; in Fig. 13, $x_e=0.2$

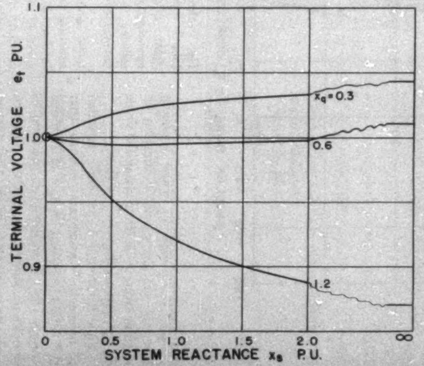

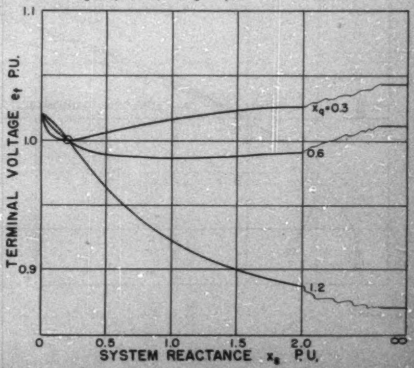

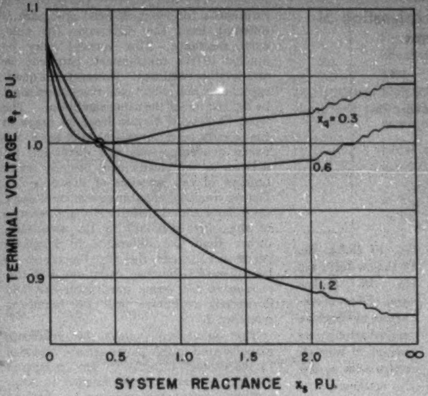

Fig. 14 (above left). Effect of synchronous-machine transient saliency on variation of terminal voltage with system reactance

Initial conditions: $e_t=1.0$; pf=1.0; i=1.0

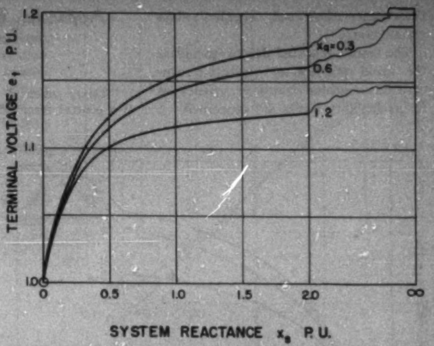

Figs. 16. Effect of synchronous-machine transient saliency on variation of terminal voltage with system reactance; $x_e=0$

Initial conditions: $e_t=1.0$; pf=0.8; I=1.0

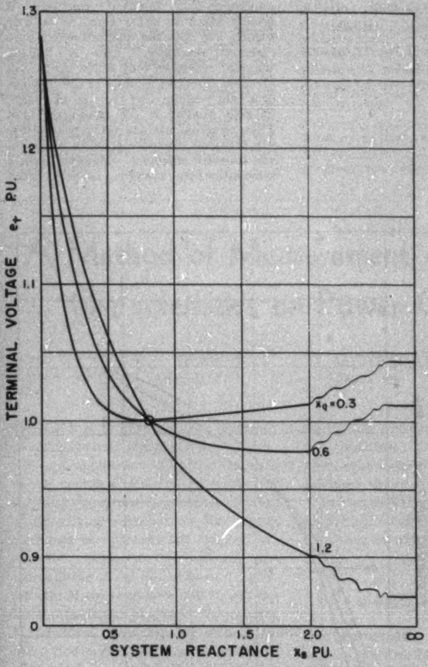

Fig. 15 (left). Effect of synchronous-machine transient saliency on variation of terminal voltage with system reactance; $x_e=0.8$

Initial conditions: $e_t=1.0$; pf=1.0; i=1.0

Figs. 12 through 15, for unity terminal pf initially, show that now the transient voltage change of a salient-pole machine is greater than would be obtained neglecting saliency, and is, moreover, in the opposite direction. There is really little resemblance between the actual change (assuming the machine actually has x_q greater than x_d') and the change calculated neglecting saliency.

Figs. 16 through 19, for 0.8 terminal pf, overexcited, show an opposite effect. Now the transient voltage change including saliency is somewhat less than that calculated neglecting saliency, and the differences are not so great.

Finally Figs. 20 and 21 are included to show a few examples of the effect of synchronous-machine rotor saliency on the transient power angle characteristic. These curves of power versus angle change in general confirm the validity of neglecting saliency in the usual transient-stability swing curve. For instance, in the range of positive increments in angle $[(\delta-\delta_0)>0]$ saliency does not seem important, and this is of course the range in which a machine whose stability is critical will usually be swinging.

Conclusion

It is not possible to dismiss completely the effect of synchronous-machine transient rotor saliency as far as variations in voltage are concerned. Saliency may be negligible in some cases, but it is suggested that in general the curves of this paper may be used to help determine whether or not saliency is significant. If it is, then it either can be properly taken into account in the study, or these curves may be of assistance in obtaining estimates of correcting factors. The effect of saliency is most pronounced in those cases where sudden changes in system reactance, as viewed from the machine in question, are involved, as compared to those cases where only angular swings are involved.

The results reported do not invalidate the usual practice of neglecting synchronous machine transient saliency as far as stability limits are concerned.

Appendix. Explanation of Terms

"Rotary saliency" as used in this paper is a general term meaning that the quadrature-axis (or interpole-axis) reactance is different from the direct-axis (or pole-axis) reactance. This concept may be applied to the subtransient, transient, or steady-state condition. However, the quadrature-axis and direct-axis reactances must be defined under the same conditions. The word "saliency" derives from its usage in the steady state since the difference between quadrature-axis and direct-axis reactance in the steady state usually arises because of the presence of salient poles. During transient or subtransient conditions, the difference in the electrical characteristics of the rotor windings in the two axes, rather than the difference in magnetic permeance, causes the two reactances to be different. Further definition and discussion of the terms quadrature-axis and direct-axis reactance will be found in reference 1.

The numerical values of reactance actually used in this paper are not intended to correspond directly to any particular machine but are merely designed to cover a range. Any actual case can be obtained by interpolation or extrapolation. The quadrature-axis transient reactance is usually taken as either equal to or only slightly less than the quadrature-axis synchronous reactance. This is because transient reactance only differs from synchronous reactance because of the presence of a field winding, and there is, of course, no field winding in the quadrature axis. Thus, no actual machine has its quadrature-axis transient reactance equal to its direct-axis transient reactance. However, such a symmetric-rotor machine is very often

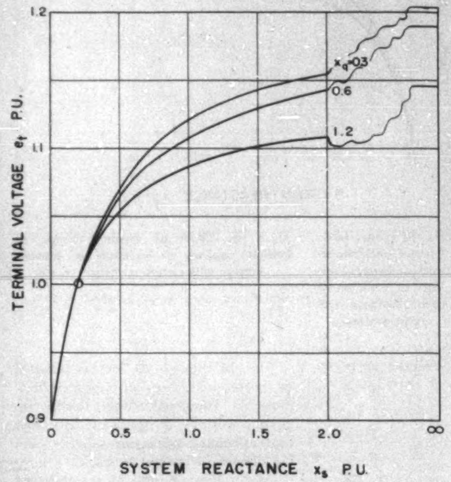

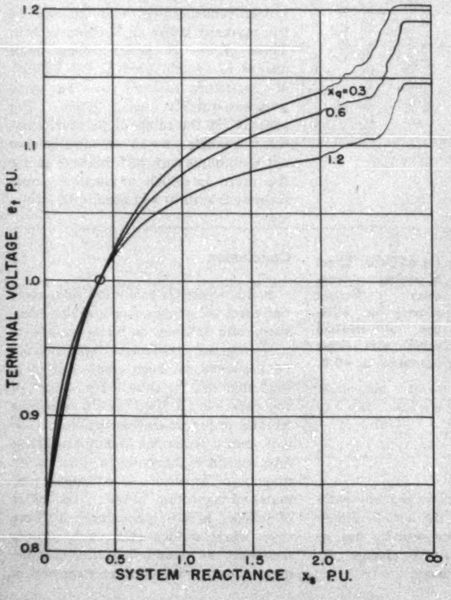

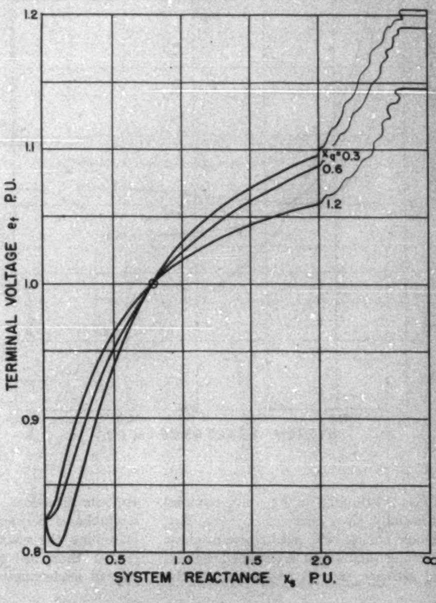

Fig. 17 (left), Fig. 18 (below left), and Fig. 19 (below right). Effect of synchronous-machine transient saliency on variation of terminal voltage with system reactance

Initial conditions: e_t=1.0, pf=0.8, i=1.0

In Fig. 17, x_s=0.2
In Fig. 18, x_s=0.4
In Fig. 19, x_s=0.8

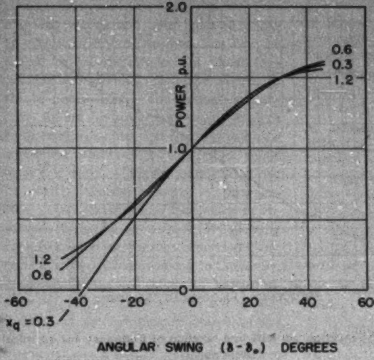

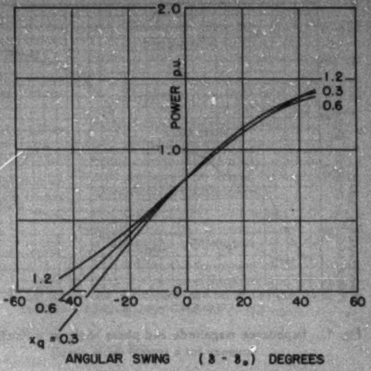

Fig. 20 (left) and Fig. 21 (right). Effect of synchronous - machine transient saliency on variation of power with angle

Initial conditions: $e_t = 1.0$, $i = 1.0$, $x_e = 0.4$
In Fig. 20, pf = 1.0 initially
In Fig. 21, pf = 0.8 initially

assumed for the purpose of simplifying the calculations in engineering studies.

The effect of transient rotor saliency on variations in terminal voltage during disturbances arising from changes of machine angle or of system reactance has been shown in this paper. The effect of transient rotor saliency on changes in terminal voltage arising from the sudden application of shunt loads has already been shown in references 2, 3, and 4, and has been more completely discussed in chapter 9 of reference 1.

References

1. SYNCHRONOUS MACHINES—THEORY AND PERFORMANCE (book), C. Concordia. John Wiley & Sons, Inc., New York, N. Y., 1951, chaps. 8, 9.

2. STARTING INDUCTION-TYPE MOTORS FROM SYSTEMS OF LIMITED CAPACITY, W. C. Johnson, Jr. *General Electric Review*, Schenectady, N. Y., Dec., 1930, pp. 712–22.

3. VOLTAGE VARIATION OF SUDDENLY LOADED GENERATORS, H. C. Anderson, Jr. *Ibid.*, Aug., 1945, pp. 25–33.

4. REGULATION OF A-C GENERATORS WITH SUDDENLY APPLIED LOADS, E. L. Harder, R. C. Cheek. *AIEE Transactions* (*Electrical Engineering*), vol. 63, June 1944, pp. 310–18.

5. POWER SYSTEM STABILITY–VOL. II (book), S. B. Crary. John Wiley & Sons, Inc., New York, N. Y., 1947, chap. 6.

6. COMPUTATIONAL AIDS TO POWER SYSTEM ANALYSIS, A. Chorlton, R. Robert, C. Concordia. *Paper No. 323*, CIGRE, Paris, France, 1954.

7. *Discussion* by L. E. Saline of SYSTEM STABILITY LIMITATIONS AND GENERATOR LOADING, H. C. Anderson, H. O. Simmons, Jr., C. A. Woodrow. *AIEE Transactions*, vol. 72, pt. III, June 1953, p. 418.

A Method of Measurement of Carrier Characteristics on Power Cables

B. J. SPARLIN
MEMBER AIEE

J. D. MOYNIHAN
MEMBER AIEE

THERE is an increasing use of carrier channels over power cables. The design and application of carrier channels require complete electrical information of the cables at carrier frequencies. By use of simplifying assumptions, the parameters can be approximated but not accurately calculated. In general, the power factor of the insulation and the resistance of the conductor and sheath can be approximated at carrier frequencies. If individual conductors are used, it appears that each phase conductor can be considered as a coaxial cable, but this has not yet been completely verified by field tests. The many unknown quantities necessary for accurate calculations of the transmission parameters of the cable make further field tests advisable. The purpose of this paper is to present a test method which has been used and some of the theoretical considerations given to the test procedure. This test method has given values which are consistent with established theory.

The general theory of attenuation and phase shift is based on transmission equations that are well known. These are

$$E_s = E_r \cosh l\sqrt{ZY} + I_r Z_0 \sinh l\sqrt{ZY} \qquad (1)$$

$$I_s = I_r \cosh l\sqrt{ZY} + \frac{E_r}{Z_0} \sinh l\sqrt{ZY} \qquad (2)$$

The characteristic impedance of a transmission line is defined as

$$Z_0 = \sqrt{Z/Y} \qquad (3)$$

where

E_s = sending-end voltage
I_s = sending-end current
E_r = receiving-end voltage
I_r = receiving-end current
$Z = (R + j\omega L)$ per unit length of line
$Y = (G + j\omega C)$ per unit length of line
l = length of line in same units

The significance of the terms Z and Y, as applied for carrier channels in equations 1, 2, and 3, are sometimes overlooked. Z is generally assumed to be $j\omega L$ of the line and Y is assumed to be $j\omega C$ of the line. In carrier applications this assumption cannot be made since R and G are not negligible. As a result, $\sqrt{ZY}$ and $\sqrt{Z/Y}$ are usually complex numbers. Very seldom does $\sqrt{Z/Y}$ take on the purely resistive value as is commonly assumed, even though it sometimes approaches this value. $\sqrt{ZY}$ is defined as the propagation constant γ, which is also defined as $\alpha + j\beta$, where

α = the attenuation constant, nepers per unit length
β = the phase shift, radians per unit length

It is significant to point out that Z_0 in equation 4 can be purely resistive only where Z and Y have the same phase angle

---

Paper 55-77, recommended by the AIEE Carrier Current Committee and approved by the AIEE Committee on Technical Operations for presentation at the AIEE Winter General Meeting, New York, N. Y., January 31-February 4, 1955. Manuscript submitted June 15, 1954; made available for printing November 18, 1954.

B. J. SPARLIN is with the Westinghouse Electric Corporation, East Pittsburgh, Pa., and J. D. MOYNIHAN is with the Sprague Electric Company, North Adams, Mass.

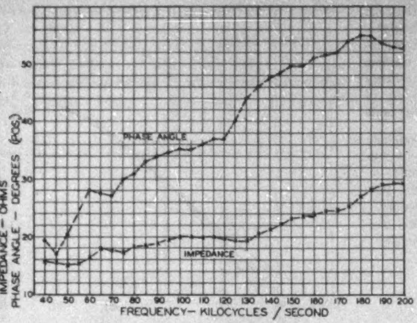

Fig. 1. Impedance magnitude and phase angle as a function of frequency for a typical cable circuit

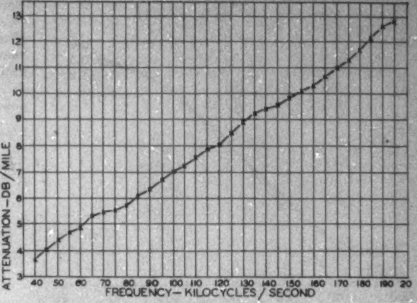

Fig. 2. Attenuation per mile as a function of frequency for a typical cable circuit

$$Z_0 = \sqrt{Z/Y} = \sqrt{(R+j\omega L)/(G+j\omega C)} \qquad (4)$$

It should be noted that equal phase angles are the essential factor, not the fact that R and G are negligible. It is further interesting to note that in the consideration of the propagation constant

$$\gamma = \sqrt{ZY} = \sqrt{(R+j\omega L)(G+j\omega C)} = \alpha + j\beta \qquad (5)$$

If R and G are assumed to be negligible as mentioned in the foregoing, the expression for γ is purely reactive and the attenuation factor becomes zero. Since it is accepted that the attenuation α can not be zero, it must be acknowledged that R and G are not negligible. If R and G are not negligible, then it will only be the exceptional case of $(R + j\omega L)$ and $(G+j\omega C)$ having the same phase angle that will yield a characteristic impedance Z_0 that is purely resistive.

There is at present little known or published information about the characteristics of cables at carrier frequencies. Therefore, the conductance which takes into account the leakage resistance, dielectric absorption losses, and displacement current is a very difficult value to calculate. Also the fact that R is normally small compared with $j\omega L$, and G is normally small compared with $j\omega C$, makes comparatively accurate values essential to arrive at a reasonable value for the phase angle of Z_0 and an attenuation factor. It is with these basic concepts in mind that the methods of measuring Z_0, α, and β are proposed.

Characteristic Impedance

There are several methods for measuring Z_0, the most common of which are the substitution method and the open-circuit–short-circuit method. The substitution method becomes somewhat cumbersome when substituting both an R component and an X component. Measuring the cable impedance and phase angle at the sending end does not give a clear indication of the magnitude of change necessary for the R or X termination at the receiving end to make the two impedances equal. This method therefore becomes a trial-and-error method. Fig. 1 shows impedance and phase angle as a function of frequency.

The open-circuit–short-circuit method is a much more direct method and for this reason it was chosen. From the equation

$$Z \text{ input} = \frac{E_s}{I_s} = \frac{Z_0(Z_r \cosh \gamma l + Z_0 \sinh \gamma l)}{(Z_0 \cosh \gamma l + Z_r \sinh \gamma l)} \qquad (6)$$

it can be shown that

$$Z_0 = \sqrt{Z_{oc} Z_{sc}} \qquad (7)$$

By using an impedance bridge which will measure the impedances Z_{oc} and Z_{sc} including their respective phase angles, it is a simple matter to calculate both the characteristic impedance and the characteristic phase angle. Measuring the sending-end voltage and current for the two conditions is not sufficient unless a reliable means of determining the phase angle is also used. If a line is sufficiently long, the input impedance will almost equal the characteristic impedance regardless of the termination. For instance, if αl is 2.3 nepers or more, the input impedance of a line will be within 2 per cent of the Z_0 even for the extreme terminations of open circuit and short circuit.

Attenuation

To measure the attenuation by measuring either received voltage or current, the line must be terminated in the same impedance as the input impedance, i.e., the characteristic phase angle and magnitude. Fig. 2 shows attenuation as a function of frequency.

The attenuation normally is given in decibels (DB) and is calculated as follows

$$\text{DB} = 10 \log_{10} (P_s/P_r)$$

$$\text{DB} = 10 \log_{10} \frac{E_s^2/(R_s+jX_s)}{E_r^2/(R_r+jX_r)} \qquad (8)$$

If $(R_s + jX_s)$ is equal $(R_r + jX_r)$, then

$$\text{DB} = 20 \log_{10} (E_s/E_r) \qquad (9)$$

It is suggested that a known voltage be applied at the sending end and this voltage be measured across the characteristic impedance at the receiving end with a frequency selective voltmeter. It is significant to point out that errors can be avoided by the use of a frequency selective voltmeter. Oftentimes, ground currents will cause a difference in potential along the sheath of the cable, and the resultant current flow in the cable will give a false reading when read on a broad-band voltmeter. The sending end can usually be monitored with a broad-band voltmeter when the applied voltage is relatively high.

Phase Shift

To measure phase shift in the field is somewhat more difficult than the two previously discussed quantities. It was found that two phases of installed cable could be jumpered at the far end so that the transmitting and receiving terminals of the cable were both at one location. Then the applied voltage and received voltage can both be applied to an oscilloscope.

As the frequency is increased, the

standing waves will pass from in phase (represented by a straight line on the scope) to 180 degrees out of phase (appearing as a straight line perpendicular to the in phase line). The frequency-scanning should be started at a low enough frequency to insure that the first in-phase frequency observed is that of a single standing wave. This frequency then can be plotted against velocity of propagation. As each in-phase frequency is observed, it too can be plotted. By plotting each frequency and recognizing that there can be no sharp discontinuity in the curve, it is possible to tell where, if any, multiples of the fundamental did not appear because of the complex reactance of the circuit.

This method leaves room for error if not executed by an individual familiar with the technique but, with a little experience, this method gives reliable results without elaborate or unusual test equipment.

Test Procedure

The following method has been used several times and has given consistent results. A step-by-step procedure is given for the sake of clarity.

1. Connect drain coils between each of the 3-phase conductors and the cable sheaths at each end of the cable.
2. Open the grounding disconnects on the cable at each end. (Allow sufficient time for cable to discharge before step 2.)
3. Connect an impedance bridge across the drain coil of one cable phase to be measured.
4. Measure impedance of this cable phase with the remote end open- and short-circuited at 5-kc intervals from 40 to 200 kc.
5. Compute the characteristic impedance Z_0 at each of the 5-kc intervals by means of the equation $Z_0=\sqrt{Z_{oc}Z_{sc}}$.
6. If either or both of the other phase conductors are of different construction, measure them as in steps 3 through 5.
7. Disconnect impedance bridge from cable.
8. Connect signal generator and vacuum-tube voltmeter to the phase to be measured. Connect variable *R*, *L*, and *C* and frequency selective voltmeter to the receiving end of this phase.
9. Terminate the cable in its characteristic impedance by adjusting *R*, *L*, and *C* to the characteristic impedance.
10. Transmit a known reference level of signal and measure the received level across the terminating impedance with the frequency selective voltmeter.
11. Steps 9 and 10 are repeated at 5-kc intervals from 40 to 200 kc.
12. Steps 8, 9, 10, and 11 are repeated for any phase conductor that is different from the first one measured.
13. Two phase conductors of the same construction are jumpered at the remote end. Assuming these are phases *B* and *C*, it is now possible to transmit locally on phase *B* and receive the signal locally on phase *C*.
14. Terminate *C* locally with the *R*, *L*, and *C* adjustment for approximate characteristic impedance termination.
15. Steps 9 and 10 are repeated at a few frequencies to ascertain that normal ground currents have not influenced the previous attenuation measurements.
16. Connect the cable input and cable output to the horizontal and vertical inputs of the oscilloscope.
17. Adjust the frequency of the oscillator to give a series of in-phase and 180-degree out-of-phase indications to determine the propagation velocity of the cable.

Conclusion

An attempt has been made to set up a test procedure that is consistent with transmission line theory. Test equipment commonly available has been used, and the results obtained have been consistent within the accuracy of the test equipment. The results are also consistent with transmission line theory and the meager amount of information presently available.

Reference

1. COMMUNICATION ENGINEERING (book), W. L. Everitt. McGraw-Hill Book Company, Inc., New York, N. Y., 1937.

Field Current Sources for Electric Defibrillation

PAUL L. BETZ
MEMBER AIEE

UNDER certain conditions, the heart may lose its rhythmic pumping action and cease to maintain circulation of the blood. This situation is known as ventricular fibrillation and may occur during surgical procedures or as a consequence of electric shock. When ventricular fibrillation occurs in the hospital operating room, a countermeasure is to open the chest and massage the heart to reestablish blood circulation and then to employ a defibrillation procedure that consists of passing a suitable electric current through the heart itself. This is done by applying electrodes to the surface of the heart and passing a 60-cycle alternating current of about 1.5 to 2.0 amperes (amp) through the heart for about 0.5 second (voltage between 120 and 135 volts). Current so applied brings the heart to rest and holds it at rest until the current is interrupted at which time the heart will usually resume its normal rhythmic pumping action provided the elapsed time of fibrillation is not excessive.

When ventricular fibrillation occurs outside of the operating room, conditions do not permit opening the chest to expose the heart for the application of electrodes. Kouwenhoven and Milnor[1] have explored a method of defibrillation that may be applied with the chest intact and under field conditions. The proposed method employs electrodes that are placed on the surface of the body and through which an electric current is passed, the magnitude of which is sufficient to accomplish defibrillation, provided the heart is not cyanotic.

Electric utility companies are especially interested in a defibrillation method which can be applied in the field, since electric shock is an ever-present hazard and is a subject to which continuous attention is given. It is recognized that much will have to be accomplished before defibrillating procedures may be practiced by nonmedical personnel but, to evaluate the possibilities of the method, it is necessary to have a source of electric current suitable for use in the field where commercial power may not be available. During the

---

Paper 55-87, recommended by the AIEE Safety Committee and approved by the AIEE Committee on Technical Operations for presentation at the AIEE Winter General Meeting, New York, N. Y., January 31–February 4, 1955. Manuscript submitted October 19, 1954; made available for printing November 18, 1954.

PAUL L. BETZ is with the Consolidated Gas Electric Light and Power Company of Baltimore, Baltimore, Md.

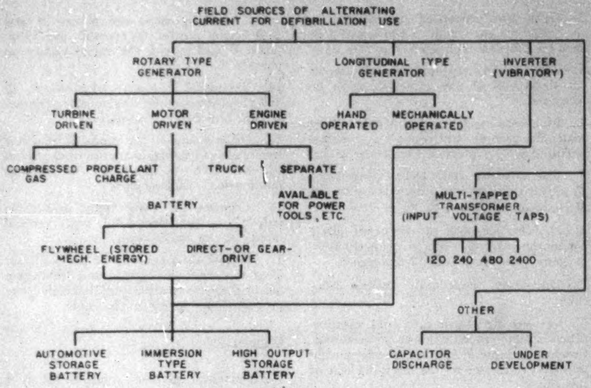

Fig. 1. Current sources for field use

past 2½ years, the author has undertaken to explore the possibilities of obtaining a suitable field power source while Kouwenhoven has concentrated on the development of defibrillation methods using electrodes applied to the surface of the body. The purpose of this paper is to outline briefly the various sources that were investigated and to point to those that appear to meet best the requirements of the field defibrillation method.

Electrical Requirements

The electrical requirements for heart defibrillation can be stated in terms of requirements as determined from animal experiments, since this method has not been applied to human subjects. Experiments were performed using anesthetized dogs[1] and from these the following requirements for the power source were obtained: voltage = 480 volts; current capability = 15 amp; frequency = 60 cycles; and load time = 1 second.

A power source meeting these requirements has been found to give satisfactory results with electrodes placed on opposite sides of the chest. Other experiments using a different electrode position, as described by Kouwenhoven and Milnor,[1] indicate that defibrillation may be accomplished with currents on the order of 4 to 6 amp at the previously mentioned voltage and frequency. The opinion has been expressed that the current necessary for human heart defibrillation will not exceed that used in the more recent experiments, i.e., it will be in the range of 4 to 6 amp. The field current sources that have been investigated are based on delivering 15 amp at the required voltage and frequency and, if the lower current values may be employed, some reduction in the size of equipment may be possible.

In addition to the electrical requirements listed in the foregoing, there is the further requirement that the power supply be available for use promptly. During ventricular fibrillation, blood circulation ceases and physiological damage may be minimized by holding the period of fibrillation to a minimum. Some delay is unavoidable in reaching a shock victim and in preparing for the defibrillation procedure. Additional time to make the power source available for use if required must be held to a minimum. Hence, a further requirement for the power supply is that it must be capable of being started or made to function within about 10 seconds and, preferably, within a shorter time period.

Current Supplies for Field Use

Fig. 1 shows the various arrangements of current sources that have been investigated and which are discussed in the following.

1. Consideration was given to the use of an a-c generator connected to a turbine driven by a compressed gas such as air or by hot gases from the burning of a propellant charge. The latter type of turbine has been developed for aviation use and it was found that it appears feasible to adapt a unit of this type to drive a generator for defibrillation use. This would require a development contract according to several manufacturers of this equipment. Estimate of the cost of development was $20,000 by one company, and $47,000 by another. Either of these expenditures would be expected to provide the first unit and succeeding units would be at considerably reduced cost. In one case, the cost of additional units was estimated at about $1,800 in lots of 10. The estimated weight of such a unit is 60 pounds.

Consideration was given to the use of compressed air to operate an air turbine instead of the turbine adapted to propellant-charge operation. Here, the weight of containers for the compressed air is a limiting factor unless extremely high gas pressure is used, in which event safety becomes a consideration. Pressure bottles would be bulky at moderate gas pressure and difficult to handle in the field. For this reason, the compressed-air unit was not given extended consideration. Possibly, a unit of this type could be developed which would meet weight and safety requirements.

2. Consideration was given to the use of storage batteries to operate a motor-generator set. The ordinary automobile-type storage battery was considered to be of too limited capacity to provide approximately 6 kw of electric output even though this might be sustained for a very short time. Consideration was given to another type of battery developed during World War II which requires immersion in water for activation. This battery has an indefinite shelf life when dry and, when immersed, provides high electric output for a single discharge. Difficulty is seen in testing defibrillation equipment employing this type of battery since a test of the equipment would require replacement of the battery and there may still be uncertainty as to the capability of the new battery.

Information was obtained on a new storage battery capable of extremely high discharge rates together with relatively low weight. This battery employs silver and zinc as plate materials and is capable of furnishing 1,350 amp for 30 seconds, or 630 amp for 5 minutes. A battery of these cells having an output of 24 volts is considered suitable for driving motor-generator devices. A battery of this type costs approximately $2,400 and weighs about 67 pounds.

Consideration has been given to the use of a fly wheel to assist the battery in meeting the high demand occurring at defibrillation. Such devices for storing mechanical energy have found limited practical applications but, in this instance, the weight of the fly wheel appears to be excessive for portability. The fly wheel becomes unnecessary in systems where use is made of the high discharge rate storage battery.

Having found the high-output storage battery which appears to be satisfactory for the proposed use, an investigation was made of the cost and weight of a motor-generator set to operate with 24 volts d-c on the motor and to have an output of 480 volts, 60 cycles a-c. It was found that such a motor-generator set could be purchased in the price range of $950 to $1,400. Thus, the cost of the silver-zinc battery and a suitable motor-generator set would be in the range of $3,350 to $3,800. The weight of the motor-generator set alone would be about 250 pounds; and total weight, including the storage battery, would be about 320 pounds.

3. Consideration has been given to the use of an a-c generator which is suitable for operation from the fan belt of a truck engine, from a power take-off on the truck, or by a separate engine. Such a generator is available having 3-phase output in 3-, 5-, and 10-kw ratings at 220 volts, 60 cycles per second. Tests on a 3-kw unit indicated that the single-phase overload capacity is sufficient to provide defibrillation current for the required time when operated at overspeed corresponding to a frequency of about 90 cycles per second and when using a transformer to step up the voltage to 480 volts. The 5-kw unit will meet defibrillation requirements at normal speed (60-cycles per second output) and, on single-phase load, this generator will supply 15 amp at 220 volts or 30 amp at 110 volts; the usefulness of the latter is described in the following. A transformer is provided to step up the voltage to 480 volts for defibrillation and also to reduce the voltage to 110 volts for other uses. A wheelbarrow-type base is contemplated together with a suitable gasoline engine to drive the generator such as a 2-cylinder 4-cycle engine. There is advantage in the wheelbarrow mounting in that the unit may be left at the work location while the truck proceeds to other operations. The cost of the complete unit is approximately $700 and the weight is approximately 530 pounds. If desired, a small hand winch can be installed on the truck to simplify movement of the unit into and out of the truck.

One matter of concern is the promptness with which this power source would be able to supply defibrillation current. To be satisfactory, the gasoline engine should start on the first attempt. Where the engine generator is a stand-by unit for defibrillation use only, there would be grave concern in regard to starting. This situation would be improved were the unit to be used frequently, such as where it would be called on to supply energy for routine field uses. A portable engine-generator set such as this could be used to operate miscellaneous hand tools, fans, lights, heaters, etc., and this might prove of great value in field operations. The set could also be used with a suitable rectifier to charge storage batteries for radio communication. Frequent use of the engine-generator set for these purposes would improve the starting reliability of the set should defibrillation use be required. There would be a good possibility that the unit would be in operation at the critical time.

4. Consideration was also given to the use of a generator of the type in which a permanent magnet is moved longitudinally through a series of coils to induce a limited number of cycles of alternating current suitable for use in defibrillation. An alternative would be to move the coils with respect to a fixed permanent magnet. In either case, the movable element could be operated by hand, by a spring, or by explosive charge. This type of device is not seen to have advantage over rotating devices such as the a-c generator already discussed. The latter has the advantage of being capable of providing more cycles of alternating current.

5. Consideration was given to the use of a vibrator-type inverter driven by a storage battery. The current requirements of such a device could not be met by the ordinary storage battery but the high-output storage battery previously mentioned could be used. There is uncertainty as to the ability of the contacts employed in the vibrator of the inverter to give reliable performance under such drastic operating conditions. For this reason vibrator-type inverters were given only passing consideration.

6. Consideration was given to the use of a multitapped transformer having input voltage taps for standard voltages up to 2,400 volts and an output winding to give 480 volts and 15 amp. The basis for using such a transformer may be found in the following statements which are believed to cover the facts:

a. Fibrillation would be unlikely to occur where the electric shock is from voltages in excess of 2,400 volts. In this connection, it is to be noted that fibrillation is induced by the passage of small currents (milliamperes) through the heart and, at voltages in excess of 2,400 volts, the current reaching the heart would be in excess of the values that produce fibrillation.

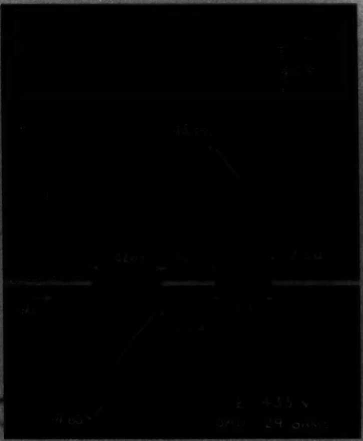

Fig. 2 (left). Capacitor discharge, 1-cycle type

Fig. 3 (below). Capacitor discharge, 2-cycle type

b. Shocks obtained from circuits at 2,400 volts and lower do not occasion current flows sufficient to open associated fuses or circuit breakers. Hence, the circuit that gave the shock would remain energized and be available after the shock.

c. A circuit exposed sufficiently to permit shock through accidental contact would be available to ground as an energizing source for the multitapped transformer.

Weatherproof transformers having input voltage taps at 120, 240, 480, and 2,400 volts and having an output voltage of 480 volts and current capability of 15 amps suitable for defibrillation use may be obtained for about $60. Such a unit would weigh about 50 pounds.

7. While the aim has been to obtain a 60-cycle output from the field power unit, consideration has been given to the design of a capacitor discharge type of device using radio *B* batteries as the current source. Devices of this type were built and tested. In one of these units, banks of capacitors were charged to 450 volts d-c and these were discharged through a programming switch to the electrode circuit. The switch in the first unit provided a discharge from one set of capacitors and then changed the connections to supply a discharge from another bank of capacitors in the opposite direction. Fig. 2 is an oscillogram of the discharge current through a dummy resistance load simulating the heart load. The results with this device in the defibrillation experiments were satisfactory when the delay between onset of fibrillation and application of defibrillation current was short (30 seconds). They were not as reliable for longer delay times as when 60-cycle current was used. This apparatus was then modified to provide 4 half-cycles of discharge, each succeeding cycle being of opposite polarity. Fig. 3 is an oscillogram of this type of discharge to the dummy load. The results with this modification were inferior to the 1-cycle device. It was concluded that simulated alternating current by capacitor discharge is inferior to a 60-cycle source.

8. Other types of energy sources are under consideration which require further development before their feasibility can be determined. These have not yet reached the stage to be included in this discussion.

Conclusions

The various current sources that have been discussed are indicated diagrammatically in Fig. 1. Following the order given in Fig. 1, the systems that appear to be most suitable for defibrillation in the field are as follows:

1. Turbogenerator unit driven by propellant charge. Units of this type would have the advantage of low weight (approximately 60 pounds). Their chief disadvantages are high development cost, minimum of $20,000, and relatively high unit cost, $1,800 each in lots of 10.

2. Motor-generator set using high-output storage batteries. The unit cost of this arrangement would be about $3,500 and the weight about 320 pounds.

3. Separate engine-driven generator. This unit would be available for defibrillation and routine uses such as battery charging, operation of power tools, lights, heating units, etc. The unit cost would be approximately $700 in single lots decreasing to about $645 in lots of 10. The weight of this unit is approximately 530 pounds.

4. The multitapped transformer having input voltage taps for 120, 240, 480, and 2,400 volts and an output winding capable of providing 480 volts at 15 amps. The cost of such a transformer is approximately $60 and the weight about 50 pounds. One disadvantage is that this equipment may not be immediately available for use as it requires connection to the source that administered the electric shock and this may be inaccessible or even undetermined at the time defibrillation is required. Where overhead lines are involved, the difficulty of connection is increased. The weight and cost considerations are quite favorable.

At the present time, it appears that the most practical unit for defibrillation is the separate engine-driven generator, item 3, which is used in routine field operations as well as for defibrillation. The matter of prompt starting is yet to be determined in relation to the requirements of defibrillation.

Reference

1. ELECTRIC DEFIBRILLATION, W. B. Kouwenhoven, W. R. Milnor. *AIEE Transactions*, vol. 74, pt. III, 1955 (*Paper 55-95*).

Supervisory Control and Associated Telemetering Equipment—A Survey of Current Practice

AIEE COMMITTEE REPORT

SUPERVISORY control had its inception in the early 1920's. The use of supervisory control increased gradually in the succeeding years as more operating companies became acquainted with it and the benefits that could be realized by its use. Its use has increased at an accelerated rate since the end of World War II, indicating a greater trend toward centralized control of power systems. The availability of improved telemetering equipment to operate in conjunction with supervisory control has accelerated the use of both because it has made possible bringing control, indication, and metering of distant substations and equipment to a centralized control point. This has resulted in reduced operating costs and improved system efficiency.

Questionnaire

A working group of the Automatic and Supervisory Control Subcommittee prepared a questionnaire regarding employment and characteristics of supervisory control and telemetering systems in use. This questionnaire was distributed early in 1953 to 119 representative operating companies throughout the United States. Eighty replies to the questionnaire were received. The purpose of the questionnaire was to determine for the benefit of both manufacturers and users the present relative usage and the possible trend of usage of supervisory control and telemetering and characteristics of existing equipments.

QUESTION 1

The first question asked the users to list the various types of stations with and without supervisory control, as shown in Table I. The purpose was to determine

---

Paper 55-128, recommended by the AIEE Substations Committee and approved by the AIEE Committee on Technical Operations for presentation at the AIEE Winter General Meeting, New York, N. Y., January 31–February 4, 1955. Manuscript submitted October 21, 1954; made available for printing December 9, 1954.

The personnel of the Working Group of the Automatic and Supervisory Control Subcommittee of the AIEE Committee on Substations are: M. E. Reagan, *Chairman*; T. J. Allen, H. Bany, J. F. Bracken, W. M. Larson, J. L. McKee, J. W. Savage, and J. J. Winsness.

Table I. Stations or Substations According to Types

	1	2	3	4	5	6
		Unattended				Attended
	Total Number	Automatic Without Supervisory Control, Per Cent	Automatic With Supervisory Control, Per Cent	Supervisory Control Only, Per Cent	Total With Supervisory Control, Per Cent	Manually Controlled, Per Cent
A-c substations						
Distribution	10,889	61.4	2.4	1.9	4.3	34.3
Bulk Power	1,266	36.8	6.1	7.6	13.7	49.5
Switching	409	46.4	12.5	18.8	31.3	22.3
Total a-c substations	12,564	58.6	3.1	3.0	6.1	35.3
Synchronous condensers	171	33.3	4.1	7.6	11.7	55.0
Hydrogenerators	738	20.3	5.6	6.8	12.4	67.0
Power rectifiers	81	61.7	13.6	0	13.6	24.7
Synchronous converters	297	27.6	9.1	0	9.1	63.3
Motor generators	105	20	15.2	5.7	20.9	59.1
Grand total	13,956	55.3	3.5	3.2	6.7	38.0

Table II. Distance and Type of Channel Supervisory and Telemetering

		Length of Channel			
	No. of Channels	Total Channel Miles	Minimum Miles	Maximum Miles	Average Miles
Leased telephone line	482	4,196	0.06	75	7.83
Owned telephone line	680	3,156	0.085	125	4.64
Power-line carrier	306	17,950	3.0	380	58.6
Telephone-line carrier	42	2,364	2.8	300	56.3
Microwave	61	5,234	4.0	450	85.7

Table III. Size of Unattended Automatic and Unattended Supervisory Stations

		Time to Get to Station			
	Range, Kilovolt-Amperes	Minimum, Minutes	Maximum, Minutes	Average, Minutes	No. of Replies
Largest unattended automatic station in use	1,250 to 200,000	15	75	25.5	77
Largest unattended automatic station considered feasible	3,000 to 300,000				43
Largest supervisory controlled station	900 to 210,000	15	60	23.3	78
Largest supervisory controlled station considered feasible	10,000 to 800,000				36

the extent of usage of supervisory control and telemetering for various applications.

The following definitions were established as a guide for answering this question:

1. A bulk power station transforms power from the transmission system to the subtransmission circuits which supply the distribution stations. The transmission circuits transmit power from the generating stations to the bulk power stations and may also transmit power between generating stations.
2. A distribution station consists of a source of supply to the primary circuits which feed distribution transformers or industrial loads. The industrial or network substations should not be included. The distribution station may or may not involve a transformation.
3. A switching station permits switching of circuits (usually at the transmission voltage level) and there are no transformations.

Table I shows the use of supervisory control as reported by 77 users involving approximately 935 supervisory systems. The majority of supervisory and telemetering is used in control of a-c substations with the highest percentage on bulk power and switching stations. Column 5 shows the total percentage of substations using supervisory control (total of columns 3 and 4). 31.3 per cent of the switching stations used supervisory control. On an over-all basis 6.7 per cent of the stations or substations were reported as supervisory controlled. Since the questionnaire was not sent to transportation companies, the information obtained on power rectifiers, synchronous converters, and motor generators is less than that obtained for the other applications.

QUESTION 2

The second question asked the users to list distances and types of channels in use for supervisory control and telemetering. Table II is a tabulation of distance and types of channels used with supervisory control and telemetering by 75 users. It shows that the majority of channels are line wire but that power-line carrier channels are very numerous and represent by far the largest number of channel miles. This is to be expected as supervisory systems are applied to more and more distant stations. The number of microwave channels show a favorable reception considering the short time that they have been available, and the indications are that this type of channel is being used for longer distances than any other types of channels.

QUESTIONS 3 AND 4

The users were asked to state the kilovolt-amperes of the largest unattended automatic station and the largest supervisory controlled station on their systems, the largest they would consider for each, and the time required for an operator to reach the station. Table III shows the range of replies to these questions. The tabulation indicates that automatic and supervisory control is already in use to control fairly large stations or substations. It also indicates that users have realized sufficient reliability and economy of operation with supervisory equipment to warrant its being applied to control much larger stations and substations.

QUESTION 5

Users were asked whether or not they considered automatic or supervisory controlled stations as reliable as those manually operated. Out of 75 replies, 79 per cent answered "yes" and 21 per cent answered "no." Out of 75 users, 4 replied that automatic or supervisory controlled stations had been changed to manual for the following reasons:

1. Two stations were temporarily changed because of policy and will later be restored to supervisory control.
2. One user discontinued use in urban areas as he could not tolerate delays.
3. One station was changed because of obsolete equipment.
4. One station outgrew circuit-breaker ratings with reclosers.

It is noted that only one user reported discontinued use of supervisory control for a reason which might be a reflection against the equipment. Details of this case were not reported by the user.

QUESTION 6

Users were asked to check the types of telemeter readings (such as kilowatts) they used with supervisory control and to

Table IV. Use of Telemetering with Supervisory Control

	Number of Users Using	
	Continuous Readings	Selected Readings
Kilowatts	32	29
Kilovars	28	25
Bus voltage	23	38
Feeder current	5	24
Position	12	29
Water level	10	8
Kilowatt-hours	11	11

list whether the readings were continuous or selected. Table IV shows the number of users of supervisory using the various types of telemeter readings. The majority of use is in reading kilowatts, kilovars, and voltages. Although not apparent from the table, it was found that out of 79 users of supervisory control, approximately 81 per cent use telemeter readings of some sort. 50 per cent of the telemeter users employ both continuous and selected readings. Approximately 30 per cent of the telemeter users employ selected readings only, while approximately 20 per cent use continuous readings only. This table shows that telemetering has become of major importance in the use of supervisory control and is an important factor responsible for its rapid growth.

Question 7

Users were asked to indicate whether or not automatic synchronizing or synchronism check is used on tie-line circuit breakers closed automatically or by supervisory control. Out of 78 users of automatic or supervisory controlled stations, approximately 76 per cent of the users employ automatic synchronizing or synchronism check equipment. This indicates that automatic synchronizing or synchronism check equipment is also an important adjunct to supervisory systems and that supervisory is extensively used to close tie-line breakers and connect a-c generators to the system.

Question 8

Users were asked to list the source of power used for supervisory control. Out of 77 users of supervisory control, 74 use batteries for control power. Eighteen of these users also have supervisory control operated from a-c station service. Of the 74 users employing batteries for control power, approximately 36 per cent use both station control batteries and separate supervisory control batteries, 39 per cent use station control batteries only, and 25 per cent use separate control batteries only. This indicates that battery control power is most extensively used primarily because of its reliability. However, it also indicates that in some cases it is preferable from the user's standpoint to use a-c station service as a control power source. Some such installations use an emergency supply such as a motor generator operated from a battery to generate alternating current for the supervisory equipment in case of failure of the normal a-c station service. The use of separate control batteries for supervisory control reduces the possibilities of grounds in the control circuit with the resulting troubles.

In some cases, it is easier to maintain separate supervisory system batteries at constant potential at both the master and remote station because of the steady drain imposed by supervisory equipment devices. Most supervisory systems are now available for operation on 48 or 125 volt d-c. This permits the use of the station control battery in many cases which, of course, reduces the initial battery costs and the resultant maintenance and replacement costs.

Conclusion

The replies to the questionnaires distributed indicate that supervisory control and associated telemetering is now being used very extensively by operating companies. The design of supervisory equipment, its utilization of modern telemetering equipment, and its adaptation to a variety of channels to cover great distances have kept pace with the requirements of the power industry. It is expected that the usage of supervisory control will increase considerably in the future because of its versatility and the recognized advantages of centralized control for efficient system operation.

References

1. American Standard for Automatic Station Control, Supervisory, and Telemetering Equipments. *ASA C37.2-1945*, American Standard Association, New York, N. Y., 1945.

2. Telemetering, Supervisory Control and Associated Circuits. *AIEE Special Publication S-12*, Sept. 1948.

Eccentricity, Vibration, and Shaft Currents in Turbine Generators

L. T. ROSENBERG
MEMBER AIEE

THE operation and maintenance of modern high-speed turbine-driven generators require a thorough knowledge of their construction, as well as the ability to recognize the symptoms and understand the causes of impending injury and failure. In the preparation of the proposed AIEE Guide for the Operation and Maintenance of Turbine Generators, it was decided certain topics that do not readily fall into any major classification could be grouped together into a miscellaneous section. Under this heading the Working Group for the Preparation of Operating and Maintenance Guide for Turbine Generators has listed:

1. Eccentricity of rotor in stator.
2. Axial position of rotor with respect to stator.
3. Vibration.
4. Shaft currents and bearing insulation.

It was further decided that the substance of this section of the proposed guide be submitted to the membership in the form of suitable papers. It was hoped this would bring forth discussions from among operators as well as manufacturers that could be incorporated into the proposed Operating Guide before final publication.

This paper discusses the four subdivisions of the miscellaneous section from the standpoint of diagnosis, causes, corrective measures, and preventive maintenance. In order to be applicable to air-cooled as well as hydrogen-cooled machines and both bracket-bearing and pedestal-bearing types, the construction features of the four largest American turbine-generator manufacturers were studied, and the recommendations of each relating to these topics were carefully considered. No attempt has been made to include the steam turbine except in so far as it may be a contributing factor to generator behavior.

Eccentricity of Rotor in Stator

The initial assembly of a turbine-generator unit involves careful alignment of the generator rotor with the turbine

---

Paper 55-121, recommended by the AIEE Rotating Machinery Committee and approved by the AIEE Committee on Technical Operations for presentation at the AIEE Winter General Meeting, New York, N. Y., January 31–February 4, 1955. Manuscript submitted October 18, 1954; made available for printing December 6, 1954.

L. T. Rosenberg is with the Allis-Chalmers Manufacturing Company, Milwaukee, Wis.

The author wishes to acknowledge the many helpful suggestions and the instruction book material received from the members of the AIEE Working Group for the Preparation of Operating and Maintenance Guide for Turbine Generators.

spindle, as well as accurate positioning of the stator with respect to the rotor. Eccentricity of the rotor is more serious on 4-pole machines than on 2-pole units, because the flux in the region of the small gap is in parallel with that in the region of the long gap rather than in series and hence subject to more variation per revolution. Even in 2-pole units, however, the flux density wave becomes higher near the pole center as it approaches the region of the small gap and the magnetic pull is appreciably greater in this region. In addition to the pulsating unbalanced magnetic forces, the changes in flux distribution cause induced currents in rotor winding, wedges, and surface, and circulating currents between parallel stator circuits with consequent increased losses and temperatures. Excessive inequality in the gap can also adversely affect the fringing fluxes at the core end region and may result in abnormal local temperatures in clamping plates or retaining rings. The maintenance of accurate centering is also important to be sure of maintaining uniform clearances at oil wipers, fans, baffles, etc., where tolerances are often small.

Concentricity is initially established by careful measurement of the air gap in at least four positions at each end of the generator. The procedure and allowable tolerances will vary somewhat depending on the air-gap length, the number of poles, whether the unit is air- or hydrogen-cooled, and whether the rotor is supported in pedestal- or bracket-type bearings.

In some bracket-bearing machines, the adjustment of the air gap as well as the clearances at oil wipers, baffles, seals, fan shrouds, etc., is accomplished at the factory prior to shipment. In other types, these adjustments may be made or rechecked during installation of the unit, and should preferably be done under the supervision of the manufacturer's erection engineer. In any case, the procedure and allowable tolerances recommended by the manufacturer should be followed in the initial installation as well as in subsequent reassemblies.

Once properly centered, the rotor is not likely to shift suddenly except in the case of accident. With separately supported pedestal bearings, settling or growth of the foundation or grouting over an extended period may disturb concentricity, as well as the alignment between rotor and turbine spindle. Abnormal wear of the babbitt will also tend to bring about these same results. Checking the gap for uniformity at regular inspection periods is therefore advisable and can often be done quickly by tapered feelers, thickness gauge, or pin gauge either in the air gap or between rotor bearing fit and outer frame ring bore if the position of the latter is previously determined relative to the stator inner frame bore. If measurements are made in the gap, care must be exercised to be sure the gauge is in contact with a tooth rather than a slot wedge and far enough from the core end to avoid the tapered or stepped end laminations if employed.

Axial Position of Rotor with Respect to Stator

The rotor should be reasonably well centered axially with respect to the stator under all operating conditions. Appreciable asymmetry not only produces an end thrust but can seriously affect the end fringing flux and produce abnormal local heating of the fingerplates and retaining rings.

If the generator has bracket-type bearings supported from the end covers, the correct axial location of the rotor can usually be obtained by an adjustment relative to the bearing center lines. These are permanently located in relation to the stator core and yoke by the machined end cover fits against the stator. In this type, the fan shrouds, seals, baffles, oil wipers, etc., may sometimes be adjusted at the factory before shipment to suit the bearing positions and in such cases should need no further checking. Adequate provision is usually made for axial movement of the coupling due to thermal changes in the turbine, and for any additional expansion of the rotor when the unit is loaded, as well as for any necessary axial clearance for disengaging the coupling.

For machines with separate pedestal-type bearings initial axial centering is often accomplished after the rotor has been lined up and coupled to the turbine by adjustment of the stator position on the base plate. If this had not been done previously at the factory, or if for any reason the stator was not suitably dowelled or keyed to the base plate, axial centering must be done when the unit is installed.

Since the method of adjustment and permissible tolerances depend upon individual design details, the manufacturer's recommendations should be followed for each unit. Once the correct stator location has been established, subsequent checking of axial positioning is seldom necessary unless either the thrust bearing or the stator has been moved from its initial setting. The adjustment of fan shrouds, baffles, etc., however, may be necessary whenever they are disturbed, or after the rotor is removed and replaced.

When the axial centering of the rotor must be rechecked, measurements should be made between stator core ends and some reference point on the rotor such as the outer end of the retaining rings if they are equally spaced from the rotor body. Measurements at several points around the periphery are recommended to allow for uneveness in the punchings.

Vibration

The vibration of a turbine-generator unit may originate from a number of widely different causes. The most common source of rotor vibration arises from physical dissymmetries in the rotor when built that result in nonuniform weight distribution around the geometric axis. To overcome roughness from this source turbo-generator rotors are carefully balanced at the factory before shipment. Touch-up balancing is often necessary after installation because of the influence of the foundations and of the turbine spindle if solidly coupled. Other causes of rotor roughness have been traced to thermal or magnetic sources and to the inequality in rotor stiffness in the direct and quadrature axes, as well as to improper adjustment of bearing clearances, oil whip, and other factors related to lubrication.

Measurement of rotor vibration is most commonly made at the bearings. There are several types of instruments in general use that accurately measure or record the amplitude of movement. Experience has shown that a single set of permissible bearing vibration amplitudes cannot be established that would safely cover all types and ranges of ratings. Consequently, the manufacturer's recommendations should be followed in each case.

Vibration in the stators of 2-pole generators sometimes results from the magnetic pull between rotor and stator in the air gap, the force being greater in the direct axis than in the quadrature axis. The rotating magnetic pull tends to deform the stator elliptically, thus creating a double frequency component of stator vibration. Adequate rigid bracing to limit the magnitude of the core distortion on large 2-pole machines proved impractical from the standpoint of shipping clearances, stator weight, and appearance. In most large modern 2-pole machines the core vibration is therefore usually isolated from the outer wrapper and foundation by means of some form of flexible support.

If the core is tightly clamped from the

ends, the laminations will be supported as a continuous ring that will have a natural frequency well above the 120-cycle forced frequency. Under this condition the amplitude of the core vibration will usually be well within safe limits, and little or no objectionable double frequency vibration is likely to be transmitted to the foundations. Occasionally, some parts of the outer wrapper plate or lagging may resonate at or near 120 cycles and the acceptable vibration amplitude of these parts will in most cases depend upon their manner of support or the nuisance value in the form of unpleasant noise, provided the core vibration is known to be safe. Proportions of 4-pole stators have been such that core vibration has seldom been troublesome.

The sudden appearance of new vibration or an increase in existing amplitude may be of greater significance to the operator than the steady continuous type of vibration. For this reason a history of vibration amplitudes is believed desirable for all machines. One of the first signs of short-circuited rotor turns may be increased rotor vibration. Removal of excitation will often indicate whether the effect is electromagnetic. Measurement of rotor resistance is seldom a reliable indication unless the exact temperature is also known. If the rotor has a temperature recorder the chart should be examined for indications of a sudden drop in rotor resistance at the time, vibration appeared. The rotor impedance with 110 volts, 60 cycles, applied to the rings is sometimes useful for detecting rotor turn short circuits provided an initial reading with no short-circuited turns is available for comparison. Most rotors will not take more than 5 to 10 amperes at 110 volts and hence can be tested from the lighting circuit if the rotor winding is not grounded.

Unlike short-circuited turns in the stator, short-circuited rotor turns do not necessarily require reinsulation immediately if a satisfactory balance can be achieved. Rotors have been known to operate for years with a few short circuits between successive turns in one or more coils. Experience has shown that short-circuited rotor turns are not usually progressive in nature and are more apt to reduce the temperatures in their respective coils than increase them. Of course, they do require more excitation amperes, and hence the rotor temperature as a whole is increased even though a temperature indicator may show the reverse.

If short-circuited turns cause a thermal unbalance, the vibration will vary with temperature and hence will lag any increase in excitation by the length of time required for heating to occur. If variation from the cold to the hot condition is not too great, weight adjustments can sometimes be made to keep the amplitude entirely within a satisfactory range for all temperatures.

Location of the slots containing short-circuited turns or coils may be possible in solid rotors without retaining ring removal by measuring the leakage flux across the top of the slot wedge with an alternating voltage applied to the collector rings and comparing the readings for the various slots. With nonmagnetic wedges a single short-circuited turn out of 20 or 30 turns will reduce nearly 50 per cent the alternating voltage induced in an exploring coil held above the slot wedge. Slots with magnetic wedges should be compared with each other as their leakage flux is quite low. An oscilloscope is often useful to measure the low exploring coil voltage if a 110-volt a-c supply is used across the collector rings. Other means are sometimes also used such as an a-c potentiometer. After location of the slots affected, thermal balancing may be possible by partial restriction of the ventilating ducts in the region of these slots. If axial ducts are not provided or accessible, the use of paint or other surface treatment for thermal balancing may be possible but this would probably be a trial and error process.

Increased rotor vibration could also indicate a displacement of rotor coil blocking or physical damage to the shaft or fans. A fiber baffle rubbing the shaft at one point has been known to cause severe shaft vibration. Such cases are unaffected by the removal of excitation and after tripping often continue during retardation.

A sudden appearance of stator vibration or noise might indicate high voltage, unbalanced load, or a loosening of the core to a point where some of the laminations have ceased to act as a rigid ring. It could also mean a loosening of some parts, either internal or external, that have become resonant at the frequency of the applied force or are being rattled about by the ventilating gas. In double-winding machines, a characteristic noise can be heard clearly when load is suddenly removed from one of the windings.

The appearance of vibration has also been traced to such external factors as the shifting of the foundation because of settling or thermal changes, coupling misalignment or uneven wear, roughness transmitted from the turbine spindle, unequal expansion of turbine and generator bearing supports, and it even has been traced to other machines in the same power plant. As an example of remotely induced vibration, internal inspection of a 35,000-kw hydrogen-cooled turbo-generator once revealed a continuously vibrating cooler tube while the unit was at rest with its rotor removed. The source of vibration was found to be a compressor operating in the basement of the power plant. Another interesting case consisted of a vibrating noise which after months of speculation was finally traced to a loose valve handle below the generator that was resonant to the minute vibration of the shell.

Shaft Currents and Bearing Insulation

The most common cause of induced shaft voltages is the inequality in reluctance of the parallel flux paths linking the rotor and the consequent pulsations in this component of flux. If both bearings are in electric contact with each other through a frame or base plate, substantial currents may flow through bearing oil films and may damage the shaft journals and the babbitt surface, as well as gears or other metallic parts in contact with the rotor or turbine spindle. Under certain conditions sludging of the lubricating oil may also occur.

By suitable combination of partings, lamination segments, and number of poles, the voltages from this source can sometimes be minimized, but the choice of these design details is greatly restricted in turbogenerators. Consequently, the outboard end of the rotor is usually insulated from ground, including the bearing, all piping connections, exciter coupling or bearings, hydrogen seal, etc.

Shaft currents can also result from a magnetized shaft, bearing pedestal, or end cover or from windings or end connections that produce axial flux in the rotor. The currents induced from these sources do not always flow from bearing to bearing, but can flow from shaft to babbitt at one end of the bearing and back again at the other. The bearing insulation will not prevent this type of circulating current. Fortunately, this condition is not common and the currents from it are not usually very great. It can often be detected by the characteristic scratches appearing at the extremities of the bearing journal, and its correction is usually possible by demagnetization of the affected parts. Cases of magnetized shafts, bearings, and end covers have been known to result from the dryout of stator windings using direct current or from double ground faults in rotors.

Bearing currents have also been found

to originate from electrostatic charges generated within the steam turbine. Pitting or abnormal wear of worm gears as well as objectionable radio and television interference have been traced to this source. The remedy in such cases is a grounding brush somewhere on the shaft or spindle.

The use of grounding brushes at both ends of the unit to short-circuit the shaft currents induced along the shaft has not been uniformly effective since the brushes themselves often have an appreciable contact potential drop. Damage to gears near the front end of the turbine has been reduced, however, by installation of a grounding brush near the gear.

With pedestal-type bearings or with bracket bearings where the outboard bracket is insulated from ground, there are various means to check the insulation of the outboard bearing while the unit is running. Perhaps the simplest consists of two successive measurements of voltage using an a-c d-c millivoltmeter, the first from a sliding contact on the shaft to ground at the outboard end of the rotor, and the second from the pedestal (or insulated bracket) to ground with a dead short circuit from a sliding contact on the shaft to the pedestal (or insulated bracket). If the bearing insulation is satisfactory both readings will be alike; if not, the second will be lower than the first.

To check the insulation of pipe joints while the unit is running, a couple of dry cells or a storage battery may be connected from the pedestal (or insulated bearing bracket if bracket type) to a point on the pipe 2 or 3 feet beyond the insulated flange. A d-c millivoltmeter connected across the 2- or 3-foot length of pipe between flange and battery connection will indicate whether any current is flowing through the insulated joint.

If the bearing is mounted within the end cover the insulation is sometimes located between the bearing pads and the bearing or between the bearing ring and end shield. In hydrogen-cooled machines seal insulation may be located between the seal and either the vents, brackets, or end shields. No separate seal insulation or bearing insulation is necessary if the bracket itself is insulated. In some types, oil seals are also insulated, and in some cases both hydrogen seals or both ends of the rotor may be insulated rather than only one. The insulation of such enclosed parts should be checked individually as each part is assembled. The insulation of thrust-bearing-type seals may be rechecked by pressing the seal ring back away from the shaft flange before the top half of the bearing is assembled. The main bearings and circular-type seals may be rechecked by lifting the rotor a few mils and sliding a thin sheet of insulation under the journal. Care must be exercised to avoid damaging oil wipers or other stationary parts by excessive lifting of the rotor. The condition of insulation with either bracket- or pedestal-type bearings can sometimes be checked while the machine is running by touching a grounded wire to the shaft to see whether a spark occurs. The absence of sparking may be an indication of faulty insulation unless the machine is known to be entirely free from shaft voltages.

The most common causes of faulty bearing or seal insulation are metallic chips or slivers in bolt holes or across small internal clearances. Embedded thermocouples, graphite or paint on insulating material or pipe flanges, and low resistance gasket material, as well as other forms of dirt, moisture, or foreign matter, have also been found to cause trouble.

References

Balancing

1. Balancing Turbine Generator Rotors, L. P. Grobel. *General Electric Review*, Schenectady, N. Y., vol. 56, July 1953, p. 22.

2. Modern Practice in the Balancing of Large Turbine-Generator Rotors, C. M. Laffoon, A. C. Hagg, C. H. Janthey, P. R. Heller. *AIEE Transactions*, vol. 70, pt. I, 1951, pp. 593–98.

3. Thermal Balancing of Large Rotors, W. F. King. *Allis-Chalmers Electrical Review*, Milwaukee, Wis., 3rd quarter, 1947, p. 8.

4. Balancing Is Easy if You Know How, W. F. King. *Ibid.*, 1946, pp. 25.

Short-Circuited Turns

5. Locating Shorted Turns in A-C Turbine Generator Field Coils, J. F. Kalbach. *Power*, New York, N. Y., vol. 93, no. 4, April 1949, pp. 80–81.

Vibration and Noise

6. Magnetic Vibrations in A-C Generator Stators, R. A. Baudry, P. R. Heller, L. P. Curtis. *AIEE Transactions*, vol. 73, pt. III, June 1954, pp. 508–16.

7. Suppression of Magnetic Vibration and Noise of Two-Pole Turbine Generators, A L Penniman, Jr , H. D. Taylor. *AIEE Transactions* (*Electrical Engineering*), vol. 60, June 1941, pp. 283–88.

8. Special Problems of Two-Pole Turbine Generators, C. M. Laffoon, B. A. Rose. *Ibid.*, vol. 59, Jan. 1940, pp. 30–33.

Shaft Currents

9. Bearing Corrosion in Turbo-Generators, F. A. Ten Broeke. *Corrosion*, Houston, Tex., vol. 4, no. 12, Dec. 1948, p. 590.

10. Shaft Currents in A-C Machinery, O. A. Olsen. *Power Generation*, New York, N. Y., vol. 53, Nov. 1949, p. 102.

11. Shaft Currents in Electric Machines, P. L. Alger, H. W. Samson. *AIEE Transactions*, vol. 43, Feb. 1924, pp. 235–45.

12. Currents in Bearings of Electric Generators, W. Buchanan. *Electrician*, London, England, vol. 75, May 28, 1915, pp. 266–67.

Analysis of Fault Currents for High-Voltage Circuit-Breaker Interruption

MARTIN J. LANTZ
MEMBER AIEE

THE most important factor in the operation of a circuit breaker under fault conditions is the current the breaker must interrupt. The purpose of this paper is twofold: To indicate and discuss the factors involved in the appraisal of interrupting duty of existing system circuit breakers; and to discuss relative magnitudes of currents for the different types of faults that a breaker must interrupt.

The basic or symmetrical rms current that the breaker must interrupt is calculated by the standard method of symmetrical components. Circuit conditions that may modify these basic current values are asymmetry of the current or d-c offset which increases the basic current value, and fault resistance which decreases the basic current.

The standard method of fault calculation is based on the AIEE general method which assumes all source voltages in phase, one per-unit internal voltage, subtransient machine reactance, and equality of positive- and negative-sequence reactance. Application of these data to the standard equations produces a current approximately equal to the theoretical current at time zero. A-c decrement is normally neglected for high-speed circuit breakers but is probably in the maximum order of 6 to 8 per cent for times of 3 to

---

Paper 55-102, recommended by the AIEE Switchgear Committee and approved by the AIEE Committee on Technical Operations for presentation at the AIEE Winter General Meeting, New York, N. Y., January 31–February 4, 1955. Manuscript submitted September 20, 1954; made available for printing November 29, 1954.

Martin J. Lantz is with the Breaker and Fault Analysis Unit, Bonneville Power Administration, Portland, Oreg.

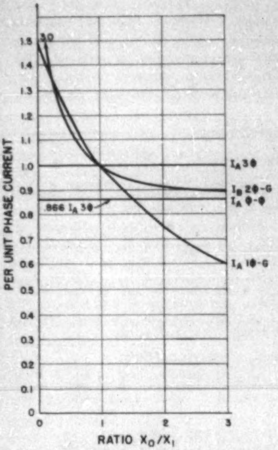

Fig. 1. Relationship of total fault current for various types of fault as a function of the X_0/X_1 fault-impedance ratio

5 cycles near generating plants.

The Appendix shows the standard equations and connotation for the calculation of the basic fault currents. These are the total currents to the fault. For ground faults, the total fault current I_g is equal to the summation of the phase currents to the fault. The circuit residual current is the summation of the zero-sequence currents in the three phases of the circuit and is equal to $3I_0$; however, this current does not flow in a single conductor to be interrupted by the circuit breaker except for a radial circuit to the fault point. For the majority of faults, the actual current to be interrupted by the first opening breaker is the phase current or current flowing through the conductor. This current is a combination of the sequence currents which are distributed according to their own network impedances. To determine the current to be interrupted by the first opening breaker, it is necessary to calculate the phase current through it by combining the various sequence currents in proper order. The second opening breaker for a 2-terminal circuit has a duty equal to that of a radial line breaker.

Fig. 1 shows the relationship of total fault currents for the various types of fault. If $X_1=X_2=X_0$, all faults are of equal magnitude except the phase-to-phase fault which is equal to 0.866 times the others. If X_0 is greater than X_1, the total phase current for the ground faults is less than the 3-phase fault current, as shown in the curve. If X_0 is less than X_1, the total phase current to the ground faults is greater than the 3-phase fault current with ideal limits of three times greater for the 2-phase-to-ground and 1.5 times greater for 1-phase-to-ground fault. The practical limits are approximately 1.35 to 1.4 corresponding to a ratio of X_0/X_1 of 0.2. From the curve it is apparent that the most severe total fault current results from either a 3-phase or phase-to-ground fault except for extreme low ratios of X_0/X_1.

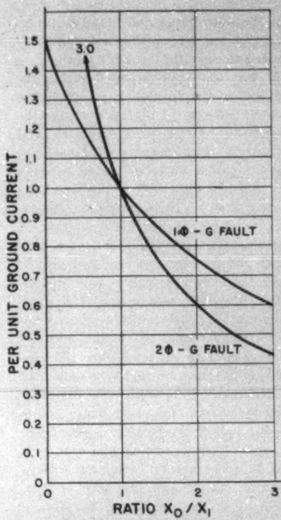

Fig. 2. Relationship of total residual fault current for single- and double-phase-to-ground faults as a function of the X_0/X_1 fault-impedance ratio

Fig. 2 shows the relationship of total residual or ground currents for the two types of ground faults. The same current limits are reached as for the phase currents for the theoretical lower ratio limit of zero. It will be noted that for the 1-phase-to-ground fault the total phase current and ground fault curves are equal.

In circuit-breaker application, it is the phase current which is interrupted in all cases. In special cases such as radial circuits, the phase current equals the residual or ground current for ground faults, since the radial current is the total fault current. This is not true when fault current is contributed from more than one path to the fault. In the appraisal of the amount of phase current interrupted by the circuit breaker, the branch current which does not go through the breaker to the fault is not interrupted and should be subtracted from the total value. This is a simple matter for the phase faults but becomes more involved for the ground faults. The phase-current distribution must be determined for the bus fault and the branch currents subtracted to determine the appropriate circuit-breaker current.

For ground faults, the ground-current magnitude is a function of all three impedance networks but its distribution is a function of the zero-sequence impedance network only. The determination of the phase-current distribution requires the sequence-current distribution of both the positive- and zero-sequence networks. The following equations may be used to determine the phase-current distribution from the sequence-current distribution.

1-phase-to-ground fault

$$\text{Branch phase current } I_A=2\times\text{total } I_0\times\frac{\text{branch } I \text{ 3-phase fault}}{\text{Total } I \text{ 3-phase fault}}+\text{branch } I_0$$

2-phase-to-ground fault

$$I_B \text{ branch phase current} =\frac{I \text{ branch 3-phase fault}}{I \text{ total 3-phase fault}}\left(\frac{a^2}{K_1}-aK_2\right)-\frac{I_0 \text{ branch 1-phase-to-ground fault}}{I_0 \text{ total 1-phase-to-ground fault}}(K_3)$$

where

$$K_1=X_1+\frac{X_1X_0}{X_1+X_0}$$

$$K_2=\frac{1}{X_1+2X_0}$$

$$K_3=\frac{X_0}{X_1^2+2X_1X_0}$$

$$a=-0.5+J.866$$
$$a^2=-0.5-J.866$$

The values of reactance are the total system sequence reactance to the point of fault. While the foregoing equations look cumbersome, they reduce down to simple calculations when the numerical values are known for a given location.

To determine the phase-current distribution for a 2-phase-to-ground fault, the data required are the 3-phase fault-current distribution and total positive-sequence impedance for a 3-phase fault and the zero-sequence current distribution any total zero-sequence impedance for a 1-phase-to-ground fault. This assumes that X_1 and X_2 are equal. The impedance constants may be computed and applied to the equation to evaluate the branch-faulted phase current for a 2-

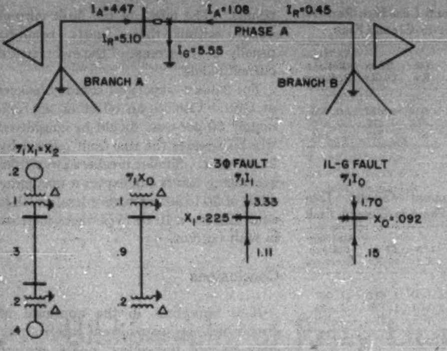

1Φ-G FAULT

$$\text{BRANCH } \Phi \text{ CURRENT} = 2 \times \text{TOTAL } I_0 \times \frac{\text{BRANCH } I\ 3\Phi \text{ FAULT}}{\text{TOTAL } I\ 3\Phi \text{ FAULT}} + \text{BRANCH } I_0$$

$$I_A \text{ BRANCH A} = 2 \times 1.85 \times \frac{3.33}{4.44} + 1.70 = 4.47$$

$$I_A \text{ BRANCH B} = 2 \times 1.85 \times \frac{1.11}{4.44} + .15 = 1.08$$

Fig. 3. Single-line-to-ground fault, phase-A current

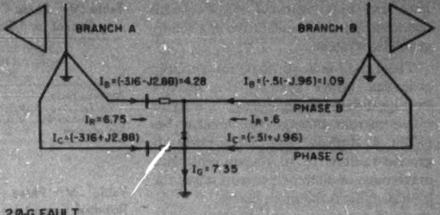

2Φ-G FAULT

$$I_B \text{ BRANCH } \Phi \text{ CURRENT} = \left(\frac{a^2}{k_1} - ak_3\right)\frac{I \text{ BRANCH } 3\Phi \text{ FAULT}}{I \text{ TOTAL } 3\Phi \text{ FAULT}} - \frac{k_2 I_0 \text{ BRANCH } 1\Phi\text{-G FAULT}}{I_0 \text{ TOTAL } 1\Phi - \text{G FAULT}}$$

$$k_1 = .225 + \frac{.225 \times .092}{.317} = .29$$

$$k_2 = \frac{1}{.225 + .184} = 2.45$$

$$k_3 = \frac{.092}{.225^2 + 2 \times .225 \times .092} = .99$$

$$\left(\frac{a^2}{k_1} - ak_3\right) = \frac{-.5 - J.866}{.29}\,(+.5 - J.866)\,.99 = -1.23 - J3.84$$

$$I_B \text{ BRANCH A} = \frac{3.33}{4.44}(-1.23 - J3.84) - \frac{1.70}{1.85} \times 2.45 = -3.16 - J2.88 = 4.28$$

$$I_B \text{ BRANCH B} = \frac{1.11}{4.44}(-1.23 - J3.84) - \frac{.15}{1.85} \times 2.45 = -.51 - J.96 = 1.09$$

Fig. 4. Two-phase-to-ground fault, phase-B and phase-C current

phase-to-ground fault which is the current to be interrupted by the circuit breaker.

An example of a simple computation is shown in Figs. 3 and 4 equation. These represent a generator and high-side grounded-neutral transformer on each end of a single-circuit transmission line. The fault is assumed on the line side terminals of the circuit breaker near the branch A bus. Assumed reactance and calculated current values are shown in per-unit values. The basic data required to determine the phase-current distribution for both single- and double-phase-to-ground faults are the phase-current (I_1) distribution for a 3-phase fault and the zero-sequence current (I_0) distribution for a single-phase-to-ground fault. These basic calculated data are shown. Application of the conversion equation permits calculation of the faulted phase currents for both types of ground faults. The residual currents $3I_0$ are also shown for comparative purposes as is the total fault current I_g. The X_0/X_1 ratio of this example is 0.41. From the curve for this ratio, a lower total phase current and a greater total ground current is to be expected for the 2-phase-to-ground fault compared to the 1-phase-to-ground fault. This is shown by the calculated values.

System Circuit-Breaker Analysis

A survey of 334 high-voltage circuit breakers on the Bonneville Power Administration solidly grounded system show the following relative interrupting duties for 3-phase and single-phase-to-ground faults. This study includes all circuit breakers of the main system except the circuit breakers at the Bonneville, Hungry Horse, and Grand Coulée generating plants. Table I shows the type of faults producing the most severe circuit-breaker duty and the number of breakers involved. Only 3-phase and single-phase-to-ground faults were studied since their duties were the most severe. The data indicate that about an equal number of the system breakers will receive their greatest duty from each type of fault. Also the data show that the relative position of the line, transformer, or other breakers does not modify the general picture of distribution of duty and type of fault. Other positions include shunt capacitor, bus tie, and bus-sectionalizing circuit breakers.

Table II shows the average and maximum ratios of phase current through the breaker for a single-phase-to-ground fault to the phase current through the breaker for a 3-phase fault where the ground fault was more severe. Table III shows the average and maximum ratios of phase fault to phase current through the breaker for a 3-phase current through the breaker for a single-phase-to-ground fault where the 3-phase fault was more severe. The 57-to 69-kv values are omitted from the all-breakers average because the grounding banks and remote ground sources result in high-fault zero-sequence imped-

Table I. Number and Type of Fault Producing Most Severe Circuit-Breaker Duty

	230 Kv		115 Kv		57 to 69 Kv	
	3-Phase Fault	1-Phase-to-Ground Fault	3-Phase Fault	1-Phase-to-Ground Fault	3-Phase Fault	1-Phase-to-Ground Fault
Line breakers	29	34	64	55	17	23
Transformer breakers	10	15	12	14	6	8
Others	8	6	15	14	2	2
Total	47	55	91	83	25	33

Table II. Ratio of I_ϕ Current for Ground Fault to I-Phase Current for 3-Phase Fault

	230 Kv	115 Kv	57 to 69 Kv	All High-Voltage Circuit Breakers
Average ratio	1.414	1.184	1.166	1.167
Maximum ratio	1.488	1.538	1.348	1.538

Table III. Ratio of I_ϕ Current for 3-Phase Fault to I_ϕ Current for Ground Fault

	230 Kv	115 Kv	57 to 69 Kv	All High-Voltage Breakers*
Average ratio	1.132	1.198	1.946*	1.170
Maximum ratio	1.400	1.563	5.000*	1.563

* These values are high because of grounding banks and remote ground-current sources.

ance and high ratios of X_0/X_1. This condition is not representative of a solidly grounded system.

These data indicate that, for a solidly grounded power system, the relative average differential in severity of duty or phase current through the breaker between a 3-phase and single-phase-to-ground fault is 13 to 19 per cent with maximums of 40 to 56 per cent when the 3-phase fault is the more severe.

The circuit-breaker duty is determined by the actual phase current passing through it to the fault. This is not the residual current for a ground fault except for the case of a radial position with no backfeed of either positive- or zero-sequence currents. Erroneous breaker duties will result when residual currents are used to determine breaker duties. A study of the fault currents where the ground fault exceeded the 3-phase fault indicates the relationship between phase currents and residual currents present in the breaker positions; see Tables IV, V, and VI.

These data indicate that unless the phase current is used for determining the breaker duty, for single-phase-to-ground faults, the average breaker duty calculated would have been 9.5 per cent too great with a maximum error of 43 per cent for approximately half the system breakers and 5.7 per cent too small with a maximum error of 44.6 per cent for the other half. It also shows that for 32 of the systems breakers the phase current on the average was 5.8 per cent greater than either residual current for a 1-phase-to-ground fault or phase current for a 3-phase fault with a maximum of 18.3 per cent greater. These data may or may not be important in the application of new circuit breakers but they are important in appraising the duties to be expected of existing system breakers. Phase current through the circuit breaker should always be used to determine the actual circuit-breaker duty. The main purpose of this paper is to discuss the factors involved in the appraisal of interrupting duty of existing system circuit breakers. The application of new breakers would be based on the same fundamental data but adequate allowance must be made for system expansion. A study of existing breakers on an expanding system should be made periodically to make sure that they may not be seriously overstressed by fault.

Table IV. Phase Current Less Than Residual Current for 1-Phase-to-Ground Fault

	230 Kv	115 Kv	57 to 69 Kv	All High-Voltage Breakers
Average ratio I_ϕ/I_g	0.904	0.912	0.885	0.905
Minimum ratio	0.626	0.675	0.570	0.570
No. of cases	56	87	25	168

Table V. Phase Current Greater Than Residual Current for 1-Phase-to-Ground Fault

	230 Kv	115 Kv	57 to 69 Kv	All High-Voltage Breakers
Average ratio I_ϕ/I_g	1.098	1.050	1.012	1.057
Maximum ratio	1.554	1.454	1.136	1.554
No. of cases	46	87	29	162

Table VI. Phase Current Greater Than Either Residual Current for 1-Phase-to-Ground Fault or Phase Current for a 3-Phase Fault

	230 Kv	115 Kv	57 to 69 Kv	All High-Voltage Breakers
Average ratio I_ϕ/I_g or $I_{3\phi}$	1.056	1.080	1.035	1.058
Maximum ratio	1.109	1.183	1.136	1.183
No. of cases	15	9	8	32

When the maximum symmetrical current possible for the breaker to be required to interrupt is determined, there are still other factors to be considered. Normally zero-fault resistance is used for ground-fault calculations; however, tower-footing resistance may limit the possible fault current reducing the breaker duty.[1] In appraising the possible fault duty of a circuit breaker, probability factors should be considered. One factor is the exposure involved. The amount of physical exposure to fault for a bus sectionalizing, capacitor, or transformer breaker is much smaller than that of a bus tie breaker, used as a line breaker, or line breakers. The chances of a fault occurring are therefore less; however, if the fault does occur, it is more likely to approach the maximum calculated value. The probability of a fault occurring on the terminals of a line breaker are remote. Since the breaker duty decreases as the fault-location distance increases from the breaker location, it is logical to apply a probability factor to line breakers especially for ground faults on lines protected by a section of overhead ground wire adjacent to the stations.

Asymmetry of fault current to be interrupted should be considered when the circuit breaker is sensitive to d-c offset, especially for high-speed breakers located near generating stations.[2] The degree of fault-current asymmetry is a function of the phase position of the voltage at the time of fault. If the fault occurs at maximum voltage, there is no offset but if the fault occurs at the zero point of the voltage wave, complete offset results. The offset of the fault current varies within these limits resulting usually in an increase of the symmetrical current values.

For 230-kv 3-cycle oil circuit breakers at Grand Coulée, an offset of approximately 50 per cent should be considered which increases the rms fault current by 22 per cent. Similar breakers away from generating plants can expect a maximum offset of 30 to 40 per cent or less, which is equivalent to a 10 to 15-per-cent increase in fault current.

Conclusions

It is important in the appraisal of circuit-breaker fault-current interrupting duty to use the actual phase current through the breaker. The most severe total fault current will result for a 3-phase fault if the X_0/X_1 ratio is greater than unity. The most severe total fault current will result for a single-phase-to-ground fault if the X_0/X_1 ratio is less than unity and greater than approximately 2/10th. Lower ratios will produce the greatest fault current with a 2-phase-to-ground fault.

All faults with the exception of the phase to phase fault are of equal magnitude if the X_0/X_1 ratio is unity. Other factors to be considered in the determination of the maximum probable fault current to be interrupted are possible fault resistance, possible asymmetry of fault current, and degree of physical exposure of associated circuits to faults.

Appendix. Standard Equations for Calculation of Basic Fault Currents

3-phase fault

$$I_1=\frac{E}{X_1}=1$$

where

$I_A=1$
$I_B=1$
$I_C=1$

Phase-*B*-to-phase-*C* fault

$$I_1=-I_2=\frac{E}{X_1+X_2}=0.5$$

where

$I_A=0$
$I_B=-J\,0.866$
$I_C=J\,0.866$

Phase-*A*-to-ground fault

$$I_1=I_2=I_0=\frac{E}{X_1+X_2+X_0}=0.333$$

where

$I_A=I_g=3I_0=1$
$I_B=0$
$I_C=0$

Phase-*B*-to-phase-*C*-to-ground fault

$$I_2+I_0=-I_1=\frac{E}{X_1+\frac{X_2X_0}{X_2+X_0}}=0.667$$

where

$I_A=0$
$I_B=-0.5-J\,0.866=1$
$I_C=-0.5+J\,0.866=1$

Nomenclature

X_1 = positive-sequence reactance
X_2 = negative-sequence reactance
X_0 = zero-sequence reactance
I_1 = positive-sequence current
I_2 = negative-sequence current
I_0 = zero-sequence current
$X_1=X_2=X_0=1$
$I_A=I_1+I_2+I_0$
$I_B=a^2I_1+aI_2+I_0$
$I_C=aI_1+a^2I_2+I_0$
$E=1$
I_A = phase-*A* current
I_B = phase-*B* current
I_C = phase-*C* current
$I_R=I_g=3I_0$ = ground or residual current
$a=-0.5+J0.866$
$a^2=-0.5-J0.866$

References

1. Effect of Fault Resistance on Ground-Fault Current, Martin J. Lantz. *AIEE Transactions*, vol. 72, pt. III, Oct. 1953, pp. 1016–19.

2. Power System Fault Current Analysis Including Study of Transient Offset, Martin J. Lantz. *AIEE Transactions*, vol. 73, pt. III, Oct. 1954, pp. 1073–78.

Bibliography of Relay Literature 1950–1952

ERIC T. B. GROSS
FELLOW AIEE

THIS bibliography is a continuation of similar bibliographies of relay literature which have been published previously and are contained in the following volumes of the *AIEE Transactions:*

1927–1939, vol. 60, 1941, 1435–47.
1940–1943, vol. 63, 1944, 705–09.
1944–1946, vol. 67, pt. I, 1948, 24–27.
1947–1949, vol. 70, pt. I, 1951, 247–50.

The papers listed include those in the field of relaying, as well as in associated fields, published in this country. Included are articles covering relaying, as well as service restoration, testing, system stability, methods of calculation, instrument transformers and other auxiliary devices, which are available in *Science Abstracts, Section B*, and in other digesting or indexing periodicals, as well as in the original magazines listed.

Depending upon the general substance of each article, the listing of the titles is subdivided into 13 sections. The entries in each section are numbered consecutively and listed by year in alphabetical order, the name of the first author determining the alphabetical position. Though some of the papers referred to may cover material in various sections, each title is listed in only one section. A list of periodicals which have been cited and their place of publication is given on page 48.

Section A. Line Protection—Distance Relaying

1. Norwegian Distance Relays—Characteristics and Experience of Operation, J. L. Braten. *Elektroteknisk Tidsskrift*, vol. 63, 1950, pp. 309–17.

2. A New Rapid Acting Distance Relay, H. Hoel. *Ibid.*, pp. 349–54.

3. High-Speed Distance Protection, A. Matthey-Doret. *Brown Boveri Review*, vol. 37, 1950, pp. 162–66.

4. Combined Phase and Ground Distance Relaying, Warren C. New. *AIEE Transactions*, vol. 69, pt. I, 1950, pp. 37–44.

5. Progress in the Field of Quick-Response Distance Protection for Extra High Voltage Supply Networks, F. Parschalk. *VDE-Fachberichte*, vol. 14, 1950, pp. 21–25.

6. Use of Compensated Selective Impedance Elements for the Detection of Faulty Phases, A. B. Chernin. *Elektrichestvo*, no. 9, 1951, pp. 12–18.

7. The Technical Basis of Resistance Measurement in the New Siemens Line Protection, H. Neugebauer. *Siemens Zeitschrift*, vol. 25, 1951, pp. 244–51.

8. Analysis of the Indications of Distance Impedance Relays on Very Long Lines, S. S. Rafili. *Elektrichestvo*, no. 6, 1951, pp. 51–58.

9. Progress in the Construction of Selective Protective Installations, G. Stark. *Elektrotechnik*, vol. 5, 1951, pp. 407–11.

10. Grapho-Analytical Method of Investigating the Performance of Distance Relays, G. I. Atabekov. *Elektrichestvo*, no. 2, 1952, pp. 23–32.

11. Influence of the Star-Delta Transformation on the Operation of Distance Relays, G. I. Atabekov. *Ibid.*, no. 5, pp. 20–23.

12. Breakdown and Relay Protection, J. L. Braten. *Elektroteknisk Tidsskrift*, vol. 65, 1952, pp. 277–86.

13. Development and Testing of an Experimental System of Discriminating Protection for Faults Between Phases and Phase to Earth on High Voltage Lines and Networks with the Neutral Completely Insulated, A. Parrini, E. Sailer, G. Segre. *Report No. 318* CIGRE, 1952.

14. Double Earth Fault Tests on the Austrian 220 kv System, W. Weller, F. Zimmermann. *Osterreichische Zeitschrift fur Elektrizitaetswirtschaft*, vol. 5, 1952, pp. 75–77.

Section B. Line Protection—Pilot Wire and Carrier Current

1. Line Tuning Equipment Used with Coaxial Cable for Carrier Current Installation on Power Lines, Howard J. Sutton. *AIEE Transactions*, vol. 68, pt. I, 1949, pp. 44–49.

2. Carrier Relaying Aids 115-kv New England Tie Lines, H. L. Goodrich. *Electrical World*, vol. 133, no. 11, Mar. 13, 1950, pp. 84–86.

3. The Intertripping of Remote Circuit Breakers on Electric Power Systems, A. P. Gordon, J. Rushton. *Metropolitan-Vickers Gazette*, vol. 23, 1950, pp. 228–32.

4. Current Transformer Difference Overcome with Percentage Type Relay, J. H. Samson, E. L. Michelson. *Electrical World*, vol. 134, Dec. 8, 1950, pp. 96–98, 111.

5. The Application of Phase-Comparison Principles to Power-Swing Conditions on Long High-Voltage Transmission Lines, G. W. Donaldson. *Proceedings*, Institution of Electrical Engineers, vol. 98, pt. 2, 1951, pp. 47–49.

6. Choice of Telemetering Systems and Channels for a Power System, C. K. Duff. *AIEE Transaction*, vol. 70, pt. I, 1951, pp. 1086–91.

7. Factors in the Choice of Microwave and Carrier Channels for Power System Operation and Dispatching, F. C. Krings. *Proceedings*, Midwest Power Conference, vol. 13, 1951, pp. 351–57.

8. Measurements and Tests on a Power Line Carrier Relaying System, R. H. Miller, A. R. Worthington. *AIEE Transactions*, vol. 70, pt. I, 1951, pp. 1005–07.

9. A New Carrier-Current Frequency-Shift System for Use with Differential Protection of Transformer Banks, R. W. Beckwith. *Ibid.*, pp. 832–35.

10. Considerations in Selecting a Carrier Relaying System, R. C. Cheek, J. L. Blackburn. *AIEE Transactions*, vol. 71, pt. III, Jan. 1952, pp. 10–18.

11. Experimental Investigation of Transient Interference from Power Line Faults on Carrier Current Equipment with Reference to Relaying, H. Elmlund, S. Engstrom, A. Hollner. *Paper 303*, CIGRE, 1952.

12. Power-Line Carrier for Relaying and Joint Usage, Part II. A Survey of Modern Power-Line Carrier Systems, G. W. Hampe, B. W. Storer. *AIEE Transactions*, vol. 71, pt. III, Aug. 1952, pp. 661–70.

13. Protective Relaying Over Microwave Channels, H. W. Lensner. *Ibid.*, Jan., pp. 240–05.

14. Pilot Relaying for Transmission Systems, S. C. Leyland, J. L. Blackburn. *Paper 310*, CIGRE, 1952.

15. A Phase-Comparison Carrier-Current

Paper 55-93, recommended by the AIEE Relays Committee and approved by the AIEE Committee on Technical Operations for presentation at the AIEE Winter General Meeting, New York, N. Y., January 31–February 4, 1955. Manuscript submitted October 20, 1954; made available for printing November 18, 1954.

Eric T. B. Gross is with the Illinois Institute of Technology, Chicago, Ill.

Relaying System for Broader Application, **N. O. Rice, J. S. Smith.** *AIEE Transactions*, vol. 71, pt. III, Jan. 1952, pp. 246–50.

16. The Protection of Teed Feeders, **J. Rushton, F. A. Stary.** *Metropolitan-Vickers Gazette*, vol. 24, 1952, pp. 247–56.

Section C. Line Protection—Ground Faults

1. Earth-Leakage Protection, **C. A. Martin.** *Transactions*, South African Institute of Electrical Engineers, vol. 41, 1950, pp. 133–204.

2. Sensitive Ground Protection, **AIEE Committee Report.** *AIEE Transactions*, vol. 69, pt. I, 1950, pp. 473–76.

3. Operating Experience with Ground Distance Relays, **M. P. Osburn, P. L. Dandeno.** *Ibid.*, vol. 70, pt. II, 1951, pp. 1508–16.

4. Ground Fault Relay Protection of Transmission Lines, **J. L. Blackburn.** *Ibid.*, vol. 71, pt. III, Aug. 1952, pp. 685–92.

5. Ground Relay Polarization, **J. L. Blackburn.** *Ibid.*, Dec., pp. 1088–95.

6. Suitable Current Polarizing Sources for Ground-Type Relays, **O. A. Lentz.** *Electrical World*, vol. 138, Dec. 29, 1952, pp. 74–76.

7. The Adjustment of Earth Fault Protection with Cable Current Transformers, **A. V. Ostrovskaya, I. M. Sirota.** *Elektricheskie Stantsii*, no. 3, 1952, pp. 30–32.

8. Sensitive Earth-Fault Protection with Cable Type Current Transformers, **I. N. Popov.** *Elektrichestvo*, pp. 3, 1952, pp. 38–43.

Section D. Line Protection—General

1. Relaying of Transmission Lines from New Sunbury Generating Station, **H. H. Green, J. A. G. Oewel, O. Ramsaur.** *AIEE Transactions*, vol. 68, pt. II, 1949, pp. 873–78.

2. Relay Protection for Medium Length High-Voltage Transmission Lines, **J. H. Kinghorn.** *Ibid.*, vol. 69, pt. I, 1950, pp. 461–67.

3. Transmission-Line Protection of Short Lines of the Metropolitan Area of a Typical System, **W. E. Marter.** *Ibid.*, pp. 468–72.

4. Unique Protection Required for Midwest Interconnection, **A. J. Nicholson.** *Electric Light and Power*, vol. 28, Nov. 1950, pp. 90–94, 96.

5. Protection of the French Electric Transmission Network, **M. Dietsch.** *Bulletin*, Association des Ingenieurs Electriciens Sortis de l'Institut Electrotechnique Montefiore, vol. 64, 1951, pp. 331–49.

6. Series Capacitors During Faults and Reclosing, **E. L. Harder, J. E. Barkle, R. W. Ferguson.** *AIEE Transactions*, vol. 70, pt. II, 1951, pp. 1627–42.

7. Short-Circuit in Parallel Cable Connections. Current Distribution and Selective Protection, **G. Schulerud.** *Elektroteknisk Tidsskrift*, vol. 64, 1951, pp. 285–95.

8. Short Circuit Protection in High-Voltage Networks, **I. Bach.** *Elektrotechnika*, vol. 45, 1952, pp. 238–50.

9. Back-up Protection in High Voltage Systems, **C. Jean Richard.** *Bulletin*, Association Suisse des Electriciens, vol. 43, 1952, pp. 425–28.

10. Automatic Reclosing on the French Power Transmission System, **L. Roche.** *Bulletin*, Societe Francaise des Electriciens, Series 7, vol. 2, 1952, pp. 501–12.

11. Simple but Foolproof Scheme of Back-Up Cable Relaying, **George Steeb.** *Electrical World*, vol. 137, June 30, 1952, pp. 76–78.

Section E. Bus Protection

Section F. Apparatus Protection

1. Shipshaw Relay Protection, **J. T. Madill, F. H. Duffy.** *AIEE Transaction*, vol. 68, pt. I, 1949, pp. 50–58.

2. Differential Relay Sensitivity Adjuster, **C. L. Headley.** *Ibid.*, vol. 69, pt. II, 1950, pp. 1203–06.

3. Back-up Protection for System Faults at Generator, **D. C. Hoffmann.** *General Electric Review*, vol. 53, no. 2, 1950, pp. 38–41.

4. Theory and Application of Transformer Differential Protection, **George W. McKenna.** *AIEE Transactions*, vol. 69, pt. II, 1950, pp. 1197–1202.

5. Note on the Performance of the Differential Protection of Transformers, **M. Poli.** *Paper 112*, Associazione Elettrotecnica Italiana, vol. 2. 1950, pp. 107–12.

6. A New Carrier-Current Frequency-Shift System for Use with Differential Protection of Transformer Banks, **R. W. Beckwith.** *AIEE Transactions*, vol. 70, pt. I, 1951, pp. 832–35.

7. Thermal Relay for Protection of Transformers on Overload (Westinghouse Type T.R.O. Relay), **H. Demoulin, L. Marique.** *Ateliers de Constructions Electriques de Charleroi*, no. 1, 1951, pp. 18–29.

8. A New Heat Operated Relay for Protection of Transformers, Cables and Other Electrical Machinery, **P. Ignacz.** *Elektrotechnika*, vol. 44, 1951, pp. 308–11.

9. Earth Fault Protection of Generators in Resistance Earthed Networks, **G. Lengyel.** *Ibid.*, pp. 335–44.

10. Instantaneous Balanced Current Protection Using a High Impedance Relay with Bar-Primary Current Transformers, **J. Rushton, F. E. Wellman.** *Metropolitan-Vickers Gazette*, vol. 23, 1951, pp. 369–78.

11. A New Type of Temperature Relay Used for Protection of Transformers, **L. Marton.** *Elektrotechnika*, vol. 44, 1951, pp. 312–19.

12. Protection of Series Condensers Against External Disturbances and Internal Faults, **R. Pelissier.** *Bulletin*, Societe Francaise des Electriciens, series 7, vol. 1, 1951, pp. 492–98.

13. Power Transformer Protection. Checking Connections of "Ratio Differential" and "Circulating Current Relays," **V. B. Shah.** *Electrical Review*, vol. 149, 1951, pp. 937–40.

14. Relay Protection of A-C Generators, **AIEE Committee Report.** *AIEE Transactions*, vol. 70, pt. I, 1951, pp. 275–82.

15. Sensitive Ground Relaying of A-C Generators, **Eric T. B. Gross.** *Ibid.*, vol. 71, pt. III, Apr. 1952, pp. 539–44.

16. Recent Achievements in the Field of Generator Earth Leakage Protection, **R. Kurdziel.** *Przeglad Elektrotechnicsny*, vol. 28, 1952, pp. 190–201.

17. Instrumentation Details of the New Siemens Differential Protection, **H. Neugebauer.** *Siemens Zeitschrift*, vol. 26, 1952, pp. 219–24.

18. Novel Frame Protection for High-Voltage Machines, **H. Steel.** *Deutscher Elektrotechniker*, vol. 6, 1952, pp. 374–76.

19. The Operation of Turbo Alternators Under Unbalanced or Out-of-Step Conditions, **A. Wust, J. Dispaux.** *Paper 106*, CIGRE, 1952.

Section G. Distribution and Network Protection

1. Protection Against Short-Circuits on the 22-kv Network in South Bohemia, **J. Heral, J. Richtr.** *Elektrotechnicky Obzor*, vol. 40, 1951, pp. 372–79.

2. Relay Protection of 33-kv Tie Feeders, **W. H. O'Connor, H. D. Ruger.** *Electrical Engineering*, vol. 71, Feb. 1952, pp. 165.

3. New Selective Protective Circuits for Medium-Voltage Distribution Substations and High-Voltage Transformer Stations, **C. Ramelot.** *Bulletin*, Association des Ingenieurs Electriciens Sortis de l'Institut Electrotechnique Montefiore, vol. 64, 1951, pp. 99–112.

4. Experience with 3-ph. Low-Voltage Interconnected Networks in Berlin, **H. Weber.** *Elektrotechnische Zeitschrift*, vol. 73, 1952, pp. 162–65.

Section H. Service Restoration

1. The Bonneville Power Administration Relaying and Reclosing Program, **Clifford C. Diemond, Donald L. Wylie.** *AIEE Transaction* vol. 69, pt. II, 1950, pp. 1039–48.

2. High-Speed Auto-Reclosing for High-Voltage Transmission Systems, **R. K. Edgley.** *Reyrolle Review*, no. 141, 1950.

3. An Improved Reclosing Relay, **L. E. Goff.** *AIEE Transactions*, vol. 69, pt. II, 1950, pp. 1480–87.

4. Consideration of Requirements and Limitations of Relaying and High-Speed Reclosing on Long and Heavily-Loaded Transmission Lines, **C. E. Parks, W. R. Brownlee.** *Ibid.*, pt. I, pp. 103–09.

5. Combined Application of Automatic Reclosing, a New Protective Relay, and an Arc-Suppression Coil, **B. Pavlovsky.** *Elektrotechnicky Obzor*, vol. 39, 1950, pp. 310–18.

6. The Fault Removal Service of the (Austrian) Interconnected Network, **K. Mayer.** *Osterreichische Zeitschrift fur Elektrizitaetswirtschaft*, vol. 4, 1951, pp. 171–75.

7. Single Pole Reclosing: Relaying Problems and Arc Extinction Times, **W. P. Dobson, V. V. Mason.** *Paper 316*, CIGRE, 1952.

8. Relay Equipment Designed for Automatic Reclosing, **E. Elmlund, T. Holm.** *ASEA Journal*, vol. 25, 1952, pp. 91–102.

9. Experience with Auto-Reclosing Systems on 220 and 150 kv Systems of Electricite de France in 1950 and 1951, **Petard.** *Bulletin*, Societe Francaise des Electriciens, series 7, vol. 2, 1952, pp. 513–15.

10. Relay Protection and Automatic Phase Reclosing on Short Circuit Between Two Phases and Short Circuit of a Phase to Earth, **M. P. Razenknop, A. B. Chernin.** *Elektricheskie Stantsii*, no. 3, 1952, pp. 33–38.

11. Rapid Reclosing Tests on a 30-kv Distribution Network, **B. Thoren.** *ASEA Journal*, vol. 25, 1952, pp. 102–08.

Section I. General and Miscellaneous Relaying

1. New Direct-Acting Relay for Ring-Type Networks, **A. Matena.** *Engineers Digest*, vol. 11, 1950, pp. 347–48.

2. Relaying Practices and Economical Switching Station Arrangements of the Bureau of Reclamation, **W. A. Morgan, R. W. World.** *AIEE Transaction*, vol. 69, pt. II, 1950, pp. 865–71.

3. Relay Maintenance of a Metropolitan Power System, **W. J. Smith.** *Proceedings*, Midwest Power Conference, vol. 12, 1950, pp. 446–50.

4. A Study of Directional Element Connections for Phase Relays, **W. K. Sonnemann.** *AIEE Transactions*, vol. 69, pt. II, 1950, pp. 1438–51.

5. Directional Relay Circuits for Protection Against Phase-to-Phase Faults, **H. Stalder.** *Brown Boveri Review*, vol. 37, 1950, pp. 166–71.

6. Analysis of the Operation of a Directional Induction Relay with Cylindrical Rotor During Transient Processes, **L. A. Gelbukh.** *Elektrichestvo*, no. 2, 1951, pp. 21–24.

7. Tendencies Regarding Machine Protection of Electricite de France. Characteristics of the French Grid and Their Effect on Line Protection, **P. Henriet.** *Bulletin*, Association des Ingenieurs Electriciens Sortis de l'Institut Electrotechnique Montefiore, vol. 64, 1951, pp. 313–30.

8. Protective Gear, **E. H. Hubert.** *Ibid.*, pp. 35–59.

9. Design Features of a Modern Induction-Pattern Overcurrent Relay, **H. S. Lewis.** *General Electric Review*, vol. 18, 1951, pp. 111–23.

10. Protective Relaying on Industrial Power Systems, **Carl M. Lathrop, Charles E. Schleckser.** *AIEE Transaction*, vol. 70, pt. II, 1951, pp. 1341–45.

11. Bibliography of Relay Literature 1947–1949, **AIEE Committee Report.** *Ibid.*, pt. I, pp. 247–50.

12. Induction Type Resistance Relay, **A. M. Bresler.** *Elektrichestvo*, no. 9, 1952, pp. 57–60.

13. Selecting A-C Overcurrent Protective Device Settings for Industrial Plants, **F. P. Brightman.** *AIEE Transactions*, vol. 71, pt. II, Sept. 1952, pp. 203–11.

14. Sub-Station Practice (book), **T. H. Carr.** Chapman and Hall, London, England, 2nd ed., 1952.

15. Reactance Relays Discriminate Between Load-Transfer Currents and Fault Currents on 2,300-Volt Station Service Generator Bus, **G. B. Dodds, W. E. Marter.** *AIEE Transactions*, vol. 71, pt. III, Dec. 1952, pp. 1124–28.

16. The Protection of Electrical Power Systems: A Critical Review of Present-Day Practice and Recent Progress, **H. Leyburn, C. H. W. Lackey.** *Proceedings*, Institution of Electrical Engineers, vol. 99 pt. 2, 1952 pp. 47-66.

17. The Application of Transductors as Relays to Protective Gear, **R. K. Edgley, F. L. Hamilton.** *Ibid.*, pp. 297–313, 344–48.

18. Generalized Distance and Differential Protection and the Corresponding Fault Location Devices, **J. Ilivici.** *Bulletin*, Societe Francaise des Electriciens, series 7, vol. 2, 1952, pp. 447–56.

19. Report of Study Committee on Protection and Relaying, **S. Margoulies.** *Paper 332*, CIGRE, 1952.

20. Report of the International Study Committee on Protection and Relaying, **S. Margoulies.** *Paper 325*, Ibid.

21. Blocking Relay for Improvement of Protection of Long 220 kv Lines, **M. F. Melnikov.** *Elektricheskie Stantsii*, no. 10, 1952, pp. 48–51.

Section J. Testing and Analyzing

1. Detection of Overheated Transmission Line Joints by Means of Bolometer, **J. R. Leslie, J. R. Watt.** *AIEE Transactions*, vol. 68, pt. I, 1949, pp. 64–69.

2. Insulator Flashover Deionization Times as a Factor in Applying High-Speed Reclosing Circuit Breakers, **A. C. Boisseau, B. W. Wyman, W. F. Skeats.** *Ibid.*, pt. II, pp. 1058–67.

3. Fault-Throwing Tests on the 132 kv Grid System Under Normal Working Conditions, **W. Casson, F. H. Birch.** *Proceedings*, Institution of Electrical Engineers, vol. 97, pt. 1, 1950, pp. 279–301.

4. Deionization Time of High-Voltage Fault-Arc Paths, **Everett J. Harrington, E. C. Starr.** *AIEE Transactions*, vol. 68, pt. II, 1949, pp. 997–1004.

5. Fault Location by Pulse Time Modulation, **R. W. Hughes, Nelson Weintraub.** *Electrical Engineering*, vol. 69, Nov. 1950, pp. 1009–11.

6. Measuring Apparatus for Relay Equipment, **B. J. Larsson.** *ASEA Journal*, vol. 23, 1950, pp. 31–36.

7. Transient Fault Locator Proves Out in Operation, **L. R. Spaulding,** *Electrical World*, vol. 133, no. 25, 1950, pp. 110.

8. A Transient Fault Locator for High-Voltage Transmission Lines, **L. R. Spaulding, C. C. Diemond.** *AIEE Transactions*, vol. 68, pt. II, 1949, pp. 1005–12.

9. Relay Testing Practices in a Power Company Serving a Large Area, **V. E. Verrall.** *Proceedings*, Midwest Power Conference, vol. 12, 1950, pp. 451–54.

10. Application of Power Line Outage Monitor, **John F. Atkinson, James D. Cooke.** *AIEE Transactions*, vol. 70, pt. II, 1951, pp. 1292–96.

11. Line Fault Location by Impulses, **C. Beguin.** *Cables et Transmission*, vol. 5, 1951, pp. 315–24.

12. The Role of Field Tests on the Network in the Development of High Voltage Equipment, **M. Laborde.** *Bulletin*, Societe Francaise des Electriciens, series 7, vol. 1, 1951, pp. 157–76.

13. Traveling Wave Relations Applicable to Power-System Fault Locators, **Laurel J. Lewis.** *AIEE Transactions*, vol. 70, pt. II, 1951, pp. 1671–80.

14., Impulse Method of Locating Cable Faults, **A. Ya. Usikov, I. Kh. Vakser.** *Elektrichestvo*, no. 10, 1951, pp. 20–23.

15. The Location of Transient Faults on Overhead Lines by Means of Apparatus Measuring the Turning of a Relay Movement. Principles and Results of Operation, **P. Devilane.** *Bulletin*, Societe Francaise des Electriciens, series 7, vol. 2, 1952, pp. 271–80.

16. Turning Relay Apparatus Used for the Location of Transient Faults, **C. Kaplan.** *Ibid.*, pp. 281–87.

Section K. System Stability

1. Stability Conditions of the Swedish Trunk-Line System, **S. Lalander, D. Jungnell.** *Svenska Vattenkraft Foreningens Publikationer*, no. 418, vol. 10, 1950, pp. 343–84.

2. High-Speed Reclosure of Circuit-Breakers, **J. R. Mortlock.** *BTH Activities*, vol. 21, 1950, pp. 188–92.

3. An Electric Analogue Method for the Direct Determination of Power System Stability Swing Curves, **W. B. Boast, J. D. Rector.** *AIEE Transactions*, vol. 70, pt. II, 1951, pp. 1833–36.

4. Methods of Assessing the Stability of an A-C Power System, **R. F. Linsell.** *Engineer*, vol. 192, 1951, pp. 332–34.

5. The Behaviour of Selective Protective Equipment During Phase Swing, **A. Thewalt.** *Elektrotechnische Zeitschrift*, vol. 72, 1951, pp. 20–23.

6. Accurate Computation of 2-Machine Stability, **Ralph D. Goodrich, Jr.** *AIEE Transactions*, vol. 71, pt. III, Aug. 1952, pp. 577–81.

7. Power System Stability Criteria for Design, **W. A. Morgan.** *Ibid.*, Jan., pp. 499–504.

8. A Note on the Equal Area Stability Criterion, **J. E. Parton.** *Proceedings*, Institution of Electrical Engineers, vol. 99, pt. 4, 1952, pp. 204–16.

9. Report of the International Study Committee No. 13: System Stability and Voltage-Load-Frequency Control, **B. G. Rathsman.** *Report 336*, CIGRE, 1952.

10. Comparison, Based on Stability Angle, of Different Types of Reclosing on Transmission Lines and Inter-Connectors, **R. Robert.** *Bulletin*, Societe Francaise des Electriciens, series 7, vol. 2, 1952, pp. 516–25.

Section L. Methods of Calculation

1. Hochspannung und Hochleistung (book), **J. Biermanns.** Carl Hanser Verlag, Munich, Germany, 1949.

2. Calculation of Short-Circuit Currents at Electrically Remote Locations, **R. T. Lythall.** *Iron and Coal Trades Review*, vol. 159, 1949, pp. 1291–94.

3. How to Calculate Relay Settings in Field, **C. L. Betts, Jr.** *Electrical World*, vol. 134, July 31, 1950, pp. 96–97.

4. Handling Power System Problems on an A-C Network Calculator, **P. O. Bobo.** *Electrical Engineering*, vol. 69, Oct. 1950, pp. 867–69.

5. Construction of Short Circuit Current Decrement Curves, **F. P. Brightman.** *Power and Works Engineer*, vol. 54, no. 7, July 1950, pp. 66–69, 118.

6. Analysis of Synchronous Machine Short Circuits, **Robert D. Camburn, Eric T. B. Gross.** *AIEE Transactions*, vol. 69, pt. II, 1950, pp. 671–79.

7. The Calculation of Currents Due to Faults Between Turns in Transformer Windings, **B. L. Coleman.** *Report*, British Electrical and Allied Industries Research Association, ref. Q/T121, 1950.

8. Construction and Operation of Austrian Network Analyzer, **W. Erbacher.** *Osterreichische Zeitschrift fur Elektrizitaetswirtschaft*, vol. 3, 1950, pp. 357–61.

9. Some Experience with a British A.C. Network Analyzer, **G. Lyon.** *Proceedings*, Institution of Electrical Engineers, vol. 97, pt. 2, Dec. 1950, pp. 697–724.

10. New Aid to Network Calculator Operation, **G. P. Wilson.** *Electric Light and Power*, vol. 28, no. 1, 1950, pp. 78–79, 120–21.

11. Network Analyzer for Electric Power Systems. *Engineering*, vol. 169, no. 4381, 1950, pp. 94–95.

12. Analysis of Subsequent Faults, **Howard K. Amchin, Eric T. B. Gross.** *AIEE Transactions*, vol. 70, pt. II, 1951, pp. 1817–23.

13. Short Circuit Power in Auxiliary Circuits of Thermal Power Stations, **H. DeMarsac.** *General Electric Review*, vol. 60, 1951, pp. 5–13.

14. Power Flow in an Interconnected System with Particular Reference to a Special Network Analyzer for Solving Related Problems, **M. R. Dunster.** *Journal*, Institution of Engineers of Australia, vol. 23, 1951, pp. 37–46.

15. The Network Analyzer as an Auxiliary of the Chief Load Dispatcher, **W. Erbacher.** *Osterreichische Zeitschrift fur Elektrizitaetswirtschaft*, vol. 4, 1951, pp. 170–71.

16. A Review of Network Analysers, Their Design and Application, **O. Hauge.** *Elektroteknisk Tidsskrift*, vol. 64, 1951, pp. 191–96.

17. An Application of Rheonomic Abstract Space to the Analysis of Electric Fault Circuits, **Y. Ishizuka.** *Report*, Waseda University, no. 15, 1951, pp. 39–47.

18. Fault Calculations (book), **C. H. W. Lackey.** Oliver and Boyd, Edinburgh, Scotland, 1951.

19. Asymmetrical Components for Fault Studies, **G. Lyon.** *Electrical Times*, vol. 120, 1951, pp. 454–58.

20. Fault Currents and Voltages in Symmetrical 3-ph. Networks, **S. Rusck.** *Teknisk Tidskrift*, vol. 81, 1951, pp. 171–73.

21. The Inrush of Magnetizing Current of Transformers, **M. S. Thacker, B. Rakesh.** *Elektrotechnik*, no. 23, 1951, pp. 93–100.

22. Faults and Fault Protection in Electrical Three Phase Systems, Vol. I. The Faults and Their Evaluation (book) (in German), **H. Titze.** Springer-Verlag, Vienna, Austria, 1951.

23. A Power System Analogue and Network Computer, **E. A. Baldini, A. P. Fugill.** *AIEE Transactions*, vol. 71, pt. III, Jan. 1952, pp. 291–97.

24. Symposium on Network Analyzers, **Eric T. B. Gross.** *Proceedings*, American Power Conference, vol. 14, 1952, pp. 381–83.

25. Unbalances of Untransposed Overhead Lines, **Eric T. B. Gross.** *Journal*, Franklin Institute, vol. 254, 1952, pp. 487–98.

26. A New Danish Network Analyzer, **J. E. Knudsen.** *Elektroteknikeren*, vol. 48, 1952, pp. 511–17.

27. Major Faults on Power Systems (book), **A. G. Lyle.** Chapman and Hall, Ltd., London, England, 1952.

28. Power System Analysis (book), **J. R. Mortlock, M. W. Humphrey Davies.** *Ibid.*

29. A New Principle is Employed for 60-Cycle A-C Network Analyzers, **E. B. Phillips.** *AIEE Transactions*, vol. 71, pt. I, 1952, pp. 18–25.

Section M. Instrument Transformers and Other Auxiliary Devices

1. Effect of Core Properties on Defects of Instrument Transformers, **N. F. Astbury, J. McFarlane.** *Engineering*, vol. 170, no. 4413, 1950, pp. 184–86.

2. A Survey of Bushing-Type Current Transformers for Metering Purposes, **G. Camilli.** *AIEE Transactions*, vol. 69, pt. I, 1950, pp. 429–40.

3. A New Line of Orthomagnetic Bushing-Type Current Transformers, **John W. Farr.** *Ibid.*, pp. 424–28.

4. A Low-Oil-Content Universal Current Transformer for Extra High Voltages, **H. Hartmann.** *Brown Boveri Review*, vol. 37, 1950, pp. 159–61.

5. New Dry-Type Insulation for Instrument Transformers, R. A. Pfuntner, R. E. Franck, F. R. D'Entremont. *AIEE Transactions*, vol. 69, pt. I, 1950, pp. 453–58.

6. Cable Type Ring Current Transformer for Earth-Fault Protection, Eric T. B. Gross. *Bulletin*, Association Suisse des Electriciens, vol. 42, 1951, pp. 503–09.

7. The Performance of Current Transformers During Overload Conditions, A. Kaltofen. *Elektrotechnische Zeitschrift*, vol. 72, 1951, pp. 707–10.

8. Application Guide for Grounding of Instrument Transformer Secondary Circuits and Cases. *AIEE Standard No. 52*, 1951.

9. The Effects of Coupling-Capacitor Potential-Device Transients on Protective Relay Operation, AIEE Committee Report. *AIEE Transactions*, vol. 70, pt. II, 1951, pp. 2089–96.

10. Frequency Errors in Negative-Sequence Segregating Networks, E. A. Livingston. *Proceedings*, Institution of Electrical Engineers, vol. 99, pt. 4, 1952, pp. 390–96.

11. Determination of the Over Current Characteristic of Current Transformer, R. Kuchler. *Elektrotechnische Zeitschrift*, vol. 73, A, 1952, pp. 480–81.

12. Unbalance of Currents of Zero-Sequence Current Transformers, I. M. Sirota. *Elektrichestvo*, no. 6, 1952, pp. 46–52.

List of Periodicals

AIEE Transactions, New York, N. Y.
ASEA Journal, Vasteras, Sweden
Associazione Elettrotecnica Italiana, Milan, Italy
Ateliers de Constructions Electriques de Charleroi, Charleroi, Belgium
British Electrical and Allied Industries Research Association, Leatherhead, England
Bulletin, Association des Ingenieurs Electriciens Sortis de l'Institut Electrotechnique Montefiore, Liege, Belgium
Bulletin, Association Suisse des Electriciens, Zurich, Switzerland
Bulletin, Societe Francaise des Electriciens, Paris, France
Brown Boveri Review, Baden, Switzerland
BTH Activities, British Thomson-Houston Company, Ltd., Rugby, England
Cables et Transmission, Paris, France
CIGRE, Paris, France
Deutscher Elektrotechniker, Berlin, Germany
Electric Light and Power, Chicago, Ill.
Electrical Engineering, New York, N. Y.
Electrical Review, London, England
Electrical Times, London, England
Electrical World, New York, N. Y.
Elektricheskie Stantsii, Moscow, USSR
Elektrichestvo, Moscow, USSR
Elektrotechnicky Obzcr, Prague, Czechoslovakia
Elektrotechnik, Berlin, Germany
Elektrotechnika, Budapest, Hungary
Elektrotechnische Zeitschrift, Frankfurt, Germany
Elektroteknikeren, Copenhagen, Denmark
Electroteknisk Tidsskrift, Oslo, Sweden
Engineer, London, England
Engineers Digest, New York, N. Y.
General Electric Review, Schenectady, N. Y.
Iron and Coal Trades Review, London, England
Journal, Franklin Institute, Philadelphia, Pa.
Journal, Institution of Engineers of Australia, Sydney, Australia
Metropolitan-Vickers Gazette, Manchester, England
Osterreichische Zeitschrift fur Elektrizitaetswirtschaft, Vienna, Austria
Power and Works Engineer, London, England
Proceedings, American Power Conference, Illinois Institute of Technology, Chicago, Ill.
Proceedings, Institution of Electrical Engineers, London, England
Proceedings, Midwest Power Conference, Chicago, Ill.
Przeglad Elektrotechniczny, Warsaw, Poland
Reyrolle Review, Durham, England
Siemens Zeitschrift, Frankfurt, Germany
Svenska Vattenkraft Foreningens Publikationer, Stockholm, Sweden
Teknisk Tidskrift, Stockholm, Sweden
Transactions, South African Institute of Electrical Engineers, Johannesburg, South Africa
VDE-Fachberichte, Frankfurt, Germany
Waseda University, Tokyo, Japan

Turbine Generator Operation and Maintenance Practice of Philadelphia Electric Company

E. I. GALLAGHER
ASSOCIATE MEMBER AIEE

THIS paper shows the practice in a typical large power system and is one of a group of papers requested by the Committee on Rotating Machinery, Synchronous Machinery Subcommittee, in connection with their work in preparing a proposed AIEE guide for the operation and maintenance of turbine generators. It is presented primarily for the purpose of focusing attention on this subject and of stimulating discussion of any points involving a difference of opinion or practice.

Description of System

The Philadelphia Electric Company system includes seven steam and one hydro generating stations with a total installed capacity of 2,286 megawatts (mw). The Company is a member of the Pennsylvania-New Jersey Interconnection which operates installed capacity of 7,756 mw. The Company's generating capacity by steam is distributed among 32 units, ranging in size from 14 to 182 mw. Seven of these generators exceed 100 mw capacity. Generator voltages are all at 13,800 volts except the latest addition which is 20,000 volts.

The 1953 system peak was 1873 mw with 978 megavars (mvar). There are five synchronous condensers of 30 mvar each and approximately 50 mvar of fixed static condensers on the system. An additional 75 mvar are available on the 60-cycle motors of the frequency converters which supply the railway and streetcar load. The system power factor varies from 84 per cent at heavy-load periods to 91 per cent during light-load periods.

Scheduling of Load

The units are loaded on an incremental cost basis. This means that only those

---

Paper 55-117, recommended by the AIEE Rotating Machinery Committee and approved by the AIEE Committee on Technical Operations for presentation at the AIEE Winter General Meeting, New York, N. Y., January 31–February 4, 1955. Manuscript submitted October 21, 1954; made available for printing November 24, 1954.

E. I. Gallagher is with the Philadelphia Electric Company, Philadelphia, Pa.

units required for generation and local area or interconnection reserve are in service. All other units are taken off the line as load conditions permit. As a result, about nine machines are put on the line every morning. Some units may be put on twice a day for short periods over the peaks. Others have a 24-hour demand and are taken off only when necessary. One unit operated continuously for over 6 months and was taken off at the manufacturer's recommendation to test the overspeed trip mechanism.

Reactive is adjusted on the generators, converters, and synchronous condensers to attain the best conditions. Generators are never operated with leading power factor; as far as possible the reactive is carried in the area where it is required. This reduces transmission line loading and losses. The maximum loading of the generator is limited by the name-plate rating for field or armature current, or maximum permissible coil temperature. None of these values is ever exceeded. Normally, the maximum loading is determined by the field or armature current. Maximum coil temperatures run up to 90 degrees centigrade (C) on some generators at full load. However, the maximum on most generators is about 70 C.

Operation of Units

The system is operated on 13- and 33-kv bus voltage schedules for the various locations. The generators carry the required voltage to maintain the scheduled bus voltage and the necessary reactive. In accomplishing this the generator terminal voltage may be 5 per cent over the rated voltage for the machine.

Voltage regulators are used on nearly all the generators. Rheostatic and the vibrating type of regulators control voltage on the older generators while the static type with fast response control voltage on the newer large generators. They have been very satisfactory. The regulators are cleaned and inspected on a routine schedule. The larger units are provided with a minimum excitation limit to prevent instability.

The fundamental generator protection is a current differential relay on the windings. Some of the generators have phase and ground overcurrent relays for back-up protection. Several units have reverse power relays which are primarily for turbine protection. On loss of field the procedure is to trip the unit immediately. Loss of field relays are being installed on the larger units.

Condensing units from 60 to 182 mw capacity are taken off nightly for as short a time as 4 hours. These units are returned to service in 20 minutes after shutdown of less than 8 hours. The limiting factor in the rate of loading the unit is the turbine conditions. The generator is not considered. Generally, units going on the line are loaded at a rate of not more than two per cent per minute of the full load rating. After they are on the line, and operating conditions are normal, larger rates of change are made. Preheating of the field in starting has been used for three large units on recommendation of the manufacturer.

Cooling of Generators

The cooling systems of air-cooled generators are operated to maintain substantially constant coil temperatures. Cooling water is adjusted manually to accomplish this. Several air-cooled systems have electric heaters in the air ducts to maintain a temperature high enough to prevent condensation while the unit is off the line. This also helps to maintain constant coil temperature.

Hydrogen-cooled generators maintain a constant ambient. This is done by holding the cold gas temperature constant, usually at about 35 C. Control is by manual adjustment of the cooling water.

The hydrogen pressure carried on any particular unit depends upon the load dispatcher's requirements for reactive. The generating station is informed of the estimated kva required from the unit, and sufficient hydrogen pressure is maintained to carry the estimated load on the generator. This procedure reduces hydrogen consumption and leakage. Normally the maximum kva required from a generator will not vary much from day to day on units capable of operating at 15 pounds per square inch gauge or higher hydrogen pressure. These, being the newer and more efficient units, will carry full load daily. In the event that more reactive is required, the hydrogen pressure can be quickly increased.

At present, there has been no occasion to operate above 15 pounds per square inch gauge hydrogen pressure except for generator capability tests. At 15-pounds-per-square-inch gauge, hydrogen leakage may amount to 250 cubic feet per day on large generators. Hydrogen consumption is watched closely and any increase is noticed immediately. Leakage is checked with an explosimeter type of detector.

Maintenance of Generators

Generator maintenance may be divided into electrical and mechanical phases. The maintenance section inspects for physical damage to the generators. They look for loose wedges, broken supports, core movement, coil distortion, tape separation, loose retainer rings, and any other visible defect. Collector rings are never ground or polished unless they are giving trouble. Nothing is done to them on the basis of appearance. Generator fields on closed cooling systems are not removed at every inspection period.

The field-winding resistance is carefully measured during complete inspections. Variations from the original value are carefully noted and any appreciable change is investigated. This has shown up loose connections in the field leads of several machines.

The station forces megger the armature and field at 500 volts every month or when possible. No routine high-voltage tests are made except when there is suspected damage or repairs or replacements in the electrical circuit. At present, several generators have difficulty with tape separation and they are given a hi-pot annually. Absorption tests are made for 10 minutes during each complete inspection period, in general with the use of 500 volts for the field, and 1,000 and 10,000 volts for the armature.

Conclusions

Since internal inspections after the first year have shown relatively little trouble, the period between complete inspections is being extended to as much as 5 years. No generator-forced outages have been attributed to operating practices.

An Anechoic Chamber for Noise Tests on Large Power Transformers

A. W. BENOIT
NONMEMBER AIEE

R. T. HEMMES
MEMBER AIEE

M. W. SCHULZ, JR.
ASSOCIATE MEMBER AIEE

THE completion in 1954 of the world's largest anechoic chamber as part of General Electric's transformer sound laboratory focussed attention on the efforts being made to reduce transformer noise. The noise produced by transformers, while not a new problem, has become increasingly important with the rapid growth of the electric power industry and the expansion of residential districts. The advantages of the unit substation and other economic factors have brought about a trend toward the installation of more, and in many cases larger, transformers in residential areas. The resulting noise complaints have made it evident that noise must be given special consideration in the design of a transformer installation. For many applications transformers with noise levels considerably below the National Electrical Manufacturers' Association (NEMA)[1] standard limits are required.

The use of cold-rolled core steel with its improved loss characteristics has permitted manufacturers to produce smaller, lighter, and less costly transformers to meet given electrical specifications, but in many cases this has caused the noise level to be higher than that of earlier units built of hot-rolled steel. It is now recognized that noise level may be a limiting design criterion.

None of the methods presently available to the transformer design engineer for reducing noise level are particularly effective when measured in terms of incremental cost per decibel (db). A 10-per-cent reduction in operating flux density in the core, e.g., results in only about 3 db reduction in noise level, but it represents an appreciable increase in cost.

Thus two factors, (1) the need for special attention to noise because of the nature of the ultimate environment of the transformer, and (2) the emergence of noise level as a critical design specification, have led both users and manufacturers of power transformers to devote considerable time and effort to the investigation of the transformer noise problem.

This paper describes some of the details of the design, construction, and operation of the first anechoic chamber built for noise testing large power transformers. It is shown how the acoustic treatment of the test area and new developments in instrumentation contribute to unprecedented accuracy in the measurement of transformer noise. Better data will provide a more complete understanding of the problem and lead to new methods for its solution.

Facilities Required

One of the main difficulties facing the manufacturer in the investigation of noise problems is the procurement of accurate data which are independent of the particular surroundings in which the measurements are made. For convenience, the sound testing activities may be divided into two categories, acceptance testing and development work.

ACCEPTANCE TESTING

The well-known NEMA standards for transformer noise are the basis of all acceptance tests although the standard limits are often modified in accordance with customer specifications. It has long been recognized that the NEMA standards are far from ideal, but they do represent a means for obtaining reasonable estimates of noise performance with a minimum of special facilities.

There are two important requirements which must be fulfilled by the space in which noise measurements are made if accuracy is to be obtained. First, the ambient noise must be low enough to keep it from contributing appreciably to the readings, and second, the reflection of sound from walls or near-by objects must be controlled to prevent excessive errors.

The NEMA standards recognize the second requirement by stating that all reflecting surfaces should be 10 feet or more from the transformer. This requirement can be satisfied by clearing a space on the factory floor; however, the noise of numerous other sources, such as transformers in the vicinity undergoing electrical test, generators supplying power to the test area, and overhead cranes, produce an ambient noise level much too high to allow satisfactory noise testing. Therefore the only alternatives are (1) to make the tests at a time when these other noise producing activities have been suspended, (2) to provide a special acoustically treated room, or (3) to make the tests at some remote outdoor site. The first two methods have been used at Pittsfield. Units up to 5,000 kva were tested in a small "noise room." The larger units were tested on the floor of the factory on week ends or holidays and required special scheduling

DEVELOPMENT WORK

Tests must be performed to provide information for transformer design engineers to enable them to calculate noise levels, to evaluate changes in the design or the manufacturing process, to determine, the physical laws governing the generation, transmission, and radiation of transformer noise, and to determine the reaction of people to noise. Frequently a variety of dynamically scaled models of transformers and associated structures such as barriers require study. The experiments usually require special measurements such as frequency analyses. The greatest possible accuracy is necessary so that small changes which may be quite important can be evaluated with a minimum number of samples.

The accuracy of a sound level reading in the presence of reflecting objects is greatly affected by the distance between the microphone and the sound source; the standard deviation increases quite rapidly with the distance. It is highly desirable in many instances to measure the sound level as a function of space but this cannot be done with uniform accuracy in a room with reflecting surfaces. For developmental purposes it is highly desirable to have available a special room with low ambient sound level, free from reflections, and providing a large working space. These needs, coupled with those for acceptance testing large power transformers on a more orderly schedule, led to the decision to build an anechoic (without

---

Paper 55-26, recommended by the AIEE Transformers Committee and approved by the AIEE Committee on Technical Operations for presentation at the AIEE Winter General Meeting, New York, N. Y., January 31–February 4, 1955. Manuscript submitted October 25, 1954; made available for printing November 15, 1954.

A. W. BENOIT (retired) was with Charles T. Main, Inc., Boston, Mass., and R. T. HEMMES and M. W. SCHULZ, JR., are with the General Electric Company, Pittsfield, Mass.

The outstanding work of Briggs Gettys in the preparation of general specifications for the sound laboratory was largely responsible for its creation. The detailed acoustical design of the anechoic chamber was prepared by the consulting firm of Bolt, Beranek and Newman, Inc., and the structural design was by Charles T. Main, Inc. The Gilbane Building Company was the general contractor. The authors regret that it is impossible to enumerate the contributions of the many persons who have been associated with the design, construction, evaluation, and operation of the sound laboratory.

Fig. 1. Exterior view of sound laboratory

echo) chamber which could accommodate the largest transformers now anticipated.

Sound Test Laboratory

A study of the trends in transformer development and other forcasts of future sound testing requirements resulted in specifications for a noise test building.

SPECIFICATIONS

It appears reasonable to expect that transformers weighing 400 tons and measuring more than 37 feet by 27 feet and 33 feet high will be built and will require noise tests. Such units may have a rating in excess of 500,000 kva. The noise test chamber must be large enough to provide safe electrical clearance from the bushings of the largest transformer and also to allow accurate sound level readings to be taken at least 6 feet from the string contour of the transformer.

It is necessary that the ambient sound level be less than 40 db on 40-db weighting. A level of less than 30 db is desirable. To simulate tests on the open ground a hard floor and reflection-free walls and ceiling are necessary. For other tests it is desirable to approach anechoic conditions.

The sound level meters and other instruments should be the most stable and accurate permitted by the state of the art. Facilities must be provided for easily checking and calibrating the instruments.

GENERAL DESCRIPTION

The sound laboratory depicted in Fig. 1, built at a cost of approximately $1,500,000 meets all of the specifications just given. As shown in Fig. 2, it consists of four major sections: the entrance chamber, the anechoic chamber, the control and storage rooms, and the auxiliary transformer rooms.

Normally a fully assembled transformer is placed on a special transfer car and transported on standard gauge rails through the entrance chamber into the anechoic chamber. The entrance chamber provides a working space and temporary storage for equipment awaiting test. The transformers to be tested can be brought into this chamber and the outer door closed before the door to the test chamber is opened. Thus the anechoic chamber is protected from adverse weather conditions. Forced-air heat exchangers in the entrance chamber are used for heating the anechoic chamber when the intervening doors are opened.

The anechoic chamber is a reinforced concrete building with all structural supporting members of the walls and roof on the outside. This provides a room 66 feet long, 56 feet wide, and 50 feet high with smooth unobstructed interior surfaces. The actual working area, after the acoustic treatment has been added, is about 7 feet less than these dimensions. The transformer and transfer car are supported by rails which rest on a massive concrete foundation which has been designed to allow maximum coverage by acoustic absorbing materials. Fig. 3 shows the interior of the anechoic chamber.

There are two consoles of instruments in the control room. One contains the sound measuring instruments and the other the controls for the power circuits which supply the excitation to the transformer being tested. There is an observation window next to each of the consoles so that the operators may view activities in the anechoic chamber.

The auxiliary transformer rooms contain the step-up transformers which are used to supply power to the transformer being tested, the circuit breakers, potential and current transformers, and other auxiliary power sources.

ANECHOIC CHAMBER

To provide a low ambient sound level and high absorption coefficient, the walls, floor, and ceiling are massive, multilayer structures covered with sound absorbing material. The doors are similar and have special hardware and gaskets to seal them. Fig. 4 shows a cross section of the walls. They consist of 12-inch reinforced concrete, 2-inch Fiberglas, 8-inch solid concrete blocks, 0.030-inch copper sheet, 6-inch air space, and 28-inch Fiberglas wedges. The concrete block wall is tied to the 12-inch wall by resilient connectors. The floor and roof are very similar except that the concrete blocks are replaced by 6-inch reinforced concrete slabs and minor changes are necessary in the method of supporting the structures.

The copper sheet provides radio-frequency shielding so that measurements may be made of the radio and television interference caused by transformers. The shield is continuous with all joints interlocked, rolled flat, and soldered. The copper sheet is omitted from the steel doors but continuous electric ground connections are provided. Even the observation windows are covered with fine mesh copper screens. All power lines entering the anechoic chamber have radio-frequency filters. Lighting fixtures are incandescent, not fluorescent, and all

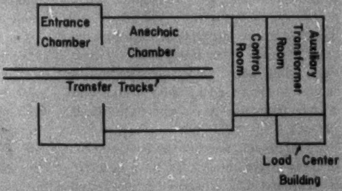

Fig. 2. Layout of buildings

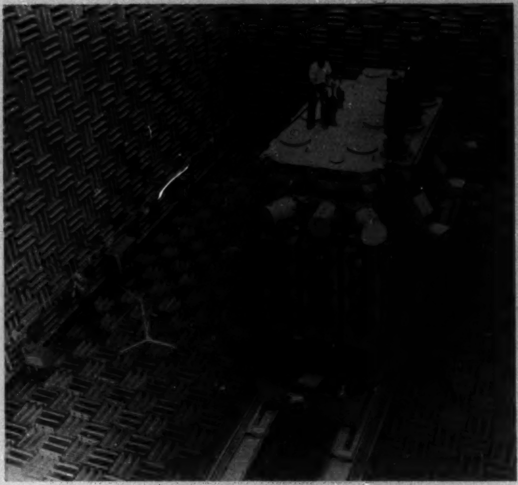

Fig. 3. Interior of anechoic chamber

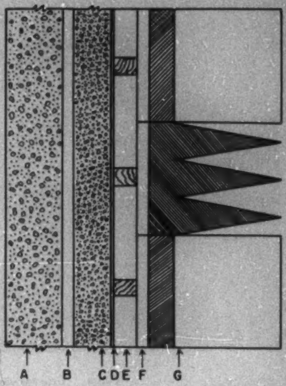

Fig. 4. Cross section of wall of anechoic chamber

A—12-inch concrete wall
B—2-inch Fiberglas
C—8-inch concrete block wall
D—0.030-inch copper sheet
E—6-inch wood frame and air space
F—2-inch angle-iron wedge support
G—28-inch Fiberglas wedges

metal parts of the acoustical treatment are grounded.

A notable feature of the building is the main door, made up of two leaves covering an opening 30 feet wide by 37 feet high. Since each leaf of the door weighs about 30 tons a sliding door was considered more practical than a hinged suspension. Each leaf is carried on power-driven wheels operating on rails. The doors consist of two 4-inch thick compartments constructed of structural steel channels and 1/4-inch thick steel plates. The outer compartment is filled with dry sand and the other is filled with Fiberglas. The seal around the door frame consists of a rubber tube which can be inflated with compressed air and a strip of foam rubber forms the seal between the two leaves of the door when they are closed.

The observation windows between the control room and anechoic chamber consist of two wood frames, one set in the 12-inch concrete wall and the other in the 8-inch concrete block wall. A 1/2-inch thick plate glass and a 3/8-inch thick plate glass are set in the first frame about 8 inches apart but not parallel to each other. In the other frame is a 5/16-inch thick plate glass. This construction is similar to that used in radio studios and greatly attenuates any sound transmitted through it.

To approach anechoic conditions, all surfaces of the room must have acoustic absorption coefficients of 0.99 or better at the frequencies of interest. This means that less than 1 per cent of the sound energy striking the surface is reflected. Fiberglas wedges are the most practical treatment which will provide this degree of absorption at a frequency of 120 cycles per second (cps), which is the fundamental noise component of most transformers.[2–4]

The wedges are installed on all the walls, the floor, and the ceiling of the anechoic chamber and cover these surfaces as completely as possible. The main doors have wedges installed on them and portable wedges are available to cover the tracks in the center of the room. Part of the door frame and the small personnel doors are covered by a Fiberglas blanket. The only surfaces which have not been treated with absorbing materials are the two observation windows and several junction boxes which contain outlets for microphone cables and auxiliary power circuits but they have a negligible effect on the acoustic quality of the room because of their relatively small size.

The working floor to support the operators and small test equipment consists of 3/32-inch galvanized stranded aircraft cable interwoven on 2-inch centers each way. The cables are individually spring-supported and are normally under a tension of 450 pounds. The floor is usually 10 inches above the tips of the wedges but may sag as much as 6 inches when supporting small groups of people. This floor does not impair the anechoic quality of the room.

To simulate the condition of a transformer installed on a reflecting surface, such as a hard floor or the ground, a removable plywood floor has been provided. This floor is supported just above the wire floor by a pipe and angle frame and is entirely independent of the spring floor.

TRANSFER CAR

For normal acceptance testing a transformer is completely assembled, filled with oil, loaded on the transfer car, and moved into position in the anechoic chamber. The transfer car has been specially designed to carry 400 tons and to support the transformer during the test. This eliminates the need for crane facilities in the anechoic chamber but it does require that the transfer car provide a dynamically rigid support, particularly at 120 cps.

Hydraulic jacks which have been built into the car bear on the rails and lift the car about $1^{1}/_{2}$ inches. Aluminum shims are placed between the car frame and the concrete foundation so that when the car is lowered it rests on a solid support. The frame of the car is a rigid structure and has been designed so that it has no modes of vibration in resonance near 120 cps.

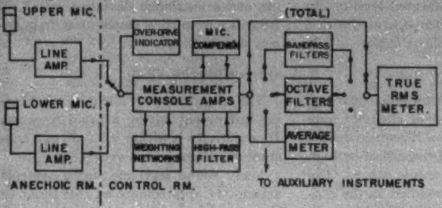

Fig. 5. Block diagram of instrumentation serving one side of anechoic chamber

Power Supply

The NEMA standards specify that transformers must be excited at rated voltage and frequency with no load applied for noise tests. It is expected that units even larger than 500,000 kva will require noise tests, hence a 12,000-kva 3-phase, 60-cycle generator has been provided to assure good voltage wave form.

A 10,000-kva bank of single-phase transformers in the auxiliary transformer room step the voltage up to the required level. They are 3-winding transformers with series-multiple arrangements for the high-voltage and intermediate-voltage windings. With suitable tap and winding connections and control of the generator voltage it is possible to provide any voltage up to 69 kv.

The generator is controlled by amplidynes which hold the voltages and frequency to better than 0.1 per cent of the values set by the operator. Instruments and appropriate instrument transformers are provided to allow the operator to read the voltage, current, and frequency of the excitation at any time.

Auxiliary power is available in the anechoic chamber to operate fans, oil pumps, or other equipment. Three-phase 60-cycle power from 92 to 503 volts is obtained an autotransformer and induction voltage regulator. A motor-generator set supplies up to 250 volts d-c.

Instrumentation

Given a test chamber of adequate quality, the burden of minimizing tolerances in sound level measurements falls upon the instrumentation. As previously shown, tests on completed large power transformers and development tests pertaining thereto both place a high premium on each db of measured level; a corresponding economic outlay for high accuracy in the measuring equipment is warranted.

The design of the measurement console must provide for high stability and convenient standardization so that in service complete reliance can be placed on each set of readings taken. Consideration must also be given to the need for obtaining large numbers of readings rapidly, since measurements may involve as many as 40 microphone positions around a transformer, with frequency analyses at many positions and possible repetitions of all measurements at several levels of excitation voltage.

Measuring Equipment Layout

Fig. 5 shows in block diagram form the layout of the basic measuring system. There are two such systems, which operate from the north and south sides of the anechoic chamber simultaneously and independently.

The two microphones shown in Fig. 5 are mounted on a single boom, Fig. 6, which automatically maintains one microphone directly above the other. The separation between microphones is made one-third of the tank height of the transformer under test. White cloth tapes are drawn taut around the outer limits of the transformer radiators to show the contour at one-third and two-thirds tank height. The wheeled tripodal stands supporting the microphone booms are then rolled toward the transformer until there is a visual 1/2-inch clearance between the contour tapes and the horizontal rings of $11^{1}/_{2}$-inch radius which surround each microphone, thus assuring the microphone distance of 1 foot specified by NEMA.[1]

The microphones feed into separate line amplifiers in the anechoic chamber. The amplified outputs are fed into the main measurement console in the control room; see Fig. 7. The right-hand panel at center height serves the north side of the anechoic chamber and provides controls for switching in either of the microphones and obtaining sound level measurements at the desired weighting, usually

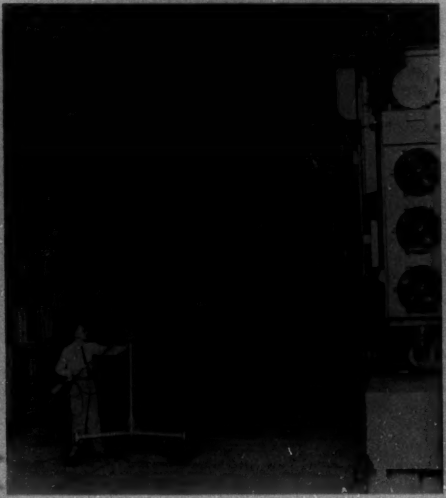

Fig. 6 (left). Microphones and supporting boom

Fig. 7 (below). Console of sound measuring instruments

40-db. Corresponding equipment at the left side of the console serves the south side of the anechoic chamber.

For rapid routine frequency analyses, a band-pass filter set is provided below the sound level measuring panels, which can be switched in to pass 120 cps and successive harmonics thereof individually as a dial switch is advanced. A standard octave band filter set, above the measurements panel, is also provided since octave band information is of increasing interest in transformer noise measurements. The output meter for indicating sound levels is a rapid-acting true rms instrument, inherently more accurate in showing the rms value of highly peaked waves than the instruments found in conventional sound level meters, as will be explained later.

It is recognized that comparative measurements will sometimes be made on transformers after installation in the field, using conventional sound level meters. To delineate the possible extent of measurement error due to waveform considerations, a true average meter has been supplied in the measurement berth. Readings from this meter are for reference purposes only, the official measured level being that supplied by the rms meter.

Thus rapidity of measurement is achieved by the use of four microphones placed semiautomatically, rapid switching, and quick-acting output meters. The end result is that two test operators are kept continuously occupied at the measurement console, recording the levels of total noise and components thereof throughout the test period.

Although rapid measurements are desirable, high accuracy is the paramount interest. Whereas an accuracy in absolute sound pressure measurements of ±2.0 db serves satisfactorily in many industrial applications, an over-all accuracy of ±0.5 db is demanded here. This in turn requires a still smaller tolerance in each of the components of the measuring system, now to be described.

MICROPHONES

Western Electric *640AA* condenser microphones were selected for all routine work in the anechoic chamber. Largely employed in industry as laboratory standards, these microphones are characterized by high stability. For example, a temperature change at the microphone from 25 to 35 degrees centigrade produces a change in sensitivity of approximately 0.1 db. The same temperature change in the case of the crystal microphone supplied with conventional sound level meters causes a change in indicated level of approximately 2.4 db, when operated with a typical 25-foot microphone cable.

AMPLIFIERS

The microphone preamplifiers and line amplifiers in the anechoic chamber were designed by the Western Electroacoustical Laboratory and are distinguished by high stability and large dynamic range. The measurement berth amplifiers in the control room were designed by the Measurements Unit of the Pittsfield High Voltage Laboratory to have high stability and very low distortion. The frequency response is within 0.1 db of being flat from 80 to 8,000 cps. All amplifiers are a-c powered and free from the effects of ordinary changes in line voltage. To remove all possibility of instability from line voltage surges, a separate generator has been provided to supply the instruments.

A thyratron guardian circuit is applied to the line amplifier to signal the test operator if the amplifier saturation level is approached during any part of the signal cycle. In the comparatively rare case where this may occur an insertion loss of 20 db is inserted at the microphone preamplifier and readings are corrected accordingly.

NETWORKS

In accordance with standard practice, three weighting networks are provided, which discriminate against high and low frequency in a manner similar to the human hearing mechanism at three levels of prevailing sound. By selection of the proper network the indicated sound level is made more nearly representative of the sensation of loudness at the ear.

The flat, 70-db, and 40-db weighting networks have been adjusted to offer an identical insertion loss at 1,000 cps and a tolerance of ±0.3 db from the American Standards Association (ASA) design objective[5] over the important frequency range from 120 to 1,200 cps. This tolerance may be contrasted with the ±2.0 to 3.0 db deviation permitted in conventional sound level meters of the same range by ASA standards.

Over the range 80 to 8,000 cps the tolerance of the amplifiers and weighting networks has also been held to ±0.3 db, based on a nondirective microphone. A separate compensating circuit has been included to apply a free-field correction for the *640AA* microphone at high frequencies, with a maximum deviation in the range 1,000 to 5,000 cps of 0.3 db from the computed correction curve. A high-pass filter is optionally available with a cutoff frequency slightly below 120 cps and a maximum deviation of 0.3 db from flat frequency response at frequencies above 120 cps.

OUTPUT METER

The output meter is a true rms indicating instrument having a rapid response. Its sensitivity is within ±0.2 db of a constant value from 80 to over 4,000 cps.

Many sound level measuring systems attempt to approximate an rms response by operating an inherently average-reading instrument on the curved characteristic of a driving circuit. The circuit may have the form of a copper oxide rectifier or a specially biased vacuum tube. A major shortcoming has been the instability of the reference characteristic with change in temperature, polarizing voltage, and age. This situation is reflected in the ASA specifications which permit an error of ±0.5 db in the rms addition of two equal voltages in nonharmonic relation. The superiority of the use of an inherently true rms meter with suitable frequency-compensating network is indicated by a maximum observed error of only 0.1 db when making this test at various points on the instrument scale.

A second consideration is the ability of the instrument to give an rms response to highly peaked waves. In this regard, ASA specifies two tests, the more severe of which requires (after inserting a constant loss between the meter terminals and driving circuit) that two voltages, each initially capable of causing full-scale deflection, be first doubled and then simultaneously applied. The permitted deviation from rms addition in conventional sound level meters is ±1.5 db. The measured error in the equivalent test on the true rms system is 0.3 db. This ability of the instrument to handle peaked waves is important in power transformer measurements, where, with fans inoperative, the noise is concentrated at discrete frequencies in harmonic relation.

FILTER SETS

The electronic band-pass filter sets for rapid routine frequency analyses were custom built by the Western Electroacoustical Laboratory to provide an attenuation of 25 to 40 db to neighboring harmonics while passing individual harmonics of 120 cps up to the sixth. At the same time, each passband is maintained within 0.5 db of flat for a frequency range of at least ±7 per cent from the center frequency. This permits checking transformers for any troublesome resonances of parts by varying the electric excitation frequency from 56 to 64 cps and identifying the offending har-

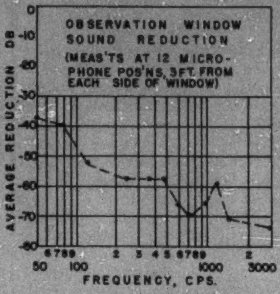

Fig. 8. Sound attenuation of observation window versus frequency

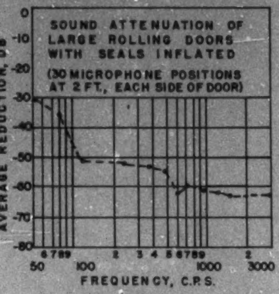

Fig. 9. Sound attenuation of main doors versus frequency

monic of noise. The octave filter sets are of standard manufacture, conforming to ASA specifications.[6]

SYSTEM CHECKS AND STANDARDIZATION

It is imperative that dependable measurements always be obtained on the first attempt. The steps taken in design to insure stability have already been outlined. There remains a possibility in an electronic system of a component failure, causing an error of several db.

To insure that such a condition would be detected during tests, means are provided in the measurement console for the routine injection of an electric signal of known strength into the microphone channel prior to every series of measurements. A resulting normal indication certifies the correct gain in the amplifying and measuring system. Similarly an acoustic check is provided daily or whenever desired by means of a small hood enclosing a calibrated loudspeaker which is slipped over each microphone in turn. While not regarded as a standard, the hood detects any change in microphone sensitivity in excess of 0.5 db.

All microphones receive accurate calibrations under anechoic conditions monthly against the Pittsfield Works Standard, another *640AA* microphone set aside for the purpose. This is compared semiannually with the General Electric Standard at Schenectady and cross checks are made with leading sound laboratories.

AUXILIARY INSTRUMENTATION

A complement of accessory equipment has been provided to cover such nonroutine measurements as may be required of the anechoic chamber. Among the items included are: crystal microphone channels for measurements at very low levels or in applications where microphones must be considered expendable; a 2,500-watt audio amplifier for core vibration studies and other purposes; a moving strip camera and oscilloscope for transient noise studies; a Bruel and Kjaer spectrometer-recorder, and other instruments for general noise analysis work.

Evaluation of Anechoic Chamber

To evaluate the effectiveness of the design of the room, extensive measurements have been made to indicate the degrees of isolation and absorptivity achieved. While much data remain to be analyzed, results can be presented with reference to several salient matters.

ISOLATION

The ambient noise level in the test room is approximately 19 db at 40-db weighting and 42 db without weighting. The effectiveness of the observation windows in providing isolation is shown by the curves of Fig. 8. It will be observed that over the frequency range from 120 to 3,000 cps the difference in average sound levels at a 3-foot distance from the two sides of the window is in excess of 52 db. The curve of Fig. 9 shows the minimum attenuation provided by the large rolling doors at the chamber entrance, with gasket seals inflated.

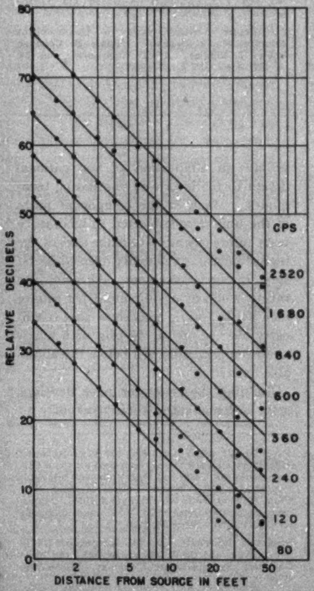

Fig. 10 (left). Comparison of measured sound level to inverse square law, Pittsfield anechoic chamber. Microphone and point sound source 20 feet above centerline of transfer tracks

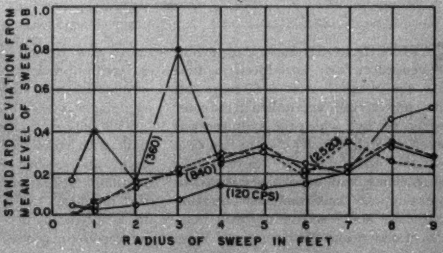

Fig. 11 (right). Variation of sound level at microphone traveling in a horizontal circular orbit about point sound source. Source 8 feet above transfer tracks at center of room. Tracks covered by portable wedges

ABSORPTION

The proximity to a true anechoic condition is indicated by the nearness of the measured curve of sound intensity versus distance to inverse square law; a point source of sound is employed. Fig. 10 shows such data taken with source and microphone on a line 20 feet above the center line of the railroad track within the chamber. The maximum measurement error involved in these data is estimated at ±0.3 db of sound level and ±1 per cent of distance. It will be noted that in the critical range from 120 to 840 cps the minimum distance at which 1 db of deviation occurs is in excess of 16 feet.

In contrast with anechoic chambers previously constructed, the purposes of this room require that it have a railroad track with massive concrete supports, extending for nearly the full length of the room along its centerline. This structure extends upward among the permanently installed absorptive wedges of the floor, with the upper surface approximately 1 foot above the tips of the surrounding wedges. To minimize reflections which might otherwise occur from this structure, particularly at the higher frequencies, a set of portable glass-wool wedges is moved over the exposed track structure when full anechoic properties are desired.

To test the effectiveness of these wedges, a point sound source was placed at various heights above the center of the working area of the room. At each height, a microphone was caused to sweep through a horizontal orbit of constant radius about the source. On a given sweep the standard deviation from the mean sound level is a measure of the nonuniformity of absorption. If the area were completely free of absorption anomalies the measured sound level would be a constant, independent of angular position. The results of measurements for a height of 8 feet above the track structure are shown in Fig. 11. It will be observed that the standard deviation from the arithmetical mean level amounts to less than 0.8 db for radii as large as 9 feet, at the frequencies of interest in testing model and full-scale transformers.

Conclusions

It has often been said that measuring a transformer's noise level does not make it quieter. By the same reasoning, more accurate readings obtained in an anechoic chamber will not make the noise any less annoying. However, more accurate data necessarily will provide a better understanding of the problem and will lead to new methods for its solution. The sound laboratory allows more rapid accumulation of data because tests can be made with greater speed and because more transformers can be made available for testing.

The elimination of reflections and the reduction of instrument errors permit the detection of changes of the order of 1 db in transformer noise level. These might formerly have been attributed to errors. Reliable evaluation of changes in the manufacturing process which affect sound level shows that only 1 or 2 db will have an important cumulative effect.

Though the sound laboratory has been in operation only a few months, it has already provided new information which will prove helpful to the users of power transformers. Dynamically scaled models of transformers and various enclosing wall configurations have been tested to give more accurate information for the design of such barriers. The possibility of using auxiliary sound sources to modify the radiation pattern of a transformer and reduce the noise in a particular direction has also been investigated.[7]

References

1. STANDARDS FOR TRANSFORMERS. *Publication No. TR1-1954*, National Electrical Manufacturers Association, New York, N. Y., May 1954.

2. THE DESIGN AND CONSTRUCTION OF ANECHOIC SOUND CHAMBERS, L. L. Beranek, H. P. Sleeper, Jr. *Journal*, Acoustical Society of America, New York, N. Y., vol. 18, 1946, pp. 140–50.

3. PERFORMANCE OF THE ANECHOIC ROOM OF THE PARMLY SOUND LABORATORY, H. C. Hardy, F. G. Tyzzer, H. H. Hall. *Ibid.*, vol. 19, 1947, pp. 992–95.

4. CONSTRUCTION AND DESIGN OF PARMLY SOUND LABORATORY AND ANECHOIC CHAMBER, Peter J. Mills. *Ibid.*, pp. 988–92.

5. SOUND LEVEL METERS FOR MEASUREMENT OF NOISE AND OTHER SOUNDS. *Publication No. Z24.3*, American Standards Association, New York, N. Y., 1944.

6. SPECIFICATION FOR AN OCTAVE-BAND FILTER SET FOR THE ANALYSIS OF NOISE AND OTHER SOUNDS. *Publication No. Z24.10, Ibid.*, 1953.

7. RECENT CONTRIBUTIONS TO TRANSFORMER AUDIBLE NOISE CONTROL, William B. Conover, Robert J. Ringlee. *AIEE Transactions*, vol. 74, pt. III, Apr. 1955, pp. 77–90.

Test Report on a Fully Supercharged Generator

STERLING BECKWITH
FELLOW AIEE

B. M. KOETTING
ASSOCIATE MEMBER AIEE

L. T. ROSENBERG
MEMBER AIEE

G. W. STAATS
MEMBER AIEE

SUPERCHARGED cooling of turbine generators was introduced in 1951 with the installation of a 60-megawatt (mw) unit having ducts milled in the rotor copper, through which the hydrogen was forced at high velocity by the use of a 2-stage centrifugal blower. Several similar machines have since been placed in operation and their combined operating experience now exceeds 6 years. Details of design and performance of these units now in service have been fully covered in previous papers,[1,2] and a generator with both stator and rotor supercharging was described a year ago.[3,4]

This fully supercharged generator was built with redesigned mechanical, magnetic, and cooling features to permit maximum utilization of this new ventilation principle. As a result, the generator is specifically designed in all respects for conductor cooling and is more than simply an adaptation of conventional design to the improved ventilating techniques. Many of the component parts of the unit were subjected to laboratory tests before assembly to make sure of the high standard of reliability deemed necessary in such machines. Although its rating is 40 mw at 30 pounds per square inch gauge (psig), tests show that it will carry over 60 mw at 45 psig with maximum temperatures well below the allowable limit.

Building the generator on a development order afforded the opportunity to

---

Paper 55-123, recommended by the AIEE Rotating Machinery Committee and approved by the AIEE Committee on Technical Operations for presentation at the AIEE Winter General Meeting, New York, N. Y., January 31–February 4, 1955. Manuscript submitted October 20, 1954; made available for printing November 24, 1954.

STERLING BECKWITH, B. M. KOETTING, L. T. ROSENBERG, and G. W. STAATS are with the Allis-Chalmers Manufacturing Company, Milwaukee, Wis.

Fig. 1. Fully supercharged generator on test

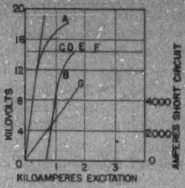

Fig. 2. Saturation and synchronous impedance curves

A. No-load saturation curve
B. Full-load amperes at zero power factor
C. Full-load amperes at 85% power factor
D. 125% load amperes at 85% power factor
E. 160% load amperes at 85% power factor
F. 200% load amperes at 85% power factor
G. Synchronous impedance curve

test thoroughly and make improvements at all stages of manufacturing without the usual concern for a required delivery date. Shop tests included many different heat runs at a wide range of gas pressures up to 70 psig as well as the usual characteristic curves, reactances, wave form, losses, vibration, and blower performance in air and hydrogen. Nearly 100 temperature measurements were made as often as every 30 minutes during each heat run by means of embedded resistance-type, thermocouple-type, and mercury thermometers placed throughout the entire machine and at various external points. The machine was equipped with pipe fittings and valves for five manometers to study the performance of the newly developed single-stage blower. The results of these exhaustive tests are given here.

Characteristic Curves and Losses

Using the initial test setup pictured in Fig. 1, the zero power factor heat runs, the no-load and full-load saturation curves, open-circuit core loss, direct- and quadrature-subtransient and zero-sequence reactances, and windage and friction loss tests were obtained.

Table I. Comparison of Short-Circuit and Conventional Generator Currents

	Fully Super-charged	Con-ventional
Three-phase symmetrical, rms amperes	11,800	21,000
Single-phase line-to-line, amperes	10,200	18,200
Single-phase line-to-neutral, amperes	13,500	24,600
Mechanical forces at instant of fault, %	31	100

The no-load and full-load saturation curves and the synchronous impedance curve are shown in Fig. 2. The calculated no-load saturation was based on ordinary silicon steel punchings because the availability of grain-oriented silicon iron was not certain at that time. The improved core material was obtained, however, and the saturation curve as well as the core loss was more favorable as a result. The improved permeability and reduced loss agree closely with comparative tests on other machines built with both types of core iron.

It was originally thought that the fully supercharged generator would require well over twice the exciter capacity of the equivalent conventionally cooled generator. Tests indicate 170 kw are required at full load, which is substantially less than twice. A good share of this improvement is credited to the carefully designed magnetic circuit which departs appreciably from conventional design.

It was anticipated that with high gas pressure overloads approaching 200 per cent (%) would be possible, so the fields were designed to permit enough excitation for this load without exceeding 250 volts. Normal generator load is therefore carried with a low exciter voltage, thus accounting for the apparently high field amperes.

The sudden short-circuit currents based upon test values of reactances are compared in Table I with those of the equivalent conventional generator. The last line of the table gives the mechanical forces during a fault in % of those of the conventional generator.

As stated in an earlier paper,[3] the generator nominal rating is based on equalling conventional machine efficiency at full load rather than on temperature limitations. The temperature tests presented in the next section confirm this condition and also show that, if desired, a portion of this temperature margin may be exchanged for even higher efficiency by operating at reduced gas pressure. This step raises the full-load efficiency as well as the fractional load efficiencies well above those for conventional cooling.

Temperatures

In the previous paper[3] it was predicted that the temperature rise of the stator coil strands for full load in 30 psig hydrogen would be that given by curve *A* of Fig. 3. Curve *B* shows the test values of temperature rise of the hottest strand as measured by thermocouples located along the length of the coil. These measure-

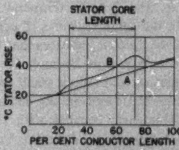

Fig. 3. Temperature distribution along stator coil at full load in 30 psig hydrogen

A. Expected temperature rise of stator coil strands
B. Test temperature rise of hottest stator coil strand

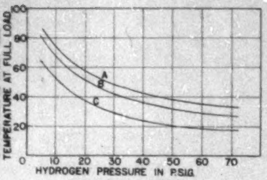

Fig. 4. Operating temperatures as a function of hydrogen pressure

A. Maximum stator strand rise by thermocouple
B. Maximum stator coil rise by detector (located at discharge end of core)
C. Rotor rise by resistance

ments were taken during operation at rated kilovolt-amperes, zero power factor, in 30 psig hydrogen. Since the thermocouples are located on the hottest strand, the temperatures measured include the effect of eddy loss in the hottest strand. Such temperatures are usually not adequately given by temperature detectors between coil sides or under slot sticks. The strand temperature rise at the discharge end of the coil is slightly less than that in the slot portion because the reduced eddy-current losses in the coil ends more than offset the increase in gas temperature.

The effect of hydrogen pressure on the operating temperatures of the fully supercharged generator is clearly given by Fig. 4. The test points through which these curves were drawn were derived from measurements of temperature rise on many heat runs at loads ranging from no load to 60 megavolt-amperes, at voltages up to 16,200, and at hydrogen pressures of 5, 10, 15, 20, 30, 45, 60, and 70 psig. These curves indicate extremely effective ventilation for this fully supercharged machine, not only at higher hydrogen pressures but even at pressures as low as 5 psig. The nearly constant 6-degree temperature difference between hottest thermocouple and hottest temperature detector in the same region is of particular significance, since it indicates that there is very little heat flow through the stator coil insulation and only a small temperature differential between the coil and the core. This fact, coupled with the low average temperature along the length of the coil, as shown in Fig. 3, and the relatively short length of the machine, assures that differential expansion will be minimized.

From the considerations of the preceding paragraph, it is apparent that this machine will have overload capacity at increased hydrogen pressures far in excess of conventionally ventilated machines. This was expected and clearly stated in the earliest publication.[1] Fig. 5 gives a comparison between expected and actual capacity as a function of gas pressure, based on a constant copper temperature corresponding to full load at 30 psig. As rotor temperature is farther below acceptable limits than stator temperature, the latter may be assumed to govern. Curve *D* shows permissible load versus pressure for a hot-spot stator copper temperature rise of 75 degrees centigrade (C), which is still 15 C below the proposed revised AIEE Standard No. *1*[5] and American Standards Association Standard *C-50.*[6] Although it is realized that the overload capacity in kilowatts can seldom be fully utilized, due to turbine or boiler limitations, the increased kilovolt-amperes available from the fully supercharged generator make it an attractive machine from the standpoint of kilovar overloads.

Temperature rises of the mechanical parts of the fully supercharged machine were also very favorable. Of special interest are the temperature rises of some of the components considered to be design innovations.[4] These may be briefly discussed as follows:

Collector Rings and Brushes. These were painted with special temperature sensitive paint. This paint indicated, after all heat runs had been completed, that no part of the rings had reached 115 C total temperature, which was the calibration of the lowest temperature paint available. The rings had operated during five heat runs for which the excitation kilowatts were 44% above full-load excitation. Tests on this unit and on other 3,600-rpm generators show that 80 to 90% of the collector ring heat loss is due to surface friction, hence resistance loss is not the limiting factor as it is on slower speed machines. The small diameter ring used on this machine reduces the major heat loss, so that cooler rings as well as brushes result. The brush holder temperature rise by thermocouple at the highest field current was 30 C.

Finger Plates. Temperatures of the individual tooth finger plates[4] were measured by thermocouples. The temperature rise at either end of the core did not exceed 43 C at full load under the lowest hydrogen pressure of 5 psig. This result is quite encouraging and proves that the high ampere conductor loading of the fully supercharged machine is no hardship for these clamping fingers.

Bushings. The radiator-type jet-cooled bushings also were highly satisfactory.

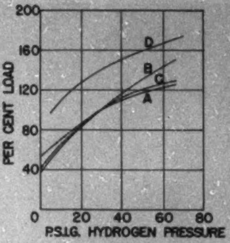

Fig. 5. Expected and actual capacity as a function of hydrogen pressure

A. Expected capacity at full-load temperatures
B. Test rotor capacity at full-load rotor temperature
C. Test stator capacity at full-load stator temperature
D. Permissible load for 75 C stator hot-spot rise

The maximum temperature rise of the bushing itself, measured by a thermocouple located at the outer extremity of the stud, was only 27.4 C at 60-megavolt-amperes, 30 psig. The temperature rise of the outer shell near the bushing was 19.4 C.

Operation of Seals and Other Design Features

Many of the design improvements merit individual comment, but as this is beyond the scope of the present paper only a few observations and test results will be given. As previously described,[3] the stator windings are suitable for a range of voltage ratings by the omission of fractional turns. One turn per phase was cut out during the shop tests. The long air gap was believed well suited for such winding modifications and the test results did not indicate excessive rotor temperatures. Utilization of this feature is only possible because of the liberal stator coil thermal margin as substantiated by tests.

One of the purposes of testing over a wide range of gas pressures was to observe the behavior of the hydrogen seals. Test floor facilities limited operation to 70 psig. At this pressure in either air or hydrogen the sight flow gauges indicated only a mere trickle of oil was being admitted to the hydrogen side of the seals. The hydrogen leakage at 70 psig was within shop safety requirements despite the many pipe connections for manometers and thermocouples that were brought out of the generator.

Vibration records were made at many points on the generator shell, bearings, and elsewhere and, as expected, were found to be well below similar measurements on the relatively large conventionally cooled machines of equal rating. Observations during assembly and tests showed that the end cover V-clamps, the air gap baffle, seals, and auxiliary parts were easy to install or dismantle and conformed in every way to expectation.

Improvements relating to the rotor were equally successful. The machine was in good mechanical balance at all loads and temperatures. The long air gap and internal cooling of the windings permitted omission of the usual rotor surface grooving. The lower noise level of the smooth rotor was especially noticeable during shop balancing runs.

Perhaps the most gratifying of all test results was the splendid performance of the new single-stage blower developed after a series of experimental tests with quarter-scale models. Pressure measurements exceeded by 20% the highest measured pressure on any of the 2-stage blowers previously tested, while power input per cubic foot per minute was materially lower. The improved blower efficiency permits this machine to operate safely in air because the air temperature undergoes only a moderate rise in passing through the single-stage blower. With adequate cooling water of low temperature, substantial loads may be carried in air.

The behavior of the axial flow coolers was also found to be highly satisfactory. As most of the test floor cooling water supply was needed for the 66-mw unit with which the load heat runs were made, the fully supercharged machine had to be tested with the limited drinking water supply. Less than 25% of rated water flow was provided, but since its temperature was somewhat below the specified value, inlet hydrogen did not exceed 40 C except during the 60 and 70 psig tests where it rose to 42 C and 43 C respectively. Inlet temperature in air at 2 psig was less than 40 C under the test conditions with reduced water flow.

The exciter for this generator is to be of the a-c commutatorless type similar to one built and tested a year ago[7] for a 35-mw unit. In addition to eliminating the commutator, brushes, and all rotating windings, the device incorporates a continuously acting voltage regulator of superior speed and reliability. Also it permits direct-connected 3,600-rpm exciters on fully supercharged generators of any capacity now contemplated.

Conclusions

It may be concluded from the foregoing that the shop tests of the fully supercharged generator confirm the complete adequacy of its design and substantiate the predictions presented in earlier papers. The new single-stage blower yielded considerably more pressure than the earlier 2-stage blowers and a substantial efficiency improvement. The excitation requirements are well below expected values and temperatures are low on both stator and rotor.

The efficiency at normal gas pressure is equal to that of the conventionally cooled unit at full load and higher at reduced loads. Because of the temperature margin, operation at low hydrogen pressures is shown to be permissible and to raise efficiencies at all loads. This pressure adjustment may be governed by temperature of the embedded resistance detectors between coil sides at the discharge end of the stator, as these temperatures are only 6 C below those of the hottest strands. If temperatures are allowed to approach within 15 C of permissible standards, an enormous overload is possible either in kilowatts or kilovars. Because of the high blower efficiency, the tests indicate operation in air to be possible at a load depending upon the temperature and quantity of cooling water available.

The fully supercharged generator is considered a great forward step because of its many economies and advantages to the utility. Among these are savings in power plant space; lower crane, foundation, and switchgear costs; reduced differential expansion; and less maintenance. Ratings up to 200 mw can be built of this design without exceeding the physical size of the 3,600-rpm conventionally cooled rotors previously built by Allis-Chalmers. High-quality rotor forgings at this size are more easily obtained than the larger sizes. The cooling ducts milled in the copper conductors permit reducing the stresses in rotor bore, tooth root, wedges, and retaining rings. The 200-mw unit could be shipped assembled from the factory without resorting to the cartridge design of the stator.

The gas volume of the supercharged generator with its compact, axially cooled stator core and external cooler housings will be a small fraction of that of the conventional type, and therefore pressure changes with load to keep efficiency high at all loads are economically possible.

With materials now available, it is safe to say that fully supercharged generators up to 300 mw are possible at 3,600 rpm. Application to 1,800 rpm is definitely feasible but will require separately driven high-speed blowers since adequate pressure at 1,800 rpm would involve a prohibitive blower diameter.

References

1. SUPERCHARGED HYDROGEN COOLING OF GENERATORS, **Sterling Beckwith.** *AIEE Transactions*, vol. 71, pt. III, Jan. 1952, pp. 168–75.

2. SUPERCHARGED COOLING OF GENERATORS, **Sterling Beckwith.** *Allis-Chalmers Electrical Review*, Milwaukee, Wis., 3rd quarter, 1951.

3. A NEW FULLY SUPERCHARGED GENERATOR, **S. Beckwith, L. T. Rosenberg.** *AIEE Transaction*, vol. 73, pt. III, June 1954, pp. 477–83.

4. ADDITIONAL DESIGN FEATURES OF THE FULLY SUPERCHARGED GENERATOR, **B. M. Koetting, G. W. Staats.** *Ibid.*, pp. 484–86.

5. GENERAL PRINCIPLES UPON WHICH TEMPERATURE LIMITS ARE BASED IN THE RATING OF ELECTRIC MACHINES AND APPARATUS. *AIEE Standard No. 1*, Feb. 1954.

6. ROTATING ELECTRICAL MACHINERY. *ASA C50-1943*, American Standards Association, New York, N. Y., 1943.

7. A NEW EXCITATION SYSTEM, **H. W. Cory, W. L. Ringland.** *Proceedings*, Southeastern Electric Exchange, Atlanta, Ga., Sept. 24, 1954.

8. VENTILATION OF INNER-COOLED GENERATOR, **R. A. Baudry, P. R. Heller.** *AIEE Transactions*, vol. 73, pt. III, June 1954, pp. 500–08.

9. DIRECT COOLING OF TURBINE-GENERATOR FIELD WINDINGS, **C. H. Holley, H. D. Taylor.** *Ibid.*, pp. 542–50.

Steam Turbine-Generator Operating and Maintenance Methods of the Southern California Edison Company

C. L. SIDWAY
MEMBER AIEE

C. M. CLEVENGER
MEMBER AIEE

Synopsis: This paper provides selected information related to the operation and maintenance of steam turbine generators, as practiced on the Southern California Edison Company system. The methods outlined are the result of years of progressive development and necessarily reflect the predominant characteristics of the system which they serve. Certain of these characteristics will be outlined as the basis for a better understanding of the existing operating methods.

The System and Its Operation

The System

Graphically, the Edison major 220-kv transmission system is wye-shaped, Fig. 1, with the principal sources of generation at the extremities of the wye, and with the major load center at the convergence. One arm of the wye, extending 250 miles northward, terminates at Big Creek, in the Sierra Nevada Mountains of Central California. In the Big Creek area some 530 megawatts (mw) of hydrogeneration are located. Five 220-kv substations are located along the four parallel transmission lines which comprise this arm of the wye, supplying power to intermediate loads. In addition, one 250-mw interconnection with the Pacific Gas and Electric Company is made at the approximate mid-point of the arm, while a 110-mw interconnection with the same utility exists closer to the Big Creek generation area.

The alternate arm of the wye crosses the Mojave Desert, extending 300 miles eastward to Hoover Powerhouse on the Colorado River. Approximately 400 mw of generation are available at this location. Of the three 220-kv transmission lines which comprise this arm of the wye, two reach the load center in Southern California without intermediate taps, while the third line has interconnection points with the state of Arizona at Davis and Parker Powerhouses and, in addition, serves two groups of pumps on the Metropolitan Water District Aqueduct between Parker and the Edison Highgrove Substation in Southern California.

The stem of the wye, approximately 20 miles in length, connects the Long Beach Steam Plant No. 3 (220 mw) and the Redondo Steam Plant No. 2 (156 mw) to the 220-kv system. Available in the same area, at 66 kv, are the Long Beach Steam Plant No. 1 (22 mw), the Long Beach Steam Plant No. 2 (174.5 mw), and the Redondo Steam Plant No. 1 (288 mw). The Etiwanda Steam Station (280 mw), located near the eastern edge of the major load center, supplies power to the 220-kv system and to the local 66-kv load.

Pacific Southwest Power Area

The Pacific Southwest Power Area, of which the Southern California Edison Company is a contributing member, embraces an area of approximately 380,000 square miles. On October 1, 1954, there existed a total installed capacity of 8,800 mw of generation, about equally divided between hydro and steam. The coincident peak during the summer of 1954 amounted to 7,737 mw.

The Edison system contains 2,187,420 kw of effective operating capacity of which 52 per cent is steam. During the first seven months of 1954, steam production amounted to 58 per cent of the system total. Edison operates in parallel continuously with three other systems and, from time to time, with two additional systems under automatic tie-line load control. It is present practice that one of the systems will assume frequency regulation of the combined systems, usually employing time-error correction, while the other systems control their ties with the frequency-regulating system, normally using tie-line bias control.

Under prevailing conditions, the load changes on the systems and interchange of power across the interconnecting ties will on occasion impose rate-of-generation changes of 25 to 30 mw per minute for periods of relatively short duration. The use of multiple plant regulation within any one of the systems has not been adopted, the load control, or frequency regulation, being assigned to one generating plant at a time. While the indicated rate of change in generation is sporadic, it does require that the regulating or controlling station be capable of manipulating its generating units appreciably.

On the Redondo Steam Plant No. 1, which has automatic combustion control, no difficulty is experienced in handling the indicated load changes. The control is less satisfactory when using some of the older steam plants where the limiting factors are often related to thermal expansion and contraction phenomena in the steam cycle and, in some cases, to the auxiliary equipment, especially the boiler feed pumps.

Load Allocation

The problem of load allocation between hydro and steam generation and between numerous and varied generating plants is complex. To attempt to detail accurately the many factors which must be evaluated to define wholly the procedure is beyond the scope of this paper. However, it may serve the intended purpose to indicate some of the more influential factors.

In hydrogeneration it is important that maximum utilization of available water be accomplished even though it is not possible to know with certainty when such water will become available, either from rains or melting snow. This requirement assumes particular significance in the case of stream-flow plants, which have no storage facilities. Adding to this problem is the need for meeting contract commitments for release of water to users in the lower valleys, and the further need for staying within maximum permissible limits for storage of water. Experience indicates that about 85 per cent of the normal runoff will occur between April 1 and July 30. Further complicating the water-use problem is the diversity of available water sources where certain generating plants in tandem arrangement effect joint use of water and where converging streams in the lower canyons add to the supply available to lower canyon plants.

Much of the planning and scheduling of steam generation and maintenance is hinged on the aforementioned factors. In the dry years, as much steam as possible is operated as base load generation, and capacity factors tend to approach unity. To make certain that sufficient

---

Paper 55-119, recommended by the AIEE Rotating Machinery Committee and approved by the AIEE Committee on Technical Operations for presentation at the AIEE Winter General Meeting, New York, N. Y., January 31–February 4, 1955. Manuscript submitted October 18, 1954; made available for printing December 8, 1954.

C. L. Sidway and C. M. Clevenger are with the Southern California Edison Company, Los Angeles, Calif.

fuel will be available for these maximum requirements for steam generation, minimum-use provisions are included in fuel contracts. During wet years, these provisions force the use of steam generation at times when the economics of the situation might not so dictate and must accordingly be considered, along with the hydro limitations, in arriving at a load allocation schedule. The steam generation plants serve as a source of kilowatt capacity to meet system load requirements, including spinning reserve requirements associated with either normal or emergency operation, although steam is not the sole source of spinning reserve. Steam generation also must provide the kilowatt-hours of energy to meet system load requirements which are beyond the ability of hydro sources to provide.

The more modern steam plants on the Edison system operate with a capacity factor approaching 90 per cent, and have on a few occasions exceeded this figure, while the older plants operate with a capacity factor less than 90 per cent. As implied previously, this factor is directly related to the water yield in hydro. The over-all steam division capacity factor for the last 4 years has fluctuated between 46 and 80 per cent. Additional items influencing the yearly capacity factor are the programmed and unprogrammed outages required to maintain the extensive auxiliaries involved in steam generation.

The sequence of loading and unloading the steam generating plants conforms to rigid economy factors. Thus, the load increases are normally made at the plant which can make them at the lowest incremental cost rate. Conversely, the load reductions are usually made on the plant operating at the highest incremental cost rate. The steam plants are responsible for the placement of assigned loads to the individual units according to incremental heat rates.

Wherever practical, block-loading increments are assigned on the basis of operating the units at the wide-open valve positions. This philosophy applies as well at the full load point of the generator, except where limited by boiler capacity. This practice is followed to minimize the effect of the throttling losses.

SYSTEM SEPARATION

During periods of general instability or persistent low speed, the system is set up to separate automatically into load areas, each area containing sufficient generation to carry the isolated load, with some spare capacity. One such load area is that associated with the group of steam generating plants. In case the automatic separation does not occur within 15 seconds and the instability still persists, a manual separation is performed at all main separation stations where such instability is being observed, without regard to the indicated frequency at the station.

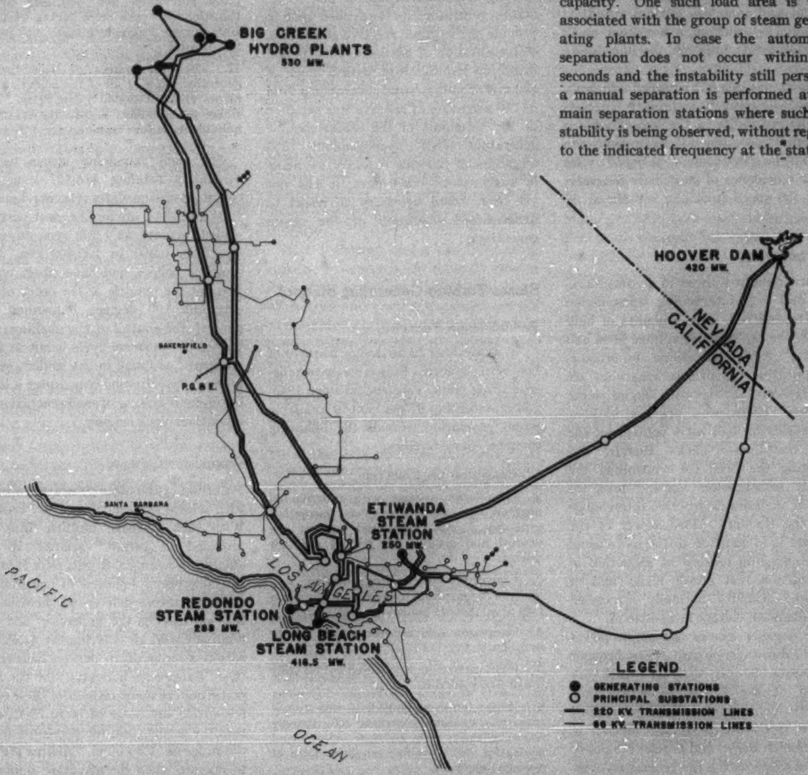

Fig. 1. Southern California Edison Company, major generating stations and transmission system

If, following the main separations, it is found that one of the steam plants is out of step with the other steam plants in the isolated steam load area, then further manual backup separations can be made to isolate the case of trouble, thereby maintaining maximum continuity of service. These delayed manual backup separations are not made until after at least 20 seconds have elapsed. Within isolated systems formed by separations, if instability still persists, the 220-kv switching centers may order load dropped or further sectionalizing.

In the generating stations with multiple generators, generators which are not obviously out of step with each other but which have rejected load and are apparently out of step with the system are kept on the line for at least 1 minute unless there is some compelling reason to do otherwise. Every effort is made to restore and maintain normal speed, as indicated by machine tachometers, on all generators remaining on the line during periods of instability.

During periods of low speed which are not accompanied by instability (suggesting the possibility of the loss of a block of generation), manual separations are made if the speed remains below 57 cycles with no evidence of immediate recovery, or if the speed is falling rapidly at 57 cycles.

VAR LOADING

With remote sources of hydrogeneration and long intervening transmission lines transferring large amounts of bulk power, the problems of voltage level and reactive generation assume importance. Complicating the picture somewhat are the high-capacity ties with the adjoining utilities. These ties operate without the benefit of load ratio control on the main transformer banks, thereby emphasizing the need for controlling the 220-kv transmission voltage level to prevent undesirable reactive interchange over the tie lines. This aspect of the problem is in addition to the more usual and compelling reasons of reduction in transmission real power losses and of increased stability normally associated with adequate voltage level control.

The existing sources of reactive power on the Edison system are: 1. synchronous condensers, 90 per cent of which are located at the 220/66-kv substations; 2. static capacitors, which are applied at the distribution voltage levels; 3. transmission lines; and 4. reactive power realized by operating the generators overexcited.

The availability of load ratio control at the majority of the 220/66-kv substations makes it possible to vary the condenser kilovar generation over a wide range and still maintain desired 66-kv bus voltage. The 66-kv stations having load ratio control are given condenser reactive generation schedules which in general call for maximum boost during the heavy-load period, and maximum buck, or a value of reactive generation which will bring the 220-kv banks to unity power factor, during the light-load period.

The steam station generators are operated close to unity power factor, generally in the range of 0.98 to 0.99 lag. Basically, they are considered as a reserve source of reactive generation. During periods when there exists an abnormal system reactive demand, or when a forced outage of a large synchronous condenser or long transmission line occurs, steam station generators are then called upon to provide the required reactive generation. Representative of the heavy-load period operating requirements, with a block of 679-mw of on-line steam generation a total of 119 megavars of reactive was supplied at the terminals of the steam turbine generators. With approximately 500 megavars of bucking capacity available in synchronous condensers, it has not yet been found necessary to resort to underexcited operation of the steam generators.

Steam Turbine-Generating Stations

BASIC DESIGN FEATURES

An analysis of basic design features of Southern California Edison steam turbine-generating plants constructed since 1945, and representing 67 per cent of available steam generation, reveals the following common characteristics:

1. Generators are 3,600 rpm.
2. Generators operate with ungrounded neutrals, and have single-phase potential-type transformers connected between the neutral and ground for ground detector alarms.
3. Generators are hydrogen-cooled, and most have maximum hydrogen pressure ratings of 30 pounds per square inch (psig).
4. Generator armature voltages are 13.8 kv or 18 kv.
5. Field excitation is provided at 250 volts d-c or 375 volts d-c.
6. With a few exceptions, field excitation is supplied by motor-generator sets, usually one per unit with common spare, and operating with rotating amplifier type of voltage regulators.
7. Generators are wye-connected and supply power to the system through main transformer banks which are delta-connected on the low-voltage winding, and wye-connected on the high-voltage winding.
8. The largest single generator carries a 1/2-psig hydrogen rating of 147,059 kva at 18 kv, with the smallest unit rated 70,588 kva at 13.8 kv.
9. With the exception of the Redondo Steam Plant No. 1, power for auxiliaries is supplied at 4,160 volts from auxiliary generators located on the shaft of the main unit, with reserve backup from the system through step-down transformers.
10. Relay protection for the main generators consists principally of generator differential protection and unit differential protection. The latter establishes a protective zone encompassing both generator and transformer and generally serves as backup for the faster generator differential relays. Negative-sequence relays are being installed on three large units on a trial basis.
11. Steam conditions on the earlier Redondo Steam Plant No. 1 units are 900 degrees Fahrenheit and 850 psig at the throttle, while the more recent units are 1000 degrees Fahrenheit and 1,800 psig at the throttle.
12. The unit system of boiler-turbine-generator exists at all of the modern steam plants except Redondo Steam Plant No. 1, where seven boilers supply the steam requirements of four turbines.

The eight remaining steam turbine generators totaling 416,167 kva with initial operating dates varying between 1924 and 1943, are for the most part air-cooled, operate at 1,800 rpm, range in size from 6,000 to 100,000 kva, have multiple boilers, and have steam conditions at the throttle of the order of 375 psig and 700 degrees Fahrenheit. In general, the control of the auxiliaries involved in the steam cycle is not as fully automatic as found in the modern steam plants; this situation constitutes a limiting factor in the use of such generation for other than block loading.

GENERATOR COOLING

Certain of the older generators operate with closed-system, forced-air cooling. With such systems, multiple fans are provided to permit variation in the amount of cooling with generator loading. The practice is followed of maintaining the temperature differential between the hot air leaving the generator and the relatively cold air entering the generator within a range of 20 degrees centigrade (C). Experience indicates that the normal armature temperatures for these units lies within the range of 60 to 75 C, and that the normal field temperatures are in the range of 70 to 90 C. Alarms are set to operate when the armature temperatures reach 85 C, with supplemental instructions not to exceed 100 C, while the alarms on the field are set at 110 C with instructions not to exceed 125 C.

The generating plants of more recent design operate with hydrogen-cooling of the generators, based on maintaining acceptable cold gas temperatures. Normally, the cold gas temperatures are not allowed to exceed 40 C. If the cold gas temperature exceeds 40 C, additional hydrogen is added. When the cold gas temperature drops below 40 C, the first step taken is to remove the more costly condensate cooler from service. If further action is required, the hydrogen pressure regulator valve is set at a lower value, and the machine pressure allowed to decrease by normal leakage. At loads below 60 mw on 78-mw units, decreases are made in hydrogen pressure to a minimum of 1/2 psig, when justified by prevailing cold gas temperature.

Emergency Procedures

With auxiliary generators located on the shafts of the main units, and also constituting the normal source of energy for the auxiliaries, any departures in speed of the main units are directly reflected in similar departures in speed of the auxiliaries. This is an important factor in establishing emergency operating procedures.

In the event of loss of field of a main generator, the following instructions apply. As soon as it has been verified that loss of excitation has occurred, most of the net load on the unit is removed as rapidly as possible, using the fast position of the load limit followed by immediate opening of the circuit breakers connecting the unit to the system. The unit speed is then re-restablished at its normal 3,600-rpm value to restore the speed of auxiliaries. This is particularly important for certain key pumps. All important supervisory instruments are checked for possible clues as to the source of trouble, or any damage which may have resulted therefrom. The system dispatcher is notified as to the location of the loss in generation.

If the supervisory instruments do not indicate that damage to the unit has occurred, an attempt is made to restore excitation to the unit, using the spare exciter where available. If successful, the unit is synchronized to the system and reloaded, meanwhile observing its performance during the loading period. If unable to restore excitation, and supervisory instruments and other checks indicate no known mechanical trouble, the unit is allowed to idle, carrying its auxiliary load, while an investigation is made. Subsequent procedure is then determined by facts established for the individual case.

The operating procedure in the event of out-of-step operation, assignable to causes other than loss-of-field, are generally identical with those indicated in the foregoing for that condition. Because the influence of out-of-step generators may be detrimental to the satisfactory operation of other machines on the line at the time, it is generally considered preferable that such unstable machines be removed from the system as rapidly as practicable to the extent permitted by spinning reserves and other emergency procedures which may be invoked. Where single generators are out of step with other generators in the same plant, ordinarily indicated by high unit speed and low kilowatt load, the unit is immediately removed from the line and resynchronized as soon as possible, following a few precautionary checks of supervisory instrumentation. When multiple generators in the plant are not obviously out of step with each other, but have rejected load and are apparently out of step with the system, usually the generators are kept on the line for at least 1 minute unless there is some compelling reason to do otherwise. Every effort is made to restore and maintain the normal speed (as indicated by machine tachometers) of all of the generators remaining on the line during period of instability.

If a generator relays on differential, and the generator is not urgently needed for system operation, the generator and all related and pertinent equipment are thoroughly checked for contributory causes before restoring the generator to service. When a generator relays on differential, and the generator is urgently needed for system operation, the following procedure applies:

1. If the relay operation is known to be faulty or accidental, and there is no accompanying voltage dip such as would be produced by a short circuit, an attempt is made to restore normal speed and voltage and, if successful, to return resynchronized to the system.

2. If the cause of the relay operation is not immediately known, the relayed equipment is inspected for evidence of trouble. If the inspection suggests that the contributory causes are related directly to the generator, thorough tests are made before restoring the generator to service. If the inspection indicates that the trouble is external to the generator, efforts are made to correct or isolate the trouble to permit restoring the generator to service. If the inspection reveals no apparent cause for the relay operation, the system dispatcher is so advised and preparations are made to restore normal machine speed and voltage and return to service.

Start-up Procedures

In the startup of steam turbine generators from a cold start, very little difference exists in procedure applicable to generators of varying age and manufacture. The essential difference being in the point of application of field to the generator. In the 1,800-rpm category, field is applied on Edison units at 350 rpm, while in the 3,600-rpm group, two selected points of field application obtain, these being 50 rpm on one block of generators and 3,000 rpm on another block, conforming to manufacturers' recommendations.

The following description is illustrative of start-up practice on a selected group of 3,600-rpm generators, and is predicated upon all of the requirements of a rather extensive procedure for preparing the turbine and related auxiliaries for operation having been met satisfactorily.

With the unit on turning gear, an inspection is made of certain critical items such as lube oil levels, hydrogen pressure and density, shaft eccentricity, and a test of admission valves for freedom of operation. The unit speed is increased to 50 rpm and tripped, and an audio check is made for possible rubbing or binding in the turbine generator. The speed is thereafter increased to 400 rpm over a 10-minute period. This speed is maintained for 30 minutes and, in the interim, the shell temperature, vibration, and eccentricity are observed on the unit recorders. If operation appears satisfactory, the speed is then increased gradually to 3,000 rpm, and field current is applied to the generator. Further increase in speed to 3,600 rpm is made and the unit placed on governor control. The time interval from 400 to 3,600 rpm requires approximately 40 minutes. Thus a total of 80 minutes have elapsed from the initial roll to the point when the unit is placed under governor control. This typical 78-megavolt-ampere generator is then synchronized to the system and loaded to 10 mw and held at that load for 20 minutes while certain major items are re-examined, following which the unit is released for normal operation. The practice of field preheating on steam turbine generators is not employed on the Edison system.

Shut-down Procedures

Under normal conditions, the existing load on the generator is removed at a rate of 1 mw per minute. When unloaded, an underspeed release test is made and the field removed from the generator. Trip tests are performed for low vacuum, low oil, and over-speed conditions. After a test of governor range, the unit speed is readjusted to 3,600 rpm and the unit tripped manually.

In the case of the older units, when the generator is off the line with the throttle valve tripped and the machine decelerating, the field current is reduced to near minimum, and this field entirely removed about 30 seconds before the unit stops rolling. It is a general rule, applicable to steam generating units on the Edison system, that it is permissible only in an emergency to increase the field current to shorten the deceleration period. In an extreme emergency, when an immediate shutdown of a unit is necessary, the turbine throttle valve, or stop valves, are tripped closed as quickly as possible and the generator circuit breakers are opened immediately. The decision to increase the generator field current to force the machine to decelerate in a shorter period or the decision to open the generator field breakers of the older generators and allow them to come to rest without a field is left to the judgment of the operating personnel on shift, who are guided by the nature of the emergency.

Generator Maintenance Procedures

It is the objective of the maintenance program, as followed by the Southern California Edison Company, to confine failures to determinable periods consistent with operating schedules to the fullest extent possible. To realize this objective requires added emphasis on the preventive aspect of maintenance and the use of test procedures which on occasion may appear to be severe, particularly to those who are remote from the over-all problem.

ROUTINE OUTAGES AND OVERHAULS

Routine outages on main units are conducted at all plants on a maximum interval of 90 days. These outages are usually confined to an 8-hour period, intended to provide an opportunity to check all functional equipment intimately related to operation of the units and is, in effect, a verification test of turbine-generator safety devices. The basic 90-day interval may be shortened if adverse insulator contamination should develop. Trip tests are performed on circuit breakers; governor operation is checked; brushes, slip rings, and commutators are closely inspected; insulators are washed or wiped; and safety devices are carefully tested. Some short-time work is accomplished during the outage. The steps outlined in the foregoing for normal shutdown constitute a part of the routine outage procedure as well as a part of the routine overhaul.

Overhauls on main units are conducted on a basic 3-year interval. On alternate overhauls, the generator rotor is removed to permit a more extensive inspection. A detailed account of items covered during overhauls is outlined in the following.

PRELIMINARY EXAMINATION

Prior to the routine overhaul, the operating records are examined for information suggesting a need for a more detailed inspection of the subject generator. Historical reference is made to the supervisory instrumentation covering main bearing vibration, bearing oil pressures, hydrogen pressure, purity, losses and temperature, and a correlation of these factors with generator loading. An inspection is also made to determine the amount of maintenance work directly required for the supervisory instruments.

MAIN BEARING AND SEALS

Bearing and seal clearances have varied sufficiently throughout the life of the generators to justify inclusion in the overhaul program. In general, maximum permissive clearance limits in the range of $1^1/_3$ to 4 mils per inch of shaft are considered satisfactory, the exact value depending on certain qualifying factors such as the age of the machine. Bearings are inspected for high spots, wear, pinching caused by excessive shims, and for foreign matter imbedded in the babbitt. The bearing insulation is carefully wiped, washed with naphtha or solvent, and dried and meggered.

BEARING OIL SYSTEM

Bearing oil pressures are compared with standard factory recommendations. This item has not been a source of trouble. An inspection is made for indication of exterior leakage around the bearings and piping, and for cleanliness of lube oil coolers, strainers, and tanks. The condition of the bearing oil is observed. More exhaustive oil analysis is made by operating personnel as a part of normal operation.

HYDROGEN SYSTEM INSPECTION

If comparison of hydrogen losses with permissible limits suggested by the manufacturer indicate excessive use, a thorough check of coolers and piping is made and corrective action is taken. Variations as great as twice normal in such losses have been experienced.

Piping and valves in the related cooling water system are inspected for visible leaks to ascertain that the valves are operable. Coolers are examined for tube deposits and wire brushed if necessary. The use of condensate has minimized the amount of cleaning required in the coolers. Hydrogen cooler vents are checked for proper functioning, for placement, and for loose or broken joints in the vent lines.

Following overhaul, the hydrogen system is tested under operating pressure by soaping in the disturbed area, or with a haloid torch and freon gas with the unit in air, the choice dependent on the type of unit. The instruments associated with the hydrogen system are calibrated each time the system is purged. Hydrogen alarms are tested before returning to service.

GENERAL CHECK LIST

Generator moisture detectors and alarms are examined. Shell temperatures are checked when returning the generator to service. The control wiring is inspected and meggered where practicable. Voltage regulators are serviced and tested. The supervisory instruments and associated remote pickups are inspected, tested, and calibrated.

On the older units, the generator bus is meggered; this test is omitted on the newer units employing numerous post-type insulators because it has not produced consistent results. Necessary testing and preventive maintenance work is performed on associated exciters, main circuit breakers, field breakers, and rheostats. Added emphasis is placed on the importance of circuit-breaker work, especially as related to possible single-phase operation of the generators.

GENERATOR STATOR, ROTOR IN PLACE

The stator winding is meggered in hydrogen. If conditions appear favorable, the established a-c overvoltage test, computed as 150 per cent of the highest a-c operating voltage, is applied. Among the determining factors in the application of the overvoltage are the general level of the megger readings, the related polarization index, and any unusual conditions observed during the megger tests. If it appears reasonably certain that application of the standard a-c overvoltage test will result in breakdown of the winding, a preliminary test using direct current may be performed.

The generator is purged of its hydrogen, and the hydrogen coolers are removed for the remainder of the inspection. The general appearance is checked for oiliness, moisture, or unsatisfactory insulating varnish. Winding is inspected for any insulation abrasion which might indicate presence of foreign material.

Coil ends are examined for possible distortion. The security of all lashings, spacer blocks, and coil support brackets is established. Coils are inspected for tape separation, progressive balling of insulation, and for excessive sponginess. Conditions found are recorded on a chart for future reference. Coils are examined for evidence of corona attack.

Any progressive armor separation in the conducting paint belt is noted. Wedges and filler strips are checked for movement or looseness. Immediate area is searched for broken pieces of laminations, wedges, or foreign metallic particles. The stator iron is inspected to the extent possible for working, and for indications of moisture or of hot spots. Tightness of core bolts and finger plates is determined by inspection and tests.

GENERATOR STATOR, ROTOR REMOVED

In addition to a more comprehensive examination of the requirements outlined in the foregoing, the generator stator is further inspected for the following conditions:

1. Coil movement in slot.
2. Damaged, missing, or loose wedges.
3. Foreign material in ventilating ducts.
4. Stator iron for indication of hot spots and moisture.
5. Iron oxide deposits adjacent to brackets.

GENERATOR ROTOR, IN PLACE

The rotor winding is meggered in hydrogen. A routine d-c overpotential test is applied to the field winding. This test voltage has been established as 180 per cent of the a-c test value formerly employed, the exact value being related to maximum operating field voltage. The coupling faces are checked with feelers for alignment, and a coupling rim check is made with feelers and a nonmagnetic dial tester. Coupling bolts and rotor fan blades are checked for tightness. Collector ring insulation, stud assemblies, and brush assemblies are checked for alignment, clearances between brush box and ring, and for wear, cleanliness, and mechanical integrity.

GENERATOR ROTOR, REMOVED

In addition to a more comprehensive examination of the requirements previously outlined, the generator rotor is further inspected for these conditions:

1. The retaining rings and centering rings are inspected for tightness and for evidence of working, burning, and for discoloration, particularly between ring fit and rotor body.
2. Clearances between wedges and retaining rings are checked.
3. The rotor surface is examined for indication of foreign matter having been in the air gap, and for evidence to local heating.
4. The winding bracing blocks are inspected for movement, and the winding for general appearance.
5. All ventilating passages are checked for cleanliness.
6. The bearing journals are inspected for wear, eccentricity, and grooving, particularly if the unit has been operated for any appreciable periods on turning gear.
7. Shaft and retaining rings are magnafluxed.

Conclusions

The policies and procedures outlined have been in effect on the Southern California Edison Company system since about 1945. During this period no generators have failed in service.

It is hoped that this exposition of the operating and maintenance procedures applying to a system involving widely separated, mixed hydro and steam generating plants, and long, high-voltage transmission lines will be of value to other power system engineers.

References

1. PROPOSED GUIDE FOR INSULATION MAINTENANCE FOR LARGE ALTERNATING-CURRENT ROTATING MACHINERY. *AIEE Standard No. 56*, May 1954.

2. ROUTINE INSULATION TESTING OF SYNCHRONOUS MACHINES, L. F. Hunt, J. H. Vivian. *AIEE Transactions*, vol. 70, pt. I, 1951, pp. 756–62.

3. A MAINTENANCE INSPECTION PROGRAM FOR LARGE ROTATING MACHINES, John S. Johnson. *AIEE Transactions*, vol. 70, pt. I, 1951, pp. 749–55.

4. OPERATION OF SYNCHRONOUS CONDENSERS ON THE SOUTHERN CALIFORNIA EDISON COMPANY SYSTEM, C. R. Canady, J. H. Drake. *AIEE Transactions*, vol. 71, pt. III, Dec. 1952, pp. 1,051–58.

Development of Small Hydroelectric Sites in Western North Carolina

H. H. GNUSE, JR.
MEMBER AIEE

IT HAS been economically possible to develop several small hydroelectric sites in Western North Carolina during the past 5 years by incorporating in the structures only those mechanical, structural, and electrical components that are actually required to produce electricity safely and reliably with a minimum of operating and maintenance expense. The use of the rock fill, earth-faced type of construction for the dams has been a major factor in providing a low-cost design. Also, the installation of supervisory control and telemetering to permit operation of the new plants by personnel located at existing plants has greatly reduced operating costs, thereby contributing to the economical development. The use of protective coatings of stainless steel on vulnerable turbine parts has been a major factor in reducing long-term maintenance costs.

Electrical Design Features

All of the recent installations have utilized remote control in some form to eliminate the need for operators at the new plants. For those plants that have been located within a radius of approximately 1 mile from an existing attended station, it has been found most economical to transmit the power output of the plant at generator voltages to the attended station where the generator oil circuit breaker is located, along with the associated metering, relaying, and synchronizing equipment. With such an arrangement, the remote station can be controlled by a 19-conductor cable of no. 19/25 American Wire Gauge utilizing the battery voltage supplied from the control station, thus eliminating even the need for a station battery at the remote plant.

Those plants that are located too distant from the control station for the economical transmission at generator voltage are controlled by supervisory and tele-

---

Paper 55-165, recommended by the AIEE Power Generation Committee and approved by the AIEE Committee on Technical Operations for presentation at the AIEE Winter General Meeting, New York, N. Y., January 31–February 4, 1955. Manuscript submitted April 2, 1954; made available for printing November 24, 1954.

H. H. GNUSE, JR., is with the Nantahala Power and Light Company, Franklin, N. C.

The author wishes to acknowledge the assistance of B. J. Fletcher, Chief Hydraulic Engineer, Aluminum Company of America, in the preparation of this paper.

metering equipment operating over a pair of telephone wires or over a single carrier-current channel. Since the application of such supervisory control and telemetering equipment has already been described,[1,2] a detailed explanation of the functions and operations of this equipment will not be given. It should suffice to point out that, consistent with the basic design consideration of limiting the installation to equipment that is actually required for safe and reliable generation, the supervisory and telemetering equipment has been kept to a minimum. With the multitude of functions that can be accomplished by supervisory control and telemetering, it is usually difficult to determine just where to stop with such an installation. It is obvious that if an unnecessarily large amount of such equipment is installed, it becomes increasingly more difficult and expensive to maintain, and the added cost of the unnecessary equipment offsets a portion of the economical gains that it should normally afford.

For these installations, supervisory control is used to accomplish the following:

1. Start and stop the unit.
2. Adjust the kilowatt output of the unit.
3. Adjust the kilovars of the unit.
4. Open and close transmission-line sectionalizing devices in the substation when such are installed.
5. Sound an alarm for operation of any of the relays or for indication of high or low reservoir elevation.

Telemetering is used for the following indications:

1. Generator kilowatt output.
2. Generator kilovar output.
3. Generator voltage.
4. Level of water in reservoir.

It will be noticed that only one annunciator alarm indication is used. This decision was based on the conviction that in case of an alarm a man must be dispatched to the station to correct the trouble, and that little added benefit would be gained by providing the operators at the control plant with specific information as to the exact nature of the relay operation. When the attendant reaches the remote plant, he can determine the cause of the operation from the station annunciator and report to the controlling station. In the meantime, the operators at the controlling station can determine the seriousness of the alarm by checking their telemetered readings or by checking to see if the machine will restart if it has been automatically shut down. The protective circuits at the remote plant are arranged so that the machine locks out for relay operations indicating serious trouble, such as operation of the differential relays, generator ground relay, low battery voltage, hot bearings, etc.

It will also be noted that no supervisory control or telemetering is used for operation of the taintor gates. They are controlled by float-operated devices which, when the lake has reached its maximum operating level, automatically position the taintor gate to discharge the stream flow in excess of the turbine discharge. Such automatic devices not only save considerable investment cost in supervisory control and telemetering but also relieve the operator at the remote station of the time-consuming chore of constantly checking the lake elevation and adjusting the taintor gate opening during periods of high flows. A high water alarm is incorporated in the annunciator circuit to sound an alarm should the water in the reservoir rise above a predetermined level, indicating that the taintor gate controls had not functioned properly.

All of the recent developments have been single unit stations. The need for station service supply when the generator is shut down has prevented the application of a unit transformer-generator installation with high-voltage circuit breaker, and it has been necessary to install the oil circuit breaker between the generator and the step-up transformer bank. Since this low-voltage oil circuit breaker could provide all the protection required except for faults within the transformer itself or on the transformer busses, which faults should be very rare in occurrence, a high-voltage oil circuit breaker has been omitted and a combination air break switch and ground switch utilized. In case of operation of the differential or case ground relay on the transformer bank, the high-speed ground switch places a fault on the line which trips the feeder breaker at a remote substation and simultaneously initiates the trip circuit to the gang-operated air break switch so that it will be opened before the line can be manually reclosed.

Generator protection is provided by a conventional neutral ground current transformer and relay and by double-primary current transformers which operate a sensitive plunger-type overcurrent relay for differential protection. By using a low ratio on this double-primary current transformer, more sensitive relaying can be obtained at much less cost than with the conventional generator differential relay.

Another somewhat unconventional electrical design feature is the use of the station service secondary voltage for supplying synchronizing potential on the transformer side of the generator breaker. This eliminates the need of additional potential transformers for this purpose and has proved entirely satisfactory in actual operation.

Mechanical, Structural, and Hydraulic Design Features

The powerhouses for these projects have been built large enough to accommodate the unit with its associated switchgear with provision for only enough unoccupied space to store the rotor when the unit is disassembled. No control rooms or offices have been included in view of the fact that the plants are all remotely operated. The switchgear and switchboards are placed on the generator floor which is usually level with the top housing of the generator stator.

For those installations where a steel pipe line is required, the design has taken into consideration the inherent self-supporting strength of the pipe to require a minimum of supporting bents. On one installation which required 2-foot diameter pipe, the bents were spaced at 64 feet, and in order to provide a uniform grade for the pipe, the supporting bents varied from a few feet to as much as 50 feet in height.

At all of the developments where a tunnel was required to divert the river during construction, the project has been designed so that this diversion tunnel is subsequently used for carrying the water from the reservoir to the powerhouse. This required that the intake be located at a very low level in the reservoir, and it therefore created considerable pressure on the intake gate. To overcome the difficulty of raising such a gate against pressure, filler valves were built into the face of some of the intake gates for filling the tunnel or pipe line to equalize the pressure before the gate is opened. This filler valve is moved by the same cable that operates the gate and therefore automatically opens first and closes last.

Tunnels are unlined except for short lengths at the intakes, at the downstream ends, and at a few locations where bad ground was encountered. It is more economical to drive the tunnels to a large section, permitting truck haulage and keeping water velocities low, than to drive small sections giving higher velocities and requiring lining. There are no inlet valves at the powerhouses at Tuckasegee, Cedar Cliff, and Bear Creek, and unwatering for maintenance is accomplished satisfactorily by use of the intake gates. No surge tanks or pressure relief valves are used at Cedar Cliff or Bear Creek even though the conduit lengths are 1,152 feet and 1,484 feet respectively. Effective control of speed and pressure rises is maintained by the governors.

Considerable savings in initial construction costs of many of these projects has been realized by designing the controlled spillway structures, such as taintor gates, to pass flows of 25 to 50-year flood magnitude with relatively inexpensive washout-type fuse plugs for larger, less frequent flows. Before the fuse plugs would be washed out, the flood flow would have reached such magnitude that the additional discharge from the lake storage through the fuse plugs would not contribute excessively to the flood peaks downstream. These fuse plugs are usually earth fills that are easily replaced when and if they are washed out.

Rock Fill Dam

The development of the rock fill dam has probably been the greatest factor in reducing construction costs of small hydroelectric projects. On small streams where the flood flows can be passed around the dam through low saddles between adjoining hills or through spillway and cascade sections cut into the rock abutments at the ends of the dam, the rock fill type of construction provides a very economical structure which in many cases costs less than one-third as much as a concrete structure.

The reason for the reduced cost is fundamental and very obvious. Rock can be quarried from the spillway and cascade area and placed in the dam for about $1.50 per cubic yard, whereas concrete would cost about $20.00 per cubic yard, depending on the availability of cement and suitable concrete aggregate. Thus, per cubic yard, the rock fill costs less than one-twelfth as much as concrete, and since the rock fill requires only about four times as much yardage as a gravity concrete dam, the economy of the rock fill dam is evident. Company studies indicate that concrete can be justified only at locations that lend themselves perfectly to a thin section arch dam. Even in such cases, the rock fill would usually be competitive.

There are many additional advantages that the rock fill construction possesses:

1. The rock fill dam can be constructed on foundations that are completely unsuitable for concrete structures. Unit loads are much less and foundation conditions less critical, thus permitting a wider choice of site and reduction of foundation treatment.

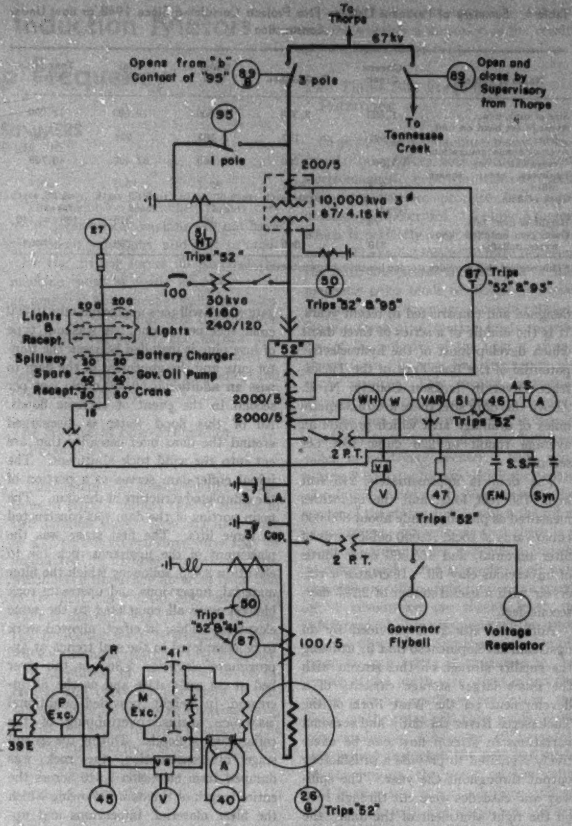
To Thorpe
67 kv
Opens from "b" Contact of "95"
89 B
3 pole
89 T
Open and close by Supervisory from Thorpe
To Tennessee Creek
95
1 pole
200/5
10,000 kva 3 ϕ
67/4.16 kv
51 NT
Trips "52"
87
50 T
Trips "52" & "95"
87 T
Trips "52" & "95"
100
30 kva
4160
240/120
20a
20a
Lights & Recept.
Lights
Spillway
30
30
Battery Charger
Spare
40
40
Gov. Oil Pump
Recept.
30
30
Crane
15
"52"
2000/5
2000/5
WH
W
VAR
51
46
A.S.
A
Trips "52"
2 P.T.
VR
V
47
F.M.
S.S.
Syn
Trips "52"
3
L.A.
3
Cap.
2 P.T.
Governor Flyball
Voltage Regulator
50
Trips "52" & "41"
87
100/5
R
"41"
P Exc.
M Exc.
39E
VR
A
45
V
40
26 G
Trips "52"

Fig. 1. Single-line a-c schematic diagram of the Bear Creek project

2. The rock fill dam of the earth-faced type is practically immune to damage by earthquakes or sabotage. The elasticity of the impervious clay fill makes it self-healing and it actually tightens and improves with age. Leakage is therefore held to a minimum. One engineer has estimated the life at one million years and states that after that he is not concerned about what happens to the structure.

3. Construction of a rock fill dam does not require much equipment other than the road building type, and requires very little high cost, expert supervision, control, and inspection, which means that more contractors are qualified to perform the work. Design costs are also less than for concrete structures.

4. The material for a rock fill dam is practically always available at the site in mountainous regions. The quality of rock is not critical since the design can be modified to use almost any type of rock and earth that is available. There are never any national emergency restrictions on the use of rock and earth such as often exist for cement and reinforcing steel.

5. Loads and stresses in the dam and foundation are low and free from abrupt changes. The water load is carried into the foundation directly by the shortest path, thus eliminating stability problems.

6. Danger from uplift is eliminated by the free draining rock fill.

The Bear Creek Development

The Bear Creek development is typical of several of the projects that have been

Table I. Summary of Pertinent Data on Five Projects Completed Since 1948 or now Under Construction

Name of Project	Queens Creek	Tuckasegee	Cedar Cliff	Bear Creek	Tennessee Creek
Size of unit, kva	1,800	3,333	7,500	10,000	12,000
Average net head on unit, feet	929	117	169	224	486
Average annual generation, megawatt-hours	5,000	13,200	24,300	32,400	40,700
Drainage area, square miles	3.6	54.7	80.7	75.3	40.1
Type of dam	rock fill, earth faced	concrete arch	rock fill, earth faced	rock fill, earth faced	rock fill, earth faced
Height of dam, feet	78	61	165	215	180 and 140
Cost per installed kilowatts, dollars	310	300	220	280	350*

*This project also provides storage benefiting downstream plants.

designed and constructed in recent years. It is the middle of a series of three dams which develop most of the hydroelectric potential of the East Fork of the Tuckasegee River in Jackson County, N. C. Above this dam site, there are 75.3 square miles of drainage area which provide an average runoff of 225 cubic feet per second.

The dam is approximately 215 feet high, 750 feet long, and the quantities measured as placed include about 850,000 cubic yards of rock, 70,000 cubic yards of filter material, and 165,000 cubic yards of impervious clay fill. It creates a reservoir with a useful storage of 2,287 day-second-feet.

Additional storage is provided by an upstream development so that by utilizing the smaller storage on this stream with the much larger storage capacity of a development on the West Fork of the Tuckasegee River the daily and seasonal variations in stream flow can be effectively regulated to provide a satisfactory output throughout the year. The spillway and cascades were cut through rock on the right abutment of the dam; the volume of these excavations was designed to provide the required amount of rock for the dam and actually an almost perfect balance was obtained in construction with no rock wasted other than a relatively small amount of unsuitable decomposed rock that was taken out of one of the cascade sections. The spillway includes one electrically operated taintor gate which will pass approximately 10,000 cubic feet per second. A washout type of fuse plug is installed between the taintor gate and the abutment of the dam to pass an additional 50,000 cubic feet per second in the event of extreme floods. All of this flood water is discharged around the dam over cascades that are cut into the solid rock abutment. The initial coffer-dam serves as a portion of the completed structure of the dam. The main portion of the dam was constructed in three lifts. The first stage was the placement of the upstream rock toe to elevation 2,435, following which the filter material, impervious and upstream rock blanket were all completed to the same elevation. This, in effect, allowed work to be completed in the seal trench at approximate elevation 2,360 in the river bed at an early date and as the fill increased in height provided additional insurance against overtopping of the coffer-dam by floods. During the second stage of construction, the rock was dumped from elevation 2,540 across the entire length of the dam, following which the filter material, impervious and upstream blanket were competed to this elevation. The final stage involved the construction of the crown from elevation 2,540 to elevation 2,580. In this section all material was brought up simultaneously.

The turbine, rated 13,000 horsepower, at 230-foot head, drives a 10,000-kva generator at 90-per-cent power factor, 4,160 volts, 400 rpm. The powerhouse is only 30 feet 6 inches by 40 feet 9 inches, yet it contains all the necessary equipment, including switchgear and switchboards, with enough storage space for the generator rotor. Of particular interest might be the method of cooling the generator which provides for the admission of outside air through a 6-foot by 6-foot inlet damper near the top of the powerhouse wall with the discharge of hot air from the generator through an opening below the generator floor level. By-pass dampers are used to warm the powerhouse during cold weather.

The switchyard is located immediately adjacent to the powerhouse and consists of a small steel structure 16 feet by 20 feet in plan. In order to save space, substation steel, and 66-kv bus, two circuits have been arranged vertically entering the station on the same bay. A motor-operated air-break switch provides for sectionalizing the transmission line which extends to the Tennessee Creek project approximately 4 miles upstream. A single-pole grounding switch and 3-pole motor-operated air-break switch are installed for protection of the Bear Creek transformer.

Fig. 1 is a single-line a-c schematic diagram of the station. Most of this arrangement is conventional except, as explained in a previous paragraph, for the differential protection of the generator, protection of the transformer bank, and use of station service supply for synchronizing potential. The relaying, supervisory, and telemetering equipment has been kept to the minimum that was considered practical to provide adequate protection and satisfactory control from the remote attended station. Table I summarizes data on five projects from 1948 to the present.

References

1. SUPERVISORY CONTROL AND REMOTE CONTROL HELP TVA CUT OPERATING COSTS, **R. M. Aspaugh, A. P. Maness.** *AIEE Transactions*, vol. 73, pt. III, Aug. 1954, pp. 863–69.

2. SUPERVISORY CONTROL OF 30,000-KVA HYDROELECTRIC PLANT, **C. W. Bohner, A. P. Maness.** *AIEE Transactions (Electrical Engineering)*, vol. 65, June 1946, pp. 337–42.

Vibration in 2-Pole Induction Motors Related to Slip Frequency

ERNEST W. SUMMERS
ASSOCIATE MEMBER AIEE

VIBRATION and noise in a 3-phase 2-pole a-c motor quite often are characterized by a pulsation or beat in the amplitude, i.e., the amplitude of the vibration and noise increases and decreases at a uniform frequency which is related to the slip of the rotor. In many applications, these pulsations are not detrimental to the performance of the machine, but they have an adverse psychological effect upon anyone in the vicinity of the machine because a noise which pulsates is much more noticeable than one which is steady. Performance can be influenced in applications where an a-c motor is built into a common frame with another machine such as a d-c generator. With this construction, the pulsations can cause a variation in commutation or in the generator output voltage.

Vibrational pulsations of this nature encountered in 2-pole motors are of the order of from 1/2 to 10 cycles per second (cps) depending upon the slip of the rotor and the type of pulsation. A normal human ear cannot hear vibrations much under 15 cps, but these pulsations are definitely audible. Therefore, it is reasoned that the pulsations are not a single fundamental frequency but must be the result of co-operation between two different frequencies at least one of which is in the audible range.

Two types of pulsations are encountered most frequently. The most common one varies at two times slip frequency, and the second varies directly with slip. The purpose of this paper is to describe the fundamental conditions which must exist to produce pulsations of the nature described and how in 2-pole a-c motors certain mechanical and electrical dissymmetries co-operate to produce vibrational driving forces which meet these conditions.

The conclusion is reached that a perfectly symmetrical machine will not have vibrational pulsations, and that to minimize the driving forces all parts of the machine must be made as symmetrical as practical both mechanically and electrically. Also, to minimize the response to the driving forces, the natural frequency of all parts of the machine must be kept away from running frequency and twice line frequency.

The Nature of Low-Frequency Pulsations

Fundamentally, low-frequency pulsations in electric motors can be caused in two different ways. First, the amplitude of a given vibrational force wave may be modulated by another vibrational force which has a frequency different from that of the first. A typical fully modulated wave is shown in Fig. 1. Here, the carrier frequency wave is modulated by a wave which has a relatively low frequency. The amplitude of the carrier wave increases and decreases uniformly or pulsates as dictated by the modulating wave, but its frequency remains constant. The general equation for a sinusoidally modulated wave is

$$a=(A_0+B_m \sin \omega_1 t) \sin \omega t \qquad (1)$$

where

A_0 = maximum amplitude of unmodulated wave
B_m = maximum amplitude of modulating wave
ω_1 = modulating frequency
ω = carrier frequency

Second, if two vibrational driving forces exist simultaneously having approximately the same frequency, they alternately aid and buck one another causing the phenomenon of beats. The frequency of the beat or pulastion is the difference between the two frequencies. Since the addition of two sine waves of slightly different frequency does not produce the same curve as when two sine waves are multiplied, the resultant wave will not look exactly the same as the modulated wave in Fig. 1, but the envelope of the amplitude will have precisely the same characteristic. Thus, it is impossible to listen to a machine and determine whether a pulsation is the result of a modulation or a beat.

Two Times Slip Frequency Pulsations

In any 2-pole a-c machine, many vibrational driving forces, both mechanical and electromagnetic, exist simultaneously and can co-operate to produce both phenomena just described. Assume a motor which is perfectly symmetrical mechanically. The radial magnetic force between the rotor and stator core at each of the magnetic poles tends to distort the core periodically as the magnetic field rotates. Since a force of attraction exists regardless of the polarity of the pole, a vibrational force of twice line frequency always results. This second harmonic driving force is independent of the number of poles, but is more prominent in 2-pole machines because the distance between poles is relatively greater. Now consider a 2-pole machine in which the center of rotation of the rotor coincides with the center of the stator, but in which the rotor is not round. This means that there is a point of minimum air gap which travels at rotor speed. In a 60-cycle 2-pole machine, the revolving field rotates at a speed of 60 revolutions per second (rps), or 3,600 rpm. If it is assumed that the rotor speed is 59 rps, and that the point of minimum air gap starts at time zero in the center of the north pole, then, when the north pole has made on revolution, the point on the rotor will have made 59/60 of a revolution. The rotor will keep falling behind and when the field has made 30 revolutions, the point on the rotor will have made 29.5 revolutions and so will line up with the south pole. When the field has made 60 revolutions, the rotor will have made 59, and the point will coincide with the north pole again. Thus, in 1 revolution of slip, the point of minimum air gap has come under the influence of maximum flux density twice

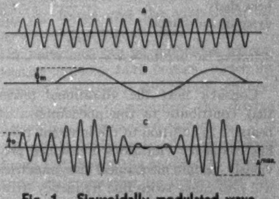

Fig. 1. Sinusoidally modulated wave

A—Carrier wave unmodulated
B—Modulating wave, 1 1/2 cycles
C—Modulated wave

Paper 55-133, recommended by the AIEE Rotating Machinery Committee and approved by the AIEE Committee on Technical Operations for presentation at the AIEE Winter General Meeting, New York, N. Y., January 31–February 4, 1955. Manuscript submitted October 21, 1954; made available for printing December 8, 1954.

Ernest W. Summers is with the Westinghouse Electric Corporation, Buffalo, N. Y.

The author sincerely appreciates the guidance and advice given to him by his associates, particularly H. C. Werner.

and, therefore, the frequency of the unbalanced magnetic pull between the rotor and stator is twice slip frequency. This vibrational driving force is superimposed on the normal twice line frequency driving force and modulates it at twice slip frequency.

A revolving point of minimum air gap can be caused by other dissymmetries such as a bent shaft, or dynamic unbalance combined with a weak shaft. With dynamic unbalance, the geometrical center of the rotor does not coincide with the axis of rotation but lies on a circle about this axis. The diameter of this circle depends upon the amount of unbalance and the stiffness of the shaft.

Electrical dissymmetries in the rotor such as a defective bar will also cause modulation. This can be explained briefly in the following manner. Normally the ampere-turns of the stator and rotor tend to balance one another except for the excitation ampere-turns. If it is assumed, however, that a rotor bar is open circuited, then the current flowing in it and, thus, the ampere-turns produced will be greatly reduced. The net unbalanced stator ampere-turns will produce an air-gap flux density greater than normal at the point of the defective bar. This increased flux density will cause a higher induced voltage and, thus, a higher current in the bars adjacent to the defective bar; hence the net effect is that the stator and rotor ampere-turns still balance one another, but the flux distribution in the air gap is altered. This change in flux distribution is most pronounced when the defective bar is under a magnetic pole and least effective when it is between poles. Since the defective bar is passed by a magnetic pole twice for each revolution of slip, the inherent twice line frequency vibration is modulated at two times slip frequency. Obviously, the motor torque will also pulsate at this same frequency.

Pulsations caused by modulation can be summarized as follows:

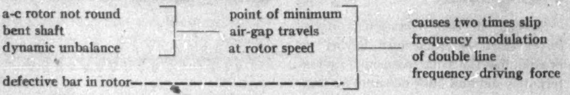

Consider next the vibrational forces that contribute to the phenomenon of beats.[1] In addition to the inherent twice line frequency vibrations mentioned previously, certain mechanical dissymmetries will also cause twice line frequency driving forces. Assume that the center of rotation of the rotor coincides with the center of the stator and that the rotor is round, but the stator is slightly elliptical. As the field rotates, it passes a point of minimum air gap twice each revolution and, thus, produces a vibrational force of twice line frequency. If the rotor and stator are both round but the rotor is not perfectly centered in the stator, the same frequency vibration results.

Several mechanical driving forces exist which can cause two times running frequency vibrations. A shaft which has noncircular cross sections, caused by keyways for example, or elliptic bearings are the two most important examples.[2] This second harmonic driving force is not particularly important except in 2-pole machines in which the harmonic differs from twice line frequency by two times slip frequency. Thus, these two driving forces alternately reinforce and interfere with each other and produce a beat. The conditions producing this beat can be summarized as follows:

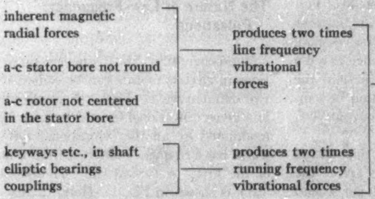

Another factor which must be included when considering the causes of the beat phenomenon is the space harmonics in the main flux wave.[3] Parasitic torques will be produced by these harmonics, but they also produce parasitic radial forces which tend to cause noise and vibration. As an example, consider the stator 5th harmonic which travels around the stator in the direction opposite to that of the fundamental. The 5th harmonic has five times as many poles as the fundamental, or ten poles. The time variation of all the stator harmonics in the air-gap flux is the same as for the fundamental since they are all produced by the same current. Therefore, with sinusoidal impressed voltages, the revolving harmonic component fields in the air-gap flux caused by the windings revolve more slowly than the fundamental field. Thus, the 5th harmonic revolves one-fifth as fast as the fundamental, or 12 rps for a 60-cycle 2-pole machine. With ten poles revolving at 12 rps, a vibrational driving force of 120 cps is produced which is exactly the same as the fundamental. In the same manner it can be shown that all of the stator harmonics will produce radial forces of twice line frequency. This is one reason why they make the pulsation worse.

There is, however, a more important aspect of the situation. The frequency of the voltage induced in the rotor by a space harmonic is equal to the line frequency times the slip of the rotor with respect to the harmonic.[4] In the Appendix it is shown that for the 5th harmonic which rotates in the opposite direction of the fundamental

$$f_2 = f_1(6 - 5S_1) \tag{2}$$

where

f_1 = frequency of the fundamental
S_1 = slip of the rotor with respect to the fundamental

For the 7th harmonic, which travels in the same direction as the fundamental

$$f_2 = f_1(-6 + 7S_1) \tag{3}$$

If a slip of 5 per cent or 3 rps for a 60-cycle 2-pole machine is assumed, the frequency induced by the 5th harmonic in the rotor is

$$f_2 = (60)(6 - 5 \times 0.05) = 345 \text{ cps}$$

The frequency induced by the 7th harmonic is

$$f_2 = (60)(-6 + 7 \times 0.05) = -339 \text{ cps}$$

Numerically, these two frequencies differ by 6 cps, or two times slip frequency. The negative sign for the 7th harmonic merely means that its motion relative to the rotor is opposite that of the 5th harmonic. Thus a point on the rotor sees two revolving fields which are aiding one another when they are in phase and bucking when they are out of phase. The net result is that a torque pulsation occurs which varies at two times slip frequency. Other harmonics such as the 11th and

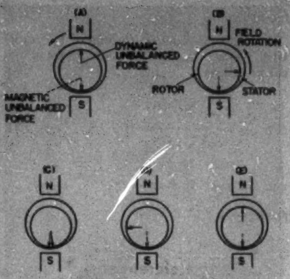

Fig. 2. Dynamic unbalance modulated by magnetic unbalance

13th, 17th and 19th, 23rd and 25th, etc., also beat with one another at the same frequency.

It is well known that the magnitude of the space harmonics can be suppressed by the proper winding pitch. The most desirable pitch is 83 per cent which reduces the 5th and 7th harmonics to about 26 per cent of that with full pitch. Since small 2-pole machines are very difficult to wind with this long a throw, the best compromise is 55 to 57 per cent which reduces the 7th harmonic to a small value. It is important to note that, if the winding is such that prominent space harmonics are present, the pulsation can occur even if the rotor, stator, and air gaps are perfect.

Pulsations Which Vary Directly with Slip or as a More Complex Function

Certain combinations of mechanical and electromagnetic forces can cause other pulsations which vary with slip. For example, assume that the rotor is dynamically unbalanced and that it is not perfectly centered in the stator, as shown in Fig. 2. When a magnetic pole (either north or south) lines up with the minimum air-gap point and the mechanical unbalance vector is 180 degrees from this point, the unbalanced magnetic pull will tend to reduce the mechanical unbalance. Assume again that the field rotates at 60 rps and the rotor at 59 rps. When the field has made 15 revolutions, the rotor will have made 14.75 revolutions, or will have slipped 1/4 revolution, as shown in Fig. 2(B). Later, when the field has made 30 revolutions and the rotor 29.5, the mechanical unbalance vector lines up with the south pole, as shown in Fig. 2(C), and the two force vectors are in space phase. The rotor keeps slipping further behind until it has slipped 1 full revolution and the mechanical unbalance vector once more lines up with the north pole, as shown in Fig. 2(E).

Note that the magnetic unbalanced force vector remains stationary in space and exists only when a magnetic pole is at the small air gap, while the mechanical unbalanced force vector revolves with the rotor. Thus, the running frequency vibration caused by dynamic unbalance will be modulated by the unbalanced magnetic force. The frequency of the modulation will vary with slip, but is not a continuous function of slip. This modulation requires that a point on the rotor and the revolving field coincide with a point on the stator periodically, and thus it has 1 degree less of freedom than the two times slip frequency modulation. For certain values of slip, the three points may never coincide. Using the same example as previously, if the revolving field has a velocity of 60 rps, and the rotor 59 rps, then a magnetic pole will pass a point on the rotor two times per second. Furthermore, the point on the rotor and magnetic field will always meet at the same points on the stator, and it is possible that none of them are the point of minimum air gap.

This depends on the initial relative position of the three points. If the initial conditions are correct, then the running frequency will be modulated at exactly slip frequency. If not, no modulation, or only slight modulation will occur at slip frequency. With the rotor speed of 49.1 rps, a pole will pass a point on the rotor 1.8 times per second and they will meet at progressively different points on the stator. Thus, the rotor and field may eventually coincide or come close to coinciding with a particular spot on the stator, but the frequency of the modulation will be less than slip frequency. It is difficult to write a mathematical expression to prove this, but a graph which shows the position of a point on the rotor and the magnetic field with respect to the stator at any instant will illustrate it. If several types of dissymmetry are involved, the situation is even more involved. Actually, an arc of the stator should be considered rather than a point because, if the rotor is off center, the gap will be small for an appreciable part of the circumference. For this reason, and the fact that the slip is not absolutely constant, the pulsation is usually slip frequency or close to slip frequency.

Often an a-c motor is combined with a generator in a unit frame 2-bearing set. Some generators such as d-c machines with half as many commutating poles as main poles, and some types of high frequency generators, have a condition where the armature and the frame are at different potentials magnetically. This can cause a d-c flux to flow through the shaft, a-c rotor, air gap, and core and back through the frame to the generator. If the a-c motor were not excited, this flux would be distributed uniformly around the a-c air gap, but with the motor excited it will be concentrated at either the north or south pole depending upon the polarity of the d-c flux. With more than two poles the magnetic attraction between the rotor and stator will remain balanced, but with two poles an unbalanced magnetic force exists because of the difference in flux density in the two diametrically opposite air gaps. This unbalanced force rotates at synchronous speed and thus passes a point on the rotor once for each revolution of slip. Now, if the rotor is dynamically unbalanced, a situation similar to the previous one exists, i.e., the unbalanced magnetic force alternately increases and decreases the amplitude of the running frequency vibration. The frequency of this pulsation is always slip frequency since it is independent of position with respect to the stator. If, in addition, the rotor is not centered in the stator, then the slip frequency pulsation also could be modulated at some lower frequency.

IDENTIFICATION AND ELIMINATION OF PULSATIONS

Whenever a pulsation is encountered, it can be determined which of the two general types it is by accurately measuring the slip and the frequency of pulsation. Further evidence can be obtained by measuring the frequency of the vibrations in the machine. If a prominent vibration of approximately twice line frequency exists, and it pulsates, then it is the first general type. However, if a predominate running frequency vibration exists which pulsates, it is the second general type.

Thus far, only the vibrational driving forces which exist have been considered, but the final amplitude of vibration is dependent upon both the amplitude of the driving forces and the vibrational response of the various parts. Therefore, the pulsations can be eliminated by correcting either or both factors. Once the type of pulsation is determined, changes can be made to minimize the driving forces, listed previously, causing it. It is impossible to eliminate all of the driving forces but, unless the mechanical or electrical dissymmetries are quite large, the forces tending to produce the pulsations will be relatively small and excessive vibration will not occur unless some part of the machine is resonant.

It is very important that the natural frequency of all parts of the machine and particularly the shaft be something other than running frequency or twice line frequency. The shaft frequency can be between the two frequencies, but it would be desirable to have it at least 10 per cent above twice line frequency.

Conclusions

It is obvious from the previous analysis that a perfectly symmetrical 2-pole 3-phase a-c motor would not be afflicted with vibration pulsations, although it still might vibrate. The conclusion is reached that to eliminate vibration pulsations the following things must be done:

1. Make stator bore, air gaps, and rotor as accurate and uniform as practical.
2. Make the shaft straight, without noncircular cross sections, and with perfectly round ball-bearing fits. These factors are of less importance if the natural frequency of the shaft is well removed from twice running frequency.
3. Keep the natural frequency of all parts, but particularly the shaft and stator core, away from running frequency and twice line frequency.
4. Make rotor symmetrical electrically, and use a stator winding pitch which suppresses the space harmonics and particularly either or both the 5th and 7th harmonics.

Appendix. Slip of Rotor with Respect to Harmonics

The slip of the rotor with respect to a stator space harmonic is equal to the difference between the speed of the harmonic field relative to the stator and the speed of the rotor relative to the stator divided by the speed of the harmonic field; thus, the slip of the rotor with respect to the 5th harmonic is

$$S_5=\frac{-\frac{2f_1}{5P_1}-\frac{2f_1}{P_1}(1-S_1)}{-\frac{2f_1}{5P_1}}=6-5S_1 \qquad (4)$$

where

P_1 = number of poles of the fundamental
f_1 and S_1 are as defined previously

The frequency of the voltage induced in the rotor by the 5th harmonic is

$$f_5=f_1(6-5S_1) \qquad (2)$$

In the same manner, the slip of the rotor with respect to the 7th harmonic can be calculated as

$$S_7=\frac{\frac{2f_1}{7P_1}-\frac{2f_1}{P_1}(1-S_1)}{\frac{2f_1}{7P_1}}=-6+7S_1 \qquad (5)$$

and for the 7th harmonic

$$f_7=f_1(-6+7S_1) \qquad (3)$$

References

1. The Nature of Vibration in Electrical Machinery, Troy D. Graybeal. *AIEE Transactions*, vol. 63, 1944, pp. 712–18.

2. Mechanical Vibrations (book), Den Hartog. McGraw-Hill Book Company, Inc., New York, N. Y., 1947, pp. 305–08.

3. Electric Machinery—Vol. II (book), M. Liwschitz-Garik, C. C. Whipple. D. Van Nostrand Company, Inc., New York, N. Y., 1946, pp. 124–270, 494–508.

4. Principles of Alternating Current Machinery (book), R. R. Lawrence. McGraw-Hill Book Company, Inc., New York, N. Y., 1940, pp. 505–10.

5. Radio Engineering (book), F. E. Terman. *Ibid.*, 1947, p. 526.

Improved Field Conductor Materials for Turbine Generators

C. H. HOLLEY
MEMBER AIEE

R. E. SAVIDGE
NONMEMBER AIEE

THE present demands for large unit ratings in 2-pole high-speed turbine generators have dictated that the field winding conductor materials be unusually strong to withstand the various mechanical stresses applied during the operation of the machine. At the same time, high electrical conductivity must be maintained so that the material can be utilized most efficiently.

Some 10 years ago the General Electric Company embarked on a program to improve existing conductor materials and to develop new alloys, which would provide design engineers with greatly improved conductor materials permitting generator design to keep pace with the industries' demands.

In the past, field conductor distortion was one of the limitations in designing a thoroughly reliable large turbine-generator field. Various authors[1–4] have adequately described the causes of and the difficulties from such conductor distortion, but this problem is again briefly stated for purposes of reference in the following.

Conductor distortion results from a cycle beginning when the generator starts to rotate after a shutdown. At this time, the field conductors, which are cold, are thrown outwards by centrifugal force and being restrained by the wedges gradually become locked in by this force at approximately two-thirds rated speed. When synchronous speed is reached, field current is applied, the generator is connected to the system, and load is picked up. During this increased application of field current, the conductors heat up and attempt to expand. However, since they have previously been locked in, due to the centrifugal force, the thermal expansion is restrained and a resulting compressive stress is applied to the conductors. At these elevated temperatures [hot-spot temperatures may vary from 100 degrees centigrade (C) to 140 C] the compressive stress applied may cause plastic deformation if:

1. The stress exceeds the elastic limit of the material as defined by the compressive stress strain curve at operating temperature.
2. The high loadings obtained at these temperatures exceed the compressive creep strength of the material.

Each of these phenomena may produce a minute but significant upsetting in the conductor material. As this cycle is repeated (i.e., beginning from a cold start) the upsetting is again introduced and the effect is additive.

The results of this conductor distortion,

Paper 55-131, recommended by the AIEE Rotating Machinery Committee and approved by the AIEE Committee on Technical Operations for presentation at the AIEE Winter General Meeting, New York, N. Y., January 31–February 4, 1955. Manuscript submitted October 19, 1954; made available for printing December 2, 1954.

C. H. Holley and R. E. Savidge are with the General Electric Company, Schenectady, N. Y.

The authors are indebted to many persons both within and without the General Electric Company. Particularly, we gratefully acknowledge the outstanding contributions of L. B. Barker of the General Electric Company and Prof. M. F. Sayre of Union College in the design and operation of the creep testing apparatus and the accumulation of test data. Special acknowledgment is due R. H. Harrington, metallurgical consultant, for his original work on Cond-Al and his guidance during the development of the alloy on a commercial scale. Appreciation is also due H. D. Taylor for his foresight in initiating this program and continued encouragement and guidance and to H. F. McCullough and M. F. Kent for their contribution in the early development stages. Also, thanks are due to J. D. Lubahn and B. M. Cain for their helpful suggestions in the preparation of this paper.

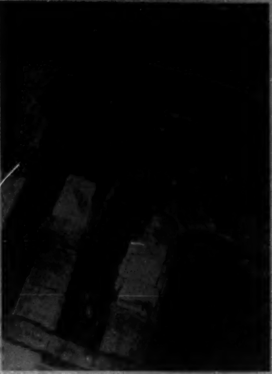

Fig. 1. View of end winding conductor distortion showing lower turns of coils pulled in towards field body

as illustrated in Fig. 1, have been observed on generators built by various manufacturers in this country[4] and in Europe.[1,2] The effect has been pronounced on field windings made with annealed tough-pitch copper and annealed electrical conductivity (E.C.) grade aluminum. The authors' company has approached the distortion problem in three ways:

1. By the development and use of improved conductor materials which have high physical properties and resistance to creep capable of withstanding any stress imposed during the operation and life of a turbine generator.
2. By the design and use of improved field winding ventilation methods which keep both the hot-spot and average field temperature to a minimum and thereby reduce the stress on the conductors due to lower differential expansion and at the same time increase the life and reliability of the insulation.
3. By preheating[4,5] which is an effective preventative of distortion in generator fields.

This paper will deal directly with item 1, i.e., the development and use of superior field conductor materials.

A 2-step development program to produce the required field conductor materials was initiated as follows:

a. An intensive test program to determine the physical properties (including compression creep at elevated stresses and temperatures) of commonly used field conductor metals and those developed under item b.

b. The development of high conductivity copper and aluminum alloys with a compressive yield strength of 12,000 pounds per square inch (psi) or better at 140 C and with negligible creep at this loading and temperature.

The results of this program have been encouraging.

Silver and cadmium bearing coppers are now available and in use that have compressive yield strengths at 140 C of about 20,000 psi, or more than three times that of annealed tough-pitch copper. These alloys undergo less than 2 per cent (%) the amount of deformation in compression creep of annealed tough-pitch copper at stress levels existing in generators with no sacrifice in electrical conductivity.

An aluminum alloy (Cond-Al) is in commercial use which has a compressive yield strength at 140 C of 15,000 psi or about four times that of annealed E.C. aluminum. Cond-Al suffers less than 1% as much deformation in compression creep as annealed E.C. at machine stress levels and 10% the creep of annealed E.C. which has been 20% cold worked and stress relieved. The electrical conductivity of Cond-Al is within 2% of E.C. aluminum.

Test Program

The foregoing analysis of the problem shows that the principal mechanical properties in question are compression yield and creep strengths. It was decided to study creep with the stress applied in compression since this most nearly duplicated the conditions in the generator, and it was desirable to avoid errors due to the Baushinger effect (the phenomenon by which plastic deformation of a metal raises the yield strength in the direction of plastic flow and decreases the yield strength in the opposite direction).

Since no commercial apparatus was available for such tests, a compression creep machine was designed.[6] In this machine the load is applied to the ends of a 1-inch by 5/16-inch by $5^{1}/_{2}$-inch specimen through a yoke arrangement. The specimen is supported on the sides just enough to prevent buckling without producing noticeable friction. Tube and push rod extensometers transmit the changes in the 5-inch gauge length from the sides of the specimen to two dial indicators above, which are graduated in ten-thousandths of an inch. The average of the two readings is used to plot the creep curves. With this equipment, a study of the compression creep properties of the commercially available high conductivity materials was begun immediately. Development alloys were run as soon as they were available.

Copper Program

A review indicated that more favorable results would be expected if the copper were strengthened by using some cold work and with the addition of silver or cadmium to raise the recrystallization (softening) temperature. Five % cold work was established as a reasonable amount for two reasons: 1. the softening temperature decreases with increasing cold work, and 2. springy copper is difficult to assemble during the winding operation. Fig. 2 shows the effect of silver on the annealing temperature of copper.[7] The commercial alloy containing 8 to 10 ounces of silver per ton of copper was chosen because the very large rise in softening temperature in the early part of this curve is adequate for the purpose.

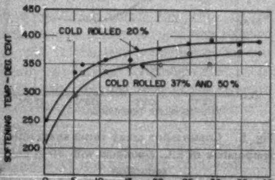

Fig. 2 (left). Effect of silver on softening temperature of copper. Data taken from reference 7

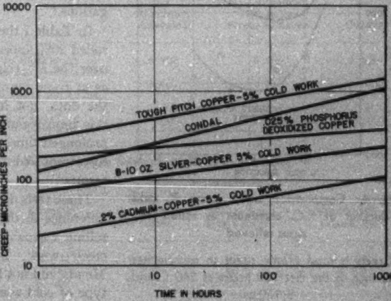

Fig. 3 (right). Compression creep of some coppers and Cond-Al at 140 C (284 F) and 8,000 psi

Table I. Mechanical Properties of Some Coppers

Material		Room Temperature Tensile			140 C—Compression		200 C Tens.	
Copper Alloy	Condition	Ultimate Strength, Psi	0.2% Yield Strength, Psi	% Elongation	Stress for 0.1% Creep in 1,000 Hours, Psi	0.2% Yield Strength, Psi	1,000-Hour Rupture Strength	1-Hour Softening Temperature, C
Tough-Pitch	Annealed*	31,000	5,800	74.0	4,700	5,800	15,000	
	Cold Drawn 5%	32,200	14,700	58.5	5,900	9,200		
	Cold Rolled 5%	32,200	19,100	57.5	7,200	10,900		350
	Cold Rolled 20%	40,850	40,850	33.5	11,800	33,000		
Silver 8 to 10 ounces per ton	Annealed*	31,100	6,240	80.5	5,200	6,400	20,000	
	Cold Drawn 5%	32,000	23,100	53	16,000	22,000		
	Cold Rolled 5%	33,700	29,600	47	17,300	28,000		450
0.2% cadmium	Annealed*	33,800	14,230	73.0	13,400	14,900	27,000	
	Cold Drawn 5%	34,400	26,200	55	17,300	19,400		
	Cold Drawn 10%	41,600	41,000	26	21,200	32,500		
	Cold Rolled 5%	33,000	22,800	56	16,700	19,400		500
0.025% phosphorus	Cold Drawn 5%	33,450	24,700	54.5	16,500	21,300		
	Cold Rolled 5%	32,425	15,390	62	8,600	9,900		
0.5% selenium	Cold Drawn 5%	31,925	14,810	56.5	6,400	10,600		
	Cold Rolled 5%	31,600	14,370	55.5	6,800	10,600		
OFHC plus 10 ounces silver	Cold Rolled 5%	37,350	33,250	41.5	17,600	29,000		
OFHC plus 0.2% cadmium	Cold Rolled 5%	34,200	25,300	46	13,800	22,000		

*Annealed at 500 C for 1 hour.

An alloy of copper with 1% cadmium was available but the 87% conductivity of this alloy was too low for this end use. Data prepared by Smart and Smith[8] show that the addition of 0.2% cadmium lowers the conductivity only about 1.5% and increases the softening temperature of tough-pitch copper by 200 C. Tests were made of a copper alloy containing the nominal amount of 0.2% cadmium. There was no reason to suspect that OFHC, phosphorous-deoxidized, or selenium-bearing copper would prove to be any improvement over tough-pitch, but since no data were available these were included in the tests.

Typical creep curves which were obtained for several of the coppers are shown in Fig. 3 and the compiled data for all the coppers tested are shown in Table I. In both comparisons the improvement in creep properties, rupture strength, and softening temperature because of the addition of silver or cadmium is obvious.

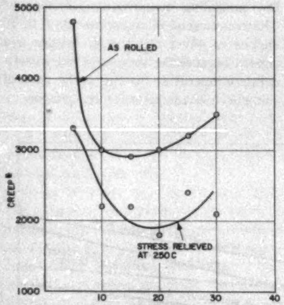

Fig. 4. Compression creep versus % cold reduction of E.C. aluminum as rolled and stress relieved

*Creep is total plastic strain in microinches per inch in the first 100 hours at 140 C and 5,130 psi

The phosphorous-deoxidized copper provides an increase in creep strength, but this high residual phosphorous reduces the electrical conductivity to about 80%. Phosphorous, cadmium, and silver all have the effect of raising the recrystallization temperature of copper.

As was expected, the 0.5% selenium copper alloy was not different from tough-pitch. Selenium has virtually no solid solubility (mixing of solids where the components are atoms) in copper and, consequently, no noticeable effect on the mechanical properties.

This investigation did not show OFHC copper with silver or cadmium to be any better than tough-pitch copper with silver or cadmium. Evidently, the effects of these two addition elements overshadow any effects which might be due to the insoluble oxides of copper. This agrees with the results of other investigations.[9]

In Table I the tough-pitch copper cold rolled 20% appears to be an improvement over the 5% cold rolled at 140 C as well as at room temperature. Other plots of the data, not included here, show that this improvement is not maintained for prolonged times at 140 C. Tensile creep tests reported by others[9] confirm these results.

These tests did not show any significant difference in the creep properties due to rolling versus drawing. In their tension creep work, Benson, McKeown, and Mends[9] did not find any effect due to the type of cold work, and this is again confirmed by our work on aluminum reported later in this paper and by recent work on our aluminum alloy, Cond-Al. It is well known that there will be a considerable difference in the response of copper to cold work due to grain size, minor impurities and their distribution, and alloying elements. Much more extensive work would have to be done to separate these variables before any significant conclusions could be drawn.

Aluminum Program

Aluminum field windings extend the design possibilities in generators by decreasing the load on the retaining rings and rotor forgings and permitting the manufacture of large diameter rotors. Aluminum has about 61% of the volume conductivity and a specific gravity of 31% that of copper so that for equal conductance only 51% as much weight of aluminum is required.

After a considerable number of genera-

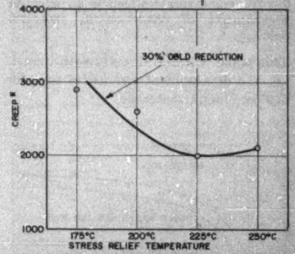

Fig. 5. Compression creep versus stress relief temperature of E.C. aluminum with 30% cold reduction

*Same as Fig. 4

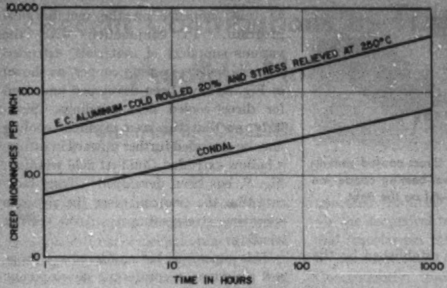

Fig. 6. Compression creep of Cond-Al and E.C. aluminum at 140 C (284 F) and 5,000 psi

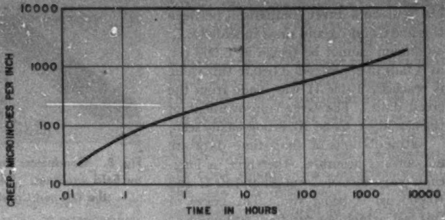

Fig. 7. Compression creep of Cond-Al at 10,000 psi and 140 C

tors had been wound with E.C. grade aluminum, it was found that these windings were susceptible to failure by compression creep, but the advantages of aluminum were so outstanding that work was begun to improve this property in E.C. aluminum. The program to improve the compression creep properties of E.C. aluminum included work on cold drawing, cold rolling, and stress relief treatments. Tests of drawing versus rolling did not show any significant difference, but it was found that E.C. aluminum could be made more creep resistant by alterations in the usual manufacturing cycle. One of the tests is described now.

Six pieces of an annealed bar were cold rolled by different amounts in 5% increments up to 30% reduction. Part of each piece was tested as rolled and part was tested after it was stress relieved at 250 C [482 degrees Fahrenheit (F)] for 5 hours, except the bar which was rolled 30%, from which additional samples were taken and stress relieved at 175 C (347 F), 200 C (392 F), and 225 C (437 F). The results are plotted in Figs. 4 and 5.

These data show that there is an optimum condition for minimum creep in all three cases. This effect was also found by Zschokke[10] in his work on some steels. In the curve for as-rolled material in Fig. 4, the strengthening effect of cold work is noticeable up to 15%. Above this the cold work has lowered the softening temperature so that 140 C is enough to produce softening during the test. In the other curve of specimens stress relieved at 250 C, the test temperature has virtually no further softening effect. The prior softening has lowered the strength and creep resistance of the specimens with greater than 20% cold work, but 250 C is not enough to soften specimens effectively with less than 20% cold work. A stress relief has taken place without appreciable softening and the strengthening effect of the cold work is still in evidence.

This effect of prior annealing is again shown by Fig. 5. It is already established that softening takes place during the test of the 30% cold reduced specimens. The maximum stress relief with minimum softening is represented by the lowest creep in this curve. For stress relief temperatures below 225 C additional softening takes place during testing; above 225 C the alloy is already too soft to give the maximum resistance to compression creep.

Part of the difference in level of the two curves in Fig. 4 is probably due to the Baushinger effect. The specimens have been made weaker in compression by the cold work in the opposite direction and stress relieving nullifies this effect. The rest of the difference must result from the softening during testing of the cold worked specimens.

The program to develop an aluminum alloy with the required properties has been described.[6] Briefly, studies of recrystallization, electrical conductivity, and rupture strength due to single addition metals[11] provided data to make trial alloys. The alloy selected after extensive tests of several compositions is now known as Cond-Al.[12]

Cond-Al is an age-hardenable alloy with the nominal composition of 0.55 iron, 0.33 magnesium, 0.12 silicon, and the remainder aluminum. The processing of Cond-Al follows the sequence of hot rolling, cold drawing, solution heat treatment, cold rolling 10 to 20%, and age hardening. After this, the alloy is ready to be wound into field coils.

The creep qualities of field coils made of Cond-Al can be seen by referring to Fig. 3. At the stress level of 8,000 psi this alloy falls between cold worked tough-pitch and cold worked silver bearing copper. The improvement in compression creep of Cond-Al over the best condition which we were able to produce in E.C. aluminum, as described in Fig. 4, is shown by Fig. 6. The first E.C. aluminum field coils used in generators were made of annealed material. The values for annealed E.C. could not be plotted in Fig. 6 since the creep rate is so fast at 5,000 psi stress that it is impossible to obtain consistent data. It was desira-

Table II. Comparison of Compression Creep Data for Three Aluminums

	E.C. Aluminum Annealed	E.C. Aluminum Cold Rolled Stress Relieved	Cond-Al
Stress for 0.1% creep at 140 C in 1,000 hours, psi	2,000	4,000	8,000
Creep in the first 1,000 hours at 140 C and 5,000 psi in 0.001 inch per inch	failed	4.6	0.6
Creep in the first 1,000 hours at 140 C and 10,000 psi in 0.001 inch per inch	failed	failed	2
Compressive 0.2% yield strength at 140 C	4,000	8,000	15,000

Table III. Tensile and Fatigue Strength of Three Aluminums

Material	Anneal	Tensile Strength, Psi	Yield Strength 0.2% Offset	Elongation, % in 2 inches	Fatigue Strength 500,000,000 Cycles, Psi
Cond-Al	none	22,800	19,300	22.0	12,000
Cond-Al	450 C	13,250	3,360	43.0	8,400
E.C. Aluminum	350 C	10,800	2,520	58.0	3,300

ble to make a direct comparison between this and Cond-Al, and since annealed E.C. aluminum cannot be tested at 5,000 psi, as it fails in compression before this value is reached, Table II was made from the creep data. The large improvement of the new alloy, Cond-Al, is now easily seen.

Extrapolations of short-time data are not always accurate; therefore, a long-time creep test of Cond-Al at 140 C and 10,000 psi is being run. The curve of this test which has run for 5,600 hours at the time of this writing, is shown in Fig. 7. The creep rate in microinches per inch per hour which is still diminishing was 1.2 at 100 hours, 0.39 at 1,000 hours, and 0.14 at 5,000 hours. A failure such as occurs in tensile creep would never be expected in this test since the specimen becomes larger in cross section and the stress decreases.

In addition to creep, generator windings may also be subject to fatigue stresses; therefore, this property was measured in Cond-Al and annealed E.C. aluminum. These results are shown in Table III. Annealed properties were measured because part of the end of the field coil is softened so that it can be formed to the shape of the rotor during the winding operation. Here again the tests show that Cond-Al is superior.

The electrical conductivity of Cond-Al is 59% International Annealed Copper Standard. The temperature coefficient of resistance of Cond-Al was found to be the same as copper, 0.00385 ohm per ohm per C between 25 and 144 C. The coefficient of linear thermal expansion is 13.1 $\times 10^{-6}$ between 68 and 212 F.

Discussion

Silver-bearing copper has been used in turbine-generator field windings for approximately 15 years. The addition of the silver has raised the recrystallization or softening temperature so that the increased creep strength, due to the previously mentioned cold reduction, is maintained at temperatures above those encountered in service. The silver-bearing alloy also has increased the rupture strength and has eliminated various types of cracking, which have been found on old machines originally wound with annealed tough-pitch copper. Thus the silver-bearing copper has enabled the generator designer to create generator fields which are limited in diameter only by stress limitations on the steel rotor forging and retaining rings, and in length by such considerations as static deflection and critical speeds as established by the bearing spans.

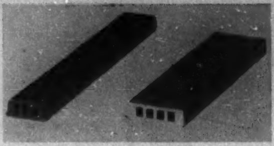

Fig. 8. Conductors for direct-cooled generator field windings. Silver-bearing copper on the left and Cond-Al on the right

The use of cadmium copper has been limited principally because of the restricted supply and higher cost. Its slightly better physical properties have made it attractive for use as amortisseur windings on large special turbine generators for such application as single-phase loading. Cadmium copper, because of its higher recrystallization temperature than silver-bearing copper, stands ready for use as field winding material when new high temperature field winding insulations, which are now being developed, are applied.

Of the various aluminum alloys so far developed, the one that stands out for this application is Cond-Al. To date, there are 31 generators running with Cond-Al field windings with an additional 20 generator fields shipped or on order. The oldest Cond-Al winding from the point of service has been operating for over 5 years. Cond-Al has been used widely in the replacement of original soft E.C. aluminum windings, some of which have been in service for 16 years, but principally it has permitted the extension of generator capability approximately 20% higher than that possible with copper windings, while maintaining conventional insulation and ventilation methods. Cond-Al, with its weight-to-conductivity ratio advantage over copper of almost 2 to 1, permits the design of larger diameter generator fields within the stress limitations on the steel retaining parts than have been possible with copper.

Cond-Al has not been used as a substitute for copper windings but has been used principally to permit the design and use of machines which were not possible with copper. However, the availability on a commercial scale of this new alloy has provided a worthy backup material should copper again become unavailable or in short supply for defense reasons.

The advent of direct-cooling[13,14] of generator stators and rotors has also had a great influence on the metallurgical program. In conjunction with the various suppliers of materials, extruded shapes of silver-bearing copper, as shown in Fig. 8, have been developed and used for direct-cooled field windings. Similarly, so that the area of direct cooling may be extended further upward in rating, a hollow extruded Cond-Al field winding, Fig. 8, has been developed. Tests indicate that the two can meet the rigorous operating stresses impressed on such a winding.

This paper may be considered as a progress report on a continuing development program. Further improvements and new alloys in both copper and aluminum are now being pursued.

References

1. Deformation of Turbo-Alternator Rotor Windings Due to Temperature Rise, G. A. Juhlin. *Journal*, Institution of Electrical Engineers, London, England, vol. 85, 1939, p. 544.

2. The Operation of Large Turbo-Alternators to Reduce Rotor Winding Deformation, R. H. Coates, B. C. Pyle. *Ibid.*, vol. 93, pt. II, Apr. 1946, pp. 192–212.

3. Turbo-Alternator Rotor Coil Shrinkage, W. D. Horsley. *Heaton Works Journal*, Newcastle Upon Tyne, England, vol. 4, no. 23, 1946.

4. Prevention of Rotor-Winding Deformation on Turbo-Generators. J. G. Noest. *AIEE Transactions* (*Electrical Engineering*), vol. 63, July 1944, pp. 514–19.

5. Field Preheating for Large Turbine-Generators, W. J. Gilson, Jr., H. D. Taylor. *AIEE Transactions*, vol. 73, pt. III, Dec. 1954, pp. 1375–83.

6. Cond-Al—A Tailor-Made Aluminum Alloy of High Creep Strength and Conductivity, L. B. Barker, C. H. Holley, R. H. Harrington, M. F. Sayre. *Metal Progress*, Cleveland, Ohio, vol. 63, no. 5, May 1953, pp. 90–94.

7. Arsenical and Argentiferous Copper. J. L. Gregg. Chemical Catalogue Company, Inc., New York, N. Y., 1934.

8. Effect of Certain Fifth-Period Elements on Some Properties of High Purity Copper, J. S. Smart, A. A. Smith. *Technical Publication No. 1567*, American Institute of Mining and Metallurgical Engineers, New York, N. Y., Feb. 1943.

9. The Creep and Softening Properties of Copper for Alternator Rotor Windings, N. D. Benson, J. McKeown, D. N. Mends. *Journal*, Institute of Metals, London, England, vol. 80, 1951–52, pp. 131–42.

10. Raising the Creep Limit by Cold Working, H. Zschokke. *Brown Boveri Review*, Baden, Switzerland, vol. 33, Sept. 1946, pp. 227–33.

11. The Effect of Single Addition Metals on the Recrystallization, Electrical Conductivity, and Rupture Strength of Pure Aluminum, R H Harrington. *Transactions*, American Society of Mechanical Engineers, New York, N. Y., vol. 41, 1949, p. 443.

12. Aluminum Alloy, R. H. Harrington. *U. S. Patent No. 2,572,562*, Oct. 23, 1951.

13. Direct Cooling of Turbine-Generator Field Windings, C. H. Holley, H. D. Taylor. *AIEE Transactions*, vol. 73, pt. III, June 1954, pp. 542–50.

14. Progress in the Design and Application of Large Steam Turbine-Driven Generators, C. E. Kilbourne, J. B. McClure. *Proceedings*, American Power Conference, Chicago, Ill., vol. 15, Mar. 1953, pp. 358–74.

Recent Contributions to Transformer Audible Noise Control

WILLIAM B. CONOVER
MEMBER AIEE

ROBERT J. RINGLEE
NONMEMBER AIEE

AUDIBLE noise from transformers has harassed electric power companies and transformer manufacturers for the last decade. Measures to reduce sound levels are expensive at best, and because of the subjective nature of noise it is often difficult to foresee a noise problem when a particular transformer installation is in the planning stage. This has necessitated corrective measures after the transformer is in service, a situation which naturally complicates their application.

Two solutions to the problem are currently being sought by manufacturers. The first approach is to reduce noise at the source by advanced transformer design. This is a long-term development, involving basic metallurgical, structural and electrical factors, some of which are scarcely beyond the research stage. The pieces of this puzzle are slowly and painstakingly being put into place. The second approach is the development of expedients which can provide immediate relief for utilities that have, or foresee the possibility of having, a critical noise problem. This paper deals with two methods which fall in the second category.

The first part will present recently acquired information on the behavior of roofless wall-type barriers. The utility of such barriers lies in their ability to give a fairly substantial reduction in noise level over a wide area, at a cost which is moderate compared to other methods of equal effectiveness. The design of such barriers—and possibly even the decision to use them—is often based on information derived from tests on a model of the specific installation.[1]

The second part of this paper deals with the cancellation of transformer noise by injecting an equal and opposite noise into the troublesome area. This is a new development which has not yet been put to the ultimate test of continuous service in the field. However, it promises to be by far the most economical and satisfactory solution for noise problems where a limited area only is involved.

The full realization of the potentialities of the barrier method, and the rapid perfection of the sound cancellation method, are assured by the availability of an anechoic chamber[2] specifically designed for the acoustical testing of transformers and transformer models. Until recently no adequate facility of this type existed. Consequently, some types of much-needed experimental work were not at all feasible, and other work had to be conducted under conditions which drastically impaired speed and accuracy.

Use of Models to Study Transformer Noise Patterns and Effects of External Barriers

Scale model transformers have been used to study the effects of external barriers on transformer noise patterns.[1] Small speakers housed in a paper enclosure were used to represent the transformer. For the studies reported here, a dynamically scaled transformer core, winding, and tank were used to provide the noise source. In Appendix I the requirements for scaling structures such as transformers have been considered in more detail. The requirements are easily met for structures with little damping by constructing exact scale models.

Models of transformers were constructed to a one-seventh linear scale. To maintain dynamic similarity to the prototype, the model is excited at a frequency of 420 cycles per second (cps), or seven times normal 60-cps excitation. The models were noise-tested to establish:

1. Noise versus distance data for transformer tanks.
2. Polar noise plots; i.e., variation of noise amplitude with azimuth angle.
3. Evaluation of the effect of external barriers upon reducing audible noise.

All measurements were made on the fundamental harmonic of transformer noise.

NOISE VERSUS DISTANCE DATA

The diminishing of noise pressure level with radial distance from the center of the tank has been plotted in Fig. 1 for models of a 125,000-kva transformer and 1,500-kva transformer. Notice that at distances far from the transformers the change in noise pressure level closely follows the square law; i.e., a 6-decibel (db) reduction with each doubling of distance. Each point plotted on Fig. 1 is the average of 20 or more measurements made about the transformer tank. Near the source, along particular radial lines, the change of pressure with distance may be greater or less than predicted by the square law. However, on the average, the noise diminishes in accordance with this law. A discussion of this phenomenon is presented in Appendixes II and III.

VARIATION OF NOISE ABOUT TRANSFORMER

Polar plots of transformer noise as a function of polar angle about the tank indicate that the source is very complicated. The complexity is very probably caused by the involved vibration modes present in the transformer tank. The fundamental and low order modes of vibration of the tank are better radiators of sound than the high order modes when compared on an equal velocity basis. The ability of the low order modes to radiate more noise for a given vibration velocity is offset by the higher velocities present in the modes that are resonant near the transformer driving frequencies. For liquid-filled power transformer tanks, the resonant frequency of the fundamental mode has been observed to be the order of 20 cps or less. For modes resonant near 120 cps, the mode spacing is the order of 20 inches by 20 inches as shown in Fig. 2. Thus, across the length the height of a small power transformer tank, several node lines may be observed for the fundamental harmonic of transformer noise. This subject is treated in more detail in Appendixes III and V. The radiation from several modes is considered in Appendix III and the node spacings for rectangular mode patterns in oil-backed plate are considered in Appendix V.

Probably because of the resonance phenomenon, the noise pattern about

---

Paper 55-31, recommended by the AIEE Transformers Committee and approved by the AIEE Committee on Technical Operations for presentation at the AIEE Winter General Meeting, New York, N. Y., January 31–February 4, 1955. Manuscript submitted October 25, 1954; made available for printing November 16, 1954.

WILLIAM B. CONOVER and ROBERT J. RINGLEE are with the General Electric Company, Pittsfield, Mass.

The authors are grateful for the many contributions to this work by their associates. Much credit is due to M. W. Schulz for analytical studies which helped form the concepts discussed in this paper. The early success of the sound cancellation experiments is due to valuable ideas by W. F. M. Gray, who also contributed much in the way of equipment construction and field tests. Model barrier and cancellation tests were supervised by K. A. Johnson whose many contributions are appreciated.

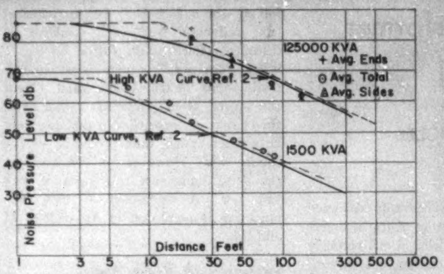

Fig. 1. Model transformer noise versus distance plot for fundamental noise frequency. Measurements taken on flat weighting network

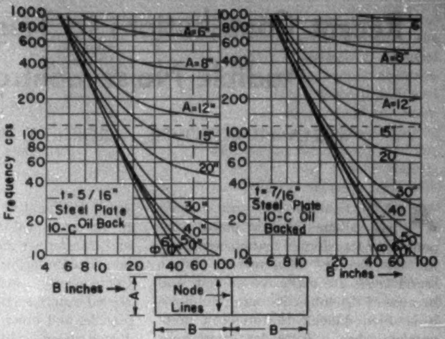

Fig. 2. Resonant frequency curves for rectangular node patterns for a steel plate with 10-C oil on one side and air on the opposite side. System is assumed infinite in extent

the transformer is subject to considerable variation, as much as 30 db for the 125,000-kva model. One might expect that the noise pattern would exhibit a 4-node or cos 2φ shape with azimuth angle φ, but the patterns as shown in Figs. 3 and 4 for the 125,000-kva model and Figs. 5 and 6 for the 1,500-kva model do not exhibit this form. The important consideration to be gained from these data is that the noise patterns about the transformer tanks are directional, being in general higher on the ends of the tank than on the sides. This means that average values of noise as determined by National Electrical Manufacturers Association (NEMA) measurement standards must be treated as the average of a pattern containing several lobes.

While the data presented in Figs 3 through 6 are for the fundamental harmonic of transformer noise, patterns of the same complexity are observed for the other frequency components of transformer noise. Test data taken at scaled heights of 7 feet and 21 feet above ground indicate that the pattern varies with elevation.

External Barrier Tests with Model Transformers

Scale models were chosen for external barrier studies because of the relative ease of construction, ease of changing barriers, and ease of making measurements. The effects of external barriers have been discussed in other papers.[1,3–7] The purpose of the tests was to study the effects of barrier shape and size upon sound attenuation. The effect of barrier height, spacing from the tank wall, and the effect of noise build-up within a hard walled cell were investigated. Tests were made upon 4-sided, 3-sided, and 2-sided enclosures.

The effectiveness of an external barrier is dependent upon three factors: the transmission loss through the wall, the transmission loss due to diffraction around the top and side edges of the walls, and the noise pressure build-up within the enclosure. It is assumed that the wall vibration due to ground-borne motion is small.

The acoustic transmission loss through various wall materials has been studied by the National Bureau of Standards.[8] Choice of a material for a wall should be governed by the amount of noise attenuation needed. As a rough rule, the acoustic transmission loss through the wall material should be at least 10 db greater than the noise attenuation required of the enclosure. It is also essential that wall resonance be avoided at the desired frequencies. Interior grade plywood 3/4 inch thick was used for the model enclosures. The acoustic transmission loss through this material at 840 cps is greater than 25 db.

The pressure build-up within an en-

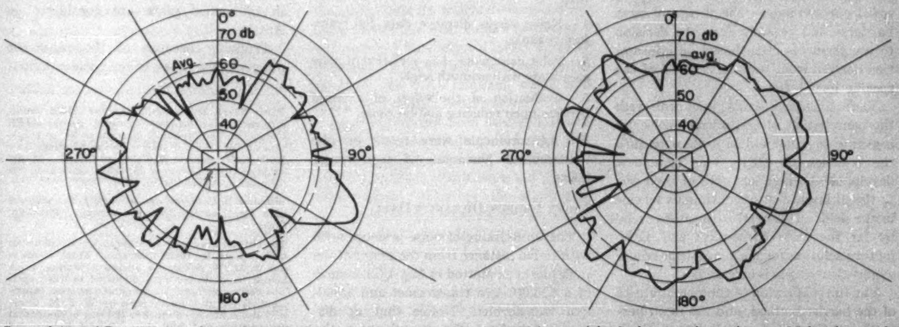

Fig. 3 (left) and Fig. 4 (right). Polar plot of fundamental frequency noise for 125,000-kva model. Scale microphone distance 84 feet from tank center. Microphone height above the ground plane is 7 feet for Fig. 3 and 21 feet for Fig. 4. Measurements taken on flat weighting network

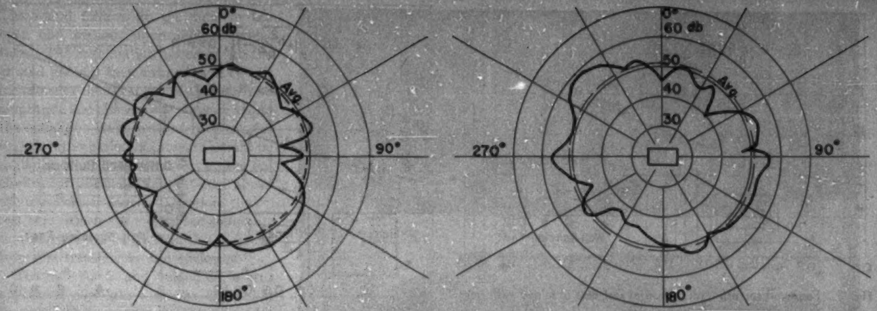

Fig. 5 (left) and Fig. 6 (right). Polar plot of fundamental frequency noise for 1,500-kva model. Microphone on 81-foot radius (to scale) from tank center. Microphone height above the ground plane is 7 feet for Fig. 5 and 21 feet for Fig. 6. Measurements taken on flat weighting network

closure represents the pressure gradients required to decelerate the air motion at the barrier wall. Another way to look at the phenomenon is to consider the multiple reflections of pressure from the hard surfaces of the walls and tank. The vibration of a transformer tank is affected negligibly by the acoustic load imposed by the air about the tank. Pressure build-up can represent a loss in possible noise reduction due to the enclosure. The increased pressure level is equivalent to a source of higher noise level.

Pressure build-up is a function of the spacing of the wall from the tank. Data upon pressure build-up are included with the barrier noise attenuation data in Figs. 7, 8, and 9 and in Tables I and II. For 4-sided enclosures, the build-up ranged from 3 to 6 db; for 3-sided enclosures, from $2^1/_2$ to 4 db; and for 2-sided enclosures, from 1/2 to 4 db.

Pressure build-up data reported were obtained by comparing noise measurements at 1-foot distance to scale from the model tanks at one-third and two-thirds tank height (NEMA test) with and without the enclosures about the tanks. Measurements were taken at 34 microphone positions about the 125,000-kva model tank, and 20 about the 1,500-kva tank, to determine each NEMA average. The data indicated that the build-up was not dependent upon barrier wall height in the range 0 to 10 feet to scale above the transformer cover. The build-ups measured for the three heights 0, 5, and 10 feet were averaged and plotted as a single point.

The pressure build-up inside the model enclosure was reduced to 0 by lining the interior of the enclosure with an acoustic treatment. A 1-inch-thick layer of *PF 615* Fiberglas spaced $1^3/_4$ inches from the wall was used as the acoustic treatment for the model. To scale, this acoustic treatment would have been equivalent to a glass wool blanket in the order of 7 inches thick spaced 1 foot from the full-scale wall. While transformer tanks and barrier walls can be scaled, it is not known if absorption coefficients for glass wools can be maintained as the scale and frequency are changed.

Test data upon 4-sided enclosures showed that the build-up increased as the spacing between the wall and tank was decreased from 11 to $4^1/_2$ feet to scale. These data are presented in Fig. 7. The high build-up experienced at the $4^1/_2$-foot spacing was probably due to the proximity of the spacing to one-half wave length of the sound. One-half wave length of 120-cps sound is 4.71 feet for a sonic velocity of 1,130 feet per second. The air loading upon the tank has negligible effect upon the tank vibration. The tank behaves as a constant displacement source so the sound pressure should increase as the wall spacing approaches $\lambda/2$.

The attenuation of sound by partial enclosures is analogous to the attenuation of light by diffraction over a knife edge. Using this analogy Fehr and Wells have presented a theoretical method for calculating the attenuation of the sound due a point or a line source by a wall. They have presented the theoretical results in curve form[9,10] which gives the attenuation in db as a function of the dimensionless parameter n. The parameter is dependent upon the height of the wall relative to the source, the height of the observer relative to the source, the spacing of the source from the wall, the spacing of the observer from the wall, and the wave length of the sound. Let R be the average distance of the wall from the source, let h be the height of the barrier above the source, and let λ be the wave length of the sound. If the observer and the source are at the same elevation, then at large distances from the source and wall the value of n may be calculated from the relation $n=h^2/\lambda R$, provided $D \gg R$ and $R \geqslant h$. D is the spacing from the wall to the observer.

The simplicity of this method for calculating sound attenuation recommends it as a means for estimating the effects of partial enclosures. Several assumptions are required to apply the theory to a transformer enclosure. The first assumption regards the source. The vibrating transformer tank is assumed to be replaced by a point source located at the geometric center of the tank. The second assumption concerns the interaction of the barrier wall upon the sound within the enclosure. To account for the effect of an acoustically hard wall upon the sound produced by the transformer, it is assumed that the magnitude of the point source is increased by the amount of the build-up. This assumption was confirmed in the tests reported in Tables I and II. The third assumption concerns the method for calculating the distance from the equivalent point source to the barrier wall. For the data reported here, the value of R was determined from an average of the distances from the tank center to the barrier measured to a side wall, to an end wall, and along the diagonal to the corner formed by the side and end wall. For all the tests reported, the spacing S between the barrier and the tank was kept uniform for the side and the end of the tank; see the sketch in Fig. 8.

The test data taken were plotted against the parameter n in Figs. 7, 8, and 9 for 4-, 3-, and 2-side partial enclosures. The value of n for each test condition was calculated in accordance with the three

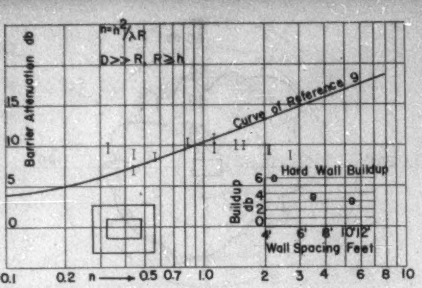

Fig. 7. Four-wall enclosure sound barrier test data obtained with transformer models

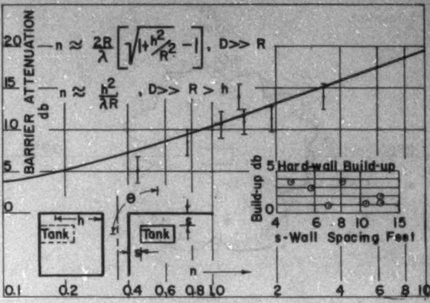

Fig. 9 (above). Two-wall enclosure sound barrier test data obtained with transformer models

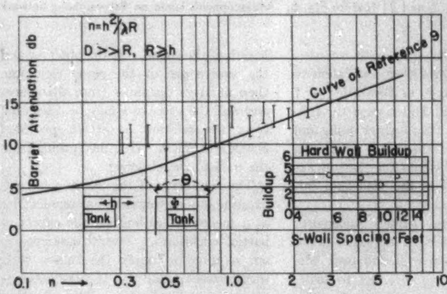

Fig. 8. Three-wall enclosure sound barrier test data obtained with transformer models

assumptions presented. The sound attenuation due to a barrier was determined by comparison of pressure measurements at 42, 84, and 140 feet to scale from the center of the tank before and after the barrier was put in place. Scaled microphone height was 7 feet above the ground plane. The attenuations reported have been corrected for the build-up within the enclosure. The actual or net attentuation is the difference of the attenuation reported and the pressure build-up reported for each barrier configuration. For example, a barrier with a reported attenuation of 10 db and a build-up of 3 db would have a net attenuation of 7/ db. A good acoustic treatment on the barrier wall would reduce the build-up to 0. The corresponding net attenuation would then be 10 db. The bar associated with each plotted attenuation data point indicates the 95-per-cent confidence limits upon the mean. The bar represents the variance due to repeat testing.

The attenuation for 4-sided enclosures is reported as the average determined at 108 positions about the circumference of the tank. Readings were taken every 10 degrees of azimuth for the three distances reported. The attenuation for 2-sided and 3-sided enclosures is given as the average of the attenuations measured at 30 positions in the 90-degree sector shown in the sketches in Figs. 8 and 9.

The data for 4-sided enclosures show that the attenuation was relatively independent of wall height or spacing for the range reported in Table I. The data plotted in Fig. 7 do not correlate with the attenuation predicted from the diffraction theory because the assumptions made do not apply to this configuration. Gettys and Conover[1] have reported similar results. It may be that the 4-sided enclosure should be considered as an open-ended tube from an analytical viewpoint,

Table I. Barrier Test Data for 125,000-Kva Model

Wall Shape	Equivalent Wall Spacing, Feet	Equivalent Wall Height Above Tank Cover* 0 Feet	5 Feet	10 Feet	Wall Lining‡	Pressure Buildup, Db	Equivalent Microphone Height, Feet
		Wall Attenuation, Db†					
4-wall	4½	8.8§	10.1	8.8	(1)	5.8	7
	7	7.0	9.7	9.4	(1)	3.4	
	11	9.8	10.4	10.0	(1)	3.1	
	7	8.2	9.9	8.6	(2)	−1.0	
3-wall	5.8	8.3‖	12.2	14.2	(1)	3.9	7
	8.2	11.0	13.3	12.9	(1)	3.7	
	10.5	11.2	11.0	13.2	(1)	2.8	
	12.3	10.1	10.8	13.7	(1)	3.8	

*Tank size of 125,000-kva model is 15½ by 37 by 27 inches high or 9.05 by 21.6 by 15.7 feet. Tank size of 1,500-kva model is 3½ by 8¼ by 13½ inches high or 2.05 by 4.8 by 7.9 feet.

†Actual attenuation of wall equals wall attenuation listed less pressure build-up.

‡(1) Refers to no lining (hard plywood). (2) Refers to 1-inch Fiberglas spaced 1¾ inches from barrier wall (PF-615).

§Average of 108 positions about tank.

‖3- and 2-wall data represent average in 90-degree sector of 30 points.

Table II. Two-Wall Barrier Test Data for 1,500-Kva Model

Equivalent Wall Spacing, Feet	Equivalent Wall Height Above Tank Cover 2.8 Feet	7.0 Feet	12 Feet	Wall Lining	Pressure Build-up, Db	Microphone Height Scale, Feet
		Attenuation, Db				
6.9	5.2	10.7	11.3	(1)	0.9	4½
12.3		8.5	10.8	(1)	1.3	4½
4.7				(1)	3.8	
4.7				(2)	0	

The sound follows up the tube to the open end without appreciable attenuation. The attenuation observed at the ground plane is then a function of the dimensions of the open end of the tube and amplitude and phase of the pressure across the opening. Even with an acoustic lining, the attenuation of pressure should be negligible as the sound travels up the enclosure for heights of only 10 feet above the transformer cover. Therefore the effect of wall height an observed sound attenuation would be small at distances far from the transformer and enclosure.

The data for 2- and 3-sided enclosures appear to correlate with the diffraction theory. The agreement of test results and calculated values for the 3-sided enclosures is best for the higher values of *n*. These correspond to wall heights of 10 feet above the transformer cover. At lower heights and *n*'s the tests give higher attenuation than the theory predicts. A definite correlation between the theory and the test data may be observed for the 2-sided model enclosures.

From these data it would appear reasonable to design 2- and 3-sided enclosures on the basis of the diffraction theory of Fehr and Wells and to allow a loss of attenuation due to the build-up within the enclosure. A properly designed acoustic lining would eliminate the the build-up.

Fig. 10 shows a 125,000-kva model transformer with a 3-wall enclosure sound barrier in place. The noise level on the open side of a 2- or 3-sided enclosure is affected by the presence of the barrier, as is shown in Fig. 11. The increase in noise level upon the open side was as much as the build-up in the enclosure. Fig. 11 shows that the presence of the barrier alters the sound field appreciably. The attenuation on the barrier side and the increase of sound on the open side of the enclosure are not constant, but vary over a considerable range. All data reported here are averages, and must be treated as such. If more precise data are required of a particular installation, it is recommended that a scale model of the installation be investigated.

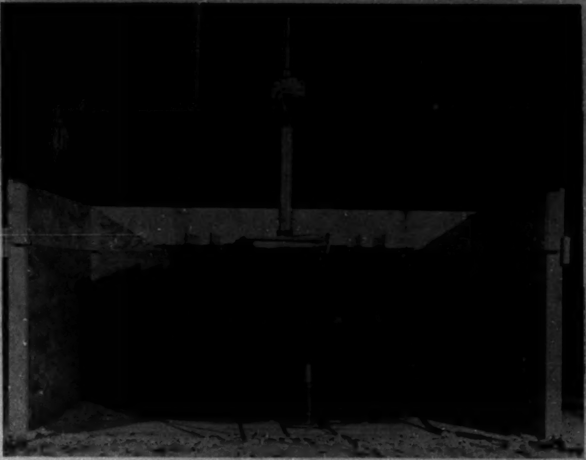

Fig. 10. A 125,000-kva model transformer with a 3-wall enclosure sound barrier in place

TRANSMISSION LOSS THROUGH BARRIER MATERIAL

Noise pressure and vibration measurements were taken about the barrier walls to determine the transmission loss through the wall. From several repeat measurements, the following data were obtained:

Sound Pressure Measurements:

Average pressure inside wall, 87.8 db (flat weighting).

Average pressure one inch from outside wall, 60.8 db (flat weighting).

(Pressure measurements were taken at one-third and two-thirds tank height.)

Wall Vibration Velocity Measurements:

Maximum observed velocity reading, 5.4 centimeters per second rms.

Average observed velocity reading, 2.1 centimeters per second rms.

The noise pressure resulting from a plane wave vibrating at 5.4 centimeters per second rms is 61 db.

It was concluded that wall vibration was not a limiting factor in the tests reported.

Sound Cancellation

Recent tests have demonstrated the practicability of projecting a "beam of silence" through the complex sound field which surrounds a transformer. Although at the present stage of development the beam is limited to a width of about 30 degrees, this is sufficient to eliminate complaints in some installations. The equipment required to do this consists of from one to four loudspeakers, a source of a fraction of a watt of electric power containing the harmonics of noise to be eliminated, and a means of adjusting the phase and amplitude of each harmonic. The cost of this equipment is a small fraction of the cost of conventional sound barriers.

THEORY OF OPERATION

To understand how sound cancellation can be obtained, it must be realized that at large distances a transformer appears to

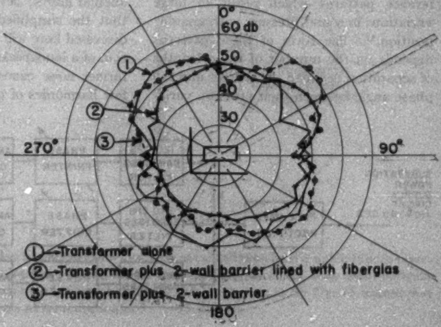

Fig. 11. Polar plot of fundamental frequency noise for 1,500-kva model with and without 2-wall sound barrier in place. Microphone on 81-foot radius to scale from tank center; microphone height 7 feet above ground plane. Measurements taken on flat weighting network

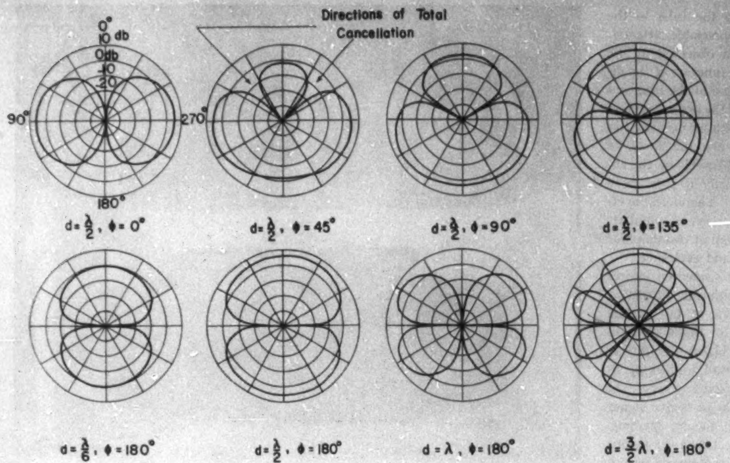

Fig. 12. Directional characteristics of a pair of point sound sources of equal strength. Sources lie on $\theta=0$-degree axis. d = distance between sources, ϕ = phase angle between source sound pressures. Sound pressure given in db with respect to pressure from either source operating alone

be a point source of sound in so far as measurements made along a fixed radial line are concerned; i.e., an observer will find a 6-db reduction in sound level each time his distance from the transformer is doubled. Furthermore, the variation of instantaneous sound pressure with time and radial distance will follow the same law as for a point source. In general, however, the sound pressure will vary with angular position, which is not true of a point source. A formal proof of these statements is given in Appendix II.

At distances several times the longest dimension of the transformer, it can be considered as a point source of sound, provided that consideration is limited to a relatively narrow radial beam. It is well known that the placement of a second point source of sound in the vicinity of the first one will give rise to interference patterns which result in large variations in sound pressure with angular position.[11] The form of these patterns depends on the number of wave lengths of separation between the sources and the phase angle between their pressure variations. Since discussions of this phenomenon in books on acoustics seem to be restricted to cases of in-phase or opposite-phase operation of the sources, a derivation for the case of an arbitrary phase angle is given in Appendix IV.

Fig. 12 shows some typical polar slots of sound pressure around a pair of point sources of equal strength. A study of these curves will indicate the effect of separation and phase angle on the sound pressure field at large distances from the sources. The important thing to notice from equation 45 and the curves of Fig. 12 is that by proper adjustment of the phase angle of a second source (e.g., a loudspeaker) the sound from the first source (e.g., a power transformer) can can be cancelled in a desired direction.

It has been pointed out that a transformer can only be considered a point source when viewed between rather small angular limits; nevertheless, it is believed that the simplified mathematical model discussed here will help to explain the action of a loudspeaker as a means of transformer noise cancellation. For the first few harmonics of transformer noise a 12-inch loudspeaker in a closed baffle is a fairly accurate model of a point source, so no simplifying assumptions are required to explain its behavior.

FIELD TESTS

The first tests of sound cancellation on an actual transformer installation were made on a 15,000-kva unit located at a substation situated on a flat open field, distant enough from sources of disturbing noise to permit quite satisfactory tests (as field tests go!). The equipment used to effect cancellation was assembled on the basis of ready availability; it by no means represents the ultimate in economy or desirability for permanent installation.

To provide a source of harmonic voltage synchronized with the sound output of the transformer, a full-wave selenium rectifier was plugged into a convenience outlet in the substation. Its output was applied to a 3-channel filter which isolated the 120-, 240-, and 360-cycle components of the rectifier output voltage from each other and permitted adjustments in the phase and magnitude of each. These frequencies were then recombined in an addition network and applied to the input of a power amplifier which in turn drove a

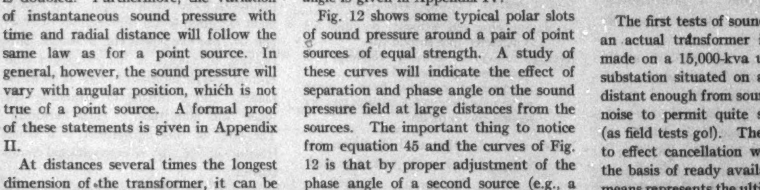

Fig. 13. Block diagram of sound cancellation equipment

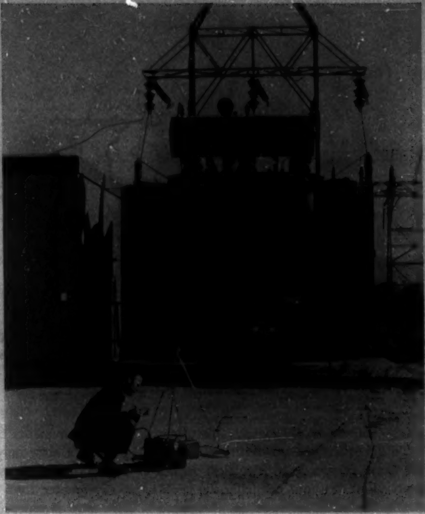

Fig. 14. Measuring sound cancellation on a 15,000-kva transformer in the field. Source of cancellation is a 12-inch loudspeaker in the small box on the side of the tank

loudspeaker. A block diagram of the system is shown in Fig. 13. Successful tests were also conducted in which the output of a vibration meter as used instead of the rectifier. The vibration pickup was fastened to a transformer radiator tube to produce a voltage containing the required harmonics.

The loudspeaker was a 12-inch direct radiator type, mounted in a plywood enclosure. It was held in place near the transformer tank with wire, its location being determined primarily by convenience. Fig. 14 shows a typical loudspeaker placement. In the tests to be described, the loudspeaker faced the tank and was located about 1/2 inch away.

The microphone of the sound level meter was mounted on a tripod at a distance of 100 feet from the transformer on a 0-degree axis arbitrarily drawn through the center of the unit perpendicular to the largest face of its oval tank. The output of the sound level meter was fed to a sound analyzer tuned to 120 cycles. The sound cancellation equipment was energized and the magnitude and phase angle of its excitation were adjusted to give a minimum reading on the sound analyzer. The audible effect of the cancellation was astonishing. Once the adjustment had been made, the transformer noise could be turned off and on at will, merely by switching the loudspeaker on and off.

Without changing the loudspeaker adjustments sound level readings were taken at different angular positions at constant radius with the speaker turned off and on. Fig. 15 shows the results graphically. At locations where the noise reduction was maximal, the balance between transformer noise and speaker noise was rather delicate. The reduction varied between 15 and 35 db momentarily, and appeared to be a function of wind velocity, although other causes are believed to be at least partially responsible. The curves were plotted from estimated average readings.

If the beam width of the silent zone is defined as that angle within which the sound reduction is 6 or more db, it will be noted that the beam width is about 23 degrees. Outside the intended angle of sound reduction, the loudspeaker does not add appreciably to the transformer noise in those regions where it is comparatively high. It does, however, tend to fill in the low-level regions and bring them up to a fairly constant sound level. This is to be expected, since the loudspeaker is very nearly a point source and by itself would therefore put out a con-

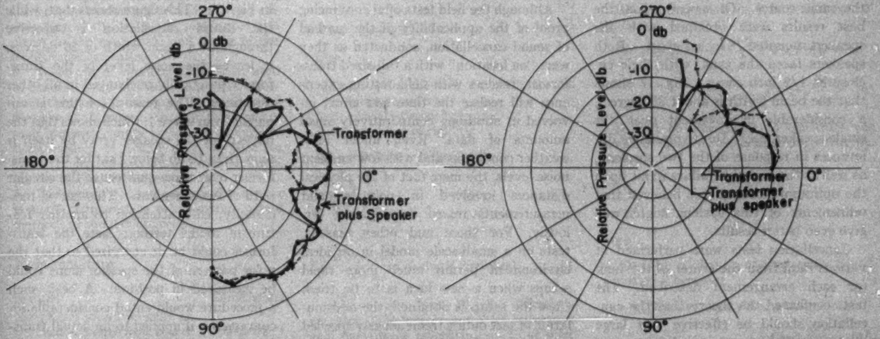

Fig. 15 (left) and Fig. 16 (right). Directional pattern of noise from a 15,000-kva transformer with and without cancellation from a single loudspeaker. Reference level (0 db) is sound pressure without cancellation at 100 feet, 0 degrees. In Fig. 15 the measurements are at 100-foot radial distance from tank and cancellation is adjusted for maximum noise reduction at $\theta = 0$ degrees. The setup for Fig. 16 is the same as for Fig. 15 except that speaker excitation was adjusted to give maximum noise reduction at $\theta = -45$ degrees

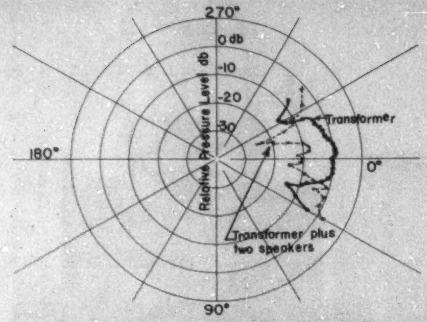

Fig. 17. Directional pattern of noise from a 15,000-kva transformer with and without sound cancellation from two loudspeakers 78 inches apart, operating in parallel. Speaker excitation was adjusted to give maximum noise reduction at $\theta = 0$ degrees

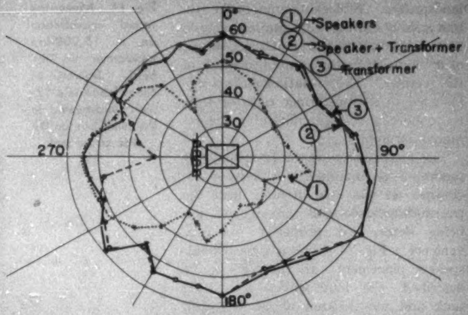

Fig. 18. Sound cancellation test with a 125,000-kva model transformer and a 4 element loudspeaker array. Polar plot is for fundamental frequency of transformer noise

stant sound level in all directions.

To determine the possibility of aiming the beam of silence by electrical adjustment alone, without changing the geometry of the loudspeaker setup, the microphone was placed on the −45-degree radial at a distance of 100 feet. Following the adjustment for minimum noise level at this location, readings were taken in other directions. The results are plotted in Fig. 16. The beam width of the silent zone is only about 13 degrees in this case, probably because of the rather sharp lobe in the sound pattern of the transformer.

To find out if the beam width in the 0-degree direction could be widened without unduly complicating the loudspeaker arrangement, a trial was made with two loudspeakers operating in parallel from the same source. Of several trials, the best results were obtained with the speakers mounted 78 inches apart. Both speakers faced the tank, with their enclosures 1/2 inch away. Fig. 17 shows that the beam width is about 35 degrees, a considerable improvement over the single-speaker test. Due to presumed differences in response of the two speakers, as well as the probable failure to hit upon the optimum location, it is believed that refinements of this system might well give even better results.

Cancellation tests were performed at various radii from the center of the tank for each arrangement described. The tests confirmed the theory that the cancellation should be effective over large distances. Tests out to distances as great as 500 feet indicated that the reduction at any point along a radial line was never less than 6 db.

The data reported here were obtained by measurements on the 120-cycle component of noise only, since in the 15,000-kva transformer used this was substantially greater than the other harmonics. However, it was found in a listening test that when the 360-cycle harmonic was also cancelled the improvement was even more impressive. This was true even though the 360-cycle tone was 15 db below the level of the 120-cycle tone before cancellation was applied.

A comparison of Figs. 15, 16, and 17 shows that the polar pattern of transformer noise is somewhat different in each test. These variations are presumed to result from changes in the vibration pattern of the transformer, in wind velocity, and in air temperature.

LABORATORY TESTS

Although the field tests offer convincing proof of the applicability of the method of sound cancellation, conducted as they were "on location" with a full-sized transformer, readers with field testing experience will realize the time and effort involved in obtaining comparatively small amounts of data. Even under ideal weather conditions and with low ambient noise levels, the mere fact of the physical distances involved in point-by-point measurements retard development seriously. For these and other reasons, tests on a small-scale model in an ideal environment permit much more rapid setups when a new idea is to be tried. Once the setup is obtained, the accumulation of test data is tremendously speeded up.

The availability of a large anechoic chamber makes possible the testing of scale models without problems of ambient noise and weather conditions. The Pittsfield Sound Laboratory has provision for the installation of a plywood floor when tests require the representation of a reflecting ground plane. The simulation, on a model scale, of an ideal site on a flat plain without reflecting structures in the vicinity is thus readily accomplished.

The one-seventh scale model transformer previously referred to was used for the sound cancellation tests conducted in the Laboratory. These tests used a 4-element array of 2-inch loudspeakers to achieve a directional source of sound. Such a source permits cancellation in the desired direction without appreciably affecting the transformer sound pattern in other directions. The behavior of the 4-element array is analyzed in the literature.[12]

The results of a typical test are plotted in Fig. 18. This figure shows that, while the sound cancellation is effective throughout a beam width of 26 degrees, it leaves the noise level of the transformer practically unchanged in all other directions. The reason for this is apparent from curve 1, which shows that the pattern for the speaker array by itself is more than 10 db below that for the transformer over three-quarters of the circular path of measurement. This curve, incidentally, calls attention to another feature of model testing: here the transformer could be de-energized so that the polar pattern of the speaker alone could be measured in position. A best, such a procedure would entail considerable inconvenience if applied to an actual transformer carrying load.

Cancellation tests were made at both the fundamental and the second harmonic of model transformer noise; i.e., at 840 cps and at 1,680 cps. At 1,680 cps, the 4-element array was equivalent to four sources of sound placed in a straight line and spaced one-half wave length apart. Since the same array was used for 840 cps and 1,680 cps, the zone of influence, at 840 cps, covered an appreciably wider angle than it did at 1,680 cps.

Conclusions

SOUND BARRIER TESTS BY MODELS

1. Sound field plots versus radial distance from scale model transformers correlate well with similar test data upon full-scale transformers.
2. Studies of the variation of sound pressure level with azimuth angle about the transformer indicate that the pattern is very complex, and is higher at the ends of the tank than at the sides.
3. Test data indicate that pressure build-up inside a hard-walled barrier subtracts directly from the attenuation possible with a given barrier configuration. For open-walled structures the build-up increases the noise proportionately on the open side.
4. Four-wall barrier data obtained do not correlate with either wall height or spacing from the tank.
5. The attenuation due to 2- and 3-wall barriers may be predicted by simple calculations.

SOUND CANCELLATION

1. By using the technique of sound cancellation, it is possible to reduce transformer noise in a given direction by 6 db or more, over long radial distances, throughout angles up to about 35 degrees.
2. At a given point, noise reductions averaging about 20 db are easily obtainable. (Complete cancellation of a given harmonic is possible for short times, but slight changes in the delicate balance of sound pressures occur momentarily, preventing continuous complete cancellation.)
3. The angular position of the beam of silence may be changed without altering the geometry of the setup, by making adjustments in the magnitude and phase of the loudspeaker excitation.
4. When one or two loudspeakers are used to cancel transformer noise in a given direction, the noise is increased in some other directions. However, in situations where such increases cannot be tolerated, a directional source of sound may be used to effect the desired cancellation without altering the original field elsewhere.
5. The cost of a sound cancellation system is small compared to other sound control methods of equal effectiveness.

Nomenclature

Symbol	Dimensions
A = phasor sound pressure at unit distance from source	$ML^{-1}T^{-2}$
c = velocity of sound	LT^{-1}
D = plate rigidity	$ML^{2}T^{-2}$
d = distance	L
$\mathbf{d}$ = vector distance	L
E = Young's modulus	$ML^{-1}T^{-2}$
$\mathbf{F}$ = body force vector	$ML^{-2}T^{-2}$
j = imaginary unit	$\sqrt{-1}$
k = wave-length constant ($=2\pi/\lambda$)	L^{-1}
L = scale factor	
n,m = integers	
p = phasor sound pressure	$ML^{-1}T^{-2}$
$R(\ )$ = real part of ( )	
$\mathbf{r}$ = position vector	L
r = radial distance	L
t = time	T
= plate thickness	L
V = plate potential energy	$ML^{2}T^{-2}$
= maximum surface velocity	LT^{-1}
v = radial velocity	LT^{-1}
$\mathbf{w}$ = displacement vector	L
W = energy	$ML^{2}T^{-2}$
α = angle between two position vectors	
θ = co-latitude in spherical co-ordinate system	
λ,μ = elastic coefficients	$ML^{-1}T^{-2}$
ρ = mass density of medium	ML^{-3}
σ = Poisson's ratio	
ϕ = phase angle, radians or degrees	
velocity potential	$L^{2}T^{-1}$
displacement potential	L^{2}
φ = longitude in spherical co-ordinate system	
ω = angular frequency	T^{-1}

Appendix I. Requirements for Scaling Structures

As a review of the use of models, it will be well to consider the requirements necessary to permit the scaling of elastic structures. Referring to article 91, page 133 of reference 13, let $\mathbf{w}$ be the vector displacement in the curvilinear co-ordinate system. The vector equation of equilibrium appears as

$$(\lambda+\mu)\nabla(\nabla\cdot\mathbf{w})+\mu\nabla^2\mathbf{w}+\rho\mathbf{F}=\rho\frac{\partial^2\mathbf{w}}{\partial t^2} \quad (1)$$

This equation may be transformed to

$$(\lambda+2\mu)\nabla(\nabla\cdot\mathbf{w})-\mu\nabla\times\nabla\times\mathbf{w}+\rho\mathbf{F}=\rho\frac{\partial^2\mathbf{w}}{\partial t^2} \quad (2)$$

$$\mathbf{w}=\mathbf{i}_1u+\mathbf{i}_2v+\mathbf{i}_3w \quad (3)$$

where

$\mathbf{i}_1$, $\mathbf{i}_2$, and $\mathbf{i}_3$ are the unit vectors in the co-ordinate system
λ and μ are elastic coefficients
μ is the modulus of rigidity

If σ = Poisson's ratio, then

$$\sigma=\frac{\lambda}{2(\lambda+\mu)}$$

and

$$E=\frac{\mu(3\lambda+2\mu)}{\lambda+\mu}\ \text{(Young's modulus)} \quad (4)$$

Observe the form of the differential operator $\nabla(\ )$; $\nabla\cdot(\ )$; and $\nabla\times(\ )$ in orthogonal curvilinear co-ordinates. From reference 14, section 1.16, page 47

$$\nabla\Phi=\sum_{j=1}^{3}\frac{1}{h_j}\frac{\partial\Phi}{\partial X_j}\mathbf{i}_j \quad (5)$$

$$\nabla\cdot\mathbf{w}=\frac{1}{h_1h_2h_3}\left(\frac{\partial}{\partial x_1}(h_2h_3u)+\frac{\partial}{\partial x_2}(h_1h_3v)+\frac{\partial}{\partial x_3}(h_1h_2w)\right) \quad (6)$$

$$\nabla\times\mathbf{w}=\frac{1}{h_1h_2h_3}\begin{vmatrix} h_1\mathbf{i}_1 & h_2\mathbf{i}_2 & h_3\mathbf{i}_3 \\ \frac{\partial}{\partial x_1} & \frac{\partial}{\partial x_2} & \frac{\partial}{\partial x_3} \\ h_1u & h_2v & h_3w \end{vmatrix} \quad (7)$$

h_1, h_2, and h_3 are defined as follows. The elementary cell bounded by co-ordinate surfaces is a rectangular box whose edges are $ds_1=h_1dx_1$, $ds_2=h_2dx_2$, and $ds_3=h_3dx_3$. The box volume is

$$dv=(h_1h_2h_3)\,(dx_1dx_2dx_3)$$

Note that the product h_iX_i has the dimension of length. Notice also that the three operators have the dimension (length)$^{-1}$. Two operations such as $\nabla\times\nabla\times\mathbf{w}$ have the dimension (length)$^{-2}$.

We now change the scale of the geometric system such that a new co-ordinate system $h_i'X_i'=Lh_iX_L$. L will be a dimensionless scale factor. For $L<1$ the new system is physically smaller than the original system. For a 1/7 scale, $L=1/7$.

Let $\mathbf{w}'$ be the displacement in the scaled system. Point for point, we desire $\mathbf{w}'$ to be linearly related to $\mathbf{w}$,$\mathbf{w}'::\alpha\mathbf{w}$. The equation of motion in the new system becomes

$$(\lambda'+2\mu')\nabla'(\nabla'\cdot\mathbf{w}')-\mu'(\nabla'\times\nabla'\times\mathbf{w}')+\rho'\mathbf{F}'=\rho'\frac{\partial^2\mathbf{w}'}{\partial t'^2} \quad (2')$$

The primes indicate the new system. The primed operators are related to their unprimed counterparts by

$$\begin{aligned}\nabla'(\nabla'\cdot[\ ])&=\frac{1}{L^2}\nabla(\nabla.[\ ])\\ \nabla'\times\nabla'\times[\ ]&=\frac{1}{L^2}\nabla\times\nabla\times[\ ]\end{aligned} \quad (8)$$

Substituting relations 8 into equation 2′ yields

$$\frac{1}{L^2}(\lambda'+2\mu')\nabla(\nabla\cdot\mathbf{w}')-\frac{1}{L^2}\mu'\nabla\times\nabla\times\mathbf{w}'+\rho'\mathbf{F}'=\rho'\frac{\partial^2\mathbf{w}'}{\partial t'^2} \quad (9)$$

It will be convenient to construct the model of the same material as the prototype. Hence

$$\lambda=\lambda'$$

$$\mu=\mu'$$

$$\rho=\rho'$$

Also, by a change of time scale $t'=Lt$, equation 9 becomes

$$(\lambda+2\mu)\nabla(\nabla\cdot\mathbf{w}')-\mu\nabla\times\nabla\times\mathbf{w}'+L^2\rho\mathbf{F}'=\rho\frac{\partial^2\mathbf{w}'}{\partial t^2} \quad (10)$$

Equation 10 cannot admit of similarity to equation 2 unless certain restrictions are placed upon the body forces. The restrictions may take the form:

1. **F**′ and **F** nontime-variant (forces such as gravity).
2. **F**′ scaled as $1/L^2$ **F** if time variant.

In the study of models, the only body force usually present is gravity. The gravity body force causes the body to assume some rest displacement. All displacement of oscillatory nature will be measured relative to the rest position of the body. It is customary to subtract the rest position displacements so that for body forces such as gravity equation 10 reduces to

$$(\lambda+2\mu)\nabla(\nabla\cdot\mathbf{w}')-\mu\nabla\times\nabla\times\mathbf{w}'=\rho\frac{\partial^2\mathbf{w}'}{\partial t'^2} \tag{11}$$

and

$$(\lambda+2\mu)\nabla(\nabla\cdot\mathbf{w})-\mu\nabla\times\nabla\times\mathbf{w}=\rho\frac{\partial^2\mathbf{w}}{\partial t^2} \tag{12}$$

The system admits of scaling in this case.

Scaling of Fluid Structures

For fluids there is no shear rigidity. With zero viscosity or for waves with no rotation the equation of motion becomes

$$\frac{K}{\rho}\nabla(\nabla.\mathbf{w})=\frac{\partial^2\mathbf{w}}{\partial t^2} \tag{13}$$

This equation is subject to the restrictions regarding body forces mentioned previously in the section on elastic structures. ρ is the mass density of the fluid; K, the bulk modulus, is defined as $p=-K\nabla.\mathbf{w}$; p is the excess pressure over the rest value. The requirements for scaling fluids, therefore, are the same as for scaling elastic solids.

Upon Scaling Compound Structures such as Braced Liquid-Filled Tanks

Consider a braced tank. Each part of the tank will have its dynamic counterpart in a scaled part of a model tank. Suppose the model deflections are to the full-scale deflections as the scale ratio **w**′ proportional to L**w**.

The resulting stresses in the model will be equal to those in the prototype. This follows since the stresses (or pressures) are dependent upon first space derivatives of displacement; i.e., functions of $\nabla(\ )$ or $\nabla\cdot(\ )$, and upon the elastic constants λ and μ, which are assumed the same for model and prototype. Therefore, the boundary stresses upon the model are exactly equal to the boundary stresses upon the prototype. Integrated over the boundary surface, the energy attributable to the boundary stresses is

$$W=\int_s\frac{\mathbf{w}}{2}\cdot\mathbf{X}dS \tag{14}$$

where **X** is the boundary stress (vector). The energy in the model will be L^3 times the energy in the prototype.

The internal energy due to elastic deflection is given by the volume integral

$$W=\int_v\frac{1}{2}(e_{ij}X_{ij})dv \tag{15}$$

where e_{ij} is the material strain.

e_{ij} model $=e_{ij}$ prototype

X_{ij} model $=X_{ij}$ prototype

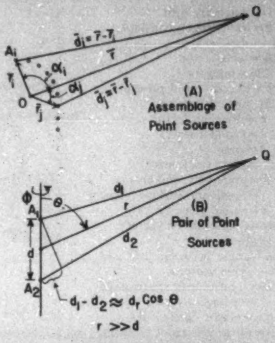

Fig. 19. (A) Arbitrary assemblage of point sources of sound of arbitrary strength, showing nomenclature of generalized position vectors. (B) Pair of point sources aligned on $\theta=0$-degree axis in spherical co-ordinates

hence the internal energy due to elastic deflections in the model would be L^3 times the internal energy of elastic deflection of the prototype.

A similar case exists for the kinetic energy

$$\text{kinetic energy}=\rho/2\int_v\left(\frac{\partial\mathbf{w}}{\partial t}\cdot\frac{\partial\mathbf{w}}{\partial t}\right)dv \tag{16}$$

provided

$\mathbf{w}'=L\mathbf{w}$ for corresponding points

then

$$\frac{\partial\mathbf{w}'}{\partial t'}=\frac{\partial L\mathbf{w}}{\partial Lt}=\frac{\partial\mathbf{w}}{\partial t}$$

Thus the kinetic energy in the model is L^3 times the kinetic energy of the prototype.

Since

$$\frac{\text{Boundary Energy Model}}{\text{Boundary Energy Prototype}}=\frac{\text{Elastic Energy Model}}{\text{Elastic Energy Prototype}}=\frac{\text{Kinetic Energy Model}}{\text{Kinetic Energy Prototype}}$$

and since

$$\frac{\text{Strains and Stresses Model}}{\text{Strains and Stresses Prototype}}=1 \tag{17}$$

provided $\mathbf{w}'\alpha L\mathbf{w}$, then the effects of liquids and individual parts upon one another in the full-size prototypes are matched by equal or scaled effects in the model.

Appendix II. Sound Pressure Field at a Large Distance from a Sound Source of Arbitrary Shape

Consider a surface of arbitrary shape, each point of which is undergoing simple harmonic vibration of the same frequency. The magnitude and phase angle of the vibration of each point are functions of position. The vibrations of the surface will communicate themselves to the surrounding medium and thus radiate sound outward. For the purpose of the analysis which follows, it is convenient to replace this surface by a suitable distribution of point sources of appropriate strength and phase angle.[15]

Examining for the moment a single one of these point sources, it can be shown[16] that the instantaneous sound pressure $p_{\text{inst.}}$ at some point Q, located a distance d from the source, is given by the real part of

$$p_{\text{inst.}}=-j\omega\rho\frac{A'}{d}\epsilon^{j(\omega t+\phi-kd)} \tag{18}$$

Letting $A=-j\omega\rho A'\epsilon^{j\omega t}$, equation 18 may be simplified to read

$$p=\frac{A}{d}\epsilon^{j(\phi-kd)} \tag{19}$$

In equation 19, A represents the complex sound pressure at unit distance from the source; ϕ stands for the phase angle with respect to some chosen reference time axis; and $k=2\pi/\lambda$, where λ is the wave length of sound in the medium under consideration.

Returning now to an assemblage of n such point sources, the total sound pressure p_t at some distant point Q will be, by superposition

$$p_t=\sum_{i=1}^{n}\frac{A_i}{d_i}\epsilon^{j(\phi i-kdi)} \tag{20}$$

In this equation d_i represents the distance between the ith source and the point Q. A_i represents the complex sound pressure due to the ith source at unit distance from it, and ϕ_i is its phase angle.

Referring to Fig. 19(A) which shows the vector distances and their symbols for the ith and jth point sources and the point Q, it is seen that

$$d_i=|\mathbf{r}-\mathbf{r}_i|=\sqrt{(\mathbf{r}-\mathbf{r}_i)\cdot(\mathbf{r}-\mathbf{r}_i)}=\sqrt{\mathbf{r}^2+\mathbf{r}_i^2-2\mathbf{r}\cdot\mathbf{r}_i} \tag{21}$$

$$=\sqrt{r^2+r_i^2-2rr_i\cos\alpha_i}$$

where α_i is the angle between **r** and $\mathbf{r}_i$.

When Q is far removed from the assemblage of point sources (i.e., when $r>>r_i$), r_i is negligible compared to r. Equation 21 may therefore be written

$$d_i\approx\sqrt{r^2-2rr_i\cos\alpha_i}$$

$$=r\sqrt{1-\frac{2r_i}{r}\cos\alpha_i} \tag{22}$$

and since the second term under the radical is very small compared to the first, equation 22 may be further simplified by using the first two terms of the binomial expansion to give

$$d_i\approx r\left(1-\frac{r_i}{r}\cos\alpha_i\right)=r-r_i\cos\alpha_i \tag{23}$$

Because it was specified that $r>>r_i$, equation 23 may be further reduced to $d_i\approx r$. Such an approximation must be used with caution, however. It is valid when applied to the d_i in the denominator of equation 20, but when multiplied by k, as it is in the imaginary exponent of equation 20, it assumes the nature of a phase angle, and because of the periodic nature of angles and their functions the same liberties cannot be taken with it here. Bearing this double standard of approximation in mind, equation 20 may be written

$$p_t \approx \sum_{i=1}^{n} \frac{A_i}{r} e^{j(\phi_i - kr + kr_i \cos \alpha_i)}$$

$$= \frac{e^{-jkr}}{r} \sum_{i=1}^{n} A_i e^{j(\phi_i + kr_i \cos \alpha_i)} \qquad (24)$$

For a given configuration of sources of given strength and phase angle, all the terms under the summation sign in equation 24 are constant except for α_i, which depends on the angular position of point Q with respect to the co-ordinate axes.

Because α_i varies with the angular position of Q, the sound pressure is in general a function of position even when Q is at a fixed distance from the origin. However, if the point Q is restricted to lie in a fixed *direction*, all terms under the summation sign are complex constants and their sum must also be a complex constant. If this constant be expressed as $B \exp j\psi$, equation 24 may be written as

$$p_t \approx \frac{B}{r} e^{j(\psi - kr)} \qquad (25)$$

This is identical in form to equation 19 for a single point source, thus indicating that, at a sufficiently large distance, a complex source of sound appears as a point source to an observer on a radial line of fixed direction.

Appendix III. Spherical Model Approximation to a Transformer Tank

The sphere appears to be another possible simple mathematical model to represent a transformer tank. It is realized that this model is far from an accurate representation because transformer tanks are frequently rectangular in plan and elevation views and because the acoustically hard ground plane requires than an image be located underground. The source is thus more pencil-like than spherical. However, at distances from the tank, the representation of the pressure waves by spherical terms becomes quite accurate.

The expression for the velocity potential for an outward travelling wave becomes in spherical co-ordinates (reference 14, pages 404 and 406)

$$\Phi(r,\theta,\phi) = \sqrt{\frac{\pi}{2kr}} \sum_{n=0}^{\infty} H_{n+1/2}^{(1)}(Kr) \times \left(a_{n0} P_n (\cos\theta) + \sum_{m=1}^{n} (a_{mn} \cos m\phi + b_{mn} \sin m\phi) P_n^m (\cos\theta) \right) e^{-j\omega t} \qquad (26)$$

where $K = \omega/c$ when c = the sonic velocity. The term $P_n^m(\cos\theta)$ is equal to

$$\frac{(\sin^2\theta)^{m/2}}{2^n n!} \frac{\partial^{n+m}(-\sin^2\theta)^n}{\partial(\cos\theta)^{n+m}} \qquad (27)$$

Functions of the simplest θ variation for $m \neq 0$ are obtained by equating m and n

$$P_n^n(\cos\theta) = \frac{(2n)! \sin^n \theta}{2^n n!} \qquad (28)$$

The radiation from a sphere vibrating with the prescribed velocity

$$V_r/r = V_n P_n^n(\cos\theta) \cos n\phi e^{-j\omega t} \qquad (29)$$

is

$$\Phi = \frac{\dfrac{V_n'}{\sqrt{Kr}} H_{n+1/2}^{(1)}(Kr) \cos n\phi \sin^n \theta e^{-j\omega t}}{K\left(\dfrac{n+1}{(KR)^{3/2}} H_{n+1/2}^{(1)}(KR) - \dfrac{1}{\sqrt{KR}} H_{n-1/2}(KR) \right)} \qquad (30)$$

where R is the radius of the sphere.

The acoustic pressure is given by

$$P = \rho \frac{\partial\Phi}{\partial t} \qquad (31)$$

$$= -j\omega\rho\Phi$$

where ρ is the mass density of the fluid.

$$P = \rho c V_n \times \frac{\dfrac{1}{\sqrt{Kr}} H_{n+1/2}^{(1)}(Kr) \cos n\phi \sin^n \theta}{\dfrac{n+1}{(KR)^{3/2}} H_{n+1/2}^{(1)}(KR) - \dfrac{1}{\sqrt{KR}} H_{n-1/2}(KR)} e^{-j\omega t} \qquad (32)$$

The noninteger order Hankel function of the first kind is defined by

$$H_\nu^{(1)}(Kr) = J_\nu(Kr) + jY_\nu(Kr) \qquad (33)$$

From page 64, reference 17

$$Y_\nu(Kr) = \frac{J_\nu(Kr) \cos \nu\pi - J_{-\nu}(Kr)}{\sin \nu\pi} \qquad (34)$$

for $\nu \neq$ integer.

For $\nu = n + 1/2$

$$Y_{n+1/2}(Kr) = (-1)^{n+1} J_{-(n+1/2)}(Kr) \qquad (35)$$

and the Hankel function of equation 33 becomes

$$H_{n+1/2}^{(1)}(Kr) = J_{n+1/2}(Kr) + j(-1)^{n+1} J_{-(n+1/2)}(Kr) \qquad (36)$$

The numerical values of $1/\sqrt{Kr} H_{n+1/2}^{(1)}(Kr)$ have been plotted in Fig. 20 for several values of n. The amplitude has been plotted in units of $20 \log \left| \frac{1}{\sqrt{Kr}} H_{n+1/2}^{(1)}(Kr) \right|$. The pressure radiated from a sphere of radius $R = 3/K$ has been plotted in Fig. 21 for several different vibration modes described in equation 32.

Two points of interest may be observed in the curves. First, notice the near-field effect in the 8- and 12-node modes. Although the pressures at the surface of the sphere for the various modes are within 10 db of each other, the pressure caused by the 4-node pattern is considerably greater than for the 12-node pattern at distances $r > 10/K$. The second point of interest is that, for the

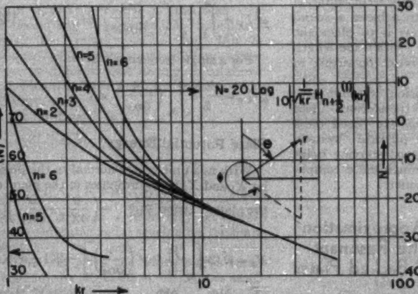

Fig. 20. Graph of magnitude of one-half order Hankel functions versus argument

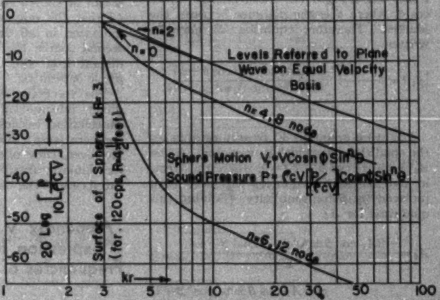

Fig. 21. Sound pressure versus distance from a sphere for several vibration modes

modes plotted, at distances $r>10/K$ the change of pressure level with distance is 6 db per distance doubled.

Appendix IV. Sound Pressure Field at a Large Distance from Two Point Sources

When only two points sources are involved, equation 20 becomes

$$p_t=\frac{A_1}{d_1}e^{j(\phi_1-kd_1)}+\frac{A_2}{d_2}e^{j(\phi_2-kd_2)} \quad (37)$$

A spherical co-ordinate system r, θ, φ will be used in which the $\theta=0$ axis is aligned so that it passes through the point sources. The origin of the co-ordinate system is placed midway between the sources. The geometry of the arrangement is sketched in Fig. 19(B).

Of primary concern is the absolute value of the sound pressure, so equation 37 is first multiplied by its conjugate p_t^*, giving

$$\begin{aligned}|p_t|^2=p_tp_t^*=&\left(\frac{A_1}{d_1}e^{j(\phi_1-kd_1)}+\right.\\&\left.\frac{A_2}{d_2}e^{j(\phi_2-kd_2)}\right)\left(\frac{A_1^*}{d_1}e^{-j(\phi_1-kd_1)}+\right.\\&\left.\frac{A_2^*}{d_2}e^{-j(\phi_2-kd_2)}\right)=\frac{A_1A_1^*}{d_1^2}+\frac{A_2A_2^*}{d_2^2}+\\&\frac{A_1A_2^*}{d_1d_2}e^{j[\phi_1-\phi_2+k(d_2-d_1)]}+\\&\frac{A_1^*A_2}{d_1d_2}e^{-j[\phi_1-\phi_2+k(d_2-d_1)]}\end{aligned} \quad (38)$$

The analysis will be restricted to the sound pressures at large distances from the origin; i.e., $r>>d$. Hence, $d_1\approx d_2\approx r$. The phase angle between the two sources $\phi_1-\phi_2$ can be replaced by ϕ. Then equation 38 becomes

$$\begin{aligned}|p_t|^2=&\frac{|A_1|^2}{r^2}+\frac{|A_2|^2}{r^2}+\\&2R\left(\frac{A_1A_2^*}{r^2}e^{j[\phi+k(d_2-d_1)]}\right)\end{aligned} \quad (39)$$

Since A_1 and A_2 have the same arguments, $A_1A_2^*=|A_1A_2|$. All terms are now real, so the bars indicating absolute magnitudes will be dropped from the A's for convenience. Also, Fig. 19(B) shows that $d_2-d_1\approx d\cos\theta$, where d is the distance between the sources. Therefore equation 39 may be written

$$|p_t|^2=\frac{A_1^2+A_2^2+2A_1A_2\cos(kd\cos\theta+\phi)}{r^2} \quad (40)$$

Equating equation 40 to zero establishes the conditions for which p_t vanishes. Then $A_2^2+2A_1A_2\cos\beta+A_1^2=0$, where the terms in parenthesis in equation 40 have been replaced by β for simplicity. Solving this quadratic for A_2

$$\begin{aligned}A_2&=\frac{-2A_1\cos\beta\pm\sqrt{4A_1^2\cos^2\beta-4A_1^2}}{2}\\&=-A_1(\cos\beta\pm\sqrt{\cos^2\beta-1})\end{aligned}$$

Therefore

$$A_2=-A_1(\cos\beta\pm i\sin\beta) \quad (41)$$

Since A_2 is real, this equation is satisfied only if $\sin\beta=0$. Therefore, $\beta=0$, π. But A_2 must be positive, so $\cos\beta$ must be negative, and β can only equal π. Hence, the conditions for zero sound pressures at large distances are

$$A_2=A_1 \quad (42)$$

$$\beta=kd\cos\theta+\phi=\pi \quad (43)$$

Thus the sound pressure can be made zero at any given distant point by properly adjusting ϕ, provided that $A_2=A_1$.

Replacing A_2 by A_1 in equation 40 in accordance with this finding, and extracting the square root, gives

$$|p_t|=\sqrt{2}\frac{A_1}{r}\sqrt{1+\cos(kd\cos\theta+\phi)}$$

A well-known trigonometric identity enables simplification of this to

$$|p_t|=\frac{2A_1}{r}\cos\left(\frac{kd}{2}\cos\theta+\frac{\phi}{2}\right) \quad (44)$$

To express the sound pressure from two equal sources as a ratio to the pressure from one source operating alone, $|p_t|$ is divided by $|p_1|=\sqrt{p_1p_1^*}=A_1/r$. Also, it is convenient to express distances in terms of wave length, so k will be replaced by $2\pi/\lambda$. The result is

$$\left|\frac{p_t}{p_1}\right|=\pm 2\cos\left(\frac{\pi d}{\lambda}\cos\theta+\frac{\phi}{2}\right);\quad (r\gg d,\ A_1=A_2) \quad (45)$$

Examination of equation 45 shows:

1. The magnitude of pressure about a pair of point sources of equal strength is always symmetrical about the $\theta=0$ axis, since $\cos(-\theta)=\cos\theta$.
2. The sound pressure pattern for a given separation and phase angle is independent of φ, the longitudinal angle is the spherical co-ordinate system as oriented here.
3. The maximum possible value of sound pressure from a pair of point sources is twice that for a single source.
4. A sound pressure of zero can be obtained in any direction by properly adjusting the phase angle between the two sources.
5. The sound pressure will approach zero at all distant locations if the separation of the sources approaches zero and they are oppositely phased; i.e., if $d\ll\lambda$, $\phi=\pi$ radians.

Although it is not obvious by inspection, it can be shown fairly easily from equation 45 that the only way to achieve a sound reduction in all directions is to place the second source less than 1/6th wave length distant from the first source operating in phase opposition.

The foregoing conclusions do not give direct information on transformer noise cancellation because they are based on a comparatively simple physical system. However, they offer a good starting point for thinking about the much more complicated case of the transformer.

Appendix V. Approximation Expression for the Resonant Frequencies of Oil-Backed Plates

This analysis relies entirely on Rayleigh's approach to the calculation of the resonant frequencies. The following assumptions were used to simplify the analysis:

1. Plates are assumed to be infinite in extent.
2. Oil is assumed infinite in extent with no obstructions, but on one side of the plate only.
3. Air loading is negligible.
4. For the sizes of plates and resonant frequencies considered the compressibility of oil will be neglected. In other words, the dimensions of the shortest span between nodes in the vibration pattern will be assumed shorter than 1/4th wave length in the oil.

The analysis proceeds with the use of a displacement potential function defined as

w displacement = −gradient of Φ

$$\mathbf{w}=-\nabla\Phi \quad (46)$$

$$\mathbf{V}=\frac{\partial\mathbf{w}}{\partial t}=-\frac{\partial\nabla\Phi}{\partial t}$$

For Rayleigh's method the energies in the plate and oil are required.

For the Fluid (Oil)

The kinetic energy is given by

$$\omega^2T_0=\rho_0/2\int_v\mathbf{V}\cdot\mathbf{V}/dv \quad (47)$$

Thus

$$\omega^2T_0=\rho_0/2\int_v\left(-\frac{\partial\nabla\Phi}{\partial t}\cdot-\frac{\partial\nabla\Phi}{\partial t}\right)dv \quad (48)$$

For a single-frequency sine wave

$$\omega^2T_0=\frac{\omega^2\rho_0}{2}\int_v\nabla\Phi\cdot\nabla\Phi\,dv \quad (49)$$

The potential energy is

$$V_0=\frac{\rho_0c^2}{2}\int_v(\nabla^2\Phi)^2\,dv \quad (50)$$

For the Tank Wall or Plate

Let $\mathbf{n}_2$ be a unit vector normal to the surface of the wall. Let $\partial/(\partial\mathbf{n}_2)$ denote derivatives in the $\mathbf{n}_2$ direction. Then if S_2 is the plate surface

$$\omega^2T_p=\int_{S_2}\frac{t_2\rho_2}{2}\left(-\frac{\partial^2\Phi}{\partial\mathbf{n}_2\partial t}\right)^2ds_2 \quad (51)$$

For a single-frequency sine wave

$$\omega^2T_p=\frac{\omega^2t_2\rho_2}{2}\int_{S_2}\left(\frac{\partial\Phi}{\partial\mathbf{n}_2}\right)^2ds_2 \quad (52)$$

Plate Potential Energy

With $\mathbf{n}_2$ a unit vector normal to the plate, let X_1 and X_2 be co-ordinates in the plane of the plate. Define $\nabla_{12}^2(\ )=\left(\frac{\partial^2}{\partial X_1^2}+\frac{\partial^2}{\partial X_2^2}\right)(\ )$

$$\begin{aligned}V_p=D/2\int_{S2}&\left\{\left[\nabla_{12}^2\left(\frac{\partial\Phi}{\partial\mathbf{n}_2}\right)\right]^2-2(1-\sigma)\times\right.\\&\left.\left[\frac{\partial^3\Phi}{\partial\mathbf{n}_2\partial X_2^2}\frac{\partial^3\Phi}{\partial\mathbf{n}_2\partial X_1^2}-\left(\frac{\partial^3\Phi}{\partial\mathbf{n}_2\partial X_1\partial X_2}\right)^2\right]\right\}dS_2\end{aligned} \quad (53)$$

$$D=\frac{E_s t_2^3}{12(1-\sigma^2)}$$

Frequency Equation

Assume a mode in the plate

$$w=w_0 \sin\frac{\pi y}{A}\sin\frac{\pi X}{B}\sin \omega t \tag{54}$$

The corresponding oil motion will be matched to the plate motion at the boundary $Z=0$. The simplified equation of motion for a fluid is in terms of the displacement potential function

$$\nabla^2\Phi=\frac{1}{c^2}\frac{\partial^2\Phi}{\partial t^2} \tag{55}$$

If a sine wave time variation is assumed, equation 55 reduces to

$$\nabla^2\Phi+K^2\Phi=0 \tag{56}$$

where

$$K=\omega/c \tag{57}$$

In rectangular co-ordinates, with trigonometric variations in x and y, the solution of equation 56 is

$$\Phi=\Phi_0 \begin{matrix}\sin\\ \cos\end{matrix}\frac{\pi x}{B}\begin{matrix}\sin\\ \cos\end{matrix}\frac{\pi y}{A}\times \epsilon^{\pm\sqrt{(\pi/B)^2+(\pi/A)^2-K^2}\,z}\begin{matrix}\sin\\ \cos\end{matrix}\omega t \tag{58}$$

Now, the radical in the exponent of equation 58 will be investigated. Let $\alpha=\pi/A$, $\beta=\pi/B$. It is possible to show that for small A and B compared to a wave length of vibration in the oil, the radical may be approximated by

$$\sqrt{\alpha^2+\beta^2-K^2}\approx\sqrt{\alpha^2+\beta^2} \tag{59}$$

and the fluid flow is essentially incompressible.

Rewriting equation 59 in more convenient form

$$\sqrt{\alpha^2+\beta^2-K^2}=\sqrt{\alpha^2+\beta^2}\sqrt{1-\frac{K^2}{\alpha^2+\beta^2}}$$

For $K^2/(\alpha^2+\beta^2)$ small, the expression may be further reduced to

$$\sqrt{\alpha^2+\beta^2-K^2}=\sqrt{\alpha^2+\beta^2}\left(1-\frac{1}{2}\frac{K^2}{\alpha^2+\beta^2}\right)$$

An arbitrary limit will be set that if the factor $1/2[K^2/(\alpha^2+\beta^2)]$ is less than 0.05 its effects will be neglected in the calculations; i.e., incompressible flow will be assumed. These equations will hold within 5 per cent for kinetic energy calculations, and within 2.5 per cent for frequency determination.

The limit for K is

$$K^2<0.1(\alpha^2+\beta^2) \tag{60}$$

Thus

$$\omega/c<0.316\sqrt{(\pi/A)^2+(\pi/B)^2} \tag{61}$$

But $\omega|c=2\pi|\lambda$, so a limit may be written on the allowable nodal spacing for the limits listed.

Table III gives the wave length versus frequency for 10-C oil at 50 degrees centigrade, where

$C_{50°}=1.325\times10^5$ centimeters per second
$=5.22\times10^4$ inches per second

Table III. Wave Length Versus Frequency for 10-C Oil at 50 Degrees Centigrade

f, CPS	λ, Inches
120	435
240	217
360	145
480	108.5
600	87
720	72.4
840	62.2
960	54.3
1,080	48.3
1,200	43.5

Most of the vibration work in transformers is concerned with the fundamental component, 120 cps. The limits on A and B at 120 cps will now be determined. Two cases are worth investigating to set a limit on the size A or B may reach and still stay within the assumptions. Equation 61 may be rearranged to make this comparative investigation

$$A<\frac{0.158\lambda}{\sqrt{1+A^2/B^2}} \tag{62}$$

Case A:

$A/B=1$

$A<0.112\lambda$

$A_{120}<49$ inches

Case B:

$A/B\to0$

$A_{120}<68.6$ inches

To summarize, so long as the square node pattern for an oil-backed plate is within 49 inches for 120 cps, the error by assuming incompressible flow will be less than 2.5 per cent. A check for a plate thickness of 1 inch indicates that at 120 cps the condition $A/B=1$ does not approach 49 inches so that the assumption is entirely justified for normal transformer tank plate thicknesses.

Returning to equation 58, the incompressible flow case is given by

$$\Phi=\Phi_0 \begin{matrix}\sin\\ \cos\end{matrix}\frac{\pi x}{B}\begin{matrix}\sin\\ \cos\end{matrix}\frac{\pi y}{A}\times \epsilon^{\pm\sqrt{(\pi/A)^2+(\pi/B)^2}\,z}\begin{matrix}\sin\\ \cos\end{matrix}\omega t \tag{63}$$

The co-ordinate system is chosen with z increasing with further traverse into the fluid. Since Φ cannot go to infinity at an infinite distance from the plate, the plus solution for the exponential is rejected. Similarly matching boundary conditions at the plate requires the sine variations in x and y.

The form of Φ must therefore be

$$\Phi=\Phi_0\sin\frac{\pi x}{B}\sin\frac{\pi y}{A}\times \epsilon^{-z\pi\sqrt{1/A^2+1/B^2}}\sin\omega t \tag{64}$$

$$w=-\frac{\partial\Phi}{\partial z}=\Phi_0\pi\sqrt{1/A^2+1/B^2}\sin\frac{\pi x}{B}\times \sin\frac{\pi y}{A}\epsilon^{-z\pi\sqrt{1/A^2+1/B^2}}\sin\omega t \tag{65}$$

At $z=0$

$$w=\Phi_0\pi\sqrt{1/A^2+1/B^2}\sin\frac{\pi x}{B}\times \sin\frac{\pi y}{A}\sin\omega t \tag{66}$$

Matching boundary conditions, it is found that Φ_0 is related to w_0 of equation 54 by

$$\Phi_0=\frac{w_0}{\pi\sqrt{1/A^2+1/B^2}} \tag{67}$$

which, when substituted into equation 66, gives

$$\Phi=\frac{w_0}{\pi\sqrt{1/A^2+1/B^2}}\sin\frac{\pi x}{B}\sin\frac{\pi y}{A}\times \epsilon^{-\pi z\sqrt{1/A^2+1/B^2}}\sin\omega t \tag{68}$$

To determine the kinetic energy in the fluid, Φ is substituted from equation 68 into equation 49 and the necessary algebra is performed. The result of the integration gives

$$\omega^2T_0=\frac{\omega^2\rho_0}{2}\left(\frac{AB}{4}\right)\left(\frac{1}{\pi\sqrt{1/A^2+1/B^2}}\right)w_0^2 \tag{69}$$

Substitution of w from equation 54 into the expressions 52 and 53 give the following expressions for the plate energies

$$\omega^2T_p=\frac{\omega^2\rho_s t_2}{2}\left(\frac{AB}{4}\right)w_0^2 \tag{70}$$

and

$$V_p=D/2\left(\frac{AB}{4}\right)[(\pi/A)^2+(\pi/B)^2]^2w_0^2 \tag{71}$$

The total kinetic energy in the vibrating system is the sum of equations 69 and 70

$$\omega^2T=\frac{\omega^2\rho_s t_2}{2}\left(\frac{AB}{4}\right)\left(1+\frac{\rho_0}{\pi\rho_s t\sqrt{1/A^2+1/B^2}}\right)w_0^2 \tag{72}$$

The resonant frequency of the nodal spacing $A\times B$ is determined from equations 71 and 72 to be

$$\omega^2=V_p/T \tag{73}$$

$$\omega^2=\frac{\pi^4D}{\rho_s t_2}\frac{(1/B^2+1/A^2)^2}{1+\dfrac{\rho_0}{\pi\rho_s t_2\sqrt{1/A^2+1/B^2}}} \tag{74}$$

Solving for f, one obtains

$$f=\frac{\pi}{2}\sqrt{\frac{E}{12(1-\sigma^2)\rho_s}}\,t_2\times \frac{1/A^2+1/B^2}{\sqrt{1+\dfrac{\rho_0}{\pi\rho_s t_2\sqrt{1/A^2+1/B^2}}}} \tag{75}$$

For steel

$E=30,000,000$ pounds per inch^2

$\sigma=0.3$

$\rho_s=7.35\times10^{-4}\dfrac{\text{pounds per second}^2}{\text{inches}^4}$

For 10-C oil at 20 degrees centigrade

$\rho_o/\rho_s=0.1126$

Change with temperature is relatively unimportant; e.g., at 60 degrees centigrade

$\rho_o/\rho_s=0.1095$

With steel and 10-C oil data, equation 75 reduces to

$$f=9.74\times10^4 t\frac{1/A^2+1/B^2}{\sqrt{1+\dfrac{0.0359}{t\sqrt{1/A^2+1/B^2}}}} \qquad (76)$$

where t, A, B, are in inches.

References

1. Acoustic Models of Transformer Installations, **Briggs Gettys, William B. Conover.** *AIEE Transactions*, vol. 70, pt. I, 1951, pp. 333–38.

2. An Anechoic Chamber for Noise Tests on Large Power Transformers, **A. W. Benoit, R. T. Hemmes, M. W. Schulz, Jr.** *Ibid.*, vol. 74, pt. III, Apr. 1955, pp. 50–56.

3. Transformer Audio Noise Problems on an Electric Power System, **C. E. Murry.** *Ibid.*, vol. 68, pt. II, 1949, pp. 740–52.

4. Audio Noise in Transformers in Residential and Commercial Areas, **C. E. Baugh.** *Ibid.*, vol. 69, pt. I, 1950, pp. 121–28.

5. Quiet Transformer Installations—A Problem for Both Equipment and Substation Designers, **I. S. Mendenhall, F. L. Taylor.** *Ibid.*, pt. II, pp. 1148–53.

6. Transformer Noise and its Confinement, **Corbett McLean.** *Ibid.*, pp. 1409–16.

7. An Investigation of Audio Noise in Substation-Type Transformers, **J. H. Vivian, R. R. Peck.** *Ibid.*, vol. 70, pt. I, 1951, pp. 328–32.

8. Sound Insulation of Wall and Floor Constructions, **V. L. Chrisler.** *Report BMS 17* and *Supplements 1* and *2*, Building Materials and Structures, National Bureau of Standards, Washington, D. C.

9. The Reduction of Industrial Machine Noise, **R. O. Fehr.** *Proceedings*, Second Annual National Noise Abatement Symposium, Chicago, Ill., Oct. 5, 1951.

10. Handbook of Acoustic Noise Control. Vol. I, Physical Acoustics, **R. H. Bolt, S. J. Lukasik, A. E. Nolle, A. D. Frost.** *WADC Technical Report 52-204*, Wright Patterson Air Force Base, Ohio, Dec. 1952, p. 312.

11. Acoustics (book), **Leo L. Beranek.** McGraw-Hill Book Company, Inc., New York, N. Y., 1954, pp. 91–96.

12. **Beranek,** *op. cit.*, pp. 96–97.

13. A Treatise on the Mathematical Theory of Elasticity (book), **A. E. H. Love.** Dover Publications, New York, N. Y., 4th rev. ed.

14. Electromagnetic Theory (book), **J. A. Stratton.** McGraw-Hill Book Company, Inc., New York, N. Y., 1941.

15. Vibration and Sound (book), **P. M. Morse.** *Ibid.*, 2nd ed., 1948, pp. 312–13, 326–32.

16. Fundamentals of Acoustics (book), **L. E. Kinsler, A. R. Frey.** John Wiley and Sons, Inc., New York, N. Y., 1950, pp. 162–67.

17. A Treatise on the Theory of Bessel Functions (book), **G. N. Watson.** Cambridge University Press, Cambridge, England, 1922.

18. Transformer Noise Measurement Methods, **AIEE Committee Report.** *AIEE Transactions*, vol. 73, pt. III, June 1954, pp. 683–92.

◆

Discussion

T. R. Specht (Westinghouse Electric Corporation, Sharon, Pa.): These tests with models and the sound cancellation method are very interesting. The comparison of the attenuations secured by 2-, 3-, and 4-sided barriers is quite useful. As I understand the paper, the barrier tests were made at only the fundamental of the sound frequency which is twice the frequency of the applied voltage. It would be interesting to know the attenuation at higher frequencies as well.

In the case of the 2-wall enclosure, the theoretical equation is satisfactory, so it is possible to calculate the attenuation at the higher frequencies. In general, the sound from a transformer contains higher harmonics. The attenuation, due to the wall, of the sound will be larger than as given in the paper because the wall attenuates the higher frequency components more than the fundamental. From Fig. 9 referring to a 2-wall enclosure, the attenuation increases about 3 db each time the frequency doubles. For a 4-wall enclosure, by comparing it to a vibrating piston set in an infinite surface, for constant sound energy radiated, the sound level at some distance from the transformer would decrease again 3 db each time the frequency doubles.

The harmonic content of the sound from transformers varies with various transformers. The harmonic index (HI) is an indication of the amount of harmonic content. Mutschler and Madden[1] give the HI of a transformer as 11.9. C. S. Murray[2] gives an HI for a 60,000-kva transformer of 5.5. I calculated some examples, assuming a sound consisting of various components, with 120 cycles and higher harmonics. The 3-db rule for the increased attenuation for the harmonics was used. The attenuation of the db_{40} sound level between the transformer and some point away from the transformer was calculated. It was observed that this attenuation is about the same for the same HI, for frequencies of the harmonics through 720 cycles. For an HI of 15, the attenuation for the db_{40} sound is 1.5 db greater than for the 120-cycle component; for HI = 12, 3 db more; for HI = 9, 4.4 db more; and HI = 6, 5.2 db more.

Sound cancellation has intriguing possibilities but it would appear that there would be difficulties in applying it in practice. If the transformer and loudspeaker are supplied from the same voltage source, the sound level of the loudspeaker would change 1 db for a 10-per-cent change in voltage and the transformer would change about 3 db. The load current produces a small amount of noise in the transformer. Changes in pressure in the tank would change the modes of vibration of tank panels. Also the loudspeaker and its power source would need to be stable with time. It would be possible for an adverse combination of these factors to make the cancellation ineffective. If there were a bank of transformers, a loudspeaker would have to be placed on each transformer, unless the transformers were grouped closely together and could be considered as a single transformer. A report on a practical installation will certainly be of real interest to all.

References

1. Harmonic Index—A Tool for Transformer Audio Noise Investigation, **W. H. Mutschler, Jr., T. F. Madden.** *AIEE Transactions*, vol. 69, pt. I, 1950, pp. 115–18.

2. *Discussion* by **C. S. Murray** of reference 1, p. 118.

William B. Conover and **Robert J. Ringlee:** Mr. Specht is correct; the model barrier data reported were for the fundamental frequency of transformer noise. For the one-seventh scale model this was 840 cps. Two check tests were made with the 2-sided enclosure at the third harmonic of transformer noise, 2,520 cps for the model. These two checks were found to agree closely with the attenuations predicted from the diffraction theory of Wells and Fehr (references 9 and 10 of the paper) using the calculation methods given in our paper. Additional tests are planned with the 3- and 4-sided enclosures at the second, third, and higher harmonic frequencies of transformer noise.

Those accustomed to using the HI as an indication of frequency composition will find Mr. Specht's analysis useful for estimating the effects of partial enclosures upon transformer noise measured upon the *A* network of the sound level meter.

Successful sound cancellation tests have been performed upon three outdoor substations. These tests have shown that the transformer noise varies slowly with time along particular radial directions. A self-compensating system is being developed to follow the variations of transformer noise.

Functional Temperature Endurance Tests on a Silicone Glass Fiber Insulation System for Dry-Type Transformers

M. L. MANNING
FELLOW AIEE

THIS paper is an outgrowth of test procedures agreed upon by the AIEE Working Group on Life of Materials, Subgroup on Functional Tests, under the auspices of the Committee on Transformers of the Power Division. Work on a 15-kv class silicone glass fiber transformer insulation system was assigned to the author. Other members of the Subgroup studied lower temperature insulation systems. Based on the activity of the Subgroup on Functional Tests, additional experimental test work on insulation systems under accelerated conditions to be correlated with actual transformer operating experience has been recommended.[1]

By substantiating data, accelerated functional tests on a silicone glass fiber insulation system are linked with dry-type transformers in service. Support is offered for the recent action by the Transformer Section of the National Electrical Manufacturers Association (NEMA) in establishing 180-degree-centigrade (C) hottest-spot temperature rise for what is classified as group 3 dry-type transformers.[2] Model transformers, 16 in number, having a composite silicone glass fiber insulation system corresponding to 15-kv-class insulation were subjected to heat, 90 per cent (%) humidity and 100% dielectric-proof voltage test-cycling at 200, 275, and 350 C obtained by circulation of current in the windings. Ordinarily in service, dry-type transformers are given only 75% test voltage, in accordance with AIEE Standard No. 53.[3]

Present-Day Practice of Evaluating Insulating Materials for Dry-Type Transformers

A review of present-day practice may be helpful. Basically four procedures are involved. First, AIEE Standard No. 1, which was revised in February 1954,[4] follows the same general material classification since its inception in 1913. Based mainly upon chemical composition, insulating materials are given classifications of *O*, *A*, *B* and *H*. Temperatures of 90, 105, 130, and 180 C respectively are suggested. They are the limiting hottest-spot temperatures at which these classes may be operated continuously with normal life expectancy. Tests are not prescribed to support the classifications. For example, a class *B* designated transformer may use class *A* structural materials as components, yet, according to AIEE No. 1, class *A* is given a 105-C hottest-spot temperature limit. But the transformer is called class *B* which signifies 150-C permissible hottest-spot temperature. The qualifying statements in this standard allow such latitude to exist.

Second, the American Society for Testing Materials standards outline methods for testing various kinds of insulating materials. Suppliers of materials follow these standards and users may duplicate the tests or devise others to be assured that desired properties of materials are obtained. The mechanical and electrical properties are set at the transformer manufacturer's discretion and are not prescribed by the standards.

Third, the American Standards Association Standards for transformers and those of the AIEE specify a limiting temperature rise for a given class of insulation. The temperature values set are in accord with those of AIEE No. 1.

NEMA has divided dry-type transformers into three groups. Group 1 allows a permissible hottest spot temperature rise, 65 C; group 2, 110 C, and group 3, 180 C.[2] This is the initial step taken by standardizing bodies to formulate a workable plan. The user of transformers is confident that in the transformer manufacturer's product these temperature limits are conservative and that considerable margins exist.

The fourth step, or plan, in use for evaluation of insulating materials is made by the transformer manufacturer. The manufacturer screens the materials, observes the characteristics of each material mechanically and electrically, allows margins above test requirements and processes these materials into a transformer insulation system. Considerable conservatism in insulation system designs exists because failures are always costly to a manufacturer, and he must protect his reputation. Users are thus protected by such a general plan of insulating material selection, which has been in use for a number of years by reliable manufacturers.

What Is Needed in New Methods

Present-day practice, as outlined, has several disadvantages. In recent years many new bonding and impregnating resins have been developed for use with base materials such as glass fiber and asbestos. The task becomes quite hopeless in establishing temperature limits on an organic or inorganic basis for numerous materials by assigning to them alphabetical letters. Furthermore, the situation becomes more complicated because of recent action by the International Electrotechnical Commission in suggesting two new insulation classes *E* and *F*.[5]

Standardizing groups dealing with transformer and manufacturing problems require freedom in choosing suitable requirements for insulation and temperature limits. The present arrangement of the AIEE in setting up the Subcommittee on Dielectrics of the Basic Sciences Committee for evaluation of materials alone, plus the Working Group on Life of Materials Committee having a subgroup under the Transformer Committee, is a step in this direction. Wasteful use of time results in having an over-all committee make basic decisions. Freedom of movement is required by dividing the responsibility with smaller committees.

A convenient procedure is necessary for screening new materials, followed by evaluation of these materials in transformer insulation systems. This paper deals with the latter plan, whereby functional testing of an insulation system is utilized after the primary selection of materials has been made. Functional tests of an insulating material system give the practical, accelerated means by which the component parts of the system are evaluated at temperatures, voltage stresses, and humidity conditions found under extreme service conditions. Tem-

---

Paper 55-44, recommended by the AIEE Transformers Committee and approved by the AIEE Committee on Technical Operations for presentation at the AIEE Winter General Meeting, New York, N. Y., January 31–February 4, 1955. Manuscript submitted October 18, 1954; made available for printing November 18, 1954.

M. L. MANNING is with the Pennsylvania Transformer Company, Canonsburg, Pa.

The author expresses his appreciation to H. M. Yorke of the Pennsylvania Transformer Company for his suggestions and assistance in the preparation of this paper and the charts.

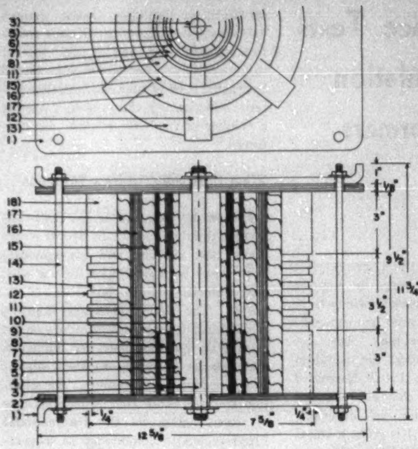

Fig. 1. Component parts of test model

1—1/8-inch aluminum clamping plate
2—1/8-inch insulation (silicone laminate)
3—5/8-inch clamping bolt
4—$1\frac{1}{2}$-inch-diameter cylinder
5—1/4-inch duct (silicone laminate)
6—1/8-inch insulation tube (silicone laminate)
7—low-voltage keepback
8—1/4-inch duct (silicone laminate)
9—low-voltage keepback
10—low-voltage winding first layer (1–7 square)
11—low-voltage winding second layer (1–7 square)
12—3/8-inch radial spacers (porcelain)
13—high-voltage winding (2—0.045 by 0.289)
14—1/4-inch clamping bolt
15—1/2-inch duct (silicone laminate)
16—3/8-inch insulation tube (silicone laminate + silicone rubber-coated fiber glass cloth)
17—1/2-inch duct (silicone laminate)
18—high-voltage keepback
Weight of low-voltage wire, 3.5 pounds
Weight of high-voltage wire, 8.2 pounds
Total weight of test model, 29 pounds

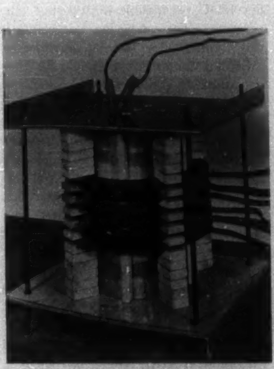

Fig. 2. 15-kv class test model

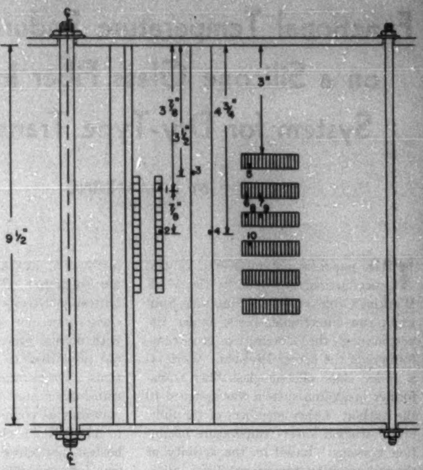

Fig. 3 (above). Thermocouple locations. The thermocouple nos. follow, with their locations

1—second layer low-voltage, second turn from top
2—second layer low-voltage, eighth turn from top
3—inside high-low voltage barrier, $3\frac{1}{2}$ inches from top
4—outside high-low voltage barrier, $4\frac{3}{4}$ inches from top
5—top section high-voltage winding, third turn from inside
6—second section high-voltage winding, second turn from inside
7—second section high-voltage winding, sixth turn from inside
8—third section high-voltage winding, second turn from inside
9—third section high-voltage winding, sixth turn from inside
10—fourth section high-voltage winding, third turn from inside

perature gradients on component materials differ in a transformer insulation structure. The only true means for determining the behavior of these materials is in a system evaluated functionally by test.

The primary screening of materials may still be classified under letters, *A*, *B*, *H*, etc., with corresponding temperature limits. This may be done without reverting to an organic or inorganic basis by test codes based on life test performance of materials. The second step is the development of test codes for the evaluation of insulation systems by functional test for transformers.

Purpose of Functional Tests for a 15-Kv Insulation System

1. To verify that a 15-kv test model is practical.

2. To devise a practical test procedure utilizing heat, voltage, and humidity cycling.

3. To obtain helpful information for devising a test code for functional temperature endurance tests of dry-type power transformers.

Test Apparatus

TEST MODELS

A test model with component parts, built at an approximate cost of $90 for labor and materials, is illustrated in Figs. 1 and 2. This model represents a typical structure for a 15-kv-class insulated high-voltage winding, with a 1.2-kv-class low-voltage winding and supporting structure. All insulation is glass fiber silicone resin bonded. The high-voltage coil is wound of two parallel conductors to permit a

Table I. Test Cycles Withstood, ±0.5 Cycle, 14 Models Total

			Models			Insulation System							
				Units		Flashover Barrier-to-Ground Plate After Humidification		Flashover Barrier After Removal of Ground Plate After Humidification		Flashover Turn-to-Turn or Section-to-Section After Humidification			
										Double Glass Fiber		Special Insulation	
Test No.	Aging Temperature, C	Duration Aging Cycles 48 Hours per Cycle	Total Units	With Thermocouples	Without Thermocouples	Unit	Cycles Withstood 48 Hours per Cycle	Unit	Cycles Withstood 48 Hours per Cycle	Unit	Cycles Withstood	Unit	Cycles Withstood
1	200	7	3	1	2–3	2–3	7			2–3	7		
2	275	7	4	1	2–3–4	2	0.5					2	7
						3	2.5					3	7
						4	6.5					4	7
		10	3		5–6–7	5	1.5	5	8.5	5	1.5		
						6	1.5	6	8.5	6	1.5		
						7	1.5	7	3.5	7	1.5		
3	350	4	4	1	2–3–4	2	0.5			2	1.5		
						3	1.5					3	4
						4	3.5					4	4

dielectric test of turn-to-turn insulation. The leads from each pair of twin sections are brought out separately to permit a section-to-section voltage test. The low-voltage winding consists of two layers to permit testing. Thermocouples, nos. 8 and 10, located in the third section of the high-voltage winding, are used to monitor the current flow (Fig. 3) to obtain hottest-spot temperature desired. Models having thermocouples, of course, were not subjected to voltage tests. Ordinarily, greater creepage of about 1-inch high-voltage winding to ground is allowed. The reason for use of the 3-inch distance in the model was to determine if creepage flashover or puncture would occur. Special turn-to-turn insulation was used on five of the test models.

TEST EQUIPMENT FOR HUMIDITY EXPOSURE AND CURRENT CONTROL

For this test a steel tank of bolted construction, 50 inches long, 25 inches wide, and 24 inches high was utilized. To obtain 90% humidity at room temperature, a pan 12 inches wide, 24 inches long, and 2 inches deep containing saturated lead nitrate salt solution was placed in the bottom of the tank. By means of a fan, recirculated air was blown over the solution and through the ducts of the transformer models. For humidity exposure, the aluminum foil wrapping was removed from the models. In Fig. 4, the tank for humidity exposure, the current regulator, and associated control equipment for monitoring current flow in the model transformer windings can be noted. Winding currents of 67, 110, and 150 amperes respectively, were required to obtain hottest-spot temperatures of 200, 275, and 350 C.

TEST PROCEDURE

To maintain the high-voltage and low-voltage barrier insulation temperature

Table II. Power Factor (High-Voltage to Low-Voltage and Ground)

Average Values, Per Cent Measured at 32 C

	Fig. 5				Fig. 7	
	Aging Temperature 200 C, PF, %		Aging Temperature 275 C, PF, %		Aging Temperature 350 C, PF, %	
Hours of Aging	Before Humidity	After Humidity, 90% RH*	Before Humidity	After Humidity, 90% RH	Before Humidity	After Humidity 90% RH,
0			7.2		5.5	
48		5.5	5.2	8.7	3.9	6.9
96	6.0	7.9	5.2	6.8	3.8	6.1
144	5.0	9.9	4.7	12.4	3.6	5.5
192	5.5	9.7	4.9	7.4	3.25	4.95
240	5.5	10.5	4.8	10.7		
288	4.8	9.1	4.8	9.5		
336	5.2	9.5	4.7	9.9		
			Second Series of Tests (Fig. 6)			
0			5.1			
48			5.3	16.2		
96			5.8	31.6		
144			5.2	19.9		
192			4.2	13.8		
240			4.5	8.5		
288			6.4	9.3		
336			5.0	11.0		
384			5.2	10.4		
432			4.9	9.5		
480			5.1	10.0		

* Relative humidity.

Fig. 4. Temperature aging of test models

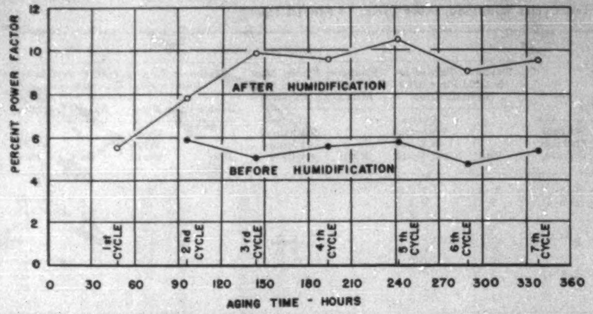

Fig. 5. Pf versus aging time before and after humidification, 90% RH at 32 C, high to low voltage and ground, 15-kv-class dry-type silicone glass fiber transformer system. This also applies in Figs. 6 through 10. Aging temperature 200 C

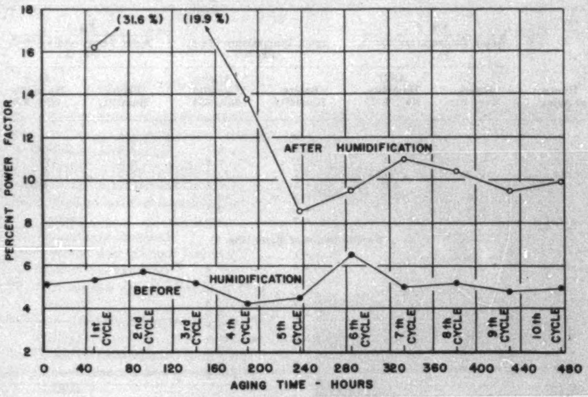

Fig. 6. Aging temperature 275 C

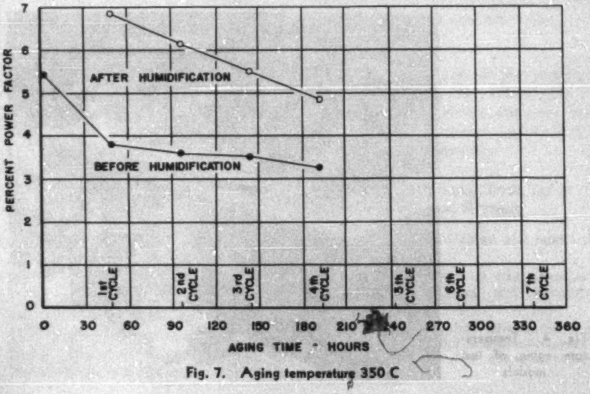

Fig. 7. Aging temperature 350 C

within 25 C of the hottest-spot winding temperatures selected, the air ducts in the structure of the models were blocked by asbestos packing. The entire model was then wrapped with aluminum foil. As many as three models were connected in series with the model having thermocouples for a particular temperature aging. A functional test cycle which follows an initial dielectric proof voltage test on all models except those having thermocouples is outlined in the following. (Of a total of 16 models three were wound with thermocouples.) Two models without aging cycles were subjected to $1^{1}/_{2}$x40 microseconds positive-polarity impulse voltage tests to determine the impulse voltage ratio.

In the functional test cycle, a cycle consists of the following:

1. Heat aging; 48 hours at a given temperature; circulation current in windings.
2. Cooling to ambient temperature 4 hours.
3. Dielectric proof tests.
4. Humidify at 90% relative humidity (RH) for 24 hours.
5. Dielectric proof tests within 1/2 hour after removal from humidity chamber.

The dielectric proof test consists of:

1. American Standards Association standard 100% test voltage for 15-kv-class insulation. Major insulation, high-voltage winding to ground and to low-voltage winding, 1 minute withstand, 31 kv. Section-to-section, 1 minute, 60 cycles, rms 7 kv. Turn-to-turn, 1 minute, 60 cycles, rms 800 volts. Layer-to-layer, low-voltage winding, 1 minute, 60 cycles, rms 5 kv.
2. Power factor (pf) test at room temperature H-LG, L-HG, HL-G.

Comments on Test Results

The heat, humidity, and dielectric proof tests were made in air in accordance with the test procedure outlined in the foregoing. Table I outlines test cycles withstood. (Ordinarily 1-inch greater creepage distance is allowed in actual 15-kv transformer barrier construction. The purpose of clearance used in the models was to determine if puncture or voltage creepage would occur under such cycling.)

Test 1 was discontinued; there was no flashover or evidence of deterioration at 200 C.

For test 2 the following conditions obtained at 275 C:

1. One model; 0.5 cycle withstood. Voltage creepage over barrier-to-ground plate after 90% humidity exposure. Special turn-to-turn insulation used; no failure through 7 cycles.
2. One model; 2.5 cycles withstood.

Voltage creepage over barrier-to-ground plate after humidity exposure. Special turn-to-turn insulation used on this model; no failure through 7 cycles.

3. One model; 6.5 cycles withstood. Voltage creepage over barrier-to-ground plate after humidity exposure. Special turn-to-turn insulation used; no failure through 7 cycles.

4. One model; 7 cycles withstood. Thermocouple unit; no voltage tests.

5. Three models; 1.5 cycles withstood. Voltage creepage over barrier-to-ground plate after humidity exposure. After voltage creepage flashover on barrier insulation, ground plates were removed. Barrier insulation did not puncture at any time even though creepage flashovers to ground occurred from 3.5 up to 8.5 cycles. Turn-to-turn insulation consisting of two wraps of glass fiber failed at 1.5 cycles after humidity exposure.

6. One model with thermocouples; 17 cycles withstood. This model withstood all heat cycling and humidification. Thermocouples were removed at the completion of 17 cycles to make voltage tests. Proof voltage tests were withstood. Flashover occurred on the barrier at 46 kv with the ground plate removed.

For test 3 the following conditions obtained at 350 C:

1. One model; 0.5 cycle withstood. Voltage creepage over barrier-to-ground plate after 90% humidity exposure. Turn-to-turn failure 1.5 cycles. (Two wraps of glass fiber used.)

2. One model; 1.5 cycles withstood. Voltage creepage over barrier-to-ground plate after 90% humidity exposure. Turn-to-turn special insulation withstood 4 cycles, the maximum cycling.

3. One model; 3.5 cycles withstood. Voltage creepage over barrier-to-ground plate after 90% humidity exposure. Turn-to-turn special insulation withstood 4 cycles.

4. One model; four cycles withstood. Thermocouple unit; no voltage tests.

In connection with the power factor before and after humidification, the average 60-cycle voltage values measured at 32 C. Table II and Figs. 5, 6, and 7 list the high-voltage to low-voltage and ground measurements. Table III and Figs. 8, 9, and 10 list the high-voltage and low-voltage to ground measurements.

For location of thermocouples, refer to Fig. 3. Thermocouple readings are found in Table IV for 200-C aging, 7th cycle; in Table V for 275-C aging, 7th cycle; and in Table VI for 350-C aging, 4th cycle.

In the impulse voltage tests two models without heat aging and with ground plates, $1^1/_2$x40 microseconds positive-polarity impulse voltage was applied to the high-voltage winding with the low-voltage winding grounded; see Table VII.

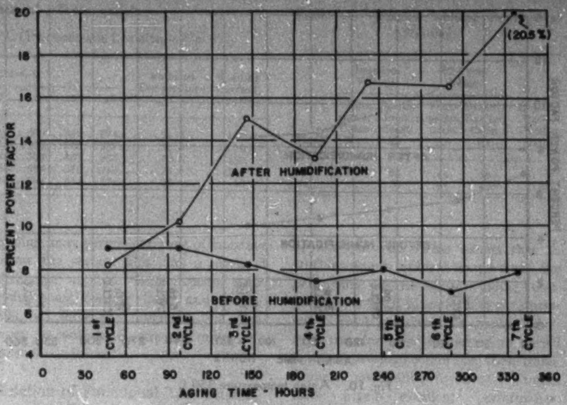

Fig. 8. Aging temperature 200 C

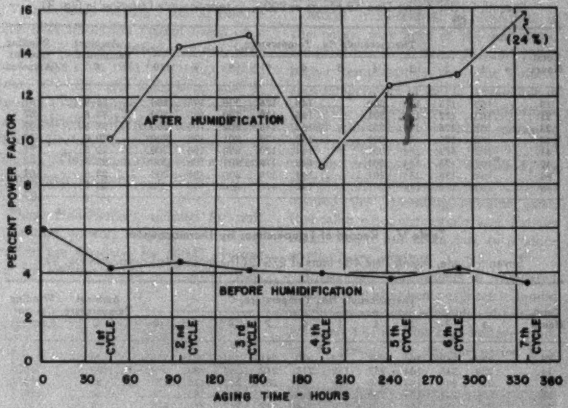

Fig. 9. Aging temperature 275 C

Table III. PF, High and Low Voltage to Ground

Average Values, % Measured at 32 C

	Fig. 8		Fig. 9		Fig. 10	
	Aging Temperature 200 C, PF, %		Aging Temperature 275 C, PF, %		Aging Temperature 350 C PF, %	
Hours of Aging	Before Humidity	After Humidity, 90% RH	Before Humidity	After Humidity, 90% RH	Before Humidity	After Humidity, 90% RH
0			6.0		6.9	
48	9.0	8.2	4.2	10.0	5.6	10.9
96	9.0	10.2	4.6	14.2	5.1	9.8
144	8.2	15.0	4.2	14.7	4.7	8.6
192	7.6	13.2	4.0	8.9	4.4	8.3
240	7.9	16.8	3.8	12.6		
288	7.0	16.8	4.2	13.0		
336	7.8	20.4	3.6	24.2		

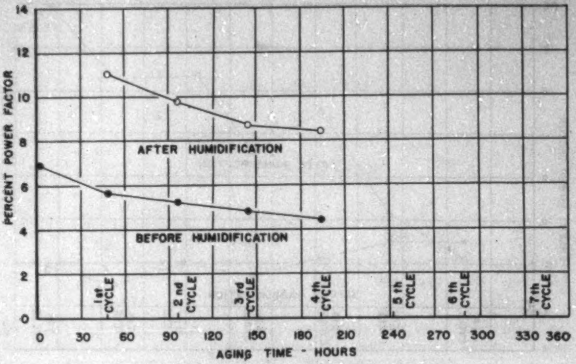

Fig. 10. Aging temperature 350 C

Table IV. Record of Temperatures by Thermocouples

Seventh Cycle, Aging Time 48 Hours at 200 C (Thermocouple Location in Fig. 3)

Total Hours	Thermocouple No., Temperature, C										Ambient Temperature, C	Winding Current, Amperes
	1	2	3	4	5	6	7	8	9	10		
19	162	175	131	200		146	176	200	195	200	23.8	67
21	163	177	132	201		145	176	200	195	200	23.8	67
24	162	176	134	201		145	146	202	195	200	23.8	67
40	162	175	134	201		143	176	201	196	200	20.6	67
41	162	175	134	201		144	176	200	195	200	22.2	67
42	162	175	134	201		143	176	201	196	200	23.8	67
44	162	176	134	201		144	176	200	196	200	23.8	67
48	162	175	134	201		144	176	200	196	200	23.8	67

Table V. Record of Temperatures by Thermocouples

Seventh Cycle, Aging Time 48 Hours at 275 C (Thermocouple Location in Fig. 3)

Total Hours	Thermocouple No., Temperature, C										Ambient Temperature, C	Winding Current, Amperes
	1	2	3	4	5	6	7	8	9	10		
12	230	242	164	257	172	220	241	254	274	278	25	110
14	229	245	164	257	172	213	242	247	280	268	25	110
15	230	245	164	256	170	214	239	247	275	275	25	110
16	229	244	164	255	172	213	245	247	282	276	26	110
18	229	245	164	255	172	213	242	247	275	276	26	110
19	229	244	164	255	172	213	245	247	275	276	26	110
48	229	244	164	257	172	220	241	254	275	275	25	110

Discussion of Test Results

Cyclic Application of Heat Aging, Cooling, Proof Voltage, Humidification and Proof Voltage

The temperature of the barrier insulation was held within 25 C of aging or hot-test-spot winding temperature. It is important that only 100% proof voltage after humidification caused creepage flashover on barrier insulation after 275- or 350-C heat aging. Flashovers did not occur after humidification at 200-C aging temperature. Neither did flashovers occur after the heat-aging portion of the cycle for the whole range of aging temperatures used. Tests on Motorettes revealed also that humidification is a factor.[6]

Models having thermocouples would withstand aging temperature and humidification indefinitely since they were not subjected to proof voltage. At 275-C heat cycling, the model having thermocouples withstood 17 cycles (34 days' heat aging, 17 days' humidification). At the completion of 17 cycles, this model withstood 100% proof voltage with thermocouples removed up to 45-kv rms maximum withstand 60-cycle voltage after drying at room temperature

Puncture of barrier insulation did not occur during any heat aging temperatures of 200-, 275-, and 350-C aging temperatures. Flashovers occurred only after humidification. Usually in design practice, about a 1-inch greater creepage distance is allowed from the high-voltage winding to ground. Use of the 3-inch creepage distance in the model was to determine if creepage flashover or puncture would occur.

General appearance and condition of the barrier insulation was good after the 200- and the 275-C aging. At 350-C aging, the silicone resin became somewhat deteriorated, but it was in reasonably good condition mechanically. This was noted when models were dismantled. No punctures were found after careful inspection. Of importance also is the fact that these models were aged in air. In nitrogen atmosphere, aging data for silicone insulation shows that for equal thermal aging, the temperature may be increased about 50 C over that of silicones operated in air (ventilated).[7]

Turn-to-Turn Insulation

Glass fiber insulation may be scuffed during the winding operation or the bond of the silicone resin to the glass may be insufficient to withstand extreme heat aging, humidification, and 100% voltage cycling. This may be the reason for the turn-to-turn strength variation found at 275- and 350-C. If the turn-to-turn failure occurs at adjacent points between sections of coils, section-to-section flashover results. If must be remembered that in service, the turn-to-turn voltage stress is much lower than the 800-volt withstand required for this proof test after 90% humidification.

At 275-C aging temperature, the turn-to-turn glass fiber insulation in three models withstood 1.5 cycles. A special wire insulation developed for 15-kv class transformers used in three models withstood the maximum test cycling of 7 cycles.

At 350-C temperature aging, failure occurred in one model using glass fiber insulation at 1.5 cycles. Failures were not found in the two models having special wire insulation.

For the low-voltage layer insulation, during all cycling, the layer insulation withstood 5 kv, 1-minute voltage proof test.

For temperatures in insulation structure as determined by thermocouples, refer to Fig. 3, which gives the location of thermocouples. Tables IV, V, and VI give values at a particular cycle.

Winding current was controlled mainly by thermocouples wound in the third

Table VI. Record of Temperatures by Thermocouples

Fourth Cycle, Aging Time 50 Hours at 350 C (Thermocouple Location in Fig. 3)

Total Hours	Thermocouple No., Temperature, C										Ambient Temperature, C	Winding Current, Amperes
	1	2	3	4	5	6	7	8	9	10		
46	275	311	225	325	227	271	340	309	357	374	21.6	150
47	275	313	226	331	228	273	351	305	363	387	22.8	150
48	275	313	226	325	229	277	349	304	357	375	22.8	150
49	275	311	227	325	231	273	355	305	345	385	24.4	150
50	275	313	226	325	228	275	355	304	354	378	24.4	150

Table VII. Impulse Voltage Applied to Windings

Model	Impulse Voltage		60-Cycle Voltage		Impulse Ratio, Withstand
	Withstand, Crest Kv	Barrier Puncture, Crest Kv	Withstand, Crest Kv	Flashover Barrier, Crest Kv	
1	59	63	44	48	1.34
2	54	59	44	48	1.23

section of the high-voltage winding on the second and on the sixth turn from the inside of the pancake winding (thermocouples 8 and 9). Note that the temperature was held within ±2 C for the 200- and 275-C settings and within ±1.5% of the 350 C setting.

Temperature maintained on the barrier insulation was within 25C lower temperature than the hottest-spot winding or aging temperatures. This was accomplished by blocking the air ducts with asbestos packing and by carefully wrapping the entire models with aluminum foil.

PF Test Values

In connection with pf test value, see the section "Test Procedure," and Table II. Pf in per cent versus aging time in hours is plotted with the use of before and after humidification conditions in Figs. 5, 6, 7, 8, and 9. After humidification, pf measurements were made within 20 minutes of removal of models from the humidification tank. Before humidification, pf measurements were made at the end of the 4-hour cooling period after the 48-hour temperature aging.

Consider, for example, the high-voltage to low-voltage and ground set of pf measurements. After humidification, pf values fluctuate as normally occurs during moisture release or curing of resin varnish. Before humidification, pf values are practically constant for the entire cycling considered. The initial pf value at 275 C aging is 5.1%. Through 10 cycles of heat aging, the per-cent pf value terminates at 5.1%. In this set of measurements the barrier insulation is predominant in the system.

Constant pf values can be noted also for the before-humidification conditions through all cycling for the high- and low-voltage winding to ground measurements.

These practically unchanged pf values are of significance. Silicone resins because of their water-repellant nature prevent penetration of moisture in small cracks of varnish film. Older kinds of bonding and impregnating resins, after exposure to 90% humidity and heat cycling, may permit entrance of moisture below the surface film. As a result of shrinkage at high temperatures, some resins may become loose and brittle. Silicones have the toughness and resiliency to withstand stresses under abnormal conditions.

Relation of Functional Test Models to Dry-Type Transformers in Service

Transformers, having a similar silicone glass fiber insulation system based on a permissible 180-C hottest-spot rise, have been in use since 1951.[8] Ratings extend from 250- through 2,000-kva, and 5- through 15-kv ratings. Typical core and coil construction for a 500-kva, 3-phase, silicone-insulated transformer appears in Fig. 11. This transformer, with a sealed-in nitrogen enclosure, is illustrated in Fig. 12.

These transformers, utilized for unit substation, network, and station auxiliary service, are designed for 150-C average rise by resistance and 30-C permissible hottest-spot rise. This means that in 40-C maximum ambient temperature, the permissible hottest-spot winding temperature is 220 C in conformity with present NEMA standards for group 3 dry-type transformers. Subjected to varied load and overload conditions, these transformers, now numbering about 100 units, have given excellent performance. Mostly, sealed-in nitrogen construction is utilized to ensure freedom from dirt and contaminating conditions.

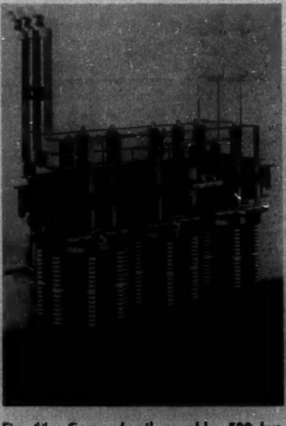

Fig. 11. Core-and-coil assembly, 500 kva, 3-phase, 150-C rise

Model transformers, as described in this paper, were aged at 275- and 350-C temperatures or at least 55- and 130-C higher temperatures than the hottest-spot temperature of 220 C permissible in dry-type transformers. Transformers would seldom be subjected in service to such extreme heat cycling, humidity, and voltage conditions as withstood by models. By functional tests, the user is assured that operating margins exist, that failures become remote, and that the manufacturer has taken care to produce a reliable transformer.

In service, transformers of ventilated construction after being exposed to humid conditions are not frequently subjected to voltages of 31 kv from high-voltage winding to ground. A dry-out period may

Fig. 12. Sealed-in nitrogen transformer, 500-kva, 3-phase, 150-C rise

be allowed or lightning arresters can be utilized. Barrier insulation flashovers, as experienced in the models having less creepage distance (high-voltage winding to ground) than that for 15-kv transformers, become of less concern when operating conditions are considered. In practice, the increased creepage distance utilized lessens the possibility of flashover. The fact remains that cycling and voltage tests did not produce holes in the silicone glass fiber barrier insulation system.

Conclusions

1. Tests demonstrate that a 15-kv class model is practical.

2. By utilizing heat, voltage, and humidity cycling, a functional test procedure on models develops voltage stresses and temperature gradients more severe than those ordinarily found for transformers in service. Tests on a model can be more numerous, varied, and accomplished at less cost than tests on complete transformers. Test data obtained by interested transformer manufacturers can be compared.

3. Silicone insulation system data are now available for a test code on functional temperature endurance tests on ventilated dry-type power and distribution transformers.

4. Failure by puncture of the silicone glass fiber barrier insulation was not obtainable in spite of the severity of the tests. At 200-C aging, no flashovers occurred from the high-voltage winding along the barrier insulation surface to the end of the plate (ground) after humidification in 7 cycles' duration of the test. A 275-C aging, flashovers occurred at 1.5 cycles, but upon removal of the end plates, up to 8.5 cycles were withstood before flashover after humidification in 10 cycles' duration of the test. At 350-C aging, flashovers occurred from 0.5 to a maximum withstand of 3.5 cycles, and end plates were not removed in 4 cycles' duration of test. If flashover occurred after humidification for a given cycle, flashover would again take place after the heat aging and humidification on subsequent cycles.

5. Future consideration should be given to increasing the high-voltage winding to ground clearance in the model used. Ordinarily, a full-sized transformer utilizes about a 1-inch greater creepage distance. But the purpose of the test was realized in determining whether creepage or puncture of the barrier would result for the clearance used. The purpose of the test cycling was to determine its adequacy rather than to test a specific transformer design.

Variable insulation flashovers, without puncture of barriers, constitute a debatable question about failure. Increased creepage distances may change the conditions entirely. Therefore, no attempt was made to plot time of variable flashovers (life) on logarithmic ordinate scale graph paper, having the reciprocal of absolute temperature scale to represent temperature aging as the abscissa.

6. After humidification only, voltage proof testing resulted in barrier flashover. Models having thermocouples withstood all heat cycling through as many as 17 cycles at 275 C (34 days of heat aging, 17 days of humidification at 90% humidity). Models having thermocouples could not be subjected to voltage tests. After thermocouples were removed on the unit exposed to 17 cycles at 275 C, a maximum voltage of 45-kv rms (45% above test) was withstood for 1 minute (high-voltage winding to ground).

7. Even though the turn-to-turn voltage strength and other requirements demanded by the tests exceeds those found for transformers in service, the fact remains that the test method dictates the margin of strength available. Development of insulating materials for wire covering can proceed accordingly.

8. Data presented in this paper for models plus the service record of 100 transformers having similar insulation systems, offer support for the recent action by NEMA in establishing for group 3 transformers a permissible 180-C hottest-spot rise. Ratings of these transformers extend from 250 kva through 2,000 kva, 5- through the 15-kv class, and designs are based on the temperatures proposed by the new NEMA standards.

References

1. Temperature Classes for Dry-Type Transformers as Determined by Functional Tests, **Paul Narbut.** *AIEE Transactions*, vol. 72, pt. III, Oct. 1953, pp. 917–23.

2. Standards for Transformers. *NEMA Publication No. TR1-1954*, National Electrical Manufacturers Association, New York, N. Y., par. TR1-2.012.

3. Proposed Guide for Operation and Maintenance of Dry Type Transformers with Class B Insulation. *AIEE Standard No. 53*, Oct. 1952.

4. General Principles Upon Which Temperature Limits Are Based in the Rating of Electric Machines and Other Equipment. *AIEE Standard No. 1*, Feb. 1954.

5. Tentative Proposal for Classification of Insulating Materials. International Electrotechnical Commission, London, England, Technical Committee No. 2, Subcommittee 2C, Aug. 1954.

6. Insulation Systems for Random-Wound Motors Evaluated by Motorette Tests, **T. J. Gair.** *AIEE Transactions*, vol. 73, pt. III, 1954 (Feb. 1955 section), pp. 1702–07.

7. Aging Evaluation of Dry-Type Transformer Insulating Systems, **H. C. Stewart, L. C. Whitman, A. L. Scheideler.** *AIEE Transactions*, vol. 72, pt. III, Apr. 1953, pp. 267–77.

8. The Application of Class-H Insulation to Transformers, **Melvin L. Manning.** *AIEE Transactions*, vol. 70, pt. II, 1951, pp. 1427–38.

◆

Discussion

Yale Goldberg (Iowa Power and Light Company, Des Moines, Iowa): When a utility man enters a discussion relative to transformers whether it be concerning design, maintenance or operation, economics are of prime importance. We are familiar with the oil-immersed transformer and the various types of insulation class *A*, class *B*, class *O*, and the comparatively new class *H*.

As the load current in any transformer is increased its temperature rises because of greater losses. The material most subject to damage by heat in a transformer is the insulation. There is insulation in the core and in the windings, but since the core losses are nearly constant for all loads, it is the insulation on the windings which causes concern. It is known that any insulating material deteriorates; that deterioration is a function of both temperature and time; that the higher the temperature the greater the rate of deterioration; and that any operation of a transformer reduces its life.

Through research, an insulation was developed such as class *H* with a suggested limiting hottest-spot temperature of 180 C. A factor such as greater safety in operation because of the use of materials less combustible, as those found in class-*A* insulation in an oil-filled transformer, is important. Oil-filled transformers are probably the most widely used type. Liquid-filled are perhaps next in number used and lastly the dry-type transformer. Safety is a watchword in every utility today. Any improvement in equipment which lends itself to safer operation is given every consideration.

Network areas are usually in dense load sections of town. In these areas large numbers of people move about. Many underground vaults are constructed in sidewalks and open gratings are used for ventilating purposes. When oil-filled transformers are used in installations such as these, there is a hazard to pedestrians passing over the vaults should an explosion occur which could throw hot oil and possibly fire. If a liquid-filled transformer in such a vault should fail or explode, there would be fumes of a pungent nature which could harm pedestrians.

We experienced the failure of a liquid-filled transformer which occurred in a transformer room beneath an alley adjacent to retail stores. There was a long delay in restoring a bank to service because of the need for airing out the vault sufficiently to permit the men to enter and clean up the damage. Many complaints were registered by adjacent store proprietors, and one could not help but wish for some dry-type or other transformer which would not be subject to similar damage. In fact, the solution to a problem of this nature may well be the use of a sealed dry-type transformer which has no combustible material in its makeup.

The use of an insulating material which can be subjected to higher temperatures such as class *H* should permit an over-all smaller transformer. Large numbers of vaults exist with fixed hatchways in their tops which will not permit passage of transformers of over certain dimensions. A reduction in the physical dimensions of transformers with an increase in kilovolt-ampere ratings would certainly appeal to the cost-conscious utility group. This is especially true today, as statistics indicate that electric loads have grown and it is generally predicted that future consumption will be even greater.

We are contemplating the conversion of some 4-kv network vaults to 13-kv network. Transformers of correct size both electrically and physically will permit the use of existing hatchways, eliminating the need for rebuilding transformer manhole tops and thereby allowing the conversion to be completed with minimum cost.

The author has presented a valuable and timely paper based on tests and practical experience. His test results are very interesting and quite comprehensive. The rugged tests on the 15-kv models are evidence that much progress has been made toward the production of a safer 15-kv dry-type transformer which should be gratifying to those utility men who work with network transformers. With continued research, production costs should be reduced and the dry-type transformer will rightfully take its place in the utility picture.

Perhaps newer types of insulation will be developed with the co-operation of the chemist and the electrical engineer which may still further reduce the physical size and still be economically practical. Perhaps gas other than nitrogen will be found for use in sealed dry-type transformers which will be even more efficient.

A. F. Phillips (Duquesne Light Company, Pittsburgh, Pa.): Mr. Manning has made a very interesting and useful contribution to the art of model testing dry-type transformers. Data on the aging of insulation are needed to demonstrate the reliability of the three groups of dry-type transformers when operating at their permissible hottest-spot limits. The test data summarized in the paper indicated that seven models, which are rated at 180 C rise (220 C total temperature), withstood 275 C for 14 days and that one model withstood 275 C for 34 days. A few tests were made at 350 C. Although it is a good start, the limited test data presented in this paper are not enough to establish the life criteria for this type of equipment. It would be desirable to increase the creepage distances so that actual failures could be obtained from which a life versus aging temperature plot could be made as the author mentions in his conclusion 5.

Data on the aging of class-*H* insulation and information on the method of calculating hottest-spot temperatures of overloaded class-*H* transformers are needed by the utilities to aid in the assignment of emergency operating ratings. Occasionally it may be necessary to operate a 220 C transformer at 275 C. It is very difficult to understand the significance of test data at temperatures over rated value if means of interpreting them in terms of per-cent load are not known. The tables in the paper list the winding currents in the models necessary to maintain the three different test temperatures, but these values cannot be translated into per-cent load on an actual transformer.

Since the author has developed the knowledge and technique of running model tests at very high temperatures, he should be encouraged to continue the work as these data are essential to the economical operation of this type of equipment.

Dr. A. A. Halacsy (I-T-E Circuit Breaker Company, Philadelphia, Pa.) The tests showed that creepage sets the limit to the voltage in dry-type transformers. Does the author think it possible and practical to build dry-type transformers for voltages higher than the 15-kv class in the light of the difficulties experienced in creepage?

W. W. Satterlee (Westinghouse Electric Corporation, Sharon, Pa.): In commenting on Mr. Manning's interesting paper, I desire to compliment the Chairman of the AIEE Working Group on Life of Materials, John L. Cantwell, for his capable guidance of the activities of the Group, and, less directly, the members of the Subgroups who have been studying the temperature classifications of insulation structures for dry-type transformers during the past few years.

Mr. Cantwell appointed the first Subgroup of four members of the Working Group in November 1952 to study the functional evaluation of insulation systems for dry-type transformers. The Subgroup agreed that there were two possible approaches to the subject: first, the testing of insulation elements, i.e., component parts for use in an insulation structure, or second, the testing of complete insulation structures as used in transformers. The first approach may be called the component method; the latter, the model method of testing.

At a later meeting this Subgroup agreed that it would work to effect a recommendation for the model method of testing to establish bench marks for temperature classes of insulation systems for dry-type transformers and the preparation of a test code for this purpose. The work of this Subgroup was completed in May 1953 with the preparation of a tentative test code, including the design of a particular model for use in laboratory testing of insulation structures. In June 1953 the Working Group agreed that the work of the Subgroup represented a step in the direction of standardization and the establishment of design codes based on model tests, because temperature limits are determined not only by the chemical structure of the insulating materials but also by the manner in which they are used in an insulation structure.

The proposed test code deals with functional testing and temperature classification rather than with the testing of components and the classification of materials. To continue this work, Mr. Cantwell appointed a second Subgroup to consider modifications of the proposed test code in accordance with suggestions of the Working Group and to set up a program for obtaining the basic data required to establish the model method of testing and the requirements of the code. Since then, members of this Subgroup have done a considerable amount of model testing of insulation structures for the purpose of establishing the workability of the proposed test code. Mr. Manning's paper represents a contributing portion of this work.

However, interpretation of the author's results is difficult. In doing this, one should keep in mind the original objective as formulated by the Subgroup. It was to give laboratory trial to the test procedure specified in the code and to the specific model recommended for the testing of a 15-kv insulation structure. It was not intended at this time to use the test code to determine the permissible operating temperature for any specific insulation structure. Due consideration of these things may help in understanding the author's results.

In the tests Mr. Manning describes, flashovers occurred in the models. Thus, if flashovers are taken as insulation failures, which is a provision of the test code, the author's results show the life of the models to be very short. For instance, at 275 C the life of group 3 transformers may be expected to run over 5 cycles of 8 to 16 days' duration instead of 3 to 4 cycles at 48 hours each.

One possible reason for the apparent short life of the models is, as the author points out, insufficient electrical clearance in the models. If so, we must acknowledge that the results of the author's tests, as related to the permissible operating temperature, are not conclusive and that additional tests designed to specifically determine the permissible operating temperature for group 3 dry-type transformers are very desirable. However, when one considers that the intended objective of the tests was to help establish the validity of the proposed test code, then the author's work constitutes a valuable addition to the entire efforts of the Subgroup. Mr. Manning deserves much credit and he is to be commended for his co-operation with the Subgroup on this overall subject.

M. L. Manning: Comments by the discussers are appreciated. A practical approach to operating problems is a necessity. In dealing with the subject, it must be remembered that data were not available for such severe temperature and humidity cycling as outlined for a test cycle in the paper for a 15-kv class silicone glass fiber insulation system. A model structure was agreed upon by the Subcommittee for laboratory trial. Numerous models must be tested in conformity with a test code, when available, to arrive at answers to all questions. The purpose of this initial paper dealing with group 3 dry-type transformers was to verify if a 15-kv class model is practical, to devise a practical test procedure, yet impose operational conditions, and to obtain helpful information for a test code by establishing a few beacon lights for possible aging temperatures. The validity of a possible test code must be established. It should be realized also that much thought and planning was required in the AIEE Working Group on Life of Materials and in the Subgroup on Functional Tests. Other members of the Subgroup studied lower temperature group 2 transformer insulation systems while the author was given the responsibility for group 3 (high temperature) insulation systems.

Of importance is the fact that only heat cleaned glass fiber base material and high temperature withstanding silicone resins and rubbers were used in my system. Unless oil and sizing is removed from glass fibers, insufficient bond strength of the resin to the fibers exists and delamination will occur at high temperatures. This fact is highly important when considering insulation systems aged in air at 275 C and 350 C. The end or failure points at such high temperature cycling are dependent upon the quality of the insulation system.

Mr. Goldberg's comments offer support to safety features desired by most operating people. Unless an insulation system considered for functional tests at high temperatures meets safety from fire and explosion hazards where human life is in danger, the system cannot be practical from a user's point of view. The insulation system described in the paper is free from volatile oils and toxicity, will not support combustion, and can be used at 220 C hottest-spot temperature in air or nitrogen. In case nitrogen leaks from a tank in a network transformer having this insulation system, load can be maintained until resealed. Conclusions that danger from fire and explosion is eliminated are verified elsewhere.[1] As Mr. Goldberg points out, by continued usage the economic picture for high temperature materials can be changed to decreased costs. A similar situation existed about 14 years ago when phenolic impregnated and bonded glass fiber materials were first introduced. Use of gases other than nitrogen to reduce dimensions of sealed transformers are under study; results are encouraging. The problems encountered by Mr. Goldberg in the application of network transformers are interesting.

Mr. Phillips emphasizes an important fact that more work is required to get possible answers to end-of-life points for insulating materials. This problem has plagued engineers for many years. For the silicone insulation system described in the paper for group 3 transformers, it is hoped that a few guideposts are established in arriving at suitable test code aging temperatures. A functional or prototype test method will assist greatly in estimating emergency temperature limits. But it must be remembered that correlation with transformers in service is necessary. Models alone cannot establish a direct relationship with transformers with respect to current density in windings, core heating, and circulatory effect of cooling by ducts. An insulation system is evaluated by a test model to give the user and manufacturer information concerning this system. Actual stresses on the insulation, both thermal and electrical, are imposed by the cycling. It is helpful to know that Mr. Phillips is in accord with the indea for continuing the work in obtaining data essential to the economical operation of transformers.

Dr. Halacsy questions the possibility of voltage creepage as setting the limit to the voltage rating of dry-type transformers. Perhaps in the models voltage creepage appeared to establish the end point but it will be recalled that the 3-inch creepage distance of the high-voltage winding to ground (end plate) was set to determine if creepage or flashover would occur. Actual 15-kv class transformers use greater creepage distances, hence the next step is to increase the distance in the models since the basic question was answered in that the barrier structure did not puncture. If certain operational characteristics such as higher impedance and dimensions are permissible, it does appear possible to build dry-type transformers higher than 15-kv class, particularly by use of perfluorocarbon gases for sealed units. Development work is proceeding in this direction.

Mr. Satterlee outlines an interesting review of the committee work in establishing the background of the paper. At a later date, the combined work of the AIEE Working Group on Life of Materials and the Subgroup will be presented. My work deals with an insulation system having a 70 C higher permissible hottest-spot winding temperature, hence the problems differ in many respects from the insulating systems studied by other members of the Subgroup.

Mr. Satterlee comments that my results are difficult to interpret in that at this time the test code was not intended to determine the permissible operating temperature for any specific insulation structure. I wish to make the point clear that no test code or bounds for aging temperature limits were in existence at the time the models were tested. The purpose of the testing was to establish the validity of requirements that might be met in formulating a test code. But we must remain practical in correlating data established by a test code with transformers in service. In this manner we can obtain better answers to insulation problems. Conclusions in the paper amplify my viewpoint. Additional tests on models will be made, utilizing increased creepage distance to obtain puncture of barrier insulation.

It is hoped this initial paper will arouse interest in obtaining good answers to end-of-life aging questions and overloads on transformer insulation systems which have been of concern to engineers for many years. Users and manufacturers of transformers must co-operate to enjoy success.

REFERENCE

1. *Discussion* by M. L. Manning of SEALED DRY-TYPE TRANSFORMERS PROVED SAFE BY TEST, E. W. Tipton. *AIEE Transactions*, vol. 72, pt. III, Aug. 1953, pp. 847–48.

An Experimental Gas-Insulated 138-Kv Current Transformer

G. CAMILLI
FELLOW AIEE

IT IS well recognized that under special conditions the dielectric strength of some gases is superior to both liquid and solid insulation. The low dielectric loss of these gases, their self-healing qualities, and relatively low cost are outstanding characteristics which are very useful in some applications. Thus compressed Freons and sulphur hexafluoride have been used in high-voltage capacitors where low dielectric loss is essential, and in X-ray transformers where reduced dimensions and nonflammability are of primary importance. Recently, compressed fluorocompounds have also found application in the production of very high voltages for nuclear physics work.

As far as the author knows, gas-insulated apparatus has never before been built for operation on a commercial power system where the equipment may be subjected to surges and lightning voltages. An experimental 138-kv gas-insulated current transformer is described which withstood all the commercial tests both at low frequencies and impulse voltages levels as specified in the American Standards Association Standards for transformers.[1] Three types of insulating mediums are discussed, solid, liquid, and gaseous, and the reasons why gas insulation was chosen are given.

The Influence of the Insulating Medium on the Type of Construction

Since solid insulation generally has higher dielectric strength than either liquid or gaseous insulators, there is no doubt that solid insulation, either in the form of resin-impregnated fibrous material or cast synthetic resins, leads to the most compact designs. In this case, however, the complete elimination of voids is of paramount importance. Another problem which needs to be considered is the dissipation of heat under normal and overload conditions. The eyebolt design in which the solid insulation (paper) is impregnated with oil as in an oil-filled cable is a good compromise. It will be noted that in this case, Fig. 1, the high-voltage winding is enclosed in a metal shield and the solid insulation is wound over the shield. In high-voltage transformers where the thickness of the insulation is

---

Paper 55-12, recommended by the AIEE Transformers Committee and approved by the AIEE Committee on Technical Operations for presentation at the AIEE Winter General Meeting, New York, N. Y., January 31–February 4, 1955. Manuscript submitted September 16, 1954; made available for printing October 28, 1954.

G. CAMILLI is with the General Electric Company, Pittsfield, Mass.

The author acknowledges with grateful appreciation the help given by C. D. Geisler in the preparation of this paper.

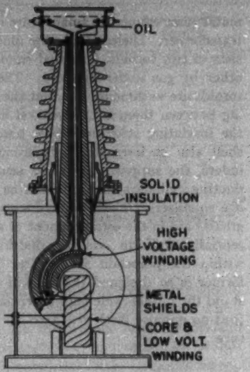

Fig. 1. Cross-sectional view of the conventional high-voltage current transformer

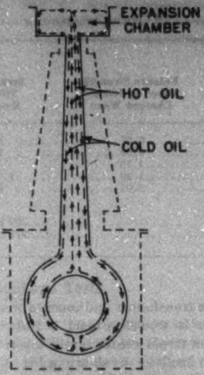

Fig. 2. Cooling diagram of the conventional high-voltage current transformer

Fig. 4. Internal view of the 138-kv gas-insulated current transformer showing the low-voltage shield and high-voltage shield

appreciable, there will be little or no heat dissipation through the solid insulation. The cooling is provided by the circulation of the oil existing between the shield and the high-voltage winding, as shown in Fig. 2.

When solid insulation with no trace of liquid is used, the casting material encloses only the low-loss dissipating elements of the current transformer. In a current transformer, most of the heating is produced by the high-voltage winding inasmuch as the low voltage winding carries only 5 amperes at full rated primary current, and the iron core operating at very low flux densities (ordinarily at less than 1,000 gausses) has little loss to dissipate.

Current transformers in which the main insulation consists exclusively of an insulating liquid have not been looked at very favorably by those familiar with high-voltage phenomena. The main objection being that particles such as lint, or bits of paper, especially if wet, may be attracted into the regions of high dielectric stresses and produce internal flashover. Therefore, it has been a generally accepted parctice to introduce between the high- and low-voltage windings some sort of an insulating barrier, or barriers, with a total thickness so proportioned that in the case of momentary complete breakdown of the liquid the solid insulation by itself is sufficient to withstand the impressed voltage for a very short time. Under some conditions, the barrier actually stops streamers and spittings, thereby preventing full spark-over. A streamer hitting a barrier in a liquid splashes a short distance and is quenched.

In the case of a gas-insulated transformer with no forced circulation, there will be no extraneous or foreign material which may float in the insulating medium; therefore, there will be no need for any discontinuity in the insulating structure. Furthermore, a streamer hitting a barrier in gas is possibly more self-perpetuating because of the longer free-path distances between molecules. It should also be recognized that owing to the wide difference between the permittivities of solids and gases the corona-starting voltage, for a given total dielectric distance, will be lowered by the introduction of a barrier into the gap.

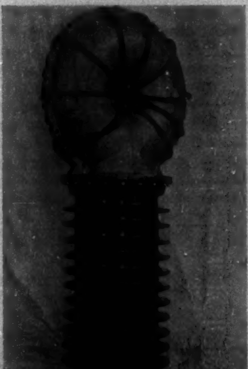

Fig. 3. External view of the 138-kv gas-insulated current transformer

It might be argued that in case of failure in the all-gas insulating structure the low-voltage winding may be brought up to the voltage level of the high-voltage winding. This difficulty can be easily overcome by enclosing the low-voltage

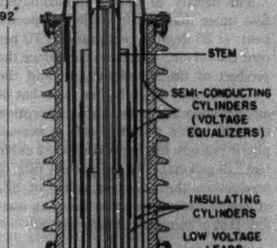

Fig. 5. Cross-sectional view of the 138-kv gas-insulated current transformer

Table I. Dielectric Tests on the 138-Kv Gas-Filled Current Transformer

Gas Pressure, Pounds Per Square Inch Gauge	Impulse Polarity	Impulse Tests Maximum Withstand Voltage, Kv-Crest	Relative Strength Based on 750-Kv Chopped Wave	Breakdown Voltage, Kv-Crest
5	+	575	0.77	600
10	+	720	0.96	745
15	+	850	1.13	
20	+	970	1.29	1,025
10	−	775	1.03	800
		60-Cycle Tests		
0		289 kv rms		302 kv rms
5		357 kv rms		371 kv rms
10		371 kv rms		

winding within a shield which is solidly connected to ground. It is interesting to note that while in a conventional liquid-insulated transformer the insulation strength is mainly dependent upon the thickness and quality of the insulating material, in a gas transformer a third variable, pressure, is introduced with a subsequent increase in the flexibility of the insulating structure.

Among the various gases, the fluorogases are of particular interest in high-voltage applications because of their generally inert character and high dielectric strength.[3] The fluorogases of most interest are the Freons, sulphur hexafluoride, and the fully-fluorinated compounds such as C_2F_8.

Characteristics of the Gas Used in This Experimental Transformer

In this experimental transformer, sulphur hexafluoride was selected as the gas which has the most advantageous characteristics.[4,5] Under normal service conditions, SF_6 is inert and nonflammable and produces no harmful effects on personnel if it accidentally escapes from the apparatus.

The density of SF_6 is approximately five times that of air while its specific heat, at 55 degrees centigrade, is 70 per cent that of air. It follows that, since the product of the specific weight and the specific heat of SF_6 is higher than that of air, SF_6 has a higher total heat absorption than air. One pound of SF_6 at atmospheric pressure fills approximately 2 cubic feet (19 gallons). At the present rate of production, the price per gallon of SF_6 at atmospheric pressure is less than one-half that of standard transformer oil.

Description of the Gas-Insulated Transformer

The transformer is of the porcelain clad type. The most striking feature is that the high-voltage winding is external to the transformer and consists of a cable which is wound around a hollow aluminum toroid located on the top of a porcelain insulator, as shown in Fig. 3. The toroid is connected to one terminal of the high-voltage winding and encloses the core, the low-voltage winding, and a grounded toroidal shield for the low-voltage winding, as shown in Figs. 4 and 5.

Both the high-voltage and low-voltage toroidal shields are split into two sections, the low-voltage shield being supported by the secondary winding and the core. The latter is held up in position by a metal stem connected to the base of the transformer. Dielectrically the unit consists of two toroids, insulated from each other by gas under pressure. The two toroids are so dimensioned that the spacing between them is the weakest link in the insulating structure. The porcelain shell also encloses three insulating cylinders, the supports for three semiconducting cylinders that function as voltage equalizers. These voltage equalizers greatly aid in the establishment of an essentially uniform voltage distribution within the porcelain shell. The transformer is so designed that it will withstand the full 60-cycle high-potential test (but no impulse test) with zero gas pressure.

Dielectric Tests

The experimental unit has been tested at both 60 cycles and impulse voltages, with the results shown in Table I. It should be noted that in accordance with American Standards Association Standards[1] the required 1-minute 60-cycle test for 138-kv transformer winding should be 277 kv, while the 1-minute 60-cycle with-

Table II. Accuracy Characteristics of the Gas-Insulated 138-Kv Current Transformer, 60-Cycle Tests

Positioning of Conductors	No. of Turns	Connection	Burden Volt-Amperes	Burden Power Factor	Secondary, Amperes	Radio Correction Factor	Phase Angle
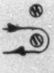	1	2,000 to 5	2.5	0.90	0.5	1.0016	+13
					1.0	1.0001	+ 9
					2.0	0.9993	+ 6
					3.0	0.9989	+ 5
					4.0	0.9987	+ 4
					5.0	0.9886	+ 4
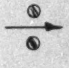	1	2,000 to 5	2.5	0.90	0.5	1.0016	+13
					1.0	1.0002	+ 9
					2.0	0.9993	+ 6
					3.0	0.9987	+ 5
					4.0	0.9987	+ 4
					5.0	0.9986	+ 3
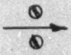	1	2,000 to 5	50	0.50	0.5	1.0079	+ 9
					1.0	1.0047	+ 5
					2.0	1.0025	+ 3
					3.0	1.0015	+ 2
					4.0	1.0009	+ 2
					5.0	1.0009	+ 1
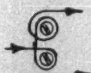	2	1,000 to 5	2.5	0.90	0.5	1.0010	+13
					1.0	0.9999	+ 9
					2.0	0.9980	+ 6
					3.0	0.9988	+ 5
					5.0	0.9984	+ 3
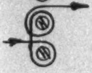	2		50	0.90	0.5	1.0075	+ 9
					1.0	1.0043	+ 6
					2.0	1.0020	+ 5
					3.0	1.0013	+ 4
					5.0	1.0003	+ 2
	10 evenly distributed over toroid	200 to 5	2.5	0.9	0.5	1.0014	+14
					1.0	1.0001	+ 9
					2.0	0.9990	+ 7
					3.0	0.9988	+ 5
					5.0	0.9984	+ 4
	10 evenly distributed over toroid		50	0.5	0.5	1.0074	+ 9
					1.0	1.0043	+ 6
					2.0	1.0021	+ 4
					3.0	1.0014	+ 3
					5.0	1.0003	+ 2

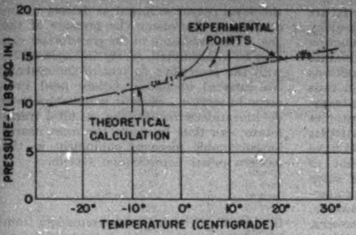

Fig. 6. Internal pressure versus temperature of the 138-kv gas-insulated current transformer

stand voltage for a 138-kv bushing should be 335 kv. Also, the high-voltage winding of the transformer should withstand impulse tests to ground of 650 kv (standard full wave) and 750 kv (chopped wave).

It is interesting to note that during the dielectric tests a transformer of this type can be repeatedly spark-discharged internally without any apparent damage. Therefore, by a few trials at various working pressures, the insulation strength can be placed, within limits, at the most desirable level This is a unique feature of the gas-insulated transformer which cannot be conveniently duplicated by the conventional liquid-filled transformers. From the foregoing test results, it appears that a working pressure of 10 pounds per square inch gauge, at 25 degrees centigrade, is sufficient to meet the various dielectric tests required.

Accuracy Characteristics

From the standpoint of its accuracy the transformer can be thought of as essentially a through-type current transformer in which the number of turns of the primary winding can be changed to maintain a constant, predetermined number of ampere-turns. By making suitable changes in the number of high-voltage turns, and in some cases by selecting the proper low-voltage tap, any standard ratio of transformation of from 1 to 1 to 400 to 1 is obtainable. To obtain good accuracy without the use of any compensating scheme, the transformer is designed for operation at 2,000 ampere-turns. Thus, the transformer can be used for a large range of primary currents.

While it is desirable that the primary winding be evenly distributed around the circumference of the toroid, the results shown in Table II indicate that the accuracy of the transformer is not influenced by the unsymmetrical positioning of the turns. For relaying service, the current transformer has an accuracy-class rating of *10L800*.

Gas-Leakage Tests

The current transformer, which was built in the fall of 1946, has shown no appreciable leakage of gas in all these years. The unit was first filled with nitrogen about June 1, 1947. For about 4 weeks, frequent readings of temperature and gas pressure were made. At the end of that time, as no leaks had appeared, the nitrogen was replaced with sulphur hexafluoride and the unit was placed in an outdoor testing area and energized at 150 kv, 60 cycles to ground. Readings of temperature, gauge pressure, and barometric pressure were made each day until September, 1948, and thereafter once each week. Fig. 6 shows that the relationship between pressure and temperature readings checks very closely with theoretical calculations, indicating that the unit can indeed be made gas-tight by using ordinary rubber gaskets. Samples of the gas obtained after the transformer was continuously energized for 3 years contained no decomposition products.

Tap for Potential Measurements

A capacitance tap can be readily added to a gas-insulated transformer. Since the dielectric constant of the gas does not change appreciably with temperature, it appears that a capacitance divider could be built which would be more accurate than the conventional apparatus which utilizes liquid-filled components.

Explosion Characteristics of the Gas-Insulated Transformer

When a failure occurs, the pressure developed in a gas-filled transformer is only a fraction of that developed in a liquid-filled unit. The pressure from the arcing of sulphur hexafluoride develops from thermal excitation of the gas rather than from the formation of a large amount of dissociation products. As mentioned, before, under breakdown conditions, the arc occurs between the two torodial shields. The pressure of a moderate cushion of gas located at the arc prevents any very rapid build-up of pressure throughout the remainder of the transformer and, therefore, it would be feasible to relieve the pressure by means of a relief diaphragm and so prevent it from reaching dangerous values.

Conclusions

An experimental current transformer has been developed in which the main insulation consists exclusively of a fluorinated gas under pressure. It appears that this type of transformer has several advantages over the conventional liquid-filled unit, especially for voltages higher than 115 kv. They weigh considerably less than comparable liquid-filled units. These units can be operated in any position; they have unlimited ratio adjustment; and their inherent insulation strength can be readily determined. While designed to operate at 10 pounds per square inch gauge, under certain conditions they can operate satisfactorily with the gas at atmospheric pressure.

References

1. TRANSFORMERS, REGULATORS, AND REACTORS. *C57*, American Standards Association, New York, N. Y., 1948 and 1949.

2. NEW DEVELOPMENTS IN CURRENT-TRANSFORMER DESIGN, G. Camilli. *AIEE Transactions*, vol. 59, 1940, pp. 835–42.

3. FLUORINE CONTAINING GASEOUS DIELECTRICS, G. Camilli, R. E. Plump. *AIEE Transactions*, vol. 72, pt. 1, May 1953, pp. 93–102.

4. GASEOUS INSULATION FOR HIGH-VOLTAGE TRANSFORMERS, G. Camilli, G. S. Gordon, R. E. Plump. *AIEE Transactions*, vol. 71, pt. III, Jan. 1952, pp. 348–57.

5. DIELECTRIC BREAKDOWN OF SULFUR HEXAFLUORIDE IN NONUNIFORM FIELDS, C. N. Works, T. W. Dakin. *AIEE Transactions*, vol. 72, pt. I, Nov. 1953, pp. 682–89.

◆

Discussion

H. R. Lucas (Canadian General Electric Company, Ltd., Toronto, Ont., Canada): Much has been said of the advantages of automation in removing the load of drudgery from human shoulders. Any development which will remove an onerous, time-consuming, and monotonous operation from a manufactured article can be classified along with automation as an ultimate benefit to humanity. Of such a nature is the development described.

In a conventional design of an oil-filled current transformer, the high-voltage coil must be insulated by taping on solid insulation which is subsequently dried and oil-impregnated under high vacuum and with great difficulty. Because of the irregular shape of the coil, it is impractical to apply the tape by machine. The work must therefore be done by hand. Several hundred pounds of tape may be applied to a single coil in a monotonous wrapping operation which may take 100 hours or more to complete. The drying and oil treatment of the masses of insulation so applied takes days and even weeks in the larger sizes of oil-filled transformers.

In contrast, the gas-filled transformer, having its insulation inserted by the mere opening of a valve, takes no longer to apply insulation to than the time required to inflate an automobile tire. Also, having a negligible quantity of hygroscopic insulation the problem of treatment to remove moisture is practically eliminated, and the time required for this operation is reduced from many days to a few hours.

From a design engineer's point of view, the desirability of knowing the exact margin of safety attained in his design must be tempered by the cost of finding out the breakdown level of an expensive sample or prototype. Limited numbers of tests are therefore performed, and fairly healthy margins of safety are used on production designs to allow for manufacturing variables and experience factor. Under no conditions can the actual breakdown level, and thus the factor of safety, of the particular transformers built for shipment to the customer be found by test. Tests done on samples show the factor of safety which would have been obtained, if the same amount of identical insulation is applied the same way to an identical structure in the production design. Variations do occur, however, in the materials themselves, the processes, and in the human element. For these reasons no manufacturer will willingly exceed the recognized insulation test levels on a transformer built for a customer, even though he knows the margin of safety in his design was 30 or 40 per cent on the prototype samples.

With the gas-filled transformer this objection is removed. Not only can the actual insulation puncture or flashover level be determined by nondestructive testing but this level can be adjusted as desired by increasing or decreasing the pressure of the gas. The insulation in the transformer can thus be co-ordinated, surely and accurately, with the protective devices of the system. No internal insulation failure need ever occur in service. Since it is not subject to deterioration with age, the gas-filled transformer can thus be made the most nearly indestructable piece of equipment in the modern power transmission system.

G. Camilli: The favorable comments from Mr. Lucas are gratifying and are very much appreciated by the author. While the 138-kv current transformer described in this paper was insulated with sulfurhexafluoride, it should be noted that new gases are being developed for electrical purposes. It is possible that some of them may have superior characteristics in which case the size of the transformer can be reduced without impairing its operating characteristics.

Results of High-Current Tests on 161-Kv Disconnecting Switches

A. M. McNERNEY
ASSOCIATE MEMBER AIEE

THE trend toward heavy power concentrations, starting in the Tennessee Valley Authority (TVA) area in 1951, led to the development of 10,000-megavolt-ampere circuit breakers for 161-kv service, with anticipation of 15,000-megavolt-ampere interrupting ratings.[1] At the same time, continuous-current ratings up to 1,600 amperes were required. The industry, however, had failed to develop disconnecting switches to meet the same service.

To stimulate the development of new designs of switches, or modifications of existing designs, the TVA announced in May 1952 a program of high-current testing of disconnecting switches. A momentary current of 62,000 amperes rms was specified to co-ordinate the switch capability with the circuit-breaker rating.[1] Manufacturers were invited to submit samples to meet the increased requirements. No limit was placed on the number of variations in design which could be submitted for test. The conditions applying to the tests and the testing equipment are described by Gostin.[2] The tests and test results on switches submitted by manufacturers as well as on old switches taken out of service are described in this paper.

Scope of Tests

The announced scope of tests to be performed on new 1,200- and 1,600-ampere switches submitted by manufacturers was as follows:

1. 60-cycle momentary current test at 62,000 amperes rms in six successive shots, each not more than of 10-cycle duration. Time intervals between the first three shots, approximately 20 cycles; between third and fourth shot, approximately 10 minutes; between the last three shots, approximately 20 cycles. (While 20 cycles was specified as the interval between test shots, the limitations of the equipment were such that the interval actually was about 70 cycles.)
2. Temperature test at continuous-current rating of switch.
3. Momentary current test at higher current values.

Momentary current and temperature tests were also made on a number of old switches which were removed from service at locations on the system where the duty had become critical. These tests were designed to determine the actual capabilities of these old switches. Special tests were made on certain new and old switches in an attempt to determine the effect of contact pressures, contact coatings, and other features on the momentary current capabilities.

Summary of Switches Tested

The following is a summation of the switches subjected to high-current tests. New switches submitted by manufactures: 11 of 1,600 amperes and 12 of

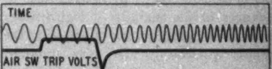

Fig. 1. Typical oscillogram of single test shot

Paper 55-9, recommended by the AIEE Switchgear Committee and approved by the AIEE Committee on Technical Operations for presentation at the AIEE Winter General Meeting, New York, N. Y., January 31–February 4, 1955. Manuscript submitted September 30, 1954; made available for printing October 27, 1954.

A. M. McNerney is with the Tennessee Valley Authority, Knoxville, Tenn.

Table I. Momentary Current Tests on New Switches

Switch Make and Type	Continuous-Current Rating, Amperes	Contacts		Blade	Test Shots			Test Results
						Rms Amperes(b)		
		No. (a)	Conformation		No.	Maximum	Minimum	
A-1	1,200	6	offset	2" IPS(c)	6	80,400	64,600	no damage*
A-2	1,200	4	offset	2" IPS	1	92,200		blade blew open and burned
A-3	1,200	4	offset	2" IPS	2	67,500	52,000	blade rose 2 1/8"*
A-4	1,200	4	in line	2" IPS	6	82,100	64,600	no damage
A-5	1,600	6	in line	3" sq by 3/16"	6	87,000	68,400	no damage*
B-1	1,200	6	in line	2" IPS	6	77,200	54,800	no damage
B-2	1,600	6	in line	2 1/2" IPS	6	85,250	74,300	no damage*
B-3	1,200	6	offset	2" IPS	6	(d)	(d)	no damage*
B-5	1,200	4	offset	2" IPS	6	51,600	43,300	minor pitting
					3	56,700	54,000	line burns
C-1	1,200	2	offset with stops	2" IPS	7	53,000	44,500	some welding at contacts
C-2	1,200	2	reverse-loop offset	2" IPS	12	62,900	51,200	no damage*
					6	79,000	60,000	no damage
					6	80,300	69,700	no damage
					9	84,500	74,600	no damage
					9	98,000	78,400	no damage
					3	106,800	89,800	pressure marks
C-3	2,000	4	reverse loop in line	3" sq by 1/4"	7	70,500	58,600	pressure marks*
C-4	1,600	4	reverse loop in line	3" sq by 3/16"	8	70,000	58,700	no damage*
					1	114,000		pressure marks
					6	82,300	65,300	pressure marks
C-5	1,600	8	reverse loop in line	3" sq by 3/16"	5	106,100	99,500	pressure marks
D-1	1,200	4	in line(e)	2" IPS	12	59,700	45,200	no damage*
					6	77,000(d)	64,000(d)	minor pitting
D-2	1,200	4	in line(e)	3 1/2" type *B*	6	73,500	52,100	minor pitting
D-3	1,600	6	in line	3 1/2" type *B*	6	65,000	55,800	no damage
					6	91,200	70,300	slight burns*
E-1	1,200	4	offset, crimped	2 1/2" by 1/2"	6	66,400	51,000	no damage*
E-2	1,600	4	offset, crimped	2" IPS	6	74,000	56,100	no damage
					6	84,100	68,200	no damage
					3	84,100	80,900	no damage*
F-1	1,200	4	offset	1 1/2" Ex. H.	6	63,700	55,100	silver transfer*
F-2	1,600	4	offset	2 1/2" Ex. H.	1	71,600		blade blew open and burned
					6	68,300	55,100	no damage*
G-1	1,200	6	offset(f)	2" IPS	6	79,400	65,400	minor pittings
G-2	1,600	6	offset	2 1/2" Ex. H.	6	74,300	63,200	no damage*
H-1	1,200	2	offset	2" outside diameter by 1/4"	1	75,000(d)		blade blew open and burned
H-2	1,200	2	offset	2" outside diameter by 1/4"	3	57,000	48,100	rear contacts burned
H-3	1,600	8	offset, button stop	3 1/2" outside diameter by 1/4"	6	71,200	58,700	slight burns*

Notes: *Switch sent to temperature test; see Tables II and III.
(a) Total number of contact fingers on jaw end.
(b) Rms value of first half-cycle.
(c) Blade reinforced with steel inner liner for stiffness. IPS stands for iron pipe size. (This also applies for Tables II, III, IV, and VI.)
(d) Oscillogram defective.
(e) Standard design, not modified for tests.
(f) First switch tested had an external hook for locking blade in position (removed on subsequent tests).

1,200 amperes. Miscellaneous switches removed from service on the TVA system: 2 of 1200 amperes, 4 of 600 amperes.

A total of 374 test shots was made on new switches submitted by manufacturers and the results are summarized as follows:

Switches	Current Rating, Amperes	
	1,200	1,600
Destroyed	2	1
Moderately damaged	1	1
Slightly damaged	4	2
Not damaged	9	7

Types of New Switches Tested

All except one of the switches submitted by manufacturers were of the rotating-blade, high-pressure contact type. The one exception was a push-pull type with multiple fingers forming the jaw.

The 1,200-ampere standard designs had single or multiple contacts on the jaw end. The conformation followed the generally used design in which the contacts form a right-angle offset between the blade and the terminal pad. This conformation is referred to as offset contacts herein. About half of the designs had bosses on the contacts or crimped conformation or even separate latches to provide means of counteracting the magnetic forces tending to blow the blade out of the contacts at high currents.

A majority of the makers offered modified designs aimed at eliminating, mitigating, or resisting the blade blowout effect. These included such features as reinforced blades, increased number of contacts on the jaws, or modified contact conformation such as in-line conformation (i.e., the blade, contacts, and terminal pads are in a straight line), or reverse-loop contacts. In the latter design, the conformation is offset but the contact forms a loop and utilizes the magnetic effect of the increased current to apply more pressure. The 1,600-ampere ratings generally incorporated the same contact designs as the modified 1,200-ampere designs. Blades necessarily were larger and the extra stiffness added to their ability to resist the blade blowout effect. Contact pressure was applied in some cases by mounting the contact fingers on beryllium straps; in others by backup springs. All except one had silver-to-silver or copper-to-silver contacts. The one exception was a copper-to-beryllium contact.

Determination of Test Current

A tracing of a typical oscillogram of a high-current test shot is shown in Fig. 1. All current values shown in the tables are amperes rms of the first half-cycle determined in accordance with AIEE Standard No. 22.[2]

Momentary Current Tests on New Switches

The most significant of the momentary current tests on switches as submitted by manufacturers are shown in Table I. Many of the test shots are omitted because it is felt that they do not contribute enough to this paper.

In making the tests on these switches as well as on subsequent tests, a single pole was mounted and adjusted on the test structure. The blade was then opened and closed, using the operating lever on the rotating insulator stack, and the lever was then wired in place to simulate the locking action normally obtained from the operating mechanism.

For the sake of simplicity, no attempt is made to tabulate the various jaw contact designs except for their general physical conformation. Rear, or hinge, contacts also are not tabulated. On the majority of the switches, the hinge contacts were duplicates of the front contacts. One make used flexible shunts. Some used nonbreak shunts or contacts. The hinge contacts obviously were not subjected to the same forces as the jaw contacts and only one make sustained damage at that location.

It will be noted from the tables that a considerable range in current was obtained in shots of the same series. While the offset of the test current delivered by the test equipment was not as consistent as expected,[2] the transient factor (ratio of rms of first loop to rms of steady state), however, averaged 1.48 for all shots and was in excess of 1.5 for the maximum shots listed in the tables. Judgment of the performance of the switches was, of course, based upon the maximum shots.

In several cases, more than the announced number of test shots was made on a particular switch. In some instances this was because of adjusting for better current or better offset values. In other instances, notably switches *C-2*, *C-4*, and *D-1*, switches were returned from the temperature test and retested in an attempt to destroy them either by higher currents or by repeated test shots.

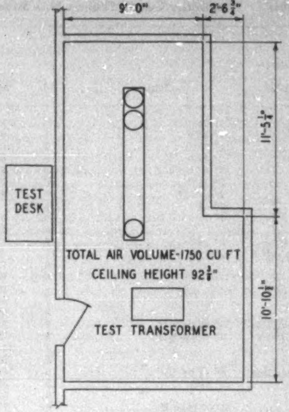

Fig. 2. Layout of temperature test room

Except for switches *H-1* and *H-2*, all damage sustained was on the jaw contacts, and the test results described in the last column of Table I refer to that location. The terms in the test results tabulation refer to the condition of the contacts when examined after each series of shots. "Minor pitting" or "slight burns" indicate the start of welding or burning action not sufficient to affect the operation or continuous-current capacity of the switch. Line burns or welding were sufficient to affect the switch, but it could still be made operative by redressing the contacts.

Temperature Tests

In making the temperature tests on the different makes and designs of switches, it was desired to obtain exactly comparative data. Existing standards are vague, at best, as to the conditions under which such tests should be made. It is well known what effect a draft within a room, or a slight cross-breeze if outdoors, will have on test temperatures of equipment.

The electric equipment for the temperature tests are described by Gostin.[3] To obtain identical conditions for each switch, the switches were tested in an interior room, the dimensions of which are shown in Fig. 2, and closed off by the only access door. The loading transformer was located in the room, and thermocouple leads and current transformer leads were run to a test desk located outside the room. The only time the room was entered during a test run was to check the ambient temperature from mercury thermometers located above and to each side of the test switch. The results of the temperature tests on new switches are shown in Tables II and III. Because of the variations in switch designs, and to simplify the tabulation, only comparative points are listed. For multiple points such as contacts, shunts, etc., the observed range is shown.

Temperature tests were made at rated current and, unless otherwise noted in the tabulation, on the same switch which had been subjected to the momentary current tests. Temperature tests also were made at rated current and at other values on two of the older switches removed from service. The results of these tests are shown in Table IV.

In all cases, switch types and numbers shown on the tables of temperature tests are the same as shown on the high-current tests. Particular attention is called to the temperature tests on switch *F 1*; see Table II. The final temperature of the center of the 1 1/2-inch extra-heavy blade was much lower than expected, especially under the conditions of the test. Investigation disclosed that the blade was heavily coated with a smooth clear lacquer, presumably for appearance. The test was rerun with the lacquer re-

Table II. Temperature Tests on New 1,200-Ampere Switches, Test Current 1,200 Amperes

Switch Make and Type	Blade Size	No. of Contacts (a)	Temperature Rise, Degrees Centigrade: Jaw Contacts Maximum	Jaw Contacts Minimum	Blade Tip	Blade Center	Blade Rear	Hinge Shunts Maximum	Hinge Shunts Minimum	Bridge Maximum	Bridge Minimum	Ambient Temperature, Degrees Centigrade
A-1	2" IPS(b)	6	20.8	18.8	20.8	28.2	21.0	17.8	15.8	18.2	16.8	30.0
A-3	2" IPS	4	16.5	15.2	17.0	27.2	16.5	16.5	16.2	18.2	16.5	29.7
B-3	2" IPS	6	15.4	15.4	16.7	25.5	23.6	17.4	17.4	21.0	20.4	29.7
C-2	2" IPS	2	20.5	19.2	20.5	25.3	17.4	15.0	14.2	15.4	15.4	26.0
D-1	2" IPS	4	23.7	21.8	28.4	28.7	27.3	28.7	19.6	(c)	(c)	21.5
E-1	2 1/2" outside diameter by 1/8"	4	27.8	23.7	27.0	29.5	29.0	28.6	27.3	32.1	28.6	20.5
F-1	1 1/2" Ex. H. (d)	4	24.5	24.0	23.3	27.6	21.4	14.4	12.2	25.9	22.6	22.5
F-1	(e)		26.8	24.2	26.4	40.3	24.3	14.1	13.8	24.7	24.7	25.0
G-1	2" IPS	6	17.8	15.7	19.1	22.6	16.9	17.7	17.7	15.2		22.5
H-1(f)	2" outside diameter by 1/4"	2	38.8	37.2	38.8	26.0	28.5	33.2	27.5	21.0	21.0	23.0

Notes: (a) Total number of contact fingers on jaw end.
(b) Reinforced blade.
(c) Series of hinge shunts replace normal bridge construction.
(d) Blade was lacquered.
(e) Retest with lacquer removed from blade.
(f) New switch, duplicate of one damaged in high-current test.

Table III. Temperature Tests on New 1,600-Ampere Switches, Test Current 1,600 Amperes

Switch Make and Type	Blade Size	No. of Contacts (a)	Temperature Rise, Degrees Centigrade: Jaw Contacts Maximum	Jaw Contacts Minimum	Blade Tip	Blade Center	Blade Rear	Hinge Shunts Maximum	Hinge Shunts Minimum	Bridge Maximum	Bridge Minimum	Ambient Temperature, Degrees Centigrade
A-2	3" sq by $^{5}/_{16}$"	6	23.3	20.3	23.0	25.1	16.8	16.0	15.8	20.3	19.8	31.5
B-2	$2^{1}/_{2}$" IPS	6	25.8	23.3	27.2	25.3	23.1	18.4	18.4	16.6	16.6	32.5
C-4	3" sq by $^{3}/_{16}$"	4	19.3	17.1	19.6	21.7	15.6	14.7	13.0	13.2	10.9	27.9
D-3	$3^{1}/_{2}$" type *B*	6	28.9	24.8	29.4	28.6	26.3	29.8	23.2	(b)	(b)	25.5
E-2	$2^{1}/_{2}$" outside diameter by $^{1}/_{4}$"	4	38.6	32.7	37.2	31.6	37.7	43.9	41.6	42.2	41.3	24.0
F-2	$2^{1}/_{2}$" Ex. H	4	25.7	24.7	25.7	25.7	19.9	14.3	13.6	20.4	20.4	25.0
G-2	$2^{1}/_{2}$" Ex. H	6	27.8	25.6	29.1	27.6	22.4	27.8	27.8	23.8	23.8	25.0
H-3	$3^{1}/_{2}$" outside diameter by $^{1}/_{4}$"	8	26.5	24.8	26.5	17.8		14.0	12.5	11.0	11.0	25.0

Notes: (a) Total number of contact fingers on jaw end.
(b) Series of hinge shunts replace normal bridge construction.

Table IV. Temperature Tests on Old Switches Removed from Service

Switch No.	Test Current, Amperes	Temperature Rise, Degrees Centigrade: Jaw Contacts Maximum	Jaw Contacts Minimum	Blade Tip	Blade Center	Blade Rear	Hinge Shunts Maximum	Hinge Shunts Minimum	Bridge Maximum	Bridge Minimum	Ambient Degrees Temperature, Centigrade
J	600	18.5	18.5	16.0	14.5	11.0	18.0		14.0	12.8	22.5
	800	30.5	30.5	25.8	22.8	17.8	32.0		23.0	20.5	23.0
4-A	600	19.8	19.0	19.8	12.5	7.2	10.0	10.0	13.5		23.0
	800	31.8	30.8	32.5	20.5	11.0	18.0	18.0	20.5		23.5

moved and the results show how the lacquer affected the temperature readings.

Tests on Old Switches Removed from Service

Old switches removed from service and subjected to momentary current and temperature tests were of the following types:

1. Rotating blade, high-pressure contact type, two offset contacts per side on single beryllium strap. Installed 1 year prior to test.

2. Rotating blade, high-pressure contact type, one cast beryllium offset contact per side. Installed about 10 years prior to test.

3. Area contact, push-pull type, pressure-applied to floating contact shoe by fixed spring. Installed about 12 years prior to test.

4(a). Area-contact type with auxiliary device for applying pressure to floating contact shoes. Installed about 14 years prior to test.

4(b). Same as 4(a) except with pressure-applying device removed.

5. Multiple shoe contacts, push-pull type, pressure-applied to floating contact shoes by fixed springs. Installed about 15 years prior to test.

6. Rotating blade, high-pressure contact type, one cast beryllium U-shaped contact. Installed about 7 years prior to test.

These switches had been removed from hydro stations or remote switching stations and had, therefore, not been subjected to contaminated atmosphere.

The results of the tests on switches 1 to 5 are shown in Table V. The designations *A*, *B*, and *C* under switch 2 are for tests on each of the three poles of switch 2. As in the case of the tests on new switches, all damage sustained was on the jaw end and the test results refer to that location. The results of the tests on switch 6 are shown under switch *J-1* in Table VI.

Table V. Momentary Current Tests on Old Switches Removed from Service

Switch No.	Continuous-Current Rating, Amperes	Blade	Test Shots No.	Rms Amperes(a) Maximum	Rms Amperes(a) Minimum	Test Results
1	1,200	2" IPS	6	51,600	43,300	fire on each shot—minor burns
			3	56,700	54,000	line burns
2-*A*	1,200	$1^{1}/_{2}$" Ex. H	5	53,600		slight burning
			1	58,800		switch blew open and burned
2-*B*			2	60,300	46,800	no damage
			1	55,700		blade tied down
			1	58,600		tie removed—no damage
			1	64,000		tie broke—switch blew up
2-*C*			2	54,600	50,400	minor pitting
			2	62,750	61,300	heavy pitting
			1	64,500		switch blew open and burned
3	600	$1^{1}/_{2}$" IPS	3	42,900	39,200	no damage
			3	46,800	44,200	transfer of metal
			3	52,200	48,800	medium burning*
4-*A*	600	swaged	6(b)	51,300	46,500	no damage
			3	50,700	49,000	small burns
			3	55,800	55,200	spot welding*
4-*B*	600	swaged	1(c)	61,300		small burns
			1(d)	49,600		contacts and blade burned
5	800	3" by 1/4"	3	49,600	40,700	slight burning
			3	44,500	44,200	no damage
			1	52,300		contacts and blade burned

Notes: *Switch sent to temperature test after dressing contacts.
(a) Rms value of first half-cycle.
(b) Switch as received had auxiliary contact pressure applying device.
(c) Contact-pressure applying device adjusted and locked in place.
(d) Contact-pressure applying device made inoperative.

Special Tests

Tests were made on several makes and ratings of new and old switches to determine the effect of contact pressure, contact coatings (such as graphite), and special features such as reinforced blades or increased number of contact fingers. These tests are tabulated in Table VI.

It will be noted that some tests from Table I are repeated in Table VI because modifications were made on switches originally tested "as received," and it seems desirable to repeat the test data for direct comparison. The switch *J* was an old switch, described in item 6 in the section entitled "Tests on Old Switches Removed from Service." Test

Table VI. Special Tests

Switch Make and Type	Continuous-Current Rating, Amperes	Contacts				Blade	Test Shots			Test Results
		No. (a)	Conformation	Pressure, Pounds	Coating		No.	Rms Amperes (b)		
								Maximum	Minimum	
A-3	1,200	4	offset	200	graphite	2" IPS	2	67,500	52,000	blade rose 2 1/8"
A-5	1,200	4	offset	200	graphite	2" IPS(c)	2	62,300	55,500	no blade movement
A-21	1,200	4	offset	200	graphite	2" IPS	2	63,800	57,300	blade rose 1 5/16"
				125	none	2" IPS	3	65,700	60,600	no blade movement
				125	graphite	2" IPS	3	65,600	63,400	blade rose 9/16"
A-22	1,200	4	offset	140	graphite	2" IPS(c)	3	65,000	63,800	blade rose 1 1/8"
				140	none	2" IPS(c)	1	64,800		blade rose 3/8"
A-23	1,200	6	offset	140	none	2" IPS(c)	3	64,400	61,700	no blade movement
		6	offset	140	graphite	2" IPS(c)	3	64,600	63,000(e)	blade rose 7/16"
		6	offset	140	graphite	2" IPS(c)	6	66,200	62,000	blade rose 5/8"
G-1	1,200	6	offset	80	none	2" IPS(d)	6	79,400	65,400	slight pits
				40	none	2" IPS(d)	3	76,500	64,300	slight pits; blade moved 3/8"; held by latch
				80	none	2" IPS(f)	3	70,500	63,300	no blade movement
H-1	1,200	2	offset	200	none	2" outside diameter by 1/4"	1	75,000(e)		blade blew open—burned
							3	57,000	48,100	rear contacts burned
H-10	1,200	8	offset	100	none	2" outside diameter by 1/4"	3	57,900	49,900	minor sparking
							4	60,700	56,900	minor sparking—no damage
J-1	600	2	offset	55	none	2" type *K*	1	50,200		blade blew open—burned
J-10	600	4	offset	55	none	2" type *K*	6	54,400	42,700	slight transfer of metal
J-11	600	6	offset	55	none	2" type *K*	6	52,400	44,400	slight transfer of metal
J-12	600	6	offset	55	none	2" type *K*	3	62,500	52,400	slight transfer of metal
							3	61,500	57,300	slight transfer of metal

Notes: (a) Total number of contact fingers on jaw end.
(b) Rms value of first half-cycle.
(c) Blade reinforced with steel inner tube for stiffness.
(d) External latch to restrict blade movement.
(e) Estimated. Oscillograph did not record.
(f) External latch removed.

J-1, see Table VI, was on the switch as removed. Subsequent tests, *J-10*, *J-11*, and *J-12* on that make, were on various combinations of replacement blade tips and multiple contacts furnished by the original manufacturer. The test results refer to the conditions at the jaw-end contacts because, as also noted in the section entitled "Momentary Current Tests on New Switches," all damage sustained was at that location. Blade movement in all cases refers to the total displacement of the blade tip.

Inspection After Tests

Upon completion of the testing program, all the switches tested were assembled at one location for a general inspection and comparison of design features. It was thought that the inspection might disclose some explanation of apparently inconsistent results in the tests.

It is evident that over- or underadjustment of the blade-operating linkage can greatly affect the blowout effect at the contacts. Sloppy fits in some linkages result in lack of control of the blade to such an extent that the blade tip will orient itself in different positions during successive opening and closing operations. Any play in the linkage also minimizes or eliminates any holding effect in the hinge end which might help to counteract the blade blowout effect.

Both the test results and the general inspection leave a doubt as to the effectiveness or desirability of blade-latching devices such as bosses or crimps on the contacts or external latches unless they are absolutely necessary for proper blade action, especially under icing conditions. Otherwise, it appears that such features constitute too much of a hazard to proper blade-closing action.

Conclusions

It is dangerous to draw definite conclusions from a limited series of tests. Even though a total of 374 test shots was made, they were spread over so many makes and types that, with a few exceptions, each received only a limited amount of testing. Factors such as variations in magnitude and asymmetry of the test current, or variations in blade adjustment or blade position, could be eliminated only by a long series of tests on each switch. However, it is believed that the high-current tests were extensive enough to justify the following general conclusions:

1. Single contacts are inadequate for high-current ratings.
2. Standard 1,200-ampere switches can be rerated to a 62,000-ampere momentary rating by one of the following modifications: reinforcing the blades to obtain greater strength in resisting the blade blowout effect; increasing the number of contacts; adopting an in-line arrangement of blade, contacts, and terminal pad; or using a reverse-loop contact construction.
3. Older type of switches, using the push-pull blade action and single, floating, area contact fingers, have higher short-time capability than the standards in effect at the time of their manufacture, as shown by the tests on switches 3, 4(a), and 5.

The temperature tests, even under the reasonably exact conditions provided, show some inconsistency especially at the center of blade of various makes utilizing the same size blade. The inaccuracies inherent in the thermocouples, differences in their mounting, errors in reading them, differences in conditions of blade surfaces and end drainage all contribute. However, the differences in the tests were within reasonable limits as compared with the gross differences between these tests and factory tests on identical switches. Standards that include exact conditions under which temperature tests at the factory are to be made, and exact conditions for preparation of the sample under test, seem definitely to be needed.

References

1. High-Speed Multiple Reclosing Oil Circuit Breaker for 161 Kv, 10,000,000 Kva, B. P. Baker, G. B. Cushing. *AIEE Transactions*, vol. 71, pt. III, Jan. 1952, pp. 22–31.
2. High-Current Testing of Air-Disconnecting Switches, B. F. Gostin. *AIEE Transactions*, vol. 74, pt. III, Apr. 1955, pp. 21–25.
3. Air Switches, Insulator Units, and Bus Supports. *AIEE Standard No. 22*, July 1952, Appendix A.

◆

Discussion

T. E. Curtis (A. B. Chance Company, Centralia, Mo.): The high-current and temperature rise tests on 161-kv disconnecting switches performed by TVA in 1952 were very worth-while and certainly made a material contribution to the industry. I helped design some of the equipment tested and I was privileged to witness some of the tests. Some specific contributions for industry are as follows.

The attention of manufacturers of disconnecting switches was focused on the need for high-current, short-time ratings on disconnecting switches of transmission voltage ratings in considerable excess of the ratings available prior to the tests. The ever-increasing short-circuit capacity of transmission networks gave rise to this requirement. The final result is that many manufacturers now have switches which do an excellent job of withstanding short-time high currents of magnitudes greatly in excess of what was considered necessary a few years ago and an additional new series of short-time current ratings has been established for disconnecting switches by the National Electrical Manufacturers Association (NEMA) Standard *SG6-1954*.[1]

In conjunction with its test program, TVA provided a facility where short-time currents in excess of 100,000 amperes could be obtained. A facility providing test currents of such magnitude had not been available to most manufacturers up to that time, and the information gained by the manufacturers was of inestimable value in determining the final design for switches of the new short-time current ratings.

The study and tests pointed out the weakness in the then existing standards for conducting temperature rise tests on disconnecting switches and have resulted in a revision of these standards to call for better controlled conditions. We feel that the method of conducting temperature rise tests used by TVA was not entirely related to service conditions and that requirements were unduly severe. However, we are in agreement with the present NEMA Standards which, in part, adopt some of the ideas of Mr. McNerney and other TVA engineers.

REFERENCE

1. POWER SWITCHING EQUIPMENT. *NEMA Standard SG6-1954*, National Electrical Manufacturers Association, New York, N. Y., 1954.

A. H. Powell (General Electric Company, Philadelphia, Pa.): The author and his associates undertook and successfully completed a program of major proportions when they made momentary and heat rise tests on a large number of switches from various manufacturers. The results, as would be expected, varied considerably and without knowing more about the particular configuration of each switch than could be included in the relatively meager information in the tables it is rather difficult to note any particular trends as far as the most suitable type of contact or method of switch blade operation is concerned. However, it was apparent, although not expressly stated, that essentially all the switches met the values which are specified in avialable industry standards quite well.

For example, Table II giving the temperature rise tests on various new 1,200-ampere switches showed that with the exception of one switch the temperature rises were all below the 30-degree maximum permitted by the standards. The author states, and quite correctly, that a very satisfactory set of test conditions was present and that differences throughout the tests were within very reasonable limits but the facts do not seem to bear out the statement that there were gross differences between the results obtained by the author and those made in the factories. It is assumed that the switches in the factory all met the 30-degree rise limit and the tests which the author made confirmed the fact that the switches apparently met this limit.

The same condition seems to be true with the momentary test. There was generally no damage such as severe pitting or welding of the switch contacts when they were subjected to their normal values as listed in the NEMA standards. These standards, until changed in 1954 by NEMA *SG6-1954*, required that a 1,200-ampere switch pass a momentary current of 40,000 amperes and a 4-second current of 25,000 amperes without damage which might affect its current-carrying ability. All of the 1,200-ampere switches shown in Table I appear to meet this requirement. More recent changes in the NEMA standard provided an additional rating for 46, 69, 115, and 161 kv, 1,200-amperes switches consisting of a momentary value of 61,000 amperes. Apparently the various switches submitted for the author's tests were designed on this basis, for the results indicate that even at the higher value the various switches did not have particular trouble.

The results of momentary tests on some of the old switches which were removed after a number of years' service were very interesting. These old and weathered switches apparently met the ratings existing at the time the switches were built quite successfully and in fact came very close to meeting up-to-date ratings which are in general above the older requirements. Temperature rise tests also indicated that the older switches were well designed.

As a general statement, it can be said that while it is certainly very worth while to check on the quality of the products that are being used in electric systems today, such as the disconnecting switches described in this paper, it should also be emphasized that switches, like practically every other device and product, are made to some industry standards. The reputable manufacturer designs and exhaustively tests the product so as to meet these standards and whatever is designed into the device in the way of excessive material, etc., is done to insure compliance with the standards in normal manufacturing routines. Obviously the amount of excess capacity included in a design by the various manufacturers will vary considerably and may not be an indication of which device is the most suitable but could very well be based on the availability or lack of suitable testing equipment and experience with the designs over years of service.

Mr. McNerney's conclusion that more comprehensive standards are needed which will specify how temperature tests are to be made is a good one. The same comment could well be made for momentary and short-time tests. However, the conclusion that standard 1,200-amperes switches can be rerated to a higher value, especially if certain modifications are made, seems to be questionable for if the switches are made to a certain standard there is no justification for expecting them to meet greater values by making minor changes in the switch design.

S. C. Killian (Delta-Star Electric Division, H. K. Porter Company, Inc., Chicago, Ill.): The tests described in this paper are very complete and the author and his associates are to be complimented on their courage in undertaking a task that was not only exceptionally large but involved many problems in setup and procedure. The paper must necessarily be of a general nature because each manufacturer's switch is not discussed by name. The author's deductions and conclusions are important and it is likely that the entire industry benefited from these tests.

One of the most significant conclusions of the paper deals with straight-line contacts. It is interesting to follow the evolution of this contact. In 1941 my company built and patented the first switches employing a rotating blade and straight-line contacts. These were 4,000- and 5,000-ampere switches and the contact design was actually ahead of its time. The switch voltage was only 23 kv and, even though the switches were tested at 120,000 amperes, the short length of the blade and its tremendous strength precluded any blade movement.

The straight-line contact feature then was only an added safety factor. However, as soon as TVA and other operating companies began to talk of short-time currents in excess of 60,000 amperes on switches involving 6-foot 0-inch long blades this straight-line contact became a necessity. All straight-line contact design for outdoor switches is now based on similar thinking.

From the foregoing we do not intend to convey the impression that the offset or angular contact is faulty. Many switches with this type of contact satisfactorily passed these tests. As the author points out, and it bears repeating, when using angular contacts the blade must embody sufficient strength and its mounting must be sturdy and not subject to "backing up" by taking loose play out of driving links, levers, and knuckles in the live mechanism, when the blade is loaded under fault conditions.

We are pleased to see that while the author states, "About half of the designs had bosses on the contacts or crimped conformation or even separate latches to provide means of counteracting the magnetic forces tending to blow the blade out of the contacts at high currents," he concludes that, "Both the test results and the general inspection leave a doubt as to the effectiveness or desirability of blade-latching devices such as bosses or crimps on the contacts or external latches unless they are absolutely necessary for proper blade action especially under icing conditions. Otherwise, it appears that such features constitute too much of a hazard to proper blade-closing action." We feel this point is well made and that the blade should be fully controlled from the hinge and not even depend on a contact stop for its correct motions and positions, much less on bosses or latches. Those utilities which operate in sleet and ice belts can testify to the difficulty of operation on device-free switches. To put bosses and latches at the crucial contact positions would intensify this ice difficulty many-fold.

The tests on the old switches are of special interest and it is pleasing to the manufacturers to know that switches we built 10 to 15 years ago will still carry current in excess of that for which they were originally guaranteed. However, in order that there be no misunderstanding, it should be pointed out again that, "These switches had been removed from hydro stations or remote switching stations and had therefore not been subjected to contaminated atmospheres." We can be certain that had the contacts of these switches been severely contaminated the results would have been much poorer.

T. A. Burdeshaw (Southern States Equipment Corporation, Hampton, Ga.): Users as well as manufacturers of air switches are indebted to Mr. McNerney and his associates for their work in staging so comprehensive a series of tests and for the excellent exposition given. The scope of Mr. McNerney's paper is very broad, so I shall confine my discussion to a small segment of it. In particular, I shall discuss elemental considerations in studying contact behavior under momentary currents of a relatively high order. This discussion qualifies to a degree conclusions 1 and 2.

Contact failure can be attributed to excessive heat generated by one or more of the following.

1. Resistance heating of the contact bodies. In testing air switches under momentary currents this cause can be eliminated from consideration. If contact members are adequate for load currents for protracted periods of time they cannot generate melting temperatures in the brief period of a momentary test.

2. Heating at the contact surfaces from film resistance. This is a more likely cause of failure at high current. Obviously, high film resistance can result in practically instantaneous temperature rise to the melting point of contact material and failure occurs. In testing new switches or old switches with clean contacts this type of failure is not too prevalent. However, tests of old switches with contacts not cleaned shows a marked increase in the rate of failure from film resistance.

Various methods have been employed to minimize the possibility of contact deterioration from film formation. Sliding or wiping engagement of contacts results in some cleaning. Extremely high contact pressures have been employed to cut through the film.

The use of silver is relatively extensive and results in a slower rate of film formation. At the same time the film formed is softer and is more easily broken down by engagement under pressure.

3. Separation of contacts. Separation of contacts during current flow is found to be a prevalent cause of failure during momentary high current tests. Two types of separation occur, both caused by magnetic forces generated by the current flow.

a. The first type, referred to as blade blowout, results in the movement of the blade in an opening arc. It may move only a minute amount or may move completely out of engagement, depending upon the force of the magnetic field as related to the blade restraining force. The use of multiple contacts does not affect the forces producing this movement. The use of a reinforced blade increases its ability to resist blowout and therefore increases the amplitude of current necessary to move the contact. Adopting a true in-line construction eliminates the blowout force. However, some so-called in-line designs actually utilize offset contacts. Reverse loop contacts change the direction of force from the magnetic field so that it acts to force the blade further closed rather than open. A position stop prevents movement in that direction so the blade remains stationary.

b. The second type of separation results from magnetic forces acting upon the contact members to push them away from the blade. These forces under some value of current exceed the force of spring pressure and the contact opens and is damaged by arc heat. Reinforcing the blades does nothing to alleviate this condition. Increasing the number of contacts permits of greater short-circuit capacity by dividing the current among several members. Obviously, an infinite current can be carried by an infinite number of contacts. The in-line arrangement in most constructions minimizes but does not eliminate contact separation. Even they have lateral offsets in the current path resulting in magnetic separation at some value of current. Reverse loop contacts utilize the magnetic field to cancel the force working to relieve contact pressure. The result is that contacts do not separate at any value of current. With this arrangement the ability of a clean contact to withstand high momentary current is limited by the cross section melting characteristics of the contact member.

It is also of interest to note that switch *F-1* shown in Table II operated at a higher temperature after removal of the lacquer coating from the blade than had been the case when coated with lacquer. In order to show the effects of surface coatings on conducting tubing we recently made a temperature rise test on a piece of $^3/_4$-inch IPS tubing under several conditions with the following results. The tubing as received from the mill in a new condition slightly oxidized and with a temperature rise of 21 degrees centigrade (C) above an ambient of 27 C was noted. With the tubing burnished a temperature rise of 25 C above an ambient of 30 C was noted. The burnished tubing was coated with clear lacquer and a temperature rise of 20 C above an ambient of 29 C was noted. The tubing was again cleaned and a coat of lamp black was applied. The temperature rise noted in this case was 16 C above an ambient of 30 C. Again the tubing was cleaned and a coating of red Glyptal was applied and allowed to dry. Under this condition a temperature rise of 15 C above an ambient of 29 C was noted.

Lester C. Hart (Hi-Voltage Equipment Company, Cleveland, Ohio): Presentation of the result of high-current tests on disconnecting switches will be appreciated by the electric power industry, which must contend with higher fault currents than were considered when many important stations on the system were built. Anyone who was present during the tests must have been impressed with the planning and organizational work necessary to conduct them. In addition to determining what the switches would safely withstand, the tests showed the value of some elements of design.

With high currents powerful magnetic forces are developed. These magnetic forces can be used to increase the short-time current capacity of a switch. This is accomplished by providing a straight-line current path from the terminal through the contacts and the switch blade, and by making a compact contact assembly with the contact fingers or shoes close together so that the magnetic field encircling them will increase contact pressure to many times normal, thus clamping all parts as one rigid structure. Motion between current exchange surfaces, even slight vibration, appears to result in arcing. The greater the current the more pronounced is the burning.

Some of the switches tested are designed to resist the magnetic forces by mechanical means. As long as these means are maintained effective the switches safely withstand high currents.

Mr. McNerney comments on existing standards for temperature tests. The industry does not have a satisfactory standard for testing outdoor switches. Such a standard which gives consideration to normal operating conditions is needed. The best switch is a careful balance of all elements of design. Under existing vague standards, a sacrifice in one or more elements is often made to meet a test condition that is never experienced in service.

Arem Foti and **J. B. Owens** (I-T-E Circuit Breaker Company, Greensburg, Pa.): Mr. McNerney's paper was most interesting to us since our company was among those that had the privilege of submitting switches for use in the reported test program. This discussion presents a further opportunity to express our gratitude for the invitation to participate.

In the past several years there has been a pronounced growth in electric transmission and distribution systems throughout the country. Increased generating capacity and the interconnection of electric utility systems have resulted in higher system short-circuit currents. Thus, the need arose for power switching apparatus and power switching equipment capable of withstanding the short-circuit currents that could be developed.

The announcement in 1952 by TVA of a program for high-current testing of disconnecting switches was very definitely one of the stimulants that awakened the industry to the need for extending the capability of outdoor air switches. It was also instrumental in the development of the 1,600-ampere continuous current rated switches required. The response of switch manufacturers in submitting switches to meet these requirements is a tribute to the industry. It is symbolic of the spirit of co-operation with which switch manufacturers and users attempt to solve their mutual problems in dealing with new conditions and new situations that continually arise.

The need for outdoor air switches to match the momentary current ratings of circuit breakers has been given recognition, as evidenced in the October 1954 revision of NEMA Standard *SG6-1954*. The re-

Table VII. Ratings for Outdoor Air Switches

Nominal Voltage Rating, Kv	No. of Insulators	Maximum Design Voltage, Kv	Impulse Withstand, Kv	Continuous Current Rating, Amperes											
				400	600	600	1,200	1,200	1,600	2,000	2,000	3,000	4,000	5,000	6,000
				Momentary Current Rating, Thousands of Amperes*											
				20	20	40	40	61	70	70	80	100	120	160	200
				Construction Classification											
7.2 (7.5)	1	8.25	95	ABCDEFGH		ABCDEFGH		ABDEGH			ABH	AH	AH	AH	AH
14.4 (15)	1	15.5	110	ABCDEFGH		ABCDEFGH		ABDEGH			ABH	AH	AH	AH	AH
23	1	25.8	150	ABCDEFGH		ABCDEFGH		ABDEGH			ABH	AH	AH	AH	
34.5	1	38	200	ABCDEFGH		ABCDEFGH		ABDEGH		ABH		AH	AH		
46	1	48.3	250	GH	ABDEGH	ABG	ABDEGH	ABG		AB					
69	2	72.5	350	GH	ABDEGH	ABG	ABDEGH	ABG		AB					
115	3	121	550		ABDEGH	ABG	ABDEGH	ABG		AB					
161	4	169	750		ABDEG	ABG	ABDEG	ABG	ABG						
230	5	242	900				ABG	ABG	ABG						
	6		1,050				ABG	ABG	ABG						
	7		1,300						AG						
	8		1,470						AG						
	9		1,675												
	10		1,800												

* Short-time current ratings include a momentary and a 4-second current rating based on test conditions described in NEMA Standard *SG-1954*, section 3.03. Divide the momentary rating by 1.6 to obtain the standard 4-second current rating. When a higher momentary current rating than shown is required, use a switch having a higher current rating.

Note: Where grounding switches are applied to the main switch, the current ratings are not necessarily the same.

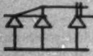
A
Vertical

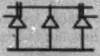
B
Double

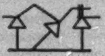
C
Tilting

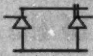
D
Side

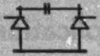
E
Center

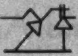
F
Tilting

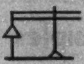
G
Grounding

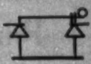
H
Hook

vised ratings for outdoor air switches are shown in Table VII.

An examination of the table will reveal the existence of a dual set of momentary current ratings for switches with a continuous current rating of 600 and 1,200 amperes in voltage ratings 46 kv and above. A reflection of these revised ratings in our own make of switches is shown in Fig. 3. The 20,000-ampere momentary rating per pair of contact fingers for the jaws of Fig. 3 evolved as a result of our own laboratory testing. This rating represents satisfactory performance and includes a reasonable margin of safety.

The appearance of the in-line jaw in Fig. 3 is directly attributable to the program outlined in this paper. Upon testing the 161-kv switch with a conventional jaw at increasingly higher test currents in our own laboratory prior to shipment for the TVA tests, we observed the tendency for the blade to be urged out of its jaw contacts. This blade "blow-open" effect is the result of electromagnetic forces set up by current passing through the offset current path of the conventional jaw. The in-line jaw was designed to remedy this condition, and it is a sound and proven solution. Removal of the offset path simultaneously eliminates the objectionable electromagnetic forces.

Summarizing briefly then, there did arise a need for extending the momentary current capability of outdoor air switches; recognition was given to this need in the eventual assignment of switch ratings to match circuit-breaker ratings; and finally a means of providing switches with jaw contact arrangements in accordance with the revised ratings was found. The TVA is deserving of credit for the active role it has played in this general program.

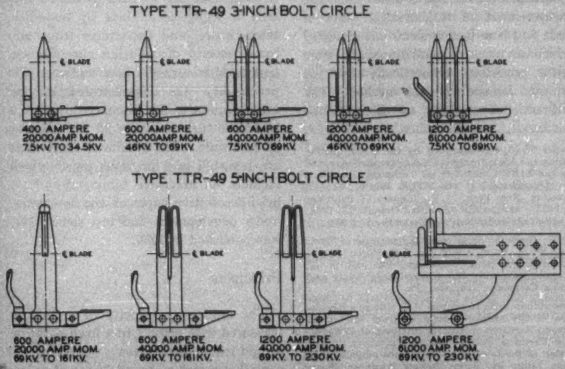
TYPE TTR-49 3-INCH BOLT CIRCLE

TYPE TTR-49 5-INCH BOLT CIRCLE

Fig. 3. Jaw contact arrangements as applied to vertical break switches

A. M. McNerney: I am deeply grateful for the interest shown in this paper as evidenced by the number of discussions and also for their generally complimentary nature. In so far as most of the discussions cover similar points, I shall consider them as a whole instead of commenting on them individually.

Several mention the new series of short-time ratings adopted by NEMA subsequent to the completion of our tests. We feel that our requirements and tests emphasized the need of such ratings and accelerated their adoption.

Comments were also made on our recommendation that definite standards be set up for conditions under which temperature tests are to be made. We are pleased that the latest edition of NEMA adopts the general features of our recommendation. Mr. Curtis states that our temperature tests were unduly severe. To that we agree, but it was only by such severe conditions that we could eliminate as many variables as possible so as to make a fair comparison between all of the makes tested. In this connection, I would like to mention Mr. Powell's comment that the paper does not bear out the statement that there were gross differences between the results obtained by me and those made in factories. That is true, the statement having been made only on the basis of what we had observed. In general, certifications of tests made in the usual large, open, and sometimes drafty test bays in factories, compared with our tests, show differences of as much as 10 degrees on parts as comparable as the center of 2-inch IPS blades.

Considerable discussion was offered on the merits of various types of contacts and our conclusions regarding means of increasing the momentary ratings of switches. Most of the switches submitted were standard designs, modified only at the jaw end. We did not try to evaluate the comparative merits of those modifications but listed those which successfully met the test. Mr. Killian's statement that angular or offset contacts require a blade of sufficient strength and a mounting sturdy enough to prevent backing up is a good one. However, multiple contacts of the angular type, if of sufficient number, seem to eliminate at least part of that problem. Whether this is due to better gripping action by the multiple contacts (for the magnetic forces are still there) we do not have sufficient data to say. However, referring to Table VI, in tests *H-1* and *J-1*, with single contacts the blade blew completely out of the jaw. The same switches with multiple contacts, tests *H-10* and *J-12*, successfully withstood the test current. We believe, although we do not have sufficient data to prove it conclusively, that multiple contacts of the angular type, even when provided with enough fingers, probably have a top limit of a 62,000-ampere rating with a reasonable added safety factor. The straight-line and reverse-loop contacts should have no difficulty matching the 15,000 megavolt-ampere 161-kv circuit-breaker rating which the industry is now developing.

Mr. Powell states that, if switches are made to a certain standard, there is no justification for expecting them to meet greater values by making minor changes in the switch design. If I understand him correctly, he questions why we should expect to find excess capacity in existing switches or increase their capacity by minor modifications. He is well justified in questioning this. However, by determining the excess capacity in existing switches or devising means of making minor modifications to increase their capacity, we were able to establish that existing switches were able to meet the short-circuit requirements at certain locations. As a result of these tests we estimate that the TVA saved in excess of $1,000,000 by not having to replace switches.

In concluding, I want to thank Mr. Burdeshaw for the tests he furnished to show the effect of various finishes and coatings on the temperature of copper tube. We are pleased to note that his test results confirm our findings on switch *F-1*, table II. This, as well as the other temperature data he furnishes, make a valuable addition to this paper.

Principles and Application of the Ultrasonic Flowmeter

R. C. SWENGEL
ASSOCIATE MEMBER AIEE

W. B. HESS
NONMEMBER AIEE

S. K. WALDORF
MEMBER AIEE

NO ONE method of measurement of fluid flow has been or probably ever will be devised that will solve satisfactorily all problems as varied as the determination of flow in ocean tides, rivers, irrigation flumes, pipelines, water and sewage systems, and myriad industrial and laboratory processes. Some basic methods, however, can be used for a wide variety of applications and it is believed that the new ultrasonic flow meter is one of these. It should find many fields of usefulness in addition to the measurement of hydraulic turbine discharge, its first application, because it has no components in the measuring section which can clog or jam; it is accurate and relatively simple, and it is basically an absolute method which permits its use without prior calibration by other means. In hydroelectric turbine testing, a single ultrasonic flow measurement and calculation is made regularly in about 15 minutes, a considerably shorter period than is possible with other test methods. For continuous service, the meter can be made to indicate and record directly in terms of velocity or quantity of flow.

This new bidirectional method measures flow velocity by determining the apparent difference in the velocity of compression waves propagating with and against the flow over a single path.[1] Apparent changes in velocity of propagation are determined by measuring the wave transit times, or differences in transit times, between two fixed points. The new method described in this paper is adaptable to widely varying conditions; however, the equipment, especially the transducers, may have to be designed for the specific application. Knowledge of the method's characteristics and present limitations may even preclude its use where other methods now offer very satisfying solutions.

Because the method is based upon the measurement of fundamental units of time and length, any electronic circuitry which can measure small intervals of time with precision, theoretically can be adapted for use with the method. The bidirectional method, as distinguished from the older upstream-downstream methods, uses but two transducers whose functions as transmitter and receiver are interchangeable. It is even conceivable that the transducers could be both transmitter and receiver simultaneously using differing frequencies or frequency-modulated signals. Or, using electronic gating and pulsing, both transducers could transmit simultaneously, then quickly revert to their receiving function to determine transit times. Another technique, alternate transmissions at a fixed frequency with differences in transit times determined by phase-angle measurement, was used in the initial application.

The validity of the new ultrasonic method was established in the laboratory where errors of 1 per cent and less were obtained with water velocities of 1 to 10 feet per second in a 5-inch by 9-inch steel conduit. These tests of accuracy also showed that the method is affected to only a negligible amount by turbidity, temperature, and departures from uniform velocity distribution normally encountered in straight flow sections. Its practicality was demonstrated by the measurement of the discharge through a hydraulic turbine intake 25 feet high by 16 feet wide. The results of these tests are reported in a previous paper which includes an extensive bibliography.[2] A brief descriptive paper on the flowmeter, under development and test since 1947, was published in 1950.[3]

Principles

The motion or velocity of a fluid is measured with respect to a fixed point or a rigid frame of reference. In the ultrasonic flowmeter a second frame of reference, the fluid itself, must be considered

---

Paper 55-28, recommended by the AIEE Instruments and Measurements Committee and approved by the AIEE Committee on Technical Operations for presentation at the AIEE Winter General Meeting, New York, N. Y., January 31–February 4, 1955. Manuscript submitted October 15, 1954; made available for printing December 23, 1954.

R. C. Swengel is a consulting engineer in York, Pa., W. B. Hess is with the Safe Harbor Water Power Corporation, Conestoga, Pa., and S. K. Waldorf is with the Pennsylvania Water and Power Company, Lancaster, Pa.

The authors wish to express their sincere appreciation of the assistance received from Robert G. Roush, Research Associate, Institute of Cooperative Research, Johns Hopkins University, in the design of the low output-impedance amplifier and from James M. Barry, System Engineer, Pennsylvania Water and Power Company, in the mathematical development of Appendixes I and II.

Nomenclature

c = velocity of propagation of sound in fluid whose flow velocity is to be measured
c_r = velocity of propagation of sound in transducer rod
d = displacement of transducers along axis of flow and length of measuring section of flowmeter
d' = actual geometric distance between transducers
f = frequency of ultrasonic signals, cycles per second
$j = \sqrt{-1}$ = mathematical complex operator
$n = v/c$
t = difference between upstream and downstream transit times $= t_u - t_d$
t_0 = transit time for a compression wave to travel in either direction from one transducer to other when there is no flow
t_d = transit time for a compression wave to travel downstream from one transducer to other
t_u = transit time for a compression wave to travel upstream from one transducer to other
v = velocity of flow of fluid to be measured
w = width of measuring section of flowmeter
Δ = difference between phase angles measured when transmitting with and against flow
β = angle of path of ultrasonic signal when leaving transmitter, with respect to horizontal reference axis
$\theta = \cos^{-1} c/c_r$ = radiation angle of terminated transducer
ϕ = angle of geometric path between transducer locations, with respect to horizontal reference axis

---

wherein the velocity of propagation is constant. When the fluid moves with respect to the rigid frame of reference, there are apparent changes in propagation velocity within the fluid relative to the rigid frame of reference. The ultrasonic flowmeter utilizes these apparent changes in propagation velocity as a means for determining the velocity of movement or flow.

To measure velocities with the new method, two fixed points on the stationary frame of reference are used. In the most elementary case, the two points are considered on the axis of flow, with a compression wave originating at one of the points and traveling to the other. If there is no flow

$$c = \frac{d}{t_0} \tag{1}$$

When the fluid moves at constant velocity and the wave is transmitted in the direction of flow

$$c + v = \frac{d}{t_d} \tag{2}$$

When the wave is transmitted against the direction of flow

$$c - v = \frac{d}{t_u} \tag{3}$$

Subtracting equation 3 from equation 2

$$(c+v)-(c-v) = \frac{d}{t_d} - \frac{d}{t_u} \tag{4}$$

$$2v = \frac{d}{t_d} - \frac{d}{t_u} \tag{5}$$

or

$$v = \frac{\frac{d}{t_d} - \frac{d}{t_u}}{2} = \frac{d}{2}\left(\frac{1}{t_d} - \frac{1}{t_u}\right) \tag{6}$$

It will be noted that the absolute propagation velocity does not appear in equation 6 for the determination of flow velocity. Fundamentally, therefore, the method can be applied to the measurement of velocity of flow of any fluid, regardless of the absolute propagation velocity which can vary considerably with temperature, pressure, and the medium. It is essential in using equation 6 that absolute elapsed transit times be measured and that they be expressed in absolute units, i.e., seconds.

For the initial development, it appeared more desirable to measure differences in upstream and downstream transit times with sinusoidal signals of a fixed frequency than to use single pulses. A change in the phase angle between the voltages on the transmitting and receiving transducers is a measure of the velocity of flow. This effect is utilized in the new bidirectional method when the measurement is made of the difference in phase angle produced by the alternate upstream and downstream transmissions over a single path. Another basic principle that needs to be considered is the condition where the transmission path is not along the axis of flow but at an angle. This is included in the development of generalized equations given in Appendixes I and II.

It will be noted in equations 30, 32, 35, and 36 in Appendix I that the absolute velocity of propagation in the fluid during measurement must be known when a technique utilizing transit time differences is used. Further, it is interesting and significant to note that the displacement of the transducers along the axis of flow is the dimension of the measuring section entering into the velocity determination. Of course, the width and height of the measuring section must be known to calculate the volume of flow.

Equation 40, in Appendix II, for calculating flow from t_d and t_u with the transmission path at an angle to the axis of flow becomes the same as equation 6 when the path between transducers is along the axis of flow because $\phi = 90$ degrees and $\sin\phi = 1$. In the foregoing analyses, only a uniform constant flow velocity is considered, an ideal not existing in practice. The ultrasonic flow meter is not affected by appreciable departure from uniform velocity distribution, the measuring signals integrating vectorially the velocities through which they pass.

Transducers for Area Measurements

In the preceding section the flow in a single plane is analyzed. In practice, it is usually desirable to measure a volume of flow which involves the determination of the average flow velocity over a cross section. To accomplish this, linear transducers were developed for use in rectangular ducts which in effect are line sources of ultrasonic radiation rather than point sources. When two such transducers are properly positioned, the received signal will have traversed all elements of the flow cross section and will have been affected by all components of the flow velocity. In the initial application of the flowmeter, which was the measurement of the discharge through one of the three bays comprising the intake of a 42,500-horsepower low-head hydroelectric turbine, velocities were averaged over a cross section of 400 square feet for flows up to 2,500 cubic feet per second.

Fig. 1. 30-foot transducer installed in turbine intake

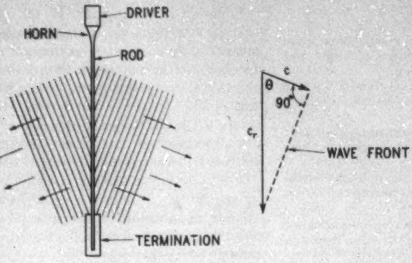
DRIVER
HORN
ROD
TERMINATION
c
θ
90°
c_r
WAVE FRONT

Fig. 2 (left). Conical wave pattern of terminated transducer

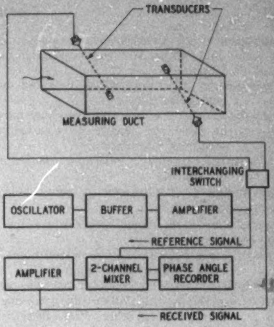
TRANSDUCERS
MEASURING DUCT
INTERCHANGING SWITCH
OSCILLATOR
BUFFER
AMPLIFIER
REFERENCE SIGNAL
AMPLIFIER
2-CHANNEL MIXER
PHASE ANGLE RECORDER
RECEIVED SIGNAL

Fig. 3 (right). Block diagram of equipment used

Fig. 1 shows this installation and may convey some impression of the large quantities of water measured. These transducers were found to be in excellent condition after being totally submerged for 1 year.

A linear transducer consists of three principal parts—the driver, the mechanical transformer or horn, and the antenna or radiator. Depending upon the frequency used, the driver may be piezoelectric for the higher frequencies or magnetostrictive for the lower frequencies The horn is a mechanical coupling or impedance-matching device between the driver and the antenna.[4] It has an exponential taper and its size is dependent upon the frequency at which it is used. The stainless steel antenna rod shown in Fig. 1 has a diameter of 1/4 inch.

Transducers may be either resonant or nonresonant, the latter being the more desirable because of their highly directional characteristics which help to eliminate the effects of echoes and other undesired transmission paths. Radiation patterns can be predicted within narrow limits from the relations between propagation velocities in the antenna and the fluid medium. As a nonresonant system, the undriven end of the transducer rod is made to absorb any acoustic energy not radiated into the fluid. This produces a radiation pattern having the form of a cone, as represented in Fig. 2. In water, c is about 4,800 feet per second, and c_r is about 17,000 feet per second in chrome stainless steel.

Appendix III gives a method for calculating the proper tilt angle when mounting nonresonant transducers. It will be noticed in Fig. 6 that, in addition to the transducers being placed on opposite walls, their driven ends are placed facing in opposite directions. This is done to have the path of every element of the ultrasonic signal pass through the same length of transducer rods and undergo the same phase shift and attenuation due to the rods. This ensures that differences in the signal components are caused by fluid velocity effects only.

Electronic Equipment

Fig. 3 is a block diagram of the equipment used for proving the validity of the method and for hydroelectric turbine testing. It utilizes continuous transmission at a fixed frequency with cyclic reversal of the direction of transmission and measurements of the phase angle between transmitted and received signals. The difference between the phase angles for upstream and downstream transmissions is the measure of flow velocity. This technique was used for testing because it appeared to be the least complicated for applications with water subject to very slow temperature changes.

The measuring system has three principal functions—transmitting, interchange of transducers, and measurement of phase angle. The power source has three features:

1. The frequency is adjustable over a range of 5 per cent and has very high stability.
2. Changes in load do not affect the oscillator frequency.
3. The reference voltage derived from the power source is not affected by any difference in impedances of the two transducers.

The oscillator chosen for the power supply is a *6AG7* in a modified Clapp circuit; see Fig. 4. A voltage having high harmonic content is taken from the plate circuit of the *6AG7* for direct comparison with the standard frequency broadcast of the National Bureau of Standards station *WWV*. The Clapp circuit offers the advantage of high stability and permits close adjustment of the operating frequency. The buffer, a *6SK7* tuned

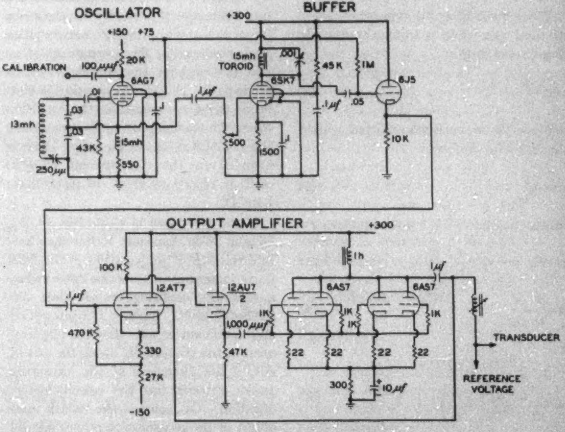
OSCILLATOR
+150
+75
CALIBRATION
100μμf
20K
6AG7
.01
.03
.03
13mh
43K
15mh
550
250μμ
.1
BUFFER
+300
15mh TOROID
.001
45K
1M
6SK7
.1μf
.1μf
.05
6J5
500
1500
.1
10K
OUTPUT AMPLIFIER
+300
1h
1μf
100K
12AT7
12AU7/2
6AS7
6AS7
.1μf
470K
330
27K
-150
1,000μμf
47K
1K
1K
1K
1K
22
22
22
22
300
10μf
TRANSDUCER
REFERENCE VOLTAGE

Fig. 4. 25-kc power supply

amplifier with a *6J5* cathode follower, eliminates the effects of load changes on the oscillator frequency.

The output amplifier comprising the balance of the circuit has an output impedance of a fraction of 1 ohm and supplies a few watts with adequate current for the highly capacitive load of a crystal transducer. An inductance is placed in series with the transmitting transducer to lower the load impedance and to obtain a better match between the amplifier and transducer. The reference voltage, Fig. 4, is taken directly from the output terminals of the output amplifier to eliminate any possibility of phase shifts within the amplifier which might occur as the result of differing transducer load impedances.

The receiving amplifier in Fig. 3 is conventional except that precautions were taken to avoid phase shifts with changes in amplitude of the received signal. This condition is readily obtained by the use of air-core inductors. The mixer circuit is also conventional, using a heterodyne oscillator to reduce the frequency of the two incoming signals to approximately 500 cycles per second. This is done to make the rise time of the square-wave pulses actuating the phase-angle circuit a negligible fraction of 1 cycle.

The phase-angle recorder circuit is similar to several commercially available types using clipping and squaring of the two sine wave voltages along with an Eccles-Jordan switching circuit to produce a pulsating direct voltage whose average value is directly proportional to the phase angle between the two voltages being compared. This voltage is recorded on a Minneapolis-Honeywell 10-inch high-speed electronic strip chart recorder calibrated in degrees of phase angle. This recorder has a very linear response which is important for the accurate determination of phase-angle differences. A phase shifter inserted in either channel is convenient for phase-angle calibration as well as for positioning the record on the chart.

The coaxial mechanical interchanging switch was designed expressly for this application. The most important feature of its design is the high degree of isolation between transmitting and receiving circuits attained by the use of thorough shielding. All contacts are of the silver wiping type to minimize any change in impedance of the coaxial cables with which it is used. A Geneva gear train on a slow-speed gear motor provides the necessary torque with the required dwells and time intervals for switching. The switching cycle for this application is 10 seconds.

Practical Considerations

With any method of measurement, certain precautions must be taken to attain a high degree of accuracy. The necessary precautions and considerations for the attainment of a high degree of accuracy with the ultrasonic flowmeter are as follows:

1. There must be accurate knowledge of the velocity of propagation of sound in the fluid to be measured when a phase-angle or other transit-time difference measuring technique is used. For water, accurate data are available.[8]
2. The approximate range of flow velocity to be measured.
3. The limiting physical dimensions of the measuring section must be known.
4. Transducers must be chosen or designed to have radiation patterns suitable for the measurement to be made.
5. No mechanical nor electric coupling between the transmitting and receiving circuits is permissible other than the acoustic path through the fluid being measured. Also, there must be no coupling between the receiving and reference voltage circuits prior to phase-angle comparison.
6. There must not be undesired acoustic echo paths in the measuring section. This is obtained when there is a linear relation between phase angle and frequency for transmissions in the measuring section in the range of frequency used for measurement.
7. Transducer radiation patterns must not be modified by the transducer mounting.
8. Equipment must be independent of surroundings and of variations in supply voltage as well as free from phase shifts arising from changes in signal levels.

Conclusions

1. The bidirectional ultrasonic method makes possible the determination of flow velocity of a fluid with accuracy even when the physical properties of the fluid are known only approximately.
2. Because the method is based on measurements of fundamental units of time and length, it requires no velocity calibration by other means or methods prior to use and is amenable to rigorous mathematical analysis.
3. The method is quite versatile because signal transit times can be measured in several ways, the transducers can have many forms, and the electronic circuitry can be varied to satisfy the designer's needs and judgment.
4. Usually the transducers can be installed without alteration of the flow section and without interference to flow.
5. The velocity-sensitive elements, having no moving parts nor openings, are practically immune to clogging and jamming.
6. A new class of transducers, the linear or antenna type, has been developed and applied. This principle of utilizing ultrasonic driving elements on radiating systems makes possible ultrasonic analogues of electromagnetic antennas and radiation patterns.
7. Extensive laboratory tests with a rectangular 5-inch by 9-inch duct prove the method's practicality and ability to measure accurately over appreciable ranges of temperature, turbidity, turbulence, and flow distortion.
8. The ultrasonic method is especially well suited to the measurement of large volumes of flow, as shown by its application to the measurement of the discharge of a 42,500-horsepower hydroelectric turbine.

Appendix I. Derivation of Velocity Equations in Terms of Transit Time Differences

The conditions shown in Fig. 5 represent flow at constant and uniform velocity $\mathbf{v}$ in a measuring section of length d and width w. In Fig. 5(A), where the direction of transmission of the ultrasonic signal is upstream, the geometric path AB between transducer locations A and B makes the angle ϕ with the horizontal reference axis. In Fig. 5(B), where the ultrasonic signal is transmitted in the opposite direction, BA makes the angle 180 degrees $+\phi$ with the reference axis.

When there is no flow, the ultrasonic signal follows the identical paths AB or BA, depending upon the direction of transmission

$$AB = BA = d' = \frac{d}{\sin\phi} = ct_0 \tag{7}$$

When there is flow at velocity $\mathbf{v}$, the vector relationship in Fig. 5(A) in polar form is

$$ct_u\underline{/\beta} + \mathbf{v}t_u\underline{/270^\circ} = d'\underline{/\phi} \tag{8}$$

For the ultrasonic signal to reach point B when there is flow, it must leave the transmitter at angle β instead of at angle ϕ.

Dividing equation 8 by t_u,

$$c\underline{/\beta} + \mathbf{v}\underline{/270^\circ} = \frac{d'}{t_u}\underline{/\phi} \tag{9}$$

Rewriting 9 in rectangular form and placing $j\mathbf{v}\sin 270$ degrees $= -j\mathbf{v}$

$$c\cos\beta + jc\sin\beta - j\mathbf{v} = \frac{d'}{t_u}\cos\phi + j\frac{d'}{t_u}\sin\phi \tag{10}$$

Separately equating reals and imaginaries in equation 10

$$c\cos\beta = \frac{d'}{t_u}\cos\phi \tag{11}$$

$$c\sin\beta - \mathbf{v} = \frac{d'}{t_u}\sin\phi \tag{12}$$

$$\cos\beta = \frac{d'}{ct_u}\cos\phi \tag{13}$$

$$\sin\beta = \frac{d'}{ct_u}\sin\phi + \frac{\mathbf{v}}{c} \tag{14}$$

Squaring equations 13 and 14, adding

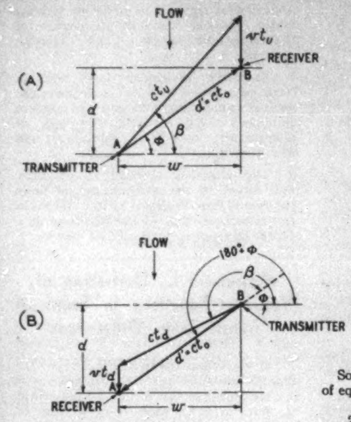

Fig. 5 (left). Vector relationships

A—upstream transmission
B—downstream transmission

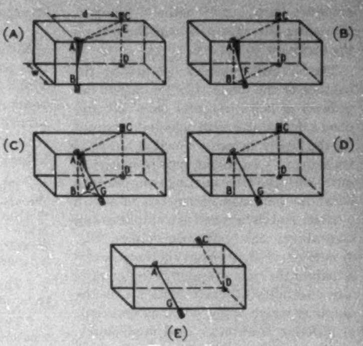

Fig. 6 (right). Determination of tilt angle for terminated transducers

them, and replacing $\sin^2\beta+\cos^2\beta$ by its equivalent, unity

$$1=\left(\frac{d'}{ct_u}\right)^2\sin^2\phi+2\frac{d'\mathbf{v}}{c^2t_u}\sin\phi+\frac{\mathbf{v}^2}{c^2}+\left(\frac{d'}{ct_u}\right)^2\cos^2\phi \quad (15)$$

Combining the first and fourth terms on the right-hand side of equation 15, replacing $\sin^2\phi+\cos^2\phi$ by its equivalent, unity, multiplying through by c^2, and rearranging terms

$$\mathbf{v}^2+\frac{2d'\mathbf{v}}{t_u}\sin\phi+\left(\frac{d'}{t_u}\right)^2=c^2 \quad (16)$$

For ultrasonic signal transmission downstream, as represented in Fig. 5(B), equation 17 can be derived by the method followed to obtain equation 16

$$\mathbf{v}^2-\frac{2d'\mathbf{v}}{t_d}\sin\phi+\left(\frac{d'}{t_d}\right)^2=c^2 \quad (17)$$

For convenience in computation and as a criterion of applicability for the several forms of equations for flow velocity, the ratio n is introduced

$$n=\mathbf{v}/c \quad (18)$$

$$\mathbf{v}=nc \quad (19)$$

In equation 16 substitute equation 19 for $\mathbf{v}$ and equation 7 for d'

$$n^2c^2+\frac{2(ct_0)(nc)}{t_u}\sin\phi+\frac{c^2t_0^2}{t_u^2}=c^2 \quad (20)$$

Multiplying equation 20 through by t_u^2/c^2

$$n^2t_u^2+2nt_0t_u\sin\phi+t_0^2=t_u^2 \quad (21)$$

$$(1-n^2)t_u^2-(2nt_0\sin\phi)t_u-t_0^2=0 \quad (22)$$

Equation 22 is a quadratic of the form

$$ax^2+bx+c=0 \quad (23)$$

The standard solution to equation 23 is

$$x=\frac{-b\pm\sqrt{b^2-4ac}}{2a} \quad (24)$$

Solving equation 22 for t_u, using solution of equation 24

$$t_u=\frac{2nt_0\sin\phi\pm\sqrt{(2nt_0\sin\phi)^2+4(1-n^2)t_0^2}}{2(1-n^2)}$$

$$=t_0\left(\frac{n}{1-n^2}\right)\sin\phi\pm\frac{\sqrt{(2nt_0\sin\phi)^2+4(1-n^2)t_0^2}}{2(1-n^2)} \quad (25)$$

The analogous equation for t_d can be derived from equation 17 by similar procedure and is identical to equation 25 except that $\sin\phi$ has a negative sign. The first term, therefore, has a negative sign in the equation for t_d, but the second terms are identical in equations for both t_u and t_d because $\sin\phi$ is squared. Therefore

$$t=t_u-t_d=2t_0\left(\frac{n}{1-n^2}\right)\sin\phi \quad (26)$$

or

$$tn^2+(2t_0\sin\phi)n-t=0 \quad (27)$$

Solving for n using standard quadratic solution of equation 24

$$n=\frac{-2t_0\sin\phi\pm\sqrt{4t_0^2\sin^2\phi+4t^2}}{2t} \quad (28)$$

Solving equation 28 for $\mathbf{v}$ after substituting $n=\mathbf{v}/c$ from equation 18 and $t_0=d/(c\sin\phi)$ from equation 7

$$\mathbf{v}=\frac{-d\pm\sqrt{d^2+c^2t^2}}{t} \quad (29)$$

Since $\mathbf{v}$ is always positive or zero, equation 29 becomes

$$\mathbf{v}=\frac{\sqrt{d^2+c^2t^2}-d}{t} \quad (30)$$

If sinusoidal signals of frequency f are used to measure t by determining the phase-angle difference Δ between the upstream and downstream transmission conditions

$$t=\frac{\Delta°}{360°}\times\frac{1}{f}=\frac{\Delta}{360f} \quad (31)$$

Substituting equation 31 in equation 30

$$\mathbf{v}=\frac{\sqrt{d^2+(c^2\Delta^2)/(360f)^2}-d}{\Delta/360f}$$

$$=\frac{\sqrt{(360fd)^2+c^2\Delta^2}-360fd}{\Delta} \quad (32)$$

Equations 30 and 32 can be replaced by simpler equations if the ratio $n=\mathbf{v}/c$ is small. In the measurement of the discharge of hydraulic turbines, $n\approx 10/4{,}800$ and $n/(1-n^2)\approx n$ to within one part in 230,400. Under such circumstances, equation 26 can be simplified to

$$t=2t_0n\sin\phi=2t_0(\mathbf{v}/c)\sin\phi \quad (33)$$

from which

$$\mathbf{v}=\frac{ct}{2t_0\sin\phi} \quad (34)$$

Since $t_0=d/(c\sin\phi)$ from equation 7

$$\mathbf{v}=(c^2t)/2d \quad (35)$$

To convert equation 35 for use where Δ is measured, substitute equation 31 in equation 35

$$\mathbf{v}=(c^2\Delta)/(720fd) \quad (36)$$

Appendix II. Derivation of General Velocity Equation in Terms of Absolute Transit Times

Subtracting equation 17 from equation 16 eliminates c

$$(2d'\mathbf{v}\sin\phi)/t_u+(2d'\mathbf{v}\sin\phi)/t_d+(d'/t_u)^2-(d'/t_d)^2=0 \quad (37)$$

Combining terms and dividing by d'

$$2\mathbf{v}\sin\phi\left(\frac{1}{t_u}+\frac{1}{t_d}\right)=d'\left(\frac{1}{t_d^2}-\frac{1}{t_u^2}\right)$$

$$=d'\left(\frac{1}{t_d}-\frac{1}{t_u}\right)\left(\frac{1}{t_d}+\frac{1}{t_u}\right) \quad (38)$$

which results in

$$\mathbf{v}=\frac{d'}{2\sin\phi}\left(\frac{1}{t_d}-\frac{1}{t_u}\right) \quad (39)$$

Substituting for d' from equation 7

$$v=\frac{d}{2\sin^2\phi}\left(\frac{1}{t_d}-\frac{1}{t_u}\right) \qquad (40)$$

This general equation becomes equation 6 when $d'=d$, because ϕ is then 90 degrees and $\sin\phi=1$.

Appendix III. Calculation of Transducer Tilt Angle

Fig. 6 shows graphically a method for determining the proper tilt angle for mounting terminated transducers in a rectangular flow section. In Fig. 6(A), both transducers are shown in a vertical position displaced along the axis of flow by a distance d. The angle CAE is 90 degrees$-\theta$, where θ is the radiation angle in Fig. 2. If the transducers were mounted vertically as illustrated, the section of flow included in triangle ACE would not be included in the velocity measuring area.

As a first step, the transmitting transducer is moved to position AF, sufficiently to make E coincide with C, where F is on the line BD. The shortcoming of this position is the omission from measurement of the flow in triangle ABF. Angle $BAF=$ 90 degrees$-\theta$. Therefore, BF can be determined from the relation $BF=AB\times\tan$ (90 degrees$-\theta$).

In Fig. 6(C), the transmitting transducer has been rotated about axis AC until the transducer coincides with the wall, assuming its final position AG. Since BFG is a right angle because of this rotation about AC and angle $GBF=\tan^{-1} w/d$ is fixed by the dimensions of the duct, BG can be determined from the equation $BG=BF/(\cos GBF)$.

In Fig. 6(D), it can be seen that the tilt angle BAG is $\tan^{-1}(BG)/(AB)$. In Fig. 6(E), the receiving transducer CD has been placed in its final position by making it parallel to transducer AG by rotation in the plane of the wall about point C.

References

1. Fluid Velocity Measuring Apparatus, R. C. Swengel. U. S. Patent applied for.

2. The Ultrasonic Measurement of Hydraulic Turbine Discharge, R. C. Swengel, W. B. Hess, S. K. Waldorf. *ASME Transactions*, American Society of Mechanical Engineers, New York, N. Y. (*Paper 54A-54*).

3. Measuring Water Velocity by an Ultrasonic Method, W. B. Hess, R. C. Swengel, S. K. Waldorf. *Electrical Engineering*, vol. 69, no. 11, Nov. 1950, p. 983.

4. Piezoelectric Crystals and Their Applications to Ultrasonics (book), W. P. Mason. D. Van Nostrand Company, Inc., New York, N. Y., 1950, pp. 163–64.

5. Properties of Ordinary Water Substance (book), N. E. Dorsey. Reinhold Publishing Company, New York, N. Y., 1940, pp. 191–93.

◆

Discussion

Fred E. Cornwell (Bureau of Reclamation, Denver, Colo.): This paper deals with a subject of vital importance to the engineer who is associated with hydroelectric installations. There is no question but that an accurate, dependable method of making flow measurements on large installations presents many problems which have not been solved satisfactorily. A method which can give results of a flow measurement in a time approaching 15 minutes would appear to offer real advantages, provided it can yield accurate, dependable results under field conditions. The authors present a very interesting approach with their ultrasonic meter.

It is difficult to evaluate the general procedure and accuracy of the instrument without further technical details and possibly test data. The authors state, "The ultrasonic flowmeter is not affected by appreciable departure from uniform velocity distribution, the measuring signals integrating vectorially the velocities through which they pass." How could variable cross-sectional areas associated with these variable velocities be integrated to give appropriate flows? The question of nonuniform velocities has been at the root of many difficulties encountered with other methods. It is stated that the instrument requires no prior calibration in that it is basically an absolute method It appears to me that some calibration, possibly as a function of conduit shape and average velocity, would be essential.

In the paper reference is made only to rectangular shapes. For anything approaching general usage, applicability to circular shapes would be highly desirable. Any work related to this question would be of interest. Test data on the discharge measurements for the 42,500 -horsepower hydroelectric turbine on which this instrument was used would be of assistance in evaluating the device. If available, similar data by alternate methods should be included.

The ultrasonic flowmeter, or future modifications of it, may be found of use by the hydraulic industry. However, before it can gain general acceptance, the hydraulic engineer will need to be convinced that it does consider realistically the difficulties which have confronted him in the past I hope that my questions will assist in clarifying some of the points involved.

J. R. Leslie (Hydro-Electric Power Commission of Ontario, Toronto, Ont., Canada): The authors are to be commended for originating and aptly describing a new technique in the hydraulic measurement field. The scheme described appears to have great promise. Could the authors answer one or two questions concerning the case of nonuniform flow? As is well known, some of the difficulties with present techniques are caused by the presence of a nonuniform distribution of velocity across the intake, owing to either turbulence or the changing cross section. Is it possible then, on theoretical grounds, to show that the method of measurement yields a true average of the velocity? Secondly, the presence of turbulence in the water should affect the amplitude of the received signal, and possibly make the instrument nonworkable. Have any measurements of signal attenuation across the channel been made?

Robert T. Knapp (California Institute of Technology, Pasadena, Calif.): The accurate measurement of the flow rate of large quantities of liquid has been serious problem for a great many years. Most of the methods of measurement found satisfactory for small flow rates are not applicable to the larger flows, principally because they are not primary measurements but require calibration, and the calibration is not possible with large flow rates because of the tremendous construction cost of suitable calibrating basins or weighing tanks. Therefore, the presentation of a new primary method of flow measurement is always of great interest to the engineering profession. This paper appears to be of particular importance because it not only proposes a new primary method of flow measurement, i.e., one which does not require calibration but also a method which does not require unduly expensive equipment or serious modification of the flow channel. Furthermore, although it basically measures the instantaneous flow rate, the measurements can be repeated so rapidly as to form a continuous record of flow rate, thus making it adaptable to unsteady as well as to steady flow.

The paper deals primarily with the general principles of the method and two quite different methods of use, one requiring prior knowledge of the velocity of sound in the flowing liquid, and the other independent of it. However, very little has been said concerning the inherent limitations of the method. Additional discussions of the following points would be valuable: Factors affecting upper limits of accuracy attainable, either in the instrumentation or caused by the flowing fluid; effect of variation in velocity across the cross section, particularly in the direction perpendicular to the direction of travel of the measuring sound waves; and methods of application to nonrectangular cross sections, in particular to circular ones.

The authors are to be congratulated upon the presentation of this paper. It is hoped that they will be encouraged to pursue vigorously the development of this new flow meter.

F. L. Lawton (Aluminum Laboratories Limited, Montreal, Que. Canada): The authors have succeeded in developing a method of measurement of fluid flows which is apparently adaptable to economic permanent installation so that the efficiency of a number of water wheels in a plant can be expeditiously determined from time to time. The authors could confirm this?

It is well known that the efficiency of water wheel runners varies over a long period of time owing to changes in the profile of the blades arising from repairs associated with pitting from cavitation. Such repairs restore the exact profile. Consequently, the efficiency of the unit varies. This becomes of importance in achieving optimum economy of water usage and maximum kilowatt-hour generation from a group of units.

It would be interesting to have the authors' opinion on the relative accuracy of the ultrasonic method as applied to the measurement of flow through relatively long penstocks as contrasted with other methods such as the salt-velocity and Gibson methods.

C. W. Watchorn (Pennsylvania Water and Power Company, Baltimore, Md.): The real significance of the paper is that a very accurate method for measuring the performance of hydro units under difficult conditions that might not be obtained satisfactorily otherwise is reported, since such information is the basis for the potential improvement in and maintenance of system operating economies that can amount to very large savings under various conditions, particularly in combined hydro and steam systems.

These savings could stem from several sources, e.g.: the knowledge as to the correct characteristics of the units provides a basis for their economical loading both as individual units and also as among the several units in a plant; the method provides a means for readily checking unit performance as a basis for possible adjustment or repairs in case there are indications of sufficient deviation from expected performance to justify such measures; and such knowledge provides the basis for the economical co-ordination of hydro and steam generation.[1]

REFERENCES

1. CO-ORDINATION OF HYDRO AND STEAM GENERATION, C. W. Watchorn. *AIEE Transactions*, vol. 74, pt. III, Apr. 1955, pp. 142–50.

R. C. Swengel, W. B. Hess, and S. K. Waldorf: Several questions of Mr. Cornwell, Mr. Leslie, and Mr. Knapp are answered in reference 2. Perpahs it will add to the scope of this paper to restate that laboratory tests on nonuniform flow of somewhat greater magnitude than expected in the turbine intake indicated no errors when the asymmetry was parallel to the plane of the transducers. Deviations of 2 per cent were found when the asymmetry was perpendicular to the plane of the transducers. The latter can be corrected by utilizing four transducers in place of the usual two. Turbulence created in the laboratory tests by various numbers and widths of steel bars in the flow stream immediately ahead of the measuring section produced no measurable errors. The turbulence did attenuate the signal slightly but not enough to warrant measurements; it is estimated that it was of the order of 5 to 10 per cent.

We realize that the method has a wider field of application to circular flow sections; however, our work was confined to rectangular sections because of the specific problem to be solved. Mathematical analysis and some experiments indicate that the method is applicable to other geometric sections; however, the precision of such measurements has not been determined. Physical problems in sound propagation and transducer design will probably vary with each conduit shape and will require additional research and development.

The ultimate accuracy of the method depends primarily upon a thorough knowledge of the sound-propagation path between transducers. Proportional changes in phase angle or transit time corresponding to changes in frequency of the sound waves for a no-flow or a stable-flow condition is one method of obtaining such knowledge. Instrumentation is secondary and depends upon the degree of reliability and accuracy desired.

Regarding Mr. Lawton's statement, there is no reason why an installation could not be made permanent and periodic efficiency tests conducted. Furthermore, we believe that with additional development of the instrumentation the measurements could be made continuous. The development of the ultrasonic method in this particular case was for turbine intakes too short for either the salt-velocity or Gibson methods. It is our opinion that comparable accuracies could be obtained on rectangular sections suitable to the three methods of measurement.

In view of Mr. Watchorn's and Mr. Lawton's experience and close association with the economic phases of power generation, their comments concerning the importance of obtaining actual performance characteristics of hydraulic turbines are greatly appreciated.

Magnetization of Transformer Cores During Impulse Testing

M. F. BEAVERS
MEMBER AIEE

J. E. HOLCOMB
MEMBER AIEE

L. C. LEONI
ASSOCIATE MEMBER AIEE

THE American Standards Test Code[1] states, in paragraph 22.121, that "Because of the nature of impulse test failures, one of the most important matters is the detection of failure." It suggests a number of indications of insulation failure such as noise within the transformer and the presence of smoke or bubbles. Another means suggested for detecting insulation failure is to compare oscillographic records of the applied voltage and neutral current waves taken during reduced and full-wave tests. Any deviation between the applied voltage wave shapes or between neutral current wave shapes obtained during the reduced full-wave or full-wave tests "indicates changes in impedance arising from insulation breakdown within the transformer, or changes in the impulse circuit external to the transformer, and the cause should be investigated."[1] Under this interpretation, if the impulse circuit external to the transformer is judged satisfactory, the transformer insulation must be considered as having failed to pass the test.

A 250-kva 2,400/4,160Y single-phase transformer was recently tested according to this accepted technique, and was reported to have failed on the basis of increases noted in the oscillograms of neutral current, as well as increased sound in the unit on repeated impulses. The oscillograms indicated that several consecutive applications of the reduced full waves produced successively increasing neutral currents. This effect had been observed by one of the authors in development tests dating back to 1945, and it led to an investigation of possible causes for nonlinear responses of this type. This paper satisfactorily explains these effects by considering the accumulation of residual magnetization which is produced when unidirectional impulse are applied.

This experience demonstrates very clearly that unless the phenomenon is recognized, any difference between the wave shapes during the reduced full-wave and full-wave tests may be falsely interpreted as indication of failure of the transformer insulation.

It is the purpose of this paper to discuss these effects more thoroughly and to establish criteria by which magnetization during impulse testing may be anticipated. Suggestions are also offered for procedures which may permit a better comparison of the waves at reduced and full-wave levels and which minimize the accumulation of residual flux.

The relative effects on the applied voltage wave and the neutral current wave with a 1-turn short circuit will be shown

Paper 55-30, recommended by the AIEE Transformers Committee and approved by the AIEE Committee on Technical Operations for presentation at the AIEE Winter General Meeting, New York, N. Y., January 31–February 4, 1955. Manuscript submitted October 20, 1954; made available for printing November 16, 1954.

M. F. BEAVERS, J. E. HOLCOMB, and L. C. LEONI are with the General Electric Company, Pittsfield, Mass.

The authors wish to thank members of the General Electric High Voltage Laboratory, particularly J. H. Hagenguth, A. F. Rohlfs, P. L. Waldon, and A. J. Welling, for their invaluable help in the experimental stages of these tests.

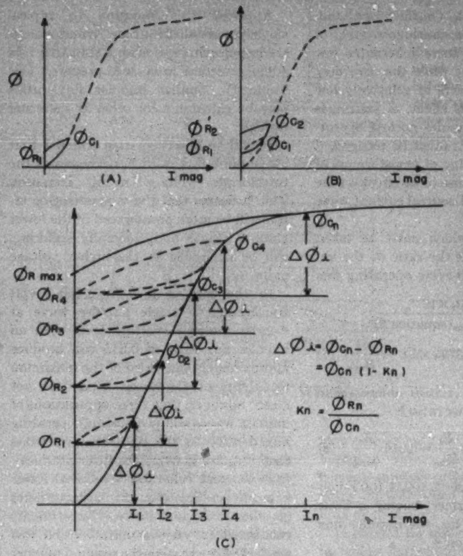

Fig. 1 (left). Sketch of magnetization curve showing cumulative effects of successive impulse waves on winding with initially demagnetized core

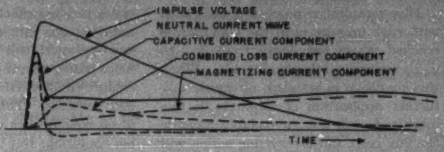

Fig. 2 (above). Typical voltage and neutral current wave shapes

to be much larger than the core magnetization effects.

Mechanics of Core Magnetization

Because impulse test waves are prescribed in transformer standards in terms of times to crest and half value, it is most practical to show the relation between volt-time integrals and core magnetization.

The degree to which transformer cores are magnetized by unidirectional voltages depends upon the voltage, wave shape, number of impulses, and the magnetic characteristics of the core. The flux produced by a single impulse depends upon the time integral of the impulse voltage wave in accordance with the general law of induction

$$e = -N\frac{d\phi}{dt}10^{-8}$$

$$\phi = \frac{-10^8}{N}\int_0^t e\,dt \qquad (1)$$

where

ϕ = total lines of flux, maxwells
e = volts
N = total active turns
t = time, seconds

The flux produced by one impulse, which will be represented by $\Delta\phi_i$, is usually considerably less extensive than the normal 60-cycle operating flux. For 60-cycle operation the flux is

$$\phi_{60} = \frac{10^8}{N}\int_0^{1/240} 1.414E_{\text{rms}} \sin \omega t\,dt$$

$$= 375{,}000\frac{E_{\text{rms}}}{N} \text{ lines of flux} \qquad (2)$$

For an impulse wave excitation, using some relatively simple approximations for the time integral of a standard type of impulse derived in the Appendix

$$\Delta\phi_i = \frac{10^8}{N}\int_0^t e\,dt = 140\frac{E_i t_i}{N} \text{ lines of flux} \qquad (3)$$

where

E_i = impulse crest, volts
t_i = time in microseconds to half crest value according to standard definitions

To illustrate the impulse magnetization process, refer to the typical magnetization curves in Fig. 1, which start from a completely demagnetized core condition.

In Fig. 1(A) ϕ_{C1} indicates the maximum flux attained by one impulse wave of such voltage as to produce a flux increment of $\Delta\phi_i$. When the impulse is over, the flux does not necessarily return to zero because of the retentivity characteristics of the magnetic circuit. Instead, the flux will decay to some point ϕ_{R1} which is the residual flux in the core after one impulse.

When a succeeding impulse wave of the same amplitude and shape is applied, the flux increment $\Delta\phi_i$ is added to the residual flux ϕ_{R1} to reach a new flux crest of $\phi_{R1} + \Delta\phi_i = \phi_{C2}$ as shown in Fig. 1(B). The flux then decays to a new residual value ϕ_{R2}. This is essentially a d-c magnetization process.

The degree to which the flux crest will build up with successive applications of the impulse wave depends on the retentivity characteristics of the particular core. If the core has no retentivity characteristics, the flux in the core would decay to zero after each impulse. Therefore, the ratio ϕ_{R1}/ϕ_{C1} would be zero and no build-up in core magnetization would result with successive impulse waves. However, if the core has retentivity characteristics it retains some of the flux from the preceding impulse wave, therefore a build-up in core magnetization is likely. If $\phi_{R1}/\phi_{C1} = k_1$, $\phi_{R2}/\phi_{C2} = k_2$, etc., and $\phi_{Rn}/\phi_{Cn} = k_n$, where n is the number of impulse waves of a given wave shape and amplitude applied, the build-up in flux crest will proceed in a step-by-step manner as shown in Fig. 1(C). This process can be expressed by the equations

$$\begin{aligned}
\phi_{C1} &= \Delta\phi_i\\
\phi_{C2} &= k_1\phi_{C1} + \Delta\phi_i = k_1\Delta\phi_i + \Delta\phi_i = \Delta\phi_i(k_1+1)\\
\phi_{C3} &= k_2\phi_{C2} + \Delta\phi_i = \Delta\phi_i(k_1+1)k_2 + \Delta\phi_i\\
&= \Delta\phi_i(k_1k_2 + k_2 + 1)\\
\phi_{C4} &= k_3\phi_{C3} + \Delta\phi_i\\
&= \Delta\phi_i(k_1k_2k_3 + k_2k_3 + k_3 + 1) \qquad (4)
\end{aligned}$$

Following this procedure, the flux crest resulting from n successive applications of the impulse wave may be approximated to a satisfactory degree.

If k is approximately constant for the region of the magnetization curve under consideration, the equation for flux crest reduces to

$$\phi_{Cn} = \Delta\phi_i(1 + k + k^2 \ldots + k^{(n-1)})$$

$$= \Delta\phi_i\frac{1-k^n}{1-k} \qquad (5)$$

Table I. Impulse Flux Ratios

Voltage Rating, E_{rms}	BIL E_i, Kv	Ratio, E_i/E_{rms}	Impulse Flux Ratio, F_i
2,400/4,160Y	60	25	0.375
7,200/12,470Y	95	13.2	0.198
14,400	95	6.6	0.099
69,000	350	5.07	0.076

This cumulative process is continued with each impulse until the condition is reached where the decay from ϕ_{Cn} to ϕ_{Rn} is approximately equal to $\Delta\phi_i$. When this condition is satisfied, obviously any further application of impulses of this magnitude will not appreciably increase the flux crest and a recycling action will occur on a minor loop which has a vertical component of $\Delta\phi_i$ and a "bias" or residual flux of ϕ_{Rn}.

Theoretically, an infinite number of impulses would be required to reach a recycling point anywhere below the "knee" of the normal magnetization curve. However, a more realistic approach is to assume that, for all practical purposes, recycling occurs when

$$\phi_{Cn}-\phi_{Rn}=0.95\Delta\phi_i \qquad (6)$$

To determine whether or not a certain transformer will exhibit this residual build-up during impulse testing and if so to what extent, it is necessary to have a magnetization curve and a hysteresis loop diagram of the type of core used in the transformer. As an example in extremes, assume a core with several joints and air gaps. Such a core will have inherently high magnetizing current but the core can be excited to a relatively high flux density without exhibiting any appreciable residual effect. On the other hand, a core made with a continuous strip of low loss steel will have inherently low magnetizing current while the core may exhibit residual effects at relatively low flux densities. This effect, of course, is of no consequence under normal operating conditions but it must be recognized during impulse testing of transformers of certain ratings because of its effect on the impulse voltage and neutral current wave shapes.

Another factor which must be taken into consideration is the ratio of the impulse flux to the 60-cycle operating flux

$$F_i=\frac{\Delta\phi_i}{\Delta\phi_{60}}=\frac{1.4E_it_i\times10^{-6}}{0.00375E_{rms}(\text{equation 2})}$$

$$=373t_i\times10^{-6}\times\frac{E_i}{E_{rms}} \qquad (7)$$

For a standard 1.5x40 microsecond wave, the impulse flux ratio is

$$F_i=373\times40\times10^{-6}\times\frac{E_i}{E_{rms}}=0.015\frac{E_i}{E_{rms}} \qquad (8)$$

For a single-phase 2,400/4,160 *Y*-volt distribution transformer, having a basic impulse level of 60 kv, the impulse flux ratio is, from equation 8

$$F_i=0.015\times\frac{60{,}000}{2{,}400}=0.375$$

Applying this equation to typical single-phase distribution transformers, the impulse flux ratios for a standard 1.5x 40-microsecond wave was prepared (see Table I). Similar impulse flux ratios may be calculated for other transformer ratings.

It will be observed from Table I that the impulse flux ratio F_i decreases as the transformer voltage rating increases. This indicates that the magnetization effect will be more pronounced in the lower voltage ratings and, generally speaking, will be negligible in the higher voltage units.

In the case of a 2,400/4,160 *Y*-volt transformer, a single impulse wave at standard impulse voltage level with an impulse flux ratio of 0.375 will produce approximately one-third of the maximum rated flux of the core. This does not mean, however, that three applications of impulse waves will produce full operating flux density in the core because, when each impulse is over, the flux will decay from its crest value to a somewhat lower value, depending upon the characteristics of the particular core. Experiments conducted on various units verified this method of calculating the residual magnetization.

So far this discussion has been con-

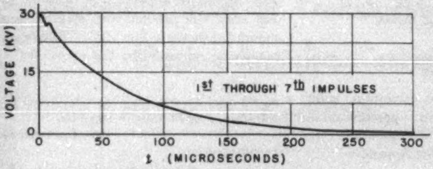

(A) APPLIED VOLTAGE WAVES

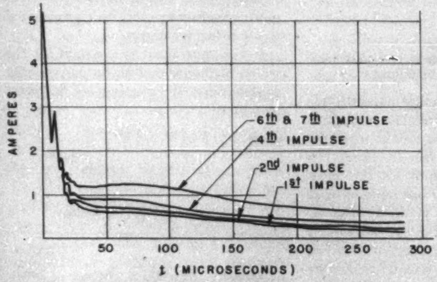

(B) NEUTRAL CURRENT WAVES

Fig. 3. Fifty % BIL, successive impulse voltage and neutral current waves for a transformer with initially demagnetized core and without intermediate demagnetization

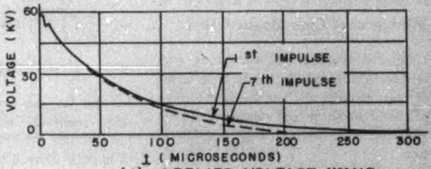

(A) APPLIED VOLTAGE WAVE

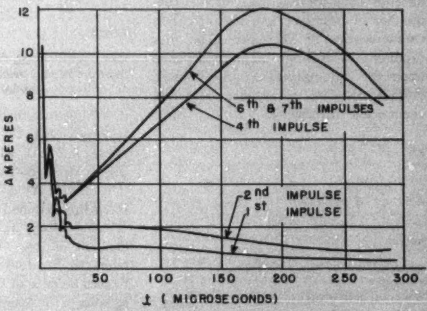

(B) NEUTRAL CURRENT WAVE

Fig. 4. One-hundred % BIL, successive impulse voltage and neutral current waves for transformer with initially demagnetized core and without intermediate demagnetization

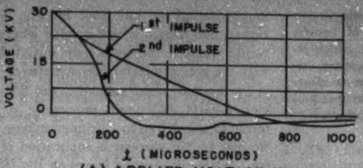

(A) APPLIED VOLTAGE WAVE

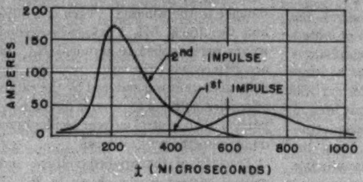

(B) NEUTRAL CURRENT WAVES

Fig. 5. Fifty % BIL, effect of magnetic saturation produced by very long-duration impulse voltage waves applied to transformer with initially demagnetized core. Note: second impulse voltage wave was attenuated by an excessive neutral current due to core saturation

cerned only with the flux produced by the voltage-time area of an impulse voltage wave and the degree of residual flux remaining after the impulse is over. To produce a certain amount of flux, a magnetizing current must flow through the windings. The value of magnetizing current required to produce a given value of flux is determined from the magnetization curve similar to that shown in Fig. 1(C).

When using the neutral-current method of fault detection during impulse testing, this magnetizing current must flow through the neutral impedance circuit; therefore, any changes in the flux crest during impulse testing will be reflected in changes in the neutral-current wave shape. When successive impulses increase the flux crest to levels above the knee of the magnetization curve, the magnetizing current may increase to values many times that of the normal exciting current, Fig. 1(C). If the loading of the impulse circuit depends primarily upon the unit being tested rather than external circuit parameters, then the voltage wave may be considerably affected.

The neutral current wave contains not only the magnetizing current component but also the capacitive current and loss current components as illustrated in Fig. 2. The capacitive current is the charging current which flows through the capacitance of the windings and is of relatively short duration. The magnetizing current component continues to increase as long as a voltage exists across the winding. It follows that the maximum magnetizing current occurs when the excitation voltage approaches zero. At this time the capacitance and loss current components will have decayed to a negligible value; therefore, the neutral current consists primarily of the magnetizing current when the impulse voltage is at or near zero.

It should be quite apparent from the foregoing that changes in the neutral current and applied wave shape may definitely be attributed to changes in core magnetization during impulse tests on certain transformer ratings, and this effect should not be misconstrued as indicative of insulation failure. It should also be stated that, since an appreciable amount of flux may be produced during each impulse, it is reasonable to assume that some degree of magnetostriction occurs which will produce an impact sound.

Experimental Studies in Core Magnetization by Impulse Voltage

To demonstrate the effect of residual magnetization on the impulse voltage and neutral current wave shapes, a series of tests was staged on the 250-kva 2,400/4,160*Y*-volt single-phase transformer referred to at the start of this paper. The basic impulse level of the primary winding was 60 kv.

Tests were started with the core completely demagnetized by slowly decreasing a 60-cycle excitation voltage to zero prior to each set of tests. Then the impulse voltage was applied to one end of the winding while the other end was grounded through a resistance shunt, paralleled by a capacitor to by-pass some of the capacitive charging current. Simultaneous oscillograms of voltage and neutral current waves were recorded.

The first series of impulse tests consisted of several applications of waves at 50-per-cent (%) basic impulse insulation level (BIL), 30-kv. Tracing of the applied voltage and neutral current waves are shown in Figs. 3(A) and 3(B) respectively.

It will be observed that recycling occurred at about the sixth impulse where the neutral current stopped increasing on successive waves. Recycling in this case occurred at a region on the magnetization curve considerably below the saturation level as indicated by the neutral current, which at the time near voltage zero (about 280 microseconds) was less than the normal magnetizing current crest.

In the next series of tests, several impulse waves at 100% BIL (60 kv) were applied, again starting from zero magnetization. Tracings of the applied voltage and neutral current waves are shown in Figs. 4(A) and 4(B) respectively. It is evident from the neutral current waves that recycling occurred at about the sixth application since the neutral current no longer increased on successive waves. Here recycling occurred above the knee of the magnetization curve because the $\Delta\phi_1$ supplied by the impulse voltage exceeded the difference between flux crest and residual-flux at the knee of the normal curve. When this condition exists, the core has accumulated its maximum residual flux, and additional impulses serve only to provide a recycling from this point as indicated by the neutral current which began to increase rapidly at 20 microseconds and reached values well in excess of the normal magnetizing current for the unit. Note also that the applied voltage wave shape was changed slightly because of the relatively heavy current drain on the impulse generator in the vicinity of 100 to 180 microseconds.

To accentuate the magnetization phenomena, long-tail voltage waves (1.8x265 microseconds) were applied to the winding. Tracings of consecutive voltage and neutral current waves are shown in Figs. 5(A) and 5(B) for the 50% voltage level. These waves saturated the core, as evidenced by the tremendous increase in neutral current and the severe drop in impulse generator voltage on other than the first application at the 50% voltage level. The fact that the neutral current peaks occur in the vicinity of zero applied voltage indicates that the magnetizing current component was dominant.

The time integral of the first applied voltage wave in Fig. 5(A) is approximately

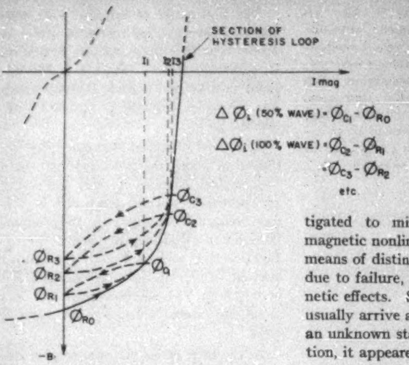
SECTION OF HYSTERESIS LOOP
I1
I2 I3
I mag
$\Delta \varnothing_1$ (50% WAVE) = $\varnothing_{C_1} - \varnothing_{R_0}$
$\Delta \varnothing_1$ (100% WAVE) = $\varnothing_{C_2} - \varnothing_{R_1}$
= $\varnothing_{C_3} - \varnothing_{R_2}$
etc
$\varnothing_{C_3}$
$\varnothing_{C_2}$
$\varnothing_{R_3}$
$\varnothing_{R_2}$
$\varnothing_{R_1}$
$\varnothing_{C_1}$
$\varnothing_{R_0}$
-B

Fig. 6. Schematic diagram showing effect of impulse waves on core which initially had maximum residual magnetism in direction opposite to that produced by impulse wave

$$800\text{ (microseconds)} \times 10^{-6} \times \frac{30{,}000}{2}\text{ (volts)}$$
$$= 12\text{ volt-seconds}$$

assuming a simple triangular shape. Since the voltage-time area for a 2,400-volt 60-cycle wave is 0.00375x2,400 = 9 volt-seconds, the impulse flux ratio is 12/9 = 1.33, which indicates that the first impulse wave was sufficient to produce a crest flux one-third greater than that produced by normal 60-cycle excitation.

From these data, it is apparent that changes in the impulse voltage and neutral current waves can be produced by changes in core magnetization and its attendant effects upon the impedance of the winding, and are not necessarily due to winding failure. This must be taken into account when analyzing the oscillograms.

Various testing procedures were investigated to minimize and control the magnetic nonlinearities, and to provide a means of distinguishing between changes due to failure, and changes due to magnetic effects. Since the transformer will usually arrive at the impulse test area in an unknown state of residual magnetization, it appeared desirable to bring the core to a known or at least a reproducible magnetic state.

The best procedure would be to demagnetize the core by gradually reducing a 60-cycle excitation voltage to zero prior to each impulse, but this necessitates access to a voltage source which might not otherwise be required or readily available in an impulse test area.

Another solution is to impulse one end of the winding with several low-voltage long-tail impulse waves sufficient to produce saturation. This constitutes a full magnetic, reproducible bias from which to initiate commercial impulse tests on the opposite end of the winding. With the core completely magnetized in a direction opposite to that in which the flux is driven by the test wave, successive impulses will drive the core towards zero magnetization as indicated in Fig. 6 rather than toward a higher value which would result if the tests were initiated with the core completely demagnetized.

To illustrate this technique, the 250-kva 2,400/4,160Y unit previously referred to was driven to maximum magnetic bias by the successive application of six 1.5x300-microsecond waves on the H_1 terminal. The applied voltage was limited to 50% of the BIL to assure no damage to the winding. Then one 50% and two 100% BIL 1.5x45-microsecond waves were applied to terminal H_1. In accordance with the usual practice, the neutral current was reduced by the ratios of applied voltages to provide direct comparison of all neutral current oscillograms on an amperes-per-volt basis.

Tracings of the applied voltage and neutral current waves shown in Fig. 7 indicated a slight difference between the neutral currents produced by the 50% and the two 100% impulse voltage applications. Even more important is the fact that the 100% neutral current waves had lower amplitudes than the 50% waves on an amperes-per-applied-volt basis. This, coupled with the observation of no change in the voltage wave, could not represent a typical response since a failure from winding to ground would produce a change in the voltage wave and in the characteristic shape of the current wave while a failure between parts of the winding would produce an increased rather than a decreased neutral current.

The mechanism of core excitation in

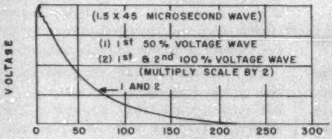

(A) APPLIED VOLTAGE WAVES

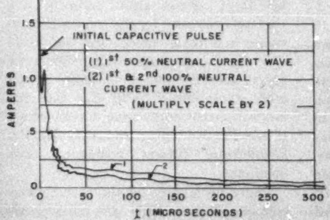

(B) NEUTRAL CURRENT WAVES

Fig. 7 (left). Consecutive 50% and 100% impulse voltage and neutral current waves for transformer which initially had maximum residual magnetism in direction opposite that produced by impulse waves

1—First 50% impulse
2—First and second 100% impulses (multiply scale by 2)

Fig. 8 (right). Consecutive 50% and 100% impulse voltage and neutral current waves showing effects of a short-circuited turn for transformer which initially had maximum residual magnetism in direction opposite that produced by impulse waves

1—First 50% impulse, no fault
2—First 100% impulse, with faulted turn (multiply scale by 2)

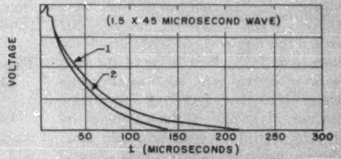

(A) APPLIED VOLTAGE WAVES

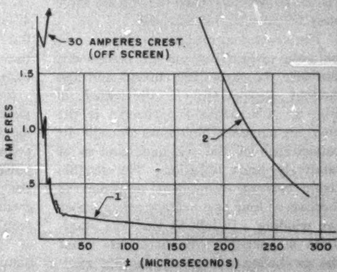

(B) NEUTRAL CURRENT WAVES

this instant differs from that observed when the core was excited by impulse from a demagnetized state. The relation of flux to magnetizing current shown in Fig. 6 is characterized by a rapidly increasing slope of the hysteresis loop; therefore, when impulse excitation reduces the flux, a point is reached where additional reduction (ϕ_{C3} to ϕ_{R3} in Fig. 6) requires very little increase of magnetizing current (I_3 to I_4) and successive impulse currents remain essentially unchanged. The primary advantage of this technique therefore results from an ability to reproduce the magnetic state of the core coupled with the relative insensitivity of the maximum magnetizing currents to repeated applications of impulse voltage while neutral current sensitivity to impulse failures is preserved.

To determine the degree of neutral current changes produced by a failure as compared to the small differences noted when the reverse remanence method is used, the core was fully magnetized in a reverse direction by the method described, and then a reduced voltage full wave (50% BIL) was applied to the opposite terminal.

Tracing 1 in Fig. 8 show the voltage and neutral current wave shapes under this condition. At this point a 1-turn short circuit was placed about the core leg over the high-voltage winding to simulate a turn-to-turn fault. A 100% BIL full-wave test was then applied, and tracings marked 2 in Fig. 8 show the voltage and neutral current wave shapes. The tremendous increase in neutral current due to the short-circuit compared to the small neutral current shift shown in Fig. 7 due to magnetization changes in the core demonstrates quite effectively that if failure of the insulation occurs or is present during the 100% full-wave test, the change in neutral current will be of an entirely different order than that due to core magnetization effects.

Conclusions

1. Changes in neutral current wave shapes between consecutive impulse tests on a transformer with perfectly good insulation can be attributed, in certain cases, to cumulative magnetization effects in the core.

2. The effect of core magnetization on the neutral current wave shape is likely to be more prominent on a low-voltage winding (e.g., 2,400 volts) than on a higher voltage winding (e.g., 15 kv) because of a higher impulse flux ratio at the lower voltage ratings.

3. The effect of core magnetization on the neutral current wave shape is likely to be more prominent on a transformer having a core with a lower exciting current due to the lack of air gaps in the magnetic circuit.

4. The effects of core magnetization on the neutral current wave shape can be minimized either by demagnetizing the core with 60-cycle excitation prior to each impulse or by first applying several low-voltage long-tail impulse waves to one terminal, thus driving the core to full saturation.

5. Although a small difference in wave shape may still exist in either of the procedures suggested in paragraph 4, a fault equivalent to a 1-turn short circuit will cause a change in the neutral current wave shape in the order of 20 to 100 times that caused by residual build-up by consecutive impulse tests.

6. When an appreciable amount of flux is produced by an impulse wave, a magnetostrictive noise is produced in the core which may be misconstrued as an indication of insulation failure.

Appendix I. Calculation of Impulse Voltage Time Integral

Eaton and Gebelein[2] propose for a typical impulse wave the equation

$$e=A(\epsilon^{-(\alpha-\beta)t}-\epsilon^{-(\alpha+\beta)t}) \tag{9}$$

where A, α, β are tabulated for various wave shapes.

Accordingly, the time integral of a standard 1.5 x 40-microsecond voltage wave is $53.8 \times 10^{-6}E_t$ volt-seconds, or

$$1.35E_t t_t \times 10^{-6} \tag{10}$$

where

E_t = impulse crest, volts
t_t = time to one-half of voltage crest in microseconds, according to the standard definition

Then, according to the general law of induction

$$\phi=\frac{-10^8}{N}\int_0^t e\,dt \tag{11}$$

the total increment of flux produced by a single impulse becomes

$$\phi_t=135\frac{E_t t_t}{N} \text{ lines of flux} \tag{12}$$

where N = number of active turns impulsed.

The time integral of an impulse wave may also be approximated by assuming the voltage crests in zero time, and that the wave decays exponentially. In this instance

$$e=E_t\epsilon^{-t/T} \tag{13}$$

For a 40-microsecond wave, the time integral becomes

$$\phi_t=145\frac{E_t t_t}{N} \tag{14}$$

A reasonable estimate for rapid calculation would be obtained by averaging equations 4 and 6 to obtain

$$\phi_t=140\frac{E_t t_t}{N} \tag{15}$$

where

E_t = crest volts
t_t = time in microseconds to $E_t/2$
N = total number of active turns under impulse

References

1. TEST CODE FOR DISTRIBUTION, POWER, AND REGULATING TRANSFORMERS. *ASA C57.12-1948*, American Standards Association, New York, N. Y., 1948.

2. CIRCUIT CONSTANTS FOR THE PRODUCTION OF IMPULSE TEST WAVES, J. R. Eaton, J. P. Gebelein. *General Electric Review*, Schenectady, N. Y., vol. 43, no. 8, pp. 322–32.

◆

Discussion

J. H. Hagenguth (General Electric Company, Pittsfield, Mass.): The authors' results clearly point out that changes in neutral current waves obtained during impulse tests on transformers are caused by changes in the impedance of the transformer. These changes, however, may not necessarily be due to failures, but can be caused by the nonlinearity of the magnetic circuit. Once recognized, of course, the procedure of testing suggested by the authors will give variations in neutral current waves which are minute compared to the variation caused by even a 1-turn fault.

It is clear that great care must be used in the interpretation of current wave-shape variations lest a perfectly good transformer may be rejected in test, although the cause of the deviation was the reaction of the physical constant of the transformer rather than a failure. During the tests the neutral resistor used to measure the winding current was paralleled by a capacitor to reduce the initial high-capacitive peak to tolerable values. It is important to point this out because the high sensitivity of detection is not reduced, as clearly indicated in Fig. 8.

P. A. Abetti (General Electric Company, Pittsfield, Mass.): Heretofore it had been generally assumed that transformers show a linear behavior when subjected to impulse voltages. This conclusion is based mostly on experimental evidence[1,3] rather than on theoretical analysis of the effect of the core steel within the frequency and flux density ranges of interest. For instance, good oscillograms proving the linearity of the transformers tested are given in reference 3. All these tests were made with power rather than with distribution transformers. Theoretical and experimental studies of the effect of the iron core have been made.[4-8] Karasev and Margolin conclude that it may always be assumed that the permeability is constant and, for most practical purposes, equal to infinity. The same assumption is employed by Heller and Veverka who obtain good agreement between calculated and measured frequencies of an experimental winding with isolated neutral consisting of identical coils varying in number from 5 to 20.

This generally accepted linearity leads to three extremely important conclusions for the calculation and measurement of impulse voltages in transformers.

1. The impulse response does not depend upon the number and polarity of the impulse waves to which the transformer has been subjected previously, i.e., unless a failure occurs, the transformer has no memory for impulse tests.
2. The impulse response depends only upon the shape, not upon the magnitude of the applied voltage wave.
3. The impulse response does not depend upon the applied power-frequency voltage.

In fact, the response obtained with applied voltages of the order of 1,000 volts by means of the transient analyzer is assumed to be equal to the response during commercial impulse testing or in the field with impulse voltages up to or larger than 1,000,000 volts and, eventually, with full power-frequency voltage.

The authors have clearly shown the limitations of conclusion 1 for certain ratings of distribution transformers and how to overcome such limitations. The question might now be raised whether conclusions 2 and 3 still hold as assumed heretofore, and the following considerations will be of help.

In the standing-wave theory the impulse response of a winding depends upon: the modes of oscillation of the winding (wave shapes and natural frequencies); and the difference between the initial and final distributions, which determines the amplitude of these modes.

If the core is nonlinear, its nonlinearity must affect either the modes of oscillation or their amplitudes to influence the impulse response. The initial distribution depends mainly upon the transformer capacitances, while the final distribution is almost linear. Changes in the core permeability could only alter the small deviations from linearity of the final distribution, with negligible effects on the mode amplitudes. More important are the effects of the core on the wave shapes and frequencies of oscillation.[6,7] If the neutral of the winding is isolated, there is magnetizing flux in the iron core, and a decrease in permeability will have two effects: the values of the lower natural frequency will be increased, while the higher frequencies will remain practically the same; and the wave shapes of the lower harmonics become more peaked, and the corresponding maximum gradients are increased.

For a 1.5x40-microsecond applied wave, an increase of the fundamental frequency will increase somewhat the maximum voltages to ground. In fact, these maximum voltages usually occur after one semiperiod of the fundamental. The shorter this period, the smaller the decay of the applied wave and, therefore, of the axis of oscillation, which corresponds to the final distribution. On the other hand the changes in wave shape will reduce the amplitude of the fundamental and this will counteract in part the aforementioned effect. The increased gradients of the lower harmonics may increase the voltages between relatively distant parts of a winding, e.g., across 10- to 50-per-cent winding. When the neutral of the impulsed winding is grounded, as in the great majority of practical cases, the natural modes of the winding do not cause any magnetizing flux. The path of the leakage flux for these modes is mostly in air and, therefore, the effect of the core on the wave shapes and natural frequencies is much smaller for grounded than for isolated neutral. In all cases the voltages between coils and between turns of the impulsed winding are not affected at all by the behavior of the core. In fact, these voltages are determined essentially by the higher harmonic modes of the winding. In a recent analysis by field theory,[8] it was shown that the presence of an iron core with infinite permeability influences the surge performance of a coil only within the range of the lower harmonics. It follows that this effect will be less for a core with finite but constant permeability and even less will be the effect of variation of the permeability.

Further evidence to substantiate these conclusions has been obtained by tests on electromagnetic models of power transformers. It will be recalled[4] that these models reproduce correctly the nonlinear properties of the iron core, since the values of B, H, and μ are the same at corresponding points and at corresponding times in the original and in the model. Since transformers behave linearly for most impulse phenomena, this important characteristic of electromagnetic models is made use of only in special investigations. For instance, the natural frequencies of the high-voltage winding of a 3-phase 30,000-kva transformer model were measured as a function of the applied voltage. It was found that the fundamental frequency with isolated neutral showed a 20-per-cent change, while the higher harmonics with isolated neutral and all natural frequencies with grounded neutral showed changes from 1 to 4 per cent of the order of accuracy of the measurements. Similar results were obtained with a model of a 667-kva single-phase transformer.

It may be concluded, therefore, that the nonlinear behavior of the core, evidenced by the authors for certain types of distribution transformers, will affect very little the oscillatory components of the impulse response. There will be no changes in the voltages across small parts of the winding, and the changes in the voltages to ground and across large parts will be small. It may be also concluded that tests with the transient analyzer and with the impulse generator reproduce satisfactorily in all cases the conditions encountered in the field.

References

1. The Recurrent Method of Examining Surge Phenomena, K. J. R. Wilkinson. *Report No. 306*, CIGRE, Paris, France, 1939.

2. Recurrent Impulse Generator, G. Dufour. *Ateliers de Construction Électrique de Charleroi*, Charleroi, Belgium, no. 1, 1950, pp. 21–25.

3. An Experimental Contribution to the Study of Transformer Insulation, R. Langlois-Bérthelot, Neuve-Eglise, Kohn, Renaudin. *Report No. 144*, CIGRE, Paris, France, 1950.

4. The Behavior of Transformer Steel In Over-Voltage Phenomena, V. A. Karasev, A. D. Margolin. *Journal of Technical Physics*, Moscow, USSR, vol. 7, 1937, pp. 804–21.

5. The Oscillations of a Transformer Winding Taking Into Consideration the Effect of the Iron Core, B. Heller, A. Veverka. *Elektrotecnicky Obsor*, Prague, Czechoslovakia, vol. 39, 1950, pp. 5–7.

6. Natural Frequencies of Coils and Windings Determined by Equivalent Circuit, P. A. Abetti, F. J. Maginniss. *AIEE Transactions*, vol. 72, pt. III, June 1953, pp. 495–504.

7. Fundamental Oscillations of Coils and Windings, P. A. Abetti, F. J. Maginniss. *AIEE Transactions*, vol. 73, pt. III, Feb. 1954, pp. 1–10.

8. Field Theory of Wave Propagation Along Coils, H. Poritsky, P. A. Abetti, R. P. Jerrard. *AIEE Transactions*, vol. 72, pt. III, Oct. 1953, pp. 930–39.

9. Transformer Models for the Determination of Transient Voltages, P. A. Abetti. *Ibid.*, June 1953, pp. 468–80.

M. F. Beavers, J. E. Holcomb, and L. C. Leoni: It is interesting to note that Mr. Abetti's theoretical studies indicate that the nonlinear behavior of certain transformer cores will have very little effect on the impulse response of the transformer.

As Mr. Hagenguth points out, great care must be used in the interpretation of current wave-shape variations lest a perfectly good transformer be rejected in test. It was suggested that the test code be studied by the appropriate committee to consider modifications which would recognize the change in the applied voltage and neutral current wave shapes caused by magnetization of transformer cores during impulse testing.

Power Distribution System Parameters

A. H. KIDDER
FELLOW AIEE

J. H. NEHER
MEMBER AIEE

THE POWER distribution engineer is frequently confronted with the need to appraise effects upon the distribution system such as would be caused by the supply of singular loads, or by proposed modifications of distribution practice relating to circuit and substation sizes, power factor (pf) correction, a change in distribution voltage, or a change in the limits of voltage regulation. For rate-making purposes he is occasionally required to appraise the costs associated with the supply of existing and possible new types of loads and customers.

The effects of each load extend through all of the circuits which, together, comprise the related power distribution system. Among other things, therefore, consistent appraisal requires evaluating directly, according to one consistent method, the effect of each load upon both the length and the weight of conductors needed at each distribution voltage level; as well as the load and the number of customers supplied per circuit, per transformer, and per substation. This paper therefore has been prepared to summarize the development of a method which holds promise of achieving the desired results, by dealing with the distribution circuit as a functional entity and in terms of its natural parameters.

List of Symbols

a = fixed component of unit cost
a_c = applying to a circuit, cost units per conductor foot
a_t = applying to a transformer, cost units per transformer
A = conductor size, circular mils (CM)
α = phase angle of voltage loss in a circuit
α_p = applying to principal lateral
α_r = applying to riser branch
b = incremental component of unit cost
b_c = applying to a circuit, cost units per pound of conductor
b_t = applying to a transformer, cost units per kilovolt-ampere (kva) of load
b_p = capitalized cost of power, cost units per watt
β = equivalent load density, thousands of kva per square mile
C = unit cost
C_c = applying to a circuit, cost units per kva
C_t = applying to a transformer, cost units per kva
Δd = length of a unit section of circuit, feet
d = distance between two points, feet
d_p = from supply point to end of principal lateral
d_r = from supply point to end of riser branch
D = total circuit length, feet
δ = current density, amperes per 1,000 CM
E = effective voltage to neutral
f = lateral distance between unit loads, feet
F = voltage adjustment factor as developed in Appendix III
F_p = applying to principal lateral
F_r = applying to riser branch
i = phase current per unit load, amperes
i_0 = applying to an existing design
1,000 I/A = current density, amperes per 1,000 CM
I_s = motor starting current, amperes
j = phasor operator $\sqrt{-1}$
K = constant resistive voltage loss per foot in conductor of a size proportional to its ampere load
K_0 = applying to an existing design
K_p = applying to laterals
K_r = applying to riser branches
L = total load delivered by a circuit in kva
(LF) = annual loss factor of a circuit
m = ampere feet per phase conductor between two points
m_p = from supply point to end of principal lateral
m_r = from supply point to end of riser branch
M = total ampere feet per phase conductor of circuit
n = a number equal to half-length of a riser branch divided by s
N = number of conductors in a circuit, including the neutral
N_p = number of phase conductors
p = power loss per phase conductor, watts
p_p = from supply point to end of principal lateral
p_r = from supply point to end of riser branch
P = total power loss per phase conductor, watts
ϕ = equivalent customer density, thousands per square mile
q = a number equal to the half-length of the principal lateral divided by f
Q = number of unit loads per unit
R = circuit resistance, ohms per conductor foot
ρ = conductor resistivity, CM ohms per foot
s = distance between lateral branches, feet
S = unit size
T_i = effective transformer current ratio, primary/secondary, including the effect of a different number of phase on each side
T_v = effective transformer voltage ratio, primary/secondary
$\Delta\theta$ = change in phase angle along a circuit (Fig. 1)
θ = angle by which currents lags the effective phase-to-neutral voltage, degrees
U = unit load, kva
v = permissible voltage loss of a circuit, per cent (%)
v_s = voltage dip due to motor starting, %
V = voltage loss per phase conductor between two points, volts
V_i = component of V in phase with the current
V_q = quadrature component of V
V_t = voltage loss in a transformer (referred to the secondary)
W = total weight of one phase conductor, pounds
X = circuit reactance, ohms per conductor foot
X_s = circuit reactance applicable to motor-starting currents, ohms per conductor foot
y = the number of a lateral counting from the extremity of a riser branch
Z = circuit impedance, ohms per conductor foot

The use of the prime (′) indicates a successively higher circuit level.

General Considerations

The principal classes of distribution system components are conductors with their associated insulation and structures; also substations, transformers, switchgear, regulators, pf corrective equipment, and metering installations. The effect of size S upon the installed cost C for an assembly of a given class seldom requires evaluating coefficients for more than the first two terms of the following complete representation

$$C=a+b_1S+\ldots+b_nS^n \tag{1}$$

It is important, however, to observe that the fixed, or a component of cost is usually appreciable. In the case of conductors, for instance, the a component of cost, which is independent of conductor size, includes practically the whole cost per foot for the associated rights of way and structures such as poles, or towers, or conduits and manholes. Hence, consistently representative distribution system parameters must permit determining the quantity as well as the size of each unit assembly under the given conditions.

The development of distribution circuit parameters begins with the prerequisite that the voltage loss between the first and last loads distributed from a common supply point must not exceed some established design limit. For the purposes of practical generalization, the following six assumptions have been made:

1. A large number of equal loads, located on rectangular properties of identical size.
2. Rectangular intersections between the through streets and the cross streets.
3. Lateral and riser main conductors erected along routes respectively parallel

---

Paper 55-19, recommended by the AIEE Transmission and Distribution Committee and approved by the AIEE Committee on Technical Operations for presentation at the AIEE Winter General Meeting, New York, N. Y., January 31–February 4, 1955. Manuscript submitted September 8, 1954; made available for printing November 8, 1954.

A. H. Kidder and J. H. Neher are with the Philadelphia Electric Company, Philadelphia, Pa.

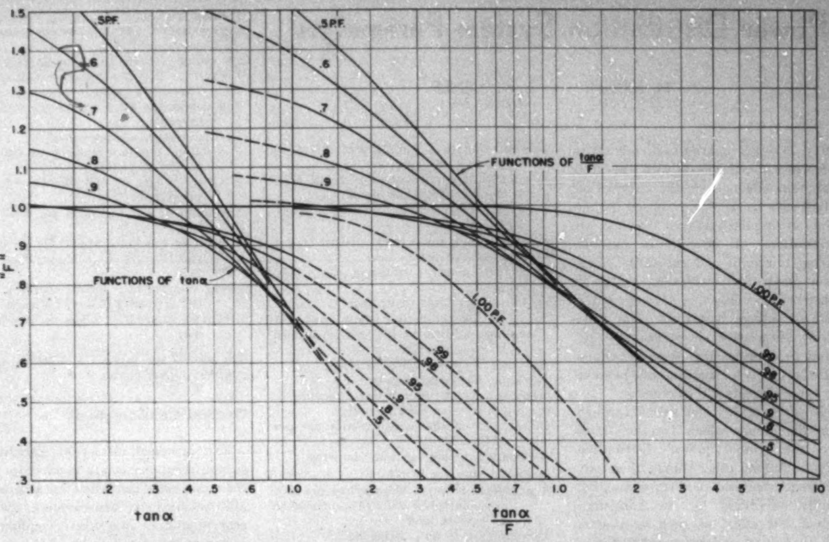

Fig. 1. Voltage adjustment factor F as functions of tan α or (tan α)/F, and pf

to the through streets and the cross streets. These are tentatively assumed to be consistently interconnected, so as to form one continuous electrical network throughout the whole area to be served.

4. Each distribution circuit includes one supply point complete with all essential equipment and accessories, plus all conductors carrying the load it distributes to the various points where it is delivered to customers, or to the supply points of other circuits in the system of which it is a part.

5. For illustrative convenience, it is assumed that the distribution system can be completely represented in terms of circuits operating at but three distribution voltage levels which will be consistently designated as the secondary-, primary-, or high-voltage levels.

6. As a practical first step, the conductor cross section is assumed proportional to the ampere load, but with the explicit understanding that the natural relationship must be determined before this analysis is considered complete.

The foregoing assumptions have the advantage of limiting the initial investigation exclusively to considering the singular effects of individual loads. After these effects have been evaluated, it will be appropriate to undertake an accounting for the characteristics peculiar to the community, as determined in part by diverse street configurations, diverse land occupancy, diverse loads, and diverse load-coincidence relationships.

Voltage Loss Characteristics

The permissible voltage loss is the amount by which the voltage delivered to the most remote load on a circuit may be less than that supplied to the circuit. This is a function of the effective impedance, the current flowing, and also the phase relationship between current and voltage.

The electrical resistance is inversely proportional to the conductor size and therefore is assumed tentatively to bear an identical relation to the load current. On the other hand, the reactance component of electric circuit impedance is determined by the spacing between conductors having different polarities, by the magnetic permeability of the conductor material and, to some extent, by the conductor diameter. Increases in conductor size decrease the reactance somewhat, but this is an effect which may be neglected in the present analysis because some overstatement of the reactance is permissible. This permits the assumption that the reactance is that for the smallest practicable conductor size at the given conductor spacing. The conductor spacing is essentially fixed by the operating voltage of the circuit, and the choice of open-wire or cable construction. Hence, the effective reactance per conductor is largely independent of its load in amperes. However, there are cases, particularly in underground cable circuits, where the required total conductor area of the circuit is divided between a number of parallel paths or cables along the given route, and the effective reactance is then inversely proportional to the number of parallel paths and the total load in that part of the circuit.

Consider, now, a section of single path main Δd-feet long and carrying I amperes of current per phase, in a physical arrangement of conductors which has an effective resistance of K/I ohms per foot and an effective reactance of X ohms per conductor foot. The impedance of the conductor becomes the phasor

$$Z=\frac{K}{I}+jX \text{ ohms per conductor foot} \qquad (2)$$

and, taking current as the reference phasor, the voltage loss in the section becomes

$$V=V_i+jV_q=I\Delta d\left(\frac{K}{I}+jX\right) \qquad (3)$$

$$=K\Delta d+jXI\Delta d \text{ volts per section}$$

The quantity K appearing in these equations represents the constant resistive voltage loss per foot in conductors having sizes proportional to their ampere loads. If the corresponding conductor area is A in CM and ρ represents the resistivity of the conductor in CM ohms per foot

$$K=\frac{I}{A}\rho \text{ volts per foot} \qquad (4)$$

$$=\frac{12I}{A} \text{ for copper conductors}$$

It will be seen from equation 3 that the voltage loss consists of two components: one, a function of the Δd-foot length of the section; the other, a function of the $I\Delta d$ ampere feet in the section. By extension, to include a number of adjacent sections having differing values of I, which change with each additional unit load picked up, it will be seen that the over-all voltage loss between any two points is a composite function of the total distance d and the m-ampere-foot total per conductor included.

In the symmetrical distribution system assumed, each unit load will be a constant of i amperes per conductor. The m ampere feet will equal the sum of the products of i by the respective circuit distances to the unit loads distributed by the circuit. The evaluation of m will be considered in due course. Meanwhile, the voltage loss between the point of supply and any point in the distribution circuit may be written as

$$V=Kd+jXm \text{ volts} \qquad (5)$$

while, for a previously installed main in which the conductor area was originally designed for a unit load current of i_0 amperes with conductors having a voltage loss of K_0 volts per foot, equation 5 becomes

$$V=(K_0i/i_0)d+jXm \text{ volts} \qquad (6)$$

The assumption of uniform current density is a useful device for determining the average conductor size needed in any situation. The fact that practical considerations discourage frequent changes in conductor size need cause no concern, because practical deviations from rigorous observance of uniform current density have little effect upon voltage loss. In fact, it is often useful to assume a uniform conductor size having the same total weight as if it had been "tapered" to operate everywhere at uniform current density. The average size would be the same in either case, and identically related to the load.

For a uniform conductor size having an effective resistance of R ohms per conductor foot, the voltage loss is given by the expression

$$V=m(R+jX) \text{ volts} \qquad (7)$$

If v represents the permissible voltage loss in % of the nominal voltage E, and θ represents the pf angle of the load, the following approximate relationship will exist for a circuit having uniform current density

$$\frac{vE}{100}=Kd\cos\theta+mX\sin\theta \text{ volts, approximately} \qquad (8)$$

For convenience, equation 8 may be replaced by

$$\frac{vE}{100}=\frac{Kd}{F} \text{ volts} \qquad (9)$$

where F is a function of both θ, the pf angle of the load, and α, the effective phase angle of the circuit impedance; the value of α being such that

$$\tan\alpha=mX/Kd \qquad (10)$$

Similarly, for a circuit having uniform conductor size throughout

$$\frac{vE}{100}=m(R\cos\theta+X\sin\theta), \text{ approximately} \qquad (11)$$

$$=mR/F \text{ volts} \qquad (11A)$$

where F is a function of

$$\tan\alpha=X/R \qquad (12)$$

Curves of F for various values of pf are given in Fig. 1, as functions $\tan\alpha$ or $(\tan\alpha)/F$. As indicated in Appendix III, these curves contain a correction for the quadrature component of voltage drop which is not compensated for in equations 8 and 11.

Elementary Distribution Circuits

The natural method of installing low-voltage, or secondary lateral mains in an urban community is to route them either along, or parallel to, the through streets. The distance between such lateral mains will be roughly equal to the s-foot distance between the through streets. Under the assumption of equal loads, each in an equal area, the points of connection to the mains may be generalized as a series of unit loads equally spaced at intervals of an f-foot distance along the laterals.

Such a system is shown in Fig. 2, in which the unit loads are indicated as dots along the lateral mains and the supply points are indicated by circles. Riser mains are also shown, perpendicular to and interconnecting the laterals. The over-all effect of interconnecting the laterals and risers is to permit the maximum practical use of each supply-point by forming a uniform and electrically continuous distribution network.

As one considers the symmetry of the network described, it will be observed that there will be certain points on each of the laterals and risers, at which there will be no current flow. The limits of the area bounded by such points of no-load transfer are indicated by the dashed lines of Fig. 2, from which it is seen that the energy fed through each supply-point is distributed throughout a diamond-shaped area. It is also apparent that the load and voltage distribution within each diamond would not be affected in any sense, if the diamond were arbitrarily separated from the network and operated independently as a circuit having the loads shown in the branch type of circuit in Fig. 3. It will be seen that the load at each extremity of the

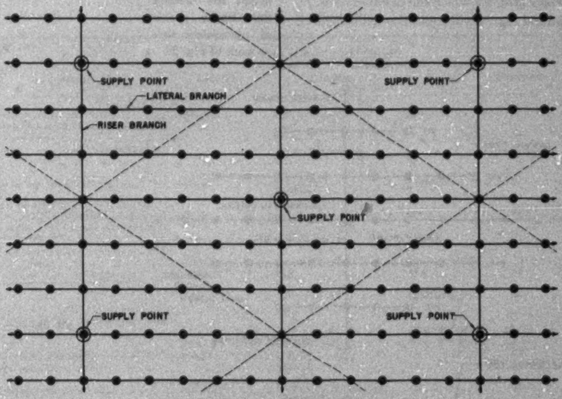

Fig. 2. Elementary distribution network

principal lateral and riser branches is but one-fourth of the unit load, since the loads located at these points are fed symmetrically from four directions. Similarly there will be a half-unit load at the extremities of each of the other laterals.

Consider the half-length of the principal lateral to be qf feet and the half-length of the riser branch to be ns feet in Fig. 3, as limited by the requirement that the permissible voltage loss shall not be exceeded. This requirement will have been satisfied approximately, if the total voltage loss between the supply point and the extremities of both the principal lateral and riser branches is held within the permissible limit. As indicated in equations 5, 6 and 7 the voltage loss will be a function of d_p and/or m_p for the principal lateral and d_r and/or m_r for the riser branch.

Under certain conditions, permissible voltage drop or other considerations may indicate that it is impractical to utilize riser branches. In this case the network reduecs to a system of laterals only, and each supply point will serve a lateral type of circuit, as illustrated also in Fig. 3. In this case it will be seen that the effective area served by each circuit is rectangular in shape.

Primary- and High-Voltage Distribution Circuits

It will be apparent that the supply points of a low-voltage or secondary grid will include transformers fed from a similar primary grid. In this case the total load of each secondary circuit and its losses becomes the unit load of the primary grid, for which the distance between lateral mains will equal the half-length of the secondary riser branches, being

$s' = d_r$ feet, the half-length of the branch-type secondary riser branch, or
$= s$ feet, the distance between streets for a lateral-type secondary (13)

and the lateral distance between unit loads on the primary will be equal to twice the half-length of the longest, or principal lateral in the secondary-circuits which it supplies, being

$f' = 2d_p$, the length of the principal secondary lateral (14)

Further, it will be noted that for alternate lateral mains the locations of the loads picked up are displaced laterally by a distance of $f/2$ from the positions of the loads on adjacent laterals. The equivalent circuit for such a grid assumes two forms as shown in Fig. 4, depending upon whether the parameter n represent an even or an odd number of laterals.

Likewise, each primary-branch circuit may include a unit-type substation, which is fed in turn from a similar type of high-voltage grid. On the other hand, construction economy may favor reducing high-voltage conductor mileage by installing larger substations and "radial-type" primary feeders to permit supplying several primary-branch circuit loads per substation. However, whether it be high-voltage branch circuit supply or primary-voltage, radial-feeder supply, the circuit routes must run along or under streets; hence the vertical distance s and the lateral distance f between loads picked up will be given by expressions identical to equations 13 and 14, in which d_r and d_p have values as determined for the grid being supplied.

For the radial type of primary circuit, the maximum feeder length (Fig. 5), is determined simply by the impedance and the load. It is, therefore, evident that the area served in this case will have the shape of a diamond whose parameters qf and ns will be equal. The use of feeder voltage regulators permits the use of longer feeders, to serve when desirable a larger area and load from such a circuit.

Circuit Parameters

It is now practical to determine the total number Q of unit loads served, the total length D feet of the circuit, the total ampere feet M, and the power loss P in watts per conductor, in terms of the foregoing relationships. The total weight of one phase conductor may be determined from the ampere feet M, by the following relationships in which w represents the

Fig. 3 (below). Equivalent circuit for one supply point in the elementary network of Fig. 2

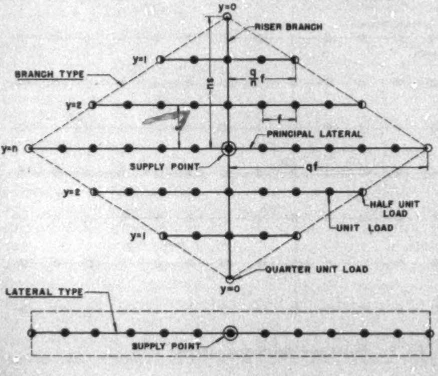

Fig. 4 (right). Equivalent supply circuit for feeding the supply points of elementary network of Fig. 2

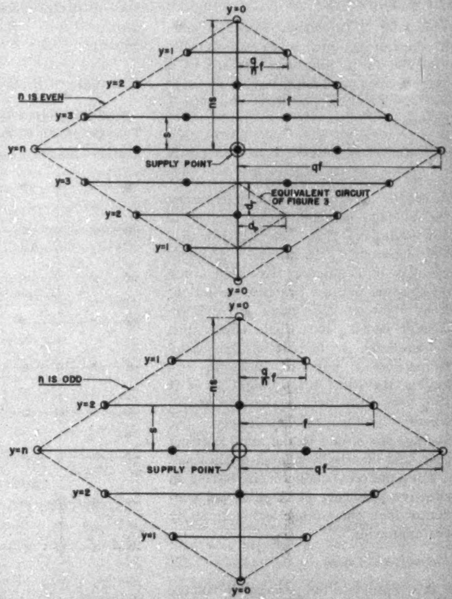

weight of the conductor in pounds per CM foot. For a circuit having a uniform current density

$$W = w_p M/K \text{ pounds per conductor}$$
$$= 36\times10^{-6}\, M/K \text{ for copper} \quad (15)$$

and for a circuit having a uniform conductor size throughout

$$W = wAD = w_p D/R \text{ pounds per conductor}$$
$$= 36\times10^{-6}\, D/R \text{ for copper conductors} \quad (16)$$

The branch, lateral, and radial type of circuits discussed are analyzed in Appendixes I and II, from which it will be seen that general parameters may be derived which are qualitatively identical for any type of circuit and voltage level. These are given in Table I.

Equivalent values of K in terms of R may be obtained from equations 8 and 10 after making the proper substitutions for d and m from Table I. These equivalent relationships are also given in Table I. In the case of a branch type of circuit it will be noted that the equivalent value of K_p for the lateral branches, equation 28, differs from K_r for the riser branch, equation 29. For cost analysis, however, it is sufficient to use the average relationship given by equation 30, which is obtained by simultaneously solving equations 26 and 27.

The values of q and n appearing in the equations of Table I are subject to certain limitations. Field conditions in a city, for instance, will require that n be an integer, since ns is a multiple of the distance between the streets along which the lateral branches are run. For a branch type of system, qf should be related similarly to the distance between the transverse streets which will carry the riser branches. For the radial system as shown in Fig. 5, it will be evident that b must be an integer and that q must be a multiple of one half, since qf must be a multiple of $f/2$.

Also, as previously indicated, the values of q and n must be such that the permissible voltage loss to the extremity of the principal lateral or riser branch shall not be exceeded. By substituting equations 14, 19, 21 and 22 in equations 9 and 11, expressions are obtained for q-maximum and n-minimum, as given in Table II. Since n-max will depend upon q, the solution for q should be made first. In the case of lateral and branch circuits equations 32 and 34, the parameter tan α on which the factor F depends is itself dependent upon q or n, which in turn involve F. A solution for F may be effected by use of equations 32(A) and 34(A) involving the parameter (tan α)/F.

Fig. 5. Radial-type supply circuit

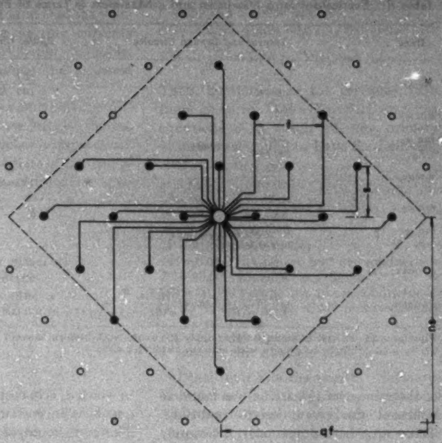

Curves of F are derived in Appendix III and given in Fig. 1, as functions of pf and tan α, or (tan α)/F.

Under certain conditions, the values of q and n thus obtained may result in a value of total current which exceeds the permissible load for a particular part of the circuit. In this case the values of q and n should be reduced observing the permissible current limitation, as well as that of approximately equal voltage losses to the respective extremities of the circuit.

For calculating the total weight of conductors, it has been necessary to assume with theoretical rigor that the conductor size everywhere in the circuit is exactly proportional to the amperes carried. The average conductor size thus derived is therefore proportional to the load, and it has been explained that the theoretical tapering of conductor sizes if of no practical significance, except as a device for determining the average size. Henceforth, the principal controlling factor is voltage loss which can be handled as rigorously and far more readily in terms of a more practical construction, such as the utilization, throughout the full length of each lateral and riser in the circuit, a uniform conductor cross-section

Table I. Distribution Circuit Parameters

Item	Type of Equivalent Circuit: Lateral	Branch	Radial	Equation
Q = number of unit loads	$2q$*	$2qn$	$2qn$	17
d_p = half length of principal lateral in feet	qf	qf	qf	18
d_r = half length of riser branch in feet		ns	ns	9
D = circuit length in feet	Qf	$Q(f+s/q)$	$\frac{Q}{3}(qf+ns)$	20
m_p = ampere feet per conductor in half of principal lateral	$q^2if/2$	$q^2if/2$	qif	21
m_r = ampere feet per conductor in half of riser branch		$n^2isq/3$	ins	22
M = ampere feet per conductor in circuit	$qfQi/2$	$(qf+ns)Qi/3$	$(qf+ns)Qi/3$	23
P = watts loss per conductor	MK	MK	MK	24
	$Qi^2Rq^2f/3$	$Qi^2Rq\left(\frac{qf}{6}+\frac{2n^2s}{5}\right)$	$Qi^2R(qf+ns)$	25
W = weight in pounds per conductor	$36\times10^{-6}\ M/K$	$36\times10^{-6}\ M/K$	$36\times10^{-6}\ M/K$	15, 26
	$36\times10^{-6}\ D/R$	$36\times10^{-6}\ D/R$	$36\times10^{-6}\ D/R$	16, 27
K_p = volts per foot	$qiR/2$	$qiR/2$	iR	28
K_r = volts per foot		$qniR/3$	iR	29
K = volts per foot	$qiR/2$	$\frac{qi(qf+ns)}{3(qf+s)}R$ (average)	iR	30

* Exception: Although the number of unit loads $Q=1$ at the lateral circuit limit $q=0$ in equation 17, all other items vanish as should be expected.

Table II. Expressions for q-Maximum and n-Maximum in Terms of Permissible Voltage Loss

Item	Lateral and Branch Circuits	Radial Circuits	Equation
q-max	$\frac{vEF_p}{100\,fK}$	$\frac{vEF}{100\,fK}$	31
tan α_p	$\frac{iqX}{2K}$	$\frac{iX}{K}$	32
$\frac{\tan\alpha_p}{F_p}$	$\frac{ivEX}{200\,fK^2}$ for q-max		32A
n-max	$\frac{vEF_r}{100\,sK}$	$\frac{vEF}{100\,sK}$	33
tan α_r	$\frac{niqX}{3K}$	$\frac{iX}{K}$	34
$\frac{\tan\alpha_r}{F_r}$	$\frac{i(vE)^2XF_p}{30{,}000\,fsK^3}$ for n-max		34A
q = max	$\sqrt{\frac{2vEF_p}{100\,ifR}}$	$\frac{vEF}{100\,ifR}$	35
n = max	$\sqrt{\frac{3vEF_r}{100\,qisR}}=0.46\sqrt[4]{\frac{fvEF_r{}^3}{is^2RF_p}}$	$\frac{vEF}{100\,isR}$	36

Equations 24, 26, and 31 through 34(A) apply to circuits with uniform current density and equations 25, 27, 35, and 36 apply to circuits with uniform conductor sizes.

of the same average size as was found to represent the given design conditions. There may be sections near the supply point, particularly in the higher voltage circuits, in which somewhat larger conductors will be needed in order to prevent overheating. However, such high-current sections can be identified readily, and a larger conductor provided if required.

Cost Considerations

It can be shown that the installed cost of a lateral or riser main may be expressed in the general form

$$C_c=\frac{DN}{L}\left(a_c+b_c\frac{W}{D}\right)\text{ cost units per kva}\quad(37)$$

in which the constants a_c in cost units per conductor foot and b_c in cost units per pound of conductor are dependent upon the type of construction involved. L represents the distributed load in kva, and N the number of phase and neutral conductors. If the neutral is of reduced size, the weight factor in equation 35 should be reduced accordingly. This cost includes conductors, devices and the allocated portion of poles and fixtures, or rear busses in the case of the secondary.

If U represents the unit load in kva at each secondary-service tapoff, and Q is the number of loads supplied

$L=QU$ kva for the secondary-circuit

whence

$L'=LQ'$ kva for the primary circuit
$L''=L'Q''$ kva for the primary-supply-circuit
(38)

Similarly for a transformer installation

$$C_t=\frac{1}{L}(a_t+b_tL)\text{ cost units per kva}\quad(39)$$

in which a_t is in cost units per transformer and b_t is in cost units per kva of load. This cost should, of course, include installation cost as well as the material costs of the transformer and its accessories, such as lightning arresters and fuses.

The capitalized cost of line losses may be determined from the following expression

$$C_{cl}=b_p(LF)N_p\frac{P}{N}\text{ cost units per kva}\quad(40)$$

in which b_p represents the capitalized cost of power in cost unit per watt, (LF) is the annual loss factor of the circuit, N_p the number of phase conductors, and P the watt power loss per phase conductor at the time of maximum load.

Similarly for a transformer

$$C_{tl}=5b_p[1+3(LF)]\text{ cost units per kva}\quad(41)$$

Equation 41 is predicated upon 0.5% iron losses and 1.5% full-load copper losses in the transformer.

Effect of Motor Starting Currents

Heretofore, we have not considered the voltage dips caused by 120-volt fractional horsepower motor-starting currents. The effect is almost entirely restricted to the secondary circuit and distribution transformer, and is greatest when caused by the starting of a motor at the end of the principal lateral. Since the secondary circuit is usually 3-wire single phase, this voltage drop involves the neutral conductor as well as one of the phase conductors.

If the neutral and phase conductors have a resistance of R ohms per foot, and if the transformer impedance be taken at a nominal value of $1.8+j2.7\%$; and I_s is the motor-starting current in amperes at 0.5 pf, we may find the resultant voltage dip v_s in % by analogy to equation 10. Thus

$$v_s=100\frac{I_s}{E}\left[qf(R+1.73X_s)+0.032\frac{E}{Qi}\right]\%\quad(42)$$

in which X_s represents the reactance in ohms per foot between the neutral conductor and the phase conductor involved.

For secondary circuit conductors having uniform cross section equal to the average size which satisfies the given conditions of load and voltage loss, the relationship between K and R will be that given in equation 28 of Table I. Thus for a secondary designed to operate at uniform current density

$$v_s=100\frac{I_s}{E}\left(2\frac{fK}{i}+1.73qfX_s+0.032\frac{E}{Qi}\right)\%\quad(43)$$

If a permissible value is established for v_s, the maximum permissible values of R or K are

$$R\text{-max}=0.01\frac{E}{qf}\left(\frac{v_s}{i}-\frac{3.2}{Qi}\right)-1.73X_s\text{ ohms per foot}\quad(44)$$

$$K\text{-max}=\frac{0.005E}{f}\left(\frac{v_si}{I_s}-\frac{3.2}{Q}\right)-0.866qiX_s\text{ volts per foot}\quad(45)$$

It will be noted that the neutral conductor resistance has an important effect on the voltage dips accompanying line-to-neutral motor-starting current surges. This effect gives added support for the usual practice of utilizing identical neutral and phase-wire sizes in secondary circuits.

Illustrative Example

To illustrate the composite effect of the relationships so far established, it is desired first to determine what would be the cost per customer for overhead secondary circuits and primary branches, in a system designed to satisfy certain assumed conditions; then, to observe how the cost would be affected respectively by moderate deviations from the assumed design conditions. The illustration need not be carried further at this stage because this will be sufficient to illustrate all of the principles involved.

For this purpose, let us consider a large group of identical single phase customers, each having noncoincident maximum demand of 1 kva at 0.95 pf, in an area where the property lines and street configurations are as illustrated in Fig. 6; to be supplied by a 3-wire 120/240-volt single-phase secondary, through 2,400-

120/240-volt distribution transformers fed by 2,400/4,160 Y primary circuits in an overhead system, having a common primary and secondary neutral and an over-all voltage spread of 10%, between the respective customers' service taps along the secondary mains.

To simplify the illustration, it is arbitrarily assumed that no special provisions for emergency breakdown service need be made, and that the single phase secondary loads are somehow balanced between the primary phases at each transformer location. The assumption of balanced 3-phase transformer loads at single-phase transformer locations has the advantage of simplifying primary-branch geometry and related calculations while maintaining the distributed load per conductor mile essentially the same as that which accompanies the normal practice of supplying adjacent single-phase loads from adjacent phases of polyphase mains. The foregoing and certain other necessary assumptions are summarized as follows:

$f=650/12=54$ feet
$s=250$ feet
$\theta=\cos^{-1} 0.95=18.2$ degrees
$U=2$ kva load at each secondary service tap-off
$i=\dfrac{2\times 1{,}000}{240}=8.3+j0$ amperes load at each secondary tap-off
$E=\dfrac{240}{2}(\cos\theta+j\sin\theta)=114+j\,37.5$ volts
$V_t=1.8+j\,2.7$, % voltage loss in the transformer
$=2.5\%$ effective at 0.95 pf
$v+v'=7.5\%$ voltage loss, total in secondaries and primaries, divided as equally as practicable
$N=N'=3$; $N_p=2$; $N_p'=3$
$K=0.012$ volts per conductor foot for copper at 10^{-3} amperes per CM
$I_s=20$ amperes and $v_s=4\%$ for 120-volt motor-starting current
$X=116\times 10^{-6}$ ohms per foot
$X_s=102\times 10^{-6}$ ohms per foot
$X'=144\times 10^{-6}$ ohms per foot
$(C_eL)/(DN)=0.123+0.31\ W/D$, cost units per secondary or primary conductor, foot-installed, complete with supports and all accessories
$C_tL=125+6.2\,L$, cost units per transformer, installed complete with accessories
$b_p=0.164$ cost units per watt; $(LF)=0.12$

By equations 31 and 32 of Table II, assuming $v=3.75\%$, it is found that $q-\max=6.6$. By equation 14 it is found that $f'=2qf=710$ feet. In this case, however, f' must be a multiple of the 650-foot length of the block as required to permit location of the primary branches along the transverse street routes. Hence the correct value becomes $q=6$ and the corresponding secondary voltage loss becomes $v=3.3\%$, which leaves a balance of $10-2.5-3.3=4.2\%$ available for allocation to the primary circuit.

By equation 41 it is found that the voltage dip due to motor-starting currents $v_s=4.2\%$ which is probably tolerable, being only slightly above the assumed limit of 4%.

Since $qf=325$ feet, or one-half the distance between transverse streets, the use of secondary-riser branches is impractical. Hence the secondary will be of the lateral type, for which it is found from the equations of Table I that

$Q=12$
$D=650$ circuit feet
$M=16{,}100$ ampere-feet per conductor
$P=193$ watts per conductor
$W=48.5$ pounds per conductor
A-average $=12/R=25{,}000$ CM (approximately no. 6 size)

and by equation 38

$L=24$ kva

Whence, by equations 37, 40, 39, and 41, the respective components of secondary circuit cost become

$C_e=11.9$ cost units per kva; $C_{el}=0.32$ cost unit per kva
$C_t=11.4$ cost units per kva; $C_{tl}=1.12$ cost units per kva

The corresponding characteristics of the associated primary branches may be found by the use of equations 13 and 14 and the following relationships

$$E'\underline{/\theta}=T_v[(1+0.005v)E+V_t] \text{ volts} \qquad (46)$$

$$i'=QiT_t \text{ amperes} \qquad (47)$$

in which V_t represents the transformer voltage loss, T_v the effective transformer voltage ratio, and T_t the effective transformer current ratio including the effect of the assumed transformation from a single-phase secondary to a 3-phase primary.

Thus, for the primary branches

$f'=650$ and $s'=250$ feet
$E'\underline{/\theta'}=2{,}360+j824=2{,}520\underline{/19.2}$ volts
$i'=\dfrac{12\times 8.3}{30}=3.3+j\,0$ amperes

Then, by the use of the pertinent relations given in Tables I and II and cost equations 37 through 41, the primary branches are found to have the following characteristics

$q'=13$
$n'=18$
$Q'=468$
$L'=11{,}200$ kva
$D'=313{,}000$ circuit feet
$M'=6.68\times 10^6$ ampere feet per conductor
$P'=80{,}000$ watts per conductor
$W'=20{,}000$ pounds per phase conductor
A' average $=21{,}300$ CM (approximately no. 7 size)
$C'_e=12.0$ cost units per kva
$C'_{el}=0.42$ cost units per kva

Upon review of the resulting primary-branch grid, it is found that an additional 8,900 feet of neutral conductor would be required for the riser branches in certain sections where there would be no secondary conductors to provide a common neutral. The cost of this neutral amounts to 0.02 cost units per kva. Thus, the total installed cost of the secondary circuit and primary-branches is 35.5 cost units per kva, exclusive of service taps from the secondary circuit to the customer's premises. The capitalized cost of power losses is also seen to be 1.86 cost units per kva, making the total cost 37.2 cost units per customer for the secondary circuit, associated primary branches and power losses.

To appraise the total cost per customer in each particular case of course, the calculations must be extended similarly, so as to evaluate the corresponding transformer component or substation component of primary-circuit cost and the higher voltage circuit costs, as well.

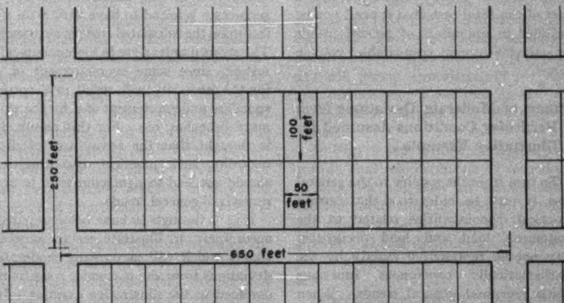

Fig. 6. Street and property lines assumed for example

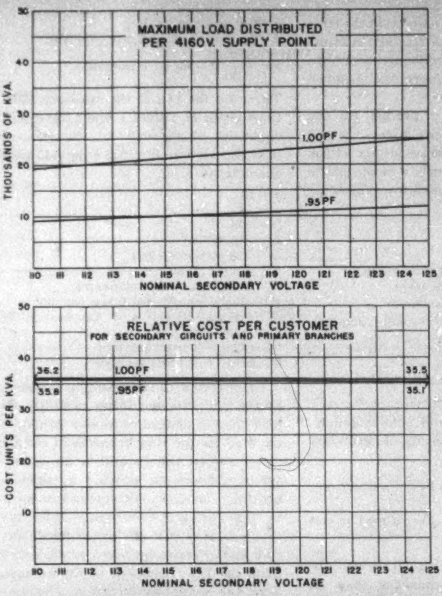

Fig. 7. Illustrative effect in new construction of nominal secondary voltage upon aerial circuit capacity and cost for 1-kva per secondary customer on a 50-by-100-foot lot, with 10^{-3} amperes per CM, 3.3% voltage loss in secondaries, 4.2% in primaries, and 2.5% in transformers

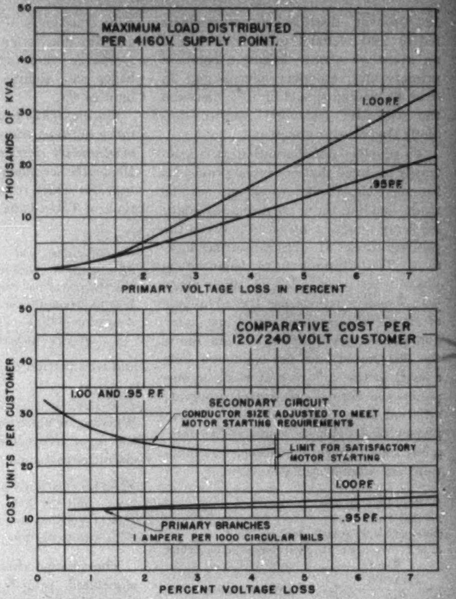

Fig. 8. Illustrative effect in new construction of voltage loss upon aerial circuit capacity and cost for 1 kva per 120/240-volt customer on 50-by-100-foot lots

These additional calculations will not be undertaken now because no new principles remain to be illustrated. It is preferred instead to consider how moderate deviations from the voltage, load density, etc., assumed for the illustration would affect the costs of the components already evaluated.

It is already apparent that the capitalized cost of power losses is so small a part of the total cost that it need not be included in appraisals of general trends for circuits having comparable voltage losses.

Effects of Moderate Deviations from Particular Conditions Assumed for Illustrative Example

To turn from the specific to the general case, it must be understood that certain practical discontinuities related to the customer's load and land occupancy may not be represented exactly by the mathematically continuous functions which represent general trends. When the customer's load, as well as the frontage and depth of his property become independent variables, it will be seen, for instance, that the expressions for q and n will almost invariably develop intermediate fractional values such as $q=6.6$, rather than the integer $q=6$ which exactly represented the conditions assumed in the illustrative example. Although this appears to introduce a substantial error at one step in the calculations, the consistent use of the theoretical value in such cases is found to have very little effect upon the calculated cost per customer. The errors involved are to some extent offsetting, since some overstatement of q for the secondary will result in a corresponding understatement of q' for the primary branches, etc. For this reason, it is thought that the advantages of disregarding such practical discontinuities should not lead to significant error in appraisals of general trends.

Figs. 7 through 10 have been prepared accordingly, to illustrate certain general trends which will accompany moderate deviations from the particular conditions assumed in the illustrative example. It will be noted that the costs given represent only the installed costs of the secondary circuit and primary branches, for the reasons given. In the preparation of these figures it was found convenient to use the general relations of Table III, which do not require separately identifying intermediate steps in the calculations. These relationships are further simplified by dealing in terms of the equivalent number of customers and the equivalent load density per square mile. By substitution of the respective secondary and primary voltages and unit costs of the illustrative example, in the general equations of Table III, it will be found that they reduce to the correspondingly less general relationships of Table IV, which apply specifically to the conditions summarized in Figs. 7 through 10.

It will be noted that Tables III and IV include expressions of the primary circuit transformer cost which was not evaluated or included in the illustrative example, or in Figs. 7 through 10. The principal effect of this omission is to make the cost per customer at unity pf appear to be slightly, but not significantly, higher than at 0.95 pf.

The principal advantage of improved pf

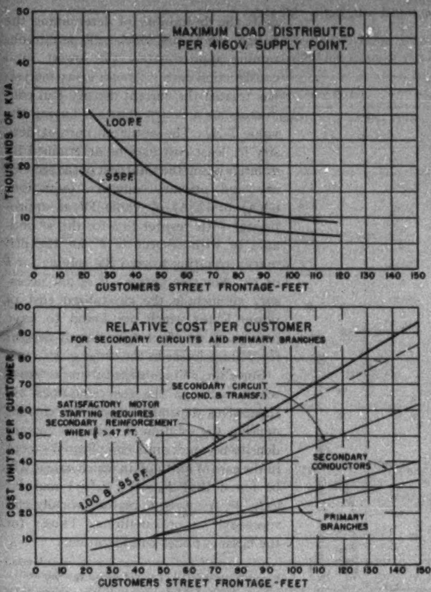

Fig. 9. Illustrative effect in new construction of customers' street frontage on aerial circuit capacity and cost for 1 kva per 120/240-volt customer, with 50-by-100-foot lots, 10^{-3} amperes per 3.3% voltage loss in secondaries, 4.2% in primaries, and 2.5% in transformers

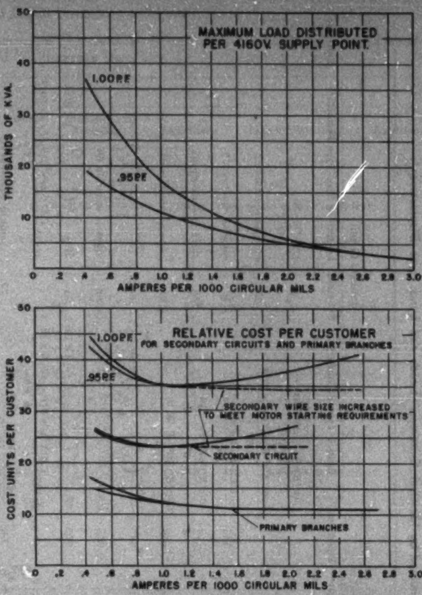

Fig. 10. Illustrative effect in new construction of current density upon aerial circuit capacity and cost for 1 kva per 120/240-volt customer on 50-by-100-foot lots, 3.3% voltage loss in secondaries, 2.5% in transformers, and 4.2% in primaries

is that of reducing the kva load per customer. The subordinate effect upon increasing the maximum load distributed per circuit is of little practical consequence at the primary circuit loads involved in this illustration.

The criteria for satisfying the motor starting limitations, and for determining the relative cost of branch-type versus lateral-type secondaries, are also included in Tables III and IV. If the load density β is not sufficiently high to require a design which is adequate for motor starting, the circuit must be reinforced by providing larger conductors and, in some cases, by designing also for some higher load density.

Variations in nominal secondary supply voltage, Fig. 7, are seen to have very little effect upon relative cost for secondary circuits and primary branches, being essentially constant for all voltages in the range from 110 to 125. A constant ratio of transformation between secondary and primary voltages was assumed.

Permissible voltage loss, in the order of 3%, Fig. 8, is seen to develop approximately the lowest cost per customer. For the primary branches this figure also shows a slight upward trend of cost per customer with increasing circuit load, because of the inherently larger average conductor size needed. The upward trend of average conductor size with circuit load operates to offset the substation economies in such a way that, in some situations, cost considerations may limit practical circuits to sizes considerably smaller than would be permitted by voltage loss limitations alone. For instance, the 4.2% voltage loss of the illustrative example would permit using 4,160-volt primary circuits, or bus-regulated unit substations, as large as 10,000 kva at 0.95 pf, which are substantially greater than has been common practice at this load density of approximately 4,000 kva per square mile.

As the customer's street frontage increases, it is seen (Fig. 9) that the cost per customer for secondary circuits and primary branches increases with an almost linear relationship, and the maximum load per primary circuit decreases as would be expected, with the accompanying decrease in load density. Load density, of course, increases inversely with the customer's land occupancy, and directly with his load.

The relative effect of current density upon aerial circuit capacity and cost is illustrated in Fig. 10, from which it is apparent that the assumed density of 1 ampere per 1,000 CM gives approximately the lowest total cost for the secondary circuit, but that a somewhat higher density will permit approximately one cost unit per customer lower cost for the primary-branch component of the primary circuit.

In Figs. 9 and 10 there is also a suggestion that reinforcement of secondary circuits, as necessary to accommodate 120-volt motor starting, need not increase the total cost per customer in new construction at load densities above 3/4 kva per customer, or 3 kva per 100 street feet.

Inference from Fig. 10, that primary branches should perhaps operate at higher current densities than secondaries, sug-

Table III. Distribution Circuit Dimensions and Costs in New Construction as Determined by Identical Customers' Loads and Land Area Displacements

	Secondary Circuit						Primary Circuit			
	Branch-Type	Equation	Lateral-Type (n = 0)*	Equation	Spot-Type (n = q = v = 0)**	Equation	Branch-Type Secondary	Equation	Lateral- or Spot-Type Secondary	Equation
$\frac{\tan\alpha_p}{F_p}$ (to find F_p from Fig. 1)	$\frac{1.25iEv\beta sX\times10^{-3}}{U\delta^2}$	48	same as equation 48				$\frac{1.04i'E'vEF_rv'\beta X'\times10^{-3}}{U'\delta\delta'^2}$	49	$\frac{1.25i'E'v'\beta sX'}{U'\delta'^2}\times10^{-3}$	50
$\frac{\tan\alpha_r}{F_r}$ (to find F_r from Fig. 1)	$\frac{0.69iEv^2E\beta XF_p\times10^{-3}}{\delta^3}$	51					$\frac{0.69i'E'v'^2E'\beta X'F_p'\times10^{-3}}{U'\delta'^3}$	52	same as equation 52	
Area served, square miles per circuit	$\frac{50(vE)^2F_pF_r\times10^{-9}}{\delta^2}$	53	$\frac{60vEsF_p\times10^{-9}}{\delta}$	54	$1/500\phi$	54S	$\frac{50(v'E')^2F_p'F_r'\times10^{-9}}{\delta'^2}$	55	same as equation 55	
Number of customers per circuit	$\frac{50(vE)^2\phi F_pF_r\times10^{-6}}{\delta^2}$	56	$\frac{60vE\phi sF_p\times10^{-6}}{\delta}$	57	2	57S	$\frac{50(v'E')^2\phi F_p'F_r' \quad 10^{-6}}{\delta'^2}$	58	same as equation 58	
Load distributed, kva per circuit	$\frac{50(vE)^2\beta F_pF_r\times10^{-6}}{\delta^2}$	59	$\frac{60vE\beta sF_p \quad 10^{-6}}{\delta}$	60	$2\beta/\phi$	60S	$\frac{50(v'E')^2\beta F'_pF_r'\times10^{-6}}{\delta'^2}$	61	same as equation 61	
Conductor feet per customer	$\frac{27.8N}{\phi}\left(\frac{1}{s}+\frac{1.2\delta}{vEF_p}\right)\times10^3$	62	$\frac{27.8N\times10^3}{\phi s}$	63	0	63S	$\frac{33.3N'}{\phi}\left(\frac{\delta}{vEF_r}+\frac{\delta'}{v'E'F_p'}\right)\times10^3$	64	$\frac{27.8N'}{\phi}\left(\frac{1}{s}+\frac{1.2\delta'}{v'E'F_p'}\right)\times10^3$	65
Pounds of copper per customer	$0.835\,\frac{iENv\beta(F_p+F_r)\times10^{-3}}{U\delta^2\phi}$	66	$\frac{1.25iENv\beta F_p\times10^{-3}}{U\delta^2\phi}$	67	0	67S	$0.835\,\frac{i'E'v'N'\beta(F_p'+F_r')\times10^{-3}}{U'\delta'^2\phi}$	68	same as equation 68	
Conductor cost per customer	$\frac{27.8Nac}{\phi}\left(\frac{1}{s}+\frac{1.2\delta}{vEF_p}\right)\times10^3+$ $0.835\,\frac{iENb_cv\beta(F_p+F_r)\times10^{-3}}{U\delta^2\phi}$	69	$27.8\,\frac{Nac\times10^3}{\phi s}+$ $\frac{1.25iENb_cv\beta F_p\times10^{-3}}{U\delta^2\phi}$	70	0	70S	$33.3\,\frac{N'ac'}{\phi}\left(\frac{\delta}{vEF_r}+\frac{\delta'}{v'E'F_p'}\right)\times10^3+$ $0.835\,\frac{i'E'N'b_c'v'\beta(F_p'+F_r')\times10^{-3}}{U'\delta'^2\phi}$	71	$27.8\,\frac{N'ac}{\phi}\left(\frac{1}{s}+\frac{1.2\delta'}{v'E'F_p'}\right)\times10^3+$ $0.835\,\frac{i'E'N'b_c'v'\beta(F_p'F_r')\times10^{-3}}{U'\delta'\phi}$	72
Transformer cost per customer	$\frac{20a_t\delta^2\times10^3}{(vE)^2\phi F_pF_r}+\frac{\beta b_t}{\phi}$	73	$\frac{16.7a_t\delta\times10^3}{vE\phi sF_p}+\frac{\beta b_t}{\phi}$	74	$\frac{1}{2}a_t+\frac{\beta}{\phi}b_t$	74S	$\frac{20a_t'\delta'^2\times10^3}{(v'E')^2\phi F_p'F_r'}+\frac{\beta b_t'}{\phi}$	75	same as equation 75	
Motor-starting limitation	$\beta\left(\frac{v_s}{I_s}-\frac{144vX_sF_p}{\delta}\right)\leqq$ $66.5\,\frac{U\delta}{iE}\left(\frac{1}{s}+\frac{0.96\delta}{v^2EF_pF_r}\right)\times10^3$	76	$\beta\left(\frac{v_s}{I_s}-\frac{144\cdot X_sF_p}{\delta}\right)\leqq$ $66.5\,\frac{U\delta}{iEs}\left(1+\frac{0.8}{vF_p}\right)\times10^3$	77	$\frac{\beta v_s}{I_s}\leqq$ $\frac{1.6\phi U}{i}$	77S				

* A lateral-type secondary circuit costs less than a branch-type when $\left[\frac{0.6a_t\delta^2}{vEF_pF_r}+\left(\frac{Nac}{F_p}+\frac{N'ac'}{F_r}\right)\right]>\left[\frac{1}{s}\left(\frac{0.5a_t\delta}{F_p}+\frac{vEN'ac'}{1.2}\right)\right]$ (78)

* A spot-type secondary costs less than a lateral-type under conditions readily recognized by comparing the sum of equations 70 and 74 with equation 74S.

gests the desirability of determining the design conditions which will permit obtaining approximately the lowest total construction cost. The previous analysis has treated the current density δ in conductors, as a design constant having the value I/A. The optimum current density for least cost may be determined by differentiating the total cost of the secondary and primary circuits (equations 69(A) to 75(A) of Table IV as appropriate) with respect to δ for the secondary, or with respect to δ' for the primary; equating to zero the solving for δ or δ'. For this purpose it is not necessary to include the capitalized cost of power losses which are found to have practically no effect upon circuit designs for voltage losses in the order of 3%.

Since the voltage adjustment factors F which occur in the cost equations are themselves dependent upon the current density, the solution of optimum current density becomes quite complicated except in the case of unity pf, in which case it will be found that $F_p=F_r=F_p''=1$ and F_r' may be expressed mathematically by successive approximations. Thus, for the circuits under consideration.

δ–optimum $=0.177\sqrt[3]{v^3\beta}$ amperes per 1,000 CM for branch-type secondary (79)

δ–optimum $=0.041\sqrt[3]{v^3\beta s}$ amperes per 1,000 CM for a lateral-type secondary (80)

δ'–optimum $=0.34\sqrt[4]{v'^3}\beta$ amperes per 1,000 CM for the primary (81)

Equation 81 is based on the assumption that the unit costs of the transformers and accessories supplying the primary circuits are $a_t'=10{,}000$ cost units and $b_t'=3.5$ cost units per kva.

By reference to Fig. 10 it is seen that the secondary- and primary-branch components of the cost curves are relatively flat at points near their minimum values. Also, in Figs. 7 through 10, it is seen that the cost per kva is practically independent of pf in the range from 0.95 to 1.00. It is therefore concluded that the current density producing the lowest construction cost at unity pf approximately represents the conditions permitting the least cost for all pf in the range from 0.9 to 1.00. It is thought possible that further investigation might indicate this assumption to be valid also at even lower pf.

In Fig. 11, the over-all effect of customers' load upon cost per customer is seen to be a practically linear relationship at constant current density. The relationship is also seen to be almost linear in Fig. 12, for the theoretically ideal condi-

Table IV. Illustrative Distribution Circuit Dimensions and Costs

For a System Supplying Identical 240-Volt 3-Wire Single-Phase Secondary Loads from Nominal 4,160-Volt 3-Phase Circuits ($E'=2{,}520$) and with Unit Costs as Assumed for Illustrative Example

Item	Secondary Circuit				Primary Circuit			
	Branch Type	Equation	Lateral Type	Equation	Branch-Type Secondary	Equation	Lateral Secondary	Equation
$\frac{\tan\alpha_p}{F_p}$ (to find F_p from Fig. 1)	$72.5\times10^{-6}\frac{v\beta s}{\delta^2}$	48A	same as branch type		$6.25\times10^{-3}\frac{vF_rv'\beta}{\delta\delta'^2}$	49A	$62.5\times10^{-6}\frac{v'\beta s}{\delta'^2}$	50A
$\frac{\tan\alpha_r}{F_r}$ (to find F_r from Fig. 1)	$4.84\times10^{-3}\frac{v^2\beta F_p}{\delta^2}$	51A			$86.5\times10^{-3}\frac{v'^2\beta F_p'}{\delta'^2}$	52A	same as for branch secondary	
Area served, square miles	$0.72\times10^{-3}\frac{v^2F_pF_r}{\delta^2}$	53C	$7.2\times10^{-6}\frac{vsF_p}{\delta}$	54A	$0.313\frac{v'^2F_p'F_r'}{\delta'^2}$	55A	same as for branch secondary	
Number of customers	$0.72v^2\frac{\phi F_pF_r}{\delta^2}$	56A	$7.2\times10^{-3}\frac{v\phi sF_p}{\delta}$	57A	$313\frac{v'^2\phi F_p'F_r'}{\delta'^2}$	58A	same as for branch secondary	
Load distributed, kva	$0.72v^2\beta\frac{F_pF_r}{\delta^2}$	59A	$7.2\times10^{-3}\frac{v\beta sF_p}{\delta}$	60A	$313\frac{v'^2\beta F_p'F_r'}{\delta'^2}$	61A	same as for branch secondary	
Conductor feet per customer	$\frac{835}{\phi}\left(\frac{100}{s}+\frac{\delta}{vF_p}\right)$	62A	$\frac{83.5\times10^3}{\phi s}$	63A	$\frac{835}{\phi}\left(\frac{\delta}{vF_r}+\frac{0.048\delta'}{v'F_p'}\right)$	64A	$\frac{835}{\phi}\left(\frac{100}{s}+\frac{0.048\delta'}{v'F_p'}\right)$	65A
Pounds copper per customer	$1.25\frac{v}{\delta^2}\frac{\beta}{\phi}(F_p+F_r)$	66A	$1.88\frac{v\beta}{\delta^2\phi}F_p$	67A	$0.87\frac{v'\beta}{\delta'^2\phi}(F_p'+F_r')$	68A	same as for branch secondary	
Conductor cost per customer	$\frac{100}{\phi}\left(\frac{100}{s}+\frac{\delta}{vF_p}\right)+$ $0.39\frac{v}{\delta^2}\frac{\beta}{\phi}(F_p+F_r)$	69A	$\frac{10^4}{\phi s}+0.585\frac{v}{\delta^2}\frac{\beta}{\phi}F_p$	70A	$\frac{100}{\phi}\left(\frac{\delta}{vF_r}+\frac{0.048\delta'}{v'F_p'}\right)+$ $0.27\frac{v'\beta}{\delta'^2\phi}(F_p'+F_r')$	71A	$\frac{100}{\phi}\left(\frac{100}{s}+\frac{0.048\delta'}{v'F_p'}\right)+$ $0.27\frac{v'\beta}{\delta'^2\phi}(F_p'+F_r')$	72A
Transformer cost per customer	$\frac{174\delta^2}{v^2\phi F_pF_r}+6.2\frac{\beta}{\phi}$	73A	$\frac{17.4\times10^3\delta}{v\phi sF_p}+6.2\frac{\beta}{\phi}$	74A	$\frac{32}{\phi}\frac{\delta'^2}{v'^2F_p'F_r'}+3.5\frac{\beta}{\phi}$	75A	same as for branch secondary	
Motor-starting limitation	$\beta\left(1-0.073\frac{vF_p}{\delta}\right)\geq$ $665\delta\left(\frac{1}{s}+\frac{0.008\delta}{v^2F_pF_r}\right)$	76A	$\beta\left(1-\frac{0.073vF_p}{\delta}\right)\geq$ $665\frac{\delta}{s}\left(1+\frac{0.8}{vF_p}\right)$	77A				
Lateral-type secondary: cost lower than branch, when	$\left[\frac{1.70\delta^2}{vF_pF_r}+\left(\frac{1}{F_p}+\frac{1}{F_r}\right)\delta\right]>\left[\frac{100}{s}\left(\frac{1.70\delta}{F_r}+v\right)\right]$			78A				

tions which permit the least total construction cost for secondary circuits and primary branches.

The average conductor sizes indicated in Fig. 12 are considerably smaller than had been expected. Therefore, it seems appropriate to review a few considerations which account in part at least for the small wire sizes developed in these illustrative calculations:

1. It will be recalled that the illustrative example included no special provisions for emergency breakdown service, such as is usually provided in cases when failure of supply to one circuit requires redistribution of its load between adjacent circuits. The permissible voltage loss in the thus temporarily enlarged circuits is considerably greater under such emergency conditions, but it seems quite probable that some additional conductor capacity, and therefore a larger average size, might be required.

2. The mechanical strength required to withstand standard wind and ice loading of the conductors, frequently establishes a minimum practical conductor strength which would require a larger copper conductor than needed to satisfy only the electrical characteristics of the circuit. Where cost and other related considerations are favorable, however, there has been a considerable use of steel-reinforced aluminum cable, copperweld, or other high-strength conductor, to provide the required mechanical strength without necessarily providing excess conductivity.

3. The consistent year-to-year growth of customers' loads requires such frequent circuit reinforcement that it is generally good practice to install somewhat larger conductors than would be sufficient for the particular loads at the time when reinforcement becomes necessary.

4. The illustration assumes complete new construction under ideal conditions such as are seldom encountered in practice.

The effect of customer's load upon distribution circuit size, also shown in Figs. 11 and 12, is of considerable interest, since it will be noted that the load limit per circuit at 0.95 pf is in each case approximately proportional to the square root of the load per customer. For several years, this particular relationship between circuit load and load density has been observed by the Philadelphia Electric Company as an empirical characteristic of its secondary-, primary-, and high-tension circuit loads.

It now seems appropriate to examine briefly the effect of current density upon the load distributing capacity of primary-branch circuits. This is shown in Fig. 13 for several values of current density as a function of load density at 0.95% pf. From a review of this figure it will be seen that the square-root relationship is approximately representative of a current density in the order of 1 ampere per 1,000 CM. With the current density adjusted for least cost, a 0.43 power relationship is obtained. The latter relationship is thought to be practically unattainable in a growing system where each new load is almost invariably accommodated by a comparatively "piecemeal" reinforcement of the existing facilities, in such a way as to provide the added capacity for the least practical additional cost.

Diverse Effects of the Community

According to the previously outlined plan, all preceding steps in this analysis have dealt exclusively with the singular effects of individual customers. Having established a method by which these singular effects may be appraised, it is now appropriate to consider the diverse community effects involved in the distribution of power to diverse customers, under diverse conditions which are unquestionably beyond the control of any single customer.

A given customer has exclusive control over the magnitude and time of his maximum demand. The almost obvious corollary is that he can have no control whatever over the corresponding actions of his neighbor, who is supplied from the same circuit. Yet, their joint use of a

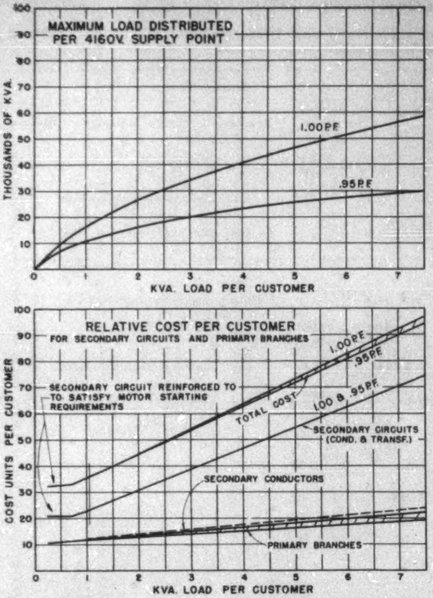

Fig. 11. Illustrative effect in new construction of load per customer on aerial circuit capacity and cost for 120/240-volt customers having 50-by-100-foot lots, with 10^{-3} amperes per CM, 3.3% voltage loss in secondaries, 4.2% in primaries, and 2.5% in transformers

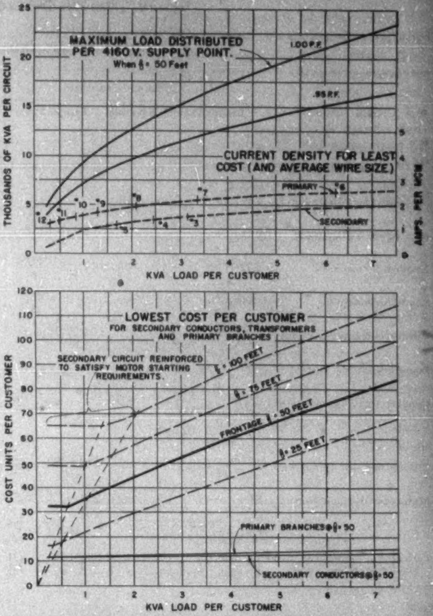

Fig. 12. Illustrative effect in new construction of designs for aerial circuits with lowest cost at 0.95 to 1.00 pf for 120/240-volt customers having lots 100 feet deep with current density adjusted to lowest cost, 3.3% voltage loss in secondaries, 2.5% in transformers, and 4.2% in primaries

common distribution circuit has certain effects to which they jointly contribute.

There was a time, in the days of 1,000-watt flat-irons and 40-watt light bulbs, when the maximum demands of neighboring residential customers were far more nearly uniform than now. With the advent of electric ranges, domestic water heaters, clothes driers and unit air conditioners, however, the loads of residential customers are becoming quite as diverse as the loads of other classes of customers supplied from the same or comparable circuits. Accordingly, it is thought that the only practical way of avoiding possible error in accounting for the diverse load characteristics of customers is to postulate the premise that no distribution circuit will serve two customers having equal or coincident load characteristics. Load diversity, however, is only one of all the community effects which must be accounted for and it should affect only the load component of distribution circuit costs.

On the other hand, random diversity of street layouts, parks, play grounds, cemeteries, rivers, railroads, airports, as well as diverse rights-of-way conditions as affected by rock, trees, and other construction handicaps, including the occasional need for expensive underground construction, are characteristics of the community which are not related to load but have substantial effects upon construction costs. Such diversities are usually subject to objective evaluation only to the extent that their composite effect can be identified by analysis of the distribution plant records for the respective accounts involved. These often-overlooked diversities can have very extensive effects upon costs, perhaps sufficient at times almost to smother the effects of load diversity.

It is therefore apparent that an accounting for the diverse effects of the community requires dealing with them in terms of two general classifications, load diversity and other diversities. Although "other diversities" directly affect the fixed components of unit costs, it will be seen that they also affect the load component of distribution circuit costs to the extent that the numbers of units increase with increasing load density.

Allocation of Construction Costs Between Diverse Loads Supplied from Given Distribution Circuit

By the method developed, it is possible to calculate both the fixed component and the load component of distribution circuit construction cost for each customer served, in terms of kva maximum demand at his meter, his land occupancy, and representative unit costs for the predominantly characteristic type of distribution circuit construction. The representative unit costs are usually obtainable from the property records for each of the particular plant accounts involved, particularly if trended to some consistent construction cost level. In such cost allocations, so long as distribution circuit sizes increase in proportion to the square

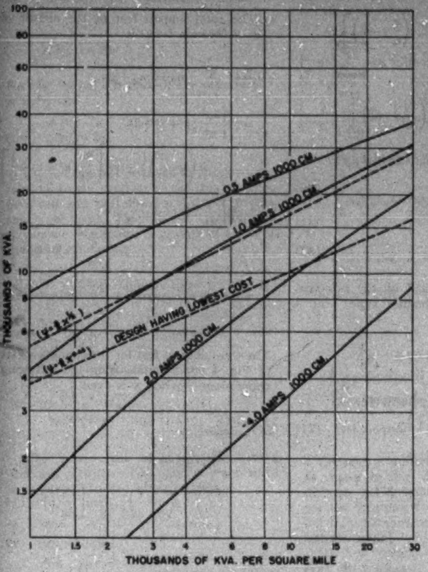

Fig. 13. Illustrative effect in new construction of load density on aerial circuit capacity for various current densities at 0.95 pf for 120/240-volt customers having 50-by-100-foot lots, 3.3% voltage loss in secondaries, 2.5% in transformers, and 4.2% in primaries

root of the load density, it is practical to assume, for copper conductors, a current density of $\delta=1$ ampere per 1,000 CM. The sum of the respective calculated fixed components and load components of construction costs for all of the customers involved will then represent the circuit which these customers would in general require if there were no diversities.

The general noncoincidence of customers' maximum demands is usually accounted for in terms of coincidence factor,[1] having values which range from zero to unity, increasing statistically with increasing load factor and to some extent inversely with the number of similar loads on the circuit. Possible questions concerning whether such factors apply accurately to circuits supplying random combinations of dissimilar loads are not properly a part of the present investigation. It is sufficient to note that the applicable load coincidence factor for any circuit will be the ratio of the maximum demand on the circuit to the sum of the customer's individual maximum demands. Since this ratio will have some value which is less than unity, it follows that the corresponding equivalent load density will also be less. The consequent effect upon calculations made according to the relationship summarized in Tables III and IV may therefore be observed by substituting the correspondingly adjusted value of load density which equals the product of β by the particular coincidence factor found applicable to the circuit in question.

The effect of load diversity upon the calculated construction cost for each of the customers on the circuit may be accounted for by proportionally reducing his load component of costs to account for the applicable coincidence factor for the circuit serving him. The sum of the calculated fixed components and the adjusted load components of construction costs for all customers served by the circuit will then be the total cost corresponding to the predominately characteristic type of distribution circuit construction, if there are no other diversities. The other diversities may then be accounted for with very little likelihood of introducing any significant inequity, by adjusting the total construction cost for each customer by the ratio of the actual cost of the circuit to the cost which has been found to represent the predominately characteristic type of distribution circuit construction.

Considerable additional investigation beyond the immediate scope of this analysis would be required to determine whether the foregoing procedure for distribution circuit cost allocation is more desirable than methods currently followed. It may, however, have some value as a basis for confirming or improving such methods.

Conclusions

1. Dealing with the distribution circuit consistently as a functional entity, and in terms of its natural parameters, has promise of becoming an extremely effective aid to judgment in certain general problems relating to distribution system design and cost allocation.

2. While the example chosen to illustrate this method of analysis must be recognized as having limited general application, the analysis does suggest that little reduction in cost per customer may be expected to accompany any "inching upward" of the secondary voltage level within the range of 115 to 125 volts.

3. Secondaries designed for the supply of load densities less than 4 kva per 100 street feet (1 kva per customer having a 50-foot frontage) must be reinforced to prevent excessive motor-starting voltage dips. It is apparently possible, however, to provide needed reinforcement (Fig. 10) without noticeably affecting the trend of cost per customer until (Fig. 12) the load density reaches about two-thirds of that at which reinforcement becomes necessary.

4. The per customer cost for secondary circuits and primary branches increases almost linearly with the customer's maximum demand and with his street frontage. In designs for least cost, as in Fig. 12, it will be noted that transformers almost entirely account for the load component of secondary-circuit and primary-branch costs per customer.

5. For the case illustrated in Fig. 12, the least cost is within 5% of 65 cost units per 100 feet for all loads up to 4/3 kva per 100 feet of the customer's street frontage plus 7.5 cost units for each additional kva of his load.

6. The empirically observed trend of load per circuit with the square-root of the load density is shown by this analysis to be generally characteristic of circuits having average current densities in the order of 1 ampere per 1,000 CM of copper conductor.

7. Economy favors permitting current density to exceed 1 ampere per 1,000 CM where practical in aerial circuit designs.

8. The curves of maximum load distributed per 4,160-volt supply point in Fig. 12, suggest that bus-regulated substations might be found to be practical in unit sizes substantially larger than has been general practice. At 1 kva per customer, which represents approximately 4,000 kva of circuit load per square mile in this illustration, it is theoretically possible to distribute as much as 7,000 kva from such a unit substation at 0.95% pf.

9. Analyses of trends in distribution plant costs might become substantially more informative if organized so as to distinguish separately between the factors which affect the fixed component and those which affect the load component of construction costs.

Appendix I. Derivation of Equations for Equivalent Circuits of Figs. 3 and 4

Referring to Figs. 3 (branch type) and 4, let y indicate the number of a lateral counting from the extremity of a riser branch. The number of unit loads picked up by a lateral is

$$q_y=\left(\frac{2}{f}y\frac{q}{n}f+1\right)-2+2\times\frac{1}{2}=\frac{2q}{n}y(y>0<n)$$

$$q_0=\frac{1}{4}\qquad (y=0)\qquad (82)$$

$$q_p=(2q+1)-2+2\times\frac{1}{4}=2q-\frac{1}{2}\qquad (y=n)$$

The total number of unit loads picked up is therefore

$$Q=2\left(q_0+\sum_{y=1}^{y=n-1}q_y\right)+q_p$$

$$=2\left\{\frac{1}{4}+\frac{2q}{n}[1+2+3\ldots(n-1)]\right\}+2q-\frac{1}{2}$$

$$=2qn\qquad (17)$$

since

$$1+2+3\ldots x=\frac{x(x+1)}{2}\qquad (83)$$

For the lateral type circuit shown in Fig. 3

$$Q=(2q+1)-2+2\times\frac{1}{2}=2q\qquad (17)$$

The half-length of each lateral is

$$d_y=y\frac{q}{n}f\text{ feet}\qquad (84)$$

and for the principal lateral

$$d_p=qf\text{ feet }(y=n)\qquad (18)$$

The half-length of a riser branch is

$$d_r=ns\qquad (19)$$

Therefore the total circuit length is

$$D=4\sum_{y=0}^{y=n-1}d_y+2d_p+2d_r$$

$$=\frac{4q}{n}f\,[1+2+3\ldots(n-1)]+2qf+2ns$$

$$=Q\left(f+\frac{s}{q}\right)\qquad (n>0)$$

$$Qf\qquad (n=0)\qquad (20)$$

The ampere-feet in half of each lateral of Fig. 3 (branch type) and in half of each even-numbered lateral of Fig. 4 is

$$m_y=if\left\{\left[1+2+3\ldots\left(\frac{q}{n}y-1\right)\right]+\frac{1}{2}\frac{q}{n}\right\}$$

$$=if\left(\frac{q}{n}y\right)^2\text{ ampere-feet }(y<n)\qquad (85)$$

For the odd-numbered laterals shown in Fig. 4

$$m_y=if\left\{\left[\frac{1}{2}+1\frac{1}{2}+2\frac{1}{2}\ldots\left(\frac{q}{n}y-1\right)\right]+\frac{1}{2}\frac{q}{n}y\right\}$$

$$=if\left\{\frac{1}{2}\left[1+3+5\ldots\left(\frac{2q}{n}y-2\right)\right]+\frac{1}{2}\frac{q}{n}y\right\}$$

$$=\frac{if}{2}\left[\left(\frac{q}{n}y\right)^2+\frac{1}{4}\right]\text{ ampere-feet }(y<n)\qquad (86)$$

since

$$1+3+5\ldots x=\frac{(x+1)^2}{4}\qquad (87)$$

The ampere-feet in half of the principal lateral in Figs. 3 (branch type) and 4 (n is even) is

$$m_p=if\left\{[1+2+3\ldots(q-1)]+\frac{1}{4}q\right\}$$

$$=\frac{if}{2}q\left(q-\frac{1}{2}\right)=q^2\frac{if}{2}\text{ approximately ampere-feet}\qquad (21)$$

and in Fig. 4 (n is odd) is

$$m_p=if\left\{\frac{1}{2}[1+3+5\ldots(2q-2)]+\frac{1}{4}q\right\}$$

$$=\frac{if}{2}\left[q\left(q-\frac{1}{2}\right)+\frac{1}{4}\right]=q^2\frac{if}{2}\text{ approximately ampere-feet}\qquad (21)$$

The ampere-feet in half of the lateral of Fig. 3 (lateral type) is

$$m_p=if\left\{[1+2+3\ldots(q-1)]+\frac{1}{2}q\right\}$$

$$=q^2\frac{if}{2}\text{ ampere-feet}\qquad (21)$$

The ampere-feet in a section of the riser branch between any y and $Y+1$ numbered lateral is

$$\Delta m_r=is\left(\frac{1}{4}+\sum_{y=1}^{y=y}q_y\right)$$

$$=is\left[\frac{1}{4}+\frac{2q}{n}(1+2+3\ldots y)\right]$$

$$=is\left[\frac{q}{n}y(y+1)+\frac{1}{4}\right]\text{ ampere-feet}\qquad (88)$$

The ampere-feet in half a riser branch is therefore

$$m_r=\sum_{y=0}^{y=n-1}\Delta m_r$$

$$=is\left\{\frac{q}{n}[1^2+2^2+3^2\ldots(n-1)^2]+\frac{q}{n}[1+2+3\ldots(n-1)]+\frac{n}{4}\right\}$$

$$=isn\left[\frac{q}{3n}(n^2-1)+\frac{1}{4}\right]=n^2\frac{isq}{3}\text{ approximately ampere-feet}\qquad (22)$$

since

$$1^2+2^2+3^2\ldots x^2=\frac{x(x+1)(2x+1)}{6}\qquad (89)$$

The total ampere-feet of the circuit of Fig. 3 (branch type) is

$$M=4\sum_{y=0}^{y=n-1}m_y+2m_p+2m_r$$

$$=if\left\{\frac{2q^2}{n^2}[1^2+2^2+3^2\ldots(n-1)^2]+q\left(q-\frac{1}{2}\right)\right\}+isn\left[\frac{2q}{3n}(n^2-1)+\frac{1}{2}\right]$$

$$=ifq\left[\frac{q}{3n}(2n^2+1)-\frac{1}{2}\right]+isn\left[\frac{q}{3n}(2n^2-2)+\frac{1}{2}\right]$$

$$=\frac{Qi}{3}(qf+ns)\text{ approximately ampere-feet}\qquad (23)$$

The total ampere-feet for the configurations of Fig. 4 are obtained from the following expressions. When n is even

$$M=if\left\{\frac{2q^2}{n^2}[2^2+4^2+6^2\ldots(n-2)^2]+\frac{2q^2}{n^2}[1^2+3^2+5^2\ldots(n-1)^2]+\frac{1}{2}\left(\frac{n}{2}\right)+q\left(q-\frac{1}{2}\right)\right\}+isn\left[\frac{2q}{3n}(n^2-1)+\frac{1}{2}\right]\text{ ampere-feet}\qquad (90)$$

and when n is odd

$$M=if\left\{\frac{2q^2}{n^2}[2^2+4^2+6^2\ldots(n-1)^2]+\frac{2q^2}{n^2}[1^2+3^2+5^2\ldots(n-2)^2]+\frac{1}{2}\left(\frac{n-1}{2}\right)+q\left(q-\frac{1}{2}\right)+\frac{1}{4}\right\}+isn\left[\frac{2q}{3n}(n^2-1)+\frac{1}{2}\right]\text{ ampere feet}\qquad (91)$$

These equations are equal to

$$M=if\left\{\frac{2q^2}{n^2}[1^2+2^2+3^2\ldots(n-1)^2]+q\left(q-\frac{1}{2}\right)+\frac{n}{4}\right\}+isn\left[\frac{2q}{3n}(n^2-1)+\frac{1}{2}\right]$$

$$=if\left\{q\left[\frac{q}{3n}(2n^2+1)-\frac{1}{2}\right]+\frac{n}{4}\right\}+isn\left[\frac{q}{3n}(2n^2-2)+\frac{1}{2}\right]$$

$$=\frac{Qi}{3}(qf+ns)\text{ approximately ampere-feet}\qquad (23)$$

For the lateral-type circuit of Fig. 3

$$M=2m_p=\frac{Qi}{2}qf\text{ ampere-feet}\qquad (23)$$

It should be noted that the foregoing expressions for Q, m, and M also may be derived on the assumption of a uniformly distributed load throughout the area. It will be apparent that the load density is $1/fs$ unit loads per square foot and since the area of the diamond-shaped area served by a branch-type equivalent circuit is 2 $qfns$

$$Q=\frac{1}{fs}\times 2qfns=2qn \qquad (17)$$

For the lateral-type circuit the area served is $2qfs$, and

$$Q=\frac{1}{fs}\times 2qfs=2q \qquad (17)$$

The ampere-feet involved in any instance is equal to the product of the total current involved and the effective distance to the center of load, which is the rectangular distance to the center of gravity of the area involved

$$m_p=\frac{2qi}{2}\times\frac{qf}{2}=q^2\frac{if}{2}\text{ ampere-feet} \qquad (21)$$

$$m_r=\frac{2qni}{2}\times\frac{1}{3}ns=n^2\frac{isq}{3}\text{ ampere-feet} \qquad (22)$$

and for the branch-type circuit

$$M=4\times\frac{Qi}{4}\times\frac{qf+ns}{3}=\frac{Qi}{3}(qf+ns)\text{ ampere-feet} \qquad (23)$$

The power loss in a system having uniform conductor size may be determined as follows. In half of each lateral

$$p_y=i^2fR\left(\frac{1^2}{2}+\frac{3^2}{2}+\frac{5^2}{2}\ldots\frac{qy}{n}\text{ terms}\right)$$
$$=\frac{i^2fR}{3}q\frac{y}{n}\left[\frac{qy^2}{n}-\frac{1}{4}\right]\text{ watts per conductor} \qquad (92)$$

since

$$1^2+3^2+5^2\ldots x\text{ terms}=\frac{1}{3}\times(4x^2-1) \qquad (93)$$

The power loss in a section of the riser branch between any y and $y+1$ numbered lateral is from equation

$$\Delta p_r=i^2sRq^2\frac{y^2}{n^2}(y^2+2y+1)\text{ watts per conductor} \qquad (94)$$

The power loss in a riser branch is therefore

$$p_r=\sum_{y=0}^{y=n-1}\Delta p_r=i^2\frac{sRq^2}{n^2}\times\left[\begin{array}{l}1^4+2^4+3^4\ldots(n-1)^4+\\2\{1^3+2^3+3^3\ldots(n-1)^3\}+\\1^2+2^2+3^2\ldots(n-1)^2\end{array}\right]$$
$$=i^2sRq^2\left(\frac{n^3}{5}-\frac{n}{3}+\frac{1}{7.5n}\right)=\frac{i^2sRq^2n^3}{5}\text{ approximately} \qquad (95)$$

since

$$1^4+2^4+3^4\ldots x^4=\frac{1}{30}\times(x+1)(2x+1)\times(3x^2+3x-1) \qquad (96)$$

and

$$1^3+2^3+3^3\ldots x^3=\frac{x^2(x+1)^2}{4} \qquad (97)$$

The total power loss in a branch type circuit is therefore

$$P=4\sum_{y=0}^{y=n-1}p_y+2p_p+2_{pr}$$
$$=\frac{i^2fR}{3}\left[\frac{4q^3}{n^3}\{1^3+2^3+3^3\ldots(n-1)^3\}-\frac{q}{n}\{1+2+3\ldots(n-1)\}+2q^3-\frac{q}{2}\right]+$$
$$\frac{2}{5}i^2sRq^2n^3=Qi^2Rq\left(\frac{qf}{6}+\frac{2n^2s}{5}\right)\text{ approximately} \qquad (25)$$

For a lateral-type circuit

$$P=2p_p=\frac{2}{3}i^2fR_q\left(q^2-\frac{1}{4}\right)=Qi^2\frac{Rq^2f}{3}\text{ approximately} \qquad (25)$$

Appendix II. Derivation of Equations for Radial Circuit of Fig. 5

Consider a uniform system of unit loads as shown in Fig. 5 where the horizontal distance between loads is f feet and the vertical distance is s feet. Each load is fed from the source of supply by an individual feeder which reaches the load through a vertical path and a horizontal path as indicated. The area which may be thus served with a maximum voltage loss will be diamond-shaped as shown, and the height and width of the diamond will be theoretically equal. If a larger area is to be symmetrically served by a number of such systems, it is apparent that the corners of each diamond-shaped area will be midway between individual pickup points horizontally or vertically. Thus, if the parameters of the area served are indicated as qf and ns as before, it will be evident that qf must be a multiple of $f/2$. Since the pickup points at the vertical corners of the diamond are spaced $2s$ apart for the staggered spacing of pickup points shown in Fig. 5, and which will be obtained for systems of the higher voltage levels, it is apparent that n must be an integer.

It will be apparent also from Fig. 5 that there is a possibility of a pickup point falling on the boundary. Hence, for purposes of calculating the maximum voltage loss, we may interpret d_p as being the maximum horizontal distance and d_r as the maximum vertical distance from the supply point in the area served. Therefore

$$d_p=qf\text{ feet} \qquad (18)$$

$$d_r=ns\text{ feet} \qquad (19)$$

$$m_p=iqf\text{ ampere-feet} \qquad (21)$$

$$m_r=ins\text{ ampere-feet} \qquad (22)$$

The remainder of the parameters are most readily obtained by considering the system as one having a uniformly distributed load throughout the area. As indicated in Appendix I, therefore, the values of Q and M will be the same as therein derived. Since each unit load is supplied by a separate feeder

$$D=\frac{M}{i}=\frac{Q}{3}(qf+ns)\text{ feet} \qquad (20)$$

and

$$P=\frac{Qi^2R}{3}(qf+ns)\text{ watts per conductor} \qquad (25)$$

Appendix III. Development of Voltage Adjustment Factor F

Let E_1 represent the phase-to-neutral voltage at the nearest customer, V_t the component of line drop in phase with the current, and V_q the quadrature component of line drop. The magnitude of the phase-to-neutral voltage at the last customer is given by the expression

$$E_2=\sqrt{(E_1+V_t\cos\theta+V_q\sin\theta)^2+(V_q\cos\theta-V_t\sin\theta)^2}\text{ in volts} \qquad (98)$$

and the permissible difference in magnitude between E_2 and E_1 is

$$E_2-E_1=\frac{vE}{100}\text{ volts} \qquad (99)$$

Since from equations 9 or 11

$$\frac{vE}{100}=\frac{Kd}{F},\text{ or }\frac{mR}{F}=\frac{V_t}{F}\text{ volts} \qquad (100)$$

from equations 98 through 100 the following relationship is obtained

$$\frac{1}{F}+\frac{E_1}{V_t}=\sqrt{\left(\frac{E_1}{V_t}\right)^2+2\frac{E_1}{V_t}\cos\theta+\frac{V_q}{V_t}\times\sin\theta+1+\left(\frac{V_q}{V_t}\right)^2} \qquad (101)$$

Solving equation 101 for V_q/V_t the following is obtained

$$\frac{V_q}{V_t}=\frac{E_1}{V_t}\left[\sqrt{\sin^2\theta+\left(\frac{V_t}{E_1}\right)^2\left(\frac{1}{F^2}-1\right)-\frac{2V_t}{E_1}\left(\cos\theta-\frac{1}{F}\right)}-\sin\theta\right] \qquad (102)$$

If $E_1=E(1-1/2\,v/100)$, from equation 100

$$\frac{E_1}{V_t}=\frac{1}{F}\left(\frac{100}{v}-\frac{1}{2}\right)=\frac{100}{Fv}\text{ approximately} \qquad (103)$$

If equation 103 is substituted in equation 102 and if it is recognized that $V_q/V_t=\tan\alpha$, where α is the effective phase angle of the circuit, the following expression results

$$\tan\alpha=\frac{100}{Fv}\left[\sqrt{\sin^2\theta+\frac{v^2}{10^4}(1-F^2)+\frac{v}{50}(1-F\cos\theta)}-\sin\theta\right] \qquad (104)$$

For $\theta=0$ (unity pf) equation 104 reduces to

$$\tan\alpha = \frac{1}{F}\sqrt{(1-F)\left(1+F+\frac{200}{v}\right)}$$

$$= \frac{14.3}{F}\sqrt{\frac{1-F}{v}} \text{ approximately} \qquad \textbf{(105)}$$

The solution of equations 104 and 105 for F at various pf in terms of $\tan \alpha$ and $(\tan \alpha)/F$ is given in Fig. 1. To eliminate a fourth variable, v has been taken at a nominal value of 3.75%. Moderate variations in v from this value will have a negligible effect except in the case of unity pf, for which Fig. 1 also becomes applicable, provided the abscissas are multiplied by the ratio $\sqrt{v/3.75}$.

Reference

1. Coincidence-Factor Relationships of Electric-Service-Load Characteristics, Constantine Bary. *AIEE Transactions (Electrical Engineering)*, vol. 64, Sept. 1945, pp. 623-28.

◆

Discussion

Constantine W. Bary (Philadelphia Electric Company, Philadelphia, Pa.): I would like to commend Mr. Kidder and Mr. Neher on their well-conceived, well-formulated and valuable paper. It is a milestone in the study of the parameters affecting the economics of power distribution systems. I was especially interested in the authors' conclusions relating to the basic concepts of a modern power distribution system and their mathematical rationalization of its cost behavior depicted in Figs. 11 and 12, as applying to the functional elements of primary branches, secondary transformers, and secondary circuits.

As a result of work done by Mr. Kidder and his associates in the Philadelphia Electric Company over 20 years ago, we have been using in our cost-of-service analyses the concepts and major parameters of power systems distribution cost behavior now so ably described in the present paper. There is no question in my mind that such concepts as the functional components of the power distribution system and such major parameters as the number of customers and their maximum demands form the cornerstones for a comprehensive structure of determining the cost behavior of a power distribution system, but there are two points which should be kept in mind by those who have occasion to build on the foundation laid by this paper:

1. It must be appreciated that the very considerable amount of load diversity which we have come to associate with supplying the usual number of residential customers per circuit diminishes quite rapidly as the number becomes less than 20 and vanishes at one customer per circuit. The relationship is one to which I have previously referred as the "first law of load diversity".[1]

2. In actual practice there is some fixed maximum size of load that can be carried at a given tap-off point, limited by the practical size of a distribution transformer installation—a fact which should be expected to introduce a point of discontinuity in the cost curves and will increase the cost per customer materially at noncoincident maximum demands beyond the range considered by the authors.

To illustrate the effect of load diversity on distribution transformer loading, let us consider a group of residential customers having equal noncoincident maximum demands of 3.5 kva per customer. According to curve D of Fig. 1 of reference 1 of the paper, the corresponding average load per customer in terms of transformer maximum demand (sometimes referred to as diversified maximum demand) would be 2.4 kva per customer in groups of 2 customers per circuit; 1.9 kva per customer in groups of 4 per circuit; 1.6 kva per customer in groups of 10 per circuit; 1.5 kva per customer in groups of 20 per circuit, and 1.4 kva per customer in groups of 25 customers per circuit. In this case, therefore, the transformer load per customer might range anywhere from 1.4 to 3.5 kva, depending only upon the number of customers served under the circumstances.

For the range of customers' loads considered by the authors, I think that the numbers of customers per transformer probably are sufficiently large so that the single parameter for the "load" or the "maximum demand" used by them in plotting the cost curves depicts the relationships within that range without risk of introducing appreciable error. Beyond 7.5 kva per customer, however, it certainly becomes essential to recognize the increasingly important trend of load diversity with the decreasing number of customers per transformer. As the maximum demands of residential customers continue to increase to levels above 7.5 kva per customer, I am inclined to believe that an adequate appraisal of the effect upon cost per customer will require dealing with two "load" parameters: one dependent upon the customers' noncoincident maximum demands above some predetermined value, and another dependent on their diversified maximum demand.

It will be noted that the load component of distribution system cost is more closely related to the load per circuit than it is to individual customer's maximum demand at his service entrance, while the fixed or area coverage component of such cost is basically dependent upon the number of customers per tap-off point. Since in actual practice there is some fixed maximum size of load that can be carried at a given tap-off point, the number of customers per tap-off will decrease with an increase in the load size of customers (especially beyond the size of 5, 7, or 10 kva per customer), and such decrease in the number of customers per tap-off point will be accompanied by an increase in the group coincident factors, in accordance with the first law of load diversity, which further diminishes the possible number of customers per tap-off point. The over-all effect of these conditions will be reflected in higher unit cost per customer of the so-called "fixed" or area coverage costs of the tap-off points, and this in turn can be traced back fundamentally to the increase in the customers' load size as measured by their noncoincident maximum demands. In our system of cost analysis, we have been reflecting this condition in the past, on an empirical basis, for customers of the small general light and power class, supplied from the secondary system, which has had for many years back a relatively large number of customers with maximum demands in excess of 5 kva.

Although empirically these conditions may be rationalized on the basis of a 50-kva or a 100-kva secondary transformer installation per tap-off point (as a practical maximum under present-day conditions depending upon local conditions), I hope that the authors will find an opportunity to pursue further their fundamental analyses of the power distribution parameters with a view to establishing a mathematical rationalization of the two load parameters, which appear to be necessary to reflect fully the behavior of power distribution costs for a wide range of customers' load requirements, beyond the 5, 7, or 10 kva per customer. The importance of realizing the existence of these two parameters will be, in my opinion, of ever-increasing significance in the economics of power distribution systems of the future, as the kva maximum demands of residential customers increase by leaps and bounds with the ever-growing use of electricity, and especially as a result of rapidly increasing saturations of residential air conditioning and, in the not too distant future, with the growth of the heat pump and other types of space heating loads, which will place such customers' maximum demands considerably beyond the 5, 7, or 10 kva per customer values, and which will be accompanied with an increase in their group coincidence factors.

REFERENCE

1. Load-Structure of a Modern Electric Utility System, Constantine W. Bary. *Proceedings*, American Power Conference, Chicago, Ill., vol. XVI, 1954, p. 401.

D. N. Reps and **H. E. Lokay** (Westinghouse Electric Corporation, East Pittsburgh, Pa.): The approach taken by the authors to solve a complex problem is a very interesting one. It is our interpretation that the principal purpose of this paper is to present methods for analyzing primary and secondary distribution system costs with the ultimate objective of obtaining maximum economy of system design and operation. The authors have chosen to present results of hypothetical examples showing the relationships of cost per customer versus kva demand per customer.

The relationships established in this paper are quite general, and we note with great interest that a somewhat different approach to distribution system cost evaluation which we have taken leads to results which closely agree with the cost picture presented in Fig. 11. A brief description of the methods employed in our study follows.

The distribution system is designed to serve load of a stipulated kva-per-square-mile load density with costs put on a dollars-per-kva basis. The uniformly distributed load, to be similar to the subject paper, could be subdivided into any desired kva demand for customer, and the total system cost can be visualized on a dollars-per-customer basis. In our analysis, we divide the system into five major components: subtransmission circuits, distribution substations, primary-feeder circuits, distribution transformers, and secondaries and services.

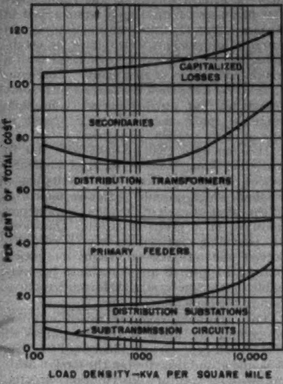

Fig. 14. Typical per-cent cost allocation to each system component and capitalized energy losses for minimum-cost systems at each load density

All the major components were included because every type of system will have a different form that each component will take. For instance, a primary-network system will require dual subtransmission supply to each primary-network distribution substation, and primary feeders will be networked. A radial primary distribution system on the other hand may have dual-transformer and dual-subtransmission-supply distribution substations, or may be a simple radial system throughout. Secondaries may be radial or banked. It will be noted that the form the system components will take determines the "service quality" and "service continuity" rendered by the system as a whole. Having stipulated in advance what these system attributes should be, it is then possible to optimize (minimize) the cost of that type of system to serve a given load density. Two, or several, system arrangements can be studied, if necessary, for purposes of economic comparisons of alternatives.

The variables or parameters entering into such a cost optimizing or minimizing procedure are: subtransmission voltage, distribution-substation size, primary-feeder voltage and the number of primary feeders per substation, distribution transformer size, secondary voltage and secondary conductor size, and pole spacings.

From the studies we have made, a typical per-cent cost allocation to each system component and capitalized energy losses for minimum-cost systems at each load density are shown in Fig. 14. This particular case is for a radial system with a 34.5-kv single subtransmission-circuit supply to single-transformer distribution substations, and radial primary feeders operating at 2,400/4,160 volts. Secondary voltage is 120/240 volts. Since Mr. Kidder and Mr. Neher consider primary circuits, distribution transformers, and secondaries only, in Fig. 15 we have replotted Fig. 14 to show only these components.

Fig. 16 is obtained from Fig. 11. To convert kva per customer to kva per square mile, we have assumed that a load of 1 kva per customer represents a load density of 2,000 kva per square mile. This relationship comes about if 1 square mile is assumed to contain ten streets in both directions, with lots of 50-foot frontage on both sides of the streets in one direction. A load density increase then involves greater demand per customer, since the area at 2,000 kva per square mile is assumed saturated with residences.

The similarity in the per-cent costs allocated to the three components from our analysis, and the authors', is apparent. This close similarity indicates that our approach to system cost determination which considers uniformly distributed load rather than load per customer, and dollars per kva rather than cost per customer, leads to the same results as the authors' analysis.

However, the minimum-cost system for a given load density might, e.g., utilize different conductor sizes and substation ratings than a load density just a relatively small increment greater. Obviously it would not be practicable to change out conductors continually, and replace substation transformers and distribution transformers with different size units to satisfy the optimum requirements for each slightly greater density as the load grows. Hence the most economical system is one which minimizes total investment over some considerable period of time. This procedure would require "overdesigning" some or all of the components at the outset to eliminate the need for costly changeovers at too frequent intervals. Such overdesigning is often mandatory if for no other reason than that ratings of equipment and conductor sizes are standardized at specific values. These considerations apply to both the authors' and our approach to the problem as presented herein.

We are in agreement with the conclusions of Kidder and Mr. Neher. An approach such as theirs to the problem of distribution system cost optimization definitely leads to a better understanding of the subject. Further investigation including the effects of load growth will shed additional light on the problem and prove exceedingly useful in distribution system planning.

A. H. Kidder and J. H. Neher: We are most appreciative of the interest shown in our paper, particularly of the discussions which raised points that deserve careful consideration. Also, one of the reviewers whose name is not known to us raised an additional point which is deserving of recognition.

Mr. Bary's emphasis of the need to

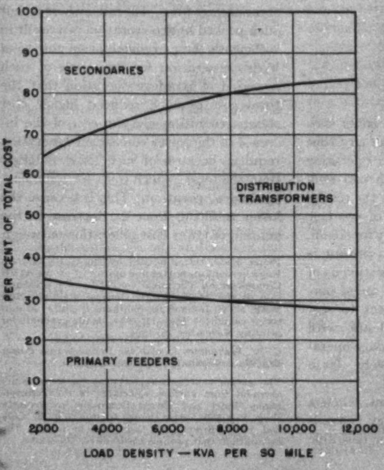

Fig. 15 (left). Fig. 14 replotted to show only primary circuits, distribution transformers, and secondaries

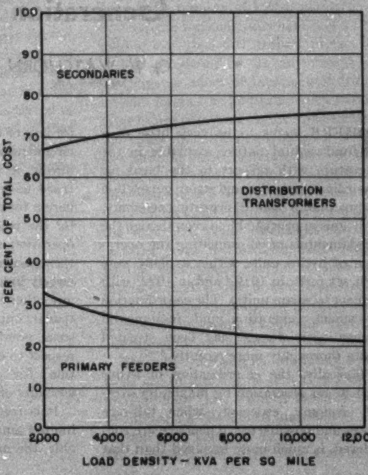

Fig. 16 (right). Fig. 11 replotted converting kva per customer to kva per square mile

recognize the effects of load diversity on distribution transformer loading, as well as the effect of the natural limit on maximum distribution transformer size, is important, and both effects can be accounted for readily by a slight extension of our analysis. If β represents the load density on a fully diversified or coincident load basis, these effects will modify the secondary equations only, and it may be shown that the only appreciable change will occur in equations 73 and 74 for the transformer cost per customer which may be rewritten as

$$\text{Transformer cost per customer} = \frac{a_t}{2Q} + \frac{\gamma \beta b_t}{\phi} \qquad (106)$$

in which $2Q$ is the number of customers per circuit, as given by equation 56 or 57, and γ represents the ratio of the coincidence factor Ω_n for $2Q$ customers to the coincidence factor for an infinitely large number of customers Ω_∞. As shown in reference 1 of the paper

$$\gamma = \frac{\Omega_n}{\Omega_\infty} = 1 + \frac{1-\Omega_\infty}{2Q\Omega_\infty} \qquad (107)$$

If the transformer size is limited to L_{max} in kva

$$2Q \leq \frac{\phi L_{max}}{\gamma \beta}, \text{ number of customers} \qquad (108)$$

In this case $2Q$ should be determined by equation 108 in the range where equation 108 yields lower values of $2Q$ than equations 56 and 57.

It is of considerable interest to know that the independent approach of Mr. Reps and Mr. Lokay develops cost trends quite similar to those which can be derived from information given in the paper. In the present state of the art, however, we think that it is important to emphasize the distinction between cost trends and costs, because it has been our experience that alternate approximate designs of distribution circuits will develop quite similar cost trends, but they may not necessarily develop identical costs in otherwise equal situations.

Although the curves in Figs. 15 and 16 have similar general trends, it will be noted, e.g., that there is considerable difference between their respective slopes as well as the corresponding absolute values represented at nearly all load densities. It is quite probable that these divergencies may be attributed in part to lack of sufficient data.

These observations therefore should not be construed to the discredit of the discussers. They merely emphasize the possibility of pitfalls which unfortunately may befall one who on occasion finds it necessary to deal with approximations. It was for this reason that we undertook to develop a method by which it would be possible to determine the number of given loads which a distribution circuit could supply under given conditions, together with the total load, the circuit length, and total conductor weight required, as necessary in order to estimate its total cost under given conditions.

In this particular case, it is unfortunate that the large number of parameters and the multiplicity of circuits involved in any distribution circuit make it necessary to deal in terms of cost as the only practical common denominator. For this reason it may be helpful to remind the reader that the first part of the paper, summarized in Tables I and II, serves to develop certain essential dimensions which must be established before costs can be evaluated with a maximum degree of confidence. Cost considerations were then introduced with some reluctance, but only as necessary to illustrate the application of the basic theory in one of many possible situations.

It is our hope that we have been able to introduce some measure or rigor in distribution circuit synthesis by developing a method which permits accurate appraisal of the effect of each of the many parameters involved in a given situation. Questions of providing for emergency breakdown service and advance provisions for anticipated load growth are thought to be amenable to solution by straightforward application of the principles outlined.

The unknown reviewer raised a point concerning the loads at the extremities of the branch-type circuit, illustrated in Figs. 2, 3, and 4, and described in the section dealing with elementary distribution circuits. We find that we had failed to point out that the loads shown in these extremities accurately represent the situation only when $qf = ns$, as at unity pf. Rigorous representation of these boundary loads at other pf's is apparently impractical at this stage and should have been acknowledged. The effect of failure to account accurately for this effect would be to overstate somewhat the amount of load which could be distributed by the circuit. The design thus derived can be checked and modified in any situation where it is found necessary to compensate for this neglected circuit reactance effect.

Co-ordination of Hydro and Steam Generation

C. W. WATCHORN
MEMBER AIEE

THERE seems to be very little of a fundamental nature available in the literature with respect to the basis for co-ordinating hydro and steam generation for maximum over-all operating economy.[1–3] This appears to be so even though the fundamentals of co-ordinating the operation of hydro units within a plant were first set forth in 1919,[4] and in 1922[5] with respect to steam units. The co-ordination of steam generation and incremental transmission losses has been treated quite thoroughly more recently.[6–11]

Basically, the co-ordination of hydro and steam generation for maximum overall economy, especially when tail-race losses and possible use of pondage are considered, is much more involved than that for any of the foregoing since, under such circumstances, the operation at any time during a period of pondage operation (used as periods of drawdown and refill herein for convenience) affects the results for the whole of that period of pondage operation, whereas, particularly for steam, the operation from instant to instant is largely independent of the operation as of any other instant. Such facts are of particular importance with respect to seasonal pondage operation, and also with respect to daily or weekly pondage operation for which comparatively large amounts of water are involved.

It is frequently thought that, when a limited amount of hydro energy is available, the most advantageous or desirable operation is to utilize such energy in the peak of the load to as great an extent as possible since such operation results in the smallest amounts of required higher cost steam generation. The fallacy here is that such peaked hydro operation can result in sufficiently large reductions in the total hydro generation for the whole of such a period of pondage operation that the total cost of such reduced higher cost steam generation and the cost of the increase in the lower cost steam generation required because of such losses is larger than the total of such costs for some flatter hydro operation. This is because the losses resulting from the increase in the amount of lower cost generation outweigh

---

Paper 55-33, recommended by the AIEE System Engineering Committee and approved by the AIEE Committee on Technical Operations for presentation at the AIEE Winter General Meeting, New York, N. Y., January 31–February 4, 1955. Manuscript submitted May 11, 1954; made available for printing November 16, 1954.

C. W. WATCHORN is with the Pennsylvania Power and Water Company, Baltimore, Md.

The author expresses appreciation for the encouragement from various associates in the Pennsylvania Water and Power Company, particularly H. A. Von Eiff. Also thanks are due to R. W. Cole and F. F. Brooks for their care in making the calculations that provide the basis for the study.

the savings resulting from the reduction in the amount of higher cost steam generation required. The optimum operation is a compromise between the operation that results in the maximum amount of hydro generation on the one hand, and the operation that results in the hydro generation that replaces the maximum possible amount of the otherwise higher cost steam generation on the other hand. Such optimum operation, in contrast with this latter operation, results rather in such losses in hydro generation in reducing the amount of higher cost steam generation required that, together with the cost for the resulting increase in the lower cost steam generation, maximum over-all economy is obtained for the whole of the period of operation.

The investigation reported here was started in an attempt to develop or discover a basis for automatically co-ordinating hydro and steam generation. The results were determined experimentally by means of what might appropriately be called a mathematical model of a combined hydro and steam system which could be operated fairly conveniently in any manner desired and for which the results could be measured to any practical degree of precision necessary. This approach was used since it appeared, after much study, that the problem could not readily be solved in any other manner.

Nomenclature

c = cost of the system steam generation, dollars per hour
g_h = generation of the hydro plant, megawatts (mw)
g_s = system steam generation, mw
q = hydro plant discharge, thousand cubic feet per second (mcfs)
r = rate of pond inflow in mcfs at time t in hours
H = head on the hydro plant, feet
I = intake losses, feet
L = system load in mw at time t in hours from the beginning of the operation under consideration
M = tail-race elevation, feet
N = incremental water value, dollars per hour per mcfs. It is a constant during the whole of any period of pondage operation of the hydro plant under consideration (used as drawdown and refill herein for convenience, but not limited thereby)
P = pond elevation at time t, feet
S = withdrawal from storage in mcfs-hours at time t as compared with zero withdrawal for a full pond
T = period of operation, hours
$\frac{dc}{dg_s}$ = system incremental steam cost, dollars per hour per mw
$\frac{dg_h}{dq}$ = incremental hydro equivalent of the hydro plant under consideration, mw per mcfs
$\frac{\partial g_h}{\partial q}$ = incremental hydro equivalent with constant head, mw per mcfs
$\frac{\partial g_h}{\partial H}$ = incremental change in hydro generation with respect to head with constant discharge, mw per foot
$\dot{q}$ = time rate of change of the hydro plant discharge, mcfs per hour
$\dot{r}$ = time rate of change of inflow into the pond of the hydro plant, mcfs per hour
$\frac{dI}{dq}$ = incremental change in the hydro plant intake losses with respect to plant discharge, feet per mcfs
$\dot{L}$ = time rate of change of the system load, mw per hour
$\frac{dM}{dq}$ = incremental change in tail-race elevation with respect to plant discharge, feet per mcfs
$\frac{dP}{dS}$ = incremental change in pond elevation with respect to storage, feet per mcfs-hour
$\ddot{q}$ = first derivative of the time rate of change of the hydro plant discharge, or the second derivative of the hydro plant discharge as a function of time, mcfs per hour^2
$\ddot{L}$ = first derivative of the time rate of change of the system load, or the second derivative of the system load as a function of time, mw per hour^2
$\frac{d^2P}{dS^2}$ = second derivative of the pond elevation as a function of storage, feet per mcfs-hour^2

Results

The investigation indicated that maximum economy may possibly be obtained in the co-ordination of hydro and steam generation when the product of the system incremental steam cost and of the difference between the ratio of the time rate of change of the load to the time rate of change of the hydro plant discharge and the incremental hydro equivalent of the hydro plant under consideration is equal to a constant during the whole period of drawdown and refill of the pond of that plant. This relationship may be expressed by the following basic hydro steam co-ordinating equation

$$\frac{dc}{dg_s}\left(\frac{\dot{L}}{\dot{q}}-\frac{dg_h}{dq}\right)=N \tag{1}$$

Further, the incremental hydro equivalent dg_h/dq in equation 1 may be expressed as

$$\frac{dg_h}{dq}=\frac{\partial g_h}{\partial q}+\frac{\partial g_h}{\partial H}\left(\frac{(q-r)\frac{dP}{dS}}{\dot{q}}-\frac{dI}{dq}-\frac{dM}{dq}\right) \tag{2}$$

Equation 2 substituted in equation 1 results in

$$\frac{dc}{dg_s}\left\{\frac{\dot{L}-(q-r)\frac{\partial g_h}{\partial H}\frac{dP}{dS}}{\dot{q}}-\left[\frac{\partial g_h}{\partial q}-\frac{\partial g_h}{\partial H}\left(\frac{dI}{dq}+\frac{dM}{dq}\right)\right]\right\}=N \tag{3}$$

which for $\dot{q}=0$ becomes

$$\frac{dc}{dg_s}\left\{\frac{\ddot{L}+\left(\dot{r}\frac{dP}{dS}-(q-r)^2\frac{d^2P}{dS^2}\right)\frac{\partial g_h}{\partial H}}{\ddot{q}}-\left[\frac{\partial g_h}{\partial q}-\frac{\partial g_h}{\partial H}\left(\frac{dI}{dq}+\frac{dM}{dq}\right)\right]\right\}=N \tag{4}$$

Although the method of co-ordinating hydro and steam generation for maximum combined economy as developed here was specifically investigated on the basis of drawdown and refill of the pond of the hydro plant over the period of operation under study, the application of that method of co-ordination to such combined operation is not limited to that basis of pondage operation; it is equally applicable to the problem of determining the most economical operation to be followed in going from any given beginning pond elevation at any time to any given ending pond elevation at some predetermined future time, e.g., in the following of a rule curve. In fact, it is particularly applicable to the problem of determining the rule curve itself such as to result in the optimum co-ordination of hydro and steam generation in the seasonal operation of a reservoir.

Further, it will be noted that, regardless of the number of hydro plants on a system, the incremental steam cost to be used at any time with respect to each of such plants should be the same except for the possible effect of incremental transmission losses. In addition, when two or more hydro plants are on the same stream, the inflow into the ponds of each of the downstream plants is flatter than the discharge of the plant immediately upstream and, also, there is a time lag between such pond inflows and plant discharges unless the upstream plant discharges directly into the pond of the downstream plant. In the latter case, the inflow into the ponds of each of the downstream plants is equal to the discharge of the plant immediately upstream except for possible additional inflow between the two plants.

These hydro steam co-ordinating equations are in such forms that they can be used directly (i.e., without modification) to interrelate the hydro and steam generation and, also, the generation among the various hydro plants of a system for

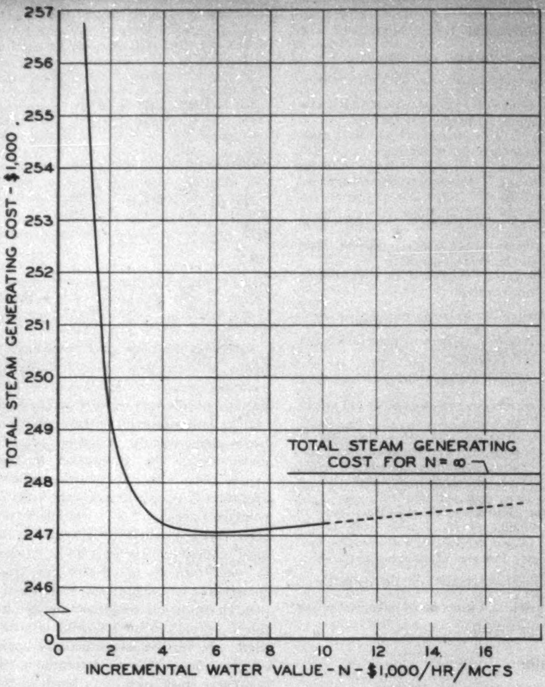

Fig. 1. Total system steam generating cost versus incremental water value N

optimum results regardless of their number, location on the system, type, etc., unless it is desired also to compensate for the effect of incremental transmission losses. This latter problem is beyond the intended scope of this paper but, considering the relatively high state of the development of methods for handling the companion problem as related to all-steam systems,[9–11] it may be expected that comparable results, as related to such losses, are also obtainable with respect to combined hydro and steam systems.

Method of Investigation

The mathematical model of the combined hydro and steam system used as the basis for this investigation may be represented by the following indicated equations

$$c=f(g_s) \qquad (5)$$

For a lossless transmission system g_s results in

$$g_s=L-g_h \qquad (6)$$

$$L=F(t) \qquad (7)$$

$$g_h=\phi(q,H) \qquad (8)$$

$$H=P\text{-}I\text{-}M \qquad (9)$$

$$P=\Phi(S) \qquad (10)$$

$$I=\beta(q) \qquad (11)$$

$$M=\gamma(q) \qquad (12)$$

$$S=\theta(q,r,t) \qquad (13)$$

$$r=\lambda(t) \qquad (14)$$

$$q=\rho(t) \qquad (15)$$

The system thus represented was operated on many different bases in an endeavor to determine a systematic basis which would result in minimum total steam generating cost over a period of time for which the operation was such that the total water used during that period was some predetermined amount. Many experiments finally indicated that optimum results are obtained when the hydro plant is operated at some constant incremental water value in accordance with equation 1 as more fully expressed by equation 3.

The relationships indicated were determined in the following manner: first, with respect to equation 5

$$\frac{dc}{dq}=\frac{dc}{dg_s}\frac{dg_s}{dq}=N \qquad (16)$$

and from equations 6 and 7

$$\frac{dg_s}{dq}=\dot{L}\frac{dt}{dq}-\frac{dg_h}{dq} \qquad (17)$$

then, rearranging

$$\frac{dg_s}{dq}=\frac{\dot{L}}{\dot{q}}-\frac{dg_h}{dq} \qquad (18)$$

which substituted in equation 16 results in equation 1.

Then, from equation 8

$$\frac{dg_h}{dq}=\frac{\partial g_h}{\partial q}+\frac{\partial g_h}{\partial H}\frac{dH}{dq} \qquad (19)$$

and from equations 9, 11, and 12

$$\frac{dH}{dq}=\frac{dP}{dq}-\frac{dI}{dq}-\frac{dM}{dq} \qquad (20)$$

Also, from equation 10

$$\frac{dP}{dq}=\frac{dP}{dS}\frac{dS}{dq} \qquad (21)$$

and from equation 13

$$\frac{dS}{dq}=(q-r)\frac{dt}{dq} \qquad (22)$$

Then, rearranging equation 22 and substituting it in equation 21 and substituting that resulting equation in equation 20 yields

$$\frac{dH}{dq}=\frac{(q-r)\frac{dP}{dS}}{\dot{q}}-\frac{dI}{dq}-\frac{dM}{dq} \qquad (23)$$

which substituted in equation 19 results in equation 2.

Equation 3 is continuous when the numerator of the first expression within the braces thereof is equal to zero at the same time that the denominator $\dot{q}$, is also equal to zero, since that expression is then in the indeterminate form and may be evaluated by differentiating both its numerator and denominator with respect to t, which reduces it to the first expression within the braces in equation 4.

There is no definite solution to equation 3 since it is solvable for all values of N, for which, however, there is only one of such values that results in the optimum over-all system operation. The value of N that results in such optimum system operation is determinable by means of successive approximations with the solution of the equation best done graphically for the purposes here. Such a solution is illustrated in the Appendix.

Table I. Computation of System Steam Generating Cost for Incremental Water Value N Equal to $6,000 Per Hour Per Mcfs

Line	Term	Derivation	Unit											
1	t		hours	0	1	2	3	4	5	6	7	8	9	10
2	$\dot{q}'$	assumed; see note *A*	mcfs per hour	−1.07	−1.00	−0.93	−0.87	−0.79	−0.71	−0.64	−0.57	−0.49	−0.41	−0.34
3	q'	see note *B*	mcfs	34.171	33.136	32.171	31.271	30.431	29.681	29.006	28.401	27.871	27.421	27.046
4	r	assumed	mcfs	30	30	30	30	30	30	30	30	30	30	30
5	$q'-r$		mcfs	4.171	3.136	2.171	1.271	0.431	−0.319	−0.994	−1.599	−2.129	−2.579	−2.954
6	S'	$S_{t-1}'+[(q'-r)_{t-1}+(q'-r)_t]/2$; see note *C*	mcfs-hours	0	3.6535	6.307	8.028	8.879	8.935	8.2785	6.982	5.118	2.764	−0.0025
7	N	assumed	$ per hour per mcfs	6,000	6,000	6,000	6,000	6,000	6,000	6,000	6,000	6,000	6,000	6,000
8	$\dot{q}''$	see note *D*; should check $\dot{q}'$ of line 2	mcfs per hour	−1.07	−1.00	−0.93	−0.87	−0.79	−0.71	−0.64	−0.57	−0.49	−0.41	−0.34
9	$\dot{q}$	$-1.07+0.05833t+0.003333t^2-0.0001852t^3$; see text	mcfs per hour	−1.070	−1.009	−0.941	−0.870	−0.795	−0.718	−0.640	−0.562	−0.485	−0.410	−0.339
10	q	$34.193-1.07t+0.02917t^2+0.001111t^3-0.0000463t^4$	mcfs	34.193	33.153	32.177	31.271	30.439	29.682	29.003	28.402	27.879	27.431	27.037
11	S	$4.1926t-0.535t^2+0.009722t^3+0.0002777t^4-0.00000926t^5$	mcfs-hours	0	3.668	6.327	8.046	8.894	8.948	8.284	6.979	5.113	2.762	0
12	P	$56-0.1S$, equation 31	feet	56.0000	55.6332	55.3673	55.1954	55.1106	55.1052	55.1716	55.3021	55.4887	55.7238	56.0000
13	M	$0.2q$, equation 37	feet	6.8385	6.6306	6.4355	6.2543	6.0877	5.9363	5.8005	5.6803	5.5757	5.4863	5.4115
14	H	$P-M$, equations 9 and 36	feet	49.1615	49.0027	48.9318	48.9412	49.0229	49.1689	49.3711	49.6217	49.9130	50.2376	50.5885
15	g_h	$-10+(0.1q-0.00001q^2)H$, equation 24	mw	138.443	134.502	131.148	128.079	125.393	123.084	121.145	119.566	118.335	117.439	116.858
16	L	$500-20t$, equation 26	mw	500	480	460	440	420	400	380	360	340	320	300
17	g_s	$L-g_h$, equation 6	mw	361.557	345.398	328.852	311.921	294.607	276.916	258.855	240.434	221.665	202.561	183.142
18	c	$20+3g_s+0.01g_s^2+0.001g_s^3$, equation 27	$ per hour	49,675.81	43,455.16	37,651.33	32,276.87	27,341.60	22,852.15	18,811.50	15,218.58	12,067.92	9,349.33	7,047.57

Notes:

A: equal to $\dot{q}''$ of line 8 for $t=0$, and assumed for all other values of t.

B; the value of q' for $t=0$ assumed, and for other values of t computed as $q_{t-1}'+[(\dot{q})_{t-1}'+(\dot{q})_t']/2$.

C: the value of S' for $t=10$ should be as nearly equal to zero as is practicable.

D: based on t, q', S', N, and Fig. 2 for all values of t.

$$\sum_{t=0}^{10} c=\$247,386.13; \quad \sum_{t=0}^{10} g_h=1,248 \text{ mw-hours}$$

$$c'=49,675.81-6,424.0844t+200.85685t^2+2.719427t^3-0.0875260t^4-0.00317448t^5$$

$$C'=\int_0^{10} c'\,dt=\$247,025.80.$$

Conclusions

Various other systematic bases for co-ordinating hydro and steam generation were determined and investigated but none resulted in as low a cost as that obtained with the application of the basic hydro steam co-ordinating equations expressed as equations 1 and 3. It was therefore concluded that these co-ordinating equations were probably the answer to the problem even though it has not been found possible to establish a rigorous basis for this conclusion. It, nevertheless, is believed that if they actually do not provide such fundamental basis for co-ordinating hydro and steam generation for maximum economy, they at least result in sufficiently close answers to be so used for all practical purposes. In any event, it is hoped that the material presented may contribute in some measure to the eventual solution of what appears to be a rather difficult and complex problem.

It is quite probable that any practical use of the equations presented should be made by means of automatic controls or some simplification of the basic method itself, because, even with but one hydroplant, it is believed that these co-ordinating equations are too complicated to be used for direct manual application. The justification of the use of these hydro-steam co-ordinating equations would, of course, depend on an evaluation of the results obtained with their application as compared with the results obtained with other bases of co-ordinating hydro and steam generation. However, in this regard, Fig. 1, in which the smaller values of *N* are for the more peaked hydro generation which frequently is thought of as being the more desirable basis for co-ordinating hydro and steam generation, shows that the total cost of system steam generation may increase very sharply under some circumstances with such more peaked hydro generation. On the other hand, this figure also shows that the optimum value of *N* is not particularly critical since the curve is fairly flat over a rather wide range of values of *N*. It is consequently believed that numerical integration and differentiation should give satisfactory results in any application of these co-ordinating equations to actual conditions.

Appendix. Determination of the Optimum Value of N

The solution of equation 3 to determine the value of *N* such that the optimum operation results is illustrated by Table I and Fig. 2.

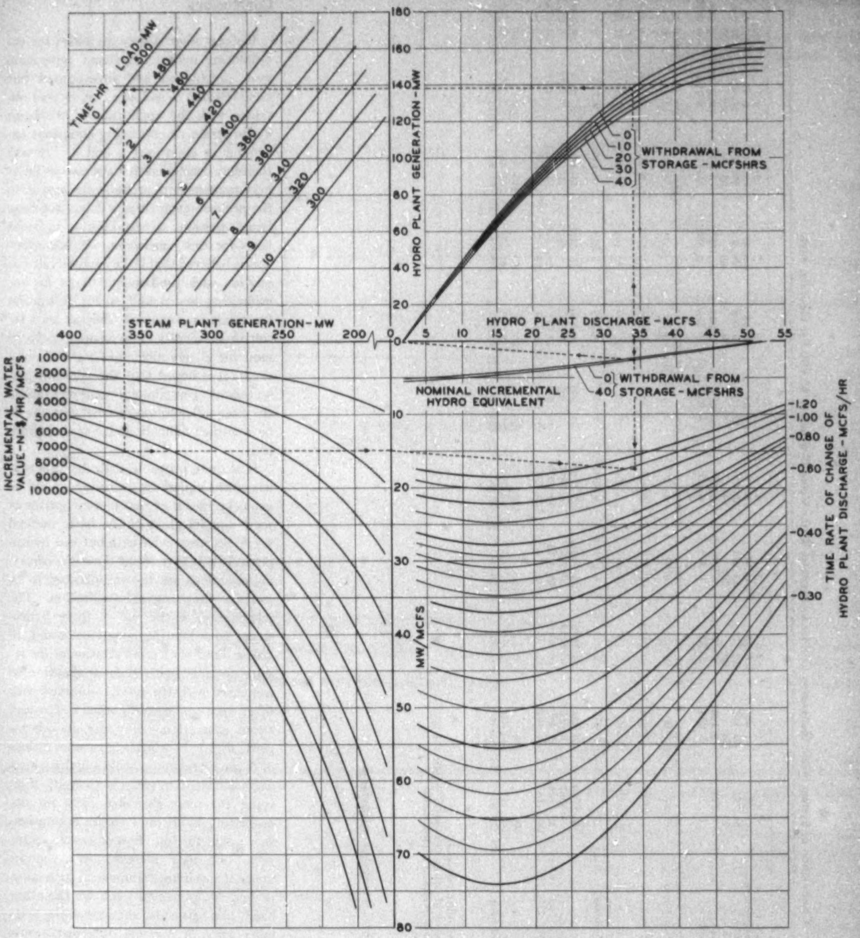

Fig. 2. Curves for the graphical solution of equation 41

The curves in the first quadrant of Fig. 2 show the hydro plant generation versus its discharge for various amounts of withdrawals from storage. They were obtained from equation 8 written as

$$g_h = -10+(0.1q-0.00001q^3)H \qquad (24)$$

where equation 9 is taken to be

$$H=56-0.1S-0.2q \qquad (25)$$

The second quadrant merely provides a graphical means of subtracting the hydro generation, obtained from the curves shown in the first quadrant, from the total system load as of various whole values of time t as given by equation 7 written as

$$L=500-20t \qquad (26)$$

These equations were found to result in the required steam generation varying over a wide enough range of system steam generating cost so that a short period of operation, 10 hours, could be used so as to minimize the necessary calculations as much as reasonably possible since all the calculations were made manually with desk calculators and, at the same time, it would be a sufficiently long enough period so as to reflect satisfactorily the effect of all the factors involved.

The curves in the third quadrant of Fig. 2 are each for various assumed constant values of N as shown. These curves are functions of the steam generation and are in units of mw per mcfs, as shown. They are obtained by dividing such assumed values of N by the incremental steam cost for the various values of steam generation shown. Then, writing equation 5 as

$$c=20+3g_s+0.01g_s^2+0.001g_s^3 \qquad (27)$$

results in

$$\frac{dc}{dg_s}=3+0.02g_s+0.003g_s^2 \qquad (28)$$

Equation 27 results in tremendously high steam generating costs for the larger values of generation, but this is of no particular significance since in this paper only the basic principles for the correct operation of combined hydro and steam systems in general are being determined rather than the correct operation of any particular system. This characteristics of such high values of steam generating costs is necessary because, based on the arithmetical method of investigation and the short period of time (10 hours) of operation used in the study to facilitate the calculations, it would thereby be sufficiently responsive to differences in total costs so as to provide a reasonable basis for a sound conclusion.

Then, to illustrate, for a required steam generation of 300 mw for which, from equation 28, the incremental steam cost is $279 per hour per mw and for a value of N of $5,000 per hour per mcfs, the corresponding value resulting therefrom and to be plotted with respect to the vertical scale between the third and fourth quadrants is 17.92 mw per mcfs and is obtained as $5,000 per hour per mcfs divided by $279 per hour per mw.

Two quantities are shown plotted in the fourth quadrant of Fig. 2: the first expression within the braces of equation 3; 2. the nominal incremental hydro equivalent which is the second expression within the braces of that equation.

Then, from equation 26

$$\dot{L}=-20 \tag{29}$$

and from equation 24

$$\frac{\partial g_h}{\partial H}=0.1q-0.00001q^3 \tag{30}$$

Then, as included in equation 25

$$P=56-0.1S \tag{31}$$

from which

$$\frac{dP}{dS}=-0.1 \tag{32}$$

For equation 14 written as

$$r=30 \tag{33}$$

and substituting equations 29 through 33 in the first expression within the braces of equation 3 results in

$$\frac{-20+0.1(q-30)(0.1q-0.00001q^3)}{\dot{q}} \tag{34}$$

which is shown plotted in the fourth quadrant of Fig. 2 as a function of q for various values of $\dot{q}$, as shown to the right of that quadrant.

Also, from equations 24 and 25

$$\frac{\partial g_h}{\partial q}=(0.1-0.00003q^2)(56-0.1S-0.2q) \tag{35}$$

Then, as included in equation 25

$$I=0 \tag{36}$$

and

$$M=0.2q \tag{37}$$

from which

$$\frac{dI}{dq}=0 \tag{38}$$

and

$$\frac{dM}{dq}=0.2 \tag{39}$$

Substituting equations 30, 35, 38, and 39 in the second expression within the braces of equation 3 yields

$$(0.1-0.00003q^2)(56-0.1S-0.2q)-0.2(0.1q-0.00001q^3) \tag{40}$$

which is also shown plotted in the fourth quadrant of Fig. 2 as a function of q for various values of withdrawals from storage S; only two are shown in the figure.

Expression 40 or the second expression within the braces of equation 3 is in the exact nature of the over-all plant incremental hydro equivalents used for many years in various studies in that it only takes into account the unit characteristics of some given head and the incremental head losses as related to the intake and tail-race and disregards the incremental head losses related to withdrawals from storage. The effect of this latter factor should also be included as shown in equation 2 which expresses the true incremental hydro equivalent. The determination that factors should be included in the expression for the incremental hydro equivalent, equation 19, to account for the incremental head losses resulting from withdrawals from storage as shown in equation 23 and that a factor should be included in the hydro steam co-ordinating equation itself, equation 1, to account for the effect of the time rate of change of the load to be supplied are new in so far as it is known to the author. These determinations proved to be the whole key to the problem as finally resolved. Then, since expression 40 is not actually the true incremental hydro equivalent, it is referred to, for convenience, as the nominal incremental hydro equivalent.

The use of Fig. 2 in solving equation 3, with equation 28 and expressions 34 and 40 substituted in it, which results in

$$(3+0.02g_s+0.003g_s^2)\left[\frac{-20+0.1(q-30)(0.1-q0.00001q^3)}{\dot{q}}-[(0.1-0.00003q^2)(56-0.1S-0.2q)-0.2(0.1q-0.00001q^3)]\right]=N \tag{41}$$

is illustrated in Table I where the first step is to assume a value for the hydro plant discharge q for $t=0$. This is shown as 34.171 mcfs in line 3 of Table I for the conditions there. A line is then drawn vertically into both the first and fourth quadrants for this value of hydro plant discharge, as shown by the dotted line in Fig. 2. Next, a line is drawn from the point of intersection of this vertical line and the curve for the nominal incremental hydro equivalent for the withdrawal from storage for the time t under consideration to the origin, as shown in the fourth quadrant. A second line is then drawn horizontally from the point of intersection of this same vertical line and the curve for the hydro generation for the same withdrawal from storage for the same time t as in the foregoing, as shown in the first quadrant, into the second quadrant to the load for the time under study, at this point for $t=0$. Next, a vertical line is drawn downward from this point into the third quadrant to the intersection with the curve there for the assumed value for N, $6,000 per hour per mcfs in this case, as shown in line 7 of Table I. Then, proceed horizontally to the right from this point of intersection to the intersection with the vertical line through the origin between the third and fourth quadrants; from which latter point of intersection a line is drawn parallel to the line originally drawn from the nest of curves of the nominal incremental hydro equivalents through the origin to the point of intersection with the vertical line originally drawn through the assumed discharge of the hydro plant. This latter point of intersection determines the value of $\dot{q}$, as shown in line 8 of Table I for $t=0$. This initially determined value of $\dot{q}$ is also entered in line 2 of Table I.

The runs for all the following values of t start with assumed trial values of $\dot{q}$, as shown in line 2 of Table I, rather than with an assumed value of hydro plant discharge as for $t=0$. The values of hydro plant discharge for these succeeding hours are computed as shown by note B to line 3 of Table I, based on the assumed values of $\dot{q}$ of line 2. The resulting withdrawals from storage, based on these values of hydro plant discharge, are then computed as shown in line 6. Based on these data of hydro plant discharge and withdrawals from storage values of $\dot{q}$ are determined from Fig. 2 in the same manner as just described with respect to $t=0$, and the values of these quantities thus determined are entered in line 8. They should check the values assumed for q of line 2 for the same value of t. If they do not, new values of $\dot{q}$ should be assumed for line 2 and the procedure repeated with respect to each value of t, in order, until the values determined with respect to line 8 check those assumed for line 2. It was found that this check was usually obtained on the second trial for most of the values of t. These calculations are repeated for the whole of the period under study and should result in zero withdrawal from storage at the end of the period of operation, or as close thereto as it is practicable to obtain, −0.0025 mcfs-hours in the case illustrated by Table I. If the withdrawal from storage at the end of the period of operation is not nearly equal to zero, a new run should be made beginning with a new trial initial value for the hydro plant discharge for $t=0$, and the whole process should be repeated until the desired conditions are met.

The middle portion of Table I, beginning with line 9, was prepared as a basis for determining the total cost of the steam generation for the whole of the period of operation with a high degree of precision so as to provide the most reliable basis practicable for a sound conclusion. The equation for q, shown on line 10 under the derivation column of Table I, was assumed as

$$q=q_1+2q_2t+3q_3t^2+4q_4t^3+5q_5t^4 \tag{42}$$

There seemed to be no basis for readily determining any theoretically exact equation for this quantity. However, this statement of the hydro plant discharge as a function of time is believed to be sufficiently close, for the purposes here, to any theoretically exact equation that may actually exist with respect to the conditions under investigation so that any differences there may be between it and what might otherwise be the correct form of equation for this quantity with respect to such conditions would not be of any practical or possibly even of any theoretical significance as to such purposes.

The equation for $\dot{q}$, shown on line 9 under the derivation column of Table I, was determined, first, from equation 42 as

$$\dot{q}=2q_2+6q_3t+12q_4t^2+20q_5t^3 \tag{43}$$

Second, as to the specific values for the coefficients $2q_2$, $6q_3$, etc., shown on Table I, they were solved for simultaneously as based on the values for $\dot{q}$, shown for $t=0$, $t=3$, $t=6$, and $t=9$ on line 8.

All the coefficients of equation 42, except q_1, are then determinable from the results obtained in the determination of the coefficients for equation 43. Since the operation is assumed to be on the basis of returning the pond to the same elevation at the end of the period of operation under study as at the beginning of such period, the total plant discharge during the whole of that period is equal to the total pond inflow during such period. Then, if for the purpose of this investigation, but not otherwise limited thereby, constant pond inflow during the period of operation is assumed, as shown by equation 33

$$\int_0^T q\,dt=\int_0^T (q_1+2q_2t+3q_3t^2+4q_4t^3+5q_5t^4)dt=\int_0^T r\,dt \tag{44}$$

from which, performing the indicated operations

$$q_1T+q_2T^2+q_3T^3+q_4T^4+q_5T^5=rT \tag{45}$$

which results in

$$q_1=r-q_2T-q_3T^2-q_4T^3-q_5T^4 \tag{46}$$

The quantity q_1 is then readily determinable from this latter equation and the coefficients are determined for equation 43 as in the foregoing. The determination of the correct values for these coefficients is very important in this study since precisely the same total amount of water will thereby be assured to be used during the period of operation for each of the various bases of operation investigated. This will then result in no one of such methods of operation being at any advantage or disadvantage as compared with any other as related to the amount of water used since, otherwise, it might be difficult to reach a sound conclusion.

The equation for the withdrawals from storage S, as shown on line 11 under the derivation column of Table I, was determined in the following manner with respect to equation 42

$$S=\int_0^t (q-r)dt=\int_0^t (q_1-r+2q_2t+3q_3t^2+4q_4t^3+5q_5t^4)dt \tag{47}$$

from which, performing the indicated operations

$$S=(q_1-r)t+q_2t^2+q_3t^3+q_4t^4+q_5t^5 \tag{48}$$

The balance of Table I is believed to be readily followed from what is shown there except possibly the determination of the total cost for the period of operation as shown at the bottom. Two of such determinations are shown, one is based on trapezoidal summation which results in a total cost of $247,386, and the other is based on a more exact integration which results in a total cost of $247,026, or a difference of $360. An investigation showed that this latter basis of determination of such cost is much more nearly correct than that based on trapezoidal summation. The equation for the rate of cost c' is based on the values of c on line 18 for the even values of t, and is shown in the next to the last line at the bottom of Table I. The coefficients for this equation were solved for simultaneously as based on such values of c.

Fig. 1 shows the total costs for the same conditions as in the foregoing except for different values of N. These results were determined in the same manner as shown on Table I and were also based on Fig. 2. Fig. 1, in which the smaller values of N are for the more peaked hydro operation, and, for which, with $N=\$\infty$ per hour per mcfs the hydro plant discharge is equal to a constant pond inflow, shows that it is necessary to make computations of the total system cost for different assumed values of N, and then to determine the value of N that results in the minimum of such cost. It is determined from this figure that, for all practical purposes, the optimum value of N is that for which Table I is computed, $6,000 per hour per mcfs. Every other systematic basis for controlling the operation that it was found possible to devise, and which were all investigated, resulted in larger total cost than the $247,026 shown determined there.

References

1. Short-Range Economic Operation of a Combined Thermal and Hydroelectric Power System, W. G. Chandler, P. L. Dandeno, A. F. Glimn, L. K. Kirchmayer. *AIEE Transactions*, vol. 72, pt. III, Oct. 1953, pp. 1057–65.

2. Short-Range Load Allocation Hydro-Thermal Electric System, John J. Carey. *AIEE Transactions*, vol. 73, pt. III, Oct. 1954, pp. 1105–12.

3. Computer Search for Economical Operation of a Hydrothermal Electric System, R. J. Cypser. *Ibid.*, pp. 1260–67.

4. Report on Technical Sections Sessions, Prime Movers Committee. *National Electric Light Association*, New York, N. Y., 1919, p. 158.

5. Dividing Load Between Units, George R. Davison. *Electrical World*, New York, N. Y., vol. 80, no. 26, Dec. 23, 1922, pp. 1385–87.

6. Intrasystem Transmission Losses, E. E. George. *AIEE Transactions*, vol. 62, 1943, pp. 153–58.

7. Co-ordination of Fuel Cost and Transmission Losses by Use of the Network Analyzer to Determine Plant Loading Schedules, E. E. George, H. W. Page, J. B. Ward. *AIEE Transactions*, vol. 68, pt. II, 1949, pp. 1152–63.

8. Total and Incremental Losses in Power Transmission Networks, J. B. Ward, J. R. Eaton, H. W. Hale. *AIEE Transactions*, vol. 69, pt. I, 1950, pp. 626–32.

9. Co-ordination of Incremental Fuel Costs and Incremental Transmission Losses by Functions of Voltage Phase Angles, W. R. Brownlee. *AIEE Transactions*, vol. 73, pt. III, June 1954, pp. 529–41.

10. A Transmission Loss Penalty Factor Computer, C. A. Imburgia, L. K. Kirchmayer, G. W. Stagg. *Ibid.*, pp. 567–71.

11. Loss Evaluation—Part II. Current- and Power-Form Loss Formulas, E. L. Harder, R. W. Ferguson, W. E. Jacobs, D. C. Harker. *Ibid.*, pp. 716–31.

◆

Discussion

F. L. Lawton (Aluminium Laboratories Limited, Montreal, Que., Canada): The author is to be congratulated on a constructive presentation which clearly sets out the problems involved in co-ordinating hydro and steam generation in a complex power system for optimum economy. The problem is a difficult one but the author has succeeded in so developing thinking that, while not a finished method or tool for application by power engineers, it is a distinct forward step, and one which has been badly needed for a long time.

D. B. Klapper (Commonwealth Edison Company, Chicago, Ill.): Mr. Watchorn's development of a procedure for co-ordinating operation of separate steam and hydro plants is a significant step in the search for methods of reducing power system operating costs. It appears that the method used by the author may possibly be extended to cover an unsolved problem arising in systems supplied entirely by steam plants. This problem centers around the determination of proper allocation of fixed total available fuel supplies of different costs and heat content; namely, the station incremental rate for a given station is not entirely dependent upon that particular station's output, but is also dependent upon anticipated loading of other steam plants within the system.

Table II

	Hydro	Steam
Energy available	variable pondage	variable heat content and storage tonnage
Cost of losses	in tail-race, etc.	in transportation of fuel to different stations

The similarity between Mr. Watchorn's problem and the one just mentioned is based on the possible analogies given in Table II.

Concerning the application of Mr. Watchorn's method to combined steam and hydro systems, it should be pointed out that the solution of equation 3 or 4 is a problem in the variational calculus, which is dependent upon the class of "admissible function" assumed as possible solutions. The trial-and-error method used to obtain minimum costs may require a large number of iterations, particularly since a considerable amount of time may be wasted finding only relative minimums rather than the absolute minimum. Even then, there may still exist some doubt as to whether another class of functions may not result in lower costs; e.g., $N=N(t)$ rather than $N=$constant as assumed in the paper. A cyclic function (of time) for N appears to be a possibility. Although this would add a considerable amount of work, it might result in final savings.

R. H. Miller (Pacific Gas and Electric Company, San Francisco, Calif.): The subject of co-ordination of hydro and steam generation is one which merits a great deal of study. Considerable interest has been shown in the past few years in economic loading of steam generating units and consideration of transmission losses in over-all economic operation of power systems.

The co-ordination of steam and hydro generation is a logical extension of this subject and the approach that the author has taken seems to be a logical one. Frequently, operation of hydro and steam is done by rule of thumb, and it has not been possible to be certain that maximum over-all economy results from such a method of operation. It is apparent from the mathematical derivations in the paper that a solution for the most economical operation of co-ordinated hydro and steam generation is complex. By resorting to curves derived from the mathematical equations, Mr. Watchorn has been able to arrive at optimum conditions for hydro and steam generation where the total hydro and steam can be considered as being lumped.

A system such as that of the Pacific Gas and Electric Company consisting of 47 hydro and 18 steam plants spread over a large geographical area presents a very complex problem. The hydro plants vary in head from less than 50 feet to over 2,500 feet and include both stream flow and storage operation.

Considering also the factors involved in water regulation such as storage rights and requirements necessary for release for domestic and irrigation uses which must be correlated, if possible, with power generation, a solution of the problem of most economic utilization of water is very difficult. All of these problems are further compounded when transmission losses are considered. It appears that the author's conclusion that the basic equations can be practically applied only by the means of a computer or by automatic controls is well founded.

It is hoped that further work will be done along the line of co-ordination of hydro and steam generation so that practical and simplified methods of solution to the problem may result as undoubtedly there are economies to be achieved.

G. J. Vencill (Union Electric Company of Missouri, St. Louis, Mo.): Co-ordination of hydro and steam generation to supply the needs of an electric power system has been necessary since the early days of the industry in order to realize economies and minimize operating costs. We have operated our facilities to what we thought was the best advantage by comining applicable data with rules of thumb and best judgment without reducing the procedure to substitution in a mathematical equation.

The method developed and presented by the author takes into account use of stored water and the effect of plant flow or tail water level with the resultant head. Many other factors must be evaluated before an answer can be obtained, and we are doubtful that a practical system of automatic controls can be devised to do this on the Union Electric system. In addition to the fundamental hydraulic factors, consideration must be given to possibility of future runoff as determined from weather conditions and weather forecasts, and to governmental regulations which affect our use of storage. The necessity of altering load schedules to accommodate a heavily loaded towboat bound upriver has upset many a well-laid plan for hydro operation. With such factors as these, in addition to variable hydro turbine efficiencies over a range of loads, and the difficulty in precise determination of steam generation incremental costs over a narrow range of output, the difficulties in reducing all the elements to a form suitable for automatic calculation seem insurmountable. Even when a perfect hydro schedule is determined by balancing all physical factors, the effect on fuel commitments, delivery schedules, use of available dump gas, etc., sometimes dictates changes. The possible combinations introduced by considering more than one hydro plant would be considerable.

Undoubtedly the rigorous exploration of the many facets of this problem by mathematical means is interesting and may lead to approximations which are useful, but the complex and indeterminate nature of many of the elements would seem to make their automatic calculation impractical.

P. L. Dandeno and W. G. Chandler (Hydro-Electric Power Commission of Ontario, Toronto, Ont., Canada): The author states in the conclusions that various other systematic bases for co-ordinating hydro and steam generation were determined and investigated but none resulted in as low a cost as his own.

The discussers, in co-operation with the G. E. Company, have been carrying on a similar program of investigation on the Ontario Hydro System (see reference 1 of the paper). This has involved the problem of scheduling three steam plants and four hydro plants on a co-ordinated basis. The digital methods originally outlined in 1954 by Glimn, Kirchmayer, Habermann, and Thomas[1] have been applied, both with and without the effect of transmission losses. Needless to say, the problem becomes less complicated when not considering transmission losses, and when the number of hydro plants to be scheduled is reduced to one only the amount of work is further reduced.

We would like to ask Mr. Watchorn whether he specifically considered the methods outlined in reference 1 of the paper. These methods have a rigid theoretical basis for their application. Admittedly, these methods at present cover only the constant head hydro problem. It has been our experience, however, that the shape of the incremental water rate curve for hydro plants remains practically invariant over a ±5-per-cent range in head with small changes, of course, in actual value of the curve as head varies. This range in head applies to a generating station with a reasonably large pondage back of it. Bearing these factors in mind, the assumption of constant head is reasonably valid and we have proceeded with good results on this basis.

We note with interest the value N employed by Mr. Watchorn which he states is the incremental water value in dollars per hour per 1,000 cubic feet per second. This is analogous to the value γ referred to in reference 1 of the paper. This value γ, multiplied by the incremental hydro plant rate (usually given in mw per cubic feet per second), gives an equivalent hydro incremental rate in dollars per mw-hour. This could be readily compared with the usual steam plant incremental characteristic in dollars per mw-hour. The latter is derived from the incremental heat rate in Btu per mw-hour and the cost of fuel in dollars per million Btu. Thus γ can be determined and is in dollars per million cubic feet. We feel that this latter method of specifying water values is a clearer one than that suggested by Mr. Watchorn and is directly comparable to the usual steam values used. By choosing γ, usually by trial and error, in such a manner that the desired amount of water is used, the standard co-ordination equations result. A typical value of γ for our Des Joachims plant, 134-foot head and 27,500-cubic-foot-per-second average daily flow, is \$9.00 per million cubic feet.

These equations could be easily solved graphically when not considering transmission losses and digital means could be employed when the more complex problem of including losses is under consideration. If losses are not included and only one hydro plant is considered, the parameters employed in the hydro-steam solutions are those which are usually met in the straight steam solution.

If Mr. Watchorn has any further comments on his reasons for establishing another set of equations, we should be most interested in hearing about them.

REFERENCE

1. AUTOMATIC DIGITAL COMPUTER APPLIED TO GENERATION SCHEDULING, A. F. Glimn, K. L. Kirchmayer, R. Habermann, Jr., R. W. Thomas. *AIEE Transactions*, vol. 73, pt. III, Oct. 1954, pp. 1267–75.

C. W. Watchorn: I wish to thank all the discussers for their contributions with respect to a very complex problem. As stated by Mr. Lawton, methods have been badly needed for a long time for the co-ordination of hydro and steam generation. However, the problem is too complicated for the human mind of itself alone to even begin to cope with it and the time is past when we should consider any way of handling it, where the hydro plants involved are of any appreciable size, other than by the application of automatic computers.

Mr. Klapper is quite right in his conclusion that the method described in the paper as being used in the investigation of the fundamental relationships to be observed in the co-ordination of hydro and steam generation for optimum results has wider application than to just that problem. What was really done was to determine the form of the relationships that should be observed among the several factors involved in such co-ordination as a special case only of the general problem for which the manner of use of the energy available from any source is a factor in its co-ordination with otherwise normal steam generation (at least as we know it today) so as to obtain maximum economy. The specific forms that such relationships will take for different conditions or situations will differ as the factors involved and their interrelationships differ with respect to each of such conditions and situations, but the fundamental basis for their determination, nevertheless, should be essentially the same as that described in the paper.

Although I am skeptical that N should be other than a constant, as assumed in the paper, Mr. Klapper's suggestion that it may actually be a variable in order to result in minimum costs is an interesting possibility. However, in the same way that practical considerations, such as the uncertainties of future loads, river flows, etc., together with the flatness of the minimum cost–N relationship itself in the vicinity of absolute minimum cost, as shown in Fig. 1, do not require that N must be determined exactly with respect to such minimum cost, it may be that any additional reductions in total cost that may be obtainable under such conditions with N as a variable as compared with its being assumed to be a constant would be of comparatively little practical significance. However, an investigation of such possibilities would be most interesting.

The complexity of the system described by Mr. Miller demonstrates the need for a systematic basis for co-ordinating hydro and steam generation. The requirements for such co-ordination, as well as the requirements for water release for purposes other than for power production, except for the effect of incremental transmission losses, are fully met by the co-ordinating equations presented in the paper. In the event that the water released for such other purposes is also to be used for generation, such use is a factor in the determination of the total withdrawals from storage from time to time, whereas, in the event the water that is thus required to be released is to be a diversion, such use is equivalent to a reduction in river flow or pond inflow, even to the extent that such latter quantities may then, in effect, actually become negative.

There is no doubt but that the problem is a difficult one as more specifically outlined by Mr. Vencill. The uncertaintites as to future loads and river flows, and, it might be added, also as to the future availability of generating capacity, including the future availability of steam capacity, etc., exist regardless of the method used for the co-ordination of hydro and steam generation, but it is believed that a minimum of difficulties, in the sense of obtaining maximum economy, will be experienced because of such uncertainties with the application of the method of co-ordination suggested in the paper as contrasted with other possible methods of such co-ordination. This is believed to be so because, regardless of the method of co-ordination used, reappraisals are required to be made from time to time for best results, and then should be followed by the necessary readjustments of the operation, which are possibly less drastic with the suggested method of co-ordination, since, according to Fig. 1, the value of N is not at all critical.

My answer to Mr. Miller's discussion relative to the problems related to the requirements for water release other than in accordance with the best use for power production applies equally to Mr. Vencill's discussion. Subject to an evaluation, as suggested in the paper, very well worthwhile benefits may very possibly be realized as the result of the application of the suggested basis of co-ordination, or of some simplified version of it, in spite of such uncertainties and resulting difficulties, thereby possibly justifying the application of such a systematized basis of co-ordination, it being recognized that it is desirable to resist the temptation to sacrifice justifiable accuracy for mere simplicity. It is not enough to develop something that is simple merely because it is simple; rather, if it is to be simple it is preferable that it be a simplification of something we really know about.

There is really no conflict of which I am aware between the current paper and that of reference 1 of the paper. The present paper had been well under way for over 2 years when reference 1 first became available in 1953. It was hoped then, when that paper first became available, that it might provide the answer to the general problem treated in the current paper which had concealed its secrets so stubbornly so long. It was soon realized that this hope was not to be so easily fulfilled, since, as stated both in that paper and by Mr. Dandeno and Mr. Chandler, it was intended that that paper was to provide for the co-ordination of hydro and steam generation and transmission losses only for the limited condition for which the head remained constant, whereas the current paper was intended to provide for the more general relationship with respect to the co-ordination of hydro and steam generation without any limitations whatsoever on the hydro plant characteristics, but treating the co-ordination of transmission losses as a separate problem beyond the scope of the paper.[1] It is believed that the equations of both papers will give the same results in the co-ordination of hydro and steam generation for maximum economy with an assumed constant head hydro plant assumed to be operated on the same bus as the system steam plants. Thus, the co-ordinating equation of the earlier paper is, in effect, a simplification of the more general equation of the current paper when the appropriate conditions obtain. Then, if for no other purpose, the more general equation provides a basis for the measurement of the effect of whatever simplifications it is desired to investigate, or, putting it another way, before we attempt to make anything simple, we should know what we are simplifying and what the effects of such simplifications are with respect to the particular surrounding circumstances.

REFERENCE

1. *Discussion* by C. W. Watchorn of AN INCREMENTAL COST OF POWER DELIVERED COMPUTER, E. D. Early, W. E. Phillips, W. T. Shreve. *AIEE Transactions*, vol. 74, pt. III, 1955 (*Paper 55-141*).

Thyrite Protection for Series Windings of Autotransformers

J. W. ALBRIGHT
ASSOCIATE MEMBER AIEE

THE application of surge voltage to the series winding of an autotransformer presents unique transient-voltage problems which are generally more severe than encountered in transformers with electrically separated windings. When a pulse is applied to the high-voltage terminal of an autotransformer, almost all of the voltage appears across the series winding, even though the turns in the series winding may be only a fraction of the total turns from high-voltage terminal to ground. The resultant high internal transient-voltage oscillations in the winding often make the problem of providing the required amount of insulation extremely difficult.

Furthermore, the magnitude of the internal voltage transients can be influenced to a large degree by the terminal conditions of the series winding during the period that the surge voltage persists. This phenomenon makes possible a situation where an autotransformer designed to withstand voltage surges of a given magnitude with certain terminal conditions, and demonstrated by factory test to have adequate insulation for that condition, could fail in service when subjected to a surge of the same magnitude if the terminal conditions were substantially different.

A practical example of a situation where the terminal condition may be significantly different in service than during the factory test is the case where a by-pass gap or lightning arrester is connected across the terminals of the series winding to limit the voltage which may

---

Paper 55-52, recommended by the AIEE Transformers Committee and approved by the AIEE Committee on Technical Operations for presentation at the AIEE Winter General Meeting, New York, N. Y., January 31–February 4, 1955. Manuscript submitted October 19, 1954; made available for printing November 26, 1954.

J. W. ALBRIGHT is with the General Electric Company, Pittsfield, Mass.

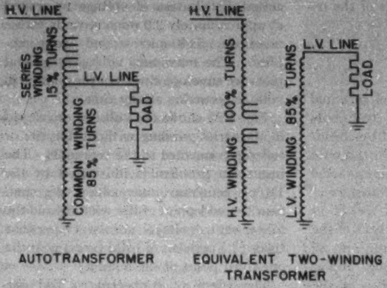

Fig. 1 (left). Autotransformer and equivalent transformer for 138- to 115-kv ratio

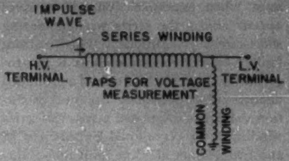

Fig. 2 (right). Diagram of electromagnetic model used for tests

appear across it. In this paper it will be shown that such a practice does not improve the internal winding stresses, but actually increases them with respect to voltage to ground, if shielding is not utilized to control the voltage distribution in the winding. Unless the autotransformer is properly designed to allow for this effect and the factory impulse test is designed to simulate the by-pass gap sparkover or lightning arrester operation, a potential service hazard can be created.

Simulation of the service conditions in text is, itself, a difficult problem. Where both the high- and low-voltage terminals are insulated for the same voltage level, an effective test can be obtained by short-circuiting both terminals together. If they are insulated for different levels, an elaborate voltage-divider arrangement is required to limit the voltage across the series winding to a value equal to that permitted by the protective device. Although the actual protective devices could be installed on the autotransformer for the test, the wave-shape changes produced on the impulse oscillograms by the operation of the devices largely destroy the usefulness of the oscillograms for failure detection purposes.

In this paper it will also be shown that shielding the series winding greatly reduces the internal transient-voltage oscillations. Shielding may be accomplished electrostatically, or by means of internally mounted Thyrite* shunting resistors interconnected with the winding. When the Thyrite is connected to the winding at regular intervals, essentially linear voltage distribution is obtained and internal transient-voltage oscillations are effectively eliminated. Control or elimination of internal voltage transients in this manner generally obviates the need for external by-pass devices connected across the series winding. However, in special cases where advantage can be gained from their use, the addition of such devices does not change the distribution of voltage within the shielded winding.

Series Winding Transients

The impulse voltages applied to the high-voltage terminals of an autotransformer are determined by the basic insulation level of the system, but the turns in the series winding are based upon the coratio, or per-unit difference in voltage rating of the series and common terminals, as illustrated in Fig. 1. It has been shown[1] that, when a surge impinges on the high-voltage terminal, practically all of the voltage appears across the series winding when a resistance representative of the surge impedance of the load connected to the autotransformer in service is connected from the common terminal to ground. This means that the impulse "volts per turn" are greater than in a comparable 2-winding transformer, and the component of the voltage transients developed in the windings which depend primarily upon electromagnetic induction are correspondingly higher. The most severe problem usually is encountered when taps are provided in the series winding.

When taps are required to change the voltage rating of the high-voltage terminal, they must be physically located in the series winding to avoid changing the voltage rating of the low-voltage terminal also. The turns tapped out must be the required percentage of the total turns in the series and common windings, but, since only a fraction of the turns are in the series winding, the percentage of the series winding turns tapped out is much greater.

For example, in an autotransformer rated 138,000 grounded wye/115,000 grounded wye with a ±5-per-cent tap range on the high-voltage terminal, the total tap range of 13.8 kv represents 46 per cent of the turns in the series winding. On minimum turns connection, the idle tap turns are equal to 86 per cent of the active turns in the winding. When this condition exists, the transient voltages developed across the tap range may equal or exceed the surge voltage applied to the high-voltage terminal.

The difficulty of insulating for such voltages, particularly in autotransformers with low coratio, has encouraged some use of applying by-pass spark gaps or lightning arresters to limit the voltage which can appear across the terminals of the series winding. It will be demonstrated that the use of such a spark gap or lightning arrester does not improve, and may actually increase, the internal voltages to ground and between parts of the winding unless special design features are incorporated to improve the voltage distribution of the winding.

For this reason, the General Electric Company has adopted the practice of applying internally mounted Thyrite resistors, interconnected to the winding at regular intervals to produce essentially linear voltage distribution. This practice has been in effect for approximately 15 years and has proved itself in service over that period.

The Thyrite is not designed to limit the voltage across the series winding but only to control the voltage distribution within the winding. Generally, the Thyrite alone will furnish the needed protection of the series winding without external by-pass devices. When the coratio is exceedingly low, or the tap range high, as in the example previously cited, the tap range may require excessive insulation even with linear voltage distribution. In such cases, an external lightning arrester connected across the high- and low-voltage terminals, combined with internally mounted Thyrite, may be used to reduce further the voltages in the series winding.

Application of Lightning Arrester

The rating of a by-pass lightning arrester applied in this manner must be adequate to assure valve reseal performance when excessive dynamic voltages appear across the series winding during short-circuit conditions. When certain fault conditions exist, such as a line-to-ground fault on the load side of a grounded neutral autotransformer, the total excitation voltage is impressed across the series winding. The combined impedances of autotransformer and line limit the excitation voltage to a value less than the prefault voltage, but the voltage may be several times higher than the normal operating voltage across the series winding.

---

*Registered trade-mark of General Electric Company.

Any by-pass arrester used must withstand this overvoltage. Failure of the lightning arrester to reseal would increase the severity of the short circuit by reducing the circuit impedance and thereby impose greater duty on the circuit breakers and other system components. As the failed lightning arrester would be required to carry power current for the duration of the short circuit, a fault lasting longer than a few cycles could physically destroy the arrester.

Since the by-pass arrester must be of higher valve rating than would be normally used for a system voltage corresponding to the normal operating voltage of the series winding, this by-pass arrester cannot be incorporated as an inherent part of the normal line-to-ground arresters protecting the autotransformer. Separate lightning arresters must be used from line to ground on the high-voltage and low-voltage lines to limit the value of incoming surges to magnitudes consistent with the basic insulation levels of the respective lines.

Tests

To demonstrate the effect of terminal conditions on series winding transients and the improvement obtained by shielding, a series of tests were conducted on a unity time scale electromagnetic model of a 2-winding core-type autotransformer with concentric windings, as shown in Fig. 2. The model had 15 per cent of the total turns in the series winding and 85 per cent in the common winding—representative of an autotransformer in the 138,000 grounded wye/115,000 grounded wye class. A total of 18 taps were provided in the series winding for voltage measurement purposes. The electromagnetic model technique is particularly suited to a study of this nature, as it permits a much more thorough exploration of points within the winding than can be done practically on an actual transformer. It has been demonstrated[2,3] that the accuracy of the models is well within the limits required for design purposes.

Fig. 3 shows the maximum voltages between parts, maximum voltages to ground, and initial voltage distribution of the series winding with five different conditions existing when an impulse is applied to the series terminal. The initial voltage distribution is not the true electrostatic voltage distribution, but the actual distribution of voltage to ground at approximately 2.0 microseconds with a nominal 1.5x40-microsecond wave applied. The maximum voltage to ground plots are envelope curves of the maximum voltage occurring at any time.

Fig. 3(A) shows the voltages developed in the series winding without Thyrite or rod gap connected to the terminals. The insulation problem is illustrated by the 120 per-cent maximum voltage to ground near the mid-point of the winding and the 57-per-cent voltage across 17-per-cent turns (2.5 per cent of total turns) near the one-third point of the winding.

The effect of connecting a rod gap across the series winding terminals is illustrated in Fig. 3(B). For this example, the rod gap was set to spark over when the applied wave reached 25 per cent of crest value. Note the initial voltage distribution in the first half of the winding is not changed. In the second half of the winding, the voltages are raised along a curve of approximately the same shape, but of reverse slope, as in the first half of the winding. This distribution is produced by the spark-over of the rod gap which raises the potential of the low-voltage terminal to a value near that of the high-voltage terminal. The maximum voltage to ground at the mid-point has increased to 155 per cent, and the maximum voltage between parts of the series winding (46 per cent), although decreased somewhat from the value in the previous case, occurs near the mid-point

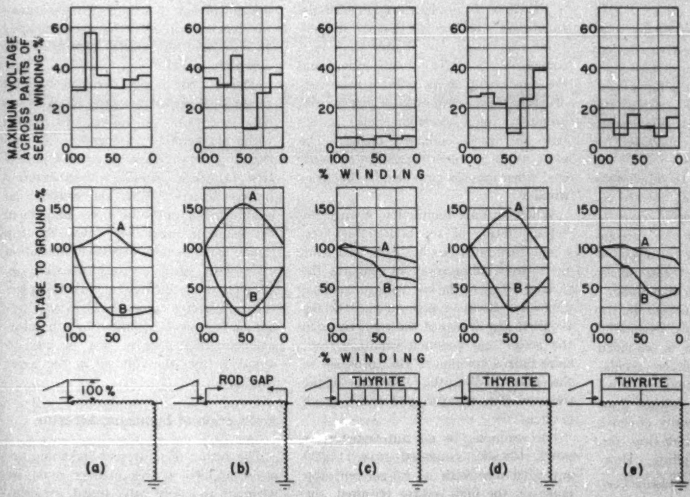

Fig. 3. Voltage distribution in series winding with 2.5x55-microsecond wave applied to high-voltage terminal

A—Maximum voltage distribution
B—Minimum voltage distribution
(a)—No protection
(b)—Rod gap across series windings
(c)—Thyrite with five interconnection points
(d)—Thyrite connected at ends only
(e)—Thyrite connected at ends and mid-point

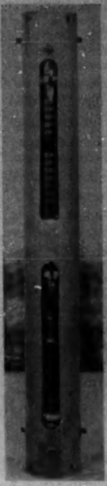

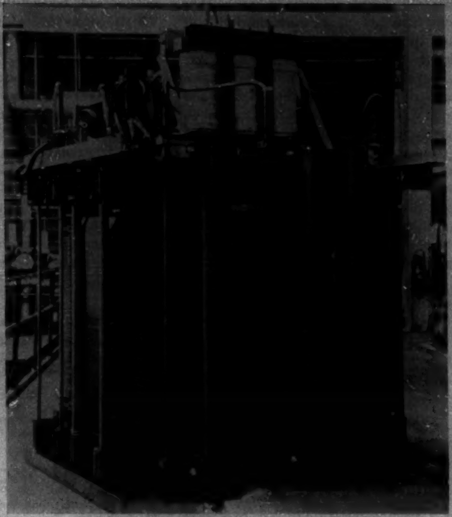

Fig. 4 (left). Thyrite stack for internal mounting in power transformers

Fig. 5 (right). Thyrite stacks applied across the winding of a 2-core 3-phase regulating autotransformer

of the winding where taps are normally located.

The spark-over of the rod gap produces an effect which is identical to that obtained by impulsing both ends of the winding simultaneously. When an impulse wave travels toward the mid-point of the winding from both ends, a reflection is produced at the mid-point which tends to double the applied voltage at that point. In this example, damping of the wave holds the reflection to less than double voltage but still permits the mid-point of the winding to oscillate to 155 per cent of the applied voltage.

Fig. 3(C) strikingly illustrates the advantage of Thyrite interconnected with the winding at several points. Both the initial and maximum voltage distribution curves are essentially uniform. The maximum voltage to ground is limited to 102 per cent, and it occurs near the line end. The voltage between parts is approximately constant throughout the winding and does not exceed 6 per cent of the applied voltage across 17 per cent of the series winding.

The effect of the interconnections between the Thyrite and winding is illustrated in Fig. 3(D). Thyrite without interconnection is similar to a lightning arrester across the terminals, and the resulting voltage transients are not significantly different from the case of a rod gap across the terminals in Fig. 3(B). The voltages to ground and between parts are somewhat less, principally because the voltage drop across the Thyrite improves the initial voltage distribution.

One interconnection between the mid-point of the Thyrite and the mid-point of the winding is illustrated in Fig. 3(E). This is an intermediate case, roughly analogous to the condition which is obtained with partial electrostatic shielding of the winding. It shows marked improvement over the case of no interconnections, but is not as effective as the multiple interconnections shown in Fig. 3(C).

Application of Thyrite

The Thyrite used in transformers is in the form of 6-inch-diameter disks, 3/4 inch thick, with nonlinear resistance characteristics similar to those used in lightning arresters. The application differs, however, inasmuch as the disks are directly connected to the winding without isolating gaps and must be able to withstand operating voltage continuously without overheating. Although this practice requires the use of several times as many disks for a given voltage as does an arrester, it has the advantage of relieving the Thyrite from dependence upon a gap structure to interrupt power-follow current before dangerous overheating occurs.

A sufficient number of disks are placed in series to limit the Thyrite temperature to a maximum of 95 degrees centigrade with the transformer delivering full load at 105-per-cent voltage. In addition to this requirement, the stack is also designed to limit the Thyrite temperature to a safe value during the factory induced-voltage test and during any system faults which may cause abnormal voltages to appear across the winding.

The adequacy of the design methods, and the stability of the Thyrite disks, have been proved by the operating record of hundreds of transformers in service for as long as 15 years without a single failure attributable to the Thyrite.

Since the Thyrite is used only to divide the voltage uniformly along the winding—not to limit the voltage across the terminals—the resistivity of the stack is not important and may vary over wide limits without affecting its performance for this application. This allows the designer complete freedom to select the number of disks in series to meet the heating requirements.

The effectiveness of the Thyrite as a voltage divider derives from its nonlinear volt-ampere characteristics[4] rather than the specific resistance of the stack. These may be expressed by

$$I = KE^N$$

where

I and E = instantaneous values of current and voltage respectively

K and N are constants depending upon the dimensions and composition of the disk

For disks used in transformers, the exponent N is in the order of 3.5; so an elevenfold increase in current merely doubles the voltage across the disk. In the application being considered, when a surge impinges on the autotransformer terminals, the current in the various portions of the Thyrite stack is different since charging current is supplied to the winding at the points of interconnection. The flat volt-ampere characteristics of the disks permit wide variations of current throughout the stack without producing a significant departure from uniform voltage distribution.

Thyrite Stacks

When a number of disks are used in series in a stack, they are mounted in a

Herkolite* tube, as shown in Fig. 4. The tube furnishes rugged mechanical support and serves as insulation to the mounting framework, tank wall, and other surrounding parts. Axial pressboard spacing strips between the Thyrite disks and tube wall provide adequate ducts for oil circulation. Copper spacing disks with extruded feet are located between all Thyrite disks to maintain electric contact while providing ventilation for maximum heat dissipation Flexible copper straps or cable are brazed to the spacing disks at the points where connection to the winding is desired.

Permanent contact pressure is maintained throughout the stack by stainless steel leaf springs at the ends of the stack. Both the spacing disks and the leaf springs are dimensioned so that they cannot protrude beyond the diameter of the Thyrite disks to produce concentrated voltage stress points which might endanger the insulation. The voltage stress at the ends of the stack is controlled by 1-inch thick contoured steel toroids designed to give optimum dielectric field conditions and insulated for maximum dielectric strength.

The rugged mechanical construction, simple electric connections, and effective insulation structure are illustrated in Fig. 5 which shows the application of Thyrite across the series winding of a 3-phase regulating autotransformer with load ratio control

Conclusions

1. The series windings of autotransformers present unusual surge voltage problems requiring special design attention.

2. Limiting the voltage across the terminals of the series winding with a by-passing rod gap or lightning arrester does not control the internal transient voltages in the winding.

3. Transient-voltage oscillations can be eliminated by shielding the winding to produce a linear surge-voltage distribution.

4. Thyrite provides an effective, safe, and practical means of obtaining linear voltage distribution.

References

1. Use of Thyrite in Power Transformers, J. R. Meador. *AIEE Transactions*, vol. 68, pt. II, 1949, pp. 959–64.

2. Transformer Models for the Determination of Transient Voltages, P. A. Abetti. *AIEE Transactions*, vol. 72, pt. III, June 1953, pp. 468–80.

3. Long-Time-Scale Models of Transformers for the Determination of Transient Voltages, P. A. Abetti, H. B. Belck. *AIEE Transactions*, vol. 73, pt. III, April 1954, pp. 345–53.

4. Thyrite A New Material for Lightning Arresters, K. B. McEachron. *AIEE Transactions*, vol. 49, pt. II, April 1930, pp. 410–20.

---

* Registered trade-mark of General Electric Company.

◆

Discussion

W. A. Williams (General Electric Company, Pittsfield, Mass.): The author has demonstrated the effectiveness of Thyrite in the shielding of the series winding in an autotransformer. As pointed out, the use of such material gives the designer a means to reduce greatly the surge voltage to ground and to provide a linear distribution of voltage across the winding when the Thyrite is connected at regular intervals into the series winding.

The step voltage regulator is a particular type of autotransformer, and the same type of shielding is employed in this apparatus. In many of the step voltage regulator applications, the use of Thyrite is identical to that described in the paper. In such cases it is not designed to limit the voltage across the series winding but merely to insure that the distribution is linear.

However, many step voltage regulators in the lower voltage range, 15 kv and below, are of single-core construction. In these designs the taps are uniformly distributed across the series winding. On certain operating connections, near the tap changer neutral, 100 per cent of the surge voltage appearing between source and load bushings may appear across adjacent taps in the winding. Therefore, some means is desirable to limit the voltage. Connecting Thyrite across the active part of the winding is an effective way to limit this voltage. The voltage drop across the Thyrite is fixed by the characteristics of the material and the surge current it passes. Hence, the insulation between adjacent taps in the winding can be closely co-ordinated with the voltage drop across the Thyrite.

W. L. Teague and **L. B. Rademacher** (Westinghouse Electric Corporation, Sharon, Pa.): In Fig. 3 the author shows the voltage distribution that occurs in the series winding of an autotransformer for various terminal conditions. Figs. 3(A), 3(B), and 3(D) demonstrate that this particular winding has an extremely bad voltage distribution. Through better design of the series winding or by using shielding as the author suggests, the stress due to the voltage distribution may be reduced considerably. With an improved distribution, either a gap or a lightning arrester across the winding will prevent excessive voltages in the winding due to the oscillations.

Better distribution can be obtained by designing the series winding to have a high through capacitance relative to the ground capacitance or by using electrostatic shielding. In the core form transformer construction, this could be accomplished by using a Hisercap[1] or a Lowgrocap winding. By the interleaved-turns arrangement of the Hisercap winding, a high through capacitance is obtained. The Lowgrocap winding obtains the same result by decreasing the capacitance to ground through the use of static plates and winding arrangement. For shell form transformers, the windings inherently have a high through capacitance as compared to the ground capacitance. Thus by using either improved coil construction or shielding, the voltage distribution can be improved to reduce greatly the stresses that may occur when the series winding is protected with a gap or lightning arrester.

The design and protection of autotransformers is extremely complicated because of the voltages that may be induced internally due to the high volts per turn that develop from surges. The designer may use many schemes to prevent overstressing of the insulation. The winding may be designed to permit oscillations and sufficient insulation applied to withstand the overvoltages, or the design may be made to avoid excessive oscillations. Generally, the simplest and least hazardous method will prove to be the most reliable. By using the better voltage distribution approach, this problem is often simplified and complications are avoided.

Reference

1. Improved Core Form Transformer Winding, E. J. Grimmer, W. L. Teague. *AIEE Transactions*, vol. 70, pt. I, 1951, pp. 962–67.

J. W. Albright: I wish to express my appreciation to the discussers for their comments, which contribute substantially to the understanding of the problem. Mr. Williams has brought out an additional benefit which can be obtained from the application of Thyrite in some particular cases. In most high-voltage autotransformers the number of Thyrite disks required to shield the series winding is such that a voltage comparable to the basic insulation level will develop across the winding if current surges of 10,000 amperes or more are considered. However, in autotransformers where the operating voltage of the winding is very low compared to the basic insulation level, as in step voltage regulators, the volt-ampere characteristics of the Thyrite may limit the voltage to less than basic insulation level for surges of this magnitude. In these cases, the internal insulation of the winding can be safely co-ordinated with the voltage permitted by the Thyrite.

It is true, as Mr. Teague and Mr. Rademacher point out, that series winding transients can be reduced by means of electrostatic shielding. Electrostatic shielding has been used successfully for many years in transformers and in autotransformers with high coratio. Numerous varieties of electrostatic shielding have been developed in addition to the static plate for shell-type windings and the interlaced turn arrangement for the core-type disk windings mentioned by the discussers. Others in commercial use include rib shields for core-type disk windings, and cylindrical shileds for concentric laper windings.

Of these, only the cylindrical shields with concentric layer windings can be designed to produce essentially straight-line voltage distribution under all impulse conditions. All of the other varieties give varying results, depending upon the winding voltage and current rating, transformer or autotransformer rating, and wave shape of the surge applied to the terminals. The most difficult conditions are encountered in the series windings of autotransformers of low coratio. Here, the capacitance of the winding to ground is approximately the same as for a full capacity winding, but the series capacitance is very low because the number of turns in the winding is reduced to only a fraction of those in a full capacity winding. Since the proportions by which the ground capacitance can be reduced, and the series capacitance increased, by the electrostatic shields are about the same as in a full capacity winding, the ratio of ground capacitance to series capacitance is much higher in the series winding, and the internal voltage transients are correspondingly greater. Therefore, although the addition of electrostatic shields will improve the voltage distribution over that obtained without shields, the transient voltage oscillations are far from eliminated. Fig. 3(E) in the paper shows a winding with a very good initial voltage distribution produced by Thyrite interconnected at the mid-point of the winding, yet the maximum voltage between parts of the winding is three times the value obtained with essentially uniform voltage distribution in Fig. 3(C).

The voltage distribution of the winding used in the paper is extremely bad as stated by the discussers. However, it is also representative of the distribution obtained in any unshielded winding. The test results illustrated in Fig. 3 clearly demonstrate the ability of Thyrite, when interconnected to the winding at regular intervals, to produce essentially uniform voltage distribution in any winding without other aids.

Another advantage of Thyrite which makes it desirable for use in shielding is the simplicity of the application. The windings have normal turn distribution; it is not necessary to distort the turn distribution by interlacing, or to add capacitive elements in the critical dielectric field. Electrostatic shielding inevitably introduces complications in the windings and insulation. Furthermore, some types, such as static plates, occupy valuable space within the winding structure and increase the short-circuit reactance. Therefore, more active materials (copper and core iron) are necessary to maintain the transformer characteristics. These complications are avoided in those cases where Thyrite can be used, as in series windings of autotransformers.

Evaluation and Application of Silicone-Organic Resin Combinations for Dry-Type Transformer Insulation

G. F. SIMMONS
ASSOCIATE MEMBER AIEE

A. L. SCHEIDELER
ASSOCIATE MEMBER AIEE

THE rapid development of synthetic insulations in recent years has provided a challenge to the electrical designer. Incentives to utilize the improved mechanical and electrical properties of these new materials have been especially great in the design of apparatus operating in gaseous mediums. Dry-type transformers have provided a fruitful field for the application of such man-made materials.

Since transformers are designed for many years of life, it is necessary to resort to accelerated aging tests of insulation when determining its possible application. Results obtained with a specified set of laboratory procedures must then be extrapolated to the variety of operating conditions encountered in service. Recognition of this fact has resulted in considerable activity within the AIEE in an effort to establish standard conditions under which insulating systems may be evaluated. Such efforts have been in the direction of specifying material use as a result of functional tests rather than on the previous basis of chemical composition.

The inadequacy of chemical composition as a criterion in evaluating insulation has been well recognized. Perhaps, it is not so apparent that, in the present state of the science, chemical composition is likewise deficient as a basis for proposing insulation systems. Systems which may appear satisfactory for use when only chemical structure is considered are often found inadequate when subjected to the variety of conditions found in service. It is the purpose of this paper to demonstrate that insulation combinations which would not meet the arbitrary classifications based on organic content of the structure may prove not only satisfactory but superior when considered in the light of their function in a given piece of apparatus. The use of such combinations has resulted in an insulating system offering outstanding characteristics for dry-type transformers.

Composite Insulating Systems

The advantages of using silicone-based products in dry-type insulating systems are well known. They are characterized by stability at high operating temperatures and resistance to the absorption and harmful effects of moisture.[1–5,9] These advantages must be weighed against the difficulties which may arise in conjunction with silicone applications. The dielectric strength, mechanical strength, and curing characteristics for a given application are, in general, inferior to those of the best organic resins. High cost is also a limiting factor in many silicone applications.

To acquire the best of silicone characteristics as well as high dielectric and mechanical strength, it has been the practice to mix basic materials such as silicone and selected organic resins and use this mixture as a general-purpose resin. This practice has resulted in insulation structures with improved over-all properties, but which do not possess either the high degree of moisture resistance and life of

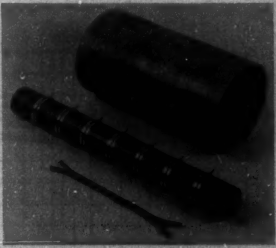

Fig. 1. Test pieces used in evaluating component insulating structures

Front—turn
Center—layer
Back—barrier

Paper 55-43, recommended by the AIEE Transformers Committee and approved by the AIEE Committee on Technical Operations for presentation at the AIEE Winter General Meeting, New York, N. Y., January 31–February 4, 1955. Manuscript submitted October 19, 1954; made available for printing November 22, 1954.

G. F. SIMMONS and A. L. SCHEIDELER are with the General Electric Company, Pittsfield, Mass.

the silicones or the superior mechanical and electrical properties of the best organic resins.

It would obviously be very desirable to obtain a material or combination of materials which retain the good features of the best silicone and organic resins without accompanying limitations. If the functional requirements of constituents within a dry-type insulating system are considered, it may be seen that such a possibility exists.

The useful life of many insulating systems containing organic materials is greatly increased by the substitution of an inert material such as nitrogen for a circulating air atmosphere. Silicone-impregnated systems, while much superior to organic structures in air, are improved only slightly by the removal of oxygen from the surrounding medium.[6] Such evidence indicates that oxygen is a primary contributor to deterioration in dry-type apparatus and that the thermal superiority of the silicones stems largely from their resistance to the effect of oxygen. It may be inferred from these results that the silicones may, in proper combination, be used to extend the life of certain organic materials.

This investigation was conducted in an effort to develop a dry-type transformer insulating system which would utilize the high dielectric and mechanical strength characteristics of selected, organic impregnants and the temperature- and moisture-resisting characteristics of suitable silicones. It was desired to accomplish this in as economical a manner as possible by using a minimum of silicone resin.

Emphasis was placed on the use of silicone resins as a surface treatment of conventional 150-degree-centigrade (C) base insulations. By this procedure, the silicone replaced the weakest link in the present 150-C system, the organic impregnating varnish. The organic constituent of the base material was shielded by the silicone resin coating from the deteriorating effects of oxygen and moisture.

Evaluation of Pertinent Properties

Two criteria[8] have been utilized in determining the aging performance of the materials under study. These are the dielectric strength at the elevated aging temperature and the power factor after exposure of the insulating component to high humidity.

Dielectric Breakdown

When a component insulation system is not subjected to an undue amount of moisture or mechanical abuse, the dry dielectric strength of the component becomes the predominating factor in determining insulation life. Such conditions will be present when the apparatus is operating in a clean, dry enclosure or when a sealed type of construction is used and maintained. Reduction of dry dielectric strength may be utilized then to estimate a reasonable maximum life for the material.

The per-cent reduction in dielectric strength which should be chosen as a criterion for end of life depends on the application and system under consideration. The manner in which a component insulation approaches failure may be just as important to the designer as the failure point. A desirable procedure is to define life as a function of the per cent of initial dielectric strength which is chosen as the failure point.

The large number of samples and amount of testing required rule out this method in many instances. A 50-per-cent criterion has been widely used as meeting most requirements for transformer applications, the implication being that a 50-per-cent reduction in dielectric strength in a transformer, as designed, will result in marginal operating conditions. The data herein are treated in terms of a 50-per-cent criterion where the time to failure at 50 per cent of initial breakdown levels has been determined. No such reduction has been observed with some of the materials considered during long periods at elevated temperatures. Those data have been analyzed in terms of desired operating temperatures.

Power Factor

The minimum life of insulation used in ventilated dry-type transformers is determined essentially by the moisture-resisting properties of the composite insulation. When the material has deteriorated because of thermal aging, by flaking, crazing or charring, it no longer provides either the mechanical bonding or the moisture resistance necessary for operation under adverse conditions. Hence, deterioration in resistance to the effects of moisture as measured by power factor on a humidified sample is a comparatively simple, but comprehensive, test for defining the minimum life of a composite dry-type transformer insulation. Resistance-to-moisture absorption may also be used to define the optimum curing characteristics of a material, provided dielectric and mechanical properties are adequate.

Construction of Component Samples

The component samples were, in instance, designed to provide a reasonable representation of the conditions to which the materials would be subjected in a transformer. The completed structures are shown in Fig. 1.

Turn Insulation

The turn insulations investigated were applied to rectangular copper wire, using

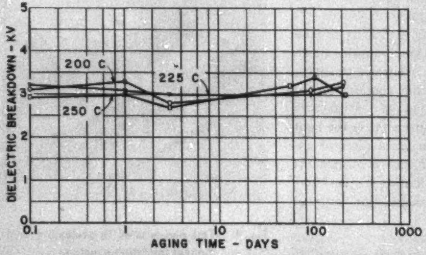

Fig. 2. Turn insulation dielectric breakdown of a silicone resin impregnated asbestos sheet and glass yarn, bonded and treated with silicone. For power-factor data see Fig. 3

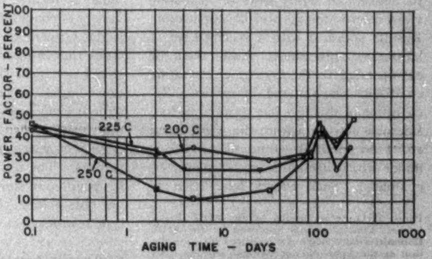

Fig. 3. Turn insulation power factor at 90-per-cent relative humidity of a silicone resin impregnated asbestos sheet and glass yarn, treated and bonded with silicone. For breakdown data see Fig. 2

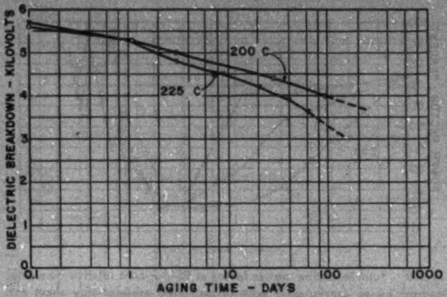

Fig. 4. Turn insulation dielectric breakdown of an acrylic ester resin impregnated asbestos sheet and glass yarn, phenolic resin treated. For power-factor data see Fig. 5

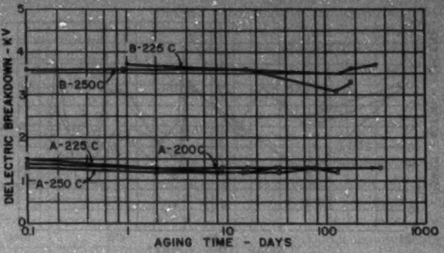

Fig. 6. Turn insulation dielectric breakdown of (A) a phenolic resin bonded glass yarn treated with silicone and (B) an acrylic ester resin impregnated asbestos-clay sheet and glass yarn, bonded and treated with silicone. For power-factor data see Figs. 8 and 9

standard factory processes.[6] The insulated wire was cut into 10-inch lengths. Two pieces were placed together in a jig and a 2-inch length on each end of the sample was spread apart. The middle 6 inches were then tied together with glass yarn and the completed samples were given a standard factory treatment with the desired varnish. The electrodes used in testing the insulation were the two copper wires.

LAYER INSULATION

The insulating material being investigated was wound on a metal mandrel after the manner of Whitman and Stewart.[7] Sheet material of desired thickness was wrapped around a metal mandrel with a 2-inch outside diameter and 18 inches long. Tinned copper electrodes 1/2 inch wide and positioned 2 inches apart were wrapped around the insulation and held in place by means of copper binding wires. The sample was then given a factory treatment with the desired varnish.

BARRIER INSULATION

Small cylinders (approximately 6 inches in diameter and of appropriate thickness) were wound with the desired materials using factory operating procedures. The completed cylinder was then given a factory treatment with the desired varnish.

Interpretation of Results

TURN INSULATION

It is apparent from the typical results illustrated in Fig. 2 that high-temperature turn insulations, utilizing silicones as the resinous constituents, possess very stable dielectric strength characteristics as a function of time and temperature. Even though long testing times were involved, the dielectric strength was not reduced. A life of 20,000 hours at the hottest spot temperature has been recommended as a criterion of minimum life for a dry-type transformer insulating system.[7] When established slopes[8,9] of life versus temperature for silicone insulated systems are considered, it becomes apparent that, on a dielectric strength basis, these components are suitable for operation at temperatures well above 200 C. It may well be that other factors, i.e., copper oxidation rather than insulation life may impose the temperature limit in silicone-insulated apparatus.

The impregnating resin must also perform the very important function of inhibiting the entrance of moisture into the system during that part of the apparatus load cycle which results in low insulation temperatures. Silicone-impregnated and treated components are, after exposure to 250 C for more than 200 days, as resistant as new materials to moisture effects measured by power factor; see Fig. 3. Actually, aging at high temperature improves the moisture-resisting properties for a considerable period.

Comparable, high-temperature turn insulation containing an organic impregnant and treated with an organic varnish[6] has been analyzed on the basis of a 50-per-cent dielectric strength criterion. These data have been reproduced in Fig. 4. On the basis of results extrapolated from

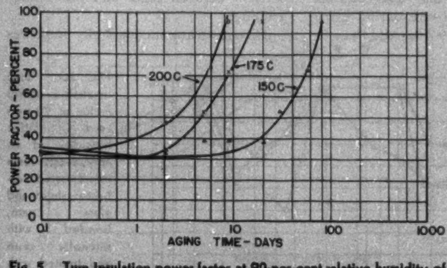

Fig. 5. Turn insulation power factor at 90-per-cent relative humidity of an acrylic ester resin impregnated asbestos sheet and glass yarn, phenolic resin treated. For breakdown data see Fig. 4

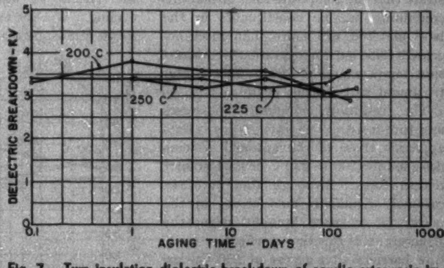

Fig. 7. Turn insulation dielectric breakdown of acrylic ester resin impregnated asbestos sheet and glass yarn, bonded with phenolic resin and treated with silicone. For power-factor data see Fig. 10

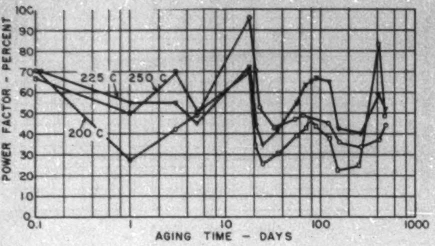

Fig. 8. Turn insulation power factor at 90-per-cent relative humidity of a phenolic resin bonded glass yarn, treated with silicone. For breakdown data see Fig. 6

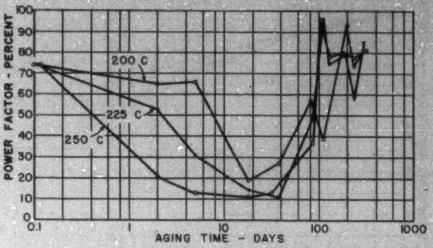

Fig. 9. Turn insulation power factor at 90-per-cent relative humidity, comprising an acrylic ester resin impregnated asbestos-clay sheet and glass yarn, bonded and treated with silicone. For breakdown data see Fig. 6

Fig. 4, the composite insulation is limited under these maximum life conditions to an operating temperature of approximately 170 C. A somewhat higher maximum operating temperature may be calculated if a less than 50-per-cent criterion is utilized.

The weakest link in this system, however, is the organic, final treating varnish, Fig. 5 reproduced from reference 6 illustrates that such a high-temperature, phenolic-varnish-treated turn insulation will not maintain its resistance to the effects of moisture throughout the minimum required life at 150 C. This is true in spite of the fact that the varnish under consideration is superior to most other organic varnishes in maintaining its properties as a function of time and temperature.

When silicone resin is substituted for the organic-treating varnish, the resulting composite exhibits dielectric strength characteristics as a function of time and temperature which are very similar to those of the comparable system where all resins are silicones. The dielectric strength versus aging times characteristics, illustrated in Figs. 6 and 7, demonstrate that the composite turn insulations containing organic constituents in the base material will more than meet accepted criterion for operation at hottest spot temperatures of 200 to 220 C after treatment with silicone resins.

The resultant composite possesses moisture-resisting characteristics which approach those of conventional systems designed for 200 to 220 C of hottest spot temperatures. Although there are occasional anomalous fluctuations in the power factor after humidification, the structures still function as effective moisture barriers after a year at 250 C; see Figs. 8, 9, and 10. It may be seen from a comparison of Figs. 9 and 10 that the use of a phenolic resin binder for the glass yarn has a measurably adverse effect on moisture-resisting properties. The phenolic resin is superior, however, to a silicone bonding resin in preventing fraying of the glass fibers both before and during aging.

Layer Insulation

Mica paper impregnated with a high-temperature polyester resin possesses dielectric strength and loss characteristics which make it very desirable for use as layer insulation and as electric padding for major insulation, i.e., barriers, in dry-type transformers. Its comparatively weak mechanical characteristics limit its use at present to applications where the material may be used in sheet form. As a consequence, it was evaluated as layer insulation. When treated with silicones, the material will perform adequately at hottest spot temperatures approaching 200 C. The life at 20,000 hours on the basis of a 50-per-cent dielectric strength criterion is at least 190 C; see Fig. 11. Its aging characteristics are very similar to those of silicone-impregnated asbestos in an air atmosphere.

The composite is also very resistant to the effects of moisture and thermal cycling. Weekly exposure during aging to an atmosphere at 90 degrees Fahrenheit of 90-per-cent relative humidity for 24 hours followed by 24 hours at room conditions resulted in approximately a 45-per-cent reduction in life on the basis of a 50-per-cent dielectric strength criterion. Although no comparative data are available, it is believed that such a reduction is small when the severe cycling is considered.

Major Insulation

The data available indicate that a 150-C major insulation is much improved by the use of a silicone treatment. Many 150-C insulation structures so treated give satisfactory operation in apparatus with hottest spot temperatures of over 200 C.

Improvements in insulation functioning brought about by this treatment are not confined to a specific base material or resin-base material combination. The merits of the final silicone treatment are apparent even with an essentially inorganic insulating structure. One insulation of the inorganic type which is an economical material based on the discovery of a controllable phospho-asbestos reaction may be formed as cylinders for barriers between high- and low-voltage windings.

Silicone treatment markedly improves

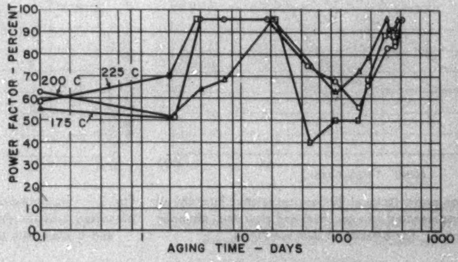

Fig. 10. Turn insulation power factor at 90-per-cent relative humidity of an acrylic ester resin impregnated asbestos sheet and glass yarn, bonded with phenolic resin and treated with silicone. For breakdown data see Fig. 7

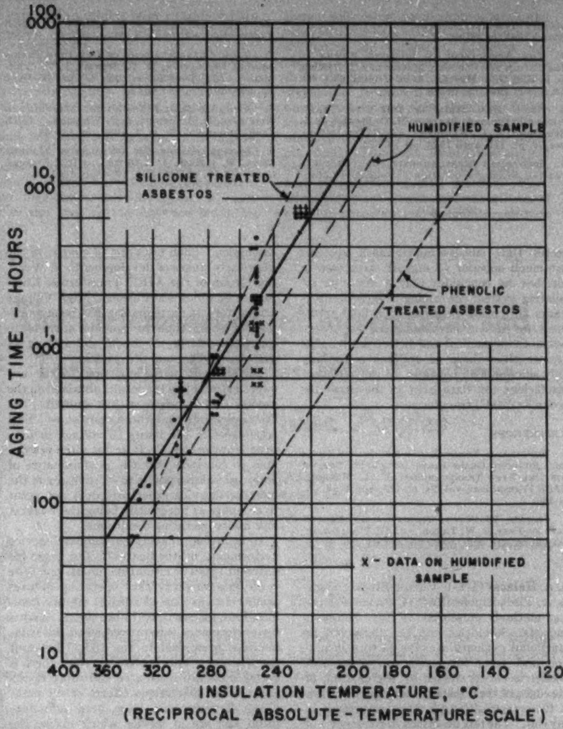

Fig. 11. Aging characteristics utilizing 50-per-cent initial dielectric strength criterion. Layer insulation is a polyester resin impregnated mica paper sheet treated with silicone. Curves for silicone-treated and phenolic-treated asbestos from reference 5

the initial dielectric properties and moisture resistance of this structure. Prolonged exposure to aging temperatures as high as 250 C are actually beneficial to its dielectric properties. The effect of thermal aging on the dielectric strength and moisture resistance of such cylinders treated with silicone are illustrated in Figs. 12 and 13. All of the composite structures, turn, layer, and barrier, remained mechanically sound throughout the aging periods. Their appearance, as aging progressed, resembled that of systems containing only silicone impregnants.

Conclusions

The results of this investigation demonstrate once more the inadequacy of existing "class" designations for high-temperature insulation. A better procedure is to consider the functional requirements of each basic material in a component insulation. Then, by proper selection, materials of different classes may be used in combination to produce superior insulating systems for many applications.

The consequences of this approach to the design of dry-type transformer insulating systems have been especially significant. It is possible to utilize the outstanding dielectric and mechanical strength characteristics of selected organic impregnants and the temperature- and moisture-resisting characteristics of good silicones. This may be accomplished in an economical manner while using a minimum of silicone.

A dry-type insulating system containing organic impregnants and using silicones as a final treatment offers the following advantages for use in circulating air apparatus.

1. The thermal stability of the system is adequate for operation at hottest spot temperatures geater than 200 C.
2. The resistance of the system to moisture is maintained throughout transformer life and is much greater than that of the usual 150 C system.
3. The insulating components will, in general, possess mechanical and dielectric strengths greater than those of systems containing only silicone impregnants.
4. The versatility and areas of dry-type transformer applications are greatly increased by the use of this insulating structure.

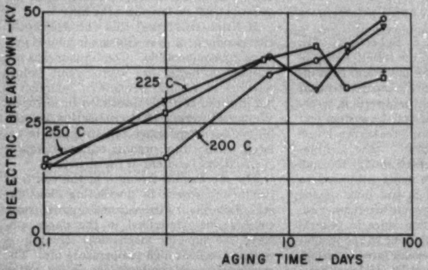

Fig. 12. Dielectric breakdown of inorganic cylinders treated with silicone

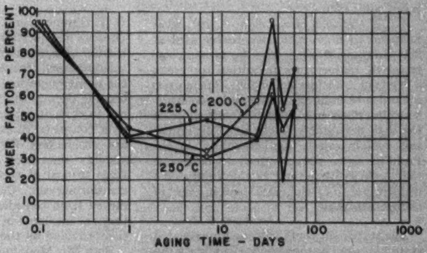

Fig. 13. Power factor at 90-per-cent relative humidity of inorganic cylinders treated with silicone

References

Silicone-Resin-Treated Magnet Coils, G. L. Moses, J. J. Torok. *AIEE Transactions*, vol. 65, July 1946, pp. 414–16.

2. Investigation of Silicone Insulation on High-Temperature Railway Motor, G. Grant III, T. A. Kauppi, G. L. Moses. *AIEE Transactions*, vol. 66, 1947, pp. 305–11.

3. Organo-Silicone Compounds for Insulating Electric Machines, T. A. Kauppi, G. L. Moses. *AIEE Transactions (Electrical Engineering)*, vol. 64, March 1945, pp. 90–93.

4. The Application of Silicone Resins to Insulation for Electric Machinery, J. DeKiep, L. R. Hill, G. L. Moses. *AIEE Transactions*, vol. 64, March 1945, pp. 94–98.

5. Aging Evaluation of Dry-Type Transformer Insulating Systems, H. C. Stewart, A. L. Scheideler, L. C. Whitman. *AIEE Transactions*, vol. 72, pt. III, April 1953, pp. 267–77.

6. Significant Measurements for Determining the Stability of High-Temperature Magnet-Wire Insulation, A. L. Scheideler. *AIEE Transactions*, vol. 73, pt. I, May 1954, pp. 177–82.

7. Aging Characteristics of Dry-Type Transformer Insulation, H. C. Stewart, L. C. Whitman. *AIEE Transactions*, vol. 67, pt. II, 1948, pp. 1600–07.

8. Aging of Class-B Insulating Material in Nitrogen, H. C. Stewart, L. C. Whitman. *AIEE Transactions*, vol. 70, pt. I, 1951, pp. 436–39.

9. Thermal Endurance of Silicone Magnet Wire, W. J. Bush, J. F. Dexter. *AIEE Transactions*, vol. 73, pt. III, Aug. 1954, pp. 1005–10.

◆

Discussion

M. L. Manning (Pennsylvania Transformer Company, Canonsburg, Pa.): This paper makes a plea for silicone-organic resins for dry-type transformer application. Most tests were conducted on a component basis in what is called a "reasonable representation" of the conditions to which materials would be subjected in a transformer. I am not sure after reading the paper whether ventilated or sealed construction is advocated in transformers for use of these resins. Emphasis is placed on the use of silicone resins as a surface treatment of conventional 150 C base insulations. In other words, the organic link in the base material is shielded from the effects of oxygen and moisture by the silicone resin coating. To back the author's plea for what might be called "the foster relatives of the silicone family," the organic resins do not possess the life of the silicone resins.

To clarify the situation for usage in transformers, I suggest the following procedure:

1. A direct comparison should be made with 15-kv class transformer models aged in air.[1] This comparison would be made using the same tests including power factor of major insulation and same construction of models. Such a structure actually simulates a power transformer, i.e., pancake high-voltage coils, axial spacers, and barrier insulation.
2. A direct comparison should be made with transformers in service. Mention is not made of the service performance of transformers utilizing the silicone-organic resins.
3. What happens if a short-circuit failure occurs in the silicone-organic-insulated transformers? By test, sealed silicone-insulated transformers have been proved safe through 600 C temperature.[2] Combustion is not supported.
4. If nitrogen atmosphere is lost, what happens to organic-silicone resins used at 220 C temperature in air, the present hottest spot temperature permitted for group 3 dry-type transformers in air? Silicone resins and rubbers used in the insulation structure described in reference 1 make use of the high heat-stable silicones. This insulation system can be used at 220 C in air. From the users' point of view, it would seem that security is desired in the ability of a transformer to carry normal load in event of nitrogen leakage.

The statement that "silicone-impregnated systems... are improved only slightly by the removal of oxygen from the surrounding medium" is contradictory to data submitted in reference 5 of the paper. The author states that silicone-impregnated systems are much superior to organic structures in air, but he concludes that a dry-type insulating system containing organic impregnants and using silicones as a final treatment for use in circulating air apparatus possesses mechanical and dielectric strengths greater than those of systems containing only silicone impregnants. It appears that insufficient test data exist in the paper for group 3 (220 C) transformers.

References

1. Functional Temperature Endurance Tests on a Silicone Glass Fiber Insulation System for Dry-Type Transformers, M. L. Manning. *AIEE Transactions*, vol. 74, pt. III, Apr. 1955, pp. 91-100.

2. Sealed Dry-Type Transformers Proved Safe by Test, E. W. Tipton. *AIEE Transactions*, vol. 72, pt. III, Aug. 1953, pp. 843–48.

A. A. Halacsy (I-T-E Circuit Breaker Company, Philadelphia, Pa.): I question if the test methods presented by Mr. Simmons and Mr. Scheideler can be considered as functional evaluation as far as turn insulation and layer insulation are concerned. Dielectric effects caused by the crossing of the edges of the adjacent wires will not show in these tests although they are present in any coil. The test described in reference 1 of M. L. Manning's discussion is certainly a better functional evaluation and should result in lower breakdown voltages. Have the authors made any comparative tests justifying their simplification?

The tests showed that creepage sets the limit to the voltage in dry-type transformers. Do the authors think it possible and practical to build dry-type transformers for voltages higher than the 15-kv class in the light of the difficulties experienced in creepage?

G. F. Simmons and **A. L. Scheideler**: Dr. Halacsy has questioned the functionality of the test samples used for layer and turn insulation tests. It must be remembered that the primary purpose of these tests is to assess the thermal stability of the system and not to evaluate dielectric breakdown levels of a complete transformer. The samples are satisfactory for determining thermal stability since they are being subjected to fields typical of those in the bulk of the transformer coil. Crossovers are further removed from consideration since in general they are insulated in addition to the insulation provided by the regular wire covering.

Both Mr. Manning and Dr. Halacsy have suggested that these insulation combinations be tested by the use of models aged in air, as described in reference 1 of Mr. Manning's discussion. Such tests are, of course, in the very early stages of development. A Working Group of the AIEE Transformer Committee in which the Pittsfield High Voltage Laboratory is participating has been working for some time to provide answers to questions relating to model size and structure, test cycles, and life criteria.

An example of the questions to be answered is raised by the results obtained on the models in the reference just quoted. Dr. Halacsy states that those tests show "that creepage sets the limits to voltage in dry-type transformers." It seems more reasonable to conclude that the predominance of creepage failures points to a deficiency in the models. Service experience does not point to creepage as necessarily being the weakest link under operating conditions.

It is rather difficult to compare service performance on the basis of a few years for different types of insulation, unless one type is so unsatisfactory that operating failures occur. In the case of silicone-organic combinations, as described in the paper, operating performance is improved when this combination is applied to the 150 C hot-spot transformer. This is obvious, since there is better moisture resistance and more resistance to the deleterious effects of temperature. Transformers have been manufactured and are in service which utilize the silicone-organic combination.

Suitable silicone-organic resin combinations, as described in this paper, are dependable for use at 220 C hot-spot temperatures, either in air or in nitrogen. It is advocated that open dry-type transformers for use at temperatures of 220 C hot spot embody these combinations. Obviously, if these insulations are good for use in air, there is no problem in the sealed dry-type transformer if air should perchance replace the nitrogen, except as to the moisture effects upon unpainted steel surfaces and the like.

It has been shown[1] that the decomposition products of even silicone insulated systems are combustible. Combustion was not supported during the short-circuit failure referred to in Mr. Manning's reference 2 because the coil was immersed in nitrogen. We would suggest that criteria for flammability of a transformer coil structure be related to the total organic and semiorganic (i.e., silicone) content of the structure.

The mechanical strength of the coil is of prime importance in preventing short-circuit failures. The silicone-organic resin combinations described in the paper embody the superior mechanical strength as well as excellent high temperature life. The organics in such combinations do not soften as do existing silicones at the high temperatures encountered during either overload or short circuit. The composite may therefore be expected to exhibit more reliability than can be obtained in presently available silicone systems.

Mr. Manning questions our statement that silicone-impregnated systems are improved only slightly by the removal of oxygen from the surrounding medium. Although the improvement is significant, it is much less than that obtained with organic resins. It is true that silicone-impregnated systems are much superior to organic structures in air from both the moisture-resistant and high-temperature-life point of view. It is also true that a dry-type insulating system containing organic impregnants, and using silicones as a final treatment for use in circulating air apparatus, possesses, mechanical and dielectric strengths greater than those of systems containing only silicone impregnants. Nothing is contradictory about the two statements since they refer to different properties. We agree that the use of silicones overcoating organic resins would not result in a better moisture-resistant and high-temperature-life condition than with pure silicone-impregnated systems. However electric and mechanical strength are of as great importance as moisture resistance and high temperature life in electric apparatus.

Dr. Halacsy questions the practically of dry-type transformers for voltages higher than the 15-kv class. Such a unit, which is now being manufactured, utilizes a gas with a higher dielectric strength than nitrogen, thus improving all insulation characteristics.

REFERENCE

1. RELATION OF TRANSFORMER DESIGN TO FIRE PROTECTION, B. D. Treanor, L. C. Whitman, *AIEE Transactions*, vol. 71, pt. III, Aug. 1952, pp. 678–81.

The Determination of Incremental and Total Loss Formulas from Functions of Voltage Phase Angles

C. R. CAHN
ASSOCIATE MEMBER AIEE

A NEW approach in the form of remarkably simple formulas for the determination of incremental transmission losses in electric power systems has been advanced by Brownlee.[1] He derived the formulas for the simplest possible transmission system of two generators connected by a single transmission line and apparently showed them to be applicable to practical power systems by heuristic reasoning, which lead him to solve some numerical cases. Brownlee's formulas are functions of the phase angles of the generator bus voltages, so that their application is restricted to those cases where the phase angles are known. Since phase angles are not presently available on the actual system, Brownlee's results are useful at this time mainly in load studies on a-c network analyzers.

The purpose of this paper is to provide a more solid foundation for Brownlee's results, showing some of the conditions which must be satisfied for their validity, to provide additional numerical examples of the successful use of Brownlee's theory, and to provide an extension of Brownlee's theory to give expressions for incremental and total losses which do not require knowledge of generator voltage phase angles. The resulting loss formulas are conventional in that they require specification of the generator power outputs only. It is believed, however, that the method of calculating incremental and total loss formulas presented here is considerably simpler than any yet advanced.

The Brownlee Formulas

The Brownlee formulas in slightly modified form are derived and presented here for reference. The sending end and receiving end power inputs to a transmission line of impedance $Z=R+jX$ are

$$P_1=\frac{V_1^2R}{R^2+X^2}-\frac{V_1V_2}{R^2+X^2}(R\cos\theta-X\sin\theta) \tag{1}$$

$$P_2=\frac{V_2^2R}{R^2+X^2}-\frac{V_1V_2}{R^2+X^2}(R\cos\theta+X\sin\theta) \tag{2}$$

where θ is the angle by which the sending end voltage leads the receiving end. The subscripts 1 and 2 denote the sending end and the receiving end respectively. If it is assumed that the two ends are maintained at constant voltage, any change in P_1 and P_2 is caused by a variation in θ. Differentiating with respect to θ and defining the transmitted power as the average of the sending end and receiving end powers results in

$$dP_L/d\theta=\frac{2V_1V_2}{R^2+X^2}R\sin\theta \tag{3}$$

$$dP_{1-2}/d\theta=\frac{V_1V_2}{R^2+X^2}X\cos\theta \tag{4}$$

$$dP_L/dP_{1-2}=2\frac{R}{X}\tan\theta \tag{5}$$

where $P_L=P_1+P_2$ is the system loss and $P_{1-2}=(1/2)(P_1-P_2)$ is the transmitted power. Integrating with respect to θ between the initial value θ_a and the final value θ_b, the equations for a finite change are obtained

$$\Delta P_L=\frac{4V_1V_2}{R^2+X^2}R\sin\left(\frac{\theta_b+\theta_a}{2}\right)\sin\left(\frac{\theta_b-\theta_a}{2}\right) \tag{6}$$

$$\Delta P_{1-2}=\frac{2V_1V_2}{R^2+X^2}X\cos\left(\frac{\theta_b+\theta_a}{2}\right)\sin\left(\frac{\theta_b-\theta_a}{2}\right) \tag{7}$$

$$\Delta P_L/\Delta P_{1-2}=2\frac{R}{X}\tan\left(\frac{\theta_b+\theta_a}{2}\right) \tag{8}$$

In the foregoing derivation the variations caused by changes in voltage magnitude have been neglected completely. This is justified by the actual practice on power systems of maintaining all busses at practically constant voltage. Thus, although a 1-degree change in the phase angle between two plants is quite small, it produces as much voltage acting to circulate current as a 2-per-cent change in the voltage magnitude at one of the plants, a quite considerable voltage change. Therefore, it is assumed in the following that voltage magnitude variations never need to be taken into account.

Paper 55-25, recommended by the AIEE System Engineering Committee and approved by the AIEE Committee on Technical Operations for presentation at the AIEE Winter General Meeting, New York, N. Y., January 31–February 4, 1955. Manuscript submitted October 18, 1954; made available for printing November 15, 1954.

C. R. CAHN is with Syracuse University, Syracuse, N. Y.

The author wishes to thank H. L. Harrington, H. B. Smith, W. D. Wilder and other members of the Niagara Mohawk Power Corporation, Buffalo, New York, for their advice and support. Particularly invaluable during the development of the theory was the counsel, both technical and otherwise, of D. W. Spence, Supervisor of the Network Analyzer Laboratory at Syracuse University, who also supplied extensive personal efforts towards the obtaining of the network analyzer data. Some of the calculations were made by D. D. Nadkarni.

The material contained in this paper was adapted from a portion of a dissertation submitted in partial fulfillment of the requirements for the degree of Doctor of Philosophy at Syracuse University, Syracuse, New York.

The Brownlee Formulas on Practical Systems

The demonstration of the applicability of the Brownlee formulas to practical systems hinges on the finding of an analytical method of exchanging generation between two plants or tie lines, all of which will be called "generators." One possibility is to take advantage of the fact that a considerable variation in the power flows has only a relatively small effect on the voltages at the loads if the generator voltages are held fixed. Then, if one generator has its voltage phase angle increased at constant magnitude, holding the voltage of another generator fixed in both magnitude and angle and holding the currents of all other generators and of all loads fixed in both magnitude and angle, the result will be an approximation to the desired condition where generation is exchanged between the two generators with no other changes in the generation or in the loads. The low impedance of the transmission system connecting the two generators allows a large change in their currents with only small voltage changes on the system. Changes in power at the other generators and at the loads are a result of the small voltage changes acting on a fixed current. If the other generators and loads were then trimmed to their proper values, the additional incremental losses would be small in comparison with those caused by the major swing.

The procedure just described for exchanging generation between two generators will now be applied to a transmission system with three points of entry, the first two being the aforementioned two generators, the third being an additional generator or load, as shown in Fig. 1. This is the most general system which must be considered since the extension to a larger number of points of entry will be evident. The results to be obtained will indicate some of the conditions which must be satisfied for the validity of Brownlee's formulas on practical systems.

The system is isolated from ground except at the points of entry, with the usual assumptions of neglecting off-nominal turns-ratios and lumping line charging in the loads being made. In terms of the open-circuit self- and mutual impedances Z_{nm} with generator 2 grounded, the relations between voltages and currents are

$$\begin{aligned} E_1-E_2&=Z_{11}I_1+Z_{13}I_3\\ E_3-E_2&=Z_{31}I_1+Z_{33}I_3 \end{aligned} \qquad (9)$$

where I_2 does not appear in the equations.[2,3]

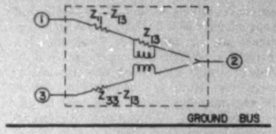

Fig. 1. Transmission system equivalent

In addition, the current I_2 is the negative of all other currents combined. That is

$$I_2=-I_1-I_3 \qquad (10)$$

Solving equations 9 and 10 for I_1 and I_2 gives

$$\begin{aligned} I_1&=\frac{1}{Z_{11}}(E_1-E_2)-\frac{Z_{13}}{Z_{11}}I_3\\ I_2&=\frac{1}{Z_{11}}(E_2-E_1)-\left(1-\frac{Z_{13}}{Z_{11}}\right)I_3 \end{aligned} \qquad (11)$$

If equations 11 are multiplied by the complex conjugate voltages E_1^* and E_2^* respectively, and the second equation 9 is multiplied by I_3^*, the complex power inputs to the three points of entry are found to be

$$W_1^*=E_1^*I_1=\frac{1}{Z_{11}}(E_1E_1^*-E_1^*E_2)-\frac{Z_{13}}{Z_{11}}E_1^*I_3$$

$$W_2^*=E_2^*I_2=\frac{1}{Z_{11}}(E_2E_2^*-E_1E_2^*)-\left(1-\frac{Z_{13}}{Z_{11}}\right)E_2^*I_3 \qquad (12)$$

$$W_3=E_3I_3^*=E_2I_3^*+Z_{31}I_3^*I_1+Z_{33}I_3^*I_3$$

Differentiating with respect to the angle of θ_1, assuming that the magnitude of E_1 and all other quantities are fixed and taking the real part to get only the real power loss, gives

$$dP_1/d\theta_1=\frac{V_1V_2}{|Z_{11}|^2}[R_{11}\sin(\theta_1-\theta_2)+X_{11}\cos(\theta_1-\theta_2)]+\left(Re\frac{Z_{13}}{Z_{11}}\right)V_1|I_3|\times\sin(\theta_1-\phi_3)-\left(Im\frac{Z_{13}}{Z_{11}}\right)V_1|I_3|\times\cos(\theta_1-\phi_3) \qquad (13)$$

$$dP_2/d\theta_1=\frac{V_1V_2}{|Z_{11}|^2}[R_{11}\sin(\theta_1-\theta_2)-X_{11}\cos(\theta_1-\theta_2)] \qquad (14)$$

$$dP_3/d\theta_1=-\left(Re\frac{Z_{31}}{Z_{11}}\right)V_1|I_3|\sin(\theta_1-\phi_3)-\left(Im\frac{Z_{31}}{Z_{11}}\right)V_1|I_3|\cos(\theta_1-\phi_3) \qquad (15)$$

where $E_n=V_n\underline{/\theta_n}$ and $I_n=|I_n|\underline{/\theta_n}$. *Re* and *Im* mean real part and imaginary part respectively. Then the rates of change of power loss and transmitted power with θ_1 are

$$dP_L/d\theta_1=\left(\frac{dP_1}{d\theta_1}+\frac{dP_2}{d\theta_1}+\frac{dP_3}{d\theta_1}\right)=\frac{2V_1V_2}{R_{11}^2+X_{11}^2}\times R_{11}\sin(\theta_1-\theta_2)+2V_1|I_3|\cos(\theta_1-\phi_3)\times\frac{R_{13}X_{11}-X_{13}R_{11}}{R_{11}^2+X_{11}^2} \qquad (16)$$

$$dP_{1-2}/d\theta_1=1/2\left(\frac{dP_1}{d\theta_1}-\frac{dP_2}{d\theta_1}\right)=\frac{V_1V_2}{R_{11}^2+X_{11}^2}\times X_{11}\cos(\theta_1-\theta_2)+1/2V_1|I_3|\sin(\theta_1-\phi_3)\times\frac{R_{13}R_{11}+X_{13}X_{11}}{R_{11}^2+X_{11}^2}+1/2V_1|I_3|\times\cos(\theta_1-\phi_3)\frac{R_{13}X_{11}-X_{13}R_{11}}{R_{11}^2+X_{11}^2} \qquad (17)$$

It is seen that equations 16 and 17 are the same as equations 3 and 4 with additional correction terms. However, the correction terms in practical cases may be expected to be small for two reasons. The first is that the magnitude of a load or generator current is normally small in comparison with the ratio of the system voltage to the self-impedance of a generator (with another generator grounded) unless large loads are supplied by large generations in the same area. The second is that the correction term in equation 16 is zero if the resistance-reactance ratio is uniform in the system. It may be expected that the resistance-reactance ratio of the self- and mutual impedances will not vary excessively for most loop interconnected systems unless there exists important transmission at different voltage levels. The first correction term in equation 17 is small for high power-factor loads, and the major cosine term is large enough so that the correction terms in this equation can be disregarded in all practical cases. Since the major term of equation 16 involves a sine of a small angle, it may be expected that the incremental losses will be more in error than the incremental transmitted power when the correction terms are neglected.

It is thus clear why the Brownlee formulas can work on practical systems. Since all other points of entry to the system besides those of the two generators between which generation is exchanged are considered as open circuits during the swing, the proper impedance to use in Brownlee's formula is the one measured with all loads and capacitors disconnected. A final verification is provided by numerical examples presented in the following.

A New Derivation of Incremental Loss Coefficients

The Brownlee formulas, having been shown suitable for application to most practical power systems, are used as the point of departure in the development of expressions more suitable to economic studies. Since phase angles are not available on present-day power systems, they cannot be used in system operation without the introduction of additional telemetering equipment, which must be highly accurate because of the small phase-angle differences involved. Also, phase angles could not be of use in economic scheduling of generation, since they could not be accurately predicted. Thus, expressions involving powers are preferable except for system planning on a network analyzer where phase angles are available. Such expressions may be obtained if it is possible to relate phase angles to generator powers. The relationship may be established from the first equation 9. The left side of the equation can be manipulated so that it becomes proportional to the major term on the right side of equation 16, while the right side of equation 9 can be manipulated into the form of the sum of terms, each of which is a coefficient times a generator or a load power.

Then, provided that the correction terms in equations 16 and 17 can be neglected, it is shown in Appendix I that the incremental loss between generators n and M is given by

$$dP_L/dP_{n-M}=\sum_{m=1}^{N} A_{nm}P_m \qquad (18)$$

where P_m is the power output of generator m, P_{n-M} is the average of P_n and $-P_M$ and a total of N generators numbered 1 to N is assumed. There are $N-1$ equations, one for each value of $n\neq M$. For $n=M$ all coefficients are zero. The A_{nm} coefficients are taken as constants evaluated from a chosen base case. As originally derived, the sum in equation 18 was extended over all generators except number M and over all loads. However, the load powers were eliminated and the output of generator M was introduced by using the approximation that the total generation equals the total load, neglecting the effect of losses as a second-order correction. Also required to eliminate the loads were the assumptions that each load power remains a fixed fraction of the total load and that the Q/P ratio of each load remains fixed. Line charging is included in the loads. The A_{nm} coefficients will be called incremental loss coefficients.

The A_{nm} coefficients are evaluated by the following procedure:

1. Select a large generator to be the swing machine M and, with its point of entry grounded, measure the open-circuit self- and mutual resistances and reactances R_{nm} and X_{nm} between the generators. A procedure for making these measurements on the network analyzer is described in the literature.[3]

2. Using values from the base case, calculate for each value of n and m

$$D_{nm}=2K_{nm}X_{nm}\times \frac{(1-s_mK_{nm})\cos(\theta_m-\theta_n)+(s_m+K_{nm})\sin(\theta_m-\theta_n)}{V_nV_M\cos(\theta_n-\theta_M)} \qquad (19)$$

where $K_{nm}=R_{nm}/X_{nm}$ and $s_m=Q_m/P_m$ is the ratio of the reactive output to power output of generator m.

3. Calculate for each n

$$(dP_L/dP_{n-M})_{\text{base case}}=2K_{nm}\times \tan(\theta_n-\theta_M)_{\text{base case}} \qquad (20)$$

4. Using the base case generator powers, calculate for each n

$$w_n=\frac{\sum_{m=1}^{N} D_{nm}P_m-(dP_L/dP_{n-M})_{\text{base case}}}{\sum_{m=1}^{N} P_m} \qquad (21)$$

5. Calculate for each value of n and m

$$A_{nm}=D_{nm}-w_n \qquad (22)$$

It has been found that greater accuracy is obtained if the portions of the reactive outputs which do not vary with exchanges of generation are included with the loads before calculating the generator Q/P ratios. In lieu of such data it is suggested that each s_m be taken as equal to either zero or its base case value, whichever is algebraically smaller.

Equation 18 may be used for finite increments also if average powers are used. From equations 5 and 8, rewritten for exchanging generation between plant n and plant M, and equation 18

$$\begin{aligned}\Delta P_L/\Delta P_{n-M}&=2K_{nn}\tan(\theta_n-\theta_M)_{\text{av}}\\&=2K_{nn}\tan\frac{(\theta_n-\theta_M)_{\text{initial}}+(\theta_n-\theta_M)_{\text{final}}}{2}\\&\approx 1/2[2K_{nn}\tan(\theta_n-\theta_M)_{\text{initial}}+2K_{nn}\tan(\theta_n-\theta_M)_{\text{final}}]=\sum_{m=1}^{N}A_{nm}(P_m)_{\text{av}}\end{aligned} \qquad (23)$$

This development assumes that the phase-angle differences are all small, as must be the case if the derivation of equation 18 is to be valid.

The application of equation 5 or 18 to the economic scheduling of generation is now outlined. At the most economic dispatch, generation may be exchanged between two plants without affecting the fuel cost input. Letting F_n be the fuel cost input of plant n, for each $n\neq M$

$$dF_n+dF_M=0 \qquad (24)$$

or

$$\frac{dF_n}{dP_n}(dP_{n-M}+1/2dP_L)=-\frac{dF_M}{dP_M}(-dP_{n-M}+1/2dP_L) \qquad (25)$$

Rearranging equation 25 gives

$$\frac{dF_n}{dP_n}\,\frac{1+(1/2)dP_L/dP_{n-M}}{1-(1/2)dP_L/dP_{n-M}}=\frac{dF_M}{dP_M} \qquad (26)$$

To a reasonable degree of approximation it may be written that

$$\frac{1+(1/2)dP_L/dP_{n-M}}{1-(1/2)dP_L/dP_{n-M}}\approx 1+dP_L/dP_{n-M}\approx\frac{1}{1-dP_L/dP_{n-M}} \qquad (27)$$

since dP_L/dP_{n-M} is normally relatively small. It may be shown that incremental loss coefficients can be applied in the same manner as total loss coefficients except in the calculation of total losses.

Derivation of Total Loss Coefficients from Incremental Loss Coefficients

The preceding incremental loss formula, equation 18, is entirely satisfactory for economic scheduling of generation and becomes inadequate only when total losses are desired, as is the case if an evaluation of annual fuel cost savings is to be made. For such purposes the derivation of a total loss formula is necessary. It is shown in Appendix II that a total loss formula of the form

$$P_L=\sum_{n=1}^{N}\sum_{m=1}^{N}P_nB_{nm}P_m \qquad (28)$$

can be derived from the incremental loss formula of equation 18. The assumption is made in the derivation that the total loss is proportional to the square of the total generation when all loads and all generations are changed proportionately. This is reasonable if the busses are maintained at nearly constant voltages. The derivation calculates the total loss for an arbitrary generation total by first multiplying all generator powers in the base case by the ratio of the actual total generation to the base case total generation. Then, starting from the scaled base case and maintaining the total generation constant, each generator in turn is changed from its scaled base case output to its value in the actual case, the incremental loss caused by the change being calculated by equation 18. The various calculated increments are added to the scaled power loss of the scaled base case to get the total loss of the actual case. The result is then rearranged in the form of equation 28.

Table I. Generation Data

			Case				
			1	2*	3	4	5
$G1$	Twin Branch	mw	43.8	93	144	195	244
		megavars	53.4	54	30	22	21
$G2$	Fort Wayne	mw	86	46	13.2	−20.9	−54.2
		megavars	−54	−18	−0.7	12	19
$G3$	Portsmouth	mw	73.5	51.5	34.6	18.2	4.9
		megavars	−13.2	−8	−6.9	−2.9	1.4
	System loss	mw	8.00	3.70	2.72	4.68	9.00

* Base case.

Table II. Base Case Data

n	V_n	θ_n	s_n
1	1.015	8.0°	−0.200
2	0.980	8.0°	−0.560
3	0.953	22.1°	−0.210

The procedure for calculating the B_{nm} coefficients from the A_{nm} coefficients is now outlined:

1. For each value of n, using the generator powers from the base case, calculate

$$a_n = \frac{\sum_{m=1}^{n} A_{nM}P_m + \sum_{m=n+1}^{N} (A_{nm}-A_{mn}+A_{mM})P_m}{2\sum_{m=1}^{N} P_m} \tag{29}$$

2. Calculate for each value of n and m with $n \geqq m$

$$\mathbf{B}_{nm} = \mathbf{B}_{mn} = (1/2)(A_{nm}-A_{nM})+a_n+a_m \tag{30}$$

3. Using generator powers from the base case, determine

$$B_{MM} = \frac{(P_L)_{\text{base case}} - \sum_{n=1}^{N}\sum_{m=1}^{N} P_n\mathbf{B}_{nm}P_m}{\left(\sum_{m=1}^{N} P_m\right)^2} \tag{31}$$

4. For each value of n and m with $n \geqq m$, calculate

$$B_{nm} = B_{mn} = \mathbf{B}_{nm} + B_{MM} \tag{32}$$

The B_{nm} coefficients calculated by this procedure will be called new total loss coefficients. Because of the additional assumption required in the derivation, the total loss coefficients will not predict incremental losses as well as the incremental loss coefficients themselves.

Examples

EXAMPLE I

The first illustration of the preceding theory is made on a simple system which has already been presented in reference 4. The impedance diagram and the base case load flows are shown in Fig. 2, and additional generation data for several other dispatches are listed in Table I, as obtained from reference 4. The system loss for each case, found by summing the I^2R loss in each line, is also listed in Table I. The base case data used for calculating the loss formula are given in Table II. The generator Q/P ratios are taken as the slopes of the linear approximations to their P-Q characteristics, as plotted from the data in Table I.

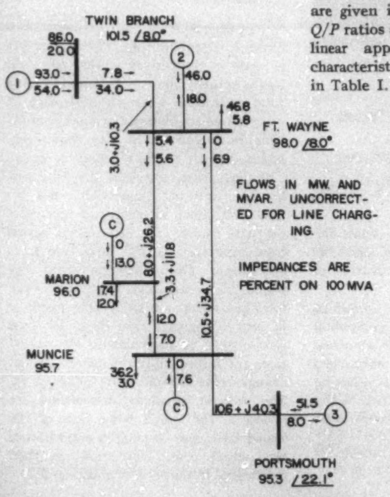

Fig. 2 (left). Impedance diagram and base case load flows

First, A_{nm} coefficients will be calculated. Generator 1 is chosen as the swing machine. The self- and mutual impedance of the generators with generator 1 grounded are calculated to be

$Z_{11}=Z_{12}=Z_{13}=0+j0$

$Z_{22}=Z_{23}=0.0300+j0.1030;\ K_{22}=K_{23}=0.291$

$Z_{33}=0.1905+j0.688;\ K_{33}=0.277$

The D_{nm} quantities of equation 19 are calculated in tabular form in Table III. From the base case data equation 20 gives

$$(dP_L/dP_{2-1})_{\text{base case}} = 2(0.291)\tan 0.0° = 0.0000$$

$$(dP_L/dP_{3-1})_{\text{base case}} = 2(0.277)\tan 14.1° = 0.1391$$

The calculation of the w_n in equation 21 is shown in Table IV. The incremental loss coefficients A_{nm} are found from equation 22 to be

$$A_{nm} = \begin{array}{cccc} & m=1 & 2 & 3 \\ n=1 & 0.0000 & 0.0000 & 0.0000 \\ 2 & -0.0345 & 0.0357 & 0.0305 \\ 3 & -0.0605 & 0.0103 & 0.3695 \end{array}$$

These coefficients are in per unit on a 100-megavolt-ampere (mva) base.

The generation data do not include cases where generation is exchanged between the swing machine and only one other. Therefore, the incremental coefficients are used to obtain total loss coefficients. The a_n quantities are cal-

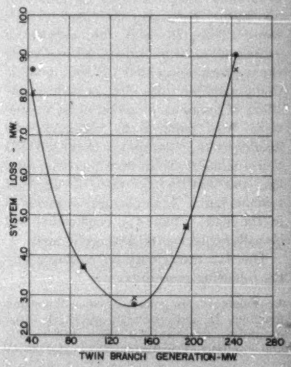

Fig. 3 (right). Comparison of calculated and actual losses

— Losses by I^2R
⊙ New total loss formula
× Kirchmayer formula

Table III. Calculation of D_{nm}

n	m	(V_mV_1) $\cos(\theta_n-\theta_1)$	$\theta_m-\theta_n$	$(1-K_{nm}s_m)$ $\cos(\theta_m-\theta_n)$	$(K_{nm}+s_m)$ $\sin(\theta_m-\theta_n)$	$2K_{nn}X_{nm}$	D_{nm}
2	2	0.995	0.0°	1.163	0.000	0.0600	0.0702
2	3	0.967	14.1°	1.027	0.020	0.0600	0.0650
3	2	0.965	−14.1°	1.128	0.066	0.0571	0.0708
3	3	0.937	0.0°	1.058	0.000	0.3810	0.4300

Table IV. Calculation of w_n

m	P_m	D_{2m}	P_mD_{2m}	D_{3m}	P_mD_{3m}
1	0.930	0.0000	0.0000	0.0000	0.0000
2	0.460	0.0702	0.0323	0.0708	0.0326
3	0.515	0.0650	0.0335	0.4300	0.2215
		$-dP_L/dP_2-1$	0.0000	$-dP_L/dP_3-1$	−0.1391
Total	1.905		0.0658		0.1150
		w_2	0.0345	w_3	0.0605

Table V. Calculation of a_n

m	P_m	A_{21} or $A_{2m}-A_{m2}+A_{m1}$	Production	A_{31}	Production
1	0.930	−0.0345	−0.0321	−0.0605	−0.0563
2	0.460	−0.0345	−0.0159	−0.0605	−0.0278
3	0.515	−0.0403	−0.0208	−0.0605	−0.0312
Total	1.905		−0.0688		−0.1153
		a_2	−0.0181	a_3	−0.0303

culated in Table V according to equation 29. Then, equation 30 is used to calculate the $\mathbf{B}_{nm}$ coefficients, e.g.

$$\mathbf{B}_{32}=(1/2)(0.0103+0.0605)-0.0303-0.0181=-0.0130$$

The resulting $\mathbf{B}_{nm}$ coefficients are

$$\mathbf{B}_{dm}=\begin{array}{cccc} & m=1 & 2 & 3 \\ n=1 & 0.0000 & X & X \\ 2 & -0.0181 & -0.0011 & X \\ 3 & -0.0303 & -0.0130 & 0.1544 \end{array}$$

The value of B_{11} is chosen to make the total loss formula fit the base case loss of 0.0370 per unit. Equation 31 gives the result: $B_{11}=0.0129$. Adding B_{11} to all $\mathbf{B}_{nm}$ coefficients gives the final matrix in per unit on 100 mva

$$B_{nm}=\begin{array}{cccc} & 1 & 2 & 3 \\ 1 & 0.0129 & & \\ 2 & -0.0052 & 0.0118 & \\ 3 & -0.0173 & -0.0001 & 0.1673 \end{array}$$

This matrix is symmetrical. These total loss coefficients may be compared with those calculated by Kirchmayer's method.[4]

A comparison between the actual loss, the loss calculated by the foregoing B_{nm} coefficients, and the loss calculated by Kirchmayer's B_{nm} coefficients for each case in Table I is given in Table VI. Fig. 3 presents a graphical comparison. It is felt that for this system the new loss coefficients provide a closer correlation between calculated and actual losses than do the Kirchmayer loss coefficients, although both are quite satisfactory.

Table VI. Comparison of Actual and Calculated Losses

Case	Actual Loss, Mw	New Total Loss, Mw	Kirchmayer Loss, Mw
1	8.00	8.65	8.06
2	3.70	3.70	3.70
3	2.72	2.77	2.93
4	4.68	4.72	4.72
5	9.00	9.02	8.65

Table VII. Open-Circuit Impedances for nm System*

	m=1	2	3	4	5	6	7	8	9	10	11	12	13	14	15	16	17
n= 1	0.0880 0.293																
2	0.0856 0.280	0.1420 0.421															
3	0.0536 0.1774	0.0542 0.1780	0.0540 0.1770														
4	0 0	0 0	0 0	0 0													
5	0.0096 0.0334	0.0096 0.0334	0.0096 0.0334	0 0	0.0476 0.1404												
6	0.0113 0.0390	0.0113 0.0390	0.0113 0.0390	0 0	0.0387 0.1160	0.0545 0.1640											
7	0.0113 0.0390	0.0113 0.0390	0.0113 0.0390	0 0	0.0387 0.1160	0.0545 0.1640	0.0965 0.306										
8	0.0154 0.0493	0.0154 0.0493	0.0154 0.0493	0 0	0.0218 0.0704	0.0295 0.0946	0.0295 0.0946	0.0500 0.1570									
9	0.0220 0.0802	0.0220 0.0802	0.0220 0.0802	0 0	0.0160 0.0499	0.0204 0.0642	0.0204 0.0642	0.0311 0.0935	0.0422 0.305								
10	0.0160 0.0513	0.0160 0.0513	0.0160 0.0513	0 0	0.0210 0.0690	0.0280 0.0925	0.0280 0.0925	0.0472 0.1527	0.0356 0.1084	0.0656 0.218							
11	0.0161 0.0508	0.0161 0.0508	0.0161 0.0508	0 0	0.0214 0.0697	0.0282 0.0934	0.0282 0.0934	0.0483 0.1544	0.0339 0.1048	0.0584 0.201	0.0890 0.296						
12	0.0161 0.0508	0.0161 0.0508	0.0161 0.0508	0 0	0.0214 0.0697	0.0282 0.0934	0.0282 0.0934	0.0483 0.1544	0.0339 0.1048	0.0584 0.202	0.0892 0.297	0.1130 0.372					
13	0.0161 0.0508	0.0161 0.0508	0.0161 0.0508	0 0	0.0214 0.0697	0.0282 0.0934	0.0282 0.0934	0.0483 0.1544	0.0339 0.1048	0.0584 0.202	0.0892 0.297	0.0950 0.312	0.1021 0.336				
14	0.0161 0.0508	0.0161 0.0508	0.0161 0.0508	0 0	0.0214 0.0697	0.0282 0.0934	0.0282 0.0934	0.0483 0.1544	0.0339 0.1048	0.0584 0.202	0.0892 0.297	0.0945 0.310	0.1007 0.332	0.1022 0.338			
15	0.0161 0.0508	0.0161 0.0508	0.0161 0.0508	0 0	0.0214 0.0697	0.0282 0.0934	0.0282 0.0934	0.0483 0.1544	0.0339 0.1048	0.0584 0.202	0.0892 0.297	0.0942 0.310	0.1001 0.330	0.1001 0.330	0.1230 0.427		
16	0.0161 0.0508	0.0161 0.0508	0.0161 0.0508	0 0	0.0214 0.0697	0.0282 0.0934	0.0282 0.0934	0.0483 0.1544	0.0339 0.0148	0.0584 0.202	0.0892 0.297	0.0942 0.310	0.1001 0.330	0.1001 0.330	0.1230 0.427	0.1350 0.493	
17	0.0860 0.282	0.0848 0.275	0.0530 0.1776	0 0	0.0096 0.0334	0.0113 0.0390	0.0113 0.0390	0.0154 0.0493	0.0220 0.0802	0.0160 0.0513	0.0161 0.0508	0.0161 0.0508	0.0161 0.0508	0.0161 0.0508	0.0161 0.0508	0.0161 0.0508	0.0900 0.304

* Upper figure is resistance, lower figure is reactance.

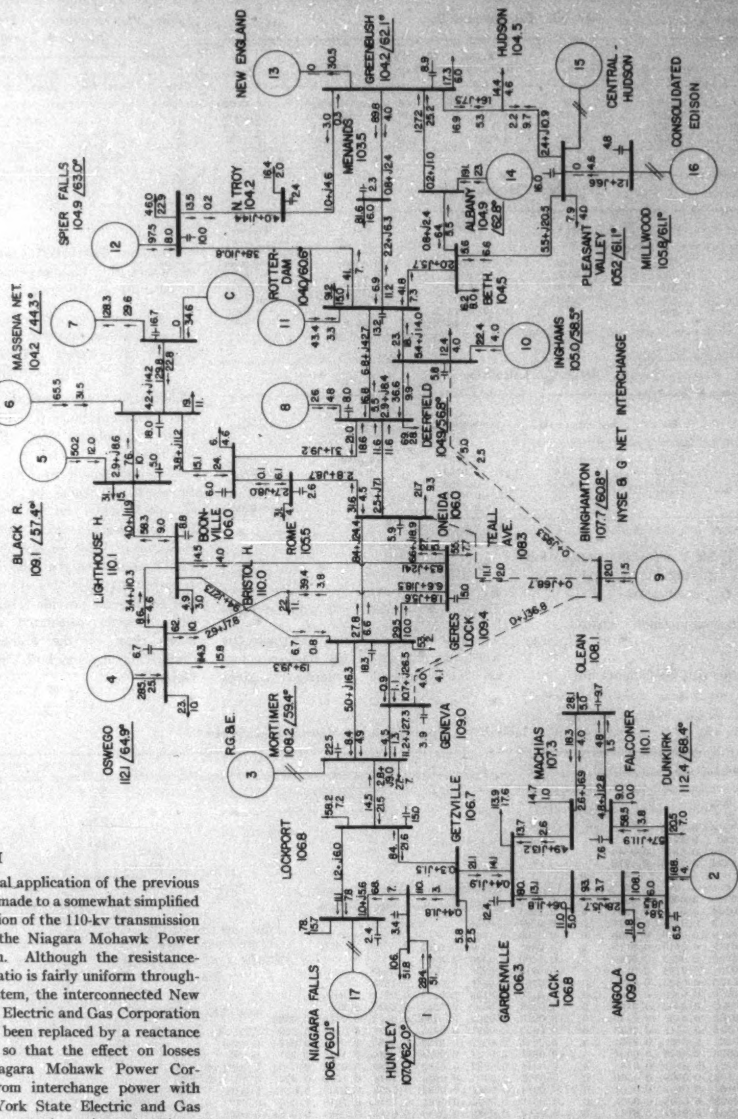

Fig. 4. Impedance diagram and base case load flows for Niagara Mohawk 110-kv system. Flows on mw and megavars. Impedances in per cent on 100-mva base

NEW ENGLAND
13
GREENBUSH 104.2 /62.1°
HUDSON 104.5
15
CENTRAL HUDSON
CONSOLIDATED EDISON
16
MILLWOOD 105.8/61.1°
PLEASANT VALLEY 105.2/61.1°
ALBANY 104.9 /62.8°
14
MENANDS 103.5
N. TROY 104.2
SPIER FALLS 104.9 /63.0°
12
ROTTER-DAM 104.0/60.6°
11
BETH. 104.5
C
MASSENA NET. 104.2 /44.3°
7
INGHAMS 105.0/58.5°
10
TAYLORVILLE 107.9 /54.1°
6
8
DEERFIELD 104.9/56.8°
NYSE & G NET INTERCHANGE
BINGHAMTON 107.7 /60.8°
9
BLACK R. 109.1 /57.4°
5
LIGHTHOUSE H. 110.1
BOON-VILLE 106.0
ROME 105.5
ONEIDA 106.0
TEALL AVE. 108.3
BRISTOL H. 110.0
OSWEGO 112.1/64.9°
4
GERES LOCK 109.4
OLEAN 108.1
R.G.&E.
MORTIMER 108.2 /59.4°
3
GENEVA 109.0
MACHIAS 107.3
FALCONER 110.1
DUNKIRK 112.4 /68.4°
2
LOCKPORT 106.8
GETZVILLE 106.7
GARDENVILLE 106.3
LACK. 106.8
ANGOLA 109.0
NIAGARA FALLS 106.1/60.1°
17
HUNTLEY 107.0/62.0°
1

EXAMPLE II

A practical application of the previous theory was made to a somewhat simplified representation of the 110-kv transmission system of the Niagara Mohawk Power Corporation. Although the resistance-reactance ratio is fairly uniform throughout the system, the interconnected New York State Electric and Gas Corporation system has been replaced by a reactance equivalent so that the effect on losses in the Niagara Mohawk Power Corporation from interchange power with the New York State Electric and Gas Corporation may be estimated. Fig. 4 is a combined impedance diagram and base case load study.

Oswego was chosen as the swing machine, and the open-circuit self- and mutual impedances of the generators with Oswego grounded were measured on the network analyzer, the results being presented in Table VII. Incremental loss coefficients were then calculated, assuming that all generators had Q/P ratios equal to zero except for Huntley, Dunkirk, and Albany. The slopes of their P-Q characteristics were used for these plants, the respective values being −0.265, −0.255, and −0.170.

Table VIII. Incremental Loss Coefficients for nm System

	m = 1	2	3	4	5	6	7	8	9	10	11	12	13	14	15	16	17
n = 1	0.0836	0.0691	0.0186	−0.0749	−0.0590	−0.0565	−0.0575	−0.0505	−0.0353	−0.0493	−0.0489	−0.0488	−0.0488	−0.0475	−0.0491	−0.0492	0.0657
2	0.0802	0.1565	0.0051	−0.0880	−0.0709	−0.0685	−0.0701	−0.0619	−0.0451	−0.0606	−0.0601	−0.0598	−0.0598	−0.0612	−0.0603	−0.0604	0.0631
3	0.0436	0.0387	0.0352	−0.0543	−0.0378	−0.0352	−0.0361	−0.0289	−0.0134	−0.0277	−0.0274	−0.0273	−0.0273	−0.0262	−0.0277	−0.0278	0.0375
4	0.0000	0.0000	0.0000	0.0000	0.0000	0.0000	0.0000	0.0000	0.0000	0.0000	0.0000	0.0000	0.0000	0.0000	0.0000	0.0000	0.0000
5	−0.0103	−0.0115	−0.0118	−0.0308	0.0476	0.0333	0.0302	0.0101	−0.0020	0.0094	0.0107	0.0108	0.0110	0.0122	0.0104	0.0102	−0.0113
6	−0.0146	−0.0161	−0.0158	−0.0380	0.0271	0.0537	0.0500	0.0171	−0.0010	0.0161	0.0175	0.0175	0.0176	0.0187	0.0168	0.0167	−0.0153
7	−0.0147	−0.0166	−0.0148	−0.0374	0.0295	0.0581	0.1396	0.0192	0.0001	0.0178	0.0190	0.0184	0.0190	0.0182	0.0183	0.0179	−0.0144
8	−0.0202	−0.0218	−0.0223	−0.0488	−0.0117	0.0007	−0.0014	0.0371	0.0020	0.0353	0.0381	0.0381	0.0384	0.0412	0.0375	0.0368	−0.0217
9	0.0008	−0.0004	−0.0009	−0.0192	−0.0082	−0.0050	−0.0059	0.0023	0.0510	0.0060	0.0057	0.0052	0.0058	0.0070	0.0055	0.0054	−0.0005
10	−0.0246	−0.0262	−0.0270	−0.0526	−0.0188	−0.0077	−0.0099	0.0250	0.0024	0.0592	0.0529	0.0533	0.0533	0.0566	0.0520	0.0516	−0.0264
11	−0.0371	−0.0385	−0.0397	−0.0647	−0.0314	−0.0202	−0.0226	0.0123	−0.0124	0.0375	0.0881	0.0891	0.0893	0.0955	0.0873	0.0865	−0.0390
12	−0.0395	−0.0408	−0.0425	−0.0674	−0.0340	−0.0233	−0.0261	0.0006	−0.0152	0.0345	0.0856	0.1253	0.0939	0.1014	0.0906	0.0898	−0.0419
13	−0.0399	−0.0413	−0.0428	−0.0678	−0.0341	−0.0234	−0.0261	0.0097	−0.0153	0.0345	0.0862	0.0946	0.1073	0.1132	0.1019	0.1007	−0.0422
14	−0.0395	−0.0408	−0.0425	−0.0673	−0.0339	−0.0233	−0.0262	0.0094	−0.0154	0.0342	0.0851	0.0928	0.1037	0.1164	0.1007	0.0997	−0.0418
15	−0.0385	−0.0398	−0.0410	−0.0650	−0.0328	−0.0224	−0.0248	0.0089	−0.0150	0.0316	0.0815	0.0886	0.0989	0.1060	0.1438	0.1428	−0.0405
16	−0.0367	−0.0379	−0.0391	−0.0618	−0.0312	−0.0213	−0.0236	0.0084	−0.0142	0.0303	0.0774	0.0843	0.0942	0.1009	0.1369	0.1662	−0.0385
17	0.0770	0.0656	0.0125	−0.0740	−0.0580	−0.0555	−0.0565	−0.0496	−0.0344	−0.0484	−0.0480	−0.0479	−0.0479	−0.0468	−0.0483	−0.0484	0.0779

Table IX. New Total Loss Coefficents B_{nm} for nm System*

	m = 1	2	3	4	5	6	7	8	9	10	11	12	13	14	15	16	17
n = 1	0.0301																
2	0.0308	0.0647															
3	0.0129	0.0062	0.0217														
4	−0.0097	−0.0139	0.0033	0.0297													
5	−0.0130	−0.0178	−0.0007	0.0162	0.0419												
6	−0.0145	−0.0194	−0.0021	0.0132	0.0323	0.0425											
7	−0.0145	−0.0197	−0.0016	0.0135	0.0334	0.0448	0.0858										
8	−0.0178	−0.0228	−0.0059	0.0073	0.0124	0.0156	0.0148	0.0279									
9	−0.0134	−0.0182	−0.0012	0.0160	0.0080	0.0066	0.0064	0.0044	0.0374								
10	−0.0211	−0.0261	−0.0093	0.0043	0.0077	0.0102	0.0095	0.0207	0.0181	0.0348							
11	−0.0276	−0.0325	−0.0159	−0.0020	0.0011	0.0037	0.0028	0.0141	0.0105	0.0237	0.0427						
12	−0.0287	−0.0336	−0.0173	−0.0033	−0.0001	0.0022	0.0011	0.0128	0.0091	0.0223	0.0415	0.0601					
13	−0.0288	−0.0338	−0.0173	−0.0034	−0.0001	0.0023	0.0012	0.0130	0.0091	0.0224	0.0419	0.0448	0.0511				
14	−0.0294	−0.0343	−0.0179	−0.0039	−0.0007	0.0016	0.0005	0.0121	0.0084	0.0215	0.0406	0.0431	0.0485	0.0543			
15	−0.0290	−0.0338	−0.0172	−0.0028	−0.0002	0.0020	0.0011	0.0118	0.0085	0.0201	0.0387	0.0410	0.0461	0.0491	0.0691		
16	−0.0280	−0.0328	−0.0162	−0.0012	0.0006	0.0025	0.0017	0.0115	0.0089	0.0194	0.0367	0.0388	0.0437	0.0466	0.0657	0.0819	
17	0.0288	0.0189	0.0095	−0.0073	−0.0128	−0.0146	−0.0147	−0.0175	−0.0012	−0.0199	−0.0260	−0.0273	−0.0274	−0.0273	−0.0270	−0.0254	0.0317

* This matrix is symmetrical.

The A_{nm} coefficients are presented in Table VIII. New total loss coefficients were then calculated from the incremental loss coefficients, the results being presented in Table IX.

Several load studies were made to determine the incremental losses when generation was exchanged between Oswego and another generator. The losses were calculated by each of the following methods:

1. Brownlee formula, equation 8.
2. Incremental loss formula (A_{nm} coefficients).
3. New total loss formula (B_{nm} coefficients).
4. Kirchmayer total loss formula.

In addition, the incremental transmitted power was calculated by equation 7. The results are presented in Figs. 5 through 12 along with the actual losses found by summing the I^2R loss in each line and the actual incremental transmitted powers.

An arbitrarily selected criterion for judging the accuracy of the various formulas was that incremental rates should be accurate to at least 1/10th mil per kilowatt-hour at the 4-mil level. According to equation 26, this means that the allowable discrepancy between actual and calculated incremental losses should not exceed 2.5 megawatts (mw) for a 100-mw swing of generation. This criterion is satisfied for all swings except for Dunkirk and Binghamton. For the Dunkirk swing and the new total loss formula is outside the acceptable range, but the Brownlee and the incremental formula are just inside. Apparently the interaction between Dunkirk and Huntley is causing the Brownlee formula to give somewhat erroneous results. For the Binghamton swing the Brownlee and the incremental formula are just on the borderline. The new total loss formula is outside the acceptable range. The failure of the Brownlee formula in this case is ascribed to the unrealistic assumption of pure reactance tie lines. Also of interest is the fact that the voltage in the neighborhood of Deerfield had to be raised with increasing Deerfield generation to prevent the generators there from operating at a leading power factor. The accuracy of the Brownlee formulas is still good in this case, but a definite error in the incremental transmission formula is observed.

A final test of the formulas was made by scaling all loads to 70 per cent of their value in Fig. 4. Two load studies were made in which some of the Oswego generation was swung to Huntley. The

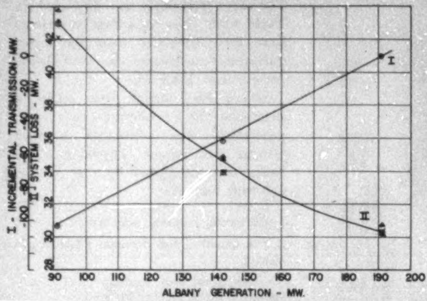

Fig. 5. Comparison of actual and calculated losses for exchange of generation between Albany and Oswego

— Network analyzer values
⊙ Brownlee angle formulas
× Incremental loss coefficients
● New total loss coefficients
△ Kirchmayer coefficients

These symbols also apply to Figs. 6 through 12

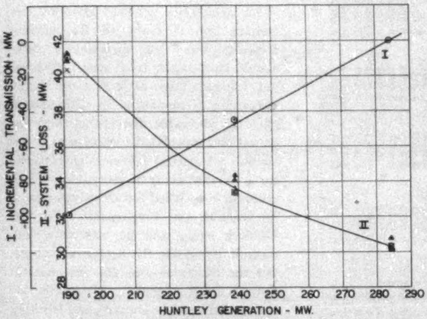

Fig. 6. Comparison of actual and calculated losses for exchange of generation between Huntley and Oswego

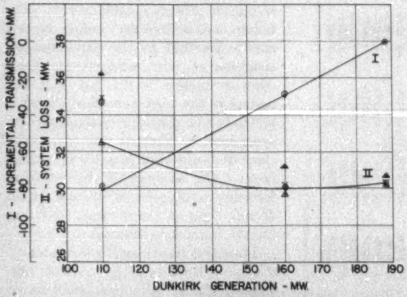

Fig. 7. Comparison of actual and calculated losses for exchange of generation between Dunkirk and Oswego

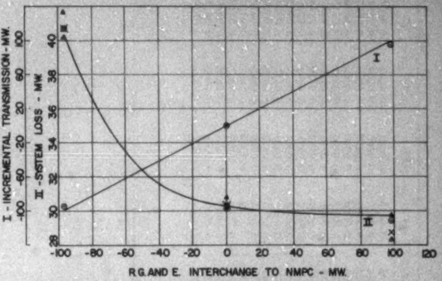

Fig. 8. Comparison of actual and calculated losses for exchange of generation between Rochester Gas and Electric Corporation and Oswego

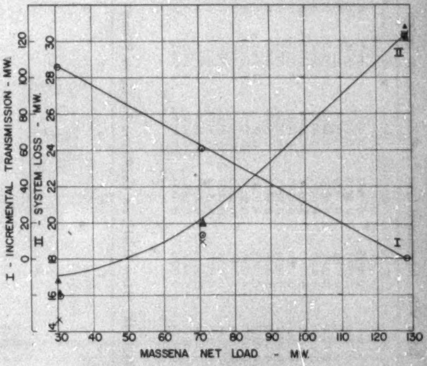

Fig. 9. Comparison of actual and calculated losses for a varying Massena net load supplied from Oswego

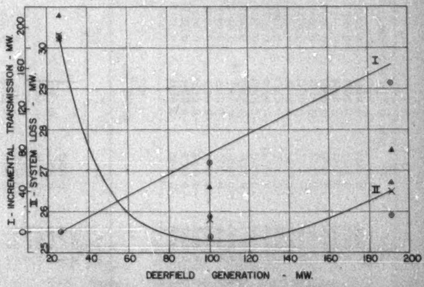

Fig. 10. Comparison of actual and calculated losses for exchange of generation between Deerfield and Oswego

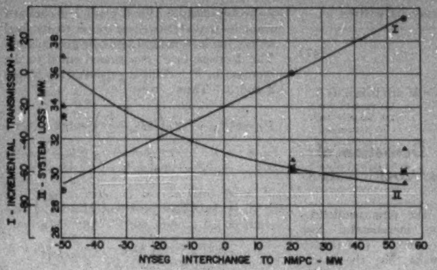

Fig. 11. Comparison of actual and calculated losses for exchange of generation between New York State Electric and Gas Corporation and Oswego

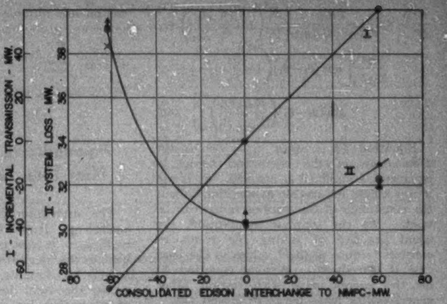

Fig. 12. Comparison of actual and calculated losses for an exchange of generation between Consolidated Edison and Oswego

results are shown in Table X. It is seen that the Brownlee formulas and the incremental formulas are in good agreement with the actual values. The Kirchmayer formula gives a somewhat closer agreement with the actual total loss than does the new total loss formula, although both are satisfactory.

In all test cases, then, the Brownlee formulas and the incremental loss formula displayed acceptable accuracy for economic scheduling purposes. As must be expected from the approximations in its derivation, the new total loss formula is less accurate than the incremental loss formula. The Kirchmayer total loss formula provided an excellent correlation with the actual losses.

Conclusions

On the basis of the preceding theory and numerical cases, it is concluded that the Brownlee theory and the new loss formulas are applicable to practical electric utility systems at least in those cases where all important transmission is at the same voltage level. The Brownlee formulas appear to be about as accurate in most cases as the Kirchmayer B_{nm} coefficients. It has also been demonstrated that incremental and total loss coefficients can be obtained with considerably less computation than has hitherto been possible, and that these coefficients display satisfactory accuracy except where a wide variation in reactance-resistance ratios is encountered. It is hoped that others interested in the problems of economic scheduling will apply the theory developed in this paper and so determine for themselves its advantages and disadvantages.

Appendix I. Derivation of Incremental Loss Coefficients

The derivation of incremental loss coefficients, already outlined in equations 19 through 22, is now presented. The correctness of the Brownlee formulas, equations 3, 4, and 5, is assumed. Additional assumptions are listed where needed.

Continuing the use of the system in Fig. 1, the law of cosines and equation 9 give

$$|E_1-E_2|^2=V_1^2+V_2^2-2V_1V_2\cos(\theta_1-\theta_2)$$
$$=(Z_{11}I_1+Z_{12}I_2)(Z_{11}^*I_1^*+Z_{12}^*I_2^*) \quad (33)$$

Differentiating with respect to θ_1 and noting that only I_1 is variable

$$2V_1V_2\sin(\theta_1-\theta_2)=Z_{11}\frac{dI_1}{d\theta_1}(Z_{11}^*I_1^*+$$
$$Z_{12}^*I_2^*)+Z_{11}^*\frac{dI_1^*}{d\theta_1}(Z_{11}I_1+Z_{12}I_2) \quad (34)$$

Ignoring the correction term in equation 16 gives

$$\frac{dP_L}{d\theta_1}=\frac{2V_1V_2}{Z_{11}Z_{11}^*}R_{11}\sin(\theta_1-\theta_2)$$
$$=2R_{11}Re\left[\frac{dI_1^*}{d\theta_1}\left(I_1+\frac{Z_{12}}{Z_{11}}I_2\right)\right] \quad (35)$$

According to equation 11

$$\frac{dI_1^*}{d\theta_1}=\frac{1}{Z_{11}^*}\frac{dE_1^*}{d\theta_1}=\frac{-jE_1^*}{Z_{11}^*} \quad (36)$$

Then, letting α_{nm} be the angle of Z_{nm}, equation 35 becomes

$$\frac{dP_L}{d\theta_1}=2R_{11}Re\left[\frac{-j}{Z_{11}^*}\left(E_1^*I_1+\frac{Z_{12}}{Z_{11}}E_1^*I_2\right)\right]$$
$$=\frac{2R_{11}}{|Z_{11}|}Re\left(V_1|I_1|\underline{/\phi_1-\theta_1+\alpha_{11}-90^\circ}+\right.$$
$$\left.\left|\frac{Z_{12}}{Z_{11}}\right|\frac{V_1}{V_2}V_2|I_2|\underline{/\phi_2-\theta_2+\theta_2-\theta_1+\alpha_{12}-90^\circ}\right)$$
$$=\frac{2R_{11}}{|Z_{11}|}\left(V_1|I_1|\sin(\phi_1-\theta_1+\alpha_{11})+\right.$$
$$\left.\left|\frac{Z_{12}}{Z_{11}}\right|\frac{V_1}{V_2}V_2|I_2|\sin(\phi_2-\theta_2+\theta_2-\theta_1+\alpha_{12})\right)$$
$$=\frac{2R_{11}}{|Z_{11}|}[V_1|I_1|[\sin(\phi_1-\theta_1)\cos\alpha_{11}+$$
$$\cos(\phi_1-\theta_1)\sin\alpha_{11}]+\left|\frac{Z_{12}}{Z_{11}}\right|\frac{V_1}{V_2}V_2|I_2|\times$$
$$[\sin(\phi_2-\theta_2)\cos(\theta_2-\theta_1)\cos\alpha_{12}-$$
$$\sin(\phi_2-\theta_2)\sin(\theta_2-\theta_1)\sin\alpha_{12}+$$
$$\cos(\phi_2-\theta_2)\sin(\theta_2-\theta_1)\cos\alpha_{12}+$$
$$\cos(\phi_2-\theta_2)\cos(\theta_2-\theta_1)\sin\alpha_{12}]] \quad (37)$$

Noting that $R_{nm}=|Z_{nm}|\cos\alpha_{nm}$, $X_{nm}=|Z_{nm}|\sin\alpha_{nm}$, $P_n=V_n|I_n|\cos(\phi_n-\theta_n)$, and $Q_n=-V_n|I_n|\sin(\phi_n-\theta_n)$, equation 37 finally becomes

$$\frac{dP_L}{d\theta_1}=\frac{2R_{11}}{|Z_{11}|^2}\left[P_1X_{11}-Q_1R_{11}+\frac{V_1}{V_2}P_2\times\right.$$
$$[\cos(\theta_2-\theta_1)X_{12}+\sin(\theta_2-\theta_1)R_{12}]+$$
$$\left.\frac{V_1}{V_2}Q_2[\sin(\theta_2-\theta_1)X_{12}-\cos(\theta_2-\theta_1)R_{12}]\right] \quad (38)$$

Now, ignoring the correction terms in equation 17

$$\frac{dP_{1-2}}{d\theta_1}=\frac{V_1V_2}{|Z_{11}|^2}X_{11}\cos(\theta_1-\theta_2) \quad (39)$$

so that dividing equation 38 by equation 39 gives

Table X. Results for 70-Per-Cent Load Level in Mw

Incremental Losses			Incremental Transmitted Power		Total Losses			
Brownlee	Incremental	Actual	Brownlee	Actual	Case	New Total	Kirchmayer Total	Actual
−2.41	−2.90	−2.6	78.1	82	1	27.2	26.0	26.7
					2	23.9	25.2	24.1

$$\frac{dP_L}{dP_{1-2}} = \frac{2R_{11}}{V_2 \cos(\theta_1-\theta_2)}\left\{\frac{P_1}{V_1}\left(1-\frac{Q_1}{P_1}\frac{R_{11}}{X_{11}}\right)+ \frac{X_{13}P_3}{X_{11}V_3}\left[\cos(\theta_3-\theta_1)\left(1-\frac{Q_3}{P_3}\frac{R_{13}}{X_{13}}\right)+ \sin(\theta_3-\theta_1)\left(\frac{R_{13}}{X_{13}}+\frac{Q_3}{P_3}\right)\right]\right\} \quad (40)$$

Equation 40 is exact in so far as the elimination of the correction terms in equations 16 and 17 is justified. It is not useful unless reasonable assumptions about the constancy of the various terms can be made. As the simplest assumption, the usual practice of taking the terms as constants equal to their values in the base case is introduced. Writing equation 40 for the general case with several other generators or loads besides the first two

$$\frac{dP_L}{dP_{1-2}} = \sum_m D_m P_m \quad (41)$$

where

$$D_m = 2K_{11}X_{1m} \times \left(\frac{\cos(\theta_m-\theta_1)(1-s_mK_{1m})+ \sin(\theta_m-\theta_1)(K_{1m}+s_m)}{V_mV_2\cos(\theta_1-\theta_2)}\right) \quad (42)$$

with

$s_m = Q_m/P_m$ and $K_{nm} = R_{nm}/X_{nm}$

Equation 41 is not useful as it stands because the summation is over all loads as well as all generators, the coefficient of generator 2 being zero. The loads may be eliminated and the power output of generator 2 introduced if the usual assumption of proportional, constant power-factor loads is made. Then, the summation over all loads may be replaced by a single term K_RP_R whose magnitude is proportional to the total load P_R. The constant of proportionality, K_R is not known, since no D_m coefficients have been calculated for the loads. However, it may be evaluated indirectly from the base case. First make the substitution

$$P_R = -\sum_{m=1}^{N} P_m \quad (43)$$

where N generators are assumed. Equation 43 assumes that the total generation equals the total load with the system losses being negligible. Then, equation 41 becomes

$$\frac{dP_L}{dP_{1-2}} = \sum_{m=1}^{N}(D_m-K_R)P_m \quad (44)$$

K_R is chosen so that dP_L/dP_{1-2} has the correct base case value, as determined from equation 5, which is rewritten as

$$\frac{dP_L}{dP_{1-2}} = 2K_{11}\tan(\theta_1-\theta_2) \quad (45)$$

Equation 44 may be rewritten as

$$\frac{dP_L}{dP_{1-2}} = \sum_{m=1}^{N} A_mP_m \quad (46)$$

with the summation extending only over the generators. A similar equation can be derived for each pair of generators, but only the N-1 equations between one generator and all others are necessary. Letting M be the chosen plant, the incremental loss formula may be written as

$$\frac{dP_L}{dP_{n-M}} = \sum_{m=1}^{N} A_{nm}P_m \quad (47)$$

All coefficients with $n=M$ are taken as 0.

Appendix II. Derivation of New Total Loss Coefficients

The derivation of the new total loss coefficients from the incremental loss coefficients is now presented. The theory behind the derivation is that the incremental loss formula may be used to calculate the total loss for some dispatch of generation by determining the incremental loss obtained every time a plant is changed from its base case value to its value in the dispatch for which the total loss is desired. Because the incremental loss formula concerns changes of generation at constant system loads, the total loss for a dispatch at a system load different from that of the base case cannot directly be calculated by the foregoing procedure. Therefore, an additional assumption is introduced, which is that, if all generations in the base case are multiplied by the factor k with a corresponding change in each load, the total loss is multiplied by k^2, corresponding to the assumption of fixed bus voltages, making currents and powers approximately proportional. Following this assumption, the base case generation is scaled by the ratio of total generation in the dispatch whose loss is desired to the total generation in the base case. The incremental loss formulas are then applied to go from the scaled base case to the given dispatch. Since the incremental loss formulas were derived assuming a fixed system load, a slight additional error is introduced by neglecting the effect of incremental losses on the output of the swing machine when the various increments are found.

The derivation is illustrated for a 4-plant system; the extension to a larger number will be evident. The incremental loss formula, with plant 4 being the swing machine, is

$$\frac{dP_L}{dP_{1-4}} = \sum_{m=1}^{4} A_{1m}P_m$$

$$\frac{dP_L}{dP_{2-4}} = \sum_{m=1}^{4} A_{2m}P_m$$

$$\frac{dP_L}{dP_{3-4}} = \sum_{m=1}^{4} A_{3m}P_m \quad (48)$$

Base case powers and power loss will be indicated by the subscript *o*. Define the ratio k by

$$k = \sum_{m=1}^{4} P_m \Big/ \sum_{m=1}^{4} P_{mo} \quad (49)$$

and define the difference in power outputs between the case for which the total loss is desired and the scaled base case as p_m

$$p_m = P_m - kP_{mo} \quad (50)$$

Then, the desired power loss is found by applying the incremental loss formulas for finite increments. First, plant 1 is changed from its scaled base case value to its final value, the incremental loss being calculated. The decrease in P_4 is assumed equal to the increase in P_1. This is repeated for plants 2 and 3. Thus

$$\begin{aligned} P_L = {} & k^2P_{Lo} + \left[A_{11}\left(kP_{1o}+\frac{p_1}{2}\right)+A_{12}kP_{2o}+ A_{13}kP_{3o}+A_{14}\left(kP_{4o}-\frac{p_1}{2}\right)\right]p_1 + \\ & \left[A_{21}(kP_{1o}+p_1)+A_{22}\left(kP_{2o}+\frac{p_2}{2}\right)+ A_{23}kP_{3o}+A_{24}\left(kP_{4o}-p_1-\frac{p_2}{2}\right)\right]p_2 + \\ & \left[A_{31}(kP_{1o}+p_1)+A_{32}(kP_{2o}+p_2)+ A_{33}\left(kP_{3o}+\frac{p_3}{2}\right)+A_{34}\left(kP_{4o}-p_1-p_2-\frac{p_3}{2}\right)\right]p_3 = \\ & k^2P_{Lo}+kp_1\sum_{m=1}^{4}A_{1m}P_{mo}+ kp_2\sum_{m=1}^{4}A_{2m}P_{mo}+kp_3\sum_{m=1}^{4}A_{3m}P_{mo}+ \\ & (1/2)(A_{11}-A_{14})p_1^2+(1/2)(A_{22}- A_{24})p_2^2+(1/2)(A_{33}-A_{34})p_3^2+ \\ & (A_{21}-A_{24})p_2p_1+(A_{31}-A_{34})p_3p_1+ (A_{32}-A_{34})p_3p_2 \end{aligned} \quad (51)$$

If in equation 51, equation 50 is substituted for p_m and equation 49 for k and the expression simplified

$$\begin{aligned} P_L = {} & C\left(\sum_{m=1}^{4}P_m\right)^2+P_1\left(\sum_{m=1}^{4}A_{1m}P_{mo}- (A_{11}-A_{14})P_{1o}-(A_{21}-A_{24})P_{2o}- (A_{31}-A_{34})P_{3o}\right)\sum_{m=1}^{4}P_m\Big/\sum_{m=1}^{4}P_{mo}+ \\ & P_2\left(\sum_{m=1}^{4}A_{2m}P_{mo}-(A_{21}-A_{24})P_{1o}- (A_{22}-A_{24})P_{2o}-(A_{32}-A_{34})P_{3o}\right)\times \sum_{m=1}^{4}P_m\Big/\sum_{m=1}^{4}P_{mo}+ \\ & P_3\left(\sum_{m=1}^{4}A_{3m}P_{mo}- (A_{31}-A_{34})P_{1o}-(A_{32}-A_{34})P_{2o}- (A_{33}-A_{34})P_{3o}\right)\times\sum_{m=1}^{4}P_m\Big/\sum_{m=1}^{4}P_{mo}+ \\ & (1/2)(A_{11}-A_{14})P_1^2+(1/2)(A_{22}- A_{24})P_2^2+(1/2)(A_{33}-A_{34})P_3^2+ (A_{21}-A_{24})P_2P_1+(A_{31}-A_{34})\times P_3P_1+(A_{32}-A_{34})P_3P_2 \end{aligned} \quad (52)$$

where C is a constant involving the base case power outputs and power loss. It will be determined indirectly. Now define the quantities

$$a_n = \frac{\sum_{m=1}^{n}A_{n4}P_{mo}+\sum_{m=n+1}^{4}(A_{nm}-A_{mn}+A_{m4})P_{mo}}{2\sum_{m=1}^{4}P_{mo}} \quad (53)$$

The numerator in equation 53 is the same as the quantities in parentheses in equation 52. Then, equation 52 may be written as

$$P_L=\sum_{n=1}^{4}\sum_{m=1}^{4}P_nB_{nm}P_m \qquad (54)$$

where for $n \geq m$

$$B_{nm}=B_{mn}=C+a_n+a_m+(1/2)(A_{nm}-A_{n4}) \qquad (55)$$

It is seen that C is identical with B_{44}. B_{44} is found by making equation 54 fit the base case loss. Thus, choose B_{44} so that

$$P_{Lo}=\sum_{n=1}^{4}\sum_{m=1}^{4}P_{no}(B_{nm}-B_{44})P_{mo}+ B_{44}\sum_{n=1}^{4}\sum_{m=1}^{4}P_{no}P_{mo} \qquad (56)$$

Generalized to the case of N plants, the foregoing derivation is outlined in equations 29 through 32.

References

1. Co-Ordination of Incremental Fuel Costs and Incremental Transmission Losses by Functions of Voltage Phase Angles, W. R. Brownlee. *AIEE Transactions*, vol. 73, pt. III, June 1954, pp. 529–41.

2. Electrical Transmission and Distribution Reference Book (book). *Westinghouse Electric Corporation*, Pittsburgh, Pa., 4th ed., 1950, pp. 314–16.

3. Analysis of Total and Incremental Losses in Transmission Systems, L. K. Kirchmayer, G. W. Stagg. *AIEE Transactions*, vol. 70, pt. II, 1951, pp. 1197–1204.

4. Loss Formulas Made Easy, A. F. Glimm, R. Habermann, L. K. Kirchmayer, G. W. Stagg. *AIEE Transactions*, vol. 72, pt. III, Aug. 1953, pp. 730–35.

◆

Table XI. Generation and Load Data, Mw

	Case 1	2*	3	4	5
Twin branch *G1*	43.8	93.0	144.0	195.0	244.0
Fort Wayne, *G2*	86.0	46.0	13.2	−20.9	−54.2
Portsmouth *G3*	73.5	51.5	34.6	18.2	4.9
Subtotal	203.3	190.5	191.8	192.3	194.7
Less actual losses	8.0	3.7	2.7	4.7	9.7
Net indicated load	195.3	186.8	189.1	187.6	185.0
Set load	186.4	186.4	186.4	186.4	186.7
Closing error	8.9	0.4	2.7	1.2	−0.4

* Base case.

Table XII. Arithmetical Calculation of Incremental Losses

Line Section	System Loss, Portsmouth to Fort Wayne, Mw: Base Case, No. 2	With 0.1 Mw to Ft. Wayne	With 0.1 Mw from Ft. Wayne
Portsmouth-Muncie	3.170222	3.182293	3.158176
Muncie-Fort Wayne	0.051899	0.052294	0.051512
Muncie-Marion	0.069542	0.070021	0.069066
Marion-Fort Wayne	0.050535	0.050383	0.050689
	3.342198	3.354991	3.329443
Loss differences		0.012793	−0.012755
Incremental loss (average)		0.12774 per unit	

Table XIII. Comparative Calculations of Incremental Loss, Portsmouth to Fort Wayne (Plant 3 to Plant 2)

	Per Cent
Actual incremental loss (from Table XI)	0.1277 or 12.77
Direct phase-angle calculation, equation 13 (ref. 1 of the paper)	
$\dfrac{4\times3.65\times0.12367}{(3.65+0.124)_2}=$	0.1268 or 12.68
New (Cahn) total loss constants	
$M_3=2(0.515\times0.1673+0.93(-0.0173)+0.46(-0.0001))=$	0.14005
$M_2=2(0.46\times0.0118+0.93(-0.0052)+0.515(-0.0001))=$	0.00108
$M_{32}=(0.14005-0.00108)+(1-0.00108)=$	0.1391 or 13.91

Discussion

W. R. Brownlee (Southern Services Inc., Birmingham, Ala.): In his justification of the phase-angle method, the author has derived certain correction terms appearing in equations 16 and 17. It appears that these are based on constant current from the third generator. In an actual power system, the current from this generator would vary, especially in its phase position, since the phase angle of the bus voltage at generator no. 3 would move forward as required to keep its power output constant when generation is being increased at plant 1 and reduced at plant 2. This influence may be quite difficult to introduce in equations, but I am confident that full recognition of this fundamental fact of power system performance would reduce the magnitude of the correction terms to a negligible value.

In his conclusion, the author avoids a positive assertion that phase-angle equations and the new loss constants based thereon are applicable to systems with superposed high-voltage transmission. It is believed that this lack of complete confidence may arise from Fig. 11 where power is exchanged between Oswego and a foreign system. The foreign ties have been represented, as shown in Fig. 4, by pure reactance. My previous paper (ref. 1 of the paper) had only a brief mention of the use of a pure reactance line for a foreign path. This concept has been found quite useful to determine the incremental losses between two plants on a particular system when some 25 per cent of the interchange between these plants may pass through a foreign system. However, when this expedient is utilized, as the author has done in Fig. 4, the system then becomes of the line type with a high-reactance path between plant 9 and the intermediate generation and the usual reactance-resistance ratio from this equivalent intermediate plant to plant no. 4. This system should be so treated by assigning all of resistance indicated between plants 4 and 9 to a section between plant 4 and the equivalent intermediate plant, assigning a reactance to this section based on the ratio shown between plants 3 and 4, and assigning the remaining reactance from the intermediate plant to plant 9. Such a calculation results in an indicated loss between the base case and a flow of 49.5 mw to Binghamton of 6.45 mw, or a total loss of some 36.6 mw, which is only slightly above the actual loss curve of Fig. 11. This illustrates the flexibility of the direct phase-angle method for dealing with high-reactance paths.

The formulas in this paper make use of incremental loss referred to the average of sending end and receiving end power, whereas previous analyses have referred this loss to the designated terminal. With the proper designations followed, the author's equation 26 is equivalent to equation 11 of my earlier paper (ref. 1 of the paper). However, the approximations shown as equation 27 may not be justifiable for substantial angles. For example, with an incremental loss from one plant to another of 30 per cent, the economic fuel ratio by equation 26 would be 1.429, whereas, by equation 27, it could be either 1.353 or 1.548. To avoid confusion, it is suggested that a bar be used over the letters representing average sending and receiving power or incremental losses referred to such power as $\overline{dP}_{12}$ or $\overline{M}_{12}$.

An interesting comparison of the use of constants calculated has been provided by the new method and those advocated by Glimn, Habermann, Kirchmayer, and Stagg (ref. 4 of the paper). The author states that the total losses are derived more accurately by the new method (based on phase angles) when compared with earlier methods which made no use of phase-angle incrementals. The information in Fig. 3 provides incom-

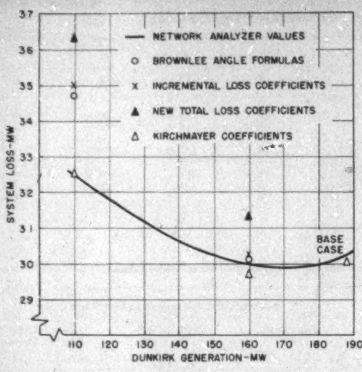

Fig. 13. Comparison of actual and calculated losses for exchange of generation between Dunkirk and Oswego

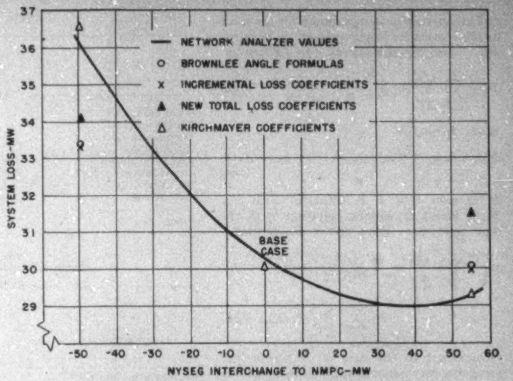

Fig. 14. Comparison of actual and calculated losses for exchange of generation between New York State Electric and Gas and Oswego

plete support of this assertion. Two of the points shown are definitely better by the new method, but the point on the left-hand side of the figure appears to show better correlation for the earlier constants. However, this point is in serious error in the paper, as is shown in Table XI. The discrepancy indicated for case 1 amounts to over 4 percent of the total system load and is greater than the total I^2R losses. Accordingly, it would not be expected that a straightforward formula would provide an adequate indication of the measured losses, and the fact that the earlier formula (ref. 4 of the paper) appeared to do so is not complimentary to that method. With this incorrect case deleted, the new formulas show better correlation than the earlier formula.

Another check on the new total loss constants may be made by comparing the incremental losses between pairs of plants of the Portsmouth-Fort Wayne-Twin Branch system. The actual incremental loss from Portsmouth to Fort Wayne was calculated by superposing a flow of 0.1 mw at Portsmouth toward Fort Wayne, with the proper change in kilovar flow, and calculating the loss in each line section before and after. A similar analysis gives the change in loss for a flow of 0.1 mw to Portsmouth from Fort Wayne, the average value being a genuine incremental. Table XII provides details of these calculations. Table XIII shows the calculation of the incremental losses by phase angles and by the new total loss constants. The new constants yield a satisfactory result, but the value calculated directly by phase angles is closer to the actual incremental loss.

The new method presented has several important advantanges over those published previously. The derivation of the constants is much simpler, and some of the more fantastic assumptions are avoided. There is still a suspicion of w' although the treacherous Q/P ratio has been properly relegated to the background. Finally, the new method is evidence of the growing conviction that adequate co-ordination of fuel and transmission requires loss constants with accuracy focused on incremental losses, rather than total losses.

A. F. Glimn and L. K. Kirchmayer (General Electric Company, Schenectady, N. Y.): Mr. Cahn is to be commended for his thorough analysis of and his contributions to methods of calculating transmission losses. In general, good loss formula results have been obtained by all the methods treated. It is particularly gratifying that the results of the so-called Kirchmayer formula give the best correlation between actual and calculated losses in the study of the Niagara Mohawk system.

The results obtained by the simplified Cahn formulas and the Brownlee formula appear to be in error principally in the swings between Oswego and Dunkirk and Oswego and New York State Electric and Gas. In the Dunkirk swing of approximately 80 mw, Fig. 13, the error in the change in loss by the Kirchmayer formula was negligible. The error was 2.2 mw by the Brownlee formula, 2.5 mw for the Cahn incremental loss formula, and 3.8 mw for the Cahn total loss formula. In Fig. 14, for the swing between Oswego and New York State Electric and Gas, it is seen that the error in the change in loss for the 100-mw swing was 3.5 mw for the Brownlee formula, 3.5 mw for the Cahn incremental loss formula, 4.2 for the Cahn total loss formula, and 0.5 mw for the Kirchmayer formula.

These errors result chiefly from the fact that neither the Brownlee formula nor the simplified Cahn formulas correctly consider the effects of intermediate load and generation when the circuits have different reactance-resistance ratios. Inspection of

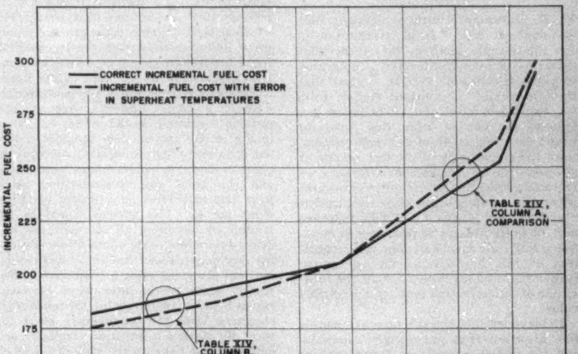

Fig. 15. Incremental fuel cost curves for station P7

Table VII shows that variation in reactance-resistance ratio need not be excessive to produce such errors.

The nature of these discrepancies has been previously pointed out in our discussion last year of Mr. Brownlee's paper (see ref. 1 of the paper). Mr. Cahn has contributed to a proper understanding of the Brownlee approach through means of equations 16 and 17, which also indicate the nature of the errors introduced by the Brownlee method. These equations, although derived for slightly different assumptions than used by Glimn and Kirchmayer, can be employed to calculate the error curves involved in the application of the Brownlee formula as presented in our discussion of the Brownlee paper. The Kirchmayer formula does not rely on any assumptions with regard to the reactance-resistance ratios of the lines in the system. The errors illustrated by Mr. Cahn's study are usually significant in systems in which the transmission lines are at different voltage levels and in which transformers appear.

Has the author had an opportunity to use his more exact approach in his study of the Niagara Mohawk system?

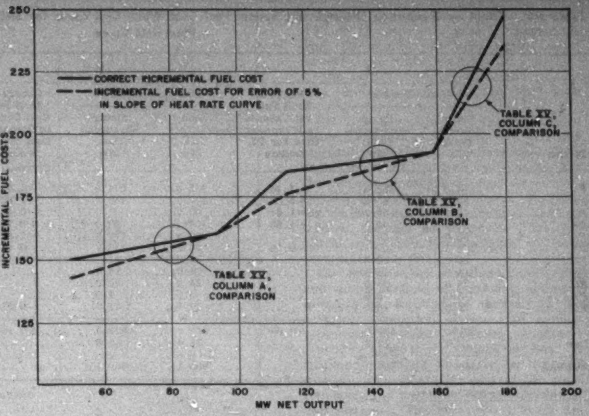

Fig. 16. Incremental fuel cost curves for station P2

R. H. Travers (Ohio Edison Company, Akron, Ohio) and **R. W. Long** (Westinghouse Electric Corporation, E. Pittsburgh, Pa.): Mr. Cahn has done an admirable job of extending Mr. Brownlee's work in the development of loss formulas to the form in which this theory can be used in system operation and in economic dispatching. The methods of approach used by both Mr. Brownlee and Mr. Cahn are unique and depend to some extend on intuition. Therefore, for a complex system, it is not feasible to present a rigorous mathematical derivation for the constants developed.

Approximations of derivation are introduced when some of the mathematical terms of an expression are dropped with the reasoning that their numerical significance is negligible. This is a device frequently utilized in many branches of applied engineering and, when it is used, it necessitates setting up some criteria of accuracy for the final results.

In this paper the "criterion for judging the accuracy of the various formulas was that incremental rates should be accurate to at least $^1/_{10}$th mil per kilowatt-hour at the 4-mil level." In terms of the resulting power dispatched to a particular station this statement is somewhat ambiguous. If the slope of the increment curve is steep, a shift of $^1/_{10}$th mil in incremental cost might mean a shift of 1 or 2 mw in power output. However, at lower loadings on that same station, a similar shift in incremental cost could change output by as much as 30 or 40 mw.

This suggests that possibly the point in the development of economic dispatching has been reached where the loss formulas are relatively more accurate than the basic fuel cost data. In the newer plants equipped with modern instrumentation in the steam end, it is possible to get well-defined input-output data from which incremental heat rate curves of good accuracy can be determined. This is not necessarily true of the older plants.

In the co-ordination equations for economic dispatch recognizing incremental transmission loss, the predominant factor is the station incremental fuel cost. To illustrate this, we have made a set of 11 economic dispatch solutions using erroneous data of various types, and calculated the resulting change in total fuel input cost to the system caused by these errors.

Fig. 15 shows the correct incremental cost curve for one station as a solid curve. The dash curve is another increment cost curve determined from data which involved errors in reading superheat temperatures. Two system comparisons are made with these data. For a 1,052-mw system generation, this station should carry 203 mw. The erroneous curve, about 4 per cent in error at the 200-mw region, yields a dispatch which allocated only 197 mw to this station, a shift of 6 mw. These 6 mw were picked up over several other stations on the system, as shown in Table XIV, column *A*. All of these incremental shifts in generation were then evaluated at bus-bar costs, and the increased fuel costs at the other stations in picking up this 6 mw was $1.20 more than the saving in fuel cost resulting from unloading station *P7* by 6 mw. This value of $1.20 may seem small but, as an error of this magnitude persists, it integrates with time and can easly reach several thousand dollars a year.

Another solution at the 596-mw system generation level where this station is loaded at 82-mw showed a shift of 12 mw, this time an increase in *P7* load caused by apparent lower bus-bar cost of about 4 per cent. Here again, evaluation of the shifts at all plans showed a net increased cost to the system of $1.31, as shown in Table XIV, column *B*. In this example no correction has been made for the increased generation which would be necessary to carry the same customer load since losses have increased.

Table XIV. Effect on Generation Dispatch and System Fuel Cost When Cost Curve for Station P7 Contains Error in Superheat Temperature

	A			B		
	Economic Dispatch Solutions		Change in Total Fuel Cost Caused by Using Erroneous Data for P7, Dollars	Economic Dispatch Solutions		Change in Total Fuel Cost Caused by Using Erroneous Data for P7, Dollars
Station	Using Correct Data, Mw	Using Erroneous Data, Mw		Using Correct Data, Mw	Using Erroneous Data, Mw	
P1	240.0	240.0		163.3	154.3	−16.16
P2	29.3	29.8	+ 1.27	17.9	17.9	
P3	169.0	169.6	+ 1.38	98.1	96.4	− 2.94
P4	0	0		0	0	
P5	124.0	124.7	+ 1.69	95.3	94.1	− 2.13
P6	129.0	131.3	+ 5.58	74.9	74.6	− 0.53
P7	203.0	197.0	−14.43*	82.4	94.6	+23.07*
P8	26.5	27.3	+ 2.41	14.8	14.8	
P9	4.9	4.9		4.6	4.6	
P10	51.5	52.4	+ 2.76	24.8	24.8	
P11	75.0	75.2	+ 0.54	20.0	20.0	
	1052.2†	1052.2†	+ 1.20	596.1†	596.1	+ 1.31

* Evaluated at correct fuel cost.
† Dispatch data not corrected for changed system losses.

Table XV. Effect on Generation Dispatch and System Fuel Cost When Cost Curve for Station P2 Contains a 5-Per-Cent Error in Slope of Heat Rate Curve

	A			B			C		
	Economic Dispatch		Change in Total Fuel Cost Caused by Erroneous Data for P2, Dollars	Economic Dispatch		Change in Total Fuel Cost Caused by Erroneous Data for P2, Dollars	Economic Dispatch		Change in Total Fuel Cost Caused by Erroneous Data for P2, Dollars
Station	Using Correct Data, Mw	Using Erroneous Data, Mw		Using Correct Data, Mw	Using Erroneous Data, Mw		Using Correct Data, Mw	Using Erroneous Data, Mw	
P1	134.3	133.4	−1.44	215.3	214.5	−1.59	240.0	240.0	
P2	82.5	85.8	+5.23*	142.1	146.2	+7.80*	169.0	171.2	+4.88*
P3	70.7	69.7	−1.61	92.2	92.0	−0.40	136.8	136.6	−0.45
P4	61.6	60.4	−1.93	98.4	98.0	−0.79	126.2	126.1	−0.23
P5	60.0	60.0		127.8	126.4	−2.83	182.9	182.3	−1.39
P6	109.3	109.2	−0.16	138.9	138.7	−0.41	146.0	146.0	
P7	20.0	20.0		52.0	51.4	−1.34	72.7	72.4	−0.78
P8	18.0	18.0		18.0	18.0		26.5	26.3	−0.48
P9	25.0	25.0		25.0	25.0		52.1	51.7	−1.10
P10	5.0	5.0		5.0	5.0		5.9	5.8	−0.22
P11	15.0	15.0		17.8	17.7	−0.28	33.0	33.0	
	601.4	601.5	+0.09	932.5	932.9	+0.16	1191.1	1191.4	+0.23
Loss	12.2	12.3		32.4	32.8		44.2	44.5	
Net load	589.2	589.2		900.1	900.1		1146.9	1146.9	

* Evaluated at correct fuel cost.

Table XVI. Effect on Generation Dispatch and System Fuel Cost When Cost Curve for Station P2 Contains a 5-Per-Cent Error in Purchase Price of Coal

	A			B			C		
	Economic Dispatch		Change in Total Fuel Cost Caused by Erroneous Data for P2, Dollars	Economic Dispatch		Change in Total Fuel Cost Caused by Erroneous Data for P2, Dollars	Economic Dispatch		Change in Total Fuel Cost Caused by Erroneous Data for P2, Dollars
Station	Using Correct Data, Mw	Using Erroneous Data, Mw		Using Correct Data, Mw	Using Erroneous Data, Mw		Using Correct Data, Mw	Using Erroneous Data, Mw	
P1	134.3	130.3	− 6.42	215.3	212.0	− 6.52	240.0	240.0	
P2	82.5	96.0	+21.69*	142.1	159.2	+32.78*	169.0	172.6	+8.04*
P3	70.7	67.0	− 5.94	92.2	91.7	− 0.99	136.8	136.5	−0.68
P4	61.6	56.8	− 7.71	98.4	97.1	− 2.57	126.2	126.0	−0.45
P5	60.0	60.0		127.8	121.8	−12.13	182.9	182.0	−2.08
P6	109.3	108.7	− 0.97	138.9	137.8	− 2.23	146.0	146.0	
P7	20.0	20.0		52.0	49.4	− 5.80	72.7	72.1	−1.56
P8	18.0	18.0		18.0	18.0		26.5	26.2	−0.72
P9	25.0	25.0		25.0	25.0		52.1	51.5	−1.65
P10	5.0	5.0		5.0	5.0		5.9	5.8	−0.32
P11	15.0	15.0		17.8	17.2	− 1.69	33.0	32.9	−0.32
	601.4	601.8	+ 0.65	932.5	934.2	+ 0.85	1191.1	1191.6	+0.26
Loss	12.2	12.6		32.4	34.1		44.2	44.7	
Net load	589.2	589.2		900.1	900.1		1146.9	1146.9	

* Evaluated at correct fuel cost.

Table XVII. Effect on Generation Dispatch and System Fuel Cost When All B Constants Pertaining to Station P2 Are Reduced by 10 Per Cent

	A			B			C		
	Economic Dispatch		Change in Total Fuel Cost Caused by Erroneous Data for P2, Dollars	Economic Dispatch		Change in Total Fuel Cost Caused by Erroneous Data for P2, Dollars	Economic Dispatch		Change in Total Fuel Cost Caused by Erroneous Data for P2, Dollars
Station	Using Correct Data, Mw	Using Erroneous Data, Mw		Using Correct Data, Mw	Using Erroneous Data, Mw		Using Correct Data, Mw	Using Erroneous Data, Mw	
P1	134.3	132.8	−2.40	215.3	213.3	− 3.96	240.0	240.0	
P2	82.5	88.5	+9.53	142.1	152.1	+19.81	169.0	171.5	+5.55
P3	70.7	68.9	−2.89	92.2	91.8	− 0.79	136.8	136.3	−1.13
P4	61.6	59.4	−3.54	98.4	97.4	− 1.98	126.2	126.0	−0.45
P5	60.0	60.0		127.8	123.6	− 8.50	182.9	181.8	−2.54
P6	109.3	109.0	−0.49	138.9	138.2	− 1.42	146.0	146.0	
P7	20.0	20.0		52.0	50.6	− 2.46	72.7	72.4	−0.78
P8	18.0	18.0		18.0	18.0		26.5	26.2	−0.72
P9	25.0	25.0		25.0	25.0		52.1	51.9	−0.55
P10	5.0	5.0		5.0	5.0		5.9	5.8	
P11	15.0	15.0		17.8	17.8		33.0	33.2	+0.65
	601.4	601.6	+0.21	932.5	933.1	+ 0.70	1191.1	1191.2	+0.03
Loss	12.2	12.4*		32.4	33.0*		44.2	44.3*	
Net load	589.2	589.2		900.1	900.1		1146.9	1146.9	

* Losses evaluated using correct B constants.

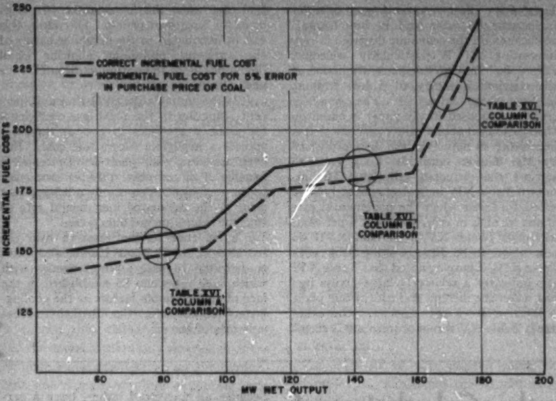

Fig. 17. Incremental fuel cost curves for station P2

This correction would tend to increase the magnitude of the error.

Fig. 16 shows similar incremental cost curves for another station. In this case, the error is caused by a 5-per-cent error in slope of the incremental heat rate curve. This type of error can easily occur, since these heat rate curves are plotted from test data and are usually someone's judgement as to the best curve which fits a cloud of test points. Here the solutions are at system net load levels of approximately 600 mw, 900 mw, and 1,150 mw. Using the erroneous incremental cost curve, increased loadings are obtained for *P2* of 3.3 mw, 4.1 mw, and 2.2 mw respectively. Evaluating these shifts for total changes in system fuel cost results in increases of $.09, $.16, and $.23, as shown in Table XV, columns *A*, *B*, and *C*. At the points where these solutions were obtained, the bus-bar costs for station *P2* were in error by approximately 2 per cent or less.

Fig. 17 again relates to station *P2* and shows an error curve for a 5-per-cent reduction in fuel cost. At the same system net load levels as before, the dispatches using this erroneous curve increase loading of the station by 13.5 mw, 17.1 mw, and 3.6 mw respectively. Because of this error in fuel cost at station *P2*, the fuel cost input to the system was increased by $.65, $.85, and $.26, as shown in Table XVI, columns *A*, *B*, and *C*.

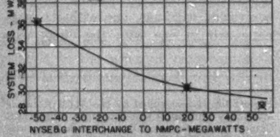

Fig. 18. Comparison of actual and calculated losses for exchange of generation between New York State Electric and Gas and Oswego

— Actual
⊙ Modified Brownlee
× Revised incremental

Station *P2* has the highest over-all incremental transmission loss penalty of any station on this system. Therefore, all the *B* constants relative to this station were arbitrarily reduced by 10 per cent and new dispatches were obtained for the same three levels of system net load as before. The resulting increases in loading of *P2* were 6.0 mw, 10.0 mw, and 2.5 mw and the changes in fuel cost to the system were $.21, $.70 and $.03, as shown in Table XVII, columns *A*, *B*, and *C*.

From these data it is apparent that a change of 10 per cent in a group of *B* constants is less serious economically than a 4 to 5-per-cent change in a plant incremental fuel cost, and in one comparison less serious than a 2-per-cent change in fuel cost. Based on these data, it appears desirable for the steam production people to examine their methods more closely so as to give better basic cost data for use in economic dispatching.

By the same token, however, efforts should be made to obtain better loss formulas because there are many instances where these formulas are being used to determine incremental losses for sale power, and these incremental losses are then used in billing calculations. For this latter purpose it is still necessary to strive for the highest accuracy possible in these *B* constants.

C. R. Cahn: I am grateful for the interesting and informative discussions. Mr. Brownlee has rightly indicated that the correction terms in equations 16 and 17 assume constant current at all generators other than the two between which generation is exchanged. An attempt to hold constant powers at the other generators leads to great analytical complication, and it becomes difficult to draw any general conclusions from the results. In some simple cases, however, the correction terms in equations 16 and 17 have been shown to give reasonably accurate corrections to the basic Brownlee formulas.

Mr. Brownlee points out that a study of Table I shows a system load nearly 9 mw more for case 1 than for the base case. Reference to the original load study shows that the increase at each load was not proportional to the base case load power. Correcting the load distribution results in only an 0.2-mw increase in losses so that the Kirchmayer-Glimn formula is still the more accurate one for this case.

Mr. Brownlee has contributed a powerful and simple method of extending his basic formulas to obtain more accuracy in the frequently recurring situation of a line-type system with different reactance-resistance ratios in the various sections. A single intermediate bus may be assumed with an appropriate division of the total resistance and reactance being made to the two sections. The incremental losses are then computed separately for each of the sections.

Illustration of the foregoing is given for the Binghamton and the Dunkirk generation swings for which the basic Brownlee formulas gave somewhat unsatisfactory results, as shown in Figs. 7 and 11. For the Binghamton swing, the total impedance is divided into $j0.1670$ between Binghamton and the equivalent intermediate bus and $0.0422 + j0.1380$ between the intermediate bus and Oswego. The latter section has a reactance-resistance ratio characteristic of the main transmission system. The comparison between actual losses and those calculated by the Brownlee formulas applied to each of the two sections is shown in Fig. 18. In addition, a new incremental loss formula was obtained using the 2-section equivalent. Losses determined with the incremental loss formula are also shown in Fig. 18.

For the Dunkirk swing the total impedance is divided into 0.0130 between Dunkirk and the equivalent intermediate bus and $0.1290 + j0.421$ between the intermediate bus and Oswego. The latter section has a reactance-resistance ratio characteristic of the main transmission system. The losses in the zero-reactance section are calculated by I^2R, assuming that the full output of Dunkirk flows in the

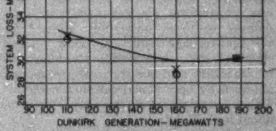

Fig. 19. Comparison of actual and calculated losses for exchange of generation between Dunkirk and Oswego

— Actual
⊙ Modified Brownlee
× Revised incremental

resistance. The incremental loss in the other section is calculated with the Brownlee formulas. The losses calculated in the foregoing manner are shown in Fig. 19 along with the actual losses and those determined by a revised incremental loss formula.

It is seen that an excellent correlation between calculated and actual losses is now obtained for both generation swings, removing any objection to the application of the Brownlee formulas and the new formulas to the system shown in Fig. 4. It is believed that use of the foregoing improvement will also enable a reliable application of the methods of the paper to systems with transmission lines at different voltage levels interconnected by transformer banks. As pointed out by Mr. Glimn and Mr. Kirchmayer, this type of system usually will have a wide variation in the reactance-resistance ratios.

The analysis by Mr. Travers and Mr. Long of the effect of various types of errors in incremental rates and in loss formula coefficients on the economic dispatch is very interesting. It is particularly welcome, since I feel that no adequate discussion of the required accuracy of a loss formula has yet been advanced. The accuracy criterion proposed in the paper is based on observations of actual utility practice. It is interesting to note that the data presented by Mr. Travers and Mr. Long seem to support the proposed criterion. The results of Table XIV indicate a relatively large excess fuel cost when the incremental rate of one plant is in error by about 4 per cent. Although Tables XV, XVI, and XVII do not appear to be directly comparable with Table XIV, it may be noted that Table XVI also indicates a relatively large excess fuel cost when the incremental rate of one plant is in error by 5 per cent. On the other hand, Table XV shows a quite small excess fuel cost when the incremental rate is in error by 2 per cent or less. Of course, this can be attributed to the parabolic nature of the economic minimum, allowing small deviations from the optimum dispatch with negligible error.

It is shown in Table XVII that a 10-per-cent reduction in the total loss coefficients for plant 2 produces in two of three instances a negligible excess fuel cost. But even assuming that plant 2 operates at a penalty of 25 per cent, a 10-per-cent error in the coefficients means only a 2.5-per-cent error in the calculated incremental rate so that the results are not unexpected.

I agree that further research into the representation of plant incremental rates is desirable to assure the accuracy with which such rates can be established in the face of such variable factors as the cooling-water temperature, the British thermal unit rate of the coal, etc.

A New Approach to the Calculation of Synchronous Machine Reactances—Part I

M. E. TALAAT
ASSOCIATE MEMBER AIEE

Synopsis: In Part I of this paper, the 2-reaction theory of synchronous machines[1] is used to derive the torque equation at any slip *s* of the unexcited synchronous motor with one equivalent damper-winding circuit in each axis. It is then shown that this synchronous motor torque equation reduces in the special case of uniform air gap and continuous damper to the torque equation of the induction motor as developed from its equivalent circuit.[2] A paramount criterion for the correctness of any resistance or reactance equations derived for synchronous machines is their reducibility in the special case of uniform air gap and continuous damper to those commonly known for the squirrel-cage induction motor.[2,3]

Equations in terms of dimensions and physical constants are derived in this paper from basic theory of coupled circuits. Also it is shown that all of these equations reduce in the previously mentioned special case of uniform air gap and continuous damper to those universally given[2,3] for the squirrel-cage induction motor. These equations are then inserted in the definitions of transient and subtransient reactances obtained by operational calculus methods.[4] The nomenclature of this paper will be found in Appendix I.

In a later paper, comparison will be made of calculated transient and subtransient reactances based on the equations given here with those given by test and reference,[5] and the discrepancies will be discussed. Also, numerical samples of calculations of the different reactances will be given, using information based on the present paper.

THERE have been many papers on steady-state and transient circuit analysis of synchronous machines, but relatively few presenting design equations for the constants which are used in the analytical theory of synchronous machines.

Needless to say, accurate theoretical analysis of synchronous machine steady-state or transient performance can be greatly jeopardized if the constants to be inserted in the analytical equations or equivalent circuits are themselves inaccurate.

It has been noticed by many designers over a period of time that the unsaturated calculated values of transient and subtransient reactances of synchronous machines, using equations presented in a previous paper[5] on this subject, have yielded results that are often lower than those obtained by test. This has made it necessary for many designers to apply an empirical factor based on experience, to increase their calculated values to approximate more closely the test values of transient and subtransient reactances.

Hence, the need arises in practical design work for a new approach to the subject. The new equations must give unsaturated calculated values which are higher than any test values. This is because all measured values have a certain degree of saturation which tends to give lower values by test than by calculations which neglect saturation.

If saturation factors referred to in the previously mentioned paper[5] were applied, the calculated results will show an even greater discrepancy from test values.

Discussion and Conclusions

In respect to the damper windings, two main points of view are followed in dealing with the calculation of synchronous machine constants. One[6,7] is to consider each two damper bars symmetrically located with respect to the direct axis or quadrature axis as comprising one damper-winding circuit in the direct or quadrature axis respectively. This makes the subsequent subtransient or starting analysis of the machine very involved, and would require the use of the network analyzer which may not be readily available, or may not be economically justified in the majority of cases.

The other point of view,[5,8] which is adopted in this paper, replaces the unsymmetrical damper winding by two equivalent windings, one with its magnetic axis in line with the direct axis

---

Paper 55-6, recommended by the AIEE Rotating Machinery Committee and approved by the AIEE Committee on Technical Operations for presentation at the AIEE Winter General Meeting, New York, N. Y., January 31–February 4, 1955. Manuscript submitted March 18, 1954; made available for printing October 27, 1954.

M. E. TALAAT is with the Elliott Company, Ridgway, Pa.

The author wishes to express his thanks to R. F. Edwards for his criticism, and for his suggestions in regard to the wording of this paper.

(pole center), and the other with its magnetic axis in line with the quadrature axis (interpole center).

This point of view simplifies the analysis of synchronous machines, and is readily applicable to the majority of cases, where a single bar material is used in the damper winding. Where more than one material is used, as in the case of many synchronous motors, one circuit can be added for each additional group of bars of one material, or an equivalent bar material figured[9] for all bars and, hence, one equivalent damper-winding circuit can still be used in each axis.

In this paper, the argument is first advanced that the paramount criterion for the correctness of any resistance or reactance equations derived for the equivalent one damper-winding circuit in each axis is their reducibility in the case of continuous damper and uniform gap, to those universally given for the reflected secondary resistance and secondary reactance of the squirrel-cage induction motor. That this reducibility must be the case is shown in Appendix II, where the induction motor torque equation is obtained by the application of the 2-reaction theory of synchronous machines to the nonexcited case with continuous damper windings and uniform air gap.

In Appendix III the magnetomotive force (mmf) distribution in each of the equivalent damper-winding circuits is studied, and certain coefficients are defined. These are then used in Appendix IV to obtain self-, mutual, and leakage reactances as well as resistance of each equivalent damper-winding circuit referred to the stator side. The results are all shown to reduce for continuous damper and uniform gap to those given for the reflected constants of the squirrel-cage induction motor.[2,3] In Appendix V, equations for the self-mutual, and leakage reactances of the field winding referred to the stator side, are derived. In Appendixes IV and V, it is clearly shown that mutual reactances derived from either side and referred to the stator side are all equal. Their relation to the armature reaction reactances in the direct or quadrature axis is given.

Results from Appendixes IV and V are then inserted in the definition of transient and subtransient reactances obtained from operational calculus methods. This yields equations for reactances which are readily seen to agree qualitatively in form with the equivalent circuits of synchronous machines for transient and subtransient conditions when one equivalent damper winding only is considered in each axis.

No per-unit (pu) system is used in this presentation. This was done in order to present, to beginners in the design field, equations for the reactances of salient-pole synchronous machines on the basis of the principle of coupled circuits and the fundamental concepts of physics with which they have some familiarity.

The equations presented are given in terms of dimensions and physical constants, and they yield values in ohms. If any pu system is to be selected by the design or application engineer, he can simply divide the values obtained by his pu impedance to get the reactances in pu.

In Part II of this paper, numerical examples of calculating the synchronous machine reactances using the equations presented here will be given. The results obtained will be compared with those given by using equations given in reference 5 and those obtained from tests on several machines. A discussion of the discrepancies will be given.

General Theory

In this paper the analysis equations developed are based on the generalized 2-reaction theory of synchronous machines, in which the following assumptions are made.[10]

ASSUMPTIONS

1. Saturation, hysteresis, and eddy currents in all magnetic circuits are neglected. This linearizes the machines. Eddy currents in electric circuits and charging currents between electric circuits or parts of circuits are also ignored.
2. The armature phase winding is distributed in such a way as to produce sinusoidal space distribution of mmf.
3. The pole structure is symmetrical about the axis of the pole. A symmetrical polyphase armature winding is assumed.
4. The variation of armature phase self- and mutual inductances contain only zero and second-harmonic sinusoidal space components.
5. The magnitude of the second-harmonic components of armature phase self- and mutual inductances are equal.
6. The variation of the mutual inductances between any armature phase circuit and any rotor circuit with respect to rotor position is purely sinusoidal.
7. The self- and mutual inductances of all rotor circuits are independent of rotor position. This neglects the effect of the slots.
8. Effective armature winding flux linkages are produced only by the fundamental component of air-gap flux density.

ASYNCHRONOUS TORQUE EQUATION

It is shown in Appendix II that by the use of Park's equations[1] the torque equation of the unexcited synchronous machine with uniform air gap and continuous damper winding at any slip s is given by

$$T=\frac{m}{4}Pe_m^2\frac{-s\alpha_d(x_d-x_d'')}{(r\alpha_d-s\omega x_d'')^2+(s\omega r+\alpha_d x_d)^2}\quad\text{watt-seconds}\qquad(1)$$

(Torque has negative sign for motor action.)

It is further shown in Appendix II that when the definitions of α_d, x_d and x_d'' are introduced in equation 1, then equation 2 results

$$T=-\frac{m}{4}P\frac{e^2m}{\omega}\times\frac{\frac{m}{2}R_{Dd}x_{ad}\frac{m}{2}SX_{aDd}}{\left(r\frac{m}{2}SX_{DDd}+\frac{m}{2}R_{Dd}x_d\right)^2+\left(x_{LD}\frac{m}{2}SX_{aDd}+\frac{m}{2}SX_{LDd}x_d-r\frac{m}{2}R_{Dd}\right)^2}\quad\text{watt-seconds}\qquad(2)$$

which is identical with induction motor torque equation as obtained from circuit theory[2] if the identities given by equations 38 to 45, inclusive, are noticed. Equation 2 leaves no doubt that any of the equations developed for the constants

$$\frac{m}{2}R_{Dd},\ \frac{m}{2}X_{LDd},\ \frac{m}{2}X_{aDd},\ \text{and}\ \frac{m}{2}X_{DDd}$$

for the equivalent 1-circuit damper winding in the direct axis as well as

$$\frac{m}{2}R_{Dq},\ \frac{m}{2}X_{LDq},\ \frac{m}{2}X_{aDq},\ \text{and}\ \frac{m}{2}X_{DDq}$$

for the equivalent 1-circuit damper winding in the quadrature axis must reduce for the case of uniform air gap and continuous damper winding to those normally given for the squirrel-cage induction motor.[2,3]

EQUATIONS FOR DAMPER-WINDING CONSTANTS REFERRED TO STATOR SIDE

In Appendix IV the following equations are derived for leakage, mutual, and self-reactances as well as resistance for each of the equivalent single-circuit damper winding. These are given

$$X_{LDd}=\frac{8fL(Nk_w)^2}{10^8P}\frac{2\pi\lambda_{bed}}{n_b(1-k_b)}\ \text{ohms}\qquad(3)$$

$$X_{aDd}=\frac{8fL(Nk_w)^2}{10^8P}\lambda_aC_{d1}\ \text{ohms}\qquad(4)$$

$$X_{DDd}=X_{LDd}+X_{aDd}\ \text{ohms}\qquad(5)$$

$$R_{Dd}=\frac{8(Nk_w)^2}{P}\frac{r_{bed}}{n_b(1-k_b)}\text{ohms}\qquad(6)$$

$$X_{LDq}=\frac{8fL(Nk_w)^2}{10^8P}\frac{2\pi\lambda_{beq}}{n_b(1+k_b)}\text{ ohms} \quad (7)$$

$$X_{aDq}=\frac{8fL(Nk_w)^2}{10^8P}\lambda_aC_{q1}\text{ ohms} \quad (8)$$

$$X_{DDq}=X_{LDq}+X_{aDq}\text{ ohms} \quad (9)$$

$$R_{Dq}=\frac{8(Nk_w)^2}{P}\frac{r_{beq}}{n_b(1+k_b)} \quad (10)$$

EQUATIONS FOR FIELD-WINDING REACTANCES REFERRED TO STATOR SIDE

In Appendix V, the following equations are derived for mutual and self-reactances of the field winding. These are given by

$$X_{afd}=X_{fDd}=X_{aDd}\text{ ohms} \quad (11)$$

$$X_{ffd}=\frac{8fL(Nk_w)^2}{10^8P}\left(\frac{C_{d1}}{C_1}\right)^2\left(2C_p\lambda_a+\frac{4}{\pi}\lambda_F\right)\text{ ohms} \quad (12)$$

EQUATIONS FOR TRANSIENT AND SUBTRANSIENT REACTANCES

By operational calculus methods[4] it can be shown that the equations for transient and subtransient reactances of synchronous machines with one damper-winding circuit in each axis in addition to the field winding are given by

$$x_d'=x_{Ld}+x_{ad}-\frac{m}{2}\frac{X_{afd}^2}{X_{ffd}} \quad (13)$$

$$x_d''=x_{Ld}+x_{ad}-\frac{m}{2}\times\frac{X_{DDd}X_{afd}^2-2X_{aDd}X_{afd}X_{fDd}+X_{ffd}X_{aDd}^2}{X_{DDd}X_{ffd}-X_{fDd}^2} \quad (14)$$

$$x_q'=x_q''=x_{Lq}+x_{aq}-\frac{m}{2}\frac{X_{aDq}^2}{X_{DDq}} \quad (15)$$

Now if values of X_{LDd}, X_{aDd}, X_{DDd}, X_{afd}, X_{fDd}, and X_{ffd} from equations 3, 4, 5, 11, and 12 are substituted in the definitions of direct-axis transient and subtransient reactances given by equations 13 and 14, then the following expressions are obtained

$$x_d'=x_{Ld}+x_{ad}\left(1-\frac{\lambda_aC_1^2/C_{d1}}{2C_p\lambda_a+\frac{4}{\pi}\lambda_F}\right)\text{ohms} \quad (16)$$

$$x_d''=x_{Ld}+x_{ad}\times\frac{2\pi\lambda_{bed}\left[(2C_p-C_1^2/C_{d1})\lambda_a+\frac{4}{\pi}\lambda_F\right]}{[\lambda_aC_{d1}n_b(1-k_b)+2\pi\lambda_{bed}]\left[(2C_p-C_1^2/C_{d1})\lambda_a+\frac{4}{\pi}\lambda_F\right]+2\pi\lambda_{bed}\lambda_aC_a^2/C_{d1}}\text{ ohms} \quad (17)$$

And if values of X_{LDq}, X_{aDq}, and X_{DDq} from equations 7, 8, and 9 are substituted in the definition of quadrature-axis transient and subtransient reactances given by equation 15, then the following expression is obtained

$$x'_q=x''_q=x_{Lq}+x_{aq}\frac{2\pi\lambda_{beq}}{\lambda_aC_{q1}n_b(1+k_b)+2\pi\lambda_{beq}}\text{ ohms} \quad (18)$$

Appendix I. Nomenclature

B_{ad} = amplitude of space fundamental component of air-gap flux density due to fundamental component of mmf due to current in phase A when its magnetic axis is in line with the pole center

B_{Dd} = amplitude of space fundamental component of air-gap flux density due to fundamental component of mmf due to equivalent single-circuit damper winding in the direct axis

B_{fd} = amplitude of space fundamental component of air-gap flux density due to field winding mmf

C_{d1} = ratio of the amplitude of the fundamental air-gap flux density produced by a sinusoidally distributed mmf whose axis is in line with pole center to that which would be produced with a uniform air gap equal to the effective air gap over the pole center[5]

C_{q1} = corresponding coefficient for the quadrature axis[5]

C_1 = ratio of the fundamental to the actual value of field form at pole center[5]

C_p = ratio of average to value of the field form at pole center[5]

D = stator core bore, inches

D_r = rotor diameter, inches

e_m = amplitude of terminal voltage per phase

e_d = direct-axis armature voltage[1]

e_q = quadrature-axis armature voltage[1]

f = supply frequency in cycles per second

g_e = equivalent air gap under pole center, inches

i_a = instantaneous current of phase A

i_d = direct-axis armature current[1]

i_q = quadrature axis armature current[1]

I_{Dd} = instantaneous current of equivalent single damper winding in the direct axis

I_{Dq} = instantaneous current of equivalent single damper winding in the quadrature-axis

I_f = instantaneous field current

$k_b = \sin n_b\alpha_b/n_b \sin \alpha_b$ (see equations 57 and 61)

k_w = stator winding factor for fundamental components, includes pitch, distribution, and skew factors

k_{Dd}, k_{Dq} = breadth factors for equivalent single-circuit damper windings in the direct and the quadrature axis respectively[8]

$$k_{Dd}=\frac{\sin^2 N_{Dd}\frac{\alpha_b}{2}}{N_{Dd}\sin\frac{\alpha_b}{2}}\text{ for even } n_b,\ N_{Dd}=1/2n_b$$

$$k_{Dd}=\frac{\sin\left(N_{Dd}\frac{\alpha_b}{2}\right)\sin(N_{Dd}+1)\frac{\alpha_b}{2}}{N_{Dd}\sin\frac{\alpha_b}{2}}\text{ for odd } n_b,\ N_{Dd}=1/2(n_b-1)$$

$$k_{Dq}=\frac{\sin n_b\frac{\alpha_b}{2}}{2n_b\sin\frac{\alpha_b}{2}}\text{ for even or odd } n_b$$

k_f = field-winding breadth factor for fundamental component of flux density distribution in the air gap. See equation 104

L = core length, inches

L_d'', L_q'' = subtransient inductances in direct and quadrature axis respectively

L_d, L_q = synchronous inductances in direct and quadrature axis respectively

L_{DDd}, L_{DDq} = self-inductances of equivalent single-circuit damper winding in the direct and quadrature axis respectively

L_{aDd}, L_{aDq} = amplitude of mutual inductances, between phase A and direct and quadrature axis equivalent damper windings

m = number of phases = 3 for 3-phase winding

M_a = amplitude of fundamental component of armature mmf, due to current in phase A

M_{Dd}, M_{Dq} = amplitude of fundamental component of mmf of equivalent damper windings in direct and quadrature axis respectively

M_f = field winding mmf = I_fN_f

N = number of stator series turns per phase

N_f = number of field series turns per pole

n_b = number of damper bars per pole

n = rpm

P = number of poles

$p=\dfrac{d}{dt}$

Q_2 = number of rotor bars

R_{Dd}, R_{Dq} = resistance of equivalent single-circuit damper windings in direct and quadrature axis respectively referred to stator side

R_f = field resistance referred to stator side

r = stator resistance per phase

r_{be} = equivalent single-bar resistance including end ring effect

s = slip

t = time, seconds

T = asynchronous average torque

x_d'', x_q'' = direct- and quadrature-axis subtransient reactances per phase respectively

x_d', x_q' = direct- and quadrature-axis transient reactances per phase respectively

x_d, x_q = direct- and quadrature-axis synchronous reactances per phase respectively

x_{Ld}, x_{Lq} = direct- and quadrature-axis leakage reactances per phase respectively

X_{LDd}, X_{LDq} = direct- and quadrature-axis equivalent single-circuit damper leakage reactances referred to stator side

X_{DDd}, X_{DDq} = direct- and quadrature-axis self-reactances of equivalent single-circuit damper windings referred to stator side

X_{aDd}, X_{aDq} = amplitude of mutual reactances between the windings of phase A and the equivalent single-circuit direct- and quadrature damper windings respectively, referred to stator side

x_{ad}, x_{aq} = direct- and quadrature-axis armature reaction synchronous reactances respectively

x_{be} = equivalent single-bar reactance = $2\pi f\lambda_{be}L10^{-8}$ (2); subscripts d and q refer to direct and quadrature axis respectively

$\alpha_d = \frac{\omega R_{Dd}}{X_{DDd}}$, $\alpha_q = \frac{\omega R_{Dq}}{X_{DDq}}$ (See equations 24 and 25)

δ = angle in electrical degrees between magnetic axis of phase A and rotor direct axis

$\theta = \omega t + \delta$

θ_n = angle between n-n bars (electrical degrees)

λ_{be} = equivalent single bar leakage permeance including end ring effects,[3] per inch; subscripts d and q refer to direct and quadrature axis respectively

$\lambda_a = \frac{6.38D}{Pg_e}$ (see reference 5)

λ_p = pole leakage flux linkage permeance due to body and tip[5] per inch

ψ_d, ψ_q = flux linkages in direct and quadrature axis respectively[1]

$\omega = 2\pi f$

α_b = angle between two bars (uniform distribution of bars)

τ = pole pitch

τ_n = distance between n-n bars

Appendix II. Development of Torque Equation of Unexcited Synchronous Machine at Any Slip s from 2-Reaction Theory

Based on the generalized 2-reaction theory presented by Park[1] with an equivalent 1-rotor circuit in each rotor axis, the following fundamental relations are obtained

$$e_d = -e_m \sin\delta = p\psi_d - ri_d - \psi_q p\theta \qquad (19)$$

$$e_q = e_m \cos\delta = p\psi_q - ri_q + \psi_d p\theta \qquad (20)$$

For no field excitation ψ_d and ψ_q are given by

$$\psi_d = -\frac{\alpha_d L_d + pL_d''}{\alpha_d + p}\, i_d \qquad (21)$$

$$\psi_q = -\frac{\alpha_q L_q + pL_q''}{\alpha_q + p}\, i_q \qquad (22)$$

where

$$p = \frac{d}{dt} \qquad (23)$$

$$\alpha_d = \frac{R_{Dd}}{L_{DDd}} \qquad (24)$$

$$\alpha_q = \frac{R_{Dq}}{L_{DDq}} \qquad (25)$$

$$L_d'' = L_d - \frac{\frac{m}{2} L_{aDd} L_{Dad}}{L_{DDd}} \qquad (26)$$

$$L_q'' = L_q - \frac{\frac{m}{2} L_{aDq} L_{Daq}}{L_{DDq}} \qquad (27)$$

At any slip s,

$$\delta = -s\omega t \qquad (28)$$

$$p\theta = (1-s)\omega \qquad (29)$$

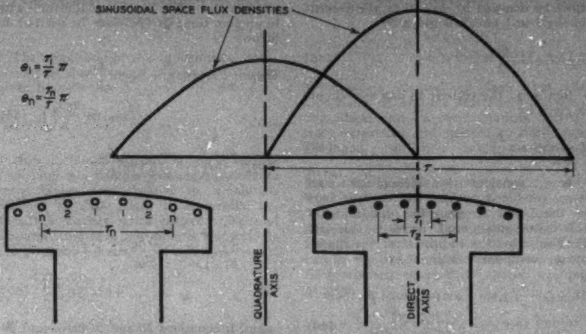
SINUSOIDAL SPACE FLUX DENSITIES
$\theta_1 = \frac{\tau_1}{\tau}\pi$
$\theta_n = \frac{\tau_n}{\tau}\pi$
τ
n
2
1
1
2
n
τ_n
τ_1
τ_2
QUADRATURE AXIS
DIRECT AXIS

Fig. 1. Pulsating sinusoidally distributed space flux density with magnetic axis in line with direct axis (pole center), or quadrature axis (interpole center)

And if complex quantities are used, then

$$p = j\omega s \qquad j = \sqrt{-1} \qquad (30)$$

$$e_d = je_m \qquad (31)$$

$$e_q = e_m \qquad (32)$$

Also, the average torque[1] will be given by

$$T = \frac{m}{8} P(i_q\psi_d - i_d\psi_q) \text{ watt-seconds} \qquad (33)$$

Now, if values of ψ_d and ψ_q from equations 21 and 22 are substituted in equations 19 and 20, and if, next, equations 29 through 32 are used, and since for uniform air gap and continuous damper winding the direct- and quadrature-axis constants are identical, then i_d and i_q will be given by

$$i_d = e_m \frac{\omega s - j\alpha_d}{(r\alpha_d - s\omega x_d'') + j(s\omega r + \alpha_d x_d)} \qquad (34)$$

$$i_q = -ji_d \qquad (35)$$

Substituting values of i_d and i_q from equations 34 and 35 into equations 21 and 22 respectively, then using the results in equation 33, the following torque equation is given for the induction motor

$$T = \frac{m}{4} Pe_m^2 \frac{-s\alpha_d(x_d - x_d'')}{(r\alpha_d - s\omega x_d'')^2 + (s\omega r + \alpha_d x_d)^2} \text{ watt-seconds} \qquad (36)$$

Torque has negative sign for motor action.

Now, by inserting the definitions of α_d and x_d'' as given by equations 24 and 26 into equation 36, and arranging terms, it follows that

$$T = \frac{mPe_m^2}{4\omega} \times \frac{-\left(\frac{m}{2}R_{Dd}\right)x_{ad}\left(\frac{m}{2}sX_{aDd}\right)}{\left[r\left(\frac{m}{2}sX_{DDd}\right) + \left(\frac{m}{2}R_{Dd}\right)x_d\right]^2 + \left[x_{Ld}\left(\frac{m}{2}sX_{aDd}\right) + \left(\frac{m}{2}sX_{LDd}\right)x_d - r\left(\frac{m}{2}R_{Dd}\right)\right]^2} \text{ watt-seconds} \qquad (37)$$

Equation 37 is identical with induction motor torque equation as obtained from circuit theory[3] if the identities given by equations 38 through 45, inclusive, are noted, and if the eddy current and hysteresis losses are neglected and unit of torque taken as watt-seconds.

$$V = e_m/\sqrt{2} \qquad (38)$$

$$r_1 = r \qquad (39)$$

$$x_1 = x_{Ld} \qquad (40)$$

$$r_2' = \frac{m}{2}R_{Dd} \qquad (41)$$

$$x_2' = \frac{m}{2}X_{LDd} \qquad (42)$$

$$x_m = x_{ad} = \frac{m}{2}X_{aDd} \qquad (43)$$

$$x_1 + x_m = x_{Ld} + x_{ad} = x_d \qquad (44)$$

$$x_2' + x_m = \frac{m}{2}X_{LDd} + X_{aDd} = \frac{m}{2}X_{DDd} \qquad (45)$$

Appendix III. Amplitude of Fundamental Component of Sinusoidal Mmf Distribution for Each Equivalent Single-Circuit Damper Winding in Direct and Quadrature Axis

If a pulsating sinusoidally distributed space flux density with its magnetic axis in line with the direct axis (pole center) is assumed (Fig. 1), then the currents induced in each two damper bars, located symmetrically with respect to the flux wave axis, are of equal magnitude and of opposite direction[6,8]. The currents of maximum magnitude are induced in the two damper bars that would be located one-half pole pitch from the flux wave axis. The current in each other two damper bars located at an electrical angle $= \theta/2$ from the flux wave axis will have a magnitude equal to $\sin\theta/2$ times the maximum magnitude.

Now, if the current of maximum magnitude be denoted by I_{Dd}, then the current in the 1-to-1 circuit is given by

$$I_{1d} = I_{Dd} \sin \frac{\theta_1}{2} \tag{46}$$

Similarly, the current in any n-n circuit is given by

$$I_{nd} = I_{Dd} \sin \frac{\theta_n}{2} \tag{47}$$

Now, consider the rectangular mmf wave produced by the two damper bars of the 1-to-1 circuit. The amplitude of this rectangular mmf wave is I_{1d}. By Fourier series the amplitude of the fundamental component is given by

$$M_{1d\max} = \frac{4}{\pi} I_{1d} \sin \frac{\theta_1}{2} \text{ ampere turn per pole} \tag{48}$$

The mmf of other pairs of bars symmetrically located with respect to the pole axis can be treated similarly.

The amplitude of the resultant space fundamental mmf of all pairs of bars in ampere turns per pole is given by

$$M_{Dd} = \frac{4}{\pi}\left(I_{1d} \sin \frac{\theta_1}{2} + I_{2d} \sin \frac{\theta_2}{2} + \ldots + I_{NDd} \sin \frac{\theta_{NDd}}{2} \right) \tag{49}$$

Substituting values of I_{1d}, $I_{2d} \ldots I_{nd} \ldots$ from equations 46 and 47, etc., and arranging terms, then

$$M_{Dd} = \frac{2}{\pi} I_{Dd} N_{Dd} (1 - A_{Dd}) \tag{50}$$

where, in general

$$A_{Dd} = \frac{1}{N_{Dd}} (\cos \theta_1 + \cos \theta_2 + \ldots + \cos \theta_n + \ldots + \cos \theta_{NDd}) \tag{51}$$

and

$$\theta_n = \frac{\tau_n}{\tau} \pi \tag{52}$$

If the case of uniform space location of damper bars along the pole face is considered, then for even number of bars per pole the following relations are true

$$n_b = 2N_{Dd} = \text{even number} \tag{53}$$

$$\theta_1 = \alpha_b,\ \theta_2 = 3\alpha_b \ldots \theta_n = (2n-1)\alpha_b \tag{54}$$

And for the odd number of bars

$$n_b = 2N_{Dd} + 1 = \text{odd number} \tag{55}$$

$$\theta_1 = 2\alpha_b,\ \theta_2 = 4\alpha_b \ldots \theta_n = 2n\alpha_b \tag{56}$$

Now if equations 53 and 54, or 55 and 56 are used in equation 51, and the resultant finite trigonometric summation evaluated and then substituted in equation 50, the following expression for M_{Dd} is obtained for both cases of even and odd number of bars per pole

$$M_{Dd} = \frac{1}{\pi} n_b I_{Dd} \left(1 - \frac{\sin n_b \alpha_b}{n_b \sin \alpha_b} \right) = \frac{1}{\pi} n_b I_{Dd} \times (1 - k_b) \tag{57}$$

By a similar reasoning, the amplitude of the resultant space fundamental mmf of all pairs of bars in the quadrature axis in ampere turns per pole can be derived as follows

$$M_{Dq} = \frac{4}{\pi}\left(I_{1q} \cos \frac{\theta_1}{2} + I_{2q} \cos \frac{\theta_2}{2} + \ldots + I_{NDq} \cos \frac{\theta_{NDq}}{2} \right) \tag{58}$$

$$M_{Dq} = \frac{4}{\pi} I_{Dq} \left(\cos^2 \frac{\theta_1}{2} + \cos^2 \frac{\theta_2}{2} + \ldots + \cos^2 \frac{\theta_{NDq}}{2} \right) \tag{59}$$

$$M_{Dq} = \frac{2}{\pi} I_{Dq} \left[N_{Dq} + \frac{N_{Dq}}{N_{Dq}} (\cos \theta_1 + \cos \theta_2 + \ldots + \cos \theta_{NDq}) \right] \tag{60}$$

And if equations 53 and 54 or 55 and 56 are used in the same manner as in deriving equation 57, the following expression is obtained for M_{Dq} for both cases of even and odd numbers of bars per pole.

$$M_{Dq} = \frac{1}{\pi} n_b I_{Dq} \left(1 + \frac{\sin n_b \alpha_b}{n_b \sin \alpha_b} \right) = \frac{1}{\pi} n_b I_{Dq} (1 + k_b) \tag{61}$$

(In deriving equation 61 for the case of odd number of bars the effect of the center bar is obtained by taking the average of the two expressions; once neglecting the center bar effect and once considering the whole bar effect.) Notice that in the induction motor case the angle $\alpha_b = \pi / n_b$ and hence, the second term k_b in the brackets of both equations, 57 and 61, reduces to zero.

Appendix IV. Reactances for Each Equivalent Single-Circuit Damper Winding in Direct and Quadrature Axis

The amplitude of the fundamental component of armature mmf due to an equivalent direct-axis damper-winding current circulating in phase A only is given by[3]

$$M_a = \frac{4}{\pi} \frac{Nk_w}{P} i_{Dd} \tag{62}$$

Therefore the amplitude of the fundamental component of flux density B_{ad} due to M_a when the magnetic axis of phase A is in line with the direct axis is given by

$$B_{ad} = \frac{4}{\pi} \frac{Nk_w}{P} i_{Dd} \frac{3.19}{g_e} C_{d1} \tag{63}$$

Similarly, from Appendix III, the fundamental component of flux density B_{Dd} due to M_{Dd} is given by

$$B_{Dd} = \frac{n_b}{\pi} I_{Dd} (1 - k_b) \frac{3.19}{g_e} C_{d1} \tag{64}$$

Now, if the fundamental armature mmf and the equivalent damper winding mmf are to yield equal fundamental flux density distribution when their respective magnetic axes are aligned, then from $B_{ad} = B_{Dd}$ the following current ratio is obtained

$$\frac{I_{Dd}}{i_{Dd}} = \frac{4Nk_w}{Pn_b(1-k_b)} \tag{65}$$

The voltage ratio between phase A and the equivalent single-circuit direct-axis damper winding when the magnetic axis of phase A is in line with the direct axis is given by[3]

$$\frac{e_{Dd}}{E_{Dd}} = \frac{Nk_w}{PN_{Dd}k_{Dd}} \tag{66}$$

From equations 55 and 56, the impedance ratio for the equivalent direct-axis damper winding is given by

$$A_{zDd} = \frac{4(Nk_w)^2}{P^2 N_{Dd} k_{Dd} n_b (1-k_b)} \tag{67}$$

Now, the total leakage flux linkage of the equivalent direct-axis damper winding is given by

$$\begin{aligned} \psi_{LDd} &= P(I_{1d} + I_{2d} + \ldots + I_{nd} + \ldots + I_{NDd}) 2\lambda_{bed} L \\ &= PN_{Dd} k_{Dd} I_{Dd} (2\lambda_{bed} L) \end{aligned} \tag{68}$$

Therefore, from the fundamental definition of reactance as flux linkage pu current, x_{LDd} is obtained as follows

$$x_{LDd} = 2\pi f \frac{\psi_{LDd}}{10^8 I_{Dd}} = PN_{Dd} k_{Dd} (2x_{bed}) \text{ohms} \tag{69}$$

Consequently, if the ratio given by equation 67 is used to refer x_{LDd} given by equation 69 to the stator side, then

$$X_{LDd} = \frac{8(Nk_w)^2}{Pn_b(1-k_b)} x_{bed} \text{ ohms} \tag{70}$$

In Appendix III, it was mentioned that in the case of the induction motor $k_b = 0$, and $x_{bed} = x_{be}$, consequently

$$\frac{m}{2} X_{LDd} = \frac{8(Nk_w)^2}{Pn_b} x_{be} \text{ ohms} = x_2' \tag{71}$$

(See references 2 and 3.)

Also, from equation 63, the flux linkage in the equivalent direct-axis damper winding due to phase A current i_{Dd} is given by

$$\psi_{Dad} = N_{Dd} k_{Dd} Nk_w \frac{4}{\pi} C_{d1} \lambda_a L i_{Dd} \tag{72}$$

Consequently, from the fundamental concept of inductance as flux linkage pu current, and by use of equation 66 for voltage ratio, the amplitude of the mutual reactance X_{Dad} between the equivalent direct-axis damper winding and phase A referred to the stator side will be given by

$$X_{Dad} = 2\pi f \frac{\psi_{Dad}}{10^8 i_{Dd}} \frac{Nk_w}{PN_{Dd}k_{Dd}} = \frac{8fL(Nk_w)^2}{10^8 P} \times C_{d1}\lambda_a \text{ ohms} \tag{73}$$

Alternatively, from equation 64 the flux linkage in phase A due to the current in the equivalent direct-axis damper winding is given by

$$\psi_{aDd} = (1-k_b) n_b Nk_w \left(\frac{1}{\pi} C_{d1} \lambda_a \right) L I_{Dd} \tag{74}$$

Consequently, if the current ratio, equation 65, is used to eliminate I_{Dd} from equation 74, and the fundamental concept of inductance as flux linkage pu current is again applied, then the amplitude of the mutual reactance X_{aDd} between phase A and the equivalent direct-axis damper winding referred to the stator side will be given by

$$X_{aDd}=2\pi f\frac{\psi_{aDd}}{10^8 i_{Dd}}\frac{4Nk_w}{Pn_b(1-k_b)}i_{Dd}$$
$$=\frac{8fL(Nk_w)^2}{10^8 P}C_{d1}\lambda_a=X_{Dad}\text{ ohms} \qquad (75)$$

Equations 73 and 75 show that the amplitude of the mutual reactances between any phase and the equivalent direct-axis damper winding calculated from either side are equal. Also, since C_{d1} goes to unity for the induction motor case, then

$$\frac{m}{2}X_{aDd}=\frac{m}{2}X_{Dad}=x_{sd}=x_m{}^{2,3} \qquad (76)$$

By reasoning similar to that used in deriving equations 73 and 75, it can be shown that the self-reactance of the equivalent direct-axis damper winding referred to the stator side will be given by

$$X_{DDd}=\frac{2\pi fL}{10^8}\frac{4(Nk_w)^2}{P^2N_{Dd}k_{Dd}n_b(1-k_b)}\times$$
$$\left[Pn_b(1-k_b)N_{Dd}k_{Dd}\left(\frac{1}{\pi}C_{d1}\lambda_a\right)+\right.$$
$$\left.PN_{Dd}k_{Dd}2\lambda_{bed}\right]=\frac{8fL(Nk_w)^2}{10^8P}\times$$
$$\left[\lambda_aC_{d1}+\frac{2\pi\lambda_{bed}}{n_b(1-k_b)}\right]\text{ohms} \qquad (77)$$

The loss in the damper winding

$$P_{Dd}=2r_{bed}I_{Dd}{}^2\left(\sin^2\frac{\theta_1}{2}+\sin^2\frac{\theta_2}{2}+\ldots+\right.$$
$$\left.\sin^2\frac{\theta_{NDd}}{2}\right)P\text{ watts} \qquad (78)$$

By the use of relations given in Appendix III it will be seen that for both odd or even numbers of bars per pole, equation 78 will reduce to

$$P_{Dd}=1/2r_{bed}I_{Dd}{}^2n_b(1-k_b)P\text{ watts} \qquad (79)$$

Now, if the current ratio given by equation 65 is used to replace I_{Dd} by its equivalent i_{Dd} in the stator side, then

$$P_{Dd}=\frac{8(Nk_w)^2}{Pn_b(1-k_b)}i_{Dd}{}^2r_{bed}\text{ watts} \qquad (80)$$

Therefore, from equation 80 the equivalent direct-axis damper-winding resistance referred to the stator side R_{Dd} is given by

$$R_{Dd}=\frac{8(Nk_w)^2}{Pn_b(1-k_b)}r_{bed}\text{ ohms} \qquad (81)$$

Notice the similarity of equation 81 for the reflected resistance with equation 70 for reflected leakage reactance. Equation 81 was obtained from the argument that the reflected resistance R_{Dd} must be such as to have the same heat loss as that of the real damper winding.

Also, for the case of induction motor $k_b=0$, and again

$$\frac{m}{2}R_{Dd}=\frac{4m(Nk_w)^2}{Pn_b}r_{be}=r_2' \qquad (82)$$

(See references 2 and 3.)

Appendix V. Field-Winding Constants

The amplitude of the fundamental component of flux density B_{fd} due to M_{fd} is given by reference 5

$$B_{fd}=N_fI_f\frac{3.19}{g_e}C_1 \qquad (83)$$

Now if B_{fd} is equated to its armature phase and its damper-winding equivalents respectively, and treated in a similar manner to that given in Appendix IV, then the current ratios between field and armature and field and damper respectively are given by

$$\frac{I_f}{i_{fa}}=\frac{4}{\pi}\frac{C_{d1}}{C_1}\frac{Nk_w}{PN_f} \qquad (84)$$

$$\frac{I_f}{I_{fDd}}=\frac{1}{\pi}\frac{C_{d1}}{C_1}\frac{n_b(1-k_b)}{N_f} \qquad (85)$$

Also, from Appendix III it can easily be seen that for the same amplitude of the fundamental component of direct-axis flux density B_d, the voltage ratio between phase A, the equivalent direct-axis damper winding and the field is given respectively by

$$\frac{e_{fd}}{E_{fd}}=\frac{Nk_w}{PN_fk_f} \qquad (86)$$

$$\frac{E_{fDd}}{E_{fd}}=\frac{N_{Dd}k_{Dd}}{N_fk_f} \qquad (87)$$

From equations 84 and 86, the impedance ratio for the field winding is given by

$$A_{zf}=\frac{\frac{4}{\pi}C_{d1}}{C_1k_f}\frac{(Nk_w)^2}{P^2N^2_f} \qquad (88)$$

Again by similar consideration to those given in Appendix IV, the flux linkage in the field winding, due to current in phase A when the direct axis is in line with magnetic axis of phase A, is given by

$$\psi_{fad}=N_fk_fNk_w\frac{4}{\pi}C_{d1}\lambda_aLi_a \qquad (89)$$

Consequently, from the fundamental concept of inductance as flux linkage pu current and by use of voltage ratio, equation 86, the amplitude of the mutual reactance X_{fad} between the field winding and phase A referred to the stator side will be given by

$$X_{fad}=2\pi f\frac{\psi_{fad}}{10^8i_a}\frac{Nk_w}{PN_fk_f}=\frac{8fL(Nk_w)^2}{10^8P}C_{d1}\lambda_a$$
$$\text{ohms} \qquad (90)$$

Alternatively, from equation 83, the flux linkage in phase A due to the current in the field winding is given by

$$\psi_{afd}=Nk_wN_fC_1\lambda_aLI_f \qquad (91)$$

Consequently, if the current ratio, equation 84, is used to eliminate I_f from equation 91, and the fundamental concept of inductance as flux linkage pu current is applied, then the amplitude of the mutual reactance X_{afd} between phase A and the field winding referred to the stator winding will be given by

$$X_{afd}=2\pi f\frac{\psi_{afd}}{10^8i_{fa}}\frac{4}{\pi}\frac{C_{d1}}{C_1}\frac{Nk_w}{PN_f}i_{fa} \qquad (92)$$
$$=\frac{8fL(Nk_w)^2}{10^8P}C_{d1}\lambda_a=X_{fad}\text{ ohms}$$

Equations 90 and 92 show that the amplitude of mutual reactances between any phase and the field winding derived from either side and referred to stator side are equal. Also, it is readily seen that

$$\frac{m}{2}X_{afd}=\frac{m}{2}X_{fad}=x_{ad}\text{ ohms} \qquad (93)$$

By similar reasoning to that used in deriving equations 90 and 92, and if the impedance ratio equation 88 is used, it can be shown that the self-reactance of the field winding referred to stator winding is given by

$$X_{ffd}=\frac{8fL(Nk_w)^2}{10^8P}\frac{C_{d1}}{C_1k_f}\left(\frac{\pi}{2}C_p\lambda_a+\lambda_p\right)\text{ohms}$$
$$(94)$$

Again, from equation 83, the flux linkage in the equivalent direct-axis damper winding due to field current is given by

$$\psi_{Dfd}=PN_fN_{Dd}k_{Dd}C_1\lambda_aLI_f \qquad (95)$$

Consequently, if equation 84 is used to eliminate I_f from equation 95 and then the voltage ratio given by equation 66 is used to refer the quantity ψ_{Dfd} to the stator side and the definition of inductance is applied, then the mutual reactance X_{Dfd} between the equivalent direct-axis winding and the field winding referred to the stator winding is given by

$$X_{Dfd}=\frac{2\pi f}{10^8}\frac{\psi_{Dfd}}{i_{fa}}\frac{4}{\pi}\frac{C_{d1}}{C_1}\frac{Nk_w}{PN_f}\frac{i_{fa}}{I_f}\frac{Nk_w}{PN_{Dd}k_{Dd}}$$
$$=\frac{8fL(Nk_w)^2}{10^8P}C_{d1}\lambda_a\text{ ohms} \qquad (96)$$

By similar reasoning, it can be shown that by using equation 64, the flux linkage in the field winding due to the equivalent direct-axis damper winding is given by

$$\psi_{fDd}=PN_fk_f\frac{1}{\pi}n_b(1-k_b)C_{d1}\lambda_aLI_{Dd} \qquad (97)$$

and in the same manner, if equations 65 and 86 are used to refer the quantity to the stator side, and the definition of inductance is applied, the mutual reactance X_{fDd} between the field winding and the equivalent direct-axis damper winding referred to the stator winding is given by

$$X_{fDd}=\frac{2\pi f}{10^8}\frac{\psi_{fDd}}{i_{Dd}}\frac{4Nk_wi_{Dd}}{Pn_b(1-k_b)I_{Dd}}\frac{Nk_w}{PN_fk_f}$$
$$=\frac{8fL(Nk_w)^2}{10^8P}\lambda_aC_{d1}=X_{Dfd}\text{ ohms} \qquad (98)$$

Equations 96 and 98 show that the mutual reactances between the field winding and the equivalent direct-axis damper winding derived from either side and referred to stator side are equal. Further, it is readily seen that

$$\frac{m}{2}X_{fDd}=\frac{m}{2}X_{Dfd}=x_{ad} \qquad (99)$$

The loss in the field winding

$$P_f=r_fI_f{}^2\text{ watts} \qquad (100)$$

Now, if the current ratio given by

equation 84 is used to replace I_f by its equivalent i_{fu} in the stator side, then

$$P_f=\left(\frac{4}{\pi}\frac{C_{d1}}{C_1}\frac{Nk_w}{PN_f}\right)^2 i_{fu}^2 r_f \text{ watts} \qquad (101)$$

Since the equivalent field-winding resistance R_f referred to the stator side must be such as to have the same heat loss as that of the real field winding, then

$$R_f=\left(\frac{4}{\pi}\frac{C_{d1}}{C_1}\frac{Nk_w}{PN_f}\right)^2 r_f \text{ ohms} \qquad (102)$$

Equation 102 gives the following impedance ratio from energy consideration

$$A_{zf}=\left(\frac{4}{\pi}\frac{C_{d1}}{C_1}\frac{Nk_w}{PN_f}\right)^2 \qquad (103)$$

By comparing equations 103 and 88 the following relation for k_f should hold if the reflected loss is based only on the fundamental component of space flux densities due to I_f or its reflected phase equivalent

$$k_f=\frac{\pi}{4}\frac{C_1}{C_{d1}} \qquad (104)$$

References

1. Two-Reaction Theory of Synchronous Machines, Generalized Method of Analysis—Part I, **R. H. Park.** *AIEE Transactions*, vol. 48, July 1929, pp. 716–30.

2. Electric Machinery (book), **M. Liwschitz-Garik, C. C. Whipple.** D. Van Nostrand and Company, Inc., New York, N. Y., 1946.

3. Reactances of Squirrel-Cage Induction Motors, **T. C. Lloyd, Victor F. Giusti, S. S. L. Chang.** *AIEE Transactions*, vol. 66, 1947, pp. 1349–55.

4. The Operational Impedance of a Synchronous Machine, **M. C. Waring, S. B. Crary.** *General Electric Review*, Schenectady, N. Y., vol. 35, 1932, pp. 578–82.

5. Calculation of Synchronous Machine Constants—Reactances and Time Constants Affecting Transient Characteristics, **L. A. Kilgore.** *AIEE Transactions*, vol. 50, Dec. 1931, pp. 1201–13.

6. Starting Performance of Salient-Pole Synchronous Motors, **T. M. Linville.** *AIEE Transactions*, vol. 49, April 1930, pp. 531–45.

7. The Direct- and Quadrature-Axis Equivalent Circuits of the Synchronous Machine, **A. W. Rankin.** *AIEE Transactions* (*Electrical Engineering*), vol. 64, Dec. 1945, pp. 261–68.

8. Starting Performance of Salient-Pole Synchronous Motors, **M. M. Liwschitz.** *AIEE Transactions*, vol. 59, 1940, pp. 913–19.

9. Starting Performance of Synchronous Motors, **H. V. Putman.** *AIEE Transactions*, vol. 46, Feb. 1927, pp. 39–59.

10. Steady-State and Transient Synthesis of 3-Phase Reluctance Motors (Synchronous Motors Withour Field Excitation), **Mostafa E. Talaat.** *AIEE Transactions*, vol. 70, pt. II, 1951, pp. 1963–70.

◆

Discussion

Dean Harrington (General Electric Company, Schenectady, N. Y.): Earlier papers form a set of classical references which pioneered in penetrating the mysteries of synchronous machine behavior. Because each considered a different facet of the problem various approaches, definitions and symbols were used. While this was adequate at the time, there is a need for a reliable and consistent present-day treatment requiring a minimum of previous reader knowledge of the subject. This paper which presents reactances in ohmic value, is a good start in this direction.

The literature had developed the concept of nonreciprocal mutual reactance between the polyphase armature and each of the many rotor circuits. In this concept, the rotor sees the mmf of the several phases of the armature. One phase of the armature, however, sees only the current of the particular rotor circuit of interest. The author has nicely avoided this confusing issue by always referring to mutual reactance between one direct-axis phase and the rotor. Since reactances are quoted and used in pu, the conversion from ohms to pu should, for completeness, be covered in Part II of this paper, or good references should be given.

The paper offers several equations for machine torque expressed in watt-seconds. While watt-seconds have the same basic units as pound-feet, nevertheless the former is generally construed as a unit of work while the pound-foot is universally accepted as a unit of torque. If metric units are preferred, the newton-meter is commonly accepted for torque. Mr. Talaat's paper should be a help to the young engineer who is attempting to become acquainted with the elusive ways of synchronous machine reactance.

Lee A. Kilgore (Westinghouse Electric Corporation, East Pittsburgh, Pa.): The author has attempted to improve on the equation for transient and subtransient reactance given 24 years ago (reference 5 of the paper), which is certainly long enough ago to try a new approach. He states that the earlier equation gave results which were too low. It happens that the earlier equation for transient reactance was an exact one if the right permeance values are used and as far as the experience of the writer and his colleagues goes, it has always given accurate results. There have been a number of important water-wheel generator jobs where a low transient reactance was specified, where it was economically profitable to be able to calculate this constant accurately and where it was never found necessary to take any excessive margins to meet the guarantees. The author's equation 16 appears to be identical with that given in the earlier paper, so it may be in the determination of the permeance factors for the field where the author has differed. However, the equation for this quantity is not given. It would be interesting to see a tabulation of test and calculated values such as were given in the original paper.

With regard to the subtransient reactance, the author makes the assumption that the axis components of current in the damper windings are sinusoidally distributed. On the direct axis this seems a particularly poor assumption in many cases. The original paper at least made an attempt to represent the true current distribution in the pole tip bar. This is a point where some further work would seem justified, since no method short of that in Linville's paper (reference 6 of the paper) has attempted to be complete, and that method is too involved for ordinary use. Again the writer's experience with the early equation has been very good with the exception of its application to synchronous motors with very high resistance damper windings where the apparent subtransient reactance on test is higher than calculated because even in one-half cycle the induced current in the outer damper has decayed appreciably and the oscillograms do not show this high decrement term in the subtransient reactance. Possibly the assumption of a sinusoidal current would fit this case better, but would not fit a low-resistance damper. The author states that the paramount criterion for the correctness of the equations are that they reduce to the conventional values for a round rotor machine. This would be desirable but certainly not the major factor, since no salient pole machine approaches a round rotor machine in this respect. Again, it would be interesting to see some test data and to know the damper bar size and resistivity.

I believe the author's approach has more value in calculating constants for synchronous motor starting than for subtransient reactance. I have used such a method, but even for this purpose widely different impedances of damper bars could lead to serious error and call for special treatment.

M. E. Talaat: I agree with Mr. Harrington that the usual unit of torque is the pound-foot; or the newton-meter in the meter-kilogram-second system of units. However, when torque is considered as the product of flux linkage and current, and when it is noted that flux linkage has the unit of volt-second and current has the unit of ampere, their product is in watt-seconds. Multiply torque in watt-seconds by 0.7376 to obtain the result in pound-feet. The watt-second is equal to the newton-meter and the conversion factor is 1.

As to the per-unit system, it is usually agreed to refer machine reactances to their unit impedance in ohms which is machine-rated phase voltage divided by rated phase current. Any reactance given in ohms and referred to the stator side can therefore be divided by this unit impedance in ohms to give the per-unit value based on machine-rated kva and voltage. In network analyzer studies made on large systems it is often found necessary to refer machines' reactances as well as transformers' and transmission lines' impedances on a common kva and voltage base, and further conversions become desirable. Reference 1 of this discussion is a good treatment of the subject.

I agree with Mr. Kilgore that equation 16 for the direct-axis transient reactance in the paper is identical in form with that given in the earlier paper. (See reference 5 of the paper.) If in searching for the truth by the use of a new approach the same equation as the old one is arrived at, then at least we know that our equation is correct in form and by the process of elimination should look for other possible sources of discrepancies between tested and calculated values. Such may be the permeance factors for the field or those entering in the calculation of the stator leakage permeances. As mentioned in the paper these points will be brought out in Part II, to follow.

However, I cannot agree with Mr. Kilgore that the subtransient reactance is a truer assumption of the current distribution in the bars than that made in the paper. The coefficient (reference 5 of the paper) $\cos (n^1-1)\tau_b/\tau_r\ \pi/2$ if examined for the case of the induction motor where $n_b = \tau_r/\tau_b$ would go to

$$\cos\left(\frac{\pi}{2}-\frac{\tau_b}{\tau_r}\frac{\pi}{2}\right)=\sin\frac{\tau_b}{\tau_r}\frac{\pi}{2}\approx\frac{\tau_b}{\tau_r}\frac{\pi}{2}$$

Since, for the induction motor the field leakage permenance λ_F goes to infinity and (reference 5 of the paper)

$$6.38\left(0.5+\frac{h_{b2}}{b_{b2}}+\frac{h_{b1}}{3b_{b1}}\right)=6.38F_b$$

represent twice the permeance per bar, then his

$$\lambda_{Dd}=\frac{\tau_b}{\tau_r}\frac{\pi}{2}6.38F_b=10\frac{\tau_b}{\tau_r}F_b$$

while his λ_{Dq} is taken to be actually that of the induction motor and is given (reference 5 of the paper) as

$$\lambda_{Dq}=20\frac{\tau_b}{\tau_r}F_b$$

where F_b is taken here for brevity to mean the leakage permeance factor per bar. This means that by Mr. Kilgore's paper

$$X_{Dd}'=\frac{1}{2}X_{Dq}'$$

for the case of the induction motor.

This shows that Mr. Kilgore's treatment of the damper winding case fails to meet the paramount criterion for the correctness of the equation of X_{Dd} (reflected damper winding leakage reactance in the direct axis), namely, that for the case of continuous damper and uniform air gap the direct- and quadrature-axis quantities should become equal to one another and identical with the induction motor constant. On the contrary, the quadrature axis reflected secondary reactance in Mr. Kilgore's paper becomes twice that of the direct axis, which is physically inconceivable.

In a typical large water-wheel synchronous machine Mr. Kilgore's $X_{Dd}'=0.069$ (in per-unit of rated phase voltage and rated phase current), and by the new method $X_{Dd}'=0.12$. The subtransient reactance by his method was $x_{du}''=0.175$, and by the new method $X_{Dd}'=0.226$ (using the same stator leakage reactance $=0.106$), while the measured value at 16.5 per cent (%) voltage was 0.217. If for the sake of comparison we accept the tested value at 16.5% voltage to be the correct unsaturated subtransient reactance and the stator leakage reactance to be true at 0.106, this leaves $0.217-0.106=0.111$ for X_{Dd}'. This means an error in Mr. Kilgore's X_{Dd}' of −38% and an error in X_{Dd}' by the new method of only +8%. The error in the subtransient reactance by Mr. Kilgore's method is −18.5% and the error by the new method is only +4%. The calculated unsaturated value should always be slightly higher than any measured value, because of saturation. This accounts for the plus sign in the percentage difference between measured value and that calculated by the new method. The machine given here for comparison had all bars located near the pole face; they all had the same configuration and they all were of copper. The ratio of bar reactance to bar resistance was 26 at 60 cycles and 75 degrees centigrade, and the machine had higher subtransient time constant than normal machines $T_d''=0.087$ second. The large discrepancy between tested value and that calculated by Mr. Kilgore's method cannot be blamed therefore on a high resistance damper winding or on a fast-decaying subtransient current, as he pointed out in his discussion, but lies in a more basic error in his equation, as appears from its failure to be true for the limiting case of the induction motor. The basis on which Mr. Kilgore has taken the factor

$$\cos (n_b-1)\frac{\tau_b}{\tau_r}\frac{\pi}{2}$$

to be the fraction of the armature mmf, acting across the subtransient leakage paths in the rotor was not indicated in his paper. In his tabulation of calculated and tested results, no mention of the test voltages during measurements was given or whether saturation was taken into consideration in his calculations, or how. In Tables I and II of his paper eleven cases out of 19, for machines with damper bars, show higher subtransient reactances by measurement than by calculation. This discrepancy is in the wrong direction since any measured value should be less rather than greater than a calculated value with no saturation taken into account.

It is probable that the measured direct-axis subtransient reactances given in Mr. Kilgore's paper were obtained from tests taken at voltages high enough to give rated current values of direct-axis transient reactances, and therefore yielded fairly saturated values for the subtransient reactances, which made them seem closer to the low values calculated by his method. This, together with the fact that in many cases a large percentage of error in calculating X_{Dd}' reflects in a smaller percentage of error in the calculated direct-axis subtransient reactance, may have been the reason why Mr. Kilgore and his colleagues did not notice the seriousness of the discrepancy between calculated and measured values.

The assumption of sinusoidal space distribution of currents in the bars located in the pole face is based on the following two assumptions:

1. That during disturbance a time-varying sinusoidal space distribution of fundamental air-gap flux density is centered along the magnetic axis of the pole for the case of direct-axis quantities and along the interpolar axis for the quadrature-axis quantities. A pulsating field is, for instance, the case in method 3 of the AIEE test code for synchronous machines[2] for determination of direct-axis subtransient reactance form a static impedance test with single-phase voltage whose magnetic axis is in line with the pole axis.
2. That the impedance per bar, composed of leakage reactance per bar and resistance per bar, is the same for all bars. This assumes that all bars are located in the pole face and have the same configuration. This neglects only the variation in harmonic differential and tooth top leakage permeances due to variations in the air gap, and which are generally small. For pole tip bars which have different configuration a special treatment will be presented in Part II of his paper.

From these two assumptions one can proceed as follows to substantiate the assumption of sinusoidal space distribution of currents in the damper bars. With reference to Fig. 1, the sinusoidally space distributed time varying flux density in the direct-axis is given by $B(x,t)=B_d(t)\cos\frac{\pi}{\tau}x$, or $B(\theta,t)=B_d(t)\cos\theta$ where $\theta=\frac{x}{\tau}\pi$.

The flux linking any two damper bars n-n that are located symmetrically with respect to the flux wave axis is given by

$$\psi_n(t)=L\int_{-\frac{\tau_n}{2}}^{\frac{\tau_n}{2}}B_d(t)\cos\frac{\pi}{\tau}x\,dx$$

$$=\frac{2}{\pi}\tau LB_d(t)\sin\frac{\theta n}{2}$$

where

$$\theta n=\frac{\tau_n}{\tau}\pi$$

Therefore the voltage induced in n-n circuit is given by

$$E_{nd}(t)=\frac{-d\psi_n(t)}{dt}10^{-8}$$

$$=\left(\frac{2}{\pi}\tau L\frac{dB_d(t)}{dt}10^{-8}\right)\sin\frac{\theta n}{2}$$

$$=E_{Dd}(t)\sin\frac{\theta n}{2}$$

Now, from basic principles

$$2r_{be}I_{nd}(t)+2L_{be}\frac{dI_{nd}(t)}{dt}$$

$$=E_{nd}(t)=E_{Dd}(t)\sin\frac{\theta n}{2}$$

Solution of this differential equation yields a current of the form

$$I_{nd}(t)=I_{Dd}(t)\sin\frac{\theta n}{2}$$

where $I_{Dd}(t)$ is the instantaneous current that would be induced in the two bars embracing a full pole pitch, and is the maximum possible current.

From a qualitative point of view, it is known that the basic principles of damping state that maximum damping effect in the direct-axis is given by the outermost bars in the pole face and zero-damping effect by a bar located at the pole center. A sinusoidal space distribution of currents in the damper bars meets this qualitative requirement.

It is therefore clearly seen that the assumption of sinusoidal space distribution of currents in the damper bars is as good an assumption as that of a sinusoidal fundamental space distribution of effective flux density in the air gap, which is one of the basic assumptions made in the development of the 2-reaction theory of synchronous machines.[1]

REFERENCES

1. CIRCUIT ANALYSIS OF A-C POWER SYSTEMS (book), Edith Clarke. John Wiley & Sons, Inc., New York, N. Y., vol. I, 1943.

2. TEST CODE FOR SYNCHRONOUS MACHINES. *AIEE Standard No. 503*, June 1945, par. 1.865, p. 36.

Gas-Pressurized 120-Kv and 161-Kv Pipe-Type Cables in Ontario

STEPHEN KOZAK
ASSOCIATE MEMBER AIEE

COLIN PRESCOTT
NONMEMBER AIEE

ADDITIONAL power requirements in the Toronto area of the Southern Ontario System led to the construction of the Richard L. Hearn Generating Station. The output of this thermal generating station is taken at 115 kv into the existing system by a 4-circuit overhead line. Where the new 4-circuit line joins the existing network, difficulty was experienced in obtaining rights of way for additional overhead circuits. Underground construction was the only practicable alternative. In 1951, approximately 1 mile of 115-kv pipe-type gas compression cable was installed, followed in 1952 by a further $4^1/_2$ miles of pipe-type cable. Two miles of the latter were of the gas compression type and $2^1/_2$ miles were the Atkinson-Fisher gas-pressurized type. It is with this latter $2^1/_2$ circuit miles that this paper is concerned.

Route

The route length of $1^1/_4$ miles traverses undeveloped land of the Don River basin, Fig. 1. Difficulty in obtaining permanent right of way on the east river bank led to the placing of part of the route on the west bank and necessitated two river crossings. The preliminary investigations of the route can be divided into three parts.

First, the river crossings were selected from several profiles of soundings, utilizing the cone penetrometer method to determine solid bearing underneath the accumulated silt. Fig. 2 is representative, and indicates that unstable bearing extended for approximately 4 feet below normal river bottom. The resultant recommendation of burial at the 237-foot elevation was modified to the 235-foot elevation, when civic authorities revealed an intention to dredge to the 239-foot elevation at some future date.

Second, a soil classification was conducted along the route by sampling at auger holes every 300 feet. A tabulation of soils, hydrogen ion concentration, and presence of free water was prepared. The information obtained was of limited use as actual excavation showed much more frequent variation, and on future projects it will not be pursued.

The third investigation was concerned with soil thermal resistivity. The results obtained by the transient needle method[1] are shown on Fig. 3. In the section from 2,500 to 3,500 feet, the natural undisturbed clay has been covered with as much as 3 feet of trash fill including ashes, bottles, and various metal scrap ranging from bottle caps to bedsteads. The low values on the chart at 3,500 to 4,500 feet are coincident with an underground water course. The high thermal resistivity for the ground surface under Bloor Viaduct at 4,600 feet may be remarked, the bridge effectively shielding the ground from rainfall. Excavation of the heterogeneous fill revealed many air pockets, no doubt partly responsible for the high thermal resistivities. After laying, 2 feet of sand backfill was used in these areas. The remainder was of the original excavation materials, suitably screened.

The minimum required 3-foot depth of cover was maintained wherever possible. However, the vertical approaches to the river crossings, coincident as they were with main railway-line crossing, necessitated much greater depth, as did certain uncharted obstructions. The vertical and horizontal bends were onerous and demanded due consideration in planning the cable pulling. The profile and splicing locations were established in cooperation with the cable manufacturer in the early stages of the project.

Choice of System

A system obtaining great mechanical integrity and yet possessing flexibility was of prime concern. Additionally, in such a relatively short route length, it was of paramount importance to have the land cable suitable for the river crossings. Both direct burial and duct and manhole systems would require special submarine construction. The direct-burial alternative was considered not sufficiently sound mechanically.

City conditions with the attendant likelihood of interference by other underground plant dictated maximum mechanical strength. City conditions also called for maximum flexibility of routing. It was decided that a system employing steel pipe was most adaptable to these conflicting requirements.

In the selection of a pipe-type system, gas-pressurized, gas compression, and high-pressure oil-filled were considered. The first two were similar in first cost and less than the high-pressure oil-filled. The Atkinson-Fisher gas-pressurized pipe-type cable was selected for the section from Gerrard Transformer Station to Bloor Street Junction.

Circuit Requirements and Cable Description

Of the two parallel circuits, one was required to operate on the 60-cycle 120-kv (nominal 115-kv) solidly grounded neutral system, the other to operate temporarily on the 25-cycle 120-kv (nominal 115-kv) system convertible to 60-cycle operation at some future date. The latter system is grounded through a resistance and is considered as ungrounded for the purpose of voltage rating. This circuit was insulated for 161-kv equivalent grounded neutral.[2] For the potheads the 138- and 161-kv classes of the AIEE standard for potheads[3] were selected. Joints were rated to be in accord with cable rating. Both circuits were required to transmit 125 megavolt-amperes at 115 kv, 60 cycles, at a design load factor of 100 per cent (%).

For these conditions of load capacity with all losses considered, a copper conductor size of 1,150,000 circular mils of annular cross section, operating at 85 degrees centigrade (C) maximum conductor temperature, was required for the pipe sections. With sheaths open-circuited, the terminal ends capacity was considerably higher for the same size. The cable dimensions are given in Table I for both 120- and 161-kv designs. For the cables in pipe, the hollow annular conductor of shaped copper segments is insulated with mass-impregnated paper dielectric, protected with bronze, polyethylene and copper tapes, and D-shaped copper skid wire. The three cores are factory cabled, with a length of lay of approximately 48 inches. The decision to cable the cores was influenced by many factors; those of prime importance being as follows:

Paper 55-50, recommended by the AIEE Insulated Conductors Committee and approved by the AIEE Committee on Technical Operations for presentation at the AIEE Winter General Meeting, New York, N. Y., January 31–February 4, 1955. Manuscript submitted October 22, 1954; made available for printing December 8, 1954.

STEPHEN KOZAK is with the Canada Wire and Cable Company, Ltd., Toronto, Ontario, Canada; and COLIN PRESCOTT is with the Hydro-Electric Power Commission of Ontario, Toronto, Ontario, Canada.

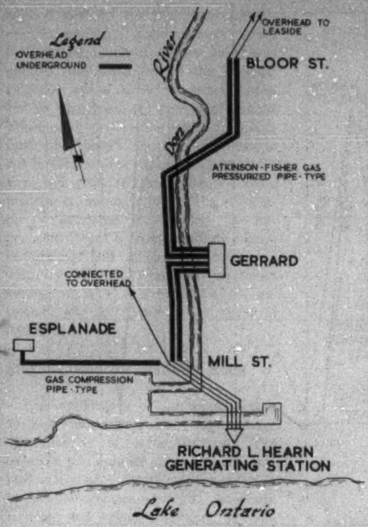

Fig. 1 (left). Schematic pipe-type cable systems

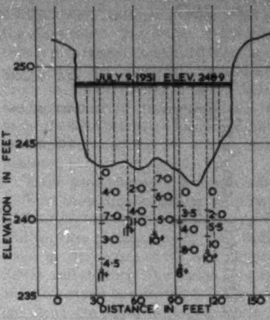

Fig. 2 (right). Profile of typical river crossing. Cone penetrometer readings indicate ultimate bearing capacity in tons per square foot

1. To mitigate end thrust on the joints during load cycles.

2. To contribute to easier pulling and avoid any danger of jamming on relatively short bends.

3. To simplify installation and reel handling, and reduce exposure time to outside atmosphere.

The terminal ends were of the same conductor construction and insulation details but were sheathed with seamless aluminum sheath.

All cables were shipped under nitrogen pressure of 25 to 30 pounds per square inch (psi) in the core; the pipe cables were additionally protected by a gas-tight reel construction. The shipping lengths of pipe cable were dictated by the route access difficulties, river crossings, and horizontal and vertical bends. The 6,000-foot route was supplied in five shipping lengths, between 1,000 and 1,200 feet in length. The pipe route was particularly difficult in respect to bends. At one river crossing vertical bends to reach specified depth were immediately followed by tight right angle horizontal bends (minimum radius 22 feet) to remain within the right of way.

Pipe Cable: Design and Manufacture

The cable design was founded on the principles of gas pressure void control in mass-impregnated paper dielectric. The use of an almost inert gas at high pressure in intimate contact with, and forming part of, the dielectric was first suggested by the Atkinson-Fisher team in their 1925 patents. Wherever possible the design incorporated manufacturing techniques already successfully developed, notably those related to the conventional oil-filled system, and which would realize to the fullest extent the economic and reliable exploitation of these principles. Experimental work on similar cables since 1950 had shown that the criteria of design, available materials and terminations, were suited to this pipe-type Atkinson-Fisher system.

Adoption of a hollow conductor has the advantage that the maximum gas pressure is coincident with the maximum electrical stress at the conductor surface. It permits the use of gas supply through the terminal ends after the fashion of oil-filled system oil feed. It also permits the use of a simple pothead design uncluttered by accessories. Coupled with the use of a tight-fitting, seamless, and pressure-retaining aluminum sheath, it allows a simple design of factory-sealed single-conductor terminal cable which has sensibly the same constructional and electrical characteristics as the cable in the pipe. For the required cross-sectional area, the annular conductor offsets skin effect to a degree comparable to a segmental conductor.

Initially, the insulant thickness for both circuits was chosen to limit the maximum operating stress to 92 kv per centimeter (cm). This premised the use of single annulus of conductor segments; subsequently a 2-layer construction was adopted which increased the conductor diameter approximately 1.5%, resulting in a maximum operating stress of 90 kv per cm.

The maximum radial stress of 92 kv per cm was chosen to provide the following factors of safety:

1. With respect to external surges $\frac{g_{ca}}{g_c} \geqq 8$

2. With respect to internal surges $\frac{g_{ct}}{g_c} \geqq 3$

3. With respect to ionization ignition $\frac{g_{cn}}{g_c} \geqq 2$

where

g_c = radial stress at the conductor surface at rated voltage rms.

g_{ct} = radial stress at the surface of the conductor at the 1-hour abscissa on the voltage-time-to-breakdown curve.

g_{ca} = radial stress at the conductor surface for impulse voltage breakdown (crest value) wherein puncture occurs on the crest or tail of the wave, thus giving minimum breakdown rather than a maximum one which would occur if the value were on the wave front.

g_{cn} = radial stress at the conductor surface at the ionization ignition voltage.

Laboratory development tests on 69-kv cable designed to the same parameters[4] confirm that the design factors of safety with respect to g_{ct}, g_{cn}, and g_{ca} are readily attainable. For an impulse test of 4.5 $(E+10)$ kv, where E is the line-to-line voltage in kv, the corresponding calculated values of radial stress at the conductor surface are 760 kv per cm and 750 kv per cm for 120- and 161-kv cable respectively. Development and type tests have indicated an impulse

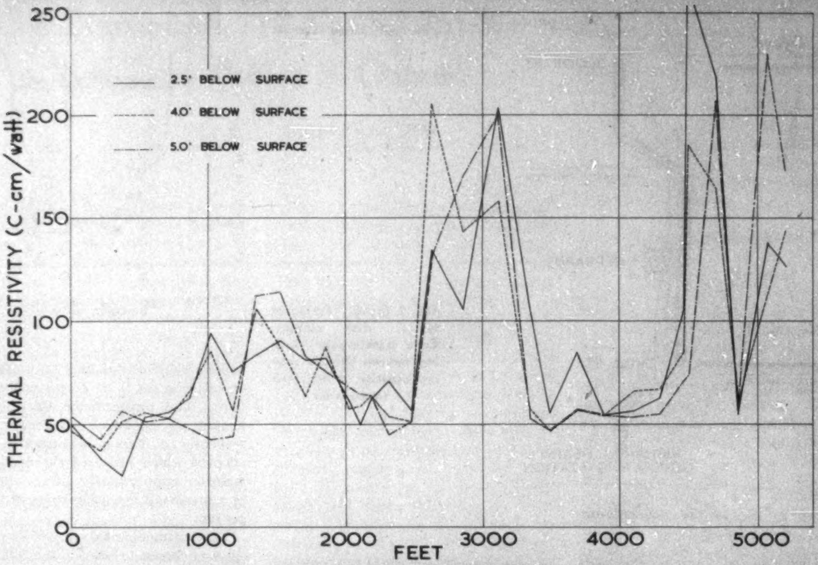

Fig. 3. Soil thermal resistivity determinations along cable route

strength for this cable corresponding to values of g_{ea} of at least 900 kv per cm, and the work of a host of contributors (see references to reference 4) has shown representative values for all high-voltage cables between 800 to 1,000 kv per cm.

The hollow conductor is constructed by utilizing a double layer, each of 16 shaped segments. The double layer had the following advantages over a single construction:

1. Better drawing and stranding when compared to that obtainable with the relatively slender segment of a single layer for this area.
2. The first layer of 850,000 circular mils was a construction used for many miles of conventional oil-filled cable and production techniques were thus in existence.
3. The double layer facilitated the fitting of a flush connector desired in the joint design by the mere removal and scarfing of the outer layer.

The selection of the 0.690-inch gas channel was influenced by item 2 in the foregoing, but included the forethought that the channel must be blown clear of any excess impregnating compound after manufacture. However, in the case of an aluminum-sheathed cable[4] with a 3/8-inch gas channel, manufactured concurrently with the subject cable, no difficulty was experienced in this respect. Unless otherwise dictated, future construction will adopt a 0.5-inch channel.

The shield construction around each core was designed to consist of 1 by 0.004-inch bronze tape intercalated with polyethylene tape; 1 by 0.004-inch bronze intercalated with polyethylene tape; and 1 by 0.070 by 0.200-inch copper skid wire with 1.5-inch lay over-all. During the processing of an experimental length, it was found that the bronze tapes tended to open up when the cores were cabled together, thereby impairing the moisture seal for installation purposes. As installation was to take place during the rainy fall season, it was decided to replace the outer tapes with two intercalated soft copper tapes which would hold down the bronze and polyethylene moisture seal.

Application of the insulant papers followed conventional practice for solid-type cables with additional close attention to paper tape widths and tensions. Superdense, relatively thin papers were

Table I. Cable Description and Dimensions, Inches

				3-Conductor Pipe-Type Cables				1-Conductor Terminal Cables			
	Conductor Diameter				Diameter			Thickness		Diameter	
Rating	Outside	Inside	Insulant Thickness	Protective Tapes*	Over Skidwire	Over Cabled Conductors	Pipe Size	Aluminum Sheath	Rubber Sandwich	Over Sheath	Over-all
120 kv	1.315	0.690	0.385	1×0.004 bronze 1×0.005 polyethylene 2×0.004 copper	2.27	4.90	$6^5/_8$ OD†×0.280	0.110	0.150	2.31	2.61
161 kv	1.315	0.690	0.565	1×0.070×0.200 copper skidwire	2.63	5.66	$8^5/_8$ OD×0.320	0.135	0.150	2.72	3.02

* Same makeup for 120- and 161-kv cables.
† Outside diameter.

applied next to the conductor for dielectric grading. Approximately 0.050 inch of 0.0025-inch superdense paper was applied, the remainder of the insulant thickness was of 0.005-inch dense papers. Cables were dried and mass-impregnated before skid wire application and cabling (and also before sheathing the single conductor terminal cables). Close attention was paid to the pressure-cooling process to ensure a dielectric as completely saturated as possible. The impregnant was a compound of polyisobutylene and mineral oil having a viscosity of 4,000 Saybolt universal seconds at 50 C and exhibiting an extremely low and stable power factor of 0.03% at 100 C.

Single-Conductor Terminal Ends

This application of aluminum sheath to high internal pressure high-voltage operation is of some interest. The superior performance of aluminum over lead or lead alloy sheathing materials[5,6] in respect to greater strength, hardness, fatigue, and creep resistance is consequently applied to the fullest economical benefit. For example, calculation for the 161-kv terminal ends show that a pressure of 700–1,000 psi is required before a stress corresponding to 0.1% elongation (proof stress) is attained. The aluminum sheath in this case is of 0.135-inch thickness and 2.72-inch outside diameter.

The application of aluminum sheath for the terminal ends was made possible by taking advantage of three developments, as follows:

1. Development of a cast-plumb technique to effect the seal between sheath and pothead and between sheath and trifurcating joint.
2. The application of an asphaltic, rubber-and-fabric tape combination, commonly known as a rubber sandwich, which permits direct burial and sheath isolation.
3. The design of a rugged gas feed pipe-line insulator capable of withstanding 500-psi internal pressure which, coupled with item 2 permitted operation of the terminal end cable with sheaths open-circuited. Adequate current-carrying capacity for the terminal ends was practical only with the sheath currents interrupted.

Terminal Design

The general layout of the terminal design is shown in Fig. 4. The porcelain shell, stainless-steel dome, and cast-plumb body are designed for the full operating pressure of 200 psi. Each pothead assembly was subjected to an acceptance test of 500 psi oil pressure for 6 hours, followed by 300-psi air pressure for 6 days. During experimental work similar porcelains have withstood 500-psi 1/2-hour cycle tests and sustained 300-psi pressures of several weeks' duration.

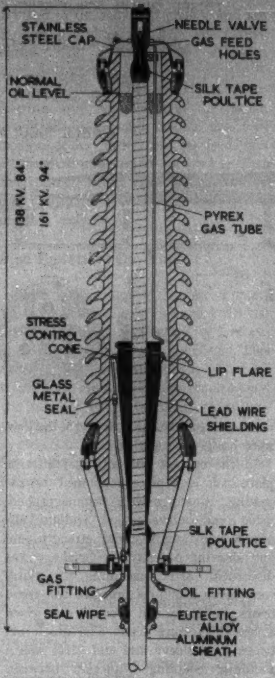

Fig. 4. Terminal design, 138-kv and 161-kv grounded neutral rating at 200-psi internal pressure

The aluminum sheath is sealed to the wiping bell by a cast plumb. First, a small wiped seal is made over asbestos packing between the sheath and bell. This seal is then reinforced by pouring a molten alloy of 63/37 tin-lead at the required temperature into an aluminum mold clamped around the sheath. The act of pouring displaces a hot palm oil flux from the mold.

On installation, the terminal is filled with oil to a predetermined level, such that a gas space is obtained at the top. The gas from the external gas supply is carried through the filling oil by a heavy-wall Pyrex glass tube. Gas is introduced to the conductor hollow core from the gas dome through a needle valve orifice. The proper oil level is realized by allowing heated compound into the bottom of the terminal while vacuum is maintained on the glass tube. The height of the glass tube is so arranged that the oil level, upon contraction to ambient temperature, drops to approximately 8 inches below the top of the tube, thereby effecting the proper balance between a compound-filled terminal and an internal volume compensator.

Design parameters of the stress control cone are those used in designs which have successfully withstood long-time 60-cycle and impulse voltage tests.[4] The radial stress on the surface of the cone for both 138 kv and 161 kv is 7 kv per cm. Longitudinal stresses are limited to 1.5 kv per cm along the stress cone profile and to 5.0 kv per cm in the terminal filling oil adjacent to the stress control cone lip flare. These stresses are in accord with other comparable empirical data.[7] Dimensions imposed on the pothead to provide adequate external flashover values provide adequate internal creepage distance and prove to be approximately three and four times the design stress criteria of 1 kv per cm for the 161-kv and 138-kv designs respectively.

Joints

Joint design was based upon the use of hand-applied preimpregnated straight-paper tapes, similar in density and thickness to the factory-applied cable insulant. They were supplied preimpregnated with cable compound in sealed containers after drying and vacuum treatment. Stepping and taping profiles were calculated by methods according to Short,[8] using the following design parameters:

Radial stress at conductor surface for rated voltage

$g_c = 92$ kv per cm

Radial stress at cable insulant surface for rated voltage

$g_s = 58$ kv per cm for 120-kv cable
$g_s = 49$ kv per cm for 161-kv cable

Radial stress at ferrule surface for rated voltage

g_f between $0.48\ g_c$ and $0.50\ g_c$

Maximum longitudinal stress along stepping profile 1.3 kv per cm.

Maximum longitudinal stress along stress cone profile 1.2 kv per cm.

These criteria result in a design strength of joint, with factors of safety to internal and external transient surges, compatible to that of the cable itself. Since cable geometry is undisturbed by the flush ferrule, the factor of safety in relation to conductor and ferrule surface stresses

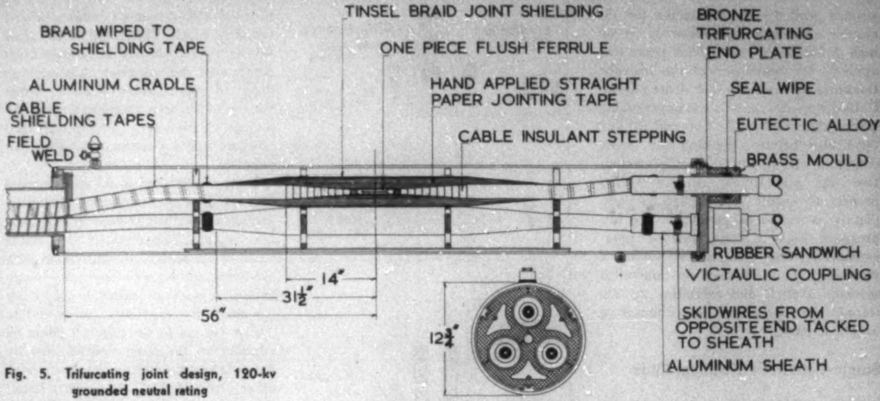
TINSEL BRAID JOINT SHIELDING
BRAID WIPED TO SHIELDING TAPE
ONE PIECE FLUSH FERRULE
BRONZE TRIFURCATING END PLATE
ALUMINUM CRADLE
HAND APPLIED STRAIGHT PAPER JOINTING TAPE
SEAL WIPE
CABLE SHIELDING TAPES
EUTECTIC ALLOY
FIELD WELD
CABLE INSULANT STEPPING
BRASS MOULD
RUBBER SANDWICH
VICTAULIC COUPLING
14"
31½"
56"
SKIDWIRES FROM OPPOSITE END TACKED TO SHEATH
12¾"
ALUMINUM SHEATH

Fig. 5. Trifurcating joint design, 120-kv grounded neutral rating

may be wholly applied to offset the uncertainties of field jointing

Features of the joint are shown in Figs. 5, 6, and 7. The completed single-conductor joints are supported in cast-aluminum cradles, which are banded with stainless-steel ribbon, spaced apart, and connected by an aluminum channel. This channel allows the joint casing to slide smoothly over the assembly. Originally, it was intended that the joint casing would serve as a temporary cap over the cable ends during the period between pulling and start of jointing, and a somewhat complex system of gasketed flanges was designed. Subsequently, the sleeve proved much too heavy and unwieldy for this purpose, and comparatively light sheet metal caps were used. Skid wires were terminated on binding posts and the posts at each end of the joint were jumpered together.

In the case of trifurcating joint, the plate was a 1-piece machined bronze casting. Castings were gammagraphed, using a radioactive isotope "Iridium 192" of approximately 50 curies' strength, and any showing porosity or shrinkage was discarded. After machining, the plates were given a 500-psi pressure test for 4 hours, surface-tinned over-all, and given a repeat pressure test. The union between joint sleeve and end plate was a Victaulic coupling. Junction between the aluminum-sheathed terminal cables and the end plate was achieved by use of the cast-plumb technique as described for the potheads.

Jointing procedure was similar in many respects to that followed for the conventional low-pressure oil-filled system. In this case, gas instead of oil was kept under a positive pressure within the hollow core and was allowed to flow from it when cut, thus preventing contamination from the atmosphere. To this safeguard was added flushing with hot compound at frequent intervals throughout the jointing. The 1-piece flush ferrule is fitted with a valve enabling the nitrogen to bleed past the soldering operation. Taping over the stepping matched the factory insulating tapes in width, thickness, and density. Once the hand-applied insulation reached the diameter of the factory insulation, wider tapes were applied to speed taping. Wherever and whenever possible, exposed insulation was temporarily wrapped with polyethylene tape to exclude mois-

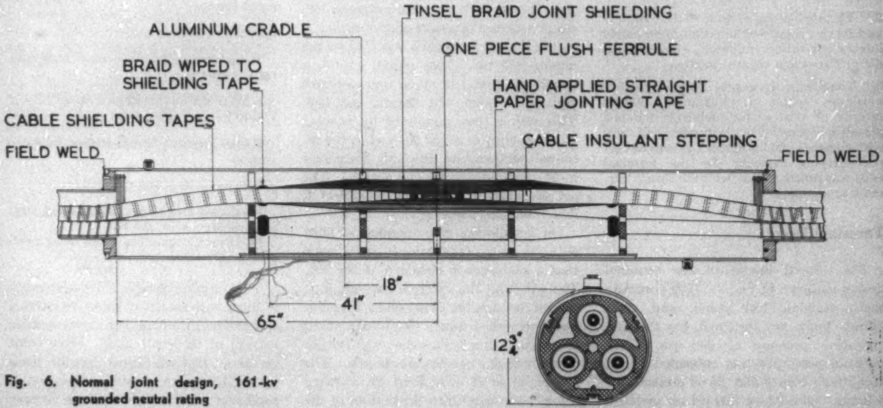
TINSEL BRAID JOINT SHIELDING
ALUMINUM CRADLE
ONE PIECE FLUSH FERRULE
BRAID WIPED TO SHIELDING TAPE
HAND APPLIED STRAIGHT PAPER JOINTING TAPE
CABLE SHIELDING TAPES
CABLE INSULANT STEPPING
FIELD WELD
FIELD WELD
18"
41"
65"
12¾"

Fig. 6. Normal joint design, 161-kv grounded neutral rating

Fig. 7. Trifurcating joint, 161 kv, showing victaulic coupling and cast-plumb seals between pipe and single-conductor aluminum-sheathed terminal ends

ture and contaminants. No effort was made to air-condition the joint bays, which were sheeted over and warmed above ambient by electric heat lamps. Almost all operations were kept confined to the joint bay so that exits and entrances were minimized. After completion of the acceptance pressure tests, the joints were directly buried.

Gas Charging and Ancillary Equipment

Both circuits, 120-kv and 161-kv, are supplied from a gas-charging cubicle located at Gerrard Street. Each phase of each circuit is fed through its Gerrard Station terminal by underground gas lines of 3/8-inch outside diameter dehydrated copper tubing, insulated and protected with a 1/16-inch wall of extruded polyethylene. A diaphragm-type valve and a high-pressure pipe-line insulator were interposed at the base of each pothead to maintain isolation of the pothead above ground and to permit control of gas to each terminal.

The insulated gas lines were drawn into conduit embedded in the concrete protective cover over the direct-buried terminal cables. Each line was purged to a dew-point value of −20 degrees Fahrenheit before connection. The steel pipe of each circuit was similarly fed at the Gerrard end at the underground trifurcating joints.

The control panel in the gas-charging cubicle was arranged so that manipulation of valves would enable gas to supply the pipe, each individual hollow core of each phase, or all four together. Fig. 8 depicts the schematic diagram of the gas connections. In normal operation the two stand-by gas bottles are disconnected from the line, and the pressure gauge on the manifold is connected to read the pressure on all three phases. Pressure alarms are connected to the pipe gas feed line and to the manifold phases, and are set for low alarm at 175 psi. These alarms are bourdon-tube actuated mercury switches.

Throughout the panel standard components were specified and the design permitted simple and flexible gas feed manipulation. Individual gas feeds can be isolated and tested for leaks. One disadvantage of the panel design rests in the multiplicity of fittings subject to possible leakage.

Pipe Protective Covering

Since factory-applied protective coatings are customarily expected to be superior to field application, a factory-applied coating was specified. This decision was strengthened by the relatively small amounts of pipe required and the number of route obstructions preventing any degree of continuous field application. Coal tar, Fiberglas reinforced enamel coating was specified as follows:

1. Pipe to be cleaned internally and externally by shot-blasting.
2. Bond coating of coal tar primer.
3. Hot coating, 1/16-inch minimum, coal tar enamel.
4. One wrap 0.015-inch Fiberglas wrap.
5. Hot coating, 1/32-inch minimum, coal tar enamel.
6. One wrap tar impregnated 15-pound asbestos pipe-line felt.
7. One wrap heavy Kraft paper.

A thin spray coating of No-Oxide export no. *2 W* pipe primer was specified for the inside of the pipe. An electrical holiday-detection test was applied at the factory just after coating application, using a spark coil type of detector, producing a maximum voltage of approximately 12 kv. All holidays, which were not numerous at this stage, were repaired.

The pipe was transported to the site of the work by rail, stored for a minimum of two weeks, and distributed direct to the work by truck. Great care was taken at all times to avoid damage to the coating, the pipe being lifted by means of an attachment to each uncoated end. Pipes were plugged at the factory to keep out dirt and water.

The first sections of pipe were welded and made ready for holiday test approximately one month after coating application. Many holidays in the coating were revealed by test—averaging 12 per 40-foot length of 8-inch pipe, and approximately 6 per length of 6-inch pipe. Reduction of the detector output voltage to the minimum value which would arc across a gap in the coating, approximately 5 kv, showed no reduction in the number of indicated holidays.

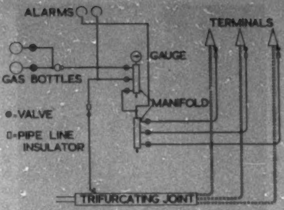

Fig. 8. Schematic diagram: gas-charging controls

Inspection of the holidays revealed some slight signs of mechanical damage: a few hair-line cracks radiating from a central point such as might have been caused by a blow. The remaining holidays coincided with small gas bubbles between the primer and the first enamel coat. Surprisingly, the hand-coated and wrapped joints were consistently the better covering by a wide margin.

It was found that a light blow, for example, a stone weighing 1 pound dropped from about 4 feet, would produce a holiday. The bond between the pipe and the coating was poor. The difference between this bond on the sample prepared for laboratory test and the pipe in the field was most marked. On the former, the enamel could be chipped off only in small flakes with the use of a hammer and chisel; on the latter the pipe could be peeled by hand. Analysis of the coating materials showed no adulteration or evidence of inferiority of the raw materials.

Patching all holidays would have been both expensive and so frequent as to constitute almost a route-long hand-wrapping job. It was decided to abandon electrical holiday detection; to patch the few places where there was obvious mechanical damage, relying on cathodic protection to back up the poor coating.

Subsequent investigations could not isolate any single reason for the poor quality of coating. One possible explanation for the bubbles is the fact that asbestos pipe-line felt has been found to give off volatiles on contact with hot enamel of 500 degrees Fahrenheit.[8] Improper curing of the primer, over-heating, and improper stirring of the enamel are all possible causes, and investigation showed that conditions would allow such occurrences, but not their persistence during coating. Evidence of mishandling

Fig. 9. Laying of 6- and 8-inch pipe in common trench

of the hot pipe immediately after coating on poorly padded racks and rollers was also evident, and could have contributed to numerous holidays, especially where the lengths were allowed to roll together while still warm. Our experience has shown that there is very little tolerance in the application recommendations, and any future job will have to be painstakingly inspected at every step.

Installation

Following pipe placement and welding of sections, Fig. 9, the welds were water-bath tested at 150 to 175 psi. Backfill consisted of a 3-inch layer of sand under and over, a 6-inch layer selected from previously excavated material, followed by machine placement of the remainder.

Advantage was taken of the proximity of the cable manufacturing plant by arranging that no cable was to be ordered on the job site unless conditions favored immediate installation. Prior to a pulling date, joint flanges were welded to each pipe section, tarpaulins erected and pipe sections wired and purged to a dew point of −20 degrees Fahrenheit, with the use of nitrogen of 0.1% oxygen content. The cabled pipe cable was transported on welded steel reels sealed by an impervious laminated gas blanket under the lagging. The large size of reel permitted only a slight positive pressure within the blanket. However, the cable cores were maintained at a positive pressure of 30 to 40 psi during shipment and during pulling operations. The three conductors were fitted with pulling eyes and end seals made gas-tight to the outer tapes by the use of a sleeve filled with low-melt alloy; see Fig. 10.

During pulling in, a nitrogen flow was maintained on the pipe from the end remote from the cable feed, and a slight amount of cable compound was used to aid the pulling in. Actual pulling tensions were not recorded in this installation, as only short lengths were involved (maximum 1,200 feet); however, it is sufficient to say that the pulls in all cases were relatively light, and no disturbance of skid wire or protective tapes was observed.

After completion of pulling in a particular length, the cable cores were blown clear with a grade of nitrogen of high purity, containing less than 0.002% oxygen, excess cable was cut off, and cable ends were capped and jumpered to the nitrogen supply. All operations were performed on the principle of maintaining the cables under pressure and/or gas flow at all times. After capping, and check of cable cores and pipe for dew point, the ends were sealed in nightcaps gasketted to the joint flanges.

Acceptance Tests

After installation was completed, each circuit was subjected to a 12-hour pressure test at 300 psi. A d-c test voltage as outlined in the Association of Edison Illuminating Companies' specifications[2] was applied for 15 minutes after completion of the pressure test. The test voltage for the 120-kv circuit was 203-kv direct current; for the 161-kv circuit the d-c test voltage was 250 kv, limited by the test set and atmospheric conditions.

Anticorrosion Protection

The cable route parallels two trunk railways systems and the installation was followed by the construction of two parallel oil pipe lines. The city street railway system also imposed an involved stray current pattern and it was decided to postpone the choice of a cathodic protection system until construction activity had subsided and a regular pattern of soil potentials had become manifest. The cable pipes were bonded to the station grounds at each terminal. An early survey indicated that a magnesium anode bed near Gerrard might, at least, provide some temporary protection, this was installed but subsequent measurements indicated that it was ineffective.

Pipe-to-soil potentials measured during the first year of service indicated peak pipe potentials of up to plus 1 volt measured to a copper sulphate cell, coincident with transit system rush hours. At this time current peaks of 3 to 4 amperes were entering one station ground, flowing through the pipe, and out at the other end.

Fig. 10. Reel of 3-conductor pipe-type 120-kv cable, showing pulling eyes and end seals

A system that would protect the pipe and, incidentally, the station grounds would require very high currents. An arrangement was sought whereby the potential required could be inserted in series between the station ground and the pipe, and at the same time have a low a-c impedance to fault currents. Such an arrangement would use the station ground bed as an anode but it was thought that the yearly loss of metal could be tolerated.

It was decided to insert 2-volt secondary cells of the automotive type in series between the pipe and the station ground beds to be kept charged by rectifiers and which would, in effect, float between the rectifier terminals supplying protective current to the pipe. Investigation showed that the cells would effectively shunt a-c fault current across the rectifier terminals and prevent undue potential rise in this event.

Experience in Service

The 2 years of operation under normal load have recorded two electrical faults on the 120-kv circuit, the second directly attributable to the first, and both line-to-ground faults. Additionally, a number of gas leaks have occurred on the circuits.

The first 8 months of operation on load were without incident, except for a gradually decreasing gas pressure, particularly on the 120-kv circuit, as indicated by the charts of daily peak loading and pressure readings; see Fig. 11. During this period some small leaks were located on loosened fittings on the ancillary equipment, and were rectified.

Continued pressure decrease in the following months demanded replenishment of nitrogen from standard cylinders, pending out-of-service availability of the circuits to investigate what appeared to be leaks of more consequence.

The first line-to-ground fault on the

120-kv circuit occurred approximately 11 months after the in-service date. The second fault occurred less than 2 hours after returning the repaired circuit to service potential and load. In the first fault the gas pressure was of the order of 125 psi, whereas the pressure on the occurrence of the second fault was 230 psi.

Location and Repair of Both Faults

On the occurrence of the first fault the pressure dropped to zero on the circuit. After immediately establishing a gas feed to the circuit to maintain a slight positive pressure, the fault resistance was burned down by passing heavy current at low voltage from the turbine generators. The fault location was indicated by linascope and oscillator, finally it was accurately located using a sensitive Murray loop bridge. The fault was located 31 feet from a joint location and 2,430 feet from the Bloor Junction terminal end. The fault was uncovered within 24 hours from the time of failure.

Externally the fault had burned a hole approximately $1^1/_4$ inches in diameter through the 0.280-inch wall of the steel pipe. Removal of approximately 2 feet of pipe revealed severe local charring of the insulation on one phase right to, and including, burnout of some of the conductor and partial charring of a second phase. The third phase was undamaged. Examination of the insulation of all three conductors immediately adjacent to the fault by "boiling out" individual tapes and application of magenta dye tests revealed no moisture present nor any ionization. Visual appearance of all paper indicated adequate compound on all tapes, and no drying out of the insulation was in evidence.

The decision was made to cut all three conductors and to remove sufficient pipe to allow making of a normal 3-conductor joint. Flanges were subsequently welded to the pipe, with the cables protected from the welding heat by packing with asbestos and foil. The joints were constructed and the sleeve welded in position without incident.

Several leaks were repaired on the circuit and the system tested at 300 psi for 7 days. A d-c test potential of 200 kv was applied without incident for 15 minutes on each phase to ground, and the circuit was restored to service.

The second electrical fault occurred without drop of pressure and was again located within the confines of the repair joint by the linascope, oscillator and Murray loop tests. On removal of the repair sleeve and on examination of the faulted phase, it was evident with little doubt that the heat of welding the flange for the first repair had damaged the cable resting on or near the bottom of the pipe. The other two cables were undamaged; also the three cables in the vicinity of the opposite flange, after very careful inspection, showed no indication of heat damage.

The repair to the faulted phase was carried out by cutting the conductor and inserting a lengthened ferrule, and taping a normal single-conductor joint. The flange and 2-foot section of attached 6-inch pipe were slid back to make room for the joint by cutting out a short section of the 6-inch pipe. This method permitted more thorough wrapping of the cables under the weld region joining the 6-inch pipe with the flange to the rest of the pipe. Alternate layers of asbestos paper and aluminum foil were wrapped many times round the cables for approximately 2 feet, and the weld performed over a standard split-backing ring. The 12-inch joint diameter sleeve from the repair joint was extended by two half sections of similar pipe welded together, and the whole assembly was finally coated and wrapped and supported on concrete pedestals. The circuit was again pressure-tested to 300 psi for 7 days, tested to 250 kv direct current for 15 minutes, and returned to service. Operation has been without further incident.

Possible Causes of First Fault

In the following are crystallized the findings of a joint co-operative investigation of the possible causes of, or conditions giving rise to, the first fault:

1. A lightning storm occurred in the area before the occurrence of the failure. A lightning stroke component counteroperating in range of the cable, recorded one lightning discharge 1 hour before the fault. Otherwise there were no system disturbances recorded within a contributable period of time.
2. A possible accident or imperfection during cable manufacture not detected by the routine tests.
3. Possible damage during shipment or installation of the particular length of cable.
4. A local hot spot due to the heterogeneous nature of the surrounding soil.

One other observed fact was the steady decrease in gas pressure throughout the 11-month period prior to the fault, as charted in Fig. 11. However, the results of test data, particularly those of Fig. 6, reference 3, and the experience and tests of others, were considered sufficient basis for allowing the pressure to drop as shown without taking the circuit out of service.

Examination, as explained previously, did not reveal any indication of heating or drying out of the insulation. Nevertheless, in an effort to obtain more data on the possibility in item 4, a number of thermocouples were attached to both pipes. Records have so far indicated no pipe temperatures exceeding 27 C. However, it has not been possible, as yet, to duplicate the circuit-loading conditions together with the soil environmental conditions which preceded the fault.

Gas Leaks

During the repairs of the electrical faults, the trifurcating joints and potheads were carefully examined and checked for gas leaks. Some potheads showed deformation of the neoprene gaskets at the top porcelain-to-cap seal, caused by uneven tightening of the cap-retaining bolts. To repair these leaks, gaskets were replaced and bolts retorqued at daily intervals.

Leaks were found at several of the cast plumbs, one on a pothead and others on the trifurcating joints. Of these, a number were rectified by recasting new metal in the original mold. Two cast plumb could not be sealed completely by this relatively simple process, and the original mold bodies were replaced with split-mold bodies of more ample dimensions.

More than 85% of the original cast plumbs are in satisfactory operation after repeated pressure tests of the system at 300 psi for long intervals during the fault repairs. This is considered, under the circumstances, reasonably satisfactory

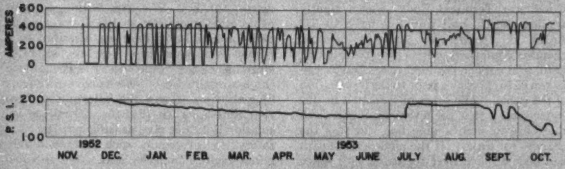

Fig. 11. Chart of peak daily load and gas-pressure 120-kv circuit

evidence of the soundness of the cast-plumb technique.

The troubles experienced and the nature of the successful remedial measures have indicated that the original molds, unless the cast is skillfully and carefully made, were of dimensions not quite sufficient to allow for all the vagaries and degrees of skill encountered in the field.

Summary

The features of this installation of pipe-type gas-pressurized cable may be briefly enumerated:

1. Seamless aluminum-sheathed terminal ends for high-voltage high-pressure operation.
2. Complementary components such as rubber-sandwich protective covering and high-pressure pipe-line insulators to permit operating aluminum-sheathed terminal ends with sheath currents interrupted.
3. Hollow-core conductor to facilitate gas feeding through high-pressure terminals, and to obtain an improvement in application of gas pressure to the dielectric.
4. High-pressure potheads without inner pressure-retaining chamber.
5. Cabling of conductors for the pipe-type cable.

The application of these features to the gas-pressurized pipe-type cable system has produced a pipe-type cable system of simple design, without encumbrances of complex accessories. It should be remarked, however, that several improvements of design details have become evident during the manufacture and installation, which when applied in future will permit further economies and refinements for more reliable field application.

References

1. Rapid Measurement of the Thermal Resistivity of Soil, V. V. Mason, M. Kurtz. *AIEE Transactions*, vol. 71, pt. III, Aug. 1952, pp. 570–77.

2. Specifications for Impregnated-Paper-Insulated Cable High Pressure Pipe-Type. Association of Edison Illuminating Companies, New York, N. Y., 1st edition, Sept. 1951.

3. Potheads. *AIEE Standard No. 48*, Jan. 1948.

4. Aluminum-Sheathed Type-SA Gas-Pressurized 69-kv Cable for Vancouver, F. G. Wollaston, H. D. Short. *AIEE Transactions*, vol. 72, pt. 3, Dec. 1953, pp. 1158–74.

5. Cables Sheathed with Aluminum. Development in Great Britain, P. M. Hollingsworth. *Paper No. 203*, CIGRE, Paris, France, 1950.

6. Seamless Aluminum Sheathed Cables, H. D. Short. *Electrical News and Engineering*, Toronto, Canada, vol. 61, No. 22, Nov. 15, 1952, p. 73.

7. Joints, Sealing Ends and Accessories for Pressure, L. G. Brazier. *Journal*, Institution of Electrical Engineers, London, England, vol. 93, pt. II, Oct. 1946.

8. A Theoretical and Practical Approach to the Design of High-Voltage Cable Joints, H. D. Short. *AIEE Transactions*, vol. 68, pt. II, 1949, pp. 1275–83.

9. Cable Through Tunnel Under Continental Divide Links Power Systems, F. M. Wilson, R. A. Nelson. *AIEE Transactions*, vol. 70, pt. II, 1951, pp. 1556–63.

◆

Discussion

R. W. Atkinson (General Cable Corporation, Bayonne, N. J.): It is useful to note a few of the comparisons between these very interesting Canadian installations and the practice which is current in the United States. The use in the terminals of a pressure resistant porcelain shell is of interest since the customary design in the United States which uses an inner "stop tube" to substain the hydrostatic pressure was developed when a porcelain shell with assured strength was not available.

The aluminum-sheathed terminal cable sections, compared with United States practice of unsheathed cable in copper pipe is noted. The method here used to prevent circulation of current in these sheaths, while effective, seems unduly expensive compared with the simple United States practice of insulating the hardware of the terminal base from the supporting structure.

The use by the authors of flush ferrules in the splices has worked nicely with their type of conductor. The use of a flush connector (ferrule) makes it very much easier to produce a joint having a dielectric strength equal to that of the cable; conversely, a connector much larger than the conductor is reasonably acceptable only if a strength considerably less than typical of the cable is expected from the joint.

It is noted that the cable saturant used is similar to that of United States practice though of lower viscosity, yet of greater viscosity than that currently used for so-called solid-type cables. We believe that the greater viscosity used in the United States has material advantage in terms of long life than does the more fluid saturant. There are some problems occasioned by the higher viscosity but these have all been proved surmountable.

L. I. Komives (The Detroit Edison Company, Detroit, Mich.): The Detroit Edison engineers would like to congratulate the authors and their respective companies on their paper. Because of our close tie with the Ontario-Hydro System and our predilection for high-voltage, gas pressure cables, we are particularly interested in their problems.

Mention was made of the use of 4-mil bronze tape intercalated with polyethylene tape which was to serve as a moisture seal. When it was found that the bronze tape tended to open when the cores were cabled together, could it have been possible to substitute a soft copper tape for the bronze tape in the rest of the order? In Detroit we are using two tapes in our seal, first a soft and then a half-hard copper tape.

The viscosity of the impregnating compound is given as 4,000 Saybolt universal seconds (SUS) at 50 C. While the viscosity is quite a bit higher than compounds usually used, in Detroit we prefer a compound with a viscosity of about 80,000 SUS at 50 C (3,000 at 100 C and 250,000 at 100 degrees Fahrenheit). We think that the higher viscosity of the compound in such pipe-type cable at operating temperatures, the less likelihood there is of quick migration of the oil from the insulation into the pipe. Was the selection of the higher viscosity based on similar reasoning?

In connection with the discussion of leaks and gas-charging controls in Fig. 8 and gas pressure chart in Fig. 11, we wonder whether the aluminum sheath mentioned in the first paragraph of the section "Single-Conductor Terminal Ends" was a tightly applied sheath, and would it have to be? Again, in Detroit we prefer a pressure chamber comprised of steel pipe, trifurcating head, and copper terminal risers, which can be tested for pressure prior to the installation of the cable. The other observation in this connection is that the fewer gas connections there are in such a pipe line, the less the chances for leaks. If the aluminum sheath had been applied over the cable with space between the shielding tape and the aluminum sheath, one connection shown in Fig. 8 to the trifurcating joint would have been sufficient. The gas pressure in the three terminal lengths would have been equalized with the pressure in the pipe through the loose aluminum sheath. At least three valves, three pipe insulators, and six connections, plus one of the manifolds, could have been dispensed with. We cannot help but feel that there would have been less likelihood of leaks in such construction.

We noted with interest that the terminals were tested with 300-psi air pressure for 6 days and that some sustained this pressure for several weeks' duration. Could the authors enlighten us as to whether they observed any cold flow or other disturbing phenomena at the jointing surface with the porcelain and hardware during these tests?

The pipe-protective covering is described in detail and mention is made that the coating proved to be so poor that cathodic protection had to be employed to protect the pipe. In Detroit, as well as in many other places in the United States, very good results have been obtained with the use of Somastic covering for such pipe lines. Is this available in Canada, and was it considered for use on this line?

With many other cable engineers who read this interesting paper, we also wondered what caused the failure on this cable after 11 months of service? We have an experimental line in which a cable similar to the Toronto cable employing 400 mils of insulation was tried for a number of months at fairly high temperatures, operating at the rated 120 kv. We had failure on this cable after operating at 100 C for a while and the cause of failure was ascribed to a turned-over paper tape next to the outer strand-shielding tape on the conductor (high-stress region). We discovered effects of ionization around the failure, and since that time have felt that the 400 mils of insulation does not give us sufficient factor of safety to overcome such comparatively minor factory imperfections. We also feel that pressure is quite important in gas cables of this type. In a self-contained gas pressure cable the temperature of the conductor is not very different from that of the pressure container (reinforced lead sheath) and thereore the number of the nitrogen molecules in the butt space near the conductor are not reduced to such a degree as can happen in a pipe-type cable under similar conditions. The expansion of the oil in the self-contained cable being restrained by the comparatively tight sheath will also increase the gas pressure in the butt space to greater extent than in a pipe-type cable of similar construction. In view of this, the ionization voltage in the butt space near the conductor in a pipe-type cable is lower than in an equivalent self-contained cable at higher temperature. We agree that results of test data do permit the dropping of the pressure to even less than 125 psi; however, we do not do this in Detroit. We do not operate our cables normally below 205 psi. The pressure may drop to 190 psi before an alarm rings, and in an emergency we may operate the cable at much lower pressure for a short time. We feel that if we do this we are definitely impairing the life of the cable.

In Detroit we believe that the high gas pressure pipe-type cable is the simplest and most economical type of cable to install and maintain. We now have over 50 miles of this cable in service at present and we are installing several additional lines.

L. Meyerhoff (General Cable Corporation, Bayonne, N. J.): It is noted that the shield construction of the cables consisted of a 4-mil bronze tape, intercalated with a 5-mil polyethylene tape, followed by two 4-mil copper tapes intercalated with each other and a 70 × 200-mil copper skid wire. This construction did perhaps insure a good mositure barrier, as suggested by the authors but it may be noted that it also resulted in a shield of extremely low electrical resistance.

In Table IX of reference 1 of this discussion there are given measured values of the shield resistance of three different cables in which the shield constructions were similar to those described. Calculation shows that the resistance of the two intercalated 3-mil copper tapes in those three cables is, on the average, 1.55 times the calculated resistance of a copper tube of 6-mil wall thickness. Assuming that the same factor is valid for the authors' cables, it will be found that r_s', the shield resistance minus skid wires, is 240 microhms per foot for the cable with 385-mil insulation and 205 microhms per foot for the cable with 565-mil insulation at 30 C. The skid wires in parallel with the tapes make the values of r_s, the shield resistance, 225 and 195 microhms per foot respectively.

According to equation 5 of reference 2 of this discussion the incremental conductor resistance ΔR_s due to shield circulating current is

$$\Delta R_s = \frac{555}{r_s} \text{ microhms per foot}$$

and, from equation 13 of reference 1 of this discussion, the incremental conductor resistance $R\Delta_s'$, due to shield proximity effect is

$$\Delta R_s' = \frac{210}{r_s'} \text{ microhms per foot}$$

Both these equations apply for triangular configuration of the conductors and will be approximately correct for three cabled conductors.

Thus, at 30 C the incremental conductor resistances due to shield loss will be

Cable with 385-mil insulation, 2.46+0.87 = 3.33 microhms per foot.

Cable with 565-mil insulation, 2.84+1.02 = 3.86 microhms per foot.

Since the conductor resistance at 30 C is 9.6 microhms per foot, the shield loss adds 35% (in terms of d-c conductor loss) to the loss of the system in one case, and 40% in the other. These values compare with about 2.5% for the shield structure as originally contemplated by the manufacturer. At operating temperature the incremental conductor resistance due to shield loss will be 12 or 14% lower than at 30 C, but obviously this does not change the general picture.

In their discussion of the reported cable failures on their system the authors mention as a possible cause "a local hot spot due to the heterogeneous nature of the surrounding soil." It is suggested that the high losses in the shields may also have contributed materially to the overheating of the cables.

REFERENCES

1. A-C RESISTANCE OF SEGMENTAL CABLES IN STEEL PIPE, L. Meyerhoff, G. S. Eager, Jr. *AIEE Transactions*, vol. 68, pt. II, 1949, pp. 816–34.

2. A-C RESISTANCE OF PIPE-CABLE SYSTEMS WITH SEGMENTAL CONDUCTORS, AIEE Committee Report. *AIEE Transactions*, vol. 71, pt. III, Jan. 1952, pp. 393–414.

Stephen Kozak and Colin Prescott: In Mr. Atkinson's remark regarding prevention of sheath currents at the terminal ends, it is not clear which method he considers expensive. The terminal hardware is simply isolated from the supporting structure perhaps very similarly to United States practice and is certainly not expensive. The pipeline insulator in the 3/8-inch outside diameter copper gas feed line, though operating at 200 psi, is far from expensive, and compares most favorably with United States practice of insulating the oil feed lines. The asphaltic and rubber sandwich corrosion protection on the aluminum sheath is necessary for corrosion protection. Isolation of the sheaths of course is a corollary function but similar precautions would be advisable regardless of what materials the buried riser pipes were formed.

As confirmed by Mr. Atkinson, the joint design employing flush ferrules permits easier attainment of joint electrical strength equal to that of the cable. Not only is the stress distribution more favorable, and the maximum value correspondingly reduced, but the smooth surface permits use of straight paper hand-applied tape, intrinsically superior to creped paper tape. Not only does a more compact and denser joint result but the quality of the paper and the type of impregnating compound is at the cable manufacturer's control.

Mr. Komives' searching observations arappreciated. In respect to the shielding tapes, Mr. Komives' remarks have prompted a review of the experimental data compiled in 1951, and the actual production specification cards for the cable. We must admit to an error in describing the make-up of the shields as detailed in the section "Pipe Cable: Design and Manufacture," and in Table I. The shield construction supplied was

One $1^1/_2$ × 0.005-inch polyethylene tape intercalated with one 1 × 0.004-inch commercial bronze tape.

One 1 × 0.004-inch soft-copper tape intercalated with one 1 × 0.004-inch commercial bronze tape.

Of several solutions investigated to better the behavior of the tapes during cabling operations, the rugged and conservative shield construction just described was adopted for this first installation. At the time, there was no indication of how the various shield constructions would handle in pulling the cabled lengths through the somewhat arduous pipe section pulls. Our findings during installation have shown that elaborate shielding and moisture seals are not necessary for cabled conductors since the cabling of the conductors proves attractive in ease of handling, pulling, and wear on skid wires and shielding tapes. Our next design would consider either Mr. Komives' construction or possibly only one semihard copper tape intercalated with polyethylene tape.

The impregnating compound was selected after many tests of its qualities, both electrical and mechanical, and several factors influenced the choice of viscosity. Primarily the viscosity of 4,000 SUS, though not as high as that preferred by Mr. Komives, was considered more than sufficiently high to prevent migration of any consequence. The hollow-core design of gas-pressurized cable with the gas permeating outwards from the core presents a cable structure not as susceptible to leaking out of the compound as does the design of cable employing the "segmental" conductor. Such concepts as consideration of the compound in suspension in the gas, the balance of pressures in the insulant structures, the surface tensions between the tapes and the compound density, and the impregnation procedure must all be assessed along with considerations of viscosity. The compound selected was the best of several studied taking all factors into account. The compound has extremely low and stable power factor, and a high dielectric strength. It is outstanding in its nonadsorption of moisture characteristic. Another factor influencing the choice of compound was its suitability of handling in the existing cable plant, in respect to the hollow-core principle; a very viscous compound would be practically impossible to blow out of the core. Yet another factor was the desire to avoid the disadvantages of lifting the cable out of the impregnating tanks prematurely. Our strong preference is toward full completion of the impregnating process under applied pressure during the cooling cycle down to room temperature.

We agree with Mr. Komives that the gas-charging panel can be simplified. Our present thinking would point to halving the number of manifolds and valves, but not for the reasons put forth by Mr. Komives. We would maintain a tight aluminum-sheathed cable and a separate feed to each pothead, if only for the reason that a pothead can be replaced or repaired without losing any of the gas in the pipe. Since nitrogen in Canada is expensive, the feature is worth while. The aluminum-sheathed terminal lengths are likewise pressure-tested before installation, are very easily handled without need of threading exposed cable through long risers, and the seals to the pipe and to the pothead are simply made. The pothead oil is contained adequately by a silk-tape poultice over the sheath, potheads can be installed at whatever time is suitable, and no welding or specialties are required. In other words, the procedure for installing terminal ends on high-pressure cable is kept almost as simple as terminating ordinary solid-type high-voltage cable.

With respect to pressure tests on pothead assemblies and the behavior of gasket surfaces, one disadvantage noted was the necessity of torquing the bolts of the gasketted joints several times in the field before applying gas pressure to the pothead. Normally these gasketted joints are fully torqued in the factory, but in this case the components had to be separated and then reassembled in the field because the pothead metal parts adaptable to our stress cone diameter could not be obtained in time. The gaskets are confined in recesses in the metal parts, and once the initial compression and set have been realized by torquing, no gasket displacement, bulging, or distortion was evident even after the severe pressure test cycles.

Unfortunately Somastic coating for the pipes could be supplied only by shipping the pipe to the United States for coating. The expense and the delay would have been prohibitive and the likelihood of damage during shipment increased. However, the coating specified would, we feel, be entirely adequate were proper quality control and determined inspection stringently observed.

Some of Mr. Meyerhoff's observations can be answered by referring to our reply to Mr. Komives, wherein we corrected our reporting of the shield assembly construction. We are not in agreement with the factor of 1.55 quoted; indeed the factor varies quite appreciably with the extent of overlay or overlap in the intercalation practice. Our test measurements of the resistance of shield assemblies consisting of two intercalated copper tapes with 75% overlay showed that the factor was 2.06 for dry tapes, and for the same construction with the tapes applied with a film of viscous cable compound, the factor was as high as 5.56. Applying the more pessimistic dry value to an effective calculated resistance of a thin-walled copper and bronze tube of 0.006-inch thickness (assuming conductivity of the bronze is 50%), the incremental conductor resistances due to shield loss are as in Table II.

Table II. Incremental Conductor Resistances

Cable	$\Delta R_s+\Delta R_s'$	R_{ac}/R_{dc}*	R_{ac}/R_{dc}†
120 kv (0.385-inch paper)	1.48+0.493=1.97	1.19	1.08
161 kv (0.565-inch paper)	1.642+0.577=2.22	1.22	1.07

* Ratio at the shield for 1×0.004-inch copper tape and 2×0.004-inch bronze tape assembly at operating temperature.

† Ratio at the shield for the formerly contemplated shield assembly of two 0.004-inch bronze tapes each intercalated with polyethylene tape.

The shield losses are therefore much less than Mr. Meyerhoff's 35% and certainly these losses do not reduce the rating as severely as Mr. Meyerhoff would imply.

The change in shielding construction after running the experimental length was not enacted without due consideration of the slight increase in losses, but with the knowledge that the conservative assumptions made in the original calculations for conductor size would permit an additional copper tape without significant reduction in rating.

Epoxy Resin Casting of Dry-Type Current Transformers

W. C. FARNETH
ASSOCIATE MEMBER AIEE

GEORGE GALLOUSIS
ASSOCIATE MEMBER AIEE

Synopsis: The use of synthetic resins and casting techniques for the embedment of electrical components is continually increasing in the United States and in Europe. This paper presents to the industry some results of approximately 3 years of work with epoxy resins and casting techniques at Allis-Chalmers Manufacturing Company.

Although the work to date has been confined primarily to a 600-volt insulation-class indoor-outdoor, dry, window type of current transformer, experience clearly indicates that the extension of the use of these techniques and materials to a higher voltage class and larger dry-type current transformer applications is not only desirable but feasible.

EPOXY resins[1] inherently possess characteristics which make them suitable for use as insulation for dry-type current transformers. These characteristics include good adhesion to metal and ceramics, good mechanical strength, good dielectric properties, good resistance to temperature variations, low moisture absorption, low shrinkage during cure, and high resistance to solvents. In addition, the epoxy resins are well suited to use in casting processes which are relatively simple and inexpensive.

Experimental castings of units of higher voltage class have been made. These units, all presenting more difficult configurations, are now being evaluated. Prototypes of such units are shown in Fig. 1. The more complex configurations of current transformers require careful design to resolve coil support and shrinkage problems as well as to keep the total amount of resin used to an economical minimum. The designer, however, has many types of epoxy resins available to him. Proper adjustment of the base resin formulation, the resin-filler proportions, and the casting process make successful new applications possible.

For the specific application of the current transformer shown in Fig. 2 the use of the epoxy resin eliminates the need for a conventional case and bushing and consequent sealing and gasketing problems. (A noncast conventional unit is shown in Fig. 3.) The epoxy resin casting technique results in a rugged unit which may be used for either indoor or outdoor applications.

The four manufactured current rat-

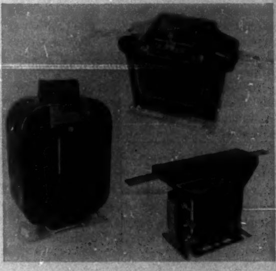

Fig. 1. Prototypes of units 600-volt insulation class and higher

---

Paper 55-34, recommended by the AIEE Transformers Committee and approved by the AIEE Committee on Technical Operations for presentation at the AIEE Winter General Meeting, New York, N. Y., January 31–February 4, 1955. Manuscript submitted October 18, 1954; made available for printing November 16, 1954.

W. C. Farneth and George Gallousis are with the Allis-Chalmers Manufacturing Company, Pittsburgh, Pa.

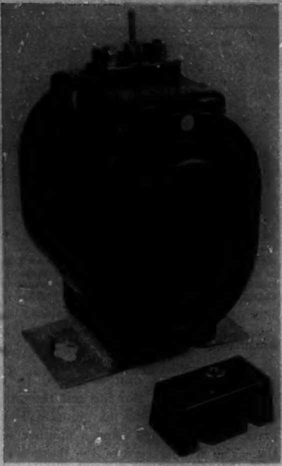

Fig. 2. Allis-Chalmers Manufacturing Company type-TWM 600-volt class cast current transformer

ings (200, 5-ampere; 400, 5-ampere; 600, 5-ampere; and 700, 5-ampere) are all satisfactory for use at 200-per-cent (%) continuous rated primary current. A typical 400-ampere unit element is shown in Fig. 4. It consists of an electric steel core insulated by means of pads and creped Kraft paper tape upon which the secondary winding is placed. Secondary terminals and a base-mounting arrangement complete the element assembly.

Casting

Smooth, inexpensive metal molds coated with release agents are used in the casting process. Each mold is provided with a bracket supporting the transformer element, an arrangement for positioning and aligning the secondary terminals, a pouring reservoir, and a clamping arrangement. The initial casting steps include the drying of the transformer and the establishment of a uniform mold and element temperature. To achieve this the transformer is inserted in the mold and the combination placed in an air-circulating oven.

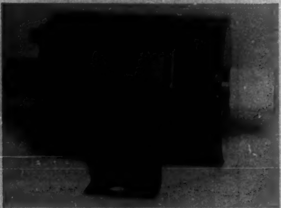

Fig. 3. Conventional outdoor window-type current transformer

The epoxy base resin to which a filler has been added is heated to the same temperature as the transformer and the mold. This step is followed by the introduction of the hardener or catalyst into the resin, the thorough stirring of the resin-hardener mixture, the careful filling of the molds, and the curing of the resin in an air-circulating oven. Upon removal from the mold the transformer is cooled to room temperature, the flash is removed, and a rating plate, customer's number plate, secondary terminal board, and base are attached.

The material evaluation tests[1] which have been performed to date are of two types, those performed on actual transformers and those performed on material samples. The tests on transformers are discussed first.

Long-Time Tests

Of primary importance in evaluation are long-time tests under actual operating conditions. On the roof of Allis-Chalmers' Pittsburgh Works, since October 1952, prototypes of the present units have been operating continuously at 200% rated current. Approximately every 3 months, measurements of capacitance, dissipation factor, insulation resistance, and resin hardness are made and recorded. These measurements indicate no significant change in the condition of the units. Values recorded on a representative 200, 5-ampere unit appear in Table I.

The primary conductor for these tests consisted of a steel bar 9 inches long fitted tightly into the primary opening of the transformer.

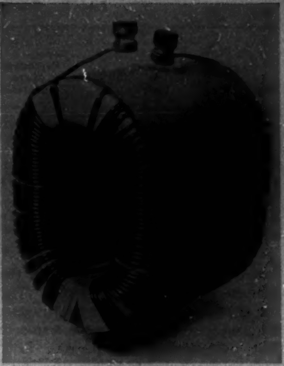

Fig. 4. Element of 400, 5-ampere type TWM

Thermal Cycling

Additional transformers underwent thermal-cycling tests for 1,008 hours. The temperature sequence of each cycle was −30 degrees centigrade (C), +75 C, and room temperature. During the tests units progressed directly from one cycle to the next, remaining in each temperature condition for 24 hours. No voltage or current was applied to the transformers during these tests. Again, as in the case of the long time tests, capacitance, dissipation factor, insulation resistance, and resin hardness were measured. The test results in Table II indicate no significant change in these characteristics. These transformers withstood a standard 2,500-volt 60-cycle one-minute applied potential test from secondary to ground after 2-cycles, and again after 14 cycles.

Thermal Aging

Thermal aging tests were also performed during which units were subjected to a temperature of 130 C for 1,500 hours. The standard 60-cycle applied potential test of 2,500 volts for 1 minute was applied after 500 hours and 1,000 hours, and was successfully withstood by each unit.

The test results presented in Table III

Table I. Representative 200, 5-Ampere Unit Long-Time Test Results

	October 1952	September 1954
Primary to secondary and ground		
Capacitance, micromicrofarads	82	54
Dissipation factor, %	0.8	1.1
Secondary to primary and ground		
Capacitance, micromicrofarads	650	650
Dissipation factor, %	3.8	0.9
Primary and secondary to ground		
Capacitance, micromicrofarads	630	603
Dissipation factor, %	2.9	0.9
Durometer hardness, shore C scale	96	97

Resistance measurements, made at the same time as the capacitance and dissipation factor measurements, were equal to or greater than 10^6 megohms throughout the test.

Table II. Thermal Cycling Test Results

Unit	Number of Cycles	Secondary to Ground Capacitance, Micro-microfarads	Secondary to Ground Dissipation Factor, %	Average Type C Shore Durometer Hardness
A	0	408	1.3	97
B	0	456	0.5	97
C	0	385	3.2	97
A	14	405	1.9	98
B	14	450	1.2	99
C	14	385	3.8	97

Resistance measurements, made at the same time as the capacitance and dissipation factor measurements, were equal to or greater than 10^6 megohms throughout the test.

Table III. Thermal Aging Test Results

Unit	Secondary to Ground Capacitance, Micro-microfarads	Secondary to Ground Dissipation Factor, %	Average Type C Shore Durometer Hardness
Before Heat Aging			
D	353	2.1	92
E	270	1.5	92
F	319	1.5	90
After Heat Aging for 1,500 Hours at 130 C			
D	360	1.4	94
E	260	1.0	95
F	325	0.5	92

Resistance measurements, made at the same time as the capacitance and dissipation factor measurements, were equal to or greater than 10^6 megohms throughout the test.

indicate no appreciable change in the characteristics of the units tested. The test at 130 C for 1,500 hours was based on the average copper rise of a 600, 5-ampere unit operating at 200-per-cent load. This rise was found to be less than 30 C. Therefore the average copper temperature of a unit operating continuously at 200-per-cent load in a 30-C ambient would be less than 60 C. Assuming a 10-degree rule of insulation life (the insulation life is halved for each 10 C increase in temperature) 1,500 hours at 130 C is approximately equivalent to 20 years at 60 C.

Artificial Weathering

Transformers were operated for 1,000 hours at 200-per-cent rated current in the artificial weathering chamber shown in Fig. 5, built expressly for this test. The chamber used was a tank above which a bank of ultraviolet lamps were positioned. The intensity of the lamps was controlled to provide an ultraviolet intensity of approximately five times the maximum intensity of the sun and an infrared intensity equal to the maximum intensity of the sun. Fresh tap water was automatically sprayed on the units for 10 minutes every hour. This test indicated no appreciable change in capacitance, dissipation factor, secondary resistance to ground, or resin hardness.

Weight Loss

Several material tests were made. The first, a good indicator of the thermal stability of material, was a test of weight loss versus time at elevated temperature. Fig. 6 shows that the weight loss after 46 days of aging in an air-circulating oven at 170 C was only 1.8 per cent for the specific resin tested.

Dielectric Strength Versus Temperature

Tests of dielectric strength versus temperature were also made on sheet sample castings of the material. These tests, performed on 80-mil-thick 6-inch square samples, in accordance with American Society for Testing Materials Standards,[2] were 60-cycle 1-minute step-by-step hold tests using standard 2-inch diameter electrodes. Creep occurred around the edge of the samples at room temperature and at 50 C in air. These tests were therefore made under oil. The other test points at elevated temperatures were obtained in an oven in air. Test results are plotted in Fig. 7. A comparison has been made on this curve between the epoxy resin tested and asphalt impregnated paper. The data indicate the resin to be superior to the asphalt-impregnated paper.

Flammability

Fig. 8 shows a unit subjected to a flammability test. For this test the unit was exposed to an oxygen-acetylene flame for 30 seconds using a number 46 tip. The temperature of the flame was approximately 3,500 C. On removal of the flame the resin continued to burn slowly for 8 seconds after which it extinguished itself. Very little smoke was evolved during this period of burning and no irritating effects were noticed. After cleaning the charred resin from the area to which the flame had been directly applied, it was found that the charring had occurred to a depth of 3/16 inch. Beyond this depth the resin was apparently still solid.

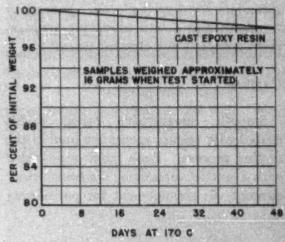

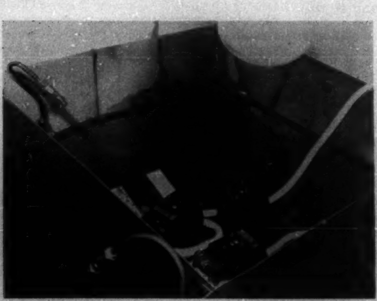

Fig. 5 (left). Units in artificial weathering chamber

Fig. 6 (upper right). Weight loss versus time at elevated temperature

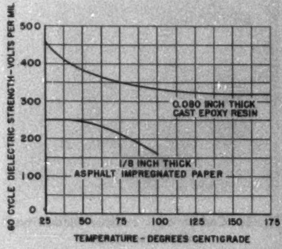

Fig. 7 (right). Dielectric strength versus temperature

Fig. 8. Application of 3,500 C oxyacetylene flame to type TWM

A number or the units were placed in an incinerator at 425 C. No unusual behavior was observed during these operations. On removal from the incinerator the physical dimensions of the units were found to be unchanged, but the charred resin was easily chipped off. From the described tests it is apparent that the operation of these units under conditions of extreme heat is satisfactory and also that the units do not constitute a fire hazard.

Quality Control

Prior to shipment, each production unit is subjected to an unusual quality control insulation test. Each unit is immersed in a saline solution to a depth slightly below the secondary terminals. The salt solution is grounded, thereby grounding the mounting feet and core and simultaneously acting as a primary conductor. A 60-cycle test voltage of 4,000 volts is then applied to the secondary terminals for 1 minute, stressing the resin from secondary to primary and ground. This test voltage, which is in excess of the 2,500-volt 60-cycle dielectric test between secondary and ground as specified by American Standards Association standards,[3] results in maximum information from a single testing operation. It checks the condition of all the resin between the secondary and the saline solution.

Summary

The use of synthetic resin and casting techniques for the embedment of electrical components is continually increasing. The use of such techniques and an epoxy casting resin has produced successful 600-volt insulation class window-type current transformers which are now in large-scale production. Material and transformer evaluation tests made to date indicate that the production of higher voltage class and larger current transformers is feasible. Several prototypes of these more complex units have been experimentally produced.

References

1. Process of Preparing Synthetic Resins, Pierre Castan. *United States Patent no. 2,324,483*, July 20, 1943.

2. Methods of Test for Dielectric Strength of Electrical Insulating Materials at Commercial Power Frequencies. ASTM *Standard No. D149-44*, American Society for Testing Materials, Philadelphia, Pa., 1944.

3. Instrument Transformers. *ASA C57.13-1948*, American Standards Association, New York, N. Y., 1948.

4. New Methods in the Manufacture of Insulations Based on Synthetic Casting Resins, H. Koller. *Paper No. 124*, CIGRE, Paris, France, 1952.

5. Instrument Transformers with Synthetic Resin Insulation, Alfred Imhof. *Paper No. 127*, CIGRE, Paris, France, 1954.

6. Cast-Resin Embedments of Circuit Subunits and Components, Alex E. Javitz. *Electrical Manufacturing*, New York, N. Y., Sept. 1951, pp. 103–118.

7. A New Dry-Type Insulation for Instrument Transformers, R. A. Pfuntner, R. E. Franck, F. R. D'Entremont. *AIEE Transactions*, vol. 69, pt. I, 1950, pp. 453–58.

8. Evaluation of Butyl Insulation for Outdoor Instrument Transformers, J. A. McDonnell, H. E. Crabtree. *AIEE Transactions*, vol. 70, pt. II, 1951, pp. 2021–25.

9. Revolutionary Advance in Instrument Transformer Design, I. F. Kinnard. *General Electric Review*, Schenectady, N. Y., June 1949, pp. 15–19.

10. Indoor-Outdoor Transformers: A New Concept in Instrument-Transformer Design, R. E. Franck. *Electric Light and Power*, Chicago, Ill., Aug. 1951, pp. 104–106, 143.

◆

Discussion

Dr. A. A. Halacsy (I-T-E Circuit Breaker Company, Philadelphia, Pa.): The authors mention that their tests indicate the feasibility of the production of higher voltage class and larger current transformers. I should like to mention some past development of such current transformers.

The idea of producing such a 15-kv class wound-type current transformer, fully encapsulated, was considered in 1949. Tests were carried out and prototypes produced in 1952 and 1953 in the factory of Eastern Power Devices, Toronto, the I-T-E Circuit Breaker Company's plant in Canada.

A prototype of a 15-kv class 300/5-ampere current transformer, having a 5-turn primary and a wound-steel core, showed a remarkable reduction in the length of a current transformer, with taped insulation from about 23 to 11 inches. This was achieved by increasing the creepage with the use of cast ribs, which would not be possible in the case of taped insulation.

Today our company is producing quite a few 15-kv epoxy resin encapsulated devices, and we can be sure that epoxy casting will be used for considerably higher voltages in the not too distant future.

Paul Wildi (Pacific Oerlikon Company, Tacoma, Wash.) and **A. Ernst** (Oerlikon

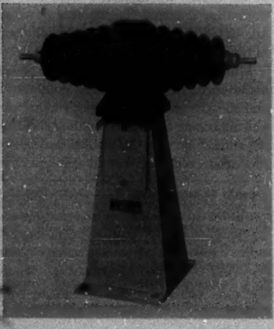

Fig. 9 (left). Line of epoxy-cast indoor current transformers for 10-kv rated voltage, with single and double secondaries

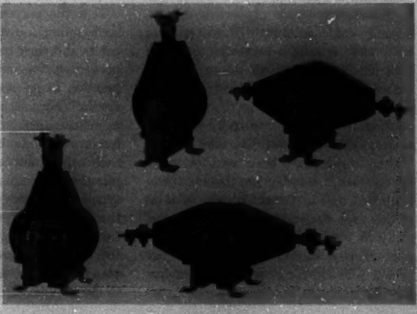

Fig. 10 (right). Current transformer for outdoor application. Rated voltage 16 kv

Engineering Company, Zurich, Switzerland): The use of epoxy resin as an insulator for dry-type current transformers is definitely an improvement over previously employed techniques. Its application is, however, not limited to low-voltage instrument transformers. The low-dissipation factor, the high dielectric strength and, when used with proper fillers, the good heat-transfer characteristics of the material, make it ideally suited for high-voltage applications. Our company adopted this technique in 1948 and is currently building epoxy cast instrument transformers up to a rated voltage of 60 kv.

Fig. 9 shows a line of indoor current transformers as built at present for 10-kv rated voltage, 16-kv maximum operating voltage, and 42-kv low-frequency one-minute withstand voltage. The design offers considerable advantage over the conventional design, specifically, high resistance to moisture, very high instantaneous current rating (300 to 500 times rated current), economy in manufacturing, and very little tendency to accumulate dust and dirt. The excellent weather resistance of the insulation material offers the possibility of using cast resin application for outdoor use.

Fig. 10 shows a current transformer with a completely embedded secondary core for use on electrical traction systems. Current transformers of this type have been in use for longer than 5 years. The one shown is rated 16 kv, 500/5 amperes, at $16^{2}/_{3}$ cycles per second.

Field experience with this new design of current transformers indicates that we have not yet reached the limit of performance of the new material. We are at present experimenting with prototypes up to a rated voltage of 380 kv.

W. C. Farneth and George Gallousis: We appreciate the discussers' comments. We are aware, of course, that other higher voltage work with epoxy resins has been in progress. This has been indicated in our references and synopsis. However, in higher voltage class applications, a conservative approach demands that transformers utilizing a new material and process be subjected not only to routine insulation tests but also to accelerated and long-time tests comparable in severity to those outlined in our paper. Results of such tests or results of field experience are a valuable addition to the information now available in this field.

Mineral-Insulated Metallic-Sheathed Cables

C. A. JORDAN
MEMBER AIEE

G. S. EAGER, JR.
ASSOCIATE MEMBER AIEE

CERTAIN inorganic materials of mineral or mineral-like nature have long been recognized as possessing properties which make them attractive for use as insulation for electric cables. Materials that have received consideration as insulants are magnesium oxide, aluminum oxide, kaolin, asbestos, powdered glass, and zircon porcelain, to mention a few. Of these, magnesium oxide is the only material (aside from low-density fibrous asbestos) that has received important practical application to date. The principal factors that have influenced this status are: 1. magnesium oxide, in proper form, makes an excellent cable insulation, and 2. it has the characteristics needed for practical cable fabrication, and field handling and installation.

The nature and properties of inorganic cable insulants in general are such as to require a protective covering over all. In the case of the cables here described, this takes the form of an impervious metallic sheath.

Mineral-insulated metallic-sheathed cables, although relatively new in the United States, have been used for many years abroad, notably on the European continent and in Great Britain. Cables of this type were first produced commercially in France in 1934. In 1937, production was started in Great Britain. World War II temporarily retarded further development in other countries, particularly in view of the relatively complex and expensive plant required for manufacture. In 1946, however, the company with which the authors are associated first produced prototype mineral-insulated high-frequency coaxial cables for military use (since standardized as the *RG-81/U* and *RG-82/U* cables of Joint Army-Navy Specification *JAN-C-17A*[1]). In 1949, this company made available in the United States 600-volt rated single-conductor and multiconductor mineral-insulated metallic-sheathed power cables, and fittings therefor. In all three countries the cable materials and constructions and the methods of fabrication, have been substantially similar; in particular, magnesium oxide has been the basic insulant employed.

It is the purpose of this paper to describe mineral-insulated metallic-sheathed cables and their terminating fittings with particular reference to United States practice, to present the principal properties and characteristics of such cables, and to indicate some of the novel and unique features and characteristics which make such cables advantageous for many applications. In this country, cables of the type under consideration are offered under the trade name Pyrotenax Safety Mineral Insulated Wiring, and have been given the generic designation by the industry as a whole (see the National Electrical Code) of type *MI*. The latter designation will be used in the following for the sake of convenience and brevity.

Cable Materials, Constructions, Sizes, and General Dimensions

MATERIALS

While a number of choices of conductor and sheath materials are theoretically possible, performance, economics, and manufacturing considerations nominate copper as the metal of principal usefulness for mineral-insulated power cables. Its electrical properties are unexcelled in practical conductor metals, and it possesses in high degree the strength and ductility essential for fabrication of this type of cable in commercially long lengths. (This will be clearer from the discussion of manufacturing methods to follow.) For these reasons, present standard type-*MI* power cables consist essentially of one or more solid copper conductors embedded in finely divided, highly compressed magnesium oxide insulation, the whole enclosed in a continuous, seamless copper sheath. Conductors and sheaths of all cables are annealed dead-soft to normalize internal mechanical stresses and to facilitate handling and installation in the field.

Mineral-insulated cables have been made abroad with aluminum conductors and sheaths, and with copper conductors and aluminum or aluminum alloy sheaths. All-aluminum type-*MI* cables have been produced experimentally in this country.

Paper 55-54, recommended by the AIEE Insulated Conductors Committee and approved by the AIEE Committee on Technical Operations for presentation at the AIEE Winter General Meeting, New York, N. Y., January 31–February 4, 1955. Manuscript submitted October 19, 1954; made available for printing December 2, 1954.

C. A. JORDAN is with the General Cable Corporation, Perth Amboy, N. J., and G. S. EAGER, JR. is with the General Cable Corporation, Bayonne, N. J.

Table I. 600-Volt Type-MI Power Cables, Standard Constructions and Sizes

No. of Conductors	Size Range, AWG Inclusive
1	16 to 4/0
2	16 to 4
3	16 to 4
4	16 to 6
7	16 to 10

In addition to the standard copper *MI* power cables, there is in regular production here at present a special small cable which has conductors of a copper-nickel resistance alloy and a sheath of copper, designed for heating service. The British regularly produce thermocouples of the *MI* type having chromel-alumel and copper-constantan couple conductors and sheaths of nickel-chrome and mild steel. They also produce standard type-*MI* thermocouple compensating cables having these same conductor combinations and iron-constantan, as well, and sheaths of cupro-nickel and mild steel. These various thermocouple cables are available in two basic diameters, 0.266-inch and 0.125-inch respectively. Aside from these cable applications, magnesium oxide insulation is used in heating elements, such as Calrod units.

Sizes and Constructions

Type-*MI* 600-volt power cables are available in single-, 2-, 3-, 4- and 7-conductor constructions, as may be required for particular applications. The standard size ranges for the various constructions are indicated in Table I.

The special 2-conductor heating cable just referred to has 0.038-inch diameter copper-nickel resistance alloy conductors, compressed magnesium oxide insulation, copper sheath over all. It has an over-all diameter of 0.246 inch, and is rated 300-volt.

As will be evident from the manufacturing methods to be described, the conductors of type-*MI* cables are not directly die-drawn. As an unavoidably inherent characteristic of this type of cable, therefore, the conductors cannot be expected to meet the exactingly high standards applicable to die-drawn wires with respect to surface finish and close diameter tolerance. This, however, involves no practical disadvantages or sacrifice in the use of such cables. Conductor size is conveniently and closely controlled by resistance measurement in lieu of conventional diameter measurement by micrometer. Conductor concentricity and uniformity of cross-sectional area are completely adequate for all practical requirements. The sheath of type-*MI* cables, being directly die-drawn, can be and is held to close diameter tolerances to ensure good match with the appurtenant terminating fittings.

Insulation Thickness

By design in multiconductor type-*MI* power cables, the separation between surfaces of adjacent conductors (thickness of insulation) is identical to that between surfaces of outer conductors and sheath. Actually, of course, multiconductor *MI* cable may be regarded most accurately as belted cable having nominal conductor and belt insulations of the same thickness, each equal to one-half of the separation between conductors or between conductors and sheath. For simplicity and clarity, however, the term "insulation thickness" will be employed to designate the combined thicknesses of insulation and belt, i.e., the separation between surfaces of metal components. Thus interpreted, the design insulation thickness of multiconductor *MI* cables is nominally the same as that of single-conductor cables.

The thickness of insulation in 600-volt rated type-*MI* power cables varies somewhat with conductor size, ranging in approximately linear relationship (with respect to cable diameter) from about 0.060 inch for the smallest size (16 American Wire Gauge (AWG)) to about 0.080 inch for the largest standard size (4/0 AWG). Strict theoretical relationships are, however, slightly modified in some instances to gain the important practical advantage of a reduction in the required number of fitting sizes (by equalizing and grouping cables of different constructions but nearly equal outside diameters) if that can be done without violating fundamental design requirements. The nominal insulation thickness of the special 300-volt heating cable is 0.043 inch. As will be seen later, magnesium oxide insulation has such properties that in each instance the design insulation thickness is adequate for the assigned voltage rating.

Sheath Dimensions

Sheath thicknesses of type-*MI* cables are determined by both mechanical and electrical requirements, i.e., the sheath must be both feasible of manufacture and rugged enough to afford requisite mechanical protection, and must also have sufficient conductance to insure proper grounding and handling of fault currents. In the case of 600-volt *MI* power cables, sheath thicknesses vary linearly with cable diameter from a nominal value of 0.023 inch for the smallest cable to 0.039 inch for the largest. A more significant picture of electrical relations will, perhaps, be afforded by Table II, which indicates the nominal area or conductance ratio of sheath to conductor for the *maximum* size of cable of each construction. The sheath area ratios, or relative sheath conductances, of smaller sizes of cable are greater than those indicated in Table II in all instances, i.e., Table II shows the *minimum* relative sheath conductances.

Table II. 600-Volt Type-MI Power Cables, Minimum Relative Areas of Outer Sheaths

No. of Conductors in Cable	Ratio of Sheath Area to Area of One Conductor
1	0.478
2	2.35
3	2.58
4	3.74
7	8.11

For single-conductor cables, sheath and conductor area equalize at 4 AWG; for that size the ratio of sheath area to conductor area is 1.02.

As will be noted from Table II, mechanical considerations dictate sheath cross-sectional areas larger than are electrically required (in terms of an arbitrary 100 per cent (%) of the conductance of a single conductor) for all multiconductor cables, and for all sizes of single-conductor cables 4 AWG and smaller. Even in the case of the larger sizes of single-conductor cables, a single-phase circuit would have a minimum combined sheath area of about 96%, and a 3-phase circuit about 143%. These relative conductances, of course, far exceed the requirements of the National Electrical Code for grounding conductors.

General

Finally, type-*MI* cables of all sizes and constructions are very compact and relatively light, which contributes greatly to ease of handling and installation.

Methods of Manufacture

With the briefly outlined history and current status of type-*MI* cables, and their salient features and dimensions in mind, it is of interest to give some consideration to manufacturing methods, not so much with the purpose of covering tedious technical detail but rather to give users a clearer appreciation of what, aside from the inherent properties of the component materials, makes type-*MI* cables what they are.

There are two variants of the general method of manufacture. Both develop from what may, for lack of a better term, be called the "starting assembly." In so far as metal parts are concerned, the starting assembly consists of a relatively large, seamless, cylindrical copper tube and one

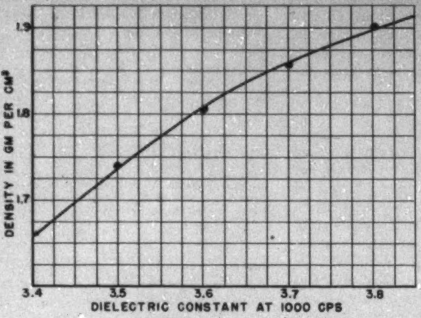

Fig. 1. Influence of density on dielectric constant

or more relatively large solid copper starting conductors, all having the same relative proportions as they will have in the finished cable.

In the older of the two methods of manufacture, magnesium oxide powder, after preliminary treatment to secure the proper condition and properties, is molded under heavy pressure into cylindrical pellets, each of which is longitudinally cored for the desired number of conductors in the cable. These pellets have, with practical clearance fits, outside diameters to fit closely into the starting tube, and core hole diameters to fit closely the starting conductors, automatically giving them the correct relative proportions for the finished cable. After complete dehydration and while still hot, the pellets, together with the starting conductors, are assembled within the starting tube, with the magnesia pellets closely stacked end to end and with the starting conductor(s) inside their core holes. It will be seen that this process affords a high degree of accuracy and uniformity of conductor spacing and insulation thickness.

In the newer of the two variants of the general method of manufacture, now coming into use because of the increased production rate it makes possible, the starting conductor(s) is placed within the starting tube, and are automatically jigged to exact position by new complex equipment which at the same time continuously and progressively feeds pretreated, dehydrated magnesium oxide powder into the tube and around the conductors, and tamps it into the correct uniform body and density from one end of the starting tube to the other. This alternate method of preparing starting assemblies also results in high accuracy and uniformity of conductor positioning and insulation thickness.

Subsequent manufacturing operations are the same regardless of the method of preparing the starting assembly. The latter is drawn down in successive stages, with the necessary intermediate anneals, to the finished size of cable in exactly the same manner as is employed in conventional wire drawing, except of course for the differences of degree occasioned by the relatively large starting size. In these drawing operations, the tube or sheath is, of course, the only component that is directly die-drawn, but fortunately it happens that the properties of dense magnesium oxide and copper, at least, are such that insulation and conductors, as well as sheath, all draw down smoothly, uniformly, and in proper relative proportions to the final cable size. The final operation after coiling the finished cable is a deep anneal to normalize internal stresses and insure proper and uniform handling properties.

This brief recital of basic manufacturing methods immediately makes it possible to understand a number of salient factors about type-*MI* cables. First, the tooling is complex and expensive, and involves a considerable time element, which makes it difficult to produce special constructions, or cables with other component materials which may or may not, when associated with magnesium oxide insulation, draw down satisfactorily in commercial coil lengths. Second, the method of manufacture lends itself only to production of solid conductors (at least there would be no practical advantage to be gained by indirectly drawing stranded conductors) and the indirectly drawn conductors characteristically differ in appearance and tolerance range from directly drawn wires, as has already been mentioned; such conductors are not necessarily inferior but merely different and in any case are completely adequate for their intended use. Finally, it is obvious that feasible continuous coil lengths of completed cables are controlled by the mass of the starting assembly and, since the starting assemblies of all *MI* cables have somewhat similar mass, feasible coil lengths of large cables are less than those of small cables. Shipping lengths are, however, commercial in all sizes and constructions, and in those comparatively rare cases where cable runs exceed available lengths the cables can readily be spliced in boxes with standard fittings.

As a natural result of the method of manufacture, which involves tremendous pressures during the drawing operations, the originally relatively dense, dry magnesium oxide insulation becomes so highly compacted that, although essentially a powder at all stages, it eventually assumes many of the characteristics of a solid. For all practical purposes of cable handling it acts as a solid, i.e., while the insulation can readily be removed from the conductors for making connections and terminations, there is little if any tendency for it to flow or chalk out when cable ends are cut and the cable is being handled and trained to position. The seemingly solid nature of the insulation also contributes much to the desirable rigid, yet flexible, handling properties of *MI* cables, and explains in considerable degree the remarkable physical properties and resistance to abuse which are inherent in this cable type.

Properties of Magnesium Oxide Insulation

Commercial magnesium oxide is obtained by calcining the natural magnesite (magnesium carbonate) or by calcining a synthetic material (magnesium-carbonate or magnesium-hydrate) produced from sea water. The electrical properties of magnesium oxide depend a great deal on the source of the magnesite, the method and degree of calcination, and the type and amount of impurities present. Experience has indicated that one of the most suitable sources of magnesium oxide for electric wires and cables is the natural calcined India magnesium oxide. Typical chemical composition of this natural magnesium oxide as used in cables is:

Magnesium oxide,	89.47%
Calcium oxide,	1.29%
Silicon dioxide,	3.88%
Ferrous oxide,	0.07%
Aluminum oxide,	0.24%
Free moisture,	0.57%*
Volatile matter (combined water and carbon dioxide)	4.48%*
	100.00%

*Expelled upon drying in normal course of manufacture.

The electrical and physical properties

of magnesium oxide depend a great deal upon the degree to which the powder is compressed. Gemant and Glassow[2] have reported that the a-c dielectric strength of compressed magnesium oxide increases appreciably as the density of the compressed powder increases.

The dielectric constant of magnesium oxide also varies with the density of the compressed powder. The magnesium oxide insulation in cables has a density in the range of 1.6 to 2.0 grams per cubic centimeter. Fig. 1 shows the variation of the dielectric constant of magnesium oxide as the density is increased. These data were taken on coaxial cables, at a frequency of 1,000 cycles per second (cps) at room temperature.

Magnesium oxide has relatively high thermal conductivity. This is advantageous for an insulation used for electric cables. The thermal conductivity is three to five times greater than that of most organic insulations used on electric wires and cables. As may be expected, the heat conductivity increases as the specific gravity (density) of the compressed powder increases.

Magnesium oxide is hygroscopic. When combined with water it forms magnesium hydroxide. The presence of free moisture quickly reduces the dielectric strength and allows an appreciable leakage current to flow. When used as an insulation in cables, arrangements must be made to prevent moisture from coming into contact with the insulation. This is accomplished by end seals which are discussed later.

Properties of Type-MI Cables

INSULATION RESISTANCE

The insulation resistance of mineral insulated cables is relatively high compared to that of most organic insulations. At room temperature it exceeds that of any extruded insulation commonly employed on cables except polyethylene. The insulation resistance decreases with increasing temperature. Fig. 2 shows typical data for single-conductor 4/0 AWG type-*MI* cable. The insulation resistance was measured at 500 volts direct current between the conductor and the sheath after a 1-minute electrification time, in accordance with the procedure of the American Society for Testing Materials (ASTM).[3] Samples were placed in an air oven for 16 hours at 120 degrees centigrade (C) for drying unprotected cable ends prior to testing, as was done prior to taking all electrical data reported in this paper.

That the data in the foregoing may be compared with those for other well-known inorganic insulations, the curve of Fig. 2 is replotted in Fig. 3. The data for alumina porcelain, muscovite mica, and high tension porcelain were reported by Lindsay and Berberich[4] and are shown in Fig. 3 for comparison purposes. The abscissas of Fig. 3 show temperature, but the values are plotted on the basis of the reciprocal absolute temperature scale, as is done in several subsequent curves in this paper. Magnesium oxide has a considerably higher resistivity than high-tension porcelain at the higher temperatures, and compares favorably with alumina porcelains. As would be expected, magnesium oxide exhibits the same general type of resistivity-temperature characteristic as the inorganic insulations reported by Lindsay and Berberich. The transition point of magnesium oxide appears to be at approximately 250 C.

POWER FACTOR

The power factor (pf) of magnesium oxide is very low compared to that of most insulations used in electrical wires and cables. The room temperature value for typical cable is generally 0.1% when measured at 60 cps, 40 volts per mil.

Typical pf data are given in Fig. 4. Measurements were made at 1,000 cps using a General Radio bridge *716A*. As will be seen later the pf of magnesium oxide insulation is substantially independent of frequency. Samples were placed in an air oven for these tests to attain the correct temperature. The samples were 5 feet long, equipped with suitable guard circuits. The pf is less than 1% up to 250 C, above which the increase is more rapid. This temperature corresponds to that observed as the transition temperature in Fig. 3.

DIELECTRIC CONSTANT

The dielectric constant of magnesium oxide insulation in type-*MI* cables is shown in Fig. 5. This value varies somewhat, as discussed previously, with the degree of compression of the powder, i.e., with its density. The dielectric constant is relatively constant for temperatures up to about 300 C, above which it increases more rapidly. These data were taken at a frequency of 1,000 cps, using a General Radio bridge *716A*. There is no sharp transition point at 250 C as observed in the case of pf and insulation resistance.

The dielectric constant is independent of frequency over the range from 60 cycles

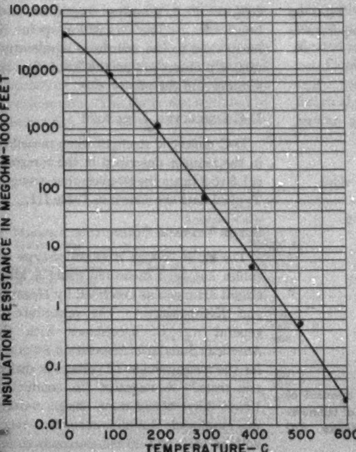

Fig. 2 (left). Insulation resistance, temperature relation for typical single-conductor 4/0 AWG type-MI cable

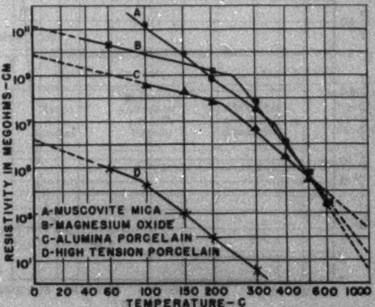

Fig. 3 (right). Resistivity, temperature properties of various inorganic insulations

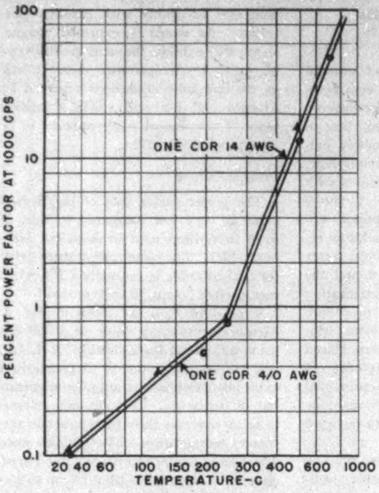

Fig. 4. Pf, temperature relation for typical MI cable

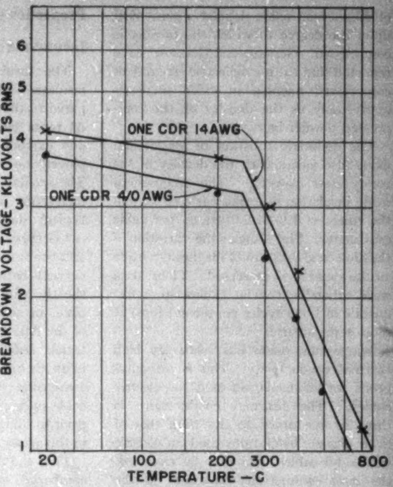

Fig. 6. A-c dielectric strength of MI cables as influenced by temperature

per second to 400 megacycles per second. This particular feature plus the low pf mentioned previously makes this insulation attractive for use in high-frequency cables, as will be discussed later.

A-C Dielectric Strength

The 60-cycle dielectric strength of magnesium oxide in type-*MI* cables is approximately 60 volts per mil when measured at room temperature, which is relatively low compared to most other insulations used on wires and cables. The breakdown voltage of typical completed cables is generally 3,500 to 5,000 volts, which is considered adequate for cable having a 600-volt rating. Performance of cable in service bears this out.

The dielectric strength of *MI* cable decreases with an increase in temperature, and at about 250 C this rate of decrease becomes greater. Typical data are shown in Fig. 6. These tests were conducted on typical *MI* cables, following generally the ASTM D 149–44 procedure.[5] Tests on 1-foot lengths were made at temperatures from 25 to 200 C in an air oven at the test temperature Tests at temperatures from 200 to 850 C were made in 5-foot lengths of cable heated by conductor current and lagged with asbestos insulation. Temperatures were measured by thermocouples strapped to the sheath which would give temperatures slightly below the insulation temperatures. An initial voltage of 40 volts per mil at 60 cps was maintained for 5 minutes, then increased 20% each 5 minutes thereafter until breakdown. The transition point is fairly close to the transition temperature (250 C) observed for the insulation resistance and the pf.

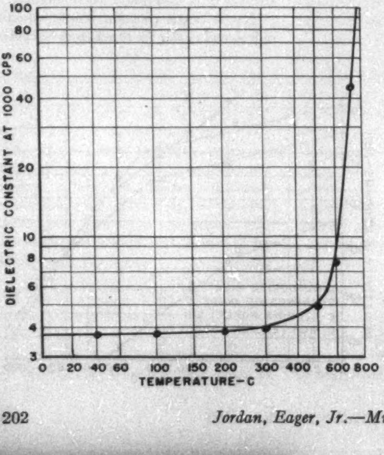

Fig. 5. Dielectric constant of MI cables, effect of temperature, single conductor 4/0 AWG

D-C Dielectric Strength

D-C dielectric strength when measured in the manner described in the foregoing is 1.5 to 2 times the 60-cycle rms strength. Typical data are shown in Table III.

Surge Voltage Strength

The surge voltage strength of type *MI* cables has been measured using a Marx circuit arranged as described by Newman and Kemppainen.[6] The procedure in general was in accordance with the American Standards Association Standard for the measurement of voltage in dielectric tests.[7] A negative (to conductor) 1.5x40-microsecond-wave surge voltage was employed; 1.5 microseconds to reach voltage peak and 40 microseconds to fall

Table III. Dielectric Strength, Type-MI Cable

Type of Cable, AWG	Room Temperature: 60 Cps, Rms Volts	Direct Current, Volts	Surge Strength, Volts, 1½x40	Switching Surge, Volts
1-*cdr* 4/0	2,800		6,000	5,000
1-*cdr* 16	2,900		6,100	5,200
1-*cdr* 9	3,500	6,900		

to one-half peak voltage. Tests were made on single-conductor cables, sizes 16 AWG and 4/0 AWG on samples approximately 10 feet long. The wave shape was observed by means of a cathode-ray oscilloscope. Measurements were conducted at room temperature. The surge voltage was initially 5,000 volts; it was raised in 5% steps until failure occurred. It has been found in surge testing that repetitive tests on the same cable sample may result in subsequent breakdowns at voltages equal to or greater than the original breakdown level. In actual service, however, a surge breakdown may cause power follow-up and permanent failure. In Table III typical surge strength data taken at room temperature are given. For comparison purposes, dielectric strengths at 60 cps are given. These were obtained following the step-by-step procedure described previously under a-c dielectric strength tests. The 1.5 x 40-microsecond surge strength of *MI* cable is about 50% greater than the 60-cycle peak voltage strength.

SWITCHING SURGE VOLTAGE STRENGTH

Switching surge voltage strength tests were made on the same *MI* cable sizes as were employed in the surge voltage tests. A switching surge which took 1,000 microseconds to reach the first peak was employed. A damped wave was used, each succeeding peak decreasing 20% from the previous one. The surge was initiated by discharging a capacitor (previously charged by d-c voltage) across the primary winding of a testing transformer. The *MI* cable specimen was connected across the secondary winding of the transformer. Wave shape was observed by means of a cathode-ray oscilloscope. Otherwise the same procedure of test was followed as described under surge voltage strength tests. The switching surge breakdown voltages are tabulated in Table III.

MECHANICAL PROPERTIES

The cable will withstand severe mechanical abuse such as bending, twisting, and impact without appreciably impairing its electrical efficiency.

Table IV indicates the reduction in dielectric strength of single-conductor 4/0 AWG cable after bending the cable at room temperature around a mandrel having three times the diameter of the cable. The dielectric strength after stretching the cable 10% of its original length at room temperature is also given. Dielectric strength test procedure was the step-by-step procedure described previously under a-c dielectric strength tests.

Another sample of 4/0 AWG cable was placed in an Amsler Universal testing machine and slowly crushed between a steel plate and a steel mandrel of the same diameter as the cable but set at right angles to it. The compressive load to cause insulation breakdown, when 1.8 kilovolts (three times the voltage rating) were maintained between conductor and sheath, was 17,500 pounds. The magnesium oxide insulation was flattened, along with the cable sheath and conductor.

Additional crushing tests comparing *MI* cable to conventional types of armored cable and wire-in-conduit are indicated in Table V. Three samples were cut from each cable, tube, or conduit under test and were placed between a flat steel plate and a V-shaped anvil hardy having a smoothly rounded edge with 1/4-inch radius, and crushed by means of a Dillon tester. The outside diameters were measured and the forces necessary to crush to one-half of the outside diameter were observed. The samples were chosen at random from various manufacturers of labeled rigid steel conduit, electric metallic tubing, and armored cable.

Table IV. Mechanical Abuse Tests, Single-Conductor 4/0 AWG

	Breakdown Voltage, Kilovolts, Rms: After Bending Around 3X Mandrel	After Stretching Longitudinally 10%
Sample *A*	2.80	2.30
Sample *B*	2.70	2.40
Sample *C*	3.20	2.50
Average	2.90	2.40
Original	3.85	3.85
Reduction, %	25	38

Impact tests were also conducted to establish the effect of a sudden blow on *MI* cable; the results appear in Table VI. These tests, in addition to *MI*, also included other conventional types of wiring systems utilizing samples chosen at random from various labeled manufacturers. In these impact tests, the cable was laid over an anvil hardy having a smoothly rounded edge with a 1/4-inch radius. Weights of 50, 20 and 10 pounds were dropped on the cable and the length of drop in feet determined which produced not more than two failures in 10 separate blows. A 3-phase 4-wire 120/208-volt a-c supply with neon lamps in the circuit was used to detect failure.

These various mechanical abuse tests indicate that type-*MI* cable has greater resistance to impact than armored cable and less than rigid steel conduit. It has greater impact resistance than electrical metallic tubing in the larger sizes, and equivalent resistance in the smaller sizes. With regard to crushing, the resistance of type-*MI* cable is greater than that of ar-

Table V. Comparative Crushing Tests

Manufacturer Identification for Armored Cable and Electrical Metallic Tubing	Armored Cable: AWG Size and No. of Conductors	Armored Cable: Weight to Crush to 1/2 OD,* Pounds	Electrical Metallic Tubing: Trade Size, Inches	Electrical Metallic Tubing: Weight to Crush to 1/2 OD, Pounds	Rigid Steel Conduit: Trade Size, Inches	Rigid Steel Conduit: Weight to Crush to 1/2 OD, Pounds	Type-MI Cable: AWG Size and No. of Conductors	Type-MI Cable: Weight to Crush to 1/2 OD, Pounds
A	14/2	733	1/2	1,283	1/2	5,333	14/2	4,400
B	14/2	783					14/3	5,400
C	14/2	800						
E			1/2	1,317				
F			1/2	1,517				
A	14/3	767	1	2,483	1	7,500	6/2	9,633
B	14/3	917					6/3	9,200
C	14/3	1,017						
E			1	2,267				
F			1	2,417				

*Outside diameter.

Table VI. Comparative Impact Tests

Description of Material	Position of Conductors or No. of Wires Within Conduit	Lowest Height to Cause Failure, Feet: 50-Pound Impact Weight	Lowest Height to Cause Failure, Feet: 20-Pound Impact Weight	Lowest Height to Cause Failure, Feet: 10-Pound Impact Weight
Type-*MI* cable, 2-conductor, 14 AWG	edgewise	2.5	5.5	
Type-*MI* cable, 2-conductor, 14 AWG	flat	2	7	
Type-*MI* cable, 2-conductor, 6 AWG	edgewise	7.5		
Type-*MI* cable, 2-conductor, 6 AWG	flat	7.5		
Electrical metallic tubing, 1/2 inch	four 14-AWG type-R, within conduit	2.5	5	
Rigid steel conduit, 1/2-inch	four 14-AWG type-R, within conduit	over 7.5*		
Electrical metallic tubing, 1 inch	three 6-AWG type-R, within conduit	5.5		
Rigid steel conduit, 1 inch	three 6-AWG type-R, within conduit	over 7.5*		
Armored cable, 2-conductor, 14 AWG		0.1	1.5	3
Armored cable, 3-conductor, 14 AWG		0.1	2	3

*Limit of test equipment.

mored cable, electrical metallic tubing, and rigid steel conduit in the larger sizes; the crushing resistances of type-*MI* cable and the smaller sizes of rigid steel conduit are equivalent.

As would be expected, the breaking strength, elongation, and stress-strain properties of type-*MI* cable are essentially those of an annealed copper wire having the same cross-sectional area as the combined areas of sheath and conductor(s). Fig. 7 is a cyclic-loading stress-strain diagram for single-conductor 12 AWG type-*MI* cable. In this test, load was cyclically applied as follows:

1. Starting from an original value of 8% of the cable's ultimate strength, load was increased to 30% of the cable strength and held for 15 minutes.
2. Load was next reduced back to the original 8% value, then raised to 50% of the cable strength and held for 1 hour.
3. Once more, load was reduced to the 8% value and again raised, this time to 70% of the cable's ultimate strength, and held for 2 hours.
4. Finally, the applied load was again reduced to the 8% value, and raised to 73% of the cable's ultimate strength and held for 1 hour.
5. Thereupon the extensometer was removed and, after returning once more to the original 8% starting load, the sample pulled to destruction.

This test was performed on a 134.5-inch gauge length in an Amsler tensile machine. The rate of both load application and removal was 100 pounds per minute.

The ultimate strength of this particular type-*MI* cable was 650 pounds. Inasmuch as the cable as a whole has a cross-sectional area of 0.0475 square inch, and the combined cross-sectional area of the sheath and conductor is 0.0216 square inch, this corresponds to a tensile stress of 13,700 pounds per square inch in the cable as a whole, and of 30,100 pounds per square inch in its metal components. This latter value is quite usual for annealed copper conductors. The *MI* insulation itself, of course, has negligible strength in tension. The final modulus of elasticity indicated by Fig. 7 is 5.9×10^6 pounds per square inch based upon the entire cable, and 13×10^6 based on its metal components alone.

In Fig. 7 the cross-sectional area of the entire cable has been taken as the stress base primarily to demonstrate that the cable responds smoothly as an integral unit to changing mechanical loads. Thus presented, it should be understood that the figure is particular to single-conductor 12 AWG type-*MI* cable. However, this figure may be translated readily to one that is universally applicable to type-*MI* cables of all sizes and constructions, merely by multiplying the ordinates of the diagram by the ratio of the cable area to the metal component area, i.e., by the ratio 0.0475/0.0216.

Resistance to Corrosion

Because copper is more resistant to corrosion than most metals in common usage, type-*MI* cable can be installed successfully in most industrial locations. However, in environments containing gaseous or liquid reagents detrimental to copper, such as some chemical and processing plants, etc., the advisability of a protective covering should be considered. This might take the form of a simple coat of acid-resistant paint, neoprene jacket, or the like. The necessity of such coverings can be judged most simply and reliably by experience with copper vessels, tubing, bare conductors, etc., in the same environment. Direct burial of plain type-*MI* cable in the earth is usually inadvisable unless it is known that electrolysis and exposure to acid-reaction materials are not involved. Cathodic protection may be effective where electrolysis is a factor, and a suitable protective covering will usually provide protection against both electrolysis and chemical corrosion.

Electrical Constants

The electrical constants of interest in engineering given applications of type-*MI* cables differ little, if at all, from those of the older conventional forms of low-voltage power cables. Cable size (aside from thermal or current rating relations discussed later), voltage regulation, and operating efficiency are all calculated in conventional manner; in fact, existing voltage drop and power loss tables will be found to serve satisfactorily. Where, however, it is desired to engineer a given job with close accuracy, the following information will prove helpful.

Resistance

The conductors and sheaths of type-*MI* cables are of high-grade annealed copper and naturally have the standard resistivity and temperature coefficient of resistance of that material. In short, the d-c resistance of a given *MI* conductor

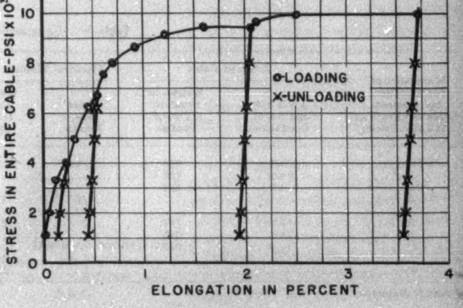

Fig. 7. Stress-strain diagram. Single-conductor 12 AWG, type-MI cable

at any given temperature is the same as that of any other good, solid, annealed copper conductor of the same size at the same temperature.

For greatest accuracy in all a-c applications, particularly in the case of the larger conductor sizes, there should be added to the d-c resistance the further effective resistance components resulting from skin and proximity effects and sheath losses. Methods for doing this are presented in the Appendix.

Contrary to first impressions in some quarters, the increased resistance of type-*MI* cables to alternating currents is moderate. Considering, e.g. a, 3-phase 60-cycle circuit composed of three single-conductor 4/0AWG *MI* cables (the largest standard size) arranged in equilateral triangular configuration with sheaths in contact and operating at a conductor temperature of 85 C, the total increment in effective conductor resistance due to combined skin and proximity effects and sheath losses is only 5.8% (see the Appendix), about the same as the resistance increase that would occur with three conventional 4/0 AWG single-conductor cables in conduit. The added losses of smaller *MI* cables, and in particular multiconductor *MI* cables, are much lower, as will be apparent from the typical examples given in the Appendix.

The principal cause of increase in effective conductor a-c resistance of single-conductor *MI* cables is, of course, the loss created by sheath-circulating currents. Inasmuch as the effect of sheath currents increases with cable spacing, it is generally desirable to group single-conductor cables of a circuit closely together if best voltage regulation and lowest power losses are important desiderata.

INDUCTIVE REACTANCE

For both multiconductor and grouped single-conductor *MI* cables, the inductive reactance from conductor to neutral is given quite simply by the following equation

$$X_1 = 0.8820 \times 10^{-3} f \log_{10} \frac{2.568S}{d} \qquad (1)$$

where

X_1 = inductive reactance to neutral, ohms per 1,000 feet
f = frequency, cps
S = effective spacing between conductor centers, inches
d = diameter of conductor, inches

The inductive reactance of *MI* cables is inherently low compared with that of older conventional cables because of relatively close conductor spacings, a factor generally helpful in improving voltage regulation, particularly at power frequencies in excess of 60 cps.

CAPACITANCE

The specific inductive capacitance of compressed magnesium oxide insulation is about 3.8, generally comparable with that of a good rubber insulation of low specific inductive capacitance. For all low-voltage, low-frequency power work, therefore, capacitance effects are of little practical significance and, as in the case of most other low-voltage cables, may be neglected. However, where operating frequencies become sufficiently high to make capacitance of possible interest, it may be evaluated by methods presented by Simmons,[8,9] Dwight,[10] and Lee.[11] Reference 8 will be found most convenient for rapid evaluation of capacitance from: 1. conductor to sheath, i.e., to neutral, for single-conductor cable; 2. conductor to neutral for 3-conductor cables; and 3. all conductors to sheath for 2-, 3-, and 4-conductor cables. Reference 9 also gives an equation for estimating the capacitance from all conductors of an *n*-conductor cable to sheath. Unfortunately, however, no satisfactory G_2 factors for 2- and 4-conductor cables (for the calculation of capacitance from conductor to neutral) have yet emerged in the literature, so far as the authors are aware, which makes it necessary to determine such capacitances empirically where required.

Temperature Capabilities

The temperature capabilities of *MI* cables are truly remarkable. Mention has already been made of the fact that the final manufacturing operation is a deep anneal, something that would be totally impossible with any other type of cable known today. Magnesium oxide insulation is stable and unaffected by temperatures up to its melting point, 2,800 C. Actually, the only temperature limit in short-time exposures is the melting point of copper itself, 1,083 C. Short of that point, *MI* cable is completely nonflammable; not only will it not burn or support combustion, but it will not develop flammable or toxic gases. In a word, it is the most nearly fireproof cable available today and, remarkably, its end temperature limit is determined not by its insulation but rather by its conductor or conductors and sheath. Its refractory properties constitute an important practical advantage for many types of applications.

The temperature limit of *MI* for continuous operation is determined only by the progressive oxidation temperature of its copper sheath. Investigation shows this to be about 250 C, i.e., provided that temperature is not exceeded, a reasonably long sheath (and cable) life may be expected. Operation at temperatures in excess of 250 C, on the other hand, appears likely to cause progressive oxidation of the sheath (oxidation, spalling of the oxide coating with expansion and contraction of the cable, and exposure of fresh metallic copper, further oxidation, etc.), and curtailed sheath life.

Pilling and Bedworth[12] have developed an equation for oxide film growth on copper in the following general form

$$W = \sqrt{Kt} \qquad (2)$$

where

W = increase in wire weight due to the combined oxygen in the surface oxide film, grams per square centimeter of wire surface
K = oxide film growth parameter (see Fig. 8)
t = time, seconds

Pilling and Bedworth give the oxide film growth parameter for oxygen from 1,000 C down to 400 C; and that for air from 1,000 C down to 700 C. The values for air obviously are less than those for oxygen. The oxide film growth parameter for copper in oxygen is reproduced in Fig. 8 from data provided by Pilling and Bedworth. To increase the usefulness of the data the growth parameter is extrapolated downward to a temperature of about 250 C. The Pilling and Bedworth equation can be translated to the following more convenient form

$$d = 21{,}100\sqrt{Kt} \qquad (3)$$

where

d = the thickness of copper converted to oxide, mils
K = the Pilling and Bedworth oxide film growth parameter
t = time, hours

Based on equation 3 and using the film growth parameters indicated in Fig. 8, the calculated decrease in copper sheath thickness as a function of time is given in Table VII. Values given are for oxygen and are somewhat higher than those for air; this is particularly true for temperatures in the range of 250 C.

Campbell and Thomas[13] have demonstrated that at temperatures below 250 C the rate of oxidation is somewhat less than predicted by equation 3. Their data indicate that the oxide film grows in accordance with the following general equation

$$W = \sqrt[3]{Kt + C} \qquad (4)$$

where

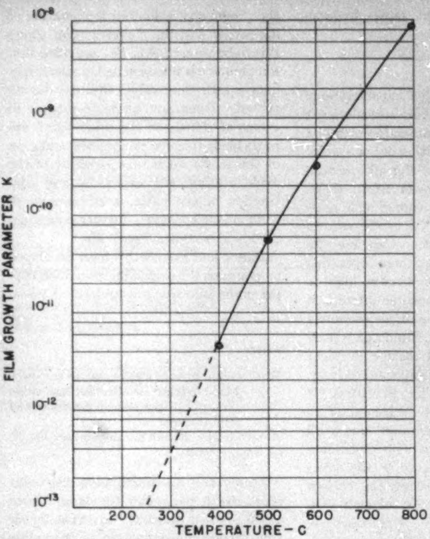

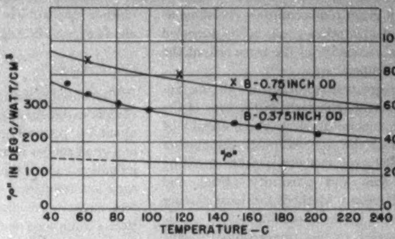

Fig. 8 (left). Oxide film growth parameter

Fig. 9 (above). Insulation thermal resistivity and sheath surface thermal resistivity as a function of temperature

W = weight of oxygen absorbed, micrograms per square centimeter
t = time, minutes
K, *C* = constants

Samples of representative type-*MI* cable were placed in an air atmosphere at temperatures of 750 and 1,000 C. The thickness of the oxide film was measured after representative periods of time. The measured decreases in wall thickness of the copper sheath are shown in Table VIII. These measured values are compared to values calculated from equation 3 with the use of the oxide film growth parameters for oxygen as presented in Fig. 8.

A design-operating temperature of 250 C is, of course, high for most ordinary cable applications (save for running through local hot spots and the like) because of deleterious effects on common building materials and hazard to personnel and, even where cable runs are suitably isolated and/or guarded, because of the heavy voltage drops and power losses associated with temperature-resistance effects, particularly for circuits of appreciable length. The resistance of copper at 250 C is 1.52 times its resistance at 85 C. This might, of course, be compensated by correspondingly larger conductor cross section, but in most instances this would be uneconomical. Most high-temperature applications of *MI*, however, are of a special nature, either involving unusually high ambient temperatures, extra-heavy current or short cable runs, or both, direct connection to electric heaters or other heat sources, or actual utilization of *MI* cable itself as a heater. All such high-temperature applications obviously require special treatment both with respect to the installation as a whole and to the necessary terminations and connections. These various considerations introduce a third operating temperature limit for *MI* in most routine applications, this time determined by ordinary practical service requirements and to an important degree by the temperature capabilities of the appurtenant terminating fittings available at present. At the moment, this latter limit is 85 C, based primarily upon the temperature capabilities of the present standard terminating fittings. This, of course, does not preclude higher local hot-spot temperatures for *MI* cables per se, provided terminations are located in cooler areas such that the combined effects of load current and ambient temperature do not cause termination temperatures in excess of 85 C. Development of terminating fittings for temperatures higher than 85 C is under way.

Table VII. Decrease in Copper Sheath Thickness as a Function of Time at Various Temperatures

Decrease in Sheath Thickness, Mils*	250 C, Years	400 C, Years	800 C, Hours
1	2.57	0.0583	0.259
2	10.3	0.233	1.04
5	64.3	1.46	6.48
10	257	5.83	25.9

*1 mil = 0.001 inch.

Current Rating

As Fig. 9 indicates, the thermal resistivity of compressed magnesium oxide insulation used in type-*MI* cables is low, being of the order of 150 C per watt per centimeter (cm)³ at a conductor temperature of 85 C, greatly facilitating flow of heat from the conductor(s) to the outer sheath.

The surface thermal resistivity of the sheath is dependent upon the degree of weathering or oxidation, upon the diameter of the cable, and apparently also to some extent upon the sheath temperature. Fig. 9 includes two curves of sheath surface thermal resistivity applicable to type-*MI* cables, one for a cable having a diameter of 3/8 inch, the other for a cable having a diameter of 3/4 inch. The surface resistivity decreases somewhat as the sheath temperature increases, but in the 80 to 85 C temperature range the indicated sheath surface thermal resistivity is about 630 and 830 C per watt per cm² for the 3/8- and 3/4-inch cable diameters respectively. The decrease of sheath surface resistivity with increasing sheath temperature may be partially explained by the blackening of the sheath (with re-

Table VIII. Comparison of Measured and Calculated Decrease in Wall Thickness, Type-MI Cable

Temperature, C	Time, Hours	Decrease in Wall Thickness, Mils* Measured in Air	Decrease in Wall Thickness, Mils* Calculated in Oxygen
750	4	2.5	2.6
750	72	9.0	10.8
1,000	2	10.8	11.8
1,000	3	13.5	14.7
1,000	7	20.3	23.7

*1 mil = 0.001 inch

Table IX. Dimensions of Cables Employed in Tests

Description of Cable	Conductor Diameter, Inch	Nominal Insulation Wall Thickness, Inch	Nominal Thickness of Copper Sheath, Inch	Diameter Over Copper Sheath, Inch
1-conductor 16 AWG	0.051	0.060	0.023	0.215
1-conductor 14 AWG	0.064	0.060	0.023	0.230
1-conductor 12 AWG	0.081	0.059	0.024	0.246
1-conductor 9 AWG	0.114	0.064	0.025	0.293
1-conductor 4/0 AWG	0.460	0.081	0.038	0.699
2-conductor 14 AWG	0.064	0.063	0.027	0.371
3-conductor 14 AWG	0.064	0.061	0.028	0.387
2-conductor 6 AWG	0.162	0.066	0.035	0.590
3-conductor 6 AWG	0.162	0.064	0.036	0.621
RG-81/U	0.063	0.129	0.027	0.375
RG-82/U	0.125	0.263	0.050	0.750

sultant increase of the effective emissivity factor) as the test proceeded, but it appears doubtful that this can be regarded as the sole reason. Increasing temperature would tend to increase heat dissipation both by radiation and convection.

The data presented in Fig. 9 were taken on *RG-81/U* and *RG-82U* cables having the dimensions indicated in Table IX. The cables were placed in a special chamber free of air drafts, so equipped that an ambient temperature of 40 C could be maintained. Conductor temperatures were obtained from conductor resistances measured by means of a Kelvin double bridge arranged so that the conductor resistance could be measured while the d-c loading current was passing through the conductor. The sheath was electrically idle. The sheath temperature and the ambient temperature were measured by suitable thermocouples placed along the length of the cable. The total watt input to the conductor was determined by measuring the conductor current and calculating the watts from the product of the square of this current and the conductor resistance. The insulation thermal resistivity ρ and the sheath surface thermal resistivity B were then calculated from the following equations

$$\rho = \frac{T_c - T_s}{0.00522w \log_e \dfrac{D_i}{d}}$$

$$B = \frac{(T_s - T_a)D}{0.00411w}$$

where

T_c, T_s, T_a = conductor, sheath and ambient temperatures respectively, C
D_i = diameter over insulation, inches
D = outside diameter of cable, inches
d = conductor diameter, inches
$w = I_c^2 R_{dc}$ where I_c is the conductor d-c current in amperes, and R_{dc} is the conductor resistance in ohms at the test temperature, watts per foot
ρ = insulation thermal resistivity, C per watt per cm²
B = surface thermal resistivity, C per watt per cm²

Rosch[14] has shown that the surface thermal resistivity of cables having outside diameters of about 1.75 inches and less is dependent upon cable diameter. As a result of this work the National Electrical Manufacturers' Association (NEMA) and the Insulated Power Cable Engineers Association (IPCEA)[15] have adopted a conventional standard, which has been used by the industry for many years, and in which the surface thermal resistivity of all types of cables is taken as a value varying linearly from 650 at cable diameter equal to zero, to 1,200 at cable diameter equal to 1.75 inches. For diameters larger than 1.75 inches, a constant value of 1,200 C per watt per cm² is used. Since all standard *MI* cables have sheath outside diameters of under 1.75 inches, the applicable NEMA-IPCEA surface thermal resistivity would be given by the expression

$$B = 314.3D + 650 \qquad (D \leq 1.75 \text{ inches}) \qquad (5)$$

where

B = surface thermal resistivity of sheath, C per watt per cm²
D = cable outside diameter, inches

Surface thermal resistivities indicated by equation 5 appear to be high in comparison with those indicated by the investigations of Schurig and Frick[16] on the heating of bare conductors. Fig. 10 shows two curves of surface thermal resistivity B, one a plot of equation 5, the other derived from curve A, Fig. 13, of reference 16. According to Schurig and Frick, their curve A is based on a 30 C rise above a 40 C ambient, at an indicated conductor temperature of 70 C. Also included on Fig. 10 are two test points taken from Fig. 9 of measured sheath thermal resistivity for the 3/8-inch and 3/4-inch diameter *MI* cables at a sheath temperature of 70 C. These latter points fall between the IPCEA and Schurig and Frick curves. It is evident from all of the available data that the IPCEA curve is at least on the conservative side when applied to *MI* cables, perhaps unduly so. Nevertheless it is accepted as a basis for the following estimates of current-carrying capacities for type-*MI* cables, together with the insulation thermal resistivity of 150 C per watt per cm² indicated by Fig. 9. Inasmuch as dielectric loss is negligible in type-*MI* cables, the following current-rating equations then become applicable

$$R_i = \frac{0.7832G}{n} \qquad (6)$$

$$R_s = \frac{2.672}{D} + 1.292 \qquad (D \leq 1.75 \text{ inches}) \qquad (7)$$

$$R_{th} = R_i + R_s \qquad (8)$$

$$I = \sqrt{\frac{\tau}{nR_cR_{th}}} \qquad (9)$$

where

R_i = thermal resistance of insulation, C per watt per linear foot
R_s = surface thermal resistance of sheath, C per watt per linear foot
R_{th} = total thermal resistance of cable, C per watt per linear foot
R_c = effective conductor resistance at operating temperature, ohms per foot
G = geometric factor for heat flow from conductor(s) to sheath (given for 1-, 2-, 3-, and 4-conductor cables in reference 8)
n = number of conductors in cable
τ = temperature rise of conductors, C, i.e., difference between conductor operating temperature and ambient temperature
I = current per conductor, amperes
D = cable over-all diameter, inches

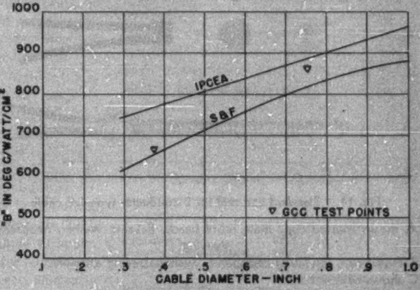

Fig. 10. Surface thermal resistivity. Comparison of IPCEA and Schurig and Frick curves and GCC experimental data

Table X. Current Ratings of Type MI Cables; Conductor Temperature 85 C, Ambient Temperature 30 C

Cable Size, AWG	Calculated Current Rating Amperes						NEC* Current Rating Amperes					
	1-Cdr† Cable	2-Cdr Cable	Three 1-Cdr Cables Grouped‡	3-Cdr Cable	4-Cdr Cable	7-Cdr Cable	1-Cdr Cable	2-Cdr Cable	Three 1-Cdr Cables Grouped	3-Cdr Cable	4-Cdr Cable	7-Cdr Cable
14	36	31	29	26	23	19	30	25	25	25	20	17.5
12	46	40	37	34	30	25	40	30	30	30	24	21
10	62	53	50	45	40	33	55	40	40	40	32	28
8	82	71	65	59	53		70	50	50	50	40	
6	107	94	85	79	71		100	70	70	70	56	
4	145	125	114	106			135	90	90	90		
3	168		131				155		105			
2	194		151				180		120			
1	224		173				210		140			
1/0	260		200				245		155			
2/0	300		229				285		185			
3/0	346		263				330		210			
4/0	399		301				385		235			

Correction Factors For Other Ambient Temperatures

20 C	25 C	30 C	35 C	40 C	45 C	50 C	55 C	60 C	65 C	70 C	75 C	80 C
1.09	1.05	1.00	0.95	0.90	0.85	0.80	0.75	0.67	0.60	0.52	0.43	0.30

*National Electrical Code.

†Cdr = conductor.

‡Cables in triangular configuration, sheaths in contact.

These equations apply strictly to a single 1-conductor or *n*-conductor isolated cable in still air. Where several cables are grouped closely together with sheaths in contact, the group may be treated with fair approximation as a single multiconductor cable having a sheath diameter equivalent to that of the circle circumscribing the entire group. Where cables are grouped with separations between cable surfaces ranging from one-quarter to one cable diameter, the group correction factors, Table IV of reference 15 are useful. For cable groupings having spacings between cable surfaces exceeding about one cable diameter, mutual heating effects become small and may be neglected, i.e., the cables treated as individual isolated cables, without serious error.

These various considerations are subject to some modification (based upon good judgment) depending upon the physical arrangement of cable groups; for instance, vertical runs have the advantage of greater "chimney" effect than horizontal runs. Finally all theoretical calculations based on the simple assumption of cables or cable groups isolated in air necessarily involve departures from the actual conditions of many practical installations wherein cables are laid in trays, racked over surfaces, etc., and hence are affected by their surroundings. These extraneous effects unfortunately are too numerous and varied to lend themselves readily to satisfactory analytical treatment, and usually must be determined empirically.

Table X shows current-carrying capacities of type-*MI* cables calculated in accordance with the methods described. These current ratings are based upon an operating temperature of 85 C and an ambient temperature of 30 C. Current ratings for other ambient temperatures may be determined readily from the correction factors included in the table. Also included in Table X in parallel column arrangement are current-carrying capacities prescribed in the 1953 National Electrical Code for type-*MI* cables, likewise based on a conductor temperature of 85 C and an ambient temperature of 30 C. These code ratings, of course, were not determined specifically for type-*MI* cables, rather they are the ratings established earlier for other, older types of cables having the same assigned operating temperature rating, and are the category into which *MI* was placed when it received code recognition.

Terminating Fittings

As previously mentioned, magnesium oxide insulation is hygroscopic, combining with water to form magnesium hydroxide. In addition to the water of constitution, the hydroxide can also absorb a certain amount of extra water which remains in the free state. This latter tends to reduce

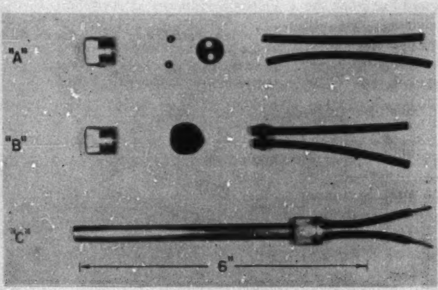

Fig. 11. Standard end seal for 2-conductor type-MI cable

A shows knurled cup, strain relief beads, Bakelite washer, neoprene sleeving
B shows cup, insulating compound, washer-sleeving assembly
C shows completed seal

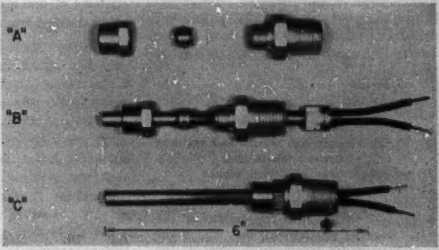

Fig. 12

A shows locknut, compression ring, and threaded gland
B shows components of A, placed on MI cable with end seal
C shows completed termination ready for attachment to enclosure

the dielectric strength and current resistance of the insulation and could ultimately cause failure. However, should a cable end accidentally become exposed to moisture during handling and installation, the longitudinal penetration into the cable ordinarily is relatively slow, and confined to a short distance from the open end. In any case, absorbed moisture can be completely eliminated and the cable restored to its original dry state by playing a torch lightly over a short section adjacent to the cable end, or simply by cropping the affected end. The efficacy of such treatment can be judged most conveniently and effectively by megger test. While hygroscopic effects thus constitute no particular problem during the handling and installation stage, it will be appreciated that installed cables must be permanently sealed at their ends to prevent subsequent ingress of water. Terminating fittings are required, therefore, to serve three principal functions: 1. Seal the cable end as mentioned. 2. Provide means for extending and insulating the individual conductors beyond the cable seal for purposes of connection to terminals or other conductors. 3. Anchor the cable to the box, fitting or enclosure to which it is attached.

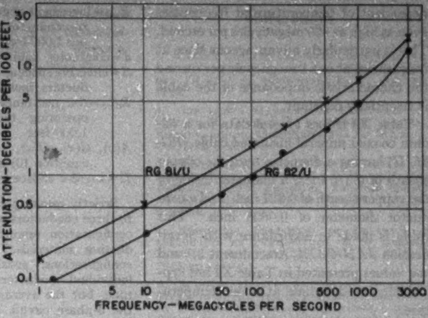

Fig. 13. Typical data showing the variation of attenuation at room temperature with frequency

Fig. 11 shows a cable seal and its component parts, in this case for a 2-conductor *MI* cable. It consists essentially of: 1. a cylindrical, knurled brass cup or pot, internally threaded at the knurled end to fit the cable sheath size for which it is intended, and having a recessed opening at the other end to receive a circular, reinforced bakelite insulating washer; 2. strain-relief insulating beads; 3. the aforementioned washer; 4. special high-temperature moisture-resistant insulating neoprene sleeving of the size required for the cable conductors; and finally 5. special plastic heat-resistant, moisture-resistant, insulating potting compound. After the sheath and insulation have been stripped from the conductors for the requisite distance (which may be much longer than that depicted in the figure), the knurled brass cup is screwed onto the end of the cable sheath, cutting its own thread in the process. The knurled cup is then completely filled with sealing compound. Next, the preassembled insulating washer and insulating sleeves (each of the latter with its strain relief bead under the washer) are slipped over the conductors and pressed home in the shouldered recess of the compound-filled knurled cup (excess compound being extruded into the sleeving and around the edges of the insulating washer), and the washer firmly secured in position by a small tool that crimps the lip of the cup thereon. This completes the cable seal proper. Seals for single-conductor and other multiconductor cables are made in identical manner except, that, aside from suitable adjustment of dimensions with those of the cable involved, the number of holes in the insulating washer and the number of insulating sleeves are co-ordinated with the number of conductors in the cable being terminated.

Fig. 12 shows the remaining components of a standard termination, which are identical in form for both single-conductor and multiconductor cables and vary only with the outside diameter of the cable involved. These components are three in number, all of brass, and consist of: 1. a threaded gland internally recessed to fit the knurled sealing cup; 2. a compression ring which fits over the cable sheath and seals it off (on the well-understood principle adapted so widely to pressure pneumatic and hydraulic tubing); and 3. a follow-up compression-locking nut. The threaded gland proper, of course, may be inserted into a box or enclosure and secured thereto by a standard locknut, or screwed into threaded bosses of various types of enclosures, in either case anchoring the cable to the device or fitting on which it terminates. Cables may be spliced, where required, by terminating them into a suitable box, and joining and insulating the conductor ends within the box. The entire standard *MI* cable line is accommodated by only four sizes of threaded glands (with associated seal ring and locknut) corresponding to conduit sizes of 3/8 inch, 1/2 inch, 3/4 inch, and 1 inch respectively. The threads of these glands are standard conduit threads.

It can be seen from this brief outline that *MI* terminating fittings are both simple in principle and simple to apply, and require no essentially new techniques. Properly installed, they very efficiently and effectively serve their intended purpose, even with standard knockout boxes and enclosures. Employment of watertight boxes and enclosures, where required, to protect otherwise exposed conductor terminal lugs, screws, etc., makes possible a completely moistureproof, vaporproof, and dustproof system.

Present standard terminating fittings have an assigned maximum continuous operating temperature of 85 C, governed by the temperature capabilities of the pot-sealing compound, insulating washer, and insulating sleeving. The possibilities of alternate potting compounds and sleevings, suitable for operation at higher temperatures, are being investigated, with currently encouraging prospects. There are also possibilities in the ceramic-soldered-to-metal type of terminal, or small cable pothead, for use under very high temperature conditions or where atomic radiation is a factor. These possibilities are being looked into and can be exploited as occasion requires.

High-Frequency Uses

The relatively low dielectric constant and the low pf of magnesium oxide make this insulation suitable for use at ultrahigh frequencies. As indicated previously, the dielectric constant is relatively constant over the frequency range of 60 cps to 400 megacycles per second. The pf is relatively constant. Both the dielectric constant and pf are practically in-

Table XI. RG-81/U High-Frequency MI Cable

Room Temperature Parameters	
Capacitance	37.1 micromicrofarads per foot
Impedance	52.5 ohms
Velocity of propagation	53.0%
Attenuation	2.1 db per 100 feet at 100 megacycles

dependent of temperature at frequencies even as high as 400 megacycles per second. This is particularly advantageous since at frequencies above 1 megacycle per second the characteristic impedance of the cable is essentially constant.

Table XI shows typical data for a 52-ohm coaxial mineral-insulated cable (*RG-81/U*) having a diameter over the copper sheath of 0.375 inch, a diameter inside of the copper sheath of 0.321 inch, and a conductor diameter of 0.0625 inch. This cable is made in accordance with Specification *JAN-C-17A*, Amendment 3,[1] and the values presented in Table XI are typical measured values at room temperature.

Measurements of attenuation on *RG-81/U* and *RG-82/U* were made at room temperature. A General Radio type-874 coaxial equipment set was used for measurements in the frequency range of 1 to 900 megacycles per second. For measurements at 3,000 megacycles per second, the *MIT CO-AX* instrument and cable test unit type *Q* was employed. Results are shown in Fig. 13.

Appendix

Skin and proximity effects and sheath losses tend to increase the effective a-c resistance of conductors in metallic-sheathed cables. Skin and conductor proximity effects are common to all cables, whether single-conductor or multiconductor. In the case of grouped single-conductor cables, sheath losses consist of two components, those due to sheath proximity (eddy) currents which flow solely within the individual sheaths, and those due to sheath-circulating currents which leave an individual sheath at one or more points and return to it at one or more others. In the case of individual multiconductor cables, sheath losses consist solely of those due to sheath proximity (eddy) currents.

Skin effect can be evaluated most conveniently by means of tables contained in most electrical handbooks[17] of a-c/d-c resistance ratios corresponding to the function

$$x = 0.02768\sqrt{f/R_{\text{d-c}}} \qquad (10)$$

where

f = frequency, cps
$R_{\text{d-c}}$ = conductor d-c resistance at operating temperature, ohms per 1,000 feet

Conductor proximity effects can be estimated by means of the following equations from Arnold[18,19]

$$R_{pc1} = 0.5K(d/S)^2 A(x) R_{d-c} \text{ (single-phase)} \qquad (11)$$

$$R_{pc3} = \frac{1.5(d/S)^2 G(x) R_{d-c}}{1 - 0.2083(d/S)^2 H(x)} \text{ (3-phase)} \qquad (12)$$

where

R_{pc1} = increment of conductor resistance due to conductor proximity effect, ohms per 1,000 feet, for single-phase circuits
R_{pc3} = increment of conductor resistance due to conductor proximity effect, ohms per 1,000 feet, for 3-phase circuits
d = conductor diameter, inches
S = effective spacing between centers of conductors, inches
R_{d-c} = d-c resistance of conductor at the operating temperature, ohms per 1,000 feet
$A(x)$, $G(x)$, $H(x)$, are functions of x (see equation 10) as given in Fig. 14
K = a-c/d-c resistance ratio (reference 17)

Strictly speaking, equation 12 applies only to three conductors in equilateral triangular configuration remote from all other conducting materials. For other conductor configurations, proximity effects on the individual conductors will differ in magnitude, but the average proximity effect for the 3-phase circuit as a whole should be indicated with practical accuracy by employing the effective conductor spacing for the particular configuration involved. Equation 11 also applies strictly only to conductors remote from all other conducting materials. Moreover, particularly in the case of grouped single-conductor *MI* cables, at least, the proximity effects indicated by both equations 11 and 12 tend to be pessimistic, i.e., too high, because these equations do not take into account sheath currents which, being of opposite polarity to the conductor currents, reduce flux linkages between conductors and hence reduce proximity effects. However, inasmuch as conductor proximity effects are relatively small for type-*MI* cables, even of the largest sizes, these equations serve with practical accuracy and tend, if anything, to be conservative.

Sheath proximity loss is attributable to eddy currents induced in the sheath by the main conductor currents. For two single-conductor type-*MI* cables connected in a single-phase circuit, the sheath proximity loss may be calculated from the following development of an equation from Arnold[20]

$$R_{ps1} = \frac{73.4f^2}{R_s}\left(\frac{D_m}{2S}\right)^2 \times 10^{-9} \qquad (13)$$

where

R_{ps1} = increment of conductor resistance, ohms per 1,000 feet
R_s = sheath resistance at operating temperature, ohms per 1,000 feet
f = frequency, cps
D_m = mean sheath diameter, inches
S = spacing between conductor centers, inches

For three single-conductor type-*MI* cables arranged in equilateral triangular configuration and carrying balanced 3-phase currents, the sheath proximity effect may be calculated from

$$R_{ps3} = \frac{110f^2}{R_s}\left(\frac{D_m}{2S}\right)^2 \times 10^{-9} \qquad (14)$$

where R_{ps3} = increment of conductor resistance, ohms per 1,000 feet, and the other symbols are the same as given for equation 13.

For three single-conductor type-*MI* cables arranged in a flat configuration, the effect of the sheath proximity losses may be calculated from the following equations from Arnold[20]

R_{ps3} (either outer cable)

$$= \frac{55f^2}{R_s}\left(\frac{D_m}{2S}\right)^2 \times 10^{-9} \qquad (15)$$

R_{ps3} (middle cable)

$$= \frac{220f^2}{R_s}\left(\frac{D_m}{2S}\right)^2 \times 10^{-9} \qquad (16)$$

where symbols are the same as given for equation 13.

The effect of sheath proximity loss for a 2-conductor type-*MI* cable may be calculated from the following equation, which is a development of a similar equation originally developed by Meyerhoff[21]

$$R_{ps1}' = 1.913 \times 10^{-4} f M_{21} \qquad (17)$$

where

R_{ps1}' = effective increase in conductor d-c resistance, ohms per 1,000 feet

$$M_{21} = 4v\left(\frac{a^2}{1+V^2} + \frac{a^6}{9+V^2} + \frac{a^{10}}{25+V^2} + \ldots\right)$$

$$a = \frac{d(m+1)}{D_m}$$

$$v = \frac{1.913 \times 10^{-4} f}{R_s}$$

m = ratio of insulation thickness (as previously defined) to conductor diameter
f, d, D_m, and R_s have the meanings given previously

In the case of 3-conductor type-*MI* cables, the effect of sheath proximity currents can be evaluated by means of the equation suggested by Simmons[8]

$$R_{ps3}' = \frac{396(2S_1)^2}{R_s D_m^2} \times 10^{-6} \qquad (18)$$

where

R_{ps3}' = effective increase in conductor resistance, ohms per 1,000 feet
S_1 = distance between center of each conductor and center of cable, inches
and all other symbols have the meanings previously given

For two single-conductor cables in a single-phase circuit or three single-conductor cables with equilateral spacing in a 3-phase circuit, the added effective conductor resistance due to sheath-circulating currents is given by the relations

$$R_0 = \frac{X_m^2 R_s}{X_m^2 + R_s^2} \qquad (19)$$

$$X_m = 0.8820 \times 10^{-3} f \log_{10}\frac{2S}{D_m} \qquad (20)$$

where

R_0 = added effective conductor resistance, ohms per 1,000 feet
X_m = mutual reactance between conductor and sheath, ohms per 1,000 feet
S = effective separation between cable centers, inches
R_s, f, and D_m have the meanings assigned previously

Equations 19 and 20 apply rigorously only when sheath proximity effects are negligible. In most practical problems, however, the error is relatively small,

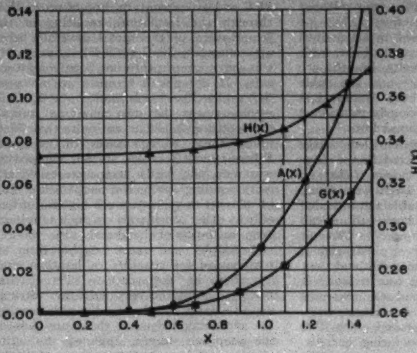

Fig. 14. Functions of x for determination of conductor proximity effects

though it is a maximum for the case of cables with sheaths touching. A more exact evaluation in such cases has been worked out by Miller[22] and Dwight.[23,24]

For other arrangements of one and two circuits of single-conductor cables, see Table VI of reference 8.

The application of these equations to type-*MI* cables may best be shown by a few typical examples. Consider first a 60-cycle 3-phase circuit composed of three single-conductor 4/0 AWG type-*MI* cables arranged in equilateral triangular configuration with sheaths in contact and operating at a conductor temperature of 85 C. For these cables the following data are applicable

$R_{d\text{-}c}$ at 85C = 0.0615 ohm per 1,000 feet
$d = 0.460$ inch
$S = 0.699$ inch
$R_s = 0.127$ ohm per 1,000 feet at an assumed temperature of 80 C
$D_m = 0.661$ inch

$$x = 0.02768\sqrt{\frac{60}{0.0615}} = 0.864$$

From handbook tables of a-c/d-c resistance ratios, the ratio corresponding to the value of x in the foregoing is 1.0029. In short, 60-cycle skin effect increases the resistance of the conductor by 0.29% or 0.0002 ohm per 1,000 feet.

For conductor proximity effect, $G(x)$ and $H(x)$ are 0.0085 and 0.338 respectively, as obtained from Fig. 14. Then

$$R_{pc3} = \frac{1.5\left(\frac{0.460}{0.699}\right)^2 0.0085 \times R_{d\text{-}c}}{1 - 0.2083\left(\frac{0.460}{0.699}\right)^2 0.338}$$

$$= 0.0057 R_{d\text{-}c} = 0.0004 \text{ ohm per 1,000 feet}$$

which is equivalent to an increase of effective resistance of 0.57%.

For sheath proximity effect

$$R_{ps} = \frac{110 \times (60)^2}{0.127}\left(\frac{0.661}{2 \times 0.699}\right)^2 \times 10^{-9}$$

$$= 0.0007 \text{ ohm per 1,000 feet}$$

which corresponds to a 1.14% increase in the d-c resistance value of 0.0615.

The effect of sheath circulating current is given by

$$X_m = 0.882 \times 10^{-3} \times 60 \log_{10} \frac{2 \times 0.699}{0.661}$$

$$= 0.0172 \text{ ohm per 1,000 feet}$$

$$R_0 = \frac{(0.0172)^2 \times 0.127}{(0.0172)^2 + (0.127)^2} = 0.0023 \text{ ohm per 1,000 feet}$$

which corresponds to an increase of 3.73% in the conductor d-c resistance.

The total 60-cycle resistance at 85 C is therefore = 0.0615 + 0.0002 + 0.0004 + 0.0007 + 0.0023 = 0.0651 ohm per 1,000 feet or 105.8% of the d-c resistance. This is commensurate with resistance increase occurring with three conventional 4/0 AWG single-conductor cables in conduit.

The example given purposely involves the largest standard size of single-conductor *MI* cable. The added losses of smaller cables and, in particular, multiconductor cables, are much lower. For instance, for size 4 AWG single-conductor cables in equilateral triangular configuration with sheaths in contact, the skin and proximity effects are negligible and the added conductor resistance due to sheath circulating currents is only 0.33% of the d-c resistance, assuming as before a conductor operating temperature of 85 C and a frequency of 60 cycles.

The added losses in the case of multiconductor type-*MI* cables are still lower. For 3-conductor 4 AWG type-*MI* cable (the largest standard size) operating at a temperature of 85 C and a frequency of 60 cycles, skin and conductor proximity effects again are negligible and the increased effective resistance due to sheath proximity currents is indicated as

$S_1 = 0.157$ inch
$R_s = 0.118$ ohm per 1,000 feet at an assumed temperature of 80 C
$R_{d\text{-}c} = 0.312$ ohm per 1,000 feet at 85 C
$D_m = 0.691$

$$R_{ps3}' = \frac{396(2 \times 0.157)^2 \times 10^{-6}}{0.118 \times (0.691)^2} = 0.000693$$

This corresponds to an increase in conductor d-c resistance of only 0.22%, a very small value.

References

1. CABLES, COAXIAL AND TWIN-CONDUCTOR, FOR RADIO FREQUENCY. *Joint Army-Navy Specification JAN-C-17A*, Washington, D. C., July 25, 1946.

2. COMPRESSED MAGNESIA AS ELECTRICAL INSULATOR, A. Gemant, F. A. Glassow. *Journal*, Franklin Institute, Philadelphia, Pa., vol. 230, no. 4, Oct. 1940, p. 471.

3. TENTATIVE METHODS OF TESTING RUBBER INSULATED WIRE AND CABLE. *ASTM Specification D470-52T*, ASTM Standards, American Society for Testing Materials, Philadelphia, Pa., 1952, pt. 6, p. 179.

4. ELECTRICAL PROPERTIES OF CERAMICS AS INFLUENCED BY TEMPERATURE, E. W. Lindsay, L. J. Berberich. *AIEE Transactions*, vol. 67, pt. I, 1948, pp. 734–42.

5. STANDARD METHODS OF TEST FOR DIELECTRIC STRENGTH OF ELECTRICAL INSULATING MATERIALS AT COMMERCIAL POWER FREQUENCIES. *ASTM Specification D149 44*, ASTM Standards, American Society for Testing Materials, Philadelphia, Pa., 1952, pt. 6, p. 928.

6. HIGH-VOLTAGE INSTALLATION OF THE PRECIPITATION STATIC PROJECT—PART IV. M. Newman, A. O. Kemppainen. *Proceedings*, Institute of Radio Engineers, New York, N. Y., vol. 34, no. 5, May 1946, p. 247.

7. MEASUREMENT OF TEST VOLTAGE IN DIELECTRIC TESTS. *ASA C68.1-1953*, American Standards Association, New York, N. Y., 1953.

8. CALCULATION OF THE ELECTRICAL PROBLEMS OF UNDERGROUND CABLES, D. M. Simmons. *Electric Journal*, East Pittsburgh, Pa., May to Nov. 1932.

9. CABLE GEOMETRY AND THE CALCULATION OF CURRENT-CARRYING CAPACITY, Donald M. Simmons. *AIEE Transactions*, vol. 42, June 1923, pp. 600–20.

10. THE DIRECT METHOD OF CALCULATION OF CAPACITANCE OF CONDUCTORS, Herbert Bristol Dwight. *Ibid.*, vol. 43, June 1924, pp. 958–65.

11. CALCULATION OF THE CAPACITANCE BETWEEN TWO WIRES OF A THREE-CONDUCTOR CABLE, Y. W. Lee. *Ibid.*, vol. 48, Jan. 1929, pp. 195–97.

12. OXIDATION OF METALS AT HIGH TEMPERATURES, N. B. Pilling, R. E. Bedworth. *Journal*, Institute of Metals, London, England, vol. 29, 1923, p. 529.

13. THE OXIDATION OF METALS, W. E. Campbell, U. B. Thomas. *Transactions*, Electrochemical Society, New York, N. Y., vol. 91, 1947, p. 623.

14. THE CURRENT-CARRYING CAPACITY OF RUBBER-INSULATED CONDUCTORS, S. J. Rosch. *AIEE Transactions (Electrical Engineering)*, vol. 57, Mar. 1938, pp. 155–67.

15. CURRENT CARRYING CAPACITY TABLES (book). Insulated Power Cable Engineers Association, Montclair, N. J., first edition, Dec. 1943.

16. HEATING AND CURRENT CARRYING CAPACITY OF BARE CONDUCTORS FOR OUTDOOR SERVICE, O. R. Schurig, C. W. Frick. *General Electric Review*, Schenectady, N. Y., Mar. 1930, p. 141.

17. STANDARD HANDBOOK FOR ELECTRICAL ENGINEERS (book), Archer E. Knowlton, editor. McGraw-Hill Book Company, Inc., New York, N. Y., seventh edition, 1941, section 4–29.

18. EDDY CURRENT LOSSES IN SINGLE-CONDUCTOR PAPER-INSULATED, LEAD-COVERED, UNARMOURED CABLES OF A SINGLE-PHASE SYSTEM, A. H. M. Arnold. *Journal*, Institution of Electrical Engineers, London, England, vol. 89, pt. II, no. 12, Dec. 1942, p. 636.

19. EDDY CURRENT LOSSES IN MULTI-CORE PAPER-INSULATED, LEAD COVERED CABLES, ARMOURED AND UNARMOURED, CARRYING BALANCED 3 PHASE CURRENTS, A. H. M. Arnold. *Ibid.*, vol. 88, pt. II, no. 1, Feb. 1941, p. 52.

20. THE THEORY OF SHEATH LOSSES IN SINGLE CONDUCTOR LEAD-COVERED CABLES, A. H. M. Arnold. *Ibid.*, vol. 67, 1929, p. 69.

21. PIPE LOSSES IN NONMAGNETIC PIPE, L. Meyerhoff. *AIEE Transactions*, vol. 72, pt. III, Dec. 1953, pp. 1260–75.

22. SHEATH CURRENTS, SHEATH LOSSES, INDUCED SHEATH VOLTAGES AND APPARENT CONDUCTOR IMPEDANCES OF METAL SHEATHED CABLES CARRY-

ING ALTERNATING CURRENTS, Miller. *Thesis*, University of Illinois, Urbana, Ill., 1929.

23. LOSSES IN GROUNDED SHEATHS OF SINGLE-CONDUCTOR CABLES, H. B. Dwight. *Electric Journal*, East Pittsburgh, Pa., 1924, p. 62.

24. PROXIMITY EFFECT IN CABLE SHEATHS, Herbert Bristol Dwight. *AIEE Transactions*, vol. 50, Sept. 1931, pp. 993–98.

◆

Discussion

Henry Richter (Ebasco Services, Inc., New York, N.Y.): This type of cable is coming into wider use for power, control, lighting, and heating tracers for freeze protection. For the first three of these applications the considerations leading to its choice may include fire hazard, ruggedness, lower installed cost than the more or less standard cables in conduit, high ambient temperatures, etc. In freeze protection circuits it may be called upon to withstand one of the worst possible conditions for insulated cables, namely, the presence of moisture and temperatures up to 250 C, or 482 degrees Fahrenheit (F).

Based on our experience with type-*MI* cables in all four of the applications just listed, it would appear that improvements in the terminations would assist materially in furthering the use of this cable, and the following remarks are directed mainly toward that end.

In the section "Properties of Magnesium Oxide Insulation," it is stated that "The presence of free moisture quickly reduces the dielectric strength and allows an appreciable leakage current to flow." A test was made using two pieces of *MI* cable with the conductors spliced and the ends of the magnesium oxide left exposed to the air. This joint was enclosed in a large conduit box with water in the bottom of the box to a depth of about 1/4 inch, the joint being about 1/4 inch above the water. The box was then hermetically sealed. The magnesium oxide thus was subjected to almost a completely saturated atmosphere. Readings of insulation resistance were taken daily and the test was continued for 90 days at room temperature. The insulation resistance dropped from an initial 200,000 ohms to as low as 20,000 ohms after several days, then climbed steadily to approximately 80,000 ohms after several weeks and continued there for the remainder of the test. If the two ends of a cable on a 480-volt circuit supplying a motor were similarly exposed to extremely high humidity it would thus appear that the maximum leakage current due to low insulation resistance would be about 20 milliamperes.

It is noted in the section "Terminating Fittings" that in the presence of moisture the mineral insulation forms magnesium hydroxide, and we are informed that this compound acts as a stop to the entrance of moisture into the magnesium oxide insulation beyond the hydroxide. This may explain why the insulation resistance of an *MI* cable exposed to moisture-saturated air for a very long time is not lower than has been noted.

At the end of the 90-day exposure, potentials of 120 volts a-c and d-c, 240 volts a-c and d-c, and 440 volts a-c and d-c were applied successively to this joint without failure or any noticeable effects. The a-c voltage was then increased in steps until flashover occurred at the end of the cable at approximately 1,500 volts, but the arc left no noticeable damage and the cable undoubtedly could have been continued in service at any of the previously mentioned operating voltages after breakdown.

Again, in the subsection entitled "Surge Voltage Strength," it is stated that a surge breakdown may cause power follow-up and permanent failure. Tests were made with a typical type-*MI* cable the unsealed end of which had been immersed in tap water for 50 days continuously, 120-volt alternating current was applied and a small arc occurred at the cable end, but when the circuit breaker was reclosed it did not trip. The cable end was immersed in water again, but for 5 minutes only. This procedure was repeated with 220 volts and 440 volts alternating current. There was no visible damage to the cable. The worst kind of fault that might be encountered in service was then reproduced at the end of the type-*MI* cable by completely coating the magnesium oxide with heavy carbon black, and thoroughly moistening the latter. This fault produced a loud report on 440 volts alternating current but all of the carbon black was burned off and the type-*MI* cable termination was left unimpaired. When the circuit breaker was reclosed there was no further trouble. The fault current in this case was limited by the relatively small capacity of the source of potential. It may be that with the heavy follow currents available from control and auxiliary power busses in generating stations an arc would result in the spattering of copper at the end of the magnesium oxide insulation, which would bridge the gap between conductors or between conductor and sheath and thus produce permanent failure, but such evidence is still to be produced.

As regards switching surges, which may reach 5,000 to 7,000 volts on control and auxiliary power circuits in generating stations and thus cause flashover at sealed as well as unsealed ends of type-*MI* cable, there are rather simple and inexpensive methods for suppressing such surges when the source of the trouble has been located. For example, a resistor, capacitor or small rectifier may be shunted across the relay coil or solenoid that gives rise to the surge. It seems still to be proved that switching surges will be of consequence in producing permanent failure of type-*MI* cables in generating stations even if the cable ends are not sealed.

In the subsection "Resistance to Corrosion," a maximum copper temperature of 85 C is noted for the more usual circuits. The temperature drop through the insulation is not likely to exceed 5 C with the conductor at 85 C, which would give a sheath temperature of 80 C (176 F). Such a sheath temperature would be excessive as regards safety to personnel if the cable is installed where it may be touched readily by workmen. In some cases the temperature of bare metal surfaces exposed to personnel in generating stations is limited to 60 C (140 F). However, lead-covered cables and armored cables have been in service in such stations for many years with maximum copper temperatures of 85 C and a temperature drop of up to 15 C through the insulation, resulting in the temperature of the metal covering being approximately 70 C (158 F). Apparently this outer temperature has been considered safe. If the sheath temperature of type-*MI* cables likewise is limited to 70 C it would appear that the maximum copper temperature should be not more than 75 C under these circumstances of exposure. Where type-*MI* cables are not exposed to workmen, the sheath temperature and the corresponding conductor temperature may be allowed to go very much higher, limited only by other considerations, such as voltage drop, oxidation of the sheath, etc.

A simpler and more reliable form of termination for type-*MI* cables than that described in the section "Terminating Fittings" would be very welcome. Stringing the beads on the conductors, forming the anchoring bulges at the inner ends of the neoprene sleeves, applying the quite plastic insulating potting compound to the brass sealing cups, and threading the washer over the numerous conductors and securing it in the cup are fussy operations for workmen. Furthermore, at an ambient temperature of 100 F or higher, such as encountered in the central and southern parts of the United States during the summer, the potting compound quickly flows out of the sealing cup when the cable is vertical and the cup mouth is downward. It may thus be difficult to keep the cup filled with compound until the washer has been secured in place at the mouth of the cup. With regard to stripping the sheath of the type-*MI* cable, it is desirable that a sheath-stripping tool for quick and easy removal of the sheath be made available.

Where type-*MI* cable is chosen because of its unusual quality in resisting fire, it is logical to require that the cable termination be able to withstand as high a temperature as the cable itself, namely 1,083 C (1,981 F), which is the melting point of the copper sheath. It is manifest that the type of cable termination described in the section "Terminating Fittings" would not meet this need.

Work is going forward further to introduce improvements in the terminations and applications of type-*MI* cable, which should facilitate its use greatly where its particular advantages make it superior to other types of cable.

The manufacturer of this radically new type of cable is to be commended for making it available, and the authors of the paper are to be congratulated for the thoroughness of their presentation.

S. J. Rosch (Anaconda Wire and Cable Company, Hastings-on-Hudson, N.Y.): I has been my privilege to have followed the history of the *MI* cable and to have seen an actual installation of several types on board a French battleship. Pyrotenax, as the *MI* cable is known in Europe and Canada, has had a fairly successful operating record and meets an indicated need under certain operating conditions. That was one of the main reasons for its broad acceptance as one of the permitted wiring methods in the 1953 edition of the National Electrical Code[1] and if used within the temperature limitations of 90 C maximum, it should perform satisfactorily under the various conditions for which it is now recognized.

It is for this reason that exception is taken to the statement by one of the authors that, given the proper type of termination, it should be possible to operate the *MI* cable at temperatures up to 250 C. It should be noted that the current-carrying capacity ratings in Tables 1 and 2 of the National Electrical Code[1] are based on continuous duty. Whereas it is possible that the magnesium oxide insulation may be operated continuously at temperatures up to 250 C, the same is not true of the over-all copper sheath or the copper conductors. From a metallurgical point of view, copper may not be operated continuously at temperatures in excess of 150 C. The term "copper" as used in the present discussion, does not include special copper alloys intended for higher-temperature operation.

Many electrical people have observed embrittlement of copper conductors connected to the base of certain gas-filled lamps. Actual measurements at the base of such lamps indicated temperatures of about 400 F (approximately 200 C). One of the solutions offered, is the use of nickel or nickel-clad copper conductors for such cases and is so stated in the Underwriters' Laboratories' standard for *AF* fixture wire.[2] When an *MI* cable should operate continuously at a conductor temperature of 250 C, the temperature of the over-all copper sheath would undoubtedly be in excess of 200 C. This combination is a condition which I consider unsafe for continuous operation, hence this word of caution. It should be noted that this general subject, the maximum safe permissible operating temperature for both copper and aluminum, is now under consideration by a special code committee.

REFERENCES

1. NATIONAL ELECTRICAL CODE. National Fire Protection Association, Boston, Mass., 1953.

2. STANDARDS FOR AF FIXTURE WIRE. Underwriters' Laboratories, Inc., Chicago, Ill.

E. G. Davies (Pyrotenax of Canada, Ltd., Toronto, Ont., Canada): In presenting this excellent paper on *MI* cables, Dr. Eager touched upon the hygroscopic nature of the insulant (magnesium oxide), but in the event that this may cause some doubts concerning the performance of these cables, attention is called to an important fact relating to this characteristic. In the normal course of installing this cable, and assuming that a length or coil has been exposed to the atmosphere for some time, the electrician in stripping away the copper sheath from the ends, to produce the required lengths of conductor tails, automatically frees the end sections of the insulation, thus returning from magnesium hydroxide to the original magnesium oxide, and a megger test on a run of *MI*. Cable thus prepared for terminating in the prescribed manner, will produce a reading of infinity.

The rigidity of these cables has been mentioned, but it should be noted that the experience referred to was in connection with a somewhat special size (outside the normal range in which these cables are produced) in fact, something in excess of 1-inch outside diameter. The flexibility of *MI* cables throughout the listed range is considered adequate for the majority of applications, and it will be noted that a radius of six times the diameter has been prescribed and approved by the National Electrical Code. (See reference 1 of Mr. Rosch's discussion.)

Replying to the remarks of Mr. Rosch, who appears to be keenly interested in striving for a temperature limit of 150 C for copper, it is to be hoped that he will not overlook the requirements demanded by certain branches of industry in such applications as vessels, machines, etc. in which lighting circuits are required to function in temperatures well in excess of 150 C. For these applications *MI* cables with suitable high-temperature terminating fittings will prove most advantageous.

An incident of World War II in England serves to prove the general robustness of *MI* cables. During a severe air raid over London, a bomb was dropped on an oil refinery on the Thames River, and the feeder cable (mineral-insulated) running under the jetty and over a section of the river was put out of commission. Upon examination it was discovered that a bomb fragment had passed under the jetty, sheering off a section of the copper sheath of the no. 4/3 conductor *MI* cable (0.730-inch outside diameter). By the application of a blow torch for a few inches either side of the fracture, thus driving out whatever moisture had penetrated the insulation, it was a simple matter to solder over the fracture, and in a very short time the cable was in service again.

C. A. Jordan and **G. S. Eager, Jr.**: Mr. Richter indicates that improvements in the terminations for type-*MI* cable would assist in furthering the use of this cable. This is recognized, and it is anticipated that future improvements will result ultimately in terminals easier for workmen to install as well as terminals suitable for operation at temperatures above 85 C. In addition, it is anticipated that improved tools to facilitate the installation of terminals will be made available. Mr. Richter's data concerning cable without terminals are extremely valuable, and they emphasize that magnesium oxide insulation, even though hygroscopic, can withstand substantial exposure to moisture and still maintain reasonable good insulating properties. The use of terminals, consequently, not only increases the margin of safety, but in addition maintains the insulation at the ends of the cable at its original insulating properties even though exposed to humidity and moisture for long periods. Mr. Richter's point concerning surge protective devices is well taken. Experience has indicated that such devices are seldom necessary on a-c circuits. For d-c circuits where voltages are 110 volts or higher, precautions may have to be taken to reduce surge voltages below the withstand values indicated.

Mr. Davies emphasizes that in making a normal installation, sufficient insulation is removed from the cable ends to ensure that the cable actually installed has insulation which has not been subjected to moisture ingress. The wartime experience enumerated by Mr. Davies is a typical example of how moisture, even though it may enter the cable due to a ruptured sheath or poor terminal, will not penetrate far because the magnesium oxide changes to magnesium hydroxide. Both the crystal structure and specific volume change, and the magnesium hydroxide formed acts as a seal to further water penetration. Experience shows that from 6 to 8 inches of the magnesium hydroxide acts as a good seal. The "fault" is thus restricted to a short section of the cable. This "sealing" action has been pointed out by Mr. Richter as well as by the authors.

Mr. Rosch's concern about the suggested maximum operating copper temperature of 250 C must not be taken lightly. His example, however, pertains to fixture wire and hinge cable where individual copper strands are in the order of 5 to 10 mils in diameter. Progressive oxidation is a surface phenomenon largely independent of wire diameter. Oxidation of metallic copper to a depth of, say, 2 or 3 mils would have a far more serious effect on a 10-mil wire (36 to 16% remaining area) than on a 100-mil wire (92 to 88% remaining area). We do not feel that this experience is applicable to type-*MI* cable where the copper sheath diameters and thicknesses are both considerably higher, and where the smallest conductor wire size is 16 American Wire Gauge (51 mils in diameter). Except at the ends of the cable, the copper conductors are not exposed to the atmosphere which is an additional factor in reducing any tendency towards excessive conductor oxidation. In our experience, continuous operation at a temperature of 250 C will not of itself produce embrittlement of copper.

D-C Machines—Method for Short-Circuit Calculations

JOHN CYBULSKI
ASSOCIATE MEMBER AIEE

JOHN P. O'CONNOR
MEMBER AIEE

IN THE U. S. Navy, problems of space, weight, reliability, and safety of electric power systems are important on the large vessels and become critical within the submarine. An optimum design with adequate protection becomes the prime goal whenever electric dynamos and their associated equipment are employed by the U. S. Navy. However, a power system of large kilowatt capacity when subjected to a fault can cause extensive damage to the bus structures, machine shafts, and circuit breakers, and possibly can disable the d c machine through flashover. In addition, the reliability of an entire system is endangered if there is incorrect circuit-breaker selectivity. On the other hand, a d-c power system which is overdesigned with a high safety factor because of lack of knowledge is also undesirable.

Because of the design advances made on d-c propulsion systems, an investigation was authorized for the study of the performance of submarine propulsion and auxiliary power equipment. Specifically, the following information on the rotating machinery was desired.

1. Maximum short-circuit current.
2. Rate of rise and decay of the short-circuit current.
3. Effect of changes in voltage, speed, and machine loading on the short-circuit characteristics.
4. Flashing characteristics.

In 1947, methods[1,2] were employed and were found to yield rather high values of short-circuit current in the Navy d-c power systems. To determine the validity of these results, the investigation was begun at the New London Naval Base where a mockup of a submarine electric system was studied under severe short-circuit conditions. Interim reports outline the experimental setup and contain the original data, progress, and development of this preliminary study. At the conclusion of this study, Naval Research Laboratory reports described the transient characteristics of d-c motors and generators, the transient characteristics of lead-acid submarine batteries, and the flashing of d-c machines caused by short circuit.[3,4]

In view of the difference between experimental and computed values of short-circuit currents using the available techniques, it was necessary that the theory of transient characteristics of d-c machines be extended to provide the accuracy necessary for attaining the optimum in shipboard system design. Although the factors contributing to the limitation of short-circuit current, namely, armature and external circuit resistance, brush-contact drop, reactance voltage, and flux distortion and destruction, were all considered, the application of these in calculating transient response from machine constants appears inadequate.

Linville[2] simplified his analysis and proposed a new method for plotting the transient currents.[5] It was still evident that more fundamental knowledge of rotating machinery was required before relations could be formulated to calculate with the required accuracy the transient response of d-c machines. A report[6] has been published which contains plots of the zero short-circuit transient resistance versus the kilowatt- or horsepower-speed product for a wide range of d-c machines. The application of these curves is suitable for estimation purposes. More recent literature contains material on related phases of this problem.[7–12] Investigation of the basic phenomena occurring during transients led to interim reports on the behavior of flux, coefficients of induction, and armature-winding resistance and brush-contact drop.[13] The purpose of this paper is to introduce new relationships to provide greater accuracy in the calculation of short-circuit current flow in d-c machines.

Nomenclature

Upper case letters denote total quantities. Exception is made for flux and flux linkages where the same size letter is used. Lower case letters denote per-unit (pu) quantities; total quantities divided by their respective base values result in a pu system.

A_t = mean section area of armature tooth, inches squared
a = number of parallel paths in the armature
B = total number of commutator segments
b = width of brush contact face in commutator segments
c = machine constant, $PZ/a\ 60$
d_s = depth of armature slot, inches
E = armature generated voltage, volts
E_r = average reactance voltage per coil, volts
F = initial over-all flux-fringing factor, approximately 1.1
g = main pole average air gap, inches
I = current, amperes
i = instantaneous current either armature or shunt field; expresses total or pu current depending on terms in the expression
K = coefficient of coupling between two circuits
K_{fs} = shunt-field mutual leakage-linkage ratio n_{fs}/n_g; for generalized values see Appendix II
K_t = permeance of the air-gap line, pu; generalized value 1.3
K_l = plus and minus sign for initial motor and generator action respectively, $1 \pm (i_{a0}/10e_0)$
K_s = steady-state load coefficient, $1-(1/3e_0)$
K_1 = permeance constant of the iron flux,[5] pu; $\phi_t/(P_a/P_p)m_{a1} - n_{b1}$
K_2 = permeance constant of the space flux,[5] pu; $1.25K_t g/(g+d_s)$
K_3 = direct armature-demagnetizing factor at steady state, $(K_s b P m_{a1})/B$
K_3' = direct armature-demagnetizing factor at peak armature current; equation 10
L = inductance, henrys
L_{g1} = inductance of shunt-field winding per pole caused by direct axis flux linkages, henrys; equation 59
L_l = inductance of shunt-field winding per pole caused by leakage linkages, henrys; equation 60
l_d = axial shunt-pole depth, inches
M_{f-a} = initial coefficient of mutual induction between the armature and shunt field, henrys; equation 27
M_{f0} = initial shunt-field magnetomotive force (mmf), $N_f i_{f0}$, ampere-turns
M_{fs0} = initial net shunt-series mmf $(M_{f0} - M_{s0})$, ampere-turns
M_{f-a}' = coefficient of mutual induction between armature and shunt field at peak time, henrys; equation 31
N = speed of machine, revolutions per minute
N_a = armature turns per pole, $Z/2\,a$
N_b = pole-face winding turns per pole
N_f = shunt-field winding turns per pole
N_s = series-field winding turns per pole
N_a' = effective number of armature-winding turns for direct demagnetization action upon the air gap as a result of an effective brush shift
n = initial coefficient of leakage between armature and shunt-field circuits
n_f = leakage-linkage coefficient for the shunt-field winding, shunt-field leakage flux linkages divided by air-gap shunt-field linkages at M_{f1}

Paper 55-112, recommended by the AIEE Rotating Machinery Committee and approved by the AIEE Committee on Technical Operations for presentation at the AIEE Winter General Meeting, New York, N. Y., January 31–February 4, 1955. Manuscript submitted October 20, 1954; made available for printing November 24, 1954.

JOHN CYBULSKI and JOHN P. O'CONNOR are with the Naval Research Laboratory, Washington, D. C.

n_s = speed at which no-load saturation is taken, pu
n_t = number of armature teeth per pole arc
P_a = initial permeance of tube a, webers per ampere-turn
P_b = initial permeance of tube b, webers per ampere-turn
P_g = permeance of the air-gap line at no load, webers per ampere-turn
p = steady-state permeance $(K_1/3e_0+K_2;\ p \leqq K_1)$, pu
P = number of poles
p_a = pole arc, inches
p_0 = initial permeance of air gap, pu; $\phi_0(i_{f0} \pm m_{s1}i_{a0})$; plus and minus sign for cumulative and differential connection respectively
p_p = pole pitch, inches
p' = effective air-gap permeance at i_a', (K_1r'/e_0+K_2)
$\mathcal{P}$ = permeance, webers per ampere-turn; generally appears as P with subscripts and superscripts
$r = r_w + r_b + r_e$, actual resistance of armature circuit at steady-state short-circuit current, pu
r_b = effective brush-contact resistance at steady-state short-circuit current, pu; $(n_0K_s^2E_rb+V_c)/E_1$
$r' = r_w + r_b' + r_e$, actual resistance of armature circuit at peak short-circuit current, pu
T_a = initial armature-circuit time constant, seconds; equation 25
T_d = decrement time constant, seconds
T_r = rise time constant, seconds
t_{pa} = time to peak armature current, seconds
V_b = total effective brush-contact drop per unit current, volts
V_c = normal total brush-contact drop, usually 2 or 3 volts
Z = number of armature conductors
$\alpha = n_0K_i^2E_rb$, reactance voltage pu current at peak armature current
$\beta = 1/T_d$, decrement factor, seconds
$\gamma = 1/T_r$, rise factor, seconds
$\Delta\mathcal{P}$ = incremental permeance proportional to a slope on no-load saturation curve
μ = permeability of air, $4\pi 10^{-7}$, henry per meter in a subrationalized meter-kilogram-second system
ϕ_a = initial flux in tube a, webers; P_aM_{f0}
ϕ_b = initial flux in tube b, webers; P_bM_{f00}
ϕ_{fa} = effective initial mutual flux linking all of shunt-field winding turns N_f per pole, webers; as created by armature-circuit direct-axis mmf
ϕ_t = iron flux for intrinsic saturation $(A_tn_t\ 125{,}000)/\phi_1$, pu
ϕ_0 = initial air-gap flux, e_0/n_0, pu; or in lines as applicable in Appendix I
ϕ_d' = direct-axis flux at peak armature current, pu; equation 11, or in lines as applicable in Appendix I
ψ_0 = initial flux linkages of shunt field, equation 42

SUBSCRIPTS

a = external armature circuit current
b = effective brush contact
c = cable, circuit breaker
d = total armature circuit
e = external to machine winding including the short circuit
f = shunt-field circuit
0 = initial condition
s = series-field winding
w = armature winding and all other machine windings in series
x = loss of air-gap flux resulting from direct magnetization plus crossmagnetization
1 = base quantity; with mmf other than M_{f1} taken at base armature current

Prime indicates value of quantity corresponding to peak armature current. Where there is no subscript or superscript, quantity corresponds to steady-state condition. Exception is made for initial inductances and mutual.

Derivation of Equations

The over-all approach in the solution of short-circuit transients, as presented in this paper, has been to develop a method for obtaining peak armature current and the corresponding field current. Then by using these values of current and the rise and decrement factors, the transient armature and field current are found.

In the development of equations the pu system has been used. The use of the pu system is dictated by convenience and by the desire to employ the same nomenclature previously used in treating the subject of short-circuit calculations. The value of any quantity in pu is obtained by dividing the quantity by its base value.

Base values for the quantities used are:

I_{a1} = base armature current, the armature current for which the reactance voltage has been determined
N_1 = base speed, speed at which the reactance voltage has been determined
M_{f1} = base mmf, the shunt-field mmf per pole at which n_f has been determined (no load)
I_{f1} = base field current, the shunt-field current corresponding to base field mmf
ϕ_1 = base flux, air-gap flux per pole corresponding to base field mmf
E_1 = base voltage, voltage generated at no load, base flux, and base speed
R_1 = base resistance, E_1/I_{a1}

The base armature current and the base speed usually correspond to a name-plate rating at which the reactance voltage has been determined. The reactance voltage for a machine with several name-plate ratings is determined at that rating for which the product of speed and current is a maximum. In general, n_f is determined at a value of shunt-field mmf that represents maximum operating air-gap flux.

EQUATIONS FOR PEAK ARMATURE CURRENT

The peak short-circuit current of a d-c machine can be written as

$$i_a' = (e_0 - e_x')/r' \tag{1}$$

where e_0 is the initial generated voltage of the machine before short circuit and r' is the total resistance at peak current. The drop in initial generated voltage at peak current caused by the loss in air-gap flux is represented by e_x'. If e_x' is defined by the equation

$$e_x' = r_x'i_a' \tag{2}$$

then equation 1 may be written as

$$i_a' = e_0/(r' + r_x') \tag{3}$$

In equation 3 all the factors tending to reduce the magnitude of the peak short-circuit current are expressed in terms of resistance and the applied voltage e_0. By writing equation 3 in a concise form, the peak armature current is

$$i_a' = e_0/r_d' \tag{4}$$

where

$$r_d' = r' + r_x' = r_w + r_e + r_b' + r_x'$$

The problem of determining i_a' now becomes one of obtaining r_b' and r_x' in terms of known machine constants In the derivation of equations the following assumptions have been made:

1. The theorem of constant flux linkages can be applied, with negligible error, to the shunt-field linkages up to the time of peak armature current.
2. The change in permeance of the air gap from its initial value can be attributed to saturation of the armature teeth alone.
3. Armature crossmagnetization caused by initial load has negligible effect on the permeance of the air gap.
4. The brushes are on neutral and any initial load will not result in an effective brush shift.
5. There is negligible change in speed of the machine from the initial speed up to the time of peak armature current.

The derivation of equations for the effective brush-contact resistance r_b' and for the total demagnetization factor, r_x' are similar in some respects to the derivations given by Linville.[2,3] The equations given here, however, include the effect of initial conditions on the magnitude of peak short-circuit current. In addition, there is a factor in the equation for shunt-field current which reflects the effect of the series field on the transient shunt-field current.

EFFECTIVE BRUSH-CONTACT RESISTANCE r_b'

With no Initial Load

In the steady-state operation of a d-c machine where there is overload or where the commutating flux is insufficient to give good commutation, it is well known that the center of current collection shifts in the direction of rotation toward the trailing brush edge. This effective brush shift results in a direct armature demagnetizing effect on the shunt field equal to the number of armature ampere-turns included in twice the angle of shift. A second result is an increase in the effective brush-contact drop which is related approximately inversely to the time in which commutation must take place. The ordinary reactance voltage E_r is based upon linear commutation over the complete brush width. On the other hand, if commutation is assumed to take place linearly over a distance of one commutator segment (at the trailing brush tip), the reactance voltage becomes E_rb, where b is the number of commutator segments spanned by the brush. The effective brush-contact resistance in pu at any given speed is then

$$r_b' = V_b/E_1 = (n_0E_rb + V_c)/E_1 = (\alpha + V_c)/E_1 \qquad (5)$$

The reduction in the time of commutation (from the time required for the commutator to travel one brush width to the time required to travel one commutator segment) is made on the assumption that the actual nonlinear commutation existing during short circuit can be represented as a linear commutation occurring in this reduced time. This results in a uniform current density in the brush over a width of one commutator segment and zero current density over the remainder.

Actually, the current distribution in the brush face under conditions of poor commutation is small at the leading brush tip and large at the trailing brush tip. An exponential distribution of current in the brush face would appear to approach more nearly the actual distribution. Linville,[3] by solving the basic equation of a coil undergoing commutation, shows that the current density in the brush face is exponential and derives the following equation for effective brush-contact resistance

$$r_b' = V_b/E_1 = \alpha/E_1\left(\frac{\epsilon^{\alpha/V_c}+1}{\epsilon^{\alpha/V_c}-1}\right) + V_c/E_1 \qquad (6)$$

It will be noted that equation 6 is similar to equation 5. The expression in parentheses in equation 6 is essentially a correction factor. When α/V_c is large, the correction factor approaches unity and equation 5 could then be used for calculating r_b'. For simplification in computation, the effective brush drop in volts, pu current V_b, is plotted in Fig. 1 as a function of α, with V_c as a parameter. It will be noted from Fig. 1 that, as α increases, r_b' can be expressed by the more simple relation given by equation 5. In the modification of equation 6 to include the effect of initial load, it will be shown that α as defined by equation 5 is only a special case for zero initial load and a more general expression will be given in the following section.

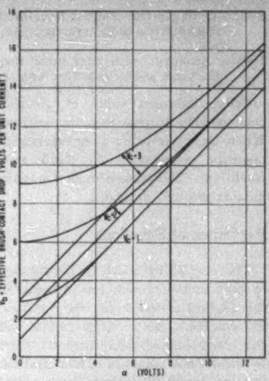

Fig. 1. Effective brush-contact drop V_b versus reactance voltage

Straight lines: $V_b = V_c + \alpha$

Curves:

$$V_b = V_c + \left(\frac{\epsilon^{\alpha/V_c}+1}{\epsilon^{\alpha/V_c}-1}\right)\alpha$$

$$\alpha = n_0K_l{}^2E_rb$$

$$r_b' = V_B/E_1$$

With Initial Load

The derivation of the foregoing equations for effective brush resistance is based on the assumption that there is no flux in the commutating region up to peak armature current. Experimental data[4] show that if a machine is short-circuited with no initial load there is a negligible flux change. With initial load, however, the interpole flux is built up to a value dictated by the load so that the reactance voltage for the initial load is compensated. Thus, it appears that for any initial load there is no effective brush drop nor shift in the point of current commutation. In the case of a generator, only that part of peak current represented by the difference between the peak current and the initial current $i_a' - i_{a0}$ can give rise to an uncompensated reactance voltage and to a shift in the center of current commutation. Hence, if linear commutation is assumed over the entire brush face, then the reactance drop for i_a' is $n_0E_ri_a'$ for the condition of zero initial current and $n_0E_r(i_a' - i_{a0})$ for initial load i_{a0}. Similarly, if the effective brush shift is b commutator segments for i_a' when the initial load current is zero, then the brush shift is $1-(i_{a0}/i_a')\,b$ when the initial load current is i_{a0}. This formulation results because at i_{a0} the brush shift is zero. Therefore, the reactance voltage pu current at i_a' for a generator is

$$\alpha = b(1 - i_{a0}/i_a')n_0E_r(1 - i_{a0}/i_a')$$

In the case of a motor with initial load, the initial commutating flux is in the wrong direction to compensate any of the reactance voltage under short circuit. When a motor is subjected to short circuit, the armature current reverses; but, as in the case of a generator, the commutating flux remains practically unchanged in magnitude and direction up to peak short-circuit current. The magnitude of the reactance voltage at i_{a0}, which is compensated by the initial commutating flux, is $n_0E_ri_{a0}$. This is equal to the voltage generated in each armature coil by the commutating pole flux when the armature current reverses. This voltage effectively increases the reactance voltage that would exist if there were no initial commutating flux. The uncompensated reactance voltage for a motor with initial load i_{a0} is then $n_0E_r[1+(i_{a0}/i_a')]$ pu current, and the effective brush shift is $[1+(i_{a0}/i_a')]b$. Hence, for a motor the reactance voltage pu current at i_a' is

$$\alpha = b(1 + i_{a0}/i_a')n_0E_r(1 + i_{a0}/i_a')$$

This equation is similar to that for a generator with initial load. Define the factor in parenthesis as follows

$$K_l = (1 \pm i_{a0}/i_a') \qquad (7)$$

where the plus sign applies for a motor with initial load and the negative sign applies for a generator with initial load. Then α at i_a' for operation as a motor or as a generator and for any i_{a0} and n_0 is

$$\alpha = n_0K_l{}^2E_rb \qquad (8)$$

and equation 6 for effective brush-contact resistance r_b' is always applicable when values of K_l as defined by equation 7 are used. In determining values for the load factor K_l, it is recommended that an estimate of i_a' equal to 10 e_0 be used. This estimate is not critical and will have negligible effect on the final computed value of i_a'.

Total Demagnetization Factor r_x'

The demagnetization of the main field, or the reduction in the air-gap flux can be attributed to three distinct effects resulting from short circuit:

1. Direct-axis armature demagnetization, which is proportional to the effective brush shift and the magnitude of armature current.

2. The series field which magnetizes or demagnetizes the main field depending on the direction of series field ampere-turns during short circuit.

3. Armature crossmagnetization, which effectively decreases the permeance of the air gap.

The constant K_s' used represents the direct-axis armature-demagnetizing mmf pu current per pole at peak armature current. As in steady state, this quantity is proportional to twice the angle of brush shift. Hence, for an effective brush shift equal to $b/2$ commutator segments

$$K_s' = bPm_{a1}/B \tag{9}$$

for the condition of no initial load. Under initial load conditions it has been shown that b becomes K_lb. Hence, under the condition of initial load

$$K_s' = K_lbPm_{a1}/B \tag{10}$$

For simplicity, the derivation for r_z' is for the case of a differentially connected generator with initial load. For other initial conditions such as operation as a motor or cumulative connection of the series field, the derivation would be parallel to that illustrated. The equation for the flux ϕ_d' at time of peak armature current in terms of the direct-axis mmf and the effective air-gap permeance p' for the case considered is

$$\phi_d' = [i_f' - m_{s1}i_a' - K_s'(i_a' - i_{a0})]p' \tag{11}$$

It is shown in Appendix I that by applying the theorem of constant flux linkages to the shunt field of a differentially connected generator the following equation results

$$\phi_0 + n_f(i_{f0} - K_{fs}m_{s1}i_{a0}) = \phi_d' + n_f(i_f' - K_{fs}m_{s1}i_a') \tag{12}$$

The determination of K_{fs} and applicable values are given in Appendix II. Solving equation 12 for i_f' gives the following expression

$$i_f' = (\phi_0 - \phi_d')/n_f + i_{f0} + K_lK_{fs}m_{s1}i_a' \tag{13}$$

Here, $\phi_0 - \phi_d'$ represents the loss in useful air-gap flux at peak armature current. The corresponding loss in voltage e_z' equals $n_0(\phi_0 - \phi_d')$, and from equation 2 the following may be written

$$\phi_0 - \phi_d' = r_z'i_a/n_0$$

Substituting this relation in equation 13, the value of shunt-field current at peak armature current is

$$i_f' = (r_z'i_a')/n_0n_f + i_{f0} + K_lK_{fs}m_{s1}i_a' \tag{14}$$

By the simultaneous solution of equations 11 and 14, i_f' is eliminated and the following equation is obtained

$$(r_z'i_a')/n_0n_f - \phi_d'/p' = K_s' + (1 - K_{fs}) \times (i_a' - i_a) - (i_{f0} - m_{s1}i_{a0}) \tag{15}$$

The initial direct-axis mmf $(i_{f0} - m_{s1}i_{a0})$ in equation 15, by using assumptions 3 and 4, can be written as follows

$$i_{f0} - m_{s1}i_{a0} = \phi_0/p_0 \tag{16}$$

Then substituting this relation and the following expressions for ϕ_0 and ϕ_d' in equation 15

$$\phi_0 = e_0/n_0 = i_a'(r' + r_z')/n_0$$

$$\phi_d' = (e_0 - r_z'i_a')/n_0 = i_a'r'/n_0$$

r_z' may be solved for, giving

$$r_z' = \frac{n_f}{1 + (n_f)/p_0} \{n_0K_l[K_s' + (1 - K_{fs})m_{s1}] + [(1/p') - (1/p_0)]r'\} \tag{17}$$

At no load, base speed and base voltage p_0 is equal to unity; in normal operation it will not differ appreciably from this value. The expression $(1/p') - (1/p_0)$ represents the change in reluctance of the air gap. When a machine is fully compensated, the value of this expression becomes negligible and may be assumed equal to zero. In the computation of r_z' which is usually not more than 30 per cent of the total resistance, r_d' it is sufficiently accurate to estimate i_a' by e_0/r' in the expression for p'. The derivation of r_z' and i_f' has been given for a differentially connected generator. The derivations for a cumulatively connected generator and for initial operation as a motor, either cumulative or differential, are similar. The equations of r_z' and i_f' for all these possible conditions of initial operation are expressed in concise form by the equations in the section entitled "Summary."

EQUATIONS FOR TRANSIENT CURRENT

The philosophy leading to current-time plots of short-circuit transients of a d-c machine is that of imposing specific boundary restrictions on the peak magnitude, rise, decrement, and steady-state magnitude of the current. These conditions are introduced into equation 18 which is the simplest form of a solution of an inductively coupled 2-loop system. That is

$$i = c_1e^{-\gamma t} + c_2e^{-\beta t} + c_3 \tag{18}$$

where

c_3 = steady-state current
$c_1 + c_2 + c_3$ = initial current
$\gamma = 1/T_r$, rise factor
$\beta = 1/T_d$, decrement factor

The peak current i_a' and i_f' are obtained by equations 4 and 34. After computation of the time constants T_r and T_d, the constants c_1 and c_2 may be determined through cut-and-try numerical reiterations until the peak armature current given by equation 18 is in agreement with the value obtained under short-circuit calculations. Simultation of equation 18 by an analogue computer will expedite these computations and display the current-time plot of the shunt-field and armature circuits. From equation 18 the time to peak is given by

$$t_{pa} = 1/(\gamma - \beta) \ln(-\gamma c_1/\beta c_2) \tag{19}$$

The initial rate of rise is given by differentiation of equation 18 and setting t equal to zero

$$di/dt = -\gamma c_1 - \beta c_2 \tag{20}$$

The factors γ and β which appear in equation 18 may be approximated by the reciprocal of the armature and shunt-field circuit time constants T_a and T_f respectively. However, a more accurate estimate of these factors can be made if the coefficient of mutual induction is introduced. In a linear inductively coupled 2-loop system, the defining equation for the time constant is

$$\tau = \frac{(\tau_a + \tau_f) \pm [(\tau_a + \tau_f)^2 - 4n\tau_a\tau_f)]^{1/2}}{2} \text{ seconds} \tag{21}$$

where

$$n = 1 - K^2 \tag{22}$$

Coefficient of leakage between two circuits of time constants τ_a and τ_f, with

$$K = M_{f-a}/(L_aL_f)^{1/2}$$

Coefficient of coupling between the shunt-field and armature circuits, with

$$M_{f-a} = PN_f\phi_{f-a}10^{-8}/I_{a1} \text{ henrys} \tag{23}$$

$$\phi_{f-a} = (K_s'K_l \pm m_{s1})(\Delta p)\phi_1 \text{ maxwells per pole per base current} \tag{24}$$

In equation 24 the plus and minus sign is used for differential and cumulative action of the series field respectively. Equation 21 provides T_r and T_d for the specific terms employed and applicable times.

It can be assumed with satisfactory accuracy that the decrement of both armature and shunt-field currents is dependent on the shunt-field inductance, while the rise time to peak is essentially a function of the armature-circuit inductance. However, the coefficients of self and mutual induction change during the short circuit because of saturation, eddy-current effects, and commutation. To effect a simple solution while taking into account as much of the actual phenomena as possible, the following procedure is used. This method restricts itself to those factors which can be obtained at various stages in a short-circuit calculation.

RISE FACTOR

Computation of the rise factor requires the time constants τ_a, τ_f and the leakage coefficient n, which exist immediately after short circuit. These initial values are determined from the following equations

$$\tau_a = T_a = L_d/r'R_1 \text{ seconds} \tag{25}$$

$$\tau_f = T_f = L_f/R_f \text{ seconds} \tag{26}$$

$$M_{f-a} = PN_f(K_3'K_1 \pm m_{s1})(\Delta p)_0\phi_1 10^{-8}/I_{a1} \text{ henrys} \tag{27}$$

In general, calculations of both armature and shunt-field inductances are for the unsaturated condition. Initial conditions of load and field excitation will often contribute to a sufficient change in saturation to make the unsaturated values inapplicable. The effects of a variable degree of saturation are difficult to calculate for the armature circuit because it is composed of the armature, compensating, series, and interpole windings. Some of these windings are in opposition so that only the respective leakage linkages contribute to the net inductance. A method for calculating the unsaturated armature-circuit inductance is shown in reference 8. Any changes in initial saturation may be taken into account for L_f and M_{f-a}, as shown in Appendix III. A solution of equation 21 for the smaller of the two roots will provide T_r when the values of T_a, T_f and n are substituted.

Therefore

$$\gamma = \frac{2}{(T_a + T_f) - [(T_a + T_f)^2 - 4nT_aT_f]^{1/2}} \tag{28}$$

with

$$n = 1 - (M_{f-a})^2/L_dL_f$$

DECREMENT FACTOR

The computation of the decrement factor is similar to that for the rise factor. In this case, the constants τ_a, τ_f, and n, which exist at the peak current, are used. Calculation of these constants, as outlined by the following equations, requires a knowledge of shunt-field and armature-circuit inductances, the respective circuit resistance, and mutual inductance at peak current

$$\tau_a = T_a' = L_d/r_d'R_1 \tag{29}$$

$$\tau_f = T_f' = L_f'/R_f \tag{30}$$

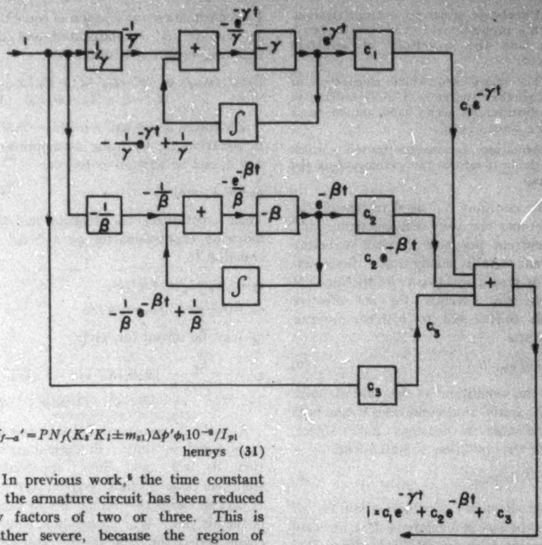
1
$-\frac{1}{\gamma}$
$-\frac{1}{\gamma}$
+
$-\frac{e^{-\gamma t}}{\gamma}$
$-\gamma$
$e^{-\gamma t}$
c_1
$c_1e^{-\gamma t}$
∫
$-\frac{1}{\gamma}e^{-\gamma t} + \frac{1}{\gamma}$
$-\frac{1}{\beta}$
$-\frac{1}{\beta}$
+
$-\frac{e^{-\beta t}}{\beta}$
$-\beta$
$e^{-\beta t}$
c_2
$c_2e^{-\beta t}$
∫
$-\frac{1}{\beta}e^{-\beta t} + \frac{1}{\beta}$
+
c_3
c_3
$I = c_1e^{-\gamma t} + c_2e^{-\beta t} + c_3$

Fig. 2. Block diagram for an analogue computer system

$$M_{f-a}' = PN_f(K_3'K_1 \pm m_{s1})\Delta p'\phi_1 10^{-8}/I_{p1} \text{ henrys} \tag{31}$$

In previous work,[5] the time constant of the armature circuit has been reduced by factors of two or three. This is rather severe, because the region of saturation in the armature circuit is small and the leakage inductances caused by the air paths predominate. As stated previously, the effects of saturation upon armature-circuit inductance are difficult to evaluate. A small reduction in the armature-circuit time constant is shown in equation 29, which utilizes the effective transient resistance In Appendix III a development is shown for calculating L_f' and M_{f-a}' at peak time A solution of equation 21 for the larger of the two roots will provide T_d when the values of T_a', T_f', and n' are substituted

Therefore

$$\beta = \frac{2}{(T_a' + T_f') + [(T_a' + T_f')^2 - 4n'T_a'T_f']^{1/2}} \tag{32}$$

with

$$n' = 1 - (M_{f-a}')^2/L_d'L_f'$$

ANALOGUE COMPUTER SOLUTION AND DISPLAY

A block diagram illustrating simulation of equation 18 on an analogue computer is shown in Fig. 2. Adjustment of coefficient boxes c_1, c_2, and c_3 is made until the conditions of initial, peak, and steady-state armature current are satisfied. From the displayed trace, the armature peak time can be obtained. In an actual short circuit, it is often difficult to ascertain accurately when the armature current peaks. It is easier to determine the time it takes the current to reach a specific percentage of the maximum and the time that elapsed before the current decays below this same percentage. These data would be of more value than the peak current and the time to peak.

To plot the shunt field current the value of armature peak time is obtained from the displayed trace or from equation 19. This peak time and the value of shunt-field current I_f' are imposed as constraints on equation 18, employing the same rise and decrement factors as those for the armature. Adjustment of coefficient boxes c_1 and c_2, which are equal to each other for the separately excited machines, is made until the foregoing boundary restrictions for the shunt-field current are contained in a transient trace.

Limitations

The equations developed for short-circuit calculations are necessarily limited in their application by the simplifying assumptions made in their derivation. In general, the assumption of constant speed is satisfactory since the time to peak armature current is small and, for large machines, the inertia of the armature is great enough to maintain the speed substantially constant up to this time. This assumption does result in higher values of calculated peak current than if the actual speed were used.

TOTAL DEMAGNETIZATION FACTOR

The assumption that the effective permeance of the air gap at peak armature current is only affected by saturation of the armature teeth caused by armature crossmagnetization is not valid under all operating conditions. At low initial flux density and low short circuit, the teeth which carry effective flux ϕ_d' may not be at intrinsic saturation. At high initial flux density and high short-circuit current not only the teeth which carry the effective flux ϕ_d' are at intrinsic saturation but also the iron below these teeth. In the latter case, the present formulation for r_z' will give a value for this quantity which is low and will result in a calculated value of I_a' which is too high. Hence, for initial voltages greater than 1 pu, it is probable that the iron below the teeth reaches intrinsic saturation and a correction in p', the effective permeance at peak current, should be made to reflect this condition. This correction on p' would result in a lower value for this quantity than is now obtained. If, however, such a correction is not made, the results will be on the safe side in that the calculated value of armature current will be high.

THEOREM OF CONSTANT FLUX LINKAGES

The assumption that the theorem of constant flux linkages can be applied to the shunt-field circuit is only valid if the resistance of this circuit is very small or if the time to peak current is small. Its use is justified on the basis that the time to peak current is small, and that the actual resistance of the shunt-field results in the loss of negligible linkages in the short time considered. The actual loss in linkages would result in lower values of peak current than the calculated values.

BRUSH-CONTACT RESISTANCE AND ARMATURE-DEMAGNETIZATION FACTOR

For the condition of zero initial load, the expression used for r_b' and K_3' are the same as those derived by Linville.[2,3] They have, however, been modified to account for the effects of initial load. Both the original derivations for r_b' and K_3' and their modifications for initial load conditions are based on simplifying assumptions that give an approximate solution. The assumption that there is on change in commutating flux up to peak current is approximately true for solid interpoles. With laminated interpoles,[4] this assumption would not be true and r_b' as now obtained should be reduced. The assumption that the center of current commutation is at the trailing brush edge at peak armature current may be justified qualitatively since it is known that undercommutation shifts the center of current commutation in the direction of the trailing brush edge. The assumption that it is exactly at the trailing brush edge at peak armature current for the condition of no initial load is justified on the basis of simplicity rather than rigor.

Linville[3] in his derivation of an expression for r_b' obtains an equation for the current density in the brush face at peak armature current. Although this current distribution is exponential in form, it is always positive and is independent of the magnitude of peak armature current. Experimentally, however, it is found that the current distribution in the brush face is a function of the magnitude of peak armature current and, at one edge of a brush may be zero or even negative.

The rigorous development of expressions for commutation losses, eddy-current, and demagnetization effects under short-circuit conditions would prove extremely difficult, it not impossible, and would lead to complicated and unwieldy expressions. For this reason, it is felt that a less rigorous analysis having the advantage of simplicity and reflecting in an admittedly approximate fashion the physical changes that occur will prove sufficiently accurate for useful engineering results.

TRANSIENT CURRENTS

In a previous paper[3] the assumption has been made that the shunt-field and armature-circuit currents peaked at the same time. This is an unnecessary restriction. As a matter of fact, the field current peaks before the armature current. The present development thus more accurately reflects the actual situation.

This method utilizes an analogue computer to enforce the computed boundary conditions for the armature- and shunt-field circuit currents and enables a rapid solution for the constants in a simple equation. A single current-time trace is obtained, uniquely fulfilling the foregoing limitations without resorting to changes in constants, curve shifting, or other manipulations mid-way in the time plot. The time to reach peak current is very indefinite in those cases where the peak current is maintained substantially constant for a relatively long time. In view of this, the time to reach 90 per-cent of the peak value and elapsed time when the current is above 90 per-cent of its maximum would be definite and useful information.

Summary of Equations

EQUATIONS FOR PEAK ARMATURE CURRENT

The equations for peak armature current are as follows

$$i_a'=e_0/r_d' \tag{4}$$

where

$$r_d'=r_s+r_w+r_b'+r_z'$$

$$r_b'=\alpha/E_1\left(\frac{e^{\alpha/V_c}+1}{e^{\alpha/V_c}-1}\right)+V_c/E_1 \tag{6}$$

$$\alpha=n_0K_1^2E_rb$$

$$r_z'=\frac{n_f}{1+n_f/p_0}\{n_0K_1[K_3'\pm(1-K_{f3})m_{s1}]+[(1/p')-(1/p_0)]r'\} \tag{33}$$

where $(1/p')-(1/p_0)$ is considered zero for a fully compensated machine. The field current I_f' existing at peak armature current is obtained from the equation

$$i_f'=i_{f0}+[(r_z'/n_0n_f)\pm K_1K_{f3}m_{s1}]i_a' \tag{34}$$

Machines under short circuit operate as generators and the action of the series field under short circuit determines the sign to be used in equations 33 and 34. If the series field, when the machine is under short circuit, aids the shunt field (cumulative connection), the minus sign should be used; whereas if it opposes the shunt field (differential connection), the plus sign should be used. It will be understood that, if a machine is operated as a cumulatively compounded motor before short circuit, during short circuit the machine will operate as a differentially compounded generator, and it is the operation under short circuit that determines the sign to be used in equations 33 and 34.

EQUATIONS FOR TRANSIENT CURRENT

The armature current is given by the following equation

$$i=c_1e^{-\gamma t}+c_2e^{-\beta t}+i_s \tag{35}$$

where

$$i_s=\frac{i_{f0}}{(r/pn_0)+K_1K_3+m_{s1}}$$

$$\gamma=\frac{2}{(T_a+T_f)-[(T_a+T_f)^2-4nT_aT_f]^{1/2}} \tag{28}$$

with

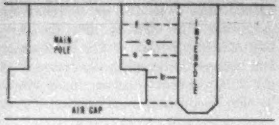

Fig. 3. Relation of shunt- and series-field windings to magnetic pole pieces

$n = 1-(M_{f-a})^2/L_dL_f$

$$\beta = \frac{2}{(T_a'+T_f')+[(T_a'+T_a')^2-4nT_a'T_f']^{1/2}} \qquad (32)$$

with

$n' = 1-(M_{f-a}')^2/L_d'L_f'$

Constants c_1 and c_2 in equation 35 are adjusted until the peak armature current i_a' is attained with the restriction that

$i = i_{a0}$ at $t = 0$

The armature current has a peak time given by

$$t_{pa} = [1/(\gamma-\beta)] \ln(-\gamma c_1/\beta c_2) \qquad (19)$$

The shunt-field circuit current is given by the following equation

$$i = c_1\epsilon^{-\gamma t}+c_2\epsilon^{-\beta t}+i_{f0} \qquad (36)$$

where for a separately excited machine, c_2 is equal to $-c_1$ and

$c_1 = (i_f'-i_{f0})/(\epsilon^{-\gamma t_{pa}}-\epsilon^{-\beta t_{pa}})$

For a self-excited machine, the constants c_1 and c_2 in equation 36 are adjusted until the current i_f' is reached at time t with the restriction that $i = i_{f0}$ at t equals zero, and $i = 0$ as t approaches infinity.

After obtaining the solution for the constants c_1 and c_2 in equation 35, the initial rate of rise of the armature current is given by

$di/dt = -c_1\gamma - c_2\beta$

In reference 14 it is shown how these equations are employed on five machines and results are compared with test data.

Appendix I. Derivation of Shunt-Field Flux Linkage Equations

For simplicity this derivation is based upon a differentially connected generator. The following assumptions are made: 1. The field windings have no partial linkages; and 2. initial armature current up to 1 pu does not effect the air gap by cross magnetization.

Initial Linkages

Initial conditions: $I_{a0} \leq 1$ pu; I_{f0}. The brushes are on neutral and there is no direct-axis armature mmf. Equation 37 expresses the flux linkages for the paths outlined in Fig. 3, where f and s represent the position of the shunt and series field windings respectively

$$\psi_0 = N_f(\phi_a+\phi_b+\phi_0) \qquad (37)$$

In terms of the path permeances, equation 37 becomes

$$\psi_0 = N_f^2I_{f0}(P_a+P_b+P_0)-N_fN_sI_{a0}(P_b+P_0) \qquad (38)$$

Equation 38 may be rewritten

$$\psi_0 = P_0N_fM_{f0}(1+n_{f0})-M_{s0}(1+n_{fs0}) \qquad (39)$$

where

$n_{f0} = N_fM_{f0}(P_a+P_b)/N_fM_{f0}P_0 = (P_a+P_b)/R_0$

$n_{fs0} = N_fM_{fs0}P_b/N_fM_{fs0}P_0 = (P_b/P_0)$

Divide equation 39 by N_f and rewrite to form

$$\psi_0/N_1 = \phi_0+P_0n_{f0}(M_{f0}-K_{fs0}M_{s0}) \qquad (40)$$

where

$K_{fs0} = n_{fs0}/n_{f0} = P_b/(P_a+P_b)$

Define

$n_f = N_fM_{f1}(P_a+P_b)/N_fM_{f1}P_1 = (P_a+P_b)/P_1$

$n_{fs} = N_fM_sP_b/N_fM_sP_1 = P_b/P_1$

Then it follows that

$K_{fs} = n_{fs}/n_f = P_b/(P_a+P_b) = K_{fs0}$

and

$n_{f0}/n_f = P_1/P_0$

Equation 40 can now be written as

$$\psi_0/N_f = \phi_0+P_1n_f(M_{f0}-K_{fs}M_{s0}) \qquad (41)$$

where calculation of K_{fs}, which is a function of position of the series field, is shown in Appendix II.

Equation 41 may be expressed with pu quantities by

$$\psi_0 = \phi_0+n_f(i_{f0}-K_{fs}m_{s1}i_{a0}) \qquad (42)$$

LINKAGES AT PEAK ARMATURE CURRENT

Peak time conditions: i_a' and i_f'. The flux linkages at peak are given by equation 43 for the paths outlined in Fig. 3

$$\psi' = N_f(\phi_a'+\phi_b'+\phi_d') \qquad (43)$$

In terms of the path permeances, equation 43 becomes

$$\psi' = N_fM_f'(P_a'+P_b'+P') = N_fI_a'(P_b'N_s+P'N_s+P'N_a') \qquad (44)$$

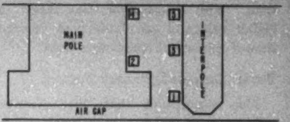

Fig. 4. Positions corresponding to actual and effective series-field windings

Equation 44 may be rewritten as

$$\psi' = N_f'P'M_f'(1+n_f')-N_sI_a'(1+n_{fs}')+N_a'I_a' \qquad (45)$$

where analogous to the previous development

$n_f' = (P_a'+P_b')/P' = (P_a+P_b)/P' = n_fP_1/P'$

$n_{fs}' = P_b'/P' = P_b/P' = n_{fs}P_1/P'$

as the permeance of the air paths a and b are not greatly influenced by peak currents.

Equation 45 may now be written as

$$\psi' = N_f[(M_f'-M_s'-N_a'I_a')P'+n_fP_1(M_f'-K_{fs}M_s')] \qquad (46)$$

Equation 46 may be expressed with pu quantities by

$$\psi' = (i_f'-m_{s1}i_a'-K_s'K_li_a')p'+n_f(i_f'-K_{fs}m_{s1}i_a') \qquad (47)$$

where further simplification employing equation 11 leads to

$$\psi' = \phi_d'+n_f(i_f'-K_{fs}m_{s1}i_a') \qquad (48)$$

Application of the constant flux linkage theorem is expressed by equating equation 42 to equation 48 which results in

$$\phi_0+n_f(i_{f0}-K_{fs}m_{s1}i_{a0}) = \phi_d'+n_f(i_f'-K_{fs}m_{s1}i_a') \qquad (12)$$

Appendix II. Calculation of Leakage-Linkage Ratio K_{fs}

Development of Equations

Usually the series field is located at either one of two positions with respect to the shunt field; these are numbered 2 and 4, as shown in Fig. 4. Without an actual series-field winding, an effective series field may result by a suitable arrangement of the connections between interpole and pole-face windings. In Fig. 4, the boxes labeled 1, 3, and 5 show the origin of those paths and their relative positions in passing around the main pole.

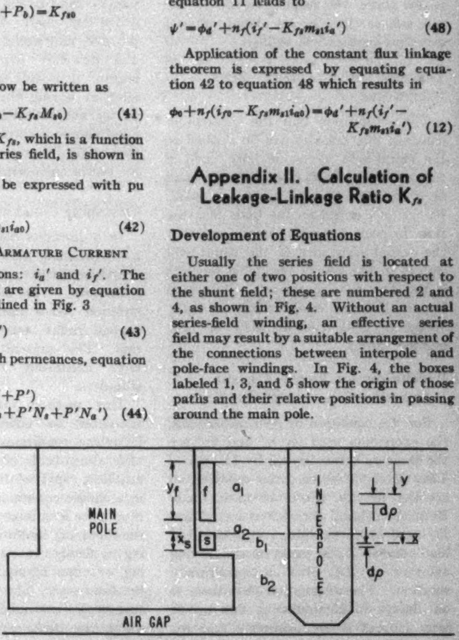

Fig. 5. Detail for development of partial flux linkage equations

By extension of the development in Appendix I to the case of partial linkages, a more accurate equation for the computation of K_{fs} should result. The following development utilizing partial linkages is offered for position 2, as shown in Fig. 5, with a differential series-field connection.

For path a_1 as a function of distance y, the turns n equal N_f/y_f, the mmf M_f equals $(M_{f1}/y_f)y$, and the permeance P equals $(P_{a1}/y_f)y$.

For the tube dP at distance y there is a

$$d\phi_{a1}=M_f dP=(M_{f1}/y_f)(P_{a1}/y_f)y\,dy$$

The partial leakage linkages $N_f\phi_{a1}$ caused by the shunt-field mmf alone are given by

$$\int_0^{y_f} n\,d\phi_{a1}=N_f M_{f1}P_{a1}/3 \qquad (49)$$

For path a_2, the entire mmf M_{f1} acts on permeance Pa_2, creating flux ϕ_{a2} linking all turns N_f

$$N_f\phi_{a2}=N_f M_{f1}P_{a2} \qquad (50)$$

For path b_1, as a function of distance x, all the turns N_f are linked, the mmf M equals $M_{f1}-(M_s/x_s)x$, and the permeance P equals $(P_{b1}/x_s)x$.

For the tube dP at distance x there is a

$$d\phi_{b1}=m\,dP=\left(M_{f1}-\frac{M_s}{x_s}x\right)\frac{P_{b1}}{x_s}dx$$

The partial linkages $N_f\phi_{b1}$ caused by the combination of shunt- and series-field mmf are given by

$$\int_0^{x_s} N_f d\phi_{b1}=N_f(M_{f1}P_{b1}-M_aP_{b1}/2) \qquad (51)$$

For path b_2, the entire mmf $(M_{f1}-M_s)$ is acting on permeance Pb_2 creating flux ϕ_{b2} linking all turns N_f

$$N_f\phi_{b2}=N_f(M_{f1}-M_s)Pb_2 \qquad (52)$$

The total initial linkages for the shunt field are obtained by summing up equations 49 through 52 plus the initial air-gap linkages $N_f(M_{f1}-M_s)P_0$

$$\psi_0=N_fM_{f1}(P_{a1}/3+P_{a2}+P_{b1}+P_{b2}+P_0)-N_fM_s(P_{b1}/2+P_{b2}+P_0) \qquad (53)$$

In a similar manner to the case in Appendix I, equations 54 and 55 may be written by inspection

$$n_{f0}=(P_{a1}/3+P_{a2}+P_{b1}+P_{b2})/P_0 \qquad (54)$$

$$n_{fs0}=(P_{b1}/2+P_{b2})/P_0 \qquad (55)$$

Therefore

$$K_{fs}=(P_{b1}/2+P_{b2})/(P_{a1}/3+P_{a2}+P_{b1}+P_{b2}) \qquad (56)$$

Generalized Values

Instead of attempting a calculation for the individual leakage-linkage coefficients, an estimate of their ratio K_{fs} is possible. Average values of K_{fs}, in general, are applicable for the numbered positions shown in Fig. 4.

The following magnitudes of K_{fs} are suitable:

Position	1	2	3	4	5
K_{fs}	0.10	0.65	0.80	0.95	0.85

Calculation of Individual Permeances

To compute the permeances of the flux paths outlined in Fig. 5, the usual assumption of infinite permeability of the iron is made so that only the air-path permeance is effective with

$$\mathcal{P}=\mu A/l$$

If it is desirable to obtain an estimate of the absolute value of n_f or n_{fs}, the value of P_1 is needed. This base permeance can be obtained in either of two ways. If a saturation curve is available, this permeance of the air gap corresponding to one pole is

$$P_1=\frac{\phi_1 10^{-8}}{M_{f1}}$$

Without a no-load saturation curve, the permeance of the air-gap line may be approximated by

$$P_g=\frac{4\pi p_a l_a 10^{-7}}{39.3gF} \qquad (57)$$

Then

$$P_1=\frac{P_g}{K_t} \qquad (58)$$

Appendix III. Calculation of Initial and Peak Time Shunt-Field Inductance

Initial Inductance

In the computation of shunt-field inductance it is possible to factor in the changes in saturation. If a no-load saturation curve is available, the calculation of the shunt-field winding inductance caused by direct-axis flux linkages is at 1 pu excitation

$$L_{g1}/\text{pole}=N_fE_1\Delta p_1/cN_1I_{f1}\text{ henrys} \qquad (59)$$

where

$$c=PZ/a60$$

$\Delta p_1=de/n_s d(i_f)$ pu, and at i_f equal to I_{f1}

In addition to the contributions of air-gap flux, there is leakage self-inductance as a result of shunt-field leakage linkages. Since it has been shown in Appendix I that these linkages are proportional to the shunt-field mmf

$$L_l/\text{pole}=n_fN_fE_1p_1/cN_1I_{f1} \qquad (60)$$

where

$p_1=e/n_si_f$ pu $=1$ at i_f equal to I_{f1}

The total initial shunt-field inductance L_f per pole is given by the sum of equations 59 and 60. If there is an initial load, the shunt-field inductance caused by the air gap can be modified. It has been found that the incremental permeance Δp (proportional to the slope of the no-load saturation curve) can be related to the permeance p (proportional to e/i_f) approximately by a cube law. The incremental permeance for the general case is

$$\Delta p_0=\Delta p_1(p_0)^3\text{ pu} \qquad (61)$$

The total initial shunt-field inductance for the general case is

$$L_f=[(p_0)^3L_{g1}/\text{pole}+L_l/\text{pole}]P \qquad (62)$$

If a no-load saturation curve is not available, then Δp_1 in equation 59 may be estimated at base speed by

$$\Delta p_1=(1/K_t)^3\text{ pu}$$

The value of Δp_0 obtained from equation 61 is also employed in determining coefficient M_{f-a} given in equation 27.

Inductance at Peak Time

In the computations of shunt-field inductance, it is possible, as before, to factor in the changes in saturation; those evidenced at peak time. The incremental permeance $\Delta p'$ is related to the permeance p' by a cube law

$$\Delta p'=\Delta p_1(p')^3\text{ pu} \qquad (63)$$

It follows that the total shunt-field inductance at peak is

$$L_f'=[(p')^3L_{g1}/\text{pole}+L_l/\text{pole}]P \qquad (64)$$

The value of $\Delta p'$ obtained from equation 63 is also employed in determining M_{f-a}' given by equation 31.

References

1. THE SHORT-CIRCUIT CHARACTERISTICS OF D-C GENERATORS, G. E. Frost. *AIEE Transactions (Electrical Engineering)*, vol. 65, June 1946, pp. 394–402.

2. CURRENT AND TORQUE OF D-C MACHINES ON SHORT CIRCUIT, T. M. Linville. *AIEE Transactions*, vol. 65, 1946, pp. 956–65.

3. TRANSIENT CHARACTERISTICS OF D-C MOTORS AND GENERATORS, A. T. McClinton, E. L. Brancato, Robert Panoff. *AIEE Transactions*, vol. 68, pt. II, 1949, pp. 1100–06.

4. FLASHING OF D-C MACHINES CAUSED BY SHORT CIRCUITS, A. T. McClinton, J. P. O'Connor. *AIEE Transactions*, vol. 72, pt. III, Feb. 1953, pp. 1–7.

5. SOLID SHORT CIRCUIT OF D-C MOTORS AND GENERATORS, T. M. Linville, H. C. Ward, Jr. *AIEE Transactions*, vol. 68, pt. I, 1949, pp. 119–24.

6. MAXIMUM SHORT-CIRCUIT CURRENT OF D-C MOTORS AND GENERATORS, AIEE Committee Report. *AIEE Transactions*, vol. 69, pt. I, 1950, pp. 146–49.

7. TRANSIENT RESPONSE OF DIRECT-CURRENT DYNAMOS, H. E. Koenig. *AIEE Transactions*, vol. 69, pt. I, 1950, pp. 139–45.

8. MEASUREMENT AND CALCULATION OF D-C MACHINES ARMATURE CIRCUIT INDUCTANCE, H. D. Snively, Paul B. Robinson. *AIEE Transactions*, vol. 69, pt. II, 1950, pp. 1228–37.

9. MEASUREMENT OF D-C MACHINE PARAMETERS, Robert M. Saunders. *AIEE Transactions*, vol. 70, pt. I, 1951, pp. 700–06.

10. ELECTROMECHANICAL ANALYSIS OF A SEPARATELY EXCITED D-C MACHINE, R. E. Vowels, W. G. Forte. *AIEE Transactions*, vol. 71, pt. I, 1952, pp. 32–42.

11. RATE OF RISE OF SHORT-CIRCUIT CURRENT OF D-C MOTORS AND GENERATORS, AIEE Committee Report, A. G. Darling, T. M. Linville. *AIEE Transactions*, vol. 71, pt. III, Jan. 1952, pp. 314–25.

12. COMMUTATION OF LARGE D-C MOTORS AND GENERATORS, T. M. Linville, G. M. Rosenberry, Jr. *AIEE Transactions*, vol. 71, pt. III, Jan. 1952, pp. 326–36.

13. TRANSIENT PERFORMANCE OF D-C MACHINERY, John Cybulski, E. L. Brancato, J. P. O'Connor. *AIEE Transactions*, vol. 72, pt. III, Feb. 1953, pp. 45–52.

14. D-C MACHINES SHORT-CIRCUIT CALCULATION AND TEST RESULTS, J. P. O'Connor, J. Cybulski. *AIEE Transactions*, vol. 74, pt. III, Apr. 1955, pp. 322–32.

D-C Machines—Short-Circuit Calculations and Test Results

J. P. O'CONNOR
MEMBER AIEE

J. CYBULSKI
ASSOCIATE MEMBER AIEE

THE wide use of d-c machinery in naval and industrial applications and the demand for reliability under all conditions of operation increases the importance of the design and operation of protective equipment. For this reason the need for a reliable method to compute the transient currents of motors and generators when a system is subjected to a fault is obvious.

The field of rotating d-c machinery includes a very wide variety of types and designs. The equations used in this paper, however, are applicable, for the calculation of fault transients, to all machines used for power applications in industry and in the U. S. Navy.

A description of the theory and the derivation of equations used in this paper have been given in a companion paper.[1] Like other equations given in the literature[2] for the computation of peak short-circuit current, the equations used here are based upon simplifying assumptions. Hence, a discrepancy between calculated and test values is expected. For this reason the accuracy of results obtained by computation is unknown unless test results are available. If test results were available on a large group of machines for comparison with computed results, a degree of confidence could be established in the validity of equations for the computation of peak short circuit of any machine in the normal power range. Reported test results in the literature, however, especially for machines of 1,000 kw and larger, are extremely meager. Confidence in the reliability of any method for the computation of short-circuit current can only be established by the confirming evidence of test results.

Test Values and Computed Results

In this paper the test results on five machines, which were part of a mock submarine propulsion plant, have been used to indicate the accuracy of computations. In a previous paper[3] test results on four of the five machines reported on here were given and were compared with the computed results obtained by the best method[3] then available.

The name-plate data of the five machines used for short-circuit tests are given in Table I, and the basic constants required for short-circuit calculations are given in Table II. A comparison of test peak short-circuit currents and the values obtained by computations are shown in Table III. A comparison of calculated and test transient currents appears in Figs. 1 through 6 inclusive.

Nomenclature

Upper-case letters denote total quantities. Exception is made for flux and flux linkages where the same size letter is used. Lower-case letters denote per-unit (pu) quantities; total quantities divided by their respective base values result in a pu system.

A = effective area of armature conductors in each slot, square inches; a_1h

a_1 = width of space taken by copper conductors in slot, inches (average $a_1 = 0.78b_1$)

b_1 = width of armature slot, inches (average $b_1 = 0.37p_a/n_1$)

C_s = number of armature conductors per slot, Z/S

d_a = diameter of armature, inches

E_0 = armature generated voltage, before short circuit, volts; $V_t \pm R_a I_{a0} \pm V_c$ (plus and minus signs are taken for generators and motors respectively)

E_1 = voltage generated at base flux, base speed, and no load, volts

f = frequency of commutation, cycles per second; $PN_1/120$

h = height of space taken by copper conductors in slot, inches (average $h = 0.87d_s$; if d_s, a_1, and b_1 are not known use average $h = 3.46ZI_c/\pi d_a j$)

i_a'' = estimate of steady-state armature circuit current, pu

I_c = armature conductor current, amperes; I_{a1}/a

I_{a1} = rated armature current at which the reactance voltage has been determined

I_{f1} = shunt field current corresponding to base field magnetomotive force, M_{f1}/N_f

i = instantaneous current, either armature or shunt field; units are in amperes or pu, depending on the context in which they are used

j = current density in armature conductors, amperes per square inch; $C_s I_c/A$; generalized value 2,500

K_l = initial load coefficient, $1 \pm (i_{a0}/10e_0)$; plus and minus sign for initial motor and generator action respectively

K_s = steady-state load coefficient, $1-(1/3e_0)$

K_2 = permeance constant of the "space flux," pu; generalized value 0.14

L_d = initial armature circuit inductance, henrys

N_a = armature winding turns per pole, $Z/2a$

N_b = pole-face winding turns per pole

N_f = shunt field winding turns per pole

N_1 = speed at which the reactance voltage has been determined, rpm

p = steady-state permeance, pu; $(K_1/i_a''+K_2)$, $p \leq K_l$

p_1 = permeance at base conditions in per unit equals one

R_a = resistance of armature winding only, ohms

R_1 = base resistance, ohms; E_1/I_{a1}

r_b' = effective brush-contact resistance at peak short-circuit current, pu

$r_x' = r_{xd}' + r_{xq}'$, an equivalent resistance to account for the loss in air-gap flux at peak armature current, pu

Table I. Name-plate Data on Five Machines

Machine	Kw	RPM	Horse-power	Constant Speed Rise, Degrees Centigrade	Volts	Amperes	Duty	Ventilation
Generator G-1, General Electric Company	1,100	750		60	415	2,650	continuous	forced
Generator G-2,* Westinghouse Electric Corporation	300	1,200		40	260	1,150	continuous	self
Motor M-1, General Electric Company		1,300	1,375	60	415	2,600	continuous	forced
Motor M-2, Westinghouse Electric Corporation		280	1,375	60	415	2,650	continuous	forced
Motor M-3, General Dynamics Corporation (Formerly Electro-Dynamic Works)		1,750	90	40	250	298	intermittent	self
* Multi-rated machine includes	300	1,200			345	870		
	150	600			260	575		

Paper 55-114, recommended by the AIEE Rotating Machinery Committee and approved by the AIEE Committee on Technical Operations for presentation at the AIEE Winter General Meeting, New York, N. Y., January 31–February 4, 1955. Manuscript submitted October 22, 1954; made available for printing December 16, 1954.

J. P. O'CONNOR and J. CYBULSKI are with the Naval Research Laboratory, Washington, D. C.

r_{xd}' = component of r_x' due to direct demagnetization

r_{xq}' = component of r_x' due to crossmagnetization

S = number of armature slots, p_pPn_t/p_a

t_{pa} = time to peak armature current, seconds; equation 19 of reference 1

t_{pf} = time to peak field current, seconds; equation 8 or 10

V_{f0} = initial voltage across shunt field circuit, volts

V_t = terminal voltage of machine, volts

V_a' = effective increase in armature winding resistance drop at base speed and current

ϕ_i = iron flux for intrinsic saturation, pu; generalized value 1.1

ϕ_1 = air-gap flux per pole corresponding to base field magnetomotive force at no load, maxwells

SUBSCRIPTS

b = effective brush contact

d = total armature circuit

e = external to machine winding including the short circuit

f = shunt field circuit

0 = initial conditions

s = series field winding

w = armature winding and all other machine windings in series

x = loss of air-gap flux resulting direct magnetization plus crossmagnetization

1 = base quantity; with magnetomotive forces other than M_{f1} taken at base armature current

Prime indicates the value of the

Table II. Definitions and Symbols for Basic Machine Constants with Values for Five Machines Used in Tests

Symbol	Quantity	Five Machines G-1	G-2	M-1	M-2	M-3
A_t	mean sectional area of armature tooth, square inches	6.21	4.85	4.5	9.95	3.1
a	number of parallel paths in armature	10	6	6	8	2
B	total number of commutator segments	345	198	138	304	85
b	number of commutator segments spanned by brush	4.03	4.05	3.65	4.73	1.64
d_t	radial depth of teeth, inches	1.74	1.907	1.685	2.47	1.34
E_1	base voltage, volts	415	520	415	345	250
E_r	reactance voltage (bar-to-bar) at base load, base speed	3.2	4.98	4.42	4.23	3.8
g	main pole air gap, inches	0.175	0.155	0.19	0.150	0.125
I_{a1}	base armature current, amperes	2,650	1,150	2,600	2,650	298
K_{fs}	shunt field mutual leakage-linkage ratio*	0.10	0.95	0.85	0.95	0.65
K_t	permeance of air gap line, pu	1.25	1.47	1.32	1.27	1.31
L_w	armature circuit inductance, microhenrys	93	250	100	300	2,300
M_a	armature ampere-turns per pole at base load	9,130	6,325	9,960	12,600	3,170
M_b	pole face winding ampere-turns per pole at base load	3,975	2,300	6,500	6,625	0
M_{f1}	shunt field ampere-turns per pole, no load, base magnetomotive force	5,020	5,000	5,400	5,100	4,510
M_s	series field ampere-turns per pole at base load	1,325	850	1,300	1,120	580
N_1	base speed, rpm	750	1,200	1,300	280	1,750
N_f	shunt field turns per pole	550	748	500	510	2,100
n_f	shunt field leakage coefficient at base field current	0.14	0.17	0.14	0.18	0.142
n_t	number of teeth per pole arc	6.9	10.25	14.14	12.2	7.74
P	number of poles	10	6	6	8	4
p_a	pole arc, inches	8.5	7.33	9.0	9.85	7.77
p_p	pole pitch, inches	14.2	11.79	14.66	15.32	10.8
R_w	resistance of armature circuit, ohms	0.003	0.00725	0.00304	0.00612	0.02145
V_c	brush drop at full load	3.0	2.0	3.0	2.0	2.0
Z	total number of active armature conductors	690	396	276	608	170

* Generalized values; see Appendix II of reference 1.

Table III. Comparison of Calculated and Test Values of Peak Short-Circuit Currents

		Initial Conditions					Accuracy of Calculated Quantities					
							Peak Armature Current			Shunt Field Current		
							Pu			Pu		
Machine	Run	E_0, Volts	N_0, RPM	I_{a0}, Amperes	I_{f0}, Amperes	R_e, Ohms	Cal.	Test	% Accuracy	I_f' Cal.	Test Peak	% Accuracy
G-1	A1e1	427	715	2,000	12.8	0.00227	8.39	7.02*	119			
	A1e2	415	715	0	10.8	0.00190	7.85	7.77	102			
	A1c	314	715	2,600	8.8	0.00227	6.71	5.70*	118			
	A1a1	214	715	2,400	5.8	0.00228	5.17	3.93*	132			
G-2	D-6	351	1,200	1,030	5.46	0.0049	7.63	7.95	96	3.18	4.00	80
	D-4	345	1,200	0	3.85	0.0049	6.50	6.39	102	2.87	3.35	86
	D-9	306	1,200	1,070	5.00	0.0049	7.10	7.47	95	2.80	3.42	82
	D-7	300	1,200	0	3.10	0.0049	5.74	5.70	101	2.43	2.75	88
	D-3	276	1,200	1,045	4.40	0.0049	6.50	6.72	97	2.48	3.02	82
	D-1	270	1,200	0	2.80	0.0049	5.29	5.07	104	2.17	2.12	102
M-1	A1e1	427	1,238	2,300	14.3	0.00204	9.95	8.47*	117			
	A1c	312	1,238	2,000	8.3	0.00202	7.45	7.05	106			
	C5c†	247	1,300	100	5.0	0.00330	4.92	4.88	101			
	C5b†	230	1,300	2,470	2.6	0.00265	3.69	3.67	100			
	A1b	216	638	2,200	13.0	0.00238	7.15	7.16	100			
	A1a2	209	950	1,900	7.2	0.00198	5.98	6.35	94			
	A1a1	208	1,240	1,700	5.8	0.00196	5.15	5.54	93			
M-2	A1e1†	390	267	2,700	11.5	0.00362	5.42	4.15*	131	4.28	4.87	89
	A1c†	279	267	2,400	5.0	0.00361	3.88	3.44	113	2.83	2.11	135
	C5b	253	280	1,745	8.3	0.00365	4.40	4.38	103			
	C5c†	248	280	100	5.4	0.00390	3.93	3.23	122			
	C1†	207	234	2,200	3.5	0.00428	2.95	2.76	107			
	A1A2†	175	204	2,500	3.3	0.00371	2.67	2.64	101	2.09	1.48	141
M-3	44F	350	2,200	0	6.3	0.00293	12.45	10.20*	122	5.46	6.32	87
	36F	292	1,800	0	6.85	0.00293	12.15	10.70*	114	5.24	7.05	74
	C-6†	256	1,800	15	2.00	0.01458	9.28	8.40	110	3.64	4.22	86
	C-7†	253	1,745	257	2.00	0.01450	9.20	8.05	114	3.73	4.22	88
	35F	250	1,800	0	4.25	0.00293	10.62	9.90	107	3.40	4.67	73
	38F	250	1,550	0	7.00	0.00293	11.03	11.75	97	5.04	6.35	80
	40F	250	2,200	0	2.95	0.00293	9.80	7.70*	127	3.27	3.30	99
	41F	250	2,100	0	3.16	0.00293	10.00	7.43*	135	3.42	3.30	104

* Flashover reduced the value of peak short circuit.

† Operating as a motor prior to short circuit.

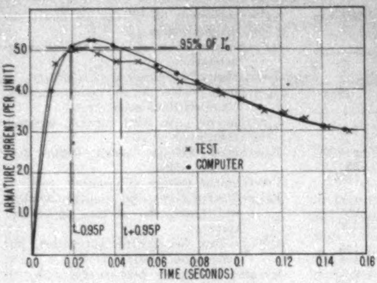

Fig. 1 (left) and Fig. 3 (right). Comparison of test and computed transient armature current. G-2 run D-1 for Fig. 1 and M-2 run Alc for Fig. 3

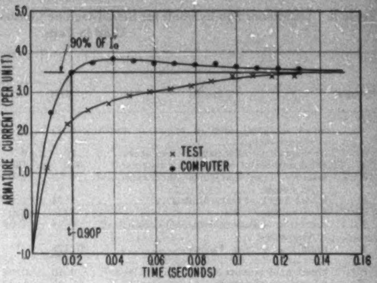

quantity corresponding to peak armature current. Double prime indicates an estimate. Where there is no subscript or superscript, the quantity corresponds to a steady-state condition. Exception is made for initial inductances and mutual inductances.

Additional symbols are defined in Tables II and IV and in reference 1.

Equations for Short-Circuit Calculations

The equations employed for short-circuit calculations have been derived in a companion paper[1] and are listed there. The peak armature current under short-circuit conditions is

$$i_a'=e_0/r_d' \qquad (1)$$

where

$$r_d'=r'+r_z'=r_e+r_w+r_b'+r_z' \qquad (2)$$

An improvement in an estimation of i_a' results when the equation for r_z', equation 33 of reference 1, is separated as follows

$$r_z'=r_{zd}'+r_{zq}' \qquad (3)$$

Then

$$r_{zd}'=\frac{n_f n_0 K_I}{1+n_f}\left[K_3'\pm(1-K_{fs})m_{s1}\right] \qquad (4)$$

$$r_{zq}'=\frac{n_f}{1+n_f}\left(\frac{1}{p'}-1\right)r' \qquad (5)$$

where the plus or minus sign in equation 4 is used when the series field opposes or aids the shunt field respectively during a short circuit. In a fully compensated machine there is no crossmagnetization and therefore the term r_{zq}' is equal to zero. Hence for a fully compensated machine the peak armature current is

$$i_a'=e_0/(r'+r_{zd}') \qquad (6)$$

When a machine is not fully compensated, or without compensation, it is first handled in the same way as a fully compensated machine. The value of the peak armature current thus obtained is a first approximation and is too high, since r_{zq}' was assumed equal to zero. This first approximation of i_a' is then used to compute r_{zq}'. If the computation of r_{zq}' results in a negative value, r_{zq}' should be assumed equal to zero and equation 6 would apply. This procedure for machines that are not fully compensated is necessary because the peak permeance p' is defined in terms of the peak armature current i_a' in the form of

$$p'=K_1/i_a'+K_2 \qquad (7)$$

Hence to determine p' and r_{zq}' a good approximation to the peak current such as given by equation 6 is employed.

From the equations listed in the companion paper,[1] the following equations applicable to the shunt field have been derived:

For separate excitation

$$t_{pf}=\frac{1}{(\gamma-\beta)}\ln\gamma/\beta \qquad (8)$$

$$di/dt=-c_1(\gamma-\beta) \qquad (9)$$

For self-excitation

$$t_{pf}=\frac{1}{\gamma-\beta}\ln(-\gamma c_1/\beta c_2) \qquad (10)$$

$$di/dt=-(c_1\gamma+c_2\beta) \qquad (11)$$

Sample Calculation

The basic constants required for short-circuit calculations are described in Table II and values of these constants are also given for the five machines tested. From the basic constants, Table II, the derived or computed constants, Table V, are obtained. Table IV-A illustrates how the computed constants are obtained for machine G-2, and

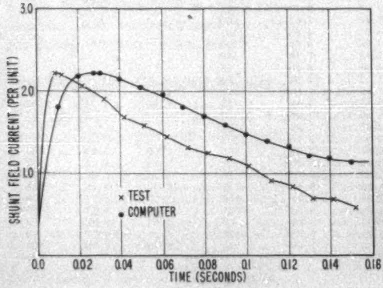

Fig. 2 (left) and Fig. 4 (right). Comparison of test and computed transient field current. G-2 run D-1 for Fig. 2 and M-2 run Alc for Fig. 4

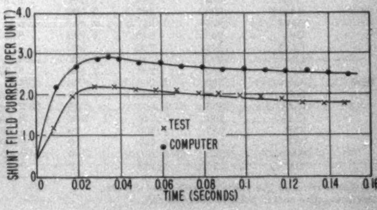

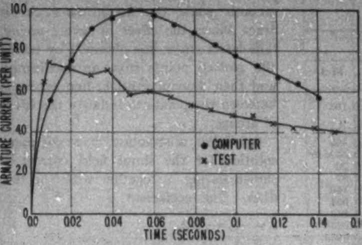

Fig. 5. Comparison of test and computed transient armature current M-3 run 41F

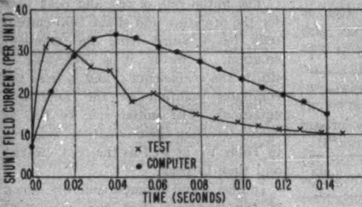

Fig. 6. Comparison of test and computed transient field current. M-3 run 41F

Table IV. Computed Constants, Short-Circuit and Field Currents, and Rise and Decrement Factors

Item	Defining Equation	Value
A: Computed Constants for Short-Circuit Calculation on G-2 Run D-1		
R_1	E_1/I_{a1}	0.452
I_{f1}	M_{f1}/N_f	6.7 amperes
m_{a1}	M_a/M_{f1}	1.265
m_{b1}	M_b/M_{f1}	0.460
m_{s1}	M_s/M_{f1}	0.170
m_{c1}	$(p_a/p_p)m_{a1}-m_{b1}$	0.323
ϕ_1	$E_1 10^8/cN_1$	6.56 × 10^6 lines
ϕt	125,000 $A_t n_1/\phi_1$	0.95
K_1	$\phi t/m_{c1}$	2.94
K_2	$1.25gK_t/(g+d_s)$	0.138
K_2'	bPm_{a1}/B (no load)	0.155
r_w	R_w/R_1	0.016
$K_{f2}m_{s1}$		0.1615
$(1-K_{f2})m_{s1}$		0.0085
E_rb		20.2 volts
B: Calculation of Peak Short-Circuit Current Run D-1 for Initial Conditions Shown in Table III		
e_0	E_0/E_1	0.52
n_0	N_0/N_1	1.00
K_t	$1\pm(i_{a0}/10e_0)$	1.00
r_e	R_e/R_1	0.0108
a	$n_0K_t^2E_rb$	20.2 volts
r_b'	equation 6 of reference 1	0.0427
r'	$r_w+r_e+r_b'$	0.0695
r_{sd}'	equation 4 with plus sign	0.0238
i_a' (approx.)	equation 6	5.57
p'	equation 7	0.666
r_{sq}'	equation 5	0.0050
r_s'	equation 3	0.0288
r_d'	equation 2	0.0983
i_a'	equation 1	5.29
i_{f0}	I_{f0}/I_{f1}	0.418
i_f'	equation 5 with plus sign reference 1	2.17
C: Calculation of Decrement and Rise Factor Run D-1 for Initial Conditions Shown in Table III		
K_s	$1-(1/3e_0)$	0.36
K_2	K_spbm_{a1}/B	0.056
r_b	$(n_0K_s^2E_rb+V_c)/E_1$	0.0089
r	$r_w+r_e+r_b$	0.0357
i_a''	$\dfrac{e_0}{r+n_0K_t(K_2K_s+m_{s1})}$	1.65
p	$\dfrac{K_1}{i_a''}+K_2,\ p\leq K_t$	1.47
i_a	$\dfrac{i_{f0}}{r/pn_0+K_2K_s+m_{s1}}$	1.73
ϕ_0	e_0/n_0	0.52
p_0	$\phi_0/(i_{f0}-m_{s1}i_{a0})$	1.24
Δp_1	$(1/K_t)^2$	0.318
Δp_0	$\Delta p_1(p_0)^2$	0.61
c	$PZ/a60$	6.6
L_{g1}	$N_fE_1\Delta p_1/cN_1I_{f1}$	2.3 henrys per pole
L_l	$n_fN_fE_1p_1/cN_1I_{f1}$	1.25 henrys per pole
L_f/P	$(p_0)^2L_{g1}+L_l$	5.64 henrys per pole
R_f	V_{f0}/I_{f0}	93 ohms
T_f	L_f/R_f	0.364 second
T_a	$L_a/r'R_1$	0.010 second
M_{f-a}	$PN_f(K_2'K_t+m_{s1})\Delta p_0\phi_1 10^{-8}/I_{a1}$	0.350 henry
n	$1-M_{f-a}^2/L_aL_f$	0.762
γ	$\dfrac{2}{(T_a+T_f)-[(T_a+T_f)^2-4nT_aT_f]^{1/2}}$	118 seconds^{-1}
p'	equation 7	0.694
$\Delta p'$	$\Delta p_1(p')^2$	0.106
L_f'/P	$(p')^2L_{g1}+L_l$	2.02 henrys per pole
T_f'	L_f'/R_f	0.130 second
T_a'	$L_a/r_d'R_1$	0.007 second
M_{f-a}'	$PN_f(K_2'K_t+m_{s1})(\Delta p')\phi_1 10^{-8}/I_{a1}$	0.0088 henry
n'	$1-(M_{f-a}')^2/L_aL_f'$	0.979
β	$\dfrac{2}{(T_a'+T_f')+[(T_a'+T_f')^2-4n'T_a'T_f']^{1/2}}$	7.7 seconds^{-1}
Armature i	$c_1e^{-\gamma t}+c_2e^{-\beta t}+i_a$	
Field i	$c_1(e^{-\gamma t}-e^{-\beta t})+i_{f0}$	

Table IV-B shows in detail the computation of the peak short-circuit current and the corresponding shunt field current for the initial conditions given in Table III for run D-1. Table IV-C shows a detailed computation of the rise and decrement factors and steady-state short-circuit armature current for this run. From the results given in Tables IV-B and IV-C a complete transient solution can be obtained on an analogue computer.

A block diagram illustrating simulation by a *GAP/R* analogue computer is shown in Fig. 2 of reference 1. Before computation begins a calibration which involves scaling of time and magnitude is made for the coefficient boxes and the display cathode-ray tube. Actual times of interest of the order of 0.2 second are represented by a computing interval of 40 milliseconds. This electronic computation is repetitive, 20 times during a second, so that the solution may be displayed on a cathode-ray tube. With a rectangular co-ordinate grid on the cathode-ray tube the calibration is made so as to simplify the reading of the magnitude and time data. A picture is taken of the displayed transient and superimposed illuminated grid, thus giving a permanent record.

From the computer solution for run D-1, the coefficients of the equation for the transient, equation 35 of reference 1, are found for the armature current to be

$c_1=-6.30$, $c_2=4.46$, $c_3=1.76$ (calculated steady-state current)

The transient as obtained by the computer and the actual test transient are shown in Fig. 1. The computer curve was obtained by abstracting data every 0.01 second from a photograph of the trace. In Fig. 1 it will be observed that the computer curve is

Table V. Computed Constants for Short-Circuit Calculations

Constants in Pu Except Where Noted	G-1	G-2	M-1	M-2	M-3
	Five Machines				
m_{a1}	1.820	1.265	1.845	2.470	0.703
m_{b1}	0.792	0.460	1.200	1.300	0
m_{s1}	0.264	0.170	0.241	0.220	0.128
m_{c1}	0.298	0.323	−0.063	0.290	0.493
ϕ_1 (maxwells)	4.82×10^6	6.56×10^6	†	12.1×10^6	2.52×10^6
ϕ_t	1.11	0.92	†	1.25	1.20
K_1	3.72	2.94	†	4.31	2.37
K_2	0.143	0.138	†	0.091	0.140
K_2' (no load)	0.213	0.155	0.292	0.308	0.054
R_1 (ohms)	0.157	0.452	0.160	0.130	0.840
r_w	0.0192	0.0160	0.0191	0.0471	0.0256
$K_{fs}m_{s1}$	0.0264	0.1615	0.2045	0.2083	0.0835
$(1-K_{fs})m_{s1}$	0.2380	0.0085	0.0362	0.0110	0.0450
L_{g1} (henrys)	1.49	2.30	1.40	3.02	10.8
L_t (henrys)	0.41	1.25	0.45	1.12	3.51
E_rb (volts)	12.9	20.2	16.15	20.0	6.24
I_{f1} (amperes)	9.13	6.7	10.8	10.0	4.30*

* For series-parallel connection of the shunt field, in runs C-6 and C-7 field coils are in series, $I_{f1}=2.15$ amperes.

† Constant not needed as m_{ct} indicates slight over compensation.

Table VI. Initial Rate of Rise, Peak Current, and Time to Peak

	Initial Rate of Rise			Peak Current, Pu			Time to Peak, Seconds		
	Pu per Second	Amperes per Second	Test D-1 Amperes per Second	Computer Constants	Basic Constants	Test D-1	Computer Constants	Computer Display	Test D-1
Armature	710	0.82×10^6	0.80×10^6	5.11	5.29	5.07	0.0278	0.028	0.022
Field	250	1,670	1,550	2.17		2.12	0.0247	0.027	0.010

Table VII. Comparison of Calculated and Test Values of Peak Short-Circuit Currents for Zero External Resistance

Machine	Terminal, Volts	Speed, RPM	Load, Amperes	Peak Armature Current, Pu: Cal.	Peak Armature Current, Pu: Test	% Accuracy
			Machines at Rated Conditions, Full Load Initially			
G-1	415	750	2,650	9.55	8.5*	112
G-2	345	1,200	870	8.57	9.0	95
M-1	415	1,300	2,600	8.02	7.5	107
M-2	415	280	2,650	6.24	5.0*	125
M-3	250	1,750	298	10.30	10.0	103
			Machines at Rated Conditions, No Load Initially			
G-1	415	750	0	8.34	7.5	111
G-2	345	1,200	0	7.28	7.9	92
M-1†	415	1,300	0	9.49	8.5‡	112
M-2†	415	280	0	7.14	6.0‡	119§
M-3	250	1,750	0	11.18	11.1	101

* Flashover reduced the value of peak short-circuit current.

† No suitable test available for extrapolation.

‡ Test peak estimated on basis of 1 pu difference between the no-load and full-load condition.

§ It is probable that at the 6.0 pu estimated value there would be flashover as there was at 5.0 pu.

smooth while the actual short-circuit trace shows the effect of severe arcing. The latter curve was obtained by taking the plotted points from an oscillogram and then drawing straight-line segments between the points to indicate the effect of arcing.

A similar abstraction of a computer solution for the shunt field current is shown in Fig. 2 together with the test data. The coefficient

$$c_1=-c_2=-2.2$$

was obtained for a separately excited field from the computer. It can also be calculated directly by evaluating equation 36 of reference 1 at the peak time for armature current.

The initial rate of rise and peak time for the armature and shunt field current may be obtained from the transient solution. However, it is preferable to utilize the coefficients c_1 and c_2 from the computer solution in the applicable equations. The initial rate of rise as calculated from these equations is shown in Table VI, as well as the peak current and time to peak.

In Figs. 3 and 4 comparisons are shown of the transient (test and computed) armature and shunt field currents respectively for machine M-2. A comparison of computed and test results on M-3 may be made in Figs. 5 and 6 for the armature and shunt field transient currents respectively.

If some of the design parameters in Table II are not available, then various approximations may be made for the resistance parameters, the peak current, and the initial rate of rise as shown in Appendix I.

Discussion of Results

Values of peak short-circuit armature current, as obtained from oscillograms and as computed, are given in Table III for 31 low-resistance short-circuit tests on five machines. A comparison of the

Table VIII. Comparison of Approximations and Test Values of Peak Short-Circuit Current

Machine at Rated Conditions, No Load Initially, Zero External Resistance

Machine	Test* i_a	Approximation of r_x': Cal. i_a'	Approximation of r_x': % Accuracy	Approximation of E_rb: a_1, Inches	b_1, Inches	h, Inches	R, Ratio	R_a, Ohms	Cal. i_a'	% Accuracy	Approximation from Fig. 8: i_a'	Approximation from Fig. 8: % Accuracy
G-1	7.5	11.90	159	0.396	0.480	1.491	6.20	0.0016	7.10	95	10.1	135
G-2	7.9	7.56	95	0.173	0.260	1.628	5.72	0.0044	6.80	86	9.3	118
M-1	8.5	10.20	120	0.183	0.235	1.470	5.90	0.0015	8.82	104	10.1	119
M-2	6.0	7.25	121	0.247	0.331	2.224	3.72	0.0033	6.71	112	10.1	168
M-3	11.1	11.00	100	0.270	0.330	1.154	3.88	0.0144	8.86	80	8.3	75

* Values taken from Table VII.

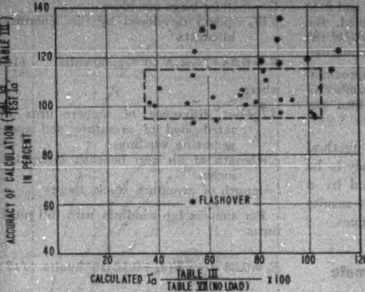

Fig. 7 (left). Accuracy of calculation of peak short-circuit current versus relative magnitude of peak short circuit

Fig. 8 (right). Peak zero resistance short-circuit current versus machine terminal voltage rating, rated conditions, no load initially

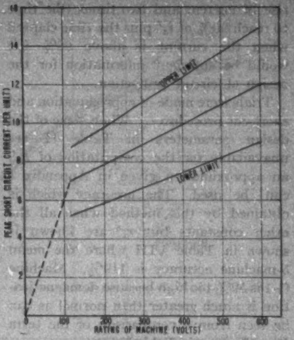

test and computed values of peak armature current for the various short-circuit runs on the machines used in this series of tests is indicative of the accuracy with which the peak short-circuit current can be computed for widely varying initial conditions of load, speed, and voltage. Over-all the calculated results obtained on the machines tested are good considering that each of these machines is of a special design for operation over a voltage range of 250 to 415 volts for shipboard service. The accuracy of the computations as shown in Tables III and VII would be better were it not for the occasional severe flashing which reduced the magnitude of the measured external current. Hence in those runs where flashing occurred the computed values are generally on the high side.

For those concerned with the design and application of protective equipment for d-c machinery, the peak short-circuit current at rated conditions and with no external resistance is considered most important. Computed and test values of peak short-circuit current for rated conditions and zero external resistance are given in Table VII. In this table the accuracy of the calculated data is given, using the test data that could be extrapolated to these conditions as a base. However, there was no test sufficiently close to full-load initial conditions for machines M-1 and M-2. For these machines a 1 pu change was employed as an estimate of the difference to be expected between the no-load to full-load test data. It is noted from Table VII that the higher currents occur for motor operation at no load and for generator operation at full load.

A graphical representation of the percent (%) accuracy obtained by computation of peak armature current is shown in Fig. 7. The abscissa in this figure represents the relative magnitude of calculated peak short-circuit current in % where the base value of peak current is that computed for rated conditions and no load. For a range of peak currents that vary in relative magnitude from 35% to 105%, the mean accuracy for all runs is 109% of the test values. If the runs where flashover occurred are excluded the mean accuracy for the remaining runs is 105%.

In some of the tests shown in Table III the transient field current was not recorded. In those cases where an oscillogram of the transient field current was taken the field current i_f' corresponding to peak armature was calculated, and is compared to the test peak field current in Table III. In the computation of the % accuracy of the field current, the test peak field current is taken as a base and the calculated field current i_f' is expressed as a percentage of the base. In general, the field current i_f' that exists at peak armature current is slightly smaller than the true peak field current because the field current peaks before the armature current. For this reason it was expected that the computed values of i_f' would be somewhat smaller than the test values of peak field current. An average accuracy of 93% was attained for the 17 runs available for comparison.

Although the computed transient curves compare favorably with the actual test data, the accuracy as to the time of the peak armature and field current is highly variable so that average figures cannot be cited. There are several reasons for errors in computed peak time. Primarily, the complex magnetic circuit with superimposed eddy-current effects cannot be simulated accurately with simple time constants. Even if more elaborate time constants are employed it remains difficult to evaluate correctly the effective inductance and resistance of the circuits at the various times. In addition, unpredictable flashing, interpole flux response, and steady-state current estimation contribute to errors in transient current plots. Therefore, instead of relying on an estimate of peak time from a current time plot, it is believed that the time interval when the computed current exceeds 90% or 95% of its peak value will, in general, include the actual test peak.

For example, in Fig. 1 a horizontal line has been drawn at the magnitude 95% of i_a', i.e.

$$0.95(5.29)=5.03 \text{ pu}$$

This line intersects the computed transient curve at two points: $t_{-0.95p}=0.019$ second and $t_{+0.95p}=0.044$ second. Those two times are indicative of the short-circuit behavior of the d-c machine. A different characteristic is illustrated in Fig. 3, where the percentage limits were dropped to 90% of i_a'. It is suggested that specifying the peak magnitude of current together with the initial rate of

Table IX. Initial Rate of Rise of Transient Currents

			$\{[d(i_a)]/(dt)\}\,10^{-4}$			$[d(I_f)]/(dt)$		
			Amperes per Second			Amperes per Second		
Machine	Run	I_a	Cal.	Test	% Accuracy	Cal.	Test	% Accuracy
G-1	A1e2	.50	2.90	3.48	83	4,770	3,100	154
G-2	D1	.60	0.87	0.80	109	1,650	1,550	107
M-1	A1c	.73	1.80	1.55	116	3,750	(no record)	(no record)
M-2	A1e1	.69	1.06	1.58	67	2,340	1,860	126
M-3	41F	.10	0.11	0.15	73	1,450	1,190	122

rise of current and two times (the time to reach 90% of i_a' plus the time elapsed when the current is above 90% i_a') would be sufficient information for the design of circuit protection.

Trials were made of approximation and short-cut procedures. When some of the design parameters in Table II are unavailable for the computation of r_x', an approximation given in Appendix I can be used. The accuracy which is obtained by this method when all the other constants but r_x' are known is shown in Table VIII where the mean 5-machine accuracy is 119%. Machine G-1 is 59% too high because demagnetization is much greater than normal as can be seen from a comparison of the term $(1-K_{fs})\,m_{s1}$ in Table V.

When the product $E_r b$ is not known an alternate procedure for computation of its value, developed in Appendix I, may be used. The accuracy obtained by this method when all the other constants are known is shown in Table VIII where the mean 5-machine accuracy is 95%.

A rough estimate of the peak armature current resulting from a short circuit at rated condition and no initial load is shown in Appendix I. The results of application of this procedure for the five machines (employing the median line of Fig. 8) are shown in Table VIII with a mean accuracy of 123%.

Approximate procedures were also applied to the calculation of the initial rate of rise of armature and shunt field current as shown in Appendix I. Comparable results to those obtained under the sample calculation were attained and are shown in Table IX with a mean accuracy of 90% and 127% for the armature and shunt field circuits respectively.

In Appendix II it is shown that by normalizing the no-load saturation curves for the five machines it is possible to employ generalized values for various constants and to develop a simple equation to represent the saturation curve.

Conclusions

Based on a comparison of test and calculated data on five machines, it is concluded that the accuracy in the computation of armature and field currents is as follows:

1. Peak armature current is within 105%±10% for 90% of the runs on the average if there is no flashover.
2. Peak field current is within 90%±20% for 90% of the runs on the average.
3. Initial rates of rise of armature and shunt field currents are variable with a mean of 90% and 127% respectively.
4. Time to peak for the armature and field current is highly variable. Instead, the time to reach and remain above 90% of the peak value will provide realistic information.
5. Peak armature current by approximation processes requiring a small number of design constants is feasible provided the reduced accuracy is acceptable.

Complete confidence in the method presented here and in the accuracy to be expected can only be established by a comparison of computed and test results on a large variety of d-c machines.

Appendix I. Approximate Calculations

The method of calculation for short circuit from design constants is reasonably accurate for all practical purposes, but is open to the objection that a large number of design constants are required, and the computation is involved and cumbersome.

Approximation of r_x'

Many design constants are used in the computation of r_x', a fictitious resistance which, when multiplied by the peak armature current, represents the loss in generated voltage. A rough approximation to this loss in generated voltage when a machine is short-circuited at any voltage, rated speed, and no load is one-third the voltage at which it is short-circuited. It is also found from tests and the equation derived for r_x' that the loss in generated voltage is almost directly proportional to the speed of the machine. Then a rough approximation of E_x', the loss in voltage due to short circuit at peak short-circuit current, may be expressed as

$$E_x' = (E_0/3)(N_0/N_1) \text{ volts}$$

Hence the generated voltage at peak short-circuit current is

$$E' = E_0(1 - N_0/3N_1) \text{ volts} \qquad (12)$$

The peak short-circuit current is then

$$I_x' = E_0(1 - N_0/3N_1)/R' \text{ amperes} \qquad (13)$$

Applying equation 13 to the machines tested at rated conditions, no load (in Table VII) the results are compared with test data and are shown in Table VIII.

Approximation of $E_r b$

At the present time, the reactance voltage E_r and the number of segments b spanned by the brush are utilized as per equation 6 of reference 1 to calculate an effective transient increase in armature winding resistance due to poor commutation. If the value of E_r, which is obtained most reliably from the manufacturer, is not available it can be calculated from any one of a number of equations, which are at best estimates. A list of some of these follow

$$E_r = 12 n_0 I_{a1} 10^{-6}/d_a \text{ volts} \qquad (14)$$

$$E_r = C_r KW_a/d_a \text{ volts} \qquad (15)$$

where

$C_r = 0.12$ for large machines
KW_a = power developed by the armature, kilowatts

$$E_r = 6.38\,AT\,l\pi d_a N_1 10^{-6}/g_c\,60 \text{ volts} \qquad (16)$$

where

AT = net difference of ampere-turns at rated load of armature and compensating windings
g_c = length of air gap beneath interpoles, inches
l = length of armature stack, inches

For simplex lap windings with full pitch turns

$$E_r = 0.33\,\frac{Z^2 N_1 I_{a1}}{Bab}(d_s + 0.1 l_e)10^{-6} \text{ volts} \qquad (17)$$

where

b = number of segments covered by the brush rounded off to the next higher integer
l_e = length of end connection for each conductor, inches

For simplex wave winding

$$E_r = 0.17\,\frac{Z^2 N_1 I_{a1}}{Bab}(d_s + 0.1 l_e)P10^{-6} \text{ volts} \qquad (18)$$

Equations 14 through 18 are different with each developed from definite assumptions and dependent on what data are available. If neither an estimate of E_r nor b is available the following method is recommended.

In the recent literature[4] there has appeared an equation

$$J/J_0 = 16\pi f a_1 h^2/3 s b_1 \qquad (19)$$

expressing a ratio of the commutation loss to the d-c loss of the armature winding. Equation 19 is based on the lag in flux reversal and nonuniform distribution of current in the conductor with assumption of instantaneous commutation where the energy involved is either lost during the commutation period at the contact surface (between the commutator segments and brushes) or within the armature conductors.

Equation 19 is rewritten to express the ratio of the increase in armature winding resistance to the d-c ohmic value

$$R = 0.054 a_1 f h^2/b_1 \qquad (20)$$

where h is in inches and a value for s, the specific resistance for copper, is used. This ratio is next incorporated as an increase in the effective transient armature winding resistance as follows

$$r_b' = (R-1)R_a n_0/R_1 + V_c/E_1 \qquad (21)$$

If it is desirable to include the effects of load, equation 21 may be rewritten as

$$r_b' = (K_l^2 n_0 V_a' + V_c)/E_1 \qquad (22)$$

where

$$V_a' = (R-1)R_a I_{a1} \text{ volts} \qquad (23)$$

Equation 22 is of the form of $(\alpha + V_c)/E_1$ so that Fig. 1 of reference 1 may be used to aid in evaluating r_b' whenever α is as small as the plotted values of α. This procedure for approximating $E_r b$ by equations 20, 22, and 23 was applied to the five machines and the results compared with test data as shown in Table VIII.

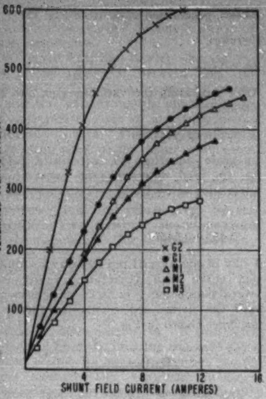

Fig. 9 (left). No-load saturation curves for five machines. Abscissa has been multiplied by 2 for M-3

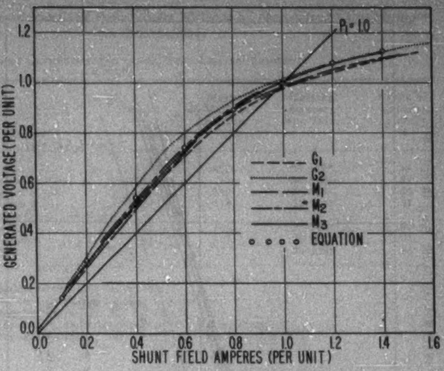

Fig. 10 (right). Normalized no-load saturation curves for five machines

Approximation of Peak Armature Current

In the preliminary design of a d-c power system only the voltage and current of machines are known and in order to have some idea of design requirements under fault conditions an estimate of the value of peak short circuit of each machine is required. It is known from experience that the maximum current of a d-c machine on "solid" short circuit is about 7 to 12 times rated current. In general, the higher values apply to 600 to 1,500-volt machines and the lower values to 125 to 250-volt machines. This rough approximation is shown graphically in Fig. 8 where peak short-circuit current, represented by the median line, is plotted against rated machine voltage. The other two lines shown in this figure have been arbitrarily drawn at 25% above and below the median line, and are suggestive of the band within which the actual maximum short-circuit current of most machines will fall. A comparison of test values of peak short-circuit current and the values as obtained from the median line of Fig. 8 are shown in Table VIII.

Approximation of Initial Rates of Rise

It is not always necessary to obtain a full solution for the transient armature current in order to compute the initial rate of rise. An approximation to the initial rate of rise of armature current may be calculated from the following equation

$$di/dt = E_0/(L_w + L_s) \text{ amperes per second} \tag{24}$$

Application of equation 24 to machine G-2 listed in Table IX results in

$$di/dt = 270/(310 \times 10^{-6}) \text{ amperes per second}$$

It is also possible to approximate the initial shunt field current rate of rise by utilizing this estimate of the initial rate of rise of armature as shown in the following development. Ratio of field to armature rate of rise is estimated by

$$N_{se}/N_f = I_{f1}(K_s'K_1 \pm m_{s1})/I_{a1} \tag{25}$$

where the plus and minus sign is for differential and cumulative action of the series field. Equation 25 written on the basis of unity coupling is rewritten as: Shunt field rate of rise is equal to

$$di/dt = I_{f1}(K_s'K_1 \pm m_{s1}) \text{ armature rate of rise}/I_{a1} \text{ amperes per second} \tag{26}$$

Application of equation 26 to G-2 listed in Table IX results in

$$di/dt = 6.7(0.155 + 0.17)870{,}000/1{,}150 = 1{,}650 \text{ amperes per second}$$

If there is no value of armature circuit inductance available, the following procedure is suggested to obtain an estimate of the armature winding inductance. Let

$$L_w = C_z L_{w1} \tag{27}$$

where

$L_{w1} = 19.1E_1/I_{a1}N_1P$ (from reference 5) machine base inductance in henrys

with generalized values for C_z (from reference 6).

Appendix II. Normalized Saturation Curves

A study was made to see whether generalized values may be employed successfully for some parameters which are now determined directly or indirectly from the no-load saturation curve of rotating machinery. No-load saturation data were obtained at base speed for the five machines tested and are shown plotted in Fig. 9. All machines begin to exhibit the typical saturation characteristic in the vicinity of base field current.

In an attempt to improve this similarity the abscissa and ordinate values of the original saturation data were divided by the appropriate base current and base voltage for each machine. This normalized data may be viewed in curve form in Fig. 10. These normalized curves show good agreement as to shape and lend themselves to the setting up of generalized values for K_1, K_2, Δp_0, and Δp_1. That these saturation curves come close to each other is attributed to design procedures whereby the operating point is generally "on the knee" of the saturation curve as a compromise between full utilization of the magnetic structure and high magnetic core losses.

Another worth-while feature in connection with the curves is the relation between the incremental permeance and static permeance. This relation was sought by obtaining the quantities E_0/I_{f0} and dE_0/dI_{f0}, at each integral current step from the data in Fig. 9. These new data were then further normalized into a pu system by employing the voltage and current base of each machine. It was found that there is an inverse correlation between K_1 and the incremental slope at base field current. In fact, when the reciprocal of K_1 is taken simply to the third power, the computed Δp_1 is in good agreement with the actual slope in pu at base field current. These

Table X. Comparison of Incremental Permeances

			Saturation Curve Slope				
			$dE_1/d(I_{f1})$		Approximation		
Machine	E_1/I_{f1}, Volts per Ampere	N_1, RPM	Volts per Ampere	Pu	K_1	$(1/K_1)^3$	% Accuracy
G-1	45.5	750	19	0.418	1.25	0.513	123
G-2	77.6	1,200	27	0.348	1.47	0.318	91
M-1	38.4	1,300	14	0.364	1.32	0.435	119
M-2	34.5	280	15	0.435	1.27	0.487	112
M-3	116	1,750	48	0.413	1.31	0.444	107

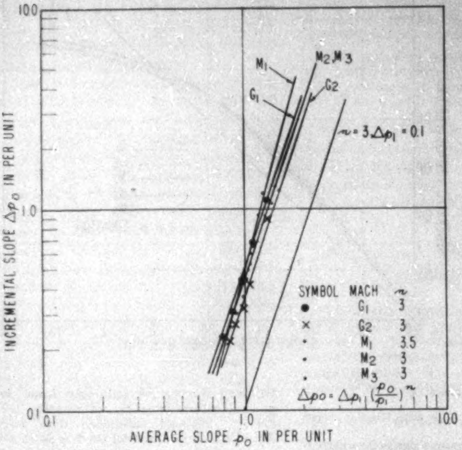

Fig. 11. Relations of incremental slope to the average slope of a no-load saturation curve

comparisons are shown in Table X.

The relation given by equation

$$\Delta p_0 = \Delta p_1 (p_0)^3 \tag{28}$$

was found by making a plot of the normalized incremental slopes versus the average slopes to the saturation curves. As shown in Fig. 11 these plots for four of the five machines were approximated by straight lines of a slope of three, indicating a cube power law. In addition, the intersection of these lines with the abscissa of 1.0 provides a check as to the magnitude of Δp_1. An assumption is made that equation 28 may be employed with p' in place of p_0 to obtain $\Delta p'$. As this relation between the incremental slope and the average slope of a saturation curve was satisfactory, the development was extended to the writing of an equation for representation of the no-load saturation curve.

Essentially equation 28 expresses

$$de/di = dp_1 (e/i)^3 \tag{29}$$

From the previous material when $i = 1$, $e = 1$, $dp = (1/K_t)^n$, where

$K_t = 1.3$, generalized value from Fig. 10

$n = 3.0$, generalized value from Fig. 11

therefore

$dp_1 = 0.455$

After separating the variables equation 29 becomes

$$\int de/e^3 = dp_1 \int di/i^3 \tag{30}$$

Integrate equation 30, substitute 0.455 for dp_1, and determine the constant of integration at $i = 1$ and $e = 1$ to arrive at

$$e^3 = \frac{i^3}{0.455 + 0.545 i^3} \tag{31}$$

A plot of equation 31 representing a saturation curve with generalized values for several parameters is in excellent agreement with the normalized curves for the five machines shown in Fig. 10.

References

1. D-C MACHINES—METHOD FOR SHORT-CIRCUIT CALCULATION, **John P. O'Connor, John Cybulski.** *AIEE Transactions*, vol. 74, pt. III, Apr. 1955, pp. 214–21.

2. SOLID SHORT CIRCUIT OF D-C MOTORS AND GENERATORS, **T. M. Linville, H. C. Ward, Jr.** *AIEE Transactions*, vol. 68, pt. I, 1949, pp. 119–24.

3. TRANSIENT CHARACTERISTICS OF D-C MOTORS AND GENERATORS, **A. T. McClinton, E. L. Brancato, Robert Panoff.** *AIEE Transactions*, vol. 68, pt. II, 1949, pp. 1100–06.

4. TRANSIENT PERFORMANCE OF ELECTRIC-POWER SYSTEMS (book), **Reinhold Rudenberg.** McGraw-Hill Book Company, New York, N. Y., 1950, p. 123.

5. CURRENT AND TORQUE OF D-C MACHINES ON SHORT CIRCUIT, **T. M. Linville.** *AIEE Transactions*, vol. 65, 1946, pp. 956–65.

6. RATE OF RISE OF SHORT-CIRCUIT CURRENT OF D-C MOTORS AND GENERATORS, AIEE Committee Report, **A. G. Darling, T. M. Linville.** *AIEE Transactions*, vol. 71, pt. III, Jan. 1952, pp. 314–25.

◆

Discussion

Donald T. Bewley (General Electric Company, Schenectady, N.Y.): Figs. 1 through 6 show that the agreement between tested and calculated transient curves is not as close as might be desired. This in itself is not as discouraging as it may seem since the sustained current is not reached before either flashover occurs or the circuit breaker operates; hence, the important items to be accurately calculated are peak armature current and maximum rate of rise of armature current. For industrial machines utilizing circuit breakers, an accurate determination of these items will assure proper selection of breakers that will interrupt the armature circuit before injury to the system apparatus occurs.

The test results indicate that the authors have made an important contribution to an accurate determination of peak armature currents. Closer agreement between test and calculated values of maximum rates of rise of armature current might be realized if a more accurate determination of machine inductance could be utilized. For the designer having machine parameters at his disposal, the determination of armature circuit inductance by the method of Snively and Robinson[1] has been found to be fairly reliable. Use of equation 27 of the present is not too reliable because of the wide variation in values of C_x for different machines.

The authors have indicated a method of including the effect of initial load on the peak value of short-circuit armature current. This is an important contribution since it shows that the effect of initial load on generating machines is to raise the peak armature current. The effect of initial load on motoring machines, on the other hand, is to lower the peak armature current. It has been the practice, in some circles, to ignore initial current and calculate the short-circuit armature current on the basis of zero initial load. Superposition of rated load on a d-c machine, expressed in pu as +1 for generators and −1 for motors, was assumed to be applicable if the no-load peak short-circuit current values were known. The results given in Table VII indicate that such a procedure would give acceptable results; therefore, for rapid calculation this method seems to be justified. Of course, test data on other machines are required to substantiate the method fully.

Mr. O'Connor and Mr. Cybulski have given us a refined method of determining short-circuit performance. They are to be complimented for their contributions.

REFERENCE

1. MEASUREMENT AND CALCULATION OF D-C MACHINE ARMATURE CIRCUIT INDUCTANCE, **H. D. Snively, Paul B. Robinson.** *AIEE Transactions*, vol. 69, pt. II, 1950, pp. 1228–37.

J. P. O'Connor and J. Cybulski: As indicated by Mr. Bewley, the transient plots in Figs. 1 through 6 do not showas close agreement in all cases as might be desired. It should be emphasized, however, that the runs selected for these transient plots are not typical but rather those that show the greatest divergence. In Table III it will be noted that the results in general are good and compare well with the test values. Where the results are poor, as in run 41F, the machine was operating at a speed 20% above rated speed, which is hardly typical of actual operating conditions. The transient plotted in Fig. 3 for run Alc is for a low value of initial voltage and the resulting value of peak short-circuit current is small and equal to the steady-state value. For the applications engineer, interested in selecting circuit breakers, initial conditions that result in a short-circuit current equal in value to the normal steady-state value of short-circuit current (about 3 pu) is of little importance.

We agree with Mr. Bewley that reasonably close agreement between test and calculated values of maximum rates of rise of armature current may be obtained when an appropriate value of armature circuit inductance is used. The values of machine inductance used in the paper were those supplied by the manufacturer. These values were checked using a-c measurements (60 cycles) and found to be in close agreement with the values given by the manufacturers. However, the value given by the manufacturer for M-3 was obviously too low (5 microhenrys). In the paper a value of 2,300 microhenrys obtained by a d-c incremental flux method was used for M-3. A subsequent measurement of machine inductance by the a-c method gave a value of 900 microhenrys. If this latter value had been used for the transient plots (Figs. 5 and 6) better agreement would have resulted. Our experience indicates that values of inductance obtained by 60-cycle a-c measurements give satisfactory results when compared to test values of the maximum rate of rise. It should be emphasized, however, that the calculated or measured value of unsaturated armature circuit inductance does not truly represent the machine inductance under all initial conditions. For example, the effect of initial load on a machine reduces the armature circuit inductance because of saturation effects.

Equation 27 is not an accurate method for calculating armature circuit inductance because of the difficulty in obtaining a reliable value of C_x applicable to a particular class of machines; it was suggested only as an approximate and convenient method when a more accurate value could not be obtained. The ease with which calculations can be made by using this equation whenever design details are unavailable for the computations indicated by Snively and Robinson needs no defense. Further, if the values of inductance as obtained by equation 27 are compared to the values obtained by the Snively and Robinson method for the large number of machines listed in reference 6 of the paper, good agreement is found. This of course is not surprising since the generalized values for C_x are based on the calculated results obtained mainly by the Snively-Robinson method.

It appears to us that for clarity in analysis and discussion two terms which cause considerable confusion in short-circuit work should be clearly defined. These terms are the initial or maximum rate of rise of short-circuit current and time to peak armature current. Measuring the current slope at time zero on an actual oscillogram of a short circuit is a matter of considerable difficulty and it is not surprising that different observers will report slopes that differ considerably. In any event, the initial slope is of little practical value unless it is representative of the average rate of rise up to a particular value of the transient armature current. If the maximum or initial rate of rise of armature current is defined and measured as the average rate of rise from the time of initiation of short circuit up to the time when a fixed fraction of peak armature current (say, one-half) is reached, then this rate of rise would have a definite meaning and would be of practical use. Similarly, the time to peak armature current means little unless it is definite and has practical utility. For example, in a short circuit where the armature current remains near its peak for a relatively long time the time to peak is indefinite and not easily discernible. For this reason it is obvious that the time to reach a fixed fraction of peak armature current (say, nine-tenths) would be more practical and desirable from the point of view of those concerned with circuit-breaker application.

Table XI. Comparison of Exact and Approximate Methods by Short-Circuit Calculations on Five D-C Machines

Rated Conditions, No Loads, Zero External Resistance

No.	Method	Required Basic Constants	Mean 5-Machine Accuracy, %	Machine Accuracy Min.-Max., %	Range of Machine Accuracy, %
1	exact	25	107	92–119*	27
2	approximation of E_rb	26	95	80–112*	32
3	approximation of r_x'	7	119	95–159	64
4	approximation B	6†	118	92–143*	51
5	median curve for r_d' (ref. 6 of the paper)	4†	155	97–248*	151
6	approximation A	4†	127	85–290*	205
7	curve for i_a'	1	117	75–168*	93

* Error on machine M-2.

† A motor requires one additional constant (horsepower).

No. 3 approximation of r_x' requires E_1, I_{a1}, N_1, R_w, E_r, b, and V_c.

No. 4 approximation B requires E_1, I_{a1}, N_1, R_w, R_a, and P.

No. 5 r_d' curves require E_1, I_{a1}, N_1, and a knowledge of pole face windings.

No. 6 approximation A requires E_1, I_{a1}, N_1, and P.

The adding or subtracting of 1 pu armature current for motor or generator respectively to account for the effect of an initial 1 pu load condition (the initial computation for peak short-circuit current being made on the basis of zero initial load) is considered to be a reasonably accurate method of estimating the peak short circuit if it is a zero external resistance short circuit and if the machine is initially at or near its rated speed and voltage. In extrapolating the test values of peak short-circuit current for the initial conditions of no-load rated voltage and rated speed for motors M-1 and M-2 in Table VII an increase of 1 pu was added to the test values obtained at rated load and rated conditions. In most cases the effect of flashing or flashover prevents exact experimental verification of this procedure.

Approximation procedures were developed in this paper in order to enable estimation of peak short-circuit currents whenever design data are limited. After completion of this paper, this work was expanded as estimates of short-circuit current are often desired during design of power systems. The various approximate procedures are compared with test data and the significant results appear in Table XI. Procedures A and B were developed. Briefly, they result from the application of empirical equations extending the approximation of E_rb in combination with the approximation of r_x' in this paper. The end result is that

$$r_d'=\frac{3}{2}(r_w+r_b')$$

approximating r_x' by one-third r_d'.

$$r_b'=\frac{V_b}{E_1}$$

with

$$V_b=\alpha\left(\frac{\epsilon^{\alpha/b}+1}{\epsilon^{\alpha/b}-1}\right)+V_c \text{ volts}$$

(with V_c assumed equal to 2 this expression may be evaluated using Fig. 1 of reference 1 of the paper)

where

$$\alpha=V_a'=(\mathfrak{R}-1)R_aI_{a1} \text{ at rated speed, no load}$$

with

$$\mathfrak{R}=0.67PN_1Q^2 10^{-9}$$

and

$$Q=350\left(\frac{KW_a 10^3}{N_1}\right)^{0.14}$$

ampere conductors per inch of armature periphery. The KW_a term is $E_1I_{a1}/1{,}000$ for a generator, 0.746 horsepower for a motor.

A system for rating all seven methods listed in Table XI with some figure of merit should take into account the number of basic constants, the absolute value of the difference between the mean machine accuracy and 100%, and the range in machine accuracy. One basis would be to assign an equal weight to each one of those statistics. A summation of the numerical value of each of the three statistics for each method would indicate a figure of merit. Assuming that the number of basic constants is most important, the

Table XII. Figure of Merit and Rating of the Methods

No. Method	Equal Weight		Unequal Weight	
	Merit	Rank	Merit	Rank
1	59	1	28.4	6
2	63	2	29.7	7
3	90	4	15.3	3
4	75	3	12.9	2
5	210	6	24.6	4
6	236	7	27.2	5
7	111	5	12.0	1

other two statistics may be given a weight of one-tenth their value. On this basis another figure of merit can be computed. Both of these rating systems were applied to the data of Table XI with the results shown in Table XII. The methods are ranked with the lowest figure of merit the best procedure. With equal weight attached to the statistics, methods 1 and 2 are best with methods 3, 4, and 7 close behind. With the greater weight attached to the number of constants, methods 3, 4, and 7 are equally good and considerably better than all the other methods. Either system for establishing a figure of merit indicates that the recommended approximations at the present time are methods 3, 4, and 7.

We wish to thank Mr. Bewley for his discussion, which emphasizes the important practical reasons for short-circuit calculations and affords us the opportunity to clarify some additional questions not treated in the paper.

Turbine Generator Stator-Winding Temperatures at Various Hydrogen Pressures

J. R. M. ALGER
ASSOCIATE MEMBER AIEE

C. E. KILBOURNE
FELLOW AIEE

D. S. SNELL
MEMBER AIEE

Synopsis: The power industry has for years accepted certain general principles upon which temperature limits are based in the rating of electrical machines and apparatus. AIEE Standard No. 1[1] sets forth the philosophy to be followed in selecting the permissible total temperatures at various locations within machines, dependent upon the class of insulation employed. The particular values of allowable temperatures and the locations at which they shall be measured in cylindrical rotor machines are stated in the American Standards Association Standard (ASA) C50.[2] Both of these standards established their recommendations many years ago, when turbine generators were all air-cooled machines and the industry's experience on the performance and life of such machines was a dominant factor in the selection of allowable temperatures.

In 1937, when turbine generators began to be hydrogen-cooled, the allowable temperatures established for air-cooled machines and the temperature differences between the measurable temperatures and the hot-spot temperatures were tacitly assumed to be correct for the new type of cooling at a hydrogen pressure of 1/2 pound per square inch gauge (psig) in spite of a load increase which was realized with hydrogen cooling. With time, the practice of operating machines at hydrogen pressures higher than 1/2 psig has become quite general. Also for some years a number of machines have had their ratings based on capacities associated with increased hydrogen pressures, and there is no industry standard which recognizes the proper allowable measurable temperatures and temperature rises. Thus there are two conditions, one applying to operating machines whose ratings have been set at 1/2-psig hydrogen for increased capabilities at higher hydrogen pressures, and another, the establishment of proper temperatures for machines rated at higher than 1/2-psig. This indicates a need for increased knowledge on the temperature behavior of turbine generators.

Several years ago, an analysis was presented of the temperatures and temperature rises in turbine generator windings, including both a theoretical approach to the problem of determining the temperature conditions and a comparison of test and calculated results on a particular machine.[3] Since that time the theoretical approach has been refined and additional tests have been made in which actual copper temperatures were measured. This paper presents the results of the last several years' work, adding to the accuracy of the theoretical approach, and giving additional comparisons between tests and calculations. Thus it is intended as a contribution to the increased knowledge needed on the temperature behavior of turbine generators. In addition, since many data are now available on the temperatures existing at 15- and 30-psig, as well as at 1/2-psig hydrogen pressures, certain principles which should apparently underlie the allowable temperatures to accompany higher than 1/2-psig ratings are proposed. These principles are offered as a basis for revision of the ASA C50 standard to take account of the increased temperature drop from hot-spot copper temperature to detector temperature at elevated hydrogen pressures.

THE almost universal use in this country of hydrogen as a cooling medium for large turbine-driven generators, and the expanding use of increased casing pressure to obtain increased outputs from a given size of machine have created a need for an extended understanding of the temperatures and temperature rises which exist throughout such structures. This need is particularly pressing with respect to temperatures in the vicinity of the armature windings because the highest temperature in contact with the insulation, the temperature of the copper of the coils, cannot be directly measured with practical devices available at present. Hence, it is now necessary to establish an allowable rise, by resistance temperature detectors, for various conditions of operation, which will give assurance that the total temperatures, which are not now directly measured, will be satisfactory.

Today the two standards AIEE No. 1 and ASA C50[1,2] exist as guides to establishing the permissible temperatures throughout large machines. The AIEE No. 1 in particular defines the philosophy underlying the proper selection of temperatures. Neither of these standards, however, takes full account of the conditions existing in hydrogen-cooled turbine generators, as both were created before the advent of these machines. Therefore, the problem that exists today concerns the application and extension of these standards to take account of conditions as they are now. In particular, what should be the allowable copper temperature (hottest spot) in the armature windings of these machines; what resistance temperature detector rise should be associated with this hottest spot; how does the use of hydrogen cooling and increased loading associated with 1, 2, and 3 atmospheres absolute casing pressure of the cooling gas affect these temperature limits; and what happens to the ambient cool gas temperatures as casing pressure changes, are questions that need answering today. But first, what is the philosophy expressed by AIEE No. 1 which may be used as a guide and an approach to the problem?

AIEE No. 1 has recently been undergoing a reappraisal and revision to include

---

Paper 55-118, recommended by the AIEE Rotating Machinery Committee and approved by the AIEE Committee on Technical Operations for presentation at the AIEE Winter General Meeting, New York, N. Y., January 31–February 4, 1955. Manuscript submitted October 15, 1954; made available for printing December 7, 1954.

J. R. M. ALGER, C. E. KILBOURNE, and D. S. SNELL are with the General Electric Company, Schenectady, N. Y.

The authors wish to acknowledge the support and encouragement given them by their associates in the General Electric Company who contributed materially to this paper, particularly L. P. Shildneck, C. H. Holley, I. J. Dilts and D. J. Herder for test information generously made available, and R. S. Neblett, H. D. Taylor, E. D. Huntley, B. M. Cain and J. H. Carter for their encouragement in the preparation of the paper and their critical review of its contents.

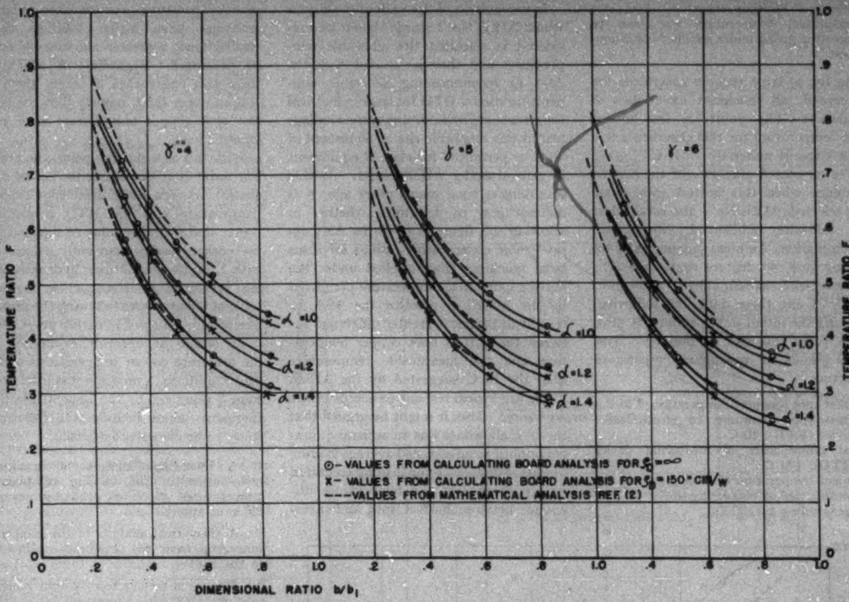

Fig. 1. Values of the ratio F for different values of b/b_1, α and γ for $r=0$, for $\rho_D=150$ C inch per watt, and for $\rho_D=\infty$. From calculating-board analysis, with values from mathematical analysis shown for comparison

knowledge gained in recent years. In its revised form, recently presented, it represents the most modern thinking on the selection of proper temperatures for various service conditions and various classes of insulation used throughout industry. To quote directly:

"This pamphlet. . .deals with the general considerations upon which the temperature rise limits in. . .standards are based. The principles... are intended to serve as a general guide in the preparation of the various standards for specific types of equipment, and it is recognized that variations from the numerical values of temperature rise given are desirable in particular cases. . .it is recognized that rating limits are most useful if they indicate feasible outputs for equipment under usual service conditions. A principal determining factor in establishing temperature rise limits is the thermal endurance of the insulating materials employed, but numerous other factors must be considered."

These other factors include consideration of the following:

"1. Insulation does not fail by immediate breakdown upon arrival at a critical temperature but by gradual deterioration with time. Therefore, the question of how hot an insulation can be operated can be answered only on the basis of how long it is desired to have it last...

2. The electrical strength of insulation cannot be directly correlated with the mechanical strength...physical disintegration [with heat or from other causes] finally results in electrical failure...In view of the important influence of mechanical stresses, thermal expansion and contraction forces impose temperature rise limitations on larger equipment, even though higher temperature rises [for a given class of insulation] have proven to be satisfactory in small machines.

3. Insulation life is dependent to a considerable extent upon the access of oxygen, moisture, dirt or chemicals to the interior of the insulation structure...Particularly favorable results are indicated from the use of chemically inert gases as cooling or protective media.

4. ...the useful life of insulation is [dependent on the] percentage time the equipment is used, and the degree of loading when used.

5. Insulation life depends on the treatment the insulation receives during manufacture and installation...

6. It is also important to realize that the physical deterioration of insulation, under the influence of time and temperature, increases very rapidly with temperature. [Tests on] Class A insulation in air-exposed rotating machines...indicate that roughly 10 to 12 C increase in temperature halves the life. For other classes of insulation [under varying conditions] a similar change in life is observed at varying temperature increments..."

The Standard outlines the following basis for the assignment of temperature limits:

"1. [It is necessary to classify] insulation systems or their component materials in terms of the limiting temperature which can be reasonably assigned to them in continuous service, or for a desired period of expected life.

2. [It is necessary to select] a reasonable value of limiting ambient temperature which, subtracted from the limiting temperature [item 1] gives limiting values of temperature rise.

3. [In order to use temperature indicating instruments, it is necessary to establish] nominal temperature differences between the temperatures read by the various practical temperature measurement methods, and the limiting insulation temperatures at the selected values of limiting temperature rise.

4. [After establishing these temperature

differences] limiting values of observable [measurable] temperature rise [can be assigned] a rating under specified conditions of test."

As far as large turbine generators are concerned, all machines have class *B* insulation. The value of the hottest spot temperature for this classification is "For Class B material. . .130 C."

For air-cooled machines of the sizes in existence when this hottest spot value was selected, AIEE No. 1 also established the following additional temperature bench-marks: Ambient temperature (of cooling gas), 40 degrees centigrade (C); hottest spot measurement allowance, 10 C. Using these data, the following, showing the intent of the standards as of some years ago, can be derived. Here RTD stands for resistance temperature detectors.

Hottest spot (copper) temperature, 130 C.
Hottest spot allowance to measurement device (RTD), 10 C.
Total temperature of measuring device (RTD), 120 C.
Ambient temperature of cooling gas, 40 C.
Allowable rise of measuring device (RTD) over cooling gas, 80 C.

In recognition of the various conditions which AIEE No. 1 stated should be considered in selecting the allowable temperatures and their associated rises, the ASA in recommending allowable temperature rise by RTD for large cylindrical rotor turbine generator armature windings placed this allowable rise at 60 instead of 80 C as permitted for class *B* equipment in general under AIEE No. 1. As this was done a good many years ago, it is difficult now to determine whether in selecting this figure of 60 C the ASA desired more conservative ratings for these large machines than applied under the hottest spot 130 C temperature permitted by the AIEE, or whether the ASA intended to permit a greater difference between the hottest spot copper temperature and the measurable temperature than the 10 C suggested by the AIEE. There are logical reasons to accept either approach. Also, it might be argued that the 10 C allowance was an arbitrary number applied to an assumed average loading condition and, since the loading condition largely determines the temperature difference between hottest spot and measured temperatures, and therefore as large machines have higher loadings than smaller ones, a greater allowance should be permitted. Regardless of which of these two approaches is taken, there is still an upper limit, namely that the hottest spot copper temperature shall not exceed 130 C.

With this as a starting point, the problem today is to determine the actual difference between the hottest spot copper temperature and the RTD measuring point; and with this value established for the various loadings currently associated with 1/2-, 15-, and 30-psig hydrogen casing pressures, to construct a modern table of temperatures following the principles so ably outlined in earlier years.

To obtain an accurate evaluation of the armature copper temperatures under load conditions, a program was instituted some 3 years ago by the General Electric Company which includes the following steps, to be discussed in detail.

1. A theoretical analysis of armature temperature in the vicinity of highest temperatures as determined by several different approaches.
2. A theoretical analysis of the temperature drop from the armature conductors to the RTD's.
3. A series of factory tests on four generators provided with thermocouples on the armature conductors as well as the usual RTD's.
4. Field tests on two of the factory-tested generators in order to evaluate the armature conductor and air-gap temperature rises under actual load conditions and to coordinate these data with the previous theory and the factory data.

This program has permitted some analytical and experimental evaluation of the several factors which determine the temperature rise of the armature winding and the temperature drop from the copper conductors to the temperature detectors.

Conclusions

1. Hottest spot copper temperature is intended by the Standards as the starting point for selecting the temperature rises associated with establishing a rating for a machine. In hydrogen-cooled turbine generator armature windings the hottest spot copper temperature selected should be a constant value, independent of the hydrogen casing pressure selected as a condition of the rating.
2. Theoretical studies, checked by tests, have produced a satisfactory method of determining the temperature difference between the hottest spot copper temperature and the temperature of the practical measuring device, the RTD.
3. These studies and tests indicate that as copper loadings, and therefore losses,

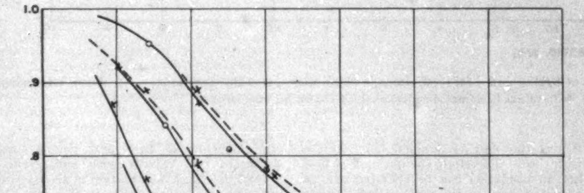

Fig. 2. Values of the ratio F for different values of b/b_1 and γ, for $\alpha=1$, $\rho_D=\infty$, for $r=0$ and $r=0.14$ inch from calculating-board analysis

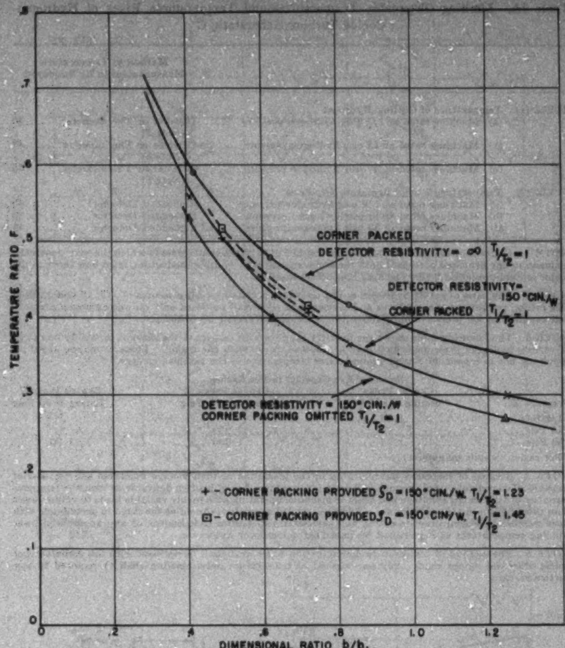

Fig. 3. Values of the ratio F for different values of b/b_1 for $\alpha=1$, $\gamma=5$, $r=0.14$ inch. For corner packing provided and for corner packing omitted. Exposed bar corner and detector surfaces at temperature of tooth iron. For three values of T_1/T_2, for $\rho_D=150$ C inches per watt, and for $\rho_D=\infty$. From calculating-board analysis

increase, which is customary practice as hydrogen casing pressures increase from 1 to 2 or 3 atmospheres, the difference between hottest spot copper temperature and the RTD temperature increases rapidly, approximately as the square of the ratio of the copper loading at the several casing pressures.

4. With the proportions used at present for economical cooler design, and holding constant cooling water conditions, the ambient temperature of the cooling hydrogen rises a few degrees as the machine loading increases at the higher casing pressures.

5. Therefore, considering conclusions 1 to 4, it is obvious that to hold constant hottest spot copper temperatures as loads increase with hydrogen casing pressure, the allowable rise of the RTD over the ambient cooling gas temperature must decrease.

6. From the theory and test data presented here, together with data from other sources, a working group under the sponsorship of the ASA C50 Committee has proposed a table of allowable cold gas and RTD rises at various loadings and hydrogen casing pressures for hydrogen-cooled turbine generators. This paper discusses their proposal, quotes the table, and advocates the acceptance of the temperatures and temperature rises given in the table.

7. With respect to machine performance and the effect of hydrogen pressure on the temperatures existing in various parts of the machine, the following points are of interest:

a. The temperature difference across the ground insulation is the principal factor in determining the differences between hottest copper temperature and RTD. Other temperature to be considered is the temperature distribution throughout the copper inside the insulation, and the thermal field adjacent to the sensitive element of the RTD.

b. The thermal field adjacent to the RTD element can be determined as a function of the geometry and materials used in the slot area.

c. With adequate packing of the space between the corners of the armature bars and the RTD, heat dissipation from the side surfaces of the RTD to the cooling gas has negligible effect on the RTD readings in slots of the width common in turbine generators (approximately 1 inch or more).

d. With adequate packing of the RTD, the temperature drop from copper to RTD, for a given loading in a given machine, is independent of the hydrogen pressure.

e. Both the total copper temperature and the RTD temperature are basically related to the local temperature of the cooling gas in the vicinity of the tooth packet adjacent to the RTD locations in the generator.

f. The hottest spot in the armature winding is located in the top coil side adjacent to the hottest RTD, about halfway up the coil side and is, usually, for loads between 100 and 125 per cent (%) of normal, between 2 and 4 C hotter than the average temperature of the top coil side.

g. The average temperature of the top coil side may be approximately determined from the reading of the adjacent temperature detector, from the equation

$$\text{top coil-side temperature} = \text{RTD temperature} + (1-F)T_3 + \Delta T_c$$

where the values of T_3 and ΔT_c may be calculated, for a given load condition, from the equations given in the derivation of equations in the section "Theoretical Analysis of Armature Temperatures," paragraph 4. The value of F may be determined for the dimensions of the given armature bar, by reference to the curves in Figs. 1, 2, and 3.

1. Proposed Revision of ASA C50 Standards

Several years ago the ASA C50 Committee established a subcommittee to review the present C50-1943 standard for rotating electrical machinery and to recommend such modifications and changes as was deemed necessary to modernize the standard. One of the subjects for revision considered by the subcommittee was Table I of the standard covering permissible temperature rises of various classes of machines, and particular attention was directed to establishing the proper temperatures and temperature rises for hydrogen-cooled turbine generators.

Based on the theoretical and experimental data presented in sections 2 to 5, plus similar data from other sources, the sub-committee prepared a table and associated notes for the proposed revision of C50. Table IA is a part of the proposed table and notes applying to stator winding temperatures at various hydrogen pressures.

The authors wish to express their agreement with the proposed table and to urge

Table IA. Limiting Observable Temperatures and Temperatures Rises of Hydrogen-Cooled Turbine Generators, C

		Method of Temperature Measurement to Be Employed	
ITEM (1)	Temperature of Cooling Hydrogen		
	(a) Machine rated at 1/2 Psig hydrogen pressure	Detector or Thermometer (Note 5)	40
	(b) Machines rated at 15 psig hydrogen pressure	Detector or Thermometer (Note 5)	44
	(c) Machines rated at 30 psig hydrogen pressure	Detector or Thermometer (Note 5)	46
ITEM (2)	Temperature Rise of Armature Windings		
	(a) Machines rated at 1/2 psig hydrogen pressure	Embedded Detector	60
	(b) Machines rated at 15 psig hydrogen pressure	Embedded Detector	50
	(c) Machines rated at 30 psig hydrogen pressure	Embedded Detector	45

NOTE 1 Conventionally cooled machines are considered to be those machines in which the heat, generated by losses in any principal portion of both the armature and field winding conductors, must flow through the major ground insulation before reaching the cooling medium.

NOTE 2 The basis of rating hydrogen cooled machines is stated for H_2 pressures of 1/2, 15 and 30 psig. The rating, guaranteed temperatures and temperature rises shall be based only on one hydrogen pressure and capabilities for pressures only above the rated pressure shall be considered.

NOTE 3 The following table shows the industry practice with respect to the ratio of capability to rating at various hydrogen pressures which may be selected to establish the rating. These ratios are based on supplying not to exceed 90°F inlet cooling water temperature to the machine coolers:

	Ratios of Kva Capacity to Kva Rating		
Pressure X	Cap. at Press. X Rating at 1/2 Psig	Cap. at Press. X Rating at 15 Psig	Cap. at Press X Rating at 30 Psig
1/2 Psig	1.00	*	*
15 Psig	1.15	1.00	*
30 Psig	1.25	1.086	1.00

* For ratios, consult manufacturer.

NOTE 4 Because of increased thermal drop in the insulation of high voltage machines and because of mechanical considerations of thermal expansion in large machines, it is often desirable to limit the temperature rises of large or high voltage machines or machines operating with highly variable loads to values lower than those shown in the above table. Hydrogen cooled generators should be operated in accordance with their selected hydrogen pressure rating and associated capabilities independent of any apparently lower winding temperatures as determined by imbedded detectors or resistance.

NOTE 5 The method of temperature determination to be used shall be optional with the manufacturer unless otherwise agreed upon. Only one method of temperature determination shall be required in any particular case.

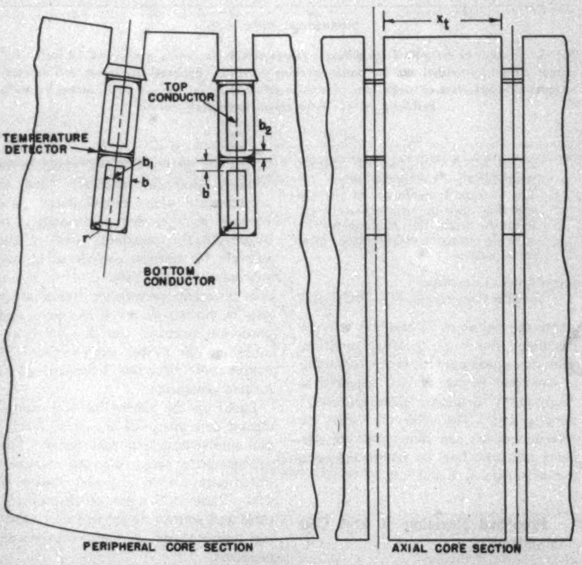

Fig. 4. Sketch of slot region and longitudinal section of a lamination package in a generator stator

its adoption. In interpreting and applying the data from this table to particular machines it should be noted that the values of limiting temperatures and temperature rises in any standard are the highest values permissible on any machine of the class, size, and type covered by the standard, and do not necessarily reflect proper operating procedures for all machines covered by the standard. Particular attention should be paid to note 4 where it is pointed out that temperatures and temperature rises lower than the values given in the standard may be advisable for certain large or high voltage, or variable load units. Especially in these cases, but also for hydrogen-cooled machines as a whole, safe operating practice should load the machines in accordance with their ratings and/or capabilities in kw, power factor (pf) and kva at various hydrogen-casing pressures. In these cases temperature rises lower than the maximum allowed in other cases covered by the standards can be established by tests in the user's plant, and if desirable these lower values can be used as guides to the performance of the unit.

2. Theoretical Analysis of Armature Temperatures

USING THE D-C CALCULATING BOARD

With generators using the multiple radial system of stator ventilation the hottest part of the armature winding is in the core discharge section nearest the center of the generator. Since the distribution of gas flow to the several vent ducts in a given section of the stator is fairly uniform, and since axial heat flow along the conductors may be accounted for in the calculation, an analysis of the heating of the armature winding and iron may be conveniently made through consideration of a unit section of the stator in the center discharge section, comprising a single slot pitch circumferentially and a single vent duct pitch axially. A sketch of a unit stator section is illustrated in Fig. 4. An analysis of the temperature rise of the armature conductors and iron above the temperature of the gas entering the radial vent ducts, for different conditions of load and hydrogen pressures, was made through use of the d-c calculating board. In this analysis the unit section shown in Fig. 4 was considered as represented by a network of thermal resistances as illustrated in Fig. 5. The losses in the unit section were assumed to be concentrated at various points as shown. On the d-c board the various thermal resistances were represented by ohmic resistances, the losses in the various sec-

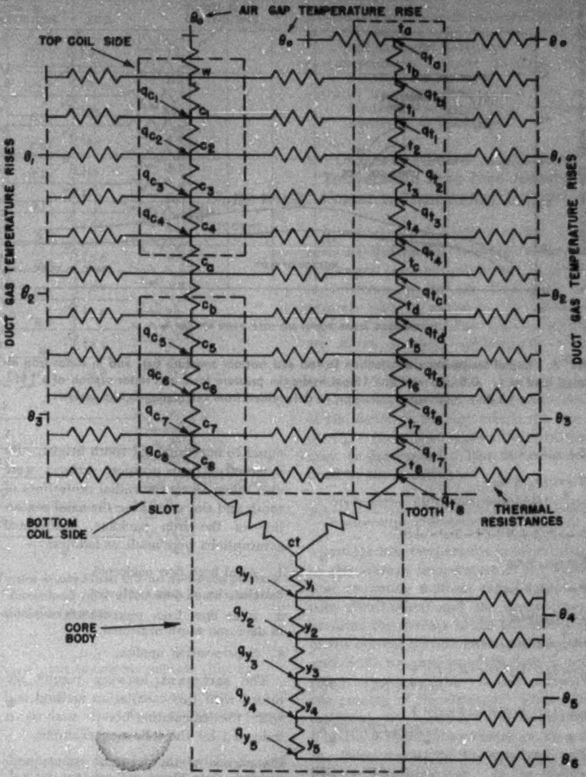
AIR GAP TEMPERATURE RISE
θ_0
TOP COIL SIDE
w
q_{c_1} c_1 q_{c_2} c_2 q_{c_3} c_3 q_{c_4} c_4 c_a c_b q_{c_5} c_5 q_{c_6} c_6 q_{c_7} c_7 q_{c_8} c_8
t_a q_{t_a} t_b q_{t_b} t_1 q_{t_1} t_2 q_{t_2} t_3 q_{t_3} t_4 q_{t_4} t_c q_{t_c} t_d q_{t_d} t_5 q_{t_5} t_6 q_{t_6} t_7 q_{t_7} t_8 q_{t_8}
θ_1
θ_2
θ_3
θ_4
θ_5
θ_6
DUCT GAS TEMPERATURE RISES
SLOT
TOOTH
THERMAL RESISTANCES
BOTTOM COIL SIDE
ct
q_{y_1} y_1 q_{y_2} y_2 q_{y_3} y_3 q_{y_4} y_4 q_{y_5} y_5
CORE BODY

Fig. 5. Thermal-electric circuit or one armature slot and tooth pitch and for a single core package, used in calculating-board analysis

tions as current flows, and temperature drops as voltage drops. The resistances were evaluated for one-quarter of a slot package, assuming no heat flow across the radial center lines of the slot and tooth and the axial centerline of the package. For the portion of the system where distributed heat flow was obtained, the thermal resistances were calculated on the assumption of parabolic temperature distribution. One-dimensional heat flow was assumed and the principle of superposition applied. Axial heat flow was not considered. Temperature rise of the gas in passing along the ducts was included. For the insulation in the coil corner, a separate analysis for the determination of the thermal resistance is shown in Appendix I.

In the calculating-board analysis, the temperature rises of the armature copper and iron were determined with respect to the temperature of the gas entering the radial vent ducts. This is the temperature of the gas in the air gap opposite the core discharge section. A method (not included here) for calculating the temperature rise of the gas in the air gap has been developed. The gap gas rise at the center of the generator is usually higher than the total gas rise through the generator, because of the rotor I^2R losses which are given up to the air gap in the center portion of the machine.

The results of the calculating board analyses are given in Figs. 6, 7, and 8. The temperature rises of the armature coil sides and iron at different radial positions, as determined from this study, for operation at rated load at 1/2- and 15-pound per square inch (psi) hydrogen pressure, are shown in Fig. 6. The average temperature rise of the top coil side is shown to be higher than that of bottom coil side, as a result of the higher eddy current losses in the top coil side. Fig. 7 gives the calculated radial temperature distribution in the two coil sides at two loads at 1/2-psi hydrogen pressure for two values of insulation thermal resistivity, corresponding to the maximum and minimum values expected to obtain in practice. Laboratory tests have indicated that the thermal resistivity of the ground insulation of a standard mica-insulated armature bar is determined largely by the density of the insulation when the bar is in final condition in the slot. It has been shown by test that the apparent thermal resistivity of the insulation may vary considerably, being as much as 170% of the dense insulation resistivity if proper care is not exercised in assembling and fitting the bar to the slot. The influence of duct gas rise on the winding temperature is also shown in Fig. 7, and is observed to be small. The calculated division of heat flow in the coil sides and iron, for operation at rated load of 1/2-psi hydrogen pressure, is shown in Fig. 8. It is observed that the major portion of the copper losses passes into the tooth iron and is dissipated from the duct iron surfaces. Also, some of the loss in the bottom coil side passes into the core body while some of the core body loss passes into the tooth. From this analysis and others for different loads and hydrogen pressures, it is evident that for closely approximating the winding temperature rises under load, the plane of division of radial heat flow in the tooth may be assumed to lie at a distance inward from the tooth root approximately equal to one-third the tooth height.

Equivalent Thermal Circuit

For convenience in predetermining the stator temperatures, equations for the numerical calculation of the temperature rises of the armature winding and iron above air gap temperature for a unit stator section were derived as shown in the following.

Calculation of Copper and Iron Temperature Rises Above Cold Gas Temperature for Thermal Circuit of Fig. 9

$$R_1=\frac{r_{bx}r_{by}}{r_{bx}+r_{by}}$$

$$r_3=\frac{r_{tx}r_{ty}}{r_{tx}+r_{ty}}$$

$$r_5=\frac{r_{cd}r_{cg}}{r_{cd}+r_{cg}}$$

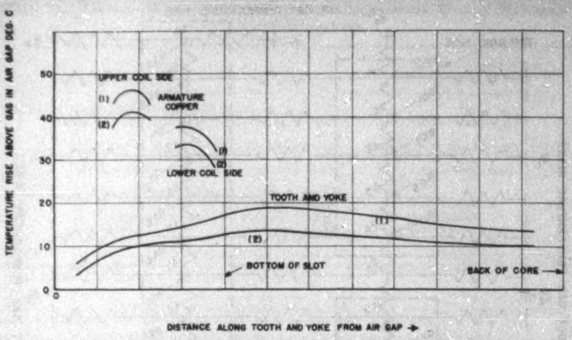

Fig. 6. Radial temperature distribution in top and bottom armature bars and in stator iron at rated load at 1. 0.5-psi; and 2. 15-psi hydrogen pressure for a unit stator section of a 111-mva 13.8-kv 3,600-rpm generator, as determined from calculating-board analysis

$A = r_3 + r_4 + r_5$

$B = r_3 + r_4' + r_{cd}$

$C = r_3 + R_1 + R_2$

$D = r_3^2(A+B+C) - 2r_3^3 - ABC$

$E = r_4 q_{ct} + r_3 q$

$F = r_4' q_{cb} + r_3 q$

$G = R_2 q_1 + r_3 q$

$q = q_b + q_t + q_{ct} + q_{cb}$

$q_1 = (1/D)\{r_3^2[G-(E+F)] + r_3(AF+BE) - ABG\}$

$q_5 = (1/D)\{r_3^2[E-(F+G)] + r_3(BG+CF) - BCE\}$

$q_7 = (1/D)\{r_3^2[F-(E+G)] + r_3(AG+CE) - ACF\}$

$q_3 = q - q_1 - (q_5 + q_7)$

$t_{ct} = r_5 q_5 + \theta_0$

$t_{cb} = r_{cd} q_7 + \theta_0$

$t_t = r_3 q_3 + \theta_0$

$t_b = R_1 q_1 + \theta_0$

$T_1 = t_{ct} - t_t$

$T_2 = t_{cb} - t_t$

$T_3 = 0.5(T_1 + T_2)$

$\Delta T_c = 0.5(t_{ct} - t_{cb})$

These equations are based upon the equivalent thermal circuit of Fig. 9. Mean values for the temperature rises of the coil sides, tooth, and core are assumed, and for the parts in which the heat flow is distributed, parabolic temperature distribution has been assumed. The surface of division for the radial heat flow in the iron has been assumed to be located inward from the tooth root by an amount equal to one-third the tooth height. By symmetry, heat division surfaces were also taken along the radial centerlines of tooth and slot and along the axial centerline of the iron package. Additional assumptions were made as follows:

1. Axial heat flow neglected.
2. Gas rise in duct neglected.
3. Heat flow from temperature detector to duct and tooth neglected.
4. Superposition applies.

The agreement between results obtained with this calculation method and with the calculating-board analysis is indicated by the following example.

Comparison of the armature copper temperature rises above air gap gas, as calculated by several methods for a 111-mva 13.8-kv 3,600-rpm generator operating at rated load at 1/2-psi hydrogen pressure, is as follows:

Average slot copper by method of reference 3, 38.5 C.

Top coil-side copper: D-c board analysis (average), 44.0 C; method described in section 2 ("Equivalent Thermal Circuit"), 40.7 C.

Bottom coil-side copper: D-c board analysis (average), 36.0 C; same method, 35.1 C.

For the calculation of the temperature rise of the bottom coil side the numerical calculation method checks the calculating board analysis closely; for the top coil side the agreement is not as close. However, from a number of calculation examples using both methods, it has been determined that the calculation method based on the equivalent circuit of Fig. 9 may be calibrated to yield results which are reasonably satisfactory.

NOMENCLATURE

Dimensions (Refer to Fig. 4)

b = thickness of coil-side insulation, including clearance space between coil side and slot wall
b' = thickness of ground insulation at top and bottom of armature bar
b_1 = over-all copper width inside insulation
b_2 = radial distance from edge of copper to center of temperature detector
r = outside radius of corner of armature bar
X_t = axial length of core package
α = ratio b_2/b

Equivalent Thermal Resistances

r_4 = path from mean copper temperature to slot wall, top coil-side
r_4' = path from mean copper temperature to slot wall, bottom coil-side
r_{bx} = path from mean core body temperature to vent duct gas (axial)
r_{by} = path from mean core body temperature to gas at back of core (radial)
r_{cd} = path from mean copper temperature to vent duct gas (axial), one coil side
r_{cg} = path from mean copper temperature to air gap (radial), top coil side
r_{tz} = path from mean tooth temperature to vent duct gas (axial)

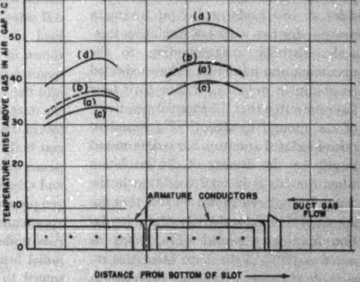

Fig. 7. Radial temperature distribution in top and bottom armature bars at normal and 110% of normal load at 0.5-psi hydrogen pressure, for a unit stator section of a 111-mva 13.8-kv 3,600-rpm generator for two values of insulation thermal resistivity (in % of value for maximum insulation density), as determined from calculating-board analysis

A—1.0 load 125% resis; duct gas rise = 0
B—1.0 load 125% resis; duct gas rise ≠ 0
C—1.0 load 100% resis; duct gas rise ≠ 0
D—1.1 load 125% resis; duct gas rise ≠ 0

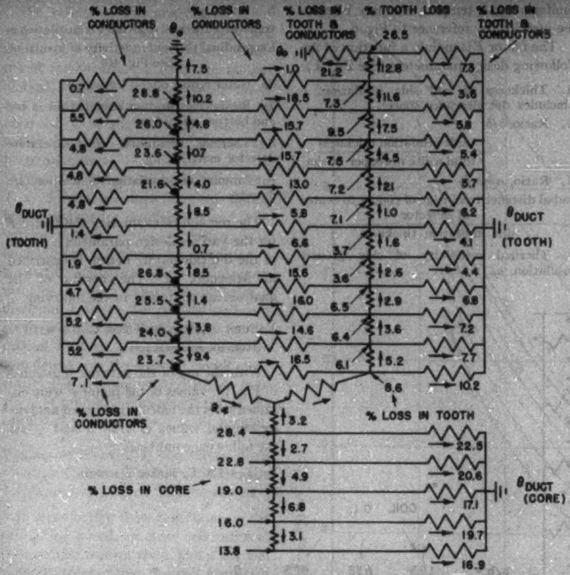
% LOSS IN CONDUCTORS
θ_0
% LOSS IN CONDUCTORS
% LOSS IN TOOTH & CONDUCTORS
% TOOTH LOSS
% LOSS IN TOOTH & CONDUCTORS
26.5
θ_0
7.5
1.0
21.2
12.8
7.3
0.7
28.8
10.2
18.5
7.3
11.6
3.6
5.5
26.0
4.8
15.7
9.5
7.5
5.8
4.8
23.6
0.7
15.7
7.6
4.5
5.4
4.8
21.6
4.0
13.0
7.2
21
5.7
4.8
8.5
5.8
7.1
1.0
6.2
θ_{DUCT}
(TOOTH)
1.4
0.7
6.6
3.7
1.6
4.1
θ_{DUCT}
(TOOTH)
1.9
26.8
8.5
15.6
3.6
2.6
4.4
4.7
25.5
1.4
16.0
6.5
2.9
6.8
5.2
24.0
3.8
14.6
6.4
3.6
7.2
5.2
23.7
9.4
16.5
6.1
5.2
7.7
7.1
10.2
8.6
% LOSS IN CONDUCTORS
9.4
3.2
% LOSS IN TOOTH
26.4
22.5
2.7
22.8
20.6
4.9
% LOSS IN CORE
19.0
θ_{DUCT}
(CORE)
17.1
6.8
16.0
19.7
3.1
13.8
16.9

Fig. 8. Distribution of heat flow in unit section of stator at rated load 0.5-psi hydrogen pressure for a 111-mva 13.8-kv 3600-rpm generator, as determined from calculating-board analysis. Flows expressed in% of total heat input

r_{ty}=path from mean tooth temperature to air gap (radial)

R_1=path from mean core body temperature to vent duct and core back gas (axial-radial)

R_2=path from mean tooth temperature to mean core temperature (radial)

R=armature bar corner resistance (see Fig. 10)

Heat Inputs

q_{c1}, q_{c2}, etc.=inputs to conductors (Fig. 5)

q_{t1}, q_{t2}, etc.=inputs to tooth (Fig. 5)

q_{y1}, q_{y2}, etc.=inputs to core body (Fig. 5)

q_b=input to core body (Fig. 9)

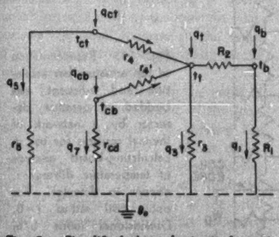
q_{ct}
t_{ct}
r_4
r_4'
q_t
R_2
q_b
t_t
t_b
q_{cb}
t_{cb}
q_5
r_5
q_7
r_{cd}
q_3
r_3
q_1
R_1
θ_0

Fig. 9. Simplified thermal circuit for unit section of stator for use in calculating temperature rises

q_{cb}=input to bottom coil-side (Fig. 9)

q_{ct}=input to top coil-side (Fig. 9)

q_t=input to tooth (Fig. 9)

q_1, q_3, q_5, q_7=heat flows in thermal circuit of Fig. 9

Temperature Rises (All Except T_1, T_2, and T_3 Are Above Cold Gas Temperature)

c_1, c_2, etc.=conductor temperature rises (Fig. 5)

t_1, t_2, etc.=tooth temperature rises (Fig. 5)

c_t=tooth root temperature rise (Fig. 5)

w=wedge temperature rise (Fig. 5)

Y_1, Y_2, etc.=core body temperature rises (Fig. 5)

θ_1, θ_2, etc.=duct gas temperature rises (Fig. 5)

θ_0=air gap gas temperature rise (Figs. 5 and 9)

t_b=average rise, core body (Fig. 9)

t_{cb}=average rise, bottom coil-side (Fig. 9)

t_{ct}=average rise, top coil-side (Fig. 9)

t_t=average rise, tooth iron (Fig. 9)

T_1=average temperature rise of top coil side above average tooth iron temperature

T_2=average temperature rise of bottom coil side above average tooth iron temperature

T_3=average temperature drop in coil-side insulation

ΔT_c=difference between average temperature rise of top coil side and average of temperature rises of top and bottom coil sides

Thermal Resistivities

ρ_i=coil side insulation (including resistivity of clearance space between coil side and slot wall) resistivity

ρ_D=temperature detector material resistivity

γ=ratio, transverse thermal resistivity of insulation ρ_i/longitudinal thermal resistivity of insulation

3. Calculating-Board Analysis of Temperature Drop from Armature Copper to Temperature Detector

A mathematical analysis of the temperature differential between armature copper and temperature detector is given in reference 4. In the following, an analysis made by use of the d-c calculating board is described, the results of which are shown to agree substantially with those of the mathematical analysis. Both analysis had for their objective the evaluation, for various design parameters, of the factor F, through which the temperature drop from copper to detector may be determined. This factor is defined by the equation

$$F=\frac{\text{temperature difference, detector to iron}}{\text{temperature difference, copper to iron}}$$

where the iron temperature is assumed to be the average temperature of the tooth iron (assuming uniform radial temperature distribution) and the copper temperature the average of the temperatures of the bottom portion of the top coil side and of the top portion of the bottom coil side, the portions which mainly influence the reading of the detector. From this definition, the required temperature differential is temperature difference, copper to detector$=(1-F)\times$temperature difference, copper to iron. In the derivation of the factor F, in both the mathematical and the calculating board analyses both the tooth iron and the top and bottom coil sides were assumed to be at uni-

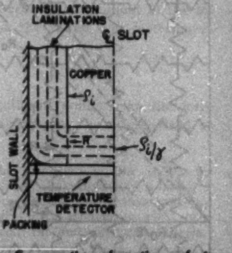
INSULATION LAMINATIONS
℄ SLOT
COPPER
ρ_i
R
ρ_i/γ
SLOT WALL
TEMPERATURE DETECTOR
PACKING

Fig. 10. Cross section of portion of top armature coil-side with corner resistance R, and transverse and longitudinal insulation thermal resistivities indicated

form temperatures. Actually, the radial temperature distribution in the coil sides and the tooth is nonuniform, as shown by Figs. 6 and 7. However, since the reading of the temperature detector is influenced mainly by the copper temperatures in the bottom portion of the top coil side and in the top portion of the bottom coil side and, since the average of these two temperatures was in most of the cases analyzed not greatly different from the average of the mean temperatures of the two coil-sides, the factor F can be equally well defined with reference to the latter temperature. The assumption of a uniform tooth temperature may likewise be justified, by reference to Fig. 6.

The factor F is mainly a function of the following design parameters (See Fig. 4.):

1. Thickness of coil side insulation, b (includes slot clearance space).
2. Ratio, b/b_1
$$=\frac{\text{side insulation thickness}}{\text{total width of copper in slot}}$$
3. Ratio, $\alpha=b_2/b$
$$=\frac{\text{radial distance from edge of copper to center of detector}}{\text{side insulation thickness}}$$
4. Thermal resistivity of side ground insulation, ρ_t.
5. Ratio, $\gamma=$
$$\frac{\text{transverse thermal resistivity of insulation } \rho_t}{\text{longitudinal thermal resistivity of insulation}}$$
(See Fig. 10).
6. Outer radius of coil corners, r.
7. Radial temperature distribution in top and bottom coil sides.
8. Thermal resistivity of temperature detector material, ρ_D.
9. Amount of ventilation of temperature detector.

The method of evaluating the factor F for the various design parameters, by use of the d-c calculating board, is described in Appendix II. The results of the analysis are contained in the following.

Values of Factor F for Coils with Corner Radius r=0

With the use of the network illustrated in Fig. 11, values of the factor F were obtained from the calculating-board analysis for several values of b/b_1, α and γ, for the following conditions:

1. $\rho_D=150$ C, inches per watt
2. $\rho_D=\infty$

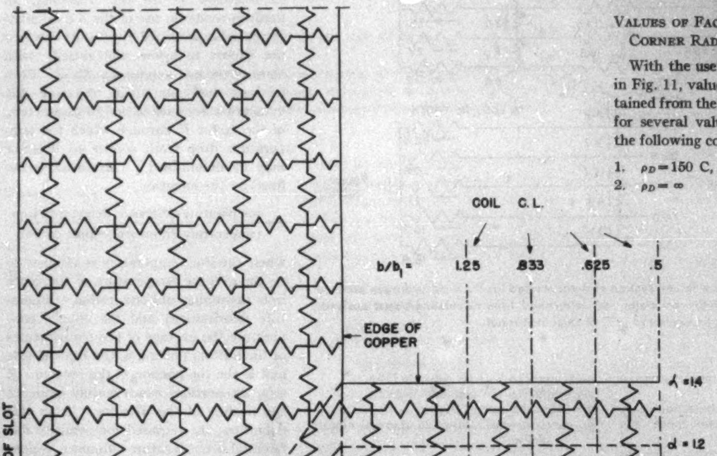

Fig. 11. Representation of top armature bar insulation and adjacent embedded temperature detector by a network of thermal resistors for use in calculating-board analysis of temperature difference, copper to detector. For outer coil radius r=0. Dimensional ratios b/b₁ and α variable. For b/b₁ < 0.5, network is extended to right

The results of this analysis for $\alpha=1$ and $\gamma=1$ to $\gamma=8$, for condition 2, are shown in Fig. 12. The values determined for condition 2 from the mathematical analysis[4] for $\alpha=1$ and $\gamma=4$, 5, and 6, are shown for comparison and are observed to be slightly higher than the values obtained from the calculating-board analysis.

Figs. 13 and 1 give values of the factor F as determined from the calculating board analysis for conditions 1 and 2 for various values of b/b_1, α, and γ, with values from reference[4] for condition 2 shown for comparison. Substantial agreement is shown between the values of F determined from the calculating-board study and the values from the mathematical analysis. Placing the temperature detector in the thermal circuit, (i.e., changing its thermal resistivity from ∞ to 150 C in per watt) is shown to reduce the calculated value of F by a small amount.

VALUES OF FACTOR F FOR COILS WITH OUTER CORNER RADIUS, $r \neq 0$ AND FOR UNEQUAL COIL SIDE TEMPERATURES

In representing these conditions on the calculating board, an outer coil radius of $r=0.14$ inch was assumed, and a thermal network representing the coil insulation for the two coil sides was used. Also, calculations were made for the following conditions:

1. The space bounded by outer corner surface, slot wall and detector sealed with a packing.
2. Corner packing omitted and the exposed coil and detector surfaces maintained at the temperature of the slot wall.

Condition 2 corresponds to an intensive ventilation of the temperature detector.

Fig. 2 gives values of F for various values of b/b_1 and γ as determined from the calculating-board analysis for $\alpha=1$ and $T_1/T_2=1$ (where T_1 and T_2 are the temperature rises of top and bottom coil sides above iron temperature respectively) for coils with $r=0.14$ with corner space packed, with values of F determined for coils with $r=0$ shown for comparison. A small increase in the value of F resulting from the rounding of the coil corners is indicated.

Fig. 3 shows the effect on the value of F of an intensive ventilation of the temperature detector, also of varying the ratio T_1/T_2 from 1.0 to 1.45, as determined from a calculating-board analysis for $\alpha=1$, $\gamma=5$. It is shown that the value of F increases slightly as the ratio T_1/T_2 is increased, and that intensive ventilation of the coil corner and of the detector edges reduces the value of F by several per cent.

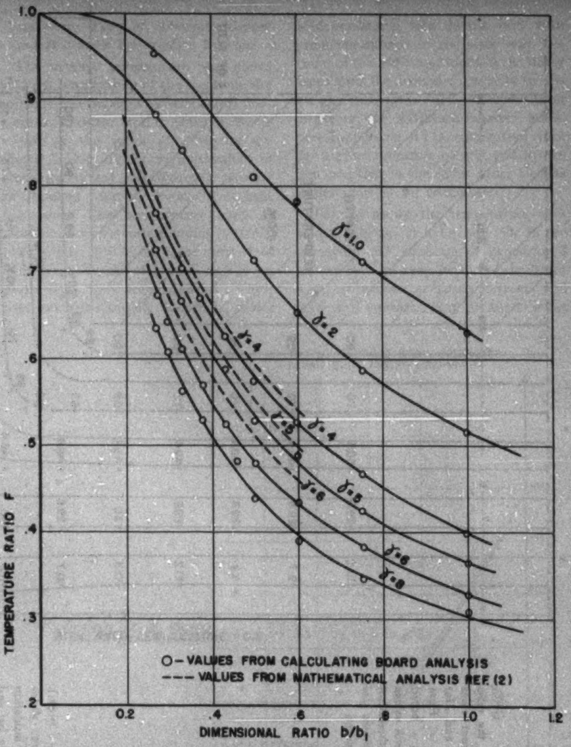

Fig. 12. Values of the ratio F for different values of b/b_1 and γ, for $\alpha=1$. For $r=0$, $\rho_D=\infty$. From calculating-board analysis, with values from mathematical analysis shown for comparison

TEMPERATURE DISTRIBUTION IN COIL INSULATION AND DETECTOR

The temperature distribution in the coil insulation and along the width of the temperature detector as determined from a calculation-board analysis for a coil with rounded corners, with corner packing provided, for assigned values of α, γ, b/b_1, and T_1/T_2 is shown in Fig. 14. In Fig. 15 the radial temperature distribution in the coil insulation along the slot centerline has been plotted, as has the temperature distribution along the detector width, for the same values of the several design parameters as in the foregoing. This has been done for corner packing provided, and for corner packing omitted, detector ventilated. From the temperature curves shown at the bottom of Fig. 15 it may be deduced that the temperature-detector element is sufficiently narrow in width (0.09 inch) to read the peak of the temperature curve, which is on the slot centerline. From the upper curves in Fig. 15 it is shown that the temperature gradient in the insulation on the radial slot centerline is nonlinear.

RESULTS

The significant points from the foregoing analysis may be summarized as follows:

1. For the condition of the coil outer corner radii = 0, the values of the factor F obtained from the calculating-board analysis were in substantial agreement with those obtained from the mathematical analysis.
2. If adequate packing of the coil corners is provided so that the effect of detector ventilation on the detector reading may be neglected, the curves given in Fig. 1 may be used with fair accuracy to predict the

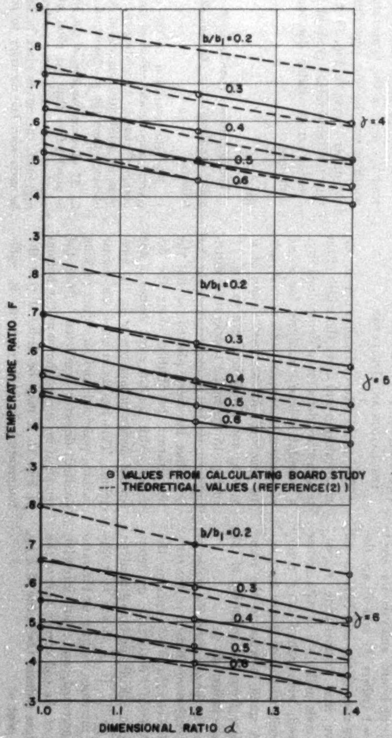

Fig. 13 (left). Values of the ratio F for different values of b/b_1, γ and α for $r=0$, $\rho_D=\infty$. From calculating - board analysis, with values from mathematical analysis shown for comparison

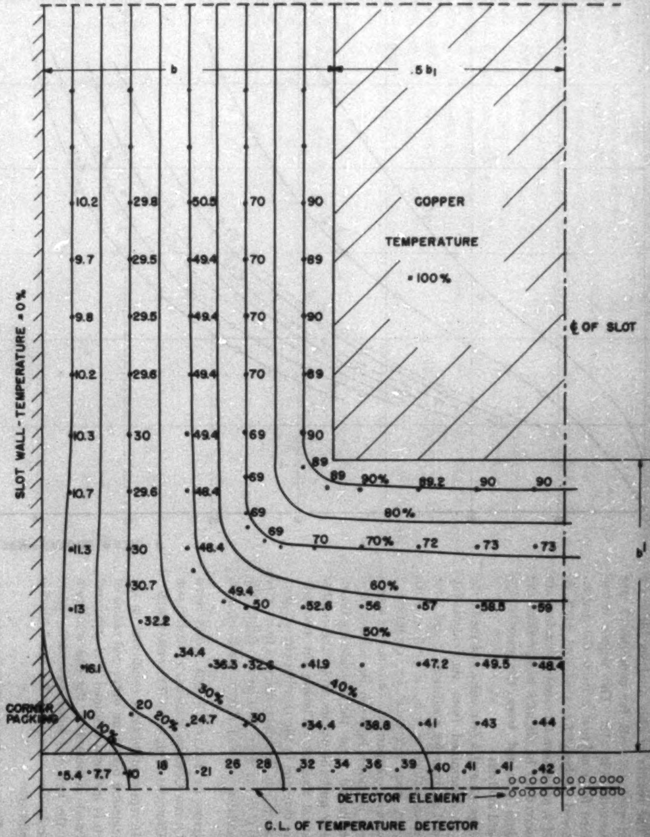
b
.5 b₁
COPPER
TEMPERATURE
=100%
℄ OF SLOT
SLOT WALL-TEMPERATURE =0%
b¹
90%
80%
70%
60%
50%
40%
30%
20%
10%
CORNER PACKING
DETECTOR ELEMENT
C.L. OF TEMPERATURE DETECTOR

Fig. 14 (right). Temperature distribution in insulation of armature bar and in temperature detector for $r=0.14$ inch, $b/b_1=0.625$, $\alpha=1$ $\gamma=5$, $T_1/T_2=1$, $\rho_D=150$ C inches per watt. Corner packing provided. Numbers represent % temperature difference, copper to tooth iron. From calculating-board analysis difference between the average of the two coil-side temperatures and the detector temperature.

3. Correction of the values of F given by the curves of Fig. 1, to take account of rounding of the coil corners, of unequal temperatures in the two coil sides, and of ventilation of the detector, may be made by reference to the curves of Figs. 2 and 3.

4. Factory Tests on Four Generators

During the past 2 years, factory heat run tests have been conducted on four 3,600-rpm hydrogen-cooled generators provided with thermocouples on the copper of the armature bars, by means of which the copper temperatures in operation at various currents and at various hydrogen pressures were determined. The ratings of the four generators (at 1/2-psi hydrogen pressure) were as follows:

Generator no. 1,	18.75 mva,	0.80 pf,	13.8 kv
Generator no. 2,	100 mva,	0.85 pf,	14.4 kv
Generator no. 3,	105.8 mva,	0.85 pf,	14.4 kv
Generator no. 4,	129 mva,	0.85 pf,	20 kv

Generator no. 1 was tested at rated pf on the load test stand at one of the General Electric plants; the other three generators were each tested under conditions of zero excitation, open circuit and short circuit.

TEST ARRANGEMENT

A diagram showing the locations of the various temperature-detecting devices employed in the tests on generator 4 is given in Fig. 16. Similar arrangements were provided for the tests on the other three generators, although the ventilating-circuit arrangements varied among the machines. The thermocouples on the armature-winding copper were located on three top neutral bars at several stations along the length of the stator, the thermocouples in each group being spaced about 2 inches apart axially, and positioned radially as shown in the inset in Fig. 16. Thermocouples molded into strips of laminac, and resistance temperature detectors attached to specially designed slot wedges, were provided for measuring temperatures in the air gap. Tooth iron temperatures were measured with thermocouples located on the axial center line and at the outer edges of the iron packages, at about one-third of the way up the tooth from the tip.

TEST RESULTS

The principal results of the tests on the four generators are summarized in Figs. 17 to 24. These results are briefly discussed in the following.

Temperature Rises of Armature Copper and Resistance Temperature Detectors

The average temperature rises above cold gas temperature of the top armature coil-side and the adjacent embedded temperature detector, in the center discharge section of the stator of generator are shown in Fig. 17 for various values of armature current and hydrogen pressure as obtained from the short-circuit heat run tests. The temperature rises at armature currents corresponding to 100%, 115%, and 125% of the rated current, at hydrogen pressures of 1/2, 15 and 30 psi respectively, have been indicated. These rises are substantially less than under load conditions, and do not vary with armature current in the same way, because of the additional losses in the stator teeth and the increased gas rise in the air gap from rotor I^2R losses under load. However, the difference between armature copper and RTD temperature rises, for a given armature current and hydrogen pressure, is the same under load as under short-circuit conditions.

Fig. 18 shows the temperature rises above cold gas of a top coil side in the armature end windings of generator 3 at two stations near the end of the stator core, at various armature currents and hydrogen pressures, from the short-circuit

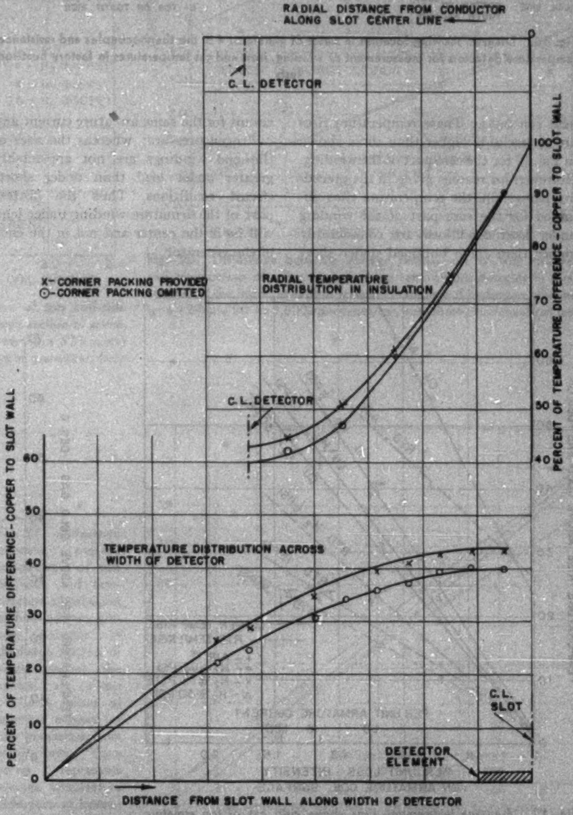

Fig. 15. Temperature distribution in armature bar insulation along radial slot center line, and across width of temperature detector, for $r = 0.14$ inch, $b/b_1 = 0.625$, $\alpha = 1$, $\gamma = 5$, $T_1/T_2 = 1$, $\rho_D = 150$ C inch per watt; for corner packing provided; and for corner packing omitted, exposed bar corner and detector surfaces at iron temperature. From calculating-board analysis

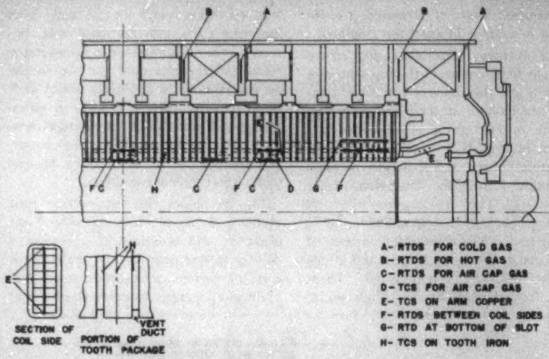

Fig. 16. Diagram showing location in stator of generator 4 of the thermocouples and resistance temperature detectors for measurement of winding, iron and gas temperatures in factory heat-run tests

heat run tests. These temperature rises are appreciably higher than those shown in Fig. 17 for the core part of the winding. However, for reasons given in the preceding paragraph, the temperature rises obtained for the core part of the winding under load conditions are considerably higher than those obtained under short circuit for the same armature current and hydrogen pressure; whereas the rises of the end windings are not appreciably greater under load than under short-circuit conditions. Thus the hottest part of the armature winding under load will be in the center and not in the ends of the generator.

Temperature Drop Through Armature Bar Insulation

The temperature drop from the average copper temperature in the top armature coil side to the average tooth iron temperature, representing the thermal drop in the top bar insulation, is shown in Fig. 19 as obtained from short-circuit heat runs on generators 3 and 4 at various armature currents and hydrogen pressures, from measurements made in the center discharge section of the core. This temperature drop is shown to be independent of the hydrogen pressure. With the use of the calculated a-c I^2R loss in the top bar, and assuming a division of losses to tooth and vent duct as calculated using the equations (given in the section "Theoretical Analysis of Armature Temperatures," paragraph 4) the thermal resistivities of the top bar insulation for the two generators were determined to be 110 and 127% respectively, of the value for bar insulation of maximum density as determined by laboratory tests. For generators 1 and 2 the thermal resistivities of the top bar insulation were similarly found to be 107 and 130% respectively, of the latter value. (In calculating the insulation thermal resistivity for generators 2 and 4, an axial heat flow in the top bar equal to 5% of the generated loss was assumed, as estimated from the curves of axial tem-

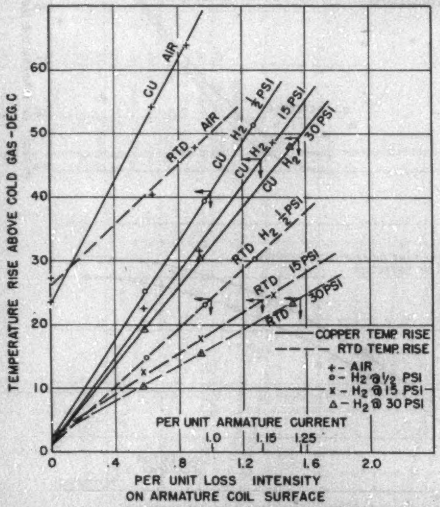

Fig. 17. Average temperature rises above cold gas of top armature coil side and adjacent embedded temperature detector in center discharge section of stator of 105.8-mva 14.4-kv 3,600-rpm generator, at various armature currents and hydrogen pressures from short-circuit heat-run tests

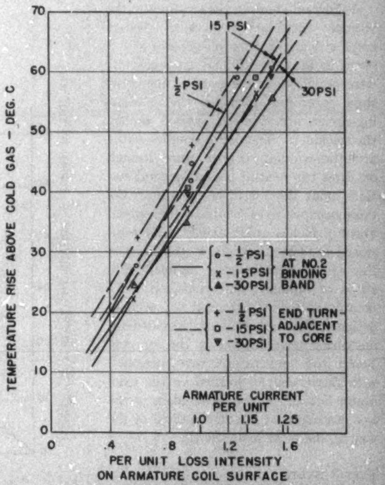

Fig. 18. Average temperature rises above cold gas of top armature coil-side at two stations in end winding of a 105.8-mva 14.4-kv 3,600-rpm generator at various armature currents and hydrogen pressures, from short-circuit heat-run tests

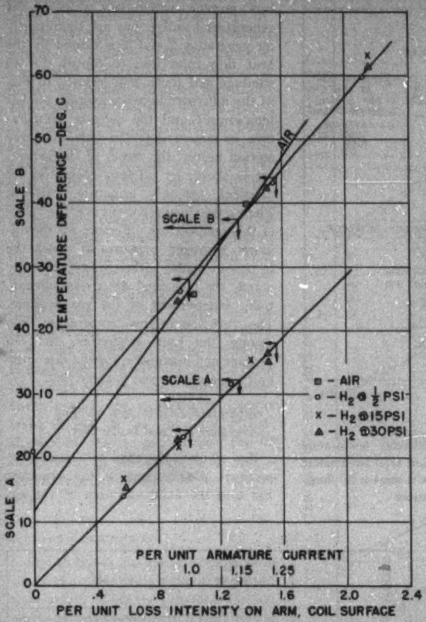

Fig. 19. Difference between average temperature of top coil-side and average tooth-iron temperature in center discharge section of stator, at various armature currents and hydrogen pressures, for a 105.8-mva 14.4-kv 3,600-rpm and a 129-mva 20-kv 3,600-rpm generator, from short-circuit heat-run tests

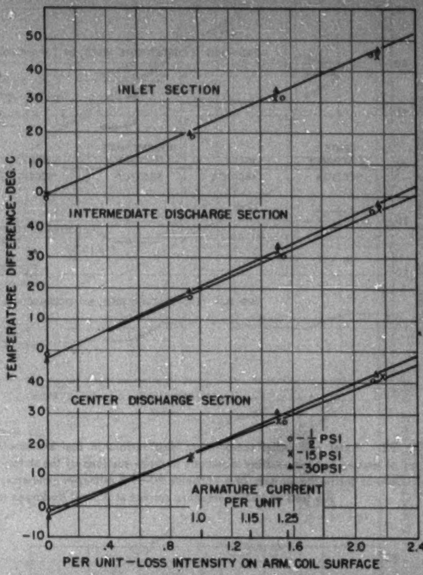

Fig. 20. Difference between average temperature of top coil-side and temperature of adjacent embedded temperature detector in three sections of the stator, at various armature currents and hydrogen pressures for a 129-mva 20-kv 3,600-rpm generator, from short-circuit heat-run tests

perature distribution determined from the tests; see Fig. 22. For generators 1 and 3 the test curves of temperature distribution indicated negligible axial heat flow, hence none was assumed in calculating the insulation resistivity.)

Temperature Drop from Average Top Bar Temperature to Temperature Detector

The differential between average top bar temperature to temperature detector is shown in Fig. 20, as measured in three sections of the stator of generator 4 at various armature currents and hydrogen pressures. It is shown to be practically the same in all sections, for the same armature current, indicating little variation in the bar conditions in different parts of the stator. Also, the drop appears to be little influenced by changes in the hydrogen pressure, indicating negligible ventilation of the temperature detector. (All four generators showed this same result.) The small negative temperature differential obtained at zero arma-

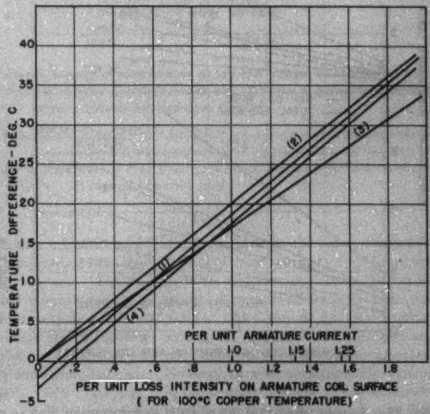

Fig. 21. Difference between average temperature of top coil-side and temperature of adjacent embedded temperature detector in discharge section of stator nearest the center, at various per unit values of armature current for four generators, from factory tests. Each curve represents average temperature difference at hydrogen pressures between 0.5 and 30 psi

Curve 1—18.75-mva 13.8-kv generator

Curve 2—100-mva 14.4-kv generator
Curve 3—105.8-mva 14.4-kv generator
Curve 4—129-mva 20-kv generator

ture current, which was obtained for generators 1 and 4, but not significantly for generators 2 and 3, is caused by the heat flow from iron to copper due to windage and tooth iron losses. In Fig. 21 the difference between average top bar temperature and the detector temperature as measured in the core discharge section nearest the center of the generator is shown for all four generators for different per-unit armature currents. The curves given represent average values of this temperature difference for the different hydrogen pressures at which the tests were made; although, as previously noted, the measured drop was substantially independent of the gas pressure. The variation in this temperature drop among the four generators, between average and maximum, for the same per-unit armature current is about 8%.

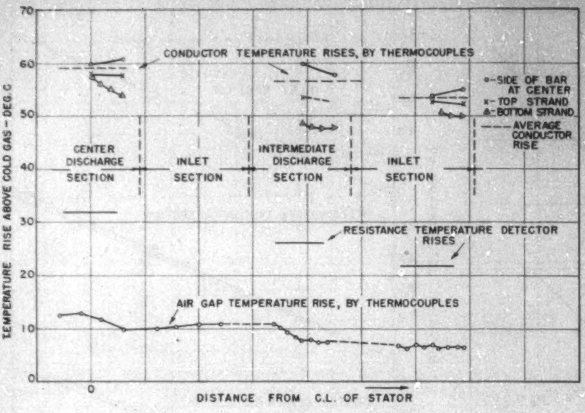

Fig. 22. Axial and radial temperature distributions in top armature coil-side; temperature rises of embedded temperature detectors in three sections of the stator; and axial temperature variation of gas in the air gap, of a 129-mva 20-kv 3,600-rpm generator, from short-circuit heat-run tests at 125% armature current at 0.5-psi hydrogen pressure

Temperature Distribution in Top Armature Bar and in Air Gap

Fig. 22 gives the axial and radial temperature distributions in top armature bar and the axial variation of the air-

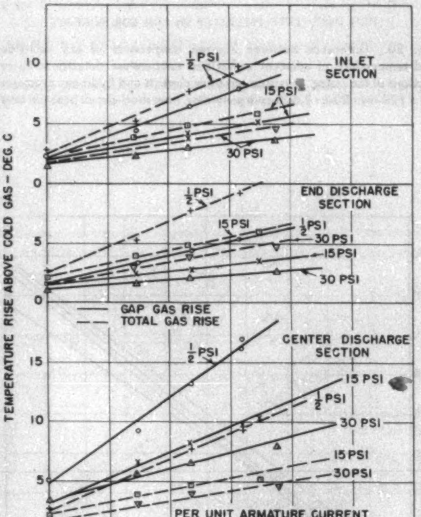

Fig. 23. Average temperature rise of gas in air gap opposite three ventilation sections of generator at various armature currents and hydrogen pressures for a 105.8-mva 14.4-kv 3,600-rpm generator, from short-circuit heat-run tests

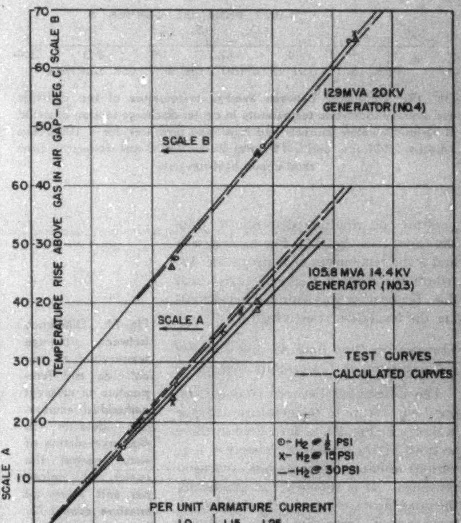

Fig. 24. Average temperature rise of top armature coil-side above gas temperature in air gap opposite center stator discharge section, at various armature currents and hydrogen pressures, for a 105.8-mva 14.4-kv 3,600-rpm and a 129-mva 20-kv 3,600-rpm generator, from short-circuit heat-run tests, with temperature rises calculated from equations shown for comparison in section 2 ("Equivalent Thermal Circuit")

gap temperature along the gap for generator 4, as determined from a short-circuit heat run test at 125% armature current at 1/2-psi hydrogen pressure. The radial temperature distribution in the top bar is shown to agree, essentially, with the curves shown in Figs. 6 and 7, as obtained from the calculating board analysis on the 111-mva, 13.8-kv generators, the highest copper temperature occurring about halfway up the coil side, and the temperature of the top strand of the bar being somewhat higher than that of the bottom strand. In calculating the average coil-side temperatures from the thermocouple readings, parabolic temperature distribution in the coil side radially was assumed. Under this assumption, the difference between maximum and average bar temperatures was in most cases only a few degrees C, hence the curves of temperature differential between copper and temperature detector given in Fig. 21 may be used without significant error, to predict from the detector readings the hot spot as well as the average temperature of the top coil side.

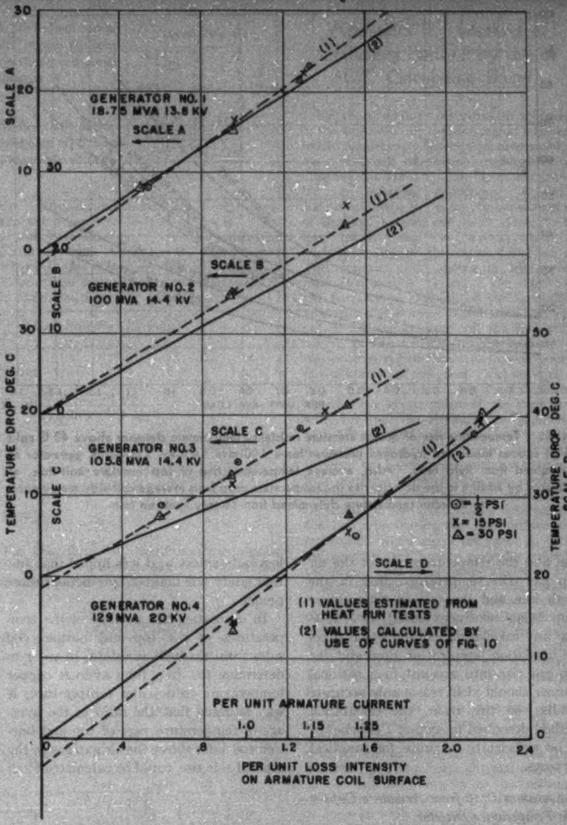

Fig. 25. Difference between average of temperatures of top and bottom coil-sides and temperature of embedded detector, in stator discharge section nearest center of generator at various armature currents and hydrogen pressures

1—As estimated from heat-run tests, using a calculated ratio of average coil-side temperature to top coil-side temperature

2—As calculated by use of the curves of Fig. 1 using values of insulation thermal resistivity determined from the tests

Air-Gap Temperatures

Fig. 23 shows the average temperature rise of the gas in the air gap at three stations axially along the generator for generator 3 at various armature currents and hydrogen pressures, as obtained from the short-circuit heat run tests. The gap gas temperature rise at the center of the generator, which represents the ambient gas rise for the hottest section of the armature winding, is shown to be appreciably higher than the total gas rise through the generator, at all gas pressures. This is caused by the temperature rise from the rotor I^2R loss, of the rotor ventilating gas which is discharged into the air gap at the center of the generator. Similar results were obtained in the tests on generators 2 and 4. For generator 1 the center ventilation section of the stator core was an inlet instead of an outlet section, as it was for the other generators, so that a different axial distribution of gap gas temperatures was obtained.

Analysis of Tests

Temperature Rise of Armature-Winding Copper

As an approximate check on the accuracy of the calculation method described in section 1 the average temperature rise of the top armature bar above air gap temperature was calculated by this method for the four generators tested, and for different armature currents and hydrogen pressures. These were compared with the temperature rises obtained from the heat run tests. Fig. 24 gives these calculated temperature rises for generators 3 and 4, with test values for the center discharge section shown for comparison. The good agreement shown between test and calculated copper temperature rises, while gratifying, should not be taken as complete proof of the accuracy of the calculation method; for, since the values of insulation thermal resistivity used in the calculations were estimated from the heat run data and, since the temperature drop in the bar insulation comprises about 90% of the copper rise above the air gap temperature, substantial agreement between test and calculated values was to be expected. However, since we are interested primarily in the temperature rise of the armature-winding copper above cold gas, and since the main components of this rise are the temperature drop in the coil-side insula-

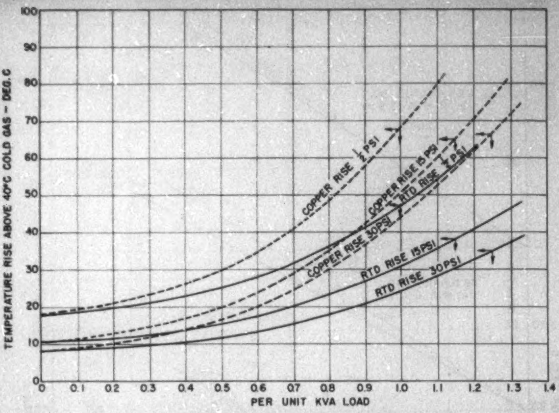

Fig. 26. Temperature rise of hottest armature resistance temperature detector above 40 C cold gas at various loads and hydrogen pressures for a 100-mva 14.4-kv 3,600-rpm generator as determined from field tests. Also, average temperature rise of top armature coil-side, as estimated by adding to the detector rise the temperature drop from average coil-side temperature to detector temperature determined from factory heat-run tests

tion and the temperature rise of the air gap gas (the temperature drop in the tooth iron and the surface temperature drop being relatively small), it follows that any calculation method which takes the insulation temperature drop and the gap gas rise into account in a rational manner should yield reasonably accurate results; on this basis, the calculation method described in section 1 is believed to be sufficiently accurate for practical purposes.

Temperature Drop from Armature Copper to Temperature Detector

To provide an approximate check on the validity of the analysis given in section 2, the temperature drop from the average temperature of top and bottom armature bars to the detector temperature was calculated for various armature currents for the four generators tested, by use of the *F* factor given by the curves of Fig. 1, using the values of insulation thermal resistivity determined from the tests, and compared with the values of this temperature drop estimated from the tests.

This comparison is given by the curves of Fig. 25. For generators 1, 2, and 4 the agreement between the values of temperature difference estimated by the use of the *F* factor given by the curves of Fig. 1, and the values estimated from the heat run data, may be considered satisfactory. However, for generator 3 the agreement is less satisfactory and it is hoped that further study will make all predictions more precise.

In estimating the average of the temperatures of the top and bottom coil sides from the heat run data, in order to determine the drop from average copper temperature to detector temperature, it was assumed that the ratio of the average of temperature rises of top and bottom coil sides above the air gap gas to the top coil side rise, could be calculated from the equations given in section 2 ("Equivalent Thermal Circuit"). This assumption was necessary since the temperature of the bottom coil side was not measured in the tests. The ratio was in most cases approximately 0.9. It was also assumed in the calculations that the thermal resistivity of the coil side insulation was the same for both top and bottom coil sides. However, even under the limitation of these assumptions it is indicated that the analysis given in section 2, when properly calibrated by tests, provides a satisfactory basis for determining the temperature of the armature-winding copper from readings of the temperature detector.

5. Field Tests on Two Generators

The temperature rises of the armature copper and temperature detectors were determined for generator under 1 actual load conditions from the factory tests. However, the other three generators, having been tested in the factory under zero excitation, under open- and short-circuit conditions only, required testing in the field to determine the armature heating under load conditions. Figs. 26 and 27 give load test data on generators 2 and 4 as obtained from field tests. Fig. 26 gives the temperature rises of the hottest armature temperature detector above 40 C cold gas at various loads at rated pf for generator 2. To the values of temperature detector rise obtained in the load tests, the pertinent values of temperature drop from average top coil-side temperature to detector temperature obtained in the factory tests (refer to Fig.

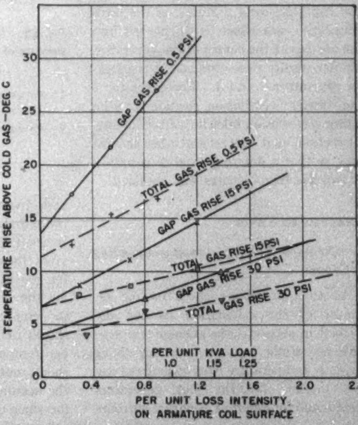

Fig. 27. Average temperature rise of gas in air gap opposite center stator discharge section, at various loads and hydrogen pressures, for a 120-mva 20-kv 3,600-rpm generator, as determined from field tests

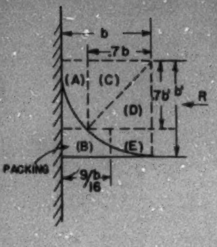

Fig. 28 (left). Division of corner insulation into several sections for calculation of corner thermal resistance R

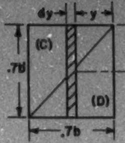

Fig. 29 (right). Calculation of thermal resistance of section (CD) of corner insulation

21) were added, giving the curves of average temperature rise of top coil side versus load shown in Fig. 26. It is observed that for the specified generator capabilities of 115% at 15 psi and 125% at 30 psi the copper temperature rises are slightly under the values estimated for rated load 1/2 psi. Considering the usual increases in cold gas temperature over 40 C obtained at these elevated loads and gas pressures, of from 4 to 6 C, the hot-spot armature-winding temperatures for these overload conditions would for this generator be only slightly higher than at rated load 1/2-psi pressure.

Fig. 27 gives curves of average temperature rise of the gas at the center of the air gap for generator 4 as determined from field tests at various loads at rated pf, and at different hydrogen pressures. Comparison of these curves with those given in Fig. 23 as obtained from factory tests at short circuit for generator 3 indicates nearly the same relationship between gap gas rise and total gas rise, except that the difference between the two rises is considerably greater under load than under short-circuit conditions, because of the increased rise of the rotor ventilating gas which discharges into the center of the air gap, from the field I^2R loss.

Appendix I. Calculation of Armature Bar Corner Resistance R

In the calculating-board analysis of the armature copper temperatures, calculation of the thermal resistance of the insulation in the corner of the armature bar is required. In the corner, referring to Fig. 10, the heat from the coil side flows both along the mica laminations and across them; also the space between the outside of the insulation, the tooth, and the detector, is sealed with packing to prevent ventilation of the temperature detector; hence the calculation of the corner resistance R is a rather complex problem.

For the resistance calculation, the corner insulation was considered to be divided into several resistances, as shown in Fig. 28. Assuming parallel lines of heat flow through the corner, the resistances ($R_A \ldots R_E$) were evaluated for the designated areas. The actual heat flow lines will be somewhat distorted from the assumed flow lines; however, this distortion will be neglected. From these assumptions, the resistance R is calculated from the equation

$$R=\frac{(R_A+R_C+R_D)(R_B+R_E)}{R_A+R_B+R_C+R_D+R_E}$$

where

$$R_A=\frac{(0.3b)\rho_t}{X_t(0.7b')}=\frac{3}{7}\,\frac{b\rho_t}{b'X_t}$$

$$R_B=\frac{9}{16}\,\frac{b\rho_t}{X_t(0.3b')}$$ (Assuming thermal resistance for material in corner space the same as for coil)

$$R_E=\frac{7}{16}\,\frac{b\rho_t}{X_t(0.3b')\gamma}$$

The heat flow will divide between regions C and D. Considering a differential element, as in Fig. 29

$$d(R_C+R_D)=\frac{\dfrac{(\rho_t dy)}{(xX_t)}\,\dfrac{(\rho_t dy)}{(\gamma X_t)(0.7b'-x)}}{\dfrac{\rho_t dy}{xX_t}+\dfrac{\rho_t dy}{\gamma X_t(0.7b'-x)}}$$

$$=\frac{b\rho_t}{X_t b'(\gamma-1)}\,\frac{dy}{\dfrac{(0.7b\gamma-y)}{(\gamma-1)}}$$

therefore

$$R_C\pm R_D=\frac{b\rho_t}{b'X_t(\gamma-1)}\int_0^{0.7b}\frac{dy}{\left(\dfrac{0.7b\gamma}{\gamma-1}\right)-y}$$

$$=\left(\frac{l_n\gamma}{\gamma-1}\right)\left(\frac{b\rho_t}{X_t b'}\right)$$

Note that as $\gamma \to 1.0$ denoting equal transverse and lengthwise resistivities

$$R_C+R_D\to\left(\frac{b\rho_t}{X_t b'}\right)$$

which is as it should be.

Evaluating R for $\gamma=4.0$ results in

$$R=0.611\,\frac{b\rho_t}{X_t b'}$$

A calculating-board study (obtained by breaking the corner up into small sections and including the proper resistivity of the corner packing) showed

$$R=0.650\,\frac{b\rho_t}{X_t b'}$$ for 100-megawatt generator

$$R=0.720\,\frac{b\rho_t}{X_t b'}$$ for 111-megawatt generator

which were quite reasonable checks on the method of calculation.

Appendix II. Method of Evaluating Factor F by Use of D-C Calculating Board

By the procedure described in reference 5, the insulation in the slot region adjacent to the temperature detector was represented by a network of thermal resistances, as illustrated in Fig. 11. The latter was drawn for the following conditions: 1. outer coil radius, $r=0$; 2. equal temperature rises of top and bottom coil sides above tooth iron temperature, i.e., $T_1=T_2$; and 3. various values of the ratios b/b_1 and α. The diagonal lines shown in the corner insulation in Fig. 11 locate the planes of the surfaces of division of the insulation into side and bottom regions; in the side region the laminations of the insulation course in the vertical direction, while in the bottom region the laminations course in the horizontal direction. The network of Fig. 11 was set up on the d-c calculating board for a given value of the ratio b/b_1 with the resistors adjusted in accordance with the specified values of α and γ. With a given potential difference maintained between the busses representing copper and iron surfaces respectively, the potential difference between the point representing the center of the temperature detector and the bus representing the iron surface was measured. The ratio of the latter potential difference to the former gave the value of the ratio F, for the assumed values of b/b_1, α and γ. For evaluation of the ratio F for unequal temperatures of top and bottom coil sides, a network representing the coil insulation for both coil sides was used, while for the condition of outer coil radius $r\neq 0$ the corner insulation was represented by a network of resistors arranged in curvilinear squares.

The resistances of the resistors of the thermal network illustrated in Fig. 11 were evaluated for unit thickness of the insulation perpendicular to the plane of the page. Denoting the transverse thermal resistivity of the coil insulation by ρ_t the resistance of a unit resistor for transverse heat flow is $R_X=\rho_t$, while that of a unit resistor for a longitudinal heat flow is $R_y=\rho_t/\gamma$. At the iron and copper boundaries, except at the corners, the resistances of the resistors are one-half the above values. For the resistors representing the region adjacent to the corner diagonals, the resistances were calculated as follows: From Appendix I, the thermal resistance of a block of insulation of unit depth in which the direction of the laminations on either side of a diagonal plane across the corners of the block differs by 90 degrees is given by the equation

$$R_{CD}=AB \tag{1}$$

where

$$A=\frac{l_n\gamma}{\gamma-1} \tag{2}$$

and

$$B=d/w \tag{3}$$

where

d = length in block in direction of heat flow
w = width of block

For

$\alpha = 1$

for which the resistances are symmetrical on either side of the diagonal, i.e., $B = 1$, the resistance of resistor *a* in Fig. 11 can be readily shown to be

$$R = (\rho_i/\gamma)\left[0.5 + \frac{A}{A+1/\gamma}\right] \tag{4}$$

while the resistance of resistor *b* can be shown as

$$R = \rho_i\left[0.5 + \frac{A}{1+A}\right] \tag{5}$$

The resistance of the corner resistors *C* and *d* in Fig. 11 is given by the equation

$$R_c = R_d = \frac{A\rho_i}{1+A} \tag{6}$$

The resistances of the unit resistors of the temperature detector are given by the equation

$$R_D = \rho_D L_D / W_D \tag{7}$$

where

L_D = length of unit resistor of detector
W_D = width of unit resistor of detector
ρ_D = thermal resistivity of detector material

For values of $\alpha \neq 1$, the resistors adjacent to the diagonals do not have symmetrical resistance values on either side of the diagonal, i.e., $B \neq 1$. For this condition, the resistances R_a, R_b, etc., are calculated in the same manner as for $\alpha = 1$, first calculating R_{CD} from equation 1, and then combining this resistance in series parallel with the resistances of the other sections of the block of insulation represented by the resistor.

References

1. GENERAL PRINCIPLES UPON WHICH TEMPERATURE LIMITS ARE BASED IN THE RATING OF ELECTRIC MACHINES AND APPARATUS. *AIEE Standard No. 1*, Feb. 1954.

2. ROTATING ELECTRICAL MACHINERY. *ASA C50-1943*, American Standards Association, New York, N. Y., 1943.

3. LOADING OF HYDROGEN-COOLED GENERATORS AT ELEVATED GAS PRESSURES, D. S. Snell. *AIEE Transactions*, vol. 69, pt. I, 1950, pp. 186–204.

4. TEMPERATURE DROP TO RESISTANCE TEMPERATURE DETECTOR IN STATOR WINDINGS OF TURBINE GENERATORS, R. P. Jerrard. *Ibid.*, vol. 73, pt. III, June 1954, pp. 665–70.

5. HEAT TRANSFER PATTERNS OF MULTICOMPONENT STRUCTURE BY COMPARATIVE METHODS, Carl F. Kayan. *Transactions*, American Society of Mechanical Engineers, New York, N. Y., vol. 71, no. 1, 1949, pp. 665–70.

6. GENERATOR STATOR COPPER TEMPERATURE INDICATOR, A. L. Brownlee, H. E. Brown. *AIEE Transactions*, vol. 72, pt. I, Nov. 1953, pp. 676–78

◆

Discussion

M. D. Ross (Westinghouse Electric Corporation, East Pittsburgh, Pa.): The authors have mentioned the recommendations of the Synchronous Subcommittee of the ASA C-50 group in regard to standard ambient temperatures. The following discussion outlines the basis for the recommended values.

When the first hydrogen-cooled turbine generators were designed, the gas-tight structure and the coolers were arranged for a maximum of 0.5-psi hydrogen pressure. A few years later, there was a demand for higher gas pressures, and a large number of machines were built with a capability rating at 15 psi. Within the last 7 years, a number of generators have been sold to operate up to a maximum hydrogen pressure of 30 psi. In all these designs, the gas coolers were arranged for an outlet gas temperature of 40 C at the half-pound maximum rating and with the specified maximum water temperature and flow. The temperatures obtaining at the outlet of the cooler with 15 psi and later with 30 psi were determined by the half-pound condition. These temperatures at the outlet of the cooler will vary somewhat with the design of the generator and the relative losses at the capability ratings. The variation may be as much as 6 C between the half-pound condition and the 30-psi condition.

It is entirely normal for the ambient temperature of hydrogen-cooled machines to increase over 40 C when the machine is operated at loads and gas pressures higher than the basic rating at 0.5 psi, but this phenomenon is not understood by many operators. It may be explained as follows.

When a machine is operated at gas pressures over 0.5 psi with correspondingly higher loads, the increase in losses in the machine is almost exactly balanced by the increase in heat transfer capability of hydrogen coolers. Therefore, the difference between the average cooler water temperature and the average hydrogen remains approximately constant. However, the ability of the hydrogen gas to absorb heat increases much faster than the losses in the machine for any given increase in gas pressure, with the result that the temperature rise of the gas decreases with increasing gas pressure. Since the average temperature of the gas must remain constant, the reduction in the gas temperature rise results in an increase in cold gas temperature, and a decrease in hot gas temperature at higher gas pressures. Fig. 30 shows the general nature of this phenomenon.

It would require coolers of nearly double the usual size to maintain a 40 C ambient at the 30-psi rating. This would increase the diameter of large machines unreasonably with no extra advantage to the operator, since present temperatures are satisfactory.

It is apparent from this discussion that the characteristics of the gas coolers now in use are quite well matched to the machines with which they are associated. While the gas temperature goes up as the higher gas pressures and capabilities, the machine internal temperatures come down to compensate for the rise in the gas pressure.

The maximum cold gas rises of 40, 44 and 46 C for 0.5, 15 and 30 psig as given in the Committee recommendations clarifies the matter of expected cooler performance with varying gas pressure.

Herman Halperin (Commonwealth Edison Company, Chicago, Ill.): It is gratifying to see the results of the extensive investigations and studies given in this paper.

In a previous discussion, I raised a question as to the magnitude of the temperature drop between the resistance temperature detector and the armature conductor at a hydrogen pressure of 0.5 psi. More importantly, emphasis was given to using the temperature rise and the total temperature of the armature conductor itself, as the criteria in determining design and operating limits for an armature at various hydrogen pressures. This practice of considering hottest spot temperature or temperature rise as the final criterion is generally used for transformers, cables, contacts of breakers, etc.

It is good to see the very close check between calculations and test results for three of the four generators covered in Fig. 25. The results of the further investigations mentioned will be of interest.

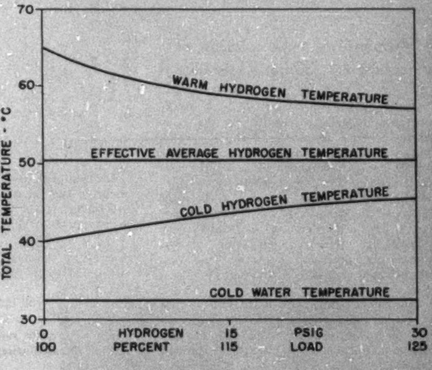

Fig. 30. In a typical hydrogen-cooled generator of conventional design, the cold gas temperature varies as shown

As a result of various discussions with generator manufacturers, I have been using a value of 20 to 25 C as the temperature drop through the armature coil insulation to the resistance detector for a hydrogen pressure of 0.5 psi. For loads in amperes over the name-plate half-pound rating, the temperature drop has been assumed to be proportional to the ratio of the heat at the increased load to the heat in armature conductor at the half-pound rating. Such data as that in Fig. 26 indicate that all these practices in Chicago have been conservative.

The implications of the discussions and data in the article are that designs of armatures are aimed at having hottest-spot copper temperatures of about 115 C or less, assuming inlet hydrogen at the proposed standard values of 40 C with 0.5 psig pressure, etc. It would be of interest to have the authors' comments on loading armatures during, say, ten 1-day summer emergencies each year to currents that would cause increases of about 10 degrees above the hottest-spot temperatures at maximum rated conditions. Also, would their analysis pertaining to this question be modified in case the inlet hydrogen temperatures are held 10 degrees below the proposed ASA range of maximum values of 40 to 46 degrees? Likewise, comments would be appreciated on loading an armature once a year during an emergency some 15 or 20 degrees above the design's hottest-spot temperature at maximum rated load, provided the resulting temperature is not over 130 C.

Regarding the proposed revision of ASA C50 standard, the term "capability" (or "capabilities") is used in notes 2, 3, and 4 of Table Ia and in section 1. It seems to me that in covering, in a commercial transaction, the expected performance of a generator for certain specified currents kilowatts, etc., and conditions, only such terms as "rating," "capacity," and "maximum rating" should be used, and the term "capability" reserved for use by the operator in determining the maximum allowable loading for a given piece of apparatus, after taking into account its particular inherent characteristics, load cycle, installation conditions, and required reliability. These remarks apply to transformers, cables, etc., as well as to generators.

J. R. M. Alger, C. E. Kilbourne, and **D. S. Snell:** The authors thank Mr. Ross for his helpful discussion, which presents a clear explanation of the reason for the increase in cold gas temperature of a generator which occurs with increasing hydrogen pressure and load, a circumstance which is not generally understood by the average operator. The authors also appreciate the comments by Mr. Halperin, which indicate general agreement with the conclusions of the paper. As Mr. Halperin suggests, a figure of approximately 115 C has been accepted by the authors as the maximum allowable hot-spot temperature in operation with cold gas temperatures of 40 to 46 C at hydrogen pressures over the specified pressure range. It is desirable that this temperature should not be exceeded, even for brief periods of operation. However, if system conditions require maximum loading, it must be realized that this operation will reduce the life expectancy of the insulation.

In operation with cold gas temperature below the proposed ASA range of maximum values (40 to 46 C) the load should be held to those values which will ensure that the hot-spot temperature rise does not exceed the rises for normal load conditions, otherwise the differential expansions of the armature coils with respect to the iron will exceed those obtained at the loads corresponding to the capabilities at the various hydrogen pressures, which will in turn reduce the life expectancy of the insulation. That is to say, the generator should be operated at all times in accordance with the capability curves of the generator, and not by endeavoring to hold constant hot-spot temperature.

Answering Mr. Halperin's comments regarding the term "capability," this term and capacity are used interchangeably in the paper and denote the kva output which may be obtained continuously at hydrogen pressures over that for which the rating is determined, for approximately the same or lower hot-spot temperatures and temperature rises. The generator capability is usually the same as the turbine capability, which is the continuous output at generator terminals when the turbine is clean and operating under specified throttle steam and temperature and exhaust pressure with full extraction from all extraction openings.

Oil Flow and Pressure Calculations for Pipe-Type Cable Systems

AIEE COMMITTEE REPORT

THE components of oil-filled cable systems are subject to thermal expansion or contraction in varying degrees; hence as the temperature of these components change with change in load, oil must flow out of or into the system if the desired oil pressure is to be maintained. Solutions for the pressure differentials thus resulting in the case of low-pressure oil-filled cables (Pirelli type) have been presented by Miller,[1] Shanklin and Buller,[2] Miller and Wollaston,[3] and Wollaston.[4]

Similar problems are encountered in high-pressure oil-filled pipe-type cable installations where it is desirable to know the maximum oil pressures which may be developed on sudden application of load, and the size of the pump and the pumping pressures which must be provided in order to maintain a minimum pressure at any point in the line when load is dropped. The solutions of these and related problems are presented in this report.

General Considerations

The pressure differentials under consideration depend upon the oil demand or the rate of change of oil content per foot of pipe. This change in oil content is dependent not only upon the expansion or contraction of the oil itself with change in temperature, but also upon corresponding volumetric changes with temperature in the conductor, insulation, and pipe. Because of the different thermal characteristics of the mediums involved, the temperature will vary discontinuously from the conductor to pipe.

Unlike the low-pressure oil-filled cable where the oil demand of the insulation, which contains the larger portion of the oil, may be determined as a mathematical function, a practical solution of the pipe cable involves dividing the system into a number of zones for each of which the average rate of temperature change with time must be determined in some manner. The zones established are the conductor, insulation, free oil space, and the pipe.

The greatest part of the thermal expansion or contraction will occur in the free oil zone through which the major portion of the heat flow is carried by thermal convection. As indicated in reference 5, the thermal drop resulting from this mode of heat transfer is concentrated in thin films at the boundary surfaces, hence the body of oil will be at substantially a uniform temperature. Actually, therefore, this method of treating the oil space is not a simplification but the best method of representation.

Paper 55-32, recommended by the AIEE Insulated Conductors Committee and approved by the AIEE Committee on Technical Operations for presentation at the AIEE Winter General Meeting, New York, N. Y., January 31–February 4, 1955. Manuscript submitted October 20, 1954; made available for printing November 16, 1954.

The personnel of the Working Group on Pipe-Type Cable Hydraulics of the AIEE Committee on Insulated Conductors are: J. H. Neher, *Chairman*, F. H. Buller, R. W. Burrell, G. N. Everest, B. J. Merrell, M. H. McGrath, M. Morris, and J. C. Parker.

Nomenclature

a = oil demand due to conductor loss, cubic inches per foot per second
a_d = oil demand due to dielectric loss, cubic inches per foot per second
B = flow resistance, pound-seconds per square inch per cubic inch per foot
c = circumference of an area, inches
D_b = diameter of by-pass piping, inches
D_c = diameter of conductor, inches
D_i = diameter oven insulation, inches
D_0 = inside diameter of pipe, inches
D_p = outside diameter of pipe, inches
D_s = diameter over shielding tapes, inches
E_s = modulus of elasticity of steel, pounds per square inch (psi)
E_0 = bulk modulus of oil, psi
f = shear force per unit area, psi
F = flow rate, cubic inches per second
F_0 = constant flow rate delivered by the pump, cubic inches per second
γ = specific gravity of the oil
h_0 = unit temperature-time transient of the oil, thermal ohm feet, degrees centigrade (C) feet per watt
Δh = change in elevation, feet
H_{ce} = steady-state thermal resistance from conductor to ambient earth, thermal ohm feet
H_{ie} = steady-state thermal resistance from mid-insulation to ambient earth, thermal ohm feet
H_{oe} = steady-state thermal resistance from mid-oil to ambient earth, thermal ohm feet
H_{pe} = steady-state thermal resistance from pipe to ambient earth, thermal ohm feet
K = ratio of pressure drop in the pipe with cables to the pressure drop for the same flow without cables
l = length of a by-pass system, feet
L = length of main pipe, feet
M = inertia in pound square seconds per square inch per cubic inch per foot
μ = viscosity, centipoises
μ_0 = initial viscosity of the oil, centipoises
N = number of by-pass systems associated with main pipe
O_l = oil requirement due to load change, gallons
O_s = oil requirement due to seasonal temperature changes, gallons
P_b = pressure differential in the by-pass systems, psi
P_f = frictional pressure drop, psi
P_h = hydrostatic pressure, psi
P_m = pressure differential in the main pipe, psi
P_0 = constant pressure impressed by the pump, psi
ΔP = elastic transient pressure increment, psi
Q = heat flow resulting from a-c losses in one conductor, watts per foot
Q_d = heat flow resulting from dielectric loss of one cable, watts per foot
s = area, square inches
t = time, seconds
t_0 = time at which load is dropped, seconds
t' = time at which the oil demand is a maximum after dropping load, seconds
τ = unit of time (Appendix II)
T_c = conductor temperature, C
T_i = mid-insulation temperature, C
T_0 = oil temperature, C
T_0' = initial oil temperature, C
ΔT_{0d} = oil temperature change due to dielectric loss, C
T_p = pipe temperature, C
u = flow velocity, inches per second
V = volume, cubic inches per foot
V_e = elastic volume change, cubic inches per foot per pound per square inch
x = distance from the closed end of the line, feet
y = distance from pipe or cable surface, inches

The basic equation for the change in oil volume ΔV in cubic inches per foot with change in temperature for three cables in the pipe is

$$\Delta V=\begin{Bmatrix}0.0060\\0.0036\end{Bmatrix}D_c^2\Delta T_c+0.0120(D_i^2-D_c^2)\Delta T_i+0.0070(D_0^2-3D_s^2)\Delta T_0-0.0003D_p^2\Delta T_p \text{ inches}^3 \text{ per foot} \quad (1)$$

in which ΔT_c, ΔT_i, ΔT_0, and ΔT_p are the temperature changes in C of the conductor, mid-insulation, the oil, and the pipe of outer diameters D_c, D_i, D_0, and D_p in inches respectively; and D_s is the diameter over the shielding tapes. The two constants appearing in the first term apply to concentric stranded or to compact segmental conductors. Equation 1 is based upon the composition of components given in Table I. It will be noted that the last term is negative since the pipe expands on increase in temperature and effectively reduces the change in volume of oil.

If a given load, which has been sustained until steady-state temperatures prevail, is removed from the cable system, the rate at which oil is absorbed per-unit length of the system is known as the oil demand and is commonly indicated as a in cubic inches per foot per second. This quantity is a function of the load dropped and the elapsed time. When a given load is suddenly applied to the system, oil will be ejected from the system at exactly the same rate, and thus the oil demand is most conveniently found by differentiating equation 1 with respect to time

$$a=\frac{d}{dt}\Delta V \text{ inches}^3 \text{ per foot-second} \quad (2)$$

This in turn requires the determination of the temperature rises ΔT_c, ΔT_i, ΔT_0 and ΔT_p as functions of time, which are directly proportional to Q, the heat liberated at each conductor in watts per foot.

The calculation of the corresponding per-unit temperature-time transients at conductor and insulation, oil, and pipe for a particular cable system may be accomplished mathematically as indicated in reference 6. However, this is a time-consuming process and these transients may be determined more readily by use of an analogue computer.[7] This has been done for the six typical pipe-type cable systems outlined in Table II and the resultant per-unit oil demands, a/Q in cubic inches per second per foot of pipe per watt per foot of conductor (cubic inches per watt-second), are shown in Fig. 1. In many cases the per-unit demand may be interpolated from these

Table I. Composition and Coefficients of Expansion of the Several Zones

Material	Coefficient of Expansion	Conductor, Per Cent: Concentric Stranded	Conductor, Per Cent: Compact Segmental	Insulation, Per Cent	Oil, Per Cent	Pipe, Per Cent
Copper	5×10^{-5}	77	79			
Paper	10×10^{-5}		10.5	50		
Oil	75×10^{-5}	23	10.5	50	100	
Steel	3.6×10^{-5}					100
Net coefficient of expansion		21.1×10^{-5},	12.9×10^{-5},	42.5×10^{-5},	75×10^{-5},	3.6×10^{-5}.

Table II. Typical Pipe-Type Cable Systems

System	Voltage	Conductor		Insulation, Mils	Pipe, Inches, Outside Diameter	Q_d, Watts per Foot	D_s/D_0^2
I	69 kv	350, MCM*	concentric stranded	285	$5^9/_{16}$	0.31	0.255
II	138 kv	350, MCM	concentric stranded	505	$5^9/_{16}$	0.82	0.342
III	69 kv	500, MCM	concentric stranded	285	$6^5/_8$	0.35	0.231
IV	69 kv	1500, MCM	compact segmental	285	$6^5/_8$	0.55	0.330
V	138 kv	1500, MCM	compact segmental	505	$8^5/_8$	1.39	0.302
VI	230 kv	1500, MCM	compact segmental	835	$8^5/_8$	2.65	0.384

* Thousand circular mils.

curves, thus avoiding the necessity for a separate determination of this quantity.

From a rigorous standpoint, the effect of dielectric losses may be handled in similar manner by setting up a separate thermal network for these losses and determining a curve of a_d. This has been done for the three systems of Table II having the largest conductor size, and hence the largest dielectric losses, as shown in Fig. 2. In many cases the effect of dielectric loss may be treated with sufficient accuracy by suitably including the dielectric loss with the conductor loss.

The calculation of pressure involves the viscosity of the oil which is dependent upon the oil temperature T_0

$$T_0 = T_0' \pm Qh_0 \text{ C} \qquad (3)$$

where T_0' is the initial oil temperature and h_0 is the unit temperature-time transient of the oil in thermal ohm feet. The sign of the second term depends upon whether load is added or dropped. Curves of h_0 for the cable systems of Table II are shown in Fig. 1. When the dielectric loss is not included with the conductor loss, equation 3 may be extended by the term ΔT_{0d} representing the temperature change in the oil from dielectric loss. Curves of ΔT_{0d} are given in Fig. 2.

In cases where a given load is dropped before the steady-state conditions resulting from that load have been attained, the corresponding oil demand that a' may be found as follows. If the load is dropped at time t_0 after its application, at a subsequent time $t' = t_0 + \Delta t$

$$a' = a_t' - a_{\Delta t} \text{ inches}^3 \text{ per foot-second} \qquad (4)$$

in which a_t' represents the value of the a curve at time t' and $a_{\Delta t}$ its value at time Δt. In calculating the maximum value of a' occurring after dropping load, it is sufficient to assume that Δt is equal to the time at which the a curve is a maximum. It will be noted that if the load has continued long enough for steady-state conditions to prevail, equation 4 becomes equal to equation 2 with change of sign.

Corresponding values of h_0' and $\Delta T_{0d}'$ for use in equation 3 are determined in similar manner.

Calculation of Oil Flow

If L is the length of the line in feet, it will be apparent that the amount of oil which will flow into or out of the line as a function of time after dropping or increasing load is

$$0_l = 4.33 L \Delta V \times 10^{-6} \text{ gallon} \qquad (5)$$

The seasonal line oil change is obtained by substituting the seasonal change in ambient temperature ΔT_a for ΔT_c, ΔT_t, ΔT_0, and ΔT_p in equation 1.

$$0_s = 3L\Delta T_a[D_0^2 - (D_c^2 + 1.3D_s^2)] \times 10^{-6} \text{ gallons approximately} \qquad (6)$$

Required Pump Capacity

The rate of oil flow after dropping or increasing load is

$$F = 0.26La \text{ gallons per minute} \qquad (7)$$

The required pump capacity is the maximum value of equation 7.

Calculation of Pressure

When oil is required by the line, the pumping pressure which must be developed is that required to maintain the desired minimum pressure at the "worst" point of the line aided or opposed by the hydrostatic pressure resulting from change in elevation along the line P_h and to overcome the friction developed in supplying the additional oil P_f. If Δh is the change in elevation at any point of the line and γ is the specific gravity of the oil, at that point

$$P_h = 0.434\gamma\Delta h, \text{ psi} \qquad (8)$$

The frictional pressure P_f varies as the square of the distance from the closed end, and is composed of two parts, that developed in the main pipe and that developed in the by-pass system. As indicated in Appendix I, P_f may be expressed by the relationship

$$P_f = P_m + P_b = 35.5x^2 a\mu \left(\frac{K}{D_0^4} + \frac{N}{L}\frac{l}{D_b^4}\right) \times 10^{-6} \text{ psi} \qquad (9)$$

in which μ is the viscosity of the oil in centipoises, x is the distance from the closed end in feet, L is the length of the main pipe in feet, l is the effective length of a by-pass system in feet and N is the number of by-pass systems. The factor K depends upon the relative size of the cables and their position in the pipe.

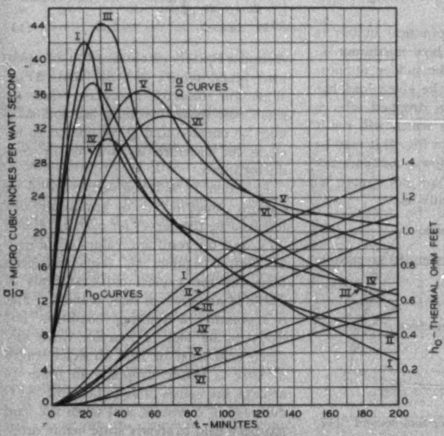

Fig. 1. Curves of a/Q and h₀ as functions of time for the pipe-type cable systems of Table II

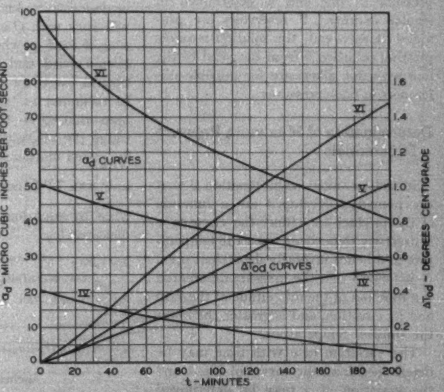

Fig. 2. Curves a_d and ΔT_{0d} as functions of time for the larger pipe-type cable systems of Table II

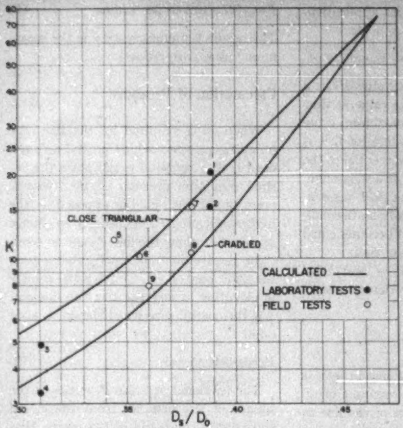

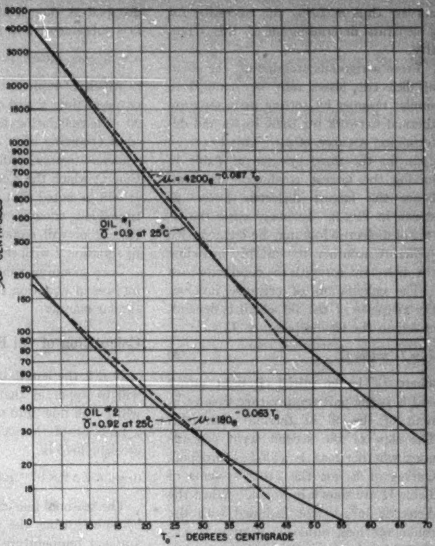

Fig. 3 (above). Calculated and measured values of the factor K as functions of the cable to pipe diameter ratio

Fig. 4 (right). Oil viscosity as a function of temperature

Curves of K as a function of the ratio D_s/D_0 are given in Fig. 3 for close triangular and cradled spacings. The development of these curves is discussed in Appendix I.

The maximum pumping pressure required is determined by plotting equations 8 and 9 over the length of line in order to determine the worst point. The calculation of the maximum internal pressures built up within the system upon the application of load and with the system discharging into a reservoir at a given back pressure at one end is determined in similar manner. If reservoirs are provided at each end, the solution requires plotting equation 9 from each end of the line with due allowance for possible differences in back pressures.

Determination of Maximum Pressure Differentials

It will be noted from equation 9 that the pressures developed are a function of the product $a\mu$. Since the viscosity μ is inversely dependent upon the temperature and hence inversely dependent upon Q, it follows that the pressure differential is a function of the magnitude of the load and its duration, and is greater the lower the ambient temperature.

The variation in a with time may be determined from the curves of Fig. 1 and the variation of μ may be determined from equation 3 and the characteristic viscosity-temperature curve of the oil, shown in Fig. 4. Oil no. 1 is typical of the oil used at present in pipe-type cable systems. Oil no. 2 is the type used in low-pressure oil-filled cables and has been included to permit consideration of an oil of lower viscosity where pressure variations would otherwise be excessive. By plotting the product $a\mu$ its maximum value may be determined for any condition of loading.

Nevertheless, as a practical matter it is desirable to know how maximum $a\mu$ will vary with Q on the sudden application of load or when the given load has been carried and then dropped after a critical length of time which will result in maximum $a\mu$. From Fig. 4, it may be seen that over the lower temperature range the viscosity of oil no. 1 may be expressed mathematically as

$$\mu = 4{,}200\epsilon^{-0.087\,T_0} \text{ centipoises} \qquad (10)$$

Thus by equation 3 extended to include dielectric loss

$$\begin{aligned}\mu &= 4{,}200\epsilon^{-0.087\,(T_0' \pm Qh_0 \pm \Delta T_{0d})}\\ &= \mu\epsilon^{-0.087\,(Qh_0+\Delta T_0 d)} \text{ centipoises}\end{aligned} \qquad (11)$$

and

$$a\frac{\mu}{\mu_0} = [Q(a/Q)+a_d]e^{-0.087\,(Qh_0+\Delta T_{0d})}$$
$$\text{inches}^3 \text{ per foot-second} \qquad (12)$$

where μ_0 represents the initial viscosity of the oil.

Since a/Q, a_d, h_0 and ΔT_{0d} are functions of time, by differentiating equation 12 with respect to time and equating to zero, we find that the maximum values of $a\mu$ will occur at the time when

$$Q\frac{d(a/Q)}{dt}+\frac{da_d}{dt} = 0.087\,[Q(a/Q)+a_d] \times \left[Q\frac{dh_0}{dt}+\frac{d\Delta T_{0d}}{dt}\right] \text{ inches}^3 \text{ per foot-second}^2 \qquad (13)$$

A similar equation is obtained on dropping load based on a', a_d', h_0', and $\Delta T_{0d}'$. When the dielectric losses are relatively small, the terms involving a_d and ΔT_{0d} may be omitted and Q considered to include the dielectric as well as the conductor losses.

Equation 13 may be solved for Q at various values of time by graphically differentiating the curves for a/Q, a_d, h_0 and ΔT_{0d} and the resultant values of $a\mu$ may be plotted against Q. This has been done for the typical cable systems of Table II as shown in Figs. 5 and 6. Fig. 6 represents a limiting condition not likely to be met in practice since any given load must be held an exact length of time t_0 before dropping in order to achieve the values of μa indicated. As Q decreases t_0 increases, and when the load has been held to steady state before dropping ($t_0 = \infty$) the corresponding value of Q is determined by differentiating equation

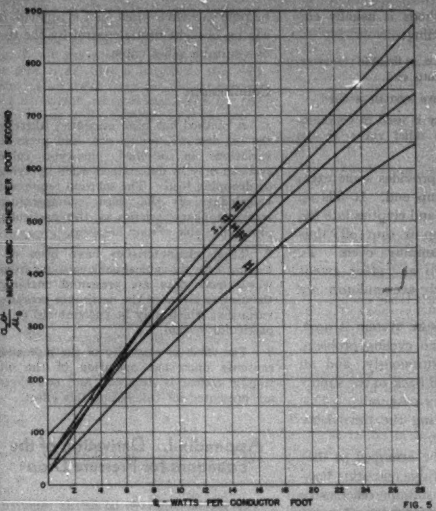

Fig. 5. Maximum value of $a\,\mu/\mu_0$ as a function of suddenly applied load

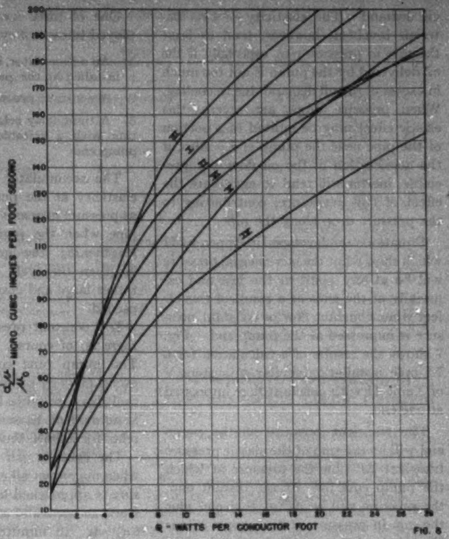

Fig. 6. Maximum value of $a'\mu/\mu_0$ as a function of load dropped

12 with respect to Q and then equating to zero.

Thus, neglecting dielectric loss

$$Q=\frac{11.5}{h_0'}=\frac{11.5}{H_{0e}-(h_0)_{\Delta t}}\text{ watts per foot}\qquad(14)$$

and

$$a\frac{\mu}{\mu_0}=4.2\frac{a'/Q}{h_0'}=\frac{4.2(a/Q)\text{ max}}{H_{0e}-(h_0)_{\Delta t}}$$

inches³ per foot-second (15)

where h_0' and a'/Q are ultimate values ($t_0=\infty$), and $\Delta t=t$ for maximum a/Q.

Effect of the Elastic Transient

When the cable system is operated at constant pressure, or over a very narrow pressure range, the pressure changes produced by a slow thermal transient will be affected little, if at all, by the elastic properties of the system. However, in a pipe cable fed by a constant-flow oil pump of considerable capacity the usual practice is to permit the pressure to drop materially below the normal operating level during cooling, then to restore it to a point somewhat above the normal operating level by means of a rapid-pumping operation.

If the flow resistance is low, the pipe will come up to pressure fairly uniformly. But if low temperatures, high oil viscosity and restricted flow areas, either in the pipe itself or in the feed line from the pump, or the by-pass system combine to produce high-flow resistance, the elastic properties of the system, and particularly the compressibility of the oil and the extensibility of the pipe, may become important.

If the pipe and its contents were absolutely rigid, a very slight oil contraction during cooling would drop the pressure to zero. Then the pump would start, and would replace the oil lost by contraction, after which the pressure would tend towards infinity unless the feed were reduced to a value equal to or less than the

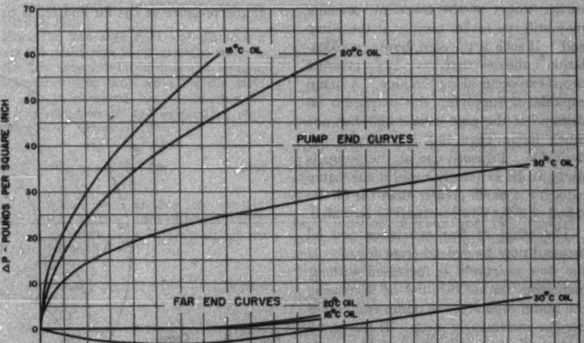

Fig. 7. Typical pipe-type cable elastic pressure transients for a 7.5-mile installation similar to system V of Table II with constant flow impressed at one end

oil demand. The elasticity of the materials involved, however, tend to limit the rate of pressure rise, especially if the oil delivered by the pump is not too much in excess of the oil demand due to cooling. When pressure drops are severe, this elastic effect may be limited to a portion of the pipe near the pump end. Also, if the acceleration of the oil flow is appreciable, inertia will tend to aggravate the effect of flow resistance, contributing to the pressure drop along the pipe.

Equations are developed in Appendix II which show what the incremental pressure will be at any point in the line and especially at the ends as a result of this effect when constant flow or constant pressure is impressed at the pump end. Fig. 7 shows the results of a calculation for a 7.5-mile installation similar to system V of Table II with constant flow impressed at one end.

The transient pressure at the pump end will be the sum of the elastic pressure transient ΔP plus the pressure at which the pump cuts in. At the distant end, the pressure will be ΔP at that end plus the cut in pressure of the pump minus P_h.

The elasticity of the system tends to maintain pressure at the far end of the line over what would exist if the pressure drop due to the flow necessary to supply the oil demand were the only factor present.

At the pump end, the pressure rises rather rapidly because the pump is feeding in more oil than the pipe can absorb because of the oil demand. Even though the pump capacity may be lower than the oil demand of the entire pipe during the earlier stages of the transient, pressure may still rise rather rapidly at the pump end. If such is the case, however, calculation indicates that very large pressure drops can occur along the pipe. A pump capable of supplying the maximum oil demand of the pipe is advisable but one much larger than this is generally not desirable. Pressure rise at the pump is likely to be extremely rapid if the pump capacity is much greater than the oil demand or if the flow resistance is very high.

The effect of flow resistance and oil demand may be judged from Fig. 7. If the flow resistance is increased without increasing the oil demand or decreasing the pump capacity, the pump end curves become increasingly steep. If the pump is shut off after an increase of 40 pounds per square inch, for instance, under the conditions shown in Fig. 7, it will run for about 1 minute with oil at 15°C, and therefore some cycling of the pumping equipment will occur.

One of three methods is usually employed to control cycling:

1. An accumulator, i.e., a flexible reservoir, is installed at the pump end.
2. A constant pressure system is used.
3. A time delay relay is used in combination with a suitable relief valve at the pump end.

The accumulator provides some extra elasticity at the pump end. It fills up as pressure increases and empties into the pipe when the pump is shut off, thus lengthening the pumping cycle. To lengthen the cycle to any great extent rather large and costly accumulators are needed.

If a constant pressure system is used, there is, of course, no cycling problem. The pump runs continuously, and all excess oil is by-passed back to the supply tank by a suitable by-pass valve. This is equivalent to setting the time delay relay for infinite time.

The controls can be arranged so that when maximum allowable operating pressure is approached a suitable relief valve starts to open, and a time delay relay, set for, say, 10 minutes' delay is started. This arrangement permits the pump to maintain a substantially constant pressure on the pipe for a limited time by bypassing back to the supply tank the excess oil which the pipe cannot absorb without pressure increase. After this time the time delay relay shuts down the pump, which procedure is found to reduce cycling frequency very greatly. It is, of course possible to control cycling frequency between almost any reasonable limits that may be desired by adjusting the time delay relay.

If the pressure at the far end tends to become excessive when load is applied, it can be brought under control by the use of a suitable relief valve.

Conclusions

1. A method has been presented whereby the oil demand, pump size, and pressure variations in oil-filled pipe-type cable systems may be determined when applying or dropping load. The solution requires a knowledge of the basic temperature transient characteristics of the particular pipe-type cable system involved.
2. These characteristics have been determined for six typical cable systems from which basic data are presented enabling the user to estimate the maximum pressure variations which may be encountered on a particular system.
3. The effect of elasticity of the pipe and contents upon the operation of the oil supply system is discussed and equations are presented for calculating this effect.

Appendix I. Derivation of the Equations for Pressure Drop

The pressure differential dP/dx required to maintain a laminar oil flow of F cubic inches per second in the main pipe having an inside diameter D_0 inches may be expressed by a modification of Poiseuille's law

$$\frac{dP}{dx}=71\frac{\mu F}{D_0^4}K\times10^{-6}\text{ psi per foot} \qquad (16)$$

where μ is the viscosity of the oil in centipoises. The factor K has been added to care for the obstructions caused by the three cables, and represents the ratio of pressure differential in the pipe with cables to the pressure differential for the same flow without cables. The value of K for a particular cable and pipe configuration may be determined approximately by the following method.

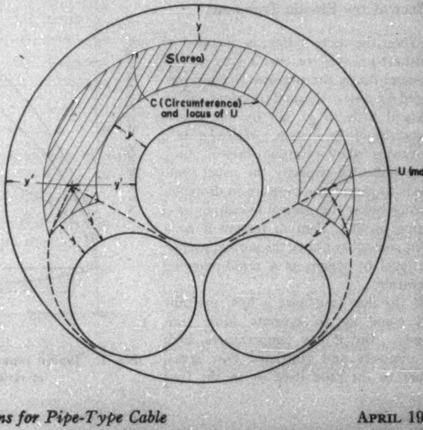

Fig. 8. Cross section of a pipe-type cable system showing factors affecting the determination of the pressure drop

Consider an oil stream of cross-sectional area s square inches and of c inches' circumference, as shown in cross-section in Fig. 8. If the pressure differential along the pipe is dP over a length dx this will result in an axial force on the oil stream of $s\ dP$ which must be balanced by the shear at the wall $cdxf$, where f is the shear force per unit area. Thus

$$\frac{dP}{dx}=12\frac{c}{s}f \text{ psi per foot} \qquad (17)$$

For laminar flow assuming that the flow velocity is the same at equidistant points from any boundary

$$f=0.145\mu\frac{du}{dy}\times 10^{-6} \text{ psi} \qquad (18)$$

where u is the flow velocity in inches per second at y inches distance from the boundary. When equation 18 is substituted in equation 17

$$\frac{dP}{dx}=1.74\mu k\times 10^{-6} \text{ psi per foot} \qquad (19)$$

where

$$k=\frac{c}{s}\frac{du}{dy} \text{ per inch-second} \qquad (20)$$

Thus

$$u=k\int_0^y \frac{s}{c}\,dy=k\int_0^y \frac{1}{c}\left(\int_y^{y'} c\,dy\right)dy \text{ inches per second} \qquad (21)$$

where s and c are functions of y. The total flow F is equal to the integral of the product of u by the differential flow area $c\,dy$

$$F=\int_0^{y'} ucdy = k\int_0^{y'} c\left[\int_0^y \frac{1}{c}\left(\int_y^{y'} c\,dy\right)dy\right]dy \text{ inches}^3 \text{ per second} \qquad (22)$$

If there are no cables in the pipe, the operations indicated by equation 22 may be solved mathematically. Thus

$$F=k\int_{D/2}^{0} -2\pi r\left[\int_{D/2}^{r} -\frac{1}{2\pi r}\left(\int_r^{0} -2\pi r dr\right)dr\right]dr = \pi\frac{D_0^4 k}{128} \text{ inches}^3 \text{ per second} \qquad (23)$$

In this case, since the lines of equal velocity are actually at uniform distances from the boundary, the substitution of equation 23 in equation 19 gives Poiseuille's law (equation 16 with $K=1$). With cables in the pipe, the assumption that the lines of equal velocity are at uniform distances from the boundary surfaces is not strictly correct. In the absence of a more rigorous treatment, however, the procedure indicated will serve as a guide, and it agrees reasonably well with experimental data.

The integrations indicated by equation 22 may be carried out graphically with the aid of a cross-section diagram drawn to scale for the particular cable configuration assumed and similar to Fig. 8. The corresponding value of K for use in equation 16 is obtained by comparing the results of this process with equation 24. Values of K thus determined for several D_s/D_0 ratios with the cables in close triangular and in cradled conformation are illustrated in Fig. 3.

The back calculation of K from field tests may be subject to considerable error because of the difficulty of measuring the oil temperature and hence determining the effective viscosity throughout the test length, and because of uncertainty as to the actual cable configurations. To obtain a check under controlled laboratory conditions, three 40-foot lengths of either standard 1$^1/_2$-inch or 2 inch pipes provided with 1/16×3/16-inch D-shaped skid wires were placed inside of an 80-foot length of standard 6-inch steel pipe in either close triangular or cradled conformation. A differential manometer was connected to a 30-foot gauge section of the 6-inch pipe and oil of 600 to 2,100 centipoises viscosity was passed through the pipe at flow rates of from 1/2 to 7$^1/_2$ gallons per minute. The results of these tests and of available field tests are summarized in Table III and are plotted in Fig. 3.

Table III. Measured Values of K

Test No.	Source	Cable Configuration	Length, Feet	D_s/D_0	μ	K
1	Phelps Dodge Laboratory	close triangular	30	0.388	590	21.7
					1,140	20.2
					1,320	19.4
					1,740	20.4
					weighted average	20.2
2	Phelps Dodge Laboratory	cradled	30	0.388	1,300	15.7
					1,480	15.5
					1,580	15.6
					2,140	15.0
					weighted average	15.3
3	Phelps Dodge Laboratory	close triangular	30	0.310	1,380	4.9
4	Phelps Dodge Laboratory	cradled	30	0.310	1,400	3.3
5	Philadelphia Electric Company	in field	6,937	0.345	69	11.7
6	Consolidated Edison Company	in field	5,810 1,250	0.350 0.380	605	10.2
7	Consolidated Edison Company	in field	13,500	0.380	530	15.4
8	Consolidated Edison Company	in field	13,500	0.380	540	10.5
9	City of Memphis	in field	52,083	0.360	310	8.0

Since the flow rate F at any distance x along the main pipe is equal to xa where a is the flow rate developed in a unit section, the pressure drop built up along the main pipe P_m is obtained by substituting xa for F in equation 16 and integrating with respect to x. Thus

$$P_m=35.5x^2\frac{K}{D_0^4}a\mu\times 10^{-6} \text{ psi} \qquad (24)$$

If the main pipe is divided into sections by N by-pass systems each of length l feet, the total pressure drop P_b built up in the by-pass systems ($K=1$) is

$$P_b=71\frac{l}{D_b^4}[1+2+3\ldots(N)]\frac{L}{N+1}a\mu\times 10^{-6} = 35.5N\frac{l}{D_b^4}La\mu\times 10^{-6} \text{ psi} \qquad (25)$$

Since P_b may be assumed to vary as x^2

$$P_f=P_m+P_b=35.5x^2\left[\frac{K}{D_0^4}+\frac{N}{L}\frac{l}{D_0^4}\right]a\mu\times 10^{-6} \text{ psi} \qquad (9)$$

Appendix II. Derivation of Equations for the Elastic Transient

The pipe and its contents may be considered analogous to a transmission line having series resistance and inductance and shunt capacitance and leakage. The flow F in cubic inches per second is analogous to electrical current and the flow resistance B in pound seconds per square inch per cubic inch per foot corresponds to electrical resistance. The inertia M in pound seconds per square inch per foot is analogous to inductance, and the elastic volume change V_e in cubic inches per foot per psi corresponds to electrical capacitance. Thus from equation 16

$$B=71\frac{\mu K}{D_0^4}\times 10^{-6} \text{ psi seconds per inch}^3 \text{ foot} \qquad (26)$$

$$M=\frac{1430\gamma}{D_0^2-3D_t^2}\times 10^{-6} \text{ psi second}^2 \text{ per inch}^3 \text{ foot} \qquad (27)$$

and

$$V_e=\frac{3\pi}{E_s}(D_0^2-1.5D_t^2)\left(\frac{2D_0}{D_p-D_0}+\frac{E_s}{E_0}\right) = 45(D_0^2-1.5D_t^2)\left(1+0.0145\frac{D_0}{D_p-D_0}\right)\times 10^{-6} \text{ inches}^3 \text{ per psi foot} \qquad (28)$$

when γ is the specific gravity of the oil, E_s is Young's modulus for the steel of the pipe (29×10^6 psi) and E_0 is the bulk modulus of the oil (0.21×10^6 psi).

The oil demand a, however, which is a fixed function of time and the thermal properties of the system, is not exactly analogous to transmission line leakage which is independent of time.

The differential equations to be solved, therefore, are

$$\frac{dP}{dx}=FB+M\frac{\partial F}{\partial t} \text{ psi per foot} \qquad (29)$$

$$\frac{dF}{dx}=a+V_e\frac{\partial P}{\partial t} \text{ inches}^3 \text{ per foot second} \qquad (30)$$

If the pipe is closed at the far end, and the pump starts supplying oil at constant rate F_0, the solution for ΔP, the transient pressure increment is

$$\Delta P=\frac{F_0 t}{LV_e}-\frac{1}{V_e}\int_0^t a\,dt+2F_0BL\times \sum_n \phi(nx)[2\alpha\beta_1+(\alpha^2+\beta_1^2)\epsilon^{-\alpha t} \cos(\beta_1 t-\theta_1)]\text{ psi} \quad (31)$$

where

$$\alpha=\frac{B}{2M}\text{ per second}$$

$$\beta_1=\sqrt{\frac{(n\pi/L)^2}{MV_e}-\alpha^2}\text{ per second}$$

$$\phi(nx)=\frac{(-1)^n}{2\alpha\beta_1(n\pi)^2}\cos\frac{n\pi x}{L}=\phi'(n)\cos\frac{n\pi x}{L}$$

$$\theta_1=\frac{\alpha^2-\beta_1^2}{2\alpha\beta_1} \quad (32)$$

At the pump end, this becomes

$$\Delta P=F_0\left(\frac{t}{LV_e}+\frac{BL}{3}\right)-\frac{1}{V_e}\int_0^t a\,dt+ 2F_0BL\sum_n(-1)^n\phi'(n)(\alpha^2+\beta_1^2)\epsilon^{-\alpha t}\times \cos(\beta_1 t-\theta_1)\text{ psi} \quad (33)$$

At the far end, this becomes

$$\Delta P=F_0\left(\frac{t}{LV_e}-\frac{BL}{6}\right)-\frac{1}{V_e}\int_0^t a\,dt+2F_0BL\times \sum_n \phi'(n)(\alpha^2+\beta_1^2)\epsilon^{-\alpha t}\cos(\beta_1 t-\theta_1)\text{ psi} \quad (34)$$

The expression

$$\frac{1}{V_e}\int_0^t a\,dt\text{ psi}$$

may be evaluated by graphically or numerically integrating the appropriate a/Q curve of Fig. 1 out to the given value of t and multiplying by Q/V_e.

If a constant pressure P_0 is impressed by the pump, the solution for ΔP is

$$\Delta P=P_0\times \left[1+2\sum_n \psi(nx)\epsilon^{-\alpha t}\cos(\beta_2 t-\theta_2)\right]+ \frac{2}{V_e}\sum_n \psi(nx)\int_0^t a(\tau)\epsilon^{-\alpha(t-\tau)}\times \cos[\beta_2(t-\tau)-\theta_2]d\tau\text{ psi} \quad (35)$$

where

$$\beta_2=\sqrt{\frac{(2n-1)(\pi/2L)^2}{MV_e}-\alpha^2}\text{ per second}$$

$$\theta_2=\tan^{-1}\frac{\alpha}{\beta_2}$$

$$\psi(nx)=\frac{(-1)^n}{\beta_2\sqrt{MV_eL^2}}\cos\frac{(2n-1)\pi}{2}\frac{x}{L} =\psi'(n)\cos\frac{(2n-1)\pi}{2}\frac{x}{L} \quad (36)$$

The expression $a(\tau)$ is the value of a at $t=\tau$. At the far end, this becomes

$$\Delta P=P_0\times \left[1+2\sum_n \psi'(n)\epsilon^{-\alpha t}\cos(\beta_2 t-\theta_2)\right]+ \frac{2}{V_e}\sum_n \psi'(n)\int_0^t a(\tau)\epsilon^{-\alpha(t-\tau)}\times \cos[\beta_2(t-\tau)-\theta_2]d\tau\text{ psi} \quad (37)$$

The expression

$$\frac{2}{V_e}\sum_n \psi'(n)\int_0^t a(\tau)\epsilon^{-\alpha(t-\tau)}\times \cos[\beta_2(t-\tau)-\theta_2]d\tau\text{ psi}$$

may be evaluated for a given value of t as follows:

1. Calculate β_2 and θ_2 for $n=1$. Also calculate α.
2. Calculate several values of $t-\tau$ over a range of time $\tau=0$ to $\tau=t$.
3. For each value of τ, evaluate $\epsilon^{-\alpha(t-\tau)}\cos[\beta_2(t-\tau)-\theta_2]$, and multiply by $Q[a(\tau)/Q]$, obtaining $a(\tau)/Q]$, from the appropriate a/Q curve of Fig. 1 taken at time $t=\tau$.
4. Evaluate this integral, using either a planimeter, or numerical method between time 0 and time t.
5. Now, multiply by $\psi'(n)$ for $n=1$.
6. Repeat calculations 1 to 5 for $n=2$ and $n=3$.
7. Add the results, and multiply the sum by $2/V_e$.

Fig. 7 shows the application of equations 32, 33, and 34 to a long pipe cable. In preparing these curves an allowance was made for a 2-second period during which the pump was coming up to speed. During this time the flow was assumed to be proportional to time.

Appendix III. Calculation of the Oil Demand and Pressures for a 69-Kv 1,500,000-Circular-Mil Oil-Filled Pipe-Type Cable System (System IV of Table II)

For basic parameters see Table IV.

Calculations of Oil Flows

Seasonal from 5 to 25 C ambient by equation 6

$$0_s=3\times 35{,}000\times 20\times 30.2\times 10^{-5} =635\text{ gallons}$$

For full load of 880 amperes continuously, by equation 1

$$\Delta V=0.0072\Delta T_c+0.0232\Delta T_i+0.1770\Delta T_o- 0.0132\Delta T_p$$

$$\Delta T_c=7.9\times 6.70=53$$

$$\Delta T_i=7.9\times 6.18=49$$

$$\Delta T_i=7.9\times 5.20=41$$

$$\Delta T_p=7.9\times 4.67=37$$

Therefore, $\Delta V=8.28$, and by equation 5, the oil expelled by sustained full load is

$$0_l=4.33\times 35{,}000\times 8.28\times 10^{-3} =1{,}250\text{ gallons}$$

Hence, the reservoir capacity should be at least

$$635+1{,}250=1{,}885\text{ gallons}$$

Required Pump Capacity

The maximum rate at which the pump may be required to supply oil will obtain if full load continuously held is increased to 1,040 amperes for 4 hours and then dropped. From Fig. 1 for system IV and equation 4 for the base load

$$a'/Q=(0-30.8)\times 10^{-6}=30.8\times 10^{-6} \text{ inches}^3\text{ per foot second}$$

and extrapolating for the additional transient load

$$a'/Q=(10.8-30.8)\times 10^{-6}=20\times 10^{-6} \text{ inches}^3\text{ per foot second}$$

Thus by equation 7

$$F=0.26\times 35{,}000[7.9\times 30.8\times 10^{-6}+ (10.2-7.9)\times 20\times 10^{-6}] =2.63\text{ gallons per minute}$$

Calculation of Pressures

Assuming close triangular configuration, from Fig. 3 $K=8$.

By equations 8 and 9

$$P_h=0.434\times 0.9\times 114=47\text{ psi}$$

$$P_f=35.5\times(35)^2\left[\frac{8}{(6.13)^4}+\frac{19}{35{,}000}\times \frac{12.36}{(2.07)^4}\right]a\mu=264a\mu\text{ psi}$$

Table IV. Basic Parameters

Diameters, Inches	Steady-State Thermal Resistances	Miscellaneous
$D_c=1.41$	$H_{cs}=6.70$	$L=35{,}000$ feet
$D_i=1.98$		$N=19$ by-pass sections
$D_s=2.02$	$H_{is}=6.18$	$l=12.36$ feet per section
$D_o=6.13$	$H_{os}=5.20$	$\Delta h=114$ feet at end of line
$D_p=6.63$	$H_{ps}=4.67$	$\gamma=0.9$ (Oil no. 1)
$D_b=2.07$		$Q_d=0.55$ watts per foot
$D_s/D_o=0.33$		$R_{dc}=8.60$ microhms per foot at 75 C R_{ac}/R_{dc} at conductor $=1.105$

Full load = 880 amperes; Q (including Q_d) $=(880)^2\times 8.60\times 1.105\times 10^{-6}+0.55=7.35+0.55=7.9$ watts per foot.

Emergency = 1,500 amperes for 15 minutes, $Q=21.6$ watts per foot, followed by 1,040 amperes for 225 minutes, $Q=10.2$ watts per foot.

If full load of 880 amperes is suddenly applied with an ambient of 5 C, the maximum value of P_f from Fig. 5, system 4 for $Q=7.9$, and from Fig. 4 for 5 C is

$$P_f=264\times225\times10^{-6}\times2,700=160 \text{ psi}$$

Thus the maximum internal pressure for a normal pressure of 200 psi at the elevated end is

$$200+160=360 \text{ psi}$$

If an emergency load of 1,040 amperes with an ambient of 5 C is dropped after the critical time which will yield the maximum value of P_f from Fig. 6 for $Q=10.2$

$$P_f=264\times94\times10^{-6}\times2,700=67 \text{ psi}$$

Assuming that a minimum pressure of 75 psi is required to suppress ionization, the minimum pumping pressure required is

$$75+47+67=189 \text{ psi}$$

which will occur 33 minutes after the load is dropped (see curve IV of Fig. 1) provided that the load was carried for the critical length of time.

The critical value of a sustained load for maximum P_f after dropping may be obtained by equation 14

$$Q=\frac{11.5}{5.20-0.17}=2.29 \text{ watts per foot}$$

The corresponding load current is

$$I=\sqrt{\frac{2.29-0.55}{1.105\times8.60\times10^{-6}}}=428 \text{ amperes or}$$

48.5 per cent full load

By equation 14 with a 5 C ambient

$$a\mu=4.2\times2,700\times\frac{30.8\times10^{-6}}{5.20-0.17}=0.070$$

Therefore, starting from steady-state conditions the maximum pressure loss which will occur on dropping load is

$$P_f=264\times0.070=18 \text{ psi}$$

References

1. *Discussion* by K. W. Miller of SYMPOSIUM ON 132,000-VOLT, SINGLE-CONDUCTOR, LEAD-COVERED CABLE, P. Torchio. *AIEE Transactions*, vol. 47, Nov. 1927, p. 213.

2. CHARACTERISTICS OF OIL-FILLED CABLE, G. B. Shanklin, F. H. Buller. *AIEE Transactions*, vol. 50, Dec. 1931, pp. 1411–12.

3. THERMAL TRANSIENTS AND OIL DEMANDS IN CABLES, K. W. Miller, F. O. Wollaston. *AIEE Transactions*, vol. 52, March 1933, pp. 98–113.

4. TRANSIENT TEMPERATURE PHENOMENA OF 3-CONDUCTOR CABLES, F. O. Wollaston. *AIEE Transactions*, vol. 68, pt. II, 1949, pp. 1284–97.

5. THE THERMAL RESISTANCE BETWEEN CABLES AND A SURROUNDING PIPE OR DUCT WALL, F. H. Buller, J. H. Neher. *AIEE Transactions*, vol. 69, pt. I, 1950, pp. 342–49.

6. A SIMPLIFIED MATHEMATICAL PROCEDURE FOR DETERMINING THE TRANSIENT TEMPERATURE RISE OF CABLE SYSTEMS, J. H. Neher. *AIEE Transactions*, vol. 72, pt. III, 1953, pp. 712–18.

7. THE DETERMINATION OF TEMPERATURE TRANSIENTS IN CABLE SYSTEMS BY MEANS OF AN ANALOGUE COMPUTER, J. H. Neher, *AIEE Transactions*, vol. 70, pt. II, 1951, pp. 1361–71.

◆

Discussion

E. H. Kirkham (Phelps Dodge Copper Products Corporation, Yonkers, N. Y.): This paper offers a new and very useful tool for pipe cable design, and the committee is to be complimented on a fine piece of work.

Since the advent of pipe cable, pipe size has been based on the allowable clearance between the cable and the pipe, clearance being defined as the distance between the inside top of the pipe and the top of the three cables in triangular arrangement.

There has been no unanimity of opinion as to what that minimum clearance should be. Recommendations ranged from 1 to 0.25 inch, and economic considerations governed exclusively. We recently had a case of a 5-mile line where a 7/8-inch clearance would admit the use of a 4-inch inside diameter pipe, but application of the equations in the paper disclosed that the use of such 4-inch pipe would result in pressures over 700 psi on increasing load. When 5-inch pipe was considered, we found that this pressure was under 300 psi.

These values would obviously have been lower with a shorter line, which leads to the generalization that for short lines the clearance should control, while for lines over about 3 miles the hydraulic characteristics might well determine the pipe size.

R. W. Atkinson (General Cable Corporation, Bayonne, N. J.): When considering the use of a larger pipe to reduce flow resistance, it might be feared that this would increase "oil demand" because of the larger volume of oil. It would appear, however, that the increased volume would be almost exactly offset by the lower rate of temperature rise within the pipe caused by the greater thermal storage capacity. Thus 10-watt power absorbed in heating 1 gallon of oil will produce exactly the same rate of expansion (milliliters per hour) as if absorbed in 2 gallons. Thus the advantage of the reduction in flow resistance by the larger pipe will be fully realized without a partial offset by increase of oil demand. Of course, the larger pipe will cause an extension in the time during which oil will flow and will require increased reservoir capacity. Even this small disadvantage is accompanied by a significant advantage in that the greater thermal storage capacity given by the large pipe will improve the peak load "ampacity."

John C. Parker (Memphis Light, Gas and Water Division, Memphis, Tenn.): It is the intent of this discussion to present the results of field tests, on one pipe-type cable circuit, which unfortunately could not be completed until after the preparation of the paper. The characteristics of this circuit are as follows:

Voltage, 115 kv
Conductor, round, compact strand, 500,000 circular mils
Insulation, 435 mils
Pipe, outside diameter, $5\,{}^{9}/_{16}$ inches
Q_d, watts per foot, 0.48
D_s/D_0, 0.339

The oil viscosity-temperature curve is the same as oil no. 1 in Fig. 4.

The average measured value of K for a 14,140-foot circuit of this cable was 4.5 for an oil viscosity of 530 centipoises and flow rates of 4.03 to 6.16 cubic inches per second.

Measured values of oil demands, a/Q and the unit temperature, time, transient of the oil, h_0 are given in Fig. 9. It should be noted that the front of the a/Q curve is dependent on the settling of the oil pressure relief devices.

The maximum measured value of a_μ/μ_0 was 234 microcubic inches per foot per

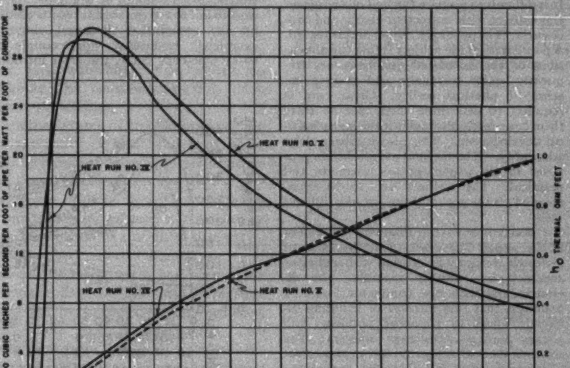

Fig. 9. Measured values of oil demands, a/Q unit, temperature time transient of the oil h_0, 115-kv high-pressure oil-filled cable

second for 8.0 watts per conductor foot when load was suddenly applied to the cable circuit, and 42 microcubic inches per foot per second for 3.5 watts per conductor foot when the load was dropped. It was surprising to find such excellent agreement of the theoretical values given in the paper and actual measurements in the field.

E. H. Grosser and **R. L. Rowan** (Commonwealth Edison Company, Chicago, Ill.): While the determination of transient oil pressures and oil flow in low-pressure oil-filled cable has been the subject of a number of papers presented before the AIEE, there have been no corresponding presentations of methods dealing with transients in high-pressure oil-filled pipe-type cables. This paper gives, we believe for the first time, methods whereby conditions in pipe-type cables may be calculated. It is true that there is a much greater pressure margin in this kind of cable as compared with the low-pressure oil-filled type, because of its higher operating pressures, so that transients that occur in dropping load, for example, cannot result in complete loss of pressure for any normal type of installation. Nevertheless, there are situations in which it becomes desirable to be able to determine pressure and flow conditions for pipe-type cable, and for these situations the Committee report should prove most valuable.

To get the temperature transient for pipe cable, it is necessary to refer to a paper by Mr. Neher (ref. 6 of the paper). It would be helpful, we think, if a set of sample calculations covering this part of the determination could be made available for the specific cable shown in the pressure transient calculations of the present report. It is suggested that this addition could be covered in the closing discussion.

F. O. Wollaston (British Columbia Electric Company, Ltd., Vancouver, B. C., Canada): It is difficult to prepare the text of a paper on this subject with consistent clarity and conciseness. The paper is a model in this regard. A peculiarity of the subject is that the dimensions of the calculated quantities are frequently quite unwieldy and convey no sense of physical reality. Great care is required to determine them and to state them completely throughout the mathematical development. This also has been done admirably. The method of calculation proposed in the paper appears adequate and practical. The authors are to be commended on the accomplishment of a difficult task.

I disagree with the following statement in the paper: "In many cases the effect of dielectric loss may be treated with sufficient accuracy by suitably including the dielectric loss with the conductor loss." I maintain that this method of handling dielectric losses in transient problems will always lead to erroneous answers. The rigorous method suggested in the paper, but not developed in detail, is the proper approach. A method of handling dielectric loss transients in Pirelli-type oil-filled cable with acceptable accuracy is given in references 3 and 4 of the paper. The basis of my criticism of the quoted statement follows. The rate of change of temperature at the first instant of a transient is a maximum in the element of the cable wherein the losses have been changed, and is zero everywhere else. For example, if the dielectric losses undergo a change, the insulation will experience at the very first instant the maximum rate of temperature change to which it is to be subjected. On the other hand, the rate of change of temperature in the conductor will be zero at the first instant. If the dielectric loss is considered to occur in the conductor instead of in the insulation, the conductor at the first moment of a dielectric loss transient will be constrained by the mathematics to undergo its maximum rate of temperature change, whereas the insulation will have zero rate of temperature change. This result is the exact opposite of reality. Nothing during the progress of the transient brings the calculated results any closer to reality. These considerations are most important in hydraulic problems, since the oil demand is directly proportional to the rate of temperature change.

Referring to the a/Q curves in Fig. 1, it will be seen that a/Q has a finite value at zero time. This value at zero time results solely from the oil demand contributed by the conductor. At this stage of the transient the cable insulation and the oil in the pipe contribute nothing to the oil demand. During the subsequent stages of the transient, the insulation and pipe oil contribute substantially to the oil demand. Because of their comparatively large volume, their contribution soon overshadows that of the conductor and the peak of the demand curve results. If the dielectric losses were assumed to occur in the conductor, the calculated oil demand transient due to dielectric loss would have exactly the same shape and per-unit value as the a/Q curves. Now turning to the a_d curves in Fig. 2, which were determined by a rigorous method, it is obvious that there is no correspondence whatever between the two sets of curves. This illustrates that the suggested approximate method will not produce results of reasonable accuracy. In many practical problems the effect of dielectric losses is minor or negligible and it is easy to fail to recognize that results obtained by the assumption discussed above are completely erroneous. For example in a 69-kv pipe-type cable, the error introduced by incorrect handling of dielectric losses would probably be negligible. In the first place, the dielectric losses are intrinsically small compared to load current losses. In the second place, the dielectric loss transient affects mainly the cable insulation, which contains only a small part of the total oil in the system. On the contrary, a substantial error might occur in problems involving 230-kv and higher voltage Pirelli-type oil-filled cable. In this case the dielectric losses would be much larger and would affect the majority of the oil in the system, that is, the oil in the insulation.

J. H. Neher: The Working Group is very appreciative of the interest with which this report has been received. As Mr. Kirkham has pointed out, it should furnish a ready means of determining whether or not a pipe size which is satisfactory from a cable-pulling standpoint will permit operation within permissible pressure limits.

Mr. Atkinson's observation that the maximum oil demand is substantially independent of the volume of oil employed had not occurred to us, although it is quite evident from Fig. 1, where it will be seen that the maximum values of unit oil demands for systems II and V are roughly the same, despite the fact that the oil volumes are in the ratio of 1 to 3. This is largely responsible for the reasonably close grouping of the curves of Figs. 5 and 6, and enables the user to compute quickly the maximum pressures which may be developed without a detailed transient temperature determination for the particular cable system under consideration.

In this connection, it will be observed that the test data submitted by Mr. Parker represents a maximum oil demand of 30 microcubic inches per second for a loss of 1 watt per conductor. The cable tested by Mr. Parker is somewhat different than any of those studied in the report and the calculated value of maximum unit oil demand is 34 microcubic inches per second. The corresponding value of a μ/μ_0 calculated approximately is equal to 270 microcubic inches per foot per second for a suddenly

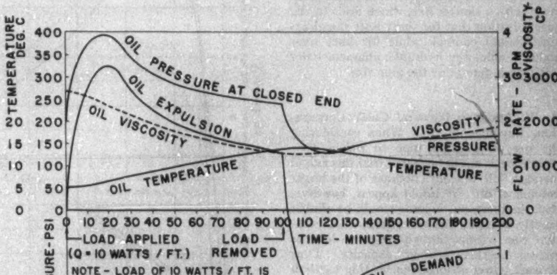

Fig. 10. **Flow conditions on pipe-type cable system with load applied and load removed, 30,000-foot 69-kv 350,000-circular mil $5^{9}/_{16}$-inch pipe, 300 psi maintained at pumphouse**

applied load of 8 watts per conductor foot as against a measured value of 234. The differences between these calculated and measured values amounting to about 15 per cent are not unreasonable considering the difficulties attendant to measurements in the field and the somewhat approximate nature of the basic calculations of the temperature transients involved.

With regard to the latter, Mr. Grosser and Mr. Rowan have suggested that a set of sample transient calculations be included. Unfortunately, space does not permit this, such calculations if made by the method of reference 6 for the four transients required for a given case would be as long as the report itself. As indicated in the report, however, these four transients were determined by an analogue computer (reference 7) and the calculations required after the computer had been set up merely involved multiplying the meter readings by an appropriate constant to obtain the transient temperature rises per unit of conductor loss at the conductor, mid-insulation, oil, and pipe.

Mr. Wollaston is quite correct in his remarks about the theoretically correct method of handling dielectric losses. This was followed in determining the curves of Fig. 2. In the case of cables of 69 kv and under, however, experience has shown that the results obtained are substantially the same whether the dielectric loss is included with the conductor loss or treated separately in a rigorous manner.

To present an over-all picture of what happens when load is picked up and dropped by a pipe-type cable system, Fig. 10 has been prepared. It will be seen that when the load is picked up, the oil pressure at the closed end builds up from an initial value of 200 psi to a maximum value of nearly 400 psi in about 20 minutes, after which it falls off in accordance with the characteristic oil demand curves. However, since the oil temperature is rising and its viscosity is lowering, the pressure will fall off at a faster rate than the oil demand since it depends upon the product of the oil demand by the viscosity.

If the load is sustained, the rate of oil expulsion will decrease to zero and the pressure will return to the initial value of 200 psi. In this particular case, however, the load was dropped after 100 minutes, resulting in a decrease in oil pressure at the closed end to 130 psi, which is less than the initial value of 200 psi, and a change in the direction of oil flow. The duration for which the load has been held before dropping has a pronounced effect upon the resulting pressure drop, and in this case the load has been held for the critical length of time which will result in minimum pressure at the closed end.

Recommendations for Improving Reliability of Stand-by Engine Generators for Microwave Communications Systems

NELSON B. THARP
MEMBER AIEE

IT IS common practice among the users of microwave communications systems to employ engine generator sets for stand-by operation during periods of interruption of the normal power source. Although this practice materially improves the reliability of systems, the engine generator set itself has sometimes proved to be a source of system outage. There are, of course, many causes for engine generator difficulties; however, the majority are traceable to several basic reasons.

The first source of trouble lies in the attempt to apply a standard engine generator unit in a service having highly specialized and rigorous requirements. This action has sometimes been the result of the user not being aware of the real operating problems involved and sometimes from the unavailability of suitable equipment. Experience has shown that standard units, although quite satisfactory for conventional use, may be quite inadequate for microwave stand-by use. Correctly applied, however, stand-by power units can attain a high degree of reliability.

A second source of trouble arises because many of the microwave system users do not have the experience and maintenance techniques vital to keep the engine generator sets in reliable operating condition. This experience comes with time, but meanwhile engine failures can decimate the continuity records of a microwave system.

Another source of trouble originates in the ambiguity or lack of defined terms and techniques describing performance and its measurement for the engine generator sets. Often, there is not a meeting of minds between the user and the engine generator manufacturer until after an installation had proved inadequate.

Considerable progress has been made in overcoming the problems by system users and by technical groups including both users and manufacturers. Two such groups are Radio-Electronics-Television Manufacturers Association (RETMA) Sub-subcommittees TR-14.3.2 and TR-14.3.3 which have proposed standards to establish consistent terminology, practical methods of measuring performance, installation procedure, and, where possible, acceptable standards of performance on engine generator sets for microwave stand-by service.

In this paper it will be attempted to outline practical requirements for purchase and installation of stand-by engine generator sets of 25-kw capacity, or less, for microwave systems. The recommendations are based on the experience of the author, users, and the proposed standards of RETMA committees on stand-by engine generators and housing for microwave. The material is substantially in agreement with the proposed RETMA standards and, in some instances, material has been quoted directly. While sufficiently rigorous to insure satisfactory operation, the requirements are close enough to standard commercial products to avoid any material increase in cost. The requirements will be presented along with a short discussion concerning the reasons for the recommendation.

Ordering and Performance Specifications

ENGINE

Duty. The engine should be capable of continuous unattended operation under rated load for a period of 30 days provided lubricating oil is supplied every 100

Paper 55-42, recommended by the AIEE Carrier Current Committee and approved by the AIEE Committee on Technical Operations for presentation at the AIEE Winter General Meeting, New York, N. Y., January 31–February 4, 1955. Manuscript submitted October 22, 1954; made available for printing November 17, 1954.

NELSON B. THARP is with the Westinghouse Electric Corporation, Baltimore, Md.

The author is grateful to George F. Thole for some of the information given in the section entitled "Battery Charger."

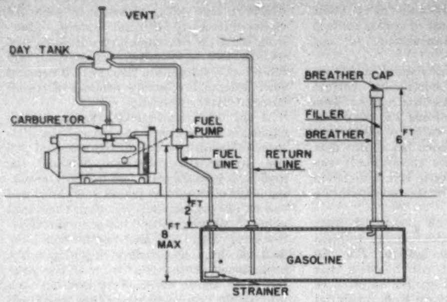

Fig. 1. Recommended installation stand-by engine generator

hours of operation and an adequate fuel supply is available.

This performance can only be expected after the proper break-in procedure, as recommended by the supplier, has been completed.

Speed. The engine shall operate at a nominal speed of 1,800 rpm or less.

Lower speed engines are preferable for durability. 1,200 rpm is desirable, 1,800 rpm is maximum.

Altitude. Standard engines should work at rated load up to 3,300 feet above sea level without any special parts.

Adjustment of carburetors should be all that is necessary for optimum efficiency at altitudes up to 3,300 feet. Equipment for altitudes above 3,300 feet should be so specified to supplier.

Ambient Temperature. The engine shall operate at full rating over the range of +40 to +125 degrees Fahrenheit (F) without auxiliary heaters. With auxiliary heaters, the engine shall operate over the range of −20 to +125 F. At −20 F, the engine shall start and deliver rated power within 30 seconds and, at 0 F, within 15 seconds.

Temperature refers to air ambient to engine including air intake to carburetor. Heaters can be crankcase or cooling-liquid heaters.

Relative Humidity. The engine shall develop rated power at relative humidities up to 85 per cent.

Although engines will generally start and operate at higher humidities, many manufacturers are reluctant to guarantee unconditionally full performance under less than full load conditions. This is because of the occasional icing condition occurring in the carburetion process. However, when the engine is operated near full load, the internal temperature and carburetion allow reliable operation at higher relative humidity percentages. With proper treatment, condensation on ignition components is not a major source of trouble.

Fuels. Gasoline engines shall operate satisfactorily on standard grades of gasoline, natural gas, propane or butane, or mixtures as specified.

Although performance should be satisfactory on standard grades of gasoline, marine or nonleaded gasoline of 80 octane is recommended. This type of gasoline will not foul the carburetor jets with residue during periods of inactivity—a common source of gasoline engine starting failure. Leaded gas accelerates carbon and lead deposits in the combustion chamber and reduces valve life. This is aggravated by the constant speed operation of most stand-by engines. Engine manufacturers recommend that engines in stand-by service be run under load about 30 minutes each week to insure starting when an actual need arises.

Air Intake and Carburetion. Both electric and thermostatic choking shall be provided for gasoline engines. Air intake shall be provided with an oil-bath air filter.

These items are generally standard and deemed necessary for reliable operation and electric and hand-crack starting.

Fuel Pump. Gasoline engines shall include a fuel pump capable of an 8-foot vertical lift. The pump shall be equipped with fuel strainer and sediment bowl and/or strainer. Means for hand-priming shall be provided.

Fuel Day (Gravity) Tank. Gasoline engines will be equipped with a properly vented, 1-quart auxiliary fuel tank to be installed between the fuel pump and the carburetor.

This tank is to insure quick starting by providing, by gravity, replacement fuel for that which evaporates from the carburetor during inactive periods. Return lines should be installed, as shown in Fig. 1.

Fuel Preheaters. Fuel preheaters shall be provided where necessary for efficient starting and operation under temperature conditions specified. An automatic gas control valve shall be provided where fuels other than kerosene or gasoline are used.

Where liquified gas fuels are used in cold climates, special facilities may be required to maintain vaporization rate. The use of liquified butane creates problems at temperatures below +60 F and liquified propane at temperatures below +14 F. A mixtures of these gases will require attention at some temperature between +60 and +14 F.

Ignition. The ignition system shall be adequately protected against failure caused by moisture condensation.

This protection may include covers and silicone treatment of exterior of ignition components. Engine should start even when covered with condensation.

Lubrication System. The lubricating-oil capacity of the engine shall be adequate to permit at least 100 hours of continuous operation on one filling. A pressure and oil-level gauge shall be furnished. Main and connecting-rod bearings shall be pressure-lubricated. A low-oil-pressure cutout switch shall be furnished which will stop the engine before damage when oil pressure falls below a safe operating value.

In general, water-cooled engines will operate over a longer time on one oil filling than air-cooled engines. This is apparently because of a somewhat more uniform cooling with liquid systems which reduces hot spots—a cause of oil deterioration.

Cooling System. Liquid-cooled engines shall be equipped with a pressure type of radiator cap designed to maintain a pressure of not less than 2 pounds per square inch. An adequate pusher-type fan, drawing radiator air away from engine, shall be provided. A thermostat shall be provided to control the operating temperature of the engine to be within the recommended range. A high-water-temperature cutout switch shall be provided to stop the engine if the maximum safe operating temperature is exceeded, as specified for the operating altitude. Maximum operating point of the high-temperature thermostat shall be 210 F. Air-cooled engines shall be equipped with a similar high-temperature cutout switch. The maximum operating temperature of the engine and cooling system shall be such that the temperature of the engine, when stopped, shall not normally rise to the operating point of the cutoff thermostat. If necessary, provisions shall be included to continue to operate the unit at no load for a period of time sufficient to meet this requirement. A suitable guard shall be provided to prevent accidental contact with fan blades, belts, or other moving parts. If an air-exhaust duct is required, suitable fastenings for the duct shall be provided on the engine (radiator frame).

Pressurized radiator caps are to increase the boiling temperatures of the cooling liquid. Pusher-type cooling fans are preferable from a safety and comfort standpoint, since heat and possible exhaust leaks around the engine are drawn away from the engines and through the radiator from where they can be safely ducted to the outside. Thermal overshoot upon stopping an engine must be prevented since restarting is impossible for a period until the engine temperature has returned to the operating range.

Governor Control. Stable engine speed, defined as a speed constant to within 0.8 per cent of final operating speed shall be obtained within 15 seconds after engine has been started. Stable engine speed shall be resumed in no longer than 8 seconds after any sudden change in load including no load to full load. During or after any change of load, the engine speed shall not vary more than 5 per cent. Belt-driven governors are not acceptable.

The limitations on governors, if met, are adequate to allow satisfactory microwave equipment operation even when the generator is supplying a flashing beacon load of 50-per-cent full load. Such a load, of course, may tend to create somewhat more wear on the governor.

Starting System. The starting system shall be sufficient to provide the minimum recommended cranking speed without overheating for 90 seconds. Starter apparatus shall be connected directly to the engine crankshaft or by gears or silent chain drive. Provisions for hand-cranking shall be included. Starting apparatus should be capable of at least five successive starts within a 5-minute period without overheating or damage, if the total operating time does not exceed 90 seconds.

Exhaust System. The exhaust system shall include means of adequate silencing and spark suppression. Exhaust outlets shall be of sufficient size to provide ready installation of commercially available exhaust assemblies. Recommended exhaust assembly and/or maximum allowable back pressure shall be furnished by the engine supplier.

Battery Charger. Equipment shall be provided which will charge starting batteries during the time the engine is running. It may be either a separate engine-driven generator or may be provided by other means. It shall have an adjustable, or automatic, charging rate to allow for the frequency and duration of the engine-operating periods in obtaining correct battery-charge replacement. It shall be capable of replacing starting loss of battery in less than 30 minutes of normal engine operation at 25 degrees Centigrade or more.

If the engine-operating periods are erratic with respect to number and duration, an automatic regulator is the only satisfactory method of getting adequate charge in a normal running period without overcharging on an extended run.

Start-Stop Control. The engine shall be provided with a manual start-stop control clearly marked and easily accessible.

To meet safety rules, this switch must not be placed over 6 feet from the rotating machine.

ALTERNATOR

The alternator shall conform to American Standards Association and National Electric Manufacturers Association motor and generator standards[1] for 50-degree-centigrade rise.

Temperature, Altitude and Relative Humidity. Requirements are the same as for the engine (see section entitled "Engine") except that the alternator shall meet performance requirements at a relative humidity of 95 per cent.

Capacity. The alternator shall be rated in kilovolt-ampere (kva) capacity at 0.8, 0.9 (lagging), and 1.0 power factor. The alternator shall be capable of carrying without damage a 1-minute load of 150 per cent of its rated amperes and a 2-hour load of 125 per cent of its rating.

The requirement for rating the alternator at various typical power factors is necessary because the actual kva capability of synchronous saturated field type of alternators changes with power factor. This is true as the phase of the load current affect the excitation field which in turn materially affects the kva capability. Many such machines rated at 5 kw and 5 kva at power factor=1 will not produce 5 kva at power factor=0.9; see Fig. 2 for example of a typical machine. Purchase orders should specify the voltage, wire arrangement (two or three wire, etc.), kva and power-factor requirements.

Voltage Regulation. Voltage output from no load cold to full load hot shall be within ±5 per cent of rated voltage on unity power-factor loads at an ambient temperature of 70 F. Normal rated voltages are in the range of 110 to 120, single phase, 3 wire, grounded neutral. Under any combinations of load (20 to 100 per cent), power factor (0.8 to 1.0), temperature (−20 F to +125 F), altitude (0 to 3,300 feet), and relative humidity (up to 85 per cent), output voltage shall not vary more than 5 per cent from rated voltage. This shall include conditions where load variations of 20 per cent are occurring at up to a 40-cycle-per-minute rate and where the generator is at either ambient or operating temperature.

The over-all 5-per-cent limitation is necessary as some engine generator guarantees refer to any one, but not any and all combinations of the load, temperature, humidity, altitude, and power factor; yet combinations of extremes often occur in actual practice.

Frequency Regulation. The output frequency shall not vary more than 1 cycle from 60 cycles with a load variation from 20 to 100 per cent.

Where the load uses a voltage regulator sensitive to power frequency, the regulator is usually cut out when the load is shifted to stand-by unit operation.

Wave Shape. Alternators shall meet the applicable American Standards Association standard[2] which requires that the deviation factor of the open-circuit terminal-voltage wave of synchronous

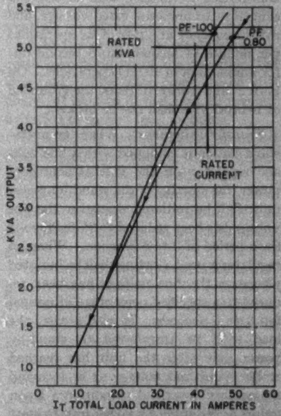

Fig. 2. Gasoline stand-by plant rated 5 kw 5 kva, power factor=100 per cent

machines shall not exceed 0.1. The definition of deviation factor of a wave is the ratio of the maximum difference between corresponding ordinates of the wave and of the equivalent sine wave when the waves are superimposed in such a way as to make this maximum difference as small as possible. An equivalent sine wave is a wave having the same frequency and rms value.

Poor wave shape of power source may in some instances cause malfunctioning of microwave equipment and serious discrepancies in measurement of voltages on some types of instruments.

Starting Control. Alternator shall be equipped with an enclosed control box (National Electrical Manufacturers Association type-1 or equivalent) for relays and contacts to provide electric cranking. Overcranking protection shall be provided which will automatically open the cranking circuit if the engine fails to start after a cranking period of 60 to 90 seconds. The cranking dropout must be reset by hand after a maintenance check to determine the cause of engine malstarting.

AUTOMATIC TRANSFER PANEL

The equipment shall be of suitable design to operate in unattended stations. Temperature, altitude, loads, and power-factor requirements are the same as for the engine (see section entitled "Engine") except that the transfer panel shall meet performance requirements at a relative humidity of 95 per cent.

Rating of Transfer Switch. The line-transfer contactor shall be capable of transferring a resistive load of 125 per cent of rated amperes, rated voltage, and rated frequency at a rate of six operations per minute (4 seconds on, 6 second off) for a minimum of 10,000 operations. On both 2- and 3-wire systems, the grounded or neutral wire shall not be broken.

Transfer Initiations. When the microwave station is equipped with a line-voltage regulator on the normal source of power, the starting of the stand-by power unit shall be initiated whenever the line voltage has been reduced to 95 to 98 volts for a period of 3 to 5 seconds. When no regulator is used, starting shall be initiated whenever the line voltage has been reduced to a specified percentage of normal for 3 to 5 seconds. In either case, the load shall be transferred to stand-by power unit after the unit has reached stable speed and voltage so as to avoid momentary overload condition. Upon failure of the stand-by power unit to start (lack of fuel, etc.), the load circuit shall not be transferred away from normal power source. No chattering of relays is permissible.

The voltage of 95 to 98 volts is chosen as it represents the minimum operating range of line voltage for the average line regulator (115 volts ±17 per cent). When no regulator is used, the minimum satisfactory operating voltage of the microwave equipment must be used to specify the line voltage for transfer initiation. Adjustable time-delay dropout is available from most stand-by suppliers covering a range from 1 to 10 seconds (±1/2 second). Also, adjustable voltage-sensitive dropout relays can be obtained which cover a range of 95 to 110 volts (±1 volt) to accomodate various conditions. Where brief overvoltage conditions are expected, similar facilities should be specified to disconnect the line power and replace it by the stand-by power unit.

Return to Primary Power. When a voltage regulator is used and the normal primary power source is restored to a value 2 to 6 per cent above the dropout voltage for a continuous period of at least 10 minutes, the load shall be transferred back to the primary power source. This transfer should not interrupt the power source by more than 1/4 second. Upon failure of the stand-by power unit while carrying load, the load shall be transferred back to the normal source immediately or at least upon restoration of normal supply. No chattering of relay contacts is permissible.

Adjustable time-delay functions are available from 10 to 30 minutes. In general, it is desirable, once the stand-by engine is started, to leave it running under load for a 20- to 30-minute period. This allows the battery to be recharged and the operating temperature to evaporate accumulated moisture in the lubricating oil. It is not desirable to run the engine any length of time without load as this accelerates the accumulation of carbon with accompanying engine inefficiency and maintenance cost increase. Fuel supply monitoring, local or remote, is desirable to avoid fuel exhaustion where each start means a 20- to 30-minute run under load.

Battery Charger. The transfer panel shall include a starting-battery trickle charger connected to the normal power source having an adjustable charge rate from 0.04 to at least 0.2 amperes. An ammeter and fuse shall be included in this circuit.

Since the condition of the battery will vary with age, the interim charging rate must be adjustable to maintain the optimum battery charge by replacing normal leakage charge. Experience has indicated that many battery failures are the result of excessive charging. Overcharging concentrates the acid which chars the separators, causing a high self-discharge rate resulting in severe sulfation of the plates. This high rate also disintegrates the positive grids, allowing the active material to fall to the bottom of the cells. This action can take place in a relatively short length of time. Accordingly, the trickle charger should be carefully set as per the battery manufacturers recommendations for the ambient temperature and operating conditions present. It is recommended that the trickle charger be run from a regulated line source if available. The generator or battery charger attached to the engine generator set should have an automatic charging-rate regulator or have the charging rate correctly adjusted for the average engine-starting frequency and average running time so as to replace the charge dissipated in the starting operation.

Alarm Contacts. An auxiliary contact shall be provided on the transfer panel which will close upon operation of the transfer switch for the purpose of activating a remote alarm.

Test Switch. A test switch, appropriately marked, shall be provided to simulate a normal source failure. The switch shall affect the control circuit only and shall have two positions—one to run the stand-by unit without transferring, and one to achieve actual transfer of load to the stand-by unit. When operating the engine without intending transfer of the load, a failure of the primary source will still cause normal transfer. When actually transferring the load, the transfer will take place with no greater than 1/4-second interruption of power to the load. The transfer back to primary source will take place automatically in normal fashion and timing as specified. The test switch shall be a momentary type that cannot be left in the test position.

Housing. The transfer panel shall be furnished with suitable terminals clearly marked for all external connections. It shall be for wall-mounting and enclosed in a National Electrical Manufacturers Association type-1 cabinet (or equivalent) with a gasketed dust-tight cover.

OTHER ELECTRIC CONTROLS

Emergency Stop Switch. The stand-by power unit shall be designed to accommodate a remote, wall-mounted 2-position switch for stopping the engine in an emergency. The circuit shall be such that, once stopped by the emergency stop switch, the engine will not attempt to restart automatically until the emergency switch is returned to normal position.

STANDARD ACCESSORIES

Each standby power set shall be supplied with the following standard accessories:

1. Starting battery of voltage and ampere-hour capacity recommended by engine manufacturer but, in every case, capable of cranking the unit at the recommended cranking speed for a period of 5 minutes at temperatures above 32 F. Batteries shall be shipped dry-charged with electrolyte included.
2. Underground fuel tank not less than 55 gallons for a 5-kw plant or 110 gallons for a 10-kw plant. Tank fittings to include suitable combination filler and vent pipe (with locking-type cap) not less than 30 inches long to allow use of measuring stick. Tank will include fitting for gas supply and return line from day tank. Tank must be suitable for direct burial.
3. Radio-noise suppression kit consisting of shielded ignition wires, caps over spark plugs and condensers shall be installed in standard equipment.
4. Special tools required for installation or normal maintenance, including a hand crank.
5. Wiring diagram installation, operation, and maintenance instructions; certified dimensional installation drawings; shipping list; and renewal parts lists.

OPTIONAL ACCESSORIES

The following accessories shall be available when needed:

1. Line ammeter and voltmeter (with meter switches if desired).
2. Vibration isolators.
3. Metal housing enclosure with removable side panels.
4. Meter-type fuel gauge.
5. Low fuel supply alarm (independent contacts to close at preset fuel level).
6. Liquid petroleum gas accessories: primary regulators, fuel preheaters, metering equipment, fuel lines, and connectors.
7. High rate position on trickle charger capable of replacing 1/2 ampere-hour capacity of the battery in 24 hours.
8. Overvoltage protection transfer operation (similar to low voltage function).
9. Automatic regulator on the engine-driven generator or battery charger to give optimum charge rate depending upon battery charge.
10. Extra-long-life lead acid or alkaline starting batteries.
11. Automatic exerciser timing unit for periodic stand-by unit operation. (A minimum of 30 minutes each week is recommended.)
12. Cathodic protection on fuel tank.

Fig. 3. Recommended installation stand-by engine generator

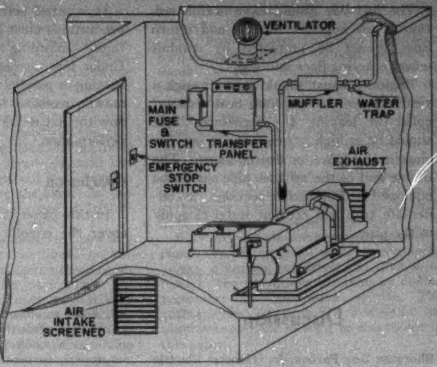

13. Engine crankcase or cooling-liquid heaters.

Installation Notes

The manner in which the stand-by unit is installed is an important factor in its reliability in microwave service. Fig. 3 shows a plan for installation which is recommended by engine generator and microwave equipment manufacturers. Following are comments on installation based on users experience and manufacturer recommendations:

A separate enclosure for the engine generator set is desirable from a safety, temperature rise, and noise point of view. The exit from the building should not be through the engine enclosure. The emergency stop switch should mount at the entrance to the engine room.

Pusher-type engine fans are recommended for exhausting engine-cooling air through fireproof ducts to the outside. This positively exhausts dangerous engine exhaust gases that have escaped. It also runs the heated air outside, preventing recirculation of air in building which tends to raise inside temperature rapidly.

Exhaust-ducting, and air inlet and outlet ports must not create too great a pressure drop or back pressure so that normal cooling-air volume is reduced. Caution should be taken to avoid locating in positions where prevailing drafts or winds interfer with normal air intake or outlet. Ports should be located so that they will not be blocked by snow, leaves, mud, etc.

The stand-by unit house must be ventilated and/or insulated to keep ambient within rated temperatures of −20 and +125 F. Batteries, relays, dry rectifiers, and other components fail rapidly beyond these limits and the manufacturers warranty will not apply. Batteries at low charge begin to freeze at about −20 F but, at full charge, the freezing point is much lower. When temperatures above 100 F are usual, lower specific gravity batteries will give better service.

In cold weather, water-cooled radiators must be protected against freezing. Some users report difficulty with ethylene glycol antifreezes penetrating into the lubrication oil and gumming or binding the pistons of the engines so that they will not start after an idle period.

In installing fuel lines, care must be exercised not to exceed the 8-foot lift ability of the fuel pump and to use large enough fuel lines on long runs to avoid excessive friction loss. The return line from the day tank to the fuel tank should terminate under the fuel surface to prevent an air circulation through the day tank to the vent. This would allow excessive evaporation of the gas from the day tank. The filler piper should discharge at bottom of fuel tank to prevent agitation of surface level on filling.

In installing engine, mount on raised base to facilitate draining oil and placement of drip pans beneath engine. A surrounding dike is desirable to confine spilled or leaking fuel. A 24-inch working space is desirable on all sides of engine.

The fuel tank should be installed underground with a minimum of 24 inches of fill over the tank. Where it is installed in wet soil, the tank should be weighted with stone or concrete to prevent its surfacing through its own buoyancy. The fuel tank should be provided with at least a 2-inch fill line with removable screen and locking cap, and a vent line with breather cap. These lines should extend well above possible snow or water line.

The fuel line should have flexible section at the engine. All fuel and return lines should be protected by conduit where entering floor and walls.

Engine exhaust should pass through a weatherproof, rodentproof, heat-resistant collar in leaving the structure. Exit should be as high as necessary to prevent clogging by fallen or drifted snow. The engine end of the exhaust pipe should be equipped with a flexible section. A condensate trap will prevent water-clogging of the pipe.

In liquified petroleum gas installations precautions must be taken to install fuel tanks according to local regulations. Under low temperature conditions, preheating or parallel manifold arrangements may be necessary to keep gas pressure and flow to that required by engine for rated performance.

Conclusion

In this paper it was not attempted to cover the equally important subject of operational maintenance since that is extensive in itself and warrants a separate discussion. The material presented does clearly indicate the necessity of obtaining and correctly installing engine generators sets well suited to the purpose intended.

References

1. Motors and Generators. *NEMA Standard MG1*, National Electric Manufacturers Association, New York, N. Y., 1955, sect. 11.9.

2. Rotating Electrical Machinery. *ASA Standard C50*, American Standards Association, New York, N. Y., 1943, par. 3.220.

◆

Discussion

Sherman Guy Forbes, Jr. (General Electric Company, Beaumont, Tex.): The paper fails to consider the one determinant that will assure reliable operation of emergency power plants using piston-type internal combustion engines as prime movers. That important ingredient of reliability is maintenance. By neglecting this important matter it fails to justify recommending specialized engine-generator sets for stand-by service in microwave communication systems.

Maintenance includes operating conditions and methods, and the type and quality of the upkeep given the individual components that make up an emergency power plant. These vital matters must be among the items considered fully to allow correct application of an engine-generator set as a part of an emergency power plant that will be dependable. If their vital importance is not weighed heavily, the best and most specialized engine-generator set will have have no reliability.

There are in reality three separate and distinct operating and maintenance problems, rather than one. The three are determined by: The engine and its auxiliaries; the generator and its auxiliaries; and the controls that make the engine-generator set a stand-by or emergency power plant.

Given the consideration due their individual peculiarities, it would appear that the basic engine-generator set can be a standard unit. Then a special unit of high cost due to small-quantity production and of dubious worth with regard to improvements in reliability will not be required.

The prime mover in either a standard or special engine-generator set will normally determine the over-all reliability of the emergency power supply. The types of sets in question employ piston-type internal combustion engines as their power source. In all such engines operating reliability is determined by the operating conditions and the upkeep of the engines. Thus these vital matters must definitely be among the items considered to allow correct application of an engine-generator set for emergency service on a microwave communications system. If they are not considered, the best and most specialized engine-generator set will have no reliability.

Without further delving into the operation and maintenance of the power plant, it is advisable to consider other subjects in the paper that affect the reliability of the power plant as a whole and which appear to be improperly correlated.

In the section entitled "Ordering and Performance Specifications" are itemized separately many conditions that cannot be so considered. Under the subtitle "Engine" duty, ambient temperature, relative humidity, and governor control should all be considered as a single item. The information about all of these is required to determine the real duty cycle and thereby the size of the engine required. Under the subheading "Alternator" specifications are set for the voltage regulation for 20% load variation occurring at a frequency of 40 cycles per minute. This disagrees markedly with the 50% load variation called for in the discussion of governor control. It is in the subsection "Frequency Regulation" that the allowable speed variation is established for the engine under the load swings given in the previously mentioned paragraphs. Furthermore, the description of the duty of the engine, and its governor control are contradictory. The first establishes a requirement for a continous rated load and the second a load that is continually varying in increments of 50 per cent (%) at an unspecified rate. In other words, during the daylight hours when the beacon is not operating full load will be but 50% of rated. This then affects what is said about relative humidity. It is stated that full load is required for reliable engine operation at high relative humidities. Finally, the engine is required to go from standstill to full load in less than 30 seconds.

Rather than break down all the engine specifications item by item, the specifications should establish the load, the duty cycle, and the special conditions of operation. These then can be used to determine the other conditions that must be met.

The paper indicates a preference for liquid-cooled engines. Such engines cannot successfully meet the rapid-start and load assumption requirements previously called for. This is because of the thermal inertia of the cooling system associated with a liquid-cooled engine. In addition, a liquid-cooled engine calls for the maintenance of a third fluid system not required with an air-cooled engine.

Where ambient temperatures permit, a liquified petroleum gas should be used as a fuel as these fuels minimize crankcase dilution, carbon deposits in the firing chambers, decomposition of the lubricating oils from chemical reactions with condensates in the crank case, wash-down of lubricating oils from the cylinder walls during starts, and starting difficulties after long periods of idleness.

It is felt that proper specifications covering operating requirements for the set must be established so that a good application can be made. Then specific operating conditions such as ambient temperatures, relative humidity, and altitude should be set up in each case in order to determine the variations of the basic set required to meet definite local conditions. With all of this specified, adequate operating and maintenance schedules can be established that will allow such sets to be truly reliable.

Nelson B. Tharp: As Mr. Forbes points out, maintenance is an important "ingredient of reliability," so much so, in fact, that the author clearly stated in the paper's conclusion that no attempt had been made to include it in this paper since to be adequately covered, it should be the subject of another paper. The fact that it was not included, however, does not in the author's mind "fail to justify recommending specialized engine generator sets for stand-by service in microwave communications systems" as Mr. Forbes states. One must purchase and install equipment before he can maintain it, and no amount of maintenance, however thorough, will overcome inherent shortcomings of misapplied equipment. The many users of engine generator sets in microwave services would object to the idea that their troubles have all been due to their poor maintenance work. The "special unit at high cost," appears to be contrary to the opinion of various engine generator manufacturers who were an integral part of the Radio-Electronics Television Manufacturers Association Committee and to the author's experience in purchasing units which meet the requirements.

With respect to the comments on the numerical arrangement of the material, it is true that a number of other arrangements could have been employed, possibly with some improvement in organization.

Mr. Forbes indicates a contradiction between the paragraphs on governor control and voltage regulation with respect to performance under varying loads. It should be noted that for voltage regulation it is required that the output voltage remain within 5% of rated voltage at load variations for 20 to 100% and specifically includes a 20% variation occurring at 40 cycles per second (beacon load). The comment on governor control (not the specification) merely points out that if the governor meets the requirements with respect to transient loads as specified for voltage regulation, even a 50% load variation from a flashing beacon will not affect the generator output to where it would interfere with normal microwave operation.

Mr. Forbes feels that there is conflict between the paragraph on duty in the section "Engine" and the one on governor control because one deals with steady loads and the other with transient loads. Both types must be considered since the engine generator will be expected to perform correctly under both conditions. Again, for governor control, the item does not set up a 50% flashing load requirement, but merely comments on the ability of the engine to do this if it meets the other transient requirements in the paragraph.

It is desirable for the engine to start and assume normal load in 30 seconds since the microwave users wish to reduce service outage to a minimum and this is the shortest reasonable time at −20 F. Some sad experiences have shown that there may be a significant difference between the time that an engine achieves rated speed and the time that it will assume rated load. Sometimes an engine will reach speed quickly, but when the load is applied will slow down to where it will fail to carry the load. In this case a warm-up period is required, resulting in delay in microwave service.

The paper was not intended to show any preference with respect to liquid or air-cooled engines. Its only purpose was to set up the engine generator performance requirements for adequate microwave service, and to comment on certain facts which may be of interest or value to a user. As long as an engine meets the requirements as set up by the microwave needs, choice of cooling is strictly the user's preference.

Mr. Forbes states that where ambient temperatures permit, liquified petroleum should be used. Although the author is inclined to agree with this statement and its supporting reasons, it was not felt that a paper of this nature has the right to say what type of power should be used, but rather should only describe what performance is necessary for adequate microwave service, and present facts on the characteristics of each various types of power sources so the user can choose for himself in the light of his particular situation.

It is hoped that someone will prepare a paper describing good maintenance techniques, operating problems, and their solutions in the operations of stand-by engine generators in microwave service. The author wishes to thank Mr. Forbes for his comments and the interest he has shown in this paper.

Fundamental Relations of System Voltage Drop and System Loads

G. M. MILLER
MEMBER AIEE

L. W. ROBBINS
ASSOCIATE MEMBER AIEE

ONE of the primary requirements of modern electric power systems is to deliver power to the loads at essentially constant voltage. With strong emphasis on fulfilling the voltage requirement, some of the important factors which affect the ability of the over-all system to deliver power are overlooked. A simple series circuit including a constant-voltage source, a series impedance, and a load impedance displays characteristics that are similar to those of an over-all electric power system. In this paper, it is explained how some of the fundamental concepts derived from a simple series circuit may be used to show the interrelations between voltage drop and load-carrying ability of a system. A clearer understanding of the factors which influence the ability of a system to deliver power will enable the engineer to plan system development and operation to make the most effective use of lines and transformers to deliver power from generation to the load.

Curves of voltage drop plotted against power delivered at constant power factor have been used for studying performance of a line section.[1,2] By considering an over-all power system as a single series impedance, similar curves give useful information on the ability of a system to deliver power at satisfactory voltage. A series circuit having a 1.0 per-unit (pu) constant-voltage source, 1.0 pu series impedance, and a static-impedance load gives general curves that may be adapted by a pu approach to estimate performance of a power system. Examples of the application of this method to an idealized system are presented to show the use of these general curves.

Conclusions

The general curves of voltage drop and power delivered through 1.0 pu impedance applied to electric power systems show the effect of such factors as the following:

1. The maximum power that can be transmitted through a power system depends on the total impedance of the system between generation and load, the resistance-reactance (R/X) ratio of the total system impedance, and the power factor of the load.

2. Supplying kilovar requirements of system load locally and power-factor improvement practices not only reduce the voltage drop in a power system but also increase the maximum power the system can deliver. An example shows that correcting load power factor from 0.8 to 1.0 more than doubles the maximum power the system being studied could deliver for a given voltage drop.

3. Convenient comparisons between normal and line-outage conditions can be made from the general pu curves by reference to different kilovolt-amperes (kva) bases determined from the total system impedance for each condition.

4. The use of several load tap-changing transformers or regulators in series can increase the maximum power a system is able to deliver at satisfactory voltage. Analysis using the general voltage-power curves provides a convenient method for comparing how effective additional regulating range or power-factor correction will be on a specific system.

Assumptions

The following general assumptions were made for this analysis:

1. The analysis is limited to steady state conditions.

2. Loads are represented by static impedances and are assumed to have constant kilowatt characteristics. This is the same assumption as made for a-c network-analyzer studies of load and voltage problems.

3. Synchronous stability problems are not considered. Where steady-state stability between synchronous machines is a problem, the stability limits may restrict power transfer to less than indicated by the voltage limits developed from this analysis.

4. Line-charging has been neglected in the general analysis. This gives more conservative results than would be obtained if appreciable amounts of line-charging capacitance were included.

Paper 55-41, recommended by the AIEE Transmission and Distribution Committee and approved by the AIEE Committee on Technical Operations for presentation at the AIEE Winter General Meeting, New York, N. Y., January 31–February 4, 1955. Manuscript submitted October 20, 1954; made available for printing November 17, 1954.

G. M. MILLER is with the General Electric Company, Schenectady, N. Y. L. W. ROBBINS is with the General Electric Company, Hudson Falls, N. Y.

The authors wish to acknowledge the assistance of P. H. Light in preparing this paper.

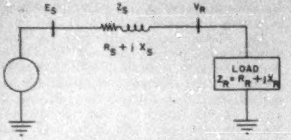

Fig. 1. Simplified equivalent circuit

5. In the application to actual systems it is assumed that adequate capacity is provided to avoid thermal limitations in components such as transformers, line conductors, and switches.

Explanation

The simple series circuit shown in Fig. 1 is made up of a source of constant voltage E_s, a system impedance Z_s, and a variable load impedance Z_r. If the load impedance is gradually reduced from some very high value, keeping power factor constant, the power received P_r increases and the load voltage V_r drops below E_s. The power increases up to a maximum and, if the load impedance is further reduced, the power received decreases until it reaches zero when the load impedance reaches zero. With E_s 1.0 pu volts and Z_s 1.0 pu reactance, Fig. 2 shows the load power and voltage as Z_r is reduced, keeping power factor constant. These curves may be calculated by solving equations 2 and 10 by longhand calculation, graphically by circle diagram, or by using the a-c network analyzer.

The point of maximum power is of some special interest. By letting k represent the ratio X_r/R_r, or the cotangent of the load power-factor angle, it is shown in Appendix I that the maximum power at a given power factor is delivered when $R_r = Z_s/\sqrt{1+k^2}$. Since k may vary, it is also shown that the greatest maximum power is delivered when $k = -X_s/R_s$ or when $R_r = R_s$ and $X_r = -X_s$. Adjusting the load impedance to equal the complex conjugate of the source impedance will be recognized as impedance-matching, as used frequently in communication and other low-power circuits. The application of impedance-matching to the fullest extent is impractical on constant-voltage power systems, but limited application of the same general principle can be made to use more effectively the capability of a system to transmit power from source to load.

The fundamental equations for power flow through impedance show that the power received at the load depends not only on the load impedance but also on the magnitude and R/X ratio of the system impedance. To cover the range of constants ordinarily encountered in electric utility systems, this analysis has been made covering system impedance R/X ratios from 0 to 0.4, and covering load power factors from 0.8 lagging to 0.98 leading.

Curves of load voltage and power received at constant power factor provide a convenient method to show the relation between system load-carrying ability, power factor, and voltage drop. Curves for loads at power factors of 0.8, 0.9, 0.98, 1.0 and 0.98 leading supplied from 1.0 pu voltage through 1.0 pu system impedance are plotted for system R_s/X_s ratios of 0 in Fig. 2, 0.1 in Fig. 3, 0.2 in Fig. 4, 0.3 in Fig. 5, and 0.4 in Fig. 6.

To show how system R/X ratio affects the ability of a system to deliver load at satisfactory voltage, a constant-voltage line A is shown on each family of curves at 0.825 pu volts. This particular value is used later in the section entitled "Example 1." It is based on the assumption that the transformer turn-ratios and the regulating range available in the system can provide rated voltage to the load as long as the pu voltage is not lower than 0.825 pu. Table I shows the maximum 0.8 and 1.0 power-factor loads the system can deliver at this voltage over the range of system R/X ratios from 0 to 0.4. Similar comparisons could be made at any other pu voltage or at other power factors.

Pu Approach

By special application of the pu system, one set of curves calculated for a source voltage E_s of 1.0 pu and a system impedance Z_s of 1.0 pu can give practical results for any power system that can be reduced to an equivalent of the simple series circuit shown in Fig. 1. Application of the method to study over-all system performance is described here, but it is equally applicable to the part of a system that is fed from a constant-voltage source. If the source voltage cannot be held constant, it is necessary to go farther back into the system until a source point is found where voltage can be maintained constant over the desired range of loads. Failure of the assumed source to maintain constant voltage would introduce sizeable errors in the maximum power delivered by the system.

When the pu system is used for system studies, a base kilovolt (kv) is usually chosen to correspond to operating voltage and a free choice of base kva can be made at any convenient number, like 50,000 or 100,000 kva. Base current and base impedance are dependent on base kv and base kva, as shown in Appendix II. For application of the pu curves, Figs. 2 through 6, to actual systems, the operating voltage at source E_s is chosen as base kv. The base kv at other voltage levels is then determined by the actual transformer turn-ratios. The most significant change from the usual procedure is to choose a base kva that will make the total system impedance Z_s equal to 1.0 pu.

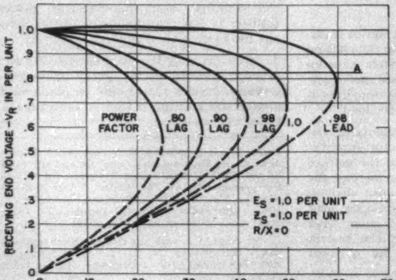

Fig. 2 (left). Receiving - end voltage and power received at constant power factor with system ratio R/X=0

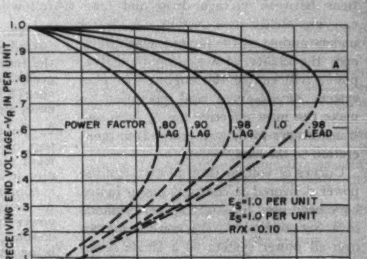

Fig. 3 (right). Receiving - end voltage and power received at constant power factor with system ratio R/X=0.10

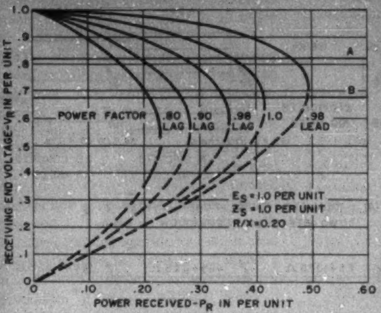

Fig. 4 (left). Receiving-end voltage and power received at constant power factor with system ratio R/X=0.20

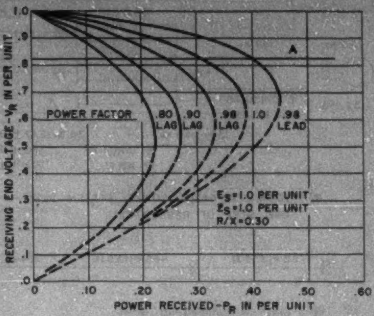

Fig. 5 (right). Receiving-end voltage and power received at constant power factor with system R/X ratio=0.30

Base kva is made dependent on system impedance and base kv. If the system impedance is changed, a different base kva is used. Comparisons between different systems are made in kilowatt power received rather than in pu, because the pu values are on different base kva.

Application

Several examples will demonstrate use of the pu curves to reach the general conclusions already stated.

EXAMPLE 1

A simple radial system having generation at one location, 138-kv transmission lines, 34.5-kv subtransmission, and 7.2/12.47-kv distribution is shown in Fig. 7(A). The transformer turn-ratios are chosen so that at no load a generator voltage 5 per cent below generator rating of 13.8 kv will give 138 kv on the transmission lines, 34.5 kv on the subtransmission, and 12.47 kv on the distribution system with the regulating transformer at the 34.5 to 12.47-kv step-down on its neutral position. The only load tap-changing equipment in the entire system is located at the 34.5 to 12.47-kv substations and has ±10-per-cent range available for regulating the 12.47-kv distribution system. For this example it is assumed that half of this regulating range is reserved to correct for contingencies giving higher than normal voltage at the primary side of these substations.

Since this simplified system is symmetrical, it can be easily reduced to a single equivalent impedance that will represent the entire system from the source of regulated voltage at the generator terminals to the load appearing at the primary of the distribution transformers out on the 12.47-kv feeders. The steps in the reduction of the system, conversion to pu, and finding the total system impedance are shown in Figs. 7(B) and (C). Since conditions of maximum load are to be considered, it is assumed that the generator voltage at peak load will be held at 14.5 kv, 5 per cent above generator rating of 13.8 kv. The generator operating voltage of 14.5 kv is chosen as base kv. The base kv for each of the other voltage levels is determined by the transformer turn-ratios from that base. It is assumed that 100,000 kva of transformer capacity is used at each transformation. The impedance for each part of the system is calculated in pu on a 100,000-kva base and the appropriate kv base. The base kv and the pu impedance for each part of the system on 100,000 kva are shown in Fig. 7(C). The total pu impedance for the system is $0.104+j0.4949$ pu or 0.506 pu on 100,000-kva.

By changing to a new kva base that will make 0.506 pu on 100,000 kva equal to 1.0 pu, the general curves calculated for 1.0 pu system impedance become directly applicable to the system being studied. Appendix II shows the derivation of the following expression for changing to the new base kva.

$$\text{base kva}_2 = \frac{\text{base kva}_1}{Z_1 \text{ in pu}}$$

$$\text{base kva}_2 = \frac{100{,}000}{0.506} = 197{,}500 \text{ kva}$$

The R/X ratio of the system impedance is 0.104/0.495 or 0.21. Since this is very close to 0.20, the curves in Fig. 4 will be used for this case.

The base kv for the 12.47-kv system established by the generator base kv and turn-ratio is 15.1 kv when the regulating

Table I. Power Received at 0.825 Pu Volts, 0.8 and 1.0 Power Factor for System R/X Ratios Between 0 and 0.4

System R/X Ratio	Pu Power Received 0.8 Power Factor	 1.0 Power Factor
0	0.172	0.467
0.1	0.153	0.403
0.2	0.145	0.355
0.3	0.137	0.312
0.4	0.130	0.278

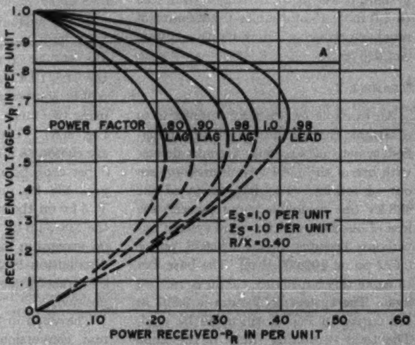

Fig. 6. Receiving-end voltage and power received at constant power factor with system R/X ratio=0.40

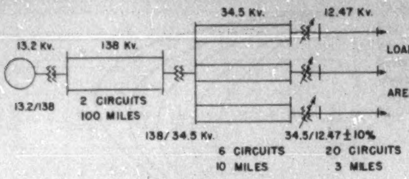
34.5 Kv.
12.47 Kv.
13.2 Kv.
138 Kv.
LOAD
AREA
13.2/138
2 CIRCUITS
100 MILES
138/34.5 Kv.
34.5/12.47 ± 10%
6 CIRCUITS
10 MILES
20 CIRCUITS
3 MILES

(A) IDEALIZED RADIAL POWER SYSTEM WITH ONE STEP OF REGULATION

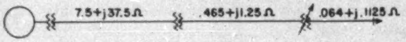
7.5+j37.5 Ω
.465+j1.25 Ω
.064+j.1125 Ω

(B) LINE IMPEDANCES IN OHMS

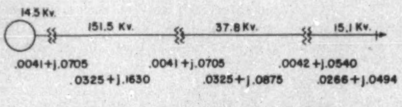
14.5 Kv.
151.5 Kv.
37.8 Kv.
15.1 Kv.
.0041+j.0705
.0325+j.1630
.0041+j.0705
.0325+j.0875
.0042+j.0540
.0266+j.0494

TOTAL Z_S = .1040+j.4949 = .506 PER UNIT

(C) BASE Kv. AND PER UNIT IMPEDANCES ON 100,000 Kva BASE

Fig. 7. Reduction of system having one load tap-changing transformation

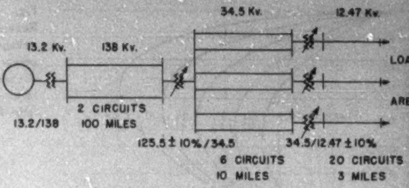
34.5 Kv.
12.47 Kv.
13.2 Kv.
138 Kv.
LOAD
AREA
2 CIRCUITS
13.2/138
100 MILES
125.5 ± 10%/34.5
34.5/12.47 ± 10%
6 CIRCUITS
10 MILES
20 CIRCUITS
3 MILES

(A) IDEALIZED RADIAL POWER SYSTEM WITH TWO STEPS OF REGULATION.

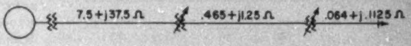
7.5+j37.5 Ω
.465+j1.25 Ω
.064+j.1125 Ω

(B) LINE IMPEDANCES IN OHMS

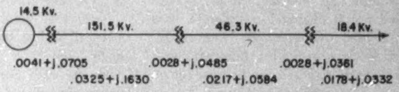
14.5 Kv.
151.5 Kv.
46.3 Kv.
18.4 Kv.
.0041+j.0705
.0325+j.1630
.0028+j.0485
.0217+j.0584
.0028+j.0361
.0178+j.0332

TOTAL Z_S = .0817+j.4097 = 0.418 PER UNIT

(C) BASE Kv. AND PER UNIT IMPEDANCES ON 100,000 Kva BASE

Fig. 8. Reduction of system having two load tap-changing transformations

transformers at the 34.5 to 12.47-kv substations are at maximum boost. Normal operating voltage of 12.47 kv is 0.825 pu, and it can be plotted in Fig. 4 as a horizontal line *A*. The intersection of this voltage line and the constant power-factor curves designates the maximum power that can be delivered at 12.47 kv at that power factor.

Evaluation of the power received shows that 28,800 kw can be delivered at 0.8 power factor, and 69,500 kw can be delivered at 1.0 power factor. For this system, power-factor correction from 0.80 to 1.0 more than doubles the amount of revenue-producing kilowatts the system can deliver.

Example 2

An example of practical interest is to determine the maximum load the simplified system of Example 1 could deliver with one of the 138-kv transmission lines out of service. The impedance of the 138-kv line is doubled to represent the loss of one line, and the total system impedance becomes $0.1365+j0.658$ pu or 0.672 pu on 100,000 kva. The base kva to make this impedance 1.0 pu is 149,000 kva. The system R/X ratio is 0.207 so the curves in Fig. 4 will again be used. The total regulating range is the same as was available in Example 1 so the same voltage line will be used.

With one 138-kv line out of service, the system can deliver 0.348 pu power on a 149,000-kva base or 51,800 kw at unity power factor. This compares with 69,500 kw at unity power factor when both lines were in service. At 0.80 power factor, 0.146 pu power can be delivered, which is 28,800 kw for the normal condition and 21,800 kw when the line is out.

Example 3

If the system used in Example 1 has load tap-changing equipment at the 138/34.5-kv transformation as well as the 34.5/12.47-kv substations, the results will be somewhat different. The system using two steps of regulation is shown in Fig. 8(A). The transformer turn-ratios are chosen so a no-load generator voltage 5 per cent below rating of 13.8 kv will give 138 kv on the transmission lines, 34.5 kv on the subtransmission lines with the 138/34.5-kv transformer tap-changers on maximum buck, and 12.47 kv on the distribution feeders with the 34.5/12.47-kv transformers on the neutral tap position.

The steps in the reduction of the system, conversion to pu, and finding the total system impedance are shown in Figs. 8(B) and (C). The generator operating voltage is chosen as base kv and is assumed to be 14.5 kv under maximum load conditions. At maximum load, the 138/34.5-kv transformers are assumed to be on maximum boost tap of 113/34.5 kv, and the 34.5/12.47-kv transformers are assumed to be on maximum boost tap of 34.5/13.72 kv. These turn-ratios give the new base kv, shown in Fig. 8(C). As in Example 1, it is assumed that 100,000 kva of transformer capacity is installed at each transformation. Fig. 8(C) shows the impedance of each part of the system calculated in pu on 100,000 kva and the proper kv base, as determined by actual turn-ratios. The total pu impedance for the over-all system is $0.0817+j0.4097$ or 0.418 pu on 100,000 kva.

The system impedance of 0.418 pu on 100,000 kva is equal to 1.0 pu impedance on a 239,000-kva base. Its R/X ratio is 0.20 so the curves in Fig. 4 apply.

The base kv for the 12.47-kv part of the system is 18.4 kv as determined by the base kv at the generator and the assumed turn-ratio. Normal operating voltage of 12.47 kv is 0.678 pu on the 18.4-kv base. A constant voltage line *B* is plotted in Fig. 4 at 0.678 pu volts. The intersection of this line and the constant

Power-factor curves show the maximum Power that can be delivered at 12.47 kv for that power factor.

The effect the second tap-changing transformation has on the load-carrying ability of the system is shown by a comparison with the results of Example 1. The results are tabulated in Table II.

The effect an additional regulator has on raising the maximum power delivered depends on where the regulator is located and on how much of the total system impedance it changes to a higher base kv. However, on any specific system, a comparison similar to Table II provides a sound basic approach for studying the economics of using additional steps of regulation or power-factor correction to raise the load-carrying ability of that system.

Summary

These three examples illustrate use of the general voltage-power curves to estimate over-all system performance. The pu approach makes it possible to obtain results on a variety of systems from one set or curves derived from a series circuit having a 1.0 pu voltage source and a 1.0 pu system impedance. The general curve and the pu approach provide a useful method for studying over-all system performance and comparing alternate plans or apparatus in planning for future system growth.

Appendix I. Calculation of Curves

In the series circuit, Fig. 1, E_s represents a source of constant voltage, Z_s represents the total system impedance, and Z_r represents the load impedance. The maximum power that can be delivered through a given transmission system or source impedance can be found by expressing the power received in terms of known parameters and solving for the maximum with respect to Z_r.[2]

The current in the series circuit is expressed as

$$I=\frac{E_s}{\sqrt{(R_s+R_r)^2+(X_s+X_r)^2}} \tag{1}$$

The power received at the load is

$$P_r=I^2R_r=\frac{E_s^2R_r}{(R_s+R_r)^2+(X_s+X_r^2)} \tag{2}$$

To find the maximum power that can be delivered at a given power factor, let k represent the cotangent of the power-factor angle or the ratio of X_r/R_r

$k=X_r/R_r$

$X_r=kR_r$

Substituting in equation 2

Table II. Comparison of Results

Load Power Factor	Power Delivered System Using One Load-Tap Changing Transformation, Kw	 System Using Two Load-Tap Changing Transformations Kw
0.8 lagging	28,800	50,200
0.9 lagging	37,500	63,900
0.98 lagging	52,900	82,000
1.0	70,100	99,500
0.98 leading	91,300	*

*This point is below the voltage at maximum power so the full tap range cannot be effectively used.

$$P_r=\frac{E_s^2R_r}{(R_s+R_r)^2+(X_s+kR_r)^2} \tag{3}$$

With k held constant to represent constant power-factor load, the value of R_r that will give maximum received power is found by taking the first derivative of P_r with respect to R_r and equating it to zero. Then, solving for R_r gives

$$R_r=\frac{\sqrt{R_s^2+X_s^2}}{\sqrt{1+k^2}}=\frac{Z_s}{\sqrt{1+k^2}} \tag{4}$$

This value of R_s in terms of Z_s and k is substituted in equation 3 and after expanding and simplifying gives

$$P_{r\ \max}=\frac{E_s^2}{2Z_s\sqrt{1+k^2}+2(R_s+kX_s)} \tag{5}$$

Since k may be variable, it is also desirable to find the value of k which gives the greatest maximum power received. This is done by taking the first derivative of $P_{r\ \max}$ with respect to k, equating it to zero, and solving for k. This gives

$$k=\pm\frac{X_s}{R_s} \tag{6}$$

The greatest maximum power received is found by substituting equation 6 in equation 5.

$$P_{r\ \max\ \max}=\frac{E_s^2}{4R_s+\frac{2}{R_s}(X_s^2\pm X_s^2)} \tag{7}$$

By inspection, this expression of received power will have its maximum value when $k=-X_s/R_s$ and equation 7 becomes

$$P_{r\ \max\ \max}=\frac{E_s^2}{4R_s} \tag{8}$$

For $k=-X_s/R_s$, the X_s term will have to be the negative quantity. When these conditions are met

$$R_r=\frac{\sqrt{R_s^2+X_s^2}}{\sqrt{1+X_s^2/R_s^2}}=\frac{R_s\sqrt{R_s^2+X_s^2}}{\sqrt{R_s^2+X_s^2}}=R_s \tag{9}$$

Since by definition $k=X_r/R_r$ and for greatest maximum power received $k=-X_s/R_s$ and $R_r=R_s$, then $X_r=-X_s$ or $X_s=-X_r$. Therefore, the system and load impedances are equal and the reactive components have opposite signs, or the load impedance and the system impedance are the complex conjugates of each other.

The voltage at the load is of primary interest in constant-voltage electric power systems. It can be calculated

$V_r=E_s-IZ_r$

In phasor form

$$I=\frac{E_s}{R_s+R_r+j(X_s+X_r)}$$

and

$$V_r=E_s\left(1-\frac{R_s+jX_s}{R_r+R_s+j(X_s+X_r)}\right) \tag{10}$$

$$V_r=E_s\left(\frac{R_r+jX_r}{R_r+R_s+j(X_s+X_r)}\right)$$

Appendix II. Calculation of Base Kva and Base Current

In balanced, 3-phase systems, the relations between system quantities in ohms, amperes, volts, and corresponding pu quantities are given by the following equations

base kva = base current, amperes $\times\sqrt{3}$ base line-to-line kv

base current, amperes =

$$\frac{\text{base kva}}{\sqrt{3}\ \text{base line-to-line kv}} \tag{11}$$

base impedance, ohms =

$$\frac{\text{base line-to-line kv}\times 1{,}000}{\text{base current}\times\sqrt{3}}=\frac{(\text{base line-to-line kv})^2\times 1{,}000}{\text{base kva}} \tag{12}$$

$$\text{pu } Z=\frac{\text{actual } Z,\text{ ohms}}{\text{base impedance}}$$

$$\text{pu } Z=\frac{\text{actual } Z\times\text{base kva}}{(\text{base line-to-line kv})^2\times 1{,}000} \tag{13}$$

From equation 13, the following expression for changing pu impedance from one kva base to another or from one kv base to another is apparent

$$\text{pu } Z_2=\text{pu } Z_1\left(\frac{\text{base kva}_2}{\text{base kva}_1}\right)\left(\frac{\text{base kv}_1}{\text{base kv}_2}\right)^2$$

Rearranging

$$\text{base kva}_2=\text{base kva}_1\left(\frac{\text{pu } Z_2}{\text{pu } Z_1}\right)\left(\frac{\text{base kv}_2}{\text{base kv}_1}\right)^2 \tag{14}$$

Equation 14 may be solved to find a new base kva that will make the pu impedance on the old base kva equal to 1.p pu on the new base. Assuming no change in base kv, the equation is simplified to

$$\text{base kva}_2=\frac{\text{base kva}_1}{\text{pu } Z_1} \tag{15}$$

References

1. PRINCIPLES OF ELECTRIC POWER TRANSMISSION (book), L. F. Woodruff. John Wiley and Sons, Inc., New York, N. Y., 1938, p. 179.

2. AC POWER TRANSMISSION AT HIGHER VOLTAGES, I. B. Johnson. *Electric Light and Power*, Chicago, Ill., Jan. 1950.

3. ALTERNATING-CURRENT CIRCUITS (book), R. M. Kerchner, G. F. Corcoran. John Wiley and Sons, Inc., New York, N. Y., 1951, pp. 133–34.

◆

Discussion

H. R. Tomlinson and R. O. Bigelow (New England Power Service Company, Boston, Mass.): The authors have provided system planners with an interesting approach for estimating, on an over-all system basis, the voltage performance of alternate methods of system expansion. This method appears applicable in those cases where voltage conditions alone are the determining factor in establishing maximum permissible line loadings; and where sufficient accuracy can be obtained by reduction of the system constants to a single lumped impedance. It seems likely that these restrictions may result in very limited applications of the method or in erroneous conclusions from a study of alternates if the limitations of the method are unintentionally exceeded.

In the first place, the practical problems of system planning invariably involve a combination of thermally limited and voltage-limited facilities which are closely interrelated. Furthermore, the importance of the thermal limitations is greatly increased as voltage-improving devices such as regulators or capacitors are installed on the system. It does not seem practical, therefore, to eliminate this interrelationship as suggested by the authors' assumption 5. Strong emphasis should not be placed on voltage requirements without giving equal consideration to the importance of delivering power within thermal limitations and with losses based on optimum design. As an example, one conclusion which might be drawn from a study based on the power-versus-voltage curves of the paper is that an increase in load capability of a system can be provided more economically with voltage-regulating equipment than with shunt capacitors installed at the locations of reactive load. This appears by comparing an investment in regulating equipment with an investment necessary for shunt capacitors to provide the same increase in load capability. Although this result verifies the fact that strictly voltage limitations can be alleviated more economically with regulating equipment than with capacitors, it completely excludes both the increased load capability provided by capacitors in thermally limited elements of the system and the reduction in losses in all elements of the system back to the source of supply. These added factors will generally be predominantly favorable to the capacitor alternate.[1]

Secondly, the method requires that the entire system be reduced to a single lumped impedance. This means that any studies based thereon must be limited to consideration of only two points on the system. In the examples given in the paper, the authors concentrate their attention on a source, either the generator terminals or some other bus, where constant voltage is maintained, and on an effective center of distribution where the load is assumed to be concentrated. No consideration is given to the intermediate substation bus voltages or gradients on intervening lines having widely different R/X ratios. Again, considering the method from the point of view of application to practical system design problems, there are very few cases were conditions at these intermediate points can be neglected.

A good example is a typical distribution feeder having a voltage gradient between the first and last customer. The application of additional regulating equipment will permit heavier loading for the same center-of-distribution voltage but there will be a steeper voltage gradient which may exceed permissible voltage limits at the extreme ends. When this type of approach is extended to include the entire supply system, it is necessary to retain, in the equivalent representation, the identity of important intermediate points between the source and the load. This is particularly true on large systems where a significant portion of the load may be delivered at transmission or subtransmission voltages. In addition, the lumped impedance approach provides no means of including diversity or of establishing which portions of the system are voltage-limited and which portions are thermally limited.

To summarize, we concur with the authors' conclusion that the use of capacitors and voltage regulators will pay large dividends by increasing permissible loadings with continued acceptable voltage service. It is also evident that the generalized curves presented in this paper provide a very useful tool for estimating purposes on those portions of a system where voltage conditions can definitely be established as the only limiting factor and where intermediate points are of no concern.

It appears questionable, however, whether this technique can be applied successfully to an entire system from generator to load, as suggested by the authors in their illustrative examples. It is recognized that general studies of this type must be based on simplified equivalents if the complexity of the mathematics is to be contained within reasonable bounds. It is equally important, however, to realize that the value of the results obtained are entirely dependent upon the accuracy with which this equivalent represents actual system conditions. It is our opinion that application of this method on such a broad scale requires an oversimplification which may lead to serious error.

REFERENCE

1. AN EVALUATION OF POWER-FACTOR CORRECTION ON A SYSTEM BASIS, H. R. Tomlinson, R. O. Bigelow. *AIEE Transactions*, vol. 73, pt. III, 1954 (Feb. 1955 section), pp. 1,677–84.

G. M. Miller and L. W. Robbins: We certainly agree that many of the details have not been included in the examples of the paper. We wonder, however, if these details are ever handled completely when projecting the system into the future, say, as far as perhaps half the life of the system being built today. At that time, the system load will be two or four times today's load. Will the increased load be carried simply by duplicating today's system or will some of the increased load be carried on today's system. Certainly, decisions made now will affect what can be done in the future. Perhaps the idealized system approach is one method of answering these questions.

Mr. Tomlinson and Mr. Bigelow very accurately pointed out that there are two ways in which comparisons can be drawn from the curves of the paper. One is the comparison between regulating equipment and power-factor improvement equipment to handle the same kilowatt load. The second comparison concerns the amount of loading that can be handled within a given system voltage pattern. It should be noted that these two comparisons correspond to a vertical and horizontal comparison respectively on the curves of Figs. 2 through 6. We agree that losses and thermal loading should be part of the engineering evaluation of the first comparison. Actually, we have found the approach of the paper particularly useful in evaluating losses for various system patterns.

In the second comparison we would like to point out one method that might be used to factor in the effect of thermally limited equipment when considering increased loading within a given system voltage pattern. We may use the first example of the paper whose total transformer impedance represents very nearly 40 per cent of the total impedance between generation and load. Normally, transformers are applied on a thermal basis and transformer bank sizes would be expected to increase proportionally to the increase in load permissible with power-factor improvement. This would result in a decrease of transformer impedance proportional to the reciprocal of the increase loading. Actually, this results in an even larger increase in the loading of the remainder of the system than is indicated in Table I. Referring to line *A* of Fig. 4, it is seen that power transmitted at 0.98 lag equals 0.27 pu and the power transmitted at 0.98 lead equals 0.46 pu. The new system reactance at 0.46 pu loading would be equal to 0.6 + 0.27/0.46 × 0.4 or 0.824 of the original system reactance. However, the 0.46 pu loading is on the new system base and corresponds to 0.46 × 1/0.824 or 0.56 pu loading on the base of the original system. A second approximation of the transformer reactance is indicated and this results in an increase loading to 0.58 pu on the original system base. From this it may be concluded that it is possible to more than double the loading on that part of the system which made up 0.6 of the original impedance by increasing the load power

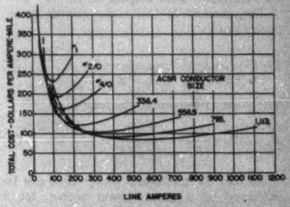

Fig. 9. Transmission costs in dollars per ampere-mile for seven steel-reinforced aluminum-cable conductors versus line loading in amperes. Fixed costs of $10,000 per mile, conductor cost, $0.50 per pound, and losses are evaluated at $300 per kilowatt

factor from 0.98 lag to 0.98 lead. In our example this corresponds to doubling the loading on all the lines.

We would like to refer to some unpublished work covering the economics of transmission line conductor size to indicate the possible economics that might be realized if the system is built to take this increased loading. Total cost has been determined on an ampere-mile basis as the function of three costs:

1. Those costs that are independent of conductor size such as right-of-way; terminal equipment; that part of the structure and insulation costs independent of conductor size; overhead ground wires and structure grounds, if required; and engineering.
2. Those costs that are a function of conductor size such as delivered cost of conductor; stringing costs; and that part of the structure and insulation costs which is a function of conductor size.
3. The cost of the power losses. This is a function of line loading and conductor size and is equal to $3\,I^2R$.

Fig. 9 shows some of the results of this study. It indicates that large conductors and heavy line loadings make for minimum line costs and it appears to justify the careful investigation of those factors affecting line loading.

Design of the Adjustable Lin-O-Phase Filter

REUBEN LEE
MEMBER AIEE

ALONG with the growth of power line carrier communications and consequent crowding of the frequency spectrum between 40 and 200 kc, the need for band-pass filters has arisen to prevent adjacent channel interference. With frequency-modulated transmission, requirements for these filters are unusually difficult, as can be seen from the response limits shown in Fig. 1. A specified maximum insertion loss of 17 decibels (db), a passband of ±3 kc, together with attenuation at ±8 kc of −100 db compared to mid-band present a technical problem unusual in two respects: Design of the filter to meet specified requirements, and measurement of the filter characteristics. In both the design and the measurements, special precautions are necessary prevent stray pickup from spoiling performance.

Electrical Design of Filter

Performance required of these filters is as follows:

1. Must adjust to any frequency from 40 to 200 kc.
2. Maximum mid-band insertion loss must not exceed 9 db at 40 kc and 17 db at 200 kc. Must be proportional at other frequencies.
3. Attenuation at frequencies must be ±8 kc from mid-band, 100 db minimum below mid-band loss.
4. Response at frequencies ±3 kc from mid-band must be within 5 db.
5. Maximum distortion must be 10 per cent (with 1,000-cycle audio and modulation index = 2.5) when tested in frequency-modulated transmitter-receiver setup.
6. Response and distortion limits must not be exceeded over a range of temperature from −20 degree centigrade (C) to +70 C, and humidities up to 95 per cent.
7. From 2 to 10 filters shall be capable of being connected in parallel across 100- to 200-ohm transmission line without interaction.
8. Absorption of local transmitter power, at any frequency, must be less than 1 per cent per filter.
9. Must be mechanically sturdy.

To prevent distortion to a frequency-modulated signal, it is necessary to consider both amplitude and phase response over the frequency range of each filter. An ideal filter would have attenuation and phase shift as shown in Fig. 2, i.e., the attenuation would be zero in the passband and infinite at all other frequencies. The phase shift would be linear throughout the passband. Then the signal at the filter output would be an exact replica of the input signal but delayed in time. Such a filter cannot be realized in practice because of inevitable coil and reflection losses.

Several types of filter have the necessary attenuation; shunt-turned band-pass configuration of Fig. 3 was chosen because of its simplicity and fairly linear phase shift over the pass band.[1] Linearity of phase shift in the Lin-O-Phase filter is sufficient to prevent distortion of frequency-modulated signals transmitted through the filter. This is indicated by the typical 100-kc carrier-frequency phase-shift curve shown in Fig. 4. Component values of inductance and capacitance are calculated from the usual design formulas which are given in the following.

For a full section, each coil has

$$L_1 = \frac{(f_2 - f_1)}{4\pi f_1 f_2} R \text{ henrys} \tag{1}$$

Each series capacitor has

$$C_1 = \frac{f_1 + f_2}{4\pi f_1 f_2 R} \text{ farads} \tag{2}$$

Each shunt capacitor has

$$C_2 = \frac{f_1}{\pi f_2 (f_2 - f_1) R} \text{ farads} \tag{3}$$

where

f_1 = lower cutoff frequency
f_2 = upper cutoff frequency
R = filter characteristic impedance

Frequencies f_1 and f_2 lie somewhat outside of the passband. Calling the frequency spread for 3-db response BW

$$\frac{f_2 - f_1}{BW} = 1.4$$

To avoid distortion, phase shift must be close to linear from f_1 to f_2. For a 14-section filter with the response of Fig. 1 and phase shift of Fig. 4, distortion was 8 per cent maximum.

The wire used in winding the coils is Litz. Coil Q changes with frequency, as shown in Fig. 5. All coils are vacuum-impregnated in high-grade wax to exclude moisture and maintain Q under extreme humidity. The need for high Q is greatest at the highest carrier frequencies. At these frequencies, mid-band loss would exceed the limit if Q were lower than 180.

The filter is made adjustable so that it may be tuned to any frequency within the range. A total of 16 different designs covers the carrier band of 40 to 200 kc, with each filter covering about a 10-per-cent frequency range. These filters are all similar in construction and differ from each other only in the values of inductance and capacitance necessary to tune the filter to the desired frequency. Tuning is accomplished by an adjustable slug within each coil. The range over which

---

Paper 55-78, recommended by the AIEE Carrier Current Committee and approved by the AIEE Committee on Technical Operations for presentation at the AIEE Winter General Meeting, New York, N. Y., January 31–February 4, 1955. Manuscript submitted October 21, 1954; made available for printing December 3, 1954.

Reuben Lee is with the Westinghouse Electric Corporation, Baltimore, Md.

The author is grateful to R. W. McCusker for doing the experimental work on which the paper is based.

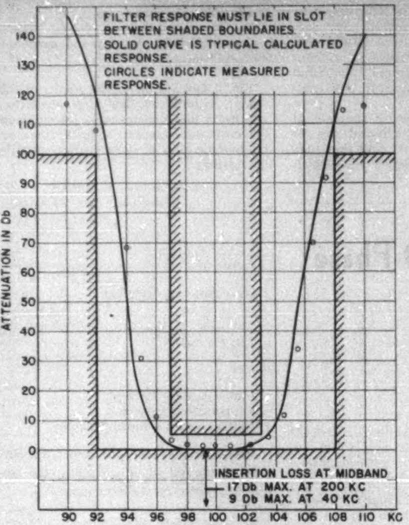

Fig. 1. Line-O-Phase filter frequency response

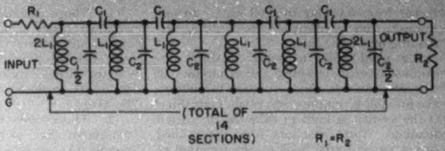

Fig. 3. Lin-O-Phase filter circuit configuration

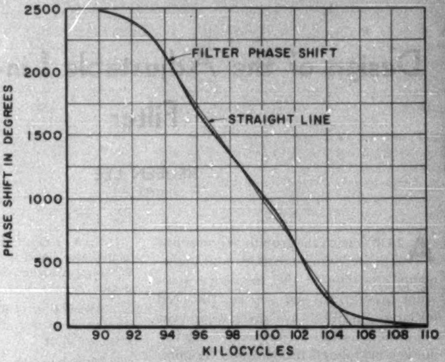

Fig. 4. Typical Lin-O-Phase filter phase shift versus frequency

the coil can be tuned is limited to 25 per cent of maximum inductance to maintain the coil Q values necessary to keep insertion loss within the desired limits.

To prevent loading of the power line with several parallel-connected filters, high filter impedance Z_0 is used, on the order of 10 to 20 kilohms. For the frequency range under consideration, a filter having Z_0 in the 10,000- to 20,000-ohm range gives convenient values of C and L. A high impedance filter operating between resistive terminations $R_1 = R_2 = Z_0$ prevents absorption of local transmitter power by the filter input sections. Filter impedance Z_0 varies with frequency, as shown in Fig. 6. The mid-shunt impedance drops to low values at frequencies below f_1 and above f_2. A transmitter operating at these frequencies would deliver most of its power into the filter if it were not for the high value of Z_0.

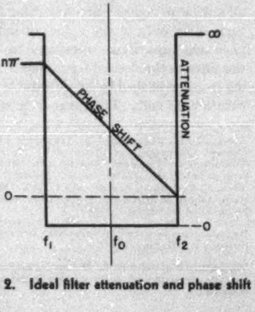

Fig. 2. Ideal filter attenuation and phase shift

Physical Design of Filter

Fig. 7 shows the Lin-O-Phase filter with the cover off and with a section of the filter shown separately. Each section is mounted on micarta angle as a separate subassembly. A core surrounding the adjustable coil has two half-cups of powdered iron cemented together. On the top half is a brass turret which supports the tuning slug. Both cups and slug are molded of finely divided iron particles and an insulating bond. Core temperature coefficient of permeability is 0.002 per cent per C. At the sides of the coil are mounted the series and shunt capacitors. Wiring between sections passes through notches in the partition. Components are not grounded to the case, but the return wire, G in Fig. 3, is insulated to eliminate ground currents which might link directly between terminals without passing through the filter.

Each filter section is completely shielded from each other section. Shielding is necessary because of stray flux from the adjustable coils. Such shielding is not necessary in fixed-frequency filters using toroidal coils; with care in manufacture, toroidal stray flux can be made negligible. The filter case itself is made of cast iron and has 15 compartments, one for each section. The first and last sections are half-sections for matching purposes. Each compartment is lined with a nonferrous metallic liner to maintain coil Q at a high value. If the nonferrous liner were omitted, stray flux from the coil would cause sufficient loss in the cast-iron case to degrade Q below an acceptable value.

The assembly is mechanically quite rugged. Of the many filters which have been shipped so far, all have withstood shipping shocks with no change in tuning or other damage.

Stray magnetic flux emanating from the top of the core in each compartment is shown approximately by the thin lines in Fig. 8. In this figure, the nonferrous liner is aluminum. Most of the flux crosses directly from the plunger to the cup core, as indicated by the short horizontal lines. Small inevitable air gaps exist around the plunger and where the cup cores are cemented together. Some of the flux from the plunger gap re-enters the cup core at some distance from the

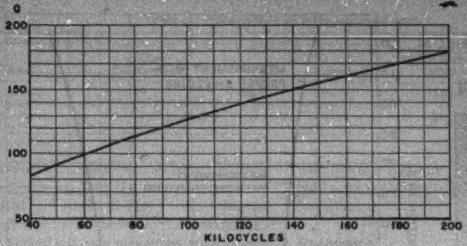

Fig. 5. Variation of filter coil Q with frequency

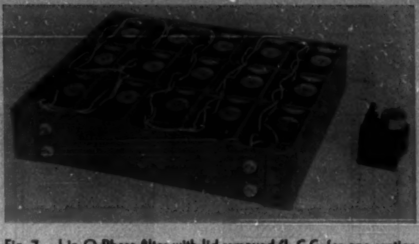

Fig. 7. Lin-O-Phase filter with lid removed ($L_1C_1C_1$ for one section shown separately)

plunger. Other flux lines strike the thick top wall of the turret and cause eddy currents to be set up in the direction shown by the arrow points and tails. These eddy currents cause most of the flux to be deflected away from the turret so that very little enters the turret except for a few mils of depth on the inner surface. The flux is further deflected away from the sides of the turret by eddy currents shown along the vertical walls and re-enters the core at the base of the turret. A few of the flux lines leak out of the small gap between the turret and the cup core where they fan out until they strike the aluminum liner. Here, again, they set up eddy currents which deflect them down toward the gap between the cup cores. A much smaller amount of flux penetrates the aluminum liner. This is represented by the single line which sets up eddy currents in the cast-iron partition wall, and which in turn deflects flux back to the iron core.

Field strength H, shown as an ordinate and causing this stray flux, is indicated qualitatively at the top of Fig. 8 with abscissa corresponding to radial distance from the center of the plunger. The turret shields the current at the top of the coil so effectively that it is not necessary to use an iron cover for the filter. The cover used with the filter of Fig. 7 is made of 1/8-inch thick aluminum.

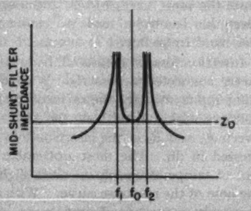

Fig. 6. Variation of filter impedance with frequency

In each compartment, stray flux strikes the nonferrous liner and sets up shielding eddy currents in a similar manner. Only a very small fraction of the total stray flux reaches the cast-iron partitions between compartments. What little flux does reach the cast iron penetrates the casting walls to a still smaller surface skin than in the nonferrous liner. Attenuation of the stray magnetizing force produced by each coil is thus effected in two stages: first, by the liner and, second, by the case. The strength of the magnetizing force at any distance x from the surface varies accordingly to the following equation

$$H=H_0\epsilon^{-\frac{x}{\delta}} \tag{4}$$

where

H_0 = magnetizing force at the surface
$\delta = 1{,}980\sqrt{\rho/\mu f}$, inches
ρ = resistivity, ohm-centimeters
μ = permeability
f = frequency, cycles

In this equation, δ is known as the depth of penetration; it is the distance from the surface at which eddy-current density is 36.8 per cent of the surface-current density. For any nonferrous metal, μ is unity and, for cast iron, it is approximately 1,000. The depth of penetration for aluminum at 100 kc is approximately 0.01 inch and for cast iron it is 0.0017 inch. Thus the pickup in the wiring from section to section is reduced to a very small amount by cast-iron walls of 1/8-inch thickness and liners 0.025-inch thick. Using the foregoing equation, the attenuation caused by copper alone is as follows

$$H=H_0\epsilon^{-0.025/0.00817}=0.045H_0 \text{ for 0.025-inch thickness}$$

$$H=H_0\epsilon^{-0.125/0.00817}=0.25\times10^{-6}H_0 \text{ for 0.125-inch thickness}$$

The shielding effect of thick walls is quite apparent. For the 1/8-inch wall, the magnetic field strength is attenuated 132 db. Because of this, it might be thought that 1/8-inch thick copper partitions would provide enough shielding. This is not sufficient because, part way through the wall, opposing eddy currents from neighboring compartments are flowing. Resultant stray flux thus tends to link other sections and by-pass the filter. Besides, this stray flux could link the wiring in the carrier receiver, which has approximately 100-db gain. At 8 kc from mid-band, the pickup with an all-copper case is large enough to limit attenuation to about 70 db and throw the filter response out of limits.

Hence, dual shielding is required: iron to attenuate stray flux, and nonferrous metal to keep most of the stray flux out of the iron and, hence, keep coil Q high. The attenuation of magnetizing force for various thicknesses of cast iron, copper, and aluminum, is given in Table I.

The tremendous calculated attenuation of 609 db with 1/8-inch thick iron walls is, of course, more than needed; but in a casting, 1/8-inch thick walls are the minimum practicable. A fabricated steel case of thinner stock would also be amply effective. In Table II are figures showing the effect on Q of a 200-kc coil with and without nonferrous liners.

Measurements

To measure the performance of a filter which meets the requirements of Fig. 1, it is necessary to observe several unusual precautions. To get accurate readings, the residual or stray voltages should be at least 20 to 30 db below the minimum expected filter output or, for this case, about 120 to 130 db or more below mid-band. Therefore, noise filters must be used in all power lines entering the measuring booth to exclude radio-frequency pickup from these lines. Not only must the booth be shielded but there must be a shield between the input and output terminals of the filter. The main reason

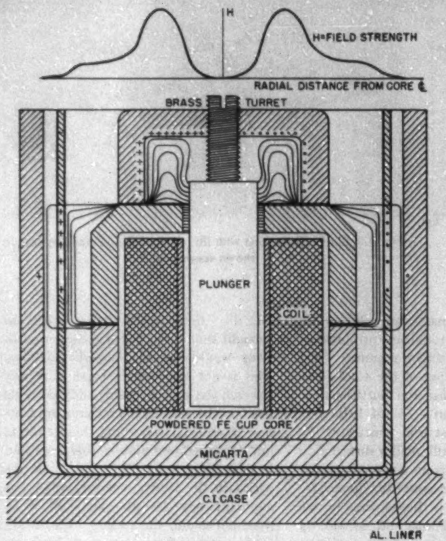

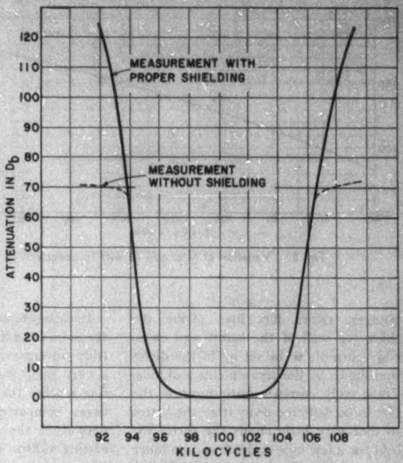

Fig. 8 (left). Approximate field strength and flux distribution in filter compartment

Fig. 10 (above). Effect of shielding on filter response measurements

for this second set of shields is to prevent the output voltmeter from picking up stray flux from the signal generator directly through the air. Fig. 9 shows the shielding which was used in making measurements on this filter. Without such shielding or with the filter cover removed, the attenuation curve apparently flattens off at about 70 db, as shown dotted in Fig. 10. Without the cast-iron case, there is sufficient pickup of stray flux from the input end sections of the filter by the voltmeter power leads to indicate even less attenuation.

Signal generator output should be a distortion-free sine wave. The signal generator power supply should be well filtered to eliminate hum. Beat frequencies caused by harmonics or hum are effectively detected by the skirts of the response curve, so that using poor input wave form may result in erroneous filter output.

Attenuation is measured conveniently on an electronic voltmeter with 11 ranges from 0.001 to 100 volts full scale. This type of meter has an electronic amplifier, the gain of which is adjusted for each range. Consistency of readings is checked by taking output at some readable point on two different scales. Starting with mid-band attenuation and proceeding to 8-kc below mid-band, it is possible to check every range in this manner. Unless such a check is made, nonlinearities in the voltmeter amplifier may cause inaccurate measurements.

Alignment of a filter of this type may be conveniently done by using an oscilloscope to indicate resonance of the shunt arms of each section with the following section short-circuited. Voltage minima and maxima occur with proper tuning of the respective alternate sections. In effect, this method means that L_1 and C_2 of each section, Fig. 3, are tuned to the upper cutoff frequency. When the following section is short-circuited, the series capacitor C_1 changes this tuning so that the filter is tuned as a complete unit to mid-band frequency $f_0 = \sqrt{f_1 f_2}$. This is not quite the same as $(f_1 + f_2)/2$, and a small correction has to be made to center the mid-band frequency.

Insertion loss is measured by a voltmeter connected across R_2. With constant input voltage, the ratio of output voltages with and without the filter between R_1 and R_2 is the insertion loss expressed in db. The most noticeable effect of temperature was to shift slightly the nose of the response curve. With the low temperature coefficient cores, this shift was approximately ±250 cycles as the temperature was changed from −20

Fig. 9. Shielding used for attenuation measurements

Table I. Attenuation of Magnetizing Force

Metal	ρ, Ohm-Centimeters	μ	δ, Inch	Db Attenuation of H By 0.025-Inch Thick	Db Attenuation of H By 1/8-Inch Thick
Cast iron	80	1,000	0.00177	122	609
Copper	1.7	1	0.00817	27	132
Aluminum	2.7	1	0.0103	21	106

Table II. Effective Q of a 200-Kc Coil

Filter Compartment, Thickness	Coil Q
1/8-inch copper	195
1/8-inch iron	76
1/32-inch iron	76
1/8-inch iron+1/32-inch copper liner	193
1/32-inch iron+1/32-inch copper liner	194

to +70 C. There was sufficient latitude in design so that the response remained within the limits of Fig. 1 when temperature was varied between these extremes.

Distortion was measured with a conventional distortion meter connected in the frequency-modulated receiver audio output. Although distortion was somewhat different at different carrier frequencies, the largest variations occurred with temperature changes. From −20 to +70 C, the distortion varied between 5 and 8 per cent at a given frequency.

Conclusion

In conclusion, it may be said that tunable frequency-modulated receiver filters with ±3-kc bandwidth and 100-db attenuation of unwanted signals are entirely practical for power line carrier frequencies with careful design. Particularly necessary is the provision of ferrous partitions between filter sections to prevent stray coupling which would otherwise by-pass the filter; nonferrous shielding is not sufficient in itself for such performance.

Reference

1. Input Filter Design for Frequency-Modulated Power Line Carrier Receivers, R. L. Filmore. *AIEE Transactions*, vol. 71, pt. III, Jan. 1952, pp. 450–54.

◆

Discussion

R. W. Beckwith (General Electric Company, Syracuse, N. Y.): The author is to be complimented on this well-written and very informative paper. At first the title suggested that each filter might be adjustable over the entire carrier spectrum of 40 to 200 kc; however, it is realized that this approach is not practical and the division of the spectrum by 16 is a good compromise.

I should like to ask the academic question of whether the author believes the ideal characteristics of Fig. 2 would permit distortion-free reception of a frequency-modulated signal or whether the loss of higher order side bands would still produce distortion.

My company has found that 100 db can also be obtained by multiple thickness nonmagnetic shielding; however, the method described in the paper is certainly one good way of achieving the desired result.

Reuben Lee: Mr. Beckwith's question on the loss of higher order side bands is, as he points out, academic, because we achieved reasonable distortion reception with the actual filter. We do know, however, that linearity of phase shift has greater influence on distortion than attenuation just outside the passband. There is no doubt that the loss of higher order side bands would cause some distortion, but the amount is negligible in comparison with that due to nonlinear phase shift.

It is interesting to note that Mr. Beckwith obtained 100 db by multiple thickness nonmagnetic shielding. Our calculations and tests indicate that these multiple shields would have to be very thick to produce the results described in the paper. This would add to the filter weight and size.

An Improved Approximate Technique for Calculating Cable Temperature Transients

F. C. VAN WORMER
ASSOCIATE MEMBER AIEE

IN THE cross section of the single conductor cable illustrated in Fig. 1, the thermal resistance, thermal capacity, and temperature of the insulation are not linear functions of the thickness of the insulation. Consequently, the rigorous solution[1] of the cable temperature transient problem is quite complicated and involves lengthy and time-consuming calculations.

An Approximate Solution

An approximate solution is obtained by lumping the constants of the cable and forming an equivalent π circuit, as shown in Fig. 2. In line with the practice followed in transmission line problems, half of the thermal capacity of the insulation may be placed with the thermal capacity of the conductor at conductor temperature and the other half may be placed with the thermal capacity of the sheath at sheath temperature.

This method of lumping half of the thermal capacity of the insulation at each side of the thermal resistance of the insulation as shown in Fig. 2 has been used by Buller.[2] Since the temperature gradient through the insulation is not a linear function of the insulation thickness, this method of allocating the thermal capacity of the insulation does not accurately represent the total heat stored in the insulation.

Nomenclature

R = outer radius of insulation
r = inner radius of insulation

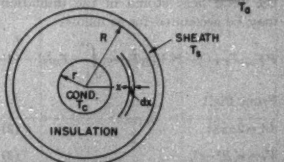

Fig. 1. Cross section of single-conductor cable in air

Paper 55-51, recommended by the AIEE Insulated Conductors Committee and approved by the AIEE Committee on Technical Operations for presentation at the AIEE Winter General Meeting, New York, N. Y., January 31–February 4, 1955. Manuscript submitted September 20, 1954; made available for printing December 8, 1954.

F. C. Van Wormer is with the General Electric Company, Schenectady, N. Y.

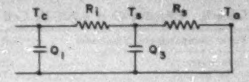

Fig. 2. Equivalent π electric circuit for the thermal circuit of cable in Fig. 1

R_i = insulation thermal resistance, degrees centigrade (C) per watt per foot of cable
R_S = cable surface thermal resistance, C per watt per foot of cable
T_C = conductor temperature, C
T_x = insulation temperature at x, C
T_S = cable sheath temperature, C
T_a = air ambient temperature, C
Q_1 = thermal capacity of conductor including oil plus part of the thermal capacity of the insulation, watt-minutes per C per foot of cable
Q_2 = part of the thermal capacity of the insulation, watt-minutes per C per foot of cable
Q_3 = thermal capacity of cable sheath plus part of thermal capacity of the insulation, watt-minutes per C per foot of cable
P = that part of the thermal capacity of the insulation to be allocated at an inner isothermal
V_i = cross-section area of insulation, square inches
q_i = insulation thermal capacity, watt-minutes per C per square inch of insulation per foot of cable
Q_i = total thermal capacity of the insulation watt-minutes per C per foot of cable
t = time, minutes
ϵ = base Napierian logarithms
P_i = insulation thermal resistivity, C centimeters per watt
$K = 0.00522 P_i$
W = watts per foot of cable at conductor

An Improved Approximate Solution

MODIFIED EQUIVALENT π CIRCUIT

The accuracy of the approximate solution using lumped constant may be improved by allocating the thermal capacity of the insulation at conductor temperature and sheath temperature so that the total heat stored in the insulation is represented.

If P represents the part of the insulation thermal capacity to be placed at conductor temperature and $(1-P)$ the part to be placed at sheath temperature, the total heat stored in the insulation may be accounted for as follows

$$PV_iq_iT_c+(1-P)V_iq_iT_s=q_i\int_r^R T_x dA \qquad (1)$$

From Fig.1

$$dA=2\pi x dx \qquad (2)$$

$$V_i=\pi(R^2-r^2) \qquad (3)$$

The temperature distribution throughout the insulation is such that

$$T_c-T_x=WK\log_\epsilon\frac{x}{r} \qquad (4)$$

and

$$T_c-T_s=WK\log_\epsilon\frac{R}{r} \qquad (5)$$

Combining equations 1, 2, and 4 results in

$$PV_iq_i(T_c-T_s)+V_iq_iT_s=2\pi q_i\times \int_r^R\left(T_c-WK\log_\epsilon\frac{x}{r}\right)xdx \qquad (6)$$

After performing the indicated operations

$$PV_iq_i(T_c-T_s)+V_iq_iT_s =2\pi q_i\left[\frac{T_c(R^2-r^2)}{2}- WK\left(\frac{R^2}{2}\log_\epsilon\frac{R}{r}-\frac{R^2-r^2}{4}\right)\right] \qquad (7)$$

By combining equations 7, 3, and 5, after simplifying, yields

$$P=\frac{1}{2\log\frac{R}{r}}-\frac{1}{\frac{R^2}{r^2}-1} \qquad (8)$$

Values of P as a function of R/r are shown in Fig. 3.

It is interesting to note that when R/r is 1.0, the value of P from equation 8 is 0.50. This condition is equivalent to an insulated cylinder of infinite radius or a plane. For this case the temperature distribution is known to be a linear function of the insulation thickness, and placing half of the thermal capacity at each terminal temperature accurate accounts for the total heat storage.

Also R/r is 1.0 when $R=r$, which corresponds to zero thickness of insulation but, in this case, the thermal capacity of the insulation is zero.

MODIFIED EQUIVALENT *T* CIRCUIT

For small conductors with a heavy wall of insulation, further accuracy is obtained by the use of a modified equivalent T circuit, as shown in Fig. 4. In this case the thermal capacity of the insulation is placed part at the conductor, part halfway through the insulation thermal resistance, and part at the sheath. Since the insulation thermal resistance between r and x in Fig. 1 is proportional to log x/r, R_i is divided in half when

$$x/r=R/x \text{ or } x=\sqrt{Rr} \qquad (9)$$

The area of the insulation between r and x is

$$V_i'=\pi(x^2-r^2) \qquad (10)$$

The area of the insulation between x and R is

$$V_i''=\pi(R^2-x^2) \qquad (11)$$

Since $x/r=R/x$, the value of P as determined from equation 8 or Fig. 3 is the same for both parts of the insulation.

The thermal capacity of the insulation is then allocated as follows

At T_c place Pq_iV_i' (12)

at T_x place $(1-P)q_iV_i'+Pq_iV_i''$ (13)

at T_s place $(1-P)q_iV_i''$ (14)

Example

The accuracy of the three approximate solutions discussed is illustrated by applying these methods to a single conductor cable in air and comparing the resulting temperature transient with the results obtained, using distributed constants in accordance with the rigorous solution given in reference 1. The cable selected for the comparison is a single-conductor 250,000-circular-mil 0.69-inch core 0.560-inch paper insulation 0.125-inch lead sheath oil-filled cable. The resulting temperature transients are shown in Fig. 5.

The solution using an equivalent π circuit, lumping the thermal capacity of the insulation 50 per cent at the conductor and 50 per cent at the sheath, gives a considerably lower temperature rise than the exact solution using distributed constants. The solution using an equivalent π circuit, lumping PQ_i at the conductor and $(1-P)Q_i$ at the sheath, gives a considerable improvement in accuracy but for this rather small conductor and heavy wall of insulation, there is still a considerable difference between this approximation and the solution using distributed constants.

The solution using the modified equivalent T circuit of Fig. 4, lumping the thermal capacity of the insulation at the conductor, sheath and at the halfway point through the insulation thermal resistance as described in the foregoing, gives a very close check with the solution using distributed constants. The method of solution using the equivalent π and T circuits of Figs. 2 and 4 and the expansion theorem is outlined in Appendixes I and II.

The four methods of calculation result in the following temperature rise equations which were plotted in Fig. 5.

Using distributed constants

$$(T_c-T_a)=4.48-3.89\epsilon^{-0.0145t}- 0.52\epsilon^{-0.1850t}-0.07\epsilon^{-0.5200t}$$

Using the modified equivalent T circuit

$$(T_c-T_a)=4.48-3.94\epsilon^{-0.01438t}- 0.45\epsilon^{-0.1296t}-0.09\epsilon^{-0.3123t}$$

Using the equivalent π circuit and

$(P)-(1-P)$ allocation of the insulation thermal capacity

$$(T_c-T_a)=4.48-4.127\epsilon^{-0.01449t}-0.353\epsilon^{-0.0637t}$$

Using the equivalent π circuit and 50–50 allocation of the insulation thermal capacity

$$(T_c-T_a)=4.48-4.275\epsilon^{-0.01341t}-0.205\epsilon^{-0.[illegible]t}$$

In the preceding example the following constants were used:

$r=0.49$ inch

$R=1.05$ inches

$P_i=600$ C centimeter per watt

$R_i=2.39$ thermal ohms, C per watt per foot of cable

$R_S=2.09$ thermal ohms, C per watt per foot of cable

$Q_{\text{oil}}=151.0$ watt-seconds per C per foot of cable

$Q_{\text{conductor}}=136.5$ watt-seconds per C per foot of cable

$Q_{\text{insulation}}=1{,}014.0$ watt-seconds per C per foot of cable

$Q_{\text{lead}}=255.0$ watt-seconds per C per foot of cable

Conclusions

For cables with large conductors and moderate walls of insulation or small conductors with thin walls of insulation, the approximate solution using the equivalent π circuit of Fig. 2 and placing PQ_i at the conductor and $(1-P)Q_i$ at the sheath, is quite accurate and is very much less laborious than the rigorous solution using distributed constants.

The process of lumping the cable thermal circuit to form a 2-part network often gives sufficient accuracy. This method has been used by several engineers.[2,3] The method of lumping the cable insulation thermal capacity described in this paper results in improved accuracy, as seen in Fig. 5, with no appreciable extra work.

For cables with small conductors and heavy walls of insulation, the approximate solution using the modified equivalent T circuit of Fig. 4 and allocating the insulation thermal capacity in accordance with equations 12, 13, and 14, is sufficiently accurate for most engineering work. The labor of solving the T circuit is somewhat greater than for the π circuit but is still greatly less than for the solution using distributed constants.

The solution of the cubic equation for the three roots of the equivalent T circuit in Appendix II is easily performed by a digital computer. There are also several long-hand methods[4–6] for the solving of cubic equations which are quite easy to apply.

As soon as the solution for the conductor temperature T_c is reached, the solution for the insulation temperature T_x and sheath temperature T_s is readily obtained, as shown in Appendixes I and II. The use of the equivalent T circuit giving an intermediate insulation temperature is particularly desirable if oil demands and oil pressure drops are to be calculated.

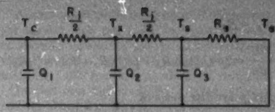

Fig. 4. Modified equivalent T electric circuit for the thermal circuit of cable in Fig. 1

Appendix I. Solution of the Equivalent π Circuit

Using the expansion theorem, the solution of the equivalent π circuit of Fig. 2 is as follows

$$T_c-T_a=W\left(R_i+R_S+\sum_p\frac{Y_p}{p\dfrac{dZ}{dp}}\epsilon^{-pt}\right)$$

$$T_s-T_a=W\left(R_S+\sum_p\frac{Y_p'}{p\dfrac{dZ}{dp}}\epsilon^{-pt}\right)$$

where

$$Y_p=pQ_sR_iR_S+R_i+R_S$$

Fig. 3 (below). Allocation of insulation thermal capacity

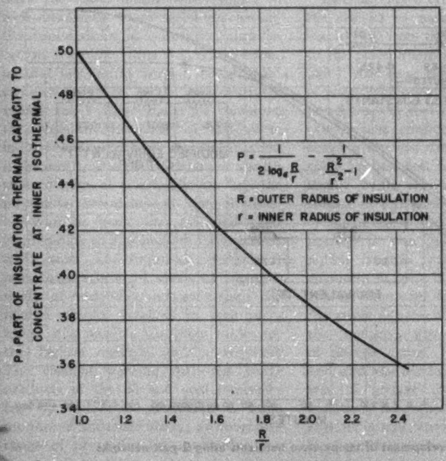

Fig. 5 (right). Calculated conductor temperature transients

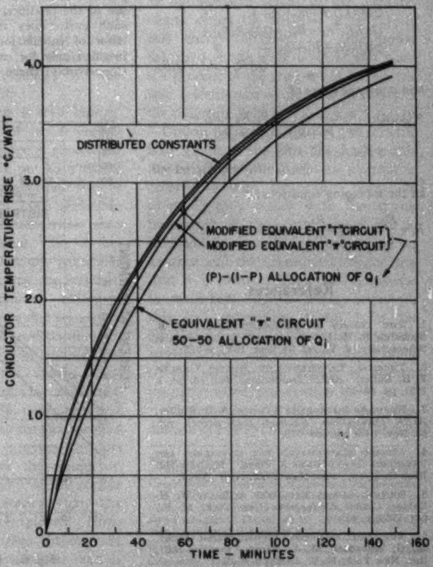

$$Y_p' = R_S$$

$$\frac{p\,dZ}{dp} = 2p^2Q_1Q_2R_IR_S + p[Q_1(R_I+R_S)+Q_2R_S]$$

and p are the roots of

$$p^2Q_1Q_2R_IR_S + p[Q_1(R_I+R_S)+Q_2R_S]+1=0$$

Appendix II. Solution of the Equivalent T Circuit

Using the expansion theorem, the solution of the equivalent T circuit of Fig. 4 is as follows

$$T_c - T_a = W\left(R_1+R_2+R_3+\sum_p \frac{Y_p}{p\frac{dZ}{dp}}\epsilon^{-pt}\right)$$

$$T_2 - T_a = W\left(R_2+R_3+\sum_p \frac{Y_p'}{p\frac{dZ}{dp}}\epsilon^{-pt}\right)$$

$$T_s - T_a = W\left(R_3+\sum_p \frac{Y_p''}{p\frac{dZ}{dp}}\epsilon^{-pt}\right)$$

where

$$Y_p = p^2Q_2Q_3R_1R_2R_3 + p[Q_2R_1(R_2+R_3) + Q_3R_3(R_1+R_2)] + R_1+R_2+R_3$$

$$Y_p' = pQ_3R_2R_3 + R_2 + R_3$$

$$Y_p'' = R_3$$

$$p\frac{dZ}{dp} = 3p^3Q_1Q_2Q_3R_1R_2R_3 + 2p^2[Q_1Q_2R_1(R_2+R_3) + Q_1Q_3R_3(R_1+R_2) + Q_2Q_3R_2R_3] + p[Q_1(R_1+R_2+R_3) + Q_2(R_2+R_3) + Q_3R_3]$$

and p are the roots of

$$p^3Q_1Q_2Q_3R_1R_2R_3 + p^2[Q_1Q_2R_1(R_2+R_3) + Q_1Q_3R_3(R_1+R_2) + Q_2Q_3R_2R_3] + p[Q_1(R_1+R_2+R_3) + Q_2(R_2+R_3) + Q_3R_3] + 1 = 0$$

In the foregoing equations:

$$R_1 = \frac{R_I}{2} \qquad R_2 = \frac{R_I}{2} \qquad R_3 = R_S$$

References

1. The Theory of Oil-Filled Cable, G. B. Shanklin, F. H. Buller. *General Electric Review*, Schenectady, N. Y., vol. 34, Sept. 1931, p. 523.

2. Thermal Transients on Buried Cables, F. H. Buller. *AIEE Transactions*, vol. 70, pt. I, 1951, pp. 45–55.

3. Notes on Emergency Ratings, A. H. Kidder. *AIEE Transactions (Electrical Engineering)*, vol. 58, Nov. 1939, pp. 599–610.

4. Applied Mathematics for Engineers and Physicists (book), Louis A. Pipes. McGraw-Hill Book Company, Inc., New York, N. Y., 1946.

5. Solving Cubics This Way is Easy, W. H. Gable. *Control Engineering*, New York, N. Y., Oct. 1954, p. 49.

6. Numerical Methods in Engineering (book), M. G. Salvadori, M. L. Baron. Prentice-Hall, Inc., New York, N. Y., 1952, pp. 8–13.

Discussion

F. H. Buller (General Electric Company, Schenectady, N. Y.): The author has presented a technique for the calculation of transients on underground cables which should give acceptable accuracy in most cases and which is actually very much simpler than the more rigorous technique involving distributed constants (see reference 1 of the paper). The equivalent π circuit with 50-50 allocation of the thermal capacity mentioned by the author has, in fact, been considered and rejected on the grounds of insufficient accuracy for the computation of thermal transients and oil demands of cables in free air or in underground ducts. If reasonable precision was desired in such cases, the method of distributed constants was used; and the author's simplification should be very welcome to engineers responsible for practical calculation in such cases.

In the case of a directly buried cable or pipe cable (see reference 2 of the paper) the over-all error involved in the use of the equivalent π circuit in question is very much reduced, since this circuit is a relatively small part of a rather large complex of thermal resistances and capacitances, which are necessary for the proper inclusion of the effect of the earth on the thermal transient. This is particularly true of oil-filled pipe cables, where a very considerable quantity of oil is involved; this oil follows quite closely the temperature changes of the pipe itself. However, even in such cases there is an advantage in using the author's equivalent π circuit, with (P) and $(1-P)$ allocation of the thermal capacity, since this can be done with practically no extra labor as compared with the use of 50-50 allocation. The use of the modified equivalent T circuit in such cases does materially increase the labor of calculation; and it is probably justified only for cables in air or in ducts. Conceivably, there may be some very exceptional problems where it might be justified for directly buried cables; but these problems would certainly be unusual ones.

An equivalent π circuit will not, in general, give the oil-demand curve its characteristic peak for cables in air or in ducts, although the maximum oil demand as calculated from an equivalent π circuit with (P) and $(1-P)$ allocation will approximate the maximum oil demand quite closely. Has the author found that the modified equivalent T circuit will, in general, give such a peak, and if so will this peak come at or close to the proper time?

J. H. Neher (Philadelphia Electric Company, Philadelphia, Pa.): The techniques for handling the distributed thermal capacitance of the insulation which the author has presented will be most useful to those of us who have been trying to develop procedures for calculating cable temperature transients which will be simple and still will have the accuracy required. In this connection, I should like to suggest a procedure using these techniques whereby the temperature transient may be readily calculated with almost any degree of accuracy.

As shown in Fig. 5, the modified equivalent T circuit is considerably more accurate than the modified equivalent π circuit during the initial portion of the transient. It will also be noted that during the latter portion of the transient the simpler π circuit has an accuracy comparable with the T circuit, which is sufficient for almost any application.

The objection to the T circuit, consisting as it does of a 3-part network, is of course that considerable labor is involved in formulating the corresponding 3-term exponential equation, and I doubt if any time will be saved by developing the temperature transient equation by this means instead of by the use of Bessel functions, as indicated in reference 1. The 2-term exponential equation for the π circuit or 2-part network, on the

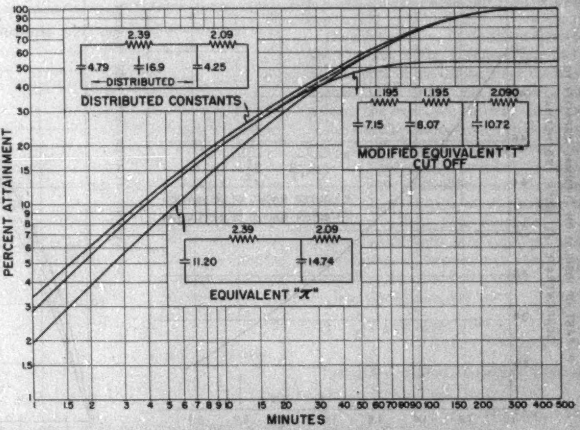

Fig. 6. Development of temperature transients using 2-part networks

other hand, is rather quickly determined, as shown in reference 3.

Considering the *T* circuit shown in Fig. 4, it will be apparent that during the initial part of the transient, its form is unaffected by the magnitude of Q_3 and R_3, since the heat flow will not have penetrated that far. Hence we may cut off the circuit at Q_3 and we have left a 2-part network which is readily solved. The resulting transient is shown in Fig. 6 of this discussion which also shows the transients calculated by the author using distributed constants and for the modified equivalent π circuit. Obviously, the cut-off network solution will not be correct during the latter part of the transient but during the initial part it will be seen to be considerably more accurate than the π circuit. It is a simple matter to develop a smooth envelope of these two curves, as shown by the dashed line, to obtain an over-all transient curve of reasonable accuracy.

Even greater accuracy during the initial portion may be obtained by suitably dividing the thermal capacitance of the insulation into three or four parts instead of two, but otherwise following the procedure as set forth by the author. This will result in a 4- or 5-part network of which only the first two sections are used, and will give increasingly greater accuracy where it may be required if the procedure is used for oil flow and pressure calculations.

The author is to be congratulated for having made a significant contribution in this respect.

F. C. Van Wormer: Mr. Buller asks if the use of the modified equivalent *T* circuit will give the oil-demand curve its characteristic peak.

The modified *T* circuit approach was applied to the example shown in Fig. 5 of an article by Shanklin and Buller in 1931[1]. The characteristic peak on the oil-demand curve and pressure drop curve was obtained.

An oil-demand peak of 62.5×10^{-6} cubic inches per second per foot was obtained at time of about 7.5 minutes. This compares with Fig. 5 of 63.8×10^{-6} cubic inches per second per foot at about 8 minutes.

A maximum pressure drop of 0.56 pounds per square inch per 1,000 feet was obtained in about 25 minutes' times. This compares with Fig. 5 of about 0.575 pounds per square inch per 1,000 feet also at about 25 minutes.

In this case the modified *T* solution gave results about 2 or $2^{1}/_{2}$% lower than the long rigorous solution. This is probably as close as some of the other data are known.

Mr. Neher's treatment of the modified *T* equivalent circuit is very intriguing and greatly reduces the labor involved in obtaining the cable temperature transient. I agree with Mr. Buller's statement that, "an equivalent π circuit or 2-part network will not, in general, give the oil demand curve its characteristic peak for cables in air or in ducts." I find that the location of the three roots by the method of reference 4 saves considerable time over the rigorous method involving Bessel functions. I wish to thank the discussers for their interest.

REFERENCE

1. CHARACTERISTICS OF OIL-FILLED CABLE, G. B. Shanklin, F. H. Buller. *AIEE Transactions*, vol. 50, Dec. 1931, pp. 1411–20.

The Co-ordination of Power and Communication Cable Characteristics

H. D. SHORT
MEMBER AIEE

FROM the very beginning of the science of electricity, sometime in the first half of the 19th century, the need for insulated conductors has kept apace of scientific developments. In the early days the cable maker was obliged to seek insulating materials from among the commodities of commerce, such as cotton and silk yarns, paper, bitumen, natural oils, gutta percha, amber, and eventually rubber. Until comparatively recent times these materials remained the standard insulants of the cable industry. Today, however, the situation is drastically changed. From our wealth of knowledge of atomic physics, and the physicists' researches in the electrical behavior of gases and oils and their combination in agglomerate formulations with paper, and improved methods of manufacture brought about by constant study of processing methods (and the related physics involved in such processes), it is possible to design cables for the highest voltages so far required. The chemist working with the waste products of the oil and coal industries has succeeded in producing a large number of materials having an enormous range of properties and possessing the prime requisites of a good insulant, some of which permit the design of cables capable of efficient operation at the very high frequencies demanded by the progress of modern living.

Electric cables are, as is well known, the arteries by means of which energy is conveyed from the source of generation to the place where it is put to a useful task. And since the present-day society is essentially one based upon economic principles, the cost of transmission is an ever-present consideration. So it becomes a *sine qua non* that any particular cable be designed to carry the required energy with the maximum efficiency consistent with these economic principles.

In the early days of electrical engineering it was held—and indeed the notion is still prevalent among some engineers in spite of the vast accumulation of knowledge to the contrary—that the prime purpose of the insulant around the conductor was to prevent the loss of electric charge from the conductor, and that the conductivity of the copper was of greater importance than the quality of the insulant employed. However, it is now known that the insulant is of much greater importance; and it may be accepted that the chief role of the insulant is not so much to form a barrier to the loss of charge as to present a medium by means of which the transfer of energy along the conductor may be efficiently effected. The conductor acts more especially as a source of free electrons as well as guides the direction of energy flow; the flow takes place because of the physical action of the displacements within the medium. The rate of this energy transfer, i.e., the power delivered or the work done in unit time, is a product of the gradient of the electric field (electric stress) and the intensity of the magnetic field.

Under the subjection of the electric field gradient the free electrons within the conductor are forced to migrate in accordance with established laws. In so doing they collide with the atomic framework of the metal giving rise to heat energy, which is observed as resistance and the subsequent copper loss. And it is of more than passing interest to recall here that the energy supplying this loss enters the metal from the insulant around it, which is under the strain of the electric field—conforming to the equipartition theory of electromagnetic wave propagation.

All the schemes available for the transmission of energy, whether by mechanical

---

Paper 55-56, recommended by the AIEE Insulated Conductors Committee and approved by the AIEE Committee on Technical Operations for presentation at the AIEE Winter General Meeting, New York, N. Y., January 31–February 4, 1955. Manuscript submitted December 29, 1953; made available for printing December 8, 1954.

H. D. SHORT is with the Canada Wire and Cable Company, Toronto, Ontario, Canada.

or electrical means, have one outstanding, common aim: the production of strain at the source of supply and its relaxation at the other end where the energy is expended. That is to say, there must occur a change from potential energy to kinetic energy, or the converse, in order for energy of any kind to be conveyed from one place to another. In the hydraulic system, pressure is developed; in the mechanical system it is the strain in the rotating shaft. Similarly, in the case of electric energy, transmission strain within the insulation is produced.

In nearly all engineering practice the energy used comes from the kinetic energy developed by a falling mass of water, or is derived from the conversion of the inherent potential energy existing between the atoms of oxygen and carbon into the kinetic energy of steam, such as takes place when water is heated by burning coal or any other organic substance. At the sending end of an electric transmission system the generators and transformers raise the potential energy of the electric field (or the strain) between the conductors to the highest possible level without occasioning too high losses or breaking down of the insulation. At the delivery end energy is expended by a relaxation of electric field forces.

Thus there occurs within the insulant a heat loss produced by the strain of the electric field which has become known as the dielectric loss. It is always necessary when dealing with high voltages or high frequencies to make sure that the proper insulating medium is chosen, and that the dielectric loss is not allowed to become so great as to cause thermal or electrical instability with eventual breakdown of the insulation sustaining the system.

The first part of the paper is restricted to a general consideration of the transmission of energy along a cable line without regard to any frequency limitation. The paper diverges in two directions, one having to do with low frequencies and high voltages and the other with high frequencies and low voltages. As one proceeds along these two lines of thought, the similarities and the disparities indigenous to the transmission of power on the one hand and intelligence on the other come more and more into common focus.

The paper is confined to the limiting case of what are known as coaxial cables, which for all intents and purposes means very much what the name implies, i.e., a cable whose conducting elements are in the form of circles having coincident lateral axes—a geometrically symmetrical system possessing the minimum electrostatic capacity and the maximum potential energy $(g^2)/(2C)$ relative to any other formation of one circle enclosed by another, and exhibiting unstable equilibrium in respect of the inner conductor which will permit it to move in any direction unless otherwise constrained.

Fig. 1 depicts the geometry of this type of cable: it is a coaxial cable in the simplest sense of having only two conductors. Quite obviously, of course, a coaxial cable could be constructed with any given number of conductors. However, from practical considerations the 2-conductor cable is of most interest and is the only one with which this paper is concerned. Although Fig. 1 shows the inner conductor to be in the shape of an annulus conforming to that of the outer conductor, it may be of a solid or cylindrical shape without upsetting the underlying physical principles involved, and very often occasions demand that it be of such a cross-sectional configuration.

Nomenclature

R = resistance per wire unit of length
L = inductance per wire unit of length
C = capacitance per wire unit of length
g = leakage per wire unit of length
Z = impedance per wire unit of length
Y = admittance per wire unit of length
Z_0 = characteristic impedance
ρ = propagation constant
α = attenuation constant, hyperbolic radians or nepers per wire unit of length
β = wave-length constant, radians per wire unit of length
f = frequency, cycles per second
λ = wave length, units of length
V = wave velocity along the cable, units of length per second
W = load impedance
E_a = design impulse voltage breakdown to neutral for the cable, kilovolts
k = dielectric constant
$\cos\theta$ = load power factor
P_n = natural load of the line
p = power transmitted at any point distance x from sending end
P_S = power input at sending end
g_c = electric stress at surface of the conductor in a cable, kilovolts per centimeter

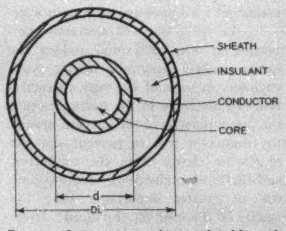

Fig. 1. Cross section of coaxial cable with annular conductor

General Consideration of the Transmission of Waves Along Cables

The fundamental parameters of the propagation of electromagnetic waves along a cable regardless of frequency are R, L, C, and g. In any infinite line, or finite line of practical linear dimensions, these parameters are reiterante and may be thought of as uniformly distributed along the cable circuit.

A combination of these parameters may be established to give two well-known complex quantities, named by Oliver Heaviside Z and Y. These complex quantities may be further dealt with by a process of mathematical deduction in accordance with the Lagrange classical method of arriving at the wave-transmission equation, and as first elucidated by Heaviside.

Thus certain additional quantities are obtained germane to all problems of a-c transmission in cables, whether the commodity transported is power in bulk to do useful work or intelligence to inform. They are

$$Z_0=\sqrt{Z/Y}$$

$\rho=\sqrt{ZY}$ hyperbolic radians per wire unit of length

two extremely important relationships, for they reveal after very little reasoning the essential characteristics which not only distinguish the two modes of transmission (low frequency and high voltage and the converse) but remain to identify and bring into prominence the respective design features which have to be considered. For, as Faraday once emphasized in discussing the velocity of electromagnetic propagation along wires or cables of different lengths, it is necessary to take into account the circumstances of the wires "being twined round a frame in a small space, or spread through the air through a large space or adhering to walls, or lying on the ground." It will be of interest to see how this state of affairs comes about. The propagation constant may now be written in the Cartesian co-ordinate or polar form best suiting our purpose: i.e.

$$\begin{aligned}\rho&=\sqrt{ZY}\\&=\alpha+j\beta=Ae^{j\theta}\end{aligned}$$

where two new terms, α and β, have been introduced. It is of more than

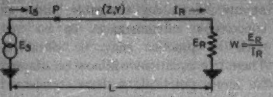

Fig. 2. Schematic diagram of steady-state transmission line

$e = E_S \cosh \rho x$

$i = I_S \cosh \rho x - \frac{E_S}{Z_0} \sinh \rho x$

where x is measured from the sending end

$e = E_R \cosh \rho x + Z_0 I_R \sinh \rho x$

$i = I_R \cosh \rho x + \frac{E_R}{Z_0} \sinh \rho x$

where x is measured from the receiving end

$(\cosh 0 = 1, \ \sinh 0 = 0)$

passing interest to note that the exponential function from which α as a transmission unit was derived was first revealed to unsuspecting electrical engineers in Montreal by the late Lord Rayleigh during the course of a lecture delivered in 1884.

The significance of Z_0, α, and β in respect to the propagation of electromagnetic energy along a cable will now be examined. Consider a single coaxial cable of length L transporting energy from the sending end to a load impedance W at the receiving end. This is shown in Fig. 2 merely to illustrate the juxtaposition of the complex quantities involved. The appropriate subscripts refer to the sending end and receiving end respectively.

The four familiar transmission equations of classical theory relating these quantities one to the other are given as a matter of reference. e and i are the voltage and current at any point P along the cable in terms of either the sending or receiving end components at a distance x from either end. Then at any point P at a distance x from the sending end

$$e = E_S \cosh \rho x - Z_0 I_S \sinh \rho x \tag{1}$$

$$= \left(\frac{E_S - Z_0 I_S}{2}\right)\epsilon^{\alpha x}\epsilon^{j\beta x} + \left(\frac{E_S + Z_0 I_S}{2}\right)\epsilon^{-\alpha x}\epsilon^{-j\beta x} \tag{2}$$

Similarly

$$i = I_S \cosh \rho x - \frac{E_S}{Z_0} \sinh \rho x \tag{3}$$

$$= \left(\frac{I_S - \frac{E_S}{Z_0}}{2}\right)\epsilon^{\alpha x}\epsilon^{j\beta x} + \left(\frac{I_S + \frac{E_S}{E_S}}{2}\right)\epsilon^{-\alpha x}\epsilon^{-j\beta x} \tag{4}$$

Hence it is at once evident that several things are happening to the wave as it proceeds along the cable. First of all, as long as W is finite, Z_0 tends to reduce the absolute value (as well as the complex value) of the voltage and alter that of the current at any point, and its complex value and the length of the line will determine to some extent the voltage regulation to be obtained in any particular case.

The second part of each equation, remembering that

$$\epsilon^{-j\beta x} = \cos \beta x - j \sin \beta x$$

shows that as the wave proceeds along the cable the absolute value (or magnitude) of both the current and the voltage at any point is decreased, in respect to the sending end conditions, according to the parameter α, i.e., attenuation is taking place. Also, the complex (or phasor) value of the current and voltage is being rotated with respect to the sending end through angles $= \beta$ radians. Fig. 3 illustrates these phenomena for the second part of each equation which involves a clockwise rotation because of $\epsilon^{-j\beta x}$. The result is a logarithmic spiral which, of course, will evolve into a circle as α is decreased. In other words, α expresses the change in the absolute value of the current or voltage, β the change of phase of the current or voltage, and Z_0 a definite reduction depending on its magnitude and hence on the cable design. However, it is not quite correct to infer that Z_0 alone is dependent on the cable design, for it is all too obvious that both α and β must also be functions of the initial design consideration. If f and λ are introduced and it is noticed that $\cos \beta x$ and $\sin \beta x$ are repeated each time βx passes through 360 degrees or 2π radians, it becomes evident that the angle between current or voltage at any point in the cable and the current or voltage at another point distance λ therefrom $= 2\pi$ radians.

Since these two points are 1 cycle apart it will take a wave $1/f$ seconds to travel the distance λ. The equation for velocity V is

$$\begin{aligned} V &= dx/dt \\ &= \lambda/(1/f) \\ &= \lambda f \\ &= 2\pi f/\beta \end{aligned}$$

As has already been stated, the transfer of energy along the cables takes place in the insulating medium, and it would be expected that the inbred properties of the medium would have some influence on the velocity of the waves. This has been clearly shown to be the case as evinced by the equation for velocity, viz. $(2\pi f)/\beta$, and it has been shown that β bears a definite relationship to two of the four initial parameters C and g, whose magnitudes are dependent upon the character of the insulating material and upon the frequency of transmission. From this point of view the wave velocity then becomes doubly dependent upon the frequency.

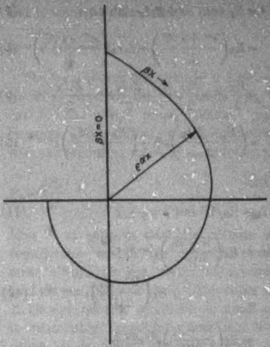

Fig. 3. Logarithmic spiral

In any chosen medium the wave velocity can never, so far as is known, exceed the speed of light: 300×10^6 meters per second. In cables the wave velocity is appreciably less, being a function, as may be readily discerned, of the dielectric constant of the medium whose influence becomes greater in these respects as the frequency is increased. Since

$$\rho = \sqrt{ZY} = \alpha + j\beta = \sqrt{(R + jL\omega)(g + jC\omega)}$$

then

$$\begin{aligned} \alpha^2 + 2j\alpha\beta - \beta^2 &= (R + jL\omega)(g + jC\omega) \\ &= Rg + j(Lg\omega + RC\omega) - \omega^2 LC \end{aligned}$$

The real and imaginary parts may be equated. Therefore

$$\begin{aligned} \alpha^2 - \beta^2 &= Rg - \omega^2 LC \\ 2\alpha\beta &= Lg\omega + RC\omega \end{aligned}$$

from which it may be shown that

$$\alpha = \left[\sqrt{\left(\frac{R^2 + \omega^2 L^2}{2}\right)\left(\frac{g^2 + \omega^2 C^2}{2}\right)} + \left(\frac{Rg - \omega^2 LC}{2}\right)\right]^{1/2} \tag{5}$$

$$\beta = \left[\sqrt{\left(\frac{R^2 + \omega^2 L^2}{2}\right)\left(\frac{g^2 + \omega^2 C^2}{2}\right)} - \left(\frac{Rg - \omega^2 LC}{2}\right)\right]^{1/2} \tag{6}$$

Referring to the other pair of transmission line equations, then taking a point P, this time at a distance x from the receiving end, we may write

$$e = E_R \cosh \rho x + Z_0 I_R \sinh \rho x \qquad (7)$$

$$= E_R\left(\frac{\epsilon^{\rho x} + \epsilon^{-\rho x}}{2}\right) + Z_0 I_R\left(\frac{\epsilon^{\rho x} - \epsilon^{-\rho x}}{2}\right) \qquad (8)$$

$$= \frac{E_R}{2}\epsilon^{\rho x} + \frac{E_R}{2}\epsilon^{-\rho x} + \frac{Z_0 I_R}{2}\epsilon^{\rho x} - \frac{Z_0 I_R}{2}\epsilon^{-\rho x} \qquad (9)$$

$$= \left(\frac{E_R + Z_0 I_R}{2}\right)\epsilon^{\rho x} + \left(\frac{E_R - Z_0 I_R}{2}\right)\epsilon^{-\rho x} \qquad (10)$$

but

$$I_R = E_R/W \text{ and } \rho = \alpha + j\beta \qquad (11)$$

$$e = E_R\left(\frac{W+Z_0}{2W}\right)\epsilon^{(\alpha+j\beta)x} + E_R\left(\frac{W-Z_0}{2W}\right)\epsilon^{-(\alpha+j\beta)x} \qquad (12)$$

$$= E_R\left(\frac{W+Z_0}{2W}\right)\epsilon^{\alpha x}\epsilon^{j\beta x} + E_R\left(\frac{W-Z_0}{2W}\right)\epsilon^{-\alpha x}\epsilon^{-j\beta x} \qquad (13)$$

Similarly

$$i = \left(\frac{I_R + \frac{E_R}{Z_0}}{2}\right)\epsilon^{\rho x} + \left(\frac{I_R - \frac{E_R}{Z_0}}{2}\right)\epsilon^{-\rho x} \qquad (14)$$

but

$$E_R = W I_R \text{ and } \rho = \alpha + j\beta \qquad (15)$$

therefore

$$i = I_R\left(\frac{1 + \frac{W}{Z_0}}{2}\right)\epsilon^{(\alpha+j\beta)x} + I_R\left(\frac{1 - \frac{W}{Z_0}}{2}\right)\epsilon^{-(\alpha+j\beta)x} \qquad (16)$$

$$= I_R\left(\frac{Z_0+W}{2Z_0}\right)\epsilon^{\alpha x}\epsilon^{j\beta x} + I_R\left(\frac{Z_0-W}{2Z_0}\right)\epsilon^{-\alpha x}\epsilon^{-j\beta x} \qquad (17)$$

Another variable has been introduced into the problem, namely load impedance W. Its significance will be more obvious later when considering practical matters in high-voltage transmission and high-frequency transmission.

Reference has been made to the copper loss in the conductors and the dielectric loss in the insulating medium, and the fact that thermal instability apart from the question of electric breakdown must not be allowed to exist. This, of course, is true of any class of cable, particularly so at high voltages because of the dielectric loss which increases as the square of the voltage, but only as the first power of the frequency.

The general equations which express the way in which the transmission line parameters enter into the physical state of affairs concerned with these losses are equation 7 and

$$i = I_R \cosh \rho x + \frac{E_R}{Z_0}\sinh \rho x \qquad (18)$$

The copper loss and the dielectric loss respectively at any point distance x from the receiving end are i^2R, in watts per wire unit of length, and ge^2, in watts per wire unit of length. Then

$$i^2R = \left(I_R \cosh \rho x + \frac{E_R}{Z_0}\sinh \rho x\right)^2 R \qquad (19)$$

$$= \left(I_R \cosh \rho x + \frac{W}{Z_0} I_R \sinh \rho x\right)^2 R \qquad (20)$$

$$= I_R^2 R\left(\cosh \rho x + \frac{W}{Z_0}\sinh \rho x\right)^2 \qquad (21)$$

$$ge^2 = (E_R \cosh \rho x + Z_0 I_R \sinh \rho x)^2 g \qquad (22)$$

$$= \left(E_R \cosh \rho x + \frac{Z_0}{W} E_R \sinh \rho x\right)^2 g \qquad (23)$$

$$= E_R^2 g\left(\cosh \rho x + \frac{Z_0}{W}\sinh \rho x\right)^2 \qquad (24)$$

If

RTH_0 = thermal resistance through which the copper loss flows

RTH_{0D} = thermal resistance through which the dielectric loss flows both in accordance with the established laws of thermal energy flow

T_R = temperature rise of the inner conductor above ambient

$$i^2 R RTH_0 + ge^2 RTH_{0D} = T_R \qquad (25)$$

since Ohm's law for steady heat flow states that the thermal resistance × watt loss = temperature rise, and hence

$$I_R^2 R\left(\cosh \rho x + \frac{W}{Z_0}\sinh \rho x\right)^2 RTH_0 + E_R^2 g\left(\cosh \rho x + \frac{Z_0}{W}\sinh \rho x\right)^2 RTH_{0D} = T_R \qquad (26)$$

The receiving end conditions are as follows:

When $W = Z_0$

$$(\cosh \rho x + W/Z_0 \sinh \rho x)^2 = (\cosh \rho x + \sinh \rho x)^2 = (\epsilon^{\rho x})^2 = \epsilon^{2\rho x}$$

hence

$$\epsilon^{2\rho x}(I_R^2 R RTH_0 + E_R^2 g RTH_{0D}) = T_R$$

When $W = \alpha$, $I_R = 0$, and $Z_0/W = 0$

$$\left(\frac{E_R^2 R}{Z_0^2}\sinh^2 \rho x\right)RTH_0 + (E_R^2 g \cosh^2 \rho x)RTH_{0D} = T_R$$

When $W = 0$ and $E_R = 0$

$$(I_R^2 R \cosh^2 \rho x)RTH_0 + (Z_0^2 I_R^2 \sinh^2 \rho x)RTH_{0D} = T_R$$

From equations 5, 6, 13, 17, and 26 the current rating under steady-state conditions, and the current and voltage at any point along the cable, under all conceivable circumstances to be met with in practice may be obtained. These five equations will now be adapted to more practical matters concerned with the initial objective of bringing into greater emphasis the similarities and disparities between high-voltage (h-v) transmission and high-frequency (h-f) transmission.

High Voltage and Low Frequency

The ordinary metallic-sheathed single-conductor power cable employed in the transporting of bulk energy represents a coaxial cable in which the inner conductor only forms part of the electric transmission circuit. Only under certain preconceived conditions does any current flow in the outer conductor, and it may normally be assumed to be at ground potential or approximately so. Spurious currents, caused by induction effects, may flow in the outer conductor, but they are not included in the power circuit transferring energy, although their effects thereon cannot always be ignored.

For successful performance in service over long periods of time, it is necessary to interpose between the two coaxial elements a suitable dielectric material. For h-v cables their material must be such that impunity from breakdown is reasonably assured, so the factors of safety relative to internal and atmospheric voltage surges must be properly chosen.

In the present state of knowledge this dielectric takes the form of a relatively solid, though not rigid, material thoughtfully designed and carefully processed in the hands of those familiar with high-voltage practices. In the case of cables to operate at high voltages it is of utmost importance that this should be so, and a reputable manufacturer long experienced in designing, making, and handling high-voltage cables is a vital factor in any project.

That is all that needs to be said here in regard to the design of h-v cables and their peculiar characteristics which distinguish them from other cables of the low-frequency class. However, it might be well to draw attention to a few other aspects of h-v cables as such.

First of all, with the original coaxial configuration in mind, it is apparent that the electrostatic capacity parameter of the transmission equations is an inverse logarithmic function of the two diameters. And for any two given diameters the symmetry of coaxial arrangement yields a minimum value of C and the maximum potential energy, which, of course, is a prime requisite of any h-v cable.

It also becomes noticeable that increasing the diameter of the outer or ground electrode further decreases C and increases the potential energy, but in so doing physical limitations and economical considerations must be taken into account. Thus the value of C and (concomittantly) the outer electrode diameter must be wisely chosen for any particular design.

From the point of view of the factors of safety in respect of internal or switching surges and atmospheric surges, C is of vital concern for it may be considered as the determinant in these matters. Nowadays there is considerable and well-deserved emphasis put upon the impulse strength of electric equipment. This is because of the need to maintain a predetermined impulse level throughout the transmission system and certain levels have been established by the various standardizing bodies. Hence the impulse voltage breakdown strength of any h-v cable is becoming the greater criterion of the dielectric design and insulant thickness, so that C is found limited to a value dictated by these circumstances, above and below which one cannot trespass. For any particular h-v rating and cable design (and conductor size) C is then, to all intents and purposes, a given quantity

$$C=\frac{1.11krgc}{2E_a} \text{ micromicrofarads per wire centimeter}$$

where r is the conductor radius.

The parameter R, or more explicitly the conductor size, for h-v cables is not usually dependent upon steady-stated current rating considerations; it is a function more especially of the voltage rating and cable design. Inductance L is largely determined in a 3-phase system by the center to center spacing of the three phases, and here again symmetry of the array is an important factor requiring attention. For all h-v cables of conductor sizes of the order of 500,000 circular mils and larger, a frequency of 60 cycles per second, and close spacing of the phases

$$\omega L=1.9R \text{ as a loose approximation}$$

Since the insulant must (for reasons not needing explanation) be of the highest grade, the value of g is about negligible in comparison with C, i.e., $g<<C$, so that for the attenuation constant an equation is found

$$\alpha=\sqrt{0.12\omega RC}$$

from which it may be noticed that the attenuation constant is to some degree related to the copper loss and the dielectric loss. Similarly, the wave-length constant may be found from the approximate equation

$$\beta=\sqrt{2.02\omega RC}$$

so that, given the load impedance W the voltage drop and regulation of any circuit may be computed from equations 7 and 13 or

$$e=E_R\cosh\rho x+\frac{Z_0}{W}E_R\sinh\rho x \tag{27}$$

These equations for α and β tell something very specific about a h-v transmission circuit transporting bulk energy, i.e., power transmission. α and β will have very low values comparatively speaking and since $\lambda=(2\pi)/\beta$ the wave length of the line is long. The long wave length gives rise to a predominant characteristic of any power cable, that of being extremely short in terms of the wave length. The small value of α means that the circuit is highly efficient in regard to the amount of power delivered compared to the input power. This is important because large amounts of power are involved, and a small drop in efficiency means an energy loss of some monetary value, the capitalized value of which could be of some consequence.

On comparatively long h-v circuits the angle between the sending end and receiving end voltages represented by β is of importance, as well as the characteristic impedance Z_0. It has, e.g., been shown that the voltage at the receiving end under open-circuited conditions could conceivably be the decisive limitation to successful operation of a long circuit. If the circuit is open at the receiving end, $W=\alpha$ and

$$E_S=E_R\cosh\rho L \tag{28}$$

From this it may be seen that at some frequency or frequencies and certain circuit lengths L it would be feasible for E_R to exceed E_S, the well-known Ferranti effect. By suitable manipulation it can be determined that as long as $\beta<1.78\alpha$ the Ferranti effect will not exist.

Now consider one other aspect of any h-v transmission line. At some particular value of I_R for a given E_R (voltage to neutral) the leading and lagging wattless components of the power received can be made equal. Then, in accordance with the equipartition theory

$$1/2CE_R^2=1/2LI_R^2$$

and

$$E_R/I_R=\sqrt{L/C}$$

and it transpires now that

$$Z_0=\sqrt{L/C}=W$$

The total power delivered in a 3-phase circuit is given by the expression $3E_RI_R\cos\theta$. At unity power factor, this becomes $3E_RI_R$, from which, together with the preceding value of Z_0, it follows

$$P_n=\frac{3E_R^2}{Z_0}$$

Now it so happens that for circuits of considerable length the absolute load must always be less than the natural load as just defined; hence the value of Z_0 should, on this score, be as small as is reasonably possible; and for h-v cables, it is about one-eighth that of overhead lines.

The relationship whereby the energy stored in the electric field is equated to the energy stored in the magnetic field will be recognized as representative of the conditions obtaining when oscillatory energy is present in a cable line, or when a lightning discharge suddenly impresses on the cable a quantity of energy which is propagated along the cable as a "pure" travelling wave or impulse; in either case R and g must be very small, relative to C and L, in so far as the manifestation of these phenomena are concerned. For oscillatory energy to persist for any finite time the losses must be relatively insignificant, i.e., Z_0 is again equal to $\sqrt{L/C}$, and it can be shown that

$$\alpha=1/2\frac{R}{Z_0}+1/2gZ_0 \tag{29}$$

$$\beta=\omega\sqrt{LC} \tag{30}$$

Now neglecting the internal inductance of the inner conductor and assuming once again the cables of a 3-phase circuit to be in close proximity, it becomes admissible within the bounds of reasonable accuracy to write

$$\sqrt{LC}=3.33\sqrt{k}\times10^{-11}$$

(where units of length are in centimeters). For overhead lines $k=1$ (the dielectric constant of dry air) in clement weather and

$$\sqrt{LC}=3.33\times10^{-11}$$

which means that the velocity of the pure wave is about that of light (300×10^6 meters per second) from the relationship

$$V=\frac{\omega}{\beta}=\frac{1}{\sqrt{LC}} \text{ centimeters per second}$$

For cables k has an upper limit of about 6; therefore an average value of $\sqrt{LC}$ would be

$$\sqrt{LC}=5.1\times 10^{-11}$$

For a h-v cable $k=3.6$ and

$$\sqrt{LC}=1.9\times 10^{-11}$$

giving a velocity for the pure travelling wave of some 99,000 miles per second.

It is now seen that in a h-v cable the energy wave of the lightning discharge travels at a much lower velocity than in an overhead line. In terms of the impulse level of the system and the conductor size

$$\sqrt{LC}=23.3\sqrt{\frac{kr}{E_a}}\times 10^{-10}$$

where r is the radius inner conductor in centimeters.

The small value of Z_0 for a h-v cable in comparison with that of an overhead circuit is of some significance when considering the effects on lightning discharges and oscillating energy phenomena. Under these circumstances equation 29 applies, the first term of which represents that part of the attenuation due to the copper loss and at low frequencies is the predominant component of the total attenuation. With low values of Z_0 the $1/2(R/Z_0)$ is high and the pure wave becomes attenuated to a larger extent than would be the case with a larger Z_0 obtaining.

Also, if a circuit is carrying a current I, as this current is suddenly interrupted the maximum value of the oscillatory voltage that may be produced is equal to IZ_0; hence a small Z_0 may be beneficial if conditions are critical.

High Frequency and Low Voltage

The characteristics defining the performance of a h-v cable in service also may be taken as governing the design and operation of cables at high frequencies, although, upon increasing frequency, it is found that the roles they play in the wave propagation mechanism vary in magnitude and effectiveness to a greater or lesser extent, owing to the several requirements which distinguish the two modes of transmission.

In the transmission of intelligence from one place to another, the fidelity of the received signal is of more concern than the loss of energy, since the energy involved in any transmission of intelligence is extremely small when compared with the transport of large blocks of power demanded by industrial and household enterprises.

As mentioned earlier in the paper, the subject matter is restricted to the symmetrical configuration of a 2-element coaxial cable, so Fig. 1 in a very simple way again shows the h-f cables in question. In contra distinction to the h-v cables, the two coaxial conducting elements now form the circuit, one being the "go" conductor and the other the "return" conductor of the usual single-phase circuit.

The five transmission line equations, equations 5, 6, 13, 17, and 26, are applicable, and at high frequencies it follows from classical theory that

$$\alpha=1/2\frac{R}{Z_0}+1/2gZ_0 \tag{29}$$

as was the case with the pure transient wave associated with the impulsive energy of the lightning discharge. However, with an increase of frequency g has a more prominent effect on the attenuation constant and at very high frequencies the attenuation component due to the dielectric loss $(1/2gZ_0)$ may be as prominent or more so than the attenuation component due to copper loss $[1/2(R/Z_0)]$. The net effect is a relatively higher attenuation constant than obtains with a h-v cable line. Once again, insulants of high quality and stability, but not necessarily of the high electric breakdown strength required by h-v cable transmission, are a paramount desideration. Here the emphasis is upon the dielectric constant and power factor of the insulant.

Since the amounts of energy are relatively small, the attenuation constant is of utmost importance, and it therefore becomes desirable to operate a h-f cable at its natural load. That is to say, the load impedance must equal the characteristic impedance or nearly so, the cable is matched to its load. Hence

$$\begin{aligned}Z_0&=W\\&=\sqrt{L/C}\end{aligned}$$

the asymptotic value of the characteristic impedance versus frequency curve, and equations 7 and 13 become

$$e=E_R\epsilon^{\alpha x}\epsilon^{j\beta x} \tag{31}$$

from which

$$e=E_S\epsilon^{-\alpha x}\epsilon^{-j\beta x} \tag{32}$$

Similarly

$$i=I_S\epsilon^{-\alpha x}\epsilon^{-j\beta x} \tag{33}$$

and

$$\begin{aligned}p&=ei\\&=E_SI_S\epsilon^{-2\alpha x}\epsilon^{-j2\beta x}\\&=P_S\epsilon^{-2\alpha x}\epsilon^{-j2\beta x}\end{aligned}$$

The current, voltage, and power are thus decreased in accordance with the exponential function involving α, i.e., $\epsilon^{-\alpha x}$, the so-called attenuation factor. The highly significant effect of the attenuation of the waves as they proceed along the line is at once apparent, as is the similarity to the h-v cable case.

Another prime aspect bearing a close parallel to h-v cable design is the necessity of elimination of ionization within the insulating medium. It is a well-known phenomenon that ionization has a depreciating effect on the attenuation of the waves, especially at higher frequencies. And whereas this phenomenon would have a salutary influence on the behavior of h-v cables subject to atmospheric transient surges, it can cause a distortion of the signal transmitted at high frequencies which would be disturbing. This, of course, is apart from any chemical or electrical deterioration which would follow excessive or malignant ionization. Nonetheless, in some cables even at very low voltages a phenomenon, discernible by a band-pass fitter as noise, may be observed which cannot be distinguished qualitatively from internal ionization magnitude below which the ionization is innocuous in so far as chemical or electrical deterioration is concerned; it nevertheless cannot be tolerated for the reason already mentioned. As with h-v cables, so in h-f cables with solid dielectrics the formation of voids which may ionize under suitable conditions in service must be brought under control during the manufacturing process and be quantitatively held to within such limits that the magnitude of any subsequent ionization will be harmless in all respects.

The energy dissipated in the voids which are initially ionized is determined by the increment of the applied voltage over the ionization ignition voltage; and it may be that the life of either a h-v cable or a h-f cable, at stresses greater than the ionization ignition voltage, is a function of the excess of the applied voltage over the ionization ignition voltage. If this excess is definitely indicated and sufficiently great, the cable life is unquestionably finite and its mortality rate high.

Once again, owing to the fact that the energy involved at high frequencies is small, comparatively speaking, it is of interest to examine that equation which expresses the steady-state current rating of the cable. In so doing it will be appreciated that that part of the energy (or signal) which fails to appear at the receiving end is converted into heat energy and causes a rise in the cable temperature.

The same current rating equation applies,* namely equation 26, and when $Z_0 = W$ as obtains by matching the cable to its load, then

$$I_R^2 RRTH_0 \epsilon^{2\alpha x} + E_R^2 gRTH_{0D} \epsilon^{2\alpha x} = T_R \qquad (34)$$

or

$$I_R^2(RRTH_0 + Z_0^2 gRTH_{0D})\epsilon^{2\alpha x} = T_R \qquad (35)$$

or, according to the Mildner equation

$$I_R^2 R\left(RTH_1 \frac{\alpha_{c1}}{\alpha} + RTH_2 \frac{\alpha_{c2}}{\alpha} + RTH_3\right) + E_R^2 gRTH_{0D} \frac{\alpha d}{\alpha} = T_R \qquad (36)$$

So it becomes evident that at the higher frequencies where α assumes much larger magnitudes it must be taken into account in determining the current rating of the cable or the power rating. The influence of Z_0 on the current rating is also revealed by equation 35.

It so happens that for any given insulating material and a symmetrical arrangement of the circular elements Z_0 is a direct function of the geometry of the coaxial circles, and hence in practice is a more or less constant quantity over a range of cable designs, reaching a practical maximum of about 200 ohms. It therefore follows that the greater limitation on the current rating of the cable is the attenuation constant α, which, as already found, is made up of two additive components—one due to the copper loss and the other to the dielectric loss. The copper loss varies at any particular high frequency as the square root of the resistivity of conductor material and inversely as the diameter of the coaxial circles, while the dielectric loss for the same geometrical relationship varies as the power factor and dielectric constant of the insulating material. And, as already said, the characteristics of the insulating material which concern the dielectric loss become the greater criterion of successful performance of h-f cables as the frequency is increased.

Hence, as with h-v cable design, the capacitance parameter C assumes a limiting value because of its dependence on the dielectric constant of the medium. Where the amounts of h-f energy to be transmitted are not too large, a dielectric constant not much greater than 2 may be suffered, providing the power factor of the insulant is relatively low (=0.0003); the solid material polyethylene is invariably used nowadays in these applications.

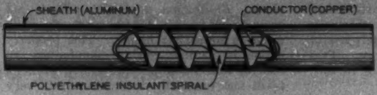

Fig. 4 (above). Helical membrane cable

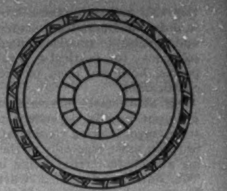

Fig. 5 (right). 120-kv oil-filled cable; outside diameter 2.65 inches

However, the efficient transmission of larger amounts of h-f energy, such as might be required for radio or video broadcasting, make the cable design more onerous. The symmetrical coaxial arrangements possess the maximum potential energy, and lowering the value of C, by increasing the diameter ratio, increases further the potential energy (or working electric stress) hence the power transmitted as well as the physical size of the cable. But the magnitude of ionization is related to the electric stress and must be kept to a minimum; consequently, there is a limit beyond which the potential energy or the working voltage cannot be raised without occasioning too bulky a cable.

Increasing the h-f energy also results in a greater power loss and higher cable temperatures as the current rating equation illustrates. Since the choice of highly conductive metals is fairly restricted, and because the asymptotic value of $Z_0 = \sqrt{L/C}$ is a fairly constant quantity consequent upon the usual load impedances involved, there remains but one other choice in designing h-f cables to carry economically the larger amounts of energy. This choice is a fairly obvious one suggested by the nature of the transmission line equations: it is to reduce to the attenuation constant to as small a value as possible.

The influence of Z_0 on the attenuation constant has been noted, and for any assigned value of Z_0 a minimum α obtains in the symmetrical coaxial arrangement for a specific ratio of the circle diameters. But this adjustment of the physical dimensions of the cable is not sufficient to result in an economically sound transmission system. Reducing the dielectric constant from somewhat over 2 to a value of 1 that obtains with air or other gases results in a decrease in attenuation of approximately 60 per cent. Therefore the solution of the problem lies in arriving at a practical cable design, mechanically robust and uniformly stable in performance, which would lend itself to commercial manufacture.

For a great many years now cable manufacturers all over the world have struggled with the problem of producing such a cable of the coaxial type. As may be appreciated, it involves the combining of the two unstable coaxial circles with the minimum amount of solid material and the maximum amount of gas into a permanently stable arrangement capable of retaining its initial symmetrical shape in any cross section throughout its duty in service and having, of course, a dielectric constant approximately equal to 1.

Fig. 4 illustrates the only cable design yet manufactured to conform to these qualifications. It was brought into commercial manufacture in England a few years ago as a result of considerable research and development work. Its design is unique and a fine example of the practice of science applied to cable making.

Fig. 5 shows a cross-sectional view of the 120-kv power cable for bulk energy transmission. As one examines closely the physical construction of these two cables, Figs. 4 and 5, some of their similarities and disparities become more tangible. In the one case—the h-v cable—the tapes are applied parallel to the longitudinal axis and in a helical formation; in the other the tape is applied at right angles to the longitudinal axis and again in a helical formation; but both make use of the tapes as their supporting structure to obtain and maintain the symmetry of the coaxial array which is so desirable.

◆

Discussion

F. H. Buller (General Electric Company, Schenectady, N. Y.): Mr. Short has presented a useful comparison between the characteristics of communication cables and power cables, and has emphasized points of similarity between these characteristics which do not manually occur to a cable engineer working in one field only. Such a comparison is valuable since it is often possible to get useful and constructive ideas from the practices which are current in a similar field. While the fundamental information is doubtedless available in the literature, it is very desirable from time to time that such comparisons be clearly drawn in order to stimulate constructive thinking, and possibly to provide immediately useful solutions to particular problems. Two points, however, seem to require further clarification.

---

* Heat flow deviates appreciably from the radial direction only when the insulant thickness becomes an appreciable fraction of the thermal wave length (thermal wave length = 1/2 electrical wave length).

Mr. Short states that conductor resistance R is not usually dependent upon steady-state current rating considerations but is a function more especially of the voltage rating and characteristic design in h-v cables. This statement is correct when conductors of the minimum permissible size are used. This minimum permissible size is a function of voltage rating (see the Association of Edison Illuminating Companies Specifications) and of type of insulation. However, the minimum permissible size usually corresponds to a very light load, a load which is, in fact, so light that it is seldom economical. The usual practice involves loads considerably greater than this, requiring the use of a much larger conductor in order to avoid overheating or excessive voltage drop. As a matter of fact, in power cable work the conductor size, and hence its resistance, is determined primarily by cable load since this is the factor which governs both heating and voltage drop; and it is only affected by the voltage rating and the cable design in so far as these factors affect maximum permissible temperature and thermal resistance.

Mr. Short states for all h-v cables of the usual conductor sizes a frequency of 60 cycles and close spacing of cables $\omega L = 1.9R$. A few spot checks indicate that this relationship does not appear to hold for single-conductor cables arranged on 6-inch centers, although it can be used as a very rough approximation for three conductor cables, or three cables pulled into one duct. Possibly, this is the thought which Mr. Short had in mind when he made this statement.

A. L. McKean (Phelps Dodge Copper Products Corporation, Yonkers, N. Y.): We should like to commend Mr. Short for his excellent summary of practical theory which emphasizes that 60 cycles and megacycles, in spite of wide divergence in frequency and application, obey the same fundamental laws of propagation and transmission.

We should like to take exception to Mr. Short's next to last paragraph which implies that the aluminum-sheathed cable with polyethylene helix separator shown in Fig. 4, developed in England, is the only design which provides a permanently stable, essentially air dielectric coaxial cable construction. There are others.

While polyethylene provides very adequate means of helical support in coaxial constructions, there is an even more suitable material available for such applications, namely polystyrene, in fully oriented tape form. Apparently, the author is not aware of styroflex, a coaxial cable which has gained world-wide recognition for its exceptional and uniform characteristics. The cable comprises a copper inner conductor, a helix of styroflex tape, and aluminum sheath outer conductor.

The reason for the exceptional qualities of styroflex lies in the stability of the styrene tape helix which surpasses polyethylene because of its extremely high modulus of elasticity. Elongation at 10,000 pounds per square inch is only 3.0 per cent; the yield point is somewhat higher. This property makes it possible, during manufacture, to control and maintain uniformity of helix pitch and pertinent diameters within very close tolerances. It also ensures stability of these uniform characteristics for the life of the cable.

Due to its outstanding properties, styroflex is presently being employed in many applications for which no other coaxial cable could be considered. Further, it is provoking reconsideration of many present-day coaxial installations and stimulating some entirely new fields of employment.

R. W. Atkinson (General Cable Corporation, Bayonne, N. J.): Both power and communication cables are ways of transmitting energy and although both obey the general transmission equations, the contrasts in characteristics are as great as the difference in purpose of transmission. Efficient power transmission by cable requires that much more than 90 per cent of the transmitted energy shall arrive for use. Efficient communication transmission permits more than 99 per cent of the energy to be lost or utilized in transmission. In power, dielectric strength, cost of energy loss, and conductor heating by the losses are controlling; in communication these are negligible. In communication the one significant property is to transmit a sufficiently accurate replica, even though attenuated a thousandfold, of the originating complex wave. This compares with the power cable requirement of substantially zero attenuation and no essential problem of distortion.

For some communication circuits, the general equation of transmission may be used in simplified form, although often being required in complete form. Seldom, however, is it necessary to treat a power cable transmission with the use of other than the simplest equations and treating its distributed constants as lumped. In the power cable the one important exception to this simple method is where it is used as a carrier to transmit communication or intelligence or where nature chooses to impose transients (lightning) when the methods of analysis become those used for communication.

Many types of material are used by both types of cable. The knowledge of dielectric constant and dielectric power factor learned from one type of cable is useful for the other but even here the numerical values are variously and significantly affected by the difference in frequency. Similar problems arise on materials that are affected by moisture absorption.

H. D. Short: I should like to thank the discussers for their contributions, and in particular Mr. Buller and Mr. McKean for their kind remarks.

Mr. Buller has referred to the statement made concerning the parameter R and mentions the Association of Edison Illuminating Companies Specifications as specifying certain minimum conductor sizes for certain operating voltages. What I had in mind was specifically the higher voltage cables of all types; and the higher the operating voltage the more the statement I made becomes a truism. In point of fact, and in spite of standardizing specifications to the contrary, we have found it obligatory to examine closely the potential gradient across the insulant when recommending a cable design to operate at voltages greater than 30 kv to neutral. And of course in this regard it is not conductor size alone that operates, but the combination of conductor dimensions and insulant thickness in the usual logarithmic fashions. So that in contradistinction to Mr. Buller's feelings in the matter we must not only look at the conductor size from the standpoint of load but also for voltages above, say, 30 or 40 kv we must ensure that the stress at the conductor surface is not unduly high, and this is especially true when dealing with solid-type cables.

Mr. McKean has confined his remarks to the h-f class of cables. We are very much aware of the German h-f cable innovation known as the styroflex design. This cable first came to our attention during the last invasion of Europe by the Allied forces—installations of it having been discovered in use by Signal Corps officers. After the war the styroflex design was very carefully studied by the English cable firm which developed the helical membrane cable.

Mr. McKean misinterprets if he felt that I implied that an aluminum-sheathed cable was the only design which provided a permanently stable, essentially air dielectric coaxial cable construction. The context of the next to last paragraph cannot be so interpreted. Mr. McKean has missed the main point I was making for the helical membrane cable. It is, as stated in the paragraph preceding it, that the helical membrane cable combines, in comparison with any other coaxial cable not excepting the styroflex design, the minimum amount of solid material and the maximum amount of gas space per unit volume into a permanently stable arrangement. This volume ratio as delineated in the paper is of great importance in reducing the attenuation.

The other main feature I was emphasizing in the paper in these respects was the unique principle involved in the helical membrane design of applying a tape at right angles to the longitudinal axis while retaining the helical formation. In the styroflex design the tapes are used parallel to the longitudinal axes as is common practice in the industry, and the tapes are simply applied with 100-per-cent overlay, a long lay, and wide butt spacing; so that it is not possible to obtain in any given case the equivalent gas space which would obtain in the helical membrane counterpart. A comparison of the mechanical characteristics of polystyrene and polyethylene which Mr. McKean has attempted is beside the point, for obviously the helical membrane cable principle can be accomplished with either material or any other suitable dielectric for that matter. Or, to put it another way, the embodiment of the helical membrane design is not necessarily confined to any one material, such as polyethylene, although the higher melting point of polyethylene in relation to that of polystyrene does present some contemporary merit in favor of the former.

The great beauty and distinct advantage of the helical membrane cable in direct comparison with the styroflex cable is its simplicity in conception and manufacture, a fact which is reflected in their comparative costs as presently marketed.

An Investigation of the Capture Effect in a Narrow-Band Frequency-Modulated System

C. D. HEDGES
ASSOCIATE MEMBER AIEE

CAPTURE effect in frequency-modulated (FM) radio transmission is that phenomenon whereby the stronger of two signals increases its predominance over the weaker signal on the same frequency in a receiver so that the weaker signal is eliminated from the receiver output. The transition in control can be very sharp when one signal becomes even slightly stronger than the other signal. That is, a small differential in radio-frequency input levels of the desired signal to the interfering signal results in a much higher ratio of signal to interference in the audio output. This characteristic of some FM systems permits the use of many more broadcast stations within a given area operating on the same carrier frequency than is possible with amplitude modulation (AM).

The amount of capture effect present in FM equipment is dependent, among other things, on the total channel bandwidth utilized. About 10 years ago, FM communication equipment was recommended for power-line carrier use; a major feature was that it possessed capture effect. This phenomenon supposedly would make it possible to work two channels back-to-back at the same station on the same frequency with less isolation between them than would be required for conventional AM channels. From a preliminary study made by the author, it was concluded that very little, if any, capture effect was present in narrow-band equipment. This is also the conclusion reached by others in previously published literature.[1,2] The investigation reported in this paper has been made to study capture effect as it relates to narrow-band FM systems used in the power-line carrier field. It was concluded, after the investigation, that a narrow-band FM system is only slightly better than an AM system of the same bandwidth with respect to rejecting interfering signals or noise.

Capture Effect Theory

From an explanation on why capture effect is present in a wide-band system, it will become evident that this phenomenon is much less effective in the narrow-band systems. When two signals, desired and interfering, pass through an FM receiver, both phase modulation (PM) and AM are produced. The AM would ordinarily be heard as a beat note in an AM receiver but the limiter circuits in the FM receiver eliminate the variation in signal due to AM. The undesired PM is not so easily eliminated. The PM results in an indirect FM signal which produces an audible output at the discriminator and the receiver output. In wide-band FM systems this interference cannot actually be eliminated but its effect can be minimized by making this undesired output appear insignificant when compared to the desired audio signal.

If the PM resultant signal is examined, it is seen that it can be represented by two carrier signals giving a resultant having the average frequency of the stronger but having its phase shifted plus and minus around its mean value at a rate equal to the difference frequency between the two carrier signals. PM may be illustrated by referring to Fig. 1. The desired carrier phasor continuously rotates through 360 degrees. The weaker undesired signal rotates relative to the desired carrier at a frequency equal to the difference frequency (F_D-F_I). AM is produced as shown. As the undesired phasor rotates around the desired phasor, PM is produced between the limits A and B. The faster the undesired phasor rotates or the faster the rate of phase change, the greater the FM. Thus, as the beat frequency increases, PM increases and therefore the undesired audio output increases. Thus, it can be shown that the degree of the indirect FM formed from PM depends upon the expression $(\Delta\theta)\,(F_D-F_I)$.[3] As already stated, F_D-F_I is the difference frequency between the two unmodulated carriers in cycles. The other factor $\Delta\theta$ is given in radians and is dependent upon the relative amplitudes of the desired and undesired carrier signals. Assume that the two signals differ in magnitude by a ratio of 2 to 1. The maximum value of $\Delta\theta$ is 26.5 degrees $[\tan^{-1}(I/D)]$ which is 0.464 radian. Assume that the difference frequency between the two carriers is 2,500 cycles. Substitution of these values into the foregoing expression results in a frequency shift of 2,500×0.464 or 1,160 cycles. The frequency variations shift at a rate of 2,500 cycles a second over a maximum shift of 1,160 cycles.

At this point it is desirable to compare the characteristics of a wide-band FM system such as is used in broadcast service with narrow-band systems as used in power-line carrier. The maximum deviation for carrier systems is approximately 2,500 cycles, and carrier FM receivers have a bandwidth of approximately 5 kc. In comparison, an FM broadcast station may employ a maximum deviation of 75 kc and the broadcast FM receiver bandwidth is approximately 150 kc. Power-line carrier systems deviate 2,500 cycles to produce 100-per-cent modulation, but in the wide-band broadcast system the carrier must deviate 75 kc to produce 100-per-cent modulation.

Returning to the example given for the conditions assumed, a shift of 1,160 cycles was present because of PM between the desired signal and the interference signal. In a wide-band receiver, the interference produced by a shift of 1,160 cycles is insignificant when compared to the audio signal developed by a swing of 75,000 cycles. As the ratio of the amplitude of desired to interference signal at the receiver input is increased or the frequency difference between the two signals decreases, the suppression of the interference signal improves. Thus, the use of wide-band FM swamps the small FM

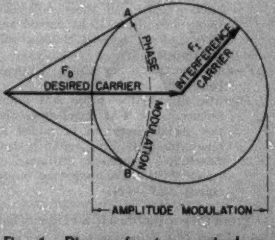

Fig. 1. Diagram for two received unmodulated carriers of different frequencies F_D and F_I

Paper 55-79, recommended by the AIEE Carrier Current Committee and approved by the AIEE Committee on Technical Operations for presentation at the AIEE Winter General Meeting, New York, N. Y., January 31–February 4, 1955. Manuscript submitted October 21, 1954; made available for printing November 18, 1954.

C. D. HEDGES is with the Westinghouse Electric Corporation, Baltimore, Md.

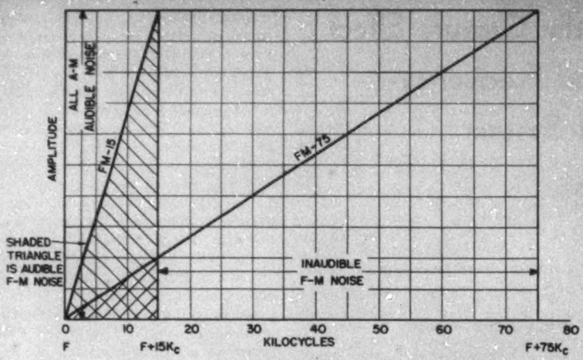

Fig. 2. Noise diagram for FM and AM receivers for various FM deviation ratios

signals developed indirectly from the interference. As the deviation ratio is decreased, the effect of the interference because of PM becomes more and more important. In a power-line carrier FM system, where the maximum shift is 2,500 cycles, it is evident that the interference caused by the calculated shift of 1,160 cycles would be too high to tolerate, almost 50-per-cent modulation. This is the same condition that exists in an AM system when the signal-to-interference ratio is 2 to 1 at the receiver radio-frequency input. Wide-band FM is required for minimum interference, and in these cases capture effect is present.

The relationship of I (interference) to D (desired signal) and frequency deviation can be shown to be as follows:

$K_1=(I/D)\,(100)$, interference modulation in an AM receiver in per cent

$K_2=(I/D)\left[\dfrac{F_D-F_I}{\Delta F}\right]\,(100)$, interference modulation in an FM receiver in percent

I = interference level

D = desired signal level

(F_D-F_I) = frequency difference between desired and interference unmodulated signals. All those difference frequencies above 15 kc should not be considered because the ear will not respond

ΔF = maximum frequency shift. Channel bandwidth equals $2\times\Delta F$

I/D = ratio of amplitudes for AM interference. For FM interference the two signals have to be added in quadrature. If, e.g., $I=0.5D$, then $\Delta\theta=\pm 26.5$ degrees or 0.464 radian $(\tan^{-1} I/D)$. The frequency swing equals $\Delta\theta(F_D-F_I)$

From these equations it is evident that wide-band FM definitely has an advantage over an AM system. If the maximum deviation is 75 kc, and (F_D-F_I) is 15 kc, the resulting interference in an FM receiver would be only 20 per cent of that obtained with an equivalent AM receiver. If the two signals have the same carrier frequency, then no audible beat effect can exist and the equivalent FM signal is zero. If the two signals differ slightly in frequency, the resulting interference is completely outweighed when the maximum deviation is 75 kc. This is an important feature of wide-band FM since the well-known beat whistle interference in an AM receiver makes reception almost impossible. However, in narrow-band FM where the deviation is limited to a low value—2,500 cycles in the case of FM power-line carrier transmitters—this advantage is greatly reduced and the capture effect of narrow-band FM over AM is very slight.

The preceding discussion was used to illustrate capture effect for the simplest case where two unmodulated carriers of different frequencies F_D and F_I arrive simultaneously in an FM receiver. For the condition when the desired and interfering carriers are modulated, PM is produced between the various desired and interfering side bands. The analysis of the interference for this case can be made by treating the resulting signals as instantaneous carrier signals (F_D-F_I). A rigorous analysis is given in Hund's book[3] on FM for this condition. See Table I for actual listening test comments made on a carrier system with both carrier signals modulated simultaneously.

Interference from Noise

In carrier systems not only is interference present from other carrier signals but there is also transmission-line random-type noise plus impulse noise due to electric storms and other sources. The analysis of this is the same as the previous discussion on capture effect theory. The reaction between each noise voltage and the carrier again produces AM and PM in which case the AM is removed by effective limiting. Since each noise signal is the same as an interference signal, then as the difference frequency increases (F_D-F_I) the interference from PM increases. This plots a triangular noise response for an FM receiver as shown in Fig. 2. In an AM receiver, each noise voltage of a different frequency will mix with the AM carrier to form a beat note. The amplitude of each beat note is the same because all distributed noise voltages have approximately the same strength and therefore, in place of a triangular noise response, there is a rectangular response. For example, a single interfering wave at the band edge in FM would give an output amplitude as great

Table I. Listening Test Comments with Transmitters T_1 and T_2 Modulated Simultaneously. See Fig. 3 for Block Diagram

T_1/T_2: Radio-Frequency Carrier Level Unmodulated, Decibels	Condition A: Unmodulated Carriers Initially Adjusted for a 300-Cycle Beat Note	Condition B: Unmodulated Carriers Initially Adjusted for a Zero Cycle Beat
0	With both signals on, neither is understandable.	
6	The desired signal T_1 is understandable but rough and distorted. Undesired signal not understandable but quite loud.	The desired signal over-rides the undesired and it is readable with practically no difficulty. The undesired signal is quite loud. When the desired signal ceases modulation, the undesired signal is also readable with practically no difficulty.
12	The interference is not tolerable but the desired channel can be understood quite well.	Desired signal is readable with no difficulty but interference is still too objectionable.
20	With both signals on, the undesired still comes in and can be heard as interference but it has practically no effect on the understandability of the desired signal. The undesired signal is a nuisance, however, along with the tone and could not be tolerated.	The desired signal is perfectly readable but the undesired signal is objectionable in the background.

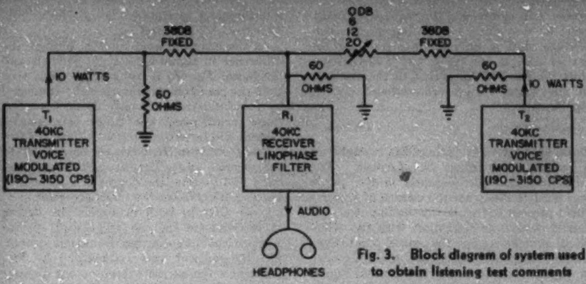
3808 FIXED
0 DB
6
12
20
3808 FIXED
10 WATTS
60 OHMS
60 OHMS
60 OHMS
10 WATTS
T1
40KC TRANSMITTER VOICE MODULATED (190-3150 CPS)
R1
40KC RECEIVER LINOPHASE FILTER
T2
40KC TRANSMITTER VOICE MODULATED (190-3150 CPS)
AUDIO
HEADPHONES

Fig. 3. Block diagram of system used to obtain listening test comments

as the same noise signal located anywhere in the AM passband. For an FM system, the suppression of noise is directly proportional to the deviation ratio. In Fig. 2, the FM-75 receiver actually accepts noise out to 75 kc and it has the usual FM triangular noise characteristic. The human ear, however, is only sensitive to frequencies within the range of audibility, up to around 15 kc, and rejects everything else. The maximum height of the audible part of the FM-75 triangle corresponding to voltage is only one-fifth of the height of that for an FM-15 triangle. Such being the case, the FM-75 advantage over FM-15 is appreciable. Then, for this consideration, it may be said that wide-band FM is superior to narrow-band transmission, but only if the input desired signal to distributed noise ratio is initially large. For impulse noise, the carrier level must be even higher than it is for distributed noise.

The requirements for a carrier communication system include the specification which requires that the equipment operate over long channels in the presence of high noise interference usually encountered on these long lines, in which case the desired carrier-to-noise voltage ratio is low. In a wide-band FM system when the signal is stronger than the noise, the audio output signal-to-noise ratio is even better than the input radio-frequency ratio but, conversely, if the noise is greater than the signal at the input, then the noise-to-signal ratio at the output is high. That is, if the noise is higher than the desired signal, the wide-band set will be captured by the noise. This would swamp the desired signal which is highly undesirable. The wide-band set shows favoritism. The ability of the narrow-band FM to reach down into the noise means that there is no capture effect because both the signal and the noise are received, neither being favored and the other excluded. Because this characteristic is not in wide-band FM, its use on a power-line system for the purpose of utilizing the capture effect feature would prove very impractical.

Experimental Results

Listening tests were conducted on standard Westinghouse type-*FD* FM equipments. Two transmitters and one receiver were employed with all units tuned to 40 kc. As previously stated, the maximum audio modulating frequency was restricted to 2,500 cycles. The maximum deviation of the carrier is 2,500 cycles for power-line carrier transmitters so the deviation ratio for this equipment is 1.

The listening test comments listed in Table I are significant because the final decision as to whether a system is actually workable is dependent upon favorable listening comments. Two conditions are included. One condition is when both unmodulated carriers are exactly on the same frequency, and the second condition is when a 300-cycle beat note exists between the carriers. This latter data are included because of the allowable drift specifications on transmitters installed in the field. From Table I it can be concluded that a reduced quality service, such as emergency voice communication, in the presence of an interference signal is possible provided the desired modulated carrier is 6 decibels or more stronger than the undesired modulated carrier. To say that communication is possible under these conditions means that the desired signal is understandable with practically no difficulty in the presence of an undesired modulated carrier, but the communication is not of the same high quality as provided by standard voice communication channels. The audible crosstalk is at such a high level that it would become annoying on constant usage. Also, when the undesired carrier is modulated and the desired carrier is not modulated, the undesired channel can be understood provided the undesired carrier level is not more than 20 decibels below the desired carrier level. This means that a listener on a desired channel would hear the desired signal satisfactorily in the presence of a modulated interference signal which results in crosstalk, but the listener will also hear the undesired channel satisfactorily when the desired channel is not modulated. This is very distracting to a conservation, but, as stated previously, emergency communication would be permitted. Likewise, an equivalent AM system with the same amount of isolation could be used as effectively.

Conclusions

There is little, if any capture effect present in the narrow-band FM equipment and this is one of the reasons that the equipment is suitable for power-line carrier application. In some applications the equipment is required to operate over long transmission lines where the noise level occasionally approaches the desired signal level. The ability of the narrow-band receiver to receive both the desired signal and the noise, neither being favored, allows the signal to be understood in the presence of the noise. In a wide-band FM system, there is appreciable capture effect which means that the over-all result is to receive the larger signal and swamp out the low signal. However, if a wide-band FM system was applied to carrier application and the noise at the receiver input was greater than the desired signal, then the noise would be received and the desired signal eliminated. Thus, for this reason, the use of wide-band FM for carrier application would be very impractical.

Emergency voice communication in the presence of an interference signal is possible provided the desired carrrier is 6 decibels or more stronger than the undesired carrier. The audible crosstalk is at such a high level for this condition that it would become annoying on constant usage. For acceptable voice communications, more than a 20-decibel difference in level between desired and interfering signals is necessary.

References

1. NBC Frequency-Modulation Field Test, Raymond F. Guy, Robert M. Morris. *RCA Review*, Camden, N. J., vol. 5, 1940–41, pp. 190–225.

2. Band-Width and Readability in Frequency Modulation, Murray J. Crosby. *Ibid.*, pp. 363–70.

3. Frequency Modulation (book), August Hund. McGraw-Hill Book Company, Inc., New York, N. Y., 1942.

Discussion

F. C. Krings (General Electric Company, Schenectady, N. Y.): The author should be commended on this addition to the application practices on power-line carrier. The listening tests contained in Table I will be of considerable value when it is desired to repeat or reuse a frequency which is already in use for FM carrier telephony. The listening tests are much more illuminating than the numerical examples used in the paper; in fact, the example in the section on "Capture Effect Theory" may lead one to an erroneous conclusion when modern carrier equipment is considered. The expression for the degree of indirect FM formed from PM of the carrier is stated in the paper as the product of the difference in signal strength times the difference in frequency. If two crystal-controlled carrier equipments are used, the maximum difference in frequency would be only 200 cycles instead of the 2,500 cycles used in the example. Then if a difference in signal level of 20 decibels is assumed, the resultant maximum shift produced by the interference is only 20 cycles. In comparing this with FM broadcast, as was done in the paper, the percentage shift is only 0.8 per cent for the carrier and is less than the 1.55-per-cent shift for the FM broadcast in the example in the paper which was labeled as insignificant.

C. D. Hedges: Mr. Krings has brought up a factor which must be clarified. The numerical example assumed in the paper was used to illustrate the degree of capture effect present in the narrow-band power-line carrier system as compared with the wide-band system under the same conditions. These conditions were that the difference in signal level between the desired signal F_D and the interfering signal F_I was 6 decibels, and also that the factor F_D-F_I was 2,500 cycles. This results in a shift of 1,160 cycles at a rate equal to the difference frequency. For the power-line carrier system, where the maximum deviation is 2,500 cycles, the interference produced is $(1,160\times100)/2,500=46.6$ per cent, which is approximately the 50 per cent stated in the paper. For the wide-band case, where the carrier deviates 75,000 cycles, the interference produced is $(1,160\times100)/75,000=1.55$ per cent.

In the example used by Mr. Krings, the difference in signal level is 20 decibels and the factor F_D-F_I is 200 cycles. It is true that the resultant maximum shift produced by this interference is only 20 cycles. For these conditions, the power-line carrier system will be subject to $(20\times100)/2,500=0.8$-per-cent interference, as compared to the desired audio output. For the wide-band FM system, the degree of interference is $(20\times100)/75,000=0.0267$ per cent.

Note that in both examples the degree of interference for the wide-band system is much less than that for the carrier system. The 0.8-per-cent value calculated by Mr. Krings for the carrier system is not directly comparable to the 1.55-per-cent value that can be calculated from the example in the paper because the conditions are not the same. In either case, however, it should be brought out that there is a significant improvement in the suppression of interference by the wide-band system over the carrier system when the same conditions are assumed. As has been previously stated, this was the reason for the numerical example.

Aluminum-Sheathed Power Cable

W. A. DEL MAR
FELLOW AIEE

E. J. MERRELL
MEMBER AIEE

IN 1886 Charles Hall developed the electrolytic process which made possible the economic production of aluminum. The process entails the consumption of about 10 kw-hours of electricity per pound of metal, and this energy represents about 20 per cent of the cost of aluminum.[1] The first commercial installation of aluminum-sheathed cable in the United States was a limited amount of telephone cable employed in 1932 on the dirigibles Akron and Macon.[2] Applications as cable sheathing were sporadic and of an essentially exploratory nature, until the threat of lead shortage in recent years sparked relatively comprehensive European usage in both the power cable and communication cable fields.[3]

In 1952, commercial production of standard lengths of aluminum-sheathed communication and power cable was undertaken at the Habirshaw Division of the Phelps Dodge Copper Products Corporation. This cable has ranged in diameter from 3/8 to $3^1/_8$ inches and has been shipped on reels in 1,000-foot lengths. Table I lists the pioneer power cable installations in the United States. When corrosion protection is required, an extruded jacket of black polyethylene is applied directly over the aluminum sheath.

Sheath Manufacture

Current manufacturing, in America, employs the draw-in and sinking method, and 2 years of experience on a considerable scale has led to the following procedure. Billets of aluminum are extruded and the tube produced is wound in long continuous lengths (multiples of 1,000 feet) on extra-large reels. These are pressure-tested and vacuum-treated, then charged with dry gas and sealed until used for cable sheathing. In the sheathing process, the required length of tube (up to 1,000 feet at present) is drawn out straight and, again, pressure-tested with dry gas. Next the cable core is drawn in. Finally, the tube is passed through a sinking die to form a suitably close fitting sheath.

The hardness or stiffness of the sheath differs at a press stop. As a result, the larger sizes tend to wrinkle some in this area when being wound on or off a reel. A practical solution to this problem is a temporary binding of two metal tapes applied over the press stop for a length of 1 foot as the cable passes from the sinking die. Such a binding is shown in Fig. 1. This is removed after installation in the field except, of course, when a polyethylene jacket has been applied over it.

The comparatively high hoop strength of aluminum sheath would seem to permit significant reduction in thicknesses from those customary for lead sheaths. However, the basic practical factor in determining sheath thickness is resistance to corrugating under normal handling procedures. This requirement results in aluminum thicknesses not far from those used for lead sheaths, being actually greater for the largest diameters. However, with the rather considerable support afforded by an extruded polyethylene jacket, reductions in aluminum thicknesses can be made to bring them close to the limit imposed by hoop stress. This is shown in Table II.

The ultimate aim for aluminum sheath production, as for lead, is continuous and direct extrusion, from press onto

---

Paper 55-53, recommended by the AIEE Insulated Conductors Committee and approved by the AIEE Committee on Technical Operations for presentation at the AIEE Winter General Meeting, New York, N. Y., January 31–February 4, 1955. Manuscript submitted October 20, 1954; made available for printing November 26, 1954.

W. A. Del Mar and E. J. Merrell are with the Phelps Dodge Copper Products Corporation, Yonkers, N. Y.

The authors acknowledge the painstaking work done by Raymond Russbach and his assistants.

Table I. Aluminum-Sheathed Power Cable Installations in the United States*

Location	Rated Voltage, Kv	Conductor Size	Type Installation	Sheath Thickness, Mils	Polyethylene Jacket, Mils	Type Joint
New York	27	2/0	1-conductor, triplexed in ducts	65	80	wiped lead sleeve
Boston	15	350,000 circular mils	3-conductor, aerial (spinner)	80	90	wiped tinned copper sleeve
Buffalo†	23	350,000 circular mils	3-conductor, aerial (catenary)	110	none	welded aluminum sleeve
New York†	15	500,000 circular mils	3-conductor, aerial	110	none	

* Total circuit footage = 32,000.
† Cable shipped but not installed.

cable core, of a seamless tube free of press stops; in other words, a screw press. Such a machine does not appear feasible at present. However, the newer European high-capacity ram presses are capable of being recharged with preheated billets within seconds so that the direct application of aluminum sheath to commercial lengths of cable is a step closer. On the other hand, press stops and billet junctions remain as significant factors for consideration. Achievement of technically satisfactory procedures in this respect is important economically.

Solid-Type Paper Cable

Necessarily, when the sheath is applied on solid-type paper cable, a small positive clearance is required to enable accommodation of impregnant expansion on temperature cycle. Otherwise, because of the high strength of the aluminum, excessive internal pressure would develop. The clearance is a function of impregnant volume and core diameter. If the cable is not shielded, this space can be ionized. Even if the cable is shielded, impregnant can migrate from the dielectric wall into the space so that some ionization may result within the insulation. Thus, aluminum sheathed solid-type cables may not exhibit as low ionization factors as newly manufactured leaded cable.

Of course, upon the first temperature cycle of any magnitude to which a leaded solid-type cable is exposed, impregnant expansion permanently enlarges the lead diameter. This results in a void volume comparable to that which must be built into the aluminum-sheathed cable originally as it is manufactured. That the void volumes are essentially equivalent is shown by the fact that aluminum-sheathed paper cable exhibits normal solid-type cable characteristics in standard accelerated load-cycle testing procedures. For example, the power-factor and ionization characteristics remained stable in the following load-cycle test run at double rated voltage on a 60-foot length of 3-conductor, 500,000-circular-mil 13.2-kv cable with an 80-mil sheath and a 90-mil polyethylene jacket. The test consisted of daily heat cycles accomplished by loading the conductors for 8 hours of each day. Voltage was on continuously. There were in succession 4 cycles to 60 degrees centigrade (C), 4 to 80 C, 4 to 100 C, 4 to 120 C and 50 to 85 C. The sample was terminated in a trifurcator fitted with porcelain potheads, laid horizontally and level with the cable run so as to prevent pothead oil from migrating into the cables. The trifurcator, shown in Fig. 2 was wiped to the aluminum sheath. Radial power factors, measured at 80 C, after the load cycle test were indistinguishable at the wipe and on the cable run.

Joining Aluminum Sheath

Joints in aluminum cable sheaths can be made by wiping, welding, or by mechanical means. Mechanical connections, i.e., flare, ferrule, threaded, with or without supplementary *O*-ring or gasket seals, are adapted to some branches of the communication field because cable dimensions are standardized at a few sizes. However in the power cable field the multiplicity of sizes requires that each application be considered separately. Welding, perhaps the most effective means of making a joint, particularly for paper cable, is in about the same category as mechanical joints for power cables. The welding is done with a tungsten arc in an argon or helium atmosphere. Argon is preferable for cable sheath work because it affords better control of the weld pool and arc. There is less clouding and the metal stays brighter in the argon envelope, enabling the welder to see the weld pool more clearly than in the case of helium. The welding head has a cup and a tungsten electrode which is water cooled to keep the electrode from melting. Flow of the argon or helium out of the cup is maintained during welding so that the arc and pool are surrounded excluding

Fig. 1. Temporary reinforcing binding at a press stop

Table II. Thicknesses of Polyethylene Jacket and of Aluminum Sheath, With and Without Polyethylene Jacket, Versus Cable Core Diameter

Cable Core Diameters, Inches*: Aluminum Sheath Without Jacket	Cable Core Diameters, Inches*: Aluminum Sheath With Jacket	Cable Core Diameters, Inches*: Polyethylene Jacket	Thickness of Sheath or Jacket, Inches
0–0.782	0–1.346		0.050
0.783–0.910	1.347–1.474		0.055
0.911–1.038	1.475–1.602		0.060
1.039–1.166	1.603–1.730	0–0.264	0.065
1.167–1.294	1.731–1.858	0.265–0.632	0.070
1.295–1.423	1.859–1.987	0.633–0.999	0.075
1.424–1.551	1.988–2.115	1.000–1.367	0.080
1.552–1.679	2.116–2.243	1.368–1.735	0.085
1.680–1.807	2.244–2.371	1.736–2.102	0.090
1.808–1.935	2.372–2.499	2.103–2.470	0.095
1.936–2.064	2.500–2.628	2.471–2.838	0.100
2.065–2.192	2.629–2.756	2.839–3.205	0.105
2.193–2.320	2.757–2.884	3.206–3.573	0.110
2.321–2.448	2.885–3.012	3.574–3.941	0.115
2.449–2.576	3.013–3.141	3.942–4.308	0.120
2.577–2.705	3.142–3.269		0.125
2.706–2.833	3.270–3.397		0.130
2.834–2.961	3.398–3.525		0.135
2.962–3.089	3.526–3.653		0.140
3.090–3.217	3.654–3.782		0.145
3.218–3.346	3.783–3.910		0.150
3.347–3.474	3.911–4.038		0.155
3.475–3.602	4.039–4.166		0.160
3.603–3.730			0.165
3.731–3.858			0.170
3.859–3.987			0.175
3.988–4.115			0.180

* This dimension is the calculated diameter of the cable core under the aluminum sheath.

Fig. 2. Trifurcator wiped to aluminum sheath

Fig. 3. Portable tungsten arc welder with accessories

Fig. 4. Screening test for the effect of moisture on tinning

the atmosphere. Fig. 3 shows a typical portable tungsten arc welder and accessories.

Wiping has been a time-honored procedure for joining the lead sheaths of power cable. Not only has it been effective but substantially the same technique is adapted to all sizes of cable. However, a prerequisite to a successful wipe is a successful and stable tinning. The tinning must be compatible with the sheath and the wipe metals. The tinning and wiping operations must not have a deleterious effect on the dielectric. Several aluminum tinning recommendations were tried on aluminum sheath without success, according to these criteria. Cadmium-zincs gave excellent bond strengths, but the tinning temperatures were too high, scorching several layers of paper except when the operation could be accomplished very quickly. The requisite speed could not be attained in the field. Tin-zincs, while effective on tube and sheet, were unreliable on cable. Clean tinning was virtually impossible to sustain while wiping.

The use of flux-assisted tinning was considered undesirable for paper cable applications, since fluxes for tinning aluminum are characteristically polar. Also, because of the exceedingly active nature of aluminum, chemically, it was deemed unwise to take a chance of leaving polar residues in the wipe region. Actually, when fluxes were employed to assist tinning, the tinning usually became unstable during wiping.

A screening test technique employed to identify the less promising tinning mixtures is illustrated in Fig. 4. Aluminum rings, 1/2 inch wide with a 140-mil wall and a diameter of $3^{1}/_{8}$ inches, were used to test bond strength. A flat, measuring 1 by 1/2 inch was made by pressing the ring over a jig 1 inch wide. The flats on a pair of rings then were filed clean and tinned with a test mixture and then coated with a film of wiping solder. The tinned surfaces of the pair were brought together under hand pressure and heated with a torch to complete the seal. Fig. 5 shows a pair of rings sealed and ready for test. The bond strength was measured at room temperature as newly made, and after aging at 90 C and 100-per-cent humidity. Fig. 6 shows a specimen in the tensile machine which applied loading at the rate of 1/4 inch per minute.

The most effective tinning solder worked with is a tin-zinc-lead combination (77.18, 20.47, 2.25). It tins cleanly at a temperature low enough not to scorch the paper tapes. No flux is necessary. It has good bond strength and is stable at wiping temperatures.

The following procedure is employed:

1. Make certain the sheath is free of oil film and like contamination. Stearine is not to be used on the aluminum.

2. Use a smooth file to remove the aluminum oxide from the sheath surface to be

Fig. 5. Test specimen prepared for screening test

Fig. 6. Testing screening specimen after aging

Fig. 7. Aluminum sheath filed preparatory to tinning

Fig. 8. Tinning the filed aluminum sheath with special solder

tinned. The filed length, as illustrated in Fig. 7, should extend well beyond the length to be wiped. This is done to minimize the possibility of interfacial corrosion at the aluminum surface, which under wet conditions and particularly in the presence

Fig. 9. Coating special tinning solder with wiping solder

of electrolyte can develop sufficient lifting force to separate a wipe.

3. Tin the entire filed section immediately, while heating the sheath with a gas torch and rubbing the aluminum surface vigorously with the stick solder; see Fig. 8.
4. Before tinning cools, coat with wiping solder (40–60); see Fig. 9.
5. Cover tinned sheath with oil-proof tape, e.g., polyethylene tape.
6. Build splice, removing sheath with a lead knife.
7. Place previously tinned sleeve in position.
8. Using ladle technique and cloths free of stearine, pack wiping metal. The wiping cloth is not to contact the tinned surface of the sheath. Discard overflow as this is likely to be embrittled by contamination with aluminum oxide. Keep pot at 290C±10.
9. Dress wipe with a hot soldering iron.

Cable Bend Tests

While for short-time tensile strength tests it is possible to make wipes stronger than the aluminum tubes which they join, this has not been the case for the most part in cable-bending tests. Moreover, when the wipes are kept wet, failure occurs by corrosion at the aluminum and tinning metal interface. Also, bend tests on welded joints show that much work must be done before the potential manhole bend life of aluminum sheath is realized.

Two test setups were employed. In one, a 5-foot sample was trained in an arc with a radius of 42 inches, terminations being a wiped pulling eye and a splice sleeve at the opposite ends. The sleeved end was held stationary in a swivel grip, and the pulling eye end was subjected to a 1-inch travel while free to swivel. In the second setup, Fig. 10, the sample was trained as for a normal manhole installation; 24-inch offset, bend radius of 12 times the diameter, with the splice centered. Both ends were wiped into pulling eyes, each of which was simultaneously subjected to 1-inch travel, opposed, but free to swivel. The splice was carried on a tripod ball-bearing mount and permitted to seek its position freely.

All samples were trained to forms so as to avoid any concentration of change of curvature. Strain in the outer skin was calculated from deflections measured with a micrometer mounted on a 6-inch chord. Each sample was charged with gas at 5 pounds per square inch, and then subjected to a continuous bend test at the rate of 1 cycle per minute. When a fatigue crack developed, the charge of gas would leak out and a relay actuated by the drop in pressure would stop the bender. A mechanical counter kept track of the number of cycles.

Bend-test results are summarized in Table III. These data emphasize the advantages of triplexing aluminum sheath cable when possible. Thereby, not only is an increased sheath life assured but more significant is the increased life which may be expected of wipes as a result of the inherently lower unit stresses on load cycle. In general, these tests indicate that the problem of designing joints for duct cables is yet in the developmental stage.

Installation Procedure

It has been the authors' experience in preparing samples for manhole bending

Fig. 10. Wiped joint sleeve on manhole bend test

tests that cables up to a diameter of approximately 1 inch may be trained to a smooth curve with a radius equal to 12 times the diameter of the cable, and that for larger cables a training radius of about 15 to 25 times the diameter should be employed. These are training radii, not radii around which cables may be pulled and then straightened during installation. Thus, when pulling cable around bends, the radius should be as generous as pos-

Table III. Bend Tests on Aluminum-Sheathed Paper Cable at Room Temperature

Test Setup	Sheath Wall, Mils	Cable Outside Diameter, Inches	Strain in Sheath, Per Cent	One-Minute Cycles to Failure	Comment
5-Foot curve	65	1.16	0.26	36,644	Length of cable without a splice.
			0.27	12,736	Wiped splice on sleeve side of center Lead sleeve. Wipe cracked adjacent to sheath.
			0.37	19,678	Wiped splice on eye side of center. Lead sleeve. Cable sheath ruptured inside curve at center.
			0.42	3,224	Wiped splices on both sides of center. Lead sleeve. Cable sheath ruptured inside curve at center.
			0.17	678	Wiped splice in middle. Lead sleeve. Splice sleeve failed in middle.
Trained			0.14	4,053	Wiped splice in middle. Lead sleeve. Wipe fatigued at top adjacent sleeve.
			0.14	1,023	Wiped splice in middle. Lead sleeve. Splice sleeve failed at one end.
	80	2.13	0.12	150,000+	Length of cable without a splice.
			0.597	795	Wiped splice totally restrained. Lead sleeve. Cable sheath ruptured in bend adjacent to eye.
			0.214	9,101	Wiped splice in middle. Aluminum sleeve. Wipes kept wet. Tinning corroded through.
			0.260	3,942	Welded splice in middle. Aluminum sleeves. Sheath fatigued adjacent to weld.
			0.106	4,916	Welded splice in middle. Aluminum sleeves. Sheath fatigued adjacent to weld.
	125	3.10	0.27	4,360	Wiped splice in middle. Lead sleeve. Splice wipe fatigued.

Fig. 11. Shipping length of aluminum-sheathed cable with wiped pulling eye and soldered end seal

Fig. 12. Experimental installation of polyethylene-jacketed aluminum-sheathed aerial cable

sible and not less than the shipping drum diameter. Requisite training curvatures can be accomplished most expeditiously with guide templates or standard tube-bending equipment.

Otherwise, installation procedure follows practices customary in handling leaded cable. The cable is shipped with standard pulling bolts or eyes and caps, as shown in Fig. 11. Light braking on the reel flange, with boards, usually affords ample tension to straighten satisfactorily power cable at least up through 2-inch outside diameter. For aerial installations where appearance is important, necessary braking of the reel may be kept to a minimum by employing a simple box straightener, mounted as close to the reel as feasible. The recommended box length is 25 times the cable diameter, with an inside clearance approximately 3 per cent of the cable diameter. A wipe of mineral oil on the cable as it enters the box will minimize friction, thereby reducing pulling tension.

Standard 2 by 8 plank is ample for a 3-inch outside-diameter cable straightener. Constructing the box with carriage bolts facilitates threading. Thus, a length of cable equal to the length of the box plus pulling grip may be straightened against a board on the ground, then swing into the opened box, the top of which is then secured by bolting. The straightener may be rigged to traverse the reel as the cable is unwound. Since the box straightener described offers little braking and can be restrained with light tackle, these are relatively simple procedures.

The high order of self-support exhibited by aluminum sheath cable permits wide spacing of trolleys and aerial suspensions. In an experimental installation a 3-conductor 500,000-mil 13.2-kv cable was pulled on trolleys spaced 15 feet apart, and the sag was insignificant as shown in Fig. 12.

Corrosion Protection

Protection of wipes and sheath from moisture and other sources of corrosion is mandatory for aluminum-sheathed cable. Table II gives the thicknesses of extruded polyethylene jacket, recommended as corrosion protection for aluminum sheathed power cable. Some million feet of paper cable have been fabricated with polyethylene jacket over lead sheath during the past 8 years. The self-lubricating property of polyethylene together with its high modulus of elasticity permit pulling dry. However, if minimum pulling tensions are desired, Bentonite polyethylene cable pulling compound is recommended. Polyethylene is admirably suited as a protective jacket for aluminum sheath, since it is both light and waterproof. The latter property is most important, because the most prevalent and perhaps the most dangerous source of corrosion is moisture in the presence of a restricted or differential supply of oxygen. This condition is almost certain to result when absorbent materials such as paper, cotton tape, wood clamps and the like are in contact with aluminum in damp locations. Under such circumstances, deep local pitting occurs very rapidly even though the water exhibits a virtually neutral test.[3] The process is essentially the formation of a local electrolytic cell. As a result of this cell formation, a very small pit is formed in which the anode is at the base. Aluminum in the pit is converted to oxides, hydroxides or salts and by progressive action the depth increases, the attack being concentrated at one place. A characteristic feature is that there may be a few tiny holes which penetrate the sheath completely, but little or no general superficial attack. This deleterious reaction becomes impossible with a polyethylene jacket because of the complete exclusion of moisture at the jacket-sheath interface; and the excellent structural properties of this material permit clamping directly upon the polyethylene, separating water-filled crevices and other dangerous moisture-containing zones in accessory hardware from the aluminum.

Economics of Aluminum Sheaths

When studying the economics of aluminum cable sheaths, it is important to remember that the cost of a sheath depends greatly on the process by which it is applied to the cable. At the present time, the only method available in the United States is by drawing the cable core into an aluminum pipe and swedging the pipe down to fit the core. This involves three processes, the extrusion of the aluminum tube, drawing the cable into the tube, and swedging. Aluminum tube, as furnished by the leading aluminum companies, costs several times the market price of ingot aluminum. Aluminum sheathed cables made by this process obviously do not realize the ultimate economic possibilities.

However, because of the work being done in Europe with presses designed to extrude aluminum directly over a cable core, in one operation, aluminum sheaths

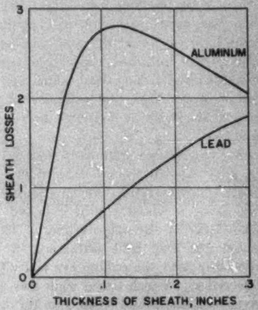

Fig. 13. Relative sheath losses versus thickness of sheath for aluminum- and lead-sheathed cables

may be put in a much more favorable economic position. Therefore, in a general appraisal of such cables it seems proper to give aluminum the benefit of the expected economic advantage of direct extrusion.

Three-conductor cables with aluminum sheaths have much higher sheath losses than cables with lead sheaths. The following study relates to cables of that type. The same principles may be applied to other types.

When cables of equal conductor sizes are compared, the lower ampacity, i.e., current-carrying capacity in amperes of the aluminum-sheathed cables because of their greater sheath losses results in lower I^2R losses in the conductors. The combined cost of these losses and the cost of the cable, by whatever method the fixed charges and operating charges are combined, are likely to be favorable to the aluminum sheathed cable. Aluminum-sheathed cables equal in ampacity to lead sheathed cables must have larger conductors and, consequently, sheaths of greater conductance in which losses are greater. It is to this more important case that this study is now addressed.

The first problem is the determination of sheath losses. There are a number of references on this subject.[4–7] The method used is that given by R. W. Burrell[7] because of its simplicity, see the Appendix. Such an equation gives a curve of the shape shown in Fig. 13 from which it appears that the losses increase rapidly with thickness of sheath and, after attaining a maximum, fall off slowly. The maximum for lead is far beyond any practical thickness.

The purpose of an economic study is to compare the present worths of expected future expenses under alternative plans. In this study, the alternative plans call for lead-sheathed and aluminum-sheathed cables of equal ampacities. The expenses to be considered are the costs of the two cables and the cost of equipment to supply the energy losses therein, both of which are taken to be capital charges and the annual costs of energy losses in conductors and sheath, both of which are operating charges. These have to be combined to obtain a total and the usual procedure is to take a certain percentage of the capital charges to include interest on investment, depreciation, taxes, and insurance. This percentage is added to the annual charges and the totals for the two plans are compared. Some engineers do not consider the cost of equipment to supply losses as a legitimate capital charge and prefer to use the sum of the fixed charges on the cables only and the operating charges. This subject is treated at some length in a series of papers.[8–11]

Aluminum-sheathed cables require corrosion protection if they are to be installed either in ducts, or to be buried underground, or to be carried aerially where unfavorable atmospheric conditions exist. The most desirable protection, as indicated in the foregoing, is black polyethylene and the recommended thicknesses of sheath and polyethylene are submitted in Table II. A typical economic comparison of lead-sheathed and aluminum-sheathed cables of equal ampacities will now be made. Each utility should make its own study using its specific conditions and should not draw too general conclusions from this example. The data are all given to three significant figures but the calculations were made with the necessary accuracy to give the final answer to that degree.

In this example, four sizes of 15-kv solid-type lead-sheathed cables of Association of Edison Illuminating Company dimensions with polyethylene jacket are considered and their ampacities determined by standard methods taking sheath losses into account. The same is done with the same sizes of aluminum-sheathed cables and ampacity curves are plotted against size for both types. By running across the curve sheet horizontally, the equivalent aluminum-sheathed cable sizes are obtained. These are as follows for three cables per duct bank:

Case	A	B	C	D
Amperes	251	330	397	482
Lead-sheathed, circular mils	212,000	350,000	500,000	750,000
Aluminum-sheathed, circular mils	220,000	380,000	575,000	over 1,000,000

These ampacities are for cables installed in ducts, three per duct bank, 75-per-cent daily load factor and are somewhat less than Insulated Power Cable Engineers Association values as sheath losses are estimated by the more accurate method cited here.

The next step is to estimate the d-c conductor losses which are as follows: Case *D* is dropped as 3-conductor cables of over 1,000,000 circular mils are not considered practical.

Case	A	B	C
Lead sheath, watts per foot	11.7	12.2	12.4
Aluminum sheath, watts per foot	11.3	11.3	10.8

The sheath losses are as follows:

		A	B	C
Lead sheath	$\frac{\text{Sheath loss}}{\text{Conductor loss}}$, watts per foot	0.00916 0.107	0.01950 0.238	0.0329 0.409
Aluminum sheath	$\frac{\text{Sheath loss}}{\text{Conductor loss}}$, watts per foot	0.048 0.542	0.104 1.17	0.185 2.00

The a-c losses, exclusive of sheath losses, are as follows:

Case	A	B	C
Lead sheath, watts per foot	11.7	12.6	13.2
Aluminum sheath, watts per foot	11.3	11.7	11.7

The total losses are as follows in kilowatts per 1,000 feet and annual kilowatt-hours per 1,000 feet assuming 50-per-cent loss factor:

Case	A	B	C
Lead sheath, kilowatts per 1,000 feet	11.8	12.8	13.6
Lead sheath, annual kilowatt-hours per 1,000 feet	51,800	56,200	59,600
Aluminum sheath, kilowatts per 1,000 feet	11.8	12.9	13.7
Aluminum sheath, annual kilowatt-hours per 1,000 feet	51,800	56,200	59,900

It will be noted that the total losses are substantially the same for lead-sheathed and aluminum-sheathed cables of equal ampacities. This simplifies the problem because the annual cost of the energy loss will be independent of the unit cost of energy and may, therefore, be neglected. The economic problem thus reduces to a comparison of the relative prices of installed lead or jacketed aluminum-sheathed cables, figures which will not be available until directly extruded aluminum-sheathed cables have become an economic reality.

Differences in cost of installation may be favorable to aluminum because of its lightness but, on the other hand, greater manhole costs may be involved with large cables as aluminum sheaths require a greater bending radius. Aerial cable fares better with aluminum sheaths, because, in most cases, the jacket may be omitted. An important field for aluminum-sheathed cables is likely to be gas or oil pressure cables of various types, as the great strength of aluminum enables higher pressure to be used than with plain lead sheaths and at a much lower cost than with reinforced lead. It is quite possible that cables of this type may eventually supersede several of the present-day varieties.[12-17]

Appendix. Burrell Method for Calculations of Sheath Losses

λ_s = ratio of open-circuit sheath loss to total d-c copper loss at 60 cycles

R_s = sheath resistance, microhms per foot

R_c = conductor resistance, microhms per foot

S = distance from conductor center to cable center, inches

C = mean radius of sheath, inches

d = diameter of conductor, inches

T = thickness of insulation, inches

$$\lambda_s = 3\frac{R_s}{R_c}\left[\left(\frac{S}{C}\right)^2\left(\frac{1}{1+0.00755R_s^2}\right)+\left(\frac{S}{C}\right)^4\left(\frac{1}{1+0.0303\,R_s^2}\right)\right]$$

$S = \frac{1}{\sqrt{3}}(d+2T)$ for round conductors

For sector conductors use 0.84 of equivalent d for round conductor.

References

1. Aluminum and the Electrical Industry, **Donald M. White.** *Electrical Engineering*, vol. 68, Nov. 1949, pp. 28–33.

2. Aluminum Cable Sheathing, **K. S. Wyatt.** *Modern Metals*, Chicago, Ill., July 1953.

3. Aluminum, **D. McAllister.** *The Electrical Journal*, London, England, April 1953.

4. Eddy Currents in Their Circular Cylinder, **F. W. Carter.** *Proceedings*, Cambridge Philosophical Society, London, England, vol. 23, 1927, pp. 901–05.

5. Eddy Current Losses in Cables, **A. H. M. Arnold.** *Journal*, Institution of Electrical Engineers, London, England, vol. 88, pt. II, 1941, p. 52.

6. Pipe Losses in Nonmagnetic Pipe, **L. Meyerhoff.** *AIEE Transaction*, vol. 72, pt. III, Dec. 1953, pp. 1260–75.

7. *Discussion* by **R. W. Burrell** of Lead-Alloy Sheaths for Underground Power Cable, **Herman Halperin, C. E. Betzer.** *AIEE Transactions*, vol. 70, pt. I, 1951, pp. 430–31.

8. Annual Carrying Charges in Economic Comparison of Alternative Facilities, **P. H. Joynes.** *AIEE Transactions*, vol. 70, pt. II, 1951, pp. 1,942–53.

9. Evaluation of Energy Differences in the Economic Comparison of Alternative Facilities, **A. P. Fugill.** *Ibid.*, pp. 1,854–60.

10. Analysis of Total and Incremental Losses in Transmission Systems, **L. K. Kirchmayer, G. W. Stagg.** *Ibid.*, pp. 1,197–1,205.

11. Economic Valuation of Power Losses, **W. R. Bullard.** *Electric Light and Power*, Chicago, Ill., vol. 29, Nov. 1951, pp. 83–87.

12. Seamless Aluminum-Sheathed Pressure Cable, **D. T. Hollingsworth.** *CIGRE*, Paris, France, 1954.

13. Aluminum-Sheathed Type-SA Gas Pressurized 69-Kv Cable for Vancouver, **F. O. Wollaston, H. D. Short.** *AIEE Transactions*, vol. 72, pt. III, Dec. 1953, pp. 1,158–75.

14. Aluminum on Power Cables Forecast, **Kenneth S. Wyatt.** *Electrical World*, New York, N. Y., July 26, 1954.

15. Aluminum for Power Cable Sheathing, **K. S. Wyatt.** *Proceedings*, American Power Conference, Illinois Institute of Technology, Chicago, Ill., vol. XVI, 1954.

16. *Discussion* of reference 12 by **K. S. Wyatt.** *Proceedings*, CIGRE, Paris, France, June 1954.

17. The Sheathing of Cables with Aluminum, **K. S. Wyatt.** *Wire and Wire Products*, New York, N. Y., Oct. 1953.

◆

Discussion

F. J. Aldridge and **P. A. Raine** (Johnson and Phillips, Ltd., London, England): We hope to be forgiven for writing from the other side of the Atlantic in a rather critical vein on the paper, but it seems to err by omission of much relevant matter. No mention is made of the fact that the paper only represents the experience of one company which, according to Table I, has only two commercially working installations of the cable. Neither does the paper attempt to confine itself to a full and detailed account of any particular aspect of the problem or to present new matter and we venture to suggest that most of the useful material in it has already appeared in one or other of our own many publications on the subject. It is perhaps unfortunate that the authors' European references do not mention either our pioneer work on the development from 1948 onwards, or the many thousands of miles of aluminum-sheathed cable we have in service.

Having made the point that one manufacturer's opinions only are presented, we examined some of them more carefully. In the section entitled "Sheath Manufacture" it is stated that "the hardness or stiffness of the sheath differs at a press stop." If by hardness the authors mean the value obtained by an impression instrument such as Vickers or Rockwell, we would disagree. If, however, they mean that the sheath is liable to fracture in that vicinity when bent, we would agree. This is not caused by hardness but by sudden transitions in grain size and shape. The only practical solution is to eliminate this suspect portion of the tube altogether, as has been our invariable practice, for we do not believe that any discriminating customer would knowingly accept cable on which a portion of the sheath was locally reinforced to protect an inherent weakness. As far as we are concerned there is no necessity to use tubes having stop marks since adequate lengths are available without them. Furthermore their elimination enables all other potentially dangerous parts of the extrusion cycle to be removed also. We feel that in accepting a tube containing billet joints, the authors are on dangerous ground, for the selection of tubes suitable for cable-sheathing involves considerably more than the mere imposition of pressure tests.

In the section entitled "Joining Aluminum Sheath," mechanical jointing is dismissed in a few words and welding is described as being in "about the same category." The authors discuss the comparative merits of helium and argon in the arc-welding process, but give no hint at all on the practical methods adopted to enable this high-temperature joint to be made on a cable without affecting the insulation. Now mechanical joints of one kind or another have been a familiar feature on aluminum-sheathed cables for many years, but a successful welded joint could represent a most desirable innovation. However, turning to Table I, we find that this type of joint has not yet been installed. If, as it appears, the method has not been tried in service then it should not be placed in the same category as the mechanical one already in general use.

This section concludes with a statement on the time-honoured method of the wiped joint, giving (with minor variations) details of the procedure first introduced by our company in 1948 and since adopted all over the world. A mechanical test for soldered joints is described which appears to be excellent, yet no test results are quoted to show that the particular tinning solder recommended is superior to any other. Could this have anything to do with the fact that Mr. Wyatt, in reference 15 of the paper, does not rate the corrosion resistance of this solder as any better than that of our 90-per-cent tin/10 per cent zinc? Incidentally, in reference 17, of the paper cadmium-zinc is recommended now admitted to be impracticable.

We note with interest that the authors could tin a tube satisfactorily with tin-zinc solder but were unable to achieve the same result when the tube contained a cable core. We cannot understand this for the many hundreds of cable jointers who have used our tinning solder here and overseas during the last 7 years have not encountered any similar difficulty.

Two further points on wiping are worthy of mention. The ladle or pot-wipe technique is not completely satisfactory for aluminum and we invariably recommend the

Table IV. Summary of Current Ratings for Aluminum-Sheathed Cables

In All Cases Equivalent Lead-Sheathed Cable Rating is 1.00

Type of Cable and Situation	Copper Conductors 0.10 Inches²	 0.50	 1.00	Aluminum Conductors* 0.10 Inches²	 0.50	 1.00
Single core (served) in air or buried	0.95	0.92	0.81	0.78	0.75	0.72
Single core (served) in ducts	1.20	1.01	0.95	0.92	0.84	0.84
Single core (sheath) bare in air	0.90	0.86	0.83	0.70	0.72	0.73
Three-core† (other than SA) served in all situations	1.00	1.00		0.78	0.80	
Three-core† (other than SA) sheath bare in air	0.96	0.98		0.75	0.78	

*The ratio of the d-c rating of a given size of aluminum conductor to that of a copper conductor of identical physical dimensions is 0.78.

†Factors relate to lead-sheathed and armored cable.

use of solder sticks to avoid it. Again the authors merely refer to "wiping solder (40/60)." Antimony is an undesirable element in such solder for use on aluminum, and either grades *40A* or *35A* of American Society for Testing Materials Specification *B.32-49*[1] should have been recommended.

In the section entitled "Corrosion Protection" the prominence given to differential oxygenation attack is commendable for it deserves wider publicity than it has hitherto received. However, the remainder of the section contains one or two surprises. The opening sentence states that protection against moisture is mandatory, yet Table I lists two aerial installations which are apparently to be erected bare. Second thoughts on this matter appear in the section entitled "Economics of Aluminum Sheaths," but the general treatment of corrosion is quite unhelpful for it gives no information to indicate where protection is necessary and where it is not required. Most surprisingly, the authors draw no attention to the fact that a wiped joint is more susceptible to corrosion than is the sheath itself and should always be protected as a matter of routine.

The section entitled "Economics of Aluminum Sheath," forecasts reductions in price when direct extrusion of sheaths is a practicable proposition, but otherwise confines itself almost entirely to the calculation of sheath losses. These calculations appear to obscure the real issue usually involved, namely, that replacement of a lead sheath by aluminum on large single-core cables materially reduces the current rating. We think that the position is shown better in Table IV, which summarizes British practice.[2]

Our only other criticism concerns Table II. We studied this Table when it appeared in reference 17 of the paper and to us it still remains an obscure and complicated method of tabulating sheath thicknesses. We would appreciate some information as to why this particular method of presentation was selected.

REFERENCES

1. *ASTM Specification B.32-49*, American Society for Testing Materials, Philadelphia, Pa., 1949.
2. ALUMINIUM SHEATHED CABLES, P. M. Hollingsworth, P. A. Raine. *Proceedings*, Institution of Electrical Engineers, London, England, vol. 101, pt. II, Dec. 1954, p. 613.

A. N. Arman (Pirelli-General Cable Works, Ltd., Eastleigh, Hants, England): Although the paper does not deal to any extent with the actual manufacture of aluminum-sheathed cables, it would seem desirable to mention a third method of manufacture, namely, the formation of sheath from rolled aluminum strip and welding the seam by means of a continuous argon-arc process. The presence of the seam may, at first sight, appear to be a disadvantage, because of the possibility of porosity or other defects. Manufacturing experience with the process has now reached such a stage in England that the continuous welding of sheaths is now being done commercially. As evidence of the quality obtainable, it may be mentioned that 23,000 yards of aluminum-sheathed 3-core 33-kv oil-filled cable has recently been satisfactorily completed using this method. When it is appreciated that this cable is finally heated in wet live steam and dried under vacuum within the sheath and that the smallest degree of porosity renders this process impossible, the high quality of the weld will be recognized.

Sheaths made by the strip-welding method have several advantages worthy of careful consideration. Strips can be joined (also by argon-arc welding) to enable sheaths of any desired length to be made. After being made, the strip joints require no special care in handling either in the forming machine or subsequently. The aluminum being rolled down (or corrugated if required) while still hot from the welding process is softer than that resulting from the cold drawing process and this gives better bending properties in the finished cable. The sheaths made in this way behave in exactly the same as those made by other processes, and I agree with the authors in most of the points they have mentioned regarding jointing, corrosion protection, etc.

The vulnerability of unprotected wiped splices and adjacent aluminum sheathing of trained duct cables as demonstrated in Table III is amply supported by experiments made in England. A more reassuring picture would have been presented if the investigation had included corrugated sheaths with wipes protected with bitumen.

The losses discussed are interesting but, I think it should be made clear that in the case of single-core cables (with fully bonded sheaths), the losses are usually considerably higher for aluminum-sheathed cables than for lead-sheathed cables. I disagree with the authors statement that the ultimate aim is continuous and direct extrusion from press onto cable core. This may be true if an extruded tube is considered to be the only sound method of approach. Experience in England is showing, however, that the welded-strip method is entirely feasible and has many advantages. Not the least of these are that the cost of the plant is only about one tenth of that required for extrusion and that sheath eccentricity (which can also be a costly item) is nonexistent.

C. C. Barnes (British Electricity Authority, London, England): This paper is of particular interest at the present time because of the persistent high-price level and steadily increasing cost of copper which tends to make the use of other metals very desirable, particularly if their use is technically feasible and they offer an economic advantage. Considerable use has been made in Europe of both aluminum conductor and aluminum-sheathed cables.

In particular, in Great Britain aluminum-sheathed cables have been widely used as an alternative to the lead-cased cable—the total length manufactured to date is in excess of 3,500 miles while, according to K. S. Wyatt, a total of perhaps 500 miles has been made in Germany.

British Standard *480-1942*[1] was revised and reissued in 1954 in two parts. Part II at the present time is confined to aluminum sheaths applied by the tube-sinking process; other techniques, however, are used in Great Britain, such as the longitudinal welding of strip formed into aluminum tube developed by the Pirelli-General Cable Works and the Research Laboratories of the General Electric Company (England) and a hot extrusion process, but this latter technique has not yet been fully developed on a commercial basis. I note with some regret that the authors have omitted to make any reference to the pioneering work of P. M. Hollingsworth and his associates who in 1947 were responsible for the first commercially successful technique for applying an aluminum sheath by the tube-sinking process.[3]

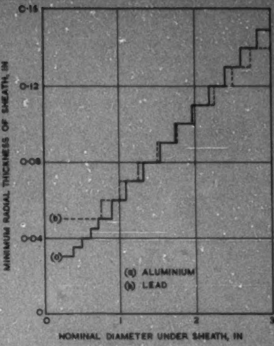

Fig. 14. Sheath thickness in relation to cable sheath diameter

Tests in Great Britain have established that bending performance alone decides the gauge of an aluminum sheath. Fig. 14 shows a sheath thickness for aluminum-sheathed cables and lead-sheathed mains cables standardized to British Standard *480-1954*. The importance of a high-grade corrosion protection for aluminum-sheathed cables cannot be overemphasized. Mr. Del Mar and Mr. Merrell make a very definite recommendation to use an extruded polyethylene jacket but, unfortunately, they do not give any test data to justify this observation.

In Great Britain the standard procedure for assessing the performance of protective coverings consists of measuring leakage currents passed by the servings on short samples of cables continuously immersed in a tank of electrolyte (usually 0.5-per-cent sodium chloride). Prior to the test the samples are subjected to a bending test and retain the final bend when placed in the tank. The electrolyte is heated daily and observations of leakage current are made at the highest and lowest temperatures, the sheath being maintained at a constant voltage of −10 volts with respect to the electrolyte. The criterion of quality is the absence of any tendency to increased leakage current, irrespective of the duration of the test. In some cases the bent sample has been supported on brick in the tank to check the mechanical ability of the covering to withstand contact with bricks or flints which may inadvertently have fallen into or been left in the cable trench.

I would welcome details of long-time tests the authors have made to assess the immunity of an extruded polyethylene sheath to aging attack by any type of soil, duct material, or any other condition likely to be encountered in the ground. Furthermore, the authors' views on the technical and economic merits of neoprene jackets for aluminum-sheathed cables will be appreciated.

The life of all buried aluminum-sheathed cables is unquestionably dependent on the perfection of the jacketing materials. In Great Britain all lead-sheathed oil-filled and/or gas-pressure lead-sheathed cables have a metallic reinforcement and, therefore, aluminum as a cable sheath is particularly advantageous when the mechanical properties of the sheathing material have to withstand internal pressure, and increasing use is being made of such cables in Europe.

REFERENCES

1. PAPER INSULATED CABLES FOR ELECTRICITY SUPPLY. *B.S.480-1942*, British Standards, London, England, 1942.

2. SEAMLESS ALUMINIUM-SHEATHED PAPER INSULATED CABLES FOR WORKING VOLTAGES UP TO AND INCLUDING 22 KV. *B.S.480-1954, Ibid.*, 1954.

3. See reference 2 of Mr. Aldridge and Mr. Raine's discussion, pp. 603–28.

Philip J. Croft (Canada Wire and Cable Company, Ltd., Toronto, Ont., Canada): The position and experience of my company has already been fully dealt with by Mr. Short and Mr. Kozak in their excellent discussion. However, there is a point in connection with bending radii and flexibility of this type of cable which is worth mentioning. In our draw-down method of manufacture, the aluminum tube, as we receive it from the extrusion press, is in a range of fixed steps as to diameter and wall thickness. The cable cores which may have to be sheathed, however, may vary infinitely in diameter, or at least in steps of a few mils.

The diameter of tube chosen for the sheathing of any particular core is limited on the lower side by our ability to draw the core smoothly and safely into the tube and, on the upper side, by the amount of cold-working considered prudent to do in the drawing-down operation. A number of standard factory procedures have been tabulated, but it is obvious that a core of the maximum diameter for a certain size of tube will receive the minimum amount of drawing down and consequent cold-working, whereas a core of a few mils larger could, according to standard-tabulated procedures, be sheathed from the next larger tube and thus receive practically the maximum amount of drawing down and consequent cold-working.

As a result of this, it has become our practice to exercise some engineering discrimination in the selection of a tube size for sheathing depending upon the end use to which the cable is to be put. For example, if the cable is intended for surface-supported power circuits in a factory or similar application in which the cable sheath to some extent takes the place of a conduit, we would permit a relatively larger amount of drawing down, since a little extra stiffness in the cable sheath enables the cable to be supported at wider intervals approximately equal to those used in supporting conduit, with consequent economy in the over-all cost of the job, while bends are usually no problem in this kind of application. For duct and manhole use, we would take steps to sheath the cable from the smallest aluminum tube into which the core could safely be drawn to minimize the amount of cold-working and preserve, as far as possible, the original ductility of the hot extruded tube. The industrial surface use of this material represents a very considerable proportion of our output, and it does seem to me that the intended end use of the cable has a large bearing upon the need for flexibility in the cable.

Herman Halperin (Commonwealth Edison Company, Chicago, Ill.): In recent years, a sharp increase in the interest in and use of aluminum as sheathing of cables has occurred in Europe and this country. This applies to certain types of installation in each of several fields of cable use. In the power-utility field in Europe, I found last fall that not only had much been done but that pioneering activity was increasing, especially since three different designs of presses to extrude aluminum sheaths directly onto cable cores were being developed. In Canada, much has been done on drawn-down sheaths on a variety of cables.

The authors have presented extensive and valuable data regarding drawn-down aluminum sheaths. In so doing, it seems to me that for some applications they have emphasized the advantages and need for extruded sheaths. Such sheaths are more ductile than drawn-down aluminum sheaths, as the elongations of the extruded sheaths in tensile tests may be three or four times as much as for drawn-down sheaths. Furthermore, it will not be necessary to use the expensive aluminum of 99.99-per-cent purity to obtain these high elongations. Incidentally, the tensile strengths of such extruded sheaths may be about one-half of that for drawn-down sheaths.

With the extruded sheaths, it appears that the thicknesses may be reduced appreciably below what the authors show in Table II, partly because there will be a reduced tendency to corrugate. With thinner sheaths, the magnitude of sheath losses in 3-conductor cables will be reduced. With extruded sheaths, the training radius for the larger cables may be much less than the 15 to 25 times the cable diameter, which the authors mention. For lead-covered cables we generally use a training diameter of eight or nine times the cable diameter. The extrusion process will make feasible the manufacture of extra long lengths. Perhaps, with the extruded sheath, the amount of voids intentionally left in solid-type cables may be reduced below what the authors describe with drawn-down sheaths.

It is appreciated that the installation of an extrusion press is very costly, and so discussions and technical and commercial studies are necessary to determine how many such presses need be installed after satisfactory presses have been developed. The European presses being developed will result in sheaths having press stops incidental to recharging. Limited information and observations on sheaths extruded by one type were encouraging as to the mechanical properties of the press-stop region of the sheath.

The results of the bend tests given in Table III are somewhat discouraging. With a sheath strain of 0.27 per cent, and a splice on the cable in three different tests, the cycles to fracture at room temperature ranged from a title to greatly less than are obtained with arsenical and tellurium-bearing alloy lead sheaths even when heated to 43 C. The authors' opinion on the cycles to fracture with extruded aluminum sheath would be of interest.

I believe that in economic studies of particularly the losses in aluminum sheaths of 3-conductor cables the cost of equipment to supply the losses should be taken into account. If there were no losses in a transmission and distribution system of a utility, then it would install 10 to 15 per cent less generating equipment and less facilities outside the stations.

C. T. Hatcher (Consolidated Edison Company of New York, Inc., New York, N.Y.): To obtain operating experience with the use of aluminum sheath cable, an installation of approximately 5,000 circuit feet of single-conductor 2/0 paper-insulated aluminum sheath, polyethylene jacket 27,000-volt triplexed cable was made during February 1954. This cable was installed instead of 3-conductor 2/0 standard lead-covered cable in the Bay Ridge section of Brooklyn along 72nd Street, between Fourth Avenue and Shore Road. This cable was energized on April 8, 1954.

This cable was installed using a special pulling compound known as Bentonite and was racked in the manholes with a minimum bending radius of 15 times the maximum outside diameter of the cable. The joints were made using the standard lead sleeve with the aluminum sheath tinned with a special solder consisting of 77-per-cent tin, 20.5-per-cent zinc, and 2.5-per-cent lead. The sleeves were wiped using standard 40-per-cent tin, 60-per-cent lead solder, with the solder temperature maintained at approximately 550 degrees Fahrenheit. After the wipes were completed and tested, the tightness at 15 pounds per square inch, the lead sleeve, wipes, and the adjacent exposed aluminum sheath were covered with a minimum of two layers, half-lapped, of 2-inch polyvinyl chloride tape. The polyethylene jacket was removed for approximately 6 inches at the point where the bonding cable and test strips were installed. The aluminum sheath was tinned with the special tinning solder described in the foregoing. The bonding cable and test strips were then attached using standard wiping solder and two layers, half-lapped, of 2-inch polyvinyl chloride tape was applied.

On December 2, 1954, an inspection was made to determine the condition of the aluminum sheath and solder wipes at a joint and bonding connection in one of the manholes. This manhole was selected for inspection because the joints had been exposed to submersion at times. The aluminum sheath, solder wipes, and lead sleeves at the joint and at the bonding point showed no signs of corrosion. There was no apparent evidence of interfacial corrosion between the aluminum and solder wipes. The joint and the bonding connection were retaped with polyvinyl chloride tape, with a coat of Roybond *A-36* metal primer before the application of the tape.

P. M. Hollingsworth (British Insulated Callender's Cables, Ltd., London, England): The comprehensive survey of aluminum-sheath characteristics and recommendations for jointing technique, corrosion protection, and the like seems at first glance rather ambitious when judged on the basis of Table I which lists the installations to date. Reference to Table I shows that of the four items mentioned, totalling 32,000 feet, only two had been installed when the paper was written, one length (unspecified) in ducts and one length (also unspecified) in air. Both of these carry a protective covering of extruded polyethylene on the sheath, but the later installations carry no such covering. It seems, therefore, that considerable undisclosed laboratory work must have been done or else much of the information has come from experience with aluminum-sheathed communication cables.

In general the data given and the opinions formed are in satisfactory agreement with conclusions that have been reached from experience in Great Britain and elsewhere derived from manufacture and installation of several thousand miles of cable which began in 1947. The great bulk of this production which covers a voltage range up to 33 kv including impregnated pressure-type cable has been sheathed by the died-down process and this type of cable is now covered by British Standard *480*, part II. There is also now a method operated in England employing strip folded round the cable cone and welded longitudinally. Finally, the direct extrusion method is being actively developed by my company.

I find myself somewhat at variance with the authors on the subject of jointing technique. In the first place, tin-zinc solder decried by the authors has been used on many thousands of joints as well as in hundreds of tests and has given every satisfaction. It certainly by no means requires such careful handling as that indicated by the rather elaborate procedure described for the tin-zinc-lead combination favored by the authors. An alternative which has been found similarly satisfactory and even easier to work is a tin-zinc-cadmium alloy.

I can confirm the excellent mechanical properties of cadmium-zinc solders and also the scorching of the insulation which prohibits their use. In that connection, the reference in the paper to the use of argon arc-welding is very puzzling since the temperatures involved must be completely destructive to the insulation unless some highly specialized procedure has been evolved. Perhaps the authors would enlarge on this point.

Statements relating to the need for protective coverings on wiped joints and sheaths seem rather contradictory as follows: "Protection of wipes and sheaths from moisture . . . is mandatory" and "Aerial cable . . in most cases the jacket may be omitted." I agree that it is essential to protect wipes and soldered joints from contact with water under conditions of immersion, but have yet to meet any case of corrosion in a wiped or soldered joint installed in normal atmospheres, rural or industrial, whether humid or otherwise. The use of extruded polyethylene for corrosion protection where this is required is to be commended and the reduction in thickness of the aluminum sheath when furnished with a polyethylene jacket is an interesting innovation.

On the subject of economics, the authors illustrate the effect of sheath losses on current ratings of 3-core cables. This effect is not noticeable on 3-core cables under British practice since, for conditions of direct laying, current densities are higher and the basis of comparison for sheath losses is between lead-sheathed and armored finish on the one hand and aluminum on the other. The same conductor sizes would therefore be used in Britain for both lead-sheathed and armored and aluminum-sheathed cables for the four ratings given in the paper. For 10-kv screened-type cables these would be 251, 330, 397, and 482 amperes for 191,000, 318,000, 446,000, and 637,000 circular mils respectively. The bases of computation for the foregoing are: Single circuit laid direct, 100-per-cent load factor; thermal resistivity of soil, 120 thermal ohms per centimeter cubed; soil temperature, 15 C, and conductor temperature, 65 C.

Under these conditions the total losses would show only very slightly to the disadvantage of the aluminum-sheathed cable. Much more significant is the increase in losses when single-core cables are employed with bonded sheaths which cause substantial reduction in ratings for conductor sizes above 400,000 circular mils.

S. J. Rosch (Anaconda Wire and Cable Company, Hastings-on-Hudson, N. Y.): The authors have made a particular point of the fact that most installations of aluminum-sheathed cables of record are of the aerial or of the indoor type but that the present paper is directed not only to these but also to aluminum-sheathed power cables intended for installation in underground ducts. It is therefore regrettable that this excellent paper does not contain any data on creep resistance of such types of cable.

Aluminum-sheathed cables are being considered as a substitute for corresponding lead-sheathed types. The literature is replete with data regarding studies of creep resistance of the latter types and, in order that a full realization may be had of the comparable behavior during load cycling in modern manholes, similar data on aluminum-sheathed power cables are highly essential. It is possible that the authors have such data as a result of the studies conducted in their laboratory and it would be appreciated if some of these data were given.

H. D. Short and **S. Kozak** (Canada Wire and Cable Company, Ltd., Toronto, Ont., Canada): The authors are to be complimented on their paper and its contributions to the furtherance of aluminum-sheathed cables. Unfortunately they neglect to mention the achievement of the firm of Johnson and Phillips, Ltd. This firm in 1948 achieved on a feasible scale the only presently commercial means of applying seamless aluminum sheath[1] to all types of insulated wires and cables. It is their development which has excited and redoubled the efforts to hasten the application of aluminum to sheathing cables. If the authors' 2 years of experience and 32,000 feet of cable installed are termed considerable, then we would say that the experience and production of Johnson and Phillips, Ltd., in England and Canada Wire and Cable Company, Ltd., in Canada can be termed astronomical.

The background of our company in production and application of aluminum to power cable sheaths extends to over 2,500,000 feet of aluminum-sheathed cables of all types including the following specific projects:

1. 57,000 conductor feet 69-kv type SA gas-pressurized cable—duct bank installation in Vancouver, B. C.

2. 25,000 conductor feet, 120-kv oil-filled cable—duct bank installation in Montreal, Que.

3. 6,300 conductor feet 301-kv oil-filled cable—tunnel installation at Kemano, B. C.

4. 1,000 conductor feet 161-kv gas-pressurized cable, direct bury, terminating ends for pipe-type cable—Toronto, Ont.

With this experience we have maintained practices which are at variance with those adopted or proposed by the authors. It has not been considered necessary to vacuum-treat or dry-gas charge the tubing after extrusion. One would expect that during draw in any benefits of vacuum treatment would be lost. We stipulate pressure tests to detect pinholes and other defects but do not pressurize the tubing during shipment or storage. We definitely do not accept lengths of tube with press stops or billet joins, believing as the authors assert that these defects remain as significant factors. Until more knowledge is accumulated on all the ramifications of press stops and billet joins, which we have found unsatisfactory on bend tests, we would prefer not to supply aluminum sheath with these imperfections remaining. The practice described by the authors of temporarily reinforcing press stops would seem to be a shortsighted and dangerous practice, not worthy of the excellent and uniform properties obtainable from continuous tubing. This type of patching would not be tolerated on lead-sheathed cables, and if only in fairness to aluminum-sheathed cables should not be permitted. Our purchase specifications prohibit press stops and billet joins, stipulate scrupulous visual, tensile, elongation, and physical tests, and permit no dents, corrugations, eccentricity flattening, scores, or gouges.

We view with suspicion the authors' claim that an extruded polyethylene covering would permit material reduction in wall thickness for the following reasons: the process of factory handling before extruding the polyethylene sheath would produce the corrugations prior to whatever advantage could be realized, unless, of course, abnormally large reels are used in the manufacturing processes; and because bending in the field could produce corrugations underneath the polyethylene which might subsequently prove damaging to the covering.

We are somewhat surprised but nevertheless very interested in the authors' claim that welding is the most effective means of making joints, particularly for paper cable. The question immediately arises as to what clearance the authors find necessary to allow for expansion of core and impregnant under the fusing heats required. We would also ask if the authors have encountered any bursting of the sheath, or bubbling of the impregnant through the molten weld metal and resulting porosity. We suspect that the authors have retreated to the welding alternate because they have not arrived at the proper method of applying the tin-zinc wiping technique. This is in evidence from the method described in the section entitled "Jointing Aluminum Sheath." One can have defective welds in the field more readily than defective wipes, especially with aluminum and, unless the welders are most expert in handling aluminum and aluminum alloys in welding aluminum it is most important to have full knowledge of the alloys and metals being jointed. It does not seem too practical to have to rely on expert welders in the field; it is much better and easier to train cable splicers in the proper technique of wiping on to aluminum.

We note the authors' assertion, in contradiction to a previous claim by their company (ref. 17 of the paper) of the unsuitability of cadmium-zinc tinning solders caused by the high temperatures necessary, but we cannot understand the authors' experience with tin-zinc solders as effective on tube and sheet, but ineffective on sheaths, although it is no doubt related to the tinning techniques employed by them.

We suspect that some foreign materials are introduced in the swaging-down, or subsequent handling processes which are not properly removed during the attempts at tinning. Are the same results obtained on sheet, tube, and sheath with the cadmium-zinc alloys? The tinning procedure should include two important steps which are not described by the authors: first, the sheath should be cleaned of any oil film, using appropriate nonresidue-forming solvents; secondly, the friction tinning should be immediately followed by vigorous rubbing of the molten tinning metal, using a stiff wire brush. This tends to break down the oxide film and flows the tinning metal into intimate bond with virgin metal. We are amazed to notice that the authors have failed to appreciate the importance of wire-brushing the tinning metal—this is the whole crux of successful wipes on to aluminum sheaths. Heat during tinning accelerates formation of the oxide film and it is essential that the tinning metal "marries" the aluminum metal and not the oxide film. This can only be ensured by the proper brushing while the tinning metal is molten. Stick wiping is preferred to pot wiping of the wiping metal. We always use a small amount of acid-free flux on the wiping cloth, taking care not to allow the cloth to come in contact with the tinned surface.

If the techniques of tinning and wiping, as we have outlined them, are followed using 90/10 tin-zinc tinning metal, aluminum sheaths can be sealed at junctures such that under any normal duty in service the wipes will perform most satisfactorily.[1]

In respect to bending tests, and contrary to the experience and opinions of the authors, our experience on similar tests using similar equipment on sheaths and tubing with copper sleeve joints and tin-zinc tinning have shown that the design of joints for duct bank and manhole applications of aluminum sheath, under Canadian and American conditions, is well beyond the development stage. In point of fact, backed by several years experience on 69-kv and 120-kv installations, joints in such applications of aluminum sheath are no more a problem than for installations of lead-sheathed cables. Employing a 48-inch-long 5-inch-diameter copper sleeve joint, $2^1/_4$-inch-diameter cable specimens, and the tinning and wiping technique just described, our laboratory bend tests have followed closely that revealed by the authors in Fig. 10. Fig. 15 illustrates in general the test arrangement we used which shows the cable trained as would be the practice for a lead-sheathed cable in a 14-foot by 9-foot manhole. Tests of this nature have been conducted introducing such variables as continuously wet wipes, duct cable movements as high as 1 inch, free and restrained lateral movement of the joint, and internal pressures as high as 25 pounds per square inch gauge. In contradistinction to the authors' experience, our test specimens under 25 pounds per square inch pressure above atmospheric have never developed wipe or sheath failures after as many as 630,000 cycles at speeds as high as 55 cycles per minute and a cable longitudinal movement of 1 inch. At the 630,000th cycle the test was stopped as it appeared that the specimen would continue under this movement for many more cycles without failure and, the 630,000 cycles represented many times the 50-year life expectancy.

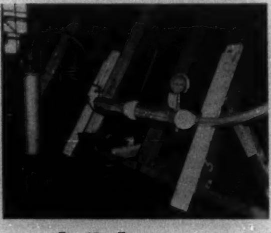

Fig. 15. Test arrangement

These test results are so at variance with those reported in the paper that we not only suspect the tinning and wiping techniques employed by the authors but also the grade of aluminum tubing metal. Could the authors state whether or not their aluminum sheathing is of the same grade as that reported in reference 2? In addition to what we have said about welded joints, we noted that Table III does not present any stronger case for the welded splice as for their type of wiped splice. It would appear that their welding method weakens the sheath metal seriously even at the internal pressure of 5 pounds per square inch gauge which they used.

In the section entitled "Solid-Type Paper Cable" the authors state that such cables may not have ionization factors as good as virgin lead-sheathed cables. Are they giving their opinion based upon their own theories or upon actual tests?

Our installation experience has not revealed any need for braking the reel to straighten the cable; our experience includes the pulling of the 301-kv all-aluminum cable.[3] Mr. Del Mar and Mr. Merrell's suggested box straightener might prove useful, but we would expect that the first few feet of a duct would achieve the same results. We confirm[1] their recommended manhole training radii of 12 to 15 times the cable diameter although we have never found it necessary to resort to special bending tools for training, except for very large cables having unusually thick sheaths. Normally the same methods as employed for lead-sheathed cables suffice for manhole training.

We share the authors' opinions in regard to corrosion protection for aluminum-sheathed cables and the dissimilar metal juncture at the wipes[1] and we have invariably used a protective coating over the wipes. However, for duct bank installations, we feel that caution should be exercised if polyethylene covering is used over the cable per se. The solvent effects of petrolatum compounds on polyethylene is well known and we would view with concern the use of such a covering in ducts into which cable has been previously installed because of the possibility of remnant quantities of unknown pulling-in greases. We should for the general case much prefer the type of covering used for the cables reported in reference 1, this being our standard practice for high-voltage cables of all designs.

Figure 11 shows a pulling eye and solder seal on an aluminum-sheathed cable. We have not found it necessary to make use of pulling eyes with aluminum-sheathed cables, our normal practice being to pull directly on the sheath or over the rubber sandwich protective covering by means of Kellem grips. They work admirably and avoid the necessity of special pulling-eye devices.

REFERENCES

1. See reference 13 of the paper.

2. SEAMLESS ALUMINUM SHEATHED CABLES, H. D. Short. *Electrical News and Engineering*, Toronto, Ont., Canada, vol. 61, no. 22, Nov. 15, 1952, p. 73.

3. THE 301-KV ALL-ALUMINUM OIL-FILLED CABLES AT KEMANO, BRITISH COLUMBIA, H. D. Short, J. T. Madill. *AIEE Transactions*, vol. 73, pt. III, Dec. 1954, pp. 1,329–43.

W. A. Del Mar and **E. J. Merrell:** We are very grateful for the excellent discussions of our paper, especially by our British and Canadian friends who have had experience with aluminum sheaths. Several discussers have deplored the absence of acknowledgement to prior workers in this field. We have purposely avoided historical references as it is very difficult to assign precedence especially where, as in this case, parallel work has been carried out in several countries. One historical reference in the beginning of the paper was mentioned to show the long lag between the first appearance of aluminum on a commercial scale and the present activity on cable sheaths.

Mr. Aldridge and Mr. Raine speak from the experience of a company which has done more than any other in English-speaking countries to develop and further the use of aluminum-sheathed power cables in those countries. They should not, however, forget the very extensive pioneer work by the Germans, especially Messrs. Felten and Guilleaume. Indeed, the German experience with aluminum-sheathed cables goes far beyond the British, and our work stems from the German much more than from the British experience.

As licencees of Felten and Guilleaume for communication cables of the type known as styroflex and as makers of another type known as spirafil, the experience of our company covers over 2,000,000 feet of aluminum-sheathed cables of diameters from 3/4 inch to $3^1/_4$ inches. Our paper, therefore, does not "represent the experience of one company which. . . has only two commercially working installations of the cable," but has a very extensive background of experience.

The purpose of the work covered by our paper was to adapt this experience with communication cables to American practice with power cables, both for installation in ducts and as supported on poles by messenger cables, neither of which subjects is covered by British publications.

The very extensive British use of aluminum-sheathed cables indoors cannot yet be duplicated in the United States because of a prohibition by the National Electrical Code, and buried cables, except for street lighting, are not used.

The statement that sheaths show no change of hardness at press stops as measured by a Rockwell instrument is, in our opinion, not strictly correct. We have found a very considerable variation of Rockwell penetration along an aluminum sheath which tends to mask any specific change at the press stop. However, looking over a large number of readings, we find a general trend toward a less penetration, in the Rockwell test, at the press stop. An example of such a case, using the Rockwell L scale and a 1/4-inch ball, showed a change from an average of 59 to 67 at the stop. In no case did we find the reverse.

The reason why we do not exclude press and billet stops from our regular production is given in our reply to the discussion by Mr. Short and Mr. Kozak. It is a purely economic question based on relative labor costs in our respective countries. The reason for the omission of details on arc welding is also given below in our reply to Mr. Short and Mr. Kozak. Suffice to say, for the present, that we flare the sheath before welding.

Our laboratory tests of mechanical joints made on our manhole bending machine, since the present paper was written, have given excellent results. While the British and Germans have made mechanical joints, we do not know whether these will stand up in such a test.

We are told that no results of our screening test are given to show which particular tinning solder is recommended as the best. That was not the purpose of the test. As stated in the paper, the purpose was to identify the less promising mixtures. After eliminating these, practical tests of the remainder determined our recommendations.

We saw the tin-zinc solder in use at the Johnson and Phillips Works in 1952 and could see no difference between their procedure and ours. The difference in our evaluation of this solder must arise either from differences in materials or from our respective views of what is good and what is bad. We are inclined to believe that it is the latter. It should be remembered that our severe manhole bending tests eliminate many joints that seem excellent by all other tests. When this test is used on large cables, there is a tendency for the cable to move from the manhole toward the joint without much bending. This puts a very severe shearing stress on the wipe of the joint and wipes which pass every other kind of test may fail grievously in this one. This is the ultimate test which a wiped joint or, indeed, any kind of joint must withstand in American practice.

The section entitled "Corrosion Protection" says that protection against sources of corrosion is mandatory. Where these sources do not exist, such protection obviously is not necessary. It is required for all duct cables and for aerial cables when installed either in a salty atmosphere near the sea or near industrial plants which may emit corrosive fumes. Under other conditions we believe that protection may not be required. The same is true of most indoor installations. Mr. Aldrich and Mr. Raine are surprised that we draw no attention to the fact that a wiped joint is more susceptible to corrosion than the sheath itself. They seem to have missed the point of our ring test which is entirely based on that assumption.

The reference to single-conductor cables with fully bonded sheaths has little or no application in United States practice, as no one here would ever bond the sheaths of single-conductor cables under conditions where the sheath losses would be appreciable. The procedures used here are described by H. Halperin.[1] Table II is based on our experience with avoidance of buckling of the sheath when bent to suitable reel radii.

Mr. Arman's description of the strip welding process is very interesting and indirectly affords us some support for our advocacy of welded joints. His comment on single-conductor cables has been answered in the foregoing.

Mr. Barnes asks for reasons for recommending a polyethylene jacket. Our tests on such jackets were completed many years ago, but our main justification is the successful use of well over 1,000,000 feet of lead-sheathed polyethylene-jacketed cables in ducts. American polyethylene does not contain polyisobutene which may explain the difference in experience in the two countries. Greases containing soap, however, should be avoided.

Mr. Barnes regrets that we have not referred to the work of P. M. Hollingsworth and his associates. If our paper had been historical, we would not only have done that but would have referred to the pioneer work in other countries, especially Germany.

Mr. Croft's discussion relates to an important precaution which should be taken in selecting tubing for draw down, with which we fully agree.

Mr. Halperin calls attention to the difference in hardness of sheaths made by the draw-down and direct-extrusion press methods. Until more experience is available with the latter, we think it safer to draw no conclusions, especially with relation to manhole life. Certainly the direct-extrusion method gives a softer and more ductile sheath which has both advantages and disadvantages.

Mr. Hatcher's experience which relates to the first item in Table I, is very valuable. We hope to have more of this kind in the near future.

Mr. Hollingsworth, who is one of the recognized pioneers in this work, is right in saying that our survey seems, at first glance, to be rather ambitious if based on the limited experience with the cables listed in Table I. He is quite correct in assuming that considerable undisclosed laboratory work and field work as well came from our experience with communication cables and, we should add, with polyethylene-jacketed lead-sheathed cables.

The tin-zinc solder which Mr. Hollingsworth has found satisfactory will not meet the conditions of American service, because cables in manholes are operated at higher temperatures than in European countries.

No trouble has been experienced with scorched insulation when using argon welding in the laboratory. A field installation using this procedure is about to be made and may lead to modifications of the laboratory procedure. We therefore postpone giving details of our procedure until it has had a practical trial.

We have answered the point about protection of wipes and sheaths from moisture and the apparent inconsistency of having an unprotected aerial cable.

Mr. Hollingsworth's data on the relative sizes of aluminum- and of lead-sheathed cables in British practice are very interesting and may be one of several reasons why aluminum sheaths have been more attractive for power cables in Britain than in America.

Mr. Rosch asked about the creep characteristics of aluminum sheaths. We have done very little work on this and refer him to the excellent paper by P. M. Hollingsworth and P. A. Raine.[2]

Mr. Short and Mr. Kozak have given an interesting outline of their company's experience with aluminum-sheathed cables, and their confidence in these is additional positive evidence of the applicability of this material for cable sheathing. Their gross footage is virtually identical with our 2,000,000 plus figure. However, whereas our shipments have been almost completely in standard 1,000-foot lengths, theirs apparently have been confined for the most part to very much shorter sections for the larger diameters because of their restriction to lengths of tubing from single billets or blooms. In this connection, while our total footage of power cable is only a fraction of our product to date, it is noteworthy that each application is purposely distinctively different in many pertinent respects. These features merit consideration where space will permit a more complete analysis of important points. Also, we can report that our applications of other types of aluminum-sheathed cables include numerous installations in a variety of environments, buried, plowed-in, submarine, and the like.

Our vacuum treatment assures the absence of moisture, a very practical consideration in respect to paper cable. The temporary reinforcement of press stops is not a patch. It is a sound precautionary procedure. It would seem the discussers have chosen to forego employment of any of the new semicontinuous ram-type aluminum extrusion presses. Would they rather confine aluminum-sheathed power-cable applications to short manhole lengths with the requisite superabundance of joints, the latter certainly just as doubtful as press stops? This is completely counter to the trend in the United States because of the high labor cost of joints.

Our purchase specifications for aluminum tube necessarily are very rigid to enable precision production of styroflex coaxial cable where dimensional control is by mils.

Mr. Short and Mr. Kozak's surmise that we use abnormally large reels on all factory operations is correct, so that the possibility of corrugations is not a manufacturing problem. Our background of field experience with polyethylene-jacketed lead-sheathed cable now has been supplemented by approximately 100,000 feet of aluminum-sheathed cable so protected, with no instability indicated to date, nor do we anticipate any.

We consider welding to be the most permanent moisture seal, all things considered

Far from retreating, but recognizing the applicability of all classes of seals, all have been under development simultaneously without prejudice. Welding aluminum admittedly requires a high skill, but a few practical precautions and intelligent design of accessories seem to suffice to make the operation feasible. Oil and other contamination cannot be tolerated. The presence of any contamination indicates itself immediately in a discolored and porous weld surface, and in this way welding is self-monitoring. We can offer the assurance that our current techniques do not result in excessive heating of the cable core as indicated by multiple thermocouples.

Unsatisfactory experience with 90/10 solder is not unique with us. Nor have we neglected to employ any of the pertinent preparatory procedures mentioned. The discussers appear to have missed reading point one of our tinning procedure, namely, "Make certain the sheath is free of oil film and like contamination. Stearine is not to be used on the aluminum."

It is difficult for us to make a comparative evaluation of the 630,000-bend-cycle figure, since so many significant factors are not given by the discussers, e.g., the maximum sheath strain, the offset, and the training radius (which from Fig. 15 appear much greater than in our tests), and sheath thickness. Instrumentation pressures, whether 5 or 25 pounds per square inch have no bearing on bend life. However, bending rates in excess of 1 cycle per minute seriously reduce the proportionate effect of stress corrosion on bend life and, therefore, are not realistic. In our opinion, a rate of 55 cycles per minute is entirely too fast.

Ionization factors are influenced by cable type, whether belted, shielded, time of storage, range of ambient during storage, etc. In some instances, tests have shown higher ionization factors for aluminum-sheathed cable samples than we have become accustomed to expect for their counterparts with lead sheaths. We do not attach any significance to this characteristic, as indicated in our paper, but mentioned it for its academic interest.

We, too, have not found the straightening block or braking necessary for duct work. These measures are desirable for those aerial applications where the best possible appearance is sought.

The discussers in referring to the solvent effects of petrolatum on polyethylene must have in mind the characteristics of polyisobutylene blends of polyethylene or low molecular weight types made in England during the war. Pure high molecular weight American grades of polyethylene exhibit outstanding stability in oils at cable sheath or jacket operating temperatures.

REFERENCES

1. REDUCTION OF SHEATH LOSSES IN SINGLE-CONDUCTOR CABLES, H. Halperin, K. W. Miller. *AIEE Transactions*, vol. 48, 1929, pp. 399–415.

2. See reference 2 of Mr. Aldridge and Mr. Raine's discussion, pp. 603–28.

A Simplified Method of Calculating Voltage Regulation Using Unit Impedance Power-Reactive Diagrams

R. M. BUTLER
MEMBER AIEE

Synopsis: The methods of analysis described provide a convenient way to calculate the voltage regulation characteristics of a transmission network as viewed from a single bulk load connected to the network. The methods apply equally well for single transmission lines and radial type of multiple circuit systems.

THE modern accepted practice for studying voltage, power, and reactive flow conditions on a transmission and subtransmission network is by use of such analytical tools as the a-c network analyzer. However, this valuable calculating aid is generally used for major system studies dealing with alternative plans for future expansion and is not always available when needed for problems of smaller scope such as determining the voltage regulation characteristics of the network as viewed from one substation. Occasionally, it is desirable to know what effect increased load or power-factor correction in the underlying distribution system will have on the voltage at a substation feeding the underlying system.

The methods discussed in the paper offer a convenient way of studying such voltage regulation problems primarily by manual calculation. If the supply system is a complex network, two simple measurements can be made when the network is set up on an a-c network analyzer for other studies. These two measurements are the open-circuit voltage E_{OC} and the short-circuit current I_{SC} at the point of interest on the network. Since steady-state voltage regulation problems are described, it is not necessary to insert the generator transient reactances into the network when measuring I_{SC}. Hence, this value of current is not the short-circuit current usually obtained in fault studies.

Using the values for E_{OC} and I_{SC}, the remaining calculations are performed manually. The advantage in using the methods described is that very little mathematical computation is required since a unique form of power-reactive circle diagram is used to give graphical solutions to the voltage regulation problems.

Summary of Method

The steps necessary in determining the voltage regulation characteristics at a load point on a power network are briefly as follows:

1. Obtain the open-circuit voltage E_{OC} at the load point in question with the load removed.

2. Obtain the impedance of the network Z_D as viewed from the load; this is the driving point impedance of the network measured at the load point.

3. Let the impedance Z_D be the equivalent impedance of the network and the voltage E_{OC} be the input or sending end voltage of the equivalent impedance.

4. Let the voltage E_{OC} and impedance Z_D be the base voltage and base ohms of the equivalent system respectively so that E_{OC} and Z_D can be expressed as 1.0 per-unit (pu) quantities. Then calculate the base kilovolt-amperes (kva) so that load power and reactive may also be expressed in pu on the calculated base kva.

5. Determine the load voltage E_2 for any value of pu power and reactive load using power-reactive circle diagrams for a unit impedance-unit input voltage circuit. E_2 will be measured on the power-reactive diagrams in pu of the sending voltage E_{OC}.

The first two steps listed for determining E_{OC} and Z_D can be performed manually if the supply system to the load is a transmission line or a radial-type supply system. Use of the network analyzer will be preferred to measure

---

Paper 55-89, recommended by the AIEE Transmission and Distribution Committee and approved by the AIEE Committee on Technical Operations for presentation at the AIEE Winter General Meeting, New York, N. Y., January 31–February 4, 1955. Manuscript submitted October 21, 1954; made available for printing November 18, 1954.

R. M. BUTLER is with the General Electric Company, Schenectady, N. Y.

The author wishes to acknowledge the assistance and contributions of J. J. Heagerty in preparation of much of the data contained in the paper.

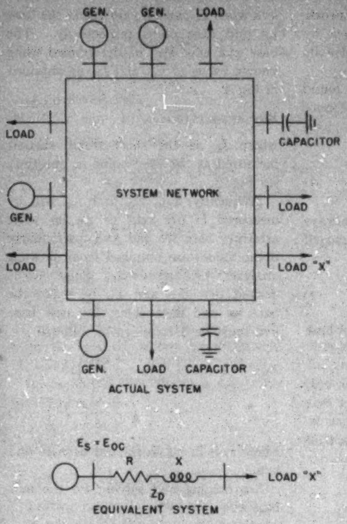

E_{OC} = OPEN CIRCUIT VOLTAGE AT LOAD BUS "X"

Z_D = DRIVING POINT IMPEDANCE OF NETWORK VIEWED FROM LOAD BUS "X"

Fig. 1 (left). Conversion of a complex network to a single equivalent impedance system viewed from a load point

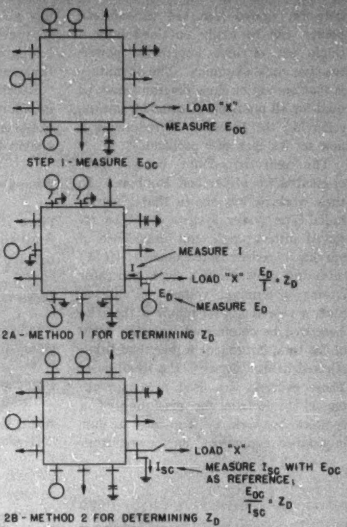
LOAD "X"
MEASURE E_{OC}
STEP 1 - MEASURE E_{OC}
MEASURE I
I
LOAD "X"
$\frac{E_D}{I} = Z_D$
E_D
MEASURE E_D
STEP 2A - METHOD 1 FOR DETERMINING Z_D
LOAD "X"
I_{SC}
MEASURE I_{SC} WITH E_{OC} AS REFERENCE;
$\frac{E_{OC}}{I_{SC}} = Z_D$
STEP 2B - METHOD 2 FOR DETERMINING Z_D

Fig. 2 (right). Measuring E_{OC} and Z_D on a network analyzer

E_{OC} and Z_D if the supply system is a complex network. Once E_{OC} and Z_D have been determined, no further use is required of the network analyzer.

Assumptions

The method used in calculating the voltage at a particular point on a network for various load conditions at that point is based upon two assumptions:

1. Changes in the steady-state load at a given point in a network will not cause a change in generator bus voltages.
2. Loads connected to the supply system network feeding a particular load of interest are assumed to have constant impedance characteristics. Changes in load at the particular point of interest will cause some variation in the voltage applied to the other loads connected to the supply system. However, it is assumed that these voltage variations will not be of sufficient magnitude to cause serious error in computation if the loads, other than the one of interest, do not have constant-impedance characteristics.

Discussion

Step 1—Conversion of Actual System Network to a Single Equivalent Impedance

The theory of converting a complex network to an equivalent single impedance is not new. The principle is stated in Thévenin's theorem which is found in many electrical engineering textbooks.

In diagrammatical form, the principle is illustrated in Fig. 1. It is seen that a system network composed of generators, circuits, and loads may all be reduced, with respect to load X, to the equivalent system shown in the lower portion of Fig. 1. The generator or input voltage to the equivalent circuit is equal to the open circuit voltage (hereafter designated as E_{OC}) measured at the load X terminal. The equivalent impedance Z_D is that impedance as seen looking into the network at load X (sometimes referred to as the driving-point impedance at load X). E_{OC} and Z_D can be manually calculated for simple radial systems or must be measured with the aid of a network analyzer for complex network systems of the type shown in Fig. 1.

When use is made of the network analyzer, E_{OC} is measured by removing the load at the point of interest while maintaining constant generator bus voltage. Z_D may be determined in two ways. The first method consists of removing the load at the point of interest, grounding all generator buses, and applying a known voltage E_D at the point of interest on the network. The phasor ratio of the voltage E_D to the current flow into the network is the driving-point impedance Z_D and is obtained in complex form on the analyzer. The second method of obtaining Z_D consists of short-circuiting the load bus while maintaining constant generator bus voltages and measuring the short-circuit current I_{SC} in complex form with the previously measured voltage E_{OC} as reference. The phasor ratio of E_{OC}/I_{SC} is the complex impedance Z_D. These measurements are illustrated in Fig. 2.

Measurements of E_{OC} and Z_D may be required for peak load conditions and for light load conditions. Ordinarily the peak load measurements will suffice. An example is given showing the manual calculation of E_{OC} and Z_D in Appendix I for a single transmission line with line-charging capacitance included. An additional example is given in reference 1.

Step 2—Conversion of the Single Equivalent Impedance to 1.0 PU

The previous discussion showed how a complex network system can be converted to a single impedance Z_D whose input voltage is E_{OC}. For convenience of computation, it is desirable to convert E_{OC} and Z_D to 1.0 pu. If all equivalent impedances as viewed from any load point on a network are converted to 1.0 pu with a 1.0 pu input voltage, the voltage regulation characteristics of the network, viewed from the various load points, can be easily obtained from a single set of unit impedance power-reactive circle diagrams. The advantage is that one set of circle diagrams may be used for all problems of a similar nature, removing the necessity of redrawing a new set for each new problem.

The unit impedance concept was originated by Miller and Robbins.[1] In their work, it was shown that a simple radial-type power system could be resolved into a single unit impedance of varying resistance-reactance (R/X) ratio and supplied by a single generator having a terminal voltage of 1.0 pu. Such a representation required that the base kva be determined from the value of the total impedance rather than being selected arbitrarily as is the usual case. These concepts are used here and extended to include the resolution of a complex network system into a unit impedance equivalent, as viewed from any single load point on the network. As previously indicated, this is done by letting E_{OC} and Z_D be the base kilovolts (kv) and ohms respectively.

Recalling a familiar expression, found in many reference sources,[2] impedance can be expressed in pu form on a 3-phase system as

$$Z \text{ in pu} = \frac{Z \text{ ohms} \times \text{base kva}}{1{,}000\ (\text{base kv})^2} \tag{1}$$

Since it is desired to make Z always equal to 1.0 pu, equation 1 is rearranged to solve for the base kva

$$\text{Base kva} = \frac{(\text{base kv})^2 1{,}000}{Z \text{ ohms}} \tag{2}$$

Substituting Z_D and making the base kv equal to E_{OC}

$$\text{Base kva} = \frac{(E_{OC})^2 1{,}000}{Z_D \text{ ohms}} \tag{3}$$

where E_{OC} is in line-to-line kv.

Hence, equation 3 determines the base kva when E_{CO} and Z_D are made the base kv and base ohms respectively. The base kva may also be determined using known values of E_{OC} and I_{SC} as obtained in Fig. 2.

$$\text{Base kva} = \sqrt{3} E_{OC} I_{SC} \tag{4}$$

where I_{SC} is the short-circuit current measured at the load point in question; see Fig. 2.

Frequently, E_{OC}, Z_D, and I_{SC} will be measured in per cent or pu on some arbitrary base kv and kva, particularly if the values are obtained from network analyzer measurements. Since it is desired that E_{OC} and Z_D be made the base kv and base ohms, the new base kva must be determined as follows

$$Z_D = 1.0 \text{ pu} = z_d \left(\frac{\text{new base kva}}{\text{old base kva}}\right) \times \left(\frac{\text{old base kv}}{E_{OC}}\right)^2 \tag{5}$$

where z_d is in pu on the old base kv and kva.

Rearranging and solving for the new base kva

$$\text{new base kva} = \frac{\text{old base kva}}{z_d(\text{pu})} \times \left(\frac{E_{OC}}{\text{old base kv}}\right)^2 \tag{6}$$

Either equations 3, 4, or 6 may be used to determine the proper base kva depending on whether values of E_{OC} and I_{SC} or E_{OC} and Z_D are given in pu form or in kv, amperes, or ohms.

Having determined the proper base kva, the power and reactive load flowing at the point in question on the network are expressed in pu on the calculated base kva as follows

$$\text{pu power load} = \frac{\text{actual kilowatts}}{\text{base kva}} \tag{7}$$

$$\text{pu reactive load} = \frac{\text{actual kilovars}}{\text{base kva}} \tag{8}$$

To illustrate the use of the foregoing relations, Fig. 3 shows the load-flow diagram of an actual 115-kv transmission network which was studied on an a-c network analyzer. It was desired that the voltage regulation characteristics of the network at the substation bus R' be determined using the principles described herein. Measurements of E_{OC}, I_{SC}, and Z_D were taken at bus R'. They are

$E_{OC} = 1.078\,\underline{/0^\circ}$ pu
$I_{SC} = 1.68\,\underline{/-86.16^\circ}$ pu
$Z_D = 0.043 + j.640$ pu

The base kv and kva of the network are 115 kv and 100,000 kva respectively.

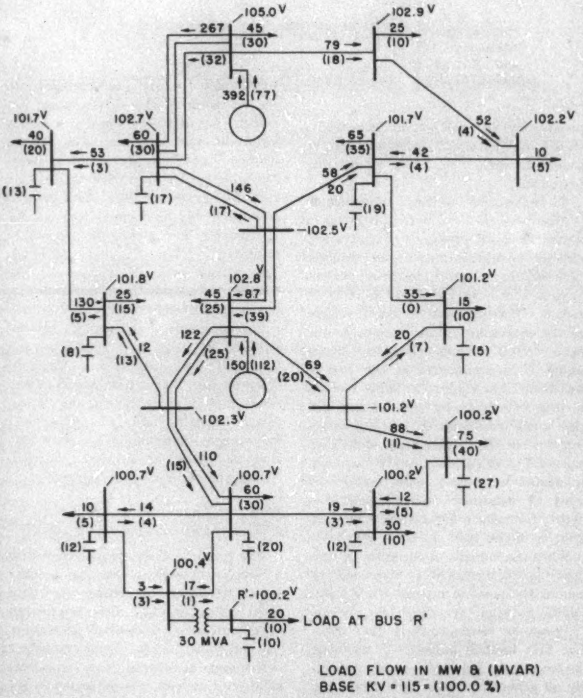

Fig. 3. Typical load-flow diagram, 115-kv system

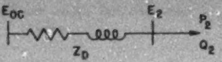

Fig. 4 (left). Unit impedance-unit input voltage equivalent circuit

E_{OC} = 1.0 PER UNIT

Z_D = 1.0 PER UNIT AT VARIABLE X/R RATIO

E_2 IS IN PER UNIT OF E_{OC}

BASE KVA = $\dfrac{(E_{OC})^2 \cdot 1000}{Z_D \text{ OHMS}}$; WHERE E_{OC} IN THIS EXPRESSION IS IN ACTUAL LINE-TO-LINE KILOVOLTS.

$P_2 = \dfrac{\text{ACTUAL KW}}{\text{BASE KVA}}$ IN PER UNIT

$Q_2 = \dfrac{\text{ACTUAL KVAR}}{\text{BASE KVA}}$ IN PER UNIT

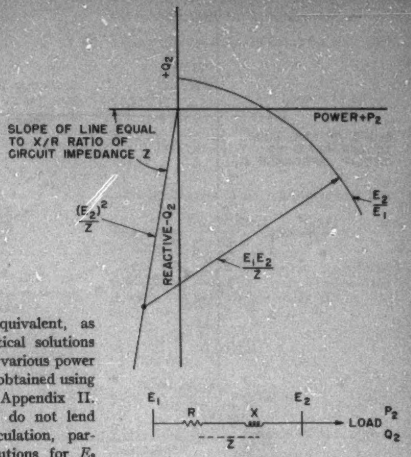

Fig. 5 (right). General construction of power-reactive circle diagram

These measured quantities were made using the methods which are illustrated in Fig. 2.

As a check on the measured value for Z_D

$$Z_D=\frac{E_{OC}}{I_{SC}}=\frac{1.078\,\underline{/0^\circ}}{1.68\,\underline{/-86.16^\circ}}$$

$$=0.043+j.640=0.641 \text{ at } X/R=14.9$$

Letting E_{OC} and Z_D be equal to 1.0 pu, and solving for the new base kva using equation 6

$$\text{New base kva}=\frac{100{,}000}{0.641}\left(\frac{1.078\times 115}{115}\right)^2$$
$$=181{,}000 \text{ kva}$$

as a check, the new base kva may also be calculated as follows, using equation 4 slightly modified

$$\text{New base kva}=E_{OC}I_{SC} \text{ base kva}$$

where E_{OC} and I_{SC} are in pu on the original network base kva and kv.

$$\text{New base kva}=1.078\times 1.68\times 100{,}000$$
$$=181{,}000 \text{ kva}$$

If a load of 10,000 kw and 5,000 kilovars were flowing to the load at bus R', these values can be expressed in pu on the new kva base using equations 7 and 8

$$\text{pu power load}=\frac{10{,}000}{181{,}000}=0.0552$$

$$\text{pu reactive load}=\frac{5{,}000}{181{,}000}=0.0276$$

Appendix I gives an example of transforming a single transmission line into a unit impedance-unit input voltage equivalent circuit using the pu system. Fig. 4 shows the final resulting pu equivalent circuit to which all original circuit configurations are transformed.

Step 3—Use of Unit Impedance Power-Reactive Circle Diagrams

The equivalent impedance of a network, as viewed from any load point on the network, can be converted to a single unit impedance equivalent, as shown in Fig. 4. Analytical solutions for the load voltage E_2 for various power and reactive loads may be obtained using the equations given in Appendix II. However, these equations do not lend themselves to rapid calculation, particularly when many solutions for E_2 are desired as a result of varying the power and reactive load. Power-reactive circle diagram solutions for E_2 can be quickly obtained particularly when the diagrams do not have to be replotted for each new problem which might arise.

The general method of constructing a power-reactive circle diagram is indicated in Fig. 5. A complete discussion of this subject is given in reference 3. It will be noted, in Fig. 5, that three quantities must be obtained in the construction of a single circle. These are:

E_2^2/Z = distance to the center of the circle from the zero co-ordinates

E_1E_2/Z = radius of the circle

X/R = slope of the line upon which the center of the circle is located

Since $E_1=E_{OC}=1.0$ pu and $Z=Z_D=1.0$ pu, the three quantities reduce to E_2^2, E_2, and the X/R ratio respectively. This is illustrated in Fig. 6.

Several circles can be plotted for different values of E_2 on the same graph, as indicated in Fig. 7. It is seen that the X/R ratio of the impedance Z_D can assume different values ranging from 20 to 1 depending on the point of measurement in a network. The circles need only be rotated in accordance with the X/R ratio of Z_D; see Fig. 8.

To eliminate the need of reproducing the circle diagrams for each new X/R ratio of Z_D, it is desirable to have a number of precalculated circles printed on transparent paper or a template. Such a template can then be rotated over standard rectangular co-ordinate graph paper so as to line up with any X/R ratio that might be encountered.

An Illustrative Example in the Use of Unit Impedance Power-Reactive Diagrams

It was shown previously that the 115-kv system network, shown in Fig. 3, could be reduced to a single equivalent unit impedance, as shown in Fig. 4. The measured and derived quantities pertaining to the equivalent circuit of the network were: $E_{OC}=1.0$ pu or $1.078\times 115=124$ kv; $Z_D=1.0$ pu; X/R ratio = 14.9; and base kva = 181,000.

Using these quantities, power-reactive circle diagrams were constructed and are shown in the lower portion of Fig. 9 for receiving voltages E_2 of 0.95, 0.90, 0.85, and 0.80 pu of E_{OC}. These pu values of receiving voltage would correspond to 118, 111.8, 105.4, and 99.2 kv respectively. The voltage regulation characteristics of the network can be plotted as a function of load at bus R', Fig. 3, where, for illustrative purposes, it has a kilovar/kilowatt ratio of 0.5 which is nearly a 90-per-cent power-factor load. A constant load line of kilovar/kilowatt = 0.5 is plotted, as shown in Fig. 9. Where the load line intersects the constant voltage circles, indicate the pu value of power required to produce the indicated values of receiving voltage E_2. The upper portion of Fig. 9 shows the voltage regulation curve of E_2 plotted as a function of pu power. The voltage regulation curve of Fig. 9, permits the determination of the receiving voltage E_2 for any specific value of power having a ratio of kilovar/kilowatt equal to 0.5. Table I gives a comparison of the voltage

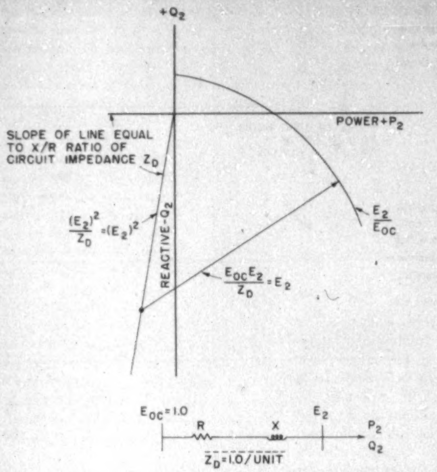
+Q₂
POWER+P₂
SLOPE OF LINE EQUAL TO X/R RATIO OF CIRCUIT IMPEDANCE Z_D
(E₂)²/Z_D = (E₂)²
REACTIVE-Q₂
E₂/E_OC
E_OC E₂/Z_D = E₂
E_OC = 1.0
R
X
E₂
P₂
Q₂
Z_D = 1.0/UNIT

Fig. 6 (above). Construction of a unit impedance power-reactive circle diagram

Fig. 7 (below). Construction of unit impedance power-reactive circle diagrams for a given X/R ratio and several values of E_2

Fig. 8 (upper right). Construction of unit impedance power-reactive circle diagrams for a given $E_2=0.9$ and two values of X/R ratio

Fig. 9 (lower right). Unit impedance power-reactive diagrams and voltage regulation characteristic for the network in Fig. 3 seen at load bus R′

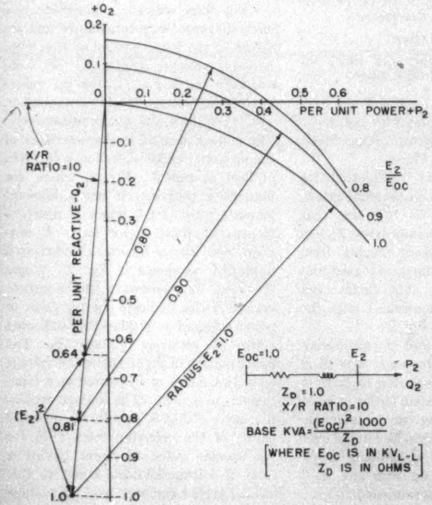
+Q₂
0.2
0.1
0
0.1
0.2
0.3
0.4
0.5
0.6
PER UNIT POWER+P₂
X/R RATIO=10
PER UNIT REACTIVE-Q₂
-0.1
-0.2
-0.3
-0.4
-0.5
-0.6
-0.7
-0.8
-0.9
-1.0
0.8
0.9
1.0
E₂/E_OC
0.80
0.90
RADIUS-E₂=1.0
0.64
(E₂)²
0.81
1.0
E_OC=1.0
E₂
P₂
Q₂
Z_D = 1.0
X/R RATIO=10
BASE KVA = (E_OC)² 1000 / Z_D
[WHERE E_OC IS IN KV_L-L, Z_D IS IN OHMS]

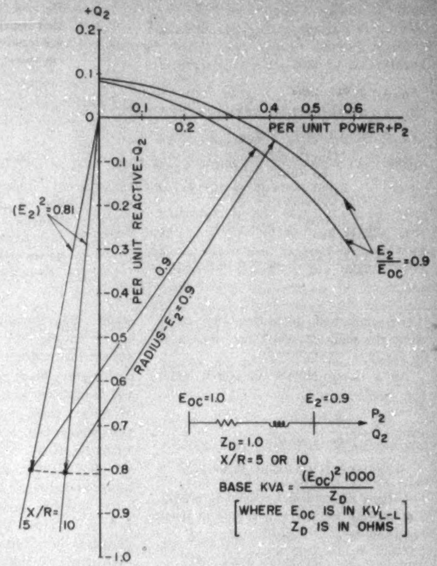
+Q₂
0.2
0.1
0
0.1
0.2
0.4
0.5
0.6
PER UNIT POWER+P₂
PER UNIT REACTIVE-Q₂
-0.1
-0.2
-0.3
-0.4
-0.5
-0.6
-0.7
-0.8
-0.9
-1.0
(E₂)²=0.81
0.9
RADIUS-E₂=0.9
E₂/E_OC = 0.9
X/R=
5
10
E_OC=1.0
E₂=0.9
P₂
Q₂
Z_D = 1.0
X/R = 5 OR 10
BASE KVA = (E_OC)² 1000 / Z_D
[WHERE E_OC IS IN KV_L-L, Z_D IS IN OHMS]

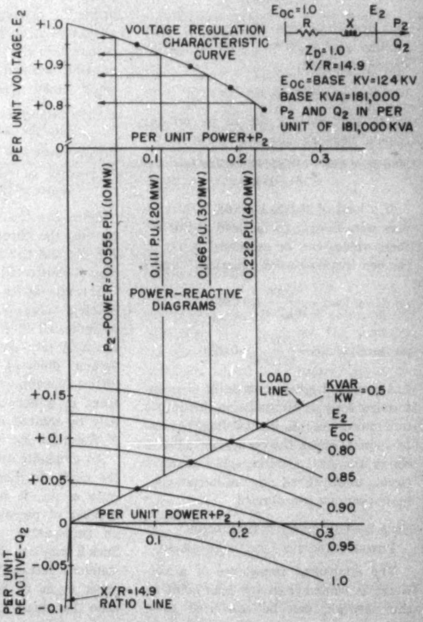

Table I. Comparison of E_2 and Measured Values

Load		E_2 (Obtained from Analyzer), Kv	E_2 (Obtained from Fig. 9), Kv
Megawatt	Megavars		
0	0	124	124
10	5	120	120
20	10	115.2	115
30	15	100.2	108.8
40	20	101.0	100.8

E_2 obtained from Fig. 9 and the actual measured values obtained from the network analyzer for several values of power. As seen, the agreement is very good. Greater accuracy can be obtained if the scale used in plotting the power-reactive diagrams is increased.

Unit impedance power-reactive circle diagrams are not restricted to the analysis of voltage regulation problems alone. They may also be used to calculate power and reactive loss on transmission lines and radial-type multiple circuit systems. In addition, they are very educational as a means of showing the effect of changing circuit X/R ratio on voltage drop or the reactive requirements at the load for maintaining a constant per-cent voltage drop.

Appendix I. Conversion of a Transmission Line to a Unit Impedance Circuit

A single 3-phase transmission line can be converted to a unit impedance circuit following steps 1 and 2 described in the paper. The transmission-line configuration is assumed as a π circuit

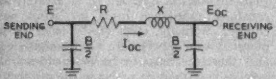

where

R = total resistance, ohms per phase
X = total reactance, ohms per phase
B = total line-charging susceptance, mhos per phase

Determine the open circuit voltage E_{OC} at the receiving end when a 3-phase voltage E is applied to the sending end terminal

$$I_{OC}=E_{OC}\frac{B}{2} \tag{9}$$

also

$$I_{OC}=\frac{E}{R+J\left(X-\frac{2}{B}\right)} \tag{10}$$

Substituting equation 10 into equation 9 and solving for E_{OC} magnitude

$$E_{OC}=\frac{2}{B}\frac{E}{\sqrt{R^2+\left(X-\frac{2}{B}\right)^2}} \tag{11}$$

Determine the driving-point impedance Z_D of the transmission line as viewed from the receiving terminal. This is done by grounding the sending-end terminal and measuring the impedance Z_D looking into the receiving terminal

$$Z_D=\frac{(R+JX)\left(-J\frac{2}{B}\right)}{(R+JX)+\left(-J\frac{2}{B}\right)} \tag{12}$$

The original transmission circuit can now be replaced by the following equivalent circuit using Thévenin's theorem

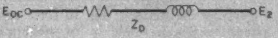

where

$$Z_D=\frac{(R+JX)\left(-J\frac{2}{B}\right)}{(R+JX)+\left(-J\frac{2}{B}\right)}$$

and

$$E_{OC}=\frac{2}{B}\frac{E}{\sqrt{R^2+\left(X-\frac{2}{B}\right)^2}}$$

The equivalent circuit can be converted to the following pu form using the methods described in step 2 of the paper

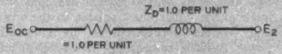

where

$$E_{OC}=\frac{2E}{B\sqrt{R^2+\left(X-\frac{2}{B}\right)^2}}=\text{base kv}$$

E = the actual sending-end voltage, 3-phase line-to-line kv

$$Z_D=\frac{(R+JX)\left(-J\frac{2}{B}\right)}{(R+JX)+\left(-J\frac{2}{B}\right)}=\text{base ohms}$$

$$\text{base kva}=\frac{(E_{OC})^2}{Z_D}\,1{,}000 \tag{13}$$

To illustrate the use of the foregoing relations, the following transmission-line constants are assumed: $R=16$ ohms, $X=80$ ohms, $B=500\times10^{-6}$ mhos, and $E=138$ kv (actual sending end voltage).

Using equation 11 and solving for E_{OC}

$$E_{OC}=\frac{2E\times10^6}{500\sqrt{(16)^2+\left(80-\frac{2\times10^6}{500}\right)^2}}$$

$$=1.02E$$

since E is 138 kv, then

$E_{OC}=1.02\times138=141$ kv = base voltage

Using equation 12 and solving for Z_D

$$Z_D=\frac{-J\frac{2\times10^6}{500}(16+J80)}{16+J\left(80-\frac{2\times10^6}{500}\right)}\text{ ohms}=16.3+J81.5\text{ ohms}=83\text{ ohms}=\text{base ohms at }X/R=5$$

Using equation 13 and solving for base kva

$$\text{base kva}=\frac{(141)^2\times1{,}000}{83}=239{,}000$$

If a load of 50,000 kw at 95-per-cent power-factor lagging were transmitted through the line, the pu value of the load would be

$$P_2=\frac{50{,}000}{239{,}000}=0.209\text{ pu}$$

$$Q_2=\frac{0.329\times50{,}000}{239{,}000}=0.069\text{ pu}$$

where 0.329 is the tangent of the power-factor angle.

Appendix II. Fundamental Power and Reactive-Flow Equations for a Unit Impedance Circuit

The following two equations have been developed in reference 4 for the following circuit configurations

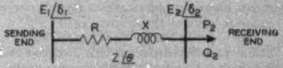

$$P_2=-\frac{E_2^2\cos\theta}{Z}+\frac{E_1E_2}{Z}\sin(\delta_{12}+\alpha) \tag{14}$$

$$Q_2=-\frac{E_2^2\sin\theta}{Z}+\frac{E_1E_2\cos(\delta_{12}+\alpha)}{Z} \tag{15}$$

where

P_2 = receiving power, pu
Q_2 = receiving reactive flow, pu
E_1 = sending-end voltage, pu
E_2 = receiving-end voltage, pu
Z = circuit impedance, pu
δ_1 = angle of voltage E_1
δ_2 = angle of voltage E_2
δ_{12} = angular difference between E_1 and E_2
θ = angle of impedance Z
α = 90 degrees $-\theta$

All quantities in equations 14 and 15 are magnitude quantities and not in phasor form. These equations are general and may be used for a unit impedance circuit of the type described in the paper. Letting $E_1=E_{oc}=1.0$ pu and $Z=Z_D=1.0$ pu, equations 14 and 15 are rewritten

$$P_2=-E_2^2\cos\theta+E_2\sin(\delta_{12}+\alpha) \tag{16}$$

$$Q_2=-E_2^2\sin\theta+E_2\cos(\delta_{12}+\alpha) \tag{17}$$

In these equations, positive load power and reactive flow is taken as flow toward the load and away from the receiving terminal of the circuit.

Equations 16 and 17 may be combined so as to eliminate the variables sin $(\delta_{12}+\alpha)$ and cos $(\delta_{12}+\alpha)$. This is done by squaring equations 16 and 17 and adding the two squared equations, which results in

$$E_2^2=(P_2+E_2^2\cos\theta)^2+(Q_2+E_2^2\sin\theta)^2 \quad (18)$$

where

$$\cos\theta=\frac{R}{Z_D}=R\text{ pu, since }Z_D=1.0$$

$$\sin\theta=\frac{X}{Z_D}=X\text{ pu, since }Z_D=1.0$$

The use of equation 18 may be illustrated using the network in Fig. 3, where it was shown that the network viewed from bus R' can be replaced by a unit impedance equivalent as represented in Fig. 4. It was determined that

$E_1=E_{OC}=124$ kv $=1.0$ pu

$Z_D=1.0$ pu on 124 kv and 181,000-kva base of $X/R=14.9$

Assume that

$P_2=20$ megawatts or 0.111 pu on 181,000-kva base

$Q_2=0.5P_2=10$ megawatts or 0.056 pu on 181,000-kva base

and solve for E_2 using equation 18

$$R^2+X^2=Z_D^2=1.0$$

$$\frac{X}{R}=14.9$$

$$R^2+(14.9R)^2=1.0$$

$$R=0.067\text{ pu}$$

$$X=14.9\times0.067=0.998\text{ pu}$$

Substituting known quantities into equation 18

$$E_2^2=(0.111+0.067E_2^2)^2+(0.056+0.998E_2^2)^2$$

Perhaps the simplest way to solve this expression for E_2 would be to substitute several trial values for E_2 into the right side of the equation, solve for E_2, and interpolate for the exact correct value for E_2. However, it was found, using power-reactive diagrams, that E_2 was 115 kv. This is equal to 115/124 or 0.929 pu of E_{OC}. Substuting this value in the right-hand side of the expression for E_2

$$E_2^2=(0.111+0.067\times\sqrt{0.929})^2+(0.056+0.998\times\sqrt{0.929})^2$$

$$E_2^2=0.868$$

$$E_2=0.93$$

This value agrees closely with the substituted value and is the correct value for all practical purposes.

References

1. FUNDAMENTAL RELATIONS OF SYSTEM VOLTAGE DROP AND SYSTEM LOADS, G. M. Miller, L. W. Robbins. *AIEE Transactions*, vol. 74, pt. III, Apr. 1955, pp. 267–73.

2. CIRCUIT ANALYSIS OF A-C POWER SYSTEMS, VOL. I (book), Edith Clarke. John Wiley and Sons, Inc., New York, N. Y., 1943.

3. POWER-REACTIVE DIAGRAMS STILL USEFUL, R. M. Butler. *Electric Light and Power*, Chicago, Ill., July and Aug. 1952.

4. POWER SYSTEM STABILITY, VOL. I (book), S. B. Crary. John Wiley and Sons, Inc., New York, N. Y., 1945.

◆

Discussion

R. D. Goodrich (Bureau of Reclamation, Denver, Colo.): This paper forms a logical link between Thévenin's theorem and circle diagram theory. Now that the connection between the two has been demonstrated it will be easy for others to suggest improvements and refinements, which are, of course, valuless without the original paper.

One more or less obvious suggestion is to utilize preplotted circles with auxiliary loci for constant watts, constant power factor, or constant real or reactive loss located on the receiving-end diagram. These loci can all be derived for constant sending-end voltage, and afford means of plotting families of auxiliary curves of, e.g., substation voltage versus substation load for various values of power factor. A number of equations for these loci are given elsewhere.[1] The data for the constant loss circles are:

Real power loss

1. Center on the B line at the distance $P_{SL}^1\cos\beta$ from the center of the power circles
2. Radius $R_{PL}=P_{SL}^1\sqrt{\cos^2\beta+P_L/P_{SL}^1-P_S^1/P_{SL}^1}$
3. P_L=loss in per unit on system base $P_{SL}^1=e_S^2/(\boldsymbol{AB})_{RP}$

Reactive power loss

1. Center on the B line at the distance $Q_{SL}^1\sin\beta$ from the center of the power circles
2. Radius $R_{QL}=Q_{SL}^1\sqrt{\sin^2\beta+Q_L/Q_{SL}^1-Q_S^1/Q_{SL}^1}$
3. Q_L=loss in per unit on system base $Q_{SL}^1=e_S^2/(\boldsymbol{AB})_{IP}$

Note that the real power loss circle shows that power is delivered to the substation with minimum loss if the reactive load is held constant at one particular value.

A word of caution is in order concerning the use of the diagram: Since Thévenin's equivalent was developed from a loaded system with certain voltages at various points in the system, results are rigorously correct only when those voltages are maintained at their original values. Both the internal voltage and internal impedance of the equivalent depend on the assumption that the loads on the system are constant impedances. But they appear in the original system representation as constant power devices supposedly independent of voltage level. Consequently deviations from the original voltage levels will cause erroneous changes in loads with a consequent error in results. This phenomenon is a familiar one in any application of an equivalent circuit "out of context."

REFERENCE

1. A UNIVERSAL POWER CIRCLE DIAGRAM, Ralph D. Goodrich, Jr. *AIEE Transactions*, vol. 70, pt. II, 1951, pp. 2042–49.

J. R. Curtin (Bonneville Power Administration, Portland, Oreg.): This paper nicely formalizes a technique which we have occasionally found very convenient in predicting the effect of single load additions or changes to a complex network. Even though an analyzer has been in use on the Bonneville system, it is not always convenient to use it to answer specific questions concerning load changes at a given point. It is easily apparent that the technique described can be very valuable to utilities having only occasional access to analyzers if the Thévenin equivalents of busses are listed for future reference.

At times we have even used the system impedance from short-circuit studies, adjusted for system impedance angle. At points remote from generation, the effect of generator subtransient reactance and generator bank reactance on the total impedance is often negligible and can sometimes be satisfactorily corrected for by reducing the system to a mesh between major generation busses, then eliminating generator and generator bank impedance. Nearby synchronous condensers will, of course, spoil the theory but that is an exception to the conditions stated in the paper.

R. M. Butler: The comments of Mr. Goodrich and Mr. Curtin are very much appreciated as they have shown ways to increase the usefulness of the method described in the paper.

Mr. Goodrich has offered a word of caution indicating that Thévenin's theorem requires all loads within the network other than the load in question to be treated as constant impedance loads for strict accuracy. Actually, most of the loads on a power system network are voltage regulated and therefore tend to be independent of voltage variations occurring in the network. Fortunately, an increase of 20 or 30 per cent in the power and reactive components of load at a given point on a network will have a small effect on the voltage levels at most of the other loads connected to the same network. The only exception would be for a condition where the load in question is electrically close to another of about equal size. Even for this condition, it has been found that the error in predicting voltage regulation usually will be quite small. I have concluded that for all practical purposes it does not matter whether the loads, which are a part of equivalent impedance, are of the constant impedance or constant kva type. Since this tends to be borne out by tests on a network analyzer, I concur with Mr. Goodrich's word of caution with the added comment that usually the error produced by the existence of constant kva load will be very small and can be neglected.

Mr. Curtin indicated that for load points electrically remote from generation it is quite permissible to use the short-circuit current as determined from 3-phase fault studies. This would seem to be quite reasonable since the generator transient reactances are a very small percentage of the total equivalent impedance to the load in question. Furthermore, for voltage regulation studies in a distribution system, the effect of generator and step-up transformer impedances is of negligible value as compared with the distribution substation transformer impedance. Hence, the suggestion of using the short-circuit current as determined from fault studies would seem to be a good way to simplify the determination of base quantities.

In using the methods described in the paper, it is necessary to know what the open-circuit voltage E_{OC} is at the load point in question. It would appear that the only way to obtain this value would be to measure it on an a-c calculating board. As mentioned in the paper, analyzers are not always available for this purpose. One way to avoid the necessity of using an analyzer to obtain E_{OC} is to assume that the presently existing peak load in question is part of the calculated equivalent impedance Z_D. Then E_{OC} is simply the voltage corresponding to the presently existing peak load. This voltage can be measured in the field. This approach is correct if it is assumed that the peak load voltage in the future will be either equal to or lower than this value next year. A prediction of next year's peak load voltage must then be based upon the additional increment of load that will be added between now and next year at the load point in question.

One of the biggest timesavers in the use of the methods described in the paper is to have a precalculated circle diagram template available for use. Such a template can be made to include constant voltage circles ranging from 1.10 to 0.80 pu in steps of 0.01 pu. Having such a template will avoid the necessity of reproducing circle diagrams many times as each new problem appears.

I have found that the methods described in the paper for predicting voltage regulation using the circle diagram template have been of considerable value in predicting the improved voltage conditions resulting from the application of capacitors and voltage regulators to points in power systems where such improvement is needed. It is hoped that utility engineers will also find this method to be of value.

Automatically Switched Capacitors in Steps on a Single Distribution Feeder

W. C. FOWLER
MEMBER AIEE

C. W. THOMAS
NONMEMBER AIEE

THE benefits deriving from the connection of static capacitors to the lines of the utility system are well established.[1,2] The disadvantages of leaving them connected at undesirable times are apparent, with the result that many installations utilize varied types of switching and control functions.[3] The maximum benefits are achieved by having capacitors located at the closest possible point to the equipment calling for reactive component of load. Some variation from this ideal may be used to take advantage of the voltage-correcting ability of the capacitors. Over-all economic factors usually determine the exact point of installation of a specific bank of capacitors.

Requirements for control of switched banks have resulted in rather large concentrations at substations. This frequently demands expensive circuit breakers and switchgear to perform the switching functions. The great disadvantage is in failure to make use of the full benefits along the lines of the distribution feeder to the approximate area of the load being delivered. Much has been accomplished in this direction by the use of time switches for control purposes, but these fail to recognize variations of the electric load which require unscheduled switching. Other forms of control are being used, but not to the extent of taking full advantage of capacitors on the feeder lines.

New forms of control units are available in which the time delay before switching is increased logarithmically as the signal strength is decreased to the contact settings. They also provide for the selection of voltage, current, watts, or vars as the signal to be used in switching.[4,5] These units present the possibility of controlling several banks of capacitors on a single feeder and having them selectively switched to fit the circuit conditions at any time.

Procedure for Testing

To investigate these possibilities, it was decided that the 4,160-volt feeder no. 2 in the system of the Public Service Company of Oklahoma offered excellent qualities to determine how well such a program might work. Fig. 1 shows the principal features of this feeder no. 2, with significant items of this test program indicated. Numerous laterals and service points are omitted as not significant.

Control signal for the capacitor bank at point *C* was obtained by measuring the kilovar load at this point on only one phase. It was assumed that unbalance between phases maintained a reasonable proportion at different times. Measurement and control signals at points *B*, *C*, *E*, *F*, and *G* were all definitely obtained from the same phase as was the voltage measurement at point *A*. Control units at *C*, *E*, *F*, and *G* were those having the

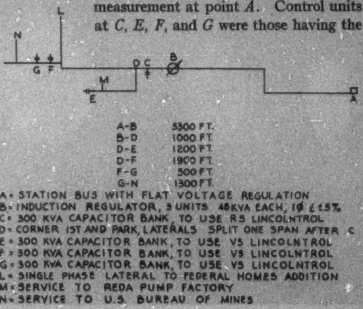
L
N
G
F
D
C
B
M
E
A
A-B 5300 FT.
B-D 1000 FT.
D-E 1200 FT.
D-F 1900 FT.
F-G 500 FT.
G-N 1300 FT.
A = STATION BUS WITH FLAT VOLTAGE REGULATION
B = INDUCTION REGULATOR, 3 UNITS 48KVA EACH, 1Ø ±15%
C = 300 KVA CAPACITOR BANK, TO USE RS LINCOLNTROL
D = CORNER 1ST AND PARK, LATERALS SPLIT ONE SPAN AFTER C
E = 300 KVA CAPACITOR BANK, TO USE VS LINCOLNTROL
F = 300 KVA CAPACITOR BANK, TO USE VS LINCOLNTROL
G = 300 KVA CAPACITOR BANK, TO USE VS LINCOLNTROL
L = SINGLE PHASE LATERAL TO FEDERAL HOMES ADDITION
M = SERVICE TO REDA PUMP FACTORY
N = SERVICE TO U.S. BUREAU OF MINES

Fig. 1. Essential points in the feeder under test

Paper 55-91, recommended by the AIEE Transmission and Distribution Committee and approved by the AIEE Committee on Technical Operations for presentation at the AIEE Winter General Meeting, New York, N. Y., January 31–February 4, 1955. Manuscript submitted October 11, 1954; made available for printing November 30, 1954.

W. C. FOWLER is with the Sangamo Electric Company, Fort Worth, Texas, and C. W. THOMAS is with the Public Service Company of Oklahoma, Bartlesville, Okla.

The authors wish to express their appreciation for the services given by other engineers of both Sangamo Electric Company and Public Service Company of Oklahoma. The design and development of the equipment, the installation of all components, the load checks and meter tests, and help in planning these tests involved both companies and numerous men in both organizations.

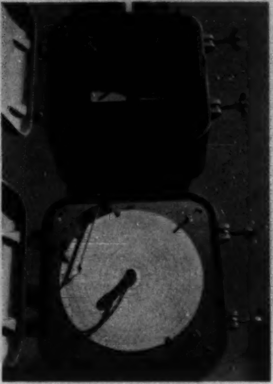

Fig. 2. Voltage control and graphic voltmeter

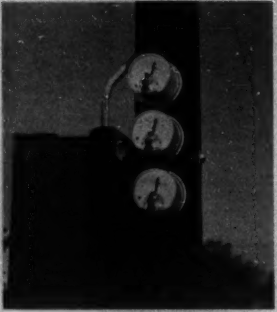

Fig. 3. Voltmeters to observe unbalance between phases

time-delay characteristics previously mentioned. The balance of load between phases was obtained by changing the connection of transformers to the extent that was practical, but no effort was made to construct additional circuits that would have been needed to divide the heavy loads found on a single-phase lateral. Voltage at the substation is maintained to approximately constant values by the switching of large banks of capacitors by the operator in that station.

Loads on the circuit consist of a mixture of industrial, small commercial, and residential customers. The first customer on the feeder is connected immediately after the regulator station, there being only one small transformer bank ahead of point *C* where reactive load is measured for control of the first capacitor bank. Special attention was given to important industrial loads at *M* and *N* and to a single-phase lateral at *L* which has become loaded with window-type air conditioners.

INSTRUMENTATION

Particular care was given to the instrumentation at all significant points. Steady-state voltage was measured with graphic thermal voltmeters at points *A*, *B*, *C*, *E*, *F*, and *G*. Where used with a control device at a capacitor installation, as in Fig. 2, the measuring element was connected through the ON contact so that an accurate record of the times of operation was obtained. Fig. 3 shows the installation of three thermal voltmeters with maximum and minimum indicating pointers, as used as point *N*, to show voltage unbalance as it developed.

Additional measurements included thermal graphic records of kilowatt and kilovar load at point *A*, as shown in Fig. 4. Fig. 5 shows the var control unit with graphic varmeter and graphic voltmeter at point *C*. Control circuit was carried one span to the switched capacitor installation on the pole following the location of the measurement point. All voltmeters were repeatedly checked with a portable precision instrument to insure accurate values when making comparisons.

Results

Figs. 6 and 7 show the nature of information obtained from these measurements and controls. Fig. 6(A) shows the results with some line-drop compensation for resistance set in the regulator, although all reactive compensation was removed. Fig. 6(B) illustrates the operation with no line-drop compensation in the regulator, with output of the regulator set for a fixed bandwidth of $124^{1}/_{2}$ to 126 volts. The voltage-controlled capacitors provided steps in voltage at each point, with the regulator acting as a vernier to bridge these steps. Fig. 7 shows voltage charts from four of the stations during the time represented by Fig. 6(B). With this combination, excellent results were obtained with bandwidths and voltage spreads less than either regulator or switched capacitors alone would achieve. Fig. 6(C) demonstrates operation that would result with no regulator in the circuit, inasmuch as the control was removed with the setting on neutral.

The var control functioned smoothly to maintain power factor of the circuit within the ability of the capacitor bank at point *C*. An average of about two

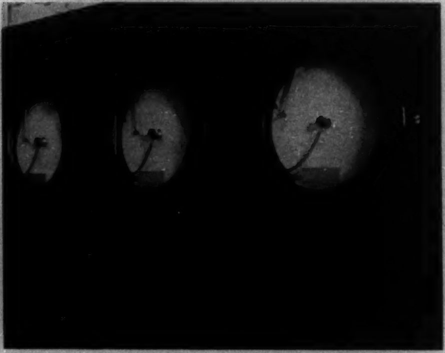

Fig. 4 (left). Meters at the substation

Fig. 5 (right). Measurement and control at point C of the circuit

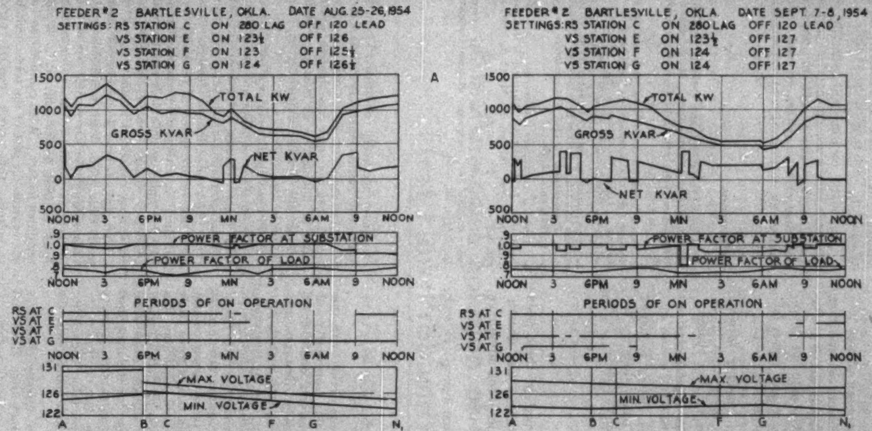

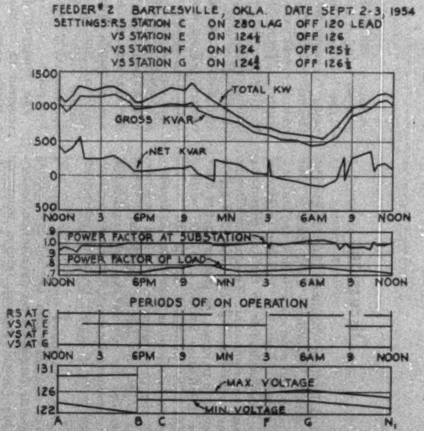

Fig. 6 (left).

A—Results with line-drop compensation in regulation

B—No line-drop compensation in regulation

C—No regulator in circuit

Fig. 7 (below). Voltage charts showing operations and results

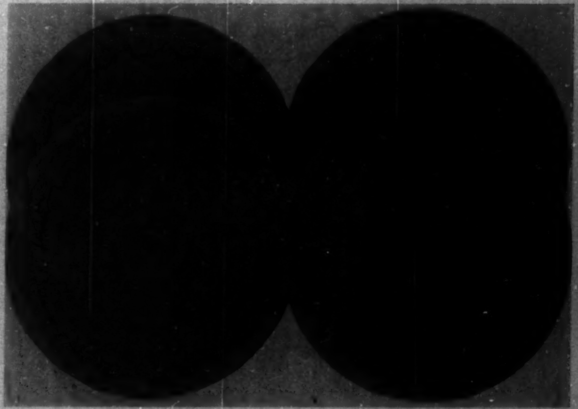

operations per day resulted to a large extent from the switching of the voltage controls under different conditions.

Voltage control at the different points performed excellently after settings were made to obtain desired switching action between the various units. Noteworthy results were found, after proper adjustments, in obtaining selective operation of the separate units as result of varying loads delivered at different times at points *L*, *M*, and *N*.

Discussion

Bandwidth of a control setting must be large enough to avoid pumping from the operation of a bank under a given control. Occasional transfers from one control point to another developed as a useful operation in having the var supply actually in the area where it was needed. With compensation set in the regulator, bandwidth on voltage controls should be greater than the range of regulation at the point of control. In this case, capacitors will be switched after the regulator has reached its limit.

Capacitors can only raise the voltages level as they are applied, and their effect in this respect decreases as it is observed closer to the source than a first observation. When using capacitors for voltage improvement, the tap settings should take into account the highest voltage that may be encountered under the conditions that may develop.

The following generalities appear to be indicated:

1. Capacitors immediately after the regulator will improve the power factor of the load handled by the regulator but require modification of compensator settings.

2. Reactive control may be connected anywhere in so far as the regulator is concerned, but must be ahead of connections serving loads that should be considered.

3. Voltage control may be connected ahead of the regulator to control capacitors connected after that unit in the circuit.

4. Voltage control installed farther from the source than the regulator should be located beyond the point for which compensation is set, when possible. Excellent results were found with voltage controls after all compensation was removed from the regulator.

Unbalanced load between phases was found as a major problem when either voltage or var control was taken as the signal and obtained from only one phase. Improvement in voltage and power-factor balancing can be obtained:

1. By balancing load carefully between phases, which includes observation of the diversity of load on the different phases.

2. By using single-phase regulators to improve voltage balance only.

3. By using automatic control to switch single-phase capacitor banks along the laterals which produce the unbalance.

Conclusions

The results developed in these tests suggest several possibilities and demonstrate certain necessities if full advantage is taken of the new controls:

1. To achieve optimum benefits in such applications, it becomes apparent that adequate measurements are needed to determine conditions of load and voltage with the installation of comprehensive control of capacitor banks.

2. The combination of regulator and automatic control units can be used to produce a narrow bandwidth and a small spread in voltage over the length of a distribution feeder. This improvement in regulation together with control of power factor offers the possibility of maximum utilization of the thermal capabilities of the various elements of a given circuit.

3. A group of automatically controlled capacitor banks can be used to provide step-voltage control. Such units contribute their share to the benefit of generation and transmission systems also, at moderate costs, as compared with large station banks.

4. Automatic controls will generally remove the capacitors, or connect them, in proper arrangements to meet the unscheduled changes of a system or load which occasionally develop without warning.

References

1. Power System Voltage Control Without Feeder Voltage Regulators, **N. N. Smeloff.** *AIEE Transactions*, vol. 67, pt. II, 1948, pp. 1,462–66.

2. An Evaluation of Power-Factor Correction on a System Basis, **H. R. Tomlinson, R. O. Bigelow.** *AIEE Transactions*, vol. 73, pt. III, 1954 (Feb. 1955 section), pp. 1,677–84.

3. Application of Shunt Capacitors at Transmission and Distribution Stations, **F. M. Porter, C. P. Zimmerman.** *AIEE Transactions*, vol. 70, pt. I, 1951, pp. 112–20.

4. Thermal Meters Control Capacitor Switching, **J. H. Patton.** *Electrical World*, New York, N.Y., vol. 141, no. 10, March 8, 1954, pp. 103, 107.

5. Lincolntrol as Used for Capacitor Switching. *Bulletin 492*, Sangamo Electric Company, Springfield, Ill., 1954.

◆

Discussion

Clark Denison (Oklahoma Gas and Electric Company, Oklahoma City, Okla.): Our studies and experience confirm the authors' statements regarding locating capacitors as near as feasible to the var consuming loads and equipment. The economic factors have shown that in our case it is highly desirable to locate the greater part of these on distribution feeders with the switched capacitors controlled so as to correct power factor to as near unity as feasible. By the same reasoning, switched capacitors on substation busses, particularly when supplied by low-voltage subtransmission, are economically sound if they are sized to fit var needs in supply lines and substations only.

We have found time switch control a very useful low-cost method of achieving desired conditions on distribution feeders. This control method insures maximum correction during system peak load periods which determine our design and capacity limitations. We feel this consideration may outweigh local feeder conditions where reactive or voltage control may seem to be a better solution.

The tests made in connection with this paper demonstrate the superiority of thermally activated reactive and voltage controls over the older instantaneous controls. These older controls were subject to excessive operations due to temporary conditions and thus were not adaptable to co-ordination with narrow control bands and selective operation as are new thermal controls. Even with these narrow control bands the tests show in two of three trials that one of the switched capacitors was not switched off, indicating that a typical feeder could logically include unswitched capacitors to the extent of the light load var demand. The tests also indicate switching time of the var controlled capacitor might be predictable enough for substitution of time clock control near the feed point.

Our company has already begun a program of combination time clock and voltage controls on substation bus capacitors to insure use during peak loads and still have the capacitors available at other times for voltage improvement during emergency operating conditions. In cases where this improvement is insufficient or where bus capacitors do not exist, it appears logical that the same combination control could be justified on at least part of the individually switched capacitors on distribution feeders.

As in most utilities our new service areas in the outskirts of cities are being served from higher voltage subtransmission and tap-changing transformers supplying trunk-type 12.5-kv distribution feeders. These areas are ideally suited to relatively large switched capacitors which should logically have combination time clock and thermally activated voltage controls with no substation bus capacitors at all.

The use of time clock control during predictable peak load conditions rather than single-phase var control would avoid application troubles due to unbalanced loads at feed points inherent in 3-phase regulated feeders. With combination voltage controls on part of the feeder switched capacitors, time clock control periods could be limited to more predictable load periods, thus avoiding many situations such as week ends, changeable weather periods, etc. By the proper co-ordination of controls the installed capacitors can be made much more adaptable to system as well as local feeder needs with the new thermally activated control devices.

W. H. Cuttino (Westinghouse Electric Corporation, East Pittsburgh, Pa.): Although automatically switched capacitors have been used on many distribution circuits for a number of years and their advantages in supplying the kilovars as needed to improve voltage conditions, release system capacity, and reduce system losses have been known, there has not been sufficient information published showing results on specific circuits. The information given by the authors should be quite interesting to the distribution engineers, particularly those embarking upon a program of adding switched capacitors.

When automatically switched capacitors are applied it is important that the bandwidth of the sensing device have sufficient spread to avoid "pumping." If several switched capacitors are applied on one distribution circuit the switching of one capacitor may affect the sensing signals at other capacitor locations. This is particularly true in the case of voltage-sensing devices and often occurs in the case of other sensing devices, depending upon their location in the circuit. The change in signal should be known at all switched capacitor locations when capacitors are switched at any one of the other locations to guard against the possibility of the capacitor switch pumping. It would be interesting to know what these values are for the circuit in the paper.

It is assumed that Mr. Fowler and Mr. Thomas do not necessarily propose using automatically switched capacitors at all locations shown in Fig. 1. It appears that one or two unswitched capacitor banks might be applied in the interest of economy with satisfactory results.

W. C. Fowler and C. W. Thomas: We appreciate the contributions made in the discussions which add to the value of the report of the tests. In connection with Mr. Denison's experienced comment on time switches, it might be mentioned that one of the banks that was automatically switched during the test period is to be operated in the future on a time schedule. However, the effectiveness in supplying vars as close as possible to the point of use is lost to a small degree in this change.

The paper gave complete results on three selected days to present typical results of various settings on "normal" days. During various "abnormal" days it was found that all banks were switched on at some times and all switched off at other times, but the conditions would not be predictable.

After the problem of unbalance was realized it was readily allowed for in setting the single-phase varmeter. The actual settings used were those found to accomplish the desired results by observing the polyphase graphic varmeter at the substation and the proportion of unbalance in reactive loads held sufficiently steady to make the operation very satisfactory. If the regulator had been in the substation it would have been convenient to measure and control the bank from polyphase measurements at that point, with a control circuit carried out to a suitable location for the switched bank.

In response to the question from Mr. Cuttino, the calculated effect of the last capacitor bank was 3 volts, which was exactly the amount observed on an instantaneous voltmeter. With compensation removed from the regulator, this unit acted to restore most of the effect of switching with the time delay of the regulator. The time delay of the thermal control was ample to allow the regulator to complete its function. The net effect found at the last bank of capacitors, after the regulator had returned to its set value, was slightly less than 3/4 volt. The effect was 1/2 volt at each of the other two banks under voltage control. Pumping did not occur until other settings were tried wherein the bandwidth on the voltage controls was reduced to a smaller value than the bandwidth on the regulator.

Mr. Cuttino suggests the merit of fixed banks in securing results at the least expense. A decision on this feature has been delayed pending minimum values of reactive load during the season of lightest loads. It appears that even 300 kilovars would be too much for the circuit to satisfy system requirements at such times. This feature of capacitor applications also identifies itself with the possible use of secondary capacitors at appropriate points where they may justify themselves. The switched capacitors should serve the purpose of handling the variations in reactive load above the minimum values.

An Analogue Solution of Cable Heat Flow Problems

E. de HAAS
NONMEMBER AIEE

P. J. SANDIFORD
NONMEMBER AIEE

A. W. W. CAMERON
MEMBER AIEE

Synopsis: Steady-state heat flow problems related to buried cables can be solved with a simple electric analogue. The soil is represented by graphite-coated paper, and the cables and sinks by fixed electrodes applied with silver paint or by movable copper cylinders. Regions with lower thermal resistivity (t/r) than the main soil body (duct banks, special backfill) are simulated by placing one or more extra sheets of graphite paper on the base paper in electric contact with it. Applications described include a duct bank problem and a double-circuit pipe-type cable placed in a rectangular box of sand. The load reduction caused by close spacing, the beneficial effect of sand backfill in poor soil, and the influence of ground water are discussed.

EQUATIONS for the heat flow from an underground cable or a group of cables have been given by Neher.[1,2] His solution is based on the Kennelly equation and works satisfactorily for various configurations. Fink[3] has applied it to cases where special backfill is used to bring the over-all thermal resistivity of an otherwise poorly conducting soil down to a more suitable design value. Exact calculation is difficult or impossible in a number of practical cases, e.g., when twin circuits are placed in a rectangular box of backfill. An electric analogue, assembled with simple equipment, may then supply steady-state solutions of sufficient accuracy.

Principle

Heat flow from a system of n parallel buried cables is basically a 2-dimensional problem in a plane perpendicular to the direction of the cables. When a steady state has been reached, the temperature satisfies Laplace's equation, and it may be written

$$\Delta T = T_n - T_A = R_{nA} W_n$$

where

T_n = surface temperature of cable n in a system of cables
T_A = temperature of a sink A
R_{nA} = thermal resistance between n and A per unit length of cable
W_n = heat transported from n to A per unit of time and per unit length of cable
ΔT = temperature rise above ambient

The same law holds for an electric flow where current is transported from a number of sources to a number of sinks

---

Paper 55-55, recommended by the AIEE Insulated Conductors Committee and approved by the AIEE Committee on Technical Operations for presentation at the AIEE Winter General Meeting, New York, N. Y., January 31–February 4, 1955. Manuscript submitted October 22, 1954; made available for printing December 6, 1954.

E. de Haas, P. J. Sandiford, and A. W. W. Cameron are with the Hydro-Electric Power Commission of Ontario, Toronto, Ontario, Canada.

The authors wish to acknowledge the stimulating discussions of these problems with colleagues at Ontario Hydro and with the other members of the AIEE Task Group on Study of Soil Thermal Resistivity, at whose request this paper is presented.

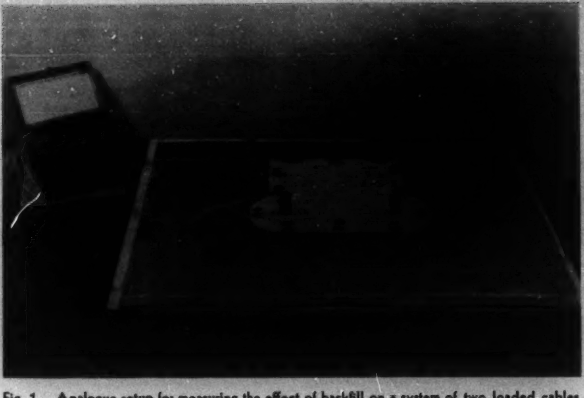

Fig. 1. Analogue setup for measuring the effect of backfill on a system of two loaded cables. The weights serve to keep the extra paper in contact with the base sheet

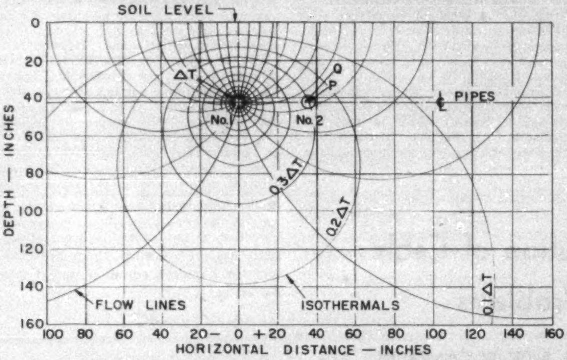

Fig. 2. Kennelly diagram of one loaded pipe. The second pipe is centered on the 0.3ΔT isothermal

$$V_n - V_A = S_{nA} I_n$$

where

$V_n - V_A$ = potential difference between n and A
S_{nA} = electrical resistance between n and A
I_n = current from n to A

The advantage of studying heat flow with an electric analogue lies in the fact that the electrical quantities reach their final (steady-state) values immediately. Besides that they are much easier to measure. Afterwards the solution is again translated into terms of heat.

Experimental Arrangement

A modification of a commercial analogue field plotter was very well suited for this model study. It uses a paper coated with a uniform layer of graphite, which is available in two varieties with approximately 10,000 and 1,000 ohms of surface resistivity. It has been found that the low-resistivity paper is best adapted for the purpose.

Desired combinations of electrodes are applied conveniently by covering the affected regions with silver paint and using fast-drying butyl-acetate as a thinner. Because the problem requires only quantitative values of the thermal resistances, there is generally no need to plot the actual field lines in the model study. It is sufficient to measure the electrical resistances with an ohmmeter or to calculate them from current and voltage; see Fig. 1.

Experimental Proof for the Validity of the Method

A simple system with well-known characteristics was set up on the board. It consisted of two circular electrodes and one straight bar, representing two cables buried below the surface of the soil; see Fig. 2. Assume that at first only one cable is loaded and dissipates heat at the constant rate of W watts per centimeter (cm), which keeps the outer diameter of the cable at ΔT degrees above the ambient. The isothermals marked $0.1\Delta T$, $0.2\Delta T$, etc., show the distribution of the intermediate temperatures. Pipe no. 2, similar to pipe no. 1 but not heated, placed at P, will attain the temperature prevalent at this point, i.e., $T_A + 0.3\Delta T$. When pipe no. 2 also becomes a heat source dissipating W watts per cm, superposition of the two heat-flow fields will raise the temperature of no. 2 to $T_A + 0.3\Delta T + \Delta T$, or $1.3\Delta T$ above the ambient (sink). The same applies to no. 1 as it is lying on the $0.3\Delta T$ isotherm of no. 2. This means in effect that the presence at this distance of a second loaded pipe increases the temperature of pipe no. 1 by 30 per cent for an unchanged dissipation from no. 1. In other words it raises the thermal resistance between no. 1 and the surface by a factor 1.30.

If the analogue method is correct, the same ratio should apply to the electrical resistances. This was investigated. The result was a measured ratio between the electrical resistances $S^*/S = 1.32 \pm 0.01$ compared with the theoretical value of 1.30, where

S = resistance from no. 1 or no. 2 to A when only one pipe is dissipating heat W
S^* = resistance from no. 1 or no. 2 to A when both pipes dissipate W

The error is principally caused by the fact that the introduction of a conducting disk at P disturbs the original field distribution around pipe no. 1.

It is conceivable that the left side of the disk 2 which is closest to pipe no. 1 is more active in increasing the effective resistance between A and no. 1 than the right side. In other words, the center of gravity of the influence of the disk is not

Table I. Thermal Resistance Between Cable and Soil Surface in Thermal Ohms (C per Watt) for a 1-Cm Long Portion of the Cable

	NELA	Neher[1,3]	Analogue
For top duct	200	305	316
For center duct	200	336	337
For bottom duct	200	336	336

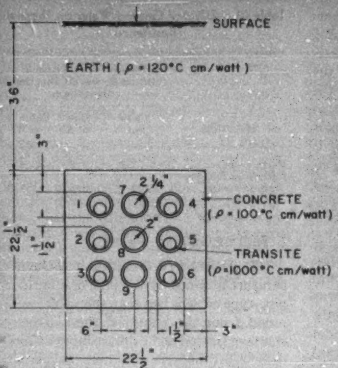

Fig. 3 (left). Duct bank with six loaded cables

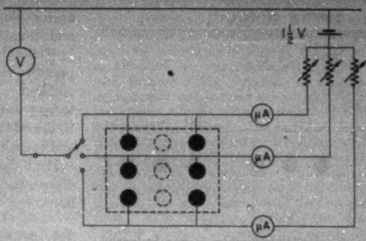

Fig. 4 (right). Electrical diagram. Current return path through graphite paper is not shown. The rheostats are adjusted until the microammeters show equal current. The resistances are calculated from voltage and current readings. If desired, the microammeter can be adjusted to unequal currents, corresponding to uneven loads

P but a point *Q*, closer to pipe no. 1. For example, if *Q* were located as in Fig. 2, the theoretical ratio would be 1.32. This type of discrepancy between theory and experiment would, however, also occur in the case of buried pipe-type cables and does, therefore, not affect the applicability of the method for solving practical problems. Consequently, the error in the use of the analogue is not above 2 to 3 per cent, which is permissible for the solution of cable heat-flow problems. At the same time it was found that edge effects are negligible when the sheet of paper is at least three times as long and three times as wide as the model.

Inhomogeneous Soil

For installations in inhomogeneous soil, the analogue should provide for paper with correspondingly varying resistivity. This is also the case if the cables are in ducts or if there is special backfill.

Although an analogue using an electrolytic tank of adjustable depths would normally be used for problems of this type,[4] the paper technique had proved so convenient for the homogeneous case that it was undertaken to modify it for use in backfill problems. Thus one or more extra sheets of graphite paper were placed on the base sheet, reducing the local resistivity to one-half, one-third, etc., of its original value. To get good contact between the sheets without disturbing the flow pattern unduly, the edges were dotted sparingly with silver paint before the sheets were laid in place.

Applications

CABLES IN DUCT

When plans were being considered for two 115-kv 125-megavolt-ampere (mva) circuits in the Toronto area, one proposal was to place the six single phases in a duct bank, as shown in Fig. 3. In such cases it is usual to apply the National Electronic Light Association (NELA) equation when calculating the current rating of the cables. The NELA equation is based on an average t/r value and does not take into account the local t/r of the soil around the duct, which in the case under consideration was 120 degrees centigrade (C) cm per watt. The concrete t/r was 100 C cm per watt. Application of Neher's equation, which does allow for high soil t/r values, would restrict the cable rating to 100 mva per circuit, where NELA permitted 125 mva. Because of this appreciable difference in capacity resulting from the two calculating methods, the analogue was used to determine which equation was suitable. A model was made with single and double extra sheets representing the duct. Resistances were measured between each cable and the sink with all cables carrying full and equal load; see Fig. 4.

If the base sheet represents a resistivity of 120 C cm per watt, the duct portion consisting of a base sheet plus one extra sheet corresponds to 60 C cm per watt, and with two extra sheets to 40 C cm per watt. As in reality the t/r value of the duct was 100 C cm per watt, the corresponding resistance values were found by interpolation. Table I gives the analogue results and the values computed from the two equations. The good agreement between the Neher values and the analogue values is evident.

EFFECT OF BACKFILL

In a case of a route for two pipe-type cables with localized areas of high t/r, up to 300 C cm per watt, the question arose whether sand backfill extending to 2 feet above cable level would be adequate; see Fig. 5. The Kennelly equation gave for one cable buried in homogeneous soil with a thermal resistivity ρ C cm per watt

$$R=0.48\rho$$

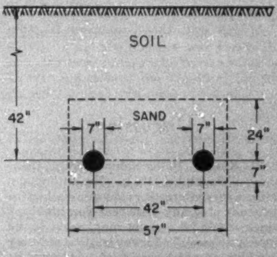

Fig. 5. Two loaded pipes in a rectangular box of sand

Table II. Thermal Resistance Between One Cable and Sink in Thermal Ohms for 1 Cm of Cable

Soil t/r, C Cm per Watt	Without Sand		With Sand 2 Feet Above Cable Level		With Sand Filling Whole Trench	
	R, One Cable Only	R′, Second Cable Loaded Also	R″/R′ Per Cent	R″	R‴/R′ Per Cent	R‴
80	38	49	100	49	100	49
160	77	98	82	80	69	68
240	115	147	68	100	48	71
320	154	196	58	114	37	73

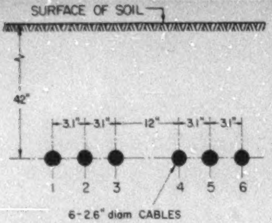

Fig. 6. Six loaded cables in one horizontal plane

where

R = thermal resistance in thermal ohms per cm length between the sheath of the cables and the sink when no other loaded cable is present

The presence of a second cable at the given distance brings R up to

$R' = 1.28R = 0.61\rho$

where

R' = as in the foregoing but with the second cable loaded to the same level as the first one

R'' = as in the foregoing but with both cables surrounded by sand, as indicated in Fig. 5

To evaluate the beneficial effect of the sand ($\rho = 80$ C cm per watt), a model was made and extra sheets of paper corresponding to the sand were placed on the base sheet. One extra sheet corresponded to sand with $\rho = 80$ surrounded with soil of $\rho = 160$; two sheets to sand $\rho = 80$ surrounded with soil $\rho = 240$, etc. Thus it was possible by a series of tests to measure the ratio R''/R in soils of various t/r. The results are given in Table II.

During the investigation it was tried out how much improvement could be obtained by filling the trench with special backfill right to the surface. The difference is apparent in poor soil where the sand acts as a short circuit for the heat flow. See Table II, where R''' represents the resistance to sink in a wholly sand-filled trench.

At full load the dissipation W from each cable amounted to 1.0 watt per cm and, thus, the figures for R, R', and R'', in Table II directly represent the temperature rise of the cable sheath over the ambient. Taking into account that the temperature of the sink may be as high as 25 C and that the rise between conductor and sheath at full load is also 25 C, it is evident that under normal full load conditions the conductor might become too hot.

Six Cables in One Plane

When the installation mentioned in the section entitled "Cables in Duct" was under consideration, the suggestion was made that the six phases be directly buried, as shown in Fig. 6. A model study was made to determine the thermal effect of close spacing.

If the thermal resistance between one single phase—no other phases loaded—and the surface of the soil is standardized at 1 thermal ohm, the resistances for all cables loaded were found between:

cable 1 or 6 and sink:	3.6 thermal ohms
cable 2 or 5	: 3.8 thermal ohms
cable 3 or 4	: 3.8 thermal ohms

From these figures it could be computed that the load-carrying capacity of phases 2, 3, 4, and 5 was only 54 per cent of the full capacity, available when the six conductors were spaced without overlapping heat-flow paths. In other words, the six cables in the given configuration do the work that four conductors of the same size could do if they were spaced sufficiently widely.

These derating factors could also have been computed from the Kennelly equation by superposing the six heat fields. An advantage of the analogue was the use of adjustable electrodes consisting of short copper cylinders mounted on adjustable arms with a small drop of mercury trapped between each electrode and the paper for good contact. In this way it was possible to observe the effects of various spacings and groupings on the resistance. This otherwise would have required many repetitions of the calculation.

Table III. Effect of Ground Water on Thermal Resistance

Heat Sink	Resistance in Thermal Ohms Between Cable and Heat Sink		
	Cable 1 or 6	Cable 2 or 5	Cable 3 or 4
Earth's surface	3.6	3.8	3.8
Earth's surface plus ground water	2.8	2.9	2.9

Effect of Ground Water

It is often observed that the actual temperature attained by the pipe of a buried-pipe-type cable is less than the value computed from the observed thermal constants of the soil and cable, using the Kennelly equation. It has been suggested that this may be caused by the ground water which may be as effective a heat sink as the surface of the earth.

To test this on the analogue another electrode was painted on the paper parallel to the one representing the earth's surface at a distance corresponding to 118-inch depth (about 10 feet of water table). It was connected electrically to the "earth's surface" electrode, thus corresponding to ground water at the same temperature as the earth's surface. The results are shown in Table III. Similar tests for other configurations show that such an additional heat sink is very effective in reducing the thermal resistance with a corresponding increase in the cable rating. Whether or not the ground water acts in this manner must, of course be determined by field tests.

References

1. The Temperature Rise of Buried Cables and Pipes, J. H. Neher. *AIEE Transactions*, vol. 68, pt. I, 1949, pp. 9–21.

2. The Temperature Rise of Cables in a Duct Bank, J. H. Neher. *AIEE Transactions*, vol. 68, pt. I, 1949, pp. 540–49.

3. Control of the Thermal Environment of Buried Cable Systems, L. H. Fink. *AIEE Transactions*, vol. 73, pt. III, Apr. 1954, pp. 406–12.

4. Electrical Analogues, G. Liebmann. *British Journal of Applied Physics*, London, England, vol. 4, July 1953, pp. 190–200.

◆

Discussion

A. H. Kidder (Philadelphia Electric Company, Philadelphia, Pa.): The authors describe a very interesting analogue method for the study of steady-state heat-flow problems which should be a useful supplement to the previously published investigations of Neher and Fink, to which they refer. It should be noted, however, that the method deals exclusively with steady-state rather than transient temperatures. The graphite-coated paper used for constructing their electrical analogy of the steady-state heat flow accurately represents a homogeneous environment. The suggested superposition of the sheets permits a corresponding increase of electrical conductivity when desired to represent approximately the use of some special back-fill, and accordingly modifies certain boundary conditions which would be difficult to evaluate mathematically. The basic principle, however, is that of steady-state heat flow in homogeneous media. The analogy is of course incapable of representing transient effects of variable cable loading, because the distributed capacity effects are not accounted for.

I am quite disturbed, therefore, by the authors' reference to the effect of ground water as an additional heat sink which they seem to think is needed to explain the fact that the actual temperature attained by a buried cable is found to be less than the steady-state value which can be computed by appropriate use of the Kennelly equation. The most likely explanation of the lower temperature attained is that the cable loads are far from constant for the great length of time necessary to achieve the steady-state temperature distribution which the Kennelly formula (see reference 1 of the paper) and their analogue are designed to represent. For ground water to be a heat sink, it must be moving so as to carry the heat away. When the improbability is considered of ground-water flow in sufficient volume to become a heat-sink, it is recognized that the only heat sink which can be counted upon is that of the atmosphere above the surface of the earth, the surface temperature distribution of which would also be modified by the presence of the buried heat source.

When Mr. Neher and I were first confronted with this problem of heat dissipation in earth several years ago, we were handicapped for some time by the generally prevalent but fallacious notion that the so-called deep-isothermal was a heat sink. I have no doubt that the authors' painting another electrode on their graphite-coated paper probably served the purpose of reconciling the analogue readings with an observed cable temperature in some situation. However, this artifice should be understood to represent nothing more than a purely empirical conclusion introduced to compensate for factors not accounted for in their attempted steady-state representation of transient phenomena.

W. A. Sinclair (The Detroit Edison Company, Detroit, Mich.): This excellent paper furnishes us with another tool for solving heat flow problems. Load reduction due to close spacing, the beneficial effect of sand backfill in poor soil, and the influence of ground water are particularly important to those of us concerned with the operation of cable systems.

The application of the analogue to the cables in duct was very interesting. At Detroit Edison we have considered the soil thermal resistivity inherent in the NELA heating constants to be 70 watt-cm units. If the results shown in Table I for the NELA equation had been corrected for the higher value of resistivity, the resultant values should check reasonably well with those given for the Neher equation or the analogue.

The second application of the analogue to the effect of backfill was extremely interesting. At Detroit Edison we have encountered areas of high thermal resistivity up to 200 C cm per watt along the route of one of our 120-kv pipe cable lines. The standard backfill called for 6 inches of yellow bank sand around the pipe. Through a portion of the area in which high thermal resistivity soil was encountered, 1 foot of yellow bank sand around the pipe was used in place of the customary 6 inches. Through the remainder of the high-resistivity area, the elevation of the pipe was lowered 1 foot which brought it nearer to the ground water level. This was an attempt to take advantage of ground water as a heat sink as described by the authors in the fourth application of the analogue. It will be interesting to see how the pipe-operating temperatures through this area compare with those obtained on the balance of the line.

Fig. 4 shows the pipes with 4 inches of sand at the sides and $3^1/_2$ inches below them. It has been common practice to surround the pipe with at least 6 inches of sand for single-pipe installations. In addition we have also filled the trench to the surface on some installations with yellow bank sand. Fig. 1 indicates that the amount of backfill adjacent to the sides and bottom of the pipe would have an important part in determining the thermal resistance of the earth path. It would be helpful if the authors could give us some data in which they considered greater amounts of sand adjacent to the sides and bottom of the pipes than were used for the effect of backfill. This could be a very important area since approximately 50 per cent of the thermal gradient horizontally out from the pipe occurs in the first 6 inches of the earth.

L. H. Fink (Philadelphia Electric Company, Philadelphia, Pa.): The application of the analogue field plotter provides a convenient means for the solution of certain cable heat flow problems which are not suited for the usual mathematical solution based on the Kennelly equation. Such a problem, for instance, is presented when the trench in which a cable system is buried is backfilled with a material of thermal resistivity differing appreciably from that of the surrounding soil. The mathematical difficulty is caused by the fact that since the contour of the backfill material does not conform to the natural isothermal lines to be found in a homogeneous region, the heat field and the flow of heat become distorted, making their mathematical description complicated and impractical. The same sort of difficulty, of course, is encountered in the solution of duct bank problems, but usually the thermal conductivity of the concrete duct bank is close enough to that of the surrounding soil for the difference to be ignored. In any case, it appears that all such problems can now be solved readily and with satisfactory accuracy by the analogue plotter. At the same time, there are cases in which the mathematical approach is still the more convenient. For instance, in the case of severe moisture migration, the resistivity of the soil may perhaps be found to vary inversely with distance from the pipe. Such a continuous variation in resistivity would be difficult to reproduce on the plotter, but Neher (see reference 1 of the paper) has shown how it may be handled readily by equation.

Despite the differences in applicability of the two methods of solution, Kennelly equation and analogue field plotter, they are basically the same, being based on the same thermal-electrical analogy. In the simple case of a uniform soil, where both are equally applicable, their respective results should check closely, and this is seen to be the case in Table I. However, because of this very fact, that the two approaches are fundamentally the same, concurrence of their results is to be expected, and neither approach can be cited as justifying the other or showing its validity.

Another consequence of this underlying identity is that certain idealizing assumptions are common to both. One such assumption is that the surface of the earth is an isothermal, having in effect perfect surface conductivity. Neher (see reference 1 of the paper) has shown that in the usual case, with an undistorted heat field, this assumption is sufficiently close to the fact as to introduce no appreciable error. However, because of the versatility of the analogue device, the authors have been able to treat a case where the error may exceed that computed by Neher. This is the example where the trench is filled to the surface with corrective backfill. As the authors observe, this provides a complete, low-resistance path between the heat source and the ground surface, through which most of the heat will flow. This concentration of heat flow directly above the source may cause the drop due to the surface resistance of the soil to be much greater at that point than at a short distance to either side. Since the analogue plotter, as described in the paper, always maintains an isothermal for the earth surface, its results in this extreme case may not be as valid as in other cases. Perhaps a substance of higher electrical resistivity could be used to simulate the ground surface.

The use of a second ground bar to simulate the effect of a water table acting as a heat sink is interesting. Such an approach would seem justifiable in cases involving a subterranean flow of water carrying off the heat by convection; whether it is permissible in other cases deserves further consideration, especially since, in dealing as we are with steady-state solutions, the thermal capacitance of the water should not be involved.

Finally, a very useful application of the device has been suggested by one of the authors. In reference 3 of the paper a set of curves was presented to show the dimensions of a trench which, when backfilled with material of a given thermal conductivity, would achieve a desired amount of improvement in over-all effective soil conductivity. Being based on the mathematical solution, difficulties of which are outlined in the foregoing, these curves represent trench dimensions conforming at least approximately to the isothermals of the undisturbed heat field and, while valid, they do not represent the most economical solution possible, either with regard to volume of backfill required or to required depth of excavation. The analogue field plotter makes it possible to determine trench dimensions which will result in greater economy of labor and material while providing a given degree of reduction in effective thermal resistance. A series of curves giving such dimensions for typical conditions would be of real value.

In demonstrating the facility and effectiveness with which the analogue field plotter can be applied to cable heat flow problems, the authors have performed a valuable service, and deserve the thanks of the engineers who deal with these problems.

F. H. Buller (General Electric Company, Schenectady, N. Y.): The authors have performed two services in presenting this paper; first, they have demonstrated clearly with examples how difficult heat flow problems, encountered in connection with buried cables, can readily be solved by the proper use of an inexpensive commercial device; and second, they have drawn attention to a device which has many other obvious applications in the study of heat-flow problems,

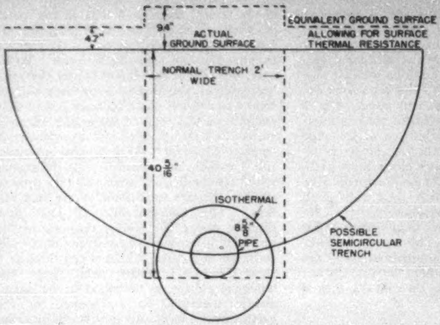

Fig. 7. Buried pipe cable, showing one isothermal and some possible trench arrangements

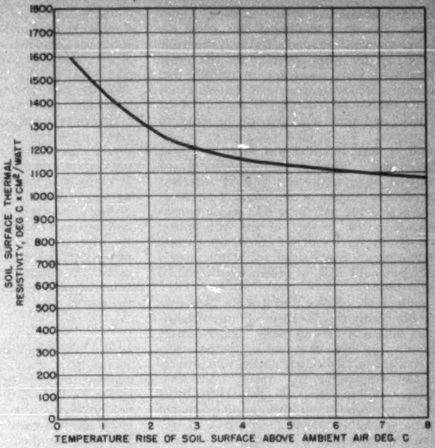

Fig. 8. Surface thermal resistivity of soil based on 32 C ambient air, wind velocity neglected

electrostatic and electromagnetic field problems, etc. It is clear that analogue computers of this character have potentially a wide application in cable practice.

A particularly valuable feature of their approach is the possibility of a detailed study of the effect of environmental modifications in improving buried cable performance. In his discussion Dr. Wiseman has stated that where soil thermal resistivity is excessive it should be reduced to a value of 80 or better by means of such modifications. Schiffreen has pointed out that environmental modifications, while helpful from the standpoint of cable rating, can be very costly. This raises the question as to how far one should go in modifying cable environment and exactly what form the modification should take for best results.

For example, a heat field can be plotted and the material between two adjacent isothermals can be replaced with some other material of, say, half the thermal resistivity of the remainder of the soil. This can be done, for instance, in the case where the "cable" is a pipe of $8^5/_8$-inch outside diameter buried at a depth of 3 feet, and the isothermal in question is the one whose highest point is at a depth of $27^3/_8$ inches below the surface of the ground (see Fig. 7). In this case, a reduction of about 16 per cent in soil thermal resistance may be expected if the soil is homogeneous and the surface thermal resistivity of the soil is negligible.

On the other hand, if a semicircular trench is excavated with its lowest point passing through the pipe center and this trench is backfilled with material having half the thermal resistivity of the surrounding soil, the thermal resistance of the system may be reduced by as much as one third, or $33^1/_3$ per cent.

These results are obtained from rather simple mathematical analyses of the problem. It may not be practical, however, to dig a trench 6 feet wide or to dig cylindrical trenches to match the isothermals of the heat field; nor are these solutions necessarily the best from the economic standpoint. Other solutions, such as backfilling a 2-foot trench with soil of low thermal resistivity, may lead to very difficult mathematical problems, perhaps necessitating important and possibly inexact approximations or, alternatively, tedious and costly numerical analyses in order to get an answer. Such solutions, however, can be very simply and inexpensively obtained with an analogue device such as that used by the authors; several possible solutions can in fact be prepared easily, cheaply, and expeditiously, and the best one selected for actual use.

A question has been raised about the effect of the soil surface thermal resistivity on the validity of these studies. This effect is in general rather slight; with a soil surface thermal resistivity of 1,200 and a soil thermal resistivity of 100, the temperature rise of the pipe mentioned would be increased only about 4 per cent by the effect of surface thermal resistivity. This increment increases as the soil thermal resistivity decreases being about 8 per cent for a soil thermal resistivity of 50.

If the soil is homogeneous and if its surface thermal resistivity is uniform along the entire surface of the soil, a very simple equation is available for evaluating the effect of soil surface thermal resistivity. The effective depth of burial becomes

$$D_{eff} = D + \rho_s/2.54\ \rho_e$$

In this equation, D_{eff} is the effective depth of burial to be used in the Kennelly equation or its variations, in inches; D is the actual depth of burial in inches; ρ_s is the thermal resistivity of the surface of the soil, and ρ_e is the thermal resistivity of the soil in the usual watt cm units. This makes the problem very easy to handle on the analogue computer.

If the pipe is installed at a 3-foot depth and the width of the trench is 2 feet and, further, if the thermal resistivity of the soil is 100 while that of the backfill is 50, and if the surface thermal resistivity of the soil is 1,200, a reasonably good approximation may be obtained on the analogue computer by placing the surface of the soil at a distance of 9.4 inches above the true depth of burial across the width of the trench, and at a distance of 4.7 inches above the true depth of burial for the rest of the soil. Such a surface discontinuity, of course, implies an approximation if the Kennelly equation is used; however, since we are dealing with a rather small correction, the approximation should be a good one.

To simplify the application of the foregoing equation, Fig. 8 has been prepared, giving the calculated value of the surface thermal resistivity of the soil for an air ambient of 32 C and on the assumption of a negligible wind velocity. A change in the air ambient will change these values only slightly, a reduction in the air ambient resulting in an increase in the surface thermal resistivity; if an appreciable wind is present there will be a tendency to reduce to some extent the surface thermal resistivity of the soil. The maximum surface rise (directly over the pipe) will usually be of the order of 3 to 5 C. It is evident from this curve that a surface thermal resistivity value of 1,200 to 1,300 is fairly representative of the surface conditions which will actually be encountered, and that the assumption of a uniform surface thermal resistivity is a reasonable one in view of the small magnitude of the correction involved.

R. J. Wiseman (The Okonite Company, Passaic, N. J.): The paper should be given consideration by engineers who are interested in the dissipation of heat from buried cable systems. Although we assume that the Kennelly equation represents the heat flow from a buried cable, some of us are none too sure that it is correct, in that the measured thermal resistivity of the soil must be modified in order to check measured cable temperatures. This analogue provides a means for a comparison of calculated and measured resistances.

I like very much the section on applications and their findings. What is needed is a comparison of the calculated values of thermal resistance of the various setups and the values found by the authors. Do they check each other's findings or is there a difference that might result in a correction factor for the calculated value? For example, in the subsection "Effect of Backfill," the authors state that the Kennelly equation gives for one cable buried in homogeneous soil a resistance of $R = 0.48\ \rho$. Is this by calculation? If so, what was found by the analogue? If the same value was obtained, then we can have more confidence in the Kennelly equation. If not, what is the correction factor to be used in the log equation to obtain the same value? How does this correction factor compare with the correction factor now used in the log equation? It has been customary in the past to assume a value of thermal resistivity ρ of 180 thermal ohm cm, but we take a value of $2/3\ \rho =$ 120 thermal ohm cm in the log equation. This is still not correct, so values of effective thermal resistivity are taken over the range of $\rho = 80$ to 100 thermal ohm cm, or (0.45 to 0.56) ρ. Is the error due to the equation or to incorrectly measuring the soil thermal resistivity?

In Table I the authors compare the thermal resistance between cable and soil surface for a duct installation. For the Neher equation and the analogue they check very well, but using the NELA duct-heating constants, the thermal resistance is very much lower; in fact, the ratio of the analogue to NELA is 1.58 for the top duct and 1.68 for the center and bottom ducts. The authors are bringing out the fallacy in the duct-heating constants. When these were first set up, they served their purpose very nicely, but since buried cable systems have become of interest, and comparison is made with a duct system, we find that a cable in a duct system, using the NELA heating constants, will carry a greater load than one directly buried. This is because in the case of the duct heating constants, they are set up for various numbers of cables in the duct bank, but do not differentiate among the several possible geometric arrangements of the ducts, the number of active ducts (yet there may be many idle ducts), the depth of burial, and the soil thermal resistivity. It would appear that the authors have taken the duct constant for 6 cables in a duct bank, namely, $6 \times 0.82 = 4.92$ thermal ohms per foot (150 thermal ohms per cm), and for the analogue they use a value of 120 thermal ohm cm for the earth around the duct bank. In Fig. 3 they give the configuration of the duct bank. From it, it is possible to compute the thermal resistance of the duct bank and surroundings, assuming the Kennelly equation to be correct. If it is assumed that 4.92 thermal ohms per foot is correct as per duct-heating constants, this is equivalent to a soil thermal resistivity of about 65 thermal ohm cm. Now, if we take a value of 120 thermal ohm cm in the same equation, we get a value of 8.18 thermal ohms per foot (250 thermal ohms per cm) or a ratio of 1.66 between the two soil conditions, which compares with the ratio of 1.68 obtained by the authors. This shows that it is not correct to use the present duct-heating constants if a comparison is to be made with a buried cable where the latter has a soil surrounding it with a thermal resistivity higher than 65 to 70 thermal ohm cm. To overcome it, we should use the Neher method for obtaining the duct thermal resistance. I hope that some day we will be able to revise the present duct-heating constants based on the Neher method. We are indebted to the authors for showing us that the Neher method does give more accurate values of thermal resistance.

William A. Del Mar (Phelps Dodge Copper Products Corporation, Yonkers, N. Y.): Paper rendered semiconducting by means of graphite or carbon black, has been used for obtaining analogue solutions of electric field problems. In such work errors were found resulting from uneven conductivity of the paper. These were eliminated by testing the paper with voltage applied so as to give equipotential lines, which on uniform paper would give some regular geometric pattern, such as a circle. Sheets which gave distorted patterns were rejected. It would be interesting to know if the authors made any such tests.

When a problem of cable ampacity (i.e., current-carrying capacity) is stated, it is usual to give a certain "ambient temperature" as a starting point.

According to Kennelly's equation, this temperature should be that of the ground at its surface. However, no one lays a thermometer on the ground for this purpose and the given ambient temperature is either that of the air or the ground at cable depth when the cable carries no load.

If the given ambient is that of the air, the thermal resistance from ground to ambient air should be included in the calculation.

If the given ambient is that of the earth at cable depth, it may differ from that at the surface, and presumably it would affect the heat flow from the cable. An extreme case may be imagined where the cable and ambient temperatures are equal but the ground surface much cooler. In that case the cable will have lower ampacity than indicated by the Kennelly equation.

The method used by the authors seems to be adaptable to ascertaining the errors introduced by these two interpretations of ambient temperature, and it is to be hoped that work will be continued along these lines.

R. W. Atkinson (General Cable Corporation, Bayonne, N. J.): The methods and materials used by the authors are well adapted to the solution of thermal flow problems. I have reported a large number of data by a similar method aimed primarily at electrical properties, particularly electrical stress.[1,2] For such a purpose, the materials used by these authors would probably present a problem because of lack of complete uniformity in resistivity. It is to be supposed, however, that the graphite-coated paper is completely adequate for the thermal analogue since gradients are not of direct consequence.

In their analysis the authors have treated the earth surface as an isothermal. To do this is not entirely correct as it may be observed where loaded cable circuits pass under a snow covered area. The snow is promptly melted in the area above the cables in weather which leaves the snow in place elsewhere. The method used by the authors may, fairly readily, be modified to take into account the gradient at the earth's surface and to allow for it.

The authors have made measurements to determine the effect on thermal resistance of a buried cable system if there is a "thermal sink," an isothermal surface below the cables unaffected in temperature by the heat from the cable system. The authors have not taken a position in advocacy of the theory but have merely evaluated it. My criticism of the theory is thus not a criticism of this paper. The isothermal surface below the surface remains isothermal only if it is not significantly affected by the heat flowing into and through it. It is very easy to conclude from temperature measurements made on loaded underground cables that there is such a sink because the enormous thermal storage capacity will introduce a time lag of weeks into the system. For measurements made in shorter time than this, the behavior will be as though there were such a "sink" as has been postulated. It seems likely to me that most of the experimental basis for the "sink" theory has resulted from this fact. It seems desirable to point out, however, that the method of these authors can also be used, with slight additions, to investigate the ultimate equilibrium point that will be reached when all of the thermal transfer is by conduction. However, to determine whether movement of underground water may be a significant factor would seem to require actual measurements made with buried heat sources and temperature measurements.

REFERENCES

1. THE DIELECTRIC FIELD IN AN ELECTRIC POWER CABLE, R. W. Atkinson. *AIEE Transactions*, vol. 38, pt. II, 1919, pp. 971–1016.

2. DIELECTRIC FIELD IN AN ELECTRIC POWER CABLE—II, R. W. Atkinson. *AIEE Transactions*, vol. 43, 1924, pp. 966–81.

E. de Haas, P. J. Sandiford, and A. W. W. Cameron: We are pleased that the paper has stimulated so much discussion on this timely subject.

We believe that the Kennelly equation is fundamentally exact, because it has been derived analytically from the basic Laplace equation for heat flow. The reason for some of the difference of opinion, as Mr. Kidder remarked, may be that the steady state is not reached for a considerable time after the cable has been loaded. Indeed, the very last portion of the temperature rise may occur only after some months from the initial loading.

We agree with Mr. Sinclair that the verification afterwards of temperatures on buried cables in correlation with the load would be very instructive. We plan to extend the model studies to larger amounts of backfill around the pipes or cables.

Mr. Fink mentions backfill economy. We have been trying to find the solution to the problem discussed in his paper[1] about the right amount of backfill to be placed around cables, but through a shortage of technical help we have not had a chance to do so.

Mr. Fink's remark regarding the surface resistance of the soil is best answered by Mr. Buller's discussion. We wish to thank the latter for his suggestions, which will make the analogue method more accurate in the case of extra backfill.

In answering Dr. Wiseman, we would say that the model studies cannot prove the truth of the Kennelly equation. As Mr. Fink remarks, the model applies the equation to more involved problems than can be solved analytically. We agree with Dr. Wiseman that the accepted present thermal resistivity values result in cables running much below the design temperature.

We thank Mr. Del Mar for his suggestion on testing the uniformity of the paper. So far, our tests have shown that the errors are smaller than 3 per cent.

The ambient temperature should be the annual maximum temperature of the ground at cable depth when the cable carries no load.

It is true, as several discussers have remarked that the NELA equation can give proper results, but this applies at only one thermal resistivity value, namely about 65 thermal ohm cm.

Mr. Kidder and Mr. Atkinson touch on the subject of heat sinks other than the surface of the soil. In the paper we have mentioned only that an analogue study can be used to evaluate the effect of such heat sinks, in case they exist. At present we think that there are not enough factors known one way or the other to enable us to discuss this point. However, the matter is well worth further theoretical and experimental study. Some field work is planned along a cable route close to Lake Ontario, where chances are good that the water table is only a few feet below the level of the cable. Geological observations have shown that in some cases the water can run perpendicularly to the cable with a speed of a few feet per day. In this case it would contribute significantly to heat removal.

In continuance of our program of model studies we have made a comparison between the observed values in the 6-cable problem (the third application in the paper) and a theoretical study, based on the principle of superposition. Agreement to within 3 per cent was reached.

Reference

1. Control of the Thermal Environment of Buried Cable Systems, L. H. Fink. *AIEE Transactions*, vol. 73, pt. III, April 1954, pp. 406–12.

Transfer of Steam-Electric Generating-Station Auxiliary Busses

D. G. LEWIS
ASSOCIATE MEMBER AIEE

W. D. MARSH
ASSOCIATE MEMBER AIEE

IN RECENT years there has been increased interest in methods of transferring steam-station auxiliary busses between normal and emergency sources. The problem has become more critical with increasing unit generator size and advancing steam conditions because of the larger motors which have slower voltage-decay characteristics and the larger auxiliary systems which generally tend toward poorer voltage regulation under bus-transfer conditions. There have been several published reports of tests made which show how voltages, currents, and speeds may vary during transfer on specific systems.[1,2] It is the purpose of this paper to discuss more generally the various kinds of bus transfer and to present a method by which it is possible to predict approximately the performance of a system under interrupted-circuit transfer conditions.

Kinds of Bus Transfers

Bus-Transfer Conditions

The large majority of modern generating stations are designed on the unit system, with two auxiliary power sources. Usually the normal source is associated with the main generating, unit as a transformer connected to the generator leads, or a main shaft-driven auxiliary generator. The second source is usually from the system, and provides power for starting up as well as for emergency conditions. It is necessary, then, to recognize two kinds of transfer between these sources: the routine transfer, made when the generating unit is started up or shutdown; and the emergency transfer, made upon failure of the normal source to provide power at adequate voltage. These two kinds of transfer have different requirements and, frequently different methods are used.

Method of Bus Transfer

Three methods of transfer may be used, characterized by the sequence and timing of operation of the source circuit breakers:

1. Continuous-circuit or paralleled transfer.
2. Interrupted-circuit transfer where there is no intentional delay between tripping the primary source circuit breaker and closing the secondary source breaker.
3. Interrupted-circuit transfer where the closing of the secondary source breaker is deliberately delayed after the primary source breaker is tripped.

Criteria for Successful Bus Transfer

The criteria for successful bus transfer are:

1. That no component of the auxiliary system shall be subjected unnecessarily to excessive duty as a result of the transfer.
2. That the performance of the auxiliary system shall be such as to permit continuous output of the main generating unit or to maintain adequate control for safe shutdown.

The most critical equipment under the first criterion is the motors which may be severely stressed by high inrush currents which can result from a nondelayed interrupted-circuit transfer. This indicates the use of a continuous-circuit transfer method; or if an interrupted-circuit transfer must be used, delay to the point where the bus residual voltage has decayed to a low enough value to prevent excessive inrush currents. In terms of bus transfer conditions, the routine cases should be done by the continuous-circuit method, the emergency case by the delayed interrupted-circuit transfer method.

Under the second criterion, the output or control of the generating unit is best assured by continuous-circuit transfer. This is feasible for the routine case in most station designs; but, where there can be a large phase difference between sources, it may not be possible to parallel them and an interrupted-circuit transfer is required. In any design, an interrupted-circuit transfer is necessary for the emergency case, and the second criterion suggests that the shorter the delay, or dead time, the better.

It is apparent that for the routine case a continuous-circuit transfer best satisfies both criteria; and unless, as previously mentioned, other factors prevent its application, it is the logical choice. But for the emergency case, the requirements of motor duty and boiler operation are in opposition, and the effect of the alternate transfer methods must be evaluated before a choice can be made.

Motor Duty

The effect of interrupted-circuit transfer on motor duty may be stated approximately in terms of the residual motor

---

Paper 55-96, recommended by the AIEE Power Generation Committee and approved by the AIEE Committee on Technical Operations for presentation at the AIEE Winter General Meeting, New York, N. Y., January 31–February 4, 1955. Manuscript submitted October 21, 1954; made available for printing November 18, 1954.

D. G. Lewis and W. D. Marsh are with the General Electric Company, Schenectady, N. Y.

Table I. Motor Constants for a 4,160-Volt Bus of a Typical Large, High-Pressure, High-Temperature Generating Unit

Motor	Type	No. of Motors	Horsepower	Kilovolt-Amperes	x	Open-Circuit Time Constant	Short-Circuit Time Constant	H
1	Boiler feed pump	2	2,500	2,160	0.16	3.6	0.12	2.5
2	Induced draft fan	2	1,250	1,140	0.16	1.0	0.058	10.0
3	Forced draft fan	2	600	530	0.16	1.25	0.048	4.5
4	Pulverizer and fan	5	300	280	0.16	0.5	0.037	7.5
5	Condensate pump	2	450	400	0.16	1.2	0.041	0.8
6	Service water pump	1	300	270	0.16	1.2	0.037	0.8
7	Circulating water pump	2	400	370	0.16	0.75	0.04	0.8
8	480-volt transformer	2		1,000	0.16*	0.5*	0.025*	1.0*
9	480-volt transformer	1		750	0.16*	0.5*	0.025*	1.0*

The values of x and H are in per unit on the individual motor kilovolt-ampere base; the time constants are in seconds. For the study of reacceleration, the secondary source is assumed to be a 12,500-kva transformer, with impedance on its own kilovolt-ampere base of 0.055 per unit.

* These values are assumed so that the transformers and their loads can be treated as equivalent motors in the calculation.

Table II. Motor Constants for Equivalent Motors Formed by Lumping Motors of Table I

Motor	Horsepower	Kilovolt-Amperes	x	Open-Circuit Time Constant	Short-Circuit Time Constant	H
1	5,000	4,320	0.505	3.6	0.12	0.685
2, 4	4,000	3,680	0.592	0.81	0.05	2.03
3	1,200	1,060	2.06	1.25	0.048	0.296
5–9	5,700	4,560	0.590	0.705	0.031	0.249

Values of x and H are in per unit on a base equal to the sum of the motor kilovolt-ampere ratings (13,620 kva).

voltage existing at the time the secondary source circuit breaker is closed. Experience has shown that if this voltage is 25 per cent of the rated voltage, or less, the inrush-current magnitude will be low enough to avoid excessive stresses on the windings. Motors of different voltage, speed, and horsepower rating vary in their ability to withstand winding stresses; but this rule is adequate to protect the most critical motors normally found on steam-station auxiliary busses.

BOILER OUTPUT AND CONTROL

The effect of interrupted-circuit transfer on boiler output and control is primarily a question of the speed-time relationships of the essential auxiliaries during the transfer. No attempt will be made to define limits of auxiliary speed and time for successful operation, because they vary widely with different boiler and boiler auxiliary designs, steam conditions, and types of fuel. But it should be possible to determine, for any particular station design, what auxiliary is limiting (pulverizer, draft fan, or boiler feed pump), at what minimum speed, and for what maximum time it may be allowed to operate without adversely affecting boiler operation. In many cases it will be possible by proper design and selection of auxiliaries to minimize the effect of reduced speed during transfer.

SELECTION OF BUS-TRANSFER METHODS

The most direct and practical way of protecting motors against excessive duty during interrupted-circuit transfer is to use an undervoltage relay on the motor bus to block closure of the secondary source circuit breaker until residual voltage has decayed to 25 per cent of normal. To predict the effect of this delay on boiler operation, however, it is necessary to know the time required for voltage decay, and the speeds of the auxiliaries during the dead time. It is also necessary to know the time required for reacceleration of the auxiliaries after the secondary source voltage has been applied. Approximate methods of determining these speeds and times as well as expressions for the transient torques and currents in the motors are presented later in the paper.

When, in the emergency case, it is determined that the speeds and times involved in a delayed interrupted-circuit transfer will not assure adequate boiler output or control, it may be necessary to resort to a nondelayed transfer. Where such transfers are truly emergency automatic operations occurring only rarely, experience indicates that motors can be expected to give reasonable service.

However, for the routine case, where it may not be possible to parallel sources, a nondelayed interrupted-circuit transfer should not be used. The frequency of transfer in the routine case would damage motor windings in a very short time. Since this transfer can be planned for times when loads are light, the use of delayed transfer will not ordinarily jeopardize boiler functions.

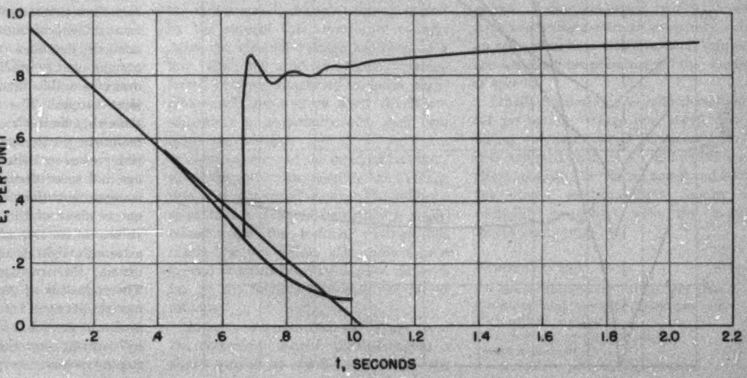

Fig. 1. Bus residual voltage decay and recovery. Motor constants given in Table II. Straight-line decay is calculated using curves of Fig. 4

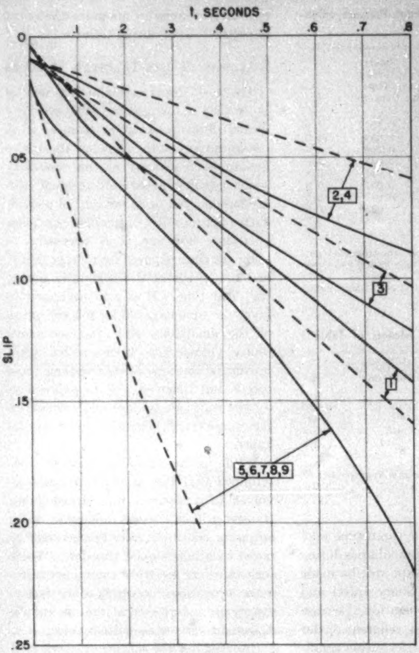

Fig. 2 (left). Motor speed decays. Primary source voltage removed at t=0. Motor constants given in Table II. Dotted curves show speed decays which would occur if motors were separately open-circuited

Fig. 3 (below). Motor speed recovery. Secondary source connected at t=0.667 second. Motor constants given in Table II

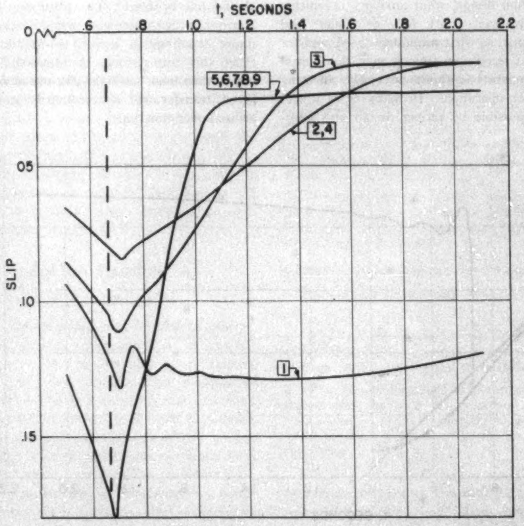

Discussion of Results

The basis for the results shown in the paper and the approximate methods which are suggested in the section entitled "Analysis" consist of a number of step-by-step calculations made using the equations of Appendix II. The calculations were made with an International Business Machines card programmed calculator, and they include a number of runs involving two, three, and four induction motors. As a starting point, typical machine constants for the auxiliaries associated with a large, high-temperature high-pressure unit were selected, as shown in Table I. The machines on this bus were then lumped into four equivalent machines, as shown in Table II.

Fig. 1 shows the decay of the magnitude of the bus residual voltage obtained from the step-by-step calculation for this case as well as a straight-line approximation obtained by using the curves of Fig. 4. Also shown in Fig. 1 is the magnitude of the bus voltage following reapplication of a secondary source at $t=0.667$ second.

Fig. 2 shows the decay in speed of the four lumped motors of Table II. Also shown are the speed decays which each of these motors would experience if they were open-circuited. This figure shows the tendency to synchronize which is maintained until the residual voltage has decayed to about 25 per cent of rated value. Fig. 3 shows the speeds of the four lumped motors following reapplication of secondary source voltage at $t=0.667$ second.

A large number of additional calculations have been made involving two and three machines. It seems reasonable that the quantities of interest, voltage, and speed decay should follow a pattern depending on certain fundamental parameters characteristic of a particular arrangement of motors. The following analysis describes the methods which may be used to predict voltage and speed decay as well as inrush current and transient torque. The analysis considers a somewhat limited range of parameters to make the predictions as accurate as possible; even so, estimates of rates of voltage and speed decay must be considered as approximations. In cases in which one or more of the motors has extreme values in its list of constants, such as extremely light load or unusually high inertia, the error may be appreciable. The equations of Appendix II give correct results even for extreme cases, so it is always possible to evaluate a situation by carrying out the complete step-by-step procedure.

Analysis

Physical Considerations

The study of bus transfer of a group of dissimilar auxiliary induction motors logically divides itself into the analysis of four periods of time:

1. The steady-state period preceding the removal of the primary source.

2. The first part of the dead time when the residual voltage is appreciable.

3. The secondary part of the dead time after the residual voltage has decayed to a negligible value.

4. The reacceleration period following the connection of the secondary source.

There is no sharp distinction between the first and second part of the dead time, since the decay of residual voltage is gradual. It is convenient, however, to analyze the two periods separately because, after the residual voltage has reached about 25 per cent of its rated value, further energy transfer between machines is negligible. In the second part of the dead time each motor can be treated separately, thus making the calculation of individual motor speeds much simpler than in the first part when the motors must be treated as a group.

The transformer feeding the auxiliary bus will normally be selected so that in the steady state prior to transfer the motor terminal voltage will have its rated value. Calculation of motor currents and slip in the steady state can be made using the familiar equivalent circuit; this calculation will not be discussed.

At the time of interruption each of the motors has a certain amount of stored energy: mechanical energy stored in the inertia of motor and load, and electromagnetic energy stored in the magnetic field. Quantitatively, the stored mechanical energy predominates; the electromagnetic energy in per unit is of the order of the current squared times the short-circuit reactance, while the mechanical energy is equal to the per-unit inertia constant of the machine. With no external source, the machines decelerate as their stored mechanical energy is used to supply the load. If all the motors and loads are identical, electrically and mechanically, they will decelerate at identical rates. No current will flow in the stator circuits, since each motor will see at its terminals a voltage equal to its own generated electromotive force (emf). This condition is just as if each motor were open-circuited. The speed decays at a rate determined solely by the load and the inertia of motor and load. The rotor flux decays exponentially according to the open-circuit time constant, and the residual voltage decays as the product of the rotor flux and the speed.

If the motors on the bus are not identical, the situation is altogether different. A motor with inertia greater than the average will decelerate more slowly and, as long as its rotor flux remains appreciable, it will act as an induction generator supplying energy to other motors having inertias smaller than the average. The effect of this energy transfer between machines is threefold:

1. The motors tend to synchronize; high-inertia motors are pulled down in speed as they supply energy to low-inertia machines.

2. The bus residual voltage decays at a rate faster than in the open-circuit case; the higher rotor currents caused by energy transfer between machines dissipate the magnetic energy in the rotors more rapidly.

3. The bus residual voltage and the individual motor fluxes all decay at very nearly the same rate. Any machine in which the flux tends to decay more rapidly than the average will receive excitation from the other machines.

There is a very short period of adjustment, about 3 cycles, immediately after the removal of the primary source. Initially, the bus frequency drops to a value corresponding to the average of the motor speeds, and then the angle of the bus voltage shifts behind the angle of the rotor flux in the high-inertia machines so that these machines supply electric torque to the low-inertia machines. This period of readjustment is included in the first part of the dead time.

After the short period of readjustment, the bus residual voltage and the motor fluxes decay at nearly equal rates. While the residual voltage is still appreciable, there is energy transfer from high-inertia machines to low-inertia machines, and the motor speeds decay at rates dictated by the rate of this transfer of energy. After the residual voltage has reached a low value, the amount of energy transferred between machines becomes negligible and the motors then decelerate separately in accordance with their own loads and inertias.

The frequency of the residual bus voltage decays at a rate equal to the average rate of motor speed decay. Calculations show that a common frequency is maintained until the residual voltage has reached a low value, after which time several frequencies may appear, depending on the relative speeds of the larger motors.

After the reapplication of voltage from the secondary source, there is again a short period of readjustment as the motor fluxes shift to positions behind the angle of the bus voltage. After this period, the motors will accelerate or continue to decelerate depending upon the bus voltage and the individual motor load characteristic. Since the motor terminal voltage will be appreciably less than its rated value because of the high motor currents, some of the motors may not develop sufficient electric torque to overcome load torque at their particular speeds. This condition may change as the less heavily loaded motors reach steady-state speed and their currents decrease to steady-state values. On the other hand, if the secondary source reactance is too high, large, low-resistance motors may not reaccelerate even after all other motors have reached steady-state speed.

Assumptions

The analysis from which the results presented in this paper are obtained is based on fundamental assumptions regarding the description of an induction machine. They are the same assumptions used by Stanley:[3]

1. Balanced rotor and stator windings are assumed.

2. It is assumed that the coefficient of mutual inductance between any stator winding and any rotor winding is a cosinusoidal function of the electrical angle between the axes of the two windings.

3. It is assumed that the rotor is smooth and that the self-inductances of all windings are independent of rotor position.

4. The effects of saturation, hysteresis, and eddy currents are neglected.

It is further assumed in the analysis that stator losses and d-c transients in the stators can be neglected, in so far as their effect on net electric torque is concerned. Appendix I contains a derivation of simplified motor equations which result from neglecting d-c stator transients. As an approximation, all motor load torques are assumed proportional to the square of speed.

Finally, in deriving simplified methods for predicting voltage and speed decay during the first part of the dead period, it is assumed that, in an induction machine operating near rated speed and load, the stored electromagnetic energy is negligible compared with the stored mechanical energy.

Nomenclature

a = motor horsepower rating, per unit
b = motor load, on motor base, per unit
e = terminal voltage
f = frequency, cycles per second
i = rotor current
p = derivative with respect to time

r = resistance of each equivalent rotor winding
s = slip
t = time, seconds
x = locked-rotor reactance
E = motor bus voltage
E' = voltage back of external reactance
H = inertia constant
I = stator current
I' = transient value of stator current
I_c = value read from the curve based on unit voltage
L = inductance
M = mutual inductance
R = resistance of each stator winding
T = time constant
T_{eff} = effective mechanical time constant
ΔT = measure of mechanical dissimilarity* between the motors
T_e = electric torque
T_m = load torque
θ = rotor position
Ψ = stator flux linkages
ψ = rotor flux linkages
Δ = difference

Subscripts

1, 2, 3 = phase arranged in order of rotor rotation
a, b, c = same as 1, 2, 3
$\alpha, \beta, 0$ = transformed components
r = rotor
s = stator
0 = at time zero
T = total
A = average
C = read from curve
e = external

All quantities, unless otherwise specified, are expressed in per unit on a base common to all machines. A convenient base is the total rated kilovolt-amperes of the motors on the bus. Weighted averages are used at several points in the analysis. It is necessary to give some consideration to the method of weighting to obtain the best estimate of the physical situation. In calculating the quantity ΔT, the per-unit motor load ab is used as a weighting factor. On the other hand, in calculating the bus average x/r ratio, it is felt that the best estimate will be obtained by using the per-unit motor rating a as a weighting factor.

BUS RESIDUAL VOLTAGE

It was pointed out earlier that if all the motors and loads on the bus are identical, each will act as if it were open-circuited, and the bus voltage will decay in accordance with the machines' open-circuit time constant. Complete step-by-step calculations of motor behavior during the dead period show that with dissimilar machines on the bus:

1. The rate of voltage decay is more rapid than the product of motor speed and an exponential decay based on the open-circuit time constant.
2. The bus residual voltage and the motor fluxes all decay at nearly the same rate.
3. The rate of voltage decay is greatest for motor combinations with the most pronounced mechanical dissimilarities.
4. If the postswitching value of residual voltage is taken as a starting point, the decay can be fairly well approximated by a straight line down to about 25 per cent of the rated voltage.
5. For combinations having the same degree of mechanical dissimilarity, the decay is roughly proportional to the average x/r ratio of the motors.

These observations lead to the conclusion that the voltage decay during the first part of the dead period can be calculated by assuming a straight line starting at the postswitching value of voltage. This postswitching value of voltage can be found with satisfactory accuracy by assuming all the motors to be lumped as one equivalent motor having average electrical characteristics, and calculating the back emf of this equivalent motor from the simple steady-state equivalent circuit. The slope of the straight line is related to the average x/r of the motors and to the degree of mechanical dissimilarity. To evaluate the relationship which exists, it is necessary to establish a measure of the mechanical dissimilarity.

If a motor decelerates with no electric torque present, its slip at any time is given by

$$s = s_0 + \frac{1}{4\pi f H}\int T_m dt \tag{1}$$

It is assumed that

$$T_m = ab(1-s)^2 \tag{2}$$

therefore

$$s = s_0 + \frac{ab}{4\pi f H}\int (1-s)^2 dt \tag{3}$$

Differentiating and separating the variables

$$t = \frac{4\pi f H}{ab}\left(\frac{1}{1-s} - \frac{1}{1-s_0}\right)$$
$$= 4\pi f T\left(\frac{1}{1-s} - \frac{1}{1-s_0}\right) \tag{4}$$

With this equation the speed decay for a single motor acting alone can be calculated. It can be seen that the significant mechanical parameter is the ratio $H/ab = T$, having the dimensions of seconds. If the load torque were directly proportional to speed, this ratio would appear in the speed equation as a time constant in the familiar sense.

In general, all of the motors on the bus will have different T ratios. Since all the H's and all the a's are expressed in per unit on a common base, it is correct to say that the ratio $[H_T/(ab)_T] = T_A$ is the mechanical parameter which expresses the central tendency or average of the bus.

Now suppose that all the motors on the bus are assigned new electrical parameters such that all motors are electrically identical with the bus average. Since all the motor fluxes decay at nearly the same rate, this step is justified. Suppose further that all the motors with T greater than T_A are lumped into one equivalent motor having $(T-T_A)$ equal to the mean $(T-T_A)$ of the individual motors; a second equivalent motor is assigned (T_A-T) equal to the mean (T_A-T) of the motors with T less than T_A. Step-by-step calculations show that this hypothetical combination of equivalent motors gives approximately the same rate of voltage decay as the combination from which the equivalents are derived. This fact provides a measure of the mechanical dissimilarity or dispersion of mechanical parameter about the average. Define the quantity ΔT

$$\Delta T = \frac{\Sigma(T_i - T_A)(a_i b_i)}{(ab)_T} \tag{5}$$

In other words, ΔT is the weighted average of the absolute magnitudes of the $(T-T_A)$ values for all the motors.

Fig. 4 shows the relationship between the bus average x/r ratio, the ratio $\Delta T/T_A$, the ratio of total load $(ab)_T$ to total rating a_T, and the slope of the straight-line approximation to the emf decay. These curves were plotted using data obtained in a step-by-step calculation as described in Appendix II.

SPEED DECAY

It is pointed out earlier that there is a very short period of readjustment following the removal of primary source voltage, followed by a period during which the individual motors tend to synchronize because of the energy transfer between high- and low-inertia machines. During both these periods, which together constitute the first part of the dead period, the individual motor speeds can be fairly well approximated by curves of the form given by equation 4, with T replaced by T_{eff} For any motor, T_{eff} will depend on the motor T, the bus average, T_A, and the bus average x/r ratio. Values of T_{eff} can be found from Fig. 5, which relates the rato T/T_{eff} to the quantities T/T_A and bus average x/r. The speed decay based on T_{eff} holds until the bus residual voltage has reached about 25 per cent of rated value. After this time, the motors act independently, and the actual motor T must be used in equation 4.

TIME FOR MOTOR REACCELERATION

Since the rates of acceleration after the reapplication of voltage are relatively

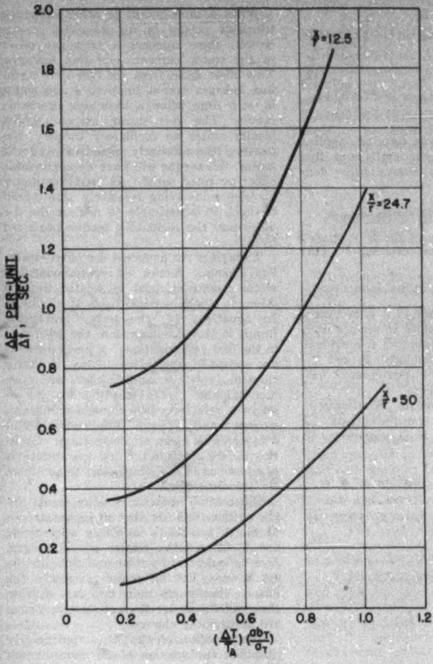

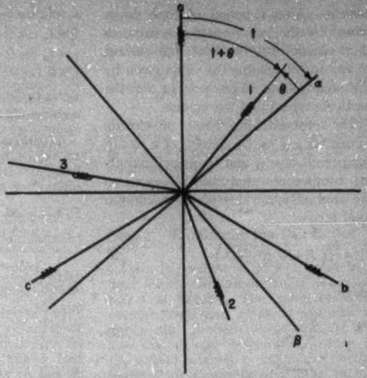

Fig. 4 (left). Correlation of calculated data. Straight-line approximation to voltage decay as a function of the parameters $(\Delta T/T_A)(ab)_T/a_T$ and (x/r)

Fig. 5 (lower left). Correlation of calculated data. (T/T_{eff}) as a function of (T/T_A). T_{eff} is effective time constant of motor speed decay

Curve a—$x/r=50$
Curve b—$x/r=24.7$
Curve c—$x/r=12.5$

Fig. 6 (above). Co-ordinate axes used to derive motor equations. The α and β axes are rotating at synchronous speed in the direction of rotor rotation

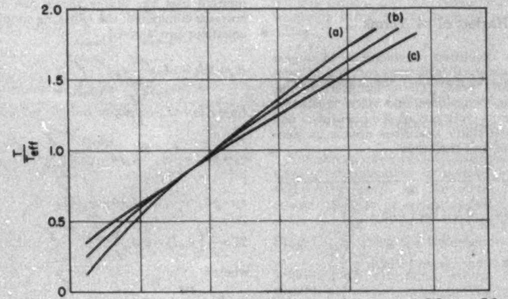

slow and since there is little exchange of energy between motors during this period, it is sufficient to analyze the speed recovery with a step-by-step calculation based on the individual motors' speed-torque and speed-current curves. In fact, such a calculation should be better than one based on the equations of Appendix II, because motor reacceleration at low terminal voltages is sensitive to differences between the idealized speed-torque curve and the actual speed-torque curve which accounts for the effects of variation of rotor resistance with frequency.

All the motors must be considered at once for the reduced bus voltage to be calculated correctly; however, similar motors may be lumped together using the method of Appendix III, so that the final number of motors to be considered may be as small as three or four. Also, as an approximation, phase differences between the various motor currents can be disregarded. The time interval associated with this step-by-step calculation can be fairly long, say 0.25 second, provided a sufficient accurate method of numerical integration is used. A suggested procedure is given in Appendix IV.

INRUSH CURRENTS AND TRANSIENT TORQUES

Appendix V gives as the expected magnitude of the inrush current (fully offset)

$$I'=\frac{\Delta E}{x} \tag{6}$$

In the worst case, ΔE is equal to the sum of the magnitudes of the preswitching bus residual voltage and the postswitching bus voltage. Then

$$I'=\frac{E_0+E'}{x\left(1+x_e\sum\frac{1}{x}\right)} \tag{7}$$

Equation 7 gives the transient value of

current. After a period of time determined by the bus average x/r ratio, or short-circuit time constant, the current to any motor reaches the value given by the steady-state characteristics for the particular speed and bus voltage.

The postswitching value of electric torque for any motor consists of a steady component plus a unit-frequency pulsating component. Appendix V gives as the approximate value of the maximum total torque

$$T_e'=\frac{E_0}{x}\left(E+\sqrt{E^2+E_0^2}\right) \tag{8}$$

where

$$E=\frac{E'}{1+x_e\sum\frac{1}{x}} \tag{9}$$

Appendix I. The Equations of the Induction Motor Referred to Synchronously Rotating Axes

Under the first four assumptions of the analysis and with reference to Fig. 6, the fundamental stator and rotor emf equations are written as follows

Stator

$$e_a=p\psi_a+Ri_a$$
$$e_b=p\psi_b+Ri_b$$
$$e_c=p\psi_c+Ri_c$$

Rotor

$$e_1=p\psi_1+ri_1=0$$
$$e_2=p\psi_2+ri_2=0$$
$$e_3=p\psi_3+ri_3=0 \tag{10}$$

In Fig. 6, the α and β axes are rotating in the direction of rotor rotation at unit or synchronous speed such that the positive α axis coincides with the center of the positive a-phase winding at time zero.

The winding self- and mutual per-unit inductances are defined by the following flux-linkage equations

$$\psi_a=L_s'i_a+M_s'(i_b+i_c)+M'\left[i_1\cos(t+\theta)+i_2\cos\left(t+\theta+\frac{2\pi}{3}\right)+i_3\cos\left(t+\theta-\frac{2\pi}{3}\right)\right]$$
$$\psi_b=L_s'i_b+M_s'(i_c+i_a)+M'\left[i_1\cos\left(t+\theta-\frac{2\pi}{3}\right)+i_2\cos(t+\theta)+i_3\cos\left(t+\theta+\frac{2\pi}{3}\right)\right]$$
$$\psi_c=L_s'i_c+M_s'(i_a+i_b)+M'\left[i_1\cos\left(t+\theta+\frac{2\pi}{3}\right)+i_2\cos\left(t+\theta-\frac{2\pi}{3}\right)+i_3\cos(t+\theta)\right] \tag{11}$$
$$\psi_1=L_r'i_1+M_r'(i_2+i_3)+M'\left[i_a\cos(t+\theta)+i_b\cos\left(t+\theta-\frac{2\pi}{3}\right)+i_c\cos\left(t+\theta+\frac{2\pi}{3}\right)\right]$$
$$\psi_2=L_r'i_2+M_r'(i_3+i_1)+M'\left[i_a\cos\left(t+\theta+\frac{2\pi}{3}\right)+i_b\cos(t+\theta)+i_c\cos\left(t+\theta-\frac{2\pi}{3}\right)\right]$$
$$\psi_3=L_r'i_3+M_r'(i_1+i_2)+M'\left[i_a\cos\left(t+\theta-\frac{2\pi}{3}\right)+i_b\cos\left(t+\theta+\frac{2\pi}{3}\right)+i_c\cos(t+\theta)\right]$$

The quantities in equations 10 and 11 can be referred to the α and β axes by means of the following transformation[4]

$$i_a=I_\alpha\cos t-I_\beta\sin t+I_0$$
$$i_b=I_\alpha\cos(t-2\pi/3)-I_\beta\sin(t-2\pi/3)+I_0$$
$$i_c=I_\alpha\cos(t+2\pi/3)-I_\beta\sin(t+2\pi/3)+I_0$$
$$i_1=i_\alpha\cos\theta+i_\beta\sin\theta+i_0 \tag{12}$$
$$i_2=i_\alpha\cos(\theta+2\pi/3)+i_\beta\sin(\theta+2\pi/3)+i_0$$
$$i_3=i_\alpha\cos(\theta+2\pi/3)+i_\beta\sin(\theta+2\pi/3)+i_0$$

Equations of the same form are applied to the stator and rotor emf's and flux linkages. In addition, the following definitions are made

$$L_s=L_s'-M_s'=\text{apparent stator self-inductance}$$
$$L_r=L_r'-M_r'=\text{apparent rotor self-inductance} \tag{13}$$
$$M=3/2M'=\text{apparent mutual inductance}$$

In the transformations 12 it is necessary to define six new variables to replace each six original variables; however, it is evident that I_0 and i_0 (and similarly Ψ_0 and ψ_0, E_0 and e_0) vanish if the restriction of balanced operation is applied.

Substituting the currents, flux linkages, and voltages from transformations 12 and the inductances from equations 13 into equations 10 and 11

$$E_\alpha=p\Psi_\alpha+RI_\alpha-\Psi_\beta \qquad \Psi_\alpha=L_sI_\alpha+Mi_\alpha$$
$$E_\beta=p\Psi_\beta+RI_\beta+\Psi_\alpha \qquad \Psi_\beta=L_sI_\beta+Mi_\beta$$
$$E_0=p\Psi_0+RI_0 \qquad \Psi_0=(L_s'+2M_s')I_0$$
$$\tag{14}$$
$$e_\alpha=p\psi_\alpha+ri_\alpha+\psi_\beta p\theta=0 \qquad \psi_\alpha=L_ri_\alpha+MI_\alpha$$
$$e_\beta=p\psi_\beta+ri_\beta-\psi_\alpha p\theta=0 \qquad \psi_\beta=L_ri_\beta+MI_\alpha$$
$$e_0=p\psi_0+ri_0=0 \qquad \psi_0=(L_r'-2M_r')i_0$$

The electric torque is given by the following[5]

$$T_e=\psi_\beta i_\alpha-\psi_\alpha i_\beta$$

The Neglect of pΨ Terms

The quantities in equations 14 appear as if observed from axes rotating at synchronous speed. The consequence of this is that symmetrical a-c stator quantities appear as constants or d-c quantities, and that d-c stator quantities appear as sinusoids at unit frequency.

When a short-circuit or other switching transient occurs in an induction motor circuit, there appears a transient offset in the stator currents and flux linkages. This offset arises from the fact that stator flux linkages cannot jump to a new value in zero time when a switching operation occurs. The d-c stator current which results causes an oscillatory torque. Because of the relatively high inertia of the motor, this torque will have no appreciable effect on rotor speed. In studying motor transients involving relatively slow speed changes, it is desirable to neglect the d-c offset and the oscillatory torque produced by it.

To neglect the transient d-c offset, stator flux linkages cannot be continuous, but stator quantities must be related to each other on a symmetrical basis at all times. In equations 14, the terms preventing jumps in stator linkages are the $p\Psi$ terms in the first two equations; a jump presents an undefined derivative. Also, if stator currents, voltages, and linkages are symmetrical and in the steady state, $p\Psi_\alpha=p\Psi_\beta=0$; relatively slow changes in voltage, current, and linkage amplitudes admit $p\Psi_\alpha=p\Psi_\beta=0$ as an approximation. Omitting the $p\Psi$ terms in the first two equations of equations 14 is a simple way to eliminate the transient offset.

Differential analyzer studies made by the authors indicate that in investigations of motor transients involving appreciable speed changes the results are not significantly affected by the omission of the $p\Psi$ terms. In the stator currents, the offsets simply do not appear. Neither the rotor fluxes nor the net electric torque are appreciably changed.

The omission of the $p\Psi$ terms greatly simplifies the solution of the motor equations. From equations 14, with the $p\Psi$'s omitted and the stator fluxes and rotor currents eliminated, the following simplified equations are derived

$$E_\alpha=RI_\alpha-xI_\beta-\frac{M}{L_r}\psi_\beta$$
$$E_\beta=RI_\beta+xI_\alpha+\frac{M}{L_r}\psi_\alpha$$
$$e_\alpha=p\psi_\alpha+\frac{r}{L_r}\psi_\alpha+\psi_\beta p\theta-\frac{r}{L_r}MI_\alpha=0 \tag{15}$$
$$e_\beta=p\psi_\beta+\frac{r}{L_r}\psi_\beta-\psi_\alpha p\theta-\frac{r}{L_r}MI_\beta=0$$
$$T_e=\frac{M}{L_r}\left(\psi_\alpha I_\beta-\psi_\beta I_\alpha\right)$$

where

$$x=L_s-\frac{M^2}{L_r}$$

Appendix II. The Equations for Several Induction Machines Fed Through a Common Reactance

Equations 15 may be modified for use in the study of several induction machines connected together and fed through a common reactance. In this case, E_α and E_β will be the motor bus emf common to all machines. They will no longer be constants, but will be functions of the total bus current, i.e., if E_α' is a constant emf back of the common reactance x_e, then

$$E_\alpha=E_\alpha'+x_e\sum I_\beta \tag{16}$$

and similarly

$$E_\beta=E_\beta'-x_e\sum I_\alpha$$

For any one motor, equations 15 give

$$I_\alpha=\frac{E_\beta}{x}-\frac{M}{L_r}\frac{\psi_\alpha}{x}-\frac{R}{x}I_\beta$$

$$I_\beta=-\frac{E_\alpha}{x}-\frac{M}{L_r}\frac{\psi_\beta}{x}+\frac{R}{x}I_\alpha \tag{17}$$

so that

$$\begin{aligned}\sum I_\alpha&=E_\beta\sum\frac{1}{x}-\sum\frac{M}{L_r}\frac{\psi_\alpha}{x}-\sum\frac{R}{x}I_\beta\\ \sum I_\beta&=-E_\alpha\sum\frac{1}{x}-\sum\frac{M}{L_r}\frac{\psi_\beta}{x}+\sum\frac{R}{x}I_\alpha\end{aligned} \tag{18}$$

A further simplification in the motor equations can be affected by omitting the stator loss terms in equation 18. Since R/x is 0.1 or smaller, the error in the currents introduced by this simplification should be 1 per cent or less. The usefulness of this approximation has been checked in differential analyzer studies with good results.

Omitting the R/x terms, and substituting the currents from equation 18 into equation 16 results in

$$E_\alpha=E_\alpha'-x_eE_\alpha\sum\frac{1}{x}-x_e\sum\frac{M}{L_r}\frac{\psi_\beta}{x}$$

$$E_\beta=E_\beta'-x_eE_\beta\sum\frac{1}{x}+x_e\sum\frac{M}{L_r}\frac{\psi_\alpha}{x}$$

Solving for the bus voltages

$$\begin{aligned}E_\alpha&=\frac{\dfrac{E_\alpha'}{x_e}-\sum\dfrac{M}{L_r}\dfrac{\psi_\beta}{x}}{\dfrac{1}{x_e}+\sum\dfrac{1}{x}}\\ E_\beta&=\frac{\dfrac{E_\beta'}{x_e}+\sum\dfrac{M}{L_r}\dfrac{\psi_\alpha}{x}}{\dfrac{1}{x_e}+\sum\dfrac{1}{x}}\end{aligned} \tag{19}$$

Equations 19 make the step-by-step solution of the multimachine problem quite simple. The third and fourth equations of the equation 15 can be solved for the rotor flux-linkage time derivatives to form a basis for whatever type of prediction equation is to be used. The flux prediction must be made for each motor. Equations 19 then give the motor bus voltages in terms of the source voltage and the predicted motor fluxes. The individual motor currents can then be found from equations 17 and the torque can be calculated. The speed is found from the acceleration equation

$$p\theta=\frac{1}{4\pi fH}\int(T_e-T_m)dt \tag{20}$$

where the mechanical torque T_m is a given function of speed. The advantage of solving for the bus voltage separately as in equations 19 is that with this arrangement the numerical difficulty of the solution increases somewhat less than linearly with the number of motors involved.

Appendix III. Lumping of Motors With Similar Characteristics

To reduce the number of machines which must be considered in studying a particular case, it is usually necessary to lump together machines with similar characteristics so that the resulting equivalent machine will have the same effect on the remainder of the system as the original machines acting individually. In this study of bus transfer, the following procedure is used:

1. All motor constants including inertia constants and loads are expressed in per unit on a common base.
2. The individual load torques and inertia factors are added together to form an equivalent load torque and inertia factor.
3. The locked-rotor or short-circuit reactances are combined as if connected in parallel.
4. The rotor resistance and the stator and rotor self- and mutual inductances are calculated using the criteria that the stator and rotor self-inductances are equal and that the equivalent machine must have short-circuit and open-circuit time constants equal to the weighted averages of the time constants of the original machines, weighting being on the basis of machine rating.

Appendix IV. Step-by-Step Method for the Calculation of Motor Reacceleration

For the purpose of this discussion, the time of reapplication of voltage will be called time zero. All the motor speeds are presumed to be known at this time.

Step 1. Starting the Calculation

Using the individual motor speed-current curves, the motor currents can be found in the form

$$I=\frac{E}{1}I_e \tag{21}$$

The voltage at the bus can be found from

$$E=\frac{E'}{1+x_e\sum I_e} \tag{22}$$

The electric torque can now be found from the individual speed-torque curves, the actual value being given by

$$T_e=\frac{E^2}{1}T_e \tag{23}$$

where T_e is the value from the curve. The first approximation to the increase in speed during the first time interval is

$$\Delta(p\theta)=\frac{\Delta t}{2H}\left(T_e-T_m\right) \tag{24}$$

This value of $\Delta(p\theta)$ is next improved by calculating the currents and torques for $p\theta=(p\theta)_0+\Delta(p\theta)$ and averaging the accelerating torque with the original value. This manner of improvement can be repeated if it appears necessary.

Step 2. Continuing the Calculation

Once the values of $p\theta$'s at $t=\Delta t$ have been found, the calculation of successive points is simpler. The value of $\Delta(p\theta)$ between $t=0$ and $t=\Delta t$ is assumed to apply also between $t=\Delta t$ and $t=2\Delta t$ and the average accelerating torque in the second interval is calculated on this basis. This torque is then used to calculate an improved $\Delta(p\theta)$ and the calculation proceeds to the next point.

Appendix V. Modified Equations for the Calculation of Inrush Currents and Transient Torques

When voltage from the secondary source is reapplied to the motor bus, each motor will experience high inrush currents and transient unit-frequency torques. To calculate the initial magnitudes of these currents and torques, equations 14 may be modified by assuming motor speeds constant and neglecting all resistances.

With these simplifications, and with stator flux linkages and rotor currents eliminated

$$\begin{aligned}&xpI_\alpha+\frac{M}{L_r}p\psi_\alpha-xI_\beta-\frac{M}{L_r}\psi_\beta=E_\alpha\\ &xI_\alpha+\frac{M}{L_r}\psi_\alpha+xpI_\beta+\frac{M}{L_r}p\psi_\beta=E_\beta\\ &p\psi_\alpha+(p\theta)\psi_\beta=0\\ &-(p\theta)\psi_\alpha+p\psi_\beta=0\end{aligned} \tag{25}$$

These equations may be solved operationally, giving for the currents and flux linkages

$$\begin{aligned}I_\alpha&=\frac{1}{x}\Bigg[E_\beta(1-\cos t)+\left(E_\alpha+xI_{\beta0}+\frac{M}{L_r}\psi_{\beta0}\right)\sin t+\left(xI_{\alpha0}+\frac{M}{L_r}\psi_{\alpha0}\right)\cos t+\frac{M}{L_r}\psi_{\beta0}\sin(p\theta)t-\frac{M}{L_r}\psi_{\alpha0}\cos(p\theta)t\Bigg]\\ I_\beta&=\frac{1}{x}\Bigg[-E_\alpha(1-\cos t)+\left(E_\beta-xI_{\alpha0}-\frac{M}{L_r}\psi_{\alpha0}\right)\sin t+\left(xI_{\beta0}+\frac{M}{L_r}\psi_{\beta0}\right)\cos t-\frac{M}{L_r}\psi_{\beta0}\cos(p\theta)t-\frac{M}{L_r}\psi_{\alpha0}\sin(p\theta)t\Bigg]\end{aligned} \tag{26}$$

$$\psi_\alpha=\psi_{\alpha0}\cos(p\theta)t-\psi_{\beta0}\sin(p\theta)t$$

$$\psi_\beta=\psi_{\alpha0}\sin(p\theta)t+\psi_{\beta0}\cos(p\theta)t$$

If it is assumed that the dead time is long compared to the machines' short-circuit time constants so that the motors may be considered as following steady-state characteristics (with slow deceleration) just prior to the reapplication of voltage, then equations 26 can be simplified to give for the currents

$$I_\alpha=\frac{1}{x}\left(\Delta E_\beta(1-\cos t)+\Delta E_\alpha \sin t\right)+I_{\alpha 0}$$

$$I_\beta=\frac{1}{x}\left(-\Delta E_\alpha(1-\cos t)+\Delta E_\beta \sin t\right)+I_{\beta 0} \tag{27}$$

in which ΔE_α and ΔE_β are the changes in motor terminal voltage through the switching operation. $I_{\alpha 0}$ and $I_{\beta 0}$ are the preswitching values of stator current.

By manipulating the terms in equations 27 it can be shown that the maximum inrush current will occur when the preswitching bus residual voltage and the newly applied voltage are 180 degrees out of phase. The magnitude of the symmetrical component of current in this case will be

$$I=\frac{\Delta E}{x}+I_0 \tag{28}$$

where ΔE equals the sum of the magnitudes of the newly applied terminal voltage and the preswitching value of bus residual voltage. To calculate the actual peak current it must be noted that the current given by the first term of equation 28 will be fully offset. For practical purposes, the I_0 term in equation 28 can be neglected.

Since slip at the end of the dead period is still relatively small, the flux linkages given by procedure 1 in Appendix III can be approximated by their preswitching values

$$\begin{aligned}\psi_\alpha&=\psi_{\alpha 0}\\ \psi_\beta&=\psi_{\beta 0}\end{aligned} \tag{29}$$

In terms of these variables, the electric torque is

$$T_e=\frac{M}{L_r}\left(\psi_\alpha I_\beta-\psi_\beta I_\alpha\right)$$

Substituting the currents and flux linkages from procedures 2 and 4 of Appendix III

$$T_e=\frac{1}{x}\left[\left(\frac{M}{L_r}\psi_{\beta 0}\Delta E_\beta+\frac{M}{L_r}\psi_{\alpha 0}\Delta E_\alpha\right)(1-\cos t)+\left(\frac{M}{L_r}\psi_{\beta 0}\Delta E_\alpha-\frac{M}{L_r}\psi_{\alpha 0}\Delta E_\beta\right)\sin t\right]+T_{e0} \tag{30}$$

T_{e0}, the electric torque prior to switching, will be small and can be disregarded. At the end of the dead time the stator currents will be small; therefore

$$\begin{aligned}\frac{M}{L_r}\psi_{\alpha 0}&=E_{\beta 0}\\ \frac{M}{L_r}\psi_{\beta 0}&=-E_{\alpha 0}\end{aligned} \tag{31}$$

Thus the initial torque can be written

$$T_e=\frac{1}{x}\left[(-E_{\alpha 0}\Delta E_\beta+E_{\beta 0}\Delta E_\alpha)(1-\cos t)+(-E_{\alpha 0}\Delta E_\alpha-E_{\beta 0}\Delta E_\beta)\sin t\right] \tag{32}$$

The torque given by equation 32 can be separated into a unidirectional torque and a unit-frequency oscillatory torque.[6] The maximum value of the unidirectional torque occurs when the preswitching bus residual voltage and the newly applied voltage are 90 degrees out of phase. This value is given by

$$T_1=\frac{EE_0}{x} \tag{33}$$

where E_0 is the magnitude of the preswitching residual voltage and E is the magnitude of the newly applied terminal voltage.

The maximum value of the oscillatory torque occurs when E and E_0 are 180 degrees out of phase at the time of switching. This value is given by

$$T_2=\frac{(\Delta E)(E_0)}{x} \tag{34}$$

For values of E_0 below 30 per cent of the value of the newly applied terminal voltage, the maximum total torque occurs when E and E_0 are approximately 90 degrees out of phase. Its value is approximately

$$T=\frac{E_0}{x}\left(E+\sqrt{E^2+E_0^2}\right) \tag{35}$$

References

1. BUS TRANSFER TESTS ON A 2,300-VOLT STATION AUXILIARY SYSTEM, **A. A. Johnson, H. A. Thompson.** *AIEE Transactions*, vol. 69, pt. 1, 1950, pp. 386–94.

2. ELECTRIC DRIVES FOR STEAM-ELECTRIC GENERATING-STATION AUXILIARIES, **W. R. Brownlee, J. A. Elzi.** *AIEE Transactions*, vol. 64, 1945, pp. 741–45.

3. AN ANALYSIS OF THE INDUCTION MOTOR, **H. C. Stanley.** *AIEE Transactions*, vol. 57, 1938, pp. 751–55.

4. TWO-REACTION THEORY OF SYNCHRONOUS MACHINES—GENERALIZED METHOD OF ANALYSIS—PART I, **R. H. Park.** *AIEE Transactions*, vol. 48, July 1929, pp. 716–27.

5. SYNCHRONOUS MACHINES (book), **C. Concordia.** John Wiley and Sons, Inc., New York, N. Y., 1951.

6. TRANSIENT PERFORMANCE OF INDUCTION MOTORS, **F. J. Maginniss, N. R. Schultz.** *AIEE Transactions (Electrical Engineering)*, vol. 63, Sept. 1944, pp. 641–46.

◆

Discussion

W. F. Mackenzie (Pennsylvania Power & Light Company, Hazelton, Pa.): The authors are to be congratulated for having presented an excellent method for calculating conditions occurring under an interrupted bus transfer. The paper provides an excellent qualitative discussion of the electrical and mechanical behavior of the equipment during the transfer. It also provides the means to obtain quantitative results for any given system. The calculations involved may be rather laborious for the engineer confronted with the design of a power plant auxiliary transfer scheme. It may be more practical to make oscillograph tests on the auxiliary system after it is assembled and design the transfer scheme from these results.

Since our company has been using the nondelayed interrupted transfer for all emergency transfers on its larger units for several years, we would be vitally interested to know the details on any motor failures that have occurred from this type of transfer.

L. R. Sellers (Tennessee Valley Authority, Knoxville, Tenn.): Mr. Lewis and Mr. Marsh have made a valuable contribution to this complex subject by their thorough analytical approach. With reference to the continuous-circuit transfer method recommended, the 0.055 per-unit transformer impedance used in Table I utilizes about 0.88 of a 250-megavolt-ampere circuit-breaker interrupting rating and all of this breaker's momentary 60,000-ampere rating. Paralleling two sources of this magnitude even for a short interval appears to be a questionable practice, particularly when the start and emergency transformer which should be connected electrically remote from the generator may be out of phase during unusual system conditions. The open-circuit method with a fixed time delay for routine transfers appears to be a better arrangement in most cases. This type of transfer can be made at full load when required.

The requirement that the residual bus voltage be limited to 25 per cent of rated voltage should be subject to a critical review since it will become unduly restrictive as the size of generating units and auxiliary motors increases. Steps leading to the establishment of this factor may have been brought about by deficiencies in motor design. Some of the motors installed recently were found to be insufficiently braced for full-voltage starting on a low-impedance supply system. Extensive transfer tests of all the auxiliaries for a 125-megawatt unit at the Tennessee Valley Authority Johnsonville plant did not indicate any apparent relation between asymmetric motor inrush and bus residual in the range of 4- to 36-per-cent residual. The higher motor impedance at 85 per cent speed as compared to the locked-rotor impedance actually tends to reduce the inrush value.

With reference to Fig. 1, the residual decay to 25 per cent in about 0.7 second is rather short for the size of motors as tabulated in Table I. Could this be attributed to an assumption that the motors were operating near name-plate rating before transfer instead of 80 to 85 per cent as in the usual case? During the transfer tests referred to in the foregoing, about 1.2 seconds were required to reach 25-per-cent residual with a total connected-motor load of 7,900 kva, including two 1,750-horsepower boiler feed motors.

Referring to Fig. 3, the poor recovery speed characteristics of a standard boiler feed motor led to the development with several manufacturers of 3,600-rpm motors with torque characteristics better matched to the pump requirements. Motors rated 2,000, 3,000, and 4,000 horsepower for use with 150-, 200-, and 250-megawatt units have been shop-tested to show accelerating torque characteristics at 75-per-cent rated volts such that they will have a definite accelerating torque above the pump requirements from zero to rated speed.

H. C. Barnes and **S. H. Horowitz** (American Gas and Electric Service Corporation, New York, N. Y.): The authors have presented an excellent theoretical examination of an interesting phase of motor protection. That operating practices which involve this problem are in use is well established.

There is no question that it is desirable to establish quickly auxiliary power from a reserve source in event of loss of the normal source from the generator. To do this quickly enough to assure safe shutdown requires automatic transfer. Any automatic scheme requires periodic testing to assure proper operation when needed. The best time to make this test is when the unit is being removed from service for maintenance or inspection. To make such a test with loadings of upwards of 200 megawatts would involve too great a service risk. To do so when removing a unit not only eliminates this risk but also saves numerous operations on the part of the operator. Also, the time of the test man is saved since the tripping is usually initiated from an emergency push button or from a protective relay contact which trips the differential, thereby testing not only the reserve transfer components but also the differential, main breaker, field breaker, and other devices. Therefore, it appears that this type of transfer will be encountered even though a transfer under actual fault conditions never occurs.

There has been some past discussion that the chance of motor damage from transfer is increasing because of the increased use of the automatic transfer as a "lazy" means of shutdown. Actually, modern generating-unit service continuity is so high that the desired test period is usually exceeded before a shutdown occurs. Therefore, there is actually little increase in the number of automatic transfers because this means is used for a routine shutdown.

After the initial shakedown period, the number of transfers because of fault conditions is very small. Also, in event of a fault, it is generally believed that the fault will act to diminish the residual voltage. Therefore, the risk of damage by reason of transfer from fault is slight.

While the paper is conclusive that theoretically there is danger of damage, practically this is questionable. Like all studies of this type, there are so many assumptions and so many variables that it always seems doubtful that the results are truly representative. For example, if it is assumed that the worst condition of full residual voltage continues, then, to cause damage, it is necessary to hit at some point considerably out of phase. If it is necessary for the angle to be greater than 90 degrees, which does not seem unresonable, then this factor alone reduces the probability 50 per cent.

Fig. 1 indicates that the inherent 20- to 25-cycle closing time of the large circuit breakers used on the incoming feeds is enough to permit voltage decay in the order of 60 to 50 per cent. This reduction means a larger angle necessary for danger and, therefore, reduces the angular area in which damage can occur. Reference 1 indicates that, at 20 cycles, the voltages are practically in phase.

Table I is fairly representative of the auxiliaries associated with a unit. However, this number of motors is in service only during full load. At the time of a normal shutdown only a few of these are in service, since the load would have been decreased to near zero and coal firing would have been discontinued. Those in service may well be practically unloaded, thereby reducing the decelerating torque and, therefore, the slip. An indication of the conditions is a typical reduction of auxiliary demand from 11,000 kw at full load to 3,000 kw at near no load. A check of planned outages of two 200-megawatt units revealed that only one forced draft fan, one boiler pump, and one circulating water pump were running. All pulverizers were down. It is, therefore, doubtful that the same motors will be stressed each shutdown. Further, pressure operation is proving so much better than suction that induced draft fans will seldom be used. This does however tend to increase the size of the forced draft fan. If larger drives are required, it is quite possible that they will be steam because of the increased over-all heat efficiency.

Even if it is assumed that the worst condition of full residual voltage at a 180-degree angle is encountered, this would appear negligible if the impedance of the source were equal to that of the load since only per-unit voltage would appear across each impedance. While this is rather impractical, there is some source impedance and the larger motor at least is nearer to this source impedance than the smaller motor. This may be insignificant but it is another factor which tends to limit the stress.

The paper states that experience has shown that residual voltage greater than 25 per cent of rated will cause excessive winding stress. Some detail of this experience would be appreciated.

Automatic transfer without intentional time delay has been in use by the American Gas and Electric Company system for over 15 years. Motor failure from mechanical winding stress has been very small. None are known to have been caused by automatic transfer. Motors of 2,500 horsepower have been in use for at least half of this period. A large number of 18,750-kva synchronous condensers have been transferred from starting to running without benefit of synchronizing or time delay and no damage has resulted. The latter may not be a fair example since it is effectively an unloaded motor, usually in hydrogen, and slip during transfer could be small. This experience does not indicate that the interrupted transfer is damaging enough to warrant much consideration.

Large motors are protected by plunger-type instantaneous relays. Seldom have these caused tripping during transfer. On a few test transfers, about 1950 it was found that a setting of 10 per cent greater than normally required for starting was needed for the 2,500-horsepower boiler feed pumps to assure 100-per-cent continuity on transfer. Even the need for this increase is questionable since it is not of too great consequence if one relay should trip as it can be readily restarted in time. The increase has not been used on the last five units and no tripping on transfer has resulted.

In speaking of winding stress, an explanation of the nature and degree of stress would be helpful. Presumably, the conductor tends to be driven through the insulation or forces out the retaining material. Is this force not distributed over the conductor area? What is the resultant pressure per square inch and how does this compare to the insulation strength in compression? Is it not reasonable that failure probably will not occur at the first stressing and that it may take several before actual insulation rupture occurs? If so, is it not possible that the required number of stresses may never be encountered in the life of the motor? If excessive inrush is encountered, the instantaneous relays would initiate tripping in about 1 cycle and clearing in another 4 or 5. Would not this tend to reduce the damage?

There has been some talk of possible shaft failure. This is not mentioned in the paper. Is this a real problem?

One of the principals of mechanical design used to be to calculate carefully the stresses and then multiply by a safety factor of roughly from 3 to 30, depending upon the damage possible. Is not some such safety factor still used, and if so, is it not sufficient to take care of these occasional stresses?

While the cost of adding time delay is insignificant, our experience has not been such to justify the nuisance value of test, maintenance burden increase, and added chance of transfer failure when needed. It may seem that these are so small as to be meaningless. It should be remembered that the ratio of really necessary gadgets per kilowatt to manpower per kilowatt is ever increasing. Therefore, any unnecessary ones should be avoided.

While we have not found it necessary, we are quite willing to change if it can be proved that our experience is unique. We would be quite interested in hearing the motor manufacturers statements as to their experience, design factors, and recommendations. If a good test procedure can be worked out which will bring this subject to conclusion, consideration would be given to make the American Gas and Electric Company system available for such tests. Perhaps a program under the joint auspices of the relay and motor committees would be feasible.

Einar Nilsson (Pacific Gas & Electric Company, San Francisco, Calif.): At our Pittsburgh steam plant one each of the boiler feed pumps, induced draft fans, forced draft fans, and condensate pumps is supplied from a single 2,400-volt bus which is connected during startup to the 2,500-volt tertiary winding of a 110/220-kv system power-interchange transformer. This is the emergency as well as the startup source of the plant. After the machine is synchronized, the station auxiliaries are normally transferred through continuous-circuit or parallel transfer to

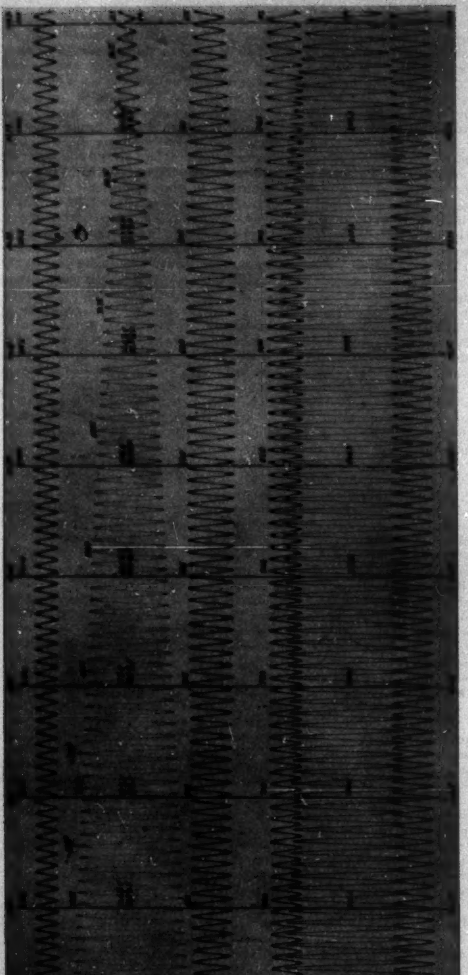

Fig. 7. Test oscillogram traces

A—Boiler feed pump current
B—Motor bus voltage
C—Condensate pump current
D—Induced draft fan current
E—Forced draft fan current
F—Supply bus voltage

the house transformer, which is directly connected to the main generator leads. The parallel transfer will be the normal procedure, delayed interrupted-circuit transfer will be the emergency case. To determine the length of the delay period or dead time required for prevention of excessive motor inrush currents or permitted for uninterrupted boiler operation, a reasonably accurate method is desirable for determining the decay characteristics of the motor voltage. The paper presents such a method. As a check on the method a test performed at Pittsburgh steam plant is being used. The test was set up on a single bus which supplied the motors of one 2,250-horsepower boiler feed pump, one 920-horsepower induced draft fan, one 900-horsepower forced draft fan, and one 500-horsepower condensate pump. Fig. 7 shows the oscillogram obtained for all motors combined. The motor loads during the test were 75 per cent of full load for each of the two pumps, 53 per cent for the induced draft fan, and 33 per cent for the forced draft fan.

In determining some of the motor constants for use in the method shown in the paper, the manufacturer's calculated values were used where available. In the case of the draft fan motors, measured values were obtained from a test of the motors. Fig. 8 shows bus voltage decay by the approximate method plotted for comparison on the same chart as the test values. The chart shows a good agreement between the two.

The author's "Criteria for Successful Bus Transfer" is a concise analysis of the problems involved. For the evaluation and the choice of the transfer method, certain critical characteristics must be known regarding the effect of dead time on boiler operation in general and fuel, feed water, and air in particular. For the benefit of the industry it is hoped that as more experience is gained with automatic transfer of station auxiliary busses, these characteristics will receive wide publicity through professional papers and articles.

C. F. Paulus (The Cleveland Electric Illuminating Company, Cleveland, Ohio): This is an excellent analysis of motor performance during interrupted-circuit transfer conditions. It nicely complements the papers mentioned in the author's references. I agree with the authors statement that in normal starting and stopping operations transfers should be made closed-circuit. I further agree that emergency transfers must be made open-circuit and the spinning motors should not be connected to the new source until their voltage has decayed to a value of 25 per cent of normal or less.

The approach suggested by the authors for calculating the time of decay for a group of motors of varying and various characteristics appears to be somewhat cumbersome and of little value in the design of power plant auxiliary systems. This is because the conditions in a power plant are different than those assumed in this paper. In the modern unitized central station with auxiliaries fed from the generator leads, it is neither necessary nor desirable to transfer all auxiliaries under emergency conditions. This transfer does not take place until the machine has been tripped. When this happens it is better to trip all mills and all but one of the fans. It is best to leave only one feed-water pump on.

At the time the emergency transfer takes place following a tripoff, the unit may have been at full load or at quarter load; the number of auxiliaries running and their loads may vary broadly. Using the author's methods to calculate the voltage decay for all these possible conditions would be a tremendous undertaking and, at best, give data which would not be directly useful. I believe that the problem can be solved by more practical means. The design of the auxiliary system for a power plant can be approached in this fashion.

To make permissible the normal transferring of auxiliaries by the closed-circuit method, transformer reactances should be so specified as to keep circuit-breaker duties within available capabilities. This problem as well as that of staying within available ampere ratings is best accomplished by using two transformers in place of one. For larger units it is generally necessary to provide two boards for each transformer. This arrangement results in four boards which makes it possible to connect only one pump, one fan, and one mill to each board. This makes it possible to transfer the auxiliary loads in four parts.

In closed-circuit transferring, the circulating current is reduced because of the greater reactance in the circuit caused by the split transformer. Failure to transfer successfully is not so serious with only a quarter of the auxiliaries being transferred. Under emergency open-circuit transferring, the inrush from the new source is not so great as to cause a low voltage problem. This inrush is further reduced by transferring only those auxiliaries which should be kept running when the machine has tripped.

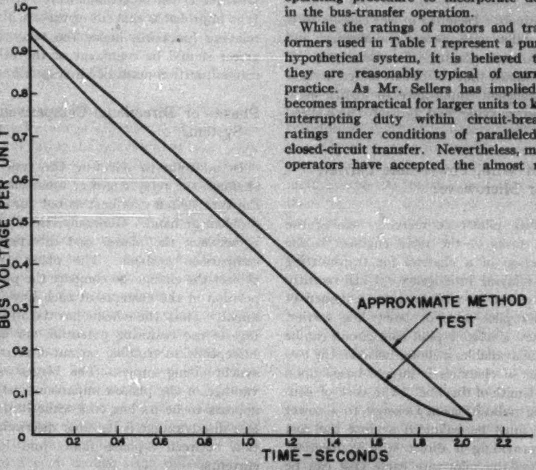

Fig. 8. Bus voltage decay against time

If the transfer to the new source is blocked until the decaying voltage on each bus has reached a value of about 25 per cent there will be no abuse of the motors. The time required to reach this value varies from board to board, and from day to day. The time in itself is of no importance. The voltage which may be fully out of phase is important. In any case, each board will be closed-in to the new source at the earliest permissible time. The likelihood of more than one board being connected to the emergency source simultaneously is very remote. There is no need to calculate the voltage decay for each motor and combination of motors.

D. G. Lewis and W. D. Marsh: We appreciate the interest shown by the several discussers, and are grateful for the many excellent ideas and suggestions presented. With reference to Mr. Mackenzie's remarks, it is certainly true that, where the design of the bus-transfer scheme can be based upon actual tests of the system involved, his is the most satisfactory method. It seems likely, however, that in some cases it will be necessary to have at least an approximate idea of what the system performance will be to select values of transformer impedance and circuit-breaker ratings.

So far as we are aware, there has been only one case of motor-winding failure that could without question be directly traced to the stresses resulting from an excessive number of nondelayed transfers. This involved two 1,500-horsepower boiler feed pump motors subjected to approximately 100 such transfers over a period of 3 or 4 years. The results were quite apparent from visual inspection of the motors which showed distortion of the coil end turns. The winding of one of these motors had failed and, as a result of the investigation, it was decided to change operating procedure to incorporate delay in the bus-transfer operation.

While the ratings of motors and transformers used in Table I represent a purely hypothetical system, it is believed that they are reasonably typical of current practice. As Mr. Sellers has implied, it becomes impractical for larger units to keep interrupting duty within circuit-breaker ratings under conditions of paralleled or closed-circuit transfer. Nevertheless, many operators have accepted the almost negligible risk involved in paralleling sources on the basis that the exposure time is extremely low. There will, of course, be designs wherein normal phase differences will not permit paralleling sources.

Mr. Sellers brings up a very important point in connection with the adequacy of motors under full-voltage starting conditions. Briefly, it should be borne in mind that in considering the ability of electric windings to withstand full-voltage starting we are dealing with a repetitive stress type of phenomenon. Starting duty is merely one of the things that wears out a winding, and a motor may be thought of as having built into it an ability to start a certain number of times before its winding will be worn out. We are not aware of any attempt to designate a specific number of starts as representing normal life for a motor winding. Such a number would vary widely with motor horsepower and speed as well as with conditions of starting voltage and load inertia. But to say that a motor is suitable for full-voltage starting necessarily implies a reasonable number of full-voltage starts. Experience indicates that modern motor windings will have an acceptable life with the number of starts found in normal power plant service. They cannot, however, be expected to have acceptable life under abnormal conditions as typified by, e.g., 30 or 40 starts per day.

The effect of nondelayed transfers is also a repetitive stress problem. However, since the stresses for any one transfer can be much greater than for a single full-voltage start, the life of a winding in terms of number of transfers must be very much shorter. Undoubtedly, the more rapid decay shown in Fig. 1 as compared to the tests conducted by Mr. Sellers is partially the result of the assumption that the motors were operating at name-plate rating.

Mr. Barnes and Mr. Horowitz have brought forth a number of interesting comments. With reference to the nature of winding stress as indicated in the foregoing, one of the more important effects is that of the bending stresses on the end turns of the winding. There are also compressive stresses existing primarily in that portion of the winding in the stator slots.

The statement that the chance of motor damage from transfer is increasing because of increased use of automatic transfer as a lazy means of shutdown may or may not be valid in any particular instance. It is quite obvious that, whether the automatic transfer relaying operates as a result of faults or not, it will be desirable to make periodic tests of the equipment. Usual practice appears to be to test generating station protective relays at intervals of from 6 months to 1 year. While it may be convenient to test the automatic transfer relays each time a unit is shut down, it is apparent that, in the case of a generator shut down once a day, this will result in from 180 to 365 times as much wear and tear on the motors. If a delayed-transfer scheme is used, this duty is drastically reduced.

There are several factors, as pointed out, that tend to reduce the inrush current on transfer below the theoretical maximum. A fault to which the motor could contribute short-circuit current would increase the rate of residual voltage decay; but in the large majority of generators which have high-resistance grounding, there would be no such contribution for a ground fault. The angle at which the reserve source is closed is, of course, a matter of probability, with a certainty that over a large enough number of transfers some will be at an unfavorable angle. The rated closing time of many circuit breakers used in auxiliary systems is 20 cycles, which from Fig. 1 would indicate a decay to more nearly 70-per-cent residual voltage. Actually, breakers of this type very frequently operate in 10 to 15 cycles, giving 80 per cent under the conditions of Fig. 1. However, this is of little significance for practical consideration since the residual voltage decay characteristics of systems vary widely depending on size of motors involved and the load at any particular time. In a similar manner, no general statement can be made as to the phase difference between residual and reserve source voltages at 20 cycles or any other time after tripping.

Relative to the question of auxiliary system loads, at the time of a normal shutdown, the fact that these loads are low is an additional factor favoring delayed transfer since boiler operation should be less critical under these conditions. Source impedance will, of course, tend to reduce motor inrush during transfer, but it is more typically one-third of the load impedance rather than equal to it as Mr. Barnes and Mr. Horowitz have chosen for their example. This would result in 1.5 per-unit voltage on the motors instead of 1.0 per-unit voltage.

It is interesting to know that in some cases it has been necessary to increase instantaneous relay settings to avoid tripping during nondelayed transfer. This would seem to be a sure indication that excessive inrush currents do exist.

Mr. Barnes and Mr. Horowitz's opinion that tripping of the motor during transfer is of little consequence is difficult to reconcile with their opening statement that it is desirable to establish auxiliary power from a reserve source quickly to insure safe shutdown. They suggest that instantaneous relaying may be a means of limiting the damaging effects of instantaneous throw over. Much of the damage has been done in the 5- or 6-cycle clearing time that would be involved but, in any case, if one is willing to accept tripping during a throw over, it would seem to defeat the entire purpose of automatic transfer. Our company has had no experience with shaft failure resulting from bus transfer.

We wish to express our appreciation to Mr. Nilsson for making available the results of his bus-transfer tests and the data showing comparison with the method of calculation presented in the paper.

Mr. Paulus' comments are particularly interesting in that they represent a different approach to the problem. Certainly Mr. Paulus' arrangement of auxiliary power system and his philosophy regarding transfer result in a very high degree of simplicity and reliability, both from the standpoint of design and operation. If it can be assumed, or known from experience, that the times involved for voltage decay to 25 per cent of normal will not be embarrassing to the boiler, there is no need to make any calculations beforehand. If desired, however, the method of the paper is flexible enough to take account of the fact that not all motors are transferred, and it should be possible to make the calculation only once or twice for the expected conditions involving the longest delays. Admittedly, if everyone were willing to shut down a generating unit under every condition for which emergency transfer is required, there would be much less need to know or be able to predict the voltage decay and recovery characteristics of auxiliary motor systems.

Line and Transformer Bank Relaying Systems

J. L. BLACKBURN
MEMBER AIEE

G. D. ROCKEFELLER
ASSOCIATE MEMBER AIEE

IN MANY power systems, connections of transmission lines and transformer banks are often encountered which require special consideration for adequate relay protection. Though these arrangements may raise difficult relaying problems, the overriding factor is the appreciable economic advantages which result. The problems can be grouped into two general classes: the 3-terminal lines, and the termination of a transmission line in a transformer bank. In this paper various cases frequently encountered together with solutions to the relaying problem are presented.

The discussion will be generally limited to relaying systems, which provide high-speed simultaneous tripping of all line terminals. Included in this classification are pilot wire, power-line carrier, and microwave relaying. In other words, it is assumed that the circuit under study is of sufficient importance to justify high-speed relaying and possibly high-speed reclosing.

Pilot Wire, Power-Line Carrier, or Microwave?

With pilot-type relaying, one of the first tasks of the relay engineer is the selection of a channel for transmitting the relaying intelligence. Until recently the choice of a channel was confined to either pilot wire or power-line carrier. Where a reliable pilot-wire circuit can be made available, a choice between the two types of channels is largely based upon the length of the line. The cost of coupling radio-frequency energy to a power line must be balanced against the cost of providing a direct wire connection. Unless the pilot-wire cable cost can be shared by other functions, a length on the order of 7 to 10 miles represents the economic limit. However, wire circuits in excess of 20 miles are in use in this country.[1]

At present, microwave is limited to key areas of the system where many functions can ride the microwave circuit. Where ten or more channels are required between any two points, it is likely that microwave will be economically feasible. It is improbable that all of these will be relaying functions, hence the relay engineer should be cognizant of the other communication needs of his system.[2]

Phase- or Directional-Comparison System?

In addition to selecting the type of channel, the relay engineer must choose the type of relaying best suited for the problem at hand. Generally, the choice is between the phase- and directional-comparison systems. The phase type utilizes the channel to compare the phase position of the currents at each line terminal. Thus, the scheme has the advantage of not requiring potential, nor is it susceptible to tripping on out-of-step or synchronizing surges. The biggest advantage of the phase-comparison system appears to be its low cost while its biggest disadvantage is its poor discrimination between 3-phase faults and load currents.

With the directional-comparison sys-

Paper 55-88, recommended by the AIEE Relays Committee and approved by the AIEE Committee on Technical Operations for presentation at the AIEE Winter General Meeting, New York, N. Y., January 31–February 4, 1955. Manuscript submitted October 19, 1954; made available for printing November 18, 1954.

J. L. Blackburn and G. D. Rockefeller are with the Westinghouse Electric Corporation, Newark, N. J.

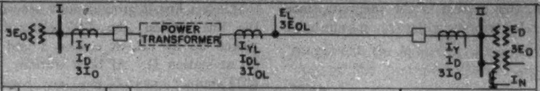

CASE	POWER TRANSFORMER CONNECTIONS	HIGH SPEED RECLOSING	DIRECTIONAL COMPARISON RELAYING						PHASE COMPARISON RELAYING	
			STATION I			STATION II				
			DISTANCE RELAYS	GROUND		DISTANCE RELAYS	GROUND		STATION I	STATION II
				MAIN	POLARIZING		MAIN	POLARIZING		
A	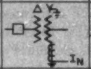	YES	E_L I_{DL}	$3I_{OL}$	I_N OR $3E_{OL}$	E_D I_D	$3I_O$	I_N OR $3E_O$	I_{YL}	I_Y
		NO	E_L I_Y	I_N	—	E_D I_D	$3I_O$	I_N OR $3E_O$	I_D & I_N	I_Y
B	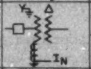	YES	E_L I_{DL}	$3I_O$ & $3E_{OL}$*	—	E_D I_D	$3I_O$ & $3E_O$	—	I_{YL}	I_Y
		NO	E_L I_Y	$3E_{OL}$	—	E_D I_D	$3I_O$ & $3E_O$	—	I_D	I_Y
C	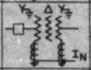	YES	E_L I_{DL}	$3I_{OL}$	I_N OR $3E_{OL}$	E_D I_D	$3I_O$	I_N OR $3E_O$	I_{YL}	I_Y
		NO	E_L I_D	$3I_O$	*	E_D I_D	$3I_O$	I_N OR $3E_O$	I_Y & I_N †	I_Y
D	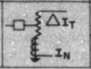	YES	E_L I_{DL}	$3I_{OL}$	I_N OR I_T OR $3E_{OL}$	E_D I_D	$3I_O$	I_N OR $3E_O$	I_{YL}	I_Y
		NO	E_L I_D	$3I_O$	*	E_D I_D	$3I_O$	I_N OR $3E_O$	I_Y & I_N OR I_T	I_Y

Fig. 1. Connection guide for high-speed simultaneous clearing of transmission lines with a transformer termination

E_D = Delta bus voltage
E_L = Delta line voltage
$3E_0$ = Residual bus voltage
$3E_{0L}$ = Residual line voltage
I_D = Bus side delta current
I_Y = Bus side wye current
I_{DL} = Line side delta current
I_{YL} = Line side wye current
$3I_0$ = Bus side residual current
$3I_{0L}$ = Line side residual current
* See Fig. 2
† See Fig. 3

tem, the direction of the fault is determined independently at each station and the result transmitted over the channel. Generally, this system is more flexible to system changes and addition of taps. A more detailed comparison of the two systems utilizing a carrier or microwave channel is given in reference 3.

Choosing the Electrical Quantities

A further job of the relay engineer is the selection of the electrical quantities for operating the relays and at what point in the system these quantities should be measured. The decision on where to measure is based on the requirements of the protective system or, if the choice is restricted, compromises may be necessary in the protection. This is one of the areas where system design can appreciably influence protective relaying.

The problems encountered in selecting the quantities are well illustrated where the transmission line terminates in a transformer bank and where either line-side or bus-side current and potential quantities may be used. Sometimes it is best to use bus-side quantities to enable the line protection system to clear bank faults, even though bank differential relays are present. However, bus quantities are not always satisfactory. Bus side zero-sequence current or voltage will not suffice for ground relaying of the line where the bank is connected wye-delta. Also, bus side current may not be satisfactory where the line is terminated in a transformer bank and high-speed reclosing is desired following line faults. If bus side current is used, the line relays are likely to trip for transformer faults and initiate reclosing. Since it is not considered desirable to reclose following a transformer fault, it is necessary to use line side current or to provide a remote trip channel to block reclosing of the remote breaker on transformer faults. To block reclosing, the remote trip signal must be received at the remote station before reclosing can be initiated by the line relays.

In some cases, the remote trip channel may also be used to block reclosing. This feature may obviate the need for blocking line relay tripping on bank faults by the use of line side quantities, if the differential relays can initiate a remote tripping signal before the line relays set up reclosing. Some delay in initiating the reclosing may be necessary to assume positive blocking for transformer faults.

One other illustration of the effect on on the protection of the point of measurement of the electrical quantities applies to the application of distance-type relays. With these relays, line side potential or its equivalent is preferable to bus voltage. This is particularly true where the bank impedance is large in relation to that of the line. Since the instantaneous elements should be set to protect a maximum of 80 to 90 per cent of the total impedance to the remote bus, a large bank impedance will limit line coverage when using bus side voltage. As an example, assume that the impedance of the line is Z and of the bank $2Z$. With the instantaneous element Z_1 set for 85 per cent of the total $3Z$, only 45 per cent of the line is covered. However, the use of bus potential will not compromise the first line protection since the carrier tripping element Z_2 is set to overreach the remote bus.

Two-Terminal Line With Transformer Termination

The electrical quantities which should be utilized for a 2-terminal line with a transformer termination are listed in Fig. 1 for four types of power transformer connections. These are generally the preferred or recommended connections, and it should be recognized that special circumstances may alter them. For each case solutions are given with and without high-speed reclosing for both phase- and directional-comparison systems. In all instances the distance relays at station I receive line voltage or the equivalent, while they use line-side current only for high-speed reclosing applications. At station II, the distance relays are always connected in standard fashion. The station II arrangement for the phase-comparison system can likewise be standard in every instance. Since the phase-comparison system is susceptible to tripping on magnetizing inrush current, a suppressor should be used where the bank is in the protective zone. The trip suppressor can be eliminated by using line-side currents but then, as suggested previously, remote tripping equipment is necessary in order to clear transformer faults at station II. Some of the special considerations are detailed in the following.

Case A

Where a delta-way bank is used with the ground on the line side, the ground relay in the directional-comparison scheme may be nondirectional at station I of Fig. 1, if bank fault tripping can be tolerated. For phase comparison the low-side current transformers at station I are connected in delta. Sensitive ground fault protection is attained by using bank neutral current at station I and comparing it with residual current at station II via the channel.

Where microwave or pilot wire is used, the channel could be employed for transfer tripping. A single impedance element per phase and a directional ground relay at station II could be set to look into the bank and clear both circuit breakers at high speed for all line faults. The relays trip the station II circuit breaker direct and the station I breaker by remote tripping. Where high-speed reclosing is desired, this system is not adequate since line relay tripping will occur on some bank faults.

Case B

Where the delta-wye bank is grounded on the bus side, special ground relay arrangements for the directional-comparison system are utilized, as shown in Fig. 2. The trip elements are energized with residual voltage and residual current respectively at stations I and II, while the reverse is true for the start or blocking elements.

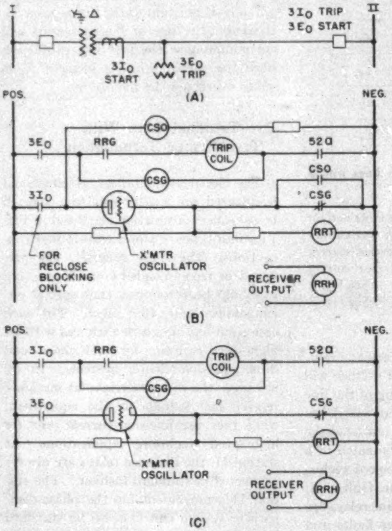
I
Y Δ
3I0 TRIP
3E0 START
II
3I0 START
3E0 TRIP
(A)
POS.
NEG.
CSO
3E0
RRG
TRIP COIL
52a
CSO
CSG
3I0
CSG
RRT
FOR RECLOSE BLOCKING ONLY
X'MTR OSCILLATOR
RECEIVER OUTPUT
RRH
(B)
POS.
NEG.
3I0
RRG
TRIP COIL
52a
CSG
3E0
CSG
RRT
X'MTR OSCILLATOR
RECEIVER OUTPUT
RRH
(C)

Fig. 2 (left). Carrier ground tripping with residual voltage 2-terminal line

A—Single line
B—Station I circuits
C—Station II circuits
RRG, RRH, RRT = Carrier auxiliary relay
CSG, CSO = D-c auxiliary elements
$3E_0$ = Instantaneous residual voltage element
$3I_0$ = Instantaneous residual current element

Fig. 3 (below). Pilot-wire protection of a line and wye-wye-delta bank

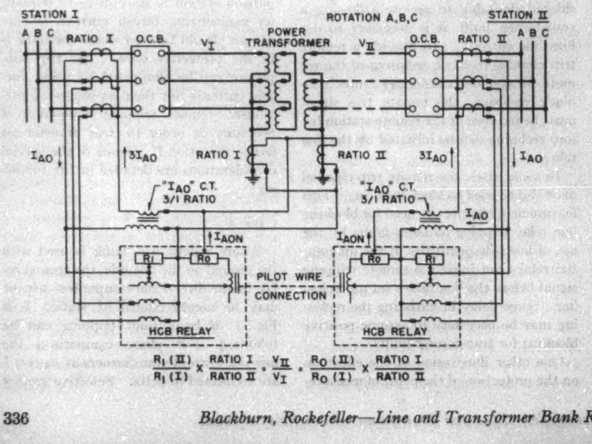
STATION I
A B C
RATIO I
O.C.B.
V_I
POWER TRANSFORMER
ROTATION A,B,C
V_II
O.C.B.
RATIO II
STATION II
A B C
I_AO
3I_AO
RATIO I
RATIO II
3I_AO
I_AO
"I_AO" C.T. 3/1 RATIO
"I_AO" C.T. 3/1 RATIO
I_AO
I_AON
I_AON
R1
R0
R0
R1
PILOT WIRE CONNECTION
HCB RELAY
HCB RELAY
R1 (II)/R1 (I) x RATIO I/RATIO II . V_II/V_I . R0 (II)/R0 (I) x RATIO I/RATIO II

When a line-to-ground fault occurs in the line section, the *CSG* element is picked up by $3E_0$ at station I and by $3I_0$ at station II. At both stations, the *CSG* contact opens to stop any possible transmission of a blocking signal and also removes the short circuit from the *RRT* coil. Since no blocking current is flowing in the holding coil *RRH*, the tripping current in the *RRT* coil causes the carrier relay contact *RRG* to close, permitting the $3E_0$ and $3I_0$ elements at stations I and II respectively to trip the breakers.

The $3I_0$ element at station I is required only if it is desired to segregate line tripping from bank tripping for reclosing purposes. Then, for faults in the bank at station I, the $3I_0$ as well as the $3E_0$ element picks up at station I. The $3I_0$ element takes preference, because of the *CSO* element, and starts transmission of a blocking signal as well as short-circuiting the *RRT* coil to prevent local tripping. The blocking signal produces holding current in the *RRH* coil at station II. This current prevents tripping even though the *RRT* coil is energized.

If the fault is beyond station II, the $3E_0$ element starts transmission at station II to block the $3E_0$ trip at station I. For this fault, no zero-sequence current is present in either circuit breaker.

Case C

Where a wye-wye-delta tertiary bank is used, the phase-comparison connections are of interest. A standard system is utilized for high-speed reclosing, but where the bank is included in the line protective zone the connections should be made as shown in Fig. 3.

The *HCB* pilot wire relay of Fig. 3 employs a composite filter whose single-phase output voltage is a function of both positive- and zero-sequence current. The open-circuit filter voltage for this special connection, but without the 3/1 I_{A0} current transformer, is

$$E_F = 2I_{A1}R_1 + I_{A0}R_1 + I_{A0N}R_0 \qquad (1)$$

Where no zero-sequence source is present within the protective zone, the filter output voltage is the same at both stations for an external fault. However, in this particular case, the neutral current at station I produces an $I_{A0N}R_0$ voltage, while the same current flowing to an external fault would normally produce at station II not only the balancing $I_{A0N}R_0$ voltage but a spurious $I_{A0}R_1$ potential as well. In Fig. 3, this latter response is eliminated by shunting I_{A0} around the R_1 resistor by means of the I_{A0} current transformer. By this means the filter response is modified and the open-circuit filter voltage becomes

$$E_F = 2I_{A1}R_1 + I_{A0N}R_0 \qquad (2)$$

By inserting the net bank neutral current into the station I filter, an equal response is obtained at both stations regardless of the current distribution, provided that

$$\frac{V_{II}}{V_I} = \left(\frac{\text{ratio I}}{\text{ratio II}}\right)\left(\frac{R_1\,(\text{II})}{R_1\,(\text{I})}\right) = \left(\frac{\text{ratio I}}{\text{ratio II}}\right)\left(\frac{R_0\,(\text{II})}{R_0\,(\text{I})}\right) \qquad (3)$$

where R_1 and R_0 are the tap values of the filter resistors, and V is the system voltage. Equation 3 states that the filter responses can be equalized either by proportioning the current-transformer ratios or the filter resistor taps, or a combination of both.

The current transformer connections in Fig. 3 apply equally well for *HKB* carrier relays. The *HKB* filter responds to both positive- and negative-sequence current as well as to zero-sequence current. The open-circuit voltage for this connection, but without the I_{A0} current transformer, is

$$E_F = K_1I_{A1} + K_2I_{A2} + I_{A0}R_1 + I_{A0N} + R_0 \qquad (4)$$

where K_1 and K_2 are constants whose values vary with settings. A comparison of equations 4 and 1 shows that the zero-sequence responses are the same in both relays. Therefore, the I_{A0} current transformer may again be used to modify the filter voltage as

$$E_F = K_1I_{A1} + K_2I_{A2} + I_{A0N}R_0 \qquad (5)$$

While an actual magnitude comparison is not made with the carrier scheme, the filter responses should be very nearly the same to insure proper time co-ordination between the start and trip fault detectors of the *HKB*. The I_{A0} current transformer should, thus, be utilized unless the spurious $I_{A0}R_1$ response is of negligible magnitude.

CASE D

The use of an autotransformer necessitates additional consideration not present with the wye-wye-delta bank of case *C*. Where the phase-comparison scheme includes the bank, the connections will be the same as in Fig. 3 except that the current-transformer ratios and filter resistor taps should be proportioned as follows

$$\left(\frac{R_1\,(\text{II})}{R_1\,(\text{I})}\right)\left(\frac{\text{ratio I}}{\text{ratio II}}\right) = \frac{V_{II}}{V_I} \qquad (6)$$

$$\frac{R_0\,(\text{II})}{R_0\,(\text{I})} = \frac{\text{ratio I}}{\text{ratio II}} \qquad (7)$$

The ratio of the neutral current-transformer should match the ratio of the local line current transformers. With this arrangement, the R_0 settings are not a function of the power-transformer voltage ratio.

If tertiary current is used instead of neutral current, the current-transformer ratios should be

$$\frac{V_I}{V_T} = \frac{\text{ratio } T}{\text{ratio I}} \qquad (8)$$

where V_T and ratio T are the voltage and current-transformer ratio of the tertiary respectively.

Three-Terminal Lines

All too frequently a 3-terminal line presents the relay engineer with difficult protection problems. This is particularly true where high-speed simultaneous tripping of all circuit breakers is required for high-speed reclosing.

One of the difficulties which occurs often is the reversal of current through station III for faults *A* or *B* of Fig. 4(A). Even though the fault is in the protective zone, the I_3 current may flow out of the line and to the fault via a tie line (not shown) between stations II and III for fault *B*.

The phase-comparison pilot wire system *HCB* offers the only possibility of simultaneously tripping all three circuit breakers under these conditions, but this is possible only if the current flowing out of one terminal is small compared to the total flowing in the other two. As a good approximation, the published characteristic curves for 2-terminal lines can be

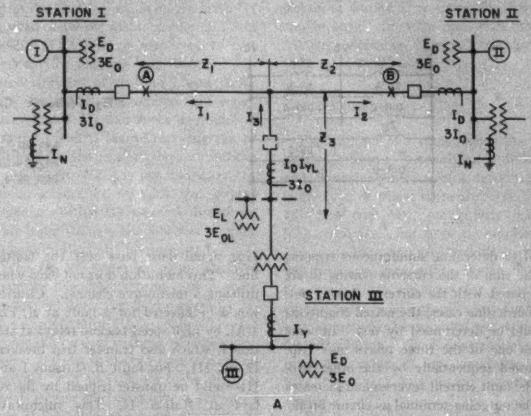

CASE	STATION III CONNECTIONS	TRIP ON BANK FAULT	STATIONS I & II			STATION III			
			PHASE	GROUND		PHASE		GROUND	
				START	TRIP	START	TRIP	START	TRIP
A	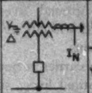	NO	E_D & I_D (Z)	$3I_0$	$3I_0+I_N$ OR $3E_0$ (DIR)	E_L & I_D (HZ-3)	E_L & I_{YL} (H3)	$3I_0$	$3I_0+I_N$ OR $3E_{OL}$ (DIR)
		YES	E_D & I_D (Z)	$3I_0$	$3I_0+I_N$ OR $3E_0$ (DIR)	—	E_D & I_Y (H3)	—	I_N
B	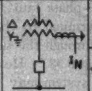	NO	E_D & I_D (Z)	$3I_0$ & $3E_0$	$3I_0+I_N$ OR $3E_0$ (DIR)	E_L & I_D (HZ-3)	E_L & I_{YL} (H3)	$3I_0$	$3E_{OL}$
		YES	E_D & I_D (Z)	$3I_0$ & $3E_0$	$3I_0+I_N$ OR $3E_0$ (DIR)	—	E_D & I_Y (H3)	—	$3E_{OL}$

B

Fig. 4. The 3-terminal line directional-comparison relaying connection guide

E_D, E_L, $3E_0$, and $3E_{0L}$ are the same as in Fig. 1
I_D = Delta current
I_Y = Wye current
$3I_0$ = Residual current
I_{YL} = Line side wye current

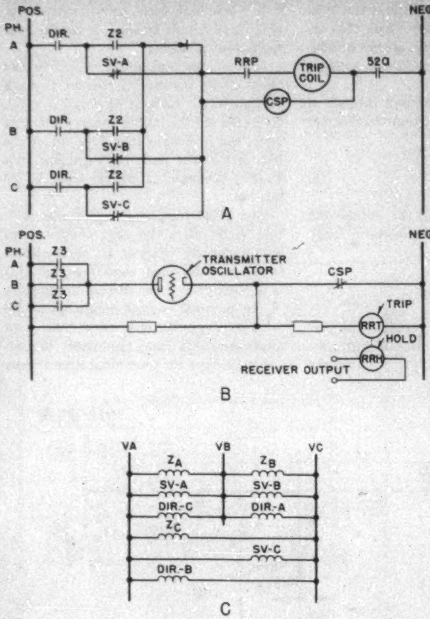

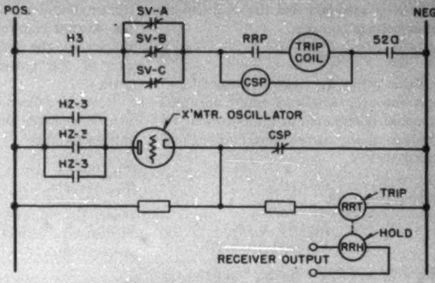

Fig. 5 (left). The addition of instantaneous voltage elements to a directional-comparison system

A—Tripping
B—Carrier control
C—Potential coil connections
DIR = Directional element
Z2, Z3 = Impedance elements
RRP, RRH, and RRT = Carrier auxiliary relay
CSP = D-c auxiliary element
SV = Instantaneous voltage element

Fig. 6 (above). Carrier and voltage-supervised tripping of a polyphase directional element

H3 = Polyphase directional element
HZ-3 = Impedance elements
RRP, RRH, RRT, CSP, and SV are the same as in Fig. 5

used to determine simultaneous tripping if the sum of the currents flowing in are compared with the currents flowing out. In borderline cases, the actual conditions should be determined by test. In some cases one of the three relays may trip, followed sequentially by the other two, as the fault current reverses and increases in the outgoing terminal as circuit breakers open. This pilot-wire system is applicable to 3-terminal lines where the pilot-wire resistance is below 500 ohms per leg and the shunt capacitance is below 0.60 microfarad per leg.

With directional-comparison or phase-comparison carrier schemes, simultaneous tripping is not possible. If the I_3 current for the case of reverse at station III is sufficiently large to operate the carrier start elements, carrier tripping will be prevented at all line terminals. If the current reversal at station III is too small to operate the start elements, circuit breakers I and II will be tripped by the carrier relays while breaker III will clear sequentially.

However, high-speed simultaneous clearing is possible with transfer tripping where I_3 reversal occurs. A transfer trip system with a power-line carrier channel is not considered feasible since the tripping signal must pass over the faulted line. This limitation does not exist when utilizing a microwave channel. Clearing would be effected for a fault at *A*, Fig. 4(A), by high-speed backup relays at station I, which also transfer trip breakers II and III. For fault *B*, stations I and III would be transfer-tripped by the relays at station II. This microwave scheme is possible because the reversal at station III occurs only for fault *A* near station I or for fault *B* near station II up to, but not at, the tap point. Thus, in most cases, instantaneous phase distance and instantaneous ground overcurrent relays can be applied without overreaching the remote stations.

Phase-comparison carrier is not widely applicable to 3-terminal lines, since the ratio of minimum 3-phase fault current through any line terminal to the maximum load current through the same terminal must be at least 3.33.[4] However, a modified 2-terminal system may be used, where the current contribution of station III is too small to pick up the fault detectors at stations I and II for a fault beyond one of these latter stations. Where there is negligible backfeed, a blocking terminal is applied at station III if slow-speed clearing of circuit breaker III is tolerable. Overcurrent relays at station III pick up for local external faults and key carrier to block tripping of stations I and II.

Another difficulty on 3-terminal lines is frequently present when applying a directional-comparison scheme to the line of Fig. 4(A). Distance elements at station III (current flowing in) do not encounter the actual impedance Z_3+Z_1 for fault *A*. Instead they see

$$Z_{\text{apparent}}=Z_3+Z_1(I_1/I_3)=Z_3+Z_1+Z_1\times(-I_2/I_3) \quad (9)$$

and similarly for fault *B*

$$Z_{\text{apparent}}=Z_3+Z_2(I_2/I_3)=Z_3+Z_2+Z_2\times(-I_1/I_3) \quad (10)$$

The minus sign on I_1 and I_2 indicates the current flows in the direction opposite from that shown in Fig. 4(A) for the faults involved.

This additional impedance is caused by the voltage drop produced by infeed current, or current not measured by the relays at station III. This distance-element underreach increases as the current contribution of station III becomes proportionately smaller. Where I_3 is very small compared to I_1 or I_2, it is not possible to set the zone-2 impedance elements to reach the station I and II busses.

When I_3 becomes too small for proper

distance-element reach, there is no need to clear breaker III from the standpoint of system stability. However, a very small current will maintain a fault arc so that, where high-speed reclosing of I and II is required, circuit breaker III must be cleared simultaneously with I and II to effect extinguishing of the arc before reclosing.

The breaker III reach may be extended by the use of the instantaneous voltage elements, whose contacts are connected in series with the directional-element contacts of the distance relays. Fig. 5 shows the simplified connections for this system. When a phase fault occurs on the line but is beyond the reach of the zone-2 distance elements, tripping can be effected when one of the voltage elements *SV* drops out. The closing of *DIR* and *SV* causes the *CSP* element to be energized. The *CSP* contact in Fig. 5(B) removes the short circuit on the tripping coil *RRT* of the receiver relay. Since the holding coil *RRH* of this receiver relay is not energized by a blocking signal from station I or II, the *RRT* coil current closes the receiver relay contact *RRP* in Fig. 5(A). Tripping of the circuit breaker then occurs through *DIR*, *SV*, and *RRP*.

The *SV* distance-element system would be applicable where the dashed bus of Fig. 4(A) is present. The line-side bus would only exist when an additional tie line is connected to station III. A set of 3-zone distance relays could then be justified on the basis that a large I_3 is available when this tie is in service. The *SV* elements are of value when this tie line is open and I_3 is supplied only by the transformer bank. For correct operation of the scheme on faults beyond stations I and II, the carrier start elements at stations I and II must operate for all faults seen by the *SV* and Z_2 elements at station III.

The relaying considerations can be quite different where the dashed circuit breaker and bus at station III of Fig. 4(A) are not present. With the line terminated in a transformer bank, the fault current source III is frequently nonexistent or very small in comparison to sources I and II. Distance-relay underreach caused by current infeed is likely to be serious. Where high-speed simultaneous tripping is required, the following two solutions are considered, utilizing directional-comparison carrier relaying.

Case A

In Fig. 4(B), the electrical quantities are listed for the case of a wye-delta bank at III, with the line side grounded and no high side breaker. The connections of stations I and II are standard. However, for phase tripping at station III, a polyphase directional relay *H*3 is utilized in conjunction with instantaneous voltage elements. The d-c circuits for this system are shown in Fig. 6. Carrier tripping occurs through the *H*3, *SV*, and *RRP* contacts. The *RRP* contact is the supervising feature of the circuit, since it will remain open if a carrier signal is received from either station I or II. Stations I and II, in turn are supervised by station III. The blocking signal from station III is initiated by the distance relay *HZ*-3 in Fig. 6. This relay is employed to prevent carrier tripping and, hence, high-speed reclosing of stations I and II for bank faults. If the remote trip signal from station III can block reclosing of stations I and II before reclosing can be initiated by the carrier relays at stations I and II, the *HZ*-3 is not necessary. A similar choice exists with the ground relays at station III where a directional relay is needed only when carrier tripping on bank faults must be prevented.

The *H3-SV* system is more sensitive than the standard scheme and is more economical than the 3-zone distance relays where source III is small. The *H*3 should not be used without voltage supervision, since it is likely to operate for an external fault too remote to be seen by the Z_3 carrier start elements at stations I and II. Should the start elements at stations I and II fail to operate, incorrect tripping of circuit breaker III will occur if voltage supervision is not used. The Z_3 settings should be made so that all external faults which cause *SV* dropout also result in the Z_3 operation.

Case B

Fig. 4(B) also lists the electrical quantities to be used with a wye-delta bank at station III when the bus side winding is grounded and there is no high side circuit breaker. The phase fault protection is the same as that of case *A*, but special consideration is necessary on the ground fault system. Since no zero-sequence current is available at station III for a line fault, carrier-supervised tripping must be effected with a voltage element $3E_{0L}$.

If the fault is internal, the directional elements in conjunction with overcurrent elements will stop carrier transmission at stations I and II so that the $3E_{0L}$ element at station III can clear the fault. If the fault is external and beyond station I, an overcurrent element at station I will operate to start carrier and block tripping of stations II and III. The $3E_0$ elements can also start carrier at stations I and II. For the fault beyond station I, the current contribution from station II may be below the overcurrent start-element pickup at station I, or circuit breaker II may be open. In either case, without the $3E_0$ start elements, incorrect tripping of station III would occur.

Conclusions

The solution of a transmission-line relaying problem is generally more difficult and expensive where a bank termination is involved or where there are more than two line terminals, particularly where high-speed reclosing is to be employed. Minor modifications to standard systems will in some cases suffice, while instantaneous voltage elements for phase or ground tripping or a transfer trip channel may sometimes be required for a satisfactory solution. The most commonly encountered problems are catalogued in Figs. 1 and 4 as a guide for convenient reference.

References

1. PILOT-WIRE CIRCUITS FOR PROTECTIVE RELAYING—EXPERIENCE AND PRACTICE, 1942–1950, **AIEE Committee Report.** *AIEE Transactions*, vol. 72, pt. III, April 1953, pp. 331–36.

2. PROTECTIVE RELAYING OVER MICROWAVE CHANNELS, **H. W. Lensner.** *AIEE Transactions*, vol. 71, pt. III, Jan. 1952, pp. 240–45.

3. CONSIDERATIONS IN SELECTING A CARRIER RELAYING SYSTEM, **R. C. Cheek, J. L. Blackburn.** *Ibid.*, pp. 10–18.

4. PHASE-COMPARISON RELAYING FOR 3-TERMINAL LINES, **H. W. Lensner.** *AIEE Transactions*, vol. 72, pt. III, Aug. 1953, pp. 697–702.

◆

Discussion

H. P. Bruncke (Northern States Power Company, Minneapolis, Minn.): The authors are to be commended for their paper and for the way in which they have outlined the various phases of the problem suggested in the title. The tabulation of types of relays for certain conditions is also very helpful.

I would like to comment on the authors' comparison between the phase- and directional-comparison relay systems. It was stated that the biggest advantage of the phase-comparison system appears to be its low cost. This is true if the protection engineer will be satisfied with just the so-called first-zone operation. In the event that backup protection is required, then the cost of the phase-comparison system will increase sharply. The phase-comparison system, of course, has the advantage that it does not require potential trans-

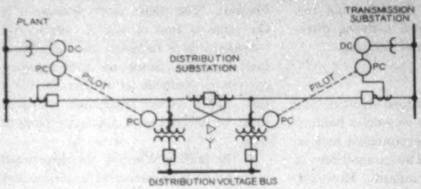

Fig. 7. Relay scheme for a transmission line with a distribution substation tapped on

DC — Directional-comparison relays
PC — Phase-comparison relays

formers. On the basis of this fact a relay scheme incorporating both the phase-comparison and the directional-comparison relays is suggested.

The authors have grouped the problems into two classes: 3-terminal lines and lines terminating in a transformer. I would like to suggest a third class, i.e., a transmission line tapped by a distribution substation. The combination relay scheme can be used for this third class. In Fig. 7 this scheme is used on a transmission line with circuit breakers at each end and with a distribution substation in the line. The distribution substation consists of two transformer banks connected to the line through air-break switches with a circuit breaker between the connection. The low side of the banks is provided with circuit breakers which will be connected to a solid distribution voltage bus. The directional-comparison relays are provided for the circuit breakers at each end of the transmission line. These will not be the carrier-current pilot type. The phase-comparison relays will be provided between the tie circuit breaker at the distribution substation and the circuit breaker at each end of the line. The relays at the distribution substation will be energized by parallel connection of the current transformers in the circuit breaker and in the high side of the transformer bank. The relays will be provided with a carrier-current pilot; thus the overall picture will be first-zone operation for each section when the phase-comparison relays are in operation and backup protection in the event that the phase-comparison relaying is out of service. The directional-comparison relays will then protect the system for faults on the transmission lines.

The authors mentioned that "system design can appreciably influence protective relaying." I believe that quite a few relay engineers have experienced the fact that usually the transmission system is laid out, and about the time the line is to be built or connections are to be made the relay engineer is consulted regarding how it can be protected. I concur with the authors that system designs should be influenced by the type of protective relaying which is available.

I agree with the authors that in the case of failures of transformer banks it is not desirable to reclose either the line or the bank; of course, with remote trip either by carrier or other means this can be accomplished very easily. Mr. Blackburn and Mr. Rockefeller mentioned that transfer trip schemes with power-line carrier channel are not considered feasible since the tripping signal must pass over the faulted line. It is agreed that there is a possibility that the signal may not reach the other end of the line; however, the chances are that a line fault will not occur at the same time that the transformer fault occurs. In all cases where transfer trip is used with power-line carrier it has been a practice to install a wave trap between the line and the transformer terminals to eliminate just such a condition as the authors refer to.

J. R. Linders (Cleveland Electric Illuminating Company, Cleveland, Ohio): The authors have presented a very worth-while and timely subject. The combined protective relay problems of transformer protection, no high-side transformer breaker, multiterminal transmission circuits, and high-speed clearing and reclosing requirements can only be solved by the complete assimilation of papers such as this. When one considers modern-day equipment reliability with its reduced maintenance requirements plus the precise knowledge of system performance gained from a-c network analyzer studies, the complex power circuits described in this paper are certain to become commonplace in the near future. I personally believe the relay engineer will be fortunate if his problems stay as simple as presented here.

It would therefore be appropriate if more background could be provided on some of the points touched on in this paper. For example, the development of equation 2 could be expanded in the author's closure or additional references provided.

In order to satisfy equation 8, the current transformer in the tertiary of a large autotransformer which we are now installing on our system would have required a ratio of 20,000 to 5. Since we have had no experience with anything near this ratio we were forced to develop an alternate solution using a directional-comparison method. It is quite possible that the contribution from this winding could have been entirely ignored, but we did not have the time to develop the significance of doing this. The relay application engineer must fully understand the principles behind relationships of all of these equations if he is to avoid pitfalls.

I believe there are additional considerations to the use of neutral currents, from autotransformers and would suggest an additional reference.[1]

The more complete solution to the 3-terminal line problem by means of transfer trip via microwave as contrasted to a carrier scheme fits in with our own plans. Since experience with this new medium is extremely limited, we believe it is essential to provide some type of fault detector to supervise the trip signal. In the case cited of the outfeed from the third terminal, a conventional fault detector responsive to conditions at this third terminal is not possible. We therefore plan on permitting tripping at station III for faults near station I or station II only when the second-zone indication from the second station as well as first-zone indication from the first station are received simultaneously at station III. Since these signals will arrive over completely separate microwave facilities, the possibility of a false tripout from any cause (including testing!) is very remote. Only experience will tell if the reliability is adversely effected by requiring two separate systems to respond properly to provide a trip signal.

The transfer trip signal originating from a transformer protective relay operation likewise cannot have the security of a local fault detector at the receiving terminal. In this case we are planning on permitting the tripping upon the reception of a single transfer trip signal. However, we plan on then immediately inspecting the line for 3-phase potential. If this exists, the trip signal was false and the breaker will be immediately reclosed, and the transfer trip equipment locked out. Since our system must obviously be set up to handle a tripout and reclosure no harm will be done. There are obviously other facets to these problems and several relay communication channels will be required to do the entire relaying job.

In conclusion I would like to return to my opening thought on the complexities of future power systems and suggest that we can simplify one area of thought communication by using standard terminology and function numbers where applicable rather than manufacturers' specific type or model designation.

REFERENCE

1. GROUND RELAYING POLARIZATION, J. L. Blackburn. *AIEE Transactions*, vol. 71, pt. III, Dec. 1952, pp. 1088–95.

Charles Morrison and **M. A. Jansen** (The Potomac Edison Company, Hagerstown, Md.): The authors have presented effectively and concisely an outline of the problems associated with the protection of 3-terminal lines and lines with transformer termination. In this connection some of our company's experience may be of interest.

Power-line carrier is used exclusively as the channel for all pilot-type relaying because we believe this type of channel is less susceptible to extraneous influence than any of the other types available. For reasons that will be amplified later phase-comparison relaying is now limited to 2-terminal metallic circuits, all relatively short. For general application, including 3-terminal lines and lines with transformer termination, we are using directional-comparison relays having modified impedance characteristics. Our experience justifies a continuation of this policy as to both relays and relaying channels.

Our first application of phase-comparison relays was made on a 3-terminal line, two terminals of which included transformers. Referring to Fig. 4, one of these was a case-A and the other a case-B terminal. Bus side currents were used in both cases, and high-speed reclosing was installed at all terminals, but was not particularly successful. Tests indicated that this was brought about partly by transformer magnetizing inrush current, actually by the difference in inrush current per phase when the case-A transformer was re-energized from the terminal at station I. Tests indicated that by desensitizing the phase-comparison relay at station I with respect to zero-phase sequence current this difficulty would be eliminated. However, in this particular situation delayed tripping was less acceptable than delayed reclosing, so this expedient was not adopted for regular operation.

Incidental to these tests we noted some delay in the reset time of the phase-comparison relays and some unaccounted-for phase-angle differences between local electrical quantities and those received from remote terminals for through faults. The first difficulty was corrected by internal changes in the relays, but before the second could be rationalized the needs of the system made it necessary to break the circuit apart as far as relaying was concerned. However, for these and other reasons we had decided by this time to use directional-comparison relaying on most of our high-voltage transmission system, and some had already been installed. Phase-comparison relaying was restricted to short 2-terminal lines without transformer termination; in fact, for this purpose phase-comparison relaying is unique, and additional terminals have been installed by us for that reason.

In addition to the two types of carrier pilot relaying in general use on our system, we have three remote trip schemes operating over frequency-shift carrier channels. These are all special applications used in connection with lines having transformer termination. Since the circumstances and equipment differ in each case these will be described individually.

CASE 1

This is a 3-terminal application having one transformer termination similar to case B, Fig. 4. The relaying quantities used for line faults are those taken from the line side of the transformer at station III. Since the line relays do not initiate tripping of any breakers for a transformer fault, high-speed reclosing is not blocked by operation of the line relays. The transformer at station III is protected from internal faults by variable percentage differential relays, which initiate tripping of the local breaker on the bus side of the transformer and block its reclosing. The differential relays at station III also function to set up the remote trip signal to stations I and II over the frequency-shift channel. Since this line is of primary importance to the power system and we had no previous experience with frequency-shift equipment, we interlocked the trip circuit of this scheme at stations I and II with the blocking circuit of the carrier pilot relays which protect the line between stations I, II, and III. The performance of this combined relaying system is as follows:

a. For a line fault the directional-comparison relays at all stations operate in the usual manner. Breakers at stations I, II, and III trip and reclose.

b. For a transformer fault the differential relays at station III operate to trip the local breaker and block its reclosing. They also initiate the transfer trip signal to stations I and II. At the same time station III line relays transmit a blocking signal to the line relays at stations I and II. The receipt of both signals at stations I and II set up the trip circuit to trip the line breakers and block their reclosing.

CASE 2

This is also a 3-terminal line having a transformer termination similar to case 1; however, the circuit itself is not considered as important as that described in case 1. At station III the quantity $3E_{0L}$ is used for ground relaying, but for the phase relays bus side quantities E_D and I_Y are used. The line and transformer are thus protected as a unit, the transformer impedance being relatively large. Although at station III this limits the line coverage of the instantaneous elements, at stations I and II it permits setting them into the transformer for full line coverage. In addition to this over-all protection, the transformer will in the near future be equipped with a rate-of-pressure-rise device which will function as a relay to trip the local breaker at station III, and, by means of a remote trip channel, the breakers at stations I and II. No interlocking signal is planned for this circuit. Breaker reclosing will be blocked when their tripping is initiated by the transformer pressure-rise device.

CASE 3

This is a 2-terminal line having an autotransformer at one terminal similar to case D, Fig. 1. However, the autotransformer at station I has both line and bus side breakers and is protected by variable percentage differential relays which trip the two breakers in case of a fault between them. Because the autotransformer is in itself a source of zero-phase sequence current to the system, I_D and I_{DL} are used for the differential relays. Over-all protection for the line and transformer is provided by time-delay overcurrent relays at station I and distance relays with instantaneous elements at station II. The transformer impedance is again relatively large and the instantaneous elements at station II can be set into the transformer impedance for full line coverage. This fact is used to advantage and by means of a remote trip frequency-shift channel nondelayed tripping is transferred to the bus side breaker at station I for the usual line faults. The bus side breaker is used to clear line faults in order to limit the duty on the line side breaker to the clearing of transformer faults beyond the reach of the instantaneous relay elements at station II.

These three applications illustrate the adaptations which may be made in the protection of a transformer as part of a line terminal. They further illustrate the use of electrical quantities suggested by the authors in Figs. 1 and 4. In connection with case D, Fig. 1, we make a qualifying comment with reference to the quantities suitable for ground-relay polarization at station I. Neither I_N nor I_T can be used indiscriminately for ground-relay polarization when supplied from an autotransformer. We realize that Mr. Blackburn has previously presented the reasons why these quantities are not satisfactory under all conditions (see ref. 1 of Mr. Linder's discussion) but we believe this should be referred to in this paper.

The authors' suggestions for correcting the underreach of distance relay elements due to current infeed on 3-terminal lines are all of considerable interest. One of these, illustrated in Fig. 5, may have an application for us, where in one instance this problem was particularly troublesome.

G. W. Hampe (Commonwealth Edison Company, Chicago, Ill.): The authors are to be congratulated on their courage and industry in tackling the grueling job of setting up preferred connections for the cases likely to be encountered in the field. With these fairly well established, I would like to discuss what to do next. The authors discussed automatic reclosures and special adaptations such as blocking automatic reclosure when transformer faults are indicated.

One trouble with the present type of automatic reclosing is that it was developed for one particular type of high-voltage system, namely a pure transmission system. In such a system there are only one or two system ties, and reclosure must be made at high speed, or the two ends of the system have lost synchronism. Many present systems, including that of my company, are dual purpose, i.e., for transmission combined with distribution. The Northern Illinois area, including Chicago, is solidly interconnected with 138-kv lines. The quick removal of one 138-kv line could cause loss of synchronism only under very special circumstances. The lines remote from the metropolitan area may have three to five terminals, some with no breakers on transformer taps. Some have single-phase 138-kv grounding switches to cause remote tripping for transformer protection. Only a few of the lines can profitably use high-speed reclosing.

The lines are generally well shielded with static wires and tower-footing resistance is fairly low. Hence in the few cases when lightning does strike it is vicious and the strokes tend to be repetitive. I pointed out in another discussion[1] that the effectiveness of conventional reclosing equipment has been low. It seems that the sustained and repetitive faults were (and will be) about 30 per cent of the total, not counting the grounding switch operations. Thus it seems that we should do some further pioneering on the subject of reclosing. Consider the following suggestions:

1. There should be no distinction in the manner of tripping. That is, reclosure could occur whether the line tripped from carrier pilot, ground instantaneous, distance (all zones), or ground backup.

2. On any trip as in item 1, the local directional- or phase-comparison carrier transmission should be turned off and held off while the local breaker opens and about 15 cycles thereafter. At the end of this period carrier control would be returned to the conventional carrier start-and-stop elements.

3. On lines requiring reclosing with speed, a carrier receiver relay should suspend reclosure until incoming signals stop, after which it is to be completed without further delay.

4. On lines not requiring speed, voltages taken from line connected potential transformers or devices should be used to determine when the line is de-energized. After it registers as de-energized, reclosure is to be completed.

5. Arrangements should be made for reclosure of a line on a sound, balanced backfeed. This could be used on all lines, but particularly on multiterminal lines. To detect the sound backfeed a relay which closes on positive-sequence line voltage V_1 or on $V_1 - V_0$ could be used.

6. On lines where automatic grounding switches are used, and possibly other multiterminal lines, use item 4 at only one terminal and item 5 at all the others. The terminal with item 4 would probably be one of low fault current capability. If it closed, and did not retrip, the major and other minor terminals would then follow by item 5. With such functions, the need for blocking reclosing by closely co-ordinated remote trip channels is considerably reduced. Remote trip channels may still be needed where high-speed reclosing is desired.

These suggestions do not exhaust the possible combinations. For reasonable effectiveness of automatic reclosing on high-voltage transmission-distribution grids automation along the lines of the foregoing seems to be needed.

REFERENCE

1. *Discussion* by **G. W. Hampe** of OPERATING EXPERIENCE WITH 230-KV AUTOMATIC RECLOSING ON BONNEVILLE POWER ADMINISTRATION SYSTEM, **D. A. Gillies.** *AIEE Transactions*, vol. 73, pt. III, 1954 (Feb. 1955 section), p. 1695.

J. L. Blackburn and G. D. Rockefeller: The discussers valuable contributions to this paper are appreciated.

With reference to Mr. Bruncke's discussion, the comparison between phase- and directional-comparison systems did not include any backup protection. A more complete discussion of this is given in reference 3 of the paper. It also happens that many applications of phase-comparison relays are made using distance-type relays for phase backup protection. Even with this complement, the cost is essentially the same as an all-directional comparison scheme. One further advantage of the phase-comparison system was brought out by Mr. Morrison and Mr. Jansen. This is the independence of the phase-comparison scheme to fault voltage which makes it particularly advantageous for very short lines. The third class of protected line suggested by Mr. Bruncke is an interesting variation of the normal 2-terminal line problem.

The last paragraph of Mr. Bruncke's discussion gives us an opportunity to clarify our nomenclature with respect to remote and transfer trip. While not a national standard, the authors have been using the term "remote trip" to signify the tripping of a remote breaker following selected relay operations, such as transformer differential relays, while "transfer trip" signifies the tripping of a remote breaker following the operation of all the protective relays at a local location. In this paper only transfer trip schemes have been outlined. We generally do not consider transfer tripping over carrier acceptable for clearing line faults because of the possibility of the fault short-circuiting or limiting the desired carrier signal. However, it has been used for phase faults where adequate ground-fault protection was obtained through a conventional carrier scheme. Remote tripping as used here refers to the clearing of the remote breaker following a transformer fault.

Mr. Linders requests that equation 2 of the paper be explained. This equation was derived from equation 1, which is the filter response of a standard connected pilot-wire relay. By comparing the two equations it is seen that the $I_{A0}R_1$ term of equation 1 has been eliminated in equation 2. This term in equation 1 results from the flow of I_{A0} current through the R_1 resistor. Referring to Fig. 3, the connection of the I_{A0} current transformer provides a shunting path which prevents I_{A0} from flowing through the R_1 resistor. The 3-unit winding is connected in the residual where $3I_{A0}$ flows and the 1-unit winding, which contains I_{A0}, is connected to shunt the R_1 resistor.

We agree that a 20,000-to-5 ratio in the tertiary of an autotransformer is impractical. It is our belief that the contribution from this winding could be neglected without any adverse effect on the relaying. However, specific data are not available to confirm this belief.

Mr. Linders' solution for clearing station III via transfer trip channels is very interesting. It would appear that the value of separate fault detectors and microwave channels for the transfer trip scheme is somewhat reduced by the application of only one signal indication for remote tripping. While a second channel is not justified economically, it is suggested that two signals be sent over the microwave channel to reduce the possibility of false tripping, particularly during testing.

The inspection for 3-phase potential appears to permit reclosing on light transformer faults which do not reduce the voltage appreciably at the remote station. This would be critical, especially if there are wide variations in normal voltage. Therefore, locking out the remote trip equipment, as outlined, should be examined carefully. The remote trip equipment may be locked out at a time when it is most valuable, i.e., when reclosing into a light transformer fault which does not lower the remote station voltage sufficiently to operate the voltage fault detectors or operate any protective relays at the remote station. Such a fault might operate the sudden pressure-type relay for tripping.

Mr. Morrison and Mr. Jansen give valuable specific applications. We will be pleased if this paper guides and aids individual thinking on each application. There was no intent to present exact solutions to these complex problems.

Operating difficulties with phase-comparison carrier relaying were mentioned. The one difficulty which the discussers did not indicate had been rectified was the unaccounted-for phase-angle differences between the local and remote signals. Mr. Morrison and Mr. Jansen did not indicate the relative magnitude of the phase shift. However, aside from normal manufacturing tolerances, some angular differences should be expected, resulting from the finite time required for both the fault and carrier signal waves to travel the length of the line. Specific field adjustments are now available in modern carrier apparatus to compensate for manufacturing tolerances and the phase shifts which vary with the line length. It is not usually expected that line length compensation will be necessary for lines less than 75 miles in length.

The blocking signal of Mr. Morrison and Mr. Jansen's case 1 should be initiated by the differential relays, since the line fault detector may not operate on all light transformer faults. Supplementing the conventional type of differential relays with a sudden-pressure relay, as mentioned in this discussion, is highly recommended for detecting light internal faults. As these pressure relays generally have a longer operating time, the blocking out of reclosing relays by their operation may not prevent reclosing where the fault is seen by the line relays.

We assume that in Mr. Hampe's third paragraph he is pointing out that in some cases single-shot reclosing is not successful because of repetitive strokes. This problem was considered beyond the scope of the present paper, but certainly seems deserving of more consideration. The problem seems to be one of distinguishing between a single permanent fault and several repetitive transient faults in rapid succession. If the differences between these two types could be identified, then a reclosing system could be designed to meet the operating requirements. In the existing schemes a minimum time interval between faults is required in order to prevent breaker pumping on permanent faults.

We choose to classify Mr. Hampe's suggestions for reclosing as follows:

1. Use the carrier blocking signal for restraining instantaneous reclosing.

2. Use dead-line or "balanced" hot-line slow-speed reclosing, or a combination of the two.

We assume that the objective of scheme 1 is to reclose as soon as the remote breaker or breakers have cleared the faults. In the conventional reclosing system, high-speed reclosing is selective, following high-speed trips, only when carrier is in service. The latter system assumes that simultaneous clearing has occurred. Mr. Hampe is attempting to obviate this assumption by confirming remote breaker clearing before initiating local reclosing.

As long as simultaneous clearing of all breakers occurs the conventional system will suffice. Therefore, Mr. Hampe's scheme is of value where sequential tripping occurs. Further, the proposed arrangement is of use only when the carrier channel is operative, since reclose restraint is dependent on the receipt of a carrier signal. It also seems reasonable to assume that where sequential tripping occurs the final breaker to clear trips by carrier. The close circuit of some of the breakers is energized at about the instant that the trip coil of the final breaker is energized.

Some or all of the difference in the times of close circuit energization can be eliminated by the auxiliary relay, which provides reclose restraint when a carrier signal is received. An additional factor is that the close circuits will be energized when the breaker mechanisms are at different positions fully closed and fully open. Thus, the actual closing times will vary and care must be taken to insure that the closing time of the first breakers to clear is long enough to allow sufficient dead time after the last breaker clears.

It appears that simultaneous closing of all breakers is not always possible with this scheme. However, the scheme appears to have merit where system stability is not a factor in the desire to reclose at the earliest possible moment.

Mr. Hampe's scheme 2, where the familiar dead-line and hot-line reclosing system is modified, seems to have merit, if hot-line reclosing on a fault arc is of great concern. His suggestion is to reclose only if the line voltage is balanced, indicating that the fault has cleared (except for three remote phase faults). This arrangement seems preferable where a line side source of 3-phase potential is available or can be economically justified.

The Induction Machine With Solid Iron Rotor

H. M. McCONNELL
ASSOCIATE MEMBER AIEE

E. F. SVERDRUP
ASSOCIATE MEMBER AIEE

THE MOST elementary type of rotor for the polyphase induction machine, the solid iron rotor, offers advantages in ease of manufacture and in high torque per ampere at standstill. In spite of these advantages, this type of construction has not been used extensively, even in applications most suited to its characteristics. This paper presents a rational method for the design of the induction machine with solid iron rotor. The method overcomes the usual difficulties encountered in treating the nonlinear magnetic properties of the rotor, emphasizing instead the same concepts used in the design of conventional machines. The formulas which are obtained refer directly to the physical dimensions of the machine and to the electric and magnetic loading of materials.

Electromagnetic Field Problem

Previous work on the electromagnetic field problem involved in the solid rotor machine has followed an approach based on modifying the results of a constant permeability theory. The work of Gibbs[1] and McConnell[2] is illustrative. A graphical treatment to find the power loss per unit of rotor surface area has been developed by Pohl,[3] in which the machine performance is obtained by cross reference to families of curves. The method of Pohl is an extension to nonlinear media of a method originated by Hay.[4]

Two aspects of this field problem appear. First is a consideration of the efforts made toward a solution of the eddy-current problem in solid iron under a pulsating excitation. Such a situation, typified by the solid iron cored toroid, produces an electromagnetic field without divergence by virtue of the geometry. Even in this case, purely analytical methods based on extension of the linear theory are quite awkward. Second, the solid rotor machine presents a 2-dimensional field problem, which is of higher complexity because the divergence theorem must be included as one of the field equations. This added complication further reduces the usefulness of any rigorous quasi-linear treatment.

Recent work using a limiting case theory[5] based on the idealized magnetic characteristic of Fig. 1 suggests that this same theory might be useful in obtaining a better understanding of the performance of the solid rotor machine. This theory was first suggested by Wolman[6] in 1932 as a method of attacking the problem of the rate of flux rise through a magnetic circuit subjected to a step function of excitation. In 1936, F. and G. Haberland[7] applied this theory to 1-dimensional situations involving sinusoidally pulsating excitation. The theory has been applied by Ganz[8] in the development of pulse transformer cores made from square loop magnetic materials. This paper extends the limiting case theory to the 2-dimensional problem of the solid rotor machine.

Nomenclature

f = stator frequency, cycles per second
g = effective air gap, meters
k_{p1}, k_{d1} = pitch and distribution factors for fundamental
m = number of phases
p = number of poles
s = slip, per unit
t = time, seconds
x', y, z = space co-ordinates referred to stator
x', y', z' = space co-ordinates referred to rotor
z_0' = depth of magnetic interface, meters
B_s = saturation flux density, webers per square meter
B_z = normal component of flux density
$B_{z1\max}$ = maximum value of space fundamental of air gap flux density
E = stator induced electromotive force per phase, volts rms
F = magnetic potential, ampere-turns
F_ϕ = magnetic potential of magnetizing current
F_L = magnetic potential of load current
H_X = tangential component of magnetic field intensity, amperes per meter
H_T = maximum value of tangential magnetic field intensity at rotor surface
I = stator current per phase, amperes rms
I_e = rotor eddy current per unit of periphery, amperes per meter
I_ϕ = magnetizing current per phase
I_L = load current per phase
J_y = axial current density, amperes per square meter
L = core length, meters
N = stator turns per phase in series
R_L = equivalent rotor resistance, ohms
T = electromagnetic torque, newton meters
X_m = magnetizing reactance, ohms
X_L = equivalent rotor reactance, ohms
α = phase angle, radians
β = phase angle, radians
δ = depth of penetration, meters
$\mu_0 = 4\pi \times 10^{-7}$ weber per ampere-meter
ρ = resistivity, ohm-meter
σ = conductivity, mho per meter
τ = pole pitch, meters
ω_0 = stator radian frequency, $2\pi f$

Method of Analysis

The analysis is restricted to balanced operation of the polyphase machine, and an equivalent circuit of the type shown in Fig. 2 is drawn to represent its electrical performance per phase. This equivalent circuit divides the total stator current into two parts, a magnetizing component

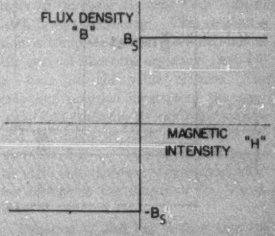

Fig. 1. Idealized magnetic characteristic

Paper 55-115, recommended by the AIEE Rotating Machinery Committee and approved by the AIEE Committee on Technical Operations for presentation at the AIEE Winter General Meeting, New York, N. Y., January 31–February 4, 1955. Manuscript submitted October 20, 1954; made available for printing November 29, 1954.

H. M. McConnell and E. F. Sverdrup are with the Carnegie Institute of Technology, Pittsburgh, Pa.

This paper is an abridgement of the thesis submitted by E. F. Sverdrup to Carnegie Institute of Technology in partial fulfillment of the requirements for the degree of Doctor of Philosophy, September 1954.

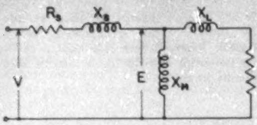

Fig. 2. Equivalent circuit, per phase star, for the solid rotor machine

and a load component. Although somewhat arbitrary, this division has a physical significance. The magnetizing current provides a magnetomotive force just sufficient to maintain the air-gap flux throughout the main magnetic circuit. The remaining component of the stator current, the load component, annuls the magnetomotive force of the rotor currents so that the required air-gap flux is not disturbed. The influence of the rotor is represented in the equivalent circuit by static circuit elements which draw a current equal to this load component.

The magnetizing impedance to be inserted in the equivalent circuit may be evaluated by standard methods. If the reluctance of the stator iron is neglected the magnetizing reactance is given by the usual design equation

$$X_M = \frac{0.9\sqrt{2}\mu_0\omega_0\tau mL(k_{p_1}k_{d_1}N)^2}{\pi g p} \qquad (1)$$

The load impedance is evaluated by the following procedure. A relation between the induced air-gap voltage E (Fig. 2) and the air-gap flux is established from Faraday's law of induction. A connection between the distribution of air-gap flux density and the magnetic potential of stator load currents is established by considering the magnetic processes in the rotor. These relationships, one between induced voltage and air-gap flux, and the other between stator load currents and air-gap flux density distribution, combine to determine both the resistive and reactive parts of the load impedance.

Air-Gap Phenomena

The voltage induced in the stator winding by the rotating air-gap flux is given by the usual equation

$$E = \sqrt{2}\frac{\tau}{\pi}(k_{p_1}k_{d_1}N)L\omega_0 B_{z1\max} \qquad (2)$$

It is assumed that harmonic voltages, which may be induced by space harmonics of the flux density distribution, are not accepted by the stator winding because of chording and distribution.

The establishment of the relationship between stator load currents and air-gap flux density distribution is a part of the rotor field analysis, to be considered in a later section. It is convenient to begin that analysis with the tangential field intensity H_x at the rotor surface as a boundary condition. This field intensity will be evaluated now in terms of the stator load current.

A rectangular co-ordinate system (Fig. 3) is fixed at the magnetic axis of the reference phase winding. The y-axis is parallel to the shaft; z is directed from the inner surface of the stator iron toward the center of the shaft; x is directed tangentially. Because of the chording and distribution of the windings, the stator currents are assumed to establish a sinusoidally distributed magnetic potential at the stator surface. Applying Ampere's circuital law to the path $ABCDA$ yields

$$\frac{\partial}{\partial x}F(x,t) = \frac{g}{\mu_0}\frac{\partial}{\partial x}B_z(x,t) - H_x\Big|_{z=g} \qquad (3)$$

in which, if the magnetic potential drop in the stator iron is neglected

$$F(x,t) = 0.9\frac{m}{p}(k_{p_1}k_{d_1}N)I\cos\left(\frac{\pi}{\tau}x + \beta - \omega_0 t\right) \qquad (4)$$

The quantity H_x at $z=g$ (equation 3) is the boundary condition to be used in the rotor field analysis. This tangential field intensity is associated entirely with currents flowing in the rotor material. The situation is somewhat analogous to the conventional induction machine in which a varying magnetic potential exists at the rotor surface because of the rotor currents, in addition to the small amount of magnetic potential required to close the main flux through the rotor iron. In the present case no magnetic field intensity is required to sustain flux in the rotor iron (Fig. 1); all the surface field intensity (H_x at $z=g$) is balanced by rotor currents.

In making the analysis it will be assumed that the field intensity at the rotor surface is a sinusoidal function with space period 2τ. Such a condition would exist truly if the air-gap flux density were sinusoidally distributed in space. However, the rotor analysis carried out on this basis shows that the resulting air-gap flux density has prominent space harmonics. The magnetic potential needed to sustain these harmonics can be obtained only from the effect of rotor currents. Therefore, the magnetic field intensity at the rotor surface cannot be truly sinusoidal. In the usual machine the air gap is so short that these higher harmonics of magnetic field intensity will

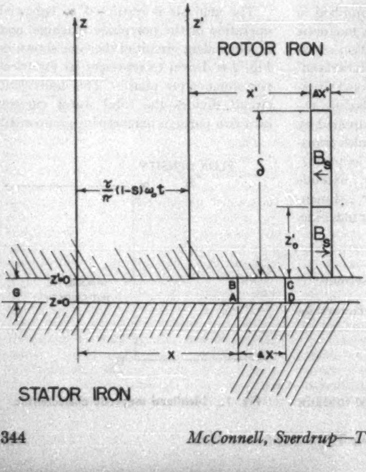

Fig. 3 (left). Stator and rotor co-ordinates, an element of rotor iron

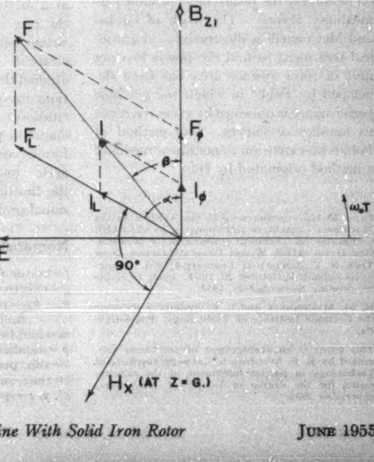

Fig. 4 (right). Phasor diagram

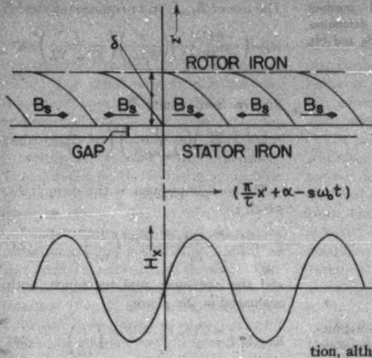

Fig. 5 (left). Traveling functions illustrating magnetic field intensity at rotor surface and magnetic state of rotor

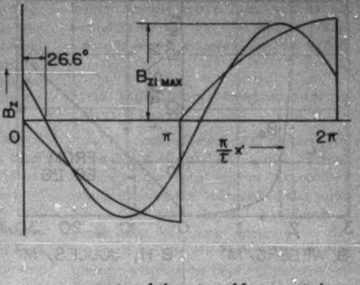

Fig. 6 (right). Air-gap flux density distribution and its space fundamental component

be neglected for the purpose of further analysis of field phenomena in the rotor. The magnetic potential required to sustain the space fundamental of the air-gap flux density will be assigned to the magnetizing current. Thus, for the fundamental components

$$\frac{\partial}{\partial x}F(x,t)=\frac{\partial}{\partial x}F_\phi(x,t)-H_x\Big|_{z=0} \tag{5}$$

in which

$$F_\phi(x,t)=0.9\frac{m}{p}(k_{p_1}k_{d_1}N)I_\phi \times \cos\left(\frac{\pi}{\tau}x-\omega_0 t\right) \tag{6}$$

$$I_\phi=\frac{E}{X_M}$$

The remaining part of $F(x, t)$ is the load component $F_L(x, t)$

$$F_L(x,t)=F(x,t)-F_\phi(x,t)$$

$$F_L(x,t)=0.9\frac{m}{p}(k_{p_1}k_{d_1}N)I_L \times \cos\left(\frac{\pi}{\tau}x+\alpha-\omega_0 t\right) \tag{7}$$

$$\frac{\partial}{\partial x}F_L(x,t)=-H_x\Big|_{z=0}$$

The quantities E, I_ϕ, I, I_L, F_ϕ, F, F_L α, β are shown on the phasor diagram of Fig. 4. The unknown angles α and β are determined from the rotor field analysis to follow.

Rotor Field Analysis

Rotor co-ordinates are denoted by primed symbols x', y', z' with the origins shown in Fig. 3. The traveling functions $f(\pi x/\tau-\omega_0 t)$ referred to stator co-ordinates take the form $f(\pi x/\tau'-s\omega_0 t)$ referred to rotor co-ordinates. The origins $x=0$ and $x'=0$ coincide once per revolution, although this has no bearing on the analysis.

A 2-dimensional field is assumed, implying that end effects are neglected. The use of a rectangular co-ordinate system implies that the rotor curvature is not important. As pointed out by Concordia[9] this procedure is justified even for 2-pole machines if the ratio δ/τ is small. These two major assumptions will be discussed in detail later.

The rotor surface is laid off in strips of width $\Delta x'$, one of which is shown in Fig. 3. Each surface element thus defined experiences a tangential magnetic field intensity pulsating at slip frequency and of amplitude H_T, where

$$H_T=0.9\frac{\pi}{\tau}\frac{m}{p}(k_{p_1}k_{d_1}N)I_L \tag{8}$$

as a consequence of equations 7. Because of the traveling excitation, neighboring elements see the same amplitude of pulsating field intensity but with a time phase displacement. The limiting nonlinear field theory of reference 6 will be applied to each rotor element individually.

The flux density at any point within the rotor may be changed only if the field intensity is zero (Fig. 1). As is shown in reference 5, this statement requires that the magnetization of the rotor elements proceed by the propagation of an interface between regions magnetized tangentially in opposite directions. At this interface the magnetomotive force of the eddy currents within the element must be balanced by the magnetomotive force externally applied to the element. Quantitative application of these arguments establishes the location of the interface within the element as a function of time. Consideration of all such elements leads to the distribution of eddy currents within the rotor. The relationship between the load component of the stator current and the rotor eddy currents is established in this way.

It is shown in reference 5 that a uniform current density exists between the element surface and the moving interface, while no eddy current flows on the other side of the interface. The density of eddy currents is

$$J_Y=-2B_s\sigma\frac{d}{dt}z_0' \tag{9}$$

when the flux density is being changed from $-B_s$ to $+B_s$. Since this density is uniform, the total eddy current contained in the element is found from

$$I_e=-2B_s\sigma z_0'\frac{d}{dt}z_0' \tag{10}$$

The field intensity at the rotor surface must balance I_e of equation 10 so that the field intensity at $z=z_0'$ is zero. Therefore

$$H_T\sin\left(\frac{\pi}{\tau}x'+\alpha-s\omega_0 t\right)=2B_s\sigma z_0'\frac{d}{dt}z_0' \tag{11}$$

Integration of equation 11 yields the depth of the interface

$$z_0'=\sqrt{\frac{2H_T}{s\omega_0\sigma B_s}}\cos\frac{1}{2}\left(\frac{\pi}{\tau}x'+\alpha-s\omega_0 t\right) \tag{12}$$

Equation 12 expresses a traveling wave function which describes the position of the interface at any value of (x', t) within the interval $0<(\pi x'/\tau+\alpha-s\omega_0 t)<\pi$. At the extreme of the interval where the argument $(\pi x'/\tau+\alpha-s\omega_0 t)$ has the value π, the process of reorienting the active layer of the rotor material from $-B_s$ to $+B_s$ is just beginning. This reorientation is complete at the other extreme of the interval where the argument $(\pi x'/\tau+\alpha-s\omega_0 t)$ has the value of zero. The traveling function illustrating the magnetic field intensity at the rotor surface and the magnetic state of the rotor are shown in Fig. 5. This pattern moves to the right with the wave of excitation, without change in the shapes of the boundaries.

Equation 12 and Fig. 5 show that the total tangential flux carried by each rotor

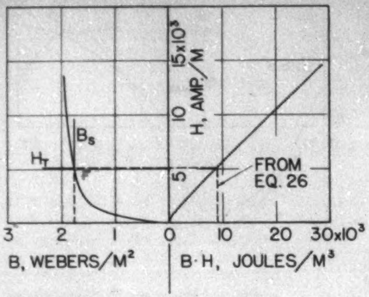

Fig. 7 (left). BH product construction to determine operating values of B$_S$ and H$_T$

element per unit of axial length varies according to the position of the element. This state of magnetization can be supported only if flux enters and leaves the rotor surface. It will be recognized most emphatically at this point that the rotor field analysis has made use of the answer to a 1-dimensional field problem to describe a 2-dimensional field. Considerable liberty has been taken with the field theory in so doing; strict conformance to field theory would demand that the divergence theorem be put into the problem initially. Instead, this theorem is used now to determine the space wave form of air-gap flux density. Essentially, this step recognizes that magnetic flux must be continuous but it treats the two rectangular components separately.

Consideration of Fig. 5 shows that

$$B_z(x',t)=2B_s\frac{\partial}{\partial x'}z_0' \qquad (13)$$

over half-cycle intervals. Thus

$$B_z(x',t)=-\frac{\pi}{\tau}B_s\sqrt{\frac{2H_T}{s\omega_0\sigma B_s}}\times \sin\frac{1}{2}\left(\frac{\pi}{\tau}x'+\alpha-s\omega_0t\right) \qquad (14)$$

Only the space fundamental of air-gap flux density is of interest because of the filtering action of the stator windings. By Fourier analysis, this fundamental component is

$$B_{z_1}=-\left(\frac{4\sqrt{5}}{3}\right)B_s\times \frac{\delta}{\tau}\sin\left(\frac{\pi}{\tau}x'+\alpha-s\omega_0t-\tan^{-1}0.5\right) \qquad (15)$$

where the maximum penetration of the field into the rotor is

$$\delta=\sqrt{\frac{2H_T}{s\omega_0\sigma B_s}} \qquad (16)$$

The air-gap flux density and its space fundamental are shown in Fig. 6.

It is noted in equation 15 that δ is fixed by $B_{z1\max}$ and the machine constants. Since in turn the fundamental of air-gap flux density is fixed by the induced voltage, it follows that δ varies but slightly over the normal operating range of the machine. Whether the handling of the divergence theorem as used in this analysis is reasonable depends upon the ratio of δ/τ, which by equation 15 is

$$\frac{\delta}{\tau}=\frac{3}{4\sqrt{5}}\frac{B_{z1\max}}{B_s} \qquad (17)$$

or about 0.1 for the usual design. Thus the use of the 1-dimensional field problem seems justified. The arguments summarized in the previous few equations also justify the use of single-phase excitation by Pohl[3] to determine the characteristics of the rotor material.

Load Resistance and Reactance; Developed Torque

Information is now available to complete the equivalent circuit. The first calculation is to determine α, since it fixes the rotor power factor (Fig. 4). Since B_{z1} must be a cosine function of time when viewed at $x=0$, it follows from equation 15 that

$$\alpha=-63.4 \text{ degrees} \qquad (18)$$

must be substituted into equations 7. Thus the load component of stator current always lags the induced voltage by 26.6 degrees. The rotor power factor is always 0.895, independent of the slip or the voltage. This result is confirmed by Gibbs.[1]

The magnitude of I_L is now computed. From equation 16

$$H_T=\frac{1}{2}s\omega_0\sigma B_s\delta^2 \qquad (19)$$

The use of δ from equation 17 yields

$$H_T=\left(\frac{9}{2\times16\times5}\right)\left(\frac{s\omega_0\sigma\tau^2}{B_s}\right)B_{z1\max}{}^2 \qquad (20)$$

The use of $B_{z1\max}$ from equation 2 yields

$$H_T=\left(\frac{9\pi^2}{4\times16\times5}\right)\left(\frac{\sigma}{B_s\omega_0}\right)\left(\frac{1}{k_{p_1}k_{d_1}NL}\right)^2 sE^2 \qquad (21)$$

Finally, from equation 8

$$I_L=\frac{1}{64}\left(\frac{p\tau}{mL^2}\right)\left(\frac{1}{k_{p_1}k_{d_1}N}\right)^2\left(\frac{1}{B_s\rho f}\right)sE^2 \qquad (22)$$

The load impedance is the ratio E/I_L, which is

$$Z_L=\frac{64mL^2(k_{p_1}k_{d_1}N)^2B_s\rho f}{p\tau}\left(\frac{1}{sE}\right) \qquad (23)$$

and the resistance and reactance, both evaluated at slip s, are

$$R_L=57.2\frac{mL^2(k_{p_1}k_{d_1}N)^2B_s\rho f}{p\tau}\left(\frac{1}{sE}\right) \qquad (24)$$

$$X_L=28.6\frac{mL^2(k_{p_1}k_{d_1}N)^2B_s\rho f}{p\tau}\left(\frac{1}{sE}\right)$$

as determined by the constant phase angle ($\tan^{-1}0.5$).

The air-gap power is the torque multiplied by the synchronous speed. Carrying out this computation for the torque yields

$$T=\left[\frac{p^3\tau}{900L^2(k_{p_1}k_{d_1}N)^2B_s\rho f^2}\right]sE^2 \qquad (25)$$

The equivalent circuit constants (equation 25) and the developed torque (equation 4) contain the saturation induction B_s as a parameter. Since the magnetic materials used in rotor construction are not exactly represented by the characteristic of Fig. 1, the value of B_s to be used is open to question. An assumption originated by Rosenberg, and discussed in detail in reference 5, proposes that the value of B_s to be used is that taken from the normal magnetization curve corresponding to the maximum field intensity. This assumption forms the basis of the method now proposed to determine the operating values of B_s and H_T.

Equation 21 may be rewritten in the form

$$H_TB_s=\left(\frac{9\pi^2}{4\times16\times5}\right)\left(\frac{\sigma}{\omega_0}\right)\left(\frac{1}{k_{p_1}k_{d_1}NL}\right)^2 sE^2 \qquad (26)$$

in which the product (H_TB_s) describes the magnetic loading of the rotor material. Thus, for a given slip and induced voltage, the value of this product is determined. It is necessary only to plot the function H_TB_s versus H_T as obtained from the normal magnetization curve. The operating value of (H_TB_s) is taken from equation 26. The construction to find H_T and B_s is illustrated in Fig. 7.

End Effects

The analysis has neglected any extra impedance introduced at the ends of the rotor. The usual procedure in conventional machines is to group the resistance and reactance of the end connections together with the squirrel-cage impedance to obtain an over-all rotor impedance. The situation in the solid rotor machine is quite different because of the nonlinearity.

Rotor currents entering the end regions cause an electric potential to appear at the ends of each rotor element. The electric field established by the moving interface (Fig. 3) must balance both the potential drop (due to eddy currents) within the element and the added potential at the ends. Thus the interface must move faster than indicated in equation 9. Consequently, a given value of H_T yields a greater depth of penetration than given by equation 16. But the depth of penetration is actually fixed by the maximum air-gap flux density, as shown in equation 17; therefore the presence of the end ring potential reduces the operating value of H_T and consequently reduces the load component of stator current. It is as though an impedance were placed in series with the rotor impedance of equations 24. The evaluation of this added impedance will be discussed qualitatively in the following paragraphs.

Throughout the analysis it has been assumed that the boundary condition at the rotor surface is a sinusoidally distributed traveling wave of tangential magnetic field intensity. The rotor current which flows in response to this surface excitation has a nonsinusoidal distribution in both density and depth. However, the total current carried by the active part of the rotor is sinusoidally distributed.

The presence of the end ring potential will alter the space distribution of rotor current density, causing it to depart from the ideal shown in Fig. 5. Still, the total rotor current will be sinusoidally distributed to satisfy both the boundary condition and the limiting nonlinear theory of eddy currents. This argument is independent of the type of end ring used.

The presence of the end ring causes a reduction in the operating value of H_T as shown previously. In addition, a change in the density of rotor currents is brought about. Therefore, the end ring both adds an impedance to the circuit and causes a change in the impedance offered by the active layer itself. This type of interaction is typical of nonlinear systems.

COPPER END RING

In the case of copper end rings, the end ring potential is sinusoidally distributed, as the end ring is made of a linear material. Since the resistivity of copper is considerably smaller than that of steel, the end ring potential will be small if the end ring and the active layer are operated at about equal current densities. Under such conditions the distortion of current density in the active layer will be of second order, so that the end ring and active layer impedances may be added directly.

STEEL END REGION: CONTINUATION OF ACTIVE LAYER

In the case of steel end regions, the sinusoidally distributed active current entering the end region encounters nonlinear magnetic material of the same kind as the active layer. The depth of penetration of these currents is determined by the current and rotor frequency, whereas the depth of penetration in the active layer is determined by the required air-gap flux (equation 17). The process in the end region is similar to conductive heating with a forced current, establishing a potential at the end ring which depends on this current, its depth of penetration, and its frequency. The phenomena in this active layer and the end regions are related in a nonlinear manner, the variables being the ratio of pole pitch to core length, the rotor frequency, and the total air-gap flux. Theoretical work on this problem is in process.

Experimental Work

The performance of the solid rotor machine was investigated experimentally using a commercial 2-phase stator. A rotor was constructed using *SAE 1020* steel with a 3/16-inch overhang on each end, which formed the end path for rotor

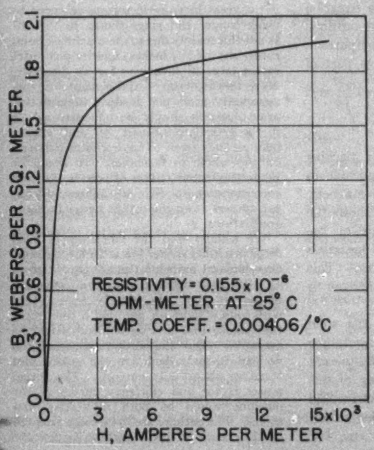

Fig. 8 (left). Electric and magnetic properties of rotor material

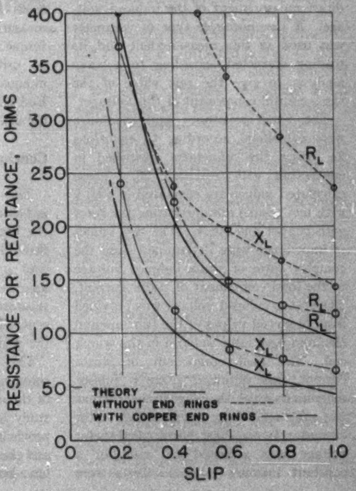

Fig. 9 (right). Calculated values and test results for rotor equivalent circuit parameters

currents. After the test program on this rotor was completed, the overhang was removed and a soft copper end ring 1/4 by $1^1/_4$ inch in cross section was soldered to each end. The pertinent machine data are as follows:

General

Rated power output, 3/4 horsepower.
Rated voltage, 440 volts.
Rated frequency, 60 cycles per second.
Number of phases, 2.
Number of poles, 4.

Stator Winding Data

Number of turns per phase connected in series, 1,080.
Winding pitch factor (fundamental), 0.940.
Winding distribution factor (fundamental), 0.903.
Winding resistance per phase at 25 degrees centigrade, 27.2 ohms.

Machine Dimensions

Stator core length, 0.0635 meters.
Pole pitch, 0.0870 meters.
Physical air gap length, 4.07×10^{-4} meters.
Stator Carter coefficient, 1.155.
Effective air-gap length, 4.70×10^{-4} meters.
Stator bore diameter, 4.375 inches.
Rotor diameter, 4.343 inches.
Ratio-active rotor length to pole pitch, 0.73.

Electric and magnetic properties of the rotor material are given in Fig. 8. This information was obtained from tests made upon a solid ring cut from the same piece used for the rotor.

The stator was equipped with a 5-turn full-pitch search coil made of no. 30 copper wire and cemented to the surface of the stator. This search coil was used to examine the wave shape of the radial air-gap flux density distribution and for a direct measurement of the induced voltage. A thermocouple type of voltmeter was used in this measurement and its reading corrected according to a wave analysis to give the rms value of the fundamental component of this voltage.

The rotor resistance and reactance were calculated according to equations 24, using the refinement described in connection with equation 26. These calculated values are compared in Fig. 9 with test results obtained using the rotor with copper end rings. The test values of impedance were determined from the complex ratio of stator-induced voltage to the load component of stator current. The stator-induced voltage was obtained from observed values of the fundamental electromotive force induced in the search coil. The load component of stator current was obtained from a phasor diagram in which the magnetizing current was subtracted from the measured stator current. In each test, the applied stator voltage was adjusted to maintain a constant induced voltage. Tests were made for two other induced voltages, 190 and 366 volts rms, with similar agreement between calculated and test values.

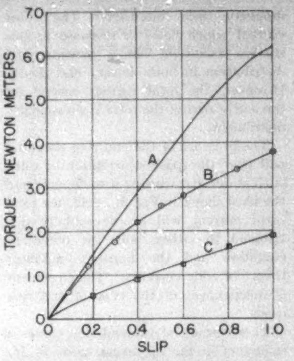

Fig. 10. Calculated values and test results for torque characteristic

Curve A, theoretical
Curve B, rotor with copper end rings
Curve C, rotor with steel end rings

Tests on the rotor without copper end rings show a considerable increase in rotor impedance. This result is consistent with the qualitative discussion of end effects. These test values are also shown in Fig. 9 for a 263-volt induced voltage.

During the tests for verification of the equivalent circuit, the torque was measured by dynamometer. These torque measurements are shown in Fig. 10. The torque calculated according to equation 25, using again the refinement outlined in equation 26, as shown for comparison. End effects account for a large part of the discrepancy noted.

Conclusions

This study of the solid rotor machine is based on a field theory applicable to the limiting case of saturable magnetic materials. As such, the study shows the way in which the dimensions of the machine and the properties of materials separately affect the performance. This separation of attributes is significant to the design process.

This and other studies of the solid rotor machine indicate the importance of the end effect. However, the present study leads to an understanding of this problem in terms of the electric field and the rotor current distribution, which have been obscure.

The general results are in agreement with those published by earlier investigators, who use with great ingenuity adaptations of the classical eddy-current theory.

References

1. Induction and Synchronous Motors With Unlaminated Rotors, W. J. Gibbs. *Journal, Institution of Electrical Engineers*, London, England, vol. 95, pt. II, 1948, pp. 411–20.

2. The Polyphase Induction Machine with Solid Rotor, H. M. McConnell. *AIEE Transactions*, vol. 72, pt. III, Apr. 1953, pp. 103–11.

3. Electromagnetic and Mechanical Effects in Solid Iron Due to an Alternating or Rotating Magnetic Field, R. Pohl. *Journal, Institution of Electrical Engineers*, London, England, vol. 91, pt. II, 1944, pp. 239–48.

4. A Graphical Treatment of The Skin Effect, A. Hay. *Ibid.*, vol. 46, 1911, p. 487.

5. Eddy-Current Phenomena in FerroMagnetic Materials, H. M. McConnell. *AIEE Transactions*, vol. 73, pt. I, July 1954, pp. 226–35.

6. On the Eddy Current Delay in Magnetic Switching Phenomena, W. Wolman, H. Kaden. *Zeitschrift für Technische Physik*, Leipzig, Germany, vol. 13, 1932, pp. 330–35.

7. The Alternating Field in Saturated Solid Iron, G. Haberland, F. Haberland. *Archiv für Elektrotechnik*, Berlin, Germany, vol. 30, 1936, pp. 126–33.

8. Application of Thin Permalloy Tape in Wide-Band Telephone and Pulse Transformers, A. G. Ganz. *AIEE Transactions (Electrical Engineering)*, vol. 65, Apr. 1946, pp. 177–83.

9. Discussion by C. Concordia of reference 2, p. 111.

Discussion

W. J. Gibbs (The British Thompson-Houston Company, Ltd., Rugby, Warwickshire, England): The most striking result of the authors' calculations and tests is the great increase in torque achieved by using copper end rings shown in Fig. 10. Is not this mainly due to the machine's being rather short ($2^1/_2$ inches) and its pole pitch rather large ($3^1/_2$ inches) for its diameter? Nevertheless, the improvement is unexpectedly good and it does suggest that some research should be concentrated on a theoretical treatment of end effects, because they seem to have a vital influence on the whole performance. It would be interesting to see curves of primary current corresponding to Fig. 10, because torque per ampere is an important figure in many applications.

We usually find the efficiency of solid rotor machines rather low. In the authors' experimental machine the air gap is given as 0.018 inch which is a normal induction motor air gap. We should expect that with such a short air gap and a solid rotor the surface iron loss on no load would be excessive. Did the authors measure the no-load losses? And are the stator slot openings abnormally narrow? The actual power factor and efficiency curves of the machine would be both interesting and useful. The authors are to be congratulated on their work in this important field.

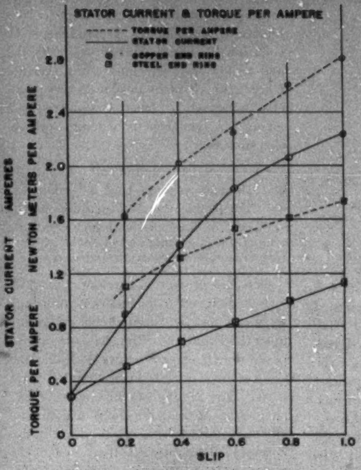

Fig. 11. Torque per ampere corresponding to Fig. 10

H. M. McConnell and E. F. Sverdrup: We are grateful to Mr. Gibbs for his contribution to the paper. His comments on end affects agree with our conclusions. A relatively short machine was used in the experimental work, although we believe that the machine chosen is fairly representative of commercial practice.

A curve showing the torque per ampere corresponding to Fig. 10 is shown in Fig. 11. Reference to manufacturers' data for this motor with its normal squirrel-cage rotor shows that the locked torque per ampere with the solid rotor, with copper and rings, is about three times the value with the squirrel cage.

The efficiency of the solid rotor machine is low if it is compared with a squirrel-cage machine of equal dimensions, considering in each case the slip required to develop name plate torque. This low efficiency is a property of any machine with high-resistance rotor. This point is emphasized to put the rotor surface loss in proper perspective. The rotor surface loss is naturally large in the solid rotor machine, but it is not predominant in causing low efficiency.

An approach to the surface loss problem can be made by classical eddy-current theory, using the residual permeability of the rotor iron and using as boundary conditions the known harmonic content of the stator magnetic potential.

Unfortunately, data are not available to show the no-load loss, the power factor, or efficiency. However, examination of Fig. 10 shows that the rotor impedance does indeed yield a current locus which is a straight line (equation 24); the theory also predicts that the power factor with respect to induced voltage approaches asymptotically the value 89.5 per cent. The tests confirm this value. The experimental machine was made up using a stator of standard manufacture, and the stator slot openings were normal.

Improved Fast-Acting Thermal Relay and Its Application as a Cage Winding Protective Relay for Synchronous Machines

JOHN BAUDE
ASSOCIATE MEMBER AIEE

THERMAL relays have been used in the past for a great variety of purposes because they are simple and reliable devices, but they are relatively slow in action. A description of design and application of a new fast-acting thermal relay for synchronous machine protection and control purposes follows. The usual application of thermal relays makes use of only the heating part of a total thermal cycle for purposes of motor control and protection. Such practice involves the simple direct or indirect heating of a bimetallic strip, which acts upon a contact-making device which in turn is arranged to stop motor operation, give an alarm, or perform any other desired function.

The thermal problem involving the relay can be studied with the help of the following equation.[1]

$$T_1=\frac{W}{h}\left(1-\frac{1}{\epsilon^{\frac{th}{MS}}}\right) \qquad (1)$$

where

M = mass of bimetallic element
S = heat capacity per gram, joules per gram per 1 degree centigrade
W = rate at which heat is applied to mass M, watts
h = rate at which heat is exchanged between the medium and the mass M per degree difference in temperature, watts per 1 degree centigrade
T_1 = temperature increase of bimetallic strip sufficient to cause deflection for contact operation
t = time in seconds to cause a temperature increase of T_1
ϵ = 2.718

The art of delaying the heating of the thermal relay's bimetallic strip during the first part of the thermal cycle has advanced to the point where appreciable close matching of machine thermal characteristics with the rate of heating of the thermal relay is obtained.

Referring to equation 1, it is obvious that thermal relays are ideal for a relatively long time out period, and it is also apparent that for a constant value of T_1 an exponential relation exists between W and t which is illustrated in Fig. 1. This means that, for relatively small values of t, the energy transfer requirement still varies in line with the existing exponential relation between W and t, and large amounts of energy are required for a short operation time regardless of whether the bimetallic strip is used as a heating current conductor or the operating element is heated indirectly. In normal motor protection practice it is not required that the thermal relay, simulating machine thermal characteristics, act very fast. If, however, the thermal relay operation can be increased to approximately 4 seconds with a reasonable operating current, say 2 to 3 amperes at 125 volts d-c such a de-

---

Paper 55-100, recommended by the AIEE Relays Committee and approved by the AIEE Committee on Technical Operations for presentation at the AIEE Winter General Meeting, New York, N. Y., January 31–February 4, 1955. Manuscript submitted October 22, 1954; made available for printing November 19, 1954.

JOHN BAUDE is with the Allis-Chalmers Manufacturing Company, West Allis, Wis.

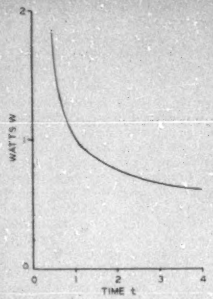

Fig. 1 (left). Energy requirement of thermal relay

Fig. 2 (right). Heating characteristic of thermal relay

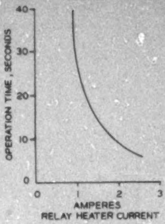

vice could help solve a difficult synchronous machine problem and provide inexpensive protection for the most vulnerable part of a synchronous motor or synchronous condenser, which is its cage or amortisseur winding. This winding is used for starting purposes and has a very limited thermal capacity which usually varies between 4 to 10 seconds at locked rotor condition. This starting winding has no outside connections. The rate of heating of this winding is substantially proportional to the slip cycles per second of the motor. In reduced voltage starting, it is also inversely proportional to the ratio of the square of the line voltage to the square of the reduced voltage during starting conditions.

The ideal cage winding protection relay should operate on a slip cycle per second basis and in accordance with the terminal voltage of the machine. At locked rotor condition the temperature rise in the cage winding of a specific motor may be well over 100 degrees centigrade per second. A fast-acting thermal relay can be arranged to simulate the thermal characteristic of the cage winding of a motor by connecting it to the control voltage source, and inserting various resistors into its circuit, which are controlled in accordance with the conditions under which the motor has to operate. The most important requirement for such a relay is reliable operation. Operating speeds up to 4 seconds with moderate power requirements are also recommended.

Fig. 2 shows the heating characteristics of a special fast thermal relay at normal ambient temperature. This relative high speed was obtained by modification of a standard relay in such a manner that the heating element was sandwiched between two bimetallic strips as shown in Fig. 3 in order to provide the necessary concentration of energy transfer from the source to the bimetallic strips.

The application of a thermal relay of this type can be expanded to include simulation of the machine's cooling characteristic if a residual current is circulated through the heater of the thermal relay after the heating period is completed. In Fig. 4 the cooling characteristic of the same relay is shown under normal ambient temperatures; in the construction of such a relay experience has shown that the shorter the heating period is compared with the cooling the more difficult it is to find a satisfactory design solution. If equation 2 for cooling is compared with equation 1 for heating, the existing design limitations can be seen more readily.

The cooling period of the total thermal cycle can be studied with the help of equation

$$T_D = \frac{1}{\epsilon^{\frac{ht}{MS}}} T_1 \qquad (2)$$

where

T_D = temperature difference between the bimetallic element and the medium at any time t

T_1 = the initial temperature before cooling

T_D will now be considered as the necessary temperature difference at which the relay will reset after heating to a time out point; it is noticed from equation 2 that the reset time t varies directly proportional with the mass M which is a design factor of the relay. The greater the mass the longer the natural reset time has to be, keeping other factors constant. A residual current during cooling will act to restore lost energy and lengthen the reset time by raising the ultimate temperature of the bimetallic element in accordance with equation 1. The typical curves of Figs. 2 and 4 show the performance of a thermal relay with all of its design factors properly balanced to meet special requirements for synchronous machine protection such as:

1. Low energy requirements.
2. Minimum trip-out time 4 seconds.
3. Controllable reset time up to 15 minutes.
4. Long life combined with high operating temperature making additional ambient temperature compensation unnecessary.

The cage protection thermal relay, Fig. 3, was designed to include an additional separately heated thermal element acting upon the same contact mechanism for purposes of an over-all check of relays during the starting period on a common time basis. The timing of this separate element is based upon normal functioning of all relays and starting of the motor under normal load conditions. If any one of the relays fails to function properly, this separate part of the cage protection relay will function to act as an incomplete sequence relay and take the motor off the line.

Application of Cage Protection Relay

The application of the combined cage protection and incomplete sequence relay is described in the following. Fig. 5 is a schematic diagram for full-voltage starting and Fig. 6 for reactor starting.

FULL-VOLTAGE STARTING SCHEME, FIG. 5

The closing circuit of circuit breaker *42* is energized by a push button, a control switch, or any automatic device having a momentarily operated normally

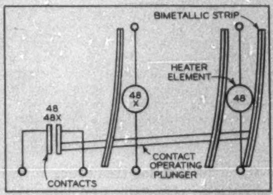

Fig. 3. Thermal relay

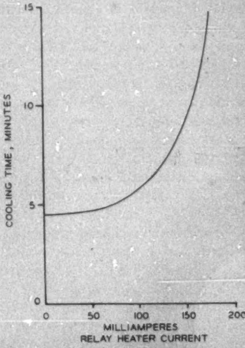

Fig. 4. Cooling characteristic of thermal relay

open or a maintained contact. The undervoltage and reverse phase relay *47* has one of its contacts connected in series in the closing circuit in order to prevent starting of the motor on low voltage. Provided that contact *47* in the closing circuit is closed, assuring proper voltage, the operation of the starting push button will pick up *42X* and energize the closing coil of circuit breaker *42CC;* upon completion of the closing cycle of the circuit breaker, relay *42Y* by action of its contacts will either lock itself in if the starting push button is of the maintained contact type or will drop out when the push button is released. This type of control is standard and is antipumping. During the starting cycle and before synchronization, the synchronous motor is protected by primary relays, including generally single-phase induction overcurrent relays with instantaneous tripping attachments, and thermal overload relays. When required, differential relays, current balance relays, and other primary protective relay may be added easily to this standard control scheme.

Cage (Starting) Winding Protection

Cage winding protection of the synchronous motor is provided by means of thermal relay *48*, which is connected at the beginning of the starting cycle into the control circuit by action of a normally open contact of auxiliary relay *13X*. The action of thermal relay *48* is controlled by two resistors *R4* and *R5*. *R4* is adjusted to provide sufficient time for starting under normal conditions. Resistor *R5* is short-circuited by the contact of a field current failure relay *40* and a normally closed contact of field contactor *41*. As soon as the starting cycle is completed and the field contactor closes, *R5* is cut into the circuit and current continues to flow through the heater element of thermal relay *48*. This current is reduced to a value which may be adjusted to delay the cooling of the thermal relay to the point where it approximates the rate of heat dissipation of the cage winding of the motor under normal running conditions. In this way maximum co-ordination of the cage protective relay with the thermal characteristics of the cage winding of the motor is accomplished. This method of co-ordinating the operation of relay *48* with the characteristics of the cage winding of the motor is carried further for cases in which the synchronous motor has been overloaded to the point of pullout or shutdown. To prevent an excessive number of unsuccessful restarts under adverse operating conditions the residual heater current of the thermal relay is increased by circulating current from the source through relay contact *48* through a normally closed contact of relay *13X* to a tap on resistor *R5* through the heater element of thermal relay *48* through resistor *R4* and back to the source. The increased residual current through the relay will delay cooling of the thermal relay further and will simulate the cage winding's rate of cooling under conditions of lockout due to overload.

Refinements

Other extra features that may be added to this cage winding protection scheme include locked rotor protection by attaching a zero speed switch to the motor, the contact of which is closed when the motor is at standstill. This contact short-circuits a portion of one of the series resistors in the relay circuit of thermal relay *48* and cuts down the operating time of this relay to a point where it matches the allowable time which the motor can operate with full voltage on its terminals but with the rotor locked. If it is impossible to equip the motor with a zero speed switch, the same thing can be accomplished by operating an underfrequency relay from taps on the discharge resistor of the motor field circuit. The contact of this underfrequency relay is connected into the circuit in the same manner as a contact of the zero speed switch just described.

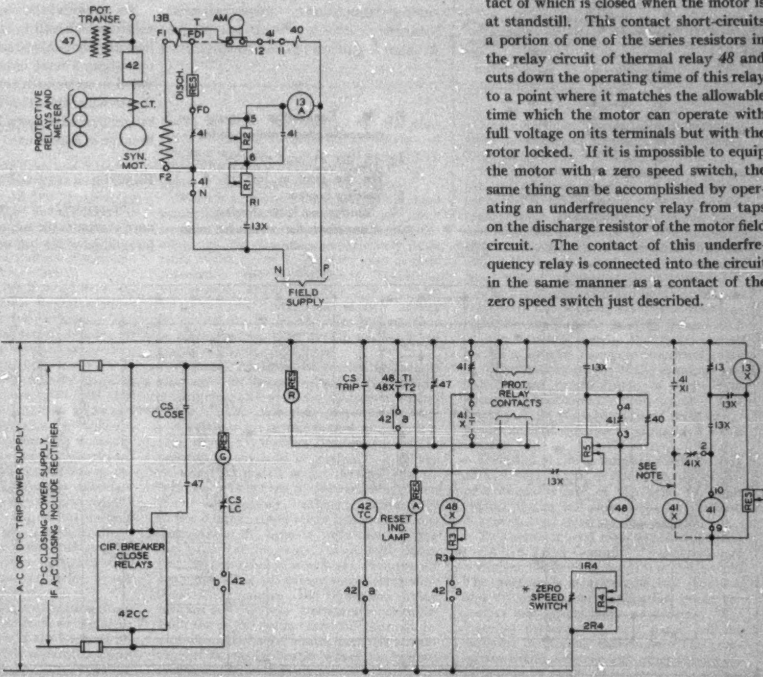

Fig. 5. Connection diagram for full-voltage motor starter

42: Running breaker
13: Field application relay
40: Field failure relay
41: Field breaker
41X: Auxiliary relay for field breaker
48: Cage winding protection relay
47: Undervoltage and reverse phase relay
13X: Auxiliary relay
Note: 41X used only when shutdown on pullout is required. Contacts 41X and 41X$_1$ must be make before break type
* Zero speed switch on motor is required if locked rotor protection is desired

Field Application

Field breaker *41* is controlled by field application relay *13*. This relay is a simple clapper-type relay which carries two coils. One of these coils, *13A*, acts as a polarizing coil and is connected into the field supply circuit by means of a normally open contact of relay *13X*. The other coil, *13B* of field application relay *13*, is connected in series with the motor field, the discharge resistor, and a normally closed contact of field contactor *41*. During the starting cycle coil *13B* therefore will be under the influence of the induced field current during the starting cycle and before the field contactor closes. The combined action of coils *13A* and *13B* provides that the two superimposed fluxes cancel each other at a certain point of each positive half-cycle, which causes relay dropout based upon time constant and air-gap adjustments. Relay *13* is adjusted to drop out at approximately 95 to 98 per cent of synchronous speed. Once the field contactor has closed under the influence of the field application relays *13*, the flux from coil *13A* is increased by cutting out a portion of its series resistance to prevent subsequent pickup on field current surges.

The control circuit of the field contactor functions as follows: At the instant the circuit breaker of the motor is closed, field application relay *13* will pick up and its normally closed contact *13*, which short-circuits the auxiliary relay *13X*, opens up. When *13X* is energized it locks itself in through a resistor and a normally open contact of the circuit breaker. This relay is necessary to set up the circuit for the closing coil of the field contactor which otherwise might pick up simultaneously with field application relay *13*. After the circuit for closing of the field contactor has been set up by field application auxiliary relay *13X*, the field contactor will close when relay *13* drops out and closes its contact *13*. A circuit in this form is set up to provide for automatic resynchronization on pullout. Under certain circumstances and with certain types of load it may be necessary to shut down as soon as the synchronous motor has pulled out of step. Shutdown is provided by the addition of a relay *41X*, the contact of which is connected in series with a normally closed contact of the field contactor. This arrangement will energize trip coil *42TC* of the circuit breaker and trip this breaker instantaneously on pullout. Tripping of the circuit breaker is accomplished either by push button or by any other automatic control device.

To check the over-all performance of all the relays during the starting period, a so-called incomplete sequence relay *48X* is provided. This relay is actually part of the cage winding relay as previously explained but consists of a separate heater element operating on the same contact assembly of relay *48*. This heater is adjusted to provide backup protection for all of the other automatic devices and the time setting is slightly longer than it normally takes to synchronize the motor.

To provide the operator with some means which will indicate when relay *48* has automatically reset after a lockout operation, a reset indicating lamp is provided in series with contact *48-48X* to indicate when this relay has reset. This arrangement cuts down lost operating time because of a lockout.

REACTOR STARTING, FIG. 6

The principle of operation of the reactance starter is the same as described in the foregoing for the full-voltage starter. The

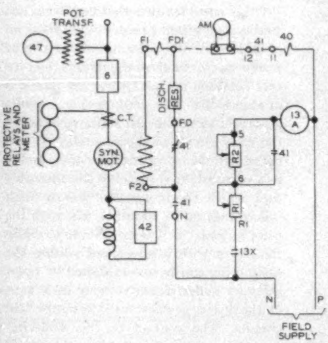

POT. TRANSF.
47
6
PROTECTIVE RELAYS AND METER
C.T.
SYN. MOT.
42
F1
FD1
AM
41
40
12
11
DISCH. RES
FD
41
F2
41
N
13 A
5
R2
6
41
R1
R1
13X
N
P
FIELD SUPPLY

Fig. 6. Connection diagram for reduced-voltage motor starter

42, 13, 40, 41, 48, 47, 13X, and * are the same as for Fig. 5
6: Starting breaker
19: Transfer and lockout relay
Δ: Connected for shutdown after pullout

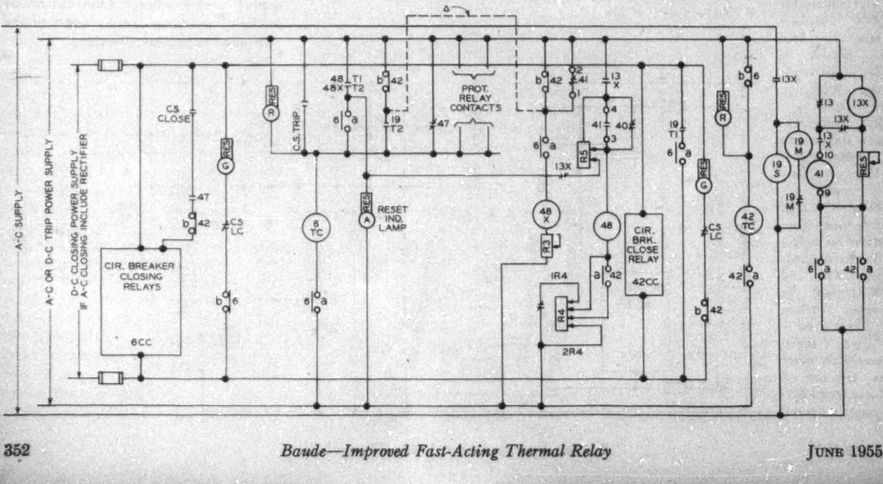

A-C SUPPLY
A-C OR D-C TRIP POWER SUPPLY
D-C CLOSING POWER SUPPLY IF A-C CLOSING INCLUDE RECTIFIER
CS CLOSE
47
b 42
CIR. BREAKER CLOSING RELAYS
6CC
RES
G
CS LC
b 6
RES
R
C.S. TRIP
6 TC
48 T1
48X T2
6 a
RES
A
RESET IND. LAMP
6 a
b 42
19 T2
47
PROT. RELAY CONTACTS
Δ
b 42
2
41
1
13 X
4
41
40
3
6 a
R5
13X
48 X
R3
1R4
R4
2R4
48
a 42
CIR. BRK. CLOSE RELAY
42CC
19 T1
6 a
RES
G
CS LC
b 42
RES
R
b 6
42 TC
42 a
19 S
19 M
19 M
13X
13
13X
13 X
10
41
9
RES
13X
6 a
42 a

main difference in operation is the fact that the starting cycle involves the closing of two circuit breakers instead of one. The operation of field application relay *13* is exactly the same as described for the full-voltage starter. The cage winding protection relay *48* is further modified in its operating characteristics by a normally open contact of the running breaker *42* which provides for the insertion of different series resistance values to co-ordinate the operation of relay *48* with the variation in the heating time of the cage winding under full-voltage conditions as against reduced-voltage operation. A timing relay device *19* is provided as a transfer and lockout relay. The purpose of this relay is to energize the running breaker closing circuit *42* after a predetermined time. This function is performed by contact *19T1* of this relay. Another contact *19T2* in series with a normally closed contact of the running breaker *42* is connected into the trip circuit of the starting breaker *6* to protect the starting reactor and open up the starting breaker in case the running breaker should not close for any reason.

The connection marked Δ can be made to provide for immediate shutdown on pullout. Relay *48X* again acts as an incomplete sequence relay and its operation somewhat parallels the function of transfer relay *19*.

The autotransformer starting scheme involves the proper co-ordination of three breakers. Starting breaker *6B*, neutral breaker *6A*, and running breaker *42* are interlocked in such a way that the neutral breaker *6A* is closed first, then the starting breaker *6B*, and after a period of time the running breaker *42* is closed and breakers *6B* and *6A* are open. The principle of operation otherwise is exactly the same as described for the reactance starter.

Conclusion

The previous description of a special thermal cage protection and incomplete sequence relay for synchronous machines outlines the practical design limits which were reached for a simple thermal relay for this type of application. Adequate protection of a synchronous machine's cage winding is one of the most important requirements for modern motor applications because it eliminates the danger of ruining the motor as the result of the operator's misjudgment of the motor's thermal capacity. Also adequate protection for the starting reactor is provided when reduced-voltage starting is used. A simple indicating lamp which indicates the position of the cage protection and incomplete sequence relay will help the operator to see exactly when the motor is ready to go through another complete starting cycle, and will be especially appreciated in industries which impose frequent overloads upon their motors.

Since the copper in the cage winding is active only during starting, the tendency exists among motor designers to decrease the amount of copper which is put into the starting winding of motors because all inactive material is eliminated as much as possible. The knowledge that efficient cage protection is always provided may be considered an important factor in altering present design practice. Furthermore, there seems to exist a discrepancy at present between the standards covering thermal capacities of starting reactors and the thermal capacity which is commonly designed into the cage winding of a motor. It seems that adequate cage protection automatically provides starting reactor protection on a precise basis which would permit revision of the present standards.

Reference

1. THERMAL PROBLEMS RELATING TO MEASURING AND CONTROL DEVICES, W. N. Goodwin, Jr. *Weston Engineering Notes*, vol. 2, no. 6, Dec. 1947, pp. 3 and 4.

◆

Discussion

H. C. Barnes (American Gas and Electric Service Corporation, New York, N. Y.): The author's coverage of the problem of motor cage windings points out the need for an improvement in motor standards. It is extremely difficult for the relay designers and engineers to protect motors adequately when such great variations exist.

On several occasions, we have endeavored to correlate thermal relay tripping times with motor thermal characteristics. The relay manufacturer is extremely evasive on the question of margin between relay time and motor thermal capability, particularly in the case of the heaters normally supplied with magnetic contactors. He will tell you that the curves are based on an "average" of motor characteristics but will not produce the curves from which the "average" is taken. His stock answer is that curves for each motor should be obtained from the motor manufacturer. The motor manufacturer will give some equally evasive answer to the effect that each motor has its own characteristics which can be determined only by tests which are economically prohibitive. With such answers determination of adequacy of protection is difficult, to say the least.

In addition to this lack of information, there are the other problems of ambient temperature, particularly if the thermal relay and motor are in widely separated areas, the difference in cooling characteristics between the relay and motor, and the difficulty in testing thermal relays because of the long wait for them to cool to ambient, all of which discourage any feeling of confidence in thermal protection of motors.

When it is realized that thermal overload protection generally consists of an effort to make the minute mass of the thermal element act just like the comparatively huge mass of the motor, it becomes evident that correlation will be difficult. Therefore, perhaps the author's approach of basically establishing a definite time and then varying it for the starting cycle or for locked rotor is more realistic than trying to match all points of the thermal curve.

Perhaps this could be carried further to eliminate the thermal relay and its inherent weaknesses and utilize synchronous timers instead. The induction overcurrent relay is a modification of this in that in general it trips in a fairly definite time once a certain percentage overload is reached. It makes no effort to match motor thermal characteristics. This type of protection has been fairly satisfactory although admittedly motor damage could result from continuous operation in the band between motor rating and pickup of the relay. A properly functioning thermal relay would, of course, permit some operating advantage where short-time overloading above the induction relay pickup setting was considered desirable. Both the definite timer, and the thermal device as applied here, would have the advantage of being applicable where no current transformers were available.

There does not appear to be a statement as to the operating tolerance of this device Such information would be of interest.

Fig. 3 appears to be intended to illustrate the advantage of placement of a bimetal on each side of the heater to take full advantage of heat availability. It is not clear just what this advantage is. It would seem that each would react to one-half the heat and each would travel the same amount. Are these additively coupled in some way?

The use of the polarized field application relay with one winding across the discharge resistor is one way of indicating the approach of synchronous speed. We have always used the simple plunger overcurrent relay in the secondary of one of the armature circuit current transformers of large synchronous condensers for this purpose. This seems to have the advantage of reduced exposure of field circuits to grounds or short circuits.

Inclusion of the incomplete start function *48* as a part of this device might be of disadvantage because of the need to await cooling if the full time is to be realized. A synchronous timer might be better.

This seems a good time to point out that the AIEE Relay Committee has established a Project Committee on Motor Protection. The purpose is to review present practices and to prepare an application guide for motors and synchronous condensers. The material presented in this paper will be valuable in guiding this work. The committee would welcome any other similar information on available protection as well as letters pointing out weaknesses of present protection. No doubt there will be a need for much consultation with manufacturers of motors, relays, industrial control, and special protective devices such as those related to lubrication and cooling. Full co-operation will be needed since the field of exploration is unlimited. Letters should be addressed to Mr. Von Roeschlaub or to me.

John Baude: I should like to thank Mr. Barnes for his discussion which emphasizes the need for a revision of motor standards. Only complete co-ordination of motor and starting reactor standards can help to realize the benefits of modern protective and control methods, of which cage winding protection for synchronized machines is only a relatively small part.

Since the cage winding protective relay is intended to protect the motor during the relatively short time of subsynchronous operation only, the relay's operating tolerance is safely within the accuracy with which cage winding thermal capacity can be predicted. In general, it will be found that the heating cycle of this type of noncompensated relay is less affected by ambient temperature changes than the cooling cycle, and both tolerances vary with the operating periods.

Since the contact mechanism of the relay requires a definite force for operation, two bimetallic strips will help to provide this critical operating force in less time than one, and the heat generated within the heater element is more protected from radiation than it would be with a single bimetallic strip.

The incomplete function heater element *48X* in Fig. 5 was included for backup protection of the heater element device *48* in Fig. 5. The cooling time of *48X* is much shorter than of that of *48* and thus will cause no needless waiting time of the operator in case of an incomplete sequence operation.

Direct-Stroke Protection of High-Voltage Switching Stations and Transformers

S. B. GRISCOM
FELLOW AIEE

J. K. DILLARD
MEMBER AIEE

A. R. HILEMAN
ASSOCIATE MEMBER AIEE

THIS paper presents results of an investigation into a phase of the lightning protection problem which has not been completely evaluated in the past: that of protection against direct strokes terminating on transmission towers and conductors immediately adjacent to high-voltage stations. Lightning protection of extensive stations in the past has been based on the premise of incoming traveling waves on overhead transmission lines, the surge having originated 1 or $1^1/_2$ miles away from the station. This broad premise encompasses two basic assumptions:

1. The station structure is so well shielded that there is practically no possibility of a lightning stroke terminating on a phase conductor within the station.
2. The first mile or so of incoming line is lightningproof or, if not, the probability of a flashover is so small that equipment failures in the event of close-in strokes can be accepted as considered risks.

Recent treatments of protection against incoming traveling waves are given in three papers[1–3] covering miniature-system studies, and two papers[4,5] covering field tests.

The possibilities of obtaining direct-stroke protection of high-voltage switching stations and transformers were studied on an actual station, the St. Lawrence River Power Project, now being undertaken jointly by the New York State Power Authority and the Hydroelectric Power Commission of Ontario. It had been determined by the engineers of Uhl, Hall, and Rich and the Commission that cable leads would be advantageous for the connections from the transformer, located on the dam, to the switching stations located on the shores. It was essential that these cables, and their associated transformers be given adequate lightning protection.

With respect to transient voltages, cables behave in a manner similar to overhead lines. However, they have much lower surge impedance and inductance and much higher capacitances, and these properties are in a direction to help the problem of surge protection. These circumstances suggested to the authors that surge protection could be studied to advantage with respect to the following points:

1. Can reliable protection be obtained against close-in direct strokes?
2. How many high-voltage lightning arresters are required?
3. What is the best placement of the arresters?

These questions have been studied at length on the Anacom analogue computer. The main object of the studies was to obtain facts pertaining to direct-stroke protection of stations and transformers. With such facts available, protective features of stations can be made on a more rational basis.

Physical Layout

Differences in local conditions resulted in two different situations: On the United States side, the cables run directly from the dam to the switching station; therefore the switching station has the initial exposure to lightning surges. On the Canadian side, the cables run from the dam to the shore and thence via overhead lines to the switching station several miles remote; therefore, the cables have the initial exposure to lightning surges. These two cases are representative of conditions that may be encountered elsewhere.

In Fig. 1, the major dimensions are shown for the 6-line 4-cable bus with four transformers on which the study was made. Cable lengths were varied from 500 to 3,500 feet in length. Fig. 2 shows an approximate physical layout and a diagrammatic representation of those circuit elements pertinent to a study of direct-stroke protection. The symbols L_1, L_2, and R_1, R_2 are the inductances and resistances of the first and second towers away from the station T_1 and T_2 respectively. L_s and R_s are the station structure inductance and resistance to ground. The letter symbols of Figs. 1 and 2 are voltage measuring points and serve to orient Fig. 2 with Fig. 1.

Direct strokes are most destructive if they occur in the one or two tower spans on the outgoing overhead lines from the switching station. Ground wires in these critical spans are three in number, and have a spacing between outermost wires greater than that of the phase conductors. This gives three desirable features: low surge impedance, practically perfect

---

Paper 55-101, recommended by the AIEE Transmission and Distribution and Protective Devices Committees and approved by the AIEE Committee on Technical Operations for presentation at the AIEE Winter General Meeting, New York, N. Y., January 31–February 4, 1955. Manuscript submitted October 26, 1954; made available for printing November 19, 1954.

S. B. Griscom, J. K. Dillard, and A. R. Hileman are with the Westinghouse Electric Corporation, East Pittsburgh, Pa.

The authors gratefully acknowledge the co-operation of J. S. Saloma of Uhl, Hall and Rich, and Dr. H. M. Ellis of the Hydro-Electric Power Commission of Ontario, for furnishing the data and other information required to make this study

shielding, and increased coupling to the phase conductor.

Circuit constants for the transmission lines, cables, ground wires in the critical spans, and rating of the lightning arresters are given in the following section.

Circuit Constants

TRANSMISSION LINES: PHASE CONDUCTORS

Inductance per foot, 0.45 microhenrys (μh).
Capacitance per foot, 2.22 micromicrofarads (μμf).
Surge impedance, 450 ohms.
Velocity of propagation, 1,000 feet per microsecond (ft/μsec).
Line insulation, 16 standard 10 by $5^3/_4$-inch insulators.
Span length, 1,000 feet.

CABLES

1,000,000-circular-mil copper, 0.925-inch paper insulation.
Inductance per foot, 0.06 μh.
Capacitance per foot, 66.7 μμf.
Surge impedance, 30 ohms.
Velocity of propagation, 500 ft/μsec.

LIGHTNING ARRESTERS

195-kv station-type lightning arrester.
Gap breakdown for slow-wave front, 600-kv crest.
Discharge voltage, 600-kv crest at 10,000 amperes used for cases *A* and *B*; 550-kv crest at 5,000 amperes used for case *D*.

CIRCUIT BREAKERS

Capacitance per bushing, 500 μμf.

TRANSFORMERS

Equivalent surge capacitance, 1,500 μμf.

SHIELDED SPANS

L_{11} = Ground wire self-inductance per foot, 0.22 μh.
L_{22} = Phase conductor self-inductance per foot, 0.45 μh.
L_{12} = Ground wire to phase conductor mutual inductance per foot, 0.77 μh.
C_{11} = Ground wire to ground capacitance per foot, 4.55 μμf.
C_{22} = Phase conductor to ground capacitance per foot, 2.22 μμf.
C_{12} = Ground wire to phase conductor mutual capacitance per foot, 13.00 μμf.
Surge impedance of ground wires = 220 ohms.
L_1 = Tower inductance, 20 μh.
L_s = Switching station inductance, 5 μh.
R_s = Switching station resistance, 1 ohm.
R_1 = Tower-footing resistance, variable from 5 to 20 ohms, 10 ohms used in most cases.

COUPLING FACTOR BETWEEN GROUND WIRES AND PHASE CONDUCTORS

35% for cases *A* and *B*.
65% for case *C*.

Anacom Procedure

Techniques used in representing the station on the Anacom have been given in detail in the literature.[1,2] In brief, the procedure consisted of setting up on the computer the proper inductances, capacitances, and resistances to represent faithfully the transient wave response of the actual circuit elements. Multipliers for the various elements were chosen to obtain wave fronts suitable to the Anacom with respect to fidelity of response and adaptability to photography on the cathode-ray oscillograph.

Fig. 1 shows the circuit used in the study. Distributed constants of the overhead lines and cables were simulated by pi-sections as illustrated in Fig. 2(B). For simplicity, only a few pi-sections are shown; in the actual setup, a sufficient number were used to assure proper response for the wave shapes encountered. Overhead lines which were so long that reflections from their ends would not return in time to affect voltages within the station were terminated in their surge impedances (represented by *Z* on lines 2 to 6 of Fig. 1). When more than two cables were used, additional cables were represented by their equivalent lumped capacitance. Transformers and circuit breakers were represented by their equivalent surge capacitance. Circuit constants for the phase conductors, cables, and ground wires are given in the section "Circuit Constants."

A major deviation from the Anacom representation used in previous studies[1-3] was the detailed representation of coupling between ground wires and phase conductor in the one or two spans entering the station. A single pi-section of this representation is given in Fig. 3, which shows both electrostatic and electromagnetic coupling. Constants shown in the figure are calculated in a manner similar to that in reference 6.

$$C_M = \frac{C_{11}C_{22}C_{12}}{C_{12}^2 - C_{11}C_{22}} \tag{1}$$

$$C_C = \frac{C_{22}^2 C_{12}}{C_{12}^2 - C_{11}C_{22}} \tag{2}$$

$$C_G = \frac{C_{11}^2 C_{12}}{C_{12}^2 - C_{11}C_{22}} \tag{3}$$

where the symbols with numbered subscripts are defined in the section "Circuit Constants." The use of two inductances each for ground wire and phase conductor permits the representation of different self-inductances while maintaining reciprocity of mutual inductance.

The 195-kv station-type lightning arrester was simulated by the countervoltage of a battery and a switch in series. The switch simulated arrester spark-over at 600 kv for slow front waves, while the countervoltage of the battery simulated arrester discharge voltage. This discharge voltage was set at a constant value of 600 kv for strokes terminating within one or two spans from the station and at 550 kv for the strokes terminating 1 or $1^1/_2$ miles

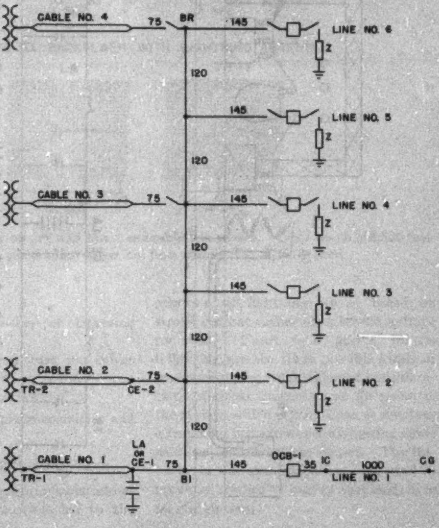

Fig. 1. Single-line diagram of the 230-kv station studied, showing circuit feet between junctions

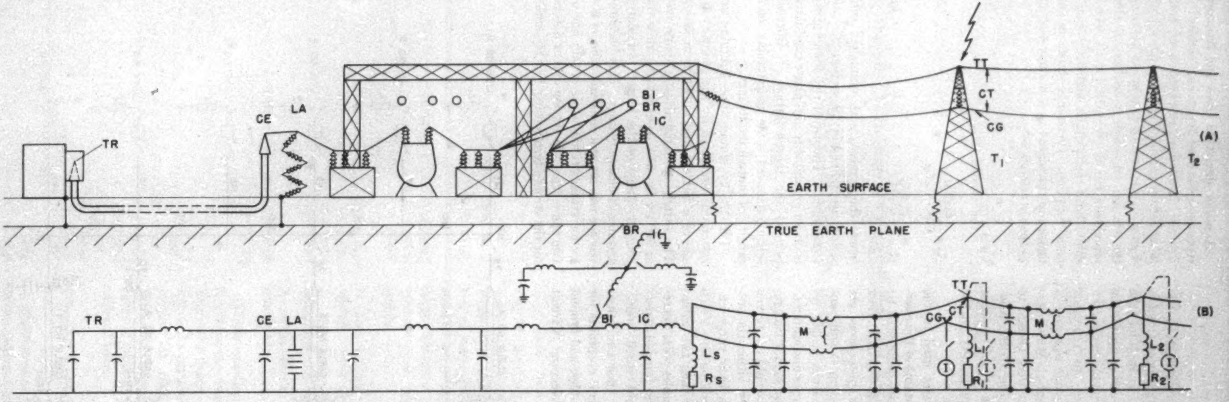
TR
CE
LA
O O O
BI
BR
IC
TT
CT
CG
(A)
T1
T2
EARTH SURFACE
TRUE EARTH PLANE
BR
TR
CE LA
BI
IC
LS
RS
M
TT
CG
CT
L1
R1
I
M
L2
R2
(B)

Fig. 2. A—Assumed physical layout. B—Diagrammatic representation of circuit elements pertinent to study of direct-stroke protection

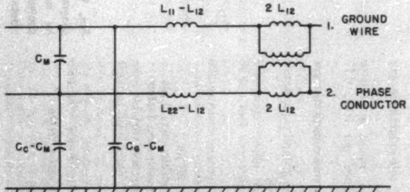
CM
CG-CM
CG-CM
L11-L12
2 L12
1. GROUND WIRE
L22-L12
2 L12
2. PHASE CONDUCTOR

Fig. 3. Single T-section of phase conductor and ground wire representation showing mutual inductance and capacitance

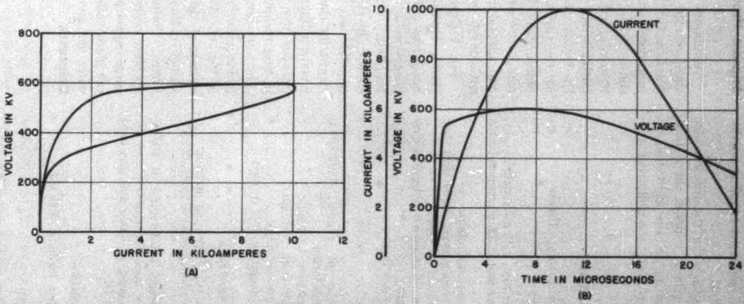

Fig. 4. Discharge characteristics of 195-kv station-type lightning arrester for 10,000 amperes, 10x20-microsecond wave discharge current

A—Volt-ampere discharge characteristics
B—Discharge current and voltage

Table I. Location of Surge Voltage Measurements

Notation	Location
TT	Tower-top-to-ground voltage at struck tower
CT	Conductor-to-tower voltage at struck tower
CG	Conductor-to-ground voltage at struck tower or at struck point
IC	Conductor-to-ground voltage at station entrance
BI	Bus potential-to-ground at incoming line bay
BR	Bus potential-to-ground at most remote point from incoming line bay
LA	Lightning arrester voltage
CE-1 and *CE-2*	Voltage at cable entrances of cable 1 and 2 respectively
TR-1 and *TR-2*	Voltage at transformers located on cable 1 and 2 respectively
OCB-1	Voltage at circuit breaker located at station entrance of line 1

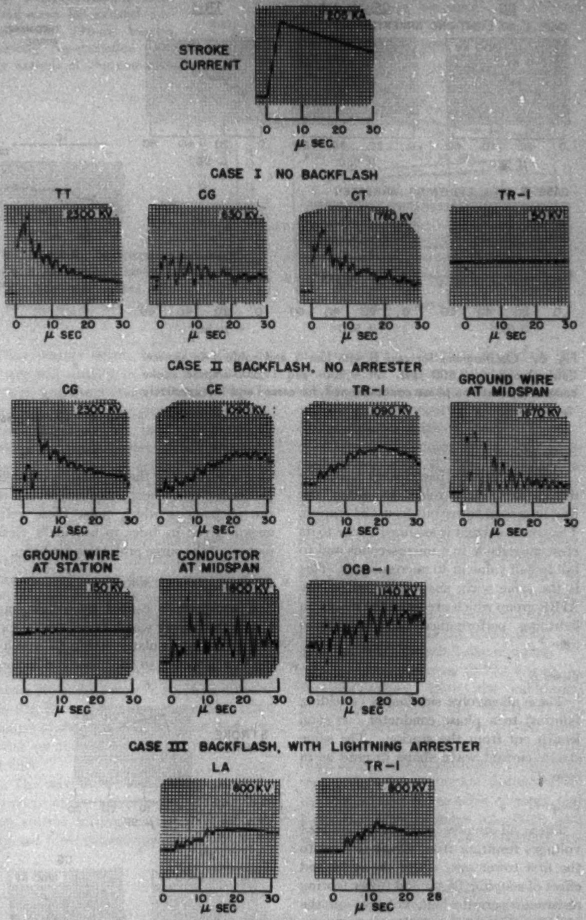

Fig. 5. Oscillograms for case A with line 1 and cable 1 in service. Cable length is 2,500 feet and struck point is first tower out from station, T_1. $R_1 = 10$ ohms

from the station. These two discharge voltages correspond to 10,000- and 5,000-ampere, 10x20-microsecond arrester discharge currents respectively. This type of arrester analogue will lead to very conservative results because the tail of the arrester voltage is held constant at the maximum discharge voltage for a long period. Fig. 4 shows the actual arrester discharge current, voltage, and volt-ampere characteristic for a discharge current of 10,000 amperes. The loop, effect in the volt-ampere characteristic causes the voltage wave to drop appreciably after crest voltage is reached. For example, at 24 microseconds, the voltage has decreased to about 57 per cent (%) of its crest value, a situation which must be taken into account in interpreting the oscillograms in those cases where the lightning arrester is connected.

Surge voltages were measured at the points identified by the letter symbols of Figs. 1 and 2. Definitions of these symbols are given in Table I. All strokes were applied to line 1 and when more than one cable was in service the entire bus was connected. Disconnects on the bus side of the breaker were open except when additional lines were simulated by closing all the switches to the surge impedance resistor *Z*.

Situations Analyzed

Since there are so many combinations of variables in the surge protection problem, a systematic appraisal of all the factors which influence the magnitude and duration of surge voltages in the station must be made. The variables are:

1. Character of the lightning wave.
2. Current magnitude in the lightning stroke.
3. Number and location of lightning arresters.
4. Number of overhead lines and cables assumed to be in service.
5. Tower-footing resistance.
6. Coupling between phase conductor and ground wires.

Character of the Lightning Wave

The idea that protection against close-in direct strokes is possible led to the selection of lightning waves based on stroke current rather than stroke voltage for study. Cases *A*, *B*, and *C*, in the following, are the three possible kinds of waves resulting from different considerations of stroke currents and the point in the system which is hit. Case *D* involves a traveling voltage wave originating some distance away from the station. The latter is the one case which has been used in previous studies[1-3] and is included here for correlation.

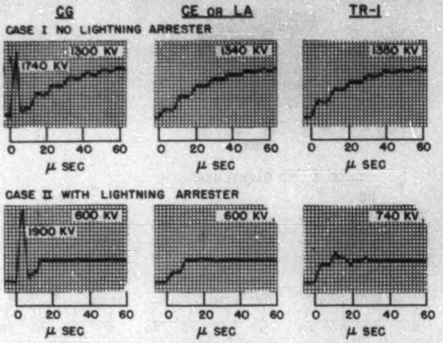

Fig. 6. Oscillograms for case B with line 1 and cable 1 in service. Cable length is 2,500 feet. A 9,200- and 11,200-ampere stroke current terminate on phase conductor at T_1 for cases I and II respectively

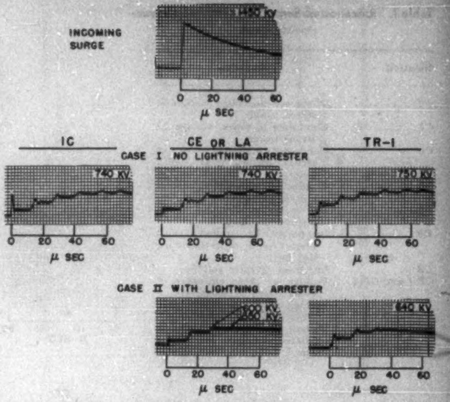

Fig. 8. Oscillograms for case D with line 1 and cable 1 in service. Cable length is 3,500 feet

Cases A

These all involve backflashes caused by direct lightning strokes to either the first or second tower out from the station. The stroke current is assumed to rise to its crest magnitude in 4 microseconds and to fall to half value in 40 microseconds. This is the same wave shape selected by the AIEE group which prepared the report on lightning performance of transmission lines.[7]

Cases B

These all involve sideflashes (shielding failures) to a phase conductor one span length out from the station. The same stroke current wave shape in used as in case *A*.

Cases C

These all involve coupled or induced voltages resulting from direct strokes to the first tower out, where the combined effect of coupling factor and tower-footing resistance permits high voltages on the phase conductors even if there is no tower-to-conductor backflash. The stroke current wave shape is the same as in case *A*.

Cases D

These all involve incoming traveling voltage waves originating 1/2 mile or so out from the station. The standard AIEE $1^1/_2$x40-microsecond wave shape[8] is used, as the most severe of the six waves used in previous studies.[1,2]

Discussion of Phenomena

Primarily, the object of the study was to obtain numerical values of surge voltages as a guide for the application of surge protective equipment. A brief review of the phenomena which cause these voltages is given in order to provide a clear picture of the surge protection problem.

Cases A: Backflashes

A backflash is caused by a lightning stroke to a tower which raises the potential across an insulator string *CT* resulting in a flashover to the phase conductor. The oscillograms of Fig. 5 show the mechanism of a backflash. After lightning strikes the tower, the tower-top potential *TT* builds up according to $L_1dI/dt+R_1I$. The first row of oscillograms in Fig. 5 shows the conductor-to-ground voltage *CG* at the struck point, the conductor-to-tower voltage *CT* across the insulator string, and the voltage at the transformer *TR-1* which would exist if no backflash occurred.

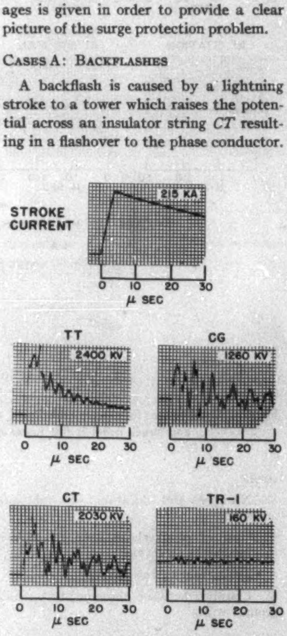

Fig. 7. Oscillograms for case C with line 1 and cable 1 in service. Cable length is 500 feet and struck point is at T_1. $R_1=10$ ohms

Depending upon the magnitude of stroke current, tower inductance, and tower-footing resistance, the voltage across the insulator string *CT* may be high enough to cause a backflash. The impulse withstand strength of the 16 insulators was determined for the particular wave form by the integration method,[1,2] which showed that 205,000 amperes are necessary to flash over the line insulation, assuming a 10-ohm tower-footing resistance. The backflash was assumed to occur at 4 microseconds, which is the point where the tower-top potential starts to decrease. When a backflash does occur, the voltage on the phase conductor *CG* rises to the tower-top potential of 2,300 kv and has the same wave shape on the tail as the tower-top potential. Shown in the second row of Fig. 5, this is the general shape of voltage waves placed on the phase conductor in all cases *A*, since L_1 and R_1 are of such relatively low impedance that the circuits connected at the station have no appreciable influence on the voltage at the struck point. Resultant voltages at other points in the station are shown in the second and third rows of Fig. 5.

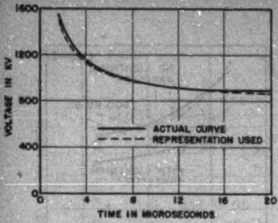

Fig. 9 (left). Impulse withstand curve for external porcelain of 196-kv bushing showing representation used for analysis of Anacom data

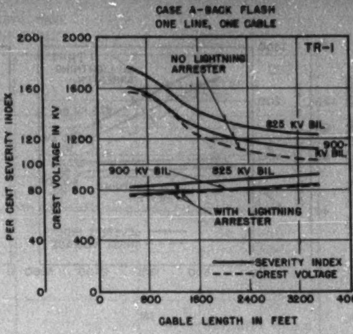

Fig. 11 (right). Stroke current of 205,000 amperes terminates 1,000 feet from station at T_1 having an $R_1=10$ ohms

Some observations from Fig. 5, while not directly pertinent to the protection problem, afford a better insight to the nature of the phenomena. Half way between the struck tower and the station, the voltage on the ground wire is highly oscillatory because of reflections from the station. But the ground wire potential at the station (actually the station steel potential) is quite low in consequence to the low ground resistance of the station. Reflections from the station and altered coupled voltage from the ground wire change the character of the traveling wave on the conductor considerably, as it moves from the struck point *CG* to mid-span and to the incoming circuit-breaker location *OCB-1*. The high-frequency components are largely suppressed by the low cable surge impedance at the cable pothead *CE*.

Also shown in Fig. 5 are the voltages at the lightning arrester *LA* and at the transformer *TR-1* with a 195-kv lightning arrester located at the cable entrance. The lightning arrester holds the crest voltage down to 600 kv at its terminals and to 800 kv at the transformer.

Cases B: Sideflashes

Sideflashes result from shielding failures which permit the lightning stroke to make direct contact with a phase conductor. They seldom occur, but when they do there will usually be a flashover to the tower, and the voltage wave entering the station will not differ greatly from that of cases *A*. However, in a few instances where the stroke current is low, the voltage may not be high enough to flash over the line insulation. These cause trouble, because they may be high enough to be dangerous to equipment insulation.

Fig. 6 shows oscillograms taken with a 4x40-microsecond current surge terminating on a phase conductor one span from the station at *CG*. Stroke current was adjusted to give a voltage at the struck point just barely insufficient to flash over the line insulation, this being the worst case. The stroke current necessary to cause flashover for the case of no arrester in Fig. 6 was 9.200 amperes, while 11,200 amperes were required to cause flashover with an arrester located at the cable entrance.

The wave shape and magnitude of the voltage at the struck point is dependent on station loading in the form of connected lines, cables, apparatus, and lightning arresters. Therefore, to obtain the same critical flashover voltage at the struck point, the magnitude of the stroke current must be varied with the number of connected circuits. Consider the case of no arresters as shown by the first row of oscillograms in Fig. 6. The voltage at the struck point *CG* initially rises at the rate of half the line surge impedance multiplied by the rate-of-rise of the stroke current. However, before maximum voltage (half the line surge impedance times the magnitude of the stroke current) is reached, a negative reflection returns from the circuit breaker and connected cable to reduce the voltage at the struck point and give the characteristic spike of voltage as seen in the oscillograms of Fig. 6. As reflections return from the cable-connected transformer, the voltage at *CG* begins to increase slowly to a second maximum value whose magnitude depends on cable length and magnitude of stroke current. Thus, for a constant distance from the struck point to the cable entrance and a constant stroke current magnitude and wave shape, the first spike of voltage has

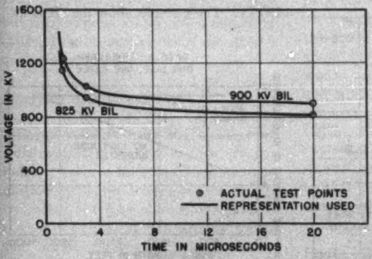

Fig. 10. Impulse withstand test points for 900-kv and 825-kv BIL transformer and curve showing representation used for analysis of Anacom data

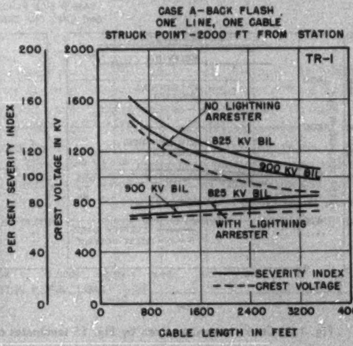

Fig. 12 (right). Stroke current of 205,000 amperes terminates 2,000 feet from station at T_2 having an $R_2=R_1=10$ ohms

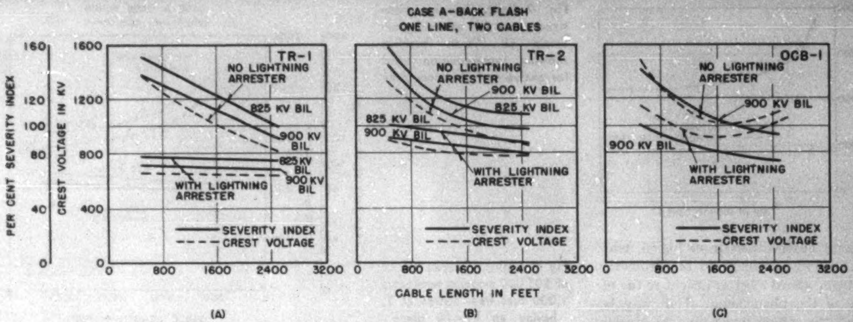

Fig. 13. Stroke current of 205,000 amperes terminates at T_1 having an $R_1=10$ ohms. The whole station bus is connected and a lightning arrester is located only at CE-1

a constant magnitude but the second slowly rising voltage magnitude and shape depend on the cable characteristics. The wave shape of this slowly rising voltage is the principal determinant of flashover since the influence of the spike of voltage is small compared with the influence of the second voltage wave. Therefore the stroke current was varied in the study to obtain the critical voltage of 1,300-kv crest for the second slowly rising voltage wave. Although this voltage varies with cable length, the variation is small and for conformity was held constant at 1,300 kv for all cable lengths.

For the case of an arrester located at the cable entrance, the first spike of voltage results from the same phenomena as mentioned for the case of no arrester. However, after this first spike, the arrester holds the voltage to approximately 600 kv, the arrester discharge voltage. Therefore, cable length has no effect on the voltage wave shape at the struck point and the wave shape of the first spike of voltage determines whether or not there is flashover of the line insulation. The critical crest voltage is 1,900 kv, which corresponds to a stroke current of 11,200 amperes.

As shown in Fig. 6, the lightning arrester analogue was set to hold 600 kv, corresponding to a crest discharge current of 10,000 amperes. As has been pointed out, the type of arrester analogue employed yields extremely conservative results with respect to the magnitude of the wave tail, and this must be considered in interpreting the voltage across the transformer *TR-1*. If a more exact analogue had been used, the shape would have been similar to the voltage wave of Fig. 4(B) with a crest of 740 kv and it would have been down to about 422 kv at 24 microseconds.

Cases C: Coupled Voltages

Coupled voltages are placed on the phase conductor by direct strokes to a tower with no backflash. These cases were studied to determine the relative severity of coupled voltages as compared to those obtained from backflashes. The Anacom set-up was exactly the same as for cases *A*, but the switch simulating the backflash was not closed. Consequently, stroke current was not applied conductively to the phase conductor; instead, stroke effects were coupled onto the phase conductor solely through the electromagnetic and electrostatic coupling shown in Fig. 3.

Surge voltage coupled on to a phase conductor *CG* for normal line constants is shown in Fig. 5, case I, and its magnitude is quite low. A more severe condition can be anticipated in which the coupling factors are increased intentionally (by aerial counterpoises) to prevent backflashes.

For the oscillogram sequence of Fig. 7, the coupling factor was increased to 65% the tower footing resistance was kept at 10 ohms, and a 500-foot cable was connected to the station. The crest stroke current of 215,000 amperes was just insufficient to cause a backflash. Crest voltage at the transformer (*TR-1*) was only 160 kv. These results show that it is un-

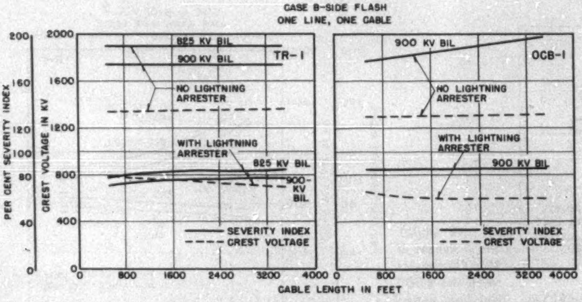

Fig. 14. Stroke current as given by Fig. 15 terminates on phase conductor at T_1

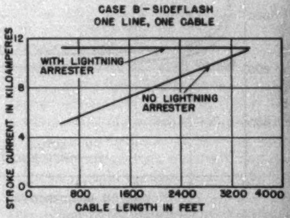

Fig. 15. Stroke current necessary to produce critical flashover voltage of 16 insulators at CG. See Fig. 14

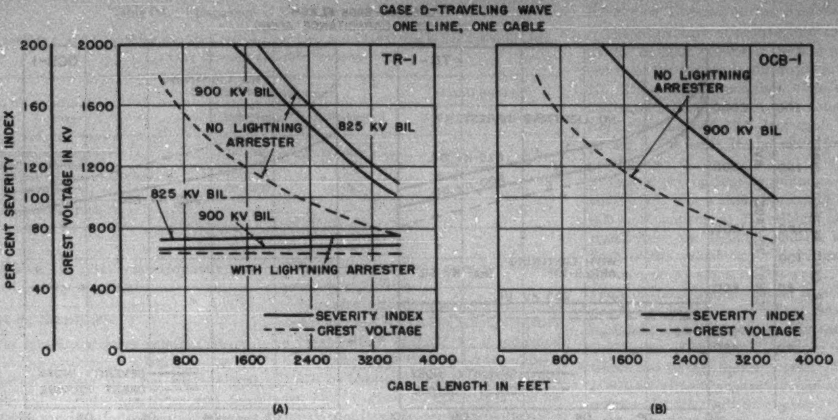

Fig. 16. Incoming surge voltage is 1,450-kv crest, $1^1/_2$x40-microsecond wave shape

necessary to consider direct strokes which do not result in backflashes.

Cases D: Traveling Voltages Waves

Studies were made of cases involving incoming traveling voltage waves to show the comparison in surge voltages caused by direct strokes close to the station and those caused by strokes some distance away. Fig. 8 shows oscillograms for the case of one overhead line and one 3,500-foot cable.

The lightning arrester was set to spark-over at 600 kv but the discharge voltage was held constant at 550 kv, which corresponds to a discharge current of 5,000 amperes. The crest voltage at the transformer *TR-1* is slightly higher than the arrester discharge voltage, but not sufficiently to alter the protection afforded. As with side flashes cases *B* the duration of arrester voltage appears to be too long, but this, as previously pointed out, is because of the characteristics of the arrester analogue employed.

Analysis of Anacom Data

Surge voltages from the oscillograms were evaluated in terms of their severity index,[1-3] a procedure based on the integration method of expressing the disruptive effect of nonstandard waves in terms of that of equivalent standard test waves. For circuit voltages of 69 kv and over, disruptive effect is given by the relation

$$\text{Disruptive Effect} = \int e^{K_2} dt$$

where e is the surge voltage as a function of time and K_2 is a constant. The % severity index (SI) is the ratio, expressed in %, of the crest voltage of the surge under consideration to the crest voltage of a surge of the same shape which will stress the insulation just to the impulse withstand curve. Or, to put it another way, % SI of a surge of any odd shape is the ratio, expressed in %, of the crest voltage of a reference wave having the same disruptive effect as the odd wave to the crest voltage of the same reference wave which will stress the insulation just to its impulse withstand curve.

In this study consideration was given to the disruptive effect of surges on the transformer insulation, and on the circuit-breaker insulation. SI's of surges on the circuit-breaker insulation are expressed in terms of the external portion of the 196-kv bushing having an impulse withstand curve as in Fig. 9. Any wave which will stress the bushings to this curve has an SI of 100%; for example, both a 1,550-kv, $1^1/_2$x40-microsecond wave chopped at 1.5 microseconds and a 900-kv, $1^1/_2$x40-microsecond wave chopped at 14 microseconds have SI's of 100%. Equating the expressions for disruptive effect of these two waves, the constant K_2 comes out to be 4.7 for the 196-kv breaker bushing. SI's of surges on the transformer were expressed in terms of the standard impulse withstand tests for both the 900-kv and 825-kv basic impulse insulation level (BIL) transformers. Therefore, for the 900-kv BIL transformer, either a 1,035-kv, $1^1/_2$x40-microsecond wave chopped at 3 microseconds or a 900-kv, $1^1/_2$x40-microsecond full wave have SI's of 100% on the transformer insulation. Based on these two standard test waves, the constant K_2 is 9.1 for the transformer insulation. Because the chopped-wave test is 15% higher than the full-wave test, the constant K_2 will be 9.1 for all transformers. The impulse withstand curves for the 900-kv and 825-kv BIL transformers are shown in Fig. 10. The curves were plotted from calculated values of SI and therefore they pass through the chopped-wave and full-wave test points, protection being co-ordinated on these two points.

Discussion of Results

SI's and crest voltages at various measurement points are plotted against cable length in Figs. 11 through 18. Tables II and III give additional data for multiple circuits for cases *A* and *B*. For the most part, the curves and diagrams of Figs. 11 through 18 and Tables II and III with their captions are self-explanatory. Discussion of each curve is

Fig. 17. Single-line diagram of circuit tested to show effect of adding lumped capacitor at TR-1

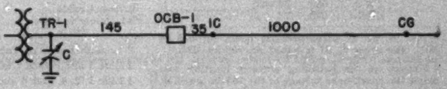

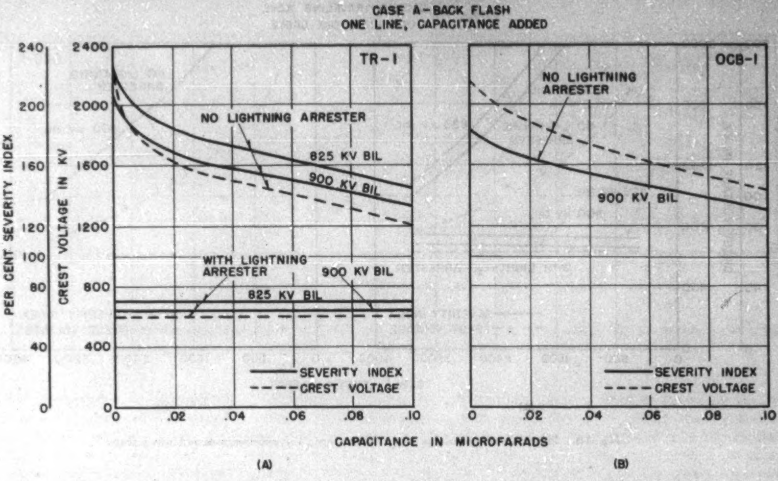

Fig. 18. Stroke current of 205,000 amperes terminates at T_1 having an $R_1 = 10$ ohms. (Refers to Fig. 17)

omitted in the interest of brevity. The curves can be used for reference purposes, and for protection problems in general. While the data are all in terms of a 230-kv system, judicious extrapolation should be possible with other operating voltages. In general, it may be expected that the SI will be higher for 138-kv systems and lower for 330-kv systems for comparable cases.

Case A: Backflash

Comparison of Figs. 11 and 12 shows that voltages at the transformer become less severe as the stroke terminating point is moved farther out from the station.

Table II. Case A, Backflash

% SI's and Crest Voltages: Four Lines (Nos. 1, 2, 4, and 6) and all Four Cables in Service: Stroke Terminates at First Tower out from Station. $R_1 = 10$ Ohms

Cable Length, Feet	Apparatus	With No Lightning Arrester		With Lightning Arrester	
		Crest, Kv	SI*, %	Crest, Kv	SI, %
500	*TR-1*	810	84 (92)	620	71 (77)
	TR-2	810	89 (97)	760	76 (83)
	OCB-1	950	88	950	89
1,500	*TR-1*	670	73 (80)	†	
	TR-2	680	76 (83)		
	OCB-1	920	73		

* The % SI in parentheses is based on 825-kv BIL; the other % SI is based on 900-kv BIL.

† Voltage at the lightning arrester location was below the spark-over voltage of the 195-kv arrester.

With one line and one cable connected, voltages at *OCB-1* were recorded only for a 2,500-foot cable. With arrester connected, a crest voltage of 1,200 kv having an SI of 144% appeared at *OCB-1*. With an arrester connected at the cable entrance, the voltage reached a crest of 1,150 kv and had an SI of 84%. However, protection of circuit breakers for other cable lengths can be estimated, from the curves of Fig. 13(C) which apply where two cables are in service. Assuming the same shape curve as in Fig. 13(C), the SI at *OCB-1* for one 500-foot cable and an arrester is 113%. The 100% SI point occurs at a cable length of 1,000 feet. Therefore, it is estimated that for case *A*, with one line and one cable, the breaker is protected for cable lengths longer than 1,000 feet.

Surge voltages at transformer *TR-2* shown in Fig. 13(B) apply for the case of an arrester located at the cable entrance *CE-1* and nowhere else in the station. Adequate protection might be afforded transformer *TR-2* for some cable lengths, depending on the transformer BIL. However, in the actual station it is desirable to place an additional arrester at *CE-2* so that protection of *TR-2* is assured if a backflash should occur on line no. 2. In this case, the curves of *TR-2* would be identical to those of *TR-1*.

Table II shows the effect of four lines and four cables in service on the voltage at the equipment terminals. With 1,500-

Table III. Case B, Sideflash

% SI's and Crest Voltages. Cable Length = 2,500 Feet. Stroke Current of 11,200 Amperes Terminates on Phase Conductor at First Tower out from Station

Connected Circuit	Apparatus	With No Lightning Arrester		With Lightning Arrester	
		Crest, Kv	SI*, %	Crest, Kv	SI*, %
1 line, 2 cables‡	*TR-1*	1,170	156 (170)	690	80 (87)
	TR-2	1,170	156 (170)	750	83 (91)
	OCB-1	1,120	169	660	88
4 lines, 4 cables§	*TR-1*	460	51 (56)	†	
	TR-2	470	57 (62)		
	OCB-1	450	56		
1 line, 1 cable	*TR-1*	720	74 (81)	660	65 (71)
Flashover to tower	*OCB-1*	570	60	480	54

* † See footnotes of Table II.

‡ Line 1 and cables 1 and 2 in service.

§ Line 1, 2, 4, and 6 and all cables in service.

Table IV. Comparison of SI's of Surge Voltages

At Transformer and Circuit Breaker for Case of One Line and One Cable in Service with Lightning Arrester at Cable Entrance

Cases	Transformer* 500-Foot	Transformer* 3,500-Foot	Circuit Breaker* 500-Foot	Circuit Breaker* 3,500-Foot
A—Backflash at first tower	75 (82)	85 (92)	113†	82†
B—Sideflash at first tower	71 (78)	78 (85)	84	86
C—Coupled voltages at first tower	19 (21)		25	
D—Traveling wave	66 (72)	79 (86)		

* See footnote of Table II.

† These are estimated values.

foot cable, the station is adequately protected without arresters.

Case B: Sideflash

The severity of surge voltages appearing at the equipment is less than for the backflash of case *A;* see Fig. 14 and Table III. With four lines and four cables in service, the station is protected without arresters; see Table III. If flashover to the tower at the struck point does occur, the severity of surge voltage at the apparatus is greatly reduced; see Table IV.

Case D: Traveling Voltage Wave

The significant fact for Fig. 16 is that the SI of surges at the transformers with an arrester in service is lower for case *D* than for cases *A* and *B*.

Effect of Capacitance in Reduction of Surge Voltage

The picture would not be complete without some calibration to the effect toward reduction of surge voltages exerted by the cable circuits. For this purpose, data for case *A* were taken on the circuit of Fig. 17, which is the same as Fig. 1 from point *CG* to *BI*, capacitance being added at point *TR-1*. These data are presented in Fig. 18 which shows that the presence of high-voltage cables makes direct-stroke protection possible.

For zero added capacitance (i.e., an open line) and with no lightning arresters, a crest voltage of 2,350 kv is indicated. Comparing the 2,350 kv with the value of 1,570 kv obtained with 500 feet of cable, see Fig. 11, gives an example of the improvement from the presence of the cable. A 500-foot cable has about 0.033 μμf capacitance. Reading from Fig. 18, a crest voltage of 1,570 kv is obtained for this value of capacitance, which checks the value from Fig. 11, taken with pi-sections representing the distributed constants of the cable.

Comparison of Voltages at Ends of Bus

Fig. 19 shows a comparison between the bus voltages at the incoming line bay *BI* and at the most remote point from the incoming line bay *BR* for case *A* with a 205,000-ampere stroke to T_1 having a 10-ohm footing resistance. One line and two 2,500-foot cables were in service for these oscillograms, which show that the crest voltage at *BR* is 20% higher than the voltage at *BI* for the case of no arrester. For an arrester connected at *CE-1* the crest voltage at *BR* is 14% higher than the voltage at *BI*.

Effect of Tower-Footing Resistance

The importance of securing low tower-footing resistances *TFR* at the first tower out from the station is illustrated in Fig. 20. These oscillograms show voltages at the transformer for cases *A*, with one overhead line and one 2,500-foot cable connected. The scale is the same for all oscillograms.

Two stroke current magnitudes were considered. For a stroke current of 145,000 crest amperes at T_1, voltages at the transformer are negligible until a backflash occurs, which is for a footing resistance of 20 ohms in this case. The value of the lightning arrester in holding down the transformer voltage when a backflash occurs is illustrated in the last oscillogram of the case I sequence which shows two voltage traces: a crest voltage of 970 kv without an arrester, and a crest voltage of 760 kv with an arrester.

The case II oscillograms of Fig. 20 were made with the same setup as case I except that the stroke current was 205,000 amperes, a value just high enough to cause a flashover with a 10-ohm tower-footing resistance. It is significant that the highest stroke current ever recorded in the field measured only 218,000 amperes. This leads to the conclusion that there is practically no possibility of a backflash occurring if the tower-footing resistance is 10 ohms or less. The effect of the lightning arrester is also shown on the last two oscillograms of the sequence.

Comparison of Cases

In terms of the surge voltages which have the highest severity on the transformer insulation, Fig. 21 shows a summary of the "worst" examples for the four general cases studied. In each case line 1 and cable 1 were in service and the stroke terminated on T_1 which had a footing resistance of 10 ohms (except case *D*,

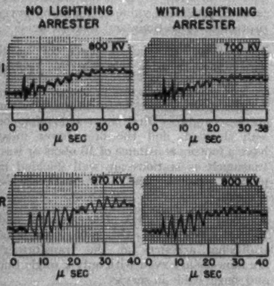

Fig. 19. Oscillograms comparing surge voltages at BR and BI

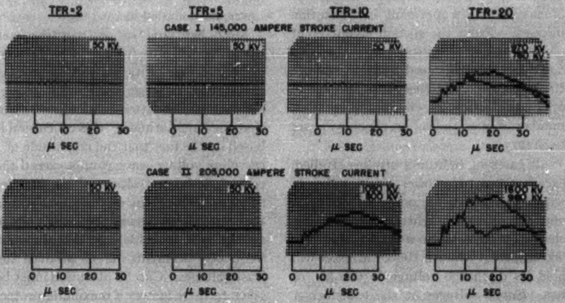

Fig. 20. Oscillograms of transformer voltages for various values of tower-footing resistance TFR

the traveling wave). The oscillograms show that the highest voltages occur for case *A* while cases *B* and *D* are of lesser severity. Case *A* is approximately 30% higher in crest voltage than case *D* which has been the commonly accepted criterion. Case *C* is of such low magnitude that it need not be considered in surge protection studies.

Analysis of Results

Data taken during the study permit a very complete assessment of lightning protection for 230-kv stations. However, a reasonable basis for station protection design must be selected from the wide range of cases studied, and due consideration must be given to certain premises. These premises are: 1. Effective shielding is provided for the switching station and on each overhead line in the one span immediately adjacent to the station through the use of three ground wires. 2. Footing resistance of the first tower out from the station is 10 ohms or less. 3. The station ground resistance is less than 1 ohm. 4. Lightning arresters are located at the cable potheads.

Strokes beyond the first span must fall in the categories of sideflashes or backflashes. In either case, the SI of the conductor-to-ground voltage wave may not exceed the line insulation strength. In the studies of cases *B* and *D*, this relation is established, and it may therefore be concluded that only the first span must be given 100% shielding, and only the first tower a low-footing resistance. Stated another way, the inductance of one span limits the incoming surge energy to protectable values.

With all lines and cables in service, the station is inherently self-protected from lightning without any lightning arresters. However, as the number of lines and cables in service is reduced, the magnitude of surge voltages appearing in the station increase. From the station layout point of view, the most critical case is that of a single outgoing line and a single cable to the transformer. Hence, it is prudent to apply protection based on the smallest number of lines and cables which will ever be in service.

All cases of lightning strokes studied, except those to a tower or ground wire with no backflash, are potentially dangerous. In all cases, lightning arrester discharge currents are in a zone (below 12,000 amperes) where a 195-kv arrester will hold its discharge voltage to 600 kv, or less. Surge voltages at the transformer exceed the arrester discharge voltage by a small amount, dependent upon the length of cable, the stroke current magnitude, and the character of the lightning wave.

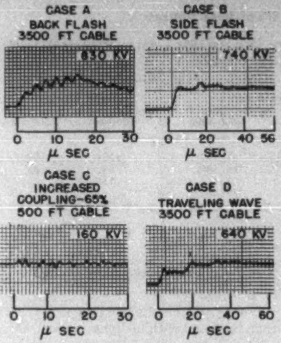

Fig. 21. Oscillograms showing summary of worst cases of surge voltages at transformer TR-1

With respect to surge voltages at the transformers, consider the shielding failure (cases *B*). On a probability basis, it is the least likely to occur. It requires a shielding failure (probability in a given span of about 1 in 5,000 years) and a stroke current in the limited range of 5,000 to 11,200 amperes (probability about four in 10) to require consideration. Thus, the over-all probability is placed at perhaps once in 10,000 years, odds which are too great to merit consideration.

Direct strokes followed by a backflash at the first tower out from the station (cases *A*) are highest in order of severity. Probabilitywise, the chances of the first tower being struck are small compared to strokes on several miles of line. However, protection against these strokes is possible when using cable connections to the transformers, so surge voltages originating from direct strokes to the first tower are included in the picture.

Most lightning surges meriting consideration will arise from strokes to towers or ground wires within about 10 miles of the station. Surges traveling a greater distance will be attenuated to an extent that they are harmless; this conclusion is based on the fact that the magnitude of a traveling voltage wave cannot exceed the critical flashover voltage of the line insulation. The point of this discussion is that strokes producing the most voltage are the least probable, and that the most frequently occurring surges produce the least voltages. Careful attention must be given to these factors if maximum protection is to be attained at minimum cost.

Figures of SI for the worst cases from Figs. 11, 14, and 16 are shown in Table IV, in which transformers with 825-kv or 900-kv BIL are shown as adequately protected for all cases considered with a 195-kv arrester located at the cable entrance. If 185-kv arresters are used, the protection margins in the case of 825-kv BIL is established as approximately as good as for 900-kv BIL with 195-kv arresters.

Circuit-breaker data are not available for the traveling wave (case *D*). However, because traveling waves produce less severe voltages than cases *A* or *B* at the transformer, it can be assumed that the same phenomena will apply at the circuit breaker. Therefore, the circuit breaker is adequately protected except for case *A* with short cable lengths. The 100% SI point for this case has been estimated to occur at a cable length of 1,000 feet. Therefore, except for cable lengths under 1,000 feet, the circuit breaker is adequately protected in all cases. If an 825-kv BIL transformer is used with an 185-kv arrester, it is reasonable to assume that the severity of the voltage wave at the 900-kv BIL circuit breaker will be low enough that the breaker will be protected for all cable lengths for all cases studied.

One of the most significant conclusions to be drawn from Table IV is that the severity of the surge voltage at the transformer produced by the worst case considered (case *A*, backflash) has an SI only 7% greater than the surge voltage produced by the traveling wave (case *D*). This leads to the conclusion that the traveling wave produces voltages only 7% less severe than the worst of close-in direct strokes, provided, of course, that the prescribed measures are taken for direct-stroke protection.

Conclusions

1. Use of cable leads to the transformers is of considerable value in lightning surge protection of stations and transformers.

2. Because of the presence of cable capacitance, reliable direct-stroke protection can be secured.

3. To secure direct-stroke protection, the stations and the first span out must be well shielded, and the first tower must have a footing resistance of 10 ohms or less. Inasmuch as stations are well shielded in present practice, the additional expense is small.

4. With 900-kv BIL transformers and 195-kv arresters at the cable entrances, additional arresters at the transformers are unnecessary even with only a single line and single cable in service.

5. With 185-kv arresters at the cable entrances and transformers of 825-kv

BIL the transformers are adequately protected, without additional arresters at the transformers.

6. When the direct-stroke protection problem is recognized and provided for, the surge voltages are only 7% more severe than those from traveling waves.

7. The circuit breaker with 900-kv BIL on the incoming line is adequately protected, provided a lightning arrester is used at the cable pothead and the cable length is longer than 1,000 feet. For the most severe strokes, the line circuit breaker may not be protected if there is only one cable and it is less than 1,000 feet long. However, the probability of strokes as severe as those studied is exceedingly remote. In any specific case, these factors should be evaluated in determining what protection should be provided.

8. Lumped capacitors, if large enough, can afford benefits similar to those afforded by cables, and the influence of capacitors, for power factor correction or other purposes, should be considered in the lightning protection problem.

References

1. Lightning Protection in Extra-High-Voltage Stations—Analyses, Anacom Study, and Results, I. W. Gross, T. J. Bliss, J. K. Dillard. *AIEE Transactions*, vol. 71, pt. III, Jan. 1952, pp. 482–92.

2. Lightning Protection in Extra-High-Voltage Stations—Influence of Multiple Circuits, I. W. Gross, L. B. LeVesconte, J. K. Dillard. *AIEE Transactions*, vol. 72, pt. III, Oct. 1953, pp. 882–90.

3. Lightning Protection in a 120-Kv Station—Field and Laboratory Studies, J. K. Dillard, H. R. Armstrong, A. R. Hileman. *AIEE Transactions*, vol. 73, pt. III, Oct. 1954, pp. 1143–52.

4. High-Voltage Impulse Tests on Transmission Lines, C. F. Wagner, I. W. Gross, B. L. Lloyd. *Ibid.*, April 1954, pp. 196–210.

5. High-Voltage Impulse Tests in Substations, I. W. Gross, S. B. Griscom, J. M. Clayton, W. S. Price. *Ibid.*, pp. 210–22.

6. Symmetrical Components (book), C. F. Wagner, R. D. Evans. McGraw-Hill Book Company, Inc., New York, N. Y., 1933, p. 185.

7. A Method of Estimating Lightning Performance of Transmission Lines. AIEE Committee Report. *AIEE Transactions*, vol. 69, pt. II, 1950, pp. 1187–96.

8. Insulator Tests. *AIEE Standard No. 41* Sept. 1944.

◆

Discussion

E. Beck (Westinghouse Electric Corporation, E. Pittsburgh, Pa.): The paper shows how the risks of damage from severe direct strokes can be reduced to a virtually negligible quantity. When the authors speak of the "idea that protection against direct strokes is possible" I do not think they mean that past practices have not provided protection; they are speaking of degrees of protection and degrees of stroke current.

Certainly protection has been afforded against direct strokes into and close to substations, even unshielded ones, in the past. Lightning-arrester engineers, as far as we are aware, have not hesitated to declare that adequate arresters applied at apparatus terminals will protect for the great majority of strokes, perhaps for all but those catastrophic strokes that occur about as often as earthquakes.

Experience bears this out. There are many unshielded stations. It is estimated that a small substation might be struck once in 10 to 15 years. Thus 1 in 10 or 15 might be struck each year. We doubt that in such substations the failure rate of protected transformers is 7 to 10%, or even half of it. A look at distribution transformers gives a similar picture. Direct strokes close to distribution transformers are quite likely and many must have occurred during the past 30 years.

The authors have shown how a cable-connected transformer can be protected against very severe strokes with arresters only at the cable entrance and not at the transformer, thereby giving protection also to the cable and adjacent switchgear. The beneficial effects of cable are effectively demonstrated. The benefit to the switchgear is important. Therefore, the paper is a contribution to the lightning protection art.

W. S. Price (American Gas and Electric Service Corporation, New York, N. Y.): Protection of station equipment against surges caused by lightning strokes adjacent to the station should be based, first, on the probability of such surges occurring, and second, on the probable severity of such surges when they do occur. Heretofore, it has been assumed that transmission lines would be so well shielded and would have such low tower-footing resistances for 1 mile out from a station that neither shielding failures nor backflashes would occur in this area. Although this assumption may be correct, a complete appraisal of the station protection problem should include a study of the severity of surges produced in the station in case a shielding failure or backflash does occur near the station. In this excellent paper the authors have, for the first time, provided a detailed picture of the severity of such surges, and have thus partially closed an important gap in our knowledge of station lightning protection.

It is evident from the oscillograms in this paper that the high-voltage cables have a profound effect on surge voltages within the station, and their presence makes direct-stroke protection possible. However, insufficient data are presented to evaluate the protection afforded by multiple lines in a station without high-voltage cables. Possibly, a similar study could be made in the future for the benefit of those of us who do not have high-voltage substation cables.

The analogue computer studies which the authors and their associates have made in the past several years have been of great value in the application of station lightning protection on a rational basis. A secondary but worth-while benefit which I have derived from these studies is the clear picture which they have given of the life and death of a surge voltage which has entered a substation containing multiple reflection points. The textbooks tell us that lattice diagrams can be used for this purpose. However, I have never seen a lattice diagram outside of its natural habitat, the textbook, and their value to protection engineers is somewhat doubtful.

Of particular interest in this respect are the oscillograms in Fig. 5 showing the mechanism of a backflash at a struck tower, and the oscillograms in Fig. 6 showing the effect of multiple reflections in the cable.

H. M. Ellis (Hydro-Electric Power Commission of Ontario, Toronto, Ont., Canada): The authors have done an excellent job of simulating the circuitry of the St. Lawrence Power Project on the analogue computer and have very capably demonstrated the usefulness of the computer in determining the severity of voltage surges which can arrive at the 230-kv cables and transformers.

Having determined the direct-stroke currents to the transmission lines which produce excessive surge voltages at the cables and transformers, perhaps the next step should be to determine the frequency of occurrence of these overvoltages. On the Canadian side a lightning outage on the several miles of transmission line between the 230-kv cable entrance and the switchyard will mean loss of one-quarter of the generation; hence, it is desirable to obtain low tower-footing resistances on the lines, i.e., 5 ohms or less, to minimize the frequency of these outages. Based on this low resistance and good overhead shielding, the lightning outage probability and the frequency of operation of the lightning protective devices at the 230-kv cable entrances becomes approximately one every 30 to 40 years for all four single-circuit lines.

Based on the infrequent operation of the lightning protective devices, the fact that there will generally be a line outage associated with this operation regardless of the type of protective device used, and the fact that the cable significantly reduces the rate of rise of the voltage surge, it appears that co-ordinating gaps located at each end of the 230-kv cables would provide adequate protection for the cables.

H. A. Cornelius (Commonwealth Edison Company, Chicago, Ill.): A paper which explains how currents so much larger than can be obtained on the basis of traveling-wave theory can reach substation equipment has been needed for several years. The authors are congratulated for recognizing this need and for supplying some helpful information. There are a few points, however, on which additional information would be useful.

It is interesting to compare the 51-kiloampere-(ka)per-microsecond rate of rise of current to a crest value of 205 ka assumed in this paper with the comments on a 1953 paper[1] for advocating the use of a 5-ka-per-microsecond 5-ka-crest current for co-ordination purposes. One discusser stated: "No record of an arrester discharge of this character has been obtained on a line properly equipped with ground wires, nor on substations with adequate provisions for shielding. It would therefore appear that for systems having a voltage of 100 kv or greater (and shielded line conductors) the steep current discharge can be neglected." Since probability calculations, based on the simultaneous occurrence of a 5-ka rate of rise to a 5-ka crest current, show that less than 1% of the currents discharged through arresters in stations to date exceed these values, how do the authors justify the use of a 51-ka rate of rise to a 205-ka crest current?

Furthermore, are not probabilities being "pyramided" unreasonably to assume the simultaneous occurrence of such unusual things as: 1. a lighting stroke which terminates on a line one or two spans out from a substation; 2. the occurrence of almost the maximum lightning current ever recorded to any object (205 ka versus 218 ka); and 3. a shielding failure, on a line having the almost perfect protection provided by three shield wires?

There are numerous 220-kv transmission lines in service equipped with two shield wires, which have such a good performance record that describing them as lightning-proof is justified. For example, on a 160-mile long line with which I am familiar nine tripouts due to lightning have occurred over a 15-year period. With such typical experience, is it not too improbable to consider seriously that a shielding failure could occur on an even better protected line?

In the section entitled "Circuit Constants" the 220-kv tower inductance was assumed to be 20 μh. This inductance value for steel towers has been used in several other papers. The basis used to determine this value has not been stated in this or the other papers. It would be of value to have the authors state how they obtained this value. Also, have any tests been made to measure the potential at the top of a typical 138-kv or 220-kv steel tower, when subjected to, say, 5 ka per microsecond or larger rates of rise of current?

In case A of section on "Discussion of Phenomena" it is stated that a 205-ka stroke to a tower having a footing resistance of 10 ohms will cause flashover of a 16-unit insulator string in 4 microseconds. The coupling factor given elsewhere is 35%. Published 1.5x40-microsecond positive wave test data give the flashover kv of a 16-unit (10 by $5^{3}/_{4}$) insulator string as 1,660 kv. Substituting values in the normal equation used to determine the current required to cause insulation flashover when the footing resistance is low

$$\text{Tower current to cause flashover} = \frac{\text{insulation flashover kv}}{\text{tower-footing resistance} \times (\text{1-less coupling factor})}$$

A value of 254 ka was obtained. Since the paper gives 205 ka, apparently some other factor has been included by the authors. An explanation will be appreciated.

Since the shielding studied in the paper extends out only 2,000 feet, it is assumed that the authors consider this adequate. There is a question as to how much line is required for its full surge impedance to become effective. A discussion of the limits which affect this problem would be helpful.

The effect of having various numbers of lines in parallel on the 220-kv bus at the time a stroke occurs to one of the lines, on the voltage imposed on one of the transformer banks, was not stated on the paper. Perhaps the authors have this information available.

REFERENCE

1. USE OF 10x20 CURRENT WAVES FOR LIGHTNING-ARRESTER TESTS, H. A. Cornelius. *AIEE Transactions*, vol. 72, pt. III, Oct. 1953, pp. 895–901.

E. C. Wentz (Westinghouse Electric Corporation, Sharon, Pa.): The authors seem to have used the SI idea with proper caution in this paper and other papers, but I think that it is well to point out its limitations. The integration-of-voltage idea is based on the assumption that the strength of insulation varies with the time of application to conform to volt-time curves drawn through the American Standards Association full-wave and chopped-wave points. Certain independent studies purport to show that insulation strength both of air and of oil-impregnated pressboard follows this rule.

Actually the relation between voltage and time to breakdown is not entirely a function of the insulating material; it is also a function of the shape of the electrodes. In general, the streamers which initiate breakdown take a long time to propagate if they start from an edge or a point such as a coil edge or lead, and lead off into regions of weaker electric field, but they initiate flashover in a small fraction of a microsecond if they start from a large rounded surface such as a large ball on the inner end of a bushing.

Insulation, of course, must be designed to meet the chopped-wave test. Insulation over edges and points will probably be weaker when longer-time voltages, such as full waves, are applied, and the designer is careful to add extra insulation to make sure it stands the full wave. Insulation over large surfaces is probably just as strong at full waves as it is at chopped waves. So if the assumption is made that the volt-time integration indicates severity, the result will be conservative for times longer than the chopped wave.

However, at times shorter than the chopped-wave value, the insulation on many broad surfaces may break down at very little higher voltage than the chopped-wave value. There is nothing in the American Standards Association Standards to tell the designer that he should make the insulation stronger at times shorter than the chopped wave. Certainly, there is nothing to tell the designer that the insulation must meet the requirements of the SI idea, and the hope that he will be careful to meet these requirements could conceivably result in disaster.

The National Electrical Manufacturers Association steep-front test values are positive points at shorter times, and if the SI idea includes these points as a base, and if all transformers are designed and tested to these steep-front values, the SI idea will be valid down to the steep-front times—no lower.

Fortunately, the applications of the SI idea have generally been at times longer than the chopped-wave values, and, as such, are conservative. I would like to ask the authors if the number of times that insulation performance at times shorter than chopped-wave times is of great enough importance to seriously limit the application of the SI idea according to the reasoning given here. From what I can read in this and similar papers there is very little data to justify steep-front tests; I would like to have the authors' comments.

J. H. Hagenguth (General Electric Company, Pittsfield, Mass.): The authors have again presented a very thorough study of the lightning protection of stations. I agree with them that a low ground resistance at the first tower and good shielding will be very beneficial in keeping lightning arrester currents low, and will help greatly in maintaining good protective margins in the stations. I recommended this in a discussion[1] some years ago. The title of the paper, it seems, is a little misleading because the direct-stroke protection of stations has been in practice for many years. The authors' real intent is to make the protection possible with a minimum of lightning arresters. This they propose to accomplish by means of cables. A cable of low surge impedance and terminated by a small capacitance acts inherently as an oscillatory circuit when excited by repeated reflections over the 1,000-foot line between the tower and the station. Thus, to use the same terminology as the paper, the voltage at the *TR* (transformer) end is about twice as great as at the *CE* (cable entrance) end until the internal cable reflections occur.

In such an oscillatory circuit the resulting *TR* voltages as compared to the *CE* voltages depend greatly on the conditions of the test circuit and the current wave applied. While the authors have chosen a tremendously high current, they have also used an unusual wave form—a straight rising front and a straight falling tail. Thus, at the instant of current crest, the inductive component of the tower voltage wave of the order of 1,000 kv suddenly collapses at the very moment when the insulators flash over. This places a very short spiked traveling wave on the conductor. Because of this short spike the voltage at the *TR* end does not exceed the voltage at the *CE* end greatly and the voltage at both ends does not rise faster so that arrester action does not occur until reflections from the *TR* end reach the cable entrance.

The resulting cable and transformer voltages depend not only on the selected current wave shape but also on the ground wire condition. Thus, with three shield wires between the station and the first tower and only one shield wire beyond the first tower, the tower voltage wave would be maintained at a higher level and for a longer time, resulting in a higher ratio of *TR* to *CE* end voltages.

Of some importance are the changes in oscillograms when the lightning arrester is applied. The wave shape at *LA* (Fig. 5) appears to be considerably modified before the arrester sparks, when compared to the voltage at *CE* without arrester sparking. However, the wave at the *TR* end appears to be exactly alike in both cases.

From the text and the conclusions, one could almost deduce that shielding is needed for only the first tower. It can be shown readily that currents of the order of 50,000 amperes and ground resistance of 30 ohms (and higher currents with correspondingly lower ground resistance) can produce severe conditions in the station if ground wires are omitted at the second tower. In that case, the ground wires do not reduce the tail of the resulting voltage wave, and also currents in excess of 20,000 amperes can flow in the lightning arrester.

The authors state that the case of a sideflash to a conductor, resulting in flashover of the insulator string, will not differ greatly from that of a stroke to a tower. This is not quite true for two reasons: First, the total current required to produce high voltages in the station may be considerably less. Second, the reflection phenomena begin in the cable with a slowly rising front and are more effective in raising the cable voltages. For instance, the wave at *CG* (Fig. 5) producing the transient in the station has about a 1,200-kv crest and a 15-microsecond tail equivalent to a tower current of 120 ka. Such currents have been measured. Since the current is building up simultaneously with the traveling phenomena on the ground wire and the conductor, the tail length will likely be greater with consequent increase in cable voltage. Also, the sudden drop in voltage due to the sudden change in rate of rise of the current wave will not occur.

For all these reasons, it is doubtful that omission of an arrester at the transformer is justified for the longer cable lengths. Before such general conclusions can be drawn, it would be necessary to conduct tests with different types of current waves for the various surge conditions as outlined in this discussion.

REFERENCE

1. *Discussion* by J. H. Hagenguth of LIGHTNING INVESTIGATION ON 132-KV SYSTEM OF AMERICAN GAS AND ELECTRIC COMPANY, I. W. Gross, G. D. Lippert. *AIEE Transactions*, vol. 64, 1945, pp. 475–76.

S. B. Griscom, J. K. Dillard, and A. R. Hileman: The remarks of Mr. Beck and Mr. Price re-emphasize and clarify some of the pertinent points covered in the paper. A complete understanding of these points is essential in applying the data to station protection problems. Dr. Ellis' deductions relative to the frequency of operation of protective devices are very interesting and corroborate the marked influence of cables on station protection. We are grateful to these discussers for these observations.

Mr. Cornelius asks about the rate of rise of stroke current. The 4x40-microsecond current wave shape used in the study is consistent with reference 7 of the paper. However, this rate of rise is not present at the arrester location at the line-cable junction. Fig. 5 shows that the rate of rise of voltage at the arrester location is 50 kv per microsecond for a backflash and Fig. 6 shows a rate of rise of 45 kv per microsecond for a sideflash. Also, for the incoming traveling wave of Fig. 8, the rate of rise at the arrester location is only 18 kv per microsecond. For such low-voltage rates of rise, arrester current rates of rise are very low. However, to be conservative, the arrester discharge voltage used in this study is based on the standard test current wave of 10x20 microseconds.

Very severe conditions were assumed for this study, as Mr. Cornelius suggests. The idea was not to recommend that protection always be based on such severe assumptions; rather it was to show that if adequate protection is provided against conventional traveling waves then it is both possible and practical in some situations to protect against severe close-by strokes.

The 20-μh tower inductance is a calculated value for a 100-foot tower (ref. 7 of the paper). It was estimated from recent high-voltage surge tests (ref. 4 of the paper) that a 100-foot tower has an inductance of about 10 μh. The towers considered here are higher than 100 feet and the value of 20 μh was chosen to be conservative and to be consistent with previous studies.

The stroke current required to cause flashover cannot be calculated from the equation given by Mr. Cornelius or from the one in reference 7. These equations assume that the coupled voltage on the phase conductor is of the same wave shape as the tower-top potential and that these two waves can be arithmetically subtracted to obtain the voltage across the line insulation. This is true at some distance out on the line from the station, but immediately adjacent to the station the coupled voltage wave will be reduced by reflections from the station. The wave shapes of the tower-top potential and coupled phase conductor voltage are different and therefore can not be arithmetically subtracted. This factor was recognized and provided for in this study. For the first time, a detailed representation of the ground wire and phase conductor, Fig. 3, was included with the station equivalent circuits so that protection against close-in direct strokes could be evaluated. Fig. 5, case I, shows the tower-top potential of 2,300 kv. The coupled voltage on the phase conductor *CG* starts to rise to a voltage of the coupling factor of 0.35 times the tower-top potential or 805 kv. However, before crest voltage of the coupled wave is reached, a negative reflection returns from the station due to the decrease in ground-wire current and station loading. Thus, as seen from Fig. 5, case I, the voltage is decreased to 630 kv and the wave shapes of the tower-top potential *TT* and the coupling voltage *CG* are different. The oscillogram of *CT* shows the resultant voltage across the insulators. For this specific wave shape, the critical magnitude so as to just cause flashover was determined by the integration method to be 1,780 kv. To obtain this voltage across the line insulation, a current of 205,000 amperes is necessary.

A transmission line possesses a surge impedance which is independent of line length. In some cases where the length is short and the front of the wave is long, reflections back and forth on this line tend to wipe out the surge impedance and, for purposes of analysis, the line can be considered as an inductance. For example, in many studies of allowable separation distance between an arrester and transformer, the drop lead to the lightning arrester of about 35 feet has been shown to be adequately simulated by its inductance. Each case must be considered separately.

Regarding the effects of multiple circuit on the reduction of surge voltage within the station, these are shown in Tables II and III and Fig. 13.

Mr. Wentz's discussion of insulation and insulation breakdown is welcomed because it shows that the SI method of analyzing nonstandard surge voltages is basically sound. This method is based on the assumption that all of the test waves are equal in severity. Although the constant K_1 is determined by equating the disruptive effect equations for the chopped wave and the full wave, Fig. 10 shows that the calculated withstand curve also coincide with the front-of-wave test point. Thus, the SI method is valid over the whole range. Most surge voltages which have appeared at the equipment terminals in this and previous studies have shown the wave shape to resemble chopped waves or full waves. Therefore, front-of-wave tests hardly appear to be justified.

The stroke current analogue used is the same as employed in previous studies and it is noted from this circuit that both the front and tail of the wave are expotential in form and not straight rising front and tail as Mr. Hagenguth concluded by looking at the oscillograms. His objection to the sudden drop in voltage at the struck tower immediately after crest is reached on the tower-top potential wave is not clear. The tower-top potential is composed of a tower inductive component and a tower-footing resistive component which are modified by reflections from adjacent towers. Immediately previous to current crest the tower-top voltage is a maximum; however, at crest current the inductive component must be zero since the rate of change of current is zero. Thus, at this point the voltage drops sharply.

Mr. Hagenguth intimates that we have chosen stroke-current wave shapes that are favorable to the protection of the transformers. Actually the reverse is true; the wave shapes and current magnitudes were intentionally chosen to produce the greatest possible transformer voltages for the particular situation investigated. In particular he apparently objects to situations wherein the inductive component of the tower voltage wave suddenly collapses at the moment the line insulators flash over. Now this is a necessary circumstance in order to impart maximum energy to the line conductors with a backflash, as examination of cases I and II of Fig. 5 shows. Compare *CG* for cases I and II. Flashover does not occur in case I and the maximum conductor voltage *CG* is only 630 kv. Flashover occurs in case II and results in a crest voltage of 2,300 kv on the line conductors. Case I may be considered as having a stroke current of 205,000 amperes and case II of 206,000 amperes.

The spikes referred to could be minimized with respect to the tail of the wave by increasing the tower-footing resistance. Since one of the main objects of the paper was to demonstrate the effectiveness of low-footing resistance, low values were used in most tests. As a matter of fact, the mechanism of protection in these cases is essentially that of limiting magnitudes by a lightning arrester and filtering ripples by the cable capacities. As Mr. Hagenguth points out, with a 30-ohm tower-footing resistance, the wave tail is greater and the protection reduced.

We do not agree with Mr. Hagenguth's observations with regard to sideflashes. The sequence of oscillograms for Fig. 6 was for 9,200 amperes stroke current and the wave at *CG* is just short of being sufficient to cause flashover. A slightly higher current would have caused flashover, eliminating the tail of the wave and giving much lower voltage throughout the station.

From the oscillographic records and resultant analysis of the voltage waves at the equipment terminals, only the first span out from the station and the station itself must be well shielded to protect the station equipment adequately against sideflashes. This is shown by Fig. 14. However, the remainder of the line should be shielded to prevent line outages.

Mr. Hagenguth expresses the opinion that more tests are required to sustain the conclusions of this paper. We believe that, we have used sufficient wave forms. Upward of 1,000 oscillograms were taken in the process of determining the "worst cases."

Measurement of Resistance and Reactance of Expanded ACSR

JOEL TOMPKINS
MEMBER AIEE

B. L. JONES
ASSOCIATE MEMBER AIEE

P. D. TUTTLE
ASSOCIATE MEMBER AIEE

Synopsis: A convenient method for the measurement of reactance and resistance of aluminum cables steel reinforced (ACSR) has been used and found to be accurate. The equipment and testing method are used to obtain accurate information concerning the a-c characteristics of all sizes of ACSR up to high values of current density, but the first use was to measure the impedance characteristics of expanded ACSR.

Expanded ACSR, 1.60 inches diameter, 1,275,000 circular mils (CM), has been found to have a d-c resistance of 0.0717 ohm per mile at 25 degrees centigrade (C), a ratio of a-c to d-c resistance of about 1.015, and a reactance at 60 cycles per second (cps) at 1.0-foot spacing of 0.347 ohm per mile per conductor. This reactance value corresponds to a geometric mean radius of 0.690 inch, or 86.2 per cent of the nominal conductor radius.

Expanded ACSR, 1.75 inches diameter, 1,414,000 CM, has been found to have a d-c resistance of 0.0660 ohm per mile at 25 C, a ratio of a-c to d-c resistance of about 1.015, and a reactance at 60 cps at 1.0-foot spacing of 0.337 ohm per mile per conductor. For this conductor, the reactance value corresponds to a geometric mean radius of 0.747 inch, or 85.4 per cent of the nominal conductor radius.

BECAUSE of the presence of the steel core in ACSR, data on the electrical charactersitics of such conductors are somewhat difficult to calculate. Data now published were based on the results of two series of measurements made by Prof. W. R. Work, the first about 30 years ago and the second a few years later. Originally W. Nesbit,[1] and later W. A. Lewis and others, made many of the calculations, using Prof. Work's test results, to complete the tables of electrical characteristics of ACSR which have been in use for some time. Prof. Work's tests were of a relatively small number of sizes of conductor, over limited ranges of current density, and much of the information in the published tables was obtained by interpolation and extrapolation. The magnetic and electrical properties of the steel core wire manufactured at the time of the tests by Prof. Work were possibly somewhat different from those of core wires manufactured today.

The electrical characteristics with which this paper is concerned are the reactance and effective resistance of cables at the frequency of 60 cps. The effective resistance is referred to throughout as a-c resistance.

To obtain accurate data on reactance and a-c resistance of ACSR as manufactured now, having standard strandings and over wider ranges of current densities than those for which data are now available, suitable laboratory equipment and a measurement method have been needed. In addition, the equipment and method are of value for determination of impedance characteristics of ACSR of special strandings.

Suitable equipment for such measurements was put into service in 1950 at the Electrical Conductor Laboratory of Aluminum Company of America. This paper describes the equipment, the development and proving of measuring techniques, and some of the results of measurements. The equipment was first used to measure the characteristics of experimental 1.75-inch-diameter 1,344,000-CM expanded ACSR. Measurements were made later of the characteristics of 1.60-inch-diameter, 1,275,000-CM expanded ACSR, and of 1.75-inch-diameter 1,414,000-CM expanded ACSR. Large quantities of expanded ACSR are being used on the 330-kv systems of the American Gas and Electric Company and the Ohio Valley Electric Corporation.

Equipment

The reactance and a-c resistance of test conductors are calculated from the readings of an a-c potentiometer used to measure the voltage drops along sections of the test conductors, with 60-cps test current flowing. Fig. 1 shows schematically the arrangement of the test conductors, potentiometer equipment, power supply transformer, and current transformer.

The a-c potentiometer comprises a Brooks inductometer, a special voltage divider, and a noninductive volt box. The detector used originally was an a-c galvanometer, with a phase-shifting transformer for the supply of voltage to the field winding. Later an electronic null detector was substituted for the galvanometer and phase shifter, with resulting simplification of operation and increased sensitivity of the potentiometer equip-

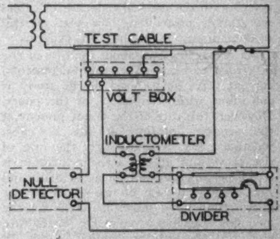

Fig. 1. Schematic diagram of test connections

Paper 55-98, recommended by the AIEE Transmission and Distribution Committee and approved by the AIEE Committee on Technical Operations for presentation at the AIEE Winter General Meeting, New York, N. Y., January 31-February 4, 1955. Manuscript submitted October 20, 1954; made available for printing November 19, 1954.

Joel Tompkins, B. L. Jones, and P. D. Tuttle are with the Aluminum Company of America, Massena, N. Y.

The authors acknowledge the valuable contributions of their associates in preparing the paper, particularly the work of J. R. Harvey on the measurement of characteristics of 1.60-inch-diameter expanded ACSR.

ment. Fig. 2 shows the potentiometer equipment.

The volt box is used to provide, for the measuring circuit, a voltage proportional to the voltage drop along the test sections of the specimen conductors. The inductometer provides a voltage proportional to, and in quadrature with, the current in the test conductors. The special voltage divider provides a voltage proportional to, and in phase with, the current in the test conductors.

The a-c potentiometer is balanced by alternate adjustment of the special voltage divider and the inductometer to provide a minimum indication of the null detector. Equations for calculating the values of resistance and reactance of each test sample, from the readings of the potentiometer, are shown in the Appendix. The averages of the individual values for each of the two samples of a pair are taken as the correct values.

Current transformers of high precision are used, and care is taken to maintain the secondary burden on the current transformers at values within their rated burdens. A 60-cps test current is furnished by special, low-voltage high-current transformers which are in turn supplied through multitapped autotransformers. Capacity for test currents up to 10,000 amperes is available. D-c resistances of test conductors are measured with a precision Kelvin double bridge with test current supplied by large storage batteries. A test current of approximately 50 amperes has been used for the measurement of d-c resistance of expanded ACSR.

The calibration of the equipment and the suitability of the measuring technique have been checked by a large number of measurements of reactance and resistance of several sizes of wire and cable of both aluminum and copper. The reactance of such homogeneous conductors, without steel cores, and the ratios of a-c to d-c resistance can be computed with acceptable accuracy. Based on the results of these numerous checks of the equipment calibration, it is believed that most measurements of resistance and reactance are accurate to approximately 1/2 of 1 per cent.

Test Method

In the measurements, two spans of the test conductor are used, each about 120 feet long. The two conductors are taken from a single continuous original length. Each span is subjected to constant tension within the limits of 15 to 25 per cent of the nominal ultimate strength of the conductor. The tension in the two spans is equalized by means of "yokes" and is maintained by a single lever loading system. The conductors are placed parallel to each other with spacings of 1.0 or 2.0 feet and are aligned so that any line perpendicular to both conductors is horizontal. The separation of the two conductors is maintained by means of spacers. After being put into place, the two spans are connected to form a single-phase return circuit. Fig. 3 shows two spans of 1.75-inch-diameter 1,414,000-CM expanded ACSR in position for tests. It also shows the return or cross connection between the two test conductors. The connections to the power supply are made at the opposite ends of the spans. Spans of multilayer test conductors are terminated in compression dead-end bodies. This type of terminal has been proved to insure proper distribution of test current between the strands of the conductors.

Measurements are made of the voltage drop along the central 100-foot sections of the 120-foot test spans. The voltage drop of each of the two conductors is measured in turn. Care was used in the placement of the voltage leads from the test conductors to the a-c potentiometer to minimize possible errors caused by extraneous voltage induced in the leads. The potentiometer equipment is located at some distance from the test conductors in another laboratory room.

Temperatures of Test Conductors

The determination of representative test conductor temperatures has been a problem. Though the laboratory room in which the test conductors have been strung has been kept relatively free of drafts, at times there have been small temperature gradients along the test conductors. Because of this possible gradient, thermocouples have been placed at different points along each test length. At relatively high values of test currents, with appreciable temperature rises, there has appeared to be a definite, though small, temperature gradient, under the test conditions, from the steel core to the outer strands. With 1,400 amperes on the 1.60-inch-diameter 1,275,000-CM expanded ACSR, the steel core temperature has been found to be 3 to 4 degrees Fahrenheit (F) higher than the temperature of the outer layer of aluminum strands. With 2.0-foot spacing between the test conductors and with relatively high values of test current, it has been found that the outer portions of one expanded conductor nearest the other conductor have had slightly higher tempera-

Fig. 2 (below). Instruments used for measurements

Fig. 3 (right). Spans of expanded ACSR in place for measurements

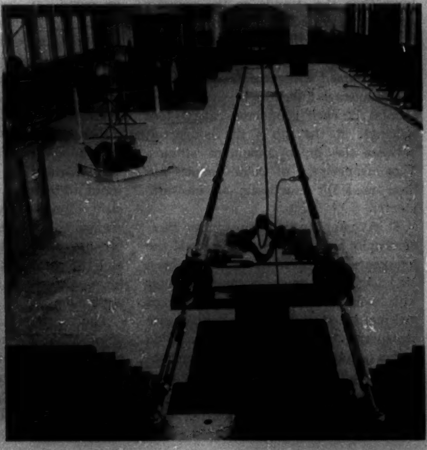

Table I. Tests of Experimental 1.75-Inch-Diameter 1,344,000-CM Expanded ACSR, to Determine if Extraneous Induction Effects Are Present

Conductor Identification	Test Length, Feet	Spacing Between Centers of Conductors, Inches	Current, 60 Cps, Amperes	Reactance of Test Length of Conductor at Given Spacing, 60 Cps, Microhms	Calculated Reactance per Mile per Conductor at 12.0-Inch Spacing, 60 Cps, Ohms	Conductor Temp. T, F	A-C Resistance of Test Length at Temp. T, Microhms	Calculated A-C Resistance Per Mile at Temp. T, Ohms	D-C Resistance Adjusted to 77 F (25 C), Microhms	Ratio A-C/D-C Resistance at Temp. T
Test A—Check for Possible End Effects										
North	100	24.0	602	7,860	0.331	81	1,330	0.0702	1,298	1.015
South	100	24.0	602	7,860	0.331	83	1,335	0.0705	1,296	1.017
North	80	24.0	602	6,270	0.331	84.5	1,072	0.0709	1,038	1.016
South	80	24.0	600	6,270	0.331	84	1,070	0.0707	1,038	1.015
Test B—Check for Proximity Effects										
North	100	24.0	1,180	7,880	0.332	188	1,625	0.0859	1,298	1.007
South	100	24.0	1,180	7,880	0.332	186.5	1,625	0.0859	1,296	1.011
North	100	12.0	1,160	6,270	0.332	187	1,630	0.0862	1,298	1.012
South	100	12.0	1,160	6,270	0.332	193	1,643	0.0869	1.296	1.010

Table II. Measurement of Reactance and Resistance of Experimental 1.75-Inch-Diameter 1,344,000-CM Expanded ACSR

Conductor Identification	Current, 60 Cps, Amperes	Reactance per 100-Foot Conductor, 24.0-Inch Spacing, 60 Cps, Microhms	Calculated Reactance per Mile per Conductor, 12.0-Inch Spacing, 60 Cps, Ohms	Conductor Temp. T, F	A-C Resistance of Test Length at Temp. T, Microhms	Calculated A-C Resistance per Mile at Temp. T, Ohms	Ratio AC/DC Resistance at Temp. T
North	301	7,920	0.334	86	1,338	0.0705	1.014
South	301	7,920	0.334	86	1,342	0.0709	1.017
North	299	7,920	0.334	153	1,533	0.0809	1.015
South	296	7,920	0.334	153	1,533	0.0809	1.016
North	599	7,880	0.332	103	1,388	0.0732	1.014
South	599	7,860	0.331	104	1,390	0.0733	1.015
North	594	7,880	0.332	153	1,529	0.0806	1.013
South	595	7,860	0.331	146	1;515	0.0800	1.015
North	1,190	7,880	0.332	104	1,390	0.0733	1.015
South	1,210	7,860	0.331	109	1,404	0.0742	1.013
North	1,195	7,880	0.332	184	1,621	0.0856	1.015
South	1,200	7,880	0.332	181	1,615	0.0853	1.016

Notes:

1. Measurements made of central 100-foot sections of samples about 120 feet long.
2. Samples at 24.0-inch spacings.
3. D-c resistances at temperature *T* based on resistance per 100-foot sample of 1,295 microhms at 77 F (25 C).

tures than the strands on the opposite side. After considerable experimentation it was decided that the representative temperatures of expanded ACSR could be determined with acceptable accuracy as the average indicated by five thermocouples in each conductor, at 20-foot spacings, at the top of the conductor, between the outer aluminum strands. This arrangement of thermocouples has been used for practically all measurements.

Thirty-gauge copper-constantan thermocouples have been used. Some of the temperature measurements have been made with a precision potentiometer with "cold junctions" in stirred baths of melting ice. Most of the temperature measurements, however, have been made with a portable potentiometer incorporating a cold-junction compensator.

D-c resistances of test conductors have been measured at room temperatures. A-c resistances normally have been measured at increased temperatures caused by the test currents, though not necessarily at equilibrium temperatures. Conductor temperatures have been determined simultaneously with the measurement of reactance and a-c resistance. To determine the ratio between a-c and d-c resistances, the d-c resistance value has been adjusted to the conductor temperature at which the a-c resistance was determined by using the temperature coefficient of resistivity of aluminum. This coefficient has been used for ACSR both because the steel carries very little current and the coefficient of resistivity of steel is approximately the same as that of aluminum.

The values of conductor temperatures obtained during measurements are probably accurate within about 3 F. It is believed that the small variations of calculated ratios of a-c to d-c resistance are largely caused by difficulties in accurately determining conductor temperatures.

Investigation of Possible Causes of Errors

It was questioned whether end effects from current connections at the ends of the spans of test conductors would influence the results of impedance measurements. It had not seemed possible that such errors could be significant with the voltage drop connections arranged as they were. To answer this question, however, measurements were made of resistance and reactance of 100-foot sections of 120-foot spans of 1.75-inch-diameter 1,344,000-CM expanded ACSR. These measurements were then repeated for a central 80-foot section of the same conductors. The test results are included in Table I. The reactance and resistance respectively per mile based on the two sets of measurements were found to be the same. It was therefore concluded that there were no significant end-effect errors in the measurements of the characteristics of the 100-foot sections. All subsequent measurements were made of 100-foot sections of 120-foot spans.

Initial impedance measurements had been made of the characteristics of expanded ACSR with the conductors spaced at 2.0 feet. The spacing, of course, was considerably less than between phases of a practical transmission line. There were questions concerning possible proximity effects at the close spacing. To determine if the proximity effect might be of importance, measurements were made both with 2.0-foot spacing and with 1.0-foot spacing. As shown in Table I, results based on the measurements at the two different spacings did not appear to be significantly different. It was therefore decided that, as there seemed to be no proximity effects discernible in closing the spacing to 1.0 foot, the proximity effect would be entirely negligible at 2.0 feet. Spacings of 2.0 feet were used for all subsequent measurements.

Table III. Measurement of Resistance and Reactance of 1.60-Inch-Diameter 1,275,000-CM Expanded ACSR

Conductor Identification	Current 60 Cps, Amperes	Reactance per 100-Foot Conductor 24.0-Inch Spacing, 60 Cps, Microhms	Calculated Reactance per Mile per Conductor, 12.0-Inch Spacing, 60 Cps, Ohms	Conductor Temp. T, F	Ambient Temperature, F	A-C Resistance of Test Length at Temp. T, Microhms	Calculated A-C Resistance Per Mile at Temp. T, Ohms	Ratio A-C/D-C Resistance at Temp. T	Note
North	605	8,160	0.347	115	82	1,500	0.0792	1.020	4
South	605	8,160	0.347	116	82	1,500	0.0792	1.017	4
North	907	8,160	0.347	81		1,390	0.0733	1.016	5
North	907	8,160	0.347	96		1,440	0.0760	1.019	5
North	905	8,160	0.347	111		1,490	0.0786	1.020	5
North	900	8,160	0.347	127		1,520	0.0802	1.018	5
North	907	8,160	0.347	140		1,580	0.0834	1.023	5
North	900	8,160	0.347	158	82	1,620	0.0855	1.014	4
South	900	8,160	0.347	158	82	1,620	0.0855	1.010	4
South	1,200	8,160	0.347	104		1,460	0.0771	1.013	5
North	1,190	8,160	0.347	113		1,490	0.0787	1.019	5
North	1,190	8,160	0.347	122		1,520	0.0802	1.019	5
North	1,190	8,160	0.347	147		1,580	0.0834	1.011	5
South	1,190	8,160	0.347	148		1,600	0.0845	1.018	5
North	1,190	8,160	0.347	165		1,650	0.0871	1.020	5
South	1,190	8,160	0.347	168		1,660	0.0876	1.017	5
North	1,190	8,160	0.347	181		1,690	0.0892	1.014	5
North	1,190	8,160	0.347	191		1,720	0.0908	1.014	5
North	1,190	8,160	0.347	209	85	1,780	0.0939	1.016	4
South	1,190	8,160	0.347	209	85	1,790	0.0945	1.020	4

Notes:

1. Measurements made of central 100-foot sections of samples about 120 feet long.
2. Samples at 24.0-inch spacing.
3. D-c resistances 1,356 microhms per 100 feet for North conductor and 1,360 microhms per 100 feet for South conductor at 77 F (25 C).
4. Measurements made at equilibrium temperatures.
5. Measurements made at temperatures below equilibrium, with temperatures increasing.
6. Nominal cross section of aluminum was 1,275,000 CM. Actual cross section was 1,277,000 CM.

Table IV. Measurement of Reactance and Resistance of 1.75-Inch-Diameter 1,414,000-CM Expanded ACSR

Conductor Identification	Current, 60 Cps, Amperes	Reactance per 100-Foot Conductor, 24.0-Inch Spacing, 60 Cps, Microhms	Calculated Reactance per Mile per Conductor, 12.0-Inch Spacing, 60 Cps, Ohms	Conductor Temp. T, F	Ambient Temperature, F	A-C Resistance of Test Length at Temp. T, Microhms	Calculated A-C Resistance per Mile at Temp. T, Ohms	Ratio A-C/D-C Resistance at Temp. T
South (black)	578	7,970	0.337	88	72	1,306	0.0690	1.021
North (black)		7,990	0.338			1,300	0.0686	1.015
South (black)	907	7,990	0.338	115	74	1,371	0.0724	1.013
North (black)		7,970	0.337	114		1,373	0.0725	1.017
South (new)	910	7,940	0.335	139	74	1,435	0.0758	1.012
North (new)		7,965	0.337	138		1,440	0.0760	1.017
South (black)	1,175	7,990	0.338	135	70	1,425	0.0752	1.011
North (black)		7,990	0.338			1,430	0.0755	1.015
South (new)	1,203	7,930	0.335	192	82	1,577	0.0833	1.011
North (new)		7,950	0.336			1,583	0.0836	1.015
South (black)	1,488	7,980	0.337	177	73	1–542	0.0814	1.011
North (black)		7,980	0.337	176		1,530	0.0808	1.006
South (new)	1,490	7,950	0.335	249	80	1,739	0.0918	1.012
North (new)		7,940	0.335	248		1,733	0.0915	1.010
South (black)	1,772	7,990	0.338	218	75	1,660	0.0876	1.014
North (black)		7,990	0.338			1,646	0.0869	1.006

Notes:

1. Measurements made of central 100-foot sections of samples about 120 feet long.
2. Samples strung on 24.0-inch centers.
3. D-c resistances at temperature *T* based on a resistance of 0.0660 ohm per mile at 77 F (25 C).
4. Nominal cross section of aluminum was 1,414,000 CM. Actual cross section was 1,399,000 CM.

The ratios of a-c to d-c resistance, shown in the lower part of Table I, for currents of about 1,200 amperes appear to be slightly lower than found in other measurements. The small discrepancies were thought to be caused by a slightly different and less satisfactory arrangement of thermocouples used for these few check measurements.

In the initial work some discrepancies were noted in the measured reactance of all-aluminum cable with different values of current. It was found that the secondary burden on the current transformers was somewhat too high for most accurate results. Subsequently, much larger secondary leads were installed between the current transformers and the measuring equipment for most of the measurements, and current-transformer ratios were selected to maintain secondary currents between about 4.0 and 5.0 amperes. These steps eliminated the discrepancies.

As may be noted in Tables I, II, III, and IV, there is close agreement between resistance and reactance values determined for each of the two test conductors of each pair. This appears to indicate that the effect of any induced voltages in the voltage drop connections was negligible.

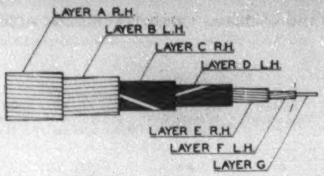

LAYER / CABLE	ALUMINUM				STEEL		
	A	B	C	D	E	F	G
1.60 IN.	28x0.1550"	22x0.1550"	2x0.1362" +FILLER	2x0.1362" +FILLER	12x0.0874"	6x0.0874"	1x0.0874"
1.75 IN.	32x0.1500"	26x0.1500"	2x0.1654" +FILLER	2x0.1654" +FILLER	12x0.0977"	6x0.0977"	1x0.0977"

Fig. 4. Constructional details of two sizes of expanded ACSR

Another Method of Measurement

In addition to the use of a potentiometer for the determination of reactance and resistance of conductors, an attempt has been made to use the wattmeter method, using sensitive galvanometer-type light-beam wattmeters with low-voltage potential windings of relatively high resistance. It was found that this method was less convenient than the potentiometer method, and would be considerably less accurate unless relatively heavy voltage-drop connections were used. With the voltage-drop connections placed for the potentiometer method, as leads to the wattmeter, a voltage drop in the leads caused by the burden of the voltage coil of the wattmeter introduced appreciable error.

Test Results With Experimental 1.75-Inch-Diameter Expanded ACSR

The reactance and a-c resistance of experimental 1.75-inch-diameter 1,344,000-CM expanded ACSR were measured at current values of about 300, 600, and 1,200 amperes. For each current value, impedance values were determined for a range of cable temperatures. Conductor spacing of 2.0 feet was used, with a tension of 7,000 pounds on each conductor. The results are shown in Table II. The reactance at 60 cps for 1.0-foot spacing, based on measured values of 100-foot test sections at 2.0-foot spacings, was found to be 0.332 ohm per mile per conductor. This value appeared to be independent of test current value and conductor temperature, and corresponds to a geometric mean radius of 0.778 inch. The ratio of a-c to d-c resistance was about 1.015. This ratio apparently was substantially independent of the magnitude of current, within the test range, and of conductor temperatures reached. There was some indication that this ratio tends to decrease slightly as conductor temperature increases. This tendency is reasonable, as the skin effect decreases with increasing resistivity caused by increased temperature. The construction of this conductor was similar to that of the 1.60-inch-diameter 1,275,000-CM and the 1.75-inch-diameter 1,414,000-CM expanded ACSR, the details of which are given in Fig. 4.

Test Results With 1.60-Inch-Diameter 1,275,000-CM Expanded ASCR

Measurements were made of the reactance and a-c resistance of this cable at currents of about 900 and 1,200 amperes over ranges of temperature at each current value. In addition, impedance values were determined at 600 amperes at equilibrium temperature. D-c resistance was measured. The measurements were made with a conductor spacing of 2.0 feet, with 7,000 pounds' tension on each conductor.

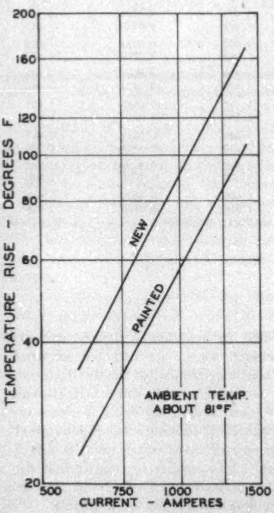

Fig. 5 (left). Temperature rise curves for 1.60-inch-diameter 1,275,000-CM expanded ACSR in free air

Fig. 6 (right). Temperature rise curves for 1.75-inch-diameter 1,414,000-CM expanded ACSR in free air

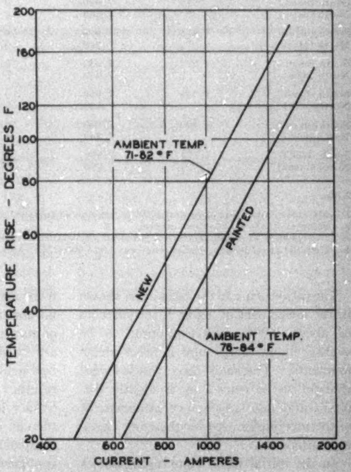

Data based on the measurements are shown in Table III.

The calculated reactance per mile, at 60 cps for 1.0-foot spacing, based on measured reactance of the 100-foot test sections at 2.0 spacing, was found to be 0.347 ohm. The ratio of a-c to d-c resistance was found to be about 1.015, and the d-c resistance at 25 C was found to be 0.0717 ohm per mile.

Test Results With 1.75-Inch-Diameter 1,414,000-CM Expanded ACSR

The a-c resistance and reactance of this conductor were determined at currents up to 1,800 amperes, all values being taken at equilibrium temperatures. The measurements were made with a tension of 9,000 pounds per conductor. This represents about $17\frac{1}{2}$ per cent of the designed ultimate strength of the cable.

The data obtained from the electrical measurements are shown in Table IV. As may be seen, the calculated 60-cps reactance for 1.0-foot spacing was found as 0.337 ohm per conductor per mile and is essentially independent of current and temperature. The d-c resistance was 0.0660 ohm per mile at 25 C and the ratio of a-c to d-c resistance approximated 1.015, slightly decreasing, as might be expected, at the higher temperatures.

Discussion

The ratios of a-c to d-c resistances of the three sizes of expanded ACSR may appear low for such large conductors. These low values may be understood by realizing that expanded ACSR is similar electrically to a hollow conductor, in which the skin-effect ratio is relatively low. With even numbers of layers of aluminum strands, losses in the steel core are very low, so that the increase in a-c resistance from this cause is also small.

The geometric mean radii of the three sizes of expanded ACSR, expressed as percentages of nominal radii, are similar (88.9 per cent for the experimental 1.75-inch cable, 86.2 per cent for the 1.60-inch cable, and 85.4 per cent for the 1.75 inch 1,414,000-CM cable).

During the measurements, data were obtained on equilibrium temperature rises of the 1.60-inch-diameter 1,275,000-CM and the 1.75-inch-diameter 1,414,000-CM expanded ACSR. These data were taken with the conductors as they were received from the cable mill, with relatively low emissivity values, and then with the conductors painted flat black, to simulate exteine weathering which could result in relatively high emissivity values. The temperature rise data are shown in Fig. 5 for the 1.60-inch-diameter 1,275,000-CM conductor and in Fig. 6 for the 1.75-inch-diameter 1,414,000-CM conductor. These curves show the temperature rises of the conductor indoors in a relatively draft-free room. Temperature rises with the conductor exposed to natural wind conditions would, of course, be lower.

Following the work on expanded ACSR, work is in progress on a program to obtain complete data on resistance and reactance characteristics of conventional ACSR of the range of sizes available, over wide ranges of current densities.

Conclusions

A convenient and accurate method with suitable equipment is available for the measurement of reactance and a-c resistance of conductors. Such characteristics of a number of sizes of ACSR, including expanded ACSR, have been measured.

Appendix. Calculation of Resistance and Reactance from Laboratory Readings

The a-c potentiometer used in this work is a modification of the customary type in that the standard current is a multiple of the actual cable current. Since the component balance voltages derived from the voltage divider and the inductometer are directly proportional to the current-resistance and current-reactance drops in the cable test length, the divider and inductometer scales may be calibrated directly for R and X. This may be done on the basis of any desired ratio of current transformation and volt box multiplier. In the present case, the instruments are calibrated on the assumption of unity ratio and multiplier. Consequently, the readings must be appropriately modified by the actual ratio and multiplier used.

The cable reactance and a-c resistance are computed as follows

$$X=\frac{G}{N}\frac{(X'+R'\tan\phi)}{\sqrt{(1+\tan^2\phi)}}$$

$$R=\frac{G}{N}\frac{(R'-X'\tan\phi)}{\sqrt{(1+\tan^2\phi)}}$$

where

X = reactance of cable test section, ohms
R = a-c resistance of cable test section, ohms
G = volt box multiplier
N = current transformer ratio
X' = reading of inductometer
R' = reading of voltage divider
ϕ = phase angle of current transformer

When the phase angle is small

$$X=\frac{G}{N}X' \text{ approximately}$$

$$R=\frac{G}{N}R' \text{ approximately}$$

Reference

1. ELECTRICAL CHARACTERISTICS OF TRANSMISSION CIRCUITS (book), William Nesbit. Westinghouse Technical Night School Press, East Pittsburgh, Pa., 3rd ed., 1926.

◆

Discussion

C. F. De Sieno (American Gas and Electric Service Corporation, New York, N. Y.): The evaluation of transmission-line losses is playing an increasingly important part in the electric utility industry. This points up the need for accurate conductor data, especially conductor resistance under various loadings and ambient temperatures. This paper therefore is an excellent step towards filling a long-standing gap in the field of electric conductors.

We are particularly thankful to the authors for the work done on the 1.6-inch and the 1.75-inch expanded ACSR because large quantities of these conductors are being used on the 330-kv systems of the American Gas and Electric Company and the Ohio Valley Electric Corporation.

H. B. Dwight (Massachusetts Institute of Technology, Cambridge, Mass.): The measurements on aluminum overhead transmission line conductors given by the authors have evidently been made with great care, and the results are without doubt very valuable.

The reactance of ACSR, except for those cables with a single layer of aluminum wire, can be computed by the geometric-mean-distance method from the dimensions of the conductor. This can be done as a predetermination of the reactance before the conductor is fabricated, and so may be useful for designs and sizes for which tests are not available.

Following the method of Example 5,[1] the 60-cycle reactance of the 1.75-inch conductor of Table IV is 7,920 microhms per 100 feet at 24-inch spacing, to be compared with the measured values of 7,930 to 7,990. For the 1.60-inch conductor of Table III, the computed value is 8,150 microhms per 100 feet, to be compared with 8,160, as measured.

This close agreement as well as other comparisons that have been made justifies the use of the calculations. More reliance should be placed on the calculations. They are not particularly short, but a geometric-mean-distance calculation needs to be made only once for a given design of conductor.

The skin-effect resistance ratio also can be computed, though not with the same precision as the reactance. The steel core does not come appreciably into the computation if the aluminum wires of right-hand and left-hand spiraling are equally balanced so that they do not produce longitudinal magnetization of the core.

If the spacing wires are not considered,

Table V. Comparison of Test and Calculated Reactance for 2- and 3-Layer ACSR, 60 Cps

Aluminum, CM	Strands of Aluminum	Layers of Aluminum	Test Results: Int. Inductance, Millihenrys per 1,000 Feet	Test Results: Reactance at 1 Foot, Ohms per Mile	Calculated Reactance at 1 Foot, Ohms per Mile	Difference from Test Per Cent
1,033,500	12+18+24	3	0.0130	0.385	0.384	−0.3
795,000	12+18	2	0.0116	0.393	0.393	0.0
795,000	10+16	2	0.0127	0.399	0.399	0.0
477,000	12+18	2	0.0116	0.424	0.424	0.0
477,000	10+16	2	0.0127	0.430	0.430	0.0

Table VI. Comparison of Test and Calculated Reactance for Expanded ACSR, 60 Cps

Diameter, Inches	Aluminum, CM	Strands of Aluminum	Layers of Aluminum	Test Reactance at 1 Foot, Ohms per Mile	Calculated Reactance at 1 Foot, Ohms per Mile	Difference from Test, Per Cent
1.75	1,344,000	2+2+30+36=70	2 Full 2 Partial	0.332	0.333	+0.3
1.60	1,275,000	2+2+22+28=54	2 Full 2 Partial	0.347	0.346	−0.3
1.75	1,414,000	2+2+26+32=62	2 Full 2 Partial	0.337	0.334	−0.9

the cable may be treated as a stranded tubular conductor. The thickness will be twice the diameter of an outer wire. For the 1.75-inch cable, the ratio t/d is 0.30/1.75=0.172. The resistance of the cable is 0.0660 ohm per mile. Reading at these values from Fig. 8-2,[1] the skin-effect ratio is 1.012.

However, all the aluminum is not within the thickness of 0.30 inch but there are four spacing wires in the region nearer the center, which indicates a higher value of the ratio. If it is assumed that strands are uniformly spread over the thickness of three layers, t becomes 0.30+0.1654=0.4654 and t/d becomes 0.266. Then from Fig. 8-2[1] the ratio is 1.026. This probably can be taken as an upper limit of the ratio, because the four spacing wires are not equivalent to a complete third layer.

By averaging the two values, an estimate of 1.019 is obtained. In a similar manner, an estimate of 1.017 for the skin-effect ratio of the 1.60-inch cable is given. These are in agreement with the measured values, 1.015.

REFERENCE

1. ELECTRICAL ELEMENTS OF POWER TRANSMISSION LINES (book), H. B. Dwight. The MacMillan Company, New York, N. Y., 1954, pp. 117–18.

W. A. Lewis (Illinois Institute of Technology, Chicago, Ill.): The authors are to be congratulated on a very clear and straightforward presentation of the test methods and results of tests made to determine the resistance and reactance characteristics of ACSR. Previous tests, including some with which I had been connected at Cornell University, were not made with equipment having the range of currents described in the paper. Therefore, the equipment represents an important extension in the available facilities, and it is gratifying that the results have been made available.

By extending the equations for the reactance of stranded conductors[1-3] to include hollow conductors of the same stranding pattern as the aluminum strands of the conductors tested by Prof. Work, it was possible to make comparisons between test and calculated values of reactance. These equations were based upon the method of geometric mean distances. For all of the conductors tested by Prof. Work, having two or three layers of aluminum strands about a central steel core, it was found that the calculated reactance for the aluminum alone checked very closely the measured values for the complete conductor. The test and calculated values are shown in Table V.

It may be concluded that, for conductors having two or more layers of aluminum strands spiraled in opposite directions about a central steel core, the effect of the steel core on the conductor reactance at spacings of 1 foot and larger, as used in the tests, is completely negligible. The inference to be drawn is that, if the current in the individual strands follows the spiral of the strands to magnetize the core, the spiralling of successive layers in opposite directions permits this effect to be almost completely neutralized.

When samples of the expanded ACSR designs referred to in the paper were being prepared for test, the conductor design data were made available to me and the equations for calculating the reactance were extended to include the effect of the filler layers with only two aluminum strands. The reactances were computed from the design data, neglecting entirely the effects of the steel core (as well as spiraling) but including the effect of stranding by the method of geometric mean distances. The computed results were given to the Aluminum Company of America for comparison with the tested values. Again the agreement was very good, as shown by Table VI.

Because of the excellent agreement in all the comparisons, it may be concluded that the reactance of multilayer ACSR may be calculated with a high degree of precision, based upon the assumptions that the steel core and the spiraling of the strands have a negligible effect and that the current in each strand of aluminum is proportional to its area. This assumption, of course, gives equal currents in all the aluminum strands if the strands all have the same diameter. The final equations have been simplified to permit their ready application.

For ACSR having only a single layer of aluminum surrounding a steel core, reactances calculated using the same assumptions did not agree with test results for completed conductors, as tested by Professor Work. Furthermore, the reactance as well as the resistance, as tested showed variations with current density, starting from a low value at small currents, increasing substantially, and then decreasing again as the current was increased. The low-current value of reactance was only slightly larger than the calculated value, neglecting the core and spiraling effects. It was concluded that the spiraling of a single layer of aluminum about the core caused a substantial effect in the measured reactance and effective resistance that depended upon the flux density in the core and decreased as the core approached saturation.

Because only a limited range of conductors of this type has been given complete tests and because of some inconsistencies among the tests, it has not been possible to prepare tables for the single-layer conductors having the same accuracy as for the multilayer conductors. The plans of the authors to make further tests are therefore very welcome. It is to be hoped that methods of including the core effects in the calculated values, with at least reasonable accuracy, can be perfected so that the resistance and reactance of special conductors such as those of unusually high strength for river crossings can be predicted in advance of actual construction.

REFERENCES

1. REACTANCE OF STRANDED CONDUCTORS, H. B. Dwight. *Electrical World*, New York, N. Y., vol. 61, April 1913, p. 898.

2. THE SELF- AND MUTUAL-INDUCTANCE OF LINEAR CONDUCTORS, E. B. Rosa. *Bulletin*, Bureau of Standards, Washington, D. C., vol. 4, no. 2, 1908, p. 301.

3. ELECTRICAL COILS AND CONDUCTORS (book), H. B. Dwight. McGraw-Hill Book Company, Inc., New York, N. Y., 1945, p. 129.

A. A. Defoe (Aluminum Laboratories Ltd., Kingston, Ont., Canada): This paper comes at a most appropriate time because during the past few months we have given consideration to the making of similar tests on some of the standard sizes and strandings of ACSR to check presently published values for the a-c resistances and reactances. The method of measurement as described by the authors is direct and fairly simple and from preliminary studies it appears evident that, if sufficient care is taken in the selection of the equipment, installation of test samples, etc., very accurate results should be obtained.

The skin effect and the internal inductance of ACSR are most difficult to calculate with any degree of accuracy owing to the presence of the steel core. This particularly applies to 1- and 3-layer aluminum conductors and especially for the higher current densities. Actual tests are, therefore, a necessity for determining the electrical characteristics of such conductors.

It may be of interest to compare calculated and test values for the a-c to d-c resistance ratio and internal inductance for the 2-layer aluminum 1,414,000-CM 1.75-inch-diameter ACSR mentioned by the authors. The calculated values for the d-c resistance and a-c to d-c resistance ratio are 0.0655 ohm per mile at 25 C and 1.01 respectively. These values compare very favorably with the test results of 0.0660 ohm per mile at 25 C and a resistance ratio of 1.015. For this same conductor, the tests give a reactance of 0.421 ohm per mile with 2-foot spacing. By calculating back, it is found that the external inductance is 1.066 millihenrys per mile and the internal inductance is 0.051 millihenry per mile. By direct calculation, the internal inductance of this conductor is found to be 0.041 millihenry per mile and this is reasonably close to that obtained from the test. However, calculations for the electrical characteristics of other conductors, especially those having one or three aluminum layers, probably would not give values anywhere nearly as close to the test values.

As stated previously, considerable attention should be given to the test setup if the highest possible accuracy in the results is to be obtained. In my opinion, the authors have given this matter the attention it deserves but, for informative purposes, it would be of interest to have their comments on two points which are as follows:

1. In the test setup, compression dead-end bodies are applied to the conductor ends to ensure proper distribution of the current between the strands of the conductors. While it would appear that this procedure is satisfactory for single- or double-layer aluminum conductors, it would seem advisable in the case of 3- and 4-layer aluminum conductors to weld the aluminum wires to the open ends of the aluminum dead-end bodies just to make certain that the current does have the opportunity to distribute itself properly in the conductor.

2. The measurement of the conductor temperature is important, as the authors have stated. From the paper, it is gathered that the thermocouples are placed at the top of the conductor and between the outer aluminum strands. Does this mean that these thermocouples are actually on the outside of the outer aluminum wires or are they between the two layers of aluminum wires?

Joel Tompkins, B. L. Jones, and P. D. Tuttle: We are grateful to the discussers for their remarks concerning the paper and the experimental work behind it.

The comment by Mr. DeSieno concerning transmission line losses is of importance. Prof. Dwight, Dean Lewis, and Mr. Defoe all noted the close agreement between calculated values of electrical characteristics and the results of measurements for ACSR with more than one layer of aluminum strands. Dean Lewis presented data showing that calculated and measured reactance values agree closely for conductors with three, as well as two, complete layers of aluminum strands. We agree, of course, that the reactances and ratios of a-c to d-c resistances can be calculated accurately for ACSR with even numbers of layers of aluminum strands. This fact will reduce considerably the amount of laboratory work necessary to revise published data on the electrical characteristics of ACSR. While it appears that the reactance of ACSR with three layers of aluminum strands can be calculated with acceptable accuracy, measurements of a-c resistance of several sizes of such cables are needed and are to be made. Measurements of reactance will be made simultaneously.

As noted by Dean Lewis, the electrical characteristics of ACSR with single layers of aluminum strands cannot be calculated with acceptable accuracy by neglecting the solenoid effect of the spiraling of the strands. Progress has been made in the development of methods of estimating the characteristics of such cables although it appears that the estimates must be dependent on experimental data concerning the characteristics of the steel cores. Confirming measurements of characteristics of several sizes of ACSR with single layers of strands are needed and are being made.

The simplified equations for the calculation of reactance promised by Dean Lewis will be welcome and helpful. The calculation by the geometric-mean-distance method is laborious for cables with many strands. A simple approximate method has been available for obtaining preliminary data. For expanded ACSR, a computation of reactance based on the equation for a single-phase return circuit composed of tubular conductors, and considering the cable as a tube of outer diameter equal to the cable diameter and of inner diameter equal to the cable diameter less four strand diameters, gave a result differing by less than 2 per cent from the experimental value. The tubular conductor concept also leads to an acceptable estimate of the a-c to d-c resistance ratio, as Prof. Dwight demonstrates.

To answer Mr. Defoe's questions, we have found that compression dead ends, properly applied, seem to meet adequately the requirements of proper current distribution. If there is any doubt, then the cable ends can be welded to be doubly sure, and compression dead ends can be readily adapted to do this. Welding has been used in preparing samples for the measurement of the characteristics of some cables with four full layers of aluminum strands.

We have experimented considerably in regard to the placement of thermocouples to insure satisfactory average readings of cable temperature. We have found no difference in the readings of couples placed between the strands of the outer layer and the couples wedged between the strands of the outer and the first inner layers. The latter position has the advantage of more mechanical security.

Capacitance-Switching Facilities at the Switchgear Development Laboratory

R. L. WILLIAMS
ASSOCIATE MEMBER AIEE

L. L. MANKOFF
ASSOCIATE MEMBER AIEE

H. N. SCHNEIDER
ASSOCIATE MEMBER AIEE

FACILITIES for capacitance-switching tests to check the performance of circuit breakers when switching the charging currents of transmission lines, cables, or large capacitor banks have been for many years a part of the circuit-breaker development program of the company with which the authors are associated. It had been recognized that severe transient voltages could be encountered when interrupting capacitive currents.[1] In order to develop an interrupter which would minimize these transient voltages[2] a bank of capacitors that provided the means for performing capacitance-switching tests was installed in the High Power Laboratory in Schenectady in 1941. This bank of capacitors had a rating of 7,800 kilovars (kvar) and was arranged for tests up to 132,000 volts. In 1948, an additional 10,800-kvar bank was added, bringing the total capacity to 18,600 kvar. In 1952, when short-circuit testing operations were transferred from Schenectady to Philadelphia[3,4] the 7,800-kvar bank was replaced with a second 10,800-kvar bank, giving a total capacity of 21,600 kvar in the present Laboratory.

With the increase in the number and length of high-voltage transmission lines and cables, and in the use of capacitor banks, the importance of this type of test-

---

Paper 55-220, recommended by the AIEE Switchgear Committee and approved by the AIEE Committee on Technical Operations for presentation at the AIEE Winter General Meeting, New York, N. Y., January 31–February 4, 1955. Manuscript submitted October 25, 1954; made available for printing December 17, 1954.

R. L. Williams, L. L. Mankoff, and H. N. Schneider are all with the General Electric Company, Philadelphia, Pa.

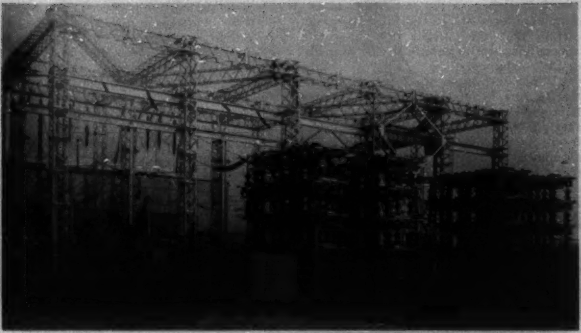

Fig. 1. Capacitor bank and high-voltage yard with 330-kv 25,000,000-kva circuit breaker undergoing capacitance-switching tests

ing has become more generally realized. It is currently being emphasized in the development program to the extent that almost as many capacitance-switching tests are being made as high-power tests.[5]

Because capacitance-switching tests utilized the same power source as interrupting capacity tests, without the actual necessity for such high-power equipment, and since this equipment is in continuous demand for power testing, it has been found advantageous to complement the capacitor bank with new facilities which utilize a synthetic circuit for investigating the capacitance-switching characteristics of developmental interrupters and breakers.

Capacitor Bank Installation

CAPACITOR BANK

Fig. 1 shows the capacitor installation in the foreground with the high-voltage yard in the rear. Power for testing is obtained from one of the two 125,000-kva short-circuit testing generators. One or both of two 100,000-kva 220-kv testing transformers are used to obtain the voltage required for capacitance-switching tests. A 330-kv 25,000-megavolt-ampere breaker is shown undergoing capacitance-switching tests.

The complete installation is built up of 7,200-volt capacitor units with a total of 21,600 kvar on a continuously rated basis. On a short-time basis (10 cycles) the units are capable of withstanding 73-per-cent overvoltages, so that switching tests may be made as high as 64,800 kvar without unduly stressing the capacitors. On this basis the capacitor bank is capable of making tests on a single-pole unit up to the equivalent of 300 miles of 330-kv line. Table I shows the range of capacitance and current available without overexcitation on the capacitors.

Physically, the capacitors are arranged in two identical, 10,800-kvar banks, with space provision for a third bank. Each bank contains 60 trays rated 7,200 volts, 180 kvar. Fig. 2 shows a close-up view of two of the trays, each containing 12 15-kvar capacitor units permanently connected in parallel. Each bank consists of two towers, with 30 trays in 4 tiers per tower. Connections progress from tower to tower and tier to tier in a helical arrangement, Fig. 3, with an insulation level above ground of 750-kv basic impulse level for the bottom tier. The insulation level between tiers is 350-kv basic impulse level. Hook-operated disconnecting switches are provided for making series-parallel combinations of units from 7.2 kv to 432 kv, thus giving a maximum of flexibility in both voltage and capacitance ranges. Fig. 4 shows the operator changing the bank connections by means of these switches.

Two high-voltage lines and two shunt (ground-return) lines for each of the two towers give a high degree of flexibility in making test connections. One high-voltage line of each bank has an insulation level corresponding to the top tier, and the second an insulation level corresponding to the bottom tier. Each high-voltage line has an automatic grounding switch which grounds the line and discharges the bank when the enclosure gate is opened. In addition to grounding switches which discharge the bank as a whole, each capacitor unit has an internal resistor which discharges it down to approximately 50 volts in 5 minutes.

The disconnecting switches for series-parallel connections are mounted on the sides and ends of the tier frames. They are so arranged that no disconnect has the voltage of more than two capacitor units (14.4 kv) so that 23-kv switches may be used. This keeps space requirements to a minimum, and the switches are easily operated from ground level.

In large commercial installations of capacitors, it is customary to equip each capacitor unit with an individual fuse which disconnects this unit from the circuit in case of an internal fault. Experience has shown that, in an installation for laboratory testing, fuses make no contribution to either continuity of service or safety of equipment. Therefore advantage is taken of the simplicity afforded by omitting the fuses. In addition, this simpler connection contributes to minimum inductance in the bank.

Tests are usually made with the test circuit breaker located in the power-test yard; see Fig. 1. Thus, both power tests and line-dropping tests may be made without shifting the location of the test breaker. Where close coupling of the capacitors and a minimum inductance is required, as in bank-to-bank testing, the test breaker is mounted on a test car located on the concrete strip immediately in front of the capacitors. On some occasions special connections within the bank have been made to eliminate even more of the inherent inductance of the bank.

A rod gap is provided to protect the capacitor bank from high transient voltages due to multiple restrikes which occur in the development of new interrupter

Table I. Maximum and Minimum Values of Capacitance and Current Obtainable at Various Test Voltages Without Overexcitation on the Capacitor Units

By Reconnection of the Units, Tests Can Be Made at 73-Per-Cent Overvoltage (for 10 Cycles Duration) at Three Times the Values of Capacitance and Current Shown

	Capacitance, Microfarads		Amperes	
Test Kv	Minimum Value	Maximum with Normal Excitation	Minimum Value	Maximum with Normal Excitation
7.2	0.077	1,105.0	0.21	3,000
14.4	0.077	276.3	0.42	1,500
21.6	0.077	122.8	0.62	1,000
28.8	0.077	69.1	0.83	750
36.0	0.077	44.2	1.04	600
43.2	0.077	30.7	1.25	500
57.6	0.077	17.3	1.67	375
72.0	0.077	11.05	2.08	300
86.4	0.077	7.67	2.50	250
108.0	0.077	4.91	3.12	200
144.0	0.077	2.76	4.16	150
216.0	0.077	1.228	6.25	100
432.0	0.077	0.307	12.50	50

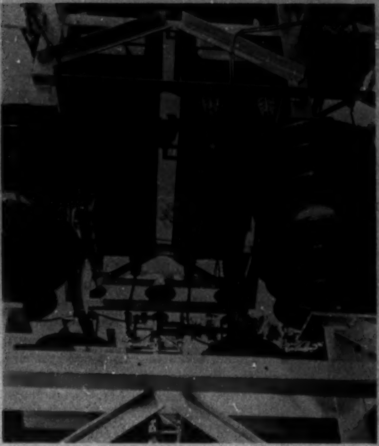

Fig. 2. Close-up of two capacitor trays, showing 12 capacitor units (180 kvar) permanently connected in parallel for each tray

Fig. 4. Side view of capacitor bank showing operation of switches for changing internal connections

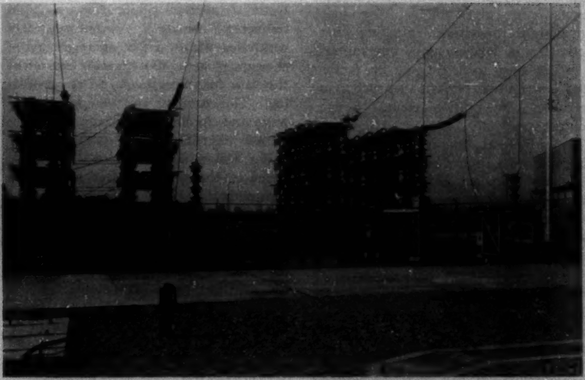

Fig. 3. Complete capacitor installation as viewed from the high-voltage yard. At the top of the picture are the four high-voltage power lines that tie into the bank. Connected to these lines are the four high-voltage grounding switches located in front of the towers. Behind and to the right of the grounding switches are the ground return or shunt lines. Interconnections between towers can be seen on the two towers on the left side of the picture

Fig. 5. Control panel for synchronous tripping of breaker under test

units. The rod gap is located on the source side of the breaker with the sparkover voltage adjusted just below the lightning-arrester level. Not only does the gap provide a high degree of protection to the capacitor bank but it also relieves the lightning arrester or surge protector at the transformer terminals of the necessity of discharging the large amounts of energy stored in the capacitor bank.

SYNCHRONOUS TRIPPING OF TEST BREAKER

In order to make a thorough capacitance-switching test on a circuit breaker, the breaker is tested over the complete range of contact-parting angles (the angle on the current wave at which contacts part). This is done to demonstrate that the breaker capacitance-switching ability is adequate for any condition encountered in service. Synchronous tripping is

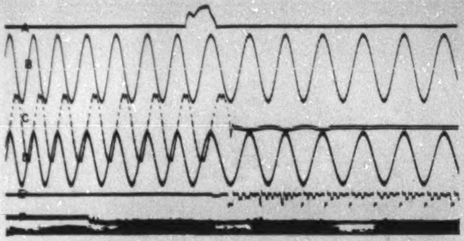

Fig. 6. Magnetic oscillogram for capacitance-switching test

Curve A—Trip current
Curve B—Generator voltage
Curve C—Current
Curve D—Voltage on source side of breaker
Curve E—Breaker travel
Curve F—Cathode-ray oscillograph timing indication

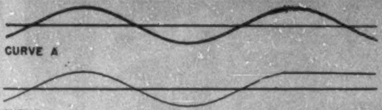

Fig. 7. Cathode-ray oscillogram for capacitance-switching test

Curve A—Voltage on source side of breaker
Curve B—Voltage on capacitor side of breaker

used to control effectively the contact-parting angle.

Synchronization of the tripping circuit is obtained by means of a control generator which is directly connected to the testing generator. This control generator supplies voltage to a phase-shifting selsyn. The selsyn triggers an electronic circuit that trips the test breaker at any predetermined point on the voltage wave. Fig. 5 shows the control panel used for synchronous control testing.

Recording of Data

Two methods of recording tests, depending upon the use to be made of the data, are employed. If the performance is to be correlated with the breaker travel, speed, pressure, etc., records are made employing both a magnetic oscillograph and the special laboratory-type 3-tube cathode-ray oscillograph producing records on a 6-inch by 40-inch film having a wide selection in time scale. Figs. 6 and 7 show typical oscillograms for such a test.

Most capacitance-switching tests do not require the elaborate oscillograms referred to in the foregoing paragraph. For these tests, all essential data are obtained by using a 4-beam cathode-ray oscillograph, having a long-persistence screen, from which a still photograph is made of the transient phenomena with a 35-millimeter camera. With this method of recording, tests are made at approximately three times the former rate, effectively tripling the availability of the test facilities for capacitance-switching tests. Fig. 8 shows a 35-millimeter record of two capacitance-switching tests, one with restrike and one without restrike.

Synthetic Circuit for Capacitance Switching

Basic Circuit

The Development Laboratory has the forementioned capacitance bank installation in the high-voltage yard to provide means of determining full-scale capacitance-switching performance of breakers. These tests are made to demonstrate that the breaker being tested can successfully handle, with adequate margin, capacitance switching. However, in the development of new interrupters it is not sufficient merely to determine successful performance for a given voltage. To evaluate adequately capacitance-switching characteristics of developmental interrupters, it is necessary to investigate the factors that contribute to performance such as interrupter configuration, contact design, contact speed, etc.

In addition to this, it has been found that for a given set of conditions there is no sharp boundary between the region where no restrikes occur and the region where restrikes occur all of the time. On the contrary, the voltage at which restrikes occur all of the time may be as much as two to three times greater than the voltage at which no restrikes occur. Also, this investigation should be made over the whole range of contact-parting angles because changes in the contact-parting angle can result in more than 100-per-cent variation of withstand voltage, and this variation changes with interrupter modifications. Since this investigation must also be made over a wide range of currents, it is apparent that, to evaluate a single modification of a developmental interrupter, many hundreds of tests must be made.

The conventional method of performing capacitance-switching tests requires the high-power facilities and large test areas of the Switchgear Development Laboratory which are in continuous demand for power testing. However, capacitance-switching tests require only a small fraction of this available power. Recognition of this fact led to the development of a synthetic circuit which is used for evaluating the capacitance-switching performance of developmental interrupters and circuit breakers. This synthetic circuit utilizes relatively low power equipment and a small test area. In essence the circuit supplies capacitive current from a low-voltage source and high test voltage from a low-current source. Synchronous isolation of the two power supplies is provided by means of a device designed for this purpose.

Synthetic circuits for investigating developmental interrupters and circuit breakers have been under consideration many times. Synthetic circuits for power testing require the application of a high-frequency, recovery voltage accurately controlled within a few microseconds of the current zero. Fortunately this is not the case for capacitance-switching testing. The recovery voltage is a 60-cycle wave and application within 100 microseconds will suffice.

Fig. 9 shows the basic circuit and wave forms of the synthetic test unit. The high-potential transformer is energized with the contacts of the interrupter closed; therefore, the high potential is impressed across the series capacitor whose 60-cycle reactance is high enough so that it will not overload the high potential transformer. To insure steady-state conditions, a minimum of 10 cycles, set by a time-delay unit, are allowed before any

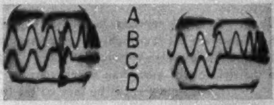

Fig. 8. Oscillogram of capacitance-switching tests photographed on 35-millimeter film showing (left) a restrike and (right) a restrike-free test

Curve A—Breaker contact parting indicator
Curve B—Line voltage on source side of breaker
Curve C—Voltage on capacitor side of breaker
Curve D—Current

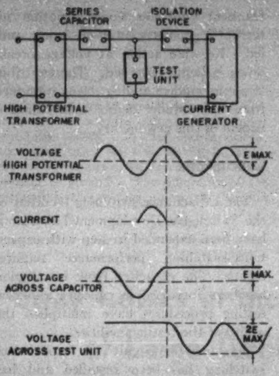

Fig. 9. Basic circuit and wave forms of the synthetic test circuit. At the top is the block diagram for the circuit. Underneath the basic circuit are the essential wave forms showing the synchronization between current and voltage and the resulting voltages across the series capacitor and the test unit

action is initiated by a synchronous-control unit. As can be seen from the waveforms the current generator is preset to fire so that current zero will occur at a voltage maximum. The current generator is fired synchronously and current begins to flow through the closed contacts. The current generator produces a half-cycle of current. At the desired time within the half-cycle the contacts part and the current continues to flow in an arc produced across the parting contacts. This arc maintains a low-impedance path for the high potential. At the end of the half-cycle of current the isolating device has removed the current generator from the circuit. The high-potential transformer voltage is then at a positive peak, and the series capacitor is charged to a voltage E_{max}. Voltage now builds up across the interrupter contacts and reaches $2E_{max}$ after 1/2 cycle.

The current generator is a bank of capacitors charged from a rectified a-c source and synchronously discharged through an inductance by means of a thyratron-trip circuit. The amount of capacitance used is governed by the range of current desired and the inductance is chosen to resonate with the capacitance at 60 cycles per second. Fine control of the amount of current obtained is achieved by adjusting the alternating voltage applied to the charging circuit.

Both the current and the voltage are displayed on a cathode-ray oscillograph. The current is measured by means of a shunt, the voltage by means of a capacitance divider across the interrupter or breaker. The contact-opening indication is obtained through the use of a switch set to fire a thyratron which in turn blanks the trace for a short interval at the time of contact opening. The composite signal, on a single trace, is obtained from a signal-mixer unit which amplifies and combines the current and voltage signal. Fig. 10 is a typical oscillogram showing current, contact indication, and voltage. The first half-cycle shown is the current wave. The remainder of the oscillogram is the voltage applied to the interrupter. In recording, the polarity of the voltage wave is reversed. This is done to position the voltage wave on the oscillograph in order to improve the readability of the test record. When it is required to record additional test data such as contact travel, interrupter pressure, etc., a 4-beam cathode-ray oscillograph is used.

The device developed to provide synchronous isolation of the two power supplies was tested extensively. In addition, to insure the reliability of the data obtained, the proper operation of this device is checked on each test. This is accomplished by means of an indicating circuit which is actuated in the event of a rare isolation failure. This circuit will blank the cathode-ray oscilloscope beam at the instant of failure, thereby recording that the test was not valid. It is to be noted that this synthetic circuit cannot be applied to interrupters that are shunted by resistors of such ohmic value that would effectively discharge the series capacitor of the synthetic circuit.

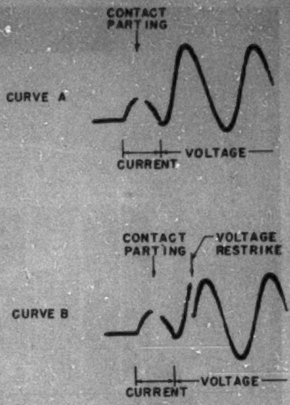

Fig. 10. Oscillogram for synthetic capacitance-switching test

Curve A—Withstand test
Curve B—Restrike

Synthetic-Circuit Installation

A permanent installation of this synthetic capacitance-switching circuit has been made in the Development Laboratory as shown in Fig. 11. This installation is divided into a control area, which is located in the upper left corner of photograph below the clock, a circuit area, which is located at rear of photograph, and two test areas, in the foreground. The circuit area contains the following components:

Fig. 11. Installation of synthetic capacitance-switching circuit. Directly in the foreground are the two test areas. Behind the test areas is the circuit area that contains the synthetic circuit. To the left of the circuit area, and underneath the clock, is the control area

Fig. 12. Control area of synthetic capacitance-switching circuit showing, from left to right, the incoming power panel, synchronous control unit no. 1 instrument panel and calibration unit, and synchronous control unit no. 2. To the extreme right is seen the cathode-ray oscillograph and 35-millimeter camera

1. Voltage regulator.
2. High-voltage transformer.
3. Series capacitor.
4. Capacitance voltage divider.
5. Isolation device.
6. Current generator.

The two test areas are interlocked so that testing can be done in one area while another test unit is being prepared in the other. The interlock circuits are controlled by the position of the single-pole double-throw high-voltage switch mounted above the rear fence of the cell areas, as shown in Fig. 11. The test-unit control wiring plugs into stationary receptacles which connect to the synchronous-control unit associated with each test area. Jumper connections in the circuit area provide for the interchanging of the synchronous-control units. The front fencing of the two test areas is removable to allow test breakers, as well as test units, to be brought into the test areas.

The control area, as illustrated in Fig. 12, incorporates the following components:

1. Incoming-power control panel.
2. Instrument panel that transmits the test data to the cathode-ray oscillograph. Data is recorded on a 35-millimeter camera mounted on the oscillograph.
3. Calibration unit.
4. Two electronic synchronous-control units which are used to synchronize the current, voltage, isolation device, test-breaker operation, and oscillograph sweep.

PHOTOGRAPHIC STUDY OF CAPACITANCE SWITCHING

In addition to capacitance-switching testing, this installation, with the synchronous-control units, has provided the means necessary to pursue a photographic study of the fundamentals of capacitance-switching phenomena. Using both still and high-speed motion photography, arcs, of the magnitude and duration encountered in capacitance-switching duty, are being investigated. The effects of transient fluid flow, contact motion, interrupter geometry, etc., are being studied. Restrike action at voltage breakdown is being observed. The contributions to understanding being obtained from this study demonstrate another benefit of this new facility.

Conclusions

The capacitance-switching facilities of the Switchgear Development Laboratory have been expanded in step with capacitance-switching performance requirements. The capacitor bank installation has been increased in capacity and new testing procedures have multiplied the utility of the testing facilities.

A synthetic circuit for capacitance switching has been installed and has proved to be a very useful tool. It has been applied to investigating many types of developmental interrupters and breakers. To date over 15,000 tests have been performed on oil-blast, air-blast, and magne-blast developmental interrupters.

The main value of the synthetic circuit is as a developmental tool. It is important to recognize that verification tests of the capacitance-switching performance of the final design of interrupter or breaker must be determined through the use of full-scale tests using equipment such as capacitor bank and high-power facilities available at the Switchgear Development Laboratory.

References

1. Effect of Restriking on Recovery Voltage, **C. Concordia, W. F. Skeats.** *AIEE Transactions (Electrical Engineering)*, vol. 58, Aug. 1939, pp. 371–76.

2. Switching Overvoltage Hazard Eliminated in High-Voltage Oil Circuit Breakers, **Lloyd F. Hunt, E. W. Boehne, H. A. Peterson.** *Ibid.*, vol. 62, Feb. 1943, pp. 98–106.

3. New High-Capacity Switchgear Laboratory, **V. L. Cox.** *AIEE Transactions*, vol. 71, pt. III, 1952, pp. 102–11.

4. Features of the Philadelphia Switchgear Development Laboratory, **W. F. Skeats, R. L. Williams.** *AIEE Transactions*, vol. 72, pt. III, Aug. 1953, pp. 770–80.

5. The Results of 7 Years' Experience with High-Capacity Outdoor Oil Breakers, **C. J. Balentine, K. G. Darrow.** *AIEE Transactions*, vol. 74, pt. III, 1955 (*Paper 55-213*).

◆

Discussion

A. E. Kilgour (Allis-Chalmers Manufacturing Company, Boston, Mass.): The authors are to be congratulated for this paper, which they have so well prepared and presented. Throughout the text there is no mention of measuring the voltage drop across the circuit-breaker contacts. It is this initial drop as the capacitors are removed from the circuit that will affect the history of breaker interruption. Important with respect to the synthetic testing at this same stage of interruption is the ratio of the kvar kva short circuit. Such has not been mentioned within the paper.

A second question follows from paragraph 5 of the section on "Basic Circuit." The second sentence beginning "The high-potential transformer voltage..." This statement seems to be in conflict with information presented in two other papers.[1,2] The conflict that arises concerns the voltage at which the breaker should be tested.

REFERENCES

1. Test Circuits for Capacitance Switching Devices, **K. G. Darrow, V. E. Phillips, A. J. Schultz R. B. Shores.** *AIEE Transactions*, vol. 74, pt. III 1955 (*Paper 55–212*).

2. Some Fundamentals on Capacitance Switching, **I. B. Johnson, A. J. Schultz, N. R. Schultz**

R. B. Shores. *AIEE Transactions*, vol. 74, pt. III, 1955 (*Paper 55-224*).

R. L. Williams, L. L. Mankoff, and H. N. Schneider: The voltage across the circuit-breaker contacts is available both in full-scale and synthetic circuit capacitance switching testing. In capacitance switching testing, using full-scale testing facilities, the voltage is measured on each side of the breaker to ground. The difference of the voltages is the voltage across the breaker contacts. Any initial voltage drop across the breaker contacts will appear on the voltage trace of the source side since the voltage of the load side will remain constant. For the synthetic test circuit as stated in the paper, voltage is measured directly across the breaker contacts. It is a property of the synthetic circuit that the initial change in voltage across the breaker contacts upon interruption is zero, corresponding to the most severe test condition with regard to kvar to kva short-circuit ratio.

There is no conflict between this paper and the two mentioned by Mr. Kilgour. They establish the voltages that should be used for the single-phase circuits equivalent to the various 3-phase conditions. The $E_{\max}$ of the present paper designates the crest value of the transformer voltage of the synthetic circuit, which may be set at the same value as that required for the single-phase equivalent circuit or for any other voltage desired. In fact, for developmental investigations, testing is done through a range of voltages far in excess of any encountered under field conditions.

Stray Losses in the Armature End Iron of Large Turbine Generators

R. L. WINCHESTER
ASSOCIATE MEMBER AIEE

Synopsis: The results of a study of stray load losses in the armature end iron of large turbine generators are presented. These losses are induced by the generator end leakage flux, and the resulting end iron temperatures limit the machine capability in the underexcited region of operation. Quantitative methods of analysis of the magnetic field distribution at the ends of the machine and the resulting losses and temperature rise are presented. Design innovations for reducing end iron losses and temperature in both conventional and direct-cooled generators are described. The results of factory and field tests supporting the principal conclusions are included.

IT WAS recognized early in the history of synchronous machines that generator operation at high lagging, unity, and leading power factors resulted in comparatively high temperatures in the structural parts at the ends of the armature core. This phenomenon has been termed "end heating" and is characteristic of the steam turbine type of alternator.

End heating is caused by losses generated in the structural parts by magnetic flux entering the ends of the armature core. This flux is caused by the resultant of the armature and field winding magnetomotive forces (mmf) and rotates in synchronism with the field. The parts affected, shown in Fig. 1, are the end laminations of the stator core, the stator core clamping fingers, the stator core flanges, and the end winding binding bands.

During the early years of electric power generation, little capacitive correction was used on transmission systems. Under these conditions, the generator supplied most of the reactive power. Most early units carried loads ranging from 0.7 to 0.9 power factor, overexcited, and performed satisfactorily with such loads. In later years, with the application of static capacitors and synchronous condensers, system power factors, during light load periods especially, have gradually shifted closer to unity.

In about 1925, the General Electric Company made turbine-generator design alterations which materially reduced the high temperatures resulting from underexcited operation. These changes consisted of using nonmagnetic steel for the structural parts, fingers, flange, and binding bands, which were previously made from magnetic steel. Additional improvement was made later by introducing the practice of chamfering the end packages of the stator core.

The reduction in temperature rise obtained by these improvements, documented by test results on many machines through years,[1] has promoted increased confidence on the parts of both the manufacturer and the operator in the underexcited capability of modern turbine generators. All turbine generators currently being built by the General Electric Company are capable of operating at rated kilovolt-amperes (kva) at 0.95 power factor, underexcited, and may be loaded to approximately 60 per cent of rated load at zero power factor, underexcited. A typical operating characteristic for one of these machines is shown in Fig. 2.

During the past few years, rather intensive, industry-wide efforts by turbine-generator designers have been devoted to increasing the specific capacity of 2-pole generators. Hampered on one hand by limits of shipping weight and dimensions and on the other hand by the mechanical limits of known structural materials, the designer has had to devise radical improvements in methods of cooling to increase the kva capacity of 2-pole turbine generators. Significant progress has been made in the design of direct-cooled generators[2-6] and in the design of multiple-circuit generators and multiple-phase generators[6] which also allow an appreciable increase in generator capacity.

The greatly increased specific capacity of these direct-cooled machines has resulted in greatly increased loadings on the generator windings. It is to be expected that the losses at the ends of the armature core will increase correspondingly. An idea of the increase in end iron temperature to be expected by simply increasing the winding loading of a large 2 pole generator may be gained by inspection of Fig. 6 of reference 1. This curve shows that a 10-per-cent increase in capability for a given generator will cause an increase in the end iron temperature of approximately 13 per cent if no other design changes are made. What, then, is to be expected if the generator rating is increased 50 per cent or even 100 per cent or more without an increase in physical size?

The results of a study directed towards gaining a better understanding of the nature of end iron losses are described.

Paper 55-130, recommended by the AIEE Rotating Machinery Committee and approved by the AIEE Committee on Technical Operations for presentation at the AIEE Winter General Meeting, New York, N. Y., January 31–February 4, 1955. Manuscript submitted October 20, 1954; made available for printing December 8, 1954.

R. L. WINCHESTER is with the General Electric Company, Schenectady, N. Y.

The co-operation of the Pacific Gas and Electric Company in carrying out tests described in this paper is gratefully acknowledged. The author also wishes to acknowledge the encouragement of B. M. Cain and C. H. Holley, and the help of H. Poritsky and S. J. Jennings whose initial work on this problem eliminated many roadblocks. Finally, C. B. Linkous, H. Kitson, and T. F. Salmon made direct contributions while on rotating engineering assignments from the General Electric Advanced Engineering Program.

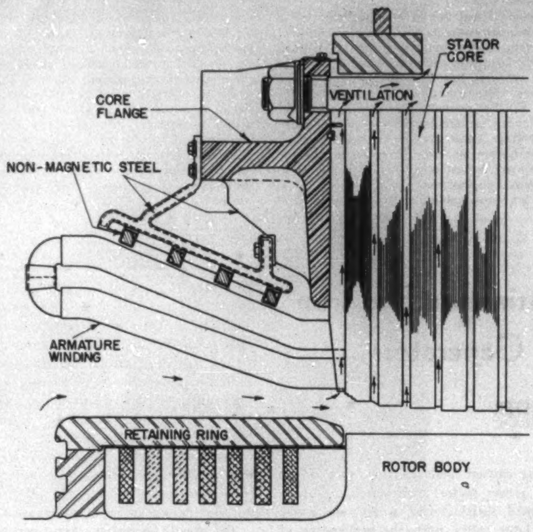

Fig. 1. Typical turbine generator end construction

This study was undertaken with the intent of learning how to design generators of increased capability with end iron temperatures consistent with those of conventional units over the entire range of operating conditions. In addition, the end losses, which appear as stray load losses become of an appreciable magnitude in up-rated generators and methods have been devised to reduce these losses. The progress which has been made towards the predetermination of end iron losses and temperature, and the loss reduction features which will be introduced in large direct cooled-generators currently being built by the General Electric Company are presented. This problem, the initial results of which are described in this paper, is just one of many similar problems inherent to the large direct-cooled generator. These problems have required, and will continue to require, thorough engineering study in advance of construction and operation to assure satisfactory and lasting operation.

Nomenclature

A_{sw} = square wave armature reaction
$\mathbf{B}$ = magnetic induction
$\mathbf{E}$ = electric field intensity
f = frequency
$\mathfrak{F}$ = magnetomotive force
$\mathbf{H}$ = magnetic field intensity
$\mathbf{J}$ = electric current density
k_p = armature winding pitch factor
k_d = armature winding distribution factor
P = number of poles
r = radius from generator centerline
V = scalar magnetic potential
x,y,z = rectangular co-ordinates
δ = depth of penetration
θ = generator peripheral angle
ρ = electrical resistivity
ρ_c = resistivity of copper
ω = angular frequency
μ = magnetic permeability
μ_0 = permeability of free space

Description of the Nature of End Iron Losses

The purpose of this section will be to discuss, from a qualitative standpoint, the nature of the losses which occur in the structural parts at the ends of the armature core. The emphasis will be placed on establishing a physical picture of the magnetic field distribution at the ends of the machine, the behavior of the conducting materials in the presence of this field, and the effect of load conditions on losses and temperature rise.

End Construction

The end construction of a typical turbine generator is shown in Fig. 1. Axial pressure is maintained on the stator core laminations by the stator core flange, which is bolted in place on extended key bars in back of the stator core. Beneath the stator core flange against the core are located the outside space blocks, or end clamping fingers, which extend as cantilevers over the core teeth between armature bar slots and maintain axial pressure on the core teeth. The armature end windings extend axially from the slots and are laced to binding bands in the usual diamond-shaped pattern. The field end windings extend axially from the rotor body and are held in place by the retaining ring. The retaining ring is shrunk onto the rotor spindle and a small air gap is maintained between the tip of the retaining ring and the rotor body.

Magnetic Field Distribution

Under normal load conditions, the generator voltage is produced by magnetic flux which passes radially across the air gap and is distributed uniformly over the length of the core and approximately sinusoidally with the peripheral angle. This air-gap flux rotates in synchronism with the field and is generated by the resultant of the armature and field winding mmf.

The end losses are generated by the end fringing flux which passes from the ends of the rotor body and retaining rings to the ends of the armature core. This flux is produced by the winding mmf, just as is the main air-gap flux, the difference being that the permanence paths are in general longer and more complicated. The end flux rotates in synchronism with the field and, therefore, sweeps past the stationary parts at the ends of the armature core at synchronous speed, inducing eddy-current losses.

Skin Effect in Conducting Materials

The losses in the various structural parts may be separated into two categories. In the first case, the eddy currents are resistance-limited, or the effective resistance to eddy-current flow is considerably larger than the effective reactance, i.e., there is little skin effect. In this case, the distribution of the magnetic field is relatively unaffected by the presence of the conducting material, and the eddy-current distribution is determined largely by the properties of the material and the magnetic field distribution.

In the second case, that of pronounced skin effect, the eddy currents are reactance-limited. In this case, the conducting material has a dominating effect on the magnetic field in its vicinity, the eddy currents being large enough to prevent the entry of magnetic flux and tending to cause the conductor to act as a shield.

The criterion to be applied to determine to which category the materials belong is the classical depth of penetration of the material. The magnetic field attenuates within a conductor (the proportions of which are large in comparison to the depth of penetration) to a value, at a point one depth of penetration below the surface, of 37 per cent of the value at the surface. The classical depth of penetration is defined as

$$\delta = \sqrt{\frac{2\rho}{\omega\mu}} \tag{1A}$$

$$= \frac{0.336}{\sqrt{\left(\frac{f}{60}\right)\left(\frac{\mu}{\mu_0}\right)\left(\frac{\rho_c}{\rho}\right)}} \text{ inch} \tag{1B}$$

The case of pronounced skin effect occurs when the dimensions of the conducting body are large in comparison with the depth of penetration, while little skin effect occurs when the dimensions are small in comparison with the depth of penetration.

EDDY-CURRENT LOSSES IN STRUCTURAL PARTS

Magnetic flux entering the end teeth of the stator core in an axial direction induces eddy currents which flow unobstructed parallel to the laminations. It has been demonstrated that a given magnetic induction entering a laminated steel body in a direction perpendicular to the laminations generates losses many times greater than the same induction entering parallel to the laminations. Eddy currents in the end teeth are largely resistance-limited except in generators with the widest teeth. The primary reason for this behavior is that the effective permeability of the stator core to axial penetration of magnetic flux is quite low because of the air gaps between laminations.

As was described previously, the binding bands, binding-band brackets and outside space blocks of the machines currently being built by the General Electric Company are made from nonmagnetic steel. The eddy currents in these parts are resistance-limited since the dimensions are small in comparison with the depth of penetration. The losses in these parts are minimized by the nonmagnetic steel construction.

On the other hand, the dimensions of the stator core flange are such that with presently used materials the currents are nearly reactance-limited. Therefore, the core flange eddy currents prevent most of the end flux from penetrating the flange and from entering the backiron. The current flowing in the flange is a small fraction of the total end winding current, the actual magnitude depending on the geometry of the end structure. Magnetic steel and cast-iron flanges behave in a similar manner except for more pronounced skin effect and higher losses than with the nonmagnetic steel construction.

With the generator operating at rated load and rated power factor, the end losses and resulting end iron temperatures are well within comfortable limits. The losses and temperature rise increase rapidly, however, as the generator loading is shifted into the underexcited region of operation[1] and, finally, actually limit the generator capability, as shown in Fig. 2. This increase in end losses and temperature is caused primarily by the changes in the magnitude and relative spatial positions of the winding mmf. As the generator loading is shifted towards underexcited operation, the locations of the peak values of the armature and field winding mmf move towards one another, and the field winding mmf decreases in magnitude. Both of these effects cause an increase in the end leakage flux and the resulting losses.

EFFECT OF NONMAGNETIC RETAINING RINGS

End losses are, in general, lowered by providing nonmagnetic retaining rings on the rotor. The presence of a nonmagnetic retaining ring tends to increase the lengths of the reluctance paths for the end leakage flux, lowering the magnetic field intensities and decreasing the losses.

Although nonmagnetic retaining rings are ideal from an electrical standpoint, there are many problems of quality control in producing these rings for large generators. As a consequence, engineering effort has been directed towards developing loss reduction features applicable to direct-cooled generators with magnetic retaining rings as well as towards solving the problems of manufacture of nonmagnetic retaining rings.

Results and Conclusions

End iron temperature rise margins in generators of conventional rating have been greatly increased by the introduction of split teeth in the end laminations of the

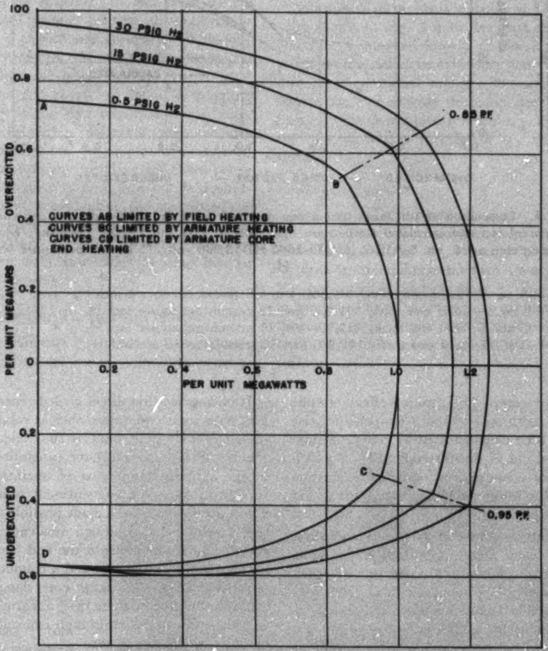

Fig. 2. Reactive capability curve for typical turbine generator

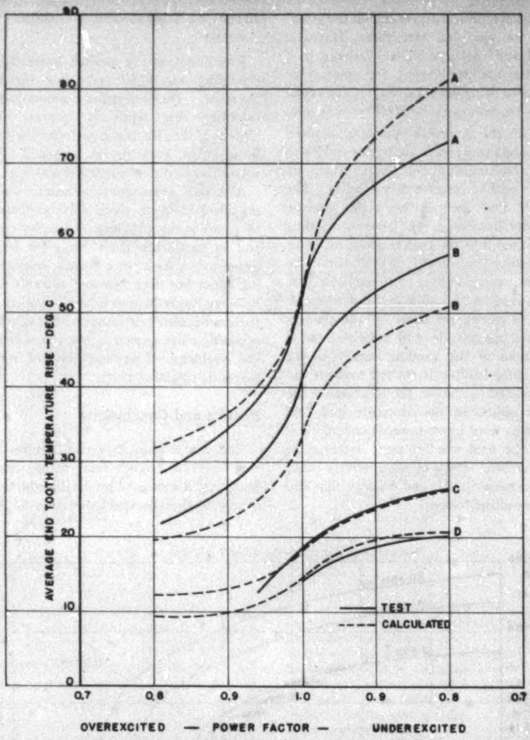

Fig. 3. Comparison of end tooth temperature rises with solid and split end teeth and comparison of test and calculated temperature rises. Pacific Gas and Electric Company, Moss Landing units no. 2, no. 5-ATB-2-129375-3600 HT-13,800 volts, 15 pounds per square inch H_2

Curve A no. 2—Solid end teeth, 112,500 kva, 0.5 pound per square inch H_2
Curve B no. 2—Solid end teeth, 112,500 kva, 15 pounds per square inch H_2
Curve C no. 5—Split end teeth, 112,500 kva, 15 pounds per square inch H_2
Curve D no. 5—Split end teeth, 112,500 kva, 30 pounds per square inch H_2

stator core. The striking effect of split end teeth on end tooth temperature rise has been demonstrated by generator field tests and is illustrated in Fig. 3 which shows a comparison of temperature rise in duplicate machines, except for solid and split end teeth.

Slotting the end teeth accomplishes, to a lesser degree of perfection, the same effect as laminating the core in a direction parallel to the magnetic flux. This loss reduction technique was first described, as far as the author is aware, with reference to the generator end loss problem, in the foreign literature.[7]

It is expected that direct-cooled generators with greatly increased specific capacities, currently being built by the General Electric Company, will have capabilities in the underexcited region of operation similar to those of conventional units. This operation has been made possible by the development of design innovations consisting of split teeth in the end laminations of the stator core and a conducting shield over the stator core flange. The introduction of these design features will also help to maintain high efficiency in direct-cooled generators.

The stator core flange shield consists of a copper shield bolted in place over the stator frame flange. This device allows the currents which otherwise flow in the flange to flow in the low-resistance shield, reducing the losses. Factory tests have been run with temporary shields of this type and are described later.

Progress has been made towards a complete understanding of the stray losses at the ends of the armature core in large turbine generators. It is hoped that the results will stimulate further investigation of this problem, and lead ultimately to a thorough understanding of the over-all generator stray load loss.

Outline of Analytical Methods and Substantiating Test Data

The analysis of end iron losses and temperature rise in large turbine generators has involved a fundamental study of the magnetic field distribution at the ends of the machine, an investigation of the flux distribution and eddy-current losses in the end teeth and fingers, and a study of the thermal characteristics of the ends of the core. The analytical methods will be outlined and the results of calculations will be compared with test data gathered on models and during generator factory and field tests.

MAGNETIC FIELD DISTRIBUTION

The magnetic field at the ends of the armature core forms a fairly complicated 3-dimensional configuration. A solution to the problem has been obtained using an electrolytic field-mapping tank especially equipped to account for the various features of the problem.

Electrolytic Tank Analogue

It is well known that 2-dimensional as well as axially symmetric Laplacian field problems may be solved by analogue methods. Among the techniques available are hand flux plotting, resistance paper, electrolytic tank, d-c calculating board, and digital computer studies. In this case the electrolytic tank seemed to be the most adaptable to the problem.

In the electrolytic tank analogue, electric voltage in the tank is analogous to the mmf in the machine, and the electric current is analogous to magnetic flux. The geometry of the generator end structure is axially symmetric, requiring a wedge-shaped tank in which the electrolyte depth varies with the radius from the generator axis of rotation.

Since the generator winding mmf vary sinusoidally with the peripheral angle, considering only the fundamental component, peripheral flux exists within the end region and should be accounted for in the analogue solution. A technique has been developed which allows the representation of the peripheral as well as the axial-radial fields in a wedge-shaped tank.

The magnetic field in the air regions at the ends of the machine may be obtained as the gradient of a scalar potential, where the potential must be a solution of Laplace's equation. Laplace's equation, in cylindrical co-ordinates, is

$$\nabla^2 V = \frac{\partial^2 V}{\partial r^2} + \frac{1}{r}\frac{\partial V}{\partial r} + \frac{1}{r^2}\frac{\partial^2 V}{\partial \theta^2} + \frac{\partial^2 V}{\partial z^2} = 0 \qquad (2)$$

where

$$\mathbf{H} = -\nabla V$$

Since the winding mmf are distributed sinusoidally with the peripheral angle, the potential V will also be sinusoidally distributed.

Let this potential be written as

$$V = V'(r,z)\cos\frac{P\theta}{2} \qquad (3)$$

Then the potential equation 2 in terms of the new potential V' is

$$\frac{\partial^2 V'}{\partial r^2} + \frac{1}{r}\frac{\partial V'}{\partial r} + \frac{\partial^2 V'}{\partial z^2} = \left(\frac{P}{2}\right)^2 \frac{V'}{r^2} \qquad (4)$$

Thus the distribution of the potential in any radial plane is independent of variations with the peripheral angle.

Equation 4 is Laplace's equation for an axially symmetric field except for the presence of the source term on the right-hand side. It may be shown that the potential distribution may be determined by any of the analogue methods applicable to axially symmetric fields providing suitable sources are located throughout the plane of the solution. In the electrolytic tank, probes were located throughout the plane of the tank and grounded through suitable resistances. The current absorbed by these probes corresponds to magnetic flux leaving the corresponding radial plane in the generator to travel in a peripheral direction. The actual field-mapping tank and pantograph plotting equipment is shown in Fig. 4.

Winding Mmf

The winding mmf are obtained by evaluating the equivalent axial and peripheral currents in the end windings. The mmf were represented in the electrolytic tank by voltage sources located on the radial centerlines of the end windings. The strengths of the voltage sources are a maximum at the ends of the core and decrease, depending on the end winding geometry, with axial distance from the core to zero outside the windings.

Magnetic Retaining Rings

Magnetic retaining rings were represented by additional current sources. Magnetic retaining rings in large turbine generators are saturated, except at very low field currents, by the large field mmf. The saturated rings may, therefore, be represented by current sources which simulate the intrinsic ring saturation level. The strengths of these sources depend only on the retaining ring material and geometry and are independent of load conditions.

Boundary Conditions

The boundaries, end teeth, rotor body, stator frame, and end shields, were represented as infinitely permeable materials. It will be shown that skin effect is of second order importance in the end teeth, hence these may be represented, as far as the magnetic field distribution in the air region is concerned, as infinitely permeable surfaces. The end shields and stator frame, generally made from magnetic steel, can only be approximated by infinitely permeable surfaces because of pronounced skin effect. Since these surfaces are relatively distant from the regions of primary interest, the approximation is of sufficient accuracy. Boundary conditions for the stator core flange will be discussed later.

The end result of the field mapping study is the determination of the magnetic field intensities in the various regions of interest for varying load conditions. Proper account must be made of the phase displacement of armature and field winding mmf in evaluating the magnetic field intensities under load conditions. The evaluation of eddy-current loss from known field intensities is described in the following.

Loss in End Teeth and Fingers

End leakage flux entering the end teeth normal to the laminations induces eddy currents, and the resulting loss is many times greater than for the same magnetic induction entering parallel to the laminations. The magnitude of the losses depends on the normal induction, determined from the field study, and the distribution of flux within the end teeth.

Axial Penetration of End Flux

It will be shown that skin effect is relatively unimportant in determining the tooth flux distribution except in generators with the widest teeth. Under this condition, the degree of axial penetration of the end flux into the core is determined by the magnetic circuit of the end packages of the stator core.

An equivalent circuit representing the end packages of the core is shown in Fig. 5. The magnetic reluctances of this network are determined from the dimensions and permeability of the core material, and the flux inputs are evaluated for the particular load condition being studied. The network can be made as detailed as necessary to obtain a reasonable approximation to the axial flux distribution. The network solution must account for the nonlinearity of the core material.

Solution of equivalent circuits of the type shown in Fig. 5 indicates that the end flux is confined largely to the first package of laminations in modern generators of conventional rating. The axial flux in the end package decreases nearly linearly with depth into the package, except for variations just below the end surface.

Tooth Loss Intensity

The tooth loss intensity and the distribution of the axial field over the width of an end tooth may be evaluated by an analysis from fundamental field theory. The geometrical configuration is shown in Fig. 6. The object here is to evaluate the tooth eddy-current loss intensity in terms of known axial fields at the end surface.

Fig. 4. Three-dimensional field-mapping tank and associated equipment

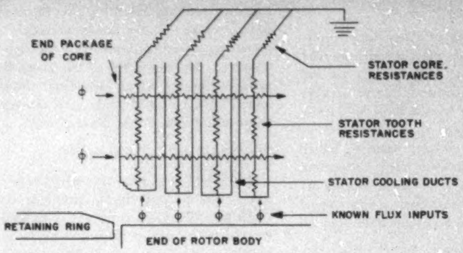

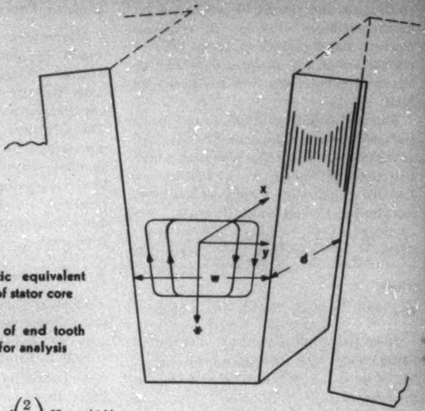

Fig. 5 (above). Magnetic equivalent circuit for end packages of stator core

Fig. 6 (right). Geometry of end tooth and co-ordinate system for analysis

It will be assumed that the end flux spanning one tooth and slot pitch enters the tooth end face uniformly over the tooth width, and that the eddy currents are 1-dimensional. The first assumption is based on the fact that the iron permeability is considerably larger than that of the air paths. The second is an approximation, but is justified on the basis that the tooth depth is considerably larger than the tooth width, and the rate of change of the axial field with the radial tooth dimension is small except over a short distance near the tooth tip. The problem will be solved first on the basis that the axial field is continuous, and then modified to account for the fact that the axial field intensity decreases with depth into the package.

Maxwell's field equations, on neglecting variations in the z direction and replacing $\partial/\partial t$ by $j\omega$ for steady conditions, are

$$\frac{\partial H_y}{\partial x}-\frac{\partial H_x}{\partial y}=J_z \qquad (5A)$$

$$\frac{\partial E_z}{\partial y}=-j\omega B_x \qquad (5B)$$

$$\frac{\partial E_z}{\partial_x}=j\omega B_y \qquad (5C)$$

Ohm's law is written as

$$\mathbf{J}=\frac{\mathbf{E}}{\rho} \qquad (5D)$$

and

$$B_x=\mu_x H_x \qquad (5E)$$

$$B_y=\mu_y H_y \qquad (5F)$$

In writing equations 5(E) and 5(F), cognizance is taken of the fact that the core permeability in a direction perpendicular to the laminations is considerably less than when parallel to the laminations because of the air gaps between laminations. Constant permeability parallel to the laminations is assumed. Differential equations for the magnetic field intensities may be derived from equations 5 in the following form

$$\frac{1}{\alpha}\frac{\partial^2 H_x}{\partial x^2}+\frac{\partial^2 H_x}{\partial y^2}=\frac{j\omega\mu_x}{\rho}H_x=j\left(\frac{2}{\delta^2}\right)H_x \qquad (6A)$$

$$\frac{1}{\alpha}\frac{\partial^2 H_y}{\partial x^2}+\frac{\partial^2 H_y}{\partial y^2}=\frac{j\omega\mu_x}{\rho}H_y=j\left(\frac{2}{\delta^2}\right)H_y \qquad (6B)$$

where

$$\alpha\equiv\frac{\mu_y}{\mu_x}$$

$$\delta\equiv\sqrt{\frac{2\rho}{\omega\mu_x}}$$

The solution of equation 6, subject to the boundary conditions of a uniform field H_0 at the face of the tooth and all the flux to be carried in the iron, is

$$H_x=H_0\left[\frac{(1+j)w}{2\delta}\,\frac{\cosh\,(1+j)\,\dfrac{y}{\delta}}{\sinh\,(1+j)\,\dfrac{w}{2\delta}}-\sum_{n=1,2,3}^{\infty}\left(\frac{4j}{\gamma^2}\right)\cos n\pi\cos\frac{2\pi ny}{w}\,\epsilon^{-\beta x}\right] \qquad (7)$$

where

$$\beta^2\equiv\alpha\left[\left(\frac{2\pi n}{w}\right)^2+j\,\frac{2}{\delta^2}\right]$$

$$\gamma^2\equiv\left(\frac{2\pi n\delta}{w}\right)^2+j2$$

The first term of equation 7 is the field distribution at some distance into the tooth, while the second term accounts for the redistribution which occurs just beneath the surface. This solution describes the behavior to be expected, i.e., the magnetic flux tends to crowd to the outside surfaces of the tooth.

The power loss intensity may be obtained as the real part of

$$P=\frac{1}{2}(j\omega\Phi)i \qquad (8)$$

where

$$\Phi=w\mu_0 H_0=wB_0$$

$$i=\int_{x=0}^{d}H_x\Big|_{y=\frac{w}{2}}dx$$

and peak values of the time-varying quantities are used. The result of evaluation 8 is

$$P=\frac{\omega^2 B_0^2 w^3 d}{24\rho}\left[\left(\frac{3\delta}{w}\right)\left(\frac{\sinh\dfrac{w}{\delta}-\sin\dfrac{w}{\delta}}{\cosh\dfrac{w}{\delta}-\cos\dfrac{w}{\delta}}\right)-\frac{24\delta^3}{\alpha^{1/2}w^3 d}\sum_{n=1,2,3}^{\infty}\frac{\gamma_r\alpha_r^2-\gamma_i\alpha_i^2}{(\gamma_r^2+\gamma_i^2)(\alpha_r^4+\alpha_i^4)}\right] \qquad (9)$$

where

$$\gamma^2\equiv\alpha_r^2+j\alpha_i^2$$

$$\gamma\equiv\gamma_r+j\gamma_i$$

The coefficient of equation 9 may be regarded as the loss which would occur if the currents were resistance-limited. The first term accounts for the redistribution of axial flux at some distance into the tooth, and the second term is a result of the reorientation just beneath the surface. Numerical evaluation of equation 9 indicates that skin effect is of secondary importance for a tooth tip to depth of penetration ratio w/δ of less than about 4. The ratio of w/δ for large turbine generators is generally less than 4; hence, it may be concluded that skin effect does not have a major part in determining tooth loss. Equation 9 was derived on the basis of uniform axial flux. Since the axial flux decreases approximately

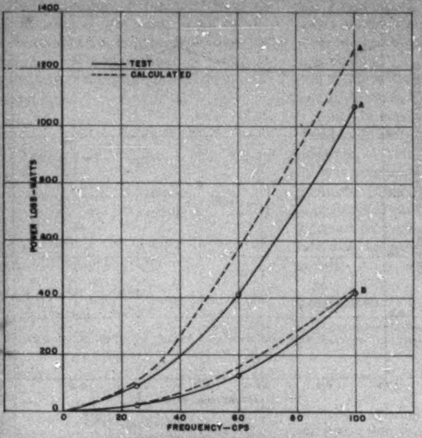

Fig. 7. Comparison of test and calculated losses in model with flux normal to laminations

Curve A—Sample, 4 by 1.5 inches
Curve B—Two samples, 4 by 0.75 by 1 inch
Normal flux density = 45 kilolines per square inch

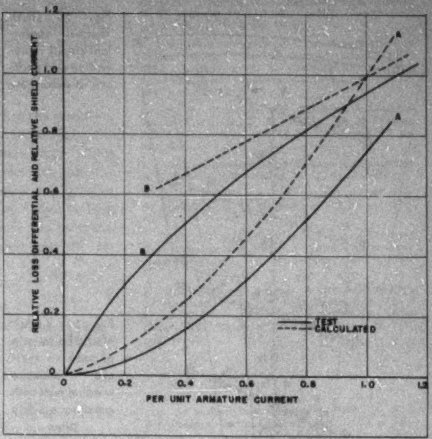

Fig. 9. Results of tests on generator with temporary copper shield

Curve A—Relative difference in stray load loss with and without flange shields
Curve B—Relative flange shield current

uniformly with depth into the package, the first term should be reduced by a factor of three.

Tests were run to evaluate loss with flux perpendicular to the laminations. First the losses in a stack of laminations 4 by 1.5 inches stacked 1 inch high were measured at varying inductions at different frequencies. The loss in two packages 4 by 0.75 inch stacked 1 inch high were also measured under identical conditions. The loss in these samples and a comparison with the losses evaluated by equation 9 are shown in Fig. 7. These data illustrate the effect of split teeth as well as confirm the method of calculation. Generator end tooth losses were computed by applying equation 9, modified to account for axial distribution, to successive radial increments of the tooth for which the axial field was nearly constant. End finger losses were calculated on the basis of resistance-limited currents.

Effect of Split End Teeth

As was mentioned previously, end tooth losses and temperature rise have been reduced significantly by the introduction of split end teeth. The end tooth is simply slotted, effectively laminating the tooth to eddy currents flowing parallel to the core laminations. Inspection of equation 9 indicates that the loss intensity with resistance-limited currents varies as the cube of tooth width. It would be expected, therefore, that placing one slot in a given tooth would reduce the loss by a factor of 4. The reduction in skin effect tends to offset part of this gain, however.

Fig. 8. Temporary copper shield mounted on stator core flange

STATOR CORE FLANGE LOSS

The dimensions of the stator core flanges of large turbine generators are such that pronounced skin effect occurs, i.e., the dimensions of the flange are large in comparison with the depth of penetration. Under this condition, the flange will act as a shield and will prevent end leakage flux from penetrating the body of the flange and entering the back iron.

In the electrolytic tank, therefore, the nonmagnetic flange was represented as a conductor having zero resistance. The flange current distribution, both radial and peripheral, is obtained directly from the potential distribution in the tank. The flange power loss was computed from this current distribution and the effective flange resistance based on the material resistivity and the known depth of penetration.

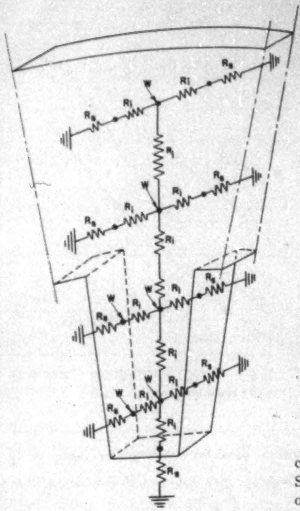

Fig. 10 (left). Thermal equivalent circuit representing end package of stator core

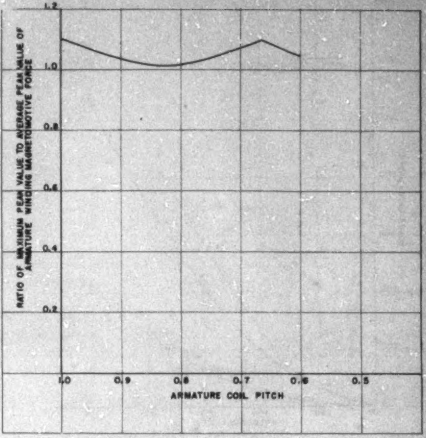

Fig. 11 (right). Variation in ratio of peak to average armature winding mmf with armature winding pitch

Because the nonmagnetic steel flange acts as a shield, the eddy-current loss can be reduced by substituting a material of lower electrical resistivity, or by covering the flange with a highly conducting shield. With constant current flowing in the flange or in the shield, the loss will vary approximately as the square root of the electrical resistivity because of the changing depth of penetration. This theory has been tested by tests on a production generator with a temporary copper shield, or amortisseur winding, located over both core flanges. This temporary shield in place on the flange is shown in Fig. 8.

The generator was tested with the shield in place and, again, with the shield removed. In Fig. 9 is shown a comparison of the relative difference in the stray load loss with and without the shield with the calculated difference in loss. The flange loss is a relatively small part of the total generator input under these conditions, but the comparison of test and calculated results is as close as can be expected.

The shield current was measured by a current transformer located on one of the radial straps. A comparison of test and calculated shield current during short circuit operation is also shown in Fig. 9. The calculated curve does not pass through zero load because of the method of accounting for retaining ring saturation.

Studies were also made of the losses in cast-iron and magnetic steel flanges. Since these do not correspond to surfaces of infinite permeability or zero resistance, it was necessary to represent the surfaces in the electrolytic tank by a network of resistances simulating magnetic conditions in the skin. The losses were found to be larger than in either the nonmagnetic steel or shielded flanges.

The flange losses can be reduced by the use of either a very high resistance or laminated magnetic shield. A magnetic shield of this type must be made from a material of very high resistance or properly laminated so that it is capable of carrying the end flux without large losses being induced in the shield itself. An additional factor of some importance is the effect of the flange or core shield on the magnetic flux distribution in the vicinity of the armature end turns and the resulting armature winding copper loss.

END IRON TEMPERATURE RISE

End tooth temperatures have been calculated using the thermal equivalent circuit, shown in Fig. 10, to represent the end package of laminations. This circuit is based on the usual approximations for 3-dimensional heat-flow problems. The tooth was represented by two nodes, with the appropriate tooth losses injected as equivalent current inputs. The iron thermal resistances are based on the core dimensions and the thermal resistivities of the core material. The surface resistances are based on the surface areas and the surface heat transfer coefficients calculated from known velocities of the cooling medium. The end finger losses are injected at the end surface nodal points.

Comparisons of test and calculated average end tooth tip temperature rises for a range of load conditions and at varying hydrogen pressures are shown in Fig. 3. The test values shown are the average of six thermocouples attached to the outside lamination at the tips of six teeth. The tests were run in the Moss Landing steam plant of the Pacific Gas and Electric Company on units nos. 2 and 5. These units are exact duplicates except that no. 5 has split end teeth. Calculated values shown are based on the methods of calculation outlined in the preceding sections.

EFFECT OF ARMATURE WINDING PITCH

It has been observed on many machines that the end teeth at or near the intersections of phase belts show the highest temperature. It will be shown that this behavior is caused by the variation of the armature winding mmf or by the harmonics of the armature reaction.

The armature winding mmf for a 3-phase generator during balanced operation can be written as

$$F=\frac{4}{\pi}A_{sw}\left(\cos(\omega t-\theta)+\frac{1}{5}\frac{k_{p5}k_{d5}}{k_{p1}k_{d1}}\cos(\omega t+5\theta)+\frac{1}{7}\frac{k_{p7}k_{d7}}{k_{p1}k_{d1}}\cos(\omega t-7\theta)+\ldots\right) \tag{10}$$

where the peripheral angle is measured from the center of a phase belt. Thus, the winding mmf consists of a fundamental sinusoidal term plus harmonics of the fundamental, the magnitudes of the harmonics depending on the winding geometry.

The magnitude of the total mmf at the location of the peak value of the fundamental term may be determined by setting $\omega t=\theta$ in this equation, which is equivalent to riding around on the fundamental term.

Then

$$F'=\frac{4}{\pi}A_{sw}\left[1+\left(\frac{1}{5}\frac{k_{p5}k_{d5}}{k_{p1}k_{d1}}+\frac{1}{7}\frac{k_{p7}k_{d7}}{k_{p1}k_{d1}}\right)\cos 6\theta+\ldots\right]$$

The ratio of the change to the peak value of the fundamental is

$$\frac{\Delta F}{F'}=\left(\frac{1}{5}\frac{k_{p5}k_{d5}}{k_{p1}k_{d1}}+\frac{1}{7}\frac{k_{p7}k_{d7}}{k_{p1}k_{d1}}\right)\cos 6\theta+\ldots \qquad (11)$$

It can be shown by direct evaluation that equation 11 has equal maximum values at the intersections of phase belts in the top and bottom layers in the armature winding. A plot of the ratio of the mmf acting at these points to the average mmf is shown in Fig. 11.

It may be concluded that the variation of end tooth temperature is caused by the variation of the armature mmf. This effect is exaggerated by the fact that the harmonic permeance paths are shorter than for the fundamental. Fig. 11 then indicates only qualitatively the temperature rise variations which may be expected.

References

1. Underexcited Operation of Large Turbine Generators on Pacific Gas and Electric Company's System, **V. F. Estcourt, C. H. Holley, W. R. Johnson, P. H. Light.** *AIEE Transactions*, vol. 72, pt. III, 1953, pp. 16–22.

2. Progress in the Design and Application of Large Steam Turbine-Driven Generators, **C. E. Kilbourne, J. B. McClure.** *Proceedings*, American Power Conference, Chicago, Ill., vol. 15, 1953, pp. 358–74.

3. Direct Cooling of Turbine-Generator Field Windings, **C. H. Holley, H. D. Taylor.** *AIEE Transactions*, vol. 73, pt. III, June 1954, pp. 542–50.

4. Ventilation of Inner-Cooled Generators, **R. A. Baudry, P. R. Heller.** *Ibid.*, pp. 500–08.

5. A New Fully Supercharged Generator, **S. Beckwith, L. T. Rosenberg.** *Ibid.*, pp. 477–83.

6. New Developments in Armature Winding Arrangement for Large Turbine Generators, **Dean Harrington, J. E. McElligott.** *Ibid.*, pp. 582–87.

7. Eddy Current Losses in the Stator Ends of Machines of Large Pole Pitch, and Means of Reducing These Losses, **H. dePistoys.** *Révue Génerale de l'Éléctricité*, Paris, France, vol. 21, 1927, pp. 215–23.

◆

Discussion

Richard T. Smith (General Electric Company, West Lynn, Mass.): Mr. Winchester has made a valuable contribution to the study of end losses through a judicious combination of theoretical work and model testing. This approach seems to be the one most appropriate, since direct measurement of generator end losses would be exceedingly difficult to carry out. The attendant problem of end temperature rises can be resolved satisfactorily by temperature measurements in the end region under various load conditions. My company has carried out this work with the help of a full load test base capable of loading the machine under test up to 18,750 kva at any power factor between zero lag and zero lead.

Tests conducted on this base during the past few years have proved conclusively the efficacy of nonmagnetic retaining rings in reducing end temperature rises during leading power-factor operation. In addition, valuable data have been obtained relative to the effects upon temperature rises of changes in materials and geometry of the end region structure.

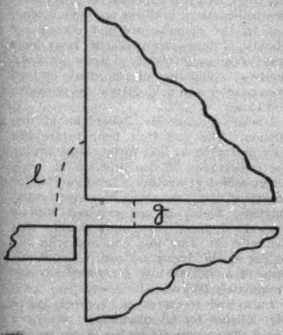

Fig. 12. End leakage flux path

That end losses may be expected to increase with increasing air gap lengths, as are being called forth by design innovations, may be shown qualitatively by reference to Fig. 12. Roughly, $B_l=(g/l)B_g$; thus, for a given per-cent increase in g, there is a somewhat smaller per-cent increase in l, thereby increasing the leakage density B_l for a given B_g.

The effect of field current in causing losses in the end region may be explained as follows: At rated load and lagging power factor the magnitude of the field mmf is sufficient to produce saturation of the magnetic retaining rings, which are then paths of relatively high reluctance, so far as the course taken by armature leakage flux is concerned. In addition, the mmf of the field end turns opposes that of the armature. As the load power factor passes through unity and thence into the leading region, the field current steadily decreases, causing the retaining rings to desaturate. As the retaining rings regain their full magnetic properties, the reluctance of the path of armature leakage flux decreases and the mmf of the field end windings is shielded from the armature. Thus the armature leakage flux increases and is accompanied by rising losses. If nonmagnetic retaining rings are used, or if the magnetic retaining rings remain saturated even at leading power factors, the resultant mmf effective in producing end loss again increases as the power factor passes into the leading region, because of the change in phase relation between the armature and field mmf, so that the losses also increase.

In addition to the work of de Pistoys (ref. 7 of the paper), some of the other contributors to the literature in this field are given in the following references.

References

1. Methods for Computing the Eddy Current Losses in Non-Magnetic Stator Flanges of Large Turbine Generators, **L. Dreyfus.** *Teknisk Tidskrift*, Stockholm, Sweden, Sept. 1932, p. 120.

2. Das Stirnstreufeld der Turbogeneratoren und die Stirnraumverluste, **R. Pohl.** *A. E. G. Mitteilungen*, Berlin, Germany, Sept. 1926, p. 326.

3. Supplementary Losses in Turbogenerators, **J. Kucera.** *CIGRE*, Paris, France, vol. 4, 1932, p. 293.

4. Frontal Stray Fields and Additional Losses in Turbogrnerators, **G. Kohler.** *Siemens-Zeitschrift*, Berlin, Germany, Dec. 1926, p. 605.

5. Recent Developments in Turbogenerators, **J. Kuyser.** *Journal*, Institution of Electrical Engineers, London, England, vol. 67, 1929, p. 108.

6. Iron Losses in Turbine Generators, **C. M. Laffoon, J. F. Calvert.** *AIEE Transactions*, vol. 48, July 1929, pp. 856–72.

7. Additional Losses of Synchronous Machines, **C. M. Laffoon, J. F. Calvert.** *Ibid.*, vol. 46, Feb. 1927, pp. 84–100.

8. Eddy Current Losses in a Conducting Plane Excited by an Alternating Current Flowing Parallel to It, **A. Mandl.** *Elektrotechnik und Maschinenbau*, Vienna, Austria, vol. 46, 1928, p. 37.

9. La Dispersion Magnetique de Conducteurs Paralleles Places Entre des Scrans de Permeabilite Infinie, **J. Kucera.** *Revue Generale de l'Electricite*, Paris, France, vol. 43, 1938, p. 355.

10. Progress in the Design and Construction of Turbine Alternators in Germany, **R. Pohl.** *Elektrotechnische Zeitschrift*, Berlin, Germany, vol. 44, 1924, pp. 729, 759.

11. Analysis of Additional Losses, **R. Pohl.** *Ibid.*, vol. 32, 1925, p. 1,182.

12. Additional Losses in Synchronous Machines and Their Measurements, **Dr. Reinhold Rudenberg.** *Ibid.*, vol. 14, 1923, pp. 37, 59.

13. The Diagnosing of Trouble in Electrical Machines, **M. Walker.** Oxford University Press, London, England, 1921, p. 99.

E. I. Pollard (Elliott Company, Ridgway, Pa.): Fig. 13 illustrates the typical construction used by my company at the ends of the stator core on turbine generators and other large synchronous machines. The fingers supporting the ends of the stator teeth are made from nonmagnetic steel bars. The fingers are in turn supported by clamping plates of magnetic steel. Magnetic steel is used in the rotor retaining rings of turbine generators. Narrow radial slots are punched in the teeth in the packages of laminations at the ends of the core, thus dividing the width of the tooth in two from the standpoint of the amount of end fringing

Table I. Maximum Temperature Rises

Ampere Conductors per Inch	Tooth Tip Rise	End Finger Rise	Clamping Plate Rise
1,020	36	25	52
590	21.5	17.5	25.5

flux linked by each section of the tooth, in the same manner as described in Mr. Winchester's paper. Fig. 13 shows a 7,500-kw turbine generator; the photograph was taken in 1946, when this construction was made our standard. Prior to this it was used by another manufacturer.

We tested two hydrogen-cooled 20-megawatt preferred standard turbine generators in 1953. To obtain sufficient kilovars for full load overexcited at zero power factor on one machine, the other was operated underexcited at zero power factor at practically zero field current in air. Thermocouples were placed on the tooth tips at the ends of the teeth, on the tips of the end fingers, and at the bore of the end clamping plate. Temperature tests were made at 0 power factor underexcited at two loads; at about zero field corresponding to 1,020-ampere conductors per inch of mean air gap periphery and at a lesser load corresponding to 590-ampere conductors per inch. Maximum temperature rises were as shown in Table I.

Since the first test was made at about zero field in air, these temperature rises are quite moderate. The tests indicate crudely what rises might be expected as the armature ampere-turn loading is increased as would be the case with direct cooling, remembering that other design changes such as longer air gaps associated with direct cooling operate to increase the amount of flux fringing into the ends of the teeth and hence their temperature rise. However, it is obvious that by dividing the end teeth into more than two sections by using more than one slot per tooth, the end tooth tip temperature can be controlled for machines of any size and loading.

After correlating these tests with a similar one made on a smaller machine, it became apparent to us that the temperature rise of the magnetic steel clamping plate would become excessive at some rating and current loading beyond our present experience, and we concluded that a copper magnetic shield over the outer surface of the clamping plate would be the most practical solution. Mr. Winchester's account of the use of a copper magnetic shield on the clamping plate is therefore most interesting to me. However, I fail to see the need for making the clamping plate of nonmagnetic steel when it is sheathed with copper, particularly when the core laminations are made of grain-oriented steel. It would be of interest if the author would report the kilowatt gain in load loss on short-circuit test realized by the use of this copper shield at full load current.

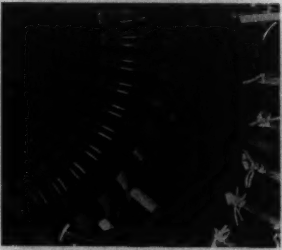
Fig. 13. Typical construction used at ends of stator core

The subject of stray losses in rotating machinery is a most interesting one. Mr. Winchester is to be congratulated for this excellent paper, which contributes to our quantitative knowledge of several of the sources of these losses.

Lee A. Kilgore (Westinghouse Electric Corporation, East Pittsburgh, Pa.): The author is to be congratulated on a rather thorough analysis of end zone losses in a large generator. I went through similar calculations with less mathematics 22 years ago and arrived at the same conclusions regarding split teeth in the end package; and such split teeth have been used on large water-wheel generators built by my company since that time and have been employed on the inner-cooled turbine generators where their use is absolutely essential.

I arrived at a somewhat different conclusion regarding end flanges or end plates. The author concludes a copper shield is best and that a nonmagnetic steel is better than magnetic. We have found that a silicon iron plate gives very low loss although a laminated shield which can handle the end zone flux is the ideal answer. With either the copper shield or the nonmagnetic steel end plate extremely high currents flow on the inner edge. The author says a small fraction of the end winding current, but the end winding current may be 50,000 amperes. It would be interesting to know what current Mr. Winchester did find flowing in the inner edge of the core flange. Even 10 per cent of end winding current in the bottom 2 inches of this plate might give over 100 watts per cubic inch and quite high temperatures. With a heavy continuous copper plate suitably shaped, the flux may be crowded out of the end plate and in spite of tremendous currents on the inner edge the temperatures would not be excessive. These copper shields have been used for a number of years by the ACEC Company of Belgium. However, a properly designed laminated iron shield can take care of this end zone flux with a minimum loss and would seem the ideal answer. The author indicates the tested values of surface temperature on the ends of the teeth, Fig. 3. The equivalent thermal circuit, Fig. 10, indicates at least an approximate method of determining the average if not the hottest temperature of the teeth. It would seem that these internal temperatures should be considerably higher than the surface temperature and it would be interesting if the author can give such figures for the full kva under excited range for the conventional construction.

G. W. Staats (Allis-Chalmers Manufacturing Company, Milwaukee, Wis.): Our company has had very favorable experience with flux traps of silicon steel, wound around the stator coil ends so as to form circumferentially laminated rings. Use of these rings in a fully supercharged generator described last year[1,2] has aided in keeping the temperature rise of the disk spring holding the individual tooth finger plates, as measured by thermocouples, down to 22 degrees centigrade at full load in 5 pounds per square inch hydrogen pressure on a machine designed for operation at 30 pounds per square inch hydrogen pressure. These tests have been described in a current paper.[3]

The author's attention is directed to a paper in the British literature[4] which discusses stray loss in some detail, paying particular attention to the end region. The paper contains a bibliography of 25 references, of which perhaps six are directly concerned with stray losses in the end region. The spirited discussion of this article is also worth reading.

REFERENCES

1. See reference 5 of the paper.

2. ADDITIONAL DESIGN FEATURES OF THE FULLY SUPERCHARGED GENERATOR, B. M. Koetting, G. W. Staats. *AIEE Transactions*, vol. 73, pt. III, June 1954, pp. 484–86.

3. TEST REPORT ON A FULLY SUPERCHARGED GENERATOR, Sterling Beckwith, B. M. Koetting L. T. Rosenberg, G. W. Staats. *AIEE Transactions*, vol. 74, pt. III, Apr. 1955, pp. 56–59.

4. STRAY LOSSES IN SYNCHRONOUS ELECTRICAL MACHINERY, P. Richardson. *Journal*, Institution of Electrical Engineers, London, England, vol. 83, 1945, p. 291.

R. L. Winchester: Mr. Smith's comments add significantly to the understanding of several of the important factors of the problem. A considerable amount of very practical data have been obtained on the full load test base of the Medium Steam Turbine Department at Lynn, Mass. The availability of such equipment makes possible a thorough full-scale evaluation of design innovations over the entire range of load conditions.

The use of nonmagnetic retaining rings results in a considerable reduction in end losses and temperature rise. All 3,600-rpm generators, 50,000 kw and larger, have been built by my company with magnetic retaining rings, and it is expected that this practice will continue until the problems attendant to the manufacture and control of quality of large, nonmagnetic rings have been adequately solved. I agree with Mr. Smith's explanation of the effect of load power factor and field current on generator end losses.

I wish to thank Mr. Pollard for his discussion. The end iron temperature rise data presented by him further substantiate the importance of the problem in large, direct-cooled generators. In answer to his questions, it is our conclusion that a nonmagnetic flange is not required with a properly designed conducting shield. The reduction in stray loss obtained with the copper shield during no-load, short-circuit tests of a 125,000-kva generator was approximately 25 kw.

I also wish to express my appreciation to Mr. Kilgore for his discussion. We have found that a periodic review of our knowledge of fundamental problems is desirable in order to maintain a quantitative understanding of these problems through the years of design improvements.

We are in substantial agreement with Mr. Kilgore's statement that a magnetic shield would seem to be the ideal answer to the problem of flange loss and temperature rise. However, a number of factors influence the choice of the type of shielding to be used. Among these are: 1. the co-ordinated mechanical design of stator frame flange, flange shield, and armature end windings and winding supports; 2. the design of a magnetic shield to minimize loss in the shield itself; and 3. the effect of the flange shield on the magnetic field near the armature end turns and the resulting extra loss in the end winding copper. Either type of shield could be used, but the conducting shield appears to us to be the better solution. We will continue our evaluation of the problem as we gain more experience with large, direct-cooled generators.

I have explored Mr. Kilgore's calculations on shield current and loss. Using Mr. Kilgore's figure of 5,000 amperes' shield current, we calculate a little less than one-third of the figure of 100 watts per cubic inch. Furthermore, if this loss is simply integrated to obtain total shield loss, adding in 50 per cent additional to account for return currents on the outer periphery, the total is found to be approximately 9 kw. This is quite low for the flange loss in a machine with a rating corresponding to Mr. Kilgore's example. This loss, dissipated over the entire shield area, would result in a very moderate temperature rise.

We have no recent operating experience with magnetic iron flanges in large, modern, hydrogen-cooled generators. Since about 1924 all of our large machines have been built with nonmagnetic stator frame flanges. Since that time we have had very satisfactory operating experience with regard to end heating in these machines.

It is well known that the internal stator tooth temperatures must be higher than the surface temperatures, since the heat is generated internally and a temperature gradient must exist in order for the heat to flow to the surface. We have examined the internal end tooth temperatures in great detail and, in the cases which we have studied, have found that, although the internal temperatures are somewhat higher, the operating margins are more than adequate for the expected service.

Finally, I would like to thank Mr. Staats for his comments. Mr. Staats and his associates are to be congratulated for the completion and successful operation of their supercharged generator.

In closing, it should be noted that a general solution to the end loss problem applicable to the machines of several manufacturers is simply not possible because of the close relationship with the details of design and construction. It is possible, however, to obtain an understanding of the losses in a given design. Through the work described in this paper and continuing efforts, we have obtained a quantitative understanding of the magnitude and distribution of end losses in our generators.

Correlation of Temperature Measurements on D-C Armatures

D. D. GERBETZ
ASSOCIATE MEMBER AIEE

J. S. EWING
MEMBER AIEE

Synopsis: The significance of the usual temperature measurements made on d-c armatures is somewhat vague, and the amount of published data on the subject is limited. This paper presents the results of a large number of laboratory tests showing the correlation among several different methods used for measuring temperatures on d-c armatures. It is believed that temperature measurements made with embedded thermocouples, read through slip rings, greatly enhance the validity of the correlations reported in this paper. Based on the data presented, it is concluded that temperature measurements made by careful resistance methods are more reliable and more nearly approximate the hot-spot values, than those made by thermometers. In the interest of brevity the scope is limited to the measurement of temperatures on the armature of d-c machines.

IT WAS evident from the number of discussions of two previously published papers[1,2] that some of the points under consideration were controversial and that additional experimental data would be most helpful toward a better understanding of the problem involved. The purpose of these papers was as follows:

1. To propose a revision of Table I of the American Standards Association Standard for limiting observable temperature rise.[3]

2. To present test data correlating thermometer and resistance rise to hot spot temperature.

3. To introduce the method of measuring temperature by resistance as a recognized standard.

Shortly after the presentation of these papers, the authors were afforded the opportunity to make a rather exhaustive study of temperature measurements on five experimental motors. The motors involved were classified as General Industrial Motors, drip-proof enclosed, continuous duty, 60 degrees centigrade rise using class-*B* insulation. These motors were self-ventilated with the fan exhausting out the end opposite the commutator. With regard to temperature measurements, these motors were felt to be representative of the present day general-purpose d-c motors. The nominal horsepower and speed rating for the motors involved are shown in Table I.

Experimental Procedure

A trial setup was made in the laboratory with thermocouples submerged in an oil bath and connected through a set of slip rings to an indicating instrument. After several modifications of the brush assembly and the junction location, it was found possible to read temperatures with a 1-per-cent (%) accuracy for a wide speed range of the slip ring assembly. With this experience as background, it was concluded to install embedded thermocouples along the armature conductor for all five sample motors. The location of these thermocouples are indicated in Fig. 1. The thermocouple leads were brought out through an axial hole in the end of the shaft to a slip ring assembly which could be directly connected to an indicating instrument. A photograph of the slip ring assembly connected to one of the sample motors is shown in Fig. 2.

The technique of making armature resistance measurements for the purposes of obtaining temperature rise was completely reviewed. After a number of trial runs had been made, a procedure was evolved

Table I. Ratings of Sample Motors

Horsepower	Rpm	Volts
40	1,750	230
60	1,750	230
100	1,750	230
150	1,750	230
200	1,150	230

Paper 55-106, recommended by the AIEE Rotating Machinery Committee and approved by the AIEE Committee on Technical Operations for presentation at the AIEE Winter General Meeting, New York, N. Y., January 31–February 4, 1955. Manuscript submitted October 20, 1954; made available for printing November 22, 1954.

D. D. Gerbetz and J. S. Ewing are with the Reliance Electric & Engineering Company, Cleveland, Ohio.

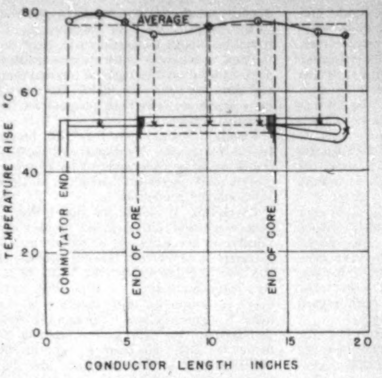

Fig. 1 (left). Location of armature thermocouples and typical temperature distribution

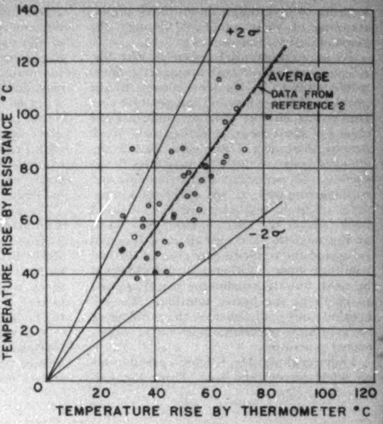

Fig. 3 (right). Resistance versus thermometer

such that measurements could be made quickly and, if necessary, repeated with a high degree of accuracy. For a description of the precautions and procedures used in making resistance measurements see the Appendix. It should be pointed out that procedures and technique outlined in the Appendix are not original with the authors, but are listed for the purpose of emphasizing the necessity of following an organized, yet practical, procedure when making resistance measurement on low-resistance armatures if accurate results are desired.

With regard to thermometer measurements, the procedure employed is the one outlined in the AIEE test code for d-c machines standard.[4]

To accumulate a large mass of data the five motors listed in Table I were subjected to a series of heat runs. Besides rated load and speed, heat runs were made on these motors at four different speeds below base speed, and at each speed several runs were made with different load settings. It would be well to emphasize that on each heat run, armature temperatures were measured by 1. A series of thermocouples located along an armature conductor; 2. Resistance measurements of the armature circuit between brushes; and 3. Thermometers located on coil heads.

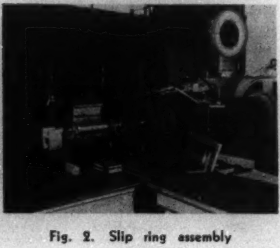

Fig. 2. Slip ring assembly

Presentation of Data

Figs. 3 through 6 show graphically the correlation of the three different types of temperature rises obtained from test data, namely:

1. Resistance versus thermometer, Fig. 3.
2. Hot spot versus thermometer, Fig. 4.
3. Hot spot versus resistance, Fig. 5.
4. Resistance versus average by thermocouples, Fig. 6.

In conjunction with the plotting of test results, it was assumed that each type of temperature measurement bore a direct relationship to the other method of measurement indicated on the graph. For example, a fixed ratio exists between the rise by resistance to the rise by thermometer. These ratios were calculated for each test and averaged. The average lines, or average ratios, are indicated on each graph. Also, the standard deviation factor σ, or rms error, was calculated for each set of data and the lines representing the two σ values are plotted on these graphs. These lines tend to bracket 95.44% of the possible test points. The average ratio and the rms error values corresponding to Figs. 3 through 6 are tabulated in Table II.

Results

The correlation of rise by resistance to thermometer indicated in Fig. 3 has several significant aspects. First, the average line shows excellent agreement with that published in Fig. 1 of reference 2. This is indicated by the dotted line on Fig. 2. It was upon that data that the recent revisions of Table I of reference 3 were based. The data of this paper therefore add additional support to the validity of this latest revision, which permits rises to be evaluated from resistance measurements as an optional method.

Secondly, it is rather obvious that the correlation from individual measurements could be in considerable error, as indicated by the dispersion of the test points and the values of the standard deviation factor σ. The reason for this scattering of test points results, for the most part, from the errors associated with thermometer measurements. This point will be made more evident after the remaining figures are discussed.

Fig. 4 shows the relationship between hot spot and thermometer. It is believed that this correlation is a better index than any previously published of hot spot based on thermometers. The explanation lies in the method of measuring hot-spot temperatures. It was felt that the number of thermocouples located in the armature and the measurement of temperature while the armature was rotating greatly improved the accuracy of measurement. Again, the dispersion of test points is believed to be partly a result of the inaccuracies of thermometer measurements.

The correlation between hot spot and resistance is shown in Fig. 5. These data are also felt to represent better the correlation between hot spot and resistance than previously published data because of thermocouple measurements and also be-

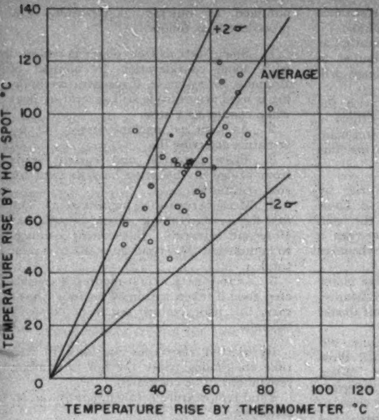

Fig. 4 (left). Hot-spot versus thermometer

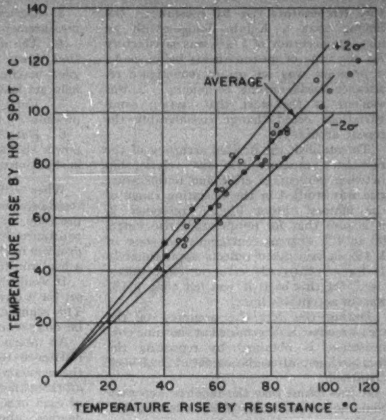

Fig. 5 (right). Hot-spot versus resistance

cause of the pains required in taking the resistance measurements. It is evident also that the dispersion of the individual test point has been greatly reduced over those charts where thermometers were indicated. A further examination of Fig. 5 substantiates the statement made by previous discussers that resistance measurements more nearly approximate the hot spot than do thermometers measurements, and that therefore more weight should be given to resistance measurements.

In Fig. 6, the rise by resistance is shown plotted against the average rise of the conductor of calculated from the thermocouple measurements. The average rise was calculated by plotting the thermocouple temperatures against the developed length of the conductors, as was done in Fig. 1, calculating the area underneath the temperature line, then dividing the area by the abscissa of the diagram. The correlation indicated in this figure is excellent; the rise as measured by resistance equals the average rise of the conductors, which is as it should be. The relatively small dispersion of the test points, as compared with previous test results, must be considered good.

Table II. Correlation of Temperature Measurement

Figure No.	Average Ratio	Rms Error, %
3	$\frac{\text{TR* by resistance}}{\text{TR by thermometer}} = 1.44$	±22.9
4	$\frac{\text{TR by hot spot}}{\text{TR by thermometer}} = 1.53$	±22.5
5	$\frac{\text{TR by hot spot}}{\text{TR by resistance}} = 1.10$	± 6.62
6	$\frac{\text{TR by resistance}}{\text{Average TR based on thermocouples}} = 1.00$	± 4.1

* Temperature rise.

Conclusions

1. Additional data correlating indirect temperature measurements with hot-spot temperatures and correlation of the various methods of indirect measurements among themselves have been presented in Figs. 3 through 6.

2. An indication of the range of possible errors for an individual measurement is indicated in Table II.

3. The correlation between resistance and thermometer shows excellent correspondence with that published in reference 2 and also with the revised Table I of reference 3.

4. The use of distributed thermocouples measured while the armature is rotating greatly enhance the validity of the data reported here over that previously published.

5. Based on the data presented, rise by resistance measurements can be made which show considerable improvement over those made by thermometers for the following reasons:

(a). The rise by resistance more nearly approximates the hot-spot temperatures as indicated by a comparison of Figs. 4 and 5.

(b). The accuracy of the measurement is strongly in favor of the rise by resistance. A comparison of Figs. 4, 5, and 6 will bear evidence to this fact.

6. Fig. 6 confirms the obvious conclusion, that the rise by resistance is a measure of the average conductor temperature throughout the machine.

Appendix. Procedures and Technique

Associated with an over-all program of temperature evaluation of d-c motors, a technique was developed to measure arma-

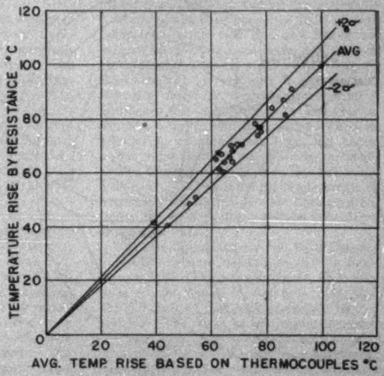

Fig. 6 (right). Resistance versus average from thermocouples

ture temperature rise by resistance. Believing that a Kelvin bridge with an absolute accuracy of 1/4% was satisfactory for the type of measurements being made, a program was set up to investigate resistance measurement technique. It was evident at the start that certain small variations could change considerably the repeat accuracy.

To establish the desired accuracy of the resistance measurement the relationship between percentage error and temperature rise was studied in the operating range of the motors. From Fig. 7, reference 2, it is seen that for temperature rise range, 60 to 100 degrees centigrade, an error of 1/4% in resistance reflects approximately 1 degree centigrade error in temperature rise. On this basis it was felt that 1/4% was an acceptable limit.

During the test the accuracy of the measurement is determined at the time cold resistance is obtained by repeating the measurement after the armature has been disturbed.

It was found that the required accuracy could be obtained only if the following precautions were taken:

1. Armature must be in the same position for hot and cold measurements.
2. Current and potential leads of the bridge must always be placed on the same commutator bars for hot and cold readings.
3. Bridge leads must be designed for surface contact.
4. Supply battery must have sufficient charge and capacity to maintain maximum sensitivity of the bridge galvanometer.

Immediately after a heat run is shut down, time, in addition to accuracy, is of the essence. It is very desirable to get a first resistance measurement within 40 seconds. This can be accomplished only if a well-organized procedure incorporating most of the following steps is followed.

1. The bridge must be adjusted prior to shut-down to read the approximate resistance expected.
2. Rapid stop should be done by dynamic or regenerative braking or other means.
3. Commutator bars used for resistance measurement should be clearly marked.
4. The use of two or more operators at shut down with the work distributed to gain maximum manpower efficiency will help get fast readings.
5. Until testers are familiar with the procedure a few trial runs will help them.
6. Data sheets, timer, bridge, and manpower should be organized before machine is shut down.

When calculating temperature rise by resistance it is very important to know precisely at what temperature the cold resistance is measured. This becomes a problem in the testing department whenever a heat run follows a check test.

It would be desirable to leave the motor set for a day before taking cold resistance. This is not always practical to do but should be done whenever possible.

An alternate method to determine cold resistance temperature is to install three thermometers on the coil surface. When all three thermometers are within 3 degrees of each other and none are more than 10 degrees above room temperature, the average reading is the value to be used for cold resistance. This limitation may vary according to the physical design and should be checked for individual cases.

The setup and procedure for measuring cold resistance are as follows:

1. Four holes are drilled in the commutator as shown in Fig. 7. Hole diameter to be such that fit will be snug with the plug fully inserted.
2. The bridge leads are plugged into the holes. For details of the plug and leads see Fig. 8.
3. Measure resistance and scribe a line on the motor shaft and bracket.
4. Remove leads, disturb armature, and reset to scribe line.
5. Replace leads and measure resistance.
6. Repeat the reading obtained in step 3 within 1/4%.

If the reading is not repeated, check items 1 to 4 listed under precautions.

Hot resistance is measured immediately after shutdown and first readings are obtained as quickly as possible. The procedure is as follows:

1. Start timer as time power is removed with some consideration to method of stopping, for example, if regenerative braking is used armature is still generating heat while coming to a stop.
2. As soon as machine stops, line up armature to scribe line.
3. Place potential and current leads from bridge in the same bars as used for cold resistance.
4. Measure resistance immediately. The first five or six readings should be taken at 10-second intervals. Subsequent readings to be taken at 20-second intervals to 6 min. total.
5. As to timing, a first reading is considered good if taken within 30 seconds; however, this may average out to be 40 to 45 seconds.

By plotting resistance rise back to zero time on semilog paper the hot or running resistance can be computed.

Total temperature is calculated by the relationship

$$T\text{ hot}=\frac{R\text{ hot}}{R\text{ cold}}\times(234.5+T\text{ cold})-234.5$$

Temperature rise is obtained by subtracting ambient temperature from the total temperature.

References

1. Temperature Rise Values for D-C Machines, AIEE Committee Report. *AIEE Transactions*, vol. 68, pt. I, 1949, pp. 206–18.

2. Temperature Rise Values for D-C Machines—II, AIEE Committee Report. *AIEE Transactions*, vol. 68, pt. II, 1949, pp. 1118–25.

3. Rotating Electrical Machinery *ASA C50-1943*. American Standards Association, New York, N. Y., 1943.

4. Test Code For Direct Current Machines. *AIEE Standard No. 501*, July 1941, pp. 6–9.

5. Temperature Limits and Measurements for Rating of D-C Machines, F. A. Compton, Jr. *AIEE Transactions* (*Electrical Engineering*), vol. 62, Dec. 1943, pp. 780–85.

6. Heating of a D-C Armature, Carl J. Fechheimer. *AIEE Transactions*, vol. 59, 1940, pp. 920–26.

7. Some Problems in the Standardization of Temperature Ratings of Fractional-Horsepower Motors, Cyril G. Veinott. *Ibid.*, pp. 1055–61.

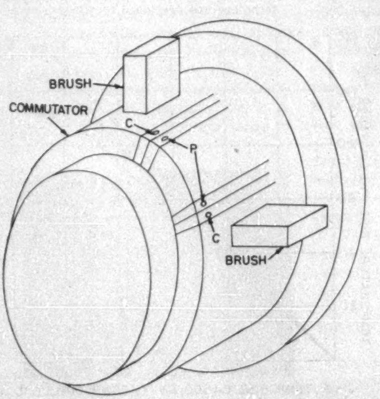

Fig. 7 (left). Commutator showing relative location of holes for current C and potential leads P from Kelvin bridge

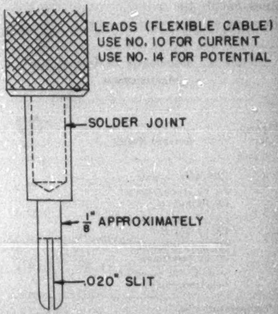

Fig. 8 (right). Typical plug for bridge leads

Discussion

E. H. Meyers (Westinghouse Electric Corporation, East Pittsburgh, Pa.): The problem of obtaining accurate readings of temperatures on machine parts has received considerable study in the last 15 years. The authors have done a fine job of developing a correlation of the results obtained by different methods of temperature measurement, and have justified the belief that consistent and accurate readings of temperature rises by the resistance measurement method can be obtained, provided sufficient care is taken.

However, it appears that the authors have also shown that, as desirable as the resistance measurement method is from the standpoint of accuracy, it is not very feasible for normal shop production testing. This is particularly true in the case of the manufacture of large machines where a given design might be built only once. For instance, it is doubtful that the production department would be receptive to the suggestion that the motor should sit for a day before taking a cold resistance or that holes should be drilled in certain commutator bars.

It appears doubtful that the importance of temperature rises on most commercial machines is great enough to justify the special methods and precautions listed by the authors. Most customers would not be willing to bear the resulting extra expense. In the case of temperature tests using thermometers it must be admitted that some of the thermometers will not give accurate values of temperature on the shutdown reading, but when the highest value of these temperatures is used from a large number of thermometers in similar locations, it is probable that the error would not be more than a very few degrees at the most. Considering the margin provided in accepted standards and the possible additional margin between the guarantees and the actual values on the machine shipped, this error becomes relatively unimportant. This is particularly true in large machines for special applications. For instance, rod mill drives may require exceptionally low-impact speed drops, tandem cold mills for steel require special speed regulations for the driving motors, blooming mill drives must have abnormal overload capacity; such requirements naturally result in low-temperature machines.

We hope that the authors' conclusions will not be interpreted to mean that the resistance method described is recommended for normal machine production tests. The methods appear to be an excellent laboratory procedure where unusual accuracy is justified, but should be limited to rather special tests.

E. C. Watson (Westinghouse Electric Corporation, Buffalo, N. Y.): The paper is a valuable contribution to the art. The authors state that the scattering of the test points is due to the errors associated with thermometer measurements. Was a series of experiments run on the same machine and under as near duplicate operating conditions as possible and, if so, what correspondence was obtained on these results? My experience has been that on such repetitive tests the thermometer measurements can be duplicated within a 2-degree-centigrade (C) rise when identical test procedures are followed. Does the rise by resistance follow a similar pattern?

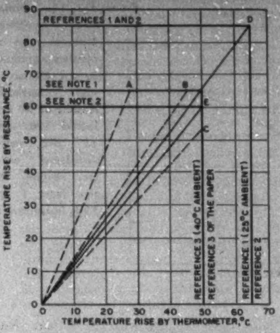

Fig. 9. Class-A machines continuous-rated

A—Maximum ratio from tests on 23 machines
B—Mean ratio from same tests
C—Minimum ratio from same tests
D—Proposed by AIEE Standards Co-ordinating Committee No. 4. Also standard for traction machines[1,2]
E—Proposed by AIEE Subcommittee on D-C Machines (ref. 1 of the paper)

Note 1. Limiting temperature rise by resistance proposed by AIEE Standards Coordinating Committee No. 4

Note 2. Limiting temperature rise by resistance proposed by AIEE Subcommittee on D-C Machines (ref. 1 of the paper)

M. A. Baker (General Electric Company, Erie, Pa.): The authors are to be congratulated on their fine paper. Their average ratio of rise by resistance to rise by thermometer correlates very well with the experience of my company in tests made on medium- and large-sized d-c machines over a number of years.

I should like to give some of the data presented to the Rotating Machinery Committee by my company in 1944. These data were originally presented to support the AIEE Committee No. 4 proposed addendum to ASA Standard C50 (ref. 3 of the paper) to increase the rise by resistance on both class-*A* and class-*B* insulated armatures and were again presented at the AIEE Summer General Meeting in 1949. While these data are not recorded in the *Transactions*, they will be found in the 1949 minutes of the D-C Machinery Subcommittee.

Fig. 9 shows the results of armature-heating data taken on 23 machines ranging from 3-kw at 1,200 rpm to 300-kw at 900 rpm with voltages ranging from 60 to 250. Both open machines with radial ventilation and axially ventilated dripproof machines were included. The ratio of rise by resistance to rise by thermometer varied over approximately the same range with both types of ventilation and enclosure. The maximum ratio of rise by resistance to rise by thermometer was 2.31 and the minimum ratio was 1.07. The amazing fact, however, is that the average of ratio of rise by resistance to rise by thermometer is 1.44, exactly the same as that determined by the authors.

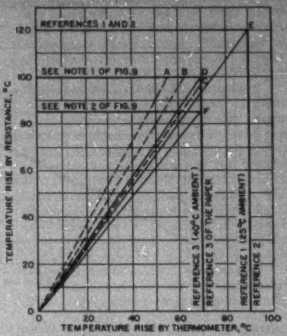

Fig. 10. Class-B machines continuous-rated

A—Maximum ratio from tests on 17 machines
B—Mean ratio from same tests
C—Minimum ratio from same tests
D—Proposed by AIEE Standards Co-ordinating Committee No. 4
E—Standard for traction machines[1,2]
F—Proposed by AIEE Subcommittee on D-C Machines (ref. 1 of the paper)

Similar data were taken on a number of class-*B* insulated d-c armatures, and on 17 heat runs made on machines ranging from 80 kw at 3,600 rpm to 5,000 horsepower at 100-rpm with voltages ranging from 220 to 600. Both the open and the enclosed types of machine were tested. These data were presented as Fig. 10. The maximum ratio of rise by resistance to rise by thermometer on these limited tests was 1.79 and the minimum 1.37. The average ratio of 1.57 is very close to the new ASA Standard C50 Table I (ref. 3 of the paper) and only slightly higher than that observed by the authors.

Many of the data presented in 1944 were taken from production tests and rise by resistance test techniques were not as well established then as they are today. Fig. 11 shows the rise by resistance to rise by thermometer ratio for d-c armatures from a number of tests made within the last year on dripproof motors and generators with axial ventilation ranging from 1 to 150 horsepower. To simplify the plotting on probability paper, the data were limited to 50 heat runs. Data which appeared erratic or questionable in any way were discarded entirely, so these results must be considered as selected data.

The minimum ratio of rise by resistance to rise by thermometer is 1.29 and the maximum is 1.79. The mean ratio of 1.48 is very close to the ratios in the new ASA C50 Table I and to the data presented by the authors. The ratios at one sigma deviation are 1.32 and 1.64 which represent an rms error of ±10.8%. It must be remembered, however, that these were selected data and

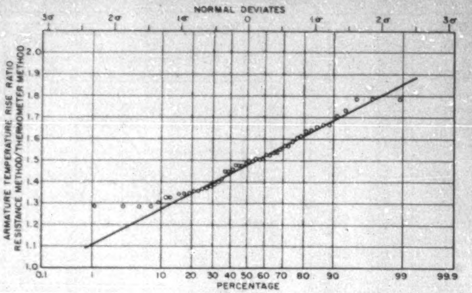

Fig. 11. Armature temperature rise ratio of resistance method to thermometer method. Results of 50 selected tests on 13 d-c self-ventilated motors ranging in size from 1 to 150 horsepower

greater variation would have been observed if all data had been used. The correlation, however, with data obtained 11 years ago and with that presented by the authors is remarkable.

REFERENCES

1. Rotating Electric Machinery on Railway Locomotives and Rail Cars and Trolley, Gasoline-Electric and Oil-Electric Coaches. *AIEE Standard No. 11*, Jan. 1943.

2. *Ibid., ASA Publication No. C35.1-1943*. American Standards Association, New York, N. Y., Jan. 1943.

3. General Principles Upon Which Temperature Limits are Based in the Rating of Electric Machines and Other Equipment. *AIEE Standard No. 1*, Feb. 1954.

M. L. Schmidt (General Electric Corporation, Fort Wayne, Ind.): The authors should be congratulated on the description of two excellent testing methods and on the proof in Fig. 6 that accurate data are obtained. It is inconceivable that there could be any significant bias or large errors in the measurement of temperature rise by resistance or the thermocouple measurements when two methods of measuring the average temperature have the 1-to-1 ratio and small dispersion shown in Fig. 6.

What I want to discuss, however, is not the test techniques or the test results but the presentation of the data. I have studied this subject of temperature measurement for many years and find that all authors, including myself, have made one of two assumptions in their statistical presentation. Some have assumed with the authors that the errors (in the statistical sense) are proportional to the temperature rise, while others have assumed that they are independent of the temperature rise. These two assumptions result in two sigma lines which diverge from the origin or which are parallel to the average line respectively.

Actually it is known that some of the errors, such as the error in taking readings and probably most of the instrument error, are independent of temperature rise and that other errors such as those due to variations in construction, ventilation, and loss distribution are proportional to temperature rise. Since some of the thermal resistances are not constant, some of the errors are probably a more complex function of temperature rise but it is unlikely that they are important over normal temperature ranges. If it is assumed that the error has two components, one independent of rise and the other proportional to rise, the equations for determining the statistical constants are

$$K\Sigma\frac{x^2}{\sigma_c{}^2+x^2\sigma_c{}^2}=\Sigma\frac{xy}{\sigma_v{}^2+x^2\sigma_v{}^2}$$

$$\Sigma(Kx-y)^2=N\sigma_c{}^2+\sigma_v{}^2\Sigma x^2$$

$$\Sigma x^2(Kx-y)^2=\sigma_c{}^2\Sigma x^2+\sigma_v{}^2\Sigma x^4$$

$$\sigma x=\sqrt{\sigma_c{}^2+x^2\sigma_v{}^2}$$

where

K = coefficient of average line $y=Kx$
σ_c = constant component of the standard deviation
σ_v = variable component of the standard deviation
σ_x = standard deviation at any point x
N = number of test points

Obviously an iterative method is the only practical method of solving the equations for K, σ_c and σ_v but in my experience the convergence is very rapid so that one iteration is all that is necessary. When this is true, the computation time is about three times that for the simpler assumptions mentioned earlier.

To show how this different approach affects the results, the proportionality factor for rise by resistance over rise by thermocouple is 0.932 instead of 0.929 and the rms error in per cent at 90 C hot spot rise is 3.66 instead of 4.94%. The first effect is negligible, being less than the probable error of the average, but the second reduces the spread of the two sigma limits from 19.8 to 14.6 C.

This is almost a limiting case, as Fig. 12 shows that the limit lines are almost parallel to the average line. Fig. 13 which is the average temperature rise by thermocouple plotted against hot-spot rise shows the slightly diverging limit lines which are obtained when the temperature-sensitive errors are approximately the same magnitude as the constant errors.

Although the sample size is too small (only five machines) to have the results mean much, there is at least an indication of the precision of the hot-spot readings in these data. The only readily recognizable sources of constant error in the thermocouple readings are tester and instrumental errors. Fig. 6 proves that there is negligible temperature-sensitive error with respect to the copper adjacent to the thermocouple, so let this unknown standard deviation be σ_{tc}. Then

$$\sigma_{HS}=\sigma_{TC}$$

and the constant portion of the average thermocouple deviation when compared to hot spot

$$\sigma_{CTC}=\sqrt{\frac{\sigma_{TC}{}^2}{8}+\sigma_{TC}{}^2}$$

For this data the value of σ_{HS} is 2 C which

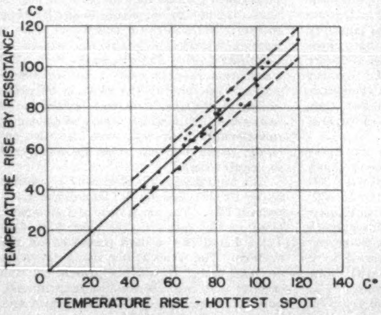

Fig. 12 (left). Temperature rise by resistance and hottest spot

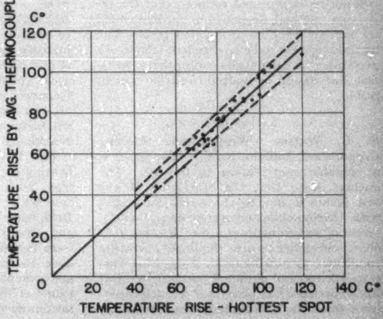

Fig. 13 (right). Temperature rise by thermocouple and hottest spot

is a little larger but quite comparable to the reported 1% calibration accuracy.

Although a comparison of rise by thermometer and rise by resistance was the primary reason for this work, the equations just shown could not be used for the thermometer data. The variations proportional to temperature were so wide and the number of points so small that σ_C^2 as calculated was negative, which is impossible. If we disregard the fact that thermometer rise must be zero when hot-spot rise is zero, and draw a line which best fits the points, it would indicate 19 degrees by thermometer when the hot spot is zero. This large apparent bias could occur because the low-temperature points were predominantly from one machine while the high-temperature points were from another machine. I should like to ask the authors if this is the case.

R. Lamborn (General Electric Company, Erie, Pa.): The authors are to be congratulated on their findings, which prove once more the superiority of the rise-by-resistance method of temperature measurement. I believe in this method. The design group with which I work has used it for more than 25 years; not as an alternative method, but as the best method for determining temperature rise. Possibly some may not be aware that the AIEE standard covering railway and other transportation equipment,[1] has specified the rise by resistance method since 1937. For the past 18 years the rise by thermometer method has had no official sanction in connection with the rating of this class of electric rotating equipment. Others also have found that when proper care is exercised, the rise by resistance method gives the designer more honest and consistent information than he ever obtained from thermometers.

I should like to enlarge upon one feature in the paper. The statement is made that by plotting resistance rise back to zero time on semilog paper the hot or running resistance can be computed. Since cooling curves are exponential in character, and since an exponential curve plots as a straight line on semilog paper, the inference might be made that in determining the so-called zero time temperature it is necessary only to lay a straight edge on the cooling curve points and read the intercept on the *Y*-axis.

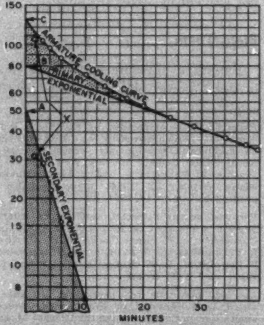

Fig. 14. Armature cooling curve analysis. Note how secondary exponential replot spots bad test point X and yields correct zero time rise C by adding intercepts A and B

Regrettably, the authors did not include a graph in their paper to show just how this worked out. In the case of transportation motors and generators, where the machines are forced somewhat harder than general purpose motors in terms of temperature rise and ventilation, the typical cooling curve is actually quite far from being a simple exponential. It seems to have two major components. The primary or longer time component has to do with the cooling rate of the armature core and windings as a unit, and upon this is superimposed the more rapid secondary exponential, probably in a large measure representing the equalization in temperature between the copper winding and the mass of the armature core.

It is of interest to note the characteristic shape of such a compound exponential when plotted on semilog paper (see Fig. 14). It is neither a straight line nor a composite of two straight lines. However, the difference between the compound exponential curve and the straight line representing the primary exponential will plot as a straight line on the same semilog paper. This fact and an appreciation of the basic concept of the relative values involved will frequently permit the engineer to discriminate between good and poor test data, and to estimate more accurately the true zero time temperature rise even though only one or two test cooling curve points may have been taken during the critical first few minutes after shutdown.

To some this will seem like a complicated procedure just to find the temperature of a motor winding. I believe, however, that to learn how to get the greatest possible performance from a given amount of material, designers will turn more and more toward this sort of approach to the problem.

I should like to ask Mr. Ewing what precautions were found necessary to obtain accurate running temperature readings from thermocouples operating through slip rings?

REFERENCE

1. GENERAL PRINCIPLES UPON WHICH TEMPERATURE LIMITS ARE BASED IN THE RATING OF ELECTRIC MACHINES AND OTHER EQUIPMENT. *AIEE Standard No. 1*, Feb. 1954, par. 1–11.

John Cybulski (Naval Research Laboratory, Washington, D. C.): The paper contains excellent procedures. It was not clear whether the temperature rise obtained by the thermometer method was gained by the subtraction of the ambient temperature from the reading or reflected some correction (in percentage or degree) by virtue of the fact that a thermometer was employed. It should be indicated in the paper that the hot-spot data were obtained by one of the thermocouples if this was the case. Was the thermocouple which provided the hot-spot data for the five machines located in a similar position in each, and did it consistently indicate the highest temperature?

Some statistical procedures were applied to experimental data obtained on five different horsepower rated machines. However, it is desirable to know the total number of heat tests taken and how many test points, identified for each machine, were used in the construction of Figs. 3, 4, 5, and 6. One would assume that the temperature rise data were selected equally from all the machines and employed for all the various temperature ratios taken. This does not appear to be the case if the number of points on Figs. 3, 4, 5, and 6 particularly are indicative of the number of tests used.

It is stated in the paper that the experimental instrumentation employing thermocouples enabled temperatures to be read with a 1% accuracy. What does this mean in relation to the accuracy of the heat test data obtained? What is the variance of this experimental error? Was a similar evaluation made under control conditions for the experimental error of resistance measurement employing a Kelvin bridge with an absolute accuracy of 1/4 %? Was a similar evaluation made using a thermometer?

It is expected that a statistical analysis of the thermometer readings and temperature ratios from each machine should firmly establish the contribution by the thermometer toward the scattering of test points. In particular, such factors as the absolute accuracy of the thermometer, the effects of the rounding off of thermometer readings, the "errors" in placement of the thermometer (thermometer is confined to the vertical position and the size of the machine determines accessibility to some extent) and the time lag for a reading all contribute to the total "measurement" error. This assumes that the same personnel took part in each method. One suspects that placement error and the response time are the major factors.

It appears that if placement could be improved and an analysis made of the inherent time lag of a thermometer some means may be developed for compensating the delayed thermometer reading. This would be analogous to the extrapolation to zero time as now accepted for the primary and secondary exponentials evidenced by the present cooling curves.

Unquestionably, the success of the thermocouple and average resistance measurements is attributed to the short time (after shutdown) necessary for good data to be obtained. If thermometers could be placed accurately and if they responded as quickly, they might be equally reliable.

D. D. Gerbetz and **J. S. Ewing**: The authors appreciate the comments and contributions made by the discussers. Mr. Meyers has pointed out instances where temperature rise is not the prime concern in certain designs because of application, and where objections might be raised to taking heat runs. Since some production departments already observe temperature rise by resistance, the added work would represent a minor modification of their test procedure. We feel the greatest gain by measurement of temperature rise by resistance is reflected in engineering information, since rise by resistance more nearly reflects the average thermal characteristics of the armature, and the value of temperature rise measured is nearer the hot spot, with the measurement more accurate.

The ability to repeat temperature measurements on the same machine serves as a good check on the accuracy of temperature measurements, as Mr. Watson suggests. We have made several repeat tests using the resistance measurement, and found that we could repeat within 2 degrees even with a different group of technicians making the test.

The data presented in Mr. Baker's discussion is a fine contribution which we are happy to include as a part of the discussion in this report.

Mr. Schmidt has shown another approach to the evaluation of the errors. In the interest of simplicity, in this report the percent error was assumed to be constant. The temperature rises from the heat runs were in general over the same range for each machine.

Mr. Lamborn points out that the cooling curve is not a straight line on semilog paper. His comments clarify what may have been misleading. He has shown an excellent method of plotting back to zero time. The curve shown indicates a first reading approximately 90 seconds after shutdown. We have found that the average time required to take a first reading is about 40 seconds, but if this for some reason required a longer time, Mr. Lamborn's method would be very useful. The precaution found necessary to obtain accurated temperature reading from *T/C* through slip rings was to introduce cold junctions in the *T/C* circuit and control the temperature of each junction. Also it was necessary to insure good brush contact.

Referring to Mr. Cybulski's discussion, for each method of temperature measurement, the ambient was subtracted from the total temperature to obtain temperature rise. The thermocouples were placed in nearly the same position for each machine. However, for each test the hot spot did not occur in the same place.

The point of view taken in this paper was to accumulate as much test data as possible over a range of machine sizes, and to correlate the data independent of the machine from which it was taken. Because of laboratory loading it was impossible to obtain an equal number of heat runs on all machines, so that some of the data may be weighted by some machines more than others; however, it was felt that the mass of data would result in good averages.

With regard to the accuracy of the thermocouples and the Kelvin double bridge, on actual heat runs, several checks indicated that we maintained our experimental limits of 1% for thermocouples and 1/4 of 1% for the Kelvin double bridge. A similar evaluation for thermometers was not made.

We agree with Mr. Cybulski that the accuracy of the thermometers could be improved by careful laboratory technique and data processing, but the care and work involved normally would not be justified in the light of the accuracy that may be obtained by resistance measurements. Not only would thermometers have to be placed accurately and respond quickly, but a number of them would have to be used as was indicated in Mr. Myers' discussion.

Effect of Shock and Vibration on Relays

AIEE COMMITTEE REPORT

Synopsis: The Project Committee has undertaken to survey the industries on their experience with the effect of shock and vibration on relays, made field and laboratory tests, and prepared a series of conclusions based on the survey and tests. It has not attempted at this time to present a universal cure for the eliminating of the effect of shock and vibration.

THE Project Committee was formed in the winter of 1950 to study the matter of relay vibration and shock resistance and methods of designing and installing relays to minimize the effect of shock and vibration. The need for such studies came from numerous cases where vibration or shock caused unwarranted protective relay operations. The complexity of the problem was fully realized as the Project Committee gathered available information, conducted tests, and coordinated the results. The studies made by the investigators have produced several interesting and valuable conclusions but have also introduced other questions yet to be answered.

Scope and Procedure

Because of the broad field of vibration and shock affecting the relays it was thought necessary to limit the study to include only the type of protective relays used in trip, control, and alarm circuits used in the power application field. The telephone-type relays were included only whenever they were part of the protective scheme. It was recognized that the design of a shockproof and vibration-resistant relay is unavoidably tied in with the construction of the panel the relay is mounted on, thus the effect of switchboard design is also considered.

The industry-wide survey to gauge the importance of the problem was also within the scope of the project. It was thought that an analysis of the survey will furnish some information as to types and construction of relays where difficulty may be encountered. The field and laboratory tests, where under controlled conditions the performance of the relays can be observed, were an important part of the study.

Survey

The electric operating companies were surveyed by questionnaires prepared by the committee and 64 operating electric utility companies were contacted. Of the 30 replies received, 28 reported 126 cases of relay operation caused by shock or vibration within the past 10 years. The analysis of these replies indicates that approximately 53 per cent of the cases were caused by shock and 47 per cent of the cases were caused by vibration. Further breakdown of the vibration shows that 80 per cent of the vibration originated from rotating machines whereas 20 per cent of the vibration was caused by transients such as passing trains, trucks, or others. Most of the difficulties reported due to shock occurred where relays were mounted on hinged panels. Some were experienced by relays in cabinets attached to circuit-breaker frames. Accidental bumping of relay panels accounted for a number of tripouts. Steel panels appeared more troublesome than the other types. No special relay construction could be singled out from the survey to prove that it is more susceptible to vibration or shocks. Auxiliary seal-in contacts appear to be responsible for some of the circuit-breaker operation caused by shock imparted to the relay. For this reason it was thought that an increased separation of main relay contacts may not prevent incorrect tripping.

Field Tests

Extensive measurements were made in steam power plants by two operating

---

Paper 55-97, recommended by the AIEE Relays Committee and approved by the AIEE Committee on Technical Operations for presentation at the AIEE Winter General Meeting, New York, N. Y., January 31–February 4, 1954. Manuscript submitted October 22, 1954; made available for printing November 18, 1954.

Personnel of the Project Committee on Effect of Shock and Vibration on Relays of the AIEE Relay Committee: L. F. FERRI, *Chairman*, A. W. ADAMS, R. E. CORDRAY, M. A. FAUCETT, T. R. HALMAN, H. F. LINDEMUTH, W. K. SONNEMANN, G. STEEB, R. I. WARD, and C. P. WEST.

The field test data were generously furnished by The Detroit Edison, Ohio Edison, and Commonwealth Edison Companies and the Niagara Mohawk Power Corporation. The extensive laboratory tests were conducted by General Electric Company, The Detroit Edison Company, and by the Electrical Engineering Department of the University of Washington under the sponsorship of the Bonneville Power Administration.

companies. The vibration frequencies and amplitudes were measured on switchboard panels, floors, and walls of power stations. The amplitude of vibration measured on steel panels by light beam type of indicators ranges from 0.2 to 2.2 mils and the frequencies varied from 30 to 190 cycles. At another location using the same type of measuring instrument, it was found that the walls were vibrating at an amplitude which increased with the distance from the floor, and readings as much as 8 mils were taken. These vibrations were transmitted to the switchboard panels and were considerably reduced when the panels were mounted on rubber. In these particular tests it was found that the steel panels had a natural frequency of less than 60 cycles and the amplitude of the vibration showed wide variations.

Laboratory Tests

Laboratory tests were conducted by one manufacturing company, one operating utility company, and the electrical engineering department of one university. The tests were mainly centered on determining the effect of shock on relays. The controlled shock was applied either by a hammer of varying weight released from different heights and hitting a fixed panel in pendulumlike fashion or by moving hinged panels through a given angle by various weights suspended on a cord from the panel through a series of pulleys. The acceleration of the panels and in some cases of the relay parts was measured or calculated and the contact bounce observed and graphically recorded. Because of the many factors influencing the tests, only general statements can be made when summarizing the results. It appears that the shock necessary to close the *a* contact of the relay cannot be defined by acceleration alone but rather by the product of acceleration and duration. It was also found that the magnitude of displacement caused by shock is proportional to the momentum and independent of the kinetic energy. It also did not appear to make any difference whether the panel was hit by a wooden or rubber mallet.

The construction of the relay has important influence on shock resistance. The clapper-type relays are generally more sensitive to shock whereas the plunger-type relays are relatively immune to shock caused by a horizontal blow. It was also observed that the shock sensitivity of the clapper-type relay varies with the position of the hinge pin with reference to the plane of the panel the relay is mounted on. For hinge-pin position perpendicular to the plane of panel, the clapper-type relay appeared to have the greatest shock resistance. The shock sensitivity of the relay with potential restraint or polarizing coil is increased if the restraint coil is de-energized.

Factors that reduce the false operation of relays are:

1. Increasing contact gap settings improves shock resistance in most cases. The amount of improvement varies with the other parameters such as a relay time which increases with gap setting. As stated before, however, the shock sensitivity of auxiliary or seal-in contacts may nullify any benefit obtained from gap-spacing increases.

2. Increased armature torques for a given relay setting improve shock resistance of all relays tested. Increased armature torque requires greater mechanical or electric restraining torque for a given relay setting. The increased restraining torque in turn improves shock resistance. Increasing restraining torque without corresponding increase in the armature torque would also result in better shock resistance relay but would reduce relay sensitivity.

3. Modification in backstop construction will result in reduced shock sensitivity. Solid backstop results in contact bounce but backstop arrangements such as ball and sleeve or other nonbounce combinations showed a consistent improvement in shock resistance over other backstop and armature variations, especially in the panel tests.

4. In general it was found that felt washers between backstop and contacts did not increase permanently the shock resistance of the relay. However, in some other instances felt-tipped backstop increased the resistance.

The changing of the natural frequency of the relay-moving element or armature has considerable effect on the shock necessary to cause false operation of the contact. The addition of mass lowers the natural frequency and an increase of spring torque raises the natural frequency. Relays with lower natural frequency are more likely to respond to shock-produced vibrations which are predominantly in the range below 100 cycles per second. The relay case and the cradle absorb a major portion of the shock applied at the door or to the panel.

Investigation of relay mountings on hinged panels reveals that harmful shock caused by slamming can be controlled by mechanically limiting the panel-closing speed. It was also found that the so-called rubber shock mounts of relays where the relay frame was mounted on rubber and the rubber in turn attached to the switchboard panel reduced the sensitivity of the relay to vibration by a ratio of 12 to 1 in the case tested, but the shock resistance was also reduced by a ratio of 2 to 1 if the shock was applied directly to the relay case.

With the hinged panel, the energy stored in rotation and translation before the impact did cause false tripping. Assuming a clockwise rotation of the contact to close upon impact of the panel, the moving element of the relay can either coast (panel hinged right-hand) or bounce on the backstop and coast (panel hinged left-hand). Thus, no conclusive statement can be made that the door hinge on one particular side will be best for all relays which may be mounted on the door. The position of the contact arm with respect to the plane of the panel appears to influence the shock resistance of the relay.

Instruments Used

There are a large number of instruments available in the industry to measure shock and vibration but it was found that only a few were applicable to meet the restrictive conditions encountered. In other cases the investigators were limited in their budget allocated for the study and the more costly instrument could not be purchased. For vibration measurements it was found that instruments using a crystal pickup and electronic amplifier furnished the most satisfactory result. The light beam type of vibration indicator also appeared to be suitable.

Different types of instruments were used for measurements of shock. The accelerometer consisting of a crystal and an amplifier were used by one laboratory. In another case a small slug-tuned coil was used as displacement pickup. The variation of the coil inductance affected the signal output of an oscillator which was amplified to supply a graphic recorder. A device consisting of a bank of leaf springs with graduated stiffness so mounted and connected that for each spring there is a certain acceleration and that is sufficient to open a contact and actuate a gas tube indicator has also been successfully used. In general it was found that the available measuring devices had to be modified to be suitable for measuring the effect of shock and vibration on relay parts under investigation.

Methods of Mitigation

On the basis of field and laboratory studies it appears that shockproof and vibration-resistant relay installation is the joint responsibility of the panel and relay designers as well as to a certain extent of those who install switchboard panels.

In designing switchboard panels and metal-clad switchgear, the following are a few of the provisions which might reduce the possibility of accidental relay operation caused by shock or vibration:

1. Use slate or composition panels where heavy shock or vibration is expected.
2. Brace steel panels by horizontal and vertical webs to add stiffness.
3. Insert shock- and vibration-absorbing layers between panels and base foundations. Similar provision can be made for wall braces. Unusual service conditions where abnormal vibration, shock, or tilting are expected require special consideration[1] and are outside the scope of this report.
4. Avoid mounting shock-sensitive relays on steel doors.
5. Provide rubber mount between relay and panel.
6. Provide door checks to control speed of closing and opening of hinged panels.

It should be noted that provision 5 is effective only in improving shock resistance if the shock is applied to the switchboard panel, but it may reduce it if the shock is applied direct to relay case.

It also appears that certain changes in relays would increase the shock resistance of the relays. Some of these suggested changes are as follows:

1. Improve backstop construction.
2. Increase restraining spring torque.
3. Increase air-gap spacing between disk and magnets.
4. Increase contact gap spacing.
5. Design clapper-type relays so the armature hinge is in a position with reference to the mounting plane to assure the greatest shock resistance.

Conclusions

1. Vibration and shock problems are real with the electric industry. Each cause appears to be of equal importance.
2. Relays on steel panels are more susceptible to vibration and shock than relays mounted on panels such as slate or composition.
3. Almost all types of relays have been reported to operate by vibration or shock, however, some relays are more sensitive than others.
4. Hinged armature (clapper-type) relays are more susceptible to shock whereas plunger-type relays are less likely to operate.
5. Some methods are available to mitigate the effect of vibration on relays. These methods can be grouped in two classes: improvements in relay design and changing in mounting. Both have been proved to be effective in overcoming the effect of vibration.
6. Shock to relays could be caused by straightline motion right angles to the panel, by motion parallel to the panel, by rotary couples applied to the panel, by rotary couples applied to the relay and by rotary couples produced by the operation of a hinged panel section.
7. Shocks resulting from the foregoing causes may be violent enough to cause relay operations and there are certain methods available to mitigate but not completely eliminate the effect of shock. These methods have been grouped in several classes: improvement in relay design, panel design, relay mounting, and modification of electric circuits.
8. The location of door hinges (left or right) will have some effect of the shock sensitivity of certain types of relays depending on the position of the contact arm.
9. Hinged armature relays can be redesigned with counterbalanced armature or with twin contacts and pivot centrally located between contacts which may eliminate the effect of shock on the relay.
10. Electric circuits may be modified so that the tripping circuit requires the closing of two independent contacts and by arranging these contacts to be in different planes.

Reference

1. Relays Associated with Electric Power Apparatus. *ASA Standard C37.1-1950*, American Standards Association, New York, N. Y., 1950.

◆

Discussion

H. C. Barnes (American Gas & Electric Service Corporation, New York, N. Y.): The committee is to be congratulated upon the completion of a fine report on a very difficult subject. Considerable ingenuity must have been required to obtain the necessary data to reach a conclusion. The material should be of great assistance to the utility engineer in laying out panels as well as to the relay designer.

The statement that "The shock sensitivity of the relay with potential restraint or polarizing coil is increased if the restraint coil is de-energized" is certainly a true one. The slightest shock even to a rear side sheet of a steel panel will cause contact closure. Normally, this is not a problem since restraint is present when the line is in service. However, it can be a problem where line side potential devices are used. These relays usually initiate second or third zone tripping through an auxiliary timer. If the contacts should close because of shock or vibration, when restraint is off, they will quite often weld because of the arc from the timer current which is drawn on the slow bounce of the contacts. Normally this does not happen because of an *a* auxiliary switch being open in the circuit breaker under the condition when the line side potential devices are de-energized.

However, this is dangerous when the breaker is out for maintenance and is closed with the disconnects open. Welding on the bounce could cause the breaker to trip and injure the maintenance man. It could also result in delay in restoring the breaker to service if no relay man is available. This can also be true if bus side bushing potential devices are used.

A worse situation could again occur under the maintenance condition where separate breaker failure relaying is provided. Should this bounce and weld, it could result in tripping an entire bus. One solution is to provide plunger-type overcurrent relays to monitor the circuit breaker rather than use auxiliary switches. These would not be picked up because no current was flowing. This is a reasonable application anyway since one of the reasons for breaker failure is the failure of the breaker to interrupt, under which condition the *a* auxiliary switches would be open and would nullify the breaker failure relaying.

Another serious case from vibration is that of the sensitive ground directional relay in the carrier start circuit. These tend to vibrate open, particularly if extreme sensitivity is used. On 250-volt d-c applications, there is often enough resistor current to cause these contacts to weld. This results in false tripping of the remote end of the line for an external fault since the contact cannot open to start carrier. Care in assuring sufficient contact wipe usually can overcome this. Also the situation is improved if the low threshold setting is avoided.

The problem of shock is likely to become greater. The trend toward economy in control buildings results in less clearance between panels. Since these spaces are often used as aisles, the relays are more apt to be bumped by ladders, pieces of conduit, crates, or whatever may be brought into the building. This is particularly true where the doors are arranged such that the space between the relay panels becomes the natural aisle. Location of critical relays high on the panel is a good preventative although not a 100-per-cent solution since they can still be kicked or bumped during such operations as replacing light bulbs. Where additional horizontal stiffening of steel panels is required, the relay mounting studs can often be used to clamp stiffening angles.

M. A. Bostwick (Portland General Electric Company, Portland, Oreg.): The committee report is both thorough and complete. However, it appears that attention may have been directed to consideration of the relay's moving contacts, neglecting spring-mounted stationary contacts.

We have successfully avoided undesirable relay operations by limiting minimum spring tensions and contacts gaps. But in one instance, we experienced an incorrect operation caused by vibration of the spring-mounted stationary contacts! The source of the vibration was a slow-moving logging train just outside the substation. This experience may be of interest to others as it directs attention to the stationary contacts which may also be a source of trouble.

A. E. Flink (Ohio Edison Company, Akron, Ohio): This is a very interesting paper and shows the need for more care in the installation of relays. Too often no attention is given to the shock and vibration which may be present when relay panels are installed. Vibration and shock do not help the bearings and jewels in any relay. Choice of a better location for relay panels can do much to reduce incorrect operations.

I have found that low restraining torque is the most troublesome and the most difficult to overcome. These relays may not operate for normal conditions but will operate for transient conditions such as bringing a machine up to speed. By determining the setting before a relay is bought, a range can be chosen so that the maximum restraining spring torque can be used. By sacrificing some sensitivity we have also been able to overcome small amounts of vibration.

The use of fast clearing and reclosing times makes it necessary to reduce rather than increase the contact gap spacing. For the last few years we have been reducing the gap spacing wherever possible. This makes the relays more sensitive to shock and vibration, but if it is not done, the control scheme may not function properly.

Donn C. Achtenberg (The Detroit Edison Company, Detroit, Mich.): The Project Committee is to be congratulated for a much needed job well done. The need for more information on the effects of shock and vibration is great.

The Detroit Edison Company has developed several shockproofing methods for various relays. These were developed partly from past experience and partly from results of tests made for the purpose of obtaining information for the Project Committee work.

On one clapper-type auxiliary relay another restraining spring is added to the one which is installed by the manufacturer. As manufactured, this relay usually has a pickup of about one-half its rated voltage. The addition of the shock-proofing spring raises the pickup to about rated voltage. For this reason, coil circuits are designed so that double-rated voltage is applied for pickup and then some kind of dropping circuit is provided to drop the voltage to be rated. On this type of relay we feel that counterbalancing the armature would be very beneficial.

One pilot-wire relay uses a polar-type element to which the contacts are attached. On this relay the contact spacing is very close. To help reduce false tripping caused by shock on this relay, the whole polar-type element is suspended on a spring arrangement within the relay case. We believe that this type of shockproofing is very desirable because it helps absorb shock and vibration both on the panel and directly on the case of the relay.

An overcurrent relay which works on the rotating disk principle is also shockproofed. On this relay, the moving contact is a beam which is unbalanced when the overcurrent element engages a gear to rise up and hit the beam. To prevent this beam from bouncing closed, a fixture is attached to the frame of the overcurrent element. The fixture is attached so that it projects directly over the beam and prevents it from operating until the overcurrent element moves over to engage the gear.

In general, we feel that if the proper measuring devices were available much valuable information could be obtained. We agree with the committee's conclusions especially numbers 9 and 10. On number 9, it is felt that, in addition to balancing armatures on clapper-type relays, it should be desirable to mount the relays within the case so that the hinged pin is perpendicular to the plane of the panel.

F. R. Bergseth (University of Washington, Seattle, Wash.): The committee has done an excellent job in preparing a report on this subject which has so many diverse ramifications and about which it is so difficult to say anything general. As a result of field and laboratory tests and analysis it may be said that attention to certain rather minor details in design and amounting of relays may result in considerably improved performance from a viewpoint of withstanding mechanical shock and vibration. One or two points mentioned in the report might well be amplified in view of the experience obtained in the laboratory tests at the University of Washington.[1]

The statement is made that the magnitude of displacement of shock is proportional to momentum and independent of the kinetic energy. A casual mathematical analysis of greatly simplified mechanical systems will reveal that the closure of a pair of relay contacts will depend upon the momentum delivered by a blow rather than the kinetic energy contained in the striking object. A multitude of test blows applied to a sample panel on which typical transmission line and bus differential relays were mounted revealed the correlation expected between momentum and relay closure for these more complex electromechanical structures just as predicted from the analysis of the simpler case. In these days, shock is usually thought of in terms of military specification and such terms as 2,000-foot-pounds shock are common and it may be surprising to note the emphasis on momentum rather than energy. It should be pointed out, however, that the military specifications envision a test blow delivered from a specific testing machine and, in this case, the momentum and kinetic energy of the blow are directly related—a specification of energy of the blow specifies the momentum equally well when the test is to be performed by a hammer blow from a given test machine.

In testing relays by means of a falling hammer type of blow, it was surprising to find that the relay performance was substantially independent of the type of cushioning surface used on the hammer—a rubber, wood, or steel surface resulted in approximately the same relay performance. Study of displacement traces made by electromechanical recorders reveals that the principal difference in the blows of a given momentum administered with different hammer faces lies in the higher frequency components. The natural frequency of the relay contact structure is low compared to the higher frequency components of displacement resulting from the use of a hard-faced hammer and little difference is noted in relay performance with these different types of blows.

A word of caution is in order here. The tests were performed at shock levels sufficient to cause false closures but not sufficient to cause relay damage such as shattered cover glasses or broken or displaced relay mechanisms. If shock intensities in these latter levels were used, it is quite probable that the nature of the striking hammer would be of considerable significance in determining the effect of a blow of given momentum. The same remarks might be made with regard to the subject of panel bracing. It was found that additional stiffening of the panel surfaces was of great help in avoiding false relay operations under shock. However, this might be just the wrong thing to do if shocks of destructive magnitudes were involved.

REFERENCE

1. A STUDY OF THE CHARACTERISTICS OF MECHANICAL SHOCK CAUSING FALSE OPERATION OF POWER RELAYS. Homer R. Forbes. *Thesis*, University of Washington, Seattle, Wash., 1953.

L. F. Ferri: The Project Committee appreciates the constructive contributions of the discussers to the subject of shock and vibration as they affect relay performance. The experience accumulated by Mr. Barnes, Mr. Bostwick, and Mr. Flink points in great detail and emphasis to the problems which, because of understandable limitations, could only be summarized in the paper. It is very apparent from their discussions that the modern high-speed relays using electromagnetic principles present in some applications a real problem because of their shock sensitivity. This problem should be a challenge to the manufacturer's design engineers. Mr. Achtenberg's solution indicates that in some specific cases modification of the relays will result in higher resistance to vibration. The committee is indeed very grateful to the contribution of Prof. Bergseth and to the fundamental research done in the laboratory under his supervision. His comments with reference to the relays responding to shock under controlled conditions are well taken and point out that some reappraisal of the basic factors may be necessary.

Practical Application of Sag and Tension Calculations to Transmission-Line Design

J. LUMMIS
MEMBER AIEE

H. D. FISCHER, JR.
ASSOCIATE MEMBER AIEE

DETERMINATION of sags and tensions in transmission lines can be greatly simplified when the accuracy of calculation is given its proper weight. It seems seldom to be appreciated that no workable mathematical equation exactly describes a suspended transmission conductor. Even if such an equation were available, inaccuracies introduced by manufacturing tolerances and field conditions would still be appreciable.

As a matter of fact, the exact relation between sag and tension is not an important one because sag, upon which ground clearance depends, is the only tangible and controllable factor. Good practice and regulatory bodies set a clearance below which the conductors must not lie; economy dictates that this clearance must not be exceeded. Maximum tensions are likewise prescribed but practical considerations generally make this a value that, while it must not be exceeded, can only be approximated. Furthermore, maximum tension is dependent upon the simultaneous occurrence of specific values of temperature, wind, and ice which from experience are known to produce safe designs but are nevertheless supposititious. As a matter of fact, because of the vibration problem, it is seldom practical to design a line for the full allowable maximum tension in any case. Thus emphasis is placed on methods of design and construction which will produce fixed clearances without exceeding safe values of tension.

In view of these limitations, methods will be shown which will produce a design within the practical limits of accuracy. The limitations of these approximate methods will also be shown as well as more precise methods which must be used under certain circumstances.

Inadequacy of Fundamental Assumptions

The usual equations used to describe a suspended conductor are the catenary[1,2] and the parabola.[2] In both it is assumed that the conductor is inelastic and flexible. In the former it is assumed that the distribution of weight is uniform along the curve of the conductor, while the latter is assumed to have its weight uniformly distributed along a horizontal projection of the curve. None of these assumptions is correct. A conductor is elastic so that the distribution of weight, while closely following that of a catenary, is dependent upon tension; furthermore, the conductor is rigid and is supported to some extent by beam action. The mathematics of an elastic and rigid catenary have been approximated[3] and, for a given tension, this curve lies somewhat above the classic catenary. Experiment seems to bear this out. However, it should be noted that any calculation involving clearance requires a transformation from maximum conditions for tension to maximum conditions for sag. Maximum condition for tension occurs during a transverse wind which is erroneously assumed to produce a uniform horizontal force upon the suspended conductor, and if ice loading is present it is assumed to be of uniform linear density throughout the span and from span to span.

The best conductor does not rigidly follow Hooke's law, and bimetallic conductors are notorious for plastic flow. While prestretching improves the elastic properties of conductors, some error arising from plastic flow is inevitable.

Where spans terminate on suspension insulators each span is affected by the action of spans adjacent. Ideally, this influence can be determined analytically but conditions are seldom ideal and some error will usually arise from this factor.

Errors Beyond Control of Design

Regardless of how accurately the design of a span is executed there are errors that are inevitable because of manufacturing and field conditions. Conductor is manufactured with a weight tolerance of ±2 per cent and the diameter tolerance is ±1 per cent, both of which have a direct bearing on the tension and which, since these variations may take place within a span, tend to invalidate the basis of design. Temperature of the conductor during sagging operations cannot be determined closer than ±5 degrees Fahrenheit (F), and this factor, too, is variable in the span. Wind is frequently present during sagging operations, and its influence on the span being sagged is indeterminable. The wind, furthermore, is usually not uniform from span to span and the influence of adjacent spans upon the span being sagged is therefore likewise indeterminate. While the influence of inelastic creep can be controlled with reasonable accuracy under laboratory conditions, it is variable and its control in the field is even more difficult as stringing operations prior to sagging frequently produce an indeterminable amount of creep and consequent error in final tension. Friction of sag blocks can be determined and compensated for if they are of high quality and in perfect working order; however, with the rough handling inevitable during construction the best blocks will vary in frictional characteristics. Finally, the transfer of the conductor from sheave to suspension clamp is done by mechanics whose carelessness or lack of knowledge, particularly where insulators must be offset to compensate for sloping spans, may introduce errors of considerable magnitude.

Equations

In view of the many sources of error outlined in the preceding discussion the catenary is taken as the form assumed by a suspended conductor. With respect to the sag the tension will be on the "safe" side, and with proper modification the equations will be as easy to manipulate as any. The basic equation for the catenary,[1] Fig. 1, is

$$y = C \cosh \frac{x}{C} \qquad (1)$$

Note that the parameter C is directly proportional to the horizontal component of the tension; a constant is the span, which must be constant in all spans separated only by vertical suspension

---

Paper 54-501, recommended by the AIEE Transmission and Distribution Committee and approved by the AIEE Committee on Technical Operations for presentation at the AIEE Winter General Meeting, New York, N. Y., January 31–February 4, 1955. Manuscript submitted June 1, 1954; made available for printing October 6, 1954.

J. Lummis and H. D. Fischer, Jr., are with the Southern California Edison Company, Los Angeles, Calif.

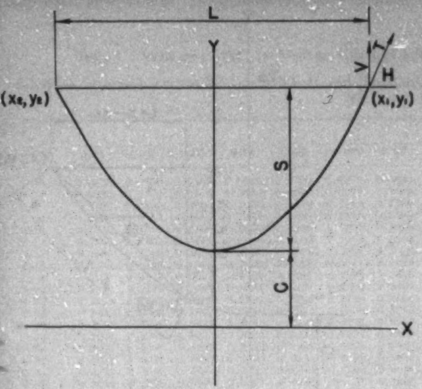

Fig. 1. The catenary

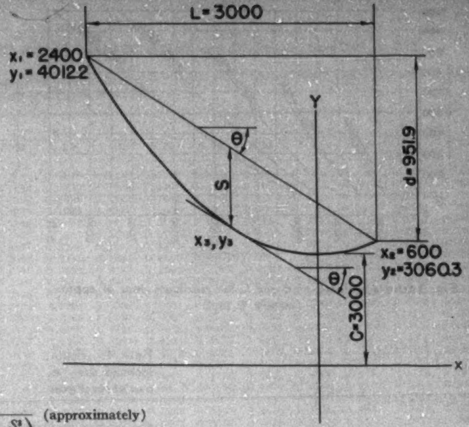

Fig. 2. Example of sag calculation

insulators. In design, therefore, C is the criterion for all sag calculations.

The variations of tension, and therefore C, for changes in temperature and loading may be determined by use of the Thomas charts,[4] Martin's table,[5] or Aluminum Company of America graphic methods.[6]

For a level span the sag is $y-C$, and using the expansion series for the hyperbolic cosine it may be shown that the sag, Fig. 1, in form for easy slide-rule operation, is

$$S=\frac{L^2}{8C}+\frac{1}{6C}\left(\frac{L^2}{8C}\right)^2+0.4\left(\frac{1}{6C}\right)^2\left(\frac{L^2}{8C}\right)^3 \qquad (2)$$

The third term of the series is never significant in the ordinary transmission span as may be seen in the following example where the span is 3,000 feet and C is 3,000

$$\frac{L^2}{8C} = \frac{3{,}000^2}{8\times 3{,}000} = 375.0$$

$$+\frac{1}{6C}\left(\frac{L^2}{8C}\right)^2 = \frac{375.0^2}{6\times 3{,}000} = 7.8$$

$$+0.4\left(\frac{1}{6C}\right)^2\left(\frac{L^2}{8C}\right)^3 = \frac{0.4\times(375.0)^3}{(6\times 3{,}000)^2} = 0.1$$

$$\text{Sag} = 382.9$$

It can be shown that the sag in an inclined span is approximately equal to the sag of a level span of the same length multiplied by the secant of the inclination of the chord. Thus, if θ is the angle of inclination of the chord, the generalized form of equation 2 becomes

$$S=\left[\frac{L^2}{8C}+\frac{1}{6C}\left(\frac{L^2}{8C}\right)^2\right]\sec\theta \text{ (approximately)} \qquad (3)$$

or

$$C=\frac{L^2}{8\left(S\cos\theta-1.33\dfrac{S^3}{L^2}\right)} \text{ (approximately)} \qquad (4)$$

The error arising from the approximations in equation 3 can be seen from the following example; see Fig. 2

$$\frac{x_1}{C}=\frac{2{,}400}{3{,}000}=0.80,\ \cosh\frac{x_1}{C}=1.3374,$$

$$y_1=4{,}012.2$$

$$\frac{x_2}{C}=\frac{600}{3{,}000}=0.20,\ \cosh\frac{x_2}{C}=1.0201,$$

$$y_2=3{,}060.3$$

$$d=\ 951.9$$

$$\tan\theta=\frac{951.9}{3{,}000}=0.3173,\ \sec\theta=1.04913$$

$$=\cosh\frac{x_3}{C}$$

Therefore, $y_3=3{,}147.4$, $x_3/C=0.3122$, and $x_3=936.6$.

Elevation of chord at

$$x_3=3{,}060.3+(936.6+600.0)0.3173=3547.9$$

$$y_3=3147.3$$

$$\text{Maximum sag}=\ 400.6$$

By Equation 3:

$$\frac{3{,}000^2}{8\times 3{,}000} = 375.0$$

$$+\frac{375^2}{6\times 3{,}000} = 7.8$$

$$\text{Maximum sag}=382.8\times 1.0491=401.6$$

The approximate equations for calculating clearances are satisfactory for ordinary conditions. However, if the maximum sag error in a span is to be kept below 1 foot, the curves shown in Fig. 3 will determine the limiting use of the approximate equations. For instance, in a 2,000-foot span with a difference in elevation of 500 feet, C must be 4,000 or greater to enable the use of the approximate equations and still keep the maximum error on the order of 1 foot. The error at the center of the span will always be small, however, with the maximum error occurring near the quarter points of the span. The calculated ground clearances will be greater than the actual clearances in that half of the span near the higher point of support, and they will be less than the actual clearances in the half near the lower point of support. The curves shown in Fig. 3 were prepared from data obtained from calculations comparing the approximate method with the exact method for varying conditions of C, L, and d.

Where the error between the calculated sags (when using approximate equations) and the actual sags exceeds a desirable limit, it will be necessary to use more precise methods. Such a method, Fig. 4, is to determine the level span of which the inclined span is a part, and then use the approximate methods in the level span.

Where l is the length of conductor in the inclined span and x_1 and x_2 are the abscissas of the upper and lower supports respectively, it follows that

$$l=2C\sinh\left(\frac{x_1-x_2}{2C}\right)\cosh\left(\frac{x_1+x_2}{2C}\right)$$

$$d=2C\sinh\left(\frac{x_1-x_2}{2C}\right)\sinh\left(\frac{x_1+x_2}{2C}\right)$$

from which it follows that

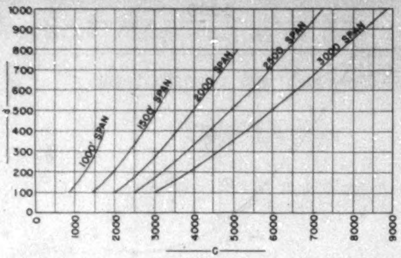

Fig. 3 (above). Limit of d and C for maximum error of approximately 1 foot

$$l^2=\left(2C\sinh\frac{L}{2C}\right)^2+d^2$$

$$x_1+x_2=C\log_e\left(\frac{l+d}{l-d}\right)$$

It then follows that

$$\frac{x_1+x_2}{2C}=\frac{1}{2}\log_e\times\left[\frac{\sqrt{\left(\frac{2C}{L}\sinh\frac{L}{2C}\right)^2+\tan^2\theta}+\tan\theta}{\sqrt{\left(\frac{2C}{L}\sinh\frac{L}{2C}\right)^2+\tan^2\theta}-\tan\theta}\right]$$

$$x_1=\frac{L}{2}+\frac{C}{2}\log_e\times\left[\frac{\sqrt{\left(\frac{2C}{L}\sinh\frac{1}{2C}\right)^2+\tan^2\theta}+\tan\theta}{\sqrt{\left(\frac{2C}{L}\sinh\frac{L}{2C}\right)^2+\tan^2\theta}-\tan\theta}\right]$$

and the level span of which L is a portion is

$$L_e=L+C\log_e\times\left[\frac{\sqrt{\left(\frac{2C}{L}\sinh\frac{L}{2C}\right)^2+\tan^2\theta}+\tan\theta}{\sqrt{\left(\frac{2C}{L}\sinh\frac{L}{2C}\right)^2+\tan^2\theta}-\tan\theta}\right] \quad (5)$$

This equation is entirely too cumbersome for practical use. However, the right-hand term can be set up in tabular or graphic form to expedite the solution. From the foregoing relationships, Table I has been prepared which gives the value of $L_e/(2C)$ for various values of $L/(2C)$ and d/L.

Vertical Clearance

A set of templates representing the curves of the catenary for various values of C may be made for use in the drafting room.[7] These of course would be constructed to the same scale as the profile. The template, when used to locate the structures on the profile, will also indicate the points of critical clearance and the calculations may then be narrowed down to those clearances which are too close to the minimum to rely on template accuracy.

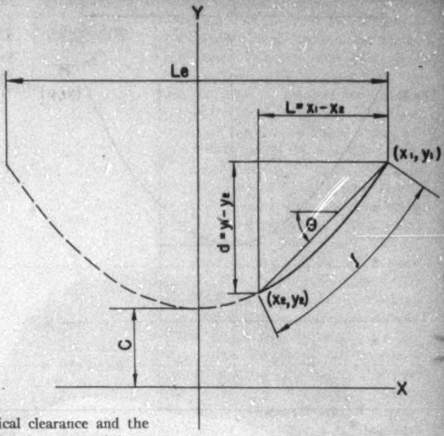

Fig. 4 (right). Inclined span as part of level span

For calculating vertical clearances at points off-center of the span a curve showing the factors K and K' to be applied to the center sag plotted versus the distance from the supports may be used. A curve of this type is shown in Fig. 5. Note that one curve is based on the parabolic value of sag and the other is the correction for catenarian sag. This curve may be used with sufficient accuracy when conditions are such that the approximate equations may be used in other calculations.

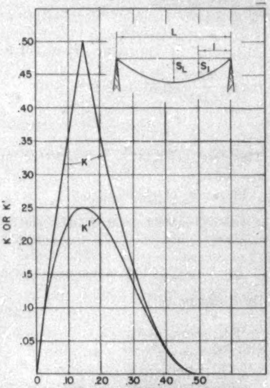

Fig. 5. Sag at intermediate points in span, where

$$S_L=\frac{L^2}{8C}+\frac{1}{6C}\left(\frac{L^2}{8C}\right)^2$$

$$S_l=K\frac{L^2}{8C}+K^1\frac{1}{6C}\left(\frac{L^2}{8C}\right)^2 \text{ for } \frac{l}{L}=0 \text{ to } 0.146$$

$$S_l=(1-K)\frac{L^2}{8C}+K^1\frac{1}{6C}\left(\frac{L^2}{8C}\right) \text{ for } \frac{l}{L}=0.146 \text{ to } 0.500$$

Swing Clearances

Clearances must also be calculated for conductors when they swing out to the side. A typical chart for determining the horizontal displacement and the rise of the conductor, due to a transverse wind, is shown in Fig. 6.

Also clearances between conductor and structure must be determined. This may be accomplished readily with satisfactory accuracy by the use of scale models. A typical model is shown in Fig. 7. To use this model, it is necessary only to calculate the swing of the insulator string and the slope of the conductor at the point of support. Then, placing the various templates in their proper position, the clearance to steel may be scaled.[8]

When the slope of the chord is known, the transverse swing of the insulator string can be computed by assuming that the vertical load imposed by the conductor is the same under wind action as in still air and that the horizontal load is equivalent to the wind force on one-half the sum of the adjacent spans. However, when the action of the wind swings the conductor to the side, the span and slope in the wind plane change[4] and this factor must be taken into con-

Table I. Value of $L_e/(2C)$ for Various Values of $L/(2C)$ Ranging from 0.02 to 0.50, and d/L Ranging from 0.01 to 0.50

Example: Assume L = 1,000 Feet, d = 400 Feet, and C = 5,000. Then L/(2C) = 0.10, d/L = 0.40, and from the Table $L_e/(2C)$ = 0.4894, from Which It Is Found that L_e = 4,894 feet

$\frac{L}{2C}$	d/L																
	0.01	0.02	0.03	0.04	0.05	0.06	0.07	0.08	0.09	0.10	0.11	0.12	0.13	0.14	0.15	0.16	0.17
0.02	0.0300	0.0400	0.0500	0.0600	0.0700	0.0800	0.0899	0.0999	0.1099	0.1198	0.1298	0.1397	0.1496	0.1595	0.1694	0.1793	0.1892
0.04	0.0500	0.0600	0.0700	0.0800	0.0900	0.0999	0.1099	0.1199	0.1299	0.1398	0.1497	0.1597	0.1696	0.1795	0.1894	0.1993	0.2092
0.06	0.0700	0.0800	0.0900	0.1000	0.1100	0.1199	0.1299	0.1399	0.1498	0.1598	0.1697	0.1796	0.1896	0.1995	0.2093	0.2192	0.2291
0.08	0.0900	0.1000	0.1100	0.1199	0.1299	0.1399	0.1499	0.1598	0.1698	0.1797	0.1896	0.1996	0.2095	0.2194	0.2293	0.2392	0.2490
0.10	0.1100	0.1200	0.1300	0.1399	0.1499	0.1599	0.1698	0.1798	0.1897	0.1997	0.2096	0.2195	0.2294	0.2393	0.2492	0.2591	0.2689
0.12	0.1300	0.1400	0.1499	0.1599	0.1699	0.1798	0.1898	0.1997	0.2097	0.2196	0.2295	0.2394	0.2493	0.2592	0.2691	0.2789	0.2888
0.14	0.1500	0.1599	0.1699	0.1799	0.1898	0.1998	0.2097	0.2197	0.2296	0.2395	0.2494	0.2593	0.2692	0.2791	0.2890	0.2988	0.3087
0.16	0.1700	0.1799	0.1899	0.1998	0.2098	0.2197	0.2296	0.2396	0.2495	0.2594	0.2693	0.2792	0.2891	0.2990	0.3088	0.3187	0.3285
0.18	0.1900	0.1999	0.2098	0.2198	0.2297	0.2396	0.2496	0.2595	0.2694	0.2793	0.2892	0.2991	0.3089	0.3188	0.3286	0.3385	0.3483
0.20	0.2099	0.2199	0.2298	0.2397	0.2497	0.2596	0.2695	0.2794	0.2893	0.2992	0.3090	0.3189	0.3288	0.3386	0.3485	0.3583	0.3681
0.22	0.2299	0.2398	0.2498	0.2597	0.2696	0.2795	0.2894	0.2993	0.3092	0.3190	0.3289	0.3388	0.3486	0.3584	0.3683	0.3781	0.3879
0.24	0.2499	0.2598	0.2697	0.2796	0.2895	0.2994	0.3093	0.3192	0.3290	0.3389	0.3487	0.3586	0.3684	0.3782	0.3880	0.3978	0.4076
0.26	0.2699	0.2798	0.2897	0.2995	0.3094	0.3193	0.3292	0.3390	0.3489	0.3587	0.3685	0.3784	0.3882	0.3980	0.4078	0.4176	0.4273
0.28	0.2899	0.2997	0.3096	0.3195	0.3293	0.3392	0.3490	0.3589	0.3687	0.3786	0.3883	0.3982	0.4080	0.4178	0.4275	0.4373	0.4470
0.30	0.3099	0.3197	0.3296	0.3394	0.3492	0.3591	0.3689	0.3787	0.3886	0.3984	0.4081	0.4179	0.4277	0.4375	0.4472	0.4570	0.4667
0.32	0.3298	0.3397	0.3495	0.3593	0.3691	0.3790	0.3888	0.3986	0.4084	0.4182	0.4279	0.4377	0.4475	0.4572	0.4669	0.4767	0.4864
0.34	0.3498	0.3596	0.3694	0.3792	0.3890	0.3988	0.4086	0.4184	0.4282	0.4379	0.4477	0.4574	0.4672	0.4769	0.4866	0.4963	0.5060
0.36	0.3698	0.3796	0.3894	0.3991	0.4089	0.4187	0.4285	0.4382	0.4480	0.4577	0.4675	0.4772	0.4869	0.4966	0.5063	0.5160	0.5256
0.38	0.3898	0.3995	0.4093	0.4190	0.4288	0.4386	0.4483	0.4580	0.4678	0.4775	0.4872	0.4969	0.5066	0.5163	0.5259	0.5356	0.5452
0.40	0.4097	0.4195	0.4292	0.4389	0.4487	0.4584	0.4681	0.4778	0.4875	0.4972	0.5069	0.5166	0.5263	0.5359	0.5455	0.5552	0.5648
0.42	0.4297	0.4394	0.4491	0.4588	0.4685	0.4782	0.4879	0.4976	0.5073	0.5170	0.5266	0.5363	0.5459	0.5556	0.5652	0.5748	0.5844
0.44	0.4497	0.4594	0.4691	0.4787	0.4884	0.4981	0.5077	0.5174	0.5271	0.5367	0.5463	0.5559	0.5656	0.5752	0.5848	0.5943	0.6039
0.46	0.4697	0.4793	0.4890	0.4986	0.5083	0.5179	0.5275	0.5372	0.5468	0.5564	0.5660	0.5756	0.5852	0.5948	0.6043	0.6139	0.6234
0.48	0.4896	0.4993	0.5089	0.5185	0.5281	0.5377	0.5473	0.5569	0.5665	0.5761	0.5857	0.5953	0.6048	0.6144	0.6239	0.6334	0.6429
0.50	0.5096	0.5192	0.5288	0.5384	0.5480	0.5576	0.5671	0.5767	0.5862	0.5958	0.6053	0.6149	0.6244	0.6339	0.6434	0.6529	0.6624

$\frac{L}{2C}$	d/L																
	0.18	0.19	0.20	0.21	0.22	0.23	0.24	0.25	0.26	0.27	0.28	0.29	0.30	0.31	0.32	0.33	0.34
0.02	0.1990	0.2089	0.2187	0.2285	0.2382	0.2480	0.2577	0.2675	0.2771	0.2868	0.2964	0.3061	0.3157	0.3252	0.3348	0.3442	0.3537
0.04	0.2190	0.2288	0.2386	0.2484	0.2582	0.2679	0.2777	0.2874	0.2971	0.3068	0.3164	0.3260	0.3356	0.3451	0.3547	0.3642	0.3737
0.06	0.2389	0.2488	0.2586	0.2684	0.2781	0.2879	0.2976	0.3073	0.3170	0.3267	0.3363	0.3459	0.3555	0.3651	0.3746	0.3841	0.3936
0.08	0.2589	0.2687	0.2785	0.2883	0.2980	0.3078	0.3175	0.3272	0.3369	0.3466	0.3562	0.3658	0.3754	0.3849	0.3944	0.4040	0.4134
0.10	0.2788	0.2886	0.2984	0.3081	0.3179	0.3276	0.3374	0.3471	0.3567	0.3664	0.3760	0.3856	0.3952	0.4047	0.4143	0.4238	0.4332
0.12	0.2986	0.3084	0.3182	0.3280	0.3378	0.3475	0.3572	0.3669	0.3766	0.3862	0.3958	0.4054	0.4150	0.4245	0.4340	0.4435	0.4530
0.14	0.3185	0.3283	0.3381	0.3478	0.3576	0.3673	0.3770	0.3867	0.3963	0.4060	0.4156	0.4252	0.4347	0.4443	0.4538	0.4633	0.4727
0.16	0.3383	0.3481	0.3579	0.3676	0.3774	0.3871	0.3968	0.4064	0.4161	0.4257	0.4353	0.4449	0.4544	0.4640	0.4735	0.4829	0.4924
0.18	0.3581	0.3679	0.3776	0.3874	0.3971	0.4068	0.4165	0.4262	0.4358	0.4454	0.4550	0.4646	0.4741	0.4836	0.4931	0.5026	0.5120
0.20	0.3779	0.3876	0.3974	0.4071	0.4168	0.4265	0.4362	0.4459	0.4555	0.4651	0.4747	0.4842	0.4938	0.5033	0.5128	0.5222	0.5316
0.22	0.3976	0.4074	0.4171	0.4268	0.4365	0.4462	0.4559	0.4655	0.4751	0.4847	0.4943	0.5039	0.5134	0.5229	0.5323	0.5418	0.5512
0.24	0.4174	0.4271	0.4368	0.4465	0.4562	0.4659	0.4755	0.4852	0.4948	0.5043	0.5139	0.5234	0.5329	0.5424	0.5519	0.5613	0.5707
0.26	0.4371	0.4468	0.4565	0.4662	0.4759	0.4855	0.4951	0.5048	0.5143	0.5239	0.5335	0.5430	0.5525	0.5619	0.5713	0.5808	0.5902
0.28	0.4568	0.4665	0.4761	0.4858	0.4955	0.5051	0.5147	0.5243	0.5339	0.5434	0.5530	0.5625	0.5719	0.5814	0.5908	0.6002	0.6096
0.30	0.4764	0.4861	0.4958	0.5054	0.5151	0.5247	0.5343	0.5439	0.5534	0.5630	0.5725	0.5819	0.5914	0.6008	0.6102	0.6196	0.6290
0.32	0.4961	0.5057	0.5154	0.5250	0.5346	0.5442	0.5538	0.5634	0.5729	0.5824	0.5919	0.6014	0.6108	0.6202	0.6296	0.6390	0.6483
0.34	0.5157	0.5253	0.5349	0.5446	0.5542	0.5638	0.5733	0.5829	0.5924	0.6019	0.6113	0.6208	0.6302	0.6396	0.6490	0.6583	0.6676
0.36	0.5353	0.5449	0.5545	0.5641	0.5737	0.5833	0.5928	0.6023	0.6118	0.6213	0.6307	0.6401	0.6495	0.6589	0.6683	0.6776	0.6869
0.38	0.5548	0.5645	0.5740	0.5836	0.5932	0.6027	0.6122	0.6217	0.6312	0.6407	0.6501	0.6595	0.6689	0.6782	0.6876	0.6968	0.7061
0.40	0.5744	0.5840	0.5936	0.6031	0.6126	0.6221	0.6317	0.6411	0.6506	0.6600	0.6694	0.6788	0.6882	0.6975	0.7068	0.7161	0.7253
0.42	0.5939	0.6035	0.6130	0.6226	0.6321	0.6416	0.6510	0.6605	0.6699	0.6793	0.6887	0.6981	0.7074	0.7167	0.7260	0.7352	0.7445
0.44	0.6134	0.6230	0.6325	0.6420	0.6515	0.6609	0.6704	0.6798	0.6892	0.6986	0.7080	0.7173	0.7266	0.7359	0.7451	0.7544	0.7636
0.46	0.6329	0.6425	0.6519	0.6614	0.6709	0.6803	0.6897	0.6991	0.7085	0.7178	0.7272	0.7365	0.7458	0.7550	0.7643	0.7735	0.7827
0.48	0.6524	0.6619	0.6713	0.6808	0.6902	0.6996	0.7090	0.7184	0.7277	0.7371	0.7464	0.7557	0.7649	0.7741	0.7834	0.7925	0.8017
0.50	0.6719	0.6813	0.6907	0.7002	0.7095	0.7189	0.7283	0.7376	0.7470	0.7563	0.7656	0.7748	0.7840	0.7932	0.8024	0.8116	0.8207

$\frac{L}{2C}$	d/L															
	0.35	0.36	0.37	0.38	0.39	0.40	0.41	0.42	0.43	0.44	0.45	0.46	0.47	0.48	0.49	0.50
0.02	0.3632	0.3726	0.3820	0.3914	0.4007	0.4100	0.4192	0.4285	0.4377	0.4469	0.4560	0.4651	0.4741	0.4832	0.4921	0.5011
0.04	0.3831	0.3925	0.4020	0.4113	0.4206	0.4299	0.4392	0.4484	0.4576	0.4668	0.4759	0.4850	0.4940	0.5031	0.5120	0.5210
0.06	0.4030	0.4124	0.4218	0.4312	0.4405	0.4498	0.4590	0.4683	0.4775	0.4866	0.4958	0.5049	0.5139	0.5230	0.5319	0.5409
0.08	0.4229	0.4323	0.4417	0.4510	0.4603	0.4696	0.4789	0.4881	0.4973	0.5065	0.5156	0.5247	0.5337	0.5428	0.5517	0.5607
0.10	0.4427	0.4521	0.4615	0.4708	0.4801	0.4894	0.4986	0.5079	0.5171	0.5262	0.5353	0.5444	0.5535	0.5625	0.5714	0.5804
0.12	0.4624	0.4718	0.4812	0.4905	0.4999	0.5091	0.5184	0.5276	0.5368	0.5459	0.5550	0.5641	0.5732	0.5822	0.5911	0.6001
0.14	0.4821	0.4915	0.5009	0.5103	0.5195	0.5288	0.5380	0.5473	0.5564	0.5656	0.5747	0.5838	0.5928	0.6018	0.6108	0.6197
0.16	0.5018	0.5112	0.5206	0.5299	0.5392	0.5484	0.5577	0.5669	0.5760	0.5852	0.5943	0.6033	0.6124	0.6214	0.6303	0.6392
0.18	0.5214	0.5308	0.5402	0.5495	0.5588	0.5680	0.5772	0.5864	0.5956	0.6047	0.6138	0.6229	0.6319	0.6409	0.6498	0.6587
0.20	0.5410	0.5504	0.5597	0.5690	0.5783	0.5876	0.5968	0.6060	0.6151	0.6242	0.6333	0.6423	0.6514	0.6604	0.6693	0.6782
0.22	0.5606	0.5699	0.5793	0.5885	0.5978	0.6070	0.6162	0.6254	0.6345	0.6437	0.6527	0.6617	0.6708	0.6798	0.6887	0.6976
0.24	0.5801	0.5894	0.5987	0.6080	0.6173	0.6265	0.6357	0.6449	0.6539	0.6630	0.6721	0.6811	0.6901	0.6991	0.7080	0.7169
0.26	0.5995	0.6089	0.6182	0.6274	0.6366	0.6459	0.6550	0.6642	0.6733	0.6824	0.6914	0.7004	0.7094	0.7184	0.7273	0.7361
0.28	0.6189	0.6283	0.6375	0.6468	0.6560	0.6652	0.6744	0.6835	0.6926	0.7017	0.7107	0.7197	0.7287	0.7376	0.7465	0.7554
0.30	0.6383	0.6476	0.6569	0.6661	0.6753	0.6845	0.6937	0.7028	0.7119	0.7209	0.7299	0.7389	0.7479	0.7568	0.7657	0.7745
0.32	0.6576	0.6669	0.6762	0.6854	0.6946	0.7038	0.7129	0.7220	0.7311	0.7401	0.7491	0.7581	0.7670	0.7759	0.7848	0.7936
0.34	0.6769	0.6862	0.6954	0.7046	0.7138	0.7230	0.7321	0.7411	0.7502	0.7592	0.7682	0.7772	0.7861	0.7950	0.8039	0.8126
0.36	0.6962	0.7054	0.7146	0.7238	0.7330	0.7421	0.7512	0.7603	0.7693	0.7783	0.7873	0.7962	0.8051	0.8140	0.8229	0.8316
0.38	0.7154	0.7246	0.7338	0.7430	0.7521	0.7612	0.7703	0.7793	0.7884	0.7973	0.8063	0.8152	0.8241	0.8330	0.8418	0.8505
0.40	0.7346	0.7438	0.7529	0.7621	0.7712	0.7803	0.7893	0.7984	0.8074	0.8163	0.8252	0.8343	0.8430	0.8519	0.8607	0.8694
0.42	0.7537	0.7629	0.7720	0.7812	0.7902	0.7993	0.8083	0.8173	0.8263	0.8353	0.8442	0.8530	0.8619	0.8707	0.8796	0.8883
0.44	0.7728	0.7819	0.7911	0.8002	0.8092	0.8183	0.8273	0.8363	0.8452	0.8541	0.8630	0.8719	0.8807	0.8895	0.8983	0.9070
0.46	0.7918	0.8010	0.8101	0.8192	0.8282	0.8372	0.8462	0.8552	0.8641	0.8730	0.8819	0.8907	0.8995	0.9082	0.9170	0.9257
0.48	0.8108	0.8200	0.8290	0.8381	0.8471	0.8561	0.8651	0.8740	0.8829	0.8918	0.9006	0.9094	0.9182	0.9270	0.9357	0.9444
0.50	0.8298	0.8389	0.8480	0.8570	0.8660	0.8750	0.8839	0.8928	0.9017	0.9105	0.9194	0.9282	0.9369	0.9456	0.9543	0.9630

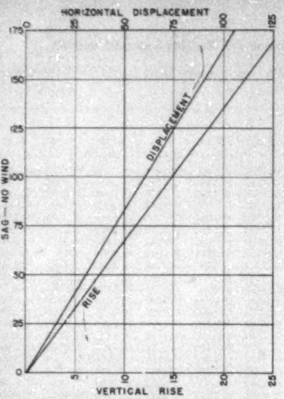

Fig. 6. Swing and rise chart for 605,000-circular-mil (CM) ACSR 30 × 19, 9,000-pound maximum tension at 25 F plus 8-pound wind

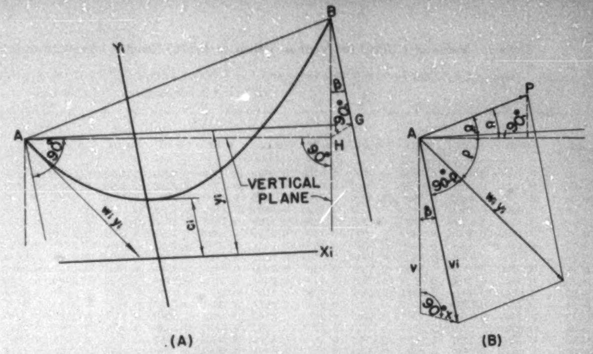

Fig. 8. Conductor lying in the wind plane

sideration for more accurate results. If it is assumed that the conductor under wind lies in a plane whose inclination to the vertical is $\cos^{-1}(w/w_t)=\beta$ where w and w_t are the unit and resultant unit weights of the conductor, the condition shown in Fig. 8(A) results. *AB* is the chord of the span and is common to the vertical and wind planes. *AH* is the span L in the vertical plane, while *AG* is the corresponding span L_t in the wind plane. The differences of elevation, d and d_t are respectively *BH* and *BG*. The conductor in the wind plane is assumed to be a catenary with parameter C_t and y_t is the ordinate at support *A*.

$$L_t=\sqrt{L^2+d^2\sin^2\beta} \qquad \text{(a)}$$

$$d_t=d\cos\beta \qquad \text{(b)}$$

and $w_t y_t$ is the resultant force at *A* from span *AB*.

In Fig. 8(B)

$$\alpha=\tan^{-1}\frac{d}{L},\ \alpha_t=\tan^{-1}\frac{d_t}{L_t},\ \rho=\cos^{-1}\frac{C_t}{y_t} \qquad \text{(c)}$$

The resultant force can be replaced by one component P along the common chord and another, v_t lying along the wind-plane vertical, thus

$$P=\frac{w_t y_t\cos\rho}{\cos\alpha_t} \qquad \text{(d)}$$

$$v_t=\frac{w_t y_t\sin(\rho+\alpha_t)}{\cos\alpha_t} \qquad \text{(e)}$$

The net vertical component acting at *A* is

$$v=\frac{w_t y_t}{\cos\alpha_t}[\sin(\rho+\alpha_t)\cos\beta-\cos\rho\sin\alpha] \qquad (6)$$

or

$$v=v_t\cos\beta-P\cos\alpha$$

where a positive sign indicates a downward force.

The net cross-line horizontal force is

$$x=\frac{w_t y_t}{\cos\alpha_t}\sin(\rho+\alpha_t)\sin\beta \qquad (7)$$

or

$$x=v_t\sin\beta$$

If there is a horizontal angle Δ in the line at *A*, then the cross-line force from span *AB* is

$$x\Delta=x\cos\frac{\Delta}{2}+P\cos\alpha\sin\frac{\Delta}{2} \qquad (8)$$

Equivalent Span

For a given set of conditions each length of span will have a different rate of tension change with change of loading

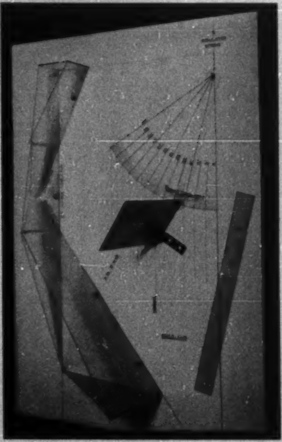

Fig. 7 (left). Model for measuring clearance to tower

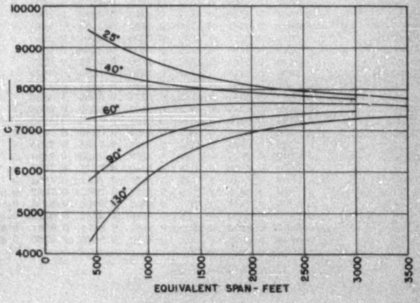

Fig. 9 (right). C Curves for 605,000-CM ACSR 30 × 19, 9,000-pound maximum tension at 25 F plus 8-pound wind or temperature. Thus, where spans are supported on vertical suspension insulators, each span will have an influence on its neighbor such that no span can be considered independently of the remainder of spans in the same section between anchor structures. On the assumptions that the suspended conductor forms a parabola, that equalizing movements of insulators are so small that they introduce no horizontal force from the suspended weight, and that the movement of the insulators can be considered axial to the conductor, Still[9] has developed an equivalent span. This span is the one which will have equivalent characteristics, in so far as tension variation with temperature and loading are concerned, as the series of spans from which it is derived. The equation is

$$L_E = \sqrt{\frac{\Sigma L^3}{\Sigma L}} \tag{9}$$

where

L_E = equivalent span
ΣL^3 = summation of the cubes of the actual span
ΣL = distance between anchor structures of the section under consideration

Using a table of cubes, confining the calculations to three significant figures, and using a slide rule for dividing and extracting the square root, the equivalent span can be determined quickly. However, it is to be noted that generally, as the number of spans increases, the equivalent span approaches the average span, and a little experience will determine when the latter figure may be used. Once the equivalent span is determined for a section of line the value of C for that section can be found from the family of curves in Fig. 9.

The equivalent span method must be used with caution as the error in the assumption made relative to the weight of the suspension-insulator string will cause the clearance to ground to be less than calculated in spans that are shorter than the equivalent, while spans longer than the equivalent will tend to have lessened clearance to lines crossing above. If a section of line contains spans of widely differing lengths heterogeneously distributed, this lack of symmetry will exaggerate the errors, as will be seen in Fig. 10 which compares the true conditions with the condition as calculated by the equivalent span method.

In Fig. 10 the spans have been sagged to a constant value of C=7,650 at 60 F and the true condition is compared with the assumed at 130 F. In Fig. 10(A) the error of the 2-span section is within practical limits of accuracy, and if these two spans are repeated indefinitely in the order 2,000, 1,000, 1,000, 2,000, etc., the errors will remain the same. If these two spans are repeated in the order 2,000, 1,000, 2,000, 1,000, etc., the errors will be reduced somewhat. Thus, where the unequal spans are well distributed, as is the usual case in practice, the errors will be minor.

In Fig. 10(B) the case of unsymmetrical nonuniformity is being approached, although if this 4-span pattern is repeated in any whole multiple the errors will be substantially reduced in all but the end spans of the section. In Fig. 10(C) and (D) the errors are attaining considerable magnitude and where the spans are as unsymmetrically distributed as in the example and if closer determination of clearance is required for critical spans it

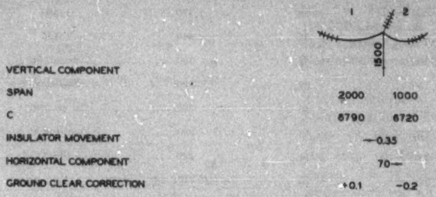
1
2
1500
VERTICAL COMPONENT
SPAN
2000
1000
C
6790
6720
INSULATOR MOVEMENT
—0.35
HORIZONTAL COMPONENT
70—
GROUND CLEAR. CORRECTION
+0.1
-0.2

(A) TWO SPAN SECTION

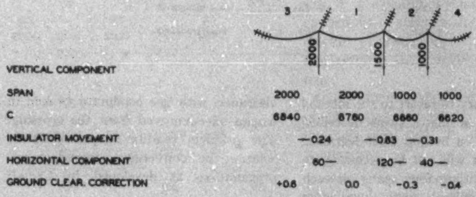
3
1
2
4
2000
1500
1000
VERTICAL COMPONENT
SPAN
2000
2000
1000
1000
C
6840
6780
6660
6620
INSULATOR MOVEMENT
—0.24
—0.83
—0.31
HORIZONTAL COMPONENT
60—
120—
40—
GROUND CLEAR. CORRECTION
+0.6
0.0
-0.3
-0.4

(B) FOUR SPAN SECTION

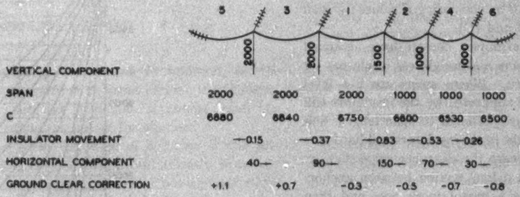
5
3
1
2
4
6
2000
2000
1500
1000
1000
VERTICAL COMPONENT
SPAN
2000
2000
2000
1000
1000
1000
C
6880
6840
6750
6600
6530
6500
INSULATOR MOVEMENT
—0.15
—0.37
—0.83
—0.53
—0.26
HORIZONTAL COMPONENT
40—
90—
150—
70—
30—
GROUND CLEAR. CORRECTION
+1.1
+0.7
-0.3
-0.5
-0.7
-0.8

(C) SIX SPAN SECTION

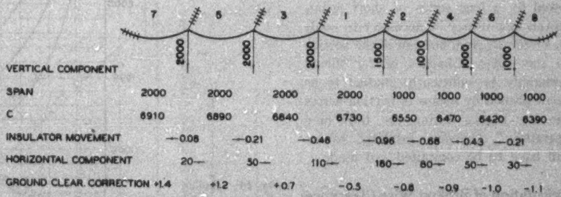
7
5
3
1
2
4
6
8
2000
2000
2000
1500
1000
1000
1000
VERTICAL COMPONENT
SPAN
2000
2000
2000
2000
1000
1000
1000
1000
C
6910
6890
6840
6730
6550
6470
6420
6390
INSULATOR MOVEMENT
—0.08
—0.21
—0.48
—0.96
—0.68
—0.43
—0.21
HORIZONTAL COMPONENT
20—
50—
110—
160—
80—
50—
30—
GROUND CLEAR. CORRECTION +1.4
+1.2
+0.7
-0.5
-0.8
-0.9
-1.0
-1.1

(D) EIGHT SPAN SECTION

Fig. 10. Example showing limitations of equivalent span method. All spans tensioned to C=7,650 at 60 F. For L_E=1,730, C=6,780 at 130 degrees. Actual condition at 130 F will be as shown in the figure for an 8-foot insulator string

Table II. Measurements of Reduction in C Caused by Broken Wire Condition

1,033,500-Circular-Mil ACSR 54×7, 14 Insulators at 5³/₄ Inches, Length of String 8.69 Feet, Before Cut the Value of C=7,470

Tower and Number	Span	Difference of Elevation	14-Span Section, Reduction in C	4-Span Section, Reduction in C
140-1				
	Conductor cut in this span			
139-4				
	1,150	+ 35	3,320	3,300
139-3				
	1,200	+ 8	2,300	2,480
139-2				
	1,196	+ 66	1,370	1,880
139-1				
	1,654	+ 37	940	1,450
138-4				
	1,500	− 32	790	insulators
138-3				
	1,180	− 39	500	restrained
138-2				
	1,570	− 40	260	to vertical
138-1				
	1,220	− 10	250	position at
137-4				
	1,301	+ 41	290	138-4
137-3				
	1,579	− 25	110	
137-2				
	1,175	− 6	0	
137-1				
	1,309	− 55	not measured	
136-4				
	1,390	+ 25	not measured	
136-3				
	1,651	−102	not measured	
136-2				

will be necessary to resort to the method of distributing insulator swing described in the section on broken wire clearance. In this case it will not be necessary to consider more than four spans on each side of the critical span since more remote spans will have minor influence. The effect of remote spans may be seen in Fig. 10 by comparing *C* values for span 1 in (C) and (D)

The examples chosen have assumed level spans and weightless insulators for simplicity. Where spans are not level the load supported by the insulators will not be proportional to span length, and the weight of the insulators and hardware will increase the clearance error slightly.

When a long section between anchors traverses a mountainous area and then enters a plain, it is likely that there will be an extensive series of long spans followed by a long series of short spans. In this case it may be necessary to grade L_E uniformly from one end of the section to the other. Changes in L_E should preferably be sufficiently gradual to be accomplished by means of friction across the sag blocks during the tensioning operation; otherwise insulator offsets will have to be computed and made.

Calculation of Broken Wire Clearance

At railroads and certain other crossings made on suspension insulators, it is frequently necessary to maintain a specified clearance with the conductor broken in a span once-removed from the crossing. The problem readily adapts itself to solution by converging successive approximations as developed by Cross[10] for determining the distribution of moments in rigid frame works. Others[11] have made the solution from a slightly different approach.

In theory there is no limit to the number of spans beyond the crossing which will influence the tension of the crossing span. However, Table II, which gives the results of a test on a 14-span section, shows that the calculations can be limited to four spans with very little error. Trial by calculation confirms the test results.

Fig. 11 shows the value of *C*, below the normal value, caused by swing of the insulator string, it being assumed that the swing is a reduction in span length. It also shows the rise of the point of support and the restoring component caused by the swing. The system is in a state of equilibrium when the difference in *C* across insulators is equal to the restoring component. Fig. 12 demonstrates this process.

Plastic Flow

Plastic flow takes place in all metals[12] and at high tensions can have considerable effect on sag. For a given set of conditions the flow in aluminum conductors is greater than in copper or steel.[12] The effect is a growth in stressed length, Fig. 13, and consequent increase

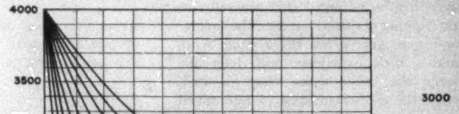

Fig. 11. Broken wire chart for 1,033,500 - CM ACSR 54 × 7, 8,000 - pound maximum tension

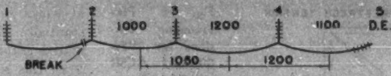

ASSUME THE CONDUCTOR BREAK OCCURS BETWEEN TOWERS 1 AND 2.
BROKEN WIRE C IS TO BE DETERMINED BETWEEN TOWERS 2 AND 3.
LENGTH OF INSULATOR STRING IS 11.0'.

FIRST APPROXIMATION:	\		\		|		|
INSULATOR SWING	11.0		5.0		0.0		0.0
REDUCTION IN SPAN		6.0		5.0			
C		2250	(530)	2780			
RESTORING COMPONENT			530				
SECOND APPROXIMATION:	\		\		\		|
INSULATOR SWING	11.0		5.0		1.8		0.0
REDUCTION IN SPAN		6.0		3.2		1.8	
C		2250	(860)	3110	(210)	3320	
RESTORING COMPONENT			530		210		
THIRD APPROXIMATION:	\		\		\		|
INSULATOR SWING	11.0		5.7		1.8		0.0
REDUCTION IN SPAN		5.3		3.9		1.8	
C		2350	(620)	2970	(350)	3320	
RESTORING COMPONENT			630		210		
FOURTH APPROXIMATION:	\		\		\		|
INSULATOR SWING	11.0		5.7		2.1		0.0
REDUCTION IN SPAN		5.3		3.6		2.1	
C		2350	(660)	3030	(200)	3230	
RESTORING COMPONENT			630		230		
FIFTH APPROXIMATION	\		\		\		|
INSULATOR SWING	11.0		5.8		2.1		0.0
REDUCTION IN SPAN		5.2		3.7		2.1	
C		2360	(650)	3010	(220)	3230	
RESTORING COMPONENT			650		230		
RISE	11.0		1.6		0.2		0.0

THE SYSTEM IS IN A STATE OF EQUILIBRIUM ON THE FIFTH APPROXIMATION AND THE CLEARANCES MAY NOW BE CALCULATED IN SPAN 2 - 3 USING C=2360.

Fig. 12. Example of broken wire calculation

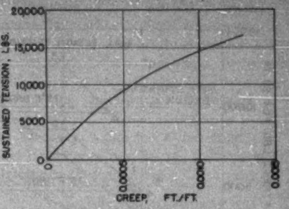

Fig. 14. Typical creep-tension curve for 795,000-CM ACSR. Total creep at 1,000 hours sustained load on unprestretched cable. Nominal ultimate tension of 27,950 pounds

of sag. The amount of flow in unimetallic conductors will vary with the installed tension, the relative tightness of stranding between layers, and the size and number of strands; also service conditions of temperature, degree, and duration of loading. Flow in bimetallic conductors will depend upon the foregoing factors and, in addition, on the proportion between metals, the temperature at time of stranding and the temperature at installation.

The influence of any one of the preceding factors, except tension, is usually small, but if their effect is cumulative the total may be appreciable. In any case it is indeterminate. The total amount of plastic flow in steel-reinforced aluminum cable (ACSR) may amount to 0.20 per cent of the conductor's stressed length; i.e., it may be equivalent to a temperature rise of about 200 F. Obviously this strains the assumptions basic to the equivalent-span principle, and it is equally obvious that a small percentage of error in the assumed total amount of creep can result in considerable error in the magnitude of the final sag.

There are in general use three methods of providing for plastic flow in conductors, each with its advantages and handicaps:

1. String the conductor at an initial tension high enough to provide for all the plastic flow to follow.
2. Prestress the conductor during the sagging operation at a tension high enough, and hold it at that tension long enough to cause all plastic flow to take place prior to final sagging.
3. Combine the two methods; prestress at a moderately high tension for a reasonable length of time, and allow for a moderate amount of plastic flow to follow.

In the first method the initial tension will be high, frequently higher than the maximum design tension, and this will impose undue loads on the supporting

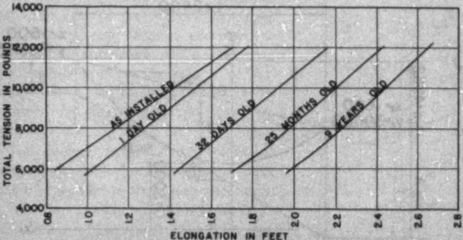

Fig. 13. Typical tension elongation curve for 1,033,500 54 × 7, 1048-foot span. Average tension 11,000 pounds between tests

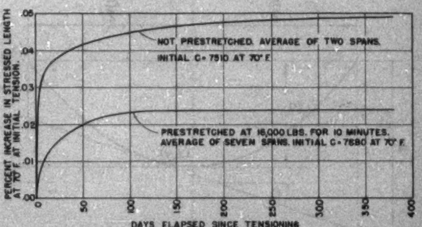

Fig. 15. Comparison of creep in 605,000-CM ACSR 30 × 19, span lengths between 1,227 feet, and 2,701 feet

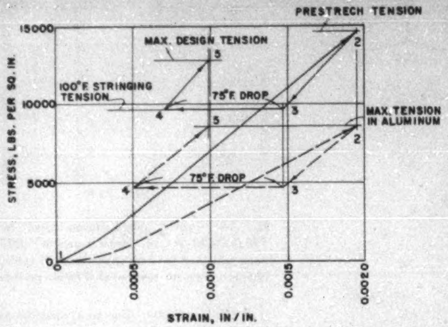

Fig. 16. Prestretching tensions for 795,000-CM ACSR 26 × 7

—— Stress-strain curve for ACSR

- - - - Stress-strain curve for aluminum

Assumed: All strands snug at stranding temperature, 100 F. Conductor tensioned at 100 F. Maximum design tension at 25 F

structures, aggravate tie-down conditions, intensify vibration troubles, and increase insulator swings at suspension angles, all for an indeterminate time extending into the operating life of the line. Plastic flow is a function of tension, Fig. 14, and because of the large amount of creep it is difficult to determine the final sag with exactitude; large amounts of creep may stretch equivalent-span assumptions beyond reasonable limits. Where sections of line successively sagged are separated only by suspension insulators, an indeterminate amount of plastic flow will take place in the first section before the second section is sagged, and the tensioning operations will thereby be hampered. Likewise, on single-circuit lines where it is necessary to level the three phases for appearance's sake, delay between sagging phases will make the leveling difficult or impossible. However, this method is generally the simplest from the construction standpoint and is frequently used for that reason.

The second method may temporarily overload anchor structures, and they may have to be supported. Tensioning equipment such as winches and cable grips will need to be stouter than normal. The conductor will tend to rise above the sag blocks at lightly loaded towers, and this condition will require precautions to prevent damage to the conductor. The "soaking" time may unduly delay construction operations. However, the advantage of the method is that the conductor, when finally sagged, is in a stable condition so that clearances can be determined accurately and without waste of structures.

The third method offers some of the constructional advantages of the first without unduly sacrificing the accuracy of the second. Somewhat heavier equipment may be required, the conductor may rise above the sag blocks at the most lightly loaded towers, and the sagging operation may be somewhat delayed. However, the anchor structures will usually withstand the tension as a temporary load, and subsequent creep will not generally be excessive; see Fig. 15.

The amount of plastic flow for a given set of conditions can only be determined from test, but the prestretching tension at which subsequent creep will be substantially eliminated can be approximated graphically, although for careful work this should be checked by test of at least 6 months' duration. The following method will give results at least sufficiently accurate to serve as a starting point for a time-elongation test.

If, in Fig. 16, the conductor is prestressed along the curves 1–2 and then sagged at stringing tension 3, the drop in temperature to minimum design value 3–4, together with the imposed maximum loading, will cause the tension to rise to the maximum design value 5. If the prestretch tension has been properly selected, the stress in the aluminum will never exceed the value attained at prestretch; and subsequent plastic flow will not take place. This procedure fails to take the time element into consideration, but if the conductor were to be held at tension 2 for a sufficient time, the results would be as predicted. Time, however, is usually costly, and, since higher tension will produce the same results, the latter element is generally more economical. For the case shown in Fig. 15, tests demonstrated that a prestretch tension of 16,000 pounds held for 10 minutes, reduced subsequent creep to 0.03 per cent as compared to 0.05 per cent for unprestressed conductor.

Since it was assumed in Fig. 16 that the unstressed length was the same for both core and envelope, it is evident that either loose stranding or prestretching at temperatures above stranding temperature will lessen the effect of the prestretch on the aluminum, while the reverse will be true when prestretching is done at temperatures below the stranding temperature.

Field Work

In the final analysis the accuracy of the design is entirely dependent upon

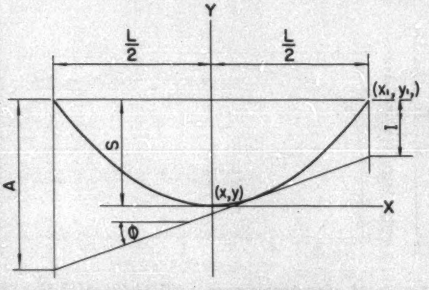

Fig. 17. Method of sagging using unequal intercepts

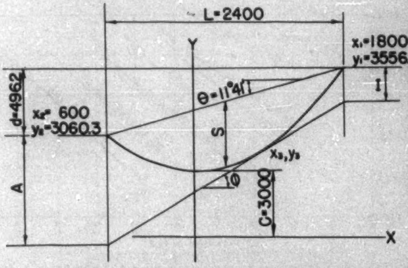

Fig. 18. Example of sagging inclined span

field operations. It is therefore necessary for the designer to prescribe the tensioning procedure. Dynamometers are ruled out wherever the section tensioned consists of more than a very few spans, because such an instrument can give the tension at only one end of the section. For longer sections the sighting method must be used, and this may be done in short spans with naked eye and sight boards, but long spans will require the use of a surveyor's transit.

So far as adjustment of tension is concerned there is no limit to the number of spans that can be sagged simultaneously by the sight method, regardless of the nature of the terrain or amount of friction in the sag blocks, provided that communication facilities are adequate and that the sag blocks are well constructed and have uniform frictional characteristics. The limitations on length of tension section will be determined by construction difficulties, and the optimum length will be reached when the cost of handling the excess conductor pulled from the section balances the savings resulting from fewer temporary anchors. Tension sections 5 miles long are common, and sections of 7 miles have been successfully sagged.

The number of saggers to a section is dependent upon the number of spans to be sagged, the quality of the sag blocks and the tension. It has been found for spans averaging about 1,100 feet, with roller-bearing sag blocks and C below 5,000, every fourth span should be sagged. Where spans average 1,400 feet and C is above 6,000, a sagger in every fifth span is adequate. Best use can be made of the least number of saggers if each conductor of a circuit is put through on identical cycle of tensions. Commonly the last sagger of a section positions his conductor while slacking back from a previously overpulled position. The next sagger, because of sag block friction, will now find his conductor low, and he therefore positions it by tightening, which in turn makes the conductor of the succeeding sagger high, etc. If this order of procedure is reversed at any stage while tensioning the next conductor, the effects of uncompensated sag block friction will be reversed between saggers on the two conductors.

For sagging purposes the conductor can be brought tangent to a line of sight which is parallel to the chord and below it by the amount S. However, it is sometimes difficult and usually inconvenient to establish such a line of sight. A more flexible method of adequate accuracy is to use unequal intercepts at the conductor supports. Consider the level parabola of Fig. 17, where

$$y_1=\frac{L^2}{8C}-y+\left(\frac{L}{2}-x\right)\tan\phi+I$$

$$y=\frac{x^2}{2C}$$

whence

$$\frac{dy}{dx}=\frac{x}{C}=\tan\phi$$

Combining these expressions

$$C=\frac{L^2}{8S}=\frac{A\pm2\sqrt{IA}+I}{2\tan^2\phi} \qquad (10)$$

Solving for S

$$S=\left(\frac{\sqrt{A}+\sqrt{I}}{2}\right)^2 \qquad (11)$$

This equation may be applied to a catenary, see Fig. 18, with considerable accuracy where neither of the factors, I or A, exceeds the other by more than two to one.

The sag by equation 3 is

$$\begin{aligned}\frac{2,400^2}{8\times3,000}&=240.0\\ +\frac{240^2}{6\times3,000}&=3.2\\ \text{Sag}&=243.2\times1.0212=248.4\end{aligned}$$

The true maximum sag for this catenary is 248.2, while the true center sag is 248.1. If $I=175.6$, the line of sight is tangent to the catenary at $x_1=810$ and $A=336.0$. By equation 11

$$S=\left(\frac{\sqrt{175.6}+\sqrt{336.0}}{2}\right)^2=249.3$$

The ratio C/L is usually 3 to 1 or greater and where this is the case it is usually safe to assume that results will be accurate when the ratio between I and A is as high as 4 to 1. However, the normal procedure is the reverse of the preceding example since it is usual to assume a value for I and from this and S compute a value of A which will determine the line of sight. Rearranging equation 11

$$A=(2\sqrt{S}-\sqrt{I})^2 \qquad (12)$$

If the preceding values for I and S are used, then $A=333.8$. These values for I and A are tangent to a catenary for which $C=3,012$, with a true center sag of 247.2 feet.

From equation 11, there follow equations which will facilitate sagging by use of an engineer's transit with methods familiar to cadastral surveyors. It is assumed that the point of observation, or transit, is at I and that the intercept A is at the distant support. The angle of the tangent ϕ, and the angle of chord θ, are considered negative when they are downward from the point of observation; d is negative when the distant point of support is below the one occupied. All other factors are always positive. Since $A=d+I-L\tan\phi$, then

$$S=\left(\frac{\sqrt{d+I-L\tan\phi}+\sqrt{I}}{2}\right)^2 \qquad (13)$$

$$\tan\phi=\frac{d+4\sqrt{IS}-4S}{L} \qquad (14)$$

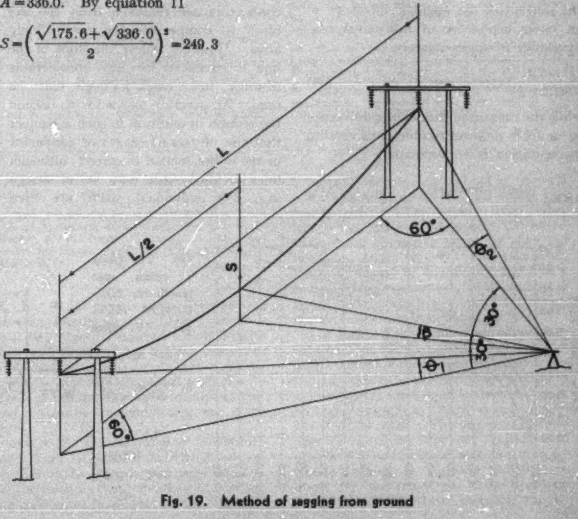

Fig. 19. Method of sagging from ground

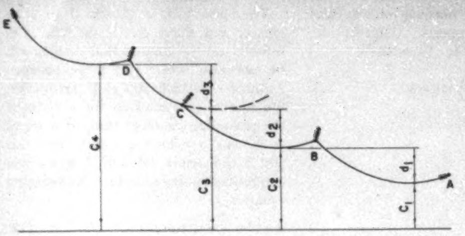

Fig. 20. Series of sloping spans

The preceding methods and equations are to be used when the transit can be mounted on a structure. This limits the method to steel-tower lines, or to wood-pole lines where sag is sufficient to make the observations from the ground at the structure, because mounting a transit on a pole is difficult and in any case a man skilled in the operation of the instrument is not apt to be skilled in climbing poles. For wood-pole lines where the span is too long for the use of sight boards, the transit may be mounted to the side of the line, and the vertical angle to the sag at the center of the span is readily computed. If the transit is placed at the apex of an equilateral triangle with the span as the base, see Fig. 19, it can be shown that

$$\tan\beta = 0.577(\tan\theta_1 + \tan\theta_2) - \frac{S}{0.866L} \qquad (15)$$

If the setup is made for the center conductor and P is the phase separation, the tangent of the angular difference to an outer conductor of horizontal configuration is approximately

$$\frac{P\tan\beta}{0.866L+P}\ \text{(approximately)} \qquad (16)$$

while the tangent of the angular difference to an upper or lower conductor of vertical configuration is approximately

$$\frac{P}{0.866L}\ \text{(approximately)} \qquad (17)$$

In general, the vertical angles will be small and tangents will be less than 0.1, so that slide-rule accuracy is adequate. For the same reason, stadia location of the apex of the equilateral triangle is sufficiently accurate. Nevertheless, the apex angle, regardless of its deviation from true 60 degrees, should be bisected to the nearest minute.

Sagging Sloping Spans

When the transmission line is in steeply sloping terrain, the difference in tension, across a supporting structure may be greater than the sag-block friction can support, and the conductor may tend to "run downhill." Where the unrestrained difference is small, the sagger may compensate for it by using judgment in adjusting the tensions somewhat tight at higher elevations and somewhat slack at lower, depending on the natural swing of the insulator strings when the conductors are removed from the sag block to compensate for most of any error. However, where the slope of the line is excessive for any considerable distance, more exact methods must be used. An accurate method is to tension the section in question in such a manner that the unstressed length of conductor in the entire section is correct, although no individual span may be at design sag. The individual spans are then corrected by adjusting the insulator strings when the sag blocks are removed. For another solution, see reference 14.

In the following discussion it will be assumed that the sag blocks are frictionless, and that the sagger will regulate his subsequent sag procedure to produce this effect. With frictionless sag blocks the condition during tensioning is as shown in Fig. 20. After the conductor is transferred to the insulators, the parameter for all spans is to be constant at C_0, the design value. The two conditions are related by the fact that the unstressed length of conductor in the section is the same for both conditions. Let a be the change in unstressed conductor length per unit change in the value of C, and assume this rate constant within the range required. Then

$$(C_0-C_1)a_1+(C_0-C_2)a_2+(C_0-C_3)a_3+(C_0-C_4)a_4=0$$

$$(C_0-C_1)a_1+(C_0-C_1-d_1)a_2+(C_0-C_1-d_1-d_2)a_3+(C_0-C_1-d_1-d_2-d_3)a_4=0$$

Let

$$d_1=\Delta C_2,\ d_1+d_2=\Delta C_3,\ d_1+d_2+d_3=\Delta C_4$$

$$C_1=C_0-\frac{\Sigma(a\Delta C)}{\Sigma a}$$

$C_2=C_1+d_1$, etc.

The values of d are found approximately by scaling the profile while the values of a are best found from a chart made for that purpose. See Fig. 21.

The amount that the insulators at support B are to be offset from a vertical line drawn through that support is $(C_0-C_1)a_1$, while the similar offset at support C is $(C_0-C_1)a_1+(C_0-C_2)a_2$, etc. If the sense of d is taken as positive when the apex of span BC is above that of span AB and negative otherwise, the positive values indicate offsets to the right and negative values to the left of the vertical through the support.

Field procedure is to sag the section to the values C_1, C_2, etc. Frictional effect of the sag blocks is eliminated during the tensioning sequence. After

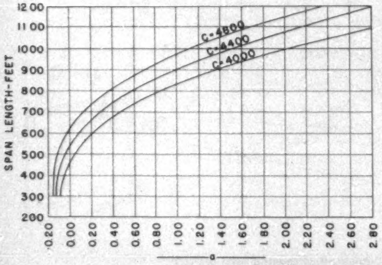

Fig. 21 (left). a versus span length for 605,000-CM ACSR 30 × 19, where

$$a=\Delta_1-\Delta_2$$

$$\Delta_1=\frac{L^3}{24C^2}-\frac{wCL}{AE}$$

$$\Delta_2=\frac{L^3}{24(C-100)^2}-\frac{w(C-100)L}{AE}$$

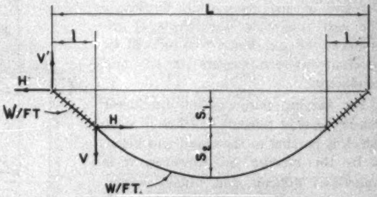

Fig. 22. Typical dead-end span

the sagging operations are completed and before the conductor is transferred from sag block to insulator at any support, the proper insulator position is marked at all supports. It should be noted that great precision in the calculations or marking is not required as small inequalities in tension will be equalized by small movements, from theoretical vertical, of the suspension insulator strings.

As an example of this process, in Fig. 20 let span $AB=800$, $BC=700$, $CD=600$, $DE=800$, and let $d_1=50$, $d_2=100$, $d_3=50$, and $C_0=4{,}400$. Then $\Delta C_1=0$, $\Delta C_2=50$, $\Delta C_3=150$, $\Delta C_4=200$, and from the curve of Fig. 21 $a_1=0.590$, $a_2=0.285$, $a_3=0.079$, and $a_4=0.590$. Also $a_1\Delta C_1=0$, $a_2\Delta C_2=14.25$, $a_3\Delta C_3=11.85$, $a_4\Delta C_4=118.00$; $\Sigma a=1.544$, $\Sigma a\Delta C=144.10$; and

$$C_1=4{,}400-\frac{144.10}{1.544}=4{,}307$$

It then follows that $C_1=4{,}307$, $C_2=4{,}357$, $C_3=4{,}457$, $C_4=4{,}507$; $a_1(C_0-C_1)=0.55$, $a_2(C_0-C_2)=0.12$, $a_3(C_0-C_3)=-0.04$, $a_4(C_0-C_4)=-0.63$; and the offset to the right at support $B=0.55$, at $C=0.55+0.12=0.67$, and at $D=0.67-0.04=0.63$.

Sag Adjustments After Installation

Occasionally the sag in a span must be adjusted after installation has been completed. This adjustment can readily be made by calculating the difference in the unstressed length of wire in the span at S_1 and S_2. The unstressed length of wire in a span is

$$=L\left(1+\frac{2.67S^2}{L^2}\right)-\frac{wL^3}{8MS}$$

where

w = weight of conductor, pounds per foot
M = modulus of conductor, pounds

Therefore, the amount of wire to be "cut in" or "cut out" of the span for change of sag from S_1 to S_2 is

$$l_1-l_2=\frac{2.67}{L}(S_1+S_2)(S_1-S_2)+\frac{wL^3}{8M}\left(\frac{1}{S_2}-\frac{1}{S_1}\right) \qquad (18)$$

or in terms of C

$$l_1-l_2=\frac{L^3}{24}\left(\frac{1}{C_1}+\frac{1}{C_2}\right)\left(\frac{1}{C_1}-\frac{1}{C_2}\right)+\frac{Lw}{M}(C_2-C_1) \qquad (19)$$

Sag in Dead-End Spans

In short dead-end spans, with low tensions, the effect of the weight of the dead-end insulator strings will be appreciable. In spans where this condition exists, such as rack spans at substations, clearances are generally kept to a minimum and the effect of the insulator strings should be accounted for. An approximate solution follows, see Fig. 22, which has proved adequate for this condition.

Taking the summation of moments about the point of support and solving for S_1

$$S_1=\frac{wl}{2H}(L-2l)+\frac{Wl^2}{2H}$$

and since $H=wC$, it then follows that

$$S_1+S_2=\frac{l}{2C}(L-2l)+\frac{(L-2l)^2}{8C}+\frac{Wl^2}{wC} \qquad (20)$$

Conclusion

The design of transmission-line tensions by precise but time-consuming methods is justified in unusual cases, but approximate and faster methods may be used to solve the problems encountered in the great majority of lines. However, these approximate methods are to be used with caution and only with a thorough knowledge of their limitations. Like a mechanic, the designer selects the tools that will most quickly produce satisfactory results.

References

1. Differential and Integral Calculus (book), **Clyde E. Love.** The Macmillan Company, New York, N. Y., 4th ed., 1943.

2. A Practical Treatise on Suspension Bridge (book), **D. B. Steinman.** John Wiley and Sons, Inc., New York, N. Y., 2nd ed., 1929.

3. The Effect of Shearing Stress on the Span Calculations of a Suspended Cable, **T. Ohtsuki.** *Journal*, Institution of Electrical Engineers, London, England, vol. 61, Oct. 1923, pp. 1079–86.

4. Sag and Tension in Overhead Lines (book), **C. G. Watson.** Isaac Pitman and Sons, Ltd., London, England, 1931.

5. Sag Calculations by the Use of Martin's Tables, **James S. Martin.** Copperweld Steel Company, Glassport, Pa., 1931.

6. ACSR, Graphic Methods for Sag-Tension Calculations, **T. Varney.** Aluminum Company of America, Pittsburgh, Pa., 1927.

7. Transmission Lines, Design, Construction and Performance (book), **Fred C. De Weese.** McGraw-Hill Book Company, Inc., New York, N. Y., 1945.

8. Measure Clearances Easily with Tower Models, **H. D. Fischer, Jr.** *Electrical World*, New York, N. Y., June 29, 1953, p. 99.

9. Electric Power Transmission (book), **Alfred Still.** McGraw-Hill Book Company, Inc., New York, N. Y., 1927.

10. Analysis of Continuous Frames by Distributing Fixed End Moments, **Hardy Cross.** *Transactions*, American Society of Civil Engineers, New York, N. Y., vol. 96, 1932, pp. 1–10.

11. Broken Conductor Effect on Sags in Suspension Spans, **Alfio Bissiri, Maurice Landau.** *AIEE Transactions*, vol. 66, 1947, pp. 1181–88.

12. Mechanics of Creep for Structural Analysis, **Joseph Marin.** *Proceedings*, American Society of Civil Engineers, New York, N. Y., vol. 68, 1942, pp. 719–35.

13. Stress-Strain Studies of Transmission Line Conductors, **G. W. Stickley.** *AIEE Transactions*, vol. 51, Dec. 1932, pp. 1052–58.

14. Design of Hillside Spans Simplified, **John M. Huston.** *Electrical World*, New York, N. Y., vol. 137, June 2, 1952, pp. 86–89.

◆

Discussion

L. T. Guess (Aluminum Company of America, Pittsburgh, Pa): I note the authors use the term "plastic flow" for the phenomenon described later in the paper as creep. I believe the term "creep" is in more common usage, especially among metallurgists, and in this case it is more specific. The definition of creep as used by metallurgists may be helpful to electrical engineers: "Creep is the flow or plastic deformation of material that occurs with time under load, after the initial deformation resulting from the application of load." Two references pertinent to the subject of creep are listed.[1,2]

References

1. A Method of Analyzing Creep Data, **R. G. Sturm, C. Dumont, F. M. Howell.** *Journal of Applied Mechanics*, New York, N. Y., vol. 58, June 1936, pp. A62–66.

2. The Creep Properties of Several Cold Rolled Aluminum Alloy Sheet Metals, **O. D. Sherby, J. E. Dorn.** *Transactions*, American Society for Metals, Cleveland, Ohio, vol. XLIII, 1951, p. 611.

H. H. Rodee (Aluminum Company of America, Pittsburgh, Pa.): This paper deals in a very practical manner with conductor sags and tensions and various associated problems. It should be of considerable interest to engineers concerned with the design and construction of transmission lines and a valuable contribution to the literature.

One of the subjects discussed in considerable detail is plastic flow or inelastic extension and its effect on sags and clearances. Of the three methods mentioned for stringing conductors to provide for this, the third is probably in most general use as the field operations will usually be less costly and less hazardous. The authors have stated that when this method is used the initial tension will frequently be higher than the maximum design tension. This statement, I believe, should be qualified to apply only to light loading conditions. I doubt that it would be true when the maximum design tension is based on heavy loading.

The inelastic extension that takes place following the installation of a conductor at initial tension without prestressing may develop gradually as a result of creep without any significant increase in loading, or it may occur quite rapidly as a result of loading with ice, snow, or wind. The customary procedure in computing sags and tensions is to provide for the inelastic extension and resulting increase in sag that will be produced by the maximum design loading. Under some conditions however, the inelastic extension or creep that develops gradually over a long period of time may result in a larger increase in sag than will be produced by the maximum design loading. Unless provision is made for this in the design, reduced ground clearance will result.

Creep is a function of stress and also a function of time. The rate of creep increases as the stress is increased, but it decreases quite rapidly with time. When plotted to a log-log scale the creep versus time relation is substantially a straight line; because of this characteristic, it is possible to determine with a high degree of accuracy the creep for long periods of time from tests extending over a few months.

As creep progresses in a conductor on a transmission line, the tension will decrease which, in turn, will cause the rate of creep to decrease. Creep is therefore to some extent self-stopping. The length of span will have considerable influence on this self-stopping action since the same unit creep will cause a larger reduction in tension in a short span than in a long span. Other conditions being equal, creep will therefore have a much greater effect on sags in long spans than in short spans.

Our laboratory has performed a considerable number of creep tests, some continuing for several years, on various sizes and types of conductors. The results show that the inelastic extension resulting from creep at normal tensions over the probable life of a transmission line will not exceed that resulting from the maximum design loading when the design is based on heavy loading conditions.

In light loading districts normal tensions are usually higher and spans longer, both of which will increase the effect of creep. On the other hand, maximum design tensions are usually lower than in heavy loading districts and the inelastic extension resulting from maximum design loading will be less. Creep will therefore usually be the predominating influence in light loading districts and should be taken into consideration in the design.

Under medium loading conditions, either the gradual creep at normal tensions or inelastic extension at maximum loading may be the predominating influence, depending upon size and type of conductor, span length and tension. For most conditions the differences will be small, and the customary practice of providing for the increase in sag after maximum design loading should be satisfactory. I believe that experience has generally confirmed this. Typical examples are given in Table III for a conductor size of 336,400-CM ACSR 30/7 and a span length of 1,200 feet. For purposes of comparison, the initial sag at 60 F was assumed the same as in both examples. The initial sags and the final sags after maximum design loading were computed by the method de-

Fig. 23 (right). Nomograph for determining control factor for conductor sagging

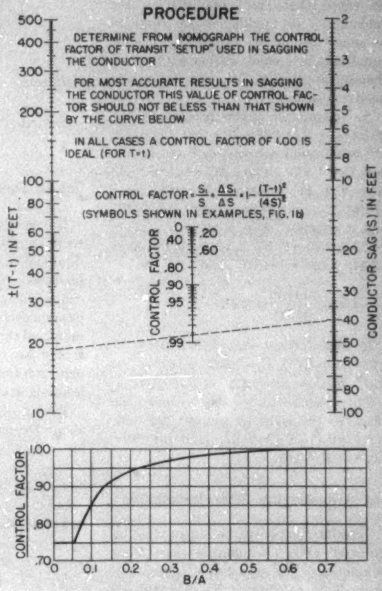

Fig. 24 (below). Sample calculations on use of nomograph to determine control factor

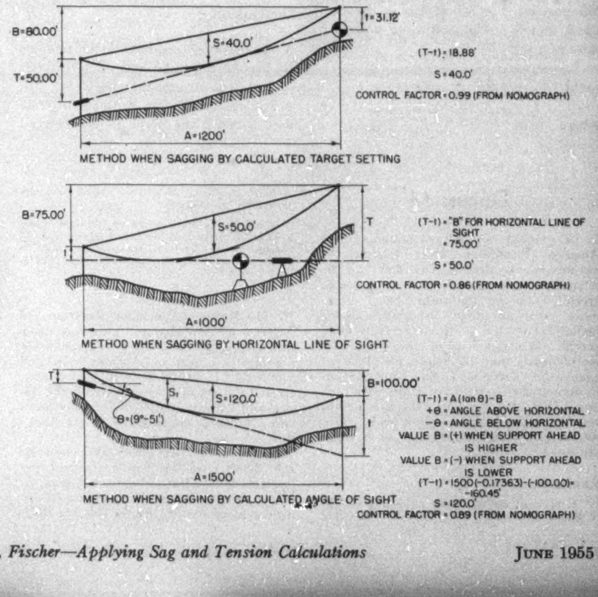
B=80.00'
T=50.00'
S=40.0'
t=31.12'
A=1200'
(T−t)=18.88'
S=40.0'
CONTROL FACTOR=0.99 (FROM NOMOGRAPH)
METHOD WHEN SAGGING BY CALCULATED TARGET SETTING
B=75.00'
t
S=50.0'
T
A=1000'
(T−t)="B" FOR HORIZONTAL LINE OF SIGHT =75.00'
S=50.0'
CONTROL FACTOR=0.86 (FROM NOMOGRAPH)
METHOD WHEN SAGGING BY HORIZONTAL LINE OF SIGHT
T
S₁
S=120.0'
θ=(9°−51')
B=100.00'
t
A=1500'
(T−t)=A(tan θ)−B
+θ=ANGLE ABOVE HORIZONTAL
−θ=ANGLE BELOW HORIZONTAL
VALUE B=(+) WHEN SUPPORT AHEAD IS HIGHER
VALUE B=(−) WHEN SUPPORT AHEAD IS LOWER
(T−t)=1500(−0.17363)−(−100.00)= −160.45'
S=120.0'
CONTROL FACTOR=0.89 (FROM NOMOGRAPH)
METHOD WHEN SAGGING BY CALCULATED ANGLE OF SIGHT

Table III

	Maximum Design Tension with National Electrical Safety Code Heavy Loading	Maximum Design Tension with National Electrical Safety Code Light Loading
Sag with maximum design loading, feet	36.8	28.3
Initial sag at 60 F, feet	25.8	25.8
Initial tension at 60 F, pounds	3,700	3,700
Final sag after maximum design loading, feet	30.0	26.8
Tension, pounds	3,180	3,550
Sag at 60 F after 10 years due to creep, feet	29.1	29.1
Tension, pounds	3,275	3,275

scribed in reference 6 of the paper, with no consideration being given to creep. Ten years was chosen arbitrarily as the elapsed time for determining the increase in sag due to creep since any further increase should be very minor because of the reduction in tension and the natural decrease in rate of creep with elapse of time. Also, it was assumed that during this time there was no increase in loading.

Paul F. Winkelman (Bonneville Power Administration, Portland, Oreg.): Some of the approximations where precise methods are not required in sag tension calculations are quite similar to our methods. However, to allow for creep and inelastic stretch, our sagging charts are based on virtual initial modulus of elasticity, whereas our maximum design templets for locating towers on the line profile are based on the final modulus of elasticity of the conductor. This virtual initial modulus curve goes through points of total elongation occurring during hold periods while increasing loads for the repeated stress-strain tests. Loads are successively held at 30, 40, 50, and 70 per cent of the conductor rated strength for periods of 1/2, 1, 3, and 3 hours respectively. In other words, this virtual initial modulus curve effectively allows for all the stretch occurring during these hold periods when used in determining stringing sags.

To duplicate the conductor elongation represented by this curve during sagging operations in the field, the sagger is required to hold the conductor 10 per cent above stringing tension for a minimum time of 15 minutes. This elongates the conductor the same amount as indicated by the virtual initial modulus for stringing tensions and removes sufficient creep to stabilize the conductor for field sagging. Furthermore, it provides for the permanent conductor set or inelastic stretch that occurs during initial maximum design loading. It also provides for a liberal amount of the additional creep that can be expected in that the final modulus of elasticity return curve is effectively offset by the creep occurring during test hold period at maximum design tension. A check of our repeated stress-strain curves indicates that this removes the amount of creep indicated by the 1,000-hour sustained load curve of Fig. 14 for 5,000 pounds or 18 per cent of rated strength which approximates our stringing tension. As the conductor will be stressed by loadings in the order of maximum design tension for only relatively short periods, the creep will be primarily controlled by bare conductor tension. These tensions would be considerably lower than the maximum design tension, particularly in heavy loading districts.

To prevent excessive errors in field sagging when the transit line of sight is tangent to the catenary too far from the point of true sag, we prepared a nomograph, Fig. 23, and a sample calculation, Fig. 24. The relation in conductor sagging error versus control factor is shown in Fig. 25. The sagging errors shown by these curves were determined by precise methods of sag calculations. By means of this control factor nomograph, the sagger can check in a moment the adequacy of his transit setup as this control factor is determined by data already available to the sagger.

In the short slack spans commonly used in substations, we determine insulator sag with the insulators installed on either one or both ends of the span for the convenience of the sagger. We determine insulator sag by a rather convenient method.[1]

REFERENCE

1. STRAIN INSULATOR EFFECT IN SUBSTATION SPAN SAGS, J. R. Stover. *Electrical World*, New York, N. Y., vol. 126, July 6, 1946.

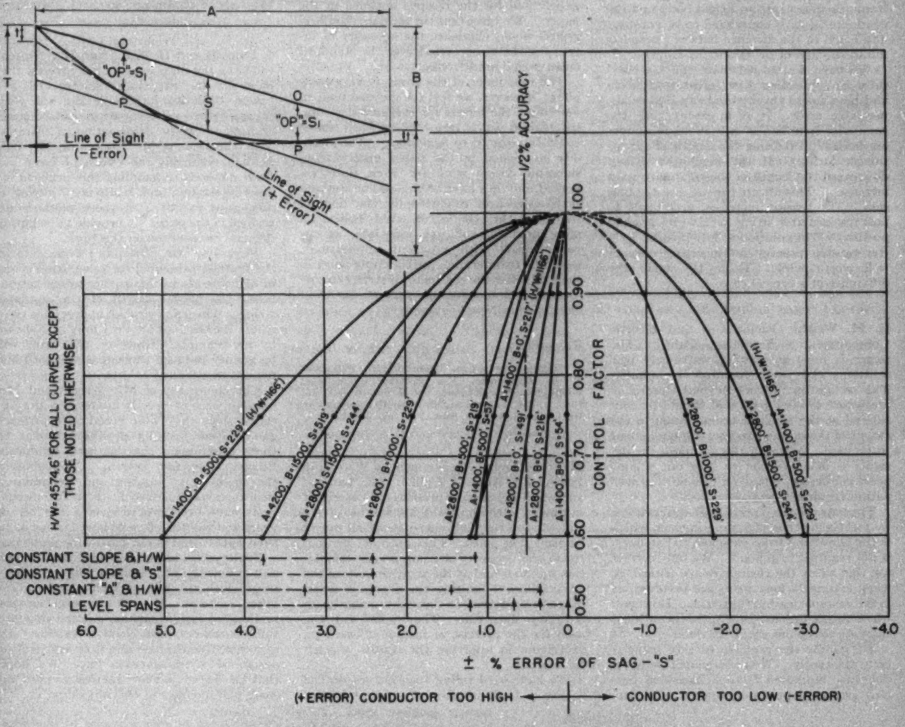

Fig. 25. Relation in conductor sagging error versus control factor

Table IV. Comparison at 120 F, 120-Foot Substation Span, 795,000-CM ACSR, 13 Insulator Units Installed With 1,005 Pounds at 0 F

	Span Constant L-2l	Span Increased by Insulator Deflection
Conductor sag, feet	2.52	1.91
Insulator deflection, feet	1.63	1.25
Total deflection, feet	4.15	3.16
Tension, pounds	600	809

W. C. Freeman (Sargent and Lundy Engineers, Chicago, Ill.): The authors have presented a comprehensive paper on transmission-line problems as a result of extensive experience.

My comments concern the section on "Sag in Dead-End Spans." The paper is not clear as to how the authors intend to use the data presented. If l is taken to be the projected length of the insulator assembly, how is this projected length obtained? If l is taken to be the actual length of the insulator assembly, which is the normally accepted method of calculating insulator deflections and conductor sags for short spans, the insulator string acts as a rigid body and the conductor span is considered to be constant and equal to the distance between supports minus the sum of the two string lengths.

We have had to calculate the sag carefully in connection with substation spans and have found this method can lead to appreciable error. It is apparent that the conductor span is L-2l only if the insulators are horizontal (l being the length of the insulator string). If the insulators deflect downward the length of the conductor span increases. This affects the sag and the tension. The tension increases and tends to pull the insulator string back to its original position. The solution is only possible by a step-by-step process but in many cases is well worth while. Table IV shows the difference in a typical case.

E. M. Wright (Pacific Gas and Electric Company, San Francisco, Calif.): The paper is most interesting, extremely well written, and well founded technically. The section on "Errors Beyond Control of Designer" is very good and should be considered at the time of design—even to the extent of the method and type of equipment to be used. With all this in mind, the designer is in a position to turn out a good practical design, based on calculations well within required tolerances.

The paper being on practical applications, we feel the method of computing sag, which is the correction from parabola to catenary, is not required in general. We only correct for this when the clearances are critical, or when extremely long spans are involved, as in the example used in the paper. However, when this is applied to a series of inclined spans we agree this should be done.

We handle the problem of side swing a little differently. We use a general series of clearance reduction factors, based on percent ground slope, to determine the reduction of ground clearance due to side swing. For horizontal displacement due to side swing, we computed stagger limitations based on the type of conductor, type or series of towers, and transmission-line separation. The stagger limitations are easy to compute and they eliminate all addition and subtraction when locating structures on profile. Determining clearance to towers by the use of a model seems a little cumbersome. We have worked out a rather complicated set of curves to be used with the profiles of the line to determine this clearance. A separate set of curves for each type of conductor and tower type is required. Although it takes a considerable amount of time to draw them, once they are made, and with trained personnel to use them, they are very practical as we often use the same conductor and series of towers on other lines.

The section on "Equivalent Span" is good; in fact we prefer this more theoretical ruling span to the empirical one. Although it takes longer to determine, it gives a more realistic approach.

The section on "Plastic Flow" is one of the best we have seen on this particular subject. We have felt for a long time that we should consider a longer creep period for all-aluminum and ACSR conductors. In general we use the first method described in the paper, and for the reasons outlined in the paper. We agree that the third method suggested would eliminate the necessity of increasing the creep period over the standard creep period in use today.

The remainder of the paper is very complete; however, we feel the method used to determine the offsets for suspension insulator strings in a series of inclined spans could be reduced to field work. The methods mentioned in the paper involve considerable design work for each tower involved, and they have to be based on assumptions as to field conditions at the time of stringing the conductor. We believe a more practical solution, especially as the paper deals with practical applications, would be to determine the clamping point in the field, after the conductor is strung to correct sag. A tool for this purpose has been developed in New Zealand.[1]

REFERENCE

1. TRANSMISSION LINE CONSTRUCTION PROBLEM. **E. B. Mackenzie.** *New Zealand Engineering*, Wellington, New Zealand, vol. 8, no. 10, Oct. 15, 1953, p. 354. Abstracted in *Water Power*, London, England, vol. 6, no. 9, Sept. 1954, pp. 358–59.

Maurice Landau (Department of Water and Power, Los Angeles, Calif.): Mr. Lummis and Mr. Fischer have presented an excellent summary of the practical application of sag and tension calculations to overhead power transmission lines. The authors demonstrate the necessity of using precise calculation methods and at the same time state the advisability of limiting the degree of accuracy of calculations to those obtainable on an ordinary slide rule. They point out the need for the exercise of judgment based on experience in applying the results of such calculations.

We have used ruling span curves similar to Fig. 9 for a number of years and have found them very satisfactory. The curves of Fig. 9 are for level spans. For transmission lines with large differences in elevation of supports we have found it advisable to prepare additional ruling span curves for spans with differences of elevation of 100, 200, 300 feet, etc. The calculations for these ruling span curves are made using the incremental method for sag tension calculations.[1,2] Use of this series of ruling span curves eliminates the necessity of special calculations for spans with large differences of elevation of supports.

The value of C for any section of the line is determined in a manner similar to that outlined in the present paper, the difference being that the ruling D (difference in elevation) is taken into account as well as the equivalent or ruling span. We have found the following approximate equation adequate for determining the ruling D

$$\text{Ruling } D = 1/2 \,(\text{average } D + \text{maximum } D)$$

REFERENCES

1. INCREMENTAL METHOD FOR SAG-TENSION CALCULATIONS, **Maurice Landau.** *AIEE Transactions*, vol. 70, pt. II, 1951, pp. 1564–71.

2. *Discussion* by **Maurice Landau** of A SIMPLIFIED SAG-TENSION METHOD FOR STEEL-REINFORCED ALUMINUM CONDUCTORS, **C. A. Jordan.** *AIEE Transactions*, vol 71, pt. III, Dec. 1952, pp. 1117–18.

J. Lummis and **H. D. Fischer, Jr.:** We wish to thank the discussers for the interest they have shown. Mr. Guess' statement is well taken. We also prefer to use the word "creep" when referring to the phenomenon of flow or plastic deformation of material. The comments of Mr. Rodee and Mr. Winkelman regarding the effects of creep and their methods of handling this problem are very interesting and, while not differing to any great extent from those methods described in the paper, do provide valuable additional information on this topic.

Regarding Mr. Freeman's comments on the method presented for calculation of sag in short dead-end spans, l is taken here as being the actual length of the insulator string. This can cause an appreciable error where the tensions are very low, as is shown by his example. However, this error will be greatly reduced when tensions are 1,500 pounds or more.

The comments of Mr. Wright and Mr. Landau were of special interest to the authors, since they were based on experience gained from meeting problems similar to those existing on the Southern California Edison Company system. Undoubtedly the methods of sagging and determining clearances as described in these two discussions have been proved over a number of years and will therefore be investigated as to their application in our particular problems.

Each system has its own specific problems and construction standards that it maintains which are different from any found on other systems. For this reason certain methods of design and construction are more suited to one system than to another. In any case, the ultimate aim is an economical design of a transmission line. We hope that the paper and the discussions open up some new avenues to this objective.

Some Utility Ground-Relay Problems

H. C. BARNES
MEMBER AIEE

A. J. McCONNELL
MEMBER AIEE

THERE are many theoretical conditions which can result in false operation of ground relays. These conditions have not been of great concern since ample margin in either pickup or time has been available, especially if sequential tripping could be tolerated.

However, these margins are being diminished by the tremendous expansion of the utility system. The available ground-relay current is being reduced by the increased number of parallel lines, by heavier ground sources at each end of a line, by grounded primary transformers tapped solidly to lines, and by higher current-transformer ratics caused by higher line loadings. The time margin is disappearing because the added facilities make a more closely knit system with the result that faults affect much more of the system, making fast clearing more desirable. The recognized value of high-speed reclosing becomes even more important as the tapped loading increases, thereby precluding sequential tripping which would interfere with high-speed reclosing.

It is the purpose of this paper to point out some of the conditions that lead to false relay operation and to present oscillographic records in verification.

The causes of incorrect or undesired ground-relay operation can be classified in various ways, and are separated into two types: incorrect information supplied to the ground relay (false residual current), and correct information supplied to the ground relay, but with system conditions which cause the ground relay to make incorrect decisions (true residual current). Thus, "false residual current" is defined as a ground-relay current that has no system counterpart, and "true residual current" is defined as ground-relay current having a true system counterpart.

False Residual Current

False residual current can be the result of poor current-transformer performance, or can be caused by certain faults and load distribution even though the current transformers perform perfectly.

CURRENT-TRANSFORMER PERFORMANCE

False residual current attributable to current-transformer performance is the direct result of the variance of the current transformer ratio-correction factor from unity or some other constant and can be caused by unbalanced burden, by differences between individual phase current transformers, or by d-c saturation of the current transformers when the primary currents are offset.

Unbalanced Burden and Differences Between Individual Phase Current Transformers

Unbalanced phase burden as a cause of false residual current can easily be illustrated by the extreme example of the open-circuited current transformer of Fig. 1 during a phase-to-phase fault. Current flows in the ground relay, although the fault does not involve ground.

With all current-transformer circuits intact, and with balanced burden, ground-relay current can still flow as a result of differences in current-transformer characteristics even though there is no primary ground current. Although false residual-current difficulties from these causes are rather rare, the possibility nevertheless exists whenever high ground-relay sensitivity is used.

D-C Saturation of Current Transformers

While d-c saturation of current transformers caused by offset currents has received wide publicity in conjunction with bus-differential relays,[1-7] there has been little attention paid to a similar phenomenon resulting in unexpected transient residual current in ground relays during phase faults or during other overcurrent conditions not involving ground. The basic reason for false transient residual current is the unequal d-c saturation of current transformers caused by unequal d-c offsets of 3-phase currents, or unequal residual magnetism.[4]

Regarding 3-phase faults, fault current must be zero at the inception of the fault and, since the instantaneous values of the 3-phase fault currents cannot be the same in all three phases, the d-c offsets of the three phases cannot be identical. For example, if a 3-phase fault occurs at the time of maximum offset of one phase, the current transformer in that phase will probably become d-c saturated causing its secondary current to be deficient. The other two current transformers being subjected to only half of the maximum d-c offset may not saturate at all; or if they saturate, they will do so later and less severely. The net result is a false residual current in the ground relay.

Similarly, unequal residual magnetism resulting from previous current-transformer history can cause false residual current. Without residual magnetism and with identical current-transformer characteristics, there should be no false residual current during a phase-to-phase fault, regardless of primary-current offset. Any deficiency in the output of one current transformer would be exactly balanced by the deficiency of the output of the second current transformer. However, unbalanced residual magnetism can cause d-c saturation of one current transformer and, to a lesser degree, of the second current transformer. Again, the net result is a false residual current in the ground relay.

Since this phenomenon is of a transient nature, the performance of high-speed relays is of principal concern. Slow-speed relays are seldom affected, except possibly when there is a high d-c time constant. As an example, consider the line relaying of Fig. 2 in which an instantaneous-ground-overcurrent relay is used to improve ground-fault protection. It is assumed that limitation of ground-fault current requires a high relay sensitivity relative to that of the phase relays. For

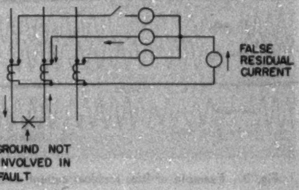

Fig. 1. False residual current caused by open-circuited current transformer

---

Paper 55-99, recommended by the AIEE Relays Committee and approved by the AIEE Committee on Technical Operations for presentation at the AIEE Winter General Meeting, New York, N. Y., January 31–February 4, 1955. Manuscript submitted October 20, 1954; made available for printing December 1, 1954.

H. C. BARNES is with the American Gas and Electric Service Corporation, New York, N. Y., and A. J. McCONNELL is with the General Electric Company, Schenectady, N. Y.

The authors are indebted to the New York State Electric and Gas Corporation, the Bonneville Power Administration, and the Niagara-Mohawk Power Corporation (Western and Eastern Division) for permission to reproduce some of the oscillograms, and to A. Hauspurg, American Gas and Electric Service Corporation, for his assistance.

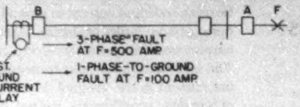
B
A
F
3-PHASE FAULT AT F=500 AMP
1-PHASE-TO-GROUND FAULT AT F=100 AMP
INST. GROUND OVERCURRENT RELAY

Fig. 2. Sensitive instantaneous ground relay used to improve ground-fault protection

the single-phase-to-ground fault magnitude of 100 amperes at F near bus A, a reasonable ground-relay setting might be 120 amperes. A 500-ampere 3-phase fault at F should theoretically cause no current to flow in the ground relay at B. However, d-c saturation of current transformers may easily cause a ground-relay current in excess of its pickup, thus causing an incorrect tripout. Overreach because of this can be prevented by increasing the ground-relay pickup or by introducing a short time delay in the ground-relay trip circuit, each of which sacrifices some protection. Also, false residual current can be reduced by inserting resistance in series with the ground relay.[8] This method requires considerable application-engineering effort and is not necessarily a complete solution. A sure solution, but seldom feasible, is to operate the ground relay from a current transformer with a magnetic circuit which surrounds all three phase currents.[9]

Although the published information on this subject indicates that the problem is very complex, the following simple equation can be used to indicate whether or not trouble can be expected

$$B_{\max}=\frac{\sqrt{2}\,10^8 ITRN_1}{A(N_2)^2} \qquad (1)$$

where

$B_{\max}$ = maximum flux density in lines per square inch
I = symmetrical primary short-circuit current, amperes rms
T = d-c time constant of primary current, seconds
R = resistance of secondary circuit of current transformer and phase relays, ohms (not including ground relay)
N_1 = primary turns of current transformer (=1 for bushing current transformer)
A = core area of current transformer, square inches
N_2 = secondary turns of current transformer

The foregoing equation was derived on the basis of infinite permeability of the current-transformer iron. Spot analytical checks with the variable permeability of the usual current-transformer iron have indicated that the results using infinite permeability are pessimistic to a minor degree. Practically, the residual flux further limits output and, therefore, the results from this method are optimistic.

With the iron used in current transformers, saturation usually occurs at flux densities over 100,000 lines per square inch, though appreciable error probably occurs only above 125,000 lines per square inch. In the example of Fig. 2, the following values are assumed:

I = 500 amperes
T = 0.01 second
R = 1 ohm
N_1 = 1
A = 4 square inches
N_2 = 20

$$B_{\max}=\frac{\sqrt{2}\,10^8\times500\times0.01\times1\times1}{4(20)^2}=$$
442,000 lines per square inch

Since 442,000 lines per square inch is large compared to 125,000, ground-relay difficulty can be anticipated.

Fig. 3 is an oscillogram of a staged, bolted, 3-phase fault (not involving ground) which was made to test an oil circuit breaker. Trace 3 shows the false residual current in the ground relays of one of the lines. Only a slight amount of true residual current appeared in the transformer neutral (trace 2).

D-C Saturation During Synchronizing

Closing out of synchronism can result in 3-phase currents comparable with short-circuit currents. Accordingly, transient residual current can appear in the ground relay because of d-c saturation of current transformers. Fig. 4 shows false residual currents appearing when a steam turbine generator was reclosed about 60 degrees out of phase with the system. In the upper oscillogram of Fig. 4, the second trace from the bottom shows residual current at one line terminal. In the lower oscillogram of Fig. 4, the second trace from the bottom shows residual current at the opposite line terminal. Both of these traces show considerable residual 60-cycle currents (false residual current) unexpected because of

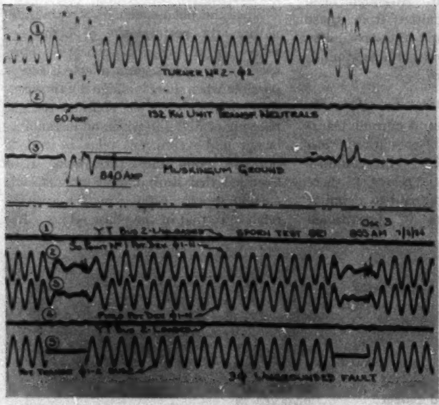

Fig. 3. Example of false residual current during a 3-phase fault

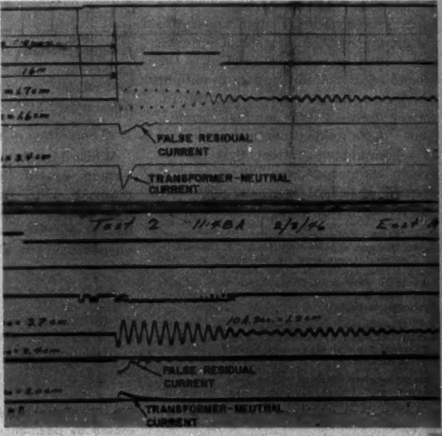

Fig. 4. Examples of false residual current during reclosing

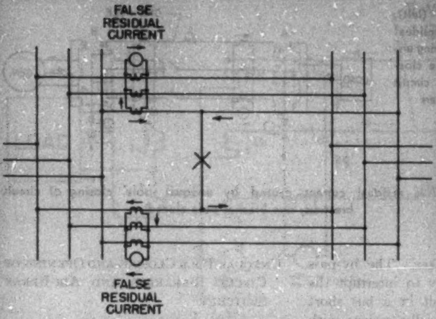

Fig. 5. False residual current during a fault involving two different phases of parallel lines

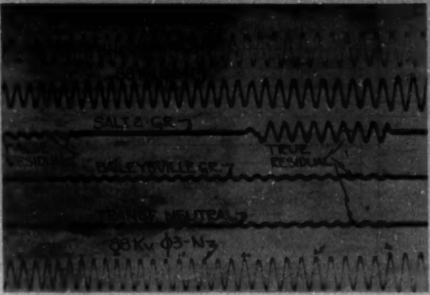

Fig. 6. Example of false residual current during a 3-phase fault involving two phases of one line and the third phase of a parallel line

the balanced 3-phase conditions. The bottom traces of Fig. 4 (transformer-neutral current) confirm that there is a negligible true 60-cycle current in each transformer neutral and, therefore, there should be a negligible true 60-cycle residual current. Inspection of Fig. 4 will show that the false residual currents at opposite ends of the line differed considerably. This can probably be explained on the basis of different residual fluxes (previous currents having been internal-fault currents), though even presumably identical current transformers sometimes differ considerably because of differences in iron characteristics.

Although the phase-comparison relays did not trip incorrectly during the test of Fig. 4, a previous test resulted in an incorrect tripout. After the previous test, it was found that the zero-sequence sensitivity was much greater than necessary. By reducing the sensitivity, successful reclosing was obtained. However, had not the reduction of ground-fault sensitivity been permissible, other measures would have been required such as introduction of time delay to the ground relays during closing.

MULTICIRCUIT FAULTS

False residual current resulting from system faults during normal system operation and not caused by poor current-transformer performance is the direct result of the inadequacy of the usual current-transformer connections to determine the actual ground current flowing. For example, Fig. 5 shows how false residual current can occur as a result of a fault between a phase of one line and a different phase of a parallel line, with ground not involved. Similarly, a 3-phase fault can result in false residual currents whether or not ground is involved.

Fig. 6 is an oscillogram of a 3-phase-to-ground fault as a result of different phases flashing over on the two circuits of a 132-kv double-circuit construction. Phase 1 on circuit no. 2 and phases 2 and 3 on circuit no. 1 flashed over during a lightning storm. It is not uncommon that different phases flash over on this type of construction, since phasing top-to-bottom is usually 1-2-3 on one circuit and 3-2-1 on the other to minimize system unbalance.

Circuit no. 2, on which only one phase was involved, tripped properly from carrier and high-speed reclosed successfully but, on circuit no. 1 having two phases involved, tripping was blocked until circuit no. 2 opened.

It can be seen from voltage trace 1 that phase 1-*N* (from potential on the 88-kv side of an autobank) was restored at 6 cycles when the Saltville circuit no. 2 (trace 3) opened. At this point, phase 2-*N* and 3-*N* voltages rose slightly but were not fully restored until the no. 1 circuit cleared at about 30 cycles. Circuit no. 1 was not connected to the oscillograph because of element limitations but clearing can be seen from the other traces. Note that very little current appeared in the bank neutral (trace 5) or the Baileysville circuit residual (trace 4) until circuit no. 2 opened at 6 cycles to change the fault from 3-phase to ground to 2-phase to ground. The residual current in circuit no. 2 (trace 3) can be seen during this period. Also, when this circuit reclosed successfully at 20 cycles, its contribution to the fault remaining on circuit no. 1 can be seen.

Analysis of the sequence components revealed that the torque to a carrier directional-ground relay on the double-faulted circuit no. 1 was in the nontrip direction. This carrier scheme utilized a separate carrier directional-ground relay which took preference over the 3-phase directional relay and, therefore, continued carrier blocking until circuit no. 2 opened. The time-delay reset of the blocking auxiliary relay further delayed tripping. A more modern scheme utilizing distance-type phase relaying would probably have operated properly since ground preference is not used and, also, since better first-zone coverage is realized.

The flow of false residual current, as shown in Figs. 5 or 6, might appear to be an advantage in that ground relays have an opportunity to operate as well as phase relays. However, there can be disadvantages such as the following:

1. Relay selectivity can be affected, resulting in a tripout of a circuit breaker or an unfaulted line.
2. Although the fault will be removed ultimately, sequential operation may result. Such operation may present the successful high-speed reclosing of both lines.

This general subject is too complicated to be dealt with in its entirety in this paper.

UNEQUAL POLE CLOSING AND OPENING OF CIRCUIT BREAKERS AND AIR-BREAK SWITCHES

Unequal pole closing of circuit breakers, a condition impossible to avoid, can cause false residual current (as well as true residual current which will be discussed later), as illustrated in Fig. 7 which shows one phase of one of two parallel lines still open. The system of Fig. 7 is shown ungrounded for easy understanding of this phenomenon. Similar false residual current can occur if the system is grounded.

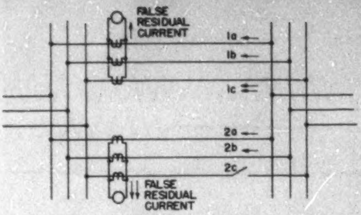

Fig. 7 (left). False residual current during unequal pole closing of circuit breakers

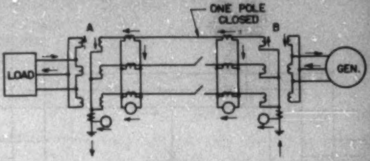

Fig. 9. True residual current caused by unequal pole closing of circuit breakers; one breaker pole closed

Fig. 8(A), while not an actual unequal-pole-closing operation, clearly illustrates the effect. This oscillogram is the result of one conductor of one of a pair of 132-kv circuits pulling apart in mid-span because of a splice failure. Trace 4 is the residual current of this line. When the conductor opened, and before it hit the ground, the false residual equivalent of phase current appeared even though there was no fault, as shown by the voltage traces 1, 3, and 6. This false residual current started carrier transmission to block tripping until the conductor hit the ground about 29 cycles later. The line relayed from backup caused by the time-delay dropout feature of the carrier-blocking auxiliary relay.

Fig. 8(B) trace 1, shows the false residual current caused by unequal pole opening and closing when switching load on a parallel line by means of a circuit breaker.

An exaggerated example of unequal pole closing or opening is when operating an air-break switch such as a line-sectionalizing switch. Also, when used as a by-pass switch, the air-break switch can be particularly dangerous, especially on opening. For example, when the first pole of the switch opens, false residual current may cause the ground relays to trip the circuit breaker. The by-pass switch would then try to interrupt the line current and result in a bus short circuit. This is especially serious with schemes cutting out bus differentials during by-pass conditions.

SYSTEM UNBALANCE

The previous example of an open phase, Fig. 7, is simply an extreme example of unbalanced phase impedance caused by lack of transposition of line conductors. False residual current can flow either during faults not involving ground or during normal load conditions. Fig. 8(B) also shows false residual current during normal load conditions (trace 1 before opening and after reclosing).

True Residual Current

It is easy to understand how ground relays can be fooled when there is no actual ground current. However, it may not be so easily understood that ground relays can also be fooled by actual ground currents. Such actual ground currents can be caused by unequal pole closing, by normal system unbalance, by induction, or by magnetizing-current inrush into power transformers.

UNEQUAL POLE CLOSING AND OPENING OF CIRCUIT BREAKERS AND AIR-BREAK SWITCHES

Unequal pole closing can cause a flow of ground current in directional-ground relays that is impossible to distinguish from an internal ground fault on the basis of relative direction alone. This is illustrated in Fig. 9, which shows the circuit conditions with one breaker pole at station *B* closed. It is apparent that a directional-ground relay at *B* would believe that there is a line fault. Not so apparent is the fact that a line relay at *A* would also believe that there is a line fault, although the relaying conditions at the two line terminals are actually identical. The line current relative to the transformer-neutral current at terminal *A* is the same as at terminal *B*. Thus, both line relays "see" what appears to be a line fault, and a high-speed directionally-relayed line might trip. It makes no difference how the relays are polarized, since zero-sequence voltage and neutral current are proportional at the grounded transformer location. Fig. 10 shows a similar circulating ground current after the second circuit-breaker pole at station *B* has closed.

Fig. 8. Example of false residual current (A) (below) when one phase conductor opened; (B) (right) during unequal opening and closing of a circuit breaker

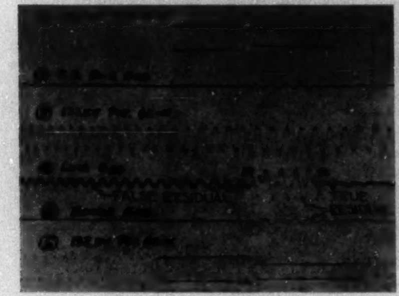

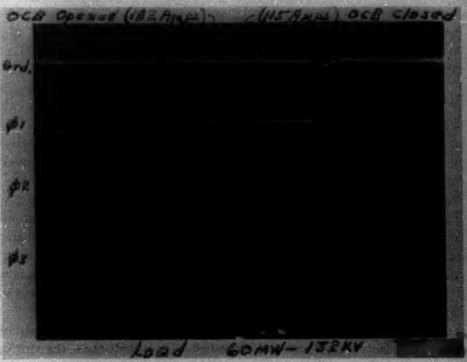

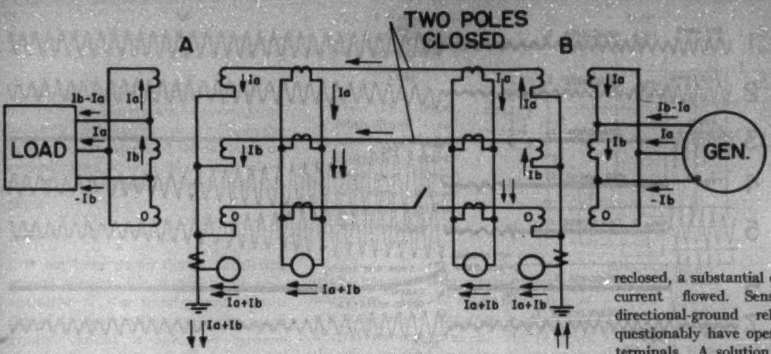

Fig. 10 (left). True residual current caused by unequal pole closing of circuit breakers, two breaker poles closed

Fig. 4 was used to illustrate the false residual current which was caused by d-c saturation of current transformers. It also illustrates the true residual and transformer-neutral current caused by unequal pole closing of circuit breakers. The two bottom traces of the oscillograms of Fig. 4 show transformer-neutral currents at opposite ends of a transmission line. When the second circuit breaker reclosed, a substantial circulating ground current flowed. Sensitive high-speed directional-ground relays would unquestionably have operated at both line terminals. A solution would have been the addition of a short time delay in the trip circuit during closing or reclosing.

Fig. 11 is an oscillogram taken to check transferred tripping. The system consisted of a 50-mile 330-kv line terminated in a 150-megavolt-ampere 330/132-kv autotransformer at each end and with breakers only on the 132-kv side. Where the circuit breaker at the local end opened, definite spikes can be seen in the transformer tertiary current and in the line ground-relay current traces as well as in the 132-kv bus zero-sequence potential. Also of interest are the high-frequency oscillations between the transformer inductance and the line capacitance as reflected in the tertiary and in the output of the potential devices on the 330-kv line where the remote circuit breaker opened.

These illustrations involve the closing or opening of load current and are particularly concerned with directional-ground-relay operation. Unequal pole closing can also cause operation of ground relays when energizing a line.

As would be expected, line-charging current enters the picture only on the longer lines. As as extreme example, consider energizing the long line of Fig. 12. Upon the closure of the first breaker pole at *A*, a ground current will flow which may be comparable with the ground

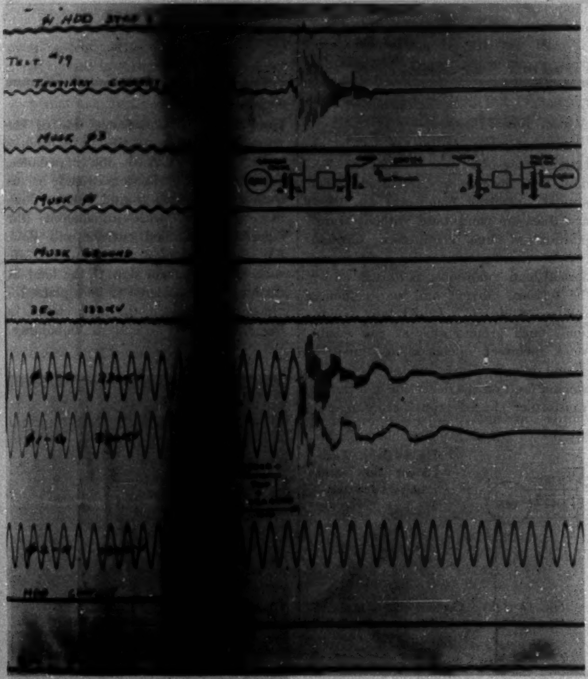

Fig. 11. Example of true residual current caused by unequal pole opening of circuit breakers

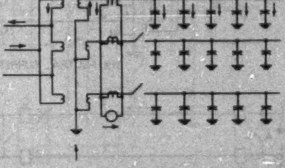

Fig. 12. Residual current when energizing a long line

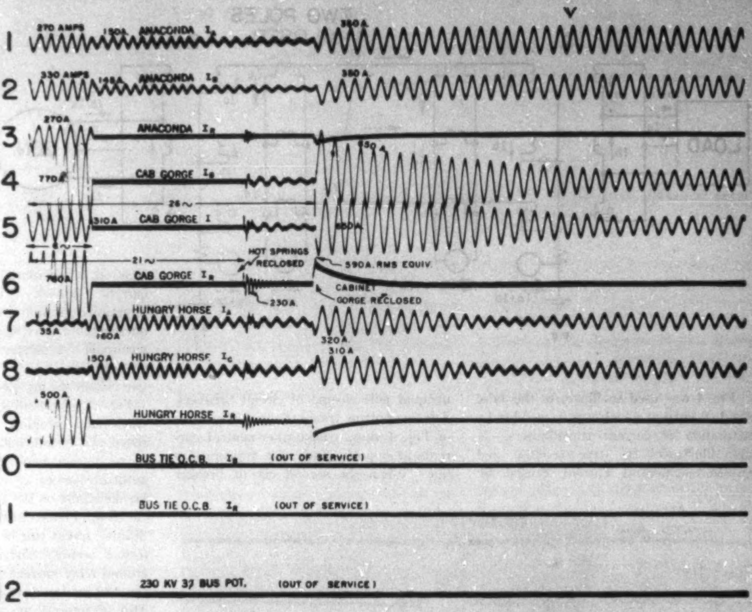

Fig. 13. Example of residual current when energizing a long line. Note high-frequency current, trace 6, when Hot Springs reclosed

current which can flow into a distant fault. More usual, however, is the ground current which flows as a result of the resonant combination of zero-sequence line capacity and the magnetizing inductance of the supply transformers.[10] Fig. 13, trace 6, illustrates such a line-energizing transient and shows that a considerable magnitude of high-frequency current is possible. In extreme cases, it has been necessary to filter out the nonfundamental-frequency currents to avoid undesired relay operation. Another solution would be the use of a harmonic-restrained relay as a fault detector.[11]

Normal System Unbalance

Unequal closing of breaker poles is an extreme case of system unbalance. Today, few systems are balanced under normal operating conditions as many new lines are being built without transposition of line conductors. Ground current can be substantial even under normal load conditions, as illustrated by the tertiary current and zero-sequence voltage of Fig. 11. Under fault conditions, such ground current can easily cause incorrect operation of sensitive ground relays. Cases are on record in which a fault on the delta side of a power transformer caused ground-relay operation on the grounded-wye side of the transformer. Fig. 14 illustrates such a fault. With balanced line impedance, the current distribution would be as indicated, with no ground current flowing. However, with unbalanced line impedances, ground current will flow. Fig. 9 can be used again to illustrate such ground-current flow if the load at station *A* is considered to be a phase-to-phase fault. Again, the open circuit in Fig. 9 represents an extreme unbalance.

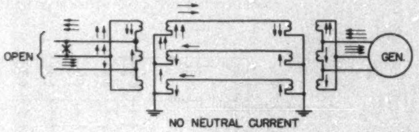

Fig. 14 (left). Fault-current flow with balanced system

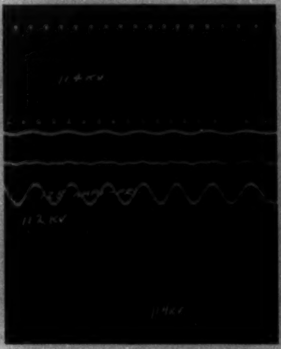

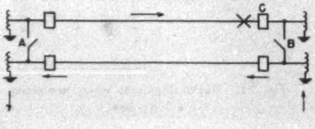

Fig. 15 (left). Ground current induced in a line by a ground fault on a parallel line

Fig. 16 (right). Example of 25-cycle current induced in a 60-cycle line

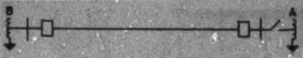

Fig. 17 (left). System conditions before energizing a transformer

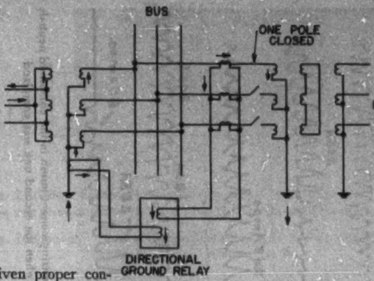

Fig. 19 (right). Magnetizing-current inrush when energizing a power-transformer integral with a line. Ground relay polarized from bus transformer neutral

Although ground current flows during normal system operation because of unbalanced line-charging current, calculations have indicated that the influence on ground relays is negligible compared to the other considerations described in this paper.

Induction

It has been shown that a circulating ground current, Fig. 9, can cause misoperation of directional-ground relays. One of the most usual causes of circulating ground current is induction between parallel lines. Fig. 15 illustrates such a case in which a ground fault on one line causes a circulating ground current in the parallel line. Oscillographic evidence of induced ground current is most convincing when the power system involves more than one frequency. Fig. 16 is an example of a 25-cycle fault inducing 25-cycle ground current in a 60-cycle system. The oscillograph was connected to observe only phenomena on the 60-cycle system. The appearance of a 25-cycle current is therefore conclusive.

Sometimes, relay sensitivities can be such that incorrect operation by induced current can be avoided. Other solutions of this problem have consisted of zero-phase-sequence overvoltage relays or phase-to-neutral-connected undervoltage relays arranged to monitor the normal ground relays. Pilot-wire or phase-comparison carrier relays eliminate the problem because they compare the currents entering and leaving the line, from whatever cause.

MAGNETIZING-CURRENT INRUSH

Energizing a Transformer

The effect of magnetizing-current inrush into power transformers on transformer-differential relays has long been known. However, its effect on ground relays has not been given proper consideration. Fig. 17 shows a portion of a system before energizing a grounded-neutral transformer at *A*. Fig. 18 shows the magnetizing-current inrush into transformer *A*, as well as the source of that current, transformer *B*. Here again is the now familiar circulating current which can cause directional-ground relays to operate incorrectly.

Little difficulty has been reported of line-relay tripouts when energizing a power transformer external to the line, although in one instance such a tripout could be definitely predicted and a harmonic-restrained relay was used to monitor the ground-relay trip circuit. A-c pilot-wire relaying or phase-comparison relaying should not be subject to incorrect operation from this cause.

If the transformer is integral with the line, i.e., no line-side circuit breaker, the relays at the energizing terminal may or may not operate unnecessarily, depending upon the location of the current transformers. For example, in Fig. 19 the direction of the residual current relative to the polarizing current is the same as for a single-phase-to-ground line fault. The directional-ground relay may therefore operate to retrip the circuit breaker. Incidentally, a-c pilot wire or phase-comparison relaying are also subject to false tripping if the protected zone includes a power transformer.

It is apparent that magnetizing-current inrush could not operate the directional-ground relay if residual current were obtained from current transformers in the high-tension bushings of the line power transformer. Even with this arrangement, false tripping can occur if the transformer is energized from the line. This could occur during high-speed reclosing where the remote circuit breaker closed slightly ahead of the local circuit breaker because of air pressure or temperature difference, etc. The local circuit breaker would then receive a trip impulse from the preclosed relay contacts when it closed. Also, undesired tripping can be avoided by polarizing the ground relay from current in the neutrals of the line power transformer, as shown in Fig. 20.

For proper operation during faults, the directional-ground relay of Fig. 20 may be polarized from the power-transformer delta. This is especially desirable if the power transformer is an autotransformer.[13] With delta-current polarizing, it would appear that there should be no magnetizing-inrush difficulty because little delta current would be expected, and any delta current which flows would be expected to be in the nontripping direction, as with the polarizing means of Fig. 20. However, magnetizing-inrush phenomena can be very complicated, and

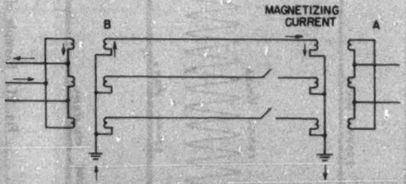

Fig. 18. Circulating ground current caused by magnetizing-current inrush when energizing a power transformer

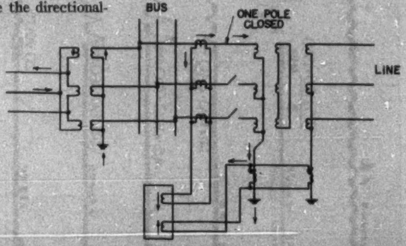

Fig. 20. Magnetizing-current inrush when energizing a power transformer integral with a line. Ground relay polarized from line transformer neutrals

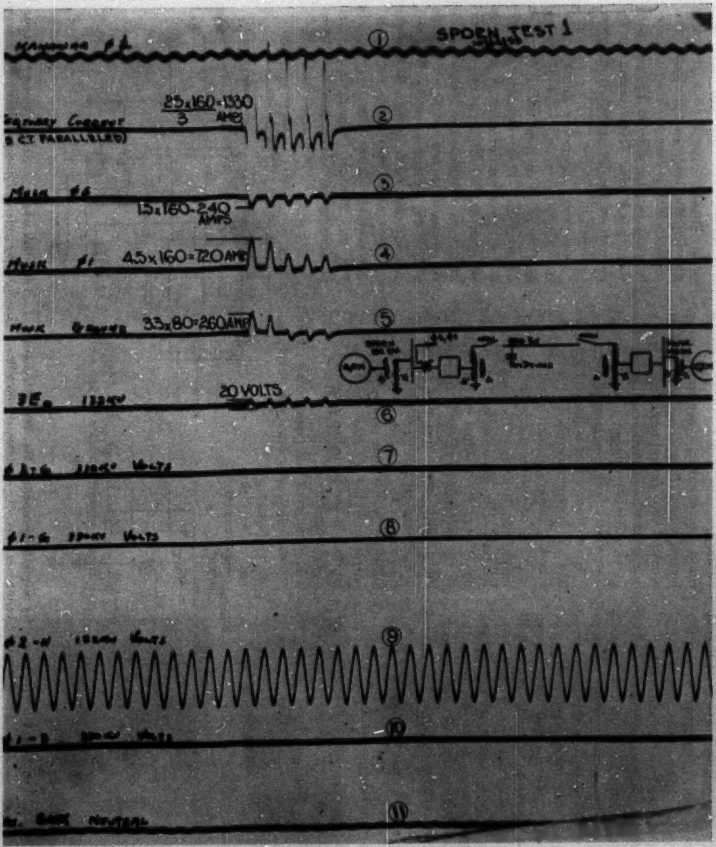

Fig. 21. Example of magnetizing-current inrush when energizing a power transformer

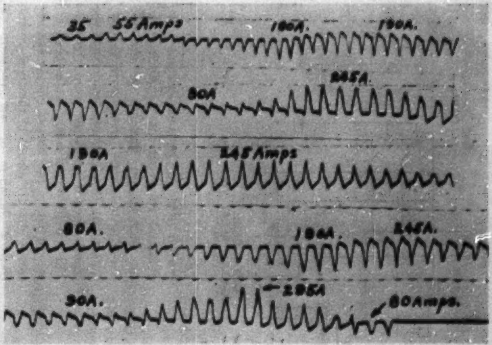

Fig. 22 (above). Example of magnetizing-current inrush in the combined neutrals of two power transformers when the second one was energized

Fig. 23 (below). Example of magnetizing-current inrush when clearing a fault

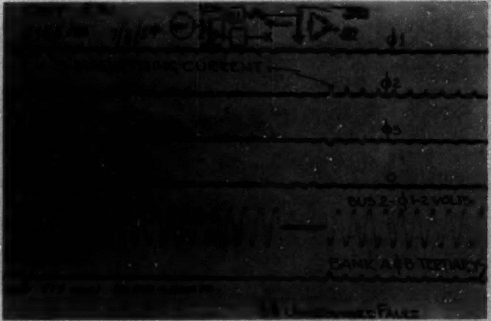

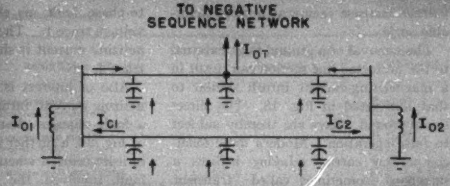
TO NEGATIVE SEQUENCE NETWORK
I_{OT}
I_{O1}
I_{C1}
I_{C2}
I_{O2}

Fig. 24 (left). Example of magnetizing-current inrush upon the inception of a phase-to-phase fault and when the fault involved the third phase

Fig. 26 (above). Effect of charging current of unfaulted parallel line on directional-ground relay operation

delta-current polarizing cannot be depended upon to prevent undesired relay operation.

Fig. 21 is an oscillogram taken during the energizing of one of the 330/132-kv 150 megavolt-ampere autotransformers of Fig. 11 from the 132-kv side with the 330-kv line disconnects open. The carrier ground relays tripped. They were connected in the residual circuit of bushing current transformers in the 132-kv circuit breaker, trace 5, and were polarized from the tertiary, trace 2. Note that the residual current, trace 5, changed direction after 2 cycles, whereas the tertiary current, trace 2, did not.

The complication of magnetizing-current-inrush phenomena is further exemplified by Fig. 22 showing the combined neutral current of two power transformers when the second transformer was energized.[10] Ground backup overcurrent relays unnecessarily removed both power transformers from service. Fig. 22 is all the same trace cut into sections to show that magnetizing-current inrush can continue long enough to operate even long time relays.

Removal of a Fault

Although the results of magnetizing-current inrush when energizing a transformer have been common knowledge, the fact that removal of a nearby fault has a similar effect on a transformer[11] has been somewhat overlooked. The only difference is that removal of a fault at current zero results in less than maximum magnetizing-current inrush because the

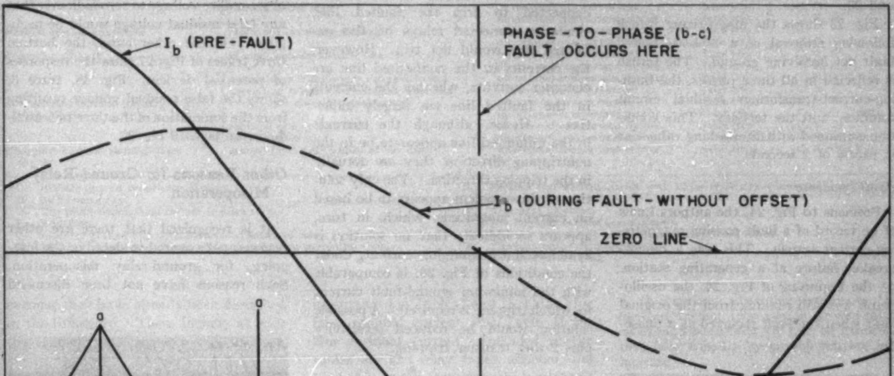
I_b (PRE-FAULT)
PHASE-TO-PHASE (b-c) FAULT OCCURS HERE
I_b (DURING FAULT-WITHOUT OFFSET)
ZERO LINE
a
c
b
VOLTAGE TRIANGLE BEFORE FAULT
a
c b
VOLTAGE TRIANGLE DURING PHASE-TO-PHASE FAULT
D.C. OFFSET
I_b (DURING FAULT AND WITH OFFSET)
MAGNETIZING CURRENT INRUSH

Fig. 25. Transformer-exciting current I_b on the inception of a phase-to-phase fault

voltage increase occurs at a more favorable angle.

The removal of a ground fault external to the protected line section can result in a magnetizing-current inrush similar to that illustrated in Fig. 18. The directional-ground relays are thereby subject to false operation. Modern directional-comparison carrier relaying utilizes a safeguard (sometimes called "transient blocking") which operates in the following manner: assume that line *A-B* of Fig. 18 is protected by directional-comparison carrier relaying. Upon the occurrence of a ground fault off the bus at station *A* and external to line *A-B*, a carrier-blocking signal is transmitted to terminal *B* to prevent tripping there. Shortly after the start of transmission of the blocking signal, an auxiliary relay operates to "seal in" the blocking signal. When the external fault is removed, the blocking signal continues for several cycles regardless of directional-relay operation and usually blankets the period during which magnetizing-current inrush might otherwise cause incorrect tripping of the line relays. In extreme cases, several cycles of transient blocking may not be sufficient, as indicated in Figs. 22 and 23.

Fig. 23 shows the magnetizing inrush following removal of a 3-phase bolted fault not involving ground. The inrush is reflected in all three phases, the bushing-current-transformer residual circuit common, and the tertiary. This condition continued with diminishing values far in excess of 2 seconds.

Fault Incidence

Previous to Fig. 24, the authors know of no record of a fault causing magnetizing-current inrush. This was a circuit-breaker failure at a generating station. At the beginning of Fig. 24, the oscillograph was still running from the original fault when the fault recurred as a phase-to-phase fault, as shown at *A* on the voltage trace 1. The characteristic magnetizing current is shown in line residual trace 3.

Also of interest is the fact that magnetizing-current inrush can occur when a fault changes character. At point *B* of Fig. 24, a further magnetizing-current inrush occurred when the phase-to-phase fault involved the third phase. The mechanism by which a magnetizing-current inrush can occur on the incidence of a fault may be of interest and is illustrated in Fig. 25.

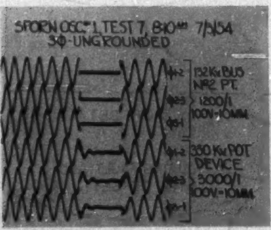

Fig. 27. Potential-transformer and potential-device responses during a 3-phase fault not involving ground

LINE-CHARGING CURRENT WITH PARALLEL LINES

Another manifestation of the effect of zero-sequence line-charging current appears in parallel lines. Fig. 26 shows the zero-sequence network with a fault near the middle of one line. If charging current is neglected, a fault location can be found which results in substantially no current in the unfaulted line. However, with line capacity considered, current will flow in the unfaulted line, as shown in Fig. 26. Comparison of the currents in the faulted and unfaulted lines would seem to indicate that, if relays were connected to trip the faulted line, similarly connected relays on the unfaulted line would not trip. However, the currents in the nonfaulted line are charging currents, whereas the currents in the faulted line are largely inductive. Hence, although the currents in the unfaulted line appear to be in the nontripping direction, they are actually in the tripping direction. The only solution of this problem appears to be based on current magnitude, which, in turn, appears to indicate that no solution is available if the charging current, under the conditions of Fig. 26, is comparable with the minimum ground-fault current for which tripping is required. A possible solution would be reduced sensitivity plus 2-way transfer tripping.

Combinations of False Residual Current and True Neutral Current

The directional-ground relay appears to be the only type that can be influenced by combinations of false residual current and true neutral current. In general, incorrect relay operation can occur if there is false residual current from any cause, e.g., Fig. 3, trace 3, simultaneously with transformer-neutral current from any cause e.g., Fig. 3, trace 2.

Particularly prone to misoperation is the directional-ground relay when used on a resistance-grounded, or other poorly grounded, system. Such a system requires high ground-relay sensitivity. Tripping can result from an external 2-phase-to-ground fault which provides adequate neutral-polarizing current and a heavy phase-to-phase component to produce false residual operating current. A potential-polarized directional-ground relay would be exposed to the same chance of misoperation.

Combinations of False Residual Current and False Residual Voltage

Again, the directional-ground relay is involved because of the two quantities required for misoperation. In general, incorrect relay operation can occur if there is false residual current from any cause, e.g., Fig. 3, trace 3, and false residual voltage caused by the imperfect performance of potential transformers or devices during faults not involving ground.

The authors have no examples of false residual voltage resulting from imperfect performance of potential transformers. The top three sinusoidal traces of Fig. 27 show the responses of potential transformers during a 3-phase fault not involving ground. The clean-cut reduction of secondary voltage to zero indicates that any false residual voltage would be negligible. On the other hand, the bottom three traces of Fig. 27 show the responses of potential devices. Fig. 28, trace 3, shows the false residual voltage resulting from the summation of the three potential-device voltages of Fig. 27.

Other Reasons for Ground-Relay Misoperation

It is recognized that there are other reasons, not covered in detail in the foregoing, for ground-relay misoperation. Such reasons have not been discussed

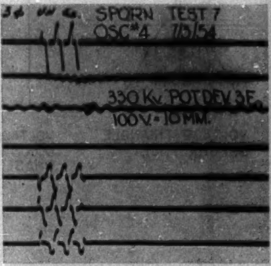

Fig. 28. Example of false residual voltage of potential devices during the 3-phase fault of Fig. 27

Table I. False Residual Current

Cause of Incorrect Operation	Circumstances	Relay Types Affected	Kind of Incorrect Operation*	Possible Solutions*
Unbalanced current-transformer burden, Fig. 1	faults not involving ground	time overcurrent	A	B, C, D
		instantaneous overcurrent	A	B, C
		directional-comparison carrier	E	B, C, F
		phase-comparison carrier or a-c pilot wire	false trip	B, C, G
D-c saturation of current transformers	faults not involving ground	time overcurrent	A	C, D
		instantaneous overcurrent	A	C, H
		directional-comparison carrier	E	C, F, H
		phase-comparison carrier or a-c pilot wire	false trip	C, G, H, I
	synchronizing or reclosing	directional-comparison carrier	false trip	C, H
		phase-comparison carrier or a-c pilot wire	false trip	C, H
	starting a motor	instantaneous overcurrent	false trip	C, K, L, M, N
Multicircuit faults, Fig. 5		phase relays on unfaulted line	U	D
		directional-comparison carrier	sequential tripping	O
Unequal pole closing or opening or system unbalance, Fig. 7	normal system or faults	instantaneous overcurrent	false trip	C, H
		directional-comparison carrier	false trip	C, H
		phase-comparison carrier or pilot wire	false trip	C, H

*A. Ground relay on unfaulted circuit trips before phase relays on faulted circuit.
B. Balance the burden.
C. Reduce sensitivity of ground relay.
D. Change time settings to obtain selectivity.
E. Start carrier blocking incorrectly.
F. Use directional-carrier start.
G. Monitor with neutral current or E_0 relay.
H. Add time delay.
I. Monitor with directional-ground relay.
J. Trip unfaulted line.
K. Use relay polarized from neutral current.
L. Monitor ground relays from relay in neutral current transformer.
M. Insert resistance in ground-relay circuit.
N. Use current transformer surrounding all 3-phase conductors.
O. Use phase comparison carrier or pilot wire.
U. Phase relays on unfaulted circuit trip before ground relays on faulted circuit.

Table II. True Residual Current

Cause of Incorrect Operation	Circumstances	Relay Types Affected	Kind of Incorrect Operation	Possible Solutions*
Unequal pole closing or opening, Figs. 9, 10, and 12	synchronizing or reclosing	instantaneous overcurrent	false trip	C, H
		directional-comparison carrier	false trip	C, H, O
	energizing long line	instantaneous overcurrent		
		directional-comparison carrier	false trip	C, H, P, Q
	opening under load	instantaneous overcurrent	false trip	C, H
		directional-comparison carrier	false trip	C, H, O
Normal system unbalance	faults not involving ground	instantaneous overcurrent	false trip	C
		directional-comparison carrier	false trip	C, O
Induction, Fig. 15	ground fault on another line	instantaneous overcurrent	false trip	C, R, S
		directional-comparison carrier	false trip	C, R, S, O
Magnetizing-current inrush, Figs. 17–20	energizing a transformer external to line	directional-comparison carrier	false trip	C, H, O, Q
	energizing transformer integral with line (bus-side current transformers)	instantaneous overcurrent	false trip	C, H, X
		phase-comparison carrier	false trip	V, H, W
		directional-comparison carrier	false trip	C, H, Q, O with V
	removal of a ground fault	directional-comparison carrier	false trip	C, H, Q, T
	fault incidence	directional-comparison carrier	false trip	C, H, O, Q
Charging current parallel lines, Fig. 26	ground fault near middle of one line	directional-comparison carrier	false trip	C, C with Y

*C. Reduce ground sensitivity of relay.
H. Add time delay.
O. Use phase-comparison carrier or pilot wire.
P. Add filter.
Q. Monitor ground trip with harmonic-restrained relay.
R. Monitor ground-trip circuit with zero-sequence overvoltage relay.
S. Monitor ground-trip circuit with phase-to-neutral-connected undervoltage relays.
T. Transient blocking.
V. Use line-side current transformers.
W. Monitor trip circuit with harmonic-restrained relays.
X. Use harmonic-restrained relay.
Y. Transferred tripping.

because they have already been described in the literature. These include at least the following.

1. Effect of steady-state current transformer exciting current on ground-relay sensitivity.[14]

2. Effect of unbalanced phase-to-neutral loading of distribution transformers on ground relays.[15]

3. Other problems involving polarizations of ground relays.[12]

4. "Neutral inversion" of potential transformers.[16, 17]

5. Another incorrect response of potential devices.[18]

Summary

The foregoing causes of incorrect or undesired ground-relay operation are summarized in Tables I and II, Table I for false residual current and Table II for true residual current. Included in the tables are the relay types affected, the kind of incorrect operation which might be expected, and the possible remedial measures.

Conclusions

1. The number of true and false residual currents and their combinations which can adversely affect ground relaying are many.

2. Unnecessary ground-relay sensitivity should be avoided. If a 2-ampere ground-relay pickup is sufficient, a lower one may not be better but rather may invite trouble.

3. In planning system expansion, ground relaying must be given careful consideration to avoid conditions where adequate ground relaying is virtually impossible.

4. If system expansion continues to demand further increases in ground-relay speed and sensitivity, it can be expected that false tripping by ground relaying will increase.

5. It may be necessary to change some operating practices. Some helpful items would be:

a. Reduction in the number of transformers operating with their neutrals grounded at a terminal to permit more uniform fault current distribution. Even this gain may not be too great since the positive- and negative-sequence components will remain. The problems of overvoltage and cost of providing insulation for ungrounded neutral operation will also limit this practice.

b. More extensive use of high-speed reclosing to minimize the effect of false tripping.

c. Increased use of devices to prevent flashover (counterpoise, static wires, etc.)

to reduce the number of occasions for false operation. An additional justification of this would be reduction of danger of equipment failure from the increasing fault-current magnitudes.

d. More extensive application of a-c pilot wire or phase-comparison carrier each of which is generally immune to the ground-relaying difficulties occasioned by the system itself. However, even these are subject to incorrect operation from false current-transformer output. Their use is also complicated by the multiple-tapped line.

References

1. New Current Transformers for Bus Differential Protection, **L. F. Kennedy, A. T. Sinks.** *AIEE Transactions*, vol. 60, 1941, pp. 1180–87.

2. Linear Couplers for Bus Protection, **E. L. Harder, E. H. Klemmer, W. K. Sonnemann, E. C. Wentz.** *AIEE Transactions* (*Electrical Engineering*), vol. 61, May 1942, pp. 241–48.

3. Instantaneous Bus-Differential Protection Using Bushing Current Transformers, **H. T. Seeley, Frank von Roeschlaub.** *AIEE Transactions*, vol. 67, pt. II, 1948, pp. 1709–19.

4. The Effect of Current-Transformer Residual Magnetism on Balanced-Current or Differential Relays, **H. T. Seeley.** *AIEE Transactions* (*Electrical Engineering*), vol. 62, Sept. 1943, pp. 164–69.

5. Considerations in Applying Ratio Differential Relays for Bus Protection, **G. B. Dodds, R. M. Smith, W. K. Sonnemann.** *AIEE Transactions*, vol. 58, June 1939, pp. 243–49.

6. Current Transformers and Relays for High-Speed Differential Protection with Particular Reference to Offset Transient Currents, **E. C. Wentz, W. K. Sonnemann.** *AIEE Transactions*, vol. 59, Aug. 1940, pp. 481–88.

7. Transient Characteristics of Current Transformers During Faults, **C. Concordia, C. N. Weygandt, H. S. Shott.** *AIEE Transactions* (*Electrical Engineering*), vol. 61, May 1942, pp. 280–85.

8. Transient Characteristics of Current Transformers During Faults—Part II, **F. S. Rothe, C. Concordia.** *AIEE Transactions*, vol. 66, 1947, pp. 731–34.

9. Earth-Leakage Relays; with Use of Ring-Type Current Transformers, **E. T. B. Gross.** *Electrician*, London, England, vol. 123, July 1939, pp. 93–95.

10. Relaying Difficulties Disclosed by Staged-Fault Tests, **W. A. Morgan, Byron Evans.** *AIEE Transactions*, vol. 67, pt. I, 1948, pp. 73–82.

11. Harmonic Current Restraint Relays for Transformer Differential Protection, **C. D. Hayward.** *AIEE Transactions*, vol. 60, June 1941, pp. 377–82.

12. Ground Relay Polarization, **J. L. Blackburn.** *AIEE Transactions*, vol. 71, pt. III, Dec. 1952, pp. 1088–95.

13. Prolonged Inrush Currents with Parallel Transformers Affect Differential Relaying, **C. D. Hayward.** *AIEE Transactions*, vol. 60, 1941, pp. 1096–1101. Disc. p. 1305.

14. Overcurrent Performance of Bushing-Type Current Transformers, **C. A. Woods, Jr., S. A. Bottonari.** *AIEE Transactions*, vol. 59, Sept. 1940, pp. 554–60.

15. Sensitive Ground Protection for Radial Distribution Feeders, **Lloyd F. Hunt, J. H. Vivian.** *Ibid.*, Feb. 1940, pp. 84–90.

16. Criteria for Neutral Stability of Wye-Grounded-Primary Broken-Delta Secondary Transformer Circuits, **H. S. Shott, H. A. Peterson.** *AIEE Transactions* (*Electrical Engineering*), vol. 60, Nov. 1941, pp. 997–1002.

17. Neutral Inversion of a Single Potential Transformer Connected Line-to-Ground on an Isolated Delta System, **Lyle L. Gleason.** *AIEE Transactions*, vol. 70, pt. I, 1951, pp. 103–11.

18. The Effects of Coupling-Capacitor Potential-Device Transients on Protective-Relay Operation, **AIEE Committee Report.** *AIEE Transactions*, vol. 70, pt. II, 1951, pp. 2089–96.

Discussion

M. Stephens Merritt (Tennessee Valley Authority, Chattanooga, Tenn.): The authors are to be commended for information on undesirable relay operations which are exceedingly difficult to isolate and eliminate. In most cases where such unwanted operations occur, such action accompanies other phenomena which, without the benefit of automatic oscillograph records of the necessary quantities, cannot be isolated as to their cause. This, among other things, points up the need for much more oscillographic equipment than is available on most power systems. It is necessary that the oscillograph operation be initiated from a very sensitive ground-relay element.

It is probable that all of these phenomena have been experienced on substantially all large electrical utility systems at one time or another even though they may not have been recognized. Except for the potential inversion listed as no. 4 in the section entitled "Other Reasons for Ground-Relay Misoperation" and the combination of false residual and true neutral current, they have all been recognized on the Tennessee Valley Authority system. Some of these spurious relay operations have been desirable, e.g.: a grounded-wye/delta stepdown transformer on the end of a short high-voltage line supplying a large industrial load developed a turn-to-turn fault in the low-voltage delta winding of one phase. The circuit was protected by means of pilot-wire relaying from the source station to the load side of the stepdown transformer for phase faults and to stepdown transformer neutral for ground faults. The unbalanced current in the phase conductor and neutral circuits as a result of the load or fault caused the pilot-wire ground relays to open the supply oil circuit breaker.

The desirable tripping results have been very few, but the highly undesirable tripping results have been many. This is especially true for the primary transmission system where most of the lines are protected by terminal comparison-carrier relay. The conditions producing these effects in most cases probably would not have been recognized except for the availability of automatic oscillographs. The recognizance of the causes has permitted some remedial measures to be taken. These measures involve:

1. Engineering design of system and stations to minimize system arrangement and operations favorable to these spurious operations.
2. Control of switching operation, especially where operation of air-break switches is involved to minimize conditions favorable to undersirable tripping on unbalanced loading or lack of simultaneous pole operations.
3. Closer adjustment of oil circuit-breaker poles in clearances than the tolerances given by manufacturer's instructions.
4. Calibrating relays available to minimum sensitivity commensurate with acceptable ground fault recognition.
5. Closer attention to application of protective relay schemes.
6. Improved characteristics effected by the manufacturers of protective relay schemes.

There yet remains much trouble on the primary transmission system from unsymmetrical oil circuit-breaker pole operation and changes in magnetization. It has not been possible in many cases to separate these phenomena since the unsymmetrical breaker pole operation is present when a tie line is closed, either automatically or when synchronizing, transformers are energized, and a fault is removed.

The methods employed by manufacturers for improvement of the relays for these conditions have been limited to substitution of high-speed induction ground-relay elements for those operating on the solenoid principle and installing in the relay coil circuits some means of energy absorption to prevent operation on short-time low-magnitude transients. The high-speed induction elements have proved effective in overriding these short-time transients with the sacrifice of about 3 cycles on low-magnitude ground faults and about 1 cycle on high-magnitude ground faults. This sacrifice in time is preferable to the unwanted operations.

The results obtained with the present relaying equipment are not satisfactory. Dissatisfaction results from continuing to get unwanted tripping where the slightly slower induction relay is not used and having greater clearing time for ground faults than should be necessary. The paper does not extend much hope of improvement without adding considerable complication by way of additional relay elements. Superpositioning of phase comparison on terminal comparison-carrier ground relaying is now being installed in a few severe cases of induction or mutual coupling but cannot feasibly be considered for general installation to remedy other difficulties. The field is still open for the manufacturers to arrive at some solution which with minor modifications to existing installations will eliminate the present deficiencies.

A high percentage of failures of high-speed automatic reclosing of oil circuit breakers on the primary transmission system has been experienced in the past. It may be that some of these which were ascribed to failure to latch, multiple lightning discharges, etc., may have been caused by the unsymmetrical circuit-breaker pole operation or transformer magnetization.

G. D. Rockefeller and **J. L. Blackburn** (Westinghouse Electric Corporation, Newark, N. J.): This paper is a valuable contribution in cataloguing the various troubles occasionally encountered in ground relaying and will be helpful to relay engineers in tracing these troubles. It should be noted that, generally speaking, these troubles occur relatively infrequently considering the large number of ground relays in successful service. This is pointed out by the authors, but merits re-emphasis lest some become unduly concerned after reading the paper.

Negative-sequence quantities are used very effectively in ground relaying to solve the difficult problem of induction. It is regretted that this was not mentioned in the paper. The amount of negative sequence induced even with untransposed lines is very small and generally negligible.[1] Thus, negative-sequence current and voltage are used to give correct directional indication for both directional-comparison carrier and for time-overcurrent type of relays.

The authors point out that saturation of current transformers usually occurs at flux densities over 100,000 lines per square inch. They suggest that the figure of 125,000 lines per square inch be used as a criterion. While a figure of 100,000 lines per square inch may be satisfactory for modern current transformers, it may not be satisfactory for some of the older current transformers. About 10 to 15 years ago, a figure of 77,500 lines per square inch represented the saturation flux density of the iron then in use.

The authors point out the value of automatic oscillographs on the power system. In fact, it would be impossible to analyze adequately the difficulties without them. This paper should encourage their more widespread use as a necessary and invaluable tool in analyzing difficult relay problems.

Some of the oscillographs are difficult to follow because of limited explanation and nomenclature. It seems that the value of the paper could be increased in this respect. Along this line, more explanation would be desirable in connection with Fig. 25.

Some of the examples presented produce transients of short duration. As relaying speed increases, examination of these transients becomes increasingly important. These cases again illustrate, we think, that there is a point of no return on increased relay speed. Perhaps there will be a trend away from demanding more speed from the relays and more emphasis on system design which tolerates faults of longer duration.

Reference

1. Determination of Inductive and Capacitive Unbalance for Untransposed Transmission Lines, R. F. Lawrence, D. J. Povejsil. *AIEE Transactions*, vol. 71, pt. III, Apr. 1952, pp. 547–56.

W. E. Marter (Duquesne Light Company, Pittsburgh, Pa.): Mr. Barnes and Mr. McConnell have presented an excellent discussion of the various difficulties which can occur in the use of ground relays and, in most cases, have suggested corrective measures.

Some recent relay operations on the Duquesne Light Company system indicate that all the problems are not yet solved. In the discussion of magnetizing inrush currents, the authors state that "Little difficulty has been reported of line relay tripouts when energizing a power transformer external to the line." I would like to add two cases to the difficulty already reported.

A 138-kv line terminates in a 100-megavolt-ampere autotransformer bank having a star-star connection and an unloaded delta tertiary winding. The bank has a circuit breaker on the 69-kv bus side, but not on the 138-kv side. The line protection is pilot wire and is fed from 138-kv breaker bushing current transformers on the source end and from 138-kv transformer bushing current transformers on the load end. The transformer was not included in the pilot-wire circuit to avoid the magnetizing-inrush problems. Despite the precautions taken, an operation of the pilot-wire protection occurred when the bank was energized by closing the 138-kv breaker at the source end of the line.

Some tests which have been run indicate that there are at least two factors involved in this problem. First, there is residual magnetism in the bank itself indicated by an oscillograph record in which the exciting current was well above the zero line for several cycles. This type of trouble is discussed in reference 1 and shows a similar condition. The second factor is current-transformer saturation and residual magnetism. The current transformers, although they are both bushing current transformers, are not duplicates since one set is on circuit-breaker bushings and one on transformer bushings.

The second case of pilot-wire relay trouble was very similar to the first, with the exception of the transformer bank connections. A 69- to 23-kv star-delta 30,000-kva bank with only a 23-kv breaker at the bank end of the line, and the bank not included in the pilot-wire protection, was energized by closing the 69-kv breaker at the source end of the line and the pilot-wire relays operated.

In both cases, pilot-wire circuit constants were well within the manufacturers limits and both pilot-wire protective equipments were equipped with phase and ground instantaneous-overcurrent interlock relays. Since one false operation occurred on a *CPD* installation and one occurred on an *HCB* operation, it can be seen that these undesirable currents do not play favorites.

I would like to make one further comment dealing with equation 1. Since system economics will dictate the I and T values, the factors which the relay engineer might improve are the R, N_1, N_2, and A quantities. Any help the current-transformer design engineers can give in increasing the A factor will be appreciated by the relay engineers.

Reference

1. The J & P Transformer Book. Darien Press, Edinburgh, Scotland.

Donn C. Achtenberg (Detroit Edison Company, Detroit, Mich.): Mr. Barnes and Mr. McConnell are to be congratulated for bringing out some information which up to now may not have been considered in analyzing false tripouts by ground relays. This is a subject which needs much discussion.

The Detroit Edison Company has experienced two faults in recent years which may possibly be explained by some of the information from this paper. In one case a 24-kv cable fault caused two 120-kv cables to trip out even though the 24-kv circuit breaker cleared instantaneously. The neutral overcurrent relay on the primary of the 120/24-kv delta-grounded-wye transformer caused the incorrect operation. Also, this neutral relay sent a remote trip signal via pilot wire to trip out the remote 120-kv breaker. The 24-kv fault involved three phases and ground and was in the substation basement. Another 24-kv fault which occurred a short time later but farther "out" did not cause the incorrect operation. It therefore appears that current magnitude is a factor. All current-transformer polarities and secondary wiring were checked and found to be all right. This may suggest, as the authors state in the section entitled "False Residual Current," that false residual current may have been present because of unequal performance by phase current transformers or unequal pole opening of an oil circuit breaker. The delta-connected primary is ungrounded. Two steps were taken to prevent a repetition of this false tripping.

1. The neutral overcurrent relay was changed from an instantaneous type to a time-delay type.
2. An extra step of time was put in to the coil circuit of the auxiliary tripping relays to give a few cycles delay in sending the remote-trip signal.

In another case, false tripping was caused during switching operations to transfer the load of a generator from one bus to another. In this instance, an actual transient voltage was observed on an oscilloscope across the operating coil of a pilot-wire relay. This relay is sensitive to both positive- and zero-sequence currents. Various "pips" could be observed as switching operations were carried out. As the authors state, unequal pole closing or opening of a circuit breaker or disconnect switch could be the cause of such false residual voltages. The duration of the energy on the operating coil was just long enough to close the contacts of the relay. While the contacts themselves opened, the arc established was enough to pick up the auxiliary tripping relay string. The auxiliary string was redesigned from one which normally drew 500 milliamperes d-c to one which draws about 54 milliamperes d-c. This allows the contacts to make momentarily without establishing an arc to cause the auxiliary relay string to pickup. Also, an extra step was put in the auxiliary string as in the foregoing case to delay pickup for a few cycles.

In connection with conclusion 3, it is the practice with this company to order neutral fuse holders for transformers on the subtransmission system if they are to be used in an area where they may be grounded. It is then determined at a later date when the details of the problem are being worked out whether or not a fuse is installed. The factors involved in this determination are the ground-relay co-ordination problem and the voltage on the unfaulted phases for a phase-to-ground fault. We are in agreement with the other conclusions drawn by the authors, especially no. 2.

J. R. Linders (Cleveland Electric Illuminating Company, Cleveland, Ohio): Mr. Barnes and Mr. McConnell are to be complimented for releasing this valuable information to the relaying profession. It will require many more hours of study to appreciate it fully. In spite of the merits of standardization of relay terminals and their calibrations, I fully support the opinion expressed in this paper that ground-relay calibrations should be hand-tailored for each application.

The basic conditions of Fig. 15 become quite complex if one or both circuits are multiterminal. With such a configuration, induced currents can sometimes exceed true fault currents for certain critical fault locations. The false residuals from two circuit faults, as in Fig. 5, can be many times greater than true line-to-ground currents on lightly grounded systems.

I am sure the authors could provide further interpretations to Fig. 21. The tertiary current is not as clean-cut as the text suggests, and it also shows a major alteration at 2 cycles at the same time as the residual-current reversal. Has anyone ever tested the actual performance of a high-speed directional element when subjected to harmonics in the polarizing winding such as shown in trace 2 of Fig. 21? I appreciate the theoretical point that the harmonics result in no net torque on the relay, but has any one made a field test of the phenomenon? Fig. 22 would be considerably more valuable if a sketch of the system and current-transformer connections were provided. As described, the phenomenon completely eludes me.

One other source of false residual currents can be present in a 3-wire current-transformer circuit which uses the station ground as the return circuit for the residual-current path. Voltage drops in the station ground network caused by the main fault-current flow can appear in the residual-relay circuit and cause incorrect performance. Modern practice of 4-wire single-point grounding of current transformer secondary circuits does not have this hazard.

The summaries in Tables I and II are valuable and impressive. Using separate communication channels for phase faults and ground faults can provide a degree of freedom which may be necessary if some of these undesirable factors unexpectedly materialize.

If I were confronted with the requirement for ground-relay sensitivities of the order considered in this paper, I would look fondly at a solution which would utilize electronic phase-comparison relays energized by air-core current transformers.

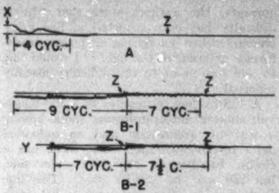

Fig. 29. Cloud discharges on 147-mile 230-kv line with no evidence of actual fault current

A recorded at Crawford Station 8/5/45. B-1 at Powerton Station 4/29/47. B-2 at Crawford Station 4/29/47. Records are from the output of current transformers in the neutrals of the 230-kv terminal transformers
X indicates a deflection equivalent to 130 amperes rms primary current
Y indicates fogged area of record
Z indicates opening of transformer L.T. breakers, as tripped by plunger-type neutral relays, either directly or by carrier remote trip

G. W. Hampe (Commonwealth Edison Company, Chicago, Ill.): This class of problems is analyzed as a group, which is very desirable. I also mentioned some problems in a general way[1] and suggested[2] potential polarization as a remedy. This, as Mr. Kennedy pointed out in his discussion, was not always applicable. It was also suggested that we might protect the three phases, wire by wire, with separate (microwave?) channels, but we have not had to do that yet.

I presented[3] a fault record, taken in May 1940, for line current transients, it is similar to the transformer neutral current in Fig. 4 of this paper, but much higher and longer. It oscillated at a slow rate (4 or 5 cycles per second) and set up an incorrect carrier trip circuit rather late, apparently because, on decaying and oscillating through the values of carrier start and stop, the start and stop elements could not co-ordinate.

I would appreciate an explanation of both the high-frequency oscillations and the slow flip-flops in the voltage traces in Fig. 11. Where line-connected potential transformers or potential devices are used, the slow transients are inevitable and the high-frequency ones quite common. Both occur when the opening of a circuit breaker de-energizes a line.

The authors referred to induction only in terms of induced ground current. It seems possible to have induced residual current without ground current. Consider 2 3-conductor cables on system no. 1 and system no. 2 in the same duct run, each with its own sheath. The phase conductors of the two cables are on systems normally electrically independent, although in the same station at one end. System no. 2 cable is one of several parallel lines between two station busses in that system, with those other parallel lines of system no. 2 geographically remote from the duct run in question. Cable no. 1 has a phase-to-ground fault, with current returning to system no. 1 neutral over the sheaths surrounding the conductors of both system no. 1 and no. 2. There would be induced voltages in the 3-phase conductors of system no. 2 cable. The resulting currents would complete their circuits over the respective phase conductors of the more remote parallel lines. The induced currents would equal an in phase, but on system no. 2 there would be no circuit for neutral or ground current. Since the three induced currents are additive with respect to a residual relay, their effect is appreciable. I used this example to explain some otherwise unaccounted-for relay operations.

To bring in rare cases, the authors might have mentioned the earth currents associated with the aurora borealis, and I can cite two cases even more remarkable. In two cases, during thunderstorms, a 230-kv line apparently discharged through the power transformer neutral at one end. This tripped the plunger-type neutral relay. The line, however, was not faulted. The line discharges as reproduced by the neutral current transformer and transmitted to the relay are shown in Fig. 29. The phenomenon, though rare, bars the use of high-speed ground relaying on that 230-kv line.

All this indicates that applying ground relays is a difficult problem, and when applying fast, sensitive, polarized ground relays, there are considerable uncertainties. At the same time, because of the relative prevalence of ground faults, good ground relaying is very desirable. Perhaps the relative popularity of rather complicated phase-fault relays is that polarizing them and computing their settings is relatively simple.

For 2-terminal pilot-wire protected lines, insurance against the vagaries of system phenomena and current-transformer performances is available,[3] provided one is willing to pay the price, which is that of a sound pilot channel. If carrier pilots are to be used (and this probably includes microwave carrier also), phase comparison seems to be more advantageous. In my experience, some installations of directional- as well as phase-comparison carrier relaying have had a perfect record. On the other installations, after much toil and trouble, both types of relaying (as of the present date) seem to have become quite immune to tripping on external faults. Several directional-comparison applications have a low efficiency on internal faults, and one directional-comparison scheme has had a completely zero efficiency up to now.

On internal line faults it is not easy to shut off a blocking carrier signal and keep it off. After the local circuit breaker opens, it often returns. From this paper some possible reasons for this behavior may be inferred, e.g., when the local trip circuit is energized from any line relay, backups included, an auxiliary relay will turn off the local carrier transmission and hold it off while the local breaker opens and about 15 cycles thereafter. At the end of this period, control would then be returned to the basic carrier controls. This could be applied to both phase- and directional-comparison schemes.

With multiterminal lines becoming more common, if not predominant, the relay engineer's troubles have only started. In discussing a companion paper[4] I make some suggestions of a general nature.

REFERENCES

1. POWER-LINE CARRIER FOR RELAYING AND JOINT USAGE—PART II. A SURVEY OF MODERN POWER-LINE CARRIER SYSTEMS, G. W. Hampe, B. Wade Storer. *AIEE Transactions*, vol. 71, pt. III, Aug. 1952, pp. 661–70.

2. *Discussion* by G. W. Hampe of SYSTEM SHORT-CIRCUIT CURRENTS, H. A. Travers, C. F. Wagner,

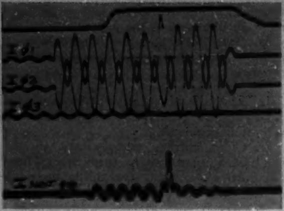

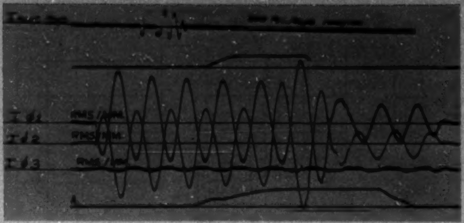

Fig. 30 (left). Phase-1 to phase-2 staged fault on an open-wire 132-kv line

Fig. 31 (right). Phase-1 to phase-2 staged fault on remote terminals of an underground pipe-type 132-kv line

C. A. Woodrow, W. F. Skeats. *AIEE Transactions*, vol. 60, 1941, pp. 1351–52.

3. A PILOT-WIRE RELAYING SCHEME UTILIZING THE PRODUCT DIFFERENTIAL RELAY, R. I. Ward, D. W. Gilman. *AIEE Transactions*, vol. 72, pt. III, Oct. 1953, pp. 911–17.

4. *Discussion* by G. W. Hampe of LINE AND TRANSFORMER BANK RELAYING SYSTEMS, J. L. Blackburn, G. D. Rockefeller. *AIEE Transactions* vol. 74, pt. III, June 1955, pp. 334–43.

Herbert G. Erdman, Jr. (Public Service Electric and Gas Company, Newark, N. J.): Mr. Barnes and Mr. McConnell are to be congratulated for their excellent presentation of one of the least understood phases of power-line relaying. We have had several cases during recent staged and actual faults on our 132-kv transmission system which involved residual current during phase faults, residual current caused by one open conductor, and incorrect tripping by carrier ground relays during a ground fault.

Fig. 30 is an oscillogram of a phase-1 to phase-2 staged fault on an open-wire 132-kv line. No ground was involved in the fault but the bottom trace indicates 160 amperes in the transformer neutral. After 6 cycles there is a rise in neutral ground current for 1/2 cycle to 1,000 amperes because of unequal circuit-breaker pole opening. The 160 amperes probably result from a combination of unequal charging current and load current in the unfaulted phase 3 and, in this case, are too small to affect relay operation.

Fig. 31 shows a phase-1 to phase-2 staged fault on the remote terminals of an underground pipe-type 132-kv cable. This is an 11-mile circuit having a reactive capacity of 40,000 kva; the 132-kv charging current is approximately 200 amperes. The cable is directly connected to a wye-delta-wye transformer bank and through a 132-kv tie breaker to the 132-kv system at the station where the oscillogram was taken.

After $6^1/_2$ cycles the 132-kv circuit breaker at the remote end of the line and 132-kv local tie breaker had opened. At this time the phase-to-phase fault was being fed only from the low-voltage (26 kv) side of the local bank. The trace of 132-kv neutral ground current shows an increase here from a very low value to approximately 1,600 amperes. An examination of the phase currents in the faulted phases discloses a phase shift at this time from almost 180 degrees out of phase to about 145 degrees. In Fig. 32 these currents are added graphically, including the current in the unfaulted phase 3, producing an indicated residual current of 1,160 amperes. Difficulty in measuring phase angle from the oscillogram makes this result approximate at best; however, the presence of such a high residual current is difficult to explain.

If the foregoing fault were moved beyond the remote terminal of the line and no ground polarizing current appeared at this terminal, directional-comparison carrier relaying would probably not cause incorrect tripping since the phase carrier-starting relays at the remote terminal would send a blocking signal; however if the carrier ground sensitivity were too high or if high-speed backup ground relays were used, false tripping could occur. In any case the co-ordination of phase carrier-starting with ground carrier-tripping elements when the magnitude of ground current is unpredictable is all but impossible.

Previous single-phase-to-ground staged faults on the same cable circuit resulted in three incorrect tripouts of other adjacent line sections. All of these lines are protected with directional-comparison carrier relaying and all tripped at their remote terminals by the operation of carrier ground relays in the absence of blocking. One case was directly traceable to a relay setting which did not cover the operating conditions at the time of the fault. At all of our stations there is only one ground source for all of the 132-kv transformer neutrals and the neutral current transformer thus measures the total neutral ground current of all the banks. Some of these stations are normally operated with the 132-kv bus split in two or more sections but have tie breakers that can be closed at any time. The remote station at which this line was terminated is normally operated with the 132-kv bus split into four sections. The carrier-starting relay is a current-polarized product-type ground relay. At the time of the fault the bus section to which the line was connected was tied to another bus section and the carrier ground relay received much more than normal energy and closed its trip contacts; the ground carrier-starting relay at the local end of the line (also a product type) did not receive enough energy to close its contacts; hence no blocking was transmitted. The co-ordination of elements satisfactory for normal bus operation was upset by emergency operating conditions.

The product-type ground relay has become increasingly difficult to set because of the split bus condition described in the foregoing. It is sometimes difficult to forsee all possible operating combinations. We are now investigating the possibility of controlling carrier with reactance ground relays which require no neutral current or zero-sequence potential for polarization.

The other two lines that tripped incorrectly during a ground fault on the cable apparently received no carrier blocking or received it too late. The carrier-starting elements on these lines are current-polarized directional-overcurrent units. These relays were thoroughly checked and subjected to further staged fault tests but no trouble could be found nor could the trouble be made to repeat itself. Sufficient oscillographic data were not obtained at the time of the initial trouble to discover any condition which might have fooled the ground relays. The fault on the cable circuit was a bolted one and was established by closing the line circuit breaker; therefore the initial surge of current was a combination of fault current and cable-charging inrush. The station bus voltage during this period showed high harmonic disturbances. It appears that high-voltage cable circuits with their high charging capacities will add to the already difficult problem of high-speed ground relaying.

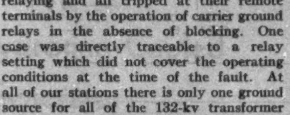

Fig. 32. Graphical addition of phase currents for the phase-to-phase cable fault

H. C. Barnes and A. J. McConnell: We particularly appreciate the corroborative evidence supplied by all of the discussers. Also, we agree with the comments on the following subjects:

1. Value of oscillographs. Merritt, Rockefeller-Blackburn.
2. Current-transformer performance. Marter, Rockefeller-Blackburn.
3. Value of time delay. Merritt, Achtenberg, Rockefeller-Blackburn.

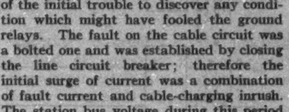

Fig. 33. Cable fault following opening of the 132-kv circuit breakers

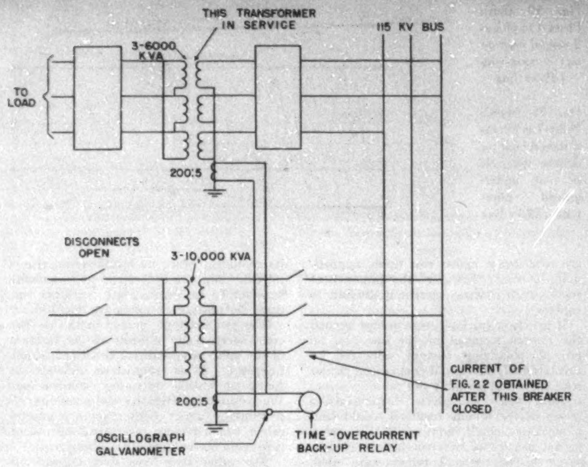
THIS TRANSFORMER IN SERVICE
115 KV BUS
3-6000 KVA
TO LOAD
200:5
DISCONNECTS OPEN
3-10,000 KVA
CURRENT OF FIG. 22 OBTAINED AFTER THIS BREAKER CLOSED
200:5
OSCILLOGRAPH GALVANOMETER
TIME-OVERCURRENT BACK-UP RELAY

Fig. 34. System and current transformer connections associated with Fig. 22

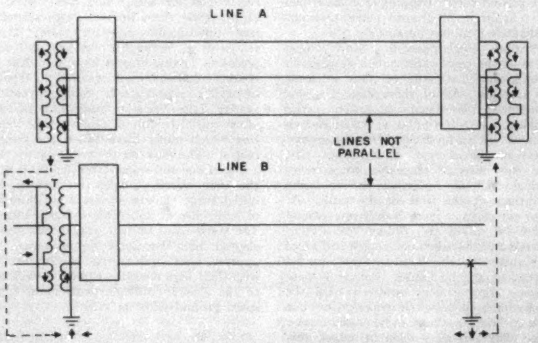

Fig. 35. Example of ground-current flow in a line which is physically and electrically separated from a ground-faulted second line

4. Insufficiency of explanation of figures. Rockefeller-Blackburn. (Fig. 25), Linders (Figs. 21 and 22), Hampe (Fig. 11).

With respect to Mr. Erdman's Fig. 31, we believe that the staged phase-to-phase fault became a 2-phase-to-ground fault at the end of 6.5 cycles. At that time, all 132-kv circuit breakers were open, the fault being supplied only through the transformer from 26 kv. The measured ground current was 1,600 amperes, and yet the only outlet (other than a ground fault) was the capacity of the 11-mile cable, the normal charging current of which is only 200 amperes. It is believed that Mr. Erdman's Fig. 32 is incorrect. It will be noted that, beginning at 6.5 cycles, the current in phase 2, Fig. 31, reaches a maximum before the current of phase 1. In Fig. 32, the current in phase 2 reaches a maximum after the current of phase 1. If the phase relationships $I_{\phi 1}$ and $I_{\phi 2}$ of Fig. 32 were interchanged, the resulting phasor diagram would be about the same as would be obtained for a 2-phase-to-ground fault.

With respect to Mr. Erdman's Fig. 30, we believe that the neutral current is simply a result of unbalanced system impedance. If the symmetrical-component method is sound, there can be no neutral current when all impedances are symmetrical.

Mr. Erdman makes a very valuable contribution by suggesting the use of ground-distance relays as a means of carrier control. Ground-distance relays of the current-compensated type require neither neutral-current nor zero-sequence voltage polarization and, consequently, are substantially unaffected by the various ground-relay ills discussed in the paper.

Mr. Rockefeller and Mr. Blackburn contributed the following additional pertinent comments:

1. The use of negative-phase-sequence quantities are effective in the solution of induction problems.
2. Older current transformers should be looked upon with suspicion. Their capabilities are about two-thirds those of modern current transformers.

Regarding Fig. 25, it is first necessary to consider that when the phase-to-phase fault occurs, E_{b-N} (see phasor diagram of Fig. 25), which is the phase *b*-to-neutral voltage, changes in the lagging direction by 60 degrees with a reduction of magnitude to one-half. By the same token, exciting current I_b (during fault without offset) lags exciting current I_b (prefault) by 60 degrees and with magnitude reduced to one-half. When the phase-to-phase fault occurs, the prefault exciting current has a negative value as shown by the solid line. Its ultimate value must be in accordance with the dotted line I_b (during fault, without offset). Since the exciting current cannot change instantaneously, there must be a d-c component called "d-c offset." Thus, for the exciting current to start in accordance with the solid line at the incidence of the phase-to-phase fault and end in accordance with the dotted line I_b (during fault, without offset), there must be the d-c offset as shown. The net result is the dotted line denoted I_b (during fault, with offset). When this exciting current causes the flux to reach the saturating point of the iron, the exciting current will increase while trying to maintain the proper flux,[1] as shown on the curve labelled "magnetizing-current inrush."

Mr. Linders desires further interpretation of Fig. 21. He suggests that something happened to the tertiary current at the end of 2 cycles. We believe that nothing occurred abruptly to the tertiary current at that time. The tertiary current was offset initially and, at the end of 2 cycles, practically all of the d-c component had disappeared. Something did occur abruptly to the phase-1 current after 2 cycles. Calculations have indicated that after 2 cycles, the phase-1 current transformer was residually magnetized so that it could not properly reproduce subsequent half-cycles of current. The current transformers in phases 2 and 3 were still able to reproduce primary current (because of lower current magnitude). Thus, the deficiency in phase 1 caused a reversal in the zero-sequence trace (Musk ground).

With further reference to Mr. Linder's discussion, high-speed directional units have been tested (in the laboratory) to show that no net torque is produced by fundamental current in one circuit and harmonic current in the other circuit. On the other hand, the same harmonic in both circuits will produce torque. We believe that Mr. Linders is suggesting the possibility of harmonic torques being produced by the combination of the tertiary current and the residual current. He is entirely correct in that certain harmonics appear in both currents. Like harmonics will produce a net torque, but the direction of that torque may be either in the tripping or the nontripping direction.

As requested by Mr. Linders, Fig. 34 shows the system and current-transformer connections associated with Fig. 22.

Mr. Linders points out another ground-relay hazard, namely, multiple grounding of the lead connecting the current-transformer neutral and the ground relay or the use of the station ground network as the fourth wire. We believe that such practices are not engaged in today, but it certainly does no harm to warn the younger men against them.

Mr. Hampe requests an explanation of the high-frequency oscillations and the slow flip-flops in the voltage traces of Fig. 11. We would guess that high frequency is a resonant oscillation between the zero-sequence line capacity and the zero-sequence short-circuit inductance of the transformer. This explanation is supported by the fact that current of the same frequency appears in the transformer tertiary. Slow flip-flops might be an oscillation between the line capacity and the magnetizing inductance of the transformer. The peculiar wave shape is explained by the nonlinearity of the magnetizing reactance, the tendency toward a flat top being caused by saturation of the transformer iron. A similarly shaped wave is shown in oscillogram 189-11, Fig. 8;[3] there the phenomenon is called a "ferrononlinear oscillation."

Mr. Hampe makes a real contribution in his discussion of induction with respect to cables in the same duct run. H. R. Paxson of the Philadelphia Electric Company, in an oral comment to the authors, noted a phenomenon akin to induction, but actually conduction. Fig. 35 illustrates the condition. *A* and *B* are nonparallel lines at different voltages. A ground fault occurred on line *B* as shown. Some of the ground current returned to transformer *T* in the normal manner. However, the remainder of the ground current found it easier to return over the phase conductors of line *A*, thereby operating the ground relays on line *A* incorrectly.

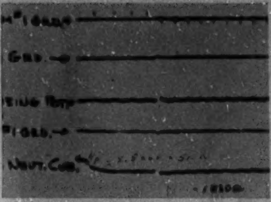

Fig. 36. Example of d-c neutral current caused by unequal pole closing of a circuit breaker

Mr. Hampe's suggestion that carrier transmission be prevented upon tripping a breaker has been used. One operating company had such a difficulty with respect to high-speed reclosing. With a fault near one line terminal, operation at the other line terminal was slow because of low ground-fault current. Carrier transmission from the fast terminal delayed tripping at the slow terminal, thereby reducing the de-energized time sufficiently to preclude successful reclosure. The solution was to prevent the "fast" line terminal from sending a carrier-blocking signal for a short period after tripping.

Fig. 36 is presented to bring the paper up-to-date. In this example, a high-tension breaker was inadvertently closed on a grounded neutral transformer, on the low side of which was a motionless generator. The transformer neutral current (bottom trace) shows an apparent d-c component lasting for at least 1 cycle. This was reproduced on the transient analyzer and was shown to result from unequal breaker pole closing. Ground relays refrained from operating incorrectly, but inadvertent ground-relay operation might have occurred.

We neglected to mention that a sometimes effective method of avoiding false residual current caused by d-c saturation of bushing current transformers is to increase the secondary turns. This method may be particularly effective because the maximum current-transformer flux varies inversely as the square of the secondary turns.

REFERENCES

1. TRANSFORMER ENGINEERING (book), L. F. Blume, G. Camilli, A. Boyajian, V. M. Montsinger. John Wiley and Sons, Inc., New York, N. Y., 1951.

2. SWITCHING HIGH-VOLTAGE TRANSMISSION LINES, I. B. Johnson, J. R. Wilson. *AIEE Transactions*, vol. 66, 1947, pp. 1,552–60.

Operation of Hydrogen-Cooled Turbine Generators

C. C. STERRETT
MEMBER AIEE

R. A. TOWNE
ASSOCIATE MEMBER AIEE

HYDROGEN-COOLED turbine generators constitute the major portion of the nation's present generating capacity. Their proper operation is necessary to assure continuity of service to the country and to protect the large capital investment involved in generating equipment. Continuous advances in the design of generators have made it necessary for manufacturers and operators to reexamine operating practices regularly.

In the late 1930's, hydrogen-cooled turbine generators were first put in operation. These units were generally based on load machines operated at 0.5 pound per square inch gauge (psig) hydrogen pressure. They were operated according to the same practices that had been developed over the years for large air-cooled generators. Successful operation was achieved in this manner for these early, relatively small units. To meet the subsequent demand for individual units of higher ratings, manufacturers gradually increased the generator physical size and utilized higher hydrogen pressures. As these larger and more efficient units were placed in service, they were generally utilized for base load operation. The older units were then often assigned to peak load operation, which subjected them to more frequent load cycling. Present operating methods must be reviewed, giving careful consideration to these additional factors, thereby providing increased assurance of continuous service, long life, and minimum maintenance.

This paper is presented to stimulate discussion which will lead to a clearer understanding of the problems involved, and to the development of acceptable operating procedures. A practical method of operating hydrogen-cooled turbine generators is described so as to satisfy present-day operating requirements. A description of the ventilation systems of hydrogen-cooled machines and a discussion of the requirements for successful operation are included. This paper applies specifically to conventionally cooled machines and not to the recently developed machines which embody coil-cooling systems wherein the coolant is brought into more direct contact with the conductors.

Description of Generator Ventilation

Figs. 1(A), (B), (C), and (D) illustrate the arrangement of a typical ventilation system for a hydrogen-cooled turbine generator. The ventilation system is symmetrical about the center of the machine. Hydrogen is circulated by means

---

Paper 55-116, recommended by the AIEE Rotating Machinery Committee and approved by the AIEE Committee on Technical Operations for presentation at the AIEE Winter General Meeting, New York, N. Y., January 31–February 4, 1955. Manuscript submitted October 26, 1954; made available for printing December 8, 1954.

C. C. STERRETT and R. A. TOWNE are with the Westinghouse Electric Corporation, East Pittsburgh, Pa.

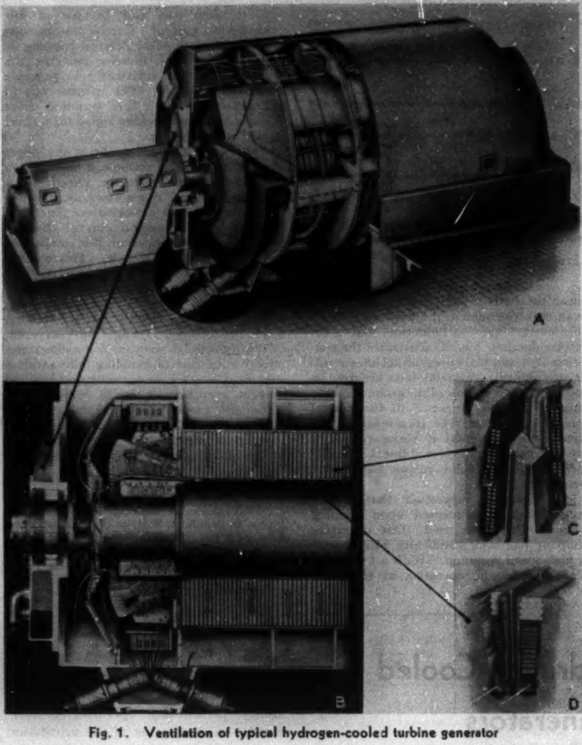

Fig. 1. Ventilation of typical hydrogen-cooled turbine generator

of blowers mounted at each end of the generator shaft. The hydrogen ventilates the rotor and the stator. The entire volume of warm hydrogen is passed through coolers mounted in the generator. The cooled hydrogen is then returned to the blowers. The hydrogen pressure usually can be increased above 0.5 psig to suit the generator loading requirements.

Temperature detectors are embedded in the stator winding to obtain a conventional indication of the temperature of the winding. The rotor temperature is determined from the average resistance of the winding. The cold hydrogen temperature is measured by means of temperature detectors located in the cooler discharge.

Requirements for Successful Operation

The successful operation of a turbine generator requires a consideration of several different factors, a discussion of which follows.

Stator Winding Temperature

The capability of the stator winding is limited by the maximum allowable temperature of the stator insulation. This temperature is maximum at points adjacent to the copper of the winding. The conventional temperature detectors inherently indicate temperatures lower than the copper temperature because of the necessary physical separation of the detector from the stator winding copper. It is a characteristic of hydrogen-cooled machines that the difference in temperature between the detector and the copper is a variable which increases at higher hydrogen pressures. Because of this variation, operation by means of detector indications is undesirable. A means of operating must be provided which effectively supervises the actual stator winding temperature.

Rotor Winding Temperature

Operation at power factors less than the nominal rated value in the overexcited region is limited by the rotor winding temperature. In this region the full rated kilovolt-amperes (kva) of the generator cannot be realized because of this limitation. An operating method must recognize this limitation. The rotor winding temperature does not limit the capability of the generator in other regions of operation.

Stator Core Temperature

Operation in the entire underexcited region is limited by extra heating in the extreme ends of the stator core where temperatures are not detected by the usual stator winding temperature detectors. Due consideration must be given to this effect.

Stator Differential Expansion

The capability of the stator winding is limited not only by total temperature but also by the effects of cyclic differential expansion between the stator coils and the stator core. Differential expansion is a function of the temperature rise of the winding. This requires that the maximum load of the machine be limited so as to limit differential expansion, and that changes in load be made so as to minimize cyclic variations in differential expansion.

The effects of high total winding temperature and frequent variations in differential expansion may result, in some cases, in separations in the stator coil insulation. The stator-coil insulation-separation problem is discussed in detail in a companion paper.[1]

Shaft Alignment

The generator and turbine shafts are solidly connected by means of a bolted flanged coupling. During operation, these shafts must be closely aligned. Misalignment may cause shaft stresses and a redisitribution of the bearing loading, both of which may be excessive and lead to a mechanical failure.

The variation in elevation of the generator shaft is a function of the temperature of its supporting members. The temperature of the bracket and the frame which support it varies directly with the cold hydrogen temperature. Consequently, the generator shaft elevation varies directly with the cold hydrogen temperature. The generator should be operated so as to minimize the possibility of misalignment between the generator and turbine shafts during load changes.

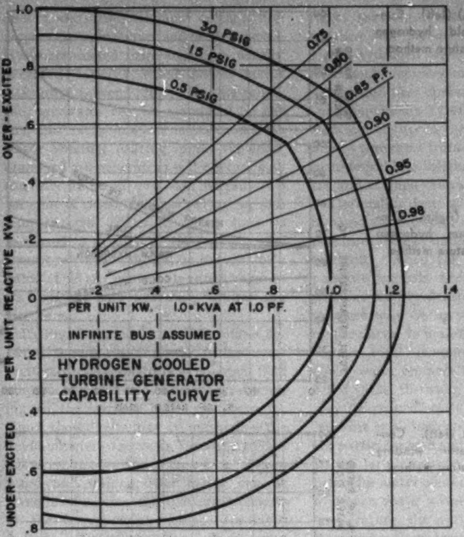

Fig. 2. Hydrogen-cooled turbine generator capability curve

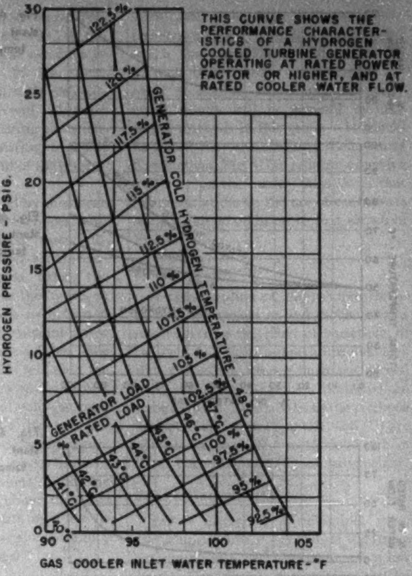

Fig. 3. Typical hydrogen-pressure regulation curve

Frame Distortion

Changes in the cold hydrogen temperature cause distortion of the frame ends, with consequent working of the mechanical joints and gaskets. This may result in increased hydrogen leakage and maintenance. The performance of the gaskets is also adversely affected by high temperatures. The generator should be operated so as to limit frame and gasket distortion.

Condensation on Water Pipes and Frame

Operation of the hydrogen coolers with water colder than the dew point of the room air will cause objectionable condensation on the water pipes and frame.

Operation by Capability Curves

A typical generator capability curve is shown in Fig. 2. This curve should be used to control the operation of the generator under all load conditions, as explained in the following.

Control of Stator Winding Temperature

Since the stator winding temperature detectors do not give a true indication of the winding temperatures, the machine should be loaded in accordance with the manufacturer's capability curve. The capability curve controls operation in the overexcited range from rated power factor to unity power factor by limiting the kva output, thus limiting heating in the stator winding. Temperature readings should be taken and recorded by the user, but their primary purpose should be to indicate incorrect operation or changes in the generator. Therefore, temperature readings are recommended as a backup protection for the hydrogen-cooling system and capability curves.

It is now standard practice to embed 12 stator temperature detectors in the armature winding. They consist of 10-ohm resistance coils located in slots between the two armature coils, and distributed around the periphery and along the length of the stator. Usually five of these resistance temperature detectors are connected to a continuous recorder which gives an indication of the stator winding temperatures. The five highest reading detectors are selected for recording. There are also two cold-gas temperature detectors, one at each end of the generator located in the cold-gas stream entering the blowers. These are generally connected to the same recorder as the stator temperature detectors.

Control of Rotor Winding Temperature

The capability curve should be used to control operation in the overexcited range below rated power factor. It limits the rotor current to a constant value as determined by heating occurring in the rotor winding.

Rotor temperature is usually indicated by a recorder which measures the resistance of the rotor field at a given time and compares it with a known resistance at a definite temperature. Calibration of the rotor temperature recorder may be obtained periodically by determining the rotor resistance from the collector ring voltage and field current with portable instruments.

Control of Stator Core Temperature

The usefulness of the capability curve as a control device is further exemplified in the underexcited region where the underexcited capability shown limits the heating in the stator-core end zones to acceptable temperatures.

Use of Capability Curve

The control of the generator according to capability curves in terms of kilowatts and kilovars may be accomplished by

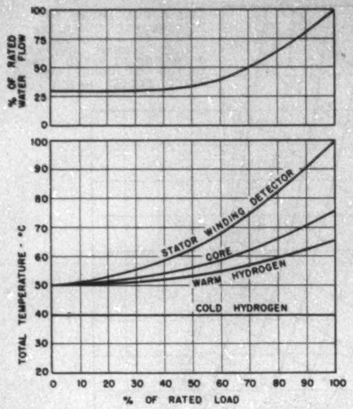

Fig. 4(A) (left). Constant cold hydrogen temperature method

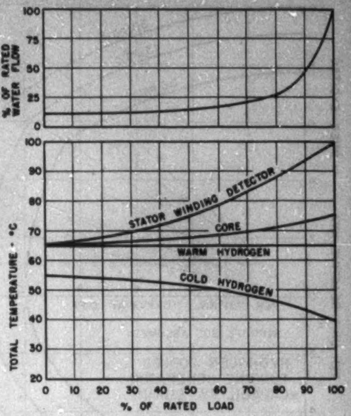

Fig. 4(B) (right). Constant warm hydrogen temperature method

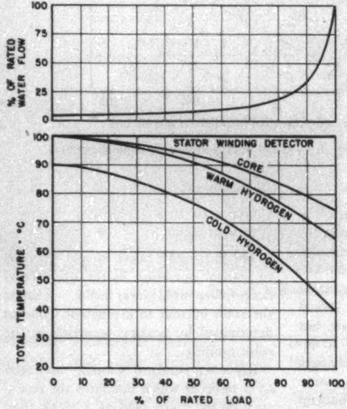

Fig. 4(C) (left). Constant stator winding temperature method

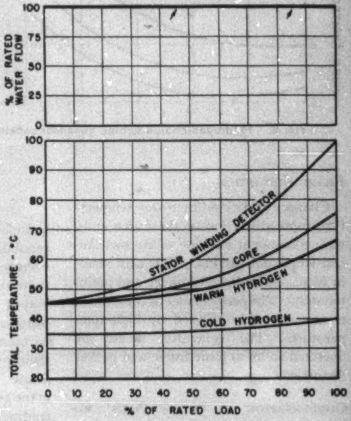

Fig. 4(D) (right). Constant cooler-water flow method

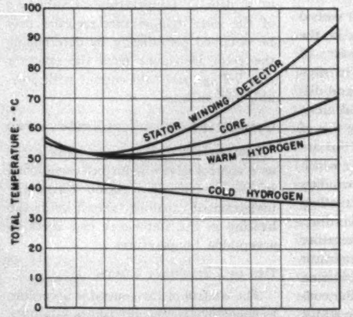

Fig. 4(E) (left). Typical method utilizing nonrecirculating condensate

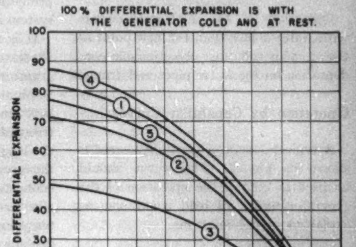

Fig. 5 (right). Relative differential expansion of stator for different methods of operation

1—Constant cold hydrogen temperature
2—Constant warm hydrogen temperature
3—Constant stator winding temperature
4—Constant cooler-water flow
5—Nonrecirculating condensate in generator coolers

meters measuring terminal voltage, line amperes, power factor, and field amperes. Hydrogen-cooled generators are usually operated between rated power factor and unity power factor. In this range, the generator can be controlled by the terminal voltage and line amperes since the stator winding heating limits the load. Standard a-c generators will operate successfully at rated kva load within ± 5 per cent of rated terminal voltage at safe temperatures. Thus, if the voltage is increased to a value of 105 per cent, the armature current should be reduced to a value of 95 per cent of its rated value to stay within safe operating limits, and vice versa.

In Fig. 2 the portion of the curve between 0 and rated power factor overexcited can be thought of as constant field ampere limits at the ratings corresponding to the various hydrogen pressures. Thus, these limits may be marked on the field ammeter to serve as operating guides. Likewise, the portion of the curve between rated and unity power factor can be thought of as constant line ampere limits at the corresponding ratings for rated voltage. Therefore, these limits may be marked on the ammeter to serve as operating guides. Since the terminal voltage may vary 5 per cent at rated kva at safe temperatures, it follows that the line ampere limits must be compensated for operation at other than rated voltage. This can be accomplished by using color bands on the meter extending ± 5 per cent of the rated line amperes. Corresponding bands may be placed on the terminal voltmeter. For example, the ammeter would have a 95-per-cent limit when the voltmeter is being held at 105 per cent of rated voltage.

USE OF HYDROGEN-PRESSURE REGULATION CURVE

A hydrogen-pressure regulation curve is shown in Fig. 3. This becomes of interest for operation at higher hydrogen pressures. This curve shows the relation between maximum load, maximum permissible cold-gas temperature, water temperature, and hydrogen pressure. The rated quantity and the rated temperature of water required by the generator gas coolers are such as to absorb full load generator losses and maintain the cold-gas temperature at 40 degrees centigrade (C) at 0.5 psig. It will be noted that, as the hydrogen pressure is increased along the 90-degree-Fahrenheit cooler-water temperature ordinate, the permissible load increases and these increments correspond to the capabilities indicated in Fig. 2. Also, this curve shows that the generator cold-gas temperature will increase above 40 C at the higher hydrogen pressures at rated water flow and temperature. It has been determined that operation with the cold-gas temperature at 48 C will not cause sufficient change in the bearing elevation, due to generator frame heating, to result in undesirable misalignment of the generator and turbine shafts.

The loading demonstrated by this curve is based on the total stator copper temperature being maintained essentially constant. When the cooler-water temperature exceeds the rated value, the machine may be derated or the hydrogen pressure may be increased, as indicated on the curve, to maintain constant stator copper total temperature. When the cooler-water temperature is less than the rated value, the water flow to the coolers may be reduced until the cold-gas temperature is as indicated by the curve for the particular load and hydrogen pressure. In the latter manner the curve becomes useful for water conservation. When the hydrogen cooler-water is above the rated temperature, the water rate may not be increased without incurring the possibility of cutting the cooler tubes.

Operation of Hydrogen Coolers

The control of the water flow to the hydrogen coolers provides a means of regulating the cold hydrogen temperature at partial loads. The water flow is maintained constant at the rated value for loads above the 0.5 psig rating. The control of the cold hydrogen temperature at partial loads involves a consideration of the requirements of stator differential expansion, shaft alignment, frame distortion, and condensation. Such a consideration indicates that operation at a constant cold hydrogen temperature should be recommended as providing the most satisfactory operating results. The basis for this recommendation is discussed in the following.

STATOR DIFFERENTIAL EXPANSION

The differential expansion between the stator winding and the stator core can be controlled to a certain extent by regulating the cold hydrogen temperature. Figs. 4(A), (B), (C), (D), and (E) illustrate the calculated generator temperatures and cooler-water flows at partial loads corresponding to several methods of control. Differential expansion is a minimum with constant stator winding temperature control, but requires prohibitive temperatures in the generator components at partial loads, and is, therefore, unacceptable. The other methods of control shown on Fig. 5 fall in a group within which the variation of differential expansion between one method and another is minor. Therefore, practically equal results will be secured by any of the methods in this group. It should be noted that the constant cooler-water flow method, Fig. 4(D), requires excessive water at partial loads. Also, note that many variations in the use of condensate are possible in addition to that shown in Fig. 4(E).

SHAFT ALIGNMENT

A consideration of the relative elevations of the generator and turbine shafts resulting from the effect of variations in the cold hydrogen temperature indicates that the cold hydrogen must not exceed 48 C if shaft misalignment problems are to be avoided. On this basis the methods of control shown in Figs. 4(B) and (C) are not acceptable. The methods shown in Figs. 4(A), (D), and (E) are satisfactory.

FRAME DISTORTION

Frame distortion is minimized when the temperatures at the ends of the frame are maintained nearly constant at a low level. The frame temperature varies approximately with the cold hydrogen temperature. Operation in accordance with methods shown in Figs. 4(B) and (C) is undesirable. The other methods are considered to be acceptable.

CONDENSATION ON WATER PIPES AND FRAME

It is desirable to avoid operation with the generator cold hydrogen temperature below 25 C to prevent condensation.

RECOMMENDED METHOD OF OPERATING HYDROGEN COOLERS

It is evident that no simple method of operating the hydrogen coolers will satisfy all of the preceding considerations. However, constant cold hydrogen temperature operation or any method which approximates this, such as shown in Figs. 4(A), (D) and (E), provides a means of control for partial load, which is a practical compromise and is, therefore, recommended.

A General Consideration of Generator Operation

As load is assumed by a generator, the cooling water should be gradually admitted to the hydrogen coolers so as to obtain a cold hydrogen temperature in the order of 35 to 40 C. As load is increased, additional water should be admitted so

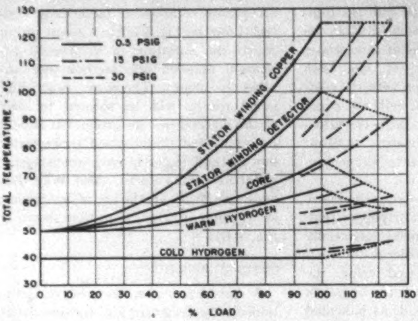

Fig. 6 (left). Typical temperatures and cooler-water flow for hydrogen-cooled turbine generator

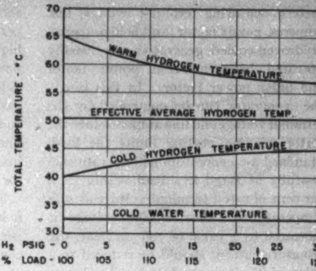

Fig. 7 (right). Variation of cold hydrogen temperature with hydrogen pressure

as to maintain the cold hydrogen temperature approximately constant.

At partial generator loads, the generator losses are reduced, permitting the coolers to be operated at less than rated conditions. A constant cold hydrogen temperature may be maintained with either a reduced water flow at the rated temperature, or an increased water temperature at the rated flow. Where the water supply temperature is considerably below the rated water temperature of the cooler, the water flow should be reduced below rated flow to maintain the recommended cold hydrogen temperature. As the cold hydrogen temperature of a generator responds slowly to changes in load, manual control of the generator temperature will be satisfactory; however, automatic control may be installed if desired. In either case, the cold hydrogen temperature should be used as the basis for regulation.

Constant cold hydrogen temperature control should be maintained up to and including the rating for 0.5 psig hydrogen pressure. For loads greater than the 0.5 psig rating, the hydrogen pressure must be increased according to the capability curve. The generator and cooler are designed so that no further increase in water flow is required for operation above the 0.5 psig rating.

Fig. 6 shows typical temperatures and cooler-water flow at various loads and hydrogen pressures. It will be noted that the stator winding copper temperature is constant for loading about the 0.5 psig rating. It will also be noted that the stator winding temperature detectors indicate unusually low temperature rises at the higher hydrogen pressures. The difference of temperature between the stator winding temperature detectors and the stator copper temperature is of the order of 25 C at 0.5 psig; and difference increases at higher hydrogen pressures, being approximately a function of the square of the current. This curve also shows that the cold hydrogen temperature increases above 40 C when the machine is operated at hydrogen pressures and corresponding loads higher than the basic rating at 0.5 psig. This behavior may be explained as follows:

When a machine is operated at hydrogen pressures above 0.5 psig with correspondingly higher loads, the increase in losses in the machine is approximately balanced by the increase in heat-transfer capability of the hydrogen coolers. Therefore, the difference between the average cooler-water temperature and the average hydrogen remains approximately constant. However, the ability of the hydrogen to absorb heat increases much faster than the losses in the machine for any given increase in hydrogen pressure, with the result that the temperature rise of the hydrogen decreases with increasing hydrogen pressure. Since the average temperature of the hydrogen remains approximately constant, the reduction in the hydrogen temperature rise results in an increase in cold hydrogen temperature, and a decrease in hot hydrogen temperature at higher hydrogen pressures. Fig. 7 shows the general nature of this phenomenon. The conventional increases in rating at higher hydrogen pressures were established by including this effect. It would require coolers of nearly double the usual size to maintain a 40 C cold hydrogen temperature at the 30 psig rating. This would increase the diameter of large machines unreasonably, with no extra advantage to the operator, since present temperatures are satisfactory.

When a generator is expected to carry loads in excess of the 0.5 psig rating regularly, it is common practice to maintain the hydrogen pressure constant at a value corresponding to this peak load. It is uneconomical to reduce this pressure for short-duration reductions in load. Under these circumstances, temperatures corresponding to the dotted lines in Fig. 6 indicate the trend of temperatures which will be obtained.

When load is being dropped from a unit prior to shut down, the water flow should be gradually reduced so as to maintain a substantially constant cold hydrogen temperature.

It should be noted that the diagrams included in this paper have been drawn so that the temperatures correspond to the proposed revision of the ASA *C50* standards[2] for hydrogen-cooled machines. Commercial machines will operate at temperature within these limits.

Summary of Operating Instructions

The generator should be operated in accordance with the generator capability curve with rated flow in the hydrogen coolers except that, for loads up to and including the 0.5 psig rating, the cooler-water flow should be regulated so as to maintain the cold hydrogen temperature at a substantially constant value in the order of 35 to 40 C.

References

1. TURBINE GENERATOR STATOR-WINDING TEMPERATURES AT VARIOUS HYDROGEN PRESSURES, J. R. M. Alger, C. E. Kilbourne, D. S. Snell. *AIEE Transactions*, vol. 74, pt. III, April 1955, pp. 232–51.

2. ROTATING ELECTRICAL MACHINERY. *ASA C50* (under revision), American Standards Association, New York, N. Y.

3. CONTROLS FOR OPERATION OF STEAM TURBINE-GENERATOR UNITS, O. N. Bryant, C. C. Sterrett, D. M. Sauter. *AIEE Transactions*, vol. 73, pt. III-A, Feb. 1954, pp. 79–88.

4. LOADING OF HYDROGEN-COOLED GENERATORS AT ELEVATED GAS PRESSURES, D. S. Snell. *AIEE Transactions*, vol. 69, pt. I, 1950, pp. 186–204.

5. A MAINTENANCE INSPECTION PROGRAM FOR LARGE ROTATING MACHINES, J. S. Johnson. *AIEE Transactions*, vol. 70, pt. I, 1951, pp. 749–55.

6. GENERAL PRINCIPLES UPON WHICH TEMPERATURE LIMITS ARE BASED IN THE RATING OF ELECTRIC MACHINES AND APPARATUS. *AIEE Standard No. 1*, Feb. 1954.

Discussion

M. S. Schneider (Cincinnati Gas and Electric Company, Cincinnati, Ohio): This is a timely paper and should be of great help to all operators of hydrogen-cooled generators. The authors apparently intend that the field loading limits should be determined by field temperature as measured by field resistance as the prime guide and the field ammeter as a check guide. The ammeter scale is to have the limits of operation indicated on it by colored marks. The capability curves in the paper are drawn for only three hydrogen pressures so I am assuming that only three marks would be required on the ammeter.

Since actual gas pressure rarely ever corresponds to the three pressures given in the paper, for the machines on our system, the operators will be required to use loading curves, which are being prepared by our Operating Engineering Section. The use of marks on the ammeter scales would result in so many points that it would be confusing.

Just last week I checked the hydrogen pressures and the resultant usage of the gas for the three units at the Walter C. Beckjord Station. The results are shown in Table I.

The quantities of gas required for higher pressures would be considerably greater and that is why the operating pressures are kept down. The system megavar requirements are such as to permit carrying field currents below rated values.

For us it would be highly desirable if curves of maximum field current versus hydrogen pressure would be provided by the suppliers of the equipment so as to give a separate field capability curve for operating over the entire overexcited region. Field temperature data should also be given for specified machines. I also wish to point out the desire for embedded temperature detectors for the clamping fingers and end iron in the stator for low excitation operation.

It is our opinion that a transmitter sending the hydrogen pressure to the control room from where the loadings of the machines are handled would be a definite aid to the operators. This intelligence should be transmitted electrically as distances are too great for satisfactory use of the pneumatic devices we now have.

I now have two questions with respect to the field temperature recorder:

1. Why do the authors suggest periodic calibration of the field temperature recorder with portable instruments and what length of period is recommended?
2. What is the recommendation for connection of the leads for the field voltage, i.e., main brushes or pilot brushes? Which gives the least trouble and has the least possibility of error?

Table I. Hydrogen Pressures at Beckjord Station

	Rating		Loading		Hydrogen Used,
Unit No.	Megawatt	H_2 Pressure, Psig	Megawatt	H_2 Pressure, Psig	Cubic Feet per Day
1	100	15	100	8	200±
2	100	30	100	10	200±
3	125	30	125	25	400±

Herman Halperin (Commonwealth Edison Company, Chicago, Ill.): In the section entitled "Operation of Hydrogen Coolers" in this interesting paper, the authors give reasons for not operating armatures with constant detector temperatures nor constant outlet-hydrogen temperatures. Have there been some unsatisfactory operating experiences or factory test observations with such practices?

The authors recommend operation with practically constant inlet-hydrogen temperatures such as 35 to 40 C at 1/2 psig pressure. We have controlled the water flow to produce inlet-hydrogen temperatures of 30 to 32 degrees throughout the load range for some of our large units. This has been done for hydrogen pressures of 10 to 15 psig as well as for operation at 1/2 psig. Comments on these practices would be of interest.

C. C. Sterrett and R. A. Towne: We wish to express our appreciation for the interesting and constructive discussions. Mr. Schneider states that we apparently intend that the field loading limits should be determined by field temperature as measured by field resistance as the prime guide, and the field ammeter as a check guide. We recommend that the capability curve be the prime guide in conjunction with the use of the field ammeter, and that the field temperature be used as a check guide. With respect to Mr. Schneider's suggestion that curves be provided showing the maximum field current versus hydrogen pressure, we agree that such curves would be a convenience to the operators when they do not wish to interpolate between the rated pressure values.

Thermocouples for supervising the temperature of the stator core end zones are available if desired. The capability curve provides a means of controlling the temperatures in the stator core end zones so that the thermocouples would serve as a check guide.

With respect to question 1, we believe that all instruments should have periodic checks made to assure their proper working order. The time interval between these checks should be in line with the operators practice with regard to other instrumentation in the plant.

With respect to question 2, the measurement of field temperature involves the accurate determination of the voltage across the collector rings. This can be measured either from the current-carrying brushes or from pilot brushes which carry no current and are used only to determine the collector ring voltage.

Pilot brushes, when properly maintained, give the most accurate indication of the ring voltage. However, these rings, because they are not carrying current, often in the course of time develop a glaze on their surface. This glaze has a high and variable electrical resistance. It, therefore, can cause an appreciable error in the voltage. This difficulty can be overcome by proper maintenance wherein the glaze is removed either by sanding the brush surface or exerting pressure on the brush, causing the glaze to be worn off by the ring itself.

Voltage determination from the current-carrying brushes is subject to an error resulting from the brush drop. This error is fairly constant and does not vary much from 3 volts. It can be compensated for at full load, and the error at light loads will be small and is also of less importance. In this case, no glaze will develop on the brush and the brush requires no maintenance to obtain constant results. We recommend the latter method of determining ring voltages because no maintenance is required and the brush-drop error can be compensated for. We feel that this is a more desirable method than the use of pilot brushes wherein lack of proper maintenance can lead to erroneous field temperature readings.

Mr. Halperin asked if there has been any unsatisfactory experience because of operation with a constant stator detector temperature or with a constant warm hydrogen temperature. We believe that the principal disadvantage of these methods is that excessive misalignment will exist between the turbine and generator shafts. This is a very real problem. Several instances of mechanical difficulties in the field due to operation in this manner have been corrected by following the recommended operating procedure.

Operation with cold hydrogen temperatures as low as 25 C are generally acceptable. Shaft misalignment can be a problem because of low as well as high temperatures. Therefore extremes in either direction should be avoided. The initial shaft alignment of the turbine-generator unit should involve a consideration of the expected temperature level of the cold hydrogen.

A Circuit Approach to the Analysis of a 2-Stage Dynamoelectric Amplifier

R. W. BURTNESS
ASSOCIATE MEMBER AIEE

THE d-c dynamo is now used in many applications as an amplifier, subject to input signals which vary as a step function, a sinusoid, or as a random-time function which is difficult to describe by a mathematical function. For this reason, its transient and frequency response has been increasingly important as the d-c dynamo has become an integral part of control systems. Dynamos with higher amplification and improved frequency response such as the amplidyne, regulex, and rototrol have been developed and are now found in many of these automatic control systems. The regulex and rototrol may be thought of as special cases of a standard d-c dynamo. An amplidyne, however, is a type of 2-stage dynamoelectric amplifier as are Rosenberg generators and certain metadynes. To improve the operation and increase the applications of the 2-stage dynamoelectric amplifier, a study of the machine from a fresh viewpoint is justified.

For many years the study of machines and of circuits was not sufficiently integrated to produce maximum usefulness and clarity in studying networks involving rotating machinery. As matrix algebra was applied to circuit problems, it became possible to study extremely complicated circuits with minimum error and maximum clarity. In 1951 W. J. Gibbs made use of the matrix method.[1] H. E. Koenig[2–4] used matrix algebra to extend the coupled-circuit viewpoint to induction motors and to d-c dynamos. In this thesis[2] he also indicated how to evaluate the parameters of the machines so that the equations could be studied with the aid of a computer.

At the present time, there are several articles that consider the amplidyne from a viewpoint of network synthesis but contain very little analysis of the amplidyne itself. The amplidyne is considered as a 2-time constant system, one time constant being that of the armature and the other being that of the field. An accurate determination of these time constants from the design of the machine is not indicated. The usual approach neglects coupling between the direct axis and the control fields, and neglects the short-circuited turns caused by commutation. The latter is an inaccurate assumption because these turns are physically situated so that the change in flux density over the area of the coil is quite large under transient conditions, and this situation exists in both quadrature and direct axes.

In the following analysis, a system of matrix algebra, largely developed by Professor M. B. Reed,[5] is used to facilitate writing equations and to give order to complex mathematical manipulation. Thus, not only the main armature circuits but also the short-circuited turns can be considered in the analysis. This paper is then an extension of the coupled-circuit approach into the area of the 2-stage dynamoelectric amplifier. The differential equations developed are general for any type of load impedance or input voltage. These variable coefficient linear differential equations are then transformed into linear differential equations with constant coefficients which can be solved by standard methods. The equations presented determine the complete transient and steady-state response for any condition of load, or any input-voltage function. With the aid of a computer, a complete study of the operation of the machine can be made.

The details of the equations of the following analysis become exceedingly complex and are not of general interest; therefore, only the outline or general method of attacking the problem and the results obtained are presented. Complete details of the succeeding equations can be found in the author's doctoral thesis. The analysis presented points out not only the two primary time constants of the machine but three others as well. Experimental verification of the analysis is included.

Definitions, Assumptions, and Reference System

Any commutating dynamo may be thought of as an amplifier, with a given input function impressed on the field terminals and the output taken from the brushes on the quadrature axis. If these quadrature axis brushes are short-circuited directly or through a series field in the quadrature axis, a strong quadrature-armature reaction flux is produced. If brushes are then placed in the direct axis, a second stage of amplification from the quadrature-axis brushes to the direct-axis brushes is produced. There may or may not be a compensating winding in this circuit to compensate for the armature reaction in the direct axis. The term, 2-stage dynamoelectric amplifier, referred to subsequently as a dynamo-amplifier, applies to this type of dynamo. The Rosenberg generator, metadyne, and amplidyne could then come under this definition. The dynamo amplifier chosen for analysis is essentially a simple amplidyne but, with the compensating terms set equal to zero, it would become a Rosenberg generator.

To develop the differential equations of a dynamo amplifier from a coupled-circuit point of view, the following is assumed to keep the mathematics rigorous. These assumptions may be modified later in the paper to conform to practice.

1. Saturation and hysteresis in the iron are negligible.
2. The machine is completely laminated.
3. The number of commutator segments is divisible by four and all armature turns are similar and symmetrically spaced.
4. The brush has the same thickness as one commutator segment plus twice the thickness of the insulation between segments.
5. The machine stator is symmetrical with respect to the direct axis and also with respect to the quadrature axis.
6. The rotor is assumed to be round and symmetrically located.

The following should also be noted:

1. An equivalent control field is used which causes the same magnetomotive force to exist as does the total of the various control fields which may be incorporated in the design of the dynamo amplifier.
2. The stator poles and stator fields are shown concentrated in Fig. 1, but in practice these poles are usually split and the winding distributed. This, however, makes no difference in the analysis when the coupled-circuit approach is used.
3. In practice, the dynamo amplifier may contain commutating windings and series

---

Paper 55-107, recommended by the AIEE Rotating Machinery Committee and approved by the AIEE Committee on Technical Operations for presentation at the AIEE Winter General Meeting, New York, N. Y., January 31–February 4, 1955. Manuscript submitted October 18, 1954; made available for printing December 15, 1954.

R. W. Burtness is with the Electro-Motive Division of General Motors, La Grange, Ill.

A more complete version of this paper was presented as a thesis in partial fulfillment of the requirements for the degree of Doctor of Philosophy in Electrical Engineering, June 1953, to the Graduate College of the University of Illinois.

Acknowledgment is made to Dr. G. H. Fett of the Electrical Engineering Department of the University of Illinois for his encouragement and assistance in this study.

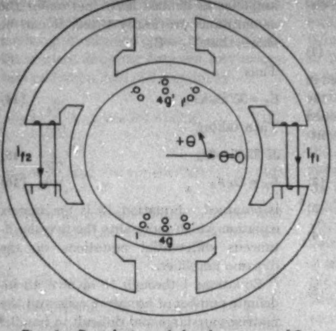

Fig. 1. Partial view of the dynamo amplifier

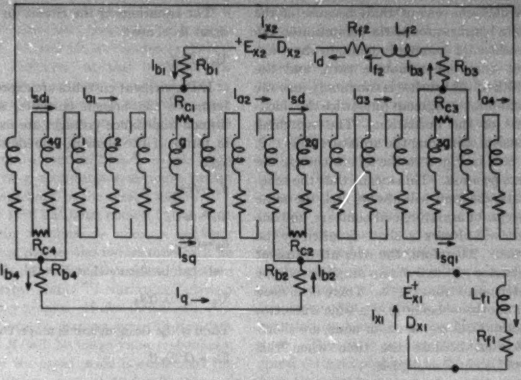

Fig. 3. Schematic diagram of the dynamo amplifier

windings. A basic dynamo amplifier is described which leads to the study of a more complex one.

Fig. 1 represents the physical picture from which a schematic diagram is drawn and which ultimately helps to keep straight the sign of the inductances which vary with time. Fig. 2 shows the width of the brushes and also the lap winding common in a dynamo amplifier. Fig. 3 shows the schematic diagram at time $=0$.

The reference system used is as follows: In any element of a network there may be current, impedance, generated voltages, and impedance voltages. These quantities are represented by I_e, D_e, E_e, and V_e respectively. The impedance D_e represents the derivative function which relates I_e and V_e such that $V_e = D_e I_e$. As illustrated in Fig. 4, an arrow is used to indicate the positive direction of current. The plus sign on the various voltages indicates the actual polarity when the voltage is a positive number.

A branch is defined as the circuit between two nodes, as indicated by large dots in Fig. 3. The same reference system applies to the branch level as to the element level. In writing the equations, the sign of the mutual inductance is included in the M term. Polarity marks are used on each inductance to facilitate the writing of signs included in the M terms when these terms are evaluated. The symbol p is used to represent d/dt.

Nomenclature

Letters denoting matrixes are written in script

Letters other than script refer to terms within a matrix

Subscript e refers to the element level

Subscript b refers to the branch level

Subscript 0 refers to the branch level after variable coefficients have been transformed into constant coefficients

The subscript $_K$ refers to the K level

Subscripts following subscripts e, b, 0, and k in script terms refer to the elements and branches described immediately following equation 16

i and j refer to armature elements where f_1 and f_2 refer to fields

R_b represents the brush and contact resistance in the director of the quadrature axis

R_c represents the brush and contact resistance in the short-circuited turns

T_{fv} = voltage transfer function

T_{fc} = current transfer function

θ = angular displacement of rotor

$\dot{\theta}$ = time rate of change of angular displacement of rotor

ω = angular frequency, radians per second

τ = time constant

Δ = determinant of D_K matrix

Development of Differential Equations

Whenever a commutating machine is operating, there is a small, high-frequency ripple caused by the switching effect as the commutator segments pass under the brushes. Thus, any transient would consist of the over-all transient response with a very high-frequency oscillation superposed on it. To get a workable solution to the problem, the small ripple effect is neglected while the effect of the short-circuited coils on the over-all transient response is taken into account. In the analysis of a dynamoamplifier it is ex-

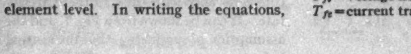

Fig. 2 (left). View of commutator of the dynamo amplifier

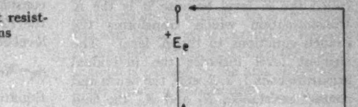

Fig. 4 (right). Reference system for voltages and currents on the element level

tremely convenient that, because of the extra brushes around the commutator, the brushes are commonly made to short-circuit only one armature turn, and the width of the brushes is commonly just one commutator segment plus twice the thickness of the insulation. The switching consists of moving the armature coils 1, 2, 3, etc., in Fig. 3 to the left to occupy the next position. This means that the schematic diagram will always look the same except for armature coil numbers, and one turn will always be short-circuited by the brush. Therefore, the over-all transient behavior of the dynamo amplifier can be determined from Fig. 3. There is no need for another schematic at a time when two commutator segments, or none, are short-circuited because the time when this could occur is negligible.

Part of the small, high-frequency ripple in the transient response is caused by the slight change in inductance and speed voltage components while each commutator segment traverses the distance between switching points. By taking $t=0$ as the time when the machine is half way between switching points and considering the inductances and speed voltage components to be constant over the time between switching instants, and of the same value as when $t=0$, a true representation of the over-all transient is obtained. Thus it is possible to solve the circuit for one position of the armature, at $t=0$, and this linear differential equation with the resulting constant coefficients will represent the over-all transient response of the machine at any time.

The equations of the system are written first on the element level, then transformed to the branch level, and then to a level containing just the currents in the direct and quadrature axes, currents in the short-circuited turns, and current in the control field. This last level is called the K level because it is the K transformation which transforms the branch equations to the K level. The element level includes the individual armature coils 1, 2, 3, etc., the brush and contact resistances R_b and R_c, the field coils, and the two external circuits. The branch level includes the four armature branches between nodes, the four short-circuited coils, the quadrature-axis short-circuited branch between nodes, the direct-axis branch between nodes, the control field, and the external driving circuit. Fig. 4 shows the reference system for voltages and currents on the element level. It is advisable to go through the development of the differential equations by means of matrix algebra to indicate the general method.

The equations of the circuit on the element level are:

$$\mathcal{V}_e=\mathcal{D}_e\mathcal{I}_e \qquad (1)$$

If the element currents are expressed in terms of the branch currents, and the branch impedance voltages are expressed in terms of the element impedance voltages

$$\mathcal{I}_e=\mathcal{A}\mathcal{I}_b \qquad (2)$$

$$\mathcal{V}_b=\mathcal{B}\mathcal{V}_e \qquad (3)$$

$$\mathcal{E}_b=\mathcal{B}\mathcal{E}_e \qquad (4)$$

It can be shown that $\mathcal{B}=\mathcal{A}'$. Thus

$$\mathcal{V}_b=\mathcal{A}'\mathcal{D}_e\mathcal{A}\mathcal{I}_b \qquad (5)$$

Then if the designation is made that

$$\mathcal{D}_b=\mathcal{A}'\mathcal{D}_e\mathcal{A} \qquad (6)$$

equation 5 becomes

$$\mathcal{V}_b=\mathcal{D}_b\mathcal{I}_b \qquad (7)$$

By a method to be described later the time-varying terms in $\mathcal{D}_b$ are transformed to constant terms and the resulting matrix is called $\mathcal{D}_0$. Thus

$$\mathcal{V}_b=\mathcal{D}_0\mathcal{I}_b \qquad (8)$$

Since it has been assumed that the machine is perfectly symmetrical and unsaturated, it can be shown that the quadrature component of current will divide equally in the two armature paths in which it flows. The direct axis current will also divide equally in the two armature paths in which it flows. Also, because of these assumptions, the over-all transient current in the two direct-axis short-circuited coils will have the same magnitude, and the over-all transient current in the two quadrature-axis short-circuited coils will have the same magnitude. Because of the references chosen, the sign of the current in the opposite short-circuited coils is reversed. These considerations make it possible to express the 12 branch currents in terms of 5 K level currents. Thus

$$\mathcal{I}_b=\mathcal{K}\mathcal{I}_K \qquad (9)$$

Equation 8 then becomes

$$\mathcal{V}_b=\mathcal{D}_0\mathcal{K}\mathcal{I}_K \qquad (10)$$

Premultiplying both sides of equation 10 by $\mathcal{K}'$

$$\mathcal{K}'\mathcal{V}_b=\mathcal{K}'\mathcal{D}_0\mathcal{K}\mathcal{I}_K \qquad (11)$$

Now define

$$\mathcal{V}_K=\mathcal{K}'\mathcal{V}_b \qquad (12)$$

Also define

$$\mathcal{E}_K=\mathcal{K}'\mathcal{E}_b \qquad (13)$$

In the particular case of the dynamo amplifier as defined here, and under the assumptions previously listed, it can be shown that $\mathcal{V}_K=\mathcal{E}_K$.

Thus

$$\mathcal{E}_K=\mathcal{K}'\mathcal{D}_0\mathcal{K}\mathcal{I}_K \qquad (14)$$

Then taking

$$\mathcal{K}'\mathcal{D}_0\mathcal{K}=\mathcal{D}_K \qquad (15)$$

$$\mathcal{E}_K=\mathcal{D}_K\mathcal{I}_K \qquad (16)$$

is obtained. Equation 16 is the matrix equation which represents the five simultaneous differential equations of the dynamo amplifier.

Equations 1 through 16 involve an indefinite number of armature coils and the matrixes are large and difficult to handle. To facilitate manipulation, the matrixes on the element level were partitioned into five groups, the numbers of which will be used subsequently as subscripts to element matrixes:

1. Rotor elements.
2. Field elements.
3. Brush resistance and contact drop in short-circuited rotor elements.
4. Brush resistance and contact drop in main rotor elements.
5. External elements.

On the branch level, the matrixes were partitioned into four groups, the numbers of which will be used subsequently as subscripts to branch matrixes:

1. Rotor branches.
2. Short-circuited branches.
3. Stator branches.
4. Main field branches.

Since the machine is assumed to be symmetrical

$$R_{b1}=R_{b2}=R_{b3}=R_{b4}=R_b$$

$$R_{c1}=R_{c2}=R_{c3}=R_{c4}=R_c$$

$$R_1=R_2=R_3=R_4=R_n=R$$

The mutual inductances of the armature coils vary with time as the coils rotate. It can be shown from Fig. 1, and the assumption of symmetry, that the mutual inductances between the armature coils consist of a Fourier series made up of only cosine terms of every other even number; 0, 4, 8, 12, etc. If it is assumed that all armature coils are full pitch coils, the angle between armature coils is $\pi/2g$. Thus the mutual coupling between elements is

$$M_{ij}=\sum_{k=0,4,8,\ldots}^{\infty} M_{ijk}\cos k[\theta-(i+j)\pi/4g] \qquad (17)$$

It can also be shown from Fig. 1, and assumption of symmetry, that the mutual inductance between armature coils and a stator field coil consists of a Fourier series made up of only odd cosine terms. Thus, the mutual coupling between any armature coil and a field coil is given by

$$M_{if_1}=\sum_{k=1,3,5\ldots}^{\infty} M_{ikf_1} \cos k(\theta-i\pi/2g) \qquad (18)$$

$$M_{if_2}=\sum_{k=1,3,5\ldots}^{\infty} M_{ikf_2} \cos k(\theta-i\pi/2g) \qquad (19)$$

Since $\mathfrak{D}_b$ contains both resistance and mutual inductance terms, it can be written as

$$\mathfrak{D}_b=\mathcal{R}_b+p\mathfrak{M}_b \qquad (20)$$

where $\mathcal{R}_b$ and $\mathfrak{M}_b$ are partitioned in the same manner as $\mathfrak{D}_b$. Thus equation 7 may be written as

$$\mathcal{V}_b=(\mathcal{R}_b+p\mathfrak{M}_b)\mathcal{I}_b=\mathcal{R}_b\mathcal{I}_b+(p\mathfrak{M}_b)\mathcal{I}_b+\mathfrak{M}_b p\mathcal{I}_b \qquad (21)$$

since $\mathfrak{M}_b$ contains terms which vary with time. Thus, $\mathcal{R}_b\mathcal{I}_b$ becomes a resistive voltage term, $(p\mathfrak{M}_b)\mathcal{I}_b$ becomes a speed voltage term, and $\mathfrak{M}_b p\mathcal{I}_b$ becomes an inductive voltage term.

Each element of $\mathfrak{M}_{b11}$, $\mathfrak{M}_{b21}$ and of each transpose involves the coupling of armature coils with armature coils, thus following the pattern

$$M_b=\sum_{i=}\sum_{j=}\sum_{k=0,4,8,12\ldots}^{\infty} M_{ijk} \cos k[\theta-(i+j)\pi/4g] \qquad (22)$$

Then, if the derivative of M_b is taken

$$pM_b=\sum_{i=}\sum_{j=}\sum_{k=0,4,8,12\ldots}^{\infty} -k\dot{\theta}M_{ijk}\times \sin k[\theta-(i+j)\pi/4g] \qquad (23)$$

Each element of M_{b13}, M_{b14}, M_{b23}, M_{b24}, and of each transpose involves the coupling of armature coils with a field coil, thus following the pattern

$$M_b=\sum_{i=}\sum_{k=1,3,5\ldots}^{\infty} M_{ifk} \cos k(\theta-i\pi/2g) \qquad (24)$$

Then, if the derivative of M_b is taken

$$pM_b=\sum_{i=}\sum_{k=1,3,5\ldots}^{\infty} -k\dot{\theta}M_{ifk} \sin k(\theta-i\pi/2g) \qquad (25)$$

Each element of M_{b33}, M_{b44}, M_{b34}, and M_{b43} is not a function of time so the pM_b term is zero.

From the examination of Fig. 3, it should be recalled that the armature coils move to the left and occupy the adjacent position in the schematic diagram each time the commutator traverses the distance between switching points. Thus, the mutual inductance between the coils and mutual inductance between each coil and the field coils will change over a complete cycle, in accordance with equations 17, 18, and 19, as θ increases from 0 to 2π. However, as this happens, the coils involved in each branch change in such a way that the coils making up each branch at any time are in relatively the same position. Thus, when looking at the circuit from a branch level, each switch of a commutator segment brings the circuit back to the same location.

Since $t=0$ has been chosen as the time when the machine is midway between switching points, the inductances will be of a value approximately midway between the narrow limits of variation between switching points. If the brush and contact resistance changes over this interval, R_b and R_c will be mean value resistances. Then, if the assumption is made that the speed is kept constant during the time of the transient, $\dot{\theta}$ becomes a constant. Thus, by taking the value of M, pM, L, and R which occur at $t=0$, considering $\dot{\theta}$ as a constant, and using the coefficients derived at this time as constant coefficients of the differential equations, the commutator ripple effect is neglected and the variable coefficient differential equations are reduced to linear differential equations with constant coefficients expressing the over-all electrical conditions in the machine.

Therefore, at $t=0$, equation 22 becomes

$$\sum_{i=}\sum_{j=}\sum_{k=0,4,8,12\ldots}^{\infty} M_{ijk} \cos k(i+j)\pi/4g=M_0 \qquad (26)$$

Equation 23 becomes

$$\dot{\theta}\sum_{i=}\sum_{j=}\sum_{k=0,4,8,12\ldots}^{\infty} kM_{ijk} \sin k(i+j)\pi/4g=\dot{\theta}S_0 \qquad (27)$$

Equation 24 becomes

$$\sum_{i=}\sum_{k=1,3,5\ldots}^{\infty} M_{ifk} \cos ki\pi/2g=M_0 \qquad (28)$$

Equation 25 becomes

$$\dot{\theta}\sum_{i=}\sum_{k=1,3,5\ldots}^{\infty} kM_{ifk} \sin ki\pi/2g=\dot{\theta}S_0 \qquad (29)$$

and $\mathcal{R}_b$ becomes $\mathcal{R}_0$.

Thus, $\mathcal{R}_0$, $\mathfrak{M}_0$, and $\dot{\theta}\mathcal{S}_0$ represent the matrixes containing the branch constants used in further development of the differential equations. The change from pM_b to $\dot{\theta}S_0$ is made to separate the term S_0, which represents a constant of the machine, from $\dot{\theta}$ which represents the presumably constant speed at which the machine is operating.

It should be noted at this point that unilateral coupling is introduced between the field and the armature. Since the armature conductors are continually moving through the field set up by the field poles, a speed voltage is produced in each conductor and thus between armature nodes on the branch level. However, when considering armature current between armature nodes, it is found that the field set up by this current is essentially stationary with respect to the field poles. The only motion is caused by commutation and is at a very high frequency. This component of magnetomotive force does not produce much flux because of eddy currents. The voltage produced in the field windings by this small amount of flux is at such a high frequency that very little change in current results because of the high impedance. Thus it is possible to neglect the speed voltages produced in the field windings by armature current, while speed voltages produced in the armature windings by field current must be considered. This indicates that each speed voltage term $\dot{\theta}S_0$ which gives field voltage in terms of armature current will be zero. The inductive voltage term M_0p will still remain bilateral because the inductive coupling between the armature branches and the field will not be affected.

The shape of the poles and magnetic path as well as the material of the machine will determine M_{ijk} and M_{ifk}. These constants can be determined from the design as indicated by H. E. Koenig.[3] In addition to the previously mentioned positions, there are several positions in the various matrixes that will be zero because of the symmetry of the machine. In equations 26 and 27, M_0 is zero when the short-circuited coils are perpendicular. $\dot{\theta}S_0$ is zero when the short-circuited coils are perpendicular to one another and also when they are in the same axis. This is true because the derivative of the mutual inductance is not changing at this point because of the symmetry of the dynamo. In equations 28 and 29, M_0 is zero when the axis of the coil is parallel to the axis of the field. $\dot{\theta}S_0$ is zero when the axis of the coil is parallel to the axis of the field. Thus equation 21 becomes

$$\mathcal{V}_b=\mathcal{R}_0\mathcal{I}_b+\dot{\theta}\mathcal{S}_0\mathcal{I}_b+\mathfrak{M}_0 p\mathcal{I}_b \qquad (30)$$

or

$$\mathcal{V}_b=\mathfrak{D}_0\mathcal{I}_b \qquad (31)$$

where

$$\mathfrak{D}_0=\mathcal{R}_0+\dot{\theta}\mathcal{S}_0+\mathfrak{M}_0 p \qquad (32)$$

Equation 9 expresses the branch currents in terms of the K level currents. The $\mathcal{K}$ matrix is written in accordance with the discussion preceding equation 7. Combining equations 4 and 13, the expression for $\mathcal{E}_K$ becomes

$$\mathcal{E}_K = \mathcal{K}'\mathcal{A}'\mathcal{E}_e \tag{33}$$

By equation 15

$$\mathfrak{D}_K = \mathcal{K}'\mathfrak{D}_e\mathcal{K} \tag{34}$$

If the foregoing matrix multiplication is carried out, equation 16 becomes

$$\begin{bmatrix} 0 \\ 0 \\ 0 \\ E_{x2} \\ E_{x1} \end{bmatrix} = \begin{bmatrix} D_{K11} & D_{K12} & D_{K13} & D_{K14} & D_{K15} \\ D_{K21} & D_{K22} & D_{K23} & D_{K24} & D_{K25} \\ D_{K31} & D_{K32} & D_{K33} & D_{K34} & D_{K35} \\ D_{K41} & D_{K42} & D_{K43} & D_{K44} & D_{K45} \\ D_{K51} & D_{K52} & D_{K53} & D_{K54} & D_{K55} \end{bmatrix} \begin{bmatrix} I_{sq} \\ I_{sd} \\ I_q \\ I_d \\ I_{f1} \end{bmatrix} \tag{35}$$

The currents of $\mathcal{I}_K$ are the currents in the quadrature-axis short-circuited turns, the current in the direct-axis short-circuited turns, the quadrature-axis current, the direct-axis current, and the main field current, as illustrated in Fig. 3 and described preceding equation 9. The D_K terms are made up of hundreds of terms which contain resistances, inductances, mutual inductances, and speed voltage coefficients, i.e., D_{K35} represents all the terms by which I_{f1} is multiplied to obtain the voltage generated in the quadrature-axis circuit.

Equation 35 gives the five linear differential equations with constant coefficients which state the over-all response of the dynamo amplifier. These equations cannot be solved in general terms because a general formula does not exist which gives the roots of a fifth or higher degree polynomial. However, once numerical values for the coefficients are obtained, the roots of the fifth or higher degree polynomial can be located. The solution to the simultaneous linear differential equations with constant coefficients is a standard procedure and either classical methods or Laplace transform can be conveniently used.

If Δ represents the determinant of D_K, and A_K represents the cofactor of D_K, then

$$\Delta \begin{bmatrix} I_{sq} \\ I_{sd} \\ I_q \\ I_d \\ I_{f1} \end{bmatrix} = \begin{bmatrix} A_{K11} & A_{K21} & A_{K31} & A_{K41} & A_{K51} \\ A_{K12} & A_{K22} & A_{K32} & A_{K42} & A_{K52} \\ A_{K13} & A_{K23} & A_{K33} & A_{K43} & A_{K53} \\ A_{K14} & A_{K24} & A_{K34} & A_{K44} & A_{K54} \\ A_{K15} & A_{K25} & A_{K35} & A_{K45} & A_{K55} \end{bmatrix} \begin{bmatrix} 0 \\ 0 \\ 0 \\ E_{x2} \\ E_{x1} \end{bmatrix} \tag{36}$$

Equation 36 then gives the differential equations of I_{sq}, I_{sd}, I_q, I_d, and I_{f1}. It can be seen that, if all values of D_K are inductive, the denominator of any D_K term will be one, and the characteristic equation of all the currents will be a fifth-order equation given by $\Delta I = 0$. From this equation the complementary function is found. There must be a negative real part to every root of the characteristic equation to insure stability. If D_{x1} and D_{x2} contain capacitance, p terms will be introduced in the denominators of some of the terms in the cofactor matrix of equation 36. These terms in the denominators will then enter into the characteristic equation and raise the order of the equation higher than the fifth-order equation $\Delta I = 0$.

The correct cofactors properly multiplied by the impressed voltages will give the forcing function which, in conjunction with the characteristic equation, will yield the particular integral. The transient and steady-state responses are then readily obtainable if the forcing function is a step function, a sine function, or another function which lends itself to standard methods of solution. If the forcing function is more complicated, the solution may have to be obtained in a series form.

Although these equations are valid for any load impedance, two common load impedances are mentioned in particular, i.e., dynamo field and dynamo armature. In the case of a dynamo field as load, $E_{x2} = 0$, and $D_{x2} = R_f + pL_f$. The equation of output current then becomes

$$\Delta I_d = A_{K54}E_{x1} \tag{37}$$

where A_{K54} is a fourth-degree expression in p as indicated in equation 35. This equation can be solved as previously indicated.

In the case of a dynamo armature as load, $E_{x2} = 0$, and D_{x2} can be approximated by a parallel combination of R_2 and C_2 which is placed in series with R_1 and L_1. In this circuit, L_1 and R_1 represent the armature inductance and resistance. The voltage across R_2 and C_2 represents the armature generated voltage. C_2 would be proportional to the moment of inertia and R_2 would be inversely proportional to viscous friction in the system. If $L_1/R_1 = \tau_1$ and $C_2R_2 = \tau_2$

$$D_{x2} = \frac{R_2 + R_1(1+p\tau_1)(1+p\tau_2)}{1+p\tau_2} \tag{38}$$

From equation 35 it can be seen that, when D_{x2} is inserted in the D_{K44} term, Δ becomes a sixth-degree polynomial in p because of the second-degree term in the numerator of D_{x2}. The denominator of D_{x2} will then become a multiplier of the right-hand side of equation 37. A_{K54} will not change because D_{K44} is not contained in A_{K54}. Thus, the forcing function becomes $A_{K54}(1+p\tau_2)E_{x1}$ and thereby involves a fifth-degree polynomial in p. Therefore, the determination of the complementary function of equation 37 with a dynamo armature load involves the solution of a sixth-degree polynomial, whereas the determination of the complementary function of equation 37 with a dynamo field involves the solution of a fifth-degree polynomial. The degree of the polynomial on the right-hand side of equation 37 necessary to determine the particular integral would be determined by the function E_{x1}.

When a dynamo amplifier is used in various systems, the transfer function is often desirable. To obtain the transfer function, E_{x2} is set equal to zero and equation 36 yields equation 37. Since

$$V_{x2} = D_{x2}I_d \tag{39}$$

equation 37 becomes

$$\frac{V_{x2}}{E_{x2}} = \frac{A_{K54}}{\Delta}D_{x2} = T_{fv} \tag{40}$$

Since the output impedance of the dynamo amplifier is usually either a dynamo field or a dynamo armature, the output current becomes very important. In a dynamo field, the flux is approximately proportional to current, and in a dynamo armature the torque is proportional to current. Therefore, a more useful transfer function relates output current to input voltage. This transfer function is obtained from equation 37

$$\frac{Id}{E_{x1}} = \frac{A_{K54}}{\Delta} = T_{fc} \tag{41}$$

The voltage transfer function, equation 40, presents a convenient way to determine the gain and phase shift as a function of frequency. The solution of the equations is not necessary. If $j\omega$ is substituted for p in equation 40, a polar plot of gain and phase shift can readily be plotted as a function of frequency.

The foregoing is a general analysis for the type of dynamo amplifier selected for study. The load is completely general and, thus, the analysis is good for any type of load which is put on the dynamo amplifier. With this analysis, it is possible to determine the complete transient and steady-state response as well as the transfer function and frequency response for the dynamo amplifier under any conditions of load and any input-voltage function. This includes the determination of all the currents in the various windings of the machine. The differential equations can be solved by standard methods and it only becomes necessary to resort to series solutions for the particular integral when the input-voltage function is of a rather complicated nature.

The foregoing analysis neglects the ripple caused by commutator action. However, if the branch equations were used directly as in equation 7, and the time-varying parameters were substituted in this equation, a standard mesh transformation could be applied. This would lead to simultaneous linear differential equations with time-varying coefficients. These equations could be solved by a point-by-point process with the aid of a computer. In this manner, the instantaneous currents could be obtained and commutation could be studied. This, of course, would be an extremely difficult problem because the instantaneous values of brush resistance and contact drop would be quite critical, and accurate methods of determining these values are not available.

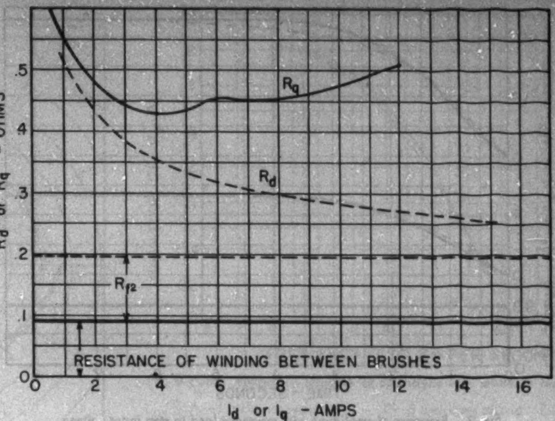

Fig. 6. Armature circuit resistance versus armature current

Experimental Verification of Analysis

When any difficult physical problem is approached from an analytical viewpoint it is usually necessary to make simplifying assumptions to make the mathematics rigorous and to simplify the analytical solution. The basic assumptions must be judiciously chosen so that the final solution will still be reasonably correct. Many electrical problems involve saturation, hysteresis, and variable parameters. Consideration of saturation in a dynamo amplifier becomes impractical from an analytical viewpoint. This is also true of hysteresis and certain types of variations in parameters such as brush resistance and contact drop. It is, therefore, necessary to make simplifying assumptions and then proceed to a rigorous solution of the mathematics involved. The mathematical solution is then used as a basis to study the problem and the effect of various changes in parameters.

After the mathematical solution is thoroughly studied, a machine can be built which has certain parameters in it that can be varied with a slight adjustment. Operating characteristics of the machine are experimentally taken and, with the use of knowledge gained from the mathematical solution, proper adjustment of the parameters is made and the desired operating characteristics are achieved. In any analytical development, it is desirable to know how accurate the basic assumptions are and what values are critical and should be closely watched. Of general interest is the knowledge of how much labor is involved in predicting operating characteristics and how accurate these results are.

Taking the forgoing requirements into consideration, the dynamo amplifier selected for experimental work was a General Electric aircraft amplidyne motor-generator *5AM61NJIC*. The motor-genera-

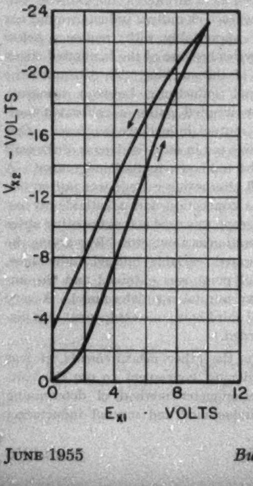

Fig. 5 (left). Amplidyne output voltage versus input voltage with resistance load

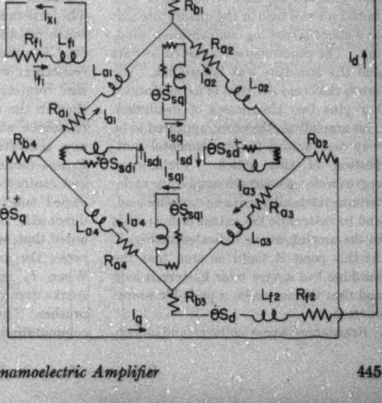

Fig. 7 (right). Equivalent circuit of amplidyne for experimental work

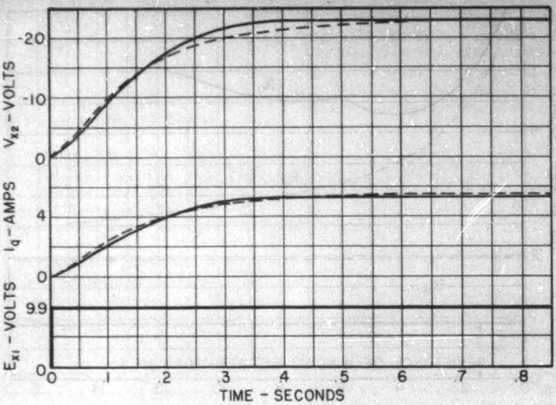

Fig. 8. Response of amplidyne with resistance load to step input voltage

- - - - Calculated curve ——— Experimental curve

This subcaption also applies to Figs. 9, 10, and 11

tor set is a 2-bearing set, the motor of which is rated at 27 volts, 88 amperes, 6,000 rpm, for 10 minutes. The amplidyne is rated at 60 volts, 1,300 watts, and 21.7 amperes. Because of the high current rating of the motor, it was not used. Instead, a 2-horsepower 3-phase 220-volt 3,480-rpm induction motor was used to drive the amplidyne. By using a motor of this capacity and considering a maximum of 30 volts, 10 amperes at the output terminals of the amplidyne, less than 1-per-cent variation in speed was expected from no load to the maximum load considered on the amplidyne. A speed check later showed about 3,548 rpm at no load and about 3,525 rpm at 30 volts, 10 amperes, or a variation of about two-thirds of 1 per cent. The amplidyne was modified so that it no longer contained a series field in the quadrature axis or a shunt across the compensating winding. The commutator contained 48 bars and the armature was lap-wound. The brush thickness was that of a commutator bar plus two thicknesses of insulation. This amplidyne, therefore, appeared to be very well suited for experimental verification of this article. Preliminary curves were taken on the amplidyne to determine its stability with a resistance load, and to determine the extent of hysteresis in the amplidyne, as indicated in Fig. 5. At this point it could be seen that the machine had a very wide hysteresis loop and that this would be a probable source of error.

Resistances, speed voltages, and inductances were all measured. It was found that obtaining measurements on the element level was impractical because of the influence of the magnetic fields of armature windings. The current in the compensating winding produces a component of flux which directly opposes the armature direct-axis flux and in the *K* level matrix, the net flux becomes important. This amounts to only about 2 per cent of the component of flux in either direction. Therefore, a few per cent error in the element level would completely destroy the accuracy of the *K* level matrix. Thus, whenever possible, measurements were made on the *K* level and values were substituted directly into $\mathfrak{D}_K$. Even with this method, a slight error is introduced because of the slight variation in speed during the transient. The resistances, with the exception of brush resistance and contact drop, were easy to measure. The armature-circuit resistances were obtained with the armature rotating, first in one direction and then in the other direction. The mean resistance was taken to compensate for any generated voltages in the circuit. It was found that the brush resistance and contact drop in the quadrature axis varied substantially from that in the direct axis, as indicated in Fig. 6. It was noted that, when I_q reached about 4 amperes, the amplidyne started to whine. When I_q reached about 10 amperes, sparks were visible at the quadrature-axis brushes. This energy loss caused by poor commutation is probably partially reflected in the high apparent value of brush resistance and contact drop. The inductance of the quadrature axis is very much higher than the inductance of the direct axis because of the opposition and close coupling of the armature winding and the compensating winding in the direct axis. Therefore, it is expected that higher voltages would be generated in the conductors undergoing commutation at the quadrature brushes, and that this would lead to poor commutation. Values of brush and contact resistance representative of the steady state current flowing in the particular circuit were taken from Fig. 6.

For determining the speed voltages present, Fig. 7 was drawn and the speed voltages were given the same polarity as impedance voltages and, thus, considered as such. The armature was rotated at about 3,548 rpm and the various speed voltages were measured with a high-resistance voltmeter and carbon brush probes on the commutator. By dividing the induced voltage by the current producing the field, $\dot{\theta}S$ is obtained. Where there was appreciable hysteresis, as there was when the main field was excited, a curve was taken of induced voltage versus exciting current after demagnetizing the field. Then the linear portion of the curve was used to determine $\dot{\theta}S$. The range of values of self-inductance measurements was from about 100 microhenrys to 500 henrys, so one method of measurement could not be consistently used to obtain all values. To measure the self-inductances of the armature short-circuited paths, the lap-wound armature was opened at a riser and an inductance bridge was used. In this measurement as well as in all others, the value of self-inductance or mutual inductance did not vary appreciably with frequency below 60 cycles because of the laminated structure of the machine. To determine the mutual inductance between armature short-circuited paths, a calibrated variable mutual inductance was used. One coil was put in series with each of the coils of the unknown mutual inductance. A small alternating voltage was put on one series connection and a cathode-ray oscillograph was used across the other series connection as a detector. By varying the calibrated variable mutual inductance, a null point was obtained and the unknown mutual was determined. A very small third-harmonic component was disregarded.

For the other measurements, it was found most convenient to use the voltmeter-ammeter method of determining self-inductance and mutual inductance.

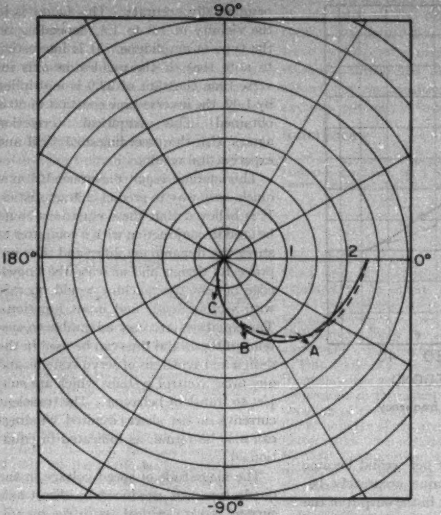

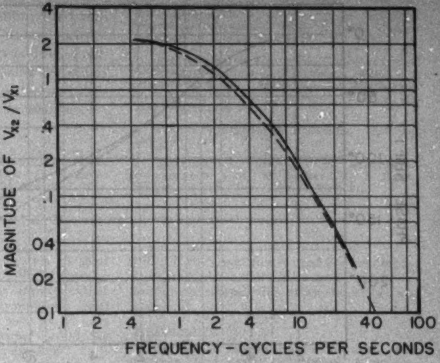

Fig. 9 (left). Frequency response of amplidyne with resistance load

A—1 cycle per second
B—2 cycles per second
C—5 cycles per second

Fig. 10 (above). Gain of amplidyne with resistance load versus frequency

The most critical inductance measurement was that of the main exciting field. It can be seen from the curve in Fig. 8 that a bow exists at the lower portion of the ascending saturation curve. Thus, at low values of alternating current, the inductance would appear unreasonably low because of the slope of the curve near the origin. By using a 60-cycle voltage of 400 volts and no biasing circuit, the current was approximately of the same peak magnitude as the current was when the field had rated direct voltage on it. A trace of the current wave shape was put on a cathode-ray oscillograph and it did not seem to differ from the trace of a sinusoidal voltage wave. The resistance was negligible, and the impedance was considered practically all reactance. In this way, a value of inductance was obtained which is considered representative of the operating current range of the exciting field, or at least it represents a kind of average over the full range of values.

The response of the amplidyne to an input step-function voltage of 9.9 volts, with a resistance load of 2.3 ohms, was chosen for prediction so that the currents involved would not cause the iron to approach the saturation point. The machine constants were then substituted into equation 35 as follows

$$\begin{bmatrix} 0 \\ 0 \\ 0 \\ 0 \\ 9.9 \end{bmatrix} = \begin{bmatrix} 0.356+0.128q & 0 & -1.21q & 0 & -26 \\ 0 & 0.096+0.36q & 0 & -0.37q & 62q \\ -1.21q & 0 & 0.436+11.5q & -0.061 & -910 \\ 0 & -0.37q & 4.58 & 2.58+1q & 0 \\ 0 & 62q & 0 & 0 & 2970+393\times 10^{3}q \end{bmatrix} \begin{bmatrix} I_{sq} \\ I_{sd} \\ I_q \\ I_d \\ I_{f1} \end{bmatrix} \qquad (42)$$

where $q=10^{-3}p$. Equation 42 was then used to determine Δ.

Thus

$$\Delta=-0.04\times 10^{-12}p^5-13.7\times 10^{-9}p^4+675\times 10^{-6}p^3+409\times 10^{-3}p^2+21.1p+143 \qquad (43)$$

The p^5 and p^4 terms involve accumulated errors from each inductance measurement and are somewhat inaccurate. They do not affect the response except at high frequency, so to calculate a predicted response, these terms were dropped. The remaining expression then has roots of −7.5, −50, and −548. An approximate solution to the characteristic equation $\Delta I=0$ is then

$$I=A_1\epsilon^{-7.5t}+B_1\epsilon^{-50t}+C_1\epsilon^{-548t} \qquad (44)$$

Upon inspection of the right-hand side of equation 37 and considering that E_{s1} is a step function that is constant after $t=0+$, the only term of A_{K54} that enters the equation is the constant term. The constant term of $A_{K54}=-142$. Then, by equating the constant terms of equation 37, the particular integral becomes

$$I_d=-9.84 \qquad (45)$$

The complete solution for I_d is

$$I_d=A_1\epsilon^{-7.5t}+B_1\epsilon^{-50t}+C_1\epsilon^{-548t}-9.84 \qquad (46)$$

From equation 39

$$V_{x2}=A\epsilon^{-7.5t}+B\epsilon^{-50t}+C\epsilon^{-548t}-22.8 \qquad (47)$$

Before the step-function voltage is applied, all the currents in the amplidyne are considered to be zero, and thus the various derivatives of the input current are zero at $t=0+$. Substitution of these conditions into equation 47, and solution for A, B, and C shows that C is extremely small, and the term $C\epsilon^{-548t}$ is negligible. Thus equation 47 becomes

$$V_{x2}=26.8\epsilon^{-7.5t}-4.03\epsilon^{-50t}-22.8 \qquad (48)$$

This equation is plotted in Fig. 8. In the foregoing manner I_q is also determined to be

$$I_q=-6.51\epsilon^{-7.5t}+0.98\epsilon^{-50t}+5.55 \qquad (49)$$

This equation is also plotted in Fig. 8.

Equation 40 shows the voltage transfer function of the amplidyne. With the resistance load previously under consideration, T_{fe} becomes approximately

$$T_{fe}=\frac{582\times 10^{-3}p+328}{675\times 10^{-6}p^3+409\times 10^{-3}p^2+21.1p+143} \qquad (50)$$

$$=862\frac{(p+564)}{(p+7.5)(p+50)(p+548)} \qquad (51)$$

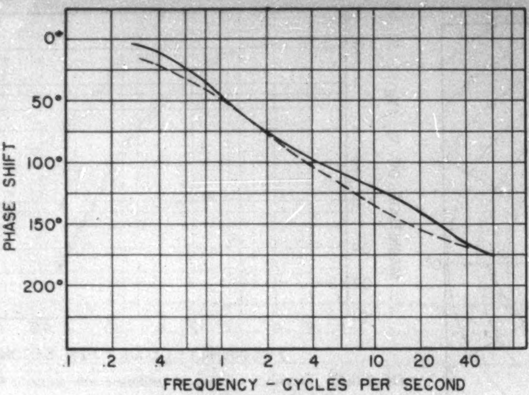

Fig. 11. Phase shift of amplidyne with resistance load versus frequency

Since the $(p+564)$ term and the $(p+548)$ term are so nearly alike, practically all the effect of these terms on phase shift and amplitude will cancel in the range below 60 cycles. Thus for this frequency range

$$T_{fv}=\frac{862}{(p+7.5)(p+50)} \qquad (52)$$

Magnitude and phase of the transfer function are plotted against frequency in the polar plot in Figs. 9, 10, and 11.

Experimental data were also taken on the amplidyne with a step-function voltage of 9.9 volts applied, and a resistance load of 2.3 ohms. A Hathaway recording oscillograph *S-14a* was used to record E_{x1}, I_q, and V_{x1}. The results are shown in Fig. 8. A frequency response was taken with the aid of a Hewlett Packard low-frequency oscillator *202 B* to generate E_{x1}, a cathode-ray oscillograph to measure voltage, and the recording oscillograph mentioned in the foregoing to record phase displacement. This frequency response is plotted in Figs. 9, 10, and 11.

Analysis of Results

Usually the amplidyne is considered as a 2-time constant system. The preceding experimental work verifies this fact when low frequencies are involved. The experimental work does not show the presence of the other three time constants which are noted in the analysis. The reason for this is that these time constants do not become effective either in phase or amplitude in the amplidyne under consideration until the frequency is above 60 cycles per second. Experimental data above 40 cycles per second became impossible to determine accurately because of noise present in the output of the machine. It is interesting to note that the inverse-time constants of each circuit, as indicated on the main diagonal of equation 42, are 2,780, 706, 37.9, 2,580, and 7.57. The inverse-time constants considered in the solution of Δ were the primary root 7.5 and the secondary root 50. It is evident that the main field is the major contributing factor to the primary root. It is also evident that the quadrature-axis inverse-time constant is the major contributing factor to the secondary root. However, it should be noted that the secondary root, which could be termed the armature inverse-time constant in a 2-time constant system, does not come directly from a specific circuit time constant, but is contributed to by several circuits and the coupling between these circuits. The secondary root is between the quadrature-axis inverse-time constant and the inverse-time constant of the short-circuited turns in the direct axis. It can, therefore, be concluded that the short-circuited turns in the direct axis have a definite bearing on the magnitude of the secondary root, and disregarding these turns can lead to considerable error in the armature time constant.

Some engineers have found that the armature quadrature-axis time constant does not give sufficiently accurate results in conjunction with the field time constant when considering the transfer function. An experimental factor has been used as a multiplying factor by which the quadrature-axis inverse-time constant is multiplied to obtain a value which is experimentally accurate. This factor is in the vicinity of 1.3 to 1.5, depending on the type of amplidyne. It is interesting to note that, if the quadrature-axis inverse-time constant of 37.9 is multiplied by 1.32, the inverse-time constant of 50 is obtained. This empirical correction agrees with the preceding analytical and experimental results.

This method is not recommended as a quick, easy way to predict characteristics. It is believed that these equations could be used in conjunction with a computer to study the dynamo amplifier and thus improve its design and increase the knowledge of how the machine would operate with various loads and input functions. The equations are very adaptable to system synthesis and thus can be used in the design and synthesis of servo systems and any other control systems which are subject to transient behavior. The transient currents in the short-circuited windings can also be found, as indicated in equation 36.

The magnitude of speed voltage in the quadrature axis produced by direct-axis current is very critical, as in the magnitude of the inductance of the main field and the magnitude of the coupling between the main field and the direct axis. The magnitude of this coupling should be small to give good stability. This coupling was negligible in the amplidyne under consideration. The armature resistance must be carefully measured as it varies widely over a common range of currents, as shown in Fig. 6. Inaccuracies in armature resistance affect both steady-state and transient results. The speed is involved in the speed voltages mentioned in the foregoing and is very important. The wide range of inductance measurements lead to measurement difficulties, but a reasonable error in quantities other than those previously mentioned does not lead to considerable error in the final results.

Conclusion

In the preceding analysis, the 2-stage dynamoelectric amplifier has been approached from a coupled-circuit point of view. Differential equations, taking into account currents in the coils undergoing commutation, have been written which are general for any type of load impedance or input-voltage function. The equations were then transformed to linear differential equations with constant coefficients. The currents in the various windings are then obtainable. The expressions for transient and steady-state response are developed along with the transfer function which gives the frequency response.

Experimental data to determine the transient and frequency response of an amplidyne were taken. Calculated and experimental curves are shown to agree within the limits of experimental accuracy. It is concluded that neglecting the armature short-circuited turns caused by commutation leads to considerable error in the value of the armature time constant. It is hoped that this analysis will serve to deepen the understanding of a 2-stage dynamoelectric amplifier as well as extend the applications of the coupled-circuit viewpoint in machine analysis.

References

1. The Modern Approach to Electrical Machine Analysis, W. J. Gibbs. *The Engineer*, London, England, Oct. 12, 19, 26, Nov. 2, 9, 1951.

2. A Circuit Approach to the Analysis of Electrical Machinery, H. E. Koenig. *Thesis*, University of Illinois, Urbana, Ill., Jan. 1953.

3. Application of Network Theory to the Analysis of Rotating Machinery. Part I—Synchronous and Asynchronous Machines, H. E. Koenig. *AIEE Transactions*, vol. 73, pt. II, May 1954, pp. 162–69.

4. Part II—Commutating Machines. *Ibid.*, pp. 169–77.

5. Mathematical Methods in Electrical Engineering (book), M. B. Reed, G. B. Reed. Harper and Bros., New York, N. Y., 1951.

◆

Discussion

Robert M. Saunders (University of California, Berkeley, Calif.): The author has undertaken a difficult but essential work in any control system component synthesis. In the inexorable demand for a transfer function for the 2-stage dynamoelectric amplifier, the systems engineer has turned to network or "black-box" synthesis as the most readily available means at hand. In his own mind the doubt always remains that his transfer function thus determined is valid only for the particular component he dealt with. Thus, it is essential that the transfer function be developed from the "inside out," so to speak, rather than from the "outside in."

Yet I am left with a definite feeling of uncertainty as to the validity of the author's results. Many of the assumptions he has made are suspect and some have even been shown to be untenable by the end of the paper, e.g., hysteresis. Others regarding eccentricity, absence of direct-axis interpoles are known at the outset to be shaky. The fact that the author was able to check his own experimental results validates his assumptions for his case only and does not provide the designer with the necessary universal means of extending himself into the unknown. On the positive side, by means of coupled-circuit theory, the author has validated the network synthesis transfer function within the assumption structure he has imposed.

G. H. Fett (University of Illinois, Urbana, Ill.): Dr. Burtness has shown that even the complicated 2-stage dynamo amplifier can be analyzed as a type of coupled electric circuit. His paper points out again how the problem of including speed voltage, mutual inductance, and load impedance voltage drops can be solved when the matrix method is adopted.

One caution must be interjected. The problem of measuring the constants required is a very difficult one to solve and the values obtained may be quite in error. The phase-shift curves obtained in Fig. 11 are more sensitive to errors in time constants than the amplitude curve of Fig. 10 and, hence, can be used to determine sources of errors. It indicates that the values of corner frequencies assumed, i.e., 7.5 and 50 radians per second, are probably too low. This is particularly true for the higher corner for which, at a frequency of about 8 cycles per second, the phase shift should be 45 degrees if the network is minimum phase; if it were nonminimum phase shift, the phase shift would be even greater. A total phase shift at this frequency would then be expected to be about 130 degrees rather than the 115 degrees actually observed. Had the high-frequency corner been found at a frequency of about 15 cycles per second, the agreement would have been excellent.

This would suggest that the higher corner frequency was caused by smaller equivalent inductance in the armature circuit, i.e., the coupling of the short-circuited winding and the remainder of the armature was actually better than the indicated measurements. Further, the uncertainties in the other measurements of inductances accumulate in this time constant, as may be noted from the form of the coefficients.

Fig. 5 shows clearly that the system is essentially nonlinear because of hysteretic effects. The comments on the measurement of the field circuit time constant also show that the system is nonlinear. Hence the answers obtained must be considered approximate not only because of the uncertainty in measurement of certain time constants but also because the time constants are not actually constants.

This does not mean that the method of attack given by Dr. Burtness is unsatisfactory. Quite the contrary. At the present state, the assumption of a linear differential equation with constant coefficients is the only feasible one in a problem so complicated. However, the desirability of consideration of the effects of the nonlinearity, especially that of the main field circuit, is apparent. Suppose that this main field circuit is expressed in terms of a describing function[1] to take into account the nonlinearity. Thus, using the notation of the paper (see equation 52)

$$T_{fs}=\frac{862}{p+50}G_{N-L}$$

where G_{N-L} is a describing function which takes into account the saturation or hysteretic effect in the main field winding but does not include the effect of harmonics.

Now G_{N-L} will be a function of both frequency and the amplitude of the signal impressed on this field. Hence, it will be describable by a family of curves, with these quantities as parameters, for a given field and magnetic circuit. So the complete transfer function which takes into account some of the nonlinear effects can be obtained by combining linear and nonlinear terms.

The form of the describing function G_{N-L} has been determined[2] for systems similar to that of the amplidyne, since the combination of hysteresis and saturation approximates backlash and saturation. The linear and nonlinear functions can then be easily combined if the co-ordinates used are log amplitude and phase shift in degrees. Has the author considered this extension of his attack?

References

1. Sinusoidal Analysis of Feedback-Control Systems Containing Nonlinear Elements, E. C. Johnson. *AIEE Transactions*, vol. 71, pt. II, July 1952, pp. 169–81.

2. Prediction of Transient Response of Nonlinear Servomechanisms by Sinusoidal Analysis, H. C. Brearley, Jr. *Thesis*, University of Illinois, Urbana, Ill., 1954.

H. E. Koenig (University of Illinois, Urbana, Ill.): There are a few significant points brought out by Dr. Burtness that are worth elaborating upon. While the starting point he has chosen may appear to be a rather complex and involved one, it does give a certain sense of continuity, elegance, and completeness. In most cases, the equations can be written for the machine and its associated network in terms of the mesh-circuit variables from inspection of the graph or connection diagram. However, when encountering an unfamiliar problem, it is sometimes necessary or desirable to write the equations in terms of the branch-circuit variables and then arrive at the mesh-circuit or node system of equations by way of the transformation of variable. By following this technique one can always proceed with complete assurance. Dr. Burtness has demonstrated how this technique is applied to the analysis of the rather complex amplidyne problem.

The author has demonstrated how by means of a change in variable it is possible to take advantage of symmetry in the coefficient matrixes in reducing the complexity of the problem. Again it is important to point out that, once the simplified set of equations have been established, it is possible to attach certain physical significance to the terms in the equations. Thus, the simplified equations can be written from inspection and it is not necessary to go through the transformations as long as the problem under consideration is similar to those of past experience. However, we are interested in developing and teaching methods of analysis which will handle the unfamiliar as well as the familiar problem. In this sense I feel the work of Dr. Burtness is quite significant.

The author has considered the commutating machine as a problem in network switching. In his analysis he pointed out the important role the commutating coils play in transient operation of the machine. In the usual treatment of this problem, the machine is assumed to have an infinite number of commutator segments and zero brush width. It is clear from Dr. Burtness' paper that the true nature of the problem does not appear under these assumptions.

This paper emphasized once more the value of matrix algebra as a tool in the study of systems of linear equations. This simple tool can and should be given to the sophomore student in electrical engineering when he is first introduced to systems of linear equations in the study of network theory.

Myril B. Reed (University of Illinois, Urbana, Ill.): The problem of designing rotating machines which have certain specified properties, when incorporated into an electric network, is an important one today. In the past, machines have been built to fit traditional forms, with the electrical properties of these machines secondary, and to a considerable extent unalterable, characteristics. Now the electrical properties are the primary specifications and the machine must be built to exhibit these properties. In other words, the problem of machine synthesis is here.

The concepts of rotating fluxes, armature reactions, etc., cannot by any at present known means be designed as an integral part of a linear-lumped network, as control system design requires. However, the scheme described by Dr. Burtness presents a major step on the way toward an effective elimination of this difficulty.

The scheme of viewing rotating machinery as electric networks with mutually coupled conductors in relative motion permits inclusion of these machines into a network as an integral part rather than as an intruder. The whole of the vast amount of network analysis and synthesis is thus placed at the hand of the machine designer. Furthermore, this method of Dr. Burtness permits the effective use of one of the major design tools coming into the engineer's hands, namely, the computer.

R. W. Burtness: I am grateful for the various discussions submitted and for the interest which has been shown in this study. It might be well at this point to re-emphasize the nature of this paper. It is rather comprehensive in its approach in that it not only is an analysis of the machine itself but also leads to the synthesis of networks involving rotating machinery. It shows what can be done to enhance the understanding of complicated electric machinery by using the coupled-circuit approach and matrix algebra. Armature short-circuited turns can be considered, various impedance loads and input voltage functions can be imposed, and machine currents and voltages can be obtained. Transient response, frequency responce, and transfer functions can be obtained also. The emphasis of the paper is on the approach to the problem of electric machine analysis and system synthesis, and not on the intricacies of measurements of the constants involved.

The purpose of this paper is certainly not to list amplidyne constants. The universal means of extending into the unknown that Mr. Saunders is looking for is the method of approach itself. It is self-evident that any experimental verification is good only for the case in question. It is, therefore, necessary to concentrate on the method of approach when making an attempt to extend into the unknown, because experimental verification for every possible case becomes a physical impossibility.

It is to be expected that the age-old problems of nonlinearity and eccentricities are present. It is encouraging to note that the experimental results check as closely as they do in spite of the nonlinearity present in the saturation curve. It is certainly expected that the results would check even more closely were the amplidyne of a more recent design involving a more linear saturation curve.

Consideration of the nonlinear components in the system is possible if the variable coefficients are not transformed to constant coefficients and a point-by-point solution to the variable coefficient differential equations is attempted. This process, however, is extremely complicated and a more feasible solution to the nonlinearity of the saturation curve is that referred to by Dr. Fett. In this way, the linear and nonlinear functions can be combined and the problem is greatly simplified over the point-by-point solution.

Dr. Koenig has pointed out that it is often possible to write the mesh or, in this case, K level equations from inspection. This is certainly true. To evaluate them in terms of the individual elements, however, becomes impossible without having developed the equations originally from the element level. Thus, starting with the development on the element level produces a more complete, accurate, and workable set of equations.

As Dr. Reed has pointed out, this method of approach is the only method at present which presents a firm step in the direction of electric machine design from the standpoint of fitting a machine to a definite network problem.

Control Circuitry for Remotely Operated Electric Utility Substations

W. A. DERR
MEMBER AIEE

W. L. METZ
ASSOCIATE MEMBER AIEE

THE number of electric utility substations which are remotely operated has been rapidly increasing since 1945. Economic and system performance considerations have been responsible for the trend to centralized control and normally unattended substations.[1-4] Except where very short distances are involved, supervisory control is employed for the remote operation of electric utility substations. Supervisory control is now being used to provide centralized control for large transmission and distribution substations. Fig. 1 shows the dispatching office of the City Public Service Board of San Antonio from which more than 75 substations are controlled over privately owned line wires, circuits leased from the Telephone Company, power-line carrier channels, or microwave channels.[5-8]

When remote control is applied to a substation it is customary to have a full complement of local control equipment such as would be employed if it was to be normally attended, so that it can be operated locally for test purposes and in emergency situations when the remote-control equipment is inoperative for any reason. In the simplest type of substation involving the control of nonautomatic circuit breakers or motor-operated switches, there are no problems in applying remote control, since the local and remote control can be directly paralleled. However, when automatic reclosing circuit breakers are to be remotely operated or when circuit breakers must be automatically synchronized or tap-changing-under-load equipment operated, problems are encountered in applying remote-control equipment. The problems basically result from the fact that two points of control are involved. These problems exist if the control can be effected from two separate sets of control devices right at the substation or if the control can be effected by local control devices as well as by supervisory control or any type of direct operating remote-control system.

In this paper schemes are presented for applying remote control to circuit break-

---

Paper 55-127, recommended by the AIEE Substations Committee and approved by the AIEE Committee on Technical Operations for presentation at the AIEE Winter General Meeting, New York, N. Y., January 31–February 4, 1955. Manuscript submitted October 21, 1954; made available for printing November 24, 1954.

W. A. Derr and W. L. Metz are with the Westinghouse Electric Corporation, East Pittsburgh, Pa.

Fig. 1. Supervisory control dispatching office of City Public Service Board of San Antonio. The operation of more than 70 substations is centralized at this location

ers having various types of commercially available automatic reclosers. The problems involved when the use of automatic synchronizing or synchronism check equipment is required are discussed and typical circuit arrangements presented. Manual and automatic operation of tap-changing-under-load transformers is also discussed. Consideration is given to remote-control cutoff or transfer means. Remote lamp indications of the position of circuit breakers and disconnecting switches and telemetered indications of the quantities usually considered essential are briefly discussed.

All of the schematic diagrams presented are based on the remote-control equipment actuating relays at the substation, contacts of these relays then affecting the required operations. These actuating relays may be considered to be operated by means of supervisory control or by direct connections to remotely located control switches.

Devices Designated in Figures

1L	Circuit-breaker local control switch
	C Contact closed in close position
	T Contact closed in trip position
	O Contact closed in off position
	SC Contact closed during and after close operation and remains closed until trip operation
1L	Tap-changer local control switch
	L Contact closed in lower position
	R Contact closed in raise position
1R	Circuit-breaker remote control relays
	C Remote close relay
	T Remote trip relay
1R	Tap-changer remote control relays
	L Remote lower relay
	R Remote raise relay
25	Automatic synchronizer or synchronism check devices
25X	Auxiliary relay to energize device 25 and prepare circuit-breaker closing circuit
25Y	Synchronizing auxiliary relay
25Z	Synchronizing auxiliary relay
27L	Undervoltage relay to permit closing in the event of dead line
27B	Undervoltage relay to permit closing in the event of dead bus
43	Transfer switch ("stayput" type)
	A Contact closed in automatic position
	M Contact closed in manual position
43L	Transfer switch (spring return type)
	A Contact closed in automatic position
	M Contact closed in manual position
43R	Remote control transfer relay
	A Automatic control
	M Manual control
43X	Auxiliary transfer toggle- or latch-type relay
	A Automatic position
	M Manual position
52	Circuit breaker
	a Auxiliary switch closed when circuit breaker is closed
	aa Electric interlock closed when circuit-breaker mechanism is in closed position
	b Auxiliary switch closed when circuit breaker is open
	bb Electric interlock closed when circuit-breaker mechanism is in the open position
	LC Latch-checking switch, closed when circuit breaker mechanism linkage is relatched
	CC Circuit-breaker closing coil
	TC Circuit-breaker trip coil
	X Circuit-breaker auxiliary closing relay
	Y Circuit-breaker closing cutoff relay
57	Primary voltage adjusting element
	L Closed to lower tap position
	R Closed to raise tap position
69	Permissive control latch-type relay for automatic recloser
	A Automatic position
	L Lockout position
69R	Permissive control relay for automatic recloser
69S	Synchronizing switch
79	Automatic recloser (capacitor type)
	H Automatic recloser holding coil
	P Automatic recloser operate coil
79	Automatic recloser (motor-driven type)
	M Automatic recloser motor
	L Automatic recloser lockout
	R Automatic recloser reset
84	Tap changer
	CS Tap-changer cam switch closed on tap
	HL Time-delay heater-type relay for automatic lower operation
	HR Time-delay heater-type relay for automatic raise operation
	LLS Lower limit switch
	RLS Raise limit switch
	TL Auxiliary lower relay
	TR Auxiliary raise relay
	XL Lower control relay
	XR Raise control relay
C	Capacitor
PR	Protective relay
R	Resistor
TM1	Telemetering selection relay for circuit no. 1
TM2	Telemetering selection relay for circuit no. 2

Circuit-Breaker Control

Without Reclosing

Except for the use of cutoff or transfer switch contacts, as will be discussed later, remote-control trip and close contacts can be directly paralleled with local-control trip and close contacts as shown in Fig. 2, when no automatic features of any kind are involved. Control of such breakers can be readily effected from more than one location because the basic trip and close functions on circuit breakers are performed by momentary contacts. Any number of momentary contacts can be paralleled to effect control. Therefore, the application of remote control to nonautomatic breakers in new or existing substations presents no problems.

With Multishot Reclosing

Fig. 3 shows local control only for a circuit breaker operated by a typical motor-driven multishot recloser. The detailed internal circuitry of the automatic recloser is not shown since the operation, while different in detail for the multishot reclosers available, is similar in basic principle.

Multishot reclosers are designed to make it possible to have a predetermined number of reclosures at predetermined time settings result if a circuit breaker is

7

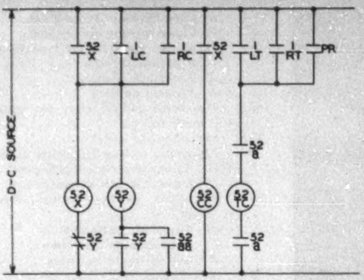
D-C SOURCE
52 X
1 LC
1 RC
52 X
1 LT
1 RT
PR
52 a
52 X
52 Y
52 CC
52 TC
52 Y
52 Y
52 aa
52 a

Fig. 2. Typical circuit-breaker schematic diagram involving local and remote control

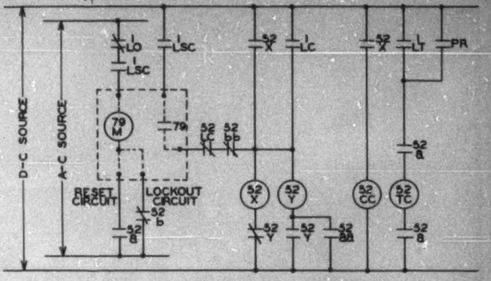
D-C SOURCE
A-C SOURCE
1 LO
1 LSC
1 LSC
79 M
79
52 LC
52 bb
RESET CIRCUIT
LOCKOUT CIRCUIT
52 b
52 a
52 X
1 LC
52 X
1 LT
PR
52 a
52 X
52 Y
52 CC
52 TC
52 Y
52 Y
52 aa
52 a

Fig. 3. Schematic diagram for a circuit breaker operated by a typical motor-driven multishot recloser with only local control

tripped by protective relay operation. They are arranged to reset to the start position if the circuit breaker remains closed on any of the automatic reclosing attempts and to travel to the lockout position if all automatic reclosures are unsuccessful. Reset can be effected after lockout if the breaker remains closed for a predetermined time interval when closed by a control switch. With reference to Fig. 3, reclosing contact *79* will close a predetermined number of times as a result of the recloser motor *79M* being energized through the complete cycle from the start to the lockout position.

Automatic recloser operation is based on circuits for its functioning being immediately established when a circuit breaker is tripped by a protective relay. When such tripping occurs the circuit-breaker control switch contacts *1LSC* and *1LO* shown in Fig. 3 remain closed and the recloser is allowed to function. The circuit breaker will be reclosed when contact *79* closes and the recloser motor *79M* will be energized through a breaker auxiliary switch contact *52b* until the lockout position is reached if no reclosures are successful. If the circuit breaker remains closed after any of the reclosures, motor *79M* is energized through breaker auxiliary switch contact *52a* until it has reset to the start position.

It is apparent from Fig. 3 that contacts *1LSC* of the circuit-breaker control switch are connected in the circuit of recloser contact *79* as well as in the circuit of the recloser motor *79M* to remove the recloser effectively from service when the circuit breaker is tripped by the control switch and to place the recloser back into service when the breaker is subsequently closed by means of the control switch. It is universal practice to employ such stayput control switch contacts in the application of all types of reclosers which are applied with only one point of manual control. It is the necessity of employing such stayput contacts to provide for proper functioning of most commercially available reclosers which makes the application of remote-control equipment to automatic reclosing circuit breakers considerably more involved than for nonautomatic circuit breakers. This is because, in general, stayput control contacts can not be paralleled and they can only be connected in series if certain operating limitations are acceptable.

When a stayput element is required in the functioning of any apparatus which can be controlled from more than one location, the control should be arranged such that a single stayput element can be controlled by momentary contacts from all control locations. All of the diagrams for remote-control operation presented are based on this fact. It is apparent that this type of operation precludes the use of stayput control switch contacts such as *1LSC* when remote control is involved.

Fig. 4 shows local and remote control applied to a circuit breaker operated by a

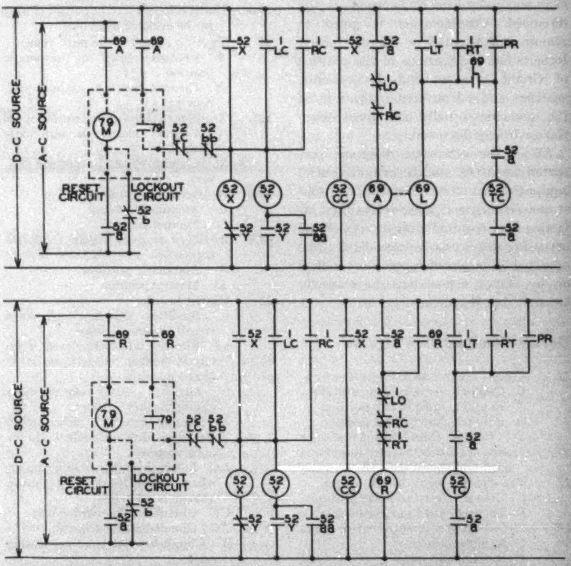
D-C SOURCE
A-C SOURCE
69 A
69 A
79 M
79
52 LC
52 bb
RESET CIRCUIT
LOCKOUT CIRCUIT
52 b
52 a
52 X
1 LC
1 RC
52 X
52 a
1 LO
1 RC
1 LT
1 RT
PR
69
52 a
52 X
52 Y
52 CC
69 A
69 L
52 TC
52 Y
52 Y
52 aa
52 a
D-C SOURCE
A-C SOURCE
69 R
69 R
79 M
79
52 LC
52 bb
RESET CIRCUIT
LOCKOUT CIRCUIT
52 b
52 a
52 X
1 LC
1 RC
52 X
52 a
69 R
1 LT
1 RT
PR
1 LO
1 RC
1 RT
52 a
52 X
52 Y
52 CC
69 R
52 TC
52 Y
52 Y
52 aa
52 a

Fig. 4 (top) and Fig. 5 (bottom). Schematic diagrams for a circuit breaker operated by a typical motor-driven multishot recloser showing methods of combining local and remote control multishot recloser. The arrangement shown provides for relay *69R* placing the recloser in and out of service at the proper time. When the circuit breaker is closed, relay *69R* is energized. If the breaker is tripped by a protective relay operation, relay *69R* remains energized to allow reclosure to be effected. If the breaker is manually tripped either locally or remotely, relay *69R* is de-energized and reclosing is prevented. Regardless of how or from where the breaker is then closed, relay *69R* is re-energized to re-establish the reclosing circuits properly. The arrangement shown in Fig. 4 is completely flexible and can readily be provided at existing as well as new substations since no control switch elements are required in addition to those employed in the customary conventional scheme where only local control is involved as shown in Fig. 3.

Fig. 5 shows a slightly different arrangement which can be employed. In this case, relay *69* is a toggle- or latch-type relay whose contacts remain in one of two positions depending on whether the *A* or the *L* coil was last energized. With reference to Fig. 5, coil *A* of relay *69* is energized when the circuit breaker is closed. If the breaker then trips from a protective relay operation, the recloser remains in service. If tripping is effected manually either by local or remote control, the *L* coil of relay *69* is energized to open the *A* contacts and close the *L* contacts. This takes the recloser out of service until the breaker is again closed. No local control switch contacts are required other than those normally needed when only local control is involved.

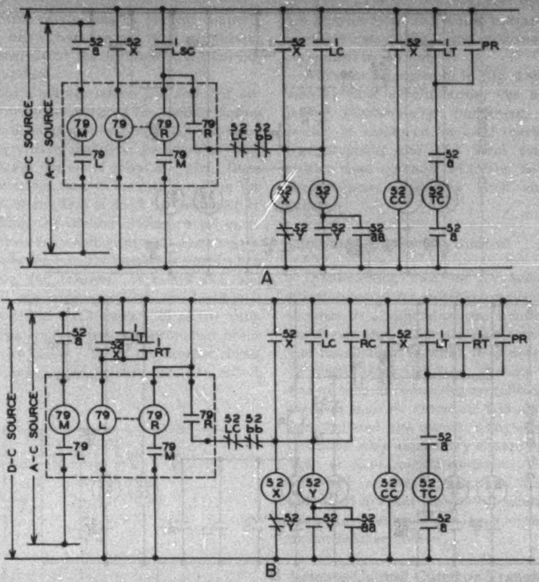

Fig. 6. Schematic diagrams for a circuit breaker operated by a motor-driven single-shot recloser

A—With only local control
B—With local and remote control

WITH SINGLE-SHOT RECLOSING

The basic circuit arrangements shown in Figs. 4 and 5, involving the use of relay *69* or *69R*, are applicable to any type of recloser. However, other arrangements not requiring the use of relay *69* or *69R* can be applied when some types of commercially available single-shot reclosers are involved.

Fig. 6(A) illustrates local control only of a breaker operated by a single-shot recloser as shown in its entirety. This recloser includes a toggle-type relay with two coils *79R* and *79L* and a motor *79M*. When coil *79R* is energized, contact *79R* closes and remains closed until coil *79L* is energized. Likewise, when coil *79L* is energized, contact *79L* closes and remains closed until coil *79R* is energized. Contact *79M* is closed after motor *79M* has been energized for an adjustable time interval.

In Fig. 6(A) a stayput contact of the control switch *1LSC* is normally employed in the reclosing circuit where only local control is involved as previously discussed. When the breaker is closed, a contact of closing relay *52X* momentarily energizes coil *79L*. This opens contact *79R* in the reclosing circuit and closes contact *79L* in the motor circuit of the recloser. If the breaker remains closed, motor-operated contact *79M* completes a circuit to coil *79R*. This results in contact *79R* closing and contact *79L* opening. The motor is thus de-energized and contact *79M* opens. If the breaker is tripped by protective relay operation subsequent to the operation just described, the breaker is immediately reclosed since contact *79R* is closed. When the reclosure is thus effected, coil *79L* is again momentarily energized by a contact of closing relay *52X*. Therefore, if the breaker immediately trips out no second reclosure can result since contact *79R* is open. If the breaker remains closed long enough for motor *79M* to close contact *79M*, the reclosing circuit is again established and subsequent automatic tripout will be followed by a single reclosure.

Fig. 6(B) is a modification of Fig. 6(A) which provides for both local and remote control of a breaker operated with the same type of single-shot recloser. Since this type of recloser contains a stayput toggle-type relay element, it is possible to eliminate any stayput contacts in the external circuitry and to employ all momentary contacts. With the arrangement shown, a circuit is completed to energize coil *79L* momentarily when the breaker is tripped locally or remotely. This results in contact *79R* being opened to prevent reclosing. The recloser otherwise functions as previously described. The arrangement shown eliminates the necessity of using relay *69* or *69R* when more than one point of control is involved. However, two separate trip contacts are required on the local control switch.

Fig. 7(A) shows local control only of a breaker operated by a single-shot recloser of the capacitor discharge type. This type of recloser contains a relay having an operating coil *79P* and a holding coil *79H*. When the breaker is closed, capacitor *C* is fully charged through resistor *R*. If the breaker is tripped by the local control switch, reclosing is prevented by the

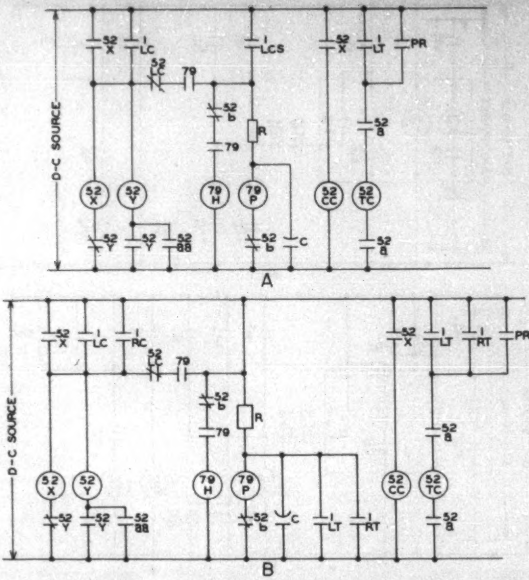

Fig. 7. Schematic diagrams for a circuit breaker operated by a capacitor discharge type of single-shot recloser

A—With only local control
B—With local and remote control

opening of stayput contact *1LSC*. If the breaker is tripped by a protective relay operation, relay *79* is operated as a result of capacitor *C* discharging through coil *79P*. Relay *79* is then held energized by its own contact completing a circuit to its holding coil *79H* through breaker auxiliary switch contact *52b* and control switch contact *1LSC*. Another contact of relay *79* completes a circuit to breaker closing relay *52X* to cause the breaker to reclose. If the breaker immediately trips, no second reclosure results since capacitor *C* cannot obtain sufficient charge to energize coil *79P* through the high resistance *R* unless the breaker remains closed for an appreciable length of time as governed by the value of resistance *R*. If the breaker remains closed long enough to charge capacitor *C* fully, a subsequent tripout will be followed by a reclosure.

Fig. 7(B) shows a modification of Fig. 7(A) which provides for both local and remote control of a breaker operated with this type of single-shot recloser. It is possible to operate this type of recloser without the use of stayput contacts on the local- or remote-control devices as shown in Fig. 7(B). Momentary contacts are used to discharge capacitor *C* when the breaker is tripped locally or remotely. This prevents reclosure when the breaker is so tripped, since relay *79* is not operated. The arrangement shown in Fig. 7(B) requires no extra relay, it being necessary only to provide two separate trip contacts on the local-control switch instead of the usual one.

With Synchronizing

Circuit breakers requiring synchronizing in normally attended stations are usually synchronized by manual means involving a synchronizing switch, synchroscope, and voltmeters. However, the closure of remotely controlled circuit breakers is frequently performed by means of an automatic synchronizer or a synchronism check device. The circuit of Fig. 8 shows a method of combining local manual synchronizing and remote automatic synchronizing where only one breaker in the station requires synchronizing prior to closing. Included in the scheme is a complete complement of automatic synchronizing equipment including the automatic synchronizer or synchronism check relay, device *25*, and the dead line and dead bus detecting relays, devices *27L* and *27B*, for closing in the event that either the line or bus is dead. The latter two devices are optional depending upon whether it is desired to have the breaker close with either the line or bus dead.

Fig. 8 shows the usual local closing circuit through the control switch *1LC* and the synchronizing switch *69S*. Remote synchronizing is initiated by relay *25X* which is energized by the remote close device *1RC*. Relay *25X* seals itself in, connects the synchronizing potentials to the synchronizer, and prepares a closing circuit to *52X* so that the synchronizing equipment can close the breaker when a condition of synchronism exists. Relay *25X* will eventually be released by the breaker auxiliary switch *52b* if the breaker closes. It can also be released by operation of the remote trip relay *1RT*. When relay *25X* releases all equipment is restored to normal.

In locally controlled substations, a common synchroscope and associated voltmeters are used regardless of the number of breakers which must be synchronized. Adequate mechanical interlocking to prevent connecting more than one set of potentials to the common synchroscope is obtained by the use of synchronizing switches with a single key for all switches. Similarly, economic considerations dictate the use of common automatic synchronizing equipment for any number of breakers in a remotely controlled substation. When more than one circuit breaker must be closed with common automatic synchronizing or synchronism check equipment, electric interlocking must be provided to insure against connecting two sets of synchronizing potentials together.

Fig. 9 shows a closing scheme for combining local manual synchronizing with remote automatic synchronizing for an unlimited number of circuit breakers in a substation. One set of synchronizing equipment consisting of an automatic synchronizer or synchronism check device and dead bus and dead line voltage relays are employed for the remote closing function. The local control follows the established practice of using separate control switches and synchronizing switches for each breaker.

In Fig. 9 relay *25Z* is normally energized through the break contact of relay *25Y*. A remote closing function for circuit breaker no. 1 is initiated by the closing of remote close contact *1RC1*. This results in energizing relay *25X1* through a make contact of relay *25Z*, a make contact of *1RC1*, and a break contact of *1RT1*. Contacts of *25X1* connect the synchronizing potentials to the dead line and dead bus voltage relays and to the synchronizing device. Another contact of relay *25X1* energizes relay *25Y* and relay *25X1* seals itself in through a make contact of relay *25Y*. The opening of the break contact of relay *25Y* in the coil circuit of relay *25Z* results in relay *25Z* releasing after a short time delay. The release time of relay *25Z* is governed by the values of capacitance and resistance connected across its coil. Release of relay *25Z* de-energizes the synchronizing start bus and prevents any other *25X* relays from being energized until relay *25X1* has released. This provides the necessary electric interlocking to prevent connecting more than one set of synchronizing potentials to the common synchronizing equipment.

Since voltage relays *27L* and *27B* are normally de-energized the breaker closing circuit must not be prepared until these relays have had time to operate. The delayed release of relay *25Z* gives these two relays time to operate if neither the bus or the line is dead by momentarily holding the breaker closing circuit open. If there is no voltage present on either the line or the bus, the breaker is closed when relay *25Z* releases. If relays *27L* and *27B* are both energized, the breaker is not closed until contact *25* of the automatic synchronizer or synchronism check device closes. When the breaker closes, the opening of breaker auxiliary switch *52b* releases relay *25Y* which in turn de-energizes relay *25X1* and restores all equipment to normal.

While the arrangement in Fig. 9 shows manual local synchronizing, the automatic synchronizing equipment can readily be employed for local operation by paralleling the *1LC* local control switch close contacts with the remote close contacts *1RC* for each circuit breaker.

Disconnecting Switch Control

Disconnecting switches for isolating transformers or for switching various bus sections in a substation are frequently motor-operated. There are remote-control installations in which it is desirable to control these switches. Remote control of such disconnecting switches is no problem since no automatic features are involved and the switch completes an operation after momentary closure of the open or close control contacts. Therefore, any number of contacts can be paralleled to effect the control similar to the arrangement shown in Fig. 2 for simple circuit-breaker control.

Remote-Control Cutoff or Transfer

The contacts of control relays which are remotely actuated can be connected directly in parallel with the contacts of local control switches as is indicated in Figs. 2 through 9. However, it is customary to provide a means of readily dis-

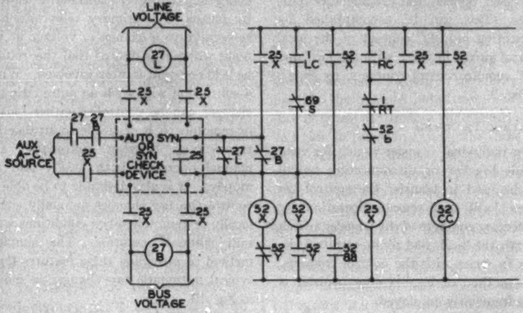

LINE VOLTAGE
27 L
25 X
27 27 B
AUX A-C SOURCE
AUTO SYN OR SYN CHECK DEVICE
25
27 L
27 B
BUS VOLTAGE
1 LC
69 S
52 X
1 RC
1 RT
52 b
52 Y
52 CC
52 aa

Fig. 8 (above). Schematic diagram showing a method of combining local manual synchronizing and remote automatic synchronizing for a single circuit breaker

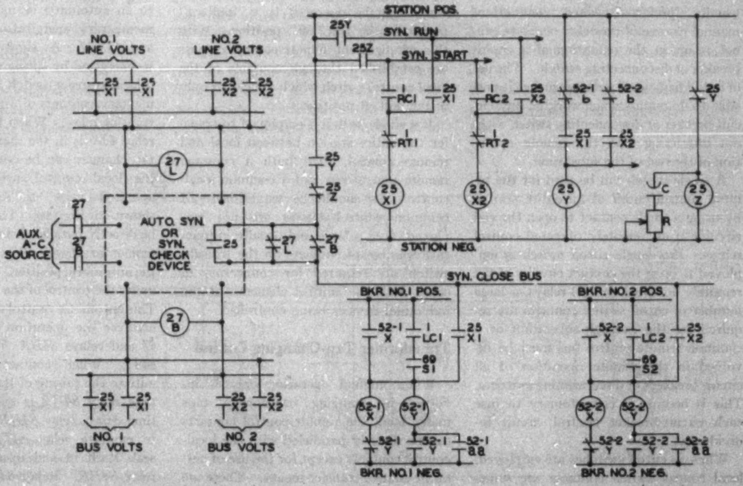

STATION POS.
25Y
SYN. RUN
25Z
SYN. START
NO.1 LINE VOLTS
NO.2 LINE VOLTS
25 X1
25 X2
27 L
27 B
AUX. A-C SOURCE
AUTO. SYN. OR SYN. CHECK DEVICE
1 RC1
1 RC2
1 RT1
1 RT2
52-1 b
52-2 b
25 Y
25 Z
C
R
STATION NEG.
SYN. CLOSE BUS
BKR. NO.1 POS.
BKR. NO.2 POS.
52-1 X
1 LC1
69 S1
52-2 X
1 LC2
69 S2
52-1 Y
52-2 Y
52-1 aa
52-2 aa
NO. 1 BUS VOLTS
NO. 2 BUS VOLTS
BKR. NO.1 NEG.
BKR. NO.2 NEG.

Fig. 9 (left). Schematic diagram combining local manual synchronizing and remote automatic synchronizing for an unlimited number of circuit breakers

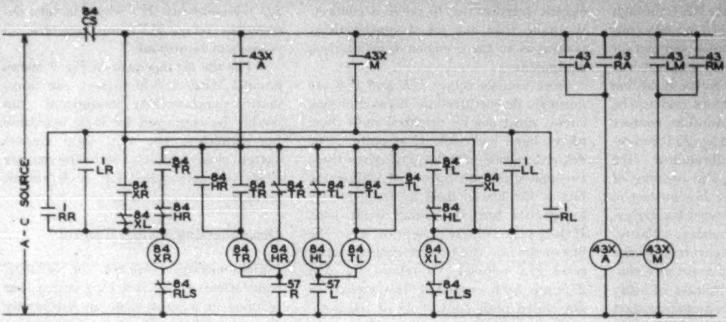

Fig. 10. Schematic diagram of tap-changer control showing local and remote manual control as well as automatic control. Arrangement shown provides for transfer between automatic and manual control being performed locally or remotely

connecting the remote-control equipment or for providing a means of transferring between remote and local control so that operations can be performed from only one or the other location. A number of different arrangements of providing such cutoff or transfer will be discussed in the following paragraphs.

REMOTE-CONTROL CUTOFF

An individual cutoff switch can be provided for each circuit breaker or disconnecting switch remotely controlled. The contacts of such cutoff switches can be connected in series with the contacts of the remotely actuated relays (contacts *1RC* and *1RT* of Fig. 2) or they may be connected in series with the coils of the remotely actuated relays. Connecting the cutoff switch contacts in series with the remotely operated relay contacts is usually preferred since inadvertent manual closure of the relay contacts cannot result in the operation of a circuit breaker or disconnecting switch. The use of individual cutoff switches makes it possible to do maintenance work on any circuit breaker or disconnecting switch without interfering with the remote operation of the rest of the substation.

A single switch can be used for the remote control cutoff of an entire station by using a single contact to open the coil circuits of all remotely operated control relays. If a single cutoff switch is employed to open the contact circuits of the remotely operated control relays, a large number of cutoff switch contacts are required for the average substation or a common remote-control bus must be involved in the remote operation of all circuit breakers or disconnecting switches. This is because it is customary to fuse each circuit-breaker control circuit individually.

When no cutoff switches are employed, local control switch contacts are sometimes used to prevent the possibility of remote closing of a circuit breaker which has been opened for maintenance purposes. This can be accomplished by connecting a *1LSC* contact of the local control switch in series with the *1RC* and *1RT* remote control contacts, as shown in Fig. 2.

CONTROL TRANSFER

An individual transfer switch for each circuit breaker or disconnecting switch can be used to transfer the control between local and remote operation by connecting contacts of the transfer switch in both the local- and remote-control circuits in series with the control contacts. This method of local-remote transfer is most frequently employed.

Individual transfer can also be effected by the use of special control switches which can be operated to a "pullout" position from the "off" position. With this arrangement remote-control circuits are established through contacts of the local control switch which are closed only in the pullout position.

If a single switch is employed to transfer the entire station between local and remote control, then both a common remote-control bus and a common local-control bus should be established. If common control busses are not employed, then a large and usually impractical number of contacts on the transfer switch are required for connecting in series with the control elements of the individual devices being controlled.

Transformer Tap-Changing Control

When manual operation only is involved in changing transformer taps under load, the remote-control contacts can be directly paralleled with the local-control contacts except for the use of cutoff or control transfer means. There are no special problems in the remote operation of such manually controlled tap changers. However, automatic control by means of a primary relay which is responsive to a change in voltage at the point where it is desired that the voltage be held constant is often involved. When a substation with such an automatic tap changer can be controlled either locally or remotely, it is desirable to arrange for transferring between automatic and manual operation both locally and remotely. It is also desirable to be able to control the tap changer manually either locally or remotely when conditions warrant manual operation. The simplest method of providing these features for a typical automatic tap changer is shown in Fig. 10.

In Fig. 10 device *43X* is a toggle- or latch-type relay which can be positioned to an automatic or manual position by momentary energization of coils *43XA* and *43XM*. As shown, these coils can be energized by spring return contacts of a local transfer switch as well as by momentary contacts of a remotely operated transfer relay. When toggle or latching relay *43X* is in the manual position, the tap changer can be controlled by either the local control switch or remotely actuated "raise" or "lower" contacts as shown in Fig. 10. These contacts can be directly paralleled since they are of the momentary type. When relay *43X* is in the automatic position, the tap changer is under the control of the automatic relays. This automatic control of the tap changer involves the operation of primary relay *57* and relays *84HR*, *84HL*, *84TR*, and *84TL*. When contact *57R* closes to initiate the raising of the voltage, heater-type relay *84HR* is energized. After a time delay, relay *84HR* closes a contact to energize relay *84TR*. Relay *84TR* seals itself in and opens the circuit to relay *84HR*. Relay *84TR* also closes a contact in the coil circuit of relay *84XR*. After a time delay, the contacts of relay *84HR* change position and this completes a circuit for energizing relay *84XR*. By means of circuits not shown the closing of the make contacts of relay *84XR* results in operation of the tap-changer mechanism to the next higher tap. The control circuits are arranged so that relay *84XR* must be energized only momentarily to have the mechanism complete a tap change. Opening of cam switch *84CS* while the tap-changing equipment is between taps results in relay *84TR* being de-energized. This restores all equipment to normal. An automatic lowering function is performed in a similar manner by closing primary relay contact *57L*.

If it is desired to have means provided to locally cutoff remote control and transfer functions, an arrangement as shown in Fig. 11 can be employed. This scheme is based on the use of a 3-position local transfer switch. With this switch in the manual position, the tap changer can be raised or lowered locally by means of the local-control switch contacts *1LR* and *1LL*. With this switch in the automatic position, the tap changer is under the control of the primary relay as previously described. With this switch in the remote position, the type of operation effected is dependent on the position of toggle- or latching-type transfer relay *43X*. With relay *43X* in the manual position, the tap-changer position can only be changed by the remotely actuated contacts *1RR* and *1RL*. With relay *43X* in the automatic position, the tap changer is under the control of the primary relay.

Remote Lamp Indication

With any remote-control system employed for the operation of circuit breakers and disconnecting switches, provisions must be made for lamp indications of the position of these devices at the remote-controlling location. When direct wire control is employed for short distances, the remote lamp indications are usually provided by direct connection to auxiliary switch contacts on the circuit breakers or disconnecting switches. In the case of supervisory control, the auxiliary switch contacts are connected to relays which are an integral part of the supervisory control system.

The use of only an *a* or a *b* auxiliary switch on a circuit breaker to provide both the red and the green lamp indications through supervisory control equipment is usually considered adequate. It is apparent that such an arrangement gives entirely accurate information except for the possibility of a broken wire to the auxiliary switch or failure of the auxiliary switch to make contact. For either of these conditions, an incorrect indication results. When the possibility of such a failure cannot be tolerated, both *a* and *b* breaker auxiliary switches can be used to provide the remote indications. When this is done, the remote indications can be made to function exactly the same as local lamp indications. If there is a broken wire to the auxiliary switches or if an auxiliary switch fails to make contact, both the remote red and green lamps are simultaneously extinguished or lighted. This latter arrangement requires somewhat more equipment than the simple arrangement based on the use of either an *a* or a *b* auxiliary switch contact.

It is customary always to use both an *a* and a *b* auxiliary switch for the remote indication of the position of a disconnecting switch. This is because a motor-operated switch can stop in an intermediate position and the use of only an *a* or a *b* auxiliary switch contact would give incorrect information if the disconnecting switch stopped in other than the extreme open or closed position. The breaker and disconnecting switch auxiliary switch contacts which are used for remote indications are usually entirely separate from those which are used for local switchboard lamp indications.

In addition to lamp indications of the position of the devices remotely controlled, it is customary to provide lamp indications of remote-control cutoff or transfer switches and various alarm conditions necessary for most efficient operation of the station. If a single remote-control cutoff or transfer switch is employed for the entire station, a single contact of the switch can be used to provide a remote lamp indication. If individual cutoff or transfer switches are provided for each device controlled, it is customary to furnish a single remote indication for reasons of economy. The intelligence for the indication is obtained by the use of a series circuit involving a contact of each cutoff or transfer switch. The contacts used in the series circuit must all be of the same type and should be closed in the "remote" position of the cutoff or transfer switch. This makes it possible to provide indication that all switches are in the remote position or that one or more switches are not in the remote position.

Following is a list of some alarm conditions which it is sometimes desirable to have reported to the controlling location.

1. High transformer temperature.
2. Low transformer oil level.
3. Low air pressure for pneumatically operated circuit breakers.
4. Tap-changer off-tap indication.
5. Low station battery voltage.
6. Faulty pilot wires for pilot-wire relaying.
7. Bus differential-relay operation.
8. Transformer differential-relay operation.

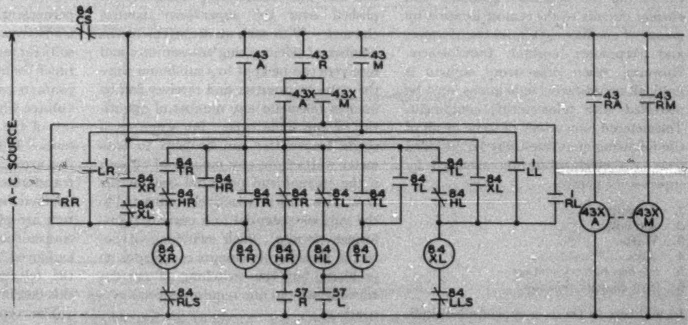

Fig. 11. Schematic diagram of tap-changer control with local transfer switch to choose between remote operation, automatic operation, or local manual operation

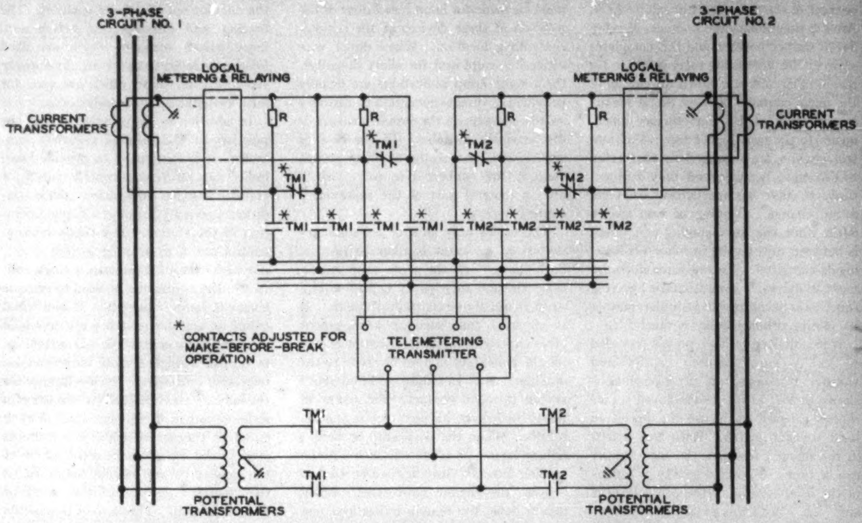

Fig. 12. Schematic diagram showing a method of selectively switching current and potential circuits to a watt-telemetering transmitter

A single alarm contact must be used for the remote indication of each such condition which it is deemed desirable to have reported to the controlling station. It is often acceptable to group alarm contacts for a common remote indication for reasons of economy.

Telemetering

Some quantitative indications are desirable for the operation of most remotely operated substations. When direct wire control is employed over short distances, the necessary quantitative information can sometimes be obtained by connecting the necessary potential and current circuits to the remote location by means of auxiliary potential transformers and step-down current transformers. However, when supervisory control is used, all quantitative indications must be provided with telemetering equipment. Telemetered indications of some or all of the following quantities may be provided from a typical substation operated by supervisory control.

1. A-c amperes.
2. A-c volts.
3. Watts.
4. Vars.
5. Station battery voltage.
6. Tap-changer position.

In addition to these, a synchronism indication must be provided if remote manual synchronizing is employed rather than automatic synchronizing as previously discussed.

To provide continuous indications of all desired quantities from a remotely operated substation requires individual channels and individual telemetering systems for each indication. Economic considerations usually preclude the furnishing of continuous telemetered indications from a remotely operated substation. Instead, it is customary to provide for selective or "on-call" telemetered indications, with the selective function being performed by the supervisory control and the telemetering being accomplished over the supervisory control channel. With such an arrangement the number of telemetering transmitters and receivers can be kept to a minimum since the same transmitter and receiver can be used to telemeter any number of quantities of the same type. For example, a single transmitter can be used to telemeter watts from any number of circuits if the current and potential coils of the transmitter can be selectively connected to the various potential and current transformer circuits. Such switching of potential transformer circuits constitutes no problem, but the switching of current transformer circuits requires special precautions.

Relays with reliable make-before-break contact adjustments must be employed for the switching of current transformer secondary circuits. Additional safeguards against the possible opening of a current transformer circuit are sometimes provided. One such additional safeguard consists of the use of auxiliary transformers in each circuit which saturate at a relatively low ohmic burden and prevent excessive voltages from appearing even if there is a failure in the make-before-break adjustment of the selective relays. Film cutouts are sometimes connected across the contacts of the switching relay. These film cutouts are chosen so that they will break down and permanently short-circuit the current transformer circuit if an open circuit results for any reason. Resistors are sometimes connected across the selective relay contacts as shown in Fig. 12 to limit the voltage which can result if there is a failure of the make-before-break relay contacts. It is apparent from Fig. 12 that this arrangement does not allow all of the transformer current to pass through the telemetering transmitter since the resistors are effectively in parallel with the transmitter. When this arrangement is employed, the design and calibration of the telemetering equipment must take this fact into consideration.

The type of telemetering equipment

employed for selective telemetering from a remotely controlled substation is governed primarily by the type of channel provided for the supervisory control. When a metallic circuit is employed, telemetering equipment whose operation is based on the circulation of a small value of direct current over the interconnecting circuit can be used. Economies in the cost of telemetering equipment can be realized when such d-c systems are used. When the supervisory control operates over a leased or privately owned telegraphic-type channel as can be obtained with telephone-line carrier, power-line carrier, or microwave equipment, the telemetering equipment must be of the pulse rate or pulse duration type.[9-11] Most of the commercially available telemetering equipment of the pulse or frequency type can usually be employed for operation over such channels.

Conclusions

The control and position indication of circuit breakers is usually the primary function of any system for the remote operation of electric utility substations. When no automatic equipment of any kind is involved in the operation of the circuit breakers, the application of remote-control equipment is simple. When automatic reclosers of any type are involved, the application becomes somewhat more complex. This is primarily because the design of commercially available reclosers is based on the use of stayput contacts in the reclosing circuit. Since stayput contacts cannot be connected in series or in parallel if a satisfactory control circuit is to result, the usual reclosing circuits must be modified when a substation is remotely operated.

Typical schematic diagrams have been presented diagrams involving the use of a number of different types of automatic reclosers. All of the schemes presented have no operational limitations since a circuit breaker can be tripped from either location and closed from the other location. The principles of operation indicated in the diagrams are applicable to automatic reclosing arrangements other than those shown.

The circuitry for circuit-breaker control becomes more involved when closing can only be effected through automatic synchronizing or synchronism check equipment, since economics dictate the use of a common set of such equipment regardless of the number of circuit breakers involved.

While circuit-breaker operation and indication is the primary function which must be performed in a remotely operated substation, individual applications may involve disconnecting switch operation and tap-changer control. In addition, various alarm functions are often provided for and telemetered indications of important electrical quantities are frequently desirable.

References

1. System Centers Its Operations in New Underground Control Room, **J. L. Davidson, J. R. Gummersoll.** *Electrical World*, New York, N. Y., Nov. 30, 1953, pp. 78–80.

2. Penelec Consolidates Communication in Strategic New Dispatching Center, **C. H. Conrad.** *Ibid.*, Dec. 28, pp. 94–95.

3. Eugene Adopts Supervisory Control, **J. I. Fuller, J. G. Kirwan.** *Ibid.*, Jan. 11, 1954, pp. 96–97.

4. Supervisory Control and Remote Control Help TVA Cut Operating Costs, **R. M. Alspaugh, A. P. Maness.** *AIEE Transactions*, vol. 73, pt. III, Aug. 1954, pp. 863–69.

5. Leased Channels for Metering and Control, **H. H. Joyner.** *Electric Light and Power*, Chicago, Ill., Dec. 1953, pp. 100–06.

6. The Combination of Supervisory Control with Other Functions on Power-Line Carrier Channels, **R. C. Cheek, W. A. Derr.** *AIEE Transactions (Electrical Engineering)*, vol. 64, May 1945, pp. 241–46.

7. Channels for Operation of Supervisory Control Equipment, **W. A. Derr, M. J. Brown.** *AIEE Transactions*, vol. 67, pt. II, 1948, pp. 1654–60.

8. Microwaves in the Electric-Power Field, **W. A. Derr, D. F. Burnside, H. W. Lensner.** *Ibid.*, vol. 71, pt. III, Oct. 1952, pp. 910–17.

9. An Electric Telemetering System, **Carl Oman.** *Radio and Television News*, Radio-Electronic Engineering Edition, Chicago, Ill., Oct. 1952, pp. 14–16.

10. A High-Speed Telemetering System with Automatic Calibration, **W. E. Phillips.** *AIEE Transactions*, vol. 70, pt. II, 1951, pp. 1256–61.

11. Remote Measurement and Control, **W. E. Rufleth.** *The Petroleum Engineer*, Dallas, Texas, Oct. 1952, pp. D-20.

◆

Discussion

S. S. Watkins (Gibbs & Hill, Inc., New York, N. Y.): The paper is a valuable contribution to the literature of electric control, because of its clear presentation of the fundamental principles that affect control problems. It will be especially useful to the engineer who must design the control of substations to satisfy operating and maintenance requirements, using commercially available equipment with a minimum of special features.

While the circuits for local and remote control of automatic reclosing are valuable in themselves as circuits for specific equipment, they have an additional value in the fundamental treatment of momentary and stayput contacts and the problems presented when more than one point of control is used. Similar methods of analysis should apply to local and remote control of the automatic starting equipment for rectifiers, motor generator sets, and hydroelectric generators.

Under "Remote Control Cutoff or Transfer" the paper mentions that it is possible to use a contact that closes in the pullout position of the local control switch, in series

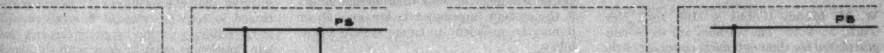

Fig. 13 (left) and Fig. 14 (right). Supervisory control circuits with the contacts of the remotely operated control relays so that the switch must be in the pullout position before remote control can be effected. Since the control switch can be placed in the pullout position only by going through the trip position, we would not usually consider this a satisfactory operating arrangement. However, this section is valuable for reviewing the different possible arrangements. Since the type of control transfer is closely related to the methods of system operation and maintenance, this subject deserves early discussion with the engineer who will operate the system.

In the discussion of supervisory control circuits under "Remote Lamp Indication," it is gratifying to note that the authors recognize a weakness in the practice of using only a single *a* or *b* auxiliary switch for both the red and the green lamp indications of circuit-breaker position. In my own organization we specify that each change of indication of a red or green indicating lamp on the control-station panel shall be initiated only by an energized circuit through an auxiliary contact of the supervised apparatus, and that loss of supervision current from any piece of supervised apparatus shall cause both lamps to be dark and shall cause the usual alarm signals to sound in the control station.

This specification for reliable indication of circuit-breaker position can be satisfied by either of the circuits shown in Figs. 13 and 14. Each circuit is in actual use and each uses three wires from the circuit breaker to the supervisory control panel. In Fig. 13 a single supervision wire is energized positive or negative for the two positions. In Fig. 14 separate red-lamp and green-lamp wires are energized positive for the respective positions. I suggest the use of Fig. 14 as a desirable standard circuit for the following reasons:

1. The standard circuit has some similarity to lamp circuits that are commonly used in local control.
2. It avoids the permanent connection of any coil to positive polarity, which, under some conditions, has caused deterioration of insulation.
3. It avoids the possibility of short-circuiting positive and negative busses in case of faulty adjustment of auxiliary switches.

W. M. Moody (Gibbs & Hill, Inc., New York, N. Y.): The authors are to be congratulated for their extensive coverage of the circuitry of remote control. My comments apply to the application problems of remote synchronizing. The authors cover quite adequately a system of interlocks to prevent connecting two sets of synchronizing potential together. Interlocks are obviously desirable, but they do not solve all the problems of remote synchronizing.

Automatic synchronizers are surprisingly accurate when they are adjusted to perform one function under a given set of conditions; but when they are required to perform two or more widely different functions, special provisions are required to obtain a comparable degree of accuracy, or careful consideration is needed to determine that the error introduced is acceptable. One of the most obvious problems is encountered where breakers of different voltage, vintage, or manufacture have appreciably different closing times. Accurate synchronizing requires that breaker closing be initiated several degrees ahead of synchronism so that by the time the breaker contacts close the voltages will be in phase. The error introduced by different closing times is usually tolerable and can be minimized by setting midway between the two closing times and by holding the allowable frequency difference to a low value; in extreme cases an auxiliary timing relay may be used to add delay to the fast-closing breaker.

More serious error is introduced when common equipment is used for different functions such as synchronizing and synchronism check. Automatic synchronizers are not synchronism check relays and will not initiate closing unless a frequency difference exists across the breaker. However, synchronizers are frequently supplemented with a time-delay voltage relay so that the two operating together will function as a synchronism check relay. The objection to this arrangement is that the setting of the synchronizer must usually be modified to accept a static phase angle and the error introduced may not be tolerable. As an example, consider the two following simplified conditions:

A transmission loop open at one end will have a static phase angle across the open breaker due to reactive drops around the loop. This angle may be as much as 30 degrees or even more, but a study of the system will usually show that the breaker can be closed without serious shock to the system or damage to equipment. If, however, closing is to be initiated by the synchronizer and voltage relay, it will be necessary to set the synchronizer to accept the static angle of, say, 30 degrees.

If now this same synchronizer is to be used for synchronizing two machines or two systems, the setting used to accept the static angle will cause an equal synchronizing error, i.e., will cause the machines to be paralleled when they are 30 degrees out of synchronism. An error this large may be sufficient to stress the generator shaft or the stator windings beyond their design limits if the system impedance is low enough or it may be sufficient to cause system instability.

To avoid situations of this nature, it is standard practice of my company to specify a synchronism check relay if the system is such that synchronism can be established over two or more circuits. The separate devices are then adjusted without compromise to perform the function for which they are intended.

Automatic synchronizers will not initiate closing if the voltage magnitudes are vastly different, but they will accept a greater difference than is generally desirable. The angular error introduced in synchronizing is usually tolerable, but large reactive surges may result. For this reason some type of voltage telemetering is usually desirable so that the dispatcher may determine that voltages are within limits before initiating synchronizing. Some type of slip-frequency telemetering is also a common requirement so that the dispatcher can determine whether the incoming machine or station is fast or slow and approximately how much.

Although remote synchronizing has several problems, the solutions to the problems are straightforward and the end result is more accurate synchronizing than is usually obtained by manual means. Experience has shown that automatic synchronizing within 1 or 2 degrees can be obtained within a reasonable test time. I should like to make two suggestions for testing automatic synchronizers:

1. A phase shifter with slip rings can be rotated at low speed to operate as a frequency changer and thereby give a constant slip frequency. Such a source is more easily manipulated, is faster, and is more accurate than using a large generator, and does not interfere with normal operation.
2. A 2-pen high-speed recorder is more accurate than a synchroscope for testing the synchronizer settings and gives a permanent record of the performances. One pen should be connected across the breaker contacts to show the instant of closure; the other should be connected to receive the difference voltage (equivalent to voltage across the breaker). The two pens together show the voltage across the breaker at the instant the contacts close, and by proper adjustment of the synchronizer the breaker will close when the voltage is zero.

W. A. Derr and W. L. Metz: We are extremely grateful for the excellent discussions of Mr. Watkins and Mr. Moody. Each of these discussions has amplified important considerations involved in the design of remotely operated electric utility substations, and are therefore valuable additions to our presentation.

Comments on the remote control cutoff arrangement employing contacts of the local control switches are given in the third paragraph of Mr. Watkins' discussion. He has inferred that the local control switch mentioned in our paper could only be placed in the pullout position by going through the trip position as must be done with standard breaker control switches. The control switch which we briefly described would be arranged so that it could only be placed in the pullout position from the off position. Therefore, the remote control could be cutoff or placed back in service regardless of the position of the breaker.

We are in complete accord with the other comments and description given by Mr. Watkins as well as with Mr. Moody's discussion of remote synchronizing.

Operation of Turbine Generators During Off-Peak High Power-Factor Periods—Practices of One Utility in a Metropolitan Area

W. J. ROBERTS
NONMEMBER AIEE

R. L. WEBB
FELLOW AIEE

BEFORE the beginning of World War II, the Consolidated Edison 60-cycle system operated with the load distributed mainly from the generating station busses with relatively low-capacity intermediate-voltage tie feeders interconnecting the major stations from north to south. The largest of the several interstation ties was rated about 40 megavolt-amperes (mva). Some operated at 13 kv and some at 27 kv.

In general, the load power factors of that time, measured at the generating station bus, varied from 0.83 to 0.85 during the day load and dropped to 0.78 to 0.80 during the early morning hours of off-peak load operation. These loads were carried with generator terminal power factors (pf) varying from 0.80 minimum during the day to 0.75 during off-peak operation. Capacitive loading consisted of the 13-kv and 27-kv distribution feeder cables plus a small amount of 4-kv distribution feeder capacitors.

Since the beginning of World War II, the 60-cycle system has experienced a peak load increase of 61 per cent with a corresponding increase of 65 per cent in generating capacity and has been equipped with a double-circuit high-voltage (138-kv) tie-feeder system between the north and south ends of the area served. In addition, one new generating station has been built to supply power directly into this tie-feeder network. Area substations supplied from the high-voltage circuits have been constructed to supply medium-voltage distribution systems direct from the 138-kv circuits.

The new 138-kv system circuits are made up of pressure-pipe type and oil-filled cable feeders. These, including the older 138-kv cables between Westchester County and the Hell Gate Generating Station, have added a total of approximately 295 capacitive megavars (mvar) to the system load at normal voltage. Also, the installation of unswitched capacitors on the 4-kv distribution part of the system have added an additional 85 mvar.

All of this increase in capacitive load has been very helpful in assisting to supply the load and system equipment demand for mvar during the high-load period of the day but it has caused the early morning light load pf of the system to increase to approximately 0.97 lagging. As the system develops, it is anticipated that the early morning load pf will soon be slightly leading.

To complicate further this over-all problem of light load operation, the generators installed during the early 1930's were 1,800 rpm units having short-circuit ratios of approximately 1.0, while since World War II, the new units have generally been 3,600 rpm machines with short-circuit ratios varying from 0.9 to 0.7, and the outlook to the future is for even lower short-circuit ratios at maximum turbine capabilities.

It is the object of this paper to review the nature of the problems associated with the foregoing trends, system loads, and generator characteristics from an operating engineer's viewpoint. The method of approaching a solution to the situation on this particular system is described herein.

System and Loads

A simplified diagram of the present 60-cycle system is shown in Fig. 1. It gives the connected generating capacity at each station and indicates the major distributing points, wherever they may be, at the generator bus or at the area substation. It shows also the day-load operating conditions and associated bus pf. In this case, the summer load conditions are given since load pf are lower at this time of the year because of the effects of rather heavy air-conditioning demands in the city. The diagram shows the medium-voltage tie circuits between the generating stations which remain unchanged, while the high-voltage circuits form a new low-impedance tie from one end of the system to the other. Voltage and angle regulators are used in the medium-voltage tie feeders to control reactive and power flow respectively between the generating stations.

Fig. 2 shows the same simplified diagram, giving typical connected generation, station loads, and bus power factors for system conditions experienced during the early morning hours when the light load of the 60-cycle system is approximately 700 megawatts (mw). In this case, a day in April was chosen since air-conditioning loading is small at that time of the year.

As already pointed out, Figs. 1 and 2 show that the 138-kv cable circuits, whose one-way distance between Hudson Avenue Station and Dunwoodie Substation is approximately 34 miles plus the 8 miles of single-circuit cable to Sherman Creek, add approximately 295 capacitive mvars to the system. Though this is quite acceptable and, in fact, beneficial during the day-load period shown in Fig. 1, it increases the average pf of the system during the off-peak morning hours to approximately 97 per cent lagging. Since it is impracticable to keep all generators operating at the system average pf, some machines operate at unity, or slightly leading, while others operate at a pf somewhat below the average, depending upon bus voltage requirements.

Considering that system development plans now in progress call for the addition of approximately 18 miles, 70 mvar of 138-kv cable circuits and that the unswitched capacitor additions to the system during the next 5 years could be approximately 75 to 100 mvar, it is expected, with the normal load increase during that same period, that the early morning hour average generator pf will become leading.

Limits of Generator Operation

Since about 4 years ago when the last large complement of high-voltage cable was added to the system, there has been some concern about the possibility that unstable operation of the system generators during the early morning may result in case certain contingencies should occur which require relatively large load pickups by the machines then in service. Since the transient stability of generators is

---

Paper 55-120, recommended by the AIEE Rotating Machinery Committee and approved by the AIEE Committee on Technical Operations for presentation at the AIEE Winter General Meeting, New York, N. Y., January 31-February 4, 1955. Manuscript submitted October 21, 1954; made available for printing December 7, 1954.

W. J. ROBERTS and R. L. WEBB are with the Consolidated Edison Company, New York, N. Y.

little affected by operating pf, the steady-state stability of the machines was determined for the most severe type of system disturbance which could reasonably be expected, with a sizable factor of safety added to it. It has been concluded, after a study of the various possibilities, that the greatest probable loss of capacity which may be expected at that hour of the morning would interrupt approximately 200-mw flow into the system. This would occur if one generator at Astoria Station is tripped automatically or if the Niagara-Mohawk tie feeders are interrupted while supplying their rated capacity into the northern end of the system. The possibility of additional capacity disconnections which might conceivably occur at the time of trouble in one element of the system, should there be an incorrect operation by one of the protective relays, is not considered in these assumed losses.

The minimum spinning capacity on the system in the early morning hours is approximately 1,000 mw. Since the maximum generator loss is estimated to be approximately 200 mw, with some possible additional loss being a possibility, this figure was increased by an arbitrary 50 per cent to allow for this additional contingency plus the differences in turbine governor performance which will result in some variation in the percentage of the load pickup by the different machines. The resulting 300-mw load change is approximately 30 per cent of the mva rating of the remaining generators on the system, or about 35 per cent of the mw rating of the same units.

In view of the aforementioned operating condition and to understand the approach made in the calculations described in the Appendix, it should be mentioned at this point that none of the generators on this closely knit system are at present supplied with high-speed excitation response equipment. A few of the recently installed units and one of the older machines are equipped with automatic voltage regulation of the motor-operated rheostat type to provide operating convenience or to improve machine stability where the short-circuit ratio of the unit is below 0.75 at maximum turbine rating. Accordingly, the stability calculations have been based upon the steady-state operating conditions only.

Since the objective of this investigation was to provide curves which would show limits of permissible operation for the system generators, it was desired to provide characteristics covering the entire range of operation from early morning light load conditions to the normal day peak load machine capability. The several generator operating limits which came under close study in this investigation are:

1. Field excitation. The excitation limits are determined by exciter capability, temperature rise in the main generator field winding at the operating hydrogen pressure, and mechanical stresses imposed on the field winding resulting from expansion and contraction forces caused by temperature variations with changes in machine loading.

2. Stator thermal capability. The stator winding temperature limit was taken as that specified by the manufacturer for the different hydrogen pressures at which the machine may be operated. The latest recommendations for resistance temperature detector indications, at all permissible hydrogen pressures, were used.

3. End-turn area heating. Heating of the metal structures in the end-turn area of the machine because of high-leakage flux which occurs when operating at high or leading pf was discussed with the respective manufacturers, and their recommendations were worked into over-all machine capability curves to avoid exceeding maximum recommended temperatures in the structural and support members at this point.

4. Steady-state pullout. The steady-state pullout loading in mw for the initial operating condition of each generator, with the imposition of the system contingency assumed, was determined by calculation over the entire operating range of the machine. A sample calculation of the type used is presented in the Appendix.

5. Loss-of-field relays. It is the practice of the authors' company to use reverse reactive current relays for generator loss-of-field protection. It becomes necessary, therefore, to limit the amount of reverse reactive kilovolt-amperes which the generators may carry, particularly at light and heavy mw loadings.

Results of Stability Calculations—Machine Thermal Limits

Curve *A-A* of Fig. 3 shows the calculated initial loading of a generator which would allow the assumed increment of load to be picked up by that machine, immediately following the assumed system contingency, without the generator becoming unstable electrically even though no change was made in the operating field current. As the initial load on the generator is increased, a point is reached beyond which the turbine cannot pick up an additional 30 per cent of its mva rating. From this point on, the new stability criterion, namely, field strength or internal voltage sufficient to carry full turbine output stably gives a new curve shown in Fig. 3 as *B-B*. Since the stability limit

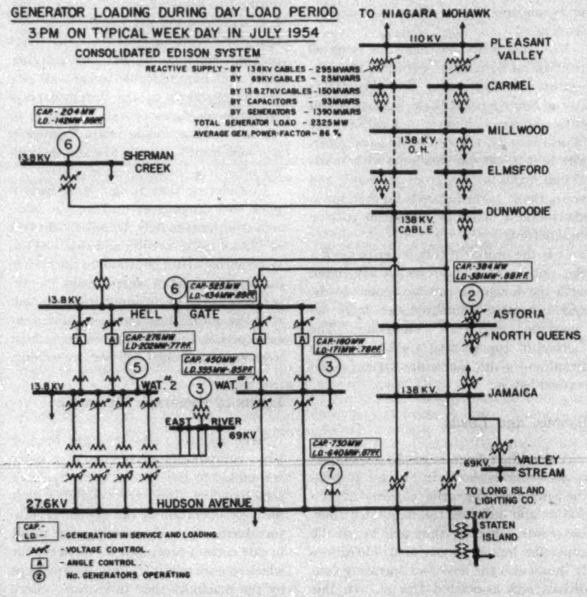
GENERATOR LOADING DURING DAY LOAD PERIOD
3 PM ON TYPICAL WEEK DAY IN JULY 1954
CONSOLIDATED EDISON SYSTEM
REACTIVE SUPPLY - BY 138KV CABLES - 295MVARS
BY 69KV CABLES - 25MVARS
BY 13 & 27KV CABLES - 150MVARS
BY CAPACITORS - 93MVARS
BY GENERATORS - 1390MVARS
TOTAL GENERATOR LOAD - 2325MW
AVERAGE GEN. POWER-FACTOR - 86 %
TO NIAGARA MOHAWK
110KV
PLEASANT VALLEY
CARMEL
MILLWOOD
138 KV. O. H.
ELMSFORD
DUNWOODIE
138 KV. CABLE
CAP. - 204 MW
LD. - 142MW .86PF
6
13.8KV
SHERMAN CREEK
CAP. - 384 MW
LD. - 381MW - .88 P.F.
2
ASTORIA
NORTH QUEENS
6
CAP. - 525 MW
LD. - 434 MW .83 PF
13.8 KV
HELL GATE
A
CAP. - 276 MW
LD. - 202 MW - .77 P.F.
CAP. - 180 MW
LD. - 171 MW - .78 P.F.
CAP. 450 MW
LD. 395 MW - .85 P.F.
5
3
3
13.8 KV
WAT. #2
WAT. #1
138 KV.
JAMAICA
EAST RIVER
69KV
CAP. - 730 MW
LD. - 640 MW - .87 P.F.
7
69KV.
VALLEY STREAM
TO LONG ISLAND LIGHTING CO.
27.6KV
HUDSON AVENUE
33KV
STATEN ISLAND
CAP. - LD. - - GENERATION IN SERVICE AND LOADING.
- VOLTAGE CONTROL.
A - ANGLE CONTROL.
② No. GENERATORS OPERATING

Fig. 1. System tie connections and generation, day load conditions, summer period

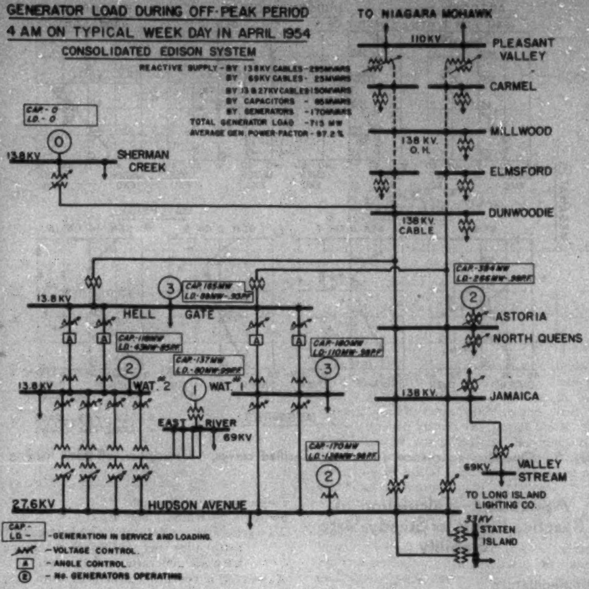
GENERATOR LOAD DURING OFF-PEAK PERIOD
4 AM ON TYPICAL WEEK DAY IN APRIL 1954
CONSOLIDATED EDISON SYSTEM
REACTIVE SUPPLY - BY 138KV CABLES - 295MVARS
BY 69KV CABLES - 25MVARS
BY 13 & 27KV CABLES 150MVARS
BY CAPACITORS - 65MVARS
BY GENERATORS - 170MVARS
TOTAL GENERATOR LOAD - 715 MW
AVERAGE GEN. POWER-FACTOR - 97.2%
CAP - 0
LD. - 0
0
138KV
SHERMAN CREEK
TO NIAGARA MOHAWK
110KV
PLEASANT VALLEY
CARMEL
138 KV. O. H.
MILLWOOD
ELMSFORD
DUNWOODIE
138 KV. CABLE
CAP-384MW
LD-266MW-98PF
2
ASTORIA
NORTH QUEENS
138 KV.
JAMAICA
69KV
VALLEY STREAM
TO LONG ISLAND LIGHTING CO.
33KV
STATEN ISLAND
3
CAP 165MW
LD-88MW-93PF
13.8 KV
HELL GATE
A
CAP-118MW
LD-43MW-85PF
CAP-137MW
LD.-80MW-99PF
CAP-180MW
LD-110MW-98PF
2
WAT. #2
1
WAT. #1
3
13.8 KV
EAST RIVER
69KV
CAP-170MW
LD-128MW-98PF
2
27.6KV
HUDSON AVENUE
CAP.-
LD. -
-GENERATION IN SERVICE AND LOADING.
-VOLTAGE CONTROL.
A
- ANGLE CONTROL.
2
- No. GENERATORS OPERATING

Fig. 2. System tie connections and generation, early morning load condition, spring period

of most generators determined in this way allows considerably more leading kilovolt-amperes to be carried than is practically necessary with present-day system loads, an additional safety margin was applied which amounts to approximately 20 per cent of the generator mva rating. This results in a new curve shown in Fig. 3 as *C-C;* see the Appendix.

It will be noted that the lower end of this curve is cut off at approximately 44 mvar leading. This is done to prevent the reverse reactive current loss-of-field relays from closing their contacts. Though the operation of this relay alone would not cause tripping of the generator, the development of a bus voltage dip causing an undervoltage relay to operate would disconnect the machine from the system. This loss-of-field relay limitation allows the generator to carry approximately 67 per cent of the loss-of-field relay setting, which is usually 35 to 40 per cent of generator mva rating. Data of these types were determined for all system generators and have been issued to the operating department for guidance in operating each machine.

Fig. 4 shows a typical characteristic giving the generator thermal limits as determined by maximum field current, stator or ampere capabilities, and permissible mvar as limited by leakage flux in the end-turn area, when operating underexcited. Care should be taken to find out whether the field current limits are determined by winding temperature or by mechanical stresses in the winding created by the forces of expansion and contraction working against the tendency for the winding to be held stationary because of high centrifugal forces. The stator winding current limit is specified by the manufacturer. He may find this limit to be determined for long machines by expansion and contraction effects rather than by actual temperature, when operating at the higher hydrogen pressures. The end-turn metal temperatures caused by leakage flux are best determined and recommended by the machine manufacturer.

Operating Experience

Curves of the type described herein have been in use as a guide to the station operators for about 5 years. They are still being used on this basis. The curves of Fig. 5 duplicate the stability limit curves of Fig. 3 for a number of generators on the system which customarily operate through the early morning hours of the day. The operating points for these machines taken during the early hours of the day are plotted beside the recommended operating characteristic. It will be noted that, in some cases, the operating experience with the system as it is today indicates that the normal operation of the machines is coming close to the characteristic determined and described in this paper.

It is anticipated, therefore, that some of the safety margin which was taken in the construction of curve *C-C* in Fig. 3 must soon be given up as the cable system is increased and the installed unswitched capacitors are increased in total mvar during the next few years. It will, of course, be possible to move curve *C-C* even farther into the leading direction should a decision be reached to install fast-acting

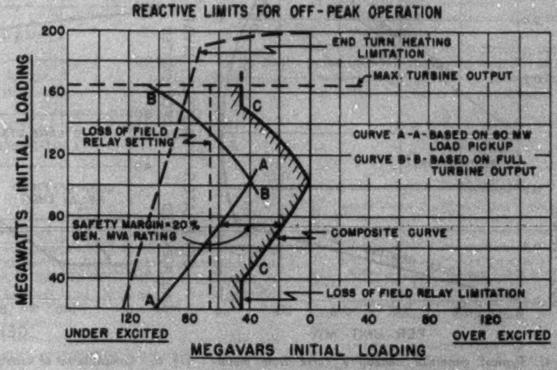

Fig. 3. Curves showing results of generator mvar capability calculations

regulators on those machines which usually operate during the early hours of the day. These machines would, of course, be those which form the most efficient combination in the several stations.

Operating Curves

Fig. 6 presents an actual set of curves used for one of the larger machines to maintain stable operating conditions during the early part of the day. The different sections of each curve may be identified to show how the limits determined and plotted in Fig. 3 are applied in the operating instructions for that particular machine, as a guide to the control room operator in loading that unit.

Conclusions

1. Turbogenerators can be successfully operated at high or slightly leading pf if operating personnel are provided with guides pointing out limits which should properly be observed. One means of doing this is described in this paper.

2. The limits of permissible minimum generator field currents can be lowered with the installation of fast-response excitation-control equipment.

3. With the application of reasonable safety factors, suitable generator steady-stability limits can easily be established for a wide range of operating conditions.

4. The use of reverse reactive current loss-of-field relays provides a means for automatically disconnecting a generator from the system, before loss of synchronism, in case minimum field current limits should not be maintained in the machine.

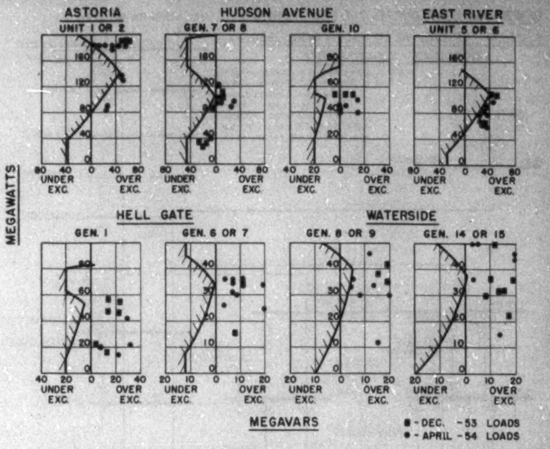

Fig. 5. Operating experience data versus specified curves, 14 machines, off-peak loading

Appendix. Calculation of Reactive Limits for Steady-State Stability

Nomenclature

P = real power, per unit (pu)
Q = reactive power, pu
P_m = pullout power, pu
E_d = pu voltage behind generator reactance
E_b = pu bus voltage
E_s = pu voltage behind equivalent system generator reactance
I = pu generator current
θ = angle by which I lags E_b
X_d = generator reactance (1/short-circuit ratio) plus any additional reactance between generator and bus, pu
X_s = external reactance measured from bus, pu
Z_L = load impedance

All pu values must be on same arbitrarily selected base

The pu system is used, with either the generator rating or 100 mva arbitrarily chosen as the base.

Then from the simplified diagram of Fig. 7, the pullout power

$$P_m = \frac{E_d E_s}{X_d + X_s}$$

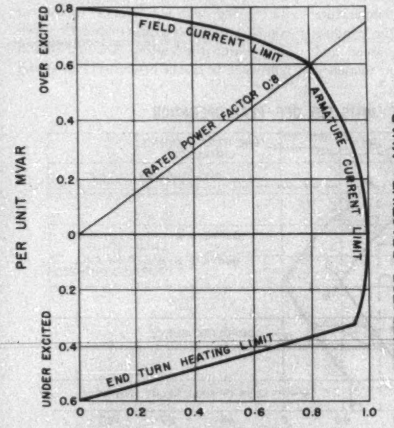

Fig. 4. Typical generator capability curve from manufacturer's data

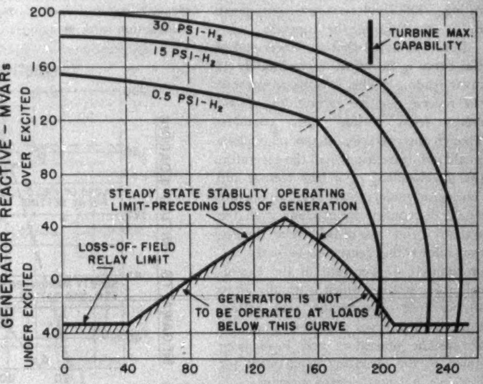

Fig. 6. Complete set of capability curves for one of the larger hydrogen-cooled system generators

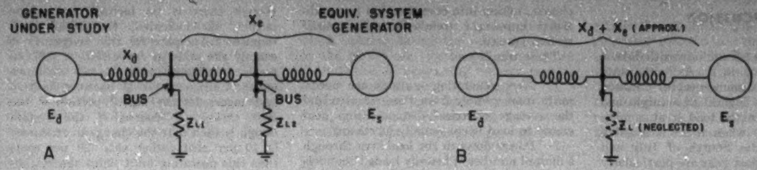

Fig. 7. Equivalent system diagram

A — Schematic diagram

B — Simplified diagram

or

$$E_d = P_m\left(\frac{X_d+X_e}{E_s}\right) \qquad (1)$$

Also

$$E_d = E_b + jIX_d = E_b + I\,(\cos\theta - j\sin\theta)jX_d$$

$$E_d = [(E_b + IX_d\sin\theta)^2 + (IX_d\cos\theta)^2]^{1/2}$$

but

$$P = E_bI\cos\theta, \text{ and } Q = E_bI\sin\theta$$

Substituting

$$E_d = [(E_b + QX_d/E_b)^2 + (PX_d/E_b)^2]^{1/2} \qquad (2)$$

Solving for Q

$$Q = \frac{[E_d^2 - (PX_d/E_b)^2]^{1/2} - E_b}{X_d/E_b}$$

or

$$Q = \left[\left(\frac{E_dE_b}{X_d}\right)^2 - (P)^2\right]^{1/2} - E_b^2/X_d \qquad (3)$$

Substituting for E_d its value in equation 1

$$Q = \left\{\left[\left(\frac{E_b}{E_s}\right)\left(\frac{X_d+X_e}{X_d}\right)P_m\right]^2 - P^2\right\}^{1/2} - E_b^2/X_d$$

When $E_b = 1$ pu

$$Q = \left\{\left[\left(\frac{X_d+X_e}{X_d}\right)(P_m/E_s)\right]^2 - P^2\right)^{1/2} - 1/X_d \qquad (4)$$

Curve *B-B* shown in Fig. 3 may be obtained from the foregoing equation either by graphical construction or by substituting values of P and solving for Q since all other quantities are known. In either case, curve *B-B* gives the limiting initial mvar for a given initial mw load, based on picking up full turbine output P_m.

When the recognized maximum contingency will result in a load pickup of 0.3 pu, the pull out power P_m should equal the initial load P plus the expected pickup of 0.3 (of generator rating).

$$P_m' = (P + \Delta P) = \frac{E_dE_s}{X_d + X_e}$$

or

$$E_d = \left(\frac{X_d+X_e}{E_s}\right)(P + \Delta P) \qquad (5)$$

where

$$\Delta P = 0.3\,\frac{\text{generator mva}}{\text{base mva}}$$

Substituting this value for E_d in equation 3

$$Q = \left\{\left[\left(\frac{X_d+X_e}{X_d}\right)(P+\Delta P)E_b/E_s\right]^2 - P^2\right\}^{1/2} - E_b^2/X_d$$

When $E_b = 1$ pu

$$Q = \left\{\left[\left(\frac{X_d+X_e}{X_d}\right)\left(\frac{P+\Delta P}{E_s}\right)\right]^2 - P^2\right\}^{1/2} - 1/X_d \qquad (6)$$

It will be found more convenient to work with equation 6 in the form given than to reduce it further. The reduction in bus voltage which takes place when load is picked up will reduce the initial load. To avoid further complication, and since the 0.3 load pickup is a rough estimate, this reduction in initial load was considered an added safety margin.

When values of P are substituted in equation 6, values of Q are obtained for plotting curve *A-A*. This curve gives the limiting initial mvar which can be carried by the generator with an initial mw load and safely pick up an increment of load equal to 0.3 of its mva rating.

To apply the foregoing to a practical case, this example will use generator 7 at Hudson Avenue Station. This is an air-cooled single-shaft 200-mva 0.8-pf 16.5-kv generator connected to a 27.6-kv bus through a 16.5/27.6-kv autotransformer. The short-circuit ratio on 200 mva, 16.5-kv is 1.00. The autotransformer reactance is 2.5 per cent on a 100-mva base. The reactance from the bus to the equivalent system generator based on calculating board studies is 18 per cent on the same base. Expressing all reactances in pu on a common 100-mva base

$$X_d = \frac{1}{1.00}\left(\frac{100}{200}\right) + 0.025 = 0.525$$

$$X_e = 0.18$$

Substituting in equation 4, for a bus voltage of 27.6 kv (1 pu) and a maximum turbine capability of 165 mw

$$Q = \left\{\left[\left(\frac{0.525+0.18}{0.525}\right)\left(\frac{1.65}{1.21}\right)\right]^2 - P^2\right\}^{1/2} - \frac{1}{0.525}$$

$$= [3.37 - P^2]^{1/2} - 1.90$$

The value of 1.21 for E_s is the calculated voltage behind synchronous reactance for the off-peak load on the equivalent system generator. For a loosely connected system, the determination of E_s will require experience and judgment. By calculating Q for $P = 1.0$, 1.2, 1.4, and 1.6, curve *B-B* is obtained.

Similarly, when known values are substituted, equation 6 becomes

$$Q = [1.24(P + 0.6)^2 - P^2]^{1/2} - 1.90$$

By calculating Q for $P = 0$, 0.4, 0.8, and 1.2 curve *A-A* of Fig. 3 is obtained.

The intersection of curves *A-A* and *B-B* is a point whose mw value is equal to the maximum turbine capability less the assumed load pickup of 30 per cent of the generator mva rating. Above this mw value, the turbine can no longer pick up a load equal to 30 per cent of rating and the criterion of stability becomes full turbine output.

Also shown in Fig. 3 are the manufacturer's end-turn heating limits, modified for the autotransformer reactive losses. The loss-of-field relay setting for this generator is 66 mvar. This setting is a function of transient stability, breaker tripping time, and available taps on the relay.[1] To prevent reaching the relay setting value, 67 per cent of the setting has been selected as the limit for operation.

To the calculated stability limits has been added an arbitrary safety factor equal to 20 per cent of the generator mva rating, to be plotted along the mvar scale so as to move the curve in the overexcited direction. No safety margins were added to the end-turn heating limits supplied by the manufacturers. For this generator, the end-turn heating does not constitute a limit in the underexcited region. The composite curve *C-C* is shown in Fig. 3 in heavy lines. It is composed of portions of the two stability limit curves referred to in the foregoing and the loss-of-field relay limit.

The schematic circuit shown in Fig. 7 may be reduced to the simplified circuit. Because of normal variations in load distribution and pf, it was considered sufficiently accurate to use $(X_d + X_e)$ for the transfer impedance and to neglect the effect of the nearly unity pf loads.

Using the simpler criterion of an infinite bus,[2] the calculated stability limits will be somewhat on the underexcited, or optimistic, side of curves *A-A* and *B-B* of Fig. 3 for the example given. To avoid confusion, the infinite bus limits are not shown.

References

1. LOSS-OF-FIELD PROTECTION FOR GENERATORS, G. C. Crossman, H. F. Lindemuth, R. L. Webb. *AIEE Transactions (Electrical Engineering)*, vol. 61, May 1942, pp. 261–65.

2. GENERATOR STABILITY AT LOW EXCITATION, B. L. Michelson, L. F. Lischer. *AIEE Transactions*, vol. 67, pt. I, 1948, pp. 1–9.

3. UNDEREXCITED OPERATION OF TURBOGENERATORS, C. G. Adams, J. B. McClure. *Ibid.*, pp. 521–28.

4. STABILITY CHARACTERISTICS OF TURBINE GENERATORS, C. Concordia, S. B. Crary, J. M. Lyons. *AIEE Transactions*, vol. 57, 1938, pp. 732–44.

Discussion

Raymond S. Watts (Commonwealth Edison Company, Chicago, Ill.): As with other companies, the Commonwealth Edison Company finds the highest pf at night and on week ends when the load is at a minimum. Week ends when there is a 3-day holiday such as the Fourth of July and Labor Day of the past year are particularly troublesome.

On these long week ends, the total system load reached a minimum of 800,000 kw, approximately one-quarter of the system peak, with a total capacity running of 1,800,000 kw of large efficient units which it is not desirable to shut down.

Previous to last year it was the practice at these periods to switch out several large high-voltage cables, set the timing device on the switched capacitors so that they would be disconnected, and operate rotary-type condensors absorbing the maximum of vars. This enabled us to keep generators at slightly lagging pf. Even when these steps were taken, the voltage remained higher than normal. In recent years, 17 large generators have been equipped with modern voltage regulators and, for the first time, switched capacitors were left on their normal cycle over these holiday week ends. Generators were allowed to go slightly leading in pf, absorbing vars from the system.

For instance, a unit at Crawford Station absorbed 10 mvar with an output of 10 mw. A unit at Fisk and one at Calumet with 78 and 40 mw respectively, absorbed as much as 5 to 10 mvar and several other units running at the time had 0 vars or unity pf. No trouble of any kind was experienced.

Safe limits of leading pf with varying loads have been determined and the machines are always operated well within these values. At such times it is the practice and the intent to have all the voltage regulators in service that system conditions will permit.

H. O. Simmons, Jr., and **C. A. Woodrow** (General Electric Company, Schenectady, N. Y.): For a specific system, Mr. Roberts and Mr. Webb have clearly evaluated an important concept: the determination of generator kilowatt-kilovar loading guides designed to give successful system performance under planned emergency conditions. As they indicate, for a metropolitan system with relatively short electrical distance between generator and load and with a number of ties between stations, the use of generator voltage regulators can be avoided by the adoption of suitable generator loading guides based solely on steady-state stability considerations. However, as the authors also indicate, this solution becomes more and more difficult as the system growth includes more kilovar generation out in the system and less and less kilovar output from the generating station itself.

The authors conclude: "The limits of permissible minimum generator field currents can be lowered with the installation of fast-response excitation control equipment." The principal purpose of this discussion is to further evaluate this conclusion, taking into consideration two additional important trends in metropolitan system growth.

These trends are:

1. New generating stations are necessarily more remote from the load area and the average electrical distance from generator to load is continually increasing.
2. Power flows to the load area through a limited number of heavily loaded channels and the loss of any one channel can create a sudden increase in the electrical distance between generator and load.

Fig. 8 illustrates conditions which may be more severe than any of those evaluated by the authors but which are readily possible, i.e., an external system having 30-per-cent system reactance (based on maximum turbine rating) as viewed from the generator terminals. Fig. 8(A) shows initial operating limits without voltage regulators, with zero kilovar safety margin, and on the somewhat dangerous assumption that the generator terminal voltage will never be less than rated voltage. Curves *A-A* and *B-B* are based essentially on the quite logical assumptions used by Mr. Roberts and Mr. Webb. No turbine will be called upon to increase suddenly its output by more than 30 per cent of rating (curve *A-A*); above 70 per cent of initial turbine output, the maximum turbine incremental demand is the difference between turbine rating and the initial turbine output (curve *B-B*). As indicated, the most critical condition develops at around 70-per-cent turbine output. Here kilovar output cannot safely be reduced below 0.3 pu. This, we feel, would be unduly restrictive for many systems.

Fig. 8(A) also illustrates another limit, curve *C-C*, which becomes significant when the loss of a channel of power flow increases the external system reactance—in this illustration, from an initial value of 30 per cent to a final value of 50 per cent. At constant excitation (no regulators), this change in reactance causes a drop in generator voltage and introduces a significant steady-state stability limitation, even though there is no increase in turbine output. As indicated, the initial limit required to prepare for this emergency is exactly the same as curve *B-B* at 0.87 pu power. At higher loads, this new reactance change limit, curve *C-C*, becomes limiting and supersedes the dotted portion of the *B-B* curve. Of course, if the system design is such that the change in reactance is 10 per cent rather than 20 per cent, then this operating limit slides appreciably to the left, perhaps slightly into the underexcited region at maximum turbine rating rather than 0.25 pu overexcited.

Most users would find it highly undesirable to accept such operating restrictions as are indicated by Fig. 8(A), and Fig. 8(B) is included to indicate the influence of adding voltage regulators to this system. The reactance change limit, curve *C-C*, disappears and curves *A-A* and *B-B* become essentially one straight line with acceptable underexcited kilovars of 0.5 pu at maximum turbine rating and considerably more underexcited kilovars at lower turbine output. Such drastic underexcitation is seldom required and, therefore, ample margin normally exists for reducing the generator voltage by 5 per cent under system light load conditions. To all intents and purposes, steady-state stability limits have disappeared. Other considerations such as generator end-turn heating and the selection of suitable loss-of-excitation protection become governing.

On the system of Fig. 8, 30-per-cent initial reactance and a maximum of 50-per-cent final reactance, transient stability problems should not develop if modern high-speed relaying and circuit breakers are used. However, installations have been made and others are contemplated where this final reactance is considerably greater than 50 per cent. In these cases, transient stability can become a limitation even with the most modern generator voltage regulations and switchgear. Kilowatt-kilovar generator operating guides can become necessary, particularly where the planned schedule includes some reduction in generator terminal voltage during system light load conditions.

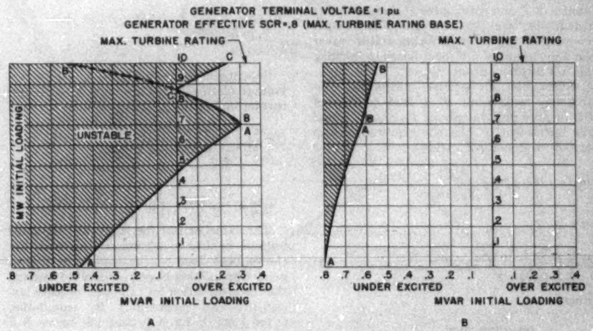

Fig. 8. Initial operating limits for steady-state stability on a 30-per-cent system

A—Without voltage regulator
B—With voltage regulator

W. J. Roberts and R. L. Webb: It is interesting to note that the experiences in Chicago, as described by Mr. Watts, are essentially the same as those in the New York City area. In fact, his early morning load level has about the same percentage characteristic with respect to the peak load level, as experienced in New York. There is little doubt that the generators which operate during the off-peak periods on the New York system will also require the addition of fast-acting voltage regulators as is now the case in Chicago.

Mr. Simmons and Mr. Woodrow have done a good job of showing the actual benefits of fast-acting voltage regulators applied to the operating characteristics of the generator referred to in the paper. We are, of course, pleased to know that they agree with the approach and assumptions used by us and we agree with them in regard to the future possibilities of voltage regulating equipment as the capacitance loading on the system increases.

Detection of Grounds in Generator Field Windings

J. E. BARKLE
MEMBER AIEE

C. C. STERRETT
MEMBER AIEE

L. L. FOUNTAIN
FELLOW AIEE

THE TREMENDOUS increase in the size of individual generating units in recent years has spurred the interest of operating engineers in at least two respects; first, because it means knowing more about the limitations and capabilities of the generator itself and, second, because of the available protective relays that will prevent the machine from exceeding its capabilities and incurring the risk of damage. There has been in the past a division of opinion among operators in their philosophy concerning keeping generators in service when some risk is involved. There are a number of different types of abnormal conditions that can occur in a generator without affecting its ability to generate kilowatts, but that do involve some risk of severe damage if the machine is kept in service. This risk is usually contingent on the slow development of the abnormal condition into a serious one or the occurrence of a second abnormality. Many operators have followed the philosophy that a generator should be kept in service to supply power to the ultimate consumer until an outage can be scheduled even though some weakness which might eventually lead to severe damage is known to exist in the machine. This practice has been influenced by shortages in reserve capacity to the extent that loss of a unit meant inadequate capacity to supply the load.

The diversification of reserve capacity by interconnections among several systems and a general increase in the amount of reserve capacity have altered this situation substantially, and it is now possible to remove a unit from service without jeopardizing the system. This reduces the necessity of assuming risks of damage to a machine to maintain service. The capital investment in a large modern generating unit is also a deciding factor. As a result, there is a greater tendency to operate generators without exceeding their capabilities, and to repair minor abnormalities as soon as they are discovered, even though a forced outage is necessary to do so. To accomplish this, the maximum capabilities must be known, and suitable instruments and protective devices must be available to detect abnormalities.

An excellent example of the recognition of a limitation of generating units is the development of a standard stating the ability of a unit to withstand an unbalanced external short circuit and the development of the generator negative-sequence current relay.[1-3] It was known that negative-sequence current in the armature of a generator would cause localized heating in the rotor structure, which if allowed to continue would cause a severe rotor failure. However, it was not until recently that the industry was able to establish a standard that relates the magnitude of armature negative-sequence current to the permissible time it can flow without causing damage. Relay engineers were then able to design a relay that permits the generator to carry its full capability in terms of negative-sequence current and then removes the generator from service to prevent damage. While this new relay is not yet widely applied, operators who are installing it are planning to connect it to trip the unit when the capability point is reached.

General Considerations of Generator Protection

Protective-relaying schemes have been developed to detect substantially all types of faults and abnormalities that might exist in generators. Schemes to detect internal faults usually take the form of some type of differential protection with parallel winding, or split-phase protection is used in some cases. Separate ground-fault relays are used where the minimum ground-fault current is below the sensitivity of the differential protection, and these relays may also operate for external faults. Some form of backup protection can be used to protect the machine against prolonged system faults.

Many specialized relays are available to detect specific abnormalities such as negative-sequence current, loss of field, motoring, out-of-step operation, single-phase operation, overspeed, overvoltage, excessive vibration, bearing insulation failure, etc. Application principles for all of these devices are discussed in the technical literature in more or less detail. In 1951, the Committee on Relays published a report[4] which included the results of a questionnaire on practices in the protection of a-c generators, and specific recommendations for modern protective schemes.

Generator Field Ground Detector

One facet of a-c generator protection that has not received sufficient study concerns detecting grounds in the field windings. There are many schemes available and in use for this purpose, and all of them have some weakness or shortcoming. The following discussion directs attention to the difficulties of detecting grounds in the field windings, and recommendations for effective protective measures are developed. The cylindrical-rotor type of generator is given primary consideration in the following, but the same statements and conclusions apply in some degree to salient-pole machines.

Paper 55-125, recommended by the AIEE Relays Committee and approved by the AIEE Committee on Technical Operations for presentation at the AIEE Winter General Meeting, New York, N. Y., January 31–February 4, 1955. Manuscript submitted October 21, 1954; made available for printing December 6, 1954.

J. E. Barkle, C. C. Sterrett, and L. L. Fountain are with the Westinghouse Electric Corporation, East Pittsburgh, Pa.

The authors acknowledge the work of M. J. Brown, Westinghouse Electric Corporation, in developing the nonlinear resistor scheme.

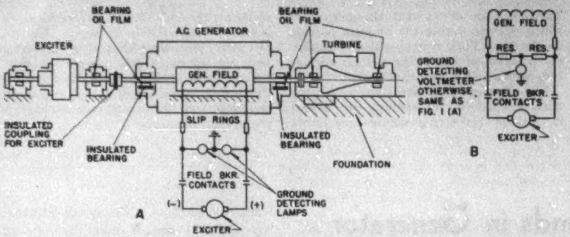

Fig. 1. A—Typical bearing arrangement on a modern a-c generator and turbine together with the field circuit equipped with lamps as a means of detecting grounds. B—Generator field circuit equipped with a voltmeter for detecting grounds; otherwise it is the same as in A

The Relay Committee report[4] makes the following statements concerning grounds on the field circuit of machines and ground detectors: "A ground on the field circuit is not serious in itself, but it indicates the presence of weakened insulation or mechanical failure, and serious damage may result if a second ground should occur. A simple form of ground indication consists of two lamps in series connected across the rotor winding with their mid-point grounded. This scheme of ground detection gives positive indication only for faults near the terminals of the field winding. More sensitive ground indication can be obtained by replacing the lamps with resistors and connecting the mid-point to ground through a sensitive relay. Complete coverage can be obtained in all cases by the use of a separate a-c supply with a low-voltage transformer. One terminal of the transformer secondary winding is connected to the field winding, while the other terminal is connected to ground through a sensitive relay." See Figs. 1 and 2.

Actually, as is developed later, none of these forms of ground indication can be considered as giving positive indication of a ground at any location in the field winding, and the use of a separate a-c supply involves some risk of further damage to the generating unit.

In the summary of replies to the questionnaire, the Relay Committee reported the following: "Thirty-five per cent provide no means for detecting a grounded field winding; 25 per cent depend on d-c ground lamps for indicating a grounded field [Fig. 1]; 15 per cent use some form of d-c voltmeter scheme; 13 per cent use both ground lamps and voltmeter; 12 per cent use an a-c relay with a transformer source [Fig. 2]." While this analysis shows considerable variation in practice, apparently 65 per cent of the operators are using some form of generator field ground detection.

The Problem

There are two factors that make the detection of generator field grounds difficult. First, the field circuit is normally isolated from ground, and even with constant voltage applied, the potential between the conductor and the rotor iron is variable, depending on the specific location in the winding. Under normal conditions, the capacitance to ground of the field winding forces a distribution of voltage so that the potential between each slip ring and the rotor iron is one-half of the applied voltage, and the potential to iron at the electrical center of the field winding is zero.

The second factor is found in the bearings of the machine. The generator designer provides insulation in both bearing pedestals so that a path for the flow of shaft current through the bearing pedestals and the bedplate does not exist. The reason for this is to prevent the damaging effect that current, even though very small, can have on the bearing surfaces. The turbine bedplate is generally a part of the station ground, and its bearing pedestals are available to connect the bedplate to the shaft electrically. Unfortunately, this connection is a poor one, because the bearing contains an oil film that can be an insulating barrier for low voltages and provides a path of low and variable conductivity at higher voltages. The conducting qualities of the bearing-oil film depend greatly on the quality and purity of the oil, clean oil being a poorer conductor than oil containing dirt or moisture.

Thus, one can conclude that the shaft and rotor of a turbine generator may be electrically isolated from the bedplate and station ground by the insulating properties of the bearing-oil film. At best, the path available to connect these parts electrically is one of questionable but probably poor conducting ability. Unfortunately, no factual data are available to indicate the magnitude of voltage that must be applied to an actual bearing-oil film to cause positive breakdown or to indicate the range of conductivities that might be encountered in practice. Both of these characteristics are highly variable and depend on many factors, including the thickness of the oil film, the area of the bearing surfaces, and the condition of the oil. Data on new clean oil are available however.

The lamps, voltmeters, or relays used to detect field-winding grounds are normally connected between the slip-ring brushes and the station ground. Even with the field winding solidly connected to the rotor iron, operation of the ground detector is dependent on the circuit between the shaft and the station ground, which includes the bearing-oil film. It is for this reason that the ability of these ground-indicating schemes to detect field-winding grounds is open to question.

Ground Detection Schemes

To show more specifically how these factors affect the operation of different schemes used to detect rotor grounds, a brief discussion is given of the principles on which the schemes are based.

LAMP AND VOLTMETER SCHEMES

The lamp and voltmeter schemes, which are the most widely used, are simple and easily understood. A typical example of each is illustrated in Fig. 1, but there are a number of variations that have been used.

The lamp scheme of Fig. 1(A) operates on the principle that the voltage to ground of each field lead is the same, and the voltages applied to the two lamps are equal. Under these circumstances, the lamps glow with equal brightness, but the brightness is a function of the excitation voltage applied to the generator field. With modern generator voltage regula-

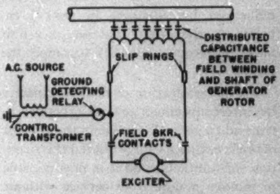

Fig. 2. Generator field circuit equipped with a-c ground relay and showing capacitance of field winding to shaft. Bearing arrangement the same as shown in Fig. 1(A)

tors, there can be considerable aperiodic variation in excitation voltage and consequently in the lamp brightness.

If the conductivity of the bearing-oil film is assumed to be excellent, and to form a good connection between the shaft and station ground, a ground at either terminal of the field winding will cause one lamp to be short-circuited and extinguished while the other lamp glows with greater brightness. It is then possible for the operator to determine that a ground has occurred and which terminal is grounded. A ground at the center of the field winding will not disturb the voltages to ground at the lamp location, and the ground is not indicated. For grounds at other locations in the winding, the degree of voltage disturbance and the probability of ground indication is between these two extremes.

On the other hand, if the oil film is assumed to be a poor conductor, insulating the shaft and rotor from the station ground, a ground at any point in the field winding will not be indicated by the lamps. The lamps in series across the excitation voltage divide the voltage equally and continue glowing with the same intensity.

The voltmeter scheme of Fig. 1(B) operates on the same principle as the lamp scheme. Under normal conditions, the voltage between the mid-point of the two resistors and ground is zero and is so indicated by the voltmeter. A ground at either terminal of the field winding causes the voltmeter to indicate a voltage equal to one-half of the excitation voltage, subject, of course, to the conductivity of the bearing-oil film. Like the lamp scheme, no indication is given of a ground at the center of the field winding.

From this brief and elementary discussion it is obvious that the lamp and voltmeter schemes are subject to ground location and bearing-oil film conductivity, and when all of the probabilities are combined, the effectiveness of the schemes is seriously in doubt.

ALTERNATING-VOLTAGE METHOD

The alternating-voltage method, one variation of which is shown in Fig. 2, was developed several years ago and is based on the principle of raising the entire field circuit to some potential above ground so that a ground at any point in the field winding can be detected. Alternating current was chosen because it is conveniently available and can be transformed to the proper magnitude. The alternating voltage is applied to one terminal of the field winding. The voltage to ground at the opposite field terminal is the sum of the alternating voltage and the d-c excitation voltage, so that part of the ground insulation is stressed at a higher crest potential than normal. A sensitive a-c relay in series with the alternating-voltage source is relied upon to indicate the ground fault.

This scheme overcomes the problem of detecting a ground at the center of the field winding, but it is still subject to failure to indicate because of poor conductivity in the bearing-oil film. In addition, the alternating-voltage method introduces a serious operating hazard that cannot be ignored. The field winding of a turbine generator has considerable capacitance to ground. The capacitance to ground of the field winding of a typical average-sized turbine generator is of the order of 0.3 to 0.7 microfarads. Again, if the bearing-oil film is assumed to be a good conductor, an alternating voltage applied to the winding-to-ground capacitance will establish a capacitive current to ground that must flow through the bearing. The bearing designer will not permit any current in the bearing because of the danger of pitting and subsequent failure.

At this point, two conflicting requirements become apparent. First, if no current is to be permitted in the bearing, the magnitude of the applied alternating voltage must be small enough that the bearing-oil film remains an insulator and prevents the flow of current. Second, if the ground detector is to operate at all, the alternating voltage must be high enough to cause conduction through the oil film when a rotor ground occurs. The variations encountered in the conducting properties of the oil film are too great to permit the choice of a voltage that meets both of these conditions. In view of the possibility of damage to the generator bearings, the alternating voltage method should be avoided as a ground detector.

DIRECT-VOLTAGE METHOD

A scheme similar to the alternating voltage scheme in Fig. 2 except for the use of a direct voltage has also been employed. The relay, of course, is then a sensitive d-c relay. This scheme eliminates the danger of bearing damage, because the direct voltage does not establish the flow of any current. There is an improvement over the lamp and voltmeter schemes of Fig. 1 as the entire field winding is at an elevated potential with respect to ground, and a fault at any point will cause a change in voltage to ground.

The detector relay still depends on conductivity in the bearing-oil film to pass sufficient current to cause operation. The principle objection is in the fact that one side of the field winding operates at a higher-than-normal voltage to ground, overstressing the ground insulation.

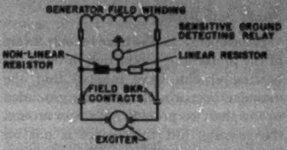

Fig. 3. Generator field circuit equipped with a nonlinear resistance bridge and a sensitive d-c relay for detecting grounds. This scheme has no null points as long as exciter voltage varies over a small range due to regulator action. Bearing arrangement the same as shown in Fig. 1(A)

NONLINEAR RESISTOR SCHEME

A variation of the voltmeter scheme of Fig. 1(B) is the d-c relay scheme shown in Fig. 3. Two resistors, one of which has constant resistance while the other is a nonlinear resistance that varies with applied voltage, are connected in series across the field winding. A sensitive d-c relay of the galvanometer type is connected from the mid-point of the resistors to ground and is the ground-detecting element.

The use of one nonlinear resistor provides a means of detecting a ground at any location in the field winding. As the resistance of the nonlinear resistor changes the location of the point in the field winding where the voltage to ground is zero also changes. Thus, the voltage to ground at all points in the winding is variable, depending on the applied excitation voltage, and a ground at any point will eventually disturb the voltages and circulate a current.

The nonlinear resistor can be replaced by a rheostat or a series of fixed resistors with pushbuttons to vary the resistance between the field leads and the relay tap. The operator must periodically move the rheostat or depress the pushbutton to move the point of zero voltage to ground in the field winding. A nonlinear resistor makes it unnecessary for the operator to take any action.

As is true with the other schemes discussed, this scheme is also dependent on the conductivity of the bearing-oil film. It does provide a means of detecting grounds at any location in the winding without applying additional voltage to overstress the ground insulation. This scheme therefore has advantages over those previously discussed.

Shaft Slip Rings

Some operators who have become aware of the problem of conduction through the bearing-oil film have insisted that the manufacturer provide a slip ring grounded to the shaft to provide a by-pass around the bearing, but this device is not an answer to the problem. The only time the brush riding on this slip ring is called upon to carry current is when a ground occurs in the field winding. Even at this time, the voltage applied to the brush is small.

The performance of brushes that normally carry no current is notoriously unpredictable. A film having good insulating properties is apt to develop on the slip ring, so that no current will flow from the slip ring to the brush unless sufficient voltage is applied to cause breakdown of the film and conduction. Thus, the slip ring in parallel with the bearing-oil film is a poor by-pass device, and it is possible that the bearing-oil film may have higher conductivity than the slip ring. If this is the existing condition, the slip ring is ineffective and by-passes none of, or only part of, the current from the bearing.

In addition to the conduction problem, the generator designer has a serious problem in finding a location to place the shaft slip-ring and brush assembly. Space on a turbine generator shaft is at a premium and considerable additional expense may be involved in adding the slip ring. For these reasons, the ability of a shaft slip ring to perform its intended function is questionable, and the expense is apt to be far greater than warranted by the advantage gained. The shaft slip ring is not a recommended solution to the problem.

Summary

All of the ground detector schemes now in use have a common shortcoming in that they depend on conductivity through the bearing-oil film to start operation. No scheme offers a positive solution to the problem. The lamp and voltmeter schemes will not operate for grounds at or near the center of the field winding because the voltage distribution is not sufficiently disturbed. The alternating-voltage method introduces a hazard because capacitive current may flow through the bearing and cause damage. The direct-voltage method eliminates this hazard but retains the objectionable feature of overstressing some of the ground insulation at a higher-than-normal voltage. The nonlinear resistor scheme enables detection of a ground at any point in the winding, but depends on the bearing-oil film conductivity for operation. The use of a shaft slip ring is not a solution to the problem, because the film on the ring surface can prevent conduction and, at best, only a portion of the current is removed from the bearing.

Experience with these schemes has been varied. Some operations have been reported, but whether the detector indicated a ground at the instant it occurred is always debatable. It is conceivable that a field-winding ground might exist for days or weeks before the bearing-oil film conductivity becomes high enough to permit operation of the ground detector. It is also conceivable that the detector might never operate. In any event, it is extremely important that operators realize that the lack of a ground detector indication does not necessarily mean that there is no ground on the winding. The ground detector must be treated as a device that may indicate a ground, but some more positive means must be used to detect grounds.

Periodic testing of the insulation with the machine at rest is one test that is frequently carried out but this is not necessarily conclusive. It is possible that a ground in the field winding will disappear as the centrifugal forces due to rotation get less and less. Therefore, some positive check should be made while the machine is still running near normal speed. This can be accomplished by momentarily by-passing the bearing-oil film and pedestal insulation with a jumper from the shaft to ground. A portable instrument or the normal ground relay protective equipment can be used to indicate whether a ground exists.

Conclusions

1. All ground detector schemes now available and in use rely on the conduction of current through the bearing-oil film for effective detection of grounds. The bearing-oil film has variable insulating properties depending on the quality and cleanliness of the oil, and in many cases it may prevent the detector from performing its function.

2. The use of a shaft slip ring to by-pass the bearing-oil film is not recommended. Because of the glaze or film that will develop on the surface of the slip ring, the bearing-oil film is apt to be more conducting, in which case, the purpose of the shaft slip ring is defeated. In addition, the expense and difficulty of finding a location on the shaft for the slip ring and brush assembly are not justified by the questionable advantage gained.

3. The alternating-voltage method is not recommended because of the danger of establishing capacitive leakage current through the generator bearings. This current can be established even though no field ground exists. Also, part of the ground insulation is overstressed because of the a-c component of voltage added to the normal exciter voltage.

4. Even when the alternating voltage is rectified into a direct voltage, the condition of overstressing the field insulation continues to exist.

5. The scheme, shown in Fig. 3, which seems to offer the best over-all protection is that using a voltage divider bridge with one leg of the bridge a non-linear resistor which will shift the zero point of ground measurement as the exciter voltage varies under regulator control.

6. In the final analysis the insulation resistance of the winding should be determined or some overvoltage means should be used to determine the insulation condition at every shutdown period of the generating equipment, in order to insure that no undetected grounds in the field winding exist.

7. Movement of the rotor coils due to rotational forces may contribute to establishing a field-winding ground. Therefore, an insulation check with the machine running at normal speed is desirable. The bearing-oil film and pedestal insulation should be by-passed with a jumper during this test.

References

1. Applications of Relays for Unbalanced Faults on Generators, **J. E. Barkle, Frank von Roeschlaub.** *AIEE Transactions*, vol. 72, pt. III, Apr. 1953, pp. 277–82.

2. Protection of Generators Against Unbalanced Currents, **J. E. Barkle, W. E. Glassburn.** *Ibid.*, pp. 282–86.

3. Generator Negative-Sequence Currents for Line-to-Line Faults, **R. F. Lawrence, R. W. Ferguson.** *Ibid.*, Feb. 1953, pp. 9–16.

4. Relay Protection of A-C Generators, **AIEE Committee Report.** *Ibid.*, vol. 70, pt. I, 1951, pp. 275–82.

◆

Discussion

H. C. Barnes (American Gas and Electric Service Corporation, New York, N. Y.): In presenting this summation of the methods of field ground detection and the problems associated with each, the authors have rendered a valuable service to utility engineering and operating personnel.

At the start of the paper, the case is argued in favor of more protection to trip a unit. This is based on the increased reserve capacity making it more permissible and the increased cost making it more desirable. This is generally true but it should be remembered that, while the system is growing rapidly, the individual unit is taking tremendous jumps in size. A 250-megavolt-ampere unit, now a common item, or a 350-megavolt-ampere unit, now in actual production, could represent a good percentage of an area's generation even though the over-all system was large enough to justify such units. Its loss could create serious local problems. The huge shafts, shells, and other parts of these large machines may present stress problems from unequal cooling or heating after a tripout, particularly with temperatures of 1,200 degrees now a reality, and higher ones no doubt on the way. Aside from these factors, there is no return on the investment when a machine is not producing, having been unnecessarily removed from service.

These comments are of no value if it is assumed that these devices trip only when there is actual trouble. However, it is irrefutable that tripping devices and associated wiring can fail or be wrong because of mechanical or electrical surges and that test men make mistakes. Therefore, false tripping is bound to occur. If an infinite number of trip devices were applied, a trip signal would conceivably be constantly present. Therefore, the need should be carefully weighed before connecting additional devices to trip. Where tripping is necessary, such as for an electrical short circuit, fast tripping should certainly occur. If a time delay is permissible, even though slight, it may eliminate trips from surges or transients even though still subject to its own or the test man's failure. If there is enough time for the operator to analyze the difficulty, then an alarm should be sufficient, particularly if supervisory personnel is readily available for consultation. Even the addition of alarms should be carefully considered since they can become so multitudinous that they are confusing.

As for field protection, generators installed on the A. G. & E. system since about 1945 have been provided with the a-c rectifier-type relay connected to alarm. These have been supplemented to d-c voltmeters with suitable test transfer switches. So far, no grounds have been experienced. There have been a few false alarms. Also, several maintenance men have discovered that the ground detector relays should have been removed from service before starting to work on the brushes. Field temperature recorders are standard, as they have been since even before the ground detectors. These indicate short-circuited turns, since they become erratic under this condition, especially if the short circuit is intermittent, as it often is on a rotating field. There have been two cases of short-circuited turns.

The most recent case of false indication was not from the relay contacts but from the indicating lamp which is part of the relay. It was noted that the lamp brilliancy was varying. Test voltmeters between the slip ring and ground indicated a voltage varying in magnitude and polarity. A voltmeter reading between the shaft at an exposed point at the turbine end of the generator gave voltages of −55, −25, +30, and +28 for the low- and high-pressure generators of two, 200-megavolt-ampere cross-compound units. They persisted even with the relay removed from service. When the shafts were grounded through a low resistance, this voltage disappeared and the lamp on the relay became normal. Apparently a capacitance charge was building up on the shaft until it was high enough to break down the oil film. This was remedied by completion of installation of shaft grounding which was provided for bearing and gear protection. Whether the glaze due to no current as mentioned in the paper will nullify this is yet to be determined. Such glaze has caused difficulty with the field temperature recorders.

Despite our rather negative experience, the field ground problem is considered serious enough to justify continued use of detection equipment supplemented by in- and out-of-service testing. The relay will continue to be connected to alarm.

H. T. Seeley and **E. J. Burdick** (General Electric Company, Schenectady, N. Y.): Throughout this paper the authors have discussed the subject of detection of generator field-winding ground faults with an overly pessimistic viewpoint, leaving the impression that the generator rotors are not and cannot be effectively grounded; that all detector schemes must therefore operate through the bearing-oil film; and that the a-c and d-c ground detection schemes overstress the field-winding ground insulation. We do not share these views but believe that automatic detection of field circuit ground faults should be used and that effective detection of these faults is available with present-day equipments.

In conclusion 1 the authors state that all ground detector schemes now available and in use rely on the conduction of current through the bearing-oil film for effective detection of grounds. No mention is made of hydro turbine-generators whose rotors are effectively grounded by the turbine without depending upon conduction of current through the bearing-oil film; nor was mention made of various resistance grounding paths located in the turbine on steam turbine units. These paths do not depend upon conduction of current through the bearing-oil film. We have found, by calculation and measurements of units in service, that water-sealing glands or carbon-packing glands effectively ground the turbine and generator rotors. If these grounding paths do not exist, the rotor can be grounded by other means.

We agree wholeheartedly with the authors' recommendation that users should measure the sensitivity of their protection rather than simply taking for granted the grounding of the generator rotors, as otherwise disappointments may occur. Such a measurement is easily made in connection with the d-c field ground detector relay and should be made a routine periodic test wherever there is any doubt as to the effectiveness of the rotor grounding path.

In the discussion of the alternating- and direct-voltage schemes of detection, the authors mention the objection that one side of the field winding operates at higher-than-normal voltage to ground, overstressing the ground insulation. It should be pointed out that the American Standards Association standards require that the field winding be given a high-potential test at 10 times rated voltage.[1] The field-winding insulation is also capable of operating continuously at a ceiling voltage of 120 per cent of rated. This higher insulation margin available in the field winding has made it possible to design a ground detection scheme that does not overstress the ground insulation.

The authors have concluded that the voltage divider bridge with one leg of the bridge being a nonlinear resistor, offers the best over-all protection. Yet this scheme relies on changes in the exciter voltage to give complete protection to the field winding. With this system, a ground fault conceivably could exist for a long period without being detected if the generator were base-loaded.

The direct-voltage scheme does not suffer the disadvantage of relying on changes in exciter voltage, since it has its own power supply and can detect field ground faults without depending on the excitation voltage. The d-c field ground detector relay, with which there have been years of successful experience, offers the best solution available today.

REFERENCE

1. ROTATING ELECTRICAL MACHINERY. *ASA C50-1943*, American Standards Association, New York, N. Y., Mar. 29, 1943.

J. E. Barkle, C. C. Sterrett, and **L. L. Fountain:** Mr. Barnes' description of the experience of the American Gas and Electric Service Corporation is of considerable interest to the authors. There was no intention in the paper itself to imply a recommendation that generator-rotor ground detectors be used to trip the machine off the line in the event of operation. In fact, the authors would agree that this is a form of relay protection that can and probably should be installed to sound an alarm and provide an opportunity for the station operator to analyze the trouble.

The philosophy Mr. Barnes proposes is a wise one to follow in any relay situation. A relay should not be connected to trip unless it is used to detect trouble that requires immediate removal of the equipment from service, and there is reasonable assurance that incorrect operations of the relay are a remote possibility. A generator-rotor ground in itself is not serious, but is undesirable. The danger lies in the occurrence of a second ground in the field winding which could cause serious damage.

Mr. Barnes also describes sporadic operation of an indicating lamp in a ground detector scheme on one of the American Gas and Electric units. This was eventually traced to the fact that the generator shaft was not grounded. When provision was made to ground the generator shaft, the shaft voltages disappeared and the lamp operation was normal.

Mr. Seeley and Mr. Burdick express favoritism for the direct-voltage method of detecting field grounds. There is no question in the authors' minds that this scheme offers a workable solution to the problem, but it is our opinion that the objections to it are sufficient to make its use undesirable. The discussers point out that the American Standards Association standards require that the field winding of a generator be given a high potential test at 10 times rated voltage and that the field-winding insulation is capable of operating continuously at a ceiling voltage of 120 per cent of rated voltage (see reference 1 of Mr. Seeley's discussion). Obviously, these requirements are designed to produce considerable insulation margin in the generator rotor.

Under normal conditions, with 250 volts applied to a 250-volt field winding, the capacitance to the rotor iron will force a distribution of voltage such that the potential at each field terminal is one-half the applied voltage. Therefore, the voltage between each slip ring and the shaft would be 125 volts. On the assumption that the d-c ground detector voltage is 125 volts, a distribution of voltage is forced so that the potential between one of the slip rings and the shaft is raised to 375 volts. This means that the insulation at this terminal of the field winding is stressed at approximately three times the normal value. While this is not sufficient to cause breakdown of the insulation, it appreciably reduces the insulation margin.

It should also be pointed out that on machine field windings rated at 375 volts, the American Standards Association standards require an overpotential test of 3,750 volts. Using the direct-voltage method of rotor-ground detection can apply a voltage to the winding insulation in a 250-volt machine that is equal to, or higher than, that normally existing in a 375-volt machine.

These discussers do not agree that the generator-rotor can be insulated from ground by the bearing-oil film but Mr. Barnes appears to substantiate the fact that this can occur by describing an actual case. There is no question that the rotor can be grounded by various auxiliary devices, but the value and desirability of these is questioned. The use of shaft slip rings was discussed in the paper and the authors do not feel that this is a reliable method of grounding. Design and manufacturing difficulties are usually encountered in attempting to provide a means for grounding the shaft.

The voltage divider bridge method described in the paper has been designed to provide ground detection equal to that of the direct-voltage method, and it does not have the disadvantage of applying higher-than-normal voltage to the rotor insulation. It seems logical to take the stand that higher-than-normal voltage should not be applied to insulation when it is not necessary to do so. In the case of a base-loaded machine where the field voltage remains constant for a considerable length of time, an artificial change in the resistance of the nonlinear resistor can be produced by having a pushbutton connected to short-circuit a portion of this resistance.

In summary, a general conclusion of the paper is that all ground-detector schemes now in use have shortcomings of one form or another. Some are erratic in operation and cannot be relied upon to detect part or all of the possible grounds. Others are objectionable from the standpoint of the effect that they might have on the generator bearings or insulation. If by some means a shaft ground is provided, the voltage divider bridge method becomes equal to any scheme which is now in use, including the direct-voltage method, and becomes superior in that it does not apply higher-than-normal voltage to the field insulation.

Rewinding A-C Generators for Improved Performance

W. G. SELINE
ASSOCIATE MEMBER AIEE

THE Shawinigan Water and Power Company has an installed capacity of 1,500,000 horsepower in six hydroelectric plants all located on the St. Maurice River in the province of Quebec. The company maintains its own electrical repair department and rewinds all its own generators. During the last 10 years nine machines totalling 240,000 kva have been rewound.

Two years ago the company had the problem of rewinding the first of a group of five generators that had originally been overrated with a temperature rise of 110 degrees centigrade (C). The problem was to reduce the rise to a more normal value without reducing the output. Some fundamental design changes were made to reduce the operating losses and a new insulation structure developed with greater thermal conductivity. Test results indicated that the new insulation had an appreciable effect on temperature reduction. Subsequently the same type of insulation was applied to another generator with different output, voltage rating, and original insulation. Again an appreciable decrease in temperature rise occurred.

This insulation is now standard in this company for all rewind jobs and the results of better heat conductivity are used to reduce temperature rise where required but more generally to increase the kilowatt output when adequate capacity is available from the turbine or the kilovar output where sufficient field and exciter capacities exist. This paper describes the operating history of the machines, their original insulation components, the new insulation and the results of rewinding on the temperature-rise-versus-output characteristic.

18,500-Kva Generators

These units are rated 18,500 kva, 6,600 volts, 0.85 power factor (pf), 120 rpm, 60 cycles, and are hydraulic-turbine-driven. They were installed in 1914 and had been guaranteed to deliver rated output with a 110 C temperature rise with no unduly harmful effects to the insulation. The exact reason for this unusual rating has been obscured by lack of records. They have the following operating history. After 10 years the end-turn cambric insulation was dry and brittle and was replaced by mica tape. There were few breakdowns over the ensuing 15 years. Subsequently, however, the frequency of failures increased to such an extent that all stator coils were reinsulated as a temporary expedient during the war. The majority of faults on these machines were turn-to-turn short circuits caused by vibrating strands. The bonding varnish on the conductor had deteriorated by heat aging and allowed the strands to vibrate and wear away the turn insulation. These characteristics are common to most failures in older machines in this company. The reinsulation process was good for 8 to 10 years, then strand vibration again caused failure.

When the decision was reached to rewind completely these units, a study was made to determine means to reduce the temperature rise but to maintain the output and to provide more heat-resistant insulation components on the conductor to eliminate the vibrating strands.

Table I. Generator Losses in Kilowatts at 18,500 Kva, 6,600 Volts, 0.85 Pf

Loss	Before Rewind	After Rewind
Windage and friction	58	66
Core	221	162
Stray load	112	88
Stator I^2R	131	122
Field I^2R	151	119
Total	673	557
Temperature rise, C	110	52

Paper 55-132, recommended by the AIEE Rotating Machinery Committee and approved by the AIEE Committee on Technical Operations for presentation at the AIEE Winter General Meeting, New York, N. Y., January 31–February 4, 1955. Manuscript submitted October 21, 1954; made available for printing December 7, 1954.

W. G. SELINE is with The Shawinigan Water and Power Company, Trois-Rivieres, Quebec, Canada.

The author wishes to acknowledge the work done on this project by Prof. W. H. Schippel, McGill University, and numerous associates in his company.

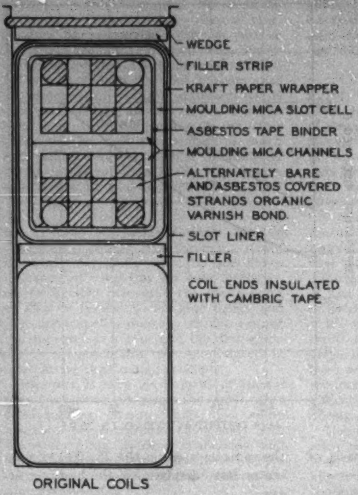
WEDGE
FILLER STRIP
KRAFT PAPER WRAPPER
MOULDING MICA SLOT CELL
ASBESTOS TAPE BINDER
MOULDING MICA CHANNELS
ALTERNATELY BARE AND ASBESTOS COVERED STRANDS ORGANIC VARNISH BOND
SLOT LINER
FILLER
COIL ENDS INSULATED WITH CAMBRIC TAPE
ORIGINAL COILS

Fig. 1 (left). Section of original stator coil for the 18,500-kva generator

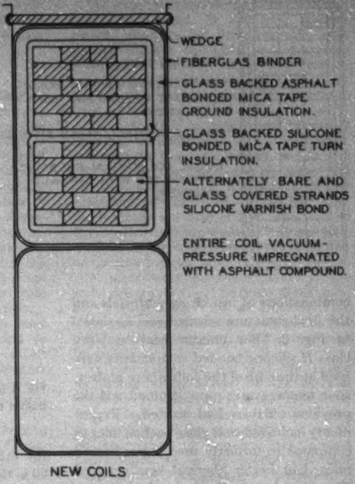
WEDGE
FIBERGLAS BINDER
GLASS BACKED ASPHALT BONDED MICA TAPE GROUND INSULATION.
GLASS BACKED SILICONE BONDED MICA TAPE TURN INSULATION.
ALTERNATELY BARE AND GLASS COVERED STRANDS SILICONE VARNISH BOND
ENTIRE COIL VACUUM-PRESSURE IMPREGNATED WITH ASPHALT COMPOUND.
NEW COILS

Fig. 2 (right). Section of new stator coil for the 18,500-kva generator

In the absence of manufacturers test data, retardation tests were made to establish and segregate the machine losses. These are shown in Table I. Analysis of these losses and the machine construction showed that the following design changes could be made to reduce losses:

1. With a more efficient insulation structure the stator conductor section could be increased to reduce the stator copper loss.
2. By increasing the stator coil pitch by one slot, the core loss could be reduced. The effect of this change on the short-circuit ratio and wave form were found acceptable.
3. As a result of change 2 the field current and losses would be reduced.
4. By more efficient stranding and transpositions, the stray losses could be reduced.

The results of these changes as established by retardation tests after rewind are also shown in Table I.

It was found however from the temperature-rise-versus-loss characteristics that these loss reductions were not sufficient to reduce the rise to a value near the 60 C standard. Hence a program of experiment and research was conducted to find an insulation structure with better thermal conductivity.

Fig. 1 shows a section of the original stator coil of the 18,500-kva generator. Numerous tests were made with various

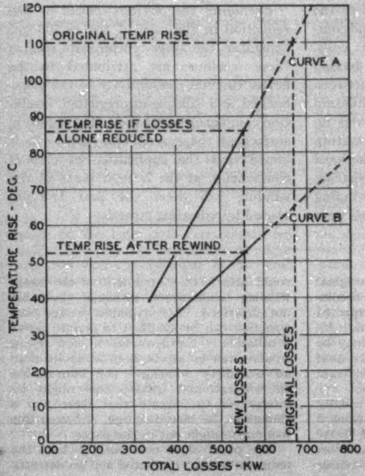

Fig. 3 (left). Temperature rise-loss curves for the 18,500-kva generator

Curve A—Original winding

Curve B—New winding

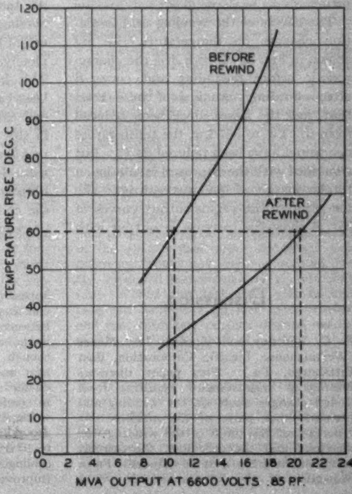

Fig. 4 (right). Temperature rise-output curves for the 18,500-kva generator

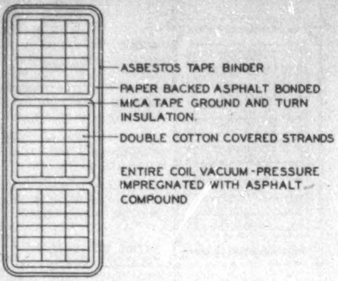
ASBESTOS TAPE BINDER
PAPER BACKED ASPHALT BONDED
MICA TAPE GROUND AND TURN INSULATION.
DOUBLE COTTON COVERED STRANDS
ENTIRE COIL VACUUM-PRESSURE IMPREGNATED WITH ASPHALT COMPOUND

Fig. 5 (left). Section of original stator coil for the 40,000-kva generator

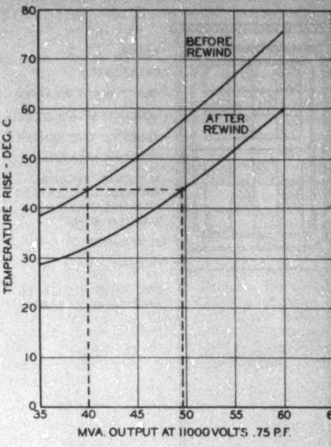

Fig. 6 (right). Temperature rise-output curves for the 40,000-kva generator

combinations of insulating materials and the final structure selected was as shown in Fig. 2. For greater heat stability class-*H* silicone bonded components were used at the core of the coils where hottest-spot temperatures were attained and the previous troubles had started. Experiments indicated that glass-backed mica as compared to formerly used paper-backed mica had better thermal conductivity. The ground and end-turn insulations were made with glass-backed asphalt bonded mica tape, vacuum-pressure impregnated with asphalt compound.

During installation all means were taken to improve the cooling characteristics of the coils. They were hot-pressed into the slots with hydraulic rams to ensure intimate contact of the insulation with the slot walls and to eliminate insulating air films. Special end-turn blocking and spacing of the coils exposed a maximum of coil surface to the cooling air.

The effects of the winding and insulation changes on temperature rise are shown in Fig. 3. Curve *A* is the characteristic before rewinding and curve *B* after rewinding. Analysis of these shows that, had the losses alone been reduced from 673 kw to 557 kw, the temperature rise would have been reduced 24 C. But combined with the improved insulation, a total reduction of 58 C was realized. The temperature-rise-versus-output curves of Fig. 4 show the increase in output with the machine considered on the basis of 60 C rise.

40,000-Kva Generator

Following the successful application of this insulation on the foregoing machine, an opportunity arrived to use the same components on a larger, higher voltage generator whose original insulation was different. This unit was rated 40,000 kva, 11,000 volts, 0.75 pf, 138.5 rpm, 60 cycles, and was installed in 1928. The original stator insulation is shown in Fig. 5. This unit had no failures until 1952. At that time inspection showed local overheating of the top end turns to the extent that the strand insulation had completely disintegrated on many coils. This heating was diagnosed as having been caused by lack of spacing between end turns, resulting in poor ventilation in this area. In this case there was no problem of general excessive temperature rise. It was planned to reduce the local heating of the top end turns by spacing the coils in this region. The rewinding procedure and insulation components were the same as used on the 18,500-kva generator but adequate for the higher voltage.

The results of this rewind on the temperature rise characteristic are shown in Fig. 6. Since the original temperature rise of this machine was normal, the benefits of the new insulation were taken in increased output. This amounted to 9,000 kva or 24 per cent over the original rating of 40,000 kva. This was mostly reactive power, as the output of the turbine was limited.

Conclusions

Excluding the obvious effects of loss reduction in the case of the 18,500-kva generator, the lower temperature rises of these machines are attributed to the better thermal conductivity of the glass-backed and silicone-impregnated insulation components, and the added radiating surface of the spaced end turns. It is hoped that the application of class-*H* components at the hottest parts of the winding will deter the past troubles caused by vibrating strands.

◆

Discussion

E. C. Whitney and **Graham Lee Moses** (Westinghouse Electric Corporation, East Pittsburgh, Pa.): This paper discusses interesting improvements resulting from design changes made on the winding and perhaps other parts of the machine. It reports that the pitch of the winding was increased and the core loss, short-circuit ratio, and field loss were all reduced. From inspection of the illustrations, it would appear that the eddy factor in the original coil was poor and numerous short circuits between bare strands would be expected if the construction was as pictured. Although not stated in the paper, it may be that an improved transposition was used on the new coil in addition to the increase in conductor cross section described.

Elimination of the slot cell will usually decrease the winding temperature from 5 to 10 degrees by detector because of better cooling of both the coil and the detector. Improved ventilation from other causes could also have contributed to the lower winding temperature, although these are not described. For example, wedge construction can be modified to permit better ventilation. Furthermore, a new clean winding can be expected to be cooler than an old dirty winding. The information on windage and friction loss might be interpreted to indicate that there was a change in the blower design, although this was not brought out in the paper.

The paper does not describe how the temperature was measured and no detector is shown in the illustration. It would be interesting to know whether the coil temperature was measured in the slot part or in the end winding. Thermal conductivity of the insulation wall is an important factor, but our experience does not indicate that the temperature by the standard AIEE detector would be affected as much as has been reported in this paper. On the other hand, the hot-spot temperature is much more affected by the thermal conductivity of the insulation than is the temperature as observed by standard detectors.

H. R. Sills (Canadian General Electric Company Ltd., Peterborough, Ont., Canada): Mr. Seline has, by the direct approach of rewinding his own machines, rather forcibly presented the user's point of view in respect to machine design and the characteristics desired. In this respect the approach is unique and the data given will be of considerable value to designers in formulating their design concepts.

However, in 1914 the majority of generators were designed primarily about their self-regulating characteristics and many machines of that period have since been rewound, using modern insulations and winding practices, for twice their original rating, but at sacrifice of their self-regulating characteristics.

The material which Mr. Seline has at his disposal for rewinding these generators was not available when the machines were built. This, of course, is the problem in evaluating insulation practices. Those that fail are already obsolete.

It is of interest to observe that in both instances the failures originated in the strands and turn insulation. The failure on the 40,000-kva generator windings was caused by carbonization of the cotton strand insulation lying in a section of the core overheated because of oil contamination. In the line terminal coils, this carbonized strand insulation was completely destroyed by internal ionization which was progressively attacking the turn and slot insulation. These coils were overheating because of circulating current losses as a result of the loss of the strand insulation.

However, the condition of the turn and slot insulation in the neutral coils where there was not ionization was such as to make it appear that, had the strands been class-*B* insulated, as is now done, they would have withstood the temperatures and there would have been no interstices for internal ionization to do its deadly work.

In Fig. 6, the curves replotted against the square of the load, and extrapolated as straight lines to no load, indicate that there has been a reduction of no load temperatures of 6 C. Is this caused by a change in pitch of the coils? If so, this leaves an improvement of 4 degrees at rated load due to improved conductivity of the insulation. It would be of interest to know how much of this should be attributed to the improved thermal conductivity obtained by pressing the coils into the slots.

The author has made a valuable contribution and I am sure it will be of much interest to machine designers. The increased loadings will produce higher thermal gradients in the insulation and it will be interesting to know how well this composite class-*H* and class-*B* insulation will sustain the test of operation.

A. W. W. Cameron and K. R. Knights (The Hydro-Electric Power Commission of Ontario, Toronto, Ont., Canada): The Shawinigan Water and Power Company is to be congratulated in taking this trial step forward in a field where too few such steps have been taken over the past 30 or 40 years. It would appear, in view of the relatively high cost and reported susceptibility of silicone insulations to deterioration in air at the higher voltages, that the company was wise in limiting the silicone application to the inner insulation of the coils where temperature and rate of deterioration are possibly the highest.

We would like to enquire whether some credit for reduced temperatures could be given to the cleaning action that resulted from replacing the windings, and whether the reduced temperatures will cause any difficulty in heating of the generator room during winter months.

It is of interest to note that glass-backed mica tape was used for the ground insulation. The author's opinion would be appreciated on whether the lower mica content obtainable with glass-backed as compared to paper-backed mica tape would limit its applicability to new generators.

We are very interested in this application of silicone-insulated compound to waterwheel generator insulation, and are hoping that the company will carry out and make available the results of a testing program to provide information on the relative rate of deterioration of these windings.

W. Hindle (Canadian Westinghouse Company Ltd., Hamilton, Ont., Canada): We would like to compliment Mr. Seline for providing some very important information on the subject of rewinding a-c generators. He has shown how it is possible to incorporate most of the improvements which have evolved since 1913 in generator design into the rewinding of some of the oldest generators in Canada.

It would be interesting to review briefly the history of the Grand Mere generating station involved in the first part of the paper. The six original machines reported by Mr. Seline, according to our records were rated 14,700-kva, 80 C rise, with a short-circuit ratio of 1.30, and the 18,500-kva 110 C rating was likely an overload rating.

In 1923, we supplied two generators of the same physical dimensions, rated 18,500-kva 75 C rise by thermometer, which tested 65 C by detector. This rating was obtained by a change in the number of slots and by increasing the amount of iron by approximately 3 per cent while still maintaining a short-circuit ratio of over 1.00. In 1940, we rebuilt one stator, supplied new field coils, modified the ventilation, and rated the rebuild 20,000-kva 60 C rise, with a short-circuit ratio of 1.00. We have no record of temperature test on this rebuild, but are of the opinion, based on design calculations and tests on similar machines, that the rise would be approximately 45 C.

The stray load loss in the author's design has been reduced, in line with modern current practices, by designing coils with thinner strands including transpositions. Mr. Seline, in a very clever way, has arranged the individual strands of the coil so that each strand is completely insulated from each other.

We note that in this rewind the coil pitch has been increased with a consequent reduction in the field current but at the expense of the short-circuit ratio. On previous designs, the limiting factor on rewinding for increased rating has been the short-circuit ratio of 1.00, and we feel that some considerable part of the improvement in rating is because of the reduction of the short-circuit ratio.

A present-day generator built on the same size frame would be rated 27,000 kva, 60 C, with a short-circuit ratio of 1.00. This generator would incorporate thermalastic insulation and the latest improvements in ventilation.

In conclusion, we feel that Mr. Seline is placing undue stress on the thermal properties of silicon varnish and that other factors have contributed such as changes in ventilation of the generators. It would be interesting to compare the rewind performance of a succeeding generator using another type of modern insulation.

J. A. Langford (Canadian-Brazilian Services, Toronto, Ont., Canada): The subject of this paper is of considerable importance to all those responsible for the operation of generators. The author has presented a very interesting account of the work of his company and he and his company are to be commended for their pioneering with silicone insulation.

Table I contains information on the losses of the 18,500-kva generators before and after rewinding. It is noted that, after rewinding, the windage and friction losses increased by about 14 per cent. Does this indicate that the quantity of air circulating through the generators was greater after rewinding?

In discussing the composition of the tape used for ground insulation, the statement is made that experiments indicated that glass-backed mica as compared to formerly used paper-backed mica had better thermal conductivity. The results obtained with the new insulation bear out the conclusions derived from experiments. From the standpoint of thermal conductivity, the only difference between glass-backed and paper-backed tape would appear to be that, for a given thickness of insulation, there would be a greater proportion of backing material in the glass-backed tape. However, this difference would not seem to account for the improved performance of glass-backed tape. Could the fact that glass-backed tape can be wound on with more tension and can, therefore, produce tighter insulation be part of the answer?

W. G. Seline: I appreciate the interest shown by the various discussers in this paper. Mr. Whitney and Mr. Moses are correct in their observation that the original coil stranding was very inefficient. The large strand sizes caused excessive eddy currents within the strands, the

Table II

Output, Kilovolt-Amperes	Guaranteed Approximate Temperature Rise, C
14,700	75
16,000	85
18,500	115

construction of the turn section did not give adequate protection against strand-to-strand short circuits, and no transpositions were made to reduce eddy currents between strands. As stated in the paper, transpositions were used on the new coils.

With regard to temperature reduction to be expected from elimination of slot cells, modified wedge design, and new clean windings, our past experience has been very discouraging. We have rewound four 35,000-kva and two 15,000-kva 6,900-volt generators where the original insulation was mica folium with a slot cell. The rewinds were made with continuous paper-backed mica-taped asphalt-impregnated coils with no slot cell. Wedges were modified by fluting for more efficient air passage. The machines were thoroughly cleaned during rewind. In the case of the 15,000-kva generators, the stator copper section was increased 5 per cent and the transpositions were employed. In all these cases the temperature rise before and after rewind remained substantially the same.

It is on the basis of this experience with mica folium and paper-backed mica tape versus the new glass-backed mica insulation structure that we conclude that the major portion of the temperature reduction comes from the better heat conductivity of the new insulation components. The increased windage and friction loss may have been the result of increased bearing friction as these underwent extensive overhauling. No alterations were made to the blowers.

Temperature measurements were made by resistance temperature detectors between coil sides at the center of the slots. The decreased temperature at this point may have resulted from the dissipation of a greater proportion of the heat from stator copper losses through the winding end turns. From experiments which approximated operating conditions, we found that the difference between the hot-spot copper and detector temperatures was of the order of 1 to 2 degrees for the new coils and 6 to 8 degrees for paper-backed mica taped coils. These experiments were made on 6,900-volt insulation.

In reply to Mr. Sills, no changes were made to the pitch of the stator coils on the 40,000-kva generator.

Regarding the discussion of Mr. Cameron and Mr. Knights, it is to be expected that the heating of the generator room will be reduced as a result of the reduction of operating losses. However, with only two of five machines presently rewound, this has not yet been noticeable.

The glass-backed asphalt bonded mica tape is approximately 0.002 inch thicker than the formerly used paper-backed tape. However, the space factor is approximately the same considering the tighter application possible and the omission of binders previously used. Compared with mica folium it eliminates the use of slot cells and bulky spacer strips between coil sides. We can see no reason why this insulation cannot be used on new machines. It is anticipated that a co-ordinated testing program will be instituted to evaluate the comparative rate of deterioration of these windings.

Referring to Mr. Hindle's review of the history of the 18,500-kva generators, our knowledge of this and the basis upon which the machines have been operated over the past 40 years is as follows:

1. The original contract stated that the coils could withstand a temperature of 150 C continuously without deterioration.
2. The original contract specified temperature rise not to exceed 55 C (above 25 C ambient) at 14,700 kva.
3. Under test the machines failed to meet the temperature rise clause and a supplemental agreement was drawn up to provide new temperature specifications, as given in Table II. The supplemental agreement also reiterated that the coils were insulated to withstand a maximum total internal temperature of 150 C. It also stated that if the generators were operated at a rise of 115 C or lower (above 30 C ambient), there would be no harmful effect on the insulation.

On the basis of this contract, the generators were rated 18,500 kva continuous operation and name plates were supplied by the manufacturer accordingly.

The two machines supplied in 1923 and the one rebuilt in 1940 were of a considerably modified design. It is agreed that a machine of greater output can be built within the same physical dimensions with an improved design and lower loss steel. This was actually the alternative available at the time of rewind. However, by only a slight modification of the electrical design and the use of these new insulation components, an equivalent result was accomplished at one-fourth the cost.

As noted in Table I, a considerable proportion of the loss reduction was in the core by increased stator coil pitch. This reduced the short-circuit ratio from 1.05 to 0.80. This was found acceptable under present system conditions.

In reply to Mr. Langford, the glass-backed tapes can be applied with considerably more tension and, undoubtedly, the resulting compactness would aid heat conductivity.

A Transductor-Type Field Ripple Detector for Synchronous Generators

H. M. McCONNELL
ASSOCIATE MEMBER AIEE

IT HAS been recognized that negative sequence stator currents in synchronous generators, if allowed to persist, may cause dangerous heating of the rotor structure due to induced currents. The problem of protecting synchronous generator against rotor heating from this cause has stimulated an active discussion among those responsible for relay application.

The present method of detecting negative sequence stator current is to employ well-known sequence-filtering networks fed by current transformers. The output of the network is used to operate a relay which actuates protective equipment if the permissible I^2T, or integrated square of negative sequence current, is exceeded. A group of recent papers[1-5] summarize the present state of development in this matter.

At the time of the presentation of these papers, it was mentioned in oral discussion that a method of detection of negative sequence currents based on the induced a-c component of field current would be desirable.[6] It is well known that a proportionality exists between these quantities. However, a conventional current transformer is not satisfactory in detecting the a-c component of field current, because of the presence of the steady d-c component which saturates the transformer.

This paper presents a circuit for the measurement of the a-c component of a current which has a considerable d-c level, with particular application to the field ripple problem at hand. The circuit consists of current transformer with an additional compensating winding supplied by a current transducer whose function

Paper 55-124, recommended by the AIEE Relays Committee and approved by the AIEE Committee on Technical Operations for presentation at the AIEE Winter General Meeting, New York, N. Y., January 31–February 4, 1955. Manuscript submitted August 11, 1954; made available for printing November 22, 1954.

H. M. McCONNELL is with the Carnegie Institute of Technology, Pittsburgh, Pa.

The work reported in this paper was supported by the Office of Naval Research, under Contracts *N7ONR 30308*, Projects *975-272* and *275*. The author is grateful for the assistance of Hugh McK. Lynch, and to Magnetics Incorporated of Butler, Pa., for some of the experimental apparatus.

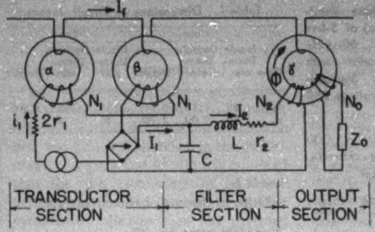

Fig. 1 (left). Circuit diagram of the transductor-type field ripple detector

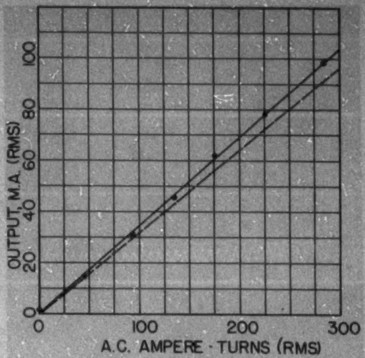

Fig. 2 (right). Steady-state output characteristic at 60 cycles, with 400 ampere-turns d-c, and 585-ohms resistive load. Dashed curve calculated by equation 7; solid curve measured

is to cancel the d-c ampere turns. The circuit is shown in Fig. 1. The cores are made in gapless (toroidal) form, of a material having essentially a rectangular hysteresis loop.

Design Objectives

The objectives in designing the circuit are to achieve: 1. a useful output current I_0 into the burden Z_0; 2. faithful response to sudden changes in either the d-c or a-c components of the current I_f; 3. acceptable linearity between I_0 and the a-c component of I_f. An approximate analysis of the circuit indicates the way in which the various circuit components must be chosen in order to meet these objectives.

Analysis

The transductor will be idealized by stating that the instantaneous current I_1, Fig. 1, is the image of the instantaneous current I_f. Reasonably close agreement between this idealization and actual performance is obtained if the resistance drop in the a-c windings of the transductor, $2r_1i_1$, is small compared with the maximum applied voltage, and the capacitor C offers low impedance to the a-c component of I_1. A detailed analysis of the transductor operation is beyond the scope of this paper; in fact, the performance of the series-connected magnetic amplifier with high-impedance control circuit is not well understood because of unexplained core behavior. An analysis of circuits of this type, making use of an idealized flux-density/field-intensity characteristic for the core material, is available in the literature.[7] It is sufficient to note here that the compensating turns of the current transformer may be adjusted to account for linear departures of the transductor performance from the ideal. Thus

$$I_1=\frac{I_f}{N_1}k_1 \tag{1}$$

where k_1 is the proportionality factor which accounts for the current ratio error of the transductor.

For perfect compensation of the current transformer

$$N_2I_{1(\text{d-c})}=I_{f(\text{d-c})} \tag{2}$$

therefore

$$N_2=\frac{N_1}{k_1} \tag{3}$$

The current transformer is idealized by neglecting its magnetizing current. Then, the ampere-turn relationship states that

$$I_{f(\text{a-c})}=N_0I_0+N_2I_{2(\text{a-c})} \tag{4}$$

The common flux ϕ of windings N_0 and N_2 require that

$$I_0Z_0=j\omega N_0\bar{\phi} \tag{5}$$

$$I_{2(\text{a-c})}(r_2+j\omega L)=j\omega N_2\bar{\phi} \tag{6}$$

The reactance offered by C at the ripple frequency $\omega/2\pi$ is not included in equation 6 because the conducting arms of the rectifier bridge effectively short-circuit C to this component of current.

Combining equations 4, 5, and 6 yields the complex ratio of transformation

$$\frac{I_0}{I_{f(\text{a-c})}}=\frac{1}{N_0\left\{1+\left(\frac{N_2}{N_0}\right)^2\left(\frac{Z_0}{r_2+j\omega L}\right)\right\}} \tag{7}$$

The rapidity with which the bias current $I_{2(\text{d-c})}$ is able to adjust to transients in the d-c level of I_f will have an effect upon the current transformer behavior. During transient intervals both the d-c and a-c components of field current change suddenly. The current transformer can by itself reproduce such asymmetrical currents in its output winding for a short time only; this time is dictated by the rate at which the average flux level of the current transformer core increases, which is in turn dictated by the burden.

It will be assumed here that the current transformer is unable to reproduce asymmetrical currents unless perfect compensation in the bias winding exists. Then a suitable transient response of the bias current I_2 will be defined as follows: the bias current should reach a level such that compensation is restored within an interval which is short in comparison with the short-circuit transient time constant (T_d') of the generator. Taking 20 cycles as a representative value of T_d', then the bias current should be able to reach the level for compensation in about 4 cycles at fundamental frequency.

Transients in the bias circuit will be calculated under assumptions that: 1. the transductor delivers a direct current I_1 proportional to the d-c component of I_f; 2. the current transformer is saturated. Then, the bias winding (N_2) may be treated as a resistance, and the circuit L, r_2, C may be considered to receive a prescribed current. Rapid response with a minimum tendency to overshoot in a circuit of this type is achieved if the damping is somewhat less than the critical value. Accordingly, a damping ratio of 0.7 will be assumed. Previous discussion of response time has indicated that about 1/15 second may be allowed between initiation of a sudden change in I_1 and a corresponding response of I_2. As shown in any treatment of second-order systems of this type, the following relationships are established

$$\left\{\begin{aligned}&\frac{r_2C}{2\sqrt{LC}}\cong 0.7\\&\frac{1}{\sqrt{LC}}\frac{1}{15}\cong 2.5\end{aligned}\right. \tag{8}$$

or

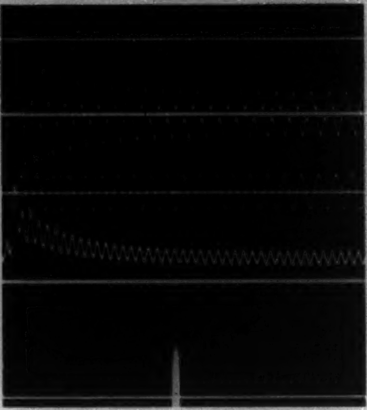

Fig. 3. Single-phase short-circuit (line to line) of 5-kva 230-volt 3-phase 60-cycle salient-pole generator with damper winding. Star-connected. No-load voltage 250 volts

Top—Output current to 1,000 ohms. Final value 86 ma, peak to peak

Second—Transductor supply current

Third—Transductor supply voltage, 60 cycles

Fourth—Current transformer bias current. Initial value 33 ma

Bottom—Generator field current. Initial value 2.29 amperes

$$\begin{cases} \sqrt{LC} \cong 0.0267 \text{ second} \\ r_2C \cong 0.0373 \text{ second} \end{cases} \tag{9}$$

Whether the conditions of equations 9 may be realized depends on whether the filter circuit Q prescribed by these equations is practical. It is found that at the ripple frequency of 120 cycles the ratio $(\omega L/r_2)$ dictated by equations 9 is about 14, which is readily obtained with commercial components.

Let it be required to design a field ripple detector for a generator in which during transients, the d-c component of field current may reach 400 amperes. The initial value of a-c component of field current under such circumstances will be less than a 400-ampere peak, by an amount equal to the initial field current. However, let it be assumed for purposes of design that the peak a-c component will be 400 amperes; the detector should be designed for an a-c level of 283 amperes rms. Let a burden of 10 volt-amperes at 1,000 ohms be required at this a-c level. These preliminary considerations fix the current transformer output at 100 milliamperes (ma) rms, and the current transformer output winding can have no more than 2,830 turns. The current transformer core must be capable of at least 100/2,830 volts per turn at 120 cycles.

Equation 7, together with the value of $Q=14$ dictated by equations 9, allows the determination of N_0 and N_2 versus the parameter (N_2/N_0) for a given value of the second parameter r_2. If r_2 is assumed to take a certain value, then N_0 and N_2 may be found such that the wire sizes, available winding spaces, and practically available choke fit the assumed value of r_2. Several trials of this nature indicate the combination best suited to the particular application considered. It is found that in the present example N_2 should be about 5,000 and N_0 should be about 2,200 if it is assumed that r_2 is 500 ohms. The corresponding value of L is 9.30 henrys. The rated value of the compensating current I_2 becomes 80 milliamperes and the rectifier must withstand 40 volts d-c. The capacitor should be about 75 microfarads, although the exact value is not critical; see equation 8.

Experimental Work

A model of the circuit has been constructed and tested. The three cores were made of 0.004-inch Orthonol tape. The dimensions in inches are shown in Table I.

Table I. Dimensions of Circuit, Inches

	Core			Box		
Core	Inside Diameter	Outside Diameter	Height	Inside Diameter	Outside Diameter	Height
α, β	1.25	1.75	0.50	1.18	1.82	0.61
γ	1.50	2.00	1.00	1.40	2.10	1.11

Other constants of the circuit are:

$N_1=5{,}000$ turns No. 32
$N_2=5{,}000$ turns No. 32
$N_0=2{,}200$ turns No. 32
$2r_1=304$ ohms, 20 degrees centigrade
$r_2=501$ ohms, 20 degrees centigrade
$L=10.5$ henrys, nominal
$C=50$ microfarads, 50 volts electrolytic

A factor k_1 was introduced in equation 1 to account for the fact that the ampere-turn ratio of the transductor is slightly less than the ideal of unity. It will be noted that both N_1 and N_2 are 5,000 turns in the model. The factor k_1 is introduced in an equivalent way in the model by placing more exciting turns upon the transductor cores than upon the current transformer core, turns being added until maximum output current is reached at rated d-c and a-c excitation levels. It was found that 72 turns on the transductor cores and 69 turns on the current transformer core achieved this result. Thus $k_1=69/72=0.958$. Rated d-c current becomes 5.80 amperes and rated a-c ripple current becomes 4.08 amperes rms. (The example design began by assuming 400 amperes in a single conductor to be the excitation level. To test the model on available machines, the nominal 70-turn exciting windings were installed. In a single conductor application it would be

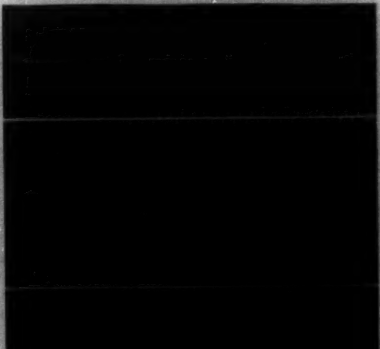

Fig. 4. Single-phase short-circuit (line to line) of 100-kva 2,300-volt 3-phase 60-cycle salient-pole generator without damper windings. Star-connected. No-load voltage 1,500 volts

Top—Output current to 1,000 ohms. Final value 230 ma peak to peak

Second—Transductor supply current

Third—Transductor supply voltage, 60 cycles

Fourth—Current transformer bias current. Initial value 50 ma

Bottom—Generator field current. Initial value 4.0 amperes most convenient to add extra turns to the current transformer compensating winding, in about 1/2 per cent taps, in order to "tune" for best compensation.)

The steady-state response of the unit at 60 cycles is given in Fig. 2. Transient response, in the situation for which the unit was designed, is shown in the oscillograms of Figs. 3 and 4. (It will be noted that the d-c component of generator field current in Fig. 4 rises to a value considerably greater than the designed level, resulting in some distortion of the output current wave form and a reduction in its rms value.)

Conclusions

The device presented in this paper is shown to be a small, inexpensive, static apparatus for the measurement of the a-c component of field current in a synchronous generator, both in the transient and steady states. It has sufficient output to operate a relay or meter. Its design is simple, and its components are readily obtained.

Probably the most serious obstacle to the application of this device to generator protection is the determination, without dangerous tests, of the amount of a-c ripple in field current per unit of generator negative-sequence current.

Accurate calculations are possible in the case of salient-pole generators. However, the presence of solid iron in the rotor forging of a turbogenerator upsets any formal calculation for those machines.

References

1. Turbine - Generator Heating During Single-Phase Short Circuits, M. D. Ross, E. I. King. *AIEE Transactions*, vol. 72, pt. III, Feb. 1953, pp. 40–45.

2. Effects of Negative-Sequence Currents on Turbine-Generator Rotors, E. I. Pollard. *Ibid.*, June, pp. 404–06.

3. Short-Circuit Capabilities of Synchronous Machines for Unbalanced Faults, P. L. Alger, R. F. Franklin, C. E. Kilbourne, J. B. McClure. *Ibid.*, pp. 394–404.

4. Protection of Generators Against Unbalanced Currents, J. E. Barkle, W. E. Glassburn. *Ibid.*, Apr. 1953, pp. 282–86.

5. Applications of Relays for Unbalanced Faults on Generators, J. E. Barkle, Frank Von Roeschlaub. *Ibid.*, pp. 277–82.

6. Backup Protection for Generators, Eric T. B. Gross, Lester B. LeVesconte. *Ibid.*, vol. 72, pt. III, June 1953, pp. 585–92.

7. Series-Connected Saturable Reactor with Control Source of Comparatively High Impedance, H. F. Storm. *Ibid.*, vol. 69, pt. II, 1950, pp. 1299–1309.

◆

Discussion

Eric T. B. Gross (Illinois Institute of Technology, Chicago, Ill.): In the discussion of an earlier paper (see reference 6 of the paper) it was reported that current transformers with air gaps, or similar equipment, have been in practical operation for relaying by using a-c currents in the rotor circuits. The transformer proposed by Dr. McConnell makes possible further improvements of such protective schemes and deserves the serious consideration of those who design, build, or use protective relays.

In this paper, particular emphasis is placed on double-frequency currents in the rotor and rotor windings. It would be of interest to learn whether the author has also considered the behavior of his device with regard to low-frequency rotor currents which are typical of other important disturbances.

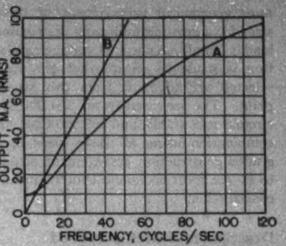

Fig. 5. Calculated performance of ripple detector circuit with 400 ampere-turns d-c and 283 rms ampere-turns a-c at various frequencies, operating into a 1,230-ohm total resistance burden. Curve A—output current. Curve B—output current capability without saturation of current transformer

H. M. McConnell: The response of the circuit to currents of frequency different from 120 cycles can be calculated from equation 7, if the output current transformer does not saturate. For constant d-c and a-c ampere-turns, but variable frequency, the output decreases with decreasing frequency because of the shunting effect of the filter section. This behavior is shown in Fig. 5, in which is also shown a line representing the capability of the current transformer core, in terms of current which can be supplied to this particular burden without saturation.

A Method for Determining Economical ACSR Conductor Sizes for Distribution Systems

A. W. FUNKHOUSER
ASSOCIATE MEMBER AIEE

R. P. HUBER
NONMEMBER AIEE

IN CONVERTING the 4-kv fringe area of the Indianapolis Power & Light Company system to 13-kv distribution, it was decided that, wherever possible, all new line construction would be made using bare steel-reinforced aluminum cable (ACSR) type of conductor. The economy of this type of conductor over copper has been well established in connection with transmission lines by the experience of many companies including the Indianapolis Power & Light Company. Since the application of ACSR was new to this company's distribution system, it was necessary to set up certain sizes as standard. The problem was in selecting as few sizes as possible to minimize stocking while still providing the most economical conductor for the loadings anticipated. It was also necessary to consider voltage regulation at the maximum allowable load conditions. A method is presented for making these selections in which a mathematical solution for determining the economic proportions of different wire sizes in a graded construction arrangement is used. It is believed that this offers a different approach to this problem from that used in other economic wire size studies.

In selecting the wire sizes for use on this system, an economic comparison of the various sizes is made in two ways. First, the most economical sizes for any value of load is determined. Second, the

---

Paper 55-159, recommended by the AIEE Transmission and Distribution Committee and approved by the AIEE Committee on Technical Operations for presentation at the AIEE Winter General Meeting, New York, N. Y., January 31–February 4, 1955. Manuscript submitted October 13, 1954; made available for printing December 15, 1954.

A. W. Funkhouser and R. P. Huber are with the Indianapolis Power & Light Company, Indianapolis, Ind.

most economical arrangement of these sizes for a growing uniformly distributed load is found. A check of voltage regulation is made to ensure that the sizes selected are adequate from this standpoint. The sizes used are no. 2/0, 266,800 circular mils (CM), and 397,500 CM. A combination using all three sizes in a graded construction arrangement proves to be the most economical for main line construction.

Description of Methods Used

The major considerations in selecting certain conductor sizes as standards are the comparisons of annual cost and voltage regulation of all sizes, and under all conditions likely to develop. Variations in load distribution, load factor, load-growth rate, loss charges, investment charges, and construction costs all affect the economical conductor sizes to be used. These factors vary from system to system and must be based on company accounting practices, operating conditions, and anticipated future conditions. Differences in voltage regulation were not evaluated in the economic comparison of conductor sizes, but data are included showing the relation of conductor size (and therefore, cost) to voltage regulation. The reduction in voltage drop is a factor favoring the larger conductor sizes when the economic comparisons are close.

In this study the economical conductor size is first established for each value of load up to a maximum allowable loading of 6,000 kva for the 13-kv circuits. One of these sizes can thus be selected for any line serving a static concentrated load within the range studied. However, most circuits have a growing load that is distributed along its entire length. To determine the most economical arrangement under these conditions, the established conductor sizes are compared individually and in various combinations to ascertain the lowest annual cost for the conditions assumed. As a further check, the regulation for the most economical combination is calculated to see if it is adequate from the voltage standpoint.

Conditions Assumed

In making up the cost comparison studies for this system, it is found that certain simplifying assumptions can be made. The cost of poles and hardware can be left out altogether. Span lengths are limited by existing pole-line spacing, service drop requirements, and joint-use telephone line specifications rather than by conductor size. The pole size is also limited by telephone contacts, and the lowest class pole used on the main distribution lines will support the largest conductor size being considered. Hardware costs are neglected since a check of the difference in cost on the system showed it to be negligible compared to the total cost per mile involved. All hardware is the same for the conductor sizes studied except for a few dead-end clamps.

The geography of the fringe service area and the location of the initial 132/13-kv substations determined the average circuit length at approximately 10 miles. The maximum circuit loading under normal conditions is limited to 6,000 kva. In determining the maximum allowable circuit loading, a value as large as practical was selected to take advantage of reduced switchgear requirements. It was also necessary to keep the number of lines to a minimum since a congestion of subtransmission lines already existed around the substation sites to be used. The limiting factors are as follows:

1. A reasonably good voltage regulation must be maintained on the 10-mile line.
2. The ratio of normal load current to available short-circuit current must allow for relay settings to give reasonable fault sensitivity.
3. The number of customers affected by a circuit outage must be taken into consideration.

It is believed that the higher voltage permits better co-ordination between oil circuit breaker, recloser, and fuse, and, with the emergency ties between circuits, the customer outage rate at this maximum circuit loading is comparable to the present 4-kv radial service.

Wire sizes are limited to a minimum of no. 2/0 since this is the smallest conductor to have still adequate thermal capacity for the maximum load. A maximum size of 397,500 CM is used since the aforementioned hardware and pole cost assumptions do not hold true for larger sizes, and it is expected that increased pole-line costs would tend to offset any loss savings. Use of an all-aluminum conductor was considered, but advantages of less sag, use of existing standard stock conductors, additional strength to allow for damaged strands, and ability to withstand high temperatures due to emergency overloads were believed to offset the slight additional cost of ACSR using a single steel strand.

For ACSR wire sizes larger than no. 4/0, the 18/1 type of stranded arrangement is used for all except the 300,000-CM size. This stranding was chosen since previous studies had shown it to be the most economical for the span lengths encountered. A 26/7 stranding is used for the 300,000-CM size since it was the only design on which data were available from the catalogue. All these larger sizes are of 2-layer construction which reduces the losses in the steel core. For no. 4/0 and smaller sizes, the 6/1 stranding using a 1-layer construction is employed. The effect of greater losses in the 1-layer construction can be seen later when nos. 3/0 and 4/0 wires never prove to be economical for any value of static loading.

Labor costs are the most difficult to establish because the time actually spent in installing wire is not usually segregated in the cost records. It is thought that labor costs would be largely determined by the weight of the conductor. In this study, labor costs for the ACSR conductor were based on estimated costs per pound for installing a copper conductor on the existing system. The values used for each size of wire are given in Table I.

Economic Comparison for Static Loads

The first step in the economic study is the determination of the annual costs of investment and losses per circuit mile for each size of conductor and for a range of loads up to the maximum allowable load per circuit. The cost values used are also given in Table I. The results of this

Table I. Costs and Load and Conductor Characteristics

Demand Charge = $150 per Kilowatt
Energy Charge = 0.004 per Kilowatt-Hour
Load Factor = 40 Per Cent
Loss Factor = 25 Per Cent
Fixed Charges = 15.5 Per Cent of Investment
Annual Cost of Losses = $32 per Kilowatt

Size	Stranding	Ohms per Mile	Cost per Pound, $		Installed Cost* per Mile of 3-Phase Circuit, $
			Material	Labor	
No. 2/0	6/1	0.895	0.2765	0.147	1,229
No. 3/0	6/1	0.723	0.2750	0.1395	1,515
No. 4/0	6/1	0.592	0.2750	0.1299	1,869
266,800 CM	18/1	0.385	0.330	0.1302	2,114
300,000 CM	26/7	0.342	0.316	0.1106	2,788
336,400 CM	18/1	0.306	0.322	0.1182	2,544
397,500 CM	18/1	0.259	0.3145	0.1078	2,882

* Cost of neutral wire not included because same size is assumed for all-phase conductor sizes.

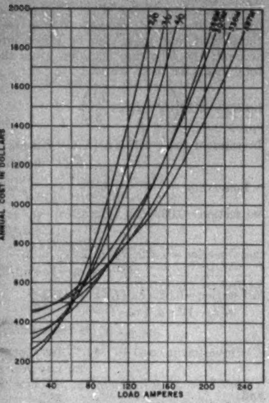

Fig. 1. ACSR distribution conductor annual cost comparison. Line length = 1 mile, static load concentrated at end of line, line cost includes conductor costs and installation labor only, loss cost = $32 per kilowatt, and fixed charges = 15.5 per cent

study are illustrated by the curves in Fig. 1. From these curves the following wire sizes are shown to be the most economical for the range of loads listed:

0 to 54 amperes, no. 2/0
54 to 96 amperes, 266,800 CM
96 to 114 amperes, 336,400 CM
114 to 260 amperes, 397,500 CM

Since the 336,400-CM and 397,500-CM curves are so close together for the range of loads for which 336,400 CM is the most economical, the extension of the use of 397,500 CM to cover this range is warranted. Thus, the entire range of loads can be economically served by three sizes of ACSR conductor, namely, no. 2/0, 266,800 CM, and 397,500 CM.

Economic Comparison for Growing Loads

The second step in the economic study is to make an accumulated annual cost comparison between established sizes and combinations of these sizes of conductor for a growing uniformly distributed load on a 10-mile line. An initial loading of 2,000 kva and a load growth of 11.6 per cent per year is taken. This allows the load to grow to 6,000 kva over a 10-year period. This initial loading and assumed load-growth rate correspond to the estimated values to be expected on the 13-kv lines when they go into service.

The cost comparisons are shown by the curves in Fig. 2. These curves show the 10-year accumulated annual cost for the various combinations with the ratio of length of large conductor to total circuit length varying from 0 to 100 per cent. The equations used in determining cost are shown in Appendix I. It is interesting to note that, in the development of equations for the determination of the most economical proportioning of sizes in a combination, the total length of line is not a factor. Only the proportion of lengths used in the graded construction arrangement is important.

For the use of one conductor size throughout, the accumulated annual cost for 266,800 and 397,600 CM are approximately equal for a 100-per-cent large conductor, as can be seen on the right-hand ordinate of Fig. 2. The accumulated annual cost of a line with a 100-per-cent no. 2/0 conductor would be substantially higher, as can be seen on the left-hand ordinate of Fig. 2. Calculations were also made for 336,400 CM, which showed it to be the most economical for use of only one size but approximately equal in cost to either 266,800 or 397,500 CM.

If the three chosen sizes are properly proportioned, combinations can be obtained which are more economical than any one size used alone, as shown in Fig. 2, and the use of all three sizes in combination is more economical than the use of only two sizes. In Appendix I, it is shown that the most economical design is obtained when 397,500 CM is used for 44.4 per cent of the total length, 266,800 CM for 26 per cent, and no. 2/0 for 29.6 per cent.

Effect of Load-Growth Rate

The effect of the load-growth rate upon the foregoing comparisons for uniformly distributed load was also investigated. Growth rates between 6 and 16 per cent were assumed and accumulated costs were calculated for both a 10-year period and the period of time necessary for a 2,000-kva initial load to grow to 6,000 kva for each rate. The ratios of wire lengths for the graded construction were taken as that found to be the most economical for the 11.6-per-cent rate. In practically all cases, the use of the three sizes of conductor in graded construction proved to be the most economical.

Effect of Change in Cost of Losses

A review of the calculations was made to determine the effect a change in cost of losses would have on the results. This could be caused by a change in demand and energy charges or by the use of a different method for loss evaluation. It was found that the relative positions of the curves in Fig. 1 remained unchanged but the points of crossover shifted to other load values. The shift of the crossover point will be inversely proportional to the square root of the change in loss cost, e.g., a 44-per-cent increase in loss costs gives $1/\sqrt{1.44}$ or 0.834, which is a 16.6-per-cent decrease in the load value. It was also found that the length of line for the smaller and medium sized conductors in a graded construction follows the same rule. The length of the larger conductor section then becomes $1-1/\sqrt{\text{change}}$.

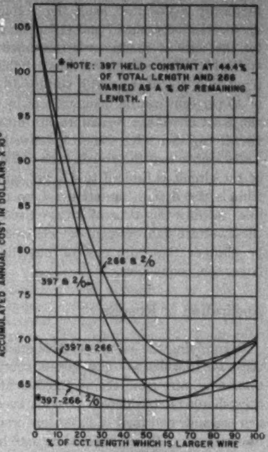

Fig. 2. Economical proportions of ACSR conductors in distribution circuits. Uniformly distributed load along line, length of circuit = 10 miles, initial load = 2,000 kva, final load = 6,000 kva, rate of growth = 11.6 per cent, and period of time = 10 years

Voltage Regulation Considerations

The reductions in voltage drop obtained with the greater investments required for conductor sizes larger than no. 2/0 ACSR are shown in Fig. 3. This curve shows that substantial reduction is obtained for investment in increased conductor sizes up until 266,800 CM is reached at which time the curve tends to bend over rapidly. The wire sizes being studied are seen to fall within the range where the most gain in voltage-drop reduction per dollar invested is found.

A check on the voltage regulation for a 10-mile line showed that, for a 6,000-kva uniformly distributed load, the voltage drop varied between 8.7 and 11.7 per cent for the various conductor arrangements studied. With substation bus voltage regulation, a primary circuit voltage drop of 10 per cent can be taken care of by a single set of voltage regulators out in the circuit together with some capacitor installations so that the drop in each section of the circuit is limited to 4.5 per cent. This is the design limitation set up for lines feeding this type of area. Use of these voltage-improvement devices would be cheaper than the cost of installing larger size conductors.

Application of Results

In applying the results of this study, the ways in which practical circuit conditions may vary from the assumed conditions should be considered. For instance, if a concentrated load of 6,000 kva were to be served at 13 kv, it would have to be much closer than 10 miles to a substation, and a single conductor size of at least 397,500 CM would have to be used.

It is believed that most of the 13-kv distribution circuits will tend to have uniformly distributed load. To allow for the possibility of loading the last half of a circuit somewhat more than the first half, it is planned to use 397,500 CM for approximately one-half the distance out from the substation on the circuit. If the last half of a line is fairly uniformly loaded and decreases to a very small load at the end of the main line run, the combination of 266,800 CM and no. 2/0 should be used for the last half of the line. Approximately one-half of the distance should be used for each size. If the load distribution is spotty with several heavily loaded spurs taking off near the end of the main line section, only 266,800 CM should be used for the last half. In determining the ratio of 266,800 CM and no. 2/0 which should be used, some thought should also be given to possible rearrangement of the line in the future so that a large enough conductor will be available at that time.

Conclusions

This study has shown that the three sizes of no. 2/0, 266,800 CM, and 397,500 CM ACSR conductor can be standardized and used in combination for the most economical circuit design for the loads to be carried by the 13-kv distribution system. Graded construction will be used for all new main line constructions with 397,500 CM used for half the distance and the other half composed of 266,800 CM and no. 2/0 in ratios determined by conditions of load distribution. Voltage regulation on long lines with heavy loads will need voltage regulator installations and possibly capacitor bank installations to hold voltage drop within prescribed limits. However, only one set of each are needed on a 10-mile circuit with a maximum allowable uniformly distributed load of 6,000 kva to give satisfactory service.

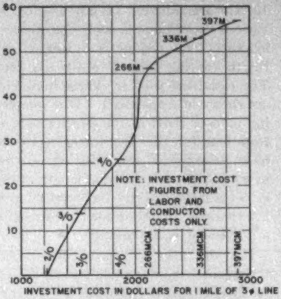

Fig. 3. Voltage-drop reduction gained per $ Invested for increasing ACSR distribution conductor size

Nomenclature

a_1 = ratio of large conductor length to total length
a_2 = ratio of medium conductor length to total length
K_1, K_2, K_3 = installed costs per mile of a 3-phase line (excluding poles and hardware) for large, medium, and small conductor respectively
L = length of circuit, miles
R = per-unit resistance
R_1, R_2, R_3 = per-unit resistance of conductors per circuit mile per 1,000 kva
I_1 = per-unit load in section
I_2 = per-unit load feeding through section
kva = initial load, kilovolt-amperes
n = number of years
r = rate of growth per year (as decimal)
C = annual cost
AC = accumulated annual cost

Appendix I. Equations for Determining Accumulated Annual Cost for Various Combinations of Conductor Sizes

Accumulated annual cost calculations were made for Fig. 2 using a circuit with graded construction and uniformly distributed load growing at a constant yearly rate. If three sizes of conductor are to be used, the following equations can be set up.

Losses for the last section are obtained using the well-known equation for uniformly distributed load where total losses are the same as if the total load were concentrated one-third of the distance out on the line. For sections where feed through of load must also be taken into account, the following equation gives the total losses for these sections

$$\text{Losses} = R(L)\left(I_2^2 + I_1 I_2 + \frac{I_1^2}{3}\right)$$

$$\text{Investment cost} = 0.155(L)[K_1 a_1 + K_2 a_2 + K_3(1 - a_2 - a_1)]$$

Loss cost

$$\text{1st section} = 0.032(R_1)(L)(\text{kva}^2)(a_1 - a_1^2 + a_1^3/3)$$

$$\text{2nd section} = 0.032(R_2)(L)(\text{kva}^2)[a_2(a_1 - 1)^2 + a_2^2(a_1 - 1) + a_2^3/3]$$

$$\text{3rd section} = 0.032(R_3)(L)(\text{kva}^2)[1/3 + a_1(a_2 - 1)^2 - a_1^2(a_2 - 1) - a_1^3 - (a_2 - a_2^2 - a_2^3/3)]$$

$$C = (\text{investment cost}) + (1+r)^{2n}(\text{loss cost}) \quad \text{for any year } n$$

and

$$AC = \int_{1/2}^{n+1/2} C\,dn$$

$$AC = n\,(\text{investment cost}) + \left(\frac{(1+r)^{2n+1} - (1+r)}{2 \log_e (1+r)}\right)(\text{loss cost})$$

To obtain the most economical (minimum cost) length for each conductor size, the following steps were made

$$\frac{dAC}{da_1} = 0 = \frac{dAC}{da_2}$$

Solving for a_2 using the two equations just obtained, substituting back, and taking $(dAC)/(da_1) = 0$

$$a_1 = 1 - \sqrt{\frac{9.7(n) \log_e (1+r)}{\text{kva}^2[(1+r)^{2n+1} - (1+r)]}} \times \sqrt{\frac{K_1 - K_2}{R_2 - R_1}}$$

Substituting back in one of the equations

$$a_2 = \sqrt{\frac{9.7(n) \log_e (1+r)}{\text{kva}^2[(1+r)^{2n+1} - (1+r)]}} \times \left(\sqrt{\frac{K_1 - K_2}{R_2 - R_1}} - \sqrt{\frac{K_2 - K_3}{R_3 - R_2}}\right)$$

then

$$a_3 = 1 - a_2 - a_1 = \sqrt{\frac{9.7(n) \log_e (1+r)}{\text{kva}^2[(1+r)^{2n+1} - (1+r)]}} \sqrt{\frac{K_2 - K_3}{R_3 - R_2}}$$

For construction using two sizes of conductor

$K_3 = 0$

$R_3 = \infty$

a_1 = same as before

$$a_2 = \sqrt{\frac{9.7(n) \log_e (1+r)}{\text{kva}^2[(1+r)^{2n+1} - (1+r)]}} \times \sqrt{\frac{K_1 - K_2}{R_2 - R_1}} = 1 - a_1$$

For construction using 397,500 CM, 266,800 CM, and no. 2/0, the proportions of each size of wire is determined as follows

$$a_1=1-\sqrt{\frac{9.7(10)\log_e 1.116}{(2{,}000)^2(1.116^{21}-1.116)}}\times\sqrt{\frac{2{,}882-2{,}114}{0.00221-0.00149}}$$

$$=0.444$$

$$a_2=\sqrt{\frac{9.7(10)\log_e 1.116}{(2{,}000)^2(1.116^{21}-1.116)}}\times\left(\sqrt{\frac{2{,}882-2{,}114}{0.00221-0.00149}}-\sqrt{\frac{2{,}114-1{,}229}{0.00513-0.00221}}\right)$$

$$=0.26$$

$$a_3=1-0.444-0.26=0.296$$

where

K_1 = \$2,882 per mile installed cost of 397,500 CM
K_2 = \$2,114 per mile installed cost of 266,800 CM
K_3 = \$1,229 per mile installed cost of no. 2/0
R_1 = 0.00149 per unit, ohms per 1,000 kva per mile
R_2 = 0.00221 per unit, ohms per 1,000 kva per mile
R_3 = 0.00513 per unit, ohms per 1,000 kva per mile
kva = 2,000 kva initial load
r = 11.6 per cent per year growth
n = 10 years

◆

Discussion

J. A. Salin (Ebasco Services, Inc., New York, N. Y.): The authors are to be congratulated on a very well written and well-presented paper. I think it is clear and very much to the point. I have compared the conductor sizes indicated to be most economical for the loads considered against similar studies that my associates and I have made and I find that within these load limits they are in substantial agreement. This is rather surprising, however, because it is our feeling that complete line costs should be used in economical wire size studies rather than the cost of conductor alone or incremental costs. I think it would be interesting to know why the authors feel that the cost of structures should be left out altogether.

As indicated in the paper, application of results is very important and, in using the results of any study, consideration must be given to the many factors which cannot be accurately evaluated in dollars. In this connection, why stop at the 397,500 CM conductor? While supporting structure costs may increase for conductor sizes larger than 397,500 CM, the increase may and usually is more than offset when the alternates such as additional line construction and perhaps even additional substations and/or transmission lines are required. Increase in pole-line costs for conductors up to 800,000 CM all aluminum on short-span construction is not great. I mention the use of conductor sizes greater than 397,500 CM because, while load densities in the area considered by the authors may not indicate circuit loads in excess of 6,000 kva, greater densities, which are becoming quite common, result in economical 13-kv circuit loads well in excess of 6,000 kva.

I am not certain whether reference to no. 2/0 ACSR as a minimum size applies to laterals or not. If so, I believe smaller conductors should be considered (say for loads under 40 amperes) as savings in investment in laterals are important since they make up a large part of the total investment in primary lines.

If conductor sizes larger than 397,500 CM and smaller than no. 2/0 are used I feel the two sizes 397,500 and 266,800 CM could be reduced to one size only. The conditions and practical considerations mentioned by the authors are certainly very important and, though it is difficult to bring them into the economical calculations, I feel they should have considerable bearing on the selection of wire size. One practical point upsetting the conclusions is that many circuits are not long radials with evenly distributed loads as were used in the analysis. Frequently, and this is an advantage from the standpoint of voltage drop and losses, circuits break up into two or more branches near the source. Another point is that circuits must be designed for emergency as well as normal operation and, while greater voltage drop and losses can be tolerated under emergency operation, ties to other circuits for emergency purposes must be adequate to perform satisfactorily when needed. Also, as the system grows, more substations will be added, and long-range plans should be carefully prepared to prevent, in so far as practical, needless and expensive conductor replacements at a later date.

J. R. Oberholtzer (Commonwealth Associates Inc., Jackson, Mich.): This paper presents an excellent analysis of the effect of proper consideration of the cost of distribution losses on system design. In the postwar era of rapid expansion, these losses have often been overlooked, sometimes necessarily so because of lack of manpower and material. The constant recognition of losses should be a part of any system-planning procedure.

It is significant to compare the current ranges for static loads for various conductor sizes, shown in the section entitled "Economic Comparison for Static Loads," with the thermal ratings of these conductors. For the first three, the maximum current is only about 20 per cent of the thermal rating. Referring to Fig. 2, the maximum load through a conductor, under conditions of growing load distributed along the line, is shown to be less than half the thermal limit for economical application.

Referring again to Fig. 2, it is noted that the use of the larger conductor to a greater extent than indicated for minimum cost will increase the accumulated annual costs only slightly. Decreased voltage drops resulting from greater use of the larger wire are not evaluated in this comparison and would tend to favor the larger size. Also, the percentage fixed-charge difference would probably be smaller if the comparison were extended over the entire life of the circuit, since loading after the first 10 years would probably be nearer the circuit rating. Considering these items, it appears that preference should be given to the largest conductor if there is any reasonable expectation that the line will become a trunk feeder to a load concentration or from a future 13-kv source. It seems that the direct route between two initial sources should have the largest conductor size throughout its length.

Although the load density in the area under consideration is not stated, the circuit dimensions indicate that it is rather light compared to the usual urban densities. Even at these light densities, adequate primary voltage is provided by one set of line regulators installed on each circuit. Considering the application of this distribution voltage at greater densities, in the order of 1,000 kva per square mile, it appears that both thermal limits and primary voltage drop will disappear as design limitations to be replaced by power loss considerations.

A. W. Funkhouser and R. P. Huber: The authors appreciate the comments of Mr. Salin and Mr. Oberholtzer which should add to the value of the paper. It is interesting to note that both discussers agree that more extensive use of larger conductor sizes for distribution systems is in order. It has been our experience in the past that wire sizes have been chosen conservatively and at times do not fit in with future requirements. They can become obstacles to good design since change-out costs often cannot be justified on the basis of economics.

Mr. Salin questions the omission of pole and hardware costs. Since our study is a comparison between sizes based on relative annual cost, any fixed charges common to all will not affect the relative position of the cost curves. For reasons set out in the text, the costs of poles and hardware would not vary on our particular system for the range of sizes considered. This permitted us to leave them out of our study.

The suggestion that greater circuit loadings and considerably larger conductor sizes might be used would be applicable, we feel, in areas with greater initial load density and greater load growth rates (approximately 100 kva per square mile and 11.6 per cent in this study) and on systems requiring considerably more new pole-line construction than was necessary in our system. Our study was limited to main line construction and, as suggested by Mr. Salin, smaller conductors will be used for laterals. At present, most existing laterals have no. 4 copper which will remain, and for new construction no. 2 ACSR will be used.

The point that the forking of a feeder circuit near the source might alter the selection of conductor sizes is well taken, but such an arrangement would be exceptional in the area studied. The method of conductor grading might still be applicable to the main branches, depending upon the permanency of the forked arrangement.

We agree with Mr. Salin that the emergency capabilities must be considered to make sure that the sizes selected are adequate from the thermal- and voltage-regulation standpoint. With the size of economical conductor being substantially above thermal limitations, as brought out by Mr. Oberholtzer, the capacity of the conductor should be sufficient in most cases. With a line-section voltage-regulation limitation of $4^{1}/_{2}$ per cent, considerable additional emergency load can be carried before a critically low voltage is reached.

As pointed out by Mr. Oberholtzer, the recognition of distribution losses is an important factor in system design. If the circuits are allowed to remain loaded up to maximum load in future years, the losses will be the predominant factor and would favor the use of larger conductor. We think that when maximum circuit loads are reached additional circuits or rearrangements with new substations will tend to repeat the load-growth cycles on feeder sections, although possibly not over as great a range as the original assumption of a 3 to 1 ratio of final to initial load. The process of adding substations and reducing circuit length as load densities grow will increase the importance of losses as compared with the thermal- and voltage-drop limitations in the selection of conductor sizes.

Distribution-Substation and Primary-Feeder Planning

W. J. DENTON
ASSOCIATE MEMBER AIEE

D. N. REPS
ASSOCIATE MEMBER AIEE

ELECTRIC utility distribution system planning is extremely difficult because plans for the addition of new facilities must keep well ahead of the time when the exact locations and magnitudes of the future loads to be served by those facilities are known. This paper presents a basis and methods for distribution system planning which take load growth into account in such a way that exact locations and magnitudes of future loads need not be known to arrive at an economic system for serving the loads when they develop. To accomplish this purpose, hypothetical, equivalent distribution systems are devised for quickly analyzing the service quality and the economic feasibility of distribution system growth plans applicable to the load areas of the actual system being studied.

The system planning concepts and methods presented in this paper are particularly applicable to urban and suburban residential areas, served predominately by overhead circuits. In such load areas some of the most fundamental planning problems center on the distribution substations, where the interrelated problems of subtransmission-system and primary-feeder design converge. Choice of distribution-substation arrangement, size, and voltage rating influences system planning in two directions: toward the source via the subtransmission circuits, and toward the load via the primary-feeder circuits.

The equivalent-system method recognizes the uncertainty of the exact magnitudes and locations of future loads in planning the locations and ratings of distribution substations, and the number and capability of the primary feeders required to distribute the power from these substations. In the equivalent system each distribution substation with its primary-feeder circuits serves an area in which load density is comparable to the values existing or forecast for the actual system being studied. Results of studies made for equivalent systems, for different values of load densities, are applicable to actual systems despite wide variations in the actual locations of individual loads in the equivalent or actual system.

Hypothetical, Equivalent Substation Areas

The hypothetical, equivalent distribution-substation areas employed in the analyses of this paper have the shape of regular polygons. The number of sides to the polygon representing a load area is equal to the number of primary feeders radiating from the primary-circuit feed point, which is assumed to be located at the center of the area. The distribution substation may be located at the feed point, or may be remotely located, with one or more express primary feeders carried from the remote substation to the feed point. For example, a hypothetical area served by six circuits radiating out from a feed point would be hexagonally shaped, with each feeder carried from the center of the hexagon along an apothem, or diagonal.

The use of hypothetical load areas and circuit patterns of symmetrical geometry greatly simplifies the comparison of alternative plans which may call for different sizes of distribution substation, different numbers of primary-feeder circuits, and different primary-feeder voltages. Such load areas and circuit patterns are abstractions because they do not exist exactly in such forms anywhere. These abstractions, however, can be made to conform with the system they are devised to represent in all of the following ways: load density, substation size; substation or feed-point service area in square miles; number of primary-feeder circuits; conductor material, and circuit impedance values; and primary-feeder voltage.

Hypothetical distribution-substation areas cannot be made to conform with actual systems in two ways: the exact duplication of circuit pattern, and the exact locations and magnitudes of loads. But as load grows, these two attributes of the system continually change, sometimes at so fast a rate that the system planner must spend all of his time with remedial measures or extensions in relatively small portions of the system, while the possibilities for system-wide engineering and economic benefits go uninvestigated.

Distribution-Substation Planning

The one phenomenon common to all distribution-system load areas is increasing load density. This is particularly true of the urban and suburban residential areas served by overhead primary-feeder circuits. Regardless of the plan adopted for serving such areas, load growth must be accompanied by (perhaps should be preceded by) an equivalent increase in distribution-substation and primary-feeder capacity. Very often, to achieve the required increases in system capability, changes in the basic system-growth plan must be made.

There are many features of the distribution substations and primary feeders that can be changed, over any reasonable

---

Paper 55-158, recommended by the AIEE Transmission and Distribution Committee and approved by the AIEE Committee on Technical Operations for presentation at the AIEE Winter General Meeting, New York, N. Y., January 31-February 4, 1955. Manuscript submitted October 26, 1954; made available for printing December 2, 1954.

W. J. DENTON is with the Westinghouse Electric Corporation, Des Moines, Iowa, and D. N. REPS is with the Westinghouse Electric Corporation, East Pittsburgh, Pa.

period of time, provided that the funds required for making the changes are available and that continuity of service to the customers is maintained while the system is being altered or expanded. Indeed, many changes are very desirable and serve to improve system economy, quality of service, and operation. Such changes may affect all of the following: primary-feeder voltage; distribution-substation size and arrangement; number of, and routing of, primary-feeder circuits; primary-feeder loading; the various applications of supplementary voltage regulators, switched and unswitched capacitors, line-sectionalizing devices, etc. Any change must eventually lead to an increase in distribution-substation capacity.

The addition of distribution-substation capacity can follow virtually an infinite variety of general plans which must fall, however, between two extremes. In one extreme, the area served from a single substation site remains fixed and the capacity of the substation grows with load density. In the second extreme, a fixed amount of transformer capacity is located on a given substation site and additional transformer capacity is located at new sites as load grows. These two extremes of distribution-system growth will be called:

1. The constant substation-area plan.
2. The constant-substation-size plan.

Between two extremes there are an infinite variety of plans which call for both the enlarging of existing substations and the addition of new substations.

As load grows, the evolution of distribution substations and primary feeders may proceed slowly at certain times, and rapidly at other times, depending on what steps are taken. Changes which occur rapidly may be embodied into the system before the load has increased by very much. During changes which evolve slowly, the load may increase appreciably.

The rate of load growth, with the attendant system-wide increase of load density, will vary not only from one system to another but also within individual substation areas. The engineering and economic factors determining the capability and pattern that a system should have at any given time depend on the rate of load growth, which unfortunately is at times a highly uncertain factor. Consequently, in order to base a system plan on some limits within which the uncertainties of load growth will lie, the various steps that can be taken to increase distribution-substation and primary-feeder capacity can be divided into two general categories: those which are accomplished while the load density remains constant, and those which are achieved usually over considerably longer periods of time during which the load density increases. The accuracy of load growth forecast will determine the accuracy of the estimated time period over which such changes should be made.

For short-range planning, the assumption can be made that load density remains constant. Even for short-range planning, however, any analysis which freezes load density will be recognized as not realistic, since load density in some urban and suburban residential areas increases appreciably even during time intervals measured in months. But a constant-density analysis, though it is academic, does serve the useful purpose of establishing certain limits on what can be accomplished when certain types of changes are made.

Nomenclature

D=load density, kilovolt-amperes (kva) per square mile
n=number of primary-feeder circuits emanating from a distribution substation site, or primary feed point. Referred to as an n-feeder pattern
kva_n=kva loading per feeder in an n-feeder pattern
kva_{nt}=total kva loading for all n feeders in an n-feeder pattern
A_n=area in square miles served by one primary feeder in an n-feeder pattern
A_{nt}=total substation or feed-point area in square miles served by an n-feeder pattern
S=radius, or opothem, of a regular polygon representing an area served by n feeders
kv=voltage at which a primary feeder operates
V_{ab}=per-cent (%) voltage drop from point a to point b
K_M=% voltage drop per kva-mile in a primary-feeder main
K_F=% voltage drop per kva-mile in a primary subfeeder
K_L=% voltage drop per kva-mile in a primary lateral
$K_1, K_2, a, b, c, d, e, a', b', c', p, q, x, y, \theta, u, v, w, P_n$ are all used in connection with particular derivations and are not intended for general use

System Changes at Constant Load Density

System planning often is centered about remedial measures which are required because of inadequate capability in the existing distribution substations and primary feeders, or poor quality and continuity of service. Usually when distribution substations and primary-feeder circuits are inadequate from a load-carrying capability standpoint, voltage drops are excessive and outages are frequent and of long duration.

Some of the obstacles that may be encountered in attempting to achieve short-range remedies, with long-range continuing benefits, are: unavailability of new substation sites and subtransmission and primary-circuit easements; prohibiting ordinances or codes or unfavorable civic sentiment toward more numerous or higher voltage circuits; and insufficient funds for investment in new facilities.

Two basic types of changes to distribution substations and primary feeders will be examined while load density remains constant: those involving an increase in primary-feeder voltage, and those for which primary-feeder voltage remains the same. Figs. 1 through 5 picture five different plans for the changing of distribution-substation size and area, or the number of primary feeders, at constant load density. Figs. 1, 2, and 3 deal with feeder-voltage increase. Figs. 4 and 5 show what can be done through two remedial measures applied at the existing primary-feeder voltage. Hypothetical substation areas having the shape of regular polygons are used to demonstrate the effects of these changes.

CONSTANT LOAD DENSITY—INCREASING PRIMARY-FEEDER VOLTAGE

Figs. 1, 2, and 3 illustrate a type of system renovation that has achieved considerable popularity—increasing the primary-feeder voltage. When such an extensive and high conversion cost project is undertaken, there are certain factors which govern what can be accomplished. It is well known that for the same kva loading the % voltage drop in a primary-feeder circuit will decrease inversely with the square of the voltage. A new voltage three times the original voltage will result in one-ninth the original % voltage drop. But when primary-feeder voltage is increased, optimum benefits may accrue if feeder loading, or distribution-substation size, is allowed to increase, at some sacrifice to the maximum possible reduction in feeder % voltage drop. Figs. 1, 2, and 3 each describe a possible plan for increasing primary-feeder voltage.

Fig. 1: At constant load density, constant substation size (and area), and constant % voltage drop per feeder, the number of primary feeders varies inversely as the square of the primary-feeder voltage. The following relationship describes this effect.

$$n \propto \left.\frac{1}{kv^2}\right|_{\text{Constant } D, kva_{nt}, A_{nt}, V} \tag{1}$$

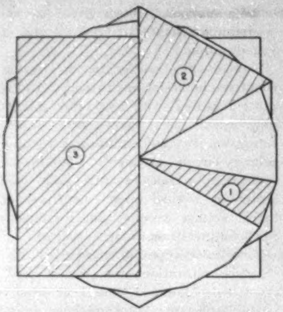

Fig. 1. Constant D, kva$_{nt}$, A$_{nt}$, V. The number of primary feeder varies as shown in equation 1. Relative values of primary-feeder voltage are:

1. kv=1.0; 2. kv=1.73; 3. kv=3.0

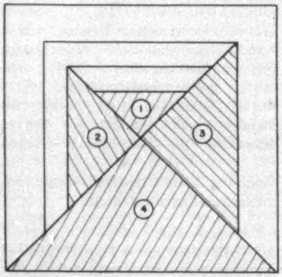

Fig. 2. Constant D, n, V. The substation loading or service area varies as given by equation 2. Relative values of primary-feeder voltage are:

1. kv=1.0; 2. kv=1.73; 3. kv=3.0; 4. kv=5.0

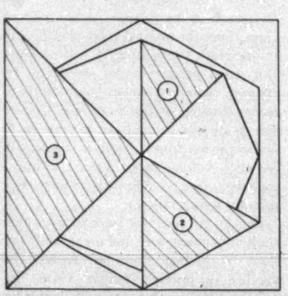

Fig. 3. Constant D. The substation loading, number of feeders, and primary-feeder voltage vary as shown by equation 3. Relative values of primary-feeder voltage are:

1. kv=1.0; 2. kv=1.73; 3. kv=3.0

Figs. 1 through 9. The regular polygons represent areas that are served from a distribution substation or feed point located at the center of the concentric polygons. The shaded sectors represent the area that can be served by one primary-feeder circuit emanating from the feed point or substation. The circled numbers with the shaded feeder-sector areas refer to the relative value of the planning parameter that is varied for that type of plan represented by the particular figure. The system-planning parameters are: Load density D; substation or feed-point loading kva$_{nt}$; substation or feed-point service area A$_{nt}$; primary-feeder voltage kv; number of primary feeders radiating from the feed point n; % voltage drop from the feed point to the end of the primary-feeder circuit V

In Fig. 1 hypothetical distribution-substation areas employing three relative values of voltage are illustrated: 1.0 kv, 1.73 kv, and 3.0 kv, with 18, 6, and 2 primary feeders required at these voltages respectively.

Fig. 2: If for an increase in primary-feeder voltage the number of primary feeders radiating from a substation or feed point remains the same, and the total % voltage drop per feeder remains the same, then each feeder can serve a larger area at the same load density. Fig. 2 illustrates that for a constant number of feeders, and % drop, at constant load density the area served by each feeder varies as the voltage raised to the four-thirds power

$$kva_{nt} \propto A_{nt} \propto kv^{4/3}\Big|_{\text{Constant } D,n,V} \qquad (2)$$

In Fig. 2 the relative areas that can be served by primary feeders operating at 1.73, 3.0, and 5.0 times the original kilovolts of relative value 1.0 are shown.

Fig. 3: Substation-revision plans provide for maximum benefits in reducing the number of feeders, Fig. 1, or increasing the substation size using the same number of feeders, Fig. 2, through the use of a higher primary-feeder voltage. However, optimum economic and service-quality benefits attendant with changeover to a higher primary-feeder voltage can usually be realized if use of the same, or somewhat fewer, primary feeders is accompanied by use of a larger distribution substation. An increase in primary-feeder voltage could result in a substation-area pattern which falls somewhere between the extremes of Figs. 1 and 2. Such a change is shown in Fig. 3.

With changeover to a higher primary feeder voltage, three results can be achieved: reduction in the number of feeders; increased substation size; reduction in the feeder % voltage drop. The extent to which all these desirable benefits can be accomplished simultaneously is given by the following relationship

$$V \propto \frac{kva_{nt}^{3/2}}{n^{3/2}kv^2}\bigg|_{\text{Constant } D} \qquad (3)$$

Fig. 3 shows changes to higher primary-feeder voltages while the % voltage drop in feeders remains constant. When the existing primary-feeder voltage is multiplied by 1.73, the number of feeders can be reduced by 25% (from eight to six in this case), while the substation size can be increased by 33%. With a changeover to three times the original primary-feeder voltage, the number of primary feeders can be reduced to half (from eight to four in this case) and substation size may be doubled.

If, however, some reduction in feeder % voltage drop is also desired when the

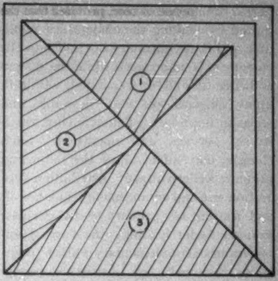

Fig. 4. Constant D, kv, n. The substation or feed-point loading and service area vary as shown by equation 4. Relative values of primary-feeder % voltage drop are:

1. V=1.0; 2. V=2.0, 3. V=3.0

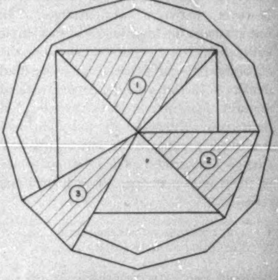

Fig. 5. Constant D, kv, V. The substation or feed-point loading and number of primary feeders vary according to the relationship in equation 5. Relative values for substation or feed-point loading are:

1. kva$_{6t}$=1.0; 2. kva$_{9t}$=1.5; 3. kva$_{12t}$=2.0

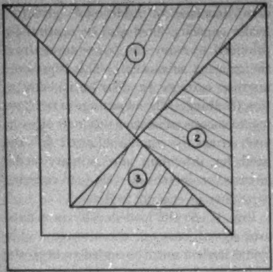

Fig. 6. Constant kva_{nt}, n, kv. As load density increases while substation load remains constant, substation or feed-point service area and % voltage drop in feeders vary as given by equation 6. Relative values of density, area, and % voltage drop are:

1. $D=1.0$, $A_{nt}=1.0$, $V=1.0$
2. $D=2.0$, $A_{nt}=0.5$, $V=0.7$
3. $D=4.0$, $A_{nt}=0.25$, $V=0.5$

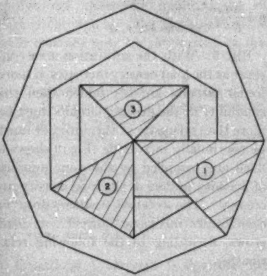

Fig. 7. Constant kva_{nt}, V, kv. As load density increases while substation load remains constant, the number of primary feeders and substation or feed-point area vary as given by equation 7. Relative values of density, area, and % voltage drop are:

1. $D=1.0$, $A_{nt}=1.0$, $V=1.0$
2. $D=2.0$, $A_{nt}=0.5$, $V=1.0$
3. $D=4.0$, $A_{nt}=0.25$, $V=1.0$

changeover is completed, then the substation-size increases cannot be as great as shown for Fig. 3, which illustrates constant % voltage drop cases. The changes illustrated in Fig. 3 are not intended to represent optimum engineering and economic improvement but only serve to illustrate what may, or may not, be accomplished with changeover to a higher primary-feeder voltage.

CONSTANT LOAD DENSITY—UTILIZING THE SAME PRIMARY-FEEDER VOLTAGE

Figs. 4 and 5 illustrate changes in substation size and the primary-feeder pattern while maintaining the same primary-feeder voltage. Such changes do not usually require the numerous, high initial cost system renovations which must accompany a changeover to a higher primary-feeder voltage.

At a constant load density, with the use of the existing primary voltage, an increase in the distribution-substation capacity at a given site can be accomplished only by increasing the number of primary feeders or increasing the loading, and consequently the % voltage drop, in the existing feeders.

Fig. 4: An increase in feeder loading at constant load density, with the attendant increase in % voltage drop in each feeder, is illustrated in this picture of a hypothetical, 4-feeder substation. An increase of 60% in feeder loading results in twice the original % voltage drop, and an increase of 110% in feeder loading results in three times the original % voltage drop. The following relationship describes this

$$kva_{nt} \propto A_{nt} \propto V^{2/3}\Big|_{\text{Constant } D,\, kv,\, n} \qquad (4)$$

An increase in % voltage drop must ordinarily be compensated for by an increased use of supplementary forms of primary-feeder voltage regulation, so that the voltage spread allocated to the primary-feeder circuit does not become excessive. Thus if the total drop is increased, additional voltage regulators must be installed at points the primary feeder so that the drop between voltage-regulated points, or between the last point on the line at which a regulator is applied, and the end of the feeder does not exceed the allowable spread-governed voltage drop in the primary feeder.

Fig. 5: A method for increasing the substation capacity at a given site, with the same primary-feeder voltage and % voltage drop in feeders, is to increase the number of feeders. The expression for this type of change is approximately given by

$$n \propto \frac{kva_{nt}}{\tan^{1/3}\left(\dfrac{180}{n}\text{ degrees}\right)}\Bigg|_{\text{Constant } D,\, kv,\, V} \qquad (5)$$

In equation 5 it will be noted that the tangent of half the angle represented by a feeder "sector" is included in the relationship. Thus the variation of kva_{nt} with n will depend to a considerable extent on the particular values of n employed before and after the change.

A typical example is shown in Fig. 5. In this case of feeder addition at constant load density and % drop, an increase from four to eight feeders permits a 50% increase in substation size. Tripling the number of feeders, from 4 to 12, permits the approximate doubling of substation size.

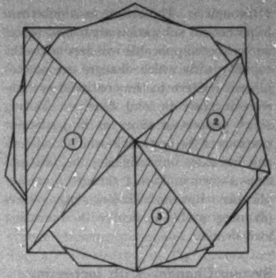

Fig. 8. Constant A_{nt}, V, kv. As load density increases while substation or feed-point area and % voltage drop in feeders remain constant, the relationship between the variable system-planning parameters is given in equation 8. Relative values of density, number of primary feeders, and % voltage drop are:

1. $D=1.0$, $n=4$, $V=1.0$
2. $D=2.0$, $n=7$, $V=1.0$
3. $D=4.0$, $n=10$, $V=1.0$

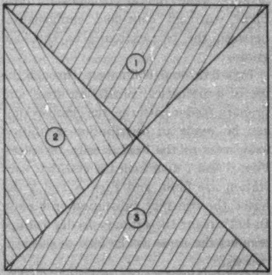

Fig. 9. Constant A_{nt}, n, kv. As load density increases while substation or feed-point area and number of feeder circuits remain constant, the relationship between the variable system-planning parameters is given in equation 9. Relative values of density, number of primary feeders, and % voltage drop are:

1. $D=1.0$, $n=4$, $V=1.0$
2. $D=2.0$, $n=4$, $V=2.0$
3. $D=4.0$, $n=4$, $V=4.0$

SUMMARY FOR CONSTANT LOAD-DENSITY CHANGES

The relationships between the substation size and the primary-feeder circuit pattern as changes are made at a constant load density have been pictured in Figs.

1 through 5. The extent to which these hypothetical substation areas and feeder patterns are applicable will depend on the rapidity with which changes are accomplished relative to the continual systemwide increase in load density. During short periods of time, or in particular portions of the system, in which load density increases only slightly, the relationships shown in Figs. 1 through 5 are applicable. But the basic long-range system planning problems deal with increasing load density.

System Changes With Increasing Load Density

Two extreme plans for making system changes at increasing load density—one calling for constant substation size, and the other for constant substation area—have already been discussed. Neither type of plan permits obtaining the maximum possible benefits in all components of the distribution system. A long-range optimum plan for any specific system will generally be one in which the system will acquire some of the benefits of both plans, through continual compromises between the two extremes as the load grows.

Figs. 6 through 9 illustrate, through the use of hypothetical substation areas and primary-feeder patterns, the changes that can be made in distribution-substation load areas as the load density increases. Figs. 6 and 7 deal with the constant substation-size plan, and Figs. 8 and 9 describe the constant substation-area plan. In both plans the primary-feeder voltage remains the same as the load density increases.

INCREASING LOAD DENSITY—CONSTANT SUBSTATION-SIZE PLAN

If the amount of capacity located at any one substation site remains fixed as the load density increases, then increments of new substation capacity that are continually added must be placed at new sites geographically located at points lying between existing substations. As load density increases, substation area decreases, so as to keep substation loading constant. The principal disadvantage of such a plan is that, as the load grows, suitable substation sites may not be obtainable. However, as one extreme representing a limit within which system growth must take place, this plan merits attention.

Constant substation-size plans may in turn be grouped into two basic schemes. In one, the number of primary-feeder circuits remains constant with increasing load density, but the % voltage drop is high at the outset when the load density is light and the substation area is relatively large. In the second scheme, primary-feeder voltage drop remains constant with increasing load density, requiring the use of more feeders per substation at the outset, when the density is low and the feeder circuits are long. These two schemes are shown in Figs. 6 and 7.

Fig. 6: With increasing load density, the use of a constant number of primary-feeder circuits supplied from a substation of constant size results in a continually decreasing % voltage drop in feeder circuits as the substation area decreases and the primary feeders are shortened. The following relationship describes this behavior

$$V \propto \frac{1}{D^{1/2}} \propto A_{nt}^{1/2} \Big|_{\text{Constant } kva_{nt},\, n,\, kv} \qquad (6)$$

In Fig. 6, when the load density in the area served by a constant-size substation has doubled and substation area is halved, voltage drop is reduced to 70% of its original value. When load density in the still further reduced substation area is four times the original value, the % voltage drop is reduced to half the original amount.

Fig. 7: With increasing load density and constant substation size, constant % voltage drop in primary feeders can be kept constant while the required number of feeders per substation continually decreases. Thus construction of new feeder circuits can proceed at a slower rate than substation addition. The number of feeders per substation, as a function of load density, is given by

$$n \propto \frac{1}{D^{1/2}} \propto A_{nt}^{1/2} \Big|_{\text{Constant } kva_{nt},\, V,\, kv} \qquad (7)$$

In Fig. 7, when the load density is doubled, the number of primary feeders required to serve the smaller area containing the same load is reduced from eight to six. When load density is quadrupled, the number of feeders is reduced to four. Note that the need to always consider a whole number of primary feeders will require use of the nearest, larger whole number of feeders if the value for n given by equation 7 does not result in a whole number.

INCREASING LOAD DENSITY—CONSTANT SUBSTATION-AREA PLAN

If the size of the area served from a given substation site remains constant as the load density increases, then additional transformer capacity must be placed at that site as the load within the area increases. Additional primary-feeder capacity must also be continually provided to carry the power away from the growing substation. This represents another extreme in distribution-substation planning. The advantage of not having to locate substations at new sites as load grows is counterbalanced by the need for providing new primary-feeder circuits or increasing the load-carrying capability of existing feeders.

Fig. 8: As the load density in a fixed area served from one site increases, additional feeders must be added to keep the % voltage drop in the feeder circuits constant. In the case shown in Fig. 8, when load density and substation load have doubled, the number of primary feeders increases from four to seven. At four times the original load density, ten primary feeders are required. The relationship between the number of feeders and the substation size for the constant-area plan is given approximately by

$$n \propto \frac{kva_{nt}}{D^{1/2}} \Big|_{\text{Constant } A_{nt},\, V,\, kv} \qquad (8)$$

Fig. 9: With the substation area constant as the load density increases, if more feeder circuits are not added then the capability of the existing circuits must be more than adequate at the outset or must be continually increased. Fig. 9 shows a fixed area supplied by the same number of primary feeders as the load density increases. The total % voltage drop in each feeder increases, however, as load grows, according to the following relationship

$$V \propto kva_{nt} \propto D \Big|_{\text{Constant } A_{nt},\, n,\, kv} \qquad (9)$$

The capability of a constant number of feeders serving a constant area as the load density increases is limited in two ways: one limit is the thermal capability of the feeder conductors, and the other is the maximum allowable % voltage drop between voltage regulated points on the feeder circuit. Provided that the existing feeder conductors are of adequate size to carry the load current, supplementary voltage regulators can be added along the feeders as load grows. Although the total voltage drop continually increases, this practice would keep the voltage spread along the feeders from becoming excessive.

CHANGES IN PRIMARY-FEEDER VOLTAGE WITH LOAD DENSITY INCREASING

Long-range system planning problems always involve increasing the load densities. Often, such planning may consider increases in the primary-feeder voltage. The increasing density examples of Figs.

6 through 9 are based on unchanged primary-feeder voltage. The effects of increased primary-feeder voltage with increasing load density can be obtained by combining the plans of Figs. 1, 2, and 3 with any one or more of those in Figs. 6 through 9. Such a procedure is one which "freezes" the load density at several values, each larger than the preceding density. The effects of various plans can then be observed from one value of load density to the next. This technique of observing dynamic or growth situations through a number of successive static representations is a standard procedure in fields of endeavor as widely diverse as power-system stability, economic theory, motion pictures, and theoretical physics.

Planning for Specific Systems or Areas

The various changes by which distribution substations and primary feeders evolve are described qualitatively in Figs. 1 through 9. The plans calling for such changes may be catalogued as follows:

1. Constant load-density planning
   a. Increasing primary-feeder voltage, Figs. 1, 2, and 3
   b. Unchanged primary-feeder voltage, Figs. 4 and 5
2. Increasing load-density planning
   a. Constant-load distribution substations, Figs. 6 and 7
   b. Constant-area distribution substations, Figs. 8 and 9

Equations 1 through 9 describe the qualitative relationships between load density, substation size and service area, number of primary feeders, primary-feeder voltage, and feeder % voltage drop for Figs. 1 through 9 respectively. The equations are gleaned from the results of the derivations presented in the Appendixes. Since these equations deal with the physical and electrical attributes of the distribution system, substitution of wide ranges of practical values for these parameters into the more complete equations of the Appendixes yields information that can be used for the planning of specific systems. Typical results of such substitutions into the equations are shown in Figs. 16 and 17. All of the system-planning factors enumerated in the foregoing, are represented quantitatively in Figs. 16 and 17. From these figures the growth of a specific system following any one of the plans can be observed.

Figs. 16 and 17 are, essentially, plots showing the number of primary feeders n per substation or feed point versus load density D within the substation or feed-point service area. The variation of n with D is shown for constant substation or feed-point loading kva_{nt} or constant substation or feed-point area A_{nt}. Fig. 16 deals with a primary-feeder voltage of 2,400/4,160 volts. Fig. 17 shows the relationships between the planning factors at 7,620/13,200 volts primary-feeder voltage. Each set (frame) of curves represents a different total % voltage drop in primary feeders. Curves for 3, 6, and 10% voltage drop are shown.

The system-planning factors, namely D, kva_{nt}, A_{nt}, n, kv, and V, may be followed by using these curves while one or more of the factors is kept constant or allowed to vary. The interrelated changes in magnitude or quantity of the six parameters are given in Figs. 16 and 17. An important system-planning ingredient not included in these relationships is time. During intervals of time over which load density increases little in certain portions of the system, the constant-density approach may be adopted for making changes. In other portions of the system, or over other periods of time during which load and density grow appreciably, the increasing-density plans may be applied.

Summary and Conclusions

Useful methods for distribution-substation and primary-feeder planning are given in this paper. The planning methods are based on the concept that actual distribution systems can be represented by hypothetical systems which are relatively simple to construct and analyze. For the purposes of system planning, these hypothetical systems are equivalent to the actual system which they represent.

Analysis of a number of primary-feeder circuit patterns of different geometric arrangement shows that distribution-substation and primary-feeder planning based on such circuit patterns are applicable to actual distribution systems. Although the ultimate locations and magnitudes of future loads will shape the growth of every distribution system, they cannot be ascertained far enough in advance to permit the exact determination of the distribution-system facilities required to serve these loads.

The exact locations of individual loads in urban-suburban areas need not be considered in studying the interrelated effect of the system planning parameters, which are the load density, distribution-substation size, primary-feeder voltage, number of feeders per substation and allowable voltage drop in feeder circuits.

The study of equivalent systems brings out the reasons for and the nature of the compromises that must be made in distribution-system design. Several plans for changes in the distribution -substation size, number of primary-feeder circuits, and feeder loading, as the load density remains constant or increases, are shown in Figs. 1 through 9. The construction of these hypothetical substation areas simplifies evaluating the effects of changes made in actual distribution systems. The quantitative relationships between the system-planning parameters are derived and are illustrated in the generalized curves of Figs. 16 and 17. These relationships can be used for quickly analyzing the service quality and economic feasibility of planning alternatives or proposed system changes.

Appendix I. Measures of Primary-Feeder Circuit Capability

In distribution-substation planning, another system component that is closely related to the substation is the primary-feeder circuit. Primary-feeder planning and design is in turn influenced not only by circuit load-carrying capability but also by the contribution that the primary feeders can make toward the quality of service, and continuity of service, rendered by the system as a whole. Because it is impossible to arrive at an optimum economic plan for distribution-system growth without specifying the quality of service to be rendered to the consumers, the primary-feeder circuits, with their contribution to both system capability and service quality, constitute a most vital part of system planning.

One very important measure of service quality is voltage spread. Voltage spread can be defined as the maximum difference in the magnitudes of the utilization voltages to which the appliances of all consumers on the same feeder circuit are subjected. In specifying the voltage spread not to be exceeded by a given distribution system design, a maximum allowable % voltage drop between voltage-regulated points is assigned to the primary-feeder circuits. This % voltage drop is determined, at maximum load, by the difference in the magnitudes of the voltages applied at the high-voltage terminals of the distribution transformers located most remotely (electrically) from each other on a section of primary-feeder circuit between voltage-regulated points.

The % voltage drop in primary-feeder circuits can be calculated to any degree of accuracy desired, but because of the continual change in load and the uncertainty of the exact load at any time an approximate method is generally used. In one such approximate method the voltage drop, actually defined as the arithmetic difference in the phasor voltages at two points, is assumed to be equal to the difference between the in-phase components of the phasor voltages at those two points. For

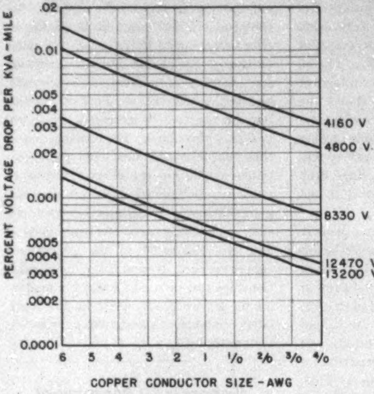

Fig. 10. % voltage drop per kva-mile for the popular copper conductor sizes. 3-phase open-wire lines with an equivalent spacing of 37 inches between phase conductors. Load power factor is 90%

a primary-feeder circuit on which one or more voltage regulators are applied, the total voltage drop in that feeder is defined, for the purposes of this paper, as the arithmetic sum of the voltage drops in each of the sections of feeder circuit between voltage regulators and between the last regulator and the end of the line.

When the operating voltage, impedance constants, and load power factor of a circuit are specified, then the total % voltage drop incurred by the load current carried in that circuit can be approximately expressed in terms of the product of kva and miles. Fig. 10 shows a plot of % voltage drop per kva-mile versus conductor size for open-wire copper-conductor primary-feeder circuits operating at several popular voltages, with the line-conductor spacing and load power factor specified. Similar information can be obtained for other conductor materials, equivalent spacings of conductors, line voltages, and load power factors. The quantity plotted on the ordinate of the curves of Fig. 10—% voltage drop per kva-mile—is an important constant in primary-feeder design, which is used to a considerable extent throughout this paper.

Another measure of primary-feeder capability is the thermal-loading limit of the circuit conductors. This limit is usually interpreted in terms of the maximum current, in amperes, that a conductor can carry. This in turn limits the kva loading at a given voltage. This paper, however, deals exclusively with the analysis of primary-feeder circuits limited in their load-carrying capability by the % voltage drop.

Appendix II. Area Coverage by a Primary-Feeder Circuit

This analysis will illustrate, for a most simple and basic case, the technique employed throughout the following Appendixes in deriving equations which relate primary-feeder % voltage drop, load density, line impedance, and line loading.

Imagine a primary-feeder circuit emanating from some feed point, and ultimately reaching every distribution transformer in the area it serves. The circuit consists of a main feeder and laterals which are tapped off the main feeder, as shown in Fig. 11. For simplicity, the feeder area is shown as a square, with laterals uniformly spaced. Each lateral carries the same kva load, consisting of distribution transformers of the same size, equally loaded and uniformly spaced.

Along with this very simple, hypothetical single-feeder pattern in Fig. 11 is shown the model used in deriving an equation for the % voltage drop from the feed point at point a to the farthest distribution transformer at point c. For the purpose of writing an expression for the voltage drop from point a to intermediate point b, it is assumed in the model that the laterals do not exist and that the main feeder is uniformly loaded between a and b. When the voltage drop along the lateral bc is written, the model "forgets" about the individual distribution transformers, and treats the lateral as a uniformly loaded line serving a rectangular area $S/2$ long and 0.2 S wide.

In constructing the model of Fig. 11 it is assumed, then, that within area S^2 the load is uniformly distributed. Consequently a given fraction of the total area served by the feeder circuit will contain the same fraction of the total load. Area becomes equivalent to kva load, so that the product of area and distance becomes equivalent to the product of kva and miles. Since the % voltage drop is equal to the product of kva, miles, and some constant, the % drop from the feed point at a to the end of the last lateral at c is approximately

$$V_{ac}=V_{ab}+V_{bc} \tag{10}$$

$$V_{ab}=K_1\int_0^{0.9S}(Sdx)x=0.405K_1S^3 \tag{11}$$

$$V_{bc}=K_2\int_0^{S/2}(0.2S)(dy)y=0.025K_2S^3 \tag{12}$$

$$V_{ac}=0.405K_1S^3+0.025K_2S^3 \tag{13}$$

With distance S expressed in miles, constants K_1 and K_2 must have the units of kva/miles² in order for V_{ac} to have the units of kva-miles. Then in order for V_{ac} to have units of % voltage drop, constants K_1 and K_2 must also contain another constant which has the units of % voltage drop per kva-mile, so that

$$K_1S^3 \text{ or } K_2S^3 \equiv \left[\left(\frac{\text{kva}}{\text{miles}^2}\right)\times\left(\frac{\%\text{ voltage drop}}{\text{kva-mile}}\right)\right](\text{miles}^3) \equiv \%\text{ voltage drop} \tag{14}$$

The quantity kva/miles² is the load density in the uniformly loaded area S^2, and the % voltage drop per kva-mile factor in equation 14 is a constant which is deter-

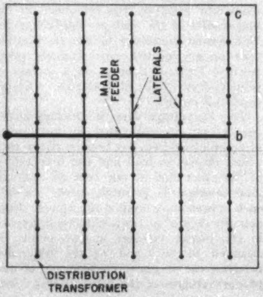

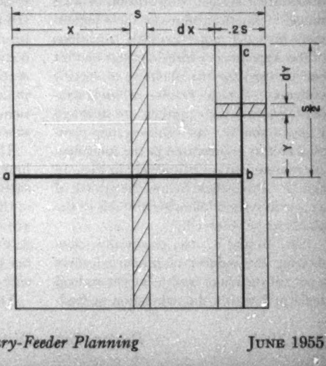

Fig. 11 (left and right). Single feeder serving a rectangular-shaped area of uniform load density, and the analytical model used to derive the relationship between % voltage drop and feeder loading in Appendix II

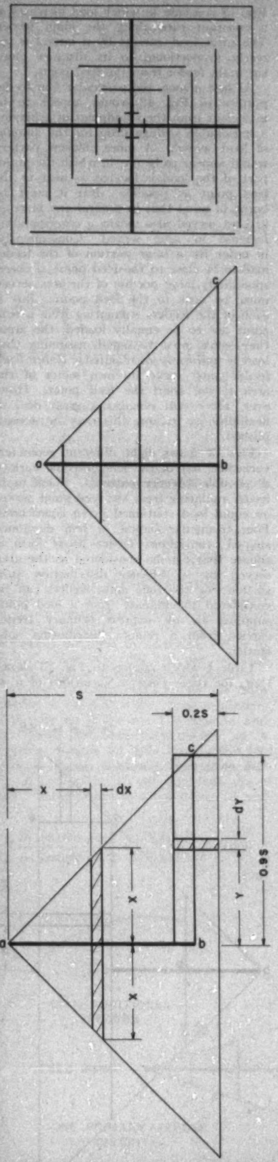
c
o
b
S
0.2S
c
X
dX
dY
0.9S
Y
a
b
X
X

Fig. 12. The 4-feeder reference pattern no. 1, with a single-feeder area and its analytical model

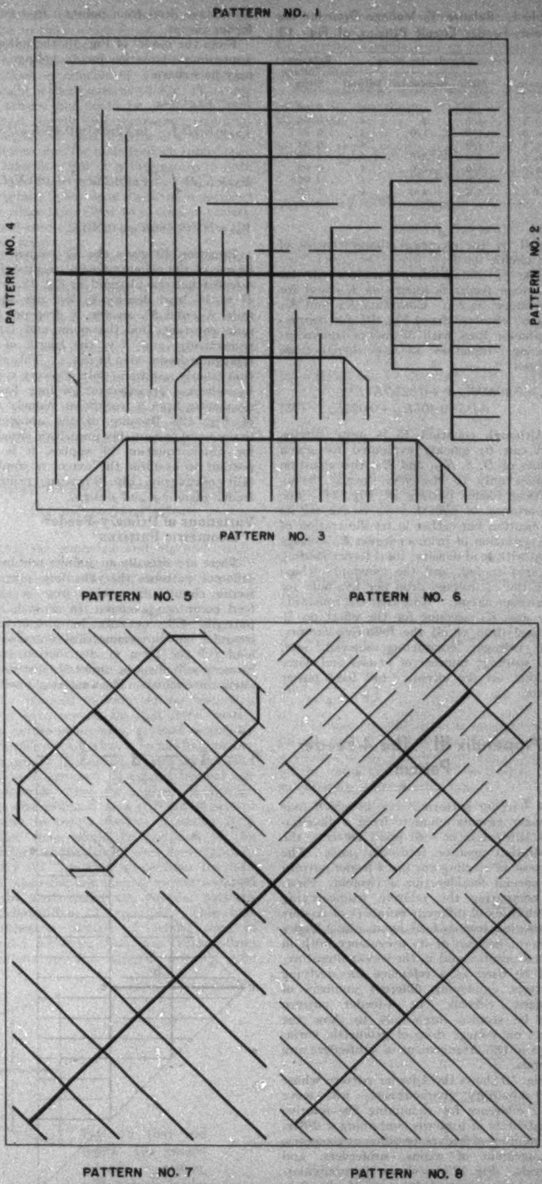
PATTERN NO. 1
PATTERN NO. 2
PATTERN NO. 3
PATTERN NO. 4
PATTERN NO. 5
PATTERN NO. 6
PATTERN NO. 7
PATTERN NO. 8

Fig. 13. Some possible variations of feeder-circuit pattern within areas served by four feeders. See Table I for the relative % voltage drops of the eight patterns

Table I. Relative % Voltage Drop for the Primary-Feeder Circuit Patterns of Fig. 13

Pattern	Conductor Sizes: Main	Conductor Sizes: Subfeeder	Conductor Sizes: Lateral	Relative % Voltage Drop
No. 1	4/0		4	1.00
No. 2	4/0	2	4	0.96
No. 3	4/0	1/0	4	0.91
No. 4	4/0		4	0.91
No. 5	4/0	2/0	4	1.06
No. 6	4/0	2/0	4	0.99
No. 7	4/0		4	0.96
No. 8	4/0	4/0	4	1.10

mined by the electrical characteristics of the circuit itself.

The % voltage drop per kva-mile for the main feeder is known as K_M and for the lateral as K_L. Constants K_M and K_L can be obtained from Fig. 10, for copper-conductor lines with 37 inches equivalent spacing. Equation 13 can therefore be written

$$V_{ac}=0.405DK_MS^3+0.025DK_LS^3$$
$$=DS^3(0.405K_M+0.025K_L) \quad (15)$$

Although equation 15 is quite simple, and can be quickly evaluated for given values of D, S, K_M, and K_L, this equation applies only to the very special, hypothetical feeder pattern of Fig. 11. The importance of equation 15 is not in its application but rather in its illustration of the variation of primary-feeder % voltage drop with load density, total feeder loading or area served, and the constants which give the % voltage drop per kva-mile for the feeder circuit. Note that the constants K_M and K_L account for the effect on % voltage drop of all the following factors: line voltage; conductor material, size, and spacing; number of phases and wires making up the circuit; and load power factor.

Appendix III. The 4-Feeder Pattern

A 4-feeder pattern is one in which four primary circuits emanate from a distribution substation or feed point to serve the substation area or feed-point area. The purpose of singling out the 4-feeder pattern for special consideration is twofold: First, in comparing the relative load-carrying capabilities of different numbers of feeders emanating from a feed point, the 4-feeder pattern, because of its prevalance both in actual practice and in the recent literature, will be used as a reference for studying patterns employing different numbers of feeders. Second, the 4-feeder pattern will be studied intensively to show the effect on voltage drop of geometric variations in the arrangement of subfeeders and laterals.

Fig. 12 shows the 4-feeder pattern whose load-capability characterisitcs will serve as a reference for examining the relative capabilities of patterns containing a different number of feeders, or different geometric arrangement of mains, subfeeders, and laterals. Fig. 12 also shows the triangular-shaped area served by one of the four mains which radiate out from the feed point, and the model which is used to derive the % voltage drop from points a to c on the feeder circuit.

From the model of Fig. 12, the following approximate equation for % voltage drop may be written

$$V_{ac}=V_{ab}+V_{bc} \quad (16)$$

$$V_{ab}=K_MD\int_0^{0.9S}(x)(2xdx)=0.486K_MDS^3 \quad (17)$$

$$V_{bc}=K_LD\int_0^{0.9S}(y)(0.2Sdy)=0.081K_LDS^3 \quad (18)$$

$$V_{ac}=DS^3(0.486K_M+0.081K_L) \quad (19)$$

Equation 19 gives the % voltage drop in one of the primary-feeder circuits of the 4-feeder pattern pictured in Fig. 12, where D is the load density in kva per square mile, K_M and K_L are the % drop per kva-mile constants for the main and lateral respectively, and S is the length of the triangular-feeder area in miles. This equation exactly applies to only one very special hypothetical arrangement of four feeders emanating from a feed point, namely that of Fig. 12. Because of the apparently limited and presumably unrealistic situation for which equation 19 applies, it is important to examine the extent of applicability of equations like 19 to actual primary-feeder planning and design.

Variations of Primary-Feeder Geometric Patterns

There are literally an infinite number of different patterns that the four primary-feeder circuits emanating from a single feed point can assume. In general, such patterns will not only be geometrically irregular and unsymmetrical but also the load (in the form of distribution transformers) will never be uniformly distributed along the circuits. The analytical model of Fig. 12 is a case in which load increases at a constant rate along the main feeder. The total load carried by a lateral is directly proportional to its distance along the main feeder from the feed point.

At first glance, the particular four-feeder pattern of Fig. 12 would appear to be inefficient from the standpoint of achieving a reasonable voltage drop for the amount of load served. A more efficient pattern would appear to be one in which the major part of the load is located as near to the feed point as possible. But it must be borne in mind that in general any increase in load served also means a corresponding increase in area served. Consequently, in order for a large portion of the feeder load to be close to the feed point, a correspondingly large portion of the area served must be near to the feed point. But if each of the feeders emanating from a feed point are to be equally loaded, the areas they serve must be equal, assuming that load is uniformly distributed. Hence each feeder must serve its own sector of the area served from the feed point. However, there still remains a great deal of flexibility as to how this may be accomplished.

Fig. 13 shows eight different geometric variations out of the kaleidoscopic variety of possible 4-feeder patterns. Each main feeder radiating from the feed point serves an equal load contained in an equal area. Four triangular-shaped, or four diamond-shaped, contiguous feeder areas form a square that can be considered as the area served by a 4-feeder distribution substation; or the four main feeders can be considered to emanate from a feed point supplied by an express primary feeder carried from a remote distribution substation.

Table I which applies to Fig. 13 shows that, for these possible variations of a 4-

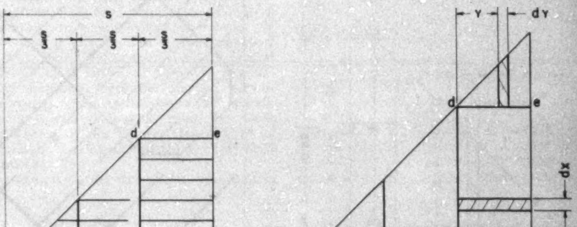

Fig. 14. Feeder-circuit arrangement and analytical model for pattern no. 3

feeder pattern, the relative % voltage drop for patterns no. 2 through 8 differs by no more than 10% from the reference % voltage drop for reference pattern no. 1, which is also the pattern of Fig. 12. The % voltage drop for each pattern was calculated in a manner similar to that resulting in equation 19 for pattern no. 1, with all load accounted for in every one of the feeder areas.

As a typical example of the voltage-drop evaluation for one of the patterns, consider pattern no. 3, shown with its analytical model in Fig. 14. The sum of the voltage drops in main, subfeeder, and lateral equals the total drop

$$V_{ae}=V_{ab}+V_{bc}+V_{cd}+V_{de} \qquad (20)$$

$$V_{ab}=DK_M\left[(S^2)\left(\frac{S}{3}\right)\right]=0.333DK_MS^3 \qquad (21)$$

$$V_{bc}=DK_M\left[2\left(\frac{S+2/3S}{2}\right)\left(\frac{1}{3}S\right)\right]\left(\frac{1}{3}S\right)=0.1852DK_MS^3 \qquad (22)$$

$$V_{cd}=DK_F\int_0^{0.678}\left(\frac{S}{3}\right)(x)dx=0.074DK_FS^3 \qquad (23)$$

$$V_{de}=DK_L\int_0^{0.388}y^2dy=0.0124DK_LS^3 \qquad (24)$$

Therefore

$$V_{ae}=DS^3(0.5182K_M+0.074K_F+0.0124K_L) \qquad (25)$$

The similarity between equation 25 for pattern no. 3 and equation 19 for pattern no. 1 is immediately apparent. The relative % voltage drops for these two patterns can be readily obtained by assigning values to K_M, K_F, and K_L. Fig. 10 can be used for this purpose in the following manner.

Assume that the main feeder for both patterns is no. 4/0 copper; the subfeeders of pattern no. 2 are no. 1/0 copper; and all laterals for both patterns are no. 4 copper. Assume all lines are 2,400/4,160 volts, 3 phases, 4 wires. Then from Fig. 10, $K_M=0.0031$, $K_F=0.005$, and $K_L=0.01$. Substituting into equations 19 and 25

$$\frac{V_{ae}\text{ in pattern no. 3}}{V_{ae}\text{ in pattern no. 1}}=\frac{0.0021DS^3}{0.00232DS^3}=0.906 \qquad (26)$$

The results obtained from computations similar to those which result in equation 26 are given in Table I.

It is possible, of course, to obtain extreme variations in relative % voltage drop for the eight feeder patterns of Fig. 13, or for any others that could be arbitrarily constructed, merely by assuming extreme nonuniformity of load distribution or other-conductor sizes for main feeders, subfeeders, and laterals. But it is interesting to note that the variety of subfeeder and lateral arrangements for these illustrative patterns is in effect equivalent to a similar variety of load-concentration patterns within the feeder areas.

Moreover, if in an actual system the main feeders carry approximately equal loads, and a reasonably small number of conductor sizes are standardized upon, then it is unlikely that subfeeder or lateral conductor sizes will differ very much, regardless of circuit arrangement, in areas of comparable load density. Equality of conductor size for different circuits in an actual system would be particularly true for the main feeder, in which most of the voltage drop is accounted for anyway, regardless of subfeeder and lateral arrangement.

Appendix IV. General Case of the n-Feeder Pattern

With the geometric and algebraic techniques employed in Appendixes II and III for the single-feeder and 4-feeder patterns serving as a background, a pattern of any number of feeders *n* emanating from a feed point will now be considered. Fig. 15 shows one feeder sector of an *n*-feeder pattern.

Note that for this general *n*-feeder case the last lateral on each main feeder is arbitrarily assumed to form the far boundary of the area served by that main feeder. This results in an area, or load served by the feeder circuit, that is somewhat smaller than would be served if the feeder load area were assumed to extend beyond the last lateral. Thus for a given % voltage drop, the assumed area ($S^2\tan\theta$) served by one of the *n* feeders is about 20% smaller than would be the case if the boundary of the feeder area were approximately 0.1 *S* farther away from the feed point than the last lateral, as was assumed for the single-feeder and 4-feeder patterns of Appendixes II and III. This new hypothetical picture of feeder area is adopted in order that the voltage-drop equations for this general *n*-feeder case yield somewhat conservative estimates for the capability of feeders, thereby allowing for extreme irregularities of load distribution and feeder-pattern geometry often encountered in actual systems.

The analytical model for the *n*-feeder pattern is also shown in Fig. 15. From this model

$$V_{ab}=K_MD\int_0^S x(2x\tan\theta)dx=0.667K_MDS^3\tan\theta \qquad (27)$$

$$V_{bc}=K_LD\int_0^{S\tan\theta}(0.2S)ydy=0.1K_LDS^3\tan^2\theta \qquad (28)$$

$$V_{ac}=V_{ab}+V_{bc}=DS^3(0.667K_M\tan\theta+0.1K_L\tan^2\theta) \qquad (29)$$

Let

$$0.667K_M=u,\text{ and }0.1K_L=v \qquad (30)$$

Then

$$V_{ac}=DS^3(u\tan\theta+v\tan^2\theta) \qquad (31)$$

where

$$\theta=\frac{360}{2n}\text{ degrees} \qquad (32)$$

Note that the area served by a single feeder can be found by dividing the feeder loading by the load density

$$A_n=\frac{kva_n}{D}=S^2\tan\theta \qquad (33)$$

The total area served by all *n* feeders of the *n*-feeder pattern is then

$$A_{nt}=n\frac{kva_n}{D}=\frac{kva_{nt}}{D}=nS^2\tan\theta \qquad (34)$$

$$S=\left(\frac{kva_{nt}}{Dn\tan\theta}\right)^{1/2} \qquad (35)$$

It is now possible to write an expression for the total % voltage drop in one of the *n* feeders of an *n*-feeder pattern, in terms of the total loading of all *n* feeders, by substituting equation 35 into 31.

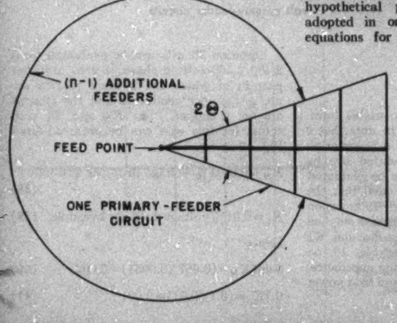

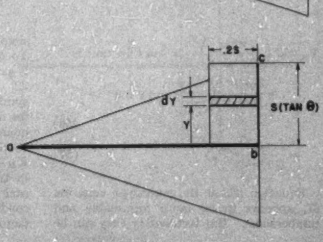

Fig. 15 (left and right). The general n-feeder pattern, with a single feeder sector and its analytical model

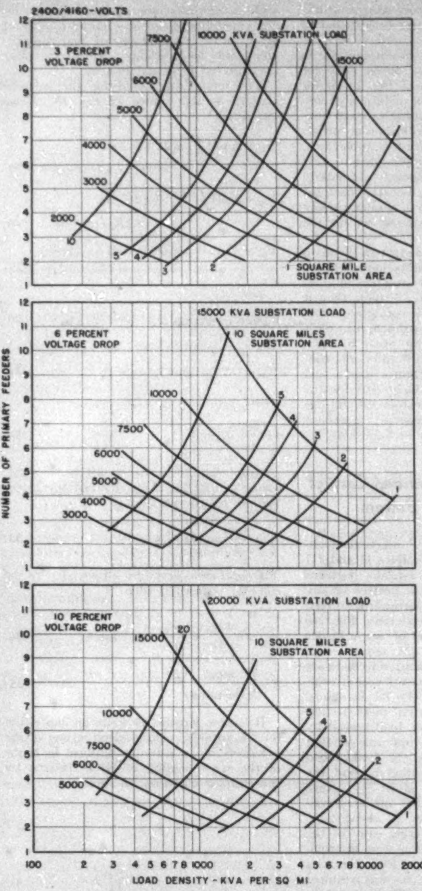

Fig. 16. Relationships between the system-planning parameters for systems employing 2,400/4,160-volt primary feeders. Number of primary feeders n versus load density D for 3, 6, and 10% feeder voltage drop V. Lines of constant substation or feed-point loading kva$_{nt}$ or constant substation or feed-point service area A$_{nt}$ are shown

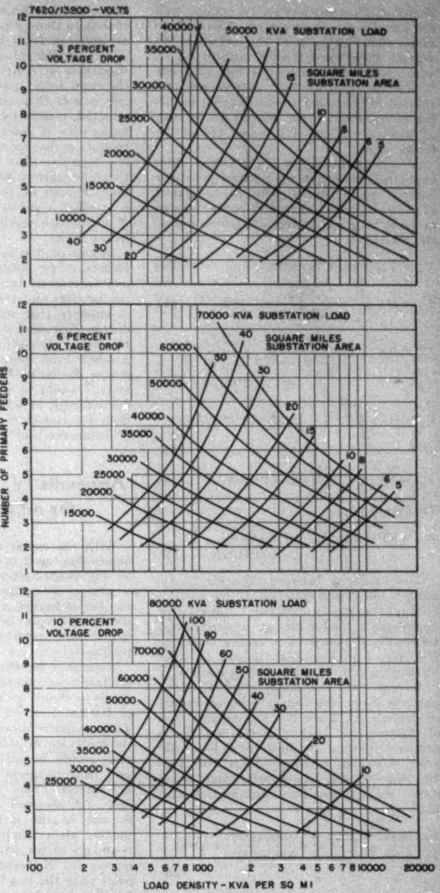

Fig. 17. Same as Fig. 16, except for systems employing 7,620/13,200-volt primary-feeder circuits

$$V_{ac}=D\left(\frac{kva_{nt}}{Dn\tan\theta}\right)^{3/2}(u\tan\theta+v\tan^2\theta)$$

$$=\frac{kva_{nt}^{3/2}}{D^{1/2}n^{3/2}}\left(\frac{u}{\tan^{1/2}\theta}+v\tan^{1/2}\theta\right) \qquad (36)$$

$$=\frac{kva_{nt}^{3/2}}{D^{1/2}n^{3/2}}(P_n) \qquad (37)$$

Equation 36, or its equivalent equation 37, appears to be quite formidable and cumbersome. But fortunately they can be simplified and put into more usable form. To do this, the first step is to note that θ is expressed as a function of n in equation 32. Hence the term represented by the symbol P_n in equation 37 can be evaluated for different values of n provided that the quantities u and v are given. In equation 30 the quantities u and v depend only on K_M and K_L. The constants K_M and K_L in turn depend, as shown in Fig. 10, on such factors as line voltage, line impedance, conductor material and size, and load power factor.

Equation 36 will now be evaluated for a 2,400/4,160-volt 3-phase 4-wire n-feeder pattern in which the n main feeders are no. 4/0 copper conductor and the laterals are no. 4 copper. The K_M and K_L constants for this case can be obtained from Fig. 10 and are

$K_M=0.0031\%$ voltage drop per kva-mile (38)

$K_L=0.01\%$ voltage drop per kva-mile (39)

Hence

$0.667K_M=(0.667)(0.0031)=0.0021$ (40)

$0.1K_L=(0.1)(0.01)=0.001$ (41)

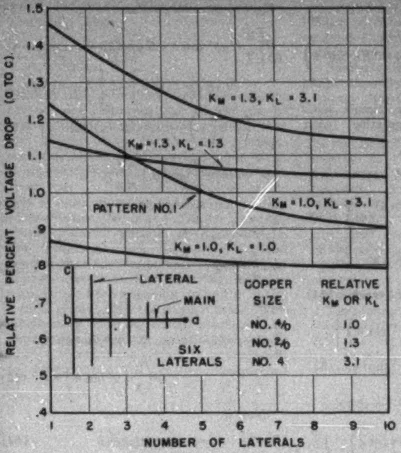

Fig. 18. Showing the effect of different combinations of main and lateral conductor sizes, and number of laterals, on % voltage drop, with pattern no. 1 as a reference

Then

$$P_n=\frac{0.0021}{\tan^{1/2}\theta}+0.001\tan^{1/2}\theta \qquad (42)$$

$$=\frac{0.0021}{\tan^{1/2}\dfrac{360}{2n}}+0.001\tan^{1/2}\frac{360}{2n} \qquad (43)$$

Now, if P_n as given in equation 43 is plotted versus n, the equation of the resulting straight line can be obtained by the "slope-intercept" method of analytic geometry. This equation is

$$P_n=(1.94n+23.1)10^{-4} \qquad (44)$$

Hence for one of the n feeders in a 2,400/4,160-volt n-feeder pattern utilizing no. 4/0 copper mains and no. 4 copper laterals

$$V_{ac}=\frac{kva_{nt}^{3/2}}{D^{1/2}n^{3/2}}(1.94n+23.1)10^{-4} \qquad (45)$$

Fig. 16 shows three sets of curves plotted from equation 45 for 2,400/4,160-volt primary-feeder circuits. The curves are a plot of n versus D for a wide range of values for kva_{nt}, which is the total loading of all n feeders comprising a pattern serving a substation or feed-point load area. Each set of curves is for a different % voltage drop. The curves for n versus D are drawn for both constant kva_{nt} or constant A_{nt}. The relationship between kva_{nt} and A_{nt} is given in equation 34.

It is interesting to note that equation 45 is not applicable to a 2-feeder pattern ($n=2$), for which $\theta=90$ degrees and $\tan\theta$ is infinite. For the evaluation of the 2-feeder pattern, two single-feeder patterns similar to the one discussed in Appendix II and pictured in Fig. 11 are combined to form a square-shaped area. The % voltage drop is then evaluated for different values of D and kva_{nt}, and the results are included in the curves of Fig. 16.

Since 7,620/13,200 volts is another popular primary-feeder voltage, Fig. 17 is a set of curves for n versus D, for different values of kva_{nt} and A_{nt} for 13.2-kv primary-feeder circuits.

Sets of curves similar to those of Figs. 16 or 17 can be obtained for any line voltage, conductor material, or size by using the relationships and methods presented in the foregoing. To aid in making estimates of the effects of such changes, Fig. 18 can be used. The general n-feeder pattern of Fig. 15, which is used to obtain the curves of Figs. 16 and 17, utilizes five laterals for each of the n main feeders. Furthermore, the conductor sizes and material in Figs. 16 and 17 are no. 4/0 copper for the mains and no. 4 copper for the laterals.

Fig. 18 shows the effect on % voltage drop of different main-feeder and lateral conductor-size combinations and different numbers of laterals. These curves are plotted with the conductor-size combination and number of laterals of Fig. 15 as a reference.

Appendix V. Effect of Supplementary Voltage Regulation on Primary-Feeder Capability

Supplementary voltage regulators or switched and unswitched capacitors are often used at various points along primary feeders to provide the equivalent of a voltage boost at their point of application. Such forms of supplementary voltage regulation are applied so as not to exceed the maximum

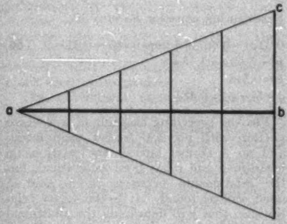

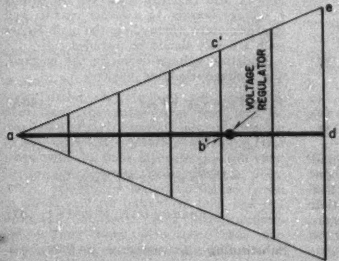

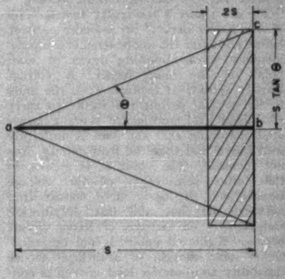

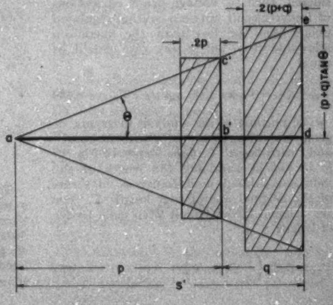

Fig. 19 (left and right). Primary feeders having equal voltage spread, with and without a supplementary voltage regulator employed in the main feeder, and the analytical model for the feeders

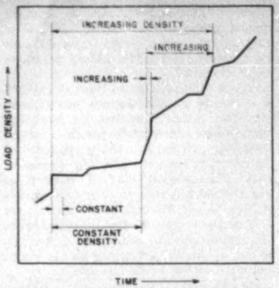

Fig. 20. Load density versus time. During certain relatively long periods the load density increases slowly, while during certain other relatively short periods the load density increases rapidly. The long-range trend, however, is one of increasing load density

allowable voltage spread on a section of primary-feeder circuit between voltage-regulated points, or between a voltage-regulated point and the end of the circuit. The following analysis will deal with the increase in primary-feeder capability provided by voltage-regulating equipment. Before proceeding with the analysis, which is based on voltage-drop considerations alone, it would be well to point out that it will be assumed throughout that thermal capability limits of feeder conductors are not reached when the addition of a voltage booster permits heavier circuit loading.

Fig. 19 shows a triangular feeder sector of one feeder area of an *n*-feeder pattern, before and after the application of a supplementary voltage-boosting device at some point on the main feeder. A voltage booster applied at a point b' on the main feeder ab will permit the feeder to carry additional load and hence serve a larger area, assuming that the load is uniformly distributed and that the load density does not increase. The point b' is chosen so that after installation of the voltage booster at b' the allowable % voltage drop between the first and last distribution transformers on sections of feeder circuit between regulated points is not exceeded. Or if some margin of additional feeder capability to allow for load growth is considered, then % voltage drops on sections of feeder circuit between voltage-regulated points may be less than the maximum allowable drop, but in any case should be equal

$$V_{ab}+V_{bc}=V_{ab'}+V_{b'c'}=V_{b'd}+V_{de} \qquad (46)$$

The purpose of the analysis diagrams, or geometric models of the "without-boost" and "with-boost" feeders, shown in Fig. 19 is to aid in obtaining the length of the voltage-regulated main-feeder S' in terms of the original main-feeder length S. For the original feeder circuit with main feeder of length S

$$V_{ab}=DK_M\left(\frac{2}{3}S^3\tan\theta\right) \qquad (47)$$

$$V_{bc}=DK_L(0.1S^3\tan^2\theta) \qquad (48)$$

$$V_{ab}+V_{bc}=DS^3\left(\frac{2}{3}K_M\tan\theta+0.1K_L\tan^2\theta\right) \qquad (49)$$

For the extended feeder circuit with supplementary voltage regulation, with main feeder of length $(p+q)=S'$

$$V_{ab'}=DK_M\left(\frac{2}{3}p^3\tan\theta\right)+DK_Mp\times\left(\frac{2(p+q)\tan\theta+2p(\tan\theta)}{2}(q)\right) \qquad (50)$$

$$=DK_M\left(\frac{2}{3}p^3\tan\theta\right)+DK_M\times[pq(2p+q)\tan\theta] \qquad (51)$$

$$V_{b'c'}=DK_L\left[(0.2p)(p\tan\theta)\left(\frac{p}{2}\tan\theta\right)\right]=DK_L(0.1p^3\tan^2\theta) \qquad (52)$$

$$V_{ab'}+V_{b'c'}=D\left(\frac{2}{3}K_Mp^3\tan\theta+K_Mpq\times(2p+q)\tan\theta+0.1K_Lp^3\tan^2\theta\right) \qquad (53)$$

Note that the last lateral on a main-feeder section is assumed to serve a rectangular area (2 $S\tan\theta$) long and (0.2 S) wide. Such an area is somewhat larger than the trapezoidal area which would have to be served in order not to infringe on the area served by a contiguous feeder in such a pattern. This assumption introduces negligible effect on the results of the analysis.

To write $V_{b'd}$ a slightly different approach will be taken. This drop will be written as the summation of the products of all the load lying beyond some point x on the main and the distance of that point x from b'

$$V_{b'c}=DK_M\int_p^{p+q}(S'^2\tan\theta-x^2\tan\theta)dx$$

$$=DK_M\tan\theta\left(S'^2(p+q)-\frac{(p+q)^3}{3}-S'^2p+\frac{p^3}{3}\right)=DK_M\tan\theta\times\left(S'^2q-p^2q=pq^2-\frac{q^3}{3}\right) \qquad (54)$$

Now $S'=(p+q)$, so that

$$V_{b'd}=DK_Mq^2\tan\theta\left(p+\frac{2}{3}q\right) \qquad (55)$$

$$V_{de}=DK_L\left(0.2(p+q)\frac{(p+q)^2\tan^2\theta}{2}\right)=DK_L[0.1(p+q)^3\tan^2\theta] \qquad (56)$$

$$V_{b'd}+V_{de}=DK_Mq^2\tan\theta\left(p+\frac{2}{3}q\right)+0.1DK_L(p+q)^3\tan^2\theta \qquad (57)$$

To find the relationship between p and q to satisfy the assumed equality of the % voltage drop between the first and last distribution transformers in each section of primary feeder between voltage-regulated points, equations 53 and 57 may be equated

$$V_{ab'}+V_{b'c'}=V_{b'd}+V_{de} \qquad (58)$$

$$D\left[\frac{2}{3}K_Mp^3\tan\theta+K_Mpq(2p+q)\tan\theta+0.1K_Lp^3\tan^2\theta\right]=L\left[K_Mq^2(\tan\theta)\times\left(p+\frac{2}{3}q\right)+0.1K_L(p+q)^3\tan^2\theta\right] \qquad (59)$$

$$\frac{2}{3}p^3+2p^2q-\frac{2}{3}q^3=0.1\frac{K_L}{K_M}\times\tan\theta(3p^2q+3pq^2+q^3) \qquad (60)$$

Let

$$0.1\frac{K_L}{K_M}=w \qquad (61)$$

then

$$\frac{2}{3}p^3+p^2q(2-3w\tan\theta)-pq^2(3w\tan\theta)-q^3\left(\frac{2}{3}+w\tan\theta\right)=0 \qquad (62)$$

Now if

$$S'=(p+q)=1\text{, then }q=1-p \qquad (63)$$

Substituting $q=(1-p)$ into equation 62 and simplifying

$$p^3\left(w\tan\theta-\frac{2}{3}\right)+2p-\frac{2}{3}=w\tan\theta \qquad (64)$$

Equation 64 will now be solved for $\theta=45$ degrees or $\tan\theta=1$, which is the 4-feeder pattern. To obtain a numerical value for w, consider a no. 4/0 copper main feeder and no. 4 copper laterals, so that $K_L/K_M=3.1$. Note that for given conductor sizes in main and laterals, and with 3-phase circuits of the same conductor spacing assumed, K_L/K_M is independent of primary-feeder voltage. Then

$$W=0.1(3.1)=0.31 \qquad (65)$$

Substituting equation 65 into 64

$$0.31p^3-0.667p^3+2p-0.667-0.31=0 \qquad (66)$$

$$p^3-5.63p+2.75=0$$

$$p=0.513$$

$$q=(1-p)=0.487$$

For the preceding example of a 4-feeder pattern with no. 4/0 copper main feeder and no. 4 copper laterals the relationship between p and q has been established, but the relationship between $(p+q)$ and S must still be found. It is this latter relationship that will determine the additional area or load that can be served by adding a voltage booster to a feeder circuit, and approximately where along the main feeder such a device should be installed.

Equating voltage drops on the original, and voltage-regulated feeders

$$V_{ab}+V_{bc}=V_{ab'}+V_{b'c'} \qquad (46A)$$

$$DS^3\left(\frac{2}{3}K_M\tan\theta+0.1K_L\tan^2\theta\right)=D\left[\frac{2}{3}K_Mp^3\tan\theta+K_Mpq(2p+q)\tan\theta+0.1K_Lp^3\tan^2\theta\right] \qquad (67)$$

Substituting the values of $p=0.513$, $q=$

0.487, and $K_L/K_M=3.1$ into equation 67, $S=0.805$. Then

$$\frac{(p+q)^2}{S^2}=\frac{1}{0.65}=1.54 \qquad (68)$$

Thus by adding a voltage booster on a feeder circuit, and allowing the circuit to be extended to pick up additional load so that the voltage drop in the two voltage-regulated sections of the circuit is the same, approximately 54% additional load can be served.

It is interesting to note that if a voltage booster is installed in the main feeder of the simple 1-feeder pattern of Appendix II, the additional area of uniform load density that can be served, such that the voltage drop from feed point to regulator equals that from regulator to end of main, is 59% greater than the original area. This relationship can be easily visualized by noting that % voltage drop is proportional to S^3. Hence if the voltage drop is allowed to double, then for the new, lengthened circuit, S becomes $2^{1/3}$ times the original value of S, and the area served by the extended circuit is $(2^{1/3})^2=1.59$ times the original area.

Similarly, if two voltage boosters permit approximately three times the original voltage drop from feed point to the last distribution transformer on the circuit, then the extended area that can be served by the feeder with two boosters is approximately $(3)^{2/3}=2.08$ times the original area served by a feeder with no voltage boosters. Thus for a primary-feeder circuit serving an area of reasonably uniform load density, the amount of load the feeder can serve varies as the two-thirds power of the number of voltage boosters plus one, applied on that feeder, provided that the current-carrying capacity of the feeder is not exceeded.

Variation in both the number of primary-feeder sectors comprising a feeder pattern and the arrangement of subfeeders and laterals has surprisingly little effect on the relative additional area at uniform load density that can be served by adding one or more supplementary voltage regulators to an existing feeder. This relative additional area can be estimated from the two-thirds power relationship just given, and is therefore about 60% greater than the original area for one regulator, and 100% greater than the original area for two regulators, provided that thermal capability limits of circuits are not exceeded.

References

1. SOME OBSERVATIONS ON THE ECONOMIC BENEFITS IN GOING FROM ONE SYSTEM VOLTAGE LEVEL TO A HIGHER SYSTEM VOLTAGE LEVEL, **D. K. Blake.** *AIEE Transactions*, vol. 71, pt. III, Aug. 1952, pp. 585–92.

2. USEFUL METHODS FOR DETERMINING PRIMARY FEED POINTS IN FUTURE DISTRIBUTION SYSTEM PLANNING, **D. L. Hopkins, D. R. Samson.** *AIEE Transactions*, vol. 73, pt. III, Aug. 1954, pp. 856–63.

3. SOME ASPECTS OF DISTRIBUTION LOAD AREA GEOMETRY, **F. C. Van Wormer.** *Ibid.*, Dec. 1954, pp. 1343–49.

◆

Discussion

B. M. Jones and **C. N. Clark** (Duquesne Light Company, Pittsburgh, Pa.): Some general comments on the planning practices of our company are offered in connection with this general subject; they do not bear directly on the technical contents of this useful and informative paper but we feel they might be interesting. Our comments concern the constant substation-size plan and the constant substation-area plan.

EXISTING SUBSTATIONS, 4 KV

Where the ultimate size of an existing substation has already been reached, our practice has been to gradually reduce the area served and provide additional capacity elsewhere, either by expanding near-by substations or installing additional substations and circuits. Similarly, for substations which have not reached their ultimate size, we just keep on providing capacity where economical until they do reach their ultimate size.

The economical factors considered in utilizing the existing substation sites to their full economical advantage are: land and buildings—utilizing to full advantage, or expanding at that site to the economical limit; available communication facilities; off street parking—proper evaluation of losses and taking cognizance thereof; storage of small repair parts; and toilet facilities. Also, for existing substations, zoning permits or municipal installation permits are much easier to obtain in many cases than for new sites.

These paragraphs referring to substations having reached their ultimate size come under the constant substation-size plan, and the substations that will be expanded to their ultimate size are initially in the constant substation-area plan, but when reaching their ultimate size will then be in the constant substation-size plan. These substations include attended, none of which we have built since 1925, and unattended automatic and semiautomatic substations, many with more than one circuit and one transformer bank.

NEW SUBSTATIONS, 4 KV

Beginning in 1947, all new 4-kv distribution substations have been of the package type, and their capacity has been used to provide relief for the existing substations by a gradual reduction in the area being supplied by the then existing substations. This practice results in the constant substation-size plan in most cases, but in some cases it is economical to expand the existing substations up to the ultimate before changing to the constant substation-size plan. Incidentally, some of this additional capacity in the existing substations is needed in attended and built-up types and in package types of installations, the latter by installing another unit in addition to the original one or by replacing the original one with a larger one.

Where successive package units are installed on one substation site, this approaches the constant substation-area plan until such time as the maximum number of units has been installed on that site, after which the area is again reduced by shifting load to other new or existing substations.

SUBSTATION SITE DIFFICULTIES, 4 KV AND OTHERS

This is an everlasting problem, and it is becoming worse as the movement to rural areas continues at an accelerated pace. Zoning requirements, public acceptance, and many other factors sometimes force the utility to depart from the perfect economical solution in some cases by installing more 4-kv substation capacity—unit types or other types—on one site. Our company has encountered instances where it could not get the site in the vicinity of the most economical location, and hence was forced to choose other alternatives.

Charles Morrison and **C. C. Wolf** (The Potomac Edison Company, Hagerstown, Md.): As is frequently the case, the use of a hypothetical and generalized method reveals certain fundamental relationships which might have been hidden in a specific approach to the solution of practical problems. The authors have not only provided the planner with some sound relationships but they have recognized certain practical aspects of planning which are sometimes overlooked. One of these is the recognition of increasing load density as distinct from increased load density.

While our own problems of distribution-substation planning are not related to load density in the usual terms of kva per square mile, we believe the authors are to be commended on their excellent treatment of the subject in the manner which is appropriate when considering urban and suburban areas. We like their inclusion of the kva-mile concept in Appendix I. During the past year we have developed what we call a linear approach to the problem of distribution-substation or feed-point planning in which kva-miles is the significant parameter. For rural distribution systems this seems to us to be the more suitable approach.

From our work we have determined that the % voltage drop per kva-mile, referring to Fig. 10, for 12.47-kv feeders is $(r\cos\theta+X\sin\theta)/1{,}555$, in which the term $(r\cos\theta+\sin\theta)$ would have the following values, based on a conductor temperature of 75 degrees centigrade, an equivalent conductor spacing of 5 feet, and a load power factor of 0.9:

No. 6 copper, 2.554
No. 2 copper, 1.202
No. 2/0 copper, 0.749
No. 4/0 copper, 0.577

Using these values we would obtain the following % voltage drop per kva-mile for 12.47-kv 3-phase feeders:

No. 6 copper, 0.00164
No. 2 copper, 0.00077
No. 2/0 copper, 0.00048
No. 4/0 copper, 0.00037

These figures agree substantially with the corresponding values taken from the curves of Fig. 10.

In Appendix V the effect of supplementary voltage regulation on primary-feeder capability is very well presented.

While again our own approach to this aspect of planning has been on a linear basis, we recognize both the need and the value of the relationships developed in the authors' presentation. It is of interest to note that on a linear basis the addition of a voltage regulator and the extension of a feeder to pick up additional load would permit a uniformly loaded line to be lengthened by about 41%, whereas the authors find that 59% additional area of uniform density can be supplied by the addition of a regulator under similar limits of voltage spread. This is not a discrepancy, but it does demonstrate the reason for our approach to the problems of primary-feeder capability where load-area geometry approaches a single dimension as it frequently does in rural distribution systems.

J. R. Oberholtzer (Commonwealth Associates, Inc., Jackson, Mich.): This paper presents a rather complete analysis of the relation between the various parameters which affect the layout of a primary distribution system. It is useful to remember these relations when analyzing specific systems so that the anticipated results of proposed changes can be estimated without excessive detailed calculations. Furthermore, the recognition of these ideal relations should prevent the system planner from drawing improper conclusions of long-range effects of system changes from a limited study of proposed immediate programs.

The relative voltage drops given in Table I, for various primary line patterns, are very nearly equal. Thus it appears that any reasonably efficient arrangement of lines will result in about the same primary voltage drop. It is noted that this analysis assumed that all lines, including the laterals, would be 3 phase. The differences between voltage drops for the various patterns might be expected to increase if the laterals were single phase, which may be closer to typical system conditions.

It would be helpful if a similar analysis could be made of the relative weight of copper required for the various patterns. This would be a good measure of the relative costs. With the patterns as they are drawn in Fig. 13 there would probably be wide variations. However, if the lateral spacing were maintained approximately equal among the patterns, which would be the case if the same distribution transformer locations were assumed, it is believed that the weight of copper would be very nearly the same.

Benefits which may be obtained by the use of supplementary regulators are outlined in the paper. The effective use of these regulators will result in heavier ampere loading of feeder conductors which will result in a rapid increase in power losses in these feeders. This should be considered in the comparison of this with other methods of increasing feeder areas.

F. C. Van Wormer (General Electric Company, Schenectady, N. Y.): In Appendixes II and III the derivations for % voltage drop in the feeder are based on only five laterals with laterals spaced $0.20S$ apart. The paper would have been of more general use and more realistic if the authors allowed any number of laterals spaced a fixed distance apart, such as a representative city block spacing.

The expression for V_{ab} in equation 11 is incorrect. It should be

$$V_{ab}=K_1\int_0^{0.9S} S(S-x)dx=0.495K_1S^3 \quad (11)$$

The expression for V_{ab} in equation 17 is also incorrect. It should be

$$V_{ab}=K_MD\int_0^{0.9S}(S-x)(S+x)dx$$
$$=0.657K_MDS^3 \quad (17)$$

The expression for V_{cd} in equation 23 is not complete since it omits the voltage drop in lateral *cd* due to the load picked up on the last branch *de* as shown in the right-hand side of Fig. 14. Consequently equation 25 is not complete and the results in equation 26 will also be affected.

The expression for V_{bc} in equation 28 is too large. The feeder area covered by the last lateral *bc* is indicated in the lower right-hand side of Fig. 15 as a rectangle instead of the trapezoidal area in the left-hand side of Fig. 15. The trapezoid area is 10% less than the rectangle. Thus equation 28 should be

$$V_{bc}=0.09K_LS^3\tan^2\theta \quad (28)$$

The authors consider feeder areas where the length of lateral is proportional to the length of the main and, in addition, the load per lateral is also proportional to the length of the main. This last factor results from the use of only five laterals, making the width of area per lateral $=0.20S$. This type of pattern is not encountered very frequently but it does simplify the mathematics. Based on these assumptions

$$V_{ac}=V_{ab}+V_{bc}=K_1\frac{DS^3}{kv^2}+K_2\frac{DS^3}{kv^2}$$
$$=\frac{DS^3}{kv^2}(K_1+K_2)$$

Thus

$$V\propto\frac{DS^3}{kv^2} \quad (69)$$

From this

$$S\propto\frac{V^{1/3}kv^{2/3}}{D^{1/3}}$$

$$\text{Feeder area } A\propto S^2\propto\frac{V^{2/3}kv^{4/3}}{D^{2/3}}$$

$$\text{Feeder kva}\propto AD\propto V^{2/3}kv^{4/3}D^{1/3}$$

or for n feeders

$$kva_{nt}\propto V^{2/3}kv^{4/3}D^{1/3}n \quad (70)$$

Equations 1 through 9 of the paper follow from these relations.

The relation $n\propto 1/kv^2$ given in equation 1 applies to a concentrated load at the end of a fixed length of line. For area coverage this relation becomes $n\propto 1/kv^{4/3}$ as seen from equation 70. The relation given in equation 3 also follows from equation 70.

In accordance with equation 3, if the feeder voltage is multiplied by $\sqrt{3}$ and the number of feeders is reduced from eight to six, kva_{nt} can be increased by 56% instead of 33% as stated below equation 3. When the feeder voltage is tripled and the number of feeders reduced from eight to four, the substation size may be increased 2.17 times.

Equation 7 should be $n\propto 1/D^{1/3}$ as seen from equation 70. Equation 9 follows from equation 69 when length S is held constant.

W. J. Denton and D. N. Reps: The remarks of Mr. Jones and Mr. Clark are very pertinent to some of the practical aspects of distribution-substation planning. The continual shifting from constant substation-area to constant substation-size plans is a frequently encountered situation in many systems. In our paper we pointed out that between these two extremes in planning philosophy there are an infinite variety of intermediate types of action which may call for both the addition of more capacity at an existing substation site and the location of more capacity at new sites. The nice feature of the picture presented by Fig. 16—for the primary-feeder voltage of 4 kv applicable to the Duquesne Light Company's situation—is that system-growth lines of either constant substation-size or constant substation-area are shown. Interpolation between these lines, moving in the direction of increasing load density, permits the planner to estimate what may have to be done to primary-feeder circuits when substation additions are made. Two parameters which can be determined from these curves are the change in the number of primary feeders required and the % voltage drop in primary feeders as load grows and distribution-substation capacity is added to the system.

As Mr. Morrison and Mr. Wolf state, the difference between considering increased, or increasing, load density is an important one. The first implies that corrective measures may comprise the only planning procedure, whereas the second indicates that preventive planning could be the goal of the distribution engineer. Corrective measures are usually a piecemeal process, and do not ordinarily result in long-range economy. The figure of 41% additional allowable line length for a uniformly loaded line after the addition of a supplementary voltage regulator is obtained in a very straightforward manner. Total % voltage drop on the line is proportional to the product of kva load and miles length. Lengthening the line by 41% will result in 141% of both the original kva loading and the miles length, and hence twice the original drop. The regulator permits a voltage spread equal to the original spread.

For the line serving load uniformly distributed in a given area, the addition of a voltage booster permits the line to be lengthened 26%. It will be noted that $(1.26)^2$ gives 1.59 times the original area, assuming that the geometric shape (say, rectangular) of the enlarged area remains similar to that of the original area.

With regard to the study of different geometric patterns for primary-feeder circuits, Mr. Oberholtzer indicates that single-phase rather than 3-phase laterals might show greater deviation in the relative % drop than the approximately ±10% obtained for the patterns shown in Fig. 13. It is difficult to find an exact sort of approach to a point such as this, because, even in Fig. 13, minor adjustments in subfeeder conductor sizes were made in order to keep % voltage drop for each pattern within the 10% limits. Presumably, then, further adjustments in subfeeder sizes could be made so that, even if single-phase laterals are considered, patterns of equal drop could still be devised. We too believe that Mr. Oberholtzer is correct when he says that the weight of conductor would not be affected to any great extent, regardless of feeder pattern, so long as the same set of distribution transformers are to be served, with reasonably equal % voltage drop for each pattern considered.

In general, the investment in overhead primary-feeder circuits, in dollars per kva load served, varies very little with either circuit capability or even circuit voltage. Most laterals are the same, standardized (and often minimum allowable) size regardless of the capability of the main and subfeeders. Since laterals form by far the largest portion of primary circuit mileage, variation in mains capability affects total circuit cost only slightly, and from the standpoint of total system cost, even less.

Mr. Oberholtzer's recognition of the increased % power loss with the use of supplementary voltage regulators is an important point. General studies we have made indicate that the % loss in primary-feeder circuits is directly related to the % voltage drop, e.g., the doubling of total drop by the addition of a regulator will approximately double the % power loss in that circuit. The inclusion of power, and energy, losses in economic studies is highly desirable. However, in planning new systems or future systems, good planning and design from the standpoint of providing good voltage for customers will virtually assure economy in losses. Moreover, there should not be a significant difference in losses in alternative system plans calling for equal service quality. However, in existing systems where voltages are too low and drops are excessive, high energy losses and poor economy are usually accompanying effects.

The first point Mr. Van Wormer raises is the use of five laterals, spaced 0.2*S* apart (*S* being total feeder length) in our derivations of Appendixes II and III. Actually the choice of number of load take-off points has no bearing on the problem, inasmuch as for the purpose of computing the total drop in the main, uniformly distributed loading was assumed. The only effect that laterals have on total voltage drop, with such an approach, is the loading of the farthermost lateral, which, we assumed, served an area of width 0.2 times the total length of the main feeder. For simplicity's sake, however, the "number of laterals" concept was used to differentiate between various possible load burdens placed on the last lateral in such a configuration. In any event, Fig. 18 shows how relative voltage drop is affected by changes in the number of laterals or conductor sizes used for main and lateral. The reference value of 1.0 for pattern no. 1 is indicated on this figure, thus permitting rapid estimation of the relative drop for patterns using other numbers of laterals and conductor sizes.

In equation 11 the expression for V_{ab} is not incorrect; it is approximate, as stated in the sentence immediately preceding this expression. Admittedly, however, Mr. Van Wormer's equation gives a closer approximation of the total % voltage drop incurred in a feeder circuit with discrete load take-off points, but with assumed continuous loading for the purposes of analysis. But equation 11 and also equation 17 are not intended for further application in computations, and hence this rougher approximation of ours is not carried into the work from which results such as Figs. 16 and 17 are obtained. Given the choice now, however, we would be more than happy to use the integral expression Mr. Van Wormer suggests. Our results comparing relative capabilities of different types of circuit patterns, voltages, and conductor sizes would not be affected to any great extent using either integral.

The expression for V_{cd} in equation 23 is indeed not complete, omitting the voltage drop in lateral *cd* due to the load picked up on the last branch *de*. Thus equation 23 should be

$$V_{cd}=0.074DK_FS^3+DK_F\left(\frac{1}{2}\right)\left(\frac{S}{3}\right)^2\left(\frac{2S}{3}\right)$$

where the second term is the missing part. Hence

$$V_{cd}=0.074DK_FS^3+0.037DK_FS^3 \qquad (23)$$

and equation 25 becomes

$$V_{ae}=DS^3(0.5182K_M+0.11K_F+0.0124K_L) \qquad (25)$$

and equation 26 becomes

$$\frac{V_{ae}\text{ in pattern no. 3}}{V_{ae}\text{ in pattern no. 1}}=\frac{0.0024}{0.00232}=1.03 \qquad (26)$$

Thus the effect of this omission is quite small, and, as a matter of fact, results in an even closer equality between the voltage drops of pattern nos. 1 and 4. There is, of course, some flexibility in the way voltage drops for the patterns of Fig. 13 can be obtained by methods of integration, since circuit configuration in "fringes" and "corners" is not intended to be exactly stipulated. This same sort of effect enters into the slight discrepancies that would be obtained from alternately considering that the last lateral serves a trapezoidal or rectangular area. Assumption of a rectangular area gives somewhat less optimistic results for feeder capability, and consequently for this reason we made the latter assumption in writing equation 28.

Relationships involving variation in the number of primary feeders emanating from a feed point become very difficult to derive, express, and manipulate. This paper represents, to our knowledge, the first attempt to approach the problem of overhead distribution-circuit general analysis with the inclusion of the number of feeders as an independent variable. The difficulty can be observed in equation 45, which shows that the number of feeders enters a general expression relating the planning parameters in the manner given by the factor $(1.94n+23.1)$ for the case illustrated for 2,400/4,160-volt circuits utilizing no. 4/0 copper mains and no. 4 copper laterals. More generally, however, the factor P_n in equation 37 houses the effect of n on all the other parameters. Realizing that few distribution engineers can devote the time required to manipulate equation 37 to suit their individual systems and plans, we computed the curves of Figs. 16 and 17 from equation 37. The distribution engineer primarily interested in what an approach such as ours can do to help him solve his problems may begin directly with Fig. 16 or 17, or from a similar figure for another primary voltage, and estimate the changes that must be made in distribution-substation size and location, number of primary feeders, or improvements in service quality, to follow a desired plan of system growth.

Equations 1 through 9 were gleaned from the general equation 37, and were easy to write only for the cases where the number of primary feeders remained constant, such as in equations 2, 4, 6, and 9. In equations 1, 3, 5, 7, and 8, where n could be an independent variable, these equations were only approximate. To find the full effect of system changes on n, Figs. 16 and 17, or similar information, should be employed.

D-C Machines: Response to Impact Excitation

J. J. BROCKMAN
NONMEMBER AIEE

C. E. LINKOUS
ASSOCIATE MEMBER AIEE

WHEN calculating the transient performance of a d-c system it is essential to know how the d-c machines in the system respond to changes in excitation voltage. Conventional d-c motors and generators have rolled steel magnet frames. Such frames have excellent mechanical strength, which adds to the serviceability of the machines, and they provide low reluctance paths for the main-pole and commutating-pole fluxes. However, they also afford comparatively low resistance paths for the eddy currents which tend to oppose any flux changes.

This paper presents a method of calculating the rise of main-pole flux and exciting current, when a step function of voltage is applied to the shunt field of a d-c machine with a solid magnet frame. The method may be extended to calculate the rise of commutating-pole flux during an increase in armature current.

Equations for flux and exciting-coil current have been developed by Dunaevskii,[1] who considers a magnetic circuit consisting of a solid section, a laminated section, and an air-gap in series combination. In his analysis he substitutes an equivalent rhombic cross-section for a rectangular one.

In the present paper, Dunaevskii's equations are applied to find the build-up of main-pole flux and exciting current when the field circuit is subjected to an abrupt change in voltage. A number of simplifying assumptions are made as follows:

1. The solid, rectangular cross-section frame may be replaced by one of rhombic section; see Fig. 1.

2. The exciting coil is wound on the solid section. Then the field due to current in the coil penetrates the solid section from all sides.

3. The length of the solid frame section, associated with a shunt field coil, is one-half the main-pole pitch, measured on the mean frame diameter; see Fig. 2.

4. The flux distribution in the laminated sections of the magnetic circuit and in the air gap is the same as the flux distribution in the solid section.

5. The static saturation curve represents the relation between frame flux and magnetic-circuit permeance under transient conditions.

6. The leakage coefficient k_l is not appreciably affected by eddy currents in the solid section or by magnetic-circuit saturation.

7. The saturation curve of the d-c machine may be approximated by several straight lines.

8. The field flux and exciting current, as functions of time, are calculated from several flux and current equations. One flux equation and one current equation are written for each straight-line portion of the saturation curve. The final flux and current expressed by one set of equations define the initial conditions for the equations that follow. However, no attempt is made to match the eddy currents. At the instant a new set of equations for flux and current becomes effective, the eddy currents are assumed to be zero.

Assumptions 1, 4, and 6 are similar to those made in reference 1. Excitation tests on two experimental choke coils with solid yokes, one rectangular and the other rhombic in cross section, produced almost identical results (see reference 1).

The equations for flux and exciting current are derived on the basis of assumption 2, i.e., the exciting coil is around the solid iron section so the field enters the iron uniformly on all sides. This is not the arrangement in a d-c machine. The field around the frame, due to increasing main-pole exciting coil current, has a rather complicated pattern. The field strength is highest on the inside radius of the frame, so that the flux enters along this surface more rapidly than it does on the outside frame surface, or the end surfaces.

When saturation effects are considered, assumptions 7 and 8 greatly simplify the calculations. However, these assumptions result in discontinuities in slopes of the calculated flux and current curves.

Nomenclature

All linear dimensions are in inches.

a = width of rhombic section, see Fig. 1
a' = width of rectangular magnet frame
b = height of rhombic section, see Fig. 1
b' = height of rectangular magnet frame section
i = instantaneous shunt field current, amperes
i_0 = shunt field current at time zero, amperes
Δ_i = change in field current between time zero and time infinity, amperes
k_l = main field flux leakage coefficient equal to the ratio of total field-flux linkage to field-flux linkage due to flux that enters the armature
l_m = half a pole pitch measured on the mean diameter of the magnet frame, see Fig. 2
N = turns per pole
P = number of poles
R = field circuit resistance per pole, ohms
t = time, seconds
T_0 = field time constant due to flux that enters the armature, seconds
T_β = frame time constant, seconds
ρ = electrical resistivity, ohm-inches
ϕ = instantaneous main-field frame flux, megalines
ϕ_0 = main-field frame flux at time zero, megalines
$\phi_1-\phi_2$ = change in field flux, megalines, corresponding to a change in field current, i_1-i_2, along a straight-line portion of the static saturation curve
$\Delta\phi$ = change in main-field flux between time zero and time infinity, megalines

Comparison of Test and Calculated Results

The main-field voltage of a 165-kw exciter was suddenly increased from 0.1 to 2.5 times normal. For test purposes,

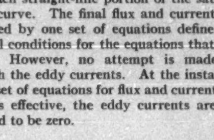

Fig. 1. Rectangular frame section and equivalent rhombus

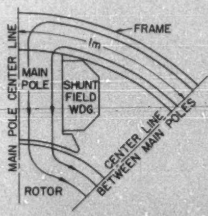

Fig. 2. Portion of the main-pole magnetic circuit

Paper 55-109, recommended by the AIEE Rotating Machinery Committee and approved by the AIEE Committee on Technical Operations for presentation at the AIEE Winter General Meeting, New York, N. Y., January 31–February 4, 1955. Manuscript submitted October 20, 1954; made available for printing November 24, 1954.

J. J. BROCKMAN is with the General Electric Company, Schenectady, N. Y., and C. E. LINKOUS is with the General Electric Company, Fort Wayne, Ind.

The authors wish to thank H. D. Snively and E. P. Smith for their very helpful suggestions in the preparation of this paper.

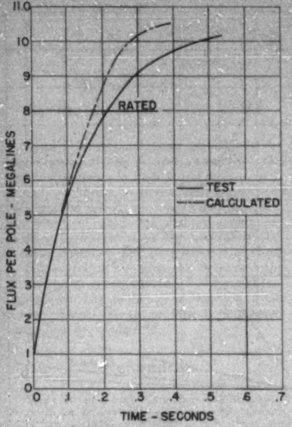

Fig. 3. Voltage build-up of 165-kw, 250-volt exciter

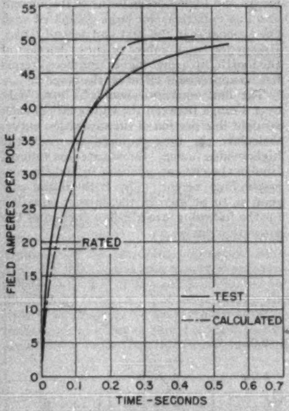

Fig. 4. Field current during voltage build-up of 165-kw, 250-volt exciter

the pole windings were connected in parallel, with an added series resistor to limit the field current to 2.5 times rated field current. Under these conditions the average rate of flux build-up for the first 0.2 second was 4.2 per unit per second. This exceptionally high rate of rise of flux permits comparison of test and calculated results under the most severe conditions. Test and calculated field flux and current curves are shown in Figs. 3 and 4.

Three 1,750-kw, 600-volt generators were identically designed except for magnet frame construction. To compare performance, one machine has a conventional solid steel frame, and the other two are laminated. Figs. 5 and 6 are plots of main-field flux and current for the rolled-steel-frame generator after the application of 1.67 times normal field voltage.

These comparisons indicate the method of calculation, including the effect of eddy currents, yields reasonably accurate predictions of the build-up of main-field flux and current. While some of the assumptions, accepted to simplify the analysis, are difficult to justify, they appear not seriously to affect the accuracy of the results.

Appendix I. Calculation of Shunt Field Flux and Current

Fig. 2 shows a portion of the main-pole magnetic circuit associated with a shunt field coil of a d-c machine. The flux path consists of a length through the solid magnet frame approximated by l_m, the laminated sections of the main-pole core and rotor, and the air gap.

For analysis, the magnetic circuit of Fig. 2 is replaced by the simplified circuit shown in Fig. 7. The length of path in the solid section l_m is the same as that in Fig. 2. The simplified circuit has a uniform rhombic cross section. The area of the rhombus is equal to the cross-sectional area of the solid frame. Its dimensions are related to those of the rectangular frame, Fig. 1, as

$$a=\sqrt{2}a'$$

$$b=\sqrt{2}b'$$

A step function of voltage is applied to the exciting winding at time zero. Prior to switching, the exciting current is assumed constant and the eddy currents are zero.

The equations for flux and exciting current, derived by Dunaevskii are

$$\phi=\phi_0+\Delta\phi\left[1-\sum_{\nu=1}^{\infty}\phi_\nu e^{-\alpha_\nu\frac{t}{k_lT_0}}\right] \quad (1)$$

$$i=i_0+\Delta i\left[1-\sum_{\nu=1}^{\infty}i_\nu e^{-\alpha_\nu\frac{t}{k_lT_0}}\right] \quad (2)$$

In these equations ϕ_ν and i_ν are given by

$$\phi_\nu=\left(\frac{T_\beta}{T_0}\right)^2\times \frac{1-\dfrac{q_\nu^2(k_l-1)}{T_\beta/T_0}}{q_\nu^3\left[(k_l-1)q_\nu+\dfrac{q_\nu-(1-\cos q_\nu)\sin q_\nu}{\cos^2 q_\nu}\right]} \quad (3)$$

$$i_\nu=\left(\frac{T_\beta}{T_0}\right)\times \frac{1}{q_\nu\left[(k_l-1)q_\nu+\dfrac{q_\nu-(1-\cos q_\nu)\sin q_\nu}{\cos^2 q_\nu}\right]} \quad (4)$$

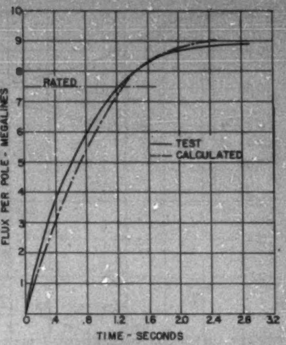

Fig. 5. Voltage build-up of 1,750-kw, 600-volt generator

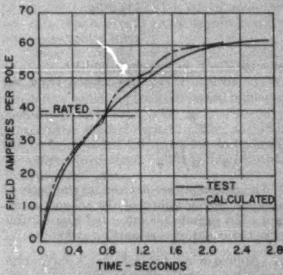

Fig. 6. Field current during voltage build-up of 1,750-kw, 600-volt generator

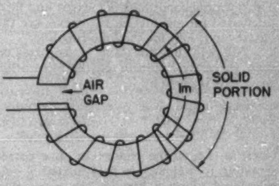

Fig. 7. Simplified magnetic circuit and exciting coil

The q_ν in equations 3 and 4 are roots of the equation

$$(k_l-1)q^2+2\frac{q\sin q+\cos q-1}{\cos q}-\frac{T_\beta}{T_0}=0 \quad (5)$$

and

$$\alpha_\nu=\frac{q_\nu^2k_l}{T_\beta/T_0} \quad (6)$$

Equations 3, 4, and 5 have been solved for numerical results using a leakage coefficient k_l of 1.15. These are plotted as func-

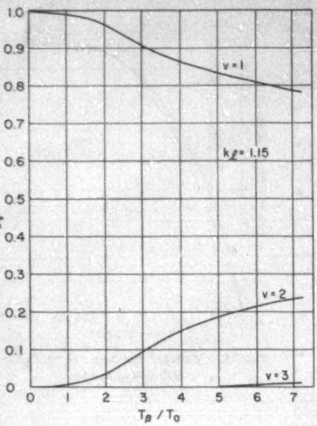

Fig. 8 (left). Coefficients for the flux equation

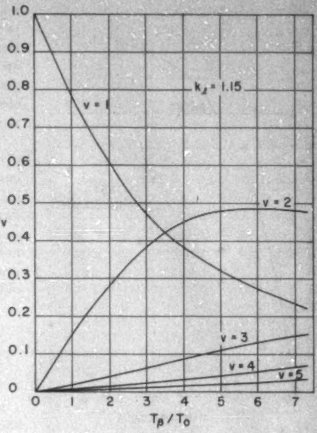

Fig. 9 (right). Coefficients for the current equation

tions of T_β/T_0 in Figs. 8, 9, and 10.

The ratio T_β/T_0 is calculated from the machine parameters as

$$\frac{T_\beta}{T_0} = \frac{l_m R}{4\left(\frac{a}{b}+\frac{b}{a}\right)\rho N^2} \tag{7}$$

The equations are derived on the basis of constant permeability of the magnetic circuit. To include the effects of iron saturation, the equations are applied as follows:

1. Approximate the machine's saturation curve by several straight lines; see Fig. 11.
2. The quantities ϕ_0, $\Delta\theta$, i_0, Δi, and T_0, have different values, corresponding to each straight-line portion of the saturation curve. The terminal conditions of current and flux, calculated for one line on the curve, are the initial conditions for the following line.
3. The field time constant T_0 decreases on each successive portion of the saturation curve. It is given by

$$T_0 = \frac{N}{R}\frac{\phi_1-\phi_2}{i_1-i_2}\times 10^{-2} \tag{8}$$

where $\phi_1-\phi_2$ is the change in flux corresponding to a change in field current, i_1-i_2, calculated along a line on the saturation curve.

Appendix II. Sample Calculations

A voltage response test was taken with an 8-pole, 165-kw, 600-rpm, 250-volt exciter. Machine constants are as follows:

a' = 20 inches
b' = 3.5 inches
k_l = 1.15
l_m = 12.6 inches
N = 250 turns per pole
R = 5 ohms per pole
T_β/T_0 = 7.25 seconds
$\rho = 5.91\times10^{-6}$ ohm-inches

The electric circuit arranged for test is shown in Fig. 12. The eight generator main-pole windings are connected in parallel. The circuit is initially at steady state.

Before closing the switch, the field current per pole is 2 amperes. From the saturation curve (Fig. 11) the initial flux per pole is 0.955 megaline. The initial linear relation, between flux and field current is useful up to 12 amperes, 5.7 megalines.

For this first region the following apply:

$T_0 = 250/5\times5.7/12\times10^{-2} = 0.238$ second
$k_l T_0 = 0.273$ second
$i_0 = 2.0$ amperes
$\Delta i = 252/5 - 2.0 = 48.4$ amperes
$\phi_0 = 0.955$ megalines
$\Delta\theta = 5.7\times48.4/12 = 23.0$ megalines

From Fig. 8 the ϕ_v are 0.783, 0.237, and 0.004. Referring to Figs. 9 and 10, the i_v are 0.225, 0.479, 0.151, 0.070, 0.034, and the α_v are 0.32, 1.82, 8.3, 13, and 23. Note that the negative exponents appearing in the fourth and higher order terms of the current and flux equations are large compared with the exponents in the first and second terms. Except for small values of time, deletion of the fourth, fifth, and higher numbered terms has no appreciable effect on the results.

The flux equation should be used only over a range between the end points of each straight-line portion of the saturation curve. Calculate the time required to reach the higher value of flux. Substitute this value of time in the current equation to find the corresponding current. This is the initial current, i_0, to be used in the current equation for the following straight-line portion of the saturation curve.

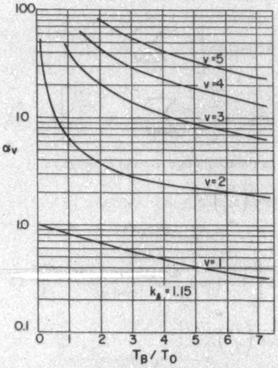

Fig. 10. Exponents for the flux and current equations

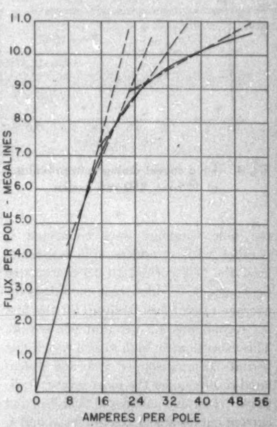

Fig. 11. Static saturation curve for 8-pole, 165-volt exciter

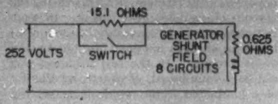

Fig. 12. Circuit arrangement for test

These calculations were carried out for four regions of the saturation curve. The results are shown in Figs. 3 and 4.

T_β/T_0 is the ratio of the solid frame time constant to the main-field time constant. Machines of standard design commonly have a T_β/T_0 equal to approximately 1.0. When calculating the performance of these machines, only two terms are needed in the flux and current equations. For v equal to 3 and greater the ϕ_v and i_v are small and the α_v are large, so these higher numbered terms become negligible.

References

1. Effects of Eddy Current on Magnetic Flux, S. Ia. Dunaevskii. *Elektrichestvo*, Moscow, USSR, pt. 2, 1951.

2. Field Transients in Magnetic Systems—A Study of Field Transients in Iron Cores Partially Laminated and Partially Solid, Ernst Weber. *AIEE Transactions* (*Electrical Engineering*), vol. 50, Dec. 1931, pp. 1234–46.

3. Transients in Magnetic Systems, C. F. Wagner. *AIEE Transactions* (*Electrical Engineering*), vol. 53, Mar. 1934, pp. 418–25.

4. Rise of Flux Due to Impact Excitation: Retardation by Eddy Currents in Solid Parts, Robert D. Pohl. *Proceedings*, Institution of Electrical Engineers, London, England, vol. 96, pt. I, 1949.

◆

Discussion

K. G. Black (General Electric Company, Schenectady, N. Y.): The authors are to be commended for obtaining a practical solution of a difficult and long-unsolved problem. They make use of a solution obtained by Dunaevskii (reference 1 of the paper) for the case of an unsaturated magnetic circuit containing a solid core of rhombic cross section and they assume that this circuit is a good approximation to the actual magnetic circuit in which the solid core is of rectangular cross section. Dunaevskii presents experimental data to demonstrate the similarity of flux responses, but for only one particular core. It is of interest to examine the validity of this approximation for other core dimensions.

The exact solution for a magnetic circuit with solid core of rectangular cross section is known for the case of flux decay, assuming the current drops to zero instantaneously. The flux decay of the exciter, for which the authors present machine constants, is calculated with the use of this exact solution. It is curve *D* of Fig. 13, and the flux decay as calculated by Dunaevskii's solution is curve *C*. For comparison with other approximations, the flux decay is calculated by two other methods. Curve *A* is based on the solution of Weber (see reference 3 of the paper) for a solid core of circular cross section, and curve *B* is calculated from a solution, suggested by Poritsky,[1] based on the assumption that the width of the frame is very large compared to the thickness. It can be seen that both curves *B* and *C* closely approximate the exact solution, curve *D*. The flux decay calculations were made on the basis of no saturation, the same basis on which the solutions were obtained.

Similar calculations were made for a 500-kw, 375-volt exciter and the results plotted in Fig. 14. The curves have the same general shape as those of Fig. 13, with the rhombic solution being the best approximation to out beyond 0.7 second.

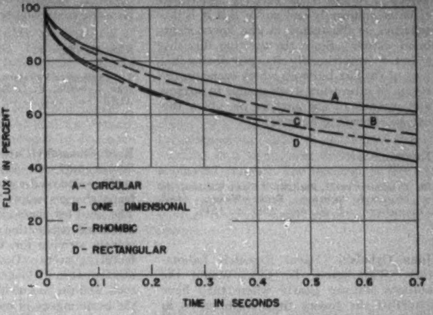

Fig. 14. Flux decay of 500-kw, 375-volt exciter

Examination of Figs. 13 and 14 lead to the conclusion that the authors are justified in proposing a method which is based upon the use of a rhombic core as an approximation to a rectangular core.

It may be noted from Figs. 9 and 11 that at the higher flux densities, and therefore in or near the region of saturation, the calculated flux build-up is more rapid than the measured build-up. This is particularly true of the 165-kw exciter. Such variance might be expected by reason of the manner in which Dunaevskii obtained his solution for flux build-up.

Dunaevskii separates the total flux into two parts; one part due to the exciting current and the other due to the eddy currents. He considers that the part due to the exciting flux is distributed uniformly across the cross section of the core. When all or part of the core is saturated, the actual flux distribution is considerably different from the uniform flux density used by Dunaevskii in his solution. If, when the core is saturated, the exciting flux could be separated from the eddy current flux, the exciting flux would be found to be distributed not uniformly, but with the highest density at the center of the core and the lowest density at the surface. This results in more eddy currents than if the exciting flux were distributed uniformly, and hence a slower build-up of flux.

Fig. 15 shows two flux build-up curves

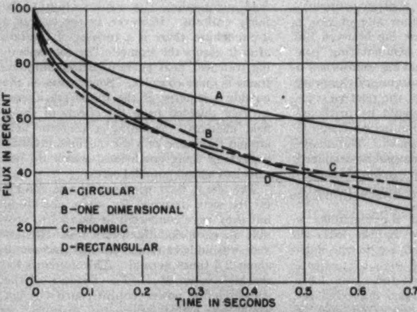

Fig. 13. Flux decay of 165-kw, 250-volt exciter

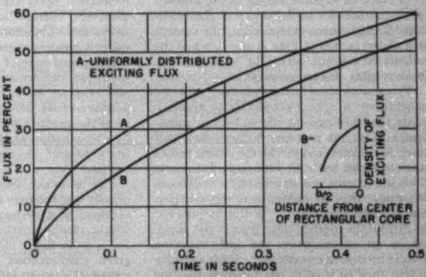

Fig. 15. Flux build-up in rectangular core

Curve A results if the exciting flux is distributed uniformly and curve B if it is distributed as illustrated in the lower right-hand corner. Since the exciting flux distribution is continually changing during that part of the flux build-up which occurs in the region of saturation, I am unable to suggest any method to the authors by which this can be taken into account.

REFERENCE

1. *Discussion* by **H. Poritsky** of FIELD TRANSIENTS IN MAGNETIC SYSTEMS, **Ernst Weber.** *AIEE Transactions,* vol. 50, Dec. 1931, p. 1246.

John Cybulski (Naval Research Laboratory, Washington, D. C.): Would the authors indicate clearly where they have extended the theory that is presented in reference 1 of the paper? Essentially the difference appears to be that a no-load saturation curve can be approximated by several straight lines and that the terminal conditions calculated for one line on the curve are the initial conditions for the following line.

It is stated in the paper that assumptions 1, 4, and 6 are similar to those made in reference 1, which leaves the impression that assumptions 2, 3, 5, 7, and 8 are different. Then it is stated that the equations for flux and exciting current are derived on the basis of assumption 2. However, in Appendix I these equations for flux and exciting current, derived by Dunaevskii are listed and employed by the authors.

There is no specific reference made to the listed references 2, 3, 4 in the paper nor to any other material in the literature on eddy-current phenomena.

In Appendix II it is stated that machines of standard design commonly have a T_β/T_0 equal to approximately 1.0 inches. However, the listing of the machine constants for the sample calculation at the beginning of this appendix has T_β/T_0 equal to 7.25 seconds. Would the authors explain this difference?

It is indicated that this method can be extended to calculate the rise of commutating-pole flux during an increase in armature current. Will the authors comment on such an extension when the interpoles are solid rather than laminated? Would it still be possible to allow a mismatch of eddy currents; that is, to assume the eddy currents to be zero at the instant a new set of equations becomes effective?

Is there an explanation as to the absence of discontinuities in the slopes of the calculated flux curves as evidenced by the smooth calculated curves in Figs. 3 and 5, while the calculated current curves in Figs. 4 and 6 have visible discontinuities?

From work done in conjunction with d-c machinery[1] it appears desirable to approximate the eddy-current effects by an equivalent circuit. It was found that a field coil may be represented by the d-c ohmic resistance in series with an inductance element. This inductance was shunted by a resistance in series with an inductance, representing the eddy-current effect. Will it be possible to extend the method described in the paper so as to approximate the eddy current effects by equivalent circuit? Such a circuit might then be used in combination with an equation describing a no load saturation curve to calculate the flux and current response continuously.

REFERENCE

1. TRANSIENT PERFORMANCE OF D-C MACHINERY, **John Cybulski, E. L. Brancato, J. P. O'Connor.** *AIEE Transactions,* vol. 72, pt. III, Feb. 1953, pp. 45–52.

R. M. Dunaiski (General Electric Company, Schenectady, N. Y.): Today's industrial applications of d-c machines are calling for faster changes in speed, current, and voltage. The need for these changes stems from the increased production that plants are constantly striving for, to offset rising manufacturing costs. Design engineers of d-c machines can no longer be content with their tools and the methods by which they gauge the performance of machines under steady-state operation, but must seek new methods with which to predict transient performance. The authors should be congratulated on providing just such a tool.

The calculation of the response of a d-c machine to impact excitation, based on eight simplifying assumptions which change the actual magnetic circuit into something having apparently little resemblance to a d-c machine, would be most questionable without experimental verification. Yet, for a variation of machine parameters over a range of about 10 to 1, the test results show fair agreement with the calculated curves. Improved correlation between calculated and test performance could undoubtedly be obtained by taking into consideration the variation in leakage flux as a result of saturation. This nonlinear characteristic, along with a better correlation of the geometric configuration of the frame, could be considered with the use of an appropriate numerical solution or some other method in lieu of the present approach to the problem.

The authors briefly mention the adaptation of their method of response calculation to the quadrature axis of a d-c machine. Here lies a fertile field for future work. The rapid advancements made in improving the response of control systems make it imperative that the machine design engineers know exactly what all their machine limitations are, and what is equally important, what can be done to improve the machine's performance. One such basic limitation, as far as improved response is concerned, is the maximum permissible rate of rise of armature current. For a given commutation margin the maximum rate of rise is dependent upon the time lag between the armature current and commutating pole field flux. Therefore, having established a desired commutation margin and knowing the required rate of rise, the relative commutation performance could be predicted and whether or not a laminated frame is justified could be determined. The analysis of the quadrature axis would be simplified by the omission of the saturable characteristics present in the excitation magnetic circuit.

The ultimate user of d-c machines is usually interested only in the over-all response of a system and not in the individual characteristics of each component. For a given figure of merit and, again, for a given commutation margin, improved response of a d-c machine can be obtained by reducing the eddy currents which tend to oppose any flux changes, or by increasing the amount of available field forcing. In some instances it may be necessary to use a combination of both methods to obtain the desired results. In the first instance, this can be accomplished, of course, by the use of a laminated frame which increases the cost of the machine. On the other hand, greater field forcing entails larger exciter capacity. It behooves the engineer to strike an economic balance between the two methods in order to insure a most economical system to the customer. The authors have provided the necessary tool with which this correlation can be made in the early stages of design.

Many engineering problems, practically unsolvable in the past, today are greatly simplified by the increased use of computer facilities. Predicting the response of a d-c machine to impact excitation is a good example of this kind of problem, and the paper should be a forerunner of many more to come destined to improve the art of machine and system design.

J. J. Brockman and **C. E. Linkous:** The authors wish to thank the discussers for their interest and their contributions toward a solution of the problem.

Mr. Black has presented an analysis and calculations to justify the substitution of a rhombic section for a rectangular one. He has also demonstrated the effect of saturation of the magnet frame.

Referring to Mr. Cybulski's comments, the authors wish to point out that Dunaevskii (see reference 1 of the paper) derives his solution for a magnetic circuit of constant permeability consisting of a solid part and a laminated part separated by an air gap. The authors have applied Dunaevskii's solution to the d-c machine and compared calculated results with experimental data.

Dunaevskii's solution for a rhombic section is in many respects similar to Weber's solution for a circular section (see reference 2 of the paper). Wagner has further modified Weber's solution by eliminating the equivalent of assumption 4 (see reference 4 of the paper).

Assumption 2, as applied to d-c machines, is much more inclusive than corresponding assumptions made by Dunaevskii and Weber. For example, in the case of a magnetic circuit with a toroidal core such as that in Fig. 7, but with a large radius of curvature, one would expect the transient field surrounding the solid section to be fairly uniform. However, in the case of a d-c machine, there is a turning of the flux after it enters the frame. The corresponding transient field pattern surrounding the frame is quite complex. Some areas on the outside perimeter of the frame are almost entirely shielded from the effects of shunt field changes. Assuming a uniform field around the frame of a d-c machine involves neglecting these conditions, which do not exist in a simple toroidal core.

The shunt field windings of the 165-kw exciter were designed for series operation, but they were connected in parallel to provide an exceptionally severe test. Resistance was added to limit the field current to about 2.5 times normal. This accounts for the high value of T_β/T_0. Because of the very high field power required, such a design would have little practical use.

The method can be extended to calculate

the rise of commutating-pole flux, including the effect of solid commutating poles. The authors have not considered its application beyond the linear range of the commutating-pole flux.

There are discontinuities in the calculated flux curves corresponding to those in the current. They are not so severe because the eddy currents influence the flux build-up much less than the field current. That is, for a given T_β/T_0, the $\phi_2, \phi_3, \phi_4, \phi_5 \ldots \phi_\nu \ldots$ terms of equation 1 of the paper are considerably smaller than the $i_2, i_3, i_4, i_5 \ldots i_\nu \ldots$ terms of equation 2.

A simple equivalent circuit for the shunt field is not readily derived from Dunaevskii's solution. Since this paper was prepared, a method has been under study to replace the effect of eddy currents by a short-circuited winding coupled to the shunt-field winding. Preliminary calculations agree very well with test results. If the method proves satisfactory, it will be described and submitted in a future paper.

Mr. Dunaiski points out that the desired response of a d-c machine may be obtained either by increasing the amount of field forcing with a solid-frame machine, or by laminating the frame. Except for very high rates of rise of main-field flux (e.g., 2.0 per unit flux per second and higher) the increase in forcing voltage required to overcome the eddy-current effect is small.

Mr. Dunaiski also calls attention to the effect of frame eddy currents on commutating-pole flux. A d-c machine should be designed to commutate satisfactorily the highest rate of rise of armature current frequently encountered in its application. If this rate of rise exceeds the commutating ability of a standard solid-frame machine, the designer may either design a solid-frame machine in a larger size, or he may use a laminated frame. The decision is one of economics, but from the user's point of view the oversized machine has the advantage of larger steady-state commutation margin.

Investigation of European Practices in Power Line Design

EDUARD FRITZ
MEMBER AIEE

IN EUROPE, power transmission cables and towers must resist, generally, the same natural forces of wind and ice as in America. It is just as necessary to consider the tension of cables at angles and at dead ends, the longitudinal pulls when ice or wind loads are not equally distributed between spans, and the exceptional case of rupture of a conductor or shielding wire.

The purpose of this paper is to review assumptions in connection with wind and ice, and other loading factors specified by European line designers, and where possible to make a comparison between American design assumptions and those employed abroad. Also included are some comments of European design requirements and the direction which changes might take. A short discussion of some of the European structural design practices differing from those in this country is also included.

Wind Pressure

The wind pressure exerted upon a conductor and transmitted to the towers is a function of the wind speed. A comparison[1] of wind speeds employed by European designers is not conclusive in connection with tower loadings because of the use of differing coefficients K in the pressure equation $P = KSV^2$, where S is the exposed surface and V is the wind speed per second. There is little disagreement in the coefficient K for flat surfaces. The variations lie in the reduction multiplier for pressures on cylinders. In this country 0.5 is used for bare cables and iced cables regardless of diameter, while in Europe the reduction multiplier varies from 0.4 to 0.7, and this variation applies with the cable diameter as well. In Germany, with emphasis on exactitude, the wind pressure coefficient first decreases with increasing diameters, then increases again to a value of about 0.5 for the larger cables. Some countries use larger values for poles and circular tower members as pipe than for conductors.

Several countries increase the unit wind pressure for spans and towers over 95 feet in height. In the light of recent failures of radio towers this 25-per-cent (%) increase seems a reasonable requirement for tall transmission towers. The low points of the conductors usually have the same ground clearance; thus it seems a refinement to increase the unit wind pressure on cables except, perhaps, for very high crossings.

The calculation of wind pressure on poles and towers is generally based upon the maximum wind speed anticipated. The peak velocity of a squall has a relatively narrow front, so a pole or tower might receive the full blast of it. However, the mean wind velocity in a long span is considerably lower than the recorded maximum velocity.

It was found in Swedish tests[2] employing 720-foot spans with a maximum velocity front width of 65 feet, that the corresponding average wind velocity of the entire span was 60% of the maximum velocity. In Sweden, as a result of this investigation and the current wind resistance K factor of 0.6 for cylinders, a unit wind pressure of 5.1 pounds per square foot is now specified on either bare or iced cables. This is but 25% of the 20.4-pound-per-square-foot pressure used for flat surfaces.

The 5.1-pound-per-square-foot unit wind pressure used is an average value which is exact for only one span length, 720 feet. For longer spans a lesser unit wind pressure might be used, as the mean velocity will decrease with increasing span lengths. The variation is probably unimportant but it suggests that steel towers on long spans might be designed for a lesser unit wind pressure than are wood poles of shorter spans. This is the reverse of American practice if an 8-pound pressure for steel is used after giving recognition to the overload factors and 4 pounds for wood.

For iced cables, some countries such as Italy use one-fourth of the unit wind pressure assigned bare cables because they consider that but half the maximum recorded wind speed will occur coincident with an iced condition. Italy is divided into three zones: plains, hills and mountains. In the plains and hills 16.4 pounds per square foot of wind are used for bare cables and 4.1 pounds when the cables are covered with 0.47 inches of radial ice. In the mountain zone 21.9 pounds is used for bare cable and 5.5 pounds for cables covered with 0.625

Paper 55-149, recommended by the AIEE Transmission and Distribution Committee and approved by the AIEE Committee on Technical Operations for presentation at the AIEE Winter General Meeting, New York, N. Y., January 31–February 4, 1955. Manuscript submitted October 18, 1954; made available for printing November 30, 1954.

EDUARD FRITZ is with Day and Zimmermann, Inc., Philadelphia, Pa.

The Pennsylvania Water and Power Company made possible in 1953 the author's trip to Europe, and the preparation of this paper. The author is indebted to the European engineers who contributed much of the material from which the article is drawn, and to foreign representatives of the Copperweld Steel International Company and the Ohio Brass Company for their help in arranging conferences and acting as interpreters.

inches radial ice. The wind under the bare condition will govern in the structural designs of the larger lines.

A corollary to reduced wind pressures on wires is the resulting smaller swing angles of insulator strings toward the tower. It has been pointed out that greater tower weight savings can be realized by shortening crossarms through a reduction of assumed insulator swing angles than will result from an equivalent decrease in the number of insulators in the string. Several countries are at present giving this their attention, first, because it will permit upgrading or increasing the voltage use of existing lines if more units can be added to the string and, second, it will reduce the cost of new lines, particularly where the torque of a broken wire is considered.

The French have been conducting a series of tests[3] on insulator and cable deviations. These tests confirm the Swedish mean wind velocity values and the fact that wind is not constant throughout space and time. Actually, the wind action results at the insulator string in a figure which represents an average value with respect to space because of the length of the spans; and with respect to time because of the inertia and elasticity of the conductors. As a result of these studies maximum insulator swing angles in France in the future will be calculated for a transverse wind push of 4.9 pounds per foot for cables of more than 1/2-inch diameter, and 6.4 pounds for cables of less than 1/2-inch diameter. These values are one-third and one-half of the pressures established by French specifications for the calculation of tower stresses.

A maximum 30-degree swing angle is at present assumed in Switzerland in spite of the Swiss design requirement of a 10.2-pound-per-square-foot wind pressure on cables. There, the swing angle is confined to 30 degrees by a generous use of suspension weights.

To those who design wood *H* frames with smaller swing angles than are to be used for steel towers, it is pointed out that the American code specifies a 4-pound-per-square-foot crossline wind load for conductors of towers and poles alike. The overload applies only to the tower capability, not to the conductor swing. Perhaps for the shorter crossarm designs at poles, reliance is placed upon that section of code which permits 30-degree swings at wood but requires 45-degree swings at steel. When poles are fitted with metallic down leads it seems that insulator swings at poles or towers should be treated alike. Surely the workman is electrically safer inside a tower cage than on the side of a grounded pole.

In 1954 Bellaschi[4] suggested a reduction of electrical clearances at higher voltage lines as well as of insulator swing angles; and at the Poles, Towers and Conductors AIEE Subcommittee meeting, much discussion concerned the form the revised code should take. The European trend would favor reducing the design swing angle to 30 degrees, provided the code includes a definition of the horizontal and vertical forces to be considered, thus restricting the location of poles or towers to sites of sufficient vertical load so that swing angles of 30 degrees will not be exceeded. This can usually be accomplished by the addition of weights at insulators.

Ice Loads

Most countries of Europe[1] include in their designs an allowance for the accumulation of ice on the conductors. In about half the countries a 12-millimeter-radial (0.47-inch) is added, as in this country, and the remainder add a constant weight of 2 kilograms per meter (1.34 pounds per foot) without regard to the cable size. In mountainous regions and in particular conditions, ice loads as great as 12 kilograms per meter (8.05 pounds per foot) have been observed and are specified.

In Europe, no direct relationship is established for increasing ice thickness requirements in terms of elevation above sea level. However, Italy does assume increased ice formation in the mountain zone, as do Switzerland and France. Sweden is divided into two ice zones, with 0.95 inches specified for the interior; and 1.34 for the coastal region. Ice in Sweden is assumed to have a specific gravity of 0.75, whereas in this country 0.92 is assumed. This reduces the ice weights in Sweden to formations of about 3/4 and $1^{1}/_{4}$ inches in terms of the vertical loadings in this country. Norway has two icing districts 1/2 inch for the usual area and 1 inch for the lake area. In one special location Norway specifies a 5-pound-per-foot load for the largest conductor. When special ice formations such as 5 and 8 pounds per foot are used in Europe, they are applied as vertical loads and to determine wire tensions at angles and dead ends, and are not coincident with wind and broken wire loads.

Broken-Wire Loads

The European countries which take into account the longitudinal pull of a conductor or shielding wire are divided into four groups,[5] as follows:

1. Those which combine wind and broken wire forces, such as Germany.
2. Those which combine ice and broken wire forces, such as Sweden.
3. Those which combine wind, ice, and broken wire forces but do not add additional longitudinal pulls, such as Great Britain, Belgium, and Norway. (America is in this group.)
4. Those which combine wind and ice, and also include longitudinal pulls due to the unbalance in conductor tensions between spans caused by uneven wind and ice loadings. These longitudinal pulls are calculated either as a function of the span and overload of ice or wind, as in France, or are given a percentage of the conductor tension as in Italy.

In Switzerland are two types of design: those with a dead end every mile, which are treated as in Italy, and those without dead ends, where a wire is broken simultaneously with ice and wind loads.

A comparison of the influence of broken-wire loads upon tower weights is complicated by the varying combinations with vertical and transverse loads; the many conductor sizes and differing conductor tensions employed, and the use of overload factors. Until recently, England appeared to apply the greatest broken-wire load: 70% of the conductor design tension plus 50% overload. This is equivalent to 1.05 times the conductor tension at the tower elastic limit. In the latest 275-kv tower designs, however, but 10% overload was assigned in connection with broken wires. This is equivalent to 77% of the broken-wire value used in this country. Belgium assigns the conductor design tension at the tower elastic limit as the broken wire load, which is the load most in use, i.e., conductor tension with no overload when 8 pounds of wind are acting on cable covered with 1/2-inch radial ice. Germany applies 50% of the cable design tension at the tower elastic limit. No ice is considered when this load is applied.

In Sweden an English translation of the design practices[6] has been prepared which is worthy of consideration. To determine conductor pulls at corners and dead ends, the resultant is computed of the assumed wind and ice loads, and to this value, the term "weight of ice in the absence of wind" is assigned. The tensile stress set up in the conductors when subjected to this load plus 30% overload is used at corners and dead ends. In the design of lines erected with reinforced security the weight of ice in the absence of wind is never considered to be less than 1.34 pounds per foot. In America for cables larger than 7/16 inch in diameter the resultant of wind and ice loading is always greater than this value.

In the tower design for breakage of a cable, the tensile force is taken as 60% of that caused by the weight of ice in the absence of wind. This reduction is stipulated "because the mechanical design of supports is based on the same permissible tower stresses irrespective of whether the conductors are intact or broken, although the actual stresses may in reality be higher when the conductors are broken." Experience shows "that this method of design is adequate to insure the stability of supports, even in those cases where breakage of conductors takes place while the conductors are acted upon the full load of ice."

At first it would appear that 60% cable tension times 1.3 overload factor or 0.78 is the broken wire multiplier. This may be so for shielding wires rigidly connected but for conductors "due regard may be paid to the reduction of the tensile stress in the conductor which can be brought about by the deflection of a suspension insulator string; or by the bending of the support or the crossarm. In general, the reduction in the tensile stress, due to the deflection of standard suspension insulator string, can be assumed to be about 50%." 50% of 60% times 1.30 overload or 0.39 of the cable design tension is the broken wire load at the tower elastic limit used in Sweden for the 400-kv line. It is the practice to break one cable on a single circuit line, two on a double and so on. For the bundled conductor lines both cables per phase are broken. This seems to be the practice everywhere, when bundled cables are used. When in Sweden the intended third cable per phase is installed to the bundled lines, only two out of the three are considered broken.

Italy adds, as longitudinal load, about one third of each cable's design tension, at which load the structure is designed up to 90% of its elastic limit. Note that under this system of loading, no broken wire torque is considered. Or as an alternate one cable may be broken at 70% of its design tension.

In France a longitudinal pull is added for each cable. This pull appears to vary with the ice or wind load. A report of a recent French line indicates that the load of one broken conductor at 40% of conductor tension was applied. In this case the conductor tension was that resulting from the application of 14.6 pounds per square foot of wind load on the bare cable.

Table I. Strength Characteristics of Steel in Europe

Class	Ultimate, Psi	Elastic Limit, Psi
ST 37	52/64,000	28,400
ST 44	62/74,000	34,000
ST 54	74/88,000	40,000
	94/11,100	54,000 (in England)

Motor Columbus of Switzerland in their designs of towers employing pipe filled with concrete as structural members are adding as longitudinal pull 5% of the maximum cable tensions for each cable. When the Swiss apply a broken wire load, they choose a value of 50% of the conductor design tension. To this they add $12^{1}/_{2}\%$ overload, which is equivalent to 0.56 times conductor design tension at tower elastic limit.

There is general agreement in Europe that the supposition of a broken wire should be questioned, particularly when applied to high-voltage lines with large conductors. Conductor failures are indeed very rare and, if they are considered as being possible, it is believed that a unit stress near the structure elastic limit should be adopted without the inclusion of other loads.

Tower Design Features

Before passing on to the tower weight summary there are several primarily structural design features practiced in Europe which differ from American procedures. First is the use of high-tensile steels. Four grades of steel are available in Europe with strength characteristics as shown in Table I.

The prevalent practice is to design for *ST 44* steel which is nearly equivalent to the American grade *A 7*. When an oversized angle is required, as a 1/4-inch thickness, and 3/16 is available in a higher grade of steel, the 3/16 section is substituted. For redundants and low-stressed members the less expensive *ST 37* is used. Variably sized and high-strength bolts are often used in the same structure to avoid gusset plates, and to permit smaller structural angles. Where there is an advantage in having fewer gauge lines at the splice, or a lesser hole reduction at the diagonals, it is not unusual to find 3/4-, 5/8- and 1/2-inch-diameter bolts in the same structure. It is estimated that 15 to 20% tower weight savings result from these practices.

Steel fabrication is very competitive among the different countries of Europe, and the design and steel weight savings are largely passed on to the utility. The British are using 94,000-pound-per-square inch (psi) steel to good advantage. Towers employing this steel, now being fabricated by a British firm for a new 230-kv line in Norway, will weigh but 65% of those of an earlier American-fabricated Norwegian line, yet designed for lighter loads. Not all of this weight-saving is the result of the use of high-strength steel however, as other design innovations not practiced in this country are being followed.

Tower designers here generally consider tower struts as hinged members, while many European designers treat them as rigid or semifixed-ended. In Switzerland the first section of a tower, if connected to a stub embedded in concrete, is assigned a column length of 0.8 times the panel length, and for sections above the bottom section 0.9 of the panel length is used. Their code permits 0.7 and 0.8 for such members. Tests, they say, sustain these values when butt splices are used, but not the overlapping splices of this country. Diagonal and horizontal struts when attached by bolts in both legs, or welded, are designed as semifixed-ended, and only single-leg bolted members are considered as hinged.

A subject, of which there seems to be agreement in Europe, but which in America is treated quite differently, is the torque distribution from a broken conductor at the end of a crossarm. If a tower has a square cross section, it is considered, here and abroad, that the torsion is divided equally on all four faces, provided that at the applied torsion level, there is a plan bracing of adequate strength, and the four tower faces have equal rigidity. For towers having a rectangular cross section, there are an infinite number of cases between square and straight line, with torsion distribution dependent in each case upon the relative dimensions of the transverse and longitudinal face and on their relative rigidity.

The British treatment of a rectangular tower as described by A. E. Percivall[7] is to consider the crossarm as a rigid beam with the torsional reactions taken entirely by the longitudinal faces. An American method, commonly used, divides the torsion equally on the four faces, but at an increased value over the square tower value depending upon the tower's width-length ratio. The British method permits thinner tower tops along the line, and results in narrow waists and tower spreads. It places all the torque above the waist in the shorter longitudinal faces, whereas in the American treatment much of the torque stress goes in the wide transverse face with its long 1/r's. It is said that the 5 to 10% lighter towers result from the British treatment.

Table II. Tower Weight Estimates

230-Kv Single-Circuit Suspension Towers; 1,300-Foot Span; Three 795,000-Circular-Mil 26/7 Steel-Reinforced Aluminum-Cable Conductors, T=11,500 Pounds; Two 7/16 Copperweld Shielding Wires, T=6,500 Pounds

		Design Loading							
		Wind		Broken Wire					
Item	Ice, Inches	Cable, Pounds	Tower, Pounds	No.	Load, Pounds		Estimated Tower Weight,*		
American Heavy Loadings							1.27†	1.33†	1.50†
1	1/2	8	12.8			National Electrical Safety Code. (1)	7,440 (1)	7,640	8,300
2	1	8	13.0				9,820	10,120	11,200
3	1 1/2	8	13.0				11,700	12,600	13,080
4	1/2	8	13.0	1	9,200	Pennsylvania Water Power Co. (2)	11,220 (2)	11,540	12,520
5	1	8	13.0	1	9,200	West-east tie (3)	12,980 (3)	13,440	14,520
6	1 1/2	8	13.0	1	9,200		14,500	14,220	16,220
Sweden								1.30†	
7	0.95	5.1	20.4			Hills		7,720	
8	0.95	5.1	20.4	1	3,450	Hills		8,860	
9	1.34	5.1	20.4			Mountain		8,800	
10	1.34	5.1	20.4	1	3,450	Mountain		9,900	
Britain							1.10†	1.50†	2.50†
11	1/2	8	20.4						12,600
12	1/2	8	20.4	1	8,050	1953 Revision (4)	10,600 (4)	12,300	
Switzerland							1.125†		
13	0.64	10.20	20.4			Hill	10,320		
14	0.64	12.75	25.5			Mountain	12,760		
Italy							1.10†		2.0†
15	Bare	16.4	25.5			Hill			9,640
16	0.47	4.1	6.4	1	8,050	Hill	8,060		
17	Bare	21.9	34.0			Mountain			11,700
18	0.64	5.5	8.6	1	8,050	Mountain	9,140		

The data on Norway and France are delayed.

* Based on Peterson equation $W=KHe\sqrt[3]{P^2}$.

† Overload factor.

With reference to the pipe-filled concrete tower designs offered by Motor Columbus of Switzerland,[9] not all of the reported savings "up to 1/2 to 2/3 of the weight of steel contained in the normal angle iron structure" are the result of the substitution of pipe and concrete. They make at least three other departures from American practice which also contribute to the weight savings: 1. the use of guys for tension members; 2. thin-walled pipe sections, 3/16-inch minimum thickness not specified; and 3. treatment of legs and struts as fixed-ended or semifixed-ended. However, much weight-saving results from the use of round sections which have better buckling resistance than angles, and the substitution of concrete for steel to support the compression load. Motor Columbus in their designs, assign a proportion of the compression load to the concrete on the basis of a steel-concrete modulus ratio of n equals 10. Their tests of field-poured concrete in pipe columns would support the use of an n ratio of 7 or even 5.

Some extra steel weight in our towers is due to our 3/16-inch minimum thickness requirement, which is intended to insure long tower life. In Italy it is felt that the emphasis should be on more adequate protective coatings rather than on the thickness of the underlying steel because the added costs of heavier than 2 ounces per square foot of galvanizing is slight, and added life through better and heavier protective coatings is not only possible, but will permit original savings of 7 to 15%, and will delay the first painting date.

Also, in Italy pipe in the towers has been used. One application was to use angle sections as corners and pipe as bracing. The pipe was flattened on the ends and bolted directly to the legs. At present, this type of construction is limited to painted structures as the inside of the pipe cannot be galvanized after flattening, and the flattening process will damage galvanizing if applied first.

Weight Comparisons

A simple tabulation of wind and ice loads is not conclusive of whether or not European design requirements lead to heavier structures than those of America. Such a listing only reveals where emphasis is placed; on wind, ice, or longitudinal pulls with or without torsion, and not the effect of coincidental load combinations and at varying overloads. Neither is a comparison of the weights of actual towers used in any voltage class conclusive, because of varying cable sizes and stringing tensions employed, and the difference in phase spacings and electrical clearances. The grades of steel available, the shape of the structure, and the knowledge and experience of the designer also leave their marks on the final tower weight.

For comparative purposes the Peterson empirical equation[10] was employed to arrive at an estimated weight for the towers of each country, using the load conditions applicable. The equation is

$$W=KHe\sqrt[3]{P^2}$$

where

He = effective height of the tower or center of gravity of the cable loads above ground

P = resultant of the cable pulls under maximum loading conditions

K = empirical constant which varies between 0.25 and 0.35 and is dependent upon the tower form

This equation is a convenient tool for evaluating the effect of changing loads on tower weights, as it states that a tower weight is proportional to its effective height and exponentially proportional to its unbalanced pulls. In each case the weight calculated is that of a 230-kv suspension tower on a 1,300-foot span without angle in the line.

For the American towers, a range of tower weights is offered, each calculated by the Peterson equation using 8 pounds of wind as crossline load acting on radial ice formations varying from 1/2 to 1 1/2 inches. Each of these climatic loading conditions is coupled with a broken or unbroken conductor condition and with the several overload capacity factors employed by utility line designers, and designers of the government agencies.

In Table II are shown these calculated tower weights. By comparing the weight of a tower meeting a European country's design requirements with an American tower of similar weight at the top of the table, one can determine to what loads, by American standards, a tower of that weight might have been designed. For instance, an American tower designed to meet the requirements of our National Electrical Safety Code[11] compares in weight favorably with the Swedish designs for the hills area.

References

1. An Inquiry on Specification or Rules According to Which Overhead Transmission Line Conductors are Designed in the Various Countries, **M. Richard.** *Report No. 230*, CIGRE, Paris, France, 1950.
2. Wind Pressure on Overhead Transmission Line Conductors, **O. D. Zetterholm, S. Sandin.** *Ibid., Report No. 202*, 1954.
3. Experimental Research on Ice-Coating and Wind Action on Single and Bundle Conductors, **R. Poyart.** *Ibid., Report No. 234*, 1952.
4. Electrical Clearances for Transmission-Line Design at the Higher Voltages, **P. L. Bellaschi.** *AIEE Transactions*, vol. 73, pt. III, Oct. 1954, pp. 1192–1200.
5. An Inquiry on the Regulations and Practices of Different Countries Which Determine the Design of Transmission Line Towers and Foundations, **M. Richard.** *Report No. 231*, CIGRE, Paris, France, 1950.
6. Swedish Electrotechnical Rules, SEN 12, Stockholm, Sweden, 1945.
7. Mechanical Design of 264 KV Transmission Lines in Great Britain, **A. E. Percivall.** *Report No. 226*, CIGRE, Paris, France, 1948.
8. New Transmission Lines with Concrete Filled Steel Tube Towers, **R. Vogell.** *Ibid., Report No. 223*, 1950.
9. Results Obtained by the Use of Tubular Lattice-Work Pylons with Flattened Joints, **M. Brunetti.** *Ibid., Report No. 217*, 1952.
10. A Formula for Estimating Tower Weights and Its Application to the Economies of Transmission Line Design, **W. S. Peterson.** *Ibid., Report No. 218*, 1950.
11. National Electrical Safety Code, National Bureau of Standards, Washington, D. C.

◆

Discussion

C. L. White (Bethlehem Steel Company, Bethlehem, Pa.): In this interesting paper various practices have been carefully reviewed and condensed into usable information for the transmission tower designer.

There seems to be a decided trend toward the use of a smaller number of insulator units in the string because of increased knowledge of insulation and flashover lightning information. Also, more study is now being given to the insulator swing angles under wind-loading deflections. This combination results in shorter crossarms and corresponding reduction in the torsion-loading on the towers from broken-wire conditions.

A few years ago, it was the practice to assume one-third of the number of wires to be broken for line-loading conditions. This resulted in designing for any two broken wires for the double circuit towers and for any one wire for single circuit lines. There is now a trend toward considering only one broken wire for double circuit towers as being satisfactory for most conditions of service.

Silicon steel appears to be the only higher strength of steel sometimes used for the construction of towers in eastern United States. This higher strength of steel is seldom used for parts other than for corner posts and then only on especially heavy structures.

American fabricating shops, in general, prefer to retain the same size of bolts throughout the same structure. Bolts of different sizes require additional operation and odd-hole punching in the shop which usually costs more than the tower weight-savings indicate. The additional handling and odd-sized hole-punching operations will also materially reduce the shop capacity. Shipments would be correspondingly delayed becaused of this feature. We also desire to use the same sized ladder or step bolts as used for the connecting bolts in order to retain the same punching for this item. United States fabricators use duplicating punch equipment which makes it economically impossible to change the size of bolt holes.

The practice of considering end-fixation factors when designing to certain unit stress values is usually well understood by the designer. The end-fixation factors are often included as a part of the specified unit stress, i.e., they are taken into account when establishing the unit stress values or the factors are applied to the unit stress values to suit the type of end-fixation for each type of member.

The distribution of torsion in a tower with a square cross section, such as exists in the usual double-circuit tower, wherein the four faces of the tower have equal rigidity, seems to be the general practice to divide the torque equally over the four faces of the tower.

In the case of single-circuit towers having a rectangular cross section in the plane of the crossarm, torsion is often distributed quite differently by various designers. Sometimes the torsion is distributed over the two parallel line faces. On other occasions, particularly with the waist-type and rotated-waist-type towers, where there is a square cross-section configuration below the waist, the torsion is distributed over the two parallel line faces down to the waist line and is then distributed equally over the four faces, if they have equal rigidity. We believe that a more exact torsional distribution is to distribute the amount of torsion to each tower face in direct proportion to its distance from the vertical axis of the tower. This will involve considerably more design effort than the procedure mentioned first.

The use of a minimum thickness of material of 3/16 inch, which is now quite prevalent, instead of 1/8 inch which was used in the past, is largely attributed to the heavier construction now required because of higher voltages, larger conductors, and longer spans. There are very few members in such towers carrying stress which can be less than 3/16 inch thick in order to satisfy strength requirement. Another factor is that angles of over 2 by 2 inches in size cannot now be obtained in thicknesses of less than 3/16 inch; while formerly much larger angles could be obtained in 1/8-inch thickness.

We agree with the author in regard to the desirability of a heavier zinc coating on transmission towers. We have no difficulty in our galvanizing shop, in obtaining on structural materials an average weight of zinc of 2.75 ounces per square foot and a minimum of 2.5 ounces per square foot, which weights are in excess of those generally specified. In regard to galvanized bolts, we usually obtain a 1.65-ounce-per-square-foot average and a minimum of 1.5 ounces per square foot, which are also in excess of the weights normally specified.

Carl Schofer (Pennsylvania Power & Light Company, Allentown, Pa.): On Sunday, September 19, 1954, at 9:01 p.m., a tornado type of storm of severe intensity crossed the Sunbury-Siegfried 220-kv line at two locations approximately 3 miles apart causing towers numbered 39/7, 40/1, and 43/2 to collapse. The intensity of the storm can be visualized from the damage done in the vicinity of tower no. 43/2 where, in a heavily wooded area down the mountainside from the tower, a path approximately 100 feet in width was torn through the timber. Trees varying in diameter from 16 to 30 inches were uprooted and thrown to the ground, indicating the high velocity of the wind.

Towers numbered 39/7 and 40/1 are adjacent towers located in a terrain practically void of trees and covered mainly with low brush and small scattered scrub pines. The vegetation therefore did not readily indicate the high velocity of the wind. However, when consideration is given to the damage done to the line, it is quite evident that the storm exerted tremendous pressure in this area. Calculations indicate that a wind velocity of approximately 170 miles per hour would be required to stress the towers to their design limits or failure point under the conditions existing at the time the collapse occurred.

The three towers involved were 4-legged steel-framed structures normally used on tangent construction on 220-kv lines. The terrain throughout this area has an elevation of approximately 1,600 feet above sea level, at which elevation heavy ice loads are anticipated during the sleet season. The line was therefore designed to withstand a 25% greater load than that which would have been imposed on the structure by 1.5 inches of radial ice on both tower and conductors with a wind pressure of 8 pounds per square foot.

This section of the line on at least two previous occasions had been loaded with $2^1/_4$ inches of radial ice on both towers and conductors with a 10 to 15-mile-per-hour transverse wind and neither the conductors nor the supporting tower showed signs of excessive loadings after the storm had subsided.

During the windstorm of September 19, tower no. 40/1 when torn loose from its foundations turned through a vertical somersault and then executed a horizontal half-roll wrapping, itself in the power conductors and overhead ground wires. When the tower finally came to rest, it was approximately 100 feet east of its foundation and about 50 feet to the right of the center line of the right of way. When it is considered that a tower of this type weighs approximately 13,000 pounds without considering the weight of the power conductors or overhead ground wires, then it can be visualized that the storm was one having wind pressures far in excess of the original design loads considered. It is therefore quite apparent that the wind velocity was considerably greater than the calculated 170 miles per hour required to bring the tower to its failure point.

Neither power conductors nor the overhead ground wires were broken by the failure. The conductor suspension clamps on the insulator assemblies on all collapsed towers slipped along the wire stripping the aluminum strands from the steel core until the tower came to rest. In the case of tower no. 40/1, this condition exerted a tremendous impact on the adjoining tower no. 39/7, causing it also to collapse.

One outstanding point regarding the design of these towers brought to light by this failure is that the diagonal lacing members on the various leg extensions which run from the tower footings to the center line of the transverse and longitudinal faces of each tower are normally under a tensile load for all conditions of tower loading and are designed as tension members. The tension load is impressed on these members by the vertical weight of the tower and the attached conductors. Transverse winds impose a small compressive load on the same members. However, under no combination of loads is this compressive load high enough to cause a change in compression members. However, during the storm the cyclonic action of the wind endeavored to lift the towers vertically from their foundations, thereby eliminating all the vertical weight while at the same time exerting a high transverse wind pressure. The load on these members then changed from a tensile to a compressive load and the towers collapsed.

Erling Ringstad (Copperweld Steel International Company, New York, N. Y.): Mr. Fritz's talks before groups of engineers in Europe created a great deal of interest. It was a fine opportunity for the European engineers to learn about American engineering practices, to compare these with their own, and to discuss reasons for differences of design, etc.

The paper should prove equally helpful to engineers in this country and Canada to give them a better understanding of European practices. It was of particular interest to me to learn about the Swedish investigation covering the narrow front of maximum wind velocity and how this is applied in the design of lines, particularly of long-span lines. This particular point and many others should be of great interest to American designers.

It was a pleasure for my company to assist Mr. Fritz in making some of his engineering contacts in Europe and we shall be similarly pleased to help other American and Canadian engineers who plan similar visits to study European engineering practices.

Eduard Fritz: I should like to express my pleasure at the interest which my paper has aroused. My position is that of an investigator relating what has been seen and read, and not of one who takes the view that all European practices are better than those in America. I do feel, however, that the practices mentioned in the paper are worthy of our consideration.

Mr. White's remarks on the fabricating shop practices in his company and the types of steel available emphasizes that often there are good reasons for the differences in practice here and abroad. The second Bethlehem method of distributing torsion in a tower is the American procedure described in the paper. Mr. White's method of recognizing fixation through an adjustment of unit stresses illustrates the point that we sometimes reach the same end but by a different route. As to minimum steel sections in our larger towers there remain many redundants without stress which could be of lighter weight were it not for our minimum section requirement.

I wish to thank Mr. Shofer for his description of the tower failures which occurred during what surely was a wind storm of tremendous pressure. It is apparent from his description of the damage done to the adjacent wooded area, that the storm had a rather narrow front, which confirms the Swedish test referred to in the paper. Those who would eliminate broken wires in our designs must not overlook the fact that when a wind of high pressure and narrow front is concentrated in one span there is always a difference in conductor tension at the adjacent towers as the slack cable in the adjacent spans is drawn into the span of heavy wind. Thus a longitudinal force including great impact is exerted at the cable supports of the adjacent towers and we have in effect a broken-wire pull of not one but several wires. In both France and Italy this is recognized when a longitudinal force in the suspension tower designs is included. However, the longitudinal forces used are not of a magnitude to withstand Mr. Shofer's tornado.

A General Transmission Loss Equation

E. D. EARLY
MEMBER AIEE

R. E. WATSON
ASSOCIATE MEMBER AIEE

G. L. SMITH
MEMBER AIEE

THE relative simplicity of the familiar quadratic form of the transmission loss equation

$$P_L = \sum_m \sum_n P_m B_{mn} P_n \qquad (1)$$

as developed by George,[1] Eaton, Ward, and Hale,[2] and Kirchmayer and Stagg[3] is made possible by four basic assumptions stated in reference 3. Some of these assumptions have been found to be the source of serious error when this simplified form of the loss equation is applied to power systems where conditions are not in agreement with the assumptions.[4] This loss equation will be referred to herein as the simplified loss equation.

It is the purpose of this paper to develop an expanded form of the loss equation, which will be referred to herein as the general loss equation, and a method of determining the values of the equation's constants which does not require any of the foregoing assumptions. Accuracy of total system loss and incremental loss values of the various sources given by this general loss equation is not adversely affected by substation loads that vary at rates which differ from each other and from the rate at which the total system load varies. Neither is it affected by variation in the ratio of reactive power to real power required to be produced at each of the various power supply sources to maintain desired voltage levels as total system load varies between maximum and minimum. (A power supply source may be a generating plant, an interconnection, a large nonconforming load, or two or more of these located close together and treated as a single source.)

Paper 55-90, recommended by the AIEE System Engineering Committee and approved by the AIEE Committee on Technical Operations for presentation at the AIEE Winter General Meeting, New York, N. Y., January 31–February 4, 1955. Manuscript submitted October 19, 1954; made available for printing November 18, 1954.

E. D. EARLY and G. L. SMITH are with Southern Services, Inc., Birmingham, Ala., and R. E. WATSON is with the Leeds and Northrup Company, Philadelphia, Pa.

The authors wish to acknowledge the substantial assistance given by H. R. Koen and R. O. Usry in the preparation of material for this paper.

To achieve the foregoing objectives, the simplified loss equation must be expanded to include additional terms. Increased difficulty in solving this more complex problem may have been a factor in preventing such development previously. The application of this new method yields equations which are readily solvable on an analogue computer. A new analogue computer has been developed,[8] which quickly evaluates the incremental transmission loss and determines the incremental cost of power delivered, thus permitting economic loading of the power system.

Form of General Loss Equation

Both total transmission loss and incremental loss of each of the power supply sources are determined jointly by the load pattern (distribution of total system load by substations) and by the distribution of system power supply by sources. The simplified form of the loss equation properly reflects the distribution of power supply by sources, but it is based on the assumption that the load pattern remains unchanged as total system load changes, i.e., each substation load remains a constant fraction of the total system load.

The assumption that all substation loads vary at the same rate with respect to variation in total system load can result in substantial error when the simplified form of the loss equation is used on systems whose substation loads do not vary in this manner. For illustration, take a system consisting of two areas connected by transmission lines with a peak period load of 500 megawatts (mw) in each area and let it be assumed that load variation in the two areas is such that, when total system load is 600 mw, the load in area *A* is 250 mw and the load in area *B* is 350 mw instead of 300 mw in each area, which would be the case if the loads in the two areas remained a constant fraction of the total system load. When system power supply is such that 100 mw are being transferred from area *A* to area *B*, the simplified form of the loss equation would compute total system loss and incremental loss of each source on the basis of transferring approximately 50 mw from area *A* to area *B*, since this equation is based on the assumption that the loads in the two areas would remain equal, or 300 mw in each area. Since on most systems there is a substantial variation in the load factor of various areas, depending on the type of load supplied, industrial, commercial, or residential, and on the type of industrial load served, it is apparent that results given by the simplified form of the loss equation, which is based on the assumption that all substation loads vary in the same manner, may be inaccurate.

Under the assumption that all substation loads remain a constant fraction of the total system load, all substation loads will become simultaneously equal to zero when the total system load is reduced to zero. Under this condition, there will be no flow of power in the transmission system, power supplied by each source will be zero, total transmission losses will be zero, and the incremental loss of each of the sources will be zero.

If each of the substation loads varies at a different rate, one load will become zero before any of the others as total system load is reduced. If these rates persist as system load is further reduced, some loads will become negative. When the net system load becomes zero, the negative loads will be equal to the positive loads, and the negative loads, which may be considered as sources of power supply, will supply power equal to the requirements of the positive loads. Under this condition, transmission losses resulting from the transfer of power from negative loads to positive loads would be supplied by system generating plants. If the net system load is further reduced until the total of the negative loads exceeds the total of the positive loads by an amount equal to the transmission losses resulting from transferring power from negative loads to positive loads, no power supply will be required from the system generating plants. This condition will be termed and referred to herein as the condition of zero system power supply.

Under the condition of zero system power supply, there will be transmission losses and, consequently, an incremental loss value for each of the power supply sources. Each term of the simplified total loss equation is a constant multiplied by the product of the outputs of two power supply sources or the square of the output of one such source. Consequently, total system losses given by the simplified total loss equation under the condition of zero power supply will be zero since the output of all power supply sources is zero, this being correct only if all loads remain a constant fraction of the total system load as it is reduced to zero, which was one of the assumptions made in deriving the equation. To make this equation applicable to the general case where all loads may vary at different rates requires the addition of a constant term K_{L0} representing total system losses under the condition of zero system power supply.

Each term of the incremental loss equations, obtained by taking the partial derivatives of the simplified total loss equation, is a constant multiplied by the power output of one of the power supply sources. Consequently, these equations will give zero as the incremental loss of each of the power supply sources under the condition of zero system power supply, which is correct only for the condition where all loads vary at the same rate with respect to variation of the total system load. To make the incremental loss equations applicable to the general case where all loads may vary at different rates requires the addition of a constant term B_{n0}, representing the incremental loss of each source under the condition of zero system power supply to each of the incremental loss equations. The general form of these equations then becomes

$$\frac{\partial P_L}{\partial P_n}=\sum_m 2B_{nm}P_m+B_{n0} \qquad (2)$$

Collectively, the incremental loss equations for all power supply sources given by equation 2, which represent all of the partial derivatives of an unknown equation, become a partial derivative system which can be solved to obtain the total transmission loss equation in its general form, which is

$$P_L=\sum_m\sum_n P_mB_{mn}P_n+\sum_n B_{n0}P_n+K_{L0} \qquad (3)$$

where K_{L0}, the constant of integration, represents total system losses under the condition of zero system power supply. The partial derivative of equation 3 gives equation 2.

It will probably be possible to determine the values of constants K_{L0} and B_{n0} from a network analyzer study of the condition of zero system power supply. Pending development of the technique of making such a network analyzer study with the required degree of accuracy, another method of determining the value of these constants will be presented. A method of determining incremental loss values for each source directly from network analyzer data will be presented later in the paper.

The importance of including the constants B_{n0} and K_{L0} in the general loss equation may be obscure since the condition of zero system power supply is an imaginary condition. However, these terms respectively give the intercepts of the incremental loss and total loss equations at zero system power supply, and B_{n0} is essential to give the proper slope to the incremental loss equation when loads vary at different rates. In this re-

Table I. Procedure for Setting Up Normalized Equations

Case	(1) B_{11} +	(2) B_{22} +	(3) B_{12} +	(4) B_{10} +	(5) B_{20} +	(6) K_{L0} =	(7) Answer
1	$2P_1$	0	$2P_2$	1.0	0	0	$(\partial P_L)/(\partial P_1)$
	0	$2P_2$	$2P_1$	0	1.0	0	$(\partial P_L)/(\partial P_2)$
	P_1^2	P_2^2	$2P_1P_2$	P_1	P_2	1.0	I^2R
2	$2P_1$	0	$2P_2$	1.0	0	0	$(\partial P_L)/(\partial P_1)$
	0	$2P_2$	$2P_1$	0	1.0	0	$(\partial P_L)/(\partial P_2)$
	P_1^2	P_2^2	$2P_1P_2$	P_1	P_2	1.0	I^2R
3	$2P_1$	0	$2P_2$	1.0	0	0	$(\partial P_L)/(\partial P_1)$
	0	$2P_2$	$2P_1$	0	1.0	0	$(\partial P_L)/(\partial P_2)$
	P_1^2	P_2^2	$2P_1P_2$	P_1	P_2	1.0	I^2R
4	$2P_1$	0	$2P_2$	1.0	0	0	$(\partial P_L)/(\partial P_1)$
	0	$2P_2$	$2P_1$	0	1.0	0	$(\partial P_L)/(\partial P_2)$
	P_1^2	P_2^2	$2P_1P_2$	P_1	P_2	1.0	I^2R

Values of P_1, P_2, $\frac{\partial P_L}{\partial P_1}$, $\frac{\partial P_L}{\partial P_2}$, and I^2R are known quantities for each case.

$\Sigma 1\times 2$ represents the summation of each entry in column 1 multiplied by the corresponding entry in column 2

$\Sigma 1\times 1$ represents the summation of the square of each entry in column 1

$\Sigma 1\times 1B_{11}+\Sigma 1\times 2B_{22}+\Sigma 1\times 3B_{12}+\Sigma 1\times 4B_{10}+\Sigma 1\times 5B_{20}+\Sigma 1\times 6K_{L0}=\Sigma 1\times 7$

$\Sigma 2\times 1B_{11}+\Sigma 2\times 2B_{22}+\Sigma 2\times 3B_{12}+\Sigma 2\times 4B_{10}+\Sigma 2\times 5B_{20}+\Sigma 2\times 6K_{L0}=\Sigma 2\times 7$

$\Sigma 3\times 1B_{11}+\Sigma 3\times 2B_{22}+\Sigma 3\times 3B_{12}+\Sigma 3\times 4B_{10}+\Sigma 3\times 5B_{20}+\Sigma 3\times 6K_{L0}=\Sigma 3\times 7$

$\Sigma 4\times 1B_{11}+\Sigma 4\times 2B_{22}+\Sigma 4\times 3B_{12}+\Sigma 4\times 4B_{10}+\Sigma 4\times 5B_{20}+\Sigma 4\times 6K_{L0}=\Sigma 4\times 7$

$\Sigma 5\times 1B_{11}+\Sigma 5\times 2B_{22}+\Sigma 5\times 3B_{12}+\Sigma 5\times 4B_{10}+\Sigma 5\times 5B_{20}+\Sigma 5\times 6K_{L0}=\Sigma 5\times 7$

$\Sigma 6\times 1B_{11}+\Sigma 6\times 2B_{22}+\Sigma 6\times 3B_{12}+\Sigma 6\times 4B_{10}+\Sigma 6\times 5B_{20}+\Sigma 6\times 6K_{L0}=\Sigma 6\times 7$

spect they are equivalent to the zero-output intercept of the familiar turbogenerator input-out curve which represents the heat input to the turbine at zero output. The value of constants B_{n0} and K_{L0} is determined by the relative rates of change of the various loads and is zero when all loads change at the same rate. Constant K_{L0} is always positive but B_{n0} may be either positive or negative. In general, B_{n0} will be positive when the loads normally supplied by source n are negative under the condition of zero system generation and will be negative when such loads are positive under the condition of zero system generation.

Method of Determining Value of Loss Equation Constants

It has been shown that the simplified loss equation can be expanded so as to cover the condition where loads vary at different rates. To eliminate the other three assumptions on which the simplified loss equation is based, as stated in reference 3, it is necessary to use an entirely different method of determining values for the general loss equation constants. This method will be outlined, then explained and illustrated in detail. The procedure is as follows:

1. A number of cases representing different system load supply conditions must be set up on the network analyzer and the following readings taken: Scalar value of line currents; bus voltage phase angle between each power supply source and each load; and transfer impedance from each power supply source to each load; see reference 4.

   The number of cases studied must not be less than $(n+2)$, where n represents the number of power supply sources, of which one-half should be for peak period load conditions and one-half for valley period load conditions. Each power supply source should be operated at maximum capability and at minimum capability, or at zero output, in one case for peak period loads and one case for valley period loads. Interconnections should be operated at maximum input to the system and at maximum output from the system.

2. The system I^2R loss for each case and value of incremental loss for each power supply source for each case must be computed. The method of computing incremental loss values from voltage phase angles between power supply sources and loads and relative rate of change of each load will be given later in the paper.

3. Equations for total system loss and incremental loss for each power supply source for each case must be set up, using the loss equation constants as the unknowns and the appropriate values of P_m and P_n as the coefficients. Since there will be n incremental loss equations and one total system loss equation for each case and $(n+2)$ cases, the total number of equations will be $(n+2)(n+1)=n^2+3n+2$, which is twice the number of unknowns, the loss equations constants.

4. The next step is to solve the equations for the values of the unknown loss equation constants. Since there are twice as many equations as unknowns, the equations must be normalized to obtain equations equal in number to the number of unknowns. The solution of these normalized equations provide a loss equation by which incremental and total losses may be computed that are in best agreement with the known values in the sense of least squares. The procedure for setting up the normalized equations for a 2-source system is illustrated in Table I.

It should be noted that the loss equation constants determined in the foregoing manner tie into incremental loss values for each power supply source and system I^2R loss for both peak period and valley period loads for $(n+2)$ cases selected to cover a wide range of system power supply conditions.

With 13 sources, the number of simultaneous equations to be solved is 105. The most advanced type of electronic digital computer offers the only feasible means of solving such a large number of equations for a reasonable expenditure of time and money. Solution of the equations is simplified by the fact that the normalized equations are symmetrical. The cost of solving 100 symmetrical equations is from $1,000 to $1,500 depending on the dominance of the diagonal terms. Use of less advanced computing equipment may cost considerably more even though the hourly equipment rental is less.

Effect of Rate of Load Change on Incremental Loss Values

Distribution of load by substations and distribution of power supply by sources are important factors in determining system I^2R loss and incremental loss values of each power supply source since these factors determine the flow of power in each transmission line. Not so generally recognized is the fact that the relative rates at which the various substation loads change with respect to a change in total system load is also an important factor in determining incremental loss of each power supply source; in fact the authors have seen no reference to this important principle in the literature. That the relative rate of change of each load does affect the incremental transmission loss of each power supply source is apparent, since the incremental change of the various loads determines the incremental change in the loading of the various transmission lines which, in turn, is one of the factors that determine the incremental loss of each power supply source.

The importance of rate of change of the various loads upon incremental loss values can be readily demonstrated by a simple example. Take the system shown in Fig. 1(A) consisting of a single generating plant and two loads, each of which is 150 mw, supplied over separate lines. The I^2R loss is computed to be 20.91844250 mw. Now let the total power delivered to the load be increased by 0.1 per cent, or 0.30 mw, and let this increase be divided between loads no. 1 and no. 2 so that each load is increased by the same 0.1 per cent, or 0.15 megawatts, which will maintain each load as a constant fraction of the total system load. Line flows for this condition are shown in Fig. 1(B). The I^2R losses are computed to be 20.96262788 mw, an increase of 0.04418538 mw for a 0.30-mw increase in total load supplied. The ratio of increment of loss to increment of generation is therefore

$$\frac{\Delta L}{\Delta P}=\frac{0.04418538}{0.30+0.04418538}=12.838 \text{ per cent}$$

In a like manner, the ratio of increment of loss to increment of generation when loads supplied are decreased by 0.1 per cent can be computed to be 12.824 per cent. The true incremental loss, which lies between the two ratios of increment of loss to increment of generation, cannot be more than 0.007 per cent different from the average of the two ratios, namely, 12.831 per cent.

Incremental loss computed in the foregoing manner will be found to be 15.648 per cent when 75 per cent of the total load change is at load no. 2 and 25 per cent at load no. 1. When 75 per cent of the total load change is at load no. 1, the incremental loss, computed in the foregoing manner, will be found to be 9.820 per cent. If load no. 1 is a 100-per-cent load-factor load and the total system load change is taken by load no. 2, the incremental loss of the generating plant will be 18.288 per cent, but if load no. 2 is the 100-per-cent load-factor load, the incremental loss will be only 6.593 per cent.

The wide spread of incremental loss values (6.593 to 18.288 per cent) for a given distribution of load and generation illustrates the important effect that the ratio of total system load change taken by each substation load, which may be quite different from the relative size of the loads, has upon incremental loss values. It also illustrates another important principle; namely, that, even though the simplified loss equation gives the correct total system loss, there is no assurance that partial differentiation will give correct incremental loss values since there are innumerable combinations of incremental loss values for the various power supply sources, depending upon the rates of change of the various loads, that will give the same total system loss. On the other hand, partial differentiation of the general loss equation may give correct incremental loss values for a given case even though the total system loss given by it is inaccurate because of the different effect the constants B_{n0} and K_{L0} have upon incremental loss and total loss. Constant K_{L0} has no effect upon incremental loss values and constants B_{n0} have a greater effect upon total loss than upon incremental loss, as illustrated by the following relationship between incremental loss and total loss

$$L=\sum_n \frac{1}{2}\left(\frac{\partial P_L}{\partial P_n}+B_{n0}\right)P_n+K_{L0} \qquad (4)$$

In addition, any inaccuracy in the determination of the value of the B_{n0} constants would be offset to a large extent by compensating changes in the value of the B_{mn} constants in so far as incremental loss values are concerned. It should be emphasized that, in the economic loading, accuracy in calculation of incremental transmission loss is of prime importance, whereas accuracy in calculation of total transmission loss is of secondary interest.

This method for determining incremental loss values will be used later in the paper and will be referred to as the $(\Delta L)/(\Delta P)$ method. Since this method uses the difference between two large numbers, all computations will be carried out with the same high degree of accuracy as that used in the foregoing illustration. In computing incremental loss in the aforementioned manner for a large number of cases, it can be stated from experience that incremental loss values computed by the $(\Delta L)/(\Delta P)$ method, when expressed as a ratio, will be correct within ±0.0003.

Method of Determining Incremental Loss Values from Network Analyzer Data

The method of determining incremental loss values for the various power supply sources from network analyzer data for use in setting up the simultaneous equations employed in determining the loss equation constants, as previously outlined, is based upon the voltage phase-angle method of determining the incremental loss incurred in transferring an increment of power from one generating plant to another while holding constant power delivered to all loads and generation at all other plants, as developed by W. R. Brownlee.[4] The same principles apply when generation is increased at one plant to supply an increment increase of a single load plus the related increment increase in losses while holding constant power delivered to all other loads and generation at all other plants.

Equation 13 of reference 4, which gives the incremental loss associated with transferring power from point 1 to point 2 on the system by the 2-step method, expressed in terms of sending-end power is

$$\frac{dL}{dP_{1-2}}=\frac{4K\tan 1/2\theta_{1-2}}{(K+\tan 1/2\theta_{1-2})^2} \qquad (5)$$

In reference 4 it is shown that the incremental loss given by equation 5 is independent of the magnitude of the transfer impedance between points 1 and 2, of the relative and absolute magnitude of the bus voltages at the two points, and of the reactive/real power ratio of the generating plant.

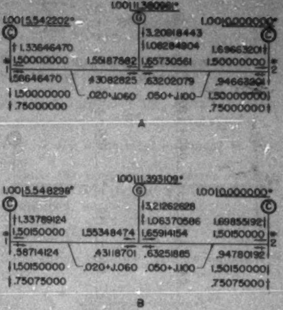

Fig. 1. System used for illustrating $(\Delta L)/(\Delta P)$ method of calculating actual incremental loss

Equation 5 can be expressed in another form which has been found more convenient for making computations

$$\frac{dP_L}{dP_{m\rightarrow n}}=1-\left(\frac{K_{mn}-\tan 1/2\theta_{mn}}{K_{mn}+\tan 1/2\theta_{mn}}\right)^2 \qquad (6)$$

where

$\frac{dP_L}{dP_{m\rightarrow n}}=(dL)/(dP_{1-2})$ of equation 5 and represents the incremental loss incurred in transferring power from source m to load n, under the conditions stated in the foregoing, expressed in terms of sending-end power

θ_{mn} = angle by which the bus voltage at the sending end m leads the bus voltage at the receiving end n

K_{mn} = reactance-resistance ratio of the transfer impedance between points m and n

When the incremental loss given by equation 6 is expressed in terms of power received at n it becomes

$$\frac{dP_L}{dP_{m\leftarrow n}}=\left(\frac{K_{mn}+\tan 1/2\theta_{mn}}{K_{mn}-\tan 1/2\theta_{mn}}\right)^2-1 \qquad (7)$$

The incremental loss from a source to the composite system load (partial derivative of losses with respect to the source) can be expressed as the summation of the incremental losses incurred in transmitting power from the source m to each of the loads n, expressed in terms of power received, divided by 1 plus the said summation of the incremental losses incurred in transmitting power from source m to each of the system loads n. In this expression, unity represents the incremental increase in power received at all loads. The per-unit incremental loss incurred in transmitting an increment of power to each of the individual loads

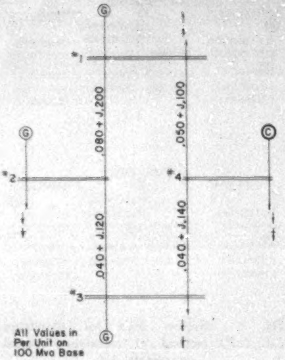

Fig. 2. Impedance diagram

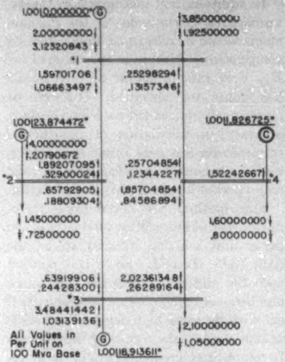

Fig. 3. Case B-1 load flow

should be represented by the incremental loss in transmitting power from source m to load n times the ratio that the incremental increase in each load n bears to the incremental increase in the total load $(dL_n)/(dL_T)$. This can be expressed in equation form

$$\frac{\partial P_L}{\partial P_m}=\frac{\sum_n \frac{dL_n}{dL_T}\,\frac{dP_L}{dP_{n\leftarrow m}}}{1+\sum_n \frac{dL_n}{dL_T}\,\frac{dP_L}{dP_{n\leftarrow m}}} \qquad (8)$$

where

$\frac{\partial P_L}{\partial P_m}$ = incremental loss of source m

$\frac{dL_n}{dL_T}$ = ratio of incremental increase of load n to incremental increase of total load

A rigorous derivation of equation 8 is given in the Appendix.

Application of Method

Some discussers[5] have criticised Mr. Brownlee's voltage phase-angle method of determining increment loss,[4] claiming that it would break down under certain combinations of phase angles, different reactance-resistance ratios in the various lines of the system, loads located on a line connecting two generating plants, and a generating plant located on a line connecting two other generating plants and having a phase angle substantially greater or less than the phase angle of the two end plants. Although Mr. Brownlee in his closure appears to have satisfactorily answered the questions raised by these discussers, it is desirable that the accuracy of the method presented in this paper for determining the value of the general loss equation constants be tested under adverse conditions and, to do this, the adverse factors referred to in reference 6 have been incorporated in the system used to illustrate the application of this method. The system selected, shown in Fig. 2, is a 3-source 4-load loop system having different reactance-resistance ratios for each transmission line, with a load located on a line connecting two generating plants and a generating plant located on a line connecting two other generating plants. In some of the cases studied, the voltage phase angle of the intermediate plant is considerably greater than that of the two end plants; in other cases studied it is considerably less.

For illustration, the value of the general loss equation constants will be determined for the system shown in Fig. 2, and incremental loss and total loss values will be computed using the general loss equation and compared with actual loss values and actual I^2R losses for a number of cases representing typical distribution of power supply by sources for peak period, median, and valley period load conditions. Load distribution for the three load periods is shown in Table II.

It will be noted that each of the loads varies at a different rate and do not remain a constant fraction of the total system load. Also, the difference in the ratio of valley load to peak load is representative of that normally found between substations serving different types of loads on a typical power system. The distribution of the change in total system load by loads is also shown in Table II.

Six representative cases of power supply by sources, three for peak period loads, and three for valley period loads, will be used in determining the loss equation constants. Power supply by sources, I^2R loss, and incremental loss of each source computed by equation 8 are shown in Table III. Fig. 3 shows the load-flow diagram for case B-1. Solution of the ten simultaneous equations for incremental loss and I^2R loss, based upon the data of Table III, gives the values for the general loss equation constants, shown in Table IV.

The assumptions on which the general loss equation is based are:

1. The variation in each substation load is a fixed percentage of the variation in system total load. This percentage is not related to the size of the load. For example, no problem is presented by a large load of 100-per-cent load factor, in which case the load variation would be zero per cent of the system total load.
2. The reactive power generation is that required to maintain the peak period and valley period bus voltage levels established in the cases studied on the network analyzer to obtain the data used in setting up the simultaneous equations for determining the loss equation constants.

Table II. Load Distribution for Three Load Periods and Distribution of Change in Total System Load

Load No.	Load Distribution, Mw			Distribution of Change, Per Cent
	Peak Period Load	Median Load	Valley Period Load	
1	500	385	270	38.34
2	200	145	90	18.33
3	300	210	120	30.00
4	200	160	120	13.33
Total	1,200	900	600	100.00

Table III. Data for Cases Used in Determination of Loss Equation Constants

Case No.	Supply by Sources, Mw			Incremental Loss,* Per Cent			I^2R Loss, Mw
	No. 1	No. 2	No. 3				
A-1	200.00	800.00	357.93	−22.62	34.16	14.45	157.93
A-2	600.00	200.00	411.33	0.93	1.75	2.17	11.33
A-3	200.00	400.00	710.73	−24.92	20.22	23.81	110.73
C-1	417.17	200.00	0	6.40	4.09	−7.21	17.17
C-2	0	200.00	469.51	−20.36	13.68	19.76	69.51
C-3	200.00	0	421.03	− 8.01	−0.08	11.91	21.03

* Computed by equation 8.

Table IV. Value of Loss Equation Constants

$B_{11}=\ 0.016576$	$B_{21}=-0.010204$	$B_{31}=-0.013611$
$B_{12}=-0.010204$	$B_{22}=\ 0.021871$	$B_{32}=\ 0.002477$
$B_{13}=-0.013611$	$B_{23}=\ 0.002477$	$B_{33}=\ 0.016792$
$B_{14}=-0.026961$	$B_{24}=\ 0.027215$	$B_{34}=\ 0.025327$
	$K_{L0}=\ 0.021524$	

Comparison of Results

A comparison of incremental loss and total system loss, given by equations 2 and 3, with actual system I^2R loss and actual incremental loss values, as determined by the $(\Delta L)/(\Delta P)$ method, is given in Table V. The 15 cases shown cover a wide range of system conditions. Peak period, median, and valley period loads are represented, and power supplied by each source covers the full range from minimum to maximum output. System I^2R losses range from a minimum of 0.9 per cent to a maximum of 11.6 per cent, and incremental loss values vary from −25 per cent to +35 per cent. The difference in bus voltage phase angle between power supply sources runs as high as 45 degrees.

The close agreement of actual values of incremental loss and total system loss with those computed by the general loss equation, as shown in Table V, fully supports the principles on which the general loss equation is based and the method of determining the equation constants. The system used to illustrate this method incorporates all of the adverse factors which the critics of the voltage phase-angle method claimed would cause this method to fail. Even better results can be expected when the general loss equation is applied to a system in which such adverse factors are not predominant. The procedure outlined by Mr. Brownlee in his closure of reference 4 for applying this method to line systems should be followed.

Conclusions

A new type of general loss equation has been developed which has the following distinctive characteristics and advantages:

1. Proper recognition is given to the effect that the difference in distribution of load by substations for maximum and minimum load conditions has upon both total system loss and incremental loss of the various power supply sources.

2. The important effect that the rate at which each substation load is changing has upon incremental loss values is recognized and taken into account in determining such values.

3. Reactive-power generation and flow is that required to maintain the system schedule of bus voltage levels during both peak and valley periods.

4. There is no restriction upon the maximum bus voltage phase angle between power supply sources, which makes the general loss equation especially applicable to interconnected systems where such angles across the system may be large.

5. It is not necessary to treat large nonconforming loads as sources of negative power supply, provided the daily variation in the nonconforming loads is followed consistently.

Appendix. Derivation of Equation 8

Consider the sum of contributions to the system transmission loss dP_L arising from increments of power $dP_{n\leftarrow m}$ received at each load from plant m as load changes $dL_n = dP_{n\leftarrow m}$ occur. The individual loads in general have different rates of change with respect to the total load.

With all other loads and sources being held constant, the total change in system loss is

$$dP_L=\sum_n \frac{dP_L}{dP_{n\leftarrow m}}(dP_{n\leftarrow m}) \tag{9}$$

With all other sources held constant, the total change in input power is

$$dP_m=dL_T+dP_L=\sum_n dL_n+dP_L \tag{10}$$

since $\Sigma\ dL_n$ is the total increment in load dL_T.

Since the increment in power received from source m at the load n is the increment in the load

$$dP_{n\leftarrow m}=dL_n \tag{11}$$

Substituting equation 11 into equation 9 gives

$$dP_L=\sum_n \frac{dP_L}{dP_{n\leftarrow m}}(dL_n) \tag{12}$$

Substituting equation 12 into equation 10 gives

$$dP_m=dL_T+\sum_n \frac{dP_L}{dP_{n\leftarrow m}}(dL_n) \tag{13}$$

Dividing equation 12 by equation 13 and then dividing numerator and denominator by dL_T gives

$$\frac{dP_L}{dP_m}=\frac{\partial P_L}{\partial P_m}=\frac{\sum_n \dfrac{dP_L}{dP_{n\leftarrow m}}\dfrac{dL_n}{dL_T}}{1+\sum_n \dfrac{dP_L}{dP_{n\leftarrow m}}\dfrac{dL_n}{dL_T}} \tag{14}$$

when all other sources are held constant.

Table V. Comparison of Results

Power Supply, Mw Source No. 1	Source No. 2	Source No. 3			Incremental Loss,* Per Cent Source No. 1	Source No. 2	Source No. 3	Total Loss,* Mw
				Peak Period Loads				
200.00	800.00	357.93	A-1	actual†	−25.76	37.41	16.36	157.93
				computed	−22.14	35.41	13.07	157.75
600.00	200.00	411.33	A-2	actual†	2.29	1.37	0.72	11.33
				computed	1.92	1.26	1.00	11.05
200.00	400.00	710.73	A-3	actual†	−25.76	21.74	23.71	110.73
				computed	−23.58	19.66	22.94	111.14
629.18	400.00	200.00	A-4	actual	5.69	9.08	−6.77	29.18
				computed	4.55	8.37	−5.90	26.78
300.00	600.00	379.01	A-5	actual	−15.57	24.48	10.49	79.01
				computed	−15.31	24.72	10.07	81.33
400.00	200.00	634.64	A-6	actual	−10.35	6.02	13.09	34.64
				computed	−10.79	6.45	13.95	36.64
				Median Loads				
200.00	400.00	348.44	B-1	actual	−13.86	17.55	10.82	48.44
				computed	−13.71	17.86	10.77	50.07
400.00	200.00	308.83	B-2	actual	− 1.56	4.66	2.74	8.83
				computed	− 1.92	4.84	3.01	9.03
327.39	400.00	200.00	B-3	actual	− 4.62	14.05	1.84	27.39
				computed	− 5.45	14.53	2.32	28.16
				Valley Period Loads				
417.17	200.00	0.00	C-1	actual†	7.33	3.83	−7.93	17.17
				computed	7.05	2.96	−7.83	16.91
0.00	200.00	469.51	C-2	actual†	−20.66	14.25	19.32	69.51
				computed	−19.56	13.80	19.29	69.90
200.00	0.00	421.03	C-3	actual†	− 7.37	−0.26	10.80	21.03
				computed	− 7.53	0.73	11.23	20.80
100.00	300.00	233.86	C-4	actual	−11.96	14.51	9.20	33.86
				computed	−11.87	14.96	9.15	35.04
300.00	200.00	107.68	C-5	actual	0.54	5.90	−1.09	7.68
				computed	0.24	5.88	−1.03	7.87
100.00	400.00	143.00	C-6	actual	−11.34	18.25	6.73	43.00
				computed	−11.44	18.89	6.59	44.82

* Actual total loss and incremental loss values are determined by the I^2R and $(\Delta_L)/(\Delta P)$ methods. Computed total loss and incremental loss values are determined by equations 2 and 3.

† Cases used for determination of loss equation constants.

References

1. INTRASYSTEM TRANSMISSION LOSSES, E. E. George. *AIEE Transactions (Electrical Engineering)*, vol. 62, Mar. 1943, pp. 153–58.

2. TOTAL AND INCREMENTAL LOSSES IN POWER TRANSMISSION NETWORKS, J. B. Ward, J. R. Eaton, H. W. Hale. *AIEE Transactions*, vol. 69, pt. I, 1950, pp. 626–32.

3. ANALYSIS OF TOTAL AND INCREMENTAL LOSSES IN TRANSMISSION SYSTEMS, L. K. Kirchmayer, G. W. Stagg. *AIEE Transactions*, vol. 70, pt. I, 1951, pp. 1197–1204.

4. CO-ORDINATION OF INCREMENTAL FUEL COSTS AND INCREMENTAL TRANSMISSION LOSSES BY FUNCTIONS OF VOLTAGE PHASE ANGLES, W. R. Brownlee. *AIEE Transactions*, vol. 73, pt. III, June 1954, pp. 529–41.

5. AN INCREMENTAL COST OF POWER DELIVERED COMPUTER, E. D. Early, W. E. Phillips, W. T. Shreve. *AIEE Transactions*, vol. 74, pt. III, June 1955, pp. 529–35.

6. *Discussion* by A. F. Glimn and L. K. Kirchmayer of reference 4, pp. 535–37.

◆

Discussion

W. R. Brownlee (Southern Services, Inc., Birmingham, Ala.): This paper presents a significant forward step in the development and verification of practical methods for the computation of incremental transmission losses as functions of generator powers. Of far-reaching importance is the new method for deriving constants which will take into account a different rate of change for each individual load on the system. Previous analyses have recommended setting up negative generators to represent loads which have different rates of change. Such an expedient is practical for a very limited number of loads and at the expense of using up valuable space in the generation matrix. The beneficial influence of the new method is apparent in Table V, where excellent performance of the constants is obtained over a wide range of generation. It is believed difficult to find a practical interconnected power system with loads of such a uniform rate of change that this factor can be ignored safely. A comparison of results using the simplified loss formula applied to the system studied by the authors would be of interest.

The method used to demonstrate incremental losses, employing very small increments of power and carrying the computation to many significant figures, is most interesting. It is believed to be the first published correlation of arithmetic incrementals with system loss constants and provides further confirmation of the adequacy of the phase-angle method. Previous analyses have employed substantial exchanges of generation and comparisons of the resulting total losses, but it has been demonstrated that a total loss comparison can conceal serious errors in the incremental loss determinations.[1]

Table VI. Values Using New Constants and Phase Angles

	From New Constants, Per Cent	From Phase Angles, Per Cent
dL/dP_{21}	27.8	27.9
dL/dP_{23}	7.9	5.8
dL/dP_{31}	21.5	22.1

The question may well arise as to whether this new loss formula, making use of different rates of change of system loads, would therefore distort the indicated incremental loss between pairs of plants for a particular system load. That is, the loads would not change at all when the generation of one plant is increased and that of a second plant reduced by the proper amount. This characteristic of the new loss formula may be tested by calculating the incremental loss between a pair of plants from the values derived by the authors for incremental losses between each plant and the load, making use of equation 16 of a previous paper.[1] These values may then be compared with those obtained from phase-angle functions. Table VI shows satisfactory conformance between the values using the new constants and the direct phase-angle quantities.

One disadvantage of this new method is the relatively high cost of solving the simultaneous equations, although such cost is justifiable if no adequate method is available at a lower cost. Experience must determine if the limitations of network analyzer technique may complicate the accurate solution of the simultaneous equations.

The concept of incremental losses existing between plants with zero generation at all of them provides an excellent physical picture of the meaning of the added terms in the loss formula. In this connection, it is noted that the simultaneous equations determine all of the constant including B_{n0} and K_{L0}. It may be feasible to calculate these additional constants directly on a network analyzer. At zero power supply, system generators would be represented by adjustable capacitors for holding voltage, and approximately half of the loads would be represented by board generators. This would require a large analyzer with, say, 30 generators or the use of divider circuits.

This new method has much to commend it. It makes no use of a grounded reference point, does not need a w' factor, and requires no separate consideration of the elusive Q/P ratios required with certain previous methods.[2] Emphasis is on incremental losses, and the basic assumptions are compatible with actual power system practices.

REFERENCES

1. See reference 4 of the paper.
2. LOSS FORMULAS MADE EASY, A. F. Glimn, R. Habermann, Jr., L. K. Kirchmayer, G. W. Stagg. *AIEE Transactions*, vol. 72, pt. III, Aug. 1953, pp. 730–37.

Charles R. Cahn (Syracuse University, Syracuse, N. Y.): This paper provides an interesting new approach to the evaluation of total loss formula coefficients using data from a number of load studies over a wide range of system conditions rather than from a single base case study. Although the method of the paper utilizes Brownlee's expression for the incremental loss, which is justified for systems on which the X/R ratios of the transmission lines are reasonably the same, the $\Delta L/\Delta P$ method could be applied instead if an automatic digital computer is used to obtain the necessary load flows.

The most obvious objection to the proposed method is the enormous amount of computations necessary to set up and solve the simultaneous equations for the unknown loss formula coefficients. However, since the loss formula is used in system operation only to provide incremental losses, I made an investigation of the possibility of directly finding incremental loss formula coefficients instead. The most general linear expression for the incremental loss resulting from an incremental exchange of generation at constant system load between source n and a selected source M is

$$dP_L/dP_n=\sum_{m=1}^{N}A_{nm}P_m+A_{n0} \tag{15}$$

where P_m is the power input to the system from source m, the A's are constants, and N is the total number of sources. There are $N+1$ coefficients to be found for each value of $n\neq M$. Values of dP_L/dP_n from $N+1$ different load studies, obtained either by Brownlee's method or by the $\Delta L/\Delta P$ method, allow simultaneous solution for the A coefficients.

The same $N+1$ load studies also allow solution for the coefficients in equation 15 for the other values of n. The matrix that has to be inverted is the same for all values of n and is only of the $N+1$ order. Of course, a least square fit to more than $N+1$ load studies is permissible.

For a system with more than four generators the incremental loss formula has a greater number of different coefficients than does the total loss formula and should therefore be more accurate, although the total loss formula has the advantage of being fitted to both total and incremental losses.

The method just described was applied to the example in the paper for purposes of comparison, using the data from Table III for the same six cases. Generator three was chosen as the swing generator ($M=3$). It was necessary to calculate from the given data the incremental loss associated with exchanging generation at constant system load between source one or two and source three. The pertinent equation is

$$dP_L/dP_n=\frac{\partial P_L/\partial P_n-\partial P_L/\partial P_3}{1-\partial P_L/\partial P_3} \tag{16}$$

as shown in reference four of the paper. Only the results for an exchange of generation between sources one and three are

Table VII. Comparison of Actual and Calculated Incremental Losses. dP_L/dP_1 Is in Per Unit

Case	Actual*	From Total Loss Formula*	From Equation 17	From Equation 18
A-1	−0.503	−0.405	−0.457	−0.444
A-2	0.016	0.009	−0.028	0.018
A-3	−0.602	−0.602	−0.602	−0.668
A-4	0.117	0.099	0.092	0.122
A-5	−0.292	−0.283	−0.340	−0.300
A-6	−0.270	−0.287	−0.340	−0.306
B-1	−0.277	−0.274	−0.326	−0.301
B-2	−0.044	−0.051	−0.092	−0.052
B-3	−0.066	−0.080	−0.122	−0.079
C-1	0.141	0.138	0.156	0.152
C-2	−0.496	−0.481	−0.498	−0.550
C-3	−0.205	−0.211	−0.257	−0.240
C-4	−0.234	−0.232	−0.278	−0.261
C-5	0.016	0.013	−0.009	0.013
C-6	−0.194	−0.193	−0.240	−0.215

*Calculated from Table V by equation 16.

included here. The incremental loss formula which best fits cases A-1, A-2, A-3, C-1, C-2, and C-3 is

$$dP_L/dP_1 = 0.07096P_1 - 0.03098P_2 - 0.07629P_3 - 0.07778 \quad (17)$$

In addition, an incremental loss formula was calculated from the B-1 load study, using slopes of the generator power-reactive characteristics at the median load level, by a direct method.[1] A constant term was added to give the best fit with the given six cases. The resulting equation is

$$\frac{dP_L/dP_1}{1-\frac{1}{2}dP_L/dP_1} = 0.0685P_1 - 0.0239P_2 - 0.0660P_3 - 0.0731 \quad (18)$$

A comparison of the various equations is given in Table VII. It is seen that the total loss formula of the paper is most accurate, presumably because of its larger number of coefficients with a small 3-source system. Interestingly, the incremental loss formula of equation 18, which is much more easily obtained than that of equation 17, also appears to be the more accurate of the two incremental loss formulas.

These results indicate the possibility of greatly simplifying the method of the paper without altering the basic approach to the problem. The possibility of including the effects of loads varying at different rates in a direct method of evaluation with an additional reduction in complexity is also shown.

REFERENCE

1. THE DETERMINATION OF INCREMENTAL AND TOTAL LOSS FORMULAS FROM FUNCTIONS OF VOLTAGE PHASE ANGLES, C. R. Cahn. *AIEE Transactions*, vol. 74, pt. III, Apr. 1955, pp. 161–76.

J. B. Ward and **H. W. Hale** (Purdue University, Lafayette, Ind.): The authors are to be complimented on a very good paper. Of particular interest is the method presented for the empirical evaluation of loss formula coefficients. We would like to comment on several statements made by the authors and on several aspects of the theory and methods presented in the paper.

Reference is made to the four basic assumptions of the so-called "simplified" loss equation and to the elimination of these assumptions by the method of the paper. Of course, examination reveals that the assumptions have been relaxed or reduced to some extent, and some of the original assumptions referred to are replaced by new ones, but to the casual reader the statement might imply that all assumptions are removed. Hence the nature of assumptions and approximations might be clarified. We would be interested in having the authors summarize assumptions relating to loads, source bus voltages, source bus angles, and source power factors which are involved in applying their loss equation to a system operating condition which deviates widely from any of the conditions utilized in evaluating the constants.

We wish to supplement the authors' presentation of an empirical method with a brief discussion of how the former loss formula methods can be generalized in form and how the four assumptions previously referred to can be relaxed to some extent.

Considerable emphasis in the paper is placed on the effect of rate of load change on incremental loss values. Implied in the authors' discussion of this matter is a particular definition of incremental loss associated with a certain plant: namely, the incremental loss of plant 1, e.g., is associated with an increment change in output of that plant alone with other plant outputs constant, the increment increase arising from an increase in total load in which all loads individually share the increase in accordance with specified constant rates of change. We would like to point out that for the purpose of achieving economic dispatch of generation the actual rate of change of system loads with respect to either total load or time is not essential. An incremental loss for each plant can be defined in terms of a variation of any one load or group of loads, independently of how total load variation is shared by the individual loads.[1,2]

The form of loss formula containing the first-degree terms and a constant is certainly more versatile than the form containing second-degree terms only. This general form arises naturally from mathematical considerations. Consider a power system with n sources and with load characteristics completely defined. The total loss may be viewed as some complicated function of n variables, namely the plant loadings. Under certain restrictions, such a function can be expanded in the form of a Taylor's series. One form of Taylor's series for a function of n-variables is shown in equation 19. Here the P's are the variables, and the coefficients

$$L(P_1,P_2,\ldots P_n) = A_0 + \sum_i A_i P_i + \sum_i \sum_j A_{ij} P_i P_j + \sum_i \sum_j \sum_k A_{ijk} P_i P_j P_k + \ldots \quad (19)$$

are combinations of various partial derivatives of the function evaluated at the origin or at some other point. Fourth and higher order terms would appear, but are omitted here. We see that the third term alone is the familiar form of loss formula, and a more accurate approximation will be obtained the more terms that are used. This is not presented as a possible method of deriving a loss formula, because the function must be known in order to take the derivatives required for writing out the coefficients; however, there may be some profit in visualizing the problem from this viewpoint and in studying the nature of the Taylor's series coefficients.

A loss formula including first-degree terms and a constant can be derived from the original loss formula. This can be done and at the same time the assumptions referred to by the authors can be relaxed to some extent without the necessity of an entirely different method. This will be presented in brief outline, without detailed steps necessary for practical accomplishment.

$$L = \sum_m \sum_n B_{mn} P_m P_n \quad (20)$$

$$L = P_1^2 B_{11} + P_2^2 B_{22} + [P_r^2 B_{rr}] + 2P_1 P_2 B_{12} + 2P_1 P_r B_{1r} + [2P_2 P_r B_{2r}] \quad (21)$$

$$\frac{\partial L}{\partial P_1} = 2P_1 B_{11} + 2P_2 B_{12} + [2P_r B_{1r}] \quad (22)$$

$$P_r = a(P_1 + P_2) + b \quad (23)$$

$$\frac{\partial L}{\partial P_1} = 2P_1 B_{11}' + 2P_2 B_{12}' + B_{10} \quad (24)$$

Consider, e.g., a system consisting of two plants and two groups of loads of different characteristics. Equation 20 shows the so-called simplified loss equation for n sources. Let us apply this equation, treating one load group as the loads in the usual way and treating the other load group P_r as an additional source. Expanded, this yields the loss formula shown in equation 21. Here the contribution of load group P_r is given by the terms within brackets. Observe that for a given P_r this contribution takes the form of a constant term and first-degree terms in P_1 and P_2. In this equation, relationship between the two load groups is not restricted to a linear one.

Equation 22 is the incremental loss associated with plant 1 as obtained by differentiating equation 21 with respect to P_1. For a given value of P_r, the last term is a constant. Let us examine the meaning of equation 22. Differentiation of equation 21 in this way implies that plant 2 output is constant and load P_r is constant. Thus the increment in loss is associated with an increase in one load group alone, with this increase being picked up on plant 1 alone. Differentiation of equation 21 with respect to plant 2 has a similar interpretation, and the resulting incremental loss values are perfectly valid in applying the established criterion for determining optimum dispatch of generation.

This form of incremental loss equation might be entirely practical to use in conjunction with an optimum dispatch computer. The P's are variables and terms associated with different load groups can be treated as parameters. It is necessary to set these parameters in accordance with the values of the loads at a given time, but rates of change of the loads are not necessary. Curve followers or some other means could control equipment simulating these parameters in accordance with any complicated load curves.

Next, let us impose a constraint on the variation of the load P_r. Specifically, assume that this load group varies in a linear fashion with the total generation as indicated in equation 23. This is approximately the same specification of load characteristics as proposed in the paper, except that there the individual load or load group is assumed to be a linear function of the total load instead of generation. Either representation will probably serve equally well as an approximation of actual load characteristics, which are of course much more complicated than the proposed straight-line relationships. If equation 23 is substituted into 21, and terms collected, a total loss formula is obtained which has quadratic terms, first-degree terms, and a constant. Differentiation with respect to P_1 will yield equation 24. Here the significance of the partial derivative is the same as that in the paper, namely, an increase in total load is shared by all loads in a specified (linear) way, and the resulting increment in loss is assigned to the one plant which picks up the increase.

We would expect that such a method of expanding the original form of loss formula to take care of various load groups would

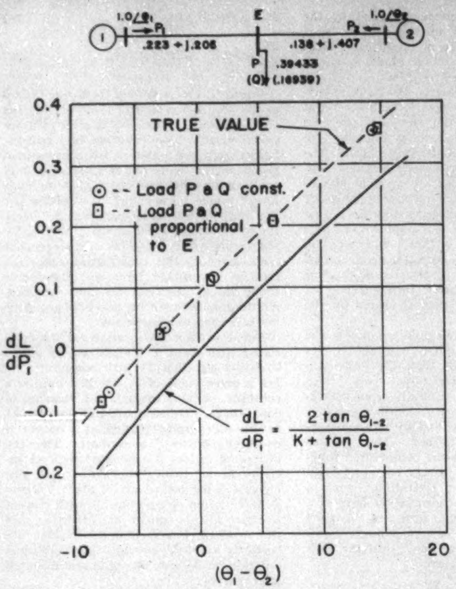

Fig. 4. Curves for incremental loss

yield adequate accuracy for many practical systems, and it might have some distinct advantages over the empirical determination of the coefficients. In the event that seasonal changes, or strikes, or some unforeseen contingency should alter the relationships between variations of the different load groups, it would not be necessary to start from the beginning and derive a new loss formula. New linear relations, such as equation 23, could be imposed and a rather minor portion of the computations repeated to obtain the new coefficients.

Finally, we would like to comment on the reference by the authors to the closure of Brownlee's recent paper.[3] In that paper, several discussions pointed out approximations inherent in Brownlee's method which were not explained in the paper. Specifically, it was pointed out that effects of the nonuniform R/X ratio and the presence of intermediate loads along lines connecting plants can introduce serious error in application of the proposed methods. In the closure referred to, the author argued that actual power system loads vary nearly as the first power of voltage and then he dispatched the related discussions very briefly with the statement: "Accordingly the load current does not change with voltage variations produced by normal exchanges of generation between sources, and thus cannot alter the incremental losses between plants." We believe this statement is not correct, and to illustrate, consider the system shown in Fig. 4. Here, two plants supply power to a single intermediate load. The two line sections exhibit a modest nonuniformity of R/X ratio. The application of the phase-angle formula for incremental loss associated with transfer of power between plants gives the solid line. The true incremental loss is given by the dotted line and, as indicated in the figure, representation of the load as power and reactive varying with the first power of voltage gives almost exactly the same true incremental loss characteristic as does constant power load. The points on the true curve were obtained by a digital solution of the system carried out to eight decimal places, and by using very small increments so that rate of change of loss is correct to three figures. The effect of intermediate loads can be an important factor, and needs further study and evaluation. The approximations of this sort which are inherent in the phase-angle method appear also in empirical evaluation of coefficients by methods of the present paper. It is shown in the paper that the methods can succeed very well in producing an accurate incremental loss formula; however, success in a single example where adverse conditions are present is of little value in discounting the potential hazards of these approximations. In the absence of complete theoretical evaluation of the assumptions, empirical evaluation requires a large amount of data.

REFERENCES

1. ECONOMY LOADING SIMPLIFIED, J. B. Ward. *AIEE Transactions*, vol. 72, pt. III, Dec. 1953, pp. 1306–11.

2. LOSS EVALUATION—PART III. ECONOMIC DISPATCH STUDIES OF STEAM-ELECTRIC GENERATING SYSTEMS, R. H. Travers, D. C. Harker, R. W. Long, E. L. Harder. *AIEE Transactions*, vol. 73, pt. III-B, Oct. 1954, pp. 1091–1104.

3. See reference 4 of the paper.

E. D. Early, R. E. Watson, and G. L. Smith: We appreciate the valuable contributions of the discussers. We note that the improved accuracy offered by the expanded form of the general loss equation presented in the paper was accepted by all the discussers, critical comment being limited to the method of determining the coefficients of the equation.

Mr. Brownlee and Mr. Cahn refer to the relatively high cost of solving the simultaneous equations, although Mr. Brownlee points out that the improved accuracy fully justifies the increased cost. Fortunately there is a much simpler method of solving the simultaneous equations at a cost that is a small fraction of $1,500 to $2,000. This method was not presented in the paper because it is not rigorous, although the results are just as accurate as those given by the rigorous method.

Equation 2 of the paper is repeated here and equation 25 is a rearrangement of equation 4

$$\sum_m 2B_{nm}P_m + B_{n0} = \frac{\partial P_L}{\partial P_n} \qquad (2)$$

$$\sum_n B_{n0}P_n + K_{L0} = L - \sum_n {}^1/_2\left(\frac{\partial P_L}{\partial P_n} - B_{n0}\right)P_n = L - P_n\sum_m B_{nm}P_m \qquad (25)$$

Comparison of equations 2 and 25 shows the left-hand side of the two equations to be identical except for the coefficients. Therefore the solution of one equation is the solution of the other when expressed in terms of a general answer. This type of general solution is equivalent to inverting the matrix in the matrix algebra solution. These equations have only $(n+1)$ unknowns and require only $(n+1)$ simultaneous equations for solution. Instead of solving 105 simultaneous equations for a 13-source system, it is necessary to solve only one set of 14 simultaneous equations in terms of a general answer, or to invert a 14 square matrix. Since the cost of solving simultaneous equations varies as the square of the number of terms, the cost of solving 14 simultaneous equations is less than one-fiftieth the cost of solving 105 simultaneous equations.

Substituting values of incremental losses for each source given by equation 8 in the general solution of equation 2 gives values for all B_{nm} and B_{n0} constants. Two values of each mutual constant will be obtained and B_{mn} may not be equal to B_{nm}, although the two values will usually be in close agreement and it is believed that they would be identical if the incremental loss values substituted were absolutely accurate.

The two values obtained for each B_{mn}-B_{nm} constant are averaged to obtain a single value for each of the mutual constants. The values of the terms $P_n\sum_m B_{nm}P_m$ are then computed and substituted in the general solution of equation 25 which gives the values of the B_{n0} and K_{L0} constants. It should be noted that in this procedure the B_{n0} values determined from the incremental loss equations are discarded and those determined by the total loss equation used in the final solution, the B_{n0} constants having a greater effect upon total losses than upon incremental losses, as stated in the paper.

Table VIII shows a comparison of the general loss equation constants given by the rigorous and nonrigorous methods and Table IX shows a comparison of incremental and total loss values given by the general loss equation with its constants determined by the rigorous and nonrigorous methods. The values obtained using the two methods are practically identical, and the values of incremental and total system losses given by the nonrigorous solution have the same high degree of accuracy as those given by the rigorous solution.

Mr. Ward and Mr. Hale request that assumptions relating to loads, source bus voltages, source bus angles, and source power factors involved in the general transmission loss equation be summarized. They are as follows:

1. The load of each substation for system peak load and minimum load conditions is determined and the assumption is made that each substation load varies between its peak load and minimum load values linearly with total system load. This assumption results in actual load distribution at system peak load and minimum load, the distribution for intermediate system loads being in error to the extent that the relationship between the variation from maximum to minimum for all loads is not linear. This assumption is considerably more accurate than the assumption that all loads remain a constant fraction of the total system load, which assumption is valid for the base load condition only.

2. Actual source bus voltages are established for both system peak load and minimum load conditions and the assumption is made that each bus voltage varies linearly with total system load from its value at peak load to its value at minimum load. This assumption is more realistic than the assumption that source bus voltages remain constant at their base load value for all other system loads.

3. No assumptions are made with regard to source voltage phase angles. In conventional methods of determining the coefficients of the simplified loss equation, source voltage phase angles are assumed to be held constant.

4. Actual load power factors, including the effect of fixed and switched capacitors, are established for each load for both system peak load and minimum load conditions and it is assumed that the power factor of each load varies from its value at system peak load to its value at minimum load linearly with total system load.

Table IX. Comparison of Incremental and Total Loss Values Given by Rigorous and Nonrigorous Loss Equation Constants

Case	Solution	Incremental Loss, Per Cent Source No. 1	Source No. 2	Source No. 3	Total Loss, Mw
		Peak Period Loads			
A-1*	rigorous	−22.14	35.41	13.07	157.75
	nonrigorous	−21.46	35.01	13.20	157.37
A-2*	rigorous	1.92	1.26	1.00	11.05
	nonrigorous	1.74	1.90	0.88	10.97
A-3*	rigorous	−23.58	19.66	22.94	111.14
	nonrigorous	−23.30	19.83	23.05	111.64
A-4	rigorous	4.55	8.37	−5.90	26.78
	nonrigorous	4.56	8.73	−6.03	27.96
A-5	rigorous	−15.31	24.72	10.07	81.33
	nonrigorous	−14.90	24.64	10.11	82.00
A-6	rigorous	−10.79	6.45	13.95	36.64
	nonrigorous	−10.84	6.99	13.93	36.62
		Median Loads			
C-1	rigorous	−13.71	17.86	10.77	50.07
	nonrigorous	−13.92	17.88	10.72	50.47
C-2	rigorous	−1.92	4.84	3.01	9.03
	nonrigorous	−1.96	5.23	2.84	9.29
C-3	rigorous	−5.45	14.53	2.32	28.16
	nonrigorous	−5.24	14.60	2.20	28.99
		Valley Period Loads			
C-1*	rigorous	7.05	2.96	−7.83	16.91
	nonrigorous	7.02	3.23	−8.13	17.89
C-2*	rigorous	−19.56	13.80	19.29	69.90
	nonrigorous	−19.32	13.87	19.22	69.59
C-3*	rigorous	−7.53	0.73	11.23	20.89
	nonrigorous	−7.62	1.18	11.04	20.25
C-4	rigorous	−11.87	14.96	9.15	35.04
	nonrigorous	−11.60	14.93	9.01	35.27
C-5	rigorous	0.24	5.88	−1.03	7.87
	nonrigorous	0.28	6.09	−1.27	7.37
C-6	rigorous	−11.44	18.89	6.59	44.82
	nonrigorous	−11.06	18.71	6.46	45.06

*Cases used for determination of loss equation constants.

Table VIII. Comparison of Loss Equation Constants Given by Rigorous and Nonrigorous Solution of Incremental and Total Loss Equations

Constant	Rigorous Solution	Nonrigorous Solution
B_{11}	0.016576	0.016229
B_{22}	0.021871	0.021352
B_{33}	0.016792	0.017010
$B_{12}=B_{21}$	−0.010204	−0.009722
$B_{13}=B_{31}$	−0.013611	−0.013633
$B_{23}=B_{32}$	0.002477	0.002694
B_{10}	−0.026961	−0.026339
B_{20}	0.027215	0.028040
B_{30}	0.025327	0.021658
K_{L0}	0.021524	0.027090

5. No assumptions are made regarding source power factors, the reactive generation at each source being that required to supply the load and maintain source bus voltages. In other methods, the ratio of reactive to real power generation (Q/P ratio) is assumed to remain at a fixed value. Recently this assumption has been relaxed somewhat by holding constant a part of the reactive generation and assuming that the remainder varies linearly with real power generation.

It will be noted that many of the assumptions of the conventional method of determining the value of the coefficients of the simplified loss equation have been eliminated entirely while others have been replaced with new assumptions that are more realistic.

Mr. Ward and Mr. Hale call attention to the fact that loads which do not vary linearly with total system load can be treated as a source of negative power supply if such loads are telemetered or can be determined with the necessary degree of accuracy by curve followers or otherwise. This is a well-known principle and three large nonconforming loads are so treated in the computer for incremental cost of delivered power described in a companion paper.[1] We do not agree that all loads can be divided into two or more groups and treated in this manner since to do so would eliminate the change in losses that would occur within the group as generation is shifted between plants and as the total load or distribution of load by groups change. Since it is necessary to represent separately each load used in the network analyzer study and since the loads not supplied directly from a generating plant bus are usually larger in number than the power supply sources, the number of loss equation constants to be determined would be increased four or more times if each load were treated as a source of negative power supply. Treating each load as a source of negative generation may be more accurate but, since the number of loss equation constants and the corresponding computer components are increased several times, use of the method does not appear to be economically feasible.

We do not agree that the method used by Mr. Ward and Mr. Hale to develop the coefficients of the general loss equation from the simplified loss equation is correct, because no consideration is given to the effect of the fixed total system loss (K_{L0}), and because individual loads are assumed to vary as a linear function of total generation rather than as a linear function of total system load. The inaccuracy of this assumption will be recognized readily when it is remembered that, for a fixed total system load, total generation and system losses can vary over a wide range as generation is shifted between generating plants. If loads are assumed to be a fixed fraction of total generation, the total system load would increase or decrease in direct proportion to total system generation and losses would remain a fixed percentage of total system generation which is incorrect.

If the correct assumption that individual loads vary as a linear function of total system load is made, namely

$$P_r = a(P_1+P_2-L)+b \tag{26}$$

$$P_S = c(P_1+P_2-L)+c \tag{27}$$

and equations 26 and 27 are substituted for P_r and P_S in equation 22, the resulting coefficients of the general loss equation will be complicated second-degree functions of

Table X. Comparison of Actual and Calculated Values of Incremental and Total Loss Values Given by Simplified Loss Equation

Case	Solution	Incremental Loss*, Per Cent Source No. 1	Source No. 2	Sou-ce No. 3	Total Loss*, Mw
		Peak Period Loads			
A-1	actual	−25.76	37.41	16.36	157.93
	computed	−20.00	40.81	17.32	174.24
A-2	actual	2.29	1.37	0.72	11.33
	computed	1.43	2.57	2.63	12.27
A-3	actual	−25.76	21.74	23.71	110.73
	computed	−21.75	23.73	27.93	124.96
A-4	actual	5.69	9.08	−6.77	29.18
	computed	4.06	10.19	−4.91	28.24
A-5	actual	−15.57	24.48	10.49	79.01
	computed	−13.87	28.75	13.47	90.97
A-6	actual	−10.35	6.02	13.09	34.64
	computed	−10.20	8.74	17.33	43.33
		Median Loads			
B-1	actual	−13.86	17.55	10.82	48.44
	computed	−11.86	20.12	12.94	50.92
B-2†	actual	−1.56	4.66	2.74	8.83
	computed	−1.30	5.49	3.85	8.83
B-3	actual	−4.62	14.05	1.84	27.39
	computed	−4.28	16.13	3.32	28.57
		Valley Period Loads			
C-1	actual	7.33	3.83	−7.93	17.17
	computed	7.60	2.08	−9.39	17.93
C-2	actual	−20.66	14.25	19.32	69.51
	computed	−16.75	14.97	21.42	65.25
C-3	actual	−7.37	−0.26	10.89	21.03
	computed	−5.96	0.25	11.96	19.22
C-4	actual	−11.96	14.51	9.20	33.86
	computed	−9.53	15.80	9.93	30.55
C-5	actual	0.54	5.90	−1.09	7.68
	computed	1.42	5.46	−1.74	6.65
C-6	actual	−11.34	18.25	6.73	43.00
	computed	−9.02	20.04	7.17	40.70

$B_{11}=0.013832$ $B_{12}=B_{21}=-0.009853$
$B_{22}=0.025740$ $B_{13}=B_{31}=-0.013646$
$B_{33}=0.020685$ $B_{23}=B_{32}=0.004981$

*Actual incremental and total loss values are determined by $\Delta L/\Delta P$ and I^2R methods.

†Base case used in the determination of B constants.

Note: See Table V for incremental and total loss values computed from general loss equation.

P_1 and P_2 and not constants, the resulting equations being so complex that evaluation by either digital or analogue computers is impractical.

It was stated in the paper that not less than $(n+2)$ cases are required to be studied on the network analyzer, where n is the number of sources, and Mr. Ward and Mr. Hale stress the importance of obtaining a large amount of data to insure accurate determination of the loss equation coefficients by the empirical method of the paper. On the other hand, it is the large amount of data used which insures the accuracy of the results obtained. When the loss equation is tied into (n^2+2n) incremental loss values and $(n+2)$ I^2R loss values covering a wide range of distribution of generation by sources for both peak and valley loads, values computed from the loss equation involve a process of interpolation between a large number of known limits and cannot be seriously in error when the values used for the limiting cases are correct.

The conventional method of determining coefficients of the simplified loss equation ties into I^2R losses for the base case only and values computed from this equation involve a process of extrapolation beyond known limits, a process subject to unlimited error unless the determination of the coefficients for the base case is based entirely upon sound theoretical principles. Although the methods used in determining these constants are considered to be based upon sound theoretical principles, so many unrealistic assumptions are made that it is necessary to introduce an empirical process in evaluating the w' or R_{LL} factor in order to force the loss equation to give correct I^2R losses for the base case, and the Q/P factor is determined entirely by empirical considerations.

The phase-angle method is used for determining incremental loss values because it is the only practical method available for determining these values from network analyzer data. Tying in with I^2R losses for each of $(n+2)$ cases offsets to a large extent any inaccuracies in the incremental loss values given by the phase-angle method. For example, in case A-2 the incremental loss values given by the phase-angle method, Table III, are completely reversed from the actual values but the values computed from the loss equation, Table V, are in close agreement with actual values.

Mr. Ward and Mr. Hale also present a discussion of the closure of a previous paper[2] designed to show that the Brownlee phase-angle method is inaccurate when used to determine incremental loss associated with the transfer of power from one source to another source, with the load held constant, over a line type system consisting of two generating plants feeding a single load over separate lines having different X/R ratios, one of which is less than unity and corresponds approximately to no. 3 copper, a conductor size not normally used on utility transmission systems.

The discussion does not appear to be applicable to the subject paper since this paper uses the phase-angle method to determine the incremental loss associated with transferring power from a source to a load while holding all other source and load powers constant. The system of the paper is a loop system with the X/R ratio of the lines varying over wide limits and with a load located between two sources. The accuracy of the results obtained, shown in Table V, speaks for the accuracy of the methods employed.

We would like to point out that the X/R ratio of the transfer impedance between sources and loads is usually limited to a small range on typical utility systems although the range of the X/R ratios of the separate lines may be large. For example, on a large utility system covering 100,000 square miles the X/R ratio of the separate lines ranges from 1.4 to 6.5 but 98 per cent of the transfer impedance X/R ratios fall in the limited range from 1.9 to 2.6 inclusive.

Mr. Cahn recognized that an independent set of equations representing incremental loss values could be set up for each source and solved to determine the B_{mn} constants. His method is similar to the nonrigorous solution presented in this closure but differs in that the solution is not tied in with system I^2R losses, which accounts to a large extent for the failure of Mr. Cahn's equation (17) to give results that are as accurate as those given by the general loss equation of the paper.

Equation 18 gives better results than equation 17, probably because I^2R losses are included in the derivation of this equation but are less accurate than those given by the general loss equation of the paper in 10 out of 15 cases. Both equations 17 and 18 represent incremental losses incurred in transferring power from one source to another at constant system load and not from a source to the load, and since this relationship is nonlinear, as shown by equation 16, it cannot be accurately represented by a linear equation such as equation 17 or 18.

Table X shows a comparison of actual and computed incremental and total loss values given by the simplified loss equation for the system of the paper, as requested by Mr. Brownlee. It will be noted that both incremental and total loss values given by the simplified loss equation are considerably less accurate than those given by the general loss equation of the paper, shown in Table V, the error in computed values being of such magnitude as to materially affect economy loading of units. Attention is directed to the fact that total losses given by the simplified loss equation are in general higher than the actual I^2R losses for peak period loads and lower than actual I^2R losses for valley period loads, which results from the inability of the simplified loss equation to take into account the shift in the system load center between peak and valley load periods when each of the loads vary at different ratios.

In applying the simplified loss equation the most recent improvements in determining the B constants were used, such as including out-of-phase components of load currents and excluding the fixed portion of Q that does not vary with generation in determining the Q/P ratio for each source.[3]

REFERENCES

1. See reference 5 of the paper.

2. See reference 4 of the paper.

3. LOSS EVALUATION—PART II. CURRENT- AND POWER-FORM LOSS FORMULAS, E. L. Harder, R. W. Ferguson, W. E. Jacobs, D. C. Harker. *AIEE Transactions*, vol. 73, pt. III-A, June 1954, pp. 716–31.

Transient Durability Testing of Valve Type Lightning Arresters

J. W. KALB
MEMBER AIEE

A. G. YOST
ASSOCIATE MEMBER AIEE

THE DESIGN testing of the valve type of lightning arresters is difficult, if for no other reason than that there is such an enormous range of performance factors which must be investigated. A lightning arrester must fulfill the following requirements:

1. Normally function as an insulator, withstanding normal system line-to-ground voltage.
2. Discharge, without damage to itself or associated equipment, transient disturbances ranging from less than 100 to many thousand amperes, and from a few microseconds' duration to several milliseconds' duration.
3. Operate as a circuit interrupter to stop the flow of power frequency follow current subsequent to unit operation resulting from transient disturbances.

Increasing the problem are the difficulties associated with obtaining substantial statistical information concerning the durations and wave shapes of surges discharged by lightning arresters. The equipment necessary to measure characteristics other than crest magnitude[1-5] is so costly as to preclude widespread installation.

Standard lightning arrester tests[6,7] are, of practical necessity, inadequate to explore all aspects of field performance. However, they are subject to reasonable duplication among different laboratories, and they form a basis of comparing relative lightning-arrester performance.

This paper describes some additional tests, as well, as alterations of standard tests, made in an effort to explore field performance characteristics. These tests are not suggested as revisions of the standard tests. In general, they involve testing techniques or possible interaction of circuit components to a degree which would render duplication among different laboratories most difficult.

Apparatus Tested

All tests were performed on standard production lightning-arrester units manufactured by the authors' company. Two types were tested. Type *GP* is designed for general-purpose station use in voltage ratings of 3 through 121 kv. Type *MP*, also designed for station use, offers better protective characteristics and greater durability than type *GP*. Type-*MP* voltage ratings are 3 through 276 kv.

Fig. 1 shows the active valve and gap elements from 4.5-kv units of these designs. The type-*MP* gap uses a separate arc-interrupting chamber to obtain more positive follow-current interrupting ability than is possible with the conventional multigap design of type-*GP* gap elements.

Circuit Voltage Drop

To accommodate power frequency test equipment of limited kva rating, the standard operating duty cycle tests permit a measurable reduction beneath open-circuit test voltage during follow-current flow. The AIEE standard[6] permits a voltage drop of not more than 10 per cent(%) of open-circuit voltage. The National Electrical Manufacturers Association standard[7] requires that the test be made using a power source of 500- to 1,000-ampere rms fault current (the current which would be obtained if the line and ground terminals of the test piece were bolted together). These test circuits result in a power circuit test condition less severe than service conditions may be because of the following conditions:

1. Follow current may be substantially less than it would be with full-rated voltage across the lightning arrester—a condition possible at high fault current locations. This reduced follow current in the test circuit results in less current-interrupting duty on the gap element and less voltage stress on the valve element.
2. The test circuit reactance, while permitting a substantial reduction in power follow current, is insufficient to result in a more severe recovery voltage transient across the gap element.

The left-hand oscillogram of Fig. 2 shows voltage and current during a standard unit operation with 10-kiloampere, 12x45-microsecond impulse on a type-*MP* lightning arrester of 4.5-kv rating. This impulse, discharged through the lightning arrester at the time indicated by the arrow, initiated the 230-ampere follow-current loop shown in the upper trace. Test circuit fault current was 1,000-ampere rms. Open-circuit test voltage was 4.5-kv rms (6.36-kv crest), and the voltage drop during follow-current flow was 6.5%.

The right-hand oscillogram of Fig. 2 was obtained with the same lightning arrester, but with open-circuit voltage increased until voltage (6.36-kv crest) during follow-current flow was equal to the lightning-arrester rating. This increased the follow-current from 230 to 295 amperes.

This 28% increase in follow current with rated voltage maintained across the test piece is evidence of the limitations inherent in the standard tests as a criterion of design adequacy. Since the 60-cycle voltage rating of the lightning arrester is a maximum value which the arrester may have to meet in service, it is necessary for the design engineer to conduct some duty cycle tests with at least full-rated voltage across the arrester

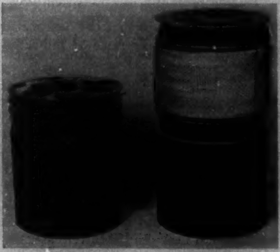

Fig. 1. The 4.5-kv valve blocks and proportionate series gap elements tested. Type GP at left, type MP at right

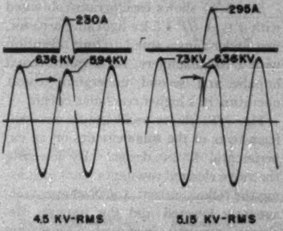

Fig. 2. Oscillograms of duty cycle unit operations on type-MP lightning arrester of 4.5-kv rms rating. Left—Standard unit operation with open-circuit voltage equal to arrester rating. Right—Open-circuit voltage increased to 5.15 kv rms so that voltage during follow-current flow was equal to arrester rating

---

Paper 55-136, recommended by the AIEE Protective Devices Committee and approved by the AIEE Committee on Technical Operations for presentation at the AIEE Winter General Meeting, New York, N. Y., January 31–February 4, 1955. Manuscript submitted October 18, 1954; made available for printing November 29, 1954.

J. W. Kalb and A. G. Yost are with the Ohio Brass Company, Barberton, Ohio.

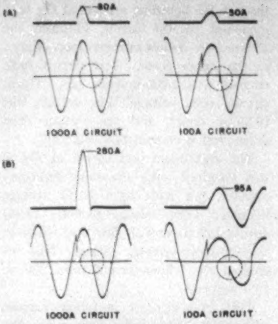

Fig. 3. A—Oscillograms showing satisfactory unit operations with type-GP lightning arrester in a 1,000-ampere fault current circuit and in a 100-ampere high-reactance circuit. Dotted circle indicates region of recovery voltage transient. B—Experimental lightning arrester of higher follow current tested in same circuits. Oscillograms show failure to interrupt power follow current in the high-reactance circuit

during follow-current flow. Without this there is no assurance that the device will perform properly in service at full-rated voltage.

High-Reactance Power Source

A design which operates properly when connected to a substantial power source may fail to interrupt follow current when energized from a higher reactance circuit, for example the end of a long, low-kva transmission line. In the latter case, the follow current and generated voltage are sufficiently out of phase to result in a more severe recovery voltage transient across the series gap element.

Fig. 3(A) shows oscillograms obtained with a type-*GP* 4.5-kv lightning arrester, first undergoing a standard unit operation with a 10-kiloampere, 12x45-microsecond impulse and, second, undergoing a unit operation in a higher reactance circuit.

Fig. 3(B) shows oscillograms obtained from tests in the same circuits on an experimental 4.5-kv design. By lowering the valve element resistance, thus increasing the follow current, the discharge voltage was lowered and the impulse discharge capacity increased. Operating duty cycle performance was encouraging because performance on the standard test was satisfactory, as evidenced by the left-hand oscillogram of Fig. 3(B). However, this same lightning arrester failed in the nonstandard, high-reactance test circuit (see right-hand oscillogram) since it failed to interrupt the power follow current. This showed its inadequacy for general service duty.

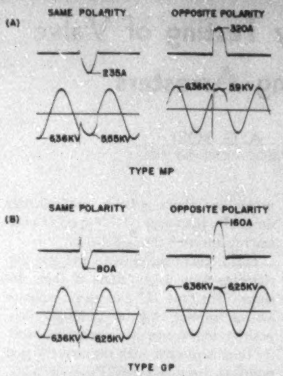

Fig. 4. A—Oscillograms of duty cycle unit operations on type-MP lightning arrester showing effect of relative polarity of the impulse and power voltage on follow-current magnitude. B—Oscillograms of the same tests made on a type-GP arrester

Polarity of Impulse

An operating duty cycle test wherein the initiating surges are the same polarity as the power frequency voltage (as specified in standard operating duty cycle tests) is not the most severe condition for valve-type lightning arresters. If the surge and power frequency voltage are of opposite polarity, the lightning-arrester discharge voltage results in energy storage in the power transformer, which when released may result in a long-duration discharge component through the lightning arrester.[8]

The oscillograms of Fig. 4 illustrate this phenomenon for both type-*GP* and type-*MP* lightning arresters. A standard 10-kiloampere, 12x45-microsecond surge was used to initiate follow current. The left-hand oscillograms were obtained during standard unit operations. The right-hand oscillograms were obtained under identical conditions, except that the surge was timed at 180 electrical degrees later. The latter condition is at least as likely to occur in service. Its greater severity is evident from the relative follow-current magnitudes.

Unfortunately, tests such as these involve considerable risk of undesirable interaction between the impulse generator and power transformer circuits.[9,10] Unless this phenomenon is sufficiently understood and controlled, duty cycle testing with impulse generator and power voltage of opposite polarity cannot be incorporated in lightning arrester standards, even though such testing would be more representative of severe service conditions.

Multiple Strokes

Field studies on a rural distribution system equipped with expulsion-type lightning arresters[11] and on 138-kv lines equipped with protector tubes,[12] showed that 22.5 and 28% of the follow-current operations respectively involved additional intermittent half-cycles of follow current. Boys camera records obtained during other investigations[13,14] showed 37 to 51% of lightning discharges as multiple in nature.

As many as 12 and 15 intermittent half-cycles of follow current on one record were obtained during the field studies on expulsion-type lightning arresters and protector tubes.[11,12] Maximum durations of records in these investigations were 1.83 and 0.67 seconds.

If mere cumulative heat storage within the mass of the valve element and its effect upon performance were the only

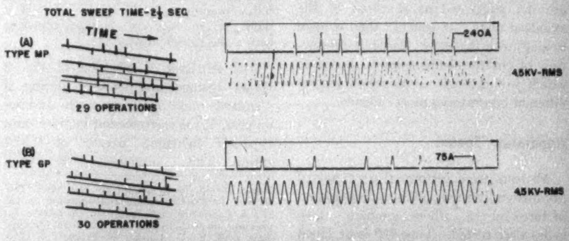

Fig. 5. A—Oscillograms of multiple-stroke test on type-MP lightning arrester. Right-hand record shows follow current and voltage during indicated portion of complete current -time record shown on left. B—Oscillograms of similar tests on type-GP arrester

Fig. 6. Combined impulse and duty cycle test equipment in the Barberton, Ohio, lightning-arrester test laboratory. Test housing surrounded by high-current impulse generator at upper left. Duty cycle test transformer at upper right

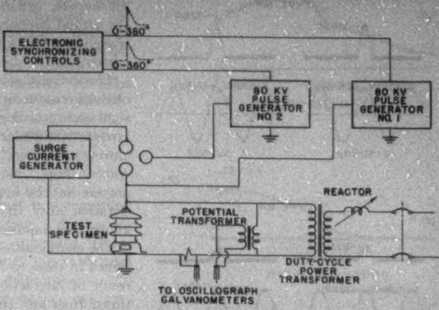
ELECTRONIC SYNCHRONIZING CONTROLS
0–360°
0–360°
80 KV PULSE GENERATOR NO 2
80 KV PULSE GENERATOR NO 1
SURGE CURRENT GENERATOR
REACTOR
POTENTIAL TRANSFORMER
TEST SPECIMEN
DUTY-CYCLE POWER TRANSFORMER
TO OSCILLOGRAPH GALVANOMETERS

Fig. 7. Diagram of test circuit used to study the effect of severe discharges through lightning arresters while they are already conducting follow current

factors involved in multiple-stroke operations, the standard operating duty cycle tests would be more than adequate to explore this aspect of service duty. The heating effect of the repeated 10-kiloampere surges is much greater than that resulting from follow current or from any repetitive surges to be encountered in service. However, the elapsed times of 30 minutes and 75 minutes permitted in the AIEE and National Electrical Manufacturers Association standards operating duty cycle tests allow redistribution of heat, within the valve element, which a multiple-stroke operation of 2 seconds' or less duration does not allow. This redistribution of heat within the valve element during the standard duty cycle tests alleviates the formation of local, unstable high-temperature regions within the valve element, which thus gives an unrealistic indication of its thermal stability.

Fig. 5 shows oscillographic records of power follow current obtained during typical tests performed to study the multiple-stroke thermal adequacy of type-*GP* and type-*MP* lightning arresters of 4.5-kv rating. These particular records show 27 and 30 separate unit operations in the elapsed time of less than 2$^1/_2$ seconds. To perform this test, it is necessary to charge the impulse generator which delivers the initiating surge at a very rapid rate. The generator capacity is therefore limited, and the repetitive surge current is approximately 3 kiloamperes of short duration. Although effort was made to maintain the power voltage polarity opposite to that of the initiating surges, this did not always occur.

Impulse Discharge Capacity with Power Voltage Applied

Most lightning arresters in stations and substations are connected to effectively grounded systems, and thus are subject to possible follow-current flow whenever the series gaps are sparked over. For this reason, the lightning arrester impulse and duty cycle test equipment in the Barberton, Ohio, laboratory, see Fig. 6 is so arranged that high current discharge capacity tests can easily be made with power voltage applied to the test piece. The following section describes one such test.

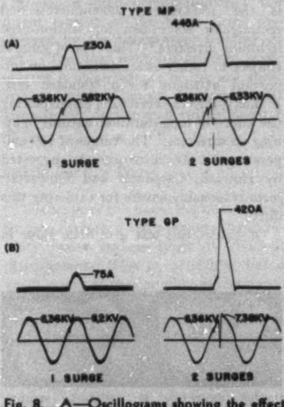

Fig. 8. A—Oscillograms showing the effect of a 10-kiloampere, 12x45-microsecond surge during follow-current flow. Circuit fault current was 500 amperes rms. B—Oscillograms of same test on type-GP lightning arrester

Impulse Discharge During Follow-Current Flow

Separate discharges of multiple lightning strokes are frequently less than 0.01 second apart.[13] It is thus likely that lightning arresters are subjected to discharges while they are already conducting follow current. Investigation of such duty is important because of the following:

1. It may result in considerably increased follow current through the valve and gap elements.
2. A high current impulse discharge during follow-current flow could reduce gap interrupting ability. This might result from

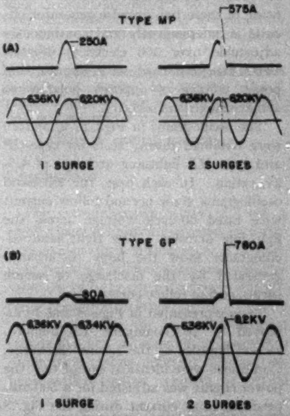

Fig. 9. Conditions identical to those of Fig. 8, except that circuit fault current was 1,000 amperes rather than 500 amperes rms

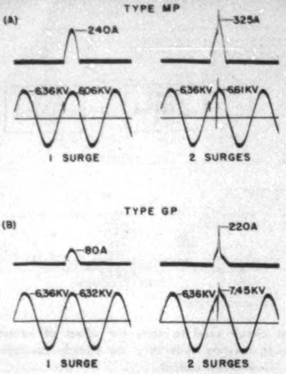

Fig. 10. A—Oscillograms showing effect of 100-kiloampere, 5x9-microsecond surge during follow-current flow on a type-MP lightning arrester. Circuit fault current was 1,000 amperes rms. B—Oscillograms of same test on type-GP arrester

undesirable arc-wandering in the simple multigap designs, like that of the type-*GP* arrester, or from damage to the interrupting chambers of high-performance gaps like that of the type-*MP* arrester.

Fig. 7 shows schematically the circuit used to represent this duty. A low-energy pulse generator is used to initiate follow current. Later, during the same follow-current loop, a second pulse generator triggers the main surge generator which discharges through the test specimen. The firing of these two impulse generator circuits is independently and continuously adjustable over 360 electrical degrees. Tests are performed with impulse and power voltage of opposite polarity to achieve maximum severity.

The oscillograms in Figs. 8, 9, and 10 were obtained during tests on type-*GP* and type-*MP* lightning arresters of 4.5-kv rating. In each case, the left-hand oscillograms show normal follow current with rated 60-cycle voltage across the lightning arrester. The right-hand oscillograms show the large disturbance generated by the discharge of severe surges during follow-current flow.

Tests represented in Figs. 8 and 9 employed a 10-kiloampere 12x45-microsecond impulse as the second discharge. Conditions were identical except that the power circuit was adjusted for a 500-ampere rms fault current during the Fig. 8 tests and a 1,000-ampere rms fault current during the Fig. 9 tests. Tests represented in Fig. 10 employed a 100-kiloampere, 5x9-microsecond impulse as the second discharge. The power circuit was adjusted for a 1,000-ampere rms fault current.

The extreme severity of these tests is obvious from comparison of the left- and right-hand oscillograms. The type-*GP* arrester particularly was subjected to currents of several times normal follow-current flow. Note that the 100-kiloampere impulse imposed less severe long-duration duty than did the longer 10-kiloampere impulse.

The enormous follow-current peaks obtained in these tests may, in part, be the result of interaction between the power transformer and surge generator capacitance. If so, they are in all probability more severe than those which would occur in service with similar surge current, time, and relative power voltage magnitude.

Fig. 11 shows a type-*MP* gap element dismantled after discharging two 100-kiloampere surges during follow-current flow. The design is self-protecting; surges of sufficient magnitude to cause damage to the arc-interrupting chamber restrike at the original spark-over gap. There are four separate arc paths on the electrodes although there were only two separate loops of follow current.

Long-Duration Discharge Capacity

A standard test to explore long-duration discharge capacity of lightning arresters is desirable in the light of present knowledge of service duty.[15,16] One such test is the 150-ampere, 2,000-microsecond rectangular wave test for station-type lightning arresters.[7] This type of surge is subject to rather exact definition, an important attribute for a standard test. It thus fulfills the need for a test exploring the effect of long-duration natural lightning on arresters. The values of 150 amperes and 2,000 microseconds suggested by Howard, Carpenter and Schwartz[15] seem reasonably severe for exploring this duty.

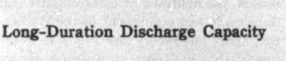

Fig. 11. Gap housing and electrodes from a type-MP lightning arrester dismantled after two 100-kiloampere discharges during follow-current flow as shown in right-hand oscillograms of Fig. 10(A)

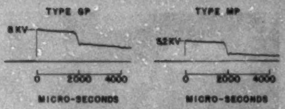

Fig. 12. Oscillograms showing voltage across type-GP and type-MP lightning arresters of 4.5 kv while discharging standard 150-ampere, 2,000-microsecond surges

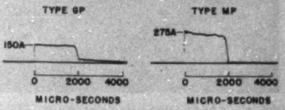

Fig. 13. Oscillograms showing current through type-GP and type-MP lightning arresters of same voltage rating with artificial transmission line charged to same voltage

Of course, this test is of little value in estimating relative switching-surge strength of lightning arresters, since it is defined in terms of current and time. The design engineer must therefore resort to additional tests, since the most severe common surge duty encountered by lightning arresters in station and substation service apparently results from switching-surge operations on long, high-voltage lines and cables.[17,18]

A switching surge is evaluated primarily in terms of voltage, not current. After the surge voltage is sufficiently high to spark-over the lightning-arrester series gaps, the resulting long-duration current magnitude is determined by line voltage, surge impedance, ground resistance, and lightning-arrester resistance. Thus the discharge current will vary greatly among different lightning arresters under identical switching-surge conditions. Figs. 12 and 13 show the effect of arrester resistance on discharge current and voltage. The tests represented by these oscillograms were made with a pi-network artificial transmission line discharging directly into type-*MP* and type-*GP* lightning arresters of 4.5-kv rating. The voltage oscillograms of Fig. 12 were obtained during standard 150-ampere long-duration discharge capacity tests on type-*GP* and type-*MP* lightning arresters. The presence of voltage after 2,000 microseconds indicates that the lightning-arrester resistance was greater than the surge impedance of the artificial transmission line. Note the greater voltage stress across the type-*GP* design. This greater voltage requires a voltage of higher charge on the artificial transmission line to obtain the same current. Actually the type-*GP* design is required to discharge about 1.9 times the energy

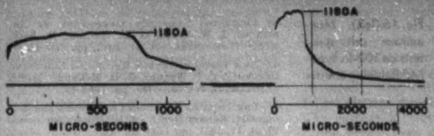

Fig. 14 (left). Oscillograms of current discharge through a 9-kv type-MP arrester. Test simulates 37 miles of 69-kv cable discharging through a 60-kv arrester

required of the type-*MP* on the standard test.

The current oscillograms of Fig. 13 illustrate the same effect in a different manner. In this case, the artificial line was charged to the voltage necessary to generate a 150-ampere surge through a type-*GP* 4.5-kv sample. Direct substitution of a type-*MP* 4.5-kv sample resulted in a 275-ampere discharge. This test, at constant generator charge voltage, would furnish a realistic comparison of switching-surge durability between the two designs because both samples were subjected to the same length of "line" charged to the same switching-surge crest voltage.

The standard 150-ampere, 2,000-microsecond test is probably an excellent choice for evaluating relative durability against long-duration natural lightning. It is a poor criterion for judging relative switching-surge performance.

Cable Tests

High-voltage cable application imposes switching-surge duty of higher current and shorter duration than high-voltage transmission lines because of the lower surge impedance and the shorter length of cables.

The ampere-time oscillograms of Fig. 14 were obtained with the pi-network long-duration surge generator and a 9-kv type-*MP* lightning arrester connected to represent a 37-mile 69-kv 1,000,000-circular-mil cable charged to 2.5 times normal line-to-ground voltage and discharging through a 60-kv type-*MP* lightning arrester. The circuit elements were so chosen that the resulting current and time values were full scale; only the voltage was reduced proportionally to the rating of the test piece. The two oscillograms are of the same current wave recorded to different time scales.

The oscillogram of Fig. 15(A) was obtained with the surge generator and a 12-kv type-*MP* lightning arrester connected to represent 18 miles of 138-kv, 1,000,000-circular-mil cable charged to 2.5 times normal line-to-ground voltage and discharging through a 121-kv type-*MP* lightning arrester.

Fig. 15(B) was obtained under identical conditions except that the duty cycle testing transformer was connected to represent a 30,000-kva, 10% impedance, 138-kv, solidly grounded transformer connected across the cable and lightning arrester. After about 700 microseconds, the discharge was carried by the transformer winding rather than the lightning arrester.

Conditions for Fig. 15(C) were identical with those of 15(B) except that a 12-kv type-*GP* lightning arrester was substituted for the 12-kv type *MP*. Thus, this circuit represented 18 miles of 138-kv cable charged to 2.5 times normal line-to-ground voltage and discharging into a 121-kv type-*GP* lightning arrester in parallel with a large-kva, wye-connected grounded transformer.

Fig. 15(B) and (C) furnish another excellent example, along with Fig. 13, of the way in which the lightning-arrester characteristic itself may determine in large measure the duty to which it is subjected. Thus, although the type-*GP* valve element would soon be destroyed by the surge of Fig. 15(B), it would not receive such a surge under the conditions represented. Its much higher impedance at these low surge currents resulted in the major portion of the surge being discharged by the transformer winding itself. The low lightning-arrester surge current is also evidence of the low surge voltage existing across the transformer and arrester during such switching-surge duty.

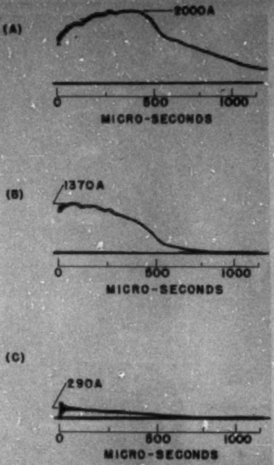

Fig. 15. Oscillograms of tests simulating discharge of 18 miles of 138-kv cable. A—Discharge through 12-kv type-MP lightning arrester. Simulates discharge of cable through a 121-kv type-MP arrester. B—Discharge through 12-kv type-MP arrester with duty cycle test transformer in parallel. Simulates discharge of cable through a 121-kv type-MP arrester protecting a large, grounded wye-connected power transformer. C—Discharge through 12-kv type-GP arrester with duty cycle test transformer in parallel. Simulates discharge of the cable through a 121-kv type-GP arrester protecting a large, grounded wye-connected power transformer

Other Service Duty

The scope of this paper has been limited to tests exploring lightning-arrester durability under various types of transient disturbances. This is, of course, but a small aspect of the complete performance characteristics of a lightning arrester. Some others, beyond the scope of this paper are the following:

1. Protective characteristics, effect of current and rate of current rise on discharge voltage, stability of discharge voltage under service duty.
2. Effect of external contamination, and effect on series gap current interrupting ability, effect on 60-cycle spark-over voltage (Fig. 16 shows a 300-kv type-*MPR* lightning arrester undergoing a 60-cycle spark-over test while subjected to a nonuniform salt spray of 300-ohms-per-cubic-inch resistivity).
3. Mechanical design, resistance to wind damage, resistance to thermal shock, pressure relief in case of electrical failure, and seal of arrester housing.
4. Stability of grading resistors.

Conclusions

The comprehensive study of even a small aspect of lightning-arrester performance as described in this paper is formidable, requiring full and sometimes imaginative use of large-capacity power and impulse generator facilities.

Tests suitable for lightning arrester standards, i.e., capable of a reasonable duplication among different laboratories, bear rather limited relation to actual service duty.

Conversely, tests approximating service duty, a necessity for the design and development engineer, will often be hard

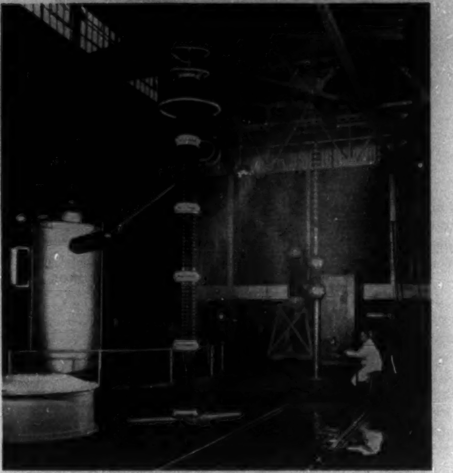

Fig. 16 (left). Nonuniform salt spray tests on 300-kv type-MP lightning arrester

to duplicate among different laboratories. Within the scope of this paper, such tests include the following:

1. Duty cycle testing with full-rated voltage during follow-current flow.
2. Duty cycle testing in high-reactance circuit to explore gap-interrupting ability.
3. Duty cycle testing with impulse and power voltage of opposite polarity, a likely service condition, and one that is more severe than impulse and power voltage the same polarity.
4. Duty cycle testing at the rate of several operations per second to obtain the local, high-temperature regions in valve elements which may occur under multiple-stroke conditions.
5. Impulse discharge during follow-current flow, a possible service condition during multiple strokes.
6. Switching surge tests, i.e., long-duration tests where impulse generator charge voltage rather than discharge current is the criterion for judging performance.
7. Evaluation of wye-connected power transformers on switching surge duty.

References

1. Advance in Technique of Lightning Measurements, **Theodore Brownlee.** *AIEE Transactions*, vol. 68, pt. I, 1949, pp. 515–19.

2. Field Research on Lightning Arrester Discharges, **G. D. McCann, E. Beck.** *AIEE Transactions*, vol. 66, 1947, pp. 625–29.

3. Field Investigation of the Characteristics of Lightning Currents Discharged by Arresters, **I. W. Gross, G. D. McCann, E. Beck.** *AIEE Transactions*, vol. 61, 1942, pp. 266–71.

4. New Instruments for Recording Lightning Currents, **C. F. Wagner, G. D. McCann.** *AIEE Transactions*, vol. 59, 1940, pp. 1061–68.

5. The Duty on Lightning Arresters for A-C Systems, **Edward Beck.** *AIEE Transactions*, vol. 70, pt. II, 1951, pp. 1134–48.

6. Report on Standard for Valve and Expulsion Type Lightning Arresters. *AIEE Standard No. 28A*, Feb. 1950.

7. Lightning Arresters. *NEMA Publication No. Lal-5*, National Electrical Manufacturers Association, New York, N. Y., Mar. 1952.

8. Estimation of Lightning Arrester Characteristics and Associated Measurement Problems, **Bror Svensson.** *Report 337*, CIGRE, Paris, France, 1946.

9. Transients During Lightning Arrester Operation in Testing Circuits and in Network Installations (in German), **K. Berger.** *Bulletin*, Schweizerischer Elektrotechnischer Verein, Zurich, Switzerland, no. 12, 1941, p. 257.

10. The Transients During Lightning Arrester Operation and Their Calculations from Consideration of the Voltage-Current Characteristics (in German), **H. Meyer.** *Bulletin*, Schweizerischer Elektrotechnischer Verein, Zurich, Switzerland, no. 4, 1942, p. 94.

11. Lightning Investigation on a Rural Distribution System, **D. A. MacCarthy, D. A. Stann, D. R. Edge, W. C. McKinley.** *AIEE Transactions*, vol. 68, pt. I, 1949, pp. 428–37.

12. Multiple Lightning Strokes—II, **K. B. McEachron.** *AIEE Transactions* (*Electrical Engineering*), vol. 57, Sept. 1938, pp. 510–12.

13. Photographic Study of Lightning, **J. H. Hagenguth.** *AIEE Transactions*, vol. 66, 1947, pp. 577–85.

14. Progressive Lightning-II **B. F. Schonland, D. J. Malan, H. Collins.** *Proceedings, A*, Royal Society of London, London, England, 1935, vol. 152, p. 595.

15. Long-Duration Surge Testing of Lightning Arresters, **S. B. Howard, T. J. Carpenter, H. Schwartz.** *AIEE Transactions*, vol. 70, pt. II, 1951, pp. 1487–92.

16. Lightning Arresters. Requirement. Which Lightning Arrester Should Satisfy, Based on Swedish Experience, **B. Grundmark.** *Report No. 330*, CIGRE, Paris, France, 1952.

17. Switching High-Voltage Transmission Lines, **I. B. Johnson, J. R. Wilson.** *AIEE Transactions*, vol. 66, 1947, pp. 1552–60.

18. Transients in Power Systems (book), **Harold A. Peterson.** John Wiley and Sons, Inc., New York, N. Y., 1951.

◆

Discussion

W. E. Eason (General Electric Company, Pittsfield, Mass.): Similar tests to those described in this lucid paper, as well as others to simulate other possible service conditions, are undoubtedly in use by manufacturers. From time to time, most manufacturers are prompted to devise a nonstandard test to fit particular conditions. Frequently the specially devised test setup and procedure involve, as the authors observe, testing techniques or possible interaction of circuit components to a degree which would render duplication among different laboratories most difficult. Moreover, the test may have been devised purely as an experimental or exploratory general test or to investigate the performance of a particular design change in one of several models of arresters. For these or other reasons, the manufacturer will refrain from suggesting a change in the Standards. Accordingly, the authors have clearly stated that the tests described in this paper are not suggested as revisions of the Standards.

Acceptance of, or a change in, an existing test is usually a long and difficult procedure because of a natural reluctance to discard the vast amounts of experience and the data of an existing test, and because of the necessity for expensive retesting if a change is accepted. Also, opposition to a proposal for a new test may come from another manufacturer with a slightly different test to simulate the same service condition. Then all manufacturers must make tests using one or more of the proposed methods. All this is expensive and time-consuming, and inevitably effects a rise in the prices of lightning arresters. It is therefore desirable that such proposals be introduced only if there is a clear need for amplification of the Standards.

I do not imply that none of the authors' suggestions warrant consideration as a possible change in the Standards. The one proposing that some duty cycle tests be made with rated voltage held during flow of follow-current is under consideration for inclusion in the forthcoming revisions of United States industry standards as well as in the proposed International Electrotechnical Commission standard. The AIEE lightning arrester standards are nearing completion after an intensive 5-year study. It is not too early to start work on the accumulation of data, to determine whether changes are justified.

I agree that long-duration test data in addition to the standard long-duration discharge tests are required to give a quantitative basis for evaluating the adequacy of a lightning arrester to discharge long lines or cable circuits. Our own continuing program to secure such data on our various designs confirms this. However, I must take issue with the authors' statement that the standard long-duration test for station-type arresters is a "poor criterion for judging relative switching-surge performance." The 1951 paper (see reference 15 of the paper) which proposed this 150-ampere, 2,000-microsecond long-duration discharge test contains evidence that the test does distinguish between arresters which withstood repeated switching-surge duty and those which failed on the same switching-surge duty. No claim has been made that the standard long-duration test exactly represents either switching-surge or long-duration lightning duty. It has been demonstrated as a test capable of standardization between independent laboratories to demonstrate the long-duration, low-current strength of an arrester. Moreover, it is a reasonable criterion for distinguishing between arresters as to their ability to withstand both long-duration lightning discharges and switching surges.

W. S. Price (American Gas & Electric Service Corporation, New York, N. Y.): Electric equipment in service on a power system is exposed to such a wide variety of electrical conditions that it would seem impossible to simulate all of these conditions in the laboratory during design work. For this reason, the actual worth of an equipment design has to be determined in many cases by the performance of that equipment in service over a period of years. However, it is inefficient and uneconomical to place equipment in service with so many "ignorance factors" included in the application that the equipment is not used at its full capability

In this timely paper, the authors describe some laboratory tests on lightning arresters exposed to various transients which might be expected to occur in service, and have pointed out that such tests are complicated and expensive and probably not capable of duplication among different laboratories. Nevertheless, such tests are extremely worth while, and should be encouraged by all equipment users, since they should ultimately permit the use of equipment on the most economical basis.

A. M. Opsahl (Westinghouse Electric Corporation, East Pittsburgh, Pa.): This is a good analysis of the problems and phenomena associated with the testing of lightning arresters. The whole range of surge conditions in service is formidable, and only a few conditions can be selected for laboratory test. In the case of surge currents, the median of the crest currents measured through arresters in service has been 800 amperes in about 5,000 measurements. In setting up tests for discharge voltage in the standard, currents of 5, 10, and 20 kiloamperes were selected with a 10x20-microsecond wave shape. These currents are about six to 25 times the median current in service. These test currents also provide range of rate of rise of current in the upper band of those that can be expected in service. The discharge voltage across the valve arrester does not change very much with various currents or with various rates of rise of current, as the standard test demonstrates.

Power follow currents and switching-surge currents fall in a lower level than the impulse currents expected from lightning. Perhaps more standard tests on the valve element in this region of current will be useful. In the past, they have been of interest only to the designer. As has been stated, the valve arrester discharge voltage does not change much with current and, conversely, the current, such as power follow, changes rapidly with applied voltage. The current in this part of the arrester characteristic rises about as the cube of the applied voltage according to the paper.

Lightning surges can occur during any part of the 60-cycle wave. An impulse current of the same polarity as the power voltage has a smooth transition from impulse current to follow current. Impulse discharges through the lightning arrester too low on the power voltage wave, too short in time, or of opposite polarity to the power voltage wave may not establish follow current through the arrester. This is a condition that can occur in service but it may be misleading if standard tests are based on such conditions. On opposite polarity power and test impulse, as the voltage across the arrester gap goes through a transient zero, a gap of high-interrupting or deionizing ability tends to quit and not restrike as the voltage rises to or overshoots the power voltage.

If the arrester gap does restrike, the energy to be absorbed is that stored in the test circuit transformer and surge generator capacitor. This is a function of the length of the surge, the capacitance of the surge generator, and the reactance of the power transformer. The duty on opposite polarity impulse and power may be more severe than testing on the same polarity but the results may also be misleading. Similarly, testing too low a voltage sample may also be misleading so the standards require that two voltage ratings be tested. For our routine power follow testing we have used longer duration current waves than those specified in the discharge voltage test. They are more certain to establish follow current and they also test for durability on the longer duration surges measured in service.

E. Beck (Westinghouse Electric Corporation, East Pittsburgh, Pa.): Several years ago some tests were made, the results of which we should like to contribute to this excellent paper. The object of the tests was to secure data pertaining to the wave shape of the current discharged through a lightning arrester from a charged conductor, in the expectation that this would resemble what might happen in the case of switching surges produced by interrupting the charging currents to an idle line or cable. I am not sure that this actually represents what happens for all switching surges, because there are many variables that enter the matter, one of which is whether the arrester is on the line or the source side of the circuit breaker and whether a voltage sufficient to discharge the arrester appears at the arrester before or after the arc in the circuit breaker is interrupted, and also what the arc characteristics are. It seems to me that variations of these cases occur. There exists a lack of factual data on the character of switching surges on systems and of the currents that arresters discharge if they are operated by switching idle lines or cable. Before jumping to conclusions, it

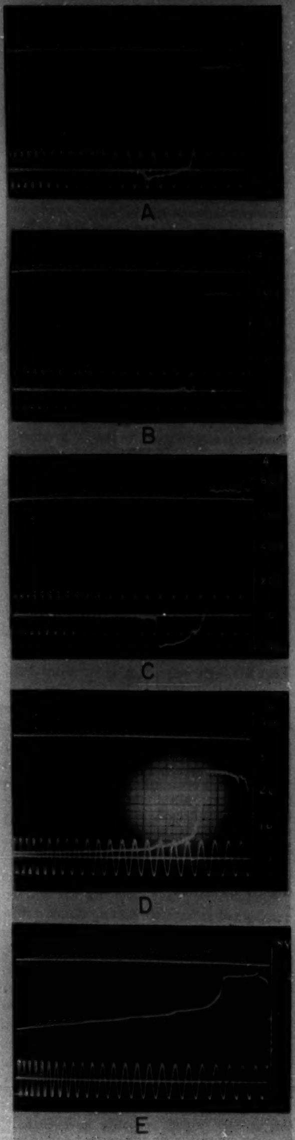

Fig. 17. Oscillograms of tests. A—Test 1. B—Test 2. C—Test 3. D and E—Test 4

seems to me we should know the facts.

Our tests may resemble the case of the arrester connected on the line side of the circuit breaker, with the line or cable charged by switching, to a high enough voltage to discharge the arrester. Also, at the moment that the arrester sparks, the circuit breaker has already interrupted so that the source is disconnected from the line. This may be the minority case, but it is the most severe as far as the arrester is concerned because it is on its own and has to dissipate all the energy that has been put into the line or cable.

The procedure in the test was to charge the cable to a definite voltage, then switch it on to a lightning-arrester element thereby discharging the cable through this arrester element. No arrester series gap is included. The test results at least show the wave shape of discharge current and the effect on the wave shape of differences in arrester impedance. The cable used was 966 feet long with a lead sheath and a surge impedance of 25.3 ohms. The cable sheath was grounded at each end and in the middle. It was charged by a rectifier.

Test 1

The cable was charged to 16 kv and discharged through a 22-ohm resistor. Fig. 17 shows the current-time oscillograms for the tests. Time runs from right to left in all the oscillograms. The wave shape in Fig. 17 (A) is practically square as is to be expected because the 22-ohm resistor almost matches the cable impedance of 25.3 ohms. The voltage appearing across the resistor in this case was 8 kv. Since the resistor's resistance was slightly less than the cable impedance, there is a small oscillation of reverse polarity.

Test 2

The cable was again charged to 16 kv and was discharged through a single station-type arrester block, the element of a 3-kv arrester. The wave, shown in Fig. 17 (C), is again practically square, because the block impedance approaches the cable impedance. The voltage across the arrester block was again 8 kv. When the current decays, the block impedance increases and there are a few added pulses of current of the same polarity as original pulse. Actually, the voltage oscillogram, not shown here, indicates that the following pulses are slightly oscillatory.

Test 3

The cable was charged to 30 kv, higher than in test 2. It was discharged again through one block. The current is now about $2\frac{1}{2}$ times higher. The voltage was about 9 kv. The initial pulse is again square, as shown in Fig. 17 (C). It is followed by a negative pulse. The arrester impedance is lower because of the higher discharge pulse.

It appears from these tests that switching surge voltage magnitude has an effect. In an actual arrester containing series gap, the arrester would probably have ceased to carry current when the current and voltage pass through zero.

Test 4

The cable was again charged with 30 kv and discharged this time through three station blocks in series, the element of a 9-kv arrester. Because of the fogging on the current oscillogram of Fig. 17 (D), the voltage oscillogram, Fig. 17 (E), is also shown. Initially the wave is square, but then, since the impedance of the three blocks in series is higher than the cable impedance, the discharge has a relatively long tail that looks like the discharge of a capacitor through a resistance.

Again, it is not the purpose of this discussion to settle the problems posed by switching surges. The real purpose is to point to some of the phases of the problem and emphasize that some fundamental data on the character of switching surges are needed to tackle the problem realistically. It should be possible to obtain such data in the field more easily than recording of lightning surges. Then some single case should be selected as a criterion.

H. A. Cornelius (Commonwealth Edison Company, Chicago, Ill.): The authors have effectively demonstrated a weakness in existing lightning arrester duty cycle test standards. In making the standard duty cycle test a 60-cycle voltage equal to the lightning arrester's voltage rating is applied, as well as the 10- by 20-impulse current wave. Present standards permit the 60-cycle voltage to decrease up to 10%, while follow-current flows through an arrester.

Several undesirable effects occur because rated arrester voltage is not maintained while power follow current flows. These effects are:

1. The magnitude of the follow current is understated, i.e., by allowing the voltage to drop to about 93%, a follow current of 230 amperes was obtained in the test. When the voltage was maintained at 100% while follow current flowed, a current of 295 amperes was obtained. This is a difference in follow current of 28%.
2. The magnitude of follow current secured under this condition is not representative of system performance requirements. System voltage will be maintained and may even be somewhat above normal on most large systems; so an arrester must be able to "seal off" against rated voltage.
3. The full heating effect of the follow current at rated voltage is not secured. Obviously the heat produced by a 128% current squared, is greater than for a 100% current squared.

Progressive improvements in the duty cycle test standards for arresters, however, have been made gradually over the years. The present AIEE Standard No. *28*,[1] permits a 10% drop below the rated voltage of an arrester, while 60-cycle power follow current flows. The present National Electrical Manufacturers Association standard, (see reference 7 of the paper) issued in March 1952, requires the use of a larger 60-cycle voltage source, one capable of delivering 500- to 1,000-ampere rms fault current to help with this problem. The weakness of the present standards, so effectively demonstrated by the author, of permitting the 60-cycle voltage to decrease during the flow of follow current, has been corrected in the draft of a new AIEE Standard No. *28*. In this draft, the 60-cycle voltage is not permitted to be less than the arrester's rated voltage during the flow of 60-cycle follow current.

Securing a test for lightning arresters which simulates the effect of repeated surges and power follow-current interruptions, such as occur in the field, on the thermal stability of arresters has been an objective for several years. The present standard duty cycle test is a poor approximation of field conditions, because of the 1-minute delay specified between successive tests in the series. Also, it is far less severe because the cumulative heat produced over a 30-minute period is less than that which may occur in service in 1 second, when a many-component stroke occurs. When 30 duty cycle tests are applied in about 2 seconds, however, as in the authors' description, the test is considered adequate and it would be desirable to include it in the revised edition of AIEE Standard No. *28*.

The present standard low-current long-duration discharge current test for arresters could be made more valuable to users and less expensive for manufacturers, by amending the method of making it. That is, instead of applying a rectangular-wave 150-ampere crest current for 2,000 microseconds to a station-type arrester, for example, as required by present standards, apply sufficient voltage to a given arrester to cause 150 amperes to flow for 2,000 microseconds. In this way, both the durability of an arrester when exposed to natural lightning and its switching-surge withstand ability can be tested under comparable conditions in all laboratories. The performance of the arrester in the field after surge voltage has caused spark-over of the series gaps, of course, will be somewhat different from that in the laboratory. In the field the long-duration discharge current magnitude will depend on: 1. the line voltage applied; 2. the line surge impedance; 3. the arrester's resistance; and 4. the arrester ground lead and ground grid resistance, as was mentioned in the paper. These factors, however, would not decrease the value of making tests on a simplified circuit in the laboratory. In closing, I wish to congratulate the authors on providing some very timely and useful information.

Reference

1. Lightning Arresters for Alternating-Current Power Circuits. *AIEE Standard No. 28*, May 1944.

J. W. Kalb and **A. G. Yost** (Ohio Brass Company, Barberton, Ohio): The authors appreciate the comments and questions of the discussers. We are certainly in agreement with Mr. Eason regarding the general objectives as well as the limitations of lightning arrester standards. Furthermore, we do not necessarily believe that any single long-duration discharge test, suitable as a standard test, can be found which is significantly better than the present 150-ampere, 2,000-microsecond test. However, a test defined in terms of current is next to meaningless when investigating switching-surge durabilities, unless all lightning arrester impedances in this current range are identical. The situation is somewhat analogous to a duty cycle test wherein the power frequency test voltage would be adjusted to give the same follow-current for all arresters. It is true that the service records of the more modern arresters, some of which meet the 150-ampere 2,000-microsecond test, are considerably better than those of earlier types. This may well be partly because of the greater immunity to long-duration natural lightning, as indicated by the ability to pass this test. However, other aspects of performance were also improved during this period, for example, the development of adequate moisture seals practically eliminated failure due to corrosion, which may have been the largest single cause of arrester failure.

We appreciate Mr. Price's interest in the tests. Of course those described in the paper represent the idea of only one manufacturer regarding the aspects of transient durability worthy of investigation. We hope this paper will encourage others to publish similar work.

We agree with Mr. Opsahl that duty cycle testing with the impulse and power frequency voltage of opposite polarity can be misleading. If power follow current is not started, conditions must be altered until it is. Once this has been done, conditions are almost certain to be more severe than those which could occur in service with presumably identical circuit parameters. There can be no doubt that the industry is far from being able to make opposite polarity duty cycle tests in different laboratories with any hope of comparable results.

We also agree that the current wave of longer duration (for example, one of 12x45 microseconds) constitutes a more severe test than does the 10x20-microsecond wave. It is used as part of our routine quality control testing.

Mr. Beck's discussion and accompanying oscillograms are most pertinent to the subject of switching-surge discharges, particularly since 966 feet of real cable were used, while the tests in the paper were made with simulated cable.

The similarity of results is gratifying, as can be seen by comparison of Fig. 17 (D) with Fig. 14. In both cases tests were made with 9-kv lightning arrester elements. The current and duration shown in Fig. 14 are much higher than those of Fig. 17 (D) but this is because the authors were attempting to represent higher cable-charging voltage, lower surge impedance, and greater length (37 miles) than were used in Mr. Beck's tests.

Mr. Beck has also shown quite aptly the effect of the arrester valve element characteristics upon switching-surge discharge magnitude, the only difference between the tests represented in Fig. 17 (B) and (C) being the number of valve blocks. This is similar to Fig. 13 of the paper, wherein the only difference between the two test conditions was that type-*GP* and type-*MP* elements were used.

We agree with Mr. Cornelius that the present duty cycle test is inadequate for exploring thermal stability or repetitive discharge strength. It must be pointed out that a repetitive discharge test could employ only weak surges for the initiation of follow-current, because impulse generators capable of delivering 10-kiloampere, 10x20-microsecond discharges cannot be charged with sufficient speed to make this test. As a multiple-stroke test, however, this constitutes no limitation, since successive current peaks of multiple discharge strokes are generally of low magnitude.

Such a test would explore a different service duty from the present standard duty cycle test wherein the repeated application of 10-kilocycle discharges constitutes a significant part of the over-all test severity. Therefore, a multiple-stroke or thermal-stability test, if employed, would supplement rather than replace the existing standard duty cycle test.

An Incremental Cost of Power-Delivered Computer

E. D. EARLY
MEMBER AIEE

W. E. PHILLIPS
MEMBER AIEE

W. T. SHREVE
NONMEMBER AIEE

THE integrated Southern Company System consisting of the Alabama Power Company, the Georgia Power Company, the Gulf Power Company, and the Mississippi Power Company serves an area of nearly 100,000 square miles and supplies a load of approximately 3,000,000 kw. Power supply sources available to this vast system consist of 18 major hydro plants, 15 major steam plants, and 11 interconnections with 6 neighboring systems. For many years, the operation of these power supply facilities has been co-ordinated through a central office known as the Power Pool Office functioning through the dispatching organizations of the four operating companies.

Co-ordination of power supply facilities was carried out by means of power supply schedules prepared in advance and supplied to each of the dispatching offices. Although important savings were realized from such co-ordination, it was recognized that advance scheduling of the operation of the various sources could not result in maximum economy since such schedules were based upon anticipated system conditions rather than those actually existing at the time. As the system load became larger and the number of generating plants increased, the additional savings which could be realized by closer supervision of power supply increased and management decided to establish a central power co-ordination office to be manned 24 hours a day to obtain maximum efficiency in such co-ordination.

During the planning and construction of this power co-ordination office, new procedures were studied to obtain increased economy of power supply with the new organization. It was concluded that the most important single improvement that could be made was to find a means of properly including the effect of transmission losses upon system power supply costs. A survey of the accomplishments in this field showed that the only existing method of doing this was by means of scheduling generation some 24 hours ahead on the basis of curves representing incremental transmission losses for a number of typical system conditions. This procedure did not offer a satisfactory solution to the problem since one of the principal reasons for establishing the new office was to eliminate advance scheduling of power supply. If the power supply co-ordinator (PSC) could take into account system conditions such as sytem load, interchange with other systems, and maximum and minimum capability of each of the generating units as they change, it would be a great aid in permitting schedules to be changed quickly to meet changed conditions and thus improve the economy of power supply.

Computer Developed to Fulfill Need

The Southern Company personnel then conceived the idea of and developed the circuits for an analogue-type computer which would quickly determine the incremental cost of power delivered for each generating unit based upon system conditions actually existing at the time. This conception embraced the idea that all telemetered information such as tie-line loadings, output of regulating plants, and output of other major generating plants should be fed directly to the com-

---

Paper 55-141, recommended by the AIEE System Engineering and Computing Devices Committees and approved by the AIEE Committee on Technical Operations for presentation at the AIEE Winter General Meeting, New York, N. Y., January 31–February 4, 1955. Manuscript submitted October 19, 1954; made available for printing December 6, 1954.

E. D. EARLY is with Southern Services, Inc., Birmingham, Ala., and W. E. PHILLIPS and W. T. SHREVE are with Leeds & Northrup Company, Philadelphia, Pa.

puter with means being provided for manually supplying to the computer other required information on current system conditions. To simplify the PSC's problem in determining the proper loading of each generating unit so as to minimize the cost of power delivered to the substations, meters showing per cent of power delivered and incremental cost of power delivered were to be located directly in front of him with selector buttons provided for selecting any unit on the system. When a selection is made the meters should provide an indication of these quantities for the selected unit. To realize these objectives, an incremental cost of power-delivered computer was designed and constructed, and has been in service on the Southern Company System since June 1954.

Operating Principles

The computer automatically determines the incremental percentage of power delivered from each source, as selected, and simultaneously calculates the incremental cost of power delivered from a particular generator located at the source. A high percentage of the required information is fed into the computer automatically and the data are "read out" manually by means of a series of push buttons provided on the center section of the computer, as shown in Fig. 1.

The only information required from the power system for computing the incremental transmission loss is the magnitude of the power at each of the sources. It should be noted that, in the case of tie lines, both magnitude and direction of power flow are required since power may flow in either direction. Large industrial loads which do not conform to the normal load pattern are introduced into the computer as sources of negative generation. This effectively prevents these loads from distorting the normal load pattern.

The magnitudes of the power in the sources which are subject to rapid or unpredictable variations are fed into the computer automatically by retransmitting means in the telemetering receiving recorders. The recorders are located on the panels which are in the background of the computer, as shown in Fig. 1. The megawatt values of the sources which are not fed in automatically are set by means of manual dials in accordance with the information received on the teletype equipment located to the right of the computer console.

The computer has been built to accomodate 30 sources although at the present time only 23 sources are required to represent the system. In some instances a source may be made up of several generating stations which are in close proximity, or it may consist of a generating station, a nonconforming load, and a tie line to an adjacent system.

The operation of the computer is relatively simple in that the operator merely pushes the button corresponding to a particular generator and the computer automatically displays the incremental percentage of power delivered from that source on one indicating meter and the incremental cost of power delivered from that generator to the load centers on a second indicating meter. These two meters, as shown in Fig. 1, are located centrally with respect to the push buttons and are calibrated respectively in per cent and mils per kilowatt-hour. The incremental cost of power delivered will hereinafter be referred to as λ. It should be noted that only the incremental percentage of power delivered is calculated for tie lines to foreign systems. The incremental cost of power delivered or, stated more exactly, the incremental cost of power delivered to the load centers is defined as the additional cost of the next increment of power delivered to the load centers taking into account not only the incremental cost of generating power at the station bus but also the attendant change in transmission loss involved in transmitting this power to the load centers.

The computer is integrated into system operation in the following manner so as to realize, as nearly as is practicable, equal λ values for all the generating units. If, e.g., additional load comes on the system, the generation of the regulating station, which is a hydro plant, is automatically increased by the action of the frequency-biased tie-line load control so that the area requirement is returned to zero. As the regulating plant approaches its upper limit of regulating capacity, the PSC redistributes the load change on the remainder of the generating units on the system so that the regulating plant generation is approximately centered in its regulating range. To determine the division of the load increase between the remaining generators which are not on automatic control, the PSC, by means of manual dials provided on the computer, inserts an increased value of generation for each of the units which are in a position to accept a load increase.

It should be noted that units having a low cost, or which are favorably located, or units which may be constrained for any reason may be operating at values below the power system λ. Units with values of λ lower than the system λ, or which are constrained, will be operating at maximum outputs and, since the outputs of these units cannot be increased, the PSC need only take into account the λ's of the nonconstrained units. After reading the λ's for the nonconstrained generating units, the PSC selects one or several of the units, the outputs of which should be increased to bring them more closely to the average value of the λ's on the nonconstrained units. The amount of load increase required for each generating unit is then determined by adjusting the manual dial to the proper value which will increase the λ of that particular generating unit to the approximate average of the λ's on the nonconstrained units. For those cases where the output of a station is telemetered to the PSC office and fed automatically into the computer, it is only necessary to snap a toggle switch from the "telemetering" to "manual" position to operate the manual dials for the various generating units in the station. After the manual dials have been adjusted to determine the megawatt increase for the various units in that par-

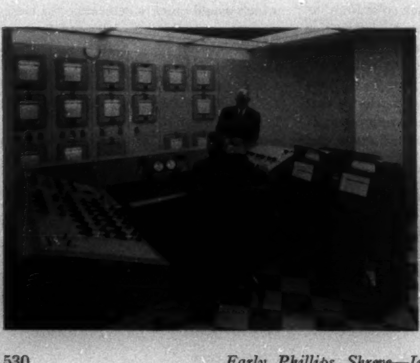

Fig. 1. Incremental cost of power-delivered computer

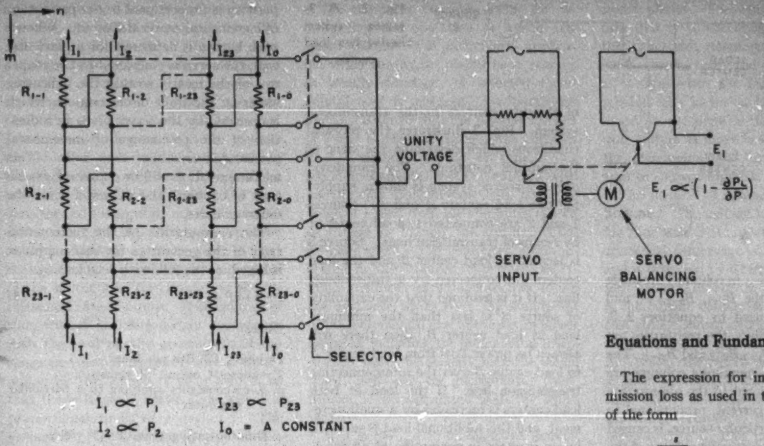

Fig. 2. Schematic diagram of matrix and incremental pescentage of power-delivered servo

ticular station, the toggle switch can be returned to the "telemeter" position. In many cases there are only a few units which economically enter into a single load increment and the entire operation outlined in the foregoing can be performed in approximately 1 minute. The same general procedure is used if the system load decreases except that the required generation changes are determined on the basis of decreases in generation.

Some of the stations on the Southern System burn either coal and/or gas in the steam generators. The gas burned is so-called dump gas and is interruptable on very short notice. Since, in general, the cost of gas is less than that of coal, a station will have a relatively low incremental rate when burning gas. When the gas supply is interrupted the PSC turns the fuel selector switch from gas to coal and the computed value of the incremental cost of power delivered automatically reflects the higher cost of the coal fuel. This will cause a change in the value of λ as read from the computer, and a readjustment of the generation of this and other stations will be required to equalize the values of λ.

The computed value of the new generation requirement, as dictated by either a system load change or a change in the type of fuel, is dispatched to the station or stations by means of the teletype referred to previously. By using the computer in the manner just described, the λ's of all nonconstrained generating units are maintained at essentially equal values. It should be noted that equal values of λ should not be interpreted to mean that λ has a constant value. The value of λ for the power system will vary as a function of total system generation. This is a well-recognized principle of electric power system operation.

The computer may also be used for obtaining an evaluation of the incremental cost of power delivered to neighboring systems and of the incremental value of power received from neighboring systems. The generator or generators supplying power to a neighboring system are those within operating range which are operating at essentially equal incremental cost of power delivered to the load centers. The λ of these generators is the system λ which was earlier described. The λ of power delivered over or received from an interconnection is the system λ multiplied by the per-cent power delivered (expressed as a decimal) as read from the computer for this interconnection. The average incremental cost of power delivered or the average incremental value of power received at an interconnection is the average of the incremental cost or incremental value as determined in the foregoing for the condition when no power is being received or delivered over the interconnection and the incremental values when such power is being delivered or received.

It has been found convenient to log the values of λ and incremental percentage of power delivered at variable intervals so that the PSC can follow the system trend and be prepared to allocate the next change in generation to the proper generator or generators. At times when the system load is relatively constant, the interval between loggings can be increased.

Equations and Fundamental Circuitry

The expression for incremental transmission loss as used in the computer are of the form

$$\frac{\partial P_L}{\partial P_m}=2\sum_{n=1}^{s}B_{mn}P_n+B_{m0} \tag{1}$$

where

s = number of sources
m = row index which assumes all values of whole numbers from 1 to s
n = column index which assumes all values of whole numbers from 1 to s
P_m = power of source m
P_n = power of source n
P_L = total transmission loss
B_{mn} = constants determined by the system characteristics
B_{m0} = constant based on the incremental transmission loss at zero system generation

The Southern System has 23 sources so that the expressions for the incremental transmission loss for particular sources are as follows:

source 1

$$\frac{\partial P_L}{\partial P_1}=2B_{1-1}P_1+2B_{1-2}P_2+2B_{1-3}P_3+ \ldots +2B_{1-23}P_{23}+B_{1-0} \tag{2}$$

source 2

$$\frac{\partial P_L}{\partial P_2}=2B_{2-1}P_1+2B_{2-2}P_2+2B_{2-3}P_3+ \ldots +2B_{2-23}P_{23}+B_{2-0} \tag{3}$$

source 23

$$\frac{\partial P_L}{\partial P_{23}}=2B_{23-1}P_1+2B_{23-2}P_2+2B_{23-3}P_3+ \ldots +2B_{23-23}P_{23}+B_{23-0} \tag{4}$$

A matrix, which is shown schematically in Fig. 2, is used in the computer to obtain analogue voltages proportional to the incremental transmission loss for each of the individual sources as typified by equations 2, 3, and 4. The resistors R_{1-1},

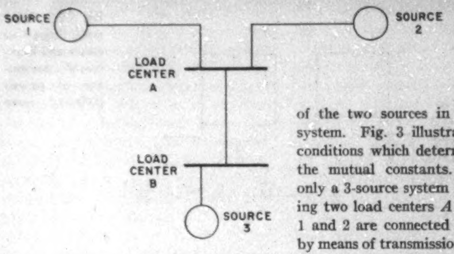

Fig. 3. A 3-source system having two load centers

$R_{2-1}, \ldots$, and R_{23-1} in column 1 are made proportional to the B_{1-1}, $B_{2-1}, \ldots$, and B_{23-1} constants used in equations 2, 3, and 4. In column 2, the resistances are proportional to B_{1-2}, B_{2-2}, and B_{23-2}. The resistances in the remaining columns are similarly proportional to the appropriate B constants. A current, proportional to the power of a particular source, is caused to flow through a particular column of the matrix. For example, the current I_1 in column 1 is proportional to P_1, and the current in column 2 is proportional to P_2, etc. A measure of the incremental transmission loss of a particular source is obtained by summing the voltages of a particular row. For example, the sum of the voltages across row 1 is $I_1R_{1-1}+I_2R_{1-2}+\ldots+I_{23}R_{1-23}+I_0R_{1-0}$ which sum is proportional to the incremental transmission loss for source 1, as expressed in equation 2. In a like manner, the sum of row 2 is proportional to the incremental transmission loss for source 2. Similarly summing over the other rows, one at a time, yields values of the incremental transmission losses for the remaining sources. When a particular source is a tie line to a neighboring system, the direction of current flow through the column reverses with a reversal of power flow.

It will be of interest to examine the B constants in some detail so that a physical significance can be assigned to them. The actual determination of these constants is developed by Early, Watson, and Smith.[1] The constants designated as B_{1-1}, $B_{2-2}, \ldots B_{23-23}$ are termed self-constants and their values are a measure of the effect on the incremental transmission loss of a given source caused by a change of power in that source. These constants are always positive in sign. The constants designated as B_{1-2}, B_{1-3}, B_{2-3}, and other similar constants where the subscript involves two sources are referred to as mutual constants. These relate the effect of a change in one power source to the incremental transmission loss of a second source. Their values may be either positive or negative depending on the relation of the two sources in the transmission system. Fig. 3 illustrates the physical conditions which determine the signs of the mutual constants. For simplicity, only a 3-source system is shown, supplying two load centers A and B. Sources 1 and 2 are connected to load center A by means of transmission lines. Source 3 is located at load center B and the load centers are connected by a transmission line. If it is assumed that the capability of source 3 is less than the minimum load at load center B, then there will always be power flow from load center A to load center B over the interconnecting transmission line. If the load at both load centers is increased by a small increment, and this additional load is supplied by an increase in generation at source 1, the incremental transmission loss for source 2 will be increased.

This is because part of the power of source 2 is being transferred to load center B over the transmission line connecting the two load centers. Since the level of power flowing over this transmission line has been raised, the incremental transmission loss associated with source 2 is also increased. If, under similar conditions, the generation is increased at source 2, the effect will be an increase of the incremental transmission loss for source 1. Thus, the mutual constants relating sources 1 and 2 are positive. If the increment in load at the load centers is supplied by increasing generation at source 3, this will decrease the power flow over the transmission line connecting the load centers and thus decrease the incremental transmission loss associated with sources 1 and 2. Since the incremental transmission losses of sources 1 and 2 decrease with an increase of generation at source 3, the mutual constants between sources 1 and 3 and also between sources 2 and 3 are negative. It is not to be implied that the foregoing explanation is intended as a rigorous proof regarding the signs of the mutual constants but is merely intended to give a physical significance to the mutual constants.

Referring to Fig. 2, the voltage derived from a row of the matrix is substracted from a voltage representative of unity and this resultant voltage is measured by an a-c potentiometer servo unit so that the position of the output shaft of the servo is proportional to unity minus the percentage of incremental transmission loss. Stating it another way, the servo shaft position is proportional to the percentage of incremental power delivered. When a push button is depressed for a particular unit, the servo is connected to the proper row of the matrix so that the indicating meter on the front of the console, which is operated by the servo, gives an indication of the percentage of incremental power delivered by that unit. This measurement, as will be explained, is also used to compute the values of λ for the different units.

The computation of the incremental rates of the generators for this computer is based on the following relations

$$I=a+bP+cP^2 \tag{5}$$

where

I = input, 10^6 Btu per hour
P = kilowatt output of generator
a, b, c = constants applying to a particular generator

Differentiating equation 5 yields

$$\frac{dI}{dP}=b+2cP \tag{6}$$

which is the expression for the incremental rate of a particular generator. It should be noted that, when equation 6 is plotted with kilowatts as the abscissa and 10^6 Btu per kilowatt-hour as the ordinate, it describes a straight line of intercept at b and a slope of $2C$.

When the generators in a multiple unit station have the same characteristics, only one incremental rate circuit is used for the station. The computer automatically divides the total generation equally among the generators in service and all computing is done on a unit basis. When a station has units of different characteristics, a separate incremental rate circuit is provided for each type of unit. For example, Gorgas Station, which has a total of eight generators, is provided with four separate incremental rate circuits. As indicated, the incremental rate curves in this installation were represented by a straight-line relationship. The principles of computing are such that incremental rate circuits can be arranged to express this relation as a series of connected straight lines of different slopes and intercepts. By this method any of the typical incremental rate curves can be followed quite closely. To convert to cost, both sides of equation 6 can be multiplied by f, the cost per 1,000,000 Btu, and the equation becomes

$$\frac{dIxf}{dP}=\frac{dF}{dP}=(b+2cP)f \tag{7}$$

Equation 7 states that the incremental

cost per kilowatt-hour is the product of the sum of b and $2cP$ multiplied by the cost per 1,000,000 Btu. Separate cost dials are provided for each station for each type of fuel which may be used in the steam generator. Some of the stations may be using both gas and coal simultaneously in a single steam generator, in which case the dial is selected for the particular type of fuel which is to be varied as a function of load. The cost dials for the steam units are calibrated in cents per 1,000,000 Btu and may be readily adjusted as the price of fuel changes. Fig. 4 is a schematic diagram of the circuit used for computing the incremental rate of a unit. The contact of slide wire S is positioned in accordance with the load on the generator and the range in volts of the slide wire is determined by the setting of slide wire S_1 so that the voltage E_1 across slide wire S is proportional to $2c$ of equation 7. The voltage E_2, Fig. 4, is thus proportional to the $2cP$ term. Slide wire S_2 is so positioned that voltage E_3 is proportional to the b term of this same equation. The sum of E_2 and E_3 is in turn proportional to $(b+2cP)$, and it is necessary to modify this sum by the cost factor f to obtain a voltage representative of the right-hand term of equation 7. This is done by applying the sum voltage to slide wire S_3 and adjusting the position of its contact in accordance with the f term, as shown in Fig. 3. The voltage E_4, which is the resultant output after the foregoing operations, is representative of the right-hand term of equation 7, or the incremental rate in mils per kilowatt-hour of the unit.

The computer provides means for coordinating the operation of hydro and steam plants. It is particularly applicable when the hydro plants have storage or weekly pondage. A selected incremental cost is assigned to a particular hydro station so that the desired amount of water is released through the turbines in a designated period of time. This pseudoincremental cost is combined with incremental transmission loss, and the value of λ read from the computer is used as a basis for loading the station, as described earlier. The computer, when operated in this manner, effectively determines the most advantageous time to use the available water from the standpoint of the incremental cost of the steam power replaced, including the incremental transmission losses associated with the steam plant, and also the incremental transmission losses associated with the hydro plant.

If it is desired to increase the amount of water released over a given period of time, the cost dial is set at a lower value which will result in a lower value of λ. This means that the station will be generating for a greater number of hours during the course of a day's time. Assigning a greater cost will result in an increased value of λ and, consequently, the amount of water released will be decreased. When it is desired to release the maximum amount of water through the turbines, the cost dial is set at zero which will normally result in the plant being fully loaded for all values of system load. Operation on some systems is based on peaking hydro plants at time of system peak to limit generation at higher cost steam plants. The computer may dictate that it is advantageous to increase the higher cost steam generation at peak loads and increase the hydrogeneration at a time when the incremental transmission loss factor is lower.[2,3] This is based on the premise that the transmission system is most heavily loaded and the incremental loss is greatest at the time of the system peak.

The method of computing λ is shown in Fig. 5. The voltage across the measuring slide wire S is proportional to the incremental percentage of power delivered, and is provided by a retransmitter on the servo shown in Fig. 2. The voltage E_4 is the output voltage of the incremental cost circuit shown in Fig. 4, and is to be balanced by the positioning of slide wire S. When the servo is balanced, the angular position of the contact arm of slide wire S is a measure of λ. For this particular computer, the range of the servo is 0 to 15 mils per kilowatt-hour. The balanced position of the slide wire is directly proportional to E_4 and inversely proportional to E_1. For example, if the voltage E_1 is doubled in value, with E_4 remaining constant, the servo will be balanced at one-half of its previous angular position. Essentially this servo is of the ratio type, which measures the ratio of the incremental rate of the generator to the incremental percentage of power delivered.

All of the variable factors in the computing circuits including the matrix elements are adjustable over wide limits of permit, taking care of future conditions which may result from changes on the power system. Factors, such as fuel cost, which may vary over relatively short periods of time have dials calibrated in

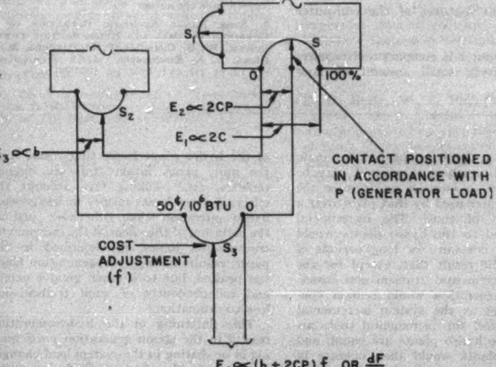
S1
S
O
100%
S2
E2 ∝ 2CP
E1 ∝ 2C
E3 ∝ b
CONTACT POSITIONED IN ACCORDANCE WITH P (GENERATOR LOAD)
50¢/10⁶BTU
0
COST ADJUSTMENT (f)
S3
E4 ∝ (b + 2CP) f OR dF/dP

Fig. 4. Schematic diagram of circuit to obtain incremental generating cost

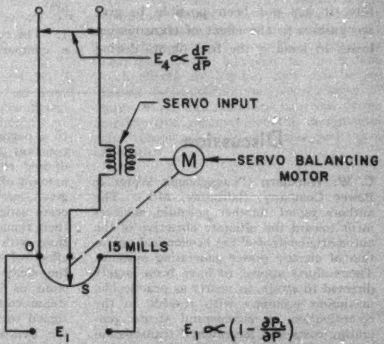

Fig. 5. Schematic diagram of circuit to obtain incremental cost of delivered power λ

the appropriate units so that they may be quickly set at new values.

The computer, as described, is of the semi-automatic type and the computed information (i.e., the required generation change) is dispatched by means of the teletype channels to the generating stations. The underlying principles are such that they can be conveniently adapted to load the power system automatically on the basis of incremental costs of power delivered in conjunction with recognized forms of load-frequency control.

All of the circuits operate directly from the 115-volt 60-cycle single-phase power supply; the power requirements being in the order of 250 watts. The accuracy of the computer is not affected by voltage or frequency variations normally encountered on electric power systems.

Operating Experience

The computer has fully lived up to all expectations. The PSC are enthusiastic about it because, as the system load changes, it tells them at what plants generation should be increased or decreased and the amount of such change. It gives them the confidence of knowing that they are doing the proper thing at all times.

The savings in production expenses resulting from the co-ordination of incremental production expenses and incremental transmission losses have been estimated at not less than $200,000 per year for the Southern Company System. During the first 4 months the computer was in operation, the severest drought conditions in the past 25 years have been experienced and it has, therefore, been necessary to operate primary fuel plants at full output during the peak-period hours to conserve hydro storages. Therefore, it has not been possible to give recognition to the effect of transmission losses in loading the fuel plants during these hours. However, the computer has been used to the full extent during the off-peak hours and the fuel plants have been loaded for equal incremental cost of power delivered. The PSC have had no difficulty in maintaining the incremental delivered cost of the various units at the same level within ±0.1 mil.

In view of the abnormal hydro conditions prevailing during this period, no studies have been made to determine the actual savings being realized. However, there are several indications that the computer is performing its duties efficiently. For example, prior to the use of this equipment, considerable difficulty was experienced during the morning loading and evening unloading period because of the overloading of transmission lines. When the loading of the plants is determined by the computer for equal incremental cost of power delivered, no difficulty is experienced from this source. This is to be expected since overloaded lines result in abnormal transmission losses. An interesting side light is that a plant on the western end of the system burning natural gas at a cost of 11 cents per 1,000,000 Btu at times operates at the same incremental cost of power delivered as another plant on the eastern end which burns oil costing 35 cents per 1,000,000 Btu; the equalizing factors being that the plant with the low-cost fuel has an incremental heat rate approximately 20 per cent higher than that of the other plant and incremental transmission losses as high as +40 per cent, while the plant burning the high-cost fuel has incremental transmission losses as low so −40 per cent.

Summary

The salient features of the computer are:

1. The computer is compact and requires a comparatively small amount of floor space and is, therefore, suitable for most dispatching offices.

2. The computer is dynamic and the results are based on actual system conditions. Constraints imposed by the system or equipment are automatically taken into account.

3. The computer, as built for the Southern Company System, can be termed semi-automatic, i.e., a large percentage of the data is fed in automatically and the computed information is read out manually. The principles used lend themselves to making the computer completely automatic in its operation.

3. For system studies or setting up future schedules, the computer may be completely divorced from the system. Generation values may then be set up by the hand-set dials, which are provided as part of the computer to determine the effects of different schedules.

4. The power requirements for operation of the computer are quite small, being in the order of 250 watts.

5. The accuracy of the computer is not affected by voltage or frequency variations normally encountered on electric power systems.

6. The values of the *B* constants in the matrix and the intercept and slope values of the incremental rate curves are adjustable over wide limits. Fuel cost dials, calibrated in cents per 1,000,000 Btu, are provided for each station for each type of fuel.

7. Push-button convenience for obtaining scheduling information eliminates human error in calculations and encourages the PSC to load the system for maximum economy of power supply.

References

1. A General Transmission Loss Equation, **E. D. Early, R. E. Watson, G. L. Smith.** *AIEE Transactions*, vol. 74, pt. III, June 1955, pp. 510-20.

2. Central Power Coordination of Southern Company System, **E. D. Early.** *Southeastern Electric Exchange*, Oct. 1, 1953. Copies may be secured from the author.

3. Short-Range Economic Operation of a Combined Thermal and Hydroelectric Power System, **W. G. Chandler, P. L. Dandeno, A. F. Glimn, L. K. Kirchmayer.** *AIEE Transactions*, vol. 72, pt. III, Oct. 1953, pp. 1057–65.

◆

Discussion

C. W. Watchorn (Pennsylvania Water & Power Company, Baltimore, Md.): The authors report another splendid achievement toward the ultimate objective of the automatic control of the economical operation of electric power generating systems. Their efforts appear to have been largely directed to attain, as nearly as practicable, maximum economy with respect to the co-ordination of incremental steam generating costs and incremental transmission losses. If the paper is correctly understood with respect to the basis described for the co-ordination of hydro and steam generation, the incremental cost assigned to a particular hydro plant would remain constant until such time when it may be desired either to increase or decrease the amount of water used by that plant over a given period of time. The incremental costs assigned to the hydro plants would then remain constant for long periods of time with the result that, except for the effect of incremental transmission losses, the steam generation would remain constant as long as the system incremental steam cost and the incremental costs assigned to the hydro plants are equal, and the hydro plants would then operate in the peak of the system load, taking all the load variations. It has been shown that such hydro operation can be very uneconomical under certain conditions because of the hydro plant losses that result from the unit, pond, intake, tail-race characteristics, etc.[1] Taking into account the effect of these losses results in less peaked hydro operation than otherwise, just as the inclusion of the effect of the incremental transmission losses, as described in the paper, results in the hydrogeneration being less peaked, but to a much greater extent and independently of such transmission loss co-ordination.

This flattening of the hydrogeneration results in the steam generation participating in or sharing in the system load changes along with the hydro. Such operation results in a variable rather than a constant system incremental steam cost.

Then, since the incremental cost to be

assigned to the hydro plants is equal to the system incremental steam cost as of the same time, it must also be variable. This requirement presents the problem as to a possible basis for such a determination. One such basis, which as of now appears to require considerable simplification if it is to have practical application but which, at least, is a start, is shown by the following equation obtained by rearranging equation 1 of reference 1

$$\frac{dc}{dg_{sh}}=\frac{N}{\dfrac{\dfrac{dL}{dt}}{\dfrac{dq}{dt}}-\dfrac{dg_h}{dq}} \qquad (8)$$

where

$\frac{dc}{dg_{sh}}$ = incremental cost to be assigned to the hydro plant, $ per hour per megawatt

N = incremental water value in $ per hour per 1,000 cubic feet per second and is a constant during the whole of any period of pondage operation of the hydro plant under consideration

$\frac{dL}{dt}$ = time rate of change of the system load, megawatts per hour

$\frac{dq}{dt}$ = time rate of change of the hydro plant discharge, 1,000 cubic feet per second per hour

$\frac{dg_h}{dq}$ = incremental hydro equivalent of the hydro plant, megawatts per 1,000 cubic feet per second. It is a very complicated function that depends on the unit characteristics, the pond, intake and tail-race characteristics, the hydro plant discharge, and the inflow into the pond, all as shown by equation 2 of reference 1.

Any justification there may be for the use of such a basis for co-ordinating hydro and steam generation would, of course, depend on an evaluation of the results obtained with its application as compared with the results obtained with the application of other bases of co-ordinating hydro and steam generation.

REFERENCE

1. CO-ORDINATION OF HYDRO AND STEAM GENERATION, C. W. Watchorn. *AIEE Transactions*, vol. 74, pt. III, April 1955, pp. 142–50.

W. H. Osterle (West Penn Power Company, Pittsburgh, Pa.): The authors and the Leeds & Northrup Company are to be congratulated on the pioneering work they have done in the very important field of economic dispatching of generation. On a system as far-flung as the integrated Southern Company System, with high transmission loss and with steam stations having such a range of fuel cost as indicated, it is indeed readily understandable that savings can be made by proper dispatching, including the effect of transmission losses.

A great deal of study is being given to this problem by other companies including my own. Although the savings are not as impressive as those of the authors' company, nevertheless they are real and worth while. The fact that attention is directed to economical plant loading and transmission losses is in itself productive of good results.

I had the pleasure of seeing the computer in operation and was greatly impressed. One fact brought out in the paper was that from the generator information fed into the computer, automatically and manually, it was possible to arrive at a total system load which was metered and shown before the eyes of the operator. As our system has only a total of 1,250 megawatts, it was exciting to see a system total of around 2,900 megawatts.

I would like to ask the authors a couple of questions about the incremental cost curves for the generator units. These are represented, as I understand it, as a straight line with kilowatts as the abscissa and input in 10^6 Btu per kilowatt-hour as the ordinate. The entire curve is multiplied by a factor in proportion to fuel cost. Now the incremental cost of the generating unit is made up of fuel cost plus incremental maintenance, or O.T.F. (other than fuel) as it is usually called. This is generally added at a fixed value expressed in decimal mils per kilowatt-hour. If the curves are drawn on total cost, i.e., fuel plus O.T.F., then the cost multiplier operates on the fuel incremental and on the O.T.F. also. Further, does this one straight line adequately represent the power station incremental cost over the entire range from minimum to maximum? Also, what is done on the loss of a mill or feed water pump? I would appreciate a little further explanation of this important item in economic system loading—how these cost relationships are put into the computer.

E. D. Early, W. E. Phillips, and W. T. Shreve: Mr. Watchorn has advanced what appears to be a very logical evaluation of some of the factors which should enter into the determination of the correct economic loading of hydro plants which are integrated into an electric system which has both hydro and steam stations.

In general, any loss factors which increase with generation will tend to lower the value of generation under a given system condition. Stating the result in another way, the effect will be to reduce peaking of a particular plant. As stated by Mr. Watchorn, superimposing the factors of incremental intake losses, incremental change in tail-race level, etc., on incremental transmission loss will, in general, operate in the same direction as the incremental transmission loss and result in a further leveling of the hydrogeneration.

The measurement and transmission of the necessary data to a computer which could solve Mr. Watchorn's co-ordination equation is quite a formidable problem. Possibly the required simplification as expressed by Mr. Watchorn will remove this objection and the method will then lend itself to solution by means which are economically justified.

Regarding Mr. Osterle's discussion, Southern Company includes incremental supplies, incremental maintenance, and ash-handling expense in incremental generating cost by expressing these costs in cents per 1,000,000 Btu of fuel burned and adding such cost to the fuel cost set on the fuel cost dials. This avoids the error that a change in fuel prices would produce if such costs were reflected in the unit heat curve, referred to by Mr. Osterle. If it is desired to express these costs in terms of kilowatt-hours rather than in terms of fuel burned, a separate dial calibrated in mils per kilowatt-hour could be used.

Southern Company considers that the accuracy of a straight-line incremental heat curve from minimum to normal full load is comparable to the accuracy of the available test and operating data for its units. However, where desired, such incremental cost curves can be represented by two or more straight-line segments having adjustable slopes, with adjustable points of intersection, and adjustable no-load intercept. Discontinuities in such curves can also be represented.

Such factors as loss of a mill or feed water pump, condensing water temperature, boiler and condenser conditions, and the many other variables affecting steam plant operation probably have a greater effect upon maximum loading and average heat rate than they do upon the incremental heat-rate curve; however, to the extent such effects are known, they can be reflected by adjusting the slopes, point of intersection, and zero load intercept of the straight-line segments of the incremental cost computer, or by adjusting fuel price, or both.

Production and Installation of Vertical Water-Wheel Generators

W. D. HOUSER
ASSOCIATE MEMBER AIEE

W. HINDLE
ASSOCIATE MEMBER AIEE

J. A. TYERMAN
NONMEMBER AIEE

Synopsis: This paper deals with the shop work on Canadian Westinghouse water-wheel generators and with their installation at various hydroelectric stations. The mechanical aspects of such machines are important to the erection as well as in the production operations. The tolerances called for are remarkably close considering the size and weight of the components and the fact that large machines are erected on site. The remarks on design are confined to those concerning components.

THE demand for power in all parts of Canada has doubled each decade since 1910. Mostly the increased load has been taken care of by building hydroelectric stations. The total installed hydroelectric capacity in Canada at September 1, 1954 was 16,000,000 horsepower. The characteristics of the equipment installed depended, of course, on the local conditions, which in no two places were exactly the same. Generators had to be built to suit and data are now available on a wide range of speeds and capacities.

Details of production and erection are described which in practice have been found to be advantageous in installing more than half of the water-wheel generators in Canada. The thrust bearing is the starting point for the mechanical engineer on a generator design and the construction of Kingsbury-type bearings will later be discussed at length. All work in the shops is, of course, planned so each component will be at the site when required by the erectors to meet the construction schedule. First to go are the foundation bolts and details which have to be placed while the forms for the concrete foundation are being built. These are followed by the frame and sole plates, spider and other rotor parts, shaft and thrust bearing, upper and lower brackets, and, finally, the exciters and air casing.

Formerly, the practice was to locate the sole plates individually. Instead, for a number of years past, considerable time has been saved by bolting the sole plates to the generator frame and allowing it to position them for location and elevation. A removable ferrule in the bolt assembly allows for the final centering of the stator. The foundation bolts are, of course, placed in pipe sleeves to permit horizontal adjustment of the sole plates. No paint is applied to surfaces coming in contact with the concrete as bare metal has better adherence.

Stator

The generator frames as now designed and constructed are the result of lengthy experience. Those used in the late 1900's were built up with sections of cast iron. They were superseded by frames of fabricated steel construction. Earlier designs were subject to warpage and cracks which required extra time to correct and added to erection costs.

Modern frames comprise a series of flat, annular, uniformly spaced rings behind the stator punchings. These rings are positioned by vertical plates, structural shapes, and pipe spacers. A steel cover wraps the rings, providing support and controlling the ventilating air. Additional web plates and rings are placed above the stator punchings to support the superstructure of the machine.

Accurate machining of the bore of the stator frame is essential for satisfactory stacking of the punchings; see Fig. 1 Bores are usually held to ±0.005-inch diameter regardless of size. Out of roundness of the bore is held to similar accuracy. The over-all height of the frame is not usually critical; however, parallelism between the top and bottom face of the frame must be held to a tolerance of 0.016 inch.

High-grade silicon steel laminations are used in all large water-wheel-driven generators where efficiency is a consideration. This iron must be accurately punched so that it will build to the correct diameter with smooth faces and slots. Subsequent to punching, the iron is annealed and burr-ground to improve the electrical characteristics and it is coated with an adequate insulating material. Two coats of sodium silicate are used as it is one of the most permanent and fire resistant types of coating available. The fingers of the iron are supported by finger plates. To prevent vibration of the iron in the slot portion, it is essential that the finger plates provide adequate support to the iron. For this purpose the use of nonmagnetic rolled steel fingers held to a heavy steel punching by spot welding has been standardized. This construction provides the maximum mechanical reliability without increasing the core loss in the generator. Vent finger plates spaced at regular intervals in the stator core are of similar construction to the end plates except that the fingerlike spacers are a much smaller nonmagnetic steel section.

After the punchings are stacked in the frame and compressed or "pulled down," Fig. 2, the through bolts are welded to the frame, top and bottom and at each intermediate frame ring, to tie the iron core securely to the stator frame. The ends of the stator slots are dressed off to remove sharp edges which might damage the coil insulation during winding. Gauging of the slots assures that the coils will fit the slots. The stator bore is checked for roundness and dimensions to make certain that it is within the required tolerance. It is normal practice to allow the stator bore measurements to average from size on to +0.030 inch with a maximum variation from the average of ±0.020 inch. However, other electrical considerations for the air-gap design often affect these tolerances.

Experience indicates one and sometimes two coil support rings are necessary to prevent movement of coil ends under short-circuit conditions. These must be accurately located so that the coil does not have to be distorted or pulled back excessively to come up against the rings. For this purpose, the rings are located by an accurate gauge which is positioned relative to the slot and has exactly the same kick as the coils. This procedure allows installing coils without undue straining which could shorten the coil life. Furthermore, coils are inspected for shape on a master gauge which assures that any spares will also fit the slots and support rings. Installation of coils or "winding" is shown in Fig. 3.

Coils and slot manufacturing tolerances are such that there is no possibility of having a tight coil that cannot be inserted in the slot. It is essential, however, that the final clearance be less than 10 mils to prevent vibration of the coil in the slot. This is accomplished by wedging

---

Paper 55-162, recommended by the AIEE Power Generation Committee and approved by the AIEE Committee on Technical Operations for presentation at the AIEE Winter General Meeting, New York, N.Y., January 31–February 4, 1955. Manuscript submitted October 18, 1954; made available for printing December 2, 1954.

W. D. HOUSER, W. HINDLE, and J. A. TYERMAN are with the Canadian Westinghouse Company, Ltd., Hamilton, Ont., Canada.

Fig. 1. 50,000-kva generator frame on a 36-foot horizontal boring mill. The openings around the frame are for mounting the air coolers

Fig. 3. Winding of the coils in the stator is one of the longest assembly operations whether in the shop, as shown, or in the field. The long leads projecting from the top of the coils eliminate individual group and series connectors

the side of the coil with a mica or a semiconducting plastic sheet. This sheet is supplied in a range of sizes from 0.010 to 0.025 inch to accommodate the tolerance range allowed.

Since 1942 it has been the practice of the Canadian Westinghouse Company to braze all connections on the armature winding including series, group, and parallel rings with a silver-phosphorus alloy. This procedure eliminates the uncertainty of soldered connections and reduces the number of connections by one-half. Slot wedges are made from cloth-base micarta strips principally because of their strength, uniformity, and dimensional stability. These wedges are notched opposite the ventilating ducts to facilitate a streamline flow of air through the duct. Depending on customer preference, the stator may be either stacked and wound in sections, in the factory, or in a complete circle in the field. In many cases it is preferable to stack and wind in the factory to reduce the assembly time and the usual congestion in the powerhouse.

In the event that the stator arrives on the job in stacked and wound sections, it is set up to correct elevation and centered, sole plates are grouted and the coils bridging the splits between sections are made up to complete the winding. This is a time when great care must be taken as stator winding should only be attempted by experienced workmen under expert supervision. The winding personnel are supplied with special rubber mallets, wedge drivers, side-mica drivers, and pullers as well as all the necessary winding information from the design engineers. Where coils are to be heated during winding (continuous taped asphalt bonded type), brazing transformers with special connectors are available.

The number of coils lifted during the closing of a split depends on a number of factors and should be determined for each particular winding. Some of the factors involved are:

1. Type of coil, i.e., mica folium, continuous taped asphalt bonded, or Thermalastic.
2. Depth of slots.
3. Throw of coils.
4. Frame size.
5. Voltage class.

The number may vary from three to six times the number of coils in the throw. The risk of possible coil damage is great if less than the recommended number of coils are lifted while a larger lift than necessary results in increased cost, time, and disturbed coils. After the coils are placed in the slots and before connecting, they are given a momentary high-potential test 1.25 times final test voltage. After connection, and before the rotor is placed in the stator, the winding is given a momentary high potential of 1.15 times final test voltage. These potential tests may be made with either alternating voltage, or the equivalent direct voltage. Each coil is tightened in its slot, as mentioned previously, based on individual measurement. Contact resistance tests with an ohmmeter check this operation.

When the complete stacking and winding is to be done at the site, the frame is set up, if possible, in its final location on the generator foundations with stacking and winding operations being carried out in position. On occasion it may be necessary to stack and wind in the erection bay, in which case the complete wound and stacked stator is moved as a unit to the generator foundations and is set to correct elevation and centered. To provide additional strength, on conventional machines, the upper bracket is usually mounted temporarily on the stator before the lift is made.

The elevations and center may be set by the turbine-shaft coupling location,

Fig. 2. Partially stacked 106,000-kva frame showing the pressing operation which is carried out for every 12 inches of iron added. The 25-ton jacks bear down on temporary pressing plates. The stator tie bolts are visible between the jacks; guide strips maintain slot alignment

when available. A piano wire plumb line with a 100-pound lead weight damped in a pail of heavy oil is suspended from the top of the stator frame. Its exact location is determined either from permanent reference plugs set in the foundations or from the turbine-shaft center. The stator frames are centered to ±0.032 inch and to level within 0.004 inch. Engineer levels, micrometer targets, and pin gauges are used. The stator is now dowelled to the sole plates.

Rotor

The rotor transmits the torque from the shaft to the field poles and consists of a spider, rim, poles, blowers, and other miscellaneous parts. The rotors fall into two general classifications:

1. Umbrella design; see Fig. 4(A).
2. Conventional design; see Fig. 4(B).

The umbrella design is usually applicable to large-diameter slow-speed machines, while the conventional design is usually confined to high-speed generators. The umbrella design provides manufacturing economies as well as reduced installation costs at the powerhouse. The rotor can be lifted separately from the shaft; see Fig. 5. Thus crane capacity is reduced by the weight of the shaft, which in the case illustrated amounted to 10 per cent of the weight of the rotor. An umbrella installation also reduces the powerhouse building costs by lowering the crane rail height required for dismantling a generator.

The bearing support bracket for the umbrella-type unit is less expensive than the supporting bracket for conventional units. Since the span of the bracket is reduced and since the stator frame does not have to support any vertical thrust from the rotor, there are further design economies.

Today spiders are either fabricated or built up of disks of plate steel. For fabricated spiders, generally only the hub section is built up from annular rings of heavy plate steel. Arms of I-beam or box sections are welded to the hub. At the ends of the arms there is a heavy post to take the "shrink" and "torque" keys, which hold the rim on the spider. After fabrication, this section is stress-relieved to assure that the dimensional accuracy of the machine will be maintained and to eliminate any danger of operating failure from residual stresses. The spider is machined on a boring mill to tolerances of 0.003 inch on the bore and 0.005 inch on the arms.

In designs where it is impossible to use the laminated rim construction because of small diameters or high centrifugal forces, the plate type of rotor is used. A noninterconnected stack of completely machined disks is used. These disks are shrunk on the shaft as an accurately machined assembly. The poles are attached directly to the plates by dovetail slots in the outer edges.

The fabricated spider involves an outer rim. The function of this rim is to contain the centrifugal force of the poles during operation and to provide a flux path between poles. A staggered assembly of sheet steel segments is used. These segments act as a link structure so that the segments are in tension with the forces transmitted to the next segment by means of the through bolts acting as shear pins. Consequently, no reliance is placed on frictional forces to hold the rim punchings when rotating.

The rim punchings must build up in a circle of sufficient accuracy to have no appreciable affect on the air gap. This frequently requires an accuracy in the rim punching segment to within 0.002 inch. Such accuracy is achieved by a compound die without any resort to indexing and its resultant inaccuracies.

In building the rim, Fig. 6, the lower end plates are set up in correct location on the spider and are supported from the floor. Temporary building keys are

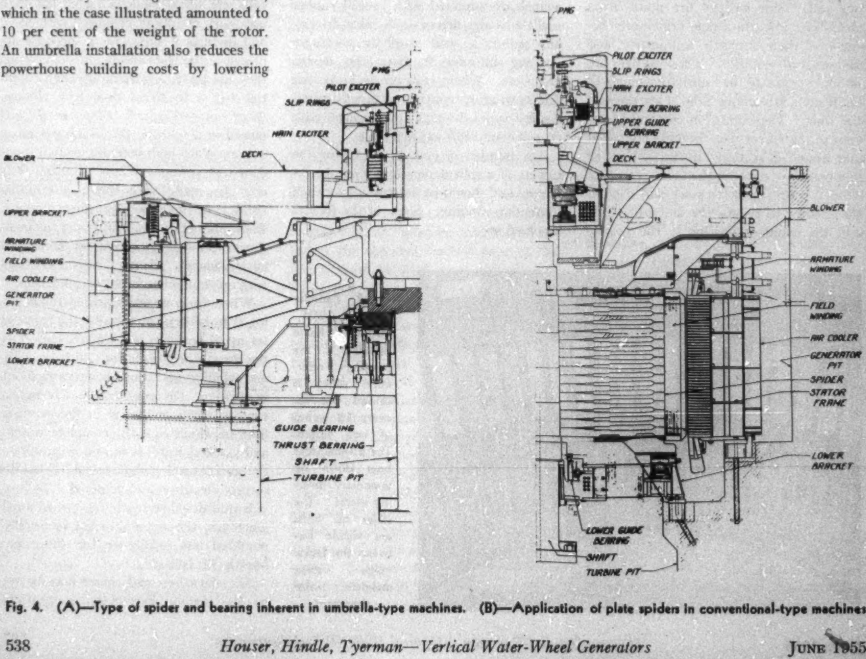
PMG
PILOT EXCITER
SLIP RINGS
MAIN EXCITER
DECK
BLOWER
UPPER BRACKET
ARMATURE WINDING
FIELD WINDING
AIR COOLER
GENERATOR PIT
SPIDER
STATOR FRAME
LOWER BRACKET
GUIDE BEARING
THRUST BEARING
SHAFT
TURBINE PIT
PMG
PILOT EXCITER
SLIP RINGS
MAIN EXCITER
THRUST BEARING
UPPER GUIDE BEARING
UPPER BRACKET
DECK
BLOWER
ARMATURE WINDING
FIELD WINDING
AIR COOLER
GENERATOR PIT
SPIDER
STATOR FRAME
LOWER BRACKET
LOWER GUIDE BEARING
SHAFT
TURBINE PIT

Fig. 4. (A)—Type of spider and bearing inherent in umbrella-type machines. (B)—Application of plate spiders in conventional-type machines

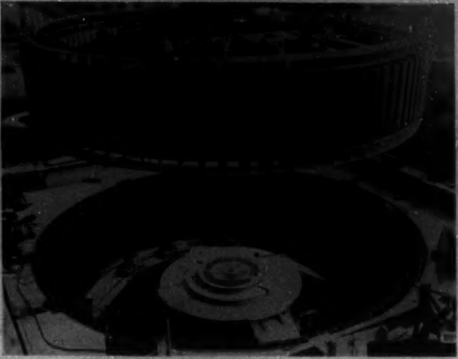

Fig. 5. The umbrella-type rotor shown ready for lowering into the stator is complete with rim and field poles, top and bottom blowers. Already installed in the lower bracket are the thrust bearing and shaft. Also visible are the hydraulic brakes sitting on the bracket arms

placed in the spider arm dovetails. As the laminations may vary slightly in thickness within the tolerances of the steel suppliers, every effort is taken to ensure proper distribution of each box of punchings so that the rim thickness will build up evenly. Stacking is carried out with the aid of accurately machined building pins. The laminations are pressed after every section of approximately 12 inches has been stacked. These methods ensure a tight, compact rim of accurate diameter. Permanent rim studs are inserted and tightened to a predetermined tension.

After the rim has been stacked the temporary dovetail keys are removed and the rim is heated by electric space heaters for the insertion of the permanent torque keys. The amount of interference is such that at moderate overspeed the rim remains tight on the spider but, at maximum overspeed, the centrifugal forces overcome the interference forces. Before the rim has cooled, the permanent rim stud nuts are checked for tightness with a torque wrench to ensure that all studs are under the correct tension. When cool, the nuts are welded top and bottom.

The field poles carry the magnetic flux generated by the field coils and mechanically position the field coils. These poles are made up of sheet steel laminations, clamped together by end plates, and riveted together. Between the pole body and the rim is a dovetail joint designed to withstand the stresses at overspeeds and to prevent any relative movement of punchings. The poles are wedged tight into the rim by the tapered dovetail keys. These poles can be easily removed, if necessary for maintenance, by removing the dovetail keys with a special puller. For ease in fitting, the dovetail keys are tinned all over and hardened on each end for driving.

First the poles alone are tried and the dovetail keys are inserted and marked. The field coils are then slipped on to the poles and these assemblies are mounted. Considerable care is taken to ensure that the field coils are tight. The pole and coil assemblies are individually weighed before shipment to facilitate weight distribution around the rotor as this minimizes balancing problems.

Shaft

The generator shaft functions to transmit the torque from the water wheel to the rotor and to support the rotating members. This shaft is made from a carbon steel forging which has been heat-treated to make a homogeneous metallurgical structure free from forging and casting stresses. It is turned and polished all over to reduce stress concentration to a minimum. Essential areas such as come in contact with other members are accurately machined and ground to ensure the satisfactory alignment of the unit. Shafts of this nature are liberally proportioned so that stresses are low and conditions of critical speeds and magnetic pull are satisfied.

The thrust collar is a continuous part of the shaft forging for umbrella-type machines; see Fig. 7. On conventional units, when a separate thrust collar is required, the collar is assembled with a light interference fit to assure accuracy of alignment and to prevent movement and fretting corrosion. The outside diameter of the thrust collar face is machined to runout of less than 0.0002 inch. The runout on the ground surfaces is also held to 0.0005 inch.

For a conventional unit the shaft is positioned vertically through the floor opening in the erecting bay of the powerhouse and is blocked at a suitable eleva-

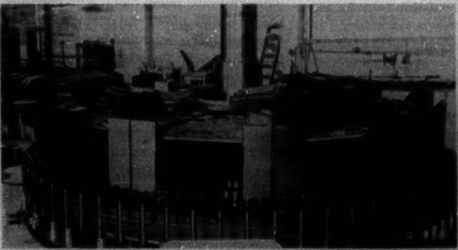

Fig. 6. Stacking rim punching. This rotor spider is shown with the rim punchings partially stacked. The pins or rods used for maintaining alignment of the dovetail slots are self-evident around the outside edge. The temporary pressing bolts shown are removed when the next pack of punchings is added

Fig. 7. All flanges on this shaft for an umbrella-type machine are an integral part of the forging. The large flange at the top end is for bolting to the underside of the rotor

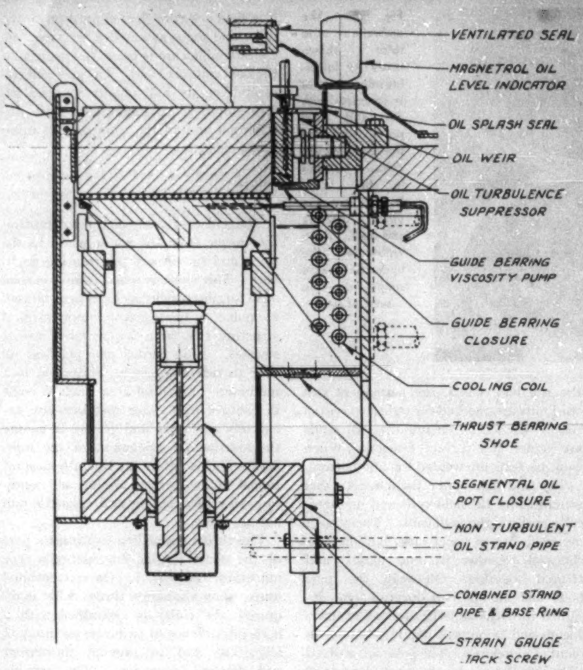
VENTILATED SEAL
MAGNETROL OIL LEVEL INDICATOR
OIL SPLASH SEAL
OIL WEIR
OIL TURBULENCE SUPPRESSOR
GUIDE BEARING VISCOSITY PUMP
GUIDE BEARING CLOSURE
COOLING COIL
THRUST BEARING SHOE
SEGMENTAL OIL POT CLOSURE
NON TURBULENT OIL STAND PIPE
COMBINED STAND PIPE & BASE RING
STRAIN GAUGE JACK SCREW

Fig. 8. Combined thrust and guide bearing assembly for umbrella-type machines, Kingsbury-type bearing

tion. The shaft at the spider fit and the hub bore of the spider are cleaned and checked for burrs or other imperfections and the fit dimensions are carefully measured as a check on the interference provided. The hub is expanded by use of space heaters to a predetermined clearance of the bore. The hub bore and shaft fits are brushed with light machine oil or a solution of molydenum disulphide and the hub is lowered down over the shaft with the use of the powerhouse crane until it is correctly positioned with the bottom against the shoulder on the shaft. Accelerated cooling on the bottom of the hub contracts this part of the hub on to the shaft first and prevents the spider from pulling away from the shoulder as it cools.

On occasion, the hub may be expanded while in a position around the shaft above the fit, with the shaft being pulled up by the crane to the correct location. This method is used where the spider is of the plate type. The shaft-lifting device provided must be suitable for lifting the total weight of shaft and spider. With the umbrella-type rotor it is not necessary to stack the rim over a pit as the shaft is not connected to the spider during this operation. Hence, the spider may be set up anywhere in the powerhouse where suitable space and permissible floor loading is available.

Brackets

The function of the main bracket is to support the weight of the rotating members through the thrust bearing and maintain alignment through the guide bearings mounted thereon. The bracket consists of a fabricated hub section which serves as the oil pot and bearing support. This hub is usually supported by four to eight radial arms which transmit the forces to the foundations. The deflection of these brackets under load must be held within limits which will assure clearances in water-wheel parts and exciters in the order of 0.10 inch.

All oil tight welds are designed with welds on both sides, each of which are checked for oil tightness. After fabrication the bracket parts are stress-relieved by heat treatment. The lower bracket is assembled in the erecting bay, placed in position and accurately centered within ±0.010 inch, and leveled to within 0.0005 inch per foot of span. Dowelling to the grouted lower bracket sole plates completes this operation. The upper bracket is centered and leveled to similar accuracy and dowelled in position to the frame prior to final assembly and then removed until the rotor is in place.

Thrust and Guide Bearing

As stated previously, the thrust bearing is the heart of the mechanical design. The Kingsbury-type bearing design, Figs. 8 and 9, has been further refined since 1948 because of new babbitting techniques, improved oil cooling and circulation, improved manufacturing practices, and metallurgical developments. The modern bearing is simple to install and adjust, reliable in service, and easy to maintain.

Bonding of babbitt to the individual bearing shoes has struck a serious obstacle in the blistering of the babbitt face by hydrogen released from the steel shoe. To circumvent this hazard, the "no bond" practice has been adopted where the babbitt is held mechanically to the steel by a network of dovetail slots. Operating experience is now proving this practice sound.

A viscosity pump designed into the trailing edge of the thrust bearing provides a unique improvement in the oil circulation. This arrangement gathers the hot oil from the trailing edge and discharges it directly into the area of the finned copper cooling coil. Without it, hot oil is picked up by the next shoe. This viscosity pump along with carefully placed baffles and liberal passages have all improved the circulation within the bearing oil pot. Foaming from turbulence at the top of the oil pot is controlled by a baffle and weir construction in conjunction with a viscosity pump built into the guide bearing; see Fig. 8. Air in the bearing oil film means increased kilowatt losses and higher bearing temperatures.

The runner plate is made from gray cast iron with chilled rubbing faces. Addition of nickel in the iron results in a close grain structure that can be lapped to a high polish. The oil absorbed in the microscopic pores of the cast iron and the flake graphite in the iron act as a solid lubricant in starting, prior to the establishment of the oil film.

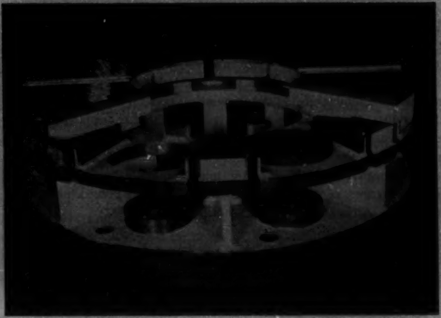

Fig. 9 (above). A 56-inch thrust bearing with two shoes and one jack screw and shoe support removed

Fig. 10 (right). Des Joachims Generating Station on the Ottawa River consisting of eight 50,000-kva 106-rpm conventional-type generators with cooling air recirculated through air-to-water coolers mounted on the frame

For the thrust bearing to give the most efficient and satisfactory service, it is imperative that the utmost care is taken in the cleaning and handling of the components during installation. The assembly must be done under proper working conditions in a clean atmosphere free from abrasive dust or dirt.

With the rotor placed in position, supported by the brakes, the upper bracket is installed and the thrust bearing base ring complete with jack screws and shoe supports already assembled is placed in its proper location in the oil pot. The bearing shoes are assembled on the shoe supports and lightly brushed with a graphite grease after which the runner plate is placed on the shoes. The thrust collar is pressed on the shaft using a pressing plate and pressing bolts. The fits are lightly coated with molybdenum disulphide to prevent galling. The circular key is inserted and the runner plate is fastened to the thrust collar. Proper load adjustment on the shoes and jack screws is now obtained through the use of strain gauges permanently located in the jack screws; these gauges may usually be adjusted within ±2$^1/_2$ per cent. For machines ordered without strain gauges, the "slugging arc" or other methods are used for adjusting the load.

The modern guide bearing has multiple, individual shoes. Separate adjustment on each shoe makes alignment easier and more accurate than with the ring-type guide bearing. Maintenance or replacement is simplified and bearing losses lowered. The individual shoe is generally set for a clearance of 0.010 inch from the journal, which is ample allowance for thermal expansion. It is usually possible to combine one guide bearing into the thrust bearing assembly. Here the periphery of the runner plate acts as the journal for the guide bearing.

Exciters

For the last number of years, direct connected exciters have been specified. One effective manner of reducing the over-all height was to use a telescopic construction in which the pilot exciter is located partially within the main exciter commutator. The armature winding of the exciter is electrically balanced to reduce the effect of unbalanced magnetic pull.

Exciters are tested in the shop where brush neutral, compensation, etc., are set to eliminate field adjustments. New designs are given a heat run and all designs are checked for ability to meet the specifications. Until recently the exciter system has taken the form of main and pilot exciters. In cases where the magnetic amplifier type of voltage regulator is specified, the direct connected pilot exciter is entirely eliminated.

General Features

Most users today prefer an enclosed ventilation system. Centrifugal blowers mounted on the rotor force the air through the core of the machine and through the air-to-water coolers on totally enclosed generators. All air passages in the machine have been improved to increase the air circulation and, in recent years, this has included new stator wedge and new vent duct designs. Air turns and splitters are put in at advantageous points to direct the air with a minimum drop in pressure. To eliminate hot spots, air coolers are arranged around the frame of the generator. These coolers are designed so that there is no possibility of air locks in the water tubes which in the past have caused considerable loss in cooling capacity.

The spider of an umbrella-type generator is connected to the top of the shaft with a circle of hollow dowels which have a light interference fit in both shaft and spider. Bolts inside the hollow dowel hold the assembly together. During assembly these dowel holes are reamed after the rotor is lowered onto the shaft. At this time, the weight of the rotor is actually carried on the brakes, with the safety blocks in place. Suitable fixtures are supplied for the rapid insertion or the removal of these dowels. It is possible to have such a rotor out for repair 4 hours after the generator is shut down.

In the umbrella machine the unit is provided with a thrust bearing lowering device. The device consists of three power-driven screws, the running nuts of which attach to and lower the thrust bearing assembly. In the lowered position, all parts are accessible for inspection and parts can be removed with a trolley supplied with the unit. On umbrella units designed for outdoor service, it is possible to remove armature coils and field poles for maintenance without opening the air casing or using overhead cranes. The field poles are removed by means of a monorail and chain block. Keys in the field pole dovetails are removed by means of a special puller.

The generator field circuit breaker is now often mounted on the upper bracket in close proximity to the exciter. This saves considerably in installation costs and dismantling of a unit as it is not necessary to disconnect heavy current-carrying field leads. The upper bracket, field circuit breaker, and exciter frames come off as a unit.

Alignment

In the umbrella installation the alignment is simplified because of the elimination of one of the guide bearings. In general, the shaft lengths are shorter which results in less throw because of the manufacturing tolerances necessary. The guide bearing located with the thrust bearing is adjustable to allow for final alignment later.

To retain permanent alignment records, it is becoming more common to work from permanent reference plugs, which are inserted while the concrete foundation is being placed. Once the shaft is in position, it is necessary to work from either the turbine shaft or the pit wall reference plugs. For alignment purposes, the generator shaft must hang freely from the thrust bearing, with the lower guide bearing left out.

The generator shaft coupling is located vertically at an elevation slightly below operating position, as it is important that any adjustment of the thrust bearing jack screws be done in a load-increasing, or upward, direction. Preliminary shaft alignment is carried out by adjustment of bearing jack screws until the coupling flanges are parallel within 0.15 mil and the flanges are in the same vertical plane.

Several upper guide bearing shoes are now tightened to prevent horizontal movement of the rotor. The rotor is rotated 360 degrees to distribute evenly the lubricant between the shoes and runner plate. The coupling flanges and the upper guide bearing journal are checked and the readings recorded. The rotor is then rotated 180, 360, and 540 degrees, with readings being checked and recorded at each position.

The shaft runout at the coupling flange should not exceed 0.00025 inch per foot of shaft from runner plate to coupling, and the out-of-parallelism between coupling flanges should not exceed 0.00003 inch per inch of coupling flange diameter at every check position. The guide bearing shoes are now removed and the final alignment and load adjustments are made. The coupling is now made up and the whole rotating assembly is checked. Once the alignment has been approved, final assembly to running clearances of the guide bearings is carried out. All bearings must be cleaned and flushed out to remove all possible foreign matter.

Dryout

The dryout of the windings depends on the insulation resistance readings, type of coil, and the urgency of the work. It is considered that, if the unit is urgently required for production of power, dryout may be omitted if stator winding insulation resistance to ground, per phase, is in the order of 75 to 100 megohms. However, if time permits, it is always good insurance to carry out the dryout until resistance readings become consistent for 48 hours, at a constant or corrected ambient temperature. A running dryout with stator windings short-circuited, is recommended.

The temperature should be brought up gradually but not in excess of 80 degrees centigrade, as measured by stator coil temperature detectors. Megger readings per phase should be taken at regular intervals and plotted on a graph. After the winding is dry, the generator may be given the final overpotential test, either a-c or d-c, at AIEE test standards[1] and placed on load.

Balancing

Although every precaution is taken in design, fabrication, and assembly to distribute the weight properly, once the machine is started up dynamic unbalance may be present. On higher speed machines, over 150 rpm, considerable success has been obtained by use of a portable dynamic balancer.

The low-speed machines are balanced by adding the necessary weight or weights by the vector analysis method, assisted by dial indicators. The shaft is painted with a thin coat of white wash in an accessible location near each guide bearing. Thousandths dial indicators are mounted to indicate the shaft at these spots. The unit is given an initial run and the throw is marked on the whitewash with a lead pencil or scribe. The indicator variations are recorded. On stopping, the high point of the throw is recorded in degrees from a reference plane. A trial weight is then applied at random and the trial run made and recorded. By vector analysis the initial unbalance is calculated and subsequently corrected by a balance weight placed directly opposite. The balancing operation may be repeated to refine the balance. On occasion, this procedure may require expanding into 2-plane balancing when dynamic unbalance is present.

General Remarks on Field Installation

Erection in the field is a continuation of factory manufacture and assembly. The large size of the machines prevents shipment as a completed unit. Engineering design and factory operations aim at reducing field work where possible, because limitations in facilities at the job site are the rule rather than the exception.

For economical and efficient erection a number of factors must be considered for each particular installation:

1. Delivery schedule of component parts: a proper sequence of shipment must be followed.
2. Manpower available: a basic crew of skilled workmen and supervisors with sufficient helpers is required.
3. Powerhouse conditions: sufficient working and storage areas are desirable as congestion makes for an inefficient operation. Cranes, compressed air, and construction power must also be available as required.
4. Overtime and shift work, while reducing erecting time, do not do so in direct ratio because of loss in efficiency. Realistic in-service dates should be laid down, as a month extra at the installation time may well result in months or years of extra life from the machine.
5. Erection equipment supplies must be adequate both from efficiency and safety standpoints, and must be of sufficient quantity for the job at hand.

Conclusion

It is safe to say that present-day designs for hydroelectric generators are a combination of improvements aimed solely at better output performance and at overcoming former operating inconveniences as well as facilitating assembly and maintenance. These latter improvements are almost entirely mechanical and are the natural outcome of years of experience on the part of both the design engineers and the operating engineers and personnel. Accurate manufacturing to close tolerances make the components for 400-ton generators as completely interchangeable as those for a washing machine motor.

The operators of expensive pieces of apparatus such as water-wheel generators are not backward in advising the manufacturer of what they consider shortcomings in any particular generator. If the shortcoming cannot be corrected in the generator in question, then at least the designer must overcome it in future designs.

As "down time" for maintenance often means a loss of potential revenue to the operator, generators that remain trouble-free mechanically save significant money each year. However, it is certain that no operator today would order a water-wheel generator expecting never to have to dismantle it for overhaul. Therefore, it is a further saving to this operator if he know that when such an overhaul comes up his machine will come apart and be able to be reassembled easily and accurately. These are goals towards which the design engineer and shop workman strive continually. No one would be satisfied today with a new machine built to 1930 design standards. Greatly improved designs are available today in generators, and more rigid and exacting purchase specifications are an indication that operators are well aware of the type of machine that is now available. The generator designer continually strives not only to keep abreast but to keep ahead of the buyers' specifications, and will be likely to continue to do so as long as we remain under the free enterprise system.

Reference

1. TEST CODE FOR SYNCHRONOUS MACHINES. *AIEE Standard No. 503*, June 1945.

◆

Discussion

F. H. Duffy (Aluminum Company of Canada, Ltd., Shipshaw, Que., Canada): The authors have done an excellent job of outlining the design and erection procedures of one manufacturer. It would be most interesting to hear from other manufacturers as to whether the same procedures are used.

One cannot help but be impressed with the close design tolerances maintained. In the industry it is often taken for granted, but the watchmaker type of work required is certainly worthy of emphasis.

Where direct current is used for test purposes it is assumed that the AIEE recommended ratio[1] is used.

Some elaboration on the use of the strain gauges for thrust bearing adjustments and the method of computing the $2^{1}/_{2}$-per-cent error in adjustment would certainly be of interest to operating personnel. When speaking of ease of assembly and fit of spare parts, it should be noted that any time the machine is dismantled or when there is a thrust bearing failure the same adjustment procedure must be followed. It might also be noted that in the erection of the unit, the trueness of the water-wheel erection has a definite effect on the ease of alignment.

Since the generator winding has been tested with high voltage and since short-circuit dryout uses about full load current, it would certainly seem more efficacious to eliminate the dryout period and generate useful kilowatt-hours by operating at slightly reduced voltage and load for the ordinary dryout time. It is probable that dielectric absorption tests are more indicative of the winding condition than any number of megger readings and these tests are easily made if a fairly high-voltage d-c test set is available.

REFERENCE

1. ALTERNATING AND DIRECT VOLTAGE ENDURANCE STUDIES ON MICA INSULATION FOR ELECTRIC MACHINERY, **Graham Lee Moses**. *AIEE Transactions*, vol. 70, pt. I, 1951, pp. 763-69. (Ratio 1.6 recommended.)

H. F. Abbott (Quebec Hydro-Electric Commission, Montreal, Que., Canada): The extent to which the authors have covered the subject of the paper, in the length permitted, is worthy of tribute. However, I have a few questions to ask, and statements to question.

BEARING CLEARANCES RELATIVE TO RUNOUT

It seems general to provide as much as 20 mils of diametral clearance for guide bearings on large generators; yet we are concerned if the machine operates with 5 thousandths shaft throw. When there is 5 thousandths shaft throw, the oil film thickness, instead of being 10 thousandths uniformly around the shaft, is momentarily $7^{1}/_{2}$ mils on one side and $12^{1}/_{2}$ mils on the other side. It would appear that the reaction exerted by an oil film as thick as $7^{1}/_{2}$ must be very small; moreover, the difference in reaction created by the oil film on one side, being such a small percentage different than on the other side, cannot provide any considerable balancing force.

Is it not true, therefore, that normally the guide bearings provide little restraint against shaft throw? Is it not the case that when a machine shaft runs smoothly without appreciable throw, that it is either because eccentric forces—centrifugal, mechanical, hydraulic side thrust, and electromagnetic—have been reduced to near zero and the throwout is independent of guide bearing restraint, or because an unbalanced electromagnetic force from the stator or hydraulic force on the turbine holds the shaft towards one side of the guide bearings so that the necessary restraint is developed to result in little throw to the shaft?

TOLERANCES

Our experience has been that machining tolerances are usually much greater than those indicated in the paper. We would also point out that it is difficult to measure ±5 mils on a 40-foot diameter stator bore.

BALANCING

I would like to inquire why the trial weight should be placed at random after the high spot is known? Why not opposite the high point to avoid the angular relation of vectors? Also should not the dynamic balance be checked at two widely separated speeds to confirm whether the counterweight is the right distance from the center to give true dynamic balance at all speeds including the overspeed condition?

DRYOUT

I would like to see the statement "temperature should be brought up gradually," qualified approximately by specific figures. The period allowed for raising temperature varies widely between manufacturers.

On the final overpotential test we do not agree that direct current is acceptable. We believe that, if the AIEE standard is revised to include direct current some further qualification would have to be coupled to the d-c test such as leakage current, or shape of the curve of leakage current versus voltage under a specified rate of build-up. We have had instances where new generators did not come near to passing the standard a-c high-potential test and they had to be completely reinsulated, although a previous d-c test, which we had been urged to accept had been carried out successfully.

VENTILATON

I would suggest that particular stress be placed on the improved distribution in the air circulation improvements made in recent years.

F. L. Lawton (Aluminium Laboratories Ltd., Montreal, Que., Canada): The authors are to be congratulated on a distinct contribution to the literature on fabrication and erection aspects of vertical hydroelectric generators. The literature is, in fact, notably lacking and hence the paper is most welcome. It is to be hoped other manufacturers will contribute papers of this type in the future, as it will then become possible to place the erection of vertical water-wheel generators on that sound engineering basis so essential to optimum performance over a long service life.

The information given in the paper on dimensional tolerances is valuable. The authors make the statement "It is essential however that the final clearance be less than 10 mils to prevent vibration of the coil in the slot." It would be most helpful if the authors would indicate, to the extent information is available, the effect of limiting such clearance to, say, 5 mils.

Referring to the rotor rim, the statement is made that "The amount of interference is such that at moderate overspeed the rim remains tight on the spider, but at maximum overspeed the centrifugal forces overcome the interference forces." Do the authors know of cases where the rim has moved on the spider?

The use of strain gauges permanently located in the jack screws of the thrust bearing is a distinct step forward, as it should enable the determination of hydraulic thrust caused by the turbine runner more easily than has been the case in the past.

The authors state "Preliminary shaft alignment is carried out by adjustment of bearing jack screws until the coupling flanges are parallel within 0.15 mil and the flanges are in the same vertical plane." Should this not be horizontal plane? Are the dimensional tolerances for shaft runout at the coupling flanges and for out-of-parallelism between coupling flanges maximum values or do some customers specify closer tolerances?

What is the authors' experience as to the most effective way of minimizing adjustments after units have been installed for a few years when, in some cases, it is found that there has been a drop in elevation or settlement of the powerhouse structure on the downstream side?

K. R. Knights (The Hydro-Electric Power Commission of Ontario, Toronto, Ont., Canada): This paper is written on a subject that is of widespread interest. We are most interested in those machine tolerances that directly affect the results of the rotational alignment erection test. Our standard field alignment tolerance, as given in the following is not more stringent than that specified in the paper except that it provides limits on the coupled generator and turbine shafts: "The overall field alignment of the coupled generator and turbine shafts as determined from a rotational test—shall be such that the centre of each or either shaft shall not deviate from the true theoretical axis more than 0.00025 inch multiplied by the distance in feet from the thrust bearing rubbing surface to the point of measurement. In addition, the true theoretical axis of the coupled shaft shall not deviate from the plumb more than an amount calculated in the same manner."

To ensure that the foregoing alignment requirements are obtained with a minimum of field delay and for other reasons, it has been found desirable to have the thrust collar provide a light interference fit on the shaft, as noted in the paper, and to have the upper and lower surfaces of the thrust collar and runner plate faced true to the bore (shall not have a rotational error as measured by a dial indicator) within a tolerance such that the cumulative error of the two surfaces shall not exceed 0.001 inch. The shaft runout and the shaft coupling contact face are also held to acceptable tolerances for this purpose.

Jack screw strain gauges have been found to provide an accurate means of distributing the load between shoes. In addition, they have been utilized to make direct measurements of hydraulic thrust. Use of these gauges is much facilitated if the leads are extended down from the upper bracket. Design of the machine, however, should permit use of the "slugging arc" method of alignment so as not to be entirely dependent on devices for this important operation; a few strain gauges have failed in service.

The practice of accurately forming coils during manufacture so as to eliminate undue strain when tying and connecting them in place is considered to be in the interest of the purchaser. It is felt that coil insulation should only be disturbed where absolutely essential, as in the closing of splits.

Thermalastic insulated windings with full coils now have been purchased for a number of large, medium-speed water-wheel generators. As noted in the paper, the splits were closed successfully by lifting approximately six times the number of coils in a throw, in view of the comparative rigidity of this type of insulation.

It is stated in the paper that the upper bracket is mounted temporarily on the stator before a lift is made. On an umbrella machine, with a light upper bracket, the question arises as to what provision is made for lifting a complete stator.

Large, single guide bearing generators have always been purchased with the following stipulation, which is meant to provide assurance of entirely stable operation under all conditions of operation and test: "The design of the generator shall be such that it will have adequate mechanical stability to operate successfully under all overspeed and fault conditions which may be experienced during operation. This requirement shall apply with the generator either coupled to or uncoupled from the turbine."

With respect to the authors' comments on stator lamination insulating material, it would be of interest to hear their views on the relative merits of sodium silicate and high temperature baked on enamel from all viewpoints, particularly with respect to moisture resistance.

Our Kingsbury thrust bearings of the original Kingsbury design have a good operating record on our system. A number of machines supplied within a recent 2-year period, however, were equipped with shoes of the thick slab type and experience with this major variation from the original Kingsbury design has not been so successful. As a result of this experience, we are in agreement with the present practice of not only eliminating the babbit bond as noted in the paper but also supplying all shoes along the lines of the original undercut design.

W. D. Houser, W. Hindle, and J. A. Tyerman: The authors wish to thank the several discussers of this paper and take this opportunity for replying to some of the points raised.

The advantages of sodium silicate or water glass over baked-on enamel or varnish as an insulation on stator laminations are that it: 1. has a thinner film for equal insulation which enhances a better stacking factor; 2. has a slower rate of deterioration; 3. is more resilient; 4. withstands higher temperature such as might occur in a stator fire; and 5. withstands higher stacking pressures as it is an inorganic inert material.

Some manufacturers are known to design rims that are loose at all speeds but are suitably restrained so that only uniform radial expansion is allowed.

We agree with Mr. Duffy that elaboration on the use of strain gauges for thrust bearing adjustment would be of interest to operating personnel, and it could well be the subject of a further paper. When reassembling a machine after overhaul, no adjustment is required if the old shoes are reused. Minor adjustment is sometimes required with new shoes because of slight manufacturing tolerances between individual shoes. With regard to strain gauge failures, we have found that improvements in the termination of the leads from the load cell have reduced the number of failures to a very low percentage. Further improvements can be expected to reduce this almost to the vanishing point.

In the case of installations that have suffered foundation settlement, shaft misalignment can usually be compensated for by adjustment of the guide and thrust bearings as they are both of the pivoted type. The settlement would have to be very severe before it would require a releveling of the stator frame.

To clear up any misunderstanding over the tolerance given in the paper for stator bore, we would like to make it clear that this refers only to the bore of the frame itself. We agree that it is not possible to hold the bore of the stacked core to tolerances of ±0.005 inch in diameter. The gauges used for measurement of large bores to the accuracies indicated are quite practical and are in daily use in our shops. The dimensional tolerances given in the paper are actually closer than that required by any known purchase specification to date and are giving satisfactory results in the field.

In designing the coil and slot sizes, the designer chooses dimensions that will result on the average in 15-mil clearance. With side mica strips available in 10-, 15-, 20-, and 25-mil thicknesses, it is possible to achieve a final clearance of not greater than 10 mils and averaging 5 mils. A small clearance is considered necessary to prevent tape migration caused by the thermal movement of the copper conductors, which can occur when the tape is prevented from moving with the copper.

Direct voltage testing has been extensively used by our field erectors for several years now, using up-to-date d-c to a-c ratios as developed by the AIEE subcommittee studying this subject. While we have had very few occasions to doubt the validity of such d-c testing, we do feel that the higher ratio now recommended by the subcommittee is a step in the right direction.

For asphalt and earlier types of coils, it is highly desirable to drive out contained moisture and solvents very slowly to avoid mechanical damage from vapour pressures. In general, the stator temperature for dryout is brought up to 80 degrees centigrade at a uniform rate over a 24-hour period.

We agree with Mr. Abbott that an oil film of 10-mil thickness will do little to restrain a shaft throw of 5 mils, but it must be realized that the clearance will be less than 10 mils at operating temperatures. However we feel that shaft throw does not originate in the guide bearing, and any serious throw should be overcome at the source, if possible, rather than call upon the guide bearing to restrain it. Guide bearings to restrain any considerable radial forces would then have to be much bulkier and more expensive than those commonly in use today.

Dynamic balancing of vertical water-wheel generators is of considerable importance and a complete explanation is too lengthy for this paper. It too could well be the subject of a separate paper.

Symposium: How Can the Utilities Best Make Use of Modern Science?

Implementation of a Research Program for the Electric Utility Industry

J. E. HOBSON
FELLOW AIEE

W. A. LEWIS
FELLOW AIEE

M. S. OLDACRE
FELLOW AIEE

IN January 1954 a paper[1] which stressed the needs of the electric utility industry for an expanded program of research was presented. This theme was expanded and supplemented in a similar paper.[2] The objective of this third paper is to summarize the comments received on the first two and to make further suggestions for a research program for the electric utility industry.

Comments on Previous Papers

The first papers were followed up by many discussions with utility executives and engineers, college faculty members and students, financiers, economists, and leaders of other industries. An extremely wide range of views was found. There was majority but decidedly not unanimous, agreement that more extensive research programs are desirable, which will investigate basic problems of the industry and provide for its long-range needs. Some utility executives were inclined to leave the job of research and development entirely to equipment manufacturers, being satisfied with whatever technical progress is offered to them. Some believed that the role of the utility companies in research should be confined to encouraging and co-operating with the manufacturers by proving and testing manufacturers' research results. Others were distressed by the duplication of efforts, facilities, and investments necessary when similar and parallel research and development programs are carried on independently by several manufacturers.

It was frequently pointed out that there is a very serious lack of knowledge about how much and what kind of research is now being performed by the utilities, and that a carefully conducted survey of present research activities would be very beneficial in evaluating the situation as it exists today. Many investigations which are really of a research character are being handled as incidentals of system operation or new construction and, thus, are not identified as part of the over-all research effort.

The members of college faculties with whom these problems have been discussed were in unanimous agreement that additional research and technical effort directed toward the problems of the utility industry would attract the increased interest of engineering students who are now inclined to believe that the power industry offers little opportunity to employees of imaginative and creative minds. Some of the financiers and bankers pointed out that an active and aggressive research program is now considered one of the essential factors in selecting companies for investment, and that the electric utility industry would perhaps more easily attract capital needed for anticipated expansions if it were more active in its research efforts. The record of the utility industry in this regard has, of course, been outstanding.

The authors were struck by two significant impressions: the wide divergence of opinion on research policies expressed by the executives of utility companies, and the inescapable feeling that too many utility engineers, as a result of their necessary concentration on everyday problems, do not have a clear understanding of what scientific research actually is or of what research might be able to do to benefit the industry.

Areas of Research for the Utility Industry

Many of the problems of particular significance to the electric utility industry may be classified under the following areas of research:

1. Long-range planning for system development.
2. Application engineering research.
3. Research in operation of utility systems
4. Apparatus development.
5. Research for the future.

Various methods for conducting research in these areas will be discussed in the following to suggest some that appear to be appropriate.

LONG-RANGE PLANNING FOR SYSTEM DEVELOPMENT

The utility industry in the past has been noted for long-range planning in providing for its continued growth. Present methods have been satisfactory, but tremendous postwar growth and rapid industrial changes indicate that new techniques of planning for the future are needed and that simple extrapolations of load curves do not give a true picture of power requirements for more than a few years ahead.

Forecasts of load growth show a disturbing diversity of opinion. Fig. 1 shows the range of estimates of peak load to 1975 as an extension of the load curve since 1945. Some estimates are based on the growth of the recent past with a doubling of load about every 10 years, or less, which will give a peak load of over 400,000,000 kw in 1975. Other estimates apply correction factors to those estimates and arrive at forecasts nearer 225,000,000 kw.

More penetrating studies must be made to analyze the factors affecting demand upon the utility industry. These will include detailed consideration of expected population growth and migration, of the agricultural, industrial, residential, and transportation needs of an area, and considerations of how the energy needs may best be met. Careful consideration of these and other basic elements will provide a much sounder basis for making long-range plans for system growth, not only for the design and building of a particular power station but also for planning 10, 15, or more years ahead.

Paper 55-144, recommended by the AIEE Research Committee and approved by the AIEE Committee on Technical Operations for presentation at the AIEE Winter General Meeting, New York, N. Y., January 31–February 4, 1955. Manuscript submitted October 20, 1954; made available for printing December 15, 1954.

J. E. HOBSON and M. S. OLDACRE are with the Stanford Research Institute, Stanford, Calif., and W. A. LEWIS is with the Illinois Institute of Technology, Chicago, Ill.

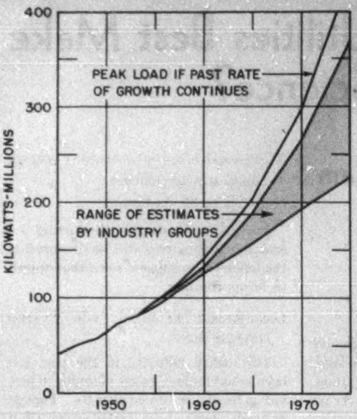

Fig. 1 (left). Prediction of peak load of the electric power industry in the United States, 1945 to 1975

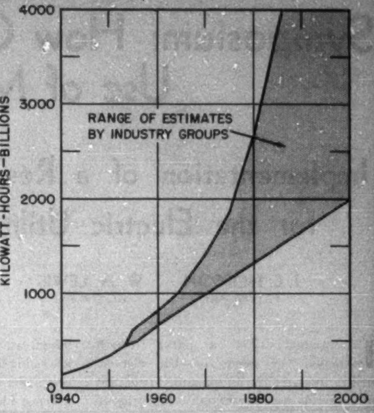

Fig. 2 (right). Prediction of output of the electric power industry in the United States, 1940 to 2000

Of equal or greater interest is the probable total energy output of the electric systems and the production in kilowatt-hours per capita. These are shown in Figs. 2 and 3. Even the most pessimistic estimates for 1975 show more than twice the present figures. This increased per-capita use should satisfy the dreams of the commercial departments but the engineering departments will need to plan far ahead to solve the problems of greatly increased generation, transmission, and distribution.

Of great importance in the future will be the changing fuel-supply picture, not only of individual utilities but for the country as a whole. Revisions currently being made by different authorities in the estimates of fuel resources make it difficult to predict how long they will be adequate for all needs at anywhere near present-day costs. One of the most penetrating of recent studies on this subject was reported by C. C. Furnas.[3] His analysis of the information presented by Palmer Putnam showed that, given expected population growth and increased energy use, the United States and the world face a shortage of conventional energy sources that will become acute in 20 to 50 years. This eventuality will have serious effects on factors of great importance to the electric utilities and must be carefully considered in present planning.

The total demand for energy in this country does not increase as fast as the demand for electric power, but is expected to about double by 1975 and quadruple by 2000 A.D. An indication of what may be expected in total energy demands and population growth is shown in Fig. 4, while the amount of energy available from various sources at costs comparable to present-day costs is shown in Fig. 5. It may be anticipated that new or more expensive energy sources will be needed in the next few decades.

The peak rate of petroleum and natural gas production in the United States will probably occur in about 10 years. When new discoveries are no longer able to keep ahead of new demands, the available supplies will have to be conserved and limited to the more exacting needs to

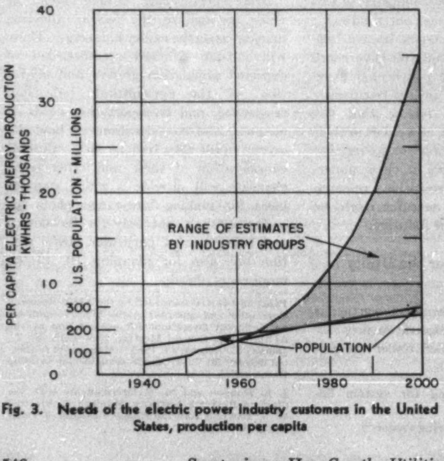

Fig. 3. Needs of the electric power industry customers in the United States, production per capita

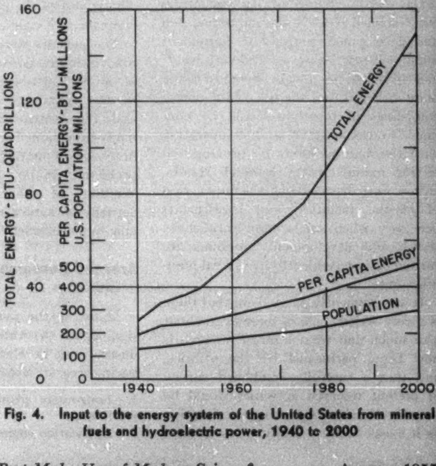

Fig. 4. Input to the energy system of the United States from mineral fuels and hydroelectric power, 1940 to 2000

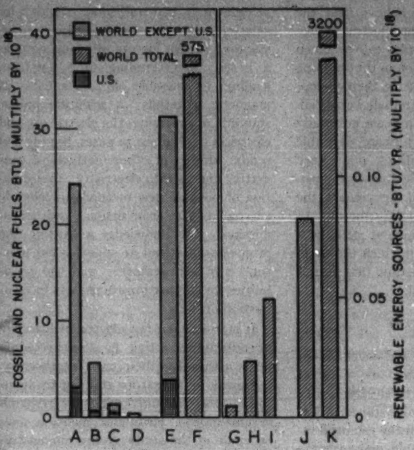

Fig. 5. Available sources of energy, nonrenewable or capital sources and renewable or income sources

A—Coal
B—Oil and gas
C—Oil shale
D—Tar sands
E—Total fossil fuels
F—World total, nuclear fuels
G—Water power
H—Wood, farm waste, and miscellaneous
I—Effective recovery from solar heat collectors
J—Total renewable or income energy sources
K—Total solar energy falling on the earth's surface

which their application is particularly suited such as liquid fuel for automobiles and airplanes, and gas for residential heating. The remaining needs will have to be satisfied by using lower grades of petroleum residues and by the increased and more efficient use of coal, lignite, and other solid fossil fuels, or by nuclear and solar energy. A possible means to release oil for power station fuel is the development of batteries or other storage devices for economically using electric energy in operation of vehicles.

The weakest part of the present position is a lack of fundamental knowledge of combustion processes, and that weakness can be overcome only by research of a basic or fundamental nature. Detailed research and economic studies of load demand and fuel use in a given area are local problems peculiar to the company or companies in the area, but the basic problems of fuel availability and fuel processing are of such magnitude and over-all importance that they could be undertaken by the energy-using industries as a whole, possibly through an industry association or other organizations which have such research as one of its major objectives. Support for industry-wide work of this type may properly come not only from the utilities but also from the suppliers of fuel and the manufacturers of equipment.

Application Engineering Research

Equipment supplied by the manufacturers makes use of the best information available to the manufacturers concerning the requirements of operation. It is well known, however, that after machinery is put into service difficulties usually develop that were not anticipated. Improved methods of determining and evaluating important characteristics are required. Investigations to improve knowledge of operating conditions and effects of environment can minimize these difficulties, reduce maintenance expense, and improve the design of subsequent equipment. Such studies are especially important when the equipment is so large or complex that it must be assembled at its final location without trial operation under controlled factory conditions. Investigations of this type may properly be called application engineering research, which has been conducted in an excellent manner by many utilities. It consists of surveys, collection of information and data, laboratory and field work, operation of apparatus under actual plant conditions, careful analysis of results, and co-ordination with similar work by other utilities and by the manufacturers, followed by distribution of results for the benefit of all. Some problems of this type will require more detailed and extensive study than many utilities are prepared to give, but they could be undertaken by technical committees of the industry, either alone or with the aid of colleges or research organizations.

In some cases, the research may require the services of scientists or engineers in special fields not normally employed by utility companies. It may be necessary to obtain information or to develop materials not now available. Thus, special laboratories and staffs may be needed. A few examples of areas where improvements are essential include new materials for very high and very low temperatures; materials for use in nuclear power applications and insulating materials suitable for the extra-high-voltage systems which will undoubtedly be needed in the future.

Discussion with utility executives and engineers has shown that much more work of this character has been done by certain leading utilities than is generally appreciated. It is also recognized that the manufacturers are making significant contributions in this area and will continue to do so. However, it is the authors' feeling that more active participation by the utilities would produce important apparatus improvements that could result in over-all economy for the industry.

Research in Operation of Utility Systems

Much has been done in investigations regarding the stability and control of interconnected systems: the proper protection of systems against disturbances such as lightning, and the protection of system operation against the effects of sudden loss of generation. However, there is a growing awareness that, with the continued growth and expansion of utility systems, research on the problems of system operation is necessary and that many of these problems pose a real challenge for further improvement.

Not only are the ordinary operating problems of interconnected systems becoming more intricate but the requirements for operating the entire system at maximum economy become so complex that conventional methods of calculation are becoming inadequate in many cases. New computing techniques are required for the quick and accurate determination of operating conditions for minimum system losses and for the allocation of those losses to particular generating stations. There is, as yet, no clear understanding of the principles which will permit the ready determination of the most economic use of water power in systems which have substantial amounts of both hydroelectric and fuel power supply. Because of the increasing complications of power systems, the trend toward automatic operation of the systems for maximum economy is clearly evident.

Only a few utilities conduct research on the effects of weather on the operation of the utility system; this subject could be the basis of discussion to show how meteorological research could pay big dividends in guiding operation and loading of the utility system and in preparing for emergencies. The Weather Bureau performs a good service in providing the basic information, but the the utility should be better prepared to apply that information to its own particular conditions.

Another problem seems to be the lack of a clear-cut basis for determining the proper financial arrangements for power interchange between interconnected systems. In the administrative side of the utility business, the best utilization of business and computing machines in the handling of customer billing, inventory control, and other data processing has not been fully realized and further research is justified. It seems evident that a much better understanding of the economics of replacing obsolescent equipment is desirable. In the establishment of rates, there is not yet an adequate and accepted basis for allocating the cost of service to various kinds of load, thereby fully justifying rate differences for separate classes of customers.

It would seem that better answers to these and similar problems would result in enormous savings because of the large volume of the utility business and would, therefore, justify extensive research effort by both utilities and manufacturers. Manufacturers of large apparatus have contributed importantly to the solution of system problems when the results affected the characteristics of apparatus or machines. Similarly, manufacturers of computing and business machines may be expected to participate extensively in research leading to the development of the most effective types of such machines for utility use. Because of the complications of mathematical and computing problems involved in many of these studies, it would seem that research organizations and colleges, which have groups of specialized personnel, could be used appropriately, effectively, and with mutual advantage.

APPARATUS DEVELOPMENT

Many utility executives have stoutly maintained that utility companies should have no part of apparatus development, but should use what has been offered by the manufacturers at a price which includes the cost of research and development. It is the belief of the authors that the primary responsibility of the utilities in apparatus development is to make sure that the job is properly done for the best interest of the utilities. Experience in other industries has frequently shown that research programs are less effective if all interested parties do not participate actively in the planning of the work, the analysis, and evaluation of the results. There is no reason to believe that the same is not true in the electric utility industry. Many examples can be given where utility participation in the planning and testing of apparatus in the development stage has been extremely beneficial.

When the manufacturers are not ready to undertake or carry forward desirable developments, the utilities may very properly initiate and conduct such projects alone, at least until they secure the co-operation of the manufacturers. In short, apparatus development must be a co-operative endeavor in which the users have an important function that is not always fully appreciated.

RESEARCH FOR THE FUTURE

The kinds of research and development discussed in the foregoing are of direct and immediate interest to electric utility companies, but in several instances it has been pointed out that all the essential information is not available and progress will be impeded if new and more penetrating information and data are not developed in both technical and economic fields.

There are several areas of knowledge on which the industry rests where the underlying scientific phenomena are unknown and where further investigation may point to a broader understanding of the physical phenomena and lead to new and entirely unexpected developments. Experience of other industries indicates that effective research on such problems may open up entirely new possibilities which will have tremendous advantages to the industry. Although the need is not so apparent, the returns may be greater than for research that is directed within narrower limits.

The important feature that these areas of research (for essential information or for underlying phenomena) have in common is the necessity for a careful scientific approach in which the abilities and skills of scientists in several fields such as chemists, physicists, metallurgists, and mathematicians as well as economists and perhaps even biologists and psychologists may be needed to make the work effective.

Several research areas for essential information in which the results may be immediately applied have already been suggested. Other basic problems of equal importance to the industry could be named. Areas of research where the industry is in need of broader fundamental knowledge have been mentioned in previous papers.[1,2] These included a comprehensive study of insulating materials in an effort to understand their behavior better and to prepare the way for the development of new and more effective insulating materials; a more precise understanding of the factors affecting corona; a better understanding of magnetism, leading to possible improvements in magnetic materials; a scientific understanding of switching, the electric arc and electrical discharges, in gases, liquids and solids; studies of other methods of converting energy into electricity; investigation of possible new methods for electric energy storage, conversion, and transmission; new knowledge regarding the properties of steam at supercritical pressures and temperatures; and the possibilities for further improvements in combustion of fuels.

It is true that a few electric utilities are already quite active in some research fields either by their own engineering, technical, or laboratory staffs or by sponsoring work at universities or research organizations. Particular mention may be made of the study groups engaged in the development and investigation of nuclear power possibilities. Others have already undertaken the installation of steam generators and turbines operating in the supercritical range. In most cases, these have been spectacular projects and have great publicity value because of their promise of large returns. It is the belief of the authors that many of the less spectacular projects are of broad significance to the industry as a whole, and have great potentialities for improvement but are now receiving inadequate attention under present conditions.

If substantial improvement is to be made in the conduct of desirable research, a suitable mechanism must be established. In the foregoing, several different methods for conducting research were discussed, and some are in actual use. The manufacturers of apparatus as well as others outside of the power industry have conducted much of the basic research but the amount of such research that can be financed on the prospect of early return in apparatus improvements or can be justified from the standpoint of public relations is definitely limited, and the authors believe that the existing methods of financing are insufficient.

Most of the electric industry research projects have been of definitely limited duration with the expectation that they will be terminated as soon as specified goals have been reached. From a long-range point of view the benefits of continuity of effort and thinking are lost although their value has been demonstrated in other industries, e.g., the chemical industry, many times over.

The importance of a cohesive group of

scientists and engineers, covering several areas of training and experience, assigned full time to the study of the industry-wide research problems becomes evident. It should be the function of such a group not only to evaluate continuously the research program of the utilities but also to examine and make recommendations for the research conducted by manufacturers, colleges, and research organizations, whether sponsored or not, and to observe contributions from foreign countries. Its members should be ever seeking new ideas and the adaptation of old ideas to new situations. Such a group would form the liaison between the application engineers of the industry and the fundamental scientists who would be most effective in carrying on the more fundamental work. This co-ordinating group could be in a position to participate in the placing of contracts for sponsored research, either directly on behalf of an industry association, or in the guidance of individual utilities in the sponsorship of work in which the company was particularly interested. The essential belief of the authors is that the implementation of basic research through temporary committees of engineers who have primary interests in other directions will not produce the most effective results.

It has been tacitly assumed in the foregoing that any such co-ordinating research group would have to serve the entire industry and would most surely have to be supported by some form of industry association, either of the utilities alone, or of the utilities and manufacturers together. Experience in other industries and in the conduct of war research has shown that research scientists, particularly in experimental fields, are most productive if they have suitable laboratory facilities at their disposal to try out new ideas in early stages and to check questionable parts of the work done by others, even if all of the work is not done under their direct supervision.

Reasoning along these lines led to the suggestion of an industry-supported laboratory in which the basic and fundamental research activities could be conducted. A research budget in the order of 1/10 per cent of the gross income of the electric utility industry was suggested as being appropriate after an early developmental period.

General Comments and Summary

Several different phases of the research program appropriate for the electric utility industry have been discussed and several methods for accomplishing the necessary research have been outlined. It is believed that no single method or form of organization, to the exclusion of others, would be fully effective or most satisfactory for the conduct of the various classes of research. The needs are many, and the type of problems suggest the possible method of approach that may be most appropriate in each case. The research subjects suggested as examples have been more or less arbitrarily assigned to the different phases of the program but they might have served equally well as examples of some other class of activity. However, consideration of all the different research activities needed seems to show that co-operative action among the utility companies with the manufacturers of equipment, the suppliers of fuel, and in special cases even with other groups is essential if a full measure of success is to be reached.

The long-term objective of any research program is to make possible improvements in the delivery of electric energy at lower cost, recognizing fully that the electric utility industry deserves to prosper only if it can deliver energy more economically in a form which can be more conveniently utilized than competitive forms of energy delivery. Therefore, economic and scientific researchers must bear in mind economic considerations in the evaluation of improvement and in the consideration of alternatives. When research is conducted through short-term projects with a specific end in view, it becomes exceedingly difficult to give proper consideration to all the background economic factors. To give effective consideration to these aspects, it is essential that there be continuity of planning, guidance, and supervision of the over-all research program.

The reaction of college faculties to the ideas and suggestions for a broader and more extensive research and development program have been expressed in the foregoing. The authors have previously indicated their belief that expanded research would have a salutary effect on college graduates and further their interest in the utility industry. Under present competitive conditions it is not sufficient to explain to college faculties and students that the utilities have challenging problems, but this situation must be illustrated by action and results if the better men are to be attracted into the industry in adequate numbers to meet the growing personnel needs. The establishment and sponsorship of appropriate research projects in college laboratories, and the active participation of utility engineers and co-ordinating scientific groups in the planning and conduct of these research projects can well be the means of restoring or creating interest in the power field to the college staffs and students. Otherwise, the gradual drift in emphasis in electrical engineering education will continue toward the electronic and communication fields, to the point where any special emphasis on the needs of the power industry will be as unheard of as specialization in electronics and radio was 30 years ago.

In comparing the electric utility industry with other industries, it appears remarkable that the industry has been able to avoid the establishment of some form of central research organization when so many other industries, with less reliance on technical background, have such organizations in existence. In a recent report[4] it has been pointed out that nearly 50 trade associations have well-staffed laboratories, for the conduct of technical research and that roughly 300 associations have invested their funds in scholarships at engineering colleges; fellowships, etc., at research institutes or the National Bureau of Standards; co-operative research in university laboratories; or privately owned commercial testing laboratories for various forms of research activities.

Although the electric utilities as regulated monopolies subject to government control do not have the same competitive urge as manufacturers, the need for continued improvement in their service to the public is just as great, and methods which have been found extremely effective in other industries should not be passed over by the electric industry without convincing proof that direct research activity would not more than justify its costs. Any doubts that the electric utilities are in a competitive field in their primary function as suppliers of energy are dispelled when attention is called to the importance given to any means that will result in lower investment cost per kilowatt capacity of equipment, or will reduce the cost of operation and maintenance. The competition between electric utility energy delivery and other forms of energy delivery and the competition between various areas of the country for industrial growth and the location of new plants make clear that the industry is subject to all of the forces of competition, and every means which will result in better service at lower over-all cost must be utilized for best results. Any private utility that does not heed this premise becomes a vulnerable target for public power, whether municipal, utility district, or federal.

The experience of many industries has

proved conclusively that long-term research carefully and intelligently conducted will frequently pay tremendous dividends. However, important projects can only be brought to fruition if carried on uninterruptedly, with continuous re-evaluation and study, and with unflagging faith in the ultimate result. Short-term projects, with limited goals, have their value, but the biggest returns can be expected from the more penetrating studies of the bigger and more lasting problems. Visionary dreams still have their place in industrial development and, if carefully nurtured, may produce new trends and revolutionary developments in human progress. The authors cannot accept the belief that the electric utility industry is so mature that it has no need for new methods, but only for improvements on existing methods. With the depletion of existing fuel resources becoming dangerously imminent, with nuclear power upon the threshhold, and with the challenge of solar energy as the ultimate means of meeting man's need for energy when other sources are either exhausted or uneconomical, the pioneering spirit which is shown by some of the utilities must spread throughout the industry. The tool of the industrial pioneer today is scientific and economic research, and the electric utility industry must find the means to utilize its full share of research potentialities to insure its continued growth and success.

References

1. RESEARCH FOR AND BY THE ELECTRIC POWER INDUSTRY, J. E Hobson, W. A. Lewis. *Electrical Engineering*, vol. 73, June 1954, pp. 516–21.

2. RESEARCH AND THE ELECTRIC POWER INDUSTRY, J. E. Hobson, W. A. Lewis. *Proceedings*, American Power Conference, Illinois Institute of Technology, Chicago, Ill., 1954, pp. 6–17.

3. ENERGY SOURCES OF THE FUTURE, C. C. Furnas. *American Chemical Society*, Washington, D. C., Sept. 14, 1954.

4. ASSOCIATION TIES WITH RESEARCH FOUNDATIONS, J. Judkins. *Trade Association World*, Kansas City, Mo., Apr. 1954.

◆

Discussion

C. Doble (Doble Engineering Company, Belmont, Mass.): The authors have made an excellent presentation of their plan for a research program for the electric utility industry. Electric power has become one of the most important single basic elements in our modern civilization. Why? Because the biggest factory or chemical plant or even the colossal atomic energy developments all are helpless without an adequate power supply. The main questions are how the utilities can produce and deliver electric power by implementing modern science into their operating requirements and how our modern civilization can make sure that an adequate and reliable supply of electric power is available.

One of the most important problems is to find and educate men who are qualified to do the job and interested to undertake it. The utilities have many important unsolved operating problems that require directed research. Experience shows that much of this directed research should be supported and directed by the utilities themselves because their actual operating experience dictates many of the requirements for new advanced design of apparatus. The equipment manufacturer cannot do the most effective design and develop the necessary new apparatus without data from this basic operating experience. Whenever the research requirements can best be met by outside research organizations, such work should be allotted by the utilities' own organization established for that purpose.

The manpower must come from colleges and it is the colleges' prime function to educate men—not to do commercial research per se. To do this job well some of the college professors must be capable of doing some of the required research. Actual contact with such research keeps them informed and alert to future trends. The type and amount of research allocated to the colleges by the power utilities should be primarily for this purpose and not competitive with commercial research. Direct financial assistance to colleges by the utilities might be done most effectively by establishing scholarships covering work which gives the students an opportunity to realize the scope and magnitude of the utilities' problem in electronics and chemistry as well as heavy currents, which is commonly thought of as the only part of utility work.

C. W. Watchorn (Pennsylvania Water & Power Company, Baltimore, Md.): It is gratifying that the authors recognize the need for more research on economical coordination of hydro and steam generation. There is a widespread feeling that either the problem is too complicated for more than rule-of-thumb procedures, or that further work is impractical. The fact is that the surface of the problem has hardly been more than scratched, and that much work still remains to be accomplished.

Theodore Baumeister (Columbia University, New York, N.Y.): It would certainly seem rational to believe that no one connected with the power industry today would challenge the value of research—even for an established art like that of electric energy generation. Change and progress are inexorable in our technological economy. There is no need today to demonstrate that research leads to an expanding industrial society. Improvements must be consciously sought and persued. For this it is necessary to have many men at work equipped with working tools. These tools cost money. Money is the practical root of the problem in the developmental efforts of the electric power industry.

The tendency up to now has been to leave the costs of research to the manufacturers, suppliers, and vendors of equipment and materials. The research effort by manufacturers has been vigorously supported, with the result that electric service is today more reliable, more plentiful, and more favorable in price to the consumer than any other service which comes to mind. The remarkable part is that the progress has been obtained without an industry-wide research program.

Some of the examples of needed research, on an industry-wide basis, are cited by the authors. Their solutions as to method may be open to debate on various grounds. However, it is essential for the industry as a whole to consider this problem in all its detail to find ways and means of supporting needed programs for progress.

Under the usual regulatory practices of the commissions it is often difficult to demonstrate the validity of the costs of research by a power company itself. If some regulatory bodies are inclined to exclude the costs of advertising household appliances as load builders, there is much uphill work still ahead for those who are research-minded. If it can be reasoned that increased power sales are of more benefit to the stockholder than to the rate payer and costs therefore are chargeable to the former, what are the prospects for finding research funds? Research by its very nature is generally doomed to negative results or to failure. If that were not the case, the answers to problems would be self-evident and no skill would be needed to find those answers. Anybody could do it. Consequently, there is a very real question posed to regulatory bodies, to utility managements and to consumers—how will the charges be allocated in any extensive research program? If the result of the research is negative and the activity must be abandoned, who is going to pay the bill?

At present it would seem that the preferred practice would be to put this burden on the owners of the business. It is doubtful, for instance, that a commission would be willing to burden future rate payers with the cost of a defunct research effort. It is much simpler to pay for research in the investment for equipment which is bought from manufacturers, who in turn have engaged in research. This might be construed as shifting the cost, with the consumer ultimately paying the bill when new equipment is bought. Why not allow research expenditures to be made directly, and consequently avoid the burden of unnecessary duplication of effort among manufacturers? There may be some merit to such argument but there is also the equally valid argument favoring research by manufacturers. While the cost of the research must ultimately be reflected in the selling price of the equipment, there is, at least in theory, the offsetting influence of competitive apparatus and prices of other manufacturers.

The solution to the industry research program which favors sponsorship by equipment manufacturers has merit when applied to specific apparatus. However, there are many types of research problems which cannot be properly or effectively handled by this method. The authors cite such problems and propose some solutions. I believe that the necessary step which must be taken is to find reasonable and acceptable ways in which funds can be set aside for carrying out the recognized research problems.

Howard P. Seelye (The Detroit Edison Company, Detroit, Mich.): The authors have made an excellent analysis of the opportunities for research which are open to the electric power industry. There is no question that there are many fields in which investigation will not only be worth while but will be essential if the industry is to maintain its position as a progressive force. In looking over the rapid progress which has been made during the past 50 years in stimulating the use of electric power and in adequately meeting the demands so produced, it cannot fairly be said that the industry as a whole has been laggard in its research. Much of it has been done by the manufacturers of course, much by the operating utilities, and much by co-operative effort. There is also a great deal of research work under way today as is witnessed by the progress being made or planned into new areas of temperatures, pressures, high voltage, atomic power, and others. No one can say just how much the utilities should have done or should be doing. The measure is the need for discoveries and how well that need is being filled rather than what per cent of income may be spent.

It is believed that the utilities could justifiably increase their activity in the research field, particularly in the direction of correlation and co-ordination of what is now being done, stimulation of more attention to those items which are of particular concern to the operating companies rather than to the manufacturers, and publicity for the efforts and results. The organization and plans of the Edison Electric Institute are directed toward just such a program. It is believed that this could eventually meet the essential needs of the situation which the authors are pointing out. It would seem much too early, however, to consider the development of another independent industry laboratory or of much of the very long-range undirected type of investigation. There are many laboratories and organizations now in existence ready and willing to undertake such work. Perhaps the industry laboratory might some time be found necessary, but for the present much valuable progress could be made by proper correlation, direction, and support of programs using the existing facilities.

J. Stuart Johnson (Purdue University, Lafayette, Ind.): There are many phases of this topic which might be discussed at this time. However, I would like to emphasize just one point concerning the stimulation of student interest in the power field. It is, in my estimation, almost a certainty that unless some means is devised to attract graduating student engineers to the utility industry, it will soon be apparent that only the men who could not locate jobs elsewhere will enter this industry. Granted, there will probably always be a few good men who are interested and enthusiastic about the power industry, but these are not nearly enough to man all utility companies. Many companies have not yet felt this shortage of quality workers, or if they have, they may have attributed it to the national engineer shortage. I am convinced, as one who has observed at firsthand the swing in student interest, that this is not the cause.

Any debate concerning the relative responsibility of the utility and the manufacturer in matters of research and development becomes entirely academic in the light of the fact that the manufacturer is not going to have power men for design either. It may be said it is his responsibility to create the interest. But who gets hurt if improved equipment is not forthcoming? He can probably turn his manufacturing efforts into other directions quite profitably.

The power industry is one of the most vital parts of our industrial America. I am deeply concerned over the possibility of its being unable to perform adequately its functions in years to come, lacking the best personnel available, and the most highly developed equipment possible. The proposal made by the authors for the establishment of a research program as individual and/or group effort represents a very real method of bringing about student stimulation as a natural by-product of its unquestioned economic contribution. I submit, however, that it will be a most profitable by-product.

G. B. Tebo (Hydro-Electric Power Commission of Ontario, Toronto, Ont., Canada): The authors quite properly emphasize the need of the electrical industry for more scientific knowledge to be gained chiefly through additional manufacturers' research, and through utility-sponsored research. But possibly too little emphasis has been placed on the changes which should take place in both the attitudes and facilities of some individual utilities if the benefits of this new information are to be fully realized.

Failure to attract engineering graduates into utility work will not be corrected by simply having the utilities encourage more research in the manufacturers' laboratories. Even a central utility-sponsored laboratory or a particular commercial laboratory will seem very remote to the graduate entering a distant utility. Nor will the flow of research information from these laboratories be of much value to a utility which lacks interest in the application of advanced scientific methods to its own immediate problems.

Some utilities have recognized that unique fields for profitable research exist within their own organizations. The logical action for such a utility was to hire a few people trained in research methods and have them assess the immediate problems by planning a research program to deal with them. This sometimes led to procurement of laboratory facilities, and the nucleus of a research establishment was created. Its size depended on the size of the utility served, and on its ability to produce results of value to that utility.

On the surface, the idea of individual company laboratories may look like unnecessary duplication. Actually, the experience of companies operating such facilities indicates that the work consists largely of day-to-day problems particular to that utility and that any findings of industry-wide interest are readily exchanged through the efficient industry associations and little tendency exists to duplicate the research work of apparatus manufacturers.

Many examples could be cited of lucrative research projects which can best be performed in the utility's own laboratory, such as:

1. An improved method of predicting daily peak load for a 3,000,000-kw system improved the accuracy of prediction by 1 per cent. This was accomplished by establishing certain local illumination-load relationships and applying advanced statistical and machine computation methods to available data. One year's saving in cost of spinning reserve repays the cost of the investigation many times over.
2. A study of wood preservation sustained for the past 25 years in the laboratory, in test plots, and in actual service has brought this science to a high state of effectiveness. The prolonged life of more than 1,000,000 poles in service pays handsome dividends to this company. Although the basic results of this pioneering effort have been of value to the whole industry, only in the utility's own laboratory could the local conditions of weather, soil, and pole species be fully recognized.
3. A striking saving in lubrication costs on a 350,000,000-dollar construction project was made by a co-operative effort of the construction, research, and purchasing departments. The lubrication recommendations of the major oil companies were studied, available materials were tested, requirements were simplified, and bulk purchases were negotiated. Over the 5-year life of this project, tangible savings on purchase of lubricants were estimated at more than 500,000 dollars. This was possible only because of the utility laboratory's long experience in the investigation of lubrication problems.

In facing the question raised by the title of this symposium, we should not overlook the opportunities for research within each utility. Nowhere else will be found the same intimate knowledge of the problems, the same sense of urgency in seeking solutions, or the same opportunities to try out and observe the solutions in actual operation. This will not retard, but should actually stimulate, the research activities of the manufacturers, the commercial laboratories, and the universities. Such local laboratories could constitute the chief source of problems for a central utility-sponsored laboratory. They would also provide an essential means of digesting and applying the results of pooled research to the operations of their own companies.

Frank E. Sanford (Commonwealth Associates, Inc., Jackson, Mich.): The authors are in substantial agreement with many others concerning the essential nature of research for the electric utility industry, but they have found a wide divergence of opinions on policies and lack of a clear understanding of the possibilities for increased research.

Perhaps the big questions may be summarized as: how to create a more favorable atmosphere for expansion of research, and how to implement or co-ordinate a program of research if it is to be expanded. These questions are closely related to three more that are basic in any further consideration: Should there be one large laboratory and staff corresponding to those of several other industries? Should more problems be assigned to the universities and to commercial research laboratories, with co-ordination through an industry committee. Or should the present arrangement be continued with major dependence on developments by individual manufacturers?

It is probable that the final answer will be found in a combination of all these possibilities, with the utility industry participating more actively in sponsoring a co-ordinated series of projects for studies in university and commercial laboratories, with projects such as the present nuclear energy developments in individual companies or groups, and with many projects handled in company organizations and co-ordinated as a result of consideration by the various engineering committees.

This combination appears most advantageous for flexibility, for its assurance of breadth in the approach to problems presented, and, very importantly, from the viewpoints of public relations and advancement of engineering education. It is possible that the electric utility industry may ultimately need a single large laboratory, but it appears much more realistic now to use present facilities in a co-ordinated program. Attempting to promote, finance, and staff such a start would be trying to leap before learning to walk.

The real and fundamental need today is to learn more about what is being done, what is considered to be needed, and with that to start building interest, understanding, and confidence. This could be done in a relatively short period of time, but it will not be a simple job and it needs more total time than is usually available to the individual members of a committee.

The first step was made toward such a plan as long ago as 1948, when the Edison Electric Institute Board of Directors approved a research program to start with addition of a research co-ordinator to its staff to aid a research committee. The duties of the committee and co-ordinator were the determination of the extent of research in progress, co-ordination of research, and the making of recommendations for additional research projects which would be considered for approval. It was then expected that the plan would be under way in January 1949.

This action followed recommendations of a committee which had surveyed the situation then and outlined a 5-year initial program. But this first step faltered and, as of today, the 5 years have passed with the discussion once more in exactly the same channel as in 1948 and before.

With time to work out of the postwar situations and the critical requirements and pressures during the smaller war which followed, it is perhaps time to try again. An initial objective should be a survey and compilation of information of activities, possibilities, and needs. Outlining ideas for short-range problems, creating a more active interest and confidence, and establishment of contacts and goals might be the only result of this initial phase. Extension and continuation to include fundamental and basic problems requiring long-range study should follow.

Improvement of present efforts should bring about immediately a higher degree of co-ordination of goals and continuity of existence. The present arrangement of specific projects which are liquidated following each effort would be blended into a program with continuity, correlation, and direction. The paper presented will prove to be very important if it will again stimulate discussion at both engineering and top management levels of the electric power utility industry.

H. H. Brown (Wisconsin Michigan Power Company, Appleton, Wis.): Since we are primarily a utility with most of our power generation coming from hydro plants, we conduct activities in collecting careful hydrological data. Besides the usual collection and analysis of rainfall, runoff, temperature, snowfall, and sunshine hours, we work on other variables. For instance, ground water levels in our drainage area have proved of value in predicting river runoff. We have found that a year with less rainfall but high water tables has produced more runoff than a year with good rainfall and low water tables. Nylon resistivity blocks buried in the ground at different levels have aided in studying the moisture in the soil between the water table and the ground surface. The 4-electrode megger resistivity routine testing has also been valuable in determining water moisture in the soil above the water table. Cyclic studies on rainfall over an extensive area like the Menominee River shed since 1911 have resulted in a major trend curve and the many contributing harmonics. Once a year our company with key personnel devotes an entire day on the review of the last year's activities. These reports are distributed to all parties concerned. We also invite some neighbor utilities to pool all the many ideas and practices. I am sure a pooling of the efforts within our nation and of those from foreign countries as well would be an interesting adventure if due funds could be established. To know the future runoff materially aids in controlling our reservoirs so as to obtain the greatest use factor of pondage without entering a winter with low reservoir levels. I think the authors' suggestion of observing foreign country practices should prove helpful.

Utilities are always fighting competition. Even though we have a monopoly in the territory we serve, we are competing with customer-owned steam turbine generation, for instance, in the paper manufacturing industry. Bottled gas has cut into our electric range and electric hot-water heater expansion programs, particularly in rural and summer resort areas. It therefore behooves us to keep abreast of the times and to give the customer the lowest possible rate consistent with a fair return on our investment.

Since I am located at the heart of the greatest research center of the paper industry, I am cognizant of the importance of research. Possibly through one of the three national utility organizations the authors' suggestions of research in the electric utility industry can become a reality.

J. E. Hobson, W. A. Lewis, and **M. S. Oldacre:** We appreciate greatly the discussers' interest. They all point out the importance of research and development in the electric utility industry, and in general agree that a more extensive research program is desirable and appropriate for the industry, even though there may not be complete agreement on the method by which the research should be accomplished. It is perhaps significant that most of the discussers, in commenting on particular research activity, have paid particular attention to recent developments, or problems that are immediately pressing and relatively little has been said about basic and long-term research for future needs. This tacit omission perhaps lends added weight to our belief that the industry is giving relatively little attention to its basic and long-term needs, and that means must be found not only to find solutions to the immediate problems but to lay a broader foundation for the developments needed for the future.

Mr. Doble stresses the point that it is the prime function of the colleges to educate men and not to do commercial research per se. We would certainly agree with this statement. However, it is generally agreed that the process of education involves not only the imparting of known facts to students but also the development of new knowledge by searching into the unknown. In this respect, we believe that it is one of the important functions of a college to carry on research in fundamental areas where the goal is the development of new information, preferably not for the purpose of meeting an immediate commercial problem but primarily for contributing to the over-all development of the art. In certain individual cases it becomes quite difficult to distinguish between fundamental research and commercial research because of the impossibility of defining specific limits. Nevertheless, the important differences in primary objective will tend to avoid any serious conflict of activity. Commercial research, by its very nature, tends to be specialized around immediate pressing problems, and the techniques developed by established laboratories in their special fields can keep them pre-eminent in their areas so that their continued existence is fully justified. When research is directed toward specific and well-defined goals, and deadlines have to be met, the pressure of research activity can seriously interfere with the educational process, and research in this area hardly belongs in educational institutions.

We agree with Mr. Watchorn that the effective co-ordination of hydro and steam generation is a complex problem, and probably extensive research will be needed for the expected results to be much better than can now be obtained by essentially rule-of-thumb procedures. Nevertheless, we believe that to obtain the maximum economy on systems having both steam and hydro generation research on this problem is justified.

Mr. Baumeister expresses some concern regarding the action that may be taken by regulatory commissions in approving research costs as legitimate charges of public utilities subject to their regulation. We believe that research is, in the final analysis, the most effective means of reducing the cost of service to the customer. Of course, in the beginning, investments in research must be made with the expectation of a future return. However, if that return is not achieved in the long run, research is not justified. In this sense, research expenditures at the present time are in the nature of an insurance policy directed toward lower costs in the future. It is of course not reasonable to look at each research project individually, because some projects will be successful, while others will not be. However, in the long run, a research program must pay for itself in lowered cost, or it should be discontinued. If this principle of research is once established, there seems little question about the justification of modest research charges as operating expenses, in the expectation of future benefits, just as higher installation costs can be justified for more efficient units because later the operating costs will be reduced. We believe that regulatory commissions can be persuaded of the logic and justice of this position. We are confident that, when the utility managements themselves are firmly convinced of the responsibility of utilities for supporting a broader research program, the regulatory bodies can be and should be persuaded to authorize the necessary charges.

Mr. Seelye believes that is is much too early now to consider the development of an independent industry laboratory or much of the very long-range undirected type of investigation. We would certainly agree with him that the need for a laboratory supported by the industry should be developed gradually, and that it would not be prudent to rush into the construction of elaborate laboratory facilities as the first step. However, it is our belief that one of the desirable early steps is the development of a research planning and co-ordinating staff for the industry as a whole that can look toward a more intensive investigation of the longer range and more basic problems of the industry which do not now appear to be receiving adequate attention. As the work of such a group becomes more effective the need for laboratory facilities in certain directions will undoubtedly become acute, and at that stage it will be time enough to initiate laboratory facilities. We do not contend that any great amount of research should be undirected. There is a place for exploratory research into new areas with no preconceived objectives, dictated primarily by the interest and curiosity of the investigator. Research of this type can be most effectively done in college laboratories where research for basic new knowledge is a principal objective. However, when early discoveries indicate interesting phenomena that give some promise of practical application, it becomes possible to develop a co-ordinated and carefully planned program of research to explore the possibilities. It is primarily in the latter area that an industry research organization and laboratory will eventually prove indispensable.

Prof. Johnson has emphasized the need for stimulating the interest of students in the power industry and it is most helpful to have his favorable opinion regarding research efforts for this purpose.

Mr. Tebo is particularly concerned about the relation of the research program to the manpower needs of the industry. We certainly do not contend that an isolated and separate research laboratory, sponsored by the industry, will so change the industry that engineers in great numbers will be attracted to all of the operating companies. However, it is our feeling that, if the industry accepts its full responsibility for an aggressive and forward looking research program at all levels including a central organization for attacking the broader problems and a more aggressive research attitude in the companies regarding their immediate problems, the working conditions within the companies will gradually be changed all along the line, and recruiting problems will become far less difficult. In short, the spirit of research becomes a method of doing business that will permeate not only the research organization but the engineering and business organizations as well, and will tend to bring the industry in step with a modern age that considers research essential to progress.

We agree with Mr. Sanford that there is now a definite need for a further look at the research requirements of the industry, and this review should be thorough, careful, and far-reaching. A desirable starting place is a survey of the research in progress and a broad evaluation of the possibilities and needs. We believe that this evaluation should most certainly include a careful study of the responsibility for the long-term research needs of the industry.

A survey of this type will largely indicate the best methods for accomplishing the desirable research. We agree that the most effective method of accomplishing the desired results will undoubtedly make use of all of the existing research tools, and we feel sure that an industry laboratory will gradually prove an indispensable part of the ultimate program.

Research in the Electric Power Industry

L. R. GATY
FELLOW AIEE

Synopsis: The electric power industry and the research it has done and is doing are reviewed briefly and areas of research which should be pursued more aggressively are discussed. The industry must provide the highest service reliability at the lowest cost consistent with sound practice. Any research that holds promise of fostering this objective should be carefully considered and encouraged either directly or indirectly.

THERE is no question of the need for research. It is the key that has unlocked many secrets of nature for the benefit of mankind. There is every reason to believe that new developments and knowledge will dwarf the progress made up to date. It was research that created the electric power industry and it is proper to examine what part the utility industry should take in an aggressive research program. Certain types of research have been and are being conducted by the utility industry and these will be continued and expanded. There are other types of research that have no place in a prudently managed utility company and these will be avoided. Between these two is a broad band of controversial activity that must be carefully considered.

Many Kinds of Research

Research is defined by Webster as a "careful or critical inquiry or examination in seeking facts or principles; diligent investigation in order to ascertain something." The author has divided research into three groups and defined them as follows: "Fundamental research" is seeking knowledge of the fundamental laws of nature without regard to the usefulness of the knowledge. "Basic research" is taking this knowledge of natural laws and applying it for the benefit of mankind. "Applied research" is seeking ways to improve a product, reduce its cost, or broaden its usefulness.

Research Being Done by Industry

Considered in the light of this definition a substantial amount of research is being carried on by the electric utility industry. Much of this research might have been carried on by industrial concerns or by universities but was initiated by the utilities before other groups became interested. Many of these projects should have been included in the category of research but were not so classed. These include work in the technical and scientific areas and frequently extend well beyond the scope of work usually associated with this industry.

A few of the research projects now

Paper 55-145, recommended by the AIEE Research Committee and approved by the AIEE Committee on Technical Operations for presentation at the AIEE Winter General Meeting, New York, N.Y., January 31–February 4, 1955. Manuscript submitted October 26, 1954; made available for printing December 9, 1954.

L. R. GATY is with the Philadelphia Electric Company, Philadelphia, Pa.

active or completed within the past few years are listed here. This partial list indicates the variety of problems being investigated by research supported either fully or partially by electric power utilities.

1. Research on graphitization of steam piping: An investigation of the phenomenon of graphite migration and means of prevention was sponsored jointly by the Edison Electric Institute (EEI) and the Association of Edison Illuminating Companies (AEIC).

2. Branch circuit overcurrent protection: An investigation of the characteristics and requirements of branch circuit protection was sponsored by EEI and AEIC and was conducted in co-operation with the Underwriters' Laboratory.

3. Pipe-type underground cable research: Factors affecting the rating and operation of high-voltage pipe-type underground cable systems were investigated by EEI and AEIC.

4. Heat pump studies: The joint AEIC/-EEI Heat Pump Committee has sponsored several studies of various phases of the problem including heat storage media. The committee is now carrying on a preliminary investigation of supplemental heat sources including solar heat.

5. Steam contamination: This research was organized to study the factors which govern the introduction of impurities into steam from the water in the boiler and the subsequent deposition of those impurities on the blades of turbines. It was sponsored by EEI, AEIC, boiler manufacturers, and turbine manufacturers and involved fundamental studies in a little-known brand of physical chemistry and the development of new measuring techniques.

In addition, active research has been carried on in the following fields as well as others not enumerated: Electronic accounting machines for billing; artificial resuscitation; load characteristics; furnace performance factors; atmospheric contamination; high-temperature steam generation; welding; and fly ash.

The Cable Engineering Section of AEIC has been very active in exploring many factors which affect cable rating, life, and operation and has received excellent co-operation from the cable manufacturing companies. Preliminary work has been done on investigating the possibility of using extra-high-voltage cable. With presently available insulation, it appears as though cable would have a very low load rating at 345 kv and could carry no load at 380 kv because of high dielectric loss. Research which pointed the way to a substantially lower dielectric loss in the cable insulation would improve the performance of existing cables and permit an extension to voltages in the 300-to 400-kv range.

In addition to these direct projects there have been many carried on by various technical committees of industry organizations. This industry is unique in its policy of free interchange of information among its member companies. Troubles and errors are frankly discussed and all information is made available to other companies having the same problems or equipment. A catastrophe may occur on one system and within a matter of hours it is known and the details are given to other companies. These troubles are discussed and analyzed at committee meetings. In addition, innovations, improved methods, better utilization of equipment and, economic simplification are discussed and the full story is made available to all interested. This atmosphere of frankness and mutual interest has created a committee organization of unusual effectiveness. It permits the entire industry to benefit from the pioneering of each member and allows the group to go forward with accurate scientific knowledge. Without this free interchange the progress to higher voltage, larger units, greater capacities, higher temperatures, and pressures would have been much slower. The industry does not call all this activity research but it is included in the definition given in this paper.

Progress Through Co-operation

There are various needs that must be weighed and evaluated. The utility industry needs a healthy and agressive equipment manufacturing industry. Both of them need alert and forward-looking groups of technical educational institutions, which provide the lifeblood of both industries through the new talent that is trained. A virile and progressive educational program contributes to progress, so ways must be found to keep educational institutions solvent to attract and hold outstanding teaching staffs. One way of doing this is to authorize research projects that will provide financial support and equally important, will stimulate interest in the power industry.

The electric utility industry has just passed its 75th birthday with every indication of a continuing dynamic growth ahead. There is a challenge for the best technical and managerial talent to carry on its traditions and fulfill its obligations. One of the reasons for this success is an extremely close relationship between the utility engineers and the engineers of the equipment manufacturers. Through the years a co-operative partnership has grown up between these two groups that has resulted in unprecedented progress in new and better products with ever increasing efficiency and reliability. The electric utility industry could not have reached its present stature without the developments that have stemmed from this teamwork and the research and standardization that has been made possible. New designs, higher efficiency, greater economy, better reliability, and simplicity of operation have all resulted from this partnership and have permitted cheaper and more reliable electric power to become one of the miracles of industrial expansion. All groups have shared in the benefits of this teamwork and any program of research must not interfere with it.

The equipment manufacturing industry has provided research laboratory facilities and personnel to carry on an aggressive program of research which includes metallurgical, chemical, electrical, thermodynamic, and other fields. This has many advantages to the manufacturer and his customers. It makes available the results to a wide group, it strengthens the sponsor, it provides excellent facilities and technical talent to investigate a problem that may develop suddenly in connection with new products or new applications, and it provides lower costs for the manufacturer that can be passed on to the customer along with a better product. Competition tends to increase the effectiveness of this arrangement and makes it far more productive than a single research center supported by many sponsors. There is nothing that provides a greater incentive than having a competitor get a temporary advantage through improvements in his product.

This research program must not be upset. It is proper that certain types of research should be conducted by the manufacturer and not by the purchaser. The customer should not be expected to do the research to improve the product he is purchasing, although he should make sure the product is the best for the application he has in mind.

The industry today is producing a kilowatt-hour for less than half the fuel required 30 years ago. This has not been brought about by any one group but through the combined efforts of the manufacturers of all types of equipment and the willingness of the utility industry to pioneer by purchasing and operating this equipment. The utility industry has been willing to pay the costs of the necessary research and take the risk of expensive changes. The field modifications made in co-operation with the manufacturer have made many contributions to progress and scientific knowledge. There appears no other feasible way of doing this type of research—a 1,000,000-pound-per-hour boiler cannot be set up in a university laboratory for research purposes, and small scale models do not yield typical results. This activity is not called research but it should be. That is undoubtedly one of the things that could have been more widely publicized in the past.

There are many similar projects which must be undertaken on a full-scale field basis and the research work is done after operation starts. Naturally there are many components that must be designed, analyzed, tested, and modified in the shop before fabrication, but the over-all operation of the device cannot be accurately determined from component information. The necessary field work and many modifications are fed back into the manufacturer's design group and used to improve future products. This type of research makes a substantial contribution to the knowledge of the art and to the welfare and prosperity of the utility business, but does not get included in the discussion of research activities.

Even though a great deal of research and promotional activity is being carried on by the utility industry and by individual electric utility companies there is certainly ample room for improvement and a substantial expansion in the amount of activity. Dynamic and continuing expansion in the industry suggests that an increase in the level of research activity would be appropriate. There are many cogent reasons why the industry should be providing a more progressive research program. One obvious reason is that inherently the utility industry must obtain a long life from its plant investment. Industrial concerns are able to write off equipment on a short-term basis, but this is out of the question for major plant investments of utility companies. Any research activity that will contribute to longer useful life and lower annual cost is highly beneficial.

New Sources of Energy

There is a new source of energy coming to the front—atomic energy. More of the national scientific talent is devoting itself to atomic energy for war and peace than has ever been devoted to a single project. The utility industry is vitally interested in this field and is actively conducting research in many directions. A large number of electric utility companies are participating in one or more study groups investigating atomic energy in all its peacetime power-producing aspects. Chemical, metallurgical, thermodynamic, mechanical, and economic factors are weighed and investigated. This work is being done in the laboratories of universities, industrial concerns, and research foundations. The recent changes in the law will permit greater use for peaceful purposes. The utility industry is now well advanced in its knowledge in this field and fully expects to continue on to the installation of large-scale atomic-energy applications.

The conversion of solar radiation to electric energy has been improved and widely heralded. How does this affect the utility industry? Some of the semi-scientific writers have envisioned a solar converter on every housetop with unlimited power available for all household uses including heating and cooling of the home. It can be said without fear of contradiction that with present knowledge, materials, and costs this is only a dream. But as research adds to knowledge and provides new materials the dreams of the visionaries are often realized or exceeded. Certainly the utility industry must keep abreast of all new developments in this field. There may be other new forms of energy or energy conversion that will appear in the future. When these are discovered through research, the electric utility industry must be ready to use them to supplement the older forms of energy conversion. This may require a research program to apply the knowledge and make the energy commercially useful but the industry should not embark on a program of fundamental research to discover such energy sources.

Progress Through Dissatisfaction

The progress made in the past 50 years can be attributed to dissatisfaction. Customers are eternally dissatisfied with what they have and want something bigger and better. This dissatisfaction extends into the factories and utilities which are always striving for better machine tools, better quality control, and better working conditions. The utilities are dissatisfied with the service they render, with the equipment they buy, with the engineers educated by the universities, with the cost of equipment and the operating expenses, and are always seeking more reliable and economical devices that will be simpler and safer to operate.

This dissatisfaction is healthy provided the desire is for something better and not just for something different. Hobson and Lewis[1] were dissatisfied with the amount of research that was being sponsored in universities by utilities and had justification for it. Their paper was a provocative and able statement of one of the important problems facing the electric power industry. Very little has been done through this channel and much more should be done. But it would be most unfortunate if this did not meet two requirements: first, it must be research which will help the utility industry to move forward; and second, it must be the type of research that can be done properly and effectively by the universities. DuBridge[2] points out the advantages of research, the needs for research, but, above all, the importance of doing the proper kind of research and not merely experimenting for the sake of obtaining financial support. Research in a university can make a substantial contribution to the understanding of natural laws and act as a stimulus to additional research by other groups. The author is dissatisfied with the amount of research the industry is doing, but is also dissatisfied with the reliability of service rendered and with the costs achieved. If such research were to make a substantial improvement in the service reliability or a substantial reduction in its costs, then the problem of the university research groups would be to find facilities and staffs to keep up with the research projects thrust upon them.

Industries hiring technical men have indicated dissatisfaction with both the quantity and quality of the engineers being educated. The electric power industry urgently needs a steady flow of good engineers capable of growth and development. It is essential to stimulate the interest of the teaching staff as well as the students in the opportunities ahead in the power field. One of the easiest and most effective ways of doing this is to provide research projects that will provide financial support for the institution and for the staff and mental stimulation for the staff and students. There are many advantages in such a program, the least of which is that it could be self-supporting and might pay off in substantial direct benefits. In addition, it provides financial support for the improvement of physical facilities, helps to obtain and hold superior teaching staffs that could not be held otherwise, and creates a real interest on the part of the men who are training and advising the students. Consequently, this will result in a more adequate flow of well-educated engineers interested in the power business. Such a plan would also provide a pool of consultants conversant with electric power industry conditions who would be available when unexpected problems arise. There have been many cases where such consultation was desperately needed but was not avilable or was unknown.

Wide Range of Power Industry

The electric utility industry is only a part of the power industry. The field includes the equipment manufacturing industry and all large industries such as mass transportation, automotive manufacturing, mining, and much of the entertainment and communication field. New techniques in the electrometallurgical field require tremendous amounts of power. The aluminum industry has some of the largest hydroelectric developments in the world. Television and radio require large blocks of power and color television will greatly increase this demand. The power requirements of the fabricating and manufacturing industry are increasing steeply with the need for higher product output with lower costs and fewer men. The large factories have extensive power distribution systems built in with the requirement that they must be flexible enough to meet future changes in manufacturing techniques and power requirements.

Co-operative teamwork between the power industry and the educators will provide handsome benefits to both parties. Research provides a medium through which this can be done. There is a broad mutual interest between the educational institutions, manufacturers, contractors, and utilities. This mutual interest should provide a strong incentive to work out a reasonable solution benefiting all parties.

Future of Industry

A brief review of the forecasted growth in electric power use by many experts presents a challenge of the first magnitude. Even if it is assumed that the growth will slow down and the load will double each 15 years, there will be eight times the load by the year 2000. The efficient supply for customers at that time will require new knowledge in the fields of generation, transmission, distribution, utilization, accounting and record keeping. Some of the problems are common to other industries but some are unique with the public utility industry. The sooner this knowledge is available the more healthy will be the growth.

Research by the electric utility industry is essential and a way must be found to strengthen and expand the research being supported by the industry. A tremendous job lies ahead even if forecasts of future growth are only partially fulfilled and every tool must be utilized to assure that this job is done well. Research wisely conceived and properly channelled will assist in this sound growth and help assure that capable technical personnel is available to the electric utility industry.

References

1. RESEARCH FOR AND BY THE ELECTRIC POWER INDUSTRY, **J. E. Hobson, W. A. Lewis.** *Electrical Engineering*, vol. 73, June 1954, pp. 516–21.

2. THE GOALS OF UNIVERSITY RESEARCH, **L. A. DuBridge.** *Electrical Engineering*, vol. 73, Sept. 1954, pp. 790–92.

◆

Discussion

Walter B. Morton (Pennsylvania Power & Light Company, Allentown, Pa.): Mr. Gaty's paper contains some thought-provoking revelations on the need for research in the electric utility industry and discusses in general terms what the electric utility industry is doing in the field of research.

I believe, however, that it might be interesting to mention a few specific examples of what some of the utilities are doing in research and what is being accomplished. While research of some nature or other has been conducted by utilities for many years, it is only since the war that many utilities have organized special research sections, divisions, or departments where specialized personnel can carry out research activities unhampered by schedules and the pressure of meeting scheduled dates.

Electric utilities have co-operated with EEI and professional societies such as AIEE, The American Society of Mechanical Engineers, and the American Society for Testing Materials in some of their research activities among which are the study of the properties of steam at high pressure and temperature, creep characteristics of metals and alloys subject to high temperatures, and resistance of metal and alloys to high gas temperatures and atmospheres.

One of the outstanding examples of the co-operation of the electric utility industry in pioneering research is the current construction of the world's first commercial size atomic power plant soon to be operated (in co-operation with the Atomic Energy Commission) by a privately owned utility. This is the Duquesne Light Company plant to be powered by a pressurized water reactor. In addition to the active construction of a working atomic power plant by one leading utility, more than 50 other utilities are actively studying the possibilities of proceeding with the construction of plants to utilize atomic power on their system. Among these is the Pennsylvania Power & Light Company.

Specifically, the Pennsylvania Power & Light Company has special research divisions in the mechanical and electrical engineering departments. These groups have conducted long- and short-range research studies to develop better design and construction methods, to make available more reliable and less expensive equipment, to improve installations for effecting economies and obtaining safety to personnel, and equipment, and continuity of service. A major objective of this research is to reduce the capital investment, the cost of operating labor, and the maintenance charges of facilities to serve the public with resulting lower cost of service.

Our company and other contiguous companies in this area pioneered many years ago in the high-voltage interconnection of large capacity utility systems to obtain the most economical use of the facilities installed by the interconnected systems. We also pioneered in the investigation and development of lightning protection for high-voltage transmission lines and our answers to these problems are now used almost universally. Our company began the development of equipment and procedures for the handling and burning of small-sized anthracite produced as a by-product and formerly discarded in culm banks as useless. Now we are the largest user of anthracite in the world, both stoker and pulverized methods of firing being developed and used as a result of our research. We developed a new design of thaw shed using hot water instead of hot air or steam for thawing badly frozen cars of coal to permit rapid unloading.

In the electrical field, co-operating with the manufacturers of equipment, our research has assisted in the development of a medium rated 500,000-kva 69-kv voltage fuse for the industry. This development was supplemented by a fault-current interrupting test at rated voltage on the Pennsylvania Power & Light Company system, which resulted in a fuse costing only 40 per cent of the then existing available heavy-duty fuse. We initiated and pioneered, as a result of considerable research, a new procedure for ice-testing air-break switches. The specifications prepared as a result of this research are now used almost universally by all disconnecting switch manufacturers and have effected improvements in the designs of several manufacturers.

We have done considerable work on the study of loading transformers on a thermal basis rather than name-plate rating, as have several other large utilities. These combined efforts have resulted in a material reduction in cost per kilovolt-ampere of transformer capacity required to serve the load and in many cases the need for additional capacity has been postponed for a long period.

We have conducted research work during the past 2 years in the development and necessary tests for the procurement of adequate 69-kv air-break switches for breaking magnetizing and network load current and, as a direct result of this research, our substation designs have been modified to effect a substantial saving in the cost of switching devices.

Immediately following World War II, after considerable research and study we were able to develop standard designs for substations; on any project we have been able to select an available design from seven standard types to fit any condition required on the system from 4 to 220 kv. This not only substantially reduced the cost of the stations but facilitated installation of rush jobs during the critical years following the end of World War II. These designs are not permanent. They are under continuous study and are modified from time to time as improvements develop as a result of research.

Another project we have in process of research, in conjunction with the equipment manufacturers, is the establishment of an adequate thermal rating for high-voltage fuses which is somewhat indeterminate at the present time. This study has not yet been completed.

I think too little emphasis has been placed on the great value of research organizations within the utilities' own forces and too little publicity has been given to the fine work that many of these groups are doing in the various utilities. The close co-operation between these groups and the manufacturers' engineers in developing improved equipment for safety, for greater reliability and for more economical installations has not been given the publicity it deserves.

As Mr. Gaty points out, most of the progress that has been made in the past 50 years can be attributed to dissatisfaction. I hope that we never become so satisfied and complacent that we will no longer find any need for these research groups that are doing so much, in co-operation with manufacturers' engineers, for the improvement in manufacture and utilization of electric equipment. It is not possible to stand still. We must go forward and continued and more intensified research will drive us forward and at an ever increasingly rapid rate.

Eric A. Walker (Pennsylvania State University, University Park, Pa.): The companion paper by Hobson, Lewis, and Oldacre[1] offers a research program to the power industry, which has as one of its themes the suggestion that a central research laboratory for the industry should be started. Mr. Gaty says that the power industry is doing a great deal of research, both by itself, through certain organizations it supports, and also through the equipment manufacturers. I believe there is one important question which has not been answered. "Do the power utilities need more and better engineers than they now are getting?" and, if the answer is affirmative, then, "Why?"

I would like to suggest that the power companies make a statement on the number of 4-year engineering graduates they need over the next 10 years to make it clear to the educators that a market exists and to allow the educators to design a curriculum to fill that market. It would be very helpful if the power companies could indicate quite clearly the type of work they expect these engineers to do. The more clearly this can be done, the better job the engineering educators can do of filling the order. Lastly, it would be extremely helpful if the power companies would indicate what they think is necessary in a 4-year educational program to make such students acceptable to the power industry. I believe they should link the courses and material they would expect the student to cover with the jobs they would expect him to fill. With these data in hand, I am sure that the educators would be much better fortified to try to steer some of their better students into the public utilities.

REFERENCE

1. IMPLEMENTATION OF A RESEARCH PROGRAM FOR THE ELECTRIC UTILITY INDUSTRY, J. E. Hobson, W. A. Lewis, M. S. Oldacre. *AIEE Transactions*, vol. 74, pt. III, Aug. 1955, pp. 545-53.

L. R. Gaty: The discussers emphasize the importance of better understanding and co-operation between the electric power industry and the engineering educators. A research program by the electric utility industry would be helpful but will not in itself correct the unhealthy situation now existing. Inauguration of an over-all industry research program should not be delayed but cannot be counted on to give more than tangible evidence that the industry is progressive and forward-looking and, therefore, attractive in providing a career for engineers

---

Manufacturer's Research in Relation to Electrical Utilities

E. E. PARKER
MEMBER AIEE

J. BAIRD
MEMBER AIEE

ENGINEERS have a twofold function. They must find ways to increase the value of present products, and they must develop new products. Similarly, any healthy industry must accomplish these same two functions and certainly the electrical utility industry is no exception. Since research and development are vital to the manufacture of products of increased value and the creation of new products, adequate work of this character is essential to the continued growth of the electrical utility industry. Thus, the question becomes immediately not one of justifying research and development but rather one of determining the appropriate areas for research and development to support the utility industry, of deciding how much should be done, and of finding out who can best do the work.

With respect to the interests of the electrical utilities, appropriate areas for research and development include:

1. Basic scientific knowledge.
2. Power generation.
3. Power transmission and distribution.
4. Power system analysis.
5. Power utilization.

To decide how much work should be done in these areas, the present situation is reviewed briefly. The availability of adequate amounts of electric power at reasonable and constantly diminishing costs has been a major factor contributing to the high standard of living in this country. The electrical utility industry has performed an amazing feat in reducing the average cost of domestic electric energy by 32 per cent[1] in the last 15 years, a period during which the cost of living has risen by 93 per cent.[2] In addition to cost reduction, there has been an increase in value of the electrical utilities product through significant improvements in reliability, voltage control, and frequency control.

Though this is an accomplishment of which to be proud, continued progress demands continued research effort. This work will be done by the utilities, consulting engineers, universities, independent research groups, and the equipment manufacturers. In this paper the electric equipment manufacturers' place in research and development programs of concern to the utility industry will be examined, by describing typical activities in each of the five areas outlined in the foregoing. Since conditions surrounding research and development in the industry are not expected to be appreciably different in the future than at present—if the special situation of atomic energy developments can be considered separately—the pattern of manufacturers, research and development now in progress should be a reliable guide for the future. Since the industry is expected to expand, it can be assumed that the amount of research and development will increase proportionately.

This paper is based on certain funda-

Paper 55-245, recommended by the AIEE Research Committee and approved by the AIEE Committee on Technical Operations for presentation at the AIEE Winter General Meeting, New York, N. Y., January 31–February 4, 1955. Manuscript submitted December 8, 1954; made available for printing March 14, 1955.

E. E. PARKER and J. BAIRD are with the General Electric Company, Schenectady, N. Y.

mental premises. These are as follows:

1. The electric equipment manufacturers are in an excellent position to make substantial contributions in research and development for the utility industry.

2. They have the double motivation of wanting to sell not only the equipment for generating and transmitting power but also the equipment that uses this power.

3. They operate in a competitive climate of the private enterprise system where proof of the worth of research and development work must be demonstrated or the work will be discontinued.

4. A great percentage of all applied research and advance development is applied to physical objects, and the manufacturers of these objects are in an excellent position to understand what work is needed and how best to do it.

5. The electrical manufacturers have reason to be proud of past contributions, although they are aware that these contributions were made possible by encouragement and active co-operation from the electrical utility industry. In many cases the utilities have assumed leadership through specifying equipment with characteristics superior to that in production.

Because of the competitive situation in the manufacture of electric equipment, it can be anticipated that the manufacturers will continue to expand their research and development activities in almost every phase of work applicable to the electrical industry as a whole. This is essential if they are to increase the value of their products and develop new products—a necessity for survival in a competitive economy.

This is not to say that the manufacturers do not welcome research programs sponsored by the utilities. They realize that in view of the ever-expanding horizons of science there is need for much research work which the equipment manufacturers are not in a position to do.

Nor is it the purpose of this paper to say that all areas vital to the growth of the industry are being adequately covered by existing research and development programs. This symposium explores ways in which research of specific interest to the utilities may be accomplished. In this paper the type of work done by the manufacturers in these five areas is discussed, and how much, on the evidence of recent accomplishments, can be expected from the manufacturers in the future.

Herein, research will be considered to mean the quest for new knowledge, new processes, and new materials. It includes basic scientific research with no definite device or application in mind, and applied research in which the feasibility of applying scientific principles for a specific purpose is proved. The term "development" is advanced development engineering including the development of an engineering model of a device.

Basic Scientific Knowledge

Conductors, insulators, and magnetic materials are three basic building blocks for all electric equipment. The nature of their behavior has never been wholly understood. Today in the electrical manufacturing companies' laboratories, there is a large amount of research devoted to obtaining better understanding of the nature of conduction, insulation, and magnetic phenomena.

Probably no utility will ever operate any equipment at 440 degrees Fahrenheit below zero, yet much research work is being done on the phenomena of superconductivity below this temperature. At temperatures near absolute zero, some metals lose all their resistance and refute many commonly held theories of conduction. New knowledge of super-conductivity may give a better understanding of how electricity is conducted at room temperatures and provide new information about the basic structure of matter.

Considerable progress has been made recently in understanding the fundamental nature of insulators and, if history is any guide, this work should eventually provide the basis for the development of better insulating materials. When chemists learn how molecules of various substances affect the characteristics of synthetic dielectrics, they may be able to synthesize improved solid, liquid, and gaseous insulators. A related area of basic electrical research, with broad implications for utilities, pertains to corona phenomena including the effect of corona on insulation. Results now being obtained should provide necessary background for the improvement of many pieces of electric equipment.

Most of the magnetic materials now in use are the result of equipment manufacturers' research and development programs. While these materials are vastly superior to their predecessors, there is still appreciable room for improvement which can only be brought about by continued work in the laboratories of the world. For example, today a much better understanding has been gained of the basic mechanism of ferromagnetism, yet in the manufacture of electrical steels there is incomplete understanding of how magnetic properties are influenced by various factor such as rolling temperature and grain size.

Significant work is being done in the area of the structure of metals. The object is to determine why metals behave as they do, with emphasis on failure under stress. In the study of certain important materials, test samples with small cross sections have, under some conditions, exhibited much higher strength per-unit area than large pieces of the same geometrical pattern. The need for knowledge of this phenomenon increases directly with the demand for larger equipment and higher design stresses. Single-crystal filaments of a large number of different metals and compounds have been grown and submitted to extensive physical tests. In the case of iron, strengths of up to 1,000,000 pounds per square inch have been obtained in single-crystal filaments. While this strength is currently of little engineering value because of the small size of the filaments, it may lead indirectly to the development of new high-strength, high-temperature alloys with vital applications in the utility industry.

Only a few examples of the manufacturers' research programs of direct or indirect benefit to the utilities have been discussed. There is also important research in the development of new light sources, arc phenomena, electron irradiation of materials, semiconduction, and nuclear science—just to name some of the more important.

Power Generation

An area where the contribution of the electrical manufacturers can be readily measured is the development of improved steam-electric generating equipment. A significant portion of the real cost-cutting enjoyed by the consumer of electric power has come about through increased steam-electric generating-plant efficiencies. Fig. 1 shows a plot of the trend of coal consumption per kilowatt-hour for steam-electric generating plants in the United States during the past 50 years. The upper curve shows the average coal consumption rate of all plants while the lower curve shows the coal requirements of the best plant in service in any particular year. These two curves are based on the utilization of coal with the heating value of 12,500 Btu per pound. Continued improvement in steam-electric generating station efficiencies is intimately tied to research in such fields as metallurgy and combustion, and to the development in equipment designs.

In addition to basic research, there is a large amount of work in the fields of material and process development as well as work to extend the knowledge of the engineering sciences, all directed toward improvement of power generation equipment. Examples of this are the search for new materials, for new knowledge of how better to apply available materials, and for improved dynamic, thermodynamic, and mechanical designs. Study of fuel combustion recently has been emphasized in the research and development laboratories of the United States. This may lead to self-pressurized combustion, eliminating induced and forced draft fans as well as reducing boiler sizes. The search continues for new thermal cycles, with increased value to the customer as the goal. Work on the commercial gas turbine falls in this area.

At least a brief comment must be made on the application of atomic energy to the utility industry. This differs from the areas mentioned in the foregoing in that the major research expenditures are being made by the Federal Government, and the magnitude of these expenditures is so very large that atomic research by manufacturing companies would be small in comparison. Governmental restrictions, while necessary, have also limited freedom of effort in this area. Despite this fact, the electrical manufacturing companies are attempting to stay abreast of the field and to create a pool of trained manpower through two approaches: conducting government-sponsored atomic energy research, and expending their own funds to solve specific atomic energy problems.

Transmission and Distribution

Two foundations upon which the modern utility system has been built are: economical and reliable transmission of power over appreciable distances at a reasonable cost, and economical systems for local distribution. The electrical manufacturers have devoted, and will continue to devote, much time and money to research and development in this area. In the past, this work has resulted in improved insulators, new understanding of corona phenomena and arc phenomena, and fundamental knowledge of power transmission and distribution system problems. Typical developments have provided high-speed and high-capacity circuit breakers, lightning-arrester improvement, and transformer designs combining greater reliability with less cost, weight, and volume.

The equipment manufacturers' laboratories for development of transmission and distribution equipment are unparalleled. They include high-voltage generators capable of producing simulated lightning strokes, high-current surge generators for studying the effect of lightning currents on transmission line equipment, short-circuit current generators for studying switchgear performance, high-capacity testing transformers, facilities for transformer noise studies, and equipment for development and testing of new materials.

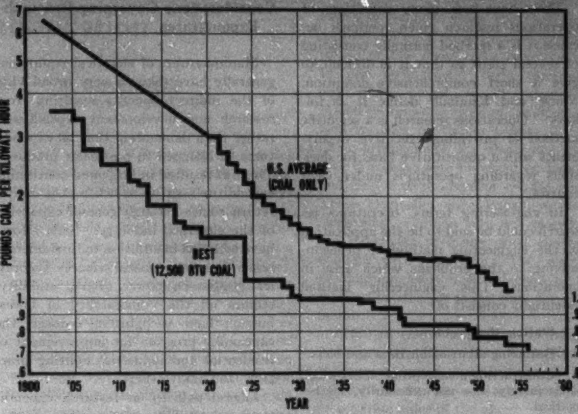

Fig. 1. United States steam-electric generating station coal rate

Much remains to be done in the study of transmission and distribution. Examples are investigations of radio noise suppression and the development and application of improved dielectrics, magnetic materials, and economical designs for higher capacity circuit breakers that will almost certainly be required in future system interconnections. The development of a computer for remote reading and automatic billing of all types of utility meters offers an engineering challenge. However, it appears doubtful that the present general pattern of transmission and distribution will be upset, although possible extension of underground systems making use of improved dielectrics and cable construction must not be overlooked.

System Analysis

System analysis, or system planning as it is frequently termed, is an area where the electrical manufacturers may be of help to the utilities, but where responsibility inherently rests with the utilities. Utility effort in this area, on the part of their own engineering staffs or through the services of consulting engineering firms, is advantageous to manufacturers since such studies normally point the need for the development of improved system equipment.

Even though basic direction for system analysis must come from the utilities, the engineering staffs of the equipment manufacturers are able to make appreciable contributions because of their specialized experience and facilities. For the utility to obtain maximum advantage from such service by the equipment manufacturers, it must maintain a competent staff capable of understanding and contributing to the solution of system analysis problems.

While most utilities individually support system analysis operations, co-operative research and development among groups of utilities has been evident. This is being done to some extent at present for regional planning, in the use of network analyzers, and in the solution of other operating problems of mutual interest such as the economics of high-voltage transmission interconnections.

The complexity of the technical and techno-economic problems, many of which have political overtones, is constantly increasing. There has been a new tool, or perhaps it is more accurate to say concept, developed immediately prior to and during World War II which holds much promise to improve the effectiveness of managers by applying a systematic approach to management problems. Thus the manager may base his decision and action on facts developed through a systematic method rather than on personal experience. It is essentially the application of engineering techniques to the problems of management. This method has become known as operation-research.

There have been many definitions of operations research given, perhaps because it is a method normally consisting of several steps so that it is difficult to give a short comprehensive definition. Morse and Kimball[3] define it as follows: "Operations research is a scientific method of providing executive departments with a quantitative basis for decisions regarding operations under their control."

In engineering terms, operations research could be said to be the application of the engineering method of problem-solving to the problems which arise in operations. This engineering method essentially consists of:

1. Stating the problem.
2. Gathering all available data and facts.
3. Constructing a conceptual model which is frequently, but not necessarily, mathematical.
4. Where pertinent, solving the mathematics and applying of boundary conditions to obtain a relationship of variables.
5. Interpreting results in view of completeness of data and simplifying assumptions.

Many of the methods of operations research already are being used by the utility industry.[4] These methods unlock a great storehouse of human knowledge which may be successfully applied to situations that up to the present time have been considered too chaotic, complex, or uncertain for any but intuitive solutions based on personal experience.[5]

Power Utilization

The very rapid increase in power consumption has been a major factor in the lower cost of electric power. For example, increased demand for power and the interconnection of power systems have permitted the installation of larger generating units with higher efficiency and lower labor and maintenance costs.

Both the wider use of existing devices and the development of new devices which depend upon electricity for power have contributed to the load growth. Devices that are important new load builders include air conditioners, television, household clothes driers, and the heat pump. In the industrial and commercial area, many developments such as new light sources and lighting techniques and new electric equipment for use in electrometallurgical and electrochemical processes contribute to power demands. Many of these devices have been the product of manufacturers' research and development efforts, thus serving the interest of both manufacturer and utility.

Considerations Governing Research Expenditures

Manufacturers of electrical equipment generally have taken a very broad view of the indirect benefits resulting from research and development expenditures rather than demanding that all expenditures be assigned to particular products. This has resulted in large and continuing expenditures in areas where the major return comes through general expansion of the electrical industry. Such efforts have included in addition to fundamental research in the physical sciences, theoretical studies on power system stability, studies on the vulnerability of transmission lines to lightning damage, the continuing program for improvement of residential and industrial lighting practices, and many others.

Liberal policies on research expenditures permit better integration of programs and allow the inclusion of work which could not otherwise be done. For example, work on improved dielectrics is supported by continuing studies on the theory of dielectrics and on corona effects in dielectrics. However, the liberal policies place an increased burden on the judgment of the personnel directing the work.

From the manufacturers' viewpoint there appear to be many areas where research and development expenditures by the utilities would be more fruitful than in direct equipment development programs of the type carried on by the electrical manufacturers. One of the many examples of utility research was the study of steam-boiler water treatment, a program that effectively augmented the work in boiler and turbine design conducted by the manufacturers. In addition to this type of research, closely correlated with manufacturers' efforts, there will continue to be many system problems in connection with the expansion of the country's power requirements. Solution of system problems will be directly dependent on research and development programs conducted by the utilities.

Looking Ahead

Research and development programs may be divided into two general classifications: an evolutionary area, and an area where new concepts alter the basic way in which a particular task is accomplished. This latter could be thought of as a revolutionary area. The evolutionary category might include all improvements in existing classes of equipment even though some of these might involve revolutionary concepts applied to the improvement of an old idea or device such as the magnetic floating of watt-hour meter rotors.

It is much more difficult to estimate or even guess what revolutionary progress will be made in the electrical utility field. There is no difficulty at all in making up a long list of revolutionary ideas; however, it is not easy to evaluate which of these ideas may ultimately lead to a practical commercial development. In the category of things that may be done but which do not look promising for the near future—either because of the state of the art, inherent limitations, or the economic environment—are such items as solar energy converters for the production of commercial blocks of power, electronic refrigeration systems, household atomic power systems, and the use by utilities of fuel cells, i.e., devices for the direct conversion of chemical to electric energy. Undoubtedly the most promising revolutionary development at the present time is the generation of electric power from atomic energy. This is a problem requiring a great deal of research and development, but there seems to be very little doubt about either the ultimate outcome or the economic justification.

Co-operation between equipment manufacturers and the utilities has brought the electrical industry to a position where it can look toward the future with unrivaled optimism. It is fortunate that this co-operation extends to the fundamental levels of research and development. It is safe to predict that the electric equipment manufacturers will continue to allocate millions of dollars per year to research and development in areas of vital interest to the utility companies. This will be done in the competitive climate of the private enterprise system where the need for demonstrating the worth of accomplishments is an effective control to assure maximum results from research expenditures.

References

1. ELECTRICAL UTILITY INDUSTRY IN THE UNITED STATES, STATISTICAL BULLETIN FOR THE YEAR 1953. Edison Electric Institute, New York, N. Y., table LIV, 1954, p. 620.

2. *Monthly Labor Review*, U. S. Department of Labor, Washington, D. C. Sept., 1954, p. 1,071.

3. METHODS OF OPERATIONS RESEARCH, P. M. Morse, G. E. Kimbal. J. Wiley and Sons, Inc., New York, N. Y., 1950.

4. THE INTEGRATED POWER SYSTEM AS THE BASIC MECHANISM FOR POWER SUPPLY, Phillip Sporn. McGraw-Hill Book Company, Inc., New York, N. Y., 1950.

5. OBSERVATIONS ON OPERATIONS RESEARCH, M. L. Hurni. *Journal*, Operations Research Society of America, Baltimore, Md., Aug., 1954, pp. 234–48.

Electric Defibrillation

W. B. KOUWENHOVEN
FELLOW AIEE

W. R. MILNOR
NONMEMBER AIEE

APPROXIMATELY 100 electric utility employees die each year as a result of accidental contacts with electric circuits. For years manual artificial respiration has been the only accepted first-aid method for victims rendered unconscious by an electric shock. Analysis of the accident statistics, however, shows that approximately a third of the shock victims who receive artificial respiration with the promptness that should give promise of success, fail to recover. There is good reason to believe that many of these failures are due to the effects of electric currents on the heart.

It has been clearly demonstrated that the heart is susceptible to electric currents. The passage of a small electric current through the heart may destroy its rhythm and throw it into a twitching state called ventricular fibrillation. In this state the circulation of the blood ceases and unless the heart action is promptly restored, death ensues. Ventricular fibrillation not only occurs in the electric-shock field, but also in surgical cases. The only known method of successfully arresting ventricular fibrillation is to send sufficient electric current through the heart to stop the twitching of the muscles. Prevost and Batteli[1] reported in 1899 that they had been successful in arresting fibrillation in the dog's heart by sending either a capacitor discharge or an alternating current through the heart. In their work they opened the chest and place the electrodes directly on the surface of the heart.

The a-c method was studied by Kouwenhoven and Hooker[2] who reported their success with the method and developed apparatus[3] for use in hospitals. With this apparatus a 60-cycle alternating current of 1.5 to 2 amperes, at 120 to 130 volts, is sent through the heart by means of electrodes placed directly on opposite sides of the heart, which must be exposed by surgery. The lives of many patients, whose hearts go into fibrillation during surgery, have been saved. Beck[4] reported in 1947 the first successful defibrillation of the human heart, with the complete recovery of the patient.

In hospitals, the alternating resuscitating current is sent through the exposed heart either in a single application of 1/4 to 1/2 second duration or in a series of five or six short pulses, each approximately 1/10 second in length. The latter method is known as serial defibrillation.

In the field it is not feasible to open the chest and place the electrodes directly on the heart. Therefore, in a field defibrillating method, the electric current must be sent through the heart by electrodes properly placed on the surface (skin) of the chest. In addition, the field method must be one that may be safely applied to a normal beating heart as the presence of fibrillation can only be detected by an electrocardiograph. Among the first to study the defibrillation problem in animals without the opening of the chest were Ferris and Williams.[5] They used sheep as the experimental animals and were successful in defibrillating the sheep's heart by sending approximately 25 amperes at 3,000 volts through the animal by means of electrodes fastened on opposite sides of the chest.

The Research

Because of the importance of this problem in the electric utility field the Edison Electric Institute in 1951 provided funds for a study of the possibility of the development of a method of recovering the fibrillating human heart which would make it unnecessary to open the chest, a method which would be safe to apply in the field as well as in the hospital, and the development of defibrillating equipment which would function in either environment. This study has been carried out at The Johns Hopkins University, and is one in which its schools of engineering and medicine, and its hospital, co-operated.

Experimental Procedure

In this study dogs weighing from 8 to 20 kilograms were used as the experimental animals. All of the animals were anesthetized with morphine and ether. A tube was inserted in the trachea and positive pressure artificial respiration using ether and air was administered. During the periods that the heart was in fibrillation, the ether was cut off, so that the condition would be similar to normal artificial respiration.

When the animal was anesthetized, the hair was removed from the chest with clippers. Two arrangements of the electrodes on the chest have been studied. In one arrangement chest electrodes, each 4 by 6 inches, of soft copper were placed on opposite sides of the chest and held in place by rubber bands. In the other arrangement the electrodes, each 5 by 5 inches, were mounted on handles and held by the operator on the chest. These electrodes were known as hand electrodes. Cardiac jelly was placed on the electrodes to insure good electrical contact with the skin. The electrocardiograph leads were attached to the four extremities for monitoring the heart action.

After an electrocardiogram of normal heart action had been taken, the heart was thrown into ventricular fibrillation by the application of a 120-volt a-c shock applied to opposite sides of the chest. The condition of the heart was checked with the cardiograph. When the heart had been left in fibrillation for the desired length of time, the resuscitating current was sent through the heart by means of electrodes on the surface of the chest. Following this an electrocardiogram was taken to determine the effect on the heart of the defibrillating current.

Results

In this section the characteristics of the heart during fibrillation are treated first. This is followed by reports of successes and failure and the hazard involved in the use of a capacitor discharge, in the use of a series of short a-c pulses (serial defibrillation) and in the use of a single long pulse of alternating current.

Fibrillation Characteristics

If the chest is open and the heart visible, the duration of the fibrillation can be estimated, to some extent, from the appearance of the heart. During the first minute the fibrillation is characterized by a vigorous fine twitching. The heart has a good tone, is of pinkish color, and only slightly or not at all dilated. At the end of the second minute the fibrillation vigor

---

Paper 55-95, recommended by the AIEE Safety Committee and approved by the AIEE Committee on Technical Operations for presentation at the AIEE Winter General Meeting, New York, N.Y., January 31–February 4, 1955. Manuscript submitted October 19, 1954; made available for printing November 18, 1954.

W. B. Kouwenhoven and W. R. Milnor are with The Johns Hopkins University, Baltimore, Md.

The authors wish to acknowledge the generosity of the Edison Electric Institute in providing funds for carrying out this investigation. The valued assistance rendered by L. Ferris, W. R. Smith, and Dr. H. B. Williams is appreciated.

is noticeably diminished, the twitching is less rapid and coarser, and the heart is rather flabby. At the end of the third minute, the twitching is slower, coarser and undulatory. The heart is cyanotic, dark in color, and definitely dilated. If fibrillation is arrested at the end of the third minute, the heart muscles may be so weakened by anoxia that it is incapable on its own of beats powerful enough to circulate the blood. It is doubtful that unless the circulation is restored in 4 minutes, there is much chance of life.

In the operating room with the chest open, the hand may be inserted into the chest cavity and the heart squeezed or massaged so as to produce effective circulation of the blood. It is possible, by means of massage, to restore an enfeebled heart to normal vigor. In fact, the circulation of oxygenated blood has been maintained in a living human being for over an hour by heart massage. Then, when the hospital defibrillating equipment became available, the fibrillation was arrested by alternating current. The patient recovered and was later discharged from the hospital with all of his faculties.

In the field it is not possible to massage the heart, but it is possible to bring the twitching ventricles to rest by the passage of alternating current through the chest even though fibrillation has continued for 3 or more minutes. In such cases it may be possible to drive the heart by the application of small electric impulses[6] to the surface of the chest, and thus aid the weakened organ in re-establishing the circulation of the blood.

Capacitor Discharge

The use of a capacitor discharge for defibrillating the heart is an intriguing one, because of the wide use of portable capacitor discharge apparatus in the flashlight photographic field. There is, however, little information in the literature on the effects of capacitor discharges on the heart.[7] Therefore, a series of experiments was first made on animals with the chest open and the heart exposed. In another series of experiments tests were made with the electrodes on the surface of the intact chest.

OPEN CHEST

A total of 135 experiments were made on the exposed heart in which it was allowed to remain in fibrillation without massage for a period of about 30 seconds. The capacitors ranged in size from 4 to 45 microfarads and the charging voltages from 150 to 1,000 volts. It was found that if the charging voltage was 600 or more volts and the energy stored in the capacitor was at least 5-watt-seconds that the discharge was effective in stopping the fibrillation, and the heart would resume normal beating. These results agree with those of Mackay and Leeds.[8]

Capacitor discharges of 5 to 12 watt-seconds at 600 or more volts were sent through the exposed heart in 57 experiments, in which the heart was allowed to remain in fibrillation, without massage, for a period of 1 to 3 minutes. In these tests there were 32 successful recoveries and 25 failures.

CLOSED CHEST

With the information obtained from the experiments on the exposed heart, experiments were carried out on dogs with the 4 by 6-inch electrodes on opposite sides of the unopened chest. Capacitors of 50, 75, 100, 175, 225, and 1,250 microfarads, charged to voltages of from 4,000 to 450 volts, were discharged through the chests of 35 dogs whose hearts had been in fibrillation from 20 to 60 seconds. There were 13 successful resuscitations and 22 failures. It was found that if the heart had been left in fibrillation for more than 25 seconds the chances of a successful recovery were very slight.

HAZARD CAPACITOR DISCHARGES

In addition, it was found that discharges of this magnitude might result in either cardiac standstill or ventricular fibrillation, when sent through the intact chests of animals whose hearts were beating normally.

CAPACITOR FAILURES

Whenever a capacitor discharge failed to arrest ventricular fibrillation, recourse was had to alternating current. It was found that in many instances, the fibrillation could be arrested by a resuscitating current from the 60-cycle supply lines, even when two or more successive capacitor discharges had failed. Therefore, our attention became focused on the use of alternating current for defibrillation. This does not mean that the capacitor discharge method has been completely abandoned. At intervals, capacitor discharges of various circuit parameters are tried to determine their effectiveness. To date, this phase of the work has not produced any encouraging data.

There are, however, an infinite number of capacitor discharges available and, in addition, there are combinations of capacitors with inductance, that may be effective. It has not been possible to investigate all of these parameters, and there is a possibility that there exists some unique combination that may prove effective. All new suggestions and ideas are being investigated.

Serial Defibrillation

All of the serial defibrillation experiments were made with the electrodes on the closed chest. In the initial tests, alternating currents of 8 to 10 amperes were sent through the chest, in a series of pulses, each of approximately 6 cycles' duration. They were applied by hand, at the rate of one pulse per second. These were effective in arresting the fibrillation, and special electronic equipment was constructed for applying the pulses of a fixed duration at an accurately controlled rate.

HAZARD SERIAL DEFIBRILLATION

The serial defibrillating current was applied to eight dogs whose hearts were beating normally. Results were surprising. In six of these cases, the application of serial defibrillation threw the dogs' hearts into fibrillation. The further study and use of serial defibrillation was therefore abandoned, because the hazard it offered to the normal heart.

A-C Defibrillation

In this method the defibrillating current was sent through the chest of the animal in a single continuous application lasting about 1 second. The current was sent through the chest in either the transverse direction, that is from the right side to the left side, or in the longitudinal, or head-to-foot, direction. Electrodes of soft copper, each 4 by 6 inches in size, were fastened to the sides of the chest by rubber bands for the transverse direction. A pair of 5-inch by 5-inch soft copper electrodes mounted on handles, and known as hand electrodes, as shown in Fig. 1 were used for the longitudinal current path. One hand electrode was placed on the upper end of the breastbone at the neck and the other hand electrode on the stomach pressing upward against the diaphragm.

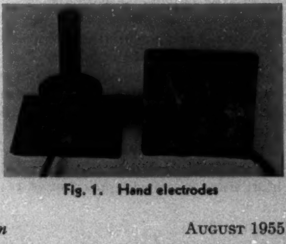

Fig. 1. Hand electrodes

CHEST ELECTRODES

The passage of a 60-cycle current of 8 to 12 amperes at 480 volts was found to be a good method of arresting fibrillation. In all, 107 experiments were made on dogs using this method. The hearts of these dogs were allowed to remain in fibrillation for various lengths of time. Artificial respiration using air was maintained during the period of fibrillation and the anesthesia was not turned on again until the heart had resumed beating and the pulse could be detected. The results of the 107 experiments are given in Table I. This table shows the duration of fibrillation before the resuscitating current was sent through the chest, the number of dogs tested, the number of cases in which fibrillation was stopped, and the number of dogs that recovered completely and were returned to their cages alive. The fibrillation was stopped by the alternating current in 68 per cent of the experiments. If the resuscitating current is sent through the animal within 1¹/₄ minutes after the fibrillating shock, the chance of a successful recovery is a 50-50 one. If it takes 2 minutes to apply the current, the chance of success is very slight.

Table I. Resuscitated Alternating Current, Transverse Direction

Chest Electrodes, Each 4 by 6 Inches, on Opposite Sides of the Chest

Duration of Fibrillation, Seconds	No. of Dogs				Percentage	
	Total	Fibrillation Stopped	Lived	Heart Beat	De-fibrillated	Lived
30	12	10	9	9	83	75
45	11	10	9	9	91	82
60	37	26	16	16	70	43
75	11	6	3	3	55	27
90	11	6	3	3	55	37
105	4	2	1	1	50	25
120	10	5	0	0	50	0
150	8	5	0	0	63	0
180	3	2	1	1	67	33

In cases where the resuscitating current stopped the fibrillation, but effective beats failed to follow, it is believed that the application of small stimulating electric currents to the surface of the chest may aid a weak heart to re-establish the circulation.

A-C HAZARD CHEST ELECTRODES

The hazard involved, in the use of a single continuous pulse of 60-a-c resuscitating current of 8 to 12 amperes was studied by applying it to 43 dogs whose hearts were functioning normally. In no instance was there any injury, and a number of the animals were kept for from one week to two months before being used in subsequent experiments. Autopsies showed no gross evidence of any trauma. The temperature rise in the heart was less than 1 degree Fahrenheit and, under the skin at the center of the electrodes 11 to 12 degrees Fahrenheit.

On the basis of 43 successful experiments, one cannot state that the method is absolutely safe to apply to a man whose heart is beating normally. The chance of its causing accidental death are, however, less than one in 1,000.

HAND ELECTRODES

The hand electrodes were not attached to the animal. The operator, wearing rubber lineman's gloves, held the electrodes, which were smeared with cardiac jelly, on the skin of the animal. One electrode was pressed against the upper end of the breastbone at the neck and the other just below the floating ribs was pressed upward against the diaphragm. Both electrodes were held either on the mid-line or very slightly to the left of it.

To date 58 tests have been made with the hand electrodes. In only four of these did the resuscitating current fail to bring the twitching heart muscles to rest. The resuscitating current values have ranged from 4 to 6.25 amperes at 450 to 500 volts, 60 cycles. If the heart has been in fibrillation for 1 minute, the length of time that the resuscitating current was applied was about 1 second; for 2 minutes of fibrillation, approximately 2 seconds.

The results obtained with the hand electrodes are given in Table II. With these electrodes, the fibrillation was stopped in 93 per cent of the experiments. Eight of these dogs, however, lived for only a few minutes after the heart had started to beat again. Perhaps these could have been saved, had there been equipment available for driving the heart. The same observation applies to other dogs, whose hearts were at standstill following the application of the defibrillating current.

Table II. Resuscitating Alternating Current, Longitudinal Direction

Hand Electrodes, Each 5 by 5 Inches, One on Breastbone at Neck and the Other on Stomach Pressing up Against Diaphragm

Duration of Fibrillation, Seconds	No. of Dogs				Percentage	
	Total	Fibrillation Stopped	Lived	Heart Beat	De-fibrillated	Lived
30	5	5	5	5	100	100
60	14	14	13	14*	100	93
75	6	4	1	1	67	17
90	24	21	7	14†	87	29
101	1	1	1	1	100	100
120	7	7	1	2‡	100	14
180	1	1	0	0	100	0

* One animal's heart beat for about 5 minutes. Its heart however, was too weak to re-establish and maintain the circulation of the blood.
† Seven animals lived for several minutes.
‡ One animal lived for about 5 minutes.

HAZARD HAND ELECTRODES

The resuscitating current has been sent through the bodies of eight normal dogs for periods from 1 to 2 seconds without causing any injury. In addition, a number of dogs, which had been used in several successive experiments, have been autopsied, and no evidence of gross trauma has been found.

Promptness

The question naturally arises: "How soon must the resuscitating current be current be applied if it is to be effective?" The answer is: "The sooner, the better." At 1 minute the chance of success is nine out of ten; at 1¹/₂ minutes one out of three; and at 2 minutes, only one out of seven. These chances may be bettered if the heart can be effectively driven by an artificial pacemaker. Promptness in getting to the shock victim is just as important here, if not more so, than it is in starting artificial respiration.

Time is important to the human brain, which is a delicate mechanism. If it does not receive oxygenated blood for a period of 5 minutes, it may deteriorate to such an extent that should the shock victim be successfully resuscitated, he will live on as a mentally deficient individual. Therefore, promptness in heart resuscitation is essential.

Summary

This paper may be summarized as follows:

1. The capacitor discharge method of stopping fibrillation was found to be unsatisfactory because of its ineffectiveness after the heart has been in fibrillation for more than 30 seconds.

2. The serial defibrillation method using pulses of alternating current was found to be dangerous to normal hearts.

3. The best method found for defibrillating the ventricles was a single application of 60-cycle alternating current lasting approximately 1 second.

4. The most effective direction of flow through the chest of the defibrillating a-c current is the longitudinal, head-to-foot direction.

References

1. Sur Quelques Éffects des Décharges Électriques sur le Coeur des Mammiferes, **J. L. Prevost, E. Batteli.** *Comptes Rendus*, Academie des Sciences, Paris, France, vol. 129, 1899, p. 1267.

2. The Effects of Alternating Currents on the Heart, **D. R. Hooker, W. B. Kouwenhoven, O. R. Langworthy.** *American Journal of Physiology*, Washington, D. C., vol. 103, 1933, p. 444.

3. A Simple Electrical Apparatus for the Clinical Treatment of Ventricular Fibrillation, **W. B. Kouwenhoven, J. H. Kay.** *Surgery*, St. Louis, Mo., vol. 30, no. 5, Nov. 1951, p. 781.

4. Ventricular Fibrillation of Long Duration Abolished by Electric Shock, **C. S. Beck, W. H. Pritchard, H. S. Feil.** *Journal*, American Medical Association, Chicago, Ill., vol. 135, 1947, p. 985.

5. Effect of Electric Shock on the Heart, **L. P. Ferris, B. G. King, P. W. Spence, H. B. Williams.** *AIEE Transactions (Electrical Engineering)*, vol. 55, May 1936, pp. 498-515.

6. Resuscitation of the Heart in Ventricular Standstill by External Electric Stimulation, **P. M. Zoll.** *New England Medical Journal*, vol. 247, 1932, p. 766.

7. Restoration of Heart Rhythm in the Mammalian Fibrillating Heart, **N. L. Gurvich, G. S. Yuniev.** *American Review of Soviet Medicine*, New York, N. Y., vol. 4, 1947, p. 252.

8. Physiological Effects of Condenser Discharges, **R. S. Mackay, S. E. Leeds.** *Journal of Applied Physiology*, Washington, D. C., vol. 6, 1953, p. 67.

◆

Discussion

G. R. Radley (Cutler-Hammer, Inc., Milwaukee, Wis.): For years I have been anxiously awaiting this report which tells how apparatus can be constructed which has a good chance of saving the life of a victim of accidental electrocution in which the circuit conditions were such that fibrillation of the heart resulted in death in spite of prompt application of even the more efficient back pressure-arm lift method of resuscitation.

At the experimental laboratory where I am employed, there are about 50 engineers. Each year new college graduates arrive who cannot immediately learn how to handle the hazards inherent in working with voltages up to 15 kv. Four persons in the last few years have met their deaths in Milwaukee from only a few seconds' contact (hand to hand) with 440 volts, even though the Schafer method of artificial respiration was begun within 2 minutes.

I propose the design shown in Fig. 2 for use in electrical laboratories. That the very minimum of time be lost in applying electrodes, two 5-inch by 5-inch plates should be attached at the two ends of a spring steel strip shaped like the capital letter J. With this design only the necktie need be removed and the shirt and undershirt unbuttoned or ripped open. With the patient lying on his back the short end of the J is hooked over his left shoulder, the long end lying against the body with the lower 5 by 5 plate contacting the abdomen ject below the lower ribs. He is then rolled over to his face in which position the lower electrode is firmly pressed against the abdomen by his body weight while the upper electrode is pressed against the back of the shoulder close to the neck and held by the spring pressure. In this position, the back pressure-arm lift method can be begun and continued with only a momentary interruption while the countershock is being applied. A hurried test for pulse is made by an assistant pressing a finger against the side of the Adam's apple, reaching in between the arms of the man who is applying the resuscitation. If no pulse can be detected, another countershock must be given. Some cases have required 10 countershocks. One life was saved after 23 shocks. Especially where several shocks are required it is necessary to maintain the resuscitation, for revival cannot be accomplished without oxygenated blood.

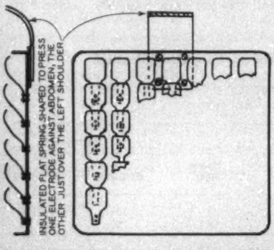
INSULATED FLAT SPRING SHAPED TO PRESS ONE ELECTRODE AGAINST ABDOMEN, THE OTHER JUST OVER THE LEFT SHOULDER

Fig. 2. Principle of yielding surface electrode for applying defibrillating current to exterior of human body. Electrodes to be covered with cloth sacks and kept inside boxes partly filled with cardiac jelly so as to be ready for instant use at all times

To obtain as large an area of contact as possible with the far from level shoulder and abdominal surfaces, I propose to cover the 5-inch by 5-inch metal electrode plates with about 50 flat springs whose upper broad ends are cylindrically curved so as to make contact through a range in position of at least 1/2 inch. These springs are made of a material, or plated with a material not affected by the cardiac jelly which lines a box pressed over the spring-covered side of the electrode while standing by for use at an unknown date.

In a laboratory it is easy to provide a circuit which shall be constantly alive with a capacity adequate for the step-up transformer which is to supply 5 amperes at 500 volts. Since the primary will require about 10 amperes at 240 volts, the control should be by means of a *DP* contactor with a 120-volt coil, operated by a timer which can be set for any value of time from 1/10 to 2 seconds' application of the defibrillating current.

Any further information relative to the construction of countershock equipment will be appreciated by the writer.

Charles F. Dalziel (University of California, Berkeley, Calif.): This paper is destined to be a bench mark in countershock resuscitation for human victims of electric shock accidents. Although the paper is largely confined to a presentation of experimental results obtained on dogs, it is evident that the authors consider that practical application to human beings is in the immediate offing. It is therefore desirable that the paper lay a proper foundation for both electrical techniques and legal technicalities.

It is only natural to anticipate that application of defibrillating shocks to human victims by laymen in the field will be both successful and unsuccessful. In the unfortunate event of failure the question is sure to be asked: "Which shock—the accidental shock or the defibrillating shock—was the responsible cause of death?" The authors' statement to the effect that with chest electrodes employing a single continuous pulse of 60-cycle a-c resuscitation current the chance of causing accidental death is less than one in 1,000 may be questioned on the basis of the experimental evidence contained in the paper. Elaboration of this conclusion might be exceedingly valuable.

The minimum shock likely to cause ventricular fibrillation is of great importance to the American Standards Association Sectional Committee on Electric Fences. Attempts are currently under way to develop satisfactory criteria for specifying the maximum allowable output from electric fence controllers. Publication of minium observed values of energy, current, voltage, and shock duration just producing ventricular fibrillation for both 60-cycle a-c and for capacitor discharges with electrodes placed on the surface of the body with the chest closed would be greatly appreciated by all of us working on this problem.

It is generally felt that translation of results obtained on animals to human beings is at most conjectural, and it would be enlightening for the authors to discuss this phase of the problem with special regard to closed-chest conditions. In the past it has been generally believed that the shock intensity required to stimulate the heart is roughly proportional to both body weight and heart weight. On this basis it would seem that the defibrillating current for man might be two to three times the values reported. Such currents might be destructive to tissues, and the corresponding voltages hazardous to the operator. On the other hand, even if no adjustment for weight is made, it would appear that the fibrillating threshold values (obtained from conversation and correspondence with the senior author) are so much in excess of the output from commercial intermittent electric fence controllers that the hazard from a single shock from these devices would appear to be entirely negligible. This leads to the possible argument that a material increase in the allowable output would be justified to increase the effectiveness of these devices, and that safety can be virtually assured by simply increasing the off period between successive shocks so as to reduce to the vanishing point the probability of a 2-year-old child ever being subjected to what the authors term serial shocks.

The authors are to be complimented on their persistence and time-consuming efforts to find the best possible solution to this most difficult and important problem. Undoubtedly counter electric shock is the most promising development in resuscitation for victims of electric shock accidents since the development of methods of artificial respiration.

Livingston P. Ferris (Ashton Plantation, Lecompte, La.): After a lapse of some years, it is good to have further experimental data concerning the effects of electric shock upon the heart, particularly its benign effect in reviving the heart from ventricular fibrillation arising from accidental electric shocks and, in rare instances, during surgery.

As a member some years ago of the Safety Committee, I urged renewed research along these lines as the only hope for substantial improvement in our record of resuscitation from accidental electric shocks. The author would agree, I believe, that these urgings had some influence on the initiation of the investigations reported on today. Therefore, it is with regret that I am not present to participate personally in this discussion.

With reference to the experiments on sheep mentioned in the author's fifth paragraph, the 3,000 volts was open-circuit before connection to the animal. Our power supply was heavily overloaded and regulation very poor, so the voltage across the animal dropped to about 900. This voltage is of interest only in estimating power supply requirements. Current alone is the significant measure of the shock. Fig. 17 of reference 5 of the paper gives a complete oscillographic record of a typical defibrillation test including before and after cardiograms, shock, currents, and voltages.

The Kouwenhoven-Milnor tests were all carried out on dogs weighing from 8 to 20 kilograms. Our tests were made on seven species of animals ranging in weight from about 1 to 100 kilograms. Our objective was to determine the relation of threshold fibrillating (not defibrillating) current to body weight and heart weight and to embrace the body weight of man. Figs. 4 and 5 (see reference 5 of the paper) show the results. A more than two-to-one difference in fibrillating current for sheep and dogs is indicated. We did not study the effect of body weight of different species on defibrillating current because our study was primarily directed at determining danger limits of current, and we could not carry the study of defibrillation nearly as far as desired. In the absence of contrary experimental evidence it would seem reasonable to expect that defibrillating as well as fibrillating current would depend to some extent upon body weight of the species of animal. The main point I wish to make on the authors' paper is that their defibrillating current for dogs should not be assumed optimum for man, and that further animal experimentation should be carried out to determine the effect of body weight. Before settling upon a value of current for reliable defibrillation of the human heart, further tests are in order on animals as large as sheep. While our study proved that 25 amperes of 60-cycle current for 1/10 second was effective for defibrillating the sheep heart, I hope that the optimum current will be less, perhaps much less. It is important to find out, and there is no way but by experiment.

Further tests should also explore the effect of duration of the defibrillating shock. There is certainly no advantage in prolonging the defibrillating shock more than necessary. I have been of the opinion that defibrillation required only the arresting of all muscular activity in the heart for some minimum time by a current sufficiently strong to overpower the disorganized forces acting on the individual fibers, then their simultaneous release to resume their natural tendency for co-ordinated action. If this be a true picture, it is a threshold current we must exceed for reliable defibrillation, rather than the prolongation or repetition of shock. The defibrillating shocks used and proposed by the authors seem much too long. If there is evidence that a lower current of longer duration can accomplish what a high short-duration shock does, the longer duration may be preferred because of the reduced power requirements. I do not see such evidence in the present paper.

The authors report increasing the duration of the defibrillating pulse with the duration of the preceding fibrillation, 1 second of pulse per minute of fibrillation. What evidence is there that increased duration of fibrillation requires a longer defibrillating pulse? Dr. King, one of my associates in the Columbia-Bell Laboratories studies, advises that he sees no physiological basis for such a relationship.

In further studies to determine the optimum characteristics of a defibrillating shock for man I should like to see the frequency of the current included, though I regard this as less important than other factors. But should we have to build special generators for field administration of defibrillating shocks, we might as well build them for the optimum frequency, if there is a substantial advantage to be gained over the common standard of 60 cycles.

The authors did not obtain encouraging results with capacitor discharges. There are so many circuit parameters that perhaps the right ones have been missed. The advantage of the capacitor discharge method, allowing the required energy to be stored slowly from low-powered circuits and discharged rapidly, may be great enough to warrant more thorough investigation before final discard. In view of the discouraging results thus far obtained, it seems desirable to pursue first the a-c method to its optimum characteristics. If the a-c power requirements turn out to be much lower than expected, then this method may be preferred for simplicity over the capacitor discharge method.

The authors report tests on what they term "serial defibrillation," a series of five or six short shocks of about 1/10 second duration occurring at intervals of about 1 second. They do not recommend it but report some hospitals using this method. I can see no reason for or advantage of "serial defibrillation" over a single pulse which may be repeated if observation shows failure. In principle, serial defibrillation seems analogous to interrupting artificial respiration to give the lungs a rest. Should one of the early pulses succeed in stopping the fibrillation, there would be some danger that later pulses would start it again. Furthermore, if we consider the use of defibrillation equipment in the accident field without the precaution of a cardiographic check, then repetition of the pulses would increase the danger of causing fibrillation when it did not preexist. This is due to the mathematical increases in probability that one of the series of pulses will strike in the sensitive T-wave (partial refractory) phase of the cardiac cycle. In this connection reference should be made to Figs. 13 and 15 of reference 5 of the paper. I believe this explains the danger reported by the authors of "serial defibrillation" shock applied to normal hearts.

The improbability of a random short shock of 1/18 second or less occurring during the short sensitive phase of the heart cycle is an important reason for trying to limit the defibrillating shock to as short a duration as possible. This is particularly true for accident cases in the field where electrocardiographic checks of heart condition seem extremely difficult. This advantage combined with the decrease in liability of fibrillation with high currents might warrant consideration of countershocks being given by well-trained personnel without check of heart by cardiograph. However, the danger of setting a normal heart in fibrillation should first be more thoroughly studied by further tests, once the optimum defibrillating shock is found.

In operating-room use of defibrillating apparatus, the misapplication of defibrillating shocks to a normally beating heart should present no problem. The subject is in expert hands, under constant observation and it should not be too difficult to add an electrocardiograph to normal equipment. Defibrillating equipment could be built-in or portable. It should be provided with safety switches and signals for protection of patient and operating personnel, and sparkproof for prevention of explosions.

When nearly 20 years ago we cautiously suggested the use of countershock apparatus in accident cases with the precaution of electrocardiographic checks on the heart, I remember the rather emphatic opposition of some resuscitation experts. This may have set back necessary studies many years. Fortunately, studies are under way again. There is much still to be investigated and I hope the fundamental studies will be continued until safe, reliable defibrillating equipment and practices are available for field cases and operating rooms. With continued close co-operation between the medical and engineering professions, I am confident that this objective can be attained.

Donald A. Picken (Ministry of Labour and National Service, Liverpool, England): First, dealing with details of the paper, it is stated that the only known method of arresting fibrillation is by induction of complete tetany. There are many ways in which fibrillation can be stopped, for example, by injection of common materials, such as ammonium chloride. The difficulty is that these materials have to be removed from the heart by irrigation. Fischer and Fröhlicher have done a great deal of work on chemical control of fibrillation and they recommend the injection of acetyl choline which, by producing a temporary nerve block, brings fibrillation to a stop. In a short time, the acetyl choline is hydrolized into products which act as stimulants. This method has been well proved by experiments.

All the information upon which the article is based is apparently deduced from experiments on dogs. The validity of comparison between dogs and human beings is extremely doubtful. Experiments which have been carried out on muscles and nerves from different animals respond in a widely different manner and I suggest that much more information is necessary on the validity of comparisons between the subjects and human beings before the results can be and human beings before the results can be of value. Much information on the effects of electric current on animals has been proved not valid for humans.

It is stated in the paper that when ventricular fibrillation obtains, blood circulation ceases and death ensues. It is not always true that blood circulation entirely ceases. In some cases over and above the fibrillating rhythm a weak heart beat of low frequency has been detected which would produce some blood circulation. Further, Jellinek suggests that fibrillation itself may be spontaneously eliminated, though not with the lower order of animals. It does occur with monkeys.

The methods suggested, while they might produce the elimination of fibrillation, are likely to have serious side effects. My investigations into fatal accidents suggest that the role of fibrillation is overemphasized and that a considerable number of deaths are due to nerve blocks rather than to fibrillation.

The possibility of causing a nerve block by currents of the magnitude suggested in the region of the thorax is considerable and it should be adopted only as a last resort. The aim of the first-aider in cases of electric shock should be to ventilate the lungs and to cause blood circulation. The use of high-frequency currents to stimulate heart beats has been tried, but the general application of current is difficult. Much simpler techniques are essential for any widespread success, and the method should deal much more generally with the effects of electric shock on human beings.

At present work is being carried out on the efficacy of the rocking-stretcher technique not only as a ventilator for the lungs, for which it is certainly adequate, but also as a means for inducing blood circulation. It has been established that a considerable degree of blood circulation does result from application of the rocking-stretcher technique, even when the heart is stationary.

Work on electricity and humans, along the lines of that being done by Djourno in Paris and that already done by Fröhlicher in Zurich is, in my opinion, essential.

The recommendation made by Djourno is one worthy of attention: when a patient is unconscious from electric shock a hollow needle should be inserted into the wall of the heart. If the heart is beating feebly this can be used to inject a heart stimulant. If the heart is fibrillating it can be used to control the fibrillation either chemically by the use of acetyl choline or electrically by the induction of tetany. This method is much less hazardous from the point of view of side effects than is the external application.

W. B. Kouwenhoven and **W. R. Milnor**: The electrode-mounting described by Mr. Radley is an interesting one and should be tried. His arrangement with one electrode on the shoulder and the other on the abdomen involves a long current path and this may require an increase in voltage to produce defibrillation.

We do not recommend repeated applications of the defibrillation current. In cases where an electrocardiograph is available and the heart is not defibrillated by the initial application, a second application should be tried. This, however, is not true in the field.

To provide good contact between the electrode surface and the body, we are planning to insert a plastic sponge about 1 inch thick between a backing piece of insulating material and the electrode. A spiral groove will be cut in the copper electrode, which will be glued to the plastic sponge. When cardiac jelly is used it is not necessary to cover the electrode surface with cloth.

It is of the utmost importance that artificial respiration be started as soon as possible and that it be maintained continuously, except during brief periods required for the application of the defibrillating current.

Professor Dalziel is correct in his statement that the application of a-c defibrillation to humans by doctors and laymen will result in failures as well as successes. We feel that the closed chest method of defibrillation should be first tried in hospitals. It should be remembered that there are many more cases of ventricular fibrillation annually in hospitals than there are in the field.

Both Mr. Ferris and Mr. Dalziel question the use of dogs as the experimental animal in this study. The dog was selected because of the large body of evidence from different kinds of medical research showing the cardiovascular physiology of the dog is analogous in many ways to that of the human heart. We are not convinced that body weight itself is an important factor in electric defibrillation. It seems more probable that the current passing through the heart, which would be determined by the voltage applied and the resistance of the pathway, is the most important factor.

In open-chest defibrillation the same voltage is used for infants and adults. The only change made is in the size of the electrodes placed on the heart. For infants the electrode diameter is 1.125 and for adults 1.75 inches. In dogs ranging from 7 to 20 kilograms, no difference was found in the response to defibrillating shocks.

In the inital stages of this work with the electrodes on the opposite sides of the chest, we applied the defibrillating current for 1 second to a heart that had been in fibrillation for 1 minute. Using the hand electrodes, we have been studying the effect of reducing the duration of the current flow, and find that durations of from 0.3 to 0.5 second are ample to bring the twitching heart muscles to rest after 2 minutes in fibrillation.

Many authors, including Mr. Ferris, have reported that the sensitivity of the heart to electric shock varies during the cycle. In the authors' study of the effects of capacitor discharges, it was recognized that if the sensitive phase was known, the shocks could be timed to pass through the dog during that period and that the time devoted to the study could be shortened. The current pathway through the animals was from right foreleg to left foreleg. One hundred and forty one discharges were sent through the bodies of 18 dogs without finding any correlation between the energy in the discharge, its position in the heart cycle, and the occurrence of fibrillation. Under the conditions of our experiments, therefore, no sensitive phase could be demonstrated.

We have only studied two frequencies as sources of defibrillating current, namely 60 and 400 cycles. The higher frequency current has been studied on 22 animals and is not a satisfactory source of supply for this purpose.

It is our opinion that defibrillating equipment should be designed to use the standard commercial frequencies because of their availability. A convenient and inexpensive source of defibrillating current is a 2-kva low-impedance transformer with primary voltage taps ranging from 120–2,400 volts.

The authors agree with Mr. Ferris, as stated in the paper, that a capacitor defibrillator would possess advantages. During 3 years we carried on intensive experimental capacitor studies, commenced in 1949, and we are still trying out new ideas and suggestions. Unfortunately we were not successful in developing an effective capacitor circuit for defibrillation.

Mr. Picken states that there are many ways in which fibrillation may be arrested. Kay,[1] working on drugs as a means of stopping fibrillation, found them to be ineffective. Fischer and Fröhlicher carried out their experiments with acetyl choline on the isolated, perfused heart. We have experimented with this drug on dogs with their hearts in place and their circulatory systems intact. In none of our experiments, under these conditions, were we able to stop fibrillation with acetyl choline.

While it is not possible to transfer directly the results of animal experimentation to humans, there exists a mass of medical evidence showing that the cardiovascular system of the dog is analogous to that of man. For example, the same voltages, currents, and circuit conditions, which in 1933 were found to be effective in defibrillating the dogs' hearts[2] are used today in hospitals on human hearts. When the human heart fibrillates the effective circulation of the blood ceases, and unless the circulation is promptly restored death will ensue.

We have experimented with monkeys and have confirmed Jellinek's finding that the monkey's heart often recovers spontaneously from fibrillation. In general this is true of animals with small hearts.

We have not had a single instance of the passage of the defibrillating current through the current pathway that we are using, causing any side effects. The method has been successfully applied to one human being whose heart went into fibrillation while undergoing anesthesia.

It is impossible to state accurately how many cases of ventricular fibrillation occur annually as the results of electric shocks. The Accident Prevention Committee of the Edison Electric Institute report that among utility employees there are approximately 50 electric shock deaths each year, where artificial respiration was started with the promptness that should have ensured a successful recovery, but failed.

The rocking-stretcher technique mentioned by Mr. Picken, should produce some circulation of the blood. The needle technique is an interesting suggestion. We suggest, however, that the shaft of the needle be covered with insulation, except for a small area near the end. Then if the needle is used as one electrode the current will be more closely confined to the heart.

References

1. The Treatment of Cardiac Arrest, J. H. Kay. *Surgery, Gynecology and Obstetrics*, Chicago, Ill., vol. 93, 1951, p. 682.

2. The Effects of Alternating Currents on the Heart, D. R. Hooker, W. B. Kouwenhoven, O. R. Langworthy. *American Journal of Physiology*, Washington, D. C., vol. 103, 1933, p. 444.

The Use of Probability in the Design and Operation of Secondary Network Systems

N. M. NEAGLE
ASSOCIATE MEMBER AIEE

D. R. NELSON
ASSOCIATE MEMBER AIEE

THE PURPOSE of this paper is to present a method of investigating the probability of the various types of outages which can occur on a secondary network system. Briefly, the results may be used in two ways: 1. To determine the principal causes of these outages. 2. To compare the effect of changes in operating procedure and system design on these outages.

Conclusions

With the aid of probability, it is possible to calculate the probability of occurrence of secondary network equipment outages, their frequency, and their duration. The data needed for a probability study are the individual network equipment outage rates. If these data are not available for the system to be studied, industry records of the equipment outage rates may be used. Placing these data in the equations shown will enable the system designer to calculate the probability of occurrence of system outages for the present and future systems.

Description of System

The secondary network is a low-voltage a-c distribution system. It is principally an underground system used to feed commercial areas; see Fig. 1. All loads, large and small, are connected to a common 120/208-volt grid supplied with power through judiciously located network transformers. These transformers are connected to one of two or more primary feeders which are so interlaced that no two adjacent transformers are supplied from the same feeder. On the secondary of the transformer is a network protector containing a fuse, an air circuit breaker and a relay. The relay operates the breaker by tripping it on reverse power flow and closing it when the voltage on the transformer secondary is greater than that on the grid. This network unit (transformer and protector) is located in a vault either singly or with several other units. Where several units are located in one vault it is called a multiunit vault.

The network system provides a high order of service to all customers, because all the loads and all the network units are connected to a common grid. The outage of any network unit means that its load is transferred to the remaining units. Because of the impedance of the interconnecting grid cables the principal portion of this load would be carried by the adjacent units. In a multiunit vault or spot network vault these adjacent units would be the remaining energized units in this vault.

System Design

The system must be designed with a knowledge of the outages that may reasonably occur on the system and the ability of the remaining energized units to carry the total load. In this the system designer has two distinct problems: 1. of supplying power to the system, and 2. of supplying power to the grid at the various load locations.

The problem of supplying power to the system is concerned with the distribution of large amounts of power over the primary feeders to the many network units. The designer must determine how many feeders are required to supply the load for all reasonable operating conditions. In this case a knowledge of the probability of feeder outages is required.

The second problem is to transform this power from the primary feeders to the grid. In multiunit vaults several network units are solidly tied together to one bus. The problem here is to provide adequate transformer capacity to carry the load on this bus during normal operating conditions. Hence a knowledge of network unit outages is important.

Definition of Terms

A single-contingency outage is defined as the outage of one unit of a group of units. A double-contingency outage is the simultaneous outage of two units in a group of units, and a triple-contingency outage is the simultaneous outage of three units in a group of units. The term outage as employed here is intended to mean the failure of a piece or pieces of equipment to carry its share of the system load.

Approach to the Problem

The explanation of the use of probability to investigate network system outages will be mainly accomplished with examples. These examples are not intended to be typical for all systems, but are used only to show how to apply the principles of probability to determine the network system outages.

Probability

The application of the theory of probability involves the determination of the chance of an event occurring in a given manner. Likewise, the theory of probability can be applied to determine the chance of two or more events occurring in

---

Paper 55-160, recommended by the AIEE Transmission and Distribution Committee and approved by the AIEE Committee on Technical Operations for presentation at the AIEE Winter General Meeting, New York, N. Y., January 31–February 4, 1955. Manuscript submitted October 20, 1954; made available for printing December 3, 1954.

N. M. Neagle and D. R. Nelson are with the General Electric Company, Schenectady, N. Y.

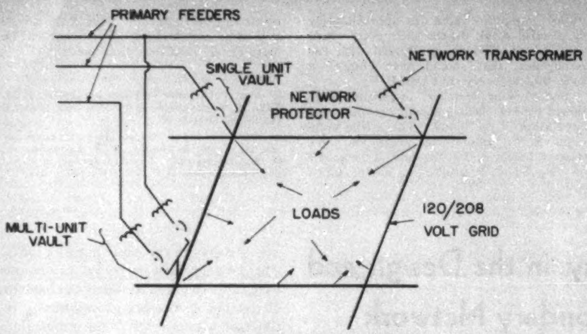

Fig. 1. The secondary network system

a particular combination, if the probability of the individual events is known. Two important fundamental theories of probability are: 1. The total probability of mutually exclusive events is equal to the sum of the individual total probabilities. 2. The probability of two or more independent events occurring simultaneously is the product of the individual probability.

Mutually exclusive events are events that cannot occur at the same time, whereas independent events are events that can occur simultaneously.

PROBABILITY OF INDIVIDUAL EVENTS

Determination of the probability of a single event occurring is rather simple. If the probability of an event occurring is P, then

$$P=\frac{\text{number of times the event occurs}}{\text{number of times the event occurs plus the number of times the event could occur but does not occur}}$$

Assuming that an event occurs 10 days during a year and will not occur the remaining 355 days of a year, then the probability of its occurrence on any particular day will be $P=10/(10+355)$ which equals 10/365 which equals 0.0274.

The first step in a study of the probability of system or vault outages is to determine the probability of individual equipment outages which will lead to vault or system outages. There are three types of individual outages that will affect the network unit (cause disconnection of the network transformer from the grid). These are:

1. Network protector failures.
2. Feeder faults.
3. Feeder maintenance.

1. Network protector failures may be of several different types. The only types of concern here are those which leave the protector open when it should be closed; i.e., leave the network protector's transformer disconnected from the system. Using data published by the Edison Electric Institute,[1] the probability of network protector outages can be determined as follows. For the period 1944 to 1946 the Edison Electric Institute report[2] on a-c network operations records 0.045 failures per protector per year. This includes failures to open and failures to close, but not fuse blowings. Of this total 64.9 per cent (%) were failures to close, making

$$0.649\times0.045=0.0292 \text{ failures to close per protector per year}$$

For use here these failure data must be placed on a time base. To do this the means of detection must be examined. Because of the inherent interconnecting load-supporting function of the network grid it is assumed that only a vault inspection or a supervisory system would determine whether a protector is open when it should be closed. Where supervisory systems are not employed the burden of detection falls upon individual inspections. If these occur once a year an average outage period for each failure might be 6 months. The outage rates would then be

$$\text{Failure to close}=0.0292\times\frac{365}{2}\text{ days}$$
$$=5.34 \text{ days per protector per year.}$$

The associated probability of any network protector being out of service at any time would therefore be

$$P_1=\frac{5.34 \text{ days per year}}{365 \text{ days per year}}=0.0146$$

If detection measures were conducted every 6 months, this probability would be reduced by 50%. The frequency of inspection is therefore the principal factor in the probability of network protector outages.

2. Faults can occur on a feeder with the failure of a cable, a joint, or a transformer. This produces a primary feeder outage by the removal of the feeder from the system by its associated protective equipment. The feeder failure rate can be determined from individual failure rates of feeder components as published in Edison Electric Institute reports. If a primary feeder were 2 miles long, had 30 joints and was connected to 14 network transformers, its total failure rate would be:

Cable failures per year $=0.068\times2$ miles $=$	0.136
Joint failures per year $=0.005\times30$ joints $=$	0.150
Transformer failures per year $=0.00274\times14$ transformers $=$	0.038
Total failures per feeder per year $=$	0.324

Assuming that approximately 2 days would be required to locate and clear the fault and return the feeder to service, the days of outage per year would be $0.324\times2=0.648$ days per year. The probability of any feeder being out of service because of fault at any time during the year would then be

$$P_2=\frac{0.648 \text{ days per year}}{365 \text{ days per year}}=0.00178$$

3. Feeder maintenance outage is the planned removal of the entire primary feeder and its associated units from service for the purpose of maintenance work. Assuming that the total time a feeder will be out of service for maintenance during any one year is 2 days, the probability of any particular feeder being out of service for maintenance at any time during the year will be

$$P_3=\frac{2 \text{ days per year}}{365 \text{ days per year}}=0.00548$$

PROBABILITY OF SEVERAL EVENTS

Knowing the individual probabilities; i.e., P_1 probability of network protector outages, P_2 probability of feeder fault outages, and P_3 probability of feeder maintenance outages, it is now possible to determine the probability of outages in the vault of N units (see Fig. 2) as follows:

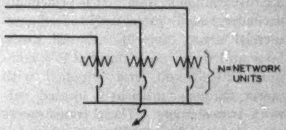

Fig. 2. N unit network vault

P_1 = probability of network protector being out of service
P_2 = probability of a primary feeder being out due to a fault
P_3 = probability of a primary feeder being out due to maintenance
P_A = probability of a network unit being out of service $P_A = P_1 + P_2 + P_3$
P_G = probability of all N units being in service
P_M = probability of M out of N units being out of service
P_N = probability of all N units being out of service
$P_G = (1-P_A)^N$
$P_M = (P_A)^M(1-P_A)^{N-M} N^C N-M$
$P_N = (P_A)^N$

P_1, P_2 and P_3 are mutually exclusive (see the Appendix) in that only one can occur at a time. Therefore, the total probability of a network unit being out of service in a vault is simply the sum of P_1, P_2 and P_3 to give P_A, the probability that one network unit in a vault will be out of service. Likewise, $1-P_A$ is the probability of one network unit being good or in service.

The probability of having two network units out of service in a vault is an independent event, as each can occur simultaneously. Therefore the probability of having two network units in service is $(1-P_A)$ $(1-P_A)$. . .while the probability of having two network units out of service in a vault is (P_A) (P_A). . . Based on this, equations can be presented which will express the probability that an outage will or will not occur in a given vault. For example, assume N units are in the vault and it is desired to know the probability that all units are good. The probability that all units are good is

$$P_G = (1-P_A)^N$$

The probability that M out of N units will be out of service is

$$P_M = (P_A)^M(1-P_A)^{N-M} N^C N-M$$

The combination factor $N^C N-M$ simply accounts for the number of ways in which this particular combination of outage can occur (see equation in the Appendix). This equation can be carried on until the probability of all units being out of service would be

$$P_N = (P_A)^N$$

These general equations are presented at the beginning of this section.

Examples

THE 4-UNIT VAULT

The easiest way to describe the use of the probability equations is with the aid of examples. First, assume that it is desired to determine the probability of the various outages in a 4-unit vault. The equipment in this vault has the values of individual probability determined earlier ($P_1 = 0.0146$, $P_2 = 0.00178$ and $P_3 = 0.00548$).

The types of outages, their probability equations, and their calculated values are as follows:

$P_1 = 0.01460$ = probability of network protector being out of service
$P_2 = 0.00178$ = probability of a primary feeder being out as result of a fault
$P_3 = 0.00548$ = probability of a primary feeder being out due to maintenance

$P_A = 0.02186$ = probability of a network unit being out of service
P_G = (all good) $= (1-P_A)^4$ $= 0.91537$
P_S = (one out) $= (P_A)(1-P_A)^3 {}_4C_1$ $= 0.08183$
P_D = (two out) $= (P_A)^2(1-P_A)^2 {}_4C_2$ $= 0.00274$
P_T = (three out) $= (P_A)^3(1-P_A) {}_4C_3$ $= 0.00004$
P_4 = (four out) $= (P_A)^4$ $= 0.00000$

0.99998

The probability of all combinations should equal 1.0.

The probability of having at least three units in service is:

$P_G = 0.91537$
$P_S = 0.08183$

0.99720 = probability that least three units are in service

The probability of having at least two units in service is:

$P_G = 0.91537$
$P_S = 0.08183$
$P_D = 0.00274$

0.99994 = probability that at least two units are in service

The value of the probability for each event occurring is a number less than 1. One way to consider these numbers is that they tell the per cent of the time a certain event will occur. For example, P_G all good, equals 0.91537 or, on the average, all the network units in this vault will be good 91.537 per cent of the time. Likewise, 8.463% of the time, one or more units will be out of service. Adding P_G and P_S evaluates the time that at least three units will be in service. Similarly, adding P_G, P_S, and P_D determines the time that at least two units will be in service. These values from the foregoing equations are 99.72% and 99.994% of the time respectively.

THE 4-FEEDER SYSTEM

Suppose it were desired to determine the availability of feeders to transmit power to the grid or, conversely, to determine the probability of feeder outages, particularly multiple contingency outages. Since a network protector outage will not disconnect a complete feeder from a system, its occurrence can be ignored for this investigation. If the system to be examined had four feeders, the associated probabilities of outage, employing P_2 and P_3 as defined earlier, would be as indicated as follows:

$P_2 = 0.00178$ = probability of a primary feeder being out because of a fault
$P_3 = 0.00548$ = probability of a primary feeder being out due to maintenance

$P_A = 0.00726$ = probability of a network unit being out of service
P_G = (all good) $= (1-P_A)^4$ $= 0.971278$
P_S = (one out) $= (1-P_A)^3(P_A) {}_4C_1$ $= 0.028404$
P_D = (two out) $= (1-P_A)^2(P_A)^2 {}_4C_2$ $= 0.000318$
P_T = (three out) $= (1-P_A)(P_A)^3 {}_4C_3$ $= 0.000000$
P_4 = (four out) $= (P_A)^4$ $= 0.000000$

1.000000

The probability that at least three feeders are in service is calculated as follows:

$P_G = 0.971278$
$P_S = 0.028404$

0.999682 = probability that at least three feeders are in service

In comparing the results of calculation on a 4-unit vault and the results on a 4-feeder system, it is obvious that the values of probability of outages have been considerably reduced. Outages are more likely in the vault because of the value of the P_1 probability of a network protector being out of service. The comparison indicates the need for a higher ratio of transformer capacity to load than feeder capacity to load. This is not the whole story, as an isolated outage confined in one vault on the system is not as serious as an outage of two whole feeders on a system.

VARIATION OF THE PROTECTOR OUTAGE TIME

The principal reason for the protector as a cause for a double-contingency outage is the duration of its outage following its failure to close. Assuming that the protector is going to be supervised so that its average outage time will not be 6 months but will be the same average duration of 2 days as that for a feeder maintenance and a feeder fault, then the probability P_1 (protector outage) is reduced from 0.0146 to 0.00016. This will reduce the value of P_A (probability of a feeder outage) from

0.02186 to 0.00742. The results of calculations in the 4-unit vault using the reduced protector outage time are:

$P_1 = 0.00016$ = probability of network protector being out of service
$P_2 = 0.00178$ = probability of a primary feeder being out because of a fault
$P_3 = 0.00548$ = probability of a primary feeder being out due to maintenance
$P_A = 0.00742$ = probability of a network unit being out of service
P_G = (all good) $= (1-P_A)^4 = 0.97065$
P_S = (one out) $= (1-P_A)^3(P_A)\,{}_4C_1 = 0.02906$
P_D = (two out) $= (1-P_A)^2(P_A)^2\,{}_4C_2 = 0.00033$
P_T = (three out) $= (1-P_A)(P_A)^3\,{}_4C_3 = 0.00000$
P_4 (four out) $= (P_A)^4 = 0.00000$
$\overline{}$
1.00004

The probability of having at least three units in service is as follows:

$P_G = 0.97065$
$P_S = 0.02906$
$\overline{}$
0.99971 = probability that at least three feeders are in service

Now, all the units are good on the average 97.065 as compared to 91.537% of the time from the calculation of the 4-unit vault. The probability of having at least three units in service in this vault is now 0.99971, which is about the same as the probability of having only two units in service, or 0.99994 in the 4-unit vault.

The 3-Unit Vault with Protector Outage Time Reduced to 2 Days

An interesting comparison can now be made using the reduced protector outage time of 2 days in a 3-unit vault as compared to the 6-month protector outage in a 4-unit vault. Following are the probabilities of the contingency outages in a three-unit vault:

$P_1 = 0.00016$ = probability of network protector being out of service
$P_2 = 0.00178$ = probability of a primary feeder being out due to a fault
$P_3 = 0.00548$ = probability of a primary feeder being out due to maintenance
$\overline{}$
$P_A = 0.00742$ = probability of a network unit being out of service
P_G = (all good) $= (1-P_A)^3 = 0.97791$
P_S = (one out) $= (1-P_A)^2(P_A)\,{}_3C_1 = 0.02193$
P_D = (two out) $= (1-P_A)(P_A)^2\,{}_3C_2 = 0.00016$
P_T = (three out) $= (P_A)^3 = 0.00000$
$\overline{}$
1.00000

The probability of having at least two units in service is as follows:

$P_G = 0.97791$
$P_S = 0.02193$
$\overline{}$
0.99984 = probability that at least two units are in service

The probability of having at least two in service is 0.99984, which is about the same probability, 0.99994, of having two units in service in a 4-unit vault. Thus the additional supervision of the protector in reducing its average outage time from 6 months to 2 days practically has reduced the need of having the fourth transformer in this multinetwork vault.

No-Feeder Maintenance

Up to this point no restriction has been placed on the occurrence of feeder maintenance. The equations have allowed feeder maintenance to occur in a similar fashion to feeder faults. As all four feeders can be taken out for faults, so the equations have allowed all four feeders to be taken out for maintenance. This is not the case in practice, as most systems will not take a feeder out of service for maintenance during peak load periods because this outage might lead to a double-contingency outage during a critical period.

The probabilities calculated in the following assume that a feeder will never be taken out of service for maintenance. This is the other extreme operating condition as compared to unlimited maintenance. Comparing the results of the 4-unit vault calculation and the results of no-feeder maintenance, shows that there has been a reduction in the total probability of contingency outage of only 0.02062, assuming that no feeders will be taken out of service in a 4-unit vault for maintenance purposes.

$P_1 = 0.01460$ = probability of network protector being out of service
$P_2 = 0.00178$ = probability of a primary feeder being out due to a fault
$\overline{}$
$P_A = 0.01638$ = probability of a network unit being out of service
P_G = (all good) $= (1-P_A)^4 = 0.93599 \quad 0.91537$
P_S = (one out) $= (1-P_A)^3(P_A)\,{}_4C_1 = 0.06245 \quad 0.08183$
P_D = (two out) $= (1-P_A)^2(P_A)^2\,{}_4C_2 = 0.00156 \quad 0.00274$
P_T = (three out) $= (1-P_A)(P_A)^3\,{}_4C_3 = 0.00001 \quad 0.00004$
P_4 = (four out) $= P_A^4 = 0.00000 \quad 0.00000$
$\overline{} \quad \overline{}$
$1.00001 \quad 0.99998$

The figures in the last column are from the calculations on the 4-unit vault.

$P_G = 0.93599$ = (all good from above for no maintenance)
$P_G = 0.91537$ = (four-unit vault calculations all good for unrestricted maintenance)
$\overline{}$
0.02062 = reduction in probability of outages with no feeder maintenance

Limited Feeder Maintenance

A more realistic approach is to assume that a feeder will be taken out of service for maintenance if no other feeder is out of service due to a fault or maintenance. This places a restriction on maintenance outages that can occur. For example, some double-contingency outages are caused by a feeder fault (P_2) and a feeder maintenance outage (P_3). If a feeder is not removed from service following a feeder fault, then P_2 (probability of a feeder fault) will not be followed by P_3 (probability of a feeder maintenance). But P_3 (feeder maintenance) can be followed by P_2 (feeder fault) to lead to a double-contingency outage. Thus, with this type of restriction on feeder maintenance certain of the combinations leading to the various degrees of contingency outages must be corrected.

For example, in order to correct the probability figures of the 4-unit vault calculation to conform to the new maintenance restriction, the terms (P_A) must be expanded as is accomplished in limited feeder maintenance. Certain terms must then be moved from one contingency to another, according to the effect of this maintenance restriction. The terms which must be moved are underscored in the following.

The terms for the outages expanded are:

$$P_G = (1-P_A)^4 = (1-P_A)^4$$

$$P_S = P_A(1-P_A)^3\,{}_4C_1 = (P_1+P_2+P_3)(1-P_A)^3\,{}_4C_1$$

$$P_D = P_A^2(1-P_A)^2\,{}_4C_2 = (P_1^2+P_2^2+\underline{P_3^2}+2P_1P_2+\underline{2P_3P_2}+2P_1P_3)(1-P_A)^2\,{}_4C_2$$

$$P_T = P_A^3(1-P_A)\,{}_4C_3 = (P_1^3+P_2^3+\underline{P_3^3}+3P_1^2P_3+3P_1^2P_2+\underline{3P_2^2}P_1+\underline{3P_2^2}P_3+\underline{3P_3^2P_1}+\underline{3P_3^2}P_2+\underline{6P_1P_2P_3})(1-P_A)\,{}_4C_3$$

$$P_4 = P_A = \text{(not of value)}$$

Terms to be added to P_S are:

$$\text{From } P_D = \left[P_3^2+\frac{P_3}{P_2+P_3}(2P_3P_2)\right]\times(1-P_A)^2\,{}_4C_2 = 0.00026$$

$$\text{From } P_T = \left[P_3^3+\frac{P_3}{P_1+P_2+P_3}(3P_3^2P_2)\right]\times(1-P_A)\,{}_4C_3 = 0.00000$$

Terms to be added to P_D:

$$\text{From } P_T = \left[\frac{P_2+P_3}{P_1+P_2+P_3}(3P_3^2P_1)+3P_3^2P_1+\frac{P_1+P_3}{P_1+P_3+P_2}(3P_3^2P_2)+\frac{P_3}{P_2+P_3}(6P_1P_2P_3)\right](1-P_A)\,{}_4C_3 = 0.00003$$

Values of 4-unit calculations corrected for the maintenance restrictions are as follows:

$$\begin{aligned}
P_G&=0.91537 &&=0.91537\\
P_S&=0.08183+0.00026 &&=0.08209\\
P_D&=0.00274+0.00003-0.00026 &&=0.00251\\
P_T&=0.00004-0.00003 &&=0.00001\\
P_4&= && \underline{0.00000}\\
& && 0.99998
\end{aligned}$$

For example, $(P_2)^2$ in P_D cannot occur as only one feeder will be taken out of service for maintenance at a time. So this term $(P_2)^2$ must be moved from P_D double-contingency outage to P_S single-contingency outage. The terms $2P_2P_3$ in P_D will not occur 100% as a double-contingency outage. If P_3 feeder fault occurs first, P_2 maintenance cannot occur. If P_2 occurs first, then P_3 can occur and lead to a double-contingency outage. Thus a portion of $2P_2P_3$ must be moved from P_D to P_S. This portion or fraction depends on the value of P_2 and P_3. As a double-contingency will not exist if P_3 occurs first, then $[P_2/(P_2+P_3)]$ $(2P_2P_3)$ is the portion of these terms to be subtracted from P_D and added to P_S. Other terms are handled in a similar fashion in the limited feeder maintenance calculation.

Interpretation of Results

As it has been pointed out, these probabilities can be expressed in terms of per cent of a year or years. From the calculation on a 4-feeder system the probability of a double-contingency outage is found to be 0.000318. Multiplying 0.000318 by 365 determines the average days outage per year

$$365(0.000318)=0.116070 \text{ day per year}$$

This term does not mean that there will be 0.11607 day of double-contingency outage each year but rather, on the average, this outage will occur 0.11607 day per year. For example, this might mean a double-contingency outage of 1.1607 days every 10 years or 11.607 days every 100 years. Obviously, if the double fault occurs only once every 100 years, this type of fault will not worry a system designer; whereas a fault of 0.11607 day (2 hours, 48 minutes) each year may be of long enough duration and occur frequently enough to be planned for by the system designer. Thus the frequency and duration of the probability of the faults is important to know. Using the 4-feeder system calculation as an example, the duration and frequency will be found.

INTERPRETATION OF SYSTEM FEEDER OUTAGES FROM 4-FEEDER SYSTEM CALCULATION

The 4-feeder system calculation consists only of feeder faults and feeder maintenance outage occurring on a 4-feeder system. Each of these individual outages P_2 and P_3 occurs for an average of 2 days' duration. When the individual outage durations are known the average duration of any contingency outage can also be determined. For the double contingency with each individual outage 2 days long the average double-contingency outage time will be 1 day long. This can be expressed as

$$\text{average duration of outage}=\frac{D_1\times D_2}{D_1+D_2}$$

where

D_1 = average outage duration of one of the failures

D_2 = average outage duration of the second failure

For the 4-feeder system calculation each duration P_2 and P_3 is 2 days and the average duration of a double-contingency outage is 1 day $(2\times 2)/(2+2)$. Dividing 0.11607 into this 1-day duration will determine the average years to obtain an average double-contingency outage of 1 day, or 1/0.11607, or 8.5 years. This means that for this 4-feeder system there will be a double-contingency outage of 1 day every 8.5 years. This same principle can be carried on into other examples to determine the average number of years between faults of a certain duration.

INTERPRETATION OF UNIT OUTAGES IN A 4-UNIT VAULT

Unfortunately the calculation on a 4-feeder system is by far the easiest to examine as only two individual faults (maintenance and feeder) each having a 2-day individual duration make up the duration of an average double-contingency fault. For the case of the vault examined for the 4-unit vault calculation there are six combinations which make up the total probability of the double-contingency outage time. Among the six combinations (see Appendix) there are three different average fault durations. Thus the total probability of a double-contingency outage (0.00274) is made up of several different durations. To examine each term, $(P_A)^2$ must be expanded as in the following interpretation of results.

$$P_D=(P_A)^2(1-P_A)^2{}_4C_2=\text{double contingency}$$
$$(P_A)^2=(P_1+P_2+P_3)^2$$
$$P_D=(P_A)^2(1-P_A)^2{}_4C_2=[P_1^2+P_2^2+P_3^2+2P_1P_2+2P_1P_3+2P_2P_3](1-P_A)^2{}_4C_2$$

The duration of the individual faults are as follows:

P_1 = protector outage average 6 months

P_2 = feeder maintenance outage average 2 days

P_3 = feeder failure outage average 2 days

The duration of the average double-contingency faults is:

1. $P_1P_1=\frac{6\times 6}{6+6}$ or $\frac{36}{12}=3$ months or 91 days

2. $\left.\begin{array}{r}P_2P_2=\\ P_3P_3=\\ 2P_2P_3=\end{array}\right\}\frac{2\times 2}{2+2}$ or $\frac{4}{4}=1$ day

3. $\left.\begin{array}{r}2P_1P_2=\\ 2P_1P_3=\end{array}\right\}\frac{90\times 2}{90+2}=\frac{180}{92}=1.96$ days

Probability of the three different double-contingency faults cause the total P_D.

1. $P_1^2(1-P_A)^2{}_4C_2$ $=0.00122$
2. $P_2P_2^2+2P_2P_3)(1-P_A)^2{}_4C_2$ $=0.00030$
3. $(2P_1P_2+P_1P_3)(1-P_A)^2{}_4C_2$ $=0.00122$

Years between the three different double-contingency faults are

1. $\frac{91}{0.00122\times(365)}=204$ years between double - contingency fault of 91 days' duration due to P_1P_1

2. $\frac{1}{0.00030\times(365)}=9.17$ years between double - contingency fault of 1 day's duration caused by $P_2P_2+P_3P_3+2P_2P_3$

3. $\frac{1.96}{0.00122\times(365)}=4.41$ years between double - contingency fault of 1.96 days' duration caused by $2P_1P_2+2P_1P_3$

The six combinations are listed under items 1, 2, and 3, and are made up of three different durations of faults, one of 91 days, one of 1 day, and one of 1.96 days. Solving for each of these individually the results are:

1 double-contingency fault of 91 days occurs every 204 years (due to P_1)

1 double-contingency fault of 1 day occurs every 9.17 years (due to P_2 and P_3)

1 double-contingency fault of 1.96 days occurs every 4.41 years (due to P_1, P_2, and P_3)

From this it can be seen that although the protectors themselves are major contributors to the double-contingency probability, these double contingencies caused by protectors are separated by many years and hence are not as important as some of the more frequent double-contingency faults. Of course, the protectors also contribute along with feeder faults $(2P_1P_3)$ and feeder maintenance $(2P_1P_2)$ to average 1.96 days of faults every 4.41 years.

Summary

Thus it is possible not only to calculate the probability of any contingency of faults on a network system or in a network vault, but also to obtain the average duration of these faults and the average years between their occurrence. Different systems or different operating procedures can thus be compared on the basis of reliability as well as economics.

The calculations have used the same probability of outage (P_A) for each primary feeder. In many systems some feeders have older equipment and may be exposed to more faults than new feeders with new equipment. Then it was assumed that these faults occur equally at any period of the day or night, or at peak load or light load. These assumptions were made in order to simplify the calculations.

It must be recognized that probability only expresses average conditions. It might take 1 year or 200 years to reach certain average conditions. Some checks have been made on an actual system, and it was found that the values obtained were reasonably consistent with what occurred on that system.

Appendix

An earlier paper[3] treated the faults P_1, P_2 and P_3 (individual outages) as independent events. After considerable discussion it appears that these individual probabilities may more properly be treated as mutual exclusive events.

Actually, it is possible for two types of outages simultaneously to affect one piece of equipment, such as the simultaneous occurrence of the disconnection of a network due to network protector failure and the disconnection of the same network unit due to a fault on the primary feeder to which it is attached. It is a moot point as to which type of difficulty is causing the outage. In practice, it does not matter because the outage would rarely, if ever, be recorded as caused by both types of difficulty. Therefore, since the recorded data from which the individual rates are determined do not or cannot account for this possible simultaneous creation of a single outage, they will probably be treated as mutually exclusive events.

The complete equation for the combination factor is

$$N^{C}a = \frac{\text{factorial } N}{\text{factorial } a \ X \ \text{factorial } (N-a)}$$

N = total number of units involved

a = number of units under consideration (i.e., either being in service or out of service)

The six combinations are:

1. P_1P_1
2. P_2P_2
3. P_3P_3
4. P_1P_2
5. P_1P_3
6. P_2P_3

References

1. A-C Network Operations, 1947–1949. *EEI Publication No. 51–6*, Edison Electric Institute, New York, N. Y., 1951.

2. A-C Network Operations 1944–46. *EEI Publication Q-22, Ibid.*, 1949.

3. Multiple Contingency Outages in a Secondary Network, **N. M. Neagle, D. R. Nelson.** *Proceedings*, American Power Conference, Illinois Institute of Technology, Chicago, Ill., March 1953.

◆

Discussion

G. H. Arapakis (Consolidated Edison Company of New York, Inc., New York, N. Y.): In the Appendix the authors refer to an earlier paper presented at the American Power Conference in 1953, in which the values of P_1, P_2 and P_3 were treated as independent events, while in their present paper they are treated as mutually exclusive events. As I see it, when they are treated as independent events the combinational probability will include a factor q, or q to some power, q being the probability that the other event or events will not happen. Since this factor q or some power of q will not in general differ greatly from unity, the numerical results obtained for the combinational probabilities will not be very different whether P_1, P_2, and P_3 are treated as independent events or as mutually exclusive events. Am I correct in this comparison? I feel that it is important since apparently there is some question as to which assumption is correct.

In their earlier paper the authors devoted considerable attention to the case of two units out of service, a valuable point since for the most part it constitutes the basis for system design. The treatment of the three probabilities P_1, P_2, and P_3 as independent events permitted a relatively simple breakdown of the double contingency into the following five possible events: 1. two network units out on failure to close but no feeder outages, 2. one network unit out on failure to close and one feeder in the same vault taken out for work, 3. one network unit out on failure to close and one feeder in the same vault going out on fault, 4. one feeder out for work and a second feeder in the same vault going out on fault, and 5. two feeders in the same vault going out on fault. The breakdown of the double contingency into these five components is very valuable since it permits us to make a comparison of their relative importance as a guide for improvement in system design and operation that will reduce the probable frequency of the double contingency.

In the paper, treating P_1, P_2, and P_3 as mutually exclusive, they are lumped together to calculate first total probabilities and then an attempt is made at separation by a regrouping of terms. The mathematical justification for this regrouping and shifting of terms from one total probability to another is not very obvious and seems rather complicated, especially if it is necessary to apply it to vault installations with more than four units. The treatment of P_1, P_2, and P_3 as independent events, which the authors followed in their earlier paper, seems to avoid these difficulties, and since there is some doubt as to which assumption is correct, I would prefer to treat P_1, P_2 and P_3 as independent events.

The calculation of the combinational probabilities of the various events enumerated in the paper is, of course, no better than the operating statistical data for outages of cables and equipment, from which one must calculate P_1, which is the average probability that a network protector fails to close, P_2 the average probability that a feeder will go out of service on fault, and P_3 the average percentage of time that a feeder is out for work or maintenance. These will vary widely for different power systems, and even for different network areas in the same system. The factors which are responsible for these variations are the type and age of cables, the length of feeders, the type and age of network equipment, and the general operating conditions which make it necessary to take a feeder out for construction or maintenance work, more frequently and for longer periods in one system or area than in another. In calculations which we have made for the Consolidated Edison System, we have found it advisable at times to use different values of P_2 and P_3 in an attempt to take into account some of these differences in design and operation.

With respect to P_1, the average probability that a network protector fails to close, the authors have used data published by Edison Electric Institute for 1944 to 1946 on a-c network operation. From these data they have calculated that 2.92% of the network protectors fail to close. The correct statistic needed for the probability calculations is the percentage of protectors that would be found open when they should be closed, assuming that one would walk in on all the protectors at the same time. The data obtained over a period of time should, of course, be corrected for the number of units inspected, and if possible allowance should be made for the fact that inspections are not made at a uniform rate but may be lumped during certain times of the year as determined by weather and other system work. Also, it should be recognized that network protectors of certain periods have shown considerably higher rates of failures, and it may be necessary to take this into account for some of the network areas affected.

I should like also to comment briefly on the value of P_2, which is used in this paper to represent the average statistical probability that a feeder will be out of service on fault. For any one feeder the length of exposure is an important variable, but the wide variety of operating conditions inherent in an actual system will cause changes in the value of P_2. If it is true then that P_2 is subject to substantial variations from its average value, the occurrence of contingencies of higher order may not be as unlikely as probability calculations based on a constant value of P_2 would indicate.

N. M. Neagle and D. R. Nelson: Whether the individual types of outage should be treated as independent or mutually exclusive events will depend upon the definition and means of recording these events. They may be treated either way depending upon the data available. Because, after considerable discussion of the matter, it was felt that most utilities would probably define and record their occurrence as mutually exclusive events, they are treated as such in this paper.

If we define a feeder outage due to feeder maintenance as the removal of a feeder from service for planned or anticipated maintenance, and a feeder outage due to fault as a completely unanticipated or unplanned occurrence, it is apparent that the two events cannot occur simultaneously. Therefore, they are mutually exclusive events. The outage of a network transformer due to network protector failure is not a clear-cut independent or mutually exclusive event. If a network protector failure exists in a vault, thereby excluding its transformer from service, and a subsequent feeder outage removes the feeder from service, it is apparent that the occurrence of one event in no way affects that of the other. Therefore, the events are independent and not mutually exclusive.

If the network protector failure is known to have occurred before the feeder outage, the outage which it creates will probably never be distinguishable as an independent event. The matter of recording an outage will probably be that it was caused by one or another type of difficulty, but rarely, if ever, as caused by two types of difficulties. Thus, unless a particular effort is made to evaluate outage causes involving network protector failures as independent events, the matter of detection and recording will invariable be that of mutually exclusive events. Therefore, all three types of outages have been treated as mutually exclusive events in the paper. The accuracy of any calculations is naturally dependent upon the accuracy of the data available. This not only refers to numerical accuracy with regard to the particular situation in question or particular types of apparatus and conditions in question, but also to the proper allocation of the outage causes as independent or mutually inclusive events. If accurate data are not available and no distinction is made in recording the detection of outages between mutually exclusive and independent events, the over-all accuracy of the calculations will probably be just as good, if the outages are treated as independent events, as it might be if they were treated as mutually exclusive events.

There are a great many factors which can be taken into account to make the data and calculations more accurate. Unfortunately, the inclusion of these factors also makes the calculations more complicated. For a true picture of the condition, where accurate data are available, it may be placed in the equations defined, or a modification thereof, depending upon the conditions to be met.

Balancing Double-Wye High-Voltage Capacitor Banks

O. R. COMPTON
ASSOCIATE MEMBER AIEE

OCCASIONALLY double-wye-connected high-voltage capacitor banks using neutral-current relaying have sufficient residual current flowing in the neutral to cause improper relay operation, thus endangering the capacitors. This paper summarizes the problem, establishes limits for the maximum allowable residual neutral current, and presents methods for balancing the capacitor bank, if necessary, to reduce the residual neutral current to the allowable limit.

When a large, high-voltage capacitor bank is composed of multiple series sections per phase and a sufficient number of parallel capacitor units per series section to meet the minimum bank size requirement, at least one capacitor unit may be removed from any series section without encountering voltages in excess of 110 per cent (%) of rated voltage on the remaining capacitors.[1] However, the loss of two or more units in any one series section can produce dangerous overvoltages within the section in which the units are lost.[1,2]

Protective relaying is often used to give indication and/or trip the bank when a sufficient number of units are lost within one series section to cause the voltage appearing across that series section to exceed 110% of rated voltage.[1] Since the majority of power capacitors used in the United States in high-voltage banks are manufactured with a 0 to + 15% tolerance, there may be sufficient inherent unbalance to cause the protective relay scheme to operate prematurely or not to operate at all when needed, depending on the magnitude and phase angle of the residual current.[3]

In addition to unbalance caused by the variation in capacitance of individual units because of the 0 to 15% manufacturing tolerance, unbalance may also arise because of:

1. Units in upper tiers operating in higher ambients owing to warm air rising from lower tiers.
2. Capacitors in top tier being subject to direct sunlight will operate at higher internal temperatures than units in lower tiers.
3. Units in top tier casting their shadows on lower tiers, thus causing units in lower tiers to operate at a relatively lower internal temperature.

Specifically this paper deals with double-wye-connected banks using neutral-current relaying since it is the most widely used system. Its popularity is the result of its low cost when compared to other schemes which are also insensitive to external system conditions and yet extremely sensitive to unbalanced bank conditions. This was also the type of relaying used on the Virginia Electric and Power Company's banks which were balanced by the method presented in this paper.

It is our purpose to present a basis for theoretically establishing a satisfactory maximum allowable neutral residual current and two methods of balancing double-wye-connected capacitor banks when it is found that the initial residual neutral current exceeds the maximum allowable limit.

Nomenclature

Z_L = impedance of phase section in which one or more units in one series section has been lost
Z_n = impedance of normal phase sections
M = number parallel units per series section
N = number of series sections per phase section
K = number of units lost in one series section
K_1 = per cent of units lost in one series section
I_a = total bank current to phase in which K units have been lost
I_{a1} = normal total bank current

Paper 55-146, recommended by the AIEE Transmission and Distribution Committee and approved by the AIEE Committee on Technical Operations for presentation at the AIEE Winter General Meeting, New York, N. Y., January 31–February 4, 1955. Manuscript submitted October 26, 1954; made available for printing December 8, 1954.

O. R. COMPTON is with the Virginia Electric and Power Company, Richmond, Va.

The author expresses his appreciation to P. B. Hendrickson for his assistance in the preparation of this paper. He also wishes to express his appreciation to J. A. Rawls, T. S. Martin, B. B. Brown, and B. F. Eldred, all of Virginia Electric and Power Company, for their encouragement and constructive criticism of this paper.

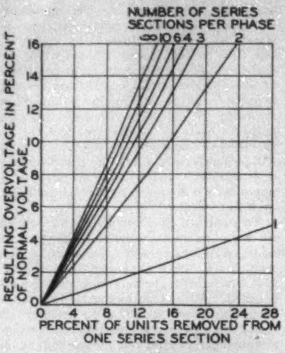

Fig. 1. Curve of overvoltage on remaining units in two series section versus percentage of units removed from that section

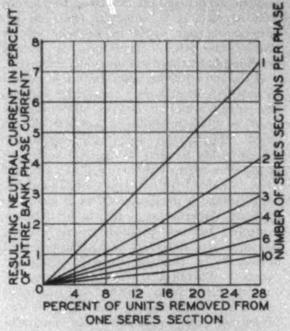

Fig. 2. Curve of neutral current versus percentage of units removed from one series section

I_L = current in phase section in which K units have been lost

I_{n1}, I_{n2}, I_{n3}, I_{n4}, I_{n5} = current in remaining phase sections

E = source line-to-neutral voltages

E_{ab}, E_{bc}, E_{ca} = source phase-to-phase voltage

e_f = voltage across series with K units lost

e_{n1} = voltage across series section under normal conditions

I_N = neutral current

$\%I_N$ = neutral current in % of normal total bank current

I_{aT} = assumed neutral current resulting from one unit being removed from top section of A phase

I_{aTa} = actual neutral current when one unit is removed from top section of A phase

I_N = actual residual neutral current with all units in service

Determination of Maximum Allowable Residual Neutral Current

Normally the neutral relay is set to pick up midway between the values of neutral currents theoretically obtained when the maximum permissible number of units and the maximum permissible number plus one unit in the same series section are lost. The maximum permissible number of units lost is defined as the maximum number that can be lost in one series section without the voltage across that section exceeding 110% of rated capacitor voltage.[1] This midway relay setting gives equal margin on either side to prevent premature relay operation when no more than the maximum permissible number are lost and to assure operation when one additional unit in the same series section is lost.

The maximum permissible number of units that may be removed from one series section may be determined by the curves in Fig. 1. The resulting neutral current may be determined for the loss of any number of parallel units in one series section by the curves in Fig. 2. The derivation of equations for Figs. 1 and 2 is shown in Appendixes I and II respectively.

The curves of Fig. 2 may also be used to establish the approximate neutral relay settings. For example, assume a double-wye-connected bank made up of three series sections per phase and eight parallel units per section. From Fig. 1 it can be determined that the maximum permissible units that may be lost is one. When two units in the same series section are lost, the bank should be relayed off. Therefore, the neutral-current relay should be set to pickup at a value of current equal to the loss of approximately one and one-half units or loss of (1.5/8)(100) = 18.75 units. Entering the curves on Fig. 2 at the loss of 18.75% units will indicate a relay setting of 1.8% of total bank current.

The relay setting in % of total bank current may be specifically determined by

$$I_R = {}^1/_2 \frac{150}{6N\left(\frac{M}{K+1}-1\right)+5} + \frac{150}{6N\left(\frac{M}{K}-1\right)+5} \qquad (1)$$

Maximum Allowable Normal Residual Neutral Current With All Units in Service

It can be readily seen that under normal conditions the maximum neutral residual current must be something less than one-half of the difference between the theoretical neutral currents obtained when the maximum permissible number of units and the maximum permissible number plus one unit are lost.

A realistic limitation of the maximum would be one-fourth of the difference in neutral currents when the maximum permissible number of units and the maximum permissible number plus one unit are lost. The maximum allowable residual current in % of total bank current may be determined by

$$I_R = {}^1/_4 \frac{150}{6N\left(\frac{M}{K+1}-1\right)+5} - \frac{150}{6N\left(\frac{M}{K}-1\right)+5} \qquad (2)$$

This value of maximum allowable residual current would provide ample margin against false tripping and at the same time avoid the trying task of obtaining a superfine degree of balance. The residual neutral-current component because of the difference in capacitance of units allowed by the 0 to +15% manufacturing tolerance will remain essentially constant for given bank. However, the residual neutral current may vary to a slight degree because of the difference in internal operating temperatures caused by the effect of upper tiers operating in higher ambients and being subjected to direct sunlight.

Variations in capacitance caused by different internal operating temperature could be substantial since the capacitance of an askarel-treated capacitor decreases approximately 1% for every 15- to 20-degree-centigrade rise in internal operating temperature. Experience has shown that units in the top tier can easily operate with internal temperature of 5 to 10 degrees centigrade above the internal temperature of units in the bottom tier.

Fortunately most high-voltage capacitor banks are so arranged that the effect of different internal operating temperatures is distributed throughout the bank

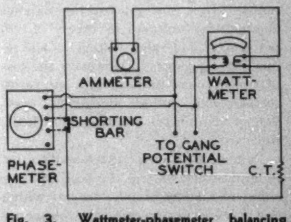

Fig. 3. Wattmeter-phasemeter balancing circuit

so that the approximate respective balance is maintained. However, there is ample margin to allow for some degree of changing unbalance caused by different internal operating temperature when the value of maximum allowable residual current specified in the foregoing is maintained.

Fig. 5. No. 5 capacitor bank, Peninsula Substation

Field Balancing of Double-Wye-Connected High-Voltage Banks

The following discussion describes the general procedure incorporated to balance the no. 4 and no. 5 double-wye-connected 24,750-kilovar 108-kv 3-phase capacitor banks at the Virginia Electric and Power Company's Peninsula Substation. Both banks are identical in design and are shown schematically in Fig. 4. Bank no. 5 is shown in Fig. 5. Each bank is made up of standard 25-kilovar 4,160-volt single-phase distribution capacitors with 15 series sections per phase and 11 parallel units per series section.

The resulting voltage rise across a series section caused by the loss of one capacitor within that section is 9%, as determined from Fig. 1. Since the loss of two units in the same series section results in a voltage exceeding 110% of rated capacitor voltage, it is necessary to relay the bank off when more than one unit is lost in the same series section.

The theoretical neutral-current flowing when one and two units are lost is 0.24 and 0.51 ampere (amp) respectively. Therefore, the neutral relay is set to pick up at (1/2) (0.24+0.51) or 0.375 amp. Likewise, the maximum allowable residual neutral-current limit is established to be (1/4) (0.51–0.24) or approximately 0.07 amp. Assuming that the maximum allowable residual neutral-current limit is established at 0.07 amp, the resulting neutral currents would range between 0.24±0.07 and 0.51±0.07 amps if one and two units were lost respectively. The exact value of the resulting neutral currents when one or two units are lost depends on the particular phase group in which the units were lost and the magnitude and phase angle of the residual neutral current.

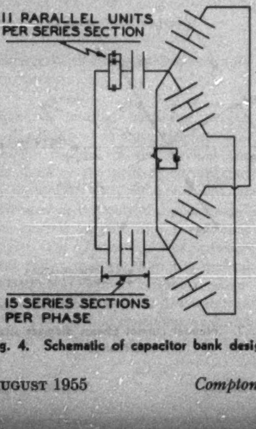

Fig. 4. Schematic of capacitor bank design

Each bank was energized to determine the initial residual neutral current. It was found that the initial residual currents were 0.295 amps for bank no. 4 and 0.265 amps for bank no. 5. It is obvious that these magnitudes of residual neutral current would cause false relay operation. For example, in bank no. 4, the loss of one unit in any one of the six phase groups could cause a resulting neutral current of 0.24±0.295 amp. With the relay set at 0.37 amp, the bank could be easily relayed off unnecessarily. Similarly, with two units lost, the neutral current in bank no. 4 could range between 0.51±0.295 amp, and this could result in two units being removed without encountering sufficient neutral current to pick up the relay and thus endangering the remaining units in the series section containing the lost units because of overvoltage operation.

The following steps constitute the general procedure followed in balancing the no. 4 and no. 5 banks at the Peninsula Substation:

1. Determine the magnitude of initial residual neutral current.
2. Determine phase angle of initial residual neutral current.
3. Determine the phase sections contributing to the initial residual neutral-current and capacitance change necessary to reduce the residual neutral current to within the maximum allowable limits.
4. Interchange high and low capacitance units to accomplish the capacitance change dictated by step 3.

Magnitude of Initial Residual Current

The magnitudes of the initial residual currents were determined by energizing each bank and measuring the neutral current on the secondary side of the 1-to-1 neutral current transformer. The initial residual neutral currents were 0.295 and 0.265 amp respectively for banks no. 4 and no. 5.

Thase Angle of Initial Residual Current

Neutral-current measurements were made on each bank with one capacitor out of one section of one phase group. This test was repeated six times to enable the phase angle of the initial residual neutral current to be determined by graphical analysis. It would, of course, have been possible to determine the phase angle with fewer measurements. For each test the bank was normal except one capacitor was removed from the series section nearest the neutral in a different phase group each time. The results of these tests are shown in Table I for bank no. 4.

It was calculated that the phase group in which the one unit was removed would supply a 0.24-amp neutral current in phase with the line current. Therefore, six vectors, each 60 electrical degrees apart and each with a magnitude of 0.24

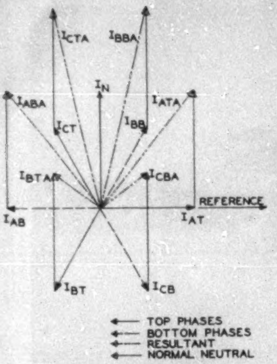

Fig. 6. Neutral current phasor diagram before interchange

amp were plotted, as shown in Fig. 6. The magnitude only was measured for each of the six conditions where one unit was removed, as described in the foregoing. This magnitude was the vectorial sum of the 0.24-amp in-phase component plus the component produced by the capacitance unbalance (initial residual current) at an unknown angle.

If a circle is drawn with a radius equal to the initial residual current, as found in the foregoing, and centered at the head of a 0.24-amp in-phase phasor, that circle will be the locus of all possible total neutral currents when one unit is removed from that phase group. A second circle with a radius equal to the total neutral current with its center at the origin is drawn which will also be the locus of all possible total neutral currents. These two circles intersect at two points; one of which is the locus of the initial neutral-current phasor.

For example, in Fig. 6, a circle with radius equal to *I* normal is drawn with the head of phasor I_{AT} as the center. Then a second circle is drawn with the center at the origin and a radius equal to the total neutral current measured when one unit is removed from the *A* phase, top group. These two circles intersect at the head of phasor I_{ATA} and, at a second point, 180 electrical degrees (through the head of phasor I_{AT}) from I_{ATA}. A line drawn from the head of phasor I_{AT} to each of these intersecting points will be the two possible normal unbalance-current phasors. These phasors are equal in magnitude and are 180 electrical degrees apart in angle. This procedure is repeated for another phase group and it becomes apparent which is the correct direction for the normal unbalance-current phasor.

Table I. Neutral Currents Prior to First Interchange, Bank No. 4

Location of Unit Removed	Neutral Current, Amp
A—top phase	0.355
B—top phase	0.110
C—top phase	0.530
A—bottom phase	0.355
B—bottom phase	0.560
C—bottom phase	0.215

The graphical analysis for determining the phase-angle relationship of the initial residual or normal unbalance current is shown in Fig. 6 for bank no. 4. This current was found to be $0.295\underline{/270^\circ}$ amp. An analysis of Table I will reveal that the loss of one unit from any section in *B*-bottom phase or *C*-top phase, of bank no. 4 would have produced a circuit-breaker trip with a relay setting of 0.37 amp. In the remaining phase groups, two or more capacitors would have to be removed from the same series section to produce a circuit-breaker trip.

Phase Groups Contributing to Unbalance

A study of the phasor diagram for bank no. 4 shows that the neutral current was high on *B*-bottom phase and *C*-top phase when one capacitor was removed from these respective groups. The neutral current was equal in both *A*-top and *A*-bottom phase groups when one capacitor was removed from either of these groups.

It was assumed that *B*-bottom phase and *C*-top phase contributed equally to the initial neutral current, i.e., 0.295/2 or 0.148 amp was contributed by each of these phase groups. The phase angle between *B*-bottom phase and *C*-top phase is about 30 degrees above and below the initial residual neutral current. Therefore, the gross current component contributed by *B*-bottom phase and *C*-top phase equals (0.148/cos 30°) or 0.171 amp.

If 0.24 amp equals the theoretical neutral current produced by the loss of one unit, the 0.171-amp component equals the current produced by the equivalent loss of 0.171/0.24 or 0.71 of a unit. This indicates that a balance could be obtained by moving 0.71/2 or 0.35 of a unit from *B*-top phase to *B*-bottom phase and 0.35 of a unit from *C*-bottom phase to *C*-top phase.

Table II. Neutral Currents After First Interchange, Bank No. 4

Location of Unit Removed	Neutral Current, Amp
A—top phase	0.330
B—top phase	0.110
C—top phase	0.328
A—bottom phase	0.201
B—bottom phase	0.375
C—bottom phase	0.022

Calculation of Number of Units to Interchange

Each unit contains approximately 4.0 microfarads (mf) of capacitance; therefore, it was necessary to interchange (0.35) (4) or 1.40 mf between the *B*-phase and *C*-phase groups. To determine which units to interchange, a capacitance bridge was used to measure the capacitance of units in the top and bottom tiers of phases *B* and *C*. Individual unit capacitance was taken of each individual unit, starting with the series sections nearest the neutral. This procedure was continued until a sufficient number of high and low units were found to make a total transfer of 1.24 mf from *B*-top phase to *B*-bottom phase and from *C*-bottom to *C*-top phase respectively. To accomplish this change in capacitance, 20 units were interchanged in the *B*-phase and 18 units in the *C* phase. After the interchange was completed, a check was made of the residual neutral current and it was found to be 0.13 amp. Therefore, it was necessary to repeat the balancing procedure.

The results of tests taken to determine the phase angle of the residual current after the first interchange are shown in Table II. Fig. 7 shows the graphical analysis for determining the new residual neutral current to be $0.13\underline{/182^\circ}$ degrees amp.

An analysis of Fig. 7 indicated that an additional transfer of 0.84 mf was needed from *B*-top phase to *B*-bottom phase.

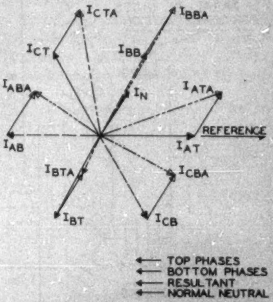

Fig. 7. Neutral current phasor diagram after first interchange

The 0.84-mf change was accomplished by interchanging 12 additional units in the *B* phase. The residual neutral current was checked after the second interchange and was found to be 0.046 amp which is within the maximum allowable residual neutral current of 0.07 amp.

The same procedure was used to balance bank no. 5. The initial neutral residual current was 0.265 amp. After interchanging 26 units in *B* phase and 18 units in *C* phase the residual neutral current was reduced to 0.098 amp. A second interchange of 12 units was made in *C* phase which reduced the residual neutral current to 0.072 amp, which is considered satisfactory.

SUBSTATION OPERATING PROCEDURE

It was first decided to lower the system voltage at the Peninsula Substation each time the banks were energized for a neutral-current measurement test to offset the voltage rise caused by the capacitors. This required considerable time for system co-ordination before each test and, as a result, tests proceeded rather slowly the first day. Since it required only approximately 3 seconds to make each current measurement, it was decided by the system operator that no voltage drop would be required before energizing the bank. The voltage reduction is more harmful than the 3-second voltage rise. After this change in procedure was made, neutral-current measurement tests were conducted very rapidly.

When making capacitance measurements prior to selecting specific units to interchange, it was found that approximately four units had to be measured for capacitance for every two units interchanged. In bank no. 4, 100 units were measured before selecting 50 to interchange; 112 units were measured in bank no. 5 before selecting 56 units to interchange. It required 4 days to attain the proper balance on both banks.

Balancing With Phasemeter and Wattmeter

Since the original balancing of the capacitor banks at Peninsula Substation, a simpler method of determining the phase angle of the neutral current has been developed. Either a phasemeter can be used to compare the phase angle of the neutral current with a reference potential, or a wattmeter for comparison of real power derived from the neutral current with each of six reference potentials. A circuit is used as illustrated in Fig. 3. The residual neutral current and one of six potentials are utilized as input quantities into a phasemeter and a wattmeter; see Fig. 3. The six potentials are 60 electrical degrees apart. With these quantities, it is possible to determine the phase angle of the residual neutral current and then proceed with the balancing, as discussed in the foregoing.

The wattmeter may have an application in normal operation. It is the practice of the operating department to inspect the capacitor installation once a week. This inspection is for blown fuses and other discrepancies. Since there are almost 4,000 capacitor-unit fuses in the installation, the inspection is quite time-consuming. A single-phase wattmeter might be installed on the control panel for each bank. A blown fuse would cause a rise in the residual neutral current of the bank which would be indicated on an ammeter on the control panel. If the inspector notes a rise in the residual neutral current, he would proceed to apply the different potentials to the wattmeter with a rotary switch. By noting the maximum wattmeter indication, he could determine which phase group has a blown fuse. The equipment for this installation would not be expensive.

Conclusions

The following conclusions are based on the characteristics and procedure for balancing high-voltage double-wye-connected capacitor banks:

1. Double-wye-connected high-voltage banks may have sufficient initial residual current to cause improper operation of the neutral-current relay used to prevent overvoltage operation of capacitor units when an excessive number of units are lost in one series section.

2. The normal residual neutral current with all units in service is the result of:

   a. A 0 to +15% manufacturing tolerance of individual capacitor units.

   b. The variation in the capacitance of units due to different unit temperatures resulting from capacitors in the top tiers operating at higher ambient temperatures than those in the lower tiers. This is because warm air rises from below; the top tiers get direct sunlight, and they cast their shadows on the lower tiers.

3. It may be found necessary to balance the bank by shifting individual capacitor units to reduce the residual neutral current to within an allowable limit to permit proper neutral-relay operation. The maximum allowable residual current is specified as one-fourth of the difference between the neutral currents obtained when the maximum permissible number of units is lost and the permissible number plus one additional unit.

4. Shifting units will counteract unbalance caused by 0 to +15% manufacturing tolerance. Unbalance caused by item *b* in conclusion 2 usually may be neglected providing the bank is arranged so that changes in capacitance caused by different internal operating temperatures will be equally distributed throughout all six phase groups.

5. Double-wye-connected capacitor banks may be easily balanced in the field by using the following procedure, when it is found that the initial residual neutral current exceeds the maximum allowable value specified in conclusion 3:

   a. Determine magnitude and phase angle of initial residual current.

   b. Determine phase groups contributing to unbalance and calculate magnitude of capacitance change in the various phase groups necessary to reduce the initial residual current to near zero.

   c. Balance bank by interchanging high- and low-capacitance units to achieve calculated capacitance change necessary to attain proper balance.

6. Balancing in the field can be eliminated if proper consideration is given to the problem by the engineers designing the bank. If the phase groups are balanced on paper and a strict unit placement program is adhered to during field erection, there should be no problem of tolerance unbalance.

7. A single-phase wattmeter or a phasemeter can be used to determine which phase group contains a blown fuse on a large bank.

Appendix I. Determination of Neutral Current

The following equations can be written by inspection of Fig. 8

$$I_{n1}+I_{n2}+I_{n3}-I_N=0 \quad (3)$$

$$I_L+I_{n4}+I_{n5}+I_N=0 \quad (4)$$

$$I_{n2}=I_{n3}=I_{n4}=I_{n5} \quad (5)$$

Solving equations 3, 4, and 5 for I_N

$$I_N=\frac{I_{n1}-I_L}{2} \quad (6)$$

Neutral current in % at normal total bank current is

$$\%I_N=\left|\frac{I_N}{I_{a1}}\right| 100 \quad (7)$$

Normal total bank current when $Z_L=Z_n$ is

$$I_{a1}=\frac{2E}{Z_n} \quad (8)$$

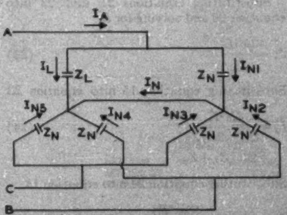

Fig. 8. Currents in double-wye-connected capacitor bank

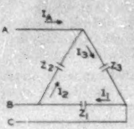

Fig. 9. Currents in equivalent delta-connected capacitor bank

Substituting equation 8 into equation 7

$$\%I_N=\frac{Z_nI_N\ 100}{2E} \qquad (9)$$

By inspection of Fig. 8

$$I_a=I_{n1}+I_L \qquad (10)$$

$$I_L=I_a\frac{Z_n}{Z_L+Z_n} \qquad (11)$$

$$I_{n1}=I_a\frac{Z_L}{Z_L+Z_n} \qquad (12)$$

Substituting equations 11 and 12 into equation 6

$$I_N=I_a\frac{(Z_L-Z_n)}{(Z_L+Z_n)} \qquad (13)$$

To solve for I_a convert double-wye network (Fig. 8) to delta network (Fig. 9)

$$Z_1=Z_n+\frac{Z_n(Z_L+Z_n)}{4Z_L} \qquad (14)$$

$$Z_2=\frac{Z_n}{2}+\frac{2Z_LZ_n}{Z_L+Z_n} \qquad (15)$$

$$Z_3=\frac{Z_n}{2}+\frac{2Z_LZ_n}{Z_L+Z_n} \qquad (16)$$

By inspection of Fig. 9

$$I_a=I_3-I_2 \qquad (17)$$

$$I_a=\frac{E_{ab}}{Z_2}-\frac{E_{ca}}{Z_3} \qquad (18)$$

From equations 15 and 16

$$Z_2=Z_3 \qquad (19)$$

Substitution equation 19 into equation 18

$$I_a=\frac{1}{Z_2}(E_{ab}-E_{ca}) \qquad (20)$$

The following voltage equalities may be written

$$E_{ab}=\sqrt{3E} \qquad (21)$$

$$E_{ca}=a\sqrt{3E} \qquad (22)$$

Substituting equations 21 and 22 into equation 20 and solving for I_a

$$I_a=\frac{3ja^2E}{Z_2} \qquad (23)$$

Substituting equation 15 into equation 23

$$I_a=\frac{3ja^2E}{\frac{Z_n}{2}+\frac{2Z_LZ_n}{Z_L+Z_n}} \qquad (24)$$

Substituting equation 24 into equation 13

$$I_N=\frac{(3ja^2E)}{(Z_LZ_n+Z_n^2+4Z_LZ_n)}(Z_L-Z_n) \qquad (25)$$

Substituting equation 25 into equation 9 and neglecting voltage and impedance angles

$$\%I_N=\frac{3}{2}\frac{(Z_L-Z_n)}{(5Z_L+Z_n)}\ 100 \qquad (26)$$

However

$$Z_n=\frac{-jXcN}{M} \qquad (27)$$

$$Z_e=\frac{-jXc(N-1)}{M}+\frac{-jXc}{M-K} \qquad (28)$$

Substituting equation, 27 and 28 into equation 22

$$\%I_N=\frac{150}{6_N\left(\frac{M}{K}-1\right)+5} \qquad (29)$$

Equation 27 in terms of % units lost is

$$\%I_N=\frac{150}{6_N\left(\frac{100}{K_1}-1\right)+5} \qquad (30)$$

Appendix II. Determination of Resulting Overvoltage

$$e_f=\frac{I_e(-jXc)}{M-K} \qquad (31)$$

$$e_{n1}=\frac{I_{a1}(-jXc)}{2M} \qquad (32)$$

$$\%e_f=\frac{e_f}{e_{n1}}\ 100 \qquad (33)$$

Substituting equations 31 and 32 into equation 33

$$\%e_f=\frac{I_e}{I_{a1}}\frac{(2M)}{(M-K)}\ 100 \qquad (34)$$

Substituting equations 8 and 25 into equation 34 and neglecting voltage and impedance angles

$$\%e_f=\frac{6MZ_n}{(5Z_1+Z_n)(M-K)}\ 100 \qquad (35)$$

Substituting equations 27 and 28 into equation 35

$$\%e_f=\frac{600MN}{6N(M-K)+5K} \qquad (36)$$

Equation 36 in terms of % units lost is

$$\%e_f=\frac{60{,}000N}{6N(100-K_1)}+5K_1 \qquad (37)$$

References

1. ENGINEERING ASPECTS OF LARGE HIGH-VOLTAGE BANKS, P. E. Hendrickson, N. R. Schultz. *Distribution Magazine*, Schenectady, N. Y., vol. 15, no. 4, Oct. 1953, pp. 20–23.

2. REPORT ON THE OPERATION AND MAINTENANCE OF SHUNT CAPACITORS, AIEE Committee Report. *AIEE Transactions*, vol. 69, pt. II, 1949, pp. 1,208–19.

3. STANDARDS FOR SHUNT CAPACITORS. *Publication Number CA1-1959*, National Electrical Manufacturers Association, New York, N. Y.

Discussion

E. C. Starr (Bonneville Power Administration, Portland, Oreg.): We have found Mr. Compton's excellent analysis of double-wye capacitor-bank currents very interesting since it extends certain considerations which led us to a somewhat different form of 115-kv bank arrangement in 1949. At that time we were considering two banks of capacitors with roughly the same rating as those described in the paper. One fact that immediately impressed us was that a sensitivity problem was apparent in any relaying scheme intended to back up the individual fuses. Whether relaying was attempted by current or voltage to ground or between floating neutrals, the % overvoltage developed corresponded roughly to the % of units removed from one layer, and the relaying quantity was disturbingly small. This promised to be further aggravated by the natural fundamental unbalance between legs and by harmonics, and inrush and external fault currents in the case of a grounded neutral.

In view of the great sensitivity required of any relay under these conditions, we were reluctant to place any more reliance for protection than necessary on relaying. A small change in calibration could permit sustained overvoltages. It seemed to us that the best possibility of avoiding overvoltage was to keep as many capacitor units as possible in parallel per layer to avoid the coincidence of failures which might lead to overvoltage. Our failure rate on capacitors which have been in service for some time is less than 0.1% per year. On this basis, and with inspection intervals of 1 week or less, the probability of overvoltage is very low.

We have adopted the grounded-neutral single-wye form of arrangement, having 25-kilovar 7,960-volt capacitors protected by individual indicating fuses. The grounded wye has the advantages of station surge protection and reduced recovery voltage during switching, and the disadvantage of complicating the relaying by inrush and harmonics. The inrush we found high enough to damage neutral-current transformers, but standard heavy-duty carbon telephone blocks on the primaries have been effective in eliminating that problem. Third-harmonic by-pass filters have been designed which are effective with one form of overcurrent relay.

A bank may have eight or nine series groups of from 20 to 30 capacitors in parallel per phase. The expectancy of three fuses blowing during 1 week in one layer of 20 in any bank is less than once in a 1,000,000 years. On this basis, we are inclined to question the need for neutral relays, although we still employ them.

N. Rex Sheppard (General Electric Company, Hudson Falls, N. Y.): Mr. Compton's paper is very well written and explains a very unique and worth-while method of balancing double-wye high-voltage capacitor banks. These comments are, therefore, not intended to discredit his very fine work. It does appear, however, that since more and more high-voltage capacitor banks are being applied, careful consideration should be given as to a preferred method of designing them.

Much experience has been gained by utilities and manufacturers since high-voltage banks were first used to any great extent a few years back. Much of this experience has been acquired since the bank referred to by the author was first designed and built. In view of this experience, it seems worth while to pose two questions:

1. Is relay protection to prevent overvoltage across individual capacitor units as a result of losing units in any particular series section justifiable in view of the probability of damage and the expense and difficulty involved in attaining an effective relay system?

2. Is it wise to break an individually switched capacitor bank into two paralleled single-wye banks with line terminals connected to a single circuit breaker and neutrals interconnected? This connection is often referred to as a double-wye bank.

It may be worth while to clarify the nature of the relay protection we are discussing. It should not be confused with the use of normal overload relays to protect the bank and system against the effects of bus faults occurring between the capacitor units and the circuit breaker. Nor should it be confused with the protection against case-bursting and service interruption afforded by individual capacitor unit fuses.

This particular type of relaying is usually thought of as providing protection against the contingencies of:

A. Overvoltage on individual capacitor units as a result of losing a given percentage of units from any one single series section. This may result since, as units fail and are removed from any one series section, the impedance of that section increases. However, since there are many sections in series, the effect of the increased impedance in one section does not decrease the phase current in the same proportion. The result of the slightly reduced current flowing through a more markedly increased impedance causes a resulting higher voltage to be impressed across the remaining units in that section. This condition is difficult to detect and protect against. It is, however, an improbable occurrence if the bank is periodically inspected. There are considerations in design which can further reduce the already small probability of incurring damage in this way.

B. An arc over across a series section as the result of a foreign object initiating a short circuit. As with any high-voltage equipment with exposed buswork and terminals, it is possible for foreign objects to initiate an arc. The difference between this and most equipments is that the arc is not line to ground or line to line, but is across only a portion of the line-to-neutral voltage. As a result, the phase current may not be increased sufficiently to cause normal overcurrent operation of the circuit breaker.

Based on observations and experiences shared with many high-voltage capacitor users throughout the country, we feel that contingency A can best be avoided by:

1. Designing the bank with as few series sections and as many parallel units in each section as possible. This can be done by:

a. Making each individually switched bank as large as possible based on the allowable voltage step. This, of course, also reduces the investment in switchgear.

b. Adopting the single-wye bank in preference to the double-wye bank.

c. Using as high a capacitor unit voltage rating as is available as a standard that will divide evenly into the required phase voltage of the banks. The small present-day difference in cost between medium-voltage (2,400 to 4,160-volt) and high-voltage (4,800 to 7,960-volt) capacitor units make this suggestion economically sound.

2. Periodically inspect the individual capacitor fuses which serve to remove as well as indicate a failed unit. When a failed unit is detected, it should be replaced along with the fuse as soon as practical to do so. It is felt that effective relaying to protect against this contingency is difficult to accomplish and may not be economically justifiable.

Contingency B may be a worth-while consideration particularly on grounded-wye banks where it is relatively inexpensive to accomplish. On grounded-wye banks, the protection can be effected by a relay system requiring a medium-voltage current transformer, a current relay incorporating inverse time-delay characteristics and a third-harmonic filter, and spark-over gaps connected across the current transformer primary. The gaps are to protect the current transformer and secondary circuit from the high voltage which might otherwise appear across it when the bank is switched on and off the line. Such a circuit is indicated in Fig. 10. On ungrounded-wye banks, the protection is similar except a potential transformer and a voltage relay are used.

Although the current or the voltage, as the case may be, is affected by system balance and capacitor bank balance, the circuits are relatively free from misoperation when set to protect against contingency B. The reason for this is that the relay need not be set nearly as fine as if designed to detect contingency A.

Most systems proposed are based on detecting the voltage at and/or current flowing through the neutral connection. The conditions at the neutral are necessarily dependent upon the vector angle and magnitude relationship of the impedances in each phase or leg of the capacitor bank. The overvoltage condition is, however, largely the result of the change in impedance in a particular series section. Therefore, with all systems proposed, except more expensive methods which measure and compare the voltages appearing across each series section (quite expensive), the relays can operate in any of three different ways:

1. They may operate as desired to guard against a predetermined overvoltage appearing across a single series section. This operation would be assured if all successive unit failures occurred in the same series section. This is a very improbable occurrence.

2. They may operate to relay the bank off the line when it is not necessary to do so from an overvoltage consideration. This may be called false operation and is likely to occur much more frequently than operation (1). This may occur when:

a. Successive faults occur in the same phase leg, but in different series sections (more likely than in same section).

b. Successive faults occur in different phase sections such that the resultant vector effect on the neutral causes relay operation (also more likely than failures in same section which might cause overvoltage).

c. Change in balance of capacitor bank because of temperature variations between one part of the bank and another. (Referred to in paper).

d. In case of a single-wye bank, the relay (being set sensitively to detect operation 1) may operate on a slight unbalance in system voltage. This is a point in favor of the double-wye connection.

3. The relay system may not operate when an overvoltage is applied in a particular series section as the result of the balancing effect of other failures in other phase legs of the bank (or banks in the case of the double-wye system). This is, just as operation 1, an improbable occurrence as a result of the high reliability of modern power capacitors and the inspection practices of most operators. It does, however, indicate a considerable limitation on relay methods.

As pointed out previously, the single-wye bank has the disadvantage over the double-wye bank in that a sensitively set relay would be affected by system voltage unbalance. There are, however, certain advantages of the single-wye bank which may well overshadow this one disadvantage. These are:

1. Twice as many units are placed in parallel in each series section. This means that twice as many units must fail in a particular section of the single-wye bank to cause the same overvoltage which might result from a given number of failures in a section of the double-wye bank.

2. The initial cost of the single-wye bank is usually considerably less than that of the double-wye bank.

It is, therefore, a worth while consideration that the single-wye bank be used in preference to the double-wye bank and that the value of relay protection to guard against individual unit overvoltage be made on the basis of its need, cost, and reliability.

By taking advantage of the added benefits of the single-wye bank, by switching high-voltage banks in as large increments as practical from a voltage step consideration, by making use of as high-voltage standard capacitor units as possible in original design, and by initiating a periodic bank inspection procedure, it is my feeling that the

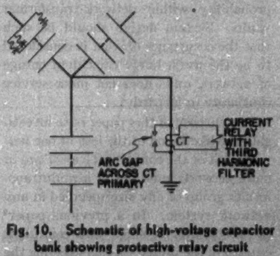
CT
CURRENT RELAY WITH THIRD HARMONIC FILTER
ARC GAP ACROSS CT PRIMARY

Fig. 10. Schematic of high-voltage capacitor bank showing protective relay circuit

user will attain the highest satisfaction from their high-voltage capacitor banks. Although I have strayed from the basic topic of this paper on balancing, I felt that the discussion would be of interest, since the fine balance is only required if relaying to protect contingency A is being considered.

O. R. Compton: Mr. Starr and Mr. Sheppard are both advocates of the single, grounded-wye-connected design for capacitor banks of large size, and I appreciate their comments very much. As Mr. Starr points out, the best form of overvoltage protection is obtained by using as many capacitors as possible in parallel and this is an inherent characteristic of the single-wye design.

It would be most helpful to the industry if a paper were prepared by Mr. Sheppard expanding the thesis he propounds in his discussion. Since the Virginia Electric and Power Company capacitor installation has been balanced by the methods described in my paper, we plan to continue operation as a double-wye bank. Future installations will be engineered in line with the latest practices of the industry.

One problem in the use of single, grounded-wye-connected capacitor banks is the possibility of telephone interference where telephone toll lines are in the vicinity. This problem will need additional exploration before the single-wye bank can come into general usage.

Coincident-Outage Probability in Secondary-Network Vaults

DAVID N. REPS
ASSOCIATE MEMBER AIEE

SINCE the advent about 30 years ago of the 120/208-volt secondary-network system of electric power distribution in commercial areas of cities, both load density and the prevalence of large, concentrated loads have continued to increase. This load growth has in turn brought about a growing tendency for added increments of network-system capability to assume the form of multiple-network-transformer installations. Moreover, the coming popularity of 265/460 volts as another secondary-network utilization voltage will accelerate future needs for multiple-transformer, spot-network installations.[1]

The allowable loading of a multiple-transformer network-unit installation may be based on the loss of one network unit or on the coincident loss of two network units. In the event of such contingencies involving the loss of network units in a particular vault or group of neighboring vaults, the network units remaining in service within that group must be capable of carrying the load. Network planning and design must therefore include evaluation of coincident-outage probability within network-transformer vaults. System design should be such that the occurrence of what it considered to be the worst likely coincident outage of network units does not place service continuity in jeopardy.

The purpose of this paper is to investigate the likelihood of the loss of one network unit or the concurrent loss of two or more network units out of a multitransformer group of any size specified in any network system. In a previous paper[2] the probability of single and coincident outages of the primary feeders serving the network units was discussed for network systems in general. This earlier analysis dealt with the factors which govern the adequacy of primary-feeder capability from the standpoint of primary-feeder outage likelihood. The present paper extends the probability analysis of network system capability into the network-unit vaults.

Causes and Effects of Network-Unit Outage

A modern secondary-network unit consists of a transformer which steps down the primary-feeder voltage to utilization voltage, and a network protector located in the low-voltage leads of the network transformer; see Fig. 1. The network protector is a special type of circuit breaker equipped with relaying which will trip the circuit breaker in the event of reverse power flow, or automatically close the breaker if the voltage across the open protector is such that power will flow from the primary feeder into the low-voltage network. The network protector also contains a set of fuses, one in each phase. Since the network-protector circuit breaker can trip only on reverse power, the fuses serve as a means for interrupting currents that are not interrupted by the network-protector circuit breaker or other means.

A primary-feeder fault results in the tripping, due to reverse-power flow, of the network protectors in all the units supplied by that feeder. Similarly, intentional de-energization of a primary feeder by tripping its circuit breaker at the source results in the opening of the network protector in every unit supplied by that feeder, due to reverse magnetizing current flow from the low-voltage system to the network transformers whose primary feeder is de-energized.

A network unit is unable to carry load if its primary feeder is de-energized, or if its network-protector circuit breaker is open. Network-unit outage will also result from blown network-protector fuses, but the effect of this cause of outage on the probability of network-unit outage is relatively small and will not be considered in this paper.

The probability of outage to a network unit is the sum of the probabilities of its primary feeder being out of service and its network protector being permanently open after having failed to close. Each of the other possible causes for network-unit outage, such as blown network-protector fuses, has a certain probability and they all can be lumped into a single value and added to the feeder-outage and protector failure-to-close probabilities to obtain the total probability of outage for that unit.

Secondary-network system designers and operators may prefer to deal with outage probabilities in terms of their likely frequency of occurrence expressed in units of years rather than with pure probability numbers which are often difficult to visualize in terms of the quantities that can be obtained from network operating experience. Hence, in the probability analyses of this paper certain approximations are introduced which permit coincident-outage frequency of network units in the same vault to be expressed in terms of such quantities as the number of network-feeder outages per year and the number of times per year that a network protector is found unable to close during a routine vault inspection.

A secondary-network system is gener-

Paper 55-161, recommended by the AIEE Transmission and Distribution Committee and approved by the AIEE Committee on Technical Operations for presentation at the AIEE Winter General Meeting, New York, N. Y., January 31–February 4, 1955. Manuscript submitted October 26, 1954; made available for printing December 6, 1954.

DAVID N. REPS is with the Westinghouse Electric Corporation, East Pittsburgh, Pa.

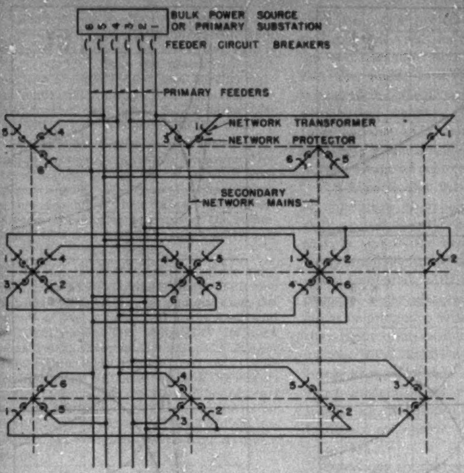

Fig. 1 (left). Part of a secondary-network system, showing six primary feeders interlaced among network vaults housing one, two, three, or four network units

Fig. 2 (right). The probability that a single network feeder outage will affect one of the units in a particular v-unit vault

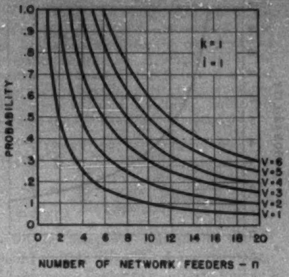

ally so designed that the loss of one primary-feeder circuit can be sustained indefinitely without excessively overloading the network units remaining in service. During such a feeder outage, single network units in certain vaults throughout the system are de-energized. In any one of these vaults, there is also some small probability that the network protector in one of the other network units will be open and unable to close. A network protector that has failed to close can in no way damage its network unit, which will be unable to carry load. However, the coincident loss of two, or more, network units in any one vault or neighboring group of load-sharing units may result in overloading the units remaining in service. The equations and computation methods presented in this paper make it possible to evaluate the risk of coincident outage of network units in vaults or groups of neighboring units.

Outages of Primary Feeders Serving a Vault

When one or more interlaced primary feeders are concurrently out of service, vaults located throughout the network area are affected. For example, during

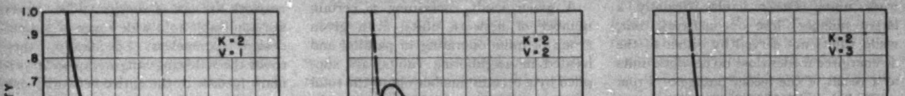

Fig. 3. The probability that the coincident outage of two network feeders (k=2) will result in the loss of one (i=1), or the coincident loss of two (i=2) network units in a particular v-unit vault

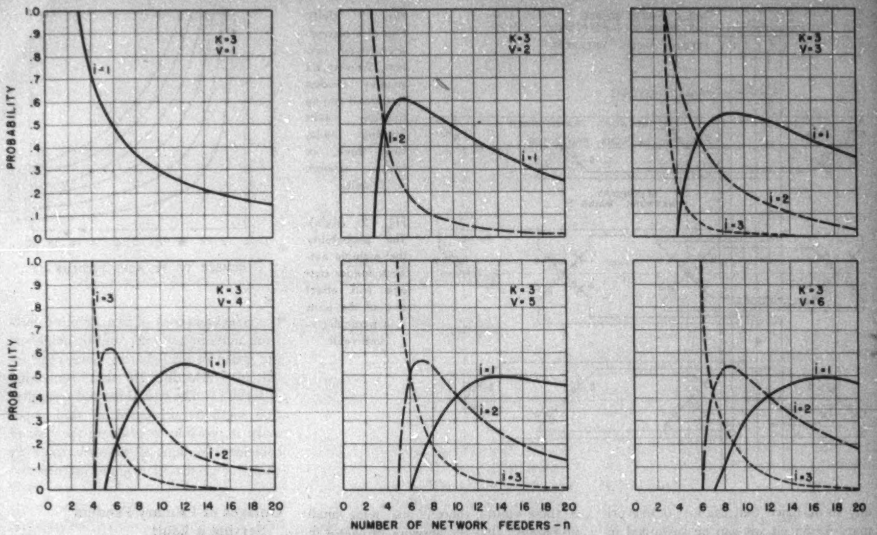

Fig. 4. The probability that the coincident outage of three network feeders (k = 3) will result in the loss of one (i = 1), two (i = 2), or three (i = 3) network units in a particular v-unit vault

the simultaneous outage of two feeders, some vaults may as a result lose two network units. Other vaults (usually a larger number) lose one network unit, while vaults not served by either of the de-energized feeders lose no network units as a result of the feeder outages. From methods described in the preceding paper[2] on primary-feeder coincident-outage likelihood, the frequency of occurrence of coincident feeder outages can be evaluated for any network system, in terms of one of more of the following factors, all of which influence or are influenced by secondary-network design:

1. Total number of primary feeders.
2. Total mileage of primary-feeder circuit.
3. The number of accidental feeder outages per year.
4. The number of accidental feeder outages per 100-mile-years of feeder circuit.
5. The total scheduled feeder-outage time per year.
6. The time duration of existing or future feeder outages.

All of these determinants of primary-feeder coincident-outage likelihood pertain to the network system as a whole. The results of an analysis based on such network-wide considerations can be extended to include coincident-outage likelihood of the network units in any given vault or within any given group of network units.

A given vault containing a certain number of network units, or a given group of units operating in parallel and located in neighboring vaults, are supplied by a certain number out of the total number of feeders to the network. In very large multiunit vaults, or in a group containing a relatively large number of network units, every one of the network feeders may be present. For instance, in a 4-feeder network, the four network units located in a particular vault would each be served by one of the total number of four network feeders. More often, however, even in multiunit vaults or groups, fewer than the total number of network feeders are represented. System-wide feeder-outage probabilities applicable to all the network feeders as a whole must be modified to apply to the fraction of the network feeders serving a particular vault or group of units.

The curves of Figs. 2, 3, and 4 are for the purpose of adjusting primary-feeder outage probabilities, computed for the entire system, for application to primary feeders serving an individual vault or group of network units. These curves can be used to find the probability for a feeder outage, or the coincident outage of two or more feeders to the same vault or group of network units when a specified number of feeders serving the entire network are out of service. The curves are applicable to a wide range of system design parameters. Specifically, they cover the following ranges: up to 20 primary feeders to the entire network; one to six network units within the same vault or group; the outage of one or the coincident outage of two or three network feeders; the loss of one or the coincident loss of two or three network units is the same vault or group as a result of network-feeder outages. The method used for deriving these curves is outlined in Appendix I. The following example will illustrate one use for the curves of Figs. 2, 3, and 4.

EXAMPLE: COINCIDENT FEEDER OUTAGES IN THE SAME VAULT

A network vault contains four units served by four different primary feeders out of a total of ten feeders to the entire network.

1. For what fraction of the total number of times during which two network feeders are simultaneously out of service will the two affected feeders be two of the four serving the vault?
2. For what fraction of the total number of 2-feeder outages will just one of the de-energized network feeders be one of the four to the vault?

1. For this case $n=10$, $v=4$, $k=2$, and $i=2$. From Fig. 3, the probability read from the $k=2$, $v=4$ curves for $n=10$ and $i=2$ is $U_{10,4,2,2}=0.15$. Thus the probability that both the affected feeders in a 2-feeder outage serve this vault is 0.15. Stating this another way, only one in 6.67 2-feeder outages will involve two feeders to this vault.

Suppose that methods[3] used for computing the average frequency of occurrence for the coincident outage of two network feeders give a period of 10 years for the network in this example. Then the average number of years between occurrences of the coincident loss of two feeders to this 4-unit vault is (10) (6.67) = 66.7 years.

2. To determine the fraction of the total number of 2-feeder outages that will involve just one feeder to the vault in question, the curves of Fig. 2 for $n=10$, $v=4$, $k=2$, and $i=1$ are used. The probability for $i=1$ when $k=2$, $v=4$, and $n=10$ is $U_{10,4,2,1}=0.56$. Thus slightly more than half the 2-feeder outages will involve one of the feeders to this vault. The average number of years between occurrences for the loss of one feeder to this vault as a result of the coincident loss of two network feeders is (10/0.56) = 17.9 years.

From the preceding example it can be seen that the curves of Figs. 2, 3, and 4 serve to determine feeder-outage probabilities in individual vaults throughout the system when feeder-outage probability for the network as a whole is given. This approach, which is first to consider network-feeder outage likelihood and then vault-feeder outage likelihood, can be very useful in secondary-network system design because it readily permits quick outage-probability evaluation of alternative network plans utilizing different numbers of interlaced primary feeders and the number of network units in vaults.

Network-Protector Failure to Close

The high reliability of modern network protectors has made network-protector failure to close purely an academic consideration in the determination of coincident network-unit outages for smaller systems. For very large systems, however, the likelihood of a protector having failed to close somewhere in the system may warrant attention. Should such an outage exist in a vault where a second network unit is out of service because its primary feeder is de-energized, two network units would be coincidentally out of service in that vault.

A network protector that cannot close may be detected under two circumstances: first, customers in the vicinity of the unloaded network unit may complain of low voltage; second, during a routine inspection of network vaults the open protector will be discovered. The likelihood of detection in the first way ordinarily is small, since the open protector may be in a multiple-unit vault in which the loss of one unit does not result in overloading of the other units; or if the open protector is located in a single-unit vault, then the neighboring network transformers are fully capable of sharing load via the secondary mains without serious decrease in the voltage at customers' loads.

For a particular network system, the accumulation of reliable data on network-protector failure-to-close frequency may be impossible because of the relatively small likelihood of such occurrences when compared with the frequency of primary-feeder outages; or because infrequent or aperiodic network vault inspections make it impossible to determine the average time duration of such outages. In the absence of data accumulated for a given system, data published by the Edison Electric Institute[2–6] may be used to obtain reasonable order-of-magnitude estimates.

Equations are derived in Appendix III for estimating the likelihood for the failure to close of a network protector in a vault, or a group of units in which one, or more, other units are out of service because of primary-feeder outages. The following example will illustrate how the equations can be used.

EXAMPLE: FEEDER AND NETWORK-PROTECTOR COINCIDENT OUTAGE

Suppose that the network system in the previous example contains 100 network units. The estimated number of network-protector failures to close is one per year. The average duration of such an outage is three months.

1. During a 2-feeder outage of 66.7 years average frequency, what is the likelihood that, in a 4-unit vault that has lost two feeders, one of the two remaining units will also be unable to carry load because its network protector cannot close?

2. How often will it be that a network protector in that vault cannot close during one feeder outage in the vault of 17.9 years average frequency?

1. For this case the quantity y in equation 24 is 3 months, or 0.25 year. Substituting into 24

$$r_{(4-2)}=\frac{(2)(1)(0.25)}{100}=0.005$$

where $r_{(4-2)}=0.005$ is the years-per-year outage rate for the two remaining protectors in the 4-unit vault. Hence, from equation 25 the period of years between occurrences for the loss of three network units in the vault, as a result of the outage of two network feeders, and the coincident failure to close of a network protector in one of the two remaining units, is

$$T_{10,4,2,(2+1)}=\frac{66.7\text{ years}}{0.005}=13{,}330\text{ years}$$

2. The period of years between occurrences, for the loss of two network units in the vault, as a result of the outage of two network feeders (one of which serves the vault), and the coincident failure to close of a network protector in one of the remaining three units is found as follows: Substitute $y=0.25$ and $(v-i)=3$ into equation 24,

$$r_{(4-1)}=\frac{(3)(1)(0.25)}{100}=0.0075$$

$$T_{10,4,2,(1+1)}=\frac{17.9\text{ years}}{0.0075}=2{,}400\text{ years}$$

In the foregoing example it will be noted that the likelihood for the outage of a primary feeder to a network unit in a vault, while another network unit in that vault is out of service because its network protector failed to close, can be reduced by shortening the time duration of network protector outages. This can be accomplished by more frequent network vault inspections for testing the operation of network protectors. The average time duration of a network protector outage will be one-half the period between inspections. By substituting values for network-protector and primary-feeder outage frequency applicable to a specific system, coincident network-unit outage frequency within any given vault can be evaluated.

Conclusion

The likelihood of coincident primary-feeder outages in a network system is influenced by several determinants of network system design. These design factors also influence coincident-outage likelihood of primary feeders within the same vault or a specified group of network units. Through the use of the equations and curves presented in this paper, the probability of coincident outage of network units within any given vault, or group of units, can be evaluated from primary-feeder and network-protector outage data or experience for the network system as a whole. Such methods of probability analysis are very useful in secondary-network system planning, because they readily permit quick outage-probability evaluation of alternative network plans utilizing different numbers of interlaced primary feeders, and different numbers of network units in vaults.

Nomenclature

n = number of network feeders
v = number of network units in one vault
N = total number of network units in system
V = total number of vaults in system
$N_{n,v}$ = number of network units in an n-feeder system with v units per vault
$V_{n,v}$ = number of vaults in an n-feeder system with v units per vault

k = number of primary feeders simultaneously out of service

i = number of primary feeders out of service in one vault

r_N = network-protector failure-to-close probability for an N-unit system

r_v = network-protector failure-to-close probability for a v-unit group

a = number of network-protector failures to close per year for the entire system

y = the outage-time duration of a network protector that fails to close, years

P_k = probability for the simultaneous outage of k network feeders

T_k = average period between occurrences of the simultaneous outage of k network feeders, years

$U_{n,v,k,i}$ = the probability that a v-unit vault will have i of its feeders out of service when k out of n network feeders are out of service

$R_{n,v,k,i}$ = the probability that i feeders to a v-unit vault are simultaneously out of service

T_v = time period between failures to close of a network protector in a group of v network units, years

$T_{n,v,k,i}$ = time period between coincident outages of i feeders in a v-unit vault, years

Appendix I. Outage Probability of Feeders Serving a Vault

Suppose that attention is centered on a particular network vault, or group of network units, containing the number v units out of a total of N units, in a system served by n interlaced primary feeders. The $(N-v)$ remaining network units in the system may be considered to have imaginary boundaries encircling them such that they are all in groups of v per group. The total number of such groups is then N/v. The fraction of this total number of groups affected in the same way by a primary-feeder outage is also the probability of such a contingency occurring in the v-unit vault or group under consideration.

Consider network systems supplied by n completely interlaced primary feeders, where n may have a different integral value for each system considered

$$n=1, 2, 3, 4, \ldots \tag{1}$$

Suppose that in each system, the network units are in groups of v, where v may have any integral value

$$v=1, 2, 3, 4, \ldots \tag{2}$$

No two units in a group of v may be served by the same primary feeder. In an n-feeder system containing groups of network units with v units in each group, there is a maximum possible number of groups for which no two groups will be served by the same combination of v out of n feeders. This number of different groups is given by

$$V_{n,v}=\frac{n!}{v!(n-v)!} \tag{3}$$

The total number of network units in $V_{n,v}$ vaults, each containing v units, is

$$N_{n,v}=V_{n,v}(v) \tag{4}$$

The quantities n, v, $N_{n,v}$ describe a hypothetical secondary-network system served by n primary feeders. Each vault contains v network units, with each unit in that vault supplied by a different feeder. The total number of vaults in the network is $V_{n,v}$ and the total number of network units is $N_{n,v}$.

The n network feeders will suffer outages such that any number k out of n feeders may be out of service at the same time, where

$$k=1, 2, 3, \ldots \tag{5}$$

When the coincident outage of two or more network feeders occurs, various vaults throughout the network area will have none, one, or more of their feeders de-energized. During such a concurrent outage of k network feeders, let i be the number of de-energized feeders in a v-unit (or v-feeder) vault, where

$$i=0, 1, 2, 3, \ldots \tag{6}$$

Two limitations are placed on the maximum value of i

$$i \leq v \text{ or } i \leq k \tag{7}$$

In this hypothetical $N_{n,v}$-unit, $V_{n,v}$-vault, n-feeder network system in which each vault houses v units, the fraction of the total number of vaults in which i feeders are lost during a network-wide outage of k feeders is represented by the symbol $U_{n,v,k,i}$ where

$$1 \geq U_{n,v,k,i} > 0 \tag{8}$$

The fractional number $U_{n,v,k,i}$ is the probability that a v-unit vault in an n-feeder system will lose i out of v units as a result of a coincident outage of k out of n feeders.

Equations can be written for expressing

n = 6
v = 1

I	II	III	IV	V	VI
I					
	II				
		III			
			IV		
				V	
					VI

$V_{6,1} = 6$

$N_{6,1} = 6$

$U_{6,1,1,1} = 1/6$

n = 6
v = 2

I	II	III	IV	V	VI
I	II				
I		III			
I			IV		
I				V	
I					VI
	II	III			
	II		IV		
	II			V	
	II				VI
		III	IV		
		III		V	
		III			VI
			IV	V	
			IV		VI
				V	VI

$V_{6,2} = 15$

$N_{6,2} = 30$

$U_{6,2,1,1} = 5/15$

$U_{6,2,2,1} = 8/15$

$U_{6,2,2,2} = 1/15$

$U_{6,2,3,1} = 9/15$

$U_{6,2,3,2} = 3/15$

n = 6
v = 3

I	II	III	IV	V	VI
I	II	III			
I	II		IV		
I	II			V	
I	II				VI
I		III	IV		
I		III		V	
I		III			VI
I			IV	V	
I			IV		VI
I				V	VI
	II	III	IV		
	II	III		V	
	II	III			VI
	II		IV	V	
	II		IV		VI
	II			V	VI
		III	IV	V	
		III	IV		VI
		III		V	VI
			IV	V	VI

$V_{6,3} = 20$

$N_{6,3} = 60$

$U_{6,3,1,1} = 10/20$

$U_{6,3,2,1} = 12/20$

$U_{6,3,2,2} = 4/20$

$U_{6,3,3,1} = 9/20$

$U_{6,3,3,2} = 9/20$

$U_{6,3,3,3} = 1/20$

n = 6
v = 4

I	II	III	IV	V	VI
I	II	III	IV		
I	II	III		V	
I	II	III			VI
I		III	IV	V	
I		III	IV		VI
I			IV	V	VI
I	II		IV	V	
I	II			V	VI
I		III		V	VI
I	II		IV		VI
	II	III	IV	V	
	II	III	IV		VI
	II	III		V	VI
	II		IV	V	VI
		III	IV	V	VI

$V_{6,4} = 15$

$N_{6,4} = 60$

$U_{6,4,1,1} = 10/15$

$U_{6,4,2,1} = 8/15$

$U_{6,4,2,2} = 6/15$

$U_{6,4,3,1} = 3/15$

$U_{6,4,3,2} = 9/15$

$U_{6,4,3,3} = 3/15$

Fig. 5. Four different, hypothetical 6-feeder network systems. The first system has vaults containing one unit each (v = 1); the second system, two (v = 2); the third system three (v = 3); and the fourth system four (v = 4). For each system, all the different possible combinations of feeders serving vaults are tabulated. From such tabulations, the fraction of the total number of vaults affected by various primary-feeder outages can be observed. This fraction is also the probability of any one vault being so affected

$U_{n,v,k,i}$ in terms of the two network design parameters n and v; the number k of network feeders simultaneously out of service; and the number i of affected feeders to a specific vault or group of network units.

To illustrate how such equations may be developed, consider the case of 6-feeder networks ($n=6$). Four different 6-feeder systems will be examined. In the first system, network units are individually located ($v=1$). In the second they are in pairs ($v=2$). In the third and fourth systems, network units are arranged in groups of three ($v=3$) and four ($v=4$) respectively. For all systems let the six primary feeders be numbered I, II, III, IV, V, and VI. Fig. 5 lists all the different combinations for six feeders serving vaults containing one, two, three, or four network units, such that in each system no two vaults are served by the same combination of feeder numbers.

After the possible combinations of feeders serving a vault with v network units are tabulated as in Fig. 5, the number of vaults losing i units when k out of six feeders are lost can be obtained by inspection. From an examination of other cases similar to those tabulated in Fig. 5, but for other values of n and v, the following equations are obtained:

For $k=1$, $i=1$

$$U_{n,v,1,1}=\frac{(n-1)!}{(V_{n,v})(v-1)!(n-v)!} \tag{9}$$

For $k=2$, $i=1$

$$U_{n,v,2,1}=\frac{2(n-2)!}{(V_{n,v})(v-1)!(n-v-1)!} \tag{10}$$

For $k=2$, $i=2$

$$U_{n,v,2,2}=\frac{(n-2)!}{(V_{n,v})(v-2)!(n-v)!} \tag{11}$$

For $k=3$, $i=1$

$$U_{n,v,3,1}=\frac{3(n-3)!}{(V_{n,v})(v-2)!(n-v-2)!} \tag{12}$$

For $k=3$, $i=2$

$$U_{n,v,3,2}=\frac{3(n-3)!}{(V_{n,v})(v-2)!(n-v-1)!} \tag{13}$$

For $k=3$, $i=3$

$$U_{n,v,3,3}=\frac{(n-3)!}{(V_{n,v})(v-3)!(n-v)!} \tag{14}$$

Values for $U_{n,k,v,i}$ computed from equations 9 through 14 are plotted in the curves of Figs. 2, 3, and 4. These curves show the probability ($U_{n,k,v,i}$) for losing i out of v feeders in a given vault should k out of n network feeders suffer coincident outages.

Suppose that the probability for the simultaneous outage of k network feeders is P_k. Methods for obtaining P_k are discussed in the first probability paper.[2] Then the probability for i feeders to a v-unit vault being simultaneously out of service because of coincident feeder outages is

$$R_{n,v,k,i}=(P_k)(U_{n,v,k,i}) \tag{15}$$

In the previous paper[2] the average number of years between occurrences of the coincident outage of k network feeders is called T_k. Hence for an individual vault, or group, containing v network units, the period in years between occurrences for the coincident outage of i network units because of k simultaneous network-feeder outages is

$$T_{n,v,k,i}=\frac{T_k}{U_{n,v,k,i}} \text{ years} \tag{16}$$

Assumptions

The analyses in Appendixes II and III are approximate, and are based on the following assumptions:

1. The total number N of network units in the system remains constant regardless of the number of primary feeders or network units out of service, i.e., $N>>1$.
2. Over a very long period of time, each network protector will experience the same number of failures to close of equal time duration.

Appendix II. Probability of Network-Protector Failure to Close

Consider a network system with a total number of N network units. For most systems in which coincident-outage probability is sufficiently large to warrant consideration, a single network unit represents a small fraction of the total number employed, i.e., $N>>1$. It will be assumed that the loss of one, or even several, network protectors still leaves very nearly the same total number in service. Hence for the purpose of the following analysis it is assumed that

$$N\cong(N-1)\cong(N-2), \text{ etc.} \tag{17}$$

For the entire system, let the number of network-protector failures to close be the quantity a per year. Then the average failure-to-close rate per protector is a/N per year. The average number of years between failures, for a given protector, located anywhere in the system is N/a years.

Let the average time interval between inspections of a network protector be ($2y$) years. Assuming that a protector discovered unable to close is immediately repaired or replaced, the average length of time during which a faulty protector remains open is y years. Hence the probability that somewhere in the system a network protector is open because it cannot close is

$$r_N=a(y)=ay \tag{18}$$

If attention is centered on a particular v-unit vault, then the failure-to-close probability for the network protectors in that vault is

$$r_v=\frac{v}{N}r_N \tag{19}$$

Substituting equation 18 into 19,

$$r_v=\frac{vay}{N} \tag{20}$$

When it fails to close, a network protector will remain open y years. Hence the average number of occurrences per year in a v-unit vault is

$$a_v=\frac{r_v}{y}=\frac{vay}{N}\left(\frac{1}{y}\right)=\frac{va}{N} \text{ occurrences per year} \tag{21}$$

The period between such occurrences is

$$T_v=\frac{1}{a_v}=\frac{N}{va} \text{ years per occurrence} \tag{22}$$

T_v is the average number of years between the occurrence of a network-protector failure to close in a group of v units in a system of N network units experiencing the quantity a network-protector failures to close per year.

Appendix III. Primary-Feeder and Network-Protector Coincident Outage

The average time period between occurrences of the coincident outage of i primary feeders to a v-unit group is given by $T_{n,v,k,i}$ years in equation 16. From equation 21 the number of occurrences per year for the failure to close of one of the network protectors in the remaining $(v-i)$ units in that v-unit group is

$$a_{(v-i)}=\frac{(v-i)a}{N} \text{ occurrences per year} \tag{23}$$

The duration of each such occurrence is y years. Hence the total time, in years per year, that such a condition will exist in the group of $(v-i)$ units is given by the probability

$$r_{(v-i)}=a_{(v-i)}y=\frac{(v-i)a}{N}(y)$$

$$=\frac{(v-i)ay}{N} \text{ years per year} \tag{24}$$

Hence the average period between occurrences involving the coincident loss of i primary feeders and one network protector out of the remaining $(v-i)$ units in a v-unit group is

$$T_{n,v,k,(i+1)}=\frac{T_{n,v,k,i}}{r_{(v-i)}} \text{ years} \tag{25}$$

References

1. SYMPOSIUM ON HIGHER DISTRIBUTION VOLTAGE FOR METROPOLITAN AREAS. *AIEE Special Publication S-66*, Sept. 1954.
2. THE PROBABILITY OF COINCIDENT PRIMARY-FEEDER OUTAGES IN SECONDARY NETWORKS, David N. Reps. *AIEE Transactions*, vol. 73, pt. III, Dec. 1954, pp. 1467–78.
3. A-C NETWORK OPERATIONS, 1936–1937. *EEI Publication No. G-1*, New York, N. Y., 1939.
4. *Ibid.*, 1938–1940. *K-4*, 1943.
5. *Ibid.*, 1941–1943. *M-1*, 1945.
6. *Ibid.*, 1944–1946. *O-12*, 1949.
7. *Ibid.*, 1947–1949. *51–6*, 1951.
8. *Ibid.*, 1950–1952. *54–5*, 1954.

◆

Discussion

G. H. Arapakis (Consolidated Edison Company of New York, Inc., New York, N. Y.): Referring to equation 15, this expression gives the outage probability of finding one or more network units in a v-unit vault out of service due to the outage of one or more feeders from a group of n feeders to a network area. However, the author fails to point out that if we wish to find the total probability of i units out of service in a v-unit vault, and this is the result of practical interest to us in system design, the expression given by equation 15 must be summed up for values of $k=i$ to $k=n$ as follows

Probability of i units out of service in a v-

$$\text{unit vault} = \sum_{k=i}^{k=n} R_{n,v,k,i}$$

$$= \sum_{k=i}^{k=n} (P_k) U_{n,v,k,i}$$

For example, in a network area supplied by a total of 10 feeders, to find the probability of one unit out of service in a 4-unit vault it would require theoretically the summation of nine terms, although practically the summation of the first two or three terms yields a sufficiently accurate answer. Similarly the probability of two units out of service will require eight terms, etc.

I would like to point out, however, that in a v-unit vault supplied by v number of different feeders, the total probability of one or more network units out of service due to feeder outages can be calculated very simply on the basis of the outage probability of the v-feeders supplying this particular vault, independently of the n feeders to the network area, as follows

Total probability of i units out of service in a v-unit vault due to feeder outages

$$= \frac{v!}{i!(v-i)!} p^i (1-p)^{v-i}$$

where $p =$ average outage probability of any one feeder from accidental causes. (This will depend on the average length of a feeder, and therefore on the size and extent of the network area.) This expression should equal to the summation of terms given in this discussion. While I have not proved this equivalence in general terms, I am satisfied that it is true from a number of numerical examples for which I have compared the two expressions.

In general, as I have pointed out, we are interested only in the total probability of finding one or more network units out of service in a particular vault. While the mathematics developed by the author are correct, I do not see what is to be gained by breaking up this total probability into a summation of terms when it can be calculated very simply and very quickly as one term from the equation which I have given here.

David N. Reps: Mr. Arapakis points out an important addition to Appendix I. The curves of Figs. 2, 3, and 4 give the first three terms of the summation to obtain the total probability for finding i out of v feeders to a given vault out of service. For example, in a 4-unit vault in a 10-feeder network the summation representing the total probability for finding one feeder out of service would be

$$\sum_{k=1}^{k=10} (P_k)(U_{10,4,k,1}) = (P_1)(U_{10,4,1,1}) +$$

$$(P_2)(U_{10,4,2,1}) + \ldots + (P_{10})(U_{10,4,10,1})$$

From Fig. 2, $U_{10,4,1,1}=0.4$; from Fig. 3, $U_{10,4,2,1}=0.55$; from Fig. 4, $U_{10,4,3,1}=0.5$. Thus the first three terms of the summation become

$$\sum_{k=1}^{k=3} (P_k)(U_{10,4,k,1}) = 0.4P_1 + 0.55P_2 + 0.5P_3$$

Mr. Arapakis also points out, and correctly so, that the terms containing P_k for $k>3$ add negligibly to the summation, because the probability for having more than three feeders simultaneously out of service is extremely small.

The reasons for my having chosen the particular way in which I present network-vault multiple-outage probability methods are severalfold. Much of the work that is being done in secondary-network system engineering design and economic analysis involves consideration of higher secondary voltages, multiple-bussing of network units, and higher primary-feeder voltages. Such changes are best investigated through the use of what I call "hypothetical equivalent" systems which exist only on paper, but over which the engineer has full control of the variables. One extremely important variable of network design is the number of primary feeders. For instance, increasing the feeder voltage permits the use of a fewer total number of feeders. This change affects not only network design and cost but also feeder-outage probability. The approach I have taken in presenting network-feeder and network-vault outage probability information lends itself to use in the comparison of alternative network designs. Such an approach not only permits answering the question "What will happen in an existing network system?" but also "What will happen in a network system that does not yet exist?"

Mechanical Alignment of Vertical-Shaft Hydroelectric Units as Practiced by Tennessee Valley Authority

C. L. NORRIS
NONMEMBER AIEE

DURING the past 20 years the Tennessee Valley Authority (TVA) has purchased and installed 74 hydroelectric generating units in 21 different power plants. Three additional units and two additional plants are under construction.

These machines vary in capacity from 7,000 kw under a head of 58 feet to 67,500 kw under a head of 330 feet. Some idea of their size can be obtained from the dimensions shown in Fig. 1. The manufacture and installation of each of these machines has followed a more or less standardized procedure as set up by the TVA personnel. This procedure provides limited running tolerances in shop machining of the shafts and thrust-bearing parts. It also provides a limited misalignment tolerance after the unit is completely assembled in the field.

Design and Specifications

Each machine is of the vertical-shaft type with the thrust bearing located below the rotor and resting on the heavy structural lower bracket of the generator which spans the turbine pit and supports the entire rotating elements. A main-shaft guide bearing is located in the turbine head cover immediately above the turbine runner; a second one is located just below the generator rotor in the generator bearing bracket. In a few cases a third is located in the generator upper bracket directly above the rotor.

The correct alignment of a hydroelectric unit begins with the inception of the job and is completed when the last part is in place. To have a correctly aligned machine the controlling tolerances and procedures must be enumerated in the manufacturing and installation specifications.

Since the majority of the machined surfaces which could cause trouble are a part of the generator contract, the generator manufacturer is usually made responsible for the shop-checking of the

---

Paper 55-163, recommended by the AIEE Power Generation Committee and approved by the AIEE Committee on Technical Operations for presentation at the AIEE Winter General Meeting, New York, N. Y., January 31–February 4, 1955. Manuscript submitted October 18, 1954; made available for printing December 3, 1954.

C. L. Norris is with the Tennessee Valley Authority, Knoxville, Tenn.

The author is indebted to R. A. Hopkins, head electrical engineer, Division of Design, Tennessee Valley Authority, for his guidance in the preparation of this paper.

combined shafts and the thrust-bearing parts. Because it is a physical impossibility to machine all mating pieces to zero tolerances, the turbine and generator shafts are checked in more than one relative position and when the best possible combination is determined each piece is match-marked at the coupling so that this same relation can be obtained when the field assembly is made. In addition to this, the generator manufacturer is made responsible for the final field alignment of the rotating parts.

Turbine Erection

For each machine the turbine has been purchased for installation by the TVA forces and the generator has been purchased installed by the generator manufacturer. Prior to start of erection the Authority submits to each interested party copies of a suggested method of erection for comments and suggestions. The differences, if any, are ironed out and in this manner erection procedures and methods which are satisfactory to all parties are outlined in advance.

Because a good alignment of machines of this type necessarily includes the embedded parts and because once the parts are embedded it would be extremely expensive to change them, the construction specifications treat each piece in detail, usually giving the size, weight, and relation to control lines and elevations. If special bracing or bolting is required this is discussed in detail, with necessary references to drawings. No concrete forms, braces, or rods are allowed to come into physical contact with the part or parts being embedded. Concrete vibrators are not allowed to be used in areas where there is danger of the vibrator striking the supporting jacks, screws, rods, braces, or the part itself. During the pacing of the concrete around the embedded parts it is usually necessary to spray water on the inside surfaces of the parts in order to hold to a minimum the distortion caused by the heat of the setting concrete. Concrete placement schedules are arranged to minimize this heat and any unbalanced thrusts. Periodic checks of the plane and concentricity of the parts are made as the erection progresses. To the uninitiated it might appear that such caution is unnecessary, but some of the necessity for good alignment can be appreciated when it is realized that the horizontal running clearances between the turbine runner and the stationary parts range from 12 to 125 mils and that normal relative speeds between these two parts range up to 75 miles per hour for some of the smaller clearances.

Once the embedded parts are in place, the remainder of the machine should be installed around these parts; therefore the turbine runner is set in place in the best possible relation with the embedded parts. The turbine shaft is set plumb and the face of the top flange level. The turbine runner and shaft are usually set about 0.750 inch below the final running position and are supported in this position by brackets built in the head cover for this purpose on propeller turbines and by the lower part of the runner which rests on a flange in the embedded parts on Francis turbines. The distance below the final running position is determined exactly by measuring between two machined surfaces in the turbine assembly. This dimension is used by the generator erector in placing the generator parts at the correct elevation.

Generator Erection

With the foundation concrete in place and with the turbine parts installed as just outlined, the generator manufacturer can proceed with the erection of the generator parts using the location of the turbine shaft flange as a control point for both horizontal and vertical dimensions, irrespective of previously established control lines or datum planes.

The soleplates for the generator-bearing bracket are set in place and grouted in using the position of the top flange of the turbine shaft to determine the location, both vertically and horizontally.

The generator-bearing bracket, shaft, and thrust-bearing assembly is made in the erection bay or on some convenient floor accessible to the powerhouse crane. For this purpose the bearing-bracket is placed on simulated soleplates and the shaft and thrust bearing are installed with the shaft resting on the thrust bearing. After the bearing and shaft have been adjusted and positioned with respect to the bracket, the entire assembly may be set in place on the permanent soleplates. The exact location of the generator shaft is determined from the position of the turbine shaft flange which has been accurately located prior to the generator erection.

When the generator shaft is in position directly above the turbine shaft and at the correct elevation, the generator shaft is rotated so that the shaft flanges can be bolted together in the same relative position, as indicated by the factory-placed match marks. To prevent damage to the permanent bolts the two flanges should be pulled together with temporary, loose-fit bolts, with the use of at least half as many bolts as there are bolt holes in the flanges. When the flanges are together the permanent bolts are installed and prestressed by stretching so that the torque necessary for any condition of loading can be transmitted through the coupling by the friction on the flange faces.

The combined shafts are then set vertical with the turbine runner positioned correctly with respect to the stationary parts, the generator stator is centered about the top portion of the generator shaft and the stator frame is bolted to the previously placed soleplates. With the stator round and correctly located, the soleplates are grouted in. The dowels between the soleplates and the stator frame are installed after the final alignment is completed.

The rotor, previously assembled in the service bay, is set in place and bolted to the generator shaft. Care must be exercised in placing the rotor so that the stator coils are not damaged. When the generator erection is completed, but before the guide bearings are set, and thrust pot closed, or the rotation check made, the thrust shoes are checked for equal loading. This should be done by an approved method acceptable to the customer and the manufacturer. To avoid the disadvantages involved in tilting the bearing bracket to plumb the shaft assembly, the shoe loading should be done in such a manner as to leave the shaft vertical and at the correct elevation

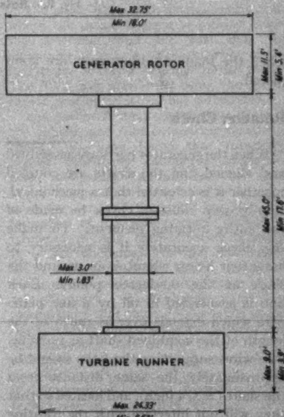

Fig. 1. Over-all dimensions of rotating elements

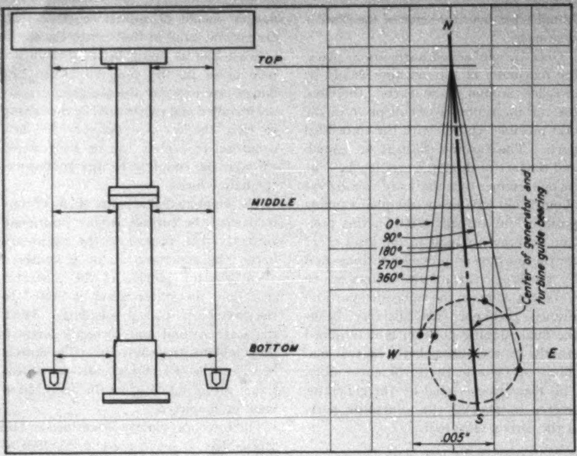

POSITION	0°	90°	180°	270°	360°
TOP					
N	.592	.590	.585	.593	.590
S	.588	.590	.595	.587	.590
W	.595	.600	.588	.594	.592
E	.585	.580	.592	.586	.588
MIDDLE					
N	.5915	.5885	.5855	.5945	.5895
S	.5885	.5915	.5945	.5855	.5905
W	.594	.601	.590	.594	.5915
E	.586	.579	.590	.586	.5885
BOTTOM					
N	.591	.587	.586	.598	.589
S	.589	.593	.594	.584	.591
W	.593	.602	.592	.594	.591
E	.587	.578	.588	.586	.589

Fig. 2. Rotation check data

when the loading adjustments are completed.

Rotation Check

When the generator parts are assembled and aligned and the shafts are coupled together it is essential that a mechanical, step-by-step rotation check be made of the entire rotating element. To make this check accurately it is necessary to hang four heavy plumb bobs around the shaft at the 90-degree points. Each bob is suspended in oil by a fine piano wire which extends over as much of the length of the combined shaft as possible. The wires supporting the bobs should be approximately the same distance from the shaft (±1/4 inch), and located so that they will not interfere with the rotating elements when the shaft is being moved from one position to the next. The arrangement should be such that a tram rod can be used in conjunction with a flashlight battery and a set of head phones so that the operator can tell when the smallest possible reading is obtained between the shaft and the wire.

At the zero position readings are taken from the shaft to each plumb wire at a minimum of three different elevations. This will determine whether or not the shaft assembly is straight and vertical. The rotating element is then turned mechanically 90 degrees at a time and similar readings are taken at the 90-, 180-, 270-, and 360-degree positions. To avoid excessive side movement or sliding on the thrust-bearing surface it has been found desirable to set up four guide shoes while the element is being turned; these shoes are to be backed away from the guide surface before readings are taken.

To avoid errors in reading the micrometers and in recording, it has been found desirable to check the quantities by adding opposite readings (see the tabulation in Fig. 2; the sum of $N + S$ or $W + E$ = the same for each position from zero through 360 degrees at any given elevation) and by plotting the shaft centers as each check is made. It is extremely important that the rotating element be free from any outside interference and that it is hanging free from the thrust bearing during the period when check readings are being made.

Fig. 2 shows a typical rotation check arrangement with check readings and results. It will be noted that in this case the shaft center, as determined from the plumb bobs on opposite sides, describes a throw-out circle on the lower end of about 0.0055 inch and that the shaft is straight from top to bottom.

The maximum throw-out as determined by this method is limited under the generator contract to a quantity determined by

$$T = 0.00075\,(L/R)$$

where

T = throw-out circle diameter, inches
R = radius of thrust-bearing runner plate, inches
L = length of shaft, inches (lower face of runner plate to center of turbine guide)

If the shaft throw-out is limited to the amount allowed by this equation the shaft alignment will usually be satisfactory; however, in no case is the actual throw-out circle allowed to be as much as the minimum clearances between the turbine runner and the stationary parts.

If the throw-out circle is greater than either of these above quantities, the remedy for each individual case is decided as the occasion arises. However, two of the more common remedies are: 1. rotating the runner plate with respect to the thrust collar, and 2. tightening the coupling bolts on one side of the coupling flanges.

When the throw-out circle has been determined, the main-shaft guide-bearing centers are set so that the shaft center will be held in the center of the throw-out circle and vertical within a tolerance of 0.001 inch in each 5 feet of shaft length.

With the shaft in the final position and with the guide bearings in place, reference points are established in the turbine head cover and the generator main bearing bracket. These points are carefully placed so that they are all equidistant from the shaft surface and readily accessible for future use without excessive dismantling of the unit parts. Records in triplicate are kept of all important settings, clearances, and tolerances.

Immediately following the completion of the assembly a thorough and complete inspection of the entire unit is made by all interested parties to determine that the unit is in starting order. All starting procedures, tests, etc., are under the direction of a co-ordinator who is familiar with the construction, erection, and operation of the machine.

During the mechanical run it is determined if the generator rotor will require additional weights for balance. If balancing is required it is desirable that this be done before the heat run is started.

Conclusions

The satisfactory and successful operation of any mechanical unit requires good alignment of the various parts.

Assuming a correct design, any installation in which the mechanical alignment is correct will give trouble-free service mechanically, whereas an installation which is not in correct alignment will give continuous trouble in the overheating of excessively worn parts, overstressing, fatigue, and it may be a contributing factor to many other troubles.

Good alignment raises production and lowers production cost due to reduced outages for expensive maintenance and repairs. Good alignment can be obtained at little or no extra cost with proper scheduling.

◆

Discussion

William J. Rheingans (Allis-Chalmers Manufacturing Company, Milwaukee, Wis.): The paper is a timely one, since the hydraulic turbine sections and the large generator and converting apparatus section of National Electrical Manufacturers Association are now working on standards for the alignment of vertical hydroelectric units. Since one of their problems is the question of rotational checks, it was interesting to note that the TVA insists upon rotational checks for all their units as a means for determining proper alignment.

The author's remarks regarding proper scheduling of parts and proper alignment checks in the shops are of great importance in obtaining proper alignment of vertical-shaft hydroelectric units.

J. F. Roberts (Allis-Chalmers Manufacturing Company, Milwaukee, Wis.): This paper is an indication of the amount of careful work that the TVA has done in connection with its great number of hydroelectric installations.

As units get larger and larger, it becomes more and more difficult to hold to extremely accurate tolerances which are required, particularly in thrust-bearing surfaces and coupling faces. It is only by taking greater care, as outlined in the paper, and carefully checking these units before they go into operation that satisfactory operating results can be obtained. If such precautions are not taken, then the penalty is either excessive wear on turbine and generator bearings, or excessive strain with possible mechanical troubles or even broken shafts at a later date.

The success which the TVA has had by developing this method of alignment and rotation checks has been a tremendous help to the industry, and similar methods are being adopted by many other users of this type of equipment. It is particularly desirable when one part of the equipment, such as the turbine, is furnished by a different manufacturer from the generator. A careful check of this type serves to locate the source of any minor inaccuracies and they can be corrected before any troubles arise, and without setting up a 3-way argument between the various manufacturers and the customer.

The tolerance for shaft throw as given by the equation in the paper is practical on shafts which are relatively short but, as the author points out, on long shafts this may result in a possible tolerance greater than the bearing clearance, in which case we must either rely on flexibility of the shafts and some bending, or else the scraping of the thrust-bearing surface, in order to get even closer tolerances.

J. Fisch (S. Morgan Smith Company, York, Pa.): The procedure used by the TVA has been applied to numerous installations. It is assumed that it has given satisfactory results in all cases. The practice noted in the section "Turbine Erection" to work out, in advance, a method of erection satisfactory to all parties concerned is to be highly recommended. No doubt progress of field work can thus be accelerated and kept under good control.

In one section "Generator Erection" temporary bolts are prescribed to pull the coupling flanges together. It is believed that this is an unnecessary refinement when the final bolts are machined to provide 2 to 3 mils' clearance in the flange holes in accordance with American Standards Association standards.

As noted in the section "Rotation Check," straightness of the shaft is determined from the four wires with plumb bobs. During rotation, wire readings are necessary only at the zero- and 360-degree positions. The throw-out circle at the turbine bearing can be established by "milking" from trammel points in the bearing housing during the four positions.

It should be mentioned that all of these alignment checks are made before the rotor is dynamically balanced. Balancing may affect the painstakingly obtained initial alignment.

Rotation checks apply primarily to units with Kingsbury-type thrust bearings. Extreme care must be exercised when rotating large units in order to avoid thrust-bearing damage.

Numerous units with spring-type thrust bearings have been installed without rotation check. After plumbing of the shaft, the unit is brought up to speed and the rotor balanced. During coasting down in speed, measurements with indicators are taken on two of the stationary thrust-bearing shoes to determine the vertical oscillations or wobble. This wobble is an indication of the perpendicularity of the thrust runner face with the shaft axis. Experience has shown satisfactory operation if the measured amplitude of the wobble does not exceed 0.002 inch.

R. B. McKeeby (General Electric Company, Schenectady, N. Y.): The author has made a worth-while contribution to a subject on which there is little published information. There has been real need for a method which could be applied practically in the over-all alignment of the hydroelectric unit. Not so long ago, the industry relied on a relatively few seasoned and experienced erectors, most of whom were in the employ of the turbine or generator manufacturers. These men command our respect for their accomplishments, which were often made under very difficult local conditions. The majority had many years of training, and were experts in their field. Men representing the two manufacturers would turn over to the operators a satisfactorily operating unit. They kept records but these were usually closely guarded and not accessible to the operating and maintenance people, who were thus left with very little knowledge of the unit they would be expected to maintain.

For this and other reasons an industry standard is needed to cover the erection of hydroelectric units. I am sure that the author's paper will encourage others to record their practical experience in this field, thus leading eventually to an industry standard.

The paper deals with vertical-shaft units where the thrust bearing is located below the generator rotor and with only the adjustable shoe type of bearing, one of the four types of thrust bearings in use today. The TVA has nine units using the spring thrust bearing which is not adjustable.

The author devotes considerable space to the difficult and time-consuming rotational check. We have found that rotational checks improperly conducted sometimes give misleading information. In some cases, this procedure has failed to reveal a misalignment, and the result has been the formation of iron oxide which cannot be tolerated in any thrust-bearing housing. It is not uncommon to find slow speed rotors of large diameter out of balance as much as 200 pounds on completion of the assembly work. We have demonstrated on several units that placing 200 pounds on the rim of a rotor when the shaft is hanging free and supported only on the thrust bearing will cause the turbine guide-bearing journal to swing out of position 10 to 20 mils. This is due principally to the flexibility of the thrust-bearing supporting bracket. If a rotational check is made on such a unit before it is balanced, the results can be meaningless, even though a satisfactory throw circle is indicated. The subsequent addition of balance weights will tip the rotor enough to generate a throw circle of 20 to 40 mils. Thus, we cannot rely on the throw circle for an indication of the runout of the thrust runner, or straightness of the shaft assembly, until the rotor is in static balance. Assuming the entire unit to be in static and dynamic balance, the displacement of the shaft, indicated by the throw circle will be restrained during operation by the turbine guide bearing, in turn causing a tipping of the thrust bearing and resulting in unequal loading of this bearing as the unit rotates. When excessive, this condition usually causes fretting corrosion on some or all of the surfaces between the thrust-bearing runner and the thrust block. The iron oxide thus formed has caused thrust-bearing failures.

The results of a rotational check are of some value if made on a unit after it has been in satisfactory operation where it is known that the generator and turbine rotors are in good balance. This method has been used for many years in locating trouble spots in a unit in operation for some time.

Several unsuccessful attempts have been made to make rotational checks on larger units. It must be realized that today there are in operation units where the total weight of the rotating element is over 2,000,000 pounds and the thrust bearing is designed to support a load of over 4,000,000 pounds. All these factors must be kept in mind in planning for the future in regard to an industry standard for checking the alignment of these units.

It is not my intention to be critical. The TVA has a large number of hydroelectric units in service, and their operating record speaks for itself. The importance of the subject justifies more papers such as this, freely discussing alignment techniques.

R. A. Baudry (Westinghouse Electric Corporation, East Pittsburgh, Pa.): The author must be commended for his clear and concise presentation. It is interesting to note that all the 74 units discussed have the thrust bearing located below the rotor, and that also most of the generators have only one guide bearing located below the rotor. This type of generator, usually called the umbrella type is well suited to accurate alignment of the rotating parts, particularly when provided with a thrust collar forged integrally with the shaft, which makes it possible to obtain easily the small throw-out specified by the author. The specified value of the throw-out indicates that the periphery of the thrust-bearing runner must have a maximum throw-out of only 0.00075 inch with respect to the centerline of the shaft. This is indeed a very small value when it is considered that some of the thrust collars are nearly 9 feet in diameter. Such a small tolerance is made possible only by the use of the most accurate type of machine tools and methods of quality control.

The tolerance of 0.001 in each 5 feet of shaft length for deviation from a vertical line indicates the high standard of quality requested by the author in the erection of machines. It would be of interest to know how this variation from a vertical line is affected by changes of the foundation with time and whether a larger variation from the vertical affects the operation of the unit as long as the guide bearings are well centered with respect to the shaft.

P. S. Johrde (Elliott Company, Ridgeway, Pa.): Since the erection procedures outlined have been tried and proven on such a wide size range of machines, they should be of interest to a great many people.

Undoubtedly, several deviations in these procedures could be brought out but these would probably be minor departures from the general line of action. We can point to a few cases where shifting foundations or the whole power plant have thrown an entire turbine-generator unit considerably out of plumb with no harmful effect upon operation. On the other hand, there are cases where the misalignment from foundation shifting was detrimental to operation. We dare not minimize the importance of alignment.

The erection procedure is for the umbrella-type of generator only. I would like to enlarge upon the subject to point out that the rection of an umbrella-type generator and its turbine can be co-ordinated to result in less total erection time than is the case with a suspended type of generator and turbine of the same rating.

Let us consider a large unit the stator of which was shipped in several sections with most of the coils installed at the factory. The lower bracket and stator soleplates can be grouted in with the aid of surveyors' instruments as soon as the foundation will permit. In both types of unit the horizontal and vertical location will have to be determined from machined stationary parts of the turbine. In either case the stator can be assembled and placed temporarily on its soleplates for completion of the winding. Meanwhile, the rotor is assembled and the turbine assembly can proceed if the scaffold for the armature winders is of the balcony type, which leaves most of the pit open for access to the turbine. Simultaneously with the rotor and stator work, the umbrella machine's lower bracket, thrust, and guide-bearing assembly, and shaft can be assembled in an erection area.

With a suspended type, the upper bracket and possibly part of the thrust bearing, upper guide bearing, and oil pot assemblies can be put together at this time.

From then, the umbrella construction proceeds speedily as outlined by the author. In pyramid fashion, the basic assemblies go together with center and levels being transferred from assembly to assembly. Finally, the upper bracket and exciter(s) are put in place using the generator rotor hub or shaft as center.

The center alignment of the stationary assemblies of the suspended type, on the other hand, should be done with the aid of a tight wire by placing the lower bracket, stator, and upper bracket assemblies in operating position with reference to the turbine shaft.

The upper bracket must then be removed and the rotor lowered into the stator until it rests on the hydraulic jacks in raised position. Next, the upper bracket is put back in place; the thrust block and bearing parts are assembled and the rotor is lowered so that it hangs on the thrust bearing.

From this operation on, the shaft coupling-up, aligning, and rotation check are accomplished approximately as described in the paper. The exciter(s) can then be positioned using the generator shaft or thrust block as center. In general, after comparing the erection of the two type generators, we can say that the umbrella type of generator and turbine required less elapsed erection time because:

1. More man hours can be spent simultaneously on the generator and turbine, i.e., less work is needed after the turbine shaft is set in position.
2. Less handling of large parts is required.
3. There is no necessity for centering all stationary elements and then disassembling part of them in order to place the rotor.

C. L. Norris: We appreciate the interesting and constructive remarks presented by the discussers. Mr. Rheingans has properly emphasized the importance of shop scheduling and alignment checks. We agree with Mr. Roberts' comment regarding the equation and also with his observations in regard to the advantages of preoperation checking.

Mr. Fisch questions the necessity for using undersize bolts for pulling coupling flanges together where American Standards Association fits are used. Using undersize bolts gives maximum assurance that the regular coupling bolts will not be scored or the nuts damaged. We have also used alternate methods such as jacking on the coupling flange and using long undersize bolts, a strong-back, and hydraulic jacks between pairs of volts. Both alternate methods are quite rapid but require additional equipment and careful planning to avoid excessive coupling flange deflection. We believe the tramming to four wires gives maximum accuracy as to the diameter and location of the shaft throw-out circle as compared to tramming to the bearing housing.

The comment in regard to the use of an indicator to measure shoe oscillations on a spring-type bearing is informative. We have not had sufficient experience with this method to evaluate its usefulness.

Mr. McKeeby's comments in regard to the erectors and their closely guarded records are in order. These gentlemen decidedly deserve credit for their skill and knowledge. We do not agree that the methods outlined in the paper apply only for one type of bearing since they have been successfully used on both the Kingsbury flat-adjustable shoe and on several spring-supported type bearings. The usual precautions taken to avoid unequal weight distribution when assembling the rotor rim have been found to give a rotor balance such that the rotation check is not materially affected provided the methods outlined in the paper are followed.

Mr. Baudry's observations are interesting in regard to shop practices required to meet close tolerances. We have operated units that do not conform to the 0.001 inch in each 5 feet of shaft length, but believe that better over-all alignment is obtained if this tolerance is maintained during the initial assembly.

Mr. Johrde's comments, comparing erection procedures of the conventional design with the umbrella-type of generator, are valuable. As stated, the paper is based on the umbrella type.

A Look to the Future of Power Transmission in the West

H. D. HUNKINS
ASSOCIATE MEMBER AIEE

A LOOK to the future of electric power markets and resources in the western states shows several problems different from those in the eastern states. These problems offer a special challenge to engineers. In contrast to the East where most load areas adjoin one another, the West is composed of widely separated load areas located in drainage basins where the economies which could not be sustained by the natural rainfall are supported by use of water from mountainous areas. Coal, used to produce most of the eastern power requirement and in many cases relatively close to major market areas, is also abundant in the West, but is located a considerable distance from the basin markets. Hydro power has in the past supplied most of the western needs, but in some areas the electric load has already exceeded this resource.

It appears desirable that the electrical industry continue investigations of comparing electric transmission with other means of transporting energy stored in the conventional fuels until economic production from other sources, such as atomic and solar energy, and tide and wind action, is assured in sufficient quantities to obviate this need. Of the four possible new sources of energy, production from nuclear reactions appears to offer the most promise.

The power demands in the Northwest have been met almost entirely from hydro power, while in northern and southern California the industry has had to produce in increasing amounts power from steam plants largely supplied by oil and natural gas transported through pipe lines. However, the future use of these fuels in enormous quantities under boilers may be limited by such already apparent factors as increasing cost of exploration, estimated future demand in relation to new discoveries, and increasing value of these resources for other uses. That these factors are recognized is shown by the fact that new west-coast power plants are being built with provisions for burning coal.

Atomic fuel having the highest energy content per pound would appear to be ideal from the standpoint of transportation over great distances in the West, if and when production costs become competitive with energy produced from hydro and conventional fuels.[1] When it is considered that atomic production of electric power is not now competitive and may face a relatively long period of development in comparison with the time it takes the electric load to double, at present rates of growth about 10 years, it appears advisable to investigate the use of the large supplies of western coal which lie along the Rocky Mountains.

As an example, consider the southern California load center which is taken as the principal load concentration in an area including Arizona and southern Nevada. Assuming continuation of the long-time growth rate, it may be necessary to supply by 1975 from thermal generation the difference between 12,500,000-kw peak load and 3,100,000 kw of hydro power representing the ultimate hydro development for this area. In 1950, the peak load was 3,900,000 kw with 2,320,000 kw supplied from hydro resources.

The estimated annual energy requirement would be approximately 71.2 billion kw-hours, including some 16.4 billion kw-hours supplied from falling water. The balance, or 54.8 billion kw-hours, if supplied from thermal generation using coal, would require about 22,500,000 tons of coal annually. Fig. 1 shows the location of coal resources in eastern Utah with existing rail lines and possible transmission-line routing to southern California.

Coal, or oil and gas made from coal, could be transported to power plants in southern California by several methods, among which shipment by rail appears at present to be the only practical one. Coal has been moved comparatively short distances by hydraulic pipe line using a water carrier, and by conveyor belt, but these methods are not considered practicable for the long distance and type of terrain involved. The conversion of coal to oil or gas for pipe-line conveyance as developed today is still too inefficient to compete economically with moving energy either by rail or by transmission line. A large portion of the energy in coal would be lost in the conversion, and gas produced from coal has too low a heat content for economical long-distance transportation. The status of these alternative methods would normally be reviewed in the light of possible new developments although no present justification is apparent.

Cost of Hauling Coal by Rail

Several excellent papers have been published which make a general comparison of electric transmission versus methods of transporting fuels.[2-4] A problem of concern has been the proper charge for hauling coal. It appears desirable to use specific freight rates for the transmission scheme and the rail haul under comparison.

Following are 18 principal factors used by the Interstate Commerce Commission in determining freight rates:[5]

1. Cost of service to the carrier.
2. Value of service to the shipper.
3. Value of the article.
4. Nature of the article—whether crude or finished, liquid or dry, etc.
5. Risk in handling the article.
6. Distance of haul (mileage scales).
7. Bulk (size) and weight of the article (density).
8. Whether special facilities or extra services are required.
9. Expense at terminals.
10. Volume of traffic, and periods of movement.
11. Method of packing and protecting the article.
12. Rates on similar articles moving under similar circumstances and conditions.
13. Rates of competing carriers.
14. Competition between producing centers or markets.
15. Whether or not the rate will be conducive to an increasing movement of the article.
16. Prospects of cars being returned loaded or empty.
17. Rates account fourth section of the Interstate Commerce act.
18. Loading (per car).

An exhaustive study should be made considering how these factors have been interpreted. Item 13 indicates that the existence of or obvious feasibility of competitive electricaly transmission could in itself be a dominant factor in establishing

---

Paper 55-184, recommended by the AIEE System Engineering Committee and approved by the AIEE Committee on Technical Operations for presentation at the AIEE Winter General Meeting, New York, N. Y., January 31–February 4, 1955. Manuscript submitted July 15, 1954; made available for printing November 24, 1954.

H. D. Hunkins is with the Bureau of Reclamation, Denver, Colo.

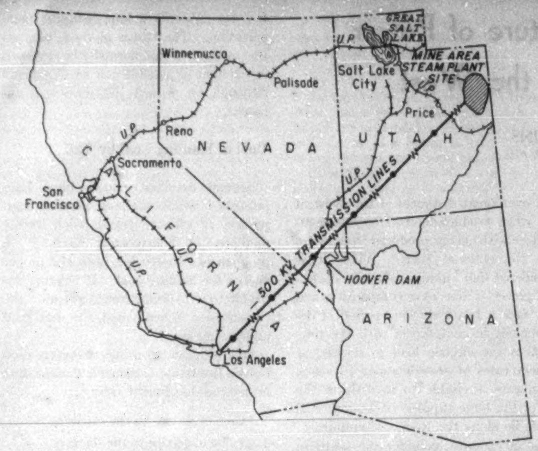

Fig. 1. Location of coal resources in eastern Utah, existing rail lines, and possible transmission-line routing to southern California

and regulating this rate. Freight rates are subject to increases as expenses of railroading increase.

Heiner, the author of an excellent paper on economics of coal for west-coast power generation assumed rail transportation as the cheapest method,[6] and felt that the export rate for hauling coal could be obtained for large movements. This rate now applies only to coal to be loaded into bunkers for water shipment and was $5.05 per ton in 1949, when the paper was written.

A rough approximation of the cost of shipping coal by rail may be made from the following 1952 rates from Price, Utah, to Los Angeles, Calif:

Slack coal, domestic rate, $6.70 per ton.
Size coal, domestic rate, $7.55 per ton.
Export rate, $5.39 per ton.

A determined rate of $5.15 per ton was used in this study and the transportation cost per kw-hour was computed to be about 2.19 mills for a coal having a heat content of 11,700 Btu per pound. The heat content of the coal in all parts of the mine area would have to be determined, as an increase or decrease in heat content would result in a corresponding change in rail transportation cost per unit of energy while electric transmission costs would remain more nearly constant. This figure includes the annual cost of step-up transformers from generator voltage to 230 kv for load-area distribution, for comparison with costs of electric transmission. The necessity of locating large new power plants away from heavily populated areas and for minimizing the number of trunk lines through and around load areas has already made the use of 230 kv economical for load-area trunk lines.

Fig. 2 shows the indexes for cost of construction of transmission lines and substations compared with the export freight rate from the Rocky Mountains to the west coast, using 1940 as the base year. By 1954 construction costs more than doubled while the export rate increased only 36 per cent (%).

Hauling 22,500,000 tons of coal annually by rail would require extensive new investment, as may be seen by the fact that in 1949 the railroads had only sufficient rolling stock to move approximately 2,000,000 tons of coal per year from Utah and Wyoming to the west coast.[6] A determination should be made as to whether extensive new railroad investment might require an increase in rail rates until the rail cost index were more in line with the construction cost index; i.e., approximately double the 1940 rate for hauling coal instead of increasing only 36%. If the 1940 rate of $4.26 per net ton were doubled, the cost of rail transport would be 3.57 mills per kw-hour on the same basis as the 2.19-mill cost estimate.

Rather than expand rail facilities to meet the full requirement, including northern California, which would under similar estimates require an additional 12,500,000 tons annually, it may be well to consider the merits of reducing this transportation load by means of electric transmission.

Qualifications of Electric Transmission

It must be assumed at the outset that an electric transmission scheme with mine-mouth plant, would have to meet certain basic requirements: first, it must meet economic competition offered by rail transportation of coal; second, it must be efficiently integrated technically and economically into the load-area power situation, beginning with the initial lines until a reasonable future time when changing economic or technical factors might change the trends in planning; third, it must provide reliability of service comparable with having the plants in the load areas and, in addition, yield side benefits in addition to strictly economic or technical advantages such as could arise from placing administrative control of the energy transportation facilities in the hands of the electrical utility.

Historically, long-distance transmission has been justified on the basis of transmitting bulk energy rather than as a means of obtaining peaking power at low-load factor. Tie lines between power systems built essentially for interchanging kw have usually been short, and built with a minimum of investment.

To meet the qualifications for bulk transmission, three principles of design are generally accepted. The first is to obtain high individual circuit loadings to work the tower steel which represents a major portion of the initial investment most efficiently. Limitations on this circuit loading are transient stability power limit and the cost of extra equipment, such

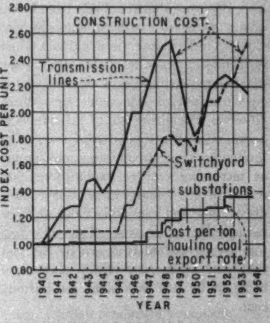

Fig. 2. Cost index for export freight rate compared with cost indexes for construction of transmission lines and substations

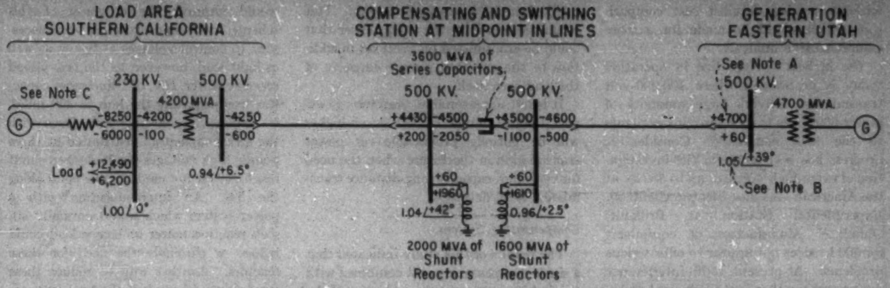

Fig. 3. Transmission of 4,200,000 kw at 500 kv over six lines 660 miles long, compensated to an equivalent length of 300 miles

A—Power shown in megawatts above the line and in megavars below the line. A positive sign indicates flow from a bus

B—Operating voltages shown in per unit of designated bus voltages. Angles given with bus voltages relative to 230-kv load area bus. The compensating station decreases over-all angle between sending station voltage and receiving station voltage

C—Receiving system represented by equivalent machine, impedance, and load. Synchronous condensers included in equivalent. Total equivalent load supplied by hydro and steam generation in load area and 500-kv transmission

as series capacitors and extra switching stations required to maintain transient stability at increased loadings. The second is to maintain a high transmission load factor in order to transmit the greatest amount of energy commensurate with the cost of stand-by capacity in the transmission system. The third is to minimize electrical losses commensurate with additional investment required in conductors and towers.

The problem then, like most engineering designs, becomes one of first determining the technical means, then balancing between the technical and economic factors. In this case, available solutions to the problems associated with long-distance transmission make such a project technically feasible. A number of papers on electric transmission show that the economic solution is approaching the point where electric transmission of bulk energy from mine-mouth plants may become less costly than hauling coal to load-area plants.[1–4]

Technical Features of Electric Transmission

A transmission system that might be considered typical on the basis of present-day technology was studied for transmitting up to 4,200,000 kw from eastern Utah, approximately a 600-mile air-line distance to Los Angeles, Calif. The total estimated load of 12,500,000 kw would be supplied principally from 3,100,000 kw of hydro capacity, 5,200,000 kw of steam capacity in the load area, and 4,200,000 kw of steam capacity at the mine. Only a-c transmission was considered. A more complete analysis of the problem should include d-c transmission.

To establish completely the practicability of such a large electric transmission system, extensive engineering and economic studies would have to be made. Studies made for this paper were of an exploratory nature to determine the present competitive position of electric transmission with respect to rail-hauling of coal in the Far West.

DESCRIPTION

Fig. 3 shows a schematic layout of the plan studied with power flow and voltages. For purposes of discussion, this scheme is divided into four components: The sending-end system, transmission lines, the compensating system, and the receiving-end system.

Sending-End System

The sending system might consist of several large power plants of from 1,500,000 to 2,000,000 kw each, located at advantageous points in the mine area, with step-up transformers connected to lines at transmission voltage. These would connect the plants to a centrally located switching station which would be the starting point of the transmission system to the coast.

The generators and prime movers, it is expected, would be the largest and most efficient available, of around 300,000 kw, with heat rate down to 9,600 Btu's per kw-hour or less, based on present-day designs. Extra units would be installed to allow for a maintenance schedule. For this study, actual cost of production within the plant was assumed to be the same whether the plant was located in a load area or at the mine.

The basis used in estimating the number of circuit breakers required at the switching stations to allow for tie breakers and spares approximating present design practice was $1^1/_2$ times (line breakers plus transformer breakers). The interrupting duty of high-speed sending-end breakers might reach 30,000,000 to 40,000,000 kva. The industry has built circuit breakers capable of interrupting 25,000,000 kva at 330 kv, and there is no indication that the limit has been reached.[7]

Transmission Lines

For transmitting 4,200,000 kw, six 500-kv transmission lines were assumed with busses at the sending end, mid-point, and receiving end. For cost estimates, single-circuit steel tower construction was assumed based on light loading. Line mileage was taken as 110% of the point-to-point distance measured from a map to allow for variations in the routing. A duplex arrangement using two steel-reinforced aluminum-cable conductors of 1,590,000 circular mils per phase was used. Detailed studies might show that a bundle arrangement having more conductors per phase and a larger total size would be more economical. The use of bundle conductors overcomes the problem of corona[8] and reduces the series compensation required, while larger conductors reduce the energy loss.

The choice of voltage would be affected by a number of factors, such as distance, magnitude of load, number of interconnecting stations, and technical and economic feasibility. Considering the distance and magnitude of load in this study, a voltage in the extra-high-voltage range was indicated, and 500 kv was selected without making detailed cost comparisons which would be made for a more comprehensive analysis.

The highest voltage line in operation today is in Sweden where 400,000-volt transmission delivers large amounts of power 600 miles from hydro power plants to the load centers.[9,10] Considerable progress has been made in the investigation of extra-high voltages up to 500 kv at the American Gas and Electric Company Experimental Station at Brilliant, Ohio.[11-17] Manufacture of equipment for 500 kv does not appear to offer serious problems. At present, radio interference during wet weather is the principal objection, but this difficulty may be overcome by the time the application foreseen in this paper occurs.

For distances greater than about 350 miles, as in the case of these studies which require transmission of power a distance of 660 miles, it has been determined that the surge-impedance loading represents a practical limit on the maximum power that should be transmitted per line.[8] A voltage of 500 kv provides a surge-impedance loading of about 625,000 kw for a single-conductor line. A duplex-conductor arrangement increases this to about 750,000 kw per line.

An annual growth of 5% of the total 1975 load would be 625,000 kw. For the purposes of this study and on the basis of present expansion of steam-power generating facilities in the load area, about one-half of this might be expected to be supplied by local plants and the other half from the remote plant located at the mines in eastern Utah. On this basis, a new line would meet the load-area needs for about $2^{1}/_{2}$ years, and the loss of a line section would not seriously limit the ability of the system to meet peak loads. In the event that one complete circuit were lost, it would represent only about 5.5% of the 1975 area load on peak. This would be less than the extra power that could be transmitted on overload in addition to the expected reserve capacity of the load area itself.

It is not unreasonable, therefore, to expect that a voltage of 500 kv or higher will be entirely practicable for power transmission in the future when the need for very high-capacity long-distance transmission lines develops.

Compensating System

The results of this study indicated that a single compensating unit combined with a switching station at the mid-point of the six transmission lines would provide an economic transient power limit and complete voltage control from no load to full load.

The compensating unit shown in Fig. 2 consisted of a series capacitor with shunt reactors on either side to form a pi-type circuit comparable to the equivalent pi-circuit for a transmission line used in network analyzer studies except with the capacitor in series and inductive reactance in shunt. This, in effect, reduced the length of the line from its physical length of 660 miles to an electrical length of 300 miles. The constants were selected to provide a surge-impedance loading close to that of the line itself. Making the shunt reactor on the output end of the series capacitor larger (with lower admittance) than the one on the input side provided an increase in transmission voltage at the compensating station. The amount of compensation could be expressed as 50% of the nominal line reactance, 69% of the imaginary component of the *B* constant, or 55% of the line mileage.

The design of the compensating system was not refined to determine whether reducing the size of the shunt reactors would improve the economy of this scheme. The shunt reactors were necessary to control voltages at heavy as well as light load, however, as the heavy-load reactive power, I^2X, of 1-line series capacitor, compensating the line to 300 miles, was about 525,000 kilovars. Even with the series capacitors distributed at three points, high voltages resulted when shunt reactors were not used at some point along the line. An interconnection with a power system which would normally absorb reactive power at heavy load could reduce or eliminate the need for these reactors. Another way to reduce these reactors would result if the transient stability power limit were high enough to permit operation well above the surge-impedance loading of the line. It was also noted that use of conductors having a higher resistance-reactance ratio, in the order of 0.10, reduced the need for the shunt reactor as the resistive component of voltage drop at heavy load tended to overcome the voltage rise at the center of the line created by flow of reactive power toward the sending end of the line. However, the high losses resulting from the use of such high-resistance conductors would not be economical. Reactive capacity would probably have to be added at the receiving end to support the voltage, and underexcited machine operation might have to be accepted at the sending station if the purchase of shunt reactors were to be avoided.

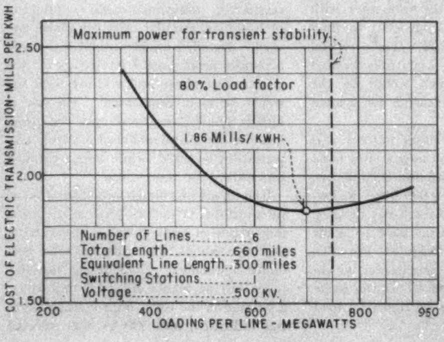

Fig. 4. Determination of economic loading

Studies were made for compensating the 660-mile line to equivalent lengths of 100, 200, 300, and 400 miles. Compensation to 300 miles provided a transient stability limit of about 750,000 kw per line for six lines in parallel and appeared to be near the economic point in amount of compensation.

The studies indicated that one intermediate switching station would be adequate after three or more lines are built in parallel. The initial system would require three switching stations, two of which could be eliminated and the equipment used at the centrally located switching station as more lines were built.

Receiving-End System

The long transmission lines would terminate at a receiving switching station where the voltage might be stepped down to 230 kv for subtransmission in the load area or the extra-high voltage lines extended to other step-down points in the area. The load kilovars would be provided as close to the load as possible by synchronous condenser or static capacitors. The transmission lines did not require kilovar support at full load.

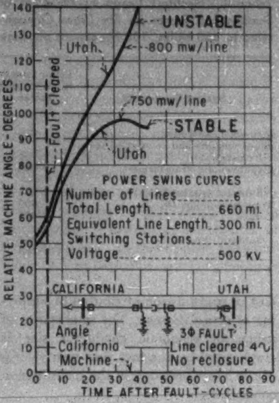

Fig. 5 (left). Power-swing curves

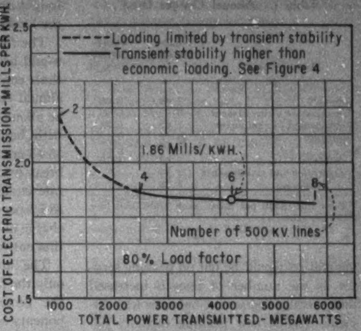

Fig. 6 (right). Effect of total load and number of lines on cost

LINE LOADING AND TRANSIENT STABILITY

Studies of economic line loading and transient stability were made to develop a workable and economical system. The first general approach was to compensate the line reactance until the voltage angle from sending to receiving end was about 30 degrees, which would occur for an equivalent length of about 300 miles. Experience has shown that several lines in parallel will usually maintain transient stability for severe faults up to about 30 degrees between the sending- and receiving-end voltages.

Economic Line Loading

The receiving-end load on this system was then varied in steps from about 350,000 to 900,000 kw per line. For each increase in power, there was a corresponding increase in the kva rating required for terminal transformers and series capacitors at the compensating station as well as an increase in the line losses. Although the amount of series compensation remained the same in ohms or equivalent length, the kva rating of the capacitors increased with the square of the current. The annual cost of equipment plus losses was computed for each loading and divided by the kw-hours that would be delivered in a year, assuming the average line loading at 80% of capacity. This gave the costs of transmission in mills per kw-hour, which are plotted in Fig. 4. The minimum cost occurred for a loading of 700,000 kw per line.

Several of these curves were obtained in the course of the study with the use of different amounts of line compensation. Compensation to an equivalent length of 300 miles was selected because the economic line loading shown in Fig. 4 was found to be close to the minimum cost of transmitting energy. Compensating the line to an equivalent length of 200 miles increased both the level of the cost curve and the distance between the minimum cost point and the transient stability limit. Studies also indicated that reduction in compensation toward an equivalent length of 400 miles might reduce the level of the cost curve a small amount, but would probably reduce the stability limit to the point that a seventh circuit would be required to transmit 4,200 megawatts.

Transient Stability

After the curves of economic loading were obtained for normal power flow, transient stability studies were made to determine the amount of power that could be carried through severe disturbances such as short circuits on one high-voltage line. The power limit for six lines was found to be 750,000 kw per line, which was in excess of the economic loading shown by Fig. 4. In view of the most economic loading and to have some margin below the 750,000-kw stability limit, the loading of 700,000 kw was considered to be a reasonable loading for the cost analysis.

Transient stability limits on power transfer were also determined for other than six lines. In each case, the relationship of economic loading and transient stability determined the maximum load and amount of compensation to be used in estimating costs. One switching station was used for the 6-line case, and as many as three switching stations were required for the 2-line case which would probably represent the initial system. In the case of six lines, three switching stations were not required. The cost of the two additional switching stations with the six lines increased the level of the economic curve and did not appreciably increase the power limit.

Future studies of this problem should consider means of increasing the transient stability power limit for less than four lines. Switching out a portion of the shunt reactors at the compensating station during the critical period of the swing would reduce excitation requirements of the transmission system and increase the height of its steady-state power-angle curve. The series capacitors could also be rearranged by high-speed switching to provide increased compensation during the swing.[18]

To be conservative, 3-phase faults were assumed near the 500-kv sending bus with 4-cycle clearing of the faulted line and no reclosing. Fig. 5 shows a typical set of swing curves in which the practical power limit was determined for the 6-line transmission system which was 660 miles long and compensated to an equivalent line length of 300 miles with one switching station at the mid-point.

Economic Features of Electric Transmission

The economics of electric transmission from remote mines may be divided into two parts. The first is associated with the broader planning and the second directly involved in the design and operation of the lines. Emphasis is placed on the influence of the various cost factors.

BROAD PLANNING

Proper planning of the division of generation between the load area and the mine would be expected to make a smooth transition from all generation in the load area to production of a large portion of the base-load energy at the mines. An increasing proportion of the load-area

Table I. Annual Charges Used

Annual Charge	Sub-stations, %	Trans-mission Lines, %
Interest	3.00	3.00
Amortization of investment	0.89	0.89
Replacement of equipment	1.62	0.74
Insurance	0.12	0.12
Subtotal	5.63	4.75
Operation and maintenance	2.15	*
Total	7.78	

* First line, $320 per mile; each additional line, $107 per mile.

generation would be put on peaking service as the number of lines is increased and existing equipment becomes less efficient. When new peaking capacity becomes necessary in the load area, costs might be reduced by designing specifically for low-load factor operation just as in the mine area special emphasis would be placed on high-load factor operation. Considerable study would have to be made along these lines in establishing the feasibility of such a scheme.

Fig. 6 shows that transmission costs would be higher during the initial stages of the project when fewer lines are in operation. The dashed portion of the curve up to four transmission lines in parallel represents maximum line-loading as limited by transient stability. It is believed that the stability limits on maximum power transfer in this range could be increased with resulting decreases in annual cost by methods discussed under transient stability.

Design and Operation

The economic factors directly involved in the design and operation of the lines are: 1. the annual charges, 2. the cost of electrical losses, 3. the economic loading and transmission-load factor, and 4. the initial costs of construction.

Annual Charges

The annual charges used in this study included interest, amortization of the investment, replacement of equipment, insurance, and operation and maintenance as shown in Table I. When expressed in percentages and multiplied by the respective construction costs, the annual fixed expenses over the life of the project are obtained. Operation and maintenance is often expressed on a unit cost in dollars per mile of line or per kva of station capacity.

With the use of these annual charges and a transmission load factor of 80%, the cost of electrical transmission was computed to be 1.86 mills per kw-hour. The estimated cost by hauling coal at a freight rate of $5.15 per ton, 2.19 mills per kw-hour, would be 18% higher.

The feasibility of electric transmission would bear heavily on the annual charge that could be obtained. The over-all annual charge used for this study would be about 6.5%, and the break-even point with hauling coal at a freight rate of $5.15 per ton would be about 7.6%. The break-even point for hauling coal at a rate equal to twice the 1940 export rate, $8.52 per ton, would occur for an annual charge of about 14.6% with a transportation cost of about 3.57 mills per kw-hour.

The annual charge used affects not only the feasibility of the project but also the economic design of system components as indicated in the recent paper on the Ohio Valley Electric Corporation (OVEC) project.[19] It was pointed out that for annual charges of less than 8%, normally accepted economic relationships to design can be altered. For a lower annual charge, greater initial investment can usually be justified, such as for larger conductors, to attain higher transmission efficiency. These factors emphasize the importance of thoroughly investigating the economic situation before the engineer can begin his work.

Cost of Electrical Losses

Table II shows the electrical losses in per cent for components of the system studied. The over-all efficiency of the transmission system was computed to be about 89.8% with 27.5% of the annual cost of transmission attributed to supplying electrical losses. The importance of using an economic conductor size is emphasized by the fact that nearly 69% of the losses occurred in the transmission conductors.

Table II. Electrical Losses in Per Cent of Sending-End Power for Six Lines Compensated to 300 Miles, 700 Megawatts per Line

System Component	Power Loss in % of Sending Power
Step-up transformers	1.002
Shunt reactors and connecting transformers	1.244
Step-down autotransformers	0.688
Subtotal (station losses)	2.934
Transmission line I^2r	7.000
Corona	0.254
Subtotal (line losses)	7.254
Total	10.188

The annual cost of generating equipment plus fuel costs were included in determining the cost of losses. For estimating the effect of increased annual charges on the cost of transmission, the cost of losses was increased accordingly.

Maximum Economic Line-Loading and Transmission-Load Factor

The maximum economic line-loading and highest annual transmission-load factor on the lines yields the lowest cost per kw-hour of energy delivered.

Economic line-loading for six lines has been discussed, and it was found that the

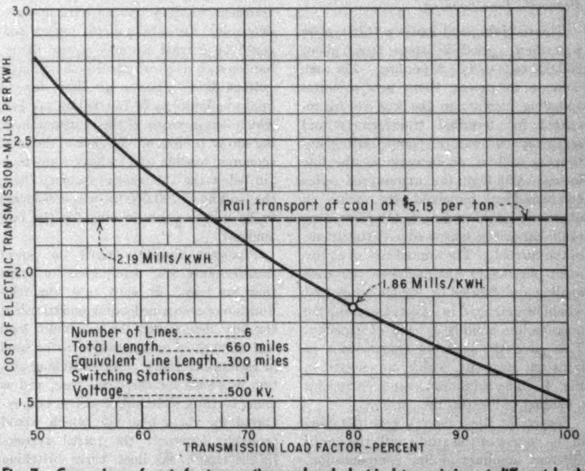

Fig. 7. Comparison of costs for transporting coal and electrical transmission at different load factors

minimum cost of transmitting energy occurred for a receiving power of 700 megawatts per line with a safe margin in transient stability. For the initial two lines that might be built, the cost of transmitting energy would be greater, as shown on Fig. 6, because of the limiting factor of transient stability on the power that can be transmitted economically. The effect of increased costs in the initial system would have to be investigated to determine whether it could be absorbed in anticipation of savings as the number of lines increases. In this respect, the timetable of installation of new lines becomes important.

Fig. 7 shows the effect of transmission-load factor on the cost of electrical transmission. An increase in load factor from 80 to 90% would decrease the cost of transmission to about 1.66 mills per kw-hour, or approximately 10.7%, based on the annual charges used in this study.

INITIAL CONSTRUCTION COSTS

In the following are listed the initial costs of construction (1952 estimates) used in this study. The increases in these costs since 1940 in relation to the increases in the cost of hauling coal were discussed under the section on cost of hauling coal by rail.

Transmission line (single circuit, including right of way and clearing), $73,370.00 per mile.

Step-up transformers, 11.10 per kva.

Step-down transformers for shunt reactors, 11.10 per kva.

Autotransformer 500–230 kv, 15.60 per kva.

Circuit breaker and bay, 420,000.00 each.

Lightning arresters, 7,500.00 per position.

Series capacitors, 27.60 per kva.

Shunt reactors, 7.20 per kva.

Synchronous condensers, 11.40 per kva.

Table III gives the percentage of total initial cost for each of the major types of equipment in the transmission system in terms of the initial construction cost. The transmission line and station costs were each near 50%. The higher annual charge for station equipment, however, made the cost of stations approximately 45.5% of the annual cost of transmitting energy with 27% for transmission lines and 27.5% for electrical losses.

Conclusions

1. On the basis of these comparisons, it appears desirable that continuing study be made on the feasibility of electric transmission as compared with other means of moving energy stored in Rocky Mountain coal over long distances between the mines and major western load areas.

Table III. Initial Cost of Equipment and Lines in Per Cent of Total Cost for Six Lines, 300-Mile Compensation

Type of Equipment	Costs in % of Total Cost
Terminal transformers	19.52
Circuit breakers	4.54
Series capacitors	14.25
Shunt reactors with step-down transformers	10.59
Lightning arresters	0.03
Synchronous condenser at receiving end	3.47
Subtotal for stations	52.40
Subtotal for lines	47.60
Total	100.00

As a result of increasing cost of exploration for oil and natural gas, estimated future demand in relation to new discoveries, and increasing value of these resources for other uses, coal may become a major source of electric energy to meet increasing loads prior to economic production by other means such as atomic and solar energy or tide and wind action.

2. The existence, or apparent feasibility, of electric transmission as a competitor with rail-hauling of coal could become a factor in determining and regulating coal freight rates.

3. Considering that extensive new railroad investment might be required to meet future requirements for hauling coal, careful investigation into the future of freight rates between Utah and southern California would be warranted.

4. On the basis of the very large physical increase in railroad facilities that might be required, principally for hauling coal, reducing this requirement by using electric transmission becomes an important consideration.

5. Electric transmission over 660 miles is apparently within present-day technology. Development of new equipment for maintaining control near abnormally large concentrations of generation during system disturbances and for operating in the extra-high-voltage range, above present usage, appears possible.

6. The practical limit on transmission-line loading over long distances appears to be restricted by transient stability for the first few lines built in parallel and then principally by the annual cost of equipment plus losses.

7. On very long lines requiring series capacitor compensation and without intermediate load points, shunt reactor compensation may be necessary to limit voltage rise even at heavy load.

8. After several parallel lines have been built for long-distance transmission, satisfactory stability performance appears possible with only one intermediate station containing both the compensating and intermediate switching equipment.

9. The influence of annual charges on the cost of electric transmission indicates that detailed investigations should be made on the economic factors involved.

References

1. Can Nuclear Power Plants Compete? *Electrical World*, New York, N. Y., vol. 138, Aug. 11, 1952, pp. 106–08.

2. System Economics of Extra-High-Voltage Transmission, H. P. St. Clair, E. L. Peterson. *AIEE Transactions*, vol. 70, pt. I, 1951, pp. 841–51.

3. Economics of Long-Distance A-C Power Transmission, S. B. Crary, I. B. Johnson. *Ibid.*, vol. 66, 1947, pp. 1092–1102.

4. Economics of Long-Distance Energy Transmission, R. E. Pierce, E. E. George. *Ibid.*, vol. 67, pt. II, 1948, pp. 1089–94.

5. The Freight Traffic Red Book, C. J. Fagg, Walter W. Weller, Arthur B. Strunk. Traffic Publishing Company, 1944.

6. Economics of Coal for West Coast Power Generation, C. P. Heiner. *Transactions*, American Institute of Mining and Metallurgical Engineers, New York, N. Y., vol. 184, Nov. 1949, pp. 388–400.

7. A New Milestone in Circuit-Breaker Interrupting Capacity—25,000,000 Kva at 330 Kv, W. M. Leeds, G. J. Easley. *AIEE Transactions*, vol. 73, pt. III—A, April 1954, pp. 304–13.

8. Corona Investigation on Extra-High-Voltage Lines—500-Kv Test Project of the American Gas and Electric Company, I. W. Gross, C. F. Wagner, O. Naef, R. L. Tremaine. *Ibid.*, vol. 70, pt. I, 1951, pp. 75–94.

9. The Swedish 380-Kv System, Ake Rusck, Bo G. Rathsman. *Electrical Engineering*, vol. 68, Dec. 1949, pp. 1025–29. Also *Report 410*, CIGRE, Paris, France, 1950.

10. Experience Gained with the Swedish 400-Kv Power Transmission and the Novel Features of the System, B. G. Rathsman, G. Jancke. *AIEE Transactions*, vol. 72, pt. III, Dec. 1953, pp. 1089–1100.

11. Corona Considerations on High-Voltage Lines and Design Features of Tidd 500-Kv Test Lines, C. F. Wagner, Anthony Wagner, E L. Peterson, I. W. Gross. *Ibid.*, vol. 66, 1947, pp. 1583–91.

12. Insulators and Line Hardware for Tidd 500-Kv Test Lines, I. W. Gross, R. L. McCoy, J. M. Sheadel. *Ibid.*, pp. 1592–1602.

13. Line Conductors—Tidd 500-Kv Test Lines, E. L. Peterson, D. M. Simmons, L. F. Hickernell, M. E. Noyes. *Ibid.*, pp. 1603–12.

14. Transformers and Lightning Arresters—Tidd 500-Kv Test Lines, F. A. Lane, J. K. Hodnette, P. L. Bellaschi, Edward Beck. *Ibid.*, pp. 1613–18.

15. Switchgear Equipment for Tidd High-Voltage Test Lines, F. A. Lane, B. W. Wyman. *Ibid.*, pp. 1619–23.

16. Instrumentation and Measurement—Tidd 500-Kv Test Lines, R. L. Tremaine, G. D. Lippert. *Ibid.*, pp 1624–31.

17. Progress Report on Tidd 500-Kv Test Project of the American Gas and Electric Company—Corona, Radio Influence, and Other Factors, Philip Sporn, A. C. Monteith. *Ibid.* vol. 69, pt. II, 1950, pp. 891–99. Also *Electrical World*, New York, N. Y., vol. 134, July 1950, pp. 76–79.

18. Location of Series Capacitors in High-Voltage Transmission Systems, S. B. Crary, L. E. Saline. *AIEE Transactions*, vol. 72, pt. III, Dec. 1953, pp. 1140–51.

19. The OVEC Project: Economic, Engineering, and Financing Problems of the 2,200,000-Kw, 18,000,000,000-Kilowatt-Hour Power Project of the Ohio Valley Electric Corporation, Philip Sporn, V. M. Marquis. *Ibid.*, vol. 73, pt. II–A, Feb. 1954, pp. 49–63.

20. A Study of Future Power Transmission for the West. United States Department of the Interior, Bureau of Reclamation, Washington, D. C., 1952.

Discussion

M. S. Oldacre (Stanford Research Institute, Stanford, Calif.): The change in the energy supply of the West and the probability that coal will become an important factor in an area now dependent on water power, petroleum, and natural gas is the most important point of the paper, even though little is presented on the relative cost and availability of various fuels and other data that must be known before effective comparison can be made of the cost transporting different forms of energy.

Papers on the economic energy source for an area are usually fairly thorough analyses of only one phase of the problem, with data for making comparisons of methods for delivering energy abstracted from other papers. The author goes beyond the usual presentation, in outlining the factors to be considered in a complete analysis, and then considering in detail the technical question in high-capacity electric transmission. It seems safe to assume that electric facilities can be provided for any reasonable extension beyond present capacity and distance of transmission and that therefore more attention should be paid to the economic factors.

All this suggests the need for a comprehensive analysis of the whole problem, and that the AIEE should take an active part in the studies of the economics of energy supply to an area. Initially, individual members or the technical committees could study various parts of the problem and co-ordinate their activities to secure a comparative analysis. The industry should sponsor a research project that could be carried on a continuing basis to obtain comparative data on the cost of energy supply to the different load centers when used in the various sources, and also to show which sources are best used for lowest over-all cost. The question of energy supply in the future is a vital one.

C. W. Watchorn (Pennsylvania Water and Power Company, Baltimore, Md.): The paper is a most inspiring one. A bold look to the future is the way to achieve real progress. It is realized that this report is a preliminary survey of uncertain future possibilities, but a few factors come to mind which perhaps should be given fuller consideration.

First, comparable reliability is doubtful with each of the author's two alternatives (see references 1 and 2 of this discussion). In the problem of maintaining comparable reliability, whether the economical solution is obtained by: 1. providing additional transmission facilities to the load area, or 2. providing additional generating capacity in the load area, over that proposed in the paper, with the mouth-of-mine steam-generating plants or by other means, the result is the same: investment costs are higher than they would be on the basis considered in the paper. Depending on the results of such an evaluation, the mouth-of-mine generation may prove much less attractive than it appears on the basis of the evaluation in the paper, where this factor may not have been evaluated.

A demonstration of the justification for the high-load factor as assumed in the paper in the evaluation of the costs of electric energy transmission with the mouth-of-mine plants would be most interesting, since this factor is of primary importance in such an evaluation.

In considering the economics of annual carrying-charge rates, the following comments are not intended to be against the public interest but rather they are intended to be in the best public interest, in advocating observance of economic laws, the violation of which can never be in the public interest, since economics is a natural force that will exact its own penalties in one way or another if its laws are violated.

Usually, the problem is presented as that of determining the relative economics of transporting energy on the one hand in the form of fuel over already existing facilities and on the other hand as electric energy over facilities that must be built; whereas, in the paper the problem is that of determining the relative economics of transporting energy over facilities not only required to be built for electric energy transmission but also largely required to be built for the transportation of energy as fuel. The differences, however, are in the details and not in the fundamentals. Charges for fuel transportation for the usual case are properly based on filed tariffs or on whatever other arrangements may be made with the transportation companies. However, the author's case is not so clear-cut in this regard, without a definite proposal for arrangements as to transportation charges for the fuel. In the absence of such a proposal, consideration should be given to what the possible freight rates or transportation charges might be.

This would be a complicated process. Nevertheless, since for the author's conditions, existing transportation facilities can move but a small portion of the total fuel required, and additional facilities are needed to move the major portion, it may be assumed that the transportation charges would be based largely on the actual costs of providing such services, i.e., the annual carrying charges, operating, and maintenance costs of such new facilities.

Upon what basis, then, private or so-called government financing, should the annual carrying charges be determined? It appears from the paper that basically the fuel transportation charges are predicted on private financing and the electric energy transmission costs on government financing. However, it is just as logical to reverse the assumptions, and base the fuel transportation charges on government financing and the electric energy transmission costs on private financing, in which case an indication is conceivable of more economy in transporting fuel than in transmitting electric energy rather than the reverse as suggested in the paper. Obviously, such conflicting results are untenable. One of the alternatives must be the more economical, independent of the assumptions. The basis for the calculations must be compatible with the facts to be determined, i.e., the question should be decided as to which alternative is really the more economical, rather than the results allowed to be a by-product of the assumptions.

A partial solution is to assume the fuel transportation and the electric energy transmission both on the same basis of either private or government financing. With such an assumption it is possible but far less likely that the fuel transportation would be indicated as the more economical with one basis of financing and the transmission of electric energy with the other than with different bases of financing, as is assumed in the paper and then as considered in the foregoing.

It is obvious that in all cases government financing results in apparently lower costs than private financing for the same job, particularly with high investment costs. This raises the question as to what magic there is in government financing and, as to why it is not used for every undertaking, thus raising all our standards of living because of the resulting lower prices. Actually, there is no magic in government financing, since the true costs or carrying charges are the same as in private financing. In government financing an allowance is usually made for interest only, the taxpayer thereby assuming the equity risk. Further, the tax provision in the allowance for carrying charges is grossly inadequate.

To continue the analysis, we may assume no public debt and all government financing on a pay-as-you-go basis, for which there would be no interest charges. Would the cost of money for government-financed projects then be zero? The answer, of course, is that it would not. The only rational evaluation is at the rate placed on it in the market place for undertakings of similar risks where it is voluntarily available from those whose money it really is in the first place, the general public's or the taxpayers'. The fact that the government may raise some of its money by borrowing cannot change this consideration in the slightest. Certainly, money made available involuntarily by way of taxes for a given project costs at least as much as that made available voluntarily by way of investments for the same project with equally competent management in both cases.

Next should be considered the treatment of taxes in the determination of the carrying charges. The noninclusion of an allowance for taxes with respect to government financing does not result in a reduction in the true cost of the project as an alternative. Rather it merely shifts the burden to the taxpayers and this cost item is carried by them when they pay their tax bills. Or, to say the same thing another way, the nonpayment or noncharging of taxes results in no over-all economic benefit to the public generally.

Thus, the relative economics of alternative projects are correctly determinable only on the basis of private financing in a free market. Whether or not the government is to finance the project, or whether rates charged for the services provided are higher or lower than if based on actual costs, are matters of public policy and are not proper considerations in the determination of the relative economics of alternative facilities (see reference 3 of this discussion).

References

1. POWER AND ENERGY PRODUCTION, C. W. Watchorn. *AIEE Transactions*, vol. 73, pt. III, Aug. 1954, pp. 901–08.

2. GENERATING RESERVE CAPACITY DETERMINED BY THE PROBABILITY METHOD, G. Calabrese. *AIEE Transactions*, vol. 66, 1947, pp. 1439–50.

3. *Discussion* by C. W. Watchorn and F. A. Allner of ALLOCATION OF THE TENNESSEE VALLEY AUTHORITY PROJECTS, Theodore B. Parker. *Transactions*, American Society of Civil Engineers, New York, N. Y., vol. 108, 1943, p. 210.

Paul H. Jeynes (Public Service Electric and Gas Company, Newark, N. J.): The paper is an excellent long-range appraisal of an interesting situation. It contains one serious weak point, which apparently is realized by its author, concerning the details of the economic comparison.

The author states that the annual charge used affects not only the feasibility of the project but also the economic design of system components as indicated in the recent paper on the OVEC project (see reference 19 of the paper), and, in conclusion 9: "The influence of annual charges on the cost of electric transmission indicates that detailed investigations should be made on the economic factors involved."

This discussion undertakes to supply the results of such detailed investigations of annual charges. The author lists annual charges as: interest, amortization of investment, replacement of equipment, insurance, and operation and maintenance.

It is not clear why both amortization of investment and replacement of equipment should be included. The investment in the initial facilities results in annual charges for return on that investment, plus depreciation expense for those initial facilities during their lifetime. When they are replaced, the capital money invested in the replacement results in annual charges for return on that capital money, plus depreciation expense for the replacement facilities, during the lifetime of the replacement facilities. But during the lifetime of facilities currently in use there is never an annual charge for future replacements; annual costs of future replacements do not begin until the replacements are made, i.e., when they are actually "used and useful."

Nor is it clear why taxes are not mentioned. Utilities encounter a variety of taxes, all of which have to be recovered in revenues. Besides federal income tax there are usually real estate, franchise, and the so-called payroll taxes; in addition there are often state income taxes, personal property taxes (sometimes applied to gross receipts in lieu of property), and sales taxes or other levies on gross receipts.

The estimate of interest at 3% is not unreasonable, but interest ordinarily constitutes only about 25% of the total return that must be earned on a project of this kind. That is, a return of about 6% may be reasonably anticipated, although somewhat more might be required to induce investors to commit their capital to this apparently risky venture. About 50% of that capital probably would be raised by means of bonds, at about 3% interest. That accounts for 0.03×0.50=$1.50 of the $6 annual return per $100 invested. The other 4.50% would represent return on equity, which is subject to income tax. Federal income taxes, at current rates, would approximate 3.97% of the gross investment.

The author's estimate of amortization of investment at 0.89% apparently is based on a 50-year life, no-salvage value, no dispersion of retirements, and reserves reinvested in the enterprise at 3%. Accepting the 50-year life estimate, assuming zero net salvage, and assuming reinvestment in the enterprise at 6% (as just discussed), the depreciation annuity would be 0.34%, i.e., if no dispersion of retirements is assumed, all property units retired exactly at age 50, none earlier and none later. However, if the more reasonable assumption is made of 50-year average life, some items having shorter and some longer lives, that figure would be increased substantially. For a typical survivor curve like the Iowa type S_0, and assuming reinvestment at 6%, the annual cost of depreciation would be 0.86%, or practically the same as suggested by the author.

Accordingly, a minimum estimate of annual costs would seem to be as follows (for substations, and similarly for transmission lines)

Return	6.00%
Depreciation	0.89%
Income Tax	3.97%
Insurance	0.12%
Operation and maintenance	2.15%
Total	13.13%

as compared with the author's 7.78%.

Utility economists frequently arrive at a figure in the neighborhood of 15% for this purpose, about double the figure suggested by the author. Of course, such a rate changes the picture entirely.

There is one conclusion that is definitely proved by the author's figures, although I am sure that this was not his intent. If we assume government financing at 3%, with no taxes, we certainly could put the competing railroads out of business, unless, of course, we also socialize the railroads, finance them at 3% interest and omit taxes. On that same basis we can also take over the steel industry, the petroleum industry, the automobile industry, or any other capitalistic enterprise intent on earning a reasonable return for its owners, and subject to taxes on that income. Comparisons on that basis are occasionally made, with the pretense that they are "economic" comparisons.

W. R. Johnson (Pacific Gas and Electric Company, San Francisco, Calif.): This is an interesting academic study of future power needs in the West. The technical assumptions upon which the transmission scheme is based are substantially an extrapolation of present developments in this country and abroad.

The author refers to the OVEC financing with total annual charges for interest, taxes, insurance and amortization to run less than 8%. The OVEC has a long-term government contract for sale of power to the Atomic Energy Commission at a high annual load factor and has consequently been able to obtain financing at a low cost. It seems unlikely that equally favorable conditions for low-cost financing can be assumed for the Utah-California transmission discussed in this paper. In spite of this, in Table I the author uses annual charges of only 5.63% for substations and 4.75% for lines, excluding operation and maintenance which are likewise not included in the OVEC 8% figure. It is evident this economic analysis is based upon the use of public credit to obtain low interest rates, and of a tax subsidy in addition by the total omission of tax costs. How can such costs properly be compared with railroad freight rates which reflect both the cost of taxes and of private financing?

Failure to compare costs on a comparable basis may result in the misallocation of resources and the use of less economical alternatives. A theoretical engineering study such as this should be completely objective in both its technical and economic approach to the problems under consideration if it is to be a real contribution to electrical engineering.

The inclusion of more representative annual charges would increase the transmission costs as shown in Fig. 7 on the order of 75%. Instead of 1.86 mills per kw-hour, as indicated for 80% load factor, a figure of 3.2 mills would be more appropriate.

In conclusions 3 and 4 the author indicates that "...extensive new railroad investment might be required to meet future requirements for hauling coal..." and that "On the basis of the very large physical increase in railroad facilities that might be required, principally for hauling coal, reducing this requirement by using electrical transmission becomes an important consideration." The implications of these two conclusions are unwarranted. The concentrated delivery of large volumes of coal to a few terminal points is well suited to railroad haulage; it would develop gradually and would not require extremely large or sudden increases in railroad facilities or investment.

Finally, it should be pointed out that the informed opinion of today is that within 20 years 10 to 15% of the electric power generation will be from atomic plants, and that in the last quarter of this century most new generating capacity will be from such plants. Estimates of fuel costs for these plants are well under even the transmission cost alone as indicated by the author. Atomic plants of this character would operate on base load, leaving the hydro and higher fuel cost plants for peaking operation. Such development would tend to make economically obsolete the mouth-of-mine, coal-fueled plants with very long transmission distances.

H. D. Hunkins: The author appreciates the discussions and finds substantial basis for agreement with many of the points discussed, among them, the suggestion by Mr. Oldacre that the AIEE should take an active part in the studies of the economics of energy supply. Such a penetrating analysis should, through research, bring out new techniques in the handling of coal fuels and methods of transporting energy. It should, through the democratic process of free discussion, result in a maximum working of the economic law ably discussed by Mr. Watchorn.

In first considering the preparation of the paper, it was clear to the author that the annual charges used in the original study made in 1952 were near a minimum. It was also noted that the relationship between the freight rate index for hauling coal from Utah to the west coast and the index of construction cost for the year 1952 were very much out of line with that prevailing in 1940 as illustrated by Fig. 2.

Since coal freight rates are regulated by a commission, and the railroads have been continuously applying for rate increases, it appears likely that with increased demands on the railroads for hauling coal, an adjustment would occur tending to restore balance between the indexes of construction costs and freight rates existing in 1940. The paper in one sense compares cost figures based on a low annual charge with a freight rate that is also considered low, and extrapolates these figures for comparing higher annual charges with higher freight rates.

In reply to Mr. Jeynes, replacement of equipment was included in the annual charges because in financing a project consisting of many major components over a relatively long period, it is recognized that all components will not have the same life span or a life span necessarily corresponding with the life of the project. The amount charged annually during the life of the project for replacement of equipment in this case is over the cost of operation and maintenance and is expected to replace partially or completely those components whose life span is less than the life of the project. It is noted that the replacement item for substations was 1.62%, while for transmission lines it was 0.74%. Some believe that a properly constructed steel tower line would have a life expectancy of 50 years which would decrease the replacement item for lines to zero in this case.

At another point Mr. Jeynes includes the replacement of equipment item as defined in the previous paragraph, plus amortization of investment in one term, depreciation, and obtains a figure considerably lower than the sum of the two items shown in the paper. It is believed that this results from the fact that the method used for computing annual charges in this paper does not permit reinvestment of funds accruing from depreciation allowance or amortization of investment. Mr. Jeynes states that his figure is based on such reinvestment.

Mr. Johnson's references to the time that electrical production from atomic fuels may be available, at a very reasonable cost, is encouraging from the standpoint of supplying future loads. Are there, however, sufficient assurances today of this future supply to warrant abandonment of investigations into the use of coal in the West? Does the philosophy that railroad growth is slow greatly improve the position of rail hauling? And can it be said without further study that mouth-of-mine plants and transmission lines would become obsolete before the end of their useful life?

An Investigation of the Economic Size of Steam-Electric Generating Units

L. K. KIRCHMAYER
ASSOCIATE MEMBER AIEE

A. G. MELLOR
MEMBER AIEE

J. F. O'MARA
ASSOCIATE MEMBER AIEE

J. R. STEVENSON
ASSOCIATE MEMBER AIEE

THIS paper records the method of analysis and the results obtained of a study made to determine the optimum economic size of steam-electric generating units that should be added to a power system. Factors such as the size of system, forced outage rate, rate of load growth, installed cost of larger generating units, the effect of a maintenance program, and the effect on the transmission system of the use of larger generating units have been taken into account. The practicability of designing and building very large generating units has not been considered in this paper as it is thought that if such large units can be economically justified the equipment manufacturers will find means of developing them.

Studies of this type based on probability methods involve an extremely large number of numerical calculations and would not be practical without the aid of automatic digital computers. It is hoped that the procedure given in this paper will provide utility engineers with a tool for determining an optimum plan for generating station additions to an individual system.

Conclusions

Based on the assumptions made in this study, the following trends may be noted from the results presented:

1. If the investment cost of large units continues to decrease with size and the forced outage rate for large units remains at the present level [2 per cent (%) or lower], the most economical pattern of system expansion is to add units of between 10% and 7% of the size of the system studied. The slope of the curve of cost per kilowatt (kw) versus size is the determining factor rather than the absolute values of investment cost.
2. If above any size the investment cost in dollars per kw remains constant, there will be very little incentive to use units above this size.
3. Any increase in the forced outage rate of large units will slow up the move to these large units.
4. For the range of rates of load growth normally encountered, the rate of load growth of a system has no appreciable effect on the size of units that can be economically justified on a system.
5. Due to the decreasing gain in investment cost and operating costs as unit sizes increase, units that are a larger percentage of system size can be justified more easily on smaller systems than on large systems.
6. Due to the decreasing gains from larger units, it appears that the rate of increase of the maximum size of units may slow down, but there is no indication that the maximum economic size of units has been reached yet.
7. Based on the factors considered in this study, it can be conservatively estimated that unit sizes of the order of 500 to 600 megawatts (mw) will be economically utilized on some power systems within the next 10 years.

System Studied

In this study a basic existing system of 2,000 mw total generating capability was assumed, consisting of 12 25-mw units, 20 50-mw units, and 7 100-mw units. All units making up the basic system and all units added to the system were assumed to be of the unit scheme type, i.e., single boiler, turbine-generator set. It was assumed that the transmission system was adequately designed to carry the full output of the generating stations to the load areas.

Expansion of the system was carried out from the basic system of 2,000 mw to a system of approximately 10,000 mw. In this expansion four basic patterns were investigated:

1. 8% to 5% expansion. The size of units was kept within a band of 8% to 5% of the total installed capacity of the system. This means, e.g., that for the basic system of 2,000 mw the first unit added to the system would be 8% of 2,000 mw or a 160-mw unit. This size of unit would be added every time new generation was required, until the unit

---

Paper 55-183, recommended by the AIEE Power Generation Committee and approved by the AIEE Committee on Technical Operations for presentation at the AIEE Winter General Meeting, New York, N. Y., January 31–February 4, 1955. Manuscript submitted October 21, 1954; made available for printing December 15, 1954.

L. K. KIRCHMAYER, A. G. MELLOR, J. F. O'MARA, and J. R. STEVENSON are with General Electric Company, Schenectady, N. Y.

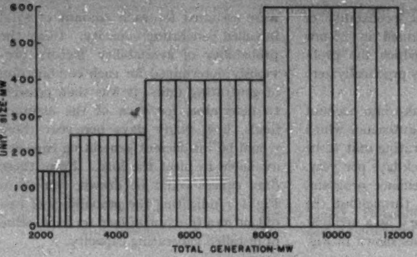

Fig. 1. Unit size as function of total generation with 8% to 5% expansion

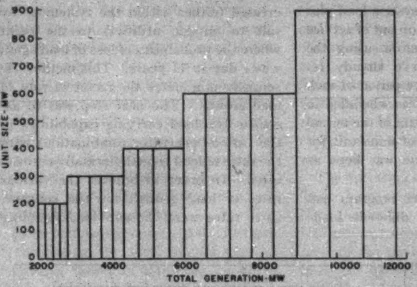

Fig. 2. Unit size as function of total generation with 10% to 7% expansion

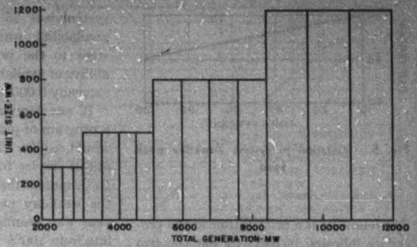

Fig. 3. Unit size as function of total generation with 15% to 10% expansion

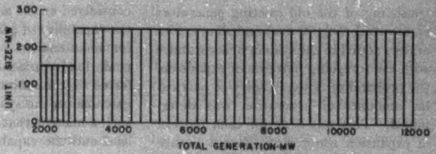

Fig. 4 (above). Unit size as function of total generation with 250-mw expansion

size was approximately 5% of the total system generation or, in this case, until the system generation totaled 3,200 mw. When this point was reached, the next unit added would be 8% of 3,200 mw or approximately 250 mw.

2. 10% to 7% expansion. The size of units added was kept within a band of 10% to 7% of the total capability of the system.

3. 15% to 10% expansion. The size of units added was kept within a band of 15% to 10% of the total capability of the system.

4. 250-mw expansion. The size of units added was initially kept within a band of 8% to 5% of the total installed capacity of the system up to units of 250-mw capacity, after which the system expansion was continued with 250-mw units regardless of system size.

To simplify the calculations, the unit sizes actually used were not exactly in accordance with the percentage bands just indicated. The sizes used were as follows and are shown in Figs. 1–4.

1. For 8% to 5% expansion, the unit sizes were 150, 250, 400, and 600 mw.

2. For 10% to 7% expansion, the unit sizes were 200, 300, 400, 600, and 900 mw.

3. For 15% to 10% expansion, the unit sizes were 300, 500, 800, and 1,200 mw.

4. For 250-mw expansion, the unit sizes were 150 and 250 mw.

Assumptions

1. The standard of reliability of the power system was such that sufficient generating capacity must be available so that the probability of loss of load would be 1 day in 11 years.

2. The combined forced outage rate was 2% for the generating unit (combined boiler and turbine-generator set). This is in line with recent experience on generating units. To determine the effect of possible lower reliability of very large units, a forced outage rate of 3% was assumed in some cases.

3. Each boiler-turbine-generator unit on the system would be out of service for 20 weekdays a year for planned maintenance.

4. The variation in system weekday peak load throughout the year was a straight line from 100% to 80% as shown in Fig. 5. This is reasonably typical for most power systems except for some systems in the south where the summer and winter peaks are approximately equal.

5. The installed cost of new generation varied with unit size as shown in Fig. 6. Above a size of 200 mw two cost curves were used, one with constant cost per kw from 200 mw up to the largest size considered, and the other showing a continuing decrease in cost per kw above 200 mw.

6. Fixed charges on the investment were 12% per year.

7. Operating labor cost in mills per kw-hour varied with size as shown in Fig. 7. Maintenance cost in mills per kw-hour varied with size as shown in Fig. 8.

8. The heat rates of the various sizes of units were as shown in Fig. 9. Above 200 mw, the heat rate was assumed to be constant as it was thought that these larger units would all use the maximum practical steam conditions and that no improvement in heat rate would be realized only from increased size. It is realized that unit heat rates, particularly in the larger size units, will almost certainly continue to improve in the future and this improvement will make the use of larger generating units more attractive.

9. The fuel cost 25 cents per million Btu.

10. The load duration curve of the system was as shown in Fig. 10. This curve is based on a system load factor of 60% which is typical of many large power systems.

11. The fuel and operating costs of units kept on spinning reserve with negligible load factors were neglected.

Method of Analysis

The method used to determine the most economical pattern of system expansion consists essentially of two parts:

1. The determination of the reserve capacity required on the system to maintain the assumed standard of reliability for each pattern of system expansion, taking into account the following factors:
   a. Size of generating units.
   b. Forced outage rate of generating units.
   c. Weekday peak load duration curve.
   d. A planned maintenance program.

2. The application of the assumed cost factors to each pattern of expansion (taking into account the reserve capacity required) to determine the most economical pattern of expansion.

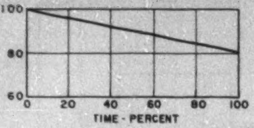

Fig. 5. Variation in system weekday peak load

The following is a brief outline of the procedure followed in carrying out the two steps. A more detailed procedure is given in Appendix I.

For each combination of generators, consisting of the old existing generators (amounting to 2,000 mw) and all new generators added to the system in accordance with the foregoing patterns of expansion, the probability of availability of particular amounts of generation was determined. This was done for each pattern of expansion using a 2% forced outage rate and also for the 8% to 5% and 10% to 7% patterns of expansion using a forced outage rate of 3% for all units over 250 mw. Since the smallest unit on the system was 25 mw, the probability of availability was determined in 25-mw steps to the point at which the probability of availability was practically zero (actually 0.00000001).

It was necessary to take into account a program of planned maintenance which would require each generating unit to be out of service for 20 weekdays per year. In planning this maintenance program, the weekday peak load throughout the year was assumed to vary as a straight line from 100% to 80% as shown in Fig. 5.

As far as system reliability is concerned, it was assumed that the total load can be considered as the actual system load plus the capability of generation out of service for maintenance. Therefore, using the peak load variation curve already referred to, the maintenance period of each machine on the system was scheduled in such a manner that the sum of the actual load and the capability of units out for maintenance at any time was kept as uniform as possible.

When this maintenance program had been established, three different loads were assumed for each amount of total installed generating capacity. Using the probability of availability factors previously determined for each combination of generating units, it was then possible to determine, for each of the assumed loads, how many days per year there would be insufficient generating capacity available to meet the load. From these data curves could be drawn, similar to Fig. 11, indicating the probability of loss of load as a function of load for each value of installed generating capacity.

First, it was assumed that whenever a new generator was added to the system the system load was immediately increased (either within the system or by sale to outside utilities) to the point where the probability of loss of load again was 1 day in 11 years. This method essentially eliminates the factor of rate of load growth. The next step was to associate the load carrying capabilities of the various generator combinations with the rates of load growth normally encountered. In order to bracket the various rates of load growth for the country, three rates were chosen: load doubling

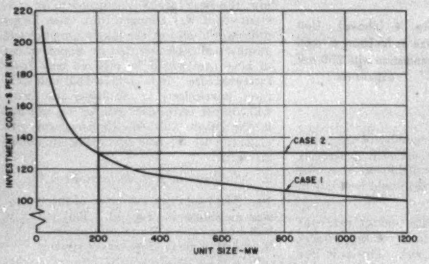

Fig. 6. Investment cost as function of unit size

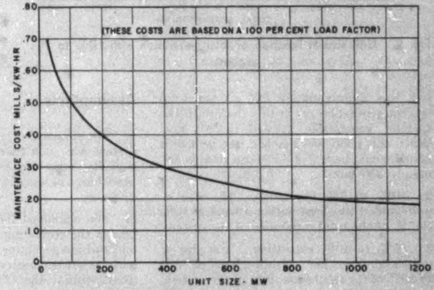

Fig. 8. Maintenance cost as function of unit size

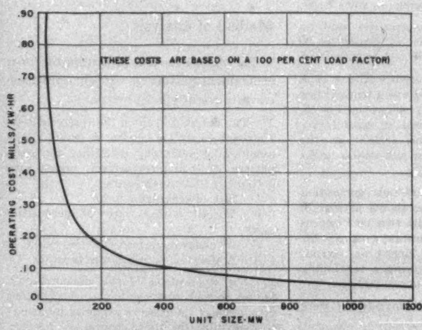

Fig. 7. Operating cost as function of unit size

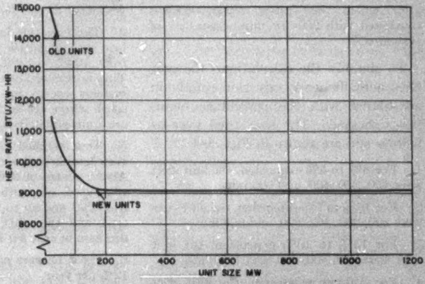

Fig. 9. Heat rate as function of unit size

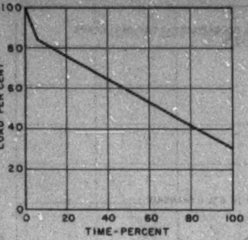

Fig. 10 (left). Load duration curve

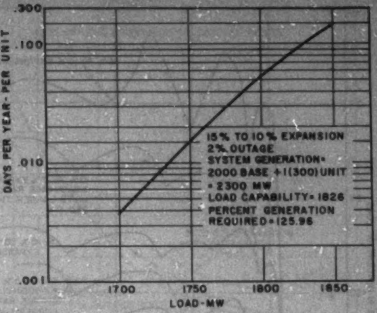

Fig. 11 (right). Probability of loss of load as function of load

in 5, 10, and 15 years. Starting with a basic system of 2,000-mw capability of generation, the load for each year was calculated for each rate of load growth until the system load was approximately 10,000 mw. In order to adhere strictly to a 1 day in 11 years loss of load probability, it was necessary in some cases to add a large block of generation when only a few additional mw of reserve were required. To be practical, in these cases, the standard of reliability was reduced to a minimum of 1 day in 7 years. No maximum standard of reliability was specified.

Table I shows the costs and the method of calculating the total annual cost of generating power in mills per kw-hour. These costs are based on the assumed curves of Figs. 6, 7, and 8 for investment, operating, and maintenance costs. Some of the units of the basic system were figured at a different investment rate than that shown in Fig. 6 as it was assumed that most of the basic system was installed at a time when investment cost was lower.

The operating costs as determined from Table I are dependent upon the utilization factor for the various machines. Utilization factor can be defined as the ratio of the kw-hours actually generated in a year by a particular machine to the maximum kw-hour capability of the machine. To calculate the utilization factor of each machine, a system load duration curve was assumed as shown in Fig. 10. This curve is based on a system load factor of 60%. It was assumed that each new unit added to the system would be base loaded. With a maintenance period of 20 weekdays per year and a forced outage rate of 2%, each new unit could supply about 90% of its total kw-hour capability. By filling in the area under the load duration curve with the generators associated with a particular load, the utilization factor for each size machine on the system was determined.

Table I. Method of Calculating Total Annual Cost of Generating Power

Mills per Kw-Hour for Each Generator Size = Base Cost (Total Capacity-Kw Divided by Peak Load-Kw × Load Factor)

		Fixed Charges +		Operating		+ Maintenance +		Fuel Costs(UF)*	=	Base Costs	×	No. Machines × Machine Rating, Mw / Peak Load × Load Factor		= Mills per Kw-Hour
Generator Size, Mw	Investment Costs, $ per Kw	Mills per Kw-Hour, 12%($ per Kw)10³/8,760		Mills per Kw-Hour		Mills per Kw-Hour		Mills per Kw-Hour		Mills per Kw-Hour per Machine				
Case 1. $ per Kw Costs Taken from Fig. 9														
25	140.00†	1.91781	+	0.900	+	0.700	+	3.75000(UF)	=	3.51781+3.75 (UF)	×	N× 25/peak load×0.6	=	
50	120.00†	1.64384	+	0.500	+	0.600	+	3.50000 (UF)	=	2.74384+3.5 (UF)	×	N× 50/peak load×0.6	=	
100	128.60‡	1.76164	+	0.300	+	0.500	+	2.40000 (UF)	=	2.56164+2.4 (UF)	×	N× 100/peak load×0.6	=	
150	138.00	1.89041	+	0.217	+	0.443	+	2.31998 (UF)	=	2.55041+2.32 (UF)	×	N× 150/peak load×0.6	=	
200	130.00	1.78082	+	0.170	+	0.400	+	2.27500 (UF)	=	2.35082+2.275 (UF)	×	N× 200/peak load×0.6	=	
250	125.00	1.71233	+	0.145	+	0.367	+	2.27500 (UF)	=	2.22433+2.275 (UF)	×	N× 250/peak load×0.6	=	
300	121.00	1.65753	+	0.126	+	0.340	+	2.27500 (UF)	=	2.12353+2.275 (UF)	×	N× 300/peak load×0.6	=	
400	116.00§	1.58904	+	0.100	+	0.300	+	2.27500 (UF)	=	1.98904+2.275 (UF)	×	N× 400/peak load×0.6	=	
500	113.00	1.54920	+	0.090	+	0.275	+	2.27500 (UF)	=	1.91420+2.275 (UF)	×	N× 500/peak load×0.6	=	
600	110.00	1.50684	+	0.070	+	0.250	+	2.27500 (UF)	=	1.82684+2.275 (UF)	×	N× 600/peak load×0.6	=	
800	106.00	1.45205	+	0.060	+	0.210	+	2.27500 (UF)	=	1.72205+2.275 (UF)	×	N× 800/peak load×0.6	=	
900	104.00	1.42466	+	0.055	+	0.195	+	2.27500 (UF)	=	1.67466+2.275 (UF)	×	N× 900/peak load×0.6	=	
1,200	100.00	1.36986	+	0.040	+	0.180	+	2.27500 (UF)	=	1.58986+2.275 (UF)	×	N×1,200/peak load×0.6	=	
												Total mills per kw-hour		
Case 2. Same as Case 1 Except That Investment Cost for All Units Above 200 Mw Kept at the 200-Mw Level														
25	140.00	1.91781	+	Same as case 1	+	Same as case 1	+	Same as case 1	=	3.41781+3.75 (UF)	×	Same as case 1	=	
50	120.00	1.64384	+		+		+		=	2.74384+3.5 (UF)	×		=	
100	128.60	1.76164	+		+		+		=	2.56164+2.4 (UF)	×		=	
150	138.00	1.89041	+		+		+		=	2.55041+2.32 (UF)	×		=	
200	130.00	1.78032	+		+		+		=	2.35082+2.275 (UF)	×		=	
250	130.00	1.78032	+		+		+		=	2.29282+2.275 (UF)	×		=	
300	130.00	1.78032	+		+		+		=	2.24682+2.275 (UF)	×		=	
400	130.00	1.78032	+		+		+		=	2.18082+2.275 (UF)	×		=	
600	130.00	1.78032	+		+		+		=	2.10082+2.275 (UF)	×		=	
800	130.00	1.78032	+		+		+		=	2.05082+2.275 (UF)	×		=	
900	130.00	1.78032	+		+		+		=	2.03082+2.275 (UF)	×		=	
1,200	130.00	1.78032	+		+		+		=	2.00082+2.275 (UF)	×		=	

*UF stands for utilization factor.
†Based on old costs.
‡Based on three generators at $100 and four generators at $150.
§Based on present and estimated future costs.

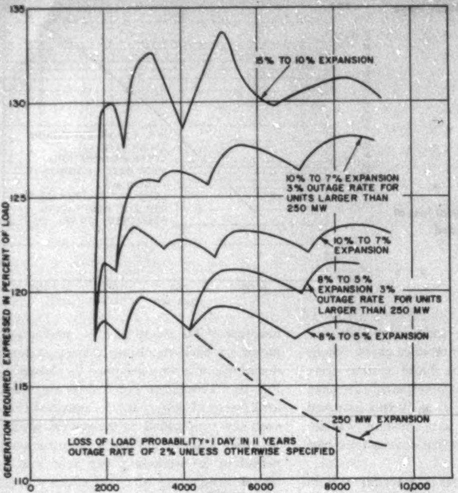

Fig. 12 (above). Reserve as function of system load with loss of load probability of 1 day in 11 years

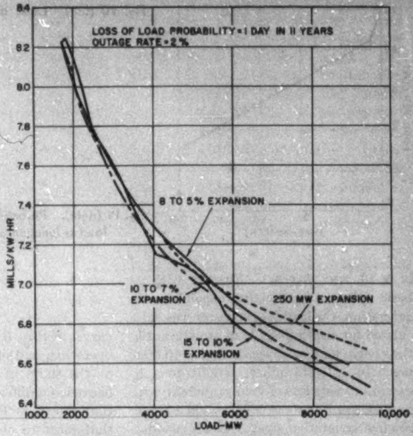

Fig. 14 (above). Cost of supplying load in mills per kw-hour (case 1 investment cost curve)

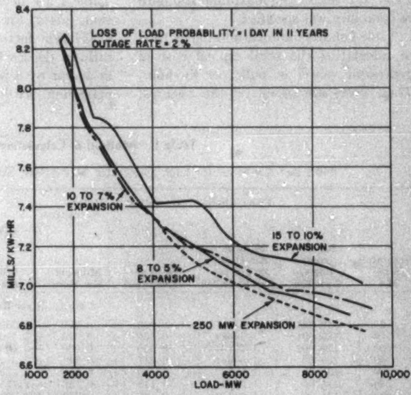

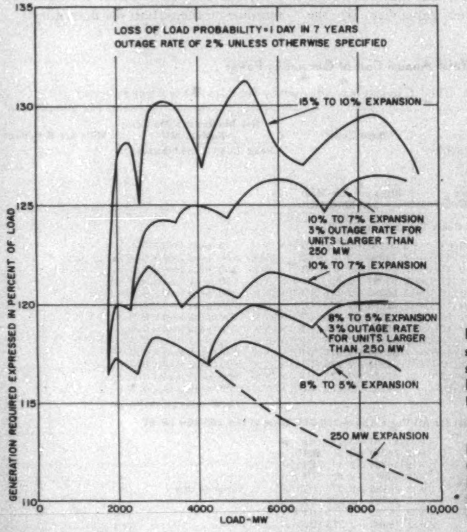

Fig. 13 (left). Reserve as function of system load with loss of load probability of 1 day in 7 years

Fig. 15 (above). Cost of supplying load in mills per kw-hour (case 2 investment cost curve)

Discussion of Results

Figs. 12 and 13 are plots of the installed generation required to meet various loads with a probability of loss of load of 1 day in 11 years and 1 day in 7 years respectively. These curves are for each of the various patterns of expansion studied and take into account a program of planned maintenance. These curves do not consider the effect on the capacity requirements of the load variations that result from changing business and weather conditions. It was found that, when the effect of these load variations is included in the calculations, the reserve requirements are increased to a larger extent with smaller % expansions than for larger % expansions.

It is apparent that there is a large difference in the reserve capacity required, depending on the size of generating units added to the system. To justify economically the use of the larger units, the extra costs associated with the increased reserve must be overcome by lower invest-

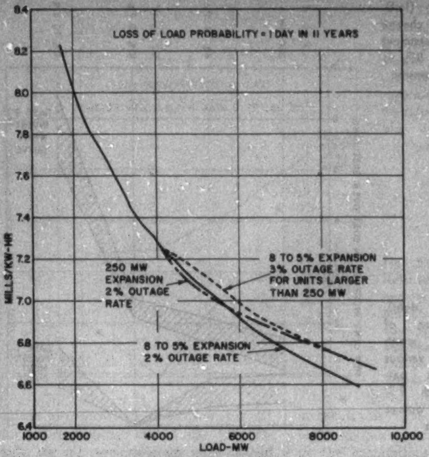

Fig. 16. **Effect of increase in outage rate for 8% to 5% expansion (case 1 investment cost curve)**

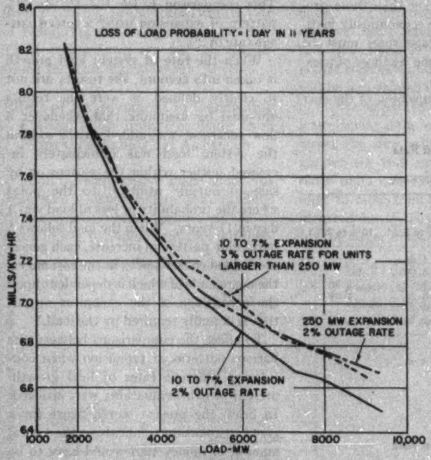

Fig. 17. **Effect of increase in outage rate for 10% to 7% expansion (case 1 investment cost curve)**

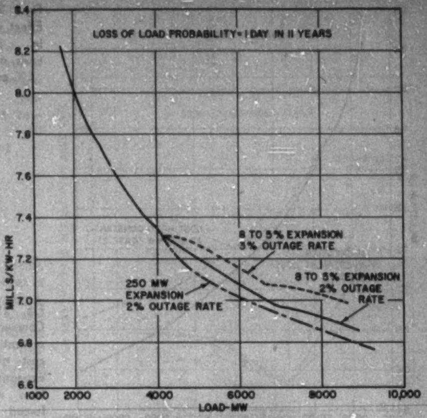

Fig. 18. **Effect of increase in outage rate for 8% to 5% expansion (case 2 investment cost curve)**

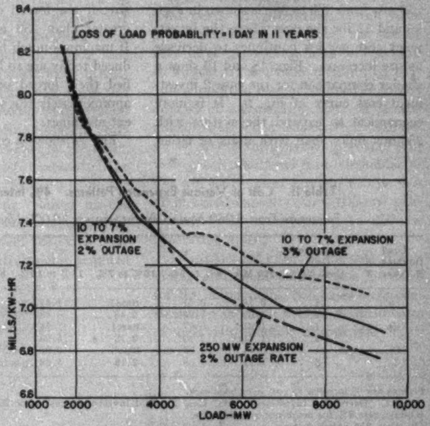

Fig. 19. **Effect of increase in outage rate for 10% to 7% expansion (case 2 investment cost curve)**

ment, operating, and maintenance costs for the larger units.

Fig. 14 compares the cost of supplying the load for the four different patterns of system expansion assuming a probability of loss of load of exactly 1 day in 11 years. These curves are based on the assumption that the forced outage rate is 2% regardless of size and that the installed cost of new units continues to decrease as the size increases. For the assumed conditions the cost curve using units of 15% to 10% of system size falls below the cost curve using units of 10% to 7% of system size for system loads above 5,500 mw.

The effect of assuming that the installed cost per kw of units above 200 mw remains constant regardless of size is shown in Fig. 15. These curves indicate that for this condition expansion with 250-mw units is generally most economical.

The results shown in Figs. 14 and 15 indicate that the most economical pattern of system expansion is very dependent on the investment cost of larger generating units. It is apparent that the future slope of the cost per kw versus size curve will be a major factor in determining the economic feasibility of larger generating units.

The effect of an increase in the forced

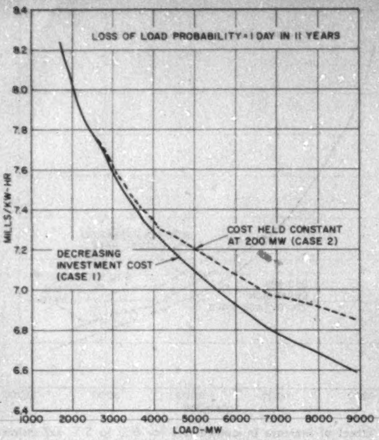

Fig. 20 (left). Effect of change in investment costs on 8% to 5% expansion

Fig. 21 (right). Comparison of present worth cost of various expansion patterns with 2% forced outage rate

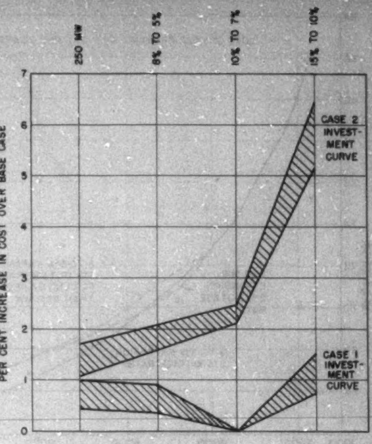

outage rate of generating units larger than 250 mw from 2% to 3% is shown in Figs. 16 and 17 for the case where the investment cost per kw continues to decrease as size increases. Figs. 18 and 19 show a similar comparison for the case 2 investment cost curve of Fig. 9. It is more economical to expand the system with 250-mw units than with units of either 8% to 5% or of 10% to 7% of the system size, if the forced outage rate for units greater than 250 mw increases to 3%. If machines much larger than those produced today are to be economically justified their forced outage rates must be approximately the same as those of present machines.

Fig. 20 shows a comparison of the cost of power in mills per kw-hour using the two different assumptions for installed cost of generation as shown in Fig. 9. This comparison is for the 8% to 5% pattern of expansion using a forced outage rate of 2%.

When the rate of system load growth is taken into account, the results are not so clearly defined as were the results obtained by assuming that whenever a new generator was added to the system the system load was immediately increased (either within the system or by sale to outside utilities) to the point where the probability of loss of load was 1 day in 11 years. When the load follows a particular pattern of increase, each generator added causes a peak in the cost curve, the magnitude of which is dependent upon the percentage of the generator output that is actually required by the load.

To effect the comparisons between the various patterns of expansion when considering different rates of load growth, present worth evaluations were utilized. In brief, the present worth figure for a given expansion indicates the total amount of money that would have to be available at the present time in order to finance completely the investment and operating costs of the generation under consideration for a given period of time.

A summary of the relative costs of the different patterns of system expansion on a present worth basis using an interest rate of 4% is shown in Table II. The figures in the table indicate the percentage increase in cost over the indicated base case. Table III is a similar comparison using an interest rate of 0%.

The cost comparisons given in Table

Table II. Cost of Various Expansion Patterns. 4% Interest Rate

Expansion From 2,000-Mw to Approximately 10,000-Mw System

Load Doubles in N Years, N	Investment Cost, Case No.*	250 Mw	8% to 5%	10% to 7%	15% to 10%	8% to 5%†	10% to 7%†
5	1	0.76	0.51	Base‡	1.52	1.68	
	2	1.52	1.98	2.48	6.43	3.30	
10	1	1.01	0.97	Base§	1.54	1.84	1.96
	2	1.71	2.10	2.13	5.93	3.23	4.38
15	1	0.44	0.30	Base‖	0.95	0.77	
	2	1.11	1.58	2.18	5.23	2.10	

Figures are % increase in cost over base case.
*Case 1. Decreasing investment cost. Case 2. Flat investment cost after 200 mw.
†Outage rate 3% for machines over 250 mw.
‡Base = 1.355 billion dollars.
§Base = 2.068 billion dollars.
‖Base = 2.624 billion dollars.

Table III. Cost of Various Expansion Patterns. 0% Interest Rate

Expansion From 2,000-Mw to Approximately 10,000-Mw System

Load Doubles in N Years, N	Investment Cost, Case No.*	250 Mw	8% to 5%	10% to 7%	15% to 10%	8% to 5%†	10% to 7%†
5	1	0.82	0.53	Base‡	1.51	1.79	
	2	1.64	2.14	2.69	6.74	3.56	
10	1	1.18	1.08	Base§	1.50	2.12	2.28
	2	1.99	2.42	2.52	6.47	3.81	5.16
15	1	0.61	0.37	Base‖	0.74	0.99	
	2	1.45	2.13	2.89	6.03	2.83	

Figures are % increase in cost over base case.
*Case 1. Decreasing investment cost. Case 2. Flat investment cost after 200 mw.
†Outage rate 3% for machines over 250 mw.
‡Base = 1.781 billion dollars.
§Base = 3.454 billion dollars.
‖Base = 5.760 billion dollars.

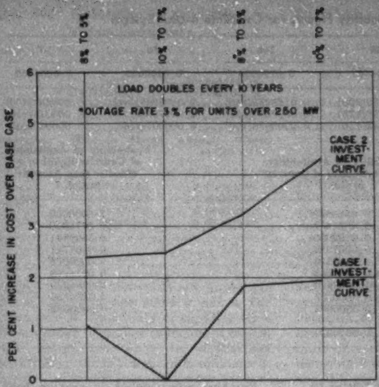

Fig. 22 (left). Effect of increase in outage rate on present worth of cost of various expansion patterns (load doubles every 10 years)

Fig. 24 (right). Relative effect of penalty in transmission system cost to provide additional transmission facilities for larger units

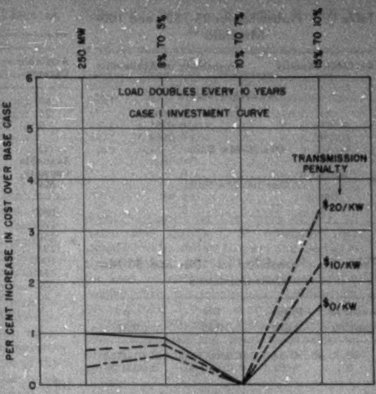

II are also shown graphically in Fig. 21 for a forced outage rate of 2%. The results for the three different rates of load growth all lie within the indicated band of results.

Fig. 22 shows the effect of an increase from 2% to 3% in the forced outage rate of generating units larger than 250 mw. These comparisons are for the case in which the load doubles every 10 years.

Effect of Improvement in Generating Station Heat Rate Resulting from Future Technological Advances

In all the comparisons made so far, the heat rates of all new generator units added to the system were assumed to be as given in Fig. 9, and no heat rate improvements in this curve resulting from future technological advances were considered in the calculations. However, it can reasonably be expected that there will be a continued improvement in station heat rates in the future as there has been in the past. This improvement in station heat rate will make larger units more attractive economically. The reason for this is that each new unit added to the system will be base loaded during the early years of operation and so the load on the older, less efficient units can be reduced. The larger the new unit that is added, the greater the fuel saving realized on the older units and this fuel saving can be used to more than offset the extra costs incurred due to the extra reserve required for the larger units.

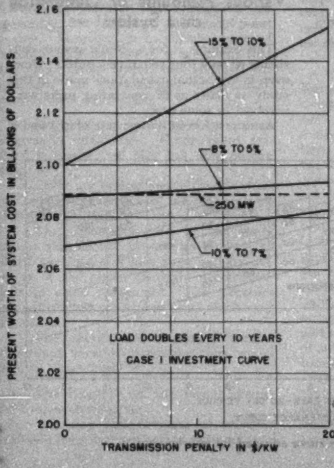

Fig. 23 (left). Effect of penalty in transmission system cost upon present worth of system cost

Effect of Larger Units on Transmission System Costs

In the results presented so far only the total costs of generating power have been considered. However, the use of very large generating units will require additional transmission facilities to provide support in case of planned or forced outages of a generating unit. It is estimated that for a widespread, well-designed system the incremental cost of providing such additional transmission facilities will be between $10 and $20 per kw of installed capacity for 1,000-mw generating units as compared to 250-mw generating units.

To explore the effect of the cost of providing additional transmission facilities for the larger units, two cases were considered by modifying the investment costs of units as a function of unit size as follows:

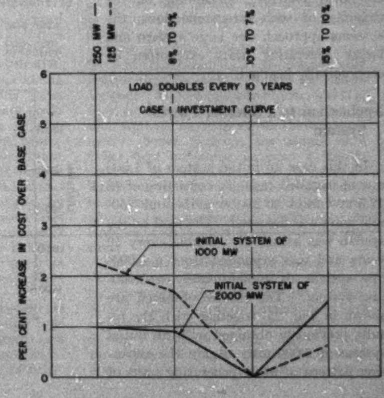

Fig. 25 (right). Effect of using initial system of 1,000 mw instead of 2,000 mw

Table IV. Probability for 25-, 50-, and 100-Mw Units

Available Capacity	Probability of Availability
Two 25-Mw Units	
50	0.9604
25	0.0392
0	0.0004
One 50-Mw Units	
50	0.98
0	0
One 100-Mw Units	
100	0.98
0	0

Table V. Probability for 100- and 50-Mw Units Combined

Available Capacity	Probability	100 0.98	0 0.02
50	0.98	0.9604(150)	0.0196(50)
0	0.02	0.0196(100)	0.0004(0)

Table VI. Probability Figures for Complete 4-Unit System

Available Capacity	Probability	150 0.9604000	100 0.0196000	50 0.0196000	0 0.0004000
50	0.9604000	0.9223682(200)	0.0188238(150)	0.0188238(100)	0.0003842(50)
25	0.0392000	0.0376477(175)	0.0007683(125)	0.0007683(75)	0.0000157(50)
0	0.0004000	0.0003842(150)	0.0000078(100)	0.0000078(50)	0.0000002(0)

(1) Available Capacity, Mw	(2) Probability of Availability of Exact Amount of Capacity in Col. 1	(3) Probability of Availability of Capacity Equal to or Smaller than Amount in Col. 1
200	0.9223682	1.0000000
175	0.0375477	0.0776318
150	0.0192080	0.0399841
125	0.0007683	0.0207761
100	0.0188316	0.0200078
75	0.0007683	0.0011762
50	0.0003920	0.0004079
25	0.0000157	0.0000159
0	0.0000002	0.0000002
	1.0000000	

1. The penalty in cost for supplying additional transmission facilities was assumed to vary linearly from $0 per kw for 250-mw units to $10 per kw for 1,000-mw units.

2. The penalty in cost for supplying additional transmission facilities was assumed to vary linearly from $0 per kw for 250-mw units to $20 per kw for 1,000-mw units.

The effect of the penalty in transmission costs on the present worth of system costs is shown in Fig. 23. In this case it was assumed that the system load doubled every 10 years. It can be seen that any appreciable extra cost in the transmission system considerably reduces the attractiveness of larger generating units. The same results are shown in different form in Fig. 24.

Interconnecting transmission facilities between systems can often be economically justified on the basis of economical power interchange and of the reduction in total reserve capacity required on the combined systems. Depending on the capacity of such interconnections, the systems approach one large system and larger generating units can often be economically justified.

Application to a Smaller Power System

In this case an initial system of 1,000 mw of installed capacity consisting of 12 12.5-mw units, 20 25-mw units, and 7 50-mw units was assumed. The load on the system was assumed to double every 10 years and was expanded from a 1,000-mw system to approximately a 5,000-mw system. The results obtained are shown in Fig. 25, together with the results previously obtained with an initial system of 2,000 mw. Again the expansion pattern of using generating units of 10% to 7% of system size was found to be the most economical but the reduction in cost by using this pattern rather than smaller units is greater for the smaller system. This result was obtained because the slope of the cost per kw versus size curve is steeper in the lower size range. There is therefore a greater gain in using units that are a higher percentage of system size on a small system than on a large one.

Summary of Factors for and Against Large Generating Units

The factors in favor of and against the use of large generating units may be summarized as follows:

Factors Favoring Large Units

1. A steep slope of the curve of cost per kw versus size.
2. Lower operating and maintenance costs per kw-hour for larger units.
3. Further improvement in station heat rate resulting from technological advances.
4. Reduction in the number of construction and maintenance crews required with larger units.
5. Interconnections with adjoining systems.

Factors Against Large Units

1. Flat slope of the curve of cost per kw versus size.
2. Increased reserve capacity required with larger units.
3. Any increase in forced outage rate.
4. Increase in capacity required in the transmission system.
5. Site limitations.

Appendix I. Example of Method Used in Determining the Probability of Availability of Various Amounts of Generation on a System[1]

This example is for a simple system consisting of only four generating units. However, in the actual calculations made in this study as many as 67 generating units were involved in some cases.

Assume a forced outage rate of 2% and a

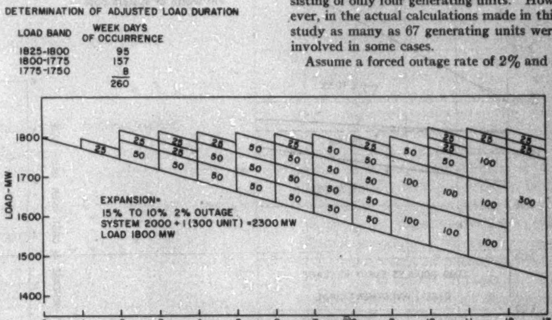

DETERMINATION OF ADJUSTED LOAD DURATION

LOAD BAND	WEEK DAYS OF OCCURRENCE
1825-1800	95
1800-1775	157
1775-1750	8
	260

Fig. 26. Load duration curve adjusted for maintenance

Table VII. Probability of Availability for Various Generations

(1) Generation, Mw	(2) Probability of Availability of the Exact Amount of Capacity Shown in Col. 1	(3) Probability of Availability of Capacity Equal to or Smaller than the Amount Shown in Col. 1
1,825	0.00015592	0.00049095
1,800	0.00020762	0.00033503
1,775	0.00004778	0.00012741
1,750	0.00005088	0.00007963

Table VIII. Load Band and Weekdays of Occurrence

Load Band, Mw	Weekdays of Occurrence
1,825 to 1,800	95
1,800 to 1,775	157
1,775 to 1,750	8

Table IX. Days per Year Not Possible to Meet Load

Generation, Mw	Probability (From Col. 3 of Table VII)	×	Weekdays of Occurrence	=	Days per Year Unable to Supply Load
1800	0.00033503	×	95	=	0.031828
1775	0.00012741	×	157	=	0.020003
1750	0.00007963	×	8	=	0.000637
			Total		0.052468

system composed of two 25-mw units, one 50-mw unit, and one 100-mw unit. The probability of availability of capacity for a given number of similar units and a chosen fixed outage rate may be determined directly from the tables given in reference 2. Table IV gives the information for the system chosen. The probability of availability of the combination of the 100-mw units and the 50-mw units may be determined as given in Table V. Similarly the probability figures for the complete 4-unit system are obtained as shown in Table VI.

The following is an example of how the planned maintenance program was taken into account in determining the reserve capacity required. In this case the installed capacity on the system consisted of 12 25-mw units, 20 50-mw units, 7 100-mw units, and 1 300-mw unit for a total of 2,300 mw. A selected portion of the probability of availability figures for this system of generation is given in Table VII. A system weekday peak load of1,800 mw was assumed and it was also assumed that the weekday peak load varied linearly with time to a minimum weekday peak of 80% of the maximum peak or 1,440 mw.

Fig. 26 shows this peak load variation and also shows how each machine on the system was scheduled for planned maintenance for 20 weekdays per year. The number on each block indicates the mw capability of a machine and outages for maintenance were scheduled so that the sum of the actual load and the capability of the units out for maintenance was as uniform as possible. With this maintenance schedule established, the number of weekdays during the year that the load plus the generation out for maintenance fell within each 25-mw load band was determined.

From Fig. 26 the information given in Table VIII was obtained. The number of days per year that it would not be possible to meet the load was then determined as shown in Table IX. This gives one point on the curve shown in Fig. 11.

The foregoing procedure was repeated for two other values of peak load; in this case 1,750 mw and 1,700 mw are two other points obtained for the curve of Fig. 11. Since the standard of reliability was assumed to be ability to carry the load at all times except 1 day in 11 years, Fig. 11 can be used to determine what load can be carried with this reliability. Reading Fig. 11 at 0.0909 day per year gives a load of 1,826 mw. Since the installed generation was 2,300 mw, the total generation expressed in terms of the load was 126% of the load.

References

1. Elements of System Capacity Requirements, C. W. Watchorn. *AIEE Transactions*, vol. 70, pt. II, 1951, pp. 1163–85.

2. Tables of Binomial Probability Distribution to Six Decimal Places, AIEE Committee Report. *Ibid.*, vol. 71, pt. III, Aug. 1952, pp. 597–620.

3. Forced Outage Rates of High Pressure Steam Turbines and Boilers, AIEE Committee Report. *Ibid.*, vol. 73, pt. III, Dec. 1954, pp. 1438–42.

4. Generating Reserve Capacity Determined by the Probability Method, Giuseppe Calabrese. *Ibid.*, vol. 66, 1947, pp. 1439–50.

◆

Discussion

O. R. Bulkley (Southern California Edison Company, Los Angeles, Calif.): The authors are to be commended for a very thoughtful and painstaking analysis of this timely subject. Based on the assumptions given, it would appear that the conclusions are reasonable, from a strictly theoretical point of view. However, in considering units of the large sizes mentioned, it is evident that other controlling factors would limit the sizes that can economically be justified. Some of these factors are:

1. Size must not run ahead of our proved progress in metallurgy. From recent evidence it seems that size has now outrun progress.
2. There are limitations to the practical and economic capacity of interconnections with other utilities.
3. The economics used in the study assume that it will always be possible to absorb the load of a new large unit by disposing of the power through interconnections to other companies. This becomes more difficult in practice as units reach very large sizes.
4. The practicability of using the largest of perhaps several alternative sizes would seem to depend on:

   a. The reserves on the prime system itself to cover outages.

   b. The size and firmness of reserves available from interconnected systems.

If the prime system has such reserves that it can cover an outage of the largest unit without shock then there is no operating problem but there may be an economic one. If the prime system has large enough ties with other systems so that it could lose the use of its largest machine without shock, there may be no problem at all. If, however, neither of these provisions is available, very large generators could be a serious handicap during forced outages.

Herman Halperin (Commonwealth Edison Company, Chicago, Ill.): This study brings out a number of interesting points, including a demonstration that probability calculations play an important part in determining the economic size of generating units. The comparisons of the various schemes could not be achieved without the use of such calculations. We have been using probability calculations as one of the important factors in determining the required reserve generating capacity, and these calculations are based on the methods developed by Adler and Miller.[1] This approach not only gives us an idea of the magnitude of outages for various time intervals but also gives information on the probable duration of outages, particularly the larger coincident forced outages.

The authors assume for the general case that the forced outage rates for unit-type installations of turbine generators and boilers would be 2%, although some calculations are based on 3%. A study of reference 3 of the paper for operating experience for turbines and boilers operating at over 1,000 pounds per square inch gauge indicates that the average combined rate of outages for the years 1950–1952, in percentage of the time that the units could be operating on weekdays, is more of the order of 3% than 2%. I hope it does definitely get down to the level of 2% or lower that the authors mention. There were lower rates of outages in 1951 and 1952 than in 1950, but other operating experiences before and after that period make it seem imprudent to use the relatively low rates of one or two years.

As is generally known, the outage rates for unit-type installations are considerably greater than for systems where the boilers are connected to a common header, which in turn supplies two or more generators. In such stations, especially when there is some reserve boiler capacity, the outage of a boiler does not cause as great a loss in capacity as with the unit-type system. Furthermore, the older and smaller units have been having lower rates of forced outages than apparently applies for the large units and boilers in unit-type installations.

For several years it has appeared to me that the sum of the load plus the allowance for overhauling plus the allowance for limitations (due to decreased summer-time load capabilities) should be a constant figure during a 12-month period. Apparently in the authors' study the effect of limitations is not considered, but they may amount to a loss of 2 to 5% in capability, or even more, in the summer as compared to the midwinter capability.

In connection with Fig. 26, where the authors show provision for overhauling on top of the range of daily load peaks during the year, it does not seem practically feasible to do what they have done. For example, in any given month of the year there may be a range in the magnitude of weekday peak loads of 10 to 15%, depending on the influence of relative darkness, temperature, and other factors on the load demands. Our studies do show that there is at present an appreciable range through the year in the monthly peak loads. In handling the allowances for overhauling and limitations, we build these allowances on top of the monthly peak demands.

In connection with the previous point, we do take a small advantage of the fact that the larger totals of forced outages are likely to persist just a day or two. This is done first by taking into account our results of studies of past loads, which show that for about 90% of the weekdays of a given month the daily peak loads have been about $1^{1}/_{4}\%$ or more below the monthly peak loads. This value, in mw, is then deducted from the indicated owned reserve that is needed according to probability calculations and other factors. The value of $1^{1}/_{4}\%$ just given applies for the winter months and the corresponding value for summer is larger.

A practical view from the standpoint of operation is to consider the possibility of relieving tight situations created by large simultaneous outages. With relatively smaller units, large simultaneous forced outages generally will not occur suddenly but will be built up to their full magnitude in successive steps in time. This makes it possible to make arrangements to return equipment to service more quickly than originally planned, in case the total of the forced outages is building up to a disturbing amount. This ameliorative measure cannot be used so effectively when the system consists of very large units where each corresponds, say, to 10% of the total system capacity.

It does not seem appropriate to comment on all the assumptions and points in this article, but a majority of them appear to be fairly reasonable. For large turbine generators, however, it seems probable that there should be an allowance for overhauling of more than the 20 weekdays mentioned. In connection with the discussion on the benefit of interconnections in reducing the reserve capacity, probability calculations, or at least some judgment, should be applied as to how much the firm power will be in case of a large outage of generating capacity. It is of interest to note that the authors use an increased rate of forced outages in one set of their calculations where the size of units goes over 250 mw.

Another point to be considered in connection with the installation of larger and larger units over a period of time is that some probability calculations need to be made to determine the possible effects of having larger than the average sized unit on the system out of service during forced outages. Two calculations on the probabilities of forced outages of a given number of units showed that, where the failed units were relatively large in size, the magnitude of the coincident forced outage was one-third bigger than for the case involving outages of just average sized units. The authors' paper demonstrates the value of using a digital computer for such studies where there are a large number of repetitive probability calculations.

Reference

1. A New Approach to Probability Problems in Electrical Engineering, H. A. Adler, K. W. Miller. *AIEE Transactions (Electrical Engineering)*, vol. 65, Oct. 1946, pp. 630–32.

C. F. Paulus (The Cleveland Electric Illuminating Company, Cleveland, Ohio): I very much enjoyed this paper, which was incisive and specific. There are several points I would like to mention.

What is included in the investment base and what rating is used in calculating the costs per kw? Possibly the equipment included should be enumerated and the rating, net or gross name plate, or capability.

The heat rate curve shown in Fig. 9 seems unduly pessimistic. This kind of curve has been shown for the last 25 years always flattening out at the size corresponding to the largest unit installed at that date. Certainly heat rates appreciably below that shown are possible. The added complications they introduce may well be justified with the larger units.

Throughout this paper there is the implication that the larger spinning reserve required with the larger units has no value; that it is an unwanted accompaniment. This extra capacity is of the highest efficiency and does have real value. The spinning reserve consists of the older units while the newest unit is fully loaded. The larger unit should be credited for the improvement in system efficiency. The larger spinning capacity on a system with larger units is useful in case of a plant shutdown. The magnitude of the net deficiency is reduced. I believe that the record of the last few years indicates that plant shutdowns are still with us.

Complete unitization of turbogenerators is still too costly. This is especially true when applied to small units. I am thinking of a system of a size where the application of the authors' formula would indicate about 100-mw units whereas units of about 300 mw appear more economical. In a plant of 600 mw, complete unitization for two 300-mw units may be justified. This would be difficult to do for six 100-mw units. The completely unitized 2-unit plant is more likely to keep some capacity on the line than is the nonunitized 6-unit plant.

The time required for an overhaul or inspection of a large unit is but little more than for a small unit. If the time required for scheduled maintenance is integrated into the reserve requirement calculations, the larger additional capacity required by larger units compared to smaller units is reduced.

A tabulation of the ratios of unit sizes to installed capacities shows that at the time the horizontal turbogenerator was introduced new units were as large as 50% of the installed capacity. The presently foreseeable growth of the electric power industry should give us confidence that additions of 20% or so are not excessive.

H. W. Phillips (Philadelphia Electric Company, Philadelphia, Pa.): This paper investigates the most economical machine sizes for future installation on an isolated system. The conclusions are reached by comparing the gain in operating economy and reduction in investment cost through the utilization of large units. The analysis fails to take into consideration the fact that the installation of a larger unit on an isolated system will, in most cases, require an increase in the spinning reserve capacity.

Experience on the Pennsylvania-New Jersey Interconnection during the last 25 years has indicated that the companies doing the best daily load forecasting have a probability of loss of load through daily load forecasting errors amounting to about once every 8 years, if 5% spinning reserve is scheduled. This frequency of loss of load once every 8 years is in line with the two analyses included in the paper covering a frequency of once every 7 years or once every 11 years. Therefore, it seems that the standards of the Pennsylvania-New Jersey Interconnection are quite paralleled with those assumed in the paper.

The hypothetical system used in the analysis has a basic load of 2,000 mw, and 5% spinning reserve would amount to 100 mw or approximately equal to the largest unit installed initially (100 mw). Based on the experience of the Pennsylvania-New Jersey Interconnection, where 30-mw units are used to make up any deficiency in spinning reserve, the daily cost for this reserve adjusted to fuel at 25¢ per million Btu would be $9.40 per mw day. This would represent an increased daily operating cost of $940 if a 200,000-kw unit were installed. If it is assumed that no additional spinning reserve is normally required on Sundays, the incremental extra spinning reserve cost would be applicable for approximately 300 days per year, and would amount to $282,000 per year. Therefore, it seems very difficult to justify doubling the size of the largest unit on an isolated system when the largest unit presently installed is equal to the daily load forecasting error hazard.

These comments have been based purely on the application of the conclusions of the paper to an isolated system; however, few electric utility companies are isolated today, and many of them have entered into pooling agreements through which the installed reserve and spinning reserve can be greatly reduced and much larger machines justified. The Pennsylvania-New Jersey interconnected system having a load of approximately 7,000,000 kw carries spinning reserve equal to $4^{1}/_{2}\%$ of the annual peak load, or 315,000 kw. This gives a probability of loss of load due to daily load forecasting errors of once every 8 years; however, two of the companies in this group have ordered units in the 225 to 275-mw class because it is possible to operate these units without additional spinning reserve. Furthermore, at the present time a 315-mw unit would be justified since it would not exceed the spinning reserve required by the daily load forecasting hazard. The probability of losing this unit at the time that the $4^{1}/_{2}\%$ load forecasting error occurred (on a 2-hour peak) would be only once in approximately 10,000 years.

Figs. 12 and 13 indicate that installed reserve of 22 to 23% would be required if the 10% to 7% expansion rate were utilized.

However, a 315,000 unit on the Pennsylvania-New Jersey system would amount to 12½% of the load of the largest system and 30% of the load of the smallest system in the area, but could be installed without increasing the Interconnection installed reserve requirement above the present figure of 10%. This is made possible through a very complete pooling agreement whereby the various companies pay at a very reasonable rate for any deficiency in their installed reserve obligation.

It is felt that if the problem were restudied, considering the possibilities available through well-co-ordinated Interconnection, the installation of units in the 10% to 7% range would prove too small and that units of greater size could be justified.

Howard P. Seelye (The Detroit Edison Company, Detroit, Mich.): A study like this may have some value in indicating trends or areas for specific investigation. It is unlikely, however, that it could be depended upon as the basis of any choice of generator size. Conditions are so different on different systems, both as to loads, transmission, interconnections, and construction costs, that a specific determination for any proposed installation is believed to be necessary.

In general, the conclusion that generators of 10% to 7% of the size of the system will be found economical is fairly well in agreement with the results of specific studies on the Detroit Edison System whereby a 260-mw unit was chosen for a system load of 2,500 mw, and a 300-mw unit as the next step a couple of years later.

Figs. 12 and 13 seem to indicate rather higher amounts of reserve generation than is believed to be necessary in practice, running from about 18% to as much as 30%. This is probably a result of the method of calculation used. Studies made for our system several years ago, using probability methods, but based on the frequency of expectation of a combination outage exceeding the load, indicated that within certain limits of practicability, the reserve required is a percentage of the load, which percentage decreases in an increasing number of units, but has little relation to the size of unit, provided that latter is not excessive compared with the size of the system. This would indicate less reserve necessary and less effect of the size of units than is indicated here. The effect of pool operation of interconnected systems has a great deal of bearing on the size of unit which may be justified. Other assumptions as to variation of cost of installation with size, variation in maintenance cost, variation in operation, variation in heat rate, etc., are all so dependent upon specific design conditions that it is hard to judge whether or not the results indicated are truly representative. As a general indication, however, of the value of reasonably large units on a system, this study is in the right direction.

M. J. Steinberg (Consolidated Edison Company of New York, Inc., New York, N. Y.): This paper describes a method of analysis relating to the economic evaluation of capacity additions to an electric system. The paper is of timely interest because of the attention currently being given to the problem of unit additions with maximum capabilities in the range of 300 mw. This problem is usually resolved on the basis of an analysis which attempts to evaluate all factors, tangible and intangible, that influence the relative economics of all alternatives under consideration. In general, the comparison of alternatives will be made with reference to a base case, which will usually be the one that requires the least investment. Differentials of annual operating savings are balanced against differential investments and final results are tabulated to show either the rate of return on added investment or the added investment that can be justified by the differential operating savings in relation to the estimated actual investment.

Attention is called to a comprehensive treatment by Skrotzki[1] of the fundamentals involved. The procedure described by the authors follows, with some modifications, the procedure recommended in the Skrotzki paper which in my opinion merits careful study by those interested in this field of activity.

The effect of unit size on installed reserve capacity requirements is of special interest. Although the literature on this phase of the problem is quite meager, there is enough to indicate that there are at least two schools of thought. One point of view is that unit size does not affect reserve capacity requirement. This stems from the policy which plans capacity additions to provide installed system reserve capacity equal to a fixed percentage of the peak load demand. The position taken is that no penalty attaches to a unit because of size, unless the size of the unit exceeds the total installed reserve capacity. This view has been upheld in a recently published article[2] which states: "It might be inferred that a larger unit would require somewhat more system reserve to provide against its outage than would a smaller one. Reserve is considered in terms of a percentage of system load, however, so if this indicates an amount as great as the size of the unit, no additional amount should be necessary..."

The opposite point of view is that system reserve capacity requirements increase with the addition of larger sized units, a characteristic which is generally the result when reserve requirements are determined by the application of probability mathematics. This is clearly demonstrated by the curves of Figs. 12 and 13 and confirmed by the curves of Fig. 27 which was prepared on the basis of uniform size unit additions. It will be observed from Fig. 27 that, with successive unit additions, there is an increase in the % reserve capacity requirement until a maximum value is reached, with the percentage values decreasing thereafter. It will also be noted that the rate of increase of reserve requirement to the maximum value varies with unit size. Thus, for a given peak load growth, the number of unit additions will decrease with unit size, while the required total capacity addition will increase with unit size, so that the total investment will also increase with unit size, and this increase in investment for the larger units must be justified by the annual savings which will result from the increased generation and improved thermal efficiency if the latter is obtained.

As between the two views on the method of determination of objective reserve capacity requirements, I favor the one which is based on the application of probability mathematics, first, because it is based on sound mathematical principles in use by the telephone industry for many years before adoption by several of the larger electric utilities, and second, because it introduces a discounting factor against the added investment for the larger size units to offset the imponderables which are inherent in long-range estimates into the future.

For most electric systems the annual generation of the initial unit addition will be affected by subsequent unit additions. In the early years of service it is expected that the initial unit will be base-loaded, with reduction in annual generation thereafter as

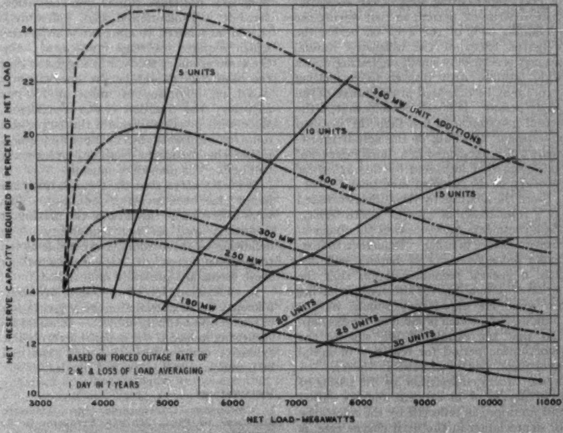

Fig. 27. Effect of unit size on installed reserve capacity requirements

Table X. Evaluation of Savings as a Function of Age

At 6% Interest

Years	Capacity Factor, %	Efficiency Factor	Relative Savings, %	Present Worth Factor	Present Worth of Annual Savings, %
1 to 5	80.00	1.00	80.00	4.2124	336.9920
6 to 10	77.23	0.99	76.46	3.1478	240.6808
11 to 15	63.19	0.98	61.93	2.3522	145.6717
16 to 20	53.49	0.97	51.89	1.7577	91.2071
21 to 25	48.20	0.96	46.27	1.3134	60.7710
26 to 30	43.39	0.95	41.22	0.9815	40.4574
31 to 35	41.08	0.94	38.62	0.7334	28.3239
36 to 40	38.17	0.92	35.12	0.5481	19.2493
41 to 45	36.13	0.90	32.52	0.4095	13.3169
45 to 50	32.91	0.90	29.62	0.3060	9.0637
Present worth of total annual savings					985.7338
Fixed charge rate					13%

Investment justified by annual savings $= \frac{985.7338}{0.13}\left[\frac{0.06(1.06)^{50}}{(1.06)50-1}\right] = 4.8028$

Ratio—justified investment to savings in first year $= \frac{4.8028}{0.80} = 6.0$

more units are added to the system. This results in non-uniform annual operating savings which decrease with service years. Conversion of the nonuniform annual savings to equivalent present worth values is a conventional procedure, which can be utilized to establish the relation between the savings in the first year of operation and the investment that can be justified for the initial unit if the simplifying assumption that annual savings will vary approximately in direct ratio to the annual generation or capacity factor is acceptable. A sample calculation along this line is given in Table X. Such a calculation is useful in evaluating differentials of operating costs of equal size units as affected by the proposals offered by manufacturers of equipment.

The rate of recovery of capital investment through operating savings is greater in the early years of the service life due to the greater utilization of the unit. Fig. 28, derived from the values of Table X, indicates the percentage recovery of the total justified investment as a function of age. It will be noted from Fig. 28 that 83% of the justified investment is recovered in a period of years representing 40% of the amortization or write-off period, so that during the remaining 60% of the write-off period the weighted effect of the estimated annual savings is relatively small, suggesting that a wide latitude with respect to estimating errors may be tolerated in this range of the study period. It is also obvious that, if the actual investment is less than the justified investment, the bulk of the actual investment will be recovered in a shorter period of time than that indicated by this figure for recovery of the justified investment.

Since the analysis by the authors is based on a comparison of present worth values, some comments on the use of this basis of comparison are in order. Reference to textbooks on engineering economics will disclose a general recommendation that the period of comparison for alternatives having the same life expectancy should be the estimated life, which is based on the assumption that the estimated life will be the amortization period for recovery of initial investment with a return thereon. A present worth comparison for the period of amortization of investment for the initial unit addition, as reflected by the allowance for depreciation in the fixed charge rate, is suggested. It is inferred that the authors have used different periods of comparison for each rate of load growth in arriving at the values shown in Tables II and III. This follows if the authors have limited their calculations to the number of years required for the system load to increase from an initial value of 2,000 mw to a final value of approximately 10,000 mw. Thus for loads doubling in 5, 10, and 15 years, the annual rates of load growth have been computed as 14.9%, 7.2%, and 4.7% respectively, requiring 12, 23, and 35 years to reach the 10,000-mw value. In view of the very small percentage differentials shown in these tables, the use of a relatively short period of comparison casts some doubt on the conclusiveness of the results. Expression of opinion on this point would be most welcome.

With reference to the same tables, it is noted that the authors have used as the base case for reference the 10% to 7% expansion, presumably because the present worth of the combined annual fixed charges and operating costs is the minimum, and this is used as the basis for the conclusion that this plan of capacity expansion is the most economical. Actually, this is not conclusive, since it is fundamental that differentials should be referred to the plan of expansion which requires the least investment. For the systems under study, it is suggested that the base case should be the one which is based on additions of units of 150-mw capacity, the smallest units considered, since with penalties against the larger size units for additional reserve capacity requirements the minimum practical investment will be for this plan of expansion.

It is also noted that the term "utilization factor" has been incorrectly defined. This term is defined as the ratio of the maximum generated load to unit capability. The definition by the authors is applicable to the terms "use factor" or "capacity factor" as these terms are generally understood.

In conclusion, I wish to extend my compliments to the authors for the presentation of a paper on a timely subject. It would be surprising indeed if the paper does not elicit extensive constructive discussion that will be beneficial to all interested parties.

REFERENCES

1. CONDITIONS CONTROLLING THE ECONOMIC SELECTION OF PRIME MOVERS, **Bernhardt G. A. Skrotzki.** *AIEE Transactions*, vol. 63, 1944, pp. 1099–1108, disc. pp. 1360–61.

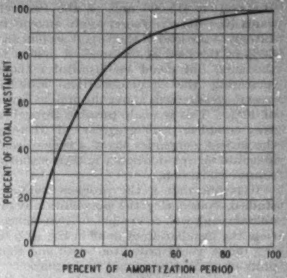

Fig. 28. Investment justified by annual savings

2. ECONOMY OF LARGE GENERATING UNITS, **H. P. Seelye, W. W. Brown.** *Combustion*, New York, N. Y., vol. 25, 1954.

C. W. Watchorn (Pennsylvania Water and Power Company, Baltimore, Md.): The paper is another valuable contribution to the growing list of examples or illustrations of the application of probability methods to power-system problems. The authors are to be most highly commended both on undertaking a very ambitious project and in making the results available to the industry. The real value or significance of the paper is in its illustration of the applicability of probability methods as a tool in the solution of economic problems of power-system design rather than with respect to the specific results reported. The material is long overdue both as such an illustration and as a demonstration of the applicability of digital computers to the handling of the vast amount of arithmetic that is inherent in such problems. This latter fact should remove much of the past reluctance as to the use of probability methods in the solution of power-system problems to which such methods are applicable.

I wish to make a few specific comments relative to various aspects of the details of such evaluations, the first regarding the determination of the timing of the installation of additional capacity. Several years ago I wrote that an acceptable and satisfactory objective level or degree of system reliability should be in the order of an average rate of failure to carry the load of 1 day in about 30 years if the effect of load variations or so-called load forecasting or estimating errors is disregarded,[1] and somewhat smaller,[2] in the order of an average rate of 1 day in about 8 to 10 years, when the effect of load variations is taken into account.[2,3] Such a basis, although possibly reasonable, is nonetheless only a matter of judgment with respect to which anyone may well take exception without there being any basis for successfully controverting any other level of objective reliability that it may be desired to propose.

More recently I proposed,[4] with concurrence by others,[5,6] that the measure of the adequacy of service continuity is the cost to the general economy of providing the service. That is, facilities should be provided up to such point that the economic burden of providing additional facilities is larger than the probable average economic gain (which is intended not to mean reductions in otherwise lost revenue[6]) that would result with increased service continuity from the installation of such additional facilities. Such a basis for the timing of the installation of additional capacity substitutes a comparison of more or less definite with and without costs as the criterion for such timing in place of an opinion as to a satisfactory level of an objective service reliability.

Also, since the studies reported are based on annual carrying charges of 12%, the cost of money involved must be in the general order of 6%.[7] It then follows that the discount rate to be used in the present worth calculations should also be about 6%;[8] there is no other choice, since it is just as essential for the discount rate that is used in the present worth calculation to be equal to that used as the cost of money in determining the annual carrying charges as it is for the I's in the equations $E=IR$ and $P=EI$ to be equal for the same condition as of any given time, because the relationships, in their respective ways, are equally rigorous. The result is that the costs of the more distant future would be discounted to a greater extent on this basis than on the basis used in the paper where two discount rates, 0 and 4%, were used. This means that the tendency may be indicated for smaller size units than otherwise to be the more economical in such a study with the timing of the installation of additional capacity based on the costs to the general economy, as just suggested.

Further, although the authors recognize the effect of load variations on the timing of the installation of additional capacity, they have chosen not to incorporate such considerations in their determination. The effect of such considerations, if included in the study, would be to tend to indicate the larger size units to be the more economical.

In addition to the bases used by the authors for determining the pattern of unit sizes to be investigated, I would suggest that an investigation of the effect of increasing and decreasing percentage patterns of size of units may have significance. Lastly, although the authors found that, "for the range of rates of load growth normally encountered, the rate of load growth of a system has no appreciable effect on the size of units that can be economically justified on a system," it nevertheless is difficult to understand why the smaller size units would not be definitely indicated to be the more economical with the smaller rates of load growth.

REFERENCES

1. PROBABILITY METHODS APPLIED TO GENERATING CAPACITY PROBLEMS OF A COMBINED HYDRO AND STEAM SYSTEM, E. S. Loane, C. W. Watchorn. *AIEE Transactions*, vol. 66, 1947, pp. 1645–54.

2. THE DETERMINATION AND ALLOCATION OF THE CAPACITY BENEFITS RESULTING FROM INTERCONNECTING TWO OR MORE GENERATING SYSTEMS, C. W. Watchorn. *Ibid.*, vol. 69, pt. II, 1950, pp. 1180–86.

3. See reference 1 of the paper.

4. POWER AND ENERGY PRODUCTION, C. W. Watchorn. *AIEE Transactions*, vol. 73, pt. III-B, Aug. 1954, pp. 901–03.

5. *Discussion* by E. E. George of reference 4, p. 906.

6. *Discussion* by M. H. Mackenzie of reference 4, pp. 907–08.

7. ANNUAL CARRYING CHARGES IN ECONOMIC COMPARISONS OF ALTERNATIVE FACILITIES, Paul H. Jeynes. *AIEE Transactions*, vol. 70, pt. II, 1951, pp. 1942–53.

8. PRESENT WORTH, OR THE TIME COST OF MONEY, AS A FACTOR IN THE ECONOMIC COMPARISON OF ALTERNATIVE FACILITIES, Paul H. Jeynes. *Ibid.*, pp. 1956–62.

L. K. Kirchmayer, A. G. Mellor, J. F. O'Mara, and J. R. Stevenson: All of the discussers have contributed to a better understanding of the problem of determining the economic size of steam-electric generating units.

In answer to Mr. Bulkley's question regarding the feasibility of building much larger generating units, we have every confidence that continued progress in metallurgy and design skill will make units larger than those now in operation economically feasible. Mr. Bulkley correctly points out that in several cases studied it was assumed that it would be possible to absorb the load of a new large unit by disposing of the power through interconnection to other companies. However, in Figs. 21 through 25, and in the conclusions of the paper, this assumption was not made, and the system load was assumed to double every 5, 10, or 15 years.

We are pleased that Mr. Halperin has indicated general agreement with our assumptions. Concerning his comments on the forced outage rate used, recent figures indicate that the reliability of large high-pressure units has been improving. We therefore feel that a 2% forced outage rate is fairly representative of most large units now in service. In connection with the treatment of maintenance outages, the approximations we made will provide the correct relative results. Also, we have been advised by several operating companies that 20 weekdays per year for maintenance are more than adequate.

In answer to Mr. Paulus' question, the investment costs used are the total installed cost of the generating unit up to the high-voltage side of the main step-up transformer. The rating referred to is net guaranteed capability of the unit. As stated in the paper, it is anticipated that unit heat rates, particularly in the larger size units, will certainly improve in the future. The effect of this improvement in heat rate is discussed qualitatively in the paper. Larger size units will be required to fully realize the potential gains resulting from much higher steam pressures.

We agree with Mr. Paulus that the extra reserve capacity required with the larger generating units has an economic value in displacing higher cost generation and our analysis has appropriately considered this effect. Also, we concur that the time required for an overhaul or inspection of a large unit is little or no more than for a small unit. This factor is reflected in the maintenance cost curves of Fig. 8.

It is our opinion concerning Mr. Paulus' comments on the cost of complete utilization that most new stations are economically utilizing the unit scheme for units approximately 100 mw and above. Also, with respect to plant outages, we believe that a 6-unit station should prove more reliable than a 2-unit station.

Mr. Phillips has commented on the effect of larger generating units on the required spinning reserve capacity. We wish to point out that the only cost of providing reserve capacity which has been ignored is the fuel cost. It is felt that with the negligible load factors involved this is a reasonable assumption, particularly as the fuel used by the spinning reserve is partly compensated for by the fuel saving on other units.

In considering the subject of interconnections, a group of operating companies may be considered as one system providing that adequate interconnecting transmission facilities and agreements exist. Thus, the 10% to 7% expansion pattern referred to the total integrated area would be a much larger percentage when referred to any operating component of the total.

We are pleased that Mr. Seelye has reported that the results of the studies undertaken by his company are in general agreement with the results of our paper. We believe that each company must conduct specific studies to obtain answers pertinent to their individual systems.

Application of probability methods to choose sufficient reserve capacity to maintain a fixed service reliability results in increased % reserve requirements as the unit size increases. This point is illustrated by reference to Figs. 12, 13, and 27.

Mr. Steinberg has called our attention to the interesting paper on this subject by Mr. Skrotzki. Our approach differs fundamentally in the treatment of reserve requirements. We have attempted to maintain the same standard of service reliability for all types of system expansion while Mr. Skrotzki's approach allows a variable standard of reliability as the system expands.

Mr. Steinberg's comments on the period of time to be used in the present worth evaluations are of interest. It is our opinion that the correct relative picture is obtained by using the selected periods, and this opinion is substantiated in part by Fig. 28.

We do not agree that minimum investment cost will necessarily be realized by expanding the initial system with 150-mw units, as this depends on the slope of the investment curve used. It is our opinion that the selection of the base used has no effect on the relative answers obtained.

We concur with Mr. Watchorn that the desirable degree of system reliability is largely a matter of judgment. However, our investigations indicate that the same relative answers will be obtained over a wide range of standards of system reliability. The measure of adequacy of service continuity as a cost to the general economy involves numerous intangible factors which are impossible to include in a study similar to ours. It is necessary that each company study their own problems and find an evaluation appropriate to their system.

Mr. Watchorn has discussed the interest rate applicable for present worth calculations. We agree that the same interest rate should be used for the present worth calculations as that used in determining the rate of fixed charges. We have explored the effect of changes in this interest rate on the present worth evaluation and found that such changes had no significant effect on the relative answers obtained in this study.

Our calculations on the effect of load variations resulting from unpredictable business and weather conditions, although not included in the paper, are in accordance with Mr. Watchorn's statement that the effect of such considerations would indicate larger size units to be more economical.

As illustrated in the paper, the economic percentage pattern of generation expansion will decrease as systems become larger and the unit costs are on the flatter portion of the investment cost curve.

In our study, the effect of the assumed variation in rates of load growth were of secondary importance. It is realized that with very slow rates of load growth smaller size units would be indicated.

The discussions have indicated that there is general agreement that probability methods are a useful tool in solution of problems of this type. The more widespread availability of digital computers will make probability and general studies of this nature more feasible by reducing the time required for calculations.

The effects of interconnections on this problem have been mentioned by several of the discussers. We agree that interconnections are important considerations. Further analytical and economic investigations of interconnection benefits are now in progress.

Pumped Storage and Hydro Generation at Flatiron Power Plant

S. M. DENTON
MEMBER AIEE

H. O. BRITT
ASSOCIATE MEMBER AIEE

THE FLATIRON Power and Pumping Plant is one of a series of plants utilizing the power drop in the transmountain water diversion of the Colorado-Big Thompson Project. The Project is a Bureau of Reclamation development which diverts water from the Colorado River on the western slope of the Continental Divide to the eastern slope to provide irrigation, hydroelectric power, and other multiple-purpose benefits. The power drop of the diverted water on the eastern slope is shown in Fig. 1.

The power installation at Flatiron consists of two 35,000-kva, 514-rpm generators driven by Francis turbines, and a 2-speed combination motor-generator and pump-turbine unit. Water is delivered to the turbines of the 35,000-kva units under a net head of approximately 1,050 feet and is discharged into the Flatiron tailrace. The water used for generation must also be used subsequently for irrigation. To release water for generation throughout the year independent of the seasonal irrigation requirements, two storage reservoirs have been provided to receive the water discharged at Flatiron. One of these is Horsetooth Reservoir downstream from the Flatiron Plant. Water from Flatiron flows to Horsetooth through a feeder canal. The remaining storage is in Carter Lake Reservoir into which water from the Flatiron tailrace is pumped by the pump-turbine unit.

It was originally contemplated that the unit would operate at the same speed in both directions of rotation and that operation would change on a seasonal basis with pumping during the winter months and generation, as a feature incidental to water releases from Carter Lake, during the irrigation season. However, the 2-speed design was adopted when it became apparent that the turbine efficiency at the expected operating heads could be increased materially by changing to 257-rpm operation when generating. The value of the additional peaking kilowatts made available by the higher turbine efficiency was sufficient to make off-peak overpumping and peak load generation a profitable type of daily operation.

Description of Unit

The motor generator and pump turbine are combined in a single unit which operates at 300 rpm when pumping and at 257 rpm in the reverse direction when generating. The motor name plate rating when operating at 300 rpm is 13,000 horsepower, 13,800 volts, and unity power factor. When operating in the reverse direction and generating, the unit is rated at 8,500-kva output, 13,800 volts and unity power factor. The unit is also capable of operating as a 10,700 horsepower motor at a speed of 257 rpm and as a 10,000-kva generator at a speed of 300 rpm; however, operation at these speeds is advantageous only under abnormal head conditions and switching for this type of operation has not been provided. Should it become necessary to operate at extreme heads for extended periods, connections may readily be changed to operate as a motor at 257 rpm and as a generator at 300 rpm.

The motor-generator is conventional in that the shaft is vertical with a thrust and upper guide bearing located above the rotor and a guide bearing below the rotor. The thrust bearing is equipped with a high-pressure oil system to provide an oil film between bearing surfaces before starting to reduce the system disturbance caused by starting. A closed cooling system has been provided which consists of two water-cooled surface air coolers inside a metal air housing. Automatic carbon dioxide fire-extinguishing equipment is included.

The unusual feature of the motor-generator is in the method of obtaining 2-speed operation. There are two electrically independent and complete stator windings, one of which is used for 300-rpm and one for 257-rpm operation. Each stator winding has three main and three neutral leads brought out of the stator frame. The six neutral leads are connected to a common bus and are grounded through a distribution transformer. The main leads are arranged so that either winding may be connected to the 13.8-kv power plant bus. Physically the rotor winding consists of 24 poles. The windings on these poles are all connected in series for 300-rpm operation. For 257-rpm operation the poles are switched so that through the creation of phantom poles the effect of a 28-pole rotor is produced. Five collector rings are used to connect the field windings to external circuits for switching, and thence to the output of a direct-connected exciter through a main field circuit breaker. In addition to changing main field connections and stator windings, the switching scheme for changing from motor to generator operation also reverses the exciter field connections to permit the exciter to build up when reversing the direction of rotation.

The pump turbine operates as a centrifugal pump in one direction and as a Francis turbine in the reverse direction. There are no wicket gates and no gov-

---

Paper 55-164, recommended by the AIEE Power General Committee and approved by the AIEE Committee on Technical Operations for presentation at the AIEE Winter General Meeting, New York, N. Y., January 31-February 4, 1955. Manuscript submitted October 21, 1954; made available for printing November 30, 1954.

S. M. DENTON and H. O. BRITT are with the Bureau of Reclamation, Denver, Colo.

The motor-generator and pump-turbine unit described was designed and manufactured by the Allis-Chalmers Manufacturing Company.

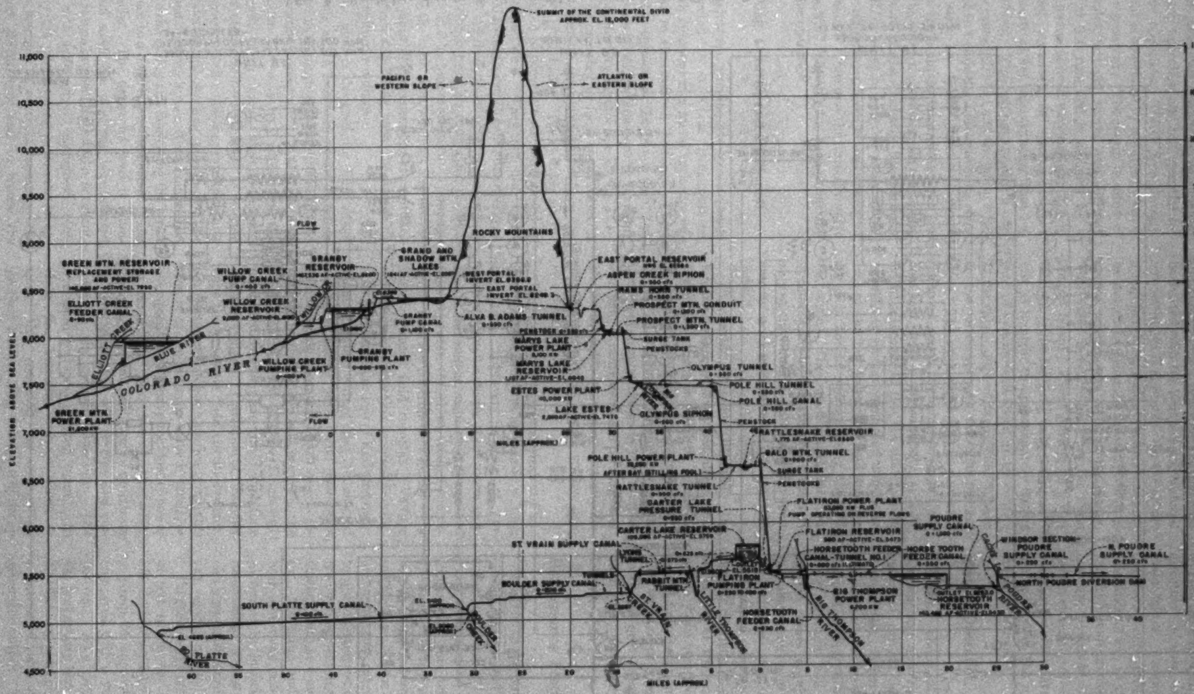
SUMMIT OF THE CONTINENTAL DIVID APPROX. EL. 12,000 FEET
PACIFIC OR WESTERN SLOPE
ATLANTIC OR EASTERN SLOPE
ROCKY MOUNTAINS
ELEVATION ABOVE SEA LEVEL
11,000
10,500
10,000
9,500
9,000
8,500
8,000
7,500
7,000
6,500
6,000
5,500
5,000
4,500
GREEN MTN. RESERVOIR (REPLACEMENT STORAGE AND POWER)
ELLIOTT CREEK FEEDER CANAL
ELLIOTT CREEK
BLUE RIVER
COLORADO RIVER
GREEN MTN. POWER PLANT 21,600 KW
WILLOW CREEK PUMP CANAL 0-400 cfs
WILLOW CREEK RESERVOIR
WILLOW CREEK
WILLOW CREEK PUMPING PLANT 0-400 cfs
FLOW
GRANBY RESERVOIR
GRANBY PUMPING PLANT
GRANBY PUMP CANAL 0-1,100 cfs
GRAND AND SHADOW MTN. LAKES
WEST PORTAL INVERT EL. 8266.0
EAST PORTAL INVERT EL. 8249.3
ALVA B. ADAMS TUNNEL 0-550 cfs
EAST PORTAL RESERVOIR
ASPEN CREEK SIPHON 0-550 cfs
RAMS HORN TUNNEL 0-550 cfs
PROSPECT MTN. CONDUIT 0-1,300 cfs
PROSPECT MTN. TUNNEL 0-1,300 cfs
PENSTOCK 0-550 cfs
MARYS LAKE POWER PLANT 8,100 KW
MARYS LAKE RESERVOIR
SURGE TANK
PENSTOCKS
ESTES POWER PLANT 45,000 KW
LAKE ESTES 2,000 AF-ACTIVE-EL. 7470
BIG THOMPSON RIVER
OLYMPUS TUNNEL 0-550 cfs
OLYMPUS SIPHON 0-550 cfs
POLE HILL TUNNEL 0-550 cfs
POLE HILL CANAL 0-550 cfs
PENSTOCK
RATTLESNAKE RESERVOIR 1,775 AF-ACTIVE-EL. 6580
POLE HILL POWER PLANT 33,250 KW
AFTER BAY (STILLING POOL)
BALD MTN. TUNNEL 0-900 cfs
SURGE TANK
PENSTOCKS
RATTLESNAKE TUNNEL 0-900 cfs
CARTER LAKE PRESSURE TUNNEL 0-550 cfs
FLATIRON POWER PLANT 63,000 KW PLUS PUMP OPERATING ON REVERSE FLOWS
CARTER LAKE RESERVOIR 108,900 AF-ACTIVE-EL. 5759
FLATIRON RESERVOIR 560 AF-ACTIVE-EL. 5473
ST. VRAIN SUPPLY CANAL
LYONS TUNNEL
TUNNELS
BOULDER SUPPLY CANAL
RABBIT MTN. TUNNEL
OUTLET EL. 5618
FLATIRON PUMPING PLANT
HORSETOOTH FEEDER CANAL-TUNNEL NO. 1
HORSE TOOTH FEEDER CANAL 0-550 cfs
BIG THOMPSON POWER PLANT 4,500 KW
HORSETOOTH FEEDER CANAL
POUDRE SUPPLY CANAL 0-1,000 cfs
WINDSOR SECTION-POUDRE SUPPLY CANAL 0-250 cfs
N. POUDRE SUPPLY CANAL 0-250 cfs
NORTH POUDRE DIVERSION DAM
HORSETOOTH RESERVOIR
CACHE LA POUDRE RIVER
LITTLE THOMPSON RIVER
ST. VRAIN CREEK
BOULDER CREEK
SOUTH PLATTE SUPPLY CANAL
SO. PLATTE RIVER
MILES (APPROX.)
60
55
50
45
40
35
30
25
20
15
10
5
0
5
10
15
20
25
30
35
40

NOTE

All water surface elevations for reservoirs refer to maximum operating water surface.

EXPLANATION

—— Underground, as buried conduit, siphon, or tunnel.

Fig. 1. Profile of the Colorado-Big Thompson Project showing power drop of diverted water on the eastern slope

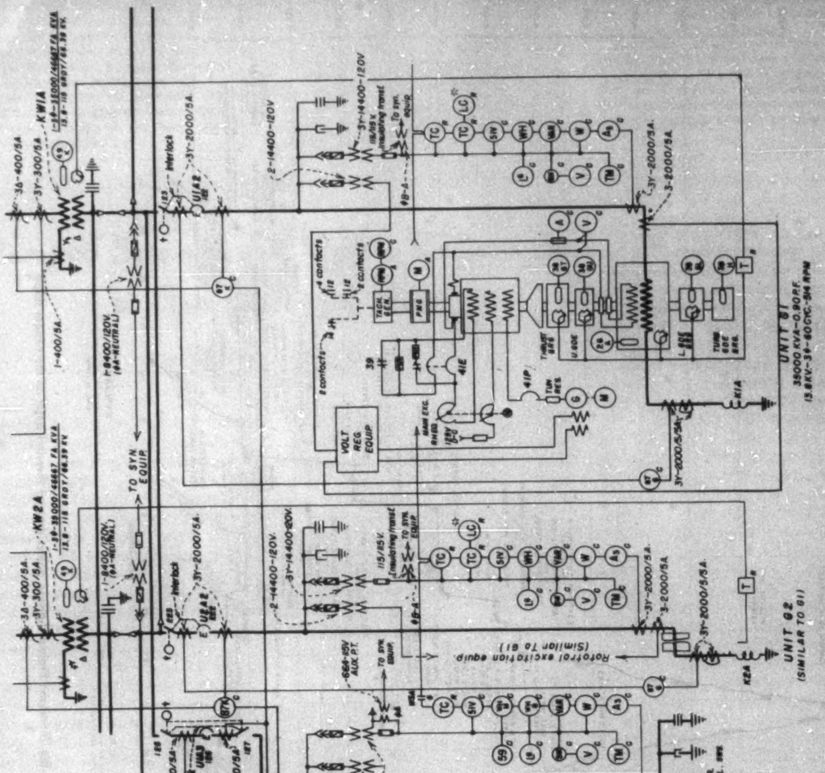
KW1A
1-3Φ-33000/46667 FA KVA
13.8-115 GRDY/66.39 KV
KW2A
1-3Φ-33000/46667 FA KVA
13.8-115 GRDY/66.39 KV
3Δ-400/5A.
3Y-300/5A.
1-400/5A.
1-8400/120V. (6A-NEUTRAL)
TO SYN. EQUIP.
Interlock
3Y-2000/5A.
2-14400-120V
3Y-14400-120V
115/115V. insulating transf.
To syn. equip.
VOLT REG. EQUIP.
TACH. GEN.
PMG
THRUST BRG.
U-GDE
L-GDE BRG.
TURB. GDE BRG.
TUR. RES.
MAIN EXC. RHEO.
3Y-2000/5/5A.
K1A
K2A
K3A
3-2000/5A.
Rotorrol excitation equip. (Similar To G1)
6.6-115V AUX. P.T.
3Y-600/5A.
3Y-14400-120V
4 contacts
8 contacts
ELECT. OPER. LEAD SEL. SWS.
DISC. RES.
UPPER GUIDE BRG.
LOWER GUIDE BRG.
TURB. GUIDE BRG.
3Y-600/5/5A.
1-50KVA 14.4/13.8KV-120/240V
UNIT G1
35000 KVA-0.90 P.F.
13.8 KV.-3Φ-60 CYC.-514 RPM
UNIT G2
(SIMILAR TO G1)
UNIT G3
8500 KVA-1.00 P.F.-13.8 KV. (G) 257 RPM
13,000 HP-1.00 P.F.-13.8 KV. (M) 300 RPM
3Φ-60 CYCLES-

Fig. 2. Single-line diagram showing switching arrangement of Flatiron Power and Pumping Plant

ernor for turbine operation. The use of wicket gates was considered detrimental to pump operation and not essential for turbine operation. Water flow through the unit is controlled by a butterfly valve in the penstock. The pump is rated at 370 cubic feet per second and 240 feet head at 300 rpm and is designed for a total pumping head varying from 170 to 300 feet. As a turbine the unit is designed to operate at net heads ranging from 140 to 290 feet. The pumping head will normally exceed 200 feet and the pump is designed to obtain the best operating characteristics for heads over this value. When the pumping head is less than 200 feet the pump is operated with the butterfly valve in the discharge line partially closed, in order to improve pump operation and prevent possible overloading of the motor. Otherwise the butterfly valve is operated full open for both pump and turbine operation.

Starting, Control, and Protection

Each stator winding has its main leads connected to a 3-pole gang-operated switch mounted in a metal enclosure adjacent to the unit air housing. These switches connect to the power plant bus and are used as lead selectors for changing from motor to generator operation. They may be operated by local manual control or by remote electrical control from the main control board. The switches are interlocked to prevent both being closed at the same time. They are also interlocked so that a switch cannot be operated unless the field circuit breaker is open and both circuit breakers connecting the unit to the 13.8-kv busses are open. To change speed the main field windings and the exciter shunt field connections are switched automatically along with the switching of armature windings.

The unit is designed for full-voltage starting as an induction motor in either direction of rotation with automatic field application equipment. In the pumping direction the unit is started with the butterfly valve closed. A water-depressing system has been included to provide for synchronous condenser operation and unwatering for starting purposes. The system operates by admitting compressed air to the casing and depressing the water surface to a level below the bottom of the impeller. The depressed level is maintained until the unit has been started and is synchronized or while it is operating as a synchronous condenser. Normally the pump casing is unwatered before starting in order to minimize the system disturbance and to reduce the duty on the motor windings by shortening the starting time. However, the unit may be started with the pump casing watered whenever this is desirable. In the generating direction of rotation the turbine may be started by using the butterfly valve to control admission of water to the casing. This valve is controlled from the main control board. When starting as a turbine using the butterfly valve, the generator is brought to approximately 80 per cent of synchronous speed under control of the valve. Full voltage is then applied to the terminals with the field breaker open. The rotor accelerates to near synchronous speed by induction motor action and field is automatically applied. As an alternate to this the unit may be brought to synchronous speed under control of the butterfly valve and synchronized at normal voltage using the synchroscope. The speed is adjusted for synchronizing by adjusting both the position of the butterfly valve and the opening in a by-pass around the butterfly valve.

To provide adequate flexibility the bussing arrangement was designed so that the motor-generator could be connected through circuit breakers to either or both of the 35,000-kva generators or to the outside system, as shown in Fig. 2. This switching arrangement also permits using all the available generating capacity for starting and reduces system voltage dips to a minimum.

The two 35,000-kva generators at Flatiron are equipped with automatic voltage regulators. However, because of the relatively small capacity of the motor-generator, the voltage regulator was omitted from this unit. Machine voltage and reactive flow are controlled manually by a motor-operated field rheostat. Voltage relays furnish protection against overvoltages resulting from loss of load and overspeed. One overvoltage relay is connected across the exciter output and operates a field-reducing contactor which inserts resistance in the exciter field circuit in the event of exciter overvoltage. This is supplemented by a relay energized by machine terminal voltage. Operation of this relay trips the generator field circuit breaker. An overspeed switch automatically initiates closure of the butterfly valve if excessive overspeeds occur from either loss of power or loss of load. Upon loss of power while pumping, the unit will rapidly decelerate to zero speed and will reverse and run away in the opposite direction. The overspeed switch will then operate to close the butterfly valve. However under this condition no overvoltage problem exists. The voltage will decay to nearly zero with reducing speed but will not build up with speed in the reverse direction because of exciter residual. Field failure, incomplete sequence, and out-of-step relay protection are provided. Operation of any of these relays trips the 13.8-kv circuit breakers. Differential relays are connected to operate for faults within either stator winding. A sensitive overcurrent relay furnishes protection for faults between the motor and generator stator windings.

Plan of Operation

During abnormal water years the combination unit may be operated for extended periods as either a pump or a generator. When the water supply is normal and the water surface elevation of Carter Lake is within its normal operating range, the unit will be operated to suit system power requirements for obtaining maximum benefit. The operation may change once or twice daily from pumping to generation. During off-peak periods pumping into Carter Lake will be in excess of irrigation storage requirements. The excess water will then be released for generation during daily peaks. The value of peaking capacity compared to the off-peak value of power will more than offset the pumping and generating losses.

Performance Tests

A model of the pump turbine was built at the factory and was tested for efficiency, capacity, and general performance. Tests were made of turbine operation at 300 and 257 rpm and pump operation at 300 rpm. The motor generator was completely assembled and partially tested at the factory. These tests included measurements for determining the speed-torque characteristic of the motor, and the various saturation curves and efficiency both as a motor and as a generator. Heat run and overspeed tests for both motor and generator operation were performed in the field after completion of installation. Pump and turbine efficiencies were determined in the field using the salt velocity method.

On the basis of preliminary calculations of test results the unit has an over-all efficiency when delivering rated output as a pump of approximately 87 per cent compared with a warranted value of 84 per cent. As a turbine-driven generator the preliminary test results show an over-all efficiency of 85 per cent compared with a warranted value of 75 per cent at rated generator output. Results of the pump-turbine efficiency tests conducted in the field agreed quite closely with the results of the model tests. In general the test results and operational performance of the unit have been gratifying.

◆

Discussion

L. R. Sellers (Tennessee Valley Authority, Knoxville, Tenn.): In this brief outline of the unique features of the Flatiron Plant, the omission of wicket gates, governor, voltage regulator, and the selection of full-voltage induction start are important from the cost standpoint and should also simplify operation.

The use of the term "motor generator" to describe this unit is usually used to designate a generator shaft driven by a motor. We have called our Hiwassee unit a generator-motor since generation was its most important function. Perhaps the designation "motor/generator" or "generator/motor" should be used to describe a single dual-purpose machine.

Information on the following additional points would be of interest:

1. Relative cost of the 2-speed motor generator as compared to a single-speed design.
2. For remote-controlled, unattended stations, does the experience at Flatiron indicate that automatic speed-matching control of a penstock butterfly valve might have possibilities, assuming induction start could not be used?
3. What are the approximate inrush kva and voltage drop for full-voltage induction start from standstill as compared to field application near synchronous speed both for 35,000-kva units in operation, and for 35,000-kva units not in operation?

For the Tennessee Valley Authority Hiwassee No. 2 pump-turbine unit which will go into service late this year, induction start at 0.50 per unit volts was selected in order to reduce transmission line drop when starting the 102,000-horsepower motor. With this voltage applied, start kva will be less than 32,000, and the calculated accelerating time is about 1.5 minutes with the pump casing evacuated and the motor thrust-bearing pressurized. This start voltage was obtained by a midpoint tap on the main transformer delta windings. The start voltage will lead the run voltage by 60 degrees, which will facilitate the transfer from the start to the run circuit breaker.

S. M. Denton and H. O. Britt: We agree regarding the terminology used in the description of the dual-purpose electrical synchronous machine forming a part of the complete unit described. The term "generator/motor" appears to be the best description of such a unit. In reply to Mr. Seller's questions:

1. It is estimated that 2-speed operation of the unit increased its cost to 45 per cent over that of a single-speed unit.
2. Our experience indicates that of the two starting methods for generator operation described in the section on starting, the first is the most desirable in that fewer adjustments and substantially less time is required of the operator. Use of the butterfly valve and by-pass for manual speed-matching is a time-consuming operation compared to synchronizing with governor speed control. Flatiron Unit No. 3 has a 6-inch by-pass valve. The butterfly valve for this unit is 76 inches in diameter. Use of a larger by-pass would speed up this synchronizing operation. For automatic operation the size and control of the by-pass would be quite important. The variation of the head under which this unit will operate would present difficult problems in the adjustment of automatic synchronizing equipment for a unit of this kind. We would expect less difficulty with either an induction motor start from standstill with automatic field application, or a turbine start with full voltage applied at some reduced speed with automatic field application (such as at Flatiron), rather than with the use of automatic speed-matching, making use of the valves.
3. Information on inrush and voltage drop under the conditions outlined in Mr. Sellers' discussion is not available.

Maximum Short Circuit and Faulty Synchronizing Torques on Generator Foundations

VERNON W. RUSKIN
ASSOCIATE MEMBER AIEE

POWERHOUSE designers must provide generator foundations of sufficient rigidity to withstand any forces that may occur as a result of short circuits or faulty (out-of-step) synchronizing. In estimating the forces on the foundations, it is usually assumed that all the air-gap torque is transferred to the sole plates. This assumption neglects the inertia and elastic deformation of the frame, and introduces a factor of safety. The calculation of the maximum foundation reactions thus reduces to the calculation of the highest air-gap torques.

Whitney and Criner[1] have established equations for the air-gap torques under various conditions of short circuit and faulty synchronizing, which checked within 10 per cent (%) of actual torque measurements on a 12,500-kva turboalternator. Later papers by Kirschbaum[2] Batchelor, Williams, and Whitehead[3] modified the torque equations for double-line-to-ground faults, and gave equations for faulty synchronizing. Unfortunately, all these equations are very involved and require a series of elaborate calculations for each particular case. A number of simple empirical expressions for the torques are therefore used by some designers, but their accuracy is doubtful.

This paper develops a new and simple method of calculating maximum air-gap torques, which can be employed to provide a practical basis for foundation design.

Direction and Nature of the Forces

The air-gap torques due to short circuits and out-of-step synchronizing are of a damped oscillatory nature[1,2], and are transferred through the frame to the sole plates. The reactions on the sole plates therefore oscillate many times per second in the directions shown in Fig. 1, and constitute severe reversing live loads on the concrete.

Depending on the instant of application and the type of short circuit or faulty

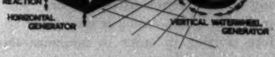

Fig. 1. Direction of forces

Paper 55-173, recommended by the AIEE Power Generation Committee and approved by the AIEE Committee on Technical Operations for presentation at the AIEE Winter General Meeting, New York, N. Y., January 31–February 4, 1955. Manuscript submitted September 15, 1952; made available for printing December 6, 1954.

VERNON W. RUSKIN is with the British Columbia Electric Company, Vancouver, B. C., Canada.

Thanks for valuable criticism and suggestions are due to A. W. W. Cameron and K. McClymont of the Hydro-Electric Power Commission of Ontario, and to J. A. Langford, A. D. Avtzine, A. Ketvirtis, and E. C. L. Green of Canadian-Brazilian Services Ltd., Toronto, Ont., Canada.

Table I. Equations to Determine Maximum Torques

Type of Fault or Synchronizing	Simplified Equations in Per-Unit Torque
Line-to-line fault	$\frac{3\sqrt{3}}{2}\ \frac{E^2}{X_d''+X_2}$
Line-to-neutral fault	$\frac{3\sqrt{3}}{2}\ \frac{E^2}{X_d''+X_2+X_0}$
Three-phase fault	$\frac{E^2}{X_d''}$
Double line-to-neutral fault	$\frac{\sqrt{3}}{2}\ \frac{E^2}{X_d''+\frac{X_2\ X_0}{X_2+X_0}}\ \frac{X_2+3X_0}{X_2+X_0}$
Three-phase synchronizing	$\frac{3\sqrt{3}}{2}\ \frac{E^2}{X_d''+X_e}$
Single-phase synchronizing	$3\left(1+\frac{\sqrt{3}}{2}\right)\ \frac{E^2}{X_d''+X_2+2X_e}$

synchronizing, the generator armature current will contain different values of positive-, negative-, and zero-sequence components, as well as a d-c transient component decaying with the armature time constant. The consequent armature reaction is counterbalanced by an immediate rise in the rotor currents, since the flux linking the rotor cannot change instantly. The additional rotor currents will decay with the rotor short-circuit time constant. The interaction between the decaying rotor and stator magnetic fields and currents produces the damped oscillatory air-gap torque.

Simplifying Assumptions

To simplify the calculation of the air-gap torque, the following factors were neglected by previous authors[1-3] and will also be neglected in this paper:

1. Armature resistance.
2. External impedance.
3. Saturation and hysteresis.
4. Harmonics due to saliency, nondistributed windings, slots, etc.
5. Decay of internal machine voltage.
6. Exciter response.
7. Gradual reduction in angular displacement between system and machine during faulty synchronizing.

The alternating currents flowing in the machine circuits cause ohmic losses, which appear as unidirectional loss torque. This contributes about 10% to the total maximum air-gap torque. On the other hand, the decay of the armature and rotor currents, represented by decrement factors, will reduce the total maximum air-gap torque by roughly 10% over the first half-cycle after the instant of short circuit or faulty synchronizing. The author therefore made the following additional assumption:

8. Over the first half-cycle, the current decrements are counterbalanced by the effect of the unidirectional loss torque, and both these factors can thus be ignored.

It will be shown later that this additional assumption does not impair the accuracy of the results for practical engineering purposes.

Effect of Saliency

Strictly speaking, the neglect of saliency in accordance with assumption 4 is completely justified only in the case of a turboalternator. For a water-wheel generator, the theoretical effect of saliency can later be approximated as explained in Appendix I for the important case of a line to line short circuit.

Effect of Load

As a further simplification, the short circuit or faulty synchronizing will be assumed to occur under no-load conditions. The effect of a fault under load conditions can later be approximated by increasing the effective generated voltage by an amount equal to the voltage drop due to the leakage reactance. Further, the external load remaining on the generator after the fault will also produce a corresponding torque, which can be taken into account by adding it to the air-gap torque under no-load conditions.

Simplified Calculation of Maximum Air-Gap Torques

In general, maximum torque will occur if the short circuit or faulty synchronizing occurs at the instant when the effect of the various d-c transient currents produced is a maximum. The interaction between the d-c transient armature field with the rotor field then produces the highest fundamental frequency torque.

Basically, the method adopted by the author to compute the maximum air-gap torque is as follows:

1. The symmetrical components of the currents and voltages at the instant of short circuit or out-of-step synchronizing are sketched, and the value of the d-c transient armature currents are obtained by inspection.

2. The symmetrical components of the currents and voltages are also sketched for the instant when the sum of the voltage times current products in all phases is maximum. This instant corresponds to the instant of maximum instantaneous power, and therefore maximum air-gap torque. It can be found by inspection and trial.

3. From these sketches, the value of all currents and voltages at the instant of maximum air-gap torque are quickly obtained, and the value of the maximum air-gap torque can be computed easily.

The practical application of this method is illustrated in Appendixes II, III, and IV.

The author analyzed various possible short-circuit and faulty synchronizing conditions and obtained a number of simple equations for the maximum air-gap torques shown in Table I. It should be noted that the equations are given in terms of per-unit torque, which is the torque corresponding to the rated kva at unity power factor and rated voltage and speed of the generator.

Comparison with Measurements and Earlier Equations

To test the simplified equations developed in this paper, they were applied to two actual examples of turboalternators, and two water-wheel generators. Table II shows that in each case the torque calculated by the simplified equations was close to, and usually slightly less than, the value obtained from the earlier elaborate equations presented by Kirschbaum,[2] Whitney and Criner,[1] and Batchelor, Williams, and Whitehead.[3]

One typical empirical equation for the line-to-line short-circuit torque is a function of voltage squared and of the reciprocal of the subtransient direct-axis reactance. Applying this empirical equation to a generator with constants as given in Table II, section *C*, the line-to-line fault torque works out to 9.5 per unit. This is approximately 13% higher than the value given by the earlier elaborate equation, and 11% higher than that given by the new simplified equation.

Table II, section *B*, compares the results with actual torque measurements by Whitney and Criner, as read from oscillograph traces in their paper.[1] Both the earlier elaborate equation and the simplified equation show better than 10% accuracy for a line-to-line fault. In the case of a 3-phase fault, the simplified equation does not agree with the measured torque as closely as the earlier equation. On the other hand, the simplified equation appears to be more accurate for a line-to-neutral fault.

Table II, section *A*, compares the results with values computed by a transient analyzer, as obtained from a paper by McCann, Warren and Criner.[4] The simplified equations appear to be at least as accurate as the earlier elaborate equations in this case. On the basis of these comparisons it was concluded that the simplified equations are sufficiently accurate for engineering purposes.

Table II. Comparison of Simplified Equations with Other Equations and Tests

Type of Machine	Type of Fault or Synchronizing	Simplified Equations Per-Unit Torque	Earlier Equations[1-3] (6,7,12) Per-Unit Torque	Remarks
A. Turboalternator				From transient analyzer[4]
$X_d''=0.097$	line-to-line	13.5	14.9	13.8
$X_d'=0.152$	three-phase	10.3	11.4	10.8
$X_d=1.17$				
$X_2=0.096$	line-to-neutral	12.3	13.7	12.4
$X_0=0.0177$				
$T_{d_0}''=0.055$	double line-to-neutral	10.3	11.5	
$T_{d_0}'=6.65$				
$R_1=0.048$				
$R_2=0.025$				
$R_a=0.00105$				
B. Turboalternator				Measured value from oscilloscope trace[1]
12,500 kva, 0.8 power factor	line-to-line	15.0	16.8	16
13.8 kv, 3-phase, 60 cycles	three-phase	11.5	13.2	13.5
$X_d''=0.087$				
$X_d'=0.118$ $X_d=1.20$ $X_2=0.087$	line-to-neutral with 0.0233 per-unit neutral reactor	10.3	11.2	9
$X_0=0.01$				
$T_d''=0.040$				
$T_d'=0.48$ $T_{d_0}=4.88$ $T_a=0.108$	line-to-neutral with 0.0097 per-unit neutral reactor	12.1	13.0	
$R_1=0.0064$				
$R_2=0.036$				
C. Salient pole generator				
78,000 kva, 0.85 power factor	line-to-line	8.8*	8.4	
13.8 kv, 3-phase, 60 cycles				
$X_d''=0.181$	three-phase	6.6	6.7	
$X_d'=0.29$				
$X_d=1.15$	line-to-neutral	5.3	5.5	
$X_2=0.215$				
$X_0=0.191$	double line-to-neutral	7.1	7.2	
$T_d''=0.05$				
$T_d'=9.5$				
$R_1=0.008$				
$R_2=0.02$ $R_a=0.002$	faulty 3-phase synchronizing	9.8	9.8	
$E=1.09$ per unit $X_s=0.085$	faulty single-phase synchronizing	9.9	10.0	
D. Water-wheel generator				
75,000-kva, 450-rpm 0.85 power factor, 13.8 kv, 60 cycles	faulty single-phase synchronizing	8.7	8.7	
$X_d''=0.189$				
$X_2=0.229$				
$X_s=0.115$				

*Includes K factor from Fig. 2.

Nomenclature

X_d'' = direct-axis subtransient reactance
X_d' = direct-axis transient reactance
X_d = direct-axis synchronous reactance
X_2 = negative-sequence reactance
X_0 = zero-sequence reactance
R_1 = positive-sequence resistance
R_2 = negative-sequence resistance
R_a = d-c resistance of stator
T_{d_0}'' = subtransient open-circuit time constant in direct axis
T_{d_0}' = transient open-circuit time constant in direct axis
X_q'' = quadrature axis subtransient reactance
e, i = instantaneous voltage and current
E = effective (or rms) generated voltage
X_s = reactance of connected system
E_m, I_m = maximum values of voltage and current
I_1, I_2, I_0 = scalar magnitude of symmetrical components
$\mathbf{I}_1, \mathbf{I}_2, \mathbf{I}_0$ = symmetrical component vectors
Faulty 3-phase synchronizing = machine connected to the system out of phase through the three poles of a breaker
Faulty single-phase synchronizing = machine connected to the system out of phase, and only two poles of the 3-pole circuit breaker are closed

Relative Values of Short-Circuit Torques

Apart from providing simple expressions for the maximum torque, the simplified equations can be used to obtain useful generalizations regarding the type of fault that produces the highest torque for a given generator.

An analysis of the simplified equations in Table I, suggests the following:

1. Since $(X_d''+X_2)$ is less than $(X_d''+X_2+X_0)$, the line-to-line short-circuit torque will always exceed the line-to-neutral short-circuit torque.

2. Taking $X_2=1/2(X_d''+X_q'')$, approximately, it can be shown that the line-to-line short-circuit torque will exceed the 3-phase short-circuit torque, provided that the ratio X_q''/X_d'' is less than 2.2. The 3-phase short-circuit torque will exceed the line-to-line short-circuit torque if X_q''/X_d'' is greater than 2.2. This ratio is less than 2.2 for all turboalternators and for most water-wheel generators. The line-to-line short-circuit torque will therefore normally exceed the 3-phase short-circuit torque.

3. Similarly, it can be shown that the line-to-line short-circuit torque will exceed the double line-to-neutral short-circuit torque provided the ratio X_q''/X_d'' is less than 3. The double line-to-neutral short-circuit torque will exceed the line-to-line short-circuit torque if X_q''/X_d'' is greater than 3. However, this ratio is less than 3 for commercial generators, so that the line-to-line short-circuit torque will normally exceed the double line-to-neutral short-circuit torque.

As a rule, the line-to-line short-circuit torque will thus exceed all other types of short-circuit torques.

Relative Values of Faulty Synchronizing Torques

Faulty 3-phase synchronizing occurs when the machine is connected to the system out of phase through a 3-pole circuit breaker. Faulty 1-phase synchronizing occurs when the machine is connected to the system out of phase, and only two poles of the 3-pole circuit breaker are closed.

1. For turboalternators, taking $X_2=X_d''$ approximately, Table I shows that the maximum single-phase faulty synchronizing torque will always exceed the 3-phase faulty synchronizing torque by about 8%.

2. For salient pole machines, taking $X_2=1/2(X_d''+X_q'')$ it can be shown that the single-phase synchronizing torque cannot exceed the 3-phase synchronizing torque by more than 8%, since X_2 is greater than X_d''. The single-phase torque will equal the 3-phase torque, when the ratio $X_q''/X_d''=1.33$ with the external system reactance $X_s=0$, and also when the ratio $X_q''/X_d''=1.65$ with the external system reactance $X_s=X_d''$. In large hydro stations the external reactance X_s does not usually exceed X_d'' and the ratio X_q''/X_d'' usually does not exceed 1.65.

As a rule, the single-phase faulty synchronizing torque for salient pole generators thus roughly equals the 3-phase faulty synchronizing torque.

It can be found by trial from the phasor diagrams that the angle of phase difference between the machine and the system which produces the highest faulty synchronizing torque is approximately 120 electrical degrees. It may be noted that a phase difference of 180 electrical degrees produces about 23% less peak torque than a phase difference of 120 electrical degrees, contrary to a fairly common misconception.

Time to Attain Peak Torque

The time taken from the instant of fault until the peak torque is reached can be obtained from the phasor diagrams used to derive the simplified equations. It is necessary only to find the displacement of the phasors at the instant of fault, and at the instant when the sum of the voltage times current products are a maximum.

SHORT-CIRCUIT TORQUES

For a 3-phase short circuit, the peak torque is reached at an instant corresponding to a displacement of 90 electrical degrees after the instant of short circuit, equivalent to 0.004 second at 60 cycles. For all other short circuits the peak torque will occur at an instant corresponding to a displacement of approximately 120 electrical degrees after the instant of short circuit, equivalent to 0.0055 second.

SYNCHRONIZING TORQUES

For 3-phase faulty synchronizing, the peak torque is reached at an instant corresponding to a displacement of approximately 120 electrical degrees after the instant of synchronizing, equivalent to 0.0055 second at 60 cycles. For single-phase faulty synchronizing the peak torque occurs at an instant corresponding to a displacement of approximately 150 electrical degrees after the instant of synchronizing, equivalent to 0.007 second at 60 cycles.

Relative Severity of Short-Circuit Faults and Out-of-Step Synchronizing

The question often arises whether out-of-step synchronizing will produce higher torques than will short-circuit faults.

THREE-FAULT FAULTY SYNCHRONIZING

A line-to-line short circuit usually produces the highest short-circuit torque. From Table I it can be seen that the 3-phase faulty synchronizing torque will exceed the line-to-line short-circuit torque, provided the connected system reactance X_s is smaller than the generator negative-sequence reactance X_2.

The connected system reactance X_s is the combined parallel reactance of all other generators on the same bus, and of the transmission circuits. In the case of unit-connected generators, X_s is the reactance of the unit transformer plus the combined parallel reactance of all other generator-transformer units, and of the transmission circuits.

In stations with generators on a common bus, and in most large unit-connected hydro stations, the connected system reactance X_s is smaller than the generator negative-sequence reactance X_2. Three-phase faulty synchronizing will then produce more severe torques than any short-circuit conditions.

However, in some unit-connected steam stations, having relatively high-voltage and high-reactance unit transformers, the system reactance X_s is greater than the generator negative-sequence reactance X_2. A line-to-line short circuit will then produce higher torques than 3-phase faulty synchronizing.

SINGLE-PHASE FAULTY SYNCHRONIZING

For turboalternators, the single-phase faulty synchronizing torque exceeds the 3-phase synchronizing torque by 8%. For salient pole machines the two torques are roughly equal. Since the 3-phase faulty synchronizing torque is often higher than any short-circuit torque, the single-phase faulty synchronizing torque will frequently exceed any short-circuit torque.

Out-of-step synchronizing is thus frequently more dangerous than short-circuit faults. It may be noted that out-of-step synchronizing is also much more likely to occur in operation than short circuits at the generator terminals. The danger of out-of-step synchronizing may be positively prevented by means of lock-out synchronizing relays, and in this case the foundations need only be designed to withstand the line-to-line short-circuit torque.

Summary

Summarizing the foregoing analysis, generator foundations can be designed on the following practical basis:

1. The reactions on the foundations oscillate in the directions shown in Fig. 1, and constitute severe reversing live loads on the concrete.
2. The assumption that all the generator air-gap torque is transferred to the sole plates introduces a factor of safety.
3. The magnitude of the maximum air-gap torque can be estimated rapidly by means of the simplified equations which are given in Table I.
4. A line-to-line short circuit usually produces the highest short-circuit torque.
5. The single-phase faulty synchronizing torque very roughly equals the 3-phase faulty synchronizing torque. The highest faulty synchronizing torque will occur when the machine is connected approximately 120 electrical degrees out of phase with the system. Out-of-step synchronizing is frequently more dangerous than any short circuit.
6. The peak air-gap torque is attained in approximately 0.004 to 0.007 second after the instant of short circuit or faulty synchronizing.

Appendix I. Effect of Saliency

The simplified equations include the effect of that part of the second harmonic torque, which is caused by the interaction of the rotating field due to the negative-sequence armature currents with the fundamental component of the rotor field. They do not include that part of the second harmonic torque which is due to saliency alone.

This is perfectly in order for turboalternators which have negligible saliency. However, for water-wheel generators, the effect of saliency can theoretically be approximated by multiplying the simplified equations in Table I, by a *K* factor, depending on the degree of saliency. In Fig. 2 the value of the *K* factor has been plotted for the important case of a line-to-line short circuit, for values of X_q''/X_d'' up to 1.6. This should cover most practical cases as this ratio is usually below 1.6 for large salient pole generators.

The value of the *K* factor was found by determining the effect of increasing the second harmonic torque by the ratio $2X_q''-X_d''/2(X_q''+X_2)$, as derived by Nickle, Pierce, and Henderson.[5]

Appendix II. Line-to-Line Short-Circuit Torque

Fig. 3 shows the phasor diagrams at the instant of short circuit and at maximum torque. Taking scalar magnitudes of the phasors, the maximum values are

$$E_m=\sqrt{2}E \tag{1}$$

$$I_1=I_2=\frac{E_m}{X_d''+X_2} \tag{2}$$

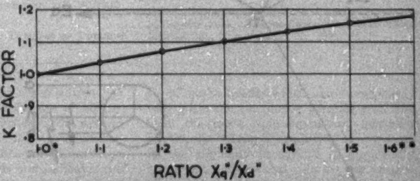

Fig. 2. Theoretical effect of saliency on line-to-line short circuit torque

* TURBOALTERNATORS
**PRACTICAL MACHINES USUALLY HAVE RATIOS BELOW 1·6

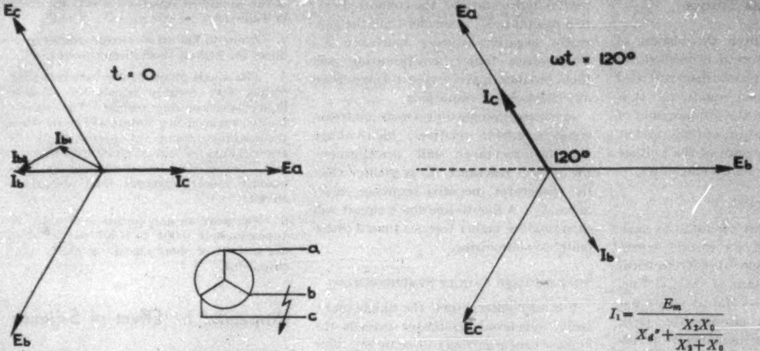

Fig. 3. Line-to-line short circuit

The angle between I_1 and I_2 is 60 degrees and combining them phasorially, the magnitude of phase current is

$$I_b = I_c = \frac{\sqrt{3}E_m}{X_d''+X_2} \tag{3}$$

At the instant of short circuit, the d-c components cancel the alternating components, hence the instantaneous value of the d-c component

$$i_b = I_b \tag{4}$$

$$i_c = -I_b \tag{5}$$

The peak torque occurs 120 degrees later, when alternating components have instantaneous values

$$i_b = \frac{I_b}{2} \text{ and } e_b = E_m \tag{6}$$

$$i_c = -\frac{I_b}{2} \text{ and } e_c = -\frac{E_m}{2} \tag{7}$$

Hence total currents

$$i_b = \frac{3I_b}{2} \tag{8}$$

$$i_c = -\frac{3I_b}{2} \tag{9}$$

The per-unit power is equal to the per-unit torque at synchronous speed, rated kva, and rated voltage

$$T = \frac{1}{3}(i_ae_a + i_be_b + i_ce_c) \tag{10}$$

which reduces to

$$\frac{3\sqrt{3}}{2}\frac{E^2}{X_d''+X_2} \tag{11}$$

The torque due to line-to-neutral, and 3-phase short circuits can be similarly derived.

Appendix III. Double Line-to-Neutral Fault

Fig. 4 shows the phasor diagrams for a double line-to-neutral fault. The scalar magnitudes of maximum positive sequence current

$$I_1 = \frac{E_m}{X_d'' + \frac{X_2X_0}{X_2+X_0}} \tag{12}$$

of maximum negative sequence current

$$I_2 = I_1\frac{X_0}{X_2+X_0} \tag{13}$$

and of maximum zero sequence current

$$I_0 = I_1\frac{X_2}{X_2+X_0} \tag{14}$$

At the instant of short circuit, the d-c components cancel the alternating components, hence instantaneous value of the d-c component

$$i_b = +\sqrt{\frac{3}{2}}(I_{b_1}+I_{b_2}) \tag{15}$$

$$i_c = -\sqrt{\frac{3}{2}}(I_{c_1}+I_{c_2}) \tag{16}$$

The peak torque occurs approximately 120 degrees later, when the instantaneous values of alternating components

$$i_b = \sqrt{\frac{3}{2}}(I_{b_2}-I_{b_0}) \text{ and } e_b = E_m \tag{17}$$

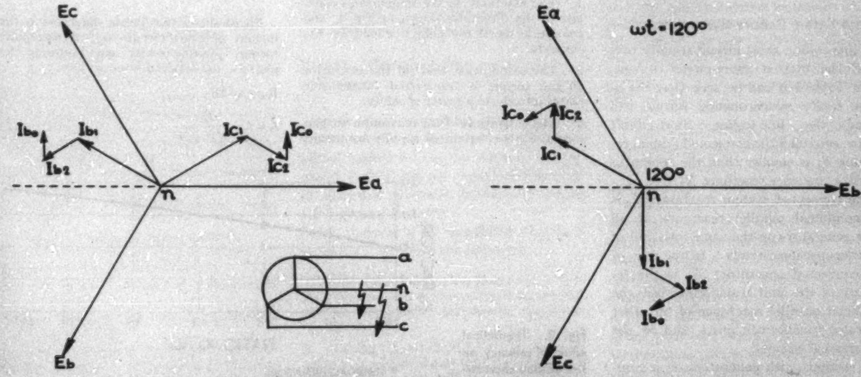

Fig. 4. Double-line-to-neutral short circuit

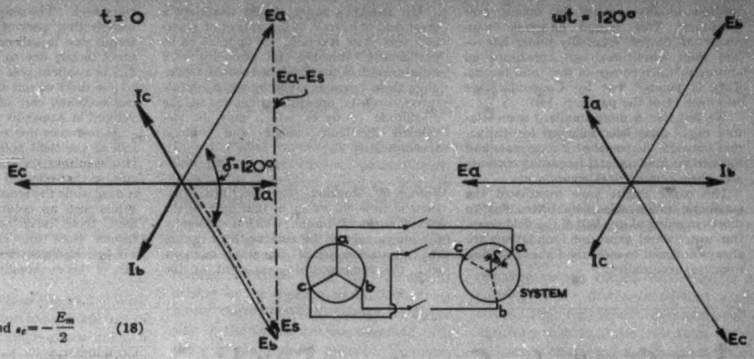

Fig. 5. Three-phase faulty synchronizing

$$i_c=-\sqrt{\frac{3}{2}}(I_{c_1}+I_{c0})\text{ and }e_c=-\frac{E_m}{2} \qquad (18)$$

Hence, total currents

$$i_b=\sqrt{\frac{3}{2}}(I_{b_1}+2I_{b_2}-I_{b_0}) \qquad (19)$$

$$i_c=-\sqrt{\frac{3}{2}}(2I_{c_1}+I_{c_2}+I_{c_0}) \qquad (20)$$

Per unit power and per unit torque is therefore

$$T=\frac{1}{3}(i_ae_a+i_be_b+i_ce_c) \qquad (21)$$

$$=\frac{\sqrt{3}E_m}{2\times 3}\left(2I_1+\frac{5}{2}I_2-\frac{I_0}{2}\right) \qquad (22)$$

And this reduces to

$$T=\sqrt{\frac{3}{2}}\times\frac{E^2}{X_d''+\dfrac{X_2X_0}{X_2+X_0}}\left(\frac{X_2+3X_0}{X_2+X_0}\right) \qquad (23)$$

Appendix IV. Three-Phase Faulty Synchronizing Torque

Fig. 5 shows the phasor diagrams for 3-phase faulty synchronizing, when the machine is 120 electrical degrees out of phase with the system. The scalar magnitude of maximum phase currents

$$I_a=I_b=I_c=\frac{\sqrt{3}E_m}{X_d''+X_s} \qquad (24)$$

At the instant of synchronizing, the d-c components cancel the alternating components, and their instantaneous values are

$$i_a=-I_a \qquad (25)$$

$$i_b=\frac{I_a}{2} \qquad (26)$$

$$i_c=\frac{I_a}{2} \qquad (27)$$

The maximum torque occurs 120 degrees later, when the alternating components have instantaneous values

$$i_a=-\frac{I_a}{2}\text{ and }e_a=-E_m \qquad (28)$$

$$i_b=I_a\text{ and }e_b=\frac{E_m}{2} \qquad (29)$$

$$i_c=-\frac{I_a}{2}\text{ and }e_c=\frac{E_m}{2} \qquad (30)$$

Hence total current

$$i_a=-\frac{3I_a}{2} \qquad (31)$$

$$i_b=\frac{3I_a}{2} \qquad (32)$$

$$i_c=0 \qquad (33)$$

Per-unit power and per-unit torque is therefore

$$T=\frac{1}{3}(e_ai_a+e_bi_b+e_ci_c) \qquad (34)$$

which reduces to

$$\frac{3\sqrt{3}}{2}\,\frac{E^2}{X_d''+X_s} \qquad (35)$$

The torque due to faulty single-phase synchronizing can be similarly derived.

References

1. DETERMINATION OF SHORT-CIRCUIT TORQUES IN TURBINE GENERATORS BY TEST, E. C. Whitney, H. E. Criner. *AIEE Transactions*, vol. 59, 1940, pp. 885–89.

2. TRANSIENT ELECTRICAL TORQUES OF TURBINE GENERATORS DURING SHORT CIRCUITS AND SYNCHRONIZING, H. S. Kirschbaum. *Ibid.* (*Electrical Engineering*), vol. 64, Feb. 1945, pp. 65–70.

3. TRANSIENT SHAFT TORQUES IN TURBINE GENERATORS PRODUCED BY TRANSMISSION-LINE RECLOSING, J. W. Batchelor, D. L. Whitehead, J. S. Williams. *Ibid.*, vol. 67, pt. I, 1948, pp. 159–65.

4. DETERMINATION OF TRANSIENT SHAFT TORQUES IN TURBINE GENERATORS BY MEANS OF THE ELECTRICAL-MECHANICAL ANALOGY, G. D. McCann, C. E. Warren, H. E. Criner. *Ibid.* (*Electrical Engineering*), vol. 64, Feb. 1945, pp. 51–55.

5. SINGLE-PHASE SHORT-CIRCUIT TORQUE OF A SYNCHRONOUS MACHINE, C. A. Nickle, C. A. Pierce, M. L. Henderson. *Ibid.*, vol. 51, no. 4, Dec. 1932, pp. 966–73.

6. SYNCHRONOUS MACHINES—III, TORQUE-ANGLE CHARACTERISTICS UNDER TRANSIENT CONDITIONS, R. E. Doherty, C. A. Nickle. *Ibid.*, vol. 46, Feb. 1927, pp. 1–18.

7. AN INSTRUMENT FOR MEASURING SHORT-CIRCUIT TORQUE, G. W. Penney. *Ibid.*, May 1927, pp. 683–91.

8. TRANSIENT TORQUES IN SYNCHRONOUS MACHINES, M. Stone, L. A. Kilgore. *Ibid.*, vol. 52, nos. 3, 4, Dec. 1933. pp. 945–53.

9. TWO-REACTION THEORY OF SYNCHRONOUS MACHINES—II, R. H. Park. *Ibid.*, no. 2, June 1933, pp. 352–55.

10. THREE-PHASE SHORT CIRCUIT SYNCHRONOUS MACHINES—V, R. E. Doherty, C. A. Nickle. *Ibid.*, vol. 49, no. 2, Apr. 1930, pp. 700–14.

11. SHORT-CIRCUIT TORQUE IN SYNCHRONOUS MACHINES WITHOUT DAMPER WINDINGS, G. W. Penney. *Ibid.*, vol. 48, no. 4, Oct. 1929, pp. 1230–41.

12. STRESS ANALYSIS IN ELECTRICAL ROTATING MACHINERY, M. Stone. *Transactions*, American Society of Mechanical Engineers, New York, N. Y., vol. 50, Aug. 1928, pp. 57–79.

13. DOUBLE-LINE-TO-NEUTRAL SHORT CIRCUIT OF AN ALTERNATOR, James B. Smith, Cornelius N. Weygandt. *AIEE Transactions* (*Electrical Engineering*), vol. 56, Sept. 1937, pp. 1149–55.

14. SYNCHRONOUS MACHINES, THEORY AND PERFORMANCE (book), Charles Concordia. John Wiley & Sons, Inc., New York, N. Y., 1951.

◆

Discussion

P. L. Dandeno and **K. R. Knights** (The Hydro-Electric Power Commission of Ontario, Toronto, Ontario, Canada): Prior papers have provided complicated equations for calculating maximum torques due to various short-circuit and faulty synchronizing conditions. Their complication has no doubt contributed to the use of certain rules of thumb now in existence, the general applicability of which are questionable. The author's one additional assumption simplifies these equations and indicates the relative magnitude of various fault torques.

It is rather remarkable, at first glance, to find that the author's method of analysis gives rise to results which agree reasonably well with the maximum torques resulting from the more rigid equations presented previously. The assumption referred to in the previous paragraph is apparently borne out in a general way by the results. The author also states that he neglects harmonics due to saliency. How does he effectively account for the second harmonic torques usually present in salient pole machines? This second harmonic component of torque, especially under line-to-line fault conditions, can constitute an appreciable percentage of the total torque. This is pointed out by Concordia (see reference 14 of the paper, p. 140).

We feel that a more standard nomenclature might have been followed for distinction between the so-called d-c currents and the various fundamental frequency currents and their symmetrical components.

The paper might have mentioned the maximum radial sole plate forces due to short-circuiting of one-half of the field poles. Our water-wheel generator foundations are always designed to meet the forces resulting from this eventuality.

Mr. Ruskin's paper should stimulate a great deal of interest in the subject of generator sole plate reaction. It appears to be particularly valuable in providing the utilities with a practical method of evaluating these forces as given by the manufacturers, and in drawing attention to the magnitude of forces which may be developed by faulty single- and 3-phase synchronizing.

Vernon W. Ruskin: The simplified equations include the effect of that part of the second harmonic torque, which is caused by the interaction of the rotating field due to the negative-sequence armature currents with the fundamental component of the rotor field. The simplified equations do not include that part of the second harmonic torque due to saliency, which is the reluctance torque due to the trapped armature flux in a salient pole machine.[5] For a line-to-line short circuit this part of the torque can be taken care of by the *K* factor developed in Appendix I.

As to forces due to short circuit of one-half of the field poles, this event requires two simultaneous grounds in the rotor circuit, so that one-half of the rotor periphery is dead while the remainder is still energized. While such an occurrence is very uncommon, there have been isolated cases of trouble from this cause. The discussers wisely design generator foundations to take care of this eventuality.

Test Circuits for Capacitance Switching Devices

K. G. DARROW
ASSOCIATE MEMBER AIEE

V. E. PHILLIPS
MEMBER AIEE

A. J. SCHULTZ
ASSOCIATE MEMBER AIEE

R. B. SHORES
MEMBER AIEE

THE energization and de-energization of capacitive kilovolt-amperes (kva) impose special switching conditions on switching devices. For example, these switching devices might be circuit breakers, disconnect switches, or load break switches which are primarily intended for resistive or inductive current interruption. Switching tests must be performed to determine the switching device rating for switching capacitive kva. As discussed in a companion paper,[1] dependent upon the predominant system component involved such as a capacitor bank, cable, or overhead line, the imposed conditions can be different and thereby result in different capacitive kva capabilities for the switching device. For conciseness, the various switching devices will be referred to hereafter simply as devices.

In the testing of switchgear, particularly at the higher voltages, laboratory facilities are usually such that only one phase of a device is tested to determine its ability to interrupt capacitive currents.[2] Consequently, it is required that the single-phase test circuit should subject the test component of the device to the same equivalent conditions as it would encounter in an actual 3-phase installation. Voltages and currents resulting from the single-phase test circuit must be interpreted relative to the 3-phase circuit.

This paper describes, defines, and demonstrates the equivalency of single-phase test circuits and test voltages and of the corresponding 3-phase kva being switched in terms of a capacitor bank, cable, or overhead line. The test circuit is defined as that which is observed from the device terminals and hence is independent of the configuration of the device itself. The paper is based in part on the results presented in a companion paper on system requirements of switchgear in switching capacitive kva.[1]

Conclusions

1. Single-phase circuits which impose exactly the same duty on any one pole of the switching device as the 3-phase circuit can be developed for most cases involving capacitance switching. These circuits may not be practical for laboratory testing of switching devices.
2. Modifications of the exact single-phase equivalent circuits can be made which result in circuits which are practical for laboratory testing. In some cases, these modified circuits do not duplicate the 3-phase conditions.
3. For any known condition of system or capacitance configuration, practical single-phase circuits suitable for laboratory testing can be synthesized even though an exact equivalent circuit cannot be derived. These synthesized circuits may only approximate the conditions of the 3-phase circuit.

Test Circuits

It is desirable to use as simple a test circuit as possible consistent with the results which are required. The use of a simple circuit for testing the capacitance switching ability of devices in the testing laboratories leads to minimizing of the test equipment, convenience in metering, and a reduction of the setup time and test samples. Usually devices are tested in the laboratories for their capacitance switching ability on a single-phase circuit

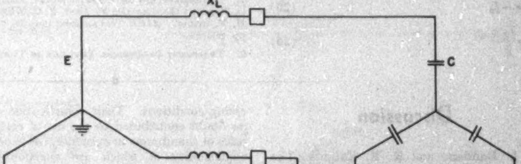

Fig. 1. Generalized circuit for switching an ungrounded capacitor bank

---

Paper 55-212, recommended by the AIEE Switchgear Committee and approved by the AIEE Committee on Technical Operations for presentation at the AIEE Winter General Meeting, New York, N. Y., January 31–February 4, 1955. Manuscript submitted October 21, 1954; made available for printing December 1, 1954.

K. G. DARROW, V. E. PHILLIPS, and R. B. SHORES are with the General Electric Company, Philadelphia, Pa., and A. J. SCHULTZ is with the General Electric Company, Schenectady, N. Y.

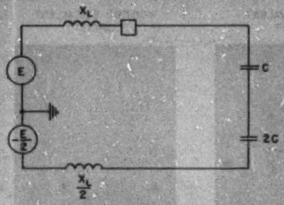

Fig. 2. Exact equivalent circuit to subject one pole of a switching device to the same duty as the 3-phase circuit of Fig. 1

with a capacitor bank as the load. With a given size capacitor bank made up of a given number of single-phase units, a device can be tested single phase to a higher equivalent 3-phase kilovar than can be tested three phase.

A circuit breaker installed on a power system may have to switch a capacitor bank, cable, or overhead line under various conditions of grounding. It is necessary to relate these actual system conditions, which are three phase, to any single-phase circuit which is used in the laboratory. The single-phase circuit should be such that it applies the same voltage across the device contacts as does the 3-phase circuit. In addition, a relationship must be established between overvoltages to ground due to restrikes in the 3-phase circuit and overvoltage to ground in the single-phase test circuit. In the following sections, the single-phase test circuits will be derived and discussed for each of the 3-phase capacitive circuit conditions under which a device may be called upon to operate.

Test Circuits Representing Unfaulted Conditions—First Pole Opening

GROUNDED CAPACITOR BANK AND SHIELDED CABLE

The simplest 3-phase condition of capacitance is the completely grounded system in which the power source neutral and the neutral of the capacitance are both tied together and grounded through connections of zero impedance. These conditions are met if the source is solidly grounded and the load is a grounded capacitor bank or a shielded cable. The three phases of the circuit are independent of each other and a single-phase circuit to test one pole of a device would consist of a duplication of one phase of the 3-phase circuit.

UNGROUNDED CAPACITOR BANKS

The capacitor bank connection most commonly found in practice is that of Fig. 1. This circuit includes an ungrounded capacitor bank and a grounded source. One pole of a device may interrupt more than 1/2 cycle before either of the other poles. A single-phase circuit may be derived which subjects one pole of a device to exactly the same conditions that it would experience if it were the first pole to open in this 3-phase circuit. This exact equivalent circuit is shown in Fig. 2 and is derived in Appendix I.

The circuit of Fig. 2 is an exact equivalent circuit in that the conditions imposed across the device terminals are in every respect identical with the conditions arising in the 3-phase circuit. Furthermore, the voltages to ground on either side of the switch are also identical with those in the 3-phase system. However, as a practical circuit for testing switching devices in the laboratories, the equivalent circuit of Fig. 2 is not convenient because of difficulties in metering, obtaining the correct voltage tap, and dividing the reactance properly.

Since the ground point in Fig. 2 is only a point of voltage reference, it may be moved without influencing the circuit; i.e., because there is only one ground point in the circuit, no current can flow in the ground connection and it may be located at any point in the circuit. As a convenience, then, ground may be moved from the 1/3 voltage tap to one terminal of the single-phase source transformer and the modified equivalent circuit of Fig. 3 results.

The equivalence of the two circuits, Figs. 2 and 3, to the actual circuit of Fig. 1 is demonstrated in the oscillograms of Fig. 4. Fig. 4(A) shows the voltages to ground on each side of the device and the recovery voltage across the device for a clearing of the first pole without a restrike. Fig. 4(B) shows these same voltages for a restrike at the crest value of the recovery voltage and a subsequent clearing at the first natural frequency current zero. Fig. 4(C) shows the voltage across the switched phase capacitor in the actual circuit and in the exact equivalent circuit for an interruption with and without one restrike. It can be seen in these oscillograms that the recovery voltage across the device is the same in all three circuits.

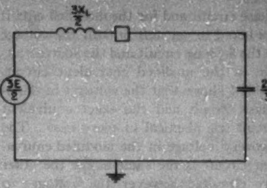

Fig. 3. Modified equivalent circuit for ungrounded capacitor banks

The voltages to ground in the circuits are different but may be interpreted by use of Table I. In Table I the voltages to ground on both sides of the device, the recovery voltage, and the voltage across the switched phase capacitor are listed for the three circuits at different times following the first interruption. These voltages are for a restrike at the crest of the recovery voltage which is interrupted at the first natural frequency current zero in a circuit with no damping. The voltages for the 3-phase circuit and the exact equivalent circuit are given in per unit of the line-to-neutral voltage in the 3-

Table I. Comparison of Theoretical Voltages* in Actual Circuit and Single-Phase Circuits for Switching an Ungrounded Capacitor Bank

	Instant of First Clearing	180 Degrees After First Clearing	Instant of Restrike	Instant of Clearing Restrike	Instant After Clearing Restrike	180 Degrees After Restrike
Actual 3-Phase Circuit						
Recovery voltage	0	3.0	0	0	3.0	6.0
Capacitor voltage to ground	−1.0	−2.0	−1.0	+3.0	+4.0	+5.0
Source voltage to ground	−1.0	+1.0	−1.0	+3.0	+1.0	−1.0
Across switched phase capacitor	−1.0	−1.0	−1.0	+3.0	+3.0	+3.0
Exact Single-Phase Circuit						
Recovery voltage	0	3.0	0	0	3.0	6.0
Capacitor voltage to ground	−1.0	−2.0	−1.0	+3.0	+4.0	+5.0
Source voltage to ground	−1.0	+1.0	−1.0	+3.0	+1.0	−1.0
Across switched capacitor	−1.0	−1.0	−1.0	+3.0	+3.0	+3.0
Modified Single-Phase Circuit						
Recovery voltage	0	3.0	0	0	3.0	6.0
Capacitor voltage to ground	−1.5 (−1.0)	−1.5 (−1.0)	−1.5 (−1.0)	+4.5 (+3.0)	+4.5 (+3.0)	+4.5 (+3.0)
Source voltage to ground	−1.5 (−1.0)	+1.5 (+1.0)	−1.5 (−1.0)	+4.5 (+3.0)	+1.5 (+1.0)	−1.5 (−1.0)
Across switched phase capacitor	−1.5 (−1.0)	−1.5 (−1.0)	−1.5 (−1.0)	+4.5 (+3.0)	+4.5 (+3.0)	+4.5 (+3.0)

*Voltages are in per unit of line-to-neutral voltage in the 3-phase circuit. Figures in parentheses are the voltages in the modified equivalent circuit in per unit of the source voltage in the modified circuit.

phase circuit and for the modified circuit are listed in per unit of both the voltage in the 3-phase circuit and the source voltage in the modified equivalent circuit. Table I shows that the voltages in the 3-phase circuit and the exact equivalent circuit are identical in every case. The recovery voltage in the modified equivalent circuit is the same as for the other two circuits; however, the voltages to ground on the source side of the switch are seen to be $1^1/_2$ times the corresponding voltages in the actual and exact equivalent circuits when expressed in the same per-unit system. The voltages to ground on the source in the modified circuit in per unit of the source voltage of the modified circuit are seen to be the same numbers as the corresponding voltages in the other circuits in per unit of the line-to-neutral voltage in the 3-phase circuit. It is also seen in Table I that the voltage to ground on the capacitor in the modified circuit corresponds to the voltages across the switched phase capacitor in the actual 3-phase circuit and in the exact equivalent circuits when they are expressed relative to their own source voltage. The voltages to ground on the capacitor are the same in per unit in all three circuits only during the periods in which current flows in the switch.

The modified equivalent circuit, then, results in the same recovery voltage across the device and the same current in the device as does the actual 3-phase circuit. The voltages to ground on the source side of the device in the modified circuit and the 3-phase circuit are the same in per unit when they are expressed relative to their own source voltages; and the voltage to ground on the capacitor in the modified circuit and the voltage across the switched phase capacitor in the 3-phase circuit are the same when they are expressed in their respective per-unit systems.

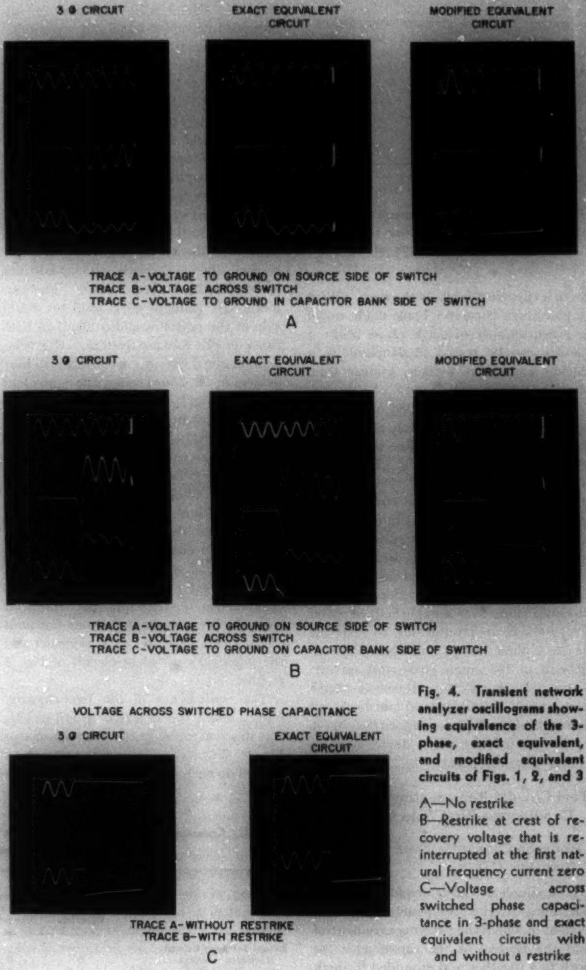

Fig. 4. Transient network analyzer oscillograms showing equivalence of the 3-phase, exact equivalent, and modified equivalent circuits of Figs. 1, 2, and 3

A—No restrike

B—Restrike at crest of recovery voltage that is reinterrupted at the first natural frequency current zero

C—Voltage across switched phase capacitance in 3-phase and exact equivalent circuits with and without a restrike

Transmission Line and Unshielded Cable

An unloaded transmission line acts like a capacitive circuit in which some of the capacitance is grounded and some of the capacitance is ungrounded. It may be represented by the circuit shown in Fig. 5, which assumes that the source is grounded in such a manner that it has an $X_0/X_1=1.0$ and that the distributed inductance of the transmission line may be neglected.

If it is assumed again, as previously, that one device pole can open more than 1/2 cycle ahead of the other two, a single-phase circuit may be derived that will impose the exact conditions on one pole that the 3-phase circuit of Fig. 5 imposes on the first pole to clear. This single-phase circuit is shown in Fig. 6. The similarity between Figs. 6 and 2 is evident. Inspection reveals that Fig. 6 would not be convenient to use as a laboratory test circuit.

Fig. 6 may be further reduced, as is proved in Appendix II, to the modified equivalent of circuit of Fig. 7. It is seen that Fig. 7 is a simple single-phase circuit with a source inductance and a capacitance to be switched; however, the magnitudes of both the source voltage and the capacitance to be switched are primarily a function of the relationship of the portion of the capacitance that is grounded and the portion of the capacitance that is ungrounded. This may be expressed in terms of the positive-sequence and zero-sequence capacitance in the circuit.

The source voltage to be used in the modified equivalent circuit of Fig. 7 is plotted in Fig. 8 as a function of the

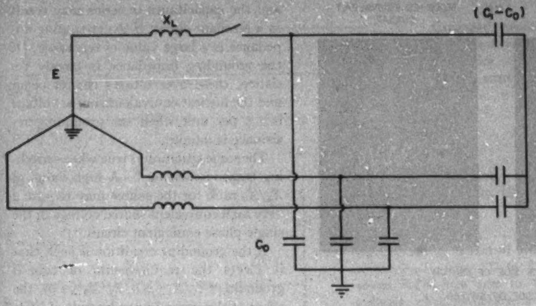

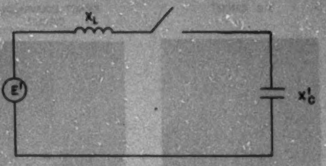

IN THREE PHASE CIRCUIT OF FIG. 5, IF

$$R=\frac{C_1}{C_0},\quad K=R-1,\quad M=\frac{X_L}{X_{C_1}},\quad A=\frac{M}{2(M+R)}$$

$$E'=E+\frac{E}{2}\left(\frac{2K}{2K+3}\right)\left(\frac{\frac{2}{3}K+1}{\frac{4}{3}K+1-M}\right)$$

$$X_C'=\left(\frac{AK+A+\frac{3}{2K}+\frac{3}{2}}{A+\frac{3}{2K}+1}\right)X_{C1}$$

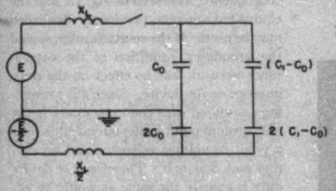

Fig. 5 (above). Generalized capacitance circuit

Fig. 6 (left). Exact equivalent circuit for generalized capacitance circuit

Fig. 7 (above right). Modified equivalent circuit for generalized capacitance circuit

ratio of the positive-sequence capacitance C_1 to the zero-sequence capacitance C_0 for an assumed circuit regulation X_L/X_{C1} of zero (a regulation of 0.10 makes less than 1-per-cent difference in the equivalent source voltage). It is seen that a source voltage of 1.0 per unit of the line-to-neutral voltage in the 3-phase circuit is required for a $C_1/C_0=1.0$ which is a circuit in which all capacitance is grounded. A source voltage of 1.5 per unit arises in a circuit for which $C_1/C_0=\infty$; i.e., all capacitance ungrounded. This confirms the circuits previously derived for the totally grounded or ungrounded capacitances. Transmission lines and unshielded cables generally have a C_1/C_0 ratio of from 1.6 to 2.0 requiring an equivalent circuit test voltage of from 1.14 per unit to 1.2 per unit.

A comparison of the results obtained by using the equivalent circuits of Figs. 6 and 7 with those resulting from the actual circuit of Fig. 5 may be seen in the oscillograms of Fig. 9. Fig. 9(A) shows a clearing without a restrike and Fig. 9(B) shows a restrike of 1/2 cycle of natural frequency duration occurring at the crest of the recovery voltage; in these figures, the voltages across the switch and to ground on either side of the switch are shown. Fig. 9(C) shows the voltages across the switched phase capacitor in the actual circuit and in the exact single-phase circuit.

The voltages resulting from these three circuits are given at various times during an opening operation in Table II. The oscillograms of Fig. 9 and the voltages listed in Table II indicate that the modified equivalent circuit does not always duplicate the conditions of the exact equivalent circuit and the actual 3-phase circuit. The modified equivalent circuit only duplicates the recovery voltage across the device prior to a restrike. If a restrike occurs, and the device clears again at a natural frequency current zero, the subsequent recovery voltage across the device is more severe in the modified circuit than in the actual or exact equivalent circuit. This is due to the fact that the latter two circuits are double-frequency circuits whereas only a single natural frequency is possible in the modified circuit. The voltages to ground in the modified circuit are not related to the corresponding voltages to ground in the other circuits.

The modified equivalent circuit of Fig. 7, then, may be used to subject one pole of a device to the same conditions that it would encounter if it were the first pole to open when switching an unloaded transmission line with complete accuracy up to the instant at which a restrike occurs. Following this instant, the conditions are only approximately the same.

Effect of Source Grounding

Up to this point this discussion has been concerned with the capacitance conditions that may be encountered and has been restricted to power sources grounded in such a manner that $X_0/X_1=1.0$ for the source. A variation in grounding impedance can only have an effect

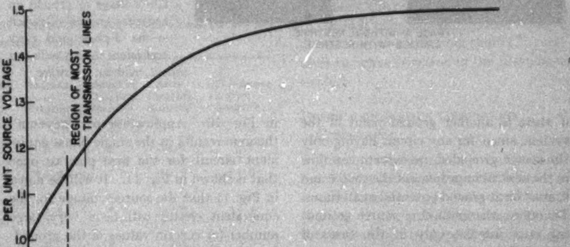

Fig. 8. Source voltages for modified equivalent circuit of Fig. 7

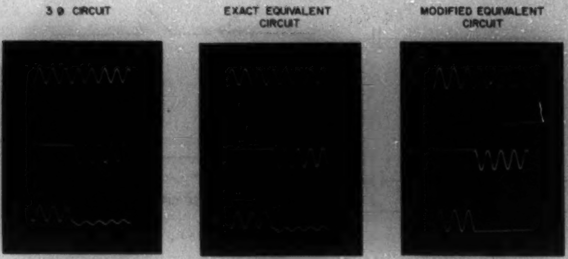

TRACE A-VOLTAGE TO GROUND ON SOURCE SIDE OF SWITCH
TRACE B-VOLTAGE ACROSS SWITCH
TRACE C-VOLTAGE TO GROUND ON LINE SIDE OF SWITCH

A

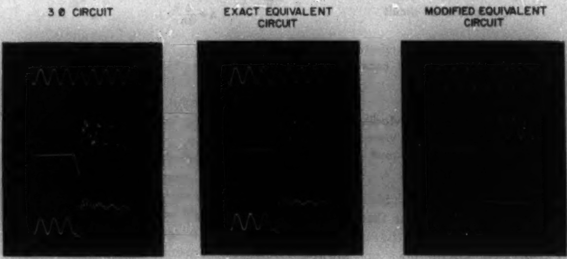

TRACE A-VOLTAGE TO GROUND ON SOURCE SIDE OF SWITCH
TRACE B-VOLTAGE ACROSS SWITCH
TRACE C-VOLTAGE TO GROUND OF LINE SIDE OF SWITCH

B

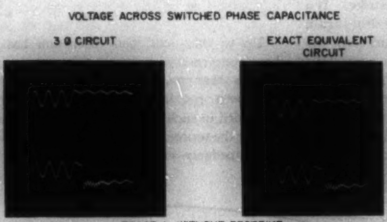

TRACE A-WITHOUT RESTRIKE
TRACE B-WITH RESTRIKE

C

Fig. 9. Transient network analyzer oscillograms showing equivalence of switching device recovery voltages in the 3-phase, exact, and modified circuits of Figs. 5, 6, and 7

A—No restrike
B—Restrike at crest of recovery voltage with reinterruption at first natural frequency current zero
C—Voltage to ground on capacitor terminal of switch in the 3-phase and exact equivalent circuits with and without a restrike

if there is another ground point in the system, since, for any circuit having only the source grounded, no current can flow in the neutral impedance of the source and it must be at ground potential at all times. Therefore, the method of source grounding is of interest only in the cases of grounded capacitor banks, cables, and overhead lines if no faults are involved. A circuit involving a grounded capacitor bank or a shielded cable and a source with variable grounding impedance is shown in Fig. 10. Application of Thévenin's theorem results in the single-phase equivalent circuit for the first pole to open that is shown in Fig. 11. It will be noted in Fig. 11 that the source voltage for the equivalent circuit will be a very large number for certain values of the grounding impedance. The reason for this can be found by referring to Fig. 10 where it is seen that with one phase open a path through the ground involving the source impedance, the grounding impedance, and the capacitance in series may result in a resonant circuit if the grounding impedance is a large value of reactance. If the grounding impedance is largely resistive, these overvoltages cannot occur and the highest equivalent source voltage is 1.5 per unit when the grounding resistance is infinite.

The same situation is true when switching transmission lines. A high value of X_0/X_1 ratio for the source may require a very high equivalent source voltage in the single-phase equivalent circuit.

If the grounding condition is such that it meets the requirements of type-B grounding ($X_0/X_1 \leq 3.0$, $R_0/X_1 \leq 1.0$), the effect of the ground impedance is of little consequence, as is seen in Fig. 12, and the equivalent circuits previously described may be used. If the source is ungrounded the grounding condition of the capacitance network has no effect on the duty imposed on the device. Since any grounding associated with the capacitance is the only ground point in the circuit, it is only a point of voltage reference and no current may flow in it. Therefore the device duty is exactly the same as would be encountered when an ungrounded bank is switched. The modified equivalent circuit of Fig. 3 duplicates the conditions for this case. For grounding conditions not described here, no generalities may be made. The duty will depend on these grounding conditions if the capacitance is grounded, and the source grounding conditions would have to be known before an equivalent circuit could be used for testing.

Test Circuits Representing Unfaulted Conditions—Second Pole Opening

Grounded and Ungrounded Capacitor Banks

If a grounded capacitor bank is being switched from a grounded source of power, the three phases are independent of each other. Therefore, the first, second, or last poles of the device to clear would experience the same conditions. The modified equivalent circuit is in this case an exact equivalent and represents a test of any pole.

When switching an ungrounded capacitor bank, it is shown in the companion paper[1] that higher voltages can exist across the second pole to clear than across the first pole. It should be remembered that this represents a condition of mechanical delay in one of the two last phases since current must be interrupted in both of these phases of the device simultaneously. This is because they are in series across the line-to-line voltage.

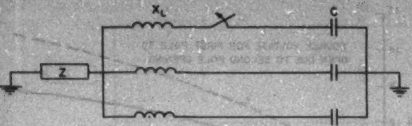

Fig. 10 (left). Grounded capacitance bank switched from impedance grounded source

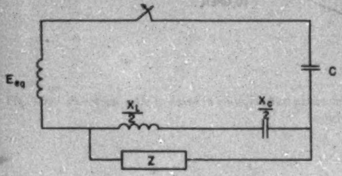

$$E_{eq}=E\angle 0+\frac{1}{1+j\left(\frac{X_L}{2Z}-\frac{X_C}{2Z}\right)}\cdot\frac{E}{2}$$

Fig. 11 (left). Exact equivalent circuit for Fig. 10

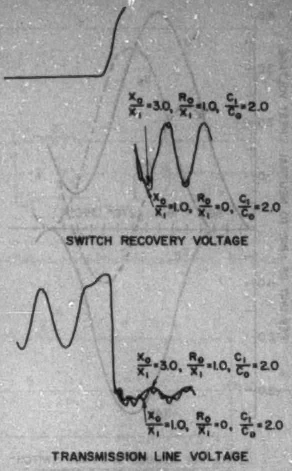

Fig. 12 (right). Effect of increasing source X_0/X_1 from 1.0 to 3.0 and source R_0/X_1 from zero to 1.0 on voltages when switching a transmission line. One restrike at crest of recovery voltage

The recovery voltage across the first phase to clear as a result of the second phase clearing 1/4 cycle later is shown in Fig. 13. It is seen that this recovery voltage reaches a crest value of 4.1 per unit which occurs 210 degrees after the current extinction in the phase in question and it reaches this magnitude only if the next phase to clear is the phase which lags the first phase to open by 120 degrees. That is, the opening phase rotation must be assumed to be phases *A-B-C* and not phases *A-C-B*.

Because of the nature of the circuit in which two phases are being opened, no exact single-phase equivalent circuit involving one switching operation is possible. However, a modified circuit may be synthesized. The recovery voltage curve of Fig. 13 is very nearly of the form (1-cos θ) for the first half-cycle. This is the form resulting from the modified test circuit. But since it takes 210 degrees for the recovery voltage to reach crest value, a lower frequency (51.5 cycles) would have to be used in the test circuit. The impedances have to be adjusted so that the proper value of current will flow. In other words, one pole of a device may be subjected to the conditions it would encounter if it were the first pole to open when switching an ungrounded capacitor bank and another pole had not yet opened mechanically. The modified test circuit may be used with a source voltage of 2.05 per unit, with a test frequency of 51.5 cycles, a source inductance 2.4 times that of the 3-phase circuit, and a capacitance equal to 0.6 times that of one phase of the 3-phase circuit.

TRANSMISSION LINE

As for the previous case, the opening of the second pole when switching a transmission line may result in a higher voltage across the first pole that opened. The higher voltage will occur during the first half-cycle of recovery voltage across the first pole only if *B* phase is the second to open. Since a current zero occurs in *C* phase before a current zero appears in *B* phase, the *C* phase pole must skip a current zero, or not yet be mechanically open, for the *A* phase recovery voltage to be increased.

Again, an exact equivalent circuit is not obtainable but a modified test circuit can be synthesized from the voltages that were measured in a 3-phase circuit. The equivalent source voltages for the modified test circuit are shown in Fig. 14 in comparison with those for the first phase to clear when no other phases are opening. These values were obtained on the transient network analyzer when switching a transmission line from a source that was solidly grounded. In the range in which most transmission lines fall, the source voltages to represent second pole opening are about 8 per cent more than those due to the first pole opening. These voltages do not appear until more than 1/2 cycle after current extinction in the first phase to clear.

EFFECTS OF SOURCE GROUNDING CONDITIONS

The equivalent circuits given above are for 3-phase circuits grounded in such a manner that the X_0/X_1 ratio of the source is unity. If the ground is increased to the limits described by type-*B* grounding, no appreciable difference will result in the equivalent circuits derived. If the source is ungrounded, the device duty is the same as for the case of ungrounded capacitance with a grounded source. This is true re-

Table II. Comparison of Theoretical Voltages* in Actual Circuit and Single-Phase Circuits for Switching Transmission Line

	Instant of First Clearing	180 Degrees After First Clearing	Instant of Restrike	Instant of Clearing Restrike	Instant After Clearing Restrike	180 Degrees After Restrike
Actual Circuit						
Recovery voltage	0	2.4	0	0	1.8	4.2
Line voltage to ground	1.0	+1.4	1.4	−2.9	−2.8	−3.2
Source voltage to ground	1.0	−1.0	+1.4	−2.9	−1.0	+1.0
Exact Equivalent Circuit						
Recovery voltage	0	2.4	0	0	1.8	4.2
Line voltage to ground	1.0	1.4	1.4	−2.9	−2.8	−3.2
Source voltage to ground	1.0	−1.0	1.4	−2.9	−1.0	+1.0
Modified Equivalent Circuit						
Recovery voltage	0	2.4	0	0	2.4	4.8
Line voltage to ground	1.2 (1.0)	1.2 (1.0)	1.2 (1.0)	−3.6 (−3.0)	−3.6 (−3.0)	−3.6 (−3.0)
Source voltage to ground	1.2 (1.0)	−1.2 (1.0)	1.2 (1.0)	−3.6 (−3.0)	−1.2 (−1.0)	+1.2 (+1.0)

*Values are in per unit of normal line-to-neutral crest of 3-phase circuit. Figures in parentheses are in per unit of modified circuit source voltage. $C_1/C_0=2$ assumed for transmission line.

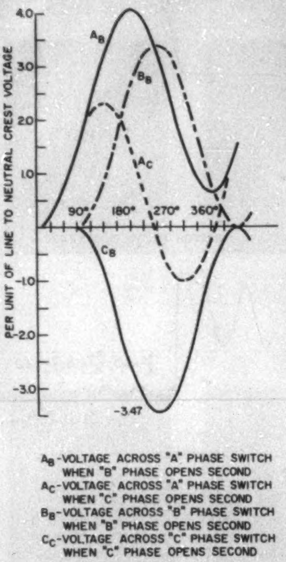

Fig. 13 (left). Recovery voltages across first pole to open when switching an ungrounded capacitance due to the opening of a second pole. The third pole remains mechanically closed

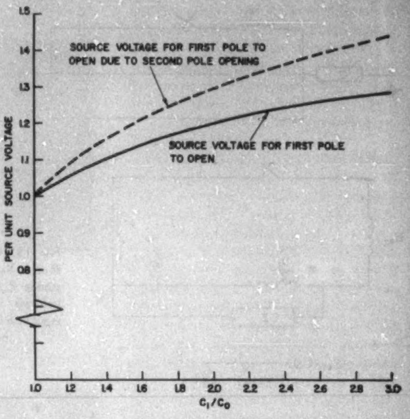

Fig. 14 (right). Recovery voltages across first pole to open when switching the generalized capacitance circuit of Fig. 5 due to the opening of a second pole

gardless of the capacitance grounding conditions. For systems not grounded in accordance with the requirements given here, the equivalent circuits for second pole opening when switching grounded capacitive circuits depend on the manner of source grounding and no generalizations can be made.

Faulted Circuits—First Pole Opening

Grounded Capacitor Banks

If the first pole to clear is assumed to be in an unfaulted phase when switching a grounded capacitor bank, as shown in Fig. 15(A), this pole may be tested in the exact equivalent circuit of Fig. 15(B). The single-phase source voltage of the exact equivalent circuit depends on the source grounding and, for the case shown in Fig. 15(B) with type-*B* grounding, the source voltage is 135 per cent of the leg voltage of the 3-phase circuit. Regardless of the manner of source grounding, the single-phase source voltage cannot exceed line-to-line voltage of the 3-phase circuit.

This circuit can be reduced to a modified equivalent circuit by combining the load impedances. For this case, the modified circuit would consist of a capacitance equal to the per-phase capacitance of the 3-phase circuit and a source inductive reactance equal to 142 per cent of the positive-sequence reactance of the source in the 3-phase circuit. The modified equivalent circuit is exact prior to a restrike and approximately correct thereafter since the modified circuit only has one natural frequency of oscillation.

Ungrounded Capacitor Banks

Two fault conditions involving ungrounded capacitor banks are of interest. If the source is grounded, a line-to-ground fault at the capacitor bank results in abnormal capacitive switching duty on the unfaulted phases of the device. A failure of a portion or all of the capacitors in one phase also changes the duty on the device.

An exact equivalent circuit to test the first pole of a device to interrupt when switching an ungrounded capacitance with a line-to-ground fault on one phase may be derived if it is assumed that this pole is in an unfaulted phase, as shown in Fig. 16(A). The source voltage in the exact equivalent circuit depends on the manner of grounding of the source. In the circuit of Fig. 16(B) the grounding impedance on the source side of the switch is such that viewed from the switch location the circuit has type-*B* grounding. The resultant source voltage in the exact equivalent circuit for this condition is 130 per cent of the leg voltage of the 3-phase circuit. The source voltage of the single-phase circuit will not exceed line-to-line voltage of the 3-phase

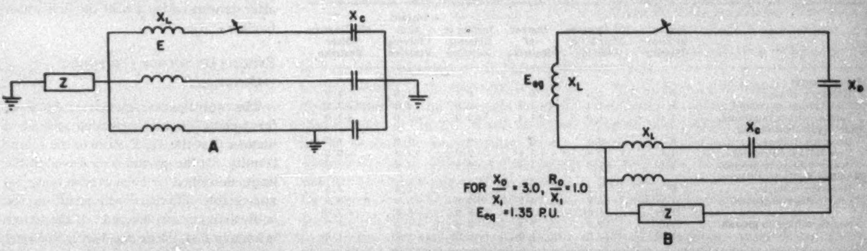

Fig. 15. A—First pole to open in an unfaulted phase when switching a grounded capacitance with a line-to-ground fault on one phase. B—Exact equivalent circuit for the 3-phase circuit of A

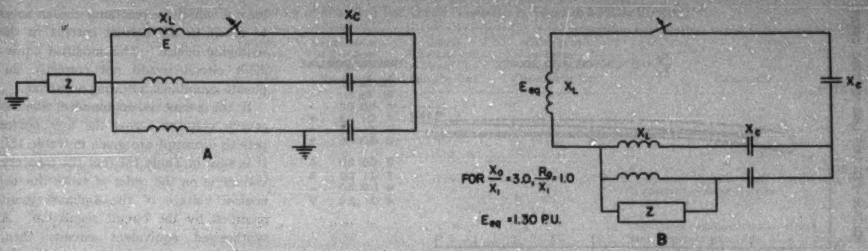

Fig. 16. A—First pole to open in an unfaulted phase when switching an ungrounded capacitance with a line-to-ground fault on one phase. B—Exact equivalent circuit for the 3-phase circuit of A

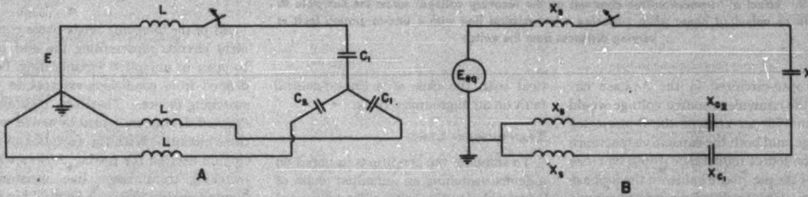

Fig. 17. A—First pole to open in a normal phase when switching an ungrounded capacitance bank in which the capacitance in one phase is more or less than that in the other two phases. B—Exact equivalent circuit for 3-phase circuit of A. Note: E_{eq} is given in Fig. 18

circuit regardless of the grounding of the source. The impedance network on the load side of the switch in this exact equivalent circuit may be combined to result in a modified equivalent circuit. This results in an equivalent load which is a capacitance whose reactance is 146 per cent of the capacitive reactance per phase of the 3-phase bank. This will result in the correct current through the switch and a recovery voltage across the switching device that is identical to that arising in the 3-phase circuit up to the time that a restrike occurs. The modified equivalent circuit is a single-frequency circuit whereas the 3-phase circuit has two natural frequencies. During and following a restrike the modified circuit is only approximately correct. It should be noted that the current and the recovery voltage across the device are less severe when there is a fault on one phase than when switching the circuit unfaulted.

UNGROUNDED CAPACITOR BANK—UNBALANCED CAPACITANCE

If a portion of the capacitance is lost in one phase of a capacitor bank, unbalancing the capacitance in the phases, the duty on the first pole of the switch to interrupt current is changed from the balanced case. Because of the series-parallel arrangement of capacitor units found in high-voltage capacitor banks, a loss of capacitor units or fuse blowing may increase or decrease the capacitive reactance.

The first pole to open in Fig. 17(A) experiences the same duty as the switch in the exact equivalent circuit of Fig. 17(B). The source voltage for the equivalent circuit of Fig. 17(B) is given in Fig. 18 as a function of the percentage of capacitive reactance unbalance and the unfaulted system regulation.

The exact equivalent circuit of Fig. 17(B) may be reduced to a modified equivalent circuit if the percentage of capacitive reactance unbalance is known. If the capacitance in one phase were short-circuited in the 3-phase circuit, the modified equivalent circuit would consist of a source voltage equal to the line-to-line voltage of the 3-phase circuit, a capacitance equal to the capacitance per phase of the 3-phase circuit, and a source inductance equal to twice the 3-phase circuit source inductance. If the capacitance

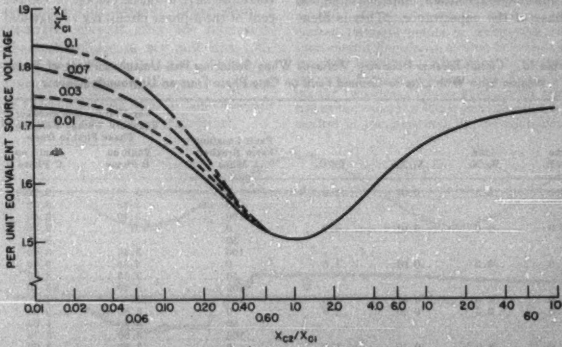

Fig. 18. Source voltages to be used in the equivalent circuit of Fig. 17(B) as a function of the capacitive reactance unbalance and the unfaulted circuit regulation

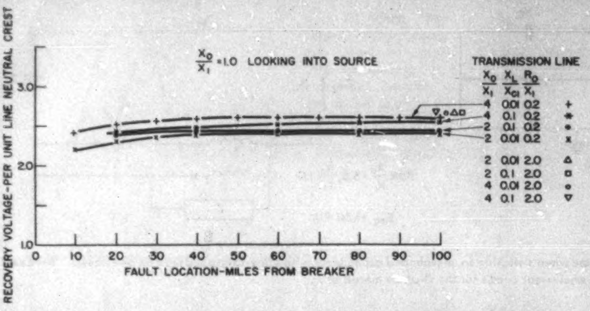

Fig. 19. Effect of transmission-line constants on the recovery voltages across the first pole to clear in an unfaulted phase when switching a transmission line with a line-to-ground fault at varying distances from the switch

were open-circuited in the 3-phase circuit, the equivalent source voltage would remain 173 per cent of the 3-phase leg voltage, and both the capacitive reactance and the source inductance would be twice that of the per-phase values of the 3-phase circuit. The modified equivalent circuit would be only approximate following a restrike because the modified circuit does not have the multiple natural frequencies present in the actual circuit.

UNGROUNDED SOURCE

If the source is ungrounded and the capacitance bank is ungrounded, the ground connection due to a line-to-ground fault has no effect on the duty on the first switch pole to interrupt. The modified equivalent circuit of Fig. 3 duplicates the duty on this switch pole under all conditions.

If the source is ungrounded, and the capacitance bank is grounded, a line-to-ground fault essentially short-circuits one phase of the capacitance. This is identical with the case of a line-to-neutral fault on an ungrounded bank.

TRANSMISSION LINES

To simulate the conditions imposed on a device switching an unfaulted phase of a transmission line with a line-to-ground fault on another phase, a circuit will have to be synthesized from the voltage conditions in the 3-phase circuit. Fig. 19 shows the crest of the recovery voltage across the first switch pole to interrupt when switching a transmission line with a line-to-ground fault on another phase at a location remote from the breaker. This information was obtained on the transient network analyzer and assumed a source that was solidly grounded ($X_0/X_1=1.0$). Fig. 19 indicates that the recovery voltage may be as high as 260 per cent of the line-to-neutral voltage of the unfaulted 3-phase circuit. The synthesized modified equivalent circuit should therefore have a source voltage of 130 per cent of the 3-phase circuit leg voltage and have a capacitive reactance chosen so as to result in the correct current in the switching device. This modified equivalent circuit would not correctly duplicate conditions following a restrike.

Table III. Circuit-Breaker Recovery Voltages When Switching First Unfaulted Phase of Transmission Line With Line-to-Ground Fault on One Phase From an Ungrounded Source

Line X_0/X_1	Line R_0/X_1	X_1/X_{c1}	C_1/C_0	Fault Location From Breaker, Miles	Per-Unit Crest of Breaker Recovery Voltage Unfaulted Phase First to Open: Fault on B Phase	Fault on C Phase
2.0	0.2	0.01	1.6	0	3.36	3.36
				50	3.38	3.38
				100	3.40	3.40
2.0	2.0	0.01	1.6	0		3.36
				50		3.38
				100	3.40	3.40
4.0	0.2	0.01	1.6	0	3.36	3.36
				50	3.38	3.38
				100	3.40	3.40
4.0	2.0	0.01	1.6	100	3.40	
4.0	2.0	0.10	1.6	0	3.80	3.60
				50	3.80	3.64
				100	3.80	3.70
4.0	2.0	0.10	1.6	0	3.80	3.60
				50	3.80	3.64
				100	3.80	3.70

If the source is ungrounded, the recovery voltages across the first device pole to interrupt are given in Table III. It is seen in Table III that the recovery voltage is on the order of twice line-to-neutral voltage of the 3-phase circuit modified by the circuit regulation. A synthesized equivalent circuit, then, should have a source voltage equal to the line-to-line voltage of the 3-phase circuit.

Effect of Shunting Resistors

All of the foregoing single-phase equivalent circuits representing the first pole to open in unfaulted circuits have been defined from conditions external to the switching device. Therefore, resistance-shunted devices may also be tested with these circuits. With the exception of the circuits derived for testing devices when switching transmission line, resistance-shunted devices may also be tested in the equivalent circuits simulating conditions arising from first pole opening when switching faulted circuits. It would not be correct to use the test circuits simulating second pole opening for resistance-shunted devices.

Summary of Results

Although exact equivalent single-phase test circuits have been derived, it is more practical to use a modified circuit for laboratory testing of capacitance switching devices. Table IV summarizes the parameters and conditions to be used in the modified test circuit for the various capacitance and grounding conditions that can be found in 3-phase circuits.

CALCULATION OF KILOVARS

The equivalent 3-phase kilovar of a single-phase capacitance switching test is calculated for unfaulted conditions as $\sqrt{3}$ (line-to-line kilovolt) (amperes test current). The line-to-line kilovolt is that on which the test voltage is based; e.g., maximum design voltage.

As an illustration, suppose single-phase tests are to be made on a 69-kv device to represent an ungrounded capacitor bank on an effectively grounded system. The maximum design voltage for the device is 72.5 kv, or 42 kv line-to-neutral. The single-phase test voltage is 1.5 (42) or 63 kv. If the test current is 160 amperes, the equivalent 3-phase kilovar is $\sqrt{3}$ (72.5) (160) or 20,000 kilovars.

Table IV. Summary of Modified Test Circuit Parameters in Terms of 3-Phase Circuit

	Voltage of 3-Phase Circuit, Per Unit	Capacitance of 3-Phase Circuit, Per Unit	Source Inductance of 3-Phase Circuit, Per Unit	Current of 3-Phase Unfaulted Circuit, Per Unit	Comments
Grounded Banks and Shielded Cables					
Grounded source					
No fault					
First pole	1.0	1.0	1.0	1.0	
Second pole	1.0	1.0	1.0	1.0	
Line-to-ground fault, type-B grounding					
First pole	1.35	1.0	1.42	1.42	equivalent circuit only approximately correct following restrike.
Ungrounded source					
No fault					
First pole	1.5	0.67	1.5	1.0	duplicates conditions across switch.
Second pole	2.0	0.57	2.4	1.0	test frequency should be 51.5 cycles, only approximate following restrike.
Line-to-ground fault					
First pole	1.73	1.0	2.0	1.94	only approximate following restrike.
Ungrounded Banks					
Grounded source					
No fault					
First pole	1.5	0.67	1.5	1.0	duplicates conditions across switch.
Second pole	2.0	0.57	2.4	1.0	approximate following restrike-test frequency of 51.5 cycles.
Line-to-ground, type-B grounding					
First pole	1.3	0.69	1.0	0.86	approximate following restrike.
Unbalanced capacitance					
Short circuit in one phase	1.73	1.0	2.0	1.94	
Open circuit in one phase	1.73	0.5	2.0	0.78	
Ungrounded source					
No fault					
First pole	1.5	0.67	1.5	1.0	duplicates conditions across switch.
Second pole	2.0	0.57	2.4	1.0	test frequency 51.5 cycles.
Line-to-ground fault					
First pole	1.5	0.67	1.5	1.0	duplicates conditions across switch.
Second pole	2.0	0.57	2.4	1.0	test frequency 51.5 cycles.
Unbalanced capacitance					
Short circuit in one phase	1.73	1.0	2.0	1.94	approximate following restrike.
Open circuit in one phase	1.73	0.5	2.0	0.78	
Transmission Line and Unshielded Cable					
Grounded source					
No fault					
First pole	1.2	$0.83C_1$	1.0	1.0	approximate following restrike.
Second pole	1.3	$0.77C_1$	1.0	1.0	
Line-to-ground, type-B grounding					
First pole	1.3	$1.0C_1$	1.42	1.42	
Ungrounded source					
No fault					
First pole	1.5	$0.67C_1$	1.5	1.0	duplicates conditions across switch.
Second pole	2.0	$0.57C_1$	2.4	1.0	approximate following restrike.
Line-to-ground fault					
First pole	1.73	$1.0C_1$	1.0	1.56	approximately duplicates conditions.

The application of devices on capacitor banks involves a further consideration. In the foregoing example, the device performance has been demonstrated for 20,000 kilovars, yet it might not be suitable for switching a capacitor bank with a 20,000-kilovar rating. Considering probable excess capacitance in the bank, possible harmonics, and operation at 10 per cent above nominal rated voltage, capacitor bank standards require their successful performance at 135 per cent of rated kilovar. As switching of a capacitor bank will normally be done when the voltage is high, the device should operate satisfactorily at 135 per cent of the nominal bank rating. Thus, the 20,000-kilovar device in the example, could be applied on a capacitor bank with a nominal rating of 20,000/1.35 or 14,800 kilovars.

Laboratory Tests

Capacitance switching tests in our Laboratory are normally made single phase using the circuit shown in Fig. 3. The device's performance over the range of currents up to its rating and at several values of tripping angle at each current value is determined. Fig. 20 shows one cathode-ray oscillogram of a high-voltage oil circuit breaker interrupting a capacitive current after one reignition. The test voltage in per unit was 1.43, based on maximum design voltage. Traces *A* and *B* are the voltages to ground on the source side and on the capacitor bank side of the breaker respectively.

Appendix I. Derivation of Equivalent Circuit

Thévenin's theorem states that any network may be represented between any two arbitrary terminals in the network by placing a generator whose voltage is equal to the open-circuit voltage between the desired terminal points in series with the short-circuit impedance as seen between the arbitrary terminals. Therefore, the 3-phase circuit of Fig. 1 may be simplified by replacing the two closed phases between the neutral of the capacitor bank and the grounded neutral of the generator by the equivalent

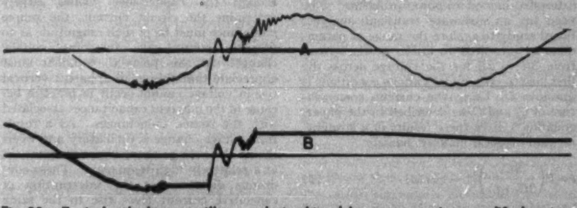

Fig. 20. Typical cathode-ray oscillogram obtained in a laboratory test using a modified equivalent circuit. Test voltage is 1.43 per unit

network given by application of Thévenin's theorem.

By breaking the 3-phase network at the neutral of the capacitor bank and looking back into the remaining two phases, the voltage between point N and ground may be determined as well as the short-circuit impedance between these two points. The voltage between point N and ground with the disconnected third phase as phase-angle reference is

$$V_n = E\left(\frac{\sin(\theta+120)+\sin(\theta-120)}{2}\right) = -0.5E\sin\theta$$

That is, the equivalent voltage behind the short-circuit impedance is equal to one-half of the phase voltage of the 3-phase circuit and is of opposite polarity to the unrepresented third phase. The short-circuit impedance is equal to the parallel impedance of two phases of the capacitor bank.

This discussion leads to the equivalent circuit of Fig. 2. Any trapped charges arising in the 3-phase circuit will appear properly in the equivalent circuit. From the equivalent circuit it may be seen that the ratio of the voltage due to the trapped charge to the source voltage is the same in either branch of the circuit proceeding from the neutral point to ground despite the time variation in the instantaneous value of the voltage sources. Consequently, whenever the switch is closed, the neutral of the capacitor bank must be at ground potential.

Since there can be no current flow in the ground connection, it serves only as a reference point for voltage measurements. The single-phase circuit may be grounded at any point as long as it is remembered that the one-third point of the source is the zero-potential point when related to the 3-phase circuit.

Appendix II. Modified Equivalent Circuit for the Generalized Capacitance Condition

The circuit of Fig. 6 may be further simplified by the application of Thévenin's theorem to the circuit in such a manner as to replace the network between the load side of the switch and ground. If it is defined that

$$R = \frac{C_1}{C_0}$$

$$K = (R-1)$$

$$M = \frac{X_L}{X_{C1}}$$

$$A = \frac{M}{2(M+R)}$$

then, on a 60-cycle basis, the load impedance between the switch terminal and ground is

$$X \text{ equivalent} = \left(\frac{A+AK+\frac{3}{2}+\frac{3}{2K}}{A+1+\frac{3}{2K}}\right)X_{C1}$$

Similarly, neglecting trapped charges, the voltage to ground on the load side of the open switch is

$$E_{\text{open}} = -\frac{E}{2}\left(\frac{2K}{2K+3}\right)\left(\frac{\frac{2}{3}K+1}{\frac{2}{3}K+1-M}\right)$$

This defines a circuit with a ground point somewhere between the terminals of a single-phase source since the equivalent voltage on the load side of the switch is in phase with the voltage on the source side of the switch. This ground point is now the only ground in the system, and it may be moved without influencing the conditions imposed on the switch. Moving ground to one terminal of the source voltage results in the circuit of Fig. 7.

It should be noted that the new equivalent circuit, while satisfying 60-cycle conditions, is not correct during transients since it has only one natural frequency oscillation while the exact equivalent circuit of Fig. 6 has two natural frequencies.

References

1. SOME FUNDAMENTALS ON CAPACITANCE SWITCHING, L. B. Johnson, A. J. Schultz, N. R. Schultz, R. B. Shores. *AIEE Transactions*, vol. 74, pt. III, Aug. 1955, pp. 727–36.

2. FLEXIBLE HIGH-POWER LABORATORY CAPACITOR BANK FOR VARIETY OF SWITCHING TESTS TO 65,000 KILOVARS, R. E. Friedrich, D. J. Burns. *AIEE Transactions*, vol. 73, pt. III, Aug. 1954, pp. 837–42.

◆

Discussion

E. W. Boehne (Massachusetts Institute of Technology, Cambridge, Mass.): The authors have presented a much-needed study of the voltages and currents associated with the switching of capacitive circuits. One is impressed with the growing need for the analysis of the resistance-inductance-capacitance circuit, lumped and distributed, in connection with power field. Many of the problems which we are approaching were encountered by the communication engineer, working in the higher frequency domain, quite a few years ago.

The essential plea of this discussion is to encourage the inclusion in AIEE papers of sufficient straightforward circuit analysis so as to bridge the gap from theory to practice and hence make it possible for the young graduate to understand and become interested in modern power problems. The need for an elaborate transient analyzer board study to explore the range of parameters as presented to arrive at the spread from $3E$ to $2E$ for the voltage across the first pole to open under various conditions is questioned. Using the current nomenclature of C_1 and C_0 as described in the paper, equation 1 gives these results in a straightforward classical manner, namely

$$e = E\left(\frac{3C_1}{2C_1+C_0}\right)(1-\cos\omega t) \qquad (1)$$

When $C_0=0$ then e becomes maximum at $3E$. When $C_1=2C_0$ then e becomes maximum at $2.4E$. When $C_1=C_0$ then e becomes maximum at $2E$.

Greater accuracy in the analysis is obtained when it is appreciated that exact results are achieved in any switching problem by introducing into the circuit, at the switch, a current equal and opposite to the current to be interrupted. When applied to the problem just given, the resulting voltage across the switch not only has the slow 60-cycle cosine component which gives rise to the foregoing peak values 1/2 cycle later but a sudden voltage change is indicated by the introduction of the capacitance current, rising sinusoidally, into the circuit inductance. This is the well-known voltage change which takes place at the breaker momentarily following the interrupting current zero and which is so important to the breaker's performance. It is the same voltage change which occurs when the capacitors are added to the circuit. Although the capacitance values largely determine the circuit current, the source inductance must be of such magnitude as to properly control the foregoing voltage change. At this point the student must appreciate that this small apparent vertical rise in voltage cannot occur in practice because of the inherent capacitances associated with the source inductances. As a result this voltage change is oscillatory and overshoots the voltage change by a like amount at a relatively high frequency. These conditions dictate that the interruption of capacitive current gives rise to the same phenomena in the circuit breaker as occurs when interrupting a short circuit except (fortunately) that everything is in miniature. Namely, the current is small, the voltage is low, and the contact parting time is small. There exists the phenomenon of rate of rise of recovery voltage, again in miniature. The success of this miniature interruption is important to the future events which can occur during the interruption.

By choosing the Thévenin approach to the circuit analysis the uninitiated may overlook these considerations. On the other hand, the cancellation approach recommended here (a form of the superposition principal) can seldom avoid giving all the true phenomena actually observed.

The second plea of this discussion concerns the advantages of the grounded bank of capacitors as compared to the ungrounded bank. In addition to reducing the circuit breaker stress from 3 to 2, the grounded bank, when properly located with respect to the line or feeder breaker, will greatly reduce the rate of rise of recovery voltage associated with the interruption of short-circuit currents. These reductions are so appreciable that circuit-breaker ratings may be greatly affected by the presence of the grounded bank behind the line or feeder breaker. This suggests that research and investigations should be made at an early date to determine the true increase in circuit-breaker rating which might be realized by the presence of the grounded bank behind the breaker. In addition, the large grounded bank on or near the bus is the ideal absorber of all incoming lightning surges. Modern capacitor banks when connected directly at the bus or line potential (not on the tertiary) cannot possibly cause the bus to rise to arrester sparking potential due to lightning. The packaged advantages of the grounded bank to the industry as a whole should indicate sufficient saving as to warrant the necessary research into the matters of effective capacitor fusing and harmonic suppression which now stand in the way of capturing the full advantages of the grounded bank. A thorough study of the multisided advantages of the large grounded bank is highly recommended.

The establishment of a switching surge committee or subcommittee of the AIEE would help many apparatus groups which all have a stake in the results and conclusions of such investigations. In a similar manner the Research Committee as well as the Education Committee have an interest and contribution to make in this area. This is particularly true when students are having difficulty finding appropriate topics for thesis study in the power area. The area of switching surge is particularly adapted to thesis study and research. It is hoped that the creation of such a committee, which cuts across apparatus lines, will afford this guidance and opportunity.

K. G. Darrow, V. E. Phillips, A. J. Schultz, and R. B. Shores: The comments of Professor Boehne point out that for this problem, as for so many others, there are several methods of attack. Since the objective of this study was to derive equivalent test circuits for capacitance switching devices, it was our feeling that the application of Thévenin's theorem to the actual circuit was superior to other methods in that the test pole of the device remained identified throughout the analysis. While we appreciate the value of the method of superposition in determining the transient voltages and currents in the circuit, the identity of the circuit elements is lost and the method does not lead as readily to an equivalent circuit.

Although a relatively small amount of mathematics is required for the solution of any specific circuit condition, when a large number of variations are to be studied the paper work reaches a prohibitive degree. For this reason, the transient network analyzer is seen to be an invaluable tool in saving the time and labor required to solve a problem. A few sample calculations to check the analyzer results with the theoretical answers are all the mathematics that are necessary.

We agree with Professor Boehne that there appear to be advantages in favor of grounding capacitor banks. This is particularly true in terms of the switching device recovery voltages when dropping a capacitor bank. A thorough investigation of the other factors involved is warranted.

Ribbon Elements for High-Voltage Current-Limiting Fuses

A. H. POWELL
MEMBER AIEE

C. L. SCHUCK
MEMBER AIEE

CURRENT-LIMITING fuses have found widespread usefulness in the following types of circuits: substation primary, instrument potential transformer, motor control, branch, auxiliary, control power, and capacitor unit.

The desirability of applying current-limiting fuses in these circuits is emphasized by the complete absence of disturbance when they operate and the benefits resulting from their current-limiting ability in the form of reduced thermal and mechanical duty on the system and connected apparatus. In expanding the ratings and in varying the physical form of the fuses to satisfy the requirements of these fields of application, some limitations as well as the flexibilities of the basic construction became evident. Long slender, mechanically inert metallic elements embedded in a granular filler have relatively fixed time-current characteristics, and high current ratings can be designed only by use of large numbers of parallel connected fine wires, requiring proportionately large internal volume, and resulting in fuse designs of large size and weight.

During the time that these fuses have been manufactured several departures from the basic design have been considered and appraised on the basis of overcoming these limitations. One of these is the use of ribbon or rectangular-shaped elements rather than round wires, the expectation being that a smaller number of ribbons would be required for a given current rating, thus permitting size and weight reductions and improved fuse construction.

Ribbon Elements at Low Voltages

That improvements might be expected to result from use of ribbon elements in high-voltage ratings was first indicated by certain design constants resulting from developmental interruption tests on low-voltage high interrupting capacity fuses.[2] The latter employ ribbon elements, design constants for which are compared in Table I with corresponding values obtained earlier in the development of high-voltage ratings employing wire elements. The values or factors of interest are respectively the tolerable volts per inch of active element and the maximum permissible amperes per arc path in interrupting high available short-circuit currents.

The use of wire elements having cross sections larger than those permitting 650 amperes per arc path results in inability of the granular filler to absorb the arc energy fast enough to avoid the development of disruptive pressure. Use of element lengths shorter than those giving 300 volts per inch results in inadequate arc voltage following melting to obtain effective current limitation.

The low-voltage fuse elements consist of ribbons including holes, the metal outside of which forms the active sections. The 900-volt-per-inch value in Table I for ribbons was computed from the actual length of ribbon consumed in low-voltage tests, not from the total ribbon length. The extraordinarily high current tolerable in each arc path with ribbon elements in low-voltage tests is apparently due to the shortness of the individual arcs, which permits some of the arc energy to be dissipated longitudinally, reducing the amount dissipated radially. The higher voltage gradient and current density values found tolerable in the low-voltage fuse designs suggested that more compact designs might be possible in at least the lower voltage ratings of high-voltage fuses.

Preliminary High-Voltage Short-Circuit Tests

To get a few indications of the possibilities of ribbon elements at higher voltage levels, four series of interruption tests were performed, with the use of single ribbon elements. The ribbons were embedded in granular quartz in a 1-inch-

---

Paper 55-217, recommended by the AIEE Switchgear Committee and approved by the AIEE Committee on Technical Operations for presentation at the AIEE Winter General Meeting, New York, N. Y., January 31–February 4, 1955. Manuscript submitted October 21, 1954; made available for printing December 3, 1954.

A. H. POWELL and C. L. SCHUCK are with the General Electric Company, Philadelphia, Pa.

The authors acknowledge contributions by W. E. Brandt and E. M. Fitzgerald, who obtained and interpreted the preliminary data on ribbon elements at high voltages.

Table I. Values from Tests

Type of Fuse	Volts per Inch	Amperes per Arc Path
Low voltage (ribbons)	900	3,800
High voltage (wires)	300	650

diameter tube composed of glass cloth impregnated with melamine resin. Particulars of these tests series are given in Table II. The test results were interpreted as indicating that:

1. A considerable range of recovery voltage and short circuit current could be interrupted by a single ribbon in a strong resilient tube.
2. Interruption of high available currents was accompanied by the development of substantial momentary pressure, and was probably made possible by the ability of the tube material to withstand such pressures.
3. The full ribbon section (not only in the region of the holes, as in low-voltage tests) combined with the fused sand so as to be converted to the slaglike formation known as fulgurite and, in view of the less sharp current-limiting action, was required at high voltage to effect interruption.
4. The use of an adequate number of holes was important in realizing volt-per-inch values comparable to those obtained in low-voltage tests.
5. The single ribbon had difficulty in interrupting available currents greater than 43,000 rms amperes even though recovery voltage gradient was moderate.

Fig. 1 shows the sample after the last test listed in Table II.

Overload Tests

In view of the results obtained in the preliminary short-circuit tests, it was thought most important to establish the ranges of voltage and current in which ribbon elements could interrupt prolonged overloads with full recovery voltage. The development of high-voltage ratings using round wire elements had emphasized the difficulty that fuses of this type, unless properly designed, have in interrupting overload currents of magnitudes that cause melting after 10 to 15 minutes. Better results were obtained with multiple rather than with single elements, evidently because of the much higher current flowing in the last element to melt and arc. If ribbons were found usable, they could be used in given current ratings in fewer numbers than wire elements, so that a lower relative overcurrent would flow in the last ribbon to melt.

Overload tests were first made with a low-voltage test circuit to determine currents causing melting after times ranging from 10 to 20 minutes. Results of these tests on numbers of ribbons from 1 to 20 are shown by the curves of Fig. 2. The curves summarize two groups of data:

1. For ribbons having holes every 1/2 inch along their length, with tube dimensions noted in Fig. 2.
2. For ribbons as in Fig. 1, modified by addition of notches and tin alloy applied to the ribbons at the center hole.

The effect of the notches and alloy in a typical case of 10 ribbons is to reduce the current which will melt the fuse in 10 minutes from 705 to 480 amperes. This results in a less inverse melting time-current curve for a given current rating. This is desirable in fuses for general application, but for fuses used in motor controls it is more important that starting current can be passed without damage to the fuse elements. Accordingly, with motor control fuses, the notches and alloy spots are not employed.

The variable of ribbon (and tube) length was found to have negligible effect on the melting current for a given number of ribbons in the range of ribbon lengths of interest (9 to 17 inches). This was true only if the ribbons were mounted straight through, rather than being arranged helically or otherwise.

With melting current data established, full recovery voltage overload tests were performed in the Switchgear Development Laboratory. In Fig. 3, some of the samples are shown in their transparent Pyrex tubes, from which excess filler has been removed, following overload tests. Samples numbered 1, 2, and 3 show 1-, 6-, and 10-element fuses melted on a low-voltage circuit. Samples 4, 5, and 6 show 1-, 6-, and 10-element fuses after overload melting tests with recovery voltages of 2,640 to 2,700 volts. Comparing sample 1 with 4, 2 with 5, and 3 with 6, differences in fulgurite formation will show how interruption against substantial recovery voltage requires elongation of the arc and a filler capable of absorbing energy from the arcs without itself becoming conducting. With recovery voltage in the order of 2,650 volts and, with the number of ribbons increasing, the average length converted to fulgurite became less, leaving unconsumed silver ribbon at the ends of the fuse tube; see sample 5 of Fig. 3.

Tests of this kind were also carried out at higher higher voltage levels to establish the territory in which successful full-recovery voltage overload interruptions could be obtained, ribbon lengths being as long as 35 inches in some tests. The results fell into the pattern shown by Fig. 4. A definite voltage "ceiling" was found to exist, regardless of ribbon length available, or the slight improvement resulting from the use of multiple elements. This indicated that the most important factor involved is the rate at which the ribbons can burn back, enabling them to cope with voltage gradients only up to a specific limiting value. These results exclude the possibility of making use of ribbon elements in the important 15-kv ratings, but definitely show their applicability in the lower voltage ratings and in current ratings hitherto possible with wire elements only in fuse tubes of considerably greater volume.

In short-circuit tests to be described, it had been demonstrated conclusively that ribbon elements required a laminated glass cloth base fuse tube to cope with the pressure developed. In directly comparable full-recovery voltage overload tests, these tubes permitted somewhat better test results than Pyrex tubes; a fact which had not been expected in view of the higher temperature withstanding rating of Pyrex. Therefore, most of the full-recovery voltage overload tests were made using melamine glass cloth tubes.

Short-Circuit Tests

Results of the overload tests had brought into focus the voltage and current ratings in which further short-circuit tests should be made of fuses with ribbon elements. At the level of 40,000 asym-

Table II. Preliminary High-Voltage Interruption Tests

Series	Test Voltage, Rms, 60 Cycles	Available Current, Rms	Thickness, Inches	Length, Inches	No. of Holes, Spacing 1/2 Inch	Performance
A	1,150	950 to 25,000	0.0025	5½	3, 5, 7	cleared
B	5,700	485	0.0038	10½	3, 5, 7, 9, 13, 19	3 holes failed; all others cleared
C	2,750	43,000	0.0038	10½	19	cleared
	5,500	27,700	0.0038	10½	19	cleared
	5,500	85,000	0.0038	10½	19	failed
	8,250	92,000	0.0038	10½	19	failed
D	23,000	31,000	0.0038	27	53	cleared
	23,000	20,000	0.0038	27	53	
	23,000	20,000	0.0038	34	67	
	27,000	33,000	0.0038	34	67	

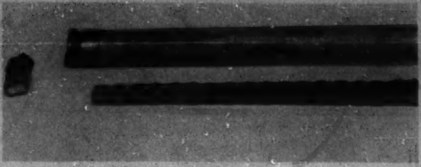

Fig. 1 (above). Developmental sample of current-limiting fuse with single silver ribbon element following interruption test. Fulgurite or slag formed shown in front of fuse tube and in section at left

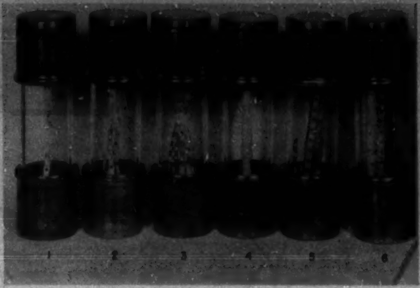

Fig. 3 (right). Developmental samples of current-limiting fuses with silver ribbon elements following overload tests

metrical amperes, a series of tests was made to compare the performance of multiple ribbon element fuses having Pyrex tubes with fuses having melamine glass-cloth tubes, at 2,650 volts, the maximum design voltage for 2,400-volt apparatus. The results, as illustrated by the oscillogram traces of Fig. 5, clearly showed that good performance depended on the use of the melamine glass cloth tubes.

In these oscillograms, the available current is shown by the dotted area and the time-current required for melting is shown by the cross-hatched area terminating at the time of the first substantial rise of arc voltage. Peak current at melting is indicated opposite the melting point on the current trace, and the decimal value opposite the peak current reached shows the fraction of the available peak current that was allowed to pass. The three tests at the top of Fig. 5 show Pyrex glass tubes incapable of withstanding the momentary internal pressure from operation of five or more parallel connected ribbons. Failures were marked by the glass being blown apart, pressure thereby being relieved, allowing the arc diameters to increase, and arc voltage to collapse. Pyrex was therefore abandoned as the tube material for ribbon element fuses.

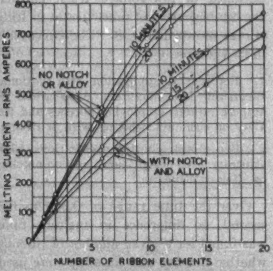

Fig. 2. Overload melting data applying to Pyrex or melamine glass cloth tubes 2$^{5}/_{8}$-inch outside diameter, 3-inch diameter ferrule, with granular quartz filler

With the glass cloth base tubes, satisfactory interruptions were obtained with numbers of ribbons up to 20 (the geometrical capacity of the 2$^{3}/_{8}$-inch inside-diameter tube), with approximately 1/4-inch spacing between ribbons; see Fig. 5, bottom, and Fig. 6, top. Tests at available currents of 60,000 rms amperes (Fig. 6, bottom) proved the ability of these rather crowded designs to interrupt 150,000 symmetrical kva on a three-phase basis. The fulgurite or slag formed in a typical short-circuit test is shown next to the fuse tube in Fig. 7. Further similar tests demonstrated the ability of longer ribbon element fuses with melamine glass cloth tubes to interrupt current equivalent to 250,000 symmetrical 3-phase kva at 5,500 volts.

Compared with typical oscillograms of short-circuit interruptions by silver wire elements, the oscillograms of Figs. 5 and 6 show that with ribbon elements the current-limiting action is somewhat less prompt following melting. With wire elements, melting is followed by an immediate reduction in current, with arc voltage rising sharply to a peak usually substantially higher than the peak of normal frequency recovery voltage. The initial rise of the arc voltage with perforated ribbon elements is seldom greater than 50 per cent (%) of this value, which might be expected on the basis of the short effective lengths of the reduced cross sections at the holes in the ribbons.

The major peak of arc voltage occurs later, at a time corresponding to melting of the full-ribbon section. This was checked in each of the short-circuit tests made, by calculation of the heating effect of the actual current flowing up to the time of the rise to the major arc voltage peak. Thereafter, the current-limiting effect is greatly accelerated, and interruption is completed at or slightly after the subsequent generated voltage zero.

The result is that in the time interval between melting of the reduced sections at the holes to melting of the full-ribbon sections, the current permitted to pass is greater than for comparable wire elements. However, the over-all current-limiting effect is quite pronounced, as may be seen by comparing the traces of actual current in Figs. 5 and 6 with the dotted areas showing the available currents.

VOLTAGE PEAKS

In the development of wire element current-limiting fuses, the rapid increase in arc voltage following melting called for special features in the fuse element design to limit the transient voltage peaks to acceptable values.[3] Cathode-ray oscillograms taken with each short-circuit test of ribbon elements provided a more detailed, but similar, account of arc voltage to that obtained with the magnetic oscillograph.

For ribbon element fuses tested at 2,650

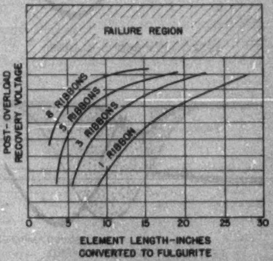

Fig. 4. Summary of full-recovery voltage overload tests on silver ribbon element current-limiting fuses

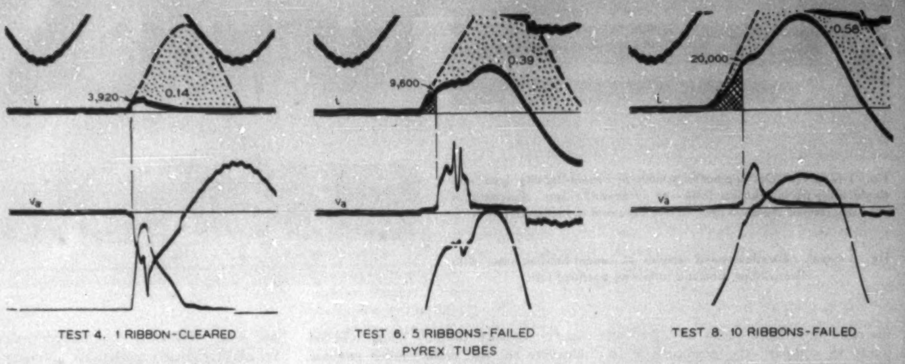

TEST 4. 1 RIBBON-CLEARED

TEST 6. 5 RIBBONS-FAILED

TEST 8. 10 RIBBONS-FAILED

PYREX TUBES

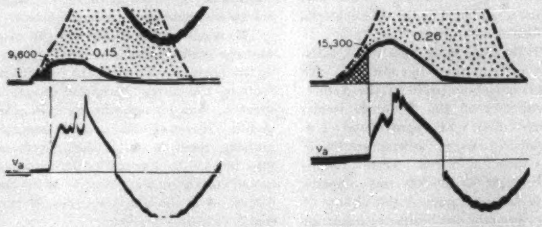

TEST 9. 5 RIBBONS-CLEARED

TEST 10. 10 RIBBONS-CLEARED

MELAMINE GLASS CLOTH TUBES

Fig. 5. Oscillogram current and arc voltage traces of short-circuit tests on multisilver ribbon element current-limiting fuses at 2,650 volts rms

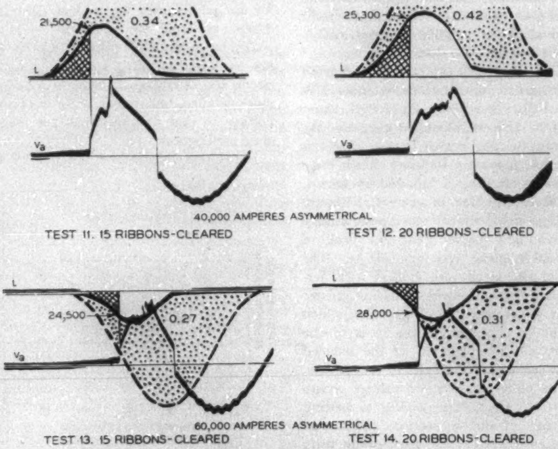

40,000 AMPERES ASYMMETRICAL

TEST 11. 15 RIBBONS-CLEARED

TEST 12. 20 RIBBONS-CLEARED

60,000 AMPERES ASYMMETRICAL

TEST 13. 15 RIBBONS-CLEARED

TEST 14. 20 RIBBONS-CLEARED

MELAMINE GLASS CLOTH TUBES

Fig. 6. Oscillogram current and arc voltage traces of short-circuit tests on multisilver ribbon element current-limiting fuses at 2,650 volts rms

and 5,500 volts, arc voltages reached respective levels only 39% and 17% higher than normal frequency recovery voltage peak (averaging all short-circuit tests). Maximum peaks in any tests were 1.76 and 1.53 of crest respectively. Analysis of the records showed no clear trend in peak voltage either with the number of ribbons or with the available current. Rates of increase did not exceed 100 volts per microsecond at any stage of the interruptions, and oscillations were substantially absent as a result of generated voltage being close to zero at the time arcing ceased.

INTERMEDIATE CURRENT INTERRUPTION

In addition to full-recovery voltage overload and short-circuit tests, interruption tests were made at intermediate levels of available current to check ability to interrupt and to obtain melting time-current data. Typical performance from tests made at 2,650 volts is indicated by data given in Table III. These, in conjunction (and close agreement) with data obtained in low-voltage tests, enabled the establishment of time-current melting curves shown in Fig. 8. The curves are in two groups:

1. For general application with National Electrical Manufacturers Association *E* ampere ratings, employing notches and tin alloy on elements, whether wire or ribbon.
2. For motor control applications with arbitrary sized designations, and no notches or alloy on elements.

Over the time range of 0.006 to 0.3 second, no difference in melting time was found for a given number of ribbons whether notches and tin alloy were used on the elements or not. For lower currents and longer times in which metallurgical changes have more chance to take effect, the curves have different

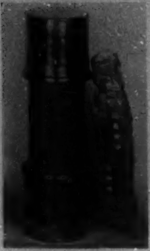

Fig. 7. Developmental sample of current-limiting fuse with silver ribbon elements. Melamine glass cloth fuse tube. Fulgurite formed in short-circuit test shown at right

shapes, as they must, since the overload melting currents are so different; see Fig. 2. In both groups the new curves applying to ribbons, shown by the dashed lines in Fig. 8, should lead to advantages from an application standpoint.

In typical high side transformer applications, the higher position of the fuse time-current curve will permit the use of feeder air circuit breakers with higher trip settings than otherwise. In motor control applications, the new curves should permit use of larger motors with given fuse sizes. The curves of Fig. 8 are matched on the basis of overload melting currents for standard National Electrical Manufacturers Association current ratings in the *A* group, and for established sizes of fuses for motor controls in the *B* group. The number of ribbons appropriate for each case are shown in Table IV, and ratios of quantities bearing on performance are listed. The lower number of ribbons than wires for a given rating is less demanding of internal fuse volume, and has enabled substantial over-all size and weight reductions in these ratings.

The near equivalence of element cross sections at the holes in the ribbons with those of the wires makes for close correspondence in the positions of the lower ends of the time-current curves; see Fig. 8. The threefold increase in section, considering the full ribbon, results in lower over-all fuse resistance, as indicated in the last column. This produces less heating with the fuse-carrying load current, even in spite of size reduction which reduce the fuse external surface available for dissipation of heat. The 3.4- to 3.9-fold increase in element surface in contact with filler grains is believed the factor principally responsible for the ability to interrupt as high as 1,500 amperes per ribbon.

TUBE STRENGTH

Pressure developed inside the fuse tube increases with the arc energy developed during interruption; and it is important to obtain a quantitative measure of the margin between the arc energy produced by rated interrupting current and voltage and that required to burst the tube. In Fig. 9, a sample is shown following a short-circuit test at higher-than-rated current and voltage in which sufficient pressure was developed to break the melamine glass cloth tube radially. Based on a hoop tension calculation and using the tensile strength rating for this material, the pressure reached approximately 4,100 pounds per square inch.

Arc energy evaluated from the oscillogram up to the time of arc voltage collapse was 101 kilowatt-seconds per inch of tube length. For designs listed in Table IV, arc energies involved in interruptions do not exceed 32 kilowatt-inches for 2,500-volt ratings and 48 kilowatt-inches for 500-volt ratings. The results are based on tests at maximum design voltages and at available currents corresponding to the interrupting ratings.

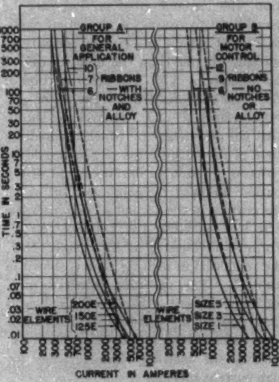

Fig. 8. Comparison of melting time-current characteristics: silver ribbon versus silver wire elements, 2,400 volt ratings

Fig. 9. Developmental sample of current-limiting fuse with silver ribbon elements. Sample shown following short-circuit test to destruction to determine limit of melamine glass cloth tube

SHORT-TIME MELTING

For both wire and ribbon elements embedded in granular filler, the melting time at moderate currents is increased by dissipation of heat through the filler. Assuming that at high available currents no heat is lost in this way during the short melting times involved, the melting time and current are related by

$$\int i^2 dt = KS^2 \qquad (1)$$

where

i = instantaneous current-amperes
t = time, seconds
K = constant
S = element cross section, circular mils

When several cycles of current are involved, equation 1 may be written

$$I^2 t = KS^2 \qquad (2)$$

where I is the rms current magnitude (symmetrical), and on conventional log-log time-current plots, the relation may be represented by a straight line of slope, 2 to 1.

In view of the high subcycle speed with which fuses of this type interrupt, and recognizing that the lower limit of con-

Table III. Intermediate Current Interruption Test Data

No. of Ribbons	Available Rms Amperes, Symmetrical	Melting Time, Cycles	Arcing Time, Cycles	Performance
6	1,600	14.0		cleared
6	3,100	0.95	1.4	no disturbance
12	3,900	5.3	1.4	
10	6,500	0.4	0.5	
12	7,230	0.5	0.8	

Table IV. Ribbon Versus Wire Elements

				Ratios, Ribbons to Wires			
				Cross Section			
Group	Rating or Size	No. of Wires	No. of Ribbons	At Holes	Full Ribbon	Element Surface*	Fuse Resistance
A	125E	32	6	0.97	3.1	3.7	0.58
	150E	39	7	0.93	2.9	3.5	0.62
	200E	48	10	0.97	3.1	3.9	0.59
B	1	32	6	0.97	3.1	3.7	0.60
	3	48	9	0.87	2.8	3.5	0.67
	5	60	12	0.76	2.4	3.4	0.72

*Full ribbon to minimum wire diameter used.

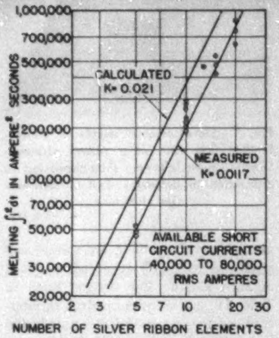

Fig. 10. Summary of short-circuit melting data indicating melting of silver ribbons at high currents faster than calculated

ventional time-current plots for co-ordination purposes is 0.01 second, Gibson[4] has proposed a "virtual-time" method for extending the melting and arcing time-current curves below 0.01 second to enable co-ordination studies involving such fast acting fuses. According to his method, the melting characteristic is simply continued downward to higher currents and shorter times at slope 2 to 1, and actual arcing time-current is assigned an equivalent or virtual value of time based on the symmetrical rms current available, i.e.

$$t_{v(\text{arcing})} = \frac{\int i^2 dt_{(\text{arcing})}}{I^2} \qquad (3)$$

The slopes of the curves for ribbons at 0.01 second, Fig. 8, are considerably higher than 2 to 1, being more nearly 3.5 to 1, for this melting time. This shows another influence at work, tending to bring about melting more rapidly than otherwise.

The constant K is proportional to the element metal's specific heat, its density, and the temperature rise required to reach melting, and is inversely proportional to its resistivity corrected or averaged through the temperature range. For small diameter silver wires, test results show K adhering to the theoretical calculated value 0.021, but for large diameter wires, a survey of melting data shows a definite reduction in this figure as wire diameter increases.

Table V. Reduction in Melting Time

ΔJ	Reduction, %
0.10J	9
0.25J	20
0.50J	33
1.00J	50

With ribbon elements the effect is even more pronounced, S being based on the cross section of silver outside the holes. In Fig. 10, a summary of measurements made from oscillograms of short-circuit tests is shown in comparison with the theoretical value of 0.021 for K. An average curve drawn through these data indicates an effective value of K of 0.0117, a reduction of 44%. The effect evidently overrides any loss of heat from the reduced sections at the holes to the full sections, and in turn to the filler, as appears to predominate at more moderate currents.

The most apparent explanation for this effect is believed to be a nonuniform distribution of the current over the ribbon or wire cross section (skin effect). If it is assumed that current is initially denser in the outer portions of the cross section, and that once these have melted the current becomes more concentrated in the inner portions, the over-all melting time can be shown to be reduced.

As a simple quantitative approximation, the element cross section may be considered to consist of two equal parts, in one of which the current density is initially greater than the uniform case J by an amount ΔJ. The other portion of the cross section then has the lower current density $J-\Delta J$. It may be shown that the percentage by which the melting time of the entire cross section would be reduced for such an initial current distribution followed by concentration of all the current in the second section after the first has melted is $100\{1/[1+J/(\Delta J)]\}$. For several values of ΔJ with respect to J, the reduction in melting time is shown in Table V. This observed reduction in K for large-element cross sections indicates that, in applying Gibson's method, some adjustments become necessary when extending the melting characteristics for high current ratings.

New Fuse Construction

The findings from the investigations described make possible more compact designs in the ratings indicated. Their reduction to practice provides an opportunity for introducing certain further improvements in design and manufacturing methods. Any time that a fuse, or any device, can be simplified and the manufacturing operations mechanized, the resulting product will be improved. The advent of the ribbon element now makes simplification of the current-limiting power fuse a reality.

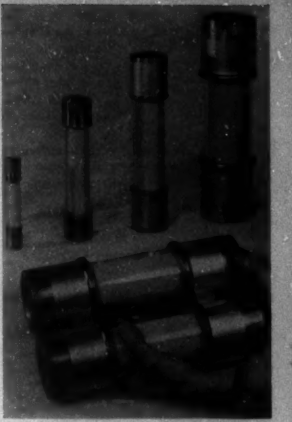

Fig. 11. Existing line of 2,400-volt current-limiting fuses. Wire elements in Pyrex tubes

ELEMENTS

The existing line of fuses, shown in Fig. 11, uses a multiplicity of silver wires. In the voltage range discussed in this paper, i.e., 2.4 and 4.8 kv, as many as 30 wires are strung straight through the tubes. The wires are made by welding together short lengths of various diameters to obtain a "stepped" section for successive melting and voltage control as described previously.[3] They are then strung through the tube and attached to contact supports at each end. A long needle and considerable skill are needed for this operation. The wires are then electrically attached by welding to the ferrules. The chances of overstressing the relatively fine (0.005 to 0.010-inch diameter) wires and the time involved in the stringing operation are obvious.

The new element described earlier, using a ribbon of silver, now makes simplification of the assembly an accomplishment. The ribbon is obtained with the thickness held to tolerances of + or −6% and is passed through rotating dies which punch out the necessary holes and notches. It is also notched to indicate the correct length and then cut into sections from a coil as required. The new-style element supports which are used only to space the elements are held in place between the ferrule and tube end. Of course, fewer ribbons are needed as compared with the wire elements, but provision is made for 10 elements for a continuous maximum rating of 200 amperes. The ferrules are silver plated, and the elements, after insertion, are positioned in the supports and then bent over the edges of the ferrules, ready for final attachment.

TUBE, FERRULES, AND INDICATOR

Most of the present line of fuses with wire elements use a heat resistant glass for the fuse tube, to which are attached copper ferrules using an antimony-lead compound. This construction is tight and strong, but as the glass is weak when subjected to tension stress such as that caused by a momentary pressure inside the tube during short-circuit interruption, a better material will result in improving the interrupting ability as was discussed earlier.

Tubes made of melamine-impregnated Fiberglas have been thoroughly investigated from several points of view including heat-withstand ability, dielectric strength, tracking characteristics, and bursting strength. It has proved to be very good and therefore it was possible to use such material for the new fuse tube, with a thinner wall than the glass to provide more volume for the filler material. The ferrules are pressed onto the tube. A light coating of cement is applied to the tube before assembly to make a watertight seal for outdoor weather condition. Fig. 12 shows the tube and ferrule assembly.

The new ferrule is made by cold working (expanding) high-conductivity copper tubing in order to obtain a smaller diameter section just below the cap to provide space for crimping the caps to the ferrules. The cap for the top of the fuse is plain, although it could include nameplate data, while the bottom cap includes means for indicating that the fuse has operated.

The indicator design has also been improved to obtain greater reliability and easier visibility. A current-sensitive restraining wire is used to hold a light weight, 3/4-inch-diameter indicator (which is in the form of an inverted cup in the recess in the cap) against the force of a compression spring. The insulator closure and holes through which the wire passes, are sealed against the entrance of moisture. The indicator element is in parallel with the main element so that when it melts during fuse operation, the current through the indicator which has been relatively small is quickly increased to a high value. The element embedded in the filler requires more current for melting than does the section in air, inside the indicator. Therefore the section in air melts first, releasing the plunger and the remainder of the element in the filler melts later, performing its function of interrupting the follow current.

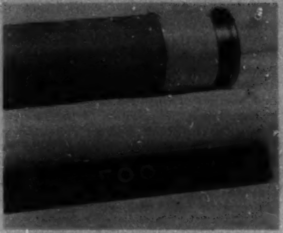

Fig. 12. One end of tube and ferrule with end cap in place ready for crimping silver ribbon elements between cap and ferrule

ASSEMBLY

The ferrules are pressed onto the fuse tube by means of a hydraulic press. The elements are located in the tube and the ends of all the ribbon elements are bent over the edges of the ferrules. This provides a direct path for the current from the elements to the ferrules.

The end cap with indicator which also includes a light gasket for sealing purposes is crimped to the ferrule, and the indicator element is pulled to the other end of the fuse and attached to the element support. The tube is then filled with the special quartz granules that provide the interrupting ability, and after the fuse is vibrated to make sure the tube is completely filled, the other cap with built-in seal is attached by crimping to the flange on the other ferrule. The cold-formed crimp and gasket provide a watertight and completely secure seal and a tight, metal-to-metal contact between the elements and the ferrules. This completes the assembly operation, in which modern manufacturing and metal-working operations have eliminated guesswork and operator skill to produce a completely reliable power fuse.

Tests and Quality Control

During the development of a new fuse with ribbon-type elements, many series of tests have been required to obtain all pertinent data and prove the conclusions. The last step in the project involves proof testing of the final design based on production tool-made samples. Such tests follow the pattern proved successful in the past and include: 1. full-capacity short-circuit interruptions, 2. low-voltage melting tests to obtain time current data, 3. full-voltage long-time interruptions with the recovery voltage maintained for approximately 30 seconds to check for postinterruption failure, and 4. a number of tests at intermediate values, particularly at maximum energy values for the rating involved. Such a series involves a large number of tests under conditions requiring accurate measuring equipment and careful control. Such tests are made on the maximum voltages and currents in each fuse frame size, and on at least two lower intermediate ratings.

The design tests are then supplemented by quality control tests, planned on the basis that all ratings will be checked every 2 years. These have proved adequate as the material in the fuse is all carefully controlled and every fuse receives a resistance check with the use of a double-bridge type of instrument. The resistances of the fuse ratings are held to within a tolerance of + or −5% to ensure meeting industry standards which provide for an over-all tolerance of 20% in melting current.

Conclusions

A new high-voltage current-limiting power fuse has been developed and the problems associated with the design and production of the fuse described. A new type of element, in the form of a flat ribbon, is used, mounted in a strong tube with a new type of ferrule to eliminate soldering and welding operations. The resulting fuse is smaller and of lighter weight for many of the ratings, and more ratings are available than in the previous line of fuses. A current-limiting, high-interrupting capacity fuse with ratings up to as much as 400 amperes at 2.4 or 4.8 kv is now a reality.

References

1. The Current-Limiting Power Fuse, D. C. Prince, E. A. Williams, Jr. *AIEE Transactions (Electrical Engineering)*, vol. 58, Jan. 1939, pp. 11–18.

2. A New High Interrupting Capacity Low-Voltage Power Fuse, C. L. Schuck. *AIEE Transactions*, vol. 69, pt. II, 1950, pp. 770–76.

3. Control of the Switching Surge Voltages Produced by the Current-Limiting Power Fuse, E. A. Williams, Jr., C. L. Schuck. *AIEE Transactions (Electrical Engineering)*, vol. 60, May 1941, pp. 214–17.

4. The Application and Standardization of High Rupturing Capacity Current-Limiting Fuses, J. W. Gibson. *AIEE Transactions*, vol. 72, pt. II, May 1953, pp. 126–32.

◆

Discussion

W. A. Gaskill (Westinghouse Electric Corporation, East Pittsburgh, Pa.): The high-voltage current-limiting fuse is relatively new in fuse art and consequently little basic design information is available. So many interrelated factors affect the interrupting ability that it is difficult to evaluate their individual effect on the performance of the fuse. Considerable design data exists on the low-voltage fuses but as the authors pointed out it is not directly applicable to high-voltage fuse design. The manufacturers must therefore spend considerable time and money in obtaining basic design information prior to developing and verifying a fuse design for production. All causes of failures of experimental fuses should be thoroughly investigated to make certain that the conclusions reached are valid.

We feel that the authors have not thoroughly investigated all possible causes of the failures they experienced. One of the most important considerations in the design of current-limiting fuses is the relationship between filler particle size and the wire or ribbon dimensions but nowhere in the paper is this discussed. A small grain size physically restricts the arc and produces a desirable high arc voltage. Also the small grains impede the flow of the silver vapors through the filler and produce a high pressure in the region of the arc. This pressure acts on the surface of the filler and produces a large radial impulse force which is transmitted through the filler to the outer tube. If a filler grain size smaller than the optimum size was used on these tests, it could well be the explanation for the failure of the Pyrex glass tube.

The use of reduced sections in fusible elements for high voltage fuses is not new. In 1944 Rawlins and Fahnhoe[1] presented a paper on a new 3-element current-limiting power fuse in which they discussed the advantages of reduced sections and the design of a fuse with the use of this principle. The spacing between reduced sections was 1/8 inch and the oscillograms showed that the initial arc voltage developed was sufficient to force an immediate reduction in current.

It is not surprising that the authors of the present paper experienced somewhat less prompt current-limiting action immediately following melting compared to solid wire elements, when it is considered that they were using a spacing of 1/2 inch between holes. The number of series arcs produced was not sufficient to produce an immediate reduction of current. This is also a possible explanation for the erratic arc voltage trace obtained on most of the tests in Figs. 5 and 6. The reduced sections in the holes melted and produced insufficient arc voltage. The current continued to increase, producing considerable energy in the region of the holes. This energy was absorbed by a relatively small volume of filler which shortly became a conductor. The formation of these conducting fulgurites reduced the arc voltage and permitted more current to flow. As the sections between the holes vaporized, the arc voltage increased. This oscillating condition between the build up of arc voltage and the reduction of arc voltage by the formation of conducting fulgurites probably accounts for the erratic arc voltage trace.

If the arc voltage produced by the melting of the reduced sections in the notches or holes is not adequate to force an immediate reduction in current, the benefit of the reduced sections is not realized. They are actually a detriment, since arc energy is being dissipated in the fuse while the remainder of the fusible element melts to produce the necessary arc voltage.

A study of the oscillograms in Figs. 5 and 6 reveals that on most of the tests the actual current deviated considerably from the available current prior to melting of the first portion of the fuse elements. If the explanation is the addition of the fuse resistance to the circuit, a larger voltage drop across the fuse during melting would be expected. The current at the instant of melting on test 13 is only one-half the available current at that time. On test 14 the two current traces coincide. The voltage appears to be of the same value on both tests 13 and 14.

Symmetrical short-circuit current tests were noticeably absent in this paper, although it was shown by Prince and Williams (see reference 1 of the paper) that the let-through current is considerably greater on symmetrical tests over 10,000 amperes than on asymmetrical tests. Also the recovery voltage conditions are more severe on the symmetrical tests.

REFERENCE

1. A NEW THREE-ELEMENT CURRENT-LIMITING POWER FUSE, H. L. **Rawlins**, H. H. **Fahnhoe**. *AIEE Transactions (Electrical Engineering)*, vol. 63, Apr. 1944, pp. 156–59.

T. J. Render (General Electric Company, Schenectady, N. Y.): When one familiar with standard low-voltage cartridge-type fuses considers the present design of the high-voltage current-limiting fuse, he cannot help but wonder why ribbon elements are not used in place of round wires. The reason for the design difference, as mentioned in the article, is the requirement of a tolerable number of volts per inch of active fuse element and the permissible amperes per arc path.

The early concept of fuse design was to have a single arc occur near the center of the wire. The ribbon-type fuse makes use of a later concept whereby a series of small arcs are formed. This provides a more uniform dissipation of the arc energy and results in a lower recovery voltage.

As shown in the paper, the phenomena of fuse-wire disintegration limited the design of fuses employing a number of parallel wires. With the introduction of ribbons, the series of arc interruptions has been shown to follow the pattern of the unduloid, producing fulgurites the full length of the multiple-arc paths. The pressures resulting from arc interruption in this manner are higher than obtained by the use of parallel wires. Hence the need for a stronger, more resilient confining medium such as the melamine glass tubing.

The new ribbon-type design of high-voltage current-limiting fuses offers many advantages over previous designs. These points are as follows:

1. A higher current rating is permitted. This means that fused starters can be built for larger motors than was previously possible.
2. The new fuse is smaller in size. This saves space in the control panel and makes handling of the fuse easier.
3. Through reduction in size, the weight of the fuse has been decreased. Since the old design of fuse was quite heavy, any weight reduction is an obvious improvement.
4. The melamine glass cloth tubing eliminates the possibility of fuse breakage due to improper handling. The presence of a glass barrel on a large, heavy fuse necessitated much additional care in its usage.
5. The peak arc voltages reached during operation of the ribbon-type fuses are considerably less than those of the wire-type fuse. Circuits are thus not subjected to as high transient voltages as before.
6. The melting time of the ribbon-type fuses under full short-circuit conditions is less than that required for the wire element fuse.
7. The melting time-current characteristics of the new fuse have a less inverse characteristic, allowing greater freedom of co-ordination of the new fuse and feeder circuit breakers. It also allows application on larger sized motors per given fuse size without danger of blowing the fuse prematurely on either starting inrush or rapid duty-cycle operations.

In view of these many advantages, the new ribbon-type high-voltage current-limiting fuse is a definite advancement in the art, incorporating all of the latest techniques concerning the phenomena of fuse element disintegration. It fills the need for a fuse which can be used with the increasingly larger motors of today's industries, and which will better co-ordinate with other protective devices of industrial power distribution systems.

A. H. Powell and **C. L. Schuck:** The authors regard the discussions as evidence of a growing interest in circuit protection by current-limiting power fuses and benefits that may be made available by their continuing development.

Mr. Gaskill expresses concern regarding some of the same design problems that have required investigation in this and earlier development work (see references 1 to 3 of the paper). An adequate treatment of the fuse filler and its optimum grain size (and grain shape) could well be the subject of a separate paper. We began such investigations in 1934 and in varying degrees have been studying the problem ever since. In 1943, in connection with the development of motor control fuses having large diameter elements, quartz sand was obtained from several sections of the country in available grades and their interrupting merits were evaluated. Screen analysis showed that each grade was composed of a range of grain sizes following a typical distribution with more or less spread. The interruption tests showed that superior performance resulted when the spread was small and when the very fine grains had been eliminated.

For the present development, the filler arrived at in the aforementioned work with large wires was employed. The relative flatness of curves of interrupting ability versus grain size in the region of interest led us to conclude that any refinement in determining an optimum grain size for ribbons could not be the key to such vast differences in performance as those obtained with Pyrex tubes versus laminated glass cloth tubes.

The use of reduced wire element sections is indeed not new (see reference 2 of the paper) but these results cannot be applied directly to ribbon-shaped elements. Further considerations are the influence of the size, shape, and spacings of reduced sections on the melting time-current characteristics, and on the over-all fuse resistance. From the interruption standpoint alone, there may be variations in holes or other shapes for the reduced sections and their spacings, which might yield advantages of different kinds in low voltage fuse designs, but for high-voltage applications, the use of 1/2-inch spacing is believed close to the optimum. This is based on results of tests with hole spacing from 1 inch down to 3/8 inch. From the melting time-current and resistance standpoints also, the 1/2-inch spacing appears most satisfactory, as closer spacing would yield less short-time capacity and higher resistance, with no improvement in short-circuit performance.

The arc voltage records are consistent in their main features and erratic only in respect to minor fluctuations with time common to the voltage drop across high-current arcs of many forms. The principal features of the arc voltage as described in the paper are believed to be characteristic of ribbon elements with reduced sections, for which the substantial difference in heat capacity of the full and reduced sections results in 25 to 30 electrical degrees' difference in their melting times on maximum available currents. Thus the full sections play the role of back-up by furnishing their length of newly formed arcs to produce the additional arc voltage needed.

In the oscillogram for test 14 of Fig. 6, the available current as Mr. Gaskill points out, does not appear to bear the same relation to the current up to the time of melting as in the other records. The current and arc voltage traces were reproduced directly from the oscillograms, but a recheck of the estimated available current indicates that it should have been sketched in somewhat higher in the first part of the loop.

Regarding test current symmetry, Prince and Williams (see reference 1 of the paper) show greater peak current when the available current is symmetrical for fuses of low ampere ratings. The present paper deals with fuses of high current ratings, for which melting currents are higher when the available current is asymmetrical. Also, the time interval until the next voltage zero is longer, making for more severe arcing. These and other factors contributing to test severity have been outlined (see reference 1 of this discussion).

Mr. Render's comments reflect the problems that users of motor starter fuses have encountered, and serve to emphasize the advances in the art which will occur as a result of the new fuse that the paper describes. The comments raised concerning the unduloid type of formation are interesting, but the fulgurite formation in the fuse, Fig. 1, is probably due more to the original element configuration. In low-current fuses with silver wire elements, melting of the elements by overload currents makes the material go into globules before separating. A similar procedure may be involved to some extent in the breakup of the ribbon when high available currents are interrupted, but then the effect is less susceptible to direct observation.

REFERENCES

1. PERFORMANCE CRITERIA FOR CURRENT-LIMITING POWER FUSES—I, E. W. Boehne, C. L. Schuck. *AIEE Transactions*, vol. 65, 1946, Figs. 5 and 6, pp. 1028–1045.
2. *Ibid.*, Part II, pp. 1034–44.

Pittsburgh Downtown 69-Kv Power Supply

Part I. Planning

V. E. HILL
MEMBER AIEE

EARLY in the redevelopment program of downtown Pittsburgh, it became evident that the existing facilities supplying electric power to this area would soon be inadequate and that major capacity additions would be required to serve this vital and rapidly increasing load.

The purpose of this paper is to describe the conditions existing in 1950 when the forecasted loads indicated that a major expansion program would be needed, and the reasons for adopting a plan involving 69-kv pipe-type cable and a new 69/12-kv substation. Two companion papers[1,2] present details of the structural and electrical design characteristics of the substation and of the electric equipment in the substation.

Load Area, Growth, and Present Downtown Power Supply

The downtown area of Pittsburgh including numerous large department stores and office buildings up to 40 floors in height is located between the Monongahela and Allegheny Rivers where they join to form the Ohio River. A geographic map of the area involved is shown in Fig. 1, and the area in question consists of about 1 square mile.

The power supply for this area in 1950 was obtained primarily from 17 12-kv cables emanating from an isolated phase switchhouse at the Brunot Island-Reed Power Stations, which are located on the Ohio River about 3 miles below the downtown area. Normal summer rating of most cables is 6,400 kva each.

Nine of the 17 cables supply three substations—Grant, Stanwix, and 13th Street—where the voltage is stepped down to 4 kv for distribution to some of the buildings. The remaining eight 12-kv cables supplied the 120/208-volt network that was started in 1926 and which has picked up most of the new loads since that time. There are two independent sections of the network known as the Area-2, 12 kv, and the Area-4, 12 kv, as shown in Fig. 1. (Several additional network feeders were authorized in 1949; subsequently five feeders were set up to carry the increasing load because of the long time involved in installing the 69-kv project.)

The area load also included some street railway's load supplied through rotary convertors and motor-generator sets at Grant and 13th Street Substations. There are two small 120/208-volt networks supplied at 4 kv, one from Grant and one from Stanwix, but these are not pertinent to this discussion; they will not be expanded and fringe areas will be cut to a 12-kv supply to prevent an increase in load on these areas.

Load growth in the area is shown in Fig. 2. Beginning about 1946, the summer peaks in this area exceeded the winter peaks primarily because of the growth of air-conditioning load and, therefore, the summer peaks are shown from 1946 on. The total load in this area in 1949 was about 75,000 kva, the growth from 1928 to 1949 being only 3.0 per cent compounded annually. Because the three substations were loaded up very nearly to capacity, most of the growth took place on the 12-kv network; it showed a growth of 8.4 per cent compounded from 1928 to 1950.

Growth of this area over the years has been less than for the system as a whole.

Paper 55-225, recommended by the AIEE Switchgear Committee and approved by the AIEE Committee on Technical Operations for presentation at the AIEE Winter General Meeting, New York, N. Y., January 31–February 4, 1955. Manuscript submitted October 19, 1954; made available for printing December 15, 1954.

V. E. HILL is with the Duquesne Light Company, Pittsburgh, Pa.

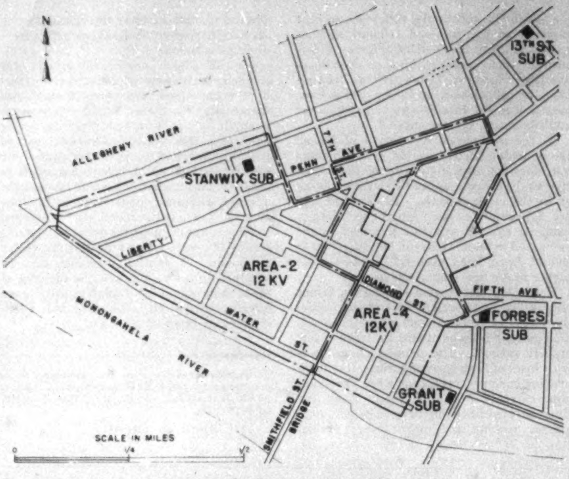

Fig. 1. Map of downtown area of Pittsburgh showing existing substations, network areas, and proposed new Forbes Substation

Fig. 3 shows the ratio of the downtown load to the total system load. This graph is based on the downtown and system winter peaks since the system peak definitely occurs in the winter time.

New Facilities Required

About 1950, the first signs of the now widely publicized redevelopment program were being observed. Several new large office and apartment buildings were either started or in the planning stage. Increased load was also expected from several existing customers. The new large office buildings at the Point, however, were still only in the talking stage. Thus, it was evident that an appreciable increase in the area load was to be expected and it was also realized that existing facilities were subject to limited expansion. The subsequent total area load growth, shown in Fig. 2, from 1950 to 1954 was at a rate of almost 6 per cent and has substantiated what was at that time a forecast of sharply increasing load growth.

Hence, a major decision for the proper method of supplying adequate capacity for long-range growth had to be made. Expansion could be provided for by three general methods as given in the following.

12-KV EXPANSION

Continued expansion at 12 kv would have required a new duct line from the Brunot Island-Reed Power Stations to the downtown area, as all the existing duct lines were very nearly filled up. Some capacity could have been obtained by replacing the old small cables with higher capacity cables, but the total amount of capacity thus gained would have been relatively limited.

Additional switching facilities would have been required at the isolated phase switchhouse on Brunot Island to take care of additional cables; as a matter of fact, many of the feeder circuit breakers now serve bifurcated cables. The switching facilities in the switchhouse were of obsolete design and could no longer be purchased. Some of the busses were being loaded above their ampere ratings. Hence, if expansion were continued at 12 kv, it would have meant an addition to the switchhouse, presumably of an entirely new design.

The only means of controlling the voltage of the low-tension network is by adjusting the generator voltages which supply the 12-kv bus at Brunot Island-Reed. In view of the fact that other 12-kv cables emanating from Brunot Island-Reed supplied residential and light industrial areas with different load cycles than the downtown area and because of tight ties with other power stations through the 69-kv transmission, it was not possible to adjust generator voltages to accommodate the network requirements as much as would have been desired. Consequently, installation of individual 12-kv feeder regulators has been considered from time to time in the past. These installations would have been both costly and cumbersome to connect.

23-KV EXPANSION

Outside of the downtown area and the area immediately adjacent to Brunot Island-Reed, the main subtransmission

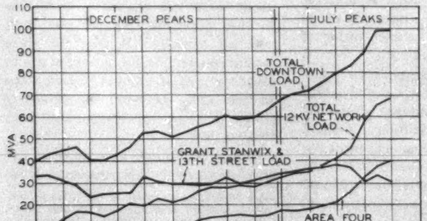

Fig. 2. Load growth in the downtown section of Pittsburgh

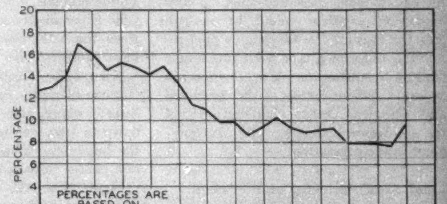

Fig. 3. Downtown Pittsburgh total load expressed as a percentage of the total system load

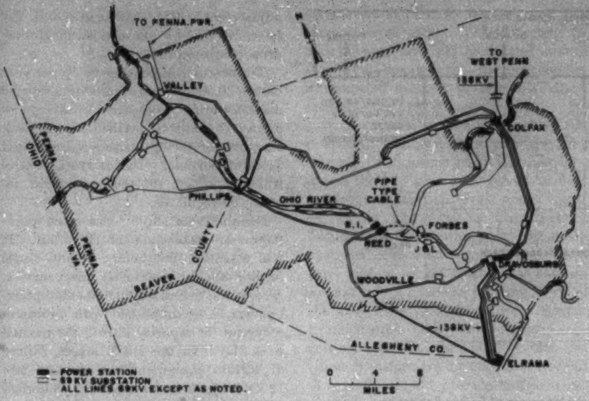
TO PENNA. PWR.
N
TO WEST PENN
138KV
VALLEY
COLFAX
PENNA
OHIO
PIPE TYPE CABLE
PHILLIPS
OHIO RIVER
B.I.
FORBES
REED
J&L
COUNTY
DRAVOSBURG
PENNA
W.VA
BEAVER
WOODVILLE
138KV
ALLEGHENY CO.
ELRAMA
POWER STATION
69KV SUBSTATION
ALL LINES 69KV EXCEPT AS NOTED.
0
4
8
MILES

Fig. 4. Location of proposed pipe-type 69-kv cable with respect to existing transmission system

voltage throughout the Duquesne Light Company system is 23 kv. Although, there are several 23-kv lines out of Brunot Island-Reed, none supply or even approach the downtown area. Nevertheless, some brief consideration was given to utilizing this voltage, either for the downtown or some of the adjacent areas.

The Brunot Island-Reed 23-kv lines are supplied by 12/23-kv step-up transformers. A 23-kv supply line for the downtown area would have meant an appreciable increase of step-up or step-down transformer capacity at Brunot Island and of step-down capacity in the downtown area. The latter would have been necessary because all the network transformers were rated at 12 kv and to replace them would have involved an enormous expense. Obviously, 23 kv had very little to offer.

69-Kv Expansion

At this time, the maximum transmission voltage, on the Duquesne Light Company system was 69 kv. It was available at Brunot Island-Reed, so that it was only natural to consider it for supply to the downtown area. This voltage is, of course, also used in metropolitan areas of other cities and has the initial merit that almost any type of cable installation would have a relatively large capacity which would take care of long-range growth.

In the interest of economy, the first consideration was to install a single radial 69-kv cable to a single transformer, with no high-tension switching. The transformer would step down to 12 kv and, by means of six stub feeders, would supply existing substations and part of the 12-kv network. This scheme would mean falling back on the emergency ratings of the existing 12-kv cables in the event that the 69-kv cable or transformer was out of service. This principle had been applied very successfully on another part of the system for many years before it became necessary to install the second line and transformer.

However, this scheme was deemed unsatisfactory in this instance for several reasons, the paramount one being that, by a relatively short extension of the proposed cable it would be possible to provide duplicate supply to the proposed substation and to an impending large steel company load which in turn would be initially supplied by means of an overhead line from an important bulk supply substation and switching point (Dravosburg). The latter was being supplied in turn by the new Elrama Power Station so that the proposed cable would provide a power outlet for the Elrama Station and a new high-capacity system transmission line for generating system requirements.

Comparative Cost Estimates

Although cost estimates for the 12- and 69-kv schemes were prepared, it was difficult to compare them because alternate facilities accompanying the 12-kv method to accomplish the same results as the 69-kv cable were difficult to define and evaluate. The cost figures obtained favored the 69-kv scheme and because this method provided more system improvement and long-range capability, it was decided to proceed with the 69-kv project. For the same reasons, it was difficult to compare losses but, again, the values obtained favored the 69-kv project.

Details of Facilities

Inasmuch as it was decided to pick up on a new 69/12-kv substation known as Forbes, one section (Area-4 in Fig. 1) of the low-tension network sup-

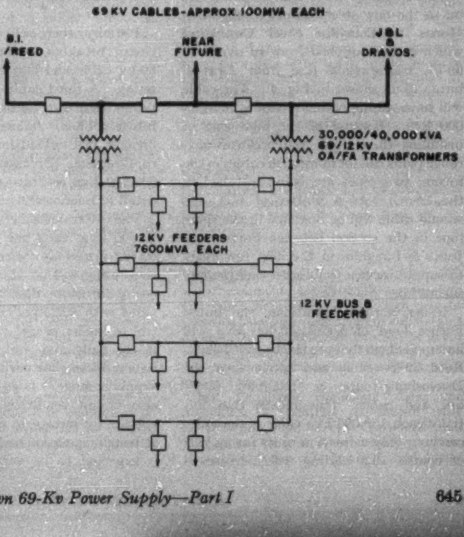
69 KV CABLES-APPROX. 100MVA EACH
B.I. /REED
NEAR FUTURE
J&L & DRAVOS.
30,000/40,000 KVA 69/12 KV OA/FA TRANSFORMERS
12 KV FEEDERS 7600MVA EACH
12 KV BUS & FEEDERS

Fig. 5. Single-line diagram of initial stage of development of Forbes substation

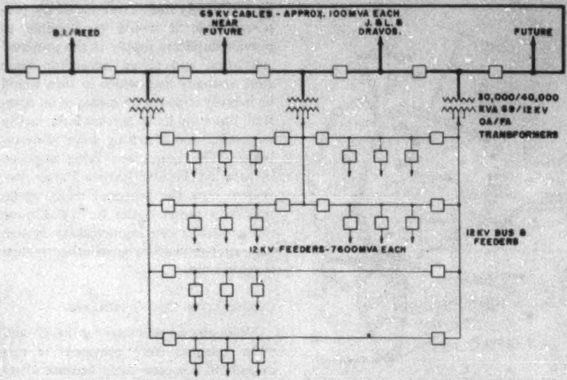
69 KV CABLES - APPROX. 100MVA EACH
B.I./REED
NEAR FUTURE
J. & L. & DRAVOS.
FUTURE
30,000/40,000 KVA 69/12 KV OA/FA TRANSFORMERS
12 KV BUS & FEEDERS
12 KV FEEDERS-7600MVA EACH

Fig. 6. Single-line diagram of ultimate development of Forbes Substation

plying a large and important segment of downtown Pittsburgh, reliability of supply and arrangement of facilities were of paramount importance. This fact plus the use of the proposed line as a system tie dictated the need for the duplicate 69-kv supply to the substation as well as adequate 69-kv switching, two transformer banks, and a more elaborate 12-kv arrangement than would normally be deemed necessary.

69-Kv Cable

A pipe-type cable with 1,500,000-circular-mil conductors is being installed from Brunot Island to the downtown substation known as Forbes, and on to the new steel company substation (Jones & Laughlin Steel Company) which is now supplied from an overhead 69-kv transmission line from Dravosburg, all as shown in Fig. 4. The cable will have an approximate rating of 100,000 kva. Because of the high cost of installing these pipes and because long-range plans call for more such cables in the future, two pipes are being installed in the trench. As a matter of fact, the second cable will be installed in the spare pipe in the section between Forbes and Jones & Laughlin in the next few years to supply service to another bulk supply substation.

Under normal conditions, the initial Forbes load of about 40,000 kva will be supplied partly over the Brunot Island-Reed 69-kv cable and partly over the Dravosburg-Jones & Laughlin 69-kv line and cable. This means that initially each 100,000-kva cable is normally carrying only a fraction of its rating but, of course, this loading will increase as the Forbes Station load grows. Then, too, either cable will have to carry the total load when the other cable is out of service. These cables will have to transmit bulk power, in either direction, for abnormal system conditions. Numerous network-analyzer studies have demonstrated the efficacy of this 69-kv tie for the latter purpose, without the need for any phase-angle control.

Forbes Substation

A very schematic single-line diagram of the initial facilities at the new Forbes Substation is shown in Fig. 5. A more detailed single-line diagram of the initial and future facilities is shown in reference 1.

Initially, there will be four 69-kv air circuit breakers, one for each incoming 69-kv cable and two bus tie breakers in series. A third cable will terminate between these two tie breakers in the near future. Thus, failure of any single breaker, bus, or transformer will not interrupt service. Breakers are rated at 3,500,000 kva and are described in more detail in reference 2.

The two transformers are rated 30,000/40,000 kva, each one oil-immersed self-cooled/forced-air-cooled. The initial station rating will be 42,000 kva (one bank out of service). Each transformer is provided with ±7.5-per-cent load ratio control to render proper voltage for changes in the daily and weekly load cycle and to compensate for variations of the 69-kv supply voltage. Load ratio control will also permit rendition of normal 12-kv voltage for outage to either 69-kv cable, although regulation under such conditions is expected to be very small. Voltage adjustment will be automatic and will be controlled by the conventional line-drop compensators.

Transformer impedance of 10 per cent on the 30,000-kva rating is within normal manufacturing tolerances involving no extra cost and was specified to keep fault currents for the ultimate station layout as low as possible. The load ratio control will compensate for the very slight increase in regulation.

Reliability of supply was again paramount in establishing the 12-kv bus. It was essential that failure of any single facility would not seriously affect service. Also, it was necessary that essential maintenance be accomplished with minimum reduction of capacity during the normal week day. In the initial stages, failure of certain equipment will remove two 12-kv cables from service, but this hazard will gradually be eliminated as the station expands, because ultimately each bus section will supply only one feeder per area. The 12-kv circuit breakers are rated at 1,000,000 kva which is ample for the duty imposed without resorting to the use of reactors which are to be avoided not only because of the expense but also because of space limitations.

12-Kv Feeders

Initially, eight 12-kv feeders consisting of 3-conductor 500,000- circular-mil shielded cables will be provided to pick up one of the two network areas. These cables will replace eight cables now emanating from Brunot Island-Reed. Of the latter, three will be utilized to provide additional capacity to the other network area which will continue to be supplied from Brunot Island-Reed, two cables will be used to provide additional capacity to the so-called North and South Side areas of Pittsburgh, and the remaining three will be used to continue a program of replacing old, small-capacity cables which have a very high failure rate.

The 500,000-circular-mil shielded cables will have a normal summer rating of 7,600 kva and an emergency rating of 10,900 kva, based on maximum copper temperatures of 81 and 96 degrees centigrade respectively. It is expected that one cable can be taken out of service at any time for connection of new loads or for maintenance. A second cable can fail without exceeding emergency ratings or causing undue low voltage.

Ultimate Development

Plans for the ultimate development of Forbes Substation provide for four 69-kv cables, three transformer banks, and 18 12-kv cables, as shown schematically in Fig. 6. As previously mentioned, the third 69-kv cable will be installed between the two existing tie circuit breakers within the next 2 or 3 years. The fourth cable is not a certainty but provision for it involves very little extra expense.

The ultimate high-tension layout at the Forbes Substation provides for a ring bus with four 69-kv lines and three 30,000/40,000-kva transformers. While ring busses are widely used because they are economical and have desirable operating characteristics, they are slightly more complicated from a relay projection standpoint and entail the hazards of dropping a section of bus should one section be out of service for maintenance and another section fail. However, owing to the desire to keep a through connection on this 69-kv line, even while performing maintenance on a bus or breaker, a ring bus was felt to be the best solution in this case. Admittedly, the through connection does not exist for certain equipment out of service in the initial development but, should experience demonstrate that maintenance outages are causing considerable operating difficulties, the ring bus can be closed without undue expense even before the additional line and transformer are needed.

Provision is being made for an ultimate installation of 18 12-kv feeders supplying three network areas. The six feeders to each network area will be divided among the various busses so that the most serious interruption will not involve more than one cable per area.

It is proposed to pick up much of the downtown load growth on this new substation. This means gradually encroaching on the two areas now served at 4 kv and, in the future, on Area-2 which is still served by 12-kv cables from Brunot Island-Reed. Actually, as previously explained, this latter area will get three new feeders when Forbes is cut in, so that it will continue to carry much of the downtown load direct from Brunot Island-Reed. Thus, the ultimate operating capability of about 85,000 kva (three transformers installed and one out of service) should provide sufficient capacity for a long time.

Consideration of 138 Kv Instead of 69 Kv

About the time that this station was being authorized, the Duquesne Light Company had also reached a decision to inaugurate the use of 138 kv in conjunction with the installation of the third Elrama generator. This meant that 138 kv would be available at Dravosburg Substation and consideration was given to installing this cable and substation at 138 kv. However, while the cable at such a voltage was readily available, isolated-phase metal-enclosed bus and air-blast switching were not sufficiently developed in the United States which precluded the use of the higher voltage.

Conclusions

While the solution to the problem of providing additional capacity to downtown Pittsburgh has been an expensive step, it has followed the general pattern adopted elsewhere of using a relatively high transmission voltage for distances of only a few miles. Even allowing for the accelerated growth in the last few years, it is anticipated that this station plus continued use of some existing facilities will provide sufficient capacity for this area for about 20 years. Moreover, the proposed 69-kv cables will fit in with other long-range development patterns for the rest of the system.

References

1. Pittsburgh Downtown 69-Kv Power Supply—Part II. Substation, E. M. Gue. *AIEE Transactions*, vol. 74, pt. III, Aug. 1955, pp. 648–53.

2. Pittsburgh Downtown 69-Kv Power Supply—Part III. Switchgear Development, P. R. Pierson. *Ibid.*, pp. 653–57.

Discussion

D. C. Vaughan (Potomac Electric Power Company, Washington, D. C.): To planners of metropolitan-type systems, papers on this subject are very valuable. The use of metal-inclosed 69-kv switchgear and air-blast circuit breakers may well permit location of a station of the type described where more conventional outdoor structures could not be tolerated. This is believed to be an extremely important development. However, the high cost of such an arrangement limits the application. As an example, using rough cost estimates developed for similar cables and switchgear in Washington, D. C., if the distance from Reed to the Jones & Laughlin Substation is less than 7 miles, it might be cheaper to install a second cable the complete distance in the spare pipe provided and connect one transformer at Forbes to each pipe without high-voltage switching. This would limit the flexibility to some extent, but it would remove a possible cause of failure. Although not a factor here, the second cable would, in many cases, be preferable because of the increased tie capacity between generating sources. We would like to make it clear that this comment is not intended as a criticism, but merely to point out that there are many cases where slightly different circumstances might lead to a different solution.

A. M. de Bellis (Consolidated Edison Company of New York, Inc., New York, N. Y.): The geography of the downtown Pittsburgh load area is similar in some respects to the downtown Manhattan load district except possibly for load density. It was in the downtown Manhattan section in New York City also, where our first 69-kv area substation was placed in service in 1951. It is noted that the Pittsburgh Substation load peak is expected in the summertime which also parallels the situation at the lower Manhattan Substation where the summer peak is about 25 per cent above the winter peak megawatts. The need for the 69-kv supply cables to transfer bulk power to large customers forced the use of a 69-kv bus at Forbes Substation. Fortunately we did not face this situation; hence we were not required to install switching at the substation.

I believe it was wise to avoid the use of reactors in the bus circuits since the station is intended to be used for network supply. Reactors have the unfortunate characteristic of creating voltage and phase-angle differences between busses and affect the load balance on the 12-kv cables under contingency operation. It is noted that automatic voltage regulators are used for the tap-changing-under-load equipment on the transformers. I would like to ask Mr. Hill what type of compensation is used in this case.

It is a bit surprising that the ultimate capacity of the substation is considered to be only 85,000 kva with two 30/40-megavolt-ampere transformers[1] remaining in service. According to the American Standards Association guides for loading transformers we would expect that the peak capacity of the substation in the summertime, on a load-cycle basis, would be more than this. I would like to ask also if consideration has been given to the future addition of more cooling equipment on the transformers to provide further increase in their capabilities.

Reference

1. American Standards for Transformers, Regulators, and Reactors. *ASA C57*, American Standards Association, New York, N. Y., May 25, 1948.

V. E. Hill: Mr. Vaughan's and Mr. deBellis' comments are certainly appropriate and much appreciated. The high cost of these high-voltage metropolitan substations dictates that careful consideration be given to every possible method of arriving at the most prudent investment consistent with satisfactory service.

Mr. Vaughan's comments about the possibility of installing the second cable in a spare pipe already provided and tapping one bank to each of the two cables, thus eliminating the expense and space consumed by the high-tension switching, certainly has attractive features. However, it appears as though this proposal has several limitations in our particular case for the following reasons:

1. Such a method is not readily adaptable to the connection of a third bank in the future, which gives a large increase in operating capability.
2. Such a method can be protected, of course, but the necessary remote tripping complicates the relaying, is subject to more troubles, and is much more expensive.
3. It provides more transmission capacity than is actually needed, although other things being equal, the second line is always valuable to back up loss of the first line.
4. The extra cable involves not only the cost of the cable but also that of two circuit breakers, one at each terminal.
5. Each cable will loop another station, thus giving rise to possible load unbalance on the two Forbes banks.
6. It now appears probable that part of the spare pipe will be utilized for a 138-kv cable; plans for the use of this spare pipe were not crystallized when the initial installation was authorized, but such use is now becoming more firm with the actual development of the system.

Probably, one of the most important features controlling the type of station in this instance is the fact that the topography of the ground, the narrowness of the streets, the absence of large ducts suitable for 69-kv cable, and results of various economic studies all dictated the use of pipe-type cable. The high cost of such construction then dictates the installation of high-capacity cable, thus making it imperative to utilize this cable for as many purposes as possible. This could only be done in our case by installing high-tension switching at Forbes.

In response to Mr. DeBellis' question concerning the type of compensation to be used at the Forbes Substation, it can be stated that it will consist of the usual line-drop compensators to simulate the impedance of the transformers and an average 12-kv feeder. The currents from the two banks will be totalized before being impressed on the compensator to actuate the tap changer of one regulator which will immediately call for a change on the other bank. Thus, the voltage adjustments on both banks will act in unison. The 12-kv feeders are all very short—a matter of fractions of 1 mile—and hence it is felt that the voltage regulation on the network should be very good.

While it has been stated that the ultimate capacity of the substation will be 85,000 kva, we would like to point out that this is merely an estimated value now; the actual value, when the three banks are in service and the load warrants it, will be based upon the usual Duquesne Light Company procedure of calculating very accurately the thermal capability of the banks based upon load cycle and field tests. It is entirely possible that station rating will be somewhat higher than 85,000 kva and, considering the extremely good reliability of transformers, it is also very likely that we will let the load exceed the operating rating somewhat before authorizing other investments to provide additional capacity for higher loads. No provision has been made for additional fan cooling or forced oil-cooling but, of course, such a possibility would always be investigated when the time arrives and the loading is such as to require more capability.

Pittsburgh Downtown 69-Kv Power Supply

Part II. Substation

E. M. GUE
MEMBER AIEE

BACKGROUND information on the Forbes Substation project is given by Hill.[1] This paper describes the problems encountered in the design of a substation, with the following ultimate requirements:

1. A 69-kv ring bus with a total of seven circuit breakers, four incoming lines, and three 30/40 megavolt-ampere 69/12-kv transformers.
2. Eighteen 12-kv feeders arranged in six bus sections with two sources to each section.
3. Equipment selected and arranged in such a manner that the substation will be compatible with the surrounding structures encountered in the downtown area of Pittsburgh, including the many improvements being accomplished under the city's redevelopment program.

Fig. 1, shows the 69-kv busses and circuit breakers rated at 2,000 amperes. All 12-kv busses and breakers are 1,200 amperes, except transformer leads which vary in size from 3,000 to 1,200 amperes depending on their location in the circuit.

Site Selection

From the inception of this project it was obvious that the availability of sites would have a great influence on the design of the station. The downtown area of Pittsburgh is highly congested and real estate values are high. After a thorough search of the desired area, only three sites were found that could be obtained at a reasonable cost. Unfortunately, all of these sites were small in area and not well suited for a conventional outdoor-type substation. However, factors other than substation costs had to be considered. These items were:

1. Location of the area to be served.
2. Route and cost of extending the 69-kv pipe-type cable.
3. Availability of street routes for the new 12-kv feeders and the cost of extending duct lines to connect the circuits to the existing system.
4. Physical appearance of the proposed substation.

Economic studies indicated the desirability of utilizing the selected site, even though substation costs were considerably greater than would be encountered with a conventional installation.

Development of the Site

The selected site contained only 17,000 square feet of usable area. It was located adjacent to the route of a proposed elevated highway and near an area selected for redevelopment. All of these factors indicated the necessity of designing an enclosed station with safety and appearance as key items.

Housing the 12-kv equipment was no problem; however, enclosure of the 69-kv switchgear without either the sacrifice of insulation level or excessive cost presented many problems. Investigation showed that standard 69-kv class insulation should be maintained, as one of the planned lines would be subject to lightning exposure within a short distance of the substation. Studies were made for a large building covering most of the site with all equipment indoors except the main transformers. This layout was discarded because of excessive cost and lack of space.

Paper 55-226, recommended by the AIEE Substations Committee and approved by the AIEE Committee on Technical Operations for presentation at the AIEE Winter General Meeting, New York, N. Y., January 31–February 4, 1955. Manuscript submitted October 19, 1954; made available for printing December 2, 1954.

E. M. Gue is with the Duquesne Light Company, Pittsburgh, Pa.

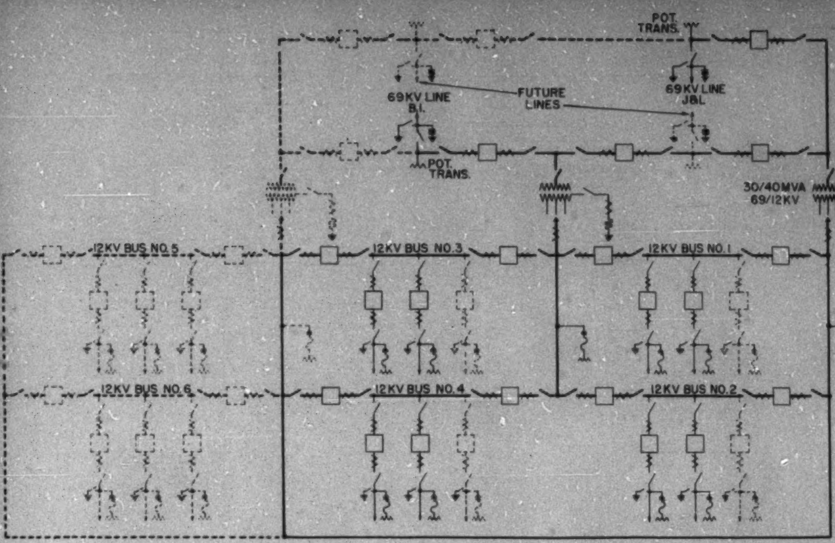

Fig. 1. Forbes Substation main single-line diagram

A 69-kv metal-enclosed bus without a specified impulse level had been used by the industry previously, so the use of such equipment at Forbes Substation was investigated. Study and laboratory tests indicated that a 350-kv impulse level bus could probably be obtained without the use of excessively large enclosures. The desired dielectric specifications for this bus were 350-kv full-wave impulse withstand with 60-cycle requirements of 160-kv dry withstand and 150-kv minimum dew flashover. Studies showed that sufficient space existed to accommodate such an installation provided the bus enclosure diameter did not exceed 43 inches. This proved to be liberal as the bus was developed with an enclosure diameter of approximately 38 inches. The design and construction of this equipment is given by Pierson.[3] Air circuit breakers were selected because of the close circuit spacing and the desire to eliminate oil-filled switching equipment in this downtown area.

Figs. 2 and 3 show plan and section views of the final development of this substation. Fronting on Forbes Street is a 3-story masonry building which houses all of the 12-kv equipment. The top floor provides space for control, relays, building heating, and ventilating equipment. The second floor houses the 12-kv segregated-phase air-blast circuit breakers arranged in six bus sections. Initially, only four sections with two feeders each are installed. Directly below is the floor which accommodates the outgoing line compartments, bank 12-kv potential transformers, station service switchgear, and the centralized air-supply system. The outgoing line compartments are of segregated phase construction and contain grounding switches and line potential transformers. These instrument transformers are used to indicate the operation of the network protectors on the transformers that are connected to the various feeders. The 12-kv cables leave the station by means of vaults located under the first floor.

The main transformers are located immediately outside of the main building and separated by masonry barrier walls. Special arrangement of radiators, bushings, and auxiliary compartments was necessary to fit the transformer to the available space. Located in the transformer wells are metal-enclosed 3-ohm neutral-grounding resistors for the 12-kv windings of the transformers. Resistor grounding was selected so as to limit ground current to a value that could be handled by existing network unit grounding switches, and at the same time limit transient overvoltages to a reasonable value.

An access roadway entering from Boyd Street and extending to Diamond Street separates the 69-kv switchyard from the transformers. The 69-kv isolated-phase air circuit breakers are arranged in two rows with space provided laterally for manholes used in terminating the pipe-type cables. Trifurcating joints are located in these holes with laterals extending to the incoming line compartments which are spaced between the circuit breakers as indicated. The line compartments also provide space for cable potheads, lightning arresters, and line-isolating and grounding switches. Because of the presence of oil, these compartments are protected by carbon dioxide fire-protection equipment. Baffle bushings are used to seal off all line compartments and circuit breakers from the main bus runs.

Askarel-filled 69-kv potential transformers are provided for each incoming line and are located in isolated-phase compartments as indicated. As a fault in the potential transformers would be cleared by line circuit breakers, no fuses are used. This decision simplified enclosure problems for this part of the station. Main transformer isolating switches are located above the driveway. All switches are remotely operated by mechanisms located at ground level or from a grating platform extending between the equip-

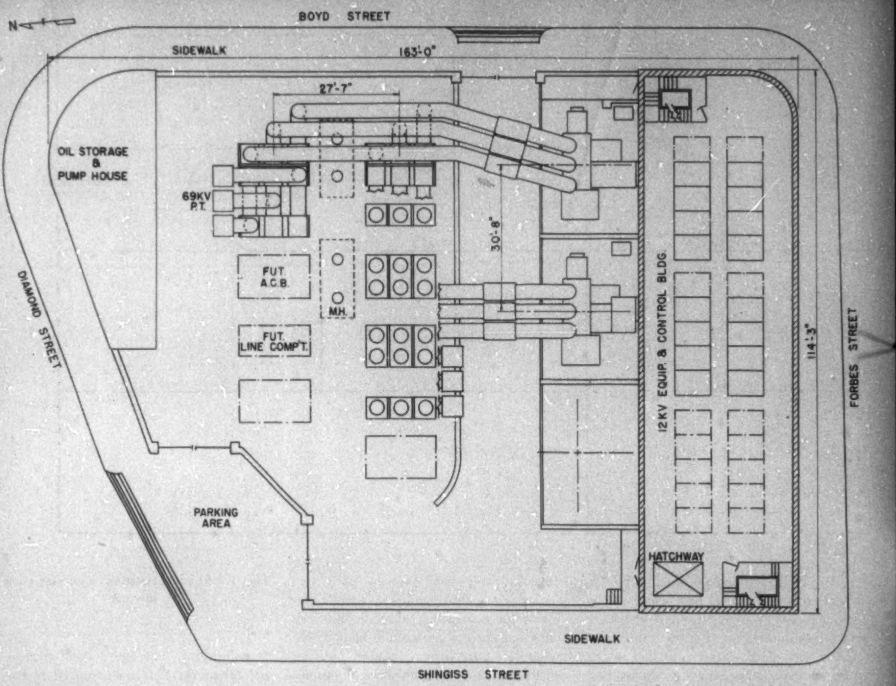
N
BOYD STREET
SIDEWALK
163'-0"
27'-7"
OIL STORAGE & PUMP HOUSE
69KV P.T.
FUT. A.C.B.
M.H.
FUT. LINE COMP'T.
30'-8"
12 KV EQUIP. & CONTROL BLDG.
114'-3"
FORBES STREET
DIAMOND STREET
PARKING AREA
HATCHWAY
SIDEWALK
SHINGISS STREET

Fig. 2. Substation arrangement, plan view

ment near the top of the circuit-breaker housings.

Located on the extreme northerly part of the station is the oil storage and pumping plant for the pipe-type cable. This building is of masonry construction and the enclosure provides a part of the masonry wall which encompasses the entire area, except for a portion in the northwest corner which is used for entrance and off-street parking. Supporting structures in the switchyard were kept to a minimum by utilizing the equipment housing as support points.

In studying Figs. 2 and 3, it should be remembered that many details have been omitted so that the main features could be clearly shown. Fig. 4 shows the station under construction.

Station Service Power Supply

Fig. 5 shows the diagram of the station service power supply system. Because of the necessity of providing reliable service to the cable oil-pumping plant and to the air supply system for the substation, it was necessary that the station auxiliary power system be very reliable. As there will be no backfeed from the 12-kv feeders from other sources, it was concluded that the station service banks should be connected to the low-tension side of the main transformers. Space was not available for a conventional installation, so it was decided to build a 225-kva unit into a separate oil-filled compartment on the main transformer tank. The unit is connected to the transformer low-tension winding through suitable re-

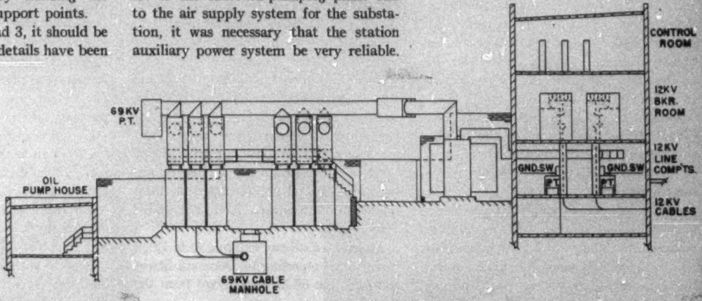
69KV P.T.
OIL PUMP HOUSE
69KV CABLE MANHOLE
CONTROL ROOM
12KV BKR. ROOM
GND.SW
P.T.
GND.SW
P.T.
12KV LINE COMP'TS.
12KV CABLES

Fig. 3. Substation arrangement, sectional view

Fig. 4. Substation during construction

sistors and fuse links. All connections to the small transformer are made internally. To minimize the exposure to the 120/208-volt winding by the external circuits, an automatic air circuit breaker is located in a compartment directly below the auxiliary transformer. Each main transformer is so equipped and service busses are provided in duplicate. The system will be operated with the auxiliary load divided between the two banks. Either of the sources are adequate for the entire station load.

Centralized Air-Supply System

Equally important with station service power was the matter of compressed air for the circuit breakers. In addition to providing air for the operation of the breakers, it was necessary to supply the constant drain caused by the bleeding of air through the 69-kv circuit breakers. This flow of dry filtered air is necessary to prevent condensation on certain parts of the circuit breaker.

As the 69-kv breakers require air at 260 pounds per square inch (psi) and the 12-kv breakers at 150 psi, consideration was given to installing separate air-supply systems. However, space limitations and cost indicated the desirability of a centralized supply for the entire station. Fig. 6 shows the schematic diagram of the system actually selected.

The major components of this system are three 15-horsepower 24-cubic-foot-per-minute free-air 1,000-psi water-cooled air compressors and two air storage units, each having a volume of 18 cubic feet and a storage pressure of 950 pounds. Air pressure is reduced to 260 and 150 psi by reducing values. Other valves for safety, control, and sectionalizing purposes are indicated on the diagram.

The distribution of air follows the same principles as that employed for station power. Normal operation will provide for half of the 12-kv and half of the 69-kv circuit breakers on one air-supply unit. The other supply unit with associated compressor will feed the other half of the switchgear. The third compressor may be used with either of the storage units. Program control will be employed so that each compressor will operate approximately the same hours per year. Storage capacity is such that, starting with a fully charged system, approximately 9 hours would have to elapse, with no compressor running, before the pressure would be too low for safe operation of a 69-kv breaker. The system as outlined is the ultimate for the station and will not be expanded as circuit breakers are added.

Relaying and Controls

The station is designed for complete remote operation and will be unattended. The only special feature of the automatic-control equipment is a selection bus that will permit the closing of a chosen number of 12-kv breakers simultaneously. Relaying including primary and backup protection is applied as follows:

1. The 12-kv lines are protected by phase and ground nondirectional, short-time overcurrent relays. Backup protection is provided by phase and ground bus overload relays.

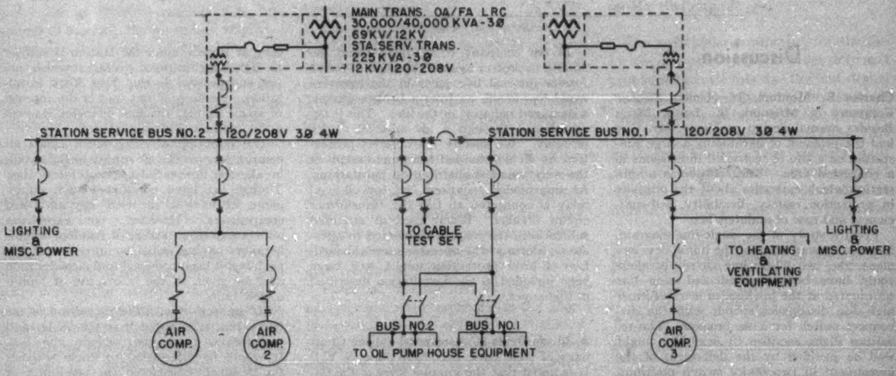

Fig. 5. Station service single-line diagram

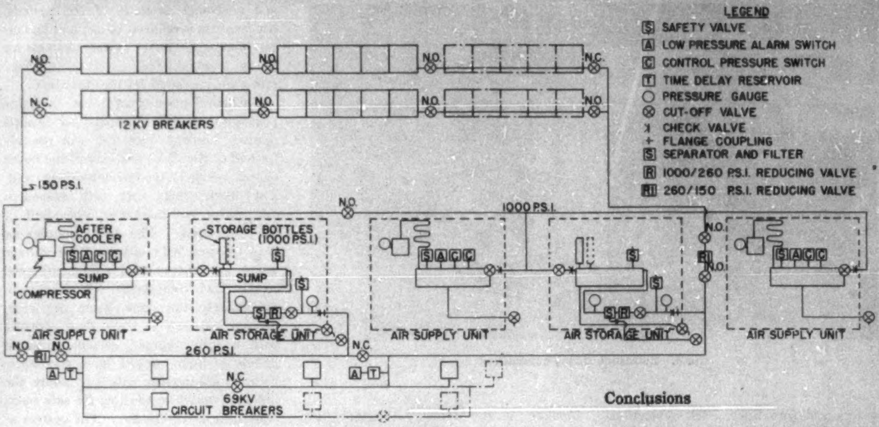

Fig. 6. Schematic diagram, air-supply system

2. The 12-kv busses are protected by variable percentage ratio differential phase relays. Secondary protection is provided by the bus overload relays discussed in the foregoing.

3. The 69/12-kv transformers are protected by variable percentage ratio phase differential relays in conjunction with magnetizing inrush desensitizers. Sudden pressure and thermal relays are provided on the transformers.

4. No separate protection is supplied for the 69-kv busses as transformer differential relays and line relays cover all sections.

5. The primary protection for both of the initial 69-kv lines consists of pilot-wire relays, as well as the necessary interlock and supervisory devices. Backup protection for the two lines is different as one line is so short that product-type ground relays could not be applied. On the Brunot Island line, reactance-type phase and product-type ground relays with the necessary instantaneous overcurrent interlock devices are used. For the short line, protection is the same except a second set of pilot-wire relays are used instead of the product-type ground relay.

Sticking 69-kv line or low-tension bank breaker protection is provided by a series of instantaneous overcurrent ground relays used to locate the defective circuit breaker. This protection was considered to be sufficient, as with isolated and segregated phase construction it is practically impossible to have a fault without involving ground.

Conclusions

This presentation includes a brief description of the difficulties involved in designing a major high-voltage substation suitable for the congested metropolitan area of a large city. It shows how the problems of appearance, safety, and compactness were solved in providing such a substation in downtown Pittsburgh. It is hoped that the data presented may be of use to others confronted with the problem of providing high-voltage installations in similarly congested areas.

References

1. Pittsburgh Downtown Power Supply—Part I. Planning, V. E. Hill. *AIEE Transactions*, vol. 74, pt. III, 1955 pp. 643–48.

2. Pittsburgh Downtown Power Supply—Part III. Switchgear Development, P. R. Pierson. *Ibid.*, pp. 653–57.

◆

Discussion

Charles E. Monfort, Jr. (Union Electric Company of Missouri, St. Louis, Mo.): Besides normal design problems, Mr. Gue had the problem of developing a large substation on a site of restricted dimensions in a congested area. The solution is a substation which embodies about the ultimate in protection, safety, flexibility, self-sufficiency, and ease of maintenance.

From a study of the single-line diagram, it would appear that, for the initial development, the two 69-kv line circuit breakers could have been omitted and each line terminated at the junction of a transformer high-side disconnect switch with the disconnect switch for a tie breaker. The resulting slight sacrifice in flexibility might well be justified by the deferment of the investment in two 69-kv switch positions. With the completion of the ring bus these breakers would, of course, have to be added.

In our company it has been found desirable to protect against exposure of transformer internal live parts in the event of rapid loss of oil, as from a broken gasket, a damaged radiator, or the like. This is accomplished through a low-oil-level device or relay. We specify low-oil-level protection at all unattended locations except at the very smallest distribution substations. At unattended locations the low-oil-level relay is connected to trip the transformer circuit breaker. Where used at attended substations, the relay is connected to operate on alarm at the operator's switchboard. Low-oil-level protection might well have been included in the installation described in this paper.

A. M. de Bellis (Consolidated Edison Company of New York, Inc., New York, N. Y.): It is noted that the impulse level of the 69-kv bus has been set at the standard value of 350 kv. This would of course be necessary at Forbes, since the station is subject to lightining impulse voltages which are not encountered in the New York installation. Because of this and in the interest of space saving, the bus diameter was set at 36 inches in our installations.

The intention of using water-cooled air compressors for the air supply to the circuit breakers at Forbes Substation is interesting. Though we have considered such equipment, we have so far used only air-cooled compressors. However, our experience with compressor units for outdoor circuit breakers having initial compression at 800 psi has not been too good and consideration may be given to the future use of liquid-cooled units.

In connection with the protection of the 69-kv bus, it is noted that the feeder and transformer protection include the bus. It would be interesting to know whether the designers considered the possibility of connecting a line and a transformer to the same 69-kv bus section, with transfer-trip equipment applied to open the remote circuit breaker for transformer short circuits. This would have saved the ultimate installation of three 69-kv air-blast circuit breakers with associated auxiliaries but would have reduced the flexibility of operation to some degree. It would also be interesting to know whether the thermal relays on the transformers are used to trip or to give alarm; also what experience has been had with transformer thermal devices for tripping and what temperature limits have been used.

E. M. Gue: Mr. Monfort has suggested that the initial installation could have been simplified, at the expense of some flexibility, by the omission of the two 69-kv line circuit breakers. The statement is true; however, the omission of breakers would have resulted in the employment of an automatic grounding switch to provide positive clearing of the remote circuit breakers for transformer faults. The modification suggested was considered and rejected partly for the foregoing reason, but mainly because of the outage time that would be necessitated by the rearrangement of the equipment. Considering the character of the load served by this station, outage time for expansion is an important factor.

Although it was not mentioned in the paper, the transformers are equipped with low-oil-level devices. The relays will sound an alarm at the load dispatcher's office by means of the remote-control system. This is our company's normal practice for unattended substations.

Mr. deBellis' comments are welcomed with interest as many of the original layouts for Forbes Substation were based on information obtained from an installation made by his company. Although insulation characteristics were necessarily different, the data served as a valuable guide in early planning. The scheme of connections as outlined by Mr. deBellis was considered and rejected. As stated in the paper, maintenance of system ties was considered very important and was the basis for the selection of a ring bus. It was considered highly undesirable to open the system ties for clearance switching on transformer outages as well as for possible transformer faults. Unfortunately metal-enclosed 69-kv disconnecting switches capable of breaking transformer magnetizing current were not available. Also, as explained in the foregoing, omission of the breakers would have required other devices. In a location such as the one under consideration, it is believed that very positive means are justified to isolate a faulty transformer in the shortest possible time.

The thermal relays on the transformers are used to control fan-cooling equipment and to give an alarm for high-temperature conditions. They are not used for tripping at this installation. In general, thermal trip is only employed at locations, such as some customer's substations, where our company does not have control or knowledge of sudden application of heavy loads. Hot-spot temperatures of 105 degrees centigrade are usually used to actuate the alarm circuit. Temperatures used for tripping vary with the specific conditions applying to a particular installation.

Pittsburgh Downtown 69-Kv Power Supply

Part III. Switchgear Development

P. R. PIERSON
MEMBER AIEE

THE planning of the Pittsburgh downtown 69-kv power supply was described by Hill,[1] the description of the substation, its arrangement, equipment, and circuitry was covered by Gue.[2] In this paper the switchgear developments involved in meeting the plans and requirements are described. Summarizing the requirements, the substation area was limited, the high-voltage circuits were subject to lightning exposure, appearance requirements were dictated by a downtown area development, and safety was of major importance.

14.4-Kv Distribution Switchgear

Conventional indoor station-type cubicles with compressed-air circuit breakers were applied on the 12-kv primary distribution circuits. These cubicle combine the main bus, the air circuit breaker, and the isolating disconnecting switches with grounded metal segregation of phases in a compact unit, as shown in Fig. 1. The cubicles include a porcelain-insulated bus, gang-operated disconnecting switches, viewing windows, illumination of disconnecting switch compartments, and interlocks between the disconnecting switch mechanism, the circuit-breaker position, and the circuit-breaker inspection doors.

The segregated phase bus provided for the 12-kv transformer to switchgear connections was designed of weatherproof construction for the outdoor portion. The indoor portion and the segregated phase bus interconnections between switch groups were not ventilated. All of these bus sections were gasketed between sections and were provided with hinged, bolted, and gasketed inspection covers. This construction keeps dust entrance to a minimum and permits maximum intervals in the inspection and maintenance schedules.

Potential transformers of the disconnecting type were connected to the 12-kv power transformer circuits. A bank of three potential transformers, star-connected, was used. Each potential transformer was placed in a separate phase-segregated compartment. Thus, phase segregation was maintained throughout the entire structure.

Combination pothead, grounding switch, and line potential transformer compartments located in the room below the indoor 15-kv switchgear provided a termination for the primary distribution feeders, connecting them to their respective breakers, indicating feeder voltage condition, and grounding the feeders during cable maintenance operations. These circuits were completed to the circuit-breaker units on the floor above with a segregated phase bus through porcelain floor tubes providing a gas or flame seal between equipment on different floor elevations.

69-Kv Switchgear

The switchgear equipment for the 69-kv circuits presented many development problems because this was the first design for metal-enclosed 69-kv service to meet the standard impulse level of 350 kv. The 69-kv circuit breakers meeting the 160-kv 60-cycle 1-minute tests had been built and installed. Associated metal-enclosed connections meeting similar 60-cycle tests were in operation. But aside from know-

---

Paper 55-214, recommended by the AIEE Switchgear Committee and approved by the AIEE Committee on Technical Operations for presentation at the AIEE Winter General Meeting, New York, N. Y., January 31–February 4, 1955. Manuscript submitted October 19, 1954; made available for printing December 3, 1954.

P. R. PIERSON is with the Westinghouse Electric Corporation, East Pittsburgh, Pa.

Contributors to the accomplishment of the design described in the paper were B. P. Baker, J. F. Peters, E. Beck, and G. Gilchrist.

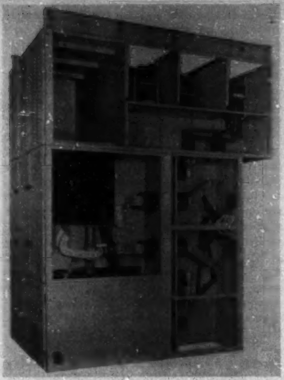

Fig. 1. Typical station-type cubicle. Compressed-air circuit breaker is in compartment at left. Main bus is at top right, isolating switch below, line compartment and switch are at lower right with provision for line connections to line terminating equipment below. Phases are segregated by grounded metal barriers

ing that the impulse withstand would be something above the 160-kv crest voltage, no information on impulse values were available. The insulators and phase-to-ground clearances used on outdoor structures were of no value as they would neither be economical nor meet the desired space limitations. As a result, it was necessary to develop, step by step, the enclosure size, bus size and shape, insulators, contour of elbows, T's and dead ends, and a suitable disconnecting switch.

69-Kv Isolated Phase Bus

Calculations showed that a round bus, about 8 inches in diameter, would meet the impulse requirements in a 36-inch inside-diameter enclosure, and that porcelain insulators having a large diameter adjacent to the bus and tapering to a smaller diameter at the grounded support might not lower this value and would probably pass a 160-kv 60-cycle test. However, neither of these items was an economical construction. The economical balance was determined by taking a number of differently sized enclosures rolled from furnace pipe steel and 4-, 6-, and 8-inch-diameter conductor tubing into the impulse laboratory and conducting a series of impulse tests. The first tests consisted of testing the conductors in a length of enclosure to determine the critical impulse withstand voltages of the various combinations with air clearances unaffected by supporting insulators. A 4-inch round conductor just met the 350-kv impulse level in a 36-inch-diameter enclosure but withstood 390 kv in a 38-inch enclosure. From these tests a 38-inch inside-diameter enclosure and a 4-inch outside-diameter round conductor were selected as the best combination, from the viewpoint of cost and space economy, for meeting the objectives in test values.

69-Kv Bus Supports

The next problem was the development of a support for this conductor which would not reduce the impulse level when introduced into the air gap between conductor and enclosure. This proved to be the most difficult problem of the entire development.

Tests of bus supports comprising mock-ups of available designs flashed over at values near 275 kv. This determined that standard types of hardware adjacent to the bus were not suitable. However, when the hardware was eliminated, all shapes and sizes of insulators had approximately the same critical withstand value. Close observation determined that the flashover was triggered by a breakdown at the point of contact between the bus and the supporting porcelain. This indicated a high concentration of stress at this point. Two approaches to the reduction of this stress condition seemed possible. The one with a background of usage was a static ring which would shield the top of the insulator and distribute the stress over a larger area. The other was a new approach consisting of carrying the stress down into the body of the insulator so that the breakdown was opposed by the puncture strength of the porcelain as compared with flashover values. The second approach was investigated because successful results would give a more economical design of insulator with hardware to which a bus could be attached.

Many combinations of parts were tested, and it was found that the depth of penetration of the hardware insert into the insulator body, the contour of the insert, the material used to secure the insert into the insulator, the projection of the insert above the top of the insulator, and the thickness and quality of the porcelain wall were all critical factors requiring coordination before satisfactory results were obtained. A satisfactory combination of factors was accomplished, and throughout the remaining test program no insulator flashovers were encountered.

Telescoping Disconnecting Switch

The previous tests adequately determined that the use of a conventional blade-type of disconnecting switch would require enclosures of unusable size; but, if a section of bus could be moved longitudinally, it would have adequate insulation characteristics in the closed position and, with proper shielding, would withstand the impulse tests in the open position. Designs of this general type had been made but were not in common use. Such a design could be enclosed in a rectangular enclosure only slightly larger than the bus and would provide space for the operating mechanism and clearance for the special shielding of contacts and blades.

Disconnecting switches of the telescoping type were designed. Each pole was placed in a separate, rectangular, isolated phase enclosure and consisted essentially of a longitudinally moving section of bus conductor telescoping into the hollow conductor of a connecting bus section or of the condenser-type bushing of the circuit-breaker compartment. Flexible fingers at each end provided the current-carrying contact between the moving blade and the fixed portion of the bus. All current-carrying contact parts were silver-plated. The blade was supported and moved through its travel by an insulator mounted on a guided platform equipped with a rack and driven by a pinion attached to the operating mechanism. Each switch enclosure was provided with a gasketed, hinged, and bolted cover for

Fig. 2. Telescoping-type disconnecting switch-pole unit with inspection door open and the switch in open position. Section of 69-kv bus with inspection cover removed is shown above. Finger contact assemblies are enclosed in static shields at insulator locations. Large static shield moves with switch blade

Fig. 3. Sample telescoping disconnecting switch, bus section, and elbow on test in impulse laboratory. Note enlarged bus section at elbow found necessary to maintain impulse level

Fig. 4. Part of factory assembly. Line entrance compartment with line disconnecting switches above are in the foreground. Immediately behind them are the 69-kv compressed-air circuit breakers with disconnecting switches above them. Interconnecting bus work is at top with potential transformer compartments at left. Note simplicity of supporting structure and walkways

accessability and a viewing window for visual inspection.

No insulation difficulties were expected from the finger clusters when enclosed in a static shield, and full impulse level was expected with the switch in the closed position because of the similarity to a continuous section of bus. These conditions were confirmed by tests. However, with the switch in the open position and the blade end terminating in a semisphere, flashovers were encountered. Larger diameter static shields restored the impulse level of the blade tip but these shields had to project beyond the blade tip where an "umbrella effect" was expected to permit sufficient protrusion for contact engagement. It became necessary to design static shields of sufficient diameter to encircle the finger cluster assembly when in the closed position, as shown in Fig. 2. Attaining the foregoing results required design of several different contours for static shields. Time and expense in the production of these shields was saved by making wooden mockups and spraying them with zinc plating. These were smoothed off and satisfactorily simulated the effects of the cast aluminum shields eventually manufactured and applied.

The over-all design of bus and disconnecting switch was confirmed by building a sample pole unit, a section of bus, and an elbow which were given a complete series of impulse and 60-cycle tests, as shown in Fig. 3. It will be noted that at the elbows and T connections a static shield approaching the theoretical optimum conductor size was found necessary to withstand the desired impulse voltage. The results of design tests are given in the following list. Approximately 2,000 impulse tests were made before the design of equipment was considered adequate and insulation level confirmed. Impulse values are corrected for weather and taken from oscillograms:

Impulse withstand, positive wave, 350 kv.

Impulse withstand, negative wave above 425-kv limit of generator (all other values are $1^1/_2$x40-microsecond positive waves).

60-cycle 1-minute withstand voltage, 160 kv.

Impulse critical flashover, disconnecting switch pole, 367 kv.

Impulse critical flashover, break jaw, hinge jaw and enclosure grounded, 367 kv.

60-cycle flashover, break jaw, hinge jaw and enclosure grounded, 177 kv.

Impulse critical flashover, hinge jaw, break jaw and enclosure grounded, 376 kv.

60-cycle flashover, hinge jaw, break jaw and enclosure grounded, 199 kv.

Impulse critical flashover, switch break distance, enclosure insulated, one jaw grounded, 386 kv.

60-cycle flashover, switch break distance, enclosure insulated, one jaw grounded, 259 kv.

Bus support insulator, dry flashover, 210 kv.

Bus support insulator, dew flashover, 160 kv.

The dew flashover test of the porcelain insulator merits description because there is no standard for this test, yet it is a condition which may prevail in isolated phase bus installations as often as once each 24 hours. This condition can occur in the morning after all parts are cooled by night temperatures. As the morning sun warms the enclosure, the moisture in the trapped air will condense on the porcelain insulators which, because of their mass, lag in temperature rise. The dew test was performed by chilling insulators in a refrigerator and then exposing them in a humid room atmosphere. The test voltage was applied after they were thoroughly dew-covered. The voltage was raised from 0 to flashover at the rate of 5,000 volts per second. At this rate of rise, tests were quite consistent, whereas at slower rates, leakage current tended to dry off the insulators, making readings erratic. An accurate reading of flashover could not be made at faster rates of rise.

Construction of 69-Kv Switchgear

Isolated phase construction was used throughout the enclosures for incoming lines, line disconnecting switches, bus connections, line potential transformers, circuit-breaker isolating switches, circuit-breaker pole units, connections to power transformers, and power transformer disconnecting switches. Isolated phase construction means that each phase is in a complete and grounded metal enclosure separated by an air space from other phase enclosures. The enclosures, except the enclosures for the circuit-breaker poles, have gasketed joints which exclude weather and dirt. Filter-type drip plugs are located at low points to relieve any water accumulation caused by condensation or unforeseen leakage. The breaker pole enclosures have to vent the gases incident to circuit interruption; these ventilators are equipped with dust filters.

The enclosures for line compartments, disconnecting switches, potential transformers and busses are constructed of aluminum sheet and structural shapes. Permanent joints between structural parts are continuous welded to provide the desired weather seal. The use of aluminum in these locations eliminates corrosion problems and reduces future maintenance to a minimum. It also permits supporting much of the equipment from the circuit-breaker enclosures. A simple, hot-dipped, galvanized I-beam structure provides supports for the balance of the equipment. The simplicity of the supporting structure is an important factor in the appearance of the installation.

The incoming line compartments were designed to enclose each phase terminal pothead, its associated lightning arrester, a disconnecting switch-pole unit, and a grounding switch-pole unit. The pothead enclosure was designed so that it can be completely removed during installation or pothead maintenance. It was also supplied with a gasketed door providing access for inspection or minor maintenance. A condenser bushing was used for the break jaw of the line disconnecting switch, thus providing a gas-tight barrier between the pothead and switch compartment. The three disconnecting switch-pole units and grounding switch-pole units associated with a 3-phase incoming line were separately gang-operated and properly interlocked so that safe operation is assured.

Isolated phase bus interconnects the various switching devices of the installation. The 38-inch-diameter enclosure is sufficiently large to permit a man to crawl through sections and perform inspection and cleaning operations with a minimum of dismantling after the original installation.

Inerteen-filled potential transformers, one per phase, connected phase to ground, are connected to the line connections between the line isolating switch and an adjacent circuit breaker. These transformers are designed for phase-to-phase potential and have full 350-kv impulse withstand.

The circuit-breaker isolating disconnecting switches are the same as the line disconnecting switches except that two 3-pole groups are mounted back to back and gang-operated from one mechanism. Key interlocks insure a safe operating sequence with the associated circuit breaker.

The 69-kv compressed-air circuit breakers are arranged with each pole in a separate housing. Louvered openings in the housing equipped with dust filters provide for the dissipation of gases resulting from breaker operations. Infrared lamps directed on the insulating supports of the breaker maintain uniform insulation characteristics during varying weather conditions.

The connections to the power transformers tap off the ring bus between sectionalizing breakers and pass through horizontally mounted disconnecting switches and continue to the power transformer primary bushings. Since gas migration barriers are not essential at these disconnecting switches, condenser bushings are not used, and the switch blade telescopes into a section of the hollow bus tubing. The gang-operating mechanism for each 3-pole transformer switch is brought down to ground level at a structure column where the operating handle and key interlocks are located. Visual inspection of the switch break is made possible from ground level by the use of a spotlight above the switch which shines through an opening in the top of the housing and can be seen through the glass inspection window in the bottom when the switch is open. When the switch is closed, the blade-moving carriage is interposed between the top and bottom openings and cuts off the light.

Walkways with guard rails and stairs to ground level at two locations are an integral part of the assembly. They provide for accessability to the disconnecting switch elevation for inspection, operation, and maintenance.

The entire switching structure was factory-assembled to insure proper co-operation of parts and permit factory high-potential tests; see Fig. 4. Shipments to the installation location were made in assembled combinations. Thus, many of the assemblies were moved directly from their means of transportation to their final location without requiring intermediate setdown space. This procedure simplified field erection and relieved much of the congestion which might otherwise have occurred. The air-supply system for both the 69-kv and 14.4-kv compressed-air circuit breakers is described by Gue.[3]

Conclusion

The construction described resulted in an assembly of switchgear using minimum lot area with a reasonable height. It has adequate insulation for the service requirements. The insulation should remain at a high level because of the material used and the dust-tight construction. The use of air circuit breakers and metal-enclosed construction contributes to safety. Field assembly was facilitated by factory assembly and shipment in subassemblies. Adequate provision was made for operation, inspection, and maintenance.

References

1. Pittsburgh Downtown 69-Kv Power Supply—Part I. Planning, V. E. Hill. *AIEE Transactions*, vol. 74, pt. III, Aug. 1955, pp. 643-48.

2. Pittsburgh Downtown 69-Kv Power Supply—Part II. Substation, B. M. Gue. *Ibid.*, pp. 648–53.

3. A New 69-Kv Compressed-Air Circuit Breaker, B. P. Baker, E. Frisch. *Ibid.*, vol. 68, pt. I, 1949, pp. 363–72.

Discussion

K. T. Ashdown (General Electric Company, Philadelphia, Pa.): Mr. Pierson's paper outlines the many engineering problems associated with the development of a metal-enclosed isolated phase bus for 69-kv service. We, too, were confronted with similar problems in the design of 69-kv enclosed gear during 1950–51. While we found that the width of this type of gear is fairly well determined by the insulation level, the depth can be varied to suit the type of insulators used.

With the flexible depth, it is possible to use standard outdoor insulators with a 350-kv-basic-impulse-insulation-level rating and therefore eliminate the necessity of designing a special type. The design selected by the author, while very special, embodies a unique and desirable feature, that of making the basic component parts of a device serve more than one purpose. This is illustrated by redesigning the top hardware to transfer the stress down into the body of the insulators so that the breakdown is opposed by the puncture strength of the porcelain as compared with the flashover values. Based on our experience in the 15-kv heavy-duty bus design, we wonder why Mr. Pierson, in designing a new porcelain, did not make the dew and dry withstand the same, i.e., equal to 160 kv. It is a proven fact that, regardless of the features of design, dew will form on the insulators under certain conditions and it is highly desirable to have an insulator that will withstand the 60-cycle 1-minute high-potential voltages when covered with dew. This is especially true at these higher operating voltages such as 69 kv.

While the insulation level is by far the major design concern in the application of enclosed conductors at this voltage, there are other features which must be taken into consideration. One of these is the thermal capacity of the bus and of other components such as disconnecting switches, etc. Thermally, there would be no question on this particular design as the 4-inch outside-diameter conductor is more than ample for the current involved. However, there is the current-carrying ability of the telescoping disconnecting switch and its associated finger contacts to be investigated.

The momentary rating of this bus is no problem because of the size of the conductor and the shielding principle of a metallic enclosure around an electric conductor. However, there still remains the momentary duty on the contacts of the disconnecting switch and how they will function under a full short circuit.

Although no direct mention was made in the paper, we assume the heat runs and momentary tests were made on the telescoping disconnecting switch to prove that they would withstand the currents encountered during a fault condition. The quantity of bracing insulators in Fig. 2 is somewhat startling. We feel that with such a construction the zero-force line principle used in our isolated phase bus can be employed. The single-insulator-per-support station would give the following advantages:

1. The number of insulators would be reduced to a minimum, thus reducing the number of creepage paths to ground.

2. More crawl space would be available for inspection and cleaning operations mentioned in the section entitled "Construction of 69-Kv Switchgear."

3. The over-all design would be thus simplified and its integrity enhanced through the use of a single-insulator-per-support station.

A. M. de Bellis (Consolidated Edison Company of New York, Inc., New York, N. Y.): It is noted that the 69-kv bus is supported in its housing on two insulators only. I trust the design is such that the insulators are held in a position where electromagnetic forces will always keep the porcelain insulators in compression.

The difficulty experienced in the design of porcelain supporting insulators has been noted. It would be interesting to know whether the insulators, as finally decided upon, were equipped with metal inserts at both ends or perhaps with none at all. It would also be interesting to know what means are provided for adjusting the porcelain-insulator pressure against the bus.

P. R. Pierson: Mr. Ashdown contributes additional information on problems of metal-enclosed 69-kv circuits. It is evident that the designs discussed had unlimited space in at least one direction, whereas the designs for the Forbes Substation had limitations in all directions.

It will be noted that the insulators were designed with unusually deep corrugations. Our tests under dew conditions indicated that a dew withstand value would have little meaning as it would vary between about 160 and 200 kv, depending on the manner in which the tests were conducted. The disconnecting switch and its associated finger contacts was equipped with the finger cluster assemblies commonly used in metal-clad switchgear where there is a background of test and service adequately demonstrating its thermal capacity and momentary rating.

The bus supporting insulators for all three phases are in line so that electromagnetic forces will keep them in compression, as suggested by Mr. de Bellis. However, the forces resulting from 3,500,000 kva at 69 kv between phases on 44-inch centers are relatively low and were no particular problem in design. The insulators were equipped with special metal inserts adjacent to the bus and flange mounting castings at the base. Jack bolts in the flange base casting were provided to align the insulator with the bus and to exert the necessary supporting pressure.

High-Current Arc Erosion of Electric Contact Materials

W. R. WILSON
MEMBER AIEE

EXCEPT for an atomic explosion, electric arcs and sparks apparently comprise the hottest regions on earth. Arcs often exist at temperatures at which all solids have melted, all liquids have vaporized, and all compounds have dissociated into the original atoms. Yet, in properly designed high-current circuit breakers, the arcing contacts operate reliably and withstand the disintegrating action of this medium. Usually made of sintered alloy materials, developed originally[1-3] in the company with which the author is associated, the contacts survive this experience many times and remain to perform their function of closing without welding, with their surfaces in condition to press together and accept their share of current at the required time.

Although there have been many investigations in the field of electric contacts, as witnessed by the 1,500 references in the bibliography[4] of the American Society for Testing Materials, surprisingly little has been published concerning the high-current region in the neighborhood of 5,000 amperes and over. Furthermore, conclusions reached from experience at low current cannot be applied at high current without specific verification. Two examples will serve to emphasize this point. The first deals with the relative life of silver and copper contacts in air. At 100 amperes, it is typical that the silver contacts will have many times the arcing life of copper contacts.[5] At 12,000 amperes, however, test data show erosion of silver and copper to be practically identical; see Fig. 1. The second example deals with life under oil. In the 100-ampere range,[5] immersing silver contacts in oil typically increases the arc erosion rate by a large factor. In the 10,000-ampere range, arc erosion of silver contacts is essentially the same in oil and air, at least at small spacings; see Table I.

The investigation of arc erosion herein described is one segment of a fundamental program which has been under way in the high-current area for several years. Other segments include investigations of clean contact resistance, long-time filming of contact surfaces in oil and in air, momentary high-current capacities (welding and exploding of contact spots), and mechanical impact strength and fatigue.

Preliminary Summary of Results

This paper reports data on arc erosion rates for the following elements listed in order of excellence as determined by test. As shown in Fig. 1, from best to poorest they are: carbon, tungsten, molybdenum, nickel, iron, titanium, copper, silver, zinc, aluminum, and tin. Data on four typical sintered alloy materials are given in Fig. 2. The ranges of practical mixtures are covered for copper-tungsten, silver-molybdenum, silver-tungsten, and silver-tungsten carbide. The erosion rate

---

Paper 55-215, recommended by the AIEE Switchgear Committee and approved by the AIEE Committee on Technical Operations for presentation at the AIEE Winter General Meeting, New York, N. Y., January 31–February 4, 1955. Manuscript submitted October 21, 1954; made available for printing December 8, 1954.

W. R. Wilson is with the General Electric Company, Philadelphia, Pa.

The author wishes to acknowledge the major contributions of C. H. Titus, who provided the initial direction of the project, and of M. A. Gusman, who conducted most of the test program. Additional contributions were made by J. R. Hopkins and C. L. Schuck. Thanks are due also to J. D. Cobine for fundamental concepts upon which much of the interpretation of the data is based.

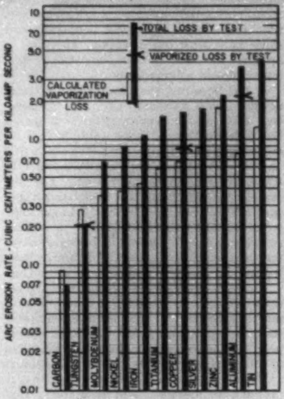

Fig. 1. Arc erosion of elements in order of excellence as determined by test. Comparison of measured erosion rates with calculated vaporization rates. Data based on half-cycle arcs of about 12,000 amperes rms on a 60-cycle base with contacts separated 1/32 inch

is given as a function of the fraction of refractory material.

Whereas understanding of the physical processes of arc erosion is nowhere near completion, in this over-all field where the rate of erosion, [cubic centimeters (cc) per kiloampere-second (ka-sec)] varies with current and material over a range of 10^6 to 1, a simple estimate including only vaporization losses permits prediction with better than order-of-magnitude accuracy of measured high-current erosion rates for the elements tested. In this estimate it is assumed that all of the electric power released at the anode and cathode (the arcing current multiplied by the sum of the anode and cathode voltage drops) goes into melting and vaporizing contact material. Perhaps the best evidence of correlation between the vaporization theory and the physical phenomenon is that the theory predicts essentially the same order of excellence of materials, from best to poorest, as was determined by test; see Fig. 1. Consideration of test results and this simple hypothesis shows that an additional source of erosion, especially for the low melting temperature materials, is that of molten metal being blown out in drops by the violent blasts of escaping vapor.

Table I. Comparison of High-Current Erosion in Air and Oil

Material	Average Loss in Grams per Arc	
	In Air	In Oil
Silver	2.025	2.114
Copper	1.490	1.300
30% copper, 70% W	0.395	0.339

Each average is based on a total of ten one-half-cycle arcs of about 12,000 amperes rms, 60 cycles.

Utility of Results

The most direct use of the results of the over-all program has been the setting up of specifications of contact performance to maintain and to improve contact reliability. Loss of material on arcing is one of the factors controlled. In addition to proof tests in the actual circuit breaker or device, any new contact material must pass exhaustive laboratory tests. The arc erosion test equipment described is economical to operate, and permits more complete evaluation and better quality control than was heretofore possible.

As the program advanced, it became increasingly evident that the physical processes of arc erosion are interwoven with those of the primary function of a circuit breaker: that of arc interruption. For example, it has been found that at least under some high-current conditions, the gaseous volume of contact material which is vaporized is so much greater than the volume between the contacts that the original insulating medium must be supposed to be almost totally displaced. Furthermore, even a minute fraction of metallic atoms will take over the arc current-carrying function from gases such as air and hydrogen. As shown by Suits,[6] as little as one part in a million of copper vapor in air will provide electrons to conduct 97 per cent of the current. As a result of these considerations, this study of high-current arc erosion has been coupled closely with other investigations aimed primarily at advancing the understanding of the fundamental processes of interruption.

There is no question, of course, as to the crucial position that electric contacts hold concerning the reliable operation of circuit breakers and contactors. The function of these devices is to interrupt the circuit by opening the contacts, and to pass load current when contacts are closed. The engineer designs and selects contacts on the basis of his knowledge of the relationships between performance and the factors which control it. He must do more than build a piece of equipment which meets certain specific tests. He must understand the various pertinent physical phenomena which may occur and design the equipment to take best advantage of their characteristics. The primary objective of this investigation has been to contribute to the basic understanding in this area.

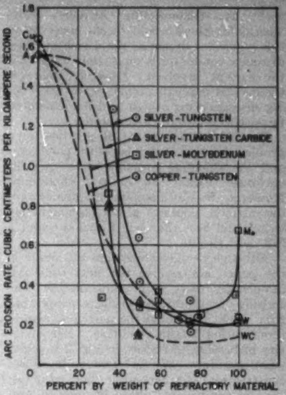

Fig. 2. Arc erosion rates for sintered alloy materials. Test basis as in Fig. 1

Test Equipment

Testing for arc erosion in the high-current range is very different from testing in the low-current range. It is typical to operate a 100-ampere contactor 100,000 times to obtain an adequate measure of the material loss. In comparison, one 20,000-ampere arc held for 0.1 second will disintegrate a section of copper bus bar 1/2 inch long, 1/4 inch thick, and 2 inches wide.

In this investigation it was desired to eliminate certain disadvantages of selecting one particular circuit breaker as being representative, and mounting each pair of contacts in it for test. These disadvantages include the difficulties of: 1. controlling arc duration, 2. eliminating or reproducing contact bouncing or vibrations so that a consistent curve of gap length versus time could be maintained, and 3. synchronizing the exact instant of contact opening with the desired point on the current wave. To eliminate these extraneous factors and to obtain arc erosion data which were reproducible and reliable, a new arc erosion-testing facility was developed and put to use.

CIRCUIT

Fig. 3 is a schematic diagram of the test equipment used. The equipment passes a single half-cycle of controlled current through an arc struck between the con-

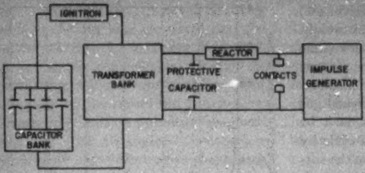

Fig. 3 (left). Schematic diagram of half-cycle, high-current arc erosion test equipment

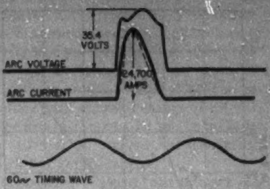

Fig. 4 (right). Typical oscillogram trace. Dotted curve of arc current calculated from equation 1

tacts. To eliminate mechanical opening stroke variations, the contacts are held stationary at a fixed gap, generally from 1/64 to 1/2 inch. A high-voltage impulse generator has often been used to break down the gap and to initiate the arc. In other cases, after comparative tests have established that the arcing region is not contaminated, the arc is initiated by means of a fuse wire. Energy for the arc which follows is derived from a large capacitor bank charged through rectifiers to several kilovolts direct current. A portion of the trigger voltage is used to fire an ignitron which discharges the capacitor bank through a transformer bank to step up the current. A reactor is used to resonate the capacitor bank to yield the desired base frequency (about 60 cycles) of the half-cycle of current. To prevent the impulse voltage from damaging the transformers, a capacitor is connected across the secondaries to form, with the reactor, a low-pass filter. Magnetic and cathode-ray oscillographs are used to record arcing voltage and current, and extensive additional instrumentation is available as needed.

Current Wave Form

Fig. 4 shows typical current and voltage wave forms traced from oscillograms. If one assumes that the arc voltage is constant and that the magnetizing reactance of the transformer is high in comparison with the secondary leakage reactance, the current wave form is given by equation 1. This expression was derived by applying the Laplace transform method to the circuit differential equations.

$$i=\frac{N(E_c-NE_a)}{L\sqrt{\frac{1}{CL}-\frac{R^2}{4L^2}}}\left(\epsilon^{-\frac{Rt}{2L}}\right)\sin\sqrt{\frac{1}{CL}-\frac{R^2}{4L^2}}\,t \tag{1}$$

where

i = instantaneous secondary current, amperes
N = transformer turns ratio
E_c = capacitor bank potential, volts
E_a = arc voltage drop, volts
L = total inductance referred to primary, henrys
C = capacity of bank, farads
R = total resistance referred to primary, ohms
t = time, seconds

Because of the exponential term in equation 1, the half-cycle of current begins like a sine wave, but gradually drops below the sine wave by an increasing amount. The calculated current form shown dotted in Fig. 4 was obtained by substituting the known value of capacitance in equation 1 together with values of inductance and resistance calculated from the performance of the circuit. The equation can be used profitably in the design of similar half-cycle equipment. It has further value in that it demonstrates that the factors causing the nonsinusoidal current wave are understood and under control.

Condition of Test

All arc erosion data reported on the graphs of this paper were taken with 1/2-inch diameter contacts with a 2-inch radius crown. The bulk of the data, such as for the elements of Fig. 1 and the sintered alloys of Fig. 2, was obtained with a 1/32-inch gap established between the contact surfaces before each arc. Generally, each pair of contacts was subjected to six arcs of one-half cycle's duration on a 72-cycle base. Because of variations in arc voltage, the crest current in the metallic arcs varied from about 20,000 to 25,000 amperes. For carbon the current was exceptionally low, reaching a crest of only 12,000 amperes. Based on the calculation method of this paper, compensation was made for these variations by reporting the data in terms of cc of material lost per ka-sec. The adjustments were a matter of a few per cent for the metals. For convenient reference, the average 72-cycle base wave was equivalent in ampere-seconds to a 12,000-ampere rms half-cycle on a 60-cycle base. Finally, because the volume of arc material lost is of more engineering importance than the weight, the weights were converted to approximate volumes by dividing by the densities of Table II. Accuracy for the sintered materials is reduced somewhat, but the original data can, of course, be recalculated by the reader if desired.

Fig. 5 presents typical curves of arc erosion in terms of material loss versus the number of arcs that had been applied in succession. Although there are appreciable variations between weight losses on successive tests, the points in general follow straight lines. These variations can often be correlated during test with pieces of contact material which gradually lose their support and then finally drop off during one of the arcs. That the erosion rate does not decrease as the number of arcs increases is evidence that composition of the sintered alloy materials does not change markedly during arcing. With the lower melting temperature materials, large protuberances which formed were filed off to maintain essentially flat surfaces.

Some data were taken, with a 2-inch gap between the contacts; see Fig. 6. The arc was initiated by means of a fuse wire and maintained for 2 or 3 cycles on a 60-cycle base.

Table II. Physical Properties of the Contact Materials

Material	Volumetric Heat of Vaporization, Gram Calories per CC	Specific Heat of Vaporization, Gram Calories per Gram	Mass Density, Grams per CC	Melting Temperature, Degrees Centigrade	Boiling Temperature, Degrees Centigrade
Graphite	32,200	14,300	2.25	3,500	4,200
Tungsten	20,900	1,100	19	3,370	5,927
Molybdenum	16,600	1,630	10.2	2,620	4,803
Nickel	15,400	1,730	8.90	1,452	2,900
Iron	13,600	1,730	7.86	1,535	2,998
Titanium	10,700	2,380	4.5	1,800	5,100
Copper	11,500	1,290	8.92	1,083	2,595
Silver	6,830	650	10.5	961	2,001
Zinc	3,410	477	7.14	419	907
Aluminum	7,500	2,780	2.7	657	2,056
Tin	4,310	590	7.30	232	2,270
Tungsten-carbide			16		

Approximate densities ρ for the alloys were calculated from $\rho=\rho_1\rho_2/f_1\rho_2+f_2\rho_1$, where f = fraction of component by weight; 1, 2 = subscripts denoting components.

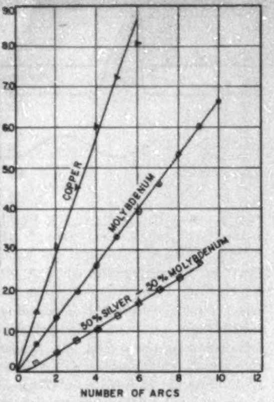

Fig. 5. Arc erosion loss as a function of the number of half-cycle arcs

In all, some 200 contact pairs have been tested. The materials came primarily from contact manufacturers, although some were supplied from within the company with which the author is associated. All materials were given metallurgical and chemical check tests.

Theory of Erosion Processes

It should perhaps first be pointed out that erosion of contacts is a complex, nonlinear space distribution type of problem involving such things as bubbles bursting through the liquid surface of the contacts in the midst of turbulent blasts of gas. Heat transfer and viscosity phenomena are involved at temperatures so high that they cannot be studied except in the arc. Consequently, calculations to be made are necessarily to establish orders of magnitude only, and to determine whether or not certain processes are active. It is not to be anticipated that the theory evolved will predict measured results with any degree of precision.

ARCING MEDIUM

In the order of 1 microsecond[7] as arcing current starts to flow, portions of the contact surfaces reach temperatures at which the metal evaporates. The gaseous volume of the metal vapor which has issued from these surfaces by the end of a high-current half-cycle arc is surprisingly large.

With copper contacts carrying the 12,000-ampere arc current, the weight of metal vaporized per operation is about 1 gram (see Fig. 5). At the typical arc temperature of 5,000 degrees Kelvin (K) and at atmospheric pressure, this weight of copper as a gas would occupy a volume of about 7,500 cc. This is a cube about 20 centimeters (cm) on a side. It therefore appears certain that the original gas or liquid between the contacts must be swept out very early in the half-cycle by this metallic gas which flows from the surfaces. Thus the arc, under the conditions of test, must flow through a gas consisting almost solely of the vapor from the contacts. This is explanation of the fact that contacts tested at high current, Table I, showed the same erosion rates in air and in oil.

ENERGY DISTRIBUTION

The classical picture of the voltage distribution in an arc is that of abrupt voltage drops which occur over microscopic distances at the cathode and anode together with a gradual linear change of voltage along the axis of the column. Because the same current flows through all drops, energy release at the contact surfaces is intense.

In working toward a more complete general understanding of arc processes, Cobine[8] has used the data presented in this paper to establish that vaporization is one of the main erosion processes at the anode of high-current arcs. He was also able to make new determinations of anode surface temperatures. In an earlier paper, Holm[9] concluded that erosion losses at the cathode of a high-current arc also results primarily from vaporization. Both investigators postulated that the electric energy dissipated in the region of the surface voltage drop (anode and cathode drops respectively) produces the vaporization, and both comment that reliable data on the magnitudes of these voltage drops are not available. The work function (energy required to "evaporate" an electron from a surface) is represented for electron flow by a voltage of about +5 at the anode and −5 at the cathode, these drops sometimes being lumped for convenience as part of the over-all anode and cathode drops.

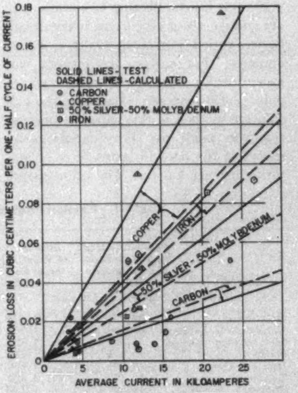

Fig. 6. Multiple-cycle arc erosion tests at 2-inch contact separation as function of current. Solid curves drawn by judgment best to fit test data. Dotted curves calculated from vaporization rate equation

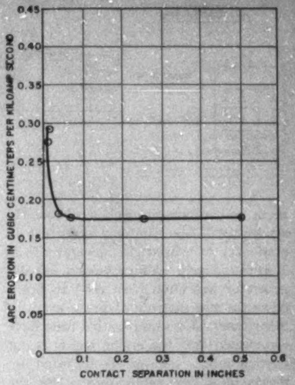

Fig. 7. Arc erosion versus spacing for silver-molybdenum sintered alloy material

There are several mechanisms whereby electric energy dissipated in the anode and cathode drops is delivered to the electrodes. The relative importance has apparently not been established as yet. At the anode, the electrons, which probably carry the bulk of the current, are accelerated through the anode drop, delivering the kinetic energy thus acquired plus the "heat of condensation" of the electrons to the anode surface. At the cathode, there is similar delivery of energy by the positive ions which carry a fraction of the current to the cathode. The cathode processes are complicated by the fact that current is also probably carried from the surface by electrons, and that the removal of each electron cools the surface by the work function. However, when these have fallen through the cathode drop they will strike arc plasma molecules and dissipate the kinetic energy as heat in the plasma immediately adjacent to the contact surface. The arc plasma must be far hotter than the contact surfaces in order to conduct current.[8] Consequently, there will be strong tendency for the heat generated near the surface to flow by ordinary heat conduction (molecular collision) through the cathode and anode drops to the surfaces. This flow will be accentuated by the extremely high axial temperature gradients near the cool electrodes. A complete mechanism for electrode phenomena would have to include explanation for (among other factors) the extremely high-speed vapor jets which have been found to issue from the surfaces.

VAPORIZATION RATE EQUATION

However, even without this complete explanation a rough energy balance can be set up on the basis of the available data. The continuous drain of vaporization energy from the region of the cathode and the anode must apparently be replaced by electric energy in nearly the same volume. This will be found consistent with the test results, Fig. 7; and it seems reasonable because of the relatively small amount of heat that could travel long distances against the flow of vaporized material and through the relatively low axial temperature gradients which exist along the column away from the surfaces.

The electric energy input near the contact surfaces is therefore

$$W=(E_c+E_a)IT \qquad (2)$$

where

W = total energy input at electrodes, watt-seconds
E_c = cathode drop, volts
E_a = anode drop, volts
I = arc current: average of absolute magnitude, amperes
T = duration of arc, seconds

The metal vaporized is

$$V=\frac{W}{\rho JH} \qquad (3)$$

where

V = volume of metal vaporized, cc
H = heat of vaporization, calories per gram
J = heat equivalent, 4.18 joules per calorie
ρ = density of contact material, grams per cc

Combining equations 2 and 3 yields the vaporization rate in cc of contact material lost per ka-sec (or kilocoulomb) of arc current

$$R=\frac{1{,}000V}{IT}=\frac{1{,}000(E_c+E_a)}{\rho JH} \qquad (4)$$

where R = erosion rate, cc/ka-sec.

This vaporization-rate equation is derived because it appears to be a rough physical constant of the material, depending for its value upon other physical constants.

Although separate values for the anode and cathode drops are difficult to obtain, an approximate value for their sum, as required by equation 4, can be obtained by measurements on short arcs. The calculations of this paper are based on the fact that both the axial voltage gradient along the column and the sum of the cathode and anode drops are reasonably independent of current magnitude. Concerning column gradients, the Ayrton[10] work shows that in carbon arc in air at 10 amperes, this gradient is about 18 volts per cm. Unpublished data taken at 10,000 amperes show that the column gradient increased only to about 25 volts per cm. For metals, the axial gradients are generally smaller than for carbon, and the gradients do not increase greatly with moderate increase in pressure.[11] Therefore, in the short gaps (initially 1/32-inch) used for the bulk of the data of this paper, the total voltage drop along the column has an upper limit of about 3 volts. The average total arc voltage, including the anode, cathode, and column drops, did not vary widely from about 29 volts at 12,000 amperes for the materials tested. Because of statistical variations and limited data, accurate values for the arc voltage are available at this time for only copper (29 volts), silver (30 volts), and molybdenum (29 volts). Therefore, with these metals the sum of the anode and cathode drops ($E_a + E_c$) averages about 26 volts. Limited data on all of the remaining materials at 12,000 amperes show individual tests varying from about 23 to 38 volts. For comparison with the low-current range, at 10 amperes the Ayrton values for the sum of the anode and cathode drops is 20 volts for silver and 16 volts for copper. Based on these facts, it is assumed, for ease in approximate calculations, that in the high-current range of stationary arcs in atmospheric air, the sum of the anode and cathode drops is 25 volts for all materials tested. Study of the data indicates that additional variables are present to the extent that more accurate determination of this factor would not improve the accuracy of correlation with measured values at this time.

Comparison of Measured Erosion Rates with Calculated Vaporization Rates

Before checking the vaporization rate equation against the data, it is of interest to see the range over which the results might lie. In a previous paper,[12] the author presented extensive data on the arcing life of silver contacts in the 10-ampere range (from 5 to 35 amperes). At 20 amperes, for example, the volume of silver lost per operation was about 10^{-9} cc. In the present tests it is 0.1 cc. This is an erosion change of 10^8 to 1 resulting from a current change of 10^3 to 1. The rate in cc per ka-sec was in the order of 10^{-5} at 20 amperes, in comparison with 1 at 12,000 amperes.

According to Holm,[9] the primary reason for this great variation in erosion rates is that most of the heat is conducted away through the contacts at low currents and moderate spacings and therefore is not available to vaporize material. As currents are raised and heat is introduced more rapidly, the vaporization region is reached in which heat conduction becomes negligible, and effectively all of the heat must be dissipated by vaporization. In Holm's work this region started in the order of 1,000 to 10,000 amperes. With certain small contacts[13] between which arcs occur at extremely small spacings, the energy input is concentrated in such a minute space that the vaporization region would occur at much lower currents. The primary assumption made throughout this paper is that only the high-current, vaporization region is being considered.

SAMPLE CALCULATION WITH COPPER

For a sample calculation with the vaporization rate equation, consider copper electrodes. Table II shows a heat of vaporization for copper of H=1,290 calories per gram. The density of copper from Table II is 8.92 grams per cc. Substituting values in equation 4 yields an erosion rate of 0.62 cc per ka-sec. The 12,000-ampere test current wave has a ka-sec value of 0.11, so the calculated volume of copper eroded is 0.068 cc. From Fig. 1, the measured value is 0.17 cc, or a discrepancy of 2.5 to 1.

This calculation considers only the amount of metal vaporized, and ignores the amount blown out in drops by the vapor as it escapes. Tests were run on some of the materials to estimate the liquid loss. An insulating cup was constructed around the arcing contact to catch most of the liquid drops. Many of these are quite large, measuring more than 1 millimeter in diameter. To permit easy escape of vapor, an inch of radial clearance was allowed between the walls of the cup and the contacts. The top extended about 1/2 inch above the upper contact surface. The total erosion rate was not altered significantly. The arrowheads on Fig. 1 represent the volume of contact material vaporized, as estimated by subtracting the weight of the drops collected from the total loss. The vaporization loss as estimated by test, then agrees very well with that from the vaporization rate equation.

PERFORMANCE OF THE ELEMENTS

For copper, it is seen that the total erosion loss is quite closely represented by the sum of the estimated loss by vaporization and the loss of liquid in the form of drops blown out as this vapor escapes. Furthermore, the liquid loss constitutes a fairly high portion of the total loss. Except for carbon, tungsten, and possibly zinc, conditions with the remainder of the elements appear to be similar, in that in each case the total loss of material is greater than that which can be vaporized by the electric energy available. With each of these elements that has been checked, the liquid loss has been substantial and in agreement with this approximate picture.

Only with carbon and tungsten does the calculated vaporization loss exceed the measured loss; see Fig. 1. The discrepancies found appear to indicate the element of error in the vaporization equation by itself. Tests with tungsten showed no detectable loss as liquid. It is difficult to make such an evaluation with carbon.

Consideration of these factors together with the melting temperatures of the elements reveals a general pattern. The amount the test erosion rate exceeds the estimated vaporization rate is indication of the amount of material lost in the liquid form. As would be expected, and as can be checked by comparing Fig. 1 and Table II, this difference tends to increase as the melting temperature decreases. With tin, which has the lowest of the melting temperatures, the entire 1/4-inch depth of the contact button turns to liquid during a half-cycle arc. Liquid loss is high. With tungsten and carbon, very little material is melted, and liquid loss appears to be negligible. It is interesting to note that the order of increasing arc erosion, decreasing volumetric heat of vaporization, and decreasing melting temperature are very nearly the same for the elements tested. Aluminum has a low melting point and a high boiling point, which would tend to maximize liquid loss; and it has a high specific heat of vaporization, which would tend to reduce vapor losses. This appears to be the explanation of the very high liquid loss indicated for this material. Zinc is the major exception to this trend of increasing liquid loss with decreasing melting temperature in that loss by liquid apparently is a small factor in comparison with vaporization. The physical properties of zinc are consistent with this action in that zinc has by far the lowest of all of the boiling points, and the lowest of the specific heats of vaporization, tending to maximize the vapor losses. It has the smallest difference between the melting and boiling temperatures, tending to minimize liquid effects. The order of excellence of the elements and the magnitude of erosion losses seem therefore to fall into position very nicely on the basis of the physical constants controlling vaporization and melting.

The possibility that a large portion of the erosion might be caused by oxidation of the surface in air should be discussed. At low current, this is an important mechanism[5] and explains the superior performance of silver (a noble metal which forms almost no oxide) in comparison with copper (a base metal which oxidizes fairly easily). However, this mechanism neglects the evidence that the erosion is controlled by phenomena at the contact surfaces, and that at high currents, the streams of metal vapor carry essentially all of the oxygen far away from those surfaces. For aluminum, with its extreme affinity for oxygen, it is quite possible that the actual liquid loss is greater than that measured, and is more nearly what is indicated by the difference between the measured erosion rate and the vaporization rate. Some of the liquid drops probably oxidize and are carried away as a gas.

SINTERED MATERIALS

One of the most striking facts concerning sintered contacts is that mixtures of two elements (such as the silver and molybdenum in Fig. 2) can exhibit lower erosion rates than either of the elements by themselves. A parallel physical concept is that, for an alloy, the melting temperature, boiling temperature, and apparently the heat of vaporization each can be greater than the corresponding values for any of the components of the alloy. Furthermore, the liquid loss from the higher melting-point refractory component will be affected by the presence of the lower melting-point conducting component.

The correct nominal composition of a contact does not ensure that its arc erosion will be acceptable. Copper-tungsten contacts of the 30%–70% type which were supposedly of equal quality have been tested and found to vary in arc erosion rate from near the tungsten value to near the copper value. One of the defects that might cause this poor performance is that of a poor bond in the tungsten matrix. If the contact were held together by the copper only, the melting of this material at relatively low temperature would permit the tungsten particles to flow away with the liquid copper.

Additional Factors

CONTACT SPACING

Fig. 7 shows that contact erosion increases at very small contact gaps. Two factors appear to combine to cause this. First, the restricted space between electrodes means that gas pressure and vapor velocity will be increased, tending to blow off more contact material. Second, because of the small spacing in relation to contact width, the fraction of heat which can flow from the cathode and anode drop region into the column, and escape without causing vaporization, is diminished.

The fact that erosion losses tend to remain relatively constant as contact gap (and total arc voltage) are increased beyond 1/32 inch is powerful evidence that the erosion losses depend on electrical energy input at the surface, and not on total arc energy. Further verification that erosion rates are reasonably constant at the higher spacings is given in the following.

CURRENT MAGNITUDE

According to the vaporization rate equation, contact erosion in cc per half-cycle should be proportional to current magnitude in the high-current range. A limited amount of erosion data was taken, ranging from 3,000 to 25,000 amperes, 60 cycles. The same type of 1/2-inch-diameter contacts was used as in the one-half cycle tests, but with 2-inch spacing. The solid curves of Fig. 6 show the best straight lines drawn by judgment to represent the test points, and the dotted curves show the estimated vaporization rates. Because the heat of vaporization is not known for the silver-molybdenum alloy, the calculated curve is based on the one-half-cycle erosion data for this material. Correlation here indicates a relatively large statistical spread between individual points, and about a 2-to-1 level of accuracy for averages. Examination of the points indicates some tendency for arc erosion loss to increase more rapidly than with the first power of current. It should be noted that in all calculations, erosion rates were assumed to be the same at 1/32 inch as at 2 inches. Current durations in these tests were several times longer than in the half-cycle tests. Under these conditions, the correlation between the vaporization rates and measured erosion values appears satisfactory. Additional verification of the approximate direct proportionality between erosion loss and current magnitude may be found in a recent paper by Spayth and Heil.[14]

POLARITY

This investigation was aimed at a-c application, but some interesting polarity effects were noted. As would be expected from low-current experience the anode of the carbon arc lost much more material (about 80%) than the cathode (about 20%). However, with silver, the polarity had no appreciable effect. Whichever contact was on top experienced about 60% of the total loss. The explanation seems to be simply that melted material falls from the top contact and lands on the bottom one. With copper, the falling material effect is present in addition to a polarity effect whereby the anode losses average about 65% of the total.

A large growth often appears on the copper anode with startling speed. At 0.2-inch spacing, during one half-cycle of arc, the anode surface melts, material gathers apparently at the anode spot, and a blunt column, rises nearly to the opposite side; see Fig. 8. It does not matter whether the anode is on the top or bottom. In one case the column rose from the anode against gravity and was in electrical contact with the cathode at the end of the test. The next arc was established without inserting a fuse wire. The current which flowed was 60% greater than any of the other arcing currents.

The same general phenomenon, but with the protuberance bridging a much smaller part of the gap, occurs at the tungsten anode. It is not seen with aluminum. The high electrostatic force caused by the anode voltage drop, and the electromagnetic pinch effect probably contribute to the formation of the column. Assuming that the bulk of the current flows to this protuberance results in an anode current density in the order of 1,000,000 amperes per square cm for copper.

Statistical variations are much greater if the losses of each electrode are considered separately. For example, in one series of tests, the loss from a tungsten cathode was zero to three significant places. The anode loss alone was sufficient to give a fairly normal erosion rate for the pair. With some of the materials, the relative erosion rates for anode and cathode shift with spacing, in a manner which at present appears to be random.

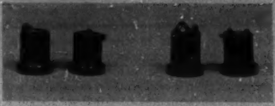

Fig. 8. Growth which appears on copper anode during one half-cycle of arcing. Anodes are marked +; the cathodes are unmarked. The molten copper rises against gravity. The mounds are about 0.16-inch high and were formed in a 0.2-inch gap. The small protuberance on the anode at the right apparently was a molten drop which fell from the cathode

Comparison with Low Currents

It is interesting to compare high-current arcing life relationships with those found in the previous investigation[13] reported by the author for the 10-ampere range. Except for the vast difference in magnitude, the primary difference is that life is inversely proportional roughly to the first power of arc current and of arc charge transfer at high current; but at low current, life was found to be inversely proportional to the 3.7 power of arc current and of arc charge transfer. This is partly because the microscopic pits which defined the termination of life with the minute arcs are of little consequence at high current. As a result, the great detrimental effect of slight bouncing at the break of circuit found at low current would not appear at high current even if arcing durations were similar. Reduction in life due to bouncing can be estimated simply by adding the charge transfer occurring during the bounce to the value inserted in the rate equation.

In both ranges the contact surfaces approach planes as the end result of arcing. The effect of crowned or radiused surfaces on life at high currents is simpler than in the low current range, because this flattening generally occurrs during the first arc. Erosion was not consistently different on this first arc, although there was tendency for it to be less. This is consistent with the reduction in loss found when contact spacing is increased.

The lack of dependence of arc erosion on line voltage, except as it affects arcing current, appears to hold in both ranges.

Conclusions

1. From the standpoint of arc erosion, the order of excellence has been determined for eleven elements. From best to poorest they are: carbon, tungsten, molybdenum, nickel, iron, titanium, copper, silver, zinc, aluminum, and tin.

2. The primary mechanism of erosion appears to be vaporization of contact material. A vaporization rate equation, based on the assumption that all of the electrical energy released at the anode and cathode goes into vaporizing contact material, yields a predicted order of excellence the same as that determined by test, except that the three poorest materials are shifted among themselves; see Fig. 1.

3. A secondary mechanism of erosion is that the great quantities of vaporized material blast drops of liquid from the surfaces as they escape. This effect is nearly absent with the highest melting temperature materials (carbon and tungsten) and tends to increase as the melting temperature decreases. Tin is the poorest of the materials because its heat of vaporization is nearly the lowest of the elements tested; its melting temperature is the lowest; and the ratio of its boiling temperature to its melting temperature is the highest. Consideration of these factors leads to a reasonable explanation for the shifted order of the three poorest materials.

4. From the standpoint of arc erosion alone, a low melting temperature is indicative of a poor material. This is closely related to conclusion 1 because, with the elements tested, the materials with low volumetric heats of vaporization also have low melting temperatures.

5. Sintered alloy contact materials sometimes have lower erosion rates than either of their component elements. Data are presented for the practical mixtures of copper-tungsten, silver-molybdenum, silver-tungsten, and silver-tungsten carbide.

6. With the sintered alloy materials, correct composition does not ensure low arc erosion. Reliable performance of arcing materials is being maintained in the author's company by extensive and continuous developmental and control testing with equipments such as are described in this paper.

References

1. SINTERED TUNGSTEN POWDER, W. D. Coolidge. *United States Patent No. 1,082,933*, Dec. 30, 1913.

2. COPPER-IMPREGNATED TUNGSTEN, N. H. Adams. *United States Patent No. 1,477,797*, Dec. 18, 1923.

3. COPPER TUNGSTEN SINTERED ALLOY, N. H. Adams. *United States Patent No. 1,552,184*, Sept. 1, 1925.

4. BIBLIOGRAPHY AND ABSTRACTS ON ELECTRICAL CONTACTS, Committee B4. *American Society for Testing Materials*, Philadelphia, Pa., 1952.

5. MATERIALS AND PROCESSES (book), James F. Young. John Wiley & Sons, Inc., New York, N. Y., 1954, "Electrical Contacts," B. W. Jones, p. 190.

6. THE DETERMINATION OF ARC TEMPERATURE FROM SOUND VELOCITY MEASUREMENTS, C. G. Suits. *Physics*, New York, N. Y., June 1935, p. 190.

7. CONDUCTION OF ELECTRICITY THROUGH GASES (book), J. J. Thomson. Cambridge University Press, London, England, vol. II, 1933, p. 564.

8. HIGH PRESSURE ARC ANODE PHENOMENA, J. D. Cobine, E. E. Burger. *Physical Review*, New York, N. Y., vol. 93, 1954, p. 653.

9. THE VAPORIZATION OF THE CATHODE IN THE ELECTRIC ARC, R. Holm. *Journal of Applied Physics*, New York, N. Y., vol. 20, July 1949, p. 715.

10. See ref. 7, p. 586.

11. GASEOUS CONDUCTORS (book), J. D. Cobine, McGraw-Hill Book Company, New York, N. Y. 1941, pp. 297, 328.

12. LIFE OF SILVER-SURFACED CONTACTS ON REPETITIVE ARCING DUTY, W. R. Wilson. *AIEE Transactions*, vol. 72, pt. III, Dec. 1953, pp. 1236–43.

13. EROSION OF ELECTRICAL CONTACT MATERIALS ON MAKE, L. H. Germer, F. E. Haworth. *Journal of Applied Physics*, New York, N. Y., Nov. 1949 pp. 1085–1109.

14. ELECTRICAL CONTACTS—PART I, F. J. Spayth, V. E. Heil. *Electrical Manufacturing*, New York, N. Y., Sept. 1954, p. 92.

◆

Discussion

J. D. Cobine (General Electric Company, Schenectady, N. Y.): This is an interesting and useful treatment of erosion from electrodes subjected to high-current arcs. The success of the author's treatment of arc electrode erosion is due both to the fact that for short arcs the column voltage drop is small relative to the anode and cathode drops and that heat conduction is an inherently slow process. Thus an energy balance can be effected without detailed attention to the fundamental physical processes involved. In fact, the very high-current arc offers a most promising field for detailed study of the arc. It is much simpler than arcs at small currents where erratic performance prevails and thousands of operations are necessary to accumulate erosion data.

It may be useful to review the basic features of the analysis (see reference 8 of the paper) of the high-current anode phenomenon referred to by the author. At the time that this analysis was developed, data on the high-current arc were very meager and it was necessary to estimate probable limits of some quantities from spark data. Since this time the data presented by Wilson on erosion and on current density by Winsor and Lee (see reference 1 of this discussion) became available. These data have greatly strengthened the position of the analysis, which is based on the best possible estimates of the probable limiting values of the various physical processes that must be present. The consequences of these limits may then be assessed.

The electric power delivered to the anode spot by the arc is

$$P_e = J_a(V_a + \varphi + V_T) \text{ watts per cm}^2 \qquad (5)$$

where J_a = anode spot current density, V_a = anode fall of potential, φ = work function of the anode material, representing power released by the "condensation" of electrons, and V_T = average energy of the electron escaping from the arc plasma (positive column) towards the anode. When the original analysis was made, it was considered reasonable to assume J_a to lie between the limits 8,000 to 50,000 amperes per cm^2. Jones, et al. (see reference 2 of this discussion) have found 8,000 amperes per cm^2 for welding arcs, we at the Research Laboratory had found 30,000 amperes per cm^2 for a 4,000-ampere arc and spark data indicated about 50,000 amperes per cm^2. The anode fall, V_a, lies between 0 and the ionization potential of the gas or vapor involved. At high currents it is reasonable to take V_a as the ionization potential of the metal atoms of the anode material. For the common metals this may be taken as 7.5 volts. The value of V_T may be taken as from 1 to 2 volts corresponding to column temperatures of 6,000 to 15,000 K respectively. Taking all the low values together and all the high values together gives the limits of electrical power input as 4.4×10^4 and 7×10^5 watts per cm^2. The anode spot also receives radiant power, P_r, and energy from the "hot" neutral atoms striking the surface whose power is P_n. The limits of P_r are 0.75×10^4 watts per cm^2 at 6,000 K and 3×10^5 watts per cm^2 at 15,000 K. The value of P_n is 0.58×10^4 watts per cm^2 at 6,000 K but is negligible at 15,000 K since the vapor there is probably completely ionized. Summing these quantities gives a minimum probable value of input power as 5.7×10^4 watts per cm^2 and a maximum probable power input as 1×10^6 watts per cm^2. It is clear that either limit represents a very high value of surface power density.

The power delivered to the anode surface by the arc must be balanced at that surface by heat conduction into the metal by radiation and by evaporation. It is easily shown that heat lost by evaporation is far greater than by the other two processes. Using the relation between temperature and mass of material evaporated, curves may be drawn for various metals which express the surface density of power carried off as function of temperature. The points at which these curves equal the maximum and minimum values of power input define the probable limits of the anode spot temperature. The probable spot temperature is considerably above the boiling point (i.e., the temperature at which the equilibrium vapor pressure equals one atmosphere). This explains the almost explosive violence with which vapor is expelled from the electrode surfaces. Since heat conduction is neglected, the analysis as presented must be confined to short time arcs, i.e., the order of one-half cycle 60 cycles per second. Since evaporation is the most powerful factor involved, the active area will be held at a relatively constant temperature. The heat flow into the metal in one-half cycle from this constant temperature surface can be shown to be relatively small, and radiation neglected. Considerable amounts of metal may be expelled by the explosion of gas pockets and splatter so that measured losses would be expected to be greater than predicted. This is well shown by the data presented by Mr. Wilson. It is more difficult to analyze the cathode spot. However, it can be shown that evaporation of metal will limit the spot temperature so that thermionic emission is of secondary importance for all but the most refractory materials. This is true even if the entire current at the cathode is carried by positive ions. In fact it is exactly the assumption tacitly made by those who calculate the energy received by the cathode as being cathode drop times current. In a long arc energy received from the cathode drop by electrons emitted cannot directly affect the cathode surface, but is used to establish the plasma.

The protuberances shown in Fig. 8 are quite interesting. As molten areas develop, surface tension and the "pinch effect" will cause a certain amount of gathering of the liquid. Arcs of the current used have total anode spot areas of the order of a square cm. It is difficult to see how the active spot could stay fixed on the top of a protuberance which continually increased in height. This is especially true if a current density of 1,000,000 amperes per cm^2 were involved. The evaporating metal from the active area would exert a considerable reaction on the surface, which should produce a depression. These depressions are seen on welding beads where the melt is piled up behind the arc foot print, and in mercury arc rectifiers. Although appearing on both upper and lower surfaces, could they not arise from drops from the upper surface, those frozen on the upper surface being too small to break free and those on the lower surface piled up by a dripping spot from above? This can be seen in welding arcs. At the cathode the current is certainly delivered to a multiplicity of cathode spots and multiple-anode spots are quite probable. This coupled with the fact that the regions of high electrostatic field are of limited extent would seem to exclude all but the smaller protuberance from anything but simple dripping.

REFERENCES

1. ELECTRIC ARC AND RESISTANCE WELDING—IV. *AIEE Special Publication S-64*, "Properties of a DC Arc in a Magnetic Field," L. P. Winsor, T. H. Lee. July 1954, pp. 49–60.

2. T. B. Jones, W. B. Kouwenhoven, M. Skolnik. *The Welding Journal*, New York, N. Y., Research Supplement, Oct. 1949.

W. R. Wilson: The author wishes to thank Dr. Cobine for his discussion. There is only one point to add. Additional data are now available as evidence that the anode protuberances are actually growths, and not drops from the opposing electrode. At the spacings of 0.5 cm with copper contacts, arc erosion appears to be unusually erratic, and during some arcs is surprisingly low. On several of these tests, the weight of the protuberance (obtained by volumetric calculation) was greater than the entire weight loss from the opposing electrode. On one, the estimated weight of the protuberance was 0.3 gram. The total weight loss from the cathode was 0.03 gram, or about one-tenth as much. Consequently, unless the anode sprays vapor which condenses on the cathode and happens to balance the weight of a drop, it seems most likely that the protuberance is a growth. Incidentally, one of these protuberances was cross-sectioned and found to be comprised of solid copper. Similar anode growths have been noted at much lower currents by Lee (see reference 1 of Dr. Cobine's discussion).

Additional data have been taken to reduce statistical deviations in Fig. 6 and to determine whether or not there is "tendency for arc erosion loss to increase more rapidly than with the first power of current." The improved data show very little deviation from straight lines. The positions of the straight lines in Fig. 6 were virtually unaffected.

The Results of 7 Years' Experience With High-Capacity Outdoor Oil Circuit Breakers

C. J. BALENTINE
ASSOCIATE MEMBER AIEE

K. G. DARROW
ASSOCIATE MEMBER AIEE

THE NEED for high-capacity circuit breakers first arose at Grand Coulee Dam in 1947 at the 230-kv level. There were then some of each of two general types of breakers in service in the Grand Coulee Dam switchyards giving satisfactory performance but having maximum interrupting ratings far short of the desired 10,000 megavolt-amperes (mva). One of these designs was the low-oil-content porcelain-clad impulse breaker and the other was the conventional dead-tank design.

Existing laboratory facilities to demonstrate breaker interrupting performance were then not adequate to prove with full-scale testing the maximum industry requirement of 10,000 mva. It was thus necessary to resort to field testing to determine the interrupting capabilities of the breaker designs in service at the Dam. In the spring of 1947 tests were made at Coulee Dam on both the impulse and the tank-type breaker designs and both breakers successfully interrupted fault duties in excess of 7,000 mva.[1,2] Two years after these tests a porcelain-clad impulse breaker originally developed for 360-kv service was field-tested at Grand Coulee Dam to take advantage of some additional installed generating capacity which increased the available short-circuit duty to 10,000 mva.[3]

The data obtained from these two series of tests contributed greatly to the background of information which was being accumulated on high-capacity breakers and led directly to the development of a porcelain-clad impulse breaker rated 10,000 mva at 230 kv. A number of breakers of this design were subsequently installed in the right switchyard at Grand Coulee Dam and one of them was later successfully field-tested at the Dam in excess of 10,000 mva.[4]

During this period all the high-capacity circuit-breaker activity was centered on the 230-kv level, but shortly thereafter a need arose for a 10,000-mva interrupting rating at 161 kv and it became evident that high interrupting capacities were going to be required at all voltages from 138 kv up through 330 kv. It was apparent that not only were all these ratings going to be required but they were going to have to be developed almost simultaneously. The immediacy and scope of the problem indicated the need for a prompt and careful analysis of existing breaker designs and a detailed review of their performance characteristics to determine the best possible design concepts for developing a line of high-capacity breakers. The design was approached as a group problem rather than as separate design approaches at particular voltage and interrupting ratings because the required operating characteristics of the breakers were so similar at all ratings and the problems of design were common.

Ampere requirements, the basis of the contact designs, were very similar at all ratings. Interrupting amperes covered a range of roughly 26,000 to 45,000 amperes with correspondingly high momentary ratings and all had to be suitable for 1,600-ampere continuous current ratings. All breakers had to have maximum interrupting time ratings of 3 cycles and be capable of reclosing in 15 cycles. Minimum oil deterioration and contact erosion were a requisite. Minimum space, weight, and oil requirements were also important design factors.

The operating and performance characteristics required for the new designs, the appraisal of performance characteristics of existing designs, and the background of high-capacity circuit-breaker knowledge acquired through laboratory, factory, and field tests led to the selection of the steel-clad impulse breaker design as the basis for the high-capacity line. This approach utilizes a steel-tank breaker structure and impulse interrupters patterned after those of the low-oil-content design.

An interrupter plan was established which was capable of extension to satisfy voltage requirements and suitable for modification for increased interrupting ratings. Tank structures and configurations were examined in order to produce similar structures at all voltage and interrupting ratings which would result in minimum space and oil requirements. Pole unit linkages required for high-speed operation were investigated in order to select a design which could be applied equally well to all ratings within the group of high-capacity breakers. Operating mechanism requirements were carefully analyzed to cover the entire line with the minimum number of operators.

The initial step in the development of this line of high-capacity breakers was the 161-kv 10,000-mva breaker described 2 years ago.[5] The 230-kv 10,000-mva rating and the 330-kv 15,000-mva rating were described subsequently.[6,7]

This paper describes briefly the new 330-kv 25,000-mva rating as well as some of the design features common to the complete line. An oil-conserving tank contour now being introduced on the 138-kv 10,000-mva and 161-kv 10,000-mva ratings is also discussed. Several novel design approaches which are covered fully in companion papers[8–10] are also identified.

The complete line of high-capacity breakers is now in service and covers the following ratings:

138 kv, 10,000 mva.
161 kv, 10,000 mva.
230 kv, 10,000 mva.
330 kv, 15,000 mva.
330 kv, 25,000 mva.

Figs. 1 and 2 show the 330-kv 25,000-mva and the 230-kv 10,000-mva ratings respectively illustrating the appearance of this line of breakers.

Design Features of the Circuit-Breaker Line

POLE UNIT

The physical size of the tank structures used on these breakers as well as the amount of oil that they require is an important economic consideration. Smaller physical size results in reduced space requirements and more economical breaker foundations. The smaller size results further in economy in the permanent oil-handling facilities required and in the amount of oil to be handled during installation and subsequent maintenance periods. Oil-conserving tank contours for the entire line were investigated to ob-

---

Paper 55-213, recommended by the AIEE Switchgear Committee and approved by the AIEE Committee on Technical Operations for presentation at the AIEE Winter General Meeting, New York, N. Y., January 31–February 4, 1955. Manuscript submitted October 25, 1954; made available for printing November 30, 1954.

C. J. BALENTINE and K. G. DARROW are with the General Electric Company, Philadelphia, Pa.

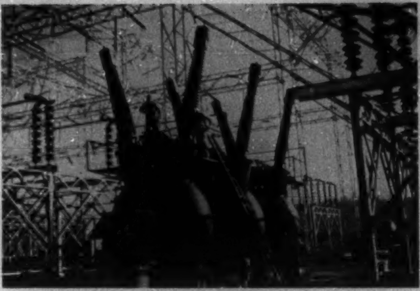

Fig. 1 (above). A view of the 330-kv 25,000-mva breaker. Special shipping members were provided to facilitate handling at the time of installation

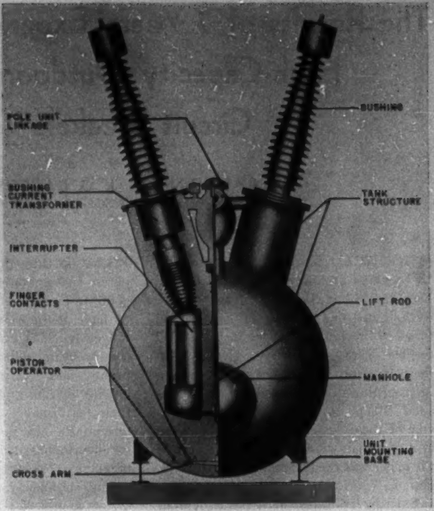
POLE UNIT LINKAGE
BUSHING CURRENT TRANSFORMER
INTERRUPTER
FINGER CONTACTS
PISTON OPERATOR
CROSS ARM
BUSHING
TANK STRUCTURE
LIFT ROD
MANHOLE
UNIT MOUNTING BASE

Fig. 3 (right). Sectional view of a single pole representative of all voltage levels from 138 kv through 330 kv. This illustrates the tank configuration and location of the major components

tain a configuration to provide these features while maintaining adequate electrical clearances. The analysis made to determine contours and to check electrical clearances is described in a companion paper.[8]

The configuration of this tank is different from that of the conventional design. The main body of the tank consists of two elliptical domed sections welded together with the supports for the bushings and current transformers and the mechanism linkage enclosure welded into the top of the assembly. The tank structure is supported by formed plates welded to its underside.

The configuration is stronger and at the same time more flexible than a cylindrical one and allows the domed sides to expand to some extent when interrupting heavy-duty fault currents. This expansion provides cushioning which results in a reduction of ground-shock disturbance. The tank supports are also designed to allow flexing to further minimize ground-shock disturbance.

A sectional view of the main oil tank structure used for all these high-capacity breakers is shown in Fig. 3. Except for physical dimensions, this illustration represents all voltage ratings from 138 kv up through 330 kv. This is illustrated in Fig. 4 which shows the relative tank sizes for the various voltages.

The breakers in service at 138 kv 10,000 mva and 161 kv 10,000 mva have been furnished with round tank designs up to the present time. This new structure de-

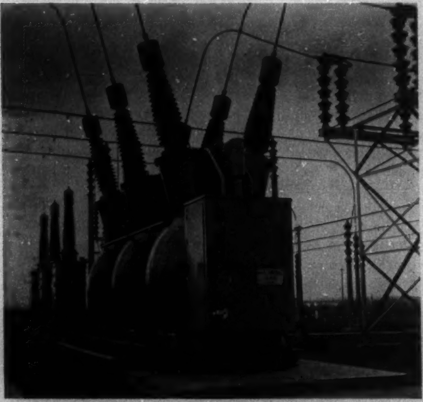

Fig. 2. An installation view of the 230-kv 10,000-mva breaker

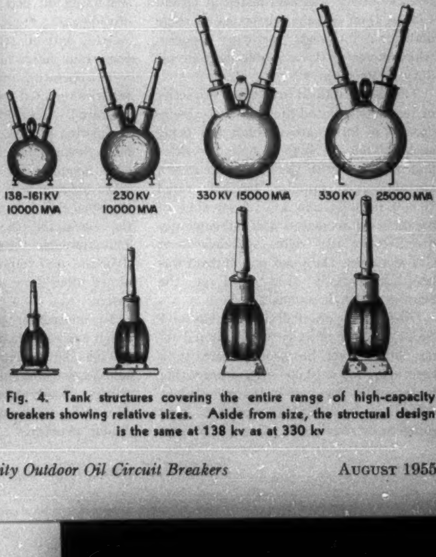
138-161 KV 10000 MVA
230 KV 10000 MVA
330 KV 15000 MVA
330 KV 25000 MVA

Fig. 4. Tank structures covering the entire range of high-capacity breakers showing relative sizes. Aside from size, the structural design is the same at 138 kv as at 330 kv

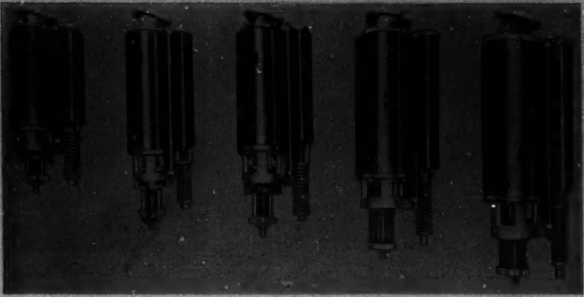

Fig. 5. Interrupters used to cover the entire high-capacity breaker range at 138, 161, 230, and 330 kv. Each interrupter is equipped with a mechanically driven piston giving impulse oil-blast action to provide constant interrupting times over the entire current range

sign has been carefully studied and sufficient clearance has been incorporated to provide adequate physical room for installation and maintenance work so that these two ratings will now be furnished with the new tank configuration, thus completing the line of high-capacity breakers in similar structures.

INTERRUPTERS

The interrupters used to span this high-capacity range evolved from the design plan for the 161-kv breaker.[8] This plan specifically provides for one fundamental interrupting unit capable of extension to increased interrupting ratings and suitable for compounding as dictated by voltage level requirements. Subsequent designs adhering to the plan were described for the 230-kv 10,000-mva breaker and the 330-kv 15,000-mva breaker. Those used for the 138-kv 10,000-mva and the 330-kv 25,000-mva ratings follow the same pattern.

The interrupters which span the range from 138 kv to 330 kv are shown in Fig. 5. All of these interrupters utilize impulse oil-blast action to provide constant interrupting times over the entire current range. A mechanically driven piston provides positive oil flow at light currents to make the action of the interrupter independent of self-generated oil-blast action at the lower end of the current range. At higher duties valving within the interrupter isolates the oil impulse piston and effects interruption entirely through self-generated oil-blast action. The mechanically driven oil piston is also used to provide a steady stream of oil while interrupting line-charging currents to prevent circuit re-establishment following initial interruption.

At 138, 161, and 230 kv two series breaks per interrupter are used. Within this range contacts are similar in design and differ only in the length of components as required by voltage applications. Longer contact structures and increased operating speeds are used at the higher voltages. At 330 kv, 15,000 mva and 25,000 mva there are three series breaks per interrupter. Both these interrupter designs have the same contacts and stroke but the 25,000 rating has heavier spring loadings and a larger diameter tube to contain more oil volume within the assembly for the higher interrupting duties.

Some of the more salient points of one interrupter, a 2-series break design, will be briefly reviewed here. This interrupter is shown in a sectional view in Fig. 6 while Fig. 7 illustrates the arrangement of the 3-series break design.

Each impulse interrupter consists essentially of three parts: the interrupter tube assembly, a mechanically operated oil piston mounted adjacent to the interrupter tube to force oil into the interrupter arcing zone, and a grading resistor to divide the voltage between the inter-

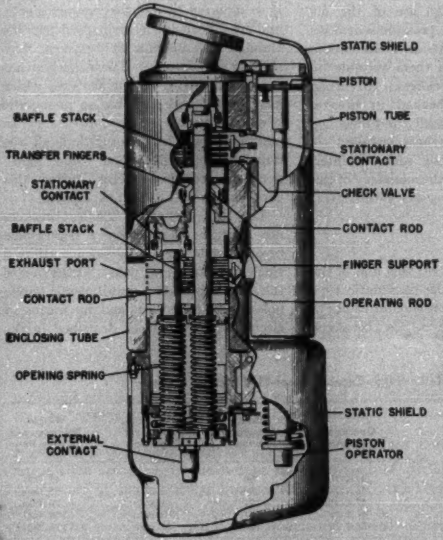

STATIC SHIELD
PISTON
PISTON TUBE
BAFFLE STACK
TRANSFER FINGERS
STATIONARY CONTACT
STATIONARY CONTACT
CHECK VALVE
BAFFLE STACK
CONTACT ROD
EXHAUST PORT
FINGER SUPPORT
CONTACT ROD
OPERATING ROD
ENCLOSING TUBE
OPENING SPRING
STATIC SHIELD
EXTERNAL CONTACT
PISTON OPERATOR

Fig. 6 (left). Sectional view of the 2-series break interrupter construction used at 138, 161, and 230 kv. This view identifies and locates the major components of the interrupter assembly

Fig. 7 (right). Sectional view of the 3-series break interrupter construction used for 330 kv. The view is representative of the 15,000-mva and 25,000-mva ratings although the latter have a larger diameter enclosing tube and heavier spring loadings

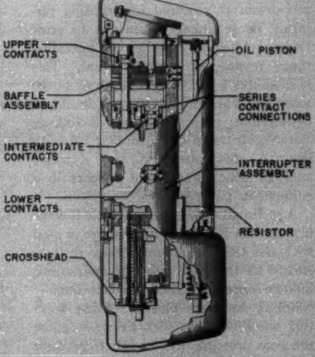

UPPER CONTACTS
OIL PISTON
BAFFLE ASSEMBLY
SERIES CONTACT CONNECTIONS
INTERMEDIATE CONTACTS
INTERRUPTER ASSEMBLY
LOWER CONTACTS
RESISTOR
CROSSHEAD

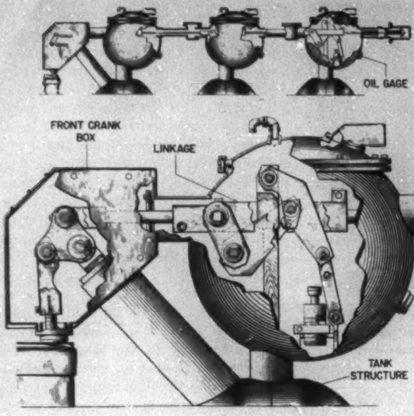

Fig. 8 (left). Sectional view of the triple-pole breaker linkage. The linkage design resulted from a thorough analysis of the mechanical system and the forces to which it is subjected. This linkage is used at 138, 161, and 230 kv. At 330 kv the same design is employed except the mechanical coupling between phases is omitted

Fig. 9 (above). The pneumatically trip-free operating mechanisms spanning all ratings from 138 kv to 330 kv. They are designed for ultrahigh speed reclosing, and employ a flux-shifting trip device to obtain high-speed tripping operations

rupters of a pole unit. The interrupter tube assembly utilizes a heavy walled insulating tube as the enclosure for two sets of series arranged simultaneously operating contacts, which provide the dual functions of current-carrying and circuit interruptions. Each set of contacts has within its arcing zone a laminated insulation structure to direct oil flow into the arc to obtain the maximum utilization of generated pressures. Both the contact opening springs at the lower end of the interrupter and the mounting adapter at the upper end which joins the interrupter to the bushing are provided with suitable electrostatic shielding.

POLE-UNIT LINKAGE

Breaker linkages are assuming more critical proportions in the over-all design of circuit breakers because interrupter loadings are continually increasing in proportion to required interrupting ratings. These linkages continue to grow larger and heavier while 3-cycle operating times remain as a requirement. This necessitates a very careful analysis of the mechanical system in order to develop a dependable, rugged, high-speed linkage suitable for use in an entire high-capacity line. A description of the dynamic analysis which was made appears in a companion paper.[9]

A sectional view of a triple-pole linkage is shown in Fig. 8. This linkage is used with the 138-, 161-, and 230-kv ratings. At 330 kv the same pole-unit mechanism linkage is used, but there is no mechanical coupling between phases. Aside from this one difference, both linkages follow the same principle of operation to produce straight line motion and give ultrahigh speed operation and long, trouble-free service through the utilization of the minimum number of components.

BUSHINGS

The bushings used in the line of high-capacity breakers follow the conventional bushing designs which have been used in outdoor breakers during the past several years.[11] The bushings are of the oil-filled, center-clamped, pressure-sealed design having certain design modifications incorporated to make them suitable for use in high-capacity breakers. All ratings of bushings were checked in breaker structures both electrically and mechanically and were further installed in breakers during lengthy series of interrupting tests to prove the adequacy of this design for high-capacity interrupting duty.

OPERATORS

The operators used on this line of circuit breakers are of the pneumatic type similar to those used on standard lines of modern outdoor high-voltage breakers. Mechanism output, however, has been increased threefold to match the requirements of the high-capacity breakers as first described on the 161-kv 10,000 mva breaker.

The mechanisms are pneumatically trip-free with a simplified mechanical system having a minimum number of moving parts. They are all designed for ultrahigh speed reclosing, as low as 15 cycles if so dictated by industry requirements, and are all capable of high-speed tripping through the use of a field-proven, flux-shifting trip device.[12] These mechanisms incorporate many of the features which have been found desirable on pneumatic operators during the past 14 years. In addition, the accessories reflect all the improvements that have been incorporated into the designs during this period as a result of field experience.

The 138-, 161-, and 230-kv breakers use a single operator for a tripole-pole breaker while the 330-kv ratings utilize a single mechanism per pole. In the case of the 330-kv breakers, simultaneous triple-pole operation is obtained by means of electric interlocking, as described in the

Table I. High-Capacity Steel-Clad Impulse Breakers

Voltage	Mva	Operating Mechanism	Tank Diameter, Inches	Oil Volume, Gallons per Triple Pole	Weight, Pounds per Triple Pole
138	10,000	*MA-19*	86	2,550	43,000
161	10,000	*MA-19*	86	2,550	44,000
230	10,000	*MA-19*	104	4,800	79,000
330	15,000	(3) *MA-18*	134	10,600	153,000
330	25,000	(3) *MA-18*	140	11,900	171,000

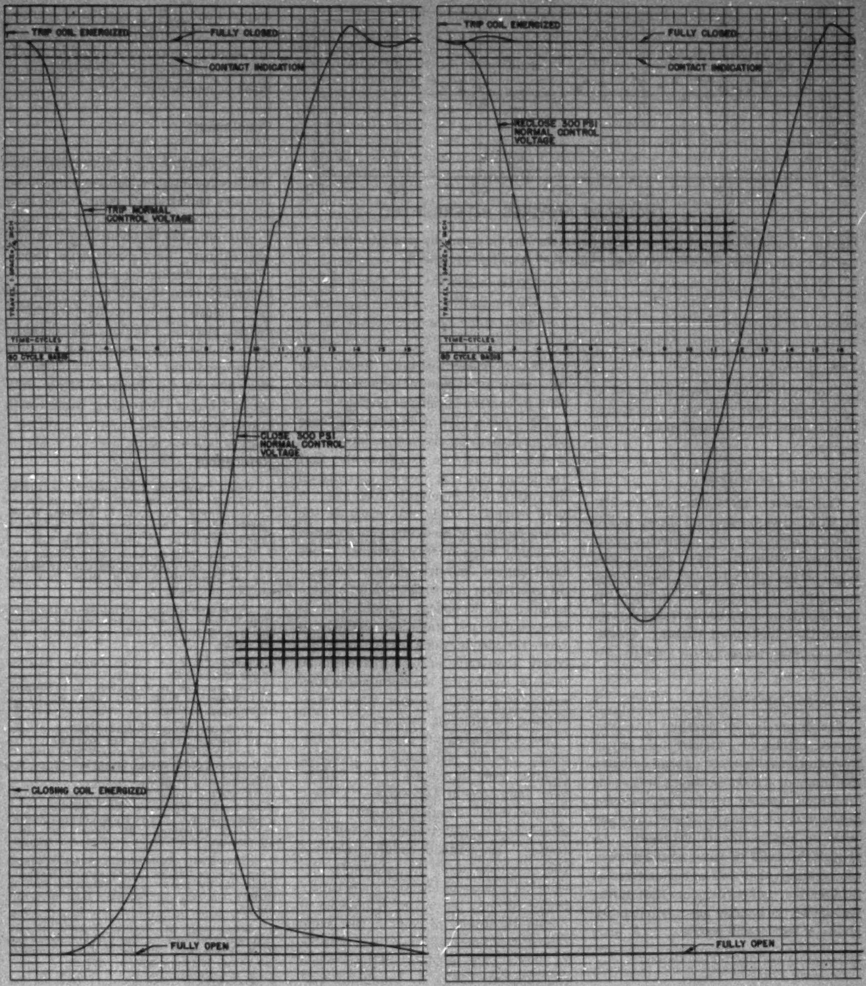

Fig. 10. Time travel chart of the 330-kv 25,000-mva breaker showing high-speed tripping, closing, and a reclosing operation in 15 cycles. This typifies the operation of all the high-capacity breaker ratings from 138 kv to 330 kv

paper on the 330-kv 15,000-mva breaker.

Table I identifies the mechanisms used on the various breakers and they are illustrated in Fig. 9. The mechanisms are similar in construction, but are of different sizes according to the output requirements of the particular breaker to which they are applied. The *MA-19* mechanism used on the 138-kv and the 161-kv breakers differs from the *MA-19* used on the 230-kv breakers only by the amount of air storage capacity required.

Design Test Performance

Proof of performance for the entire line of breakers has been obtained through a complete series of electrical and mechanical design tests to insure that all industry standards have been satisfactorily met.

Insulation Tests

All the breaker ratings have demonstrated margins of at least 10 per cent in excess of that required by industry standards on both 60-cycle and impulse voltage withstand tests.

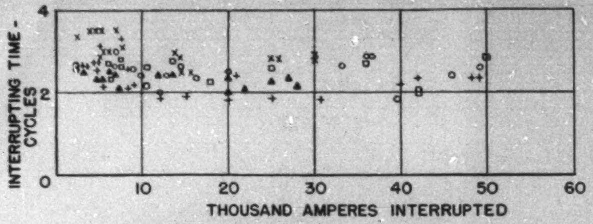

Fig. 11. A plot of interrupting times versus current showing the essentially constant interrupting time characteristics of all ratings at all magnitudes of current

○ 138 kv
□ 161 kv
▲ 230 kv
× 330 kv—15,000
+ 330 kv—25,000

Thermal Tests

The breakers have been subjected to 1,600-ampere heat runs with a maximum temperature rise on any design of 24 degrees.

Operational Timing Tests

Time travel charts taken on the 330-kv 25,000-mva breaker are shown in Fig. 10 for closing, opening, and reclosing operations. Although these charts were taken on the 330-kv breaker, they are representative of the operation of the entire line of high-capacity breakers and demonstrate that high-speed tripping, closing, and 15-cycle reclosing are readily obtainable.

Mechanical Life Tests

The entire line of breakers has been proved suitable for extended field service by operational life tests. On all designs a minimum of 5,000 operations was made on closing, opening, trip-free, and reclosing duties with no damage to any parts and with no readjustments necessary. Although this is far in excess of the number of operations that will be encountered in field service, it offers evidence that during the life of the breaker maximum dependability of service will result.

Interrupting and Short-Time Current-Carrying Tests

The interrupters have been subjected to extensive fault-current and line charging-current interrupting tests. Over 10,000 such tests were made to prove the suitability of the designs for service conditions. The approach which produced a family of interrupters for the line proved to be invaluable during this testing since it allowed the experience gained on any one design to be profitably applied to all the others. Momentary and short-time current-carrying tests were also made in excess of required values with no contact burning or pitting.

Fig. 11 is a plot of interrupting times versus currents for the various interrupter designs. It may be seen from this that the arcing times at various currents on all ratings are practically identical. A very extensive study was made of the characteristics of these interrupters while switching capacitance currents. Since the transient dielectric characteristics of an interrupter are controlled by a large number of dependent variables, it is necessary to use statistical methods to prove the adequacy of a particular design. Many thousands of tests have to be made in developing the optimum performance of a circuit breaker when interrupting line-charging currents.

To obtain adequate proof of performance, special capacitance switching facilities were developed at the Switchgear Development Laboratory.[13] These facilities included both a synthetic testing circuit and capacitor banks for full-scale testing. The synthetic circuit accelerated the development of the interrupter designs for successful interruption of capacitance currents by making it possible to obtain thousands of tests in the same time it would normally have been possible to obtain only hundreds of tests while the capacitor banks, by simulating field conditions, served as a control on the synthetic circuit. A companion paper[10] describes these facilities.

During the final proof testing of a breaker of each rating the interruption of heavy fault duties produced no visible signs of distress. Tests demonstrated that the interrupter contacts which are faced with arc-resistant material could successfully interrupt as many as 70 faults with an integrated duty of 465,000 amperes and still be capable of carrying current. The interrupter designs and the tank configuration resulted in greatly reduced ground-shock disturbance on all types of interrupting duty.

Conclusions

A considerable fund of knowledge has been accumulated on high-capacity circuit breakers during the 7 years which have elapsed since the first field test was made to determine the feasibility of developing such ratings. As a result of the knowledge gained during this time, high-capacity breakers can be built today which will meet industry requirements with ample design margins. During the development of this high-capacity line, enough background has been accumulated to make possible the design of higher voltage and higher interrupting ratings with proven components.

References

1. Field Tests for Development of 10,000-Kva 230-Kv Oil Circuit Breakers for Grand Coulee Power Plant, **C. L. Killgore, W. H. Clagett.** *AIEE Transactions*, vol. 67, pt. I, 1948, pp. 271–83.

2. Unusual Performance of Standard 230-Kv Impulse and Tank-Type Oil Circuit Breakers on Field Tests, **E. B. Rietz.** *Ibid.*, pp. 267–70.

3. Development and Testing of an Improved High-Voltage High-Capacity Impulse Circuit Breaker, **E. B. Rietz.** *Ibid.*, vol. 69, pt. I, 1950, pp. 15–26.

4. Field Tests at Grand Coulee Dam on 10,000-Mva 230-Kv Low-Oil-Content Impulse Circuit Breaker, **A. F. Darland, C. L. Killgore, C. J. Balentine, E. B. Rietz.** *Ibid.*, vol. 70, pt. II, 1951, pp. 1377–85.

5. A 161-Kv 10,000 Megavolt-Ampere Steel-Clad Impulse Breaker—The First of a Line of High-Capacity High-Voltage Breakers, **C, J. Balentine, J. M. Milne.** *Ibid.*, vol. 72, pt. III. Apr. 1953, pp. 312–21.

6. A 230-Kv 10,000 Megavolt-Ampere Steel-Clad Impulse Breaker—Another Rating in a Line of High-Capacity High-Voltage Breakers, **C. J. Balentine, J. M. Milne.** *Ibid.*, Oct., pp. 1050–56.

7. A 330-Kv 15,000 Megavolt-Ampere Steel-Clad Impulse Breaker to Guard the Nation's First 330-Kv Lines, **C. J. Balentine, Earl B. Rietz.** *Ibid.*, vol. 73, pt. III, June 1954, pp. 559–67.

8. Application of Volume Theory of Dielectric Strength of Oil Circuit Breakers, **W. R. Wilson, A. L. Streater, E. J. Tuohy.** *Ibid.*, vol. 74, pt. III, Aug. 1955, pp. 677–88.

9. Dynamics of High Capacity Outdoor Oil Breaker, **P. Barkan.** *Ibid.*, pp. 671–76.

10. Capacitance Switching Facilities at the Switchgear Development Laboratory, **R. L. Williams, L. L. Mankoff, H. N. Schneider.** *Ibid.*, June 1955, pp. 375–81.

11. A New Line of Oil-Filled Apparatus Bushings, **B. N. Bowers, D. L. Johnston.** *Ibid.*, vol. 67, pt. I, 1948, pp. 729–33.

12. Operating Mechanisms for High-Capacity High-Voltage Oil Circuit Breakers, **E. B. Rietz.** *Ibid.*, vol. 72, pt. III, Apr. 1953, pp. 256–63.

13. New High-Capacity Switchgear Testing Laboratory, **V. L. Cox.** *Ibid.*, vol. 71, pt. III, Jan. 1952, pp. 102–11.

Discussion

R. E. Friedrich (Westinghouse Electric Corporation, East Pittsburgh, Pa.): The authors have presented an excellent picture of the degree of development attained on a line of high-capacity low-oil-content dead-tank oil circuit breakers. The wide acceptance by the industry of oil breakers of this general type indicates an appreciation of their inherent advantages and economy.

It is of considerable interest to note that the "lenticular" shape of tank has been chosen not only for the 230- and 330-kv ratings but for the 138- and 161-kv ratings as well. Although the authors state that the space in the smallest of these tanks in the line is adequate for installation and maintenance work, it would appear that the personal comfort and efficiency of a normal size man ($5^1/_2$ to 6 feet tall) working inside the tank may have been sacrificed for the sake of only a moderate saving in oil volume. However, at 230 kv and above, the advantages of reduced oil volume provided by this tank shape are very worth while.

It is also of interest to note that in this line of breakers a single mechanical operator is utilized on all ratings except that at 330 kv where one on each pole is used without benefit of mechanical tie between the three. Although electric interlocking is applied, presumably to assure simultaneous energization of the closing and tripping impulses, the question arises as to whether the contacts make and break in all three poles sufficiently simultaneously to preclude the possibility of operating or relaying difficulties. We should like to know why the satisfactory experience gained with a single mechanism on the lower voltage ratings did not dictate the same design at 330 kv.

C. J. Balentine and **K. G. Darrow**: We wish to thank Mr. Friedrich for his comments on the paper.

The amount of working space available in the 138-kv lenticular tank shape was given careful consideration. Before the first circuit breaker was built a sample was made to check the amount of physical clearance inside the tank structure to satisfy ourselves before proceeding with the manufacture of the design. When the first triple-pole breaker was available in the factory, several users had their own personnel make an inspection of the working conditions inside the tank to assure themselves that installation and maintenance work could be comfortably accomplished in the space available. They were more than satisfied with the internal working conditions.

The idea of electrically co-ordinating single-pole operators is not new. The scheme was initially used on the porcelain-clad low-oil-content impulse breakers and has been proved by over 20 years of satisfactory field operating experience.

With the single mechanism per pole which is used on the 330-kv breakers it is possible to adjust the breakers so that both closing and reclosing operations are held to a maximum variance between poles of less than 0.5 cycle. On tripping operations the maximum spread between poles is less than 0.2 cycle.

It was decided to use single-pole operators on the 330-kv breakers in order to apply three standard mechanisms rather than a single one entirely new. As a result, the 330-kv breakers are being furnished with a mechanism which has been proved by field experience rather than a new mechanism with its attendent potential operating difficulties.

Dynamics of High-Capacity Outdoor Oil Circuit Breakers

PHILIP BARKAN
ASSOCIATE MEMBER AIEE

THE increased requirements imposed on modern high-capacity outdoor oil circuit breakers make necessary the utilization of analytical methods wherever possible to achieve optimum performance. The complex linkage mechanism of these oil circuit breakers, Fig. 1, can, by a judicious selection of parameters, be reduced to a simple system composed of a single mass and a single spring for the purpose of calculating circuit-breaker motion and velocity as functions of time. Calculations employing this approach correlate well with test data.

The possibility of representing a complex circuit breaker by the simple system shown in Fig. 2 is extremely attractive in that the solution can be obtained in concise form. By such an analysis it is possible to determine the effect upon the time required to trip the breaker of: 1. the mass of each component of the moving system, 2. spring preloading, 3. spring stiffness, 4. resistance produced by motion of parts moving in oil, and 5. electromagnetic forces and trip latch restraining forces which vary with time. By comparing calculated breaker motion under idealized conditions with actual test data, a measure is obtained of the extent to which actual performance deviates from the ideal.

This simplified analysis can be regarded as a stepping stone to more elaborate analyses which, by virtue of their complexity, require automatic computers for their practical solution. While the more elaborate analyses are more accurate and of greater scope, they do not detract from the value of the simplified approach by which many of the important relationships governing breaker operation can be summarized in an extremely concise fashion.

Description of Typical Linkage Mechanism

To provide specific features as a basis for discussion, reference is made to Fig. 1 which shows a representative linkage configuration of a high-capacity outdoor oil breaker. Interrupters for the three poles of the breaker are immersed in oil in tanks 1, 2, and 3. The interrupters are held closed by the linkage mechanism which in turn is restrained by means of a trip latch. This latch is normally tripped magnetically. At the initiation of a trip signal the latch moves out of the way, allowing the interrupter springs, opening springs, and gravity to accelerate the linkage. A small amount of contact wipe is introduced so that by the time the interrupters reach contact part position they are moving at a substantial velocity. Interrupter motion is halted after several inches of travel by travel stops. The remainder of the breaker linkage continues to move out until the lift rod has reached the fully open position.

Method of Analysis

To reduce the circuit breaker of Fig. 1 to a dynamically equivalent, simple mass-spring system shown in Fig. 2, it must be assumed that the linkage is completely rigid, i.e., possesses only one degree of freedom. The method of approach employed is briefly as follows:

1. The complex, distributed mass of the linkage is reduced to a single lumped mass moving with the motion of one particular link. This mass, defined as "effective mass" of the breaker linkage, is developed from relationships based on the requirement that both the actual system and its

---

Paper 55-215, recommended by the AIEE Switchgear Committee and approved by the AIEE Committee on Technical Operations for presentation at the AIEE Winter General Meeting, New York, N. Y., January 31–February 4, 1955. Manuscript submitted October 25, 1954; made available for printing December 9, 1954.

Philip Barkan is with the General Electric Company, Philadelphia, Pa.

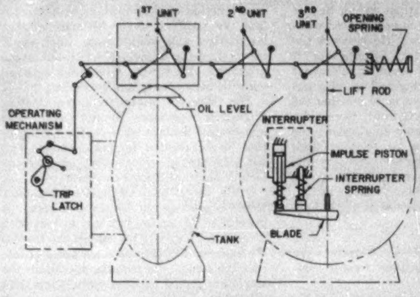

Fig. 1. Schematic representation of linkage of a high-capacity outdoor oil circuit breaker

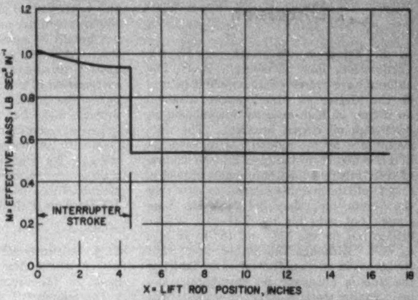

Fig. 3. Effective mass of linkage referred to lift rod datum

simplified equivalent have the same kinetic energy at all times. By virtue of this requirement the effective mass of any linkage component can be calculated by the methods described in Appendix I. By properly selecting the reference datum in the linkage at which the effective mass is developed, it is shown in Fig. 3 for a typical high-voltage breaker that the breaker effective mass is very nearly constant (±4 per cent) during the interrupter stroke and is a second constant during the remainder of the stroke. For trip operation, the assumption of constant mass results in only negligible error.

2. It is convenient to divide the total breaker stroke into three increments for the purpose of representing the operation of the interrupter springs, opening springs, and gravity. In each increment either a simple spring or a constant force can be developed which closely approximates the actual system. These relationships are developed in Appendix II, resulting in the approximate energy equations shown in Fig. 4.

3. The differential equations of motion are developed for the simplified spring-mass system shown in Fig. 2.

4. The equations are solved for circuit-breaker motion under various operating conditions.

Calculation of Ideal Performance

It is of value to calculate the circuit-breaker motion under idealized conditions. This establishes the ultimate performance possible, and by comparison with experimental data indicates the extent to which actual performance deviates from the ideal. The performance of the simplest possible system is calculated from the following differential equation of motion

$$M\ddot{X}+KX=P_0 \qquad (1)$$

Details of the solution of this equation are given in Appendix III. In developing equation 1, the following assumptions have been made:

1. The linkage is subjected to no external forces other than those produced by the interrupter springs, opening springs, and gravity.

2. No frictional losses exist.

3. No opposing drag force is developed by the motion of parts in oil.

4. The trip latch moves out of the way instantaneously, so that the breaker is immediately accelerated by the full spring force.

5. Effects of distributed mass and flexibility within the linkage are negligible.

6. Vibrations of the interrupter and opening springs are negligible.

7. The breaker effective mass is constant within the limits of validity of equation 1.

8. Within the limits of validity of equation 1, the spring characteristics are equivalent to those of a single spring with constant gradient.

9. The impulse pistons shown in Fig. 1 do not influence the motion of the remainder of the linkage mechanism.

The result of employing equation 1 in the calculation of circuit-breaker motion is shown in Fig. 5, curve *A*. This may be regarded as the best possible performance of the particular breaker design.

Influence of Various Factors on Opening Performance

By introducing additional terms and by varying the constant coefficients in equation 1, the effect of various factors

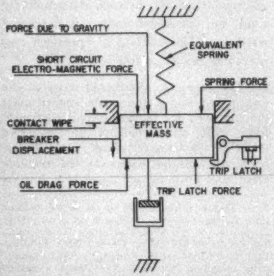

Fig. 2. Single mass-spring system, dynamically equivalent to circuit breaker

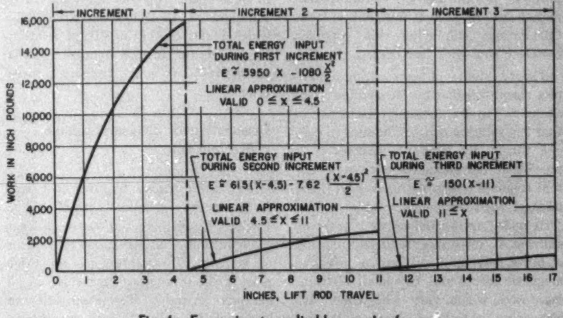

Fig. 4. Energy input supplied by opening forces

Nomenclature

a, b = velocity limits within which linearized approximation is valid
C = amplitude of electromagnetic force
C_1, C_2 = constants in linearized approximation of drag force
C_D = dimensionless drag coefficient ($\cong 1.2$ for flat plate)
E = energy
F_a, F_b = drag forces corresponding to velocities a and b
F_D = drag force produced by motion in a dense medium
g = acceleration due to gravity
I_θ = moment of inertia of rotating link about its center of rotation
I_{cg} = moment of inertia of link about its center of gravity
K = spring gradient
$M = W_e/g$ = effective mass
P_0 = spring force when $X = 0$
Q = projected frontal area of breaker parts moving in oil
S_e = contact wipe distance
T = time for trip latch restraining force to drop to zero after beginning of trip latch motion
t = time from the beginning of an increment
s = linear distance along trajectory of center of gravity of a link moving in a complex manner
W_e = see definition of M
W_Y, W_z = actual weight of linkage components of circuit-breaker mechanism
X = displacement at reference datum
X_0 = initial value of X at beginning of an increment
Y = linear displacement of Yth link
Z = displacement along trajectory of center of gravity of a link
γ = angular displacement of a link about its center of gravity
$\eta = \sqrt{K/M}$
θ = angular displacement of a rotating link about a fixed center
ω = current angular frequency

---

upon circuit-breaker performance may be established:

Effect of Oil Drag

This work can readily be extended to include the effects of oil drag, produced by the motion of the interrupters, blades, and lift rods in the oil medium. As the worst possible condition, the total frontal area of the breaker parts moving in oil may be considered equivalent to a flat plate of the same frontal area. The drag force is

$$F_D = C_DQP\dot{X}^2 \tag{2}$$

It is possible to obtain a simple solution for the equation of motion, including the type of oil drag force described by equation 2, by making a linearized approximation as is described in Appendix III. The resulting motion determined by such a calculation is shown in Fig. 5, curve *B*.

It is significant to note in Fig. 5 that during the first few inches of interrupter stroke the effect of oil drag is almost negligible. Later in the stroke, however, the effect of oil drag is significant. Since the early portion of the interrupter stroke is frequently of greatest interest, it is possible in these cases to neglect the effect of oil drag and to employ the simpler relationships of equation 1.

Calculations of the entire breaker stroke employing this method correlate well with test data as is shown in Fig. 5. Since the time at which motion begins in the actual breaker is more complex than considered here, the measured curve has been shifted along the time axis so that it coincides at 2-inch stroke with the calculated curve including oil drag. By considering the following additional factors, the travel curves can be made to correlate well on an absolute time basis:

1. The trip latch response is not actually instantaneous as has been assumed up to now. This is discussed in the next section.
2. The effect of distributed mass and flexibility within the breaker linkage has not been considered. This is beyond the scope of this paper but has been considered with a multidegree-of-freedom linear system.
3. The time required to build up the magnetic field in the flux shifting magnetic latch is approximately 1/10th cycle.

Effect of Trip Latch Restraining Force

In the breaker closed position the trip latch exerts a force equal and opposite to the spring preloading. Upon the initiation of the trip signal the latch begins to rotate away. Because of flexibility in the breaker linkage and in the trip latch mechanism and because of the kinematics of the trip latch, the force does not immediately drop to zero as a step function. From strain gauge studies it has been found that the trip latch restraining force drops off more nearly as a third-degree function of time. The effect of this manner of trip latch operation upon the time required for the breaker to reach contact part position may be evaluated by the single-degree-of-freedom system.

The differential equation of motion (equation 1) is thus modified to become

$$M\ddot{X} + KX = \frac{P_0}{T^3}t^3 \tag{3}$$

The solution of this equation is developed in Appendix III.

This equation may be used to establish interrupter position and velocity while the trip latch is still influencing the motion, or until $t = T$. For subsequent motion the system reverts back to the simple system described in item 1 of the preceding section, and equation 1 may be employed to complete the remainder of the interrupter stroke. The calculated effect of trip latch release time upon the time required for the interrupter to reach contact parting position is shown in Fig. 6. It is seen that trip latch time is an important component of the total time required to move the breaker to contact parting position.

Effect of Design Changes on Contact Parting Time

Of considerable interest to the designer is the effect of possible modifications upon the time required for the breaker to reach contact parting position. The effects of changes in total effective mass, equivalent spring stiffness and spring preloading may be concisely summarized by means of the equations which have been developed.

Applying the initial conditions of zero velocity and zero displacement, equation 1 may be employed to determine the change in time required to move the breaker to contact parting position as a function of the change in one or more of the indicated parameters. The relationship is found to be

$$\Delta t = \sqrt{\frac{M}{K}}\cos^{-1}\left(1 - \frac{S_eK}{P_0}\right) - \sqrt{\frac{M_i}{K_i}}\cos^{-1}\left(1 - \frac{S_eK_i}{P_{0i}}\right) \tag{4}$$

By consideriug the change in time rather than the absolute value of time, the equation assumes greater validity. Equation 4 has been employed to develop the curves shown in Fig. 7.

Test data showing the effect of changes

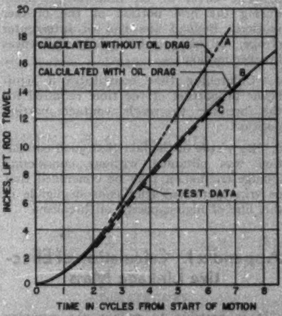

Fig. 5. Circuit-breaker opening motion

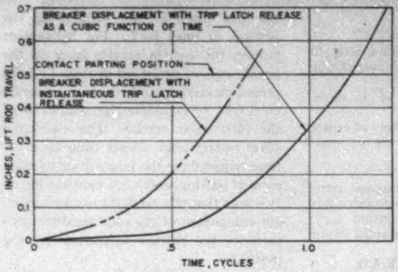

Fig. 6 (left). Effect of trip latch release time on circuit-breaker motion

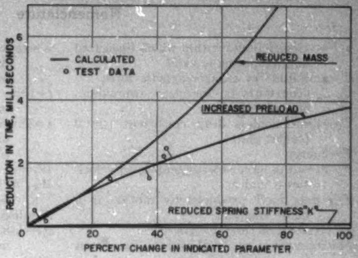

Fig. 7 (right). Effect of design changes on contact parting time

in spring preload are also shown in Fig. 7. Correlation between calculation and test is seen to be reasonably good. It can be seen from Fig. 7 that large changes in existing design parameters are required to produce even modest reductions in opening time.

Conclusions

The complex mechanism of a high-voltage circuit breaker can be analyzed by relatively simple mathematics. The results of the analysis correlate reasonably well with test data. The analysis can prove invaluable in circuit-breaker development by making possible prediction of performance under specified operating conditions and by helping to establish the best means of improving performance.

As a result of the analysis the following conclusions can be made about trip operation:

1. Changes in effective mass and spring preload must be substantial to achieve even modest reduction in the time required for the interrupters to reach contact parting position.
2. The time to contact parting position is virtually independent of the spring gradients.
3. The effect of oil drag is negligible during the first portion of the breaker motion. Beyond the end of interrupter stroke, oil drag substantially influences breaker motion.
4. Unlatching time constitutes a significant proportion of the time required for the breaker to reach contact parting position.
5. By virtue of the fact that good correlation was obtained without considering linkage friction, it may be concluded that on trip operations friction is negligible in this line of high-capacity oil breakers.

Appendix I. Calculation of Effective Linkage Mass

It is possible to reduce the complex linkage to a single lumped mass for the purpose of analysis by the following method:

1. Kinematic relationships between the links are determined by graphical or trigonometric methods.
2. On the basis of the kinematic motion relationships and the masses of the parts, a reference datum is selected at the location of the linkage components which contain the major proportion of the kinetic energy of the breaker. This datum will be either the one at which the parts have the greatest mass or undergo the greatest displacements. In high voltage oil circuit breakers this datum will normally be the lift rod-blade-interrupter datum.
3. The effective mass of each moving part referred to the datum is found by imposing the condition that the kinetic energy of the part, original and equivalent, must be the same. The relationships are derived below.
4. The effective masses are summed to obtain total effective mass of the breaker.

Calculation of Effective Mass of Parts Moving in Pure Translation

Conservation of energy requires that

$$\text{Kinetic energy} = \frac{1}{2}\frac{W_Y}{g}\dot{Y}^2 = \frac{1}{2}\frac{W_e}{g}\dot{X}^2$$
$$= \frac{1}{2}\frac{W_Y}{g}\left(\frac{dY}{dX}\right)^2\dot{X}^2$$

Therefore

$$\text{Effective mass} = \frac{W_e}{g} = \frac{W_Y}{g}\left(\frac{dY}{dX}\right)^2 \tag{5}$$

Calculation of Effective Mass of Parts Moving in Pure Rotation (e.g., Mechanical Output Crank, Bell-crank, Beam)

Conservation of energy requires

$$\frac{1}{2}\frac{I_\theta}{g}\dot{\theta}^2 = \frac{1}{2}\frac{W_e}{g}\dot{X}^2$$

Therefore

$$\frac{W_e}{g} = \frac{I_\theta}{g}\left(\frac{d\theta}{dx}\right)^2 \tag{6}$$

Parts Moving With Combined Rotation and Translation

Some links do not move in either simple translation or rotation but undergo complex motions. The motion of such a link may be regarded as a combination of translation of its center of gravity and rotation about its center of gravity. The effective mass of such a link is then

$$\frac{W_e}{g} = \left[\frac{W_z}{g}\left(\frac{dz}{dX}\right)^2 + \frac{I_{c\theta}}{g}\left(\frac{d\gamma}{dX}\right)^2\right] \tag{7}$$

In the particular circuit breaker employed

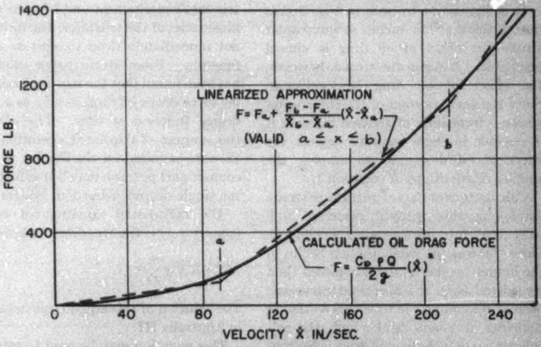

Fig. 8. Oil drag force and linearized approximation

in this analysis over 75 per cent of the total effective mass is contributed by the lift rod, blade, and the interrupters. Thus, the effect upon the effective mass of the nonlinear kinematics of the remainder of the breaker linkage is minimized by the selection of the lift rod as the datum, as is illustrated in Fig. 3. Note that the effective mass of the breaker is constant within ±4 per cent during the first $4^1/_2$ inches of interrupter stroke. Since in Fig. 3 the rate of variation of effective mass with lift rod position $(dM)/(dX)$ is maximum near zero stroke where the velocity is always quite small, it can be shown that the effect of the $(dM)/(dX)$ term upon the opening motion is very nearly negligible. The effective mass is a second constant value, within a fraction of a per cent, during the remainder of the breaker stroke.

Appendix II. Development of Equivalent Springs

It is convenient to divide the total breaker stroke into three increments and to develop either a simple equivalent spring or a constant force to provide the energy input into the system during each increment. These increments are:

1. From initial displacement until the end of the interrupter stroke, energy is supplied by the interrupter springs, opening springs, and by gravity.
2. From the end of the interrupter stroke until the opening spring force drops to zero, energy is supplied by the opening springs and by gravity.
3. From the point at which the opening spring force drops to zero to the end of the linkage stroke, energy is supplied solely by gravity.

It is possible to approximate closely the actual energy input during each increment by an equivalent linear spring. The equation for the energy of a linear spring is of the form

$$E=P_0(X-X_0)-\frac{K}{2}(X-X_0)^2 \qquad (8)$$

This equation by virtue of its form automatically conforms with the actual energy at the beginning of each increment where the energy input is zero. The constants P_0 and K are selected either by applying the conditions that the energy be equal at two arbitrarily selected values of the datum stroke or by the method of least squares error. The energy curves for each increment and the linear spring approximations are given in Fig. 4.

Appendix III. Solution of Equations of Motion

It has been shown that, within any limited portion of the circuit-breaker trip stroke, the breaker can be considered as a constant, lumped mass driven by a spring with a constant gradient. Therefore a series of solutions may be developed, each valid within a specific increment, of the total stroke. By applying the final conditions from one increment as the initial conditions for the succeeding increment the entire trip operation of the breaker may be considered by linear, one-degree-of-freedom differential equations.

The following basic equation is, with some modifications, employed throughout this analysis

$$M\ddot{X}+KX=P_0 \qquad (1)$$

or, if

$$\frac{K}{M}=\eta^2$$

$$\ddot{X}+\eta^2X=\frac{P_0}{M}$$

and the general solution is

$$X=\frac{\dot{X}_0}{\eta}\sin\eta t+X_0\cos\eta t+\frac{P_0}{K}(1-\cos\eta t)$$

and

$$\dot{X}=\dot{X}_0\cos\eta t-\eta\left(X_0-\frac{P_0}{K}\right)\sin\eta t$$

Equation With Drag Force Term

This approach may be extended to take into consideration a drag force of the following form

$$F_D=C_DQ\rho\dot{X}^2 \qquad (2)$$

A linearized approximation of the drag force may be employed, with a high degree of accuracy, by replacing the second-degree relationship by a series of straight-line segments as shown in Fig. 8. Any desired degree of accuracy can be obtained by proper selection of the number of straight-line segments. Between any two velocity limits the drag force is described by a linear equation of the form

$$F_D\cong F_a+\frac{F_b-F_a}{\dot{X}_b-\dot{X}_a}(\dot{X}-\dot{X}_a)$$

which can be reduced to

$$F_D=C_1+C_2\dot{X}$$

where

$$C_1=F_a-\left(\frac{F_b-F_a}{\dot{X}_b-\dot{X}_a}\right)\dot{X}_a;\quad C_2=\frac{F_b-F_a}{\dot{X}_b-\dot{X}_a}$$

The differential equation for circuit-breaker motion with the addition of the oil drag force is then

$$M\ddot{X}+C_1+C_2\dot{X}+KX=P_0 \qquad (9)$$

and the solution is

$$X=e^{-\frac{C_2}{2M}t}\left[A\sin\sqrt{\frac{K}{M}-\left(\frac{C_2}{2M}\right)^2}\,t+B\cos\sqrt{\frac{K}{M}-\left(\frac{C_2}{2M}\right)^2}\,t\right]+\frac{P_0-C_1}{K} \qquad (10)$$

(valid for $a\leq\dot{X}\leq b$)

where

$$A=\frac{\dot{X}_a+\frac{C_2}{2M}\left(X_a-\frac{P_0-C_1}{K}\right)}{\sqrt{\frac{K}{M}-\left(\frac{C_2}{2M}\right)^2}};$$

$$B=X_a-\frac{P_0-C_1}{K}$$

This solution is valid within specified velocity limits. When the velocity of the breaker extends beyond these limits a new equation is employed, using as the initial conditions the end conditions from the previous calculation.

Equation Including Trip Latch Restraining Force as a Known Function of Time

The differential equation of motion including a term for the manner in which the trip latch relieves is

$$M\ddot{X}+KX=P_0\left(\frac{t}{T}\right)^3 \qquad (3)$$

where T = time for trip latch restraining force to drop from P_0 to zero.

This equation is valid for

$$0\leq\frac{t}{T}\leq1$$

Applying boundary conditions of zero displacement and zero velocity at zero time, the solution is

$$X=\frac{6P_0}{\eta^3T^3K}\sin\eta t+\frac{P_0}{K}\left(\frac{t}{T}\right)^3-\frac{6P_0}{\eta^2T^3K}\left(\frac{t}{T}\right) \qquad (11)$$

If, as is true in most practical cases, $\eta T<<1$ then $\sin\eta t$ may be approximated by the first three terms of its power series. This gives upon simplification the relationship

$$X=\frac{1}{20}\frac{P_0}{K}\frac{\eta^2}{T^3}t^5 \qquad (12)$$

and by differentiation

$$\dot{X}=\frac{1}{4}\frac{P_0}{K}\frac{\eta^2}{T^3}t^4 \qquad (13)$$

Equation Including Short-Circuit Forces

If again the analysis is restricted to the first portion of the circuit-breaker stroke (i.e., interrupter stroke) linear equations can be employed to gain insight into the effect of the electromagnetic forces produced by any specified current value. The electromagnetic force can be represented by an equation of the form

$$F=2C\sin^2\omega T \qquad (14)$$

where C is a function of current amplitude and the breaker configuration. By a trigonometric identity this is equal to

$$F=C(1-\cos2\omega T)$$

Then the resulting differential equation is

$$M\ddot{X}+KX=P_0+C(1-\cos2\omega T) \qquad (15)$$

and the solution is

$$X=\left(X_0+\frac{P_0+C}{K}+\frac{C}{K-4\omega^2M}\right)\cos\eta t+\frac{\dot{X}_0}{\eta}\sin\eta t-\frac{C}{K-4\omega^2M}\cos2\omega T \qquad (16)$$

References

1. THE RESULTS OF 7 YEARS' EXPERIENCE WITH HIGH-CAPACITY OUTDOOR OIL CIRCUIT BREAKERS,

C. J. Balentine, K. G. Darrow. *AIEE Transactions*, vol. 74, pt. III, Aug. 1955, pp. 665–71.

2. A NOTE ON THE EFFECT OF TRANSIENT FORCES, T. M. Charlton. *The Engineer*, London, England, Feb. 29, 1952, pp. 300–02.

3. STARTING FRICTION IN MECHANICAL LINKAGES, C. Thumim. *Product Engineering*, Albany, N. Y., Oct. 1951, pp. 151–55.

4. SPRING ACTUATED LINKAGE ANALYSIS TO INCREASE SPEED, R. C. Van Sickle, T. P. Goodman. *Ibid.*, July 1953, pp. 152–57.

5. CALCULATION OF HIGH SPEED VALVE MOTION WITH FLEXIBLE OVERHEAD LINKAGE, P. Barkan. *Transactions*, Society of Automotive Engineers, Philadelphia, Pa., vol. 61, 1953, pp. 687–700.

◆

Discussion

Bayard E. Quinn (Purdue University, Lafayette, Ind.): One of the characteristics of a circuit breaker that is of considerable interest to a customer is the time required to interrupt the current. The sales department can be quite optimistic concerning this characteristic, leaving to the engineering department the problem of designing a breaker to perform in the promised manner. It is therefore obvious that the engineering department must have a procedure for designing a breaker by which the promised characteristics can be realized. It is also necessary to be able to make reasonable predictions concerning the performance of various breaker mechanisms that may be considered.

The problem of predicting mathematically the performance characteristics of a circuit breaker can be approached in many ways. A force analysis can be made by which Newton's laws can be applied, or energy relations can be utilized through the use of LaGrange's equation. If a classical approach is used without making any simplifying assumptions, differential equations of great complexity are soon encountered. This is usually due to the nonlinearity of the mechanisms that have to be analyzed, together with the number of links that are involved. At this stage it is sometimes possible to enlist the aid of an automatic computer, although the ease with which some of the more complex differential equations can be thus solved may be overestimated. Without the use of an automatic computer the solution of the equations may require so much time that the effort required to obtain a solution cannot be economically justified.

It is apparent that Dr. Barkan has recognized these difficulties in his analysis of the dynamic characteristics of the outdoor oil breaker. He has reduced the entire mechanism to an equivalent spring-mass system as indicated in Fig. 2. Recognizing that the equivalent mass and the applied forces vary considerably during the displacement of the mass, he has divided the total travel into three intervals, and has considered only those forces that are of significant magnitude within an interval. It is thus possible to ignore the oil drag when the velocity is low and in this manner avoid unnecessary mathematical complications. When the oil drag is significant, a linear approximation is introduced to avoid a squared velocity term in the differential equation. The complementary solution for the equation thus obtained is therefore the same as that for free-damped vibration. By considering the energy input during the travel of the mass as shown in Fig. 4 an equivalent spring constant is determined. Linear differential equations are thus used to describe the entire motion of the mechanism.

The method for calculating the effective mass as indicated by equations 5 and 6 involves the use of $(dY)/(dX)$ and $(d\theta)/(dX)$, and no further explanation is given of the method whereby these quantities have been obtained. I suggest that the effective mass be computed by using the ratio of the velocities that are indicated earlier in equations 5 and 6 instead of using the relationships that are finally given.

Of particular interest to the designer is equation 4 in which a relationship is given for all of the quantities considered during the initial motion of the blade. The effect of varying these quantities (effective mass, preload, spring stiffness) is shown in Fig. 7. It appears from this figure that a reduction in spring stiffness results in a reduction of the opening time. This is contrary to my experience. In order to discuss the effect of changing the spring stiffness it is desirable to give some explanation as to the effect that this change has on the preload since the preload will be affected if other conditions are unchanged. Fig. 7 also indicates that reduction in opening time is relatively insensitive to a change in spring stiffness. This is true for a certain range of numerical values, but there are conditions under which a much greater sensitivity to spring stiffness may be encountered. I have frequently found it useful to plot the solution to equation 1 in dimensionless form, from which information of the type shown in Fig. 7 can be obtained.

Dr. Barkan is to be commended for making a very straightforward analysis of a problem containing many complications. The simplifications have been made where the greatest benefit can be realized. The experimental results shown in Fig. 5 indicate that a high degree of accuracy is still retained in the analysis. From a theoretical viewpoint this accuracy can be expected, since approximations concerning the forces are introduced into the problem as slight variations in the behavior of the second derivative. In the two integrations that subsequently follow these variations are minimized. The use of reasonable linear approximations can thus be justified.

The results obtained in this paper should be valuable to the designer because the effects of varying the different components of the mechanism can be computed. The results should also be valuable to those who are interested in predicting mechanism performance because they indicate the accuracy that can be obtained by using the type of analysis previously described.

Philip Barkan: The points raised by Professor Quinn indicate the need for further explanation of some of the concepts presented in the paper: The development of the effective mass requires the use of kinematic analysis in determining the relative motions between the links, as represented by the terms $(dY)/(dX)$ and $(d\theta)/(dX)$ in Appendix I. For complex linkage systems, the kinematic analysis is conveniently carried out by a graphical approach. By this method, several positions of the linkage are constructed graphically, and displacement of various links relative to the reference datum X are measured and plotted. The resulting curves are graphically differentiated to obtain the required values $(dY)/(dX)$ and $(d\theta)/(dX)$ as functions of X. Where a substantial number of kinematic analyses are to be made, the evaluation of these terms can be carried out more accurately and more conveniently by the use of high-speed digital computers, employing trigonometric relationships for the 4-bar linkage which are developed in references 1 and 2.

The results presented in Fig. 7 show the effects upon contact parting time position of varying one parameter at a time. Thus, as the spring gradient is varied, the spring preload is held constant. Physically this would require the introduction of suitable spacers under the different springs to produce the same spring preload on all tests. Under such circumstances, the fact that the spring force drops off less rapidly with increasing stroke, for a lower gradient spring, means that the accelerating force and velocity are greater. Thus, the time required for the breaker to reach a specified stroke is correspondingly less, as is indicated in Fig. 7. As Professor Quinn has pointed out, the influence of spring gradient upon the time required to reach a specified stroke is not always as small as shown. It is only true if $X_k/X_s<<1$, where X_k is the stroke between closed position and the specified position and X_s is the difference between the spring free length and its compressed length in the breaker. As X_k/X_s becomes increasingly large, the influence of spring gradient becomes increasingly more important. The results shown in Fig. 7 are restricted to a range of spring gradients which are practical for consideration with high-capacity outdoor circuit breakers. No completely general implication on the influence of spring gradient was intended.

REFERENCES

1. KINEMATIC ANALYSIS, J. Kaplan, B. Pollick. *Machine Design*, Cleveland, Ohio, Jan. 1954, pp. 153–60.

2. ANALYSIS OF THE FOUR BAR LINKAGE (book), J. A. Hrones, G. L. Nelson. John Wiley and Sons, Inc., New York, N. Y., 1951, pp. xi, xii.

Application of Volume Theory of Dielectric Strength to Oil Circuit Breakers

W. R. WILSON
MEMBER AIEE

A. L. STREATER
ASSOCIATE MEMBER AIEE

E. J. TUOHY
AFFILIATE MEMBER AIEE

A NEW LINE of steel-clad impulse oil circuit breakers[1] has recently been developed and put into production by the company with which the authors are associated. These breakers are enclosed in lenticular tanks, Figs. 1 and 2, instead of the conventional cylindrical tanks. The new tanks reduce the size and weight of the breakers and reduce the quantity of oil to be handled during maintenance procedures. Because of significant changes in the electric field between the high-voltage interrupters and ground metal, an investigation was initiated early in the development program to apply recent advances in field mapping techniques[2] to the problem of determining the optimum shapes and dimensions for the tank and for the electrostatic shields on the interrupters. The purpose of the investigation was to obtain optimum over-all arrangements with adequate dielectric strength.

The results of the investigation have had definite practical application. The electrostatic shield curvatures and shapes were determined initially in the electrolytic tank, and required no subsequent modifications which were significant from an electrostatic field standpoint. It was found that electric stresses were so low on inside surfaces of the tank that breakdown does not initiate from these surfaces. Consistent with a previous paper,[3] it was found that breakdowns would not initiate from certain surfaces on which electric stresses were the highest in the breaker. Instead the breakdowns would initiate from other surfaces on which the electric stresses were as much as 40 per cent (%) less but which exerted these lower stresses through a much greater volume of oil.

To summarize, it was found possible to predict 60-cycle withstand voltages with good engineering accuracy while the designs were still on the drafting board. Because the electrolytic models could be made and modified so inexpensively, many variations in design were investigated, with the best being selected and constructed for full-scale test and subsequent use in production.

Summary of Over-all Investigation

To establish how the investigation depended upon prior work, and why certain additional concepts and information were needed, a chronological synopsis of the over-all program seems necessary. The first step was to construct 3-dimensional models of various shapes under study; see Fig. 2. These were filled with filtered water, and by application of electrolytic field analysis techniques, flux plots such as Fig. 3 were obtained showing the distribution of voltage throughout the oil circuit breaker. However, because such flux plots are difficult of interpretation except in a plane of symmetry, a 2-pointed probe was developed so that the field gradients could be determined at any point in the breaker regardless of the direction of the field or whether it happened to occur at the surface plane of symmetry of the electrolyte. Use of this probe required development of a special electronic amplifier which would measure the small voltage difference between the points of the probe even though both points were at relatively high voltage. In this manner, it was found practical to determine maximum electric field intensities wherever they occurred in the breaker with an accuracy of a few %.

This, of course, raised the question as to how much electric stress [kilovolts per centimeter (kv/cm)] oil could stand at the surface of the various electrodes. In 1915 F. W. Peek[4] published a series of curves showing that the oil dielectric strength (defined as the maximum electric field strength in kv/cm existing anywhere in the gap just before breakdown) varies over a wide range with the shape of the electrodes. He found that the oil at the surface of a small sphere would seem to withstand much more electric stress than that at the surface of a large sphere. This did not mean that for equal spacings oil between small spheres would break down at higher voltage than oil between large spheres. It did mean that improvement made by increasing radii and reducing stress would not be as great as if dielectric strength were independent of configuration. Peek's data were limited because only certain classical shapes were studied and the relationships between the curves were such that it was not at all clear how to apply the dielectric strength data to other more general shapes.

The next step of the investigation was to attempt to develop an understanding of these dielectric strength functions that would be of sufficient accuracy to permit extension of the data to the general shapes of electrodes found in circuit breakers. The results of this program were quite unexpected. It was found[3] that the primary factor controlling the dielectric strength of oil at 60 cycles was the volume of oil under relatively high stress. Small volumes had high dielectric strengths and high statistical variations. Large volumes had lower dielectric strengths and were much more consistent. Purely

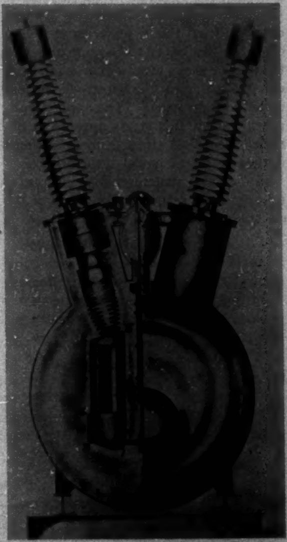

Fig. 1. Lenticular tank breaker showing location of regions at which stress measurements were made

---

Paper 55-219, recommended by the AIEE Switchgear Committee and approved by the AIEE Committee on Technical Operations for presentation at the AIEE Winter General Meeting, New York, N. Y., January 31–February 4, 1955. Manuscript submitted October 21, 1954; made available for printing December 8, 1954.

W. R. Wilson, A. L. Streater, and E. J. Tuohy are with the General Electric Company, Philadelphia, Pa.

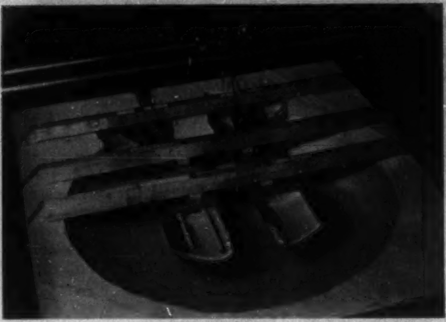

Fig. 2. Electrolytic model of lenticular tank breaker

from statistics, the various fundamental curves presented by Peek could be calculated from the dielectric strength (118 kv/cm) and standard deviation (18 kv/cm) of 1 cubic cm of oil. A curve of dielectric strength versus an equivalent volume of oil under stress was presented and is used throughout this paper as the basis for calculations. The equivalent volume of oil is that in which the electric stress is higher than 90% of the maximum stress in a given region. This equivalent volume is obtained either by approximate calculation or by means of the electrolytic field analyzer. The oil dielectric strength obtained from this volume curve is concluded in this paper to be approximately the electric stress at which corona streamers initiate from the electrode surface under consideration. The applied voltage at which this stress appears is obtained from field strength measurements in the electrolytic model of the breaker.

In dielectric structures with clearances that are large relative to the radii of the electrodes, the breakdown voltage is significantly higher than the corona starting voltage. This additional voltage, here termed the streamer extension voltage, is needed to lengthen the corona streamers until they can bridge the entire gap.

One of the principal objectives of this paper is to establish that this streamer extension voltage can be obtained approximately from the slope of the needle gap curve in oil. The hypothesis is that once the streamer extends out into the oil for a few inches from a curved electrode it assumes the same characteristic as a streamer which has extended from a needle. In short, the streamer extension voltage is found merely by multiplying the slope (kv/cm) of the needle gap breakdown curve by the estimated distance from the head of the streamer to the opposite electrode. The total withstand voltage is therefore

$$\text{Withstand voltage} = \text{corona starting voltage} + \text{streamer extension voltage} \quad (1)$$

That this hypothesis is approximately correct for at least several different electrode configurations has been established by comparing calculated withstand voltage curves with test data on large parallel disk gaps, Fig. 4, on large spherical ended rod gaps, Fig. 5, and on several circuit breakers, Table I.

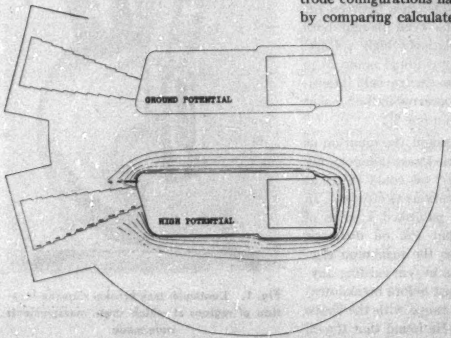

Fig. 3 (left). Field plot of lenticular tank breaker

The remainder of this paper presents the details of the streamer extension voltage derivation and of the application of the over-all method of calculating 60-cycle withstand voltage in specific oil circuit breakers.

Nomenclature

d = probe tip spacing
E = measured gradient expressed as the ratio, kv/cm/kv
g = oil dielectric strength (from volume curve), kv/cm
k = oil factor
K = ratio of model dimensions to breaker dimensions
R_1, R_2 = radii of curvature of electrode surface in two mutually perpendicular planes at the region of gradient measurement
R_s = radius of equivalent sphere that would produce the same field pattern near the surface as appears near the electrode under study, cm
V = calculated withstand voltage
V_c = corona starting voltage
V_p = ratio of probe voltage to the total interrupter to tank voltage
V_R = reference withstand voltage, kv rms
X_c = electrical clearance along probable path of failure, cm

Physical Picture and Calculation Method

Scope

Although this paper is directed primarily to the dielectric strength of oil circuit breakers, the calculation method is developed for more general application. The method deals primarily with large electrical spacings. Curves of dielectric strength versus spacing, see Fig. 6, can be divided into three regions:

1. The small spacing region through which the dielectric strength drops rapidly with increasing spacing.
2. The moderate spacing region through

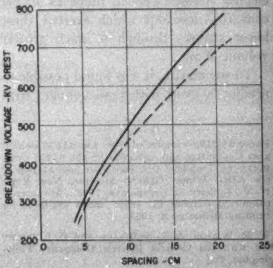

Fig. 4 (right). Disk gap breakdown voltage in oil. Solid curve from Peek's tests; dotted curve calculated

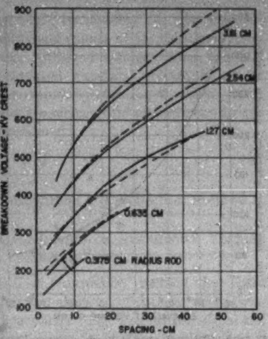

Fig. 5. Rod gap breakdown voltage in oil. Solid curves from Miner's tests; dotted curves calculated

which the dielectric strength is relatively constant.

3. The large spacing region through which the apparent dielectric strength increases gradually and some corona is presumed to appear before spark-over.

The previous paper[3] dealt primarily with moderate spacings and, to a lesser extent, with small spacings.

It is because this general investigation was undertaken to aid in estimating circuit-breaker high-potential withstand voltages that most emphasis has been placed on the large spacings. It is fortunate that reproducibility and accuracy are best in this region. The basic dielectric strength which is calculated by this method is the critical voltage, or the average withstand voltage, when the breakers are in good condition and contain good, normal oil.

Considering more general electrode configurations, reducing clearances, and reducing electrode dimensions result in marked increases in statistical deviations. Successive tests may differ in withstand voltage by two to one. In fact, the dielectric strength curves become so steep that for electrodes of small radius a few % of error in the radius might make 50% error in the withstand voltage. This region is not involved in the problem under study, except that the calculation method and physical picture are supported by the fact that they predict both the instability and the large increases in dielectric strength.

Corona Starting Voltage

It has been assumed almost universally in the literature that corona conditions around a relatively isolated electrode are determined by the electric field strength at the surface (this field strength being calculated as if no space charge were present). Proceeding on the basis of this assumption, corona would start on the surface of a given sphere whenever the field strength reached a certain value, regardless of whether that field strength were impressed by a large voltage to a distant electrode or by a smaller voltage to a closer conductor. It is quite possible that the amount of corona that would grow to a flashover at a diameter spacing might not even be visible around an isolated sphere. There also may be a transition area in oil (as there is in air) in which the corona starting gradient changes by a small amount as separation is increased to approach complete isolation. For these reasons, the corona starting voltage as herein defined for calculation purposes may be slightly different from the corona starting voltage determined visually or by definitions based on corona intensities measured electronically. The definition of corona starting gradient or oil dielectric strength used in this paper is the same as that used by Peek[4]: it is the minimum gradient on the curve of dielectric strength versus spacing. As such it is determined by the first streamer of corona which is of sufficient intensity to cause failure if an opposing electrode is inserted at moderate spacing in such a way as not to disturb the field. This concept of a constant corona starting gradient at large spacings, regardless of the precise spacing, is a convenient physical picture which is at least very close to being exact and which is supported by the fact that existing data can be calculated by its use.

Table I. Accuracy of Dielectric Strength Calculations of Developmental Oil Circuit Breakers

Circuit Breaker	% Error
161-kv cylindrical tank multibreak	+2
161-kv cylindrical tank impulse	+1
230-kv cylindrical tank multibreak	−5
230-kv lenticular tank impulse	+4
330-kv lenticular tank impulse	−2

By simple proportion, the corona starting voltage can be obtained from flux plot gradients and equation 2.

$$V_c = \frac{g}{E} \qquad (2)$$

Streamer Extension Voltage

As needle gaps are tested at increasingly large spacings, the slope of the breakdown voltage versus spacing curve reaches a relatively constant value of about 6.0 kv/cm; see Fig. 7. This means that, for each additional cm of gap at high spacing, 6.0 kv of additional voltage is required to lengthen the streamers sufficiently to bridge the gap. The hypothesis made in this paper is that once corona has started from a pair of smooth electrodes and extended out into the oil, the same additional voltage applied to the electrodes is required to bridge the gap between the streamers as would be required for a needle gap above its corona starting voltage, and in which the same gap between corona streamers remains to be bridged.

Fortunately, in the application to circuit breakers this additional voltage is generally in the order of one-fifth of the corona starting voltage, so a 25% error in the calculation would cause only about a 5% error in the final result. A good first

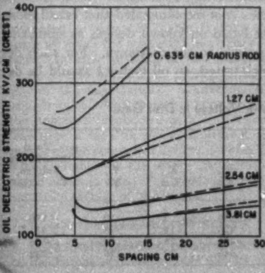

Fig. 6 (left). Oil dielectric strength versus spacing in rod gaps. Solid curves from test data of Fig. 5; dotted curves calculated

Fig. 7 (right). Needle gap breakdown voltage in oil

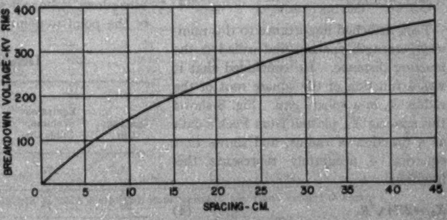

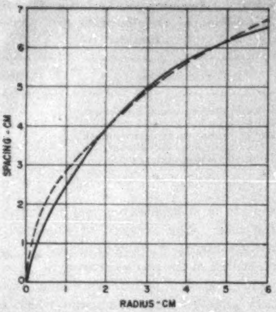

Fig. 8. Sphere gap spacing at which the breakdown gradient is a minimum. Solid curve from test; dotted curve $=2.74\sqrt{R_s}$

approximation would be merely to neglect the length of the first corona streamer and assume that the additional voltage equals the entire clearance between smooth electrodes times the 6.0 kv/cm slope of the needle gap curve. However, the typical shape of the dielectric strength versus spacing curves permits an improvement to be made to this picture. As indicated in Figs. 6 and 7, the streamer extension voltage is not required unless spacings are higher than those which give the broad minimum in dielectric strength. In fact, if these curves remained horizontal instead of assuming a rising slope no additional voltage would be required. It became apparent by inspection that the streamer extension voltage should be added above a spacing about 50% larger than that at which the minimum appears.

The corresponding physical picture is that the initial corona streamers at corona starting voltage extend into the oil an effective distance about 50% greater than the minimum-strength spacing X_m. Thus the effective gap X_s between heads of the streamers equals the total clearance along the probable path of failure minus 1.5 times the minimum-strength spacing

$$X_s=X_c-1.5X_m \qquad (3)$$

Peek attached importance to this minimum-strength spacing and called it the ionizing distance. He concluded that it was a function of the square root of the radius R_s in a sphere gap. Fig. 8 shows this spacing X_m plotted from Peek's data as a function of radius, and shows that equation 4 accurately represents this function

$$X_m=2.74\sqrt{R_s} \qquad (4)$$

Miner's[6] data for spherically ended rods also show the minimum-strength spacing to be a function of the square root of the radius, but the actual distances are 25% greater on the average. This degree of error will affect the calculated withstand voltage by only a few %, because the value 1.5 X_m is generally a small part of the total spacing, and the entire streamer extension voltage is generally a small part of the total withstand voltage.

For electrode shapes different from spheres, an equivalent sphere radius R_s is selected for want of a more accurate method and in the belief that final answers will not be affected by more than a few %. The value of R_s is selected as the radius of the equivalent sphere that would exhibit the same rate of change of gradient perpendicular to the surface as would appear at the surface of the electrode under study, provided that both surfaces have the same surface gradient. Simple electrostatic calculations show that the sphere which is equivalent to a cylinder in this respect has twice the radius of the cylinder.

On the basis of these concepts the streamer extension voltage V_s, for the general case, can be calculated by multiplying the slope 6.0 kv/cm by the unbridged gap X_s

$$V_s=6.0X_s=6.0(X_c-4.1\sqrt{R_s}) \qquad (5)$$

TOTAL WITHSTAND VOLTAGE

The total calculated withstand voltage V_B then is the sum of the corona starting voltage (equation 2) and the streamer extension voltage

$$V_B=V_c+V_s=\frac{g}{E}+6.0(X_c-4.1\sqrt{R_s}) \qquad (6)$$

MODIFICATION FOR BREAKDOWN TO TANK

The streamer extension voltage was derived on the basis of the needle-to-needle breakdown voltage curve. For the case of an electrode inside a tank, the corresponding classical configuration would be a point to a sphere surrounding the point. The closest available data are for the point-to-plane configuration. For both oil and air the point-to-plane breakdown voltage is approximately 80% of the point-to-point breakdown voltage (Peek[4]). It is apparent that the point-to-sphere breakdown voltage should be slightly lower than that for a point-to-plane gap, and a value of 70% has been selected purely on the basis of judgment. It is believed that this assumption will again cause no more than a few % error in the final calculated withstand voltage.

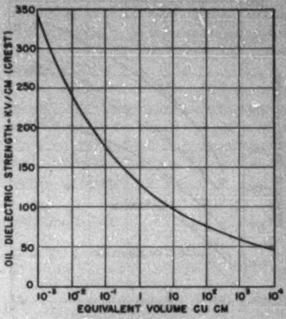

Fig. 9. Oil dielectric strength versus volume enclosed by 90% equigradient surface

The only change this brings about is to multiply the coëfficient of the streamer extension voltage in equation 6 by 0.7. The resulting equation 7 is offered for use in oil circuit breakers for calculating withstand voltage between interrupter and tank. Whereas crest voltages have been used up to this point, equation 7 is expressed in terms of rms voltages

$$V_R=0.707\frac{g}{E}+3.0(X_c-4.1\sqrt{R_s}) \qquad (7)$$

In practical applications it is recommended that equations 5, 6, and 7 not be used for absolute magnitudes. Under some circumstances it may be desirable to obtain the dielectric strength versus volume curve and the needle gap curve for the particular oil used in the design. In any case, to compensate for oil-handling practices, practical surface finishes, approximations in the method etc., it is recommended that calculations be based on known designs as similar as possible to the unknown. For each design tested, an oil factor k should be de-

Table II. Calculation of Breakdown Voltage in Disk Gaps

Spacing, Cm	Equivalent Volume, Cubic Cm	g, Kv/Cm	E, Kv/Cm/Kv	V_c, Kv	X_c, Cm	V_s, Kv	Total Breakdown Voltage, Kv (Crest)
5	275	72	0.252	286	5	0	286
10	76	85	0.201	423	14	28	451
15	75	85	0.179	476	24	89	565
20	75	85	0.156	546	32	136	682

termined by dividing the test value of withstand voltage by the calculated reference withstand voltage. Then the final calculated withstand voltage V can be determined by equation 8, where k is the average oil factor for all pertinent designs considered

$$V = kV_R \tag{8}$$

Verification of Calculation Method

CALCULATION OF BREAKDOWN VOLTAGE BETWEEN DISKS

This calculation method has been checked against test data for several configurations. Fig. 4 shows calculated and test curves for voltage breakdown in a disk gap. The test curve is from Peek's[4] Appendix 5, "Strength of Oil at Large Spacings." Data for the calculated curve were obtained in three steps as outlined in previous sections.

1. To determine the corona starting voltage, the volume of oil enclosed by 90% equigradient surfaces and the values of the highest gradients at points around the electrodes were found by measurements made on models of the disks in the electrolytic field analyzer. Gradients were measured with a 2-pointed probe and corrected to maximum values at the electrode surface with equation 9. From the equivalent volume, the oil dielectric strength g was determined by using Fig. 9. The corona starting voltage was then calculated from equation 2. For example, the corona starting volage was calculated for a disk separation of 10 cm. The volume of oil enclosed by the 90% equigradient surfaces was found to be 75 cubic cm. From Fig. 9 the oil dielectric strength g is 85 kv/cm. The maximum dielectric stress E was found to be 0.201 kv/cm/kv so the corona starting voltage was

$$V_c = \frac{85 \text{ kv/cm}}{0.201 \text{ kv/cm/kv}} = 423\text{-kv crest}$$

2. The streamer extension voltage was obtained by determining values for the length of the probable breakdown path and the radius of an equivalent sphere, as required by equation 6. From the gradient measurements it is apparent that the streamers start from the curved edges at a substantial angle and do not traverse a straight line between the two disks. The exact path of the breakdown is not calculable at this time so it was estimated as shown in Table II from the angle at which the streamers leave the surface. An error of 25% in this estimated length would produce an average error of 5% in the final results. Continuing the sample calculations for the 10-cm spacing, the estimated breakdown path X_c is 14 cm. The edge of the disk was cylindrical so the radius of the equivalent sphere is twice the 2.5-cm. radius of the edge. Substituting these values in equation 6 yields a streamer extension voltage of 28-kv crest

$$V_s = 6[14 - 4.1\sqrt{(2)(2.5)}] = 28\text{-kv crest}$$

3. The total breakdown voltage is the sum of the corona starting voltage 423 kv and the streamer extension voltage 28 kv, or 451 kv. The results of similar calculations for the remaining spacings are listed in Table II. It is important to note that large changes in equivalent volume produce relatively small changes in dielectric strength. This means that equivalent volumes do not have to be determined with more than nominal accuracy. The correlation between the test and calculated voltages of Fig. 4 is considered satisfactory.

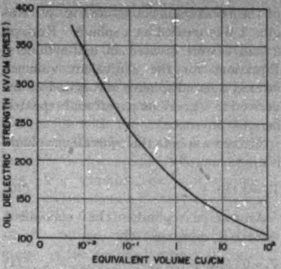

Fig. 10. Oil dielectric strength versus volume for Miner's rod gap data

CALCULATION OF BREAKDOWN VOLTAGE BETWEEN RODS

Further verification of the calculation method was obtained from Miner's[5] data on spherically ended rods; see Fig. 5. Miner's tests show that the breakdown voltage curves are discontinuous as the needle gap characteristic is approached, and all electrode shapes have about the same breakdown voltage. If the value of calculated breakdown voltage happens to lie below the needle gap breakdown, the latter value should be used instead of the calculation.

Preliminary to calculations, an approximate relation between gap voltage and maximum dielectric stress in the gap was determined by electrolytic field analysis techniques assuming the tank walls to be 30 diameters away from the rods. Data for the calculated curves were obtained by the same method used for disk gaps with one exception. By comparing Miner's data on spherical ended rods and Peek's sphere gap data, it became apparent that at moderate spacings the oil used by Miner had higher dielectric strength than that used by Peek.[4] For example, compare Peek's 1.27-cm radius spheres with Miner's 1.27-cm radius rods. For a gap spacing of 2.54 cm the spheres break down at 185 kv whereas the rods break down at 252 kv. The difference in field configuration is negligible. By the method of the previous paper,[3] the dielectric strength of a unit volume of the Miner oil was found to be 174 kv/cm and to have a standard deviation of 28 kv/cm. A curve of oil dielectric strength versus volume for the oil used by Miner, Fig. 10, was therefore derived in the same manner as presented in the previous paper for the oil used by Peek. Values of g from this curve were used in the calculation of the rod gap breakdown curves in Fig. 5.

Application to Oil Circuit Breakers

FORM OF PRESENTATION

Calculations and measurements for typical regions in a developmental breaker are shown in Table III and samples of each calculation involved in determining the withstand voltage at region 3 of Fig. 1 are included in the following development.

CONSTRUCTION OF BREAKER MODELS

For each breaker analyzed a scale model was made of the interrupter, bushing, and

Table III. Summary of Calculations of Critical Withstand Voltages for Developmental Lenticular Tank Circuit Breaker. Model Scale One-Third

Region	Type of Electrode	Equivalent Volume, Cubic Cm	Oil Dielectric Strength, Kv/Cm Crest	Electric Stress, Kv/Cm/Kv	Electric Stress at Lowest Reference Withstand Voltage,* Kv/Cm Crest	Corona Starting Voltage, Kv/Rms	Streamer Extension Voltage, Kv/Rms	Reference Withstand Voltage, Kv/Rms
1	Sphere	12.0	98	0.143	99	484	110	594
2	C†	1,070	56	0.0915	63	433	80	513
3	C	640	57	0.0993	69	406	84	490
4	C	340	64	0.0587	41	770	96	866
5	C	375	62	0.0885	61	496	108	604
6	C	5,900	50	0.0383	26	925		> 925
7	C	1,500	55	0.0484	33	805	84	854
Tank (bushing well edge)		20	91	0.0180	12	3,580		> 3,580

*Calculated, after remainder of table completed, from reference withstand voltage of region 3.

†C stands for cylinder.

breaker tank; see Fig. 2. The potential distribution along the bushing porcelain was obtained from flux plots such as Fig. 9 of reference 6. The required potential distribution was enforced by connecting resistors between stripes of silver which were painted around the wood model at ten equally spaced points along the model length. The model diameter at the center of each silver stripe was equal to the scale factor times the mean diameter of the 1-inch porcelain wall of the full-size insulator. Although this representation is not exact, Green's law demonstrates that the approximation is very good except for the immediate vicinity of the stripes. The interrupter models were scaled-down reproductions of the actual interrupters with shields in place, except that the models had no mounting bolt holes or sharp edges. Tests made on the completed breakers with and without lead foil covering the holes and indentations demonstrated that these nonuniformities were placed so that the withstand voltage was not affected.

DETERMINATION OF GRADIENT

The gradient is determined by measuring the voltage between probe tips when the probe is in the electrolyte. This voltage divided by the spacing between tips yields the average gradient over the probe tip spacing. Equation 9 derived to correct this to electrode surface gradient in the breaker takes into account the curvatures at the electrode surface and the model scale factor. In equation form the gradient is

$$E=\frac{V_p}{d}K\left(1+\frac{(R_1+R_2)}{2R_1R_2}d\right) \qquad (9)$$

Substitution of dimensions, scale factor, and probe voltage in equation 9 yields a gradient of $E=0.0993$ kv/cm/kv for the reference region of the sample calculation.

EQUIVALENT VOLUME

The equivalent volumes found in large oil circuit breakers are beyond the range of the dielectric strength versus volume curve of the reference paper.[3] Following the practice of basing calculations on dielectric structures that are as similar as possible to the device under study, the Peek[4] equation for the dielectric strength of cylinders was used to extend the range see Fig. 9. In the oil circuit breakers the regions of high stress happen to be around electrodes which are nearly spheres or cylinders. To illustrate this, and to show the location of the regions at which stress measurements were made, Fig. 1 shows a typical interrupter with its upper and lower shields in place. A field plot of one of the breakers is shown in Fig. 3. Region 1 was treated as a sphere. Regions 2 and 3 were treated as half-cylinders. Equations for the equivalent volumes around isolated spheres and cylinders are derived in a previous paper[3] and repeated here for reference.

Around a sphere the equivalent volume is approximately

$$V_e=0.4R^3 \qquad (10)$$

Around a cylinder the equivalent volume is approximately

$$V_e=0.75LR^2 \qquad (11)$$

Since regions 2 and 3 on the shields are treated as half-cylinders, only half the volume in equation 11 is used. R is the radius of the curved edge of the shield and L is the distance along the shield edge where the gradient is at least 90% of its maximum value.

The oil dielectric strength g is read from the extended volume curve; see Fig. 9. For the sample calculation, from Fig. 9 the oil dielectric strength for region 3 is 57 kv/cm corresponding to the equivalent volume of 640 cubic cm calculated from equation 11.

CORONA STARTING VOLTAGE

The corona starting voltage is calculated from the first term of equation 7. For region 3 this becomes

$$V_c=0.707\times\frac{57}{0.0993}=406 \text{ kv rms}$$

STREAMER EXTENSION VOLTAGE

The streamer extension voltage is the second term of equation 7. X_c is the length of the probable breakdown path and R_s is twice the cylinder radius. For region 3, $V_s=84$ kv. In all cases X_c was taken as the shortest distance from the region under consideration to the tank.

REFERENCE WITHSTAND VOLTAGE

The reference withstand voltage is the sum of the corona starting voltage and the streamer extension voltage, equation 7. For region 3 this is $V_R=490$ kv. As can be seen in Table III the reference withstand voltage at region 3 is the lowest value for that particular circuit breaker. The higher reference withstand voltages at the other regions are a measure of the additional overvoltage required for breakdown at these higher strength regions.

It must be emphasized that only the relative values of these reference withstand voltages have significance. For simplicity, they have been calculated on the basis of the dielectric strength of the oil used by Peek[4] in 1915. The higher dielectric strength of the oil tested by Miner at a later date shows how the overall results can change depending on the particular conditions of tests.

Accuracy of Calculations

Transformer and circuit-breaker oil can be refined and filtered by special means so that dielectric strengths can be raised far above the levels typical of normal production. For example, where one design of circuit breaker has about 18 inches of minimum strike distance, X-ray transformers[7] have been built and operated successfully at an even higher voltage with a minimum oil strike distance of 5 inches. It is apparent, therefore, that any estimate of accuracy of calculation must depend on the characteristics of the oil used in the test.

In the company with which the authors are associated, certain procedures to maintain cleanliness are observed when circuit breakers are assembled for high-potential test. Oil of controlled quality is pumped into the breakers. The dielectric strength in the 0.1-inch American Society for Testing Materials test gap[8] is determined along with other properties. With the conventional oil-filtering techniques using blotting paper, there is a quite definite practical limit of dielectric strength which is reached and maintained. Under these conditions, any particular design of breaker tested to breakdown will exhibit breakdown voltages which will have some variation from day to day but which will have a relatively stable average value.

Again adhering to the concept of basing calculations on dielectric structures which are as similar as possible to the unknown, the oil factor k was first determined by averaging the ratios of test withstand voltage to calculated reference withstand voltage for the first two breakers that were analyzed. This value of k was used to predict the breaker dielectric strength of the next design, and then after test data were accumulated a new value of k was calculated including the third design. Although this process was continued through five designs, the original value of the oil factor k did not change by more than a few %.

About the most difficult value to determine was the average test withstand voltage for the breakers. The reason for this was simply that the standardized bushing flashover voltage for the air end was generally lower than the internal oil withstand voltage of the breaker. For some breakers, overvoltage bushings were used and adjusted for approximate fit. For others the breaker dielectric strength data were taken by repeated 1-minute applications of test voltages below the critical air flashover voltage. Because of statistical variations, breakdown might occur through the oil or through the air. The percentage of oil breakdowns was recorded. Then, by simple probability methods, the critical or average withstand voltages were calculated from a single standard deviation value. Because many 1-minute applications of voltage were often required to obtain a single breakdown through the circuit breaker oil, and often none would occur, these data are limited.

Using one single average oil factor k for five circuit breakers, the critical withstand voltages for the pertinent regions such as shown in Fig. 1 were calculated for the five breakers. The calculated and test values are compared in Table I.

These percentages indicate the error which would be expected in the next breaker to be analyzed. It is obvious from the method of calculation that these errors are exactly the same as the deviations of the individual oil factors from the average. Therefore, if just one breaker were used as the reference in the determination of the oil factor, it can be seen from Table I that the worst error in calculating the breakdown voltages of the other four circuit breakers would be 5+4=9%.

As was stated in the previous paper[3] on the volume effects, caution should be exercised in extrapolating to a new dielectric structure which is radically different from the reference design. The data of Table I demonstrate that data and performance gained with cylindrical tank breakers can be translated to lenticular tank breakers by this method. However, extrapolation to the withstand voltage of a high-voltage oil circuit breaker from the calculated and test values of withstand voltage for a relatively low-voltage oil circuit recloser would not be expected to give reliable results. There are undoubtedly other effects which are active but which are not taken into account in this theory. The good correlation between test and calculated values should not be accepted as proof that the principles posed are entirely correct. The calculation method takes into account three factors that are undoubtedly important: peak electric stresses, volume of oil under stress, and clearance to tank. Because over-all variations of these quantities are not great, it is not too surprising that a function which depends upon these factors in approximately the correct manner will be useful in yielding fairly accurate practical results.

Additional Design Considerations

On entering this field for the first time, one might naturally think that electric breakdown would start from the region of highest electric stress in the breaker. Consistent with the reference withstand voltages of Table III, this does not turn out to be even approximately true in practice. For example, consider regions 1 and 3 in the sample breaker of Fig. 1 and Table III. At the lowest reference withstand voltage, the maximum electric stress at the rounded corner at region 1 is 99 kv/cm. Around the rest of the bottom periphery of the shield (region 3) the maximum electric stress is only 69 kv/cm. The minimum electrical clearance from region 1 out of the paper to the tank wall is not much different from the clearance from region 3 to the tank. When breakdown occurs, the two ends of the arc leave carbonized markings on the metal surfaces. In none of the tests witnessed was there any evidence of streamers being initiated from the high stress region 1. On the other hand, when sufficient voltage was applied to cause breakdown, the streamers would often initiate from region 3.

At various points around the shields there are small irregularities and relatively sharp edges introduced for convenience in mounting. As placed, these edges, which cause extremely high localized electric stresses, do not initiate breakdown. The explanation for this is that the dielectric strength of oil is much higher around surfaces with small radii of curvature than it is around surfaces with large radii of curvature. This is the factor for which the volume theory[3] supplies quantitative relationships. The relatively small volume of oil under stress in region 1 (12 cubic cm in comparison with 640 cubic cm in region 3) results in the region 1 having a sufficiently high dielectric strength (98 kv/cm in comparison with 57 kv/cm) to withstand the higher electric stress it experiences. As developed in the previous paper,[3] this unexpected behavior of commercial oil results at least in large part from the extremely large statistical variations which are evident when the oil is tested in small volumes.

In all of the many tests witnessed, the breakdown paths have correlated well with the calculations. The breakdowns occur only from the two or three regions with the lowest reference withstand voltage and they are distributed in a random manner throughout these regions. Consistent with the fact that the length of the streamer path X_c has relatively little effect on calculated withstand voltages, streamers often start out from a point in a low margin region in apparent ignorance of the fact that, in the direction taken, the tank happens to be a relatively great distance away. However, the streamer, initiated by conditions at the shield surface, will often continue to grow in a relatively straight line through a surprisingly large distance until the tank is struck and breakdown established.

A corollary of this is that the breakdowns are initiated on the interrupter surfaces and not on the tank surfaces. Although this conclusion has not been established by direct observation, the evidence supporting it is strong. Basically the reason is that the same quantity of flux that issues from the small surface area of the interrupters distributes itself over the large surface area of the tank. Therefore, the flux densities and electric stresses on the tank surfaces are very low. For example, the stress along the relatively sharp corner of the bushing well of Fig. 1 is so low that it is estimated that voltage would have to be increased many times before a streamer could initiate there. Further strong evidence to support this conclusion is simply that the carbonized spot, which marks the terminals of the breakdown arc, never seems to be found on the sharp edges which exist on the tank surfaces. In order to be sharp, the surface must have small area, and the chance of a streamer receiving its direction from the interrupter surface and landing on one of these sharp edges is obviously remote. There is, of course, a limit to how far a rodlike projection could be permitted to protrude from the tank wall in toward the interrupters.

Consideration of equation 7 and the factors which make up its terms yields a simple summary of the over-all effects of the important variables. It is apparent that increasing spacing X_c has two effects:

1. The gradient E will decrease, thereby increasing the corona starting voltage V_c.
2. Each cm of additional spacing X_c will increase the streamer extension voltage V_s by 3.0 kv.

Increased electrode radius of curvature will have three effects:

1. In the practical range, the maximum stress will decrease.
2. Because of the increased volume of oil under stress, the oil dielectric strength g will decrease.
3. The streamer extension voltage will decrease slightly.

One of the most important conclusions from these factors is that there is an optimum radius of curvature for a shield in a given location. In so far as it has been possible to verify, the shields in the line of steel-clad impulse circuit breakers possess these optimum dimensions.

Conclusions

1. A calculation method has been developed for determining the 60-cycle dielectric withstand voltages for oil-circuit-breaker designs while they are on the drafting board.

2. The calculated withstand voltage is the sum of a corona starting voltage and a streamer extension voltage.

3. The corona starting voltage is determined from the oil dielectric strength (kv/cm determined by the volume theory[3]) and the electric stress determined from scale models in an electrolytic tank.

4. The streamer extension voltage is determined from the slope of the needle gap curve in oil. The hypothesis is that, once the streamer extends out into the oil for a few inches from a curved electrode, it assumes the same characteristic as a streamer which has extended from a needle.

5. The calculation method checks known data on disk gaps and spherically ended rod gaps with satisfactory accuracy; see Figs. 4 and 5.

6. As predicted by the calculations, breakdown does not occur at the regions of highest electric stress in the breaker. The occurrence of a breakdown is controlled by a combination of factors including the peak electric stress, the volume of oil which feels this stress, and the distance to the opposing electrode.

7. Breakdowns in general initiate from the interrupter and travel to the tank. Consequently, minor irregularities on the tank surfaces are not detrimental.

8. For the new line of steel-clad impulse oil circuit breakers, electrostatic shield curvatures and general shapes were determined initially in the electrolytic tank and verified by full-scale performance tests. In so far as it has been possible to check, these dimensions are optimum.

9. When based on known performance of dielectric structures which are similar to the unknown, as in comparing cylindrical tank and lenticular tank breakers of different voltage ratings, accuracy is in the range of 5 to 10%.

References

1. THE RESULTS OF 7 YEARS' EXPERIENCE WITH HIGH-CAPACITY OUTDOOR OIL CIRCUIT BREAKERS, C. J. Balentine, K. G. Darrow. *AIEE Transactions*, vol. 74, pt. III, Aug. 1955, pp. 665–71.

2. SOME ENGINEERING APPLICATIONS OF THE ELECTROLYTIC FIELD ANALYZER, H. K. Farr, W. R. Wilson. *Ibid.*, vol. 70, 1951, pp. 1301–09.

3. A FUNDAMENTAL FACTOR CONTROLLING THE UNIT DIELECTRIC STRENGTH OF OIL, W. R. Wilson. *Ibid.*, vol. 72, pt. III, Feb. 1953, pp. 68–74.

4. DIELECTRIC PHENOMENA IN HIGH VOLTAGE ENGINEERING (book), F. W. Peek, Jr. McGraw-Hill Book Company, Inc., New York, N. Y., 3rd ed., 1929.

5. OIL BREAKDOWN AT LARGE SPACINGS, Douglas F. Miner. *AIEE Transactions*, vol. 46, 1927, pp. 248–55.

6. OPERATION OF BUSHINGS IN CARBONIZED OIL, W. R. Wilson, L. Wetherill. *Ibid.*, vol. 70, pt. II, 1951, pp. 1398–1407.

7. SOME STUDIES ON THE DIELECTRIC STRENGTH OF INSULATING FLUIDS, E. E. Charlton, F. S. Cooper. *American Journal of Roentgenology and Radium Therapy*, Springfield, Ill., vol. 41, no. 1, Jan. 1939.

8. METHODS OF TEST FOR DIELECTRIC STRENGTH OF ELECTRICAL INSULATING MATERIALS AT COMMERCIAL POWER FREQUENCIES. *ASTM Specification D149-44*, American Society for Testing Materials, Philadelphia, Pa., pt. III, 1944.

◆

Discussion

W. M. Leeds (Westinghouse Electric Corporation, East Pittsburgh, Pa.): After some 25 years of observing the exasperating inconsistency of electrical breakdown in high-voltage oil circuit breakers on 1-minute insulation tests, it comes as somewhat of a surprise to read this paper in which it is claimed that an equation has been developed which will enable one to predict the breakdown value for a new circuit-breaker design with an accuracy of 5% or better. Even though the factor *k* is introduced in equation 8 to cover miscellaneous items such as variations in oil-handling practices, surfaces, finishes, etc., it is still claimed in the section on "Accuracy of Calculations" that *k* varies only a few % between different designs of the same general type. The authors admit that "any particular design will have some variation from day to day, but will have a relatively stable average value." Actually these variations from day to day may sometimes be much more than 5% so that breaker testing sometimes appears to be more a question of testing the quality of the oil rather than the integrity of the rest of the breaker insulation.

I mention these points because consideration of random oil impurities under commercial handling conditions can lead to a somewhat different and perhaps equally plausible explanation of the volume theory of dielectric strength from that given by the authors based on the so-called "weak-link" theory.

This paper unfortunately omits almost all reference to the time factor in the application of voltage. In considering a steel chain under tension, time under test may be relatively unimportant, since it would be expected that if the weakest link in the chain will withstand a given load for 5 seconds it may well hold up for 5 minutes or longer at the same load. But not so with oil. Many times it has been observed that a circuit breaker holds voltage on a 1-minute test for 30, 40, 50, 55, seconds and then a flashover occurs just before the 60 seconds are up. What happened? It is hardly to be expected that the curvature of the shields would change or the spacing to the walls grow less. Did the oil just get tired of holding voltage after 55 seconds? Does it not seem logical that under normal test conditions particles of some contaminant such as water or cotton lint or suspended metal particles may gradually float into the field, changing the gradient at a critical point so that a streamer darts out and results in breakdown? Evolution of gas in the oil or release of gas from electrode pores by the electric field are other examples of time-dependent phenomena which may cause delayed breakdown.

Now carrying the reasoning a little further, in a circuit-breaker tank where there are a number of possible breakdown paths of approximately the minimum spacing to the walls, corresponding to a large oil volume under 90% stress or more, would it not be reasonable to suppose that, granting a few impurities in the oil, there would be an observable increase in the probability that one or more particles would drift or be drawn into the highly stressed locations and cause breakdown than would be the case in a different design with high electric stress concentration at just a very few locations?

I should like the authors to comment on this, and also to state the rate of application of voltage used in the basic test work, and to explain how 1-minute hold test results can be related to those tests where the voltage is continuously raised to the point of breakdown.

G. M. L. Sommerman (Westinghouse Electric Corporation, East Pittsburgh, Pa.): The equivalent volume theory or weak-link probability theory of electrical breakdown advanced by the authors leads to the inverse dependence of dielectric strength (expressed as a maximum potential gradient) on the equivalent volume of oil under stress shown in Figs. 9 and 10. There is much experimental evidence for this in rapid-rate-of-rise breakdown tests on insulating liquids, such as those of Peek. Even the results of Miner (reference 5 of the paper), who used the hold-test procedure from 1 to 10-minute durations on oil with hemispherically ended rod electrodes, when analyzed by Wilson, Streater, and Tuohy, yield the inverse dependence of strength versus stressed oil volume shown in Fig. 10.

As shown in Mr. Wilson's previous paper (reference 3 of this paper), this same probability theory leads to another conclusion; i.e., the deviation in electrical breakdown results is less when a large volume of liquid is under high stress than when only small liquid volumes are so stressed. In looking for recent data on oil breakdown which included deviations in the experimental results, we have found informative values in the work of A. Roth.[1] Roth's tests were made on technically pure oil at 50 cycles per second (generally accepted as equivalent to 60 cycles per second for liquids) and a voltage rise of 10% in 10 seconds. Electrodes investigated included concentric cylinders, equal-diameter parallel cylinders, cylinder-to-plane, equal spheres, sphere-to-plane, point-to-point, point-to-plane, and parallel 4-edged prisms. The results for oil-breakdown-strength dependence on electrode configurations, size, and spacing are remarkably similar to those of Peek for similar electrode configurations, especially when the longer voltage-application times used by Roth are considered.

What I wish to emphasize here, however, is that Roth's values of percentage deviations in breakdown strength usually increase rather than decrease when increasing equivalent volumes of highly stressed oil are considered in tests with various electrode sizes or spacings. This is contrary to the prediction of the equivalent volume theory. Thus, for moderately widely spaced spheres or parallel cylinders (spacings of 5 to 10 cm, comparable to the electrode diameter), the equivalent volume as defined by the authors increases with increasing electrode diameter. Therefore, when the diameter of such electrodes is increased, the equivalent volume theory predicts lower maximum breakdown stresses and lower deviations in the results. The measured deviations in the results actually increase significantly with increasing electrode diameter in most cases.

In these cases it is true, as stated in the foregoing, that Roth's maximum breakdown-stress values for the oil do decrease with increasing electrode diameter (increasing equivalent oil volume). For "isolated" cylinders and spheres (spacings greater than two diameters and one diameter respectively), increasing the electrode spacing does not appreciably change the equivalent oil volume as defined. The theory predicts unchanged values of maximum breakdown stress (except for the voltage increment for streamer extension) and unchanged deviations in the breakdown test results. The deviations measured by Roth always decrease significantly with increasing electrode spacing in the range from 10 cm to 30 cm (in many cases, beyond 30 cm) for the electrodes cited. It is true for the large spacing region, also, that the measured maximum breakdown stress increases (at least slightly) as the spacing increases; this is in accordance with the prediction of the equivalent volume theory as amended by the supplementary streamer extension voltage hypothesis.

The increase in percentage deviation in the maximum breakdown strength of oil found by Roth for increasing electrode diameter may be explained by thinking in terms of the larger electrode areas in contact with oil at or near maximum stress, and by postulating electrode imperfections such as microscopic points or minute pores, and/or imperfections arising from solid particles from the oil either on the electrodes initially or driven there by the electric field as the test voltage is raised. From the principle of simplicity, we can assume (for a given degree of care in fabricating electrodes and/or a given density of solid particles in the oil) that the surface density of these types of imperfections will be independent of spatial co-ordinates in the high-stress regions of the electrodes. Thus, the probability of occurrence of a damaging imperfection will be proportional to the electrode area adjacent to oil at high stress. Therefore, the probability of obtaining measured breakdown strengths which are much less than the mean strength in a set of tests will increase with the "equivalent electrode area." (The equivalent electrode area might be defined as the surface area for which the electric stress is within, say, 10% of the maximum.)

Such an electrode-surface-imperfection theory would be another of the weakest-link probability type. It would be consistent with the observed larger deviations in breakdown values as well as the observed lower maximum breakdown stresses for technical-grade mineral oil in Roth's tests with the electrode types described in this discussion. It would also account for the lower measured breakdown values obtained by Peek and others when oil is tested between disks of increasingly large diameters.

The quality factor analogous to k in equation 8 would become a factor related not only to oil quality but also to electrode surface quality. The oil quality might include resistance to microscopic ionization due to electron emission from the microscopic points on the electrodes, or the somewhat more severe corona in oil from larger imperfections or particles on the electrodes, as well as the usual dependence on moisture, particles, etc., in the commercial oils. Oil-failure mechanisms consistent with this thinking would also explain the observed decreases in oil breakdown strength and observed increases in deviation of measured oil strengths with increasing time of voltage application.

As another point of this discussion, we might consider the streamer extension voltage introduced by the authors to explain the greater maximum breakdown strength of oil with greater electrode spacings for the "isolated-electrode" range of spacings. From the values given in the authors' example for a large oil circuit breaker of a certain design, it is seen that this streamer extension voltage (84 kv rms) is more than 20% of the corona starting voltage (406 kv rms) and therefore more than 17% of the total calculated withstand voltage. These percentages should be true for the actual withstand voltage of the circuit breaker as well as the reference withstand voltage. Since the authors state later in the paper that the breaker-design confirmatory withstand tests were usually run at about 90% or more of the limiting voltage and that oil failures were sometimes observed in these breaker-design confirmatory tests, the following question arises.

Is corona in the oil observed in these oil circuit breakers when they are tested at the design-limiting voltage? Corona in oil at these test voltages is certainly indicated by the authors' treatment of the problem, at least according to my reasoning which indicates that the test voltage is from 7 to 17% above the corona starting voltage. If the answer to this question is "maybe," it would be worth while to try to measure the corona starting voltage by the various means now available for measuring 60-cycle-per-second corona. If the answer is "yes," it is indicated that another means is available for checking design calculations, quality of fabrication, quality of materials, etc. Also, it means that there is another property of the oil to be investigated and maintained, i.e., the ability of the oil to withstand corona discharges, at least for 1-minute-hold tests.

Reference

1. Hochspannungstechnik (book), A. Roth. Springer-Verlag, Vienna, Austria, 3rd ed., 1950, pp. 129–35.

Dr. Amandus H. Sharbaugh (General Electric Research Laboratory, Schenectady, N. Y.): For several years we have been interested in measuring an electric strength of liquid systems which will be dependent upon the molecular constitution of the liquid.[1] To do this it has been necessary to eliminate several external causes of premature breakdown of the liquids; e.g., it is necessary to use highly polished electrode surfaces and carefully filtered liquids. Furthermore, continuous monitoring of the breakdown gap by a microscope is necessary to insure the absence of suspended material in the high field region. When using electrode spacings of the order of 0.002 inch and pure liquid hydrocarbons, it has been observed by us and others[2] that single particles of dust as small as 0.0001 inch in diameter can cause lowering of the breakdown voltage by as much as 100%. As proposed in the present paper, it therefore seems reasonable that the rupture voltages measured in commercial oils may be determined by the volume of liquid under high stress, since it is likely that a uniform suspension of dust particles obtains in such samples. The relative importance of the area and the separation of the electrodes in determining this volume needs to be investigated.

References

1. Electric Strength and Molecular Structure of Saturated Hydrocarbon Liquids, R. W. Crowe, A. H. Sharbaugh, J. K. Bragg. *Journal of Applied Physics*, New York, N. Y., vol. 25, 1954, p. 1480.

2. High Values for the Electrical Breakdown Strength of Liquids, W. D. Edwards. *Journal of Chemical Physics*, New York, N. Y., vol. 20, Apr. 1952, p. 753.

W. R. Wilson, A. L. Streater, and E. J. Tuohy: The discussers seem primarily to request expansion of the concepts and data of the subject paper and of its forerunner which introduced the statistical volume theory of the dielectric strength of oil. Furthermore, at the Winter Meeting at least four of the presentations of papers on dielectric phenomena included reference to these basic probability concepts. Among these was a paper by Dr. Gauster,[1] which was largely a discussion of the first statistical volume theory paper.[2] In these various comments no disagreement was indicated with the primary hypothesis that probability effects are a major factor determining the average dielectric strength of commercial oil around electrodes of different geometries. However, the composite of these comments indicates the desirability of presenting certain test and analytical data, not previously published, to clarify exactly why and on what basis some of the steps were taken in the quantitative approach.

Early Stages

The investigations reported in the two statistical volume theory papers actually started in 1944 in an area of liquid dielectrics so markedly different in dimensions that it would seem, at first glance, that there could be no pertinent connection. The present investigation concerns the dielectric strength of oil circuit breakers; the former was concerned with the microscopic pool of liquid dielectric at the edges of liquid-impregnated paper-foil capacitors. As alternating voltage is raised on such capacitors this pool of liquid finally breaks down, defining a corona starting voltage. A large amount of data had been taken in fundamental investigations[3,4] of this phenomenon when the striking fact was noted that capacitors with short lengths of foil and paper had much higher average corona starting voltage than capacitors with long

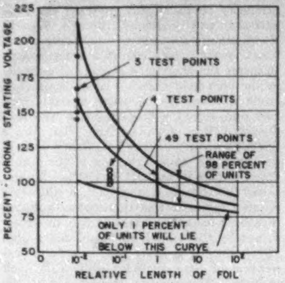

Fig. 11. Decrease of capacitor corona starting voltage with length of foil

lengths of foil. Another way of stating this is that for identical dielectric thickness the corona starting voltage decreases with increasing capacitance.

As demonstration that the effect is large and significant, Fig. 11 shows that short capacitor rolls had 60% higher average corona starting voltage than rolls that contained 100 times the foil edge length. In each case the nominal metal-to-metal clearances and electrostatic flux plots were identical. The fact revealed was that the dielectric strength of the liquid in the pool at the foil edge dropped in a regular manner as the length of foil edge under electric stress was increased. Furthermore, as is indicated by Fig. 11, deviations from the average were reduced very significantly.

These facts find their explanation in very simple weakest-link probability relationships which are important throughout the field under discussion. If there are ten capacitors, each of unit foil length, and they are tested separately, the average corona starting voltage for the ten will certainly be higher than the value of the weakest one. If, however, all ten are tested connected electrically in parallel, thus representing one capacitor of ten times the length, the dielectric strength will be that of the weakest unit. It is obvious, therefore, that the average corona starting voltage must drop as the length of foil increases. The early paper on weakest-link phenomena[5] defines the mathematical relationships which tell as a function of standard deviation approximately how much this decrease should be.

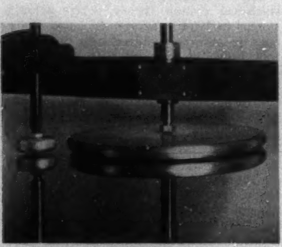

Fig. 12. One-inch- and 10-inch-diameter Rogowski gaps

The example referred to there is that of Fig. 11 of this discussion. Fig. 1 of the first statistical volume paper[2] presents the results of the mathematics in graphical form for general use. This phenomenon has a direct and important manifestation in the design of capacitors, and its existence is firmly established.

The writer of the first paper[2] spent 7 years working directly on development programs in a high-voltage dielectric testing laboratory in the transformer plant in which F. W. Peek had taken his original data. An additional 6 years were spent at a switchgear plant in work closely associated with this type of activity. Just as Dr. Leeds comments, the exasperating inconsistency of electrical breakdown was observed. However, the very presence and persistence of the wide statistical variations leads mathematically to the large reductions of dielectric strength of oil with increasing regions under stress that are the subject and conclusion of the two papers under discussion.

BASIC EXAMPLE

It will be helpful to present one complete basic example of this weakest-link phenomenon in bulk oil so that it can be used in discussing various points throughout the closure. The two uniform field gaps (based on the Rogowski contour) shown in Fig. 12 were immersed in the same oil at the same time and tested by applying rapidly rising 60-cycle voltage alternately, first on one gap and then on the other. The results of one typical run of such tests are shown as a probability plot in Fig. 13. The two sets of data are given in Table IV.

The fact of major importance here is that even though the metal-to-metal clearances were identical at 0.254 cm the smaller gap broke down at 36 kv average rms while the larger gap with 100 times the region under stress broke down at only 23 kv average rms.

Using the data given in Table IV and equation 1 of reference 2, the breakdown of the larger gap can be calculated from that of the smaller gap

$$g = 200 - 2.5 \times 33.4 = 117 \text{ kv/cm} \qquad (12)$$

The calculated breakdown voltage for the larger gap is then

$$117 \times 0.254/\sqrt{2} = 21 \text{ kv}$$

in comparison with the 23-kv test value.

This calculated gradient for the large area gap can also be read directly from the probability plot, Fig. 13, at the $1/N+1 = 1\%$ point for the small area gap. This simple method indicates the basic causes of the reduction much more directly than does the equation.

ERRORS

The calculation method is clearly stated to apply only to small extrapolations from structures of known performance. In spite of this, the error in the foregoing 100 to 1 extrapolation is only 10%. One reason is that for small extrapolations the calculations involve only an adjustment increment (see equation 12) subtracted from the established value. If, e.g., the total adjustment due to statistical factors were 10%, and if it were 20% in error, the resulting calculated value would be in error by only 2%.

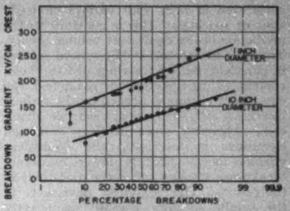

Fig. 13. Probability plot of Rogowski gap data for 1-inch- and 10-inch-diameter gaps at 0.254-cm spacing

The ratio of volumes in the basic example was selected purposely to emphasize errors. In this vein, the authors have also noted, as commented upon by Mr. Sommerman, that standard deviations do not seem to drop as much with increasing volume as is indicated by normal probability. Of course, when electrode radii are made sufficiently small with respect to spacing, they act like needles, and standard deviations are markedly reduced. This, is, however, a different field than that now being discussed. Table IV shows this type of error for the uniform field gaps. From normal probability, one would expect (see Fig. 1 of reference 2) that the standard deviation would drop from 33.4 kv/cm to 13.5 kv/cm instead of only to 27.1 kv/cm. The reason is not understood. As was stated in the original paper, normal probability is only approximately correct, and "more complete statistical analysis will probably be made." Additional uncertainty lies in the fact that the reduction of statistical deviations generally experienced as spacing is made large is neither explained by nor inconsistent with the statistical volume theory. Although these unanswered problems concerning standard deviations may constitute clues to the future investigator seeking more precise statistical relationships, they do not seem to influence the calculation of breakdown voltages over small extrapolations. This was one reason for basing the equivalent volume curves on test data and thereby eliminating dependence upon statistical mathematics.

These same data indicate the large errors that may result if the correction term is permitted to become large. If an attempt is made to calculate the dielectric strength of the small area gap of Table IV from the data for the large area gap, the factor A becomes so large that it is well off scale on Fig. 1 of reference 2. By extrapolation it is estimated that the adjustment

Table IV. Breakdown Test on Uniform Field Gaps at 0.254-Cm Spacing in 10C Oil

Diameter, Inches	Breakdown Gradient, Kv/Cm	Standard Deviation, Kv/Cm
10	127	27.1
1	200	33.4

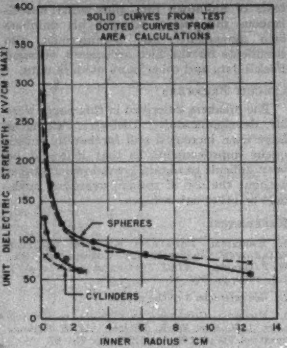

Fig. 14. Comparison of calculated and test curves of dielectric strength for isolated spheres and cylinders

Table V. Dielectric Strength of 1-Inch-Diameter Uniform Field Gaps in Unagitated and Agitated 10C Oil

Spacing, Cm	No. of Tests	Average Breakdown Gradient, Kv/Cm Crest	Standard Deviation, Kv/Cm Crest	Difference in Breakdown Gradients by Test, %	Calculated Difference in Breakdown Gradients (Volume Theory), %
Unagitated Oil					
0.254	120	202	35.6	5	11
0.508	120	193	24.8		
Agitated Oil					
0.254	40	137	33.7	14	15
0.508	40	118	33.4		

increment $A\sigma$ is substantially larger than the breakdown voltage for the large area gap and that the error of calculation is in the neighborhood of 2 to 1.

AREA VERSUS VOLUME

It is a real puzzle to establish with certainty whether the statistical relationships actually depend upon the volume or upon the surface area under relatively high stress, or perhaps on some combination of the two. In the circuit-breaker calculations, checks indicate that either could be used with about equal success. The reason is that for most electrodes it is difficult to get a large increase in area without also finding a corresponding large increase in volume. For example, the uniform field gaps of Table IV have the same ratios of area and volume. For sphere gaps of different radii but of the same spacing (referred to in the discussion of Gauster's paper[1]) area and volume calculations give exactly the same values. With the capacitors of Fig. 1, it is impossible to tell whether the proper variable is length, area, or volume.

These tests, and the electrodes of classical shapes discussed in the original paper,[3] indicated that the weakest-link or probability effects were important. The hypothesis was made that the effects were so important that they masked all the variables and that approximate calculations could be made based on them alone. On carrying out the calculations, volume was selected simply because Peek's empirical data and curves were fitted much better by the statistical volume calculations than by statistical area calculations. By choosing different standard deviations both methods could be made to work fairly well for relatively large radii.

Actually area was tried first because it was simpler. Fig. 14 compares calculated and test results. Exactly parallel to the equivalent volume calculations, the dielectric strength curves for spheres at diameter spacing were calculated by forcing the curve to pass through the two points at $R=1.27$ and $R=6.25$. Area varies as the radius squared, so a standard deviation ($\sigma=21$ kv/cm in comparison with $\sigma=15.7$ kv/cm for volume) could be calculated, on which the entire sphere gap curve could be based. Fig. 14 shows that the correlation is again remarkably similar to that obtained by the volume hypothesis.

Still parallel to the equivalent volume calculations, it was assumed that one-quarter of the surface area of a sphere at diameter spacing was under relatively high stress. From this the isolated cylinder curves were calculated. However, these curves showed insufficient variation of dielectric strength with radius. When a higher value of standard deviation was assumed, the entire cylinder curve was too low and the sphere gap curve did not match well. When looked at by itself, the cylinder gap curve could be matched with a higher standard deviation, but the value (about 37%) appeared much higher than encountered in test (although this could result from combined surface defects and oil defects). It was postulated that the actual performance is probably a combination of volume and area effects, but that the accuracy of the data and of the calculation method were not adequate to attempt separation. Both effects were lumped together in the statistical volume calculations.

These volume calculations check very well, as shown in Fig. 3 of the original paper.[3] The major reason is simply that for spheres the volume varies as the cube of the radius and surface as the square. For cylinders the volume varies as the square of the radius and surface area as the first power. Similar calculations for dielectric strength for sphere gaps as spacing is reduced show that higher standard deviations are required to check Peek's data on the area basis than on the volume basis. As is indicated in the two papers, these correlations may possibly turn out to be a fortuitous combination of effects which happens to work rather than a verification of the exact hypothesis made.

Mr. Sommerman's statement that statistical deviations should increase with surface area and decrease with equivalent volume is not understood as stated. From normal probability considerations, both should decrease.

Attempts at direct experimental determination as to whether area or volume is most important were made by testing uniform field gaps at different spacings. However, dielectric strength reduces so gradually with increased volume that predicted results for a 2-to-1 change in spacing are small. Furthermore, the equivalent volumes calculated for spheres and cylinders occupy such thin layers that plane parallel gaps separated by these distances are apparently influenced by floating particles which can bridge the gap (see reduced dielectric strength at very small spacings showed by Farmer[4]). Consequently, a volume effect may conceivably be in control for small radii but be gradually replaced by an area effect with relatively flat electrodes.

Table V lists two series of tests with uniform field gaps at different spacings. The first, with unagitated oil, shows some drop in dielectric strength with increased spacing. According to the area theory, there should be no drop. The second, with oil agitated before each test, shows appreciable drop with increased spacing, which is almost exactly as predicted by the volume calculations. Analysis of the data showed that this difference in dielectric strength is statistically significant. Thus it appears that volume effects may be more important with some oils than with others.

PURIFIED OILS

With highly purified oil in small volumes, Dr. Sharbaugh obtains dielectric strengths in the thousands of kv/cm as contrasted with 50 kv/cm for commercial oil around large cylinders. Furthermore, his purified oil has markedly lower statistical deviations.

What causes the great difference between the highly purified and the commercial oil? At least one important factor is proved by Dr. Sharbaugh to be particles floating in the oil. One such particle can reduce dielectric strength till it compares with that for very small volumes of commercial oil. Just as statistical mechanics yield composite pressure and temperature effects resulting from random velocities of myriads of electrons, no one of which is known, so the statistical volume or area mathematics seems to yield composite effects of myriads of particles and other impurities, each having unknown individual effect.

OIL FLOW

We have also noted oil flow around the gaps under stress. Undoubtedly this is one factor that contributes to the high statistical deviations, and is therefore included in the statistical theory calculations. However, the velocity of flow appears to be relatively small around uniform field electrodes in comparison with electrodes with relatively small radii. Perhaps effects of self-induced oil flow can be separated from the other variables in the future. It is doubted that Dr. Leeds believes that variations disappear on impulse, where there is no time for oil flow.

TIME DELAY

Concerning time delays of breakdown in 60-cycle 1-minute hold tests, Dr. Leeds asks if the oil just gets tired and then breaks down. Exactly the same phenomenon is encountered with air. At high altitude, delays of minutes are common[7] until a cosmic ray or other ionizing force happens to exert itself at the right spot. What little volume effect appears in atmospheric air at small spacings and with small spheres is probably caused largely by such variations. The number of free electrons released in air is proportional to the volume of air under stress. By analogy, this is at least one hypothetical process that might contribute to time delays in oil and not depend upon flow of oil into the region. Although it is outside the scope of this paper, reduction of average dielectric strength with time is one factor predicted by the weakest-link mathematics, if there is variation from test to test of the same material. A 1-minute test might be expected to yield an average breakdown voltage at least as low as the minimum found in ten short tests of 6 seconds each. However, no attempt has been made to establish the importance of this factor in comparison with others, and there is no reason at present to expect good correlation with it alone.

CORONA

We agree with Dr. Leeds that the 60-cycle high-potential test, after design performance has been established, is primarily a test of the oil rather than of the circuit breaker. Mr. Sommerman, however, seems to be concerned over the deterioration of the oil due to corona which might appear for 1 minute during a high-potential test. Even if such a corona were to occur (which cannot be established either way from the papers), it would seem that such oil deterioration would be infinitesimal compared with that caused by normal power interruption.

Concerning Dr. Leeds' question about there being more probability of impurities drifting into a large volume field than a small volume field, statistical volume effects are relatively small in comparison with the effects of shield radius on the electric field and of clearance to tank. The probability of breakdown or of corona streamers starting reduces extremely rapidly toward zero as the electric stress is reduced. All effects are combined to produce a breaker which will withstand the particular voltage desired for it.

OIL FACTOR

The oil factor k has caused so much speculation that the final value obtained by averaging the five breaker performances should perhaps be given. By chance, this arbitrary factor, introduced to include variations from Peek's oil, turned out to be $k = 1.00$. This was withheld previously because of concern that a false impression of a higher level of accuracy than was warranted for absolute values might be created. Perhaps this point has now been made with adequate emphasis.

It is assumed that Peek's oil was of slightly less strength, but his rapid-rise tests of unknown rate, plus other miscellaneous differences, brought his numbers into agreement. Mr. Sommerman also comments on the nice agreement between Peek's data and other more modern data.

CIRCUIT BREAKERS

The breakers described in this paper were all developmental. Dielectric strengths have been increased still further by subsequent improvements so that it would be very difficult to obtain breakdown averages without the use of special, oversized bushings or other subterfuges.

REFERENCES

1. EMPIRICAL EQUATIONS FOR THE 60-CYCLE SPARK-OVER GRADIENTS IN COMMERCIAL OIL, W. F. Gauster. *AIEE Transactions*, vol. 74, pt. I, July 1955, pp. 301–11.

2. See reference 3 of the paper.

3. PHYSICAL CONCEPTS OF CORONA IN CAPACITORS, J. R. Nye, W. R. Wilson. *AIEE Transactions*, vol. 72, pt. III, Aug. 1953, pp. 781–87.

4. DEVELOPMENT OF CORONA MEASUREMENTS AND THEIR RELATION TO THE DIELECTRIC STRENGTH OF CAPACITORS, R. J. Hopkins, T. R. Walters, M. E. Scoville. *AIEE Transactions*, vol. 70, pt. II, 1951, pp. 1643–51.

5. THE MATHEMATICS OF WEAK LINKS, W. R. Wilson. *The Journal of the Amateur Mathematician*, Pittsfield, Mass., vol. 2, no. 2, July 1947.

6. THE DIELECTRIC STRENGTH OF THIN INSULATING MATERIALS, F. M. Farmer. *AIEE Transactions*, vol. 32, pt. II, 1913, pp. 2097–2131.

7. CORONA IN AIRCRAFT ELECTRIC SYSTEMS AS A FUNCTION OF ALTITUDE, W. R. Wilson. *AIEE Transactions (Electrical Engineering)*, vol. 63, Apr. 1944, pp. 189–94.

Short-Circuit Currents and Circuit-Breaker Recovery Voltages Associated with 2-Phase-to-Ground Short Circuits

W. F. SKEATS
FELLOW AIEE

IT HAS been shown[1–3] that under certain conditions both the current in one phase of a 2-phase-to-ground short-circuit, Fig. 1, and the normal-frequency recovery voltage for this phase may exceed values arising from any other type of fault at this location except that, in the process of clearing, a 3-phase grounded fault passes through a stage in which it is a 2-phase-to-ground fault and is therefore subject to the same currents and voltages. Also, the normal-frequency recovery voltage of whichever phase clears first can approach line-to-line voltage when the zero-phase-sequence impedance approaches a pure resistance of high ohmic value. Although these facts have been little recognized in circuit-breaker application, with the result that the recognized currents and voltages are lower than those indicated in references 1, 2, and 3, there appears to be very little resultant adverse experience. In this paper the facts in regard to current and voltage magnitudes are reviewed and some factors that may be responsible for the lack of adverse experience are discussed. The body of the paper consists of a series of summary statements regarding the excess currents and the excess voltages which may occur in connection with a 2-phase-to-ground fault, followed by the conclusions. A more detailed discussion supporting the statements made in the paper is given in the Appendix.

Excess Currents

With certain values of neutral resistance, either in the fault or in the source neutral, the currents in one phase of a 2-phase-to-ground fault may exceed those corresponding to either single-phase-to-ground or 3-phase short circuits by values up to 15 per cent. Values are

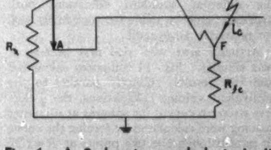

Fig. 1. A 2-phase-to-ground short circuit

Paper 55-221, recommended by the AIEE Switchgear Committee and approved by the AIEE Committee on Technical Operations for presentation at the AIEE Winter General Meeting, New York, N. Y., January 31–February 4, 1955. Manuscript submitted October 21, 1954; made available for printing December 8, 1954.

W. F. SKEATS is with the General Electric Company, Philadelphia, Pa.

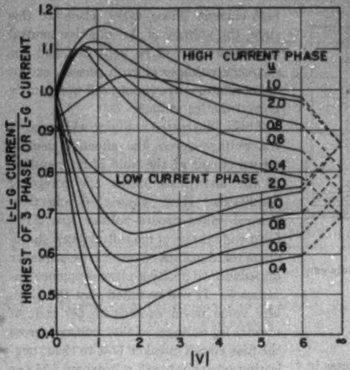

Fig. 2 (left). Ratio of 2-phase-to-ground short-circuit currents to highest of 3-phase current or single-phase-to-ground with v=0

$u+jv=(r_0+jx_0)/(r_1+jx_1)$

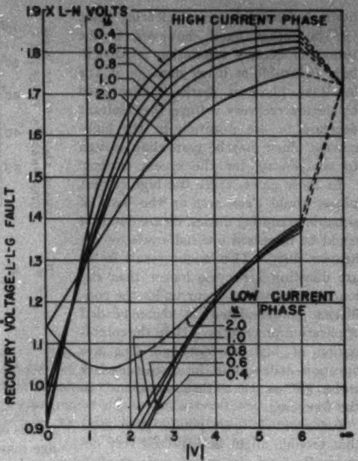

Fig. 3 (right). Recovery voltage of first phase to clear of 2-phase-to-ground short circuits

$u+jv=(r_0+jx_0)/(r_1+jx_1)$

given in curve form for a wide range of conditions in Fig. 2.

The normal-frequency recovery voltage in the phase in which this excess current occurs, if this phase clears first, lies in the range from a little above leg voltage to values above line-to-line voltage, depending upon the ratio of zero-phase-sequence resistance to positive-phase-sequence reactance (provided positive-phase-sequence resistance is negligible). Values are shown in curve form in Fig. 3.

The values of neutral resistance giving rise to these high currents are not likely to occur except in tower-footings or other fault-grounding resistances in high-voltage transmission lines.

With present circuit-breaker ratings, only a few miles of transmission line are necessary to reduce short-circuit currents to the point where the 15-per-cent increase will be insufficient to bring the short-circuit current up to that available at the station. Specific values are given in Table I.

Where the transmission line has a low-resistance ground wire solidly tied in to the station neutral, 2-phase-to-ground short-circuit currents in the first few miles of line may exceed the current available from other types of short circuit at the particular fault location. Unless the ground-return current is forced through a higher resistance than that of the ground wire itself, e.g., as by the falling of a conductor directly to earth, the 2-phase-to-ground currents cannot exceed the current available from other types of short circuit at the station bus.

Where an excess current of this sort occurs, it occurs only in one phase, and the current and recovery voltage of the other phase are both low.

The phase angle between the currents in the two phases under the conditions producing the excess current is such that current zero in the high-current phase follows current zero in the low-current phase by an average value of about 45 degrees and current zero in the low-current phase follows current zero in the high-current phase by an average of about 135 degrees. Thus, with equal interrupting duties on the two phases, there would be a 3-to-1 probability that the low-current phase would clear first and, with the existing lower duty on the low-current phase, this probability tends to be increased, with the amount of the increase depending on the characteristics of the breaker. As soon as this happens, the current and recovery voltage of the high-voltage phase are reduced to those of a single-phase-to-ground fault, which are within those contemplated in recommended application procedures.

Here, it should be noted that, on one hand, the excess current during the early part of the arcing period which would occur in this case in the high-current phase may have adverse effects upon the performance of the breaker, even though both current and recovery voltage are reduced to values within normal

Table I. Range of Resistance Values Causing 2-Phase-to-Ground Short-Circuit Currents in Excess of 3-Phase Short-Circuit Current When Single-Phase and 3-Phase Short-Circuit Currents Are Equal

			Neutral Resistance Values Calculated for Maximum Design Voltage, Ohms				
Voltage, Kv	Megavolt-Amperes	Corresponding Reactance at Maximum Design Voltage, Ohms	Minimum for 5-Per-Cent Current Increase	For Maximum Current Increase	Maximum for 5-Per-Cent Current Increase	No Increase	Miles of Transmission Line Beyond Which Current Will Not Exceed 3-Phase Current
69	1,000	5.26	0.37	2.00	6.15	9.10	1.05
	1,500	3.50	0.24	1.33	4.10	6.06	0.70
	2,500	2.10	0.15	0.80	2.46	3.63	0.42
	3,500	1.50	0.10	0.57	1.75	2.60	0.30
115	1,500	9.76	0.68	3.70	11.40	16.90	1.95
	3,500	4.18	0.29	1.59	4.90	7.23	0.84
	5,000	2.93	0.20	1.11	3.43	5.07	0.59
138	3,500	6.01	0.42	2.28	7.03	10.40	1.20
	5,000	4.20	0.29	1.60	4.92	7.26	0.84
	10,000	2.10	0.15	0.80	2.46	3.63	0.42
161	5,000	5.72	0.40	2.17	6.70	9.89	1.14
	10,000	2.86	0.20	1.08	3.35	4.95	0.57
230	5,000	11.72	0.82	4.45	13.70	20.30	2.34
	10,000	5.86	0.41	2.22	6.86	10.10	1.17
	15,000	3.91	0.27	1.49	4.58	6.78	0.78
287.5	15,000	6.08	0.42	2.31	7.12	10.50	1.22
330	15,000	8.17	0.57	3.10	9.56	14.10	1.63
	25,000	4.90	0.34	1.86	5.73	8.48	0.98

limits before the normal clearing time. On the other hand, however, if the timing of contact separation is particularly favorable or if arc duration in the low-duty phase is markedly shortened by the low recovery voltage, the resultant decrease in arc duration in the high-current phase may be more than enough to compensate for the excess current.

In those cases where the high-current phase would clear first on the basis of equal interrupting duties, its arc duration could be increased one half-cycle by the heavier duty. This might result in an arc duration 1/8 cycle longer than the longest that would occur under the conditions contemplated in recommended application procedures. Here the combination of high current and long arc duration will result in circuit-breaker stress greater than that mentioned in the foregoing.

Summarizing these points, it appears that trouble might be expected very occasionally from the excess currents of 2-phase-to-ground short circuits, but the many conditions outlined in the foregoing which must be met for such currents to be realized and to have an adverse effect on breaker performance may be expected to render such troubles extremely rare, as experience has indicated them to be.

Excess Normal-Frequency Recovery Voltages

Fig. 3 shows the normal-frequency recovery voltages which would be developed in clearing a 2-phase-to-ground fault is there were an interval of one or more half-cycles between the clearings of the two phases.

Values up to line-to-line voltage exist for the low-current phase, and even higher values for the high-current phase.

The highest values, especially for the low-current phase, however, exist when the zero-phase-sequence impedance differs substantially in phase angle from the positive-phase-sequence impedance (large values of v).

In such cases, as shown in Fig. 4, the angle by which current zero in the low-current phase leads the current zero in the high-current phase becomes very small with two results:

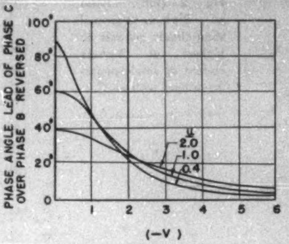

Fig. 4. Phase-angle relationship between phase B and phase C

$u+jv=(r_0+jx_0)/(r_1+jx_1)$

1. The probability that on the basis of equal interrupting duties, the low-current phase would clear first becomes very high, about 98 per cent at $v=6$.

2. The failure of the high-current phase to clear promptly in those cases where it would normally clear first results in an arc duration only a few degrees longer than would be the case for both phases with a slightly later contact separation, and consequently does not represent an important increase in maximum duty in this respect.

The conditions which give rise to high values of normal-frequency recovery voltage may be most conveniently examined by studying the voltage of the effective neutral return circuit. The effective neutral return circuit is determined by considering the circuit to consist of one section in which positive-, negative-, and zero-phase-sequence impedances are all equal, and a second section which has no positive- or negative-phase-sequence impedance, but a zero-phase-sequence impedance equal to the difference between the zero-phase-sequence impedance and the positive-phase-sequence impedance of the actual system, the difference between negative- and positive-phase-sequence impedances being considered negligible, as it usually is. The second section is then the effective neutral return circuit. Since the circuit currents and the voltages across open breaks in the circuit are dependent upon only the magnitudes of the phase-sequence impedances and not upon their arrangement or relative location in the circuit, this conception will yield quite general results, and it has the advantage that it permits easy visualization of the factors determining these currents and voltages. In accordance with the rules of phase-sequence representation, the impedance of the effective neutral return circuit is made equal to one-third of the zero-phase-sequence impedance which it represents.

That part of the recovery voltage which accounts for the values which are indicated in Fig. 3 to be above the crest of leg voltage (neglecting oscillatory overshoot) is dependent upon a large change in the voltage across the neutral return circuit. Early in the development of this change, a current zero occurs in the high-current phase. If interruption in the high-current phase takes place at this time, the voltage of the effective neutral return circuit will be kept low and the recovery voltages of both phases, except for oscillatory overshoot, will not greatly exceed the leg voltage.

This is illustrated in Fig. 5, which shows the voltage across the effective neutral return circuit at the time of interruption of the last phase under the foregoing conditions. Here values of effective-neutral-return-circuit voltage are given for a wide range of magnitude and phase-angle relationships of zero-phase-sequence impedance to positive-phase-sequence impedance. It will be noted that the absolute value never exceeds 25 per cent of normal leg voltage, so that voltage across the first circuit-breaker pole to clear, neglecting overshoot, will not exceed 125 per cent of normal leg voltage, and will usually be held well below this value since the voltage of this phase will usually be well past its crest at the time of interruption and, by the time of the next crest, the effective-neutral-return-circuit voltage will have returned to zero.

Summarizing, normal-frequency recovery voltage approaching and even exceeding line-to-line voltage may appear on the first phase to clear of a 2-phase-to-ground fault, but if the two phases interrupt on closely adjacent current zeros (less than 90 degrees apart), neither phase will develop normal-frequency recovery voltages appreciably in excess of leg voltage.

Conclusions

1. Two-phase-to-ground short circuits may result in currents up to 15 per cent higher than those associated with either 3-phase or single-phase-to-ground short circuits. The occurrence of such high currents, however, requires a combination of so many unfavorable circumstances that they are very infrequent in service. There is no adverse experience known to the author which is attributable to such currents.

2. Two-phase-to-ground short circuits may result in normal-frequency recovery voltages equal to or higher than line-to-line voltage if the two phases are not cleared within a fraction of a half-cycle of each other. When they are so cleared, however, normal-frequency voltages appreciably above normal leg voltages are not developed in either phase.

Appendix. Detailed Discussion

Current and Voltage Magnitudes

In a 2-phase-to-ground short circuit, there are two conditions under which both 3-phase and single-phase-to-ground short-circuit currents may be exceeded. The

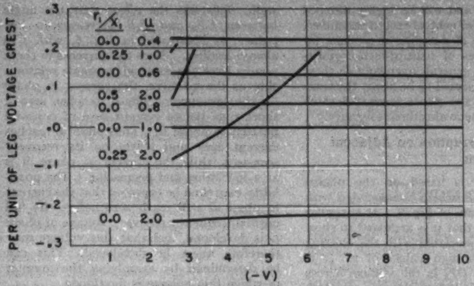

Fig. 5. Neutral voltage at clearing of phase B when phase B clears promptly after phase C

$u+jv=(r_0+jx_0)/(r_1+jx_1)$

Further extension of upward-sloping curves results in values of x_0/x_1 less than 0.4, which are extremely rare in practice

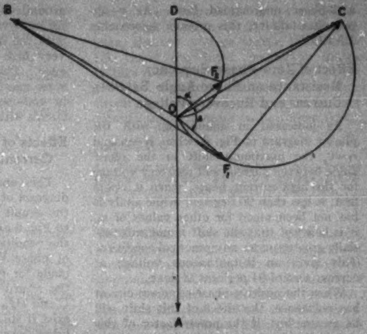

Fig. 6. Phasor diagram indicating voltages and currents associated with 2-phase-to-ground short circuits when $x_0=x_1$. Current magnitudes are proportional to F_2B and F_2C. Recovery voltage in high-current phase is given in phase and magnitude by F_1B. Recovery voltage magnitude in low current phase is given by F_1A

$$\alpha=\text{arccto}\,\frac{2r_0}{3x_1}$$

$$\beta=\text{arccot}\,\frac{r_0}{3x_1}$$

first condition occurs when the zero-phase-sequence impedance of the circuit is less than 23 per cent of the positive-phase-sequence impedance, which is very rare in occurrence. The second condition occurs when there is a difference in phase angle between the zero-phase-sequence and positive-phase-sequence impedances, as when the zero-phase-sequence impedance has appreciable resistance, e. g.; for such a difference has the effect of increasing the current in one phase and decreasing it in the other. The current in the increased phase may exceed both the 3-phase and phase-to-ground currents by as much as 15 per cent.

This is illustrated in the phasor diagram of Fig. 6, which is associated with the circuit diagram shown in Fig. 1. For the sake of simplicity and clarity a circuit is assumed in which positive-, negative-, and zero-phase-sequence impedances are equal and wholly reactive from generator neutral to point of fault, but there is resistance in the neutral return circuit. This resistance may be either in R_{fe} or R_n of Fig. 1, or divided between them.

When fault current exists in phases B and C, the voltage of point F of Fig. 6 with respect to the source neutral is at O when $R_n+R_{fe}=0$, and at D when $R_n+R_{fe}=\infty$. It can be shown that for intermediate values it lies on the semicircle of OF_2D. The current in phase B will therefore be proportional to the length of phasor F_2B, lagging it by 90 degrees in phase angle. This phasor has its maximum length in the position shown, where it is approximately 1.15 times OB.

Assuming phase B to be cleared first, the voltage at point F with respect to the source neutral after phase B has cleared will be at O when $R_n+R_{fe}=0$, and at C when $R_n+R_{fe}=\infty$. It can be shown that for intermediate values it lies on the semicircle of OF_1C. The voltage across the phase-B breaker contacts upon clearing is therefore represented by the phasor F_1B. It has a maximum value equal to 1.823 times phase-to-neutral voltage. The maximum angle between F_2B and F_1B is 19 degrees, 28 minutes, so that the power-factor angle will be reduced by no more than this amount when it is initially 90 degrees.

For numerical determination of the currents and recovery voltages with nonsimultaneous clearing, it is convenient to work with the phasorial ratio of zero-phase-sequence impedance to positive-phase-sequence-impedance, here designated $u+jv$. Then, u and v are determined by the equation

$$u+jv=(r_0+jx_0)/(r_1+jx_1)$$

In terms of u and v, the two phase currents are given by the following equations

$$i_b=\frac{E}{Z_1}\sqrt{\frac{3+3u+3u^2-3\sqrt{3}v+3v^2}{1+4u+4u^2+4v^2}}$$

and

$$i_c=\frac{E}{Z_1}\sqrt{\frac{3+3u+3u^2+3\sqrt{3}v+3v^2}{1+4u+4u^2+4v^2}}$$

In the usual power system case, the zero-phase-sequence impedance has a lower phase angle than the positive-phase-sequence impedance so that v will in general be negative. This means that i_b will in general be the higher current, but reversal of the sign of v simply results in interchanging magnitudes between i_b and i_c. The function is therefore plotted in Fig. 2 with the absolute value of v as abscissa. Curves are plotted for values of u from 0.4 to 2 and for values of $|v|$ from 0 to 6; however, for values of u less than 1, the values are divided by $3/(2+u)$ to show the relationship with the short-circuit current as now calculated. It will be noted that for values of u equal to 1, the 2-phase-to-ground short-circuit current exceeds the 3-phase and single-phase-to-ground short-circuit currents for values of $|v|$ from 0 to 5, reaching a maximum of 1.15 when $|v|$ lies between 1.0 and 1.5. When u is less than 1, the range over which the single-phase-to-ground current is exceeded is shorter and the percentage by which it is exceeded is less, but excess still exists. Even with u as high as 2, corresponding to a phase-to-ground current only 75 per cent of the 3-phase current, the 3-phase current is exceeded slightly over a considerable range of values of $|v|$. For all values of u, the current approaches 86.6 per cent of 3-phase current as $|v|$ approaches infinity.

The recovery voltages for the phase clearing first are given by the equations

$$e_b=E\sqrt{\frac{3+3u+3u^2-3\sqrt{3}v+3v^2}{4+4u+u^2+v^2}}$$

and

$$e_c=E\sqrt{\frac{3+3u+3u^2+3\sqrt{3}v+3v^2}{4+4u+u^2+v^2}}$$

Here the same remarks apply with regard to v and the relative magnitudes of the 2-phase voltages as in the case of the currents discussed in the foregoing, and it will be noted that the higher voltage goes with the higher current and vice versa.

This voltage is plotted in Fig. 3 for the same range of u and v as were the currents in Fig. 2. It will be noted that this voltage rises quite steeply as v departs from zero, reaching maximum values in the range from 1.8 to 1.85 times normal leg voltage, exceeding normal line-to-line voltage by about 7 per cent as a maximum. As v approaches infinity, the voltage decreases to $\sqrt{3}$ in all cases.

The maximum values of voltage and current do not coincide but their product rises to very high values under some conditions, as indicated by the curves of Fig. 7, where values of 1.58 E^2/X_1 and 1.81 E^2/X_1 are reached by the curves for $u=0.4$ and $u=1.0$ respectively. These compare with values of 1.0 for a single-phase-to-ground or a 3-phase-to-ground fault for which Z_0 is equal to Z_1 in both phase angle and magnitude, and 1.5 for the first phase to clear of a 3-phase ungrounded fault. As v approaches infinity, this product approaches $1.5\ E^2/X_1$.

Effect of Zero-Phase-Sequence Resistance on Phase Angle Between Current and Recovery Voltage

As indicated in connection with the phasor diagram of Fig. 6, when $x_0 = x_1$ and $r_1 = 0$, the maximum shift in the phase angle between current and recovery voltage for the high-current phase, when it clears first, is less than 20 degrees; while analysis has not been made for other values of x_0, it is believed that the shift is not substantially greater under any practical condition. This gives an instantaneous voltage at current zero of 94 per cent of peak.

When the positive-phase-sequence circuit has resistance, the effect of this shift will be greater but, if the power factor of this circuit is 15 per cent, the instantaneous voltage at current zero will drop only to 88 per cent of peak when the shift is a maximum. Furthermore, during the recovery transient the voltage will be rising toward crest value so that the benefit of this reduction will be partially lost.

The benefit from the shift may therefore be expected to be between zero and 10 per cent, depending on the positive-phase-sequence power factor and the ratio of zero-phase-sequence resistance to positive-phase-sequence reactance.

Effect of Zero-Phase-Sequence Resistance on Oscillatory Overshoot

In many field circuits the oscillation does not rise above normal crest voltage so that further damping results only in a slight decrease in rate of rise of recovery voltage. As a reasonably good approximation for those where overshoot does occur, the circuit governing this overshoot may be considered to consist of two parts. One delivers a voltage equal to normal phase-to-ground voltage ±15 per cent and has its oscillation unmodified. The other accounts for the increase above phase-to-ground voltage and will be highly damped for most values of neutral-return resistance, with the degree of damping decreasing for very high values of neutral-return resistance. Thus, in general, overshoot in these cases may be expected to be about the same in volts as for the phase-to-ground short circuit with no neutral-return resistance.

Effects of Interruption on Adjacent Current Zeros

This analysis is based on the phasor diagram of Fig. 8, which is associated with the circuit diagram of Fig. 1. It is similar to Fig. 6 except that it is arranged to show the conditions associated with the clearing of phase C with high values of v. It is made for $v = 6$. OF_2 is the voltage across the return circuit before clearing of phase C and OF_3 is the same voltage as it would exist if steady-state conditions were established between the clearing of phase C and that of phase B.

For a given value of Z_0, the same currents and the same voltages across open breaker poles will appear regardless of how Z_0 is apportioned between the neutral return circuit and that part of the circuit in which the individual phase currents flow in separate conductors. It is easier to visualize current and voltage relationships, however, if a part of Z_0 equal to Z_1 is assumed to be associated with the separate-conductor part of the circuit and the remainder with the common return part, for then the magnitude and phase angle of the current in any one phase are determined by the phasor representing the voltage drop in the impedance of that phase and the positive-phase-sequence impedance, and the current in the neutral return part of the circuit is determined in phase and magnitude by the voltage across this part of the circuit and its impedance.

From inspection of Fig. 8 it is apparent that as neutral return circuit impedance increases, the length of the phasor OF_2 increases also, bringing F_2 closer and closer to D. While Fig. 8 applies to the special case in which x_0 is equal to x_1, this fact applies to all other values of x_0 as well. This has the effect that the angle between CF_2 and F_2B decreases to low values, as illustrated in Fig. 4, with CF_2 always leading. Since the currents in these phases have the same phase-angle relationship as the voltages, the current in phase C, the low-current phase, reaches zero a short time before current zero of opposite polarity in phase B. Thus phase C reaches current zero and starts on its recovery transient while the current in phase B is at a low value and decreasing. The possibility may then be expected that the current in phase B will reach zero before the full normal-frequency recovery voltage of phase C is developed, and that this voltage may therefore never be developed. This can be determined by examining the manner in which this voltage is developed.

This is best done in terms of instantaneous voltages at the time of current zero in phase C. If $r_1 = 0$, these instantaneous voltages are equal to the projections of their phasors on the phasor F_2C. To give a convenient picture of the phenomena, this assumption is made in this discussion, but the numerical analysis upon which the final results are based considers values of r_1 from zero to $0.5\ x_1$.

When phase C clears, the phasorial position of the fault point shifts from that corresponding to a 2-phase-to-ground fault F_2 to that corresponding to a single-phase-to-ground fault F_3. The corresponding instantaneous voltages taken at the time of clearing in phase C are $O'F_2$ and $O'F_3'$. Since the voltage across the phase-C terminals is that between point C and the fault point, this shift must take place in the development of any high normal-frequency recovery voltages associated with phase C.

A part of this shift which corresponds to the rate of change of current in phase C times an inductance equal to those of phase B and the effective neutral return circuit in parallel takes place quickly, but the remainder takes place at a rate determined by the reactance-resistance ratio of the single-phase short-circuit impedance and is accompanied by a change in fault current. It will be noted that in Fig. 8 the change involves a change in polarity of the voltage $O'F$. When $x_0 = x_1$, the reactance of the effective neutral return circuit is zero, so that the current is at all times proportional to the voltage and, hence, passes through zero with the voltage. After the clearing of phase C, this current is also the phase-B current; hence for this par-

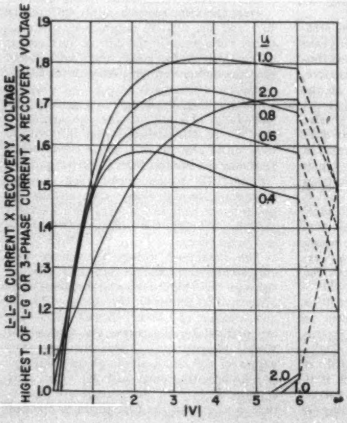

Fig. 7 (left). Product of current and recovery voltage for 2-phase-to-ground short circuits

$u + jv = (r_0 + jx_0)/(r_1 + jx_1)$

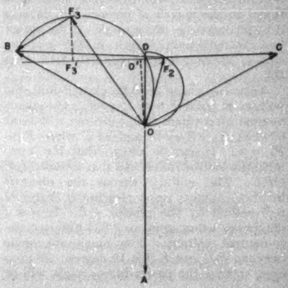

Fig. 8 (right). Phasor diagram indicating voltages and currents associated with clearing the light current phase of a 2-phase-to-ground short circuit

$u = 1$
$v = 6$

ticular case, the phase-B current zero occurs at the time of zero voltage in the equivalent return circuit and, if interruption takes place at this time, the normal-frequency recovery voltage across phase C does not exceed leg voltage.

For other values of x_0 this relationship is not exactly true but, as shown by the values of Fig. 5, it does not deviate too much. The voltage across the effective neutral return circuit does not exceed 25 per cent of leg voltage, and the phase-C breaker voltage does not exceed leg voltage to any important extent, since the phase-C generator voltage is already well past crest at the time of interruption and the effective neutral return circuit voltage will have dropped substantially to zero by the time of the next crest. Furthermore, since the normal-frequency recovery voltage in phase B is given by the length of the phasor FB, this voltage cannot greatly exceed leg when the voltage at F is kept low. It may thus be concluded that where the high-current phase interrupts promptly after the low-current phase, the high normal-frequency recovery voltages associated with the clearing of phases B and C will not be developed.

REFERENCES

1. SOME EFFECTS OF UNBALANCED FAULTS, R. D. Evans, S. H. Wright. *Electrical Engineering*, vol. 50, June 1931, pp. 415–20.

2. SYMMETRICAL COMPONENTS AS APPLIED TO THE ANALYSIS OF UNBALANCED ELECTRICAL CIRCUITS (book), C. F. Wagner, R. D. Evans. McGraw-Hill Book Co., Inc., New York, 1933, first ed., pp. 230–31.

3. DETERMINATION OF GROUND FAULT CURRENT AND VOLTAGES ON TRANSMISSION SYSTEMS, E. M. Hunter, E. Pragst, P. H. Light. *General Electric Review*, Schenectady, N. Y., 1939, pp. 353–56 and 479–85.

◆

Discussion

Otto Naef (American Gas and Electric Service Corporation, New York, N. Y.): Perhaps one additional reason for little adverse circuit-breaker experience with 2-phase-to-ground short circuits is the fact that the short-circuit duty available at the station bus is in most cases well below the breaker rating. However, we have had at least one serious breaker failure within the last few years where excessive recovery voltage during interruption of a 2-phase-to-ground fault may have been a contributory cause.

In any case, Mr. Skeats' interesting and very exhaustive analysis has again demonstrated the fallacy of carrying out single-pole factory tests and grounded 3-pole factory tests at rated line-to-ground voltage. To prove adequately circuit-breaker performance on ungrounded and grounded 3-phase and 2-phase faults by single-pole tests, the test voltage should be at least 1.5 times the rated maximum design voltage to ground. This is a requirement of the new American Standard[1] on power circuit breakers, but recognition by the manufacturers appears to be rather slow.

REFERENCE

1. SCHEDULES OF PREFERRED RATINGS FOR POWER CIRCUIT BREAKERS. *ASA C37.6* American Standards Association, New York, N. Y. Feb. 1955.

W. F. Skeats: Mr. Naef is quite correct in suggesting that an additional reason for lack of adverse experience with 2-phase-to-ground short circuits is low available short-circuit duty at the station bus. Mr. Naef's mention of a failure in which excessive recovery voltage during interruption of a 2-phase-to-ground fault may have been a contributory cause is very much appreciated. I hope that any such occurrences on systems will be brought to light to make it possible to evaluate the actual seriousness of those conditions.

Since high-voltage circuit breakers normally operate all three poles within a very short time of each other, it is to be expected, in accordance with conclusion 2, that recovery voltages appreciably above normal leg voltage will be developed infrequently.

Design Problems and Field Tests Concerning Circuit Breakers for Switching Long 230-Kv Lines

D. M. UMPHREY
MEMBER AIEE

D. J. MARSDEN
MEMBER AIEE

PROBLEMS associated with switching long high-voltage transmission lines are not new and the designs employed in attempts to accomplish satisfactory solutions are varied, depending partly on circuit breaker construction. Those designs which depend upon the self-energizing ability of the arc to provide current interruption may include such auxiliary devices as pumps, low-ohmic or high-ohmic resistors, each of which is intended to reduce or to eliminate current restrikes or to reduce the effect of current restrikes to the system, should they occur.

The purpose of this paper is to explain operating characteristics of these devices under various circuit arrangements and to describe why the decision was made to apply a new low-ohmic resistor design to an existing high-speed 230-kv multibreak circuit breaker. The modified breaker is operated on a system with reduced basic impulse insulation level (BIL) of 825 kv. Results of field tests employing this breaker-resistor combination while switching a 241.6-mile transmission line at 250-kv sending voltage will be described.

The Line-Switching Problem

Excessive transient voltages are the principle concern in switching long lines. Such voltages are usually the result of commutation of line capacitance with respect to supply voltage by restriking of line circuit breakers. Experience has shown that restrikes in circuit breakers will usually produce higher voltages on long lines than on relatively short lines. Although simple theory indicates that the generation of high transient voltages with resultant equipment damage while switching lines is a simple and to be expected occurrence, years of experience with hundreds of 115 through 230-kv circuit breakers of the type discussed in this paper have not demonstrated any appreciable normal-service overvoltage damage. The following explanation indicates some of the reasons why these circuit breakers have not produced extreme overvoltages to the extent that simple theory and probability indicate they should.

Fig. 1 indicates a simple circuit commonly referred to in explaining production of overvoltages while switching capacitive

---

Paper 55-223, recommended by the AIEE Switchgear Committee and approved by the AIEE Committee on Technical Operations for presentation at the AIEE Winter General Meeting, New York, N. Y., January 31–February 4, 1955. Manuscript submitted October 20, 1954; made available for printing December 9, 1954.

D. M. UMPHREY and D. J. MARSDEN are with the Federal Pacific Electric Company, San Francisco, Calif.

The authors wish to express their appreciation to the engineers of the United States Bureau of Reclamation and the Bonneville Power Administration for making available system facilities as well as the supervision of tests. Engineers of the latter were principally responsible for the instrumentation and the excellent oscillographic records taken. Also, we wish to express appreciation to fellow employees for their efforts in the construction and application of the resistors.

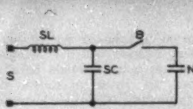

Fig. 1. Schematic diagram of inductance-capacitance circuit usually employed in explaining capacitance switching overvoltages

loads. *S* represents an a-c source having an impedance *SL* which is assumed to be predominately inductive. *SC* represents a minimum capacitance normally associated with the source or bus terminals of circuit breaker *B*. For simplicity, *NC* is assumed to be a lumped capacitance of very large magnitude as compared to that of *SC*.

Fig. 2(A) indicates voltage and current values which can occur in the circuit described. Capacitive charging current I_S for *NC* is interrupted at the time it reaches zero magnitude and normal steady-state voltage rise through *SL* is then terminated, so that E_{NC} is left at crest value and E_{SC} suddenly diminishes. Resulting voltage change *A* occurs as a recovery voltage across switch *B* and has a rate of rise corresponding to the system natural frequency. This small but rapid recovery voltage across the interrupter tends to cause arcing to persist until a later current zero, when added contact gap length is available for more effective deionization.

Plain-break circuit breakers, or circuit breakers which depend on an arc-actuated pumping system for deionization, thus tend to interrupt only after the arc in the interruptor has reached a greater length. Such tendency is of advantage in reducing probability of restrikes since the latter are more likely to occur if the arc path is shorter at the time when normal-frequency charging current is interrupted. Low-energy pumps have been observed to cause very early interruption of capacitive currents so that dielectric strength of the arc path at a time 1/2 cycle later may not be sufficient to withstand twice normal crest voltage without restriking.

Again, in Fig. 2(A) a restrike is indicated to occur after a zero current interval of 1/2 cycle. Timing chosen for the restrike is such as to produce maximum overvoltage. Frequency and magnitude of restrike current is controlled in this case by inductance *SL* and capacitance *NC*. The abscissa of the restrike portion of Fig. 2(A), enclosed in the

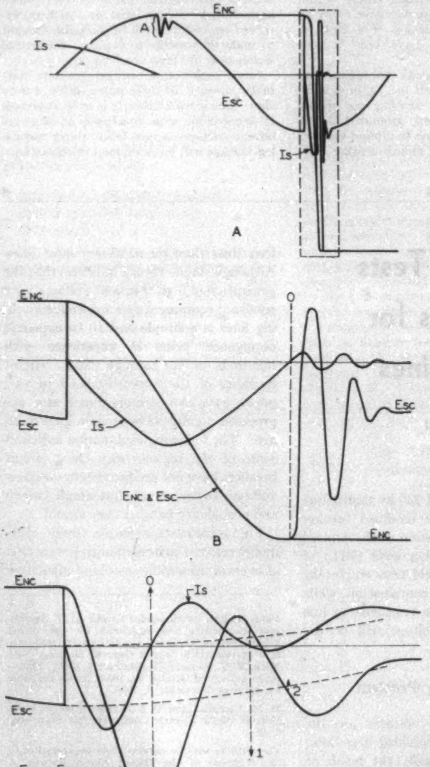

Fig. 2. Voltage and current relationship preceding and following circuit-breaker restrike

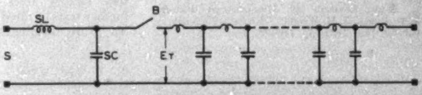

Fig. 3 (above). Schematic diagram of electrical characteristics applying to switching phenomena of long transmission lines

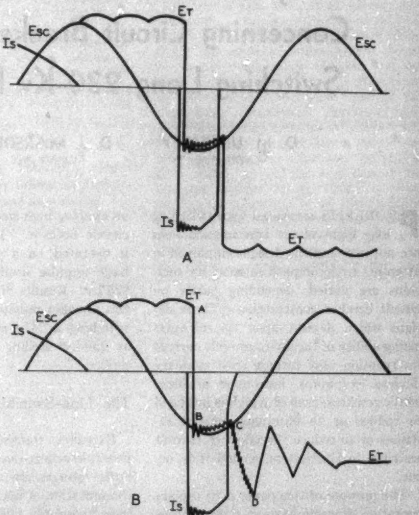

Fig. 4. Effect of corona on voltage and current relationship during the switching of long transmission lines. Timing of restrike current is shifted slightly in figure for clarification

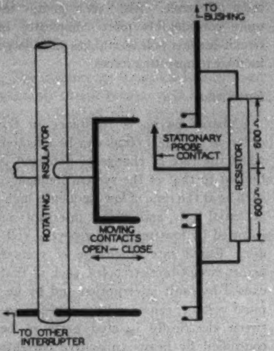

Fig. 5. Schematic diagram of half-pole assembly for a resistor-equipped 6-break rotary-type circuit breaker

dashed brackets, is shown considerably extended for clarity in Fig. 2(B).

Restrike current is assumed to stop at the first current zero, indicated by time 0 in Fig. 2(B), so E_{NC} is left approximately three times crest potential negative. Note that small capacitance SC is also charged at the same potential at this instant and that the damped oscillation of E_{SC} occurs at a frequency determined by inductance SL and minor capacitance SC. Recovery voltage across the interrupter is the difference between E_{NC} and E_{SC}.

The rate of rise and crest value of recovery voltage across switch B are each approximately twice the corresponding values which would appear following interruption of a solid fault across NC. Also, the rate of decay of restrike current near current zero is approximately twice that which would occur just prior to current zero for a solid fault. The interrupting ability of any circuit breaker would be stressed far beyond normal if it succeeded in providing necessary dielectric recovery rate to permit interruption at the first current zero of restrike current for the circuit described.

Overvoltages of greater magnitude, if produced by subsequent restrikes, would require a greater rate of increase in interrupter dielectric strength. Furthermore, short-duration and limited arc energy in restrike current pulses limits deionizing action of most oil interrupters to values considerably below normal. Interrupters using low-energy flushing type pumps would have more tendency to interrupt the restrike current as indicated in Fig. 2(B), leaving E_{NC} at approximately three times normal crest value. Most interrupters would interrupt a restrike current such as this at one of the more favorable times as indicated by points 1 and 2 in Fig. 2(C). Lengths of the vertical dashed lines indicate magnitude of possible recovery voltage across the circuit breaker for each possible interruption time.

From this discussion it follows that if the restrike current is interrupted at the first current zero the line is left highly charged and further restrikes are apt to produce higher overvoltages. Continuation of restrike current for several natural frequency half-cycles occurs in most interrupters and therefore explains why destructive overvoltages on the rather common circuit outlined are rarely encountered.

Circuit-breaker interrupter damage produced while switching closely adjacent capacitor banks should not be confused with the overvoltage problem discussed here. The former is not necessarily associated with overvoltage and damage produced is usually not due to dielectric breakdown outside of the normal interrupter arc path.

Effect of Long Line on Circuit-Breaker Restrike Mechanism

Transient switching phenomena occurring on long lines are more complex than that for short lines or lumped capacitances but circumstances are more favorable for permitting circuit breakers to produce high transient line voltages.

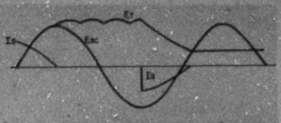

Fig. 6. Voltage and current relationship applying to ignition and interruption of shunt resistor current

In Fig. 3 S represents an a-c source having an impedance SL assumed to be predominately inductive. SC represents capacitance normally associated with the source or bus terminals of circuit breaker B. In practice the capacitance SC may vary from a minimum of bus and terminal capacitances of connected apparatus to the capacitances of many lines, and perhaps cables connected directly to the bus. Transmission line T is represented by distributed series inductance and shunt capacitance units. Surge impedances for overhead lines vary from 400 to 600 ohms depending upon conductor size and line configuration.

Fig. 4(A) indicates typical current and voltage relationships at the sending end of a 230-kv transmission line approximately 240 miles long at the time of a restrike delayed as indicated. The line surge impedance is similar to an energy-absorbing resistance from the instant the restrike voltage surge is initiated at the source terminal until the surge has traveled the length of the line and returned. The restrike current loop shown in Fig. 4(A) indicates this effect during the time required for the surge to traverse the line length and return, approximately 1/6 cycle.

The source impedance SL, Fig. 3, is usually less than one-fifth of the surge impedance of the line being switched so that source potential is affected little at the instant of restrike and parallel lines on the source bus further stabilize the bus potential at this instant. The resulting wave front as applied on the source terminal at the instant of restrike is relatively steep and, if the wave shape is not changed, an abrupt voltage rise should occur at the source terminal approximately 1/6 cycle after initiation of the restrike. This should cause restrike current

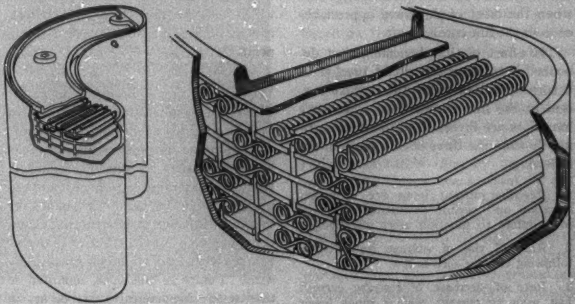

Fig. 7. Cutaway section of resistor, showing construction

Fig. 8. View of 230-kv switchyard at Hungry Horse showing two 3-pole 230-kv circuit breakers. Test breaker on right

to approach zero at a rapid rate as shown in Fig. 4(A). Interruption of the restrike at the first current zero of restrike current would then be difficult because of the rapid rate of decrease of restrike current and simultaneous high rate of rise of voltage.

Actual test records indicate performance similar to that shown in Fig. 4(B) rather than as shown in Fig. 4(A). Note in Fig. 4(B) that the rate of decrease of restrike current as it approaches zero is much less than the rate of rise. The slope of the voltage E_T between points A and B as applied to the line at initiation of restrike, is much steeper than the slope C-D of the same wave after it returns. Corona resistance apparently dissipates considerable energy from the voltage wave front as the latter travels from the source terminal to the open end of the line and returns. This is particularly true when the crest of the wave appreciably exceeds the line corona limit.

The effect of the phenomena just described is to allow the circuit breaker to extinguish rather easily the restrike current at the first current zero when very long lines are involved. This results primarily from the three effects given in the following:

1. Restrike current loops are of longer duration and permit deionizing action of interrupters to function more effectively.
2. Rate of rise of voltage immediately following current zero is low.
3. Rate of decrease of restrike current just prior to current zero is much lower than the case for restrikes on shorter lines.

From the foregoing it follows that, for long lines, restrike current interruption, will occur at the first current zero, leaving the line charged at high potential, which in turn is apt to result in even higher transient voltages should further restrikes occur. Therefore, for long lines wherein these effects are of definite concern, certain considerations must be given to breaker design to safely permit line switching.

Selection of Solution to Long-Line Switching Problem

Some of the factors which must be considered before modifying a circuit breaker design are: cost, reliability, freedom from excessive maintenance, and the increasing performance requirements of high-voltage circuit breakers as applied on modern utility systems. In general, the design which is chosen must be at least competitive in all respects from the user's standpoint.

PUMPS

Low-energy pumps are not considered to be of sufficient advantage to merit consideration and in some respects they can be a detriment as already indicated. High-energy pumps capable of maintaining pressure in the order of 50 pounds per square inch gauge in interrupting chambers have been proved effective in one or two porcelain-clad oil circuit-breaker designs. Pumps of this type, mounted so that severe mechanical stress occurs in the bushings during operation, do not seem advisable. Also, such pumps require considerably more complexity in circuit-breaker pole assemblies and a large increase in operating forces.

RESISTORS

Resistors having a resistance in the order of 1,000,000 ohms can be effective when the rate of change of potential is limited to that of the system frequency, such as at the time of low-frequency high-potential tests, and current interruptions followed by low-frequency recovery voltage. Rapid rate of change of voltage across circuit-breaker poles, such as that caused by fault interruption and by impulse voltage, causes voltage division between electrically isolated parts to be controlled by heavy capacitive currents so that such resistors have little beneficial effect.

Resistor Chosen

Resistors were chosen with an ohmic value of 2,400 ohms for the following reasons:

1. They can be readily accommodated in the existing high-voltage circuit-breaker design without serious modification.
2. The resistors can be applied so that voltage division between the upper four breaks can be maintained under nearly all conditions. This is particularly true because of the rather high distributed capacitance designed as part of the resistors.
3. Resistors designed with adequate thermal capacity and distributed electrical capacitance can improve circuit-breaker performance during heavy-fault interruption as well as when switching long lines.
4. Relatively low resistance lowers the voltage which the circuit breaker should withstand without restrike during line dropping operations.
5. Tests indicate a tendency of such resistors to shorten arcing time during the interruption of low-fault currents. However, this is of little advantage because of the short arcing time inherent in the design without resistors.
6. Resistors can be applied so that they carry current for less than $1^1/_2$ cycles during an opening operation and less than 1/4 cycle during a closing operation. Thermal duty on the resistor design is thus very light.
7. The breaker design is such that resistor current can be interrupted in interrupter chambers rather than in open oil, as is customarily the case. Resistor current can thus be interrupted much more promptly following fault-current interruption.
8. The resistors, as applied, do not impair the high-voltage circuit-breaker performance in any way. This does not imply that the added equipment will not require a proportionate increase in maintenance, etc.

Description of Resistor as Applied to an Existing Circuit-Breaker Design

The resistors are applied as two separate units per circuit-breaker pole so that one unit is mounted with each bushing-supported interrupter assembly. The schematic electrical half-pole assembly, including the resistor is shown in Fig. 5. The normal load current path from the bushing is through the upper stationary contact to the left into the upper moving contact assembly, then down and to the right into the lower stationary contact assembly and again down and to the left through the lower moving contact assembly to the other half-pole interrupter.

The resistor is connected between the upper and lower stationary contact assemblies with a center tap from the resistor to a probe associated with the upper contacts. The purpose of the probe is to provide equal division of recovery voltage between the upper and center interrupters during interruption.

The bottom contact is set to close slightly ahead of the upper contacts so that the resistor assembly for each pole can be checked by measuring resistance externally between bushings while slowly closing the circuit breaker until the lower contacts touch. Further movement in the closing direction causes the resistors to be by-passed. Normally the bottom contact closes less than 1/10 cycle in advance of the upper contacts and, in opening, the delay of this contact in parting is negligible.

Table I. Summary of Data, 1952 Line-Dropping Tests

System Diagram	Test No.	Miles Line	Bus Kv, ϕ to ϕ	Line, Amperes	Restrikes			Maximum Crest Per-Unit Line-to-Neutral Voltage Receiving End*		
					ϕA	ϕB	ϕC	ϕA	ϕB	ϕC
Fig. 10(A)	1	241.6	230	180	none	none	none	1.1	1.1	1.3
	2	241.6	242	191	none	none	2	2.4	2.2	2.5
	3	241.6	253	202	none	none	3	1.7	2.0	2.8

* Steady-state circuit voltage at receiving end was approximately equal to 300 kv when sending end was held at 253 kv.

ϕ stands for phase in all the tables.

The function of the interrupter component associated with the bottom contacts is normally to provide an arc-generated oil-pumping facility for medium and heavy fault currents. In addition, this component acts very effectively as an interrupting unit for low inductive, capacitive, and load currents. It also acts effectively in interrupting the remnant resistor current immediately after fault, load, or line-charging currents have been interrupted. This appears to be a very satisfactory solution to the common complaint that low ohmic resistors maintain fault arc ionization for several cycles after interruption and effectively reapply voltage to the fault path several cycles before the main circuit-breaker contacts actually close, so that the fault arc deionizing time during high-speed reclosing operation is seriously reduced. The total fault arc deionizing time reduction resulting from the use of the low ohmic resistor application described here is only 2 cycles maximum beyond that permitted by the normal high-speed circuit breaker without resistors. The start of resistor current flow during a closing operation at full voltage does not precede the main contact-making time by more than 1/4 cycle.

Fig. 9. Typical oscillogram showing energization of 241.6-mile 230-kv line by resistor-equipped breaker

Line-Charging Current Interruption with New Resistor

Line-charging current is usually interrupted without immediate resistor current flow, as indicated in Fig. 6. However, the voltage across the circuit-breaker pole may reach a value of double normal line-to-ground crest voltage at a time 1/2 cycle after such interruption, and this potential will nearly all appear across the bottom interrupter associated with the source bushing. A resistor current arc will then be established in this interrupter and the corresponding unit on the other half-pole assembly so that the total voltage across the circuit-breaker pole will be impressed on the two resistor units in series. The resistors then provide the double function of dividing the total voltage between the four remaining interrupters and reducing the line remnant potential, as indicated in Fig. 6.

Protection of Resistors Against Effects of Impulse Voltages

Lightning strokes are frequently repetitive so that a circuit breaker must often withstand severe impulse voltages during interruption of faults initiated by earlier discharges in the same stroke series. Based on the requirement for such performance, the resistors were designed so that each of the two pole units would withstand a 900-kv $1^1/_2$x40-microsecond impulse. Distribution of steep wave front impulse voltages through the resistor is controlled almost entirely by capacitance rather than by the resistor itself. This design requirement for improving impulse strength of resistors is similar to that required for transformer windings in that relatively large values of series-distributed capacitance as compared to shunt capacitance-to-ground are desirable in either case. Fig. 7 indicates the resistor construction. Note that the

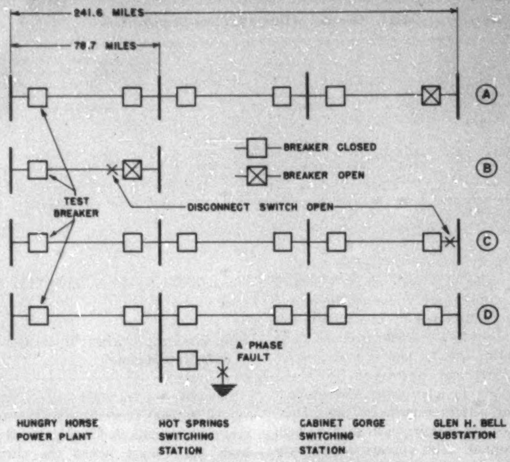

Fig. 10. Line-switching arrangements used for tests

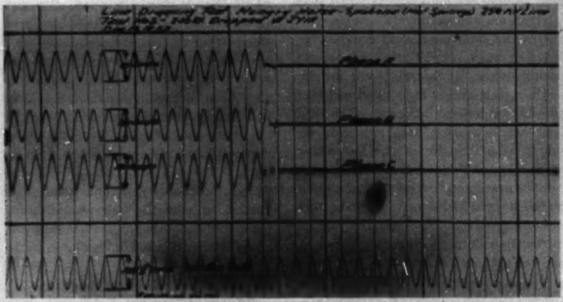

Fig. 11. Sending end oscillogram showing the most severe restrike condition without resistors in circuit breaker

Fig. 12. View through manhole showing resistors, interrupters, and moving contacts of test breaker

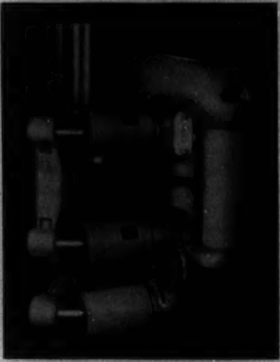

Fig. 13. View showing resistor mounted on interrupter and center tap connection between resistor and upper interrupting chamber

capacitance between the noninductively wound "pads" provides more series distributed capacitance than would have been the case if conventional single-layer resistor construction had been used.

Design Consideration for Performance During Heavy-Fault Current Interruption

An important consideration in the design of resistors for this application is temperature rise. Energy may be dissipated at rates in the order of 20,000 kw in a single resistor unit during very short time intervals and nearly all of this energy is stored in the thermal capacity of the resistance wire during such intervals. The sudden reduction of tank pressure following the interruption of heavy faults can cause hot oil on the surface of the resistance material to flash into vapor which may result in disastrous mechanical damage to the resistor assembly in addition to lowering the resistor dielectric strength. Therefore, from a thermal standpoint, a six-times factor of safety is applied to the resistor design for the worst operating condition. This is accomplished by taking advantage of the unusually short intervals of resistor current flow and by providing adequate thermal storage.

Description of Test Circuit Breaker

The 230-kv circuit breakers originally supplied at the Hungry Horse power plant were standard Pacific Electric type-*RHE-90* breakers rated at 230/196-kv, 900-kv BIL, 800-ampere, 3,500-mva, 3-cycle, 20-cycle reclosing time. The two breakers as well as the Hungry Horse switchyard are shown in Fig. 8. Inasmuch as these breakers are intended for future single-pole reclosing service, three type-*MO-5* spring-operated mechanisms were supplied for each breaker. Operating characteristics are similar to the conventional single *MO-5* mechanism and 3-pole breaker combination with closing time approximately equal to 8 cycles and contact parting times of the order of 1.5 cycles. Speed of contact separation of each break in the arcing zone is at the rate of 20 feet per second. The spring type of mechanism permits very close synchronization of all breaker poles even though the mechanical connecting link is not present. An indication of this is illustrated by Fig. 9, which is a typical oscillogram of a breaker closing operation

Table II. Summary of Data, Test Series A, B, C and D, May 12–13, 1954

System Diagram	Test No.	Miles Line	Bus Kv, φ to φ	Line, Amperes	Angle Set	Charging Current Interrupting Time, Cycles*			Resistor Current Interval, Cycles†			Re-strikes	Maximum Crest Per-Unit Line-to-Neutral Voltage, Sending End			Maximum Crest Per-Unit Line-to-Neutral Voltage, Receiving End			Per-Cent Crest Voltage Left on Line, Sending		
						φA	φB	φC	φA	φB	φC		φA	φB	φC	φA	φB	φC	φA	φB	φC
Fig. 10-B	A-4:26	78.7	242	60	0				1.6	1.1	1.6	none	1.0	1.0	1.0				49	66	47
	A-4:28	78.7	242	60	15				2.0	1.6	1.6	none	1.0	1.0	1.0				57	48	60
	A-4:30	78.7	242	60	30				1.6	1.1	1.5	none	1.0	1.0	1.0				52	67	59
	A-4:32	78.7	242	60	45				1.6	1.1	1.5	none	1.0	1.0	1.0				48	62	58
	A-4:40	78.7	242	60	60				1.1	2.1	1.7	none	1.0	1.0	1.0				66	47	25
	A-4:41	78.7	242	60	75				1.0	1.5	1.1	none	1.0	1.0	1.0				66	47	64
	A-4:42	78.7	242	60	90				1.6	1.1	2.1	none	1.0	1.0	1.0				48	58	41
	A-4:44	78.7	242	60	105				1.6	1.7	1.6	none	1.0	1.0	1.0				57	39	49
	A-4:46	78.7	242	60	120				1.6	1.1	1.6	none	1.0	1.0	1.0				36	81	73
	A-4:47	78.7	242	60	135				0.8	1.3	1.6	none	1.0	1.0	1.0				72	51	48
	A-4:49	78.7	242	60	150				1.0	1.1	1.5	none	1.0	1.0	1.0				55	67	59
	A-4:52	78.7	242	60	165	2.0	2.4	2.1	1.6	1.1	1.7	none	1.0	1.0	1.0				52	60	48
	A-4:54	78.7	242	60	180	2.5	2.3	2.1	1.6	1.6	1.6	none	1.0	1.0	1.0				52	48	52
Fig. 10-B	B-6:25	78.7	250	61	0	2.4	2.6	2.0	1.6	1.7	2.6	none	1.0	1.0	1.0				76	50	48
	B-6:28	78.7	250	61	15	2.5	2.3	2.1	1.6	1.6	2.1	none	1.0	1.0	1.0				48	44	17
	B-6:30	78.7	250	61	30	2.4	2.2	2.0	1.6	1.6	1.7	none	1.0	1.0	1.0				60	38	52
	B-6:32	78.7	250	61	45	2.5	2.3	2.1	1.5	1.6	1.7	none	1.0	1.0	1.0				54	46	63
	B-6:36	78.7	250	61	60	2.0	2.3	2.1	2.1	1.1	1.6	none	1.0	1.0	1.0				53	81	71
	B-6:38	78.7	250	61	75	2.0	2.6	2.2	2.2	1.4	1.2	none	1.0	1.0	1.0				27	46	62
	B-6:40	78.7	250	61	90	2.1	2.5	2.3	1.6	1.1	1.2	none	1.0	1.0	1.0				64	48	63
	B-6:42	78.7	250	61	105	2.0	2.4	2.3	1.6	1.1	1.6	none	1.0	1.0	1.0				50	61	45
	B-6:44	78.7	250	61	120	2.6	2.0	2.2	1.1	1.6	2.2	none	1.0	1.0	1.0				61	47	45
	B-6:46	78.7	250	61	135	2.6	2.0	2.3	1.1	1.6	1.2	none	1.0	1.0	1.0				61	47	64
	B-6:49	78.7	250	61	150	2.6	2.0	2.3	1.1	1.6	1.6	none	1.0	1.0	1.0				50	61	56
	B-6:51	78.7	250	61	165	2.6	2.1	2.0	1.4	1.6	2.1	none	1.0	1.0	1.0				35	59	58
	B-6:53	78.7	250	61	180	2.3	2.6	1.9	1.6	1.1	2.1	none	1.0	1.0	1.0				46	47	53
Fig. 10-C	C-5:13	241.6	242	200	0	2.5	2.4	2.6	1.2	1.2	0.8	none	1.2	1.1	1.1				13	4	8
	C-5:33	241.6	242	200	15	2.6	2.4	2.7	1.1	0.7	0.7	none	1.1	1.2	1.1	1.0	1.0	1.0	17	22	17
	C-5:36	241.6	242	200	30	2.6	2.4	2.7	1.2	0.8	0.8	none	1.1	1.1	1.0	1.0	1.0	1.0	10	25	19
	C-5:38	241.6	242	200	45	2.5	2.4	2.7	1.2	1.3	0.8	none	1.1	1.1	1.1	1.0	1.0	1.0	19	6	9
	C-5:42	241.6	242	200	60	2.7	2.5	2.3	1.3	0.8	1.3	none	1.1	1.1	1.1	1.0	1.0	1.0	3	16	11
	C-6:22	241.6	242	200	75	2.8	2.6	2.4	1.2	0.7	1.3	none	1.1	1.1	1.2	1.0	1.0	1.0	5	7	2
	C-12:21	241.6	242	200	75	2.7	2.5	2.2	0.8	0.8	0.8	none	1.1	1.1	1.1	1.0	1.0	1.0	4	2	27
	C-12:37	241.6	242	200	90	2.8	2.7	2.5	0.8	0.8	0.7	none	1.4	1.2	1.1	1.3	1.0	1.0	10	2	23
	C-12:40	241.6	242	200	105	2.9	2.8	2.7	0.8	0.8	0.7	none	1.3	1.2		1.1	1.0	1.1	1	2	4
	C-12:43	241.6	242	200	120	2.9	2.8	2.6	0.8	0.7	0.8	none	1.4	1.1	1.2	1.4	1.0	1.0	9	8	13
	C-12:45	241.6	242	200	135	3.0	2.9	2.7	0.7	0.7	0.7	none	1.5	1.1	1.2	1.5	1.0	1.2	7	8	10
	C-12:50	241.6	242	200	150	2.9	2.8	2.6	0.8	0.7	0.7	none	1.2	1.4	1.2	1.0	1.4	1.1	4	23	18
	C-12:53	241.6	242	200	165	2.7	2.5	2.8	0.7	0.8	0.8	none	1.1	1.2	1.5	1.1	1.0	1.5	13	13	9
	C-12:55	251.6	242	200	180	2.6	2.5	2.7	0.7	0.7	0.7	none	1.1	1.2	1.4	1.0	1.0	1.4	29	20	18
Fig. 10-C	D-1:09	241.6	250	208	0	2.8	2.7	2.5	0.7	0.7	0.7	none	1.1	1.1	1.1	1.0	1.0	1.0	12	8	18
	D-1:24	241.6	250	208	15	2.9	2.7	2.5	0.7	0.7	0.7	none	1.1	1.1	1.1	1.0	1.0	1.0	11	4	39
	D-1:27	241.6	250	208	30	2.9	2.7	2.5	0.7	0.7	0.7	none	1.1	1.1	1.1	1.0	1.0	1.0	8	0	19
	D-1:29	241.6	250	208	45	3.0	2.8	2.6	0.7	0.7	0.7	none	1.1	1.2	1.1	1.0	1.0	1.0	13	12	13
	D-1:33	241.6	250	208	60	3.0	2.9	2.6	0.7	0.7	0.7	none	1.5	1.2	1.2	1.6	1.0	1.1	17	5	14
	D-1:35	241.6	250	208	75	2.5	2.8	2.7	1.2	0.8	0.7	none	1.2	1.2	1.2	1.0	1.2	1.0	5	0	11
	D-1:37	241.6	250	208	90	2.6	2.4	2.7	1.1	0.7	0.8	none	1.1	1.1	1.1	1.0	1.0	1.0	2	15	11
	D-1:39	241.6	250	208	105	2.5	2.4	2.7	1.2	1.2	0.7	none	1.1			1.0	1.0	1.0	10	5	9
	D-1:42	241.6	250	208	120	2.6	2.5	2.7	1.2	1.2	0.8	none	1.1	1.1	1.2	1.0	1.0	1.0	11	4	3
	D-1:44	241.6	250	208	135	2.6	2.5	2.4	0.7	0.7	0.7	none	1.0	1.1	1.1	1.0	1.0	1.0	26	8	17
	D-1:47	241.6	250	208	150	2.7	2.6	2.4	1.2	0.7	1.2	none	1.0	1.0	1.1	1.0	1.0	1.0	14	4	1
	D-1:49	241.6	250	208	165	2.7	2.5	2.3	0.7	0.7	1.2	none	1.1	1.0	1.1	1.0	1.0	1.0	0	11	1
	D-1:53	241.6	250	208	180	2.8	2.6	2.4	0.7	0.7	0.7	none	1.1	1.1	1.0	1.0	1.0	1.0	21	12	16

* Time from energization of trip coil to interruption of charging current.

† Time from interruption of charging current to interruption of resistor current.

in which the 241.6-mile 230-kv test circuit was energized. The circuit breakers were equipped with the conventional six series break interrupters previously described.

Description of Field Tests

Switching the 241.6-mile line between the Hungry Horse power plant in Montana and the Glen H. Bell substation near Spokane, Wash., is recognized as very severe duty, especially with regard to the proposed high sending bus voltage of the order of 250 kv. To check circuit-breaker performance a series of field tests were made co-operatively with the Bonneville Power Administration and the Bureau of Reclamation.

Table III. Summary of Average Data, 1954 Test Series A-D

Miles Line	Average Interrupting Time for Charging Current, Cycles*			Average Resistor Current Interval, Cycles†			Average Per-Cent Crest Voltage Left on Line		
	φA	φB	φC	φA	φB	φC	φA	φB	φC
78.7	2.3	2.3	2.1	1.5	1.4	1.7	54	54	53
241.6	2.7	2.6	2.6	0.9	0.8	0.8	11	9	13

* Time from energization of trip coil to interruption of charging current.

† Time from interruption of charging current to interruption of resistor current.

Tests, 1952

To check operation of the standard circuit breaker without resistors, three line-dropping tests were made from the Hungry Horse power plant on December 13, 1952. The three tests were made with a sending bus voltage of 230, 242, and 253 kv. Measurements at Hungry Horse included the three line currents and one phase of bus voltage. Measurements at Spokane included the three line-to-neutral

Table IV. Summary of Data Test Series SF, May 12–13, 1954

System Diagram	Test No.	Load Current Before Fault, Amperes	Fault Current, Amperes, φA	Charging Current, Amperes*		60-Cycle Recovery Voltage, Kv, φ to φ	Interrupting Time, Cycles†			Resistor Current Interval, Cycles‡			Restrikes	Maximum Crest Per-Unit Line-to-Neutral Voltage, Sending End			Per Cent of Normal Crest Voltage Left on Line-Sending End		
				φB	φC		φA	φB	φC	φA	φB	φC		φA	φB	φC	φA	φB	φC
Fig. 10-D	SF-1-3:25	340	850	220	280	260	2.4	2.8	2.6	1.3	0.8	0.8	none	1.0	1.2	1.1	0	10	4
	SF-2-5:49	340	830	220	240	253	2.9	2.8	2.6	0.2	0.7	1.2	none	1.0	1.1	1.1	0	36	15
	SF-3-6:02	345	840	210	240	260	2.6	2.5	2.3	0.8	0.7	0.7	none	1.0	1.0	1.1	0	40	42

* After breaker at receiving end cleared fault.
† Time from energization of trip coil to interruption of fault or charging current.
‡ Time from interruption of fault or charging current to interruption of resistor current.

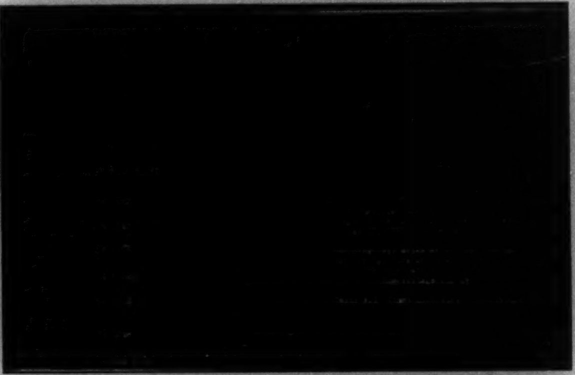

Fig. 14. Oscillogram showing de-energization of 78.7-mile line at 242 kv, breaker equipped with resistors

Fig. 15. Oscillogram showing de-energization of 241.6-mile line at 250 kv, breaker equipped with resistors

voltages. Table I includes the measured results of these tests. Examination of Table I indicates the appearance of severe transient voltages at the receiving end of the line. These voltages resulted in the external flashover of the line side bushings of phase *C* of the receiving end breaker. The bushings are rated 173-kv, 800-kv BIL. As indicated by system diagram Fig. 10(A), the receiving end breaker was open during the test and was therefore subjected to the same overvoltages that resulted in bushing flashover. The sending end oscillogram covering test 2 is shown in Fig. 11.

Tests, 1954

Inasmuch as results of the December 1952 tests indicated that improvement in performance was desirable when switching long unloaded transmission lines, it was decided to modify the breakers at Hungry Horse by the addition of low ohmic value resistors. Fig. 12 is a view through the modified test circuit-breaker tank manhole showing the resistor, interrupters and moving contacts. Fig. 13 is a close-up view of a similar resistor and interrupter assembly showing the resistor center tap connection to the upper interrupting chamber.

After resistor installation, switching tests were performed on May 12–13, 1954 with results as indicated in Tables II, III, and IV. Typical oscillograms are represented by Figs. 14, 15 and 16.

TEST SERIES A

With the system arranged as in the diagram of Fig. 10(B) the Hungry Horse-Hot Springs 78.7-mile line was energized and de-energized. On de-energizing operations the test breaker contact parting time was varied 15 electrical degrees for each operation, completing the 360-degree range, in order to check interrupting performance through all electrical conditions. Bus voltage for these tests was maintained at 242 kv with a resulting 60-ampere charging current.

TEST SERIES B

The same conditions obtained as in series *A* except for an operating voltage of 250 kv and a 61-ampere charging current.

TEST SERIES C

With the system arranged as in the diagram of Fig. 10(C) the Hungry Horse-Bell substation 241.6-mile line was energized and de-energized. The same conditions applied as for series *A* with the operating voltage maintained at 242 kv with resulting 200-ampere charging current.

Test Series D

The same conditions obtained as series *C* except for an operating voltage of 250 kv and a 208-ampere charging current.

Test Series SF

Two 75,000-kw water-wheel generators at the Hungry Horse power plant were isolated, except for the 241.6-mile single-circuit line connection to Spokane, and loaded to their capacity. Referring to Fig. 10(D), the test sequence consisted of: 1. application of solid single phase-to-ground fault at Hot Springs substation by closing circuit breaker at Hot Springs, 2. open Bell substation line breaker, and 3. open Hungry Horse test breaker. Operations were conducted so that the Hungry Horse breaker did not operate until the system had readjusted following disconnection at the Spokane end. Complete voltage and current characteristics were recorded at both ends of the transmission line.

Test Results

The resistor-equipped breaker performance throughout this series of tests was highly satisfactory. Capacitive current interruption was prompt and without restrikes. Residual resistor current interruption time was very short. System voltage was held to low and entirely safe values.

More Severe than Normal Operation Tests

Test observers have often noted that the first few operations, during a series of line-dropping operations in rather quick succession, produced fewer restrikes and lower overvoltages per operation than the remaining tests. This may explain to a degree why tests sometimes indicate rather dangerous overvoltages, whereas hundreds of circuit breakers over a period of many years have been switching high-voltage lines with no apparent damage to connected apparatus including the circuit breaker performing the switching. The increase in frequency of restrikes and overvoltages during a number of tests in rapid succession may be due to carbon in the arc path not being given sufficient time to precipitate so that the dielectric strength of the oil gradually degrades.

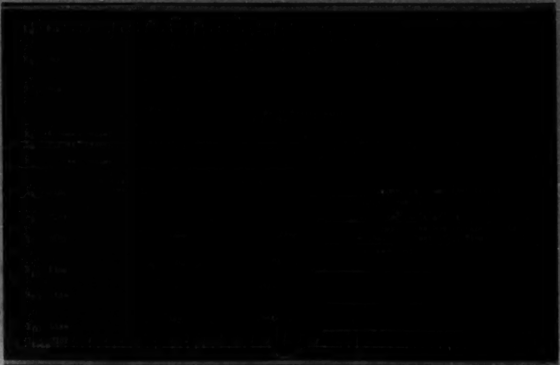

Fig. 16. Oscillogram showing de-energization of 241.6-mile line at 242 kv, with single line-to-ground fault at 78.7 miles; breaker equipped with resistors

Conclusions

A resistor has been designed specifically for application to high-voltage high-speed circuit breakers. Increased distributed capacitance is employed to improve dielectric strength for withstanding steep wave front high-voltage lightning or switching surges. Dangerous gassing of the oil surrounding the resistor during interruption of severe faults is prevented by adequate resistor thermal capacity.

The resistors described have demonstrated excellent performance in withstanding severe impulse tests, in successfully switching long high-voltage lines with operating voltages beyond the upper limit of the breaker rating, and in withstanding the stress of severe fault interruption duty as described elsewhere.[1] However, they add some complexity to the conventional circuit breaker and probably will increase maintenance requirement for circuit breakers on which they are installed. Consequently, they are recommended only for switching high-voltage capacitor banks, cables, and overhead lines over approximately 180 miles long. They may be readily installed in the field, when required, in conventional breakers for which they were designed.

References

1. Field Tests on 138-Kv High-Speed Oil Circuit Breaker at Philip Sporn Power Plant, Otto Naef, R. D. Hambrick. *AIEE Transactions*, vol. 74, pt. III, Aug. 1955, pp. 710–27.

2. *Discussion* by E. C. Starr of The Interruption of Charging Current at High Voltage, W. M. Leeds, R. C. Van Sickle. *AIEE Transactions*, vol. 66, 1947, p. 381.

3. Electrical Transmission and Distribution Reference Book. Westinghouse Electric Corporation, Pittsburgh, Pa., 1943.

◆

Discussion

E. C. Starr and **E. J. Harrington** (Bonneville Power Administration, Portland, Oreg.): It is generally recognized by the industry that if reductions in basic insulation levels below those in common use could be effected, appreciable savings would result. Practical reductions in BIL are to a considerable extent determined by the control that can be exercised over dynamic, lightning, and switching-surge overvoltages.

One of the most common types of switching overvoltage is that produced by a circuit breaker restriking during the interruption of line-charging current. While in most cases the transient overvoltages generated on the station bus are much lower than those produced on the line, they may in some cases reach dangerous magnitudes and in general are always undesirable because of the disturbances they may cause locally as well as elsewhere on the system.

To exercise control over this type of switching surge overvoltage, the Bonneville Power Administration specifies that all high-voltage circuit breakers purchased for line-switching service shall interrupt line-charging current with limited restrike characteristics. Restrikes during such interruptions may not occur beyond 1/2 cycle after the beginning of a current interruption of 1/4 cycle or more. Reestablishment of current through a control or damping resistor incorporated in the breaker is not considered a restrike.

Some circuit breaker designers and many users consider the use of resistors an undesirable means of improving breaker performance. We entertain no objections to such expedients provided breaker per-

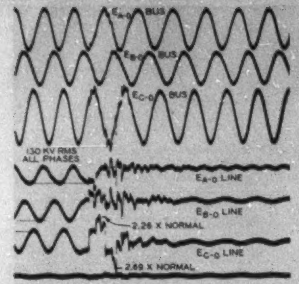

Fig. 17. De-energizing 241.6-mile line at 225 kv. Oscillogram showing restrike generated overvoltages at the sending end. Breaker not equipped with resistors

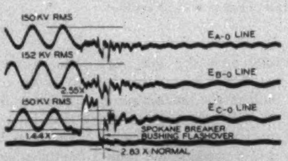

Fig. 18. Hungry Horse-Spokane line. Spokane (receiving end) oscillogram showing restrike generated overvoltages during line-dropping operation of Hungry Horse. Sending end voltage 242 kv

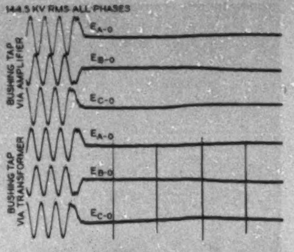

Fig. 19. Receiving end oscillogram of voltages showing de-energization of 241.6-mile line at 250 kv, breaker equipped with resistors. These are receiving end voltages corresponding to those at the sending end shown in Fig. 15

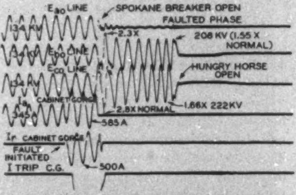

Fig. 20. Receiving end oscillogram showing de-energization of 241.6-mile line at 242 kv, with single line-to-ground fault at 78.7 miles; breaker equipped with resistors

formance, reliability, and service periods are in no way compromised by their use. The paper describes the design and application to a breaker of resistors which have markedly improved its line-dropping performance. Fig. 17 is an oscillogram obtained during a line-dropping operation with the use of the same line as used for the tests described by the authors. In this case the same type of breaker was used with no resistor equipment and the switching was done from the Spokane end of the line. The oscillogram was taken at the Spokane end and shows that the breaker performance was characterized by delayed restriking which produced transient overvoltages on the line up to 2.7 times normal at the switched end.

Fig. 18 is an oscillogram taken at the Spokane or open end of the line during an interruption of line-charging current with an unmodified circuit breaker at the Hungry Horse end. Fig. 11 is the sending end oscillogram taken during this same test. The receiving or open end oscillogram shows restrike generated overvoltages more than 2.8 times normal at this end. This transient voltage was of a nature and of sufficient magnitude to cause flashover of the breaker bushing at the open end. The 60-cycle withstand voltage of this bushing is known by test to be somewhat higher than the measured transient voltage that caused flashover. It appears that insulation subjected to a voltage above the corona formation level and then rapidly reversed may flash over even though the applied line-to-ground voltage is less than the insulation 60-cycle withstand value. This could be due to the trapped charge created by the ionization prior to reversal. The total voltage across the insulation at the instant of reversal then tends to approach the peak-to-peak value rather than the line-to-ground voltage. Further study may show that certain classes of insulation are prone to lowered dielectric strength when subjected to rapidly reversed overvoltages, thus making the presence of such transients even more undesirable than usual.

Fig. 19 is an open-end oscillogram taken during a line-dropping operation with the circuit breaker after the resistors had been added. Fig. 15 is the sending end oscillogram taken during the same test. It may be readily seen that no appreciable overvoltages were generated at either the sending or receiving ends.

The fault tests mentioned in the paper were used as a means of subjecting the circuit breaker to line-dropping duty more severe than the preceding Hungry Horse line-dropping tests. During the fault tests, the Hungry Horse generators were carrying full load at unity power factor; consequently, their excitation was much higher than when supplying line charging only. Application of the fault was an expedient to achieve rapid sequential operation of the breakers at both ends of the line and to simulate one type of normal duty. The Hungry Horse breaker was in this manner called upon to perform a line-dropping operation on the two unfaulted phases with induced overvoltage against a much stiffer bus and one whose voltage did not sag when the line-charging excitation was lost. Fig. 20 is the receiving end oscillogram corresponding to the test shown in Fig. 16. This oscillogram is of particular interest as it shows transient overvoltages of up to 2.8 times normal on the unfaulted open phases. These overvoltages appeared during the interruption of load current by the circuit breaker at the receiving end and were largely due to the long-line inductive drop recovery oscillation combined with coupling to the faulted phase. They were not generated by restrikes in the test breaker at Hungry Horse, but would have been reduced substantially if the Spokane breaker had been resistor-equipped.

The resistors described by the authors have been in service for nearly a year now and, to date, the circuit breaker performance has been entirely satisfactory. Similar resistors have been added to one other breaker of this type on the Bonneville Power Administration system, and similar performance obtained. Modification of additional breakers in the 230-kv class is planned.

P. E. Richardson (United States Bureau of Reclamation, Denver, Colo.): This paper is of particular interest because it covers a successful solution of the long-lines switching problem by the application of low ohmic resistors to a standard circuit breaker, as demonstrated by the results of tests conducted on an identical breaker before and after modification.

Because operation at above-normal voltage is commonly necessary in systems composed of long lines to remotely located hydroelectric plants, and because relaying of a fault near the receiving end of a long line frequently requires sending end breakers to operate at voltages over those held prior to the fault, the tests were conducted at voltages of 105 and 110 per cent of rated voltage.

Test series *SF* demonstrates this latter condition. In these tests the 242-mile 230-kv line was loaded at 145 megawatts at unity power factor, or at slightly more than its surge impedance loading, prior to the application of the line-to-ground fault. Receiving end voltages were at rated level and sending end voltages at 105 per cent of rated. Relaying of the line was modified to simulate that following a fault near the receiving end. After opening of the receiving end breaker and just prior to the opening of the sending end, or test, breaker, voltages on the unfaulted phases at the sending end bus were 110 to 112 per cent of that held prior to the fault.

Under heavy-load conditions it is necessary to hold bus voltages at Hungry Horse as high as 253 kv in order to retain nominal receiving end voltage.

These conditions indicate the requirement of many hydroelectric systems for circuit breakers capable of interrupting both long-line charging and fault currents at 110 per cent of rated voltage and over. While manufacturers are aware of this problem and have provided for its solution, suitable coverage of the situation should be provided by the standards.

Of interest is the completeness of the tests, the full coverage of the results made possible by the isolation of an extensive portion of 230-kv system, and the excellent instrumentation and recording provided by Bonneville Power Administration facilities, indicated by the data in Table I. In addition to records of breaker performance and sending end quantities, records were also obtained of receiving end conditions.

Table II indicates very satisfactory performance of the test breaker in interrupting line-charging current. There were no restrikes as defined by: "no resumption of main current following 1/4 cycle of current interruption." By-passing of the resistor occurred in several of the tests but not more than once in any phase and not later than 0.2 cycle after initial current interruption.

G. B. Cushing (Westinghouse Electric Corporation, East Pittsburgh, Pa.): This is an interesting account of how an oil circuit breaker of somewhat unusual contact construction has been adapted in the field to the problem of switching capacitive currents. The interrupters of each terminal have been equipped with arc-shunting resistors with the result that overvoltages are significantly reduced. Such resistor applications have numerous precedents many of which are reported in the literature.[1-4] However, this one is particularly intriguing because of its unique physical arrangement.

Having had experience with both resistor- and pump-equipped interrupters I would be among the first to admit that without the substantiating data which can be obtained in a testing laboratory the development and field installation of effective pumps to supplement an existing design would present difficult and possibly overwhelming problems. However, properly designed pumps incorporating a delay feature to avoid acting at too short a contact separation afford control of overvoltages which is acceptable for many applications. The simplicity of their construction assures long life with no increase in maintenance requirements.

Resistor units, on the contrary, are subject to many hazards. Thermal overloads, for example, arise with out-of-step switching where voltages are abnormally high and arcing more persistent. When the temperature rise becomes excessive, the insulating oil is vaporized and flashover may follow with explosivelike effects on the unit. Insulation troubles may also develop in a more subtle manner. Over a period of time carbon will precipitate on horizontal insulating surfaces, creating creepage paths that may then develop into breakdowns. Undoubtedly, such factors have been considered by both user and manufacturer. The added maintenance responsibilities are possibly an insignificant price to pay for the excellent control of overvoltages afforded by the resistor units.

In regard to the construction of the resistor assemblies, several questions arise. The confinement of the coils in small horizontal compartments would appear to adversely affect heat dissipation and at the same time introduce manufacturing difficulties. Did factors other than the electrical characteristics necessitate this arrangement? Are the many pads in each resistor wound from one continuous wire or is it necessary to interconnect them during assembly. Also, what is the material used in this structure which supports the pads?

Since there is no mention of derating, one might assume that the 3,500 megavolt-ampere short-circuit rating is maintained. Requisite proof is the successful interruption of currents of approximately 8,800 amperes. However, the only short-circuit tests on this breaker, those in Table IV, fall far short of this rating, barely exceeding the 800-ampere continuous current rating. What other tests have been made to prove the adequacy of electrical clearances in the presence of the gas bubble formed during high-current interruptions? How has the interrupting time of the resistor current been checked for the condition of minimum inductive reactance?

REFERENCES

1. Switching Overvoltage Hazard Eliminated in High-Voltage Oil Circuit Breakers, Lloyd F. Hunt, E. W. Boehne, H. A. Peterson. *AIEE Transactions (Electrical Engineering)*, vol. 62, Feb. 1943, pp. 98–106; discussion p. 421.

2. Resistors for 138-Kv Cable Switching, E. K. Sadler, T. M. Blakeslee. *AIEE Transactions*, vol. 66, 1947, pp. 39–50.

3. The Interruption of Charging Current at High Voltage, W. M. Leeds, R. C. Van Sickle. *Ibid.*, pp. 373–382.

4. Oil Circuit Breaker For Switching 115-Kv Shunt Capacitors, W. M. Leeds, J. H. Pehrson, C. F. Cromer. *Ibid.*, vol. 72, pt. III, Oct. 1953, pp. 1066–72.

K. G. Darrow (General Electric Company, Philadelphia, Pa.): This is an excellent analysis of the line-switching problem. The authors express a dubious opinion of pistons or pumps in selecting a solution to the long-line switching problem. It would appear that whether a pump was selected or not might be due to the configuration in the basic circuit-breaker design. The horizontal break instead of the vertical break might discourage the use of a piston from a mechanical standpoint. However, in circuit breakers employing vertical movement of the crossarm the pump is a perfectly straight forward approach and the mechanical stress introduced on the bushing is only a small fraction of the force introduced by interruption itself. We have found the pump a distinct asset to the interrupting process. Not only has it been valuable for switching capacitive currents, but it has proved equally valuable at higher currents, shortening arcing times and supplying clean oil across the contacts. Many thousands of tests have not uncovered any of the detrimental effects which the authors claim.

We recognize the value of the resistor in switching capacitive currents. We have used this approach for over 10 years in our own designs where capacitive currents of any magnitude were to be switched. It is a useful accessory and one which lends itself to calculation so that performance may be predicted to a considerable extent. The resistor, however, is not without its pitfalls. The authors mention the thermal problem and state they have applied a 6-time factor of safety. My question is, "Six times what?" because we must first agree what normal operation of the resistor may be. While the duration of resistor currents which are claimed to be $1^1/_2$ cycles on opening and 1/4 cycle on closing, there can be a number of these operations in succession with little time for cooling between operations.

Once the resistor becomes a part of the design, it also takes part in full-scale short-circuit interruptions. In fact we consider this a necessary part of the design proof. We note no such tests on this design. They have stated that the resistor will probably increase the maintenance requirements. We fail to see how a properly designed resistor should increase the frequency of maintenance. Finally, we have always contended that proof of line-switching performance requires a greater number of tests because proper results must be obtained statistically. The authors point out that they experienced no restrikes during these tests, but it would appear to us that this number of tests could hardly be expected to demonstrate restrike free performance.

J. E. Conner (Southern California Edison Company, Los Angeles, Calif.): The authors' explanation of the long-line switching problem and its effect on circuit breaker restrike mechanism is a model of clarity and should be extremely valuable to those whose concept of this problem is vague. The extensive wave form diagrams, with expansion of the regions of interest, contribute immeasurably to a better understanding of the text. It is particularly interesting to note that very early interruption of the small capacitive current associated with line switching has certain inherent disadvantages which should be recognized. In discussing the line-switching problem, the authors state that if a choice is necessary between the extremes of very early extinction of the capacitive current and extinction at a somewhat later time, the latter is a much more favorable condition from the standpoint of limiting overvoltages and reducing the probability of circuit-breaker restrikes. It seems paradoxical that permitting restrike current to persist for several natural frequency half-cycles is a desirable circuit interrupter characteristic.

The distinction drawn by the authors between the short-line or lumped capacitance-switching phenomena and the long-line switching problem points out that definite reasons exist for treating the latter in an individual manner. In the section pertaining to the effect of the long line on circuit-breaker restrike mechanism, it is interesting to observe that theory would dictate a rather poor possibility of interruption at the first restrike current zero, while in actual practice modifying effects, such as corona, take precedent and actually make this early interruption a distinct probability. As the authors indicate, this early extinction is not without disadvantages.

As one solution to the problem of switching long lines, the authors discuss at some length the use of resistors shunting the normal circuit-breaker interrupters. Resistors having an ohmic value of approximately one megohm have been excluded from consideration, based on the fact that such resistors will not maintain correct voltage distribution at the higher frequencies encountered in connection with fault interruption or other impulse phenomena. For reasons outlined in the paper, resistors of low ohmic value (2,400 ohms per pole) have been chosen as the solution to the long-line switching problem. Considering for a moment the use of resistors as a means of controlling internal voltage distribution, and not the specific problem of long-line switching, there seems to be some disagreement among circuit-breaker authorities as to the proper resistance values which will establish satisfactory voltage distribution throughout the necessary range of operating conditions. While it is realized that many different electrostatic configurations exist in the various types of breakers, and ideas regarding the maximum rate of rise of transient recovery voltage are widely divergent, it would seem that some area of agreement on this point could be reached.

The desirability of maintaining uniform and proper voltage division among interrupters is recognized by all circuit-breaker designers; however, the literature reveals few facts to substantiate the choice of any particular resistance value. It would appear that this problem could be attacked systematically by the use of a low-voltage repetitive pulse technique, which, with its flexibility of control, would make it possible to determine rapidly, for any range of voltage wave fronts likely to be encountered in service, the optimum resistance value for establishing the desired voltage distribution. The authors' comments on the feasibility of this would be appreciated.

In reviewing the reasons for the choice of low ohmic resistors to cope with the problem of long-line switching, it would appear that the third and fifth reasons are not consistent. In a companion paper (see reference 1 of the paper) an extensive field test program on a similar type of breaker rated 10,000 megavolt-amperes at 138 kv is described. It is stated that the influence of the resistor is most noticeable in the case of high-recovery voltage rates and low current and that it is negligible at high currents. It would be interesting to have the authors point out the area of improvement in performance attributable to the resistors which does not appear in reduced arcing time. Improved performance on low fault current interruption is unquestionable.

One of the major considerations in applying resistors of low ohmic value to high-voltage oil circuit breakers has been the need for adequate thermal capacity to prevent damage to the resistor itself during certain types of severe switching operations. It is the considered opinion of some of the engineers of the Southern California Edison Company, that what little damage has been sustained on resistor-equipped circuit breakers on our system has been due to switching out-of-step system conditions where double normal voltage was impressed across the breaker. Failure under these conditions would be due to the inability of the resistor to withstand four times the normal power dissipation. The authors state that a design factor of safety of six has been incorporated in this design for the worst operating condition, which, however, has not been specified. It is significant that the thermal capability requirements of this resistor are minimized by reducing the time of current flow to a maximum of about $1^1/_2$ cycles.

The authors are to be complimented on incorporating in their resistor design the principles of capacitance grading, found so successful wherever steep-front voltages are to be reckoned with.

Otto Naef (American Gas & Electric Service Corporation, New York, N. Y.): The authors are to be commended for their contribution to the art of resistor switching and resistor design.

A resistor of the same type as described in the paper was recently tested in a 138-kv circuit breaker at the Philip Sporn power plant on both line-dropping and interrupting performance. The favorable results obtained during the 230-kv tests at the Hungry Horse power plant were confirmed. The tests have furthermore proven the ability of the resistor to withstand the stresses imposed by severe interrupting duty.

Resistors, like other accessories in circuit breakers must be designed for the severest conditions likely to occur unless they become a potential source of trouble. It is therefore good to know that each of the two resistors was designed for the full-impulse withstand voltage of the whole circuit breaker, and also for twice the normal resistor current. Such severe conditions occur if during an opening operation only one resistor cuts in and the other resistor remains shunted by the current in the arc path of its associated interrupter.

The authors mention a thermal safety factor of six. How is this to be understood?

I would consider a resistor in danger when the wire attains a temperature of about 300 degrees centigrade, at which oil begins to vaporize. The stream of gas bubbles that commences to form at this temperature may lead to flashover between turns long before the resistor material starts to melt.

A. E. Kilgour (Allis-Chalmers Manufacturing, Milwaukee, Wis.): The authors are to be congratulated on their preparation and presentation of this paper. The oil pump in the vertical breaker has been successfully applied. It has been accepted by the user as a practical means of controlling low-current magnitudes. The addition of mechanical load due to the pump depends on its design and is commensurate with other circuit breaker components which are peculiar to individual manufacturers. The most important application of this pump is to have an effective oil flow to control the insulation build-up, rather than merely a large size. It certainly is appreciated that the rotary breaker presents a more difficult problem of applying a pump than the vertical breakers. An illustration of an effective oil pump is demonstrated by Finneran, et al.[1]

The present paper indicates that resistors are to be employed on a 230-kv circuit breaker to handle the line-charging currents. It is not indicated whether this is because of the special location or that it will be a standard procedure within this breaker design. If it is an accepted standard procedure, then it seems to be at variance with a similar breaker design, but for application on the 138-kv breaker, as presented in the companion paper (see reference 1 of the paper).

REFERENCE

1. 138-KV LINE-DROPPING FIELD TESTS, D. L. Finneran, L. J. Linde, R. D. Allen, A. E. Kilgour. *AIEE Transactions*, vol. 73, pt. III-A, Aug. 1954, pp. 809-16.

D. M. Umphrey and D. J. Marsden: We thank the discussers for their contributions, which add considerably to the value of the paper.

As Mr. Starr and Mr. Harrington point out, any proposed reduction in system BIL must first seriously consider the control that can be excercised over switching surges as well as other transient system voltages. The proposal that insulation may have a lower dielectric strength when subjected to rapidly reversed voltages warrants further study. The additional test records presented help to describe more completely the long-line switching problem.

Mr. Richardson indicates that heavy-load conditions make it necessary to hold voltages in the order of 253 kv at the Hungry Horse power plant. Consideration should perhaps be given to the fact that this will result in sending end circuit breaker recovery rms voltages in the order of 270 to 280 kv under certain switching conditions. This constitutes rather severe duty for standard 230-kv breaker designs.

Regarding Mr. Cushing's questions, the resistor coils were arranged in the horizontal configuration primarily to obtain more series distributed capacitance and to provide greater thermal storage ability in the space available, as outlined in greater detail in the paper. Each resistor is an assembly of four groups of pads each of which is wound from a single length of wire. The pad groups are joined by mechanical means. The supporting structure is manufactured from National Electrical Manufacturers Association *XX* paper-base phenolic material which, when properly applied, has exhibited excellent dielectric characteristics through the years. For proof of adequacy of design under short-circuit conditions we refer to reference 1 of the paper.

Mr. Darrow questions whether the resistor was selected in preference to a pump for mechanical reasons. Actually it appears to be very difficult to install a high-energy pump in any conventional tank-type circuit breaker for reasons outlined in the paper. The 6-times factor of safety questioned in three of the discussions is based on a high-speed open-close-open operation with full-fault kva. Six times the value of energy absorbed by the resistor in this fashion will not raise the temperature of the resistor wire over the vaporization point of the surrounding oil. Concerning the number of tests being insufficient to prove that no restrikes will occur, we believe from experience that the successful performance of the breaker under the rather severe field test conditions described adequately provides the required evidence of no restrike performance.

The proposal by Mr. Conner that low-voltage repetitive pulses be used to determine voltage division under various resistance and electrostatic configurations is worthy of study. Such a study, if found to be economically practical, might result in considerable improvement in the measurement of voltage division between multibreak contacts. The improvement in heavy-fault current interruption is associated with more positive division of recovery voltage across the interrupting breaks. Extremely severe fault interruption duty and attending pressure surges can produce transient reduction in dielectric strength so that improved voltage division, such as may be obtained by the use of low-ohmic resistors, may prove very beneficial in safeguarding interrupting ability.

We agree with Mr. Naef that the resistor is in danger if the wire should attain a temperature at which the surrounding oil begins to vaporize. The resistor design covered by the paper takes this factor into account, as explained earlier. This is accomplished by the combination of adequate thermal storage in the resistance wire plus very short resistor current duration.

In reply to Mr. Kilgour's question regarding application of the resistor, it is intended for economic reasons that resistors should be used only for those applications requiring the switching of high-voltage capacitor banks, cables, and overhead lines exceeding 180 miles long.

A 69-Kv Compressed Air Circuit Breaker for 5,000,000 Kva

R. E. KANE
ASSOCIATE MEMBER AIEE

J. K. WALKER
ASSOCIATE MEMBER AIEE

Synopsis: This paper covers the development of a 5,000,000-kva compressed air circuit breaker rated 69,000 volts with 2,000-ampere continuous current-carrying capacity. The breaker is completely metal-enclosed for outdoor installation. It has six condenser bushings extending through the roof for connection to the customer's bus structure and for mounting of current transformers and potential devices. Verification tests included interrupting demonstrations at 66, 44 and 22 kv, to prove the breaker capable of handling the high currents required for 5,000,000 kva. Additional interrupting tests, with varying rates of rise of the recovery voltage, were made to prove further the ability of the breaker to interrupt and to indicate the factor of safety built into the breaker.

EXPANDING electric utility distribution systems in large cities has necessitated the development of a 69-kv compressed air circuit breaker with a new and higher interrupting rating of 5,000,000 kva. New York City, Philadelphia, and Pittsburgh already have 69-kv breakers with interrupting ratings of 3,500,000 kva of the compressed air type, and a need for 5,000,000 kva in the New York area has already been anticipated. The ever-increasing electrical loads due to popular use of electrical appliances such as air donditioners, television sets, etc., plus the expanding industrial loads, have made necessary the use of 69 kv in the center of large metropolitan districts, as a distribution voltage. The use of compressed air circuit breakers in the center of large cities appears to be the logical solution to the problem of safer installations. Air breakers eliminate the use of oil and at the same time isolate any internal breaker trouble with a sheet-metal-grounded framework completely enclosing the breaker. The oil storage problem, complicated by insurance regulations and local ordinances is nonexistent, and the handling and filtration of oil is no longer required.

This paper is concerned with the development of a 5,000,000-kva compressed air circuit breaker rated at 69 kv. The problems of modifying an existing 3,500,000-kva compressed air circuit-breaker interrupting assembly to make it capable of handling 5,000,000 kva will be covered. The method of testing the new breaker and the electrical circuits set up during test to vary the rate of rise of recovery voltage impressed on the test breaker will be described. The use of the test data obtained to prove the capability of the new breaker to interrupt short-circuit currents under very difficult external circuit conditions should be of considerable interest to electrical engineers. Fig. 1 shows a view of the new breaker.

Interrupter

An orifice type of interrupter was employed as shown schematically in Fig. 2. Compressed air passing from the air reservoir up the blast tube causes the lower moving contact to separate from the lower stationary contact and to draw an arc. Interruption of the arc inserts the shunting resistor. This resistance in the circuit reduces the amount of current that must be interrupted by the upper contact as well as controlling the rate of the transient recovery voltage. Compressed air causes the upper moving contact to part from the upper stationary contact, thereby interrupting the shunting resistor current. This contact structure has been in operation for a number of years at 69 kv on 3,500,000-kva breakers.[1] It formed the basis for extending the interrupting capacity to 5,000,000 kva. Larger orifices for both the lower and upper contacts were used in order to handle the increased current (42,000 amperes at 5,000,000 kva as compared to 29,000 amperes at 3,500,000 kva). Other changes in contact configuration were made to reduce the clogging effect of the arc, to reduce back pressure, and to eliminate copper vapor in the arcing zone, in order to arrive at a structure capable of successfully handling 5,000,000 kva.

Interrupting Tests

A testing procedure was selected which would subject the circuit breaker to conditions normally imposed on a breaker,

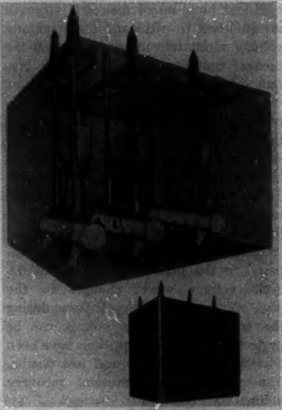

Fig. 1. 69-kv compressed air circuit breake

Paper 55-218, recommended by the AIEE Switchgear Committee and approved by the AIEE Committee on Technical Operations for presentation at the AIEE Winter General Meeting, New York, N. Y., January 31–February 4, 1955. Manuscript submitted October 21, 1954; made available for printing December 3, 1954.

R. E. Kane and J. K. Walker are with the Westinghouse Electric Corporation, East Pittsburgh, Pa.

The authors wish to thank their colleagues J. E. Schrameck and B. P. Baker of Westinghouse Electric Corporation, East Pittsburgh, Pa., who contributed a major part in the successful completion of this development and in the writing of the paper.

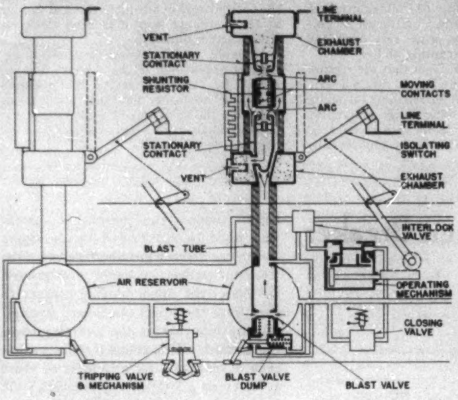
VENT
STATIONARY CONTACT
SHUNTING RESISTOR
STATIONARY CONTACT
VENT
BLAST TUBE
AIR RESERVOIR
TRIPPING VALVE & MECHANISM
BLAST VALVE DUMP
BLAST VALVE
LINE TERMINAL
EXHAUST CHAMBER
ARC
ARC
MOVING CONTACTS
LINE TERMINAL
ISOLATING SWITCH
EXHAUST CHAMBER
INTERLOCK VALVE
OPERATING MECHANISM
CLOSING VALVE

Fig. 2 (left). Schematic of 69-kv compressed air circuit breaker

Fig. 3 (right). Calculated recovery voltages of 69-kv grounded and ungrounded circuits

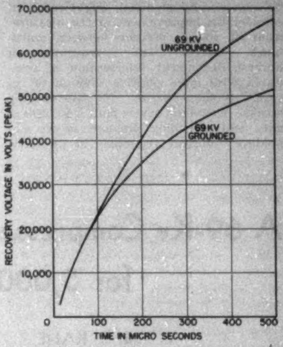

such as full line voltage, full short-circuit current, and proper rate of rise of the transient recovery voltage. It was thought desirable to use the 12-ohm resistor normally supplied with the 3,500,000-kva interrupter on the proposed 5,000,000-kva circuit breaker.

It can be shown that the maximum rate of rise of recovery voltage that will appear across the lower orifice is determined by the circuit breaker resistor when the breaker is applied on a circuit of a given short-circuit capacity. Therefore, the application of this breaker is determined when it is tested on a laboratory circuit producing rates of rise of recovery voltage which are actually greater than those it will be required to interrupt in service. This is true provided the breaker insulation and build-up of dielectric strength are sufficient to withstand the maximum voltage ultimately appearing across the breaker contacts after short-circuit current interruption.

When calculating the rate of rise of recovery voltage under short-circuit conditions, cable or line-charging current is small with respect to short-circuit current and the breaker shunting resistor current. Therefore, the capacitance of the circuit can be neglected in circuit calculations. Similarly, since the time duration of the transient recovery voltage is short compared to the period of the normal 60-cycle voltage wave, changes in the peak voltage of the 60-cycle wave during the transient recovery voltage can be neglected. These assumptions have been checked by calculation and test results. The expression for transient recovery voltage then becomes

$$e=E\left(1-\epsilon^{-\frac{R}{L}t}\right) \qquad (1)$$

where

e = transient recovery voltage, volts at any time t, after current zero
E = crest voltage of the normal 60-cycle voltage wave, volts
ϵ = 2.718, natural logarithm base
R = ohmic value of the shunting resistance across the lower orifice
t = time, seconds, after the current zero at which interruption by the lower orifice occurs
L = inductance, henrys, of the circuit under short-circuit conditions determined from the circuit rms voltage and short-circuit kva

From equation 1, the transient recovery voltage for a grounded system operating at 69 kv and capable of producing a 5,000,000-kva short-circuit may be calculated. Such calculations were made and a curve of the transient recovery voltage versus time was plotted as shown in Fig. 3. Calculations for this curve were made on the assumption that a circuit breaker having a 12-ohm resistor across the lower orifice would be used. Similar calculations were made of an ungrounded system; see Fig. 3. The difference in the curves exists because, on a 3-phase system in the event of a breaker-opening operation the first phase to clear on an ungrounded system is subjected to 87 per cent of the line-to-line voltage, whereas on a grounded system the percentage is only 57 per cent. However, the short-circuit current which must be interrupted is the same in either case.

It follows that the 5,000,000-kva short-circuit interrupting capacity of the circuit breaker is demonstrated when 42,000 amperes rms are interrupted, provided the voltage appearing across the interrupter at any time after current zero is greater than the voltage from Fig. 3 at any corresponding time after current zero. This shows that the circuit breaker has developed sufficient dielectric strength across its interrupter to withstand the maximum voltage applied by the circuit at any instant and will not break down. The test circuit used to demonstrate this condition is shown schematically in Fig. 4.

Grounded Circuit

A series of single-pole tests was made with the circuit breaker grounded as shown in Fig. 4 at test voltages of 66, 44, and 22 kv. A 12-ohm resistor R was used without any capacitance C for the first tests. A 66-kv circuit was used as this is a standard transformer connection in the laboratory. Also, 66-kv exceeds normal line-to-ground voltage of 40 kv on a 69-kv circuit and thus is a test under more severe conditions than the breaker would experience in service. The maximum current available, which measured 25,000 amperes, was interrupted at 66 kv and the maximum current available at 22 kv, which measured

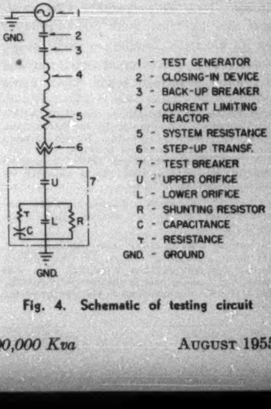
GND.
1
2
3
4
5
6
7
U
T
C
L
R
GND.
1 - TEST GENERATOR
2 - CLOSING-IN DEVICE
3 - BACK-UP BREAKER
4 - CURRENT LIMITING REACTOR
5 - SYSTEM RESISTANCE
6 - STEP-UP TRANSF.
7 - TEST BREAKER
U - UPPER ORIFICE
L - LOWER ORIFICE
R - SHUNTING RESISTOR
C - CAPACITANCE
T - RESISTANCE
GND. - GROUND

Fig. 4. Schematic of testing circuit

48,500 amperes, was also interrupted. A current interruption of 48,500 amperes is the equivalent of 5,800,000 kva at 69 kv. This is well over the required 5,000,000-kva rating. During all of these tests, cathode-ray oscillograms were taken.

The foregoing data are valid proof of circuit breaker performance at 69 and 22 kv and show that the recovery voltage as produced by the laboratory circuit was greater in time relation than the recovery voltage which would appear across the breaker when applied on a 69-kv grounded circuit in service. Accordingly, the 22-kv voltage-time relationship taken from a cathode-ray oscillogram of the test was plotted as shown in Fig. 5 and combined with the two curves from Fig. 3. To refer to Fig. 5, it is apparent that the breaker interrupted on a duty greater than it would be subjected to in service on a grounded 69-kv circuit. It maintained this condition for approximately 50 microseconds after current zero.

Since the circuit-breaker resistor had been selected so that the maximum voltage which could ever appear across the resistor in service would be less than crest voltage, it followed that the 66-kv tests demonstrated the integrity of the breaker insulation and dielectric recovery.

The application of recovery voltage to the interrupter due to the shunting resistor, as shown by equation 1, increases at a decreasing rate. Also, the rate of increase in dielectric strength between the contacts is always greater than the voltage applied across the resistor because of the flow of clean air between the contacts. It follows that the dielectric strength between the contacts is always greater than the voltage which would occur in service. As proof of this conclusion another test was made on the 22-kv laboratory circuit using capacitance in place of the shunting resistor to produce an oscillatory recovery voltage peaking at a time more than 50 microseconds after current zero. The results of this test are shown by the plotted curve for $X_c = 845$ ohms in Fig. 6. Again, the interrupter successfully withstood a recovery voltage greater than it would be subjected to in service and for a period of from 100 to 250 microseconds after current zero.

The tests had demonstrated the ability of the breaker when applied on a 69-kv grounded circuit but, as shown in Figs. 5 and 6, were not sufficient if the breaker should be applied on an ungrounded circuit. Table I lists some typical interrupting tests.

Table I. Interrupting Tests

Grounded Test Circuit, Resistor Tests, R=12 Ohms

Test Voltage, Kv	Current Interrupted, Amperes	Restored Voltage, Volts	Equivalent Kva at 69 Kv
66	7,000	56,500	800,000
66	13,100	59,000	1,500,000
66	25,000	60,000	3,000,000
22	38,600	19,000	4,600,000
22	44,500	19,000	5,300,000
22	48,500	20,000	5,800,000
Grounded Test Circuit, Capacitive Reactance Tests: $X_c = 255$ ohms, $r = 1.25$ ohms			
22	41,000	20,400	4,900,000
22	44,600	20,600	5,330,000
22	46,800	20,000	5,600,000
Grounded Test Circuit, Capacitive Reactance Tests: $X_c = 845$ ohms, $r =$ zero			
22	43,300	21,000	5,170,000
22	45,500	19,000	5,440,000
22	48,500	21,000	5,800,000
Ungrounded Test Circuit, Capacitive Reactance $X_c = 880$ ohms			
22	33,500	20,400	4,000,000
22	39,500	20,400	4,720,000
Ungrounded Test Circuit, Capacitive Reactance $X_c = 1{,}900$ ohms			
22	32,400	20,700	3,870,000
22	41,000	20,700	4,900,000
22	41,000	20,700	4,900,000
Ungrounded Test Circuit, Resistance=6 ohms			
66	496	62,000	59,000
66	14,000	61,000	1,670,000
Ungrounded Test Circuit, Resistance=24 ohms			
22	41,000	20,800	4,900,000
22	49,100	20,600	5,860,000
22	51,000	20,000	6,100,000

Low-current interrupting tests and capacitor-switching tests have been previously reported.[1]

Ungrounded Circuit

A series of single-pole tests was made on the circuit breaker to simulate an ungrounded circuit. Tests were made employing various values of capacitive reactance shunting the lower orifice as well as tests using different shunting resistance with the object of obtaining higher rates of rise of the circuit recovery voltage. Table I shows the test results obtained.

The first of these tests was made with a shunting capacitive reactance of 880 ohms, and a typical cathode-ray oscillogram was measured and plotted, as shown in Fig. 7. Another series of tests was made with capacitive reactance of 1,900 ohms and a typical cathode-ray oscillogram was measured and plotted in Fig. 7. Additional tests were made without any capacitive reactance in the circuit. A typical cathode-ray oscillogram of the resistance tests, showing the highest initial rate of rise of recovery voltage (test resistance $R = 24$ ohms) was plotted in Fig. 7.

From Fig. 7 it can be seen that the highest circuit recovery voltage for a capacitor shunt was obtained with a ca-

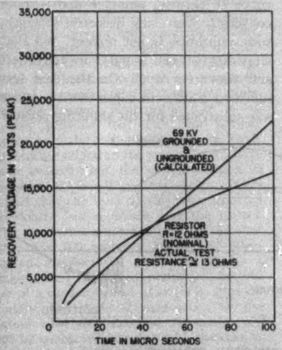

Fig. 5. Recovery voltage for a grounded test circuit with circuit-breaker contacts shunted by resistance

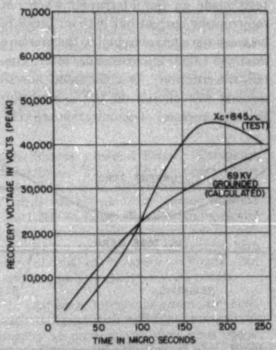

Fig. 6. Recovery voltage for a grounded test circuit with breaker contacts shunted by capacitive reactance

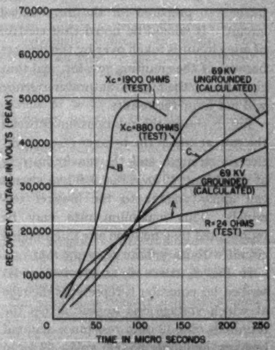

Fig. 7. Recovery voltage for an ungrounded test circuit with breaker contacts shunted by resistance and capacitive reactance

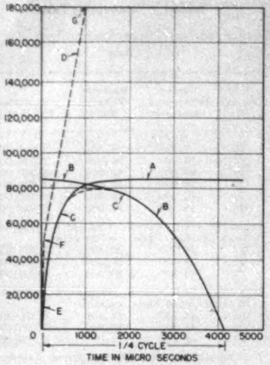

Fig. 8 (left). Dielectric strength for 5,000,000-kva compressed air circuit breaker

Fig. 9 (right). Cathode-ray oscillogram showing current flow through a noninductive shunt connected in series with breaker lower orifice

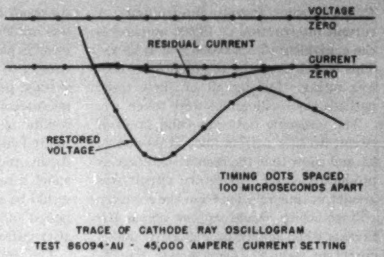

pacitive reactance of 1,900 ohms. This curve demonstrates successful interruptions at very high currents. Thus the breaker proved itself capable of interrupting a high short-circuit current and of developing a dielectric strength across its contacts greater than that of a calculated 69-kv ungrounded circuit for a period of up to approximately 150 microseconds after current zero. Once the breaker has withstood the circuit transient recovery voltage for the first 150 microseconds after current zero, the capability of the breaker for an ungrounded system has been demonstrated.

Test Results

The results obtained for the ungrounded circuit apply for the grounded circuit as well, and demonstrate additional margin for the grounded circuit only. Therefore, the summary curves as shown in Fig. 8 have been prepared for the ungrounded circuit. It should be noted that control of any circuit is taken over by the breaker because of the shunting resistor, and that circuits—of the highest natural frequency will not limit the results.

Fig. 8 shows the relationship between the rate at which the breaker recovers dielectric strength and the maximum rate at which any 69-kv 5,000,000-kva circuit can apply voltage to the breaker terminals. This maximum rate may be represented by a fault on any ungrounded circuit with an infinite recovery rate.

In Fig. 8, curve *A*, as previously described by equation 1, represents the rate at which voltage can appear across the terminals of a 12-ohm resistance-shunted breaker, assuming 85,000 volts, 69 kv$\times\sqrt{2}\times$87 per cent, instantly applied and indefinitely maintained. Curve *B* represents 1/4 cycle of a 60-cycle wave which is the circuit voltage for the first 1/4 cycle following arc extinction. Curve *C* represents the voltage-time characteristic of the most severe circuit as controlled by the 12-ohm resistance shunted breaker. It results by subtracting the ordinates of curve *B* from 85,000 volts and then subtracting this difference from the ordinates of curve *A*. Curve *D* represents the rate at which the breaker recovers dielectric strength. At any time after current zero, if curve *D* lies to the left and above curve *C*, the arc cannot be re-established since the voltage applied by the circuit will not be sufficient to cause breakdown through the dielectric strength developed within the breaker. Point *E* on curve *D*, Fig. 8, was taken from curve *A* of Fig. 7. Point *F* and the portion of curve *D* between points *E* and *F* were taken from curve *B* of Fig. 7. Thus the portion of curve *D* up to point *F* verifies the breaker's ability to develop sufficient dielectric strength to withstand 50 kv in approximately one-half of the time available when interrupting currents equal to or in excess of its rating. Point *G* of curve *D* was determined from voltage withstand tests made on the interrupter when not interrupting current but with air pressure between the contacts equal to the pressure existing 1,000 microseconds after current interruption. One thousand microseconds was chosen on the assumption that the processes of deionization are very slow and that all ionization must be swept out of the arcing space by the air blast moving at acoustical velocity. This is a most pessimistic assumption. The validity of the dielectric strength between points *F* and *G* may be established by reference to Table I and Fig. 9 which demonstrate that deionization occurs within a very few microseconds after current zero and that unsuccessful interruptions, if any, occur within the same few microseconds after current zero.

Fig. 9 shows a trace of a cathode ray oscillogram taken when interrupting 45,000 amperes with both the restored voltage and the residual current in the arcing space measured. This indicates a small residual current which is almost all capacity current. A leakage or ionizing current through the arcing space would be shown in phase with the oscillating restored voltage or by displacement from the 90-degree relationship between applied voltage and capacitance current. Since this condition does not exist, ionization, which must determine dielectric strength, is not present. Therefore, it can be concluded that the portion of curve *D*, between points *F* and *G*, is of constantly increasing dielectric strength, since ionization is not present, and that all points between *F* and *G* are to the left and above curve *C*. On the next test sufficient additional capacitive reactance was substituted for the shunting resistor

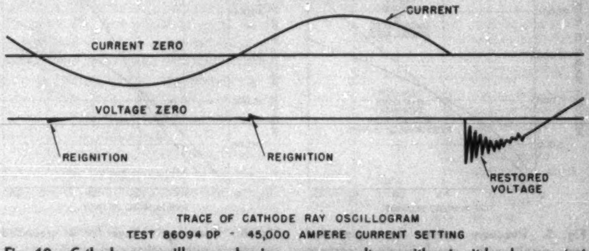

Fig. 10. Cathode-ray oscillogram showing recovery voltage with circuit-breaker contact shunted by capacitive reactance

to give a severity of test where the interruption by the breaker was problematic. Fig. 9 is a trace of a cathode-ray oscillogram taken from this test when interrupting 45,000 amperes and demonstrated that unsuccessful interruptions, if any, occur within the few microseconds after current zero. As shown in Fig. 10, two unsuccessful attempts at interruption were made before final extinction. It is to be noted that the first two attempts showed reignition in the region corresponding to that between the points *E* and *F* of Fig. 8. This feature of never failing once point *F* has been reached has always characterized this breaker and successful interruptions always have resulted if the breaker developed sufficient dielectric in a region corresponding to that between points *E* and *F*.

Conclusions

Successful interruption of 5,000,000 kva with an ample margin of safety has now been demonstrated for a 69-kv compressed air circuft breaker. The laboratory testing circuit was made more difficult than any known field circuit for a grounded or ungrounded system and the breaker still interrupted its full current rating. No demonstration of flame was noticeable even at 5,000,000 kva. Normal breaker operation is very quiet so that installation in a metropolitan district would not be objectionable from the noise standpoint. Absence of oil makes the circuit breaker desirable for crowded districts.

Breaker-operating air pressure is still only 260 pounds per square inch as no need was found to increase the pressure even though the interrupting capacity was increased. Also, modification of existing breakers already in the field is definitely possible so that future expansion needs may be easily met for those customers already having 69-kv compressed air circuit breakers.

Reference

1. A New 69-Kv Compressed-Air Circuit Breaker, B. P. Baker, E. Frisch. *AIEE Transactions*, vol. 68, pt. I, 1949, pp. 368–72.

Discussion

R. L. Webb (Consolidated Edison of New York, Inc., New York, N. Y.): The need for a 5,000,000-kva 69-kv air-blast circuit breaker has developed at our East River generating station in New York City. As time goes on it will become necessary for us to modify many existing 3,500,000-kva breakers now in service to provide the 5,000,000-kva capability. We are pleased to see the development of the new breaker along the lines which will make it relatively simple to change existing breakers to the higher rating.

In regard to the interrupting tests, the novel method used for impressing voltage across the first contact to open we trust has provided conditions which adequately simulate those in actual service.

It has been determined that the recovery voltage rate on the circuits on which these 5,000,000-kva circuit breakers will be applied is in the order of 5,000 volts per microsecond. This is without including any effects from the breaker itself. Does the author anticipate that the breakers will perform satisfactorily on such a circuit?

We are much interested in the breakers' ability to interrupt cable-charging current, since this would be a regular type of duty at the East River station. The application of the first breakers ordered will eventually require approximately 250-ampere cable-charging current interruption. It is, of course, possible that this will become larger at a later date when more cable circuits are added to the system. We have been assured that the circuit breaker is capable of handling this duty. It is stated that the tests on this were reported previously (see reference 1 of the paper). The maximum amperage reported at that time was 180 amperes which was interrupted satisfactorily at 60 kv across a single pole. This was performed by the use of a capacitor load in series in approximately 300 ohms of resistance. In the actual case this external resistance will not be connected in series with the capacitance of the cable. Only the 12-ohm resistance of the interrupter will be effective in controlilng recovery voltage. Do the authors consider this sufficient?

G. D. Floyd (Hydro-Electric Power Commission of Ontario, Toronto, Ontario, Canada): I found this paper difficult to read, and containing several sweeping conclusions which do not follow directly from the information in the paper available to the reader; indeed some of them are predicated on unknown or little known information regarding the performance of circuit breakers. It may be that the conclusions are sound but this is not evident from the context. A number of these conclusions could be given as examples. To refer to but one, in the section "Grounded Circuit," I am unable to agree that "...it followed that the 66-kv tests demonstrated the integrity of the breaker insulation and dielectric recovery." What is "integrity of breaker insulation?"

I compliment the authors on development of a compromise test for circuit-breaker duty which is supported by factual information. The increase in duty in circuit breakers now required makes it imperative that such compromise tests be developed, as no high-power laboratory can economically be built to test these breakers directly, and system tests are not always possible, and are difficult to arrange in any case. The method of using lower than normal voltage is apparently limited to cases where a resistor can be applied across the contacts. What is the possibility of making this test and arriving at consistent results if capacitor coupling is used across the contacts?

R. B. Shores (General Electric Company, Philadelphia, Pa.): The authors have done a fine job in increasing the capacity of their 69-kv air-blast circuit breaker from 3,500 to 5,000 megavolt-amperes and in devising test circuits to prove its performance on systems with extremely high rates of rise of recovery voltage. But could the authors clarify several points:

1. Air-blast circuit breakers are commonly designed with sufficient storage tank capacity to perform two close-open operations without replenishment of air. Have the performance characteristics of Fig. 8 and Table I been established by using air pressure corresponding to the second opening operation or on the basis of 260 pounds per square inch in the tank?

2. With reference to Fig. 8, I understand that point *G* of curve *D* was obtained when the unit was not interrupting current but with air pressure between the contacts equal to the pressure existing 1,000 microseconds after current interruption. Does this not mean that static air pressure was used, or was the breaker adjusted to give the desired pressure with actual air blast across the contacts?

3. I am also interested in the statement in Table I that low-current interrupting tests and capacitor-switching tests were previously reported on the breaker in 1949. Since those tests, however, design changes have been made in orifice, in contact configuration, and in the exhaust chamber. The 1949 low-current tests, and particularly capacitor switching tests, can therefore hardly be considered acceptable for the redesigned breaker.

It would be most desirable if the industry could arrive at some general standards for the rating of air-blast breakers from the standpoint of the rate of rise of recovery voltage they should handle. Comparisons between air-blast breakers, particularly between American versus foreign designs, are extremely difficult to make. The American air-blast designs too frequently are based on handling the severest rate of rise of recovery voltage which can be encountered under any system condition. This design approach eases the application engineer's job but adds substantially to the circuit-breaker cost and can even reflect into the air system costs as a result of increased orifice sizes or of additional interrupting nozzles.

A. E. Kilgour (Allis-Chalmers Manufacturing Company, Milwaukee, Wis.): The authors are to be congratulated for their interesting paper.

The axial blast breaker with its isolated disconnects is a reliable method of circuit interruption. This basis means of interruption has been successfully employed by the Allis-Chalmers company in their metal-clad switchgear units since 1942 for both indoor and outdoor application.

It is also interesting to note that our experience with this type of breaker at a somewhat lower voltage also indicates values of 13 ohms to be in the proper order of magnitudes for the shunting resistor.

The interrupting data presented does show most current magnitudes and interesting recovery voltage data, but nothing is stated in regard to the type of fault applied, the time of interruption, or the point of contact part during these tests. This information is vital when breaker ability is changed, and should not be left to the reader's imagination. It is realized that no heavy short-circuit tests were conducted at this time, but that does not justify the omission of a limited amount of oscillographic information.

R. E. Kane and **J. K. Walker:** The authors wish to thank the discussers for their interest in the paper and for their highly valued remarks. Mr. Webb anticipates recovery voltage rates on the Consolidated Edison system of 5,000 volts per microsecond. Such recovery rates will not affect breaker performance as control of any circuit is effectively taken over by the breaker-shunting resistor. In connection with the capacitor-charging current tests previously made, it should be noted that only the limitations of the laboratory testing facilities at that time prevented tests being made over 180 amperes. However, a new bank of capacitors is now available and tests from 250 to 500 amperes, without the use of resistance in series with the capacitors, is now contemplated. The removal of resistance in series with the capacitors is not expected to affect test results to any marked degree.

In reply to Mr. Floyd's question, the phrase "integrity of breaker insulation" was used to convey the thought that breaker insulation in general, and the micarta insulation surrounding the interrupter in particular, was unimpaired and completely sound after having withstood many laboratory interrupting tests.

Mr. Shores covers the operating pressure of the breaker, which is normally 260 pounds per square inch. However, all high-current interrupting tests were made at pressures of 260 and 215 pounds per square inch. The 215-pound pressure represents the existing air pressure after the first breaker operation. Another point mentioned was the curve in Fig. 8 which includes point *G*. Static air pressure at 150 pounds per square inch across breaker contacts was used to determine point *G*. A pressure of 150 pounds was selected as this is the actual pressure on the contacts during and after arc interruption as measured on test magnetic oscillograms of high-current interruptions. Another point covered was the validity of charging current tests made on a $3^{1}/_{2}$-megavolt-ampere breaker, which were said to apply to the 5-megavolt-ampere breaker. Since the contact structures of the two breakers are very similar, with only minor modifications to contact configuration, it is felt that the availability of the strong air blast more than offsets any possible ill effects of contact changes. However, additional capacitor-switching tests at higher currents are planned for the future.

Mr. Kilgour expressed an interest in magnetic oscillograph records of the test results. Magnetic records were recorded on all tests made on the breaker. Time of interruption on all tests listed in Table I was constant within the range of 4.4 to 5.4 cycles while arcing time never exceeded 1 cycle. All tests were made on a single-pole unit and Table I lists grounded and ungrounded tests. Fig. 4 shows the test circuit used. The point of contact parting, on symmetrical currents, was such that the breaker had to handle a full half-cycle of current or more before interruption. On asymmetrical currents, all interruptions on a small half-cycle of current were repeated until a large half-cycle of current was interrupted. Very heavy short-circuit tests were conducted with currents in excess of 50,000 amperes being interrupted.

Field Tests on a 138-Kv High-Speed Oil Circuit Breaker at Philip Sporn Power Plant

OTTO NAEF
MEMBER AIEE

R. D. HAMBRICK
ASSOCIATE MEMBER AIEE

Synopsis: The continuing and rapid expansion of the 138-kv transmission system of the American Gas and Electric (AG&E) Company and of its superimposed 330-kv system in terms of installed capacity and interconnections has created a demand for 138-kv circuit breakers rated considerably in excess of 5,000 megavolt-amperes (mva). At key points of the system 10,000-mva breakers are being installed in large numbers, and existing breakers are relocated to positions remote from large concentrations of power. The new breakers were purchased on the strength of single-pole factory tests made at full voltage and reduced interrupting current, and at full current and reduced voltage up to the limit of available testing facilities. Though this kind of 2-part test is never a complete substitute for full-capacity tests, it was felt that satisfactory performance under field conditions could reasonably be predicted on the basis of such tests. Some of the 5,000-mva breakers recently installed are from a manufacturer who lacks facilities for factory testing. The field tests described in this paper were made to prove this breaker up to its full rating, and then to increase the short-circuit duty until the limit of either the breaker or the system was reached. The limitation proved to be the available system short-circuit capacity, which resulted in a maximum breaker duty of 6,900 mva. It is believed that this is the heaviest fault interruption ever made at the 138-kv breaker rating. This interruption involved all power available at the site, including that received from other large stations through incoming lines. A comparison of this value with the 3,500 mva interrupted 10 years ago during field tests at the Philco generating station points to the rapid growth of the AG&E system during this period.[1]

Objective of Tests

WHILE the primary objective of the tests was to check circuit-breaker performance under short-circuit conditions, a series of tests was also carried out to obtain performance data on charging and dropping open-circuit transmission lines. A related objective was to study the effect of large fault currents on the two 132/330-kv autotransformers installed at the Philip Sporn Station, to measure the voltage gradient of the station grounding, and to obtain data on the 132-kv and 330-kv bushing potential devices during the voltage dips associated with the short circuits. Valuable information was also obtained on current transformer and relay performance.

The test program was laid out so as to cover practically the whole range of possible short-circuit conditions on the AG&E system. According to location and type of fault the network parameters which chiefly determine the severity of an interruption vary:

1. Highest rates of rise of transient recovery voltage are associated with faults on a single generator-transformer unit.

Paper 55-222, recommended by the AIEE Switchgear Committee and approved by the AIEE Committee on Technical Operations for presentation at the AIEE Winter General Meeting, New York, N. Y., January 31–February 4, 1955. Manuscript submitted October 21, 1954; made available for printing December 16, 1954.

Otto Naef is with the American Gas and Electric Service Corporation, New York, N. Y., and R. D. Hambrick is with the Federal Pacific Electric Company, San Francisco, Calif.

The authors wish to acknowledge the fine cooperation and efficient organization of the personnel of the Federal Pacific Electric Company, Appalachian Electric Power Company, Ohio Power Company, Philip Sporn Plant, and the Operating and Electrical Engineering Divisions of the American Gas and Electric Service Corporation.

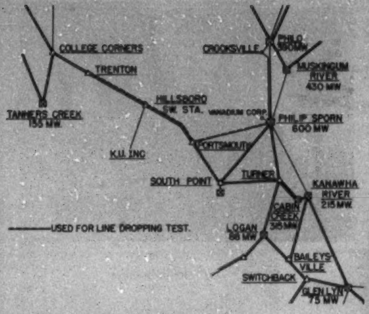

Fig. 1. Simplified diagram of AG&E Company 132-kv transmission system

Fig. 2. Philip Sporn Power Plant viewed from 132-kv switchyard

2. Highest values of normal-frequency recovery voltage are associated with ungrounded 3-phase faults.
3. Highest currents and unequal voltage distribution between interrupters, unless shunted by resistors or capacitors, are associated with single-pole faults.
4. Repetitive reclosing duty is associated with the majority of line breakers.

The tests were selected to cover each of these conditions of maximum severity and any practical combinations thereof.

System Setup During Tests

Fig. 1 shows the central portion of the 132-kv transmission system of the AG&E Company showing the principal lines and connected generating capacity at the time of the tests. The Philip Sporn Plant shown in Fig 2 was chosen as a test site because its capacity of 600 megawatts exceeds that of any other station on the system, and its central location and great number of interconnections assure maximum contributions from adjacent stations. At the same time it is sufficiently distant from important load centers to minimize the effect of sudden voltage dips. The interrupting duty was adjusted to the desired values by varying the number of generators and lines connected to the fault bus as well as the number of grounded transformer neutrals, as shown in Table I.

During the tests with reduced capacity (system setups 1, 2, and 3) all generators and lines directly contributing to the short-circuit current were connected to the no. 2 station bus, which in turn was connected to the fault bus through the backup and test breakers. The other generators and lines terminated on the no. 1 station bus and indirectly contributed to the short-circuit current through the tie lines with other stations. To prevent the dropping out of plant auxiliaries of units feeding the no. 2 station bus, these auxiliaries were temporarily connected to auxiliary transformers fed from the no. 1 bus, whose voltage never dipped below 80 per cent (%) during fault operations.

During the tests with full capacity (system setup 4) all transformer neutrals were grounded and the no. 1 and 2 station busses were tied together as a normal operating condition. Every generating unit and synchronous condenser of the system was connected, save the second 215-megawatt unit at Kanawha, the no. 5 110-megavolt unit at Glen Lyn, and the no. 2 155-megavolt unit at Tanners Creek which were temporarily out for repairs or maintenance. But for these unavoidable outages the total short-circuit duty would have exceeded 7,000 mva. The two 330/132-kv autotransformers substantially contributed to the total short-circuit current through their tertiary windings. The high-voltage side of these transformers was open, because the 330-kv system was not yet in operation. Since the tests were carried out on a Saturday the system was lightly loaded. To compensate for the corresponding reduction in generator excitation the normal load distribution was changed and the Sporn Plant operated at near full capacity. Of the plant auxiliaries, which were fed from their usual unit-connected auxiliary transformers, only the fuel feed pumps and the belt conveyer motors twice dropped out during the 3-phase full-capacity tests.

Switching and Physical Arrangements

Fig. 3 shows the test site with the 10,000-mva backup circuit breaker and the test breaker (right) installed side by side on concrete foundations some 50 feet outside a vacant bay of the 132-kv switchyard. The test circuit was connected to the no. 2 station bus through an isolating switch. The fault bus was mounted on three insulator stacks directly behind the test breaker. Ungrounded 3-phase faults and single-phase line-to-ground faults could be set up in rapid succession. The voltage between the insulated fault bus and the ground terminal was measured by a 132-kv single-phase potential transformer. Heavy copper leads connected the ground terminal to four widely distributed points of the ground mat of the 132-kv switchyard. The neutrals of the four step-up transformers at the power plant and of the two autotransformers in

Table I. System Setup

System Setup No.	Number of Generators at Sporn	No. of Lines	Transformer Neutrals at Sporn	Connected Circuits
1	1	none	1 grounded	none
2	2	4	2 grounded	2 South Point 1 Portsmouth 1 Muskingum
3	4	6	1 grounded, 3 ungrounded, 2 grounded. 330/132-kv autotransformers	2 South Point 2 Turner 1 Muskingum 1 Philo
4	4	10	4 grounded, 2 grounded. 330/132-kv autotransformers	all 10 circuits

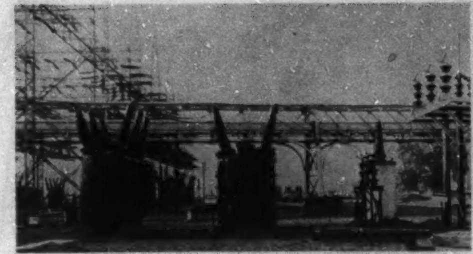

Fig. 3. Test site

Fig. 4. Test circuit breaker

the 330-kv switchyard were tied in to the ground mat through six overhead ground wires and two buried ground cables having lengths of 2,300 and 1,600 feet respectively. This considerably reduced current flow and ground potential gradients during line-to-ground faults.

A temporary wood-pole line led from the fault bus through a disconnecting switch to a tower on the Portsmouth circuit and permitted the carrying out of line-dropping tests under conditions identical to those existing for a line breaker. Fire-fighting equipment and floodlighting for night work were installed in proximity to the test breaker, but actually neither was used.

The magnetic and cathode-ray oscillographs and the breaker control and relay panels were installed adjacent to the dispatching room in the control building, thus permitting direct communication between the test personnel and the system operators. The distance between the fault bus and the control building was approximately 300 feet.

Test Circuit Breaker

The test circuit breaker, Fig. 4, is one of a number of similar breakers already installed on the AG&E system. It is a Pacific Electric type-*RHE-78* 138-kv 1,200-ampere 3-cycle common base-mounted oil circuit breaker. The breaker is operated by a type-*MO-5* spring-operated mechanism which was adjusted to provide the standard 20-cycle reclosing duty. The design of these breakers is similar to the line of standard circuit breakers, but with the following modifications which have been incorporated in designs for the higher interrupting capacity ratings.

The breaker poles are contained in 78-inch-diameter tanks instead of 64-inch-diameter tanks that are now standard for Pacific Electric breakers for the 138-kv voltage rating. The larger diameter tank was considered advisable for the higher interrupting duty expected on the AG&E system because of the larger air space available above the oil, the larger air space aiding in reducing the maximum tank pressure developed during high-capacity interruptions.

The breaker is equipped with a contact structure designed to handle the momentary and 4-second currents required by the higher interrupting capacities. The stationary contact assembly is of the sliding contact design consisting of six separate contact fingers arranged in a cluster such that arcing occurs on the front faces of the contact instead of the normal current-carrying surfaces. The moving contact is a round, hard-drawn copper bar with a combined contact and arcing tip attached to the engaging end of the blade. A sintered silver-tungsten alloy is used as the contact material for both the stationary and moving contacts. Fig. 5 is a schematic diagram showing the current path through the breaker and Fig. 6 is a view of the stationary and moving contact arrangement for one bushing position.

Fig. 7 shows details of the stationary contact structure. The interrupting elements are fiber baffles and are contained in rolled, paper-base phenolic tubes mounted horizontally at each contact position as shown in Fig. 8. The top interrupter accomplishes interruption by means of self-generated oil flow and the center and lower interrupters function as a unit; the lower interrupter acts as a pressure generating device and provides oil flow for the center interrupter.

To obtain performance data on a new resistor design during high-capacity fault interruptions, the interrupters of pole 3 of the test breaker were equipped with a 1,200-ohm linear resistor connected between the top and center contact assembly. The center tap of the resistor unit is connected to a probe located near the end of the top interrupter. The performance of the resistor-equipped interrupters in switching lines at higher voltages has been determined by previous field tests but not under fault conditions as severe as proposed for this series of tests. The resistor design is described in another AIEE paper.[2]

Test Program and Testing Procedure

Short-circuit tests were carried out on two Saturdays, June 26 and July 3; line-dropping tests were made on Sunday, June 27. The first Saturday was devoted to testing with interrupting currents from 2,000 up to 13,400 amperes, while on the second Saturday the currents ranged between 15,000 and 27,600 amperes. A summary of the number and character of tests and the maximum fault mva interrupted on the different setups is given in Table II.

To assure smooth and rapid progress in carrying out these tests a detailed memorandum on the necessary switching operations was prepared by the Operating Division. Prior to each day of testing

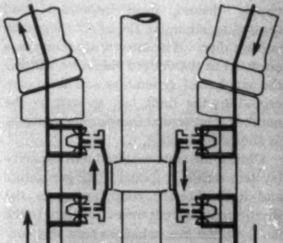

Fig. 5. Current path through test circuit breaker

Fig. 6. Arrangement of stationary and movable contacts

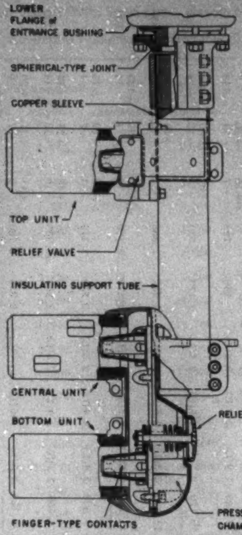

Fig. 7. Details of stationary contact structure

Fig. 8. Interrupter shielding

the final schedule was decided upon and a tentative time set for each test. On both June 26 and July 3 the tests were consistently ahead of the schedule. The actual time for running off the 31 short-circuit tests amounted to only 10 hours 11 minutes. Oil handling and inspection of contacts between tests on these 2 days required an additional 7 hours.

Visual observation of circuit-breaker performance was possible from two locations outside the fence of the switchyard. A public-address system had been installed to announce the type, estimated duty, and exact time of each test, as well as to communicate preliminary results obtained from oscillograms.

Standard close-open–15-second–close-open duty cycles, being of little significance in actual operation, were not included in the test program except as part of the normal and more severe AG&E reclosing duty cycle, open-close-open–15 seconds–close-open–150 seconds–close-open. The reclosing time on all open-close operations was slightly less than the standard 20 cycles. A plan to reduce it to 15 cycles could not be carried out be-because of lack of time to make the necessary adjustments.

The operating sequence of the test and backup breaker was controlled by means of an adjustable cam switch. On straight opening operations and the first opening of a reclosing operation, the trip impluse to the test breaker was initiated by the cam switch. The second opening of a reclosing operation was initiated by instantaneous relays. For backup protection, both the test and backup circuit breakers were provided with time-delay overcurrent relays, set to trip about 2 cycles after a normal interruption. On straight opening operations, the backup breaker was also tripped by the cam switch. In an attempt to obtain the highest recovery voltage rate possible during this series of tests, for system setup 1, which is characterized by an exceptionally small decrement of the d-c component of the short-circuit current, the cam switch was adjusted to delay tripping of the test breaker to provide as symmetrical a current as possible at the time of interruption.

Since it was desirable to check breaker performance under normal operating conditions, no attempt was made to score exceptionally high interrupting duties by large amounts of pretripping, as has often been practiced in field and laboratory tests. Such practice requires interruption to occur at the end of the first major current loop and is nearly always accompanied by a considerable decrease in severity. With the exception of test 12A, the cam switch was adjusted to initiate test breaker tripping similar to that normally expected of an instantaneous relay. For test 12A, the test breaker was pretripped approximately 0.2 cycle. During some of the heaviest test duties the current at contact parting time was from 43.5% to 49.5% asymmetrical, which

Table II. Test Summary

System Setup No.	No. of 3-Phase Ungrounded Faults: Open	Open-Close-Open	Maximum Mva 3-Phase Basis	% Asymmetry at Maximum Fault	No. of 1-Phase Grounded Faults: Open	Open-Close-Open	Open-Close-Open–15 Seconds–Close-Open–150 Seconds–Close-Open	Maximum Mva 3-Phase Basis	% Asymmetry at Maximum Fault
1	3	1	918	100	6			1,050	78
2	2	2	2,985	63	6			3,350	58
3	2	1	4,930	58	2			5,050	47.5
4	1	1	5,490	55	2	1	1	6,900	49.5
Total no. of tests	8	5			16	1	1		

Table III. 138-Kv Short-Circuit Tests at Philip Sporn Plant; Results of 3-Phase Ungrounded Faults

Equipment Tested: RHE-78 138-Kv 1,200-Ampere Oil Circuit Breaker. Phase 1: Oil Circuit Breaker Pole 3, Standard Interrupters, Equipped With Resistors. Phase 2: Oil Circuit Breaker Pole 2, Standard Interrupters. Phase 3: Oil Circuit Breaker Pole 1, Standard Interrupters

System Setup and Date	Test No.	Time	Oil-Circuit-Breaker Operation	Symmetrical RMS Amperes			% Asymmetry			Total Rms Amperes			Interrupting Time, Cycles			3-Phase Mva		Tank Pressure, Pounds per Square Inch			Recovery Rate, Volts per Microsecond
				Phase 1	Phase 2	Phase 3	Phase 1	Phase 2	Phase 3	Phase 1	Phase 2	Phase 3	Phase 1	Phase 2	Phase 3	Symmetrical	Asymmetrical	Phase 1	Phase 2	Phase 3	
June 26, 1954 Setup 1	1	7:06 a.m.	open	2,000	2,000	2,115	9	50	33	2,010	2,450	2,330	2.7(L)	3.4(L)	3.4(L)	500	610	+67 −10	+59 −14	−14	2,000
	1R1	7:10	open	2,000	2,000	2,115	17	50	26	2,055	2,450	2,250	2.4(L)	3.2(L)	3.2(L)	500	610	+23 −7	+59 −14	−14	2,000
	2	7:14	open (1)	2,080	2,000	2,115	82	25	55.5	3,180	2,120	2,720	2.1(L)	2.6(S)	2.6(S)	520	795	+12 −2.5	+24 −14	+20 −14	
			close-open (2)	2,080	2,125	2,115	77.5	100	17.5	3,080	3,675	2,180	2.4(L)	3.2(L)	3.2(L)	530	918	+20 −7	+59 −14	+20 −14	
	2R1	7:15½	open	2,040	2,000	2,115	34.5	19	63	2,265	2,070	2,835	1.9(L)	3.2(L)	3.2(L)	530	708	+15 −7	+40 −14	−14	
June 26, 1954 Setup 2	5	3:00 p.m.	open	8,920	8,680	8,690	30	10	43	9,680	8,750	10,120	2.5(S)	2.5(L)	2.4(L)	2,170	2,530	+67 −10	+60 −13	−14	1,000
	5R1	3:25	open	8,920	8,900	8,890	63	7	53	11,950	8,940	11,110	2.3(L)	2.5(S)	2.5(L)	2,230	2,985	+75 −10	+40 −13	+110 −14	330
			open (1)	9,090	9,320	8,690	40	14	57	10,400	9,480	11,160	2.6(L)	2.2(S)	2.6(L)	2,170	2,790	+95 −10	+35 −14	+130 −14	1,000
	6	3:40	close-open (2)	8,720	8,900	8,690	17	30	19	8,960	9,660	9,000	2.4(L)	2.4(L)	2.3(L)	2,225	2,410	+12 −1	+29 −7	+15 −4	
			open (1)	8,720	9,320	8,690	29	55	33	9,420	11,830	9,560	2.2(S)	2.6(L)	2.6(L)	2,330	2,955	+45 −10	+28 −13	+43 −14	250
	6R1	3:55	close-open (2)	8,915	9,100	9,310	39	14	46.5	10,180	9,250	11,130	2.3(L)	2.6(L)	2.6(L)	2,325	2,780	+41 −7	+24 −7	+20 −9	
July 3, 1954 Setup 3	7	8:10 a.m.	open	14,690	15,390	15,480	20.5	16	39	15,280	15,770	17,720	2.15(S)	2.0(L)	2.15(S)	3,870	4,430	+77 −14	+33 −14	+20 −12	667
	8	8:30	open	15,220	15,680	15,480	40	10	50	17,430	15,830	18,960	2.1(L)	2.4(L)	2.4(L)	3,870	4,740	+114 −13	+33 −14	+72 −14	330
			open (1)	15,220	15,390	15,220	58	34.5	24	19,720	17,070	16,060	2.5(L)	2.15(L)	2.5(L)	3,805	4,930	+132 −12	+40 −14	+55 −14	
	8R1	8:55	close-open (2)	14,690	15,100	14,960	0	45.5	55	14,690	17,900	19,000	2.5(S)	2.5(L)	2.3(L)	3,740	4,750	+15 −0	+40 −14	+10 −7	
July 3, 1954 Setup 4	13	3:03 p.m.	open	17,300	18,500	17,800	55	45.5	13	21,960	21,750	18,100	2.4(L)	2.15(L)	2.4(L)	4,325	5,490	+205 −14	+60 −14	+90 −11	667
			open (1)	17,300	18,500	17,800	43	0	48	20,150	18,700	21,450	2.15(L)	2.4(L)	2.4(L)	4,450	5,360	+132 −10	+127 −14	+130 −13	330
	14	3:25	close-open (2)	17,300	18,500	17,800	22	45.5	18	18,080	21,750	18,330	2.6(L)	2.6(L)	2.3(L)	4,625	5,435	+40 −8	+29 −7	+7 −2	

Table IV. 138-Kv Short-Circuit Tests at Philip Sporn Plant, Results of Single-Phase-to-Ground Faults

Equipment Tested Same as for Table III

System Setup and Date	Test No.	Time	Oil-Circuit-Breaker Operation	Phase Tested	Symmetrical Rms Amperes	% Asymmetry	Total Rms Amperes	Interrupting Time, Cycles	3-Phase Mva Symmetrical	3-Phase Mva Asymmetrical	Tank Pressure, Pounds per Square Inch	Recovery Rate, Volts per Microsecond
June 26, 1954 Setup 1	3A	8:26½ a.m.	open	1	2,685	29	2,900	2.1(S)	670	725	+6 −1	1,700
	3AR1	8:28	open	1	2,685	65.5	3,660	2.0(L)	670	915	+15 −7	1,300
	3AR2	8:35	open	1	2,685	38.5	3,050	2.0(L)	670	760	+15 −5	
	3B	9:30	open	3	2,820	33	3,100	2.9(L)	705	775	+43 −14	2,600
	3BR1	9:32	open	3	2,820	0	2,820	3.0(S)	705	705	+35	2,600
	3BR2	9:36	open	3	2,820	78	4,200	2.6(S)	705	1,050	+20	
June 26, 1954 Setup 2	4B	1:06 p.m.	open	3	9,720	28	10,450	2.0(L)	2,430	2,610	+43 −14	667
	4BR1	1:14½	open	3	9,930	50	12,160	2.1(L)	2,480	3,040	+110 −14	667
	4BR2	1:20	open	3	9,720	19	10,060	2.3(S)	2,430	2,510	+43	
	4A	1:43½	open	1	10,000	45	11,850	2.3(L)	2,500	2,960	+115 −10	667
	4AR1	1:45½	open	1	10,370	58	13,400	2.0(S)	2,590	3,350	+12 −6	500
	4AR2	1:53½	open	1	10,180	53	12,750	2.3(S)	2,540	3,180	+67 −9	
July 3, 1954 Setup 3	9A	7:10 a.m.	open	1	16,280	28	17,500	2.25(S)	4,070	4,375	+77 −12	667
	9B	7:36	open	3	16,770	47.5	20,210	2.4(L)	4,190	5,050	+72 −14	667
July 3, 1954 Setup 4	11A	1:45 p.m.	open	1	21,530	44	25,300	2.1(L)	5,380	6,325	+114 −18	500
	12A	2:11	open (1)	1	22,600	49.5	27,600	2.0(L)	5,650	6,900	+85 −18	approximately 330
			close-open (2)	1	21,180	26	22,530	2.4(S)	5,295	5,630	+41 −11	
	11B	2:35	open	3	22,060	12	22,400	2.05(S)	5,510	5,600	+43 −14	500
			open (1)	2	22,730	0	22,730	2.4(S)	5,680	5,680	+155 −14	
			close-open (2)	2	22,320	24	23,550	2.3(L)	5,580	5,885	+14 −8	
	15	4:00	15 seconds close-open (3)	2	22,320	43.5	26,130	2.0(L)	5,580	6,530	+45 −14	
			150 seconds close-open (4)	2	22,320	24	23,560	2.0(L)	5,580	5,890	+50 −14	

is normal for 3-cycle interruption of a short-circuit current that is fully offset at its inception. Initiating the fault at random with respect to the current wave produced also a few wholly symmetrical interruptions, some in the highest current range. With the exception of test 15, all single-phase-to-ground tests were made alternately on pole 1 and pole 3 in order to determine the comparative performance of the standard interrupters and the interrupters equipped with resistors.

Line-dropping and line-charging tests were made first on a 58-mile section between the Philip Sporn Plant and Portsmouth and then, after adding to it the Portsmouth-Trenton section, on a total length of 157 miles. All tests were 3 phase and the normal charging currents were 25 and 72 amperes respectively.

Instrumentation

Fault Tests

Two 7-element magnetic oscillographs were used to record fault currents, bus voltages, test circuit-breaker travel, tank pressures, and d-c closing and tripping impulses. Four additional portable oscillographs, as well as the automatic station oscillograph, recorded ground

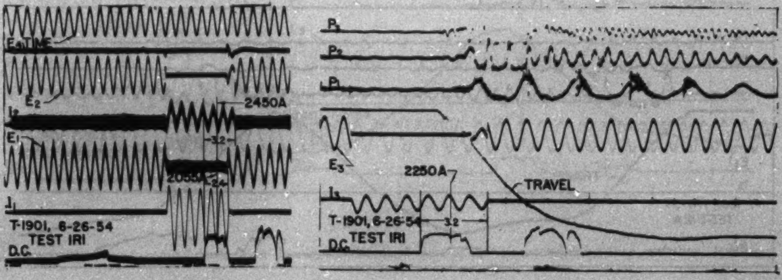

Fig. 9. 3-phase ungrounded fault, opening operation, test 1R1

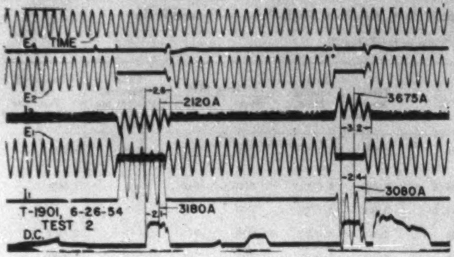

Fig. 10 (left). 3-phase ungrounded fault, open-close-open operation, test 2

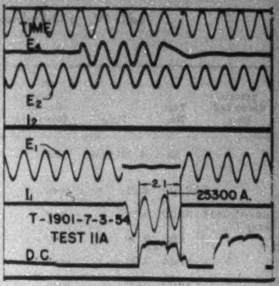

Fig. 11 (right). 1-phase line-to-ground fault, opening operation, test 11A

potentials, and relay, potential device, and autotransformer performance.

Bus voltages to ground were measured by the existing 138-kv potential transformer connected to bus no. 2. Fault-bus-to-ground voltage during 3-phase ungrounded faults was measured by a 132-kv potential transformer. Fault currents were measured by means of three special 4,000/5 ratio bushing-type current transformers located in the test breaker. Test breaker travel was measured by an electrical recorder located on pole 1.

Tank pressures were measured by means of electromechanical pressure transducers located on each of the three poles of the test breaker. Each transducer was associated with a preamplifier and a d-c amplifier for recording with the magnetic oscillograph. In addition to the electromechanical pressure transducers, a mechanical peak pressure indicator was located on each pole of the test breaker.

A cathode-ray oscillograph with an associated high-speed drum-type camera was used for recording recovery voltages across the contacts of either pole 1 or 3 of the test breaker. The potential was obtained from capacitor voltage dividers located at the capacitance taps of both bus-side and line-side bushings.

LINE-DROPPING TESTS

Two 7-element magnetic oscillographs were used to record line-charging currents, line voltages to ground, bus voltages to ground, and closing and tripping impulses. Line-charging currents were measured by standard 1,200/5 ratio bushing-type current transformers located in the test breaker. Bus voltages were measured by the existing 138-kv potential transformer connected to bus no. 2. Line voltages were measured by means of capacitor voltage dividers located at the bushing capacitance taps on the line side of the test breaker and the associated d-c amplifiers for recording with the magnetic oscillograph.

For instrumentation purposes, the test circuit-breaker ground at the test site was selected as the reference ground and all control and instrument cables were connected at the control site to terminal

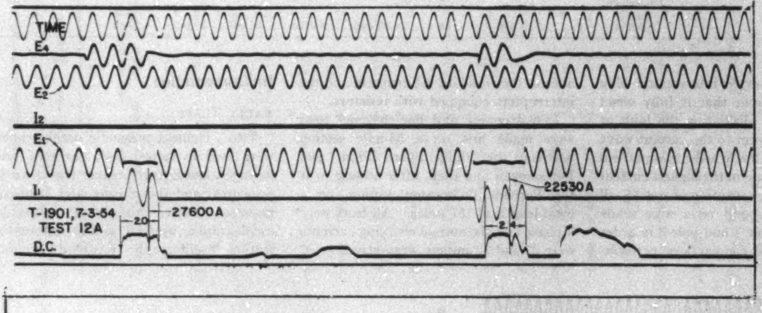

Fig. 12. 1-phase line-to-ground fault, open-close-open operation, test 12

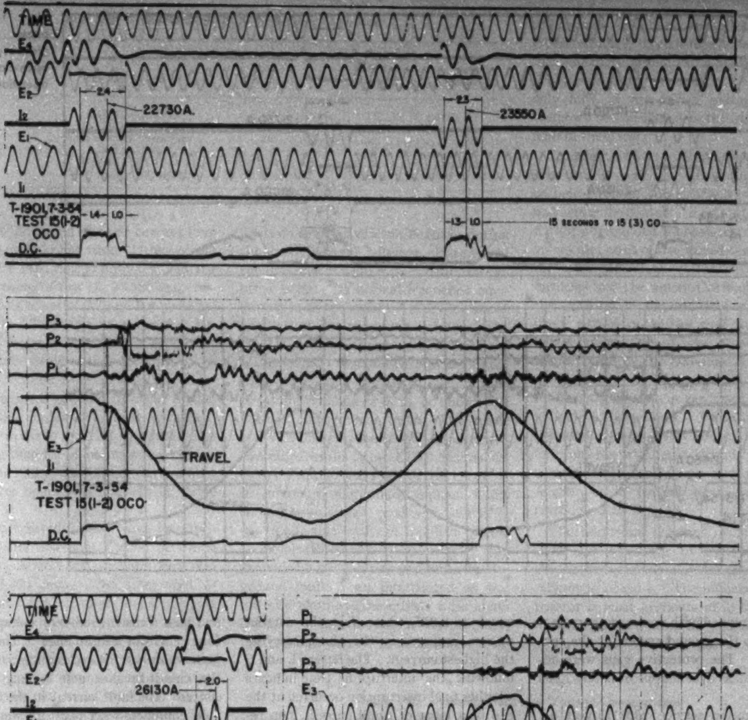

Fig. 13. 1-phase line-to-ground fault, open-close-open–15-second–close-open–150-second–close-open operation, test 15

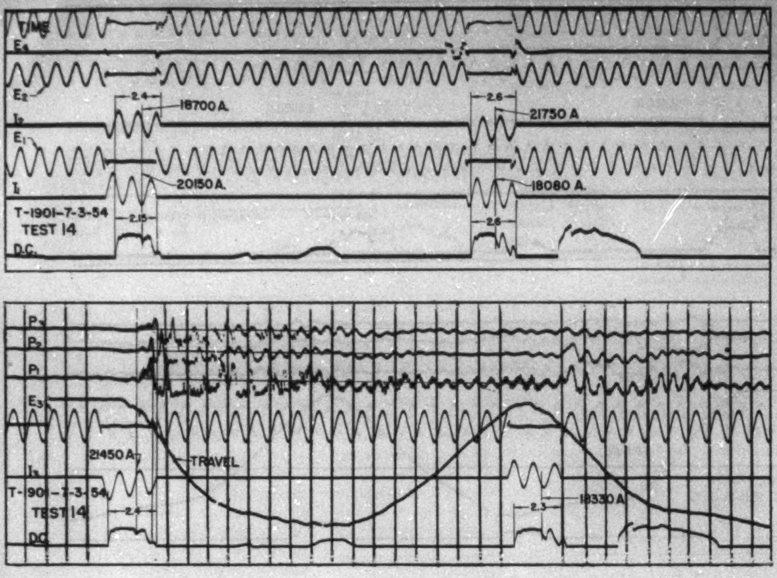

Fig. 14. 3-phase ungrounded fault, open-close-open operation, test 14

blocks equipped with protective gaps connected to the ground system at the control site. The protective gaps were adjusted to flash over at approximately 1,000 volts.

The station service 230/115-volt a-c supply is operated with one corner of the delta-connected transformers grounded, and since interconnected instruments were located both at the test site and at the control site it was necessary to provide an isolated power supply. Two distribution transformers were connected back to back as isolating transformers with an insulation level of 2,400 volts.

A d-c to a-c inverter was operated from the station battery to provide 115 volts a-c to the instruments and control devices requiring a completely reliable power source during the tests. This precaution especially was necessary during full-capacity 3-phase faults as station service power is normally obtained from bus no. 1 and/or bus no. 2.

Results of Short-Circuit Tests

The test data obtained from the oscillograph records is given in Tables III and IV. The 3-phase symmetrical and asymmetrical mva values listed in Tables III and IV were computed at the normal operating bus voltage of 145 kv and are equal to $0.25I$, where I is the current in rms amperes in the phase carrying the highest current. The letters L and S following the interrupting time indicate whether final interruption occurred at the end of a large or small current loop respectively. The percentage of asymmetry indicated in these tables is given for the current wave at the time the moving contact is flush with the end of the stationary contact and corresponds to 1.4 cycles after energizing the trip coil. For the purpose of determining arcing time, 1.4 cycles should be subtracted from the interrupting time. Typical oscillograms of short-circuit tests are shown in Figs. 9 through 14.

Interrupting Time

The 3-cycle interrupting time was exceeded only in 3-phase tests in the range of low currents (2,000 to 3,700 amperes) and high transient recovery voltage rates (one generator and no lines). The maximum value was 3.4 cycles and occurred in the circuit-breaker pole having no resistors. The fault current in the breaker pole equipped with resistors was interrupted well below 3 cycles under the same conditions.

Table V indicates the influence of the resistor on interrupting time, single-phase and 3-phase tests being consolidated. The influence of the resistor is most noticeable in the case of high recovery voltage rates and low current and is negligible at high currents.

Interrupting Duty

The maximum interrupted current was 27,600 amperes which occurred during single-phase-to-ground test 12A on the first opening of a high-speed reclosing operation. Interruption occurred in 2.0

Table V. Influence of Resistor on Interrupting Time

Current Range, Amperes	Interrupting Time, Cycles: With Resistor Avg.	Interrupting Time, Cycles: With Resistor Max.	Interrupting Time, Cycles: Without Resistor Avg.	Interrupting Time, Cycles: Without Resistor Max.	Recovery Rate Range, Volts per Microseconds
2,000 to 4,200	2.2	2.7	3.0	3.4	1,300 to 2,300
8,750 to 13,400	2.32	2.6	2.41	2.6	250 to 1,000
15,000 to 27,600	2.28	2.6	2.29	2.6	330 to 667

Table VI. Total Number of Circuit-Breaker Operations

Type Operation	Current Range	Pole 1 (Phase 3)	Pole 2 (Phase 2)	Pole 3 (Phase 1)
Opening	2,000 to 13,400	17	11	17
Opening	14,000 to 27,600	9	11	11
	Total opening operations	26	22	28
Closing	2,000 to 14,000	3	3	3
Closing	16,000 to 36,420	2	5	3
	Total closing operations	5	8	6

cycles at the end of a major current loop with 0.6-cycle arcing time. Other severe tests were 11A, 25,300 amperes, and the third opening of test 15, 26,130 amperes, with arcing times of 0.7 and 0.6 cycle respectively. Interruption occurred at the end of a major current loop in each case.

The duty cycle of test 15, open-close-open–15 seconds–close-open–150 seconds–close-open, was selected in order to test the breaker under the most severe reclosing duty in use in the AG&E system. The reclosing time for all immediate reclosing tests was 19.6 cycles. The total number of breaker operations is given in Table VI.

The integrated 3-phase mva for all 3-phase faults was 55,226 mva, of which 63% was above 4,000 mva and 29% was above 5,000 mva. The integrated 3-phase mva for line-to-ground faults was 35,120 mva for pole 3, 21,340 mva for pole 1, and 23,985 mva for pole 2.

It is recognized that the duty on a circuit breaker on closing in on a high-capacity fault can be as severe as the interruption of a high-capacity fault. The maximum making current of the backup breaker occurred on test 11A and was 35,400 rms amperes. The maximum making current of the test breaker occurred during the third operation of test 15 and was 32,800 rms amperes.

RECOVERY VOLTAGE

The normal-frequency (line-to-line) recovery voltage during the tests varied from 134 kv to 147 kv. The higher normal-frequency recovery voltages were obtained on single-phase tests during system setup 1 where an isolated machine was being used as the source of fault current. The lowest normal-frequency recovery voltages were obtained during 3-phase tests at maximum capacity, system setup 4, and occurred on the second opening of a high-speed reclosing operation, test 14.

The normal-frequency recovery voltage across the contacts of the circuit-breaker pole opening first during an ungrounded 3-phase fault is the sum of the line-to-ground recovery voltages E_1, E_2, or E_3, as the case may be, and the fault-bus-to-ground voltage E_4. The voltage E_4 appears on the magnetic oscillograms during the brief interval between clearance of the first pole and arc extinction in the two other poles. Its normal-frequency component is of the order of 40 kv, or about one-half of line-to-ground voltage. The total 60-cycle recovery voltage across the contacts of the first pole to clear amounted therefore to approximately 150% of line-to-ground voltage or 87% of line-to-line voltage during these tests. This result confirms and emphasizes the requirement contained in the latest AIEE Standards[3] that circuit breakers which are expected to interrupt ungrounded 3-phase faults should be so tested, or should have 87% of line-to-line voltage applied across terminals in case of single-pole tests. Had grounded 3-phase faults or double-line-to-ground faults been interrupted as was initially planned (these tests were abandoned in order to shorten the program) the voltage across circuit-breaker contacts would still have exceeded line-to-ground voltage, though to a lesser extent than during ungrounded 3-phase faults. Single-pole testing of circuit breakers with only 58% of line-to-line voltage must therefore be considered unrealistic in the light of these tests.

Transient recovery voltages were measured during single-phase-to-ground faults on pole 1 (phase 3) and pole 3 (phase 1), and across the contacts of pole 1 (phase 3) during ungrounded 3-phase tests. Crest values and rates of rise varied throughout the tests depending on the natural frequencies and the amount of damping in the external circuit and in the breaker itself. These quantities were influenced by the system setup, type of fault, and the presence of a 2,400-ohm resistor in pole 3 (phase 1) of the circuit breaker. Asymmetry at current zeros was another variable in these tests. Table VII gives transient voltage crests and rates of rise for every test with fault current for which a cathode-ray oscillogram was obtained. A number of typical oscillograms are reproduced in Fig. 15.

The horizontal columns in Table VII show the influence of system setup; the vertical columns show the effect of the resistor in phase 1. The influence of the resistor is most pronounced in the range of small currents such as prevailed with system setup 1. This is also the region of

Table VII. Transient Recovery Voltage Characteristics

Phase Measured	Phases Clearing		System Setup No.			
	First	Last	1	2	3	4
			Ungrounded 3-Phase Faults			
3	1*	2, 3	Test 1 182† 154 3100† 2000	Test 5R1, 6R1 91 91 330 250	Test 8 77 330	Test 14 79‡ 330§
			Test 1R1 200† 154 3100† 2000	—	—	—
3	2	1*, 3	—	Test 6 190 1000	Test 7 175 667	Test 13 142 667
3	3	1*, 2	—	Test 5 154 1000	—	—
			Grounded Single-Phase Faults			
*	1*	—	Test 3A, 3AR1 100 86 1700 1300	Test 4A, 4AR1 108 117 667 500	Test 9A 111 667	Test 11A, 12A 105‖ 500
3	3	—	Test 3B 89† 154 3000† 2300	Test 4B, 4BR1 104 100 667 667	Test 9B 107 667	Test 11B 111 500
			Test 3BR1 100† 158 3000† 2300	—	—	—

*Shunt resistor of 2,400 ohms in this phase.

†Reignition preceding final current zero.

‡Transient recovery voltage crest in % of normal line-to-ground voltage crest.

§Rate of rise in volts per microsecond.

‖Oscillogram for test 12A foggy; rate of rise approximately 330 volts per microsecond.

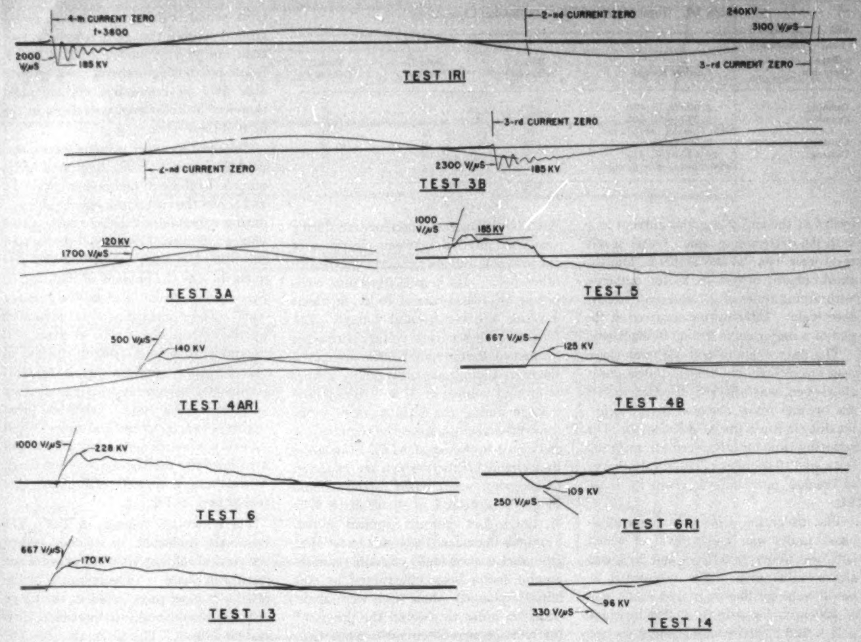

Fig. 15. Transient recovery voltage across one circuit-breaker pole during fault tests

highest recovery voltage transients, since no transmission lines were connected in this setup. For ungrounded 3-phase faults, tests 1 and 1R1, the transient in the unmodified pole, phase 3, consisted of a slightly damped oscillation having a single natural frequency of 3,600 cycles. The resistor-equipped pole, phase 1, always cleared first. Though no cathode-ray oscillograms were taken on this phase, the influence of the resistor is evident from the reduction it caused in interrupting time, which was from 0.5 to 1.3 cycles shorter than the interrupting time of phases 2 and 3. The transient voltage crest during these tests was 154 per cent of the normal line-to-ground voltage crest, and the recovery rate was 2,000 volts per microsecond. These values would have been still higher if the current had been wholly symmetrical at the final current zero.

The oscillograms for fault tests 1 and 1R1 show two short current pauses followed by reignition. The one preceding the last current zero produced a transient crest voltage of 240 kv, which equals 200% of normal line-to-ground voltage crest. The recovery voltage rate was 3,100 volts per microsecond. These higher transient values may be explained by the lesser damping of the shorter arc, and are believed to resemble more nearly the circuit transient recovery voltage unmodified by the breaker. The height and steepness of this transient is the more remarkable as it occurred after phase 1 had cleared, which left the recovery voltage divided between the breaker poles of phase 2 and phase 3.

Single-phase-to-ground faults with system setup 1 produced transient crest values and recovery voltage rates in phase 3 (no resistor) that were similar to those experienced during the corresponding ungrounded 3-phase tests when the resistor-equipped pole, phase 1, cleared first. However, if phase 3 had cleared first (there was no such 3-phase test) the transient in that phase would probably have exceeded the corresponding single-phase value by about 50%, as was the case in test 5 with system setup 2. The average frequency of the transient on single-phase tests was about 3,600 cycles as shown in Fig. 15, test 3B. The resistor-equipped pole, test 3A, Fig. 15, reduced the transient to a 100-kv crest voltage and 1,700-volt-per-microsecond recovery rate, and there were no previous reignitions. Interrupting time was from 0.5 to 1.0 cycles shorter than in the unmodified pole. The oscillations had not altogether disappeared, since the resistance was about twice the value required to make the transient aperiodic.

For faults made with system setups 2, 3, and 4, which are characterized by higher currents and connected transmission lines, the influence of the resistor was found to be negligible, as indicated by a comparison of the fourth and fifth horizontal columns in Table VII. Test 5 was an ungrounded 3-phase fault where the measured phase 3 was the phase to clear first (the only test of its kind). It produced a transient crest voltage and recovery voltage rate about 50% higher than those of the corresponding single-phase faults. There was also the expected 50% increase in normal-frequency recovery voltage. Crest values and recovery rates measured in phase 3 when that phase and phase 2 cleared last, as shown in the top column of Table VII, were slightly less than the corresponding single-phase values, which was also to be expected. The test data contained in the second horizontal column of Table VII with phase 2 clearing first must be considered anomalous. Because of the unbalance caused by the resistor-equipped pole, the associated unmodified pole was subjected to higher voltage transients than would prevail under normal conditions.

An interpretation of the test results indicates that the circuit breakers at the 138-kv switchyard of the Philip Sporn Plant are subjected to the following transient recovery voltage conditions:

1. Transformer circuit breakers are required to interrupt up to 1,000 mva on the occurrence of a bus fault. The natural frequency of the recovery voltage transient will be somewhat higher than the 3,600 cycles observed during the tests because there will be no bus sections connected to the transformer side of the breaker. Transient crest voltage and recovery voltage rate are expected to reach 250% of normal line-to-ground crest voltage and 3,600 volts per microsecond respectively.

These values apply to the recovery voltage transient across the contacts of the first pole to clear an ungrounded 3-phase bus fault. Higher recovery voltage transients occur at current zeros preceding final interruption. The transients may be different for other conditions than those existing at the Philip Sporn Plant, which has a 2,300-foot transmission line connecting transformer and circuit breaker.

Table VIII. Tank Pressures Recorded by "Lead Pellet" Pressure Indicator

Test No.	Phase Tested	Tank Pressure, Pounds per Square Inch: Phase 1	Phase 2	Phase 3
4B	3			170
4BR1	3			115
4BR2	3			80
4AR2	1	130		
5	3-phase	105	210	80
5R1	3-phase	180	180	125
9A	1	65		
9B	3			125
7	3-phase	80	80	80
11B	3			150
13	3-phase	125	130	35

2. Transmission-line circuit breakers are subjected to a heavily damped oscillation attaining crest values up to 160% of normal line-to-ground crest voltage in the case of an ungrounded 3-phase fault. Recovery voltage rates may be expected to range from 750 to 1,000 volts per microsecond, depending on the actual system setup.

In the unlikely event of the breaker clearing a line fault with all other transmission lines disconnected, much higher values of transient recovery voltage are to be expected.

3. Transient crest values and recovery voltage rates on transformer circuit breakers can be greatly reduced by the addition of suitably dimensioned shunt resistors to the interrupters.

TANK PRESSURE

The peak values of positive and negative tank pressures measured during each test with the electromechanical transducers are recorded in Tables III and IV. The maximum recorded tank pressure of approximately 200 pounds per square inch occurred in pole 3 (phase 1) during test 13 during a three-phase ungrounded fault. The highest average pressure for all three poles on a 3-phase fault occurred during test 14 and was approximately 130 pounds per square inch. Test 14 produced the most noticeable ground shock observed throughout the tests.

One problem associated with the use of the electromechanical transducer is that of mechanical shock sensitivity. This factor must be recognized in interpreting the pressure records during interruption. An indication of the magnitude and duration of the mechanical shocks affecting the transducers is given by the pressure records of poles 1 and 3 in Fig. 3, test 15, which carried no current. Pole 2 transmitted shock to the two other poles by way of the mechanical linkage and the foundation. Some of the oscillatory fluctuations are probably due to vibrations of the soil and tank structure. The electromechanical transducers were designed to have normal sensitivity in the range of all negative pressures and in the positive pressure range up to approximately 50 pounds per square inch. Above 50 pounds per square inch the the positive pressure sensitivity has been reduced to facilitate recording up to 250 pounds per square inch with the same

Table IX. Line-Dropping Tests at Philip Sporn Plant, June 27, 1954

Equipment Tested Same as for Table III

Test Setup	Test No.	Time	Interrupting Time, Cycles*: Phase 1	Phase 2	Phase 3	Restrikes	% Voltage Due to Restrike: E1	E2	E3	% Crest Voltage Left on Line: E1	E2	E3
Sporn-Portsmouth line. 58 miles. Charging current 25 amperes. Bus voltage 145 kv. Crest voltage to ground 118.5 kv. See Note 1.	L1	10:55 a.m.	2.5	1.85	1.6	1, phase 2		139		73	139	86
	L2	10:57	3.0	1.3	1.55	none				40	158	119
	L4	11:04	3.2	1.5	1.4	none				67	116	79
	L5	11:08½	3.1	1.4	1.7	none						
	L6	11:11	1.65	1.5	1.4	none						
	L7	11:17	2.7	1.55	1.4	none						
	L8	11:20	3.2	1.6	1.3	none						
	L10	11:26½	3.2	1.5	1.4	none						
	L11	11:30½	2.7	1.6	1.4	none						
	L12	11:33	3.0	1.8	1.55	none						
	L13	11:40	3.1	1.4	1.3	none						
	L14	11:43	3.0	1.8	1.6	none						
	L15	11:46½	2.8	2.1	1.5	1, phase 2		160		68	160	150
	L16	11:48	3.0	1.7	1.5	none						
Sporn-Portsmouth-Trenton line. 157 miles. Charging current 72 amperes. Bus voltage 145 kv. Crest voltage to ground 118.5 kv. See note 2.	L17	12:42 p.m.	3.2	1.4	1.7	none				37	143	115
	L18	12:45	3.4	1.5	1.9	none				28	134	110
	L20	12:52	3.0	2.65	1.55	2, phase 2		220 236	163	28	130	100
	L21	12:57	3.1	2.15	2.85	1, phase 2 2, phase 3		134	214 192	39	70	26
	L22	1:00	3.3	1.5	1.8	none						
	L23	1:06	3.4	1.5	1.9	none						
	L24	1:10	3.3	1.5	1.7	none						
	L26	1:22½	3.0	2.65	1.6	2, phase 2	121	202 202	159	72	121	100
	L27	1:28	3.25	1.9	1.8	none						
	L28	1:30½	2.4	1.6	1.45	none						
	L29	1:40	3.0	1.7	1.5	none						
	L30	1:48	3.2	2.2	1.6	1, phase 2	180	152	128	8.5	117	128

*Interrupting time is total time including reignitions and restrikes and resistor current of phase 1.
Note 1. Tests L3 and L9 were closing operations.
Note 2. Tests L19, L25, and L31 were closing operations

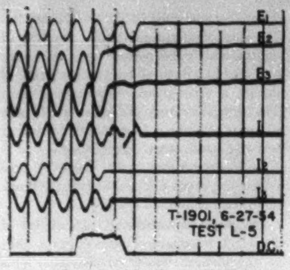

Fig. 16. 58 miles, test L-5

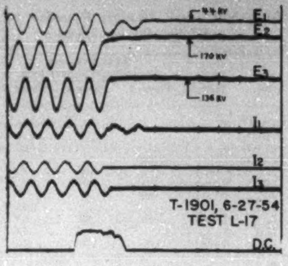

Fig. 18. 157 miles, test L-17

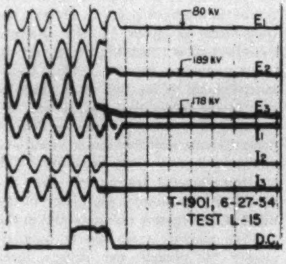

Fig. 17. 58 miles, test L-15

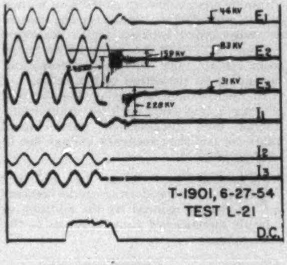

Fig. 19. 157 miles, test L-21

Figs. 16–19. 3-phase line-charging current interruptions

I_1, I_2, I_3: Phase 1,2,3 current
E_1, E_2, E_3: Phase 1,2,3 line-side-to-ground voltage

transducer. The undamped frequency of the transducer is 2,000 cycles per second which insures more than adequate frequency response for pressure surges up to 1 millisecond wave-front rise time.

The oscillograms show that after final arc extinction the tank pressure falls rapidly from its highest positive peak to a smaller negative peak which, in most cases, is followed immediately by another high positive peak. If restrikes after final interruption are to be avoided, the circuit breaker must be able to cope with the decrease in dielectric strength in the arc path caused by the negative tank pressure.

Some idea of the top air pressure and flow velocity through the vent pipe can be obtained from observations made on pole 3 of the test breaker during the higher capacity tests. The vent pipe of pole 3 overhung the foundation pad and the gas blast was sufficient to dig a 4-inch-deep hole in the 1-inch loose gravel surrounding the pad by the end of the tests. The entrance of the vent pipe on the pole top has a simple baffle to eliminate oil being forced through the vent pipe during interruption. However, some oil is trapped by the baffle, and during a high-speed reclosing operation the trapped oil is forced out of the vent pipe. It was noted during the tests that on each of the higher capacity reclosing tests approximately a cup of oil was lost through the vent pipes.

In addition to the electromechanical pressure transducer used for transient pressure recording, a peak pressure mechanical transducer was used. The mechanical transducer consists of a piston having a 90-degree conical point which penetrates a lead pellet, the depth of penetration being a function of the pressure acting on the piston. For single pressure surges of a rate of rise corresponding to that produced by 1/2 cycle of a 60-cycle wave, the peak pressure recorded by the mechanical transducer agrees quite closely with that recorded by the electromechanical transducer. As the rate of rise of the pressure surge increases, the accuracy of the mechanical transducer decreases because of the effect of inertia of the mechanical piston. Repetitive pressure surges or alternating surges cause the lead pellet to receive multiple impacts from the piston, and indicated pressures are greater than the actual magnitudes.

The time schedule during the tests did not permit changing lead pellets after each test and many of the tests were reclosing tests. Peak pressures recorded under these conditions have not been included in the summary of the mechanical pressure transducer record given in Table VIII.

Results of Line-Dropping Tests

The test data obtained from the oscillograph records are given in Table IX, and include interrupting time, restrikes, % voltage to ground due to restrikes, and % crest voltage left on the line upon completion of charging current interruption. Voltage values are entered in Table IX for all tests during which restrikes occurred and for typical tests which were restrike-free. Typical oscillograms are shown in Figs. 16 through 19.

INTERRUPTING TIME

The interrupting time indicated in Table IX is the total time of interrupting both charging current and resistor current; it also includes all reignitions and restrikes. Table X is a summary of the charging-current interrupting time in cycles.

For evaluation of arcing time during charging-current interruption, contact-parting time obtained with the low-voltage timing tests should be used. The design of the tulip-type, sliding contact assembly is such that the conical end of the moving contacts part contact with the curved arcing surface of the stationary contacts approximately 0.6 inch before the end of the moving contact is flush with the end of the stationary contact assembly. The contact-parting time for charging-current interruptions is 1.2 cycles and should be subtracted from the indicated interruption times to obtain the arcing time. During charging-current interruption, at the time the charging

Table X. Charging Current Interrupting Time, Cycles

System Connection	Pole 1, Phase 3		Pole 2, Phase 2		Pole 3, Phase 1	
	Avg	Max	Avg	Max	Avg	Max
58-mile line	1.47	1.70	1.61	2.10	2.87	3.20
157-mile line	1.78	2.85	1.75	2.65	3.13	3.40

Fig. 20 (left). Interrupters and movable contacts after final test

Fig. 21 (right). Typical condition of stationary and movable contacts after final test

current is zero the system voltage is at crest value, the line has been charged to the same value, and no voltage difference exists between the stationary and moving contacts. Depending on the value of the current wave at the instant of contact parting, very short arcing time can occur. This is evident from the 0.1-cycle arcing time for tests L2, L8, and L13. A sufficient number of tests was made on a 3-phase basis so that the contact-parting time covered the complete range of possible parting times during 180 electrical degrees and insured charging-current interruption under all conditions. From past experience with breakers of the same design as the test breaker, it has been noted that the point on the current wave at which contacts part has no discernible influence on the performance of the breaker in charging-current interruptions.

Charging-Current Interruption Performance of Pole 3

The influence of resistors in pole 3 was most noticeable in the case of charging-current interruption. No restrikes occurred and no overvoltages were produced other than that induced by restrikes on phase 2 during tests L30 and L26. Current reignition through the resistor occurred on almost all tests and is normally expected for this design. In all cases the line is left charged at a voltage much less than crest value. Since the remaining poles were not modified by resistors, the voltage swings of phase 1 due to resistor current reignition induced corresponding voltage swings, but of reduced magnitude, in the other two phases, and caused the lines of phase 2 and 3 to be left at a higher crest voltage than normal.

Charging-Current Interruption Performance of Poles 1 and 2

The present series of tests confirmed the performance of the standard interrupters as demonstrated by previous tests and operating experience. Infrequent restrikes occur but do not produce serious overvoltages or damage to connected equipment.

One restrike occurred during test L1 and L15 while switching 58 miles of line, both on phase 2, and produced voltages of 139% and 160% respectively. In switching 157 miles of line, restrikes occurred during tests L20, L21, L26, and L30. The maximum voltage of 236% was produced by two restrikes on phase 2 during test L21.

Test Circuit-Breaker Inspection

At the conclusion of tests scheduled for system setup 1, it was considered advisable to inspect pole 3 of the test circuit breaker as the resistor installation was of an experimental nature. Results of the inspection indicated no change in the installation and the tests scheduled for setup 2 were begun. Oil samples from pole 3 tested 34 kv. No inspection was considered necessary upon the completion of tests scheduled for setup 2 prior to the line-dropping tests.

Inspection of the contacts and interrupters of all three poles was made Monday, June 28. The stationary and moving contacts showed very slight erosion and required no dressing. The interrupter baffle plates also indicated very slight erosion and required no replacements. Oil samples tested 24 kv.

Upon completion of tests scheduled for setup 3, the contacts and interrupters of

TOP
CENTER
LOWER

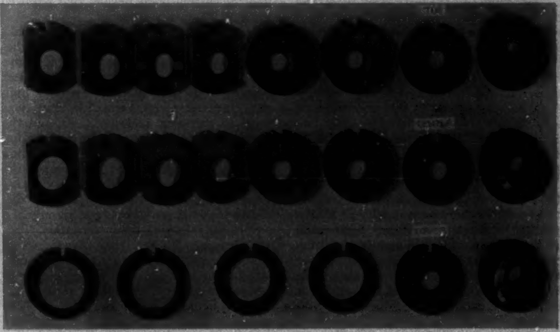

Fig. 22. (Left) stationary and movable contacts and (right) interrupter baffle plates disassembled after final test

all three poles were inspected. The contacts and baffle plates indicated more erosion than at the previous inspection but did not necessitate redressing or replacement before proceeding with the full-capacity tests on the same day.

An inspection of contacts and interrupters of all three poles was made Sunday, July 4, upon completion of the final tests. The stationary contacts were eroded slightly on the arcing surface but the normal current-carrying surfaces were in good condition and considered serviceable. The moving contacts were eroded on the conical arcing surface and the ends of the blade tips were eroded back approximately 1/16th inch. The normal current-carrying surfaces of the moving contacts were in good condition. Contact pressure between the stationary and moving contacts was normal. The interrupter baffle plates showed considerable erosion on the first three plates nearest the stationary contacts but were considered to be in sufficiently good condition so that further interrupting duty would be possible before replacement.

Carbonization of the oil in all three poles did not appear to be excessive. Oil samples tested 30 kv in pole 3 and 28 kv in poles 1 and 2 upon completion of all tests.

There appeared to be no great difference between the condition of contacts and interrupter baffle plates in each pole or between those associated with each bushing position. Fig. 20 shows the interrupters of pole 3 in place after final tests, Fig. 21 a typical condition of stationary contact assembly and moving contacts, and Fig. 22 the condition of stationary and moving contacts and interrupter baffle plates from bushing position 3 disassembled after final test. Parts from all other bushing positions were found in a similar condition.

Conclusions

1. A high-speed oil circuit breaker has been tested under maximum capacity fault conditions at the 132-kv switchyard of the Philip Sporn Power Plant. The test circuit breaker interrupted faults up to a maximum of 6,900 mva under the most severe system conditions with a minimum of system disturbance and within the rated interrupting time of 3 cycles.

2. The addition of low ohmic linear resistors to the interrupter assemblies reduces the interrupting time under system conditions giving low values of fault currents and high recovery voltage rates, and provides restrike-free operation during line-charging current interruptions.

3. The current through a transformer circuit breaker does not reach zero for several cycles after the inception of a fully offset bus fault; see Fig. 10. This condition, caused by an initially high a-c decrement and a low d-c decrement, justifies a small time delay in tripping transformer breakers so as to prevent possible damage to the circuit breaker.

4. Information was obtained on the normal-frequency and transient recovery voltage characteristics existing at a large power site under various fault conditions.

5. The condition of the contacts and interrupters upon completion of a test program involving a large integrated value of interrupted mva proves the design of the test breaker to be more than adequate from the standpoint of requiring a minimum of maintenance and replacement of parts.

6. The ease of interrupter and contact inspection and accessibility of all parts of the breaker is shown by the short time required for complete inspection during the progress of tests. This is an important factor in decreasing the outage time under operating conditions.

7. The advantages of field testing under conditions which duplicate actual operating conditions were brought forth during this series of tests in that the complete breaker was subjected to full-capacity faults and the over-all performance could be observed and analyzed. In laboratory testing, usually at reduced voltages and only upon a proportionate part of the interrupting assemblies, these conditions cannot be fully duplicated.

References

1. FIELD TESTS AND PERFORMANCE OF HEAVY-DUTY HIGH-SPEED 138-KV CIRCUIT BREAKERS—OIL AND AIR-BLAST, **Philip Sporn, Harry P. St. Clair.** *AIEE Transactions*, vol. 64, 1945, pp. 401–10.

2. DESIGN PROBLEMS AND FIELD TESTS CONCERNING CIRCUIT BREAKERS FOR SWITCHING LONG 230-KV LINES, **D. M. Umphrey, D. J. Marsden.** *AIEE Transactions*, vol. 74, pt. III, Aug. 1955 pp. 698–705.

3. TEST CODE FOR POWER CIRCUIT BREAKERS, *AIEE Standard No. C37.9*, Dec. 1953.

Discussion

C. J. Balentine (General Electric Company, Philadelphia, Pa.): The authors have presented a complete account of a set of field tests on a 138-kv circuit breaker, describing not only breaker performance but also the system setup and the instrumentation used during the tests. These tests produced a maximum duty of 6,900 mva on a breaker which was initially rated 5,000 mva. Based on these results and the initially assigned rating, what will be the new name-plate rating of the breaker? Throughout the tests, one pole of the breaker was equipped with shunting resistors but the other two poles were not. Do the test results indicate that the breaker should be equipped with resistors as standard accessories?

Reference is made in the paper to some 138-kv 10,000-mva breakers as follows: "The new breakers were purchased on the strength of single-pole factory tests made at full voltage and reduced interrupting current and at full current and reduced voltage up to the limit of available testing facilities. Though this kind of 2-part test is never a complete substitute for full-capacity tests, it was felt that satisfactory performance under field conditions could reasonably be predicted on the basis of such tests." Fig. 3 showing the test breaker on the site also shows the 138-kv 10,000-mva breaker used for backup protection during the tests. The rating of this breaker was not established with 2-part testing. Interrupting tests were made on it up to 50,000 amperes at 53.5 kv on a single interrupter. This voltage is much greater than that normally imposed on a 138-kv interrupter and the current is far beyond that required for a 10,000-mva rating.

It is stated that 78-inch diameter tanks are used instead of 64-inch diameters because the larger air space available above the oil aids in reducing maximum tank pressure. In spite of this, relatively high tank pressures were recorded, there was some oil throw on reclosing tests, and the blast of escaping gas during interruption dug a 4-inch hole in the gravel surrounding the pad. It would seem that during the interruption of even high-capacity faults there should be no oil throw and any discharge from the vent should consist only of a puff of gas following the interruption.

Conclusion 7 cites the advantages of field testing over laboratory testing. Actually field testing is only a supplement to laboratory tests. During field testing, the number of tests is always limited. The system setup is very inflexible as compared to laboratory testing facilities. It is not possible to make overvoltage tests in the field to establish design margins nor is it possible to make the many overcurrent tests required to determine the mechanical strength of interrupter structures.

Capacitance switching performance cannot be established on such relatively few tests. To adequately prove the suitability of a design for this type of service, many tests must be made with varying angles at relatively small increments of current over the entire capacitance switching range.

Field tests do a fine job of checking the performance of a breaker for a given set of conditions but they do not give the broad coverage required for general application to meet all kinds of service conditions.

A. E. Kilgour (Allis-Chalmers Manufacturing Company, Hyde Park, Mass.): It is only through the courtesy and co-operation of the utilities that any manufacturer can field-test anywhere near full interrupting capacity. Even when this opportunity to test in the field is available the interrupting capacities to date have not been near the larger circuit-breaker interrupting abilities. As an example, in this particular 138-kv 10,000-mva breaker test program, test values ranging from 54 to 69% of full capacity were realized. The field test program as conducted, however, serves well to illustrate the value of today's laboratory test procedures as practiced by manufacturers. Therefore, proper credit should be given to the good job of interpolating tests and the program that is being carried on to test breakers adequately in the laboratory.

It is an accepted fact that a resistor properly employed can reduce the possibilities of restrike and therefore can be considered as a contribution made by the breaker during interruption of the circuit. However, attention must be directed to the fact that the surge impedance of the line being interrupted by the breaker and the surge impedance from the generating source to the breaker are dictated by the system parameters and create the influence or possibility of restrike, over which the breaker directly has little or no control. The relative merits of condition to restrikes are ably presented in Dr. E. W. Boehne's paper.[1] This discussion is considered pertinent here because the present paper does not indicate whether this breaker will be furnished with or without a resistor as a standard item.

It is not understood why there should be such a variance in measuring contact-parting time. In the section entitled "Results of Short-Circuit Tests" 1.4 cycles of contact-parting time is given and in the section on "Results of Line-Dropping Tests" 1.2 cycles for contact is given. The variable is indicated to be due to the conical shape of the contacts. Our experience indicates that if a direct current is passed through these contacts during the testing adjustment period, our breakers, employing tulip bayonet contacts, give a very consistent contact-parting time, and are not directly dependent upon line-charging or interrupting-current value. It would appear to me that current magnitude should have little or no effect on the contact-parting time until after the contacts have parted and an arc has formed. These values as presented therefore appear to be inconsistent.

Conclusion 3 appears to be questionable. If the prime purpose of the breaker is considered to be protection, normally if any time delay is created it is to the detriment of the equipment which the breaker is attempting to protect. The exception to this is when through relaying sequence controlled time is for system stability or backup protection and therefore is in order.

Conclusion 4 is very interesting because comparatively little actual field data have been published regarding the rate of rise of recovery voltages during system interruption. It would certainly be advantageous to have more of this type of information available to the manufacturers, even though some papers which have been published showing the expected rate of rise of recovery voltages as indicated by board studies are of some value. However, there are considerable differences in R^3V magnitudes, depending upon the method of measurement. No mention has been made as to the particular method employed. From the data given, it appears that the slope from current zero was used. Is this correct?

The authors are to be congratulated for their fine presentation of an interesting breaker test story.

Reference

1. Traveling Wave Protection Problems—I. A Graphical Analysis with Special Application to the Switching of Lines and Cables, E. W. Boehne. *AIEE Transactions*, vol. 73, pt. III-B, Aug. 1954, pp. 920–28.

R. E. Friedrich (Westinghouse Electric Corporation, East Pittsburgh, Pa.): This paper, which describes direct field tests on a 138-kv circuit breaker to quite high values of current, is a definite contribution to the circuit-breaker art. Considering such variables as arcing time, interrupted current, degree of asymmetry of the current, and the size of the last half-cycle of current prior to interruption, it is evident from 3-phase test 14 that this breaker can be given a rating of 4,625 mva on a symmetrical basis or 5,435 mva on an asymmetrical basis. However, it does not appear to be a fair conclusion to state that greater amounts of fault power up to the maximum of 6,900 mva were interrupted under the most severe conditions. Certainly on test 12 involving a current of 27,600 amperes the arcing time was near the minimum of only 0.6 cycle. The tests at maximum kilovolt-amperes would be more conclusive had they been made under controlled conditions such as are available in a high-power laboratory, which permits tripping of the test breaker to give maximum arcing time with interruption occurring at the end of a large half-cycle of current.

It is interesting to compare the arc energy involved in phase 2 of the close-open operation on 3-phase test 14 involving the interruption of 21,750 amperes in 2.6 cycles with that involved in the opening operation on the single-phase test 12A in which 27,600 amperes were interrupted in 2.0 cycles. On both tests the last half-cycle of current was a large loop and the % asymmetry at contacts part approximately the same, 45.5% on the former and 49.5% on the latter. A simple graphical analysis assuming the same linearly increasing arc voltage for both tests shows the arc energy on the 21,750-ampere interruption to be more than three times that on the 27,600-ampere test. The lower current test can be considered to have been the more severe from the standpoint of mechanical shock. Likewise, since the arc energy is approximately proportional to the square of the arcing time, it would appear that test 14 was more severe than any of the tests which involved greater amounts of current.

Data obtained on field tests such as described in this paper are always a valuable supplement to but never can completely supplant design data obtained in the laboratory. Here conditions affecting the severity of the tests can be accurately and easily controlled, and the number and variety of tests which can be made are relatively unlimited without the pressure attendant upon keeping within limited time schedules.

The statement that the 78-inch-diameter tank was considered advisable for the higher interrupting duty expected on the AG&E system because of the larger air space available above the oil "which aids" in reducing the maximum tank pressure developed during high-capacity interruptions is of considerable interest, especially since the modern trend is to keep the oil content at a minimum value. One manufacturer, by the use of inverted surge chambers containing air and located at the lower end of the breaker tank, has been able to reduce both the tank diameter of a 13-kv 10,000-mva breaker to 62 inches and the maximum tank pressures during heavy fault interruptions.

Both the value and attendant disadvantages of using low-ohmic resistors are well known in the industry. It would be of interest to know whether the authors have concluded that they will be standard equipment on breakers of this and similar ratings.

J. E. Conner (Southern California Edison Company, Los Angeles, Calif.): The authors are to be congratulated on an excellent and very thorough report of their field test program. The extensive material presented is an invaluable contribution to the oil-circuit-breaker literature and is particularly significant at this time. With installed system capacities increasing rapidly, and breaker interrupting ratings now completely beyond the capabilities of any existing test facilities, it is particularly important that manufacturers and utilities co-operate, wherever system conditions permit, in staging tests of this nature. The information obtained from tests made under typical system conditions is impossible to obtain in any other way. These data serve to provide the circuit-breaker designer with the essential link required to correlate his developmental experiences with the requirements of actual field service. Considering the extended ratings presently being assigned to high-capacity oil circuit breakers on the basis of part pole tests, it is imperative that the designer have every available opportunity to proof-test the soundness of his over-all designs by actual system test.

The participating companies responsible for sponsoring this program are also to be complimented for their foresight in initiating a field test program of this magnitude. The amount of organization and preparation required to institute this type of test program is rather universally recognized and respectfully acknowledged. What is not so apparent is the intensive thought and study that must precede the final decision to subject an entire power system of this size to the shock and possible abuse of an extensive series of high-capacity fault-current interruption tests. This decision must be preceded by an awareness that all connected system apparatus is being tested as well as the circuit breaker itself. However, as the authors have pointed out, a great deal of valuable secondary information is accumulated which could not otherwise be obtained.

It has been a number of years since similar field tests on high-voltage oil circuit breakers were conducted on the Southern California Edison Company system. Therefore, the comments on this paper are based, not on recent testing experiences, but on a definite and continuing interest in the design and developmental progress in the circuit interruption field. In line with the general rapid expansion of the electric power industry, our company is also witnessing considerable increases in installed capacity with attendant requirements for oil circuit breakers of greater interrupting ratings at locations of large power concentrations. At the present time new breakers being purchased for installation on the 220-kv transmission system have an interrupting rating of 10,000 mva. Older breakers of lower interrupting ratings are being moved to points in the system where requirements are less severe. Some of these 10,000-mva breakers have been subjected to extensive testing in the manufacturer's laboratory, while others have not. In the latter case, these test facilities are unavailable to the breaker manufacturer.

As of this writing, the maximum short-circuit capacity of the 220-kv system is approximately 6,000 mva. At the present rate of growth, it is anticipated that this figure will reach 7,800 mva by January 1, 1957, and will approach the 10,000-mva figure within a period of 10 to 15 years. In order to prove that these recently purchased 220-kv 10,000-mva breakers are entirely adequate for the present and anticipated needs of the system, the Edison Company is contemplating a complete program of fault-current interruption and line-charging and -dropping tests in the near future.

It is particularly encouraging to note that the authors have investigated so thoroughly the rate of rise of transient recovery voltage at the time of circuit interruption. The recovery voltage data, for various circuit arrangements, presented in this report should be invaluable to the circuit-breaker designer and manufacturer. Since actual test rates of rise were measured for specific system conditions, this material should serve as an excellent guide in establishing reasonable values to be used in design testing in the laboratory.

As pointed out in this paper, it is general practice to conduct part pole tests on individual interrupters of a breaker pole by testing at full voltage and reduced interrupting current and then at maximum rated interrupting current and reduced voltage. The results of these tests are then extrapolated to produce an over-all interrupting rating for the complete breaker. The validity of this extrapolation of part pole test results is dependent upon maintaining uniform voltage distribution among interrupters at the maximum rates of rise of transient recovery voltage that are to be encountered in actual service. Once these rates of rise are known, and satisfactory voltage distribution among interrupters has been established for the complete breaker pole, it is important that similar rates of rise of transient recovery voltage be used in conducting interruption tests in the laboratory on individual interrupter elements. From the data presented in this paper it would appear that the maximum recovery voltage rates are associated with system conditions that produce relatively low fault currents. Fortunately for the development engineer, these conditions of high recovery voltage rates can be quite readily duplicated in the testing laboratory.

In reviewing the part of this paper dealing with instrumentation, it was noted that two apparently independent oscillographs were used to record the major test circuit and test breaker parameters. The increased labor of analysis with two separate oscillographic records for each test must be quite apparent, particularly when one notes that the two recording devices did not have a mutual timing or speed control arrangement. The use of a modern, multichannel magnetic oscillograph, with provisions for all measurement traces on a common time base, would have greatly simplified the work of test analysis and facilitated inspection of the oscillograms both during and after the test.

A study of the transient tank pressure measurements both from the authors' tabulations and from the oscillograms raises certain questions regarding the electromechanical pressure transducers and their associated equipment required to obtain a suitable signal level for recording. A case in point is the 3-phase ungrounded fault current test 14, shown in Table III, and mentioned briefly by the authors in the section of the paper devoted to tank pressure. It is reported that the highest average tank pressure of 130 pounds per square inch recorded for a 3-pole test occurred during test 14. Both the oscillogram and Table III verify this; however, it is noted that on the immediately following close-open operation at approximately the same interrupting duty, the average pressure recorded for the three poles was only 25 pounds per square inch. The oscillogram for this test would indicate that the recording equipment had recovered reasonably well from the effects of the initial opening operation. It would be very interesting to have the authors' comments on this point. The problem of using extremely low signal level transducers in an environment of intense electric and magnetic fields is a difficult one that the authors seem to have solved to their satisfaction.

This discussion has not commented on the performance of the test breaker during this series of interruption and line-charging and line-dropping tests. This does not indicate in any way a lack of interest in this most important aspect of the program, but only reflects the feeling that the breaker's performance left little to be desired. It would appear both from the tabulated results and the oscillograms that the breaker manufacturer and designer can be justifiably proud of the excellent performance record of their breaker as demonstrated by this extensive field test program.

Otto Naef and **R. D. Hambrick:** We would like to express our appreciation for the interesting comments presented in the discussions and we are gratified to see so much interest aroused in the problem of correlating laboratory and field testing experience. We do not wish to minimize the importance and advantages of controlled laboratory testing, though realizing that available facilities are not always used to the fullest extent for testing at maximum severity over as broad a range of conditions as possible.

We question Mr. Balentine's claim that the 138-kv 10,000-mva rating of the circuit breaker he mentions was established without recourse to 2-part testing and therefore involved no extrapolation. The normal frequency recovery voltage for single-phase testing is $145\times1.5/\sqrt{3}=126$ kv, or 63 kv per interrupter, assuming equal division of potential by resistor control. The actual test voltage of 53.5 kv was therefore only 85% of what is required, though the current was in excess of the rated value. Furthermore, only one of the two interrupters in the same tank was subjected to this high duty, and the over-all effect and the interaction between interrupters were not observed.

Several questions were raised concerning a new name-plate rating for the test breaker. Although test results indicate that the maximum interrupting ability of the breaker has not been determined by this series of tests, the name-plate rating will undoubtedly remain the same. Further tests will be necessary to demonstrate satisfactory performance at the next highest standard rating.

Resistors are not considered as standard accessories for this breaker provided 250% maximum line-to-ground voltage during line-dropping operations is considered one of the criteria for satisfactory performance. Resistors will be provided for applications requiring restrike-free performance.

We agree with Mr. Kilgour and his reference to Dr. Boehne's paper that circuit parameters create the necessary conditions during which restrikes can occur, but cannot agree with his conclusion that the breaker has little or no control over whether or not a restrike will occur. It should be obvious that one function of the breaker is to create favorable conditions within the breaker proper during line switching operations that preclude or minimize the occurrence of a restrike.

Conclusion 3 carries with it no recommendation as to what the relay time of a transformer breaker should be, but calls attention to the fact that because of inherent circuit characteristics over which it has no control the breaker may be stressed beyond its capabilities if tripped instantaneously on the occurrence of a bus fault. The recovery rate was measured by a tangent to the curve passing through the point of zero recovery voltage.

Mr. Kilgour has questioned the variable contact-parting times used. It should be pointed out that under low-voltage conditions normally used for contact-parting-time determinations, the test breaker is consistent in the contact-parting time indicated as 1.2 cycles. This condition still prevails under fault interruptions. However, the value of 1.4 cycles, corresponding to the time the end of the moving contact is flush with the stationary contact assembly, which is 0.2 cycle after the contacts part, is used as being a more realistic indication of the effectiveness of the interrupter during fault conditions inasmuch as the interrupter can begin to function effectively only after the end of the moving contact is flush with the end of the stationary contact assembly. This condition does not prevail during line charging-current interruptions, as described in the paper, and the indicated contact-parting time of 1.2 cycles is applicable.

The authors have no quarrel with Mr. Friedrich's comparison of arc energies, based on a widely accepted method of computation but not necessarily applicable in every case. They wish to point out that the calculated ratio of arc energies in tests 14 and 12A would be reduced to 2.4 if contact-parting time were determined by the instant of physical separation (1.2 instead of 1.4 cycles) as Mr. Kilgour suggests, and as appears to be the norm among most manufacturers.

It should further be noted that the arc energy which is generated during a fault interruption is influenced by a number of factors other than current and arcing time, a few of which are the rate at which ions are removed from the arc path during the high-current portion of the current wave, the pressure within the interrupter, and the length of the arc—such factors being influenced directly by the particular interrupter design involved. The interrupting units in this instance are of a design that minimizes the arc energy generated during the high-current wave and thus reduces the quantity of noncondensable gases produced during the interruption. We are confident that the circuit breaker could have interrupted 6,900 mva and probably considerably more at the most unfavorable instant of contact separation but we acknowledge that documentary proof is yet to be obtained.

It is interesting to note that another manufacturer of high-capacity circuit breakers recognizes the problems attendant upon oil column movement and disturbances during interruption. The addition of an inverted surge tank is indeed an interesting although not a novel solution to the problem.

We agree that reduced oil volume is a highly commendable and worth-while design goal. However, it is felt that the efficiency and reliability of performance should be the prime consideration.

We wish to thank Mr. Conner for his very pertinent and helpful comments concerning laboratory and field testing. We are looking forward with genuine interest to the results of the 220-kv field tests contemplated by the Southern California Edison Company. In answer to his question concerning the pressure transducers, it is a matter of record that on immediate reclosing duty cycles at higher interrupting capacities, there is a sufficient quantity of disassociated oil gaseous products remaining from the first interruption to reduce the pressure surges resulting from the second interruption.

We hope that the interest shown in the problem of correlating laboratory and field testing results will serve as a stimulus for the various standardizing activities to re-examine and publish test codes that will accord field testing its rightful place in determining breaker ratings. As in the past, the field experiences of circuit-breaker users must provide the final criteria of circuit-breaker performance.

Some Fundamentals on Capacitance Switching

I. B. JOHNSON
MEMBER AIEE

A. J. SCHULTZ
ASSOCIATE MEMBER AIEE

N. R. SCHULTZ
MEMBER AIEE

R. B. SHORES
MEMBER AIEE

THERE are a number of switching devices on electric power systems which must handle the switching of capacitive kilovolt-amperes (kva). Some of these devices are primarily designed to interrupt heavy inductive short-circuit currents or load currents; others are designed to handle only capacitive current or magnetizing current of relatively few amperes. Generally the capacitive kva to be handled by any switching device can be classified as to the predominant system component involved, such as overhead lines, cables, and shunt capacitor banks. Because of the differences in capacitance configurations and grounding conditions that can be encountered, each of these system components can impose different switching voltage conditions on the switching device and as a consequence different capacitive kva capabilities of the switchgear can be obtained.

Industry performance standards for rating the capacitive kva ability of switchgear have not been established. Each manufacturer at present may evaluate the capacitive capability of switchgear on a basis that is not common to all. Not only do questions of system voltage conditions arise but also, in so far as equivalent single-phase test circuits are used in the evaluation, do questions on the equivalence of the test circuit, of the test voltages, and of the 3-phase kva being switched.

Although many investigators have studied various phases of the subject of capacitance switching,[1-5] it is the purpose of this paper to present the results of a more complete investigation of the voltage conditions that may be encountered by switchgear in the interruption of capacitive kva of overhead lines, cables, and shunt capacitors, factoring in the effect of system configuration. In a companion paper these results are used to evaluate test circuits and to interpret results in establishing the capacitive kva capabilities of switchgear.[6] This investigation of system requirements was facilitated by the use of the transient network analyzer.

Conclusions

UNFAULTED CIRCUITS

1. Under fault-free conditions, the recovery voltage across the first pole to interrupt is different when switching grounded capacitor banks, overhead lines, and ungrounded capacitor banks. Assuming no re-establishment of the arc, the peaks of the recovery voltages are 2.0, 2.4, and 3.0 per unit (pu) of normal line-to-neutral crest voltage respectively when the system is effectively grounded (type-B grounding).

2. Restriking in the interrupting device can greatly increase the recovery voltage values over those imposed on the switch if no restriking takes place.

3. The recovery voltage across the first pole of a switching device to interrupt can be increased by the opening of a second pole depending on the capacitance configuration.

4. No appreciable change in the recovery voltage across the switch occurs as a result of system grounding conditions, providing the system remains within that region defined as effectively grounded.

5. If the system is not effectively grounded but is grounded through a high reactance or resistance, recovery voltages in excess of those given in conclusion 1 can occur across the first pole to interrupt for grounded banks, cables, and transmission lines. System grounding has no effect on the voltages associated with switching an ungrounded capacitor bank.

6. If the source is not grounded, a recovery voltage of 3.0 pu occurs across the first pole regardless of the capacitance configuration.

FAULTED CIRCUITS

1. The recovery voltages involved in switching an unfaulted phase of an ungrounded capacitor bank with a line-to-ground fault on one phase are not as high as those associated with switching under fault-free conditions if the source is effectively grounded.

2. The failure of capacitor bank units in one phase of an ungrounded bank can increase the recovery voltage across the first pole to clear if it is in one of the sound phases. The recovery voltage can be as high as 3.46 pu as against 3.0 pu for the unfaulted case. If the first pole to open is in the faulted phase, the recovery voltage is the same as in the unfaulted case.

3. When switching a faulted transmission line, the recovery voltage across the first pole to open, if it is in an unfaulted phase, is increased over the unfaulted case. The recovery voltage will be 2.6 pu instead of the value of 2.4 pu associated with switching unfaulted transmission lines.

4. When switching a grounded capacitor bank or a shielded cable, the withstand recovery voltage across the first pole to open, if it is in an unfaulted phase, is increased to

---

Paper 55-224, recommended by the AIEE Switchgear Committee and approved by the AIEE Committee on Technical Operations for presentation at the AIEE Winter General Meeting, New York, N.Y., January 31–February 4, 1955. Manuscript submitted October 21, 1954; made available for printing December 10, 1954.

I. B. JOHNSON, A. J. SCHULTZ, and N. R. SCHULTZ are with the General Electric Company, Schenectady, N.Y., and R. B. SHORES is with the General Electric Company, Philadelphia, Pa.

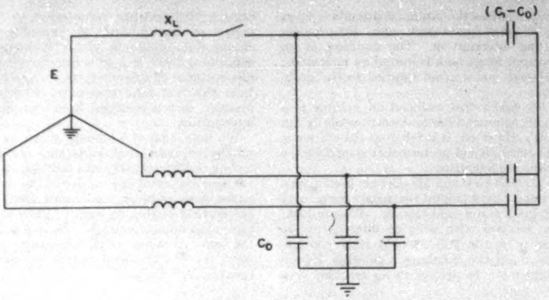

Fig. 1. A generalized capacitance circuit

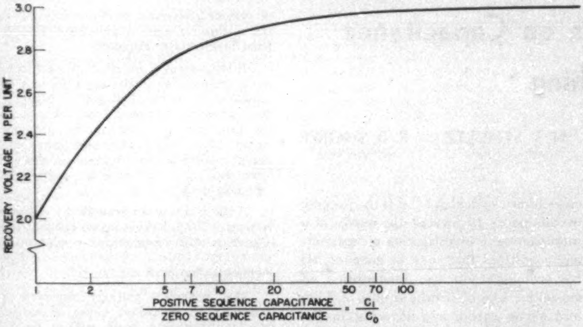

Fig. 2. Crest of recovery voltage across first pole of switch to open when switching capacitive current in circuit of Fig. 1 without restriking

2.6 pu as against 2.0 pu associated with the unfaulted case. This assumes an effectively grounded source.

Three-Phase Capacitive Circuits

In power systems, switching devices may be called upon to de-energize three basic types of capacitive circuits. These are:

1. All capacitance solidly grounded. In some instances capacitor bank neutrals are grounded and the neutral of the capacitance of most cables, in effect, is grounded.

2. A portion of the capacitance grounded. Transmission lines and some cable circuits have both phase-to-phase (ungrounded) and phase-to-ground capacitances. That is, the ratio of the positive-sequence capacitance to zero-sequence capacitance is greater than unity and, in effect, only a portion of the total or positive-sequence capacitance is grounded.

3. All capacitance ungrounded. A major portion of the shunt capacitor bank installations does not have the neutral grounded.

A generalized capacitance circuit energized from a grounded source that will fit any of the foregoing conditions is shown in Fig. 1. The circuit of Fig. 1 contains both grounded and ungrounded capacitances which are defined in terms of positive- and zero-sequence quantities. In this circuit, the zero-sequence capacitance C_0 is the grounded capacitance, and the positive-sequence capacitance C_1 is the sum of the grounded and the ungrounded capacitances. Thus, when all the system capacitance is solidly grounded the ungrounded capacitance C_1-C_0 is 0, or the circuit has a C_1/C_0 ratio of 1.0. When all the system capacitance is ungrounded, the grounded capacitance C_0 is 0, or the circuit has a C_1/C_0 ratio of ∞. For a transmission line, which involves both grounded and ungrounded capacitances, the C_1/C_0 ratio falls in the range of 1.6 to 2.0.

The testing of switching devices to evaluate their ability to switch capacitive currents may be done with single-phase circuits. For this reason, it is necessary to know the voltages between the contacts of a switching device following the opening of the first and second poles in the interruption of a 3-phase capacitive circuit. It is especially important to evaluate the variation of these voltages with changes in the parameters of the system.

Fig. 2 shows the effect of the C_1/C_0 ratio on the crest of the recovery voltage across the first pole of a switch to open. The recovery voltage is plotted in pu of the crest of normal line-to-neutral voltage. It is assumed in all cases that the switch interrupts at the instant the current goes through 0 and that the regulation involving the source inductance is negligible. Fig. 2 shows that the crest of the recovery voltage increases from twice to three times normal line-to-neutral crest value when the C_1/C_0 ratio changes from 1.0 to ∞.

Not only is the duty on a switch when interrupting capacitive currents determined by these capacitance grounding conditions but also by the grounding conditions of the source as well. Of considerable importance is the effect of system faults on the switching duty in the unfaulted phases which may experience capacitive currents. It has been shown that capacitive switching performance of

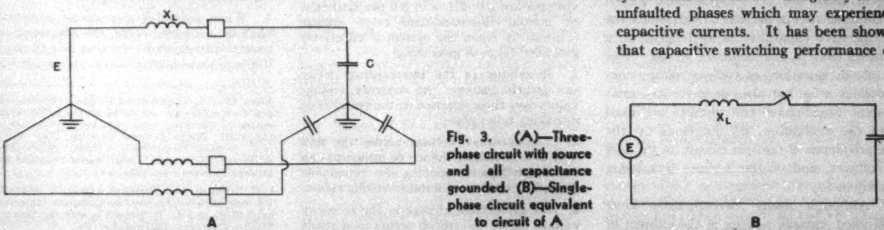

Fig. 3. (A)—Three-phase circuit with source and all capacitance grounded. (B)—Single-phase circuit equivalent to circuit of A

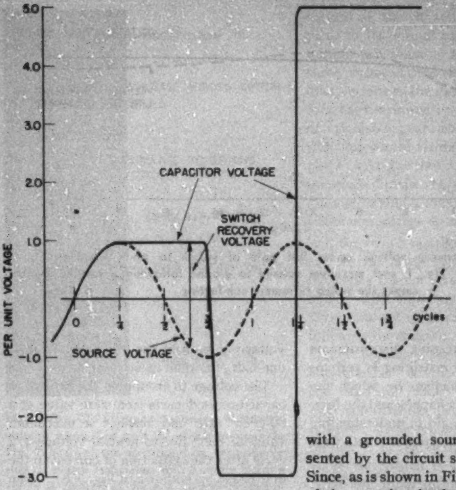

Fig. 4 (left). Voltages in the circuit of Fig. 3(B) illustrating build-up of voltage by successive restrikes

Fig. 6 (right). Oscillograms showing recovery voltage across first pole of switch to open in Fig. 1 and voltage to ground on capacitance side of switch associated with a single restrike which causes the switch to remain conducting

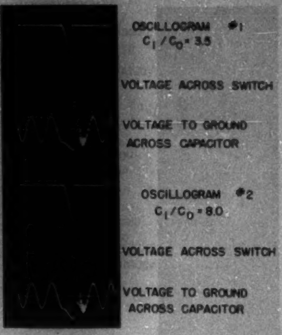

a circuit breaker is appreciably affected by the available short-circuit kva at the switch location.[7] Furthermore, the degree to which the switching device restrikes, if at all, will have a bearing on the duty imposed on the device. Each of these effects will be considered individually in the following sections.

Unfaulted Circuit—First Pole Opening

GROUNDED CAPACITOR BANKS

The switching of a grounded capacitor bank or a shielded cable from a system with a grounded source may be represented by the circuit shown in Fig. 3(A). Since, as is shown in Fig. 3(A), the neutral of the capacitor bank and the neutral of the power source are both always at the same potential, the circuit of Fig. 3(A) is essentially three single-phase circuits and each of the phases is independent of the others. That is, a switching operation in one phase is not influenced by the presence of the other phases. The results of switching one phase of the capacitor bank, therefore, may be analyzed on a single-phase basis as shown in Fig. 3(B).

Fig. 3(B) will be recognized as the classical circuit for the analysis of capacitance switching. For the sake of completeness the analysis of the single-phase circuit will be reviewed in the following paragraphs.

Fig. 4 shows the voltage on the source side of the switch and on the capacitor in the interval during which the switch in Fig. 3(B) is in the process of interruption. Since, in a purely capacitive circuit, the current leads the voltage by 90 degrees, the instant of current extinction, which is at a current zero, must occur while the voltages on each side of the switch are at a maximum. Because the switch has opened, and the capacitor is separated from the source, the charge on the capacitor cannot dissipate itself and remains on the capacitor. In other words, following current extinction, a trapped voltage equal in magnitude to the crest value of the 60-cycle source voltage remains on the capacitor.

The source voltage continues to undergo a 60-cycle variation. Therefore, a voltage, increasing with time, appears across the switch, as shown in Fig. 4. This recovery voltage beginning with a zero value reaches a maximum value of

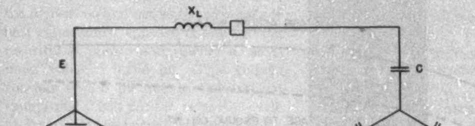

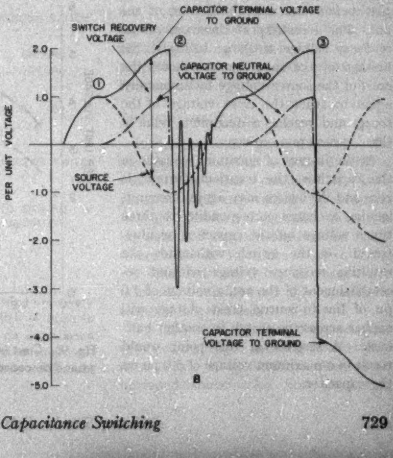

Fig. 5. (A)—Three-phase circuit with grounded source and ungrounded capacitance. (B)—Voltages in A for first pole of switch to open illustrating:

1. Successful interruption
2. Restrike at maximum recovery voltage followed by continued conduction of current
3. Restrike at maximum recovery voltage with subsequent clearing at first natural-frequency current zero

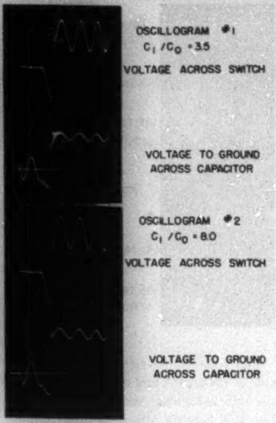

Fig. 7. Oscillograms showing recovery voltage across first pole of switch to open in Fig. 1 and voltage to ground on capacitance side of switch associated with a single restrike which is cleared at the first natural-frequency current zero

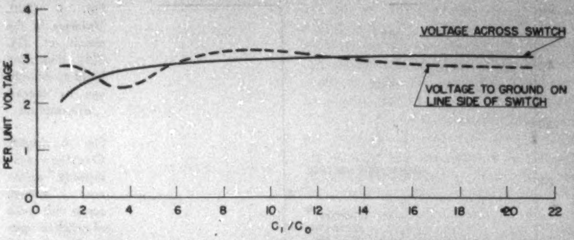

Fig. 8. Crest of recovery voltage across first pole of switch to open when switching capacitive current in Fig. 1 and maximum voltage to ground following a restrike which causes the switch to remain conducting

twice the crest of the source voltage 1/2 cycle after the current zero at which arc extinction occurred.

If the switch cannot withstand the recovery voltage at any time during this half-cycle, a re-establishment of the arc occurs reconnecting the capacitor to the source. As a consequence, the voltage on the capacitor changes from the trapped voltage condition. Because of the inductance in the system, the voltage on the capacitor oscillates past the value of the source voltage and overshoots by an amount equal to the recovery voltage just before the re-establishment of the arc. For a restrike at the crest of the recovery voltage, as shown in Fig. 4, the voltage of the capacitor overshoots the crest of the source voltage by an amount equal to twice the crest voltage of the source and reaches a maximum value of three times crest voltage.

At the instant of maximum voltage on the capacitor, the transient current is zero and the switch may again interrupt, leaving a charge corresponding to three times voltage on the capacitor as illustrated. If the switch withstands the resulting recovery voltage without re-establishment of the arc, a voltage of 4.0 pu of line-to-neutral crest voltage will appear across the switch in another half-cycle. A restrike at this point would result in a maximum voltage of 5.0 pu on the capacitor.

Although the foregoing discussion on the phenomenon of restriking is perhaps idealized, the mechanism by which the build-up occurs does happen and the foregoing analysis is an aid in understanding the more complex circuits that were studied.

UNGROUNDED CAPACITOR BANK

If the neutral of the capacitance is ungrounded, as shown in Fig. 5(A), the opening of a switch in one phase does not entirely isolate the capacitor in that phase from the system as in the previous case. If it is assumed that the first phase to clear does so at the instant of zero current and that the other two phases remain conducting, then a charge resulting in crest line-to-neutral voltage is trapped on the capacitance in the switched phase. In each of the other two capacitances a charge resulting in one-half of crest voltage is trapped, since, at the instant of crest voltage in the switched phase, the voltage of both of the other phases is at one-half of normal crest value.

The voltage to ground on the neutral of capacitances departs from zero value at a 60-cycle rate and reaches a maximum value of crest line-to-neutral voltage 1/2 cycle after the extinction of current in the first phase, as is shown in Fig. 5(B). The line terminal of the switched capacitance must remain at 1.0 pu voltage above its neutral because of its trapped charge. With respect to ground, however, it rises to a maximum value of 2 pu voltage; and, at this instant, the system voltage reaches a maximum value of opposite polarity to that at the instant of current interruption, resulting in a voltage across the open switch of three times normal line-to-neutral crest voltage.

During this process the switching device will do one of three things:

1. It will withstand the recovery voltage and therefore successfully clear the circuit.
2. It will re-establish an arc at some instant

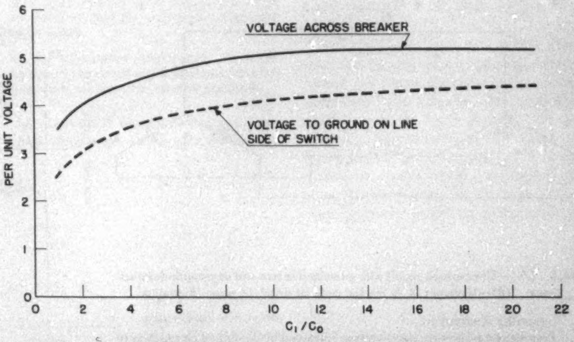

Fig. 9. Crest of recovery voltage across first pole of switch to open and maximum voltage to ground on capacitance side of switch in Fig. 1 following a single restrike which is cleared at the first natural-frequency current zero

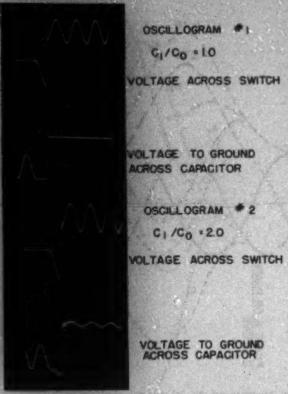

Fig. 10. Oscillograms showing recovery voltage across first pole of switch to open in Fig. 1 and voltage to ground on capacitance side of switch associated with a single restrike which is cleared at the first natural-frequency current zero

Oscillogram 1, grounded capacitance

during this process and continue to conduct until a subsequent 60-cycle current zero occurs. Fig. 5(B) shows a restrike at the crest of the recovery voltage. This may be compared to oscillogram 2 of Fig. 6.

3. It will restrike and clear at a natural frequency current zero as is shown in the latter part of Fig. 5(B). This is demonstrated in oscillogram 2 of Fig. 7.

If no restrike occurs, the voltage of three times normal is the highest across the switch contacts and the capacitance terminal voltage of 2 pu to ground will not be exceeded. If no restrike occurs, the highest voltage across the terminals of any capacitance appears in one of the unswitched phases and reaches a maximum value of 1.366 pu. This voltage consists of 0.5 pu due to the trapped charge and 0.866 pu due to the 60-cycle excitation on the unswitched phases.

If the switch is unable to withstand the crest value of the recovery voltage of three times line-to-neutral crest, a restrike occurs. If, on this restrike, the switching device continues to conduct until the next 60-cycle current zero, not interrupting at the zeros due to the natural frequency oscillation, a maximum voltage of three times normal line-to-neutral crest appears from line-to-ground on both the capacitance side and the source side of the switch as shown in Fig. 5(B). On the occurrence of the restrike, the voltage conditions in the circuit are such that the neutral of the capacitance instantly returns to its normal condition of zero potential and remains there as long as all three phases of the switch continue to conduct current to the capacitances. Therefore, the maximum line-to-ground voltage of 3 pu also appears across the line-to-neutral capacitance terminals in the switched phase. At the same time, each of the unswitched phases experiences a transient voltage having a maximum value of $1^{1}/_{3}$ times normal line-to-neutral voltage.

If the switch restrikes, it may interrupt the current again at one of the natural-frequency current zeros. The latter part of Fig. 5(B) shows an interruption at the first natural-frequency current zero following the restrike. This results in the highest possible voltages obtainable with one restrike. At the instant of restrike, the capacitor bank neutral returns to zero potential as mentioned previously; however, it now remains there for a period of only 1/2 cycle of the natural frequency while the switch is conducting current. After the interruption of current at its first zero, the voltage to ground of the neutral of the capacitance jumps immediately to a value of 1 pu opposite to its polarity prior to the restrike. The interruption of the current in the switched phase again leaves a trapped charge on the capacitances. Because the circuit conditions until the time of current interruption at the natural-frequency current zero are exactly the same as in the previous case where conduction continued, the voltage due to the trapped charge resulting from the restrike on the switched phase of the capacitance corresponds to the transient voltage of three times normal that which occurred in this previous case. This voltage of three times normal (due to the trapped charge) plus the neutral displacement of 1 pu results in a voltage to ground on the switched phase of the capacitance of four times normal line-to-neutral crest voltage. Because of the normal excitation of the two unswitched phases, the neutral undergoes a voltage variation at power frequency of 1 pu or, 1/2 cycle after the restrike, the line terminal of the switched phase capacitance reaches a value of 5 pu voltage to ground. At this instant, the voltage across the open switch is six times line-to-neutral voltage.

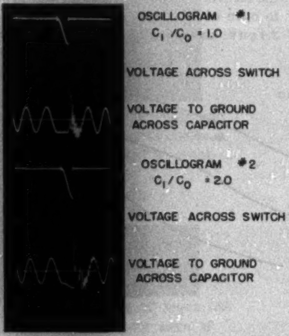

Fig. 11. Oscillograms showing recovery voltage across first pole of switch to open in Fig. 1 and voltage to ground on capacitance side of switch associated with a single restrike which causes the switch to remain conducting

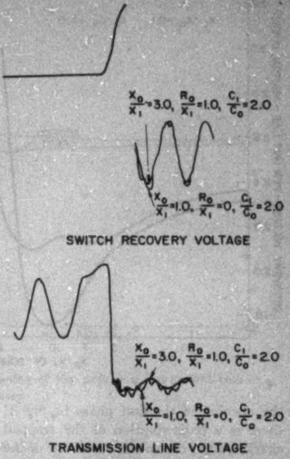

Fig. 12. Effect of source grounding conditions on recovery voltage and voltage to ground when switching a transmission line with one restrike and clearing at first natural-frequency current zero

TRANSMISSION LINES

It was previously pointed out that the capacitance network associated with a transmission line consists of both grounded and ungrounded capacitances. Because of this, voltages due to switching unloaded transmission lines lie somewhere between the values obtained in the previous cases involving all capacitance neutrals grounded and all capacitance neutrals ungrounded.

To illustrate the foregoing, consider the circuit in Fig. 1 showing the first pole of a switch to open when switching an unloaded transmission line. Following

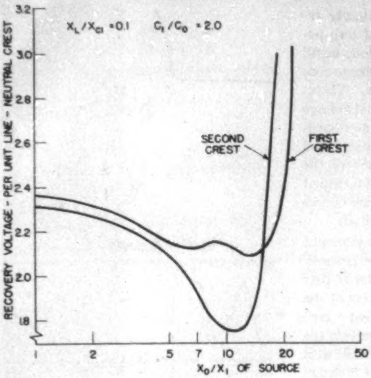

Fig. 13 (left). First and second crest of recovery voltage across first pole of switch to open when switching unfaulted transmission line with a reactance grounded source

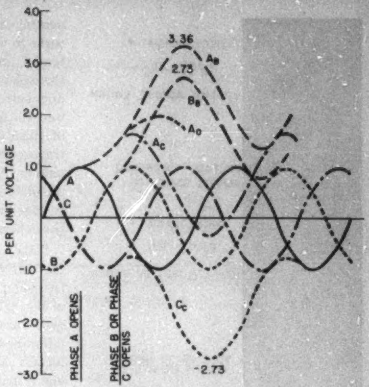

A_B - VOLTAGE TO GROUND ON "A" PHASE CAPACITOR TERMINAL WHEN "B" PHASE SWITCH OPENS SECOND

A_C - VOLTAGE TO GROUND ON "A" PHASE CAPACITOR TERMINAL WHEN "C" PHASE SWITCH OPENS SECOND

A_0 - VOLTAGE TO GROUND ON "A" PHASE CAPACITOR TERMINAL WHEN ONLY "A" PHASE SWITCH OPENS

B_B - VOLTAGE TO GROUND ON "B" PHASE CAPACITOR TERMINAL WHEN "B" PHASE SWITCH OPENS SECOND

C_C - VOLTAGE TO GROUND ON "C" PHASE CAPACITOR TERMINAL WHEN "C" PHASE SWITCH OPENS SECOND

Fig. 15 (right). Voltages due to opening of second pole when switching an ungrounded capacitance

the opening of the first phase in Fig. 1, there is a redistribution of the trapped charge on the capacitance network of the transmission line. This redistribution of trapped charges plus the capacitance-coupled effects from the 60-cycle voltage variations of the two unswitched phases, results in a voltage on the switched phase of the transmission line that is a function of the relative magnitude of the capacitances, or a function of the ratio of the positive-sequence capacitance to the zero-sequence capacitance (C_1/C_0).

The crest voltage across the switch in pu of the line-to-neutral crest voltage is given in Fig. 2 as a function of the C_1/C_0 ratio. Note that as the C_1/C_0 ratio varies from 1.0 to ∞ (all capacitance neutrals grounded to all capacitance neutrals ungrounded), the maximum recovery voltage varies from 2.0 to 3.0 pu. These numbers are the same as those given previously for these two specific cases. The voltages to ground on the transmission line vary from 1.0 to 2.0 pu for the same conditions.

Generally transmission lines and unshielded cables will have a ratio of C_1/C_0 in the range from 1.6 to 2.0. Accordingly the recovery voltage across the first pole to open of a switch varies from 2.28 to 2.4 pu as shown in Fig. 2. The voltage to ground on the transmission line terminal of the open switch for this range of C_1/C_0 would fall between the limits of 1.28 to 1.4 pu respectively.

SUMMARY OF RESULTS

To summarize the foregoing discussions on the switching of capacitor banks, cables, and overhead lines, the results from a transient network analyzer setup are given in Figs. 8 and 9. The circuit used was the same as that shown in Fig. 1. With the capacitance (C_1-C_0) held fixed, the capacitance C_0 was changed in steps so as to vary the ratio of C_1/C_0 from 1.5 to 21. The capacitances also were adjusted so as to produce ratios of C_1/C_0 down to 1.0.

The results in Fig. 8 are based on the initiation of a restrike in the interrupting switch after an initial clearing so as to produce the maximum transient line-to-ground voltage as a consequence of the restrike and on the assumption that the transient oscillation so produced is not interrupted until it has been damped, and interruption occurs at a power frequency current zero. In Fig. 9 the results are based on a restrike as for Fig. 8, except that the recovery voltage across the switch and the voltage to ground on

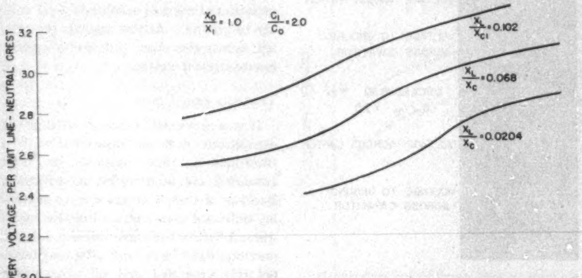

Fig. 14. Crest of recovery voltage across first pole of switch to open when switching an unfaulted transmission line with a resistance grounded source

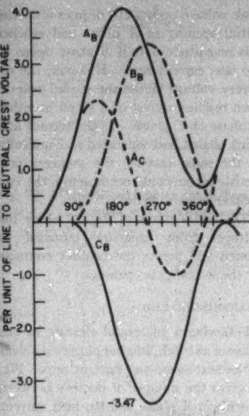

Fig. 16. Recovery voltages due to opening of second pole when switching an ungrounded capacitance

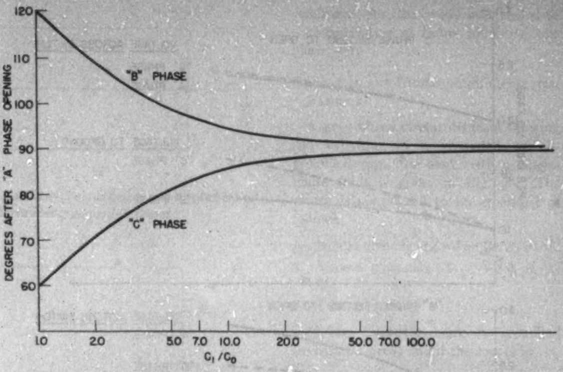

Fig. 18. Interval in electrical degrees between opening of first pole and first current zero in other two phases

the capacitance side of the interrupting switch are those obtained when the transient produced by the restrike is interrupted at the first natural-frequency current zero after initiation of the restrike. Representative oscillograms of the data plotted in Figs. 8 and 9 are shown in Figs. 6, 7, 10, and 11.

In comparing these data with the values mentioned in the previous discussions, it should be mentioned that the transient restriking voltages and the recovery voltages, depending on the restrike, may be lower than theoretical upper limits by a factor of about 10 per cent because of damping in the analyzer circuit.

Source Grounding Conditions

Up to this point consideration has been given to capacitance conditions only. It has been assumed that the source has been grounded in such a manner than the X_0/X_1 of the source is equal to unity. For the circuit studied, as in Fig. 1, there is no appreciable change in the results if the source grounding does not exceed the conditions for an effectively grounded system or a type-*B* grounding ($X_0/X_1 \leq 3.0$, $R_0/X_1 \leq 1.0$.)[4] This is illustrated in Fig. 12 where the voltages due to switching and restriking in one phase when switching a transmission line are plotted superimposed for $X_0/X_1 = 1.0$ and for type-*B* grounding of the source.

If the conditions of type-*B* grounding are exceeded, as, e.g., by adding a grounding reactor, very high voltages may result when the first pole opens when switching a grounded capacitor bank, cable, or transmission line. With one phase open, a path through ground involving the grounding reactance and the capacitance may result in a series resonant circuit. Fig. 13 shows the magnitude of the first and second crests of the recovery voltage across the first pole of an interrupter when switching a transmission line as the X_0/X_1 ratio of the source increases. For example, it is well known that opening one phase in a system grounded with a ground-fault neutralizer results in a very high voltage.

If the grounding impedance is largely resistive, the recovery voltage varies between the ground and ungrounded conditions as the grounding resistance is increased. This is shown in Fig. 14 where the change in the recovery voltage across the first switch pole to clear is given as a function of the R_0/X_1 ratio of the circuit.

If the source is ungrounded, the recovery voltage across the first switch pole to open is independent of the grounding conditions of the capacitance. The circuit recovery voltages are the same as in the case of the ungrounded capacitance and grounded source. The voltages to ground in the circuit, however, are a function of the grounding of the capacitance.

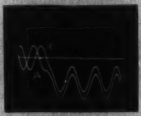

VOLTAGE FROM "A" PHASE AND "B" PHASE CAPACITOR TERMINAL TO GROUND WHEN "B" PHASE OPENS SECOND

A = 3.3 P.U.
B = 2.6 P.U.

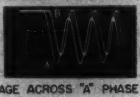

VOLTAGE ACROSS "A" PHASE AND "B" PHASE SWITCHES WHEN "B" PHASE OPENS SECOND

A = 4.0 P.U.
B = 3.3 P.U.

Fig. 17. Oscillogram of voltages due to opening of second pole when switching an ungrounded capacitance

Unfaulted Circuits—Second Pole Opening

Grounded Banks

It has been previously shown that in a circuit with a grounded capacitor bank or a shielded cable, and a grounded source, the phases are independent of each other under switching conditions. That is, each pole of a switch experiences the same duty whether it is the first, second, or last to open.

Ungrounded Banks

After the first phase has opened when switching an ungrounded capacitor bank, there is a shift in the currents in the other two phases. Since the remaining two phases of the capacitor bank are con-

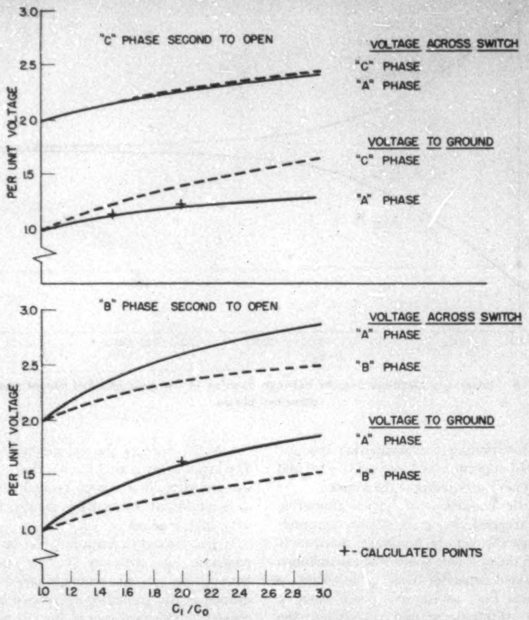

Fig. 19. Voltages due to opening of second pole when switching an unfaulted transmission line as measured on transient network analyzer

nected in series across a phase-to-phase voltage, the same current flows in both of them and leads the phase-to-phase voltage by 90 degrees. This current now has the same phase relationship as that of the source voltage on the first phase to clear, and has its first current zero 1/4 cycle after the current zero in the first phase to clear. With the same current flowing in the remaining two phases, interruption of current in these phases occurs simultaneously. If physical separation of the switch contacts in these phases takes place at nearly the same instant, the capacitor bank will be separated from the system, both electrically and mechanically, at the instant of current interruption. In this case, the voltage across the open switch contacts will be governed by the stray capacitances of the capacitor bank to ground and through the switching device.

If, however, one of the last two switch poles is mechanically delayed in opening, the capacitor bank as a whole unit will be subjected to the voltage variations of the last phase connected to the source. Because of the trapped charges on the capacitor bank, the first and second poles of the switch to open can be subjected to a high voltage across their contacts.

The voltages to ground on each side of the switch contacts following the second pole clearing are shown in Fig. 15. The voltages due to either *B* phase or *C* phase opening second are shown. As a reference, the voltage due to the first switch pole to open, assuming a delayed second pole opening, is shown. It will be noted that the highest capacitor bank voltages due to the second pole opening occur on the terminal of the first phase to clear. Even though the same current flows in the last two phases, higher voltages result if *B* phase is second to open mechanically assuming interruption at the first current zero in *B* phase after interruption in *A* phase. The trapped charge on *C* phase capacitor adds to the voltage of *C* phase but the trapped charge on the *B* phase capacitor subtracts from the *B* phase source voltage.

The voltages that appear across the switch contacts are shown in Fig. 16. It is seen that the recovery voltage across the first pole to open reaches a peak of 4.1 pu of the line-to-neutral crest. This peak voltage occurs 210 degrees after the initial opening in *A* phase and reaches this magnitude only if *B* phase opens at the next current zero. However, the recovery voltage across the second pole to open reaches a crest of 3.47 pu in either *B* phase or *C* phase. If the second and third phases had separated mechanically at the same instant, the voltages previously given would occur across the two breaker poles in series.

The oscillograms of Fig. 17 show the voltages from capacitor terminal to ground and across the breaker contacts for the second pole opening.

TRANSMISSION LINE

Following a successful clearing in one phase of a switch, another phase may clear at the next successive current zero. Fig. 18 gives the number of degrees between clearing in *A* phase and the next current zero in *B* and *C* phases as a function of the C_1/C_0 ratio of the circuit. It can be seen that for any practical value of C_1/C_0 associated with a transmission line a current zero occurs in *C* phase before one does in *B* phase.

The voltages due to the second pole opening are shown in Fig. 19. Several calculations are shown together with results obtained from the transient network analyzer. Here it is seen that the severest voltages are associated with the first phase that opened (*A* phase) and occur when *B* phase opens second. These voltages are only slightly higher than those occurring with the opening of the first pole (2.6 pu as against 2.4 pu for $C_1/C_0=2.0$) and can only occur if the first current zero in *C* phase is skipped assuming second pole opening occurs within 1/2 cycle of first pole opening.

EFFECT OF SOURCE GROUNDING

For the second pole opening, the effect of source grounding is about the same as for the first pole opening. Up to the limiting grounding impedance of $X_0/X_1 \leqq 3.0$ and $R_0/X_1 \leqq 1.0$, the numbers given in the preceding sections are not appreciably changed.

Faulted Circuits

Even though faults may exist on one or two phases of a 3-phase system, a circuit breaker in clearing the fault may be required to interrupt capacitive current in the unfaulted phases. This investigation is concerned with the effect of the fault on the voltages encountered when switching these capacitive currents. Because of the large number of combinations of faults, system and capacitance grounding

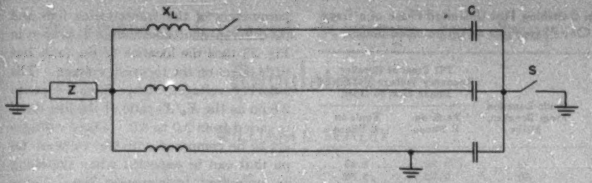

Fig. 20. Generalized 3-phase circuit showing the switching of grounded or ungrounded capacitance with a single-phase fault and impedance grounded source

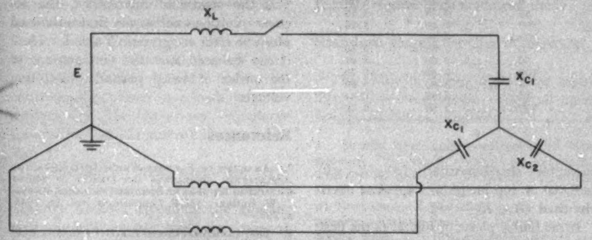

Fig. 21. Generalized 3-phase circuit showing the switching of unbalanced capacitance. X_{C2} can be greater or smaller than X_{C1}

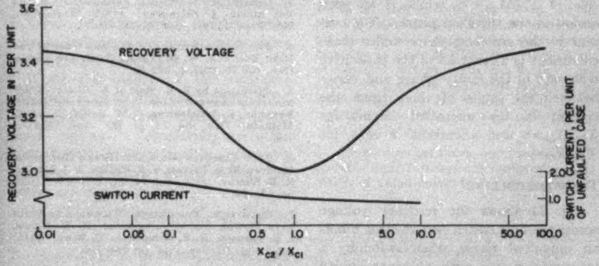

Fig. 22. Current and recovery voltage associated with first pole of switch to open for the circuit of Fig. 21

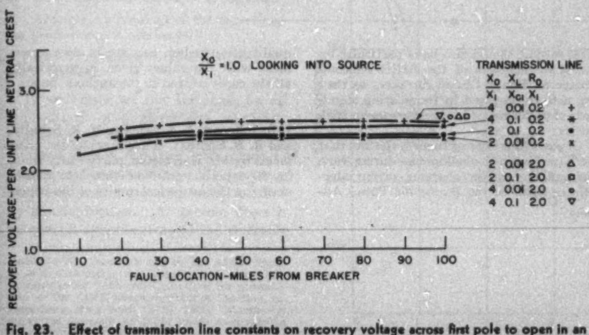

Fig. 23. Effect of transmission line constants on recovery voltage across first pole to open in an unfaulted phase when switching a transmission line with a line-to-ground fault at various distances from the switch

conditions, etc., this study was limited to a consideration of faults involving one phase only.

GROUNDED AND UNGROUNDED CAPACITOR BANKS

A generalized circuit diagram showing the switching of a grounded or ungrounded capacitor bank with a single-phase fault is given in Fig. 20. The source is considered to be grounded as follows:

1. Solidly grounded ($Z=0$ or $X_0/X_1=1.0$).
2. Type-*B* grounding ($X_0/X_1=3.0$, $R_0/X_1=1.0$).
3. Ungrounded ($Z=\infty$).

If the capacitor bank is grounded (switch *S* closed) and if the source is

1. grounded solidly, the duty on the first unfaulted switch pole to open is the same as for the unfaulted case since the three phases are independent of each other.
2. grounded in accordance with type-*B* grounding, the voltages and currents in the first unfaulted phase to open are no more than about 30 per cent greater than for the unfaulted case.
3. ungrounded, referring to the first unfaulted phase to open, the maximum voltages across the switch are twice normal line-to-line voltage (1.73 pu) for a circuit with zero regulation. It has been shown that the crest of the recovery voltage for the same circuit with no fault is 3.0 pu; thus the effect of the fault is to increase the maximum recovery voltage by about 15 per cent. The voltage to ground on the switched capacitor is 1.73 pu compared to a value of 1.0 pu for the unfaulted case. The current in both unfaulted phases is about 1.73 times normal.

If the neutral of the capacitor bank is not grounded (switch *S* of Fig. 20 open), and if the source is

1. grounded solidly, the voltage and currents of the unfaulted phases are the same as for the unfaulted case.
2. grounded in accordance with type-*B* grounding, the voltages associated with the switching of an unfaulted phase are no more than approximately 30 per cent greater than for the unfaulted case with a solidly grounded source. The currents are slightly less than for the unfaulted case.
3. ungrounded, the recovery voltage and currents are the same as for the unfaulted case with the neutral of either the capacitor bank or of the source grounded. With only one point of the circuit grounded, no current can flow in the ground which is merely a point of voltage reference. Of course, it should be pointed out that the voltages to ground before the switch opens in this circuit are not the same as in the unfaulted circuit with either neutral grounded but are 1.73 pu.

One other type of fault that is of interest is the failure of a portion of the capacitance in one phase. Such a case is

Table I. Circuit-Breaker Recovery Voltages When Switching First Unfaulted Phase of a Transmission Line With a Line-to-Ground Fault on One Phase From an Ungrounded Source

Line X_0/X_1	Line R_0/X_1	X_1/X_{C1}	C_1/C_0	Fault Location From Breaker, Miles	PU Crest of Breaker Recovery Voltage Unfaulted Phase First to Open: Fault on B Phase	PU Crest of Breaker Recovery Voltage Unfaulted Phase First to Open: Fault on C Phase
2.0	0.2	0.01	1.6	0	3.36	3.36
				50	3.38	3.38
				100	3.40	3.40
2.0	2.0	0.01	1.6	0		3.36
				50		3.38
				100	3.40	3.40
4.0	0.2	0.01	1.6	0	3.36	3.36
				50	3.38	3.38
				100	3.40	3.40
4.0	2.0	0.01	1.6	100	3.40	
4.0	2.0	0.10	1.6	0	3.80	3.60
				50	3.80	3.64
				100	3.80	3.70
4.0	2.0	0.10	1.6	0	3.80	3.60
				50	3.80	3.64
				100	3.80	3.70

shown in the circuit diagram of Fig. 21 where the capacitive reactance in one phase is different from that in the other two phases. The capacitive reactance in the odd phase X_{C2} can be larger or smaller than the reactance of the sound phases X_{C1}, depending on the manner in which the unbalance arises.

If the first switch pole to open is in one of the sound phases, the recovery voltages of Fig. 22 can appear across its contacts. These recovery voltages are plotted as a function of the ratio of the capacitive reactance in the faulty phase to the capacitive reactance in the sound phases, X_{C2}/X_{C1}. Note that for either all of the capacitance short-circuited in one phase ($X_{C2}/X_{C1}=0$) or for an open circuit in that phase ($X_{C2}/X_{C1}=\infty$), the recovery voltage is twice line-to-line voltage.

Also shown in Fig. 22 are the currents in the switched phase in pu of the values for normal balanced conditions. These currents range from 1.73 pu for one phase capacitor short-circuited ($X_{C2}/X_{C1}=0$) to 0.866 pu for one phase capacitor open-circuited ($X_{C2}/X_{C1}=\infty$).

If the faulty phase of Fig. 21 is the first to open, the crest of the recovery voltage is always 3.0 pu of normal line-to-neutral voltage except, of course, for the trivial case of $X_{C2}/X_{C1}=\infty$ which is an open circuit in the switched phase. The current in the switched phase under these conditions is a function of the capacitive reactance in the faulty phase and varies between the limits of three times the current in the unfaulted circuit for $X_{C2}/X_{C1}=0$ and a current of zero for $X_{C2}/X_{C1}=\infty$.

TRANSMISSION LINE

Fig. 23 shows the recovery voltage across the first switch pole to clear if it is an unfaulted phase when switching a transmission line with a line-to-ground fault on one phase. The recovery voltages are shown for different impedance parameters of the transmission line and for different fault locations. It is seen in Fig. 23 that the location of the fault has little effect on the recovery voltage. The recovery voltages change from 2.4 pu to 2.6 pu as the X_0/X_1 ratio of the line itself is varied from 2.0 to 4.0. These voltages are to be compared with the value of 2.4 pu that can be expected when switching an unfaulted transmission line. These data were obtained by means of the transient network analyzer.

If the source is ungrounded, the recovery voltages across the first unfaulted phase to clear are given in Table I. Here it can be seen that the voltages are of the order of twice normal line-to-line voltage.

References

1. ANALYSIS OF FACTORS WHICH INFLUENCE THE APPLICATION, OPERATION AND DESIGN OF SHUNT CAPACITOR EQUIPMENT SWITCHED IN LARGE BANKS, J. W. Butler. *AIEE Transactions*, vol. 59, 1940, p. 795.

2. TESTS AND ANALYSIS OF CIRCUIT BREAKER PERFORMANCE WHEN SWITCHING LARGE CAPACITOR BANKS, T. W. Schroeder, E. W. Boehne, J. W. Butler. *AIEE Transactions (Electrical Engineering)*, vol. 61, Nov. 1942, pp. 821–31.

3. CAPACITOR SWITCHING PHENOMENA, R. C. Van Sickle, J. Zaborszky. *AIEE Transactions*, vol. 70, pt. I, 1951, pp. 151–58.

4. THE INTERRUPTION OF CHARGING CURRENT AT HIGH VOLTAGE, W. M. Leeds, R. C. Van Sickle. *Ibid.*, vol. 66, 1947, p. 373–82.

5. *Discussion* by E. C. Starr of A 161-Kv 10,000-MEGAVOLT-AMPERE STEEL-CLAD IMPULSE CIRCUIT BREAKER, C. J. Balentine, C. M. Ratliff, Jr., G. C. McBride. *Ibid.*, vol. 72, pt. III, Apr. 1953, p. 319.

6. TEST CIRCUITS FOR CAPACITANCE SWITCHING DEVICES, K. G. Darrow, V. E. Phillips, A. J. Schultz, R. B. Shores. *Ibid.*, vol. 74, pt. III, Aug. 1955, pp. 624–35.

7. SWITCHING CAPACITIVE KILOVOLT-AMPERES WITH POWER CIRCUIT BREAKERS, N. E. Dillow, I. B. Johnson, N. R. Schultz, A. E. Were. *Ibid.*, vol. 71, pt. III, Jan. 1952, pp. 188–200.

8. PREFERRED VOLTAGE RATINGS FOR A-C SYSTEMS AND EQUIPMENT. *EEI Publication No. R-6, NEMA Publication No. 117*, New York, N.Y., May 1949.

◆

Discussion

E. J. Harrington (Bonneville Power Administration, Portland, Oreg.): I would like to compliment the authors on an excellent and most timely paper. The subject of capacitor switching and the interruption of transmission-line charging current is of interest to the industry at the present time. This subject should also be of particular interest to members of the AIEE Subcommittee on Power Circuit Breakers as they are actively engaged in formulating standards of performance for breakers under such duties.

Of particular interest to me is the fact that we have obtained oscillograms during various capacitor and line charging current interruption tests on the Bonneville Power Administration system that are in close agreement with the values given in practically all the cases treated in the authors' paper.

I. B. Johnson, A. J. Schultz, N. R. Schultz, and R. B. Shores: We appreciate the comments by Mr. Harrington, particularly those on the experimental data from field studies verifying the analytical results of the paper.

Increased Current Ratings for Step Regulators

WILLIAM C. SEALEY
FELLOW AIEE

REGULATORS, like other transformers, have a rated name-plate current. Like the transformers, they have overload capabilities without sacrifice of normal life, when the ambient temperature is below 30 degrees centigrade (C) or when full load is not carried continuously. Such overloads are described by the American Standards Association[1] (ASA) and are illustrated in Fig. 1.

In addition to these overloads, regulators have a further increase in overload capacity without exceeding the guaranteed temperature rise, when they raise or lower the voltage less than the full range of operation. The losses of a regulator decrease as the load tap changer moves toward its neutral position. This decrease in losses makes it possible to increase the current ratings on the tap voltages closer to the neutral position.

While the ability of the regulator windings to carry the load current without exceeding a safe temperature is the most important consideration, other factors must be considered in applying a regulator. Factors which affect the design of a regulator are:

1. Desired overcurrent rating on the reduced taps.
2. The voltage of the desired reduced taps.
3. The short-circuit duty required on each tap.
4. Short-time overload capacity required.
5. Arcing duty required of the tap-changing mechanism on overloads.
6. Ease of changing from one current rating to another.

These values are not the same for all applications of a given size regulator. Consequently different designs would be required if each regulator were made to fit each application exactly. This practice would not permit the advantages obtained by standardization. At present there is no general agreement as to the desirable characteristics of a standard regulator. At least five different types of standard regulators have been made and used.

Standard Regulator Characteristics

The following types of standard regulators have been made. They all meet specific service requirements.

1. Simple single-core regulator with 100-per-cent (%) rated current on all taps. There is no provision for taking advantage of the inherent increased thermal capacity on the reduced taps. This is the least expensive regulator and fits service requirements when a ±10% range is always required.
2. Single-core regulator provided with adjustable limit switches and designed so that 160% of rated current may be carried on the 5% tap and intermediate overcurrents on intermediate taps. The short-circuit capacity is less than 25 times normal on overcurrent ratings. This is a larger, more expensive regulator than that described in item 1 and may be limited in its application on the reduced range taps by the short-circuit limitations.
3. Single-core regulator provided with adjustable limit switches and designed so that 200% of rated current may be carried on the 5% tap. Full rated kilovolt-amperes (kva) may be carried on all taps from 5% to 10%. Full 25 times short-circuit current for 2 seconds can be carried on all taps. This is a larger more expensive regulator than that described in item 1 or 2 but it provides maximum performance in all respects.
4. Regulator provided with a series autotransformer and series parallel connection for 200% current rating on the 5% tap connection. No provision is made for increased current capacity on the intermediate taps. This regulator is generally used for higher current ratings and is usually comparable to the regulator of item 3 in cost and performance except that it does not provide overcurrent ratings on the intermediate taps.
5. Regulator provided with auxiliary series autotransformer to provide 200% current capacity on the 5% taps and intermediate ratings on intermediate taps. The best application of this circuit is to provide overcurrent reduced voltage taps to existing regulators by adding an external autotransformer. It is inherently the most expensive unit. It provides full kva performance on all taps in all respects.

Each of these specific regulators is representative of a general class. They may be though of as representing one point on a curve in which performance is plotted against size and cost. For the purpose of comparison, these five kinds of voltage regulators will be considered. Three of them are single-core regulators and two are 2-core units.

A single-core regulator even without rated overcurrent capacity has inherent continuous overcurrent capacity on reduced voltage taps. Let

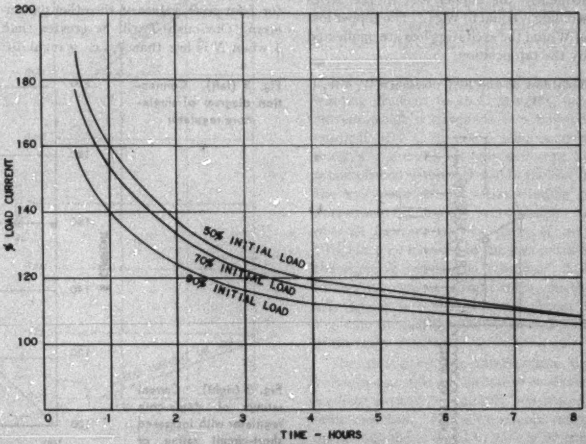

Fig. 1. ASA overloads for a regulator

Paper 55-353, recommended by the AIEE Transformers Committee and approved by the AIEE Committee on Technical Operations for presentation at the AIEE Southern District Meeting, St. Petersburg, Fla., April 13–15, 1955. Manuscript submitted January 10, 1955; made available for printing March 4, 1955.

William C. Sealey is with the Allis-Chalmers Manufacturing Company, Milwaukee, Wis.

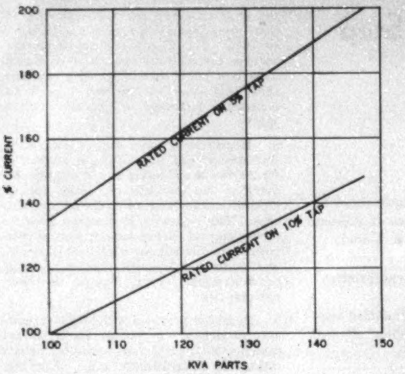

Fig. 2 (left). Current ratings of single-core regulator; both windings same kva rating

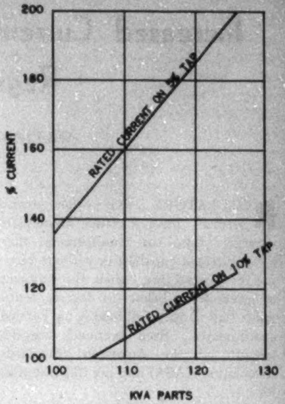

Fig. 4 (right). Current ratings of single-core regulator with reduced gradient of series winding

W_1 = watts copper loss of the exciting winding on the full 10% tap connection
W_2 = watts copper loss of the series winding on the full 10% tap connection
W_3 = watts copper loss of the preventive autotransformer and bushing leads
G = gradient between hot-spot copper and top oil temperature
F = no-load loss or excitation loss
N = per-unit portion of tap range in use
T = oil rise at rated current on the 10% tap

When operating on reduced tap, the current in the exciting winding with full load current in the line is proportional to the portion of the tap range in use. Consequently the copper loss in the exciting winding is equal to W_1N^2. The current in the series winding is equal to the line current but it flows through only the used portion of the series winding. Consequently the copper loss in the series winding is equal to W_2N. The copper loss of W_3 and the excitation loss are unaffected by the tap position.

Total loss on the 10% position $= W_1+W_2+W_3+F$

Total loss on the reduced voltage tap $= I^2(W_1N^2+W_2N+W_3)+F$

where I is the current expressed as a per unit of rated current on the 10% tap. The oil rise is proportional to the total loss to the 0.8 power. The copper gradient is proportional to the current to the 1.6 power.

The hot-spot temperature rise of the regulator on any tap =

$$\left(\frac{I^2(W_1N^2+W_2N+W_3)+F}{W_1+W_2+W_3+F}\right)^{0.8} T+GI^{1.6}=H \quad (1)$$

An inspection of equation 1 shows that on the reduced voltage taps where N is less than 1, the temperature rise at rated current will be less than when $N = 1$. This equation can be solved graphically for I for given values of the other parameters. Obviously I will be greater than 1 when N is less than 1, i.e., a regulator has inherent increased current capacity on its reduced range taps.

For constant kva output the current I is inversely proportional to N, i.e., $I = I_1/N$. Substituting in equation 1 for I

$$H=\left(\frac{I_1^2\left(W_1+\frac{W_2}{N}+\frac{W_3}{N^2}\right)+F}{W_1+W_2+W_3}\right)^{0.8} T+\left(\frac{I_1}{N}\right)^{1.6} G \quad (2)$$

An inspection of equation 2 shows that the temperature rise increases as N becomes smaller, i.e., for a regulator rated on constant kva, the maximum heating occurs on the lowest rated tap position. The inherent kva capacity on the higher range taps will always be greater than the rated kva on the lowest tap for any single-core regulator.

Fig. 3 (left). Connection diagram of single-core regulator

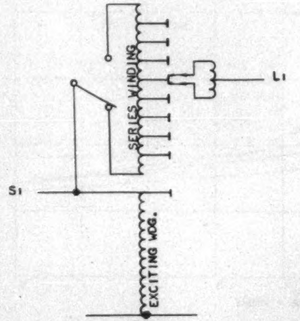

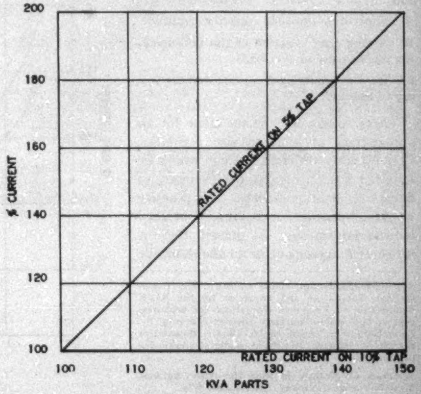

Fig. 5 (right). Current ratings of single-core regulator with increased short-circuit rating of series winding

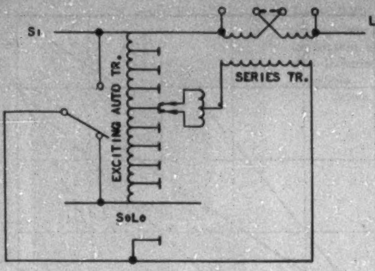

Fig. 6 (left). Diagram of 2-core regulator with exciting autotransformer and 2-winding series transformer

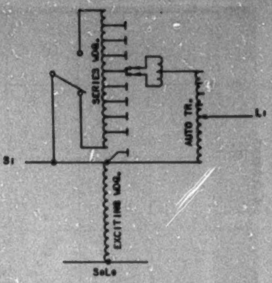

Fig. 8 (right). Circuit diagram of 2-core regulator with series autotransformer

The following values of loss are typical of a standard regulator:

No-load loss F	0.3
W_1	0.3
W_2	0.38
W_3	0.02
Total	1.00
Top oil rise	50 C
Gradient hot-spot copper to top oil	15
Total hot-spot rise	65 C

On the 5% tap, $N = 0.5$. The total losses $= I^2(0.25W_1 + 0.5W_2 + W_3) + F$. The hot-spot temperature rise on the 5% tap $=$

$$\left(\frac{I^2(0.25W_1+0.5W_2+W_3)+F}{W_1+W_2+W_3+F}\right)^{1.8} 50+GI^{1.6}=65\text{ C} \quad (3)$$

Substituting the typical values previously given and solving equation 3 either graphically or by trial and error, it is found that $I = 1.33$. This means that on the 5% tap this regulator can carry 133% of rated current without exceeding the guaranteed temperature rise. Expressed in round numbers this is taken as 135% for a typical value. Limit switches can be provided on the mechanism to limit its travel to ±5% when it is desired to take advantage of this increase in current.

A greater increase than 35% can be secured by increasing the rating of the series winding so that it is proportional to the current. The current rating obtainable is shown by the curves of Fig. 2. The short-circuit current rating is 25 times normal for 2 seconds on the 10% tap. It is equal to 25/1.35 or 18.5 times normal on the increased ratings on the 5% tap.

The advantage of this connection is that it merely needs the addition of a limit switch to provide the increased current rating. Such switches can be made for changing the setting in a few minutes. Increased current ratings intermediate between 1.35 and 1.00 times rated current on the 10% tap can be provided on the intermediate taps by suitable construction of the adjustable limit switches.

The arcing duty on the tap changing mechanism is increased. The regulator is suitable for ASA overloads except that in some cases the tap-changing mechanism may be the limitation to the safe, overloads. This connection and proportions would be the choice where the combination of reduced short-circuit duty and increased current ratings meet service requirements and where no further reduction in short-circuit requirements is permissible.

Single Core With Decreased Gradient

Another way of increasing the capacity of the single-core regulator of Fig. 3 is by decreasing the gradient of the series winding so that it is equal to 15 C on the maximum current rating on the 5% tap. Since the maximum permissible oil rise according to the ASA standards is 50 C, this means that the copper losses on both the 5% and 10% connections at their rated currents are equal. That is

$$I^2(0.25W_1+0.5W_2+W_3)=W_1+W_2+W_3$$

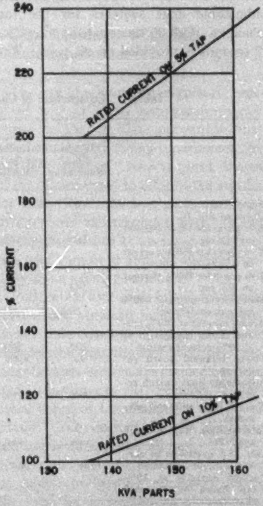

Fig. 7. Current ratings of regulator of Fig. 6

Solving for I

$$I=\sqrt{\frac{W_1+W_2+W_3}{(0.25W_1+0.5W_2+W_3)}} \quad (4)$$

An inspection of equation 4 shows that I must always be less than 2, whenever W_1, W_2, and W_3 have positive finite values.

For the values previously given

$$I=\sqrt{\frac{0.3+0.38+0.02}{0.075+0.19+0.02}}=\sqrt{\frac{0.70}{0.285}}=1.57$$

which is a typical ratio. Expressed in round numbers this is taken as a ratio of 1.6, i.e., the current rating on the 5% tap is 1.6 times the current rating on the 10% tap.

This requires a reduction of the series winding gradient to 15 C at 160% load current which corresponds to a hot-spot gradient of 7 C at 100% load current. Such a reduction in gradient can be accomplished by an increase in the size of the kva parts of the series winding of approximately 20%, representing an over-all increase in kva parts of only 10% since no increase in the kva parts of the exciting winding is required. Still further increase in current rating on the 5% tap can be accomplished as shown in Fig. 4 by further increase in the kva parts of the series winding.

The rating on the intermediate tap voltages can also be increased an intermediate amount by suitably constructed limit switches. The short-circuit rating on the 5% tap is equal to 25/1.6, or only 15.6 times rated current for 2 seconds.

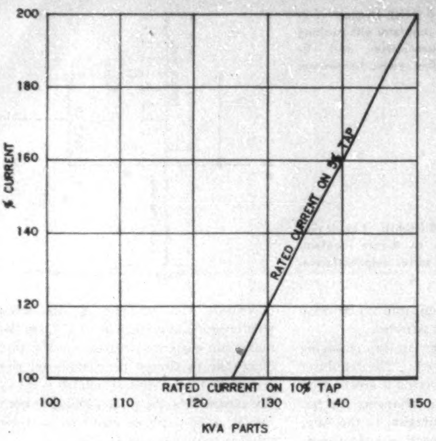

Fig. 9. Current ratings of regulator of Fig. 8

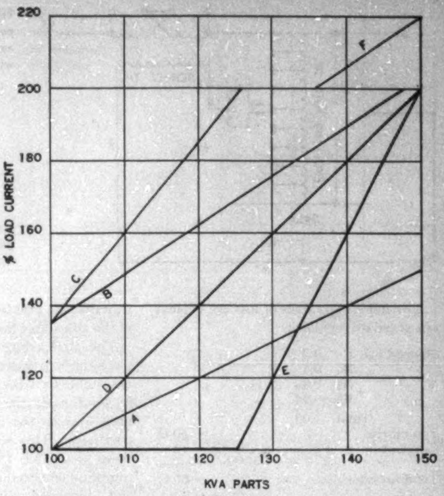

Fig. 10. Current ratings on the 5% tap of various regulator constructions

The increase in current increases the duty on the arcing contacts of the mechanism.

The regulator is suitable for ASA overloads except that in some cases the tap-changing mechanism may be the limitation to the safe overloads. This connection and proportions would be the choice where the reduced short-circuit duty is acceptable and where the increase in current meets service requirements.

Single-Core Regulator With Increased Size of Series Winding Copper

The curves of Fig. 5 are drawn for a regulator in which the size of the series winding is increased proportionally to the current rating, leaving the shunt winding unchanged. The gradient from copper to oil is designed for 15 degrees on the maximum current rating.

The loss in the series winding will be reduced. In an extreme design these values might be obtained: $W_1=0.3$; $W_2=0.15$; $W_3=0.01$. For the same oil rise

$$I=\sqrt{\frac{0.3+0.15+0.01}{0.075+0.075+0.01}}=\sqrt{\frac{0.46}{0.16}}=1.7$$

i.e., the current on the 5% tap might be 1.7 times the current on the 10% tap for the same oil temperature rise.

However, this type of unit is rated on the basis of 25 times rated current for 2 seconds on all taps. This means that the temperature rise may be different on different taps at their rated loads but must never exceed ASA temperature rises. At 200% rated load on the 5% tap the current in the exciting winding is equal to full load current, so the curve is not extended beyond this point.

This connection has the advantage of intermediate increases in rating on the intermediate taps by the use of suitably adjustable limit switches for the tap changer. Full 25 times rated current for 2 seconds is provided on all taps. The regulator is suitable for ASA overloads. The tap changer should be applied so it is not the limitation on ASA overloads. This construction would be applied where it is desirable to have full short-circuit duty on all taps at their increased ratings.

All of the connections described so far have the advantage of obtaining the increased current on the reduced tap by merely changing the position of the limit switch trips which can be made as a

Table I. Comparison of Characteristics of Various Systems

	Single Core Regulator	Reduced Gradient in Series Winding	Increased Section in Series Winding	2-Core Exciting Auto	2-Core Series Auto	Single-Core Regulator Not Overloaded
Figure No.	3	3	3	6	8	
Curve of Fig. 10	*B*	*C*	*D*	*E*	*F*	*A*
Kva parts for 135% current on 5% tap	100	100	118	136	134	135
Kva parts for 160% current on 5% tap	119	110	130	136	140	160
Kva parts for 200% current on 5% tap	148	126	150	136	150	200
Short-circuit rating at 200% current on 5% tap	18.5	15.5	25	25	25	25
Arcing current at 200% current in tap changer in % of 10% current rating	200	200	200	100	100	200
Power terminal board required	no	no	no	yes	yes	no
Adjustable limit switch required	yes	yes	yes	no	no	no
No. of core and coil elements	1	1	1	2	2	1
Intermediate tap ratings available	yes	yes	yes	no	yes	yes
Can ASA overloads be carried without limitation	no	no	yes	yes	yes	yes
Current capacity at 10% tap based on thermal characteristics for 200% current unit on 5% tap	148	125	135	100	100	200

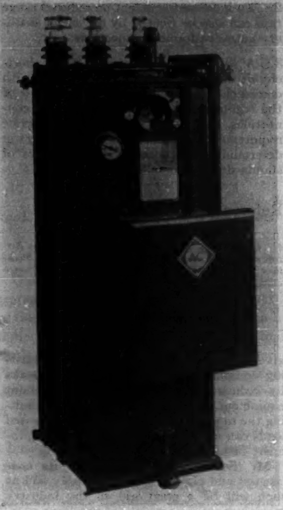

Fig. 11 (left). Typical regulator showing location of position indicator with adjustable limit switch

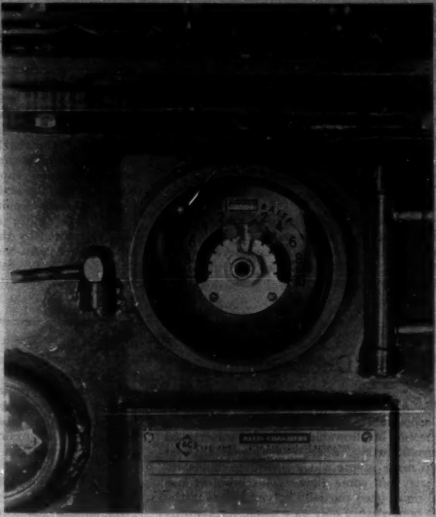

Fig. 12 (right). Regulator position indicator with adjustable limit switch pins

simple adjustment to the control circuit. They all employ a single core and coils which makes the construction simple. They all increase the duty on the arcing contacts as the current rating is increased. They are particularly applicable to the smaller regulators where core and coils are a less significant part of the total cost compared to the mechanism and control.

Tapped Autotransformer With Series Transformer

The circuit for a tapped autotransformer and 2-winding series transformer with series parallel winding is shown in Fig. 6. The kva parts of the exciting autotransformer are equal to 36% of the regulator kva parts. The kva parts of the series transformer are equal to the kva rating of the regulator.

Twice the 10% rated current capacity can be obtained at 5% range by a series parallel connection of the series winding as shown in the figure. Intermediate current ratings on intermediate taps are not obtainable with this connection. This connection has the advantage that the arcing current on full 10% rating is only 10% of the line current. On the 5% connection it is only 5% of the line current. Full short-circuit capacity is obtained on both connections.

The structure is larger and more complicated than the kva parts size indicated because the kva are divided between two transformers. It has the disadvantage that a terminal board or tap changer is required in the power circuit. It will meet ASA overloads without limitation. Its kva parts are shown in Fig. 7. It is particularly applicable to heavy current ratings where it permits the use of a smaller tap changer.

2-Core Regulator With Series Autotransformer

The use of a standard regulator combined with a series autotransformer is shown in Fig. 8. The autotransformer may be connected to any tap between 5% and 10% voltage. Its kva parts, shown in Fig. 9, are equal to 50% of the regulator kva. The total kva parts are equal to 1.5 times the regulator kva. It can be supplied either as an integral part of the regulator or it can be added externally to an existing regulator.

Full rated kva and full short-circuit current are obtained on all tap connections. The structure is larger and more complicated than the kva parts size indicates because the kva are divided between two transformers. It requires a terminal board or tap changer in the power circuit. The current in the load tap changer is the same for all taps. It is applicable not only to new units but may be added to existing regulators where the need for increased current on a reduced tap arises on an existing regulator. The circuit is sometimes advantageous to limit the current in the tap changer, permitting a smaller tap changer to be used.

Other autotransformer connections are available but none of them have advantages for general use over those described so they have not been included.

5% Tap Ratings

Fig. 10 shows a comparison of the kva parts required to produce different current ratings on the 5% tap. There is a wide variation in the kva parts required for a given current on the 5% tap and a wide variation in characteristics. Curve *A* is shown for comparison purposes, it represents a normal regulator operated as a maximum rated device on all taps. A comparison of the characteristics of various systems is given in Table I. It will be noted that no one system is in first place in all respects.

The smallest kva parts or the maximum current rating is only one phase of the process of selecting the regulator performance and type of construction which is best suited to the application.

Limit Switches

The limit switches, Fig. 11, may be adjustable to provide a decreased range of operation through a manhole in the cover or externally without removing the regulator from service. Fig. 12 shows a typical construction for the latter type where the adjustment is made by moving a pin from one position to the desired position. In some cases, the "lower" limit switch can be set for a greater range than the "raise" limit switch because the increased current will occur only when the regulator is raising the voltage.

Conclusions

1. Any single-core regulator can carry increased current on its reduced voltage tap without exceeding the guaranteed temperature rise. 135% of full load current on the 5% tap is a typical value.

By a 10% increase in the physical size the current capacity on the 5% tap can be increased to 160% of rated current on the 10% tap without increasing the capacity on the 10% tap. An increase in current capacity on the 5% tap to 200% can be accomplished but it will be accompanied by an increase in the continuous current capacity on the 10% tap also. The short-circuit capacity of the regulator may restrict the advantage which can be taken of the increased thermal capacity. By increasing the physical size and cost, any desired increase in short-circuit capacity may be secured. The ability to carry ASA overloads may be limited by the capacity of the load tap changer. An increase in capacity on the 5% tap is accompanied by an increase in capacity on the intermediate taps also.

2. An increase in current on reduced range taps can also be secured by the use of auxiliary autotransformer connections.

3. A wide variety of overload and short-circuit characteristics can be secured with corresponding variations in size and cost of the regulators by the use of different connections and design proportions. Service requirements should be the major factors in determining the selected characteristics of standard regulators.

Reference

1. Guide for Loading Step-Voltage and Induction-Voltage Regulators. *ASA Publication No. C57.35-1948*, American Standards Association, New York, N.Y., 1948.

Discussion

W. A. Munson (Westinghouse Electric Corporation, East Pittsburgh, Pa.): The question of allowable overload, or increased current rating, when operating at reduced tap range is one which has plagued the industry for some time. The problem has at times been partially solved by using the oil temperature only as a guide for loading. This, however, has not been entirely correct and as such has probably been detrimental to the equipment.

The method presented by the author enables taking into account not only the oil temperature but also predicting, with a fair amount of accuracy, the coil temperature characteristics. Therefore, a more realistic picture of regulator operation at a reduced tap range can now be predicted.

As summer loads continue to increase at a rate higher than anticipated, the method given by the author will enable using existing equipment to handle the heavy peaks by reducing the total tap range without equipment damage. Thus, by merely limiting the range of the regulator, the increased loads can now be handled and larger equipment installed when convenient.

Mr. Sealey's method, due to its conciseness and clarity, is easy to apply and as such will be a great aid to the industry in evaluating the problem of regulator overload ability.

Behavior of High-Voltage Busses and Insulators During Short Circuits

R. M. MILTON
MEMBER AIEE

FRED CHAMBERS
MEMBER AIEE

IN the near future, the maximum fault current on the 161-kv busses at some of the generating plants and switching stations of the Tennessee Valley Authority will require the use of oil circuit breakers having an interrupting capacity of 10,000 megavolt-amperes (mva). It was felt that tests should be made to determine how these 161-kv busses and their supports would react mechanically when subjected to high fault currents. Similar information was needed also on the performance of 161-kv disconnecting switches. Accordingly, plans were made and suitable temporary test equipment was installed for conducting the tests and collecting data. This article relates to the tests made on busses and insulators; the test facilities and the disconnect switch tests are not described.

Many of the 161-kv busses are of $3^1/_2$-inch aluminum tubing spaced 9 feet apart and supported by pedestal insulators spaced 38 feet apart. Some of the 161-kv busses are supported in the underhung position with the top insulator cap being bolted to the steel structure, and this results in the maximum lever arm being applied to the top insulator cap when force is exerted on the bus.

Joints in the $3^1/_2$-inch aluminum tubing busses have been made either with bolted connectors or by butt welds (in an atmosphere of nitrogen). The ability of this welded-butt connection to stand up under such heavy fault currents was something that needed to be checked.

A wealth of information is available from the various insulator manufacturers on bus-stacking insulators, but practically all of the mechanical strength data are based on a steady pull. This is in contrast to the way that the force would actually be suddenly applied as a result of short-circuit currents. The approach to this investigation was to obtain as much realistic data as practicable by simulating as nearly as feasible the conditions that exist if a bus is suddenly subjected to the magnetic forces caused by a short circuit and to observe any distortions, distresses, or failures of the busses, bus connections, and bus supports.

Description of Test Setup

To subject the insulators to tests representative of conditions actually encountered in service, two concrete foundations were poured, spaced 38 feet apart. Anchor bolts were cast in each foundation for bolting down two independent insulator stacks used to support the two parallel busses. It was felt that such a mounting would be more rigid than those encountered in actual service and would subject the insulators to the somewhat more adverse but comparable conditions.

Paper 55-11, recommended by the AIEE Switchgear Committee and approved by the AIEE Committee on Technical Operations for presentation at the AIEE Winter General Meeting, New York, N. Y., January 31–February 4, 1955, and for representation at the AIEE Southern District Meeting, St. Petersburg, Fla., April 13–15, 1955. Manuscript submitted August 16, 1954; made available for printing October 27, 1954.

R. M. Milton and Fred Chambers are with the Tennessee Valley Authority, Chattanooga, Tenn.

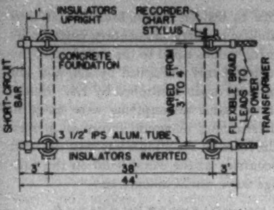

Fig. 1. Arrangement of insulators and busses during tests

The two insulator stacks, used to support one of the busses, were mounted in the upright position with a 3½-inch-high steel base between the bottom insulator and the concrete foundation. The other two stacks supporting the second bus were mounted upside down in order to simulate insulators mounted in the underhung position. Here again a base was provided between the bottom units and the foundation. Each insulator stack consisted of four standard strength basic impulse insulation level stacking units, each 14½ inches high. These units were selected at random from stock, and most of them had previously been in service.

The busses were 3½-inch iron pipe size aluminum tube, alloy *63S-T6*, and each piece was approximately 44 feet long. The bus on the upright insulators was in one continuous piece with no welds. The bus supported on the inverted insulators had a butt weld in the middle third of the span. No sleeve was provided on the inside of the tube to add strength at the weld.

The tubes were rigidly clamped to the insulators on the ends toward the power transformer, while slip-type supports were provided at the opposite end. The busses overhung the insulators as indicated in Fig. 1.

Flexible shunts were connected between the busses at a point 3 feet outside the insulator supports at the transformer terminals and these were kept as straight as possible to eliminate inherent forces. One foot beyond the insulators on the end away from the transformer, a short-circuiting bar was connected between the two busses. Flexible shunts were used to connect the short-circuiting bar to the tubular busses so the insulators would be free to move. Thus, the insulators nearest the power transformers were subjected to forces amounting to 52.6 per cent of the total force exerted on the 42-foot loop.

To record insulator movement, a graphic recorder was provided at the upright stack located near the transformer. The chart traveled at a speed of 3 inches per second. It was started prior to the test so that it would be up to speed. A 7-inch arm attached to the tubular bus adjacent to the bus clamp was used to support the stylus.

It was intended originally to have each bus supported on three insulator stacks, thereby providing two 38-foot spans per bus, but calculations indicated that the impedance of such a circuit would be so high that the current output of the power transformers would be too low. The actual arrangement used consisted of only one span as described in the foregoing, and as indicated in Fig. 1. Two motion-picture cameras were used to take pictures during the tests. They made 62 pictures per second and were started automatically at the beginning of each test.

The test current was provided by two furnace transformers temporarily installed with their 12.5-kv primary windings in parallel and their low-voltage windings (about 190 volts open-circuit) connected in series to provide the single-phase currents. The 12.5-kv circuit was so short that the system was practically an infinite bus as far as the a-c component was concerned. Practically all of the impedance to the busses being tested was reactance so that the current decrement was practically all composed of the d-c component. A slight amount of a-c decrement resulted from the heating of the low resistance in the circuit.

Details of Individual Tests

Single-phase currents were used for the tests, and the forces were calculated from the equation

$$\text{Force in pounds} = \frac{5.4 \times I^2 \times \text{length in feet}}{\text{spacing in inches} \times 10^7} \qquad (1)$$

The current reading is the maximum peak value of the first loop as taken from the calibrated oscillograph film.

Fifteen test shots were made in all, with the initial tests made at the lowest value of current obtainable from the transformer taps. A synchronous timing device was used to hit the voltage wave

Table I. Tabulation of Test Results

Test No.	Bus Space, Inches	Initial Peak, Amperes	Symmetrical Peak, Amperes	Calculated Forces: Initial, Pounds per Foot	Calculated Forces: Symmetrical, Pounds per Foot	Maximum Deflection, Inches
1	48	68,800	39,500	53.3	17.6	11/16
2	48	58,000	36,100	37.8	14.6	3/4
3	48	65,700	40,600	48.6	18.6	13/16
4	48	69,600	42,500	54.5	20.4	15/16
5	48	73,400	43,200	60.6	21.2	1 1/16
6	48	76,500	47,100	65.8	25.2	1 1/16
7	48	78,100	49,400	68.6	25.2	1 1/8
	Bus section shows sign of failure at point of weld. Permanent deflection of 6½ inches noted. Bus rolled over to maintain parallel position and decreased spacing.					
8	42	77,300	50,200	76.8	32.6	1 1/8
9	42	86,400	49,400	96.0	32.6	13/16
	Bus badly bent at point 1 inch from weld, 7 inches out of line. Bus replaced.					
10	36	91,300	48,800	125.0	37.2	1 3/16
	Bottom insulator of inverted stack failed; was completely shattered. Bottom insulator replaced with heavy-duty type.					
11	36	87,000	49,700	113.5	38.4	1 1/4
	Heavy-duty insulator replaced with standard insulator.					
12	48	75,300	44,500	63.8	23.2	3/4
13	48	59,900	47,900	40.4	26.8	3/4
14	48	79,000	44,900	70.2	23.4	3/4
15	48	63,000	47,000	44.7	25.8	3/4

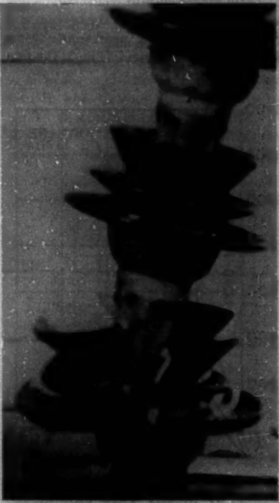

Fig. 2. Insulator failure

Table II. Apparent Forces Imposed on Insulators

Kind of Insulator Stack	Force Imposed by 10,000-Mva Fault on 38-Foot Span: Accepted Factor of 37.4, Pounds	Force Imposed by 10,000-Mva Fault on 38-Foot Span: Factor of 30.7, Pounds	Withstood Force, Pounds	Broke With Force, Pounds
Inverted standard-duty units	1,900	1,558	2,117	2,756
Inverted with one heavy-duty unit	1,900	1,558	2,502	
Upright standard-duty unit	1,900	1,558	2,756	

at zero and obtain the maximum offset. The functioning of the device was unfortunately erratic, and the results were not as uniform as expected. The controls were arranged to open the circuit automatically in less than 10 cycles after the short circuit was established. Table I gives a résumé of the pertinent data. Tests 1 through 7 were all made under similar conditions with a bus spacing of 48 inches. The current was gradually stepped up between shots by changing transformer taps. For test 7, all taps had been cut out and in order to secure more current and forces for subsequent tests, the bus spacing was reduced to 42 inches. The insulator anchor bolts were tightened between shots, the busses examined for bending, and the insulators inspected.

Tests 8 and 9 were made with still higher currents and without insulator failure; however, the welded bus was so badly bent that it was replaced with one having no welds. The bus spacing was reduced to 36 inches, and test 10 was made at a still higher current which completely shattered the porcelain in the bottom unit of the inverted stack nearest the transformer. This is shown in Fig. 2, the first picture taken by the motion-picture camera showing the break.

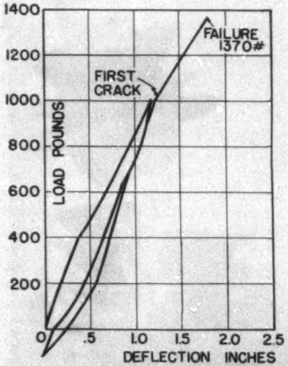

Fig. 3. Deflection and destruction test curve applying to standard 4-unit basic impulse insulation level insulator stack

The broken insulator was replaced with a high-strength insulator, and test 11 was conducted under the same conditions. There were no insulator failures during this test but the initial peak current was not quite as high as that in test 10. As all transformer taps had been cut out and as the bus spacing could not be further reduced (the busses almost swung together in this test), it was decided to try a few reclosing shots.

The bus spacing was increased to 48 inches, and shots 12 and 13 were taken in succession as quickly as the controls would permit; however, shot 13 was approximately 75 cycles after shot 12, and furthermore, the offset was poor. Shots 14 and 15 were taken in an effort to improve on the previous two shots, but they resulted in no improvement. These last tests were of no real significance as the last shot in each instance was delayed so long that the swing of the busses had been largely dampened out.

Force Calculations

The maximum force between parallel conductors spaced on 9-foot centers (standard for 154 kv on the Tennessee Valley Authority system) imposed by a 3-phase 10,000-mva fault (38,000 amperes at 154 kv) occurs on the middle bus at the time the middle bus voltage wave is 45 degrees past zero. According to the accepted equation, the forces would then amount to

$$\frac{5.4\times 0.867(\sqrt{2}\times 2\times I)(\sqrt{2}\times 2\times I)}{\text{spacing in inches}\times 10^7}=\frac{37.4\times I^2}{\text{spacing in inches}\times 10^7} \quad (2)$$

or 50-pounds-per-foot length of bus. This is somewhat higher than would actually be encountered under these conditions because in this accepted equation, the maximum value of the crest of the first loop is obtained by multiplying the rms of the steady-state value by the square root of 2 and then doubling this figure (no decrement assumed). It is the accepted practice to test oil circuit breakers for their ability to carry momentary currents by using values equal to the calculated symmetrical rms multiplied by 1.6, and this product again multiplied by 1.6. Hence, if the same assumptions were made in determining magnetic forces on busses, the force on the middle bus with the fault occurring at the worst point on the voltage wave would amount to

$$\frac{5.4\times 0.867(1.6\times 1.6\times I)(1.6\times 1.6\times I)}{\text{spacing in inches}\times 10^7}=\frac{30.7\times I^2}{d\times 10^7}=41 \text{ pounds per foot} \quad (3)$$

The accepted equation for calculating magnetic forces was used as a basis for these tests. Accordingly, if bus supports are 38 feet apart and a maximum force of 50 pounds per foot for a 10,000-mva short circuit is used, each bus support is subjected to a force of 1,900 pounds.

With the currents actually measured during the tests in the basic equation

$$F=\frac{5.4\times I^2}{d\times 10^7} \quad (4)$$

it is found that the inverted insulators

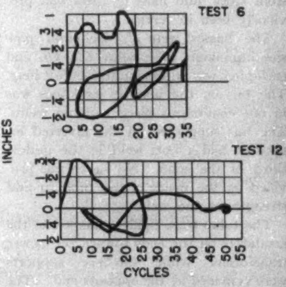

Fig. 4. Insulator deflection chart made during tests 6 and 12

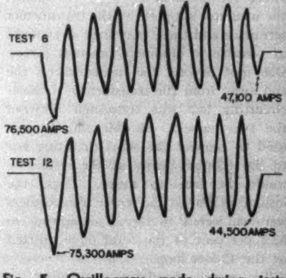

Fig. 5. Oscillograms made during tests 6 and 12

nearest the power transformers apparently withstood an initial force of 96 by 42 by 0.526 = 2,121 pounds in test 9 without breaking. During test 10 the bottom insulator in this inverted stack failed when subjected to a force of 125 by 42 by 0.526 = 2,761 pounds. The inverted stack with a heavy-duty unit at the bottom withstood a force of 113.5 by 42 by 0.526 = 2,507 pounds. A summary of the forces that would appear to be imposed on the insulators and results are given in Table II.

Fig. 3 shows a typical load stress deflection and destruction test curve made with the force applied as a steady pull on a 4-unit insulator stack, equivalent to those used to support the busses in the tests described herein. There is such a wide variation between the test results contained in Tables I and II (calculated forces and actual deflection) and Fig. 3 (actual force and corresponding actual deflection) that it is reasonable to doubt that the force effective at the insulators was as much as the calculated forces shown in Table II.

Shown in Fig. 4 is a reproduction of the insulator deflection chart made during tests 6 and 12. Fig. 5 shows a reproduction of the oscillograms of the same two shots. An examination of pictures made from the motion-picture film during test 12 shows that the busses continued to bend outward for approximately 6 cycles, and this is checked very closely by the deflection curve made on the chart, which moved at the rate of 3 inches per second. The oscillogram for test 12 shows a good offset with the wave back to symmetrical configuration at the end of about 5 cycles. It seems reasonable to consider the busses as being bent outward by a series of successive forces, each proportional to the square of its half-cycle of current; however, these successive forces are not transmitted entirely to the insulators because they are partially consumed by bending the busses and initiating the movement of the insulators from rest. Since the accepted rate of decay for short-circuit currents gives an average current from inception to steady state of approximately 1.25 times the steady-state value, these successive forces as applied to the insulators would then be equal to a current 1.25 times the peak of the steady-state current. The insulators in turn deflected as they picked up stress.

Table III. Torsion on End Insulator Stacks

Mid-span Deflection, Inches	Calculated Twist with no Restraint by Insulators		Calculated Twist Assuming Insulators Restrain $33^1/_3$ Per Cent	
	Degrees	Minutes	Degrees	Minutes
3	1	15	0	50
6	2	25	1	37
9	3	38	2	26
12	4	55	3	17
15	6	00	4	00
18	7	12	4	48
21	8	25	5	37

With this method of computation, it is found in test 6 the force on the busses, which is effective on the insulators, was 39 pounds per foot, or a total of 860 pounds on the insulator stack. In the insulator deflection chart (Fig. 3), it is shown that this force should cause the insulator stack to deflect 1.05 inches, whereas it actually moved 0.9 inch. In test 12, the effective force on the insulators was 34.8 pounds per foot, or 770 pounds on the insulator stack. The chart shows that this will produce a deflection of 0.75 inch, and this is the value actually measured. In test 10 the effective force on the insulators was 55.8 pounds per foot, or 1,230 pounds on the insulator stack. The chart shows this to be more than the strength of the stack, which agrees with the test results, since the bottom unit failed during the test. This theory presents a strong argument that will be hard to disprove as the results agree so favorably with the calculations.

This theory is suggested for high-voltage long-span tubular busses which permit the high initial forces occasioned by the few first half-cycles of current to be partly used in bending the busses and deflecting the insulators. The proposed equations for obtaining the forces on the insulators would be, for a single-phase circuit

$$F=\frac{16.86\times I^2}{d\times 10^7}\times S \qquad (5)$$

and for a 3-phase circuit

$$F=\frac{14.60\times I^2}{d\times 10^7}\times S \qquad (6)$$

where

F = force, pounds
d = spacing, center to center of busses, inches
I = symmetrical rms short-circuit current, amperes
S = one-half of sum of adjacent spans, feet

The foregoing proposed equations should not be used to calculate the forces on busses as these forces would be determined by using the equation suggested earlier in this article. Furthermore, the proposed equation for determining forces on insulators does not apply if the busses have excessive sag or nonreinforced butt welds in the middle third of the span. It will be noted, Fig. 4, that maximum deflection in test 12 occurred during about the first 7-cycles of time. In test 6, however, the deflection during the first 7 cycles was not as great as it was a few cycles later. As previously stated, the bus in test 6 had a butt weld in the middle third and the heat when welding had softened the metal near the weld; consequently it had more sag than the bus in test 12. The second peak in the deflection curve was due to the whip which occurred when the excessive sag at mid-span reached its maximum swing. This condition did not occur in test 6 as the strength of this bus had not been reduced and there was no whip from excessive sag.

Because of the long spans, and height, and the considerable weight of the insulator stacks, the "natural period" of mechanical vibration of both the bus insulators and the total bus are so low when compared to the period of 60 cycles, that no resonance from the alternating current could be expected. There was no evidence during any of the tests of the 60-cycle magnetic forces getting in phase with the natural period of the busses used on any of the tests.

Torsion Stresses

Fig. 6 is a reproduction of the insulator deflection chart made during test 7. During this test the chart remained stationary, and plainly shows the torsional stresses imposed on the insulators as the busses swing outward and then inward. Torsional stresses are a problem only to the insulators supporting the ends of the busses. The bus used during this test was the one with the weld which had excessive sag and this increased the deflection and torsion. Unfortunately no similar chart was obtained during tests on a nonwelded bus. However, the reverse movement in test 12 indicates that tor-

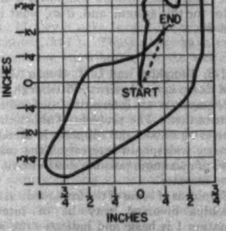

Fig. 6. Insulator deflection chart made during test 7

sion was present in a substantial amount during that test.

Table III shows the amount of twist imposed on an end insulator stack for various deflections at mid-span. These calculations apply to a $3^1/_2$-inch iron pipe size aluminum tube bus supported on insulators spaced 38 feet apart with one end clamped rigidly to the insulator and the other end equipped with a slip-type support, free to move.

One column shows the twist imposed on the insulator at the end of a bus assuming no restraint by the insulator. The other column shows what this twist would be assuming the insulators restrained the bus by $33^1/_3$ per cent. This percentage is an assumption based on observation and it is recommended that further tests and studies be made to determine this value more accurately.

Conclusions

It would appear that the present accepted equation for calculating forces on high-voltage long-span busses is not consistent with the method used in determining the momentary rating of oil circuit breakers, as it gives too high a value.

It would also appear that the present method used to determine the forces on insulators supporting high-voltage long-span tubular busses results in values excessively high, and that consideration should be given to the use of the proposed equations 5 and 6.

It is suggested that the size tube used in long-span tubular busses be selected on the basis that sag will not be excessive. It is also suggested that no welds be made in the middle third of the bus unless reinforced with a sleeve or equivalent for maintaining the original strength of the tube.

◆

Discussion

A. S. Mickley (Philadelphia Electric Company, Philadelphia, Pa.): This paper is a considerable addition to the test data available for the design of high-voltage busses to withstand short-circuit forces. Before these tests are accepted as a basis for modifying the present convention equations, however, it might be well if the authors would clear up a few questions on the analysis of their data:

1. Full offset on the initial crest was not obtained in all tests, since the fault initiating device was admittedly erratic. However, in the case of equations 5 and 6, the same empirical constant is used to explain all tests (1.25 times the symmetrical peak), regardless of the actual degree of offset obtained. Should not the varying offsets obtained under test be taken into account in arriving at an empirical constant to be useful for a design calculation assuming a predetermined offset?

2. The authors would apply their equations to an infinitely long bus. Has any attempt been made to correct the data for the relatively short test bus used and for the effect of the corner connections?

3. Equation 3 is presented as applicable to the calculation of bus stress. Have the test data been analyzed on the basis of this equation, and, if so, what comparison can be made between the calculated stress, the yield strength of the material, and the observed deformation of the busses?

4. Have the authors computed a stress factor for this system, and, if so, what is its value?

Joel S. Tompkins and **L. T. Guess** (Aluminum Company of America, Pittsburgh, Pa.): This paper is an interesting and valuable contribution. The problem of short-circuit stresses on busses and supports is becoming of more widespread interest as the magnitudes of maximum possible short-circuit currents increase.

Emphasis of some of the fundamental relationships involved may be of interest. Equation 1 is basic and indicates the magnetic force between two long parallel wires in a single-phase circuit. If a peak value of current is used, a value of maximum force results from the equation. If an rms value of current is used, the resulting force value is an average. It can be seen that, with a symmetrical alterating current, the force varies at a double frequency, 120 cycles per second (cps), between zero and maximum with the average force equal to one-half the maximum force. With an offset wave, the average force is somewhat less than one-half the maximum force. As noted in the paper, the use of equation 2 results in a value of maximum force.

While the use of equation 2 would result in the correct value of maximum force, it does not appear that it should be used to calculate stresses or deflections of long busses or supports. The maximum stress in a tubular bus under short-circuit conditions depends on the deflection of the bus. Similarly, the maximum stress in bus supports depends on the deflection of the supports. The natural frequencies of a long span of high-voltage bus and of the bus and its supports are much lower than 60 cps. As noted in the paper, the bus can be considered as being deflected by a series of successive impulses, which are at double frequency (120 cps). The net movement of the bus would be more nearly a function of the average force than of the maximum force.

A tubular bus and its supports form a mechanical system which has mass, elasticity, and some damping. The relationships involved in the dynamic response of the system to a suddenly applied force are complicated, though the response can be calculated if the constants of the system and the characteristics of the force are known. In general, the difference between the externally applied force and the internal resisting force, because of the stiffness of the system, is effective for accelerating the mass of the system. This may be expressed in general terms as

$$F_M - kx = ma = m\frac{d^2x}{dt^2}$$

where

F_M = effective magnetic force
k = effective spring constant of the system
x = effective displacement from the at-rest position
m = effective mass of the system
a = effective acceleration of the system

From this equation, it may be seen that when a constant magnetic force is first applied the displacement is zero and the acceleration is a maximum. However, as there is no displacement initially, there are no bending stresses in the bus or its supports. The shearing stresses which would occur would normally be negligibly small. If the mechanical system is critically damped, and if the magnetic force is large in relation to the effective mass of the system, the deflection will soon reach and remain at its maximum value (assuming deflection within the elastic range). The velocity and acceleration will then be zero, the right-hand portions of equation 2 will be zero, and the magnetic force will be balanced by the resistive forces of the system. As the damping in the mechanical system would probably be smaller than critical, there could be some overshoot of the displacement with attending increased bending stresses. This possibility of overshoot is recognized in the paper and is indicated in Fig. 4. The maximum bending stress is a function of the maximum deflection.

This equation is of course an oversimplification for a bus system. Normally, the maximum bending of the bus would occur quite quickly after a short circuit, so the bus would reach its maximum bending stresses quickly. Becuase of the large mass of the supports, these would reach their maximum bending stresses more slowly, though probably the maximum would be reached during the short circuit.

Because of the relatively large mass and low natural frequency of the supports, it appears that the normal maximum deflection and bending stresses could be estimated approximately by using values of average magnetic force as calculated using initial rms current values. This force would be roughly one-half of the maximum force as calculated by equation 3. It is interesting to note that equations 5 and 6, derived by the authors using a somewhat different analysis, result in values about half of those resulting from equation 3.

Because of the probability of overshoot of the bus, the maximum bending stresses in the bus probably would be somewhat greater than would be estimated by using average magnetic force, but it appears improbable that the stresses could be as great as would be estimated by using maximum force. The use of force as calculated by equation 3 would result in excessively high bending stresses, it is believed. The maximum bending stresses probably would be between a value calculated using the maximum force and a value calculated using the average force.

The comments concerning the welding of tubular aluminum bus are of interest. For maximum bending strength, welds should be located outside of regions of high bending stresses, and the strength of welds can be increased materially by the use of internal reinforcing sleeves. A basis for estimates of reduction of strength of welded bus is available.[1,2]

REFERENCES

1. MECHANICAL PROPERTIES OF ALUMINUM ELECTRICAL BUS, G. W. Stickley, C. O. Smith. *AIEE Transactions*, vol. 73, pt. III, Apr. 1954, pp. 100–06.

2. PRACTICAL CALCULATION OF SHORT-CIRCUIT STRESSES IN SUPPORTS FOR STRAIGHT, PARALLEL BAR CONDUCTORS, Schurig, Frick, Sayre. *General Electric Review*, Schenectady, N. Y., vol. 29, 1926, pp. 534–44.

C. G. Adams (General Electric Company, Schenectady, N. Y.): In reporting the results of their extensive tests, the authors have made an important contribution by focusing attention on the severe mechanical stresses imposed on bus insulators by the high values of short-circuit currents which are associated with interrupting duties presently encountered on important high-tension busses. Using their proposed equation for effective force, it appears that, in spans whose lengths are in the order of magnitude of that tested, there are forces sufficient to cause breakage of insulators at 15,000 mva interrupting duty on a 161-kv bus with 9-foot spacing. Test results have been correlated with calculations employing the proposed equation. It would be useful to have the authors' comments on several points involving the extension of the use of the equation from test conditions to the design of high-voltage busses.

Referring to equation 5, the effective force is interpreted to mean that force which, if applied slowly and steadily to the top of an insulator, would result in an insulator deflection and stress comparable to that obtained with a fully offset short-circuit current. For this type of short circuit, the pulsating components of force are 60 and 120 cps. Since the test bus appears to have a natural frequency of about 2 cps and the insulator stack about 6.6 cps, the pulsating components of force are not effective in producing insulator stress. The average forces are the only ones that need to be considered. For purposes of easy comparison, a force equal to the average force due to the symmetrical alternating current may be defined as 1 per unit (pu). It can be calculated from equation 1, when I is defined as the rms value of the symmetrical current. One pu force when slowly and steadily applied will produce 1 pu insulator stress. If the bus structure were to be considered equivalent to a single mass restrained by a single spring with very little damping, the sudden application of 1 pu force would result in a maximum transient insulator stress of about 2 pu, since the top of the insulator would overshoot its steady-state position by nearly 100 per cent. But, the average force due to a fully offset current wave, with no d-c decrement, is three times the average force due to a symmetrical current having the same a-c component, or it is 3 pu. This force, suddenly applied, would result in a maximum insulator stress of 6 pu. The time rate at which the average force changes from 3 pu to 1 pu, in relation to the natural frequency for the system, is important in determining the maximum insulator stress. This time rate of decay is largely determined by the effective X/R ratio of the circuit. In the authors' tests from observation of Fig. 5, the X/R ratio of the test circuit is approximately 6. Equation 5 suggests that the maximum insulator stress is 3.12 times the stress produced by the application of the average force due to the symmetrical current. The ratio of maximum insulator stress to the stress produced by the slow and steady application of 1 pu force may be defined as the insulator stress factor. Would the variation of circuit X/R ratio have a significant effect upon the proposed equation? Also, what would the authors consider the effective X/R ratios of their high-tension busses to be?

Referring to Fig. 6, a large insulator deflection appears to occur in a direction tangential to the bus direction. This tangential deflection combines with the lateral deflection to produce the total insulator deflection. In the center spans of a long uniformly supported bus, a tangential deflection could reasonably be expected to be small, if not entirely absent. Also, in a simply supported bus, if one end were relatively free to move through the insulator clamp, again substantially no tangential deflection should occur. Since a tangential deflection appeared to a rather great degree in the test pattern, would the authors describe the test bus clamping arrangement? In their opinion, would the method of clamping influence their test results appreciably?

Considering only lateral deflection of a uniformly supported bus, an insulator stress factor of 1.8 has been calculated from an analytical investigation for a circuit X/R ratio of 6.28 for a single application of short-circuit current. This is to be compared to the value of 3.12 from test results on a simply supported bus where a large amount of tangential deflection appeared to be present. A stress factor of 3.41 was calculated for the same uniformly supported bus, when the alternating current was applied with a circuit X/R of 25.12 for 6 cycles followed by the reapplication of the same current 25 cycles later at a point to obtain nearly the maximum insulator stress. Where high-speed reclosing is employed on lines radiating from high-voltage busses that may be subjected to high values of short-circuit current, it would appear that this should be factored into the determination of maximum insulator stress. The authors' comments on the practical necessity for taking rapid reclosing into account would be pertinent.

S. C. Killian (Delta-Star Electric Division, H. K. Porter Company, Inc., Chicago, Ill.) The authors are to be commended on their paper since it fills a long-felt want. We have all been aware of the fact that, in most cases, calculated forces on busses were not transmitted into insulators undiminished. It has been understood that when making short-circuit calculations on busses, "Part of this instantaneous force will be absorbed by the intertia of the bus system so a safety factor is naturally present."[1] This is particularly true in power circuits where the d-c component decays rapidly, making any similarity to the long, steady load in a testing machine even less of a possibility. No actual measurements or calculations had been made on this problem, however, and here in this paper for the first time we have a measure of the decrease in insulator loading due to this effect.

The authors are correct in their statement that 37.4 factor used in short-circuit equations is high for any average power circuit condition. This factor has been understood to be high since, "Some decrement will be present, even in the first half-cycle peak. On the other hand, generator overexcitation will tend to increase wave amplitude. Since these factors oppose each other, it is reasonable to suppose that the ratio is approximately correct. Their use makes bus calculation conservative."[1] Power circuits do have a generally accepted 1.6 value instead of a doubling factor. This builds a safety factor into all power short-circuit calculations and it should be recognized as such or, as the authors suggest, new equations with smaller constants used.

Equations 5 and 6, based on an average current multiplier of 1.25, do give very close agreement with test results as the authors point out. It would seem, however, that these equations would apply only to insulator stacks 4 standard units high and with bus spans of about 40 feet. Is it not reasonable to assume that with stronger busses and shorter spans, such as are used in lower voltage work, more of the initial force will be transmitted into the base of the bus support since neither the conductor or insulator are so limber? Could we generalize by saying that such equations as 5 and 6 would be applicable to insulator stacks 4 high and above since even if heavier units are used the extra height will likely compensate for the individual insulator stiffness. Forty-foot spans are representative enough to apply in a general manner. On lower voltage busses where heavier busses and stiffer insulators are used, some value should be used between the 14.6 constant and the 30.7 or 37.4 value.

In a very general sense, this paper teaches that a standard stack of insulators, 4 units high, can withstand a force two to three times as large under short-circuit as it can under steady loading. This is very valuable information.

REFERENCE

1. MECHANICAL FORCES ON BUSES DUE TO FAULT CURRENTS, S. C. Killian. *Electrical World*, New York, N. Y., Dec. 12, 1942.

R. L. McCoy (Locke Insulator Corporation, Baltimore, Md.): The authors have made a significant contribution to the electrical industry by making and reporting on this series of high current tests done on sections of actual bus mounted conventionally on practical high-voltage bus supporting insulators. This paper illuminates the frequently made error of calculating the maximum instantaneous force developed in the span and comparing this value with the strength rating of the proposed insulator as developed from steady, slowly increasing applied cantilever loads.

A true appraisal of the situation requires the analysis of many obscure factor involved in any particular case. These can often be only roughly approximated. However, valid judgments deliberately slanted towards the conservative side can usually evolve a safe and economical design.

It appears from the description of the test setup used in these tests that the flexibility usually involved in mounting the insulator was largely eliminated. This flexibility adds to that of the insulator and tends to reduce the stress imposed on the insulator and further lowers the natural period of the entire bus structure. As the authors point out, this makes the results pessimistic with respect to the insulator's ability to withstand the forces imposed.

Since high-capacity equipment, such as is involved in this study, is usually protected by extremely fast-acting oil circuit breakers, the nature of the forces imposed on the insulators becomes one of cantilever impact, and the inertia effects of the bus and insulators become important factors to consider. Where fast reclosing is practiced, consideration should be given to the reclosing time relative to the natural period of the bus structure, so that these do not coincide in period and phase if the bus should still be short-circuited on subsequent reclosures.

In connection with the authors' comments on Fig. 6 showing the deflection chart made during test 7, it would appear that longitudinal components of the trace could result from longitudinal movements of the bus, i.e., movements of the bus parallel to the length of the bus, as well as from torsional forces at the top of the insulator resulting from sidewise deflection or sag of the bus.

These tests demonstrate the marvelous ability of modern high-voltage switch and bus insulators to take repeated severe punishment under actual short-circuit conditions. In connection with disconnect switch construction there has been in recent years a demand for stiffer insulators to hold switch parts in closer alignment. It should be noted here that the perceptible degree of flexibility which is inherent in the design of the multipart cap-and-pin-type switch and bus insulator permits to to roll with the punch that the severe short-circuit imposes and still support the bus adequately time after time. Units of more rigid construction must withstand greater stresses since they do not yield as much and allow inertia to cushion the blow. It is interesting to note that in test 7 the 4-unit stack of standard strength units in the underhung or weaker position withstood without failure to the equivalent of a 15,000-mva short-circuit on a 154-kv system with a center to center bus spacing of 9 feet and an equivalent span of 22 feet under the very adverse conditions of an extremely rigid support and a weakened and badly bent bus section.

J. M. Sheadel (Ohio Brass Company, Barberton, Ohio): The short-circuit tests and the analysis of the results as presented by Mr. Milton and Mr. Chambers fill a real need in high-voltage station insulator studies. Such high-current tests can be made by power systems with far better realism than can be accomplished by insulator manufacturers.

It had been recognized in the past that the usual methods of calculating high-voltage short-circuit stresses incorporated a number of safety factors and that an additional margin normally was not necessary for insulators. The test analysis presented in this paper indicates the size of this margin for this particular test arrangement. This information will be most useful in making future calculations.

Since the insulators were mounted directly on a concrete base, the test stresses may have been more severe than actual conditions impose. In service, the insulator stacks are often mounted on steel structures to that part of the force from short-circuit conditions will be lost in the deflection of the structure.

This investigation supports the conclusion that standard cap-and-pin-type bus insulators still meet the severe requirements of this growing power system. Use of standard insulators contributes to effective manufacturing and minimizes stocking problems.

The discussion of torsion stresses and the data summarized as Table III introduce another factor. Were the indicated midspan deflection of 21 inches and the assumed 33$^1/_3$-per-cent twist restraint by the insulators based on test observations or on calculations? If torsion stresses caused by short circuits may be critical, then it will be a distinct service to the industry for additional tests to be made to determine the safety factors.

R. M. Milton and **Fred Chambers**: We deeply appreciate the discussions which serve to call particular attention to some of the phases of this problem. Reference has been made to the use of the term "stress factor" and we believe that this term may be rather widely used in this connection as the general problem is explored (of course, our tests covered only the specific problem described). Possibly the general equation (for 3-phase busses) would be

$$F=K\,\frac{37.4I^2}{d\times 10^7}$$

with K being used to designate the stress factor.

In determining stress factor there are many variables that will have to be evaluated and it is thought that this will probably be extremely difficult to do precisely. Others may also find it desirable to run some tests for their specific problem in order to check the calculations. In the accepted equation for forces between busses, the rms current is raised by a factor of $\sqrt{2}$ to obtain the peak of the steady-state loop and then the peak of the first loop is assumed to be double the peak of the steady-state loop for a maximum offset wave. (Actually, it is improbable that the peak of the first loop will be greater than 1.8 times the peak of the steady-state loop.) This is the basis for the accepted equation 2. In determining the possible rms fault currents at various locations, it is usual to take into account the possible overexcitation that may be applied to its generating units.

Some of the discussers recognized that equation 3 was given to illustrate the calculated forces that would exist if the same assumptions were made that are permitted in consideration of circuit-breaker application. We did not, as Mr. Mickley understood, advocate the use of equation 3 for calculation of bus stresses. Direct comparison cannot be made correctly for the consideration of circuit-breaker application and bus forces. For circuit-breaker application, consideration must be given to the maximum momentary values of currents while the maximum bus forces are experienced at a time when no phase is carrying the maximum current (3-phase). Equations 5 and 6 are based on a maximum offset current wave and on using a 1.25 multiplier times the symmetrical peak current. This value is based on the square root of the average of the squares of each loop from initial short circuit to steady state when the initial loop has maximum offset. The resulting equation checked very closely with the results of the steady pull test. Equations 5 and 6 should, as Mr. Mickley suggests, be revised (downward) if the current wave is considered to be different from maximum offset; however, we were interested in investigating the worst possible condition.

We realized that, in order to consider the forces that are actually transmitted by busses to insulators, the following were among those factors that needed to be considered:

1. The maximum rms short-circuit current with all lines and equipment in service and any expected overexcitation applied to generators.

2. Taking the peak of the first loop as 1.8, instead of 2, times the peak of the steady state (possibly the forces between the busses would be more realistic if this were done).

3. The characteristics of the busses themselves and the mechanical arrangement that determines the ability of the busses to transmit average values of forces to the insulators instead of instantaneous values. This would include:

a. The spacing of the busses and bus supports.

b. The characteristics of the busses themselves, such as size, weight, shape, and the elastic and damping characteristics of the busses. The magnetic forces cause the busses to bow outward and store energy to result in transferring the forces to the insulators in more of an average value form than as instantaneous amounts. Also the bowed-out busses receive less magnetic forces due to their increased separation. Mr. Tompkins gave some very interesting comments and suggested a general equation which should be very helpful in approaching the problem of evaluating these factors.

c. The natural "period" of the busses and of the bus supports. This could cause some very high values being applied to the insulators if the bus period were to be about the same as the frequency of the current loops.

d. The amount of sag that the busses may have, which would result in some "whipping" because when the magnetic forces are applied there would then be some lifting of this sagged bus.

4. The expected duration of the fault current. It is normal to expect to clear a bus fault by differential relay in 6 to 8 cycles.

5. The X/R ratio of the system at the point of fault. As Mr. Adams indicates, with a low X/R ratio, the d-c component may disappear in 2 cycles, whereas with a high X/R ratio it may continue for 15 or 20 cycles. Hence, the square root of the average of the squares of the loops for the

first 6 cycles will be higher for the higher X/R ratio.

6. The insulator mounting which may be on steel members that will themselves absorb some of the force. On the other hand, the "period" of the insulators and their mounting could be changed to result in about the same period as the busses themselves and worsen the situation.

Some of the variables, such as those listed in the foregoing, could be determined but some of them could not be defined sufficiently close for design purposes, so the tests were made for the specific conditions that required immediate investigation.

As a result of the tests, it was concluded that the stress constant K for the conditions investigated is 0.39. Possibly only minor changes in some of the conditions could result in a materially different stress constant. Doubtless, there would have been some additional tortional and tangential forces on the insulators that had slip-type supports if these had been replaced with rigid clamp-type supports.

The insulators were assumed to restrain the tortional deflection by about $33^1/_3$ per cent. This assumption was based on the calculated angle deflection for a symmetrically loaded beam and then this was compared with the estimated actual deflection. The estimates of actual deflection were based on a study of the motion pictures that were made at 62 frames per second and the movement of the stylus. Less attention was paid to tortional forces because they would theoretically only occur to the end insulators and these insulators would normally expect to have a maximum of one-half of the total forces that are incurred by the insulators located between equal spans.

The X/R ratio of the system at the location of the tests was of the order of 15 to 1. The X/R ratio at points on the Tennessee Valley Authority system where a 10,000-mva fault may be possible will probably be more nearly of the order of 30 to 1. Other conditions during the tests, however, were more rigid than would be encountered at locations of a 10,000-mva fault because the insulators were mounted in concrete, instead of being mounted on steel members that would have some flexibility (unless their flexibility resulted in a "period" about equal to the period of the bus); the insulators were subjected to torsional and tangential forces in addition to lateral forces, whereas only the latter forces would be encountered in actual service, except for the end insulators where the total forces are only about one-half of the others; the fault currents were applied for over 8 cycles in each case, whereas an actual fault may be cleared in some 4 cycles for a close-in line fault and 6 cycles for a bus fault.

Mr. Killian seems to have made a sound speculation that the stress factor determined from this test would not be exceeded if the bus supports were to remain spaced 38 feet apart and all other conditions unchanged except for additional units used in the supporting stacks for higher voltage insulation.

No instantaneous (20-cycle) reclosing tests were made. Tests 12 and 13 and tests 14 and 15 attempted to duplicate reclosing conditions; however, the reclosing was not made until some 75 cycles later and it was not made at the worst point on the voltage wave. We virtually discounted the value of these tests. In considering reclosing it is, of course, important to know the exact position and direction of movement of the bus at the moment the circuit breaker recloses, in addition to other factors. Further study is certainly indicated for this phase of the problem.

The Tennessee Valley Authority does not have any circuit breakers to reclose automatically following a bus differential operation. Of course, a close-in fault on one of the lines may cause currents approaching 10,000 mva to flow, and possibly high-speed reclosing may be used on the circuit breakers for the lines. The worst reclosing condition occurs when the mechanical forces, stored in the bus assembly, are additive to the magnetic forces caused by the fault current and if the reclosing is made at the instant that these magnetic forces are a maximum. This would represent a compounding of assumptions. The probability would be great that the fault current contributions would be divided on the busses and only the cross bus which supplies the faulted line would carry all of the current. In Tennessee Valley Authority plants, these cross busses are parallel for only a short distance and the supports are more closely spaced than on the main busses.

It is hoped that others who investigate these problems will make their findings known to the rest of us who have considerable interest in the matter.

Intermittently Increased Kilovar Output of Large Capacitor Banks

P. M. MINDER
ASSOCIATE MEMBER AIEE

THE AIEE has made recommendations for permissible 60-cycle overvoltage operation of power capacitors.[1] Operation at overvoltage of capacitors means an increased kilovar (kvar) output proportional to the square of the voltage increase. So far, little use has been made of the economics offered by this overload capacity.[2] The overload capacity of capacitors can be used advantageously for two temporary system requirements: 1. a short-time comparatively large kvar increase for system stability in emergency cases; and 2. a longer time comparatively small kvar increase for intermittent extreme voltage or power-factor improvement.

Two methods of applying an overvoltage on all or part of the capacitors of a large bank are described. Both methods are similar in that they are applicable only to multiseries group capacitor banks. Under certain conditions both methods can be of great economic advantage since the temporary kvar increase is accomplished only by the addition of a few small capacitor switches.

Overload Characteristics of Power Capacitors

Some specific values of the AIEE recommendations for short-time 60-cycle overvoltage operation are the following:

1. 1.8 times rated voltage for 15 seconds.
2. 1.7 times rated voltage for 1 minute.
3. 1.55 times rated voltage for 5 minutes.
4. 1.1 times rated voltage for 24 hours.

The permissible number of overvoltage applications for 1 minute or less is limited to 200 to 300 during the life of the capacitor. For longer periods of 5 minutes or more, a greater number of applications is permissible providing the average kvar does not exceed the kvar rating of the capacitor. If the range between 5 minutes and 24 hours is interpolated, one arrives at

1. 1.2 times rated voltage for about 6 hours.
2. 1.3 times rated voltage for about 1.5 hours.

These figures are often considered to be quite conservative.

Series-Short-Circuiting Method

The first method of temporarily increasing the kvar output of a capacitor

---

Paper 55-356, recommended by the AIEE Transmission and Distribution Committee and approved by the AIEE Committee on Technical Operations for presentation at the AIEE Southern District Meeting, St. Petersburg, Fla., April 13–15, 1955. Manuscript submitted January 6, 1955; made available for printing March 15, 1955.

P. M. MINDER is with the Line Material Company, South Milwaukee, Wis.

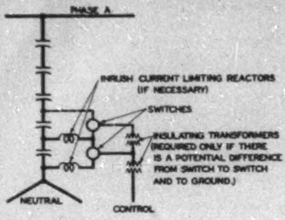
PHASE A
INRUSH CURRENT LIMITING REACTORS (IF NECESSARY)
SWITCHES
INSULATING TRANSFORMERS (REQUIRED ONLY IF THERE IS A POTENTIAL DIFFERENCE FROM SWITCH TO SWITCH AND TO GROUND.)
NEUTRAL
CONTROL

Fig. 1. Series-short-circuiting method

bank is the series-short-circuiting method. The principle of this method is to have one or more series groups in all three phases short-circuited, preferably the ones closest to the neutral. Fig. 1 shows this schematically. By short-circuiting some but not all series groups of a multiseries group capacitor bank, higher than normal voltage is applied across the remaining series groups which results in an increased kvar output of the whole bank. The short-circuited series groups do not produce any kvar. This is a disadvantage which, however, is offset by the extreme simplicity of this method.

The cost of this kvar increasing method is very small. The only equipment involved is small 15-kv capacitor switches, some low-cost current-limiting reactors, and possibly some insulating transformers. If the neutral of the bank is floating and if the switches are not grounded, the control power for the electrically operated switches should be supplied through one or several cascaded insulating transformers. Likewise, if more than one series group in each phase is equipped with a short-circuiting switch and if a potential difference exists between the frames of the series groups, an insulating transformer should be applied between the controls of the switches in the same phase.

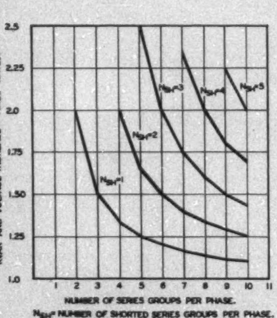

Fig. 2. Series-short-circuiting kvar increasing

For a typical example on a 69-kv 9,900-kvar grounded-neutral single wye bank consisting of six series groups of 6,640-volt capacitors, the cost of the switches and reactors to short-circuit one series group in each phase, thereby obtaining a 20-per-cent increase in kvar, would be slightly over 1-per-cent of the cost of the total bank. For an ungrounded neutral bank of the same rating the cost would be slightly over 2-per-cent of the total bank cost because of the need for insulating transformers.

The insulating transformers should have a 120 to 120-volt ratio and the insulation between the two windings should be of the 15-kv class. Depending on the design of the switch control, two transformers may be required: one for the on and one for the off operation of the switches. Such insulating transformers, two units in one tank with three low-voltage bushings and three high-voltage bushings, are a standard part of the voltage divider switching (VDS) scheme and are available on the market.[3]

Fig. 2 shows a graph of the kvar increase as a function of the number of series groups with the number of short-circuited series groups as a parameter. With the series-short-circuiting method, the ratio of the kvar increase above rated kvar is the same as the increase in voltage above rated voltage of the series groups which are not short-circuited. The square relationship between kvar increase and voltage increase is lost for the bank as a whole because the short-circuited series groups do not produce any kvar. To study the use of the graph, take as an example a capacitor bank with five series groups per phase. If two series groups in each phase are equipped with a short-circuiting switch, the kvar output can be increased to 1.66 times the rated kvar of the total bank for a safe duration of about 1.5 minutes. If only one series group in each phase is short-circuited, the kvar increase is 25 per cent, and this increase can be utilized safely for about 3 hours.

As an illustration of the economic advantages of this series-short-circuiting method, Fig. 3 shows a very favorable example, namely, a large bank consisting of five series groups and four steps of which three steps are switched by the VDS scheme, and the addition of a fifth step is under consideration. If this fifth step is not required for periods longer than 3 hours and sufficient time is allowed between increased output periods, the additional step can be obtained simply by the insertion of one small capacitor switch in each phase. This procedure eliminates the expense of additional capacitors. The reason for the requirement of only three switches per short-circuited series group in a multistep bank is that with the use of the VDS method all series groups are connected in parallel, energized or not energized. In VDS banks, as in this example, the cost per additional kvar can be an extremely small fraction of the cost of an original kvar. It is understood that the rated current of the total bank is not allowed to exceed the rated current of the short-circuiting switch.

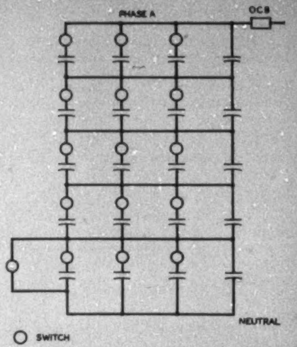

INSULATING TRANSFORMERS, CONTROL WIRING AND POSSIBLE INRUSH CURRENT LIMITING REACTORS ARE NOT SHOWN.

Fig. 3. Series-short-circuiting method applied on VDS bank of four steps

If each step is switched separately or if only 1-step banks are applied, switches are required for each step. Even so, if this short-circuiting scheme is applied on a system-wide basis, a considerable amount of kvar can be gained for intermittent duty at a very low cost.

Series-Parallel Method

The second scheme to apply overvoltage on a capacitor bank is the series-

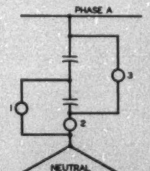

TO GET 4 TIMES RATED KVAR SWITCHING SEQUENCE CLOSE 1, OPEN 2, CLOSE 3.

TO GET RATED KVAR SWITCHING SEQUENCE OPEN 3, CLOSE 2, OPEN 1.

CONTROL WIRES NOT SHOWN.

○ SWITCH.

Fig. 4. Series-parallel method

parallel method. Its principal idea is to switch in parallel two series groups which normally are in series, so that double-rated voltage is applied on all capacitors. Therefore, the kvar output is four times rated kvar. This scheme is especially effective for increasing the system stability for a short emergency period. Fig. 4 shows a schematic for the series-parallel scheme. Its advantage over the series-short-circuiting scheme is that all capacitors contribute to the increased kvar but its disadvantage is the larger amount of switches required and a more complicated scheme in general.

To get four times rated kvar, the following switching sequence has to be applied:

1. Close switch 1.
2. Open switch 2.
3. Close switch 3.

To get rated kvar the switching sequence has to be:

1. Open switch 3.
2. Close switch 2.
3. Open switch 1.

To make this switching scheme foolproof, provisions have to be made so that switches 2 and 3 can never be closed at the same time. This requires interlocking. An advantage of this scheme is that the bank is always connected in wye, regardless of producing rated or four times rated kvar output, and therefore has all the advantages of a wye-connected bank.

Of course, the series-parallel method can be used on capacitor banks with an even number of series groups greater than two, and each two series groups can be converted into one parallel series group. However, this may lead to a somewhat impractical and complicated layout.

Benefits can be derived from using the series-parallel method on only two out of a total of three or four series groups per phase. Then, the total kvar output of the whole bank with three series groups can be increased to 200 per cent and the overvoltage across the unchanged series groups would also be 200 per cent. With a total of four series groups and the series-parallel method applied on two series groups, the kvar of the total bank can be increased to 1.6 times rated kvar and the overvoltage across the two unchanged series groups would be 1.6 times rated voltage. Of course, the series-parallel method can be applied on two series groups for banks with an even larger number of total series groups than four. However, beginning at a total number of five series groups, the series-short-circuiting method is more advantageous since it accomplishes the same result with less equipment and with generally less complexity.

Conclusion

This paper has brought to attention a so-far neglected use of the overload capacity of power capacitors. Under certain circumstances, and using capacitor banks with more than one series group, the two methods described here can result in considerable economy if an intermittently applicable kvar increase of the bank is desirable. The first method is the series-short-circuiting method which is extremely simple and inexpensive but somewhat limited in the kvar increase. The second one is the series-parallel method which requires more equipment, is more complicated, but results in a larger kvar increase.

It is not believed that any such method is in use at present, but it is hoped that this paper will arouse some interest among the electric companies to utilize every dollar's worth out of a capacitor bank.

References

1. Guides for Short-Time 60-Cycle Overvoltage Operation of Power Capacitors, **AIEE Committee Report.** *AIEE Transactions*, vol. 71, pt. III, Jan. 1952, pp. 493–95.

2. Capacitor Switching Scheme Temporarily Raises Kvar Output, **R. E. Marbury.** *Electric Light and Power*, Chicago, Ill., Nov. 1953.

3. How Georgia Power Cuts Equipment Costs with New Switching Method for Capacitor Banks, **H. H. Strozier, B. H. Schultz.** *Electrical World*, New York, N. Y., Mar. 22, 1954.

◆

Discussion

L. W. Robbins (General Electric Company, Hudson Falls, N. Y.): One of the principal reasons for applying capacitors to a power system is to reduce system losses. It has been shown[1] that loads can be corrected to nearly 1.00 power factor with substantial savings in system investment. Some studies not yet published indicate that maximum economy of system losses and system equipment result when loads are corrected to 0.98 power factor lead or more. Since the methods presented by Mr. Minder can only be used occasionally over the life of the equipment, they should not be compared directly with the alternative of using added shunt capacitors which can be operated at all times to reduce system losses and improve system performance.

In the conclusion Mr. Minder refers to the "neglected use of the overload capacity of power capacitors." It should also be pointed out that use is already being made of the overload characteristics of power capacitors. In large capacitor banks such as discussed in the paper, it is industry practice to fuse each capacitor unit. A single failed capacitor unit removed from the capacitor bank results in a nominal overvoltage on the remaining units. In general, the capacitor banks are designed in such a manner (and the user schedules his inspection of the equipment in such a manner) as to prevent exceeding the overload characteristics referred to be Mr. Minder. Obviously, changes may be required in the method of design and the method of inspection during operation if this overvoltage characteristic is to be used for other purposes.

The series-short-circuiting method, when used across a single section, does not introduce transient voltages that are not already encountered with normal unit failure and the resulting fuse operation. When more than one section is short-circuited the similarity no longer exists and each application should be checked carefully.

Under ideal conditions the series-parallel method subjects the capacitors to a transient peak voltage of three times normal peak voltage. Referring to the paper, it can be seen that if the step of closing switch 1 could be performed simultaneously in each phase, the energized section must pass from a steady-state voltage of one times normal to a steady-state voltage of two times normal. The resulting transient voltage oscillates between one times normal and three times normal before the steady-state voltage of two times normal is reached. With unequal closing of switch 1, even greater overvoltages may result. Such overvoltages probably exceed overvoltages encountered from other causes and definitely exceed the two times normal voltage frequently felt to be the maximum voltage which electric equipment should be subjected to.[2]

References

1. An Evaluation of Power-Factor Correction on a System Basis, **H. R. Tomlinson, R. O. Bigelow.** *AIEE Transactions*, vol. 73, pt. III-B, 1954 (Feb. 1955 section), pp. 1677–84.

2. Switching Capacitive Kilovolt-Amperes with Power Circuit Breakers, **N. E. Dillow, I. B. Johnson, N. R. Schultz, A. E. Were.** *AIEE Transactions*, vol. 71, pt. III, Jan. 1952, pp. 188–200.

P. M. Minder: In replying to Mr. Robbins it should be remembered that any allowable overvoltage below 1.5 times rated voltage can be applied any practical number of times.[1,3] Voltage increases below this value are the rule with the series-short-circuiting method. Therefore, this method is very well suited when an extreme power-factor correction is desired for a limited period of time for as many times as necessary.

It is true that any overvoltage due to a disconnected unit is added to the overvoltage applied for kvar increasing (except if the open unit is in the short-circuited series group). However, this is something which can easily be accounted for by shorter inspection intervals or adjustment of the unbalance detection. Moreover, it is felt that the small additional overvoltage increase does not appreciably shorten the capacitor life even if it were to go unnoticed for a long time. The reliability of present-day capacitors makes this a minor problem.

With respect to the transient voltages, these are no larger in the system than when switching on additional kvar in the conventional way. The transient voltages at the capacitor units will not exceed the very short-time values recommended in reference 1.

REFERENCES

1. See reference 1 of the paper.
2. CAPACITOR UNITS. *AIEE Standard No. 18*, Dec. 1951.

Some Factors Influencing the Temperature Rise of Armature Windings

M. M. LIWSCHITZ-GARIK
FELLOW AIEE

EXPERIMENTAL data showing the influence of the volume of air in radial vents, voids in the slots, and copper loss upon the performance of water-wheel generators have been published by F. L. Lawton.[1] The aim of this paper is to investigate the influence of these and several other factors upon the temperature rise of the stator winding of salient-pole synchronous machines.

Method of Investigation

Two methods are available for the investigation of the temperature rises and the heat flow in the electric machine: the equivalent circuit method and the analytical method based on Fourier's equation of heat flow. Both methods have advantages and disadvantages. Both require an estimation of the copper losses in the windings, i.e., of the temperature rises of the windings, in order to determine the temperature rise of the air in the radial vents, in the gap, and at the end windings. Since the designer can estimate the copper loses with reasonable accuracy, an error in this estimation will produce only a small error [of 1 to 2 degrees centigrade (C)] in the computation of the air temperature rises. Such an error in the air temperature rises has little influence on the end results of the computation of the temperature rises of the windings.

The disadvantage of the equivalent circuit is that it requires the estimation of the copper losses, not only for the determination of the temperature rises of air but also for the computation of the temperature rises of the windings themselves. An error in the latter estimation may introduce a considerable error in the temperature rises of the windings and a repetition of a large part of the tedious calculations may become necessary in order to account for the wrong estimation.

The advantage of the analytical method based on Fourier's equation is that the knowledge of the copper losses for the computation of the temperature rises of the windings is not required. On the other hand, in order to simplify the differential equations of the heat flow, it is expedient in the Fourier equation method to neglect the radial thermal resistance of the iron between teeth and core. This is not necessary when the equivalent circuit method is used. Computations made by both methods show that normally only a very small error is made when the radial thermal resistance of the iron between teeth and core is neglected.

The method used for the present investigation is the Fourier equation method. It is explained in the Appendix, the basis of which is a paper presented at the Congress International d'Electricite.[2,3] This paper gives a comparison between calculated and tested temperature rises for a large number of machines of different types showing that the method yields satisfactory results. The Appendix is an enlargement and improvement of that paper.

Factors Investigated

The influence on the temperature rises of the stator winding and iron by the following factors is investigated in this paper:

1. Air volume through the radial vents.
2. Air volume through the end windings.
3. Voids in the slot portion (embedded part) of the winding.
4. Thickness of the insulation in the slot and end windings.
5. Transverse (axial) heat conductivity of the laminations.
6. Copper losses.
7. Iron losses.

Results of the Investigation

The results of the investigation are shown in Figs. 1 through 14 and Tables I through VII. The point 100 per cent (%) refers to a typical water-wheel generator of 35,000 kva, 112.5 rpm, 13,200 volts, 3 phases, 60 cycles, and 0.9 power factor with the following data:

Bore diameter, 293 inches
Core length, 45 inches
No. of stator slots, 360
Radial vents, 24
Width of a vent, 3/8 inch
Length of the end winding, 35 inches
Cross section of copper in the slot, 2.2 inches^2
Thickness of insulation, 0.216 inch
Core loss, 270 kw
Total stator copper loss, 231 kw
Stray load loss, 153 kw
Field winding loss, 84 kw
Friction and windage loss, 129 kw
Air volume, 88,400 feet^3 per minute

The heat-transfer constants are:

0.037 watt per inch^2 per C in the vent (average value)
0.024 watt per inch^2 per C between the end windings

The heat conductivities are:

Insulation, 0.0065 watt per inch^2 per inch per C
Air, 0.00063 watt per inch^2 per inch per C.
Wedge, 0.0043 watt per inch^2 per inch per C.
Iron in radial direction, 1.0 watts per inch^2 per inch per C
Iron in axial direction, 0.025 watt per inch^2 per inch per C
Copper, 9.1 watts per inch^2 per inch per C

The losses and air volume just given yield the following air temperature rises:

In the vent at the teeth, 12.7 C
In the vent at the core, 18.1 C
In the gap, 3.7 C

INFLUENCE OF AIR VOLUME THROUGH RADIAL VENTS

Figs. 1 and 2 and Table I show the influence of a reduction of the air volume in the radial vents. Fig. 1 shows the

---

Paper 55-275, recommended by the AIEE Rotating Machinery Committee and approved by the AIEE Committee on Technical Operations for presentation at the AIEE Middle Eastern District Meeting, Columbus, Ohio, May 4–6, 1955. Manuscript submitted January 31, 1955; made available for printing March 18, 1955.

M. M. LIWSCHITZ-GARIK is with the Polytechnic Institute of Brooklyn, Brooklyn, N. Y., and is a consulting engineer to the National Electric Coil Company, Columbus, Ohio.

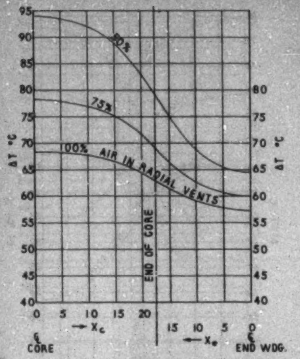

Fig. 1. Influence of the air volume in the radial vents on the temperature rise of the stator winding

temperature rise along the stator winding between the middle of the core and the middle of the end winding; see Fig. 15 also. It can be seen that a reduction of air volume in the radial vents raises the temperature level of the whole winding, i.e., even of the end windings. A reduction of the air volume by 25% increases the temperature rise of the winding in the middle of the core by about 10 C, and a reduction of the air volume by 50% increases the temperature rise of the winding in the middle of the core by about 25 C. The temperature rise of the end winding is lower than that of the embedded part of the winding, as it should be.

Fig. 2 shows the end points of the curves of Fig. 1, i.e., the temperature rises of the winding in the middle of the core ($\Delta T_{\text{middle core}}$) and in the middle of the end winding ($\Delta T_{\text{middle end winding}}$), and, in addition, the error in the reading of the resistance temperature detector (RTD), the temperature rise shown by the RTD, and the temperature rise of the iron in the middle of the core (ΔT_{Fe}, middle core). Though the readings of the RTD are considerably smaller than the actual temperature rises, the increases, due to a reduction of the air volume in the radial vents, are about the same as for the actual temperature rises, i.e., about 10 C and 25 C for an air volume reduction of 25% and 50% respectively. For the computation of the error in the RTD reading, a ratio of longitudinal to transverse thermal conductivity of 5 was assumed.[4,5]

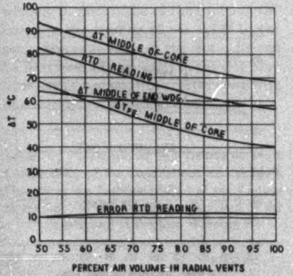

Fig. 2. Influence of the air volume in the radial vents on the temperature rise of the winding and iron in the middle of the core and on the error and reading of the RTD

Table I. Influence of the Air Volume in the Radial Vents on the Heat Flow From the Embedded Part of the Copper to the Iron, to the Air in the Gap and in the Vents, and to the End Winding

	Per Cent		
Air volume in the radial vents	100	75	50
$Q_{cu\text{-}Fe}$	61.2	58.5	51.6
$Q_{cu\text{-}g}$	7.3	7.5	7.8
$Q_{cu\text{-}v}$	25.2	23.9	21.5
$Q_{cu\text{-end winding}}$	6.3	10.1	19.1

It is seen from Fig. 2 that a reduction of the air volume in the vents causes also an increase of the temperature rise of the stator iron. For the machine considered, this increase is about the same as for the stator winding in the middle of the core.

The main consequence of a reduction of the air volume in the radial vents is a decrease of the air velocity and of the heat-transfer constant to the air in the vents. The increase of the temperature rise of the air in the vents due to the smaller air volume also has some influence.

Table I shows the heat flow from the embedded part of the stator winding to the iron ($Q_{cu\text{-}Fe}$), to the gap through the wedges ($Q_{cu\text{-}g}$), to the air in the radial vents ($Q_{cu\text{-}v}$), and to the end winding ($Q_{cu\text{-end winding}}$). A reduction of the air volume through the radial vents reduces the amount of heat flowing from the embedded copper to the iron and to the air in the radial vents, but increases the amount of heat dissipated by the end winding and the air in the gap.

Table II. Influence of the Air Volume Between the End Windings on the Heat Flow From the Embedded Part of the Copper to the Iron, to the Air in the Gap and in the Vents, and to the End Winding

	Per Cent		
Air volume between the end windings	100	65	30
$Q_{cu\text{-}Fe}$	61.2	63.9	70.5
$Q_{cu\text{-}g}$	7.3	7.5	7.9
$Q_{cu\text{-}v}$	25.2	26.0	27.7
$Q_{cu\text{-end winding}}$	6.3	2.6	−6.1

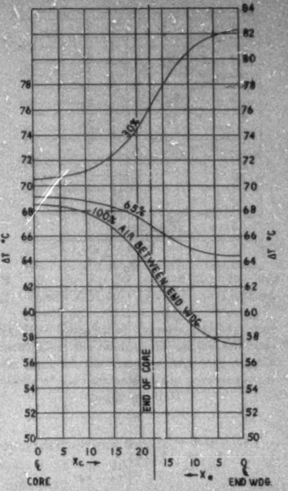

Fig. 3. Influence of the air volume between the end windings on the temperature rise of the stator winding

Influence of Air Volume Between End Windings

Figs. 3 and 4 and Table II show the influence of reducing the air volume

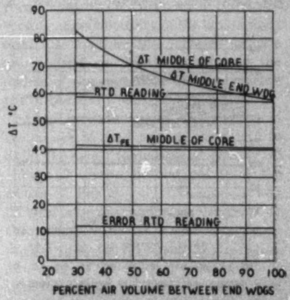

Fig. 4. Influence of the air volume between the end windings on the temperature rises of the winding and iron in the middle of the core and on the error and reading of the RTD

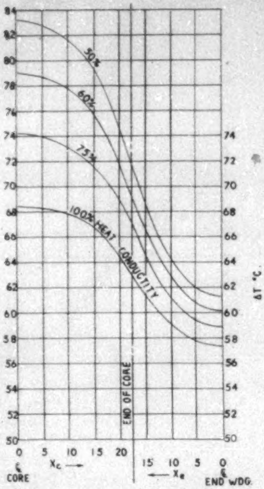

Fig. 5. Influence of voids in the slot on the temperature rise of the stator winding

through the end windings. Fig. 3 shows the temperature rise along the stator winding between the middle of the core and the middle of the end winding. It can be seen that a reduction of air volume between the end windings cause only a little increase of the temperature rise of the winding in the middle of the core, but the increase of the temperature rise of the end winding itself can be considerable. A large reduction of the air volume between the end windings may lead to a temperature rise of the end winding higher than that in the middle of the core where the temperature detector is placed. A temperature rise distribution such as that corresponding to 30% air volume is undesirable because it requires a heat flow from the end winding to the embedded part of the copper (see Table II), a condition which must be avoided.

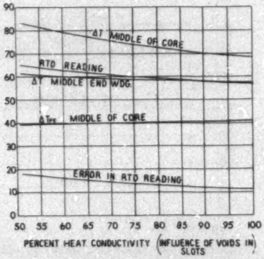

Fig. 6. Influence of voids in the slot on the temperature rises of the winding and iron in the middle of the core and on the error and reading of the RTD

Table III. Influence of Voids in the Slot, on the Heat Flow From the Embedded Part of the Copper to the Iron, to the Air in the Gap and in the Vents, and to the End Winding

	Per Cent			
Heat conductivity between copper and iron	100	75	60	50
$Q_{cu\text{-}Fe}$	61.2	56.1	51.8	48.0
$Q_{cu\text{-}g}$	7.3	7.9	8.4	8.8
$Q_{cu\text{-}v}$	25.2	27.7	29.8	31.6
$Q_{cu\text{-end winding}}$	6.3	8.3	10.0	11.6

Fig. 4 shows the end points of the curves of Fig. 3, i.e., $\Delta T_{\text{middle core}}$ and $\Delta T_{\text{middle end winding}}$, and also the error in the reading of the RTD, the temperature rise shown by the RTD, and $\Delta T_{\text{Fe middle core}}$. There is little change in the error of the RTD reading and in the temperature rise of the iron due to a reduction of the air volume between the end windings.

As in the previous case of an air volume reduction in the radial vents, the main consequence of the air volume reduction between the end windings is the decrease of the air velocity and of the heat-transfer constant to the air between the end windings.

Table II shows the heat flow between the embedded part of the stator winding and the iron, the air in the gap (through the wedges), the air in the vents, and the end winding. As the air volume between the end windings decreases, more heat flows from the embedded part of the winding to the iron and to the air in the gap and vents, and less heat flows to the end winding. At 30% air volume, heat flows from the end winding into the embedded part of the winding ($Q_{\text{cu end winding}}$ is negative).

INFLUENCE OF VOIDS IN SLOT PORTION (EMBEDDED PART) OF WINDING

Voids in the slots decrease the heat conductivity between copper and iron.

Table IV. Influence of the Thickness of Insulation on the Heat Flow From the Embedded Part of the Copper to the Iron, to the Air in the Gap and in the Vents, and to the End Winding

	Per Cent		
Thickness of insulation	100	125	150
$Q_{cu\text{-}Fe}$	61.2	62.2	64.6
$Q_{cu\text{-}g}$	7.3	7.2	7.2
$Q_{cu\text{-}v}$	25.2	24.4	24.2
$Q_{cu\text{-end winding}}$	6.3	6.2	4.0

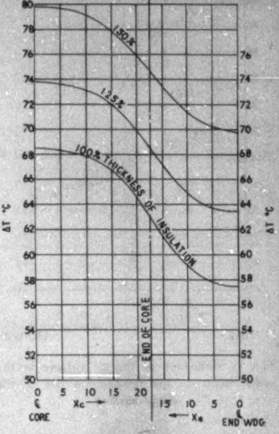

Fig. 7. Influence of thickness of insulation on the temperature rise of the stator winding

Figs. 5 and 6 and Table III show the influence of reducing the heat conductivity. Fig. 5 shows the temperature rise along the stator winding between the middle of the core and the middle of the end winding. It can be seen that voids in the slot influence the temperature rise of the end winding relatively little, but influence the temperature rise of the embedded part of the winding considerably. Even a small amount of air in the slot may cause an increase of the temperature rise in the middle of the core by 5 to 10 C.

Fig. 6 shows the end points of the curves of Fig. 5, i.e., $\Delta T_{\text{middle core}}$ and $\Delta T_{\text{middle end winding}}$, and also the error in the reading of the RTD, the temperature rise

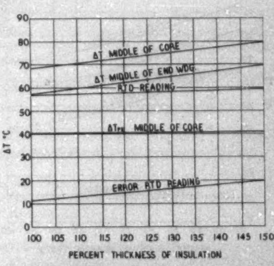

Fig. 8. Influence of thickness of insulation on the temperature rises of the winding and iron in the middle of the core and on the error and reading of the RTD

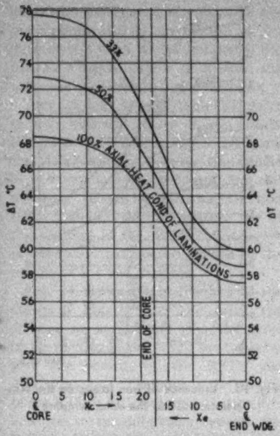

Fig. 9. Influence of the transverse heat conductivity of the laminations on the temperature rise of the stator winding

shown by the RTD, and $\Delta T_{Fe\ middle\ core}$. With increasing voids, i.e., with decreasing heat conductivity between copper and iron, the temperature gradient between copper and iron increases and, therefore, the error in the reading of the RTD increases. As a consequence, the RTD readings change relatively little with increasing voids. Voids in the slot must be avoided since they may cause large errors in the readings of the RTD and thus lead to the wrong assumption that the temperature rise of the winding stays within the permissible limits. It is understood that voids must be avoided also in the end windings, though they do not influence the temperature rise of the winding in the middle of the core and the errors in the reading of the RTD to the same degree as voids in the slot. As can be seen from Fig. 6, voids in the slot have little influence on the temperature rise of the iron in the middle of the core.

Table V. Influence of the Transverse Heat Conductivity of the Laminations on the Heat Flow From the Embedded Part of the Copper to the Iron, to the Air in the Gap and in the Vents, and to the End Winding

	Per Cent		
Transverse heat conductivity of the iron	100	50	33.3
Q_{cu-Fe}	61.2	56.7	52.6
H_{cu-g}	7.3	7.8	8.3
Q_{cu-v}	25.2	27.2	29.2
$Q_{cu-end\ winding}$	6.3	8.3	9.9

Table III shows the heat flow between the embedded part of the stator winding and the iron, the air in the gap (through the wedges), the air in the vents, and the end winding for different values of heat conductivity between the copper and iron. As the latter heat conductivity decreases, less heat flows from the embedded copper to the iron and more heat flows to the end winding and to the air in the vents and gap.

INFLUENCE OF THICKNESS OF INSULATION IN SLOT AND END WINDINGS

The thickness of the insulation of a winding should not be larger than necessary for dielectric and mechanical reasons, because thicker insulation means a decrease of the heat conductivity between copper and iron for the embedded part of the winding and copper and air for the end winding.

Figs. 7 and 8 and Table IV refer to three different values of the thickness of the insulation. Fig. 7 shows the temperature rise along the stator winding between the middle of the core and the middle of the end winding. It can be seen that an increase of the thickness of the insulation raises the temperature rise of the whole winding between the middle of the core and the middle of the end winding. The embedded part of the winding and the end winding are raised by about the same amount of 5 to 6 C for a thickness increase of 25% and 11 to 12 C for a thickness increase of 50%.

Fig. 8 shows the end points of the curves of Fig. 7, i.e., $\Delta T_{middle\ core}$ and $\Delta T_{middle\ end\ winding}$, and also the error in the reading of the RTD, the temperature rise shown by the RTD, and $\Delta T_{Fe\ middle\ core}$. As in the case of voids within the slots, the error in the reading of the RTD increases with increasing thickness of insulation so that the readings of the RTD show only small changes with increasing thickness of insulation. Corresponding to a change of the insulation thickness of 25%, there is an increase of the actual temperature rise in the middle of the core of 5.4 C, while the RTD will show an increase of only 1.1 C. It is seen from Fig. 8 that the temperature rise of the iron is affected very little by the thickness of insulation.

Table IV shows the heat flow between the embedded part of the stator winding and the iron, the air in the gap (through the wedges), the air in the vents, and the end winding for different thicknesses of insulation. As the thickness of the insulation becomes larger, less heat flows from the embedded copper to the end winding. The largest amount of the embedded copper loss still flows to the iron.

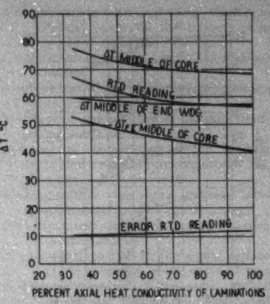

Fig. 10. Influence of the transverse heat conductivity of the laminations on the temperature rises of the winding and iron in the middle of the core and on the error and reading of the RTD

INFLUENCE OF TRANSVERSE HEAT CONDUCTIVITY OF LAMINATIONS

Tables I through IV show that about two-thirds of the heat developed in the embedded part of the winding flows into the iron and axially through the iron to the air in the vents. Therefore, it can be expected that an increase or decrease of the axial (transverse) heat conductivity of the laminations will influence the temperatures rises of the winding and iron.

Figs. 9 and 10 and Table V refer to three different values of the transverse heat conductivity of the laminations. Fig. 9 shows the temperature rise along the stator winding between the middle of the core and the middle of the end winding. It can be seen that a decrease of the transverse heat conductivity of the laminations causes a considerable increase of the temperature rise of the winding in the middle of the core while the temperature rise of the end winding is influenced little. The temperature rise of the winding in the middle of the core may increase 5 to 8 C in the case of loose laminations.

Fig. 10 shows the end points of the curves of Fig. 9, i.e., $\Delta T_{middle\ core}$ and $\Delta T_{middle\ end\ winding}$, and also the error in the reading of the RTD, the temperature rise shown by the RTD, and $\Delta T_{Fe\ middle\ core}$. The error in the reading of the RTD is influenced little by the transverse heat conductivity of the laminations and so the RTD readings show for different values of conductivity the same differences as the actual temperature rises, $\Delta T_{middle\ core}$. The influence of the

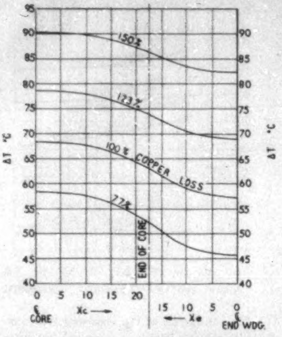

Fig. 11. Influence of copper losses on the temperature rise of the stator winding

transverse heat conductivity of the laminations on the temperature rise of the iron in the middle of the core is still larger than that on the copper in the middle of the core.

Table V shows the heat flow between the embedded part of the stator winding and the iron, the air in the gap (through the wedges), the air in the radial vents, and in the end winding. A decrease of the transverse heat conductivity of the laminations reduces the heat flow from the copper to the iron and forces a larger portion of heat to flow to the air in the gap and in radial vents and to the end winding.

INFLUENCE OF COPPER LOSSES

The copper losses to be considered are the I^2R d-c losses and all additional copper losses due to the alternating current. It can be expected that the magnitude of the copper losses will influence the temperature rise of the winding considerably and, to a lesser degree, the temperature rise of the iron.

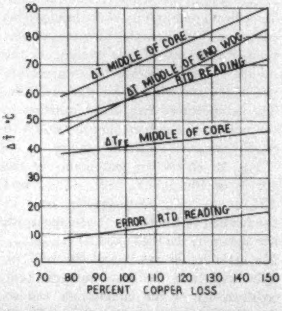

Fig. 12. Influence of copper losses on the temperature rises of the winding and iron in the middle of the core and on the error and reading of the RTD

Table VI. Influence of Copper Losses on the Heat Flow From the Embedded Part of the Copper to the Iron, to the Air in the Gap and in the Vents, and to the End Winding

	Per Cent			
Copper losses	77	100	123	150
$Q_{cu\text{-}Fe}$	56.1	61.2	64.6	66.5
$Q_{cu\text{-}g}$	8.0	7.3	6.8	6.6
$Q_{cu\text{-}v}$	26.6	25.2	24.4	23.7
$Q_{cu\text{-}end\ winding}$	9.3	6.3	4.2	3.2

Figs. 11 and 12 and Table VI refer to four different values of the copper losses. Fig. 11 shows the temperature rise along the stator winding between the middle of the core and the middle of the end winding. It can be seen that an increase of the copper losses raises the temperature rise of the whole winding, from the middle of the core to the middle of the end winding.

Fig. 12 shows the end points of the curves of Fig. 11, i.e., $\Delta T_{\text{middle core}}$ and $\Delta T_{\text{middle end winding}}$, and also the error in the reading of the RTD, the temperature rise shown by the RTD, and $\Delta T_{\text{Fe middle core}}$. Because the temperature gradient between embedded copper and iron increases with increasing copper losses, the error in the RTD reading also increases with increasing copper losses. As a consequence, the RTD readings show for different values of copper losses smaller differences than the actual temperature rise ($\Delta T_{\text{middle core}}$). For example, corresponding to an increase of the copper losses by 50%, there is an actual increase of the temperature rise of the winding in the middle of the core equal to 21.8 C, while the RTD shows an increase of only 15.1 C.

The change of the temperature rise of the winding in the middle of the core, $\Delta T_{\text{middle core}}$, is not proportional to the change of the copper losses. For copper losses equal to 77% there is a decrease in $\Delta T_{\text{middle core}}$ of 14.5%, and for copper losses equal to 150% there is an increase in $\Delta T_{\text{middle core}}$ of 31.5%. It is seen from Fig. 12 that a change of the copper losses may cause a considerable change of the temperature rise of the iron in the middle of the core.

Table VII. Influence of Iron Losses on the Heat Flow From the Embedded Part of the Copper to the Iron, to the Air in the Gap and in the Vents, and to the End Winding

	Per Cent			
Iron losses	50	75	100	130
$Q_{cu\text{-}Fe}$	68.3	64.9	61.2	57.3
$Q_{cu\text{-}g}$	6.5	7.0	7.3	7.8
$Q_{cu\text{-}v}$	22.6	23.9	25.2	27.0
$Q_{cu\text{-}end\ winding}$	2.6	4.2	6.3	7.9

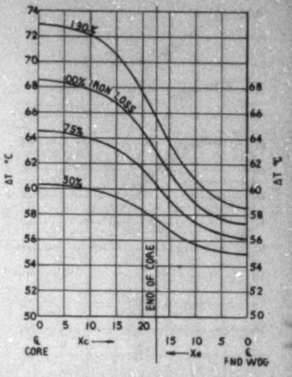

Fig. 13. Influence of iron losses on the temperature rise to the stator winding

Table VI shows the heat flow between the embedded part of the stator winding and the iron, the air in the gap through the wedges, the air in the radial vents, and the end winding. An increase of the copper losses increases the amount of heat flowing from the copper to the iron, while the amount of heat flowing to the end winding and the air decreases.

INFLUENCE OF IRON LOSSES

Just as a change of the copper losses influences the temperature rise of both copper and iron, a change of the iron

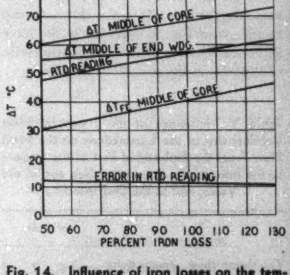

Fig. 14. Influence of iron losses on the temperature rises of the winding and iron in the middle of the core and on the error and reading of the RTD

losses also influences both, although the temperature rise of the copper is influenced to a lesser degree and that of the iron to a higher degree than when the change is effected by the copper losses.

Figs. 13 and 14 and Table VII refer to four different values of iron losses. Fig. 13 shows the temperature rise along the stator winding between the middle of the core and the middle of the end winding. It can be seen that the iron losses influence the temperature rise of the winding in the middle of the core considerably, but not very much in the middle of the end winding.

Fig. 14 shows the end points of the curves of Fig. 13, i.e., $\Delta T_{\text{middle core}}$ and $\Delta T_{\text{middle end winding}}$, and also the error in the reading of the RTD, the temperature rise shown by the RTD, and $\Delta T_{\text{Fe middle core}}$. The error in the reading of the RTD is little influenced by the iron loss and so the differences between the RTD readings and the actual temperature rises are nearly the same for the same change of iron losses. As could be expected, the relative change of the temperature rise of the iron is larger than that of the copper for the same change of iron losses.

Table VII shows the heat flow between the embedded copper and the iron, the air in the gap through the wedges, the air in the radial vents, and the end winding. An increase of the iron losses reduces the amount of heat flowing from the copper to the iron and increases the amount of heat flowing to the air and the end winding.

The values of temperature rises and heat flow shown in Figs. 1 through 14 and Tables I through VII refer to a specific machine, the data of which were given previously. These values themselves and their changes with changing parameters (volume of air in the radial vents, voids in the slots, etc.) will not be the same for all types of salient-pole machines. On the contrary, they will vary depending on a number of factors, such as distribution of losses, ratio of core length to pole pitch, etc. Yet, the foregoing computations give a general idea about the influence of the considered parameters upon the temperature rises for all salient-pole machines.

List of Symbols

A_1, A_2 = integration constant
A_{az} = area of axial cooling vents of a stack, inches^2
A_c = area of the inner cylinder of a stack of laminations, inches^2
A_c' = area of the outer cooling surface of a stack of laminations, inches^2
A_s = area of both sides of a stack of laminations, inches^2
b_v = width of a radial vent, inches
f = cross section of the copper (of both coil sides, without ground insulation), inches^2
h = heat-transfer constant, watts per inch^2 per C
h_1 = heat-transfer constant from the end windings to the air at the end windings
h_2 = heat-transfer constant from the coil to the air in the radial vent
h_{az} = heat-transfer constant from the surface of the axial vents to the air
h_c = heat-transfer constant from the inner cylinder surface of the stack to the air in the gap
h_c' = heat-transfer constant from the outer surface of the stack to the air
h_s = heat-transfer constant from the side surfaces of the stack of laminations to the air in the vent
k = heat conductivity of the heat conductor, watts per inch^2 per inch per C
k_1 = heat conductivity of the insulation of the end windings (including air layers)
k_2 = heat conductivity of the insulation in the slot (including air layers)
k_{co} = heat conductivity of copper
k_g = heat conductivity of the laminations in axial direction
l' = length of a stack of laminations, inches
L = length of the core (including radial vents), inches
L_1 = length of the end winding, inches
L_{Fe}' = iron loss in a stack of laminations, watts
N = number of slots
u = circumference of the heat conductor (of both coil sides in 2-layer windings, measured in the middle of the ground insulation), inches
u_1 = circumference of both coil sides, measured in the middle of the end winding insulation, inches
u_2 = circumference of both coil sides, measured in the middle of the ground insulation, inches
uw/f = heat transferred through the surface per unit volume, watts per inch^3
v_0 = heat developed in unit volume of the substance at ambient temperature, watts per inch^3
v_{10} = heat developed in a cubic inch of the copper of the end windings, watts
v_{20} = heat developed in a cubic inch of the copper embedded in the slots, watts
w = heat transferred by the embedded part of the winding (average value for a stack of laminations and a vent), watts per inch^2
w_1 = heat transferred to the air by the end windings, watts per inch^2
W_{az} = heat transferred to the air by the axial vents in a stack of laminations
W_A = heat transferred to the air in a radial vent by the winding
W_c = heat transferred to the air by the inner cylinder surface of a stack of laminations
W_c' = heat transferred to the air by the outer surface of a stack of laminations
W_s = heat transferred to the air by the side surfaces of a stack of laminations, watts
α = temperature coefficient of the heat conductor ($\alpha = 0.004$ for copper, α is assumed equal to 0 for iron)
δ_1 = thickness of the end-winding insulation, inches
δ_2 = thickness of the slot insulation, inches
ΔT = temperature rise
λ_1 = thermal conductivity of the end winding, watts per inch^2 per C
λ_A = thermal conductivity of the winding in the radial vents (equation 32), watts per inch^2 per C
ϑ = temperature rise above ambient temperature, C
ϑ = temperature rise of winding or iron as a function of x
ϑ_1 = temperature rise of the outer surface of the insulation of the end windings
ϑ_2 = temperature rise of the outer surface of the slot insulation in the radial vent
ϑ_{av} = temperature rise of the copper, average value as found by resistance test
ϑ_{A1} = temperature rise of the air at the end windings
ϑ_{A2} = temperature rise of the air in the radial vent at the root of the tooth
ϑ_{A3} = temperature rise of the air at the inner cylinder surface
ϑ_{A4} = temperature rise of the air at the outer surface of the core
ϑ_{A5} = temperature rise of the air in the axial vents
ϑ_{A6} = temperature rise of the air in the radial vent at the middle of the tooth
ϑ_{Fe} = temperature rise of the iron of a stack of laminations (average value)
$\vartheta_{Fe,m}$ = temperature rise of the iron in the middle of the stack
ϑ_{min} = temperature rise of the copper in the middle of the end winding
ϑ_{max} = temperature rise of the copper in the middle of the core
ϑ_s = temperature rise of the side surfaces of a stack of laminations
$\vartheta - \vartheta_2$ = temperature gradient between the inner and outer surfaces of the insulation in the vent
$\vartheta - \vartheta_{Fe}$ = average temperature gradient in the slot insulation within a stack of laminations

Appendix. Heat Flow and Temperature Rises of Copper and Iron in Electric Machines

The method of calculating the heat flow and temperature rises of copper and iron described here is applicable to stators and rotors of machines with radial, as well as with axial, cooling. It is applicable to distributed, as well as to concentrated, windings.

The assumptions on which the theoretical derivations are based are:

1. The height and width of the coil are small in comparison to its length so that there is no heat flow within the cross section of the coil.
2. The radial heat conductivity of the iron is large so that the thermal iron resistance between teeth to core can be neglected.

With these two assumptions, the heat-flow problem becomes a linear one.

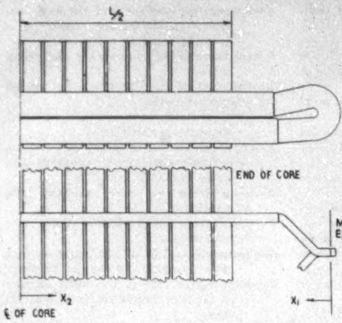

Fig. 15. Embedded part of a coil and its end winding. System of co-ordinates

Equation of Heat Flow

For the unidimensional heat flow, the heat balance under steady-state conditions is given by

$$v_0(1+\alpha\vartheta)-\frac{uw}{f}+k\frac{\partial^2\vartheta}{\partial x^2}=0 \qquad (1)$$

Equation 1 means that the heat developed in the unit volume of the heat conductor is equal to the sum of the heat conducted to the neighboring space elements and the heat transferred through its surface.

Temperature Rises of Stator Copper and Iron

Applying the equation of heat flow, equation 1, to the stator of the electric machine, the end winding and the part of the coil embedded in iron are to be considered separately. Subscript 1 will be used for the end winding and the origin of the co-ordinates will be placed in its middle. Subscript 2 will be used for the part of the coil embedded in iron, and subscript Fe will be used for the iron. The origin of the co-ordinates for the embedded part of the coil will be placed in the middle of the machine. The length of the iron (including vents in the case of radial ventilation) is assumed to be L; see Fig. 15.

End Winding

The heat transferred per unit surface of the end winding is proportional to the difference between the temperature rise of the conductor material ϑ and the temperature rise of the outer surface of the insulation of the end winding ϑ_1, i.e.

$$w_1=\frac{k_1}{\delta_1}(\vartheta-\vartheta_1) \qquad (2)$$

The heat w_1 is transferred to the air (in general to the cooling medium). It is true that

$$w_1=h_1(\vartheta_1-\vartheta_{A1}) \qquad (3)$$

It follows from equations 2 and 3 that with

$$\lambda_1=\frac{k_1h_1}{k_1+h_1\delta_1} \qquad (4)$$

w_1 becomes

$$w_1=\lambda_1(\vartheta-\vartheta_{A1}) \qquad (5)$$

Combining equation 5 with equation 1

$$\frac{\partial^2\vartheta}{\partial x_1^2}-a_1^2\vartheta+b_1=0 \qquad (6)$$

where

$$a_1^2=\frac{1}{k_{co}}\left(\lambda_1\frac{u_1}{f}-\alpha v_{10}\right) \qquad (7)$$

$$b_1=\frac{1}{k_{co}}\left(v_{10}+\lambda_1\frac{u_1}{f}\vartheta_{A1}\right) \qquad (8)$$

The solution of the differential equation 6 is

$$\vartheta=A_1\epsilon^{a_1x_1}+B_1\epsilon^{-a_1x_1}+\frac{b_1}{a_1^2} \qquad (9)$$

The temperature rise of the conductor ϑ as a function of x_1 is symmetrical with respect to the middle of the end winding, i.e., with respect to $x_1=0$. This yields $A_1=B_1$ and the differential equation 9 becomes

$$\vartheta=2A_1\cosh a_1x_1+\frac{b_1}{a_1^2} \qquad (9A)$$

Embedded Part of Winding and Stator Iron

The heat transferred from the surface of the winding material to the iron within a stack of laminations of the length l'($l'=L$ for axial ventilation) is

$$W_{Fe}=\Lambda_{Fe}(\vartheta-\vartheta_{Fe}) \qquad (10)$$

where

$$\Lambda_{Fe}=\lambda_{Fe}u_2l'N \qquad \lambda_{Fe}=\frac{k_2}{\delta_2} \qquad (11)$$

The iron losses in a stack of laminations will be denoted by L_{Fe}'. Then the total heat in the stack is $W_s=W_{Fe}+L_{Fe}'$. This heat is to be carried away by the cooling medium.

Because the axial heat conductivity of the laminations is small, the temperature rise of the side surfaces of the stack of laminations is smaller than that in the middle of the stack. In accordance with the assumption that the radial heat conductivity of the iron is very large, the temperature rise ϑ_{Fe} is the same for the inner and outer cylinder surfaces of the stack.

The heat transferred to the air by the side surfaces is

$$W_s=h_s(\vartheta_s-\vartheta_{A2})A_s \qquad (12)$$

The heat transferred to the air by the inner cylinder surface of the stack is

$$W_c=h_c(\vartheta_{Fe}-\vartheta_{A3})A_c \qquad (13)$$

The heat transferred to the air by the outer cooling surface of the stack is

$$W_c'=h_c'(\vartheta_{Fe}-\vartheta_{A4})A_c' \qquad (13A)$$

and the heat transferred to the air by the axial vents of the stack is

$$W_{ax}=h_{ax}(\vartheta_{Fe}-\vartheta_{A5})A_{ax} \qquad (13B)$$

Under steady-state conditions, the heat produced must be equal to the heat transferred to the cooling medium, i.e.

$$\begin{aligned}W_F+L_{Fe}'&=W_s+W_c+W_c'+W_{ax}\\&=h_s(\vartheta_s-\vartheta_{A2})A_s+h_c(\vartheta_{Fe}-\vartheta_{A3})A_c+\\&\quad h_c'(\vartheta_{Fe}-\vartheta_{A4})A_c'+\\&\qquad h_{ax}(\vartheta_{Fe}-\vartheta_{A5})A_{ax}\end{aligned} \qquad (14)$$

With the aid of equation 14, it is possible to set up the equation of heat flow in the stack of laminations and to determine the temperature rise across the stack as a function of the co-ordinate x, the origin of which is placed in the center line of the stack. Then ϑ_{Fe} can be eliminated from equation 14 and the equation for the heat flow in the embedded part of the winding set up.

The total heat transferred through the side surfaces of the stack is

$$\begin{aligned}W_s=W_{Fe}+L_{Fe}'-h_c(\vartheta_{Fe}-\vartheta_{A3})A_c-\\h_c'(\vartheta_{Fe}-\vartheta_{A4})A_c'-\\h_{ax}(\vartheta_{Fe}-\vartheta_{A5})A_{ax}\end{aligned} \qquad (15)$$

and the heat transferred per unit volume is

$$w_s=\frac{W_s}{\left(\frac{A_s}{2}\right)l'} \qquad (16)$$

Therefore the equation of heat flow for the stator iron is

$$w_s+k_q\frac{\partial^2\vartheta}{\partial x^2}=0 \qquad (17)$$

The solution of this equation is

$$\vartheta=-\frac{w_s}{2k_q}x^2+A_x+B \qquad (18)$$

The constants A and B can be determined from the boundary conditions

$$x=-\frac{l'}{2} \qquad \vartheta=\vartheta_s \qquad (19)$$

$$x=+\frac{l'}{2} \qquad \vartheta=\vartheta_s$$

Thus

$$A=0 \qquad B=\vartheta_s+\frac{w_sl'^2}{8k_q} \qquad (20)$$

and

$$\vartheta=\vartheta_s+\frac{w_sl'^2}{8k_q}\left[1-\left(\frac{2x}{l'}\right)^2\right] \qquad (21)$$

ϑ_s is different for the different stacks of laminations. Setting $(d\vartheta)/(dx)=0$, the maximum temperature rise of the iron of the stack is obtained

$$\vartheta_{Fe,m}=\vartheta_s+\frac{w_sl'^2}{8k_q} \tag{22}$$

The average temperature rise of the iron of the stack is

$$\vartheta_{Fe}=\vartheta_s+\frac{w_sl'^2}{12k_q} \tag{23}$$

Thus, independent of the magnitude of the quality $(w_sl'^2)/(8k_q)$

$$\vartheta_{Fe,m}=1.5\vartheta_{Fe}-0.5\vartheta_s \tag{24}$$

The average temperature rise ϑ_{Fe}, as well as the maximum temperature rise $\vartheta_{Fe,m}$ is different for the different stacks of laminations. From equations 23, 16, and 15

$$\vartheta_{Fe}=\vartheta_s+\frac{1}{\Lambda_s}[W_{Fe}+L_{Fe}'-h_c(\vartheta_{Fe}-\vartheta_{A3})A_c-h_c'(\vartheta_{Fe}-\vartheta_{A4})A_c'-h_{ax}(\vartheta_{Fe}-\vartheta_{A5})A_{ax}] \tag{25}$$

where

$$\frac{1}{\Lambda_s}=\frac{l'^2}{12k_q\frac{A_s}{2}l'}=\frac{l'}{6A_sk_q} \tag{26}$$

Substituting equations 10, 25, and 26 into equation 14

$$W_{Fe}=\Lambda_{Fe}\left[c\vartheta-\frac{1}{\Lambda}L_{Fe}'-\frac{1}{d\Lambda}h_sA_s\vartheta_{A2}-\frac{1}{\Lambda}(h_cA_c\vartheta_{A3}+h_c'A_c'\vartheta_{A4}+h_{ax}A_{ax}\vartheta_{A5})\right] \tag{27}$$

where

$$c=\frac{\Lambda_p}{\Lambda_p+d\Lambda_{Fe}} \qquad d=1+\frac{h_sA_s}{\Lambda_s}$$

$$\Lambda_p=h_sA_s+d(h_cA_c+h_c'A_c'+h_{ax}A_{ax}) \tag{28}$$

$$\frac{1}{\Lambda}=\frac{d}{\Lambda_p+d\Lambda_{Fe}}$$

The heat which flows through the insulation into a radial vent is

$$W_A=\frac{k_2}{\delta_2}(\vartheta-\vartheta_2)u_2Nb_v \tag{29}$$

This heat is carried away by the air. Therefore

$$W_A=h_2(\vartheta-\vartheta_{A6})u_2Nb_v \tag{30}$$

It follows from equations 29 and 30 for W_A

$$W_A=\lambda_A(\vartheta-\vartheta_{A6})u_2Nb_v \tag{31}$$

where

$$\lambda_A=\frac{k_2h_2}{k_2+h_2\delta_2} \tag{32}$$

The heat conduction from the coil to the air in the vent is different from that from the coil to the iron in the slot. An exact mathematical treatment would make it necessary to consider both coil parts separately and to set up two different differential equations for the heat flow. However, for the sake of simplicity, an average value for the heat transferred over the length $l'+b_v$ (stack + vent) will be introduced

$$w=\frac{W_A+W_{Fe}}{u_2(l'+b_v)N} \tag{33}$$

With this value of the transferred heat, the differential equation of the heat flow in the coil part embedded in iron becomes the same as for the end winding (equation 6) and its solution is

$$\vartheta=2A_2\cosh a_2x_2+\frac{b_2}{a_2^2} \tag{34}$$

where

$$a_2^2=\frac{1}{k_{co}}\left(\lambda_2\frac{u_2}{f}-\alpha v_{20}\right) \tag{35}$$

$$b_2=\frac{1}{k_{co}}\frac{u_2}{f}\left(\frac{\lambda_{Fe}L_{Fe}'}{\Lambda}\times\frac{l'}{l'+b_v}+\lambda_2\frac{b_v}{l'+b_v}\vartheta_{A6}+\lambda_{Fe}\frac{l'}{l'+b_v}\times\frac{c}{\Lambda_p}(h_sA_s\vartheta_{A2}+dh_cA_c\vartheta_{A3}+dh_c'A_c'\vartheta_{A4}+dh_{ax}A_{ax}\vartheta_{A5})+\frac{f}{u_2}v_{20}\right) \tag{36}$$

$$\lambda_2=\frac{b_v\lambda_A+cl'\lambda_{Fe}}{l'+b_v} \tag{37}$$

The differential equation 9 for the end winding must yield at $x_1=L_1/2$ the same temperature rise and the same temperature gradient $(d\vartheta)/(dx)$ with opposite sign, as differential equation 34 yields at $x_2=L/2$. It follows from this for the integration constants A_1 and A_2

$$2A_1=\left(\frac{b_2}{a_2^2}-\frac{b_1}{a_1^2}\right)\frac{a_2}{e}\sinh\frac{a_2L}{2} \tag{38}$$

$$2A_2=\left(\frac{b_1}{a_1^2}-\frac{b_2}{a_2^2}\right)\frac{a_1}{e}\sinh\frac{a_1L_1}{2} \tag{39}$$

where

$$e=a_1\sinh\frac{a_1L_1}{2}\cosh\frac{a_2L}{2}+a_2\sinh\frac{a_2L}{2}\cosh\frac{a_1L_1}{2} \tag{40}$$

With these values of the integration constants, the temperature rises of the copper in the middle of the machine and in the middle of the end windings become

$$\vartheta_{\max}=\frac{b_2}{a_2^2}+2A_2 \tag{41}$$

$$\vartheta_{\min}=\frac{b_1}{a_1^2}+2A_1 \tag{42}$$

The average temperature rise of the winding, as determined by the resistance test, is

$$\vartheta_{av}=\frac{2}{L+L_1}\left(\int_0^{L_1/2}\vartheta dx_1+\int_0^{L/2}\vartheta dx_2\right)=\frac{2}{L+L_1}\left(\frac{2A_1}{a_1}\right)\sinh\frac{a_1L_1}{2}+\frac{b_1L_1}{2a_1^2}+\frac{2A_2}{a_2}\sinh\frac{a_2L}{2}+\frac{b_2L}{2a_2^2} \tag{43}$$

To determine the average temperature rise of the stack of laminations ϑ_{Fe}, the assumption is made that the temperature rise of the winding within the stack is constant and equal to the temperature rise in the middle of the stack ϑ_m. Equations 10 and 27 yield then

$$\vartheta_{Fe}=(1-c)\vartheta_m+\frac{c}{\Lambda_p}[h_sA_s\vartheta_{A2}+d(h_cA_c\vartheta_{A3}+h_c'A_c'\vartheta_{A4}+h_{ax}A_{ax}\vartheta_{A5})]+\frac{L_{Fe}'}{\Lambda} \tag{44}$$

The average temperature rise of the side surfaces of the stack of laminations is then, according to equations 25 and 27

$$\vartheta_s=\vartheta_{Fe}+\frac{1}{\Lambda_s}[h_cA_c(\vartheta_{Fe}-\vartheta_{A3})+h_c'A_c'(\vartheta_{Fe}-\vartheta_{A4})+h_{ax}A_{ax}(\vartheta_{Fe}-\vartheta_{A5})]-\frac{\Lambda_{Fe}}{\Lambda_s}c\left(\vartheta_m-\frac{h_sA_s}{\Lambda_p}\vartheta_{A2}-\frac{d}{\Lambda_p}(h_cA_c\vartheta_{A3}+h_c'A_c'\vartheta_{A4}+h_{ax}A_{ax}\vartheta_{A5})\right)+\frac{L_{Fe}'}{\Lambda_s}\left(\frac{\Lambda_{Fe}}{\Lambda}-1\right) \tag{45}$$

The maximum temperature rise of the stack of laminations is, according to equation 24

$$\vartheta_{Fe,m}=1.5\vartheta_{Fe}-0.5\vartheta_s \tag{46}$$

References

1. IMPROVEMENTS IN PERFORMANCE OF HYDROELECTRIC GENERATING UNITS ON THE 2,000,000-HORSEPOWER SAGUENAY SYSTEM, F. L. Lawton. *AIEE Transactions*, vol. 65, 1946, pp. 900–10.

2. L'ECHAUFFMENT DES MACHINES ELECTRIQUES, M. Liwschitz. *Congres International d'Electricite*, Paris, France, 1932, pp. 2–37.

3. ZUR FRAGE DER ERWARMUNG ELEKTRISCHER MASCHINEN, M. Liwschitz, H. Raymund. *Wissenschaftliche Veroffentlichungen aus dem Siemens Konzern*, Berlin, Germany, vol. 12, 1933, pp. 64–88.

4. DIE TEMPERATURVERTEILUNG IN DEN NUTEN VON ZWEISTABWICKLUNGEN, Wilhelm Peters. *Ibid*, vol. IV, 1925, pp. 197–213.

5. TEMPERATURE DROP TO RESISTANCE TEMPERATURE DETECTOR IN STATOR WINDINGS OF TURBINE GENERATORS, R. P. Jerrard. *AIEE Transactions*, vol. 73, pt. III-A, June 1954, pp. 665–70.

Effect of Skew on Induction Motor Magnetic Fields

C. E. LINKOUS
ASSOCIATE MEMBER AIEE

INDUCTION motor designers must account for the saturation of the various components of magnetic reactances to make accurate predictions of the motor's performance. To predict the saturated value of these component reactances is difficult because the superposition principle can no longer be applied with accuracy. When saturation is present, to be rigorous, the net field must be studied not the component fields.

To determine the net field under saturated conditions, it should first be dealt with as though there were no saturation. To find the net field with no saturation, it is valid to find the field of each component of reactance and superimpose them in the various areas of interest.

In studying a particular motor, the author found it convenient to separate fluxes, having a portion of their path in the iron, into three components: the slot leakage flux, the air-gap space harmonic leakage flux, and the air-gap space fundamental flux. It is this latter flux with which this paper is concerned.

Designers have long recognized that the space fundamental air-gap flux varies with axial position because of skewing the rotor slots with respect to the stator slots, but to the author's knowledge nothing has been published giving quantitative data showing how much this flux may vary. It is important that designers have a knowledge of this effect because it not only affects the degree of saturation but also affects iron losses and noise.

Nomenclature

$2a$ = magnitude of major axis of ellipse
$2b$ = magnitude of minor axis of ellipse
B = magnetic induction
I_1 = stator current
I_2 = rotor current
I_M = magnetizing current
L = length of stack
N = amplitude of backward wave of magnetic induction
P = amplitude of forward wave of magnetic induction
${}_fR_2$ = forward rotor resistance
${}_bR_2$ = backward rotor resistance
s = slip
t = time
x = axial distance of a plane from the end of the stack which has the leading end of the rotor bars
X_2 = rotor leakage reactance
X_m = magnetizing reactance
α = the skew, electrical degrees
θ = electrical angle away from center of the reference winding pole in the direction of rotation
λ = electrical angle away from major axis of ellipse in the direction of rotation
τ_f = electrical angle by which the forward magnetizing current, referred to the reference windings, leads the voltage applied to the reference winding
τ_b = electrical angle by which the backward magnetizing current, referred to the reference winding, leads the applied voltage
ψ = electrical angle by which the major axis of the ellipse is located from the reference winding. Measure in the direction of rotation
ω = angular velocity of applied voltage
NL = no load
FL = full load
MT = maximum torque
SS = standstill or locked rotor
axial plane = a plane perpendicular to the axis or, in other words, a plane parallel to the plane of the laminations
reference mmf = the peak value of a space sine wave of magnetomotive force (mmf) which would produce the flux required to balance the line voltage for a balanced polyphase motor with no skew or, in other words, the mmf that would produce the design flux density
maximum mmf = the actual maximum mmf divided by the reference mmf defined in the foregoing

VARIATION OF NET ROTATING FIELD IN UNBALANCED POLYPHASE AND SINGLE-PHASE MOTORS AT A PARTICULAR AXIAL LOCATION

Techniques have been established for many years for resolving an unbalanced polyphase or a single-phase motor into forward and backward rotating sinusoidal fields of constant amplitude and angular velocity.[1–6] Let it be assumed that the fundamental flux density waves at a particular axial location have been found by these techniques to be

$$B_f = P \cos(\omega t - \theta + \tau_f) \tag{1}$$

$$B_b = N \cos(\omega t + \theta + \tau_b) \tag{2}$$

where

B_f = magnetic induction of the forward field at the angular location θ
B_b = magnetic induction of the backward field at the angular location θ
P = peak value of the forward magnetic induction wave, positive sequence
N = peak value of the backward magnetic induction wave, negative sequence
ω = electrical angular velocity
t = time
θ = angular location of a point on the stator measured from the center of a reference winding pole, positive in the direction of rotation
τ_f = a phase angle for the forward wave for a voltage applied to the reference winding of $V_m \cos \omega t$
τ_b = a phase angle for the backward wave for a voltage applied to the reference winding of $V_m \cos \omega t$

These waves are represented by rotating vectors in Fig. 1. At any instant, these two vectors may be added to get a resultant vector representing the net field. The projection of the resultant vector along the line labeled major axis in Fig. 1 is

$$(P+N) \cos\left(2\pi - \omega t - \frac{\tau_f+\tau_b}{2}\right)$$

The projection of the resultant vector along the line labeled minor axis in Fig. 1 is

$$(P-N) \sin\left(2\pi - \omega t - \frac{\tau_f+\tau_b}{2}\right)$$

These are the same form as the well-known expression for an ellipse in parametric form and, therefore, the tip of the resultant vector traces out an elliptical locus. The expression for the angular velocity of the resultant vector is

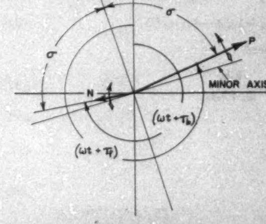

Fig. 1. Vectors representing the forward and backward rotating fields

---

Paper 55-270, recommended by the AIEE Rotating Machinery Committee and approved by the AIEE Committee on Technical Operations for presentation at the AIEE Middle Eastern District Meeting, Columbus, Ohio, May 4–6, 1955. Manuscript submitted January 31, 1955; made available for printing March 16, 1955.

C. E. LINKOUS is with the General Electric Company, Fort Wayne, Ind.

The author wishes to express his gratitude to M. L. Schmidt and F. W. Suhr, General Electric Company, for the many helpful ideas and suggestions contributed to this study.

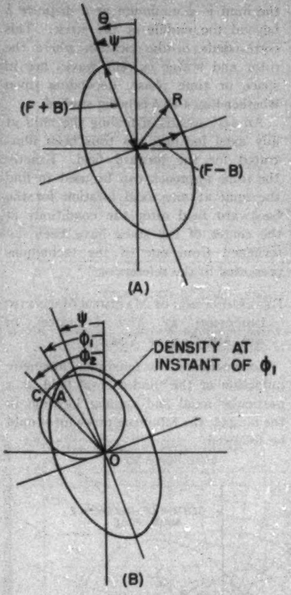

Fig. 2. Locus of rotating vector representing the resultant field

very interesting. It is developed in Appendix II.

The locus is shown in Fig. 2(A). The angle of tilt of the major axis of the ellipse away from the reference pole is

$$\psi=\frac{\tau_f-\tau_b}{2} \tag{3}$$

Thus the ellipse shown in Fig. 2(A) gives the amplitude of the wave of magnetic induction as the peak of the wave crosses any particular angular position. However, this is not in general the maximum magnetic induction which that location experiences. This can be seen from Fig. 2(B).

The plot of a sine function in polar co-ordinates is a circle. The construction of Fig. 2(B) shows that the magnetic induction at the angle ϕ_2 is greater at the instant the peak of the sine wave crosses the angle ϕ_1 than when the peak of the sine wave crosses the angle ϕ_2. It is greater by the ratio OC/OA. Thus, to find the locus of maximum magnetic induction, the envelope of the circles having a diameter from the origin out to any point on the ellipse must be found.

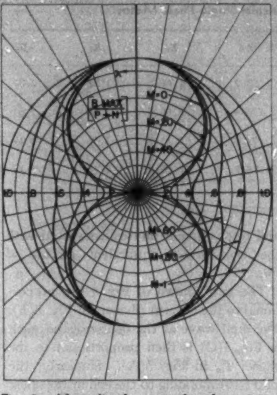

Fig. 3. Normalized curves for determining the maximum magnetic induction

Locus of Maximum Magnetic Induction at a Particular Axial Location

The maximum magnetic induction is found in Appendix I to be

$$B_{\max}=\sqrt{P^2-2PN\left\{1-2\cos^2\left\{\tan^{-1}\left[\left(\frac{P-N}{P+N}\right)\times\tan\left(\theta-\frac{\tau_f-\tau_b}{2}\right)\right]\right\}\right\}+N^2\times}$$
$$\cos\left\{\theta-\frac{\tau_f-\tau_b}{2}-\tan^{-1}\times\left[\left(\frac{P-N}{P+N}\right)^2\tan\left(\theta-\frac{\tau_f-\tau_b}{2}\right)\right]\right\} \tag{4}$$

Equation 4 is cumbersome so a set of curves has been made to facilitate finding the plot of this equation. The equation has been normalized to the following extent: $(P-N)/(P+N)$ is called M, and $[\theta-(\tau_f-\tau_b)/2]$ is called λ. This means angular position is measured from the axis of the ellipse instead of from a reference pole.

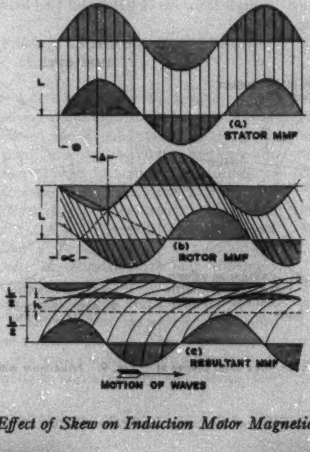

Equation 4 then becomes

$$\left(\frac{B_{\max}}{P+N}\right)=\sqrt{M^2+(1-M^2)\cos^2[\tan^{-1}(M\tan\lambda)]}\times\cos[\lambda-\tan^{-1}(M^2\tan\lambda)] \tag{5}$$

Equation 5 is shown plotted in Fig. 3 for various values of M. The curve shows that at the major and minor axes of the ellipse the maximum magnetic induction is equal to the peak value of the sine wave as the peak crosses those axes. At all other locations, the maximum induction is greater than when the peak of the sine wave crosses that location. In the figure, $M = 0$ corresponds to the backward and forward fields being equal, and $M = 1$ corresponds to the zero backward field.

Variation of the Mmf Across the Stack of an Induction Motor Due to Skew

The several mmf's in a balanced polyphase induction motor with skew are shown in Fig. 4. The situation shown is the rotor skewed at an angle α with respect to the stator. Fig. 4(A) shows the traveling wave of the stator mmf. The two shaded waves are at each end of a stack of length L. Fig. 4(B) shows the opposing rotor mmf which is leading the stator mmf at the center of the stack by an angle Δ. Fig. 4(C) shows the result-

Fig. 4 (left). The mmf waves in a polyphase induction motor

Fig. 5 (below). Transformer equivalent circuit

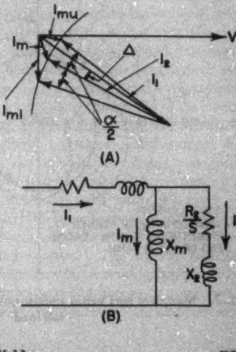

Table I. Parameters of the Particular Single-Phase Motor

Load	Current	Speed	X_m	X_2	${}_fR_2$	${}_bR_2$
No load	$2.89\,\underline{/-78.1}$	1,795	73.7	4.74	1.78	2.65
Full load	$4.33\,\underline{/-44.8}$	1,745	75.4	3.66	1.80	2.61
Maximum torque	$11.4\,\underline{/-34.4}$	1,525	77.3	2.11	1.85	2.57
Locked rotor	$19.9\,\underline{/-68.1}$	0	78.9	1.60	2.18	2.18

ant mmf. For reasons of symmetry, the time- and space-phasing of the rotor currents are the same at the center of the stack when there is skew as when there is zero skew, except for a difference caused by the higher leakage reactance. For the same reason, the time-phasing of the currents obtained from the transformer equivalent circuit of an induction motor represents conditions at the center of the stack. Thus, the angle Δ in Fig. 4 is the same angle as that between stator and rotor current phases associated with the transformer equivalent circuit of Fig. 5.

The mmf shown in Fig. 4 are proportional to the current phasors in Fig. 5(A). The mmf wave at the center of the stack in Fig. 4(C) is then proportional to the phasor I_m in Fig. 5(A). Similarly, the mmf corresponding to the end of the stack with the leading and lagging ends of the rotor bars are proportional to the phasors I_{ML} and I_{MU} respectively. Note that the mmf is a minimum at a distance h beyond the middle of the stack. This corresponds to the location where the rotor and stator current waves are in space or time phase, depending upon whether Fig. 4 or 5 is being studied.

An easy means of finding the mmf at any axial location has thus been illustrated for the forward field. Exactly the same approach can be used to find the mmf at any axial location for the backward field after the conditions at the center of the stack have been determined from one of the techniques presented in the references.[1–6]

Determination of Maximum Magnetic Induction at Any Location in the Air Gap of Yoke

To determine the maximum magnetic induction of the fundamental field at a particular axial and angular location in the air gap, the following procedure could be followed:

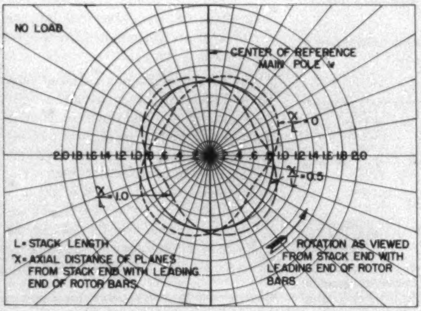

Fig. 6. Maximum mmf versus angular position for three axial planes at no load

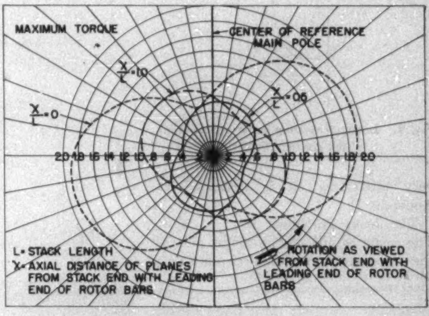

Fig. 8. Maximum mmf versus angular position for three axial planes at maximum torque

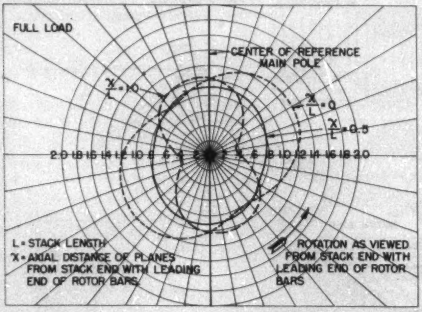

Fig. 7. Maximum mmf versus angular position for three axial planes at full load

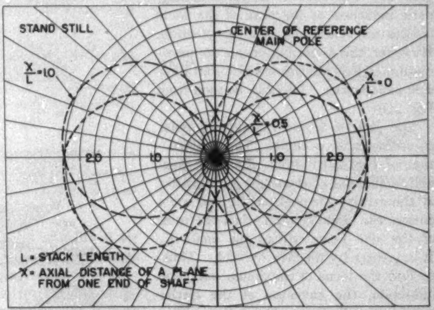

Fig. 9. Maximum mmf versus angular position for three axial planes at standstill

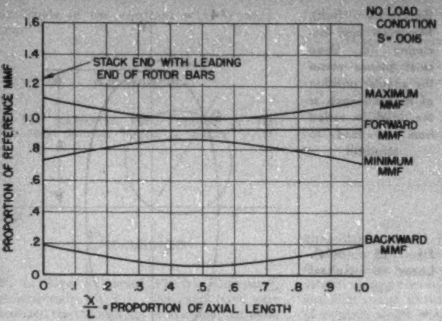

Fig. 10. Variation of several significant mmf's with axial position in the stack at no load

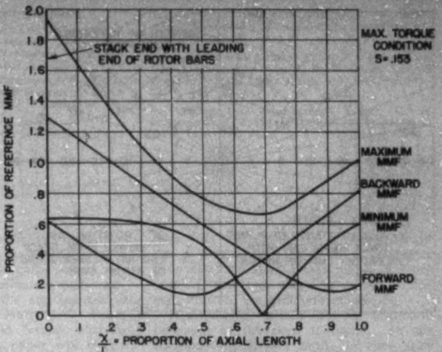

Fig. 12. Variation of several significant mmf's with axial position in the stack at maximum torque

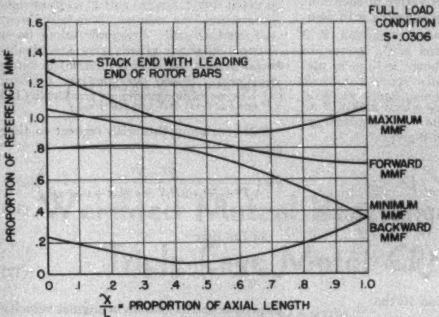

Fig. 11. Variation of several significant mmf's with an axial position in the stack at full load

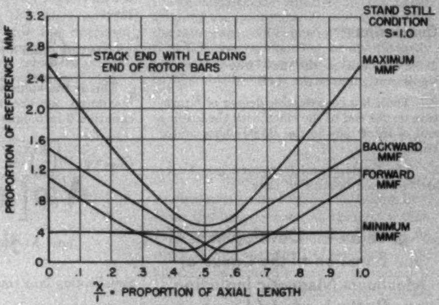

Fig. 13. Variation of several significant mmf's with axial position in the stack at standstill

1. Determine the forward and backward stator and rotor currents with respect to a reference winding at the center of the stack from the transformer equivalent circuit.

2. Rotate the rotor current phasor through an angle corresponding the accumulated skew at that location, and calculate the forward and backward magnetizing currents. The forward and backward flux fields will be proportional and in time or space phase with these magnetizing currents. The author has found it convenient to normalize these magnetizing currents by letting the current which would balance the line voltage flowing through X_m be equal to unity. Then the normalized magnetizing currents are equal to the normalized fundamental magnetic induction field and no further conversion need be made.

3. From the time phase angles of the magnetizing currents, determine the location of the major axis of the ellipse by equation 3.

4. Determine the magnetic induction at the particular angular location by using the curves of Fig. 3.

If the curve of magnetic induction in the yoke is desired, the curve of normalized magnetic induction for the air gap need only be rotated 90 electrical degrees.

Fields in a Particular Single-Phase Motor

A 1/2-horsepower 4-pole 60-cycle-per-second single-phase induction motor was chosen for a quantitative study. The stator punching had 36 slots and the rotor was skewed 21.6 electrical degrees as determined by mechanical measurement (20 electrical degrees would be one stator slot). The rotor slots were closed and had a 15-mil bridge. The conditions were investigated with only the main winding excited at no load, full load, maximum torque, and standstill.

The input currents were determined by test measurements. The circuit parameters were determined by a combination of test measurements and design formulas. They are as tabulated in Table I. The motor was operated at a 1/3-horsepower rating to obtain these data. The results of this study are shown in Figs. 6 through 14.

Figs. 6 through 9 show how the maximum (with respect to time only) air-gap mmf varies with angular position for three axial planes at no load, full load, maximum torque, and locked rotor respectively. The three axial planes are the two ends and the middle of the stack.

Figs. 10 through 13 show the variation of several significant mmf across the stack at no load, full load, maximum torque, and locked rotor respectively. The maximum and minimum mmf as shown on these curves are the maximum or minimum with respect to both time and angular position. The angular position at which they occur is not specified. Fig. 14 shows how the maximum mmf (with respect to both time and angular position)

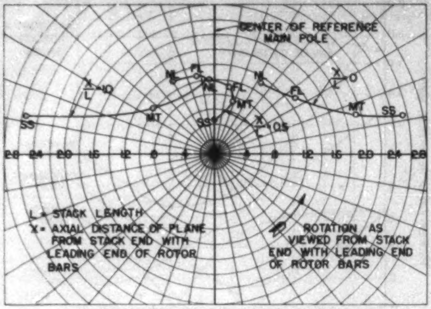

Fig. 14 (left). Maximum mmf occurring for three axial planes versus the angular position of its occurrence as the load is varied from no load to standstill

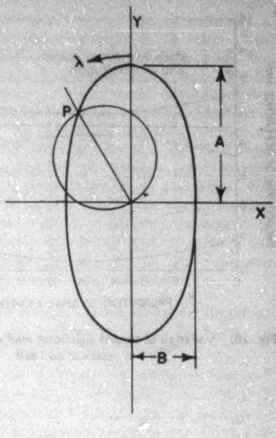

Fig. 15 (right). Locus of resultant vector

varies in magnitude and angular position as the load is varied from no load to locked rotor for the two end planes and the middle of the stack.

Conclusions

1. Skew causes the flux wave to vary significantly across the stack.
2. There is a considerable degree of saturation on the end of the stack with the leading end of rotor bars in the single-phase motor studied.
3. The fundamental frequency iron losses are increased because of skew.

Appendix I. Development of the Equation of the Locus of Maximum Magnetic Induction at a Particular Axial Location

It has been shown that the net field at a particular axial location in an unbalanced polyphase motor or a single-phase motor is a traveling sine wave whose amplitude and angular velocity varies, and that the magnitude varies in an elliptical manner. Fig. 2(B) shows that the maximum induction experienced at a point on the stator bore is not generally the peak of the sine wave as the peak passes that location. The expression for the locus of the maximum induction will be developed here.

Let the major and minor axes of the ellipse be denoted by Figs. 2(A) and (B) respectively. See Fig. 15. The ellipse can be expressed in parametric form as

$$y=a\cos\gamma \tag{6}$$

$$x=-b\sin\gamma \tag{7}$$

The equation for the magnetic induction at the instant the peak of the sine wave passes point P is

$$B=\sqrt{a^2\cos^2\gamma_P+b^2\sin^2\gamma_P}\times \cos\left[\lambda-\tan^{-1}\left(\frac{b}{a}\tan\gamma_P\right)\right] \tag{8}$$

The problem is to find the value of γ_P which will make B a maximum at the angle λ. Substituting this value of γ_P into equation 8 will then give the expression for $B_{\max}$.

Taking the partial derivative of equation 8 with respect to γ_P and equating it to zero gives

$$\gamma_P=\tan^{-1}\left(\frac{b}{a}\tan\lambda\right) \tag{9}$$

This is the value of γ_P which makes B a maximum at the angle λ. Substituting equation 9 into equation 8 gives

$$B_{\max}=a\sqrt{\left(\frac{b}{a}\right)^2+\left(1-\frac{b^2}{a^2}\right)\times \cos^2\left[\tan^{-1}\left(\frac{b}{a}\tan\lambda\right)\right]}\times \cos\left[\lambda-\tan^{-1}\left(\frac{b^2}{a^2}\tan\lambda\right)\right] \tag{10}$$

Substituting into equation 10 that

$$a=P+N \tag{11}$$

$$b=P-N \tag{12}$$

$$\lambda=\theta-\psi=\theta-\frac{\tau_f-\tau_b}{2} \tag{13}$$

gives

$$B_{\max}=\sqrt{P^2-2PN\left\{1-2\cos^2\left\{\tan^{-1}\left[\left(\frac{P-N}{P+N}\right)\times \tan\left(\theta-\frac{\tau_f-\tau_b}{2}\right)\right]\right\}\right\}}\times \cos\left\{\theta-\frac{\tau_f-\tau_b}{2}-\tan^{-1}\times \left[\left(\frac{P-N}{P+N}\right)^2\tan\left(\theta-\frac{\tau_f-\tau_b}{2}\right)\right]\right\} \tag{14}$$

Appendix II. Development of the Angular Velocity of the Vector Representing the Resultant Field

It follows from Fig. 1 that the location of the resultant vector at any time t is

$$\theta=\tan^{-1}\times \left(\frac{P\sin(\omega t+\tau_f)-N\sin(\omega t+\tau_b)}{P\cos(\omega t+\tau t)+N\cos(\omega t+\tau_b)}\right) \tag{15}$$

Differentiating this with respect to time gives

$$\dot{\theta}=\left(\frac{P^2-N^2}{P^2+N^2+2PN\cos(2\omega t+\tau_f+\tau_b)}\right)(\omega) \tag{16}$$

At the time

$$\omega t=\frac{1}{2}(\pi-\tau_f-\tau_b) \tag{17}$$

the vector has its maximum angular velocity of

$$\dot{\theta}_{\max}=\left(\frac{P+N}{P-N}\right)(\omega) \tag{18}$$

Substituting equation 17 into equation 15 shows that

$$\theta=\frac{\pi}{2}+\frac{\tau_f-\tau_b}{2} \tag{19}$$

when the angular velocity is maximum. Note that this is the angle at which the amplitude of the resultant wave is minimum.

Similarly, at the time

$$\omega t=-\frac{1}{2}(\tau_f+\tau_b) \tag{20}$$

the angular velocity has its minimum value of

$$\dot{\theta}_{\min}=\left(\frac{P-N}{P+N}\right)(\omega) \tag{21}$$

Substituting equation 21 into equation 15 shows that

$$\theta=\frac{\tau_f-\tau_b}{2} \tag{22}$$

when the angular velocity is minimum. Note that this is the angle at which the amplitude of the resultant wave is maximum.

References

1. The Revolving Field Theory of the Capacitor Motor, Wayne J. Morrill. *AIEE Transactions*, vol. 48, Apr. 1929, pp. 614–32.

2. A Suggested Rotor Flux Locus Concept of Single-Phase Induction-Motor Operation, C. T. Button. *AIEE Transaction (Electrical Engineering)*, vol. 56, Mar. 1937, pp. 331–32.

3. Single-Phase Motor Theory—A Correlation of the Cross-Field and Revolving-Field Concepts, C. T. Button. *AIEE Transactions*, vol. 60, 1941, pp. 507–12.

4. Symmetrical Components as Applied to the Single-Phase Induction Motor, F. W. Suhr. *AIEE Transactions (Electrical Engineering)*, vol. 64, Sept. 1945, pp. 651–56.

5. Operation of 3-Phase Induction Motors on Unbalanced Voltages, J. E. Williams. *AIEE Transactions*, vol. 73, pt. III-A, Apr. 1954, pp. 125–33.

6. Symmetrical Components (book), C. F. Wagner, R. D. Evans. McGraw-Hill Book Company, Inc., New York, N. Y., 1933, chap. XVII.

Discussion

P. L. Alger (General Electric Company, Schenectady, N. Y.): Designers have long realized that spiralling, or skewing, the slots of an induction motor increases the reactance and affects the performance in many ways, besides reducing the magnetic noise and locking tendency. Despite its importance, no one until now has made any thorough analysis of this subject. This paper is therefore of great interest and importance to all motor designers. Mr. Linkous has brought out very clearly the large amount of flux distortion produced by skew, and has provided methods for clearly visualizing and calculating its effects, which should be immediately useful in machine design.

It is my opinion that the skew reactance flux is in large measure the cause of the shaft vibrations and corresponding noise phenomena that occur during the starting period of typical single-phase motors. It seems probable, therefore, that further analysis along the lines of this paper will enable many of the features of small motor performance that are now obscure to be accurately calculated.

C. E. Linkous: I thank Mr. Alger for his comments. The curves for the distribution of mmf at standstill are for the excitation of a single winding, which of course is not an actual operating condition. However, the mmf will be badly distorted due to skew under heavy current no matter how many windings are excited. It is my opinion, too, that these very high mmf's contribute to the shaft vibrations.

It should be realized that the distortion increases as the skew increases. In the fractional-horsepower range the skew may vary from about 15 electrical degrees for a 1/2-horsepower 2-pole to 45 electrical degrees for a small 4-pole business-machine motor.

The calculations reported in the paper assumed the rotor currents were confined to the rotor cage. Of course, with a cast rotor cage this may or may not be a sufficiently accurate assumption, depending upon many casting conditions.

Weighted Mutual Reactances for a Triple-Cage Motor Circuit

E. R. MARTIN
FELLOW AIEE

At a symposium on double-cage motors held at Toledo in 1952,[1] the motor designers had difficulty in calculating the performance of the 75-horsepower motor which had been built and tested by Westinghouse Electric Corporation.

Following are some of the many reasons why the calculated and test results did not check very well, the test conditions being then unknown:

1. Considerable time was taken to obtain the locked rotor test, thus the rotor became hot.
2. The rotor currents in the three cages are considerably out of phase and it is difficult to calculate the mutual effects.
3. Different designers do not use the same method of calculating coil end and zigzag reactances, or of taking account of changes in reactance due to saturation.

The author thought it should be possible, with the information available, to take account of all the variables involved and set up a circuit that would give close results. This led to a different method of handling the mutual reactances, which is the main contribution of the paper. Results obtained are close to test values, without making unreasonable assumptions for the effects of saturation.

Analysis of Rotor Bar Temperatures Under Locked Test

The average time to take locked readings was 5.7 seconds. During this time the outer cage bars (hereafter referred to as 2) are loaded 84,000 to 65,000 amperes per square inch. At the latter value, the bars will rise 100 degrees centigrade (C) in about 0.5 second with no heat loss. Curves are shown giving the effect of different loading for copper and 50-per-cent (%) conductivity aluminum with no heat loss; see Fig. 1. The curve for copper is used for estimating the temperature rise in the stator winding, and those for aluminum are used for the rotor. The surrounding rotor iron will start taking heat from the bars as soon as there is a temperature difference between them. A method was suggested of calculating the conduction of heat from the aluminum to the iron, and calculations were made. Since the aluminum shrinks away from the rotor teeth when it cools a model was made up and tested. It was found that heat was transmitted from a brass bar to a small stack of 0.75×0.75 lamination only five-eighths as fast with about 0.002 (the approximate shrinkage) clearance in the hole as compared to a tight fit. The temperature rises in the outer bar and surrounding iron with no other heat conduction were calculated on this basis and are shown in Fig. 2, which also shows the slot shape. These computations are not included since they would take considerable space; but the information in Fig. 2 will indicate that the enormous amount of heat cannot get into the iron fast enough to avoid a considerable rise in the aluminum bar temperature.

The middle cage bar (to be designated

Paper 55-273, recommended by the AIEE Rotating Machinery Committee and approved by the AIEE Committee on Technical Operations for presentation at the AIEE Middle Eastern District Meeting, Columbus, Ohio, May 4–6, 1955. Manuscript submitted February 3, 1955; made available for printing March 21, 1955.

E. R. Martin is with the University of Michigan, Ann Arbor, Mich.

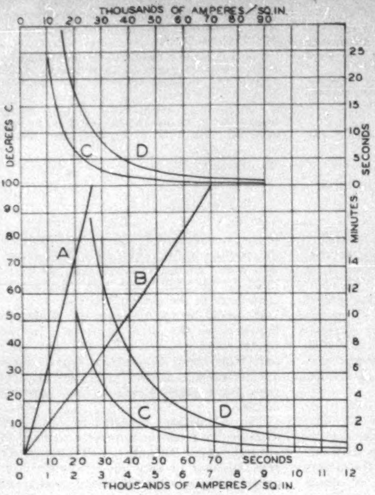

Fig. 1 (left). Curves for no-heat loss from conductors. Temperature rise in C over 25 against seconds at 10,000 amperes per square inch

A—50% conductivity aluminum

B—100% conductivity copper

Time against amperes per square inch for 100C rise above 25

C—50% conductivity aluminum

D—100% conductivity copper

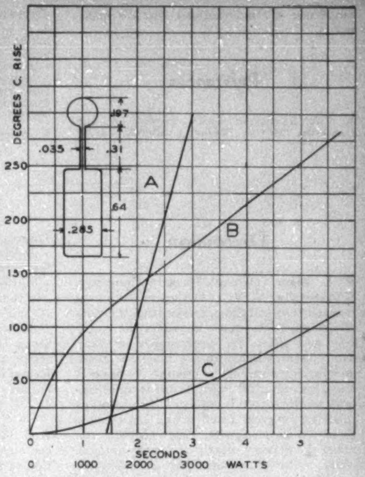

Fig. 2 (right). Bar 2, aluminum, carrying an average effective current of 1,940 amperes, rotor-locked

A—Watts per bar for temperature rises above 25 degrees C

B—Temperature rise above 25 C for bar 2 against seconds

C—Temperature rise above 25 C for rotor teeth, against seconds. Assuming no heat conducted elsewhere

as (3) or bridge between the outer and inner cage bar (4) will also be heavily loaded and will be losing heat to the rotor iron. At the same time it will conduct heat from bar 2 to bar 4 at the rate of 4.6 watt-seconds per second per degree difference in temperature. Accordingly, bar 2 is assumed to reach a temperature of 175 instead of 280 as shown in Fig. 2. Other temperatures used are shown on the circuit diagram, Fig. 3.

Reactances and Saturation

If the current at starting is known, the ampere-turns per slot can be calculated. At 563 amperes, there will be 281.5 amperes per circuit, or 2,815 ampere-conductors per slot. This will be 2,815 ampere-turns acting across the 0.150 slot opening, giving a maximum flux density of 84,600. No appreciable ampere-turns can be absorbed by the iron at this density, so no saturation will be allowed for the stator slot reactance. The pitch is 1 to 12 so there are only four slots in which both coil sides carry current of the same phase, for each of the three phases. In the other slots the current is less.

Bar 4 carries about 825 amperes, so it can produce a maximum flux density of 106,000 across the 0.035 slot. The iron on each side of the slot can absorb only about 15 ampere-turns, so no saturation will be used for bar 4. The only saturated path at starting is the bridge over the tunnelled slot 2, which may be 0.002 to 0.004 thick at the center, and it will be carrying a flux density much beyond the range of the magnetization curves. This flux will be thrown in with the zigzag reactance, which is calculated as 0.114 ohm unsaturated. This value is split 59% for the rotor and 41% for the stator. The reductions for saturation are to 63% for cold start, 70% for hot start, and 85% for pull-out. These values, the only ones in these calculations are arbitrary values. A skew reactance of 0.0175 ohm is considered constant in each circuit.

Mutual Reactances and Method of Weighting

When locked, the rotor bar currents will be of different value and phase. It would be convenient to use a value of self-reactance plus two mutual reactances in each bar circuit. In circuit 2, I_2X_2 is the self-reactance drop, I_2X_{2m3} is the mutual-reactance drop in bar 2 caused by I_3, and I_2X_{2m4} is the same for the effect of I_4. The slot reactances are calculated nearly the same by everyone, and the following permeances should be easily verified. $K_2=0.66$, $K_3=4.5$, and $K_4=11.215$. These multiplied by 0.044 for this motor give reactances, $X_2=0.029$, $X_3=0.198$, and $X_4=0.493$. The motor constants are $K=(100)^2\times3\times60\times10^{-8}=0.018$. $K_s=(20.05\times8)/60=2.67$ for the stator. $K_r=(20.05\times8)\ (0.958\times0.914)^2/50=2.45$ for the rotor. $K_{rt}=KK_r=0.044$.

The mutual effect of bars 3 and 4 on bar 2 will use the permeance of a round slot with the current at a point on the circle or outside it, and this is 1.55. Since all the flux across the slot will not cut all of bar 2, it can be seen that half can be assumed to cut all the bar. So, $0.044\times1.55/2$ gives 0.0341 ohm as the mutual reactance between bars 3 or 4 and 2, and also between bar 2 and 3 or 4, when the currents are equal and in phase. Bar 4 sets up flux across slot 2, all of which cuts bar 3, and also a flux across slot 3, only half of which may be assumed to cut bar 3. So the mutual reactance between bars 3 and 4 is $0.044(1.55+0.5\times0.31/0.035)=0.263$ ohm.

To avoid handling reactance drops not in phase, the following procedure is used. Say I_2 and I_3 differ by θ degrees. Mutual reactance to be put in circuit 2 for voltage induced by I_3, is $0.0341\times I_3\cos\theta/I_2$, and that to be put in circuit 3 for the effect produced by I_2 is $0.0341\times I_2\cos\theta/I_3$.

The circuit is set up and calculated with the best assumed values of total reactance for each circuit, then the currents and phase angles are found, the reactances corrected, and the circuit recalculated. If the first values are too far off, a third calculation may be necessary to get mutual reactances which will not change.

This, of course, is not strictly correct, but it greatly simplifies the calculations.

Circuit for Starting Hot

In Fig. 3, the circuit is shown with the various final values of resistance and reactance, together with the currents and voltages in the equivalent circuit. Rotor bar currents can be found by multiplying by 5.25, the turns ratio. The actual voltage induced in a bar is $E_0/87.5$, the divisor being the effective conductors in series per phase. The equivalent impedance of the three bar circuits in parallel is $Z' = 0.1554 + j0.094 = 0.182$. The values in the common circuit are added to this, giving $Z_r = 0.1759 + j0.2106 = 0.275$. The starting torque, hot, is $3(549)^2(0.1759) = 159{,}000$ synchronous watts which gives 2.79 per unit torque or 624 pound-feet. I_1 is 563 amperes and I_r is 549 amperes. Test values were 563 amperes and 622 pound-feet.

It is probable that the rotor averages 50 C higher than the stator, in which case the air gap would close down 0.0025 on each side, but this was not used.

The circuit was tried starting cold to check the test values extrapolated back to zero time. Resistances were reduced to 25 C values, which gives 1.25 times the calculated value for R_4, to take account of unequal current distribution. When the current shifts towards the air gap, the slot reactance will also be reduced. However, for bar 4 this correction applies to only a small part of its total so it is neglected both here and in the hot-start calculations. The mutual reactances changed slightly for bars 2 and 3 and increased from 0.1656 to 0.248 for bar 4. See totals of bar reactances in Fig. 3. The zigzag reactance was reduced to 63% for increased saturation. The calculations then gave 639 amperes at start and 607 pound-feet of torque which closely checks the test values of 650 and 605.

Break-Down or Pull-Out Torque

Under this condition, the current in bar 4 is higher than at rotor-locked, being 233 amperes (as compared to 154 amperes) in the equivalent circuit, or 5.25×233 or 1,225 amperes in the bar. This would give a maximum flux density of 158,000 across the 0.035 gap if all the ampere-turns were used on the gap. However, at this density, the adjacent iron will absorb an appreciable amount and the maximum density will be reduced to about 135,000. This will reduce the total flux about 6.3% by flattening the peak of the sine wave. This affects the major item of slot-4 reactance, the middle term in $K_4 = 0.805 + 8.86 + 1.55$, so this is changed to $K_4 = 0.805 + 8.3 + 1.55$. This times 0.044 gives 0.47 instead of the unsaturated value of 0.493 for slot-4 reactance, a rather small reduction.

Using the reduced X_4 and 85% of the X_{zz} and the d-c value of R_4 with all resistances at 65 C except R_1, which was taken at 35 degrees, the pull-out calculations gave $I_1 = 346$ and the torque 530 pound-feet against test values of 362 amperes and 528 pound-feet for 0.15 slip. Seventy-five per cent of zigzag reactance was also tried and this gave 352 amperes and 540 pound-feet of torque, but it was assumed that the change from starting should be greater than that. However, it does bring the current closer.

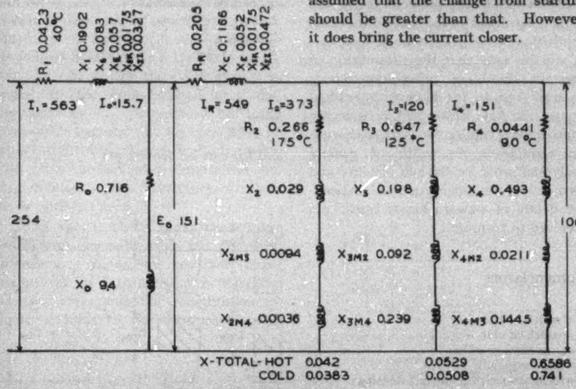

Fig. 3. Triple-cage circuit of 75-horsepower motor starting hot. This shows all values of resistance and the components of reactance, the assumed temperature of the resistance, and the currents and voltages for the different parts of the circuit

Full-Load Torque

The full-load calculations gave 94.2 amperes and 105% torque at 0.01667 slip. Since there is no load loss in this circuit, the efficiency is high. The total reactance is low and the power factor is high, which indicates that one or more of the reactances are not correctly calculated for this motor.

Alger and Wray[2] used for this motor 0.171–0.083 or 0.088 for the stator end-turn reactance instead of 0.057. If this value were used the current would be reduced to 93.5 amperes. The stray load loss by test was 927 watts, which would add 0.036 ohm to the stator circuit. If this were also added the current would drop to 92.7 amperes and the torque to 102%, which is close to test values. However, the full-load calculations do not give as much trouble as the others, so not much attention is given it here. It may be that a higher stator coil-end reactance should have been used, the zigzag and skew reactances combined, and both reduced drastically for starting.

Summary

Another method has been presented for calculating the starting and pull-out performance of double- and triple-cage motors, in which the mutual effect of the rotor bars on one another is based on the physical conception of the conditions. Effects of saturation were investigated and found to require practically no correction except in the case of the zigzag reactance. Since the rotor slot reactances can be figured accurately, the method used, though it entails some extra labor in making computations, leads to a greater assurance concerning the accuracy of the slot reactance values than can be said of the resistances.

Another check on the circuit that can be made is to draw a phasor diagram. Subtracting I_1Z_1 from E_1 leaves E_0 the induced voltage per phase. The flux density in the air gap can then be calculated for the locked condition and the equation $F = 8.85\ BIL\ \cos\theta \times 10^{-8}$ used to get the average pounds force per rotor slot, where B is the effective flux density in the air gap, I is the phasor sum of the actual rotor bar currents, or 549, L is the length of bar in inches, and θ is the angle between the rotor current and the induced voltage. This force multiplied by 60, the number of bars, and by 11.08/24, the rotor radius in feet, gives 619 pound-feet as compared to 622 test. This shows that the stator reactance is about right, since E_0 gives an air-gap flux density that will check the starting torque.

The circuit was tried on a 7.5-horsepower double-cage motor for which satisfactory data were at hand and the greatest discrepancy was 36.25 pound-feet starting torque against 35 test. It is not often that a motor is tested so carefully and completely as was this 75-horsepower motor; therefore the opportunity to try a circuit on it was too inviting to resist.

References

1. SYMPOSIUM ON DESIGN OF DOUBLE-CAGE INDUCTION MOTORS. *AIEE Transactions*, vol. 72, pt. III, Aug. 1953, pp. 621–62.

2. DOUBLE AND TRIPLE SQUIRREL CAGES FOR POLYPHASE INDUCTION MOTORS. P. L. Alger, J. H. Wray. *Ibid.*, p. 642.

Computation of Skin Effect in Bars of Squirrel-Cage Rotors

M. M. LIWSCHITZ-GARIK
FELLOW AIEE

IN A previous paper[1] equations were derived analytically for the ratio of a-c to d-c resistance and for a-c to d-c inductance in the more commonly used bars of large squirrel-cage rotors. Different methods can be used for the determination of these ratios. In certain cases, Poynting's vector can be applied; in other cases, the method shown in the aforementioned paper can be used. Where only the ratio of a-c to d-c resistance is of interest, the equation

$$\frac{r_{ac}}{r_{dc}}=\frac{1}{c}\int_c \frac{G^2\,dc}{G_0^2} \tag{1}$$

leads to the desirable results.

No matter which method of calculation is applied, the actual width of the bar does not appear in the ratios r_{ac}/r_{dc} and l_{ac}/l_{dc}, i.e., the actual width of the bar does not influence the skin effect. However, the skin effect depends largely upon the ratio of the widths of the various parts of the bar. For example, the ratio of the width at the top to the width at the bottom affects considerably the magnitude of the skin effect in the tapered bar.

Since the actual width of the bar does not influence the magnitude of the skin effect, the question arises whether or not the "depth of penetration" is influenced by the shape of the bar. It is easy to define a depth of penetration for the straight bar; see Fig. 1 (A). If this depth of penetration remains the same for other bar shapes, the problem of computation of r_{ac}/r_{dc} and l_{ac}/l_{dc} becomes a very simple one, for it resolves itself to the calculation of only d-c resistances and d-c coefficients of self-inductance (as shown in the following). The further advantage of this fact would be that it would make possible the determination of the skin effect in bars of any shape, i.e., in bars for which no straightforward mathematical solution is possible.

E. zur Nieden[2] used the assumption of the same depth of penetration as in the straight bar in order to calculate the skin effect in a tapered bar and in a ⊥ bar. The results obtained were compared with those determined by a graphical method. The comparison shows a close agreement, especially for the tapered bar. In the following, a comparison will be made for two bar types between the results obtained from the accurate equations derived in the previous paper and those determined on the basis of the same depth of penetration as in the straight bar. It will be seen that the assumption of constant depth of penetration yields accurate results for bars with gradual changes in the width and satisfactory approximate results for bars with sudden changes in the width. A general analytical proof for the admissibility and accuracy of the assumption of independent depth of penetration is much too involved to be useful.

Nomenclature

b_b = width of bar
b_s = width of slot
c = cross section of bar
f_1 = line frequency
G = local alternating current density
G_0 = direct current density
h = total height of bar
h_{pr} = depth of penetration with respect to a-c resistance
h_{px} = depth of penetration with respect to a-c inductance
l_{ac} = a-c inductance of bar
l_{dc} = d-c inductance of bar
r_{ac} = a-c resistance of bar
r_{dc} = d-c resistance of bar
s = slip of the rotor with respect to the fundamental rotating flux
λ_{ac} = a-c permeance
λ_{dc} = d-c permeance
ρ = bar resistivity, microhms per inch[3]

Definition of Depth of Penetration for Straight Bar

It has been shown in the previous paper[1] that for the straight bar shown in Fig. 1 (A)

$$\frac{r_{ac}}{r_{dc}}=\varphi(\xi) \tag{2}$$

$$\varphi(\xi)=\xi\,\frac{\sinh 2\xi+\sin 2\xi}{\cosh 2\xi-\cos 2\xi} \tag{3}$$

$$\frac{l_{ac}}{l_{dc}}=\psi(\xi) \tag{4}$$

$$\psi(\xi)=\frac{3}{2\xi}\,\frac{\sinh 2\xi-\sin 2\xi}{\cosh 2\xi-\cos 2\xi} \tag{5}$$

where

$$\xi=0.316h\sqrt{\frac{b_b}{b_s}\,\frac{f_1}{\rho}}\sqrt{s} \tag{6}$$

h_{pr} can be defined as

$$\frac{r_{ac}}{r_{dc}}=\varphi(\xi)=\frac{h}{h_{pr}} \tag{7}$$

i.e.

$$h_{pr}=\frac{h}{\varphi(\xi)} \tag{8}$$

and h_{px} can be defined as

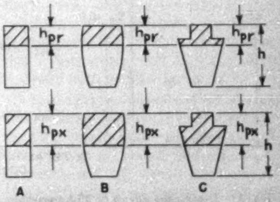

Fig. 1. Explanation of the depth of penetration

Paper 55-271, recommended by the AIEE Rotating Machinery Committee and approved by the AIEE Committee on Technical Operations for presentation at the AIEE Middle Eastern District Meeting, Columbus, Ohio, May 4–6, 1955. Manuscript submitted January 31, 1955; made available for printing March 13, 1955.

M. M. LIWSCHITZ-GARIK is with the Polytechnic Institute of Brooklyn, Brooklyn, N. Y., and consulting engineer to the National Electric Coil Company, Columbus, Ohio.

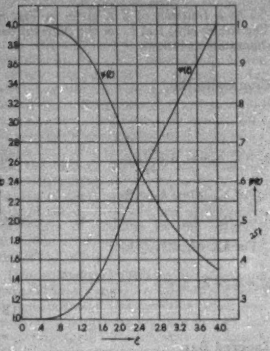

Fig. 2. Quantities $\varphi(\xi)$ and $\psi(\xi)$ as functions of (ξ)

$$\frac{l_{ac}}{l_{dc}}=\psi(\xi)=\frac{h_{px}/3b_s}{h/3b_s}=\frac{h_{px}}{h} \tag{9}$$

i.e.

$$h_{px}=h\psi(\xi) \tag{10}$$

The values of $\varphi(\xi)$ and $\psi(\xi)$ as functions of ξ are given in Fig. 2.

The Ratios r_{ac}/r_{dc} and l_{ac}/l_{dc} for Any Bar Shape

The assumption that the depth of penetration is independent of the shape of the bar means that equations 8 and 10 apply to any bar shape with h being the total height of the bar. Thus, the three bar shapes shown in Fig. 1 having the same total height will have the same values of the depths of penetration h_{pr} and h_{px} for given values of f_1, s, ρ, and b_b/b_s. It follows from this that the ratio r_{dc}/r_{ac} for any one of the three bar shapes is equal to the cross-hatched area determined by h_{pr}, divided by the total area of the bar, and that the ratio l_{ac}/l_{dc} is equal to the d-c inductance of a bar with the cross-hatched area determined by h_{px}, divided by the inductance of a bar with total bar area.

With the depth of penetration independent of the shape of the bar, the computation of r_{ac}/r_{dc} for any bar shape reduces to the determination of the ratio of two areas and the computation of l_{ac}/l_{dc} reduces to the determination of the ratio of two d-c inductances. The computation becomes simple, since no Bessel or hyperbolic functions are involved.

Table I. Comparison of Computations for Tapered and Composite Bars

Cycles	r_{ac}/r_{dc} Equations Derived Analytically	r_{ac}/r_{dc} Equations Derived on Independency of Depth of Penetration	l_{ac}/l_{dc} Equations Derived Analytically	l_{ac}/l_{dc} Equations Derived on Independency of Depth of Penetration
		Tapered Bar		
60	5.0	4.99	0.408	0.414
45	4.25	4.21	0.480	0.478
30	3.33	3.38	0.598	0.589
15	2.05	2.07	0.796	0.801
5	1.17	1.16	0.969	0.964
		Composite Bar		
60	8.88	8.63	0.378	0.387
45	7.55	7.40	0.451	0.488
30	5.70	5.81	0.583	0.635
15	3.01	2.73	0.815	0.850
5	1.30	1.2	0.975	0.975

The calculation with the depths of penetration h_{pr} and h_{px} leads to simple equations for the tapered bar, for the bar composed of a straight bar and tapered bar, and also for the ⊥ bar. These equations are given in the Appendix.

To prove the admissibility and accuracy of the assumption of independent depth of penetration, a comparison is made for the tapered bar and the composite bar in Table I. The values of r_{ac}/r_{dc} and l_{ac}/l_{dc} are calculated using the equations derived analytically in the foregoing paper and the equations of the Appendix based on independency of depth of penetration.

The dimensions of both bars are given in Fig. 3. Copper (at 75 degrees centigrade) is assumed as the bar material. The ratio b_b/b_s is assumed to be 1. The calculations were made by slide rule. For the Bessel functions, the curves used were given in the foregoing paper. The depth of penetration method yields for the tapered bar the same results as the analytically derived equations, and this holds for any bar the width of which changes gradually. However, the results of both computation methods do not agree entirely with each other in the case of the composite bar. This is because the depth of penetration method does not take into account the sudden change of the field intensity at the spot where the width of the slot changes suddenly.

The depth of penetration method yields somewhat higher ratios of r_{ac}/r_{dc} and l_{ac}/l_{dc} than the analytical method when h_{pr} and h_{px} contain a sudden change in the slot width. For these cases, a small correction factor can be used in order to take into account the sudden change of the slot width. This factor by which h_{pr} and h_{px} must be multiplied is given in Fig. 4.

Examples of Calculation

Prof. W. V. Lyon[8] has discussed the application of functions of complex hyperbolic angles to the calculation of skin-effect problems. He demonstrated the method of a ⊥ bar, the dimensions of which are shown in Fig. 5. The results of his calculations with complex hyperbolic functions are

$$r_{ac}/r_{dc}=2.01,\ x_{ac}/r_{dc}=3.19$$

These results will be compared with those obtained by the depth-of-penetration method.

From equation 6 for 60 cycles, copper at 100 degrees centigrade, and $b_b = b_s$

$$\xi=0.316\times0.564\sqrt{\frac{60}{0.910}}=1.45$$

From Fig. 2 and equation 8

$$\varphi(\xi)=1.34,\ h_{pr}=0.564/1.34=0.42>h_d=0.282$$

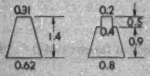

Fig. 3 (left). Dimensions of the two bars for which a comparison of calculation methods has been made

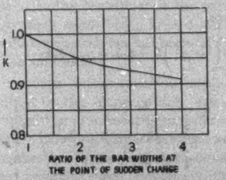

Fig. 4 (above). Correction factor for depths of penetration h_{pr} and h_{px}

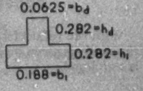

Fig. 5 (right). Dimensions of the ⊥ bar calculated using complex hyperbolic functions and the depth-of-penetration method

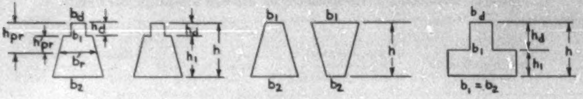

Fig. 6. For derivation of r_{ac}/r_{dc}

For $b_1/b_d = 3$, the correction factor for h_{pr} and h_{px} is 0.925, Fig. 4, i.e.

$$h_{pr} = 0.925 \times 0.42 = 0.388$$

From equation 17

$$h_{pr}' = 0.388 - 0.282 = 0.106$$

$$\frac{r_{ac}}{r_{dc}} = \frac{0.188 \times 0.282 + 0.0625 \times 0.282}{0.188 \times 0.106 + 0.0625 \times 0.282} = 1.89$$

From Fig. 2 for $\xi = 1.45$, $\psi(\xi) = 0.906$. From equation 10

$$h_{px} = 0.906 \times 0.564 = 0.511 > h_d = 0.282$$

With the correction factor 0.925, $h_{px} = 0.925 \times 0.511 = 0.472$ and from equation 25

$$h_x = 0.472 - 0.282 = 0.190$$

$$b_x = b_1 = 0.188, \ \beta = 1, \ \epsilon = 1$$

From equations 19 and 18

$$c_x = 0.188 \times 0.190 + 0.0625 \times 0.282 = 0.0533, \quad c_{bx} = 0.0357$$

$$\lambda_{ac} = \frac{1}{0.0533^2}\left(0.0357^2 \frac{0.190}{3 \times 0.188} + 0.0357^2 \frac{0.282}{0.0625} + 0.0357 \quad 0.282^2 + 0.0625 \frac{0.282^3}{3}\right) = 3.32$$

Therefore

$$x_{ac} = 4\pi \times 10^{-9} \times 3.32 \times 2\pi \times 60 \times 2.54 = 0.399 \times 10^{-4} \text{ ohms per inch}$$

Since

$$r_{dc} = \frac{0.91 \times 10^{-6}}{0.282(0.0625 + 0.188)} = 0.1287 \times 10^{-4} \text{ ohms per inch}$$

$$\frac{x_{ac}}{r_{dc}} = \frac{0.399 \times 10^{-4}}{0.1287 \times 10^{-4}} = 3.1$$

The difference between the two methods of calculation is only 6 per cent and 3 per cent respectively.

Appendix. The Ratios r_{ac}/r_{dc} and l_{ac}/l_{dc} for Composite Bar, Tapered Bar, and ⊥ Bar on the Basis of the Depth of Penetration

With the value of h_{pr} from equation 8 and the symbols given by Fig. 6, the ratio r_{ac}/r_{dc} is as follows.

Composite Bar

(a) $h_{pr} \leq h_d$

$$\frac{r_{ac}}{r_{dc}} = \frac{\left(\frac{1+\beta_0}{2}\right) b_2 h_1 + b_d h_d}{b_d h_{pr}}, \ \beta_0 = \frac{b_1}{b_2} \tag{11}$$

(b) $h_{pr} \geq h_d$

$$h_{pr}' = h_{pr} - h_d, \ b_r' = b_1 \frac{\beta_0 h_1 + (1-\beta_0) h_{pr}'}{\beta_0 h_1} \tag{12}$$

$$\frac{r_{ac}}{r_{dc}} = \frac{\left(\frac{1+\beta_0}{2}\right) b_2 h_1 + b_d h_d}{\left(\frac{b_1 + b_r'}{2}\right) h_{pr}' + b_d h_d} \tag{13}$$

Tapered Bar

$$b_r = b_1 \frac{\beta_0 h + (1-\beta_0) h_{pr}}{\beta_0 h} \tag{14}$$

$$\frac{r_{ac}}{r_{dc}} = \frac{\left(\frac{1+\beta_0}{2}\right) b_2 h}{\left(\frac{b_1 + b_r}{2}\right) h_{pr}} \tag{15}$$

⊥ Bar

(a) $h_{pr} \leq h_d$

$$\frac{r_{ac}}{r_{dc}} = \frac{b_1 h_1 + b_d h_d}{b_d h_{pr}} \tag{16}$$

(b) $h_{pr} \geq h_d$

$$h_{pr}' = h_{pr} - h_d$$

$$\frac{r_{ac}}{r_{dc}} = \frac{b_1 h_1 + b_d h_d}{b_1 h_{pr}' + b_d h_d} \tag{17}$$

With the value of h_{px} from equation 10 and the symbols given in Fig. 7, the d-c and a-c permeances become as follows: Fig. 7 and equation 7 of the foregoing paper yield the following general equation for the permeance

$$\lambda = \frac{1}{c_x^2}\left(c_{bx}^2 \frac{h_x \epsilon}{3 b_1} + c_{bx}^2 \frac{h_d}{b_d} + c_{bx} h_d^2 + b_d \frac{h_d^3}{3}\right) \tag{18}$$

where

$$c_x = \left(\frac{b_1 + b_x}{2}\right) h_x + b_d h_d = c_{bx} + b_d h_d \tag{19}$$

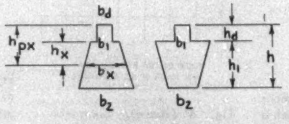

Fig. 7. For derivation of l_{ac}/l_{dc}

ϵ as a function of β is given in Fig. 8. The values of h_x and b_x for the different bar shapes are as follows.

Composite Bar

For λ_{dc}

$$h_x = h_1, \ b_x = b_2, \ \beta = \frac{b_1}{b_2} = \beta_0 \tag{20}$$

For λ_{ac}, when $h_{px} \leq h_d$

$$h_x = 0, \ h_d = h_{px} \tag{21A}$$

For λ_{ac}, when $h_{px} \geq h_d$

$$h_x = h_{px} - h_d, \ b_x = b_1 \frac{\beta_0 h_1 + (1-\beta_0) h_x}{\beta_0 h_1}, \ \beta = \frac{b_1}{b_x} \tag{21B}$$

Tapered Bar

For λ_{dc}

$$h_d = 0, \ h_x = h_1, \ b_x = b_2, \ \beta = \frac{b_1}{b_2} = \beta_0 \tag{22}$$

For λ_{ac}

$$h_d = 0, \ h_x = h_{px}, \ b_x = b_1\left(\frac{\beta_0 h_1 + (1-\beta_0) h_{px}}{\beta_0 h_1}\right), \quad \beta = \frac{b_1}{b_x} \tag{23}$$

⊥ Bar

For λ_{dc}

$$h_x = h_1, \ b_x = b_1 = b_2 \tag{24}$$

For λ_{ac}, when $h_{px} \leq h_d$

$$h_x = 0, \ h_d = h_{px} \tag{25A}$$

For λ_{ac}, when $h_{px} \geq h_d$

$$h_x = h_{px} - h_d, \ b_x = b_1, \ \beta = 1 \tag{25B}$$

The ratio l_{ac}/l_{dc} is the same as the ratio $\lambda_{ac}/\lambda_{dc}$.

References

1. Skin-Effect Bars of Squirrel-Cage Rotors, M. Liwschitz-Garik. *AIEE Transactions*, vol. 73, pt. III-A, Apr. 1954, pp. 255–58.

2. Calculation of Bars for Skin-Effect Motors, E. zur Nieden. *Elektrotechnic und Maschinenbau*, Vienna, Austria, 1933, pp. 129–34.

3. Internal Impedance, Waldo V. Lyon. *Electrical Engineering*, vol. 68, Jan. 1949, pp. 88–89.

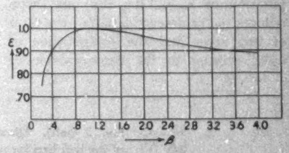

Fig. 8. Quantity ϵ as function of β

Discussion

P. L. Alger (General Electric Company, Schenectady, N. Y.): I concur fully in the accuracy and generality of the methods for calculating the effective impedance of odd-shaped squirrel-cage bars that are presented in this paper. However, I do not feel that the methods shown are the most suitable for design use. For the methods outlined enable the over-all resistance and reactance to be determined, but they do not show the division of the losses between the various parts of the squirrel cage, nor do they offer any means of allowing for the magnetic saturation which may occur across a narrow part of the conductor.

In practice, especially with cast aluminum squirrel cages, composite bars with a small section above and a large section below, connected by a narrow leakage slot or neck, are frequently used. To calculate the impedance of such a squirrel cage, at a particular frequency and impressed voltage, it is necessary to determine the fraction of the total current flowing in the neck, and also in the lower bar, and thence to determine the degree of saturation and the corresponding effective width of the neck; and this in turn will affect the over-all impedance of the squirrel cage. Also, in order to determine the temperature versus time relations, and thence the permissible stalled time of a motor, it is necessary to know the distribution of losses between the various parts of a composite bar, and the effects of changing temperatures on this distribution.

With these purposes in mind, it seems to me preferable to calculate the performance of composite squirrel-cage bars by means of an extended equivalent circuit.[1,2] There are two ways of using such an extended equivalent circuit.

One way is to divide the bar into sufficiently small sections, so that the current distribution can be assumed to be uniform within each section. In this case, simple transmission-line theory applies. The second method, which I prefer, is to divide the bar into only two, three, or at the very most four sections, such as the top bar, the neck, and the bottom bar of a cast aluminum double squirrel cage. In this case, the current distribution cannot be assumed uniform, and skin effect ratios must be applied to both the resistance and inductance of each bar section. However, for all practical cases, the three bar sections taken separately are sufficiently small so that the skin effect ratios can be expressed as an infinite series, of which only the first one or two terms need be considered. Hence, it is readily possible to develop simple algebraic equations for the factors J and K to be applied to the self- and mutual reactances and resistances of the separate bar sections, and thus to adjust the values of impedance in a simple equivalent circuit, taking full account of whatever frequency, temperature, and saturation may be present. By this method no curves, tables, or complex mathematical equations are needed, while at the same time the entire performance of the squirrel cage is easily visualized and readily adjusted to suit any desired change in design or other conditions.

REFERENCES

1. CIRCUIT ANALYSIS METHOD FOR DETERMINATION OF A-C IMPEDANCES OF MACHINE CONDUCTORS, D. S. Babb, J. E. Williams. *AIEE Transactions*, vol. 70, pt. I, 1951, pp. 661–66.

2. DOUBLE AND TRIPLE SQUIRREL CAGES FOR POLYPHASE INDUCTION MOTORS, P. L. Alger, J. H. Wray. *Ibid*. vol. 72, pt. III, Aug. 1953, pp. 637–45.

M. Liwschitz-Garik: I am grateful to Mr. Alger for commenting on my paper. His comments, I believe, are based on a misunderstanding. The method of "fictitious depth of penetration," as dealt with in my paper, applies to single-cage rotors, while Mr. Alger has in mind multicage rotors. I agree with Mr. Alger that for these latter rotors other methods for calculation of skin effect should be used and I do not apply the depth of penetration method in designing multicage rotors.

Basic Sequence Networks

H. S. KIRSCHBAUM
MEMBER AIEE

THE most general type of series fault occurring in a 3-phase transmission system is one in which three unequal impedances are introduced in the three line conductors between two points in the system. In this case, while it is possible to write the equations relating the sequence components of voltage and current at the fault, there is no simple way to interconnect the sequence networks because the mutual impedance terms in the equations are nonreciprocal and, as a consequence, any interconnections of the sequence networks would require the use of ideal amplifiers. If, however, the series fault is symmetrical with respect to the phase whose sequence components are being used as a reference (generally phase a), the mutual impedance terms become reciprocal and the sequence networks can be interconnected in a simple manner. Heretofore, only one such interconnection has been presented, e.g., Fig. 21(t) of reference 1. This figure is reproduced here as Fig. 1. This interconnection can be used on a network analyzer only for those cases in which the real part of Z_a exceeds or equals the real part of Z_b. It is not valid when the real part of Z_b exceeds the real part of Z_a, since this would require a negative resistance in the interconnection. For the sake of simplicity, "the real part of" will be dropped from the foregoing statement in the remainder of the paper. It is in such cases (e.g., lines b and c open) that each problem has been treated as a special case.

A network interconnection will be presented in this paper which can be used when the aforementioned interconnection is not physically realizable. It will further be shown that a great many of the generally used interconnections for shunt and series faults are but special cases of either one or the other of the two general interconnections presented.

The Shunt Representation

For the sake of completeness, the network interconnection of Fig. 1 will be derived. It has been called the shunt representation because for some of the simpler types of faults, the sequence networks are connected in parallel with each other.

Fig. 2 shows a portion of a 3-phase

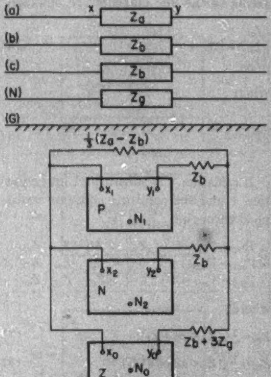

Fig. 1. Series unbalance and equivalent network interconnection from reference 1

Paper 55-278, recommended by the AIEE Transmission and Distribution Committee and approved by the AIEE Committee on Technical Operations for presentation at the AIEE Middle Eastern District Meeting, Columbus, Ohio, May 4–6, 1955. Manuscript submitted February 4, 1955; made available for printing March 21, 1955.

H. S. KIRSCHBAUM is with Ohio State University, Columbus, Ohio.

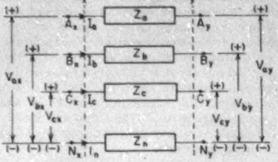

Fig. 2. Series unbalance showing positive sense of current and voltage

system with three unequal line impedances and an impedance in the neutral line. The portion of the system to the left of point x is balanced as is also the portion of the system to the right of point y. These two portions may also be interconnected through a perfectly balanced interconnection. At the fault location, Kirchoff's voltage equations may be written in matrix form

$$\begin{Vmatrix}(V_{ax}-V_{ay})\\(V_{bx}-V_{by})\\(V_{cx}-V_{cy})\end{Vmatrix}+\begin{Vmatrix}I_nZ_n\\I_nZ_n\\I_nZ_n\end{Vmatrix}=\begin{Vmatrix}Z_a&0&0\\0&Z_b&0\\0&0&Z_c\end{Vmatrix}\begin{Vmatrix}I_a\\I_b\\I_c\end{Vmatrix} \qquad (1)$$

Also, the line currents can be written in terms of the symmetrical components of phase-a current as

$$\begin{Vmatrix}I_a\\I_b\\I_c\end{Vmatrix}=\|T\|\begin{Vmatrix}I_{a0}\\I_{a1}\\I_{a2}\end{Vmatrix} \qquad (2)$$

where

$$\|T\|=\begin{Vmatrix}1&1&1\\1&a^2&a\\1&a&a^2\end{Vmatrix} \qquad (3)$$

By multiplying through equation 2 with the inverse of $\|T\|$, the symmetrical components of phase-a current in terms of the line currents are obtained

$$\begin{Vmatrix}I_{a0}\\I_{a1}\\I_{a2}\end{Vmatrix}=\|T\|^{-1}\begin{Vmatrix}I_a\\I_b\\I_c\end{Vmatrix} \qquad (4)$$

where

$$\|T\|^{-1}=\frac{1}{3}\begin{Vmatrix}1&1&1\\1&a&a^2\\1&a^2&a\end{Vmatrix} \qquad (5)$$

If equation 2 is substituted into equation 1 and the resulting equation multiplied through by $\|T\|^{-1}$

$$\begin{Vmatrix}(V_{ax0}-V_{ay0})\\(V_{ax1}-V_{ay1})\\(V_{ax2}-V_{ay2})\end{Vmatrix}+\begin{Vmatrix}I_nZ_n\\0\\0\end{Vmatrix}=\begin{Vmatrix}Z_{a0}&Z_{a2}&Z_{a1}\\Z_{a1}&Z_{a0}&Z_{a2}\\Z_{a2}&Z_{a1}&Z_{a0}\end{Vmatrix}\times\begin{Vmatrix}I_{ac}\\I_{a1}\\I_{a2}\end{Vmatrix} \qquad (6)$$

where

$$Z_{a0}={}^1\!/\!_3(Z_a+Z_b+Z_c) \qquad (7)$$

$$Z_{a1}={}^1\!/\!_3(Z_a+aZ_b+a^2Z_c) \qquad (8)$$

$$Z_{a2}={}^1\!/\!_3(Z_a+a^2Z_b+aZ_c) \qquad (9)$$

As stated previously, these equations admit no simple interconnection of the sequence networks because of the nonreciprocity of the mutual impedance terms. If, however, Z_c is set equal to Z_b, Z_{a0} becomes ${}^1/_3(Z_a+2Z_b)$ and Z_{a1} and Z_{a2} each become ${}^1/_3(Z_a-Z_b)$.

Equation 6 can then be written, after some manipulation as

$$\begin{aligned}&(V_{ax0}-V_{ay0}-3Z_nI_{a0})\\&\quad=\frac{1}{3}(Z_a-Z_b)(I_{a0}+I_{a1}+I_{a2})+I_{a0}Z_b\\&(V_{ax1}-V_{ay1})\\&\quad=\frac{1}{3}(Z_a-Z_b)(I_{a0}+I_{a1}+I_{a2})+I_{a1}Z_b \qquad (10)\\&(V_{ax2}-V_{ay2})\\&\quad=\frac{1}{3}(Z_a-Z_b)(I_{a0}+I_{a1}+I_{a2})+I_{a2}Z_b\end{aligned}$$

These equations are satisfied by the interconnection shown in Fig. 3, which can be used to calculate all the sequence quantities on either side of the fault.

The Series Representation

This representation has been called the series representation because under certain special conditions of fault the sequence networks are connected in series. It is complementary to the shunt representation in that it can be used where the former is physically unrealizable and vice versa.

The network equations for Fig. 2 can be written in the alternative form

$$\begin{Vmatrix}I_a\\I_b\\I_c\end{Vmatrix}=\begin{Vmatrix}Y_a&0&0\\0&Y_b&0\\0&0&Y_c\end{Vmatrix}\times\begin{Vmatrix}(V_{ax}-V_{ay})\\(V_{bx}-V_{by})\\(V_{cx}-V_{cy})\end{Vmatrix}+I_nZ_n\begin{Vmatrix}Y_a\\Y_b\\Y_c\end{Vmatrix} \qquad (11)$$

where

$$Y_a=\frac{1}{Z_a},\text{ etc., } \ldots \qquad (12)$$

As before

$$\begin{Vmatrix}(V_{ax}-V_{ay})\\(V_{bx}-V_{by})\\(V_{cx}-V_{cy})\end{Vmatrix}=\|T\|\begin{Vmatrix}(V_{ax0}-V_{ay0})\\(V_{ax1}-V_{ay1})\\(V_{ax2}-V_{ay2})\end{Vmatrix} \qquad (13)$$

If equation 13 is substituted into equation 11 and the resulting equation multiplied through by $\|T\|^{-1}$

$$\begin{Vmatrix}I_{a0}\\I_{a1}\\I_{a2}\end{Vmatrix}=\begin{Vmatrix}Y_{a0}&Y_{a2}&Y_{a1}\\Y_{a1}&Y_{a0}&Y_{a2}\\Y_{a2}&Y_{a1}&Y_{a0}\end{Vmatrix}\times\begin{Vmatrix}(V_{ax0}-V_{ay0})\\(V_{ax1}-V_{ay1})\\(V_{ax2}-V_{ay2})\end{Vmatrix}+I_nZ_n\begin{Vmatrix}Y_{a0}\\Y_{a1}\\Y_{a2}\end{Vmatrix} \qquad (14)$$

where

$$Y_{a0}=\frac{1}{3}(Y_a+Y_b+Y_c)\neq\frac{1}{Z_{a0}} \qquad (15)$$

$$Y_{a1}=\frac{1}{3}(Y_a+aY_b+a^2Y_c)\neq\frac{1}{Z_{a1}} \qquad (16)$$

$$Y_{a2}=\frac{1}{3}(Y_a+a^2Y_b+aY_c)\neq\frac{1}{Z_{a2}} \qquad (17)$$

As before, if $Y_a\neq Y_b\neq Y_c$, there are nonreciprocal mutual admittances in equation 14 and there is no simple interconnection of the sequence networks which can satisfy these equations. However, if $Y_c=Y_b\neq Y_a$, the mutual admittances Y_{a1} and Y_{a2} are equal to each other. For this case

$$Y_{a0}=\frac{1}{3}(Y_a+2Y_b) \qquad (18)$$

$$Y_{a1}=Y_{a2}=\frac{1}{3}(Y_a-Y_b) \qquad (19)$$

Equation 14 can then be written after some manipulation

$$\begin{aligned}I_{a0}=&[(V_{ax0}-V_{ay0}-3Z_nI_{a0})+(V_{ax1}-V_{ay1})+\\&(V_{ax2}-V_{ay2})]\frac{1}{3}(Y_a-Y_b)+\\&(V_{ax0}-V_{ay0}-3Z_nI_{a0})Y_b\\I_{a1}=&[(V_{ax0}-V_{ay0}-3Z_nI_{a0})+(V_{ax1}-V_{ay1})+\\&(V_{ax2}-V_{ay2})]\frac{1}{3}(Y_a-Y_b)+\\&(V_{ax1}-V_{ay1})Y_b \qquad (20)\\I_{a2}=&[(V_{ax0}-V_{ay0}-3Z_nI_{a0})+(V_{ax1}-V_{ay1})+\\&(V_{ax2}-V_{ay2})]\frac{1}{3}(Y_a-Y_b)+\\&(V_{ax2}-V_{ay2})Y_b\end{aligned}$$

These equations are satisfied by the interconnection shown in Fig. 4 which can be used to calculate all the sequence quantities on either side of the fault. It will be noticed that, when the interconnection of Fig. 3 yields a negative impedance in the element ${}^1/_3(Z_a-Z_b)$, the interconnection of Fig. 4 yields a positive impedance in the element ${}^1/_3(Y_a-Y_b)$, and vice versa.

At this point some comments with regard to Figs. 3 and 4 are in order. The method used in deriving these network interconnections resulted in a separate identification of the neutral terminals

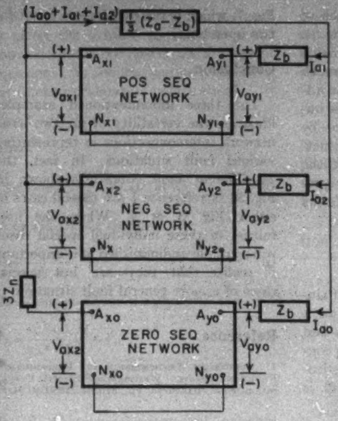
(Ia0+Ia1+Ia2)
1/3 (Za−Zb)
(+)
Ax1
Ay1
POS SEQ NETWORK
Vax1
Vay1
Nx1
Ny1
(−)
Zb
Ia1
Ax2
Ay2
NEG SEQ NETWORK
Vax2
Vay2
Nx
Ny2
Ia2
3Zn
Ax0
Ay0
ZERO SEQ NETWORK
Vax2
Vay0
Nx0
Ny0
Ia0

Fig. 3 (left). Equivalent shunt interconnection for series unbalance

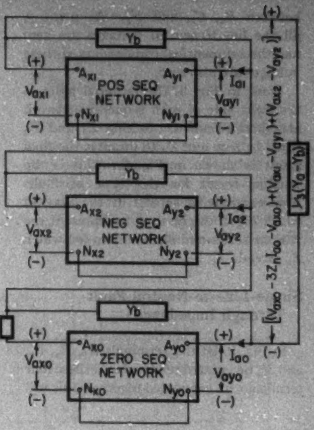
(+)
Yb
Ax1
Ay1
POS SEQ NETWORK
Vax1
Vay1
Ia1
Nx1
Ny1
(−)
Ax2
Ay2
NEG SEQ NETWORK
Vax2
Vay2
Ia2
Nx2
Ny2
3Zn
Ax0
Ay0
ZERO SEQ NETWORK
Vax0
Vay0
Ia0
Nx0
Ny0
[(Vax0 −3ZnIa0 −Vax0)+(Vax1 −Vay1)+(Vax2 −Vay2)]
1/3(Ya−Yb)

Fig. 4 (right). Equivalent series interconnection for series unbalance

N_x and N_y in both the positive- and the and negative-sequence networks. Manifestly, however, it is impossible for these terminals to have any potential difference between them other than zero. For this reason, in all of the network interconnections to follow, these are connected together in the positive- and negative-sequence networks and may be considered to be one and the same terminal. With regard to the zero-sequence network in Figs. 3 and 4, the question might be raised whether it is necessary to show that I_{a0} flows from N_{y0} to N_{x0} in order to show that $3Z_n$ is validly placed between these points. If the x and y planes of Fig. 2 are connected together by Z_a, Z_b, Z_c, and Z_n as shown and by no other impedances, then it is obvious that the zero-sequence currents I_{a0}, I_{b0}, and I_{c0} must each flow from N_{y0} to N_{x0} and that Z_n could be connected between terminals N_{x0} and N_{y0}. However, if there is a balanced connection between x and y some place within the network, not all of the zero-sequence current will flow from N_{y0} to N_{x0}. Hence it is necessary to place $3Z_n$ in series with either A_{y0} or A_{x0}. In this case, N_{x0} and N_{y0} are then connected together. This connection does not imply however that N_{x0} and N_{y0} are actually at the same potential.

To show how these two networks can be used to represent a great variety of both series and shunt faults, some examples will be given in the following sections.

Line-to-Line-to-Neutral Short Circuit

In Fig. 2, let the terminals A_y, B_y, C_y, and N_y be isolated terminals, i.e., not connected to any part of the system. If these four terminals are connected together and Z_b, Z_c, and Z_n are set equal to zero and Z_a is allowed to be infinite, the result will be a line-to-line-to-neutral short circuit

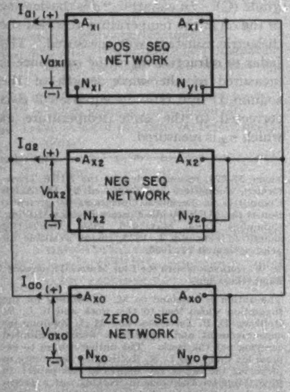
Ia1 (+)
Ax1
Ax1
POS SEQ NETWORK
Vax1
Nx1
Ny1
(−)
Ia2 (+)
Ax2
Ax2
NEG SEQ NETWORK
Vax2
Nx2
Ny2
Ia0 (+)
Ax0
Ax0
ZERO SEQ NETWORK
Vax0
Nx0
Ny0

Fig. 5. Interconnection for a line-to-line-to-neutral fault

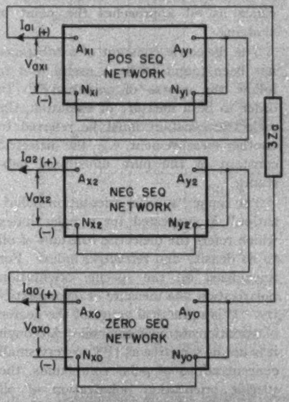
Ia1 (+)
Ax1
Ay1
POS SEQ NETWORK
Vax1
Nx1
Ny1
(−)
Ia2 (+)
Ax2
Ay2
NEG SEQ NETWORK
Vax2
Nx2
Ny2
3Za
Ia0 (+)
Ax0
Ay0
ZERO SEQ NETWORK
Vax0
Nx0
Ny0

Fig. 6. Interconnection for a single-line-to-neutral fault through impedance

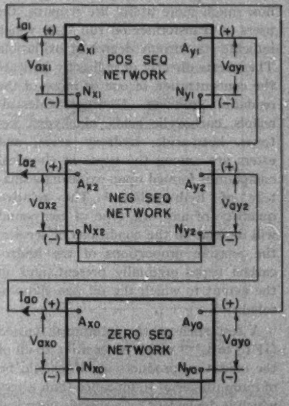
Ia1 (+)
Ax1
Ay1
POS SEQ NETWORK
Vax1
Vay1
Nx1
Ny1
(−)
Ia2 (+)
Ax2
Ay2
NEG SEQ NETWORK
Vax2
Vay2
Nx2
Ny2
Ia0 (+)
Ax0
Ay0
ZERO SEQ NETWORK
Vax0
Vay0
Nx0
Ny0

Fig. 7. Interconnection for two lines open

between B_x, C_x, and N_x. At point y, all the line-to-neutral voltages are zero and the symmetrical components of these voltages are also zero.

Thus, in Fig. 3, the terminal pairs at the right side of each sequence network are short-circuited. Setting Z_b and Z_n equal to zero and Z_a to infinity, the final result is shown in Fig. 5. This is the familiar result for this type of fault. This example is typical of the way in which Fig. 3 can be used to represent the various series and shunt faults for which Z_a exceeds Z_b.

Single-Line-to-Neutral Fault Through Impedance

In Fig. 2, let the terminals A_y, B_y, C_y, and N_y be isolated terminals. If these four terminals are connected together, this will correspond to a short circuit at each of the right-hand terminal pairs of Fig. 4. If now Z_b and Z_c are allowed to approach infinity and Z_n is allowed to approach zero, Fig. 6 will be the result. The admittance 1/3 Y_a is equivalent to the impedance $3Z_a$ which is expected to be found in series with the 3-sequence networks. This example is typical of the way in which Fig. 4 can be used to represent the various series and shunt faults for which Y_a exceeds Y_b.

Two Lines Open

As a final example let Z_b and Z_c go to infinity and let Z_a and Z_n go to zero. This is a case where Y_a exceeds Y_b and Fig. 4 must be used to represent this condition. When the necessary substitutions are made in Fig. 4, the result is Fig. 7, which is the well-known result for two open lines.

Conclusion

The three aforementioned examples illustrate the versatility of the two basic network interconnections in representing various fault situations. In fact, the 24 different fault conditions shown in Fig. 21 of reference 1 are special cases of either Fig. 3 or 4. While the usefulness of these individual special cases will continue undiminished, it is important to realize that they are but special cases of a more general fault situation.

Reference

1. ELECTRICAL TRANSMISSION AND DISTRIBUTION REFERENCE BOOK. Westinghouse Electric Corporation, East Pittsburgh, Pa., 4th ed., 1950, p. 24.

Interpretation and Significance of Tests Indicating the Concentration of Polar Compounds in Transformer Oil

R. W. JOHNSON
NONMEMBER AIEE

TRANSFORMER oil before it is put into service consists of nonpolar hydrocarbons. Oxidation results in the formation of polar compounds. To predict how much more useful life remains, the users of transformer oil run tests which indicate its current degree of oxidation. These tests directly or indirectly indicate the concentration of one or more of the oxidation products. Hydroperoxides, alcohols, carboxylic acids, aldehydes, ketones, keto-acids, hydroxy acids, and esters are among the types of chemical compounds formed upon oxidizing a mixture of hydrocarbons.[1] The relative quantity of any one type of compound will depend on the conditions of service, the relative proportions of the hydrocarbon types originally present, and on the extent to which the oil has deteriorated.

A test such as the interfacial-tension (IFT) test,[2–4] which is sensitive to all of the oxidation products of oil, should be of more universal significance than a test which is dependent on a specific chemical property, such as the ability to react with potassium hydroxide. However, while the IFT test is sensitive to very small amounts of polar compounds in oil, it progressively looses sensitivity and significance as oil approaches the point of sludging.

The dielectric constant of a substance has been found to be a useful tool to follow the course of oxidation.[5–7] In order to be a measure of oxidation, the dielectric constant must be referred to another measurement, e.g., the dielectric constant of the pure unoxidized substance.

The name "specific orientation polarization" is suggested for a polar index which refers the dielectric constant of oil to its density and refractive index. For unoxidized oil the specific orientation polarization is a measure of its aromaticity. It is a practical gauge of the degree of oxidation of transformer oil. Although it is not as sensitive as IFT to very small concentrations of polar compounds, the specific orientation polarization of oil increases in significance as the oil approaches the end of its useful life.

Definitions

The specific orientation polarization of a substance is defined by

$$p_o = p - p_d \tag{1}$$

where

$$p = \frac{\epsilon - 1}{\epsilon + 2}\,\frac{1}{d} \tag{2}$$

which is the Clausius-Mosotti equation[8] in its original form, and

$$p_d = \frac{n_D^2 - 1}{n_D^2 + 2}\,\frac{1}{d} \tag{3}$$

which is the Lorentz-Lorenz equation.[8]

ϵ is measured near 25 degrees centigrade (C). In equation 2 d is the density of the oil at the temperature at which the dielectric constant was measured. The index of refraction n_D of the substance is measured at the wave length of the sodium D line (s). In equation 3 d is corrected to the same temperature at which n_D is measured.

Paper 55-279, recommended by the AIEE Transformers Committee and approved by the AIEE Committee on Technical Operations for presentation at the AIEE Middle Eastern District Meeting, Columbus, Ohio, May 4–6, 1955. Manuscript submitted February 4, 1955; made available for printing March 31, 1955.

R. W. JOHNSON is with the Line Material Company, Zanesville, Ohio.

The author is indebted to M. I. Zwelling for the suggestion which lead to this work and to L. R. Rollison, D. F. Davidson, and M. I. Zwelling for encouragement and suggestions which facilitated carrying out the work. The author wishes to express his thanks to L. R. Rollison for assistance in preparing the tables and figures in this paper; to R. F. Matz for assistance in working out a procedure for determining dielectric constants; and to R. A. Hinshaw for some of the refractive index measurements.

The specific refraction[8] of the substance is given the symbol p_d instead of the conventional R because of the analogy of equation 1 to the conventional equation for (molar) orientation polarization[8]

$$P_o=P-P_d \tag{4}$$

where

$$P_o=4/3\pi N\frac{\mu^2}{3kT}=20.4D^2 \text{ at } 25 \text{ C} \tag{5}$$

from the Debye theory[8]

$$P=\frac{\epsilon-1}{\epsilon+2}\frac{M}{d} \tag{6}$$

the Clausius-Mosotti equation,[8] and

$$P_d=\frac{n_\infty^2-1}{n_\infty^2+2}\frac{M}{d}+P_A \tag{7}$$

Nomenclature

$P_o=P-P_d$ = (molar) orientation polarization
$P=\frac{\epsilon-1}{\epsilon+2}\frac{M}{d}$ = molar polarization
$P_d=\frac{n_\infty^2-1}{n_\infty^2+2}\frac{M}{d}+P_A$ = (molar) distortion polarization
$p_d=\frac{n_D^2-1}{n_D^2+2}\frac{1}{d}$ = specific refraction = specific distortion polarization
$p=\frac{\epsilon-1}{\epsilon+2}\frac{1}{d}=P/M$ = specific polarization
$p_o=p-p_d$ = specific orientation polarization
P_A = atomic polarization
X = mole fraction
f = weight fraction
μ = dipole moment, electrostatic units
$D=\mu 10^{18}$ = (permanent) dipole moment, Debye units
n_∞ = refractive index extrapolated to infinite wave length light
n_D = refractive index, sodium D line
N = Avogadro's number
k = Boltzman constant
M = molecular weight
ϵ = dielectric constant
d = density (grams per centimeter^3)
C_{cell} and D_{cell} = capacitance and dissipation factor readings before introduction of the sample into the cell
C_{mea} and D_{mea} = readings with the sample
p_o''' is the p_o value of the oxidized oil
p_o' is the value of the same oil before oxidation
subscript 1 or ′ refers to less polar component
subscript 2 or ″ refers to more polar component
subscript 3 or ‴ refers to the mixture
TAC = 1,000 TAN/56.1 = total acid concentration in micromoles per gram
TPC = $(p_o-p_o^{\text{initial}})10^4$ = (minimum) total polar concentration in micromoles per gram

Experimental

The capacitance and dissipation factors[9] were measured with a General Radio Company type-*716C* capacitance bridge. The power-factor cell was equipped with a guard electrode but a guard circuit was not used. The cell was used with a 43.0-milliliter sample, which put the liquid level above the bottom of the guard electrode and made the capacitance reading independent of small changes in sample volume. The cell was calibrated with benzene. It had an interelectrode capacitance of 90.4 micromicrofarads and a stray capacitance of approximately 14 micromicrofarads.

The dielectric constant[9] was calculated from

$$\epsilon=\frac{C_{mea}+90.4-C_{cell}}{90.4}$$

and the dissipation factor from

$$D=\frac{D_{mea}C_{mea}-D_{cell}C_{cell}}{C_{mea}+90.4-C_{cell}}$$

The oil samples were dried before testing by heating at 105 C for 1 hour. With other oil samples it was found that these conditions would reduce the dissipation factor of "used" oils considerably but had very little effect on the dielectric constant. The dielectric constant can decrease

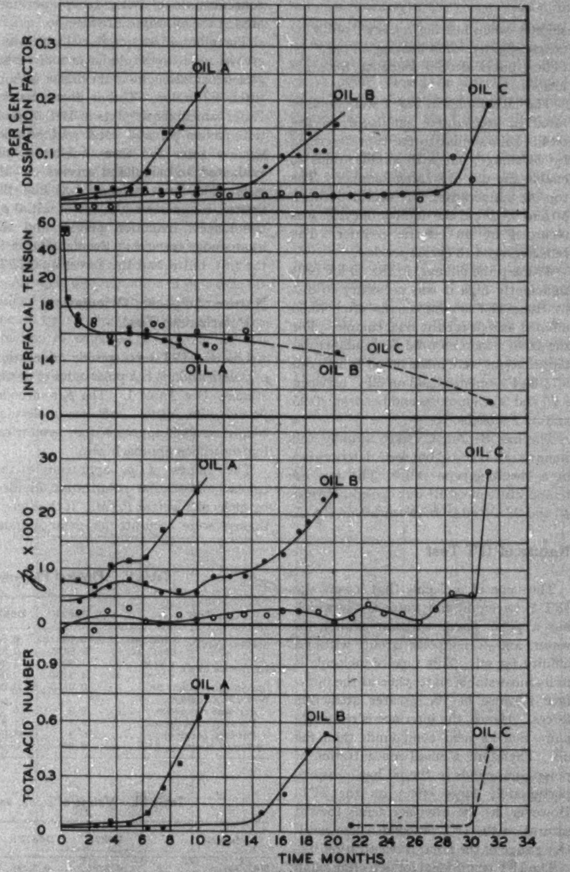

Fig. 1. Deterioration of three inhibited transformer oils in simulated service oil life cells. Specific orientation polarization p_0 total acid number, dissipation factor, and IFT versus deterioration time in months

Table I. Values for p_o and $20.4D^2/M$

Substance	p_o*	$20.4D^2/M$†
Methanol	0.903	1.84
Ethanol	0.850	1.28
Water	0.775	3.84
t-Butyl alcohol	0.720	0.795
Tetralin	0.0561	0.0735
Carbon tetrachloride	0.0101	0.0000
Benzene	0.0050	0.0000
2,2,4-Trimethyl pentane	0.0011	
n-Octane	−0.0024	0.0000
Cyclohexane	−0.0035	0.0000

*Calculated from refractive indexes, dielectric constants, and densities found in the literature.[14,16–19]

†Dipole moments used were either from tables in Glasstone[8] or Amis[12] or else were calculated by vector addition of dipole moments of groups.[8]

slightly when heating a "new" oil or increase slightly when heating a "used" oil (The t-butyl alcohol solutions were not heated.)

The oil samples in Fig. 1 were deteriorated in accelerated, simulated service, oil life cells similar to the type described by Zwelling[10] but with modifications to enable the use of smaller samples. The top oil temperature was cycled between 50 and 98 C and the number of cycles was recorded by an electric counter. The cells averaged 13 cycles per day.

To keep the oil level in the oil life cells sufficiently high it was necessary to discontinue IFT measurements after 13.75 months except for the final sample. For the same reason no total acid number determinations were made on oil B between 8.75 and 15 months and on oil C between 8.75 and 20.25 months and between 20.25 and 31.2 months.

The oils B^1 and C^1 were initially the same as oils B and C but were deteriorated in a Zwelling-type cell.[10] The top oil temperature of oil B^1 was cycled between 40 and 98 C; oil C^1 between 40 and 108 C.

Nature of IFT Test

The type of molecule that lowers the IFT between oil and water is one which has a polar group with an affinity for water and a nonpolar group with an affinity for oil. This type of molecule is in its most stable state when at the interface because of the greater attractive forces. Hence, the interface is relatively more rich in polar compounds than the oil. Therefore, a small concentration of polar compounds in the oil has a disproportionately large effect on the IFT. However, as the interface tends toward saturation the IFT becomes a less sensitive gauge of the polar concentration.[11]

The IFT test is ideal for detecting small amounts of contamination in new transformer oil, or detecting the oxidation products of oil in the early stages of deterioration. It has not lived up to early expectations, however, as an indicator of the sludging propensity of oil. When oil is near the sludging point the concentration of polar compounds is so high that the IFT value is more nearly an indication of the quality or types of oxidation products formed than it is a gauge of total polar contamination. The asymptote which the IFT approaches as oil oxidizes depends on the degree of refinement of the oil. The reason for this is probably that the less aromatic oils produce oxidation products of lower molecular weight and it is possible, therefore, to have a higher concentration of polar groups per unit area at the oil-water interface.

The more aromatic oils, which have a greater tendency to sludge at a given degree of oxidation, have the higher asymptotic IFT value. This is illustrated by Fig. 1 which shows plots of IFT dissipation factor, p_o, and total acid number against time for three inhibited oils evaluated in simulated service oil life cells. The least aromatic oil had the lightest initial color, the lowest initial p_o, the longest induction period, and the least sludge formed at the completion of the test, but it had the lowest final IFT.

Nature of Specific Orientation Polarization Test

Like the IFT test, specific orientation of polarization p_o is a polar index of a substance. See Table I. The p_o's of compounds like water and low molecular weight alcohols approach one; symetrical hydrocarbons approach zero.

The values of p_o approximate the (molar) orientation polarization divided by molecular weight P_o/M. If the Debye theory[8] were accurate for polar liquids, p_o would nearly equal $20.4\ D^2/M$. (See equation 5.)

The Debye theory has been found to be adequate for measurements made with gases, nonpolar liquids, and dilute solutions of polar compounds in nonpolar liquids. However, it is not in harmony with data on polar liquids.[12] A quantitative explanation of the discrepancy between p_o and $20.4\ D^2/M$ for polar liquids, Table I, would best be based on a modern theory of polarization, e.g., Onsager's or Kirkwood's.[12] However, the discrepancy can be qualitatively rationalized by noting that polar liquids like water are associated. The molecular weight of a liquid will increase with association but the dipole moments can either add to or cancel each other.

In spite of the limitations of the approximations involved relating p_o to the dipole moment, it is possible to make a reasonable estimate of the concentration of polar compounds from the p_o of an oxidized oil. To calculate a minimum polar concentration it is probably conservative to assume a dipole moment of 2.2 Debye units for oxidized oil molecules. Based on oxygen absorption and dielectric constant measurements Balsbaugh[6] calculated an effective dipole moment of 1.4 for the oxidation products from two highly refined oils and 1.8 Debye units for the oxidation products from an underrefined oil.

Notice in Table I that when the dipole moment D is zero p_o may have either a small positive or a small negative value. The difference between $20.4\ D^2/M$ and p_o at this end of the scale is due to the fact that equation 3 involves neither atomic polarization nor the refractive index at infinite wave length. (See equation 7.) For p_o to be consistent with the Debye

Table II. Physical Properties of Oils Studied by Balsbaugh[7]

Test		D6F2R	D6E7FR	D6E5FR	D6E4FR	D6E3FR	D6E2AFR
Specific gravity	20C/4C	0.8801	0.8402	0.8674	0.8823	0.9057	0.9445
	65C/4C	0.8673	0.8252	0.8544	0.8698	0.8770	0.9345
Refractive index	N_D^{20}	1.4900	1.4644	1.4790	1.4888	1.5050	1.5345
	N_D^{65}	1.4735	1.4482	1.4630	1.4717	1.4880	1.5178
Specific dispersion, 20C		0.0125	0.0102	0.0108	0.0120	0.0134	0.0172
Waterman analysis:							
Per-cent aromatics		9.9	0	4.6	10.9	20.7	37.5
Per-cent naphthenes		19.3	11.8	26.9	24.9	25.1	11.0
Per-cent paraffins		70.8	88.2	68.5	64.2	54.2	51.5
Dielectric constant, 85C		2.20	2.095	2.16	2.19	2.26	2.395

Table III. Values of p, p_d, and p_o Calculated From Data in Table II

Sample	D6F2R	D6E7FR	D6E5FR	D6E4FR	D6E3FR	D6E2AFR
20C, p_d	0.3285	0.3280	0.3220	0.3275	0.3280	0.3295
65C, p_d	0.3240	0.3245	0.3235	0.3220	0.3285	0.3245
Estimated 85C, d	0.8616	0.8185	0.8486	0.8642	0.8642	0.9301
Estimated 85C, p	0.3320	0.3270	0.3290	0.3290	0.3425	0.3410
Estimated 85C, p_o	0.008	0.002	0.006	0.007	0.014	0.016

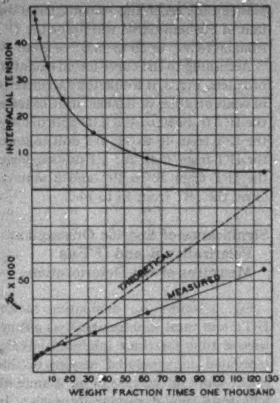

Fig. 2. IFT and specific orientation polarization p_0 as a function of the weight fraction of t-butyl alcohol in transformer oil

theory, P_A/M would have to equal the difference between p_d and $[(n_\infty^2-1)(n_\infty^2+2)](1/d)$. The two factors do tend to cancel. In the case of paraffinic and napthenic compounds, the dispersion effect (n_D not equal to m_∞) is the more important. Cyclohexane and n-octane have negative p_o's.

Unsaturated bonds will cause a dispersion factor of larger magnitude. The absorption bands are at a longer wave length, although still in the ultraviolet. Specific dispersion is used as a gauge of the aromaticity of a mixture of hydrocarbons.[13] However, the increased atomic polarization[14] of unsaturated hydrocarbons more than compensates for the increased dispersion, e.g., benzene.

As far as evaluating transformer oils is concerned, the failure of p_o to be consistent with the Debye theory is fortunate in two respects. First, it enables the p_o of a new oil to be an index of its degree of refinement. Second, it makes the p_o value of a partially oxidized oil of greater utility than P_o/M would be even if it could be measured conveniently.

The greater the degree of refinement of an oil the lower will be its initial p_o. The p_o of an oil increases with its aromatic content. This is illustrated in Tables II and III; the data in these tables are from reference 7. It should be noted, however, that the p_o values in Table III are approximate. The dielectric constant was measured at a higher temperature than the density (or refractive index) and the dielectric constant could be estimated from a graph with a precision of only 0.005 to 0.01 unit. This makes the calculated p_o's uncertain to at least ±0.002.

The second respect in which the inconsistency of p_o with the Debye theory is fortunate is that it allows the p_o value to be a practical test for estimating the life expectancy of a used oil. Oils with a high aromatic content will produce sludge at a lower degree of oxidation than one of low aromatic content. Moreover, the p_o of the more aromatic oil is larger than the less aromatic oil. Thus if all oils were removed from service when $p_o = 0.020$ (this would correspond roughly to an acid number of 0.4 for a moderately refined oil), then the oils with the greater tendency to sludge would be allowed the lowest degree of oxidation.

Any utility which is now measuring power factor and IFT of oil can determine p_o with very little additional effort. The density of the oil must be known in order to calculate the IFT value from the scale reading of a Du Nouy tensiometer. The dielectric constant can be calculated from the capacitance reading at the time the power factor of an oil is measured. Refractive index measurements can be made easily and rapidly.

A rough approximation of p_o can be obtained without refractive index measurements by assuming that the specific refraction p_d, equation 3, is 0.325. If this approximation is used, it is better to use the density of the original oil in equation 2, if it is known, rather than the density measured at any later time. Even though the specific refraction is approximately the same for oils otherwise greatly different in properties, nevertheless during oxidation the index of refraction is more nearly constant than the specific refraction.

Specific Orientation Polarization p_o and IFT as a Function of Concentration

Fig. 2 shows a plot of the p_o of a solution of t-butyl alcohol in a transformer oil as a function of the concentration, in weight fraction, of the t-butyl alcohol. It is shown in Appendix I that the p_o of a mixture of a polar compound and a nonpolar liquid should be directly proportional to the weight fraction of the polar compound. The dashed line is the theoretical relationship for these two components: $p_o = 53+(795-53)f$. At least in the case of t-butyl alcohol the Debye theory is adequate up to a p_o of 0.015.

Fig. 2 also shows a plot of the IFT of the same solutions as a function of concentration. It illustrates the progressive loss of sensitivity of the test at increased concentrations.

That the IFT test suffers a loss of sensitivity at low values is well known. However, it is probably not generally realized just how insensitive the test is at low values. It would be useful to

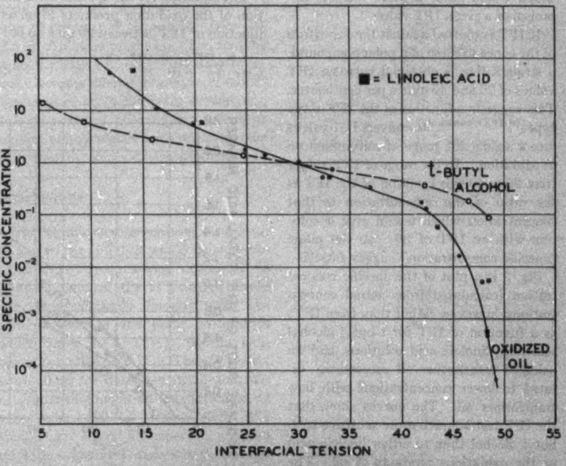

Fig. 3. (Logarithm) specific concentration versus IFT of transformer oil solutions of t-butyl alcohol, linoleic acid, and oxidized transformer oil

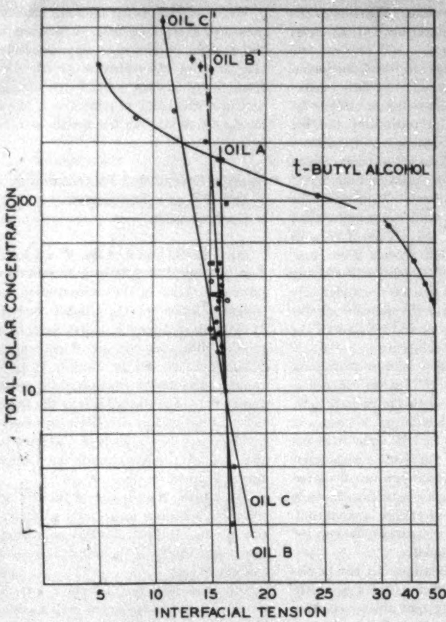

Fig. 4. Relationship of specific orientation polarization p_0 and IFT tests. Total polar concentration TPC versus IFT for oils A, B, B¹, C, and C¹, and solutions of t-butyl alcohol

translate IFT values to some function of the IFT which would be approximately a linear function of concentration and which would allow a more realistic appraisal of a given IFT value.

If IFT is plotted against the logarithm of the concentration of a polar compound, a straight line is obtained between IFT values of 20 and 40 dynes per centimeter. This suggests a function of the IFT of the type $\epsilon^{(30\text{-IFT})/\text{constant}}$ to convert IFT values into a significant gauge of contamination or oxidation. In the range of IFT values from 20 to 40 this function of the IFT is the ratio of the concentration to that concentration which would give a solution with an IFT of 30. So the name "specific concentration" suggests itself.

Fig. 3 is a plot of the specific concentration (calculated from actual concentrations, however, rather than from IFT) as a function of IFT for t-butyl alcohol solutions, linoleic acid solutions, and an oxidized transformer oil successively diluted to lower concentrations with new transformer oil. The curves show that the IFT test is much more sensitive to t-butyl alcohol than to either linoleic acid or the oxidations products of oil. The reason for this is probably that only in the case of t-butyl alcohol is the diffusion of the solute into water large enough to lower the surface tension of the water as well as the IFT between water and oil.

The equation for the specific concentration of the oxidation products of oil as a function of IFT between 20 and 40 is

$$C=\epsilon^{\frac{30-IFT}{6.1}}=10^{\frac{30-IFT}{14}} \tag{8}$$

Notice that according to equation 8 one unit of contamination will lower the IFT from 50 to 30; or 30 to 25.8; or 20 to 19.

According to the curve for oil oxidation products, Fig. 3, it would take an increase in concentration of 0.00009 unit to lower the IFT from 50 to 49; 0.03 unit to lower the IFT from 40 to 39; 0.2 unit to lower the IFT from 30 to 29; 1.1 units to lower the IFT from 20 to 19; and 8 units to lower the IFT from 15 to 14.

Significance of Specific Orientation Polarization p_0 and IFT as Measures of Oil Deterioration

Fig. 1 shows p_0, dissipation factor, IFT,[4] and total acid number[15] as a function of time for three inhibited oils deteriorated in simulated service oil life cells. Only in the case of oil A were all four tests run at regular intervals. In the case of oil B, the p_0 test was used to indicate the end of the induction period and acid nunber measurements were resumed to follow the rate of oxidation during the postinduction period. The only acid number in the case of oil C which indicated oxidation had taken place was with the final sample. The time interval between the end of the induction period and the cutoff point was less than one sampling period, 1.25 months.

Fig. 4 shows the relationship between the IFT test and the p_0 test for these three oils and the t-butyl alcohol-oil mixtures. Fig. 5 is a plot of the square root of the total acid number against p_0 for oils A, B, B¹, C, and C¹. For small values the square root of the total acid number increases linearly with p_0. At larger values the square root of the total acid number increases at a slower rate.

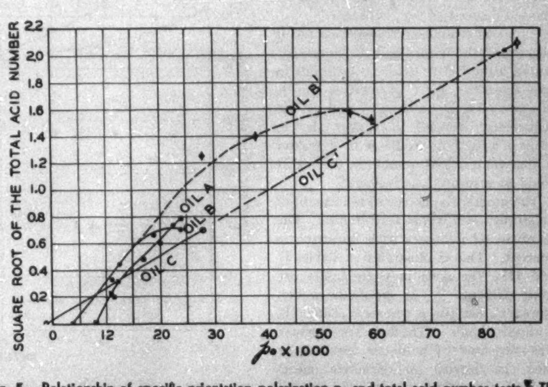

Fig. 5. Relationship of specific orientation polarization p_0 and total acid number tests. The square root of the acid number versus p_0 for oils A, B, B¹, C, and C¹

Table IV. Values of TAC, TPC, and TPC/TAC for Various Oils

Oil	$p_o \times 10^4$	TAN	TAC	TPC	TPC/TAC
A	120	0.10	1.8	43	24
A	173	0.23	4.1	96	23
A	200	0.37	6.5	123	19
A	240	0.62	11.0	163	15
B	110	0.11	2.0	72	36
B	126	0.20	3.7	88	24
B	187	0.43	7.7	149	19
B	225	0.53	9.5	187	20
B	241	0.49	8.7	203	23
B¹	460	1.54	27.5	422	15.4
B¹	522	1.94	34.6	484	14.0
B¹	553	2.46	43.7	515	11.8
B¹	594	2.36	42.1	556	13.2
C	280	0.47	8.4	291	35
C¹	860	4.41	78.5	871	11

One possible explanation of this is that acid formation is a second-order reaction with respect to the primary polar oxidation product. Or in other words, acid formation is possible only after the collision of two polar molecules or two polar molecules and one nonpolar molecule. The decrease in the rate of increase of the square root of the total acid number with respect to p_o could be the consequence of sludge formation. That is, sludge formation removes a larger fraction of acid molecules in the oil than it does the predominate polar type.

If this theory is correct, oil A should have been free of sludge at a p_o of 0.0120 and acid number of 0.10 but not at a p_o of 0.0173 and acid number of 0.23. Oil B should have been free of sludge at a p_o of 0.0126, acid number 0.20; possible sludging at $p_o = 0.0187$, acid number 0.43; and definite sludging at $p_o = 0.0225$ and acid number 0.53. The curve B¹ is apparently not a continuation of curve B. Perhaps under different deterioration conditions sludge did not form until a higher acid number was reached. Oil C, a highly refined oil, had produced a measurable, but insignificant, amount of sludge at the cutoff point. Oil C¹ had produced a considerable amount of sludge by the time p_o reached 0.0860 so the point for C¹ should have fallen below the curve for C instead of on it. Perhaps the deterioration conditions for C¹, 10 C higher maximum oil temperature, and a different type of deterioration cell favored a higher acid formation and a lesser sludge formation.

To evaluate the p_o test and total acid number test against each other, it is useful to translate each to comparable concentration terms. They both can be conveniently converted to a concentration in micromoles per gram of oil. The acid number value can be converted to total acid concentration TAC, the acid concentration in micromoles (technically microequivalents) per gram of oil, by dividing by the molecular weight of potassium hydroxide and multiplying by 1,000. The p_o value of an oil can be converted to total polar concentration TPC by assuming a dipole moment of 2.2 Debye units for the oxidation products. The units of TPC are also micromoles per gram of oil. The dipole moment, 2.2, chosen is probably higher than a "typical, effective" dipole moment for the oxidation products of oil. This choice was made in order to be able to consider the calculated total polar concentration minimum probable values.

From Appendix I

$$p_o''' = p_o' + (p_o'' - p_o')f_2$$

$$\mathrm{TPC} = \frac{(\text{polar})\text{micromoles}}{\text{gram of oil}} = \frac{g_2/M_2}{g_1+g_2}10^6$$

$$= \frac{f_2}{M_2}10^6$$

$$p_o''' = p_o' + (p_o'' - p_o')\frac{(\mathrm{TPC})M_2}{10^6}$$

$$(p_o''' - p_o')10^6 = (\mathrm{TPC})(20.4D^2 - p_o'M_2)$$

$$20.4D^2 = 101$$

and $p_o'M_2$ can be either positive or negative but in any case is small. For oil A it is probably near +3 and for oil C it is probably near −0.4. So a satisfactory approximation of TPC is

$$\mathrm{TPC} = 10^4(p_o''' - p_o')$$

Values of TAC, TPC, and TPC/TAC for oils A, B, B¹, C, and C¹ are given in Table IV. Since TPC is probably a minimum concentration of polar compounds, acids apparently account for much less than 10 per cent of the soluble, nonvolatile, oil oxidation products. The amount of acids relative to other oxidation products increases during the course of oxidation at least up to the point of sludging. A highly refined oil produces a smaller amount of nonvolatile acids relative to the other nonvolatile oxidation products.

Conclusions

The significance, sensitivity, and limitations of the IFT test would be more obvious if IFT values were converted to some function of the IFT which would vary approximately linearly with the concentration of the polar compounds which lower the IFT, e.g., specific concentration: $\epsilon^{(30\text{-IFT})/6.1}$. The IFT test is excellent for detecting small amounts of contamination in an unoxidized oil or vice versa. An oil with a high IFT should have a good life expectancy but an oil with a low IFT does not necessarily have a poor life expectancy.

Since the amount of acids relative to other polar compounds formed during the oxidation of oil is dependent on the nature of the original oil and the conditions of deterioration, it is believed that the p_o test will allow a more accurate prediction of the remaining useful life of a transformer oil than the acid number test.

Although the p_o of an unoxidized, uncontaminated oil is a measure of its aromaticity, or degree of refinement, it is not necessary to know the initial value to estimate the life expectancy of an oxidized oil.

It is believed that experience with the use of the p_o test in predicting the useful remaining life of a transformer oil will result in criteria that closely approximate the following, which are suggested by the results from the long-term simulated service tests:

1. **Large fraction of original life remaining:** $p_o < 0.0100$.
2. **Small fraction of original life remaining:** $0.0100 < p_o < 0.0150$.
3. **Negligible useful life remaining:** $p_o > 0.0175$.

A rough, but useful, approximation to p_o can be obtained without refractive index measurements by assuming that the specific refraction is equal to 0.325±0.005.

Appendix I. Specific Orientation Polarization p_o of a Two-Component Mixture

According to Glasstone,[8] p. 548

$$P''' = X_1P' + X_2P''$$

$$= \frac{\epsilon'''-1}{\epsilon'''+2}\frac{1}{d_3}(X_1M_1 + X_2M_2)$$

From the definition of mole fraction

$$X_1 = \frac{g_1/M_1}{\frac{g_1}{M_1}+\frac{g_2}{M_2}},\ X_2 = \frac{g_2/M_2}{\frac{g_2}{M_1}+\frac{g_2}{M_2}}$$

so

$$\frac{g_1\frac{P'}{M_1}}{\frac{g_1}{M_1}+\frac{g_2}{M_2}} + \frac{g_2\frac{P''}{M_2}}{\frac{g_1}{M_1}+\frac{g_2}{M_2}}$$

$$= \frac{\epsilon'''-1}{\epsilon'''+2}\frac{1}{d_3}\left(\frac{g_1}{\frac{g_1}{M_1}+\frac{g_2}{M_2}} + \frac{g_2}{\frac{g_1}{M_1}+\frac{g_2}{M_2}}\right)$$

but

$$p = \frac{\epsilon-1}{\epsilon-2}\frac{1}{d} = \frac{P}{M}$$

so

$$p'\frac{g_1}{g_1+g_2} + p''\frac{g_2}{g_1+g_2} = p'''$$

$$p''' = p'f_1 + p''f_2$$

In a similar manner it can be shown that since molar refractions are additive if concentrations are expressed in mole fractions (Glasstone,[8] pp. 531–532) specific refractions are additive in an analogous manner if concentrations are expressed in weight fractions, namely

$$p_d''' = p_d' f_1 + p_d'' f_2$$

but

$$p_o = p - p_d$$

$$p_o''' = p''' - p_d''' = (p' - p_d')f_1 + (p'' - p_d'')f_2$$

$$p_o''' = p_o' f_1 + p_o'' f_2$$

since

$$f_1 + f_2 = 1$$

$$p_o''' = p_o'(1 - f_2) + p_o'' f_2$$

$$p_o''' = p_o' + (p_o'' - p_o')f_2$$

or if

$$p_o' = 0$$
$$p_o''' = p_o'' f_2$$

References

1. Oxidation of Lubricating Oils, **H. H. Zuidema.** *Chemical Reviews*, Baltimore, Md., vol. 38, 1946, pp. 197–226.

2. The Interfacial-Tension Test and Its Significance in Appraising Performance of an Insulating Oil, **G. W. Gerell.** *Bulletin No. 146*, American Society for Testing Materials, Philadelphia, Pa., May 1947, pp. 4–7.

3. Application of the Interfacial-Tension Test in Grading Oil in Transformers Relative to Serviceability, **F. F. Walsh.** *Ibid.*, pp. 7–10.

4. Method of Test for Interfacial Tension of Oil Against Water by the Ring Method (Tentative). *ASTM D-971-48T*, American Society for Testing Materials, Philadelphia, Pa., 1948.

5. A Dielectric Study of the Autoxidation of Ethyl Sorbate, **S. E. Voltz, M. W. Rigg.** *Journal of Physical Chemistry*, Baltimore, Md., vol. 58, no. 7, 1954, pp. 537–41.

6. Symposium on Electrical Insulation. *American Chemical Society*, Cincinnati, Ohio, Apr. 1940, "Electrical Insulating Oil Deterioration, Chemical and Electrical Tests," **J. C. Balsbaugh et al.**

7. Symposium on Electrical Insulation Materials. *American Chemical Society*, Atlantic City, N. J., Sept. 1941, "Influence of Oxidation on the Dielectric Properties of Hydrocarbons and Hydrocarbon Oils," **J. C. Balsbaugh et al.**

8. Textbook of Physical Chemistry (book), **S. Glasstone.** D. Van Nostrand Company, Inc., New York, N. Y., 2nd ed., 1946, pp. 528–56.

9. Method of Test for Power Factor and Dielectric Constant of Electrical Insulating Materials (Tentative). *ASTM Standard D150-47T*, American Society for Testing Materials, Philadelphia, Pa., 1947.

10. Oil Life Measured in Six Months by New Deterioration Cell, **M. I. Zwelling.** *Electrical World*, New York, N. Y., vol. 134, Aug. 19, 1950, p. 73.

11. **S. Glasstone,** *op. cit.*, pp. 481–96.

12. Kinetics of Chemical Change in Solution, (book) **Edward S. Amis.** The Macmillan Company, New York, N. Y., 1949, pp. 44–70.

13. Effect of Solvent Extraction on Aromaticity of Lubricating Oils, **G. H. von Fuchs, A. P. Anderson.** *Industrial and Engineering Chemistry*, Easton, Pa., vol. 29, Mar. 1937, pp. 319–25.

14. The Dielectric Constants, Polarizations and Dipole Moments of Some Alkylbenzenes, **A. P. Altshuller.** *Journal of Physical Chemistry*, Baltimore, Md., vol. 58, no. 5, May 1954, pp. 392–95.

15. Method of Test for Neutralization Value (Acid and Base Numbers) by Electrometric Titration. *ASTM Standard D664-49*, American Society for Testing Materials, Philadelphia, Pa., 1949.

16. Spreading of Hydrocarbons and Related Compounds on Water, **J. E. Shewmaker, C. E. Vogler, E. R. Washburn.** *Journal of Physical Chemistry*, Baltimore, Md., vol. 58, no. 11, Nov. 1954, pp. 945–48.

17. Table of Dielectric Constants of Pure Liquids, **A. A. Maryott, E. R. Smith.** *NBS Circular 514*, National Bureau of Standards, Washington, D. C., Aug. 1951.

18. Handbook of Chemistry (book), **N. A. Lange.** Handbook Publishers, Inc., 4th ed., 1941, pp. 762–864.

19. Handbook of Chemistry and Physics (book), **C. D. Hodgman.** Chemical Rubber Publishing Company, 34th ed., 1952, pp. 666–1228.

◆

Discussion

G. M. L. Sommerman (Westinghouse Research Laboratories, East Pittsburgh, Pa.): This paper contains a valuable analysis supported by experimental results showing the advantages and limitations of several methods for evaluating the extent of oxidation of commercial transformer mineral oils. The IFT test (a physical test) is shown to be a sensitive means for detecting the presence of hydrophilic polar materials in mineral oil when the concentration of such materials is small. The acid-number test (a chemical test) is shown to indicate, as expected, only a small percentage of the total polar compounds in an oxidized oil as determined by the p_o (specific orientation polarization) test (a test based on electrical and physical properties).

In regard to the conclusion that "An oil with a high IFT should have a good life expectancy . . .," it should be noted that overrefined mineral oils may have high IFT but poor life.

From the author's data and reasoning on the difference in the results of the TAC (acidic material) test and the TPC (polar material) test, it is obvious that better correlation would be secured if the saponification numbers were measured, and if values of TSC computed therefrom were compared with the values of TPC. In fact, it was noted by Stoops[1] that when transformer mineral oils were oxidized the increases in dielectric constant due to formation of polar compounds did correlate with the increases in saponification number.

It would add to the value of the data in Table IV and Fig. 1 if the times when sludging was actually noted to occur were indicated thereon, and if the frequency of the voltage used in the measurements was stated.

In regard to the background for the orientation polarization test, it may be of interest to cite some of the literature which appeared prior to the references given in the paper. The work of Stoops[1] has already been mentioned. In three papers by the writer,[2–4] it may be noted that:

1. Equation 10 of reference 2 was derived to permit computation of $\epsilon_1 - \epsilon_0$ from μ, M, and the weight fraction of a polar solute in a nonpolar solvent even though the molecular weight of the solvent (which could actually be a mixture of a large number of hydrocarbons) was not known.

2. In reference 3 the specific polarization was defined and shown to be nearly equal to 0.33 for a wide variety of hydrocarbons and refined petroleum products.

3. Equation 4 of reference 3 defined the difference between the specific polarization and the specific refraction; also, the value of this entity as a measure of polar compounds in petroleum products of widely differing (and unknown) molecular weights was stated.

4. In reporting the results of aging tests at 120 C on nine viscous mineral oils it was stated in reference 4 that the increases in oil power factor were accompanied by proportional increases in dielectric constant. For these oxidized viscous oils it was found that $\Delta\epsilon_{60C} \simeq \Delta PF_{60C}$ at 60 cycles per second.

From this last result for viscous oils, I now compute $p_o = 0.02$ for viscous oils aged to the point where PF_{60C} reaches 0.07, a value unsuitable for many electric equipment applications. It thus appears that the numerical values for p_o stated in Mr. Johnson's conclusions for the fraction of oil life remaining of transformer mineral oils may be approximately true for more viscous mineral oils. It should be noted that more precise numerical limits would depend on the service requirements of the particular apparatus involved; also, that mineral oils with little life remaining may be rejuvenated by well-known techniques not involving acids or solvents, and that such oils may be reused for extended additional times.

REFERENCES

1. Development of Polar Characteristics in Insulating Oils, **W. N. Stoops.** *Journal of Applied Physics*, New York, N. Y., vol. 2, 1932, pp. 322–28.

2. Behavior of Dielectrics Under Alternating Stress, **G. M. L. Sommerman.** *Journal*, Franklin Institute, Philadelphia, Pa., vol. 219, 1935, pp. 433–58.

3. The Science of Petroleum (book). Oxford University Press, London, England, 1st ed., 1938, chap. on dielectric constants by G. M. L. Sommerman.

4. Properties of Saturants for Paper-Insulated Cables, **G. M. L. Sommerman.** *AIEE Transactions (Electrical Engineering)*, vol. 56, May 1937, pp. 566–76.

R. W. Johnson: I would like to thank Mr. Sommerman for his comments. He has pointed out that it is possible for an overrefined oil to have a high IFT but a poor life expectancy. I should have concluded that an oil with a high IFT should have a large fraction of its original life remaining rather than "should have a good life expectancy." Mr. Sommerman's comment can be generalized for all oil tests which are a measure of the concentration of oxidation products. Tests like IFT, TAN, $\Delta\epsilon$ can directly indicate only whether or not a measurable fraction of the oil life was used up. The number of years of useful life remaining can only be inferred from a test value if one has knowledge or makes assumptions regarding the rate of change of the property and the extreme value permissible for the particular oil tested. It is possible to estimate these qualitatively from the degree of refinement of the oil, and the degree of refinement of the oil from the color and the relative values of TAN, IFT, and $\Delta\epsilon$.

Some, but not all, of the necessary assumptions to translate p_0 into a life expectancy in years (rather than the fraction of life remaining) are automatically taken into account because of the relationship between p_0 and aromaticity. Highly refined oils in general have the best inhibitor response. Unless it is inhibited a very highly refined oil will have a poor life expectancy. An underrefined oil will have a poor life expectancy whether or not it is inhibited. Underrefined oils have high p_0's. Therefore, an oil with a low p_0, 0.002 or less, will have a good life expectancy only if inhibited and not previously subjected to deterioration. However, an oil with a high p_0, 0.0175 or more, would be expected to have a poor life expectancy in any case.

The capacitance and dissipation factor measurements used to calculate data for Table IV and Fig. 1 were made at 60 cycles per second.

The acid numbers at which oils A and B started to sludge are not known. Because of the construction of the cells it was possible to observe only that fraction of the oil removed for testing. The only sludge measurements made were at or after the cutoff point. However, the conclusions drawn from Table IV and Fig. 5 are consistent with the final sludge measurements. At the cutoff point oil A had produced more sludge than oil B. This is as expected since oil A was "apparently sludging" at an acid number of 0.23 whereas oil B did not "appear to be sludging" until an acid number of 0.4 had been exceeded.

It is possible to make a semiquantitative estimate of the relative amount of sludge formed up to the cutoff point by oils A and B from TPC and TAC values and the assumed relationship between $\text{TPC}/\sqrt{\text{TAC}}$ and sludge. At 6.25 months oil A had a $\text{TPC}/\sqrt{\text{TAC}}$ value of 32. At 10.6 months the TPC was 163. Presumably, if no sludge had been formed the TAC would have been $163^2/32^2$ or 26 micromoles per gram of oil. The difference between 26 and the actual TPC, 11, should be a measure of the amount of sludge formed up to the cutoff point. Similar calculations for oil B at 15 and 20.2 months give $15.8-8.7=7.1$ micromoles of acid per gram of oil used up in sludge formation. Therefore, one would expect that up to the cutoff point oil A would have formed roughly twice as much sludge as oil B.

Sludge measurements indicate that oil A produced about 3.3 times as much sludge as oil B. At the cutoff point oil B had deposited 113 units of chloroform soluble sludge. In the following 12 months with the oil at room temperature an additional 84 units of sludge were formed. In this 12-month period the soluble sludge (precipitable with pentane) decreased from 0.025 per cent to 0.023 per cent. No sludge measurements were made on oil A until 4 months after the cutoff point. The oil was at room temperature during this period. The total amount of sludge produced by oil A was 652 units. The soluble sludge was 0.023 per cent. Oil C at the cutoff point had formed 47 units of sludge. The soluble sludge was 0.0015 per cent. Although oils A and B precipitated sludge after the cutoff point at room temperature, they were subject to a pressure fluctuation, 0 to 5 pounds per square inch gauge, 13 times a day. The sludge would not necessarily have formed at a constant pressure.

There are several points in the paper which have not been questioned, but which should nevertheless be discussed. There are two sentences that I wish I had omitted from the original manuscript. The initial linear relationship between TPC and the square root of TAC can be explained on the basis of a first-order rather than a second-order reaction. The explanation requires the following assumptions:

1. The initial oxidation product (probably hydroperoxide) has attained a steady-state concentration. (This should be true if hydroperoxide formation were a slow reaction compared to the reactions which use up hydroperoxides.)
2. Acids are formed from the predominate constituents by a first-order reaction. Let X, P, and A represent the concentrations of hydroperoxides, polar compounds (other than acids), and acids respectively.

$$X \xrightarrow{k_1} P \xrightarrow{k_2} A$$

$$dP/dt = k_1X - k_2p = K - k_2p \tag{9}$$

$$dA/dt = k_2P \tag{10}$$

$$P = (K/k_2)(1-\epsilon^{-k_2t}) \tag{11}$$

$$A = Kt - (K/k_2)(1-\epsilon^{-k_2t}) \tag{12}$$

$$P + A = Kt \tag{13}$$

$$\frac{P+A}{A} = \frac{Kt}{Kt-(K/k_2)(1-\epsilon^{-k_2t})} \tag{14}$$

$$\epsilon^{-k_2t} = 1 - k_2t + (k_2t)^2/2! - (k_2t)^3/3! + \ldots \tag{15}$$

when $t << 1/k_2$

$$\epsilon^{-k_2t} \simeq 1 - k_2t + (k_2t)^2/2 \tag{16}$$

$$\frac{P+A}{A} \simeq \frac{Kt}{Kt-Kt+Kk_2t^2/2} = \frac{2}{k_2t} \tag{17}$$

From equations 13 and 17

$$(P+A)^2/A \simeq 2Kt/k_2t \tag{18}$$

Since TPC is approximately equal to $P+A$ and TAC is equivalent to A with concentrations expressed in microequivalents per gram

$$\text{TPC}/\sqrt{\text{TAC}} \simeq \sqrt{2K/k_2} \tag{19}$$

It should be noted that even if it were not for sludge formation eventually $\text{TPC}/\sqrt{\text{TAC}}$ would increase with time. There can be little doubt, however, that sludge formation, or some other process removing acids, comes into play before this effect becomes important. According to equation 14, TPC/TAC should continually decrease with time; in the case of oil B the ratio increased after an acid number of 0.43 was reached. Notice that the approximation in equation 16 is accurate to within 10 per cent when k_2t is 0.30 or less; but according to equation 14 if k_2t is 0.3 or larger TPC/TAC is 9 or less.

A discussion of Figs. 3 and 4 is in order. It was surprising to me that the IFT results with t-butyl alcohol solutions deviated so radically from other IFT measurements. IFT is not only comparatively more sensitive to changes in t-butyl alcohol concentrations at high concentrations but it is also, compared to higher molecular weight polar solutes, less sensitive at low concentrations. This result perhaps should have been expected. According to Traube's rule (reference 11 of the paper, p. 496) in dilute solutions the higher members of a homologous series are more effective in lowering the surface tension of water. The concentration necessary for a given lowering of surface tension is diminished by a factor of one-third for each additional CH_2 group. This can be explained by the greater mutual attraction of the higher molecular weight molecules. The lowering of surface or IFT depends on adhesive forces rather than cohesive forces; but for equal bulk-phase concentrations the substance with the greater cohesive force will have the greater concentration at the interface and thus give a greater lowering of surface or IFT.

Perhaps one of the reasons the dielectric constant of oil has not been more widely used in the past to follow the oxidation of transformer oil was the fear that water might cause erratic results. Actually attempts to dry oxidized oil by heating usually will increase rather than decrease p_0. Water is soluble only to the extent of about 50 parts per million in unoxidized transformer oil at room temperature. This concentration of water would increase p_0 about 0.0002. If the oxidization products of a transformer oil had an effective dipole moment of 2.2 Debye units and a molecular weight of 300 and if the unoxidized transformer oil had a p_0 of 0.0055, then when the p_0 of the oil reached 0.02 the weight fraction of oxidation products would be 0.05, or 50,000 parts per million.

Because of the approximate relationship between the refractive index and density of an oil it is possible to get approximate p_0 values eliminating one or the other measurement. In the paper the possibility of calculated p_0 without density measurements was overlooked. It can be shown that

$$p_0 = \frac{0.975(\epsilon - N_D^2)}{(\epsilon+2)(N_D^2-1)} (\pm 1.5 \text{ per cent})$$

if

$$p_d = 0.325 \pm 0.005$$

or

$$p_0 = 0.232\,\frac{(\epsilon - N_D^2)}{(N_D^2-1)} (\pm 4 \text{ per cent})$$

assuming 2.2 as a typical value of ϵ or

$$p_0 = (\epsilon - N_D^2)/5.2 (\pm 6.5 \text{ per cent})$$

assuming in addition 2.2 is the typical value of N_D^2.

Combination Load-Flow and Stability Equivalent for Power System Representation on A-C Network Analyzers

W. T. BROWN
MEMBER AIEE

W. J. CLOUES
ASSOCIATE MEMBER AIEE

ONE of the major problems encountered when an extensive power system is to be represented on an a-c network analyzer is that of developing proper equivalents for those portions of the power system which are not to be represented in detail either because of limitations of the analyzer or because of a desire for simplification of the over-all system. Several methods are currently available for developing fairly satisfactory equivalents for load-flow studies. There is no correspondingly satisfactory method available for developing an equivalent for stability studies where there are several points of interconnection between that portion of the system to be retained as real and that portion to be represented by an equivalent. Stability equivalents which have been used have not been identical in performance to load-flow equivalents. Modification of the a-c analyzer setup has been necessary whenever it is desired to change from a system representation suitable for a load-flow study to one suitable for a stability study.

A method is presented for developing a new equivalent which can be used interchangeably for both load-flow and stability studies. Included also are the results of an investigation made with the use of an a-c network analyzer to test the validity of the proposed new equivalent. Several of the methods available for developing load-flow equivalents are summarized briefly. The present practice of developing equivalents for stability studies is discussed.

The proposed new equivalent is by no means a rigorous replacement which can be used indiscriminately for stability studies. It is designed particularly for those cases where it is thought that the steady-state conditions of the system retained as real will vary appreciably, depending upon the type of equivalent used. Neither the proposed new equivalent nor any equivalent which has been used in the past should be employed where it is thought that approximate representation during transient conditions of those machines in the system being represented by an equivalent will alter appreciably the swinging of the machines in the system retained as real. A greater tendency towards instability will be indicated when the new equivalent is used in those instances where the conclusion as to stability will depend upon whether or not the actual system is represented in detail. Conclusions regarding stability obtained with the use of the new equivalent will, therefore, tend to be conservative.

Methods Currently Available for Developing Load-Flow Equivalents

Several methods are currently available for developing load-flow equivalents.[1] These are summarized briefly in the following primarily to facilitate the discussion of the proposed new equivalent.

METHOD 1

The system to be shown as an equivalent is represented by net loads or generation at the interconnection points adjusted so as to establish line loadings of predetermined values. This method has limitations since proper line loadings, especially for future conditions, cannot be estimated with any reliable degree of accuracy.

METHOD 2

The system to be shown as an equivalent is represented by an equivalent network which retains the identity of all of the generator busses and of the neutral bus to which all load impedances are connected. This results in a network containing $(n/2)(n-1)$ branches where n represents the total number of terminals to be retained as real. This equivalent is rigorous, assuming that loads can be represented by fixed impedances. Measurements of the transfer impedances between the n points retained as real can be made on an a-c network analyzer in the following manner: Apply a voltage between one particular point and the ground bus to which all other $(n-1)$ points have been connected. Measure the current flow to the ground bus from each of the $(n-1)$ points. The transfer impedance between the one particular point and one of the $(n-1)$ points is equal to the applied voltage divided by the current measured at the $(n-1)$ point.

A change of loads will negligibly modify the transfer impedances between the interconnecting points and the generating busses but will result in an appreciably different set of values for the transfer impedances to the neutral bus. New transfer impedances to the neutral bus must be measured for each load level that is to be studied. The chief disadvantage of this type of equivalent is in the relatively large amount of analyzer equipment required because of the retention of all generator busses as real.

METHOD 3

The system to be shown as an equivalent is represented by replacing its line impedances with an equivalent mesh network and by establishing net loads or generation at the terminals of the equivalent. Transfer impedances for the equivalent mesh network are measured in the manner described under method 2, with loads omitted from the system on which the measurements are made. Net loads and generation are determined by the use of distribution factors. Measurements for distribution factors are made on an a-c network analyzer by connecting to ground the terminals of the system to be shown as an equivalent. A current is impressed on each of the load and generator busses which are to be eliminated and the current flow to ground from each of the ground terminals is measured. Distribution factors are obtained by calculating the per-cent contribution of each of the load and generator busses to the various terminals of the equivalent. The loads and generation assigned to the various load and generator busses are then reassigned to the terminals in accordance with the distribution factors.

This method for obtaining load-flow equivalents is fairly versatile inasmuch as equivalents can be developed without prior knowledge of line loadings and

---

Paper 55-282, recommended by the AIEE Transmission and Distribution Committee and approved by the AIEE Committee on Technical Operations for presentation at the AIEE Middle Eastern District Meeting, Columbus, Ohio, May 4–6, 1955. Manuscript submitted February 3, 1955; made available for printing March 9, 1955.

W. T. BROWN and W. J. CLOUES are with the Philadelphia Electric Company, Philadelphia, Pa.

changes in load levels or generation in the equivalent can be readily made during a study once the basic distribution factors are known.

Present Practice With Respect to Stability Equivalents

There appears to be no general method for developing equivalents for stability studies where there are two or more points of interconnection between the system to be retained as real and the system to be represented by an equivalent and where it is necessary, because of lack of analyzer equipment, to combine several generators into one equivalent generator. One common method of obtaining a stability equivalent is to measure an equivalent with all generator transient reactances connected together. This results in what is hereafter termed a conventional stability equivalent, in which all generation appears back of transient reactance and all loads are reflected to both the point back of transient reactance and to the terminals of the equivalent. Methods 2 or 3 described for load-flow equivalents may be followed in obtaining this conventional stability equivalent.

One major disadvantage of the resulting equivalent is that the magnitude of the exports or imports at each of the interconnecting points will not be correct unless the vector voltages back of the individual generator transient reactances would be identical to each other if the system were shown in detail. The equivalent will usually give incorrect results from a load-flow point of view. It also may lead to incorrect conclusions with respect to stability problems, particularly where initial line loadings affect the relative phase angles of the generators in the portion of the system retained as real.

Proposed Combination Load-Flow and Stability Equivalent

The combination load-flow and stability equivalent presented here is basically a combination of the load-flow equivalent described under method 3 and the stability equivalent described in the section entitled "Present Practice with Respect to Stability Equivalents." A detailed description of the mechanics of obtaining the new equivalent is given in the Appendix. A-c network analyzer investigations utilizing this new equivalent are discussed in the section entitled "A-C Analyzer Investigations of Combination Load-Flow and Stability Equivalent." Principal steps involved in obtaining the new equivalent are as follows:

1. Compute a load-flow equivalent in accordance with method 3. A suggested method for handling off-nominal turn-ratios of transformers is given at the conclusion of this section.

2. Measure the n transfer impedances between the n interconnection points and the point back of generator transient reactances with all transient reactances tied together at a point designated by g. Compute the distribution factors, or factor, for the point g for all load points.

3. Convert the n impedances of step 2 to an equivalent mesh of $(n/2)(n-1)$ branches between the interconnection points, losing the identity of point g.

4. Compute a new mesh which, when combined with the mesh of step 3 will result in network equivalent to the load-flow mesh of step 1.

5. Impedances to be used for the new equivalent consist of the computed mesh of step 4 plus the transfer impedances of step 2.

6. Place a generator at point g with an assigned megawatt output equal to the total generation minus the load reflected to point g, as computed from the distribution factors obtained in step 2. The inertia of the generator should equal the combined inertia of all of the generators which are represented by the equivalent. The magnitude of the voltage of this equivalent generator should be approximately equal to the average of the estimated voltages of the individual generators of the equivalent weighted in accordance with the reciprocal of their respective transient reactances.

7. Net loads for each of the interconnecting points as computed for the load-flow equivalent of step 1 should be adjusted for the net generation assigned to the equivalent generator. This adjustment is accomplished by increasing all loads by the amount of the net generation assigned to the equivalent generator. The amount each load should be increased should be directly proportional to the reciprocal of the corresponding impedance arm as calculated in step 2. Where the voltages of the interconnection points are known, the megavar component of the assigned loads should be adjusted during the analyzer studies until the desired voltages are obtained.

8. The proposed new equivalent consists of the impedances of step 5, the generation of step 6, and the loads of step 7. The final result is an equivalent which appears to have the reactances of a conventional load-flow equivalent, the same net generation back of transient reactance and the same total load on the equivalent n points as a conventional stability equivalent, and the net loadings and generation within the equivalent adjusted so as to cause proper phase-angle relationships among the n equivalent points.

The performance of the proposed combination load-flow and stability equivalent with respect to its interconnection to the system shown as real is, for all practical purposes, identical to the performance of the load-flow equivalent of method 3. The performance of the combination load-flow and stability equivalent with respect to its synchronizing power output during transient conditions is similar to the performance of an equivalent developed in accordance with the principles discussed in the section entitled "Present Practice with Respect to Stability Equivalents."

Frequently a system for which an equivalent is desired has transformers with turn-ratios deviating from the turn-ratios which correspond to the nominal base voltages. These off-nominal turn-ratios are represented on an a-c network analyzer by adjustable autotransformers. Approximate recognition of the presence of these off-nominal turn-ratios when making measurements for an equivalent

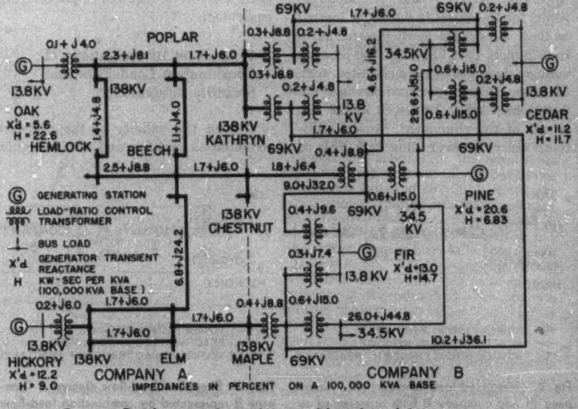

Fig. 1. One-line impedance diagram of hypothetical 2-company system

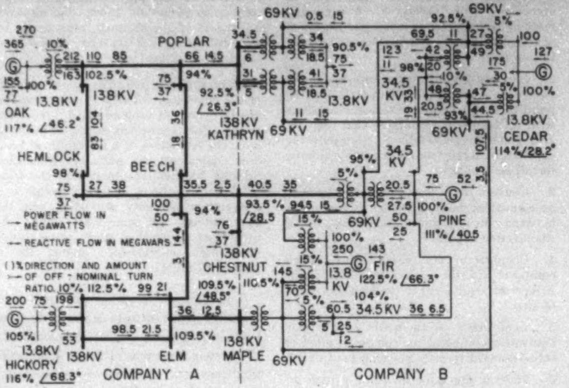
POPLAR
OAK
13.8KV
117% ∠46.2°
138KV
HEMLOCK
98%
BEECH
94%
KATHRYN
69KV
138KV
CHESTNUT
109.5% ∠48.5°
110.5%
ELM
109.5%
MAPLE
138KV
HICKORY
13.8KV
116% ∠68.3°
105%
COMPANY A
COMPANY B
34.5 KV
95%
PINE
111% ∠40.5
100%
FIR
13.8 KV
122.5% ∠66.3°
104%
34.5KV
CEDAR
13.8KV
114% ∠28.2°
100%
93%
98%
92.5%
90.5%
93.5% ∠28.5
→ POWER FLOW IN MEGAWATTS
→ REACTIVE FLOW IN MEGAVARS
( )% DIRECTION AND AMOUNT OF OFF-NOMINAL TURN RATIO. 10%

Fig. 2. A-c network analyzer load-flow diagram showing power flows, voltages, and off-nominal turn-ratios of transformers. Company A and company B both represented as real

can be made in the following manner:

With all generators removed and with the autotransformers set at their operating values, apply a voltage of 100 per cent between one of the terminals to be retained as real and the common bus to which the ground terminals of the autotransformers are connected. Insert additional autotransformers at each of the remaining open-circuited terminals which are to be retained as real and adjust each autotransformer so that the voltage on the free end of the autotransformer is 100 per cent. Measurements for transfer impedances and for distribution factors are made in the manner described in the Appendix, steps 2 and 7. Metering points for the currents should be located on those sides of the newly inserted autotransformers that have the 100-per-cent voltage during the open-circuited test. Calculate the transfer impedances and the loads which are to be placed at the terminals of the equivalent. Insert autotransformers between those terminals of the equivalent which had compensating autotransformers during the measurements and the system to be retained as real. Settings of these transformers should be reversed from the settings used during the measurements. The foregoing method is based on the supposition that the turn-ratios around closed loops within the system to be represented by the equivalent are at, or near, unity. Measurements could be made with no compensating autotransformers utilized, provided recognition is given to the various base voltages which exist at the terminals of the system because of the off-nominal turn-ratios.[2] Autotransformers, however, will still be required in the resulting equivalent.

A-C Analyzer Investigations of Combination Load-Flow and Stability Equivalent

To test the validity of the proposed combination load-flow and stability equivalent, a hypothetical 2-company power system was investigated on an a-c network analyzer. The investigations consisted of a load-flow run and of stability runs for both companies of the hypothetical 2-company power system represented as real, one company represented as real and one company represented by by the proposed combination load-flow and stability equivalent, and one company represented as real and one company represented similar to that which would be obtained if a stability equivalent were used as described in the section entitled "Present Practice with Respect to Stability Equivalents."

Conclusions regarding the performance of the proposed combination load-flow and stability equivalent when used to represent one company of the aforementioned hypothetical 2-company power system and conclusions regarding the performance of a conventional stability equivalent are as follows:

For load-flow studies:

1. Use of the combination load-flow and stability equivalent will give results almost identical to those obtained when the entire power system is represented in detail.
2. Use of the conventional stability equivalent will give results which are at marked variance with those obtained when the entire power system is represented in detail.

For stability studies:

1. Use of the combination load-flow and stability equivalent will give results which agree closely (showing, however, a slight tendency towards greater instability) with those obtained when the entire power system is represented in detail.
2. Use of the conventional stability equivalent may, in critical cases, lead to the conclusion that a system is stable when the system actually is unstable.

Fig. 1 is a 1-line impedance diagram of the power system which was studied. Fig. 2 shows the megawatt and megavar line loadings, bus voltages, and off-nominal transformer turn-ratios for the base conditions under which the stability runs

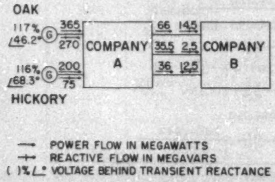
OAK
117% ∠46.2°
365
270
COMPANY A
66 14.5
35.5 2.5
36 12.5
COMPANY B
116% ∠68.3°
200
75
HICKORY
→ POWER FLOW IN MEGAWATTS
→ REACTIVE FLOW IN MEGAVARS
( )% ∠° VOLTAGE BEHIND TRANSIENT REACTANCE

Fig. 3. Simplified load-flow diagram. Company A and company B both represented as real

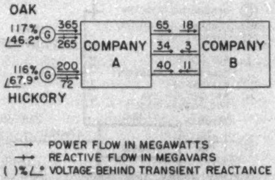
OAK
117% ∠46.2°
365
265
COMPANY A
65 18
34 3
40 11
COMPANY B
116% ∠67.9°
200
72
HICKORY
→ POWER FLOW IN MEGAWATTS
→ REACTIVE FLOW IN MEGAVARS
( )% ∠° VOLTAGE BEHIND TRANSIENT REACTANCE

Fig. 4. Simplified load-flow diagram. Company B represented by combination load-flow and stability equivalent

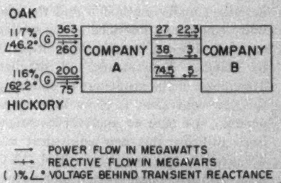
OAK
117% ∠46.2°
363
260
COMPANY A
27 22.3
38 3
74.5 .5
COMPANY B
116% ∠62.2°
200
75
HICKORY
→ POWER FLOW IN MEGAWATTS
→ REACTIVE FLOW IN MEGAVARS
( )% ∠° VOLTAGE BEHIND TRANSIENT REACTANCE

Fig. 5. Simplified load-flow diagram. Company B represented by conventional stability equivalent

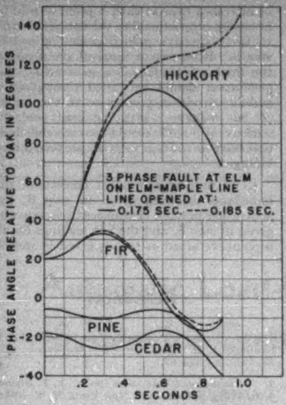

Fig. 6. Power-angle curves. Company A and company B both represented as real

were made. Simplified load-flow diagrams showing only the generation and associated vector voltages of company *A* and the power flows and voltages on the three tie lines interconnecting company *A* with company *B* are shown in Figs. 3, 4, and 5. These three diagrams show a-c analyzer readings with both company *A* and company *B* represented as real, a c analyzer readings with company *B* represented by a combination load-flow and stability equivalent, and a-c analyzer readings with company *B* represented by the previously mentioned conventional stability equivalent respectively. The conventional stability equivalent was simulated on the a-c analyzer by connecting together the points behind the transient reactances of the generators of company *B*, with company *B* otherwise represented in detail. Transformer turn-ratios and load impedances for company *B* were at the same values as those used in the load-flow run where the transient reactances were not connected together.

Examination of Figs. 3 and 4 will indicate the relative closeness with which the results of load-flow studies obtained with use of the combination load-flow and stability equivalent agree with the results obtained when company *B* is retained as real. Fig. 5 indicates that use of the conventional stability equivalent creates unreal loadings on the interconnecting lines and a smaller phase angle between the two generators of company *A*. The effect of this decreased angular difference between generators tends to make the system more stable than it actually is.

For the stability studies, a 3-phase fault was placed on company *A*'s terminus of one of the three interconnecting tie lines. The fault was cleared and the tie line opened at 0.175 second for one set of runs and at 0.185 second for a second set of runs. Plots of the swing curves were obtained with both companies retained as real, Fig. 6, with company *B* represented by a combination load-flow and stability equivalent, Fig. 7, and with company *B* represented by a conventional stability equivalent, Fig. 8. Fig. 6 shows that the system is stable with a clearing time of 0.175 second and unstable with a clearing time of 0.185 second. Fig. 7 shows that the results obtained with the use of the combination load-flow and stability equivalent are almost identical to those obtained when both companies are retained as real with, however, a slight tendency towards greater instability. Fig. 8 shows that the use of the conventional stability equivalent gives incorrect results indicating, for the conditions studied, stability where instability actually is present.

Appendix. Procedure for Obtaining Combination Load-Flow and Stability Equivalent

A suggested step-by-step procedure for obtaining the combination load-flow and stabilty equivalent is given in the following.

1. Represent on an a-c analyzer all transmission circuits of the system for which an equivalent is desired, omitting all load and generating units. If an a-c analyzer is not available, a d-c calculating board may be used by representing system reactances only.

2. Measure the transfer admittances between all points which are to be connected to the system which will be shown as real, thus reducing the network to an equivalent mesh of $(n/2)(n-1)$ branches where n is the number of interconnection points. Measurement of the transfer admittances associated with a single n point may be made by applying a voltage between one of the n points and a common bus to which each of the remaining $(n-1)$ points are connected. The transfer admittances between the single point and the $(n-1)$ points are equal respectively to the current metered between each of the $(n-1)$ terminals and the common bus divided by the applied voltage. Computation of transfer admittances rather than transfer impedances is suggested so as to facilitate succeeding computations.

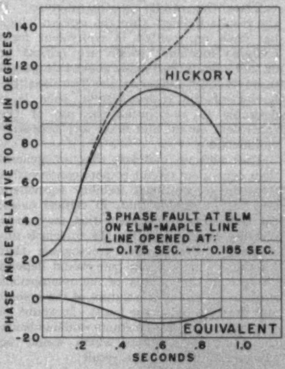

Fig. 7. Power-angle curves. Company B represented by combination load-flow and stability equivalent

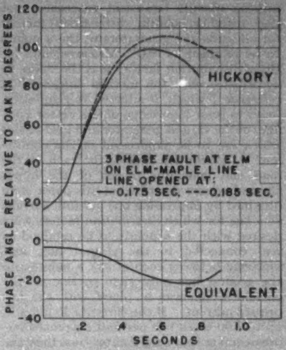

Fig. 8. Power-angle curves. Company B represented by conventional stability equivalent

3. Tie all generator transient reactances together and measure the n transfer reactance arms between the common generator point designated as g and each n point which is to be retained as real, the n points being tied together for these measurements.

4. Reduce the network of n reactance arms obtained in step 3 to a mesh of $(n/2)(n-1)$ admittances eliminating the common generator point g. This step is recommended so as to facilitate the computations of step 5.

5. Compute a new mesh of $(n/2)(n-1)$ branches by subtracting the admittance values of step 4 from the corresponding admittance values of step 2. Convert the admittances of the new mesh to impedances. Any negative resistances which appear in the transfer impedances so computed may be assumed, by necessity, to be zero for the analyzer setup. This assumption should not affect appreciably the required performance of the equivalent since accurate transfer characteristics rather than accurate loss representation is desired from the equivalent.

6. The mesh computed in step 5 plus the arms obtained in step 3 are the reactances used in the combination load-flow and stability equivalent.

7. With the original setup of the trans-

mission circuits (transient reactances not tied together) obtain distribution factors for all loads and generators to the *n* points to be retained as real. Measurements for these distribution factors may be made in accordance with the method suggested in reference 1 which, if adhered to rigorously, requires prior knowledge of the vector voltages of the various generator and load busses which are to be suppressed in the equivalent. Distribution factors for each of the load and generator busses of the hypothetical system described in this paper were obtained by impressing one per-unit current at a bus for which distribution factors were desired with the *n* points to be retained as real connected to the ground bus, and metering between each of the *n* points and the ground bus only that portion of the current which was in phase with the impressed current. If the currents do not add up to 1.00 when one per-unit current is impressed at a load or generator bus, then the current values should not be used directly as distribution factors but should be adjusted proportionately so that the distribution factors will account for 100 per cent of the load. By applying these distribution factors to the megawatt loads and generation of the various internal busses, net megawatt loadings on all *n* points can be determined.

8. Tie all generator transient reactances together and obtain distribution factors for the total amount of load which would appear at the point *g* back of transient reactance, the *n* points and the point *g* being tied together during this measurement. (It is only necessary to measure the distribution factors associated with the point *g*.) For the combination load-flow and stability equivalent the load reflected to this point *g* plus all of the generation is assumed to appear at point *g*. This will usually result in a net generation at *g*. An estimated average voltage back of transient reactance should be used for the equivalent generation.

Increase the net megawatt loadings on the *n* points as determined in step 7 by the amount of the net generation to be put at the point *g* in back of the transient reactances as determined by step 8. The amount of increased load at each *n* point should be inversely proportional to the reactance arms to the respective points as determined in step 3. If on one or more of the *n* points the final net loading is a generation, this generation should be varied throughout a stability study in proportion to the square of bus voltage. Megavar loads on the various *n* points should be scheduled as necessary to obtain desired predetermined voltages.

10. The new equivalent consists of the impedance network given in step 6, the generation in back of transient reactance as given in step 8, and the net loadings on all *n* points retained as real as given in step 9.

References

1. EQUIVALENT CIRCUITS FOR POWER-FLOW STUDIES, J. B. Ward. *AIEE Transactions*, vol. 68, 1949, pp. 373–82.

2. TRANSFORMER ENGINEER (book), L. F. Blume. John Wiley & Sons, Inc., New York, N. Y., 1938, pp. 112–18.

◆

Discussion

C. H. Hoffman (Public Service Electric and Gas Company, Newark, N. J.): There has always been some confusion between stability equivalents and power-flow equivalents. The fact that a conventional stability equivalent does not ordinarily give the correct power-flow picture has previously been accepted as simply an unfortunate but necessary approximation. The Brown-Cloues technique, although somewhat more involved than the ordinary measurement, produces a single equivalent which does both jobs as well or better than the old approach. This is particularly advantageous in those stability studies where it is desired to measure power flow at various locations at selected times during the swing. Since even the flows at time zero are incorrect with the conventional stability equivalent, it has always been hard to develop confidence in readings taken at other time steps. The authors have shown in this excellent paper that these suspicions of inaccuracy were justified.

There is no necessity, however, of discarding all old studies made with the conventional equivalents, since the example in the paper is a rather extreme case, with the boundaries of the equivalent extending quite close to the point of fault. In most studies the part of the system of greatest interest is represented in detail, and only remote portions of the system are suppressed in equivalents. Errors of representation of more remote areas have less influence on results than in the case of the example in this paper.

In step 4 of the Appendix, is it not possible (and preferable) to make the required network reduction by means of measurements similar to those necessary in step 3? Concerning step 8 of the Appendix, it may not be clear to all readers that the distribution factors are for the original network loads and not for the distributed loads at the *n* points obtained in step 7.

C. C. Young (General Electric Company, Schenectady, N. Y.): Because it is sometimes impossible or impractical to represent in sufficient detail all of the interconnected companies of a power system for a-c network analyzer studies, a method of representing a portion of a power system for both load-flow and stability studies is very desirable. Any method which satisfactorily achieves this result is a real contribution to the field of power system analysis.

One point which cannot be overemphasized is that any equivalent circuit involves making some assumptions about the system to be simplified. The equivalent cannot accurately represent the system unless the assumptions are reasonable. Thus, if two generators in a system do not swing together during a transient disturbance, then the assumption that they do swing together in itself creates an error which may invalidate the results of the analysis. If the results indicate that the system which has been represented in equivalent form contains machines which are critical or or that assumptions made about this system may directly influence the transient behavior of the entire system, then it is desirable to re-examine the use of the equivalent circuit and make any necessary modifications.

The authors indicate that in general their equivalent circuit is more conservative than the conventional stability equivalent and they conclude that, in critical cases, the conventional representation may show stability where, actually, the system is unstable. It would seem reasonable that whether or not this is true would depend directly on the validity of the assumptions made as well as on the nature of the system and the location of the fault. It would be very interesting if the authors would indicate the general conditions which would be expected to produce this result.

W. T. Brown and **W. J. Cloues:** We agree in general with the remarks made by Mr. Hoffman and Mr. Young, and wish to take this opportunity to thank the discussers for their very worth-while comments.

Mr. Hoffman brings attention to the fact that the example chosen is a rather extreme case, with the boundaries of the equivalent extending quite close to the point of fault. Admittedly, the example may be considered extreme from a stability point of view, but it is not necessarily extreme from a load-flow point of view. Regardless of the location of a fault, a conventional stability equivalent cannot be relied upon to give correct prefault line loadings on all lines of the system shown in detail. The conventional stability equivalent thus cannot necessarily be used successfully when a load-flow study is to be made concurrently with a stability study, even though the faults to be studied are far removed from the boundaries of the equivalent.

Mr. Hoffman is correct in stating that it is possible, and preferable, to make the required network reduction mentioned in in step 4 of the Appendix by means of measurements similar to those necessary in step 3. Mr. Hoffman's comments on step 8 should serve to clarify that particular step.

Mr. Young's question regarding what the general conditions are under which the use of a conventional stability equivalent may show stability where, actually, the system is unstable is quite apropos. The statement we made regarding the possible wrong conclusions which might be drawn from the use of a conventional stability equivalent, as well as the statement that use of a combination load-flow and stability equivalent may be expected to give more conservative results than those obtained by use of the conventional stability equivalent, was prompted by observations of the results of various stability runs made when testing the sample system. These statements can be supported by the following reasoning: Correct initial angles of the machines in the system retained as real will be obtained by use of the combination load-flow and stability equivalent. Conversely, use of a conventional stability equivalent will give, because of the relatively lower transfer impedances of this equivalent, initial machine angles which are closer together. The closer together the initial machine angles are, the greater is the tendency towards stability. This foregoing reasoning supports the statement that a conventional stability equivalent might show stability where instability actually is present. On the other hand, it is believed that, when computing the swinging of the machines in the system retained as real, the use of an equivalent represented by a single machine having only one degree of freedom will tend to make the machines in the system retained as real more unstable as compared to the results obtained if the machines represented by the equivalent are shown in detail thus giving several degrees of freedom to the system which is normally suppressed by the equivalent.

In short, it is reasoned that either type of equivalent generally will tend to give conservative results (greater instability) during the transient period, but that the final result, namely stability or instability, will be modified by the all-important initial angles, and the initial angles most assuredly will depend upon the type of equivalent used.

Automatic Load-Frequency Control System for Central Station Power

GUSTAVE EHRENBERG
ASSOCIATE MEMBER AIEE

THE goal of completely automatic control for large power system interconnections can be realized only by a control system that is capable of solving the following load regulating problems:[1-3]

1. It must tie an area together so that all systems within the area can accommodate large load swings with a minimum capital investment.
2. At the same time, each system within an area must be capable of regulating its own generation under normal load conditions.
3. All power generated in the system interconnections must be manufactured at a minimum cost.
4. Cyclic swings on tie loadings between interconnected areas must be held to a minimum.

The load-frequency control system described in this paper represents a sound modern approach to an economical solution of these problems, using the most advanced control techniques. The system has the following advantages:

1. It is a completely integrated control system intended not to supplement less advanced forms of control but to replace them entirely.
2. It applies electronic techniques that have been tried and tested in the process industries.
3. It is designed to control both the proportional (fringe) and reset (sustained) types of variation; but adjustments are provided so that any amount of each control mode, or any combination of both modes, is available without the use of additional equipment.
4. It incorporates an automatic incremental loader that eliminates the necessity of making slope and break point adjustments as the stations go through the loading cycle.
5. It makes provision for including a penalty factor computer.
6. The control scheme is basically simple: the system concentrates all control functions in the servos, see Fig. 1, and uses instruments only for monitoring purposes.
7. The physical arrangement of equipment simplifies interwiring connections and maintenance, and facilitates system expansion.

The fundamental parts of this system were tested recently at Denison Dam, Tex., over a period of a year, in a power system serving the entire state, with excellent results. By regulating the output of only two 37.5-kva generators, the load dispatcher was able to hold the frequency of this 1,000-megawatt power system within ±.03 cycle, and this in spite of rapid load swings caused by the fluctuating demands of large steel mills in the southern part of the state.

Fig. 2(A) shows a curve that represents approximately 1 hour's operation, with the new control system holding the system frequency; the opposite curve shows generator output (figures to the left are read directly in megawatts; figures to the right in frequency). The upper portion of this curve shows the system control operating with a wider proportional band than does the lower portion, thus effectively cutting down on the amount of fringe control. It can be seen that the frequency band becomes wider and the actual fluctuation of the generator units is greater as a result of this widening of the proportional band, thus offering reasonable support of the contention that high-speed control actually works the generator units less than does the more relaxed type of sustained control. Fig. 2(B) shows the new load-frequency control system holding base load on the plant, while another station on the system is holding power system frequency using a sustained type of frequency control system only. A comparison of the curves of Figs. 2(A) and (B) demonstrates the effectiveness of the new control system.

Control Theory[4]

The instrument engineer assigned the task of designing a control system for large power system interconnections is

Fig. 1. Electronic servo unit

Paper 55-496, recommended by the AIEE System Engineering Committee and approved by the AIEE Committee on Technical Operations for presentation at the AIEE Summer General Meeting, Swampscott, Mass., June 27–July 1, 1955. Manuscript submitted March 25, 1955; made available for printing April 21, 1955.

Gustave Ehrenberg is with the Minneapolis-Honeywell Regulator Company, Philadelphia, Pa.

The adjustable break point described in the section entitled "Fundamental Circuitry" was suggested by George Foster, Metrotype, Inc.

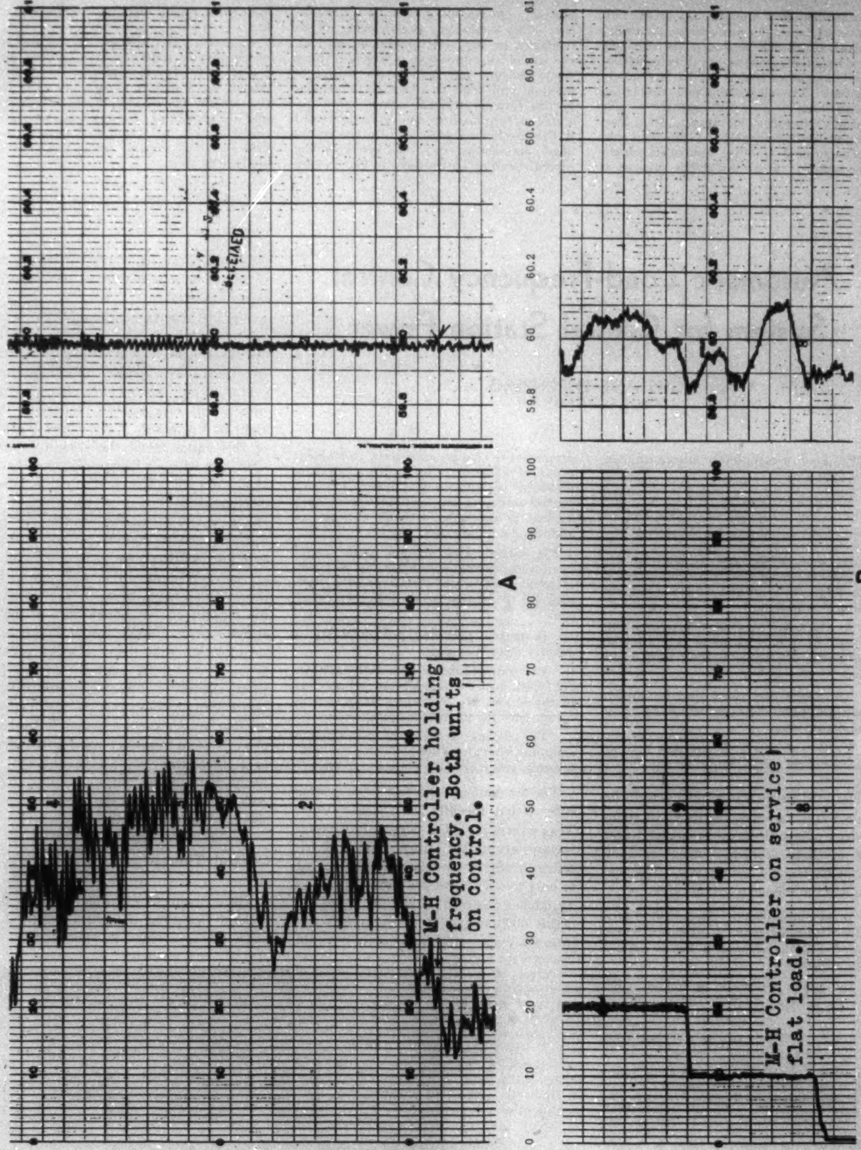

Fig. 2. Megawatt and frequency curves

A—M-H holding frequency
B—M-H holding base load and another plant holding frequency

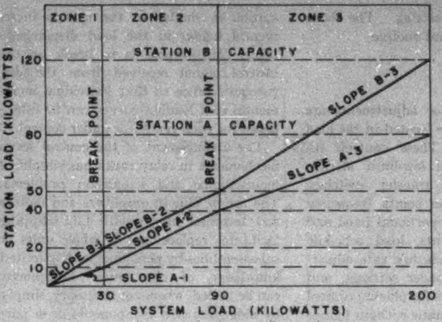

Fig. 3. Typical incremental loading curves

faced with a choice of three different control methods:

1. The reset (sustained) mode.
2. Two separate control systems, one using the reset (sustained) mode operating on a pulse-type signal; the other using the proportional (fringe) mode with a continuous type signal; with both modes being combined at the generators.
3. The reset (sustained) plus proportional (fringe) mode combined in one control unit, and transmitted directly as a combined signal to the stations, or separately to the stations and combined at the generator governor.

The first system was found to be inadequate for general process control many years ago; and, as a result, a number of packaged control units combining both the proportional and reset control modes were designed at little extra cost. The second system is just as unsound economically, for the simple reason that pulse type of control as a rule requires two separate telemetering channels—one for raise and one for lower—to deliver the reset control signal; and still another channel is required to deliver the continuous signal of proportional control. In some systems of this type two additional telemetering channels are required.

The merits of the third system of control, which uses only one telemetering channel, from an economic as well as an efficiency standpoint, should be obvious. This control system has proved its worth in other industries whose control problems are no different essentially from those of the power industry. The benefits of the combined control modes are so well established, in fact, that it should no longer be necessary to analyze a power system to determine the type of control for which it is best suited. In the opinion of the writer, the advantages of proportional control are such that it should be used throughout the power industry, the only question being the degree of its use. An explanation of how these two modes interact and are used separately helps to understand the control theory underlying the new system.

Proportional and Reset Control Action

When a sudden transient occurs in the power system, the proportional signal, a fast-speed signal, is directly proportional to the magnitude of the transient and the rate of disappearance of the signal is in a direct ratio to the rate of disappearance of the transient. The reset signal, a slow-speed signal, operates simultaneously, but at such a slow rate that its effect is negligible in the case of a sudden transient.

If the transient is of longer duration, the proportional plus reset action is the same as before, with this difference: as the system returns to a balanced condition and the proportional signal disappears, the reset part of the signal continues to feed into the incremental loader to compensate for the disappearance of the proportional part of the signal. Furthermore, the reset signal continues to drift in the direction necessary to correct the unbalance, and assumes a new position when the system is at balance.

If the proportional control signal is split from the reset signal, the reset signal is transmitted through the incremental loader, as described here. The proportional signal, however, by-passes the incremental loaders and is transmitted separately and directly to the desired generating unit, where it is combined with the reset signal.

When the controller combines both modes, the combined corrective signal is sent to an incremental loader on which curves have been laid out for the various stations, according to the load requirements of the power system. These curves are based upon the heat rates of the various generators in the system, and they may include a penalty factor which can be varied manually by dials or automatically when a transmission-loss computer is provided in the control system.

Incremental Loading

The incremental loader divides the combined corrective signal into separate control signals according to the incremental heat rate curves of each station. A pair of typical incremental loading curves is shown in Fig. 3. These curves indicate the ratio used to apportion the control signal between stations *A* and *B* so that each station gives the optimum output for any given system load. Thus, in the example illustrated in Fig. 3, for a load of 30 kw the control signal is apportioned between the two stations in a 2-to-1 ratio; for a load of 90 kw in a 5-to-4 ratio; for a load of 200 kw (total controlled system load) in a 3-to-2 ratio. The loader is flexible in design, so that it can accommodate any number of breakpoints up to 30; furthermore, the breakpoints can be positioned in any grouping along the curve so as to provide the most accurate segmental simulation of the actual incremental heat rate curve. The incremental loader is easily adjustable by means of dials mounted on the dispatcher's console.

The separate signals from the incremental loader are telemetered to the various stations on control. Within each station, a signal is sent to a station incremental loader that is similar to the system loader, except that it does not provide for penalty factor adjustments. Curves have been set up in each station loader for the individual generators within the station and separate control signals are sent out to the governor speed adjustment motors of each generating unit. This signal is compared with generator governor position and any deviation results in an increase or decrease in generator output sufficient to correct for the initial deviation of net interchange (power transfer) and/or system frequency and/or time error.

Measuring and Computing

The measuring and computing system consists of a series of sensing elements that are used to measure the net interchange of power, system frequency, and time error. The telemetered signals from the various interchange points are added together and sent to a totalizer called net interchange. The net interchange from the power totalizer is compared with schedule by the net interchange measuring circuit; similarly, system frequency is compared with frequency set point, and timer error is compared with time error set point. Any resulting error is applied as input to the area requirement computer. The net error signal, which is the algebraic sum of the net interchange, frequency, and time error signals, is then sent to the controller, which incorporates proportional and reset actions, either combined or separately.

Alarm

The alarm system consists of failure alarms, deviation alarms, and high-limit and low-limit alarms, which monitor various elements in the control system. All telemetering receivers are provided with failure alarms, which may be used to "trip" the system off control, and to provide visual and audible indication of telemeter receiver failure. All tripouts hold the system generation at its last controlled condition. Another characteristic of all trip-type alarms is that the system must be returned to control manually. The frequency measuring circuit is provided with high-low alarms which are adjustable over the sensing span; they are generally used to trip, but may also be used to provide visual-audible alarm.

The net interchange and the area requirement circuits are equipped with high-low alarms, which are adjustable over a very wide range for visual-audible indication; they may also be used to trip the system off control. Each generating station is provided with high and low load alarms which function to block the control signal received from the allocator circuit whenever the control signal calls for a station generation output in excess of either load alarm setting. The alarm indication is visual and audible.

Equipment

All system operator adjustments are mounted on a console located in the load dispatcher's office. These controls include high-limit and low-limit alarms, manual-to-automatic transfer switches, load and frequency set points, frequency bias adjustments, proportional band and reset rate adjustments, load schedule "start timer," load schedule rate adjustment, incremental loader settings, and null balance indicators for placing control from manual to automatic without bumping the system.

The incremental loader adjustments allow the dispatcher to change the loading curves on his stations at will. If a station is placed on automatic control, the incremental loader will automatically place the station on its loading curve, which, of course, takes into account the total load on the system at that particular moment. The number of slope adjusting dials for setting these curves is determined by the number of break points that the user desires. The break point dials provide a method of grouping the break points to the right or left, as may be required to establish the proper loading curves.

Also located in the dispatcher's office are recorders, mounted on a panelboard, which are used to monitor the control system. These instruments record net interchange and schedule, frequency, time error, area requirement, tie-line loadings, and station generation and schedule. All other measuring and control components, such as alarm amplifiers, telemetering equipment, and servos, are mounted on relay racks that may be located in a low-cost area of the plant.

The incremental loader located in each station is similar to the system incremental loader in the load dispatcher's office. Its purpose is to break up the control signal received from the dispatcher's office so that individual incremental cost loading curves can be established for each generator under control.

The arrangement of the control servo mechanisms in relay racks has simplified maintenance and expansion problems. The use of plug-in amplifiers and motors and terminal blocks with fan stripping facilitates replacement of whole units or subassemblies by personnel with a limited knowledge of electronics. Equipment can be added, whenever necessary, simply by mounting new components on a partially filled relay rack or by adding a new relay rack to the assembly. Since instruments are used exclusively for monitoring purposes, installation of additional instruments does not present any problem. The use of standard consoles and standardized components and subassemblies in the consoles likewise facilitates adding new components and replacing old ones.

Fundamental Circuitry

The individual circuits of which the load-frequency control system is composed are elementary and compounding them is a relatively simple matter. A simplified schematic diagram is shown in Fig. 4.

The net interchange signal from the power totalizer is continuously measured and recorded by the net interchange measuring circuit and recorder respectively. Similarly, the system frequency is continuously measured and recorded by the frequency measuring circuit and the frequency recorder, as is the time error signal.

The computing circuit is composed of the frequency and net interchange and time error bridges and the area require-

---

Errata

The following corrections should be made in the paper entitled "A New Approach to the Calculation of Synchronous Machine Reactances—Part I" by M. E. Talaat, which appeared in the April 1955 issue of *Power Apparatus and Systems*, pages 176–83.

1. The symbol C_a^3 in the last line of equation 17 should be C_1^3.

2. A bracket should enclose the capital X's in equation 45.

3. The paragraph starting at the end of page 182 should read as follows: "However, with regard to the subtransient reactance, I cannot agree with Mr. Kilgore that his paper[6] gives a truer assumption of the current distribution in the bars than does the present paper."

4. The symbol n^1 in line 5, column 1, page 183, should be n_b.

5. The second sentence of the last paragraph of column 1, page 183, should read as follows: "The subtransient reactance by his method was $x_{du}''=0.175$, and by the new method $x_{du}''=0.226$ . . ."

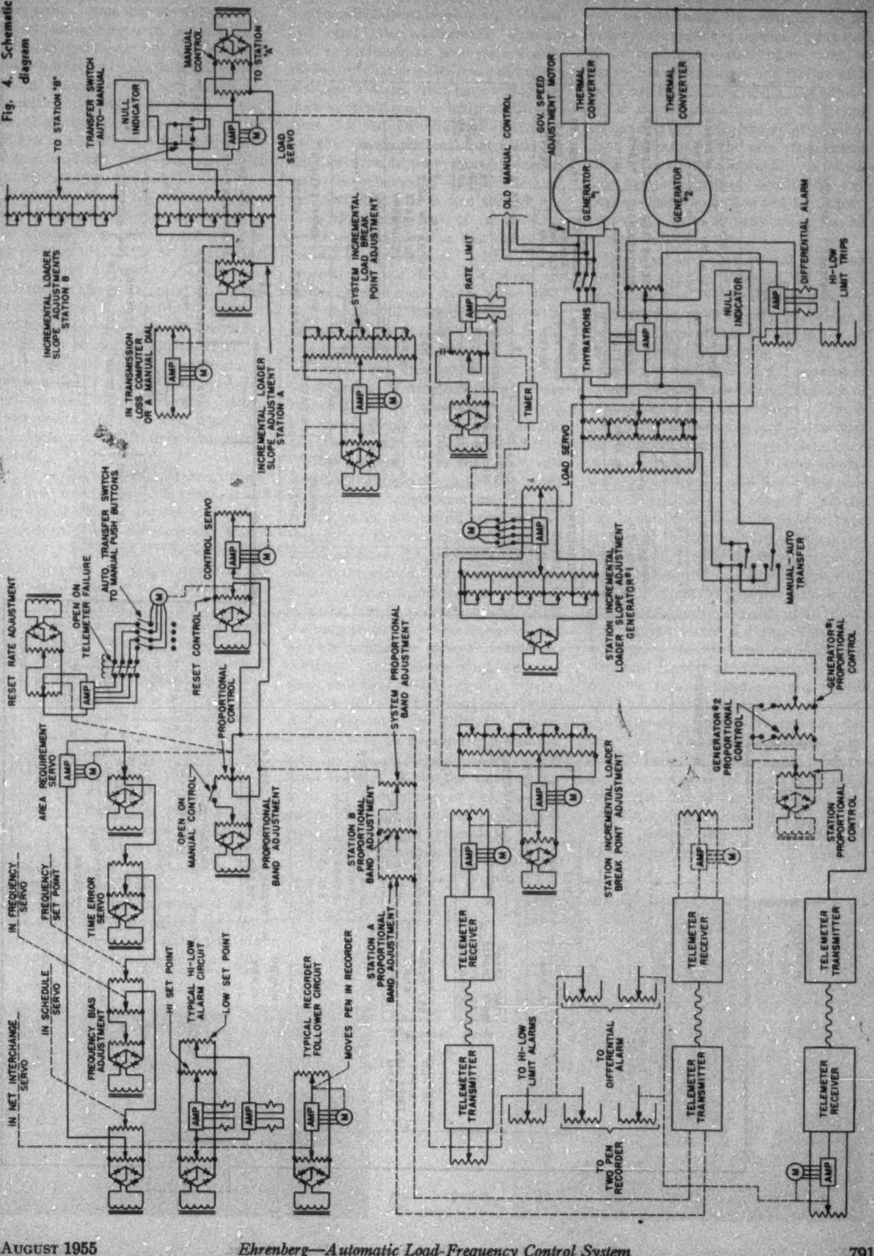
TO STATION "B"
TRANSFER SWITCH AUTO-MANUAL
NULL INDICATOR
MANUAL CONTROL
TO STATION "A"
AMP
M
LOAD SERVO
INCREMENTAL LOADER SLOPE ADJUSTMENTS STATION B
IN TRANSMISSION LOSS COMPUTER OR A MANUAL DIAL
INCREMENTAL LOADER SLOPE ADJUSTMENT STATION A
SYSTEM INCREMENTAL LOAD BREAK POINT ADJUSTMENT
AUTO. TRANSFER SWITCH TO MANUAL PUSH BUTTONS
OPEN ON TELEMETER FAILURE
RESET RATE ADJUSTMENT
RESET CONTROL
CONTROL SERVO
PROPORTIONAL CONTROL
OPEN ON MANUAL CONTROL
PROPORTIONAL BAND ADJUSTMENT
AREA REQUIREMENT SERVO
SYSTEM PROPORTIONAL BAND ADJUSTMENT
STATION B PROPORTIONAL BAND ADJUSTMENT
STATION A PROPORTIONAL BAND ADJUSTMENT
IN FREQUENCY SERVO
FREQUENCY SET POINT
TIME ERROR SERVO
IN SCHEDULE SERVO
FREQUENCY BIAS ADJUSTMENT
IN NET INTERCHANGE SERVO
HI SET POINT
TYPICAL HI-LOW ALARM CIRCUIT
LOW SET POINT
TYPICAL RECORDER FOLLOWER CIRCUIT
MOVES PEN IN RECORDER
OLD MANUAL CONTROL
GOV. SPEED ADJUSTMENT MOTOR
THERMAL CONVERTER
THERMAL CONVERTER
GENERATOR #1
GENERATOR #2
RATE LIMIT
TIMER
THYRATRONS
NULL INDICATOR
DIFFERENTIAL ALARM
HI-LOW LIMIT TRIPS
LOAD SERVO
STATION INCREMENTAL LOADER SLOPE ADJUSTMENT GENERATOR #1
MANUAL-AUTO TRANSFER
GENERATOR #1 PROPORTIONAL CONTROL
GENERATOR #2 PROPORTIONAL CONTROL
STATION PROPORTIONAL CONTROL
STATION INCREMENTAL LOADER BREAK POINT ADJUSTMENT
TELEMETER RECEIVER
TELEMETER TRANSMITTER
TELEMETER RECEIVER
TELEMETER TRANSMITTER
TELEMETER TRANSMITTER
TELEMETER RECEIVER
TO HI-LOW LIMIT ALARMS
TO DIFFERENTIAL ALARM
TO TWO PEN RECORDER

Fig. 4. Schematic diagram

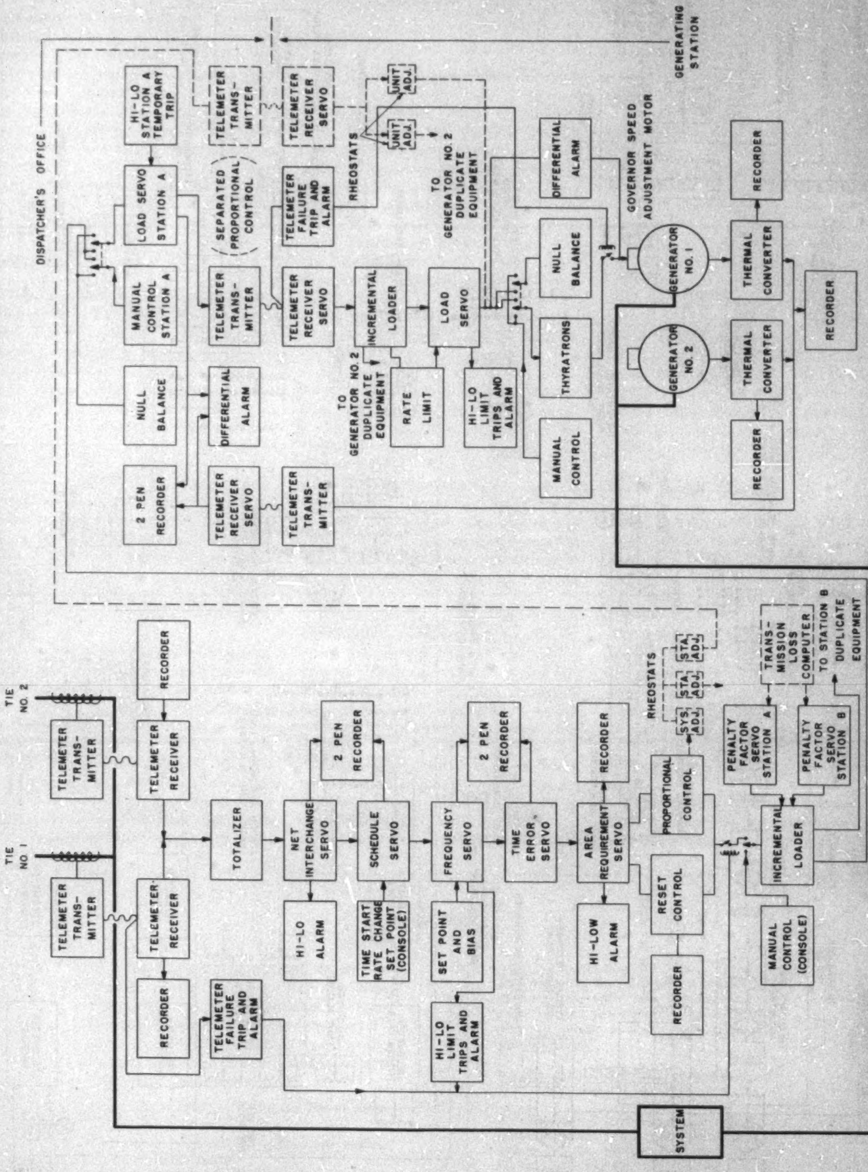
DISPATCHER'S OFFICE
GENERATING STATION
HI-LO STATION A TEMPORARY TRIP
LOAD SERVO STATION A
MANUAL CONTROL STATION A
NULL BALANCE
2 PEN RECORDER
TELEMETER TRANS-MITTER
(SEPARATED PROPORTIONAL CONTROL)
TELEMETER TRANS-MITTER
DIFFERENTIAL ALARM
TELEMETER RECEIVER SERVO
TELEMETER RECEIVER SERVO
TELEMETER FAILURE TRIP AND ALARM
TELEMETER RECEIVER SERVO
TELEMETER TRANS-MITTER
RHEOSTATS
UNIT ADJ.
UNIT ADJ.
TO GENERATOR NO. 2 DUPLICATE EQUIPMENT
INCREMENTAL LOADER
TO GENERATOR NO. 2 DUPLICATE EQUIPMENT
RATE LIMIT
LOAD SERVO
HI-LO LIMIT TRIPS AND ALARM
DIFFERENTIAL ALARM
NULL BALANCE
THYRATRONS
MANUAL CONTROL
GOVERNOR SPEED ADJUSTMENT MOTOR
GENERATOR NO. 1
GENERATOR NO. 2
RECORDER
THERMAL CONVERTER
THERMAL CONVERTER
RECORDER
RECORDER
TIE NO. 2
TIE NO. 1
TELEMETER TRANS-MITTER
TELEMETER RECEIVER
RECORDER
TELEMETER TRANS-MITTER
TELEMETER RECEIVER
RECORDER
TELEMETER FAILURE TRIP AND ALARM
TOTALIZER
NET INTERCHANGE SERVO
2 PEN RECORDER
HI-LO ALARM
SCHEDULE SERVO
TIME START RATE CHANGE SET POINT (CONSOLE)
FREQUENCY SERVO
2 PEN RECORDER
SET POINT AND BIAS
HI-LO LIMIT TRIPS AND ALARM
TIME ERROR SERVO
AREA REQUIREMENT SERVO
RECORDER
HI-LOW ALARM
PROPORTIONAL CONTROL
RESET CONTROL
RECORDER
RHEOSTATS
SYS ADJ
STA ADJ
STA ADJ
TRANS-MISSION LOSS COMPUTER
TO STATION B DUPLICATE EQUIPMENT
PENALTY FACTOR SERVO STATION A
PENALTY FACTOR SERVO STATION B
INCREMENTAL LOADER
MANUAL CONTROL (CONSOLE)
SYSTEM

Fig. 5. Block diagram

ment servo. Note that the slide wires in the frequency, time error, and net interchange bridges are actually retransmitting slide wires driven by the balancing motors in the frequency and net interchange measuring circuits respectively. Thus, the slide-wire position in each of the bridges is a continuous function of the system frequency, time error, and of net interchange (power transfer).

The slide wire in the net interchange servo forms a bridge with a slide wire in the schedule servo, which constitutes the set point to be held on net interchange. Similarly, the frequency servo slide wire and the frequency set point slide wire form another independently powered bridge. The voltage on the frequency bridge may be varied by the manual frequency bias adjustment. The frequency bridge is tied in series with the independently powered time error servo bridge, which uses a center tap resistor since no adjustable amount of time error is required.

Any deviation of the net interchange slide wire from its schedule results in an error signal which is applied to the area requirement servo. Similarly, any deviation of the frequency or time error slide wires from their set points results in an error signal which is also applied to the area requirement servo.

The area requirement servo is shown in Fig. 4 with its slide-wire center tapped. Since the net interchange and frequency and time error bridges respond separately to their respective variables and apply separate error signals to the area requirement servo, the servo is able to compute the algebraic sum of the error signals and provide an output to the controller proportional to this sum. Thus, any combination of error signals will provide a positive or negative area requirement output; if the signals are equal and opposite in polarity, they cancel and the area requirement output is zero.

The control circuit includes a proportional bridge, a reset servo, and a control servo. The proportional and reset slide wires are each powered by an adjustable voltage which provides proportional band and reset rate adjustments. Primary reset rate adjustment, however, is accomplished by changing the gear ratio of the reset servo motor, since large voltage reductions would result in loss of sensitivity. Note that the retransmitting slide wires going to the proportional bridge and the reset servo are driven by the area requirement servo balancing motor, and that the reset slide wire is tied through the proportional slide wire to an amplifier which actuates a motor that drives the control servo slide wire. Although the proportional and reset slide wires are driven simultaneously in the same direction, the effect of the reset servo upon the control servo is negligible except in the case of sustained load swings.

Thus, if the area requirement servo should swing off zero and then back to zero quickly, the control servo slide wire will move rapidly in the same direction and then return to approximately its original position. The reset slide wire would not have had the time to move from its position by a significant amount. All generators in the control system, since they follow the control systems rigidly, would increase the generation to take care of the sudden load swing and then return to their original output.

In the case of a sustained load swing, the proportional slide wire swings off zero and the generators increase output accordingly; at the same time, the reset servo continues to drift its slide wire to compensate for the sustained load change. As the reset slide wire drifts, the area requirement servo moves in the direction of zero, and the proportional slide wire returns to zero. When the area requirement servo is once more at zero, the reset control slide wire is at a new position to satisfy the increased system load.

Since both proportional band and reset rate are adjustable, the controller can be tuned to the system to provide a comparatively smooth operating curve when a flat tie line or frequency or a tie line with frequency bias is being held. The adjustments are not critical and can be backed off considerably when the point of minimum excursion of the area requirement circuit, bordering on instability, is found. The area requirement circuit will still have negligible excursion and the adjustments will then be satisfactory for all system conditions.

The combined proportional and reset signals are applied, through the control servo slide wire, to the incremental loader. Since the combined signal is apportioned by the incremental loader according to the predetermined loading or heat rate curves, any station with a flat segment of loading curve will not receive a change of control signal for that segment. This is not a great disadvantage in a system that has sufficient generating units and capacity to compensate for the loss of proportional action from one station with a constant output for a flat segment. In the case of smaller systems, the disadvantage is offset by the fact that the station incremental loading curve can be compromised to add sufficient slope to the station with the flat segment, so that this station will receive a proportional signal at all times. Furthermore, a control system using such a compromise curve can send out the combined signal on one telemetering channel. On the other hand, a control system using a split signal requires two telemetering channels. Also, a theoretically flat incremental load curve which is continually forced off its theoretical value by a proportional signal that is directly transmitted has no better economy factor than a compromised curve.

The present control system provides for either method of control. By a simple

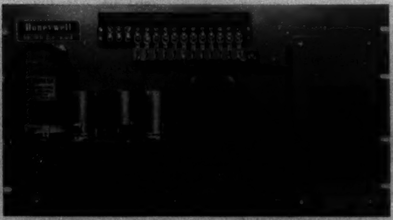

Fig. 6 (left). Electronic alarm unit

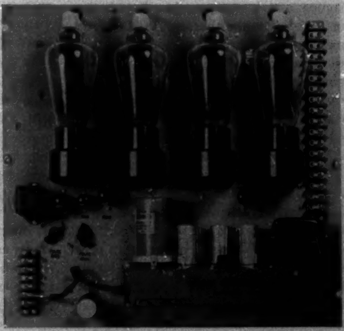

Fig. 7 (right). Thyratron relay

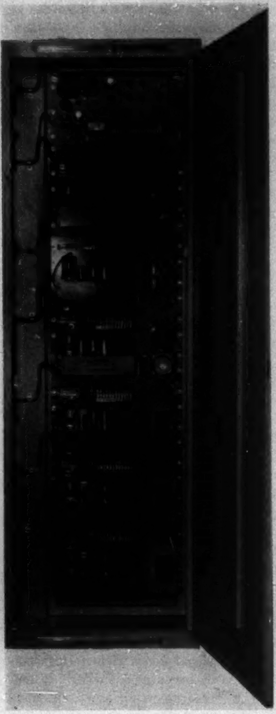

Fig. 8. Relay rack with servos

modification, as is shown by the dashed lines on the schematic, it is possible to separate the proportional control signal from the reset control signal. The proportional signal is then sent through a separate telemetering channel to each station and is then combined with the reset signal on the thyratron side of each unit load servo through the station proportional servo and the individual unit proportional band rheostats. In this system, the reset control signal alone drives the control servo slide wire and the incremental loader settings will not affect proportional band adjustments.

The incremental loader operates as follows: The incremental loader slide wire is tapped, and the segmental resistance values between taps can be adjusted from the dispatcher's console by means of percentage calibrated dials to vary the break points and slopes in the load curves for each station. For example, if the total resistance of both the control servo slide wire and the incremental loader slide wire is 100 ohms, the tapped slide wire can be adjusted so that 80 per cent (%) of its length has a resistance of 10 ohms, and 20% has a resistance of 90 ohms. A 10% full-scale movement of the control servo slide wire therefore would cause the incremental loader slide wire and the ganged slope slide wires to move 80% of full scale. In a system with five break points, if the incremental curves of the stations fluctuate greatly over 10% of the curve and are relatively flat over 90%, four break points may be set within the fluctuating 10% portion and one break point is used to set off the 90% straight line portion.

The other tapped slide wires ganged to the incremental loader slide wire each adjust the slope of a station curve and drive a station load servo. Note that the slope adjustment slide wires and the load servo slide wires each have independent voltage sources, and that the voltage source on a slope slide wire can be adjusted by a transmission-loss computer slide wire. This adjustable voltage is directly proportional to a penalty factor, since a varying voltage applied in this manner effectively multiplies. This combination of penalty factor and incremental loading could result in completely automatic transmission loss and heat loss control for a central power system when an automatic transmission-loss penalty factor computer is available.

The separate telemetering signals are received at each station by a telemeter receiver in combination with a servo whose slide wire is in a bridge circuit of the receiver. The telemetered signal is thus translated to a slide-wire position. Another slide wire on this servo drives a station incremental loader, which has one break point setting slide wire and one slope setting slide wire for each generator in the station. Each slope setting slide wire is tied into a bridge circuit with a load servo, instead of being independently powered as are the system slope setting slide wires.

The load servo, in turn, has one of its slide wires arranged in a follower circuit with a slide wire on the speed adjustment motor of the generator governor. Any unbalance of this bridge is sensed by an amplifier which actuates thyratrons to supply power to drive the speed adjustment reversible d-c motor. A load servo is interposed between the incremental loader and the governor speed adjustment slide wire so that only one slide wire need be mounted at the generator governor. If the governor speed adjustment position is sufficiently nonlinear with respect to the kilowatt output of the generator, the load servo slide wire, which drives the speed adjustment motor, may be tapped to function linearly; no adjustment is required on the governor mechanism.

Fig. 9. Relay rack with alarm units and thyratron relays

Alarm Circuitry

The load servo also includes slide wires for high-low alarm limits and for differential alarm limits. The differential alarm amplifier is located in a bridge circuit between the governor slide wire and one of the isolated slide wires on the load servo. If the governor motor does not operate within an adjustable band limit, the differential alarm amplifier senses the deviation and pulls in its relays.

A separate slide wire on the load servo is used to limit the rate of change of the generator. This slide wire is independently powered and is connected in series to a capacitor and adjustable resistance; an amplifier is provided to sense the voltage drop across the adjustable resistance. If the load servo is driven too far too fast, the surge of direct current through the capacitor and resistance is sensed by the amplifier, which pulls in its relays. If the load servo is driven very fast for only a small distance, the voltage will not allow sufficient current to pass through the capacitor to energize the amplifier. If the load servo is driven slowly for a long period of time, the rate of change of voltage across the capacitor will be such that only a small current will pass through the resistor, again not enough to energize the amplifier. The resistor can thus be adjusted to set the rate limit required for each generator. The relays of the rate limit amplifier can also be connected to an adjustable timer which will open the load servo driving motor and hold it open long enough to allow the boilers to settle down. The timer will then close the circuit to the load servo driving motor, placing the unit again under normal control.

Feedback for Monitoring Purposes

The output of all the generators in the station is summed up in a signal which is transmitted through a telemetering transmitter to a telemeter receiver in the load dispatcher's office. The signal drives a slide wire in a load servo, which in turn positions the second pen of a 2-pen recorder. The first pen of this recorder is used to record the station command signal. The total station output servo also drives another slide wire which forms a differential alarm bridge with a station command servo slide wire. If the station total load does not follow the station command signal within adjustable differential limits, as set by the dispatcher, an alarm is sounded. A block diagram is shown in Fig. 5.

Placing the System in Operation

The method for placing the control system in operation with no units on control is relatively simple. The dispatcher sets all the loading curves and break points into the incremental loader. He places his incremental loader on manual control, and adjusts it to the approximate point that he believes will balance the present system load. He instructs the station operator of the first station to be placed on control to place his units on automatic control. The station operator will have already set the loading curves and break points into the incremental loader for the station; transfer switches on the console will be turned to the OFF position. The operator merely turns the transfer switch of the first unit to come on control to automatic; the rate at which the unit moves is determined by an interrupter that was adjusted at the time of system installation. The unit moves to the position dictated by the incremental loader, at which time it is switches to the incremental loader; the interrupter will be taken out of the circuit and the unit is now on control.

This operation is repeated for all units within the station and for all stations within the system. When the entire system is on manual control, the dispatcher moves his system incremental loader manually by push button until the area requirement recorder reads zero, at which time he turns his transfer switch to automatic, placing the incremental loader on the controller. The system is now on automatic control.

Should an operator desire to remove a unit from control, he turns the manual dial of that unit to the desired load and moves the transfer switch of that unit to manual. The unit is removed from the station incremental loader, and will again, through an interrupter circuit, travel to the desired load at the proper rate of load change. If the station operator desires to operate the units without thyratrons, he turns the transfer switch to the OFF position, and then the units can be controlled by means of the conventional speed adjustment switch supplied by the turbine manufacturer.

Fig. 6 shows the electronic alarm unit, Fig. 7 the thyratron relay. Fig. 8 shows the relay rack with servos, Fig. 9 the relay rack with alarm units and thyratron relays.

References

1. Techniques in ndling Load-Regulating Problems on Interconnected Power Systems, C. Nichols. *AIEE Transactions*, vol. 72, pt. III, June 1953, pp. 447–60.

2. Area-Wide Generation Control, Nathan Cohn. *Electric Light and Power*, Chicago, Ill., vol. 31, June 1953, p. 167; July 1953, p. 97; Aug. 10, 1953, p. 77.

3. Design and Operation of System-Wide Automatic Load-Frequency Control, H. A. Bauman, C. N. Metcalf, J. G. Noest, J. B. Carolus. *AIEE Transactions*, vol. 73, pt. III, Oct. 1954, pp. 1312–19.

4. Principles of Industrial Process Control (book), D. P. Eckman. John Wiley and Sons, Inc., New York, N. Y., 1945.

A Study of Carrier-Frequency Noise on Power Lines

Part IV. Conclusion of Field Measurements

J. D. MOYNIHAN
MEMBER AIEE

B. J. SPARLIN
MEMBER AIEE

THIS is the final paper of a series. The first paper[1] dealt with the theoretical considerations preliminary to any field tests and the consideration of measuring techniques. The second and third papers[2,3] dealt with the results and interpretation of field measurements that had been made. This paper deals with the field measurements that have been made since the last paper, and rounds out the coverage of all of the presently used transmission voltage classes. This paper also includes the determination of the change in power-line noise as a function of bandwidth.

Correction for Bandwidth

The effect of bandwidth on the magnitude of noise present at the detector was discussed in parts I and III. Part I of this study showed that the response of a noise meter to impulse noise was affected as follows

$$E_{av}=2mA_0G_0 \tag{1}$$

where

m = repetition rate of impulses
A_0 = volt-time area of impulse
G_0 = mid-band gain of noise meter

This indicates that the average value of

Paper 55-458, recommended by the AIEE Carrier Current Committee and approved by the AIEE Committee on Technical Operations for presentation at the AIEE Summer General Meeting, Swampscott, Mass., June 27–July 1, 1955. Manuscript submitted February 16, 1955; made available for printing April 20, 1955.

J. D. Moynihan was with the Westinghouse Electric Corporation, East Pittsburgh, Pa., at the time the paper was written, and is now with the Sprague Electric Company, North Adams, Mass. B. J. Sparlin is with the Westinghouse Electric Corporation, East Pittsburgh, Pa.

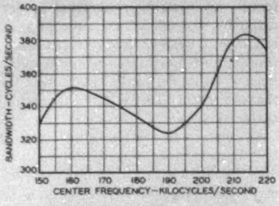

Fig. 1. Bandwidth versus center frequency of narrow bandwidth receiver used to determine bandwidth correction factor

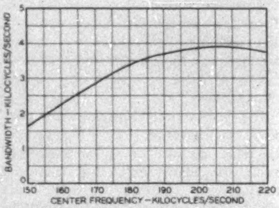

Fig. 2. Bandwidth versus center frequency of wide bandwidth receiver used to determine bandwidth correction factor

impulse noise is independent of bandwidth.

$$E_{\max}=2\sqrt{2}\,A_0G_0B_0 \tag{2}$$

where B_0 is the bandwidth of the noise meter. Therefore, the peak value of impulse noise will be directly proportional to the bandwidth.

Part I also showed that the average and peak values of the response of a noise meter to random noise was proportional to the square root of the bandwidth. Therefore, considering the average value of noise, the response will vary from

$$E_{av}=K_1B_0^{1/2} \tag{3}$$

for random noise to

$$E_{av}=K_2B_0^{0} \tag{4}$$

for impulse noise where K_1 and K_2 are constants. It therefore appears that the response of a noise meter to a combination of random and impulse noise will be

$$E_{av}=K_3B_0^{\alpha} \tag{5}$$

where α is between 0 and 1/2.

Considering the peak value of noise to be measured, it was shown in part I that the peak value response of a noise meter for random noise is

$$E_{\max}=K_4B_0^{1/2} \tag{6}$$

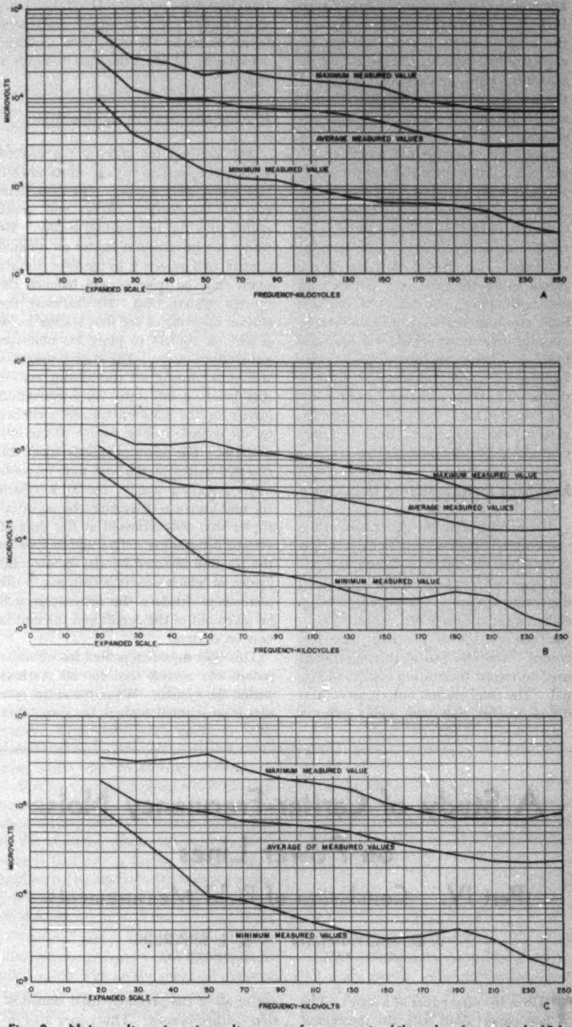

Fig. 3. Noise voltage in microvolts versus frequency in kilocycles for typical 69-kv class of lines

A. Average noise values
B. Quasi-peak noise values
C. Peak noise values

This subcaption also applies to Figs. 4 through 7

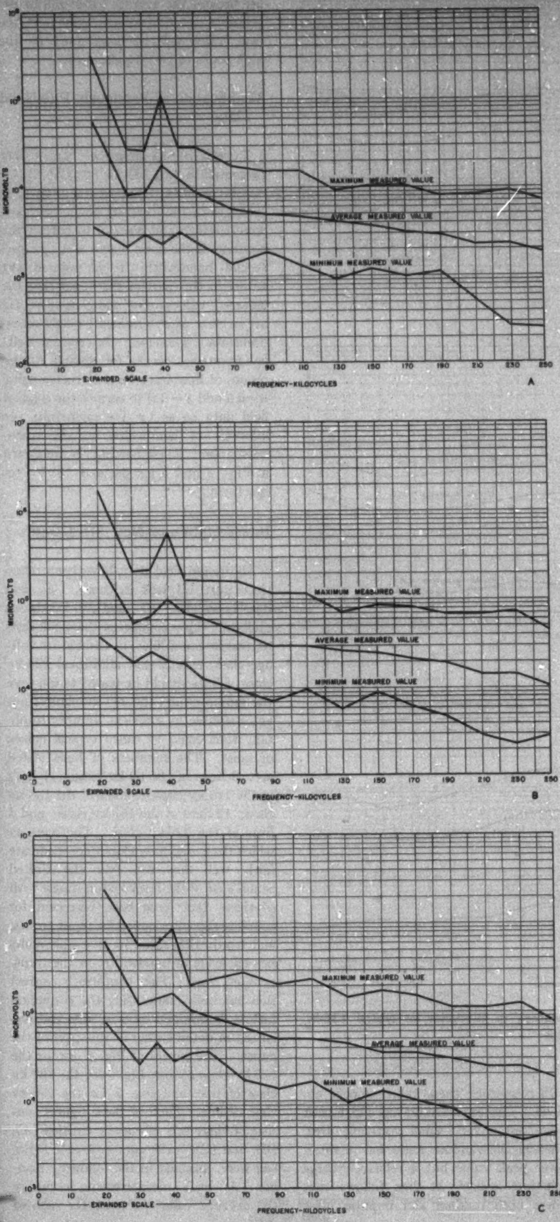

Fig. 4. Noise voltage in microvolts versus frequency in kilocycles for typical 110-kv class of lines

and the peak value response of a noise meter for impulse noise is

$$E_{max}=K_5B_0^{1} \tag{7}$$

where K_4 and K_5 are again constants of proportionality.

When the noise existing on a power line is measured, the bandwidth power will be between 1/2 and 1 because of the combination of random and impulse noise. Thus the peak value of response will be

$$E_{max}=K_6B_0^{\beta} \tag{8}$$

where β is between 1/2 and 1.

In part III, α was assumed to be 1/4 and β was assumed to be 3/4. Using these two factors, all of the data presented in part III had been corrected to a 1-kc-per-second bandwidth.

Since part III was written field tests have been conducted to determine typical values of α and β. The method used was to measure the average and peak values of noise with equipment of widely varying bandwidth. A Stoddart model *NM-10-A* noise meter, which has a frequency range of 15 to 250 kc per second, was used for the narrow bandwidth receiver. A Stoddart model *NM-20-B* noise meter, which has a frequency range of 150 kc per second to 25 megacycles per second, was used for the wide bandwidth receiver. Since the two noise meters overlap in frequency coverage, from 150 to 250 kc per second, this appeared to be an acceptable solution to the problem. Both meters are capable of measuring both average and peak values of noise. The bandwidth, from 150 to 220 kc per second, of the Stoddart *NM-10-A* which was used, as a function of frequency, is shown in Fig. 1. Fig. 2 shows the same information for the Stoddart *NM-20-B*. The field tests were conducted in substations on existing coupling capacitors. The inputs of the two meters were connected in parallel and a signal generator was used to calibrate the meters at each frequency of measurement. After calibration, the meters were connected across the drain coil of the coupling capacitor and the average and peak values of noise were measured with both meters. From these measurements, the value of α and β were determined by substituting in equations 5 and 8 and solving simultaneously. Thus

$$\alpha=\log_e\frac{(E_{\text{av wide band}})(B_{\text{narrow band}})}{(E_{\text{av narrow band}})(B_{\text{wide band}})}$$

$$\beta=\log_e\frac{(E_{pk\text{ wide band}})(B_{\text{narrow band}})}{(E_{pk\text{ narrow band}})(B_{\text{wide band}})}$$

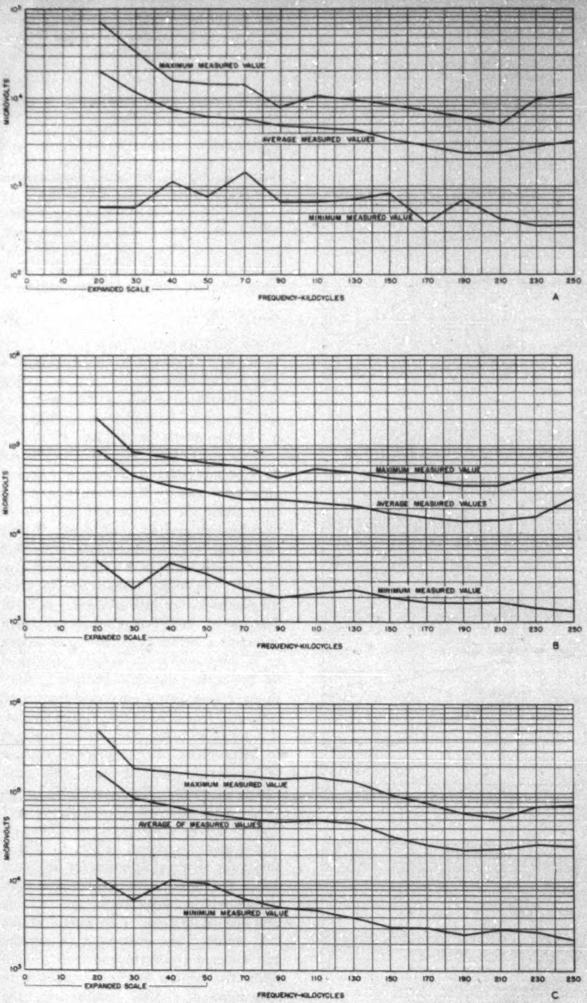

Fig. 5. Noise voltage in microvolts versus frequency in kilocycles for typical 138-kv class of lines

where

E_{av} = measured value of average noise
E_{pk} = measured value of peak noise
B = bandwidth, cycles per second

From the measurements made, it was determined that, for all application purposes, α could be taken as 0.5 and β as 1.0.

In retrospect, these values appear obvious. The impulse noise has a high peak value but a very small volt-time area, whereas the random noise has a much lower peak value but a relatively large volt-time area.[4,5] It then follows that where both random and impulse noise are present the average value will be determined by the random noise and the peak value will be determined by the high peaks of the impulse noise.

Modification of Previously Published Data

Typical voltage-frequency curves were presented in part III for 69- and 138-kv classes of lines. It was stated at that time, that the correction factors used were $\alpha=0.25$ and $\beta=0.75$ to correct the readings of the noise meter to a 1-kc-per-second bandwidth. It is pointed out earlier in this part of the paper that the assumed values of α and β in part III are in error as determined by field measurements. Therefore, the typical voltage-frequency curves for 69-and 138-kv classes of lines have been corrected using $\alpha=0.5$ and $\beta=1.0$ to correct the original field data so as to give microvolts per kilocycle of bandwidth on the transmission line. These new curves are shown in Figs. 3 and 5 for 69- and 138-kv respectively.

Interpretation of New Field Data

Additional field data have been taken since part III was written. This field data is on 115-, 161-, and 230-kv classes of lines. This completes the field tests on transmission lines, as defined by voltage class, except that additional 220-kv class of lines should be tested to improve the sampling and the 345-kv class is not yet available in sufficient number to obtain what could be called typical values of noise. The numbers of lines tested are: 9 lines of the 69-kv class; 11 lines of the 110-kv class; 8 lines of the 138-kv class; 12 lines of the 161-kv class; and 3 lines of the 220-kv class. The lines on which these measurements were made are fairly well dispersed over the United States east of the Rocky Mountains. All of these data have been corrected for coupling capacitor networks, input probes, and bandwidth so as to give microvolts per kilocycle of bandwidth on the transmission lines. The bandwidth correction has been made using the correction factors determined by field tests and discussed in detail earlier in this part of the paper. The curves of Fig. 4 are for the 115-kv class of line, Fig. 6 for the 161-kv class of line, and Fig. 7 for the 230-kv class of line. Each of these figures consists of three sets of curves, entitled (A), (B), and (C). The curves of each figure (A) were obtained in the following manner. At each measurement frequency the average values of noise for each of

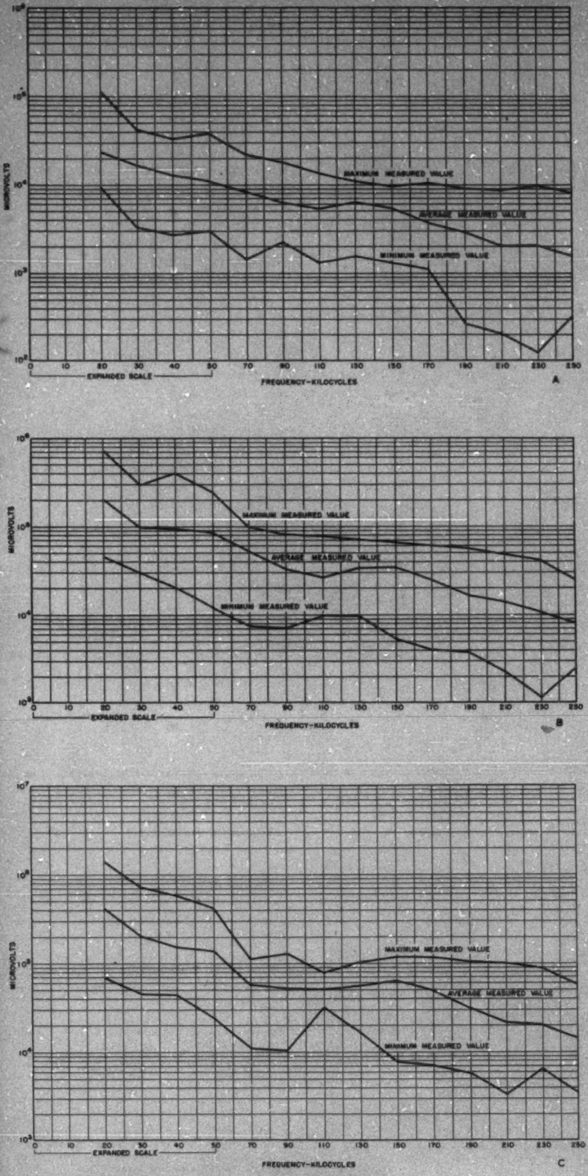

Fig. 6. Noise voltage in microvolts versus frequency in kilocycles for typical 161-kv class of lines

the individual tests on that class of line were averaged together. The maximum and minimum measured values were also recorded. Then these were plotted as a function of frequency as a family of curves subtitled (A) for each voltage class. The same was done for quasi-peak values of noise on each class of line and plotted as a family of curves titled (B). The family of curves subtitled (C) are for the peak values of noise.

A detailed explanation of Fig. 4(A) will apply to Figs. 3 through 7 except for the differences in voltage class and whether the noise value under consideration is average, quasi-peak, or peak. The curves for the average value of noise existing on 115-kv class transmission lines were collected. At each frequency for each line, the corrected average value of noise was read and recorded. From this, the average of all of the values at one frequency was determined and also the maximum and minimum values occurring at that frequency were recorded. After this had been done for all of the lines in the 115-kv, Fig. 4(A) was plotted. The maximum and minimum curve on this figure is a composite of all of the lines. One line may contribute the maximum value read at one frequency and the minimum value read at another frequency. Thus, all average measurements on all lines of this voltage class that were studied fell on or between the maximum and minimum curves shown. As was pointed out in part III of this paper, but it is believed worth repeating here, the wide separation between the maximum and minimum measured values might lead one to feel that the noise level cannot be tied down to a reasonably close figure. The authors feel that this conclusion is not correct as will be pointed out.

Since noise is essentially a constant-current function[5] instead of a constant voltage function, the impedance across which the measurements are made will determine the magnitude of noise voltage. Even though transmission-line theory[6] shows that the impedance can approach infinity for a single line under the proper termination, the impedance across which the measurements are made will be of about 200 ohms or less because of multiple lines and/or power equipment at the point of measurement. Therefore, the maximum impedance will not be much more than the average taken for a large number of lines. On the other hand, if one line or piece of equipment presents a low impedance at the measuring point, the impedance will be low irrespective of the other lines or equipment because all the lines and equipment are in parallel.

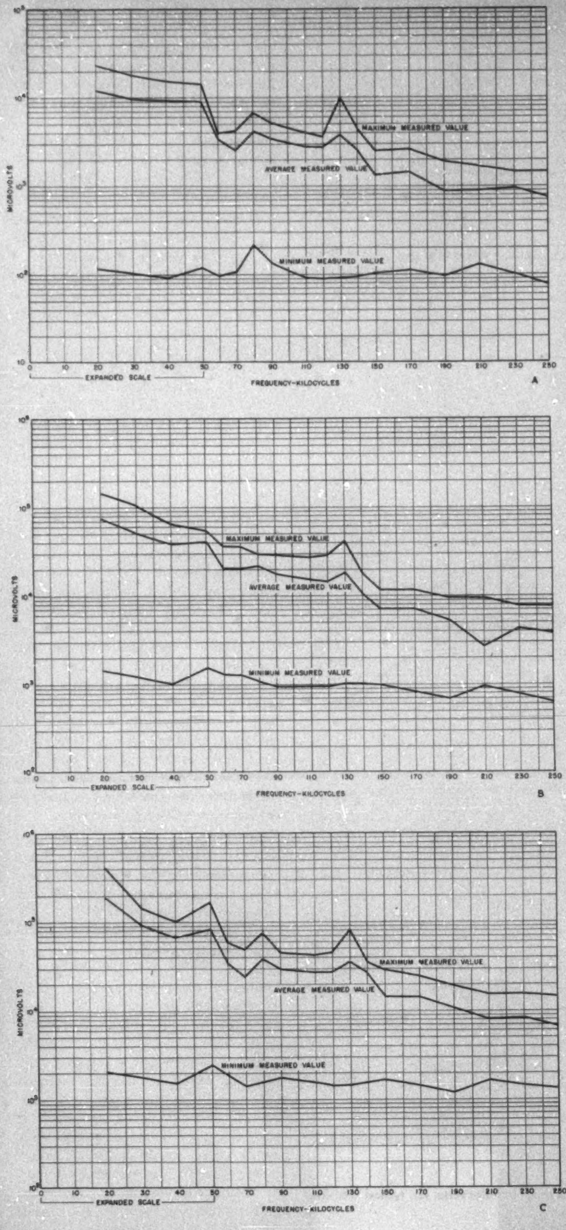

Fig. 7. Noise voltage in microvolts versus frequency in kilocycles for typical 220-kv class of lines

Since this effect occurs only at certain frequencies at a given measuring point, the noise versus frequency curves will have dips or valleys in them. It is the composite of all these dips or valleys that makes up the minimum-voltage curve as shown in Figs. 3 through 7.

All of the measurements that were used in obtaining these typical voltage-frequency curves were made on nonstorm days. Therefore, it is felt by the authors that these curves are typical values that might reasonably be expected on a transmission system on nonstorm days.

As might be expected with a finite number of test samples, the curves are not smooth; however, if a smooth curve were drawn using the curves presented as a guide, the noise would vary inversely with the frequency. This has been shown to be the theoretical case which has been verified by many measurements.

Conclusions

The conclusions which can be drawn are as follows:

1. Field tests show that the peak value of noise is proportional to bandwidth.
2. Analytical investigations have shown that quasi-peak values vary the same as peak values with changes in bandwidth.
3. Field tests show that the average value of noise is proportional to the square root of bandwidth.
4. Field tests verify the theoretical conclusion that noise varies inversely with the frequency.
5. Accompanying curves show the value of noise to be of the same order of magnitude for all voltage classes tested.

References

1. A Study of Carrier-Frequency Noise on Power Lines. Part I—Theoretical Considerations and Measuring Techniques, **R. C. Cheek, J. D. Moynihan.** *AIEE Transactions*, vol. 70, pt. II, 1951, pp. 1127–34.

2. Part II—Results of Field Measurements. *Ibid.*, pp. 1325–34.

3. Part III—Interpretation of Field Measurements, **J. D. Moynihan, B. J. Sparlin.** *Ibid.*, vol. 72, pt. III, June 1953, pp. 573–81.

4. Radio Influence Tests in Field and Laboratory—500-Kv Test Project of the American Gas and Electric Company, **G. D. Lippert, W. E. Pakala, S. C. Bartlett, C. D. Fahrnkopf.** *Ibid.*, vol. 70, pt. I, 1951, pp. 251–69.

5. Instruments and Methods of Measuring Radio Noise, **C. V. Aggers, Dudley E. Foster, C. S. Young.** *AIEE Transactions (Electrical Engineering)*, vol. 59, Mar. 1940, pp. 178–92.

6. Communication Engineering (book), **W. L. Everitt.** McGraw-Hill Book Company, Inc., New York, N. Y., 2nd ed., 1937.

Grounding Grids for High-Voltage Stations. II—Resistance of Large Rectangular Plates

ERIC T. B. GROSS
FELLOW AIEE

RICHARD B. WISE
NONMEMBER AIEE

A PREVIOUS paper[1] dealt with the calculation of the resistance of square grounding mats used in high-voltage stations. Such grounding mats are installed where rocky soil makes other grounding methods unworkable. The term mat applies to a system of conductors buried in a crisscross fashion parallel to earth and at a depth of 1 to 2 feet below its surface. The larger the number of meshes, the lower is the grounding resistance; the optimal condition being attained for a buried flat plate.

The buried plate is not a practical or economical solution of the problem. However, in any calculations concerning the resistance of a rectangular grid, it is necessary to know the values for a plate of corresponding size since the plate is the limiting case of the mesh system.

Data are available for the resistance of square grounding grids for different numbers of meshes.[1] The results of this investigation serve as a check of previous calculations, and provide data for the investigation of rectangular grids.

Grounding resistance is defined as the resistance between one electrode system in ground and another grounding electrode at infinite spacing. For a known value of resistivity of earth, ρ, this resistance to ground has been shown to be equal to $\rho/(2\pi C)$ where C is the combined capacitance of the grounding electrode system and of its image with respect to the surface of earth.

The computation of the grounding resistance of a rectangular plate therefore resolves itself into that of the calculation of a capacitance. Such capacitance calculations of rectangular plates have been attempted, but they were not rigorous attacks[2] or they involved some oversimplifying assumptions in their formulation.[3] This investigation attempts to verify the accuracy of some of the known results through the use of a somewhat modified method of calculation. In addition, the influence of the depth of the grounding plate is evaluated.

Whenever expedient, all computations were performed on the electronic digital computer located at the Computer Center at the Armour Research Foundation of Illinois Institute of Technology. Eight significant digits were used throughout all computations, and because of ease of programming checks throughout the solution, the occurrence of errors is virtually eliminated.

Calculation of Capacitance of Square Plate

Review of Method of Subareas

An approximate method of calculation, Maxwell's "method of subareas," is used throughout this investigation. The essential theory involves the division of the electrode system carrying electric charge into n subareas A_i $(i=1, 2, \ldots, n)$, each of which is considered as carrying a charge density q_i $(i=1, 2, \ldots, n)$ and has the following characteristics:

1. Such small area that q_i is essentially constant.
2. Such small dimensions that the potential V_{ij} produced by the charge on A_i over the area occupied by A_j is essentially constant and may be chosen to calculate the potential of A_j because of the charge on A_i. Similarly the potential V_{ii} produced by q_i over A_i itself is constant.

Since the potential V_{ij}, produced on A_j by the constant charge density q_i on A_i, is proportional to q_i

$$V_{ij}=K_{ij}q_i$$

and the total potential

$$V_j=\sum_{i=1}^{n} V_{ij}=\sum_{i=1}^{n} K_{ij}q_i;\ (i=1,2,\ldots,n)$$

Since the charges are in equilibrium over this charged conducting electrode system, the potential is constant everywhere on it, therefore

$$V_0=\sum_{i=1}^{n} K_{ij}q_i$$

or

$$\sum_{i=1}^{n} K_{ij}\frac{q_i}{V_0}=1$$

where V_0 is the potential of the electrode system.

The capacitance C is given by

$$C=\frac{Q}{V_0}=\sum_{i=1}^{n} A_i\frac{q_i}{V_0}$$

where Q is the total charge of the electrode system.

Thus, the problem consists of the evaluation of $(n+1)$ linear equations in the $(n+1)$ variables, q_i/V_0 $(i=1, 2, \ldots, n)$ and C.

Obviously, the finer the subdivision, the more accurate are the results. However, the labor necessary for determination of the K_{ij} values and for the solution of a set of linear algebraic equations increases considerably as n becomes larger.

Evaluation of Coefficients K_{ij}

Since the most expeditious form of the subareas used in both rectangular and

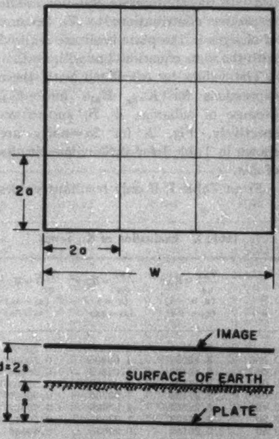

Fig. 1. Buried plate with 18 subareas

Paper 55-281, recommended by the AIEE Substations Committee and approved by the AIEE Committee on Technical Operations for presentation at the AIEE Middle Eastern District Meeting, Columbus, Ohio, May 4–6, 1955. Manuscript submitted January 24, 1955; made available for printing March 7, 1955.

Eric T. B. Gross is with the Illinois Institute of Technology, Chicago, Ill., and Richard B. Wise is with the Armour Research Foundation of the Illinois Institute of Technology, Chicago, Ill.

The authors wish to express thanks to the Armour Research Foundation of Illinois Institute of Technology for making available the facilities of the Computer Center in the performance of the computations made in this study. The International Business Machines Corporation card programmed calculator (CPC) made possible much more accurate computation than has been previously feasible.

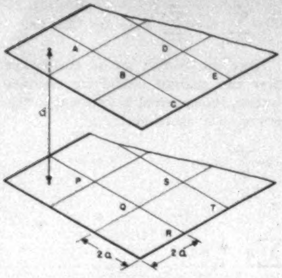

Fig. 2. Plate and image

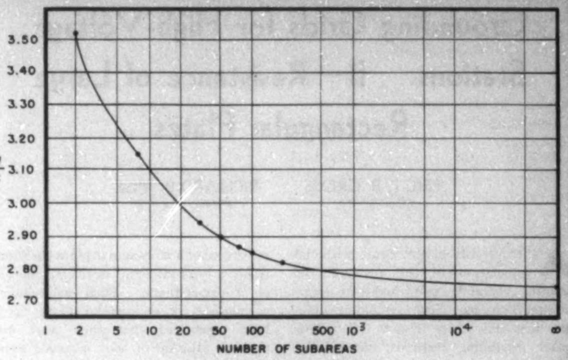

Fig. 3. Effect of number of subareas

square plate calculations is that of a square, square-shaped subareas of side $2a$ centimeters are assumed throughout. A typical configuration is shown in Fig. 1.

The potential V_P existing at the center of subarea P, Fig. 2, is comprised of that contributed by the charge q_P upon subarea P plus that contributed by all other subareas in the plate and its image with respect to the surface of earth.

Expressions are derived in Appendixes I, II, and III for the K_{ij} values needed in the determination of the individual potential contributions. The result is expressed in terms of the distance d between the plate and its image and a, half the length of a subarea side. Thus, the contributions to the potential V_P, Fig. 2, because of the charge of each subarea in the image, would be obtained by substituting the appropriate value of d/a into the appropriate equation. The respective contributions to V_P because of charges in the plate itself are realized with the same equations but with $d=0$.

The values as calculated with these expressions for K_{AP}, K_{BP}, and K_{CP} because of subareas A, B, and C respectively, Fig. 2, for $2a$=unity are shown in Table I for various magnitudes of d/a.

From Table I, if only resultant values for d/a ranging below 0.20 are considered (since, practically speaking, this is the highest value necessary for grounding grid applications), a number of observations may be made:

1. The major contribution to V_P, as is further evidenced in the sample problem Appendix IV, is from K_{PP} and K_{AP}, i.e., from subarea P and its own image.
2. The value of K_{BP} varies from 1.031 to 1.038 as the distance between plates is varied. These values differ by less than 0.7 per cent (%).
3. The reciprocal of the distance between centers of subareas P and R is 0.500. This value differs from the calculated 0.505 for K_{CP} for any value of d by 1.0%.

Accordingly, various simplifying assumptions may now be made:

1. The effects of changes in d/a need be taken into consideration only for the determination of K_{AP}.
2. If the distance between centers of subarea P and another subarea j is greater than $2a$, then K_{jP} may be approximated as $2a/r$, regardless of the value of d, where r is this distance between centers as measured on the face of the plate.
3. Taking into account the previous two assumptions, the coefficient for every subarea in the plate may now be combined with that of its respective image, defining a new coefficient. That is, set $K_{jP}' = 2K_{jP}$ $(j \neq P)$ and $K_{PP}' = K_{PP} + K_{AP}$.

Because of symmetry, some subareas in a rectangular or square plate calculation would carry the same charge density. Therefore, all subareas of equal charge density are denoted by the same letter (a, b, c, ...) and numerical subscripts are used to distinguish them. Also, by virtue of geometric symmetry of the plate, the mutual coefficients K_{ij}' and K_{ji}' are proportional, with the constant of proportionality being the ratio of the number of subareas of densities q_i and q_j.

Because subareas of side $2a$ cm are assumed, a computation will actually yield the values of $C/2a$ with C in electrostatic units (esu) or cm and $q_i/(2aV_0)$ $(i=1, 2, \ldots, n)$ also in esu. For the computation of resistance values, the reciprocal of C is used. Therefore, for a square of side W, results are tabulated for W/C. Thus, if the resistivity ρ is expressed in ohm-cm, the total resistance is given by

$$R = \frac{\rho}{2\pi C} \text{ ohms}$$

EFFECT OF NUMBER OF SUBAREAS

The first requirement for establishing the method involved the determination of the minimum value of n necessary for an accurate solution. This was accomplished by repeatedly solving for the capacitance of a square of side W cm, dividing it into more and more smaller and smaller subareas.

Beginning with $n=2$, the calculations were proceeded until the results began to level off at $n=72$. The resultant W/C for $n=72$ was 2.865. Although this

Table I. Evaluation of K_{ij} Terms

$\frac{d}{a}$	$\frac{V_{AP}}{q_A} = K_{AP}$ $(x_1 = -a)$ $(x_2 = +a)$	$\frac{V_{BP}}{q_B} = K_{BP}$ $(x_1 = a)$ $(x_2 = 3a)$	$\frac{V_{CP}}{q_C} = K_{CP}$ $(x_1 = 3a)$ $(x_2 = 5a)$
0	3.52540	1.03805	0.50509
0.005	3.50982	1.03805	0.50509
0.01	3.49422	1.03803	0.50509
0.02	3.46323	1.03798	0.50509
0.05	3.37195	1.03760	0.50505
0.10	3.22545	1.03626	0.50492
0.20	2.95328	1.03095	0.50441
0.50	2.29158	0.99656	0.50086
1.00	1.58672	0.90148	0.48884

Table II. Effect of Number of Subareas Used in Computation for Square Plate at Zero Depth

No. of Subareas	$\frac{W}{C}$
2	3.5255
8	3.1533
18	3.0090
32	2.9373
50	2.8891
72	2.8654
98	2.8450
200	2.8084

A	B	C	D	E	E	D	C	B	A
B	F	G	H	I	I	H	G	F	B
C	G	J	K	L	L	K	J	G	C
D	H	K	M	N	N	M	K	H	D
E	I	L	N	O	O	N	L	I	E
E	I	L	N	O	O	N	L	I	E
D	H	K	M	N	N	M	K	H	D
C	G	J	K	L	L	K	J	G	C
B	F	G	H	I	I	H	G	F	B
A	B	C	D	E	E	D	C	B	A

Fig. 4 (above). Subdivision of square plate, 200 subareas

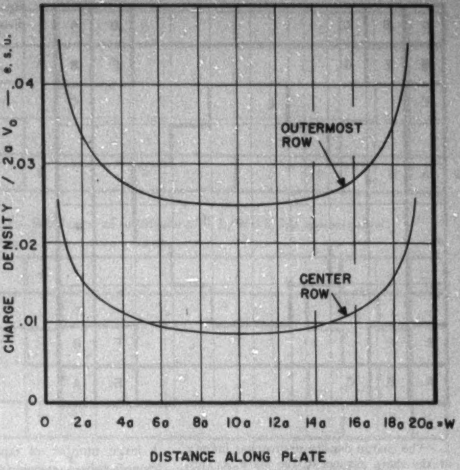

Fig. 5 (right). Charge distribution in square plate

value was only 0.8% less than the result of $W/C=2.889$ for $n=50$, it was felt that the 4.7% discrepancy between this result and the value of $W/C=2.735$ attained by Dwight,[4] using another method, merited further investigation.

Therefore the calculation was repeated for $n=98$ yielding a resultant W/C of 2.845, a further decrease of 0.7%. Since this calculation was extremely long and tedious, it was only after long deliberation that it was decided to continue to a higher value of n.

The last approximation assumed $n=200$ and resulted in $W/C=2.808$. As is evidenced by referring to Table II and the plot in Fig. 3, these results are continually decreasing, and if n is assumed to approach infinity, the value of W/C actually does seem to approach that offered by Dwight.[4]

This conclusion somewhat substantiates that offered by Reitan,[3] whose computations are similar to those of this paper. However, the effect of adjacent subareas was not taken into consideration by Reitan (i.e., K_{QP} in Fig. 2 was assumed as $2a/r$), resulting in lower values of W/C than computed here for the same values of n. His maximum number of subareas used was only 72(36).

The subdivisions used for the computation with $n=200$ are shown in Fig. 4. Because of symmetry, this calculation required the assumption of 15 different charge densities $q_a, \ldots, q_o$ and necessitated the solution of a system of 16 equations. Even with the aid of the automatic computer, the labor involved in the evaluation of these coefficients was tremendous.

Therefore, it is obvious that it would not be appropriate to consider values of n greater than 200. It may also be concluded that while this method is very convenient in the determination of capacitance for certain configurations, it does not lend itself very well to that of a solid plate because of its slow convergence. Thus, if the method is to be used at all, some further observations must be made to simplify the procedure.

SIMPLIFICATION OF PROCEDURE

Let us investigate the calculated charge distribution referring again to the calculation for $n=200$, with a square of side W cm. The resultant values of $q_a, \ldots, q_o$ refer to the charge densities at the centers of the corresponding subareas. Assume a plane intersecting the face of the plate perpendicularly along the center of a row of these subareas. A good approximation of the charge distribution along this row may be realized by plotting the value of charge density at the center of each subarea this plane crosses, and then joining these points with a smooth curve. Such curves are drawn in Fig. 5. The upper curve shows the calculated charge distribution along an outer row of subareas *a, b, c, d, e, e, d, c, b, a* and the lower curve shows the distribution along the center of the plate through subareas *e, i, l, n, o, o, n, l, i, e*. Curves for the charge distribution through other rows indicate similar relationships. From this figure, and from the values shown in Table III, a few observations may be made:

Table III. Results for Square Plate Assuming 200 Subareas

$\frac{d}{W}$	0	0.0005	0.0025	0.005	0.01
$q_a/2aV_0$	0.0452	0.0453	0.0459	0.0466	0.0479
$q_b/2aV_0$	0.0295	0.0296	0.0297	0.0299	0.0302
$q_c/2aV_0$	0.0272	0.0272	0.0274	0.0276	0.0281
$q_d/2aV_0$	0.0259	0.0260	0.0261	0.0264	0.0268
$q_e/2aV_0$	0.0254	0.0254	0.0256	0.0258	0.0263
$q_f/2aV_0$	0.0151	0.0150	0.0149	0.0148	0.0144
$q_g/2aV_0$	0.0134	0.0134	0.0133	0.0132	0.0130
$q_h/2aV_0$	0.0125	0.0125	0.0124	0.0123	0.0122
$q_i/2aV_0$	0.0122	0.0122	0.0121	0.0120	0.0118
$q_j/2aV_0$	0.0117	0.0117	0.0116	0.0116	0.0116
$q_k/2aV_0$	0.0108	0.0108	0.0108	0.0107	0.0107
$q_l/2aV_0$	0.0105	0.0105	0.0104	0.0104	0.0104
$q_m/2aV_0$	0.0099	0.0099	0.0099	0.0099	0.0098
$q_n/2aV_0$	0.0096	0.0096	0.0096	0.0095	0.0095
$q_o/2aV_0$	0.0093	0.0092	0.0092	0.0092	0.0092
W/C, esu	2.808	2.806	2.799	2.789	2.771
W/C, feet per centimeter (ft/cm)	0.09212	0.09206	0.09188	0.09150	0.09091

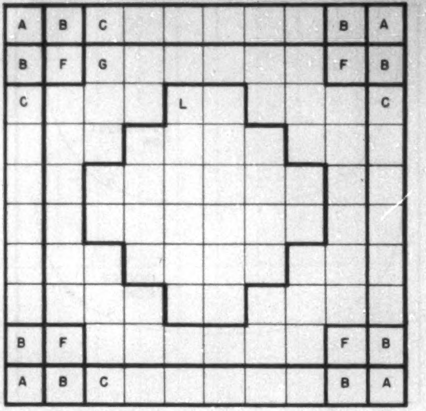

Fig. 6. Modified subdivision of square plate, 200 subareas

1. The charge density approaches infinity at the sharp corners of the plate, as substantiated by theory.
2. The value of charge density flattens out near the center along the outer edges of the plate.
3. The charge density remains essentially constant throughout the interior region.

The use of nonuniform subdivisions seems at once apparent as a means of simplifying the computation. This procedure has been attempted in the calculation of capacitance of a circular annulas with rather disappointing results.[8] The accuracy of the capacitance values so obtained seemed to be influenced only by the number of subareas and was relatively insensitive to variances in the size, or shape, of the subdivisions.

Since the number of subareas seemed to be of prime importance, and taking into account the relative flatness of the center portions of the curves of Fig. 5, it was decided to modify this method. A large number of equal-sized square-shaped subareas would be assumed and the additional assumption made that certain groupings of adjacent subareas would be of equal charge density. This, in effect, allows the computation to involve a large number of subdivisions, but eliminates the added difficulty of solving for a very large number of unknowns.

Noting in Table III the subareas of similar charge density, these subdivisions were grouped together and assumed equal; see Fig. 6. The $n=200$ computation was then repeated, this time with only six unknowns.

The subsequent results, attained at considerably less effort than the original computation, are recorded in Table IV together with the original results. This simplification yielded almost identical values as before and the resulting value of $W/C=2.811$ deviated only 0.1% from the initially calculated value of 2.808.

Hence, it has been shown that for all subsequent computations dealing with rectangular plates, fairly accurate results may be obtained through the use of these simplifying assumptions.

Table IV. Comparison of Results for Square Plate at Zero Depth

	Original Calculation	Modified Calculation
$q_a/(2aV_0)$	0.045	0.045
$q_b/(2aV_0)$	0.030	0.030
$q_c/(2aV_0)$	0.027	
$q_d/(2aV_0)$	0.026	0.026
$q_e/(2aV_0)$	0.025	
$q_f/(2aV_0)$	0.015	0.016
$q_g/(2aV_0)$	0.013	
$q_h/(2aV_0)$	0.012	
$q_i/(2aV_0)$	0.012	0.012
$q_j/(2aV_0)$	0.012	
$q_k/(2aV_0)$	0.011	
$q_l/(2aV_0)$	0.010	
$q_m/(2aV_0)$	0.010	0.010
$q_n/(2aV_0)$	0.010	
$q_o/(2aV_0)$	0.010	
W/C	2.808	2.811

Calculation of Capacitance of Rectangular Plate

METHOD OF SOLUTION

Using the simplifications of Maxwell's original method of subareas as listed in the previous section, this analysis is now extended to the rectangular plate. Calculations are performed covering the length-to-width ratios encountered in the usual switchyard proportions, still keeping in mind the use of these results as the limiting case of a rectangular grid. Accordingly, for a plate of width W feet and length L feet, results are achieved for various depths.

RESULTS OF CALCULATIONS

For a length-to-width (L/W) ratio of 1.5, a configuration consisting of 108 subareas was used. Six different charge densities $q_a, \ldots, q_f$ were assumed. Following the preceding indications, a fast drop of charge density was assumed near the corners and very little change in adjacent subareas within the interior of the plate.

Similar assumptions were used for $L/W=2$. One hundred subareas were assumed, again using only six different charge densities. The results are listed in Tables V and VI, and are very much in line with expectations.

Table V. Results for L/W = 1.5

$\frac{d}{W}$	$\frac{q_a}{2aV_0}$	$\frac{q_b}{2aV_0}$	$\frac{q_c}{2aV_0}$	$\frac{q_d}{2aV_0}$	$\frac{q_e}{2aV_0}$	$\frac{q_f}{2aV_0}$	W/C (esu)	W/C (ft/cm)
0	0.0504	0.0331	0.0289	0.0175	0.0169	0.0130	2.305	0.07562
0.0008	0.0506	0.0331	0.0290	0.0175	0.0169	0.0130	2.303	0.07555
0.0041	0.0512	0.0333	0.0292	0.0173	0.0168	0.0130	2.294	0.07528
0.0083	0.0520	0.0335	0.0294	0.0171	0.0168	0.0130	2.284	0.07495
0.0167	0.0536	0.0339	0.0298	0.0167	0.0166	0.0129	2.266	0.07434

Table VI. Results for L/W = 2

$\frac{d}{W}$	$\frac{q_a}{2aV_0}$	$\frac{q_b}{2aV_0}$	$\frac{q_c}{2aV_0}$	$\frac{q_d}{2aV_0}$	$\frac{q_e}{2aV_0}$	$\frac{q_f}{2aV_0}$	W/C (esu)	W/C (ft/cm)
0	0.0513	0.0328	0.0288	0.0177	0.0145	0.0145	1.960	0.06430
0.001	0.0515	0.0329	0.0288	0.0177	0.0145	0.0145	1.958	0.06424
0.005	0.0522	0.0331	0.0290	0.0176	0.0144	0.0144	1.952	0.06404
0.01	0.0530	0.0333	0.0293	0.0174	0.0143	0.0143	1.944	0.06378
0.02	0.0546	0.0337	0.0297	0.0171	0.0142	0.0142	1.928	0.06325

For $L/W=3$, the charge distribution was not so easily predictable. Thus, it was decided to solve for this L/W ratio twice, first assuming a drop in charge density in the outer row along the length, without too much change inside; and second assuming a more or less constant charge distribution in the outer row along the length with more of an abrupt change diagonally away from the corners.

A configuration consisting of 150 subareas was used for both runs. Grouping for the first solution is shown in Fig. 7, and that of the second in Fig. 8. The comparative charge densities are listed in Table VII for the case of $d=0$. The better assumption is immediately apparent. It can be seen that in run 1, the values of q_c and q_d turned out to be essentially equal, indicating that the charge density remains almost constant away from the corners even in the longer span of this plate. The rather abrupt drop from 0.017 to 0.013 when progressing from q_e to q_f also indicated that there really was more of a change in the interior areas. The answers of run 2 bear all this out with the resulting interior charge densities q_x, q_y, and q_z slowly decreasing while the charges along the middle of the outer row q_w, now assumed constant away from the corner, taking the identical value as that calculated for the two assumed charges q_c and q_d of run 1.

Significantly, the deviation between resulting W/C values in these two runs is almost negligible with W/C for run 1 coming to 1.536 and that of run 2 to 1.535. This result proves that the actual selection of equal charge distribution groups is not critical as long as it is based on realistic assumptions. The complete results for run 2 are shown in Table VIII.

With the use of experience gained through the previous work, the calculation was then repeated for $L/W=4$. The subdivisions for this calculation, using 200 subareas, are shown in Fig. 9 with the results in Table IX. A convenient plot of all the results is contained in Fig. 10.

Table VII. Comparison of Results for L/W = 3

Configuration of Fig. 7		Configuration of Fig. 8	
$q_a/2aV_0$	0.049	$q_u/2aV_0$	0.049
$q_b/2aV_0$	0.031	$q_v/2aV_0$	0.031
$q_c/2aV_0$	0.026	$q_w/2aV_0$	0.026
$q_d/2aV_0$	0.026	$q_x/2aV_0$	0.018
$q_e/2aV_0$	0.017	$q_y/2aV_0$	0.015
$q_f/2aV_0$	0.013	$q_z/2aV_0$	0.012
W/C (esu)	1.536	W/C (esu)	1.535
W/C (ft/cm)	0.05038	W/C (ft/cm)	0.05036

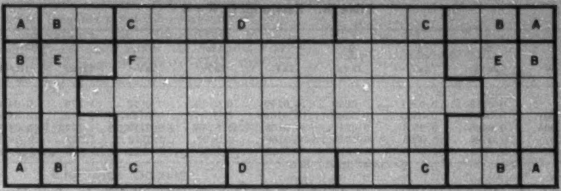

Fig. 7. Subdivision of rectangular plate L/W = 3, first approximation

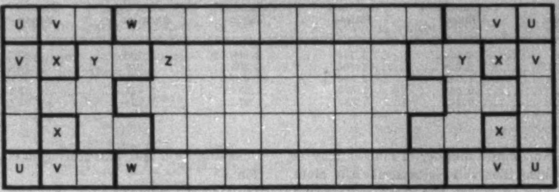

Fig. 8. Subdivision of rectangular plate L/W = 3, second approximation

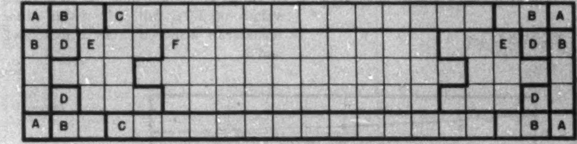

Fig. 9. Subdivision of rectangular plate L/W = 4

COMPARISON WITH OTHER WORK

There is no definite information available concerning the exact capacitance of a rectangular plate. However, since the capacitance of any plane area is greater than that of any portion of this area, definite bounds of this value for the condition $d=0$ may be obtained. Maxwell[6] shows that for an elliptic plate of eccentricity e

$$\frac{x^2}{a^2}+\frac{y^2}{b^2}=1,\ e=\sqrt{1-\frac{b^2}{a^2}}$$

$$Q=a\,\frac{V}{F(e)} \tag{1}$$

where

Q = total charge on the plate

$F(e)$ = an elliptic integral of the first kind with argument e

Thus, limits may be calculated by evaluating the capacitance of an inscribed and circumscribed ellipse. Let the length and width of the rectangular plate in Fig. 11 be L and W. The major semiaxis and minor semiaxis of the inscribed ellipse then are $L/2$ and $W/2$. Substituting in equation 1 yields

$$W/C_{\text{inscribed}}=2kF(e)=2kF(\sqrt{1-k^2}) \tag{2}$$

where

$$k=\frac{W}{L}$$

Table VIII. Results for L/W = 3

$\frac{d}{W}$	$\frac{q_u}{2aV_0}$	$\frac{q_v}{2aV_0}$	$\frac{q_w}{2aV_0}$	$\frac{q_x}{2aV_0}$	$\frac{q_y}{2aV_0}$	$\frac{q_z}{2aV_0}$	W/C (esu)	W/C (ft/cm)
0	0.0489	0.0311	0.0259	0.0175	0.0147	0.0124	1.535	0.05036
0.001	0.0490	0.0311	0.0260	0.0175	0.0147	0.0123	1.534	0.05033
0.005	0.0497	0.0313	0.0261	0.0174	0.0146	0.0123	1.529	0.05016
0.01	0.0504	0.0315	0.0263	0.0172	0.0145	0.0122	1.523	0.04997
0.02	0.0519	0.0318	0.0267	0.0169	0.0143	0.0121	1.512	0.04960

Table IX. Results for L/W = 4

$\frac{d}{W}$	$\frac{q_a}{2aV_0}$	$\frac{q_b}{2aV_0}$	$\frac{q_c}{2aV_0}$	$\frac{q_d}{2aV_0}$	$\frac{q_e}{2aV_0}$	$\frac{q_f}{2aV_0}$	W/C (esu)	W/C (ft/cm)
0	0.0473	0.0299	0.0240	0.0169	0.0139	0.0113	1.276	0.04186
0.001	0.0474	0.0300	0.0240	0.0169	0.0139	0.0113	1.275	0.04183
0.005	0.0480	0.0301	0.0241	0.0168	0.0138	0.0113	1.722	0.04172
0.01	0.0487	0.0303	0.0243	0.0166	0.0137	0.0112	1.267	0.04157
0.02	0.0502	0.0306	0.0247	0.0163	0.0136	0.0111	1.258	0.04129

Table X. Comparison Between Calculated and Other Available Results for Zero Depth

	W/C, Esu				
$\frac{L}{W}$	Circumscribed Ellipse	Inscribed Ellipse	Calculated Values	Results Using Equation 5	Deviation of Calculated Results from Equation 5
1	2.221	3.142	2.808	2.735	2.67%
1.5	2.028	2.704	2.305	2.211	4.25%
2	1.046	2.156	1.960	1.879	4.31%
3	0.553	1.670	1.535	1.471	4.35%
4	0.345	1.384	1.276	1.224	4.25%

An infinite number of ellipses may be defined that will circumscribe the plate. If the ellipse of the same eccentricity, $e=\sqrt{1-k^2}$ is chosen, since $(L/2,\ W/2)$ lies on any circumscribed ellipse, the equation of this ellipse may be written

$$\frac{(W/2)^2}{a^2}+\frac{(L/2)^2}{a^2k^2}=1$$

Solving for a and substituting in equation 1

$$\frac{W}{C}\text{circumscribed}=\frac{2k^2}{\sqrt{1+k^4}}F(\sqrt{1-k^2}) \tag{3}$$

Table X shows that the calculated values of W/C fall well within these boundaries achieved from equations 2 and 3.

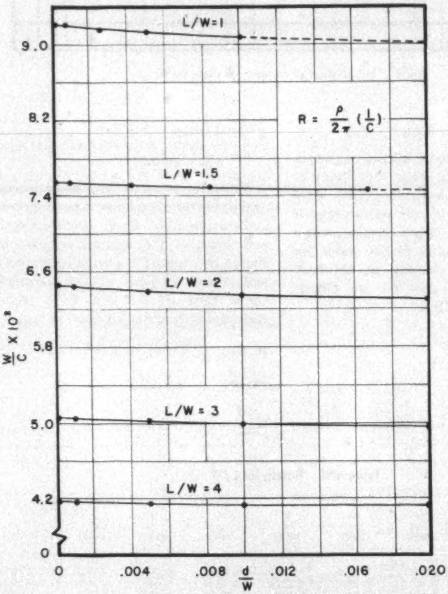

Fig. 10. Effect of depth upon grounding resistance

As previously mentioned, an approximate method (about 8% too high) of solution for the reciprocal of the capacitance of an isolated thin rectangular plate a cm by b cm has been presented by Dwight[4] where

$$\frac{1}{C}=2\left(\frac{1}{a}\ln\frac{a+\sqrt{a^2+b^2}}{b}+\frac{1}{b}\ln\frac{b+\sqrt{a^2+b^2}}{a}+\frac{a}{3b^2}+\frac{b}{3a^2}-\frac{(a^2+b^2)\sqrt{a^2+b^2}}{3a^2b^2}\right) \tag{4}$$

This equation may be altered to the following (a similar expression has been offered by McCrocklin and Wendlandt[7] containing, however, an error in the second term)

$$\frac{W}{C}=(2)(0.92)\left(k\ln\frac{1+\sqrt{1+k^2}}{k}+\ln(k+\sqrt{1+k^2})+\frac{1}{3k}+\frac{k^2}{3}-\frac{(1+k^2)\sqrt{1+k^2}}{3k}\right) \tag{5}$$

where

C = capacitance of the plate and its image, esu
W = width of plate, cm
L = length of plate, cm
$k = W/L$

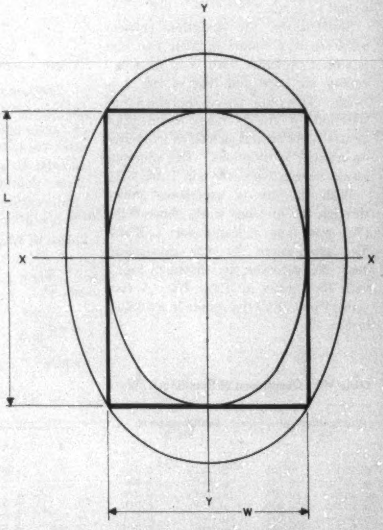

Fig. 11. Inscribed and circumscribed ellipses

Thus, values of W/C are obtained in terms of W/L by substituting the appropriate values of k into equation 5. However, this result is realized through the use of the "average potential method," an approximate means of solution in which the charge density is assumed uniform over the surface of the plate and then an average potential calculated. The accuracy of this method varies considerably for different types of conductor configurations.

As previously indicated, the trend of the values obtained with the method of subareas, as the number of subareas is increased, seems to be approaching those attained by equation 5. However, this observation is somewhat arbitrary; the only definite conclusion that can be formulated being that the values of W/C as herein computed are close to the true figures, certainly within 5%.

As for any checks on the calculated results of W/C for d other than zero, there has been experimental work[7] with a small plate, measurements being taken at different depths in a natural lake. Unfortunately, the results provide not more than a very approximate check because the depths used in the test were much too large. It is impossible to read the curves[7] accurately for the much smaller values of depth which are important for the practical application to switchyard grids.

Conclusions

1. Maxwell's method of subareas was used in calculating the capacitance of a flat rectangular plate and its image with respect to the surface of earth. The calculations were carried out for plates of various L/W ratios, assumed buried in ground at different depths and parallel to the surface of earth.

2. There exists a simple relationship between the capacitance, as referred to, and the resistance of a plate to ground. By using this relationship, the resistance to earth of a buried rectangular plate may be obtained. These values may be used as the basis of the limiting case for investigations concerning the resistance of rectangular grounding grids for high-voltage stations.

3. The calculated results, Fig. 10, show that the grounding resistance decreases as the plate is located deeper in earth. As the L/W ratio is increased, the effects of a change in depth become less pronounced. Accordingly, for the order of magnitude of depth to be used for a grounding mat, this change in resistance may be neglected if the L/W ratio is greater than 4.

4. The method of subareas is a very powerful tool in the calculation of capacitance. However, for the case of the solid rectangular plate, the necessary time required for the numerical work, in order to obtain really accurate results, becomes much too long for practical consideration. This necessitates the introduction of simplifying assumptions for the computations. The subsequent results using the modified method are accurate to within 5%.

Appendix I. Potential at Point Above Center of Uniformly Charged Square

Refer to Fig. 12. If the charge density of the uniformly charged square A of side $2a$ is q_A, the total charge on an incremental area $dxdy$ of A is $q_A dxdy$. Each of these increments of charge contributes to the potential at point P, a distance r from it, an increment of potential $dV_{AP} = (q_A dxdy)/r$, and therefore

$$V_{AP} = \int_{y=-a}^{y=+a} \int_{x=-a}^{x=+a} \frac{q_A dxdy}{r}$$

$$= q_A \int_{y=-a}^{y=+a} \int_{x=-a}^{x=+a} \frac{dxdy}{\sqrt{x^2+y^2+d^2}}$$

$$= q_A \int_{-a}^{+a} \ln \frac{(\sqrt{x^2+a^2+d^2}+a)}{(\sqrt{x^2+a^2+d^2}-a)} dx \qquad (6)$$

Set

$$\frac{x}{a} = u$$

and

$$1 + \frac{d^2}{a^2} = k^2$$

Then

$$V_{AP} = aq_A \int_{-1}^{+1} \ln \frac{(\sqrt{u^2+k^2}+1)}{(\sqrt{u^2+k^2}-1)} du \qquad (7)$$

Equation 7 may be solved by letting

$$\sqrt{u^2+k^2}+1 = m$$

$$\sqrt{u^2+k^2}-1 = n$$

and integrating by parts with the aid of nos. 145, 167, and 170, Hodgman.[8] Accordingly, the total potential at point P is

$$V_{AP} = (2a)q_A \left\{ 4 \ln \frac{\sqrt{k^2+1}+1}{k} - \sqrt{k^2-1} \left[\arcsin \frac{(2-k^4)}{k^4} + \frac{\pi}{2} \right] \right\} \qquad (8)$$

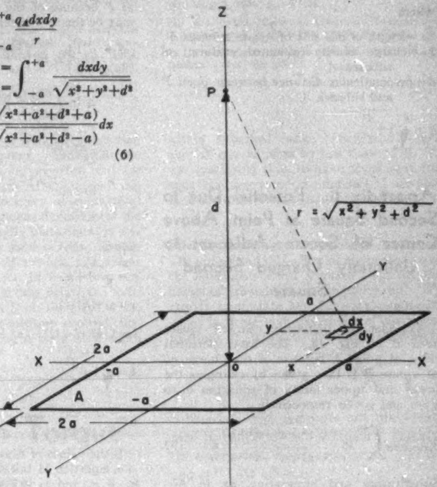

Fig. 12 (right). Point above center of square

Fig. 13 (below). Point above adjacent square

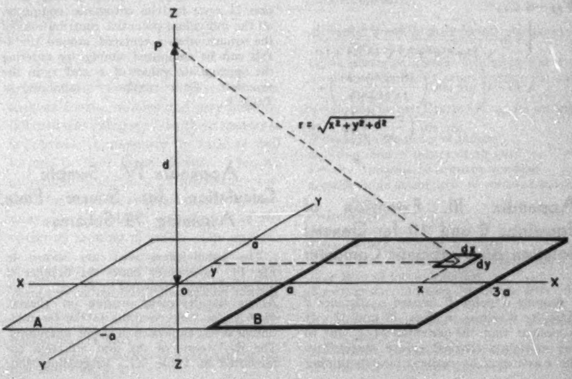

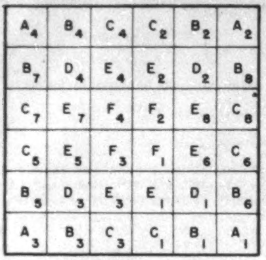
A_4 B_4 C_4 C_2 B_2 A_2
B_7 D_4 E_4 E_2 D_2 B_8
C_7 E_7 F_4 F_2 E_8 C_8
C_5 E_5 F_3 F_1 E_6 C_6
B_5 D_3 E_3 E_1 D_1 B_6
A_3 B_3 C_3 C_1 B_1 A_1

Fig. 14. Subdivision of square plate, 72 subareas

Table XI. Determination of Coefficients for First Equation, Potential on a_1, Square Plate Assuming 72 Subareas

Due to a	$K_{ij}'/2a$	Due to b	$K_{ij}'/2a$	Due to c	$K_{ij}'/2a$	Due to d	$K_{ij}'/2a$	Due to e	$K_{ij}'/2a$	Due to f	$K_{ij}'/2a$
a_1	7.0510	b_1	2.0740	c_1	1.0100	d_1	1.4142	e_1	0.8944	f_1	0.7071
a_2	0.4000	b_2	0.3922	c_2	0.3714	d_2	0.4851	e_2	0.4472	f_2	0.5547
a_3	0.4000	b_3	0.5000	c_3	0.6698	d_3	0.4851	e_3	0.6325	f_3	0.4714
a_4	0.2828	b_4	0.3124	c_4	0.3430	d_4	0.3535	e_4	0.4000	f_4	0.5547
		b_5	0.3922	c_5	0.3714			e_5	0.4472		
		b_6	2.0740	c_6	1.0100			e_6	0.8944		
		b_7	0.3124	c_7	0.3430			e_7	0.4000		
		b_8	0.5000	c_8	0.6698			e_8	0.6325		
$\frac{K_{aa}'}{2a}$	8.1338	$\frac{K_{ba}'}{2a}$	6.5572	$\frac{K_{ca}'}{2a}$	4.7884	$\frac{K_{da}'}{2a}$	2.7379	$\frac{K_{ea}'}{2a}$	4.7482	$\frac{K_{fa}'}{2a}$	2.2879

where

$2a$ = length of one side of square subarea A
q_A = charge density (assumed uniform) of subarea A
d = perpendicular distance between point P and subarea A

$$k=\sqrt{1+\frac{d^2}{a^2}}$$

Appendix II. Potential Due to Second Square at Point Above Center of Square Adjacent to Uniformly Charged Second Square

Consider the uniformly charged square area B of Fig. 13. The total potential V_{BP}, at point P because of the charge q_B of square B is then given by changing the lower and upper limits of equation 6 to $x=a$ and $x=3a$ respectively

$$V_{BP}=q_B\int_a^{3a} \ln \frac{(\sqrt{x^2+a^2+d^2}+a)}{(\sqrt{x^2+a^2+d^2}-a)}dx \qquad (9)$$

Substituting and integrating, as in Appendix I

$$V_{BP}=(2a)q_B\times \left\{2\ln\frac{(\sqrt{k^2+9}+1)^2(\sqrt{k^2+9}+3)k}{\sqrt{k^2+8}(k^2+8)(\sqrt{k^2+1}+1)^2}-\sqrt{k^2-1}\left[\arcsin\left(\frac{18-8k^2-k^4}{k^2(k^2+8)}\right)-\arcsin\left(\frac{2-k^4}{k^4}\right)\right]\right\} \qquad (10)$$

Appendix III. Extension of Equations 8 and 10 for General Solution on Automatic Computer

Assume a point P located a distance d over the x-axis as in Figs. 12 and 13. It is evident that the potential at P due to any uniformly charged square centered on the x-axis may be realized by substituting the appropriate lower and upper limits into the evaluated integral of equation 6. If these limits are denoted as x_1 and x_2 respectively, the equation for the potential at P because of the charge q_j of square j may be finally written as follows

$$\frac{V_{jP}}{(2a)q_j}=\frac{1}{2}\left\{u_2\ln\left(\frac{r_2+1}{r_2-1}\right)-u_1\ln\left(\frac{r_1+1}{r_1-1}\right)+2\ln\left(\frac{u_2+r_2}{u_1+r_1}\right)-\sqrt{k^2-1}\times\left[\arcsin\frac{(u_2^4-s_2^4)-\sqrt{t_2^4-4u_2^4s_2^4}}{k^2(r_2^2-1)^2}-\arcsin\frac{(u_1^4-s_1^4)-\sqrt{t_1^4-4u_1^4s_1^4}}{k^2(r_1^2-1)^2}\right]\right\} \qquad (11)$$

where

$$r=\sqrt{u^2+k^2}$$

$$s=\sqrt{r(k^2-1)}$$

$$t=\sqrt{k^2(r^2-1)^2-(u^4+r^4)}$$

$$k=\sqrt{1+\frac{d^2}{a^2}}$$

$$u=\frac{x}{a}$$

If the values of x_1 and x_2 are set as $-a$ and $+a$, equation 11 takes the form of equation 8; if x_1 and x_2 are set as $+a$ and $+3a$, equation 11 takes the form of equation 10, etc. Accordingly, by programming equation 11 once for the automatic computer, all the individual potential contributions of the square areas j centered around the x-axis can be computed simply by entering the appropriate values of x_1 and x_2 in the equation. These results are tabulated in Table I.

Appendix IV. Sample Calculation for Square Plate Assuming 72 Subareas

The subdivisions used are shown in Fig. 14. Symmetry limits the number of unknown charge densities to six, $q_a, \ldots, q_f$. As in the foregoing section on theory, $V_{ij}=K_{ij}'q_i$, thus resulting in the formulation of seven equations in seven unknowns. The K_{ij}' terms of the first equation are tabulated in Table XI. Proceeding similarly for subareas b to f and adding the capacitance equation

$$8.1338\frac{q_a}{2aV_0}+6.5572\frac{q_b}{2aV_0}+4.7884\frac{q_c}{2aV_0}+2.7379\frac{q_d}{2aV_0}+4.7482\frac{q_e}{2aV_0}+2.2879\frac{q_f}{2aV_0}=1$$

$$3.2786\frac{q_a}{2aV_0}+11.2017\frac{q_b}{2aV_0}+6.2217\frac{q_c}{2aV_0}+3.6064\frac{q_d}{2aV_0}+5.9468\frac{q_e}{2aV_0}+2.7887\frac{q_f}{2aV_0}=1$$

$$2.3942\frac{q_a}{2aV_0}+6.2217\frac{q_b}{2aV_0}+12.2051\frac{q_c}{2aV_0}+3.2409\frac{q_d}{2aV_0}+7.2620\frac{q_e}{2aV_0}+3.2067\frac{q_f}{2aV_0}=1$$

$$2.7379\frac{q_a}{2aV_0}+7.2129\frac{q_b}{2aV_0}+6.4818\frac{q_c}{2aV_0}+8.8620\frac{q_d}{2aV_0}+8.5423\frac{q_e}{2aV_0}+3.9102\frac{q_f}{2aV_0}=1$$

$$2.3741\frac{q_a}{2aV_0}+5.9468\frac{q_b}{2aV_0}+7.2620\frac{q_c}{2aV_0}+4.2712\frac{q_d}{2aV_0}+14.3374\frac{q_e}{2aV_0}+5.3926\frac{q_f}{2aV_0}=1$$

$$2.2879\frac{q_a}{2aV_0}+5.5774\frac{q_b}{2aV_0}+3.2067\frac{q_c}{2aV_0}+3.9102\frac{q_d}{2aV_0}+10.7852\frac{q_e}{2aV_0}+12.6132\frac{q_f}{2aV_0}=1$$

$$8\frac{q_a}{2aV_0}+16\frac{q_b}{2aV_0}+16\frac{q_c}{2aV_0}+8\frac{q_d}{2aV_0}+16\frac{q_e}{2aV_0}+8\frac{q_f}{2aV_0}-\frac{Q}{2aV_0}=0$$

Solving

$$\frac{q_a}{2aV_0}=0.05336$$

$$\frac{q_b}{2aV_0}=0.03562$$

$$\frac{q_c}{2aV_0}=0.03374$$

$$\frac{q_d}{2aV_0}=0.01884$$

$$\frac{q_e}{2aV_0}=0.01744$$

$$\frac{q_f}{2aV_0}=0.01594$$

$$\frac{Q}{2aV_0}=\frac{C}{2a}=2.09394$$

since $W=(6)(2a)=12a$

$$\frac{W}{C}=\frac{6}{2.09394}=2.8654$$

References

1. Grounding Grids for High-Voltage Stations, **E. T. B. Gross, B. V. Chitnis, L. J. Stratton.** *AIEE Transactions*, vol. 72, pt. III, Aug. 1953, pp. 799–810.

2. Calculation of Resistances to Ground, **H. B. Dwight.** *AIEE Transactions (Electrical Engineering)*, vol. 55, Dec. 1936, pp. 1319–28.

3. An Approximate Calculation of the Electrical Capacities of Rectangular and Annular Areas, **D. K. Reitan.** *M.S. Thesis*, University of Wisconsin, Madison, Wis., 1949.

4. Calculation of the Resistance to Ground and of Capacitances, **H. B. Dwight.** *Journal of Mathematics and Physics*, Massachusetts Institute of Technology, Cambridge, Mass., vol. 10, 1930–31, pp. 50–74.

5. Calculation of the Capacitance of a Circular Annulus by the Method of Subareas, **Thomas James Higgins, Daniel Kinseth Reitan.** *AIEE Transactions*, vol. 70, pt. I, 1951, pp. 926–31: Discussion by Ernest Weber, pp. 931–32, and closure, pp. 932–33.

6. A Treatise on Electricity and Magnetism, Volume I (book), **J. C. Maxwell.** Oxford University Press, Oxford, England, 3rd ed., 1892, pp. 148–54, 237.

7. Determination of Resistance to Ground of Grounding Grids, **A. J. McCrocklin, Jr., C. W. Wendlandt.** *AIEE Transactions*, vol. 71, pt. III, Dec. 1952, pp. 1062–64.

8. Mathematical Tables from Handbook of Chemistry and Physics, **Charles D. Hodgman.** Chemical Rubber Publishing Company, Cleveland, Ohio, 8th ed., 1946.

9. Capacity of Rectangular Plates and a Formula for Capacity of Aerials, **G. W. O. Howe.** *Radio Review*, Dublin, Ireland, vol. 1, Nov. 1920, pp. 710–14.

10. Grounding Resistance of Rectangular Plates, **R. B. Wise.** *M.S. Thesis*, Illinois Institute of Technology, Chicago, Ill., Dec. 1954.

11. Grounding Electrode Characteristics from Model Tests, **H. R. Armstrong.** *AIEE Transactions*, vol. 72, pt. III, Dec. 1953, pp. 1301–06.

12. Analytical Expressions for the Resistance of Grounding Systems, **S. J. Schwarz.** *AIEE Transactions*, vol. 73, pt. III-B, Aug. 1954, pp. 1011–16.

13. Let's Look at Station Grounding, **S. J. Schwarz.** *Electrical World*, New York, N. Y., vol. 143, May 2, 1955, pp. 55–58.

14. All Steel Network Grounds Substation, **G. Appleman, S. J. Litridges.** *Ibid.*, pp. 59–61.

15. Steel Ground Grid Works Well, **W. F. Dunkle.** *Ibid.*, pp. 63–65.

◆

Discussion

S. J. Schwarz (Sverdrup and Parcel, Inc., San Francisco, Calif.): As the authors state, their investigation was conducted to establish the limiting value for the resistance of ground grids. It may be added that the same limiting value also applies to the ground resistance of rodbeds. The practical importance of the authors' commendable work on the subject is illustrated in reference 12, where general equations for the ground resistance of ground mats and rodbeds were developed as a tool in predicting the resistance of square, rectangular, or oddly shaped grounding systems and for evaluating the influence of the various design data on best efficiency at economical costs. One of the influencing factors is the resistance of the metallic plate equal in size to the area covered by mesh or rods. Thanks to the authors' extensive work, the values resorted to in reference 12 have now won added reliance, even if they may have to be increased by 3% to 4% on the basis of the present paper. The authors showed, furthermore, that burying a plate at a depth within practical range lowers the resistance at ground level by less than 1.7%. It was gratifying thus to have proof that the equations suggested in reference 12 are also in this respect within slide-rule accuracy.

Eric T. B. Gross and Richard B. Wise: The purpose of this series of papers has been the establishment of a sound basis for the design of grounding mats in rocky soil. We greatly appreciate Mr. Schwarz' comments which indicate that the results of our investigations are useful to the design engineers.

Optimum Design of Induction Torque Motors and Servomotors

GERALD WEISS
ASSOCIATE MEMBER AIEE

ELECTRIC motor design is largely a trial-and-error procedure. Given a set of requirements, the engineer makes a guess at the solution. He then verifies his design by a paper analysis or by the construction and test of a sample. If the design meets the original requirements, a solution has been obtained but the engineer has no assurance that this is the best solution. However, in special cases, it is possible to determine certain motor parameters by direct synthesis, rather than by trial and error. Such a special case is the topic of this paper.

In certain applications of induction motors the performance at standstill is of predominant interest. Control motors, such as torque motors and servomotors, fall into this category. In these motors it is desirable to maximize the ratio of stall torque to stall input power. This requirement leads to a simple design formula for the rotor resistance, and, furthermore, permits direct calculation of the optimum number of poles. The analysis is based on two concepts not previously used in induction motor theory, namely, the concept of "torque-per-watt" (T/W) and of "T/W efficiency."

Nomenclature

A_w = total winding area for all phases = 1/2 total slot area
C_m = a motor parameter defined in text
c_1 = air-gap factor (Carter factor) for primary
c_2 = air-gap factor (Carter factor) for secondary
D = outside diameter of motor
D_g = diameter of motor at air gap
d = wire diameter of primary winding
e_s = allowable static error of servo at output shaft
f = frequency
H = net stack height of motor
I_2 = secondary current of motor
J = moment of inertia of servo at motor
K_A = gain of servo amplifier
K_E = transfer function of servo error detector
K_F = viscous damping coefficient of servomotor
K_T = torque coefficient of servomotor
K_V = velocity constant of servo

Paper 55-506, recommended by the AIEE Rotating Machinery Committee and approved by the AIEE Committee on Technical Operations for presentation at the AIEE Summer General Meeting, Swampscott, Mass., June 27–July 1, 1955. Manuscript submitted April 1, 1955; made available for printing June 14, 1955.

Gerald Weiss is with The W. L. Maxson Corporation, New York, N. Y.

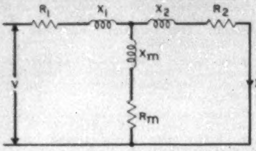

Fig. 1. Equivalent circuit of the polyphase induction motor at standstill

k_e = over-all space factor of primary winding over bare copper
k_d = distribution factor of primary winding
k_s = saturation factor of iron in motor
k_w = ratio of A_w to total primary cross-sectional area
L_e = primary end turn length per turn
L_g = air-gap length
m = number of phases
M = zero-speed slope of speed-torque curve with rated excitation
M_1 = zero-speed slope of speed-torque curve, positive-sequence component
M_2 = zero-speed slope of speed-torque curve, negative-sequence component
M_c = zero-speed slope of speed-torque curve, arbitrary control-field voltage
N_1 = primary turns per phase
N_m = a number proportional to maximum required servo speed
N_s = synchronous speed of motor
n = gear ratio between servomotor and output
p = number of poles of motor
R_1 = motor primary resistance
R_2 = motor secondary resistance referred to primary
R_m = motor mutual resistance referred to primary (core loss)
T = motor stall torque, balanced and rated input
T_1 = motor stall torque, positive-sequence component
T_2 = motor stall torque, negative-sequence component
T_c = motor stall torque, arbitrary control-field voltage
T_F = static friction of servo
V_1 = motor excitation, positive-sequence component
V_2 = motor excitation, negative-sequence component
V_{CF} = motor excitation, control-field voltage
V_{MF} = motor excitation, main-field voltage
W = total motor power input at stall
W_1 = primary motor power dissipation at stall, per phase
W_2 = secondary motor power dissipation at stall, per phase
W_m = mutual motor power dissipation at stall, per phase
X_1 = motor primary leakage reactance
X_2 = motor secondary leakage reactance, referred to primary
X_m = motor mutual (air-gap) reactance, referred to primary
y = torque-per-watt efficiency
Z_2 = a quantity related to motor parameters
α = complement of the phase angle between V_{CF} and V_{MF}
θ_I = servo input command
θ_O = servo output command
μ = permeability of free space
ξ = damping ratio of servo
ρ = resistivity of primary winding
τ = time constant of servomotor
ω_n = undamped natural frequency of servo

SUBSCRIPTS

i = ideal value of
max = maximum value of
opt = optimum value of

Induction Motor Performance at Standstill

The equivalent circuit of the polyphase induction motor with balanced inputs and rotor blocked is shown in Fig. 1. The effect of the space harmonics is neglected. The stall torque is given by the equation

$$T=\frac{p}{4\pi f}mI_2{}^2R_2 \tag{1}$$

i.e., the stall torque is proportional to the power dissipated in the secondary resistance R_2. The ratio of the stall torque to stall power is therefore proportional to the fraction of total power dissipated in the rotor. The problem of maximizing the ratio of stall torque to stall power then resolves itself into an electric-network power-matching problem.

Let the ratio of stall torque to stall input power be called T/W. Then

$$\mathrm{T/W}=\frac{p}{4\pi f}\,\frac{mW_2}{m(W_1+W_2+W_m)} \tag{2}$$

It is convenient to nondimensionalize the foregoing expression by defining an ideal T/W as the T/W which would be attained in a motor if all the power were transferred across the air gap, i.e., $W_1=W_m=0$

$$(\mathrm{T/W})_i=\frac{p}{4\pi f} \tag{3}$$

The ratio of the actual T/W to an ideal T/W is defined as the T/W efficiency of the motor

$$y=\frac{\mathrm{T/W}}{(\mathrm{T/W})_i} \tag{4}$$

$$y=\frac{W_2}{W_1+W_2+W_m} \tag{5}$$

The required motor design is then attained in two steps. First the motor parameters are selected to obtain maximum T/W efficiency, i.e., by maximizing equation 5. A quantity $y_{\max}$ is then obtained which is a function of the number of poles and of the over-all motor dimensions, and the T/W is now given by the relation

$$\mathrm{T/W}=\frac{p}{4\pi f y_{\max}}\cdot y_{\max} \tag{6}$$

By proper selection of the number of poles and of the over-all dimensions equation 6 can then also be maximized.

Design for Maximum T/W Efficiency

Equation 5 can be rewritten in terms of the motor parameters

$$y=\frac{1}{1+\dfrac{R_1[(R_2+R_m)^2+(X_2+X_m)^2]}{R_2(R_m{}^2+X_m{}^2)}+\dfrac{R_m(R_2{}^2+X_2{}^2)}{R_2(R_m{}^2+X_m{}^2)}} \tag{7}$$

It is noteworthy that the primary leakage reactance X_1 does not enter into this relation.

Consider how the T/W changes as the individual parameters (considered on a unit-turn basis) are changed. An increase of R_m will lower y, therefore it is desirable to make R_m zero; this is obviously impossible because there is an irreducible minimum to the core loss. Similarly, the primary copper resistance R_1 should be reduced to zero; here an irreducible minimum is set by the available copper winding area. The secondary leakage reactance X_2 should also be made zero; this is not possible either, and, in any case, secondary leakage is difficult to control. The mutual reactance X_m should be made infinitely large to maximize y; here a limitation exists because a minimum mechanical clearance is required for the air gap. Thus the four parameters R_m, R_1, X_2, and X_m must have finite values. The remaining parameter, the secondary resistance R_2, can then be adjusted to obtain a maximum T/W efficiency for a given set of R_m, R_1, X_2, and X_m. Since the secondary resistance of an induction motor can be varied over a wide range, this is a practical procedure.

The optimum secondary resistance is now obtained by differentiating equation 7 with respect to R_2 and setting the derivative dy/dR_2 equal to zero. The result of these operations is

$$(R_2)_{\mathrm{opt}}=\sqrt{\frac{(X_m+X_2)^2+R_m\left(R_m+\dfrac{X_2{}^2}{R_1}\right)}{1+\dfrac{R_m}{R_1}}} \tag{8}$$

This expression is considerably simplified by neglecting R_m; this is a reasonable procedure because at stall the core losses of an induction motor are very small compared to the other losses.

$$(R_2)_{\mathrm{opt}}=X_m+X_2 \tag{9}$$

R_m can then also be neglected in the expression for y, equation 7

$$y=\frac{1}{1+\dfrac{R_1}{R_2X_m{}^2}[R_2{}^2+(X_m+X_2)^2]} \tag{10}$$

By substituting the optimum value of

R_2 in equation 10, the maximum T/W efficiency is obtained, namely

$$y_{\max}=\frac{1}{1+2R_1\dfrac{X_m+X_2}{X_m^2}} \tag{11}$$

The secondary leakage reactance X_2 is usually much smaller than the mutual reactance X_m so that the following simplified expressions can be used

$$(R_2)_{\text{opt}}=X_m \tag{12}$$

$$y_{\max}=\frac{1}{1+2\dfrac{R_1}{X_m}} \tag{13}$$

$$y=\frac{1}{1+\dfrac{R_1}{X_m}\left(\dfrac{R_2}{X_m}+\dfrac{X_m}{R_2}\right)} \tag{14}$$

The maximum T/W efficiency is then a function of a single parameter R_1/X_m. This ratio is independent of the number of turns of the primary winding if all other factors remain equal. It is dependent only on the dimensions of the machine and on the desired number of poles.

To investigate whether the selection of R_2 is critical, equation 14 is plotted in Fig. 2, and it can be seen that the maximum is broad and noncritical. The shaded region represents the range which yields T/W efficiencies within 10 per cent of maximum. In the worst case, where $R_1/X_m \rightarrow \infty$, a 59-per-cent variation from the theoretical maximum is permissible. In other words, a tolerance of 59 per cent or more is permitted in the realization of equation 12, and the T/W efficiency is still within 10 per cent of attainable maximum. This noncritical relationship justifies previous simplifying assumptions, such as neglecting R_m and X_2. Equation 12 is a practical design equation even for the smallest motors where it is difficult to calculate motor parameters precisely.

The mutual reactance X_m is computed from the equation[1]

$$X_m=32\pi\mu_0 fm\frac{HD_g k_{d1}^2 N_1^2}{c_1c_2k_sL_gp^2} \tag{15}$$

All the parameters in the foregoing equation can be calculated or estimated for a given motor, and the secondary resistance is then known from equation 12. The remaining problem is to synthesize a secondary which will have this resistance. This step in the procedure is covered in the existing literature.[2,3,4]

Optimum Number of Poles

With the computation of optimum secondary resistance, the first step of the optimizing procedure has been completed. The second step is to optimize the number of poles and the air-gap diameter.

The primary copper resistance of the motor can be approximated by the d-c resistance, namely

$$R_1=\rho\frac{2H+L_e}{\dfrac{\pi}{4}d^2}N_1=\rho m\frac{2H+L_e}{k_cA_w}N_1^2 \tag{16}$$

so that the fraction R_1/X_m becomes

$$\frac{R_1}{X_m}=\frac{\rho}{32\pi\mu_0}\,\frac{2H+L_e}{H}\,L_g\,\frac{c_1c_2k_s}{k_ck_{d1}^2}\,\frac{p^2}{fD_gA_w}$$

For a motor of fixed outline dimensions it is approximately correct to assume that

$$C_m=\text{a motor constant}$$
$$=\frac{\rho}{32\pi\mu_0}\,\frac{2H+L_e}{H}\,L_g\,\frac{c_1c_2k_s}{k_ck_{d1}^2} \tag{17}$$

so that

$$\frac{R_1}{X_m}=\frac{C_mp^2}{fD_gA_w} \tag{18}$$

The T/W and T/W efficiency are then written

$$y_{\max}=\frac{1}{1+\dfrac{2C_mp^2}{fD_gA_w}} \tag{19}$$

and

$$\text{T/W}=\frac{p/4\pi f}{1+\dfrac{2C_mp^2}{fD_gA_w}} \tag{20}$$

Assuming the parameter C_m constant, the T/W is thus a function of the number of poles and of the expression (D_gA_w). Both of these quantities can be optimized for optimum motor performance. The procedure for this step depends on the particular application. Two different kinds of application are now considered, a torque motor and a servomotor.

Design of a Torque Motor

A torque motor (sometimes called a torquing motor, or torque generator) is a device which produces a mechanical output torque accurately proportional to a given input voltage or current. There are various types of torque motors depending on the desired variation of torque with angular position. This discussion is limited to motors in which the torque is independent of angular position. A typical application for such a motor is in the control of a gyroscope. In such application the rotor is directly coupled to the load, no gear stepup is feasible. Strictly speaking one cannot speak of a stator and rotor because either may move: all that can be said is that the secondary is free to rotate with respect to the primary. Usually only a limited angular rotation is possible and the motor never picks up speed; it is always stalled for all intents and purposes. A further property of such applications is that "inside-out" designs, where the primary is on the inside and the secondary on the outside, are possible.

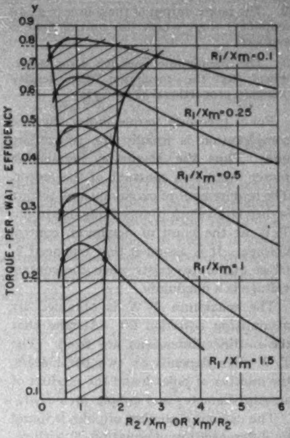

Fig. 2. T/W efficiency versus rotor resistance

Two-phase induction motors are frequently used in such applications because they are capable of delivering a torque accurately proportional to an input voltage, and because the torque is theoretically independent of rotor position. Induction motor torque is of course proportional to the square of the applied voltage; the required linear relationship between torque and voltage is obtained by keeping the voltage on one of the phases fixed, and by varying the other voltage. If saturation effects are neglected, the torque is then exactly proportional to the variable voltage.[4] The phase with fixed excitation is called the main phase or main field; the phase with variable excitation is called the control phase or control field.

In most torque-motor applications it is vital to obtain the greatest possible stall torque. This could be done merely by pumping more power into the motor, thus increasing both main-field and control-field voltages. However the permissible power input is limited by three considerations:

1. The allowable temperature rise, limited by the type of insulation, the maximum ambient temperature, and the available cooling.

2. The power output of the source (e.g., an amplifier) from which the control field is supplied.

3. The permissible linearity error determined by the maximum flux density (roughly proportional to power).

For a precision torque motor the last consideration is usually the controlling one. Thus the maximum permissible power input is a constant of the motor. The requirement of maximum stall torque is then equivalent to specifying maximum T/W at the point of maximum control voltage. It is assumed that balanced 2-phase excitation exists when the control voltage is a maximum.

The maximum T/W is obtained by maximizing equation 20. Assume that the outline dimensions are fixed. The T/W then depends on two parameters, the number of poles p and the product of air-gap diameter and copper area D_gA_w.

The optimum number of poles is found by differentiation of equation 20 with respect to p

$$p_{\text{opt}}=\sqrt{\frac{fD_gA_w}{2C_m}} \qquad (21)$$

Note that this corresponds to $R_1/X_m=1/2$ and $y_{\max}=50$ per cent. Of course the number of poles must be integral and even and may be subject to further restrictions if the primary lamination is already fixed. Therefore equation 21 is not exact and the relations are only of theoretical interest. A corresponding theoretical upper limit to the T/W is obtained by substituting equation 21 in equation 20

$$\text{T/W}=\frac{\sqrt{D_gA_w}}{8\pi\sqrt{2fC_m}} \qquad (22)$$

This equation indicates that it is required to maximize the product D_gA_w. Assume a radial air-gap motor, and consider two cases: the conventional motor with the primary surrounding the secondary, and the inside-out motor. It is obvious that the inside-out motor yields the largest D_gA_w because A_w is then approximately proportional to the square of the air-gap diameter

$$A_w=k_w\frac{\pi}{4}D_g^2 \qquad (23)$$

and

$$D_gA_w=k_w\frac{\pi}{4}D_g^3 \qquad (24)$$

If D_g is made as large as possible, say $D_g=0.9\ D$, then for the inside-out design

$$(D_gA_w)_{\max}=0.729k_w\frac{\pi}{4}D^3 \qquad (25)$$

When restricted to a conventional design, the relationship between the copper area and the air-gap diameter is approximately

$$A_w=k_w\frac{\pi}{4}(D^2-D_g^2) \qquad (26)$$

and

$$D_gA_w=k_w\frac{\pi}{4}(D_gD^2-D_g^3) \qquad (27)$$

Maximizing equation 27 by the usual differentiation process yields the optimum air-gap diameter

$$(D_g)_{\text{opt}}=\frac{\sqrt{3}}{3}D=0.577D \qquad (28)$$

and

$$(D_gA_w)_{\max}=0.385k_w\frac{\pi}{4}D^3 \qquad (29)$$

It is seen that the inside-out design yields a value of D_gA_w greater by 1.88 times the value obtained with a conventional design. The maximum obtainable T/W is approximately 38 per cent larger for the inside-out design.

A definite design procedure is now laid out:

1. The air-gap diameter is selected. If inside-out construction is permitted, then it is used.
2. The primary copper winding area is estimated, and the optimum number of poles is computed from equation 21.
3. A primary lamination is designed for the selected air-gap diameter and poles. The primary copper area is measured and checked against the estimate.
4. For a given air gap and stack length the mutual reactance can now be computed on a unit-turn basis. This determines the secondary resistance.
5. The secondary structure is designed for the computed resistance.

In practice the number of poles is rounded off downwards from the theoretical optimum, not upwards. The reason for this is that an increase in the number of poles tends to reduce the T/W efficiency faster than indicated by equation 12 because of several effects which were not considered in the analysis. If the number of slots is held constant, an increase in the number of poles will increase the space harmonics of the winding, and this reduces the stall torque and the T/W. If this is counteracted by increasing the number of slots, the size of the slots will decrease and so will the copper space factor; furthermore the effective air gap will increase. In addition, the larger number of slots are more difficult to wind, especially in a conventional type motor.

Design of a Servomotor

SERVOMOTOR CHARACTERISTICS

The servomotor differs from the torque motor in that it is required to operate over a range of speeds. Performance at stall is therefore no longer the only determining factor. Gearing is commonly used between the motor and load, and any torque amplification can thus be obtained. The allowable power dissipation is determined by the allowable temperature rise. The servomotor must operate at standstill under a prescribed duty cycle. The stall power input can then be regarded as a constant of the motor.

It is essential that such a motor does not "single-phase." That is, when the control-field voltage is reduced to zero, it should not develop a positive torque at any speed.[4] This requirement is met if the torque-speed characteristic peaks at a negative speed. This characteristic is determined by the relationship between the secondary resistance and the remaining motor parameters, and it is necessary to examine whether this relationship is consistent with the requirement for maximum T/W efficiency. It is shown in Appendix II that the two requirements are generally consistent; i.e., a motor, the secondary resistance and number of poles of which are optimized for application in a positional servo, will not single-phase provided that the secondary resistance R_2 is not smaller than the air-gap reactance X_m. In other words, inasmuch as a 60-per-cent tolerance is allowed on the relation $R_2=X_m$, optimum servomotor design requires that the upper half of this tolerance be used; R_2 may be larger than X_m, but not smaller.

A possible criterion for the design of certain servomotors would be maximum power output. With the power dissipation limited by thermal considerations, this is equivalent to a design for maximum power efficiency. However, power output and power efficiency are usually not of primary importance for small servomotors. Therefore consider a motor design based on the accuracy and stability requirements of the servo itself. The important characteristics of a servomotor are:

1. The maximum stall torque T. The ratio of stall torque to control-field voltage is called the torque coefficient K_T.
2. The maximum speed, or the synchronous speed N_s.
3. The damping coefficient K_F. The negative slope of the torque-speed characteristics constitutes the equivalent of viscous damping. The damping varies with speed and control-field voltage. From the

point of view of the servo, the damping at zero speed and zero control-field voltage is significant. In Appendix I it is shown that, at zero speed, the damping coefficient equals one half of the slope of the torque-speed characteristics for balanced inputs.

4. The moment of inertia J of the rotor. The ratio of rotor inertia to damping coefficient is called the motor time constant

$$\tau=\frac{J}{K_F} \tag{30}$$

5. The static friction of the motor. This is sometimes expressed as a starting voltage, i.e., the control-field voltage necessary to overcome static friction.

SERVO CHARACTERISTICS

For the purpose of designing a servomotor, a simple position servo with ideal characteristics will be assumed. A block diagram is shown in Fig. 3. An output shaft θ_O is slaved to an input θ_I by means of the error detector, motor amplifier, motor, and gear train. Neglecting all nonlinearities and higher order terms, the differential equation of the servo is given by

$$Jn\ddot{\theta}_o+K_Fn\dot{\theta}_o+K_TK_AK_E\theta_o=K_TK_AK_E\theta_I \tag{31}$$

or, in normalized form

$$\ddot{\theta}_o+2\xi\omega_0\dot{\theta}_o+\omega_0^2\theta_o=\omega_0^2\theta_I \tag{32}$$

where

$$\omega_0=\sqrt{\frac{K_TK_AK_E}{Jn}} \tag{33}$$

$$\xi=\frac{K_F}{2J\omega_0}=\frac{1}{2\omega_0\tau}=\frac{K_F}{2}\sqrt{\frac{n}{JK_TK_AK_E}} \tag{34}$$

Two other important characteristics are the static error e_s and the error $1/K_v$ to a constant velocity input. The static error depends on the total static frictional load and is given by

$$e_s=\frac{\text{static friction}}{K_TK_AK_E} \tag{35}$$

The velocity constant, the reciprocal of the error to a constant velocity input, is

$$K_V=\frac{\omega_0}{2\xi}=\omega_0^2\tau=\frac{K_TK_AK_E}{nK_F} \tag{36}$$

The maximum speed of the input command which the servo can follow is dependent on the maximum motor speed and the gear ratio. Therefore the approximate relation for the gear ratio is

$$n=\frac{N_s}{N_m} \tag{37}$$

where N_m is related to the required maximum following speed by a safety factor.

In designing such a servo, the gear ratio is determined by the maximum required following rate. The amplifier gain is determined by the allowable static error. Assume that this servo does not have to have high dynamic accuracy. That is, both the natural frequency and the velocity constant are unimportant. However, good damping is required. Having selected a motor size of the required power-handling ability, it is now desired to optimize the motor for maximum damping ratio.

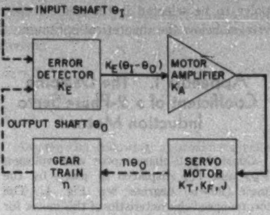

Fig. 3. Simple positional servo

Some assumption must be made regarding the source of the inertia and static friction. First, it is assumed that all the inertia resides in the motor. This is a reasonable assumption for a large class of servos, for example instrument size servos. The situation with respect to friction is less clear cut. Two extreme cases are:

1. All the friction is in the load.
2. All the friction is in the motor.

These two extremes result in two different forms for equation 35

$$e_s=\frac{T_F}{nK_TK_AK_E} \tag{35A}$$

$$e_s=\frac{T_F}{K_TK_AK_E} \tag{35B}$$

The two cases lead to somewhat different optimum motor design, and a compromise between these two will result in the best motor for an actual servo.

OPTIMIZING THE SERVOMOTOR

For the purpose of this optimizing procedure it is sufficient to approximate the damping coefficient by half the ratio of stall torque to synchronous speed; see Appendix I

$$K_F=\frac{T}{2N_s}=\frac{(\mathrm{T/W})W}{2N_s} \tag{38}$$

The synchronous speed is related to the number of poles by

$$N_s=\frac{2f}{p} \tag{39}$$

Substituting into equation 34 equations 37, 38, 39, 6, and the appropriate equation 35

$$\xi=\frac{\mathrm{T/W}}{\sqrt{J}}\frac{W}{4N_m}\sqrt{\frac{e_s}{T_F}}\propto\frac{py}{\sqrt{J}} \tag{40A}$$

$$\xi=\frac{\mathrm{T/W}}{\sqrt{N_sJ}}\frac{W}{4}\sqrt{\frac{e_s}{T_FN_m}}\propto\frac{p^{3/2}y}{\sqrt{J}} \tag{40B}$$

In either case the T/W efficiency must be maximized, so that y can be replaced by the expression in equation 19. Furthermore, the moment of inertia is proportional to the fourth power of the airgap diameter. The damping ratio is then proportional to

$$\xi\propto\frac{p}{D_g^3\left(1+2\frac{R_1}{X_m}\right)}=\frac{p}{D_g^3\left(1+\frac{2C_mp^2}{fD_gA_w}\right)} \tag{41A}$$

$$\xi\propto\frac{p^{3/2}}{Dj^3\left(1+2\frac{R_1}{X_m}\right)}=\frac{p^{3/2}}{D_g^3\left(1+\frac{2C_mp^2}{fD_gA_w}\right)} \tag{41B}$$

The optimum number of poles is found by the usual differentiation procedure

$$p_{\mathrm{opt}}=\sqrt{\frac{fD_gA_w}{2C_m}} \tag{42A}$$

$$p_{\mathrm{opt}}=\sqrt{\frac{3fD_gA_w}{2C_m}} \tag{42B}$$

The best number of poles is an even integer somewhere between equations 42(A) and 42(B). The best ratio of R_1/X_m will be somewhere between 1/2 and 3/2, and the resulting T/W efficiency will be between 25 and 50 per cent. Note that the best number of poles is somewhat larger than for the torque motor.

With the number of poles theoretically optimized, equations 41 become

$$\xi\propto\frac{A_w^{1/2}}{D_g^{5/2}} \tag{43A}$$

$$\xi\propto\frac{A_w^{3/4}}{D_g^{9/4}} \tag{43B}$$

For the conventional motor the copper winding area is expressed in terms of the motor diameters by equation 26

$$\xi\propto\frac{(D^2-D_g^2)^{1/2}}{D_g^{5/2}} \tag{44A}$$

$$\xi\propto\frac{(D^2-D_g^2)^{3/4}}{D_g^{9/4}} \tag{44B}$$

The minimum possible diameter is called for. This minimum will be determined by such considerations as the ease of winding and the number of slots required for the poles determined by equations 42. For this minimum diameter, the copper winding area is essentially a constant so that the variation of damping ratio with rotor diameter for small

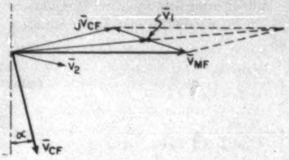

Fig. 4. Unbalanced motor excitation voltages

changes in rotor diameter becomes

$$\xi \propto \frac{1}{D_g^{5/3}} \tag{45A}$$

$$\xi \propto \frac{1}{D_g^{5/4}} \tag{45B}$$

Again a direct design procedure has been established for a motor of a given frame size. Rotor diameter and air-gap length are reduced to the smallest possible size. The number of poles is then determined from equations 42, using C_m as defined in equation 17. A lamination can then be laid out; the mutual reactance X_m is also now determined. The required rotor resistance is obtained from equation 12.

In selecting the number of poles, the remarks made in the case of the torque motor also apply to the servomotor. That is, the number is always rounded off downwards from the theoretical optimum. For example, if several even integers are located between the "optima" of equations 42(A) and 42(B), the smallest is selected.

Conclusion

In the design of induction torque motors and servomotors the T/W concept is useful in determining optimum motor design. In these motors the T/W efficiency must be maximized. This requirement leads to the very simple relationship: optimum secondary resistance = air-gap reactance.

Some approximations were made in arriving at this equation. However, the optimum is so broad that errors of 50 per cent are insignificant, and the relationship is useful even for the smallest motors. To ensure that there is no positive single-phase torque, the rotor resistance should err on the high side.

A more detailed analysis of these control motors leads to equations for the optimum number of poles. The particular equation used depends on the type of motor and its application, but the method of analysis is the same. The number of poles to be selected is the nearest even integer below the theoretical optimum.

Appendix I. The Damping Coefficient of a 2-Phase Servo Induction Motor

Consider a 2-phase motor with voltages V_{MF} and V_{CF} displaced in phase by the angle $(90-\alpha)$ degrees; see Fig. 4. The torque-speed characteristics of this motor for balanced excitation (i.e., for $V_{CF}=V_{MF}$ and $\alpha=0$) is given; see Fig. 5. Let the stall torque be denoted by T, and let the slope of this curve at zero speed be denoted by M. It is desired to find the relationship between the zero-speed slope of the torque-speed characteristics for $V_{CF}\neq V_{MF}$, and T and M. The motor performance is analyzed by the method of symmetrical components[6]

$$V_{MF}=V_1+V_2 \tag{46}$$

$$jV_{FC}=V_1-V_2 \tag{47}$$

These equations are not exactly correct except at zero speed where the motor impedance to positive- and negative-sequence excitation is identical; since only the zero-speed slope is of interest, equations 46 and 47 are satisfactory.[5] Solving for V_1 and V_2

$$V_1=\frac{1}{2}(V_{MF}+jV_{CF}) \tag{48}$$

$$V_2=\frac{1}{2}(V_{MF}-jV_{CF}) \tag{49}$$

The absolute values of V_1 and V_2 are

$$V_1=\frac{1}{2}\times\sqrt{(V_{MF}+V_{CF}\cos\alpha)^2+(V_{CF}\sin\alpha)^2} \tag{50}$$

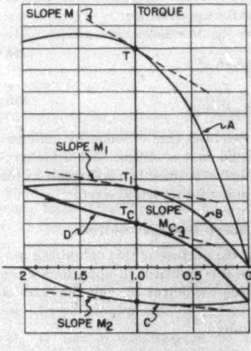

Fig. 5. Intercept and slope of torque-speed characteristics for unbalanced voltages

A—Characteristics for balanced excitation, $V_{CF}=V_{MF}$, $\alpha=0$
B—Positive-sequence component
C—Negative-sequence component
D—Resultant torque-speed curve

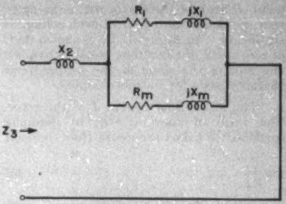

Fig. 6. Parameter Z_3 (for zero-source impedance)

$$V_2=\frac{1}{2}\times\sqrt{(V_{MF}-V_{CF}\cos\alpha)^2+(V_{CF}\sin\alpha)^2} \tag{51}$$

Neglecting saturation and changes in self-heating, stall torque is proportional to the square of the excitation. Imagine that the motor is replaced by two mechanically coupled motors, one excited with balanced positive-sequence voltages of magnitude V_1 and the other by balanced negative-sequence voltages of magnitude V_2. Then the stall torques and the zero-speed slopes of the torque-speed characteristics for the two motors are given respectively by

$$T_1=\frac{(V_{MF}+V_{CF}\cos\alpha)^2+(V_{CF}\sin\alpha)^2}{4V_{MF}^2}T \tag{52}$$

$$T_2=\frac{(V_{MF}-V_{CF}\cos\alpha)^2+(V_{CF}\sin\alpha)^2}{4V_{MF}^2}T \tag{53}$$

$$M_1=\frac{(V_{MF}+V_{CF}\cos\alpha)^2+(V_{CF}\sin\alpha)^2}{4V_{MF}^2}M \tag{54}$$

$$M_2=\frac{(V_{MF}-V_{CF}\cos\alpha)^2+(V_{CF}\sin\alpha)^2}{4V_{MF}^2}M \tag{55}$$

The net torque is the difference of the two component torques

$$T_c=T_1-T_2=\frac{TV_{CF}\cos\alpha}{V_{MF}} \tag{56}$$

which yields the well-known result that the stall torque is proportional to the control field voltage.[4] However, it is interesting to note from Fig. 5, that, when the torques are subtracted, the slopes of the two speed-torque characteristics become additive. Therefore the slope of the resultant characteristic becomes

$$M_c=M_1+M_2=\left[1+\left(\frac{V_{CF}}{V_{MF}}\right)^2\right]\frac{M}{2} \tag{57}$$

In determining the stability of a feedback control system for small oscillations, the performance for very small control voltages is of interest. It is therefore sufficient to define the motor damping coefficient as the slope of the speed-torque characteristic for $V_{CF}=0$. This is obtained from equation 57

$$K_F=M_{c(V_{CF}=0)}=\frac{M}{2} \tag{58}$$

The assumption $K_F = M$, made in many textbooks on servomechanisms, is not correct.

Appendix II. Condition for Single-Phase Operation

Chang has shown that the servomotor with zero voltage on the control field does not develop a positive torque at any speed, provided that

$$R_2 > |Z_s| \tag{59}$$

where Z_s is defined in Fig. 6 for a motor operated from a zero-impedance source.[6] In terms of the motor parameters the condition becomes

$$R_2 > \sqrt{\frac{(R_1R_m - X_1X_m - X_1X_2 - X_2X_m)^2 + (R_1X_m + R_mX_1 + R_1X_2 + R_mX_2)^2}{(R_1+X_m)^2 + (X_1+X_m)^2}} \tag{60}$$

In the previous analysis the following conditions for an optimum servomotor were derived

$$R_2 = X_m \tag{12}$$

$$\frac{1}{2} < \frac{R_1}{X_m} < \frac{3}{2}$$

Assume the following approximate relations

$$R_1 = X_m$$

$$X_1 = 0.3X_m$$

$$X_2 = 0.1X_m$$

$$R_m = 0.1X_m$$

Substituting into equation 60

$$R_2 > 0.7X_m \tag{61}$$

and the motor will not run single phase if R_2 is optimized for maximum T/W efficiency. However, it was stated previously that the relationship of equation 12 is not critical and that an error of 50 per cent is permissible. It appears desirable to stipulate that only the upper half of the tolerance be used; i.e., R_2 should be equal to or larger than X_m, not smaller.

References

1. ELECTRIC MACHINERY (book), M. M. Liwschitz-Garik, C. C. Whipple. D. Van Nostrand Company, Inc., New York, N. Y., 1946, vol. II, p. 164.

2. *Ibid.*, pp. 215–20.

3. THE POLYPHASE INDUCTION MACHINE WITH SOLID ROTOR, H. M. McConnell. *AIEE Transactions*, vol. 72, pt. III, Apr. 1953, pp. 103–11.

4. OPERATING CHARACTERISTICS OF 2-PHASE SERVOMOTORS, R. J. W. Koopman. *AIEE Transactions*, vol. 68, pt. I, 1949, pp. 319–29.

5. ELECTRIC MACHINERY (book), A. E. Fitzgerald, C. Kingsley. McGraw-Hill Book Company, Inc., New York, N. Y., 1952, p. 470 ff.

6. *Discussion* of reference 4 by S. S. L. Chang.

Application of Statistics to Motor Testing

J. L. OLDENKAMP
ASSOCIATE MEMBER AIEE

IN TESTING groups of similar motors, a considerable variation in test results has been observed. Because of this, several questions have arisen:

1. Is this variation in test results caused by differences between supposedly similar motors, differences between testing personnel, or by the inability to control and duplicate test conditions?

2. How many motors must be built to evaluate a design and rating, and can this number be reduced by repeating the performance test?

3. Do all lines of fractional horsepower (hp) motors tend to have the same variation in their test results, or will some types of motors be more uniform than others?

The problem was attacked by the use of a statistical analysis, the most logical approach for a problem of this type. The results are useful in that they give the error in estimating the performance characteristic as a function of the number of motors tested and the number of times the motors are tested.

Method of Analysis

The problem of evaluating the variation in performance tests was attacked by testing three types of motors—six motors of each type—three times. The motors were tested in a different order by different testers each time. None of the testers were aware that they were merely duplicating previous tests. The types of motors selected were: 12-watt shaded pole motors, 1/4-hp d-c motors, and 20-watt a-c series motors.

The results were evaluated by means of an analysis of variance.[1-9] It was necessary to assume the variation was composed of three parts: variation between motors, bias on the part of the testers (a tendency to read always high or low), and experimental error caused by the inability to control all test conditions; see Table I for no-load test data for the 1/4-hp d-c motors and the analysis of variance for these data. By equating the expected values of the mean squares to the numer-

Table I. No-Load Speed for 1/4-Hp D-C Motor

Motor	No. 1	No. 2	No. 3	No. 4	No. 5	No. 6
Test						
No. 1	2,020	1,985	1,950	1,950	2,050	2,000
No. 2	2,045	2,020	1,970	1,995	2,080	2,035
No. 3	1,990	1,985	1,940	1,960	2,030	2,010

Table II. Analysis of Variance, No-Load Speed

Source of Variance	Degrees of Freedom	Sum of Squares	Mean Square	Expected Value of Mean Square	Ratio F
Testers	2	5,023.33	2,511.6	$6\sigma_T^2 + \sigma_e^2$	30.63*
Motors	5	19,769.16	3,953.83	$3\sigma_M^2 + \sigma_e^2$	48.22*
Residual	10	820.01	82	σ_e^2	1
Total	17	25,612.5			

* Significant at the 99 per cent confidence level.

Paper 55-286, recommended by the AIEE Rotating Machinery Committee and approved by the AIEE Committee on Technical Operations for presentation at the AIEE Middle Eastern District Meeting, Columbus, Ohio, May 4–6, 1955. Manuscript submitted October 15, 1954; made available for printing April 4, 1955.

J. L. OLDENKAMP is with the General Electric Company, Fort Wayne, Ind.

The author wishes to acknowledge the help of J. A. Zoellner and J. L. Dolby for their assistance in developing the method of analysis. Also, M. L. Schmidt is to be acknowledged for his aid and consultation. The author expresses appreciation to D. R. Kinsey and Elizabeth Rose who performed the many computations needed in the analysis of this paper, and to R. J. Solga who assisted in obtaining test data.

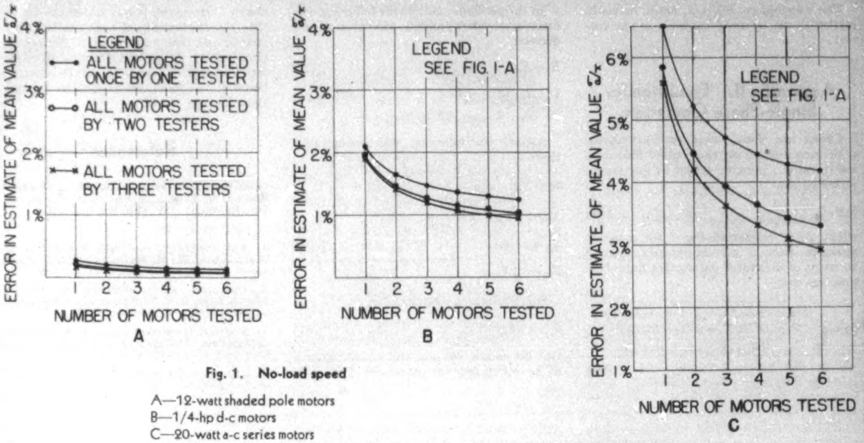

Fig. 1. No-load speed

A—12-watt shaded pole motors
B—1/4-hp d-c motors
C—20-watt a-c series motors
The subcaption also applies to Figs. 2, 3, and 4

ical value, see Table II, it was possible to calculate the three standard deviations:

σ_M = standard deviation caused by differences between motors.
σ_T = standard deviation caused by differences between testers.
σ_0 = standard deviation cuased by experimental error or inability to repeat test readings.

Knowing the magnitude of the three components of error for the selected sample taken from the total population, it is possible to calculate the deviation of the sample average from the average of the total population. The estimate of the standard deviation σ_a of the average obtained when M motors are tested T times, from the true average of the total population given by

$$\sigma_a^2 = \frac{\sigma_M^2}{M} + \frac{\sigma_T^2}{T} + \frac{\sigma_0^2}{MT} \qquad (1)$$

For clarification see Appendix I. This equation, when modified to give deviation in per unit or per cent, reads

$$\frac{\sigma_a}{\bar{x}} = \sqrt{\frac{\sigma_M^2}{M} + \frac{\sigma_T^2}{T} + \frac{\sigma_0^2}{MT}} \Bigg/ \bar{x} \qquad (2)$$

where $\bar{x}$ is calculated average of the samples.

With the aid of equation 2 it was possible to plot per-cent error ($\sigma_a/\bar{x}$) as a function of sample size (the number of motors tested) and the number of times the group of motors were tested.

Discussion

The curves of Figs. 1 through 5 indicate the error in estimating the performance characteristics for the three lines of motors. The performance characteristics covered are no-load speed, full-load speed, full-load efficiency, full-load watts input, and locked rotor torque, locked rotor torque is covered for shaded pole motors only.

Figs. 1(A), (B), and (C), give the error of estimate of no-load speed for the three types of motors. It can be seen that the shaded pole motor is associated with the smallest error and that the a-c series motor is linked with the largest error. This should be expected since induction motors have no brushes; brushes are a source of variable friction and voltage

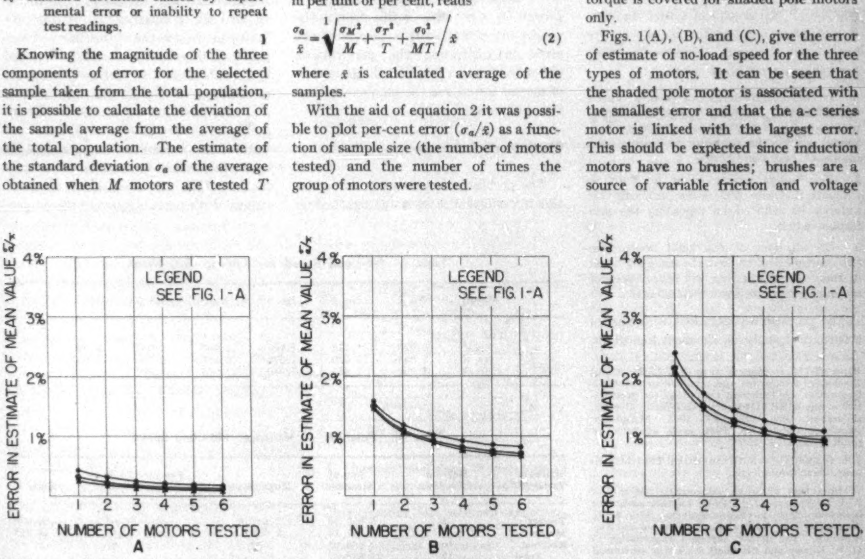

Fig. 2. Full-load speed

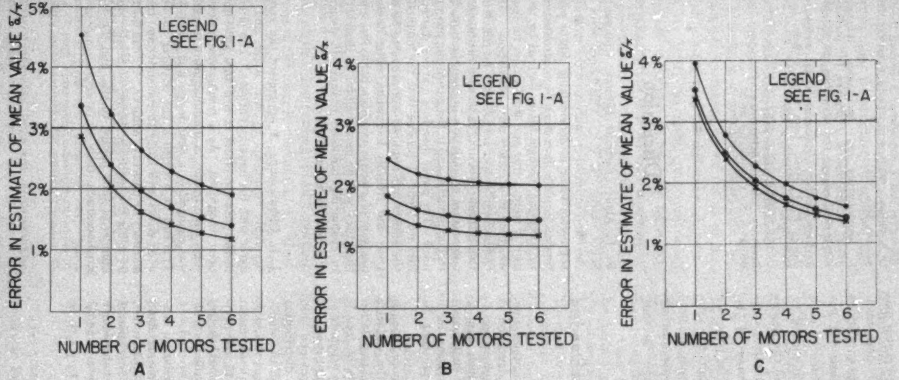

Fig. 3. Efficiency

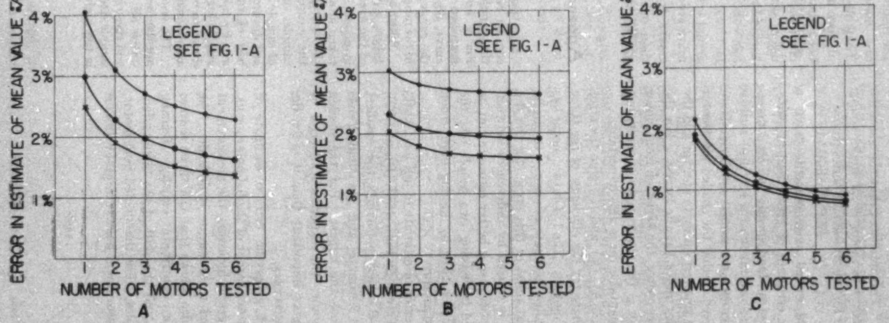

Fig. 4. Watts input

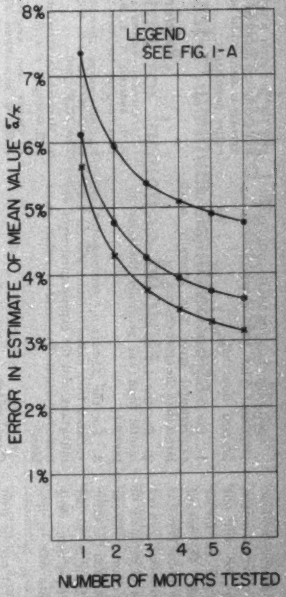

Fig. 5. Locked rotor torque, 20-watt shaded pole motors

drop. In estimating the average no-load speed of the 20-watt a-c series motor, the error is 6.5 per cent for only one motor tested once, and 3 per cent for six motors tested three times. This means that, if only one a-c series motor test was made to determine no-load speed: 68 per cent of the time the error of estimate of no load speed will be less than ± 6.5 per cent; 95.4 per cent of the time the error of estimate will be less than ± 13 per cent . . . $2\sigma_a/\bar{x}$; and 99.74 per cent of the time the error of estimate will be less than ± 19.5 per cent . . . $3\sigma_a/\bar{x}$.

By observing Fig. 1(C) it can be seen that the error of estimate is reduced more by having one tester test two motors once than by having three testers test one motor. This indicates that the variation from motor to motor is the major source of error for the 20-watt a-c series motor.

Figs. 2(A), (B), and (C) indicate that full-load speed measurements have a smaller estimate of error than measurements of no-load speed; full-load measurements are taken at a specified torque. These curves are similar to those of no-load speed in that the shaded pole motor has the smallest estimate of error and the a-c series motor has the largest. For the a-c series motor, the variation from motor to motor is the major cause of error, but experimental error is also important.

Figs. 3(A), (B), and (C) give the error of estimate for the efficiency of the three lines of motors. The 1/4-hp d-c motor has the smallest estimate of error. It can be seen that most of this error (for the d-c motor) is caused by differences between testers, because a better estimate can be obtained by having two people test the same motor than by having one person test two motors.

The error of estimate of full-load watts input is given by Figs. 4(A), (B), and (C). The a-c series motor has the smallest error of estimate, and the shaded pole motor has the largest. For the shaded pole motor, the experimental error is much more important than it is for the other two types.

Fig. 5 gives the error of estimate of locked rotor torque of shaded pole motors. As the graph indicates, the measurement of locked rotor torque is difficult. The graph also shows that the three sources of error contribute equally. Bearing friction and the skill of the tester affect the results. For the shaded pole motor, this measurement has the largest estimate of error.

Each type of motor has its own peculiar problem. The test characteristics examined show that:

1. For the 12-watt shaded pole motor, the experimental error was generally much larger than the other errors.
2. For the 1/4-hp d-c motor, the experimental error was generally the least important.
3. For the 20-watt a-c series motor, the variation from motor to motor was the most important, and the experimental error was more important than error caused by tester bias.

Conclusions

In the performance testing of motors the results vary from motor to motor and are biased by the testing personnel. They also vary because all the conditions of test are not held constant. It has been shown that the magnitude of each component of error can be calculated by use of statistical methods, and the deviation of the test results from the true average can be estimated. In view of the fact that for 32 per cent of the time the actual error may be larger than the estimate given by the graphs, it may be necessary to build several samples, rather than one, when a new design is being developed.

Appendix I. Estimate of Standard Deviation

The standard deviation σ of a population, can be regarded as the rms deviation of the population from its average value $\bar{x}$. For a normal distribution which can be described by the familiar bell-shaped curve, 68 per cent of the population lie in the range of $\bar{x}\pm\sigma$, and 99.74 per cent lie in the range of $\bar{x}\pm 3\sigma$.

When a sample of one of a population is taken, e.g., one motor test, the estimate of the average value of the total population is poor. However, if a sample of four is taken in a random manner, the estimate of the average will be greatly improved. If the entire population were grouped into samples of four units and the distribution of sample averages were plotted, the standard deviation of these averages σ_a would be half of the individual standard deviation σ. By taking a sample size of 16, the deviation of the sample average could be reduced to one-fourth of the individual standard deviation.

The true average of the population cannot be determined for the case at hand unless all motors are tested by all testers, and these results are averaged. Any smaller sample size will give an average value which is too high or too low. Equations 1 and 2 give the rms error which will be made if a finite number of motors are tested and this average is assumed to be the average of the entire population.

References

1. STATISTICAL THEORY IN RESEARCH (book), **R. L. Anderson, T. A. Bancroft.** McGraw-Hill Book Company, Inc., New York, N. Y., 1952.

2. EXPERIMENTAL DESIGNS (book), **W. Z. Cochran, G. M. Cox.** John Wiley & Sons, Inc., New York, N. Y., 1950.

3. METHODS OF STATISTICAL ANALYSIS (book), **C. H. Goulden.** *Ibid.*, 1952.

4. DESIGN AND ANALYSIS OF EXPERIMENTS (book), **O. Kempthorne.** *Ibid.*

5. STATISTICAL METHODS (book), **G. W. Snedecor.** Iowa State College Press, Ames, Iowa, 1950.

6. STATISTICAL DESIGN AND ANALYSIS OF EXPERIMENTS FOR DEVELOPMENT RESEARCH (book), **D. S. Villars.** William C. Brown Company, Milwaukee, Wis., 1951.

7. INTRODUCTION TO STATISTICAL ANALYSIS (book), **W. J. Dixon, E. J. Massey, Jr.** McGraw-Hill Book Company, Inc., New York, N. Y., 1951.

8. INTRODUCTION TO MATHEMATICAL STATISTICS (book), **P. G. Hoel.** John Wiley & Sons, Inc., New York, N. Y., 1947, p. 158.

9. INDUSTRIAL EXPERIMENTATION (book), **K. A. Brownlee,** Chemical Publishing Company, Inc., Brooklyn, N. Y., 1949, pp. 56–57.

Discussion

P. L. Alger (General Electric Company, Schenectady, N. Y.): This paper gives a clear and interesting analysis of the separate sources of error in determining motor performance. We have long been accustomed to accepting a single figure derived by test as if it were a true and final value, far outweighing in accuracy any calculation. Mr. Oldenkamp's paper reveals how far different this is from the truth, in view of the numerous sources of variation in manufacture, in test equipment, and in the measuring process itself. The paper therefore marks a distinct forward step. I believe that the methods the author has outlined will prove to be of great and steadily increasing value in the analysis of electric machine behavior, and that they will be most helpful to designers in evaluating proposed changes in design and manufacturing methods.

J. L. Oldenkamp: I appreciate the very favorable comments by Mr. Alger, and I agree with his remarks entirely. Too often in the past the errors in test data have not been recognized. As a result, wrong decisions were made: a manufacturing process was changed or a new design was rejected. This can be avoided if the engineer knows what errors he is likely to encounter and the accuracy he desires to achieve. He can then, by using the methods shown, determine the number of tests needed to give him the desired accuracy.

The Transient Stalled Temperature Rise of Cast-Aluminum Squirrel-Cage Rotors for Induction Motors

G. M. ROSENBERRY, JR.
ASSOCIATE MEMBER AIEE

IT IS usually necessary to protect motors against stalled rotor conditions. Information concerning the temperature rise of various parts of the motor during stall is necessary so that a control may be provided to remove the motor from the line before the critical member approaches a dangerous temperature. Or, conversely, the motor must be designed with adequate stall-time capacity so that a practical control may be used to protect it.

This paper is concerned only with the stalled temperature rise of rotors of the squirrel-cage type for induction motors. In the past, the most commonly used method of calculation has been based on the assumption that all heat is stored in the conductor. Although this approach has the advantage of simplicity, comparison of calculated values with test results shows that the calculated values are very conservative. For cast-aluminum rotors temperatures computed by the approximate (or simplified) method may be as much as five or more times greater than the test temperatures. The magnitude of the discrepancy depends upon the motor design, the duration of the test, etc. The need for a more accurate approach, which accounts for the important variables, is obvious.

A more precise method of analysis of the transient rotor temperatures under stalled rotor conditions is presented in this paper. Heat storage in all important parts of the rotor is accounted for. Heat dissipation from the rotor to the stator and to the ambient is also included. Calculations and test results are compared for one motor.

Special terms, where used, are defined. Most dimensions are defined in Figs. 1 and 2. The units used are watts, seconds, inches, and degrees centigrade (C). (Any other consistent set of units may be used.)

Nomenclature

A = area of the cross section of the heat-conducting path per slot (tooth) or fan blade, inches^2
A_R = surface area of one end ring including fan blades, inches^2
B = ratio of effective length of bar to total length, lumped circuit approximation
C = thermal capacitance of section (includes all slots) watt-seconds/C
D = rotor diameter, inches
L_R = length of rotor stack, inches
L_P = length of fan blade, inches
N_P = number of fan blades
N_R = number of rotor slots
P_{ad} = periphery of boundary between section a and d, inches
R = thermal resistance, for all slots, C/watts
V = volume fan blades or end ring, one end, inches^3
W = watt loss in section (including all slots)
c_p = specific heat watt-seconds/pounds-C
d = radial depth of section, inches^2
h = surface or contact heat transfer coefficient watts/inches^2-C
k = thermal conductivity, watts/C-inches
t = time, seconds
w = width of section (peripherally) per slot at outer end (radially), inches
w' = width of section at end closest to shaft, inches
$\bar{w}$ = average width of section $1/2(w+w')$
α = thermal diffusivity $(k/\rho c_p)$, inches^2/seconds
θ = temperature rise above initial temperature, C
ρ = density of material, pounds/inches^3

Subscripts

a, b, c, d, e, f, g, h apply to sections in the plane of the rotor punching; see Fig. 1
1, 2 apply to axial subdivisions as shown in Fig. 2
A refers to characteristics of aluminum conductor
F refers to characteristics of iron punching material
P refers to fan or paddles
R refers to end ring

Method of Analysis

The rotor configuration analyzed is shown in Figs. 1 and 2. This is a double squirrel-cage type of rotor slot. The rotor conductor is cast integrally with the end ring and fan blades. This rather complex distributed system is simplified by breaking it up into a lumped system. The plane of the rotor punching is divided into eight sections as shown in Fig. 1: three for the conductor a, b, c; three for the tooth d, e, f; and two for the yoke below the rotor slot g, h. This division is done for one tooth and one slot only, since all are identical. Similarly, only one-half (axially) of the rotor need be considered since it is symmetrical about the central plane. This half of the rotor is divided into two equal sections as shown in Fig. 2, designated as 1 and 2. The end ring and fan blades are the last two sections. Thus the rotor is divided into a total of 18 heat storage units.

Additional assumptions made in the analysis are as follows:

1. The heat inputs do not vary with time.
2. The thermal properties of the rotor materials do not vary with temperature or position.
3. Heat transfer axially through the iron is negligible.

When the 18 heat storage units are connected by the appropriate thermal resistances, an equivalent lumped thermal circuit is obtained. For convenience, this thermal circuit is represented schematically by the analogous electrical circuit, as shown in Fig. 3. Numerical values are shown, for the motor used as an example, to give an idea of the magnitudes of the resistances and capacitances.

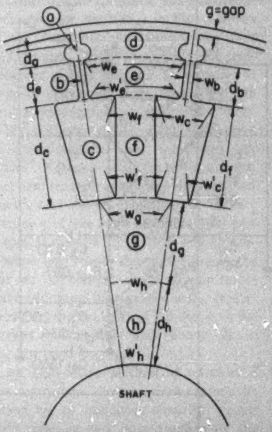

Fig. 1. Rotor-punching and slot layout

Paper 55-255, recommended by the AIEE Rotating Machinery Committee and approved by the AIEE Committee on Technical Operations for presentation at the AIEE Electrical Utilization of Aluminum Conference, Pittsburgh, Pa., March 15–17, 1955. Manuscript submitted December 16, 1954; made available for printing January 26, 1955.

G. M. Rosenberry, Jr., is with the General Electric Company, Schenectady, N. Y.

The inputs W are the watt loss in the various parts of the conductor and end ring. The thermal capacities C are calculated from equations of the form

$$C = c_p \rho V, \frac{\text{watt-seconds}}{\text{C}} \tag{1}$$

where V is the volume of the element.

Of the two types of thermal resistances, the first is a contact or surface phenomenon such as the contact resistance between the conductors and iron or the surface heat transfer off the end ring. These resistances are of the form

$$R = \frac{1}{hA}, \frac{\text{C}}{\text{watts}} \tag{2}$$

where A is the area of the heat conduction path. The other type of resistance accounts for the temperature drop in the conducting material such as aluminum or iron. This resistance is of the form

$$R = \frac{l}{kA}, \frac{\text{C}}{\text{watts}} \tag{3}$$

where l is the effective length of the conduction path required to give the correct transient temperature rise. The philosophy used in this paper to determine the effective length l is to study the exact solution for an insulated bar under different conditions of excitation. By comparing the exact solution to the solution for a single resistance-capacitance element, a value of l is determined which gives the correct average temperature for the time range of most interest. The analysis and results for two cases are given in Appendixes II and III.

The development of equations for the individual resistances and capacitances are given in detail in Appendix I. The magnitude of the values for the watt inputs may be calculated from the equivalent circuit for the double squirrel-cage motor; see, for example, reference 1.

An electronic differential analyzer was used to obtain the solution of the thermal circuit. The equations for the thermal circuit, in a form suitable for use on a differential analyzer, are indicated in Appendix I.

Results

Fig. 4 gives the results of calculations and a test on one motor. The motor used was a 4-pole 50-horsepower National Electrical Manufacturers Association design B, polyphase induction motor. All calculations and tests were made for the case of full voltage stall with balanced voltages applied. The test temperatures are shown by the solid line and the calculated results dashed. It can be seen that the agreement between test and calculations is good in both the magnitude and the shape of the time-temperature curves.

The bar temperature rise, based on the assumption that all heat is stored in the bars (all parts of the bar at the same temperature), is shown by curve A in Fig. 4. When the more precise method is used, temperatures, after 50 seconds, are only one-fifth of those given by the approximate method. Curve B is similar except that the heat is stored in the bars plus the teeth (all parts at the same temperature). In the time range of most interest, this improved method gives results closer to the true temperature although it is low for shorter times (50 C low at 20 seconds). These differences would be more pronounced for a National Electrical Manufacturers Association design C motor. Curve C is a similar curve calculated for the end ring under the assumption that it is isolated from the bars and fan blades. The variation in temperature rise throughout the rotor is shown by the calculated curves, Fig. 5.

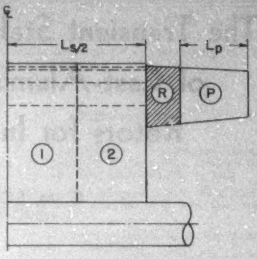

Fig. 2. Cross section of rotor, side view

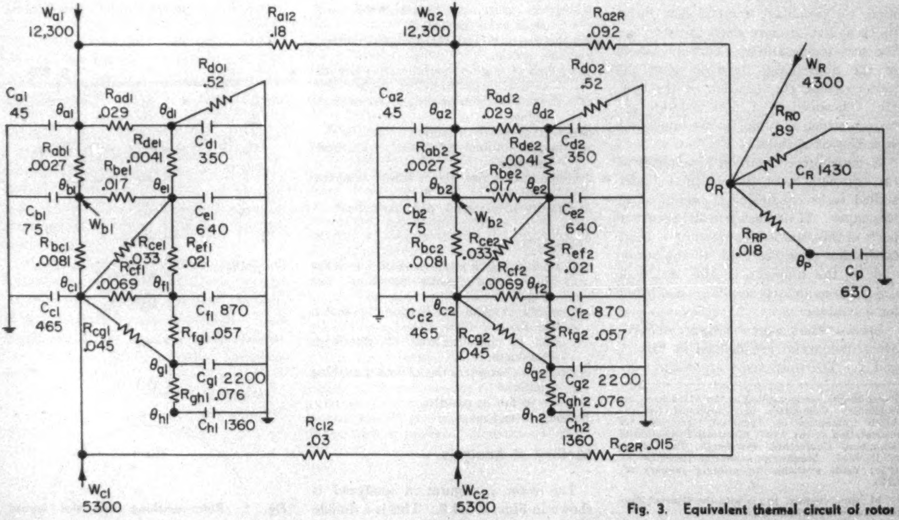
W_{a1} 12,300
R_{a12} .18
W_{a2} 12,300
R_{a2R} .092
R_{d01} .52
R_{d02} .52
W_R 4300
C_{a1} 45
θ_{a1}
R_{ad1} .029
θ_{d1}
C_{a2} .45
θ_{a2}
R_{ad2} .029
θ_{d2}
R_{RO} .89
R_{ab1} .0027
R_{de1} .0041
C_{d1} 350
R_{ab2} .0027
R_{de2} .0041
C_{d2} 350
C_R 1430
θ_R
θ_{b1}
R_{be1} .017
θ_{e1}
θ_{b2}
R_{be2} .017
θ_{e2}
C_{b1} 75
W_{b1}
C_{e1} 640
C_{b2} 75
W_{b2}
C_{e2} 640
R_{bc1} .0081
R_{ce1} .033
R_{cf1}
R_{ef1} .021
R_{bc2} .0081
R_{ce2} .033
R_{cf2}
R_{ef2} .021
R_{RP} .018
θ_P
C_P 630
θ_{c1}
.0069
θ_{f1}
.0069
θ_{f2}
C_{c1} 465
C_{f1} 870
C_{c2} 465
θ_{c2}
C_{f2} 870
R_{cg1} .045
R_{fg1} .057
R_{cg2} .045
R_{fg2} .057
θ_{g1}
C_{g1} 2200
θ_{g2}
C_{g2} 2200
R_{gh1} .076
R_{gh2} .076
θ_{h1}
C_{h1} 1360
θ_{h2}
C_{h2} 1360
R_{c12} .03
R_{c2R} .015
W_{c1} 5300
W_{c2} 5300

Fig. 3. Equivalent thermal circuit of roto

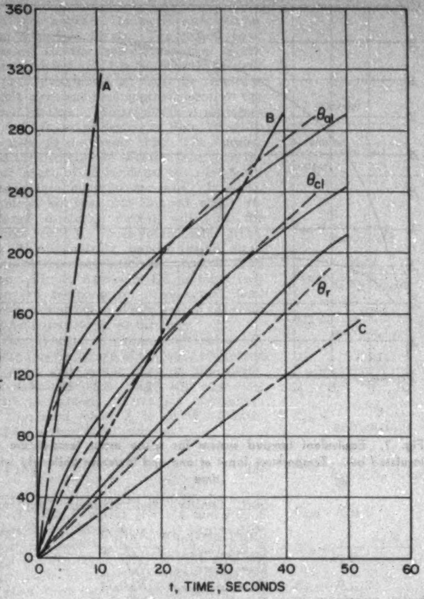

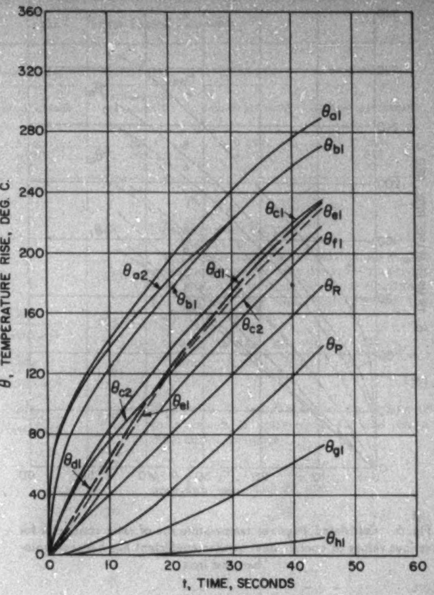

Fig. 4. Transient rotor temperature rise. Solid curves are tested, dotted curves calculated

θ_{a1}, top bar
θ_{c1}, bottom bar
θ_R, end ring
A, calculated using bars only
B, calculated using bars plus teeth
C, calculated end ring temperature, ring isolated from rotor

Fig. 5. Calculated transient temperature rise of various parts of rotor

The effect of the contact heat transfer coefficient between aluminum and iron h_{ad} is shown in Fig. 6. The correct value is, of course, a function of manufacturing processes. A magnitude of 1.0 was used for the motor calculated in this paper.

Discussion

The ultimate justification of assumptions made in the analysis comes from the comparison of calculated and test temperatures. It is shown in Fig. 4 that the correlation is quite good for all practical purposes. It would be possible to obtain slightly better results by dividing the rotor into more sections and by accounting for the change in losses with time, but the additional complication would be too great for a small gain in accuracy. Calculations have shown that the magnitude of the axial heat flow in the rotor iron is small compared to that in the conductors. This is because of the high contact resistance between laminations.

Some interesting conclusions may be drawn from Fig. 5, which shows calculated temperatures in various parts of the rotor. The end ring is the coolest part of the conductor since the current density is much lower there. The center section of the rotor is the hottest although not very much hotter than the end section. The axial coupling is rather loose. Thus if the center section is calculated alone, the results will not be significantly different unless the rotor is very short. This offers one method of simplifying the analysis. The only important result that would be lost is the end ring temperature, and it is usually not limiting. Comparison of curves *C* and θ_r in Fig. 4 shows the contribution of the bar loss to the end ring temperature rise. In this case, the actual end ring temperature is 45 per cent greater than if it were isolated.

Inspection of the rotor yoke temperature near the shaft (θ_{h1}) in Fig. 5 shows that it contributes very little to the thermal storage. After 45 seconds, the temperature rise is only 12 C because 45 seconds is not sufficient time for much heat to propagate that far in silicon steel.

Fig. 6 illustrates one of the advantages of cast-aluminum over fabricated bar rotors. For cast conductor rotors the contact heat transfer coefficient between conductor and iron is much higher. Where a value of 1.0 or more is obtained for cast rotors, it may be 0.2 more or less for fabricated bar rotors depending upon the bar fit. Of course, cast-aluminum rotors have additional advantages in the greater flexibility in the choice of bar shape, in the rugged construction and, above all, in the low cost.

An alternative method of solution of the equivalent thermal circuit would be to set up an analogous electrical circuit with resistors and capacitors, apply the current inputs, and read the desired volt-

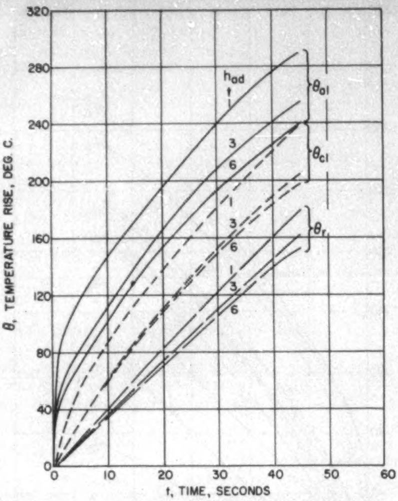

Fig. 6. Calculated transient temperature rise of rotor conductor for various values of contact heat transfer coefficient h_{ad} between rotor bars and iron

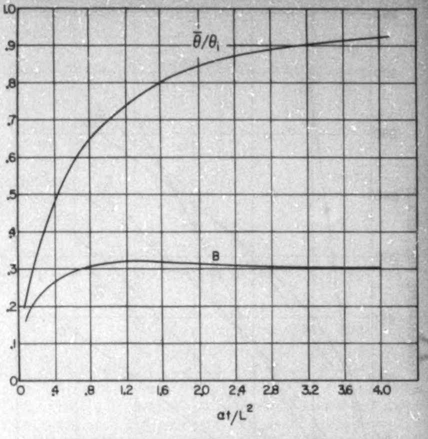

Fig. 7. Equivalent lumped system for space mean temperature in insulated bar. Temperature input at one end increases uniformly with time

ages in the circuit with a recorder. Application of appropriate scale factors makes it possible to use practical circuit components.

The magnitude of the resistances to the ambient, Fig. 3, shows that heat dissipated in this fashion is negligible. In other words, the problem is simply one of thermal storage.

The same general approach could be used for computation of transient rotor and stator temperatures while running under severe duty cycle loads. In this case, the heat dissipated to the ambient would become more important.

Appendix I. Analysis

Development of Circuit

The general approach to the development of the equivalent thermal circuit was discussed earlier in the paper in the section "Method of Analysis," where the 18 different heat storage units, as indicated in Figs. 1 and 2, are pointed out. The equivalent thermal circuit, Fig. 3, represents each of these heat storage units by the usual symbol used for an electrical capacitor. Each of the capacitors are interconnected by appropriate thermal resistors required by the physical arrangement of the rotor, Figs. 1 and 2. Thus the circuit shows two identical rotor sections connected by the axial thermal resistances of the rotor bars. The end ring and rotor fan blades are shown at the right. The axial heat flow through the punchings is negligible, and these connections are not shown. Half of the axial conductance of the middle part of the conductor b is lumped with the top and bottom bars a and c to simplify the circuit further. The heat inputs to the various parts of the conductor are shown as arrows and indicated by the symbol W with appropriate subscripts.

Equations for Circuit Elements

The capacity of the heat storage elements is in general the product of the specific heat, density, and volume. They are

$$C_{a1}=C_{a2}=c_{pA}\rho_A A_a N_R L_s/4 \quad (4)$$
$$C_{b1}=C_{b2}=c_{pA}\rho_A A_b N_R L_s/4 \quad (5)$$
$$C_{c1}=C_{c2}=c_{pA}\rho_A A_c N_R L_s/4 \quad (6)$$
$$C_{d1}=C_{d2}=c_{pF}\rho_F A_d N_R L_s/4 \quad (7)$$
$$C_{e1}=C_{e2}=c_{pF}\rho_F \overline{\mathbf{w}}_e d_e N_R L_s/4 \quad (8)$$
$$C_{f1}=C_{f2}=c_{pF}\rho_F \overline{\mathbf{w}}_f d_f N_R L_s/4 \quad (9)$$
$$C_{g1}=C_{g2}=c_{pF}\rho_F \overline{\mathbf{w}}_g d_g N_R L_s/4 \quad (10)$$
$$C_{h1}=C_{h2}=c_{pF}\rho_F \overline{\mathbf{w}}_h d_h N_R L_s/4 \quad (11)$$
$$C_R=c_{pA}\rho_A V_R \quad (12)$$
$$C_p=c_{pA}\rho_A V_p \quad (13)$$

The thermal resistances are computed from equations of the form

$$R=\frac{1}{hA}+\frac{l}{kA} \quad (14)$$

The first term involves the thermal contact

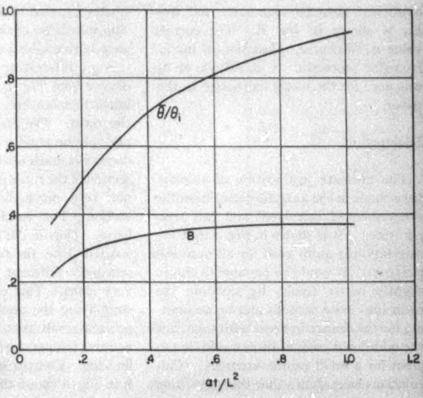

Fig. 8. Equivalent lumped system for space mean temperature in insulated bar. Step input of temperature at one end

resistance between conductor and iron or from a surface to air. The second term accounts for the temperature drop in the material itself and l is the effective length of path determined so that the resultant circuit gives the best approximation to the actual system. The results of Appendixes II and III, as presented in Figs. 7 and 8, are used to determine this. The number B is the ratio of the effective length to the total length of an insulated bar that has a temperature input at one end. It is determined so that the lumped single resistance capacitor circuit will give the correct result for space mean temperature. Fig. 7, Appendix II, applies for an input temperature that increases linearly with time. Fig. 8, Appendix III, is for a step input of temperature. The actual temperature-time curve of any part of the rotor ties between these two extremes.

The abscissa of these curves is $\alpha t/L^2$, where L is the length of the bar, t the period of time, and α the thermal diffusivity. For aluminum, α is 0.136; for steel 0.01 inch² per second. Thus, for conduction in aluminum where L is about 0.5 inch, and for a time of 20 seconds

$$\frac{\alpha t}{L^2}=10.9 \tag{15}$$

This is well past the knee of the curve for B. Fig. 7 would give 0.3 and Fig. 8 about 0.38. Since the actual temperature input is closer to that for Fig. 7, 0.3 is used for B. This value is also used for short paths in iron. For longer paths, 0.2 is used since $\alpha t/L^2$ is much smaller. If desired, the resistance may be adjusted to give a more accurate value for any particular motor.

The thermal resistances are

$$R_{ab1}=\frac{0.3d_b}{k_A N_R w_b L_s/4} \tag{16}$$

$$R_{bc1}=\frac{0.7d_b}{k_A N_R w_b L_s/4}+\frac{0.3d_c}{k_A N_R w_c L_s/4} \tag{17}$$

$$R_{ad1}=\frac{1}{h_{ad} N_R P_{ad} L_s/4}+\frac{0.15w_d}{k_F N_R 2d_d L_s/4} \tag{18}$$

$$R_{be1}=\frac{1}{h_{ad} N_R 2d_e L_s/4}+\frac{0.15w_e}{k_F N_R 2d_e L_s/4} \tag{19}$$

$$R_{ce1}=\frac{1}{h_{ad} N_R w'_e L_s/4}+\frac{0.3d_e}{k_F N_R w'_e L_s/4} \tag{20}$$

$$R_{cf1}=\frac{1}{h_{ad} N_R 2d_f L_s/4}+\frac{0.15w_f}{k_F N_R 2d_f L_s/4} \tag{21}$$

$$R_{cg1}=\frac{0.7d_c}{k_A N_R w_c L_s/4}+\frac{1}{h_{ad} N_R w_g L_s/4}+\frac{0.2d_g}{k_F N_R w_g L_s/4} \tag{22}$$

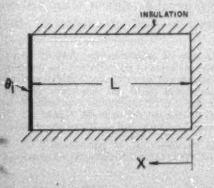

Fig. 9 (left). Insulated bar

Table I. Some Typical Constants

Material	k, Conductivity watts per C-inch	C_p Specific Heat watt-seconds per pound-C	ρ, Density pounds per inch³	α, Diffusivity inches² per second
Aluminum	5.18	407	0.093	0.136
Motor grade steel	0.58	209	0.276	0.010
Copper	9.75	176	0.326	0.17

$$R_{dg1}=\frac{1}{h_{dg}\pi D L_s/4} \tag{23}$$

$$R_{de1}=\frac{0.3d_e}{k_F N_R w_e L_s/4} \tag{24}$$

$$R_{ef1}=\frac{0.7d_e}{k_F N_R w_e L_s/4}+\frac{0.2d_f}{k_F N_R w_f L_s/4} \tag{25}$$

$$R_{fg1}=\frac{0.8d_f}{k_F N_R w_f L_s/4}+\frac{0.2d_g}{k_F N_R w_g L_s/4} \tag{26}$$

$$R_{gh1}=\frac{0.8d_g}{k_F N_R w_g L_s/4}+\frac{0.2d_h}{k_F N_R w_h L_s/4} \tag{27}$$

$$R_{a12}=\frac{L_s/4}{k_A N_R(A_a+A_b/2)} \tag{28}$$

$$R_{a2R}=R_{a12}/2 \tag{29}$$

$$R_{c12}=\frac{L_s/4}{k_A N_R(A_c+A_b/2)} \tag{30}$$

$$R_{c2R}=R_{c12}/2 \tag{31}$$

$$R_{R0}=\frac{1}{h_{R0}A_R} \tag{32}$$

$$R_{RP}=\frac{0.2L_p}{k_A N_p A_p} \tag{33}$$

Resistances for the second section are the same as those given for the first section. Some of the typical constants are shown in Table I. Surface heat transfer coefficients may be determined from reference 2.

The values for watt input to the circuit may be determined from a calculation of the double squirrel-cage performance as indicated, for example, in reference 1.

$$W_{a1}=\frac{\text{top bar loss}}{4} \tag{34}$$

$$W_{c1}=\frac{\text{bottom bar loss}}{4} \tag{35}$$

$$W_R=\frac{\text{end ring loss}}{2} \tag{36}$$

Numerical values are indicated in Fig. 3 to give an idea of the order of magnitude of the various elements.

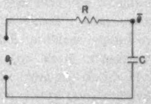

Fig. 10 (above). Lumped circuit approximation for insulated bar

Equations for Circuit

Equations suitable for setting up on an analogue computer may be readily derived from Fig. 3 by writing the nodal equations. For example, the nodal equation for the node at θ_{a1} is

$$C_{a1}\frac{d\theta_{a1}}{dt}+\frac{\theta_{a1}-\theta_{a2}}{R_{a12}}+\frac{\theta_{a1}-\theta_{b1}}{R_{ab1}}+\frac{\theta_{a1}-\theta_{d1}}{R_{ad1}}=W_{a1} \tag{37}$$

This may be rearranged to the following form which is convenient for use on a differential analyzer

$$\theta_{a1}=\int\left(\frac{W_{a1}}{C_{a1}}-\frac{\theta_{a1}}{R_{a1}C_{a1}}+\frac{\theta_{a2}}{R_{a12}C_{a1}}+\frac{\theta_{b1}}{R_{ab1}C_{a1}}+\frac{\theta_{d1}}{R_{ad1}C_{a1}}\right)dt \tag{38}$$

where

$$\frac{1}{R_{a1}C_{a1}}=\frac{1}{R_{a12}C_{a1}}+\frac{1}{R_{ab1}C_{a1}}+\frac{1}{R_{ad1}C_{a1}} \tag{39}$$

= sum of coefficients of other temperature terms plus $1/RC$ to ambient if one exists.

The other equations are of the same form and may be written down from inspection of the circuit, Fig. 3.

Appendix II. Equivalent Lumped System for an Insulated Bar, Linear Temperature Input at One End

The system to be analyzed is shown in Fig. 9. This is an insulated bar (or slab) with a temperature input at one end at time zero. The space mean temperature rise of the bar, above the initial uniform temperature, will be determined with a temperature input at time zero of the form

$$\theta_i=Dt \tag{40}$$

where D is a constant, the rate of temperature rise of the surface at $(X=L)$. The approximation is developed for the space mean temperature so that the heat stored in the thermal capacitance will be correct.

The exact solution for this case was found in reference 3. This gives the temperature distribution for various values of the time variable $(\alpha t/L^2)$. The space mean temperature $\bar{\theta}$ was determined for each of these values and then plotted versus $\alpha t/L^2$ in Fig. 7.

The equivalent lumped thermal system, to be developed, is indicated schematically in Fig. 10. The thermal storage C is for the entire bar

$$C=\rho c_p LA \tag{41}$$

The resistance R is

$$R=\frac{BL}{kA} \tag{42}$$

where B is the ratio of the total length L to the effective length which gives the correct result for average temperature. It is this value of B which must be determined.

The differential equation for the circuit of Fig. 10 is

$$C\frac{d\bar{\theta}}{dt}+\frac{\bar{\theta}-\theta_i}{R}=0 \tag{43}$$

The temperature input is given by equation 40 and at time zero; $\bar{\theta}$ is zero. The solution is

$$\frac{\bar{\theta}}{\theta_i}=\left[1-\frac{RC}{t}(1-e^{-t/RC})\right] \tag{44}$$

It is now necessary to evaluate R so that this equation gives the same result as the exact solution. Let

$$G=\frac{t}{RC} \tag{45}$$

be the correct exponent for a given value of $\bar{\theta}/\theta_i$. Let

$$H=\frac{\alpha t}{L^2} \tag{46}$$

be the value for the exact solution which gives the same value of $\bar{\theta}/\theta_i$. Solving for t from equations 45 and 46, gives

$$t=GRC \tag{47}$$

$$t=\frac{HL^2}{\alpha} \tag{48}$$

Eliminating t from these two equations and solving for R gives

$$R=\frac{L^2}{\alpha C}\,\frac{H}{G} \tag{49}$$

Substituting equation 41 for C and

$$\alpha=\frac{k}{\rho c_p} \tag{50}$$

gives

$$R=\frac{L}{kA}\,\frac{H}{G} \tag{51}$$

Comparison of equations 42 and 51 shows that

$$B=\frac{H}{G} \tag{52}$$

This is the desired result. A curve of B versus $\alpha t/L^2$ is shown in Fig. 7.

Appendix III. Equivalent Lumped System for an Insulated Bar, Step Input of Temperature at One End

The solution for this case follows exactly the procedure used in Appendix II. The only difference is the temperature input at $(X=L)$. For this case it is a step function of magnitude θ_i at time zero.

The exact solution is taken from reference 4 and plotted in Fig. 8.

For the step input of temperature, the solution of the circuit of Fig. 10 is

$$\frac{\bar{\theta}}{\theta_i}=(1-e^{-t/RC}) \tag{53}$$

This is the only equation different from Appendix II, so the same procedure is followed except that equation 53 is used in place of equation 44. The equivalent resistance is, as before

$$R=\frac{BL}{kA} \tag{54}$$

The factor B is plotted versus $\alpha t/L^2$ in Fig. 8.

References

1. Double and Triple Squirrel Cages for Polyphase Induction Motors, P. L. Alger, J. H. Wray. *AIEE Transactions*, vol. 72, pt. III, Aug. 1953, pp. 637–44.

2. Heat Transmission (book). William H. McAdams. McGraw-Hill Book Company, Inc., New York, N. Y., 2nd ed., 1942.

3. Heat Transfer (book), Max Jakob. John Wiley and Sons, Inc., New York, N. Y., vol. 1, 1949, Table 13-5, p. 268.

4. See ref. 2, p. 35.

◆

Discussion

C. G. Veinott (Reliance Electric & Engineering Company, Cleveland, Ohio): I thought I might like to say a few words. We have done quite a little work using an equivalent circuit as a thermal network in order to study temperatures in motors. Practically all our work to date, however, has been in studying steady-state conditions; for this purpose we have found a d-c network analyzer extremely useful and we have had remarkable correlation with test results. We were very much interested in Mr. Rosenberry's paper which involves transient heating requiring 18 capacitors to represent the 18 heat-storage elements. We studied his equations from the standpoint of setting them up on our own electronic differential analyzer (GEDA), but found it would take many more amplifiers than the ten provided in our computer. We would be interested in knowing what kind of a differential analyzer you used in solving these equations.

It seems pertinent to add that the paper shows how much more complicated the problem of designing electric machines is today than it was only a few years ago, and how much we are going to have to depend upon computers.

G. M. Rosenberry: The equations given in the paper were solved on a Reeves Electronic Analogue computer. Since there were 18 first-order differential equations, 18 integrators were necessary. An additional 18 amplifiers were used to provide the proper coefficients and signs. By neglecting the axial variation in temperature, this requirement would be reduced to eight integrators. For some shapes of rotor conductors, it may be practical to use less than eight.

An extension of the d-c network analyzer, mentioned by Mr. Veinott, to provide capacitors and constant current generators makes possible the direct solution of the transient equivalent thermal circuit. This is more convenient than the use of a differential analyzer since it is not necessary to compute the coefficients of the differential equations.

Design Problems and Operating Experience With Aluminum Distribution Conductors in the Philadelphia Electric Company

C. E. NELSON
MEMBER AIEE

K. S. GARRETT
ASSOCIATE MEMBER AIEE

MORE than half the investment of an electrical utility is in transmission and distribution, and of that major division the greater part will be found in distribution. While construction costs have been increasing, generating station operating economies and substation simplification have operated to stabilize the cost of electric service to the customer.

Much has been done to check the spiraling transmission and distribution costs, such as the following: use of higher voltages for transmission, rerating of existing equipment to secure the maximum use, and eliminating nonessentials. However, in 1950, new extensions for new customers and replacement of existing facilities were involving double the costs of 1940.

To prevent that portion of distribution between the substations and the customers' meters from assuming a disproportionate share of the expense of supplying electricity, Philadelphia Electric Company engineers concentrated on the use of new materials and new designs for increased economy. Appealing possibilities lay in the use of aluminum but, because of lack of information about such application of the material and because of the pressure to keep construction apace with community growth, there was reluctance to change. On two or three occasions prior to 1950, experimental installations had been planned for the system, but in each instance because of inability to clear up important details, these plans were abandoned.

The Korean War changed this situation. For essential jobs, the Defense Electric Power Administration approval was received quite readily, but copper conductors, especially the bare or weatherproof types, were not available from the suppliers. In spite of the war, new residential housing and industrial and commercial building did not slacken appreciably. Accordingly, to insure service to new developments on our system (in 1951 there were more than 20,000 housing units projected or under way), the Philadelphia Electric Company decided on the general use of aluminum in distribution. Allocations were received from the Defense Electric Power Administration and orders placed.

Initial Design Considerations

By this action, the solution of design problems surrounding the use of aluminum conductors was given tremendous impetus. First-hand experience in the use of aluminum conductors was very meager, but the material was known to have physical, metallurgical, and electrical characteristics which would require special attention if it were to be used successfully. Lack of agreement, however, on the relative seriousness of some of the problems and on the remedial measures, complicated and delayed development of a satisfactory plan of procedure.

Accordingly, a study was made of the physical strength, electrical conductivity characteristics, susceptibility to atmospheric and galvanic corrosion, and of the physical behavior during temperature cycling when aluminum was used with fittings of other metals. From these studies, and collateral laboratory and field tests, a reasonable understanding of the problem was believed to have been achieved. Convinced, that complete answers to the problem would not be available in the early stages of the application, the company decided to begin design work on a very conservative basis and to refine, simplify, and economize as experience warranted.

Although higher load densities than usually experienced were anticipated in the new housing developments, the established design principles of co-ordinating the conductor sizes with acceptable voltage drops did not appear to require substantial changes. On this basis, for the primary mains and taps, secondaries, and services, aluminum conductors were used of capacities equivalent to those formerly chosen when copper was used in corresponding applications. The primary mains became 4/0 steel-reinforced aluminum cable (ACSR), the ties between mains 1/0 ACSR, and no. 4 ACSR was selected for branches. For secondaries, 4/0 all-aluminum was used with the common neutral being 1/0 ACSR bare. For residential services, the size selected was no. 4 aluminum cable of varying constructions, larger sizes being used for commercial and industrial loads. Because of local requirements, bare ACSR was utilized for the 33- and 4-kv lines in the suburban areas while covered ACSR was used for 13.2-kv and 2.4-kv lines in Philadelphia. Initially, covered wire was used for all secondaries and services excepting neutral conductors. (See Table I for lists of strandings and specific applications adopted as standard.) New sag and tension tables were prepared for the all-aluminum conductors, and stringing tensions based on a maximum design tension of 45 per cent of ultimate strength were incorporated in the design.

Taps, terminations, and dead-end construction were given careful, detailed treatment. The first problem considered was the joining of aluminum to copper. To minimize conductor distortion during installation of connectors and during load cycling, and to provide permanent connections of adequate pressure, plated copper connectors of large contact area were selected. Attention was then turned to measures to prevent corrosion at joints. Since available connector platings did not provide a surface entirely compatible with aluminum, the danger of both galvanic and atmospheric corrosion was present. It appeared that protection against both could be gained by excluding moisture and air from the connection area. For this purpose, a grease compounded to minimize oxidation, to have long life, and to provide an abrasive characteristic to cut through the ever-present aluminum oxide was applied over the conductor before the connector was installed and later over the entire connection. Further to guard this vulnerable area, the connection was thoroughly taped.

There appeared to be no satisfactory means of terminating aluminum conduc-

---

Paper 55-249, recommended by the AIEE Transmission and Distribution Committee and approved by the AIEE Committee on Technical Operations for presentation at the AIEE Electrical Utilization of Aluminum Conference, Pittsburgh, Pa., March 15-17, 1955. Manuscript submitted December 16, 1954; made available for printing January 20, 1955.

C. E. Nelson and K. S. Garrett are with the Philadelphia Electric Company, Philadelphia, Pa.

tors at devices. In most cases, the device terminals were neither of suitable physical design nor of proper material for the attachment of aluminum conductors. Pending the development of more satisfactory terminals by the manufacturers, short jumpers of copper were used between the primary and the cutout, the cutouts and transformers, and between transformers and secondaries; see Fig. 1. The aluminum-to-copper connections at the primary and secondary taps were protected against corrosion and physical distortion in the manner already described and as an added precaution, the physical arrangement of the two conductors was such as to prevent washing of copper salts onto the aluminum.

Start of Construction

Construction work was begun in various areas of the Company following these procedures and the following quantities of aluminum were installed between March 1, 1952, and December 1, 1954:

Overhead-line conductors, all voltages, approximately 20,000,000 feet

Overhead 3 by no. 4 service entrance cables for services, approximately 600,000 feet

Overhead 3 by no. 4 triplex service drop (1, ACSR; 2, solid aluminum), approximately 2,750,000 feet

2 by no. 8, 3.5-kv street-lighting cable, approximately 190,000 feet

No. 4 and no. 2,600-volt rubber and neoprene cable for multiple street lighting (337,000 trench feet), approximately 688,000 feet

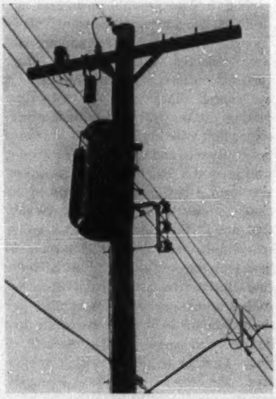

Fig. 1. Typical bare aluminum primary and secondary construction at transformer pole

Table I. Standardized Aluminum Conductor and ACSR Sizes: Their Stranding and Use

Aluminum		Usage	
Size	Type	Philadelphia Division	Suburban Divisions
No. 2/0	7-strand all-aluminum bare	neutral wire on rear bus and services	neutral wire on rear bus and services
No. 2/0	7-strand all-aluminum WP*	rear bus on houses, and services under 100 feet	rear bus on houses, and services under 100 feet
No. 4/0	7-strand all-aluminum WP	rear bus on houses pole line secondary, and services under 140 feet	rear bus on houses pole line secondary, and services under 140 feet
No. 4	ACSR 7-strand, aluminum 1-strand steel, bare		street-lighting and primary
No. 1/0	ACSR 6-strand, aluminum 1-strand steel, bare		primary, 13.2 and 33-kv
No. 4/0	ACSR 6-strand, aluminum 1-strand steel, bare		primary, 13.2 and 33-kv
No. 4	ACSR 7-strand, aluminum 1-strand steel, WP	street-lighting primary, pole line secondary, and 13.2-kv	pole line secondary
No. 1/0	ACSR 6-strand, aluminum 1-strand steel, WP	primary, secondary, 13.2-kv and services over 100 feet	pole line secondary and services over 100 feet
No. 4/0	ACSR 6-strand, aluminum 1-strand steel, WP	primary, secondary, 13.2-kv, and services over 140 feet	pole line secondary and services over 140 feet
No. 4	Triplex-service drop cable (two No. 4 all-aluminum insulated conductors and one No. 4 bare 7/1 ACSR neutral)†	service loops	service loops
No. 8	Duplex 3.5-kv aluminum rubber-covered cable	lamp-lead series street-lighting	lamp-lead series street-lighting

* WP = weatherproof. The three types of weatherproof covering will be neoprene, polyethylene, and TBWP. TBWP will not be used on all-aluminum conductor.

† The three types of weatherproof covering on this type of cable will be polyethylene, insulating neoprene, and rubber-and-neoprene.

No serious difficulties were encountered in the field, although modifications were made in original designs which have resulted in labor and material savings, two being of substantial importance. The taping of greased tap connections on bare conductors was found to be of doubtful value, if not actually harmful, and this time-consuming procedure was eliminated. The removal of the secondary conductor covering at dead ends was also an expensive operation, especially in the case of triple-braid weatherproof (TBWP) coverings, and was discontinued after tests indicated that adequate sags could be maintained by simply bending the covered conductor around the spool of a secondary rack and fastening it back on itself with two U-bolt clamps.

Development of New Secondary Construction

In the fall of 1953, after approximately 18 months of satisfactory experience with aluminum conductors, the question of possible further economies in materials and labor was investigated. Changes in the design of secondaries appeared to be the most promising field. The major portion of aluminum secondaries being erected were covered 4/0 conductors with a bare 1/0 neutral, but there was little saving with these materials as compared with 2/0 covered copper construction. However, 4/0 bare all-aluminum conductors cost only 40 per cent as much as the same conductor when covered, and also showed an appreciable saving over bare copper of equivalent electrical characteristics.

The Company's standard secondary construction provides for racks with 8-inch spacing with the bare neutral in the top position. Field tests showed that with this spacing and 150-foot span lengths, the bare secondaries could readily be short-circuited, by wind or sudden shock to the supporting pole, etc. It was shown, however, that this hazard could be eliminated by using spacers at 50-foot intervals. The addition of spacers suggested their use also as a terminal point for services to customers. Because of unequal property widths and irregularities of lot lines, and in order to maintain minimum service runs, this possibility was particularly attractive.

The spacer as finally developed consisted of two $1^3/_4$- by 18- by 3/16-inch pressed Fiberglas strips with three slots on 8-inch centers extending from the edge to the center of the strip, to accommodate the three wires of the secondary bus. The two strips are slid over the wires from opposite sides of the bus and bolted together with two bolts, thus forming a simple, inexpensive, and rugged separator. When a service is to be connected to this separator, a bridle consisting of a loop of 3/16-inch round stainless-steel wire is added. This bridle is held by the same bolts which fasten the two parts of the separator together. See Fig. 2 for an

Table II. Connectors and Dead-End Clamps for Aluminum and ACSR Conductors

Connector	Application
Connector, tap, parallel-groove, aluminum alloy body, galvanized steel bolt; for no. 8 to no. 1/0 ACSR main to no. 8 to no. 1/0 ACSR tap conductors.	...on secondary neutral and branches, service taps, and customer's service-entrance connections: aluminum to aluminum; aluminum to copper
Connector, tap, parallel-groove, aluminum alloy body, galvanized steel bolt; for no. 2/0 to no. 4/0 ACSR or all-aluminum mains; to no. 8 to no. 1/0 ACSR or all-aluminum taps.	...on primary circuit branches and on secondary branches and service taps: aluminum to aluminum.
Connector 2-bolt, tap, silicon bronze with copper or high-conductivity copper alloy spacer bar and silicon bronze bolts, completely tinplated; for no. 1/0 and no. 2/0 all-aluminum or no. 1/0 ACSR conductors.	...on primary and secondary circuits: aluminum to aluminum; aluminum to copper.
Connector, 2-bolt, tap, silicon bronze with copper or high-conductivity copper alloy spacer bar and silicon bronze bolts, completely tinplated; for no. 4/0 all-aluminum or ACSR conductors.	...on primary and secondary circuits: aluminum to aluminum; aluminum to copper.
Connector, split-bolt, tap, silicon bronze with copper or high-conductivity copper alloy spacer bar and bell-mouth washer, completely tinplated; for up to no. 1/0 all-aluminum conductors.	...secondary branches and service taps: aluminum to aluminum; aluminum to copper.
Connector, split-bolt, tap, silicon bronze with copper or high-conductivity copper alloy spacer bar and bell-mouth washer, completely tinplated; for no. 4 stranded all-aluminum or no. 4 ACSR.	...connections to customer's service entrance: aluminum to aluminum; aluminum to copper.
Connector, split-bolt, tap, silicon bronze, with copper or high-conductivity copper alloy spacer bar and bell-mouth washer, completely tinplated; for no. 4 solid-aluminum conductors.	...connections to customer's service entrance: aluminum to aluminum; aluminum to copper.
Connector, U-bolt, aluminum alloy body with galvanized steel bolt; for dead-ending no. 4 solid aluminum or no. 4 ACSR.	...primary or secondary dead ends.
Connector, U-bolt, aluminum alloy body with galvanized steel bolt; for dead-ending no. 1/0 and no. 2/0 all-aluminum or 1/0 ACSR.	...primary or secondary dead ends.
Connector, U-bolt, aluminum alloy body with galvanized steel bolt; for dead-ending no. 4/0 all-aluminum or no. 4/0 ACSR.	...primary or secondary dead ends.

installation that shows this arrangement.

Considering the savings in the cost of bare versus covered aluminum, when the cost of spacers utilized for separation is deducted, the net saving effected by using bare aluminum amounts to approximately 15 cents per circuit-foot of 3-wire 115- to 230-volt secondary, or approximately $22.00 per span of 150 feet. Additional savings with this type of construction are in service lengths which are kept to a minimum since they can be installed substantially at right angles to the line in practically all instances. Such use of bare conductor is extensive, but covered conductors continue to be used where the secondaries are installed through trees or on the rear of houses.

Primary-Design Changes Few

As greater economy was sought in secondary construction, so was it sought in designs for primary voltages. Particular attention had been given to the use of all-aluminum conductors in place of ACSR. Reliability and strength considerations, however, have continued to weigh the decision in favor of steel-reinforced conductors, notwithstanding possible substantial savings with all-aluminum conductors. Improvements in installation techniques and changes in construction details therefore have been the principal additions to earlier economies over equivalent copper designs.

Developments in Connectors

Throughout this period of the rapid growth of our aluminum distribution system, close attention to design and installation of connectors and splices continued. Basic investigations regarding the behavior of aluminum conductors at joints, and of the connectors of various body metals and platings, were discontinued with the establishment of the industry-wide research initiated by the Edison Electric Institute. However, screening of the host of available plated copper and aluminum alloy connectors has been carried on continuously. This screening has been performed on the basis of criteria substantially representing refinements of that applied in the Company's initial considerations. Performed by joint groups of engineering and operating representatives, this process has resulted in a substantial reduction in the variety of connectors initially utilized.

The present list of approved tap connectors and dead-end clamps embraces split-bolt designs with bell-mouth washers, 2-bolt types in tin-plated copper and bronze, and parallel groove and U-bolt types employing aluminum alloys. Typical applications are shown in Table II. Rejection of many earlier designs has been due to troubles in service and to relative inconvenience in installing them. The list approved at present also reflects increasing acceptance of aluminum alloy designs for both aluminum-aluminum and aluminum-copper connections, because of promise of better connections and because of reduced cost as compared to formerly specified plated types.

For splicing application, compression methods developing substantially 100 per cent of conductor strength and conductivity have been adopted as standard.

Challenging Problems

Some drawbacks and problems have appeared to challenge the engineer and operator in obtaining the maximum possible economy in the use of this metal. Heading the list is the solution to the connector problem. Better connectors and installation procedures are employed than was the case 2 years ago. However, the lack of basic knowledge in the matter leaves us unsure of our criteria for selecting connectors from the many types and designs available.

A number of construction and maintenance problems have been troublesome:

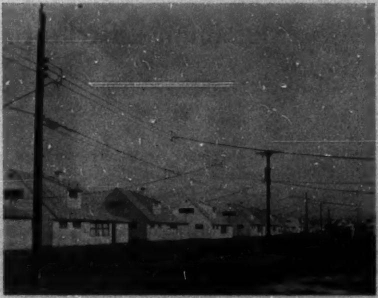

Fig. 2. Rear property distribution pole line, showing bare primary and secondary, and services terminated on spacers

1. Time for repairs to ACSR conductors is excessive, especially on our 2.3- and 4-kv systems which are worked energized. In particular, extra protective coverings, which are very difficult to apply, are required when working on 2.4 and 4-kv conductors at dead ends.

2. Cutting in dead ends in existing ACSR conductors of 2.4 and 4-kv circuits for installation of sectionalizing devices is a major operation.

3. With 95 per cent of the system consisting of copper conductors, stocks of both copper and aluminum supplies must be maintained in storerooms and on trucks.

4. The coils of the bulkier aluminum do not fit the collapsible reels on trucks, and reducing coil sizes to fit the reels results in excessive wastage. A particular example of this occurs in the case of 3 by no. 4 triplex-service drop cable.

Terminals on many devices are unsuitable for the attachment of aluminum, and present use of copper jumpers increases costs and creates joining problems.

Conclusions

To date, aluminum has given satisfactory performance in carrying load, and there has been a steady, if in cases not appreciable, reduction in construction costs as crews have become more experienced in work involving aluminum.

In comparison with costs of copper construction, economies are effected in the use of ACSR for subtransmission lines as these lines are not worked energized. There are no economies on 2.4 and 4-kv construction unless the installation is made in new territory and completed before the circuits are placed in service. The development of splicing methods and of line accessories which would eliminate the necessity for handling the steel strands in ACSR separately would be an important contribution in reducing present construction and maintenance costs on these lines.

General equipping of line devices, transformers, cutouts, arresters, etc., with terminals suitable for both aluminum and copper would be of substantial benefit.

Continuance of industry-sponsored research into the problems affecting aluminum connector design and the preparation of performance specifications should be a most valuable contribution to the fuller realization of economies and conveniences that are potential in the use of aluminum in distribution.

◆

Discussion

Robert E. Larson (Aluminum Company of America, Pittsburgh, Pa.): The authors should be complimented on their most constructive paper on the use of aluminum distribution conductors. Perhaps one of the most interesting construction features brought out in the paper is the use of bare aluminum secondaries with mid-span service drop taps. A more economical construction method for secondaries and service drops would be difficult to imagine.

It is stated in the paper that the development of splicing methods which would eliminate the necessity for handling the steel strands in steel-reinforced aluminum cable (ACSR) separately would be an important contribution in reducing present construction and maintenance costs. Alcoa is working on a development which, it hopes, will eliminate the use of the steel sleeve in splicing the sizes of ACSR normally used in distribution. It is anticipated that this splice will develop from 95 to 100 per cent of the rated strength of the conductor. Due to technicalities involved, additional information on this splice cannot be given at this time.

Aluminum-to-aluminum connections operate better when made with aluminum connectors than with connectors of other metals as the pressure changes resulting from differential expansion versus temperature are minimized. Test data from Alcoa's aluminum research laboratories show that the changes in pressure versus temperature can be further minimized by the use of aluminum bolts with aluminum connectors and clamps. Also, the lower modulus of elasticity of aluminum provides a spring follow which tends to compensate for creep and plastic deformation of conductors as might result from high operating temperatures or severe initial bolting pressure. In addition, the possibility of galvanic corrosion is minimized. Therefore, for the ultimate in performance in aluminum-to-aluminum connections, aluminum connectors plus the use of a good joint compound are recommended.

For copper-to-aluminum bolted connections, aluminum connectors with the proper use of a good joint compound may well be used where there is little or no atmospheric contamination. Under seacoast or heavy industrial conditions the use of copper-bushed aluminum connectors is recommended for copper to aluminum connections. Again the proper use of a good joint compound is essential. Copper-bushed aluminum clamps have given a good account of themselves over a period of 35 years through a wide range of conditions.

Eight Years' Experience With All-Aluminum Distribution Systems

H. E. CARPENTER
MEMBER AIEE

R. E. THORNTON
MEMBER AIEE

THE USE of all-aluminum conductors in electrical systems is not new. A company on the Pacific Coast has had such conductors in service since 1902. The company with which the authors are associated installed in 1948 approximately 80 miles of 477,000-circular-mil (CM) all-aluminum conductors in 4.16-kv 300-ampere primary feeders. This material had been recovered from an electric railway system and had been in service for 40 years previously as a trolley feeder.

For the past 8 years the conductor used by the Oklahoma Gas and Electric Company in all new residential and light commercial distribution lines has been steel-reinforced aluminum cable (ACSR) or all-aluminum. Prior to that time no all-aluminum, with the exception of that just mentioned, had been used. However, ACSR had been used only in transmission and long-span rural lines for the past 28 years.

The real impetus to the use of aluminum as a distribution conductor was a study made in 1947 of the distribution

---

Paper 55-256, recommended by the AIEE Transmission and Distribution Committee and approved by the AIEE Committee on Technical Operations for presentation at the AIEE Electrical Utilization of Aluminum Conference, Pittsburgh, Pa., March 15–17, 1955. Manuscript submitted December 17, 1954; made available for printing January 26, 1955.

H. E. CARPENTER and R. E. THORNTON are with the Oklahoma Gas and Electric Company, Oklahoma City, Okla.

transformer and secondary economics wherein various combinations of transformers and secondaries of various sizes and materials were considered.[1] This study definitely pointed to the conclusion that advantage should be taken of the relative price of aluminum as compared to that of copper.

Types of Aluminum Conductors Used

Aluminum conductors used for services is no. 4 solid all-aluminum neoprene-covered. No. 6 of the same type was also used for some time but its installation has been discontinued.

Aluminum conductor used for secondaries is mainly no. 1/0 7-strand, bare all-aluminum. Also, some no. 1/0 ACSR and some no. 3/0 all-aluminum have been used.

For primaries, 2.4, 4.16, 7.2, and 12.5 kv, the following are used:

1. Feeders of 266,000, 336,400 and 477,000-CM all-aluminum.
2. Mains of 266,000 centimeter cm and no. 3/0 all-aluminum.
3. Branch laterals of no. 4 ACSR.

For street lighting the following are used:

1. Aerial series circuits of no. 4 ACSR.
2. Aerial multiple circuits: 1. Pilot wires and supply laterals for street intersection lighting of no. 4 ACSR. 2. Supply circuits for high level arterial street lighting of no. 4 all-aluminum neoprene-covered, lashed to a *6A* copperweld-grounded neutral for support.
3. Underground series circuits of rubber-insulated, neoprene jacketed no. 4 all-aluminum.
4. Underground multiple laterals of 600-volt, rubber-insulated, neoprene-jacketed no. 4 all-aluminum and no. 6 bare copper neutral.

USAGE

It is estimated that the Company now has a total of over 11,250 miles of all-aluminum and ACSR in place as primaries of the 2.4-, 4.16-, 7.2-, and 12.5-kv class secondaries and services in the system. Today aluminum of the all-aluminum and ACSR types in the urban and rural systems are being installed at an average rate of approximately 902,000 pounds per year.

Design and Construction Data

PERTINENT PREMISES

The more pertinent premises on which the designs are based are as follows:

1. Heavy-loading conditions.

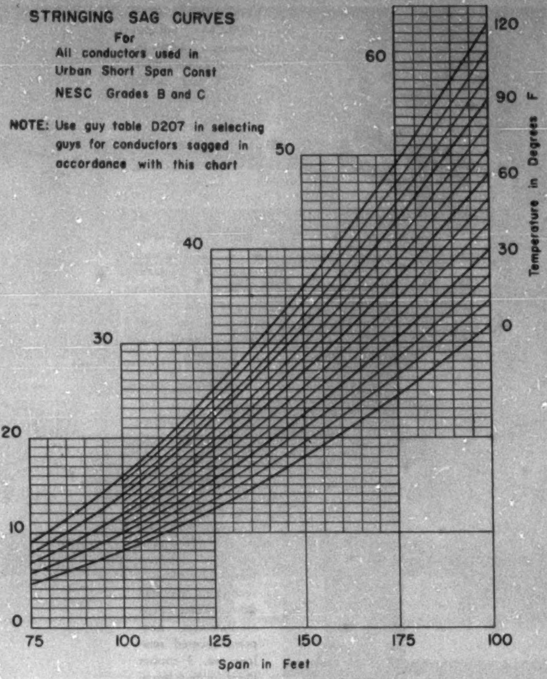

Fig. 1. Short-span universal sag chart for 75- to 200-foot spans

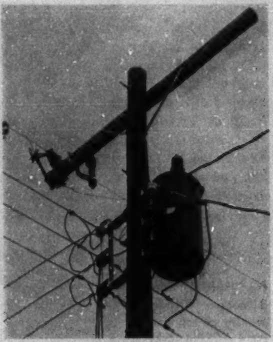

Fig. 2. No. 4 ACSR 7.2-kv primary; no. 0 all-aluminum 120/240-volt secondary; no. 4 all-aluminum neoprene-covered open services; no. 4 all-aluminum neoprene-covered, on no. 6 ACSR bare services (triplex)

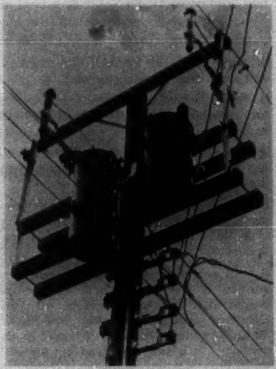

Fig. 3. Open-wye primary, no. 4 ACSR, no. 0 all-aluminum bare 120/240-volt secondary with no. 4 aluminum bare teaser for 3-phase; no. 4 all-aluminum neoprene-covered service; no. 4 all-aluminum neoprene-covered on no. 6 ACSR bare service (triplex)

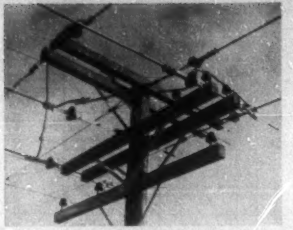

Fig. 4 (left). 477,000-CM all-aluminum 4.16-kv feeder corner; three no. 4 bare copper secondary

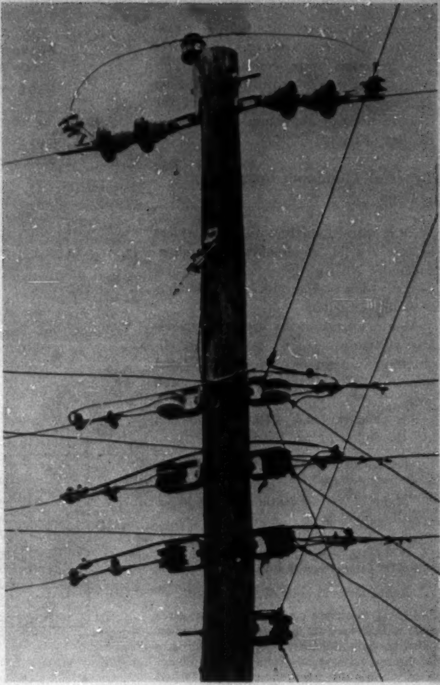

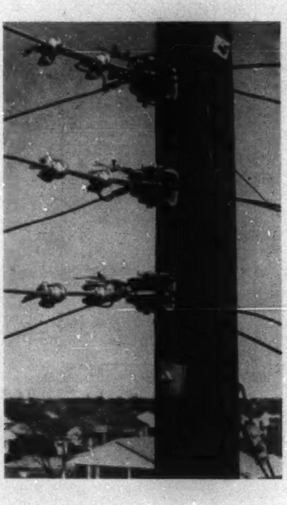

Fig. 5 (left). No. 1/0 all-aluminum secondary dead-ended on 4-inch spool rack; no. 4 all-aluminum neoprene-covered services

Fig. 6 (right). No. 4 ACSR, bare, 2.4-kv primary; no. 3 copper, bare, 120/240-volt secondary on right side of pole; no. 0 all-aluminum bare, 120/240-volt secondary on left side of pole; no. 4 all-aluminum neoprene-covered services; no. 3 copper street-lighting lateral

2. Bare conductor for primary, secondary, and aerial street-lighting circuits.

3. Primary conductors on a ridge pin or on arm with minimum horizontal spacing of 29 inches.

4. Secondary and low-voltage street lighting conductors on racks with 12-inch spacing.

5. Services to residential and small commercial establishments of the triplex cable type, no. 4 bare ACSR and two no. 4 neoprene-covered all-aluminum.

6. All urban distribution conductors regardless of size, materials or voltage are sagged alike and in accordance with the Company's universal sag chart; see Fig. 1. The all-aluminum conductors sagged in accordance with this sag chart are stressed under heavy-loading conditions in the design span as in Table I.

Table II shows those all-aluminum and ACSR conductors which the Company now considers standard for overhead distribution in urban areas. Triplex 3-conductor service cables are being used extensively.

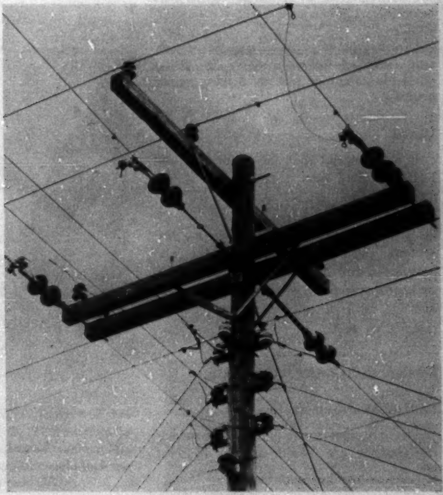

Fig. 7 (right). No. 3 copper 4.16-kv primary on top arm; no. 4 ACSR 4.16-kv primary on buck arm; no. 3 copper, bare, 120/240-volt secondaries; no. 4 all-aluminum neoprene-covered services

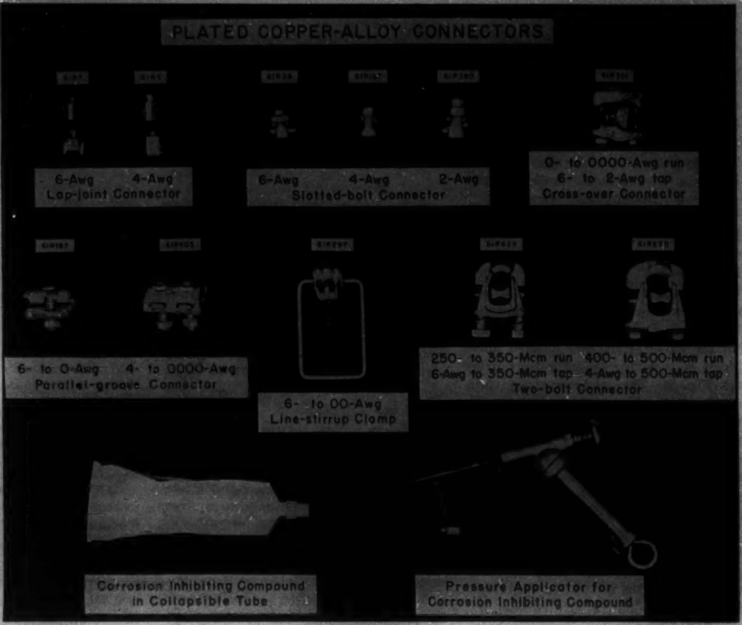
PLATED COPPER-ALLOY CONNECTORS
6-Awg 4-Awg
Lap-joint Connector
6-Awg 4-Awg 2-Awg
Slotted-bolt Connector
0- to 0000-Awg run
6- to 2-Awg tap
Cross-over Connector
6- to 0-Awg 4- to 0000-Awg
Parallel-groove Connector
6- to 00-Awg
Line-stirrup Clamp
250- to 350-Mcm run 400- to 500-Mcm run
6-Awg to 350-Mcm tap 4-Awg to 500-Mcm tap
Two-bolt Connector
Corrosion Inhibiting Compound
in Collapsible Tube
Pressure Applicator for
Corrosion Inhibiting Compound

Fig. 8. Plated copper alloy connectors and compound applicators

These cables consist of two no. 4 aluminum, neoprene-covered, spiralled for support, on a bare ACSR (6/1) supporting member which also serves as a neutral.

CONSTRUCTION DETAILS

Some of the more pertinent details of the construction methods are as follows:

1. The conductors are spliced by means of compression devices.
2. Secondary conductors are supported on conventional secondary brackets and dead-ended on a 4-inch porcelain spool bracket. Protective armor is used only at the dead ends.
3. No. 7 strong aluminum alloy is used as a tie wire on conductors up to and including 1/0. No. 4 soft aluminum alloy is used on aluminum conductors larger than 1/0.
4. Armor rod is used on aluminum conductor in long-span rural distribution lines but is not used on short-span urban lines.

Figs. 2 through 7 show typical installations of aluminum in 2.4/4.16-kv and 7.2/12.5-kv primaries, secondaries, and services.

Fig. 2 shows the no. 4 ACSR 7.2-kv primary, no. 0 all-aluminum bare secondary, no. 4 all-aluminum neoprene-covered open-wire service, and no. 4 neoprene-covered triplex service cable.

Fig. 3 shows the no. 4 ACSR open-wye 12.5-kv primary, no. 0 all-aluminum bare secondary with a no. 4 ASCR bare teaser for 3-phase no. 4 all-aluminum neoprene-covered open-wire service and it shows no. 4 neoprene-covered triplex service cable.

Fig. 4 shows a corner in a 477,000-CM all-aluminum 4.16-kv feeder, and a three No. 4 bare copper primary lateral.

Fig. 5 shows the no. 0 all-aluminum secondary dead-ended on 4-inch spool rack, and no. 4 all-aluminum neoprene-covered services.

Fig. 6 shows no. 4 ACSR bare 2.4-kv primary, no. 3 bare copper secondary and street-lighting lateral on right side of pole, no. 0 all-aluminum bare secondary on left side of pole, and no. 4 all-aluminum neoprene-covered services.

Fig. 7 shows no. 3 copper, 4.16-kv primary on top arm, no. 4 ACSR primary on buck arm, no. 3 copper secondary, and no. 4 all-aluminum, neoprene-covered services.

These construction illustrations were made primarily to show that the aluminum conductors are added throughout the system without regard to the materials in place.

Table I. Stress Under Heavy-Loading Conditions in Design Span

Conductor Size	Percentage of Ultimate Strength
1/0	41.5
3/0	35.6
266,800 CM	29.4
336,400 CM	27.4
477,000 CM	25.5

Connectors

All connectors being used in the distribution system, on copper and/or aluminum conductors, have copper alloy bodies, tin-plated. The adoption of this type of connector was the result of experience with the many other types which have been developed in the past few years.

For some time after the use of aluminum for a distribution conductor was begun, special connectors, aluminum-to-aluminum, aluminum-to-copper, and copper-to-copper, for the various wire sizes were used. This made necessary a large-store stock of connectors and the carrying of a large assortment of connectors on service trucks and line trucks. This multiplicity of connectors resulted in confusion and many misapplications. Much of the difficulty was overcome by the adoption in 1948 of copper-alloy-body tin-plated connectors, each suitable for a reasonable range of conductor sizes. The connectors are used indiscriminately in making connections regardless of the conductor materials being joined.

Considerable difficulty was experienced for some time in getting the linemen and servicemen to use protective compound in connections. They were not convinced that it was necessary and the method used in applying the compound was unsatisfactory. For applying the compound, we now provide collapsible tubes or small grease guns having an applicator nozzle; see Fig. 8. The workmen take their choice of the two methods and one or the other is reasonably satisfactory to them. The men have seen enough cases of trouble where protective compound had not been used to be convinced that it is necessary, and we believe they are consistently applying it.

When hot-line tap connectors are used, a line-stirrup clamp is placed on the conductor and the tap connection is made to the stirrup. This type of connection is made only on low-capacity connections on 7.2/12.5-kv circuits. Fewer would be used if connectors which could be readily installed with hot sticks were available. Connectors now being used on our distribution lines are shown in Fig. 8.

Trouble Experienced

Connector Trouble

Many cases of connector trouble on aluminum conductor have been experienced, the more usual types as follows:

1. Conductors burned down at connections.

2. "Light flicker" or "no lights" calls caused by loose connection or high-resistance connection caused by corrosion of the material.

3. Damage to customers' equipment caused by unbalanced voltage due to an open or poor connection in a secondary neutral.

Sufficient connector trouble had been experienced on two 12.5-kv circuits built in the early days of the Company's use of aluminum that within the last year these circuits were inspected and completely reconnectored. Considerable connector trouble has been experienced on primary, secondary, and service connections. The majority of the cases of trouble have been on aluminum-to-copper service entrance connections, and most of these were found on flicker complaints.

It is the opinion of the authors that most of the cases of connector trouble have resulted from the misapplication of connectors or lack of use of protective compound. For example, failures were experienced when cadmium-plated connectors purchased for ground connections were applied to current-carrying secondaries and services. However, considerable trouble has resulted because of error in judgment which led to specifying poorly designed connectors or because a good connector was not available. It is the authors' opinion that the best connectors developed so far are those especially made for a definite size and type of conductor, but that their better performance is more than offset by stocking and misapplication problems. A serious problem in the making of connections would be solved if a satisfactory connector for use with hot-line tools were available. There is no evidence that a concerted effort on the part of the manufacturers is being made to meet this need.

Table II. All-Aluminum and ACSR Conductors Used in Urban Overhead Distribution Lines

Wire Size	Type	Strands Alum	Strands Steel	Covering	Copper Equivalent
6*	alum	1		neoprene	8
4*	alum	1		neoprene	6
4	ACSR	7	1	bare	6
1/0	alum	7		bare	2
3/0	alum	7		bare	1/0
266,800 CM	alum	7		bare	3/0
336,400 CM	alum	19		bare	4/0
477,000 CM	alum	19		bare	300,000 CM

*For service drops only.

Conclusions

Experience with aluminum conductor material causes the Company to classify it as acceptable. At this stage of development the authors believe that improvements in connectors should be made; however, there have been no difficulties of a magnitude which would cause a return to the use of copper with the present price differentials.

With a continuation of price differentials which have persisted since 1946, aluminum will for many years be the conductor for use in distribution systems; and engineers should be diligent in extending its use wherever practicable.

Reference

1. Distribution Transformer and Secondary Conductor Economics, Bryce Brady. *AIEE Transactions*, vol. 68, pt. I, 1949, pp. 483–90.

◆

Discussion

J. D. Padgett, Jr. (Texas Electric Service Company, Fort Worth, Tex.): I prepared a discussion for H. E. Carpenter's and R. E. Thornton's paper and it ties in closely with C. E. Nelson's and K. S. Garrett's also.

We have approximately the same theory as R. E. Thornton does for the use and application of aluminum and of course, our problems are very similar, being geographically located approximately the same, but I would like to point out some of the differences between their practices and ours.

For service wire, we use a stranded aluminum neoprene-covered single conductor.

At an earlier date, during World War II, I believe, we had some very unsatisfactory experiences by using a solid, neoprene covered conductor. The wire would break, and the insulation would remain intact That problem may have been licked by now. We do use some triplex.

It was interesting that both of you use the triplex service conductor but we shied away from it, not knowing the life expectancy. We feel that possibly some time in the future, we will approach something like an ice storm and have to go out and change in wholesale fashion all of these services when they begin to break down.

We like to rely on the air insulation, even though the conductor covering has broken down as an insulator. Our present studies indicate that 1/0 all aluminum does not have sufficient tensile strength, coupled with other economic features, to suit us as a secondary conductor base. We expect to standardize on 2/0 all-aluminum secondary for possibly anything above 30 to 40 kva per thousand foot.

Our larger sizes of primary conductor, 4/0, 336, and 477 are all aluminum. The smaller sizes, of course, are ACSR, but we like the all aluminum in those larger sizes because of the simplified guying as well as the simplified joints or splicing.

We use ACSR and all aluminum, all bare exclusively for the overhead distribution system.

If anybody wants to buy copper he has to have a good reason. We are presently in the process of investigating the use of a universal sag chart.

Interestingly, I note that we are completely 180° away from Mr. Thornton on our armor rods and armor. We generally use preformed line guards for all aluminum at all supports except dead-ends and preformed armor rods for ACSR supports, and we also use the 3-inch spool insulator for the dead ends and use no armor of any kind at the dead end.

We have used some armor tape and have found that the No. 7 strong alloy tie-wire doesn't work too well with that, so we don't buy it any more. We buy only the soft drawn. We haven't been quite so fortunate in getting the linemen to use the inhibiting grease. We hope that we will. Also, we have only been using aluminum extensively about 5 years and we haven't been bothered with any electrolytic action because it hasn't rained in that long down there. That might be funny up here, but it is not down there.

We use a spring-loaded hot line clamp, copper alloy with tin plating, in the smaller sizes. We use for a larger size, where it is necessary to tap with a smaller conductor, an aluminum bodied-clamp. The bolted connectors generally, as Mr. Thornton pointed out, are pretty much what we use and we are going more and more to the compression type and that looks like the way we are going.

In response to a request through Ebasco Services, we received a letter. I would like to read this and would very much appreciate anyone's discussion on it as to their problems, or their experience, how they solve it, or what they think about it.

In part, the letter reads, "I would like to suggest that you seriously consider various strandings of ACSR as alternates to the all-aluminum particularly for some of the larger sizes.

"For many years, we have been offering a stranded ACSR with less strength than our more standard strandings.

"A number of companies have gone to 18/1 stranding, and 36/1 strandings as alternates to the all-aluminum in distribution and transmission circuits due to its superior sag characteristics.

"Many people have been somewhat hesitant about using ACSR for distribution work since they realize normally a composite joint has to be made that will anchor both the steel and the aluminum. However, in these special strandings, tests have proven that joining methods similar to those used on all aluminum for tension splicing would produce satisfactory results, holding power up to 80 or 90 per cent."

C. T. Hatcher (Consolidated Edison Company of New York, New York, N. Y.): I did have a question or two that I would like to ask. It is quite interesting to me to have heard these two papers, the Philadelphia and the Oklahoma paper, because we are extremely interested, in New York in the use of aluminum and so for the last year or two, we have given serious consideration to its use. We had some opposition from our construction forces in the use of it.

I was quite interested in what R. E. Thornton said. I understood him to say, that he uses it anywhere in his system regardless of location.

I don't know whether I understood him correctly. Does that mean that if you have a particular span of copper wire down, that you will put an aluminum section back up, and if so, do you put it up with the same sag? Are you sagging the aluminum the same as you are the copper?

That seems one of the main objections our construction people have regarding its general use. They say it is very nice to pick out a particular location in which to use it where everything is all aluminum, but they don't like the idea too much of intermingling it with copper.

I might also apply that same question to K. S. Garrett from Philadelphia: Is their installation particularly an isolated one, a localized one, or is it generally being used throughout?

One other thing that has been worrying us in the engineering as well as from the construction end, is the question of the dead-ending of aluminum. It is apparently more expensive, more cumbersome to do with, let us say, the lack of present-day splicing means.

Both of the authors have pointed that out and I would like to reiterate that particular point, that a good tension splice is required.

K. S. Garrett: To answer Mr. Hatcher, who, asked about our stopping of the use of copper or the use of aluminum indiscriminately throughout the system.

In general, I would say that we are buying little or no copper. We have continued to use some that we had for replacements, but when that has been depleted, I believe that we will use aluminum as indiscriminately as described by some of the other authors.

I appreciated the discussion primarily because it certainly expanded and embellished some of the things I might have said about our own experience.

I have only one other thing that I might add to my paper and that is that around a spreader which we have is most of our economy in distribution. I didn't describe it in detail. I would like to say that it is made of laminated fiber glass. It is designed so that it will withstand a 1,000-pound pull on the bail which should be greater than the load that would be put on any of the services which we install.

It has been tested under water and with high potential to see if it will track, and it has withstood all of these tests very satisfactorily, but I would like to warn everyone, and there have been several who have shown an interest in it, that if they get the manufacturers to make it for them and it isn't a stock item, to be very careful about their source of laminated fiber glass; the company that has made these for us has run into a terrific amount of trouble.

I would say that of the five, six, or seven suppliers of laminated fiber glass, only one could stay within these dimensions and get the strength required.

R. E. Thornton: This is certainly a heart-warming experience to find that there is so much interest in a thing that was so ill-received in the early days. I would like to comment briefly before I close my paper on the separator that Mr. Garrett has commented on.

I am going to follow with a great deal of interest the life history of those separators to see what happens in the way of chafing.

I would like to ask him if, at the point of clamping, you put a ribbon or some other protection on the line conductor?

K. S. Garrett: We do not put any liner, tube, or covering over the conductor. Before using them, we took these spreaders and put them on aluminum wire and ACSR and put them through a rather long life test on a vibrating machine; we found that they should last for a great many years in service.

R. E. Thornton: That is interesting because we are going to the idea which is not new, of course, of supporting the insulated secondaries on a bare steel messenger, using a bare all-aluminum neutral, spinning in the field, and taking the service away from the messenger.

However, that is getting back to the insulated conductors again which we had forsaken.

I am glad to hear that Alcoa is doing something about the splicing-sleeve situation and the statement that all aluminum connectors should be used. We will go along with that.

Right now, we are in a transition period where we have to meet the problem of the unlike metals so we had to take some middle ground, and we are doing that by using the copper alloy, tin-plated connections.

J. D. Padgett brought up the matter of the solid neoprene-covered service wire breaking. Yes, we had that trouble, too, at first. In fact, we thought in one of our towns in western Oklahoma where there is a lot of wind, we had some sort of insulated symphony. We would run a service to a house and right away, we would begin to get calls about the hum and the noise. Then we began to get some no-light calls. The neoprene was strong enough that the no. 6 solid aluminum, which we were using at that time, and which we no longer use, was breaking within the covering, and the covering was maintaining the service in the air but not maintaining the service electrically. We found out that our service crews were pulling up these services well beyond any reasonable tension.

We were getting vibration on the house, and then we were getting the failure of the aluminum. We have incorporated specifications in our books now that will not allow them to increase the tension and we have had no more trouble.

As to C. T. Hatcher's question about anywhere. We do not go in and pick up a piece of copper that has come down and splice in a piece of aluminum. We will make the repair with a like material. If we have to make a one-span extension of a secondary, for example, we have left a little choice to the line foreman. We give the distribution engineers a little leeway and they can say whether or not it will be a copper one-span extension or whether or not they will leave the dead-end in place on the copper and make a one-span aluminum extension.

He also mentioned dead-ending methods.

In the clamps we use to make a conventional dead-end, we are through with the bimetallic washer.

On the secondary with a single phase primary on top we have used no automatics on aluminum. Our experience on copper caused us to abandon those some years ago.

We are using a clamp-type connector and making a conventional turn-back rabbit-tail dead-end.

K. S. Garrett: What do you people do about terminating aluminum in cut-outs, lightning arresters, and distribution transformers?

R. E. Thornton: We are happy to find that our friends in the manufacturing business are doing something about this, and I have an amusing experience of which I would like to tell you. I think that it will graphically illustrate the situation.

I happened to be in our storeroom one day and there was a 25-kva transformer. Just below the secondary stud terminals was a large diamond, and one side was labelled *A*, and was silver or aluminum color. The other half of the diamond was labelled *C* and it was copper-colored.

The studs were tinned or silvered. I went back to the office and called the representative of the Allis-Chalmers' people and said, "I am sure glad to see you get on the bandwagon. That is mighty fine."

I had to tell him what I had seen. He was very happy, but imagine my chagrin when I found out that General Electric Company had dressed down one of their men in the manufacturing plant because they had used that diamond with the *A*, *C* on it to indicate that that would take either copper or aluminum. I understand that has been changed now.

In summary of this discussion, it appears that there are problems associated with the use of aluminum conductors in distribution systems which are generally associated with the points of connection and dead-ending. It is also apparent that there is a determination on the part of the manufacturers and the users of the material and accessories to solve these problems.

Development of a Welded Aluminum Bus for Substations

C. E. ASBURY
MEMBER AIEE

C. J. HARTMAN
MEMBER AIEE

THE DESIGN and use of aluminum busses in major transmission substations permits a reduction in cost compared to other types of bus construction. This paper reviews several design aspects in the development of this type of construction.

Early Designs

Some substations containing aluminum busses and cross connections designed by Commonwealth Associates, Inc., early in 1931 used connections of the bolted type and most of the fittings were very large in size compared to copper fittings. A cross section of one of these 138-kv substations is shown in Fig. 1, and that of a 46-kv substation in Fig. 2, both of these stations being on the same site. The performance and record of these earlier designs have been very satisfactory from an operating and maintenance standpoint. There have been no corrosion problems on these installations in the midwestern part of the country.

During the depression years when there was a limited amount of construction, design activity using aluminum busses was also limited. Station designs from 1936 to 1942 also had bolted connections except for the joints in the bus itself, which were made by using shrink-fit connectors. An insert was placed in dry ice while the tubing was heated in an oil bath and scoured with a wire brush. The insert and tubing were hurriedly placed together to form a joint.

In 1946, when aluminum became available after the wartime shortage, similar installations were made except for a slight change in the method of shrink-fitting the bus connections; see Fig. 3. The inserts were placed in dry ice but the tubing was heated by the use of strip heaters encased in a heavy asbestos piping insulation. This gave better control of the heat, and considerable time was saved in the bus assembly by the use of this method. In about 1952, heliarc welding of the aluminum tubing was started for extensions to existing substations with aluminum busses.

One-Line Diagrams

Most of our present major transmission substations using aluminum busses have been designed with two main busses with or without a transfer bus or as a ring bus. The major electrical connections for a typical 2-main bus arrangement are shown in Fig. 4 for a 138-kv substation. Two 138-kv busses are used with disconnect switches which make it possible to connect any line or generator to either of two busses.

The flat horizontal bus construction using aluminum busses permits the use of a simplified station structure with a minimum of supporting members which reduced the over-all cost (Fig. 1, 2, and 3). Pedestal-type bus supports may be used which require little structural steel and with aluminum busses these supports may be spaced farther apart than when some other types of bus material are used.

Present Designs

At present Commonwealth Associates are designing major substations using aluminum main bus and cross connections where practically all of the fittings are being made and connected together by heliarc welding. Several different assemblies have been designed and after considering their advantages and disadvantages, certain types of connections and arrangements have been selected to reduce the amount of construction labor required and to speed up the field assembly.

The subassemblies have been designed with simplicity in mind and to provide rigidity and ruggedness desirable for a major bus. The bus arrangements have been worked out to reduce as far as practical the number of assemblies and subassemblies required. Some of the more common types of the subassemblies are shown in Figs. 5 through 14.

It will be noted that several saddle arrangements are used in fabricating the assemblies. This improves the ruggedness and rigidity of the bus to withstand higher short-circuit currents and other types of shock loading that may occur. A considerable amount of field labor is saved during construction by the use of these types of connections. The

---

Paper 55-257, recommended by the AIEE Switchgear Committee and approved by the AIEE Committee on Technical Operations for presentation at the AIEE Electrical Utilization of Aluminum Conference, Pittsburgh, Pa., March 15–17, 1955. Manuscript submitted December 15, 1954; made available for printing January 26, 1955.

C. E. Asbury and C. J. Hartman are with the Commonwealth Associates, Inc., Jackson, Mich.

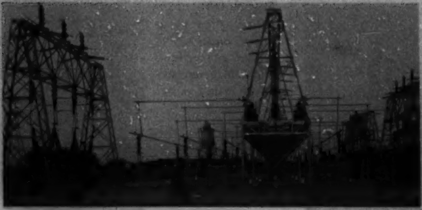

Fig. 1. 138-kv substation aluminum busses with bolted connections

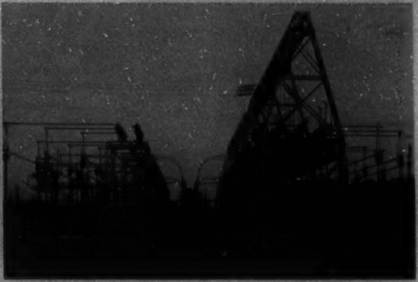

Fig. 2. 46-kv substation aluminum busses with bolted connections

designs allow a considerable amount of shop fabrication on an assembly line basis making it possible to realize appreciable savings over the cost of performing the labor in the field.

Figs. 5, 6, and 7 show the construction of an A-frame assembly for supporting one end of a cross bus. The A-frame is made from two assemblies; the V-shaped assembly at the top and the pipe-and-saddle one at the bottom. The two assemblies together form a telescoping A-frame which allows for horizontal leveling of the cross bus. It also provides for closure of the cross bus on the end at the top of the A-frame. The terminal on the end of the cross bus tube in Fig. 7 is also a telescoping arrangement which allows for a vertical alignment of the A-frame. All the field welding can be done on the ground except those welds required on the main bus at the bottom of the A-frame. The assemblies are welded in the shop. The use of saddles on the bottom of the pipe assembly on the A-frame is an easy method of positioning the A-frame on the cross bus.

Figs. 8 and 9 show an expansion assembly. It is completely shop assembled and is shown in Fig. 9 mounted in the main bus. The double loop on top and at the bottom of the assembly is necessary to divide the currents and short-circuit stresses equally. The expansion loops are placed in the main bus at approximately 100-foot intervals. The expansion of the bus is approximately $1^{1}/_{2}$ inches per 100 feet from 0 to 100 degrees Fahrenheit. The main bus is made continuous by inserting a sleeve, then welding the pieces together.

Fig. 11 shows two saddles used for supporting the main bus. It will be noted that one saddle has fixed holes while the other has a slot to provide for expansion. One fixed saddle is used for approximately each 100 feet of bus. The remainder of the saddles allows the bus to move, to take care of the expansion. Fig. 10 shows several types of fittings required to take care of differences in over-all heights of equipment and to make connections on various sizes of tube.

Fig. 12 and 13 shows various types of terminals used. Most of the fittings on cable are the compression type, some welded as well as compressed. Fig. 14 shows how some of these fittings are used.

All current-carrying parts which are bolted together use galvanized 1/2-inch diameter, quenched and tempered American Society for Testing Materials standard,[1] fine-thread series bolts with hex head and nut and Belleville spring washers with a minimum of 1-mil plating.

No-Ox-Id paste is used on all bolts, nuts, washers, and surfaces of bolted and nonstrain compression connections. Strain compression fittings are dipped in Penetrox or zinc chromate before the unit is compressed. After the joint or connection is completed, the whole surface is coated and thoroughly sealed against moisture with No-Ox-Id paste.

Relative Cost

Considerable thought has been given to the design of subassemblies to permit shop welding on an assembly line basis. Jigs and fixtures can be used for this type of work to give the proper alignment which will further speed up the field assembly. Only a relatively small number of field welds are required in the final assembly. Many of the assemblies are similar in design (for example, each crossover bus connection to an airbreak switch, Figs. 5, 6, and 7) and since each of these is assembled in the shop by the use of jigs and fixtures, they are interchangeable in the field and no particular fitting problems are involved in the installations. The technique of welding aluminum connections makes it unnecessary to purchase expensive bolted connectors and there is more assurance of a good electrical connection. It is estimated that on some of the present designs as much as 60 per cent in savings may be realized in material and labor as compared to copper bus designs using bolted connections.

Short-Circuit Tests

Short-circuit tests were performed on some of the major components to ascertain that the mechanical strength of the welds and members of the structure was adequate and also to determine any hot spots which might develop either around the welds or on some of the fittings, especially where sharp bends were involved. Since the tensile strength of most aluminum alloys is decreased appreciably at high temperatures it was essential that the likelihood of such temperature occurring in some of these components be determined before proceeding with construction. Some of the assemblies tested are shown in Figs. 15 and 16. It did not appear necessary to test long parallel runs of bus structures since the forces involved on these members during short circuits can be calculated and an ample safety factor provided in the design. This avoided the necessity of making a rather bulky test setup which would have been expensive to test.

TEST PROCEDURE

Resistance measurements were taken before and after the short-circuit tests to determine if there had been any major changes in the resistance. Dimensional measurements were also made prior to and after each test to determine any permanent movement or deformation of the samples. These horizontal measurements were taken at 3 and 5 feet from the top

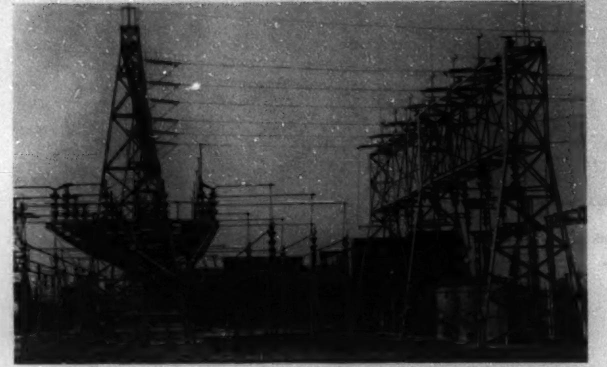

Fig. 3 (left). 138-kv substation aluminum busses with bolted connections. Shrink fit connectors in main bus

Fig. 5 (right). A-frame assembly

of the A-frame assembly; see Fig. 15. Distances were also measured between the slip joint and approximately the middle of the loop on the expansion assembly; see Fig. 16.

Temperature readings were taken just prior to and immediately following each short-circuit test with thermocouples located at points 1, 2, 3, 5, and 6 as indicated for A-frame test sample with thermocouple 4 being used to read ambient temperature. Thermocouples were located at points 1, 2, and 3 on the expansion joint with thermocouple 4 used for ambient air temperature during the measurements. Numerous locations on the test samples were marked with Tempilstiks (300 and 500 degrees Fahrenheit), crayons which turn black when their critical temperature is reached.

Two series of short-circuit tests were made on each sample, one ranging around 16,000 amperes and the other at about 23,000 to 26,000 amperes, the limit of the test facilities. Test currents were applied for 2 seconds then were off for 2 seconds and on for 2 seconds on each sample. The sample was then permitted to cool to approximately ambient temperature and the same test current permitted to flow for approximately 4 seconds. Tests were also made by preloading the A-frame assembly to simulate as far as practical the horizontal stresses that would occur on the A-frame due to forces between the top of the A-frame and the bus connection to a switch. Following each of the tests the aluminum samples were examined carefully by touch to determine any hot spots where thermocouples might be desirable. Locations of thermocouples 5 and 6 were determined by this process, and in general these read the highest temperature.

Test Results, A-Frame

There was no deformation detectable on the test sample and no hot spots which reached a sufficiently high temperature rise to be of concern. The highest temperature observed on the test specimen was about 75 degrees centigrade (C) at both point 5 and point 6. Part of the heating at points 5 and 6 was caused from transfer of heat from the test leads at these points. The 500,000-CM bare copper cable used for the test connections became quite hot during the test and, owing to such a high differential of temperature between the test lead and the test sample, much heat was transferred into the terminal of the test sample. The ambient temperatures during some of these tests were quite high, in the order of 50 to 57 C, on which the weather bureau reported as the hottest day on record for that area.

Measurements were taken with a thermocouple bridge with the thermocouple reading ambient temperature only about 2 feet from the ground and near the samples being tested. The tests were made in the substation yard, which was covered with white stone that reflected the solar heat. There was no change in color on any of the Tempilstik markings.

The tube used for the A-frame assembly felt the hottest on the outside of

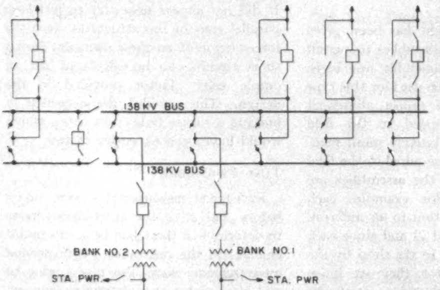

Fig. 4 (left). One-line wiring diagram. Major electrical connections for 2-main bus arrangements for 138-kv substation

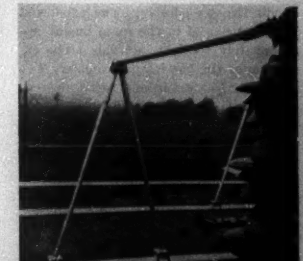

Fig. 6 (right). A-frame assembly with cross bus and terminal

Fig. 7. A-frame assemblies with cross busses

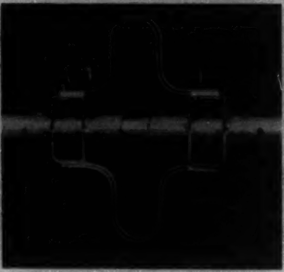

Fig. 8. Expansion joint assembly

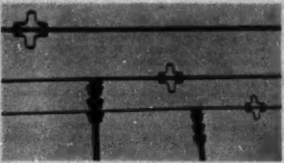

Fig. 9. Expansion joint assembly mounted in main bus

Fig. 10. Miscellaneous aluminum fittings

the A-frame during the test and this was probably because of the crowding of the current to the outside (skin effect) due to the opposing magnetic fields. The tubes appeared to be slightly hotter near the top near point 3 than at the bottom near point 2. The welds during all tests appeared to be cooler than other parts of the test samples, probably because welds connect a smaller part to a much larger piece of metal so that the larger mass conducts the heat away from the point of the weld as compared to the heat in the smaller cross-section material.

Test on Expansion Joint

There were no excessive temperature rises in any parts of the assembly, the highest temperature being only about 60 degrees with an ambient air temperature of about 57 C. Comparing the test prior to the application of short-circuit current with that immediately afterward the temperature rise appeared to be only 2 or 3 degrees in all cases. Some tests were made when the ambient temperature was about 32 to 34 degrees which showed a rise of 4 or 5 degrees during the application of short-circuit current.

Measurements of the sample indicated that the expansion joint moved outward slightly, possibly 1/16 inch, which is believed of no consequence since the top loop may have had a slight prestress which tentatively moved it slightly when the additional force was applied.

It will be noted that the temperature rise on both samples during the short-circuit test was well below any temperature which will materially affect the characteristics of aluminum. Tests have indicated that the change in tensile strength of aluminum is very small even when exposed to temperatures of 125 C for continuous periods of 10,000 hours or more.[2,3]

Experience with Erection in the Field

Because of the weight of aluminum tubing, a considerable amount of time and field labor is saved because in a great number of cases one man can do the work that would require two or more men when copper is used.

The technique of welding aluminum becomes much easier as experience is gained. It has been observed in the assembly that as the welders become more experienced, they make welds more rapidly. The use of a few simple jigs saves considerable assembly time by practically eliminating the necessity of the aligning of the busses in the air.

Fig. 11. Bus support fittings

Fig. 12. Miscellaneous compression-type terminals

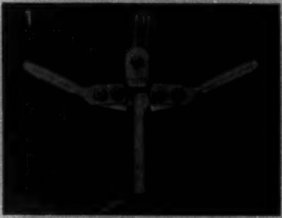

Fig. 13. Compression-type terminals

Fig. 14. Installation of compression terminals and fittings

Some specific examples illustrate how time and labor are saved doing field assembly. Three or four 30-foot pieces of tubing with an expansion joint shown in Fig. 7 and the bus support fittings in Fig. 10 are welded together on the ground. This makes approximately 100 feet of tubing and fittings which may then be hoisted, by about six men, as a unit to the top of the bus supports, and bolted in place. Another example is the installation of a piece of $1^1/_2$-inch aluminum tubing 23 feet long bent on both ends and weighing approximately 22 pounds. This

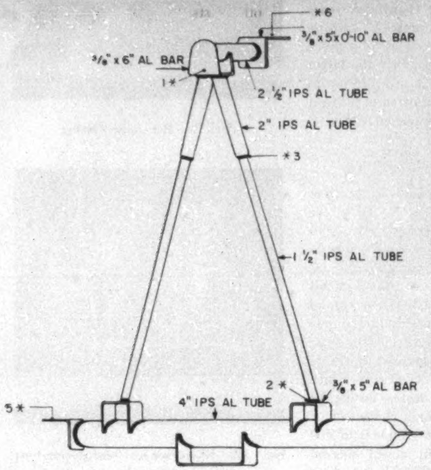

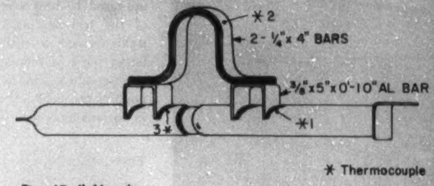

Fig. 15 (left). A-frame assembly showing thermocouple locations for short-circuit tests

Fig. 16 (above). Expansion joint assembly without lower loop showing thermocouple locations for short-circuit tests

piece of tubing was picked up by one man on the ground, and handed to another standing on a steel structure 22 feet above the ground. The man on the steel structure swung the other end of the tubing to a third man on the ladder 15 feet horizontally from him. The two men then fastened the tubing at both ends. The over-all time of placement amounted to only a few minutes. The cross connection shown in Figs. 6 and 7 was completely assembled on the ground and the only welding necessary to be done in the air was in the connections to the bus.

All-aluminum cables are used to make connections in numerous places throughout the substation, using fittings of the high-compression type shown in Figs. 12, 13, and 14. Labor can be saved by making a great many of these connections on the ground rather than in the air, and a further saving could be made if improvements are made in compression tools.

Conclusions

Experience indicates that welded aluminum can be used successfully for substation bus construction and that if properly designed it will give excellent service and will result in an appreciable saving both in material and in installation labor for major stations. Short-circuit tests which were performed on representative structure members showed that this design will withstand the high short-circuit currents likely to be encountered on present-day systems as well as on the systems being planned in the foreseeable future.

References

1. Specifications for Quenched and Tempered Steel Bolts and Studs with Suitable Nuts and Plain Washers. *ASTM Standard A325-53T*, American Society for Testing Materials, Philadelphia, Pa., 1953 Supplement, pp. 215–20.

2. Mechanical Properties of Aluminum Electrical Bus, G. W. Stickley, C. O. Smith. *AIEE Transactions*, vol. 73, pt. III-A, Apr. 1954, pp. 100–06.

3. Effect of Heating at 300 and 500 F on the Properties of Aluminum and Copper Wires. *Wire and Wire Products*, New York, N. Y., Mar. 1952.

4. Sewaren Welded Aluminum Bus Proves Practical and Economical, D. M. Quick. *Electric Light and Power*, Chicago, Ill., vol. 27, Dec. 1949, pp. 58–62.

5. Aluminum Substation Design, B. J. Fletcher, L. T. Guess. *Ibid.*, Nov. 1949.

6. Alcoa Aluminum Bus Conductors. Aluminum Company of America, Pittsburgh, Pa., 1948.

◆

Discussion

E. E. Ramm (Ohio Edison Company): The joint efforts of Commonwealth Associates, the aluminum industry, and the Ohio Edison Company have made it possible for a practical economical installation of welded aluminum bus in addition to two of the Ohio Edison Company's 138,000-volt major substations. In this discussion some of the results and experiences of construction will be given.

In the early 1940's a rigid aluminum bus was used in one of our major substations. Shrink-fit connectors were used in the bus runs with bolted fittings for connections. The shrink-fit connectors were difficult to install and took considerable time. The bolted fittings were massive and their weight caused considerable deflections in the bus runs. No trouble has been experienced with the connections from a conductivity standpoint in this installation to date.

The recent improvements in the inert-gas-shielded arc-welding process made the rigid aluminum bus installation very attractive. It eliminated the bolted-type connectors and made the installation simple. In 1953 it was decided to make several installations of welded aluminum bus.

Little experience with aluminum welding was available and as a result welders had to be trained. Several welders were sent to school for a week. These men, in turn, have taught other men and have found no trouble in training our regular welders for aluminum welding. The first welds took considerable time due to training of welders, obtaining proper welding equipment, and finding the necessary procedures to obtain good efficiency. Welding practices and procedures have now been developed so that satisfactory welding times are now being obtained. Examples of some of the welding times using the shop jig-welded components are: joining of 4-inch (iron-pipe size) tubing, 45 minutes; welding the expansion joint as in Fig. 9 in the paper, 2 hours; and welding the "A-Frame Assembly" Fig. 5, 45 minutes.

The welding equipment used is an a-c welder with a water-cooled gas-shielded electrode. Manual feed of the welding rod is preferred to automatic feed as it adapts itself more readily to overhead and vertical welding. The use of the crater-eliminator attachment on the torch was discontinued with experience and the additional welders which have been purchased are without the attachment. Temperature has no effect on welding conditions other than the freezing of the coolant and this has been corrected by using an antifreeze solution. Barriers for shielding the welds from wind have to be used for welding out of doors.

Wherever possible the compression-type fitting has been used on stranded aluminum cable. Welding to the stranded cable has been quite difficult. The compression joint is much faster although sometimes it is impossible to get the press to all of the locations required. There is need for the development of lighter and more flexible presses.

Although no final figures for labor for these welded installations are available, it is apparent that there is some labor saving due to ease in handling the lighter weight of material. There is definitely a reduced cost of material and structure required with welded aluminum bus.

Experience with the two 138,000-volt substation installations using welded-aluminum-type bus has led to the decision to construct a 23,000-volt substation with welded aluminum bus.

D. H. Sandell (Aluminum Company of America, Pittsburgh, Pa.): The authors are to be complimented for presenting some valuable design and test information and demonstrating again the sound application of welded aluminum bus for substations. This paper has shown the versatility and flexibility of aluminum construction for substations by the custom design permitted using standard materials. The allowance of liberal manufacturing tolerances on materials used in this type of construction contribute to the savings realized in the procurement of these materials.

The authors were apparently designing for a minimum of field fabrication. Circumstances may lead design engineers to specify field or shop fabrication of connectors and supports for one job using welded aluminum bus as shown in Figs. 5, 8, and 11 and on another job specify fittings supplied by a manufacturer so as to keep shop as well as field fabrication to a minimum. For engineers who wish to specify accessories fabricated by a manufacturer there are available fittings for connectors and supports that can be used for welded construction. Many times these fittings serve a dual purpose, for example, as both a connector and a jig for holding the conductor in place while welding.

It should be noted that the different aluminum alloys used for the job described in this paper are easily weldable.[1] For example, the *6063-T6* aluminum alloy pipe was easily welded to the 1/4 by 4-inch *EC-O* flexes. The *1100* and *6061-T6* aluminum alloys used for this construction were welded with similar ease.

The combination of steel bolts and Belleville spring washers used for bolted electrical joints with aluminum bus as described by the authors has an excellent record for 25 years of service. Recent tests have shown that steel bolts and Belleville washers are not the only materials that can be used for making good bolted electrical joints. Results of this testing show that adequate bolting pressure is maintained after extended periods of heating and cooling cycles by the use of aluminum bolts and plain flat aluminum washers.

REFERENCE

1. Welding Alcoa Aluminum. Aluminum Company of America, Pittsburgh, Pa.

C. E. Asbury and **C. J. Hartman**: We sincerely appreciate the discussions which have been submitted by Messrs. E. E. Ramm and D. H. Sandell and wish to thank each of them very much for their comments. We hope that our paper together with their discussions will play an important part in accelerating the development of a welded aluminum bus for substations.

Aluminum Widely Used in Power Switchgear

J. L. TALENTO

IN RECENT years aluminum and its alloys because of their availability and many desirable properties have become increasingly important as engineering materials. Aluminum is now widely used in the manufacture of switchgear products. Its applications in switchgear vary from small rivets and hardware to important structural and current-carrying parts. These applications may be divided into three catagories as follows:

1. Electrical or current-carrying applications.
2. Mechanical or structural applications.
3. Nonmagnetic applications.

Figs. 1 through 11 illustrate these various applications and appropriate comments as to reasons for use are included.

Properties of Aluminum and Its Alloys

Properties of aluminum and its alloys which make them desirable for use in switchgear are described in the following.

Electrical Conductivity (EC)

EC aluminum has a volume conductivity of 61 per cent (%) International Annealed Copper Standard. When compared with this standard on the basis of mass instead of volume the conductivity of EC aluminum is over 200% Because of its good conductivity EC aluminum is widely used as electrical bus. Number 6063 alloy which has a conductivity of 51% International Annealed Copper Standard together with relatively high strength is used for tubular conductors.

Nonmagnetic Characteristics

Since aluminum alloys are nonmagnetic they are used in many electrical applications where nonmagnetic materials are required. The most important of these uses is as bus enclosures and barriers in high-current applications where the nonmagnetic characteristics prevent overheating.

Light Weight

The specific gravity of aluminum alloys varies from 2.57 to 2.95. EC aluminum has a specific gravity of 2.71 and a density of 0.098 pound per inch^3 (lb/in^3). For most practical applications aluminum alloys may be considered as having a density of 0.10 lb/in^3, and pure copper a density of 0.324 lb/in^3, while structural steel has a density of 0.284 lb/in^3.

As these figures show, aluminum weighs approximately one-third as much as

---

Paper 55-264, recommended by the AIEE Switchgear Committee and approved by the AIEE Committee on Technical Operations for presentation at the AIEE Electrical Utilization of Aluminum Conference, Pittsburgh, Pa., March 15–17, 1955. Manuscript submitted December 16, 1954; made available for printing February 8, 1955.

J. L. Talento is with the General Electric Company, Philadelphia, Pa.

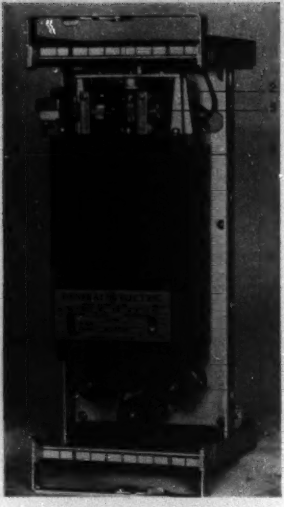

Fig. 1. Power directional relay. These alloys chosen because of strength, good machinability, nonmagnetic characteristics

1—Shaft	3—Barrel
2—Mount	4—Cap

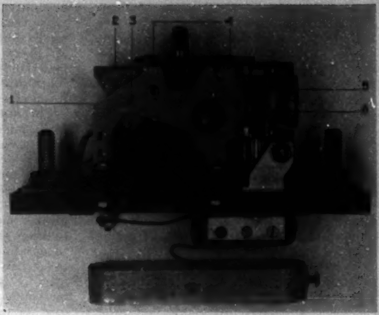

Fig. 2. Aircraft circuit breaker. Alloys chosen because of strength, light weight, ease of fabrication, nonmagnetic characteristics

1—Frame
2—Bell crank
3—Stop plate
4—Rivets
5—Clamping washer
6—Latch bracket

copper or steel, and it therefore finds use in many applications where conservation of weight is important.

Mechanical Properties

Mechanical properties of aluminum alloys vary over a wide range depending on their chemical composition, degree of cold working, and heat treatment. There are two classes of wrought aluminum alloys; the nonheat-treatable alloys whose strength is increased by cold working, and the heat-treatable alloys which acquire their high strengths by heat treatments.

Tensile strengths of wrought aluminum alloys vary from 12,000 pounds per square inch (psi) for annealed EC aluminum to over 85,000 psi for heat-treated 7075 alloy. Yield strengths vary from 4,000 psi for EC aluminum to over 75,000 psi for heat-treatable 7075 alloy. Ductility varies from approximately 45% elongation for annealed EC aluminum to less than 5% elongation for some of the heavily cold worked alloys.

Cast-aluminum alloys have tensile strengths from 20,000 psi to over 45,000 psi, yield strengths from 8,000 psi to over 40,000 psi, and elongations from less than 1 to over 15%. Variations in section size, casting methods, and heat treatment greatly alter these properties.

Strength-to-Weight Ratio

One of the basic uses for aluminum is in applications where conservation of weight is important. Heat-treatable aluminum alloys have high strength-to-weight ratios. Specific tensile strengths and specific yield strengths are used to compare strength-to-weight ratios of various materials. These values are obtained by dividing the tensile and yield strengths of the materials by their corresponding specific gravities.

Table I compares densities, mechanical properties, and conductivities of three commonly used wrought-aluminum alloys with those of other engineering alloys. The effect of cold working of aluminum can be seen from the difference in properties between the annealed and hard-rolled tempers of EC and 5052 alloy. Effect of heat treatment is shown by differences in properties of annealed and heat-treated tempers of 2024 alloy.

Moduli of Elasticity

Young's modulus of elasticity or ratio of stress (lb/in^2) to strain (inch per inch) in the elastic range is approximately 10,000,000 psi for aluminum alloys, 17,000,000 psi for copper, and 30,000,000 psi for steel. A section of aluminum will deflect three times as much as the same section of steel under similar conditions. This factor must be considered in any designs where deflection is important.

Corrosion Resistance

Aluminum, because of its high affinity

Table I. Physical and Mechanical Properties of Metals and Alloys

Material	Specific Gravity	Density, Lb per Inch^3	Tensile Strength, 1,000 PSI	Specific Tensile Strength, 1,000 PSI	Yield Strength, 1,000 PSI	Specific Yield Strength, 1,000 PSI	Elongation, % in 2 Inches	Electrical Conductivity, % IACS*
Magnesium-annealed	1.74	0.063	27	15.50	14	8.05	16	38.6
Magnesium-hard	1.74	0.063	37	21.30	27	15.50	9	38.6
5052-O	2.68	0.097	27	10.05	12	4.48	30	35.0
5052-H38	2.68	0.097	41	15.30	36	13.40	8	35.0
EC-O	2.70	0.098	12	4.44	4	1.48	†	62.0
EC-H19	2.70	0.098	27	10.00	24	8.88	†	62.0
2024-O	2.77	0.100	27	9.75	11	3.97	22	30.0
2024-T4	2.77	0.100	68	24.60	48	17.30	19	30.0
1020 steel-hot rolled	7.85	0.284	61	7.77	39	4.97	37	11.5
1020 steel-cold rolled	7.85	0.284	75	9.55	64	8.15	20	11.5
302 stainless-annealed	7.93	0.286	80	10.10	35	4.42	60	2.2
302 stainless-hard	7.93	0.286	180	22.70	150	18.90	10	2.2
70-30 brass-annealed	8.53	0.308	47	5.00	15	1.76	62	28.0
70-30 brass-hard	8.53	0.308	76	8.92	63	7.39	8	28.0
Copper-annealed	8.96	0.324	32	3.57	10	1.12	50	100.0
Copper-hard	8.96	0.324	50	5.58	45	5.02	12	100.0

*International annealed copper standard.

†This material is commonly used in wire sizes for which the typical elongation in 10 inches is about 23 per cent for EC-O and 1.5 per cent for EC-H19.

Fig. 3 (above). Direct-acting tripping device for air circuit breaker

1—Dash pot cylinder. Good castability, corrosion resistance, machinability, dimensional stability
2—Cover
Plunger not shown. Corrosion resistance, ease of fabrication

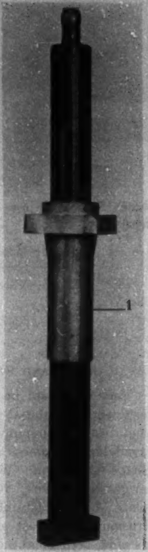

Fig. 4 (right). Oil circuit-breaker bushing

1—Bushing support. Good castability and machinability. Bushing supports also made from wrought and forged aluminum depending on cost of particular part

for oxygen and the formation of a tightly adherent protective oxide film, in general shows good resistance to corrosion. Numerous inorganic and organic finishes can be applied to aluminum to increase its resistance to corrosion. Most important of these finishes are anodizing, electroplating, and painting.

Aluminum and its alloys in the presence of an electrolyte are very susceptible to galvanic attack when in contact with other metals that are more cathodic. Water contaminated with various salts is generally the electrolyte. Some of the heat treatable aluminum alloys, especially those in which copper is a major alloying element, have areas of different potential and are thus susceptible to galvanic attack even though they are not in contact with other metals.

Table II shows the relative position of common metals in electromotive series. Metals at the top are more cathodic than metals below them. Lower metals are preferentially attacked in galvanic corrosion.

Forming and Drawing Characteristics

Aluminum and its alloys are generally considered to be among the most workable of the common metals. As with other metals there are certain basic principles as to choice of alloy, temper, tooling, and degree of permissible deformation which should be followed to obtain optimum results.

Joining Characteristics

All wrought-aluminum alloys can be readily joined by resistance-welding

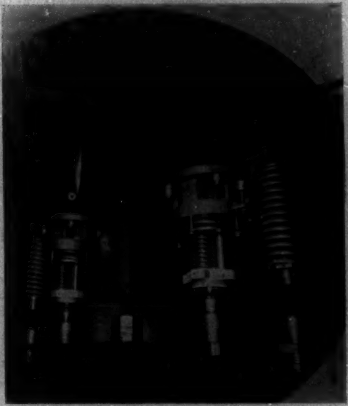

Fig. 6 (below). Interior of oil circuit breaker showing interrupters, contacts, and crossarm. Aluminum used because of light weight, high strength, good machinability. Light weight of primary importance in reducing inertia of moving parts and increasing speed of operation; also important factor in ease of assembly, especially on the larger power circuit breakers

1—Cross arm
2—Contact tip
3—Crossarm-interrupter
4—Bottom interrupter support
5—Spring support
6—Adapter
7—Bottom impulse support

Fig. 5 (left). Metal-clad switchgear

1—Bus barrier
2—Insulator support plate
3—Washer
Used because of strength and nonmagnetic characteristics
4—Primary support casting. Good castability, strength, natural aging properties

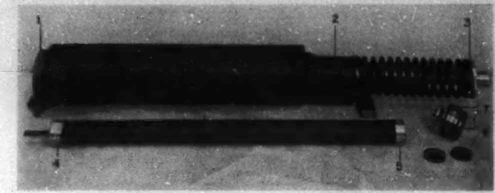

Fig. 7. Impulse cylinder and grading resistor. Reasons for use: light weight, strength, machinability

1—Cap
2—Bottom support
3—Spring support
4—Upper resistor cap
5—Lower resistor cap
6—Valve stop
7—Valve body

methods. Gas and arc welding are, however, usually limited to the nonheat-treatable alloys and the aluminum-magnesium-silicon alloys.

Furnace and torch-brazing techniques have been developed for some of the aluminum alloys, notably the nonheat-treatable alloys and the aluminum-magnesium-silicon alloys.

MACHINABILITY

Most wrought-aluminum alloys have excellent machining characteristics. With proper selection of tooling and lubricants, some aluminum alloys can be machined ten times as fast as steel.

AVAILABILITY AND RELATIVE COST

Very important in the selection of an engineering material are its availability and cost. Aluminum and its alloys are available in practically every known shape and form. Wrought alloys are available as wire, rod, tubing, sheet, plate, bar, structural shapes, and extrusions, while cast alloys are available as sand, permanent mold, or die castings. Forgings are also available.

Aluminum alloys compare favorably with copper alloys when considered on a price-per-pound basis while a distinct cost advantage can be realized when considered on a volume basis. However, compared with steel, the initial cost is considerably higher.

Any substitution of aluminum for other materials to take advantage of reduced costs is made only after thorough engineering evaluation, and assurances that there is no decrease in product quality. In many instances both improved product quality and cost reductions can be realized by the substitution of aluminum.

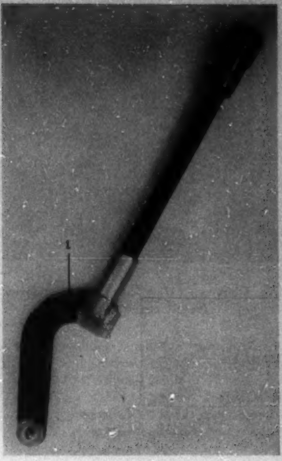

Fig. 10. Rod and coupling

1—Coupling. Used because of high strength, light weight, good weldability

The following list summarizes the properties of aluminum and aluminum alloys which make them very desirable engineering materials.

1. **Good electrical conductivity.**

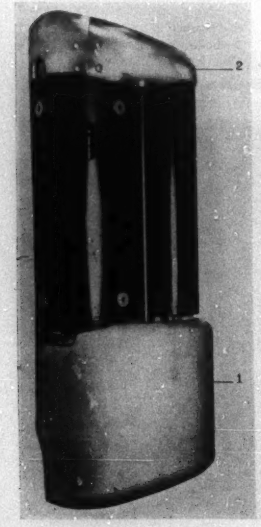

Fig. 8 (left). Interrupter with static shields. Light weight, castability, nonmagnetic characteristics most important

1—Lower interrupter shield
2—Upper interrupter shield

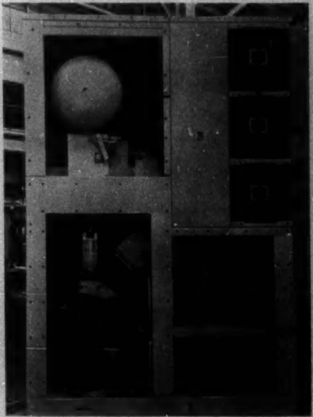

Fig. 9 (right). Air blast circuit-breaker cubicles

1—Channel bus. Used because of high conductivity and light weight
2—Phase barriers
3—Covers
Aluminum selected for phase barriers and covers because of strength, ease of fabrication, and nonmagnetic characteristics

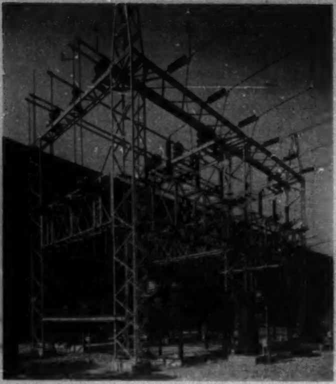

Fig. 11. Outdoor station equipment. Aluminum used because of good conductivity and light weight

1—Tubular connectors
2—Strain clamp
3—Aluminum cable steel-reinforced
4—Tubular bus conductors

Table II. Electromotive Series of Metals

Position	Metal
1	gold
2	platinum
3	mercury
4	silver
5	copper
6	lead
7	tin
8	nickel
9	cadmium
10	iron
11	chromium
12	zinc
13	aluminum
14	magnesium

2. Nonmagnetic characteristics.

3. Light weight.

4. Good mechanical properties.

5. High strength-to-weight ratio.

6. Good corrosion resistance. Anodizing, plating, painting.

7. Good forming and drawing characteristics.

8. Property of being readily welded or brazed.

9. Good machinability.

10. Good availability and favorable cost of wrought products, cast products, forgings, and extrusions.

In view of these many attributes it is small wonder that aluminum has found wide usage in switchgear products. In general, these uses may be divided into three classifications as follows:

1. Electrical aluminum is used in many current-carrying applications where advantage is taken of its light weight and good conductivity. These parts are normally silver-plated on contact surfaces to minimize oxidation and contact resistance.

2. In mechanical or structural use, the light weight, high strength-to-weight ratio, ease of fabrication, good machinability, corrosion resistance, and availability of aluminum alloys make aluminum especially adaptable to many mechanical, structural, and decorative or protective applications.

3. Many switchgear applications require materials which are nonmagnetic. Aluminum has found wide use as bus barriers and housings in high-current applications.

Typical applications of aluminum in switchgear are shown in the figures. The illustrations are chosen not on the basis of importance but merely to show the variety of aluminum applications in switchgear. The applications vary from small rivets and hardware to important structural and current-carrying parts. Wrought-alloy designations are those of The Aluminum Association.[1]

The illustrations show that aluminum and its alloys can be and are widely used in switchgear. This does not mean, however, that indiscriminate substitutions of aluminum for other metals can be made. Aluminum, like all other metals and alloys, has certain limitations, the most important of which are as follows:

1. Because of the larger volume of aluminum which must be used to obtain the equivalent d-c resistance of copper, aluminum conductors cannot be used in many existing designs where space is limited.

2. Aluminum has a low annealing temperature and therefore care must be taken in applying aluminum where elevated temperatures may be encountered.

3. Aluminum forms brittle intermetallic compounds with most metals so that joining to other metals by other than mechanical means is a sometimes serious problem.

4. Galvanic corrosion must be considered and protected against when using aluminum in contact with other materials.

In spite of these limitations, aluminum is now playing and will continue to play an important part in the manufacture of switchgear products. It is estimated that in the next 5 years aluminum consumption will be greatly increased in the design of switchgear.

Reference

1. ALUMINUM ASSOCIATION ALLOY DESIGNATION SYSTEM FOR WROUGHT ALUMINUM. The Aluminum Association, New York, N. Y., Oct. 1, 1954.

◆

Discussion

William Deans (I-T-E Circuit Breaker Company, Philadelphia, Pa.): I agree with the author. He mentioned a phase barrier of aluminum. That might have been surprising to some of you.

I thought I might report on some tests we ran years ago. It might be felt that an arc atmosphere is not very healthy for aluminum. It happens that it is not any worse than for copper. One usually thinks that aluminum, having a lower melting point, would be consumed by the arc more readily than copper. However, we have run tests putting copper in competition with aluminum where we have held the arc stationary and the removal of metal was comparable.

Also, some years ago, we ran tests on isolated phase bus, where we initiated an arc at the start of a run and allowed it to do what it wanted and then captured it at the end of the 20-foot run.

We ran tests on copper housing, aluminum housing, and manganese steel. The manganese steel suffered the most.

The arc, when it runs down to be motorized by the electromotive action of the currents, just leaves little footprints in the inner surface of the housing. When it gets to the end of the run, you may expect danger. I think the explanation based on physics is this: that aluminum and copper are of a high electric conductivity and also a high thermoconductivity. The foot or terminus of the arc is, therefore, not held captive.

The heat is conducted away from that point so that you can't develop a cathode spot. Therefore, the arc plays around as it is acted on by either mechanical action of the air or the electromotive action due to the current. With the high thermoresistivity terms, as for instance of manganese steel, the arc is allowed to stay in one place and develops a cathode spot and then it is captured.

With the aluminum and copper housings

we could see no effect whatsoever, but with the manganese steel, when it reached the end of the run and we held it on for 2 seconds (this was a 4,000-ampere arc) an area became white-hot and grew in diameter until it was about 10 inches in diameter at the end of the 2 seconds. It looked as though it was about ready to fall out. I say that in support of Mr. Talento's use of aluminum as an arc barrier. Don't be afraid of it.

J. L. Talento: I would like to thank Mr. Deans for his confirming remarks and would like to add that results of tests conducted by our engineers prior to the use of aluminum for phase barriers were in general quite similar to those described by Mr. Deans.

Nontension Aluminum Connectors

O. A. BOYER
MEMBER AIEE

EMERSON KORGES
ASSOCIATE MEMBER AIEE

CONNECTORS intended for use on aluminum conductors have generally been quite similar in design to those proved satisfactory for use on copper conductors. It has been recognized that in the event that different metals were chosen for conductor and connector, thermal expansion problems would exist, and that galvanic corrosion problems would be created. These problems are encountered when aluminum and copper conductors are joined by many of the usually available types of connectors. Economic pressure, as well as recurring scarcities of copper has forced the use of aluminum as a conductor material, although it was realized that connector problems would be encountered especially in coastal areas.

Owing to increasing difficulties experienced in maintaining satisfactory service life of connectors installed on aluminum conductors in the Gulf Coast area, a test program designed to investigate the behavior of commercially available connectors under severe conditions of changing load, high humidity, and contamination was undertaken. Consideration of equipment available for control and operation of the test led to the selection of no. 4 American Wire Gauge as the best-suited conductor size. Connectors were also uniformly available for this conductor size. As the operating current for this test, 100 amperes was selected although it was realized that this value is considerably higher than would normally be carried by no. 4 conductors in ordinary service. Cycling time was set as one hour on and one hour off, which was chosen to give maximum effect of thermal expansion due to heating and cooling of the conductors and connectors.

It was felt that outdoor operation of the test would be desirable in order to obtain the true effects of such atmospheric variables as dust, rain, dew, and ambient temperature. Corrosion was known to be most severe in coastal areas subject to salt spray which is carried by the wind, and to duplicate this condition a weekly application of sea water to each of the connectors under test was included.

Performance of each connector under test was based on its resistance, which was measured by a laboratory-type double bridge. Connection was made for purposes of resistance measurement at points on the conductor 1 inch from either side of the connector. Resistance values read in microhms were taken at weekly intervals, and used in plotting the performance curves presented.

The first test was put in operation early in 1952 at Texas College of Arts and Industries. This was an indoor test consisting of 22 joints, and was primarily to determine what the tests might do, and what additional facilities were necessary for a proper test. An attempt was made to evaluate the comparable time ratio between the test and actual service. This had not been agreed upon before the tests were started. The test confirmed the belief that tests on the basis described were practicable and could afford much information. The preliminary test was not complete in several respects. It did show clearly the needs for additional information both in the matter of time and in test specimen. It also proved that equipment and test samples were available for the proper test.

Test 1

On June 26, 1952, an outdoor test rack was built with a total of 72 joints installed. These joints show a very high mortality rate; the high failure rate particularly of the joints without contact aids indicated that it was not advisable to test any more joints without a contact aid; and it was suggested that a sealer or cover might serve to protect the joint and retain the contact aid.

Fig. 1 shows a curve of resistance plotted against time with the connectors grouped by classes as: 1. hot line tap, 2. compression, 3. parallel groove clamps, 4. average of all connectors on test, and 5. split bolt. These curves show increased resistance by classes with some very erratic behavior. The apparent erratic behavior is believed to be a result of the increasing resistance producing an internal arc which in turn resulted in a form of weld that reduced the resistance for a period of time.

Fig. 2 shows curve of failures plotted against time which agrees well with the resistance curve, indicating a definite failure pattern, but covering too short a period to be of particular significance.

This test was concluded on October 3, 1952. Twenty-nine joints had failed as of October 3, and several others had deteriorated to a point where failure was near. This meant that maintaining a constant current was nearly impossible. A failure of a joint was considered when the joint failed mechanically, when resistance increased to produce an effective open circuit, or when the joint became unstable to a degree that would indicate extreme distress.

All test joints had been installed with torque wrenches, or with the recommended procedure of the manufacturer. Contact aids were used with a group of joints and an equal group were installed without contact aids. Three identical

---

Paper 55-248, recommended by the AIEE Transmission and Distribution Committee and approved by the AIEE Committee on Technical Operations for presentation at the AIEE Electrical Utilization of Aluminum Conference, Pittsburgh, Pa., March 15–17, 1955. Manuscript submitted December 13, 1954; made available for printing January 20, 1955.

O. A. Boyer is with the Central Power and Light Company, Corpus Christi, Tex., and Emerson Korges is with Texas College of Arts and Industries, Kingsville, Tex.

The co-operation is appreciated of the following manufacturers, who have furnished test samples and counsel in the processing of these tests: Burndy Engineering, Inc., Jasper Blackburn Corporation, James R. Kearney Corporation, Thomas & Betts Company, Ideal Industries, Inc., Kaiser Aluminum & Chemical Company, Bethea Company, Inc., Preformed Line Products, Penn Union Electrical Corporation, Fargo Manufacturing Company, Joslyn Manufacturing Company, A. B. Chance Company, Dow-Corning Corporation, F. H. Moloney Company, Minnesota Mining & Manufacturing Company, and The Line Material Company.

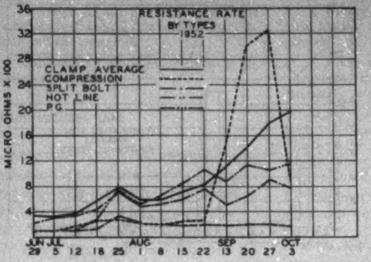

Fig. 1 (left). Resistance rate, test 1

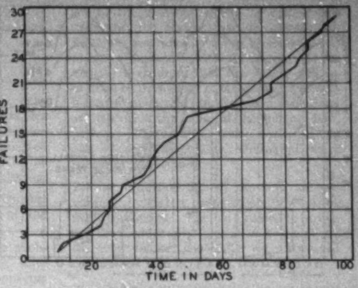

Fig. 2 (right). Failure rate, test 1

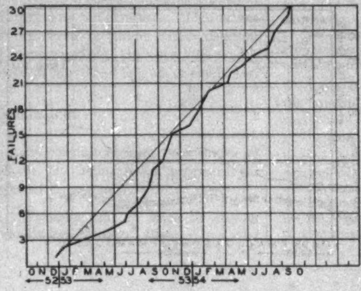

Fig. 3 (left). Failure rate, test 2

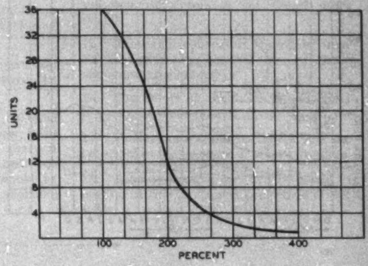

Fig. 4 (right). Resistance increase, test 2

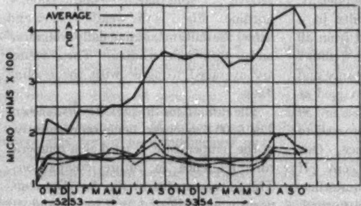

Fig. 5 (left). Resistance change by coverings

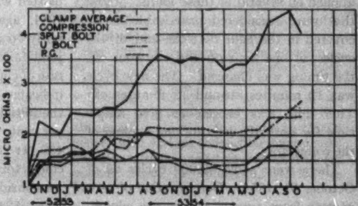

Fig. 6 (right). Resistance change by types

series of joints, one of each type from the two groups, were made in each case. One of these series was uncontaminated, except for accumulation from the open air. The other two series were treated with sea water, one by spray, and one by sponge. None of these joints were covered with any protective coatings nor sealers. These represented typical bare connectors.

Test 2

A canvass of all possible suppliers of contact aids and sealers was made with not very many samples readily available. The coverings available were: 1. Krylon, 2. Glyptal, 3. Airseal, 4. Tape, 5. Alum-a-life, and 6. Weatherwrap. Some of these have been found without apparent value; others have considerable value. It is believed that the truly usable material is not on the market at this time. Desirable qualities are ease of installation, permanence, the quality of being readily visible, removable, and compatible with grease and insulating materials.

Four contact aids were used: 1. No-oxide, 2. Penetrox A and Penetrox A-5, 3. Fargolene, 4. Kearnalene. These are all readily available and suitably packaged. Since these tests have been in operation, some new contact aids have been placed on the market. The most promising of these at this time are Nyolith Contax, and Penaseal.

The new test 2 was arranged to compare connectors by different classes, such as 1. split bolt, 2. parallel groove, 3. compression, and 4. hot line, as well as with different coverings. Contact aids were used in all connector installations except for 12 which were made in the factory, on which the detail was not furnished. Readings were to be made on the same basis as for the previous test. A sufficient number of test specimens were to be used to give reasonable answers to the many questions which arose. On the second test rack, set up on October 3, 1952, torque wrenches were used on all bolted connectors, and the factory-approved compression tools were used with the compression joints. Factory instructions were followed in detail. No copper-to-copper joints were used on this test. All joints are either copper-to-aluminum, or aluminum-to-aluminum.

This test rack consisted initially of some 85 joints and has since been en-

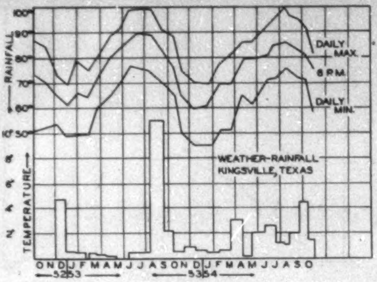

Fig. 7 (left). Weather conditions

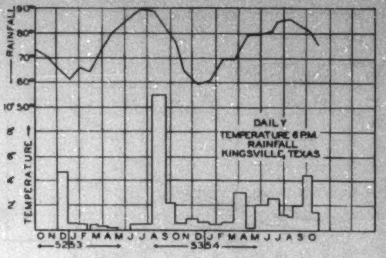

Fig. 8 (right). Weather conditions

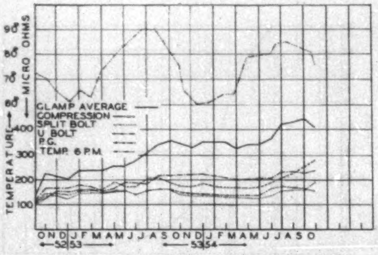

Fig. 9 (left). Temperature - resistance by coverings

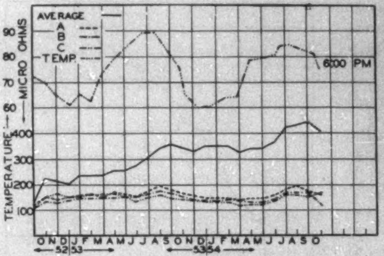

Fig. 10 (right). Temperature - resistance by types

larged to a total of 135. Coverings were applied on several of these joints: those that were considered practicable to be covered in the field. At the end of 473 cycles, at one hour on and one hour off, the timing was changed. The new cycle was 12 minutes on and 12 minutes off. This time was chosen to give ample time for both the heating and cooling of the connectors.

There were some 42,000 cycles as of October 31, 1954. Deterioration of connectors from several causes are plainly discernible. It has been estimated that from the loading standpoint this is perhaps more than normal conductor life expectancy. No direct evaluation of the time effect has been formed. In the majority of cases, the coverings are showing signs of age. Some have disintegrated and act more as a gatherer of moisture than as a sealer to keep the joint dry. None will stand a great deal of joint heating.

Examination of the curves plotted from data obtained from these connectors will help to explain the developments that have have been observed. Curves are drawn from data obtained from connectors that are still active. All data concerning a given connector are removed when the connector fails. A record is maintained of failures showing the history to the point of failure.

Fig. 3 shows the failure rate of test 2, plotted with total failures to October 31, 1954, against time. This results in a fairly straight line when viewed from all joint failures. Fig. 4 from test 2 shows rate of change of connector resistance and indicates that 36 connectors remained at the initial resistance, 28 increased to 150 per cent, and one connector increased to 400 per cent of original resistance. One connector increased to 1200 per cent. If we consider this an exception and eliminate it, the curve will become normal. Fig. 5 shows the resistance, in microhms, of all connectors. The average curve is based on all connectors on test. This curve serves as a base to which any one or more connectors may be compared. Additional curves show comparative values of groups of connectors prepared identical except that different coverings were used on each of the three groups represented. In the groups are connectors of the compression, the split bolt, and the parallel groove type.

Curve *A* is based on connectors, approximately one half of which are covered with tape and approximately one half with Glyptal. Curve *B* is of connectors covered with Airseal, and curve *C* of those covered with Krylon. Fig. 6 shows the resistance in microhms against time, and possible comparative resistances of groups of connectors; and includes all types on the test as follows: 1. parallel groove, 2. split bolt, 3. compression, 4. hot line. Fig. 7 is the weather curve and shows the daily maximum, daily minimum and a 6:00 p.m. reading. These values are averaged to agree with the reading dates.

The rainfall for the period is also shown. The 6:00 p.m. curve, being representative of the temperature, is used as a temperature reference in future comparisons. This is represented in Fig. 8. The comparison as indicated in Figs. 9 and 10 shows the temperature curve superimposed over curves 5 and 6 respectively; and indicates the change in resistance of the connectors seasonally. With the increase in temperature each year as the hot season approaches, and the corresponding reduction in resistance during the cooler months, it may be pointed out that the seasonal changes appear to show a cumulative increase in resistance from year to year. During the past 2 years plus, a great deal has been learned about these connectors. Application of the facts learned from the tests to date have shown economies by the following:

1. Reducing outages, burndowns, and trouble calls.
2. Reducing the stocks of connectors to be carried.
3. Allowing in many cases the use of less expensive connectors.

4. Providing a basis for training methods for workmen to help obtain uniform installations and use practices.

5. Reduction of number of tools to be carried on trucks.

Observations

Some observations that should be made and supplied to the industry for any value that they may carry are: Joints vary in resistance to follow a curve similar to the temperature curve, but exaggerated. The rate of decrease in resistance with the dropping of temperature is not as great as the increase in resistance during the period of increasing temperatures. This makes for a progressive failure. This condition of connectors is not the same as is experienced in equivalent lengths of conductor.

Conclusions

Some conclusions have been drawn as follows, but listing is not necessarily in order of importance:

1. Aluminum can be made to serve in seriously contaminated areas.

2. A contact aid must be used in any joint having one or more aluminum conductors.

3. A cover to exclude atmospheric contamination will delay the action of contaminants in any aluminum joint.

4. Many forms and types of joints are available; some are complicated, and some simple. In general, the complicated schemes have not been found worthy of their added difficult installation problems.

5. The joint can be made to carry current equivalent with a similar section of the conductor.

6. Stranded conductors offer some problems more serious than those for solid conductors. The reason is that a connector may transfer current to a limited number of strands, and they in turn may overheat to the point of failure; also the voids in the strands tend to bring moisture and contaminants into the joint.

7. When the resistance of a joint increases, the resultant heating tends to drive the contact aid out of the joint.

8. How much advantage the metallic bearing contact aids have has not been determined. It was reasoned that if installations were made good for the life of the conductors, a 50-year joint would be needed. No experience or test is available to give this answer.

9. In the split-bolt group of connectors, value of the spacer bar is questioned. First, no assurance is given of its value in place; and second, with the average workman, it is doubted that the spacer will be in place on a majority of occasions. Perhaps inconsistencies and inaccurate installations are too often the cause of the failures laid, perhaps, to some other cause. All washers and spacers should be eliminated from split-bolt connectors.

10. Compression splices have certain advantages. With a proper tool they can be made uniformly. They are easier to cover, and the contact aid can be made to penetrate the joint better, especially with stranded conductors.

11. Bolted connectors have the advantage of being removable. Reuse of aluminum split-bolt connectors is not found practicable.

12. Aluminum connectors should be used on all connections having one or more aluminum conductors.

13. Connectors of aluminum having mass in excess of the copper is advantageous.

14. Platings on copper or bronze are not beneficial in the presence of sea atmosphere.

15. Taps and connectors can be made to operate satisfactorily over preformed armor rods.

◆

Discussion

John E. Dean (Colorado Agricultural and Mechanical College, Fort Collins, Colo.): The authors are to be congratulated on their contribution to the knowledge of nontension connectors for aluminum. The test would seem to prove conclusively the value of contact aids. Manufacturers of contact aids are to be complimented on their achievements to date and should be encouraged to develop better materials.

The objection may well be raised that the tests were too severe both as to heating and the direct application of a corrosive agent. It is well to remember that the results reported here are in the nature of an accelerated life test. That significant data had to be collected in the shortest possible time consistent with reliability of results.

Many utility engineers are concerned about the lack of interest on the part of graduates in the power fields as a career. These tests, conducted on a college campus and sponsored by an alert utility, are an excellent example of one way to correct this unfortunate situation. I am sure that many promising young men would choose utility engineering were they exposed to the challenge existing in that field. It seems to me that many utilities are overlooking an excellent opportunity by not sponsoring testing or research on the campuses of engineering schools. Such a program could be planned to assist promising students financially and arouse their interest in utilities as a source of employment following graduation. The departments of electrical engineering are ready and willing to encourage such a program. Are the utilities?

Thomas J. Higgins (University of Wisconsin, Madison, Wis.): This is a clearly described, detailed account of the authors' tests. The engineer who deals with aluminum conductors should find the conclusions helpful.

H. G. Gossman (The Dayton Power and Light Company, Dayton, Ohio): A tremendous amount of work has been done in working up this study. I feel that a great deal of good information was probably lost by grouping the results by types of connections. Within any one type of connection results will vary greatly depending on design, the materials of which the connector is made, the connection compound used, and even whether the conductor is stranded or solid.

Attempting to measure individual resistances of connectors, from a point 1 inch out on the conductor, is laborious and prone to the introduction of considerable error. It is much easier to measure a fixed length of conductor, say 1 foot, and then express the graphed result as a resistance ratio. If a group of connections are under test, spacing the connections 1 foot apart will facilitate group readings and the resistance ratios will then represent the group average.

From my own experience in connection testing, I am certain that a 12-minute-on, 12-minute-off schedule is too short a time interval fully to heat or fully to cool the conductor.

Again, speaking from my own testing experience we consider a connector to be a failure whenever the connection resistance exceeds 50 per cent of the resistance of 1 foot of conductor in the connection.

On this basis many of the connectors in Figs. 1 and 6 must be considered poor before load cycling started.

Quoting from an extensive test of all possible combinations of No. 4 AWG aluminum and No. 6 stranded, tinned copper with various connection compounds, average initial connection resistances for various types of connectors varied as follows:

		Microhms
1.	Slotted service connectors	30 to 200
2.	Parallel groove clamps	10 to 330
3.	Tubular compression	−40 to +40
4.	Vise-type or split bolt	−20 to +50
5.	Compression copper *H*-sector	−20 to +20
6.	Compression aluminum *H*-sector	−10 to +25
7.	Compression aluminum *C*-sector	−40 to +20

Load-cycle testing early in 1954, confirmed our opinion that all but one of the commercial connection compounds resulted in poor connections. The one good compound was unacceptable for field work for several reasons. We proceeded to develop our own compound which we have been using since. It has proved itself superior as to initial resistance after extensive load cycling without wire brushing of the conductor through the compound.

D. C. Hubbard (A. B. Chance Company, Centralia, Mo.): The paper presented by Mr. Boyer and Mr. Korges is of special interest. It presents additional factors heretofore given little or inadequate emphasis. The paper further substantiates data previously presented urging the use of aluminum bodied connectors and contact aids.

The data presented are based on carefully executed and thoughtfully considered test programming. The authors and their associates at Texas College of Arts and Industries deserve special credit for the manner in which they isolated extraneous factors. Occasionally such factors lead investigators to assume conclusions which may have resulted from unconsidered causes.

We are in general agreement with the statements itemized in the authors' conclusions. We suggest some qualifications to a few comments from which assumptions too broad in scope might be drawn and to which we feel attention should be directed.

In the matter of contact aids, extensive tests indicate a suitable contact aid is essential in corrosive areas and that they are beneficial in so-called noncorrosive areas. The word suitable is the key point. For example, the contact aid must not itself contribute to corrosive attack on the elements being connected and it must have durability.

Similarly, covers to exclude atmospheric corrosion must be durable. The question of pockets under such covers is a matter of concern and unless such spaces are adequately avoided during normal application, corrosion inhibiting compounds are indicated under the area so covered. We suggest that joint covers are neither alternates nor equal substitutes for contact aids.

The problem discussed in conclusion 6 again points to the desirability of connectors designed to contact each outside strand of an aluminum conductor with a minimum of current transfers for the maximum number of strands.

Conclusion 7 points to a suggested qualification for contact sealing paste. Conductor manufacturers have urged that conductor temperatures should not exceed 100 C even for relatively short periods. We propose that a contact sealing paste should satisfactorily maintain its consistency with substantially no bleeding or flowing over the same working range allowed by conductors. We believe the resistance to flow is of greater importance than the characteristic to heal over scratches because of the problem stated in this item.

Conclusion 8 raises the question regarding the merit of metallic inclusions in contact aids. We agree with the authors that test time available to date may not assuredly predict fifty years of performance. However, measurements using the same compound base with and without metallic additions indicate observable improvement in joint performance with proper metallic additions. Tests demonstrate dramatically that such additions, when present in the contact aid, must not contribute to corrosive attack to copper or aluminum in either marine or industrial atmospheres. And, obviously, the carrier or compound base must be inert to copper and aluminum.

We are in qualified agreement with conclusion 9. Several investigators have shown that thin spacers were inadequate under specified conditions. Some of these investigators have indicated that relatively thick spacers are advantageous and overcome the objections heretofore raised.

We strongly endorse the conclusions drawn in conclusions 12 and 13 regarding the use of aluminum bodied connectors.

Preformed armor rods applied over cleaned conductors at tap locations have shown definite advantages for the connection. Resistance to damage from surge currents and from vibration fatigue is effectively increased by the armor. In contaminated areas, corrosion inhibiting contact sealing paste may be necessary between the conductor and the rods as well as between the rods and the clamp. This was clearly demonstrated in one coastal test.

H. P. Dupre (Burndy Engineering Company, Inc., Norwalk, Conn.): I would like to compliment the authors on attempting to set up a life test for copper-to-aluminum connectors. The industry has long recognized that the present methods of testing for corrosion protection can only be used for comparison purposes. We are glad to see that the findings of the authors bear out the laboratory testing which we have performed on copper-to-aluminum connections. The fact that the aluminum conductors can best be protected by employing an all-aluminum massive connector has been checked out by both methods.

We thoroughly agree with conclusion 10 which states that compression connectors are advantageous. In fact, we have recently introduced a complete line of one-piece compression connectors for distribution aluminum and aluminum cable steel reinforced splices.

However, the results shown on Figs. 1 and 10 seem to indicate that compression sleeves produce questionable results. Is this due to some individual results caused by experimental types which were tested, and could you give us a more detailed summary as to the individual types that produced these results?

E. W. Greenfield (Kaiser Aluminum and Chemical Corporation, Spokane, Wash.): I would like to ask if you think your tests emphasize the role of corrosion unduly over that due to what I call thermal ratcheting?

Do you think the temperature attained by your conductors and your connectors was actually high enough to simulate what might happen in the thermal ratcheting of heavily loaded lines?

I say that only because I noted the short length of time of your load cycle. I think it was 12 minutes, and 100 amperes were used on a No. 4 conductor rated at 4 amperes.

The second point I have to mention is that in the test stations that we discussed before in Mr. Everhart's and my paper, there are numerous connectors. There are line splicers, tap connectors, copper taps, all types of hardware in aluminized material, and in galvanized material.

I would say at least a hundred items in each of the test areas concerned with accessories are under test also. We have made no mention of them. That does not mean that we are ignoring them.

We are measuring resistances of splices; we are accumulating data, and hope as an accessory paper to bring those results out.

E. W. Everhart (Kaiser Aluminum and Chemical Corporation, Spokane, Wash.): Are some of your erratic experiences in the chart due to a few connectors, or did all of your connectors act erratically?

O. A. Boyer and Emerson Korges: Conditions chosen for the operation of the test were deliberately made as severe as might ever be encountered in actual service. These include maximum conductor load, severe corrosive conditions and frequent cycling of load to promote thermal expansion and flow difficulties.

It is felt that contact aids of maximum durability should be developed. Migration of contact aid is not desirable as it aids in depletion of the material in the joint. Materials used should also be durable in that their evaporation should not be pronounced at maximum operating temperatures.

Metallic or other inclusions used in contact aids should not corrode or produce corrosion in contact with the conductor materials since some of the contact aids used may eventually disappear and leave only the inclusions in the joint. Joint protection or covering materials that have proven successful to date have been of the type requiring hand-forming over the connectors. Objection may be made to the time required for application of this type of covering and development of a suitable long-life material that may be sprayed on seems desirable.

In regard to spacers, it is still believed that these are undesirable except possibly as a shaping device to properly clamp a stranded conductor. Operation of this test is continuing and additional information is being developed.

Mr. Hubbard mentioned one point that I would like to elaborate on just a little bit. I believe he suggests the use of spacers. He and I have discussed that a number of times.

If it is a stranded conductor of big diameter so you need a spacer to keep the conductor from distorting, then we will go along with you. If you use them simply as a spacer to keep the conductors apart, we don't agree.

We don't think it has any particular value. In fact, we have about 200,000 figures to indicate that that is not so.

Mr. Greenfield asked the question of whether or not we believe that our thermal effect on the conductor was given a reasonable chance compared to the corrosion. We are primarily concerned with corrosion in our area, and this started as a test of self preservation.

We had to serve the customer. We weren't concerned with the bigger current-carrying capacities. We were concerned with something that would stay up there for a while and we figured definitely that we could get something that would in time give us enough load current; but first, we had to get something that would physically stay in place. That was the reasoning behind our selection of the current and the cycling.

As you know, there is no indication of why we chose the 12 minutes. We have some ampere-reading curves, and in fact we keep an ammeter on the circuit all the time that shows us that in approximately

8 minutes the connectors are stable. We give them four minutes more, both in the cooling and heating.

As far as the 100 amperes are concerned, we think we have enough time.

Now, whether we are abusing them enough from a load standpoint, we are not in a position to say. From a manufacturing standpoint, we know that is not true. From a user standpoint, we know that we would have a voltage drop. If we put much more service than that in the house, we would have some other troubles that would necessitate doing something about it or changing it. So from an operating standpoint, they are sufficient. From a manufacturing standpoint they are not, and we think that manufacturers are the ones that can and should do the particular work that Mr. Greenfield mentioned.

We have no quarrel with him. We just say, "Well, that is your place, and we will take your word for that particular part of it."

I do have a question or two that I would like to ask the group. We are having a lot of trouble with connectors in trying to get them so that our boys can tell for sure what size they are. One manufacturer will label them as No. *2*, and one fellow will label them as No. *2 solid*, another fellow will label them as No. *2 stranded*, and another fellow will label them as No. *2 ACSR*, or any of the other sizes. That is about the worst situation that you can get into because we have all of those combinations on our system. If you will check just a little bit, you will find that there are some sizes only 0.002 or 0.003 difference in diameter. One case in particular is the two utility sizes from No. *2*, in *solid* to No. *4 ACSR*. There is only 0.007 difference in size.

Where is the designation that is going to make it possible for anyone to catalogue sizes of connectors in the field so that they will work?

My suggestion is that the suppliers seriously consider the idea of marking in decimals, the maximum and minimum sizes the connector will take, and forget about the size wire they will take. Give us something to work on.

Then we in turn can put a chart up and say, "This wire is a certain size." All one has to do is go over and pick out the connector that will cover that particular phase of it. That is something that has not been done, and I think we have had some tests that may have hurt some of the suppliers of materials on our tests, because I think they were coded wrong or read wrong. If a man as academic as Professor Korges and as methodical as he is will make a mistake without any pressure on him, I know that many workmen in the field will make mistakes, too.

So there are things we need some help with and you fellows can give us that help.

We have now experienced some 50,100 cycles on our tests. Some of our connectors are staying in good shape. Some of them are all rotted. We have no complaint with them. They haven't changed resistance.

To answer Mr. Everhart, we have some connectors that have remained constant since the first day they were on. The culprits are a few who are nonconformists, and who have not been constant from the start, and will probably continue not to be, although they stay in the circuit. How we are going to eliminate those particular ones gracefully, I don't know, but we have a standard material list, and a great big black pencil, and that is the only way we know of to get around those particular factors.

The Use of All-Aluminum Conductor on Transmission Lines

E. M. WRIGHT
FELLOW AIEE

E. G. LAMBERT
ASSOCIATE MEMBER AIEE

THOUGH the use of all-aluminum conductors is not new, it seems logical at this conference to bring out its distinct advantages for use on transmission lines over all other types of conductor, when it is used for the proper purposes and under proper conditions.

The first recorded use of the all-aluminum conductor in the Pacific Gas and Electric Company system was in 1899. Several 60-kv lines built over 50 years ago with all-aluminum conductor are still in operation, most of them still operating with the original conductor, splices and fittings, in heavy-, medium-, and light-loading areas, as well as in heavy fog and salt-contaminated air. None of these conductors has given any appreciable trouble, except from comparatively few splices which were the original wedge-grip type without sealing compound. The old served splices have given practically no trouble. No investigations have been made as to the tensions in the older lines, but observations indicate that they are now fairly low. No armor rods or dampers were used previous to 1920 and none has since been added on the pin-type lines.

At the present, out of over 12,000 miles of transmission circuit in the Company system there are approximately 2,900 circuit miles, or 7,300 tons, of all-aluminum conductor in use. By the end of 1960 it is expected that there will be approximately 3,600 miles, or 11,000 tons, of this type of conductor. The accumulation of all-aluminum conductor since 1900 is shown in Fig. 1. Fig. 2 shows the circuit miles installed, or proposed, in each 5-year period to 1960. Table I shows the sizes of conductors now in use on the earlier lines.

Approximately 275 circuit miles of odd sizes have been removed from the older lines between 1899 and 1911 owing to abandonment of the lines or increase in size of conductor. In the last few years, large quantities of 715,500, 954,000, and 1,113,000-circular-mil (CM), all-aluminum conductor have been installed.

In general, the use of all-aluminum conductor has been confined to the light-loading area; however, there is one installation of a 60-kv line in the California heavy-loading area which is of interest. Normally, steel-reinforced aluminum cable (ACSR) is used in the heavy-loading area, but during World War II, owing to the shortage of steel and copper, all-aluminum conductor was installed in a heavy-snow loading territory where snow depths during the winter are often over 15 feet. On this 28-mile single-circuit, pin-type, wood-pole line, starting at an elevation of 4,000 feet and ending at an elevation of 7,500 feet, the 336,400-CM all-aluminum has given perfect service. The general span length is 260 feet but there are spans from 150 to 500 feet. The line was designed for California heavy-loading, 1/2-inch ice, 6-pound wind, zero-degree Fahrenheit (F), with a normal tension of 16.7 per cent (%) of ultimate at 60 F and a maximum tension of 50% of ultimate. The Company is not planning the use of all-aluminum conductor in the heavy-loading area although it should operate properly if designed for the expected loads.

All-aluminum has also been used in the California medium-loading areas which are assumed to be at 1/4-inch ice, 6-pound wind, and zero F. The use here has been restricted to sizes of 4/0 and over,

---

Paper 55-250, recommended by the AIEE Transmission and Distribution Committee and approved by the AIEE Committee on Technical Operations for presentation at the AIEE Electrical Utilization of Aluminum Conference, Pittsburgh, Pa., March 15–17, 1955. Manuscript submitted December 15, 1954; made available for printing January 20, 1955.

E. M. WRIGHT and E. G. LAMBERT are with the Pacific Gas and Electric Company, San Francisco, Calif.

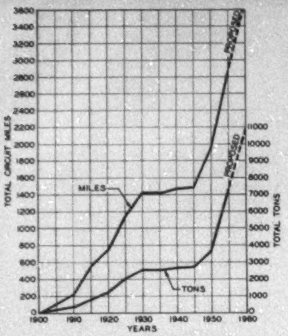

Fig. 1. Accumulated circuit miles and tons of all-aluminum conductor Pacific Gas and Electric Company transmission system

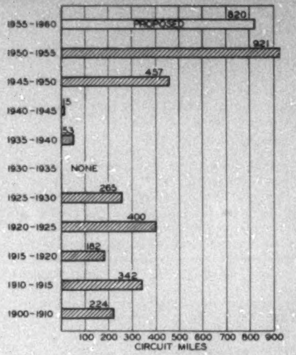

Fig. 2. Circuit miles of all-aluminum conductor installed in each 5-year period

and on 60-kv wood-pole lines. Under medium-loading conditions the conductor is strung to a tension resulting in a final tension at maximum loading condition of 50% of the ultimate conductor strength, and approximately 16% for final normal (60 F) conditions. In designing all-aluminum conductor wood-pole transmission lines for these conditions, a ruling span of 600 feet is generally used. On long spans the conductor is normally strung to the ruling span tension. Stringing to these tensions for a span in excess of 2,000 feet still results in a safety factor of unity at maximum loading conditions. It is probably better practice, however, to dead-end and design the tension in these spans independently, maintaining a constant safety factor throughout the line, although no trouble has occurred where these long spans have been strung using the ruling span tensions.

The greatest use of all-aluminum on 60 to 70-kv lines has been in the light-loading district. The California light-loading district has for the maximum loading condition an 8-pound wind at 25 F, no ice. Detailed studies have been made on the economics of all-aluminum on 60-kv lines in the light-loading district and it was found that without a doubt all-aluminum is more economical, with the same safety factors, than any other type of conductor. This study was made while conductor cost comparison was not as favorable to all-aluminum as it is now.

All-aluminum sizes from 2/0 up to 397,500 CM have been used on 60-kv pin-type and suspension-type lines. Normally the 60-kv lines are strung so that the final tension at maximum loading conditions is approximately 40% of the ultimate strength of the conductor. The normal tension at 70 F under these conditions is approximately 18% of the ultimate strength with a ruling span of 600 feet.

The use of all-aluminum conductor in sizes larger than 4/0 on pin-type insulators presents one problem which has not been entirely solved. Armor rods are installed at all support points, and the conductor is enlarged by the armor rod so much that the top, and particularly the side grooves, are not wide or deep enough to hold the conductor securely in place. The top groove has been enlarged recently by most insulator manufacturers, and it has been necessary to use the top groove, instead of the smaller side groove, for light angles to hold the armored conductor in place. The clamps of the clamp-top insulators have also recently been enlarged, which may prove the solution for straight-line and light angles.

The use of all-aluminum on suspension-type construction presents more of a problem in that the lighter conductor swings farther under the same wind conditions than ACSR or copper. This generally requires longer crossarms, but because of the decreased vertical loads and, in general, decreased line tension, the same structure designed for the heavier conductors can be used, and it is often possible to install either a conductor of larger capacity on the same structure or to reduce guying on wood structures.

There has been some objection to the use of all-aluminum as well as ACSR conductor in areas near the coast where salt-contaminated fog conditions prevail, but evidence has not been found to support this objection. There are samples of 350,000-CM all-aluminum conductor, one 19-strand installed in 1902, and one 7-strand installed in 1906. Initial operation of the two circuits of these conductors was at 60 kv. Portions of both circuits are still in operation at 60 kv, or 12 kv. The circuits were strung on wood poles with approximately 35 miles of each circuit adjacent to the west shore of San Francisco Bay where they were exposed to salt-contaminated fog as well as salt foam from salt-evaporating ponds. There has been some corrosion of these conductors, as evidenced by discoloration and the presence of salts of aluminum in the strand interstices, but careful examination discloses no measurable reduction of the cross section of the strands. This is not presented as proof that all forms of aluminum will perform equally well or that equally good performance will prevail under other conditions.

The use of all-aluminum conductor on 110-kv and 220-kv lines has been limited entirely to the light-loading district. On the 110-kv wood-pole lines the conductor is strung as on 60-kv pole lines, i.e., the maximum final tension is approximately 40% of the ultimate strength. On 110-kv tower lines all-aluminum conductor sizes 266,800, 336,400, and 397,500 CM are also strung so that the maximum final tension is approximately 40% of the ultimate. The normal final tensions at 70 F are approximately 30% of the ultimate with a ruling span of 1,000 feet.

The largest all-aluminum conductor used so far on 110-kv tower lines has been 715,500 CM. Approximately 40 circuit miles of this size have been strung. The lines are designed with a ruling span of 1,000 feet and strung so that the maximum final tension is 3,540 pounds, or 28% of the ultimate. This results in a normal final tension at 70 F of 2,400 pounds, or 19% of the ultimate. These percentages of the ultimate tension are considerably lower than those used on the smaller aluminum conductors. The reason for

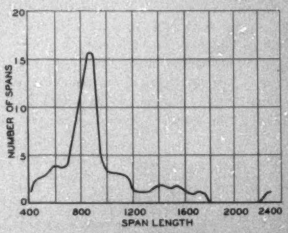

Fig. 3. Frequency of various span lengths, Morro Bay–San Luis Obispo, 110-kv tower line

Table I. Conductor Sizes

Size MCM* or AWG†	Year First Used
3/0	1899
4/0	1899
2/0	1908
471	1908
350	1910
266.8	1923
397.5	1923
336.4	1924

* Thousand circular mils.
† American Wire Gauge.

Table II. Comparison of All-Aluminum and ACSR Conductors for 220-Kv Transmission Lines

	All-Aluminum				ACSR		
Size, thousand circular mils	795	954	1,113	1,272	795	954	1,113
Stranding	61	61	61	61	54/7	5,4/7	5,4/19
Ultimate strength, pounds	14,330	16,860	19,660	22,000	28,500	34,200	40,200
Copper equivalent, thousand circular mils	500	600	700	800	500	600	700
Maximum design tension, 25 F, 8-pound wind, zero-inches ice, pounds	6,375	7,500	7,500	7,500	7,500	7,500	7,500
Safety factor	2.25	2.25	2.62	2.93	3.8	4.56	5.36
Normal design tension, 70 F pounds	4,410	5,160	5,240	5,640	5,300	5,610	6,120
Sag in a 1,200-foot span, 130 F, feet	35.5	34.3	38.4	42.5	38.9	43.0	45.7
Weight per 1,000 feet, pounds	746.3	895.5	1,045	1,193	1,024	1,229	14,31
Cost of conductor, dollars per circuit mile	4,170	4,930	5,660	6,410	4,940	5,810	6,950

this is that the 110-kv steel towers normally used are designed to withstand a maximum tension of 3,540 pounds. These steel towers were originally designed for use with all-aluminum and ACSR conductors up to a size of 397,500 CM, and for copper conductors up to 250,000 CM. When it was desired to install larger conductor sizes the same towers were used. The safety factor of the installed 715,500-CM all-aluminum conductors at maximum tension is therefore approximately 3.6, instead of the usual 2.5 as used on the smaller all-aluminum.

It has been possible to replace existing copper conductor, 3/0 in one case and 250,000-CM in another, with 715,500-CM all-aluminum (450,000-CM copper equivalent) on existing 110-kv twin-circuit tower lines without any changes whatever in the steel structures. This cannot always be done, as in rough country the difference in the coefficients of expansion, and wind loading between copper and aluminum lightens the weight on some suspension strings at low temperature to the point where changes in the structure or the use of dead ends, hold-down insulator strings, or weights may be required to take care of upstrains.

An example of the use of 715,500-CM all-aluminum conductor on 110-kv steel towers is the recently completed line from the new Morro Bay steam plant to San Luis Obispo, a distance of 16 miles. This line is in fairly rough country extending from the coast to approximately 10 miles inland. The line averages 5.6 towers per mile and the spans vary in length from 450 feet to a maximum of 2,280 feet; see Fig. 3. Twisted tapered armor rods are used at all suspension points and 6-pound Stockbridge-type dampers are installed at each end of each span with spacing and quantities according to the span length. All suspension and dead-end clamps are of the aluminum alloy type.

The highest voltage so far used in the Company transmission system is 220 kv, and it is in this voltage class that the savings in the use of all-aluminum conductor have, so far, been the greatest. All of the recent 220-kv lines in the light-loading district were designed for the use of either 954,000-CM or 1,113,000-CM all-aluminum conductor. These sizes have been installed on twin-circuit steel towers at a maximum design tension of 7,500 pounds; the tension being at 25 F with an 8-pound wind. The twin-circuit suspension-type structures are designed for two broken wires and a 1,200-foot ruling span with this maximum tension, which is not too much for all-aluminum conductors from 954,000 CM and larger. In fact, it is possible to replace 500,000-CM copper, or 795,000-CM ACSR with 954,000-CM or 1,113,000-CM all-aluminum, gaining substantially in capacity without appreciably changing the stresses on the towers. It does not seem logical to install conductors having an ultimate strength of 28,000 pounds (795,000-CM ACSR) when the economical strength of the tower is for a maximum tension of 7,500 pounds in the conductor. Where loads to be carried require a conductor with a capacity larger than 500,000-CM copper equivalent, the all-aluminum becomes more favorable. Of course, the safety factors in the conductors are smaller with all-aluminum thus used, but with proper protection with armor rods and Stockbridge dampers no trouble from vibration is expected. To sum up, where the strength of the aluminum is sufficient, it is felt that there is no need for the extra weight or the extra cost of steel.

Table II shows a comparison of ACSR and all-aluminum conductors in the sizes which are now being used or contemplated on 220-kv lines on the Company transmission system. This table is based on using the conductor on towers designed for a maximum conductor tension of 7,500 pounds, as previously mentioned. The advantage of dropping the steel cost out of the conductor when the strength of the steel core is not required is apparent. The safety factors vary from 2.25 for 795,000 CM to 2.93 for 1,272,000 CM. The normal tension at 70 F range from 31% of the ultimate strength for 795,000 CM to 25% for 1,272,000 CM.

A distinct advantage in the use of all-aluminum conductor on 220-kv lines is in changing existing conductor to get more capacity. If 795,000-CM ACSR is replaced with 954,000-CM all-aluminum at the same sag, the safety factor shown in Table II will be increased from 2.25 to 2.55. A corresponding increase in safety factor can be obtained when substituting in other sizes. This, of course, will stress the towers less longitudinally, and, in many cases will permit the use of existing towers that might otherwise be overstressed from the added wind and longitudinal load. Details have been worked out for changing 500,000-CM copper (the "rope-lay" type having considerable corona loss) to 954,000-CM all-aluminum (600,000-CM copper equivalent), or 1,-

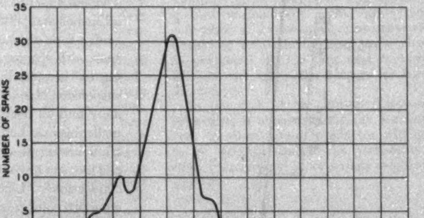

Fig. 4. Frequency of various span lengths, Morro Bay–Gates 220-kv tower line

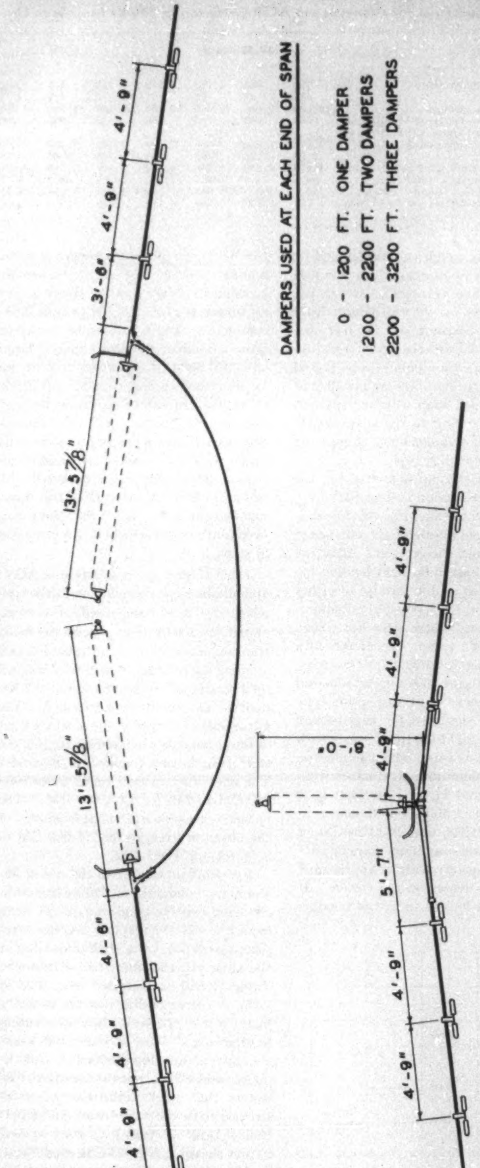

Fig. 5. Vibration dampers, armor rods, 220 kv

113,000-CM all-aluminum (700,000-CM copper equivalent) on a 220-kv twin-circuit line built in 1921, for a net cost of approximately $4,300 and $5,200 respectively per circuit mile, including the cost of conductor. For this cost there are appreciable gain in capacity and reduction in corona losses.

A twin-circuit 220-kv tower line with one circuit strung has recently been completed from the Pittsburg steam plant, 30 miles northeast of the San Francisco Bay area, to Panoche Substation, in the San Joaquin Valley, a distance of 125 miles. For 95 miles this line is parallel to and 75 feet from another tower line of the same voltage and tower types built in 1947. The older line has two circuits of 795,000-CM ACSR (500,000-CM copper equivalent); the new circuit 1,113,000-CM all-aluminum (700,000-CM copper equivalent). In rough country the new steel towers cost approximately $2,400 per mile more than the towers in the older line. In fairly flat country, the steel towers in the new line cost approximately the same as those in the old line. The additional cost for towers in rough country is partly because of the required use of dead-end structures to take care of upstrain under cold-weather and wind conditions. It was also required that the towers in the new line be set opposite the old towers, thus removing the flexibility of location which could easily eliminate some, if not all, of the dead-end structures. The use of hold-down insulator strings, or weights, would also reduce this difference of cost if this method had been used.

Another example of the use of 1,113,000-CM all-aluminum conductor is the recently completed 220-kv line from the Morro Bay steam plant to Gates Substation, a distance of approximately 70 miles. This line is in rough country as well as rolling foothills extending from the Pacific Coast east to the San Joaquin Valley. The line averages 4.2 towers per mile and the spans vary in length from 315 to a maximum of 2,800 feet; see Fig. 4. Twisted tapered armor rods are used at all suspension points and 12-pound Stockbridge-type dampers are installed at each span with spacing and quantities according to the span length; see Fig. 5. All suspension clamps are made of aluminum alloy and all dead-end clamps are of the malleable iron-bolted type with aluminum alloy keeper pieces permitting all dead-end loops to be continuous, without bolted connections. Line splices are made with standard compression-type sleeves.

A further comparison of ACSR and all-aluminum conductor will emphasize some additional points. The use of all-aluminum instead of ACSR of the same capacity is justified not only from the first cost of the conductor itself, but also from the cost of material, labor, fittings, and installation. On the all-aluminum the compression-splicing sleeves cost less, can be installed in about one-tenth of the time, and the centering of sleeve is not so critical. The cable and armor rods have less diameter, and in some cases take a smaller dead-end and suspension clamp. Vibration dampers are smaller and cost less. The conductor is lighter; hence transportation and installation cost less.

The introduction of a single strand of steel in an aluminum conductor as a safety measure brings up a point not generally considered. In several cases in the company system the steel has actually been the offending member. In two cases where 4/0 ACSR was installed, falling trees or limbs stripped or partially stripped the aluminum strands, or damaged the conductor to the extent that the steel strand was carrying all or most of the current. These were in spans over canyons or otherwise not easily seen; at least they were not discovered. At a later date, when the circuit was being used to carry heavier loads while other lines were out of service, the steel burned off, causing a failure in the circuit which was relied on to carry the load. Other failures occurred because of poor centering of the ACSR compression sleeve which caused the steel to carry so much current that burn-downs were caused at times when extra load was put on the line.

In the design of a transmission line, it is questionable whether the conductor should have a larger safety factor than the structures when the structures are rigid steel. It is certainly not economical to pay for strength that is seldom if ever used. It can even be considered dangerous to have this extra strength which, if used, at some time might cause failure of steel structures or guys on wood-pole lines. This type of failure would cause longer outages and more costly repairs. The weakest link in a line should be the easiest and quickest to repair. If the mechanical loads developed in a conductor on a line do not exceed the designed structural strengths, taking into account the type of structure, there seems to be no need for a stronger conductor. The economical structure design should be the key to the problem.

All-aluminum conductor in light-loading areas has given good service so far and, with its homogeneous make-up, high elastic limit, and low cost both for conductor and material, it should be more economical than any other type. It has no dangerous disadvantages when used with the proper safety factors.

◆

Discussion

Jordan Lummis (Southern California Edison Company, Los Angeles, Calif.): This paper gives a very thorough and interesting discussion on the economics of all-aluminum conductors. The possibility of increasing the capacity of a steel-reinforced aluminum cable (ACSR) line by using all-aluminum conductor is something that should be considered in every case where the problem arises. The same solution probably can be used on many existing copper lines.

The authors' experience with all-aluminum lines exposed to contaminated atmosphere is very significant and should act as a dash of cold water in the face of current hysteria on the subject. On the other hand, as the authors carefully note, this does not prove "that all forms of aluminum will perform equally well" and it seems highly probable that uninhibited ACSR would not have given such satisfactory service because of interaction between the zinc on the core and the aluminum.

Southern California Edison Company's experience with all-aluminum conductor has been limited to about 100 circuit-miles of 4/0 on 66-kv and 33-kv wood-pole lines. These lines were installed before the days of improved relay operation and were burned down with nearly every fault. ACSR, on the other hand, seldom suffered damage to the steel under any fault conditions, with the result that incidental damage to supporting structures was uncommon. Most of these circuits have since been replaced with copper or ACSR conductors and although relay operation is vastly improved, there are lines in some portion of nearly every 66-kv network which may be damaged by flashover. Thus, all-aluminum appears more attractive on the 220-kv systems where clearing time is much faster.

The authors' experience of hazard arising from the steel core is quite contrary to the Edison Company's. In one case of ice loading up to 15-inch diameter on a line designed for 1/2 inch of ice, the steel core was all that prevented long-sustained outage of an important 220-kv line in an area almost inaccessible to repair crews during the storm season. ACSR has held up conductors where the aluminum was annealed by forest fires. If the right kind of an airplane hits a line squarely enough it will chop apart any conductor, but cases where the core has minimized the damage are numerous. The following case history is typical: At 4:03 p.m. on June 24, 1951, a 220-kv line relayed. At 4:31 p.m. the line was tested and stayed in. At 5:52 p.m. a report was received that an airplane may have been the cause of the trouble and since the line was needed only for standby, it was de-energized pending determination of the trouble. At 7:38 p.m. it was found that a Cessna Model *140* had bumped into a 3,600-foot span of 605,000-cm ACSR 30×19, had stripped 28 strands of aluminum from the center conductor for 2 feet 9 inches and all the aluminum from the west conductor for 11 inches. The line was repaired the next day during the off-peak period. The significant points are that this circuit remained mechanically stable until repair was made at a convenient time, meanwhile remaining available for emergency service as evidenced by the fact that it carried 250 amperes across the damage for 1 hour 21 minutes.

In the case of the Edison Company's system, it is apparent that the low initial cost of all-aluminum conductor will have to be weighed against the probability of more frequent and more serious mechanical damage.

Eduard Fritz, Jr. (Day & Zimmermann, Inc., Philadelphia, Pa.): My former company, Pennsylvania Water and Power, Holtwood, Pa., also have transmission lines constructed with all-aluminum cables. Their four all-aluminum circuits are of 300,000 cm, conductivity 19 strand, and operate at 70 kv, 25 cycle. The four circuits occupy two double-circuit tower lines on the same 100 foot R/W, each line being 40 miles long. The operating record of these lines has not been of a standard one could classify as better than tolerable.

The first pair of circuits were placed in operation in 1910 with towers on 500-foot average spans. There are many longer spans, the longest being 1,400 feet. Fifty feet away is the second double-circuit line, built in 1914 with its final circuit strung in 1917.

Over the years, these four circuits have experienced many burn downs from lightning, sleet, wind updrafts, kites, buzzards, and overheating at joints. Several 3-circuit outages have occurred as the free ends of the burned-off phase made contact with the adjacent circuits. Some of the troubles, as lightning flashovers, have been almost eliminated by improved shielding and adequate tower grounding, while other troubles, such as bird contacts, could be eliminated if greater tower clearances were provided. Many total interruptions result from the rapid fusing of the all-aluminum cables, as burndowns will occur under heavy load currents, even if fast relaying were provided.

Since 1914 sleet melting has been resorted to in an effort to prevent sleet formations. In spite of this, there have been four occasions since 1932 when burndowns have occurred, due to sleet, three when the circuits were reported clear of ice, and one before the de-icing could be started.

Now for the favorable part. The original cables were strung to 500-pound tension, which means that although the average span's tension at heavy loading is 50 per cent of the ultimate, in the longer spans it should reach the cables so called elastic limit. Nevertheless, these circuits have never been resagged. If nonelastic creep has occurred, it is not noticeable.

In 1945 we measured slightly less d-c resistance for the entire line than if the cable were new, and a cable sample cut from the 1910 circuit, tested higher ultimate strength than the catalogued value. The lines are without armor rods or dampeners, yet no metal fatiguing has been discovered. There has been no depreciation in these conductors.

I wish to congratulate E. M. Wright and E. G. Lambert for a very informative paper. Also, they have made an able case for the use of all-aluminum cables as compared to steel-reinforced aluminum cable (ACSR) and for lighter conductor tensions. I would, however, like to call attention to two characteristics of all-aluminum which will tend to offset the advantages which they have pointed out.

For lines of 110 kv and lower voltages, greater conductor clearances and spacings must be provided for all-aluminum line or burndowns will be all too frequent.

The coefficient of thermal expansion of all-aluminum is 0.0000128, for ACSR 24/7 stranding about 0.0000102. If a circuit is to be loaded near its thermal limit, assuming both lines have the same 60° sag, taller towers must be provided for all-aluminum lines or dangerous crossing clearances may result.

If the line is nearly straight, the sum of these two disadvantages may offset the saving in conductor cost and in the lighter weight corner structures.

If many line angles occur, all-aluminum lines can be cheaper, but will operate satisfactorily only if adequate clearances are provided and attention is paid to the salient features as described by the authors.

Where sleet is a problem, ACSR cables usually continue to function even if several aluminum strands are burned off, whereas sleet melting may be necessary for all-aluminum lines.

It is offered for your consideration, that for lines of prime security, there is greater opportunity for savings with the use of a conductor which rarely fails than through the use of the cheaper all-aluminum where provision for broken wires in the towers should be provided.

Mr. Rodee (Aluminum Company of America): In addition to its engineering value, this paper has considerable historical interest. It referred to the first use of aluminum in 1899, which was among one of the first installations of aluminum conductors on overhead lines.

Since steel-reinforced aluminum cable (ACSR) was not developed until several years later, the question of making a choice between aluminum or between all-aluminum and ACSR did not exist at the time these early installations were made. And during the years that followed, ACSR to a very large extent replaced all-aluminum for use on overhead lines, and because of its higher strength, permitted the use of longer spans with intended savings in supporting structures. It brought out in this paper, however, that these economies can be fully realized only when it is possible to utilize the higher strength of ACSR. When faced with the problem of changing conductors on an existing line to obtain increased carrying capacity, the maximum advantage will be obtained by using a conductor with the highest possible ratio of current-carrying capacity to weight within the limitations of the strength of the existing structures.

In our all-aluminum conductor, or in some cases, ACSR with a small percentage of steel will usually be found to most nearly meet these requirements.

There is one question I would like to ask concerning the procedure used to install the all-aluminum conductors on these lines.

With the relatively high normal tensions mentioned in the paper, an appreciable amount of creep over a period of time may be expected. I would like to ask in what way provision was made to take care of this during stringing of the conductors or, stated another way, what allowance was made for the increase in sag resulting from this creep?

E. M. Wright and **E. G. Lambert**: In answer to Mr. Rodee, we compute initial tensions. We string with initial tensions and sags. We compute these tensions using the stress-strain curves which are furnished by the manufacturers. We assume in computing these tensions that the conductor will be loaded at maximum loading conditions, in our case an 8-pound wind, 25 F, for a period of 30 days. We do not prestress any of our all-aluminum, or for that matter, our ACSR.

We would like to say again that the main use of all-aluminum in our system has been in the light-loading area. In the California light-loading area there is no snow loading, ice loading, nor sleet loading and there is very little lightning.

So you might say that the conditions are mainly ideal for the use of this type of conductor.

In the heavy-loading areas, we normally use ACSR except for the one case mentioned before, and for a couple of other cases on short lines.

We thank those who made comments on the paper.

The Application of Business Machines to Electrical Utility Load Forecasting

JAMES G. GRUETTER
NONMEMBER AIEE

THIS paper describes the use of punched-card accounting equipment by the Bonneville Power Administration (BPA) in the calculation and tabulation of load forecasts. Although the procedures described were developed to meet particular needs of an electrical utility wholesaler, it is believed many elements of the system can be utilized by electrical utility load forecasters in general.

BPA, like most electrical utilities, uses load estimates both for operational and planning purposes. Load estimates are used, e.g., on a short-term basis as a guide in co-ordinating the operation of storage reservoirs, and for long-term planning of transmission, generation, and customer service facilities. The load-forecasting function, however, is entirely centered within one section which is responsible for the preparation of all load estimates used by the various organizational groups, such as the system engineering, budget, operations, customer service, and rate departments. This centralization of the load-forecasting function makes it possible to assign the responsibility for load forecasts to specialists. The use of a basic estimate by all departments also has the advantage of eliminating duplication of work and preventing the contradictions and discrepancies that inevitably occur when load estimates are simultaneously and independently prepared by various departments. In addition, the repetitive use of one basic estimate for all purposes makes it advantageous to use machine methods.

Load estimates are prepared for one primary purpose—as a guide to management. Having established a single basic estimate which has no primary purpose other than giving management a picture of the predicted loads as they are actually expected to develop, the estimate then can be adapted by management to suit any specific use. For example, the basic

---

Paper 55-450, recommended by the AIEE System Engineering Committee and approved by the AIEE Committee on Technical Operations for presentation at the AIEE Summer General Meeting, Swampscott, Mass., June 27–July 1, 1955. Manuscript submitted March 28, 1955; made available for printing April 15, 1955.

JAMES G. GRUETTER is with the Bonneville Power Administration, Portland, Oreg.

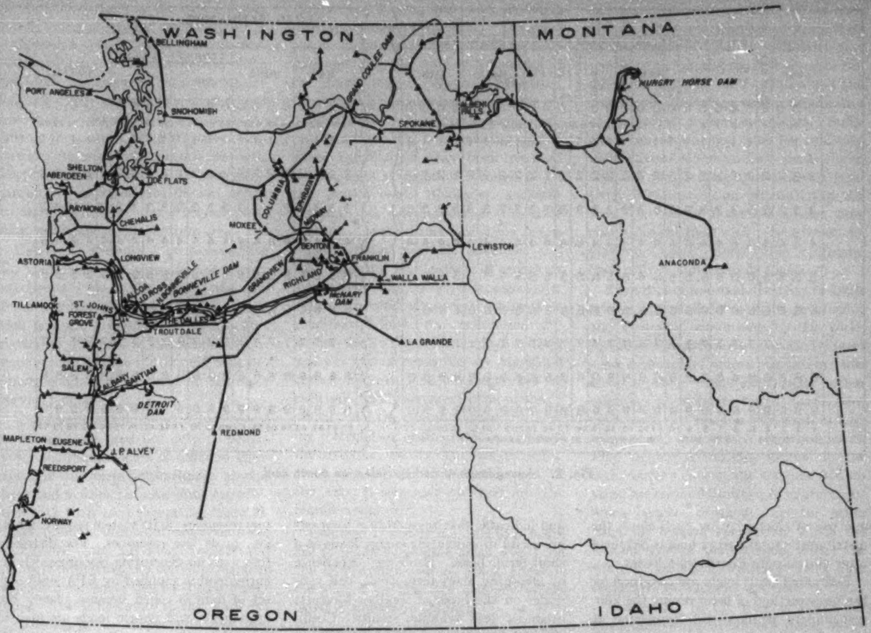
WASHINGTON
MONTANA
OREGON
IDAHO
BELLINGHAM
PORT ANGELES
SNOHOMISH
GRAND COULEE DAM
HUNGRY HORSE DAM
SPOKANE
ALBENI FALLS
SHELTON
ABERDEEN
TIDE FLATS
RAYMOND
CHEHALIS
COLUMBIA
EPHRATA
MIDWAY
MOXEE
BENTON
FRANKLIN
LEWISTON
ANACONDA
ASTORIA
LONGVIEW
ALCOA
J.D. ROSS
N. BONNEVILLE
BONNEVILLE DAM
GRANDVIEW
RICHLAND
WALLA WALLA
TILLAMOOK
ST. JOHNS
FOREST GROVE
THE DALLES
TROUTDALE
MCNARY DAM
LA GRANDE
SALEM
ALBANY
SANTIAM
DETROIT DAM
REDMOND
MAPLETON
EUGENE
J.P. ALVEY
REEDSPORT
NORWAY

Fig. 1. Location of major substations and transmission lines of BPA

estimate could be increased for planning service facilities in order that the safety factor so essential to adequacy and continuity of service could be given due consideration. Likewise, for revenue estimating or rate making a downward bias could be applied so that due caution might be observed in predicting future financial returns. In this manner the basic load estimate, itself unchanged, can be adapted for any purpose useful to the utility. This concept of load estimating considers the preparation of the basic load estimates to be a technical function, and the application of bias to the estimate to be a policy function.

Uniform Preparation of Individual System Load Estimates

As a wholesaler of electric power to 87 different distribution systems, 12 federal agencies, and 17 industries, BPA's problems in the preparation of load estimates differ to a degree from those of its utility customers. The load of most utilities consists of the total requirements of their residential, farm, commercial, and industrial customers. The power wholesalers' total load, however, is determined primarily by the total requirements (load less generation) of its utility customers. Similarly, the total BPA area load estimate is essentially the aggregate of 87 system load estimates of its utility customers.

The BPA service area, Fig. 1, embraces most of the states of Oregon and Washington, northern Idaho, and western Montana. Over this territory there are 6,565 circuit miles of transmission lines from which the utility customers are served at 322 different points of delivery. In order to schedule and provide the required transmission and substation facilities, load estimates are needed for each distributor at every point of delivery. When a distributor is served at more than one substation separate estimates must be prepared. The aggregate of separate estimates by delivery points equals the distributor's total load. Two or more distributors may be served from the same substation and generally several distributors are served from the same main system transmission line. Because the load estimates of so many different distributors must be combined to determine required substation, transmission, and generation facilities, all the estimates should be prepared in accordance with the same basic procedures. All distributors in the BPA area have therefore been provided with a load estimating manual which describes uniform methods and procedures, and contains basic worksheets to be used as a guide in the preparation of load forecasts. Both the power wholesaler and the retailer co-operate in the preparation of distributor load forecasts. The study is generally prepared in three parts: 1. a jointly prepared economic analysis and load study; 2. the distributor's plan of service for his area; 3. BPA's plan of service to the distributor. Parts 2 and 3, of course, must dovetail. The standard method used in the preparation of load studies consists of grouping the ultimate consumers into broad classifications, such as residential, farm, commercial, industrial, irrigation, space heating, street lighting, and other special classifications. By estimating the number of consumers to be served in future years and the aver-

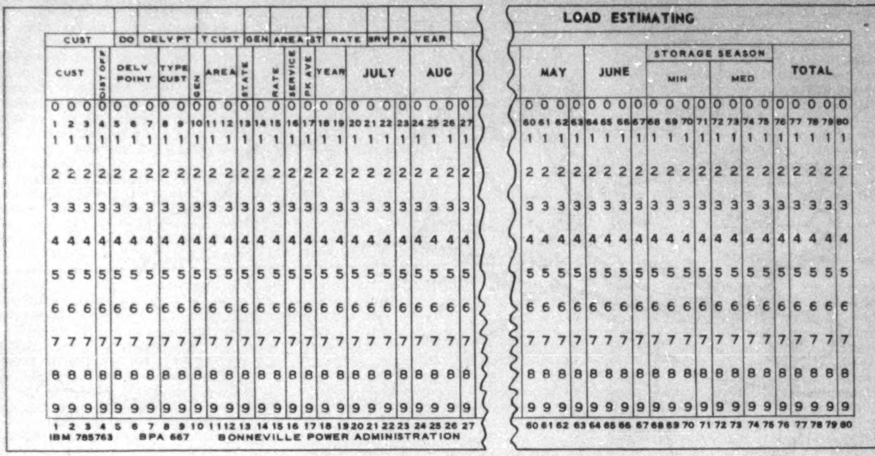

Fig. 2. Arrangement of coding system on punch card

age use of electricity by each class, the distributor's total energy load is obtained after allowing for distribution losses.

Estimated peak loads are obtained by the basic method of determining the kilovolt-ampere demand per consumer at time of peak load by each class of consumer. The contribution to the peak load per consumer is multiplied by the number of consumers for each class. The total coincidental peak load obtained is then checked against the historical trend of the system's load factors. Large industrial consumers and certain special loads must be treated individually.

Considerable diversity exists between the peak loads of the BPA distributors because their service areas cover three distinct geographic zones. Some systems, e.g., experience summer irrigation pumping peaks; others, winter space heating peaks. The standard procedure therefore provides for estimates of both winter and summer peak loads in all cases.

It is interesting to note in respect to estimating winter loads that total energy loads in the BPA service area at the present time vary about 23,000 kw per degree of change in temperature during the winter months, with the amount of the temperature-responsive load increasing each year. Studies indicate a high degree of correlation of energy loads and temperatures, with the coefficient of correlation ranging between 0.8 and 1.0. The measure of dispersion about the regression lines as measured by the standard error of estimate S is comparatively small and indicates that temperature forecasts are useful in estimating energy loads on a short-term basis. However, experience in preparing short-term peak load estimates on the basis of weather forecasts produces less reliable results. Coefficients of correlation for peak loads have been less than those for energy loads and the standard error of estimate has been larger.

Preparation of Estimates for Punched Card Accounting: The Coding System

Because the same basic estimates are used by different departments for a variety of purposes in which the statistics are grouped in a large number of combinations, it is apparent that the estimates constitute a suitable medium for machine tabulation. A workable coding system must be sufficiently flexible to provide information which is required most frequently and is capable of presenting those tabulations which would be most time-consuming if done by hand. A wide selection of information and many arrangements are possible in the design of the coding system. Each utility has unique problems to which it can adapt a system. The procedure described here in the interest of advancing this technique is only one of many possible applications.

Three sets of data are coded for each distributor with generating facilities of its own: 1. its own load estimates; 2. its system resources; 3. its system requirements, i.e., loads less resources. For distributors with no generating resources, whose entire load is supplied by BPA, only one set of data is coded because system requirements and system loads are identical. From this information it is possible to obtain either the total BPA system load or the total area load. The aggregate of all requirement estimates constitute the loads which BPA, as the wholesaler, must be prepared to supply. Total area load estimates are also determined by adding the total of the system load estimates of distributors with generation to the total requirements of nongenerating customers. Both peak and energy estimates are prepared by months for each distributor in the BPA service area for a 10-year period. The peak and energy data are punched on cards, each card listing the 12 months of a fiscal year. A description of the coding system and its arrangement on the punch card, Fig. 2, together with an explanation of some of the studies and uses to which the coded statistics are applied, follows.

The first three of the 80 columns on the punch card are reserved for customer and distributor identification. Customers, after being arranged alphabetically, are assigned numbers ranging from 001 through 999. Every electric distributor in the Pacific Northwest and every BPA customer, whether an industry, federal agency or utility, is assigned an identification number so that total Pacific Northwest area loads, resources, or requirements on the BPA system, as the case may be, can be machine-selected and tabulated.

Column 4 is used to designate the particular BPA area or district office in which the loads, resources, or requirements are located. This information is used primarily for administrative purposes to permit the central office to make comparisons between the various districts. Pertinent information may be sent, as required, to the respective district offices to assist them in customer service planning within the administrative area.

Columns 5 through 7 are reserved for the identification of substations or delivery points. As in the case of the customer identification series, 999 identification numbers are available. Thus, estimates for 10 years in the future can be readily compiled for the 322 different delivery points for purposes of customer service planning.

Columns 8 and 9, designated "type of customer," are used not only to distinguish the requirements of different categories of customers but to classify system load and system resource data for utilities with their own generating facilities. Load, resource, and requirement data are subdivided into privately owned and publicly owned utilities, and into member and nonmembers of the Northwest Power Pool. This is necessary so that data can be selected in accordance with operating and contractual arrangements.

Column 10 is used to indicate whether or not a utility has generating resources of its own. Since hydro generation supplies approximately 90 per cent of the energy load in the area, steam and hydro resources are distinguished, with hydro capabilities being calculated and punched for both minimum and median month stream flow conditions.

The full operating year may be divided into three periods. In the summer there is sufficient natural stream flow to operate all hydro plants at full capacity. The fall and winter season is characterized by freezing at the higher elevations and a consequent low natural stream flow. At this time it becomes necessary to supplement the natural flow by drawing down the storage reservoirs. In the spring the runoff from melting snows is used to refill the storage reservoirs.

As the most critical time from the standpoint of resources is the 6- or 7-month storage-release period from roughly September through April of each year, the total energy load during this period must be related to the available resources in the same period. The number of months included in the period differs between minimum and median month hydroelectric conditions, and with different levels of storage development. The average of the monthly energy loads for both minimum and median month included in the storage-release periods is calculated for each utility and punched into the individual card by the International Business Machines *602-A* calculating punch. These calculations have been reserved for the eight columns 68 through 75 on the punch card. Similarly, available resources are calculated over the same periods. Comparisons are thus made between total available resources and total loads for any individual month or averaged over any series of months under either minimum or median stream flow conditions. Both the minimum and median month requirements data (system load less system resources) are calculated and entered into a requirements card for each individual customer by the summary punch. All the common indicative coding information, such as the number of the customer, the district office, the delivery point, the major substation area, or the state, is summary punched into the requirements card.

Columns 11 and 12 are used to indicate the 44 major substation areas, Fig. 1, on the BPA system out of which power is distributed to the 322 delivery points listed in columns 5 through 7.

There are a great many factors affecting line loadings, such as seasonal diversity of loads, diversity of stream flows, variations in loadings arising from the operation of a co-ordinated system of storage reservoirs, and contractual arrangements. Since it is necessary in transmission studies to select a number of different months throughout each year under different stream flow conditions in order to determine the heaviest loadings on different parts of the system, the combining of substation loads by machine methods is almost a necessity. Some lines are most heavily loaded under minimum year stream flow conditions; others are subject to maximum loadings when median month conditions are experienced. For example, a line carrying power to a distributor which serves part of its system load from its own hydro generation must carry more power when the capability of the distributor's hydro generating facilities are at a minimum; conversely, when the local generation is at the median level less power needs to be transmitted. At the same time that the requirements of some distributors on the BPA system are reduced under median month stream flow conditions, the BPA system has more power available for sale, both as a result of the reduced demands of distributors and the increased capability of its own system. Power is therefore contracted on an interruptible basis to industrial customers in an amount roughly equal to the difference between the minimum and the median month storage season capabilities of the federal generating plants. Sufficient generation may also be available under favorable stream flow conditions to displace considerable quantities of relatively high-cost steam generation in the area. So, under favorable stream flow conditions the lines which serve steam replacement and interruptible industrial loads will be most heavily loaded.

Examples of seasonal diversity in loads arising out of differences in geographic and economic conditions in the widespread service area are numerous. Winter space heating and summer irrigation loads have already been mentioned; other examples are summer tourist loads, cannery loads that reach a maximum at harvest times, and winter lighting loads. Pine logging operations, located in the high country east of the Cascade Mountains, are normally subject to winter shutdown because of snow. On the other hand, fir logging operations, which are located west of the Cascades where the winters are comparatively mild, are carried on throughout the year.

A diversity in the time of maximum line loadings also arises as a result of operating a co-ordinated system of storage reservoirs since the several generating plants are peaked at different times of the year. For example, heaviest west to east load flows ordinarily occur in July and August when the downstream plants generate at their maximum on natural stream flow while upstream plants in the eastern part of the system are storing water to be used during the ensuing winter. Conversely, the heaviest east to west flows occur in January during the period in which natural stream flows are at their lowest and the storage reservoirs are being drafted.

Columns 11 and 12 are also used when the ultimate delivery is not made over the BPA system but over the facilities of another utility. To indicate the transferring utilities, identifying numbers have been assigned. "Wheeling" loads, served over the facilities of other utilities, may thus be compiled by the respective transferring agents as required, e.g., in compiling reports and estimates for the Federal Power Commission and the Northwest Power Pool.

It has been found necessary, from time to time, to obtain load and resource data on the basis of its location by state. Column 13 is used for this purpose.

Columns 14 and 15 are used to indicate the appropriate rate to be applied to requirement data for use in rate studies and pay-out analyses. Each rate has been assigned an identifying code number. Some of the BPA rates are 1-part and some are 2-part, with the bill depending on both the peak and energy amounts. But since both peak and energy loads can be machine-sorted and tabulated by rate schedules the calculation of revenue estimates is facilitated. Some of the BPA 2-part rates provide that the monthly billing demand shall be the highest measured or computed demand experienced during any of the preceding 11 months. By printing all months it is a simple matter to pick out the "ratcheted" demand. In the same way annual summaries of energy loads can be obtained by the machine and punched into the "total" space on the card (columns 77 through 80) to facilitate the determination of total energy charges.

Column 16, entitled "service," is used to indicate the physical and contractual arrangements made for the delivery of power. When loads are served directly over BPA facilities the major substation area is also entered into the columns reserved for that purpose. When loads are served by transfer or wheeling arrangements over the facilities of other utilities the area column, as has been previously mentioned is also used to indicate the particular transfer agent.

Four basic types of service arrangements are coded; direct; coincidental transfer; noncoincidental transfer; and transfer service for other utilities, also known as reverse wheeling arrangements. When a customer is served on a coincidental transfer basis, BPA has the responsibility for simultaneously supplying the utility making the ultimate delivery, the transfer agent, with an equivalent amount of power. Therefore in relating system loads to generation the requirements of coincidental transfers must be included in the federal load. In other reports these loads would be omitted from the total BPA load and included in the load of the utility making the ultimate delivery. When loads are served on a noncoincidental basis, the transferring agent is responsible for coincidentally providing the generation. BPA has the option of later repayment on the basis of 2 kilowatt-hours for 1 delivered. Therefore, in relating total system load to generating capability, these loads are omitted. On the other hand, they are included for revenue analysis. Transfer service loads provided for other utilities (reverse wheeling), while not included in summaries for revenue purposes except for calculation of service charges, or in load-resource analyses, are required in tabulations used for planning transmission and customer service facilities.

The remaining columns require little explanation. Column 17 is used to classify into peak and average all load, resource, and requirement data. Columns 18 and 19 are used to indicate the year. Space is then provided to record the basic data for each of the 12 months of the operating year from July through the following June. The remaining columns, previously described, are reserved for recording the average of the energy loads over both the minimum and median month storage periods and the operating year totals.

Conclusion

The method described, which has been successfully employed over a period of years, makes it possible to conduct with a high degree of accuracy many investigations and studies which otherwise could not be considered with a limited staff. A primary object in designing a coding system is flexibility. With this in mind, it is desirable as a first step to determine all the purposes to which the system is to be applied. The broadest application of the method is possible when a single basic estimate is used for all purposes, so that information required for a particular report or study, which may range from a revenue analysis to an a-c analyzer study, can be readily machine-selected and tabulated.

Effects of Corona on Traveling Waves

C. F. WAGNER
FELLOW AIEE

B. L. LLOYD
ASSOCIATE MEMBER AIEE

THE EFFECT[1] of corona on traveling waves is to retard any given point on a voltage wave above the corona threshold value by an amount proportional to the distance traveled. This suggests that the effect is equivalent to a reduction in velocity. If a linear circuit, with negligible series and shunt resistance, can be characterized by assigning to it a certain inductance L per unit length and capacitance C per unit length, then a wave impressed upon such a circuit will propagate along the circuit with a velocity v, such that

$$v=\frac{1}{\sqrt{LC}} \tag{1}$$

This relation indicates the possibility of explaining corona effects by an increase in capacitance. Most previous investigators based their analysis of wave distortion upon the energy loss associated with the voltage wave and used the available power-frequency loss data as a foundation upon which to build. Boehne,[2] however, suggested that with increasing voltage the corona envelope and hence the effective capacitance increases. With increasing voltage the velocity decreases, which accounts for the increasing retardation.

There has been some attempt to determine the increase in capacitance of conductors under corona at power frequencies by measuring the increase in charging current. However, the space charge surrounding the conductor is probably quite different under this condition than if a unidirectional surge were applied. Prompted by a desire to explain the results obtained during the tests with traveling waves at the Tidd[1] power station, the authors undertook laboratory tests in parallel with the field tests by stringing a conductor of small diameter along the center line of a long metallic barrel. The results of these tests showed conclusively that an increase in capacitance took place when the conductor was surged. Encouraged by these tests, other tests were subsequently made on full-scale conductors adjacent to a large flat screen. The

---

Paper 55-453, recommended by the AIEE Transmission and Distribution Committee and approved by the AIEE Committee on Technical Operations for presentation at the AIEE Summer General Meeting, Swampscott, Mass., June 27–July 1, 1955. Manuscript submitted March 28, 1955; made available for printing April 19, 1955.

C. F. Wagner and B. L. Lloyd are with the Westinghouse Electric Corporation, East Pittsburgh, Pa.

The authors wish to acknowledge the valuable assistance of C. P. Saalbach for performing the digital computer studies, J. W. Skooglund and C. A. DeSalvo for assisting with the analytical work, and the personnel of the Engineering Laboratories for assisting with the laboratory tests.

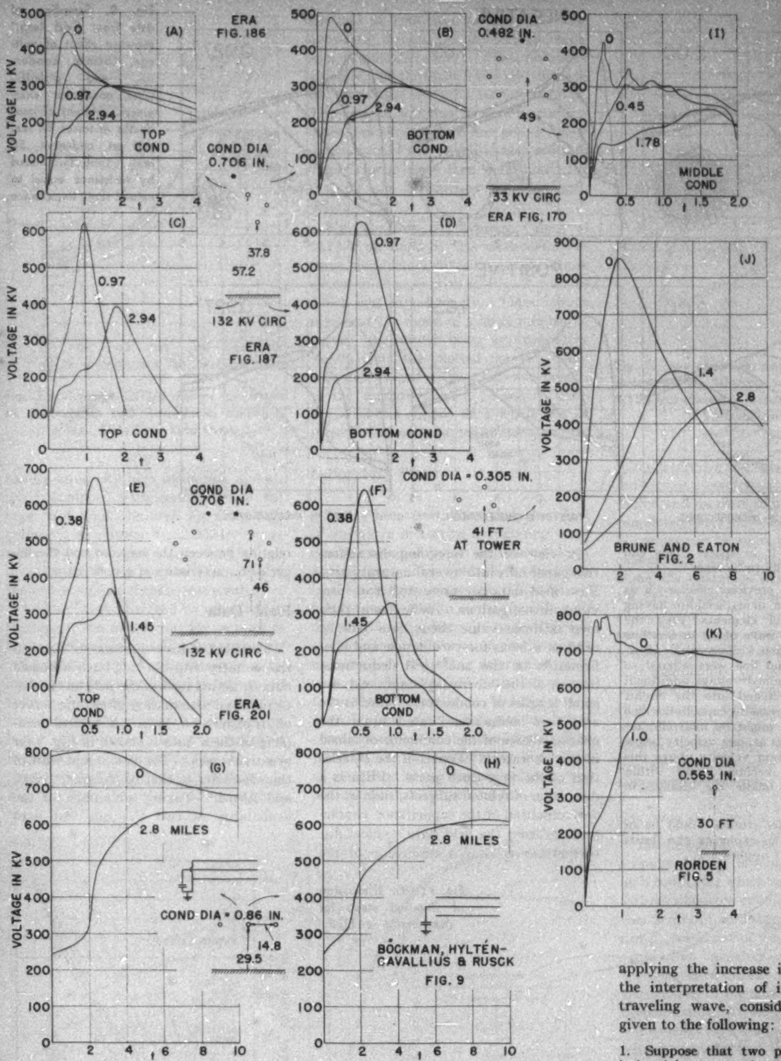

Fig. 1. Distortion of negative impulses as a function of distance traveled. All time scales in microseconds. Numbers on curves represent distance traveled from point of origin

tests under these conditions also show that the corona characteristics can be described adequately as an increase in capacitance.

Having demonstrated the increase in capacitance occasioned by corona, this is only a part of the problem. While equation 1 is correct, it must be observed that it is rigorously correct on a circuit of distributed constants only when the medium is homogeneous, such as an aerial line below corona in which the medium is air or in a cable in which the medium is rubber or some other suitable dielectric. In applying the increase in capacitance to the interpretation of its effect upon a traveling wave, consideration must be given to the following:

1. Suppose that two parallel conductors isolated from ground were loaded by shunt capacitors in such a manner that the distributed capacitance were increased without changing the inductance. One might apply equation 1 to such a system and conclude that the propagation velocity is decreased correspondingly. However, it is fundamental that any electrical disturbance in air propagates with the velocity of light. It would be expected then that as a wave of charge travels along the line some dis-

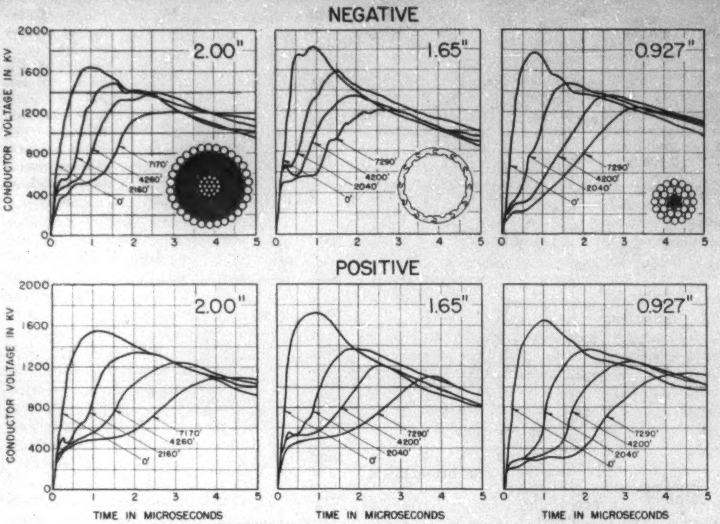

Fig. 2. Sampling of data from Tidd tests,[1] showing effect of voltage, distance, conductor, and polarity. One conductor energized. Height of conductor at tower 86 feet and at mid-span 50 feet. Line terminated by resistance equal to natural surge impedance

turbance precedes it in space. This can be shown analytically to be true.

2. Neglecting the previous effect such as might be the case in an artificial line having a large number of elements, then the propagation of the wave along such a line would follow equation 1 rigorously. However, if the artificial line were altered so that at a predetermined voltage additional capacitors were switched into the circuit (simulating the increase in capacitance due to corona), then it might be inferred that the wave propagates at one velocity below this point and a lower velocity above this point. There are certain limits within which the waves follow the change in capacitance.

3. Digital computer studies would be of considerable value in exploring the limits to which equation 1 applies.

In view of the foregoing discussion, this paper falls into several natural parts. First field data are presented from previous investigations. Aside from their own intrinsic value these data will be used as a basis for verification and confirmation of the analytical deductions. Second is the laboratory data, tests on small lengths of conductor. Third is the analytical deductions based upon the characteristics of the conductor obtained in the laboratory. Fourth is the correlation of the first three parts. Fifth is a discussion of related subjects, such as the determination of the capacitance characteristics from the field data, typical distortion curves, and a discussion of the relation between the impulse and the 60-cycle characteristics of a conductor.

Field Data

A number of investigators,[1,3–9] both in this country and abroad, have obtained data by actual tests in the field on the distortion and attenuation of electric waves on transmission lines. A typical sampling of these data is shown in Fig. 1 for negative waves. The most recent work of this character is that of Wagner, Gross, and Lloyd.[1] Taking advantage of the availability of two $1^1/_2$-mile test lines

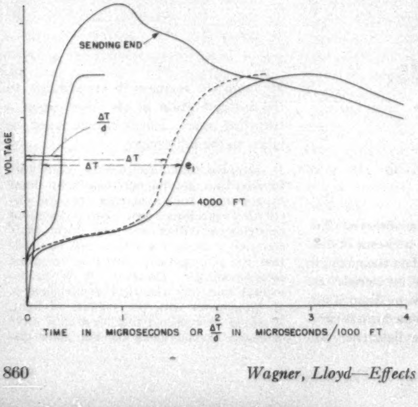

Fig. 3 (left). Illustration of detailed steps for determining (ΔT)/d

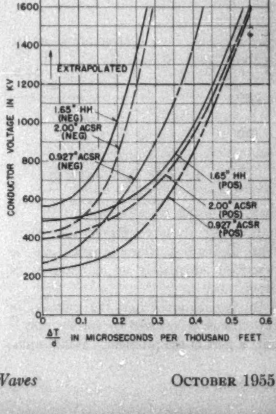

Fig. 4 (right). Average (ΔT)/d curves for surges on single conductors for the three conductors shown in Fig. 2. Data from Tidd tests[1]

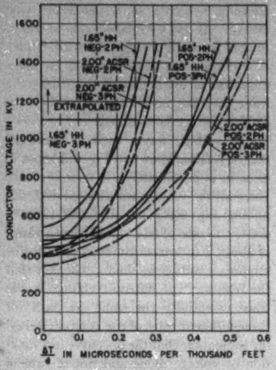

Fig. 5. Average (ΔT)/d curves for surges on 2-conductor and 3-conductor combinations. Data from Tidd tests[1]

having unusually high insulation and already equipped with conductors of the type that would be used for extra-high voltage transmission, a 2,000-kv surge generator was set up in the field for application of surges to the line. Fig. 2 shows a sampling of these test results.

As previously observed by other investigators, it was found that for each set of test conditions the wave for any particular voltage above the corona threshold voltage appeared to be retarded in time by an amount proportional to the distance traveled by the wave. To isolate this factor the Tidd test data were replotted in terms of a new quantity $(\Delta T/d)$. The significance of this quantity is shown in Fig. 3. Both the voltage at the sending end and at 4,000 feet are plotted. The horizontal distance at any voltage, such as e_1, is indicated as ΔT. These distances are shown by the dashed line and indicate the time lag of the wave for any voltage. The time ΔT was then divided by the distance d in thousands of feet giving a new quantity, $(\Delta T)/d$, which is also plotted. These curves were then determined for each of the conductors and for each polarity.

Fig. 4 shows the average values of $(\Delta T)/d$ obtained by this method for the three conductors tested, namely those shown in cross section in Fig. 2, each of which was surged singly. These curves represent the mean of a large number of curves, the spread being approximately ±0.05 from the plotted curves. They were determined without previous benefit of the analytical work presented here. Fig. 5 shows similar data when two or three phases were surged simultaneously.

Laboratory Tests

It has been postulated that the effect of corona in distorting a traveling wave can be explained by an increase of shunt capacitance. The field data discussed in the foregoing show the distortion of voltage waves due to corona, but they do not provide a fundamental understanding of the manner of variation of this shunt capacitance. To aid in interpreting and understanding the field data, laboratory tests were undertaken to determine the variation of shunt capacitance when corona exists on the conductor. The justification for representing the effect of corona as a varying capacitance was also established in these tests.

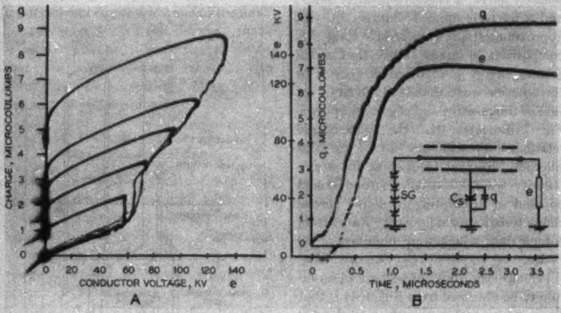

Fig. 6. Corona characteristics of 6 feet of 0.156-inch-diameter copper tube inside a 24-inch cylinder. Positive polarity

(A) q-e nest for different voltages

(B) e-time and q-time curves for the maximum q-e curve of (A)

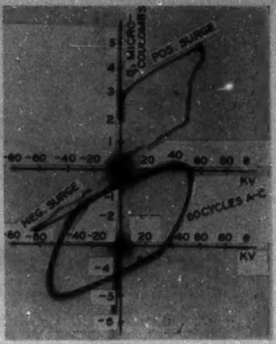

Fig. 7. q-e curves for positive and negative surges and for 60-cycle voltage. 6 feet of 0.156-inch-diameter copper tube inside a 24-inch cylinder

To determine the surge corona characteristics of a conductor, it was necessary to find and measure some quantity which completely describes these characteristics. If corona can be represented as a shunt capacitance which varies with voltage alone, the charge on this variable capacitor can be used to describe the corona characteristic. This charge-voltage (q-e) relation was the quantity which was measured in the laboratory.

It was planned to obtain tests on practical transmission conductors at practical spacings to ground. However, it was felt that tests should first be run on smaller scale setups to develop some fundamental concepts and to develop measuring techniques.

Cylindrical Ground Plane

The first group of tests was made in the Impulse Laboratory in East Pittsburgh on a conductor which was strung inside a 24-inch diameter cylinder. The cylinder was tied to ground through a mica capacitor C_s, see insert of Fig. 6. The voltage across this capacitor is proportional to the integral of current and thus measures the charge q in the portion of the cylinder between the guard rings.

The conductor voltage e was measured with a conventional double-layer, wire-wound resistance divider, 2,000 to 6,000 ohms, 2 to 6 feet in length. Oscillographic measurements were made using a cold-cathode oscillograph.

Data were obtained in two different forms, charge versus time and voltage versus time, and charge versus voltage. In the latter form, which proved more useful, the voltage across C_s was applied to

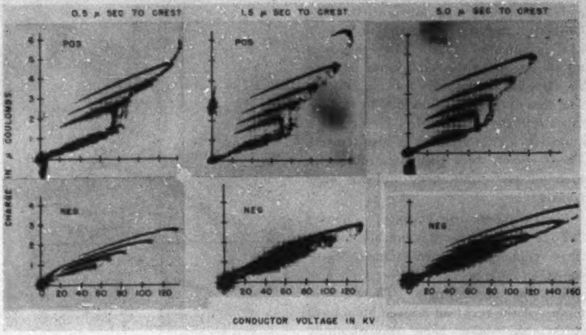

Fig. 8. Effect of time to crest upon q-e curves. 0.156-inch diameter copper tube 12 inches from flat ground plane

the vertical plates of the oscillograph by means of a short wire down the center of a hollow metal tube. This concentric-lead minimized extraneous pickup. A short cable was connected from the voltage divider to the horizontal plates of the oscillograph. The resulting trace provided a plot of charge versus voltage without the necessity of replotting this *q-e* relation from charge-time and voltage-time oscillograms.

Considerable difficulty was encountered in the laboratory in making the charge measurements. These difficulties can be readily appreciated by those who have attempted to measure impulse voltages by means of an air-capacitor divider. Considerable laboratory time was required to rid the charge-measuring circuit of its tendency to oscillate and its affinity for pickup so that adequate results could be obtained. It is necessary to keep the length of the charge and voltage measuring leads down to an absolute minimum when making a direct *q-e* measurement. The length of the charge-measuring leads must be kept to not more than a few feet to prevent the inductance of the leads from oscillating with the variable capacitance or C_s. The length of the voltage-measuring lead must be kept very short to prevent voltage being applied to the horizontal plates at a later time than voltages applied to the vertical plates.

Typical data obtained from this series of tests are shown in Figs. 6 and 7. Fig. 6(A) shows a number of *q-e* traces at different voltages which were made on the same film. With increasing voltage (going in a counterclockwise direction) all traces start with a slope equal to the natural capacitance. After the corona voltage has been exceeded, the individual traces follow essentially the same path until the crest voltage of the particular surge is reached. As the voltage decays on the tail of the wave, the *q-e* trace approaches zero voltage along a line with a slope approximately equal to the natural capacitance until a relatively low voltage is obtained. Fig. 6(B) shows a volt-time and a charge-time trace corresponding to the *q-e* curve of Fig. 6(A) having the highest voltage.

If i_c is defined as the current into the conductor-to-cylinder capacitance, the energy stored in this capacitor is

$$W=\int ei_c dt=\int edq \qquad (2)$$

Hence, the energy removed from the voltage wave by corona is the area enclosed by the *q-e* curve.

Fig. 7 shows a comparison of the *q-e* characteristics obtained with a positive-polarity surge, a negative-polarity surge, and a 60-cycle applied voltage, all with approximately the same crest voltage. A comparison of areas shows that much greater energy is involved in 1 cycle of the 60-cycle wave than is involved in the sum of the positive and negative impulses. Fig. 7 indicates that the space-charge relations for oscillatory waves are considerably different from those for a unipolarity wave. Extreme caution should be used in attempting to derive corona characteristics for unipolarity waves from corona data which were obtained at 60 cycles.

Perhaps the most important observation to be obtained from Fig. 6(A) is that the same *q-e* path is traced by all the different voltage waves so long as the voltage on the conductor continues to increase. This suggests the possibility of determining a single *q-e* curve for increasing voltages on a particular conductor. If this *q-e* relation can be shown to hold for all practical surge wave fronts, this relation can be used in the predetermination of distortion of the front of a wave traveling on a conductor when the corona voltage is exceeded.

The voltage waves used in obtaining the *q-e* relation shown in Fig. 6(A) rose to crest in approximately 1.5 microseconds. Since all the voltage waves used in determining Fig. 6(A) had the same time to crest, the rate of rise varied over a range of about 2 to 1 from the maximum to the minimum voltage applied. The fact that the fronts of the different voltage waves trace essentially the same *q-e* path for these different rates of rise is an encouraging indication that the *q-e* curve is a function of voltage alone and not of rate of change of voltage. This was further investigated by obtaining tests similar to Fig. 6(A) with surge waves having about 0.5 microsecond to crest. Except for the minor oscillations which were still present in the test setup, the *q-e* traces for the two different times to crest for increasing voltage were identical. Hence, at least for the cylindrical ground plane arrangement, the *q-e* characteristics were shown to be dependent on voltage alone and not rate of change of voltage for a considerable range of rates of rise.

VERTICAL GROUND PLANE—IMPULSE LABORATORY

The tests just described were made with a cylindrical configuration and measurements were made by means of a cold-cathode oscillograph. It was eventually desired to obtain *q-e* characteristics on practical transmission conductors at the Trafford High-Voltage Laboratory. Due to the physical arrangement of the Trafford Laboratory, it was known that it

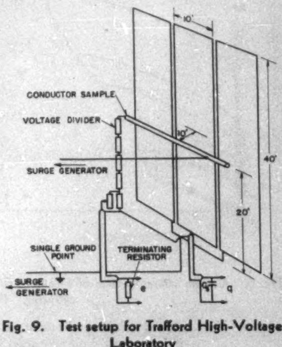

Fig. 9. Test setup for Trafford High-Voltage Laboratory

would be necessary to use a portable hot-cathode oscillograph in order to keep the measuring leads very short. To gain some experience with the flat ground plane configuration and to develop suitable measuring techniques using the hot-cathode oscillograph, another small scale setup was made in the Impulse Laboratory. An 8-foot by 12-foot ground plane, made up of wire mesh, was built in the Impulse Laboratory. The conductor was strung parallel to the screen with a spacing to the screen of from 6 to 18 inches. The ground screen was again divided into three sections to eliminate end effects, and only the center section was used for charge measurements. The charge measurements were made in a manner similar to that described previously, and the voltage measurements were again made by use of a resistance divider.

Typical results obtained in this series of tests are shown in Fig. 8. The oscillograms shown in Fig. 8 are not as good in quality as those shown in Fig. 6 for three reasons:

1. The large ground screen was more susceptible to oscillations and pickup than was the cylindrical ground screen.
2. The hot-cathode oscillograph was not as suitable for these measurements as was the cold-cathode oscillograph.
3. The oscillographs were recorded on 35-millimeter film.

The oscillograms shown in Fig. 8 are included because they again illustrate the independence of the q-e characteristic upon the front of the wave. Fig. 8 shows the q-e characteristics obtained for positive- and negative-polarity surges with three different times to crest: 5 microseconds, 1.5 microseconds, and 0.5 microsecond. It will be noted that for each polarity the same charge-voltage characteristic is traced on the rising part of the voltage wave for all the different times to crest. This provides further evidence that the charge-voltage characteristic obtained with increasing voltage is a function of voltage alone.

Vertical Ground Plane—Trafford High-Voltage Laboratory

After the preliminary testing in the Impulse Laboratory, the final laboratory tests were preformed at the Trafford High-Voltage Laboratory using a practical transmission conductor and practical spacings from the conductor to the ground plane. The test setup is shown in Fig. 9. The ground plane was made of wire mesh screen, and was 40 feet high and 25 feet wide. Again the screen was divided in three sections to eliminate end effects, and only the center 10-foot width was used for the charge measurements.

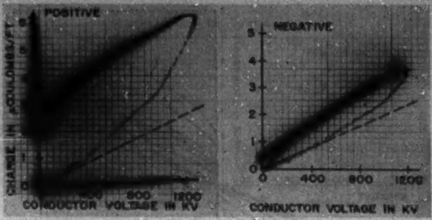

Fig. 10. Corona characteristics of 0.927-inch steel-reinforced aluminum-cable conductor. Configuration shown in Fig. 9

The conductor was strung in a horizontal position parallel to the screen, 10 feet from the screen and 20 feet above the floor. The conductor used in these tests was a 0.927-inch steel-reinforced aluminum-cable (556,500-circular-mil) conductor. It was planned to obtain the corona characteristics of a large number of transmission conductors, but the laboratory time did not permit.

The measuring techniques were similar to those described earlier for the smaller scale setups. The charge in the variable capacitance from the conductor to the ground screen was determined by measuring the voltage across the screen-to-ground capacitor C_s. The conductor voltage was measured by use of a special capacitance-compensated resistance-type voltage divider.[10] Measurements were made with the same hot-cathode oscillograph which was used in the previous tests. Considerable modifications had been made in the timing circuits, sweep circuits, and beam-control circuits before these tests were begun. A 1 by 1-oscillograph camera was also available for these tests.

Typical q-e curves obtained in this series of tests are shown in Fig. 10 for positive- and negative-polarity applied waves. Because of the width and the darkness of the return trace on the q-e curve, it was not practical to superimpose a number of q-e plots on the same film. The dashed lines which have been drawn on the oscillograms in Fig. 10 represent the natural capacitance from the conductor to the ground screen. The slope of this line was verified by measuring a q-e characteristic of a surge wave below the corona level and greatly increasing the sensitivity in both the charge and voltage directions. By determining the slope of the natural capacitance line with different values of screen-to-ground capacitance, it was also possible to determine the stray capacitance from the screen to ground, which was included in the charge calibration.

The q-e characteristics for a number of different crest voltages have been replotted in Fig. 11. Fig. 11 again shows that essentially the same q-e characteristic is traced by the different waves as long as the voltage continues to rise. The replot shown in Fig. 11 will later be used in establishing a correlation of field and laboratory data and will also be used in establishing a surge corona analogue.

The tests in the laboratory were remarkably consistent as contrasted with similar a-c tests in which either corona loss or radio influence was measured. This statement applies to both the impulse tests in the field and to the impulse tests in the laboratory. Perhaps this comparison is more apparent than real because in the impulse tests much higher ratios of applied voltage to corona threshold voltage were used than in the corona-loss and ratio-influence tests. The variance in a-c corona loss decreased as the ratio of applied voltage to corona threshold voltage increased.

The effect of water on the conductor was investigated in the screen tests with small configurations. Water had no effect upon the loss loop in the q-e curves. This is further substantiation of a similar result obtained in the field tests[1] which indicated that rain had no effect upon the attenuation and distortion of traveling waves.

Theoretical Analysis

Elimination of Electromagnetic Effects Moving With the Velocity of Light

Any analytical approach to the solution of waves on transmission lines that travel with a velocity less than that of light must take into consideration that the velocity of any electrical effect in free space equals that of light. The conventional treatment of traveling waves frequently supposes, without specifically saying so, that rectangular waves of charge and current, traveling with the velocity of light, have electric and magnetic fields associated with them that rise instantly from zero to a constant value as

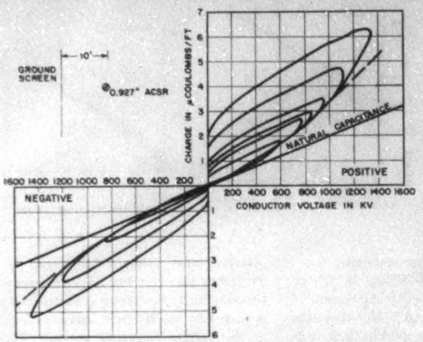

Fig. 11. Replotted nest of q-e curves for a 0.927-inch steel-reinforced aluminum-cable conductor. Configuration shown in Fig. 9

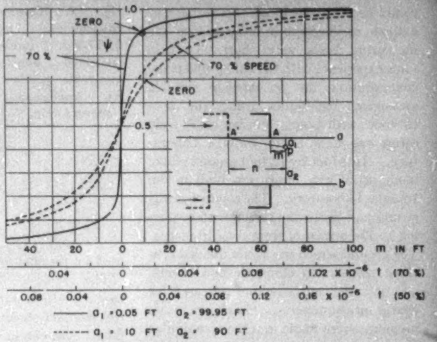

Fig. 12. Electrostatic potential of two rectangular waves of charge moving with velocities less than that of light

the heads of the waves pass a particular point. By application of the classical methods of treatment this can be shown to be the case.

When the waves travel with a velocity less than that of light recourse must be made to the so-called "retarded potentials" to calculate the effects. This method is illustrated in Fig. 12. The insert in this figure shows two parallel geometric lines (as contrasted with electric conductors). Upon a is a positive rectangular wave of charge whose position at a particular instant is shown by A. A similar negative charge resides on b. Both of these waves are moving with a velocity v expressed as a fraction of that of light, and both have corresponding currents associated with them. Suppose for the moment that this velocity is 70 per cent. If the position of the charge on a at any instant is A', then by the time that the presence of the charge at A' is felt at point p the wave has moved along the line to A, where $A'A$ is $0.7\ (A'p)$. The electrostatic potential at a point due to a charge q at a distance r from the point is q/r. By summing up such contributions of all the charges to the left of A', the total potential ψ at point p is obtained for the head of the wave in the position given by A. This has been done for both the positive and negative waves, for $a_1 = 0.05$ feet and $a_2 = 99.95$ feet and the results are plotted by the solid line. The potential of a corresponding point adjacent to line b would have a value of ψ just the negative of the value at point p. These potentials are plotted as a fraction of the potentials eventually obtained after the wave has moved to the right a great distance. The potential between these two points adjacent to the two lines is the quantity that is frequently referred to as the "voltage between conductors." It can be seen that the significant rise in potential occurs in a very small distance, 80 per cent of the change taking place in a distance of 20 feet.

If one wished to obtain the transverse electric field, one could determine a similar curve for slightly different values of a_1 and a_2 and then take the limit of $(\Delta\psi)/(\Delta a)$ as Δa becomes very small. For the present case the transverse field is not of particular interest although the potential is. The longitudinal field is of some concern. In Fig. 13, ψ is plotted for $a_1 = 10$ feet, $a_2 = 90$ feet, and $v = 0.7$. While this gives the potential at point p for different positions of the wave, it should be evident that for any given position of the wave this should also be the potential of different points along the line for which the a_1's and a_2's are the same. It would only be necessary to reverse the positive and negative abscissas. The slope or gradient of this curve E_{sx} then gives the longitudinal component of the electric field.

The magnetic field can be obtained in a somewhat analogous fashion. For this purpose the retarded vector potential **A**, is obtained. The potential at a point due to a current **i** a distance r from the point is equal to **i**$/r$. By summing up such contributions for all of the current to the left of A', the total potential **A** at point p is obtained for the head of the wave in the position given by A. It is to be observed first that since all elements of **i** that contribute to **A** are parallel to lines a and b, **A** will have a longitudinal component only. There will be no transverse component. Next it will be observed that since the limits of integration are the same as for the charges and since the distance r enters into the relation in an identical manner, **A** is proportional to ψ, and has the same wave form. Thus there are two identical waves, ψ and **A**, traveling along the line. The longitudinal electric field due to the currents E_{mx} is proportional to $-(d\mathbf{A})/(dt)$. The negative sign means that it is directed oppositely to the currents and is opposed to E_{sx}. First, because E_{mx} is a time derivative of **A** and, second, because the amplitude of the current wave I is equal to the product of charge and v, E_{mx} is proportional to the square of the velocity of the wave. When the actual numerical work is carried out it is found that

$$E_{mx} = v^2 E_{sx}$$

Thus the total longitudinal electric field is

$$E_x = E_{sx} + E_{mx} = (1-v^2)E_{sx}$$

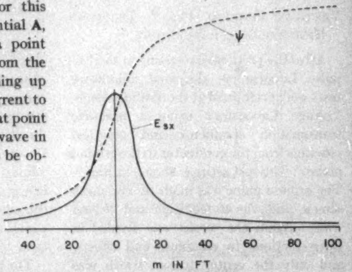

Fig. 13. Longitudinal electric field due to two waves of charge moving with a velocity of 70 per cent of light. $a_1 = 10$ feet and $a_2 = 90$ feet

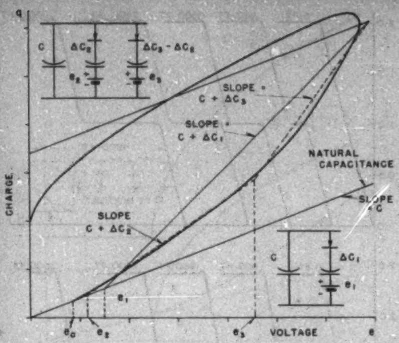

Fig. 14 (left). Analogue approximation of charge-voltage characteristics of short length of conductor

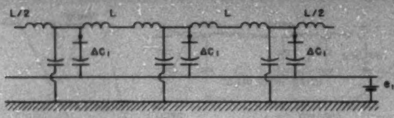

Fig. 15 (above). Analogue of a long line using the approximation of corona conditions indicated in Fig. 14

When the wave travels with the speed of light $v=1$ and E_x is zero, the electric field due to the charge just annuls the electric field due to the current. At very low velocities, E_x approaches the field arising from the charge alone. This is not to say that ψ, when expressed in terms of distance along the line, does not change with speed. The extent to which it changes is illustrated in Fig. 12. For $a_1=0.05$ and $a_2=99.95$ feet the difference for v equal to 0 and $v=0.7$ is negligible (see the circle which is plotted for $v=0$), and for $a_1=10$ feet and $a_2=90$ feet the difference between $v=0$ and $v=0.7$ is indicated by the two dashed curves.

It was originally postulated that the charges and the currents were flowing on geometric lines without making any reference to the nature of the conductivity. Now if it is assumed that the rectangular waves of charge and current are flowing on metallic conductors, an inconsistency arises in that a longitudinal electric field cannot exist on a good conductor. Actually a charge separation would occur of such nature as to tend to annul this field. On the a conductor, a positive charge would be pushed slightly ahead of the front of the wave and a negative charge just behind the front of the wave. The net effect would be to round the corners and slope the fronts of the charge and the current waves and at the same time make the front of the ψ wave more steep. In other words, the wave shape of ψ and q would be brought into closer agreement. Certainly it can be said that the difference between the two waves would be less than the departure of the ψ curves of Fig. 12 from a rectangular front. For the practical configurations of transmission lines this difference is negligible. One can proceed with assurance and assume that the curve of ψ is of the same wave shape as the charge and that the usual line constants on a per-unit length can be used.

ANALOGUES

From the laboratory experiments on short lengths of conductor that have been discussed previously, it has been shown that the charge on a conductor under impulse conditions for the rising portion of the curve is a function of the voltage only. The charge is independent of the rate of rise of voltage or the wave shape of the impulse. As the voltage applied to the conductor increases from zero, the charge increases linearly with voltage along a slope corresponding to the "natural capacitance" C of the conductor as indicated in Fig. 14. When the corona threshold voltage e_0 is exceeded, the slope of the curve becomes steeper and the curve increases until the maximum voltage of the applied wave is reached. As the voltage decreases, the curve follows an essentially straight line. For the lower values of crest voltage the slope of the return path corresponds quite closely to the natural capacitance but at the higher crest voltages the slope becomes progressively larger.

As a first approximation, the curved portion of the rising characteristic can be represented by a straight line whose slope will be designated $C+\Delta C_1$ and whose intercept with the straight line representing the natural capacitance will be designated e_1. The downward portion of the curve can be represented by another straight line having a slope equal to C. These approximations can be represented for both increasing and decreasing voltages by the analogue shown in the lower right-hand insert. Because of the greater importance of the rising part of the characteristic and the complexity of obtaining an analogue having closer correspondence to the actual characteristics for decreasing voltage, this simplified analogue is regarded as sufficiently satisfactory for most purposes. For a more accurate representation of the rising portion, the characteristic can be represented by the two dashed straight lines. The analogue for this approximation is that shown by the upper left-hand insert. For more accurate approximations, a larger number of shorter straight lines can be used and additional elements added to the analogue. Fig. 15 shows how this analogue can be inserted to form the equivalent for a long line.

DIGITAL COMPUTER CALCULATIONS

The laboratory tests showed that the surge corona characteristics can be presented by a shunt capacitance which varies with voltage alone. It remains to develop methods for interpreting a known q-e characteristic in terms of distortion of a traveling wave.

If was felt that calculations performed on a digital computer would be most helpful in providing an understanding of the effect of a nonproportional q-e relation. A sample traveling wave problem was programmed for an International Business Machines *701* digital computer. The transmission line selected for study was 4,800 feet in length with a natural surge impedance of 400 ohms and a natural velocity of propagation of 1,000 feet per microsecond. The line was represented by 480 equal pi sections such as shown in Fig. 15, each section representing 10 feet of conductor length. For one group of calculations the corona capacitors were deleted.

The voltage wave applied to the sample line rose linearly to crest in 1 microsecond, and was flat beyond 1 microsecond. A more detailed description of the digital representation is given in Appendix I.

The results of the digital computer calculations are shown in Figs. 16 and 17. The data in Fig. 16 were obtained with the corona capacitor removed. The purpose of these calculations was to verify the ability of the computer to make accurate calculations on a traveling wave problem whose solution was already known. If the line were composed of uniformly distributed inductance and capacitance, the applied wave would travel undistorted until it reached the

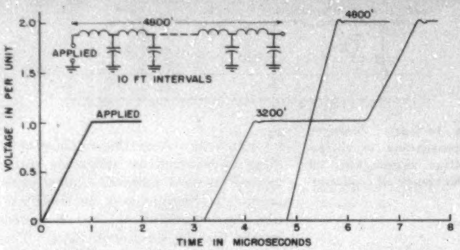

Fig. 16 (above). Results of digital computer calculations of a traveling wave on a line without corona

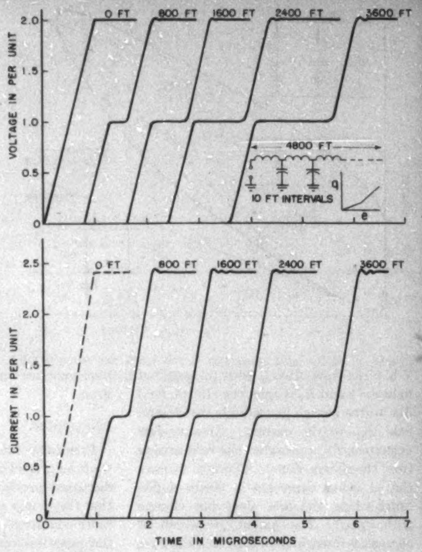

Fig. 17 (right). Results of digital computer calculations of a traveling wave on a line with corona

open end of the line where a reflection would occur. The voltage at the open end of the line would be twice the applied voltage and have exactly the same wave form. The voltage at an intermediate point along the line would be exactly the same as the applied voltage until the reflection from the open end reached the point. Fig. 16 shows that the digital computer reproduces the expected result within plotting accuracy except for a slight rounding off when the wave first begins to rise and a very small oscillation near the crest of the wave. It was concluded that the digital computer was capable of making the desired calculations with sufficient accuracy.

Fig. 17 shows the digitally calculated currents and voltages obtained when the shunt capacitance was allowed to vary in a manner to produce the *q-e* curve shown in the insert. Referring to the insert, with increasing voltage, the charge increases along a line representing the natural capacitance until the conductor voltage reaches the corona threshold voltage of 1.0 per unit. Above this voltage the slope of the *q-e* curve is twice the natural capacitance. Otherwise the representation of the transmission line was similar to that described previously. The voltage wave indicated by the wave form at 0 feet was applied. Fig. 17 shows the conductor voltages and line currents at the sending end, at 800, 1,600, 2,400, and 3,600 feet. To eliminate the possibility of confusion arising from the similarity of the wave shapes in Figs. 16 and 17, it should be noted that in Fig. 16 the stepped character of the wave at 3,200 feet is due to a reflection from the open end whereas in Fig. 17 it is due to corona. The significance of these calculations is discussed in the following section.

Velocity in Terms of Q-E Relation

In the discussion of field data, it has been suggested that the effect of corona is to retard each point on the front of the wave by an amount proportional to the distance traveled. This is equivalent to postulating a velocity for each point on the wave which is a function of voltage alone. It has already been shown that this relation holds for the Tidd test data.[1] Fig. 17 shows that this same concept applies for the digitally calculated voltage waves.

Fig. 17 shows that above corona the time required for a given level of voltage to propagate a specified distance along the line is greater than the propagation time for a level below corona by a factor of $\sqrt{2}$. Doubling the slope of the *q-e* curve results in a velocity which was decreased by $\sqrt{2}$. This suggests the possibility of rewriting equation 1 in the following manner

$$v=\sqrt{\frac{1}{L(C+\Delta C)}}=v_L\sqrt{\frac{1}{1+\frac{\Delta C}{C}}} \qquad (3)$$

where v_L is the velocity of light and $C+\Delta C$ is the slope of the *q-e* curve at any point as distinguished from the slope of the straight-line approximation that has been postulated in the analytical considerations to this point. It is shown in Appendix II that equation 3 is indeed rigorously correct under the following conditions

$$\frac{\partial e}{\partial t}\geq 0 \qquad (4)$$

$$\frac{\partial e}{\partial x}\geq 0 \qquad (5)$$

$$\frac{dq}{de}\geq 0 \qquad (6)$$

$$\frac{d^2q}{de^2}\geq 0 \qquad (7)$$

Equations 4 and 5 indicate that the velocity concept expressed in equation 3 is applicable only for the front of the voltage wave and not for the tail where the voltage is dropping. Equation 6 imposes this same limitation that the velocity concept does not hold for the tail of the wave. Equation 7 imposes the limitation that the slope of the *q-e* curve must not decrease at any point with increasing voltage, i.e., the curve must not have a point of inflection. This last limitation is necessary to prevent the mathematical occurrence of multivalued voltage waves as a function of time or distance.

Fortunately the laboratory data in Fig. 11 and the test data in Figs. 4 and 5 indicate that equation 7 is satisfied for practical transmission conductors and practical configurations. The velocity concept in equation 3 can then be applied to predict the distortion of the front of a voltage wave traveling on a conductor whose corona characteristics are known.

Distortion of Voltage Waves From Q-E Curves

In Fig. 18(A) the fundamental *q-e* curve characterizing the conductor is shown. The slope of this curve is given by the $C+\Delta C$ curve. The $C+\Delta C$ curve in turn permits the determination of the velocity characteristics from equation 3.

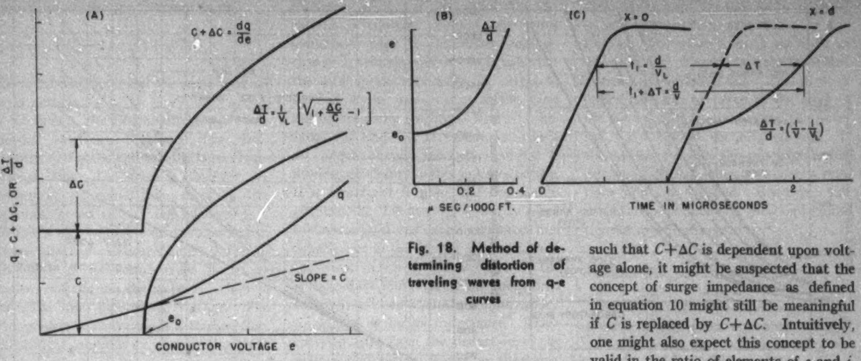

Fig. 18. Method of determining distortion of traveling waves from q-e curves

Now turning to Fig. 18(C) an arbitrary volt-time curve is shown which is applied at $x=0$. Assuming that the traveling wave has moved a distance d, the undistorted portion of the wave below the corona threshold voltage e_0 requires a time $t_1=d/v_L$ to travel this distance. A point on the voltage wave above e_0 will require the time $t_1+\Delta T$. This total time is related to the instantaneous velocity corresponding to the particular point on the voltage wave by the relation

$$t_1+\Delta T=\frac{d}{v} \tag{8}$$

Substituting the value for v from equation 3, there results

$$t_1+\Delta T=\frac{d}{v_L}\sqrt{1+\frac{\Delta C}{C}}$$

or

$$\Delta T=\frac{d}{v_L}\sqrt{1+\frac{\Delta C}{C}}-t_1=\left(\sqrt{1+\frac{\Delta C}{C}}-1\right)\frac{d}{v_L}$$

or

$$\frac{\Delta T}{d}=\frac{1}{v_L}\left(\sqrt{1+\frac{\Delta C}{C}}-1\right) \tag{9}$$

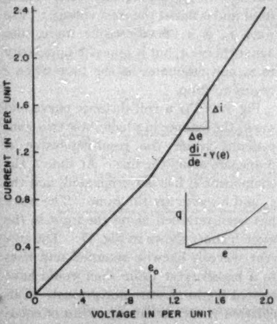

Fig. 19 (left). Current-voltage relations from digital computer calculations shown in Fig. 17

The curve for $\Delta T/d$ is plotted in Fig. 18(A). For convenience this curve is replotted in Fig. 18(B). To determine the retardation ΔT for any voltage it is merely necessary to multiply the value in Fig. 18(B) by the distance traveled. This provides the curve shown in Fig. 18(C) for $x=d$. Thus a method is available for determining the distortion of a wave traveling on a line whose q-e characteristic is known.

VOLTAGE-CURRENT RELATIONS

Once the distortion of the voltage wave has been determined, it is important to know the distortion of the associated current wave. It is well known that, for a line with uniformly distributed inductance and capacitance that does not change with voltage, there exists a constant ratio of voltage to current associated with a particular wave

$$Z=\frac{e}{i}=\sqrt{\frac{L}{C}} \tag{10}$$

where Z is the surge impedance.

If the capacitance varies in a manner such that $C+\Delta C$ is dependent upon voltage alone, it might be suspected that the concept of surge impedance as defined in equation 10 might still be meaningful if C is replaced by $C+\Delta C$. Intuitively, one might also expect this concept to be valid in the ratio of elements of e and i, i.e.

$$\frac{di}{de}=\frac{1}{z}=\frac{1}{Z}\sqrt{1+\frac{\Delta C}{C}} \tag{11}$$

It is shown in Appendix III that equation 11 is rigorously correct within the same limits which were imposed upon equation 3. Integration of equation 11 with respect to e yields

$$i=\frac{1}{Z}\int_0^e\sqrt{1+\frac{\Delta C}{C}}\,de \tag{12}$$

It is interesting to apply equations 11 and 12 to the digital computer results shown in Fig. 17. Analysis of the current waves in Fig. 17 shows that above the corona level the rate of current rise is greater than that below the corona level by a factor of $\sqrt{2}$. The current in Fig. 17 has been plotted against voltage, and the results are shown in Fig. 19. The curve in Fig. 19 applies for any combination of voltage and distance co-ordinates for the assumed q-e variation. The current is dependent upon the voltage alone.

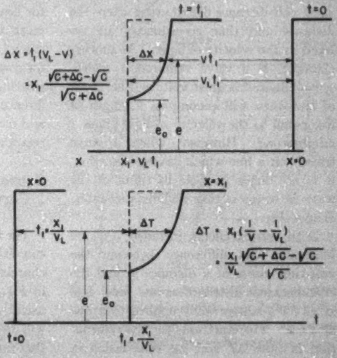
t = t_1
t = 0
$\Delta X=t_1(V_L-V)$
$=X_1\frac{\sqrt{C+\Delta C}-\sqrt{C}}{\sqrt{C+\Delta C}}$
ΔX
Vt_1
V_Lt_1
e_0
e
X
$X_1=V_Lt_1$
X = 0
X = 0
X = X_1
$t_1=\frac{X_1}{V_L}$
ΔT
$\Delta T=X_1\left(\frac{1}{V}-\frac{1}{V_L}\right)$
$=\frac{X_1}{V_L}\frac{\sqrt{C+\Delta C}-\sqrt{C}}{\sqrt{C}}$
e
e_0
t
t = 0
$t_1=\frac{X_1}{V_L}$

Fig. 20 (right). Illustration of difference between volt-time and volt-distance curves

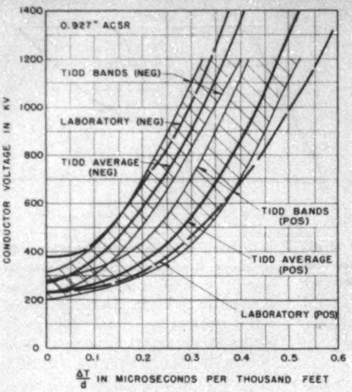

Fig. 21. Comparison of retardation curves obtained in the field with similar curves computed from laboratory data

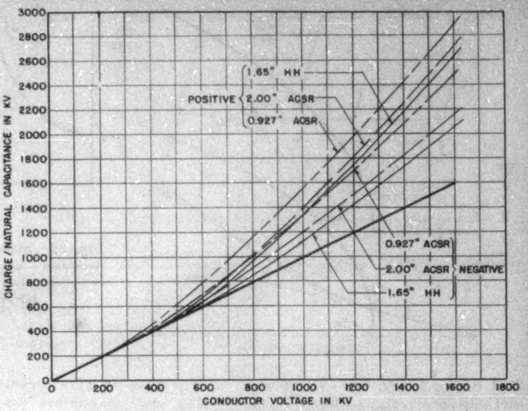

Fig. 22. Retardation curves of Fig. 4 converted to q-e curves

The slope of the current-voltage curve above corona is greater than the slope below corona by $\sqrt{2}$. This checks with equation 11 since $1+\Delta C/C=2$. It is apparent then that the use of equation 11 or 12 and the volt-time curves shown in Fig. 17 makes possible the calculation of the associated current waves. This applies generally to any q-e relation. Having found the voltage distortion of a traveling wave the corresponding current can be obtained through the application of equation 12.

Difference Between Volt-Time Curve and Volt-Distance Distribution

It is customary to think of a traveling wave as being a function of time or distance interchangeably. For example, a volt-time curve will result in exactly the same volt-distance distribution where the distance and time co-ordinates are related by the velocity of light. As another example, if a wave required 1 microsecond to reach crest voltage, the front of the wave will encompass a length of line equal to the velocity of light times 1 microsecond. However, when a wave travels on a line which causes distortion, it is no longer possible to think of the wave in terms of time and distance interchangeably.

With corona effects included, Fig. 20 illustrates the difference between the volt-time curve at a distance x_1 and the volt-distance distribution at time $t_1=x_1/v_L$ for a square wave applied to a line at $x=0$. The equations for the retardation in time ΔT and the retardation in distance Δx are shown in the figure. These equations make it clear that ΔT and Δx are no longer related by a constant but are related by the variable $\Delta C/C$. Extreme care must be used in relating the volt-time curve and the volt-distance distribution.

Correlation of Laboratory and Field Data

Fig. 4 shows the $\Delta T/d$ curves obtained during the Tidd tests for the 0.927-inch steel-reinforced aluminum-cable conductor for both polarities. These curves have been replotted in Fig. 21. The total variance[1] is indicated by the shaded areas. Fig. 11 shows the q-e curves obtained in the laboratory for the same conductor. By methods that have just been presented, the front portions of the curves for both polarities having the maximum crest voltage were converted to $\Delta T/d$ curves. These are also plotted in Fig. 21 for comparison with the field data. Considering the vagaries of corona and the difference between field and laboratory setup and measurements, it is felt that the correlation is quite satisfactory.

Conversion of Field Data to q-e Curves

The field data shown in Fig. 4 have been converted to the more fundamental q-e characteristic, and the results are shown in Fig. 22. This form of the data is less useful than the retardation curves, but will be quite helpful to those doing further fundamental work on this subject.

Effect of Corona on Tail of Voltage Wave

The preceding discussions explain the distortion of the front of a traveling wave in terms of theoretical considerations and fundamental corona characteristics obtained in the laboratory. If the wave is flat at its crest voltage, the distortion of this flat tail can also be determined. No mention has been made of distortion accompanying a wave tail which decreases with time.

Fig. 23 is included to provide an understanding of the effects present on the tail of the wave. A transmission line is assumed to have the q-e characteristic shown in (A). The volt-time curve e shown by the solid lines in (B) is applied to the line at $x=0$. The crest voltage of e is $2e_0$. Consider the wave to be resolved into two components. The component e_p is a wave which consists of the linearly rising front and is flat at the crest voltage. The wave e_n is a linearly rising wave, also flat at the crest, but is opposite in polarity to e_p and originates at the time when e begins to drop.

Fig. 23(C) is a volt-distance curve and shows the manner in which these two components, hence the resulting wave e, propagate along the line. At time t_1 the component e_n has not originated, and the e_p and e waves are the same. The wave has been retarded along the front in the same manner shown in Fig. 17. The current wave is likewise retarded and rises to a higher crest value than would have existed if corona were not present. Calculation of the current by means of equation 12 shows the crest current to be

$$i_p\text{ (crest)}=i\text{(crest)}=\frac{e_0}{Z}(1+\sqrt{2})$$

Crest current occurs at the same time as crest voltage.

At time t_2, the entire voltage wave has moved out onto the line. The component e_p is subjected to additional retardation along the front. However, e_n originates at some time after e_p has reached its flat crest. The effect of e_n is to lower the voltage e on the conductor, hence the capacitance effective for e_n is the slope C, the return trace of the q-e curve, rather than the slope $2C$ which is effective for increasing voltage. The component e_n then travels with the velocity of light, and has an associated current

$$i_n=\frac{e_n}{Z}$$

and a crest value

$$i_n\text{ (crest)}=-\frac{2e_0}{Z}$$

It will be seen that adding currents i_p and i_n results in a current which does not drop to zero along the tail but drops linearly to the constant value.

$$i_s=\frac{e_0}{Z}(\sqrt{2}-1)$$

This current exists all along the line from the origin to the point just behind the tail of the wave e. It should be noted that the voltage along this section of the line is zero. At a later time t_3 it is apparent that this same current i_s exists from the origin to the tail of e at its new position.

A current existing along the line without an associated voltage may seem contradictory until it is recognized that the current is constant through the series inductance back to the source, and no change in voltage results. It is true that the total inductance from the origin to the tail of the wave varies as the wave tail moves along the line. However, because the elements of inductance which are added already have the current i_s flowing, no change in flux linkages occurs. It is important to note that the energy put into the line at $x=0$ is exactly equal to the energy stored in the inductance and capacitance in the line for all positions of the wave shown in Fig. 23(C). As the voltage wave moves along the line, stored energy is left behind in the corona capacitor ΔC and in the line inductance. These energies arise from the distortion of the voltage and current waves as they progress along the line.

Up to the time t_3 the retarded front of e_p has not overlapped e_n. When this overlap occurs, the resolution suggested earlier is no longer valid. A portion of the component e_n tends to travel into a region of e_p where the conductor voltage is actually rising. Hence, a portion of e_n tends to travel in a region where the surge impedance is determined by the slope $2C$ of the q-e curve, and the remainder, in a region where C determines the surge impedance. A complex form of continuous reflections probably occurs in the overlapping region, and the authors have not yet been able to reach an analytical solution to this problem. This is a fruitful area for further investigation.

The field tests shown in Figs. 1 and 2 do provide an evaluation of the effect of overlapping of the tail and the retarded front. If the tail is relatively long compared to the front, the tail can be assumed to propagate without retardation or distortion. The wave front is set back as shown in Fig. 3 until the retarded front intersects the original tail. This point of intersection can be taken as the crest of the distorted wave, and beyond this point the wave follows the original tail. It should be noted that this procedure is not rigorously correct, since the energy relations are not satisfied. However, this procedure is a sufficiently good approximation for most purposes.

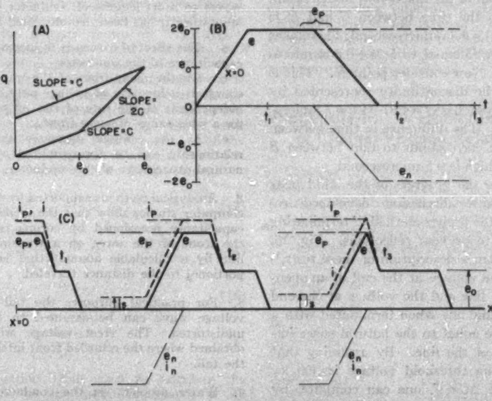

Fig. 23. Illustration of corona effects on the tail of a voltage wave

Reflections

At first thought one would expect that a wave in the corona region on reaching an open-ended line would double, because the abrupt change at this point is from the surge impedance of the line (whatever it might be) to an infinitely large impedance. Actually this does not occur. A similar modification must be made in the theory when the line is terminated by a resistance equal to its natural surge impedance.

To analyze these conditions considera-

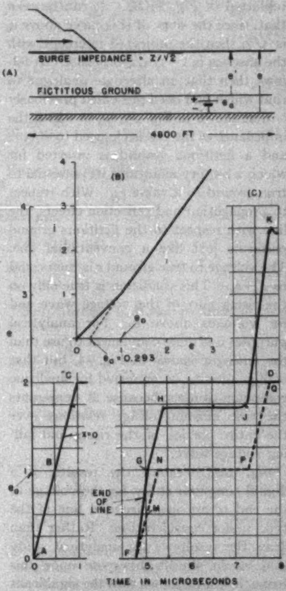

Fig. 24. Comparison of digital computer calculations and analytical calculations of the voltage appearing at the end of an open-circuited line under corona

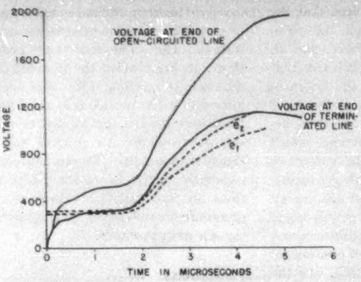

Fig. 25. Voltages measured at the end of an open-circuited line and a line terminated by its natural surge impedance together with a computed comparison between them

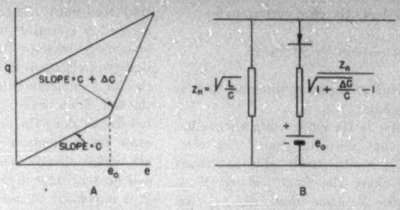
q
SLOPE = C + ΔC
SLOPE = C
e_0
e
A
$Z_n = \sqrt{\frac{L}{C}}$
$\frac{Z_n}{\sqrt{1+\frac{\Delta C}{C}}-1}$
+
−
e_0
B

Fig. 26 (above). Analogue for a reflectionless termination (B) for a line having the q-e relationship shown in (A)

tion must be given to the current-voltage relations at the point of reflection. The essential features of the phenomenon will be brought out by considering the special type of line that had previously been discussed in connection with the digital computer studies, a line in which $\Delta C = C$. The current-voltage relationship for this line is plotted in Fig. 19. This curve is replotted in Fig. 24(B). It can be seen that, since the slope of this curve above e_0 is $\sqrt{2}$, then the projected intercept with the abscissa is $1-1/\sqrt{2}$ or 0.293. It follows then that an alternate analogue to that which had been presented previously is that shown in Fig. 24(A), in which the impedance of the line is changed to $Z/\sqrt{2}$ and a fictitious ground is inserted for which a battery maintains its potential to true ground to a value e_a. With respect to propagation and reflection effects, the line with respect to the fictitious ground performs just like a conventional line. The voltage to true ground e is then equal to $e'+e_a$. This condition is true only on the rising part of the voltage wave and for voltages above e_0. For analytical purposes it is more convenient to use than the analogue shown in Fig. 14, but that of Fig. 14 is to be preferred for analogue computer studies because it represents the true current-voltage relations over the entire portion of the rising and falling voltage wave.

Fig. 24(C) shows the results of a digital computer study for the voltage at the end of an open-circuited line of the type under consideration. Rather than draw the results of an analytical study that would almost superpose upon this curve, it will be shown how the significant points of this curve can be computed. The line was 4,800 feet long and the constants were adjusted so that below corona the velocity of propagation was exactly 1,000 feet per microsecond. The voltage *OBCD* was applied at $x=0$. As the wave travels along the line two levels of voltage develop, that of $e_0=1$ and at a later time the value $e=2.0$. As the first level reaches the end of the line only the component $e'=1-0.293=0.707$ doubles. The reflected voltage to true ground is then (2) $(0.707)+0.293=1.707$. This checks the level of *HJ*. Similarly when the flat portion *CD* reaches the end, the part that reflects is $2-0.293=1.707$. Again the voltage to true ground is (2) $(1.707)+0.293=3.707$, which also checks exactly.

The curve *FNPQ* is the form that the original wave would have had at $x=4{,}800$ feet had the line been continuous. Point *F* is at 4.8 microseconds. Because of the doubling effect below e_0 point *G* occurs at time corresponding to *M* and is $4.8+0.25=5.05$ microseconds. That portion of the curve between *MN* will be delayed because all of the line is now above e_0 and therefore the time between *G* and *H* is $\sqrt{2}(0.25)=0.354$ microsecond. This makes the point *H* equal to $5.05+0.354$ microsecond. Now consider point *K*. This is simply the discontinuity represented by point *C*, which is $\sqrt{2}(4.8)+1.0=7.8$ microseconds. The difference in time between *J* and *K* corresponds to that between *B* and *C* which is 0.5 microsecond.

During the progress of the Tidd tests considerable discussion developed regarding the proper method of terminating the line to prevent reflections. Fig. 25, taken from a description of these tests,[11] shows the voltage at the end of an open-circuited line and the voltage at the end of the same line when terminated with a resistance equal to the natural surge impedance of the line. By assuming that the corona threshold voltage is 300 kv and that $\Delta C = C$, one can compute, by methods just described, the volt-time curve of the wave approaching the end of the line if there were no reflection. This is the dashed curve e_f. When the line is terminated by a resistance equal to the natural surge impedance, the voltage at the end of the line e_s is

$$e_s = \frac{2R}{R+Z}(e_f-300)+300$$

$$= \frac{2}{1.707}(e_f-300)+300$$

This curve likewise is indicated in Fig. 25. Considering the crude approximations made, the agreement is quite close. This illustrates that under corona conditions the natural surge termination is not quite correct.

Fig. 26(B) shows the correct reflectionless termination for a line having the *q-e* characteristic shown in Fig. 26(A). This relationship is developed in Appendix IV. This termination will also be useful in analogue computer studies to represent an infinitely long line, but is rigorously correct only for the rising portion of the wave.

Conclusions

1. As a result of the application of impulse waves to short lengths of conductor in the laboratory it has been demonstrated that:

a. The effect of corona is to increase the capacitance of the conductor.

b. On the rising front of the wave, the charge is a function of voltage only and is independent of the rate of rise of voltage for a wide range of surge fronts.

c. As the voltage decreases the *q-e* relationship can be approximated by the natural capacitance of the conductor.

2. Analytical methods supported by digital computer studies show that the increase in capacitance occasioned by corona retards the front of the wave on a transmission line by a calculable amount that is proportional to the distance traveled.

3. For practical purposes the tail of a voltage wave can be assumed to travel undistorted. The crest voltage will be obtained where the retarded front intersects the tail.

4. Water droplets on the conductor do not affect its *q-e* characteristics, which

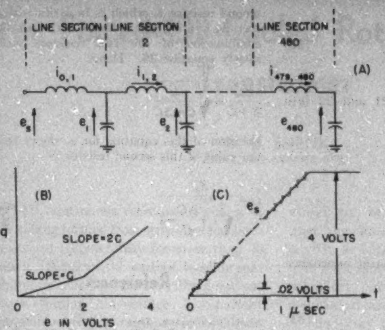

Fig. 27 (left). Elements of a transmission line under corona used in the digital computer studies

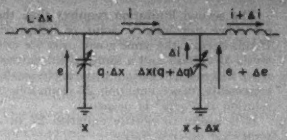

Fig. 28 (right). Schematic diagram of an element of a transmission line under corona

verifies the field tests that rain does not influence the effect of corona in distorting traveling waves.

5. Various types of analogues to represent the effect of corona have been presented. These are:

a. A device to represent the increase in capacitance which is inserted in the incremental length of conductors.

b. A combination of resistors, a battery, and a rectifier to represent a reflectionless infinitely long line.

c. A somewhat simplified adaptation of (b) consisting of a single resistor and battery that can be used for analytical work only above the corona threshold voltage.

Appendix I. Digital Computer Analysis

The transmission-line representation shown in Fig. 27(A) consists of 480 line sections, each section representing 10 feet of line. The q-e characteristic of the capacitors is shown in (B). The constants were selected so the velocity of propagation is 1,000 feet per microsecond and $Z=400$ ohms. The triangular-front wave applied at the sending end is approximated in the stepwise manner shown in Fig. 27(C). Each voltage step is 0.02 volt high; 200 steps are required to represent the wave front. The crest of the applied wave is 4 volts which is twice the corona voltage. Equations 13 through 16 are used to determine the voltages and currents for each line section, where N is the number of the particular line section of concern and ΔC is the capacitance increase due to corona.

$$\Delta i_{N-1,N}=\frac{1}{2}\,\frac{e_{N-1}-e_N}{L}\,\Delta t \tag{13}$$

$$\Delta i_{N-1,N}=\frac{e_{N-1}-e_N}{L}\,\Delta t \tag{14}$$

$$\Delta e_N=\frac{i_{N-1,N}-i_{N,N+1}}{C}\,\Delta t \tag{15}$$

$$\Delta e_N=\frac{i_{N-1,N}-i_{N,N+1}}{C+\Delta C}\,\Delta t \tag{16}$$

Equation 13 is used to calculate the current in the series inductance if all preceding current increments in the section were zero. Once a nonzero current change has been obtained for the line section, equation 14 is used for all subsequent current calculations. With equations 15 and 16 the voltage at the capacitor of each line section is calculated. Equation 15 is used below corona and equation 16 above corona. The time interval chosen was 0.005 microsecond and the computer printed voltage and current every 0.05 microsecond for line sections 0, 40, 80, 120, etc.

The first time interval calculation consists of raising e_s to the value of the first voltage step and determining the incremental current change in every line section using equation 13. Only line section 1 will contain current since $e_1, e_2, \ldots e_{480}$ will remain at zero potential. From these line currents the voltage changes are calculated using equation 15.

The incremental currents in the next interval are obtained by raising e_s to the second voltage step and assuming all other line voltages remain at the values calculated in the first interval. These incremental currents are added to the previous currents to obtain the currents in the second interval. From these currents the second interval voltage increments are determined. These increments are added to the voltages of the preceding interval to obtain the voltages in the second interval. This procedure continues until e_s reaches the crest of the wave; for subsequent intervals e_s is kept constant at crest voltage.

Appendix II. Velocity in Terms of Charge-Voltage Relation

Consider an elemental length of transmission line shown in Fig. 28 with uniformly distributed inductance, and shunt capacitance which varies with voltage alone. The differential equations relating current and voltage can be readily written

$$\Delta e=-L\frac{\partial i}{\partial t}\,\Delta x$$

$$\frac{\partial e}{\partial x}=-L\frac{\partial i}{\partial t} \tag{17}$$

$$\Delta i=-\frac{\partial q}{\partial t}\,\Delta x$$

or

$$\frac{\partial i}{\partial x}=-\frac{\partial q}{\partial t}=-\frac{dq}{de}\,\frac{\partial e}{\partial t} \tag{18}$$

where $q=q(e)$. Differentiating equation 17 with respect to x, equation 18 with respect to t, and eliminating the term $(\partial^2 i)/(\partial x\partial t)$

$$\frac{\partial^2 e}{\partial x^2}=L\,\frac{dq}{de}\,\frac{\partial^2 e}{\partial t^2}+L\,\frac{d^2q}{de^2}\left(\frac{\partial e}{\partial t}\right)^2 \tag{19}$$

Assume as a trial solution to equation 19

$$e=f(x-vt) \tag{20}$$

where $v=v(e)$, $x-vt\equiv u$. The first and second partial derivatives of equation 20, when substituted into equation 19, must yield an identity if equation 20 is a solution to the differential equation. Performing these operations yields

$$\left[\frac{d^2f}{du^2}-\left(\frac{df}{du}\right)^2 t\,\frac{d^2v}{de^2}\right]\equiv L\,\frac{dq}{de}\,v^2\times$$
$$\left[\frac{d^2f}{du^2}-\left(\frac{df}{du}\right)^2 t\,\frac{d^2v}{de^2}\right]+\left(\frac{df}{du}\right)^2\times$$
$$\left(1+t\,\frac{df}{du}\,\frac{dv}{de}\right)\left(2L\frac{dq}{de}\,v\,\frac{dv}{de}+L\frac{d^2q}{de^2}\,v^2\right) \tag{21}$$

For equation 21 to be an identity

$$L\,\frac{dq}{de}\equiv\frac{1}{v^2} \tag{22}$$

$$2L\frac{dq}{de}\,v\,\frac{dv}{de}+L\,\frac{d^2q}{de^2}v^2\equiv 0 \tag{23}$$

From equation 22

$$\frac{dq}{de}=\frac{1}{Lv^2} \tag{24}$$

Differentiating

$$\frac{d^2q}{de^2}=\frac{-2}{Lv^3}\,\frac{dv}{de} \tag{25}$$

Substituting equations 24 and 25 into 23 gives

$$2L\,\frac{1}{Lv^2}\,v\,\frac{dv}{de}+L\left(\frac{-2}{Lv^3}\,\frac{dv}{de}\right)v^2\equiv 0 \tag{26}$$

Equation 21 is an identity, and equation 20 is a solution of the differential equation 19 when

$$v=v(e)=\sqrt{\frac{1}{L\,\dfrac{dq}{de}}} \tag{27}$$

The foregoing equations are rigorously correct if $dq/de>0$ and $d^2q/de^2>0$. The first limitation is required to prevent v being imaginary. In passing from the rising to the falling portion of a q-e curve, it is necessary to pass through a region where dq/de is negative. The velocity concepts developed in this Appendix do not apply for the tail of the wave, i.e., where $\partial e/\partial t$ or $\partial e/\partial x$ is negative.

The second limitation requires that the *q-e* curve not have a point of inflection. If this occurs, the same v will exist for two levels of voltage and a multivalued voltage wave will result. Such a wave is physically impossible, hence equation 20 cannot be a solution if d^2q/de^2 is negative.

It is useful to rewrite equation 27 in a somewhat different form

$$v=\sqrt{\frac{1}{L(C+\Delta C)}}=\sqrt{\frac{1}{1+\frac{\Delta C}{C}}}\sqrt{\frac{1}{LC}}$$

$$=\frac{v_L}{\sqrt{1+\frac{\Delta C}{C}}} \tag{28}$$

where C is the natural capacitance below corona and

$$C+\Delta C=\frac{dq}{de}$$

Appendix III. Current-Voltage Relations

If a transmission line consists of uniformly distributed inductance L and constant capacitance C, the relation between voltage and current is known as the surge impedance

$$\frac{i}{e}=\frac{1}{Z}=\sqrt{\frac{C}{L}} \tag{29}$$

If the capacitance varies with voltage, let it be assumed that

$$\frac{di}{de}=Y$$

where

$$Y=Y(e) \tag{30}$$

Equation 30 will be tested to determine whether it satisfies equations 17 and 18.

If $q=q(e)$ and equation 20 is correct

$$\frac{\partial q}{\partial t}=\frac{dq}{de}\,\frac{df}{du}\,\frac{\partial u}{\partial t}=-\frac{\frac{dq}{de}\,\frac{df}{du}\,v}{1+t\,\frac{dv}{de}\,\frac{df}{du}} \tag{31}$$

$$\frac{\partial i}{\partial x}=\frac{di}{de}\,\frac{\partial e}{\partial x}=Y\,\frac{\frac{df}{du}}{1+t\,\frac{df}{du}\,\frac{dv}{de}} \tag{32}$$

Substituting equations 31 and 32 into 18 yields

$$Y=v\frac{dq}{de}=\sqrt{\frac{\frac{dq}{de}}{L}}$$

$$Z=\frac{1}{Y}=\sqrt{\frac{L}{C}}\sqrt{\frac{C}{C+\Delta C}}$$

Hence if Z_n represents the surge impedance below corona

$$\frac{di}{de}=\frac{1}{Z}=\frac{1}{Z_n}\sqrt{1+\frac{\Delta C}{C}} \tag{33}$$

Equation 33 provides a concept of surge impedance when the shunt capacitance varies. For a known *q-e* characteristic and known voltage wave, the current can be calculated analytically or graphically by

$$i=\frac{1}{Z_n}\int\sqrt{1+\frac{\Delta C}{C}}\,de \tag{34}$$

Again it should be emphasized that the foregoing relations are not valid for $dq/de<0$ or $d^2q/de^2<0$.

Appendix IV. Reflectionless Termination of a Line Under Corona

Assume a line has the *q-e* characteristic shown in Fig. 26. Below e_0 the surge impedance is

$$Z=\sqrt{\frac{L}{C}} \tag{35}$$

Above e_0 the surge impedance is

$$z=\sqrt{\frac{L}{C+\Delta C}} \tag{36}$$

Fig. 26 shows the reflectionless termination to consist of two resistors $Z\equiv Z_n$ and a second resistor z_c which is in series with a rectifier and battery. Above e_0 the parallel combination of the two resistors must satisfy equation 36. Hence

$$\frac{Zz_c}{Z+z_c}=\sqrt{\frac{L}{C+\Delta C}}$$

Solution of this equation for z_c shows that the value of this second resistor is

$$z_c=\frac{Z_n}{\sqrt{1+\frac{\Delta C}{C}}-1}$$

References

1. **High-Voltage Impulse Tests on Transmission Lines, C. F. Wagner, I. W. Gross, B. L. Lloyd.** *AIEE Transactions*, vol 73, pt. III-A, Apr. 1954, pp. 196–210.

2. *Discussion* by **E. W. Boehne.** *Ibid.*, vol. 50, June 1931, pp. 558–59.

3. **Surge Phenomena (book), Electrical Research Association.** The British Electrical and Allied Industries Research Association, London, England, 1941.

4. **Propagation of Surge Generator Waves Up to 850 Kv on a 132-Kv Line, M. Böckman, N. Hylten-Cavallius, S. Rusck.** *Paper No. 314*, CIGRE, Paris, France, 1950.

5. **Experimental Studies in the Propagation of Lightning Surges on Transmission Lines, O. Brune, J. R. Eaton.** *AIEE Transactions*, vol. 50, Sept. 1931, pp. 1132–38.

6. **Lightning Arresters as a Criterion for Insulation Levels, Harold L. Rorden.** *Ibid.*, vol. 69, pt. I, 1950, pp. 84–96.

7. **Distortion of Traveling Waves by Corona, H. H. Skilling, P. de K. Dykes.** *AIEE Transactions (Electrical Engineering)*, vol. 56, July 1937, pp. 850–57.

8. **Lightning Laboratory at Stillwater, New Jersey, R. N. Conwell, C. L. Fortescue.** *AIEE Transactions*, vol. 49, July 1930, pp. 872–76.

9. **Traveling Waves on Transmission Lines With Artificial Lightning, K. B. McEachron, J. G. Hemstreet, W. J. Rudge.** *General Electric Review*, Schenectady, N. Y., Apr. 1930, p. 254.

10. **Voltage Divider for Measuring Impulse Voltages on Transmission Lines, S. B. Griscom, B. L. Lloyd, A. R. Hileman.** *AIEE Transactions*, vol. 73, pt. III-A, Apr. 1954, pp. 228–37.

11. **Measuring Equipment and Techniques Used for High-Voltage Impulse Tests on Lines and Substations, J. W. Skooglund, W. H. Kolb, T. L. Dyer, Jr.** *Ibid.*, pp. 223–28.

The Forced-Oil-Cooled Rotary Welding Transformer

W. E. SHENK
ASSOCIATE MEMBER AIEE

THE continuous resistance welding of tubing formed from strip steel has been practiced commercially for more than 50 years. Some of the earliest welding machines for this purpose used direct current from special low-voltage high-current generators. This method is still employed, the most notable example in this district being the Youngstown Sheet & Tube Company's 26-inch pipe mill. Later, alternating current supplied by stationary transformers came into prominence and is still used in some of the older installations. The Republic Steel Corporation has a large pipe mill in Youngstown using a stationary welding transformer.

The use of either a d-c generator or a stationary transformer involves the same problem of transmitting the heavy current through brushes or other types of sliding contacts into the rotating welding electrodes. Even in the most carefully designed circuitry, the voltage drop and losses from the power supply to the electrodes represent a substantial, even predominant portion of that available at the generator or transformer. In the alternating case, the power factor is also very poor because of the unavoidably high reactance of the secondary leads. Furthermore, the sliding contacts present a very serious maintenance problem.

These shortcomings as well as the tremendous cost and size of such equipment led to a search for a better solution to the problem. About 1918, the American Transformer Company had an order to build a welding transformer. Thomas M. Hunter of that company came to the conclusion that a rotating transformer could be built to handle the welding current required, thus eliminating the need for sliding contacts to carry the heavy current to the electrodes. The first practical rotary welding transformer was the result, and a U. S. patent[1] was granted to Hunter and Snodgrass in 1923 covering this device.

The Hunter-Snodgrass transformer was successful, but, after a period of use, various modifications were seen to be desirable to improve its usefulness in the application. It was very soon evident, for example, that this air-cooled design would not be suitable for larger units since the dimensions of the transformer have to be kept to a minimum. The next unit built embodied water-cooling of the secondary conductors and a more rigid mechanical structure.

The rotary welding transformer has no sliding contacts carrying the heavy welding current. The electrodes, circular in shape, are mounted directly on the terminals of the transformer secondary in such a manner that an adequate low-impedance contact can be made. The relatively small current from the power line is conducted into the primary through brushes sliding on collector rings. Primary voltage is commonly varied to adjust welding current by means of a variable autotransformer or an ignitron contactor with phase shift control, or a combination of these methods. This is a compact and efficient welding current supply.

The early rotary transformers were either air-cooled in the very small ratings or water-cooled in the larger sizes since compactness of design is a very important factor. Practical transformers[2] of this type were built in the water-cooled design in ratings from 35 to 2,700 kva and corresponding welding current ratings from about 14,000 to 180,000 amperes, mostly for use at 60 cycles. By 1941, the possibilities of improvement in the water-cooled design had been about exhausted and welding at higher than power line frequency was becoming important. The use of these higher frequencies made it desirable to provide more effective cooling of the primary winding and also to reduce the space between primary and secondary windings in order to reduce leakage reactance.

In the water-cooled transformer, heat developed in the primary must be radiated or transmitted by conduction through the high-voltage primary insulation to the water-cooled secondary. (The use of water cooled hollow conductors in the primary is not practical since it leads to larger primary conductor space for a given rating.) Furthermore, difficulty had been experienced occasionally from the insulation becoming wet due to condensation or actual water leaks. These factors led to the consideration of an insulating cooling fluid. The possibility of using forced air or other gases for cooling was considered, but leakage reactance and compactness requirements could not be met. Therefore, forced cooling by oil or askarel appeared to be the only satisfactory means that would permit primary conductors to be cooled by direct contact with the coolant.

The first rotary transformers[3] of the forced-oil-cooled type were designed by Hunter and the writer in 1946 and put into service in 1947–48 at the Youngstown Sheet & Tube Company, the National Tube Company and the Michigan Steel Tube Products Company. These transformers, six in number, have operated practically continuously ever since.

Electrical and Mechanical Requirements

The rotary welding transformer is the heart of the electric weld tube mill. A typical mill for the production of welded steel mechanical tubing and the smaller pipe sizes is shown in Fig. 1. The large circular electrodes of the transformer can be seen in the welder section approximately at the middle of the mill. In this mill, steel strip is formed into tubular shape, welded, sized, and cut to length continuously.

The welder section of a pipe mill is shown in Fig. 2. This mill is designed for the production of 4.5- to 12-inch standard pipe. The transformer is capable of delivering 125,000 amperes continuously to the 48-inch-diameter electrodes and into the welding load.

The transformer for such a welder must meet certain electrical and mechanical requirements, and must be capable of delivering sufficient current to weld the range of wall thicknesses and tube sizes that it is practical to make in a single size of mill and in sufficient magnitude to weld at the required speeds. It must be capable of delivering this current continuously. The impedance must be as low as possible within the size limitations imposed by practical mill design. The impedance through the transformer to

---

Paper 55-523, recommended by the AIEE Transformers and Electric Welding Committees and approved by the AIEE Committee on Technical Operations for presentation at the AIEE Summer General Meeting, Swampscott, Mass., June 27–July 1, 1955. Manuscript submitted March 31, 1955; made available for printing June 1, 1955.

W. E. Shenk is with The McKay Machine Company, Youngstown, Ohio.

The author acknowledges the guidance and helpful advice of Thomas M. Hunter, of the American Transformer Company, Newark, N. J., who first conceived the rotary transformer, and who still strives for perfection in its development.

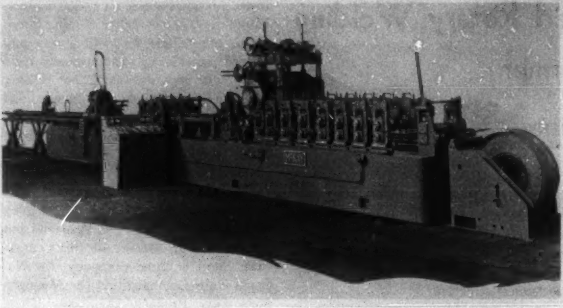

Fig. 1. Typical electrical weld tube mill. Size range 1/2- to 3-inch outside-diameter tube

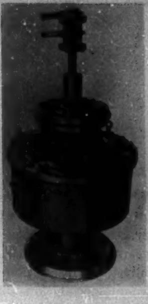

Fig. 3. 100-kva oil-cooled rotary transformer

any point on the periphery of the electrodes must be the same, so that welding current will not vary as the transformer and electrodes rotate. The design must provide for adequate cooling to all current-carrying parts and at the same time insure adequate protection against the moisture that is always prevalent around a tube mill.

The mechanical requirements practically dictate the proportions. Sufficient rigidity must be built into the throat and electrode structure to sustain the required welding pressure with negligible deflection of the electrodes. The relation of the weld line to the electrodes must be maintained, hence a thrust bearing must be mounted on the throat as close to the electrodes as possible so that thermal expansion of the parts will have a minimum effect. The diameter of the throat must be kept to a minimum so that the bearing and its housing will not be too large. Any excess here requires a corresponding increase in electrode diameter. The body diameter likewise must be kept to a minimum consistent with good electrical design.

These requirements necessarily lead to a compromise. The efficiency suffers if the transformer size is held down too much by mechanical considerations, while the welder becomes not only too large and expensive, if only electrical characteristics are considered, but it may also not be able to do its job as well. Furthermore, the very nature of the load, of which the electrodes must be considered a part, makes it useless to reduce the transformer impedance beyond a certain point. The nature of this compromise design will become apparent in the description of the oil-cooled rotary transformer.

Forced-Oil-Cooled Rotary Transformer

The standard ratings of the rotary transformer are shown in Table I. The kva ratings are output values and represent all of sizes built to date. Two larger transformers have been designed one for 200,000 amperes, 1,200 kva, and one for 300,000 amperes, 2,500 kva. The kva rating is somewhat flexible, particularly in the larger sizes. Since the copper losses are more than 90% of the total loss in all cases, the current rating dictates the size, and there is considerable latitude in the secondary voltage that may be obtained by juggling the primary copper and iron without changing external dimensions. The same basic transformer, for example, to deliver 125,000 amperes into a pipe with 1/2-inch wall would have approximately one-half the kva rating that it would need to deliver the same current into a pipe wih 1/4-inch wall. It would, of course, be capable of welding the lighter pipe at twice the speed. This design change would involve a change in the primary and core, and the frequency would also be raised to 120 or 180 cycles so that the weld would be continuous at the higher speed.

The first design[3] and that used now for ratings of 100 kva and lower is shown in Fig. 3 and depicted schematically in Fig. 4. It can be seen in Fig. 4 that the 1-turn secondary consists of two concentric copper castings and an annular copper plate. The entire transformer is built around a steel shaft for rigidity. The primary is wound on a toroidal core completely enclosed by the secondary. Thus the secondary forms the case as well as

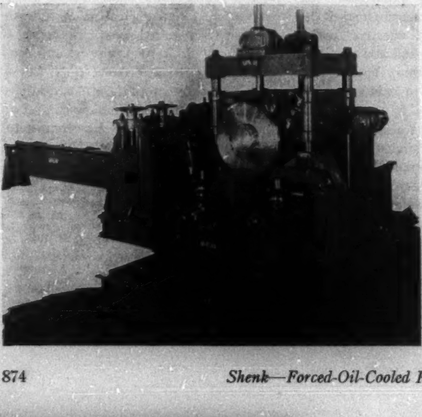

Fig. 2. Welder for pipe mill. Size range 4½- to 12-inch pipe

Table I. Ratings of Forced-Oil-Cooled Rotary Transformers Based on Full-Load Ratings at 30-Degree-Centigrade Oil Rise

Size, Kva	Frequency	Primary Volts	Secondary Volts at Electrodes	Secondary Amperes
50	60/180	440/480	2.3	21,800
75	60/180	440/480	2.5	30,000
100	60/180	440/480	2.8	35,800
150	60/180	440/480	3.1	48,300
200	60/180	440/480	3.2	57,000
300	60/180	440/480	4.0	75,000
500	60/180	440/480	4.0	125,000

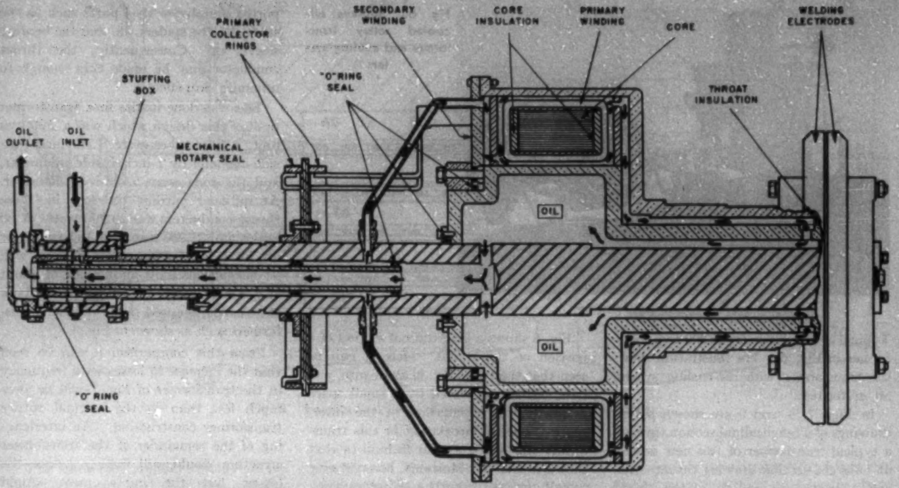

Fig. 4. McKay oil-cooled rotary welding transformer. Section showing oil circulation

the winding. This arrangement practically eliminates all stray fields except, of course, at the electrode and the primary leads.

The diagram clearly shows the oil circulation through the primary, throat, secondary, and out. All conductors carrying current are in direct contact with a rapid flow of oil. Many heat runs have shown that the hot-spot rise does not exceed 5 degrees centigrade over the oil rise, and the average primary copper rise is within 1.5 degrees centigrade over the oil rise.

The oil is pumped from a closed storage tank, Fig. 5, through a water-cooled heat exchanger and flow-meter to the transformer. The return is directly to the tank. The amount of cooling water used is regulated thermostatically and the system is provided with overtemperature and flow failure protection.

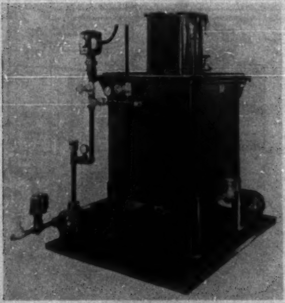

Fig. 5. Typical oil storage and cooling system

The electrodes are not cooled by the oil system. In service in the tube mill, water is continually poured on the electrodes to cool them.

The copper thickness in all parts of the secondary of this transformer is dictated principally by mechanical considerations, while the diameters of throat and bodies of secondary castings are dictated principally by electrical design. Skin effect causes the current to flow on the interior of the outer secondary and annular end plate and on the exterior of the inner secondary, so that the thickness required for mechanical strength in these parts is more than enough to accommodate the current.

Table II lists the depth of penetration in inches for copper for commonly used frequencies. If a transformer is, to be designed for 180 cycles, only about 1/4 inch of copper thickness is required or indeed is of any electrical use. At 60 cycles, 1/2 inch is more than enough. Consequently, the castings and the copper parts are made only enough thicker than these figures to give them sufficient mechanical stability and strength. It follows from these skin effect considerations, that only increasing the diameters of the secondary parts will increase the current-carrying capacity.

In this type of rotary transformer about 60% of the losses and also of the impedance is in the throat where the secondary circuit is constricted to pass through the bearing. To maintain this ratio in larger units, all dimensions would have to increase in proportion. This is not desirable or practical, consequently the efficiency of the larger units would be poorer than that of the smaller ones. This can be overcome by a change in design that reduces the throat impedance to a fraction of its value in the transformer of Figs. 3 and 4, and over-all efficiency in the large units can then be kept in line with that of the smaller ones. At the same time, a much stronger throat structure is obtained that is better able to support the welding pressures required of the large units. This structure[4] is used for ratings of 150 kva and larger.

Table II. Depth of Penetration, δ_T, Inches for Copper at Various Temperatures C

Frequency	δ_{20}	δ_{75}
50	0.367	0.403
60	0.336	0.368
100	0.260	0.285
120	0.237	0.260
150	0.212	0.233
180	0.194	0.211
300	0.150	0.165
360	0.137	0.150

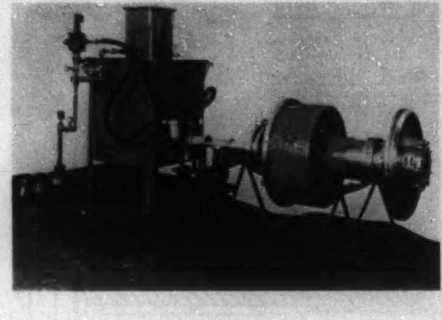

Fig. 6. **300-kva oil-cooled rotary transformer and cooling system**

Typical of this design is the 300-kva transformer in Fig. 6. The illustration shows the transformer with its cooling system set up for test.

In Figs. 7, 8, and 9 are shown patent drawings of a longitudinal section through a typical transformer of this new design, an enlarged section showing throat detail and a transverse section of the throat respectively.

Fig. 7 shows a schematic arrangement of the 500-kv transformer, the general appearance of which is quite similar to that of Fig. 4. The inner and outer secondary castings, 12 and 13 of the figure, however, do not have the tubular extensions forming the throat connection to the electrodes. Instead, the throat conductors consist of a number of concentric tubes and rods connecting the inner and outer secondary with the copper alloy supports for the welding electrodes.

Fig. 8 shows a longitudinal section of a portion of the throat. Here it can be seen that the tubes, 52, in the figure, and rods, 55, are separated by a small space permitting oil circulation in the interspace. The oil circulation in this transformer starts in a similar fashion to that shown in Fig. 4. However, after flowing radially inward from the primary cavity to the throat, the flow is divided among the 32 tubes of the throat. It flows in the interspace between tubes and rods to the cavity at the end of the rods. From this point the flow returns around the tubes to the inner secondary cavity.

In this type of throat construction the conductors are not required to carry mechanical loads. Instead the loads are supported mainly by steel parts such as the shaft, 10, the spiders, 48, and the bearing sleeve, 45. Consequently, the throat conductor may be made thin enough to minimize skin effect.

This was done in the first transformer built of this design which was a 500-kva unit. The tubes were 1.250-inch outside diameter by 1-inch inside diameter, and the rods were 0.750-inch diameter. At full-load current the loss in these throat conductors was 29,200 watts at 60 cycles and 31,300 watts at 180 cycles, or an increase of 7%. Test data as well as calculations show an increase of about 82% for the same frequencies in the type of construction used in the smaller transformers such as shown in Fig. 3.

From this comparison it can be seen that the increase in losses with frequency in the transformer of Fig. 7 will be very much less than in the original rotary transformer construction. An interleaving of the remainder of the transformer structure would still further reduce the losses, but the improvement would hardly warrant the complication and expense involved in the structure.

All rotary transformers are insulated with micarta where mechanical strength is needed as in the supports and clamps for the primary coil, core insulation, throat insulation, etc. In Figs. 7, 8, and 9 the heavily cross-hatched sections consist of solid insulation of this type.

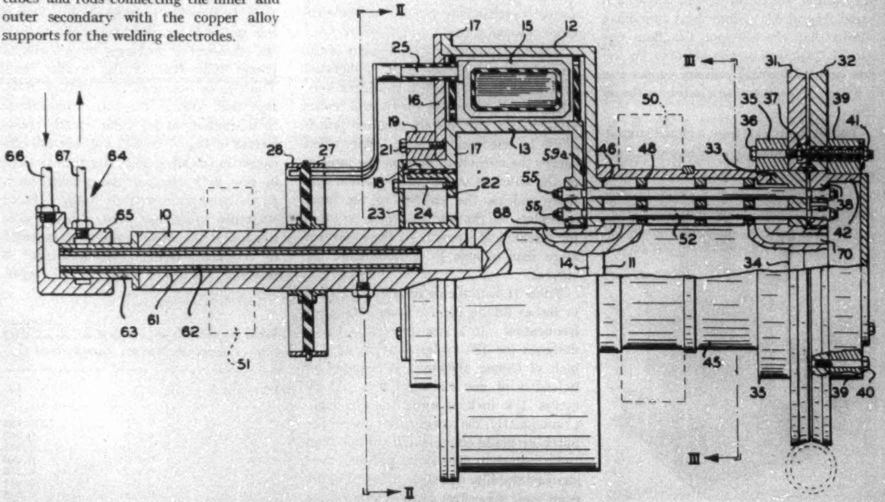

Fig. 7. **Patent drawing of 500-kva oil-cooled rotary transformer**

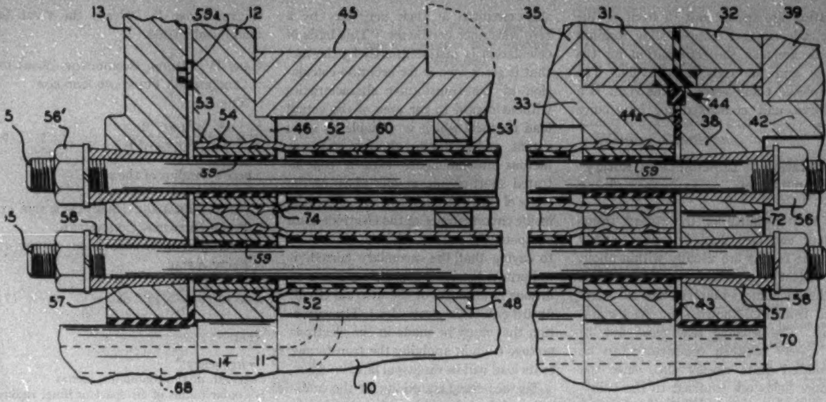

Fig. 8. Longitudinal detail of throat of 500-kva rotary transformer

The laminated primary conductors are taped with untreated glass tape and varnished after winding. Corrugated fiber similar to that used in small distribution transformer ducts is used as a barrier insulation between the outer secondary casting and the outside of the primary, and likewise between the inner secondary and the inside of the primary toroid. This insulation provides free passage for oil in contact with both primary and secondary while still acting as a barrier between them.

The creepage distances are made great enough and the insulation level is high enough to allow the transformer to take very safely a full-voltage high-potential test without oil, which is the regular test practice. Megger tests are made before the high-potential test to check dryness of the insulation and again afterwards. The transformer is then filled with hot-vacuum dried oil which is recirculated through a vacuum filter until a minimum of 28-kv oil test has been obtained. This procedure insures a dry and clean transformer. The insulation will perhaps seem more than is required, but since in operation much of this insulation must withstand continually changing stresses as well as acceleration, enough material has been used to ensure adequate strength for all operating conditions.

In Fig. 10 three transformers are shown in process of assembly. At the left, a 75-kva unit is ready to receive its primary coil and electrode assembly. In front of it on the floor is one-half of annealed core for a 500-kva transformer ready for insulation. To the right of the core a completed 300-kva primary assembly is shown.

At the center of the picture a 150-kv transformer has a few of the throat tubes and rods assembled to show their location. On the floor, throat tubes, rods, and in-

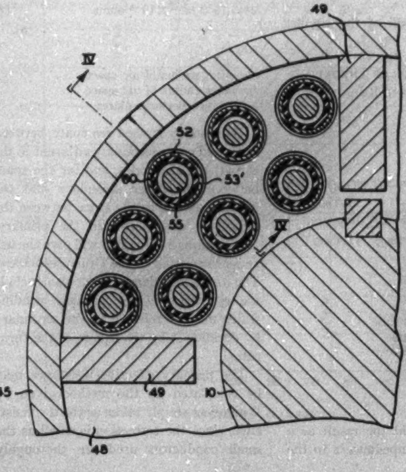

Fig. 9 (left). Transverse detail of throat of 500-kva transformer

Fig. 10 (below). Three rotary transformers in process of assembly

sulation are spread out in front of the electrode support, copper alloy forgings which are also the termination for the tubes and the rods respectively. The completed transformer at the right is a 300-kva unit connected for impedance tests.

Calculation of Impedance of Rotary Transformer

The impedance of the rotary transformer can be calculated quite closely and the results are usually within about 3% of test data. The internal impedance of the conductors involved can be calculated from well-known skin effect equations. The leakage reactances due to the spaces between conductors can be calculated quite closely also, since the leakage fields are confined to the transformer and are all circular in shape.

The general expression for the internal impedance of a flat thick plate or a cylinder of large ratio of diameter-to-wall thickness is

$$z=\frac{\rho l}{b\delta}(1+j)\coth\left(\frac{a}{\delta}+j\frac{a}{\delta}\right) \tag{1}$$

where

ρ = resistivity
l = length of the current path
b = width of the current path
δ = depth of penetration
a = thickness of conductor measured perpendicular to the direction of the current flow

In this expression $\coth\,[a/\delta+j(a/\delta)]$ approaches unity as the ratio a/δ increases.

$$\text{for } \frac{a}{\delta}=2,\ \coth\left(\frac{a}{\delta}+j\frac{a}{\delta}\right)=0.976+j0.027$$

$$\text{and for } \frac{a}{\delta}=3,\ \coth\left(\frac{a}{\delta}+j\frac{a}{\delta}\right)=1.0047+j0.00139$$

Since in all parts in the smaller transformer, Fig. 3, and all parts except the throat conductors in the larger ones, the depth of penetration is less than half of the conductor thickness, equation 1 reduces to

$$z=\rho l/b\delta(1+j) \tag{2}$$

Equation 2 can therefore be applied to the calculation of the internal impedance in all parts of the transformer secondary circuit except the subdivided throat conductors in the larger transformers. The internal impedance of these concentric tubes and rods can be calculated by well-known equations involving Bessel or Hankel functions.

In calculation of the transformer impedance, the electrodes are assumed to be short-circuited at their periphery by a zero resistance conductor. This basis of calculation is justified partly by the fact that it gives a basis for accurate calculation of the transformer characteristics without regard to the area of the actual load contact, which is variable to some extent, and partly by the fact that numerous measurements with a concentrated short-circuit at one place at the edges of the electrodes have shown that the inside circumference of the electrode is an equipotential surface. This is equivalent to saying that the secondary current is uniformly distributed under welding conditions in all parts of the internal circuit until it enters the electrodes. The correction that must be made in the electrode voltage drop in applying the transformer to its load will be discussed later.

The necessary equations for the calculation of the internal impedance and leakage reactance are as follows.

Case I. Axial Current Flow in Cylindrical Conductors

$$z=\frac{\rho l}{2\pi r\delta}(1+j) \tag{3}$$

where

ρ = resistivity, ohm-inches
l = length of cylinder
r = mean radius

$$\delta=3.15\sqrt{\frac{\rho\times10^{6}}{f}}=\text{depth of penetration}$$

Case II. Radial Current Flow in Circular Plates

$$z=\frac{\rho}{2\pi\delta}\ln\frac{r_2}{r_1}(1+j) \tag{4}$$

where r_2 and r_1 are radii of the circular plate.

Case III. Outer Tube of Throat Concentric Tube and Rod Conductors

$$\frac{z}{R_0}=-\frac{j^{3/2}mt(q+r)}{2q}\times\left\{\frac{J_0(mqj^{3/2})H_0^{(1)\prime}(mrj^{3/2})-H_0^{(1)}(mqj^{3/2})\times J_0'(mrj^{3/2})}{J_0'(mqj^{3/2})H_0^{(1)\prime}(mrj^{3/2})-H_0^{(1)\prime}\times(mqj^{3/2})J_0'(mrj^{3/2})}\right\} \tag{5}$$

where

r = outside radius of the tube
q = inside radius of the tube
$t=r-q$ = wall thickness

$$m=\sqrt{\frac{2}{\delta}}$$

Equation 5 will yield the result as a ratio of the internal impedance z to the d-c resistance R_0. Hence the z can be readily calculated.

Case IV. Inner Conductor (Rod) of Concentric Tube and Rod for Throat

$$\frac{z}{R_0}=\frac{mr}{2}j\frac{J_0(mr^{3/2})}{j^{3/2}J_0'(mrj^{3/2})} \tag{6}$$

where r = radius of the rod.

Case V. Leakage Reactance due to Field Between Concentric Cylindrical Conductors, Current Flow Axial

$$x=3.19fl\ \ln\frac{r_2}{r_1}\times10^{-8}\text{ ohms} \tag{7}$$

where

f = frequency
l = length of the conductor, inches
r_2 = outer radius of air space or inner radius of outer conductor
r_1 = inner radius of air space

This equation is used for the throat and for a portion of the leakage reactance due to the leakage flux between primary and secondary. In calculating the reactance between the cylindrical portion of the outer secondary and the primary, r_1 is taken as the radius of the winding. Likewise, in calculating the reactance due to the leakage between the inner secondary and the primary, r_2 is taken as the inner radius of the primary.

Case VI. Leakage Reactance due to Field Between Parallel Concentric Circular Plates, Current Flow Radial

$$x=3.19\,ft\ \ln\frac{r_2}{r_1}\times10^{-8}\text{ ohms} \tag{8}$$

where

r_2 = outer radius of air space
r_1 = inner radius of air space
t = distance between plates

Equation 8 is used for space between inner and outer secondary adjacent to the throat, the electrodes, and for the space between the outer secondary and the primary as well as the space between the secondary end plate and the primary.

Equations 3 through 8 will give the impedance referred to the 1-turn secondary. The total impedance must also include the resistance of the primary winding which may be referred to the secondary by dividing it by the square of the turns ratio.

The primary effective resistance may be calculated by the method given by Dwight[5] or simply taken as the d-c resistance, since the correction is small as the small conductors used are thoroughly

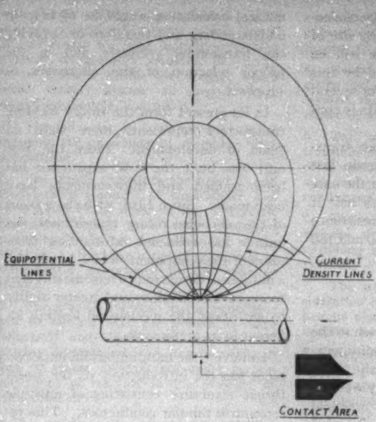

Fig. 11 (left). Possible distribution of current in tube welding electrode

Fig. 12 (below). Welding rate curves for low-carbon steel

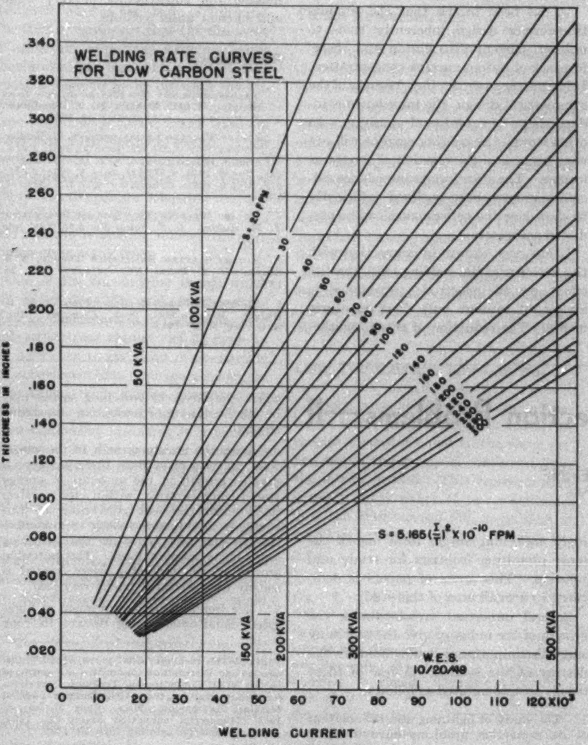

transposed. In any case the entire primary resistance is of the order of 10% of the total resistance for the transformer and the small error involved in using d-c resistance will hardly effect the end result.

Electrode Impedance Under Welding Conditions

The electrode impedance under actual welding conditions is extremely important, particularly in a large transformer. Properly, it should be considered a part of the load impedance since its value is influenced by the contact with the load, but whether it belongs to the load or the transformer it must be taken into account if a correct match is to be made between the power source and the welding load.

In Fig. 11, a representation of the possible current flow pattern in a typical electrode is shown. This does not attempt to represent the flow accurately. About all that can be said for it is the following:

1. The circle at the center of the electrode is an equipotential line.
2. The current converges to a small area at the bottom of the electrode where it contacts the tube.
3. Careful measurements with a very sensitive voltmeter made on a pair of short-circuited electrodes seem to show that for at least so far as the half radius, the equipotential lines are confocal ellipses.
4. The top of the electrodes is at the same potential as the center.
5. There is a difference in potential along the horizontal axis.

These observations are the justification for the figure.

Measurements made under welding conditions as well as simulated welding conditions indicate that the bulk of the voltage drop occurs within a few inches of the weld contact. Certainly at one-half the electrode radius from the weld contact this is true. There appear to be only two factors that can influence this impedance: 1. The spacing between the electrodes. 2. The length of the circumference that is contacted by the load.

Very little can be done about either factor. Electrode spacing is usually not over 1/4 inch and is frequently as little

Table III. Typical Power Loss in Welding Electrodes

Frequency	Current	Kw	Kilovars
60	21,800	1.76	2.60
180	21,800	2.70	7.70
60	200,000	148.00	220.00
180	200,000	228.00	648.00

as 1/16 inch, but this whole range has a relatively small effect on the reactance due to the large proportion of the total leakage field that is within the conductors. The length of the arc contacted can be varied from 1/4 inch for welding very small tubes to perhaps 4 inches on large pipe, but again this is not readily changed. According to much empirical information which is presented in chart form in Fig. 12, the same welding current is required for the same wall thickness regardless of tube diameter for the same speed of welding. Since, however, we may have a tube diameter range of perhaps three or four to one using the same wall thickness, the obtainable contact length being shorter for the small tube than the large, it follows that the electrode impedance may be considerably larger when the smaller tube is welded.

In effect, it is nearly true that the electrode impedance is a fixed number of ohms regardless of size or transformer rating. In the case of the 50- or 100-kva transformer this impedance is not very important, but in a 300- or 500-kva unit it is comparable to the transformer impedance. In the case of a transformer to deliver a welding current of 200,000 amperes or more, the electrode impedance becomes so important that it is hardly worth while to reduce the transformer impedance as far as might be wished because the size and hence the cost go up rapidly for a very small over-all gain.

Typical values of electrode impedance obtained from measurements made with an electrode short circuit simulating actual welding conditions are: $(3.7+j\,5.5)\times 10^{-6}$ ohm at 60 cycles, and $(5.7+j\,16.2)\times 10^{-6}$ ohm at 180 cycles.

These values are representative of electrodes that might be used on any size of transformer. Their significance will be clearer if the power represented by this impedance at 60 and 180 cycles for several typical full-load welding currents is considered, as shown in Table III.

In the case of the 21,800-ampere transformer, at 50 kva, this electrode loss amounts to 4% or 5%, while in the case of the 200,000-ampere 1,200-kva unit it amounts to about 12% to 19% resistance and 18% to 54% reactance for 60 and 180 cycles respectively.

Summary and Conclusions

The paper presents one approach to the problem of delivering large welding current to weld tubing continuously. The logical development of the rotary welding transformer from its earliest practical form to the modern forced-oil-cooled transformer has been outlined briefly.

It has been shown that the toroidal transformer design inherently leads to uniform current distribution and therefore lack of serious current concentration. It has also been shown that, because of the symmetrical design, the impedance is independent of rotational position. In other words, the welding current will not vary because of the rotation of the transformer. The transformer impedance calculations have been outlined sufficiently to show how the performance can be predicted accurately.

It has been shown, in connection with the problem of the welding load, that its effect on the electrode impedance is known at present only from measurements. The reduction of this to mathematical calculation would be of help in understanding and therefore in applying the transformer correctly and in the proper selection of the alternator to supply it.

In its present form the rotary welding transformer represents more than 35 years of development. Since the first unit was built the field experience has been studied and improvements have been made. Since 1946, with the advent of the oil-cooled rotary transformer, the author has collected information from users of the equipment, which has led to a number of design improvements directed to improved reliability and greater ability to withstand the mechanical loading inherent in its application.

However, the most important improvement was the introduction of the novel throat structure consisting of multiple concentric tubular conductors. This reduces the impedance substantially thus making the construction of very large and efficient units possible.

References

1. Transformer and Application of the Same to Heating, **T. M. Hunter, H. E. Snodgrass.** *U. S. Patent No. 1,478,262*, Dec. 18, 1923.

2. Rotary Welding Transformer, **T. M. Hunter.** *U. S. Patent Nos. 1,811,886*, June 30, 1931; *1,916,-218*, July 4 ,1933; *1,934,856*, Nov. 14, 1933; *1,979,-881*, Nov. 6, 1934; *1,979,882*, Nov. 6, 1934; *2,241,-015*, May 6, 1941; *Canadian Patent No. 399,117*, 1941.

3. Rotary Welding Transformer Structure, **T. M. Hunter.** *U. S. Patent No. 2,561,739*, July 24, 1951.

4. Rotary Electric Resistance Welder, **W. E. Shenk.** *U. S. Patent No. 2,616,016*, Oct. 28, 1952.

5. Electrical Coils and Conductors (book), **H. B. Dwight.** McGraw-Hill Book Company, Inc., New York, N. Y., 1945.

Traveling Wave Protection Problems—II

E. W. BOEHNE
FELLOW AIEE

DURING the past 25 years the study of lightning and of the means of preventing its destructive effects on electrical equipment have played a significant role in the development of widespread electrical systems. As lightning, our enemy no. 1, is gradually becoming subdued, our enemy no. 2, switching surges, appears in ever greater proportion as the possible ultimate factor in dictating the insulation level of electrical equipment. This has a direct bearing on the ultimate cost of electrical equipment. Accordingly, switching surges form one of the most promising frontiers for study and solution. This series of papers is dedicated to a small area of this study.

Several important trends during the growth of the industry give the switching surge the importance it now holds in the destiny of the system. A few of these trends are enumerated as follows:

1. The study of lightning and the solution of its protection problems have made it possible, in many cases, to reduce the level of insulation behind the bus to a point where the stress of switching surges may be the ultimate criterion of insulation strength.

2. With the steady growth in the megawatt capacity of systems there has been a parallel growth in the amounts of energy stored momentarily within the system itself. The transient conversion of this energy from inductive storage to capacitive storage and vice versa is the switching surge in its simplest form. This potential growth of the switching surge hazard is usually unappreciated but is very real.

3. The trend in the improvement of high-speed circuit-interrupting devices to cope

---

Paper 55-475, recommended by the AIEE Transmission and Distribution Committee and approved by the AIEE Committee on Technical Operations for presentation at the AIEE Summer General Meeting, Swampscott, Mass., June 27–July 1, 1955. Manuscript submitted March 29, 1955; made available for printing June 20, 1955.

E. W. Boehne is with the Massachusetts Institute of Technology, Cambridge, Mass.

with larger short-circuit currents could produce interrupting forces which might be too strong for light inductive currents causing considerable amounts of energy to be trapped within the system, which could quickly appear as surge voltage unless adequately controlled.

4. The advance in high-speed reclosing increases the possibility of switching surge phenomena.

5. The steady growth in the trend to add considerable amounts of capacitance kva to systems (long lines, cables, and static capacitor banks), with their attendant switching, leads to the possibility of restriking, a switching surge phenomenon of considerable importance to the industry today.

6. The gradual increase in the capacitive kva to neutral with the growth of large industrial and distribution systems employing ungrounded load transformers can lead to severe overvoltages under certain conditions of relaying in the presence of open conductors.

The study and analysis of switching surge phenomena is not as simple and as straightforward as the study of lightning. The fact is significant that the discovery of numerous important switching surge phenomena has been the result of field troubles followed up by intensive investigations. The 3-phase resistance, inductance, capacitance circuit under transient conditions still holds many secrets. Their revelation and study require the utmost in co-operation between the private utility and the parties delegated to study the phenomena. Analogue simulation of field circuits is making noteworthy contributions in many cases.

One of the encouraging trends which will speed discovery and understanding of surge phenomena is in the greater ease with which case studies can be made in the field even to the point of re-enacting the actual switching occurrence suspected of trouble. Such studies impress upon the user the statistical fact that all electrical equipment operating in a network is exposed to the transient potentials generated within the network, and accordingly each piece of apparatus is subject to a calculated risk over and above the rigid specifications required at the time of its purchase. As a result of studies of switching surges several important trends in system operation and design are noted which will eventually mold standards. A few are listed as follows:

1. The recognized superiority of the grounded system as being freer of switching hazards.

2. The importance of grounding the neutrals of load transformers in large distribution and industrial systems.

3. The desirability of gang-operated disconnecting switches to avoid, although momentarily, the creation of single-phase isolated open conductor in 3-phase circuits subject to series resonance conditions.

4. Relaying practices which avoid energizing unloaded, ungrounded load transformers through long transmission circuits where open conductors are a possibility.

5. The superiority of flat spacing of transmission line conductors as a means of minimizing double line-to-ground faults and arcing grounds in the event of broken conductors.

6. The recognized need for a new standard impulse wave to represent the nominal switching surge on industrial and utility systems.

7. The accepted need for special consideration of the capacitor switching problem as dictated in more exacting circuit-breaker performance specification.

8. Of greater importance, a keen awareness of the need of further study of the overvoltage problem in many areas dictates that analogue tools of greater precision and availability are needed, together with personnel trained in their use.

Circuit Representation

An important phase of both the analysis of switching problems and their representation in analogue circuits is the proper circuital representation of the essential circuit elements. The simpler and more obvious of these were discussed in Part I of this paper.[1] It is the purpose here to discuss the circuital representation of a bus forming a common connection to several lines and windings. This has an important bearing upon the magnitude of the voltage which can appear on the bus under various switching operations. The logical approach is to consider the individual ingredients one at a time before considering their interconnection.

Long Transmission Lines on Bus

A long transmission line on the bus behaves, under surge conditions, exactly as though a resistor equal to the surge impedance of the line were connected from the bus to ground. This representation is exact under either of two conditions: 1. if the transmission line, regardless of length, is terminated at the far end in the equivalent of its surge impedance or, 2. up until the moment of a reflected wave from the far end of the line. Accordingly, if a voltage wave of magnitude E approaches a switching station on one of q identical long lines connected to the bus, then the surge voltage e of the bus will be given by the relation

$$e=\frac{2E}{q}=\frac{\text{twice the traveling wave voltage}}{\text{number of identical lines on the bus}} \qquad (1)$$

This stems from the solution of e from the equivalent circuit[1] shown in Fig. 1. Where the magnitude of the traveling wave E is limited by the flashover of the line, say seven times the normal crest of the line to neutral voltage E_m, then

$$e=\frac{14E_m}{q} \qquad (2)$$

from which the total number of lines radiating from the bus would have to be only 5 to hold the bus to 2.8 E_m and avoid arrester operation. This is shown in Fig. 2.

When one of q lines, radiating from a simple switching bus, is open at the far end and this line is switched from the bus (there being no windings on the bus) the voltage which can appear on the line at the home end due to one restrike is given by the following relation; see reference 2 and the Appendix.

$$e_m=2(E_1+E_2)\left(\frac{q-1}{q}\right)-E_1 \qquad (3)$$

where

q = total number of connected transmission lines radiating from the switching bus

E_1 = voltage trapped on the line due to normal current zero interruption

E_2 = instantaneous bus voltage at moment of restrike

When E_2=0.95 E_m (a practical point for restriking, maximum gradient for linear contact separation) and E_1=1.05 E_m, then (E_1+E_2)=2 E_m. Now, when five lines radiate from the bus (q=5) the

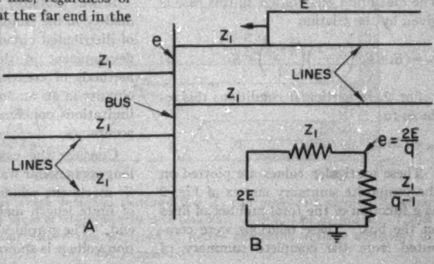

Fig. 1. A—Bus with q-connected lines and wave E approaching bus on one line only. B—Lumped circuit equivalent of A showing development of bus wave potential. See curve 1 in 2 for plot

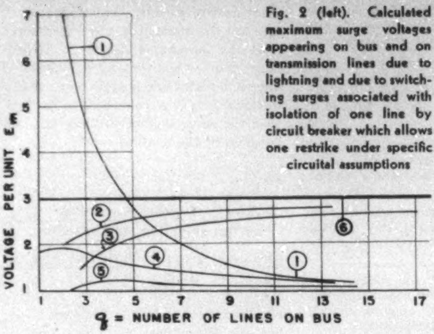

Fig. 2 (left). Calculated maximum surge voltages appearing on bus and on transmission lines due to lightning and due to switching surges associated with isolation of one line by circuit breaker which allows one restrike under specific circuital assumptions

1—Magnitude of lightning voltages appearing on bus due to waves entering station over transmission line whose impulse flashover is limited to seven times crest of normal line to neutral voltage

2—Maximum line voltage at home or source end due to one restrike. One grounded winding on bus

3—Maximum line voltages at home or source end due to one restrike. No windings on bus

4—Maximum bus voltage due to one restrike during isolation of one of lines on bus. One grounded winding on bus

5—Maximum bus voltage due to one restrike during isolation of one of lines on bus. No windings on bus

6—Maximum line voltage at far end of isolated line when one restrike occurs at source end

value of the line voltage at the home end becomes

$$e_m = \left[\left(\frac{4\times 4}{5}\right) - 1.05\right] E_m \qquad (4)$$

$$e_m = 2.15E_m$$

and the voltage at the far end of the line is

$$e_m = 2(E_1 + E_2) - E_1$$

with this value for E_1 and E_2 it becomes

$$e_m = 2.95E_m$$

The maximum bus voltage in this case is given by the relation

$$e_m = (E_1 + E_2)\left(\frac{q-1}{q}\right)\left(\frac{q+2}{q}\right) - E_1 \qquad (5)$$

For these particular conditions this reduces to

$$e_m = 1.21E_m$$

These particular values are plotted on the composite summary curves of Fig. 2 as a function of the total number of lines on the bus. These relations were computed from the complete summary of equations in the Appendix, and derived as a result of the new graphical studies of traveling wave and switching surge phenomena presented in the figures. It should be clearly pointed out that the results shown in Fig. 2 were computed on the basis of a rational set of assumptions regarding voltage conditions at the moment of restrike and upon a particular set of line terminations when more than one line was involved. Attenuation of waves and secondary phenomena were omitted. The results are indicative of the general nature and trend of the relative magnitudes of lightning and switching surges as a function of bus loading. Moreover, the equations presented permit the recomputation of the relative maximum voltages which might be expected under other values of initial voltage, surge impedances, or line and winding arrangements.

Of still greater value is the opportunity to utilize the graphical techniques to develop corresponding voltage and current equations for any particular circuital arrangement. Practice in this area and correlating the computed results with field experience (arrester operation, outages, etc.) should be a rewarding adventure toward a more scientific approach of the protective art. Station design and protection criteria should be influenced.

It was probably the realization of the duality in the simple graphical treatment of distributed circuits[3,4] which led to the development of the so-called slope-line methods of treating lumped parameter circuits in an analogous manner with no limitations concerning nonlinearity[5,6] or accuracy.

Consider the case of Fig. 3, where a long rectangular wave E traveling on line Z_1 meets the winding represented by Z_2 of finite length and grounded at the far end. The graphical solution of the junction voltage is shown in Fig. 3 for the case where $Z_2 = 3\ Z_1$. Note the exponential nature of the junction voltage. A comparison with the junction voltage of the same line terminated in a pure inductance, as shown in Fig. 4, is of interest in showing the "smooth" solution. Here the reflected wave or junction voltage is initially $2E$ in magnitude and decays exponentially to zero, which eventually recognizes the grounded nature of the circuit. A comparison of the two solutions is of interest.

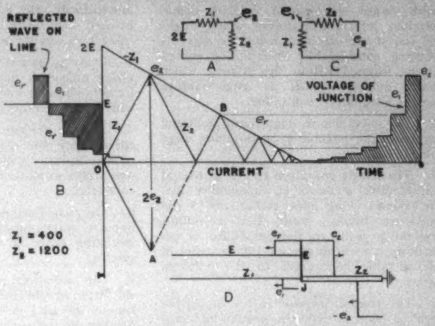

Fig. 3 (above). Calculated surge voltage appearing on bus at junction of line Z_1 and grounded winding Z_2 when rectangular wave of E approaches junction over line. Compare lumped parameter solution of Fig. 4

Returning to Fig. 3, a word of explanation is in order. Here it is first sought to solve graphically the voltage e_2 of Fig. 3(A). Hence in the volt-current diagram of Fig. 3(B), E and $2E$ are plotted. From the origin 0 Z_2 is constructed having a slope proportional to Z_2, and from $2E$ $-Z_1$ is plotted at the negative slope proportional to Z_1. It follows that the intersection of Z_2 and $-Z_1$ satisfies the solution[1] of Fig. 3(A) which is also the magnitude of the wave e_2 which enters Z_2. Neglecting attenuation, this wave e_2 will reflect at the grounded terminal and return to the junction as a negative wave. Accordingly, the solution Fig. 3(C), must

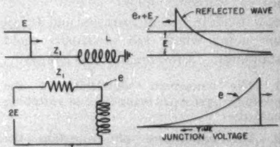

Fig. 4. Development of junction voltage where line terminates in pure inductance. Compare with wave solutions of Figs. 3 and 5

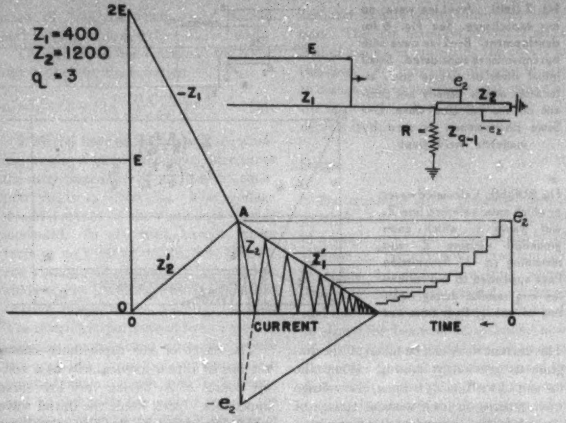

Fig. 5. Calculated surge voltage appearing on bus which has total of three identical lines connected and one grounded winding Z_1. Rectangular wave E approaches station on one of lines. (Alternate caption: Calculated lightning potential of transmission line tower when lightning wave E, running down leader stroke Z_1, impinges upon tower of surge impedance Z_2 with radiating ground wires having effective surge impedance R. Magnitude of e_2 will be modulated by wave front characteristics in relation to height of tower)

be satisfied to determine the effect of this first reflection from the neutral. Accordingly 2 e_2 is graphically constructed. The small negative wave e_1 which is pushed out on the line Z_1, and which reduces the potential of the junction by its magnitude, is computed by constructing line A B at the slope of Z_2. Where it intersects $-Z_1$ at B determines the magnitude of e_1. The reflected wave e_2' now returns positively on Z_2 to the grounded terminal where it reflects negatively to repeat the process in diminishing exponential fashion. It becomes apparent that the bottom half of the pantograph diagram is unnecessary and may be omitted.

It is important to observe the unidirectional nature of the terminal voltage, in spite of the fact that the wave in the winding is racing back and forth, changing polarity with each reflection and giving rise to the observed characteristic oscillatory behavior within the winding. It is because of this internal oscillatory behavior within the winding that sometimes the transformer is represented externally by lumped capacitance and inductance with pessimistic results concerning the nature of the terminal voltages due to an incoming wave.

Consider now the case of a bus having both lines and windings. Fig. 5(A) represents a bus having q identical long lines and r identical windings and a wave of E magnitude enters on one of the lines. The presence of the $(q-1)$ long lines is represented on the bus as a resistor to ground equal to the parallel value of the surge impedance of the remaining lines or

$$R = \frac{Z_1}{(q-1)} \tag{6}$$

Similarly

$$Z_2 = \frac{\text{surge impedance of one winding}}{\text{number of windings}}$$

Z_1 = surge impedance of incoming line

On approaching the junction the wave observes the parallel value of R and Z_2 which will be called Z_2' where

$$Z_2' = \frac{R \times Z_2}{R + Z_2} \tag{7}$$

Similarly, waves reflected from the grounded terminal in the winding approach the junction and observe the parallel value of R and Z_1 which will be called Z_1' where

$$Z_1' = \frac{R \times Z_1}{R + Z_1} \tag{8}$$

With these data it is possible to construct the graphical solution of the junction voltage as shown in Fig. 5. Here the intersection at A of $-Z_1$ from $2E$ and Z_2' from 0 determine the initial waves e_2 which enter each winding. When all windings are grounded these waves return negatively to the junction. The remainder of the pattern is the same as explained for Fig. 3 except that Z_1' replaces Z_1. The solution is shown at the lower right and is in correct quantitative relation to the magnitude of the incoming wave E for the particular number of lines and windings and their respective surge impedances, as shown in Fig. 5. Such diagrams make it possible not only to visualize the solution but to see the relative importance of each parameter; see the Appendix for the equations of line and bus voltage for this case. The travel

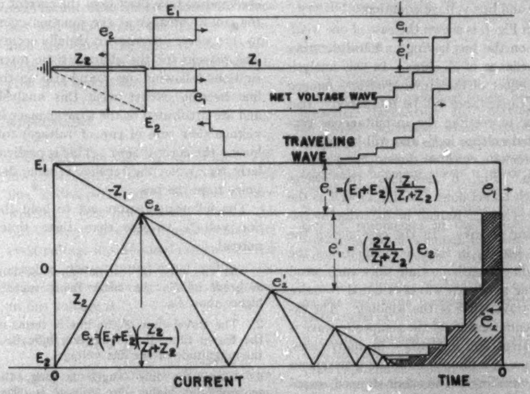
E_1
e_2
Z_2
Z_1
e_1
e_1'
NET VOLTAGE WAVE
e_1
E_2
TRAVELING WAVE
E_1
$-Z_1$
e_2
$e_1 = (E_1+E_2)\left(\frac{Z_1}{Z_1+Z_2}\right)$
e_1
$e_1' = \left(\frac{2Z_1}{Z_1+Z_2}\right) e_2$
0
e_2'
Z_2
$e_2 = (E_1+E_2)\left(\frac{Z_2}{Z_1+Z_2}\right)$
E_2
0
CURRENT
TIME
0
e_2

Fig. 6. Calculated waves which enter the switched line Z_1 and grounded winding Z_2 when the two are separated by breaker which permits one restrike. $Z_1 = 400$ ohms and $Z_2 = 1{,}200$ ohms. From such diagrams values were obtained to derive composite voltage equations in the Appendix

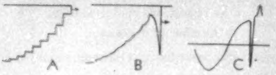

Fig. 7 (left). A—Line wave, no bus capacitance. See Fig. 6 for development. B—Line wave with bus capacitance considered. Small initial sliver of voltage soon attenuates and is usually not present on the reflected wave. C—Same phenomenon as seen by magnetic oscillograph

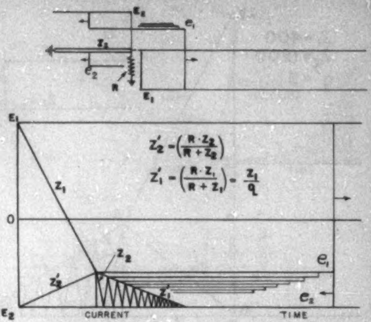

Fig. 8 (right). Calculated waves e_1 which enter switched line Z_1 and waves e_2 which enter grounded winding Z_2 and remaining $(q-1)$ transmission lines appended to bus following one restrike during isolation of one of lines from bus

time of waves on windings is essential to a detailed numerical solution. Some are given in reference 7. In general, the time intervals between voltage changes on the diagrams of Figs. 3 and 5 are the times required for the wave to travel twice the length of the winding. For grounded neutral windings this is the same time as represented by the period of the natural frequency of the winding. Many of these are given in reference 8. It should be pointed out that these approximations describe with good engineering accuracy the potentials of the bus. In some cases the potentials within the windings may become somewhat higher than the terminal voltages. In the case of open neutral windings with simultaneous surges on all three phases the neutral potentials can reach or even exceed twice the line terminal voltages. No open neutral cases are analyzed here.

Line-Dropping from Busses with Grounded Windings

To complete the comparison between the relative overvoltages due to lightning and as the result of one circuit breaker restrike when dropping a line from the bus (as presented in Fig. 2 for the switching station with no connected windings) the same cases will be considered of Figs. 3 and 5 for one restrike during the dropping of one line; see the Appendix for line and bus voltage equations.

In Fig. 6 is shown the case of one winding on the bus having an effective surge impedance of Z_2 ohms. In this analysis the effect of the presence of any lumped bus capacitance will be postponed. Just prior to restrike the instantaneous generated voltage is E_2 and will be assumed to remain constant during the phenomenon. Fig. 6 describes the waves which travel down the line as well as the waves which retreat in the winding following restrike. In the case shown the line length, in time, is many times the winding length in time since each tread of the stair-step waves is equal to twice the travel time of the winding. The exponential nature of the composite wave is apparent and it justifies, in many cases, the use of a lumped inductance to replace the winding. The stair-stepped exponential wave which travels down the line is accompanied by a current wave of similar shape, namely, the voltage wave divided by the line surge impedance Z_1. This current wave can be taken off the diagram as previously shown.[1] When the far end of the line Z_1 is open, the voltage wave returns on itself without change of sign while the current wave returns with a change of sign since the terminal current is zero. It is important to note that the actual voltage at any point on the line at any time is the algebraic sum of all the waves at that point and the original bound charge E_1. The ultimate magnitude of the voltage wave is (E_1+E_2) which doubles at the far end, giving rise to a terminal potential of

$$e=2(E_1+E_2)-E_1=E_1+2E_2 \tag{9}$$

When both E_1 and E_2 equal E_m then we have the theoretical 3 E_m. As the waves return to the junction and enter the winding the reflections at the grounded end hold the terminal voltage down and not until several internal reflections within the winding take place does the current in the circuit breaker at the junction come to zero where interruption usually occurs. The reasons for the characteristic interruptions following one round trip on the line become clearer with this analysis and are attributed to the slow changes in voltage (low rate of rise of voltage) following the current zero. This is particularly true when the breaker is some distance from the bus.

The following factors act to hold the line voltage to less than three times normal.

1. At the time of restrike E_2 is seldom as great as E_1, the latter being slightly higher than E_m.
2. The travel time of the line in terms of the travel time of the winding influences the magnitude of the line voltage.
3. When the line length is long, the tendency for higher line voltage is offset by the attenuation factors due to corona and leakage.
4. There are sinusoidal changes in the generated voltage.

The effect of bus capacitance causes the bus to appear momentarily as a voltage source of E_1 having very low surge impedance. As a result the initial wave which moves out on the line approaches a magnitude of (E_1+E_2) but dies away at a rapid rate, depending upon the time constant as viewed at the terminal capacitance, and expressed in the exponential decay

$$\epsilon^{-\left(\frac{Z_1+Z_2}{Z_1\times Z_2\times C}\right)t} \tag{10}$$

As a result the bus first holds its voltage but quickly gives way to the foregoing wave solution. Accordingly, the initial wave which moves down the line will appear as shown in Fig. 7.

When the bus has additional connected lines the diagram of Fig. 6 is modified as shown in Fig. 8. Here the resistance R is the parallel value of the surge impedances of all lines radiating from the bus exclusive of the line being switched. The graphical analysis uses the apparent junction impedances as viewed by waves approaching the junction on both the line Z_1 and winding Z_2

$$Z_1'=\left(\frac{R\times Z_1}{R+Z_1}\right) \tag{11}$$

$$Z_2'=\left(\frac{R\times Z_2}{R+Z_2}\right) \tag{12}$$

Fig. 8 presents a radically different picture. Here the initial wave moving down the line is large in comparison. In many respects Fig. 8 is the conjugate of Fig. 6. For the case of one restrike the equation for the maximum bus voltage becomes

$$e_m=E_2+2(E_1+E_2)n\left(\frac{1+nq-n}{(1+nq)^2}\right) \tag{13}$$

where $n=Z_2/Z_1$ (the ratio of surge impedances) and q is the total number of lines on the bus.

When $n=3$ this relation gives a maximum of 1.93 E_m when $q=2$. Should both n and $q=1.0$, $e_m=(E_2+E_m)=1.95E_m$.

The maximum line voltage at the home end is given by the equation

$$e_m=E_2+(E_1+E_2)\left(\frac{1+q-n}{1+nq}\right) \qquad (14)$$

With five lines on the bus and one winding, having a surge impedance three times the surge impedance of one line, this equation yields $e_m=2.58\ E_m$. This voltage should increase as the number of lines is increased. In all cases, except where there is no winding on the bus, the far-end voltage will approach 3 E_m. A close study of Fig. 2 will show important quantitative trends as bus loadings increase. The relative importance of bus versus line arresters becomes clear, particularly since the open-line circuit breaker stands as a point of maximum reflection for lightning and as the open far end to receive the switching surge of the distant breaker or line disturbance.

Important Case

A case of special importance arises when a cable-line section is isolated from a large bus by a circuit breaker which allows just one restrike, the cable being adjacent to the bus. Under the conditions of a large bus the initial wave on the cable following a restrike will be (E_1+E_2) which can be close to 2 E_m or even greater because of the capacitive coupling of the idle phase conductor with energized conductors. Following a restrike, this wave will increase at the cable-line junction causing the voltage entering the line to be

$$2(E_1+E_2)\left(\frac{Z_L}{Z_C+Z_L}\right) \qquad (15)$$

where the L and C refer to line and cable respectively.

This wave then doubles at the far end of the open line causing the maximum open circuit wave voltage to be

$$e_m=4(E_1+E_2)\left(\frac{Z_L}{Z_C+Z_L}\right)-E_1 \qquad (16)$$

When $E_1=1.05\ E_m$ and $E_2=0.95\ E_m$ and the ratio of the line-to-cable surge impedance is 8 to 1, this voltage can reach over six times normal for just one well-timed restrike. Without line arresters, flashover usually occurs under this condition. The line arresters absorb a great deal of energy in protecting the circuit in this case. For long lines, attenuation due to corona will reduce these peak values at the open end. Short lines are more vulnerable in this case.

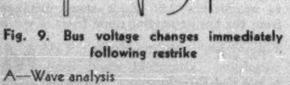

Fig. 9. Bus voltage changes immediately following restrike

A—Wave analysis
B—As viewed by fast cathode-ray oscillograph
C—As seen by slow magnetic oscillograph

Scope

The graphical study presented here is an attempt to encourage the development of a simple analytical tool as an aid to the solution and visualization of practical field problems involving traveling waves. Analogue computers, digital machines, and transient analyzers are powerful tools to study the behavior of systems; however, correct answers are dependent upon the proper circuital representations of the field circuits. Such computing tools tend to mask the answer to the question, why? concerning the physical behavior of systems. As far as possible these powerful analytical tools should be paralleled with simple and more direct methods available to the student equipped with a paper, pencil, a straight-edge and the ability to reason.

The interpretation of field or analogue phenomena as observed by the cathode-ray oscillograph or oscilloscope requires correlation with wave analysis. The diagrams presented here are essentially as would be seen at specific time intervals by an observer viewing the entire system. However, the cathode-ray measurements are made at a specific point on the system and cover the full time span of the disturbance. This difference in the mode of observation must be correlated to interpret and understand the phenomena behind the time diagrams of the oscillograph. One such sample conversion is presented in Fig. 9.

Applications

Consider the bus voltage (Fig. 6) following a restrike in the case where one line is dropped from a bus fed by one winding. Just prior to the restrike, the bus voltage has been approaching its crest voltage in sinusoidal fashion and has reached the instantaneous voltage E_2. Immediately following restrike the change in bus voltage is

$$E_B=(E_1+E_2)\left(\frac{Z_2}{Z_1+Z_2}\right) \qquad (17)$$

as graphically shown in Fig. 6. Now, when $Z_2=3Z_1$, for a practical case, and $E_2=0.9\ E_1$, then

$E_B=1.43E_1$

Now, when $E_1=1.05\ E_m$ (as is reasonable) where E_m is the crest of the normal line to neutral voltage, then

$E_B=1.5E_m$

Hence the bus voltage collapses momentarily from $+0.945\ E_m$ to $-0.555\ E_m$. This collapse is important to the turn insulation of the windings and is somewhat eased by the presence of bus capacitance which allows the change to take place exponentially. As shown in Fig. 6 and in Fig. 9, the multiple reflection of this change of voltage within the winding builds the bus voltage back up close to E_2. This is followed by the reflection from the far end of the switched line causing the bus voltage to rise still higher than E_2. These events are shown in Fig. 9 as they would be observed by both a cathode-ray oscillograph and a magnetic oscillograph. In a similar manner the student can construct the volt-time diagrams for any point on the system. The graphical solutions using the slope-line methods are a great aid in summarizing accurately the effects of multiple reflections. In a similar manner the current at any point can be studied by taking the current waves from the diagrams as shown in Figs. 9 and 10 of part I of this paper.[1]

The methods and diagrams of these papers are applicable to many special cases where multiple reflections take place on short lengths of line. Of special interest is the rise of transmission line tower potentials due to a direct stroke of steep wave front. Such a case is shown in Fig. 5 with the alternate caption employed. The parameters are redefined for this special case in items 2 through 6 of the nomenclature.

Conclusions

1. A technique for the graphical analysis of lightning and switching surges has been presented facilitating the development of simple equations which express the magnitude of the surge potentials which may be expected on lines, towers, and terminal equipment under a given set of circuital connections.

2. It is shown that, rather than using lumped parameters in the analysis, the representation of windings as short terminated lines of higher surge impedance together with the consideration of small local capacitances immediately available on the bus, when necessary, is better and more conservative.

3. When lumped parameters must be used to represent the large bus it is clear that capacitance should be used in preference to inductance. Such representation more accurately describes the surge characteristics of the large bus, and it further points up the fact that it is difficult to raise the surge potential on a large bus to arrester spark-over values.

4. As the number of lines connected to the bus increases, the lower the bus potentials become for both lightning and switching surges originating with circuit-breaker restriking (Fig. 2).

5. As the number of lines connected to the bus increases, the higher the line potentials become for switching surges originating with circuit-breaker restriking; see Fig. 2. This partially explains the difference of opinion concerning the magnitude of overvoltages produced by line-dropping tests when made without consideration of the nature of the bus from which the line is being switched.

6. The application of the graphical analysis of tower potentials due to a direct stroke may be rewarding. The effect of tower height, footing resistance, number of ground wires, etc., can be readily visualized by constructing a dynamic model of the graphical constructions.

7. The desirability is evident of increasing the surge impedance of the bus to reduce the switching surge potentials due to restriking. In this light the role of the internal resistors in modern circuit breakers takes on a new significance.[3]

8. The advancement of a technique, available at the student level, which permits the analysis of connected distributed circuits under surge conditions to be better understood should encourage greater research in the area of wave analysis.

9. The correlation of analytical studies with field experience is the greatest practical opportunity to the protection engineer. There is little doubt that serious effort on the part of field engineers in this regard will lead to the empirical determination of some of the parameters to be used in such studies. Encouragement is needed of more field investigations concerning the behavior of large and small switching stations under controlled surge generation. Such experience combined with a strong technical approach to the problem will give the best results in the shortest time.

Appendix. Composite Equations

Nomenclature

q = total of identical long lines on the bus

Z_2 = net surge impedance of grounded winding or short grounded line or short grounded cable on bus or transmission tower surge impedance in special cases

Z_1 = surge impedance of one incoming line or stroke impedance of a lightning discharge in special cases

$R = Z_{(q-1)} = (Z_1/q-1)$ effective surge impedance of $(q-1)$ lines on the bus, or surge impedance of ground wires as viewed by a lightning stroke to a tower in special cases

$Z_2' = (R \times Z_2/R+Z_2)$ = effective surge impedance of composite bus as viewed from one line or effective surge impedance as viewed by a direct lightning stroke to a tower in special cases

$Z_1' = (R \times Z_1/R+Z_1) = Z_1/q$ = effective surge impedance of bus as viewed from one winding or effective outgoing surge impedance as viewed from a tower in case of direct stroke to tower

$n = Z_2/Z_1$

e_m = peak instantaneous voltage due to surge phenomena

E_m = crest value of nominal line to neutral voltage of the system

E_1 = bound charge trapped on Z_1 due to interruption of capacitive current. Taken as 1.05 E_m in problems in this paper

E_2 = instantaneous bus voltage at moment of restrike. Taken as 0.95 E_m in problems in this paper

e_1 = initial voltage entering line Z_1 following restrike or due to reflected wave from grounded neutral following a lightning surge

e_2 = initial voltage entering winding Z_2 following restrike or lightning

e_1' = second increment of voltage entering line Z_1. Due to first reflection from grounded terminal of winding following a restrike

e_r = reflected voltage wave from junction

Bus Voltages Due to Line-Dropping, One Restrike

One Grounded Winding Plus q Lines on Bus, Fig. 7

$$e_m = E_2 + 2e_1\left(\frac{Z_2'}{Z_1+Z_2'}\right)$$

$$e_m = E_2 + 2(E_1+E_2)n\left(\frac{1+nq-n}{(1+nq)^2}\right)$$

$$e_1 = (E_1+E_2)\left(\frac{1+nq-n}{1+nq}\right)$$

$$e_2 = (E_1+E_2)\left(\frac{n}{1+nq}\right)$$

$e_1+e_2 = E_1+E_2$ (usually taken as 2 E_m for problems in this paper)

When $n = 3$ and $q = 5$ and $E_1 = 1.05$ E_m and $E_2 = 0.95$ E_m

$$e_m = 1.56E_m$$

When $n = 3$ and $q = 2$ and $E_1 = 1.05$ E_m and $E_2 = 0.95$

$e_m = 1.95E_m$ (highest point on curve)

One or More Grounded Windings Plus Switched Line Only on Bus, Fig. 6

When Z_2 is less than Z_1 ($n<1.0$)

$$e_m = E_2 + 2e_1\left(\frac{Z_2}{Z_1+Z_2}\right)$$

$$e_m = E_2 + 2(E_1+E_2)\left(\frac{n}{(1+n)^2}\right)$$

$$= E_m\left(0.95 + \frac{4n}{(1+n)^2}\right)$$

When Z_2 is greater than Z_1 ($n>1.0$); the usual case

$$e_m = E_2 + 2e_1'\left(\frac{Z_2}{Z_1+Z_2}\right)$$

$$e_m = E_2 + 4(E_1+E_2)\left(\frac{n^2}{(1+n)^3}\right)$$

$$e_m = E_m\left(0.95 + \frac{8n^2}{(1+n)^3}\right)$$

When $n = 2$

$e_m = 2.14$ E_m (highest point on curve)

Dropping One of q Lines From Bus; No Windings

$$e_m = \left[-E_1 + (E_1+E_2)\left(\frac{Z_1}{Z_1+Z_2}\right) + 2(E_1+E_2)\left(\frac{Z_1}{Z_1+Z_2}\right)\left(\frac{Z_2}{Z_1+Z_2}\right)\right]$$

$$e_m = (E_1+E_2)\times\left[\left(\frac{q-1}{q}\right)\times\left(\frac{q+2}{q}\right)\right] - E_1$$

When $q = 4$ and $E_1 = 1.05$ E_m and $E_2 =$ 0.95 E_m

$e_m = 1.20E_m$ (highest point on curve)

Line Voltage Due to Line-Dropping, One Restrike

One Grounded Winding Plus q Lines on Bus; See Fig. 7

Home end, at restriking breaker

$$e_m = E_2 + e_1$$

$$e_m = E_2 + (E_1+E_2)\left(\frac{1+nq-n}{1+nq}\right)$$

When $q = 5$ and $n = 3$ and $E_1 = 1.05$ E_m and $E_2 = 0.95$ E_m

$$e_m = 2.58\ E_m$$

Changing $q = 10$, $e_m = 2.76$ E_m
Far end

$$e_m = 2(E_1+E_2) - E_1$$

When $E_1 = 1.05$ E_m and $E_2 = 0.95$ E_m

$$e_m = 2.95\ E_m$$

One or More Grounded Windings Plus Switched Line Only on Bus; Fig. 6

When Z_2 is less than Z_1 ($n \gtreqless 1.0$).
Home end

$$e_m = E_2 + e_1$$

$$e_m = E_2 + (E_1+E_2)\left(\frac{Z_1}{Z_1+Z_2}\right)$$

$$e_m = E_2 + (E_1+E_2)\left(\frac{1}{1+n}\right)$$

When $n = 1/2$ and $E_1 = 1.05$ E_m and $E_2 =$ 0.95 E_m

$$e_m = E_m(0.95+4/3) = 2.28\ E_m$$

Changing $n = 10$, $e_m = 1.95$ E_m.
As n approaches zero (many windings) e_m approaches 2.95 E_m a short distance from the bus depending upon front of wave distortion
Far end

$$e_m = 2(E_1+E_2) - E_1$$

When Z_2 is greater than $2 \times Z_1$ ($n>2.0$).

Home end, Fig. 6

$$e_m = E_2 + \left(\frac{2e_1Z_2}{Z_1+Z_2}\right) + e_1'$$

$$= E_2 + (E_1+E_2)\left(\frac{4Z_1 \times Z_2}{(Z_1+Z_2)^2}\right)$$

$$e_m = E_2 + (E_1+E_2)\left(\frac{4n}{(1+n)^2}\right)$$

When $n=3$ and $E_2=0.95\ E_m$ and $E_1=1.05\ E_m$

$$e_m = 2.45\ E_m$$

Far end

$$e_m = 2(E_1+E_2) - E_1 = 2.95\ E_m$$

DROPPING ONE OF q LINE FROM BUS, NO WINDINGS

Home end

$$e_m = 2e_1 - E_1$$

$$e_m = 2(E_1+E_2)\left(\frac{Z_1}{Z_1+Z_{q-1}}\right) - E_1$$

$$= 2(E_1+E_2)\left(\frac{q-1}{q}\right) - E_1 \qquad (3)$$

When $q=4$ and $E_1=1.05\ E_m$ and $E_2=0.95\ E_m$

$$e_m = 1.95\ E_m$$

As q approaches infinity, e_m approaches $2.95\ E_m$ a short distance from the bus.

Far end

$$e_m = 2(E_1+E_2)\left(\frac{q-1}{q}\right) - E_1$$

In this case the same as home end.

The far end voltages neglect the additional rise in transmission line voltage due to the Ferranti effect or to induced electrostatic components from the energized phases. Wave attenuation is also neglected. The longer the lines the greater the wave attenuation. Since the first reflections at the far end are opposite in polarity to the natural rise of line voltage mentioned in the foregoing, it can be expected that the longer the line the lower the far-end surge voltage due to one restrike. The natural rise in line voltage at the home end due to the presence of the energized phase conductors will increase the value of E_1 just prior to restrike. These equations can be used to demonstrate the effect of this rise in line voltage.

References

1. Traveling Wave Protection Problems—I. A Graphical Analysis with Special Application to the Switching of Lines and Cables, E. W. Boehne. *AIEE Transactions*, vol. 73, pt. III-B, Aug. 1954, pp. 920–28.

2. *Ibid.*, Fig. 13, p. 924.

3. Methodes Graphiques Generales de Calcul des Propagations d'Ondes Planes, L. Bergeron. *Memoires*, Société des Ingenieurs Civils de France, Paris, France, 1937.

4. Du Coup de Belier en Hydraulique au Coup de Foundre en Electricité; Methode Graphique Generale (book), Louis Jean Bergeron. Dunod, Paris, France, 1950.

5. Graphical Analysis of Transient Phenomena in Electric Circuits, Kalman J. de Juhasz. *Journal*, Franklin Institute, Philadelphia, Pa., Sept. 1939.

6. Electrical Analogues and Electronic Computers, a Symposium. *Transactions*, American Society of Civil Engineers, New York, N. Y., "Storage and Water Hammer Problems," Henry M. Paynter, vol. 118, 1953, p. 962.

7. Voltage Oscillations in Armature Windings Under Lightning Impulses, E. W. Boehne. *AIEE Transactions*, vol. 49 Oct. 1930, pp. 1587–1615.

8. Traveling Waves on Transmission Systems (book), L. V. Bewley. John Wiley & Sons, Inc., New York, N. Y., 1951.

Electromagnetic Unbalance of Untransposed Transmission Lines

II. Single Lines With Horizontal Conductor Arrangement

ERIC T. B. GROSS
FELLOW AIEE

S. W. NELSON
STUDENT MEMBER AIEE

Synopsis: Various configurations of single-circuit overhead lines without and with ground wires have been considered in a previous investigation of unbalance factors m_0 and m_2.[1] In this part of the study, electromagnetic unbalance has been calculated and balance factors plotted for single-circuit overhead transmission lines with horizontal conductor arrangement and two ground wires, so located in many different positions that the protective angle differs from the 30 degrees of the earlier analysis. Since many new lines have been built with a smaller protective angle, the arrangements covered in the investigation may become valuable for application considerations. All computations have been made on an International Business Machines card program calculator, and the basic procedure is given in the Appendix.

Basic Configuration

MANY single-circuit transmission lines have horizontal configurations with two overhead ground wires. The tower structures are essentially wood-pole H frames laid out in symmetrical manner with the ground wires and phase wires forming two equilateral triangles and a protective angle of 30 degrees. In order to improve the protective value of the ground wires, not only steel towers but recently also wood structures have been constructed with varied locations of the two overhead ground wires relative to the phase wires.

A typical new 230-kv tower structure is shown in Fig. 1. The simplified construction of this tower makes it economical to have a protective angle which is smaller than the customary 30 degrees. This transmission tower is in use on the new 230-kv system of the Public Service Company of Indiana.[2–4]

Standard tower structures used in many transmission lines which are in operation have been investigated to determine the extremes on ground wire location. Recent information[5] on ground wire positions, phase wire spacing, and conductor diameters for high-voltage lines of various voltages has been reviewed in order to cover all practical cases.

The rectangular, shaded areas of Fig. 2 represent the area of ground wire location considered in the computations on the CPC. The dimensions of this area are given with reference to the phase wire spacing S, since it is an important dimension; S increases when higher voltages are considered.

The area inside the dashed 30-degree protective triangle has little practical use since lines would hardly be designed with protective angles that are larger than 30 degrees. The crosshatched trapezoidal areas shown in Fig. 2 represent bounds for the locations of ground wires. However, the entire shaded area of Fig. 2 was investigated to find the general trend of the magnetic unbalance with variable ground wire locations. The following cases were considered:[6] S between 10 and 30 feet. For each value of S, two typical values of phase wire size were used.

Paper 55-477, recommended by the AIEE Transmission and Distribution Committee and approved by the AIEE Committee on Technical Operations for presentation at the AIEE Summer General Meeting, Swampscott, Mass., June 27–July 1, 1955. Manuscript submitted March 24, 1955; made available for printing May 9, 1955.

ERIC T. B. GROSS is with the Illinois Institute of Technology, Chicago, Ill., and S. W. NELSON is with the Armour Research Foundation of Illinois Institute of Technology, Chicago, Ill.

The authors wish to express their gratitude to the Armour Research Foundation for making available the facilities of the Computer Center for this study.

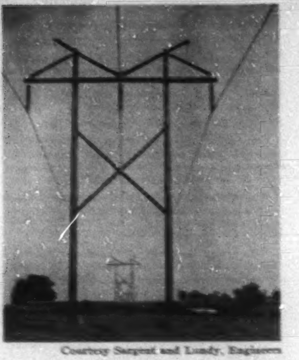

Courtesy Sargent and Lundy, Engineers

Fig. 1. 230-kv transmission line, protective angle 23 degrees

In line with present practice, steel-reinforced aluminum-cable ground wires having a geometric mean radius (GMR) of 0.0217 foot were considered. As shown by Fig. 2, results were calculated for a range of ground wire locations for each value of *S*. In the horizontal direction, the ground wire spacing *W* varied from 0.4 *S* to 2.0 *S*. The vertical height variation *G* of the ground wire above the level of the phase wires ranged from 0.2 *S* to 1.7 *S*. The ground wires *w* and *x* lie in all cases on a horizontal line above the phase wires and are equally displaced from the vertical center line, Fig. 3. To calculate the limiting cases without[3] ground wires, the ground wires can be moved to a very great distance above the phase conductors, thus eliminating their effects without changing the programming on the computer.

Method of Computation

From the basic voltage equations for a single-circuit overhead transmission line with two ground wires,[1] somewhat simplified unbalance equations have been developed in the Appendix for the horizontal configuration here considered. Since the solution by use of a computer was desirable, the development presented in the Appendix has been accomplished with this in mind. The unbalance equations were programmed for and solved on a card program calculator, which is a fairly large-scale digital computer.

The program consisted of 420 cards, needed to calculate points for one zero-sequence m_0 and one negative-sequence m_2 unbalance curve. A general-purpose control board was used in the computations. This is an 8-digit floating decimal system which eliminates the necessity for scaling. Numbers ranging from 10^{-50} to as high as 10^{50} can be used with this system.

To test the accuracy of the equations and program, results were compared to previously calculated data for the configuration with a 30-degree protective angle.[1] If the spacing between ground wires approaches zero, the unbalance factors should compare to the case of one ground wire located above the horizontal configuration. The results of both the 30-degree case and the limiting case with small spacing *W* compared satisfactorily.

Discussion of the Curves

Figs. 4 through 9 give the m_2 and m_0 unbalance factors for various line configurations. Each set of curves is for a different value of *S* and geometric mean phase wire radius R_p. The independent variable along the abscissas of a set is the ratio of *W* to *S*. The parameter determining the curves of each set is *G*, expressed as a multiple of *S*. Fig. 3 indicates how the variables used in the calculations have been defined. In all cases GMR_g equals 0.0217 foot corresponding to steel-reinforced aluminum-cable ground wire of size 266,800 circular mils and about 1/2-inch outside diameter.

Most applications will use ground wires between 0.7 *S* and *S* above the level of the phase wires. Supplementary data for such conductor arrangements and for *S* between 10 and 30 feet were computed and the results tabulated for *W/S* between 0.6 and 2; see Tables I and II.

Each set of curves has been plotted in the figures over the whole range of ground wire spacing from *W*=0.4 *S* out to *W*=2.0 *S*. Some of these locations are not practical, especially when the ground wire height above phase conductors and the spacing *W* between them are small. However, the complete curves are presented to show the general trend of unbalance for variations in ground wire locations. A small black dot which lies on each of the unbalance curves indicates the 30-degree protective angle point for that particular case. In most conditions, this is the maximum angle that is practical; thus only the section of the curve to the right of this dot is of practical importance.

For *G*=10 *S* the unbalance appears on all sets as a horizontal line. When *G*=10 *S*, both m_0 and m_2, rounded off to two significant figures, did not change with variations in ground wire spacing. The results did also not change appreciably with increased ground wire height above this value. Thus, the curves for *G*=10 *S* can be considered as approximately equal to the resulting unbalance of a horizontal line configuration without ground wires. These curves check very closely to results *obtained* previously,[3] calculated from unbalance equations derived for the horizontal conductor configuration without ground wires.

The unbalance factor m_2 shows a definite trend for variations in ground wire location. A reduction in *G* above the phase wires causes a *drop* in the m_2 factor. An increase in *W* reduces m_2, while an increase in phase wire size also increases the negative-sequence unbalance factor.

The zero-sequence unbalance curves show similar trends for variations in the ground wire location. The zero-sequence curves are shown in Figs. 7 through 9. For the larger values of *G*, m_0 is generally reduced when *W* is decreased. It is apparent from the figures that a gradual transition occurs for smaller values of *G*. The unbalance reaches a low minimum for ground wire positions somewhere between the phase wires. For the range of variables considered, the maximum value of m_0 is on the order of 30 times its minimum value as compared to the m_2 maximum to minimum factor of only 2. By noting the position of the dot, the 30-

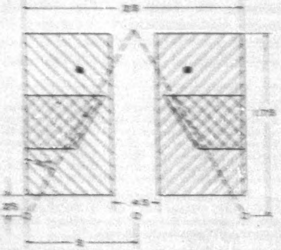

Fig. 2. Area of ground wire locations

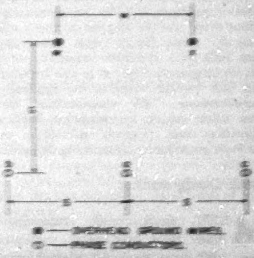

Fig. 3. Arrangement of conductors

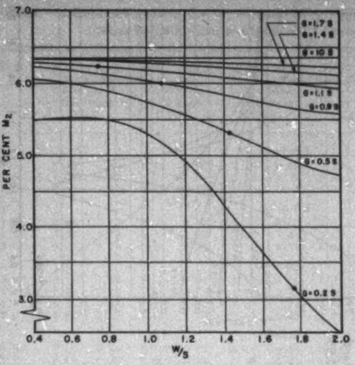

Fig. 4(A) (left, top). Unbalance factor m_2 for conductors of S=10 feet and GMR$_a$=0.02 foot

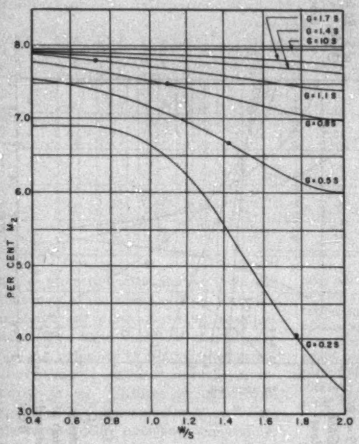

Fig. 4(B) (left, center). Unbalance factor m_2 for conductors of S=10 feet and GMR$_a$=0.04 foot

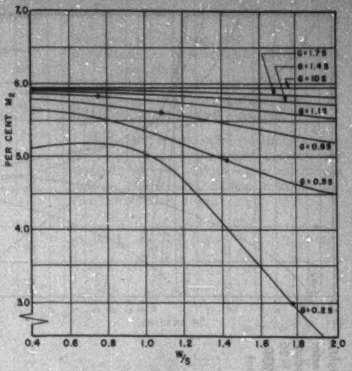

Fig. 5(A) (right, top). Unbalance factor m_2 for conductors of S=18 feet and GMR$_a$=0.02 foot

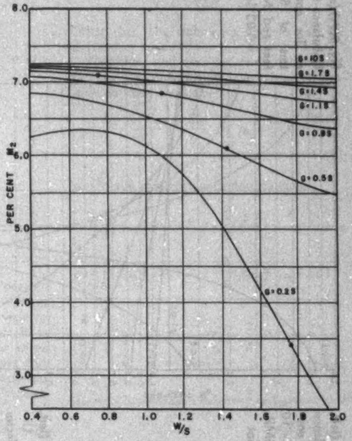

Fig. 5(B) (right, center). Unbalance factor m_2 for conductors of S=18 feet and GMR$_a$=0.04 foot

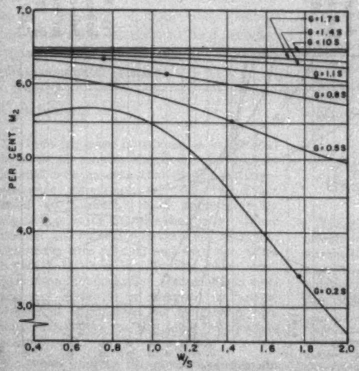

Fig. 6(A) (left). Unbalance factor m_2 for conductors of S=26 feet and GMR$_a$=0.03 foot

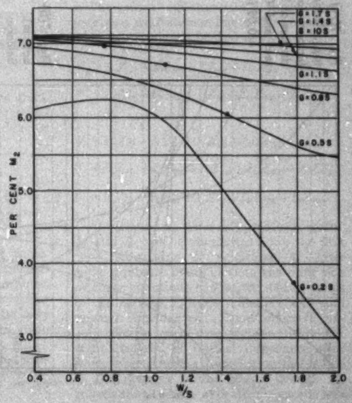

Fig. 6(B) (right). Unbalance factor m_2 for conductors of S=26 feet and GMR$_a$=0.05 foot

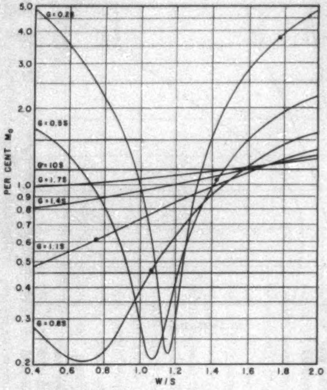

Fig. 7(A) (left, top). Unbalance factor m_0 for conductors of S=10 feet and GMR_a =0.02 foot

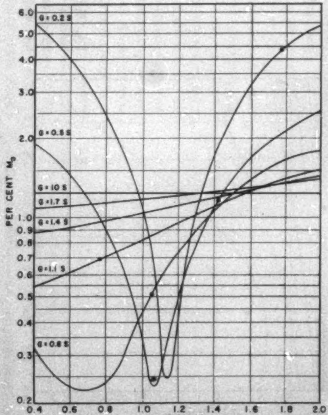

Fig. 7(B) (left, bottom). Unbalance factor m_0 for conductors of S=10 feet and GMR_a= 0.04 foot

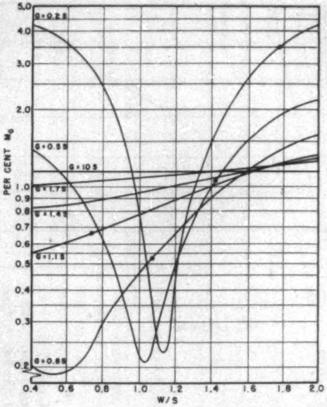

Fig. 8(A) (right, top). Unbalance factor m_0 for conductors of S=18 feet and GMR_a =0.02 foot

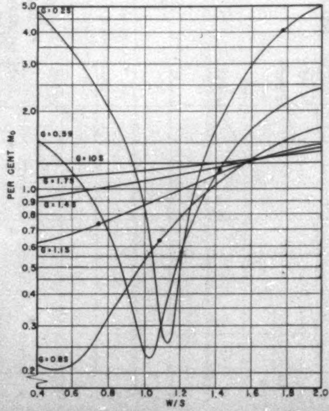

Fig. 8(B) (right, bottom). Unbalance factor m_0 for conductors of S=18 feet and GMR_a = 0.04 foot

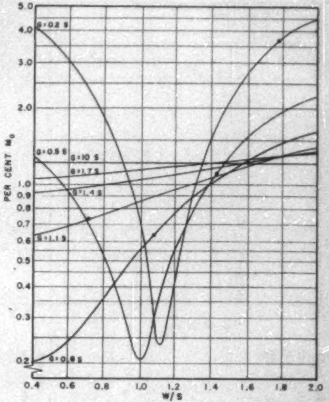

Fig. 9(A) (right). Unbalance factor m_0 for conductors of S=26 feet and MGR_a =0.03 foot

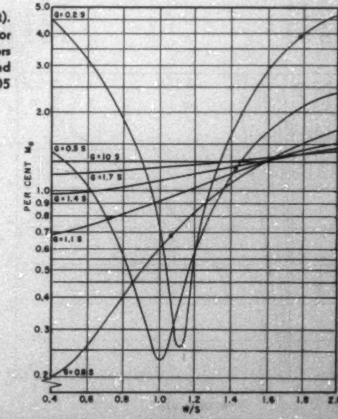

Fig. 9(B) (right). Unbalance factor m_0 for conductors of S=26 feet and GMR_a = 0.05 foot

Table I. Unbalance Factors for S=10, 14, and 18 Feet; GMR$_a$=0.02 and 0.04 Foot; Ground Wires 266,800-Circular-Mil Steel-Reinforced Aluminum Cable

W/S	S=10 Feet				S=14 Feet				S=18 Feet			
	0.02 Foot GMR$_a$		0.04 Foot GMR$_a$		0.02 Foot GMR$_a$		0.04 Foot GMR$_a$		0.02 Foot GMR$_a$		0.04 Foot GMR$_a$	
	m_2%	m_0%	m_2%	m_0%	m_2%	m_0%	m_2%	m_0%	m_2%	m_0%	m_2%	m_0%
G=0.6 S												
1.2	5.70	0.49	7.12	0.56	5.49	0.53	6.76	0.59	5.34	0.55	6.52	0.62
1.6	5.36	1.33	6.72	1.51	5.18	1.31	6.39	1.48	5.05	1.30	6.17	1.46
2.0	5.11	1.97	6.41	2.22	4.94	1.91	6.11	2.14	4.83	1.87	5.90	2.09
G=0.7 S												
1.2	5.83	0.57	7.29	0.64	5.61	0.60	6.91	0.67	5.46	0.63	6.65	0.70
1.6	5.57	1.23	6.98	1.38	5.37	1.22	6.63	1.36	5.23	1.21	6.39	1.35
2.0	5.37	1.74	6.74	1.96	5.19	1.70	6.40	1.90	5.06	1.67	6.18	1.86
G=0.865 S												
0.8	6.14	0.31	7.67	0.34	5.90	0.35	7.26	0.39	5.74	0.38	6.98	0.43
1.2	5.99	0.70	7.48	0.78	5.76	0.72	7.09	0.81	5.60	0.74	6.82	0.83
1.6	5.81	1.14	7.27	1.28	5.60	1.14	6.90	1.27	5.45	1.14	6.64	1.27
2.0	5.67	1.52	7.10	1.70	5.47	1.49	6.74	1.66	5.33	1.47	6.49	1.63
G=1.0 S												
0.8	6.20	0.50	7.74	0.56	5.96	0.54	7.33	0.60	5.79	0.57	7.05	0.63
1.2	6.08	0.79	7.60	0.88	5.85	0.81	7.20	0.91	5.68	0.83	6.92	0.92
1.6	5.95	1.12	7.44	1.25	5.73	1.12	7.05	1.24	5.57	1.12	6.79	1.24
2.0	5.84	1.41	7.31	1.57	5.63	1.39	6.93	1.54	5.47	1.38	6.67	1.53
G=1.1 S												
0.8	6.25	0.62	7.80	0.71	5.97	0.57	7.37	0.74	5.81	0.69	7.12	0.76
1.2	6.20	0.86	7.69	0.96	5.88	0.88	7.26	0.97	5.75	0.88	6.90	0.99
1.6	6.12	1.12	7.54	1.27	5.80	1.12	7.13	1.25	5.63	1.13	6.86	1.27
2.0	5.91	1.38	7.32	1.52	5.71	1.35	7.10	1.50	5.55	1.35	6.74	1.48
G=1.4 S												
0.4	6.33	0.82	7.85	0.88	6.08	0.83	7.40	0.92	5.90	0.82	7.20	0.93
0.8	6.30	0.89	7.82	0.98	6.07	0.90	7.38	1.00	5.88	0.89	7.18	1.02
1.2	6.28	1.00	7.80	1.12	6.02	1.00	7.36	1.12	5.85	1.02	7.12	1.13
1.6	6.24	1.17	7.74	1.28	5.92	1.15	7.30	1.28	5.77	1.15	7.00	1.44
2.0												
G=1.7 S												
0.4	6.34	0.98	7.86	1.08	6.10	0.97	7.41	1.12	5.92	1.02	7.23	1.10
0.8	6.32	1.03	7.84	1.13	6.09	1.03	7.40	1.16	5.90	1.06	7.20	1.15
1.2	6.30	1.10	7.83	1.21	6.08	1.12	7.38	1.22	5.88	1.12	7.18	1.22
1.6	6.27	1.18	7.80	1.30	6.04	1.18	7.37	1.31	5.87	1.18	7.12	1.29
2.0	6.25	1.26	7.75	1.40	6.00	1.26	7.34	1.40	5.85	1.28	7.11	1.37

degree protective angle marker, it is clear that most of the region of large variation in m_0 falls out of the range of the practical data. For large values of ground wire spacing, reduction in ground wire heights above the phase conductors causes an increase in m_0. Changes in phase wire spacing and phase wire size do not affect the zero-sequence unbalance appreciably. Increase in phase wire size causes a slight increase in m_0. There is little change in m_0 as a function of phase wire spacing, but what there is seems to be a decrease in zero-sequence unbalance for increased phase conductor spacing.

Conclusions

1. Zero-sequence unbalance m_0 is affected to a much greater degree by changes in ground wire spacing than is the negative-sequence unbalance m_2. On the other hand, m_2 is affected more appreciably by phase conductor changes than is m_0. Since voltage and current requirements determine the phase wire spacing and wire size, there is little freedom of altering phase configuration economically. Transmission towers can, however, be designed with some degree of freedom as far as ground wire location relative to the phase conductors is concerned.

2. When keeping the ground wires in an area with a protective angle of 30 degrees or less, the practical condition of minimum zero-sequence unbalance is in the vicinity of the equilateral configuration. If it is desirable to reduce m_2, the ground wires could be shifted a little further apart and placed lower. This change would cause an increase in m_0 so that an optimum balance must be established.

3. It is difficult to draw definite conclusions on any one configuration since the rate of change, of zero-sequence and negative-sequence unbalance factors as a function of spacing, varies considerably for different ground wire heights above the phase conductors.

4. The curves and tables permit the quick evaluation of m_2 and m_0 for all practical locations of ground wires and for conductor separations between 10 and 30 feet.

Appendix. Derivation of Unbalance Factor Equations*

The electromagnetic unbalance of single-circuit untransposed overhead transmission lines with two ground wires can be computed from the general voltage equations.[7] Unbalance factors will be shown to be only functions of the geometric variables given in Fig. 3. These variables are defined as:

S = phase wire spacing, feet
G = distance of ground wires above phase wires, feet
W = ground wire spacing, feet
GMR$_w$ = GMR of ground wires, feet
GMR$_a$ = GMR of phase wires, feet

Since the ground wire positions are to be varied in a symmetrical manner, the distance between various wires will have a definite relationship. These relations derived, from Fig. 3, are

$$D_{bw}=D_{cz}=\sqrt{G^2+\left(S-\frac{w}{2}\right)^2} \qquad D_{wz}=W$$

$$D_{cw}=D_{bz}=\sqrt{G^2+\left(S+\frac{w}{2}\right)^2}$$

$$D_{ac}=D_{ac}=S \quad (1)$$

$$D_{aw}=D_{az}=\sqrt{G^2+\left(\frac{w}{2}\right)^2} \qquad D_{bc}=2S$$

With this, the unbalance factors can be derived in terms of the original variables.[1,7]

Negative- and zero-sequence unbalanced factors for untransposed overhead transmission lines are defined as

$$m_2=\frac{I_{a2}}{I_{a1}}=\frac{-Z_{21}}{Z_2}=\frac{-Z_{21}}{Z_1} \qquad m_0=\frac{I_{a0}}{I_{a1}}=\frac{-Z_{01}}{Z_0} \quad (2)$$

where the sequence impedances equal

$$Z_1=\frac{1}{3}(Z_{aa}+Z_{bb}+Z_{cc})-\frac{1}{3}(Z_{ab}+Z_{ac}+Z_{bc})$$

$$Z_0=\frac{1}{3}(Z_{aa}+Z_{bb}+Z_{cc})+\frac{2}{3}(Z_{ab}+Z_{ac}+Z_{bc}) \quad (3)$$

$$Z_{21}=\frac{1}{3}(Za_a+aZ_{bb}+a^2Z_{cc})+\frac{2}{3}(a^2Z_{ab}+aZ_{ac}+Z_{bc})$$

$$Z_{01}=\frac{1}{3}(Z_{aa}+a^2Z_{bb}+aZ_{cc})-\frac{1}{3}(aZ_{ab}+a^2Z_{ac}+Z_{bc})$$

The general equations for a single-circuit overhead transmission line with two ground wires has been established as

$$\begin{aligned}
V_a&=I_aZ_{aa}+I_bZ_{ab}+I_cZ_{ac}+I_wZ_{aw}+I_zZ_{az}\\
V_b&=I_aZ_{ab}+I_bZ_{aa}+I_cZ_{bc}+I_wZ_{bw}+I_zZ_{bz}\\
V_c&=I_aZ_{ac}+I_bZ_{bc}+I_cZ_{aa}+I_wZ_{cw}+I_zZ_{cz}\\
0&=I_aZ_{aw}+I_bZ_{bw}+I_cZ_{cw}+I_wZ_{ww}+I_zZ_{wz}\\
0&=I_aZ_{az}+I_bZ_{bz}+I_cZ_{cz}+I_wZ_{wz}+I_zZ_{ww}
\end{aligned} \quad (4)$$

As has been done in previous work,[1] I_w and I_z can be eliminated from the first three equations of equations 4. After some algebraic manipulation, the right side of these equations can be written in terms of I_a, I_b, and I_c times effective self- and mutual impedances. These effective impedances in each case include either the complete self- or mutual impedance with no ground wire less a correction factor due to the presence of the ground wires. By substituting these effective impedances

---

*Note: In accordance with current editorial practice, phasor quantities are not differentiated from general mathematical composition, but are set throughout in light-face italic type.

Table II. Unbalance Factors for S=22, 26, and 30 Feet, GMR$_a$=0.03 and 0.05 Foot, Ground Wires 266,800-Circular-Mil Steel-Reinforced Aluminum Cable

W/S	m_2%	m_0%	m_2%	m_0%	m_2%	m_0%	m_2%	m_0%	m_2%	m_0%	m_2%	m_0%
	S=22 Feet				S=26 Feet				S=30 Feet			
	0.03 Foot GMR$_a$		0.05 Foot GMR$_a$		0.03 Foot GMR$_a$		0.05 Foot GMR$_a$		0.03 Foot GMR$_a$		0.05 Foot GMR$_a$	
G=0.6 S												
1.2	5.97	0.62	6.59	0.66	5.84	0.64	6.43	0.68	5.74	0.66	6.30	0.70
1.6	5.66	1.40	6.24	1.49	5.54	1.39	6.10	1.48	5.45	1.39	5.98	1.47
2.0	5.41	1.98	5.98	2.10	5.31	1.95	5.84	2.07	5.22	1.93	5.73	2.05
G=0.7 S												
1.2	6.09	0.70	6.72	0.74	5.96	0.71	6.56	0.76	5.85	0.73	6.42	0.77
1.6	5.85	1.30	6.46	1.38	5.73	1.30	6.31	1.38	5.63	1.30	6.18	1.37
2.0	5.67	1.77	6.25	1.88	5.55	1.80	6.11	1.86	5.45	1.74	5.99	1.84
G=0.865 S												
0.8	6.39	0.44	7.05	0.47	6.25	0.47	6.87	0.50	6.13	0.49	6.72	0.52
1.2	6.25	0.82	6.89	0.86	6.11	0.83	6.72	0.88	6.00	0.84	6.58	0.89
1.6	6.09	1.22	6.71	1.29	5.95	1.22	6.55	1.29	5.85	1.23	6.41	1.30
2.0	5.95	1.56	6.57	1.65	5.83	1.55	6.41	1.64	5.72	1.54	6.28	1.63
G=1.0 S												
0.8	6.45	0.63	7.11	0.67	6.30	0.66	6.93	0.69	6.18	0.67	6.78	0.71
1.2	6.34	0.90	6.99	0.96	6.20	0.92	6.81	0.97	6.08	0.93	6.67	0.98
1.6	6.22	1.20	6.85	1.27	6.08	1.20	6.68	1.27	5.97	1.21	6.55	1.27
2.0	6.11	1.47	6.74	1.55	5.98	1.46	6.58	1.54	5.87	1.45	6.44	1.53
G=1.1 S												
0.8	6.47	0.75	7.14	0.78	6.35	0.76	6.92	0.82	6.25	0.77	6.82	0.82
1.2	6.39	0.96	7.07	1.00	6.27	0.95	6.87	1.03	6.16	0.96	6.72	1.03
1.6	6.30	1.22	6.90	1.29	6.17	1.18	6.75	1.31	6.08	1.21	6.63	1.28
2.0	6.23	1.42	6.86	1.52	6.11	1.40	6.63	1.52	5.91	1.43	6.54	1.50
G=1.4 S												
0.4	6.60	0.90	7.26	0.97	6.39	0.92	7.11	0.97	6.35	0.94	6.88	0.98
0.8	6.57	0.97	7.23	1.03	6.38	1.00	7.10	1.03	6.30	1.00	6.87	1.05
1.2	6.53	1.10	7.20	1.15	6.36	1.10	6.93	1.16	6.25	1.10	6.79	1.17
1.6	6.48	1.25	7.12	1.28	6.28	1.23	6.90	1.31	6.18	1.23	6.75	1.30
2.0	6.38	1.38	7.05	1.43	6.25	1.35	6.83	1.45	6.14	1.38	6.68	1.44
G=1.7 S												
0.4	6.61	1.08	7.27	1.13	6.40	1.06	7.12	1.15	6.36	1.08	6.90	1.14
0.8	6.60	1.12	7.26	1.18	6.39	1.11	7.11	1.19	6.32	1.13	6.92	1.18
1.2	6.59	1.18	7.24	1.26	6.38	1.18	7.08	1.25	6.28	1.20	6.87	1.25
1.6	6.57	1.25	7.15	1.35	6.35	1.26	6.98	1.33	6.26	1.28	6.82	1.32
2.0	6.54	1.32	7.12	1.43	6.31	1.33	6.92	1.40	6.24	1.35	6.77	1.40

into equations 3, the sequence impedances can be expressed by equations 5. Primes are used to distinguish sequence impedances of configurations with two ground wires from those without ground wires

$$\begin{aligned}Z_1' = Z_1 - \frac{1}{3M}[&(Z_{aw}+aZ_{bw}+a^2Z_{cw})(Z_{aw}+a^2Z_{bw}+aZ_{cw})Z_{ww}+(Z_{ax}+aZ_{bx}+a^2Z_{cx})(Z_{ax}+a^2Z_{bx}+aZ_{cx})Z_{ww}-\\&(Z_{aw}+aZ_{bw}+a^2Z_{cw})(Z_{ax}+a^2Z_{bx}+aZ_{cx})Z_{wx}-(Z_{ax}+aZ_{cx}+a^2Z_{cx})\times(Z_{aw}+a^2Z_{bw}+aZ_{cw})Z_{wx}]\end{aligned}$$

$$Z_0' = Z_0 - \frac{1}{3M}[(Z_{aw}+Z_{bw}+Z_{cw})^2Z_{ww}+(Z_{ax}+Z_{bx}+Z_{cx})^2Z_{ww}-2(Z_{aw}+Z_{bw}+Z_{cw}+Z_{cw})(Z_{ax}+Z_{bx}+Z_{bx})Z_{wx}]$$

$$\begin{aligned}Z_{01}' = Z_{01} - \frac{1}{3M}[&(Z_{aw}+a^2Z_{bw}+aZ_{cw})\times(Z_{aw}+Z_{bw}+Z_{cw})Z_{ww}+(Z_{ax}+a^2Z_{bx}+aZ_{cx})(Z_{ax}+Z_{bx}+Z_{cx})Z_{ww}-\\&(Z_{aw}+a^2Z_{bw}+aZ_{cw})(Z_{ax}+Z_{bx}+Z_{cx})Z_{wx}-(Z_{ax}+a^2Z_{bx}+aZ_{cx})\times(Z_{aw}+Z_{bw}+Z_{cw})Z_{wx}]\end{aligned} \qquad (5)$$

$$Z_{21}' = Z_{21} - \frac{1}{3M}[(Z_{aw}+a^2Z_{bw}+aZ_{cw})^2Z_{ww}+(Z_{ax}+a^2Z_{bx}+aZ_{cx})^2Z_{ww}-2(Z_{aw}+a^2Z_{bw}+aZ_{cw})(Z_{ax}+a^2Z_{bx}+aZ_{cx})Z_{wx}]$$

$$M = \begin{vmatrix} Z_{ww} & Z_{wx} \\ Z_{wx} & Z_{ww} \end{vmatrix} = Z_{ww}^2 - Z_{wx}^2$$

The complexity of these equations may be reduced for easier computation by the use of symbolic representation. Let

$$\begin{aligned}A_w &= (Z_{aw}+Z_{bw}+Z_{cw})\\ B_w &= (Z_{aw}+aZ_{bw}+a^2Z_{cw})\\ C_w &= (Z_{aw}+a^2Z_{bw}+a^2Z_{cw})\\ A_x &= (Z_{ax}+Z_{bx}+Z_{cx})\\ B_x &= (Z_{ax}+aZ_{bx}+a^2Z_{cx})\\ C_x &= (Z_{ax}+a^2Z_{bx}+aZ_{cx})\end{aligned} \qquad (6)$$

Expressions 6 can be evaluated using the known values[1] of the complete self-impedance Z_{ii} and mutual impedance Z_{ik}, namely

$$Z_{ii} = \frac{0.830}{(100\ \mathrm{GMR})^2} + \frac{0.2860}{3} + j\left(\frac{2.8880}{3} + 0.2794 \log \frac{1}{\mathrm{GMR}}\right) \qquad (7)$$

$$Z_{ik} = \frac{0.2860}{3} + j\left(\frac{2.8880}{3} - 0.2794 \log D_{ik}\right)$$

Substituting the expressions 7 into equations 6 leads to

$$\begin{aligned}A_w &= 0.2860 + j\,2.888 - 0.2794 \log (D_{aw}D_{bw}D_{cw})\\ B_w &= 0.2421 \log D_{bw}/D_{cw} + j\,0.1397 \log (D_{bw}D_{cw}/D_{aw}^2)\\ C_w &= 0.2421 \log D_{cw}/D_{bw} + j\,0.1397 \log (D_{bw}D_{cw}/D_{aw}^2)\end{aligned} \qquad (8)$$

$C_w = -B_w^*$ (conjugate of B_w negative)

By use of equation 1

$$A_x = A_w,\ B_x = C_w = -B_w^*,\ C_x = B_w$$

Equations 8 show that the last four expressions 6 are either A_w or B_w. By substituting corresponding parts, equations 5 reduce to

$$Z_1' = Z_1 + \frac{1}{3M}\{[(B_w)^2+(B_w^*)^2]Z_{wx} + 2(B_w)(B_w^*)Z_{wx}\}$$

$$Z_0' = Z_0 - \frac{2}{3}\,\frac{(A_w)^2}{Z_{ww}+Z_{wx}}$$

$$Z_{01}' = Z_{01} - \frac{1}{3}\,\frac{A_w(B_w-B_w^*)}{(Z_{ww}+Z_{wx})} \qquad (9)$$

$$Z_{21}' = Z_{21} - \frac{1}{3M}\{[(B_w)^2+(B_w^*)^2]Z_{ww} + 2(B_w)(B_w^*)Z_{wx}\}$$

Sequence impedances without ground wires have been previously evaluated.[1] By substituting the relations of equations 1, which pertain to the horizontal configuration, the equations reduce to

$$Z_1 = \frac{1.612}{(100\ \mathrm{GMR}_a)^2} + j0.12134[\log S - \log \mathrm{GMR}_a + 0.231]$$

$$Z_0 = \frac{1.612}{(100\ \mathrm{GMR}_a)^2} + 0.2860 + j[2.888 - 0.12134(2 \log S + 0.462 + \log \mathrm{GMR}_a)]$$

$$Z_{01} = j0.02804;\ Z_{21} = -j0.05608 \qquad (10)$$

In order for equations 9 to be in proper form for the card program calculator, imaginary and real components must be separated. By defining a few more symbols, final expressions for the sequence impedances can be written. With new symbols

$$\begin{aligned}A_w &= a_1 + jb_1\\ (Z_{ww}-Z_{wx}) &= a_2 + ja_3\\ Z_1 &= C_1 + jK_1\\ B_w &= a_2 + jb_2\\ (Z_{ww}+Z_{wx}) &= a_4 + ja_4\\ Z_0 &= C_0 + jK_0\end{aligned} \qquad (11)$$

Substituting equations 11 into equations 9 and rearranging, the final forms of the sequence impedance equations result. Equations 12 are now in ideal form for digital computer solution

$$Z_1' = C_1 + \frac{2}{3}\left(\frac{a_2^2\ a_3}{a_3^2+b_3^2} + \frac{b_2^2\ a_4}{a_4^2+b_4^2}\right) + j\left[K_1 - \frac{2}{3}\left(\frac{a_2^2\ b_3}{a_3^2+b_3^2} + \frac{b_2^2\ b_4}{a_4^2+b_4^2}\right)\right]$$

$$Z_{21}' = \frac{2}{3}\left(\frac{b_2^2\ a_4}{a_4^2+b_4^2} - \frac{a_2^2\ a_3}{a_3^2+b_3^2}\right) - j\left[0.05608 - \frac{2}{3}\left(\frac{a_2^2\ b_3}{a_3^2+b_3^2} - \frac{b_2^2\ b_4}{a_4^2+b_4^2}\right)\right]$$

$$Z_{01}' = \frac{2}{3}\,b_2\left(\frac{b_1a_4 - a_1b_4}{a_4^2+b_4^2}\right) + j\left[0.02804 - \frac{2}{3}\,b_2\frac{a_1a_4+b_1b_4}{a_4^2+b_4^2}\right)\right] \qquad (12)$$

$$Z_0' = C_0 - \frac{2}{3}\left(\frac{a_1^2a_4 - b_1^2a_4 + 2a_1b_1b_4}{a_4^2+b_4^2}\right) + j\left[K_0 - \frac{2}{3}\left(\frac{b_1^2b_4 + 2a_1a_4b_1 - a_1^2b_4}{a_4^2+b_4^2}\right)\right]$$

A summary of the symbols used in equation 12 indicates that the only variables are G, W, S, GMR$_w$, and GMR$_a$ defined by Fig. 3.

$$a_1=0.2860$$

$$a_2=0.2421 \log D_{bw}/D_{cw}$$

$$a_3=\frac{1.612}{(100\ \mathrm{GMR}_w)^2}$$

$$a_4=a_3+0.1908$$

$$b_1=2.888-0.2794 \log (D_{aw}D_{bw}D_{cw})$$

$$b_2=0.1397 \log (D_{bw}D_{cw}/D_{aw}^2)$$

$$b_3=0.12134 \log D_{wx}/\mathrm{GMR}_w$$

$$b_4=1.9254-b_3 \tag{13}$$

$$C_1=\frac{1.612}{(100\ \mathrm{GMR}_a)^2}$$

$$C_0=C_1+0.2860$$

$$K_1=0.12134\left(\log \frac{S}{\mathrm{GMR}_a}+0.231\right)$$

$$K_0=2.888-0.12134[\log (S^2\mathrm{GMR}_a)+0.462]$$

where

$$D_{cw}=\sqrt{G^2+\left(\frac{w}{2}\right)}$$

and

$$D_{bw}=\sqrt{G^2+\left(S-\frac{w}{2}\right)^2}$$

then

$$D_{cw}=\sqrt{G^2+\left(S+\frac{w}{2}\right)^2} \text{ and } D_{wx}=W$$

The unbalance factors given by equation 2 can then be found by using the results of equations 12. Since the maximum unbalance for a particular line configuration is of most importance, only the absolute values of the unbalance factors have been computed. They are defined by the following

$$m_2=\frac{Z_{21}'}{Z_1'} \qquad m_0=\frac{Z_{01}'}{Z_0} \tag{14}$$

References

1. Electromagnetic Unbalance of Untransposed Transmission Lines, Eric T. B. Gross, M. Harry Hesse. *AIEE Transactions*, vol. 72, pt. III, Dec. 1953, pp. 1323–36.

2. 230-Kv Wood-Pole Transmission-Line Design, J. J. Trainor, L. B. LeVesconte. *Ibid.*, vol. 73, pt. III-A, June 1954, pp. 522–28.

3. Full Scale Structure Tests of 230-Kv Wood H Frames, W. A. Schulz. *Proceedings*, American Power Conference, Chicago, Ill., vol. XV, 1953, pp. 282–90.

4. Characteristics of H-Frame Wood-Pole Structures for 230-Kv Lines, F. E. Wolosewick. *Electric Light and Power*, Chicago, Ill., vol. 32, no. 11, Sept. 1954, pp. 96–102.

5. Modern Transmission Design Adapt Engineering Advances, Transmission Line Characteristics, Structure Configuration Diagrams. *Electrical World*, New York, N. Y., vol. 140, no. 8, Aug. 1953, pp. 121–50.

6. Magnetic Unbalance of Lines with Horizontal Conductor Arrangement, S. W. Nelson. *M.S. Thesis*, Illinois Institute of Technology, Chicago, Ill., Jan. 1955.

7. Unbalances of Untransposed Overhead Lines, Eric T. B. Gross. *Journal*, Franklin Institute, Philadelphia, Pa., vol. 254, 1952, pp. 487–97.

Protection of Personnel Against Electrical Shock Hazards in Central Office Communications Equipment

RAY V. JONES
ASSOCIATE MEMBER AIEE

WHILE the safety of employees has always been a consideration in the design of communications equipment, until recent years hazards from electrical shock have not been a serious problem since the voltages used were relatively low. Direct current of 48 volts or less has been employed for circuit operation and signaling, with some application of 130 volts. Alternating current has been employed for ringing subscriber bells, sometimes in combination with direct current, but the values have been low enough to be considered well below the limits for safety.

With the introduction of electronic facilities, higher voltages were introduced, although in many instances these higher voltages were not hazardous since it was not possible under normal conditions for a dangerous amount of current to be passed through the human body as a result of accidental contact with energized parts. In other cases, however, it was necessary, in order to insure safety to those operating and maintaining the equipment, to consider protection against possible shock hazards specifically in the design. This paper outlines the various precautions taken in the design of Bell System central office communications equipment to reduce to a minimum the possibility of dangerous electrical shock.

In the central office, primary power is in general received from commercial mains at a nominal 120 or 240 volts. Motor-generator sets or rectifiers are then used to float batteries for supplying the desired direct current. Alternating current for ringing purposes is also produced by motor-generator sets. No voltages higher than 48 or 130 are distributed throughout the office. Where such high voltages are required they are derived within the equipment with which they are to be used.

Equipment directly connected to commercial power service, including engine-alternator or battery-driven alternator sets to supply this power regularly or during emergency, have live parts insulated, guarded, or enclosed in cabinets. The power supplies in question generally involve operating voltages of less than 150 volts to ground. Warning signs are not considered necessary.

In the case of power used for signaling, switching, and operation of other communications equipment, the protective treatment provided is adapted to the level of voltage involved and is discussed here in three voltage categories. Such power includes battery supply, ringing, stepped-up alternating and rectified direct voltages, and stepped-down alternating voltage not directly connected electrically to the commercial power service.

Voltages Up to 150 Volts

No special precautions other than design layouts to minimize accidental short circuit or personnel contact are applied for cases involving up to 150 volts to ground rms a-c or nominal d-c, and not over 300 volts rms a-c across any bare parts. Enclosure in cabinets is employed when the type of equipment makes such enclosure desirable. When not enclosed certain live parts are protected by insulation.

Voltages From 150 to 600 Volts

For cases of 150 to 600 volts to ground rms a-c or d-c, and not over 1,000 volts rms a-c across any bare parts, insulation,

---

Paper 55-426, recommended by the AIEE Safety Committee and approved by the AIEE Committee on Technical Operations for presentation at the AIEE Summer General Meeting, Swampscott, Mass., June 27–July 1, 1955. Manuscript submitted February 24, 1955; made available for printing April 1, 1955.

Ray V. Jones is with the American Telephone and Telegraph Company, New York, N. Y.

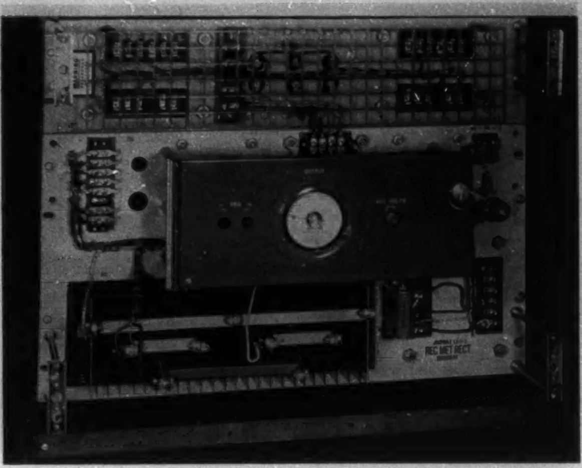

Fig. 1. TD-2 radio relay system, 24-volt regulated rectifier; front view, cover removed, hinged meter panel closed

isolation, and guarding are employed. For installations of this voltage range, it was formerly the usual practice to provide a door switch to disconnect the power supply automatically when a cover was removed or a door opened. However, experience over an extensive period has led to the conclusion that maximum safety and reliability, and greater maintenance flexibility, can be secured by concentrating attention on insulation, isolation, guarding, and effective warnings rather than placing dependence upon automatic door switches. The use of such protective devices was not particularly satisfactory where it was necessary for testing and adjusting purposes to operate the equipment with the cover removed and with normal power applied. There is a tendency for the attendant to block the safety switch rather than to apply operational safety precautions if the voltages involved are not in a range which he considers particularly hazardous. Where a circuit runs through several cabinets, door switches in series add to the complication and the opportunity for failure. Door switches may also interrupt important circuits if a cover is removed or a hinged door is opened before the load is transferred to reserve equipment. Where carrier or other multichannel systems are involved, a single power unit improperly shut down may cause nation-wide trouble on hundreds of channels. While the use of door switches affords a measure of protection to unauthorized or uninformed personnel, this obviously increases the difficulties of authorized maintenance men checking circuits under operating conditions.

High-voltage bare parts are isolated. If voltages must be checked, these parts are so arranged that they will be accessible to probes while protected against accidental contact. Supplemental enclosures or shields will be used and locations of higher voltages presenting possible hazard, such as 300 to 600 volts, will be marked with the maximum voltage involved if this appears to be practicable and useful. Pin jacks are brought out where necessary to make reading points accessible. High-voltage points requiring checking only at long intervals are protected by removable barriers fastened with screws or clips.

Appropriate warning signs are provided consisting of a metal plate or decalcomania reading "Warning—Hazardous Voltages" with the word "Underneath" added where appropriate. If the removal of an outer cover exposes live parts, the warning is applied to the outer enclosure. If all high-voltage parts are segregated and are under another inside cover or an inside guard, the warning is located on the inner cover or associated with the guard. The warning designation is placed in a prominent location visible both when guards are in place and when they have been removed for equipment repairs after power has been disconnected.

This voltage range covers most of the plate voltage rectifiers and other power sources operating at 130 volts output or higher since they will have voltages higher than 150 volts to ground across parts. By improving the isolating and guarding, and omitting the door switch, it is believed that greater safety during field operation is secured and accidental opening of working circuits is minimized. Point-to-point voltage readings specified in maintenance instructions are also facilitated.

Fig. 1 shows a rectifier for the *TD-2* radio relay system which exemplifies an equipment arrangement for the class of voltage under discussion.

High-Voltage Panel: For this rectifier the components above 150 volts are segregated on the upper panel (shown in Fig. 1); values of 600 volts are not exceeded. The panel is covered by a transparent plastic grid, further details of which are given later. By the use of this type of grid accidental contacts with live parts are prevented, but meter readings can be taken if necessary by the insertion of test probes through the grid. A warning sign is provided and located in such a position that attention will be drawn to it even with the grid in place. The sign remains on the panel when the grid is removed. The removal of the grid may be necessary in order that defective components may be replaced but the rectifier should be disconnected from its power source before the removal of a grid and not reconnected until the grid is replaced.

Low-Voltage Panel: The terminals and equipment on the lower panel and the hinged meter panel (shown in Fig. 1) operate at less than 150 volts to ground, and are not considered hazardous to a maintenance man working on the equipment. During normal operation a grounded metal cover encloses all live parts so nothing carrying voltage can be touched. Normal operation does not require removal of this cover.

Voltages Over 600 Volts

Power supply and other equipment involving voltages over 600 volts to ground rms a-c or d-c, or over 1,000 volts rms a-c across any bare parts, usually have a limited number of parts at high voltage, associated with other parts operating on low voltage. *L* carrier is an example of this class.

The high-voltage apparatus is isolated in a supplementary enclosure equipped with an automatic door switch and marked with a warning including the value of the maximum voltage. If some of the high-voltage equipment cannot be isolated, live parts are separately guarded and marked. Pin jacks are brought out to facilitate taking of high-voltage readings where these are necessary under operating conditions. A warning sign is provided on the inner enclosure to caution against possible interruption to service as well as against high voltages. In addition to the sign, there is stamped on the cover adjacent to the sign the approximate maximum value of the voltage across equipment terminals or to ground, such as 2,500 volts. The remaining lower voltage apparatus, if any, belonging to the high-voltage plant, is protected in accordance with the methods previously given, depending upon the classification of the apparatus which is outside of the inner enclosures. Usually an outer enclosure not equipped with a door switch will be supplied. There may, however, be cases where all the equipment is high voltage, or where only the high-voltage equipment need be enclosed, in which event a single enclosure only is used and the protection recommended in the previous paragraphs is applied.

Interlocks on High-Voltage Control Equipment

In certain types of plants it is necessary to perform maintenance operations on high-voltage equipment while the plant remains in service, and consideration is given to the use of key interlocks instead of door switches. One example is a 250-volt storage battery rectifier plant for plate supply. This includes a 56-cell battery plant added to the regular ±130-volt supply. Duplicate battery sections are provided, each in a separate locked cabinet, so that one section may be entirely disconnected for routine maintenance purposes while the remaining section floats across the rectifier carrying the office load. A key interlocking system prevents access to a cabinet without disconnecting its battery from the circuit. Each section is equipped with an ON and OFF switch, which is mechanically interconnected with three lock mechanisms. One lock prevents the switch from being operated to its OFF position until a master key has been inserted and turned. Two cabinet keys, one each for the front and rear cabinet doors of the section, are held in the other locking mechanisms until the switch is turned to the OFF position. The switch cannot be operated to its ON position again until both cabinet keys are restored to their proper locations in the supplementary locks. With the switch once thrown to its OFF position, the master key is "seized" and cannot be withdrawn so that the switch in the other section cannot be opened. This feature is provided in order to guard against disconnecting the load. When one of the cabinet doors is opened its key is "seized" until the door is again closed and locked. Thus the operation of the ON and OFF switch to its ON position is prevented if one of the cabinet doors is open. With the switch operated to the OFF position, the battery section is ungrounded and the maximum voltage obtainable is less than 120 volts. This particular system uses eight interlocks. More extensive plans have been developed for higher voltage systems for other uses.

Checking Voltages

The arrangements just discussed should permit safe maintenance and checking of all except the highest voltage units without taking the power plant out of service. The high voltages can also be checked while operating to the extent that pin jacks are provided, but the equipment must be shut down for other maintenance activities. Where jacks are not provided for taking certain infrequent high-voltage readings, temporary wiring to meters may be installed in some cases and the door reclosed while taking readings. It is preferable that the meters be located behind transparent panels, and that temporary high-voltage caution signs be placed to warn personnel in that vicinity. If the voltmeter has a multiplier, this should be connected so that the meter will be on the grounded side, if any.

Use of Series Resistors With Pin Jacks

The highest voltage standard portable instrument ordinarily available will be one having a maximum reading of 600 volts. On "high-voltage" equipment it will often be possible to read operating voltages by permanently installed panel voltmeters forming part of the equipment. Where point-to-point voltages of equipment over 600 volts to ground must be checked, consideration is given in the design to bringing out pin jacks to read a definite fraction of the high voltage to ground. One way of doing this is to put high series resistors between the voltage sources and the pin jacks which will act as built-in multipliers for the particular meter to be used. This should limit the current to about 1/2 mil, which is harmless even if the meter terminals should be accidentally touched.

It would also be possible to bring out the pin jacks from voltage dividers or potentiometers but this is not considered suitable under most conditions. Readings would be wrong if there is trouble in the divider and the high voltages up to full value would be put on the voltmeter if the divider connection to ground should be open. This would create a serious hazard to the attendant. For high-voltage, low-current supplies, as are used for cathode-ray tube accelerating anode potentials, consideration is given to providing inherent current-limiting features.

Protective Grids

A red-tinted plastic insulating grid has been made available for use in protecting against accidental contact with parts connected to voltages principally in the 150- to 600-volt class. This grid has ribs approximately 1/8 inch in cross section so spaced as to provide openings about 3/4 inch square through which test probes can be inserted. The grid is preferably located in such a position as to provide a clearance of 3/4 inch to 1 inch between the grid and live parts but in no case is this clearance less than 1/4 inch. It is held in place with clips so arranged as to permit ready removal of the grid if replacement of circuit components becomes necessary.

Test Probes

Two special test probes with enclosed voltage multipliers have been made available. One of these provides a multiplier for use on voltages up to 3,000 volts. It is suitably insulated so that a craftsman can manipulate it in taking readings without introducing a shock hazard. The other test probe is intended for use on up to 12,000 volts and has an enclosed 240-megohm series resistance. This type of device is intended for use in connection with video amplifiers and certain radio transmitters. It is arranged to be clipped to the point at which a reading is desired and the meter end of the attached lead is arranged to be hooked to the associated meter with a special safety connecting device to give full insulating protection from the inner live parts if the connector should be inadvertently attached or removed from the meter while the probe is connected with working voltages. The probe proper is highly insulated for protection in case it is necessary to hold the probe in position manually while taking a reading.

Another test probe for use on lower voltages has been made available. Although this device is not intended primarily as a means of insuring against high-voltage shock, it is, however, insulated to avoid contact by the user with the metallic inner parts of the tool. The contact member is surrounded by a retractable spring-loaded insulated tube which prevents undesired contacting with circuit elements. The contact member is not thrust forward to the opening of the tube for making connection with a circuit element until pressure is exerted against the spring toward the equipment under test. The tip of the contacting member is of hardened steel sharply serrated to produce several sharpened points. This feature tends to prevent slippage off the desired point of contact.

Means for Disconnection

All devices in any of the three voltage classes have means provided for disconnecting them locally without the necessity of going to a distant fuse panel. If a flexible cord is plugged into a power supply outlet this may be used. A toggle-type or other enclosed switch which indicates power ON or OFF may be employed. In some cases a fuse of the "Saf-to-fuse" or similar enclosed type may be used to disconnect the equipment locally for maintenance.

Discharging of Capacitors

If capacitors are of sufficient size to store harmful energy the circuit is normally provided with drainage resistors or other means to insure that any high-voltage charge leaks to ground promptly after power is removed. If this is impracticable they are marked with a warning and instructions are provided to cover a suitable method of discharging.

Mechanical Layout of Components

In locating parts, such as potentiometers, which may require adjustment by screw drivers or other tools while voltage is applied, care is taken to provide a free path for the tool so it will not come into contact with live parts during adjustment or in the event that it should slip off the screw head. The same applies to location of live parts which must be reached by voltmeter probes. Such probes are insulated for most of their length.

System-Planning Practices

AIEE COMMITTEE REPORT

THE SYSTEM Planning Subcommittee, Committee on System Engineering, in 1953 surveyed representatives in the electrical utility industry in regard to their system planning practices. All of those queried had representatives on the System Engineering Committee. Twenty-two responded.

This report presents the results of the survey. It does not purport to be conclusive or representative of the entire industry. However, it is believed to reflect the present practices of a group of utilities which have given definite support to the concept of system planning.

Definition of System Planning

The following definition of system planning was prepared early in 1953 by an Edison Electric Institute subcommittee and has been widely circulated through both Edison Electric Institute and AIEE channels. It appears to be generally acceptable and was used (without the last sentence) as a basis for the survey covered in the present report.

> System planning is the preparation of a rational program for the development of an electric power system, so that it can evolve in an orderly and economic manner. It includes forecasting and analyzing loads, rationalizing standards of service, anticipating trends in equipment design and coordinating the various elements of the system into a well-designed whole; it is particularly concerned with plans for changes and additions to generation, transmission, substations, and distribution facilities. It is not concerned with the problems of day-to-day operation or design except to the extent that these problems affect future system development. Briefly, electric system planning is the process of determining when, what facilities should be provided where in order to assure adequate electric service at minimum average annual cost to the community.

Purpose of Survey

Electrical utility system planning is a relatively new concept, as compared with design and operation. The purpose of the survey was to determine the present practices, trends, and individual company philosophies with regard to this function. This would include information indicative of the interest and responsibility of engineering, operating, and management personnel in planning. It was not intended to set up a standard pattern for a system planning organization but rather to point out for management consideration both similarities and differences in methods and viewpoints.

Survey Data

The questionnaire and a summarization of the data are presented in the Appendix. The detailed information obtained is interesting as an indication of the thinking of the respondents. However, it is the attitude and philosophy behind the answers that is most significant. Therefore, this report will deal principally with these matters under the following headings:

1. General.
2. Scope of planning.
3. Administrative control.
4. Responsibilities of the planning group.
5. Staffing of planning group.
6. Conclusions.

General

In the case of every company responding to the survey, management had recognized system planning as a necessity, and had provided in some way for its accomplishment. It appears to be ac-

---

Paper 55-529, recommended by the AIEE System Engineering Committee and approved by the AIEE Committee on Technical Operations for presentation at the AIEE Summer General Meeting, Swampscott, Mass., June 27–July 1, 1955. Manuscript submitted April 14, 1955; made available for printing May 12, 1955.

The personnel of the Working Group on System Planning Practices of the AIEE Committee on System Engineering are R. G. Hooke, *Chairman*, O. B. Charlton, G. C. Conner, A. P. Fugill, W. A. Gallotte, O. L. Giersch, J. R. Hango, R. F. Lawrence, L. B. LeVesconte, S. H. Lull, M. H. MacKenzie, E. L. Michelson, W. H. Osterle, L. R. Patterson, C. E. Parks, J. H. Rixse, Jr., T. W. Schroeder, J. J. Tesar, D. C. Vaughan, H. J. Vick, Jr., W. C. Westrate, G. S. Whitlow, and S. N. Witts.

cepted that "the preparation of a rational program for the development of an electric power system, so that it can evolve in an orderly and economic manner" is one of the most important factors to be considered by management. While the application of planning has been in practice from the days of the first Edison system, it has only recently been recognized as a function separate from design, construction, operation, and maintenance. As systems have become more complex, the number of alternative possibilities for action have become more numerous and the analysis of these alternatives, more time-consuming. This has led to establishment or changes in planning organization to provide management with the information upon which to make decisions. Illustrative of this is the fact that eight of 17 companies answering this question reported the setting up of planning organizations within the past 5 years.

It is apparent that each company is working out the practical application of system planning according to its own individual situation. There is a liberal mixture of planning committees with planning groups or departments; there are also numerous different allocations of responsibility for generation, bulk-power transmission, and distribution planning. The one common denominator, in addition to recognizing the need for planning, is recognition that planning requires a high degree of co-ordination. Perhaps the situation is the result of the fact that only recently have many managements become aware of the value of careful planning studies. The organization of planning departments seems to have evolved from the work done by the growing number of engineers whose efforts are in this area and whose recommendations form the basis for important decisions. For these engineers a practical working concept of planning has long been a necessity.

Scope of Planning

Assignments of the planning department vary considerably as to the system components studied. It was reported that 68 per cent (%) were involved to some degree in the planning of both generating stations and the transmission and distribution systems. All but one made both long-range plans of a general nature and more specific short-range plans for immediate application. As to the length of time covered by long-range plans, about half were for 10 or more years. There is a tendency to consider long-range planning in terms of a percentage of present load, e.g., 150%, 200%, and 300%, rather than to establish an exact time schedule.

Administrative Control

The administrative control of planning organizations shows a wide variation between companies. Nevertheless, the interest of management is demonstrated by the fact that the department is generally responsible to a high-level executive. In over half the cases, this was the person responsible for engineering. Existence of joint committees and the many cases of joint responsibility clearly reflect the need for close co-ordination which the planning leadership can initiate and assure. In five cases the department reported directly to a company officer. The survey could not determine the effectiveness of any particular method of administrative control.

Responsibilities of Planning Department

A general concept of the planning department implies that its responsibilities include system resources (generation, transmission and interconnection capacity) and the integration of these resources into an economic whole. It is primarily responsible for studies of the necessity for additions to system facilities and for economic comparisons of plans in roughly half of the companies reporting, and jointly responsible in another one-fourth.

In all companies the planners are engaged in studies of the transmission system, and in over three-fourths of the companies they have the primary responsibility for forecasting the need for and the general nature of transmission facilities to be required.

In more than half of the companies, the primary responsibility of the planning organization extends in some degree through the distribution substation, but the data show that there is a great variation in this respect.

That management considers it important that the plans be translated into dollars to assist financial planning can be seen from the fact that nearly all of the system planning departments have some responsibility for annual and long-range construction budgets and forecasts.

Responsibility for establishing standards for service reliability, reserves, and equipment ratings is in most cases shared jointly with others. Many believe that planning engineers can best act as coordinators in this area.

In forecasting system and area loads, about half of the planning departments have primary responsibility, but in only a few cases does this extend to detailed forecasting of distribution feeder loads. The latter is usually handled jointly by planning and distribution engineering groups.

Staffing of Planning Department

No attempt was made to draw general conclusions as to the proper size of a planning organization. The whole process of application of system planning in the electrical utility field is in a state of flux and growth. However, the summary, Table I, of the range of the 22 companies reporting may be of interest.

With some exceptions, the factors which appear to affect the ratios in Table I are the scope of the work performed within the group, whether the company was engaged in wholesale or retail operations, the type of supervision or administrative control, and the rapidity of load growth. No data were available to relate planning manpower adequately to revenue, investment, or rate of growth. This, however, is clearly a matter for each operating company to evaluate for itself, not only in relation to present and future load but also in relation to per cent of investment which may be affected by the activities of the planning department. Planning is a form of insurance of economic and logical development of a system and perhaps it can be evaluated as such.

Conclusion

The survey disclosed an increasing awareness on the part of management of the need for system planning. It also indicated that the majority of respondents consider this work most effectively handled if specifically assigned to a department organized for the purpose. Such a department is considered an important source for the information necessary to guide the huge future investment required by growing loads.

Appendix. Answers to Questionnaire on System Planning

I. Administrative Control

a. Is planning work under the direction of a particular department? If so, please name the department.

All of the organizations operating at the retail level reported that they had a system planning group. Only one wholesale power organization, dealing in transmission and marketing of power, reported that each branch did its own planning. One other wholesale organization had

Table I. Summary of Reports on System Planning

	Man Years per 100-Megawatt (mw) Load		
Classification	Minimum	Maximum	Median
Engineers	0.30	1.60	1.05
Technical assistants	0.06	0.50	0.24
Clerical	0.06	1.38	0.18
Total planning staff	0.60	3.25	1.49

planning divided between a central office and regional groups. Another had planning divided between the generation and transmission departments and commercial and distribution department.

Fourteen planning organizations are part of the engineering organization, two are part of the operating departments and five are independent.

b. If planning work is handled by a separate department, which officer of the company is responsible for its control?

Of the five companies engaged in retail distribution and where planning is a separate department, control is as follows:

Vice-president of engineering, operation, and construction
Vice-president of engineering and operations
Vice-president of operations
Assistant vice-president of operations
Executive engineer

One wholesale power organization had two planning groups reporting respectively to the vice-presidents of the generation and transmission and the commercial and distribution departments.

c. Are planning committees used? If they are, how are the memberships and assignments determined?

Six companies reported that they used standing committees for certain planning functions. Two of these companies specifically mentioned load forecasting as done by a committee upon which the system planning group was represented. In five cases there were committees containing representatives of the planning, engineering, operating, and production departments presumably for discussion and agreement on system plans.

Two companies reported the use of special committees to study major projects. Three other companies emphasized the use of conferences or informal discussion with other groups. It appears well recognized that planning, because of its broad effect, requires an unusually high degree of interdepartmental co-ordination.

d. If planning is a separate function, how long has it been so recognized?

Up to and including 5 years, 8
From 5 to and including 10 years, 2
Over 10 years, 7

This would appear to indicate that at least the system planning department in most utilities has been changed in recent years, either because of the increased size of the company or to improve organizational lines.

e. Where do planning assignments originate?

In nearly all cases, the answers indicated that many of the assignments originated within the planning department. One company stated, "Engineering Planning Section is charged with forecasting insufficiencies and initiating their solutions." Another answered, "Planning assignments generally originate within the System Development Division as an automatic step in the fulfillment of its duties. Some assignments originate in other divisions as the result of operating experience or as the result of problems which arise in these divisions and which can be more conveniently studied by the System Development Division." The unique viewpoint of one company was that "Planning assignments originate in the Engineering Department as a result of operating problems."

Many companies reported that planning engineers were sometimes given special problems by higher levels for study.

f. Is planning based on definite service standards which are prescribed by management?

No standards, 5
Based on standards considered as one of several factors, 6
Based on standards informally approved, 7
Based on standards formally approved, 5

Two companies listed as not having service standards modified their replies by saying, "not as yet." One company listed under "formally approved" stated that this applied to their underground system, but that there were no definite standards on overhead.

The answers appear to indicate that often in lieu of fixed standards, a balance is drawn between cost and expected service improvement.

II. Scope of Work

a. Does one group handle both electric system and generating station work?

15, YES
7, NO

Two companies answering YES stated that their participation was limited to such considerations as date required, general area of installation, and size. One company listed as NO above states that the planning division has a separate group handling generation as system resources.

b. Does the planning group handle both long- and short-range work?

21, YES
1, NO

The NO reply was modified by the statement that it applied to plans of less than two years' range.

c. At the present time, how far ahead has long-range planning been extended? If this is not considered sufficient, how far in the future is it thought long-range planning should extend?

Less than 10 years, 10
10 to 15 years, 8
Over 15 years, 3

This is approximate, since many replies represented a considerable spread, depending upon the type of planning. Several replies giving 200% load as their range were listed in the 10-to-15-year group, since the industry rate is about double load in 10 years. Many companies reported longer times for generating and transmission facilities than for distribution facilities.

Table II. Analysis of Answers to Question III

	Responsibility		
	Primary	Joint	Not Involved
a. General			
1. Design details	3	6	13
2. Requisitioning of equipment	2	2	20
3. Preparation of detailed construction estimates	1	3	20
4. Work on annual or long-range construction budgets or forecasts	13	8	3
5. Establishment of service standards and reserves	7	14	3
b. Load forecasting			
1. Forecast system load	12	3	9
2. Forecast area loads	15	4	3
3. Forecast distribution feeder loads	4	9	5
c. Low-voltage a-c networks			
1. Determination of equipment ratings	3	6	6
2. Determination of when new capacity is needed	4	6	5
3. Plans for supply stations	7	6	2
4. Plans for high-voltage feeders	5	7	3
5. Location and size of network transformers	2	4	9
6. Size and number of secondary mains	2	3	10
d. General distribution systems			
1. Determination of new equipment ratings	4	7	7
2. Determination of when new capacity is needed	8	8	2
3. Preliminary routes and size of supply lines to substations	11	2	5
4. Location and capacities of distribution substations	12	3	3
5. One-line diagram of distribution substations	7	6	5
6. Determination of short-circuit duties	7	5	6
7. Plans for relay protection	5	3	10
8. Preliminary routes and size of principal distribution feeders	4	5	9
9. Routes and size of distribution laterals	1	3	14
10. Size and location of distribution transformers	1	0	17
11. Size and location of capacitor banks	7	5	6
e. Transmission system*			
1. Determination of equipment ratings	5	15	3
2. Determination of when new capacity is needed	18	5	0
3. Preliminary routes and capacities of lines	15	8	0
4. Study of stability problems	18	5	0
5. Study of voltage regulation and reactive	17	6	0
f. Generating stations			
1. Determination of equipment ratings	7	9	6
2. Determination of when new capacity is needed	12	6	4
3. Prepare economic comparison of alternate plans for additional capacity	11	6	4

* Other duties were: To be primarily responsible for location and size of capacitor banks; and to determine economic size of conductor and overvoltage due to switching (on an extensive wholesale system).

Table III. Analysis of Answers to Question VI, a

Company No.	Engineers		Technical Assistants		Clerical Workers		All Classifications	
	Total	Per 100-Mw Load	Total	Per 100-Mw Load	Total	Per 100-Mw Load	Total	Per 100-Mw Load
1	13	0.75	4	0.23	3	0.17	20	1.15
2	15	1.36			3	0.27	18	1.63
3	24	1.32	1	0.06	4	0.22	29	1.60
4	2		1		1		4	
5	4	1.00			1		5	
6	5	1.32	1	0.26	0.5	0.13	6.5	1.71
7	1	0.50	1	0.50			2	1.00
8	8	0.44			3	0.16	11	0.60
9	53	1.66	3	0.10	6	0.19	62	1.93
10	53	1.46	15	0.41	50	1.38	118	3.25
11	8	1.09	1	0.14	1	0.14	10	1.37
12	4	1.00	1	0.25	1	0.25	6	1.50
13	11	1.60	3	0.43	4	0.57	18	2.60
14	7	1.40					7	1.40
15	6	1.55					6	1.55
16	9	0.60	4	0.25	2	0.12	15	0.97
17	3				2		5	
18	2	0.30	1	0.15	1	0.15	4	0.60
19	25	0.83	3	0.10	2	0.06	30	0.99
20	25				4		29	
21	2	0.5 to 0.67					2	0.5 to 0.67
22	13	1.30			4	0.4	17	1.70

The range in years of planning was generally less where load was growing rapidly.

III. Division of Responsibility

To what detail does the system planning group go in economic comparison and development of the preferred plan? Is it primarily responsible, jointly responsible, or not involved in the following?

See Table II. It will be noted that there are 24 answers from 22 companies. Two wholesale organizations answered for two divisions each.

Other duties were:

To determine need for voltage regulators, transient torques due to faults or synchronizing out of phase, method of grounding generator neutral, and short-circuit stresses in cables and busses.

To determine whether plant shall be of the base-load, peaking, or seasonal type.

To make economic studies of new projects.

IV. Other Routine Work

What routine work is handled by this group other than already covered?

Many items were mentioned here which were considered prerequisites for the work brought out in questions in Section III. These have been omitted in the listing of some of the more interesting answers to the question following:

1. Analyze trouble logs for preparation of data on service continuity. An annual report is issued to show trend of improvement.
2. Prepare progress reports on construction for management perusal.
3. Answer industry questionnaires, and Federal Power Commission and Public Utilities Commission reports.
4. Maintain population growth data, maintain data on interchange and area power pools, prepare studies of per capita use and utilization of equipment.
5. Make technical studies of operating problems.
6. Analyze system losses.
7. Supervise budget preparation.
8. Assemble job estimates prepared by other groups to obtain total cost and write request for authorization for funds, giving reasons for construction.
9. Carry on all network analyzer studies.
10. Act in an advisory capacity to the engineering, operating, administrative, and legal departments, furnishing from time to time such data and technical calculations as may be requested.
11. Represent company on planning and engineering problems dealing with intercompany matters on an interconnected system.
12. Supervise day-to-day dispatching. Provide data and technical information necessary for the dispatching group to carry on the day-to-day operation.

V. Degree of Responsibility

What is the degree of responsibility of the system planning group?

Somewhat unsatisfactory replies, due probably to the wording of the question, indicate that planning departments are generally responsible for forecasting any deficiencies in the ability of the existing system to meet expected increases in load, and either preparing plans or reviewing plans made by others for elimination of these deficiencies. In some cases, alternate plans are submitted to a committee with recommendations as to the preferred one. In other cases, only the preferred plan is submitted to either a committee or to management for final authorization or approval.

VI. Personnel

a. How many are engaged in planning work?

See Table III.

b. Are engineers in the planning department required to have prior experience in other departments of the company? If such prior experience is not required, is it considered desirable?

Required, 6
Not required but desirable, 15
Prefer to train in department, 1

Two companies stated that prior experience with other departments was not required, but that all engineers receive some training in other departments.

c. Is the planning group expanding faster or slower than other engineering and operating groups?

Faster, 8
Same, 9
Slower, 5

It is doubtful if these figures indicate any trend.

d. Does the planning group include a relay engineer?

YES, 10
NO, 12

However, one YES was qualified by the answer, "not as such." It will be noted that under question III, d, 7 five of the planning groups are primarily responsible for relay protection and three jointly responsible.

VII. General Comments

The following are representative of the general comments received:

"Planning work in our company is included in the duties of system operation and, therefore, the Electric Department. This brings the planning group in close contact with the Load Dispatching and the Transmission and Distribution group. General Engineering does not take part in planning except as work is assigned to them by the planning group, such as investigating a proposed plant site or hydro project from the construction angle. We normally use two engineers from Transmission and Distribution on all transmission problems, system arrangements, transmission estimates, board studies, etc. In our company, the Electric Department includes Generation, Operations and Transmission and Distribution. General Engineering is a separate department and handles design details, detailed cost estimates and construction of plants."

"It should be pointed out here that the personnel reported in VI*a* rely on regular conferences with the Superintendent of Engineering and the Assistant Superintendent of Engineering and other senior engineers for planning work."

"It is also important that all other departments do originate and contribute planned improvements through the Superintendent of Engineering."

"The System Planning Division of the General Manager's Department is a relatively new (1950) organization. The division works jointly with and is gradually assuming planning functions from various divisions of the Operating Department. These divisions previously assumed planning functions in addition to construction-operation functions."

"Negotiations with larger customers (7,500 HP and over which are usually served from the Transmission System) are handled jointly with the Commercial Department."

"It is anticipated and desirable that a larger share of budget functions be assumed by the System Planning Division."

"System Planning includes Communications planning and Load and Frequency Control planning. Another group operates the A.C. Network Analyzer and prepares reports on the studies. The engineers are also consultants on technical matters for other departments."

"Much of our planning is carried on in consultation with Consulting Engineers, particularly on generating plant studies and occasionally on load studies."

"Other general duties are kept to a minimum. However, it is obvious that those who made the plan must follow through some of the details and operating results . . . all applications for loads above 100 Kw which may require expansion of facilities at any voltage are cleared through the planning office."

"Planning group is primarily responsible for maintaining the statistical parameters of the system."

Quadriphase—A New Approach to Time Division Multiplexing

W. E. EVANS NONMEMBER AIEE
R. F. LOWE ASSOCIATE MEMBER AIEE

THE commercial microwave communication industry has supported a more or less continuous controversy on time division versus frequency division multiplexing. One of the conclusions which may be drawn from these discussions is that time division has certain theoretical advantages. That is, whenever a multichannel communication system is pushed to its ultimate performance by the length of the system, or by simultaneous and continuous loading of a high percentage of the channels, time division multiplex can produce higher signal-to-noise ratio and lower crosstalk.

However, the master timing or synchronization of a time division multiplex system presents many practical problems. Generally this master timing has required either complex wave forms such as the saw-tooth or a sharp "timer pip" spike, or multiple complex networks to delay a master pulse wave form by various amounts. Most time division synchronizing systems have required very precise, very stable plate and bias voltages. Until now, it has been found that excellent design, top quality components, regulated power supplies, and good maintenance were required to achieve the theoretical advantages of time division multiplexing.

New Concept of Synchronization

To overcome these practical drawbacks, a completely new approach to the synchronization problem has been taken In the conception of the quadriphase system, simplicity of design, operation, and maintenance has been a prime requisite. The designers were faced with two questions:

1. What is the most simple wave form: the easiest to generate and to carry from the master generator to several slave units?
2. What component is the simplest, the least expensive, and the most trouble-free?

The answers to these two questions are really quite obvious. The simplest wave form is a low-frequency sine wave; the most elementary component is the resistor. These two, the sine wave and the resistor, form the heart of the quadriphase system.

The sine wave is not generally considered as a good timing signal because of its wide variations in slope. However, the portion of a sine wave in the immediate vicinity of the zero axis is very linear and can be used as an accurate time base.

The segment *a-b* of Fig. 1 is the part of the sine wave with a slope steep enough and linear enough to be used as an accurate timing signal. The remaining problem is to make use of only the linear portion. To accomplish this, the phase

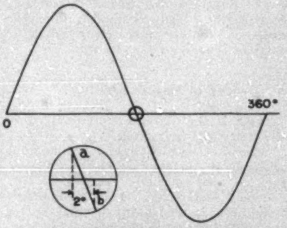

Fig. 1. Sine wave showing the linear portion usable for timing

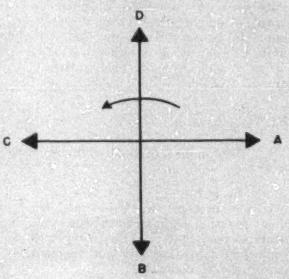

Fig. 2. Vector representation of the master synchronizing signal

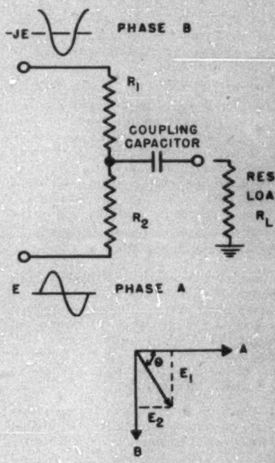

$$E_1 = \frac{E\ R_1\ R_L}{R_1\ R_2 + R_2\ R_L + R_1\ R_L}$$

$$E_2 = \frac{E\ R_2\ R_L}{R_1\ R_2 + R_2\ R_L + R_1\ R_L}$$

$$\tan\ \theta = \frac{R1}{R2}$$

Fig. 3. Schematic diagram and explanation of operation of a phase-dividing network

---

Paper 55-517, recommended by the AIEE Carrier Current Committee and approved by the AIEE Committee on Technical Operations for presentation at the AIEE Summer General Meeting, Swampscott, Mass., June 27–July 1, 1955. Manuscript submitted March 28, 1955; made available for printing May 5, 1955.

W. E. Evans and R. F. Lowe are with the General Electric Company, Syracuse, N. Y.

The authors wish to acknowledge the development of the original concept of the quadriphase system by H. P. Thomas and P. G. Smee of the General Electric Company, Syracuse, N. Y.

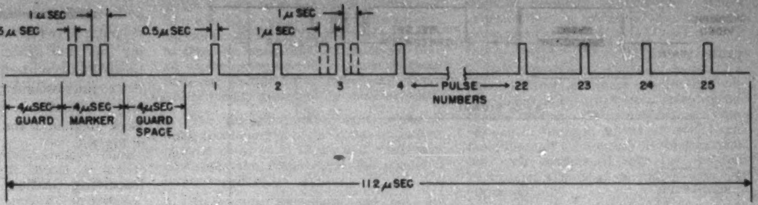
1 µSEC
0.5 µ SEC
0.5 µSEC
1 µ SEC
1 µ SEC
1
2
3
4
PULSE NUMBERS
22
23
24
25
4µSEC GUARD
4µSEC MARKER
4µSEC GUARD SPACE
112 µSEC

Fig. 4. One frame of the composite multiplexed signal showing pulse number 3 modulated 100 per cent

of the sine wave must be shifted by finite increments through 360 electrical degrees. More precisely, the phase of the master sine wave must be shifted so that its zero point at which the voltage is going from negative to positive will occur at the beginning of the time space allocated to each channel of a multichannel system. It is neither practical nor in keeping with the simplicity requirements to achieve this by employing a completely different phase-shifting network for each channel.

A single sine wave can readily be made into two such waves phased exactly 180 degrees apart by a conventional paraphase amplifier or phase inverter. If each of these two waves is shifted 90 degrees by a stable, temperature-compensated resistance capacitance network, we then have four sine waves of exactly the same frequency and phased in quadrature, i.e., "quadriphased." These may be represented in vector form as shown in Fig. 2.

With these four sine waves as a master timing signal, it is possible to use networks containing only resistors to form a sine wave of any desired phase. This is illustrated in Fig. 3, which shows two resistors connected in series from phase *A* to phase *B*. The voltage developed across the load is a sine wave whose phase is dependent upon the relative value of the two resistors. It is shown in Fig. 3 that the output phase of the divider is completely independent of loading as long as the load is resistive. Thus there is a "phase divider." With this simple type of device it is possible to produce a sine wave of any desired phase.

Only a very small portion of the sine wave in the immediate vicinity of the zero axis (much less than the total linear portion indicated in Fig. 1) will be used for the actual timing of the channel pulses. Therefore, the amplitude of the quadriphase voltages is not critical; regulated plate voltage is not required in any part of the quadriphase system.

System Design Considerations

The frequency chosen for the master sine waves will be equal to the frame repetition rate, which is the sampling rate for each channel. To keep audio distortion low, it is desirable to have the sampling rate approximately 3 times the maximum audio frequency to be transmitted. Using this criterion, the frame rate and thus the oscillator frequency must be in the range from 8 to 10 kc for telephone voice channels which normally have a bandwidth of about 300 to 3,000 cycles per second. If the time allocated to each channel is chosen at 4 microseconds, and if a like time is provided for the marker and for the guard space on either side of the marker, a 25-channel system requires a total of 28 intervals of 4 microseconds or 112 microseconds per frame. Fig. 4 shows one frame of the composite multiplex signal for such a system using pulse position modulation. This frame period results in an oscillator frequency of 8,929 cycles per second.

Transmitting Section

MASTER SYNC GENERATOR

Fig. 5 is a block diagram of the master sync generator. The tuned plate circuit of the master oscillator employs a toroidal coil with a *Q* of approximately 200 assuring excellent frequency stability. Negative feedback is employed for amplitude stability. The output of the oscillator drives a paraphase amplifier to

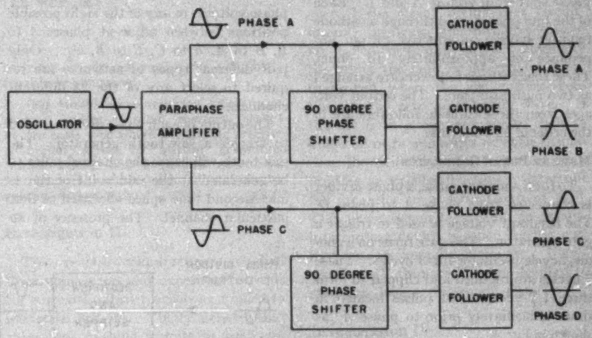
OSCILLATOR
PARAPHASE AMPLIFIER
PHASE A
PHASE C
90 DEGREE PHASE SHIFTER
90 DEGREE PHASE SHIFTER
CATHODE FOLLOWER
CATHODE FOLLOWER
CATHODE FOLLOWER
CATHODE FOLLOWER
PHASE A
PHASE B
PHASE C
PHASE D

Fig. 5. Master sync generator

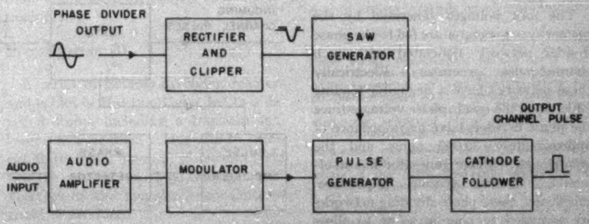
PHASE DIVIDER OUTPUT
RECTIFIER AND CLIPPER
SAW GENERATOR
OUTPUT CHANNEL PULSE
AUDIO INPUT
AUDIO AMPLIFIER
MODULATOR
PULSE GENERATOR
CATHODE FOLLOWER

Fig. 6. Channel-pulse generator and modulator

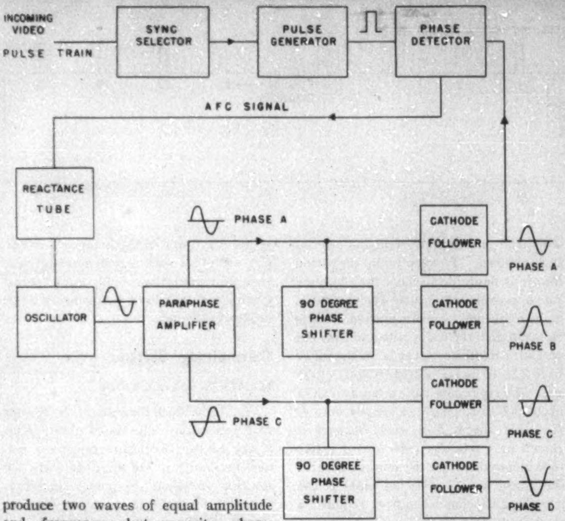
INCOMING VIDEO
PULSE TRAIN
SYNC SELECTOR
PULSE GENERATOR
PHASE DETECTOR
AFC SIGNAL
REACTANCE TUBE
PHASE A
CATHODE FOLLOWER
PHASE A
OSCILLATOR
PARAPHASE AMPLIFIER
90 DEGREE PHASE SHIFTER
CATHODE FOLLOWER
PHASE B
CATHODE FOLLOWER
PHASE C
PHASE C
90 DEGREE PHASE SHIFTER
CATHODE FOLLOWER
PHASE D

Fig. 7. Receiving sync generator

produce two waves of equal amplitude and frequency, but opposite phase. (Vectors *A* and *C* of Fig. 2.) Vectors *B* and *D* of Fig. 2 are obtained by 90-degree phase shift from vectors *A* and *C*. Each of the four phases is fed through a cathode follower having an effective output impedance of approximately 10 ohms. These four cathode followers are arranged as two push-pull pairs. The output voltages from these cathode followers are in the order of 35 volts rms.

Marker Pulse Generator

To form a marker pulse, a phase divider is connected from phase *A* to phase *D*. The resultant voltage is used to trigger a gate generator. This gate turns on a one-megacycle oscillator for 3 cycles. These 3 cycles are rectified and clipped to form three 1/2-microsecond pulses located in time, immediately prior to phase *A*, as shown in Fig. 4.

Channel Pulse Generator and Modulator

The four voltages generated by the master sync generator are fed to the phase divider network associated with each channel-pulse generator. Electrically these networks have a negligible loading effect upon the quadriphase voltages since the phase dividers have an impedance of approximately 30,000 ohms and the quadriphase voltage generator has an effective 10-ohm driving impedance. Physically, these phase-dividing networks are arranged to plug in so as to allow connection of the networks to the quadriphase voltages in any of the eight possible positions between adjacent phases *A* to *B*, *B* to *A*, *B* to *C*, *C* to *B*, etc. Only four different types of networks are required to select any of the 25 different channels.

The output of each phase divider is used to trigger a saw-tooth generator. The saw-tooth will cause the channel pulse to be generated at the mid-point of the 4-microsecond time space allocated to that particular channel. The presence of an audio modulating signal causes the channel pulse to be formed earlier or later during this time space. Maximum deviation from the center position is limited to ±1.1 microsecond. Nominal 100 per cent modulation is ±1 microsecond. A block diagram of the modulator is shown in Fig. 6.

Receiving Section

Receiving Sync Generator

The receiving synchronizing equipment as shown in Fig. 7 contains an oscillator, paraphase amplifier, and cathode followers similar to the transmitting equipment for generating the quadriphase voltages. The oscillator, however, is controlled by an automatic frequency control circuit and reactance tube to maintain synchronism of the quadriphase voltages with the received pulse train. A marker selector is employed to detect the marker pulse (by virtue of its make-up of three 1/2-microsecond pulses closely spaced). The recurrence rate and the phase of this separated marker are used to derive the automatic frequency control signal.

Demodulator

The quadriphase voltages are connected to the phase-dividing networks for each of the individual channel demodulators. The output sine wave of each network is used to trigger a gate generator whose output is a positive gate of 4 microseconds' duration. This gate is used to bias the video input section of the demodulator to allow it to accept any channel pulse occurring during the gate interval, but to reject all others. The modulation on the channel pulse is detected by means of a balanced phase

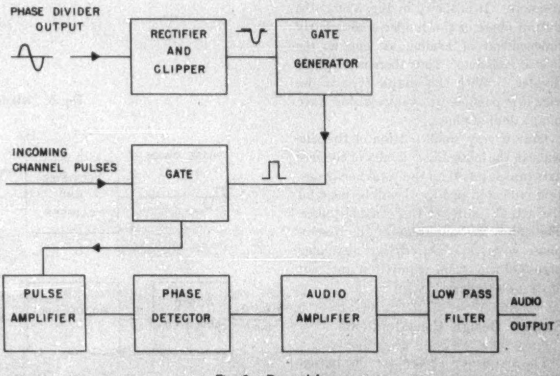
PHASE DIVIDER OUTPUT
RECTIFIER AND CLIPPER
GATE GENERATOR
INCOMING CHANNEL PULSES
GATE
PULSE AMPLIFIER
PHASE DETECTOR
AUDIO AMPLIFIER
LOW PASS FILTER
AUDIO OUTPUT

Fig. 8. Demodulator

detector. A low-pass filter is used to remove any high-frequency components present in the detector output as a result of the sampling process. Fig. 8 is a block diagram of the demodulator.

Conclusions

1. The system described employs pulse-position modulation. It should be noted that the quadriphase principle of synchronization is equally applicable to systems utilizing pulse length, pulse amplitude, or pulse code modulation.

2. Because of the simplicity of the timing signal, fewer tubes are required for its generation, which inherently reduces both manufacturing and maintenance costs.

3. The simple form of the timing signal makes it easy to detect electronically any failure or false operation of the synchronizing equipment and to transfer automatically to stand-by equipment. This means that all vacuum-tube circuits common to more than one channel of a microwave system can be readily protected by stand-by units.

4. The negligible effect upon channel-pulse positioning of plate voltage variations of as much as 10 to 15 per cent completely eliminates the requirement for regulated power supplies.

5. Since only the phase and not the amplitude of the timing voltage affects channel pulse position, tube-aging can be detected during routine maintenance long before any faulty operation of the system occurs.

6. Simple plug-in arrangement of the phase-dividing networks provides the utmost in flexibility in changing channel assignment of a particular facility when rearranging system channel layout or when expanding an existing system.

7. Eight-position, plug-in feature of phase-dividing networks results in only four different networks for a complete 25-channel system. These networks are comparable in function to the channel band-pass filters of a frequency division system, but each consists of only two resistors instead of a number of inductances and capacitors.

8. A time division multiplex system using the quadriphase system for channel timing is simpler to maintain, has fewer tubes, and is affected less by line voltage variations than any previous time division system. It is more than adequate to meet today's high standards for microwave system performance and reliability.

Review of the Factors Concerned with the Use of Protective Devices Shunting Reactors

AIEE COMMITTEE REPORT

Scope

THIS report is limited primarily to a study of factors concerned with the use of protective devices for shunting current-limiting reactors, including neutral grounding reactors, as normally applied in American transmission and distribution practice. The study was undertaken because of a growing interest in the subject and because there is very little published information available. It is hoped that the recommendations which the Working Group is making will be useful to those seeking guidance in the use of protective devices shunting reactors. The work of the group was divided into several separate investigations, each of which is described in some detail in the Appendixes. These investigations are outlined in the following.

Investigation I

A questionnaire was sent out to 45 power companies and from the results it was possible to conclude that:

1. Very little trouble has been associated with the use of current-limiting reactors.

2. Cable faults, apparently accompanied by transient overvoltages, were indicated as being largely responsible for what little trouble has occurred.

3. No trouble was reported where protective devices shunted reactors, except in two cases, one where a lightning arrester connected across a neutral grounding reactor failed, and a second where the terminals of a resistor-shunted cable-feeder reactor flashed over.

Investigation II

Two reactor manufacturers studied their application and experience records for current-limiting reactors as applied to industrial systems. They concluded that there was nothing unique in such applications distinguishing them in any way from the typical power company installations which were the subject of the questionnaire.

Investigation III

A series of failures involving reactors and cables in Havana, Cuba, led to a detailed study, including a transient-analyzer investigation. This study indicated that the forcing of current zero was the only way in which transient overvoltages of the magnitude encountered could be produced.

The results of the preceding investigations indicated that the majority of the cases of trouble were due to system transient overvoltages. Circuit changes that produce the highest transient overvoltages are known to involve arc paths. The arc path may be in a fault or it may be in a circuit-interrupting device such as a circuit breaker. If intermittent arcing takes place in a fault to ground, the phenomenon is called an arcing ground. However, if the arcing occurs in a circuit-interrupting device, the voltages produced are called switching surges. Normally the arc in the fault or interrupter is extinguished when the arc current goes through the zero point of its wave. If the arc is in a confined space, such as under oil or in apparatus or cable insulation, the deionizing agents present may produce an expulsion action to interrupt the arc prior to a normal current zero. This phenomenon in a fault or circuit-interrupting device is called forcing current zero or chopping of the arc. Investigations IV through VI were devoted to studying these arcing conditions.

Investigation IV

A general study using an analogue computer was made of transient overvoltages due to arcing grounds on circuits involv-

---

Paper 55-557, recommended by the AIEE Protective Devices Committee and approved by the AIEE Committee on Technical Operations for presentation at the AIEE Summer General Meeting, Swampscott, Mass., June 27–July 1, 1955. Manuscript submitted March 30, 1955; made available for printing May 6, 1955.

This report was prepared by the Working Group of the AIEE Fault Limiting Devices Subcommittee of the AIEE Committee on Protective Devices. Personnel of the Working Group are: J. C. Russ, *Chairman*, G. D. Bruer, G. B. Dodds, W. H. Eason, F. R. Longley, L. E. Sauer, O. L. Sidenfaden, R. S. Smithley, C. L. Wagner, and G. W. Walsh.

ing current-limiting reactors. From the study, it was concluded that:

1. Highest overvoltages occur on ungrounded systems. A resistance shunt will reduce the transient voltage across the reactor but will not reduce the voltage to ground.

2. Even on solidly grounded systems, high overvoltages can occur under certain conditions. One case studied showed the cable capacitance to be resonant with the reactor under arcing fault conditions, with the result that overvoltages as high as 400 per cent (%) occurred. These voltages can be reduced by properly designed shunt resistors.

3. Forcing current zero in circuits which have reactors can produce overvoltages many times worse than arcing grounds in which the current is extinguished at normal current zero.

4. Reactors installed on cable systems either grounded or ungrounded are more likely to be subjected to higher voltages than on other systems since cable insulation has the "expulsion" action necessary for the extinguishing and reigniting of the arc which produces the arcing ground phenomena. This expulsion action also may force current zero in the arc.

Investigation V

A review of experience with forced current zero and investigations of faults through solid dielectrics by one manufacturer indicates that:

1. Circuit breakers can force current zero but the overvoltages resulting are not likely to exceed three times the normal line-to-neutral voltage.

2. Where arcs occur through solid insulation, as in cable faults, the deionizing gases can produce an expulsive interruption, forcing current zero at a much higher rate than circuit breakers. This expulsive action will not occur when the ground-fault current is of sufficient magnitude to blow a large hole in the insulation during the first half-cycle.

3. The circuit is predominantly reactive under the fault or switching conditions.

Investigation VI

A review of the literature on forcing current zero and on postconductivity as a cause of circuit-breaker restriking indicates that:

1. Circuit breakers can force current zero but American circuit breakers are usually designed so that they do not.

2. In rare cases, where chopping is suspected, a resistor should be installed shunting the reactor.

3. Reactors, although they do have an effect on postconductivity, do not increase the severity of circuit-breaker duty.

Table I. Questionnaire Data on Reactor Applications

Voltage Range, Kv	Protection	Generator Neutral		Generator Phase Leads		Generator Phase Leads, Duplex		Load Bus Tie		Synchronization Bus Tie		Generating Station Tie		Transformer Neutral		Overhead Feeder		
		App	Tr	App	Tr	App	Tr	App	Tr	App	Tr	App	Tr	App	Tr	App	Tr	Br
2.3 to 7.2	none	2		1				9	many	1		3		3	1	6	many	B
	Q							1								1		F
	S															1		F
	T															1		F
																5		B
	U			1														
	V	1																
	*															1		B
11.0 to 16.5	none	6		9	1			11	1	6		11		5		2		B
																5	1	F
	Q	2						1		1						2		B
	QR													1				
	QY																	
	R													1	1			
	S	1														1		F
																2		B
	T															1		F
																1		BF
	TU															1		F
	TV					1												
	U							1				1				1		F
	V	2				1												
	W																	
	X	1														1	12	?
	X_1															1		?
	*							1						1		1		B
22 to 69	none	1	several					5		1		2		4		1	5	B
																1		?
	Q											1		1		1		B
	QT															1		B
	T															3		B
	TU															1		B
	U															1		B
	W_1							1										
	*													1				
100 to 220	none							1						1				
	Q													1				
	R													2				
	S													1				
	U							1				1						
	*													1				
	W_2													1				

App = no. of applications
Tr = no. of troubles
Br = breaker location
B = bus side of reactor
F = feeder side of reactor
*Arrester protection; type not specified
Q = shunt resistor
R = shunt lightning arrester
S = shunt air gap
T = arrestor connected L-G on feeder side of reactor
U = arrestor connected bus-to-ground
V = customary rotating machine protection—arrester & capacitor
W = high-frequency absorber
W_1 = arrester on transmission lines and banks
W_2 = shunt capacitor
X = arrester on cable riser connecting to O.H. feeder
X_1 = arrester on line and bus sides of reactors
Y = arrester on O. H. feeders

Investigation VII

A study of the requirements for protection of neutral grounding reactors reveals that:

1. The practice regarding protection of transformer neutrals is well established. It consists of shunting the reactors with arresters or resistors having characteristics that will protect the neutral insulation level.

2. Rotating machines having direct exposure to lightning may need additional surge capacitors (in addition to those normally used for winding protection) at the machine terminals to protect the machine neutral.

3. From a switching-surge standpoint, high transient overvoltages on rotating machines and their neutrals are avoided if the system is grounded so that X_0/X_1 is less than 10, although lower values of X_0/X_1 will further limit transient overvoltages.

4. Overvoltages can occur when an arc is extinguished at other than normal current zero, but inasmuch as the probability of such overvoltages being excessive is very remote, the use of protective equipment shunting machine neutral reactors for this purpose is usually not considered justified.

Conclusions

The Working Group has reached the following conclusions as a result of its studies:

SERIES CURRENT-LIMITING REACTORS

1. Series current-limiting reactors have an excellent record for reliability. There has been very little trouble associated with their use.

2. The great majority of applications have no protective device shunting the reactor.

3. In a preponderance of cases where trouble has occurred it has been in connection with cable feeders or with overhead feeders served by cable risers. In such applications it appears that arcing grounds through cable insulation can, under certain circumstances, force current zero with resulting overvoltage at the reactor.

4. Properly designed shunt resistors or lightning arresters will protect series current-limiting reactors, even in the most adverse circumstances, and will control switchgear and bus overvoltages which might otherwise result from the presence of the reactor in the circuit.

NEUTRAL GROUNDING REACTORS

1. Transformer neutral reactors are normally equipped with shunting resistors or arresters.

2. When rotating machine neutrals need protection, the requirements are more universally met by adding protective capacitors to the machine line terminals than by adding devices in shunt with the neutral reactor.

Recommendations

SERIES CURRENT-LIMITING REACTORS

1. Where there is exposure to lightning, standard protective practices should be followed, with the precaution that adequate lightning arresters are connected to ground on the line side of the reactor.

2. Protective shunts are not recommended for installation across series current-limiting reactors except where a user is unwilling to assume the small calculated risk of trouble developing in applications involving cable feeders or overhead feeders with cable risers.

Table I. (Continued)

Voltage Range, Kv	Protection	Cable Feeder			2-Cable Feeders, Duplex			One Overhead 1-Cable Feeder, Duplex			Transformer Phase Leads		Transformer Phase Leads, Duplex		Duplex in Generator Station Tie with Transformer on Mid-Point		Synchronous Condenser Neutral		Tertiary of Auto-transformer	
		App	Tr	Br	App	Tr	Br	App	Tr	Br	App	Tr	App	Tr	App	Tr	App	Tr	App	Tr
2.3 to 7.2	none	6	2	*B*							3									
		1		*F*																
	Q	1		*F*																
	S																			
	T	2		*B*																
	U																			
	V																			
	*																			
		1		*BF*	1		*B*				2		1		1		1		1	
11.0 to 16.5	none	14	6	*B*	1		*F*													
		2		*F*																
	Q	3	2	*B*							1									
	QR																			
	QY							1		*B*										
	R	1																		
	S																			
	T	1	0	*B*																
	TU																			
	TV																			
	U	1		*B*																
	V																			
	W	1		*F*																
	X																			
	X_1																			
	*																			
22 to 60	none	4		*B*							2									
		1		*BF*																
	Q	1		*B*																
	QT																			
	T																			
	TU																			
	U																			
	W_1																			
	*																			
100 to 220	none	1		*F*																
	Q																			
	R																			
	S																			
	U	1		*B*																
	*																			
	W_1																			

Table II. Application, Protection, and Failures

Reactor Application	Total No. of Companies Using Application	Voltage, Kv	Protected or Unprotected	No. of Companies Having Application	No. of Companies Having Trouble	No. of Trouble Cases
Column no.	2	3	4	5	6	7
Cable feeder	22	2.3–7.2	protected	3	0	0
			unprotected	7	1	several*
		11.0–16.5	protected	6	1	1
			unprotected	17	7	18†
		22–220	protected	2	0	0
			unprotected	5	0	0
Overhead feeder	21	2.3–7.2	protected	9	0	0
			unprotected	6	0	0
		11.0–16.5	protected	12	1	12‡§
			unprotected	7	0	0
		22–69	protected	7	0	0
			unprotected	2	1	5
Load bus tie	19	2.3–7.2	protected	1	0	0
			unprotected	9	2	many
		11.0–16.5	protected	3	0	0
			unprotected	11	1	1
		22–220	protected	2	0	0
			unprotected	5	0	0
Generating station tie	17	2.3–220	protected	3	0	0
			unprotected	16	0	0
Generator neutral	14	2.3–16.5	protected	6	0	0
			unprotected	7	0	0
		22	unprotected	1	1	several
Transformer neutral	13	2.3–7.2	unprotected	3	1‖	1
		11.0–16.5	protected	3	1	1
			unprotected	5	0	0
		22–220	protected	5	0	0
			unprotected	4	0	0
Generator phase leads	9	2.3–7.2	protected	1	0	0
			unprotected	1	0	0
		11.0–16.5	unprotected	9	1	1
Transformer phase leads	8	2.3–69	protected	1	0	0
			unprotected	7¶	0	0
Synchronizing bus tie	6	2.3–69	protected	1	0	0
			unprotected	8	0	0

*All trouble cases occurred on a cable riser to an overhead feeder during periods when the overhead feeder was disconnected from the riser.

†One case of trouble caused by a fault on a cable riser to an overhead feeder.

‡Protection was lightning arresters connected to ground.

§All trouble occurred on feeders having cable risers.

‖Reactor normally shunted by 400-ampere fuse.

¶In one case reactor normally shunted by breaker.

NEUTRAL GROUNDING CURRENT-LIMITING REACTORS

1. All transformer neutral reactors should be equipped with shunting arresters (resistors may be used in the lower voltage ranges).

2. The neutrals of reactor grounded rotating machines usually need no protection from switching surges if the system is grounded so that X_0/X_1 is less than 3. For values of X_0/X_1 greater than 3 it may be necessary to apply protective equipment, shunting the reactor where the system constants are such as to permit transient overvoltages to occur.

3. Where there is lightning exposure it is recommended that the machine neutral be protected by increasing the machine terminal capacitance to ground to at least 1/2 microfarad per terminal.

Appendix I. Report on Questionnaire

Objectives

A questionnaire was prepared by the Working Group for circulation among a sample group of power companies with the following objectives in mind:

1. To obtain information concerning the various methods in which reactors are connected to power systems.

2. To determine what type of surge protective devices, if any, are used in conjunction with the reactors.

3. To determine the incidence of troubles arising from surge voltages.

4. To determine whether the protection was adequate in all cases where surge protective devices were used.

5. To determine which types of application are considered to require special consideration of surge overvoltages.

The questionnaire was sent to 45 power companies, and replies were received from 34. Table I presents in detail the data obtained from the replies to the questionnaire.

Summary

REACTOR CONNECTIONS

The reactor applications reported on include applications in:

1. Cable feeders.
2. Overhead feeders.
3. Load bus ties.
4. Generating station ties.
5. Synchronizing bus ties.
6. Generator neutrals.
7. Generator phase leads.
8. Transformer neutrals.
9. Transformer phase leads.

TYPES OF SURGE PROTECTIVE DEVICES

Some type of surge protective device was applied by some companies to all of the listed applications. The types of surge protective devices reported on include:

1. Shunt resistor.
2. Shunt lightning arrester.
3. Shunt air gap.
4. Shunt capacitor.
5. Arrester connected line-to-ground on feeder side of reactor.
6. Arrester connected bus-to-ground.
7. Arresters on transmission lines and banks.
8. Arrester on cable riser connecting to overhead feeder.
9. Arrester on both line and bus sides of reactors.
10. Arrester on overhead feeders.
11. Arrester protection, type not specified.
12. Customary rotating machine protection consisting of arrester and capacitor.
13. High-frequency absorber.

INCIDENCE OF TROUBLE ARISING FROM SURGE VOLTAGES

There were relatively few trouble cases, by far the majority of which occurred on reactors installed in cable feeders or in overhead feeders having cable risers.

ADEQUACY OF SURGE PROTECTION

In general the protection was adequate where surge protective devices were used.

Discussion of Replies to Questionnaire

APPLICATIONS, PROTECTION, AND FAILURES

A summary of the information obtained from the replies to the questionnaire is given in Table II. Only those reactor applications which were reported by several companies are tabulated, but every case of trouble reported is included. Information concerning applications reported by only one or two companies can be obtained from Table I.

A brief explanation of the significance of the figures presented in columns 2 and 5 of Table II will perhaps be useful in avoiding confusion. Column 2 lists the total number of companies which make use of any particular application. On the other hand, column 5 lists the number of companies reporting the use of a reactor application in various voltage ranges, and separates protected and unprotected reactors. Thus, in any given application, a company could be tabulated as many as six times in column 5 if the company had that particular application both protected and unprotected in each of the three voltage ranges. However, in column 2 each company using a particular application would be counted only once.

APPLICATIONS

Table II indicates that cable and overhead feeder reactors are the most extensively used application of reactors, with load-bus tie and generating-station tie reactors second in importance. Generator and transformer neutral reactors are next in importance and the three remaining applications, generator and transformer phase leads, and synchronizing bus tie reactors were reported by relatively few companies.

Protection

Column 5 of Table II shows that with but two exceptions the majority of the companies provide no surge protective devices for their reactor applications. The exceptions are transformer neutral reactors and overhead feeder reactors.

In the case of the transformer neutral reactor application in the 22- to 220-kv voltage range, five companies use surge protection, and four do not. However, this was not the case in the lower voltage ranges, for in the 11- to 16.5-kv range only three companies use protective devices while five use none, and in the 2.3- to 7.2-kv range none of the three companies having the application provide any surge protection. In the overhead feeder applications, the companies using surge protection outnumber those with no protection, at all voltage levels; in the 2.3- to 7.2-kv range eight companies supply protection and six do not; in the 11- to 16.5-kv range 12 companies use protection and seven use none; and in the 22- to 69-kv range seven companies provide protection while only two do not.

The majority of companies replying to the questionnaire specifically state that they do not feel that surge protective devices are required on their specific reactor applications. However, a great majority of the troubles which were reported occurred on unprotected applications.

Failures

There were comparatively few troubles with reactors due to surge overvoltages reported in the questionnaires. No trouble of any kind was reported on synchronizing bus tie, generating station tie, and transformer phase lead reactor applications. One company reported a single case of trouble with a generator phase lead reactor, and one company reported several cases of trouble with a generator neutral installation. Three companies reported trouble with load bus tie reactors; two of these companies reported one case of trouble each, while the third reported "many" trouble cases. Each of two companies reported one case of trouble with transformer neutral reactor applications.

The great majority of troubles reported were with cable feeder applications and overhead feeder applications in which cable risers were used. In the case of the cable feeder application, seven companies reported a total of 18 trouble cases. In addition to these, one company reported a single case of trouble on a reactor in an overhead feeder which was caused by a fault on the cable riser of the circuit, and another company reported "several" trouble cases which occurred during periods when the overhead feeder was disconnected. (Only the cable riser was involved.) In these two instances, since the cable riser rather than the overhead feeder was involved in the trouble, the trouble data have been included with the cable feeder trouble data in Table II, columns 6 and 7. The application data, however, columns 2 and 5, have been included with the other overhead feeder data.

In the overhead feeder application, two companies reported 17 cases of trouble, exclusive of the two instances just described. One company reported an estimated 12 cases of trouble, all occurring on overhead feeders having cable risers, and lightning arresters at the risers. This company did not supply sufficient information to determine whether the cable risers played any part in the failure of the reactors. The second company reported five trouble cases, but did not state whether cable risers were involved.

Of the 18 companies reporting trouble due to surge overvoltages, only three had trouble with reactors equipped with surge protection of some kind. One company had a single case of trouble involving a transformer neutral reactor having a shunt lightning arrester, one company had one case of trouble with a cable feeder reactor equipped with a shunt resistor, and the third company reported an estimated 12 cases of trouble with overhead feeder reactors on circuits having lightning arresters at the cable risers of the feeders.

Details of Reactor Troubles Reported

Cable Feeder Reactors

Case 1, Table III. The 13.8-kv bus is effectively grounded by grounding one generator neutral solid. The calculated data for the last case of network cable trouble are

$I_a = I_g = 2{,}460$ amperes (line to ground)

$$\frac{X_0}{X_1} = 1.055$$

$$\frac{R_0}{X_1} = 0.355$$

The circuit breakers are known to have difficulty interrupting currents in the range of 3,000 to 5,000 amperes, and the arcing time may be 4 to 5 cycles on a 60-cycle basis. No damage or burning was apparent on the circuit-breaker contacts in any case of fault. In the last case of network cable trouble, the reactors flashed to ground and between phases. The network feeders have induction regulators on the line side of the reactors. In all cases of trouble, flashovers occurred to ground across about 5 inches of air, and ultimately spread to all three phases. Arc and fire severely damaged the breaker mechanism and buswork.

Table III. Cable Feeder Reactors

Case No.	Circuit Voltage	No. of Installations in Use	No. of Troubles	Protection
1	13.8 kv	20	3	none*
Subtransmission Network	13.8 kv	4	4	none*
2	12 kv	300	1	none
3	13.8 kv	333	1	none
4	11 kv	220	2	none
5	11.5 kv	28†	1	none
6	13.8 kv	14	1	resistor shunting reactor
7	13.8 kv	70	5	none

* Bus arresters installed in 1947.

† None of these installations are in service at present.

All of the troubles reviewed in the foregoing have occurred at one station. There have been at least two cases on subtransmission cables at two other stations, which were attributed to overvoltages due to reactors, but details are lacking. One failure on subtransmission and two failures on network feeders occurred after bus arresters were installed in 1947.

The Working Group feels that the reactors definitely contribute to the overvoltages which have caused flashovers. No line arresters are installed, since all feeders are entirely in cable. One set of bus arresters is installed on one end of the bus. The bus arresters were installed about 1947. It seems significant that the failures which occurred are 100 to 200 feet from the lightning arresters. The installation of additional arresters on the bus is contemplated, as well as Thyrite resistors on the reactors. The Thyrite resistors seem effective at all overvoltages as against the lightning arrester, which is effective only above flashover. Also a matter to be concerned about is that the lightning arrester may blow up on sustained overvoltages.

Case 2, Table III. A multiple flashover of the reactor occurred during a severe fault on this cable. The exact cause of the flashover is unknown.

Case 3, Table III. No comments on this trouble.

Case 4, Table III. For the two failures listed, the reactors failed mechanically on a cable short circuit within a mile of the reactor. It was found that the reactors were of 1920 vintage and were not physically strong enough to withstand the stresses that could be applied.

Case 5, Table III. Surge flashover caused by external 3-phase-to-ground fault on the 11.5-kv system.

Case 6, Table III. Reflection of incoming surge caused 3-phase flashover on cable feeder terminals of reactor.

Case 7, Table III. In May 1942 band *C* phase reactors were burned out by a flashover caused by lightning. In July 1947, the potheads and cables of two feeders having reactors and fed from the same bus were damaged by a flashover caused by lightning. These two trouble cases occurred on radial feeders terminating in 13.8/4.16-kv transformers. Since 1947, lightning arresters have been installed at the potheads on the source of the lines. Since then, no failures have been reported.

The other three cases of trouble occurred at installations where two cables are fed through one circuit breaker and reactor. The cables terminate on the same bus at the far end. Twice a cable fault on one cable resulted in a flashover of the potheads near the reactor on both cables. In the third case a flashover of the breaker bushings at the far end of one cable resulted in a simultaneous flashover of the potheads on both cables near the reactor.

Overhead Feeder Reactors

Case 1, Table IV. These troubles occurred 15 years ago or earlier, and information now on hand concerning them is not very

Table IV. Overhead Feeder Reactors

Case No.	Circuit Voltage	No. of Installations in Use	No. of Troubles	Protection
1	26 kv	4	4 or 5	none
2	12.5 kv	28	1	none
3	4.16 kv	61	several	none
4	12 kv	69	12 estimated	arresters at cable risers

complete. However, they involved flashovers of reactors at times of lightning storms, and the flashovers were probably initiated by lightning surges or system disturbances caused by lightning.

These troubles led to the replacement of two sets of reactors. The original reactors had bare conductors, whereas the new reactors had asbestos covered conductors and Thyrite shunt resistors.

Case 2, Table IV. Line-to-ground fault in outgoing cable to 12.5-kv overhead line caused overvoltages to appear on reactor, flashing it over and destroying it.

Case 3, Table IV. Several cases of trouble have occurred at the time of dropping of the charging current of 4.16-kv regulators through a reactor-cable combination. The oil circuit breakers in question were old and slow, and showed evidence of restriking. The trouble was cured by the installation of lightning arresters at the regulators.

Case 4, Table IV. All of the failures have been on overhead feeders connected to the reactors by cables varying in length from 150 to 500 feet. The only lightning protection on these circuits is the distribution type of lightning arrester at the risers and interconnected with the cable sheath and the system neutral. Practically all of the failures were turn-to-turn failures at the line end of the reactors. These failures occurred on reactors which were approximately 25 to 30 years old. Practically all failures occurred during lightning storms.

LOAD BUS TIE REACTORS

Case 1, Table V. Whenever a heavy fault occurred, usually close to the substation, the reactor would flash over as the faulted feeder cleared. In about 1927, the 2.3-kv bus reactor was replaced by a 13.2-kv reactor, type *CLS*, form *B*, each phase rated 152 kva, 200 amperes, 762 volts. It was tapped down so that about two-thirds of the coil remained in the circuit. This reactor was never flashed over by the clearing of 2.3-kv fault. In 1941, the 2.3-kv bus was changed to 4.16-kv grounded *Y*, and the reactor was removed.

Case 2, Table V. The one case of trouble occurred during the clearing of a line-to-ground fault on the adjacent 13.2-kv system. The reactor flashed turn to turn, and to ground. At the same time, the shunt lightning arrester of a 13.2-kv neutral reactor exploded; see case 1 in Table VI.

Case 3, Table V. Surge flashovers on reactor, disconnect switches, and connecting cables. This installation is no longer in service.

GENERATOR NEUTRAL REACTORS

Circuit Voltage	No. of Installations in Use	No. of Troubles	Protection
22 kv	2	several	none

During the 10 years of operation with reactor grounding of generators (1928–38) at two stations, several cases of surge flashovers occurred on the neutral busses. After the installation of resistance grounding at both stations, no trouble of any kind was experienced.

TRANSFORMER NEUTRAL REACTORS

Case 1, Table VI. The one case of trouble occurred during the clearing of a line-to-ground fault on the adjacent 13.2-kv system. The shunt arrester across one of the transformer neutral reactor installations exploded. At the same time, a 13.2-kv load bus tie reactor flashed turn-to-turn and to ground; see case 2 in Table V.

Case 2, Table VI. The only case of trouble involved a reactor that is connected between ground and the neutral connection of two 12,500-kva transformers that energize a 4.15-kv distribution bus. The reactor is normally shunted by a 400-ampere fuse. Heavy ground faults are thus limited in magnitude to protect regulators from excessive ground-fault current. A solid ground in the station caused the reactor to flash over to ground.

Calculations indicate that a solid ground fault in the station will initially equal 26,000 amperes symmetrical. The fuse will interrupt this current and cause the reactor to limit the steady current to 7,400 amperes. The initial transient probably caused about 10,000 volts to be impressed across the reactor, which flashed to ground.

GENERATOR PHASE LEAD REACTORS

Circuit Voltage	No. of Installations in Use	No. of Troubles	Protection
12 kv	30	1	none

A flashover to ground occurred on one phase of a generator phase lead reactor during abnormally high flow of reactive current through it. There was oscillographic evidence of high-frequency components in the current prior to the flashover.

Cause and Nature of Reactor Failures

Table VII indicates the major causes of the troubles reported on reactors. It shows that of 41 specific cases, 20 were reported as caused by lightning, and 18 by fault currents. One other assigned cause was breaking charging current through a reactor with slow circuit breakers.

Of the types of failures, 13 were flashovers between turns, nine were flashovers to ground, and two were mechanical failures. Several companies reported troubles on associated equipment, such as shunt lightning arresters exploding, cable potheads failing, and flashovers on neutral bus and cable faults, which were attributed to surge overvoltages due to the presence of the reactors.

Table V. Load Bus-Tie Reactors

Case No.	Circuit Voltage	No. of Installations in Use	No. of Troubles	Protection
1	2.3 kv	1	many	none
2	13.2 kv	1	1	none
3	6.9 kv	1	1	none

Table VI. Transformer Neutral Reactors

Case No.	Circuit Voltage	No. of Installations in Use	No. of Troubles	Protection
1	13.2 kv	3	1	shunt lightning arrester
2	4.15 kv	1	1	none

Complete Tabulation of Replies

In Table I, a complete presentation of all data obtained from the questionnaire, is shown every reactor application reported, the applications being tabulated in four voltage ranges; in each voltage range the number of companies employing each application and the type of surge protection, if any, are indicated. In the case of overhead and cable feeders, the location of the circuit breaker with respect to the reactor is also shown. The types of protection are indicated by letter symbols. Table II was derived from Table I.

Appendix II. Data on Reactors in Industrial Applications

An attempt was made to collect data for industrial applications similar to that obtained by questionnaire from the power companies. For this purpose, two of the reactor manufacturers studied their records for current-limiting reactors installed in industrial systems.

The majority of such reactors are types *H* and *J*, Table I, in cable and overhead circuits. Also quite a few are used as starting reactors for motors. The other major group used are the types *D* and *E*, bus tie and synchronizing bus reactors. There are very few cases where the other classifications are used. Types *A*, *B*, *C*, and *F* refer to generating stations, and since only the largest industrial systems have their own generation, very few of these installations exist. There are also very few cases of type *G*, reactors in transformer neutrals, since most industrial systems are either ungrounded or resistance-grounded.

Information on the protective schemes used on reactors in industrial systems is very meager. There are no recorded cases where protective devices were applied to protect the reactors themselves. There are cases where arresters are mounted adjacent to the reactors, but these are primarily for protection of other equipment. There are also a limited number of neutral grounding reactors supplied with shunting

Table VII. Reactor Troubles

Initiating Cause and Type of Failure

	Number and Type of Trouble												
	Flashover												
	Turn-to-Turn		To Ground		Phase-to-Phase		Not Specified		Mechanical Failure		Other		
Initiating Cause	No. of Companies	No. of Troubles	No. of Companies	No. of Troubles	No. of Companies	No. of Troubles	No. of Companies	No. of Troubles	No. of Companies	No. of Troubles	No. of Companies	No. of Troubles	Total Number of Troubles
Lightning	1	12					3	8					20
Fault Currents	1	1	2	8			4	3+many	1	2	1 1	1* 3†	18+many
Breaking Charging-Current Through Reactor with Old Slow Circuit Breakers											1	several‡	several
Not Specified			1	1			1	1			1	1‖	3
Unknown											1	several	several
Totals	2	13	3	9			8	12+many	1	2	5	5+several	41+many

‖Shunt arrester on transformer neutral reactor exploded.
*Cable potheads near reactors flashed over.
†Breaking charging current of cable risers to overhead feeders caused faults on cable risers.
‡No comment as to type of trouble.
§Surge flashover on neutral bus in station with reactance grounded generators.

resistors to reduce the X_0/X_1 ratio of the system.

There is a complete absence of reported cases of trouble either to the reactor or to other equipment caused by the misapplication of the reactor. This might be explained by the fact that files containing such data are destroyed after 5 years so that any cases reported in the past must have occurred at least 5 years ago. The absence of reports in the last 5 years indicates either no failures or that the industrial engineering departments of the manufacturers were not consulted. It may be that local utilities supplying industrial systems are consulted without the manufacturer's engineers being involved. In any event the information is very meager, to say the least, on this phase of the investigation.

It was concluded that in view of the general lack of detailed information, further investigation of industrial applications was not warranted and that industrial applications should follow practices established by the utilities.

Appendix III. Failures on 13.8-Kva Cable Circuits with Reactors in Havana, Cuba, and Transient Analyzer Study for Station

Seven cases of trouble on 13.8-kv cable circuits with reactors have been experienced at Consolidated Steam Electric Station in Havana, Cuba, since 1930. Two similar cases have occurred, one at each of two other stations.

At the Consolidated station the disturbances have resulted in 13.8-kv bus faults probably due to communication of the arc from the line side of the circuit breaker to the bus side of the breaker within the breaker cell. Flashovers have also occurred in the current transformer compartments and in the reactor compartments, both of which are isolated from the breaker cell and are on the line side of the breakers. All cases have occurred with Westinghouse type-*CO-11* breakers, although Westinghouse type-*CO-1* and *O-111A* breakers are also installed. The *CO-1* breakers have been installed in a maximum of 12 positions compared to about 25 positions for the *CO-11* breakers since the early 1920's. The *O-111A* breakers have gradually replaced about 75% of the *CO-11* breakers in the last 5 years.

Analysis of the information available on the last two cases of trouble indicated cable failures and about 1/2 mile from the Consolidated station were the initiating cause. Flashovers in the cells occurred across about 5 inches of air. Flashovers in the reactor compartments occurred between turns of the reactors, between reactors on different phases, and between reactors and grounded parts of the compartment. The reactors are stacked vertically for the three phases and range from 1.5% to 7.5% for different circuits. Most failures have occurred on circuits with 7.5% reactors. The calculated ground current ranged from 2,500 to 3,000 amperes, and X_0/X_1 was approximately unity while R_0/X_1 was approximately 0.36. It is known that the *CO-11* circuit breakers, being plain break breakers, have arcing times of 3 to 5 cycles for currents in the range of 2,000 to 5,000 amperes. The extent of damage to the cables at the point of fault is not known exactly for the last two cases, but it is known that from 1/2 square inch to several square inches of lead sheath have been destroyed on some of the cables. No damage to breaker contacts has ever been experienced. It is estimated that a voltage of approximately nine times phase-to-neutral on a crest basis might be necessary to flash across 5 inches of air.

A transient analyzer study was made for the Consolidated station. No overvoltages in excess of 150% were produced for any type of fault on either the faulted or unfaulted phases for restriking in the circuit breaker, restriking in the fault, or dropping capacitive circuits. The only manner in which overvoltages of any consequence could be produced was by chopping current zero. Overvoltages up to 7.5 times phase-to-neutral voltage on a crest basis were produced by chopping current zero. The maximum value of overvoltage was limited by the interrupting ability of the synchronous switch. However, the magnitude of all overvoltages was reduced to two times phase-to-neutral voltage on a crest basis or less by the addition of Thyrite resistors in shunt with the current-limiting reactors. Even though the likelihood of *CO-11* breakers chopping current zero was seriously doubted at the time of the study, the use of Thyrite resistors shunting the reactors appeared to be a possible solution to the problem. The application of Thyrite resistors therefore was recommended on all reactors at the Consolidated station.

Further consideration of the *CO-11* plain-break circuit breaker possibly chopping or forcing current zero led to concern that the *O-111A* deion grid breakers, being more efficient interrupting devices, would be more prone to the phenomenon than the *CO-11* breakers. Search of the literature on the subject and discussions with breaker designers resulted in formulation of no definite opinions. Two papers were found particularly interesting because they indicated that the magnitude of overvoltage did not necessarily depend on the magnitude of the current chopped, although rms currents chopped were less than 100 amperes. Also, reactors were important elements according to both papers. One designer felt that possibly the *CO-11* breaker in the particular cases at the Consolidated station may be able to force current zero at the values of fault current calculated, while no other breaker may have such an interrupting characteristic. Continuing study of these aspects of the problem is under consideration.[1,2] The Working Group felt that the possibility of the expulsion extinction of the fault by

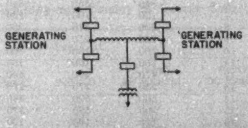

Fig. 1. Connections for duplex reactor in generating station tie

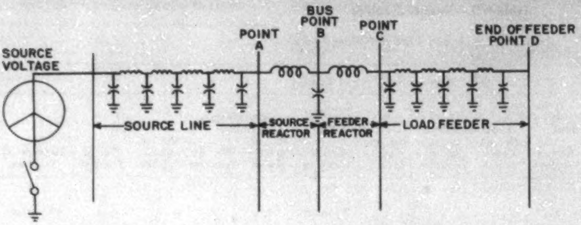

Fig. 2 (left). System for ANACOM study

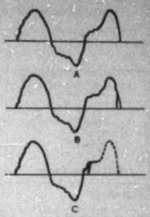

Fig. 3 (right). Examples of forcing current zero

the solid cable insulation should be considered as a source of transient overvoltage.

Appendix IV. Study of Transient Overvoltages Due to Arcing Grounds on Circuits Involving Current-Limiting Reactors

A study was made on the analogue computer (ANACOM) to determine the nature of the transient overvoltages on a system due to arcing grounds. The primary purpose of the study was to determine the effect of current-limiting reactors on the system, and what effect shunting resistors across the reactors would have on the transient overvoltages. In this study various fault conditions and system constants were examined in an attempt to find a general type of reactor application where trouble due to transient overvoltages might be expected to occur.

Description of System

Fig. 2 shows the general system set up on the ANACOM, a single-phase representation, but the actual system was set up on a 3-phase basis. The source was represented by a voltage connected to a distributed constant line. Four π sections were used for the line, which was connected to a so-called source reactor at point *A*, Fig. 2, and the reactor to a bus at point *B*. A feeder reactor was connected to the bus and to a load feeder at point *C*. The load feeder was represented by four π sections and the end of the line designated as point *D*.

The fault condition studied was an arcing ground fault on one phase. The fault consisted of the original fault occurring at the 60-cycle peak of the voltage wave and clearing at the first current zero. Two arc restrikes were considered occurring at the peak transient value of the voltage wave and clearing at the first current zero. The position of fault on the system was varied to obtain the maximum overvoltages.

System Variables

The constants and conditions of the system were varied to determine their over-all effect on the overvoltages on the system. The variables are as follows.

1. Fault location: Arcing grounds, as just described, were applied at points *A*, *B*, *C*, and *D*, see Fig. 2.
2. System grounding: Cases were taken with the source grounding switch, Fig. 2, open and closed.
3. Feeder length: The length of the load feeder was varied from zero to 24 miles.
4. Reactor resistor: The effect was studied of shunting the reactors with a resistance equal to the surge impedance of the lines or cables.
5. Type of circuit: The constants of the source line and load feeder were varied

Table VIII. Combination of System Variables for Each Case Studied

Case No.	Type of Circuit	Grounding	Length of Load Feeder, Miles	Fault at Point	Shunting Resistor Across Reactor
1	cable	grounded	12	*A*	no
2	cable	grounded	12	*B*	no
3	cable	grounded	12	*C*	no
4	cable	grounded	12	*D*	no
5	cable	ungrounded	12	*A*	no
6	cable	ungrounded	12	*A*	yes
7	cable	grounded	12	*A*	yes
8	cable	ungrounded	12	*B*	no
9	cable	ungrounded	12	*C*	no
10	cable	grounded	0	*A*	no
11	cable	grounded	24	*A*	no
12	cable	ungrounded	24	*A*	no
13	cable	ungrounded	24	*A*	yes
14	cable	ungrounded	0	*A*	yes
15	cable	ungrounded	0	*A*	no
16	overhead	grounded	12	*A*	no
17	overhead	ungrounded	12	*A*	no
18	overhead	ungrounded	12	*A*	yes

Table IX. Resultant Transient Voltages for Each Case Studied

	Point A		Point B		Point C		Point D		Across AB Reactor		Across BC Reactor	
Case No.	Faulted Phase	Unfaulted Phase	Faulted Phase	Unfaulted Phase	Faulted Phase	Unfaulted Phase	Faulted Phase	Unfaulted Phase	Faulted Phase	Unfaulted Phase	Faulted Phase	Unfaulted Phase
1	170	100	260	100	370	100	390	110	220	0	200	0
2	140	100	240	100	210	110	210	110	160	0	220	0
3	130	100	100	100	290	100	310	110	170	0	190	0
4	160	100	180	100	230	110	230	110	150	0	140	0
5	360	460	290	290	400	430	420	450	320	240	300	220
6	340	350	340	380	350	430	350	440	160	70	160	70
7	120	100	120	100	140	100	150	100	70	0	60	0
8	500	510	530	500	580	530	570	530	400	100	360	100
9	220	250	220	250	240	230	240	230	90	30	100	30
10	160	100	160	100	180	120			160	30	110	30
11	160	100	160	100	210	100	240	110	140	10	130	10
12	470	490	450	470	490	460	530	500	340	220	320	220
13	280	270	270	290	270	330	270	360	160	70	160	70
14	500	590	480	590	480	590			0	0	0	0
15	490	590	510	600	530	600			260	90	240	70
16	110	100	120	100	120	100	130	100	120	0	90	0
17	340	460	350	460	430	470	480	510	300	100	230	90
18	360	400	340	430	350	460	350	490	180	60	160	60

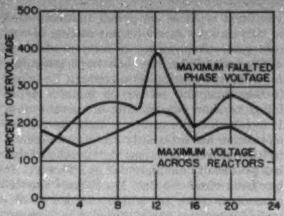

Fig. 4. Fault voltages as a function of feeder length

to represent either cable or overhead circuits.

6. Rate of current decay: The effect of forcing current zero was compared to the more normal case of extinction at current zero.

Results

Table VIII gives the combination of the system variables mentioned in the foregoing, which were used for each case studied. The resultant voltages for each is given in Table IX. The values given in Table IX are given in per cent of normal line-to-neutral crest voltage. The effect of the system variable *s* is as follows.

1. Fault location: Cases 1 through 4 give the results of faults at points *A* through *D* respectively for a grounded system. These cases show that a fault at *A* gives slightly higher voltages than at the other locations.

2. System grounding: Cases 1 and 5 compare grounded and ungrounded operation for fault at *A*. Cases 2 and 8 show the same for fault at *B*. Cases 3 and 9 show the same for fault at *C*. All except case 9 show that ungrounded operation gives the highest overvoltages. The data obtained for case 9 seem suspicious based not only on these results, but also from previous experience, so there is an inclination to disregard this case.

3. Feeder length: Cases 10, 1, and 11 are for feeder lengths on a grounded system of 0, 12, and 24 miles respectively. Since case 1 showed higher voltages (370% to 390%) than are usually expected on solidly grounded systems, a system of resonance condition was suspected. This point was investigated further with the results shown in Fig. 4. The feeder length was varied in smaller steps and the overvoltages obtained are shown. The resulting curve resembles a reasonance curve with its maximum around 12 miles. This seems to indicate that this length of cable represents a critical value of capacitance which sets up an oscillatory circuit with the reactors. This point was further checked by varying the source line length and the ohmic value of the reactors, with similar results obtained.

Cases 15, 5, and 12 are the same for an ungrounded system, and all these voltages are of the same relative magnitude and, as expected, are higher than the grounded case.

4. Reactor resistor: Cases 1 and 7 are for a 12-mile feeder on a grounded cable system, without and with resistors shunting the reactors respectively. These cases show that the voltages are materially reduced when the resistors are used. Cases 5 and 6 are for a 12-mile feeder on an ungrounded system without and with resistors, and they show that while the line-to-ground voltages are not changed, the voltages across the reactors are materially reduced.

5. Type of circuit: Cases 1 and 16 compare a grounded cable system with a grounded overhead system respectively. In this case the overvoltages on the cable system are higher. Cases 5 and 17 compare the same for ungrounded system, and there is essentially no difference between the cable and overhead circuits.

6. Rate of current decay: The effect of forcing current zero on the magnitude of the transient overvoltages appears in Table X, which shows the voltages obtained on the system with the system constants as given for case 1, Table VIII. The data for case 1, Table X are a duplication, for purposes of comparison, of the data for case 1, Table IX. Case 1*A*, Table X, is for the condition of the arc being extinguished just before the 60-cycle current zero on the second restrike. Case 1*B* is for the condition of the arc being extinguished just after the initiation of the second restrike. Fig. 3 shows the fault current for these three cases. The data are examples of one system condition only. If the fault location had been taken at *B*, *C*, or *D*, the overvoltages would probably have been higher. However, the results show that forcing current zero greatly increases the magnitude of the overvoltages, not only from phase to ground, but also across the current-limiting reactors.

Conclusions

The conclusions from these data are first, that the highest overvoltages occur on ungrounded systems, and that shunting the reactors with resistors will reduce the voltage across the reactors but not the line-to-ground voltages. This was to be expected since it is known that even without reactors, overvoltages to ground of the order of 500 to 600% occur on ungrounded systems.

The second conclusion is that even on grounded systems, high overvoltages can occur if certain conditions are met. From the data it was shown that with a 12-mile cable feeder, overvoltages of the order of 400% are obtained. It was determined that this condition exists because the capacitance of the particular length of cable is resonant with the feeder reactor for the particular arcing ground condition on the system. However, it was shown that if a resistor equal to the surge impedance of the cable were shunted across the reactor, the overvoltages would be materially reduced.

It can be concluded that forcing current zero in circuits which have reactors can produce overvoltages many times worse than arcing grounds in which the current is extinguished at normal current zero.

The last conclusion, and the one for which the study was conducted, is that if a system were chosen in which special care is taken in the application or protection of reactors (that is, one in which trouble might occur), it would be on a grounded cable system for three reasons:

1. Trouble is expected on ungrounded systems and thus proper protection is provided.

2. While on grounded systems trouble is not expected, certain system resonance conditions as given in the foregoing can cause high overvoltages.

3. On cable systems the chances of having arcing ground faults are the greatest. Cable circuits have the expulsion action necessary for the extinguishing and reigniting of the arc which produces the arcing ground phenomena. This expulsion action also may force current zero in the arc.

Appendix V. Experience of One Manufacturer with Forcing Predominantly Reactive Currents to Zero Before Normal Current Zero

Following a number of cases of flashover of cable pothead terminals adjacent to current-limiting reactors and reactor winding flashover at the same time cables were faulted to ground, it was suggested that high voltages were being produced in the reactors by the low power factor fault current being forced to zero ahead of normal current zero.

The stored magnetic energy of a circuit is in phase with the current, and since the power factor of a faulted circuit is very low the back electromotive force approaches maximum as the current approaches zero. The value of voltage generated is directly proportional to the current and its equivalent frequency. The maximum frequency will depend on the natural period of oscillation of the circuit. The highest frequencies are most likely to appear on open-wire circuits, but such circuits have only their circuit breakers to force quadrature current to zero, so overvoltages are not likely to exceed three times voltage to neutral. While the natural frequency of cable circuits would be lower, the solid insulation of the cable provides a good expulsion interrupter; a high rate of forcing results if the fault current is not so high that it can blast a large hole through the insulation on the initial half-cycle. Maximum voltage will be produced by forcing the initial half-cycle of current which will approach full asymmetry

Table X. Relative Transient Overvoltages Resulting from Forcing of Current Zero

		Overvoltages at					
Case No.	Fault Current	Point A	Point B	Point C	Point D	Across AB Reactor	Across BC Reactor
1	Fig. 4(A)	170	260	370	390	220	200
1A	Fig. 4(B)	530	350	360	390	340	380
1B	Fig. 4(C)	530	300	310	340	230	220

and provide the maximum expulsion per ampere. Consider a 3% reactor in a circuit which has a natural period of 20 times the fundamental. Forcing of the first cycle to zero of only three times normal circuit current would produce 3.6 times line-to-neutral voltage across the reactor This is quite common in arc furnace operation. If full assymmetrical short-circuit current extinguishes at the first current zero, approximately double-circuit voltage will occur.

In interrupting transformer exciting current, the hysteresis and eddy currents provide sufficient energy loss to limit the rate of discharge. A recent AIEE paper shows some tested results that check very well with calculated values. They seem to approach about five times normal as a limit. In disconnecting motors about the same overvoltages as for transformers occur, except in cases where the motor is stalled or the circuit breaker at starting makes a prestrike and extinction, in which case it approaches the air-core reactor. An induction regulator is a locked rotor motor and may be expected to produce similar overvoltages when current zero is forced. In air-core or current-limiting reactors there is very little to slow down the discharge of magnetic energy unless the coil is shunted by a suitable resistor, arrester, capacitor, or gap.[3,4]

During the past year, in conjunction with some other short-circuit tests, an attempt was made to obtain some comparative tests on the forcing characteristics of various insulating materials. Fig. 5 and Table XI show the circuit and results. One of the gap electrodes, which were 1 inch in diameter, had through its length a 5/8-inch hole covered with 0.0015-inch-thick copper foil to simulate cable sheath, and a piece of 0.0126-inch copper wire was threaded through a hole in the insulation sample to initiate the arc.

The highest voltages indicated on the magnetic oscillographs located at *A* and *B*, Fig. 5, came at the opening of the backup circuit breaker, which apparently did a consistent job of forcing.

The cathode-ray oscillograph produced a consistently poor record. However, assuming the width of the "fog" to be twice normal, the high-frequency peaks were evaluated as indicated in Table XI. The fact that the highest overvoltages were observed with the asbestos sheet, test *F*, confirms experience in developing a fault-burning set several years ago. At that time there was great difficulty in maintaining an arc after breakdown of asbestos-insulated control wire, and finally a high-frequency transformer had to be added to maintain ionization for faults involving asbestos insulation in order to obtain sufficient burning to locate the fault.

Appendix VI. Some Observations on Forcing of Current Zero by Circuit Breakers and of Postconductivity in Breakers

A considerable amount of information appears in the literature concerning the nature of current changes near current zero during circuit-breaker interruption of the arc. A few references concerning forcing of current zero, chopping, and postconductivity in breakers are of particular interest in the study of switching reactors.[5–8]

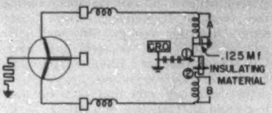

Fig. 5. Circuit for testing forcing characteristics of insulating materials

Forcing of current zero and chopping are terms denoting the various rates of changes of current attending premature current zero in some circuit-breaker operations. These phenomena are interesting in the study of reactor protection as they may produce voltages of appreciable magnitude across reactors. In 1952 was reported some of the most recent work on the general subject confirming results of past studies of chopping in high-voltage circuit breakers.[1] In the Young paper the mechanism of arc extinction in high-voltage breakers is discussed, and records of voltage, current, and arc resistance near current zero for an air-blast circuit breaker are given to illustrate the process and to show how the current may be brought to zero prematurely. Sudden changes of arc resistance are shown to occur near current zero, when the rms current is low, as for reactive loaded circuits such as unloaded transformers and shunt reactors. The way in which this condition can give rise to current oscillations and sudden interruption of current (current chopping) is illustrated. It is shown that the process is affected by circuit constants and by the circuit-breaker characteristics. The maximum instantaneous value of current being chopped in any particular circuit breaker is substantially independent of the rms value of current being interrupted and is a function of the effective capacitance across the circuit breaker. According to this work, the same mechanism exists for current-chopping in oil-break circuit breakers. In the oil-break circuit breaker, however, the dielectric does not build up as quickly and the voltages which must be produced by current chopping would not go as high as in air breakers before a restrike or a reignition occurred. As reported, chopping was actually produced in the oil-break circuit breakers but in practice conventional types of oil circuit breakers used in this country rarely permit forcing of current zero. As a matter of fact, hundreds of oscillograms taken by one large manufacturer in the testing of oil circuit breakers (other than the piston or impulse type) failed to show any forcing of current zero. It is felt that the piston or impulse type of oil breaker has inherently a greater tendency to force current zero, but that proper design has practically eliminated it as a factor. It has been observed that the greater the degree of violence by which the arc is disturbed, the more likely chopping is to occur. In any case, the maximum current that could theoretically be chopped appears to be in the range of 30 to 50 amperes.

It is generally considered that the circuit constants of practical systems along with the characteristics of available circuit breakers leave little possibility for the occurrence of dangerous overvoltages due to chopping or forcing of current zero. However, rare cases of trouble are difficult to explain otherwise. It has been suggested that in such cases the circuit be damped by placing a resistor across the breaker. When reactors are involved, a resistor may be placed across all or part of the reactor during the switching operation.

For some time, postconductivity has been recognized in circuit breakers. This conduction is caused by the ionization remaining in the breaker contact region following extinction of the arc. Its effect is to damp oscillations in the recovery voltage across the circuit-breaker contacts. Although the conduction current may become large enough to initiate breaker restriking, harmful voltages do not result from such restriking. In general, the effect of postconductivity current is to reduce the transient recovery voltage in breakers. One study indicated that although reactors near circuit breakers caused high natural frequencies in the recovery transients and thereby had some effect on postconductivity currents, they did not increase the severity of circuit breaker duty.[9]

Appendix VII. Protective Devices Used with Neutral Grounding Reactors

The use of protective devices with neutral grounding reactors falls into two general

Table XI. Forcing Characteristics of Insulating Materials

Material	Fault, Amperes		Times Normal Volts			Test No. 86,035
		1	2	A	B	
No. *296 M*	616	3		2	2	*A*
Silastic	616		2	2	2	*B*
No. *239 M*	616	No record		3	2	*C*
Hard fiber	600	No record		2	1.2	*D*
Glass melamine	600	1.5		2	2	*E*
1/8 asbestos sheet	600	7		2.2	2.5	*F*
5/16 asbestos lumber	1,200	2		1.0	1.0	*G*
5/16 asbestos lumber	2,500	2		1.0	1.0	*H*
No. *296 M*	2,500	1		1.2	1.0	*I*
No. *477 M*	4,820	4		1.2	1.2	*J*
No. *296 M*	510	2.5		1.2	2.0	*T*
No. *477 M*	510	2.5		2.2	2.5	*U*
1/8 hard fiber	510	2.5		1.3	1.3	*V*
5/16 asbestos lumber	510	2.0		1.5	1.5	*W*
1/4 porcelain	510	2.0		1.2	1.3	*X*
Glass melamine	510	1.8		2.0	1.3	*Y*
Fiber board	510	2.0		2.0	2.0	*Z*
No. *239 M*	510	2.0		2.2	2.0	*AA*

classifications, transformer neutral protection and rotating-machine neutral protection. The practice regarding protection of transformer neutrals is well established and consists of merely paralleling the reactor with an arrester or resistor having characteristics that will protect the transformer neutral insulation.

In the case of rotating machine neutrals grounded through reactors, overvoltages of two types must be considered: lightning surges and switching surges. Overvoltages on machine neutrals from lightning can occur only when the machine is connected to overhead lines directly or through a grounded autotransformer or double-wye transformer. Machine neutral protection against lightning surges is generally accomplished by the surge protective equipment installed at the machine terminals for winding protection although at 11.5-kv and over it may be necessary to add additional surge protective capacitors to the machine terminals. It has been common practice to shunt neutral reactors with nonlinear resistors or lightning arresters to limit overvoltages. However, with the advent of lower surge impedance machines, it is difficult to design a shunt that will properly protect the reactor. In the relatively few applications where the terminal equipment does not automatically protect the neutral, the addition of another surge capacitor at the terminals is regarded as the most convenient method of protecting the neutral.[10]

As for switching surges, the occurrence of transient overvoltages on the system will impose overvoltages on the machine neutrals. Where machines are grounded with neutral reactors, the ratio of zero-sequence reactance to positive-sequence reactance is normally equal to or less than 10. In such cases transient overvoltages from circuit-breaker restriking during circuit interruption or from faults in solid dielectrics will be limited to safe values. For higher ratios of X_0 to X_1 it is necessary to apply protective equipment shunting the neutral reactor except where a study indicates that system constants will not permit excessive transient overvoltages to occur.[11-14]

Overvoltages at the neutral can occur when an arc is extinguished at other than normal current zero. In the case of machine neutrals the machine capacitance reduces the overvoltages from this source to values lower than in the series reactor case. Accordingly, the possibility of excessive voltage is very remote and the use of protective equipment shunting machine neutral reactors to protect against this contingency is usually not considered justified.

References

1. Some Researches on Current Chopping in High-voltage Circuit Breakers, **A. F. B. Young.** *Proceedings*, Institution of Electrical Engineers, London, England, vol. 100, pt. II, no. 76, Aug. 1953.

2. Line Dropping and Reactor Load Interruption Tests with a Brown-Boveri 220 Kv Air Blast Circuit Breaker in the Stadsforsen Power Station (Sweden), **P. Baltensperger.** *Brown Boveri Review*, Baden, Switzerland, June 1952, *Paper 2252E*.

3. Transient Voltage Rise in Transformers Due to Interruption of Exciting Current, **A. Srinivasan, F. J. Vogel.** *AIEE Transactions*, vol. 66, 1947, pp. 1632–36.

4. Overvoltages Resulting from the Disconnection of High-voltage Motors, **P. Baltensperger, H. Meyer.** *Brown Boveri Review*, Baden, Switzerland, vol. 40, no. 9.

5. The Geometry of Arc Interruption, **E. W. Boehne.** *AIEE Transactions*, vol. 60, 1941, pp. 524–32.

6. Switching Overvoltage Hazard Eliminated in High-Voltage Oil Circuit Breakers, **Lloyd F. Hunt, E. W. Boehne, H. A. Peterson.** *AIEE Transactions (Electrical Engineering)*, vol. 62, Feb. 1943, pp. 98–106.

7. A Study of Conduction Phenomena Near Current Zero for an A-C Arc Adjacent to Refractory Surfaces, **T. E. Browne, Jr., A. P. Strom.** *Ibid.*, vol. 70, pt. I, 1951, pp. 398–409.

8. Contribution to the Study of Post Arc Current in High-voltage Circuit Breakers. *Paper No. 130*, CIGRE, Paris, France.

9. Transient Recovery Voltages and Circuit-Breaker Performance, **R. C. Van Sickle.** *AIEE Transactions (Electrical Engineering)*, vol. 61, Nov. 1942, pp. 804–13.

10. The Protection of Transmission Systems Against Lightning (book), **W. W. Lewis.** John Wiley & Sons, Inc., New York, N. Y., 1950, p. 346.

11. Effect of Restriking on Recovery Voltage, **C. Concordia, W. F. Skeats.** *AIEE Transactions (Electrical Engineering)*, vol. 58, Aug. 1939, pp. 371–76.

12. Application Guide for the Grounding of Synchronous Generator Systems, AIEE Committee Report. *Ibid.*, vol. 72, pt. III, June 1953, pp. 517–30.

13. Application Guide on Methods of Neutral Grounding of Transmission Systems, AIEE Committee Report. *Ibid.*, Aug. 1953, pp. 663–68.

14. Shunt Resistors for Reactors, **F. H. Kierstead, H. L. Rorden, L. V. Bewley.** *AIEE Transactions*, vol. 49, July 1930, pp. 1161–78.

15. Shunt Resistors for Reactors—II, **F. H. Kierstead, L. V. Bewley.** *Ibid.* (*Electrical Engineering*), vol. 53, Mar. 1934, pp. 411–18.

16. Switching Surges on High Voltage Cable Lines, **E. L. Michelson, Charles McNamara.** *Electric Light and Power*, Chicago, Ill., Feb. 1954.

The Limiter—Its Basic Functions in Network Distribution Systems

C. P. XENIS
FELLOW AIEE

TESTS on network cable insulation, design considerations, dimensional information, and characteristics of limiters in use on low-voltage network distribution systems of many electric utilities are described in the companion papers.[1-7] This paper summarizes the operating objectives which the limiter must meet, and co-ordinates the material on the various phases of this subject as covered in these papers.

The basic problem and designs developed for the purpose of protecting network cables under fault conditions have been discussed by the author in a previous paper.[8] While there has been no major change on the subject, the thermal properties of cable insulation currently manufactured have been studied in considerable detail by the Limiter Standardization Task Group of Accessories Subcommittee of the AIEE Insulated Conductor Committee for the purpose of developing standards for the guidance of users and manufacturers.

Fault Currents on Network Systems

When a fault develops on a set of mains in the network system, short-circuit current is supplied through various branches of the grid, as shown in Fig. 1 with the maximum current flowing to the fault from points *A* and *B*. Beyond points *A* and *B*, less current flows in the mains from the various directions as in the case of fault currents coming from *C* toward *A*, from *D* toward *B*, from *E* toward *A*, and from *G* toward *B*. In many cases the fault "burns clear" and, consequently, the fault currents are interrupted before permanent damage has occurred to the cables feeding the maximum fault current from *A* to *F* and from

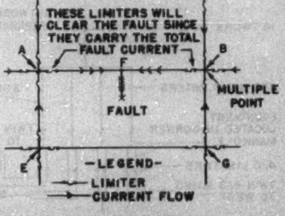
C
D
THESE LIMITERS WILL CLEAR THE FAULT SINCE THEY CARRY THE TOTAL FAULT CURRENT
A
B
F
MULTIPLE POINT
FAULT
E
G
-LEGEND-
LIMITER
CURRENT FLOW

Fig. 1. Fault-current distribution

Paper 55-443, recommended by the AIEE Insulated Conductors Committee and approved by the AIEE Committee on Technical Operations for presentation at the AIEE Summer General Meeting, Swampscott, Mass., June 27–July 1, 1955. Manuscript submitted March 15, 1955; made available for printing April 8, 1955.

C. P. Xenis is with the Consolidated Edison Company of New York, Inc., New York, N. Y.

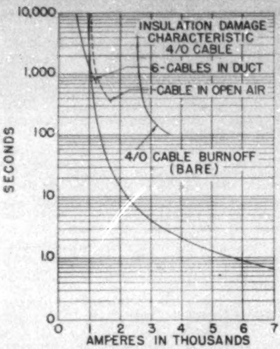

Fig. 2. Time-current characteristic of a 4/0 limiter

B to *F*. However, when the fault does not burn clear, temperatures ranging up to the melting point of copper may be reached particularly in the cable conductors from *A* to *F* and *B* to *F* if no limiter protection is provided. The result of such temperatures is the complete volatilization and destruction of organic insulation, and further spreading of the fault in a multiplicity of directions. The purpose of the limiter is to disconnect the faulted cables at *A* and *B* before the associated cable conductors have reached temperatures which are destructive to the insulation.

Limiter designs in current use have been based on the premise that fault current on the mains cables must not be interrupted too rapidly. Rapid interruption of these currents may be accomplished by fast fuse operation, but this would cause unnecessary mains interruption. Many operating conditions on the system, such as loss of one or more of the sources of supply, starting up of large motors or backfeeding into a primary fault, may cause currents to flow through certain mains sections in the grid which, while of large magnitude, are of relatively short duration and can be safely carried by the grid without endangering cable insulation. Hence, the maximum temperature which cable insulation can stand safely has been used as the basis for the selection of the proper limiter characteristic.

Fig. 2 illustrates the current-time characteristic of limiters for 4/0 cables as recommended by the Task Group. It provides protection to cable insulation over a broad range of short-circuit currents. In the range below 900 amperes, the characteristic shows that no protection is provided. These relatively low values of short-circuit current are usually the result of single-phase faults. This situation develops when two phases of a 3-phase fault have cleared either by limiter operation or because the fault burned clear in the other phase cables. Therefore, since the heat generated in the conduit is materially reduced because only part of the circuit carries current, the cable damage characteristic is definitely less pessimistic than indicated in the curve. Years of experience with limiters have demonstrated that under operating conditions the insulation has been adequately protected on the cables supplying the fault current.

When network mains backfeed into the primary system and the network protector is incapable of interrupting the backfeed current because of a defect, the fuses on the network protector are called on to clear that fault. These fuses are capable of carrying approximately twice the continuous current rating of the transformer and, therefore, have a relatively slow characteristic when interpreted in terms of name-plate rating of the equipment. The fuses must be capable of carrying, without interruption, large values of current to be supplied to the network under contingency operating conditions within the overload capabilities of the transformer and network protector for relatively short periods of time. Fig. 3 shows that, when a primary fault occurs, the network feeds current to the fault through several sets of limiters in parallel, then through the network protector and its fuse, then through several parallel connected cables to the transformer terminals, and through the transformer. The current carried by each limiter varies even in the section between the transformer and the network protector. Part of this unequal distribution of current in these parallel-connected cables is caused by unequal lengths of cable and part by proximity effect.

The limiter design must be such that there is co-ordination between the blow-

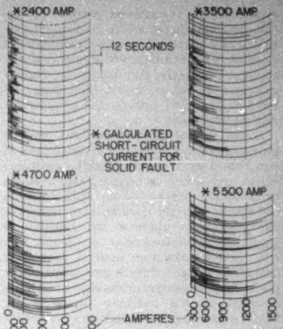

Fig. 5. Arcing fault current, 4/0 bare copper cable

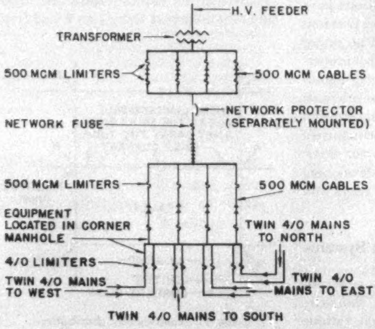

Fig. 3 (left). Current distribution diagram under backfeed conditions

Fig. 4 (right). Selection between network protector fuse Z-25 and 500,000-circular-mil limiter lug

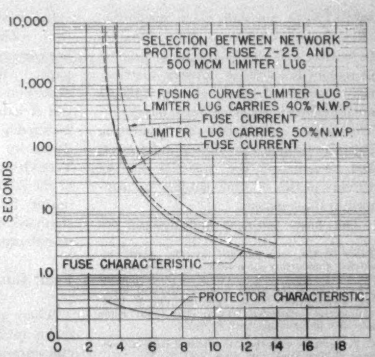

ing of the limiters and the network protector fuse. The basic design calls for the network protector fuse to blow before the limiters, unless a particular limiter carries in the order of 50 per cent or more of the fuse current.

Fig. 4 illustrates the analysis of this selectivity problem between limiters of conventional designs and one type of fuse. It will be seen that reasonable selectivity between the network protector fuse and the limiters is available in this arrangement. However, if a much faster limiter characteristic were to be used, it would be necessary to install additional sets of cables in the tie from the network system to the network protector to reduce the current per limiter and thus permit adequate selectivity.

Arcing Faults

Solid faults develop under field conditions when the molten mass of copper, lead, or both establishes a weld between conductors. This solid type of fault also develops when construction tools are accidentally driven into a conduit, thus establishing solid contact between the various cables in the conduit. Under conditions of a solid fault, currents approximating the maximum calculated values are established which, except for limiter protection, will cause the rapid destruction of cable insulation on cables between the fault and point of supply; see A to F and B to F in Fig. 1. The destruction and volatilization of insulation of the cable length involved will establish additional faults and bring the fault to points A and B, Fig. 1, and in some cases the fault will continue in several directions beyond these points. It is the purpose of limiters to prevent the development of this type of serious fault.

When the fault is not of the solid type, described in the foregoing, it consists of an intermittent arc, the current flowing being of a fluctuating type and of much lower magnitude than the calculated short-circuit value, unless of course a weld is established converting the fault into a solid short circuit. To investigate the arcing type of fault, a series of tests were made in circuits having various values of impedance and charts taken of the current flowing through an arcing fault. Fig. 5 illustrates the currents measured in four circuits which in the absence of arc impedance could supply fault currents of 2,400, 3,500, 4,700, and 5,500 amperes. With arcing faults, the cables supplying the fault current are subject to a temperature rise resulting from the fluctuating values of current permitted by the arc, which, of course, is far below the value that would have been reached if the fault were a solid short circuit. It is interesting to note that when a fault is in the arcing stage the resulting current is of a highly fluctuating nature and amounts to only a fraction of the calculated short-circuit value. At times, the current to the fault approximates the normal current-carrying capacity of the cable.

It will be concluded by an examination of the foregoing results that the proposed limiter characteristic offered by the Task Group and discussed in this series of papers is not intended to and cannot interrupt arcing currents of low magnitude. The arcs resulting from these relatively low fault currents will consume cable at the point of the fault but are not sufficient to overheat the cables supplying the fault current. Were the limiter characteristic to be speeded up to the point where faults would be cleared in the arcing stage, the serious operating difficulties discussed in the first part of this paper might result.

Discussion appears on pages 944–50.

Elements Determining Limiter Characteristic

The companion papers cover the various phases of the problem and indicate the approach to the solution of each phase of the problem. In review, the basic of the proposed limiter characteristics is the following:

1. The limiter characteristic must be fast enough to prevent the destruction of the insulation on the cables supplying the fault currents.

2. The characteristics must be slow enough to permit selectivity with the associated network protector fuse under normal and contingency operating conditions. It must be slow enough to permit transfer of current through network mains under contingency operating conditions which can be safely met by the thermal capabilities of the mains cable insulation.

References

1. Overload Classifications for Network Cables, R. C. Graham. *AIEE Transactions*, vol. 74, pt. III, Oct. 1955, pp. 916–19.

2. High-Temperature Classification of Rubber and Rubberlike Insulation of Network Cables by Oven-Heating Tests, W. H. Couch, C. J. Crowdes. *Ibid.*, pp. 930–34.

3. Time-Current Damage Characteristics, Cable in Duct, L. F. Porter. *Ibid.*, pp. 919–21

4. A Mathematical Method for Determining Insulation Damage Curves for Network Cable, R. H. Kolks. *Ibid.*, pp. 934–38.

5. Co-Ordination of Secondary Network Protection, E. L. Leinbach, A. S. Brookes. *Ibid.*, pp. 922–24.

6. Limiters—Their Design Characteristics, Function, and Application, F. Heller, I. Matthysse. *Ibid.*, pp. 924–30.

7. Characteristic Properties of Secondary Network Cables, S. J. Rosch. *Ibid.*, pp. 939–44.

8. Short-Circuit Protection of Distribution Networks by the Use of Limiters, C. P. Xenis. *Electrical Engineering*, vol. 56, Sept. 1937, pp. 1191–96.

Overload Classifications for Secondary Network Cables

R. C. GRAHAM
ASSOCIATE MEMBER AIEE

IN 1937 some unpublished experimental data showed that the rubber insulations then used on 600-volt underground secondary network cables had an approximate temperature limit of 265 degrees centigrade (C) as the point of permanent visible damage and the design characteristics of cable limiters were accordingly selected to provide the desired zone of protection on that basis. During the subsequent years new rubber insulating compounds and nonmetallic coverings have been developed which are today utilized extensively in network cables. Further, it is recognized that future development will undoubtedly provide still different network cable insulations and coverings than what are considered today's standard types.

Because of this situation the Limiter Standardization Task Group, Accessories Subcommittee, AIEE Insulated Conductors Committee, felt that among its many assignments and objectives a major phase of their work should be as follows:

1. To investigate and recommend proper damage temperature classifications for the conventional types of network cables now in use, these data to be used in the design of the appropriate cable limiter.

2. To investigate and recommend a practicable and reproducible standard test procedure that a cable manufacturer and/or user could follow to classify any new or additional network cable materials or design.

3. To record any observations in connection with items 1 and 2 which might be useful in future investigations of a similar nature.

Therefore, this paper reports on the Task Group's activities in connection with these particular phases of the problem. More specifically, this paper summarizes the results of current overload tests on network cable samples in air as conducted by several cable manufacturers at different intervals during the years 1951–1953. Some 65 cable samples were tested by the various cable manufacturers to determine the proper overload or "roasting temperature" rating to be used for limiter design characteristics.

Test Procedure and Samples

The two most popular network cable designs[1] in use today are nonmetallic sheathed constructions:

1. Stranded copper conductor, *GR-S* synthetic rubber insulation, sometimes referred to as *RH-RW* heat- and moisture-resistant compound, conforming to Underwriters' Laboratories' requirements and American Society for Testing Materials (ASTM) Specification *D 754*,[2] enclosed in an over-all sheath or jacket of polychloroprene (neoprene) compound conforming to ASTM Specification *D 752*.[3] Insulation and sheath dimensions comply with the conventional Insulated Power Cable Engineers Association (IPCEA) thicknesses for 600-volt rated power cables.[4] This cable generally has a maximum continuous temperature rating of 75 C.

2. Same as item 1 except ozone-resistant rubber insulation either of the oil-base type conforming to ASTM Specification *D 574*[3] or of the butyl synthetic rubber (*GR-I*) base type conforming to IPCEA Appendix 0.[4] The oil-base insulated cable generally has a maximum continuous temperature rating of 75 C and the butyl base 80 C according to industry specifications.

Network cable sizes vary from no. 2/0 American Wire Gauge (AWG) to 500,000 circular mils and it was decided to make all tests on no. 4/0 AWG which seems to be the most popular.

In addition to these two major cable design classifications, some very limited and preliminary data were also obtained on no. 4/0 AWG sizes utilizing a polyvinyl-chloride thermoplastic insulation (no further coverings), a specimen similar to sample 1 except that a commercially pure lead sheath replaced the neoprene jacket, and a sample similar to 1 except that a high natural rubber submarine type of insulation compound replaced the *RH-RW* compound.

The test method in all cases was in general accordance with the procedure illustrated in Fig. 1 and described in Appendix I. This procedure is recommended as a standard method for conducting overload temperature classification tests on rubber or rubberlike insulated network cables. It is believed to be a relatively simple method that is both practicable and reproducible. It will be noted that these current overload tests are conducted on cable samples in ambient air rather than in an oven, duct, or the like.

Test Results and Observations

Table I summarizes damage temperatures as recorded from visible observation of all samples after overload tests. Damage temperature may be defined as the minimum or threshold temperature at which there was visual evidence of deterioration of the insulation and/or sheath. Fig. 2 illustrates some typical effects obtained at the threshold temperature and at temperatures higher than the point of threshold damage. Porosity

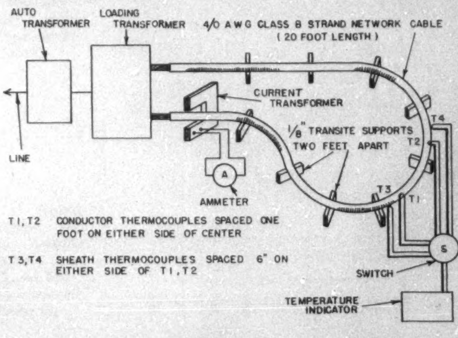
AUTO TRANSFORMER
LOADING TRANSFORMER
4/0 AWG CLASS B STRAND NETWORK CABLE (20 FOOT LENGTH)
CURRENT TRANSFORMER
1/8" TRANSITE SUPPORTS TWO FEET APART
T4
T2
T3
T1
LINE
A
AMMETER
T1, T2 CONDUCTOR THERMOCOUPLES SPACED ONE FOOT ON EITHER SIDE OF CENTER
T3, T4 SHEATH THERMOCOUPLES SPACED 6" ON EITHER SIDE OF T1, T2
S
SWITCH
TEMPERATURE INDICATOR

Fig. 1 Typical test setup for overload tests on network cables

---

Paper 55-444, recommended by the AIEE Insulated Conductors Committee and approved by the AIEE Committee on Technical Operations for presentation at the AIEE Summer General Meeting, Swampscott, Mass., June 27–July 1, 1955. Manuscript submitted March 8, 1955; made available for printing April 12, 1955.

R. C. GRAHAM is with the Rome Cable Corporation, Rome, N. Y.

The author and the Task Group are indebted to the following cable manufacturers for the samples, tests, data, and other information reported in this paper: Anaconda Wire and Cable Company, General Electric Company, Habirshaw Cable and Wire Division of Phelps Dodge Copper Products Corporation, General Cable Corporation, The Okonite Company, Simplex Wire and Cable Company, and Rome Cable Corporation.

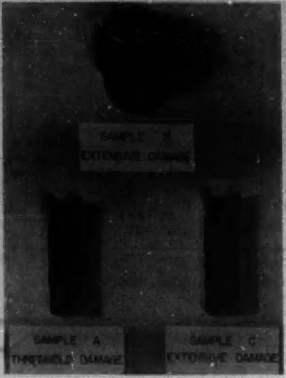

Fig. 2. Typical effects obtained on cable insulation submitted to overload conditions

and undue hardening or softening of the insulation next to the conductor were generally observed above the threshold temperature.

Correlation of Physical Tests with Damage Temperature

Physical (tensile and elongation) tests were also made on the cable samples subjected to the current overload tests in air with the following observations recorded: Fig. 3 indicates an approximate maximum deterioration of 60 per cent (%) in tensile strength of *RH-RW* insulations at the damage temperature. Fig. 4 shows an approximate maximum deterioration of 65% in elongation of *RH-RW* insulations at the damage temperature. Fig. 5 indicates an approximate maximum deterioration of 30% in tensile strength of ozone-resistant oil-base insulations at the damage temperature. Fig. 6 gives an approximate maximum deterioration of 25% in elongation of ozone-resistant oil-base insulations at the damage temperature. Fig. 7 shows an approximate maximum deterioration of 60% in tensile strength of ozone-resistant butyl insulations at the damage temperature. Fig. 8 indicates an approximate maximum deterioration of 45% in elongation of ozone-resistant butyl insulations at the damage temperature.

The abscissas of Figs. 3–8 represent conductor temperature. Physical tests were made upon samples of cable subjected to 4 hours at the indicated temperature as described in Appendix I. The measured current values and sheath temperatures given in Table II are typical of the data obtained on the overload test procedure described in Appendix I.

Table I. Damage Temperatures

Manufacturer Identification	General Type of Insulation	Damage Temperature Threshold, C (Visible Damage)
RH-RW Insulation With Polychloroprene Sheath (Samples Were No. 4/0 AWG With 5/64-Inch Insulation and 3/64-Inch Sheath)		
C		270
E		290
F		260
H		275
I		260
K		270
Range		260 to 290

The Task Group has selected 260 C as the damage temperature to be used in limiter design for this class of insulation. This classification is termed class *L 260*.

Ozone-Resistant Insulation With Polychloroprene Sheath		
A	oil-base, *GR-S*	250
B	oil-base, *GR-S*	over 230
N	butyl	260
O	butyl	over 220
R	oil-base, *GR-S*	240
S	butyl	240
Range		220 to 260

The Task Group has selected 220 C as the damage temperature to be used in limiter design for this class of insulation. This classification is termed class *L 220*.

High-Rubber-Content Submarine Insulations With Polychloroprene Sheath		
D	60% rubber	260
G	50% *GR-S*	280
Miscellaneous Cables		
M	*RH-RW* with lead sheath	240
	Polyvinyl-chloride thermoplastic	150

Due to the very meager data the Task Group was unable to select a damage temperature for limiter design on the above types of cable.

General Comments

1. It is felt that the best criterion of judgment as far as damage temperature is concerned is visible examination of the insulation next to the conductor.

2. There was a wide variation in physical properties (tensile and elongation) between different manufacturers' compounds. The value of such physical tests to be used for insulation classification is doubtful.

3. In all cases at the damage temperature the polychloroprene sheath was considerably less affected than the insulation next to the conductor. The damage temperature for the polychloroprene sheath was 270 C (as measured at the conductor) or higher in every case.

4. There is some inconclusive evidence that a lead sheath instead of polychloroprene may reduce the damage temperature by approximately 20 C. There is also some inconclusive evidence that natural in place of *GR-S* synthetic rubber in similar insulation compounds may reduce the damage temperature by approximately 20 C.

5. In most cases, a current of approximately 800 amperes was required to reach a conductor temperature of 240 C on no. 4/0 AWG under the test conditions described here. Any differences in current loading to

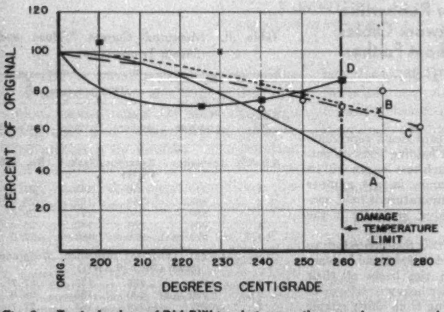

Fig. 3. Typical values of RH-RW insulation tensile strength as removed from cable submitted to overload temperatures

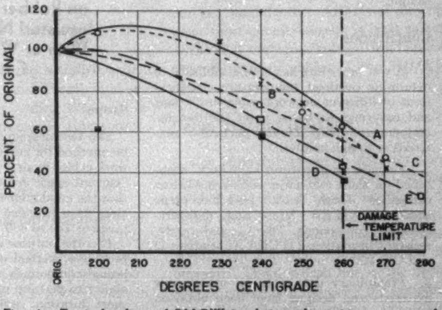

Fig. 4. Typical values of RH-RW insulation elongation as removed from cable submitted to overload temperatures

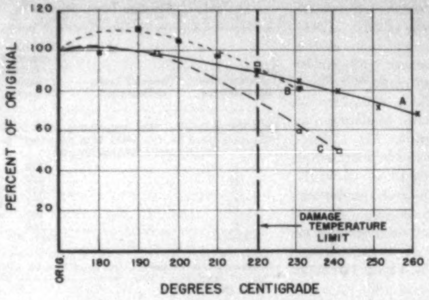

Fig. 5. Typical values of ozone-resistant oil-base (tensile) insulation as removed from cable submitted to overload temperature

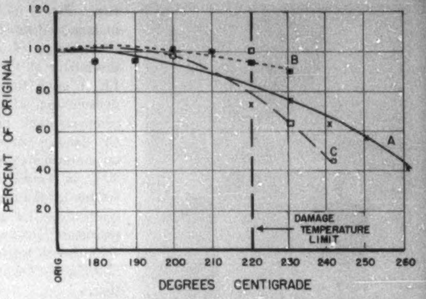

Fig. 6. Typical values of ozone-resistant oil-base (elongation) insulation as removed from cable submitted to overload temperature

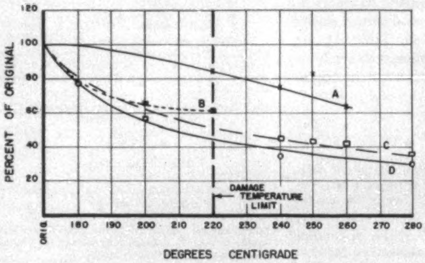

Fig. 7. Typical values of ozone-resistant butyl (tensile) insulation as removed from cable submitted to overload temperature

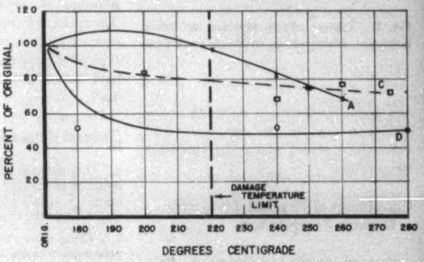

Fig. 8. Typical values of ozone-resistant butyl (elongation) insulation as removed from cable submitted to overload temperature

give the same conductor temperatures for different compounds and samples are believed to be largely due to the differences in values of thermal resistivity and emissivity of the materials employed in the cable construction.

6. The extreme deformation at 150 C of the polyvinyl-chloride insulated sample prohibited any further evaluation of this sample.

Conclusions

1. A test procedure has been established to determine overload temperature classifications of different network cable insulations and coverings as based upon the damage temperature limits of the particular materials or design involved.

2. Damage temperatures have been established for these two major rubber insulation categories (both with polychloroprene sheaths): *RH-RW* heat- and moisture-resistant compounds, 260 C, and ozone-resistant insulations (IPCEA Appendixes D and O[4]), 220 C.

3. Preliminary data only on other cable materials and designs have been obtained which may be used on future evaluations.

4. Observations have been recorded that may be studied further in similar investigations in the future.

Appendix I. Recommended Procedure for Overload Temperature Classification Tests (Current Loading Tests) on Rubber or Rubberlike Insulated Network Cables With or Without Further Coverings.

Scope

The test procedure provides a reproducible method for current loading tests on network cables in air. Each test length will be "current-aged" for 4 hours, in such manner that the conductor temperature is held constant at a specified value, generally in the range of 180 to 300 C.

It is the purpose of this test procedure to provide a method of classifying cable insulating compounds on the basis of their ability to perform under heavy overloads of short duration, resulting from short circuit and other fault conditions. This will enable the prospective user to determine the degree of protection obtained with limiters of known characteristics.

General

The manufacturer shall make tests on each insulation he offers for network cables so that classification can be determined. The cables to be tested shall have a con-

Table II. Measured Current Values and Sheath Temperatures

Sample No.	Current Load, Amperes	Temperature, C		
		Conductor	Jacket Surface	Ambient
RH-RW Insulation, Neoprene Jacket (No. 4/0 AWG)				
1	840	230	142	27.0
2	868	240	162	26.9
3	880	250	177	28.0
4	904	260	180	25.0
5	910	270	183	27.0
Ozone-Resistant (Oil-Base) Insulation, Neoprene Jacket (No. 4/0 AWG)				
1	750	220	133	27.7
2	780	230	135	28.0
3	787	240	147	27.7
4	797	250	150	30.5
5	808	260	153	29.0

ductor size of no. 4/0 AWG with ASTM class-*B* stranding. The type of insulation shall be indicated by the manufacturer, such as natural rubber, synthetic rubber, oil-base, butyl rubber, etc. The thicknesses of insulation and jacket shall be those recommended by the manufacturer for network cable service. The manufacturer should state the applicable ASTM specification applying to the insulation and sheath or/and the manufacturer's own specifications. If the manufacturer supplies the cable, insulation, or sheath to his own specifications, copies of these specifications should be furnished.

Test Procedure

Each test length shall be at least 20 feet. Tensile strength and elongation measurements shall be made on samples of insulation and sheath before and after test. The sample shall be mounted horizontally in air at least 12 inches away from any other external objects, supported by the ends, and at intermediate points so that 24 inches of cable are exposed between supports. At each support point the cable will rest on a straight strip of transite or similar material having a bearing surface 1/8-inch wide.

The test length shall be heated by passing direct current or 60-cycle-per-second alternating current through the conductor. Conductor temperature shall be measured with thermocouples inserted between strands at two points along the conductor approximately 1 foot from the center of the sample. Jacket temperature shall be measured with two thermocouples attached to the jacket surface at points approximately 6 inches from the points where the conductor thermocouples are located. Ambient air temperature shall be measured with thermocouple or thermometer at same level as cable and 2 feet distant. Load current shall be measured and recorded.

The load current shall be adjusted so that the conductor temperature is held constant within ±5 C during a 4-hour period. The desired conductor test temperature shall be reached within 1 hour, but not sooner than 45 minutes of starting time. Room temperature shall be measured and recorded. After 4 hours of current aging, the current shall be cut off and the cable allowed to cool to ambient temperature without being disturbed.

The manufacturer shall make a number of exploratory tests in accordance with the foregoing so as to arrive at a threshold temperature at which the cable insulation has been visibly damaged. This point shall be judged by visual inspection (sight, smell, and feel) of the insulation next to the conductor. He will then make tests at or near this temperature, the results of which will be used for the final classification.

Deformation shall be determined on the insulation and jacket at the points of support by measuring the thicknesses of the insulation and jacket at the points of minimum thickness and comparing with measurements made on samples as received. Tensile strength and elongation measurements shall be made separately on samples of the insulation and of the sheath of cables subjected to this test. These data are for additional information purposes only. The values of load current and the conductor and sheath temperatures shall also be reported for information purposes only.

Classification

These tests are made to determine the visible damage threshold temperature of the particular insulation being investigated for the purpose of determining limiter design characteristics. Short lengths of the cable so tested shall be cut and the insulation stripped for examination. As a result of visual examination, flexing by hand, and looking for excessive softening or hardening of the insulation, as well as other defects, the compound will be classified for damage temperature rating.

Damage temperature may be defined as the minimum or threshold temperature (expressed in C) at which there is visual evidence of deterioration of the insulation and/or sheath. In no case shall damage be so extensive as to cause deformation of the insulating wall to one-half of its original value or indicate impending failure.

Note: It must be understood that this classification of cables is no figure of merit or demerit but a criterion sought for the purpose of co-ordination between cables and limiters.

References

1. A PROGRESS REPORT ON PERFORMANCE OF SECONDARY NETWORK CABLES, E. C. DeBaene, F. M. Hull, R. H. Hiester. *AIEE Transactions*, vol. 73, pt. III-B. 1954 (Feb. 1955 section), pp. 1688–91.

2. *ASTM Specification D 754–54T*, American Society for Testing Materials, Philadelphia, Pa.

3. *ASTM Specification D 752–54T, Ibid.*

4. *IPCEA Standard S-19-81*, Insulated Power Cable Engineers Association, Montclair, N. J.

5. *ASTM Specification D 574*, American Society for Testing Materials, Philadelphia, Pa.

◆

Discussion appears on pages 944–50.

Time-Current Damage Characteristics, Cable in Duct

L. F. PORTER
ASSOCIATE MEMBER AIEE

THIS is one of several papers on the subject of the cable limiter: its function, application to the network, design and tests, and classification of cables to be protected by limiters. The selection of a limiter to protect cable from "roasting" under short-circuit conditions requires knowledge of the time-current damage characteristics of the installed cable. Such information is most directly and accurately obtained by testing the cable in duct under conditions closely approximating actual field installations.

Summary

This paper presents data obtained from a number of in-duct tests made in 1937 as a basis for limiter designs and, in addition, there are included data of supplementary check tests, which were made in 1952 on the more modern rubber-neoprene cables for comparison with the earlier in-duct tests. All the in-duct data are from tests made on nonleaded *RH/RW* type of underground cable and limited to no. 4/0, 500,000-circular-mil (CM), and 750,000-CM cables installed in 4-inch concrete duct. It is shown that *RH/RW*, neoprene-jacketed cables of current manufacture withstand heating from short-circuit current at least as well as the 1937 vintage of rubber-braid underground network cables of the *RH/RW* type.

Cable Heating In-Duct

The temperature rise in duct for some typical cables in no. 4/0, 500,000-CM, and 750,000-CM sizes is shown in Figs. 1, 2, and 3 respectively. In all cases the load was equally balanced among the phase conductors and the neutral carried no current. The dot-dash line in the upper part of each figure indicates the temperature limit beyond which immediate visible insulation damage occurred. In

---

Paper 55-434, recommended by the AIEE Insulated Conductors Committee and approved by the AIEE Committee on Technical Operations for presentation at the AIEE Summer General Meeting, Swampscott, Mass., June 27–July 1, 1955. Manuscript submitted March 17, 1955; made available for printing May 11, 1955.

L. F. PORTER is with the Consolidated Edison Company of New York, Inc., New York, N. Y.

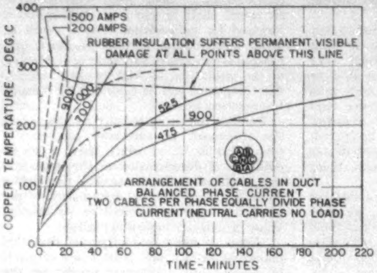

Fig. 1 (left). Time - temperature characteristic for six no. 4/O R/B cables in duct

- - - - One 4/0 cable in air

Fig. 3 (right). Time - temperature characteristic for three 750,000-CM R/B cables in duct

- - - One 500,000-CM cable in air

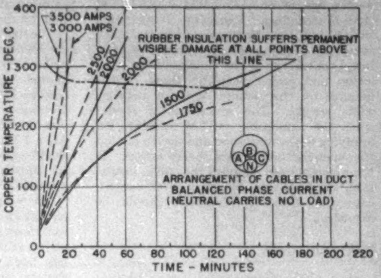

areas below this line there was no appreciable damage visible. The broken lines show temperature rise for a single cable in open air.

Time-current damage characteristics of the cables have been obtained by plotting the damage points for the insulation obtained as described in "Summary." These damage characteristics for each of the sizes tested are shown in Fig. 4. Here, also, the damage observed on a single cable in open air has been included. These damage characteristics have been used as the basis for limiter designs to provide short-circuit protection from fault currents. The broken line, indicating cable damage of a single cable in open air, is presented as a guide for estimating damage which might occur in the case of a single-phase fault in duct. Since most short-circuit currents in the lower values are apt to be under single-phase fault conditions, this curve may be a closer approximation of the lower limit of damage for which limiter protection is required. This situation develops when two phases of a 3-phase fault have cleared and the third phase is left drawing current.

Fig. 5 shows time-temperature curves for each of several current values for six no. 4/0 rubber-neoprene cables tested in duct in 1952 under conditions identical with the 1937 tests.

Fig. 6 shows constant-temperature curves plotted against time and current from the 1952 in-duct tests. Superimposed on these curves is the time-current damage characteristic for no. 4/0 cable shown in Fig. 4; also included is the no. 4/0 limiter characteristic to show its relationship to the constant-temperature curves in the lower current values. It will be noted that the 220-, 260-, and 300-degree-centigrade curves are closely grouped in the area below 1,000 amperes and that the no. 4/0 damage characteristic which was obtained from the 1937 in-duct tests lies on and between the 220- and 260-degree-centigrade curves.

Referring again to the constant-temperature curves, it is important to note they refer only to six no. 4/0 cables, with type *RH/RW* insulation, equally loaded and installed in 4-inch concrete duct. Other insulations or other duct material may result in a different temperature rise. Limited information indicates that some oil-base compounds and/or fiber duct will cause a somewhat greater temperature rise than was observed in these tests.

Test Setup and Procedure

All in-duct tests were performed by pulling the cables into a 4-inch concrete duct installed in a sand-filled box approximately 2 feet high by 3 feet wide and 18 feet long, shown in Fig. 7. In each of the tests, the cables were arranged in the configuration shown and tied at intervals so as to get a maximum temperature rise and to assure a definite location of the thermocouples after the cables were pulled into the duct. Temperatures were measured on each cable near the mid-point. The thermocouples were inserted just under the insulation of cable so as to be in contact both with the copper strands and the cable insulation. The insulation was then taped in place over the thermocouple junction. All temperatures indicated in the data were the maximum read in each test. All tests were performed with constant current and starting at room ambient temperature. Observation of the condition of the cable during the test was made through a "window" in a section of the sandbox.

Conclusion

The time-temperature damage characteristics presented here are a reliable basis

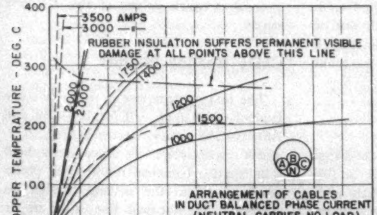

Fig. 2 (left). Time-temperature characteristic for three 500,000-CM R/B cables in duct

Fig. 4 (right). Insulation damage characteristic for rubber-insulated cable

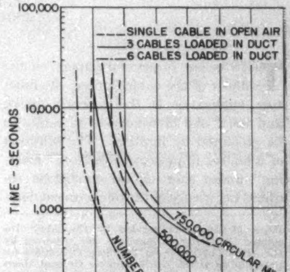

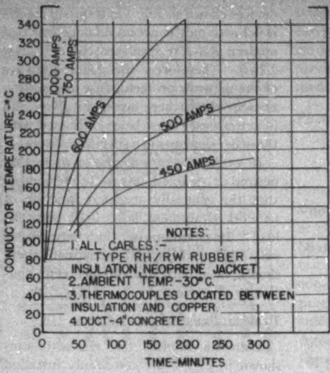

Fig. 5 (left). Time-temperature curves for six no. 4/0 cables equally loaded in duct

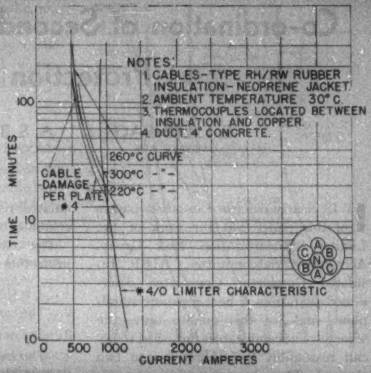

Fig. 6 (right). Constant-temperature curves for six no. 4/0 cables equally loaded in duct

for limiter design within the limitation described, namely: class *RH/RW* insulation for cable sizes 4/0, 500,000 CM and 750,000 CM installed in 4-inch concrete duct. Other classes of insulation and other duct materials may show somewhat different damage characteristics.

Since testing to date covers only one class of the network cables commonly in use and the characteristics of cables change in time with technical developments and since this type of testing is both costly and time-consuming, supplementary methods of classifying rubber insulated cables with respect to their ability to withstand high temperatures and a method of estimating in-duct heating of cables subjected to short-circuit current are given in companion papers.[1-3] Graham describes the classification of cable with respect to its ability to withstand high temperature on the basis of in-air tests. Couch and Crowdes describe a relatively quick and convenient method of temperature classification of insulation. Kolks indicates that if heating constants are known the in-duct heating of cable may be estimated with a fair degree of accuracy.

Fig. 7 (right). Test duct installation

References

1. Overload Classifications for Secondary Network Cables, R. C. Graham. *AIEE Transactions*, vol. 74, pt. III, Oct. 1955, pp. 916–19.

2. High-Temperature Classification of Rubber and Rubberlike Insulation of Network Cable by Oven-Heating Tests, W. H. Couch, G. J. Crowdes. *Ibid.*, pp. 930–34.

3. A Mathematical Method for Determining Insulation Damage Curves for Network Cables, R. H. Kolks. *Ibid.*, pp. 934–38.

◆

Discussion appears on pages 944–50.

Co-ordination of Secondary Network Protection

E. L. LEINBACH
MEMBER AIEE

A. S. BROOKES
ASSOCIATE MEMBER AIEE

IT IS clearly described in other papers of this panel that the work of the Limiter Standardization Task Group, Accessories Subcommittee, AIEE Insulated Conductor Committee determined that from a heat-resistant standpoint, and for this quality only, the secondary network cables furnished today can reasonably be separated into two classes.[1] The damage point of one, labeled class *L260*, is about 260 degrees centigrade; that of the second, labeled class *L220*, is about 220 degrees centigrade.

The object of this paper is to show, for each class, the necessity of co-ordinating all network protective devices and the manner in which co-ordination can best be effected, and to define in a general manner the bands of protection obtainable with several combinations of devices. Only 4/0 conductors and limiters are discussed. The information presented here applies approximately to other popular sizes of cable, 350,000 circular mils and 500,000 circular mils, when projected on an area of conductor basis.

Conclusions

1. A high degree of protection is available for most networks, but precautions must be observed in order to obtain it. Certain "light" networks will be outside the positive protection area but much can be done for their maximum protection if all components are properly co-ordinated.

2. A high degree of protection is not automatically obtained by the random installation of several protective devices presently available. Instead, the characteristics of the protective devices to be used in each network area must be examined and co-ordinated to achieve the highest degree of protection for that area.

Discussion

IDEAL PROTECTION

Perfect co-ordination of protective devices used in the a-c network will result in the following: Upon initiation of a secondary fault in the network, the protective devices will clear in the proper sequence and in the proper time so that the fault will be isolated and de-energized before damage greater than the "calculated risk" is incurred. In addition, customer outage will be at a minimum.

The components of this co-ordinated protection are:

1. The class of secondary cable.
2. The cable limiter.
3. The network protector fuse.
4. The insulation of the transformer and its associated equipment.
5. The station circuit breaker.

The co-ordination of these elements assumes that sufficient short-circuit current is available to properly activate the protective devices and that the short-circuit current is limited to the point that the interrupting ability of the devices under consideration is not exceeded.

Complete protection of the secondary cable would be obtained by the time-current characteristics of cable and cable limiter indicated in Fig. 1 (the limiter characteristic shown is, of course, ideal, and is not presently available). The characteristics of the network protector fuse must be such that the transformer associated with the protector will be well able to carry not only its normal and emergency load for the desired time but also high motor starting currents which may be superimposed on these loads. At the same time, the fuse must have such characteristics as will permit it to blow ahead of the heaviest loaded cable limiter in each phase in the event that the protector fails to open on a primary fault. For faults in the secondary cable the associated limiters must blow ahead of the network protector fuse. (In the case shown, the limiter is one of a probable group of eight.) The station breaker setting is sufficiently high so that all secondary protective devices will operate well ahead of it.

While the co-ordination of protective devices shown in Fig. 1 is termed "ideal," it is based on the actual damage curve of modern *RH-RW* insulated cable[2,3] (class *L260*). Therefore, the characteristics of the network protector fuse and station breaker shown here are qualitative, and in actual cases must be co-ordinated with the other elements in a specific network.

In evaluating the degree of protection desired or obtained, it is well to remember that the generally accepted function of network equipment is to hold onto the load. Investment in the network is very high, and for that investment there should be practically 100 per cent continuity of service.

TYPICAL PRESENT PROTECTION

Elements having the characteristics shown in Fig. 2 are commonly installed in the average network today.[2,3] It is obvious that the degree of protection is definitely less than in the ideal arrangement.

Curve *B* shows the time and current at which class *L260* 4/0 cable is damaged to a visible degree. At this damage point, the judgment of the observer determines whether or not it is to remain in service. Some of the cables presently in use, particularly those using oil-base insulation,[2] have a damage characteristic less favorable than that shown (i.e., less tolerant of high temperatures).

Curve *C* shows the clearing time of the 4/0 limiter presently installed on many networks. It is apparent that when sufficient current is available the limiter will clear before the insulation is damaged. There is a band, however, where no protection is afforded and the operators of the many "light" networks (those consisting of small transformers widely

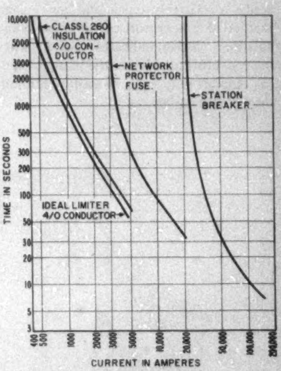

Fig. 1. Ideal protection

Paper 55-445, recommended by the AIEE Insulated Conductors Committee and approved by the AIEE Committee on Technical Operations for presentation at the AIEE Summer General Meeting, Swampscott, Mass., June 27–July 1, 1955. Manuscript submitted March 25, 1955; made available for printing April 12, 1955.

E. L. LEINBACH is with The Detroit Edison Company, Detroit, Mich., and A. S. BROOKES is with the Public Service Electric and Gas Company, Newark, N. J.

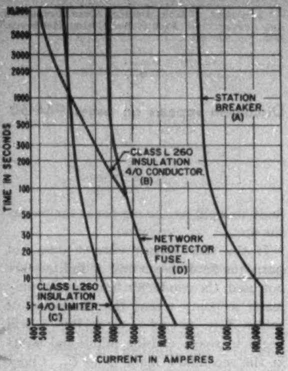

Fig. 2. Typical present protection

spaced and connected by small secondary ties) around the country can well afford to examine their systems in this regard. It should be remembered further that the amperes here designated are actual amperes, not calculated. Prior to specifying limiter characteristics substantially faster than those shown in Fig. 2, however, careful investigation should be made to determine:

1. That under foreseeable operating conditions the emergency overload carried by the limiter will not seriously damage the cable insulation adjacent to the limiter terminals.

2. That heavy starting loads on the network, such as large motors, will not blow the cable limiters. In other words, the limiter must not act as a fuse.

Curve *D* shows the clearing time of a fuse size and type commonly used with 500-kva transformer banks. The fuse is not ideal but is quite satisfactory as long as network cables are equipped with limiters, and there is suitable selectivity between the cable limiters and the network protector fuse. Fuses of somewhat different characteristics are often used, and their curves must be substituted for those shown in an actual case. Also, in the actual case what appears to be good selectivity between the fuse and the other components may be upset by insufficient or misplaced transformer capacity.

The foregoing gives a very general picture of a given combination of protective devices. The intention of this paper is to point out what is desirable, what the advantages and shortcomings of commonly used devices are, and to suggest to the operator of a network that an examination of the apparatus he has is desirable in order to determine for his system what degree of protection he can expect. The penalties of inadequately co-ordinated protection are likely to be service interruptions, damaged equipment, and perhaps explosions and fires.

PROTECTION ON CLASS-L220 INSULATION

The curves in Fig. 3 are similar to those in Fig. 2, except that the cable here shown is of the currently used oil-base or class-*L220* variety. (This curve may be shifted slightly some time in the future but is acceptable in its present form for comparison purposes.) It is readily apparent that the band of protection is considerably less than that shown in Fig. 2. Again, it is up to the operator to evaluate the components and the band protection he has, since it is well known that in some significant respects oil-base compounds are superior to some other types. This is not true, however, in regard to resistance to abnormally high temperatures.

PROPOSED PROTECTION

The assignment of the Task Group required two major steps:

1. The analysis of all the components of network protection and their relationship to each other.

2. The design and standardization of a family of cable limiters which would give the maximum protection possible and yet remain within reason as to size and cost.

The curves in Figs. 1, 2, and 3 show the analysis of the components in use at the present time as compared to protection which would be ideal. The curves in Fig. 4 show the time-current damage characteristics of two types of modern 4/0 cables. Curve *C* is the limiter matched with class-*L260* cable and curve *D* is the limiter matching class-*L220* cable.[3]

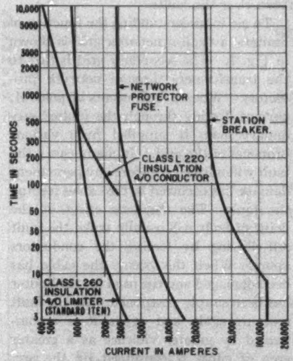

Fig. 3. Typical present protection with class-L220 insulation

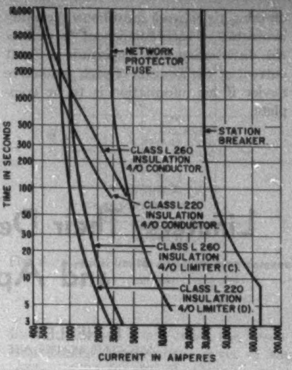

Fig. 4. Proposed protection

The limiter used for curve *D* is not a standard item at present. Enough experimental work has been done, however, to assure a limiter with time-current characteristics similar to that used for curve *D*, Fig. 4. This will provide a much improved band of protection for the *L-220* class of cables. It is again apparent that the cable is not protected perfectly, but with the proposed new limiter, curve *D*, the band of protection has been materially improved.

These four curves are the basis for network protection and all other devices should be co-ordinated about these combinations. Knowing what type of cable he has, the operator of a network can then either check the devices on his system for co-ordination or design new protection for it.

Summary

The information presented here shows that the protective devices generally used in networks of all sizes do not automatically co-ordinate to give either the best protection against secondary faults or the best operating characteristics in every network. The purpose of this paper is to draw the attention of network operators to these facts and to point out the desirability of scrutinizing each network area rather carefully in order to evaluate the degree of protection it is receiving. In addition, the advancement in the art of limiter protection is shown, which will make a much more accurate band of protection possible. The operator in examining his network must know the characteristics of each component as well as the distribution and magnitude of fault current at the location of each protective device if his information is to be complete.

References

1. Overload Classifications for Secondary Network Cables, R. C. Graham. *AIEE Transactions*, vol. 74, pt. III, Oct. 1955, pp. 916–19.

2. The Limiter—Its Basic Functions in Network Distribution Systems, C. P. Xenis. *Ibid.*, pp. 913–15.

3. Limiters, Their Design Characteristics and Application, Fred Heller, Irving Matthysse. *Ibid.*, pp. 924–30.

◆

Discussion appears on pages 944–50

Limiters, Their Design Characteristics and Application

F. HELLER
ASSOCIATE MEMBER AIEE

I. MATTHYSSE
MEMBER AIEE

SINCE publication of the original paper on limiters by C. P. Xenis,[1] a wealth of experience has been obtained, not only in the operation and use of limiters but also in the operation of secondary network distribution systems. This operating experience has resulted in a review of the limiter and types of secondary cable used in network systems as well as the theory of operation of such systems. Before describing the work which was recently done in this field, the function of the limiter will be reviewed.

Function of the Limiter

In the original theory of underground distribution, the success of a secondary network depended upon the system being designed to have sufficient short-circuit capacity to burn clear a solidly faulted cable. Possibly because of their recollection of this theory, many utility company engineers feel that limiters are unnecessary in those parts of their secondary network where they believe the short-circuit capacity is sufficiently high to burn clear faulted cables. However, even when a fault burns clear, the possibility of further trouble is not removed. The cables have been seriously damaged at the point of fault and for all intents and purposes can be considered defective. It is only a matter of time before the fault will reoccur because of operating conditions such as rain or melting snow which may flood ducts and manholes. At best, when a fault burns clear, it should be regarded as a temporary extinguishing of an arc. Furthermore, fault currents of such magnitude and duration that will burn clear a fault may elevate the copper temperature to a point where it will completely destroy all the cable insulation, thereby causing great volumes of smoke with possible fires and explosions, if the fault is not burned clear. It is the function of the limiter to clear and disconnect cable sections before they reach this damage point.

In some cases, solid cable roasting faults were tolerated in nonlimitered secondary networks in spite of the smoke and cable damage.[1,2] It was argued that the fault would eventually burn clear before spreading past the junctions at each end of the cable. Recent experiences by operating utilities have shown that major faults were not self-clearing even though the calculated short-circuit current available was more than ample to burn clear the faults.

To aid in understanding the function of limiters, a typical network grid is shown in Fig. 1. The secondary grid is tied to the transformers through network protectors. When a fault occurs at point *A*, current flowing through the faulted secondary main is supplied from various branches of the grid. In many cases, the fault will burn clear before any permanent damage has occurred to the cables feeding the fault. The magnetic effect at the point of fault will usually make the fault self-clearing by forcing the conductors apart. When this occurs the cable has been damaged and the need for the limiter has been simply postponed. As the fault reoccurs again and again, it is accompanied by greater violence as a greater area of cable is consumed by the arc. With the exposure of the copper conductor, there is a strong possibility for the fault to weld as the copper is melted by the arc.

If the short-circuit current does not burn the fault clear and if limiters are not used, the conductor temperature may reach a point where the insulation of cables *B* to *A*, and *C* to *A*, Fig. 1, will begin to roast, causing additional faults in the secondary main *B* to *C*. Under these conditions, it can be seen that current to fault *A* is supplied from three directions at points *B* and *C*. It is possible for the fault to spread and reach points *B* and *C* and then extend beyond these points in several directions, causing extensive damage. Under these conditions, when limiters are installed at points *B* and *C*, the limiters at each end of the faulted cable will clear and disconnect the secondary cable main *B*–*C* from the grid before the cable insulation is roasted. Thus, the fault is isolated and cannot spread. If limiters are not used, the only methods to control this condition are to cut the secondary mains around the faulted area or to drop the entire secondary network.

Self-clearing faults are accompanied by arcing which may cause smoke and cable damage at the point of the fault. Limiters were not designed to clear arcing types of faults which occur in network systems. C. P. Xenis discusses in some detail this particular operating consideration.[2] The sustained type of fault, in which the computed value of short-circuit current can be expected to flow, is one having negligible fault impedance. This

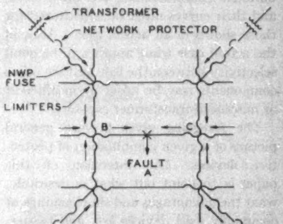

Fig. 1. Typical network grid

Paper 55-473, recommended by the AIEE Insulated Conductors Committee and approved by the AIEE Committee on Technical Operations for presentation at the AIEE Summer General Meeting, Swampscott, Mass., June 27–July 1, 1955. Manuscript submitted March 28, 1955; made available for printing May 9, 1955.

F. Heller and I. Matthysse are with the Burndy Engineering Company, Norwalk, Conn.

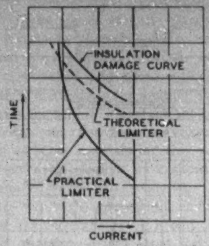

Fig. 2. Typical limiter and insulation damage curves

type of fault is only possible where there is no arcing at the fault, and may occur when the conductors come solidly into contact, leaving no chance for an arc to establish itself, or when a mass of molten metal freezes at the fault resulting in a "welded" type of fault. This is the one type of fault that invariably results in cable roasting unless it is cleared by limiters or by cutting of the cable. This is readily apparent when it is realized that the resistance of the welded fault is much lower than that of an equal length of the conductor itself. Thus, when a welded fault develops, the available tremendous short-circuit currents will raise the conductor temperature to the point where the cable insulation will be roasted. Thus, even in those sections of a network where there is ample short-circuit capacity to burn clear certain types of faults, limiters are the only protective means to isolate a faulted cable and prevent spreading of the fault.

Limiter Operating Characteristics

To design a limiter properly, it was necessary to first determine the cable insulation damage characteristic. The initial tests presented detailed information on the insulation damage curves for various types of cable.[1] This work has been re-evaluated and found to be substantially correct.[2,4]

In addition to its main function of coordinating with the cable insulation damage, the limiter must not hinder but allow for the successful operation of a network system by not clearing on:

1. Faults which will clear without damaging the cable insulation (but probably will restrike at a later date).
2. Overloads due to motor startings, transfer of load because of a primary fault, or temporary overloading during contingency operating conditions.
3. Overloads due to loss of secondary conductors caused by clearing of other limiters.
4. Reverse current supply through the network protector.
5. Faults on other secondary cables.

Fig. 2 illustrates a typical insulation damage curve of time plotted against current. In addition, the ideal and practical limiter curves are shown. The dotted line, drawn just safely below the insulation damage characteristic curve of the cable, would be the ideal time-current characteristic curve for a limiter to provide protection to the cable size involved. This curve, however, cannot be obtained because the limiter must be simple, economical, rugged enough to withstand normal operating conditions during the installation and life of the cable, and be practical to manufacture. Inasmuch as the limiter is a form of insurance, its use can only be justified when the insurance is not too costly.

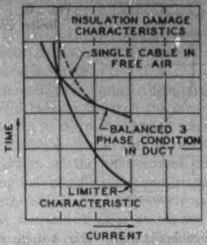

Fig. 4. Typical limiter and insulation damage curves

Fig. 3 illustrates the time-current characteristic curves for a range of limiter sizes in addition to insulation damage curves for a number of cable sizes. Note that the limiter curve actually crosses the insulation damage curve for balanced 3-

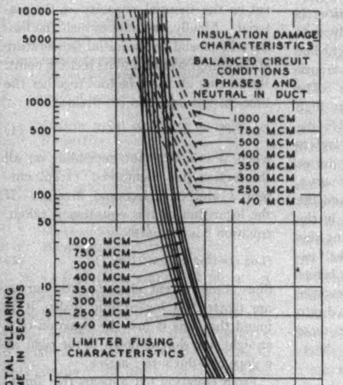

Fig. 3 (left). Cable limiter time-current characteristic curves

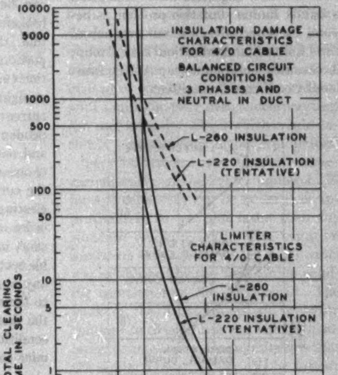

Fig. 5 (right). 4/0 limiter and insulation damage curves

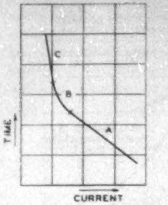

Fig. 6. Basic limiter curve

phase cables in duct. Fig. 4 sheds some light on this paradox by illustrating the insulation damage curves for both the balanced 3-phase condition in duct and for a single cable in free air. The limiter curve does not cross the curve for cable in free air in Fig. 4. In practice there would be little likelihood of the limiter not protecting the cable insulation since low-magnitude faults can be expected to be single phase (or badly unbalanced if 3 phase). The heat generated in the duct by such faults is much less than for a balanced 3-phase fault of the same current per conductor. Therefore, more time is required for a single-phase fault to bring the insulation to the roasting point than for a 3-phase fault. It can then be assumed that the cable insulation damage curve for a single-phase fault would be more like the dotted curve for the single conductor in free air curve than the solid curve as shown in Fig. 4. Operating experience has confirmed this viewpoint. However, if the network has been designed so that there is insufficient capacity to clear limiters, engineers have considered a lighter limiter, but this problem is beyond the scope of the present program of the Limiter Standardization Task Group; Accessories Subcommittee; AIEE Insulated Conductor Committee.

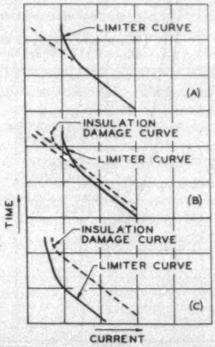

Fig. 7. Typical limiter curves

Recent operating experiences, coupled with the work of the Task Group, have cast some doubt on the ability of the standard limiter to provide complete protection for ozone-resistant rubber insulations, as it does for mineral-base insulations (RH-RW).[3] Where the threshold of damage for mineral-base insulated cable occurs at 260 degrees centigrade, damage to ozone-resistant insulated cable occurs at 220 degrees centigrade. Hence, these insulations have been distinguished by the Task Group by designating them as classes *L260* and *L220* respectively. Fig. 5 illustrates the tentative time-current characteristic insulation damage curve for class-*L220* cable. It therefore would appear desirable to design a lighter limiter with a faster fusing characteristic, especially at the low-current end of the curve, in order to prevent damage to class-*L220* cables.

Theory of Limiter Design

When the Task Group recommended an investigation into the practicability of designing and manufacturing an economical lighter limiter, it was necessary to review the basic theory of limiter design. In this manner, it could be determined which design factors had to be modified. A review of this theory will help to clarify the reason for the difference between the ideal and practical limiter time-current curves, Fig. 2, as well as the method used in designing the lighter limiter.

Limiter time-current characteristic curves as drawn on log-log paper, Fig. 6, can be easily analyzed if the curve is broken into sections. It is easily seen that they have relatively straight-line portions at both ends joined by a transition curve or "knee" in the middle. The straight portion *A*, Fig. 6, at the high current end is the simplest part. It is dependent on only a relatively few factors and may be predicted with a fair degree of accuracy. In this portion of the curve, the current is usually very high and the clearing time is very short, being in the order of 0.1 second or less. During this short interval, the current heats the fusible section up to its melting point before any appreciable amount of heat escapes to the surroundings, or is conducted into the heavier end masses. Under these conditions the following factors determine the blowing time:

1. Imposed conditions.
   - a. Current.
   - b. Initial temperature (slight effect).
2. Limiter design
   - a. Melting point of limiter material.
   - b. Resistivity.
   - c. Resistance-temperature coefficient.
   - d. Thermal capacity.
   - e. Cross-sectional area.

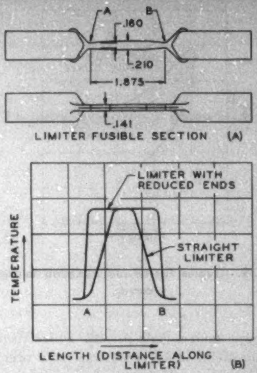
A
B
.160
.210
1.875
.141
LIMITER FUSIBLE SECTION (A)
LIMITER WITH REDUCED ENDS
STRAIGHT LIMITER
TEMPERATURE
A
B
LENGTH (DISTANCE ALONG LIMITER) (B)

Fig. 8. Typical limiter heating characteristic

All of these factors are known values. The following qualitative discussion will show how they affect the time-current curve. The rate of heat generation at any instant is proportional to I^2R in which R is dependent on the resistivity, the cross-sectional area, and the resistance-temperature coefficient. All of this heat goes to elevating the temperature of the limiter fusible section, since in this part of the curve no heat is dissipated. The temperature rise is therefore dependent on the thermal capacity of the material. Finally, the time to melt the limiter will depend on the initial temperature of the limiter section and its melting point. By putting all these factors together the time-current equation is obtained

$$I^2t = kA^2 \qquad (1)$$

where k is a constant depending on all the factors just mentioned, except current I and cross-sectional area A. If the logarithm of this equation is taken, equation 2 is obtained

$$(\text{Log } t) = (\log kA^2) - 2(\log I) \qquad (2)$$

Since time-current characteristic curves are plotted on logarithmic scales, it is found that this is just the equation of a straight line sloping down to the right at a slope of 2-down to 1-across.

From equation 1 it appears that limiters alike in all respects except for cross-sectional area would have parallel straight portions of their curves separated from each other by amounts, measured on the current scale, proportional to the increase of area of the limiter.

It can be argued that the discussion is incomplete because the limiter clearing action is not complete when the melting point is reached. In other words, current flows after reaching the melting point to supply the heat of fusion and the heat of vaporization. Furthermore, arcing begins at some stage during this process. However, calculations have shown that computed values from equation 1 agree fairly well with experimental values and that any correction, even if only for the heat of fusion, brings about less agreement with actual experiments. This is probably true because the circuit is interrupted almost immediately upon reaching the melting point. At this point, the fusible section of the limiter has no mechanical strength and its weight and other factors, such as turbulence of the gases and magnetic forces, cause it to become severed. Arcing, however, is an important factor, but time-current curves are usually obtained in the laboratory at very low voltages so that arcing time is negligible. At higher voltages the arcing time increases, but within the rated voltage of a limiter the arcing time is only a fraction of a cycle.

It has been shown that the high-current part of the limiter time-current curve is simple to predict because the action takes place so fast that no appreciable heat is lost by dissipation to the surroundings. At lower currents and long times, this heat loss cannot be neglected. Therefore, this portion of curve *C*, Fig. 6, is dependent upon the following factors:

1. Imposed conditions
   a. Current.
   b. Initial temperature (slight effect).
   c. Ambient temperature (slight effect).
2. Limiter design
   a. Melting point of limiter material.
   b. Resistivity.
   c. Resistance-temperature coefficient.
   d. Thermal capacity.
   e. Cross-sectional area.
   f. Heat conductivity.
   g. End masses.
   h. Shape of limiter.
   i. Heat-dissipation factors.

In view of these additional factors, a complete mathematical solution is extremely difficult to present. However, from experimentation and experience a qualitative concept of what occurs in this portion of the curve can be obtained.

Consider first a straight limiter section, such as a piece of wire, having considerable length. Because of this great length the masses of metal at each end receive very little heat by conduction from the center of the limiter. However, due to the heat dissipation into the surroundings by radiation, conduction, and convection, the limiter will take longer to blow than would be indicated by the extension of the lower straight portion of the curve. In other words, the low-current end of the time-current curve is bent to the right, Fig. 7(A), by the heat-dissipation factor and thus there is not a 2-to-1 slope in this region of the curve.

Curves of this type are obtained for the burn-off characteristics of insulated cables or bare wires since their great length renders the end effect negligible. Similar curves are also obtained for the insulation damage characteristic of cables except that in this case the temperature reached is not the melting point but the temperature value which would permanently injure the insulation. Nevertheless, the insulation damage characteristic curves and the limiter curves have the same 2-to-1 slope for the right-hand straight portion. This would seem to make a limiter ideal to protect a cable against insulation damage by selecting the limiter whose curve was just below the insulation damage curve.

However, the limiter must reach the melting point before it clears. Since this is considerably above the insulation damage temperature, the limiter will dissipate considerably more heat per unit of length than the cable, thereby resulting in a bending of the curve with a lower knee than the insulation damage curve. If this limiter curve were selected it would cross the insulation damage curve, Fig. 7(B), and provide no protection at currents below the point of intersection. Therefore, a smaller limiter has to be selected which overprotects, Fig. 7(C), since it would clear sooner than needed in the high-current portion of the curve.

The limiter design problem is further complicated by end effects. Obviously the limiter, unlike the cable, cannot be made so long that the ends draw no appreciable heat from the center section. Therefore, the heat conducted into the end masses slows the melting time still further, thereby bending the upper end of the time current curve towards the right and lowering the knee. To compensate for this heat drain on the limiter design, it was found necessary to devise a way to have a long "effective" length and at the same time keep the cost of the limiter to a minimum. This was accomplished by reducing the cross section of the fusible section, Fig. 8(A), near each end where it joins the tubular barrel.[1] By increasing the resistance at points *A* and *B*, Fig. 8(A), and at the same time lowering the heat conductivity, the temperature gradient, Fig. 8(B), along the fusible section was reduced. This tended to cancel the effect of the cool ends and make the fusible section behave more like a cable with considerable length.

In designing the limiter, there must be a careful balance between the cross-sectional area in the center and at the ends of the fusible section so that, in the working portion of the time-current curve, melting will usually occur at the center. Nevertheless, at very high currents the fusible section will clear at the reduced section at the ends which will make the limiter clear sooner that if it were a truly long limiter.

Therefore, when the problem of designing a lighter limiter to protect class-*L220* cable was presented, it was apparent that the limiter design had to be modified to one incorporating a longer effective length in the fusible section.[3] This design change would bend the low-current end of the time-current curve to the left as required. Initial experimental tests on size 4/0 indicate that a lighter limiter can be economically manufactured. The final design of the lighter limiter may include heat reservoirs as well as a reduced cross-sectional area in the fusible section. In addition to testing for the proper time-current curve, tests were also run to insure that the heat generated in the fusible section of the limiter would not roast the cable insulation during normal operating and overload conditions.

All initial tests were conducted on experimental limiters manufactured from one piece of copper tubing which was flattened in its center section. This center section was modified to obtain the desired characteristics. To keep the cost of the lighter limiter to a minimum, it was decided to use the 1-piece construction instead of possibly resolving the problem with a multiple-piece design incorporating low melting-point alloys which would result in a substantially higher cost limiter.

Fig. 5 illustrates the tentative time-current curve of the lighter limiter *L220* for 4/0 cable. It can be noted it is approximately 20 per cent faster than the standard limiter (*L260*). The tentative insulation damage curve for *L220* cable was established by the Task Group pending completion of the duct tests.[4] The work of the Task Group will probably continue until complete and reliable insulation damage curves are obtained so that the lighter limiter design can be further investigated for other cable sizes.

Application of Limiters

At the time a network system, which uses all new equipment and cable, is in-

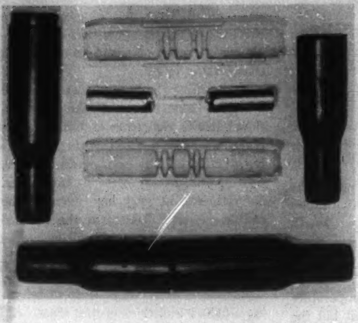

Fig. 9 (left). Straight limiter

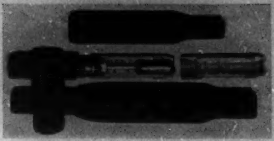

Fig. 11 (right). Molimiter

stalled the question may arise as to why it is necessary to install limiters. Operating experience has shown that secondary faults rarely occur during the early life of a network system. When faults have occurred, they have usually been traced to external damage, such as workmen cutting through cables, or a cable insulation defect which occurred during the installation or manufacture of the cable. As the network system approaches the end of its life, anywhere from 20 to 40 years, the rate of fault occurrence rapidly increases until the decision is made to recable the system. Obviously, the replacement of a network system is not an overnight job and is usually planned to take place over a number of years. It is during this period that limiters provide the maximum amount of protection.

The limiter is a connector, in addition to being a device for protecting the cable insulation from roasting. Therefore, when installed, the cost of protection is minimized since labor, which is the major cost, is already provided for during the construction of the network. The cost of going back into the network years later, just to install limiters, is usually prohibitive due to the high cost of labor. Therefore, it is normal practice to install limiters during the installation of a new or expanded network. In some cases where limiters were not initially used, they are installed whenever work has to be performed in manholes and vaults.

In a secondary network system, it is usually necessary to tie together a multiple of cables at junction points. There are many different types of limiters used in such installations but they all have the same basic design characteristics. The limiter combines a fusible section with a connector element and is made from one piece of copper tubing. In most cases, the portion of the limiter accommodating the conductor is connected to the conductor by crimping the tubular barrel to the conductor with a press. The limiter is rated by cable size and its time-current characteristic is obtained by flattening the center section of the tubing and blanking out the proper section. To quench the arc which occurs when the limiter clears and prevent it from reforming, heat-resistant shells incorporating barriers enclose the limiter. There are many different types of limiters available:

Straight limiter: Is used to splice two conductors together. In Fig. 9, note the 1-piece tubular construction, arc quenching shells, and insulating sleeves which fit snugly over the cable insulation.

Limiter lug: Terminates cable to bus bar. Normally installed in vaults where bus bar is used to join the secondary side of two or more transformers. Note the screws in the shell, Fig. 10, which prevents the cleared limiter from falling down and causing additional faults.

Molimiter: Terminates cable to a multiple outlet preinsulated mechanical-type connector which is used as a junction point to join secondary mains and services. Fig. 11 illustrates a Molimiter installation.

Limiter tap: incorporates a limiter lug modified to terminate cable to a cable ring bus. U bolt and saddle as shown in Fig. 12 make a neat compact installation. Insulating sleeve and hood keep taping to a minimum.

Limiter crab: Incorporates limiters into a multiple outlet preinsulated compression-type connector. Used to join secondary mains and services. 3-way–3-way type is shown in Fig. 13. The 5-way–5-way type has a 500,000-circular-mil (CM) conductor running through the center which is used to join two limiter crabs together, thus forming a ring bus with limiter tap elements. Fig. 14 illustrates this crab with the limiter taps, 500,000-CM conductor, heat-resistant shells, and finally the completely insulated assembly.

Network protector fuse: Fig. 15 shows types *Y* and *Z* fuses which were designed to co-ordinate with limiters. Type *Y* has the 2-hole mounting while type *Z* is drilled for 4-hole mounting.

Co-ordination of Limiters and Network Protector Fuses

Various phases of this problem have been discussed in other papers.[1,6] Since the design and application of limiters is closely allied with the design and applica-

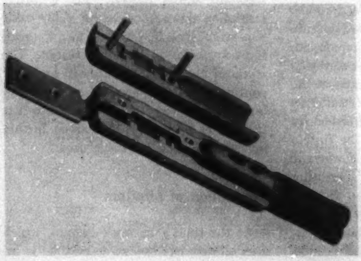

Fig. 10 (left). Limiter lug

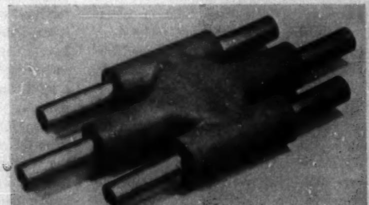

Fig. 12 (right). Limiter tap

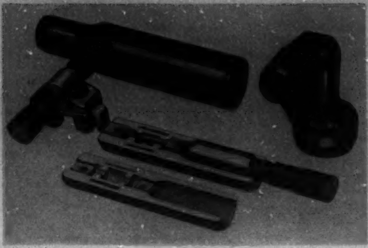

Fig. 13 (left). 3-way – 3-way limiter crab

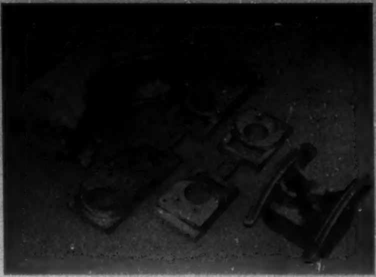

Fig. 15 (right). Type-Y and -Z network protector fuses

tion of network protector fuses, it may be best to review this co-ordination problem.

The selection of the proper size and type of network protector fuse is an important consideration in the design of a secondary network. Fuses which are too light can result in unnecessary blowing and overheating of the network protector, thus making it necessary to use external mounting, or they may even lead to cascading of all fuses in the network. If the fuses are too heavy, the network transformers may become damaged or limiters may blow before the fuse operates.

In analyzing the problem of co-ordination, two factors must be considered:

1. In the case of a primary fault, when the network protector does not function because of mechanical failure, on reverse current, the network protector fuse should clear before any of the limiters blow.
2. When a secondary fault occurs in the network, the limiters should clear the fault from the system before the network protector fuse opens if the fault does not clear.

Fig. 16 illustrates the time-current characteristic curves of a network protector fuse as well as the associated limiters. A typical case has been illustrated of a 500-kva transformer and 1,600-ampere network protector with four 500,000-CM secondary leads per phase feeding the network grid. In selecting the proper size network protector fuse, allowance for a possible unequal distribution of current in the four secondary mains should be considered. It has been the practice to design for at least 40 per cent of the network protector fuse current to be fed through one of the four limiters.[1] Therefore, in analyzing the problem of secondary co-ordination on a primary fault, the fuse size selected must be chosen so that it will blow before a limiter carrying up to 40 per cent of the reverse current.

In Fig. 16 curves 1 and 2 are for the 500,000-CM limiter and network protector fuse respectively. Curve 4 is for the 500,000-CM limiter replotted in terms of the current through the network protector fuse, assuming 40 per cent of this current is carried by the limiter.

Proper selectivity with limiters can only be obtained by selecting a network protector fuse having the same general shape for its time-current characteristic curves as that of the limiter. Selectivity is extremely important in that it minimizes the possibility of cascading network protector fuses, or clearing secondary faults by use of the network protector fuse. Fuses should be selected only after carefully analyzing the problem of co-ordination with limiters.

There are many types of fuses which have been used in network protectors for a variety of reasons. Some offer a limited range of selectivity with limiters, while others do not offer any co-ordination with limiters. There may be reasons for using each type, but before selecting the size and type a co-ordination analysis of

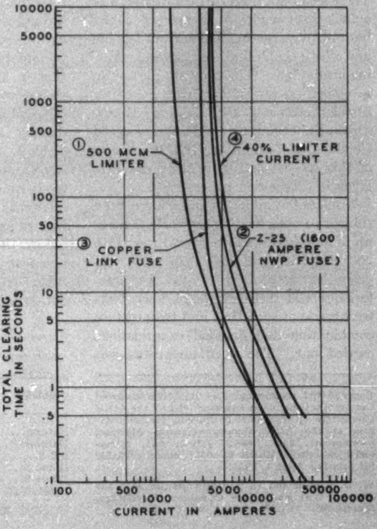

Fig. 16 (right). Co-ordination curves for limiter and network protector fuse

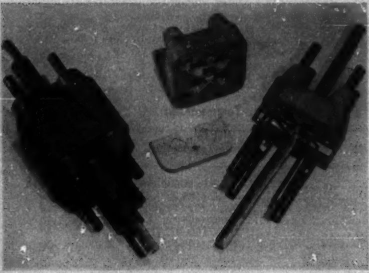

Fig. 14 (left). 5-way – 5-way limiter crab the two criteria just mentioned should be made. For example, a copper link fuse, curve 3, sometimes used in a 1,600-ampere network protector, crosses the 500,000-CM limiter curve, Fig. 16. In this case, the copper link fuse will clear on a secondary fault before the limiter when the fault current is in excess of 11,000 amperes.

Summary

1. Standard limiters rated by cable size are in general use, and are available in a wide variety of sizes and types, to prevent roasting of RH-RW type of insulation (*L260*).

2. It appears to be feasible to economically manufacture a lighter limiter to prevent roasting of *L220* cable when used in network systems.

3. The availability of limiters, coupled with means of making cable connection, justifies their use preferably during the initial installation of a network system.

4. When limiters are used, co-ordination studies between network protector fuses and limiters should be prepared in order to select the proper size and type of fuse.

References

1. SHORT CIRCUIT PROTECTION OF DISTRIBUTION NETWORKS BY THE USE OF LIMITERS, C. P. Xenis. *Electrical Engineering*, vol. 56, Sept. 1937, pp. 1191–96.

2. OVERLOAD CLASSIFICATIONS FOR NETWORK CABLES, R. C. Graham. *AIEE Transactions*, vol. 74, pt. III, Oct. 1955, pp. 916–19.

3. THE LIMITER—ITS BASIC FUNCTIONS IN NETWORK DISTRIBUTION SYSTEMS, C. P. Xenis. *Ibid.*, pp. 913–15.

4. TIME-CURRENT DAMAGE CHARACTERISTICS, CABLE IN DUCT, L. F. Porter. *Ibid.*, pp. 919–21.

5. CO-ORDINATION OF SECONDARY NETWORK PROTECTION, E. L. Leinbach, A. S. Brookes. *Ibid.*, pp. 922–24.

◆

Discussion appears on pages 944–50.

High-Temperature Classification of Rubber and Rubberlike Insulation of Network Cable by Oven-Heating Tests

W. H. COUCH
NONMEMPER AIEE

G. J. CROWDES
FELLOW AIEE

OVEN-HEATING tests on rubber and rubberlike insulations for network cable were made for the purpose of classifying their ability to withstand high temperatures for short periods of time. These tests are useful as comparisons of actual tests made on completed cables both by oven heating and current loading and offer a simple and easy method of rating insulations. The tests are part of an investigation carried out by the Limiter Standardization Task Group; Accessories Subcommittee; AIEE Insulated Conductors Committee. Other aspects of this subject and correlating data are given in companion papers.[1–7]

Insulated conductors only have been subject to oven heating for various times up to 30 minutes and temperatures up to 260 degrees centigrade (C) [500 degrees Fahrenheit (F)]. Physical characteristics and dielectric breakdown tests were made at each time and temperature combination and detailed examinations carried out. The oven apparatus was carefully designed to provide adequate volume and heating capacity to reduce temperature lag.

There is good qualitative comparison between the oven tests and cable and duct tests made by current loading. As would be expected, the oven tests produce damage at somewhat lower temperatures (approximately 10 to 25 C), since the insulation is heated at uniform temperature throughout and is without the protection afforded by the jacket. The insulation damage temperatures found are given Table I.

This method of classification is relatively quick and easy to do. It requires a minimum of apparatus. Because of these factors Appendix I gives a proposed procedure for high-temperature classification tests, by oven heating, on rubber or rubberlike insulated network cables without coverings.

General

For the past 2 years the Task Group has been working on the characteristics of limiters and their co-ordination with cable performance. The operation of networks involves the hazard or rather includes the near certainty that cables may carry large currents for short periods of time. Earlier networks depended on the cables being self-protecting and burn-off characteristics were of considerable interest. The use of limiters changed this but did not lessen the need for a knowledge of the high-temperature characteristics of the cable and co-ordination with the limiter behavior. This co-ordination has not always been present in past installations, and there have been cases of sufficient mismatch where the limiter did not protect the cable involved.

This situation is further complicated by the variety of cables available having insulations of different high-temperature behavior patterns. Since co-ordination is essential, further knowledge was required and studies have been made on the various aspects of the problem. The pertinent parts appear to be:

1. Intrinsic high-temperature behavior pattern of the cable insulations now in use under various time-temperature parameters and their classification.

2. Thermal characteristics of network cables.

Table I. Insulation Damage Temperatures

Rubber	Designation	Damage Temperature	Time, Minutes
Natural	oil base	180 C (356 F) to 200 C (392 F)	10 to 15
Natural	mineral base, class *AO*	220 C (428 F)	15
GR-S	oil base	200 C (392 F)	15
(Buna S)	low water absorptive	240 C (464 F)	15
(Buna S)	*RH-RW*	260 C (500 F)	30
Butyl	low water absorptive, heat and ozone resisting	240 C (464 F)	30

Paper **55-432**, recommended by the AIEE Insulated Conductors Committee and approved by the AIEE Committee on Technical Operations for presentation at the AIEE Summer General Meeting, Swampscott, Mass., June 27–July 1, 1955. Manuscript submitted March 8, 1955; made available for printing April 1, 1955.

W. H. COUCH and G. J. CROWDES are with the Simplex Wire and Cable Company, Cambridge, Mass.

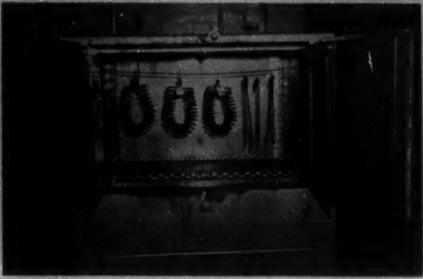

Fig. 1. Model 845A Precision-Freas oven

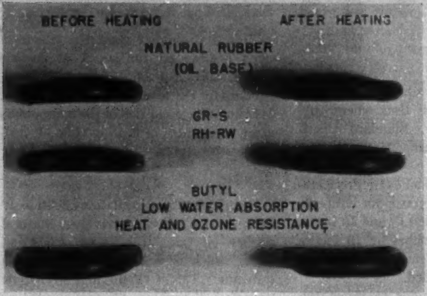
BEFORE HEATING
AFTER HEATING
NATURAL RUBBER
(OIL BASE)
GR-S
RH-RW
BUTYL
LOW WATER ABSORPTION
HEAT AND OZONE RESISTANCE

Figs. 2–6. Effect of oven heating, run no. 1. Insulation: 30 minutes at various temperatures

Fig. 2. 180 C

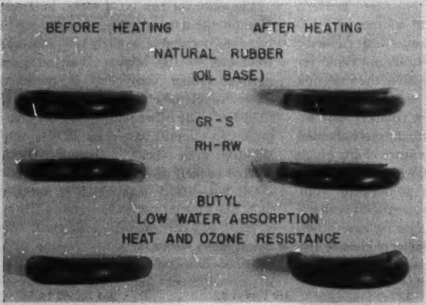
BEFORE HEATING
AFTER HEATING
NATURAL RUBBER
(OIL BASE)
GR-S
RH-RW
BUTYL
LOW WATER ABSORPTION
HEAT AND OZONE RESISTANCE

Fig. 3. 200 C

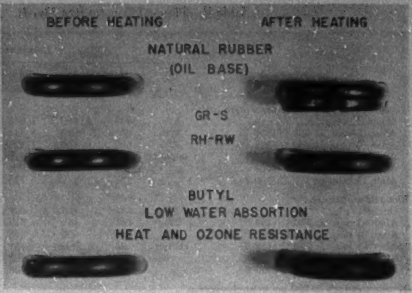
BEFORE HEATING
AFTER HEATING
NATURAL RUBBER
(OIL BASE)
GR-S
RH-RW
BUTYL
LOW WATER ABSORTION
HEAT AND OZONE RESISTANCE

Fig. 4. 220 C

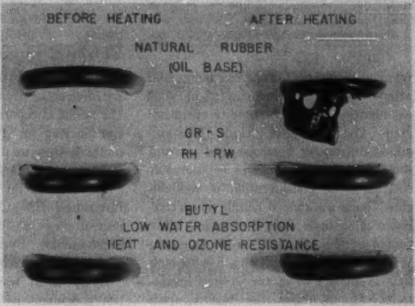
BEFORE HEATING
AFTER HEATING
NATURAL RUBBER
(OIL BASE)
GR-S
RH-RW
BUTYL
LOW WATER ABSORPTION
HEAT AND OZONE RESISTANCE

Fig. 5. 240 C

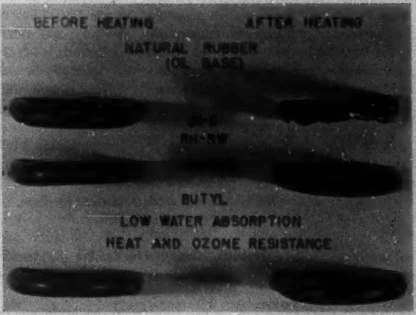
BEFORE HEATING
AFTER HEATING
NATURAL RUBBER
(OIL BASE)
GR-S
RH-RW
BUTYL
LOW WATER ABSORPTION
HEAT AND OZONE RESISTANCE

Fig. 6. 260 C

3. Mathematical determination of the temperature rise of a-c secondary network mains.
4. Overload tests on cables in air.
5. Tests on cables in ducts.
6. Characteristics of various limiters.
7. Co-ordination of secondary network protection.

This part of the study is concerned with the intrinsic high-temperature characteristics of the various cable insulations now in use as indicated by tests after oven heating.

Test Procedures

The data reported here are from two separate sets of tests run. The first of these was made on seven different insulations including natural and synthetic rubbers. The second set of tests contained refinements in test procedures and the measurement of additional pertinent characteristics on three of the component types in most use today.

The earlier tests consisted in the meas-

Table II. Physical Data for Run No. 1

	Compound						
	1	2	3	4	5	6	7
Tensile strength, pounds per square inch							
Original	928	658	1,280	1,618	1,710	1,075	864
After 15 min. at 180 C (356 F)	220	688	815	1,346	1,465	984	860
After 15 min. at 200 C (392 F)	323	590	356	1,198	1,430	925	750
After 15 min. at 220 C (428 F)	melted	331	melted	1,110	1,410	645	659
After 15 min. at 240 C (464 F)		194		1,089	1,290	383	534
After 15 min. at 260 C (500 F)		157		778	900	129	180
Elongation, per cent							
Original	368	331	475	600	600	625	488
After 15 min. at 180 C (356 F)	225	181	450	612	500	650	356
After 15 min. at 200 C (392 F)	293	118	500	593	550	600	312
After 15 min. at 220 C (428 F)	melted	94	melted	481	631	550	262
After 15 min. at 240 C (464 F)		68		468	619	456	268
After 15 min. at 260 C (500 F)		68		256	518	281	250
Tensile strength at 200-per-cent elongation, pounds per square inch							
Original	527	516	432	677	576	377	570
After 15 min. at 180 C (356 F)	202		290	637	659	362	695
After 15 min. at 200 C (392 F)	281		150	602	594	500	653
After 15 min. at 220 C (428 F)	melted		melted	626	558	330	618
After 15 min. at 240 C (464 F)				635	555	230	456
After 15 min. at 260 C (500 F)				675	495	109	160

urement of physical properties before and after oven heating and careful physical examination at each time-temperature step. The later tests include these and added durometer hardness and a-c and d-c dielectric strengths.

After some consideration it was decided to use a standard sample which consisted of a single class-*B* stranded, alloy coated conductor, size No. 8 American Wite Gauge, insulated with a 4/64-inch (0.0625-inch) wall of the desired insulations. In all cases the test samples were without outer coverings.

The samples were placed in a preheated oven at the various temperatures for the required period of time, then removed and allowed to cool to room temperature for at least 24 hours before being tested for tensile strength, elongation, durometer hardness, and a-c and d-c dielectric strength. Samples of 10 to 12 feet were used for dielectric strength tests; the samples were coiled on 2-inch-diameter mandrels. Samples for physical tests and examination were hung straight in the oven; see Fig. 1. All results reported are the mean of two samples except for the d-c dielectric strength tests where only one result is reported. Standard American Society for Testing Materials test methods were used.

The oven was a model *845A* Precision-Freas oven having a maximum temperature range of 260 C (500 F) and an inside measurement of 37 inches by 19 inches by 25 inches. Pyrex glass inner observation doors were provided.

Every effort was made to insert the test specimens as promptly as possible and to keep the oven doors open for as brief a time as necessary. The oven, in addition to a 1,200-watt heater for normal use, has two "booster" heaters, one of 1,200 watts and another of 2,400 watts. It is felt this added heat capacity is necessary in order to obtain rapid recovery of temperature after the insertion of samples. Actual measurements of oven temperature show recovery was accomplished in 3 to 5 minutes as indicated by a recording temperature chart which normally lags the temperature of the air heating medium.

Test Results

RUN NO. 1

The various compounds tested were:

1. Oil base, ozone resisting, natural rubber insulation.
2. Oil base, ozone resisting, *GR-S* rubber insulation.
3. Mineral base, performance grade, 30-per-cent natural rubber insulation *AO*.
4. Low water absorption, *GR-S* rubber insulation.
5. Low water absorption, heat resisting, *GR-S* rubber insulation, *RW-RH* type.
6. Low water absorption, ozone resisting, heat resisting, butyl rubber insulation.
7. Low water absorption, ozone resisting, heat resisting, butyl rubber insulation.

Figs. 2 through 6 show the effects of oven heating on run no. 1 at various temperatures. Table II gives the physical data for the seven compounds. Table III shows the condition of the compounds after 15 minutes of heating time at various temperatures.

RUN NO. 2

In this run three insulations commonly in use were chosen, namely: natural rubber oil base, *GR-S—RH-RW*, and butyl which is water, heat, and ozone resistant. Tables IV through VIII show the effect of heat on different conditions for these three insulations.

Discussion of Results

The data for run no. 1 given in Table II show the natural rubber insulations to be more perishable at high temperatures than any of the others. The oil base natural rubber compound is rendered unserviceable after 15 minutes at 180 C (356 F). The other natural rubber compound (a mineral base class *AO*) is only slightly more heat resistant. Both started to melt at 180 C (356 F).

Oil base *GR-S* compound is another

Table III. Condition for Run No. 1 After 15 Minutes of Heating Time at Temperatures Noted

Compound	180 C (356 F)	200 C (392 F)	220 C (428 F)	240 C (464 F)	260 C (500 F)
1	emitted smoke, on verge of melting	smoked, distorted due to melting	smoked, completely melted leaving copper bare	complete destruction	complete destruction
2	OK	smoked, small blisters all over surface	smoked, blisters larger, small cracks upon bending	smoked, blistered cracks open on bending	smoked, all blistered, cracks open on bending
3	surface tacky, on verge of melting	smoked, surface melting	smoked, surface brittle, inside tacky	smoked, surface brittle, inside melted	smoked, fell apart when removed from oven
4	OK	OK	surface brittle, small surface cracks on bending	smoked, surface started to wrinkle and crack on bending	smoked, surface wrinkles, small surface cracks on bending
5	OK	OK	OK	OK	smoked, few wrinkles surface cracks on bending
6	OK	OK	slight softening	smoked, on verge of melting	smoked, melted a little, small holes appeared
7	OK	OK	slight softening	smoked, on verge of melting	smoked, melted a little, small holes appeared

Table IV. Effect of Heat on Tensile Strength, Pounds per Square Inch

	Oil Base	RH-RW	Butyl
Original	794	797	833
Heated in air oven for			
5 min. at 180 C (356 F)	758	813	818
15 min. at 180 C	668	784	820
30 min. at 180 C	568	785	819
15 min. at 200 C (392 F)	557	785	811
5 min. at 220 C (428 F)	739	848	861
10 min. at 220 C	621	738	782
15 min. at 220 C	428	767	815
30 min. at 220 C	287	675	802
30 min. at 240 C (464 F)	220	644	633
30 min. at 260 C (500 F)	149	650	382

Table V. Effect of Heat on Per-Cent Elongation

	Oil Base	RH-RW	Butyl
Original	294	575	559
Heated in air oven for			
5 min. at 180 C (356 F)	307	532	407
15 min. at 180 C	263	529	444
30 min. at 180 C	244	525	400
15 min. at 200 C (392 F)	257	544	425
5 min. at 220 C (428 F)	343	518	443
10 min. at 220 C	282	532	413
15 min. at 220 C	175	562	350
30 min. at 220 C	100	552	337
30 min. at 240 C (464 F)	62	587	331
30 min. at 260 C (500 F)	31	512	350

Table VI. Effect of Heat on Durometer Hardness (Measured at Room Temperature)

	Oil Base	RH-RW	Butyl
Original	61	68	57
Heated in air oven for			
5 min. at 180 C (356 F)	63	69	57
15 min. at 180 C	61	69	58
30 min. at 180 C	62	69	60
15 min. at 200 C (392 F)	61	66	60
5 min. at 220 C (428 F)	60	70	58
10 min. at 220 C	60	69	61
15 min. at 220 C	53	66	56
30 min. at 220 C	55	68	58
30 min. at 240 C (464 F)	43	64	53
30 min. at 260 C (500 F)	20	63	43

perishable insulation and is little more heat resistant than the two of natural rubber. Other *GR-S* insulations are much more heat resistant with the *RH-RW* type best. Under this test they do not appear to be harmed very much until 260 C (500 F) is reached when the surface wrinkles and becomes brittle enough to crack when bent.

The butyl compounds also stand heat very well. At 260 C (500 F) in the oven test they tend to melt, develop pores, and swell a little. At 240 C (464 F) the butyl insulations soften but do not appear to be harmed.

Run no. 2 added durometer hardness and dielectric strength to the test schedule. It is interesting to note that deterioration of physical properties is accompanied by a corresponding decrease in dielectric strength. Since the times are short, oxidative deterioration is unlikely and the deterioration is probably due in most cases to the formation of pores at the very high temperatures. As shown in Table VIII, pores were developed in the natural rubber oil base compound at 200 C (392 F); in the butyl compound at 220 C (428 F). In the *RH-RW* compound there were no pores even after 30 minutes at 260 C (500 F).

Table VII. Effect of Heat on Dielectric Strength, Volts per Mil

	Oil Base		RH-RW		Butyl	
	A-C	D-C	A-C	D-C	A-C	D-C
Original	478	1,150	733	2,240	495	1,430
Heated in air oven for						
5 min. at 180 C (356 F)	430	1,170	478	2,120	430	1,210
15 min. at 180 C	438	1,380	448	1,850	450	1,210
30 min. at 180 C	390	1,130	438	2,280	430	1,080
15 min. at 200 C (392 F)	455	690	498	1,670	423	1,045
5 min. at 220 C (428 F)	440	1,430	483	2,200	380	145 (flaw)
10 min. at 220 C	368	650	493	2,500	448	1,360
15 min. at 220 C	270	495	465	1,805	425	1,450
30 min. at 220 C	288	505	448	2,330	430	1,470
30 min. at 240 C (464 F)	170	317	435	2,030	428	1,360
30 min. at 200 C (500 F)	0	0	445	2,340	250	440

Noticeable swelling occurs when the oil base compound is heated to 220 C (428 F). The butyl compound also swells but not as much. There is no swelling of the *RH-RW* (*GR-S*) compound at any of the temperatures tried. See Table VIII.

Durometer hardness, given in Table VI, shows that permanent softening occurs after 15 minutes at 220 C (428 F) for the oil base compound. The butyl compound showed indications of softening at 240 C (464 F) and further softening at 260 C (500 F). The *RH-RW* (*GR-S*) compound shows only slight evidence of permanent softening at the same temperature.

Conclusions

It is felt that the oven-heating procedure provides a quick and convenient method for the classification with respect to the intrinsic high-temperature behavior of insulations for secondary network cables. This method, when carried out on insulation only, undoubtedly gives temperatures lower than obtained in service for the same times. This is due to the oven temperature being constant with absence of temperature gradient and to the help afforded by outer coverings normally present. The temperatures indicated can be correlated qualitatively with those on cable in duct obtained with current loading.

On the basis of the tests reported here, the following comparison of compound types can be made:

1. *RH-RW* (*GR-S*) compound retains its physical and electrical breakdown properties to a higher temperature than either the butyl or oil base compounds. Indications are that *RH-RW* (*GR-S*) is serviceable after being heated for 30 minutes at 260 C (500 F).

2. The butyl compound shows a loss of physical properties and dielectric strength at temperatures higher than 240 C (464 F).

3. The physical and electrical properties of oil base compound show deterioration at a lower temperature. Signs of physical deterioration appear at 180 C (356 F) in 10 to 15 minutes and 220 C (428 F) will render the compound practically useless.

Appendix. Proposed Procedure for Preliminary High-Temperature Classification Tests, by Oven Heating, on Rubber or Rubberlike Insulated Network Cables Without Covering

Scope

The purpose of this test procedure is to provide the manufacturer with an optional screening test in the form of a convenient short-time high-temperature test method to be used in classifying insulating compounds. The results obtained by this method are approximate. For final classification, the test results must be confirmed by the current loading test method.

General

The tests shall be made on no. 8 stranded 4/64-inch wall insulated conductor. The type of insulation shall be indicated such as natural rubber, synthetic rubber, oil base, butyl rubber, etc. The American Society for Testing Materials specification applying to the insulation and/or the manufacturers' own specifications shall be noted. If a manufacturer supplies the cable insulation to his own specifications, copies of these specifications shall be furnished.

Test Procedure

1. Test samples for visual inspection shall be at least 12 feet long wound on 2-inch mandrels. Straight samples shall be used for the physical tests.

Table VIII. Effect of Heat on Appearance of Compounds

	Oil Base	RH-RW	Butyl
Original	smooth and black	smooth and slight brown	smooth and black
Heated in air oven for			
5 min. at 180 C (356 F)	no change	no change	no change
15 min. at 180 C	no change	no change	no change
30 min. at 180 C	no change	no change	no change
15 min. at 200 C (392 F)	blisters and pores	no change	no change
5 min. at 220 C (428 F)	scattered pores	no change	no change
10 min. at 220 C	shiny, porous	no change	slight tackiness
15 min. at 220 C	very porous	no change	slight tackiness (few pores)
30 min. at 220 C	swollen, porous	shiny smooth	slight tackiness
30 min. at 240 C (464 F)	soft, swollen porous, surface cracks	hard shiny surface cracks, cracks when bent	melting, tacky some pores
30 min. at 260 C (500 F)	swollen and empty shell, breaks on touch	dry, hard, wrinkled, cracks when bent	melting, tacky, increased porosity

2. Tensile strength, elongation, durometer hardness, and a-c and d-c dielectric strength tests and a visual inspection shall be made both before and after the samples have been subjected to the high-temperature oven tests.

3. The heating medium shall be a circulation air oven having a temperature range to at least 260 C (500 F) and equipped with pyrex glass observation doors. Sufficient heaters shall be provided to reduce temperature recovery to 5 minutes maximum as indicated by the recording chart when the doors are opened to insert samples. The oven shall be preheated to the desired temperature.

4. Testing methods for determining specific properties before and after exposure to heat shall conform to the requirements prescribed in the method of test of the American Society for Testing Materials covering the specific property to be determined. The inspections shall consist of a visual examination for softening, blistering, swelling, porosity, hardening, and other defects.

5. The room temperature shall be measured and recorded.

6. The samples shall be suspended in the preheated oven at the required temperature for a period of 1/2 hour. They shall then be removed and allowed to cool to room temperature for at least 24 hours before being tested. The results shall be averages of a minimum of three tests.

Tests

A number of exploratory tests shall be made in accordance with the foregoing so as to establish a starting temperature and an approximate temperature range for a more critical study. The starting temperature shall be a multiple of 20 C which is near the maximum which the insulation will withstand without failure. Check tests at the maximum withstand temperatures shall be made, the results of which will be used for tentative classification.

References

1. The Limiter—Its Basic Functions in Network Distribution Systems, **C. P. Xenis.** *AIEE Transactions*, vol. 74, pt. III, Oct. 1955, pp. 913–15.

2. Overload Classifications for Secondary Network Cables, **R. C. Graham.** *Ibid.*, pp. 916–19.

3. Time-Current Damage Characteristics, Cable in Duct, **L. F. Porter.** *Ibid.*, pp. 919–21.

4. Co-ordination of Secondary Network Protection, **E. L. Leinbach, A. S. Brookes.** *Ibid.*, pp. 922–24.

5. Limiters, Their Design Characteristics and Application, **Fred Heller, Irving Matthysse.** *Ibid.*, pp. 924–30.

6. A Mathematical Method for Determining Insulation Damage Curves for Network Cables, **R. H. Kolks.** *Ibid.*, pp. 934–38.

7. Characteristic Properties of Secondary Network Cables, **S. J. Rosch.** *Ibid.*, pp. 939–50.

Discussion appears on pages 944–50.

A Mathematical Method for Determining Insulation Damage Curves for Network Cables

R. H. KOLKS
MEMBER AIEE

SINCE 1937 limiters have been recognized as devices for protecting a-c network secondary cables against excessive damage from faults and overloads. The general principles of design and application of limiters were originally discovered by C. P. Xenis.[1]

In general it can be said that the "blowing curve" of the limiter should closely follow the damage characteristic of the cable it protects. In accordance with this principle, the characteristics of the original limiters were based upon actual tests made upon cables installed in ducts and subjected to various amounts of current. In these tests damage of the insulation was largely determined from physical examination and appearance.

Since the original development of the limiter there has not been any substantial change in the design characteristics of the types commonly available and in most cases operation has been satisfactory as contemplated. However, in recent years, along with the greatly expanded development of new rubber and rubberlike compounds for cables, there have been some reports of cases where cables were not sufficiently protected by the limiters. As a result of these reports it was considered desirable to investigate damage characteristics of some of the newer insulations, and cables more thoroughly. Partly as a result of these experiences the Limiter Standardization Task Group, Accessories Subcommittee, AIEE Insulated Conductor Committee was formed to investigate the subject and to perhaps arrive at an acceptable standard for limiters.

The present paper reports a small portion of the work of The Task Group and has as its purpose a mathematical investigation to determine the damage characteristic of a particular installation of cable. Given the temperature of the conductor at which damage could be expected, and the thermal, electrical, and physical characteristics of the cable and surrounding structure, it was desired to develop a simple mathematical equation for the time-current curve of the cables. It was considered that this would be a method supplementary to the experimental method.[3] The method reported herein

---

Paper 55-474, recommended by the AIEE Insulated Conductors Committee and approved by the AIEE Committee on Technical Operations for presentation at the AIEE Summer General Meeting, Swampscott, Mass., June 27–July 1, 1955. Manuscript submitted March 23, 1955; made available for printing May 26, 1955.

R. H. Kolks is with the Cincinnati Gas and Electric Company, Cincinnati, Ohio.

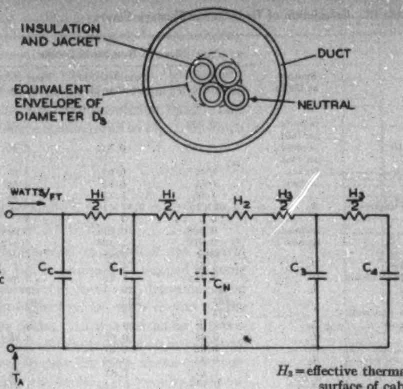

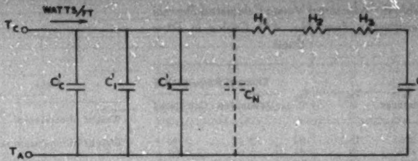

Fig. 1 (left). Equivalent thermal network

Fig. 2 (above). Simplified thermal network

was considered worthy of study in that it was hoped that it would present some information as to the quantitative effects of various factors which might be useful to manufacturers or users. It was also felt that, if future developments should result in the production of limiters having several different characteristics for the same size of cable, this method would perhaps assist the user in selecting the particular limiter which would suit his own conditions.

Discussion

In determining the damage characteristics of network secondary cables, periods of time up to 4 hours and temperatures of conductors up to 300 degrees centigrade (C) should be considered. The temperature at which the cable would be damaged in a period of 4 hours and the corresponding value of current were considered to be the factors which would largely determine the design of the limiter. Accordingly, the first part of this investigation was concerned with determining the accuracy with which the 4-hour temperature rise could be determined by calculation.

Steady-state temperature rise of cables installed in ducts can be expressed by the well-known equation

$$T_c = T_a + NI^2R(H_1+H_2+H_3+H_4) \qquad (1)$$

where

T_c = temperature of conductor, C
T_a = ambient temperature, C
N = number of conductors carrying current
I = current, amperes
R = a-c resistance of conductors, per foot
H_1 = thermal resistance from loaded conductors to outer surface of cables, C per watt per foot
H_2 = effective thermal resistance from outer surface of cables to inner edge of the duct, C per watt per foot
H_3 = thermal resistance through duct wall, C per watt per foot
H_4 = thermal resistance of duct bank and surrounding earth, C per watt per foot

For the particular problem under consideration, the temperature rise of the duct bank and surrounding earth were assumed to be negligible. The ambient temperature was accordingly assumed to be the temperature of the duct bank as measured in a near-by empty duct. The ambient temperature would therefore include the heating effects of the other cables in the duct bank.

Following the procedure of Buller and Neher,[3] the cables were assumed to be concentric with the duct, which simplified the calculations to the extent that it was not necessary to take into account the flow of heat through the direct contact between cables and duct. It was not found necessary to make any corrections later to the calculations due to the direct contact of cables with duct, inasmuch as reasonably close agreement was obtained between calculated and measured temperatures.

Network secondary cables are generally single-conductor type, with from three to seven cables installed in one duct. In the case of four cables in a duct a random arrangement and the inclusion of a neutral add complications which make the accurate calculation of H_1 and H_2 very difficult. The calculations were therefore limited to considerations of compact groupings of cables in a duct. Accordingly, the equation for H_1 in the case of four cables in a duct was taken to be the same as for a 3-conductor belted cable as given by Simmons[4]

$$H = \frac{0.00522\rho G_1}{N} \qquad (2)$$

where

ρ = thermal resistivity of insulation and sheath, C per watt per centimeter[3]
G_1 = geometric factor for 3-conductor belted cable with belt thickness = 0
$N = 3$

This equation also neglects the effect of the neutral upon H_1. For the case of seven cables in a duct, see Appendix I.

In arriving at an equation for H_2, an examination of the literature on cable calculations indicated that the commonly used value of 1,200 watts per C per square centimeter at normal operating temperatures was not sufficiently accurate at the 200 to 300 C copper temperature being considered. The following equation, as given by Buller and Neher,[3] gave more accurate results

$$\frac{1}{H_2} = \frac{0.092(D_s')^{3/4}(\Delta T)^{1/4}(P)^{1/2}}{1.39+D_s'/D_d} + \frac{0.0213}{\log_{10}\dfrac{D_d}{D_s'}} + 0.102D_s'\epsilon(1+0.0167T_m) \qquad (3)$$

where

D_s' = diameter of circle enclosing cables in duct, inches
D_d = inside diameter of duct, inches
P = air pressure, in atmospheres, assumed = 1
ϵ = emissivity of outer surface of cables = 1

Table I. Thermal Characteristics of Materials

Material	Specific Heat K, Watt-Hours per Pound per C	Resistivity, C per Watt per Centimeter[3]	Specific Gravity G per Centimeter[3]
Copper	0.048		8.89
Fiber duct, wet	0.22	470	1.05
Rubber *RH-RW*	0.16 to 0.24	325 to 610	1.05 to 1.30
Oil-base rubber	0.22	500	1.17
Neoprene	0.18	425	1.5
Concrete	0.082	115	2.3

Table II. Measured Versus Calculated Thermal Resistances, Four No. 4/0 Cables in Fiber Ducts

I, Amperes	T_a, C	T_c, C	Thermal Resistance H	
			Measured	Calculated
525	15	184	2.42	2.44
475	13	154	2.66	2.54
325	13	75	3.12	2.91
250	12	48	3.36	3.14
200	10	35	3.83	3.30

Table III. Calculation of Time-Current Damage Curves

Item	Symbol or Units	Size and Number of Cables		
		Seven No. 4/0	Four 500,000 Circular Mils	Four 750,000 Circular Mils
Weight of conductor	pounds per foot	0.653	1.54	2.32
Weight of insulation sheath	pounds per foot	0.165	0.311	0.40
Insulation thickness	inches	5/64	6/64	7/64
Jacket thickness	inches	3/64	4/64	4/64
A-c/d-c resistance ratio		1.05	1.13	1.21
Conductor resistance, 265 degrees	R	1.03×10^{-4}	0.47×10^{-4}	0.336×10^{-4}
Number of loaded cables	N	6	3	3
Conductor diameter	inches	0.528	0.814	0.998
Cable diameter	inches	0.778	1.126	1.342
Duct material		fiber	fiber	fiber
Inside duct diameter, inches	D_d	4.5	4.5	4.5
Equivalent diameter of cables, inches	D_s'	2.334	2.42	2.89
Ambient temperature, C	T_a	25	25	25
Conductor temperature, C	T_c	265	265	265
Temperature rise, cables to duct wall, C	T	135	113	106
Average duct air temperature, C	T_m	151	128	128
Thermal resistance	H_1	0.28	0.61	0.58
Thermal resistance	H_2	0.82	0.87	0.73
Thermal resistance	H_3	0.35	0.36	0.35
Total thermal resistance	H	1.45	1.83	1.66
Thermal capacity	C_c	0.188	0.222	0.334
Thermal capacity	C_1	0.198	0.187	0.240
Thermal capacity	C_n	0.064	0.136	0.192
Thermal capacity	C_2	0.485	0.485	0.485
Equivalent thermal capacity	C_c'	0.188	0.188	0.188
Equivalent thermal capacity	C_1'	0.179	0.156	0.198
Equivalent thermal capacity	C_n'	0.052	0.0905	0.125
Equivalent thermal capacity	C_2'	0.059	0.0465	0.0511
Time constant	S	0.478	0.515	0.708
Total equivalent thermal capacity	SH	0.693	0.943	1.175
Current equation plotted in Fig. 4		$517\sqrt{\frac{1}{1-\epsilon^{-1.44t}}}$	$965\sqrt{\frac{1}{1-\epsilon^{-1.06t}}}$	$1{,}195\sqrt{\frac{1}{1-\epsilon^{-0.85t}}}$

T = temperature drop between envelope enclosing cables and inner surface of duct

T_m = average temperature of air in duct, C

Since T_m and T are dependent upon H_1, H_2, and H_3, it was found necessary to arrive at the correct value for H_2 from equation 3 by the method described in Appendix II.

The thermal resistance of the duct can be obtained from the equation for a cylindrical element as follows

$$H_3 = 0.00522\ \rho \log_e \frac{D_o}{D_d} \tag{4}$$

where

D_o = the outer diameter of duct, inches

ρ = specific resistivity of duct material, C per watt per centimeter[3]

Determination of Temperature Rise Curve

To obtain the temperature rise curve for cables in ducts, the electric analogue method[5] was considered. The equivalent thermal network was therefore developed as shown in Fig. 1, where

C_c = thermal capacity of the conductor and any portion of the insulation which can be assumed to attain the same temperature as the conductor

C_1 = thermal capacity of the remaining portion of the insulation and jacket

C_2 = thermal capacity of the duct

C_4 = thermal capacity of the duct bank and the surrounding earth

Practical experience indicates that the duct bank does not change very much in temperature in a period of 4 hours, and therefore C_4 may be taken as infinite. The thermal capacities are shown lumped at the mid-points of their individual thermal resistances.

Rigorous mathematical solution of this network for the thermal transient has been covered in a number of previous AIEE papers, involving, however, a considerable amount of laborious calculations. The electric analogue computer[5] would provide a convenient and simple means for obtaining a solution providing one were available.

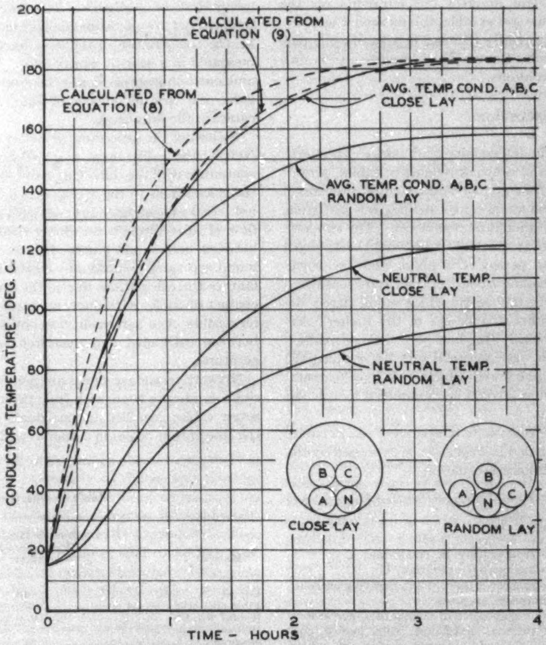

Fig. 3. Measured versus calculated temperature rise curves

The method was therefore adopted of simplifying the network by transferring intermediate capacities in the network to approximate equivalents at the extremities, much in the same manner as is done in the case of transmission lines. This procedure is illustrated in Fig. 2, in which

$$C_1'=C_1\frac{H_1/2+H_2+H_3}{H_1+H_2+H_3} \tag{5}$$

$$C_3'=C_3\frac{H_3/2}{H_1+H_2+H_3} \tag{6}$$

The thermal capacity of the neutral cable can be assumed as lumped at some logical point in the circuit, depending upon its physical location with respect to the other cables. In this particular illustration, it is assumed to attain a temperature approximately the same as the outer surfaces of the cables. The equivalent neutral capacitance then becomes

$$C_n'=C_n\frac{H_2+H_3}{H_1+H_2+H_3} \tag{7}$$

The various thermal capacities are determined from the equation

$C=WK$

where

C is in watt-hours per C per foot
W = weight, pounds per foot
K = specific heat, watt-hours per pound per C

Values of specific heat, thermal resistivity, and density of various materials which may be useful in calculations of this nature are given in Table I.

For the simplified network shown in Fig. 2 the equation for the temperature at any time t is

$$T_c=T_a+NI^2R(H_1+H_2+H_3)(1-\epsilon^{-t/SH}) \tag{8}$$

where

t = time, hours
$S=C_c'+C_1'+C_3'+C_m'$ in watt-hours per foot per C
$H=H_1+H_2+H_3$

Temperature Rise Tests

In an effort to determine the accuracy with which temperature rise of network cables could be obtained by means of the approximate mathematical expressions discussed previously, a number of tests were made at the Cincinnati Gas and Electric Company. These tests were made upon cables installed in a normal $4^1/_2$-inch fiber duct, encased in concrete, and having a length of about 30 feet. The cables were all no. 4/0 copper conductor, insulated with 5/64-inch type-*RW-RH* insulation, and having a 4/64-inch neoprene sheath over-all. In one series of tests, four cables were installed in the duct, bound together for 15 feet to represent "close lay," and in the remaining 15 feet the cables were permitted to lie in a random manner, representing "random lay." Thermocouples were connected to the copper conductors in the centers of each of the 15-foot stretches, and terminated in a multipoint thermocouple recorder. Current was circulated through three of the conductors connected in series, and held constant for about 4 hours, or until the maximum measureable temperature of 200 C was reached. The fourth conductor did not carry any current and was installed only for the purpose of representing the neutral cable.

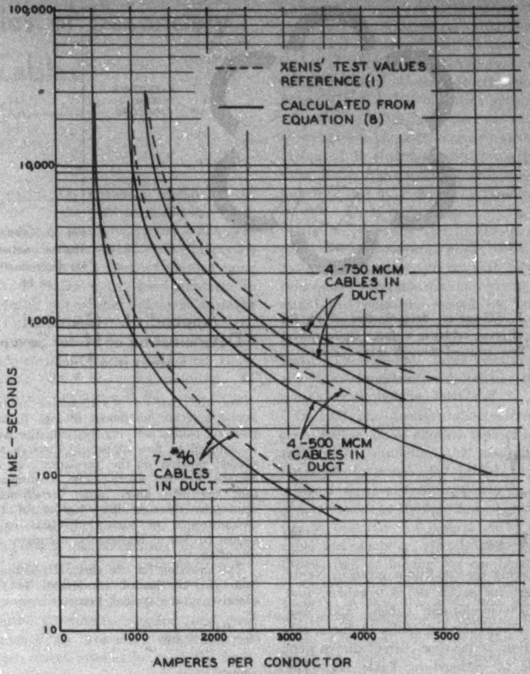

Fig. 4. Time-current damage curves

Table II shows the measured value of thermal resistance for several values of current in comparison with the calculated values. The agreement seems to be reasonably close, particularly for the high values of current.

Fig. 3 shows typical temperature rise curves for the case of four no. 4/0 cables in a $4^1/_2$-inch fiber duct and a current of 525 amperes maintained constant for 4 hours. In this same figure the temperature calculated by means of equation 8 is plotted and shows that for short periods of time considerably higher values of temperature are obtained by use of this equation than were actually obtained. One reason for the higher temperature rise is due to having assumed a constant value of conductor resistance throughout the period. In order to correct for the change in resistance, equation 8 was modified as follows

$$T_c=T_a+F\left(\frac{1}{1-\alpha F}\right) \tag{9}$$

α = temperature coefficient of resistance for copper per C
$F=NI^2RH\,(1-\epsilon^{-t/SH})$

This equation is also shown plotted in Fig. 3, and in this case the agreement with the observed rise is much closer.

Time-Current Damage Curves

For plotting time-current curves, equation 8 can more conveniently be expressed in the form

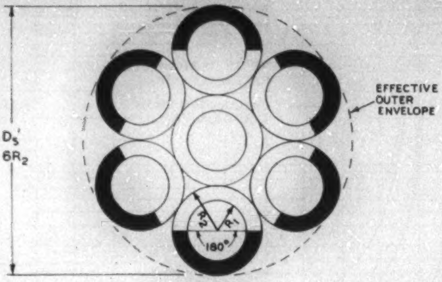

Fig. 5. Graphical determination of H_1 for case of seven cables in a duct. Uniform heat flow assumed through shaded areas

R_1 = Radius of conductor
R_2 = Outer radius of cable

$$I=I_0\sqrt{\frac{1}{(1-\epsilon^{-t_iSH})}} \tag{10}$$

where

$$I_0=\sqrt{\frac{T_c-T_a}{NRH}} \tag{11}$$

Taking the conditions given in Xenis' paper[1] for seven no. 4/0 cables, four 500,000-circular-mil cables, and four 750,000-circular-mil cables in ducts, calculations of the time-current curves were made as outlined in Table III. The curves as calculated are compared with Xenis' curves in Fig. 4, and show close agreement for low values of current and somewhat lower calculated values of current in the higher current range. The calculated curves can be brought much closer in agreement by using the average conductor resistance during the temperature rise period rather than the resistance at the end of the period as assumed for equation 11. This factor appeared to be rather difficult to express mathematically, and for practical purposes it was believed that this correction would not need to be made, particularly since limiters presently available considerably overprotect in this portion of the curve.

1. Given the maximum temperature of the conductor beyond which excessive damage can be expected, the time-current damage curves of network cables installed in ducts can be calculated with reasonable accuracy by the methods outlined.
2. The mathematical method should prove to have some value in that it permits certain factors to be evaluated which would be extremely laborious by the experimental method.

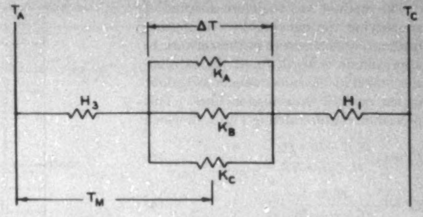

Fig. 6 (above). Thermal network for determination of H_2

Appendix I. Graphical Determination of H_1 for Seven Cables in a Duct

For the case of seven cables tightly bound together, as shown in Fig. 5, and with six cables carrying current, the heat is assumed to flow uniformly through the shaded portion of the insulation, as indicated in the figure. The assumption that the heat flows under steady-state conditions through 180 degrees of the circumference of each individual cable seems to be a reasonably accurate assumption.

The equation for the thermal resistance from the six loaded conductors to the effective outer envelope becomes

$$H_1=\frac{0.00522}{3}\log_e\frac{R_2}{R_1}$$

where

R_2 = over-all radius of cable, inches
R_1 = over-all radius of conductor, inches

Appendix II. Calculation of H_2

Typical example for the case of four no. 4/0 cables in a $4^1/_2$-inch duct

$D_s'=1.75$ $H_1=0.73$ $T_c=240$ C
$P=1$ $H_3=0.35$ $=1$
$D_d=4.5$ $T_a=40$ C

From equation 3

$$H_2=\frac{1}{K_a+K_b+K_c}$$

where

$$K_a=\frac{0.092(D_s')^{3/4}(T)^{1/4}(P)^{1/2}}{1.39+D_s'/D_d}$$

$$=\frac{0.092(1.75)^{3/4}(T)^{1/4}}{1.39+\frac{1.75}{4.5}}=0.0785(T)^{1/4}$$

$$K_b=\frac{0.0213}{\log_{10}\frac{4.5}{1.75}}=0.052$$

$$K_c=0.102D_s'(1+0.0167T_m)$$
$$=0.102\times1.75(1+0.0167T_m)$$
$$=0.1785(1+0.0167\ T_m)$$

Estimating $H_2=1.20$, then from Fig. 6

$$T=(T_c-T_a)\frac{H_2}{H_1+H_2+H_3}$$
$$=\frac{200\times1.20}{2.28}=105$$

$$T_m=T_a+\frac{T}{2}+\frac{H_c(T_c-T_a)}{(H_1+H_2+H_3)}$$
$$=40+\frac{105}{2}+\frac{0.35\times200}{2.28}=123.2$$

and

$$\begin{array}{ll} K_a=0.0785(105)^{1/4}= & 0.251 \\ K_b= & 0.052 \\ K_c=0.1785(1+0.0167\times123.2) & \underline{0.546} \\ & 0.849 \end{array}$$

$$H_2=\frac{1}{0.849}=1.18$$

Recalculating, assuming $H_2=1.18$

$$\begin{array}{ll} T=104.5 & \\ T_m=123 & \\ K_a=0.0785\ (104.5)^{1/4} & 0.251 \\ K_b= & 0.052 \\ K_c=0.1785(1+0.0167\times123) & \underline{0.546} \\ & 0.849 \end{array}$$

$H_2=1.18$

References

1. Short Circuit Protection of Distribution Networks by the Use of Limiters, C. P. Xenis. *Electrical Engineering*, vol. 56, Sept. 1937, pp. 1191–96.

2. Time-Current Damage Characteristics, Cable in Duct, L. F. Porter. *AIEE Transactions*, vol. 74, pt. III, Oct. 1955, pp. 919–21.

3. The Thermal Resistance Between Cables and a Surrounding Pipe or Duct Wall, F. H. Buller, J. H. Neher. *Ibid.*, vol. 69, pt. I, 1950, pp. 342–49.

4. Calculation of the Electrical Problems of Underground Cables, D. M. Simmons. *Electrical Journal*, East Pittsburgh, Pa., vol. 29, 1932.

5. The Determination of Temperature Transients in Cable Systems by Means of an Analogue Computer, J. H. Neher. *AIEE Transactions*, vol. 70, pt. II, 1951, pp. 1361–71.

◆

Discussion appears on pages 944–50.

Characteristic Properties of Secondary Network Cables

S. J. ROSCH
ASSOCIATE MEMBER AIEE

Synopsis: This is one of several papers[1-7] on problems associated with low-voltage secondary network cables. The data reported in this paper deal specifically with characteristic properties of such cables determined on an industry basis. These data are intended to be representative of insulations produced during the past decade, the emphasis being on nonmetallic-sheathed cables for low-voltage secondary network systems.

Historical

ALTHOUGH some nonmetallic-sheathed cable (30-per-cent rubber-insulated, braided cables) had been used for network systems in underground ducts as far back as 1919, the trend towards nonmetallic-sheathed cables had its beginning about 1930. In 1934 the writer presented an unpublished paper on a somewhat broader aspect of nonmetallic-sheathed cable for use in ducts. In that period network cables consisted mainly of conductors with rubber insulation protected with a heavy cotton braid treated with moisture-resisting bituminous compounds. In some constructions a rubber-filled tape was placed directly under the braid, while in others the braid was applied directly over the unvulcanized rubber insulation, the cable being vulcanized in that condition and the braid then treated with preservative compounds. This latter construction was based on the theory that rubber under compression could better withstand the deteriorating or swelling action of liquid media with which the cable would come in contact in underground ducts. It was contemplated that the primary function of the fibrous coverings was to provide mechanical protection during cable installation and that these coverings would deteriorate eventually due to bacterial action on the alternately wet and dry cellulosic coverings.

Basic reliance for good operating performance was therefore placed on the nature of the rubber insulation itself. Accordingly the rubber insulation was designed to have good physical properties both initially and after accelerated aging tests of various types, good resistance to moisture and other liquid media as might be found in sewage and manhole waters, and good resistance to short-time overloads of high currents (about ten times normal loading for a few minutes). In some types an attempt was made to produce a rubber insulation having a low explosibility range.

In actual operation, a large percentage of the faults burned clear rapidly. Occasionally, if not "cleared" promptly, the fault ultimately would be surrounded with molten metal. Under the latter fault condition it was not unusual to find that not only was quite an axial length of the original faulted cable destroyed but the sustained current flowing over the cable length generated excessive heat and damaged, by "roasting," the length between street intersection and the fault. A partial preventive means for such occurrences was achieved with the development and application of the cable limiter.[8]

With the availability of greater quantities of neoprene at a price considerably below that prior to 1941, the use of fibrous outer coverings was abandoned in favor of a neoprene sheath applied directly over the rubber insulation and generally with a firm bond between the two materials. The nature of the rubber insulation also underwent a radical change. It no longer was based on natural but on synthetic rubber of the *GR-S* (BUNA-S) types developed in the United States during World War II. The insulation generally used was of the heat- and moisture-resistant types with emphasis on good retention of some of the original physical properties, so as to meet the concept of what was required of such cable during overload conditions. Subsequently, other types of insulation, generally referred to as oil-base types, consisting of a blend of natural or synthetic rubbers with factice (vulcanized vegetable oils) and having an established operating record on other types of low- and high-voltage uses, were tried on some of the utilities' network systems. These oil-base types were generally also furnished with a neoprene sheath.

In 1951 some consideration also was given to the use of another type of synthetic rubber insulation, that made from butyl (also known as *GR-I*) rubber, which, although developed during World War II and only made available in limited quantities at that time for general use by the cable manufacturer, already had established itself as having the combination of excellent electrical properties and resistance to moisture, acids, and alkali, as well as resistance to oxidation and heat. Comparatively little of this insulation has been used for network cables up to the present time, due primarily to the limited availability of butyl rubber.

Before leaving the historical portion of this subject, a word about lead-covered rubber-insulated secondary network cables may be in order There is no question but that a seamless metallic sheath applied by any of the well-known methods still constitutes the only truly impermeable barrier against the intrusion of

Table I. Physical Properties of Oil-Base Ozone-Resisting Rubber Insulations Before and After Aging

	Brand Designation								
Nature of Test Conditions	1	2	2a*	3	4	5	6	7	8
Tensile Strength, pounds per square inch									
As received	735	888	763	943	588	748	700	857	711
After 96 hours in 70C oxygen bomb	645	455	726	496	590	721	769	885	737
After 250 hours in 70C oxygen bomb	732	396	626	487	483	841	753	897	711
Elongation, per cent									
As received	200	550	231	488	250	215	371	385	408
After 96 hours in 70C oxygen bomb	b†	b†	142	b†	b†	b†	275	287	285
After 250 hours in 70C oxygen bomb	b†	b†	117	b†	b†	b†	216	257	200
Stress at 200-per-cent elongation, pounds per square inch									
As received	735	435	770	608	551	739	640	598	514
After 96 hours in 70C oxygen bomb	b†	b†	b†	b†	b†	b†	726	766	646
After 250 hours in 70C oxygen bomb	b†	b†	b†	b†	b†	b†	741	844	711

*Replacements furnished by manufacturers of brands 2.
†These test specimens broke below 200-per-cent elongation.

Paper 55-441, recommended by the AIEE Insulated Conductors Committee and approved by the AIEE Committee on Technical Operations for presentation at the AIEE Summer General Meeting, Swampscott, Mass., June 27–July 1, 1955. Manuscript submitted March 25, 1955; made available for printing April 8, 1955.

S. J. Rosch is a Consulting Cable Engineer with the Anaconda Wire and Cable Company, Hastings-on-Hudson, N. Y.

Table II. Physical Properties of RH-RW Rubber Insulations Before and After Aging

Nature of Test Conditions	Brand Designation										
	9	9a*	10	11	12	13	14	15	16	17	18
Tensile Strength, pounds per square inch											
As received	822	1,124	1,048	947	947	1,003	937	756	1,061	1,192	681
After 96 hours in 70C oxygen bomb	783	1,183	1,115	1,051	793	1,130	835	804	1,189	1,310	621
After 250 hours in 70 C oxygen bomb	747	1,196	1,188	875	689	1,102	1,179	596	1,108	1,027	597
Elongation, per cent											
As received	462	612	448	420	438	390	382	515	607	325	542
After 96 hours in 70C oxygen bomb	453	610	390	342	347	375	267	503	522	312	460
After 250 hours in 70C oxygen bomb	392	594	395	290	b†	358	378	362	473	235	525
Stress at 200-per-cent elongation, pounds per square inch											
As received	426	418	381	443	294	554	652	319	407	720	458
After 96 hours in 70C oxygen bomb	440	441	502	568	506	671	758	366	524	835	519
After 250 hours in 70C oxygen bomb	522	477	595	635	b†	748	878	465	587	905	503

*Replacemenets furnished by manufacturers of brands 9.

†These test specimens broke below 200-per-cent elongation.

air, moisture, and other deleterious chemical influences into the cable interior as well as the cable insulation. This type of protection would be excellent were it not for the fact that the metallic sheath, regardless whether of lead or aluminum, is also vulnerable to ultimate attack by chemical or galvanic corrosion. Once this has occurred, the metallic sheath loses its 100-per-cent impermeability and environmental influences ultimately attack the underlying insulation leading to subsequent failure. If arcing occurs during the initiation of the failure, the sheath metal begins to melt, flows about the duct interior, and occasionally "freezes" to the duct, thereby making cable withdrawal a difficult and costly operation.

Even at present there is no industry standard for the characteristic properties or specification details for a standard type of low-voltage network cable. Obviously, different types of rubber-insulating compounds yield different characteristic properties from a physical and electrical point of view. What follows is an attempt to assemble the most recent data obtained by a number of reliable investigators, mainly under the sponsorship of the Limiter Standardization Task Group, Accessories Subcommittee, AIEE Insulated Conductor Committee, in the hopes that from these data some guidance may be obtained as to the type of insulation that best approximates the most desirable over-all characteristic properties wanted in an efficient secondary network cable.

Insulations—Physical Properties

It should be noted at the outset that physical properties for a given type of compound, before and after being subjected to some type of accelerated testing conditions, may vary considerably with the products and processes of the various manufacturers. Therefore, to obtain a true picture, data must be presented for the products of more than one manufacturer for each class of material. The purpose of this paper is to present not only the data gathered during the investigation but also from other sources which have a bearing on the properties of the three basic insulations under discussion.

Table III. Physical Properties of a Variety of Possible Network Rubber Insulations After 15 Minutes' Oven Heating at Various Temperatures

Nature of Test Conditions	Type Designations							
	a	b	c	d	e	f	g	h
Tensile strength, pounds per square inch								
Original	928	658	1,280	1,618	1,710	1,075	864	2,190
At 180C (356 degrees Fahrenheit (F)	220	688	815	1,346	1,465	984	860	2,835
At 200C (392 degrees Fahrenheit (F)	323	590	356	1,198	1,430	925	750	1,800
At 220C (428 degrees Fahrenheit (F)	melted	331	melted	1,110	1,410	645	659	1,230
At 240C (464 degrees Fahrenheit (F)		194		1,089	1,290	383	534	1,560
At 260C (500 degrees Fahrenheit (F)		157		778	900	129	180	1,050
Elongation, per cent								
Original	368	331	475	600	600	625	488	525
At 180C	225	181	450	612	500	650	356	337
At 200C	293	118	500	593	550	600	312	200
At 220C	melted	94	melted	481	631	550	262	137
At 240C		68		468	619	456	268	168
At 260C		68		256	518	281	250	125
Stress at 200-per-cent elongation, pounds per square inch								
Original	527	516	432	677	576	377	570	1,045
At 180C	202		290	637	659	362	695	1,630
At 200C	281		150	602	594	500	653	1,800
At 220C	melted		melted	626	558	330	618	
At 240C				635	555	230	456	
At 260C				675	495	109	160	

Key to nature of insulations:
a = Oil-base ozone-resisting natural-rubber insulation.
b = Oil-base ozone-resisting *GR-S*-rubber insulation.
c = Mineral-base performance-grade 30-per-cent natural-rubber AO insulation.
d = Low-water absorption *GR-S*-rubber insulation.
e = Low-water absorption heat-resisting *GR-S*-rubber insulation, *RH-RW* type.
f = Low-water absorption ozone- and heat-resisting butyl-rubber insulation.
g = Low-water absorption ozone- and heat-resisting butyl-rubber insulation.
h = Neoprene insulating compound.

Tables I and II were taken from the DeBaene-Anderson paper,[9] and are based on tests made on single-conductor no. 8 American-Wire-Gauge 7-strand cable, with a 4/64-inch wall of "rubber" insulation without any protective covering. These data are significant because they deal with properties of a substantial number of oil-base and *RH-RW* types of rubber insulation.

Tables III and IV were taken from the Crowdes-Couch paper[3] and represent an entirely different approach to determine the physical properties and behavior of these three types of insulation and others, both prior to and after more strenuous but shorter time oven-aging periods. The materials tested were the same as used for Tables I and II and, in addition, 30-per-cent natural-rubber (AO performance) and butyl-rubber types of insulation.

Table V supplements Table III and shows another physical property, namely, the physical appearance after each period of 15 minutes' heating at the same temperatures used in Table III. Similarly, Table VI supplements Table IV since it not only shows the physical appearance of the three basic insulations subjected to the oven-aging reported in Table IV but also the temperatures at which the insulation damage occurs.

Fig. 1 shows another aspect of the physical properties of 16 commercial lengths of network cable varying in type

Table IV. Physical Properties of Three Possible Network Rubber Insulations After Various Conditions of Oven Aging

Nature of Test Conditions	Natural Rubber Oil-Base Type: Actual Value	Natural Rubber Oil-Base Type: Per Cent of Original	GR-S RH-RW Type: Actual Value	GR-S RH-RW Type: Per Cent of Original	Butyl Type: Actual Value	Butyl Type: Per Cent of Original
Tensile strength, pounds per square inch						
Original	794		797		833	
After heating in oven						
At 180 C for 5 minutes	758	95.5	813	100.4	818	98.3
At 180 C for 15 minutes	668	84.0	784	98.2	820	98.5
At 180 C for 30 minutes	568	71.5	785	98.3	819	98.4
At 200 C for 15 minutes	557	70.2	785	98.3	811	97.3
At 220 C for 5 minutes	739	93.0	848	106.2	861	103.2
At 220 C for 10 minutes	621	78.3	738	92.5	782	93.8
At 220 C for 15 minutes	428	53.8	767	96.2	815	97.6
At 220 C for 30 minutes	287	36.1	675	84.5	803	96.3
At 240 C for 30 minutes	220	27.7	644	80.6	633	75.9
At 260 C for 30 minutes	149	18.7	659	82.5	382	45.8
Elongation, per cent						
Original	294		575		559	
After heating in oven						
At 180 C for 5 minutes	307	104.2	532	92.6	407	72.9
At 180 C for 15 minutes	263	86.0	529	92.0	444	79.3
At 180 C for 30 minutes	244	83.0	525	91.4	400	71.6
At 200 C for 15 minutes	257	87.3	544	94.5	425	76.0
At 220 C for 5 minutes	343	116.6	518	90.0	443	79.2
At 220 C for 10 minutes	282	95.8	532	92.6	413	73.9
At 220 C for 15 minutes	175	59.5	562	97.8	350	62.6
At 220 C for 30 minutes	100	34.0	562	97.8	337	60.3
At 240 C for 30 minutes	62	21.0	587	102.0	331	59.3
At 260 C for 30 minutes	31	10.5	512	89.1	350	62.6

of insulation or outer covering. It qualitatively assesses the temperature at which various degrees of insulation damage occur as a result of current overloads for 4-hour periods. Fig. 1 is based on the Graham[2] paper and similar data presented to the Limiter Standardization Task Group Committee.

Insulations—Dielectric Strength Properties

Table VII is based on the Crowdes-Couch paper[3] and represents both a-c and d-c dielectric strengths in volts per mil of the three basic types of insulation the physical properties of which were described in Tables IV and VI. The data are given for samples initially, and after having been subjected to different oven-heating tests.

Insulations—Effect of Water on Electrical Properties

Table VIII is based on the DeBaene-Anderson paper[9] and represents the effect of various periods of immersion in water at 50 degrees centigrade (C) on electrical properties of eight different makes of oil-base rubber-insulated conductors. These are the same insulations whose physical properties are given in Table I. Of interest is the effect of 300 volts d-c negative and positive potential respectively after prolonged immersion in water at 50 C. Part of the data is concerned with the "life-in-immersion test." Failure under this test is considered to have occurred for any of the three following reasons: insulation punctured during application of the measuring voltage, power factor of a specimen increased beyond 20 per cent, or the leakage current through the insulation became so high that the 3-kva test transformer could not maintain the desired voltage.

Table IX is similar to that in Table VIII except that the insulations tested were the same *RH-RW* types, the physical properties of which are given in Table II. Another difference is that the periods of immersion in 50 C water were greater than for the oil-base insulations reported in Table VIII.

Discussion

Analysis of the data in the present paper leads to numerous possible observations which may be summarized by the following:

1. From the point of view of emergency overload conditions and the resulting temperatures to which secondary network cables may be subjected for comparatively short periods, there seems to be little question but that the *GR-S* type of *RH-RW* insulations will withstand higher temperatures than the ozone-resisting oil-base and butyl-rubber types. However, Fig. 1 also indicates that, if the overload temperatures can be confined to values not exceeding

Table V. Physical Appearance of Insulations Reported in Table III After 15 Minutes' Oven Heating at Various Temperatures

Temperature, C	Type Designations: a	b	c	d	e	f	g	h
180 (356F)	Emitted smoke, verge of melting	O.K.	surface tacky, verge of melting	O.K.	O.K.	O.K.	O.K.	O.K.
200 (392F)	Smoked, distorted due to melting	smoked, small blisters all over surface	smoked, surface melting	O.K.	O.K.	O.K.	O.K.	surface brittle, cracks on bending
220 (428F)	Smoked and completely melted, conductors bare	smoked, blisters larger, small cracks upon bending	smoked, surface brittle, inside tacky	surface brittle, small surface cracks on bending	O.K.	slight softening	slight softening	smoked, surface brittle, cracks on bending
240 (464F)	Complete destruction	smoked, blistered, cracks open on bending	smoked, surface brittle, inside melted	smoked, surface starting to wrinkle and crack on bending	O.K.	smoked, verge of melting	smoked, verge of melting	smoked, surface brittle, cracks on bending
260 (500F)	Complete destruction	smoked, all blistered, cracks open on bending	smoked, fell apart when removed from oven	smoked, surface wrinkles, small surface, cracks on bending	smoked, few wrinkles, surface cracks on bending	smoked, melted a little, appearance of small holes	smoked, melted a little, appearance of small holes	smoked, surface brittle, cracks on bending

Key to nature of insulations:
a = Oil-base ozone-resisting natural-rubber insulation.
b = Oil-base ozone-resisting *GR-S*-rubber insulation.
c = Mineral-base performance-grade 30-per-cent natural-rubber AO insulation.
d = Low-water absorption *GR-S*-rubber insulation.
e = Low-water absorption heat-resisting *GR-S*-rubber insulation, *RH-RW* type.
f = Low-water absorption ozone- and heat-resisting butyl-rubber insulation.
g = Low-water absorption ozone- and heat-resisting butyl-rubber insulation.
h = Neoprene insulating compound.

220 C, the ozone-resisting oil-base and butyl-rubber insulations should also give satisfactory service. The only practical method currently available for controlling temperature is by suitable limiters. It is for that reason that the Task Group tentatively established the need for two limiters, *L220* and *L260*, designed for temperatures of 220 C and 260 C respectively.

2. Tables I and II indicate very definitely that there is no distinct pattern of physical properties for either the oil-base or *RH-RW* insulations. These properties vary considerably, both initially and after various accelerated-aging tests, with the formulations used by different manufacturers of these products.

3. Similar observations may be made from Tables III through VI, even though the form of samples tested and the nature of their composition and type of tests used were radically different. The short-time evaluation approach developed by Crowdes and Couch[3] offers considerable promise as a new tool for the initial determination whether some new compound offers possibilities as a suitable network insulation in either the *L220* or *L260* class.

4. Further examination of Tables III through VI reveals that, although oil-base and butyl-rubber insulations properly belong in the *L220* class, the butyl-rubber types appear to retain a greater per cent of their original physical properties, particularly elongation.

5. Statements have been made,[10] and the opinion still prevails in some quarters, that a seamless metallic sheath in place of a neoprene sheath on rubber-insulated cables would yield greater service life. Whereas it is true that an impermeable barrier such as a lead sheath would protect the underlying insulation from the effects of water and oxidation, it cannot protect the same insulation from high temperatures caused by overload conditions encountered during the operation of secondary network systems. A metal enclosure may retain overload temperatures longer than a nonmetallic sheath and aggravate the damage caused by temperature. Sample *M* of Fig. 1 indicates this because, even though the only lead-covered construction of the 16 subjected to the current-overload tests, it is the only *RH-RW* insulation of the 7 tested to show that some noticeable physical damage had occurred at 240 C. It is possible that the same insulation-damage temperature would have been obtained on cable *M* if it had also been tested in a neoprene instead of a lead sheath.

6. Table VII seems to confirm that, from a retained dielectric strength point of view, placing ozone-resisting oil-base and butyl-rubber insulations in the *L220* class and the *RH-RW* insulations in the *L260* class was a judicious decision on the part of the Task Group.

7. Since good resistance to effects of prolonged immersion in water at some elevated temperature is considered one of the desirable properties of a network cable, the data in Tables VIII and IX are of considerable interest. It is regrettable that they did not include data on several types of butyl-rubber-insulated cables but such data will doubtless be made available in

Table VI. Physical Appearance and Damage Temperature of Insulations in Table IV After Various Conditions of Oven Aging

Nature of Test Conditions	Natural-Rubber Oil-Base Type	GR-S RH-RW Type	Butyl Type
Effect on physical appearance			
Original	smooth and black	smooth and slight brown	smooth and black
After heating in oven			
At 180 C for 5 minutes	no change	no change	no change
At 180 C for 15 minutes	no change	no change	no change
At 180 C for 30 minutes	no change	no change	no change
At 200 C for 15 minutes	blisters and pores	no change	no change
At 220 C for 5 minutes	scattered pores	no change	no change
At 220 C for 10 minutes	shiny and porous	no change	slight tackiness
At 220 C for 15 minutes	very porous	no change	slight tackiness (few pores)
At 220 C for 30 minutes	swollen and porous	shiny smooth	slight tackiness (few pores)
At 240 C for 30 minutes	soft and swollen, porous surface cracks	hard shiny, surface cracks, cracks when bent	melting and tacky, some pores
At 260 C for 30 minutes	swollen and empty shell, breaks on touch	dry, hard, and wrinkled, cracks when bent	melting and tacky, increased porosity
Resulting damage temperatures			
10 to 15 minutes	180 C to 200 C		
30 minutes		260 C	
30 minutes			240 C

Table VII. Dielectric Strength of Insulations in Table IV After Various Conditions of Oven Aging

	Dielectric Strength, Volts per Mil					
	Natural Rubber Oil-Base		GR-S RH-RW		Butyl	
Nature of Test Conditions	A-C	D-C	A-C	D-C	A-C	D-C
Original	478	1,150	733	2,240	495	1,430
After heating in oven						
At 180 C for 5 minutes	430	1,170	478	2,120	430	1,210
At 180 C for 15 minutes	438	1,380	448	1,850	450	1,210
At 180 C for 30 minutes	390	1,130	438	2,280	430	1,080
At 200 C for 15 minutes	455	690	498	1,670	423	1,045
At 220 C for 5 minutes	440	1,430	483	2,200	380	145(flaw)
At 220 C for 10 minutes	368	650	493	2,500	448	1,360
At 220 C for 15 minutes	270	495	465	1,805	425	1,450
At 220 C for 30 minutes	288	505	448	2,330	430	1,470
At 240 C for 30 minutes	170	317	435	2,030	428	1,360
At 260 C for 30 minutes	0	0	445	2,340	250	440

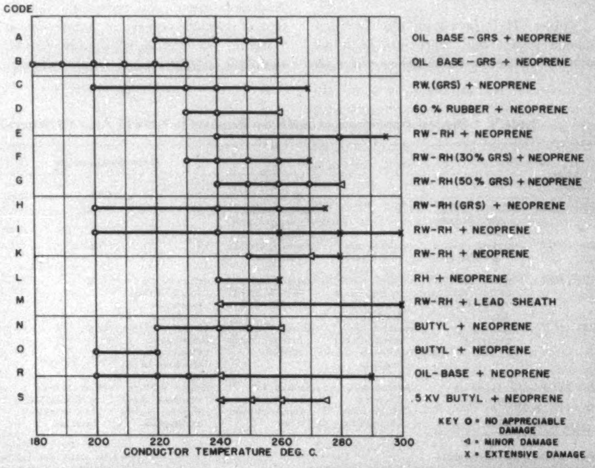

Fig. 1. Effect of 4-hour heating by current loadings on damage characteristics of secondary network cables

Table VIII. Effect of Prolonged Immersion in Water at 50 C on The Electrical Properties of Oil-Base Ozone-Resisting Rubber Insulations

Nature of Test Conditions	Brand Designation 1	2	2a*	3	4	5	6	7	8
Life in immersion test, months									
a	1	7	18	13	15	13	15	21	23
b	1	9	19+	11	15	14	18	22	24
c	1	9	10+	13	7	14	16	22	25
Dielectric strength, volts per mil									
As received	417	574+	560+			542+		389+	
After 25 months' immersion									
a	129k	53k		32	37	77	46	117	96
b	140k	57k		33	52	66	84	117	105
c	133k	56k		31	27	75	66	121	114
Power factor @ 40 volts per mil									
After 14 days' immersion, per cent	2.8	3.5	3.7	2.3	2.7	3.1	6.9	2.0	2.8
Stability factor, per cent	1.1	0.0	0.0	0.0	0.1	0.0	0.2	0.0	0.0
Increase in specific-inductive-capacitance between 1 and 14 days' immersion, per cent	5.5	6.1	5.0	4.7	5.2	3.5	6.8	2.6	2.2

Key to symbols:
* Replacement furnished by manufacturer of brand 2.
k—These specimens were tested early, brand 1 after 13 months' immersion and brand 2 after 15 months' immersion.
a, b, c—Refer to 300-volt negative d-c potential, 300-volt positive d-c potential, and a control sample without potential respectively.
D-c—Where used, was applied continuously.
Stability factor = Difference between per-cent power factor measured at 80 volts per mil and at 40 volts per mil after 14 days' immersion.

the future. The data in Tables VIII and IX do indicate that *L260* (*RH-RW* types as a class) has a decided superiority in resistance to prolonged immersion in water at 50 C over that of *L220* (represented by the oil-base) as a class.

There still exist varying opinions as to the importance of different criteria used to evaluate good moisture resistance of a rubber or rubberlike insulation for operation on an a-c system in wet locations. The tests most generally used include the "mechanical" moisture-absorption or gravimetric test, in addition to those in Tables VIII and IX. The mechanical moisture absorption of such compounds is generally expressed in terms of milligrams per square inch of surface exposed, after 7 days in distilled water at 70 C. No up-to-date mechanical moisture-absorption data on the *L220* or *L260* types of insulation have appeared in any of the references cited. However, from rather extensive data available to the author, the three types of insulation appear to have the range of mechanical moisture-absorption values as shown in Table X.

Similar data, from tests in progress, indicate that, under the 60-cycle power factor, under the stability factor and under the change in specific-inductive-capacitance (*EM-60*) test, butyl-rubber insulations as a class show a better range of values than either *RH-RW* or oil base, particularly when measured in water at 70 and 80 C, temperatures which may not be unusual in an a-c network. On the basis of resistance to moisture, the three types of insulation appear to be in the following order of merit: butyl (*L220*), *RH-RW* (*L260*), d an oil-base (*L220*).

Table X. Range of Mechanical Moisture-Absorption Values

Class of Insulation	Minimum	Maximum
L220, Oil-base	40	90
L220, Butyl	3	15
L220, *RH-RW*	14	20

8. With the daily progress in rubber technology, it is probable that one or both of the *L220* insulations may be improved to an extent as to merit their rating being improved to the *L260* classification. However, it must be emphasized that, with the future availability of the *L220* limiter design, the *L220* insulations should yield performance equal to that with *L260* insulations protected by the *L260* limiter.

Conclusions

From the data presented, it is possible to arrive at a number of interesting conclusions:

1. Up to the present, there has not been available an industry standard as to what constitutes suitable characteristic properties for a nonmetallic-sheathed network cable.
2. Each of the three basic insulations varies considerably from the others in performance under a wide variety of criteria.
3. From an over-all point of view, the decision of the Limiter Standardization Task Group Committee to establish classes *L220* and *L260* is fully justified.
4. Regardless of the superiority of the *L260* insulations over the *L220* types in ability to withstand higher overload temperatures, with the proper limiter protection, both classes of insulation should yield satisfactory service.
5. For a-c network systems not protected by limiters, the *L260* insulation should give better operating performance.

Table IX. Effect of Prolonged Immersion in Water at 50 C on the Electrical Properties of RH-RW Rubber Insulations

Nature of Test Conditions	Brand Designation 9	9a*	10	11	12	13	14	15	16	17	18
Life in immersion test, months											
a	2	21+	9	15	16	27	32	32	32	34+	34+
b	4	21+	9	16	24	27	22	32	34	34+	34+
c	5	21+	11	19	26	28	32	32	34	34+	34+
Dielectric strength, volts per mil											
As received	385	511		493		343	520+	484	488	520+	520+
After 28 months' immersion											
a	100		157	157	100	151					
b	95		169	163	102	149					
c	93		167	166	154	149					
After 32 months' immersion											
a							227	138	162		206
b							209	141		222	212
c							233	145			199
Power factor at 40 volts per mil after 14 days' immersion, per cent	3.41	3.42	3.34	3.24	3.51	2.98	0.90	1.04	3.49	1.00	1.07
Stability factor, per cent	0.81	0.22	1.74	0.09	1.45	0.73	0.69	0.09	0.42	0.43	0.00
Increase in specific inductive capacitance between 1 and 14 days' immersion, per cent	2.8	−1.6	4.2	8.6	1.9	2.8	4.8	2.0	2.9	1.2	3.2

Key to symbols:
*Replacement furnished by manufacturer of brand 9.
a, b, c—Refer to 300-volt negative d-c potential, 300-volt positive d-c potential, and a control sample without potential respectively.
D-c—Where used, was applied continuously.
Stability factor = difference between per-cent power factor measured at 80 volts per mil and at 40 volts per mil after 14 days immersion.

6. It should be possible to develop acceptable industry standards for the *L260* and *L220* network cables. If this is done, it is possible that individual performance standards would have to be provided for each of the three types of insulation because their individual characteristic properties under the various test criteria vary considerably from each other.

References

1. The Limiter—Its Basic Functions in Network Distribution Systems, **C. P. Xenis.** *AIEE Transactions*, vol. 74, pt. III, Oct. 1955, pp. 913–15.

2. Overload Classifications for Secondary Network Cables, **R. C. Graham.** *Ibid.*, pp. 916–19.

3. High-Temperature Classification of Rubber and Rubberlike Insulation of Network Cable by Oven-Heating Tests, **W. H. Couch, G. J. Crowdes.** *Ibid.*, pp. 930–34.

4. Time-Current Damage Characteristics, Cable in Duct, **L. F. Porter.** *Ibid.*, pp. 919–21.

5. A Mathematical Method for Determining Insulation Damage Curves for Network Cables, **R. H. Kolks.** *Ibid.*, pp. 934–38.

6. Co-ordination of Secondary Network Protection, **E. L. Leinbach, A. S. Brookes.** *Ibid.*, pp. 922–24.

7. Limiters, Their Design Characteristics and Application, **Fred Heller, Irving Matthysse.** *Ibid.*, pp. 924–30.

8. Short-Circuit Protection of Distribution Networks by the Use of Limiters, **C. P. Xenis.** *AIEE Transactions (Electrical Engineering)*, vol. 56, Sept. 1937, pp. 1191–96.

9. Moisture Studies on Ozone-Resisting and Type RH-RW Rubber Insulations, **E. C. DeBaene, C. A. Anderson.** *AIEE Transactions*, vol. 73, pt. III-B, 1954 (Feb. 1955 section), pp. 1746–54.

10. Economics and Comparison of Reliability of Leaded and Nonleaded Secondary Distribution Systems, **E. L. Leinbach, C. P. Xenis.** *Ibid.*, pp. 1478–81.

11. A Progress Report on Performance of Secondary Network Cables, **E. C. DeBaene, F. M. Hull, R. H. Hiester.** *Ibid.*, pp. 1688–91.

◆

Discussion

Joint Discussion

L. J. Weed (Boston Edison Company, Boston, Mass.): I should like to preface my discussion of the group of papers covering the protection of secondary network cables by the use of limiters, with a few remarks concerning the specific interest the Boston Edison Company has in this subject, and to clarify our position in this discussion.

We started our secondary network without limiters but decided to install them about the time we began to tie street mains together. The decision to install limiters was based on the protection they afforded against faults which might result in fires and explosions or extensive destruction of cable. We also felt that we would be in a better position in damage suits resulting from manhole explosions or other causes if we could point out that we had taken the best known means of protecting our secondary network system.

We found that the limiters did a satisfactory job except in the following cases:

1. Where there was insufficient short-circuit current in fringe areas.
2. On nonleaded cable with half-size neutral.
3. In the case of arcing faults.
4. On phase-to-ground faults, or where limiters on two phases had blown and the third phase failed to blow.

We had several manhole explosions and fires on nonleaded cables with half-size neutral and even on lead-covered cables where calculated short-circuit current was more than adequate to blow limiters.

These troubles resulted in unfavorable newspaper publicity and agitation by city officials and our management to do something to correct this situation.

We studied several methods of affording better protection against faults in the secondary network system such as the use of smaller limiters, that is, no. 1/0 limiters in no. 4/0 cable and no. 4/0 limiters in 500,000-CM cables, but discarded this idea because of the expense and work involved in changing existing limiters, and the troubles that might arise from unnecessary blowing on overload and the possibility of incorrect coordination with other limiters or with the network protector fuse.

Another idea which was discarded as being too expensive and physically impractical was to change all nonleaded cable to lead covered or to add more neutral capacity.

It was finally agreed that the most practical solution would be to install transformer vaults between existing vaults which would provide additional capacity for future load requirements, and thereby increase the available short-circuit current and reduce the length of cable between vaults. Also, it was agreed that an attempt be made to obtain limiters with more satisfactory characteristics, either by redesigning the present limiter or by obtaining a new type of limiter with different characteristics.

To determine what characteristics a limiter should have in order to clear arcing faults more rapidly and thereby minimize manhole explosions, a study is being made to provide the necessary test facilities to obtain actual data on various types of faults on secondary network cable installed in a simulated duct line and energized from a suitable network transformer and protector as in actual practice. When these data become available we expect to be in a better position to determine what steps should be taken to minimize the danger of manhole explosions.

Basic Function in Network Distribution Systems

Paper 55-443 would be improved if the claim that "years of experience under operating conditions shows the insulation is adequately protected" were modified. It may be possible that the limiter is satisfactory on the systems of some companies but the experience of my company, however, has been unsatisfactory especially when single-phase faults lingered.

The author gives the impression that troubles in this class also are of minor importance, and that attempts to solve the problem will be futile. My experience has been that faults in this class can be serious, and I understand that experiences on some other systems have been similar. It would be a disservice to the industry to discourage engineers from seeking a solution on the assumption that such solution would likely be impractical. There are indications that a solution may be found.

In general, the paper is good, provided it does not give the impression that when the AIEE recommended limiters are used serious trouble will not occur, nor should the impression be given that there is little hope that the present limiter can be improved.

The inadequacy of the present limiter should be clearly stated, even if it is desirable to add that at present it is the best available. That may offer some enterprising engineer a challenge. It would be embarrassing to say that it cannot be done, and then have someone do it.

Overload Classifications

As we use practically all lead-covered cable with performance-type rubber insulation, American Society for Testing Materials (ASTM) specification *D-755*, with a maximum operating temperature or 60 C in the no. 4/0 and 500,000-CM sizes, in reference to paper 55-444 we would like to inquire whether the standard limiter of the new special limiter would be recommended for such cables.

We question the use of a 4-hour period as the proper length of time to determine the damage characteristics of the insulation, as faults should be cleared normally in a matter of seconds.

Time–Current Damage Characteristics

In reference to paper 55-434, we would like an expression of opinion as to where the curve for damage characteristic of performance-type rubber ASTM specification *D-755* with lead sheath would fall.

The Boston Edison Company has considered making some short-circuit tests on cables pulled into ducts in a manner similar to the setup described in this paper in order to determine the time required for limiters of various types to blow on certain types of faults with various amounts of short-circuit current flowing. When these tests have been made we hope to have some better information on which to base our requirements for cable protection.

Co-ordination of Secondary Network Protection

I believe we are all in agreement with the conclusions arrived at in paper 55-445.

While it is in general true that we should "hang onto the load," we should not do so at the expense of possible manhole explosions which may result in personal injury and property damage and produce bad publicity in the newspapers. Such explosions have occurred on our system in cases where limiters have not blown fast enough, or at all, due to current being limited by arc resistance or other causes.

We do not see the necessity for two limiters with characteristics so close together and suggest the use of the limiter shown on curve *D*. We also suggest that study be given to an even faster blowing limiter.

Design Characterics and Application

In regard to paper 55-473, it has been our experience that arcing faults are by far the most common type of fault and we feel that something should be done toward designing a limiter to clear this type of fault. We agree that the limiter will protect the cable against the welded type of fault, but as such faults are in the minority we are not accomplishing the maximum protection to the secondary network system with the present limiter.

We do not agree that the standard limiter gives complete protection for the *RH-RW* type of insulated cable, for reasons stated in the foregoing and elsewhere in these discussions.

The co-ordination problem is well stated but its solution would be affected by a change in the design of the limiter.

Discussion of Paper 55-443

A. Bodicky (Union Electric Company of Missouri, St. Louis, Mo.): Mr. Xenis discussed the difference between a solid fault and an arcing fault which is substantiated by our own experience. Solid faults are difficult to produce and none of our failures were of a solid type. A study of 13 failures, where completed information was available, involving 20 blown limiters out of a total of 78 limiters, indicated the results shown in Table I of this discussion on the triplexed 500,000-CM nonleaded cable with a no. 4/0 bare neutral wire installed in the same duct.

Unless the fault clears itself, it takes a theoretical 7,000 amperes of fault current to blow one limiter. If the damage is more extensive, then a 11,000-ampere fault current will blow two limiters. In the meantime the 4/0 bare neutral wire will burn clear so that the third-phase conductor has no direct path to the neutral.

The largest damage, where about 140 feet of cable was burnt, occurred after a 46,000-ampere theoretical fault current opened two limiters from one end and the 4,400-ampere fault current from the other end was not sufficient to blow the limiters.

Since a 500,000-CM limiter will open on an average fault current of approximately 1,500 amperes, the actual fault current during a failure is only about one fifth that of a theoretical maximum value.

Table I. Theoretical (Calculating Board) Maximum 3-Phase Fault Current, Amperes

	No. of Ends	Max.	Min.	Avg.
No blown limiters, fault cleared with only small burn on cable	8	52,000	8,500	20,100
No blown limiters, cable burnt	7	11,000	3,100	7,900
One limiter blown	4	15,500	6,600	10,600
Two limiters blown	6	96,000	8,800	44,200
Three limiters blown	1			31,600

Discussion of Paper 55-444

G. S. Eager, Jr. (General Cable Corporation, Bayonne, N. J.): The procedure for overload temperature classification tests recommended by the AIEE Study Subcommittee on Standardization of Limiters and presented by Mr. Graham in Appendix I provides a very satisfactory means of differentiating between various types of insulations used on secondary network cables in so far as their behavior during overload conditions is concerned. This test provides a means of obtaining very reproducible results as long as reasonable laboratory testing precautions are observed. In addition, this test should prove to be very useful in the future as a means of classifying new insulations and cable constructions for secondary network applications and should aid the user in establishing whether a particular brand of cable is suitable for his system which is equipped with a particular type of limiter. Further, since a compound of a given classification may be improved over a present one, this procedure could serve as a means to justify reclassification of an *L220* compound to *L260*.

During the investigation by the AIEE subcommittee this test procedure has been applied principally to *RH-RW* (*GR-S* type) and ozone-resisting (oil-base and butyl) types of insulations having neoprene jackets as over-all coverings. It is important that this work be extended to study the performance and to classify cables having other insulations (such as *RHW* rubber, silicone rubber, and asbestos *VC*), and other jackets (such as lead and thermoplastic).

It is to be noted that the deformation of the insulation wall shall not be more than one half of its original thickness when subjected to the standard test. Although the author does not present actual test values observed on the 65 cable samples evaluated, it is assumed that the cables complied with this stipulation within their respective ratings of *L260* and *L220*. The author does report that one polyvinyl chloride insulated and jacketed sample did exhibit excessive deformation at the low temperature of 150 C. It is felt that this deformation requirement is extremely important in selecting compounds as it provides a means of finding those insulations which soften excessively during overload periods so common in secondary network systems. Such deformation reduces the dielectric strength and mechanical properties thereby producing weak points which may lead to premature cable failures. Hence, when test data are reported in the future, care should be taken to report the deformations observed.

The wide variation in physical properties (tensile and elongation) between compounds of various manufacturers is noted and the author correctly concludes that it is difficult to correlate these properties sufficiently well to use them as a criterion for classification purposes. However, it is extremely important that these properties be carefully recorded as they do give an excellent indication of the deterioration of the insulations which supplements the visible data and may demonstrate excessive deterioration not noticeable by visible observation.

E. C. DeBaene (Detroit Edison Company, Detroit, Mich.): The AIEE Limiter Standardization Task Group is to be complimented on the constructive approach used to provide a solution to a troublesome problem. If current limiters used in network circuits are to serve their intended function of protecting cable then surely they must operate on current overload before significant damage to the cable occurs.

The work reported in Mr. Graham's excellent paper provides a method and presents data which should prove of great value not only as a guide for improved limiter design, but also as an aid to the consumer in selecting a limiter to match the class of cable being installed in networks. Also, it will serve the wire and cable manufacturers with a guide for classifying new cable developments.

In reviewing this paper a few questions of a practical nature arise. These are

1. As described in the paper, the classification tests are to be made on new cable. The question then arises as to whether one can assume that the temperature at which the threshold of damage occurs for a given type of rubber insulation remains the same after years of exposure to service conditions. It is possible that the temperature required to produce significant damage to insulation may change significantly for cables operating near their maximum current-carrying capability or for cables operating in wet locations.
2. Frequently, as networks are extended, cables of different types and vintages are spliced together. It is possible, therefore, to have several different types of insulation, some having unknown threshold of damage characteristics, all protected by the same limiter. It would seem that these cables having unknown or different damage characteristics will cause trouble to consumers in co-ordinating an effective plan of protection.

Perhaps the solution to these problems lies in obtaining more data on service-aged cables of recent vintage and on older types of cables using the methods and definitions of damage threshold described in Mr. Graham's paper.

R. J. Wiseman (Okonite Company, Passaic, N. J.): I have read the various papers which have been presented dealing with the types of cables used for secondary networks. I have also endeavored to interpret the papers in their practical application. As I understand it, we are concerned with the degree of damage to a cable when a failure occurs and a short-circuit current flows through the fault. The order of magnitude of this current and its time of duration are most important because the conductor will heat up very rapidly, reaching temperatures which greatly exceed the vulcanizing temperature of the insulation. Therefore, we automatically are aging the insulation. We all know that aging of rubber compounds is an accumulative effect and we have a permanent change in the physical properties of the compound. However, in this case we are not concerned with the aging due to normal temperatures applied to the cable, but with temperature far above these temperatures, even well beyond the vulcanizing temperature; that is, in the range that will cause the destruction of the rubber compound. Thus, we are accepting the possibility of the insulation being damaged and its life greatly shortened.

The paper reports tests in which destructive effects of the temperature on the insulation depend upon the type of rubber compound. It is indicated that there is a difference between so-called oil-base, dry-mineral, and butyl compounds so it is proposed to have limiters of two capacities, one to operate at 220 C and the other at 260 C, the idea being that the insulation thus will be prevented from reaching permanent damage. This is not true. As stated before, we have exceeded the vulcanizing temperatures and, therefore, are quick-aging the compound. It is no longer a desirable insulation. Furthermore, it is difficult to appreciate why two sizes of limiters are suggested. The actual currents to cause a temperature of 220 C or 260 C to occur are very close together. For example: If we calculate the current necessary to obtain a 220 C and 260 C conductor temperature for a single cable in air, assuming a starting temperature of 25 C, we get the currents shown in Table I of this discussion for a no. 4/0 American Wire Gauge (AWG) and 500,000-CM conductor.

The differences in currents are not great between the two temperatures, and in addition, as the time of duration increases, the difference becomes less. It is difficult to picture a fault current so closely controlled that it would exceed a value to cause the conductor to reach 220 C but not 260 C; therefore, I cannot see why two limiter sizes are desired nor why we differentiate between the various compounds. All compounds will have been affected by the fault current and the cables should be replaced if they are allowed to reach these temperatures too frequently. It would seem the desirable thing to lower the temperature at which the limiter will function, say to 200 C, and to have one limiter only. I do not know if it is possible to so design a limiter.

Table I of this discussion was calculated on the basis of a single cable in air. Actually in service, the cables are installed in ducts, and there may be several in a single duct as referred to in the papers by Mr. Kolks and Mr. Porter. As we do not expect all of the cables to carry the fault current, the assumption of a single cable in air to estimate the probable fault current to reach the limiting conductor temperature is valid. Mr. Porter has shown this very nicely in his Figs. 1, 2, and 3. He shows the temperature-time curve for various currents. Perhaps the limiters should be designed on the basis of current for a specific conductor size.

Table I

	4/0 I (Amps)		500,000 CM I (Amps)	
Time (Min)	220 C	260 C	220 C	260 C
1	3,380	3,570	6,960	7,300
5	1,590	1,680	3,230	3,380
10	1,183	1,230	2,390	2,500
15	1,000	1,055	2,040	2,135
20	924	975	1,845	1,930
30	824	872	1,635	1,710
60 (1 hour)	734	776	1,430	1,495
120 (2 hours)	712	750	1,365	1,430
Ultimate	708	748	1,355	1,420

It is a bit difficult to compare his curves with Table I as he gives the curve of temperature rise with time for specific currents, whereas the table gives the current that will give the specified temperature for a given time. However, it appears that for the same temperature and time, they are not too far apart.

Discussion of Paper 55-445

R. C. Graham (Rome Cable Corporation, Rome, N. Y.): The authors have presented a good practical approach on how actually to start using some of the new information presented at the Summer General Meeting on network cable circuits, particularly as to the degree of protection that may be expected.

It is to be hoped that this very forward step will initiate others into making their own analysis and subsequent application of these useful facts. It is also hoped that this will be the start of even further forward steps towards more "adequate" network systems. For example, the cable itself is one of the key elements of the system and it might be desirable similarly to analyze the degree of protection and proper co-ordinating procedure for other than the *L220* and *L260* cable designs such as used on various systems today.

From a cable manufacturer's point of view it is readily conceivable that a satisfactory lower temperature cable design such as an *L180* or a higher temperature design such as an *L300* could be produced. What would be the value of such ratings, and is there, or will there be, an actual need for such ratings?

I. Matthysse (Burndy Engineering Company, Inc., Norwalk, Conn.): I have had the pleasure of working with the authors on the AIEE Subcommittee on Standardization of Limiters so that I can readily appreciate the many possibilities that exist for misunderstanding of the function and application of limiters. The authors have clarified many of these questions regarding co-ordination but there is one point they made that may need additional clarification.

They state that there is a band where no protection is afforded by the present limiter on the secondary cable in common usage, which has the class-*L260* insulation. This is illustrated for 4/0 cable in their Fig. 2, showing that for fault currents of less than about 1,000 amperes, the insulation would be damaged before the limiter would clear.

While this is theoretically true, practical considerations indicate a different situation. Curve *B* of Fig. 2 is for the condition of all three phases equally loaded in the duct. Low-current faults seldom involve more than one phase at a time, so that the heat is generated in the conduit at a much slower rate than for a balanced 3-phase fault. Consequently, the time to reach the damage point is appreciably longer than shown by curve *B*. Practical experience with limiters has shown that they do offer adequate protection even in this low-current region.

On the other hand, for the class-*L220* insulation such as oil-base insulations, a faster limiter must be used if full protection is desired, as the authors have indicated. Although it is tempting to use such a faster limiter even when the higher temperature class-*L260* insulation is used, the problems of selectivity and co-ordination, which become more critical with the faster limiter, can be avoided if the present standard limiter is used.

T. Niessink (Commonwealth Associates, Inc., Jackson, Mich.): One phase of network protection which may be outside the scope of the paper involves the degree of protection obtained from the relays on the station circuit breaker for faults within and on the secondary side of the network transformer. The characteristic curve for the station breaker in the paper shows satisfactory protection because it is assumed "that sufficient short-circuit current is available properly to activate the protective devices." It is questionable as to whether this is a typical case.

In a network in which each underground primary feeder supplies several network transformers, little if any protection is provided by the station breaker for faults on the secondary side of the network transformer. If the relays at the station breaker are set to operate for these fault currents the relays will not have sufficient load ability due to the high impedance of each network transformer in comparison to the total primary feeder load. The low currents (using overcurrent relays) or the high impedance (using impedance-type relays) associated with a single line-to-ground fault on the network transformer secondary aggravate the situation.

Installation of separately mounted fuses in the underground vault and connected between the primary feeder and the network transformer would require extra vault space and increased primary feeder exposure to faults. Consideration has been given to the use of "weak-link" type of fuses in the high-voltage side of the network transformers but this would introduce problems of fuse replacements and may increase the size of the network transformers.

Another solution would be the use of a transfer tripping scheme by which the station breaker would be tripped by faults not cleared by the secondary protective devices. This would require the use of a separate control circuit between the station and the various network transformers. The cost, complexity, and maintenance of this control circuit are discouraging.

Little, if any, literature appears to be available on the methods now being used to solve this problem. Apparently, it is assumed that this unprotected zone is a calculated risk. The only practical and least expensive solution seems to be the use of fuses with a possible increase in size of the network transformer.

W. T. Peirce and **Victor Siegfried** (United States Steel Corporation, Worcester, Mass.): This paper and its companions give a good picture of the value of limiters in protection of network systems and their associated cable. We wish to commend the thoroughness of the project.

We have had occasion to compute temperature rise of conductors under faulted conditions and find some discrepancy in the *L260* curve at higher values of current,

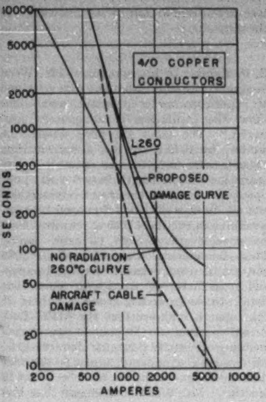

Fig. 1. Temperature rise of conductors

which should be pointed out to those using these data, inasmuch as the shorter times involve temperatures which could well fuse the copper. Obviously, at short times the *L260* curve, representing a 260 C copper temperature, must be optimistic if calculations based on no radiation give corresponding temperatures above 1,100 C, the approximate melting point of copper. The difficulty of determining such short times and of determining damage could explain the difference.

The curves of Fig. 1 of this discussion are plotted for 4/0 copper conductors to suggest a compromise damage curve. The top curve is *L260* from the paper. The middle curve is the result of calculations based on no radiation for time to reach 260 C copper temperature, and show an appreciably lower time to reach this condition than does *L260*. At longer times and lower currents, *L260* may be valid, with radiation a substantial factor. However, at time values below 100 seconds it would seem to be more desirable to follow the no-radiation calculations, where radiation should be limited in its effect. The proposed damage curve is arbitrarily drawn between the two extremes to reconcile these two conditions.

For confirmation of this view, a dotted curve is shown for damage on aircraft cable.[1] These data concern wire types used at lower voltages, and lie below the network cable curves. Inasmuch as criteria of damage may be more conservative on aircraft, the agreement with our proposed damage curve is quite reassuring.

REFERENCE

1. SHORT-TIME CURRENT RATINGS FOR AIRCRAFT WIRE AND CABLE, B. W. Jones J. A. Scott. *AIEE Transactions (Electrical Engineering)*, vol. 65, Oct. 1946, pp. 644–8.

Discussion of Paper 55-473

O. A. Lentz (Commonwealth Associates, Inc., Jackson, Mich.): This paper, together with Mr. Xenis's paper (55-443), indicate that the basic function of the limiter is to disconnect faulted cable sections before associated cable conductors have reached temperatures which are destructive to the insulation. To accomplish this a limiter must successfully interrupt all fault currents up to the maximum value obtainable on any given system. It seems rather unusual that no mention is made in the paper in regard to interrupting rating of the limiters.

It is realized that arcing and fault resistance may limit the short-circuit currents to lower than the calculated values in the majority of cases, however, as the paper points out, "weld" type of faults may occur in which the resistance of the welded fault is lower than an equal amount of conductor. For this condition the fault current will approach the theoretical calculated value. Tests[1,2] have indicated that short-circuit currents of 50 to 90 per cent of calculated bolted fault conditions could be expected on low-voltage networks. Since many networks will have calculated short-circuit currents for bolted fault conditions in the range of 100,000 to 150,000 amperes rms at either 120/208 or 277/480 volts, it seems that any consideration of standards for limiters should emphasize to some degree their interrupting ability.

Inspection and maintenance of underground network equipment while energized require that the protective devices interrupt any and all short-circuit currents without any undue stress, to prevent possible injury to personnel or to prevent further explosions or equipment damage.

REFERENCES

1. FAULT VOLTAGE DROP AND IMPEDANCE AT SHORT CIRCUIT CURRENTS IN LOW VOLTAGE CIRCUITS, O. R. Schurig. *AIEE Transactions*, vol. 60, 1941, pp. 479–86.

2. ARCING FAULT CURRENTS IN LOW VOLTAGE A-C CIRCUITS, C. F. Wagner L. L. Fountain. *AIEE Transactions*, vol. 67, 1948, pp. 166–72.

Discussion of Paper 55-432

P. D. Tuttle (Aluminum Company of America, Massena, N. Y.): This paper should provide a firm basis for formulating a quick and simple procedure for classifying rubberlike insulations for high-temperature duty. It would be helpful if the authors mentioned the exact designation number of the ASTM test method they had in mind for each of the various properties. Besides the convenience, there would be no misunderstanding in the minds of those evaluating the proposed procedure.

The reasons for the choice of the no. 8 AWG stranded conductor are not clear; an explanation may completely nullify the following remarks. With a stranded conductor, any insulation stripped for test is corrugated on one side. The ASTM tests require that these corrugations be buffed off, a time-consuming and troublesome operation, in order to obtain a tensile test specimen or a pile of the insulation for a durometer test.

Since no hardness test is mentioned in ASTM Designation *D470-52T*, I assume the method of test for this property is that outlined in Designations *D314-52T* and *D676-49T*. It would seem, where a comparison is required, that a 1/2-inch pile of insulation is practically mandatory where one of the harder rubberlike materials is involved. Hence considerable preparation would be necessary in removing the corrugations, a consequence of the stranded wire, and it seems a solid wire would be an advantage from this point of view.

Neoprene insulation would come under the "rubberlike" classification of insulation and it is exceedingly difficult to strip this compound cleanly from a plain copper conductor, especially a stranded one. Furthermore, the amalgamation technique of removal of the complete (uncut) insulation is not suitable for aluminum or plain copper wire and a larger test wire would facilitate obtaining good test specimens of the insulation. Finally, it would seem that the proposed test should be independent of the base metal.

Since the suggested test procedure is concerned with insulation properties or standards and is not an acceptance test of wire as purchased (where no control is had of the wire size available for test), I should like to propose, based on the foregoing remarks, the selection of a wire size larger than no. 8, say at least the no. 6 mentioned in *D470*. This wire should be specified as solid and of circular cross section. I feel this will not only facilitate the preparation of test specimens of the insulation, but will also minimize the effect of the choice of base wire.

Discussion of Paper 55-474

R. J. Wiseman (Okonite Company, Passaic, N. J.): This paper is a very good contribution to the symposium on networks as it suggests formulas that may be used to estimate the conductor temperature where a heavy current is being carried on several cables in a duct. Actually, this is not the condition that exists when a cable failure occurs. Up to failure, the cable carries its normal current, when suddenly a very heavy fault current flows, causing an increase in temperature of the faulted conductor. In view of the indefiniteness of the magnitude of the fault current and its time of duration, it would seem that we are not too far wrong if we assume a single cable as carrying the current, and as a close enough approximation, we can assume the cable to be in air. Actually, in practice, there will be a slightly slower temperature rise or a slightly higher current to obtain the permissible temperature. This is shown in Figs. 1–3 of Mr. Porter's paper.

The Okonite Company took part in a round-robin study on the effect of high temperatures on various types of insulation. Measurements were made of conductor, surface, and ambient temperatures for various currents. From these data, it was possible to calculate the insulation thermal resistivity and the surface thermal resistivity. To our surprise, we found that for for all three insulations, one oil-base and two mineral-base compounds, we obtained a value of 1,000 thermal ohm-centimeters for the insulation rather than the value of 500 thermal ohms used for normal operation. For the neoprene jacket, we obtained a surface thermal resistivity of 300 thermal ohms per square centimeter whereas we usually have values of 600 to 1,200 thermal ohms per square centimeters, depending on the cable diameter. Although the thermal resistance of the insulation is doubled, the surface thermal resistance can be a half to a third, resulting in a total thermal resistance less than that used for normal operation. Table II of Mr. Kolks' paper shows a decreasing value of thermal resistance with increasing conductor temperature. This decrease in thermal resistance will permit a higher current with a slightly higher rate of decrease in current with time.

I would like to suggest that the other cable manufacturers who took part in the round-robin tests analyze their data to get the true values of insulation thermal resistivity and neoprene thermal resistivity for temperatures in the order of 250 C to 300 C. It would appear that we cannot use those values that are used for normal operation.

Discussion of Paper 55-441

G. S. Eager, Jr. (General Cable Corporation, Bayonne, N. J.): This paper presents useful information on some of the properties of secondary network cables. Concerning the mechanical moisture absorption, data on cables from many suppliers indicate that the range of mechanical moisture absorption of oil-base compounds is 25 to 90 instead of 40 to 90 milligrams per square inch; and the range of *RH-RW* is 8 to 20 instead of 14 to 20 milligrams per square inch.

With reference to electrical moisture stability, the author states that "butyl-rubber insulations as a class show a better range of values than either *RH-RW* or oil base, particularly when measured in water at 70 and 80 C, temperatures which may not be unusual in an a-c network." Although the conductor temperature may normally reach this temperature range, it is highly unlikely that water surrounding the cables would reach this temperature, particularly for any length of time. Consequently, tests conducted at 70 to 80 C must be considered accelerated and not representative of field operating conditions. Our tests have indicated that when tested in water at 50 C results on some butyl compounds have been poorer than what is normally obtained with *RH-RW*. Compounding studies have indicated that in many cases extremely good aging properties in butyl are obtained at the expense of electrical moisture stability although it is possible, with sufficient knowledge of how to proceed, to obtain reasonably good aging and electrical moisture stability properties. At least one of the *RH-RW* (*L260*) compounds discussed by Mr. Rosch has now qualified as *RHW* insulation (*GR-S*). This compound is more stable in water at 75 C than most butyl compounds and it is questionable whether the butyl compound should be given the first rating.

Mr. Rosch mentions briefly, in discussing insulations in use in the 1930's, the desirability of employing rubber insulations which have low explosiveness in order to minimize the risk of explosions caused by gases evolved when the cables are subjected to fault conditions. Nothing is said about the newer types discussed more extensively in the paper. We feel that this property is extremely important and should be taken into consideration when cables are selected for secondary network systems. Results of tests conducted by us on insulations of the classes discussed by Mr. Rosch indicate that *RH-RW* insulations evolve the least quantity of gas and oil-base insulations the most. Butyl insulation evolves a richer, more readily exploding gas than that evolved from either the *RH-RW* or oil-base insulations.

A. Bodicky (Union Electric Company of Missouri, St. Louis, Mo.): From 1939 to 1942 we installed about 33 miles of the so-called high-temperature moisture-resistant natural-rubber-base insulation, tape, and braided cable on our network system. Since 1942 we have installed some 22 miles of *GRS-RH-RW* neoprene-jacketed cable for our three single-conductor twisted 500,000-circular-mil cable with a 4/0 bare neutral. To date we have had 33 failures on the natural rubber and only two on the *GRS* type of cable (both due to adjacent d-c cable fires) with a resulting failure rate of 5.5 failures per 100 mile-years on the natural rubber and 1.6 failures per 100 mile-years on the *GRS* neoprene type of cable. About 70 per cent of the early failures on the natural rubber were due to the high temperature caused by adjacent steam mains. In the majority of the cases the natural rubber cable was roasted when removed.

In 1942, an 8-month oven test at 110 C during working hours also showed the superiority of the *GRS* over the natural-rubber insulation.

R. C. Graham (Rome Cable Corporation, Rome, N. Y.): In regard to moisture resistance, the author states: "The tests most generally used include the 'mechanical' moisture-absorption or gravimetric test." It is assumed that this statement is in particular reference to the subject of network cables which are classified as "power" cables. If this is true it should be understood that except for butyl insulation (Insulated Power Cable Engineers Association Appendix 0) the so-called mechanical or gravimetric test is not required or recommended for power cables by any industry specification such as those of the American Society for Testing Materials or the Engineers Association. In fact, the only moisture resistance test recommended by these industry groups for power cables in Engineers Association's Appendix N and the Society's *D 470* is the *EM-60* electrical stability test. Therefore, we cannot agree that most moisture tests include the mechanical or gravimetric method. Moreover, considerable evidence obtained by other investigators indicates that the mechanical test has little actual significance in determining whether or not a cable is suitable for operation in wet locations.

In the author's "Discussion," and again in his "Conclusions," reference is made regarding the superiority of the *L260* over the *L220* classifications, and that improvements may be forthcoming. In this connection it should be emphasized and remembered that the AIEE Study Subcommittee on Standardization of Limiters agree (Appendix I of Paper 55-444) that this classification is no figure of merit or demerit but a criterion sought for the purpose of coordination between cables and limiters.

The author has presented a good historical review and discussion of the published literature which should add to our knowledge of the subject.

C. P. Xenis: In his comments, Mr. Weed disagrees with the statement that: "Years of experience under operating conditions show the insulation is adequately protected." The facts are very simple. A limiter, by definition, has a current-time characteristic selected to protect cable insulation on the length between the multiple point (usually the street intersection) and the fault from being damaged by temperatures in excess of 250 C resulting from excessive overloads due to cable faults. This characteristic was adopted in 1937 and has been publicized in technical papers and manufacturers' catalogues since that date. In the preceding group of papers on this topic, it is shown that the AIEE Task Group working on the subject are recommending essentially this same characteristic. All available experience supports the fact that the design conditions have been met in practice. Mr. Weed's statement that this experience may be true on the systems of some companies and not others is basically fallacious, because, after all, it takes amperes and time to cause a limiter or any other type of fuse to blow in accordance with its design characteristic. If one could conceive of a network system which cannot develop a short-circuit current in excess of 1,500 amperes under solid fault conditions in the vicinity of the network transformers, then, naturally, no limiters could be blown and none should be used, since under such conditions it would be impossible to roast the insulation. It seems to me that Mr. Weed confuses two separate and distinct items, namely: (*a*) roasting of the insulation between the fault and the multiple point and (*b*) fusion of cable conductors at the point of the fault, due to an arc between phases and to ground.

If one wanted protection to limit arcing at the fault, then fast-acting fuses or circuit breakers should be used. This would be a simple matter, and has in several instances been tried and abandoned due to unnecessary load interruptions under operating conditions, which defeat the basic objective of the network system, namely, service reliability.

In his verbal discussion during the meeting, Mr. Weed discussed a case of mains trouble in Boston which resulted in a serious explosion. In this case he revealed that there were at least two errors in design: (*a*) that fiber conduit was used, which, as is well known, will burn under the action of the arc and generate a large amount of gases in the vicinity of the arc; and (*b*) that there was insufficient neutral cable capacity which would cause overheating of the neutral under single-phase fault conditions, which will burn the insulation on the other cables in the conduit. He indicated that the limiters did blow and prevented the cable from roasting, clearly showing that had they not been there, it would have roasted the insulation between the fault and the multiple points at the adjacent street intersections. This would have brought the fault to those points and in some cases might have caused the fault to spread in several directions beyond the multiple point. Since the limiters were blown, we must conclude that the fault must have caused some welds or solid short circuits which resulted in the development of the calculated short-circuit currents, caused the blowing of the limiters, and prevented an extremely serious condition.

Mr. Bodicky's comments are based on excellent factual information and give a very clear story of performance. Our experience in New York City parallels his experience closely.

Mr. Bodicky's comments bring out the fact that under arcing faults, as explained in the paper, arc impedance and the fluctuation of current result in a major reduction in the average value actually carried by the cables supplying the fault and consequently carried by the limiter. He reports no roasted cables. In those cases where he had one or more limiters blown, he has obtained the protection provided by them. If he had these faults on a network not equipped with limiters, he would have experienced "roasted" insulation. This is the very serious type of condition which generates explosive gases over the full length of cable, and can cause extensive damage and spreading of the fault.

Closing Remarks

R. C. Graham: In regard to Dr. Eager's comments, he is correct in that the actual tests values as reported in the paper for the *L260* and *L220* ratings complied with the deformation requirement. Although only one test was made on thermoplastic insulations, it seems reasonable to assume that any sustained overload temperature above the softening or melting point of such insulating materials will result in excessive deformation.

The author is indebted to Mr. DeBaene for his kind remarks and agrees that there are yet unsolved problems which future investigations may clarify.

In connection with Mr. Weed's statements, it seems premature to conclude that the new *L220* limiter can be recommended for lead-sheathed network cables. Undoubtedly, further testing with the recommended procedure will disclose the proper classification for lead-sheathed cables. After many exploratory tests a 4-hour test period was finally selected by the committee upon the advice of other cable users, to correlate with other available data on "induct" tests, and to provide a procedure that would permit a reasonable reproducibility in results.

L. F. Porter: In summary, this paper describes "roasting" tests made at constant current on nonmetallic sheathed cables with *RH-RW* type of insulation installed in concrete duct for the purpose of determining the ability of this type of installation to withstand abnormally high overload currents, which may develop under fault conditions. In answer to Mr. Weed's question, we have no information as to how the time-current damage characteristic of leaded cable would compare with that of nonleaded cable, but it is pertinent to note that a metallic sheathed cable will have a slightly higher heat loss. If Mr. Weed is primarily interested in the heating of cable by current supplying faults in the arcing stage, data obtained from constant-current tests would appear of very limited value to him. Arcing currents are known to be fluctuating in nature and vary widely from minimum values as low or lower than the normal rating of the cable to the maximum values of the calculated short-circuit current, when the molten mass of metal or cable movement causes a solid short circuit. Damage to cables during street construction with digging equipment also may cause solid short circuits.

E. L. Leinbach and A. S. Brookes: We appreciate the comments and discussions presented and take this opportunity to reply to some of them.

The question of "positioning" the time-current damage curves of cable coverings is obviously subject to many variables, radiation being one of them. Mr. Peirce and Mr. Siegfried are certainly theoretically correct and quite likely are practicably correct in the high-current short-time range in those published.

The effect of the suggested correction would be to swing the lower end of the *L260* curve down which would reduce the overprotection of the insulation by the limiter in that range. It should be pointed out that the *L260* curve was derived and verified by a large number of tests in ducts which simulated actual service conditions.

The majority of these tests were made at times 400 seconds to 4 hours at currents which produced visually the "threshold of damage."

The operators of light networks containing but a few (3–5) primary feeders can well appreciate Mr. Niessink's concern over the lack of backup protection given a fault on the secondary by the station circuit breaker in the event the network protector does not function. Since all feeders are adding current into the fault, it would mean tripping out the entire network for each secondary fault of this nature, if protected by some scheme involving the station breakers. This is hardly the philosophy of network operation. Well co-ordinated secondary limiters and fuses, together with sufficient transformer capacity, seems to be the only presently acceptable method of protection.

Two completely opposite viewpoints are presented by Mr. Matthysse and Mr. Weed. One holds that the present limiter does clear properly in even the low-current ranges while the other feels that a much faster limiter is necessary.

We cannot completely agree with either. It is true that phase-to-ground faults generate less heat, but it is also true that phase-to-ground faults usually burn into 3-phase faults quite rapidly and then you have protection only "if sufficient current is available properly to activate the protective devices." In light networks it is possible to get just the wrong combination of fault current and time to fall outside the protection band.

It is just as true that vault and manhole explosions resulting in personal injury and property damage are to be avoided if at all possible. It must be recognized, however, that there is no type of protection presently available which will remove an arcing fault from the system thereby eliminating the cause of explosions and at the same time permit the use of time-tried network equipment in a manner which maintains service 99.99 per cent of the time. It appears that good material, good workmanship, and maintenance are the best answers to the arcing fault problem.

The proposed *L220* limiter provides for oil-base and similar compounds the same degree of protection that the *L260* provides for *RH-RW* compounds and still permits its full use to hold onto the network load. Slightly faster limiters could probably be tolerated but there is no good reason for becoming involved in co-ordination difficulties if arcing faults cannot be separated anyway; and it certainly appears that they cannot.

It is our hope, as it is Mr. Graham's, that we have emphasized the need for others to make an analysis of the degree of protection they have on their own systems so that they can decide either to live with what they have or to do something about it. As he further indicates, the Limiter Task Group has developed existing information into a usable form for both utilities and manufacturers. There is no reason why new types of cable or other equipment cannot be worked into existing systems if they prove desirable from a use standpoint.

F. Heller and I. Matthysse: The interrupting capacity of limiters as pointed out by Mr. Lentz, was not discussed in the paper. Perhaps the best indication of the interrupting ability of limiters is their service record over the past 15 to 20 years. Although many thousands of limiters have blown under all varieties of fault conditions, we know of no instance of failure of the limiter to interrupt the fault current successfully. Furthermore, all of these interruptions were accomplished with no visible external damage to the limiters.

On the other hand, laboratory tests at 220 volts alternating current have revealed that up to 30,000 amperes may be interrupted with no external disturbance other than a loud report. Higher currents may result in the splitting of the rubber jacket and fragmentation of the heat-resisting shell. However, it appears that although higher currents are accompanied by increased external disturbance, the limiter will not fail to interrupt the fault current. In addition to the operating experience over the past years, many companes have reported the clearing of limiters on fault currents which theoretically exceed values in excess of 50,000 amperes. Such a report is even included by Mr. Bodicky in his discussion of paper 55-443 by Mr. Xenis.

In view of the record of performance in service, one must conclude that in a 120/208-volt network, cable fault currents rarely exceed 30,000 amperes. Although the maximum calculated volted fault current may well exceed 1,000 amperes, such a calculation appled to a fault on a man cable would be much less. It appears, therefore, that the present limiters have adequate interrupting capacity for 120/208-volt network systems.

Mr. Weed has expressed the desire for a limiter to clear arcing-type faults. Limiters do clear arcing-type faults of such magnitude and duration as would otherwise roast cable insulation remote from the fault. However, the arc may persist for a considerable period of time before the limiter clears the fault, and in time a considerable amount of smoke may be evolved in the vicinity of the arc. The eventual clearing of the limiter prevents insulation damage remote from the fault, but it is not intended to prevent the damage due to fusion by the arc at the fault.

A limiter may be designed to operate faster to reduce the duration of the arcing, but in doing so, problems of limiter coordination and selectivity will arise. Faster limiters may bow needlessly on overloads and heavy starting currents, and under fault conditions, limiters other than those in the faulted cables may blow. A limiter can be made very little faster before such problems become serious.

Although damage in the vicinity of an arcing fault is serious, the destructiveness of a solidly welded fault in a system not protected by limiters is of much greater magnitude. Such destructiveness may be spread out over a wide area causing extensive loss of service and costly damage. It is this type of destructiveness that the limiter prevents. The fact that some limiters associated with an arcing fault are blown is a sign that more extensive damage was prevented by limiter action.

It may be possible to design a device to prevent arcing damage. In military aircraft, for example, differential current protection devices are used which operate only when the conductor itself is faulted. Such devices use a system of relays and circuit breakers which would be too costly to install in the ends of every cable in an underground secondary network. It remains a challenge to design a device which will operate as satisfactorily as a limiter in a secondary network and yet eliminate arcing damage.

Mr. Weed questions the ability of the standard limiter to give complete protection to *RH-RW*-type insulation. No doubt he is referring to the crossing of the insulation damage characteristic curve and the limiter curve. For currents less than that at the intersection of these curves, it appears that the insulation would be damaged before the limiter blows. However, the curves are for balanced 3-phase faults, while faults at currents of this magnitude are very greatly unbalanced. Such faults are most probably single phase, and the unfaulted conductors in the conduit act to absorb heat and retard the temperature rise of the faulted conductor. Experience shows that, under these conditions, the limiter does offer protection even for these low currents. Therefore, to design the limiter to protect fully against a balanced 3-phase low-current fault appears unjustified.

W. H. Couch and **G. J. Crowdes:** We appreciate Mr. Tuttle's comments with respect to the paper. Table I of this discussion gives the exact designation numbers of the ASTM test methods used for this evaluation.

Table I

ASTM Designation	Title
D 470-52T	Tentative Method of Testing Rubber Insulated Wire and Cable
D 412-51T	Tentative Method of Test for Tension Testing of Vulcanized Rubber
D 573-52	Accelerated Aging of Vulcanized Rubber by the Oven Method
D 676-49T	Tentative Method of Test for Indentation of Rubber by Means of a Durometer
D 149-44	Dielectric Strength of Electrical Insulating Materials at Commercial Power Frequencies

The reason for the size no. 8 stranded conductor stems from a number of considerations. This size was originally chosen by the committee not only because it was convenient for this particular work, but also because it was the size used in some of the earlier investigations of secondary network protection.

From our point of view, the size no. 8 is convenient to work with, since our dielectric strength samples could be made to fit into the conditioning oven, whereas a larger size would be heavier, bulkier, and much harder to handle. We did not feel that sizes smaller than no. 8 would be particularly acceptable or representative of power work nor would we feel that solid conductors represent any great percentage of network cable in use. It is possible that further refinements of this test for their experience in our committee will result in the choice of a different size of wire.

S. J. Rosch: In reply to Dr. Eager, our measurements of the mechanical moisture-absorption values of the oil-base compounds which we have examined, showed a range of 40 to 90 milligrams per square inch. We are happy to note that there are some that have values of 25 milligrams per square inch although we have not seen any to date. The same comments apply to the *RH-RW* insulations.

As regards electrical moisture stability, the author can only report on data with which he is familiar. The latter shows clearly that butyl-rubber-insulated cables show a greater degree of electrical stability in water at elevated temperature of up to 80 C than the oil-base or *RH-RW* compounds. Admittedly, the tests used were of an accelerated nature but since the same conditions were imposed on all of the insulations under test, the results must be considered as comparable. Undoubtedly there are formulations available of butyl, oil-base, and *RH-RW* compositions which may show radically different results but on the basis of the actual results obtained and reported in the paper, the conclusions drawn are in order. Dr. Eager cites the case of one *GR-S* type *RH-RW* compound which was recently approved as an *RHW* insulation to prove his point that the latter is more stable in water at 75 C than butyl rubber. I have data on an approved type of butyl *RHW* which I feel would readily negate the comments made by Dr. Eager, but these comments will be confined to the data contained in the paper.

I am in agreement with Dr. Eager's comments on the importance of a low explosiveness range as one of the desirable properties for a secondary network insulation and confirm the statement that certain types of commercially available *RH-RW* compounds evolve the least amount of gas, whereas oil-base rubber compounds give off the greatest amount of gas. We have not as yet carried on a similar investigation into the gas-evolving properties of butyl rubber compounds specially compounded so as to be suitable for the type of service conditions encountered in secondary networks. This phase of the problem will undoubtedly form the basis for the committee's additional work, should the existence of the committee be extended.

Mr. Bodicky's comments are sincerely appreciated since they add an additional link in the chain of data which proves that *GR-S* compounds designed for short-time high-temperature operation possess greater heat stability than do similar compounds made of natural rubber.

As regards Mr. Graham's comments, in an evaluation of a butyl-rubber compound from an important industry laboratory one of the yardsticks which figures very prominently deals with mechanical moisture absorption. Regardless of the merits and applicability of this test, there is no denying that if a given class of compound shows the best results on the electrical stability test in water at elevated temperatures, and also exhibits the lowest degree of physical moisture absorption by the mechanical or gravimetric tests, such class of compound may well receive the superior rating as to stability in moisture. If Mr. Graham will examine conclusion 4, he will note that the reference to superiority does not give the connotation he implies. The paper actually states that: "Regardless of the superiority of the *L260* insulations over the *L220* types in ability to withstand higher overload temperatures . . ." The truth of this statement is borne out by the data presented in the paper.

Voltage Dip and Synchronous-Condenser Swings Caused by Arc-Furnace Loads

C. CONCORDIA
FELLOW AIEE

Synopsis: This paper shows that the angular swings produced in a synchronous condenser by sudden application of an arc-furnace load do not in general increase the magnitude of the voltage dip produced. In addition, a criterion for stable operation of the condenser is given in terms of the system, buffer reactor, and arc-furnace transformer reactances.

THIS paper gives the results of a study made to determine the magnitude of the angular swing produced in a synchronous condenser by sudden application of an arc-furnace load and the effect of this swing on the magnitude of the voltage dip.

In some arc-furnace installations objectionable voltage dips have been reduced by the use of a buffer-reactor and synchronous-condenser combination as shown in Fig. 1. The synchronous condenser reduces the magnitude of the voltage dip due, e.g., to a secondary short circuit (i.e., a short circuit at the arc-furnace electrodes) by providing a parallel impedance path, so that a substantial part of the current is drawn from the synchronous condenser rather than from the system. To make the condenser more effective and economical, a buffer reactance is often inserted between the arc-furnace transformer bus and the system. This causes the system to take an even smaller share of the current. Further to reduce the reactance of the synchronous condenser a capacitor has sometimes been inserted in series with the condenser. In some cases when series capacitors have been used, trouble has been experienced because of the gap across the capacitor arcing over on secondary short circuits just when the capacitor is needed to reduce the consequent voltage dip. This capacitor arc over has usually been explainable on the basis of the normal transient voltage resulting from the short circuit. However, several questions which involve the possibility of condenser swinging have been raised in connection with some of these cases.

1. It is desired to know if, in a particular application, the condenser swing will increase the voltage dip. If it does, not so much would be gained by increasing the buffer reactance as might be calculated neglecting the swing.

2. The fear has existed of possible condenser instability if the buffer reactance is increased too much. This was given in one case[1,2] as a reason for modifying an existing system by inserting a capacitor in series with the synchronous condenser rather than simply by increasing the buffer reactance slightly.

3. It has been suggested that the transient series-capacitor voltage might itself be aggravated by condenser swings, especially when the condenser excitation is low.

4. It has been suggested that some of the disturbances observed might have been caused by the condenser temporarily going out of step.

To throw some light on these questions, a simple system as shown in Fig. 1 was set up on a mechanical differential analyzer and disturbed by the application of secondary short circuits. Resistance had to be included in the short circuit to produce any condenser torque and thus any condenser swing. This secondary fault resistance was varied over a wide range to produce the maximum swing. Two conditions of condenser excitation were considered: the condenser was assumed to be operating initially with normal no-load field excitation and then initially with zero field excitation (with unit terminal voltage in both cases) for each short circuit applied. A condenser voltage regulator of average characteristics (see equations 9, 10, and 11) was assumed to be in operation in most cases. However, a few cases without a voltage regulator were studied.

Conclusions

Within the range of system parameters studied, the following conclusions may be drawn:

1. The condenser swing did not increase the voltage dip appreciably. To the contrary, the voltage dip calculated with zero secondary resistance (and thus no condenser swing) was always greater than that produced by any finite value of secondary resistance, including that value which resulted in the maximum condenser swing. Since the condenser armature current was also practically unaffected by the swing, the voltage across a capacitor in series with the condenser armature would not be affected significantly.

2. The possibility of condenser instability seems remote if the criterion of conclusion 4 is observed. The buffer reactance was increased to a value such that the total system reactance viewed from the arc furnace and excluding the condenser was 50 per cent on the arc-furnace kilovolt-ampere base. Even this high value did not show any signs of instability. Thus the buffer reactance can very probably be considerably increased, if necessary, beyond the values which have been used, as long as the condenser has sufficient capability to maintain voltage in the steady state.

3. In the case[1,2] in which a series capacitor was used because it was desired not to increase the buffer reactance, it seems probable that the buffer reactance could have been considerably increased without any increase in the probability of instability.

4. A suggested criterion for stable operation, as far as disturbances arising at the arc furnace are concerned, is that the buffer (and system) reactance be kept smaller than the effective reactance of the arc-furnace transformer and secondary leads. This criterion is seen to be independent of the condenser reactances.

Nomenclature

e_2 = constant voltage at infinite bus back of total system reactance x_2
e_{dt} = direct-axis component of e_t
e_0 = value of condenser terminal voltage e_t before disturbance = 1.0
e_q = voltage back of x_q
e_q' = condenser field flux
e_{qt} = quadrature-axis component of e_t
e_I = field current-resistance drop

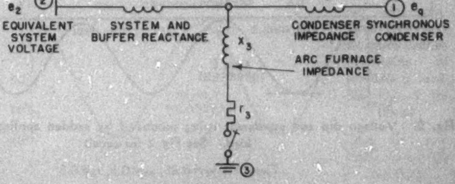

Fig. 1. Arc furnace, synchronous condenser, and buffer reactor

---

Paper 55-448, recommended by the AIEE Transmission and Distribution Committee and approved by the AIEE Committee on Technical Operations for presentation at the AIEE Summer General Meeting, Swampscott, Mass., June 27–July 1, 1955. Manuscript submitted February 7, 1955; made available for printing April 14, 1955.

C. CONCORDIA is with the General Electric Company, Schenectady, N. Y.

The differential analyzer study upon which this paper is based was made by Mrs. M. A. Fuller.

E_I = field applied voltage

E_I' = output of voltage regulator, given by equation 11

E_I'' = exciter field voltage

$E_0' = E_0''$ = the value of E_I before the disturbance = 1.0 or 0

i_d = direct-axis component of synchronous-condenser armature current

i_q = quadrature-axis component of synchronous-condenser armature current

M = condenser rotary inertia = 862 radians

r_3 = resistance of arc furnace, or load resistance (varied)

t = time, radians (1 second = 377 radians for a 60-cycle-per-second electric power system)

T_d = a damping torque coefficient = 0.2 per unit

T_{d0} = condenser open-circuit field time constant = 3,457 radians

T_s = synchronous component of electrical torque

x_2 = reactance of system plus buffer reactor = 0.25 or 0.50

x_3 = reactance of arc-furnace transformer and secondary leads, or load reactance = 0.50 or 0.25

x_c = series capacitor reactance (varied). (The series capacitor is placed in series with the condenser, so its reactance is subtracted from each component of condenser reactance. Stator transients are not considered)

x_d = condenser direct-axis synchronous reactance = $2.0 - x_c$

x_d' = condenser direct-axis transient reactance = $0.48 - x_c$

x_q = quadrature-axis reactance of synchronous condenser = $1.2 - x_c$

Z_{11} = absolute magnitude of driving-point impedance viewed from e_q

Z_{12} = absolute magnitude of transfer impedance between e_q and e_2

α_{11} = complement of impedance angle of Z_{11}

α_{12} = complement of impedance angle of Z_{12}

δ = condenser angle relative to system, radians

μ = regulator gain = 20

System Considered

A 1-line diagram of the system considered is shown in Fig. 1. The following assumptions have been made:

1. The synchronous-condenser amortisseur will be neglected except for the inclusion of a rather small (constant) damping torque coefficient. This assumption should cause the angular swings to be somewhat greater and less well damped, the voltage dip to be, if anything, very slightly greater, and the maximum armature current to be somewhat smaller than for an actual machine. It is a pessimistic assumption as far as the angular swing is concerned, and makes very little difference in the voltage dip.

   It is of interest that many people have used subtransient rather than transient reactance to determine voltage dip. Dips calculated from either reactance will correlate equally well with acceptable voltage-dip performance limits, in view of the fact that the magnitude of the load change used to calculate the dip is in itself purely a conventionally chosen number. However, it is necessary to use transient reactance if one is to obtain a realistic economic evaluation of the benefits of synchronous condensers and series capacitors. If subtransient reactance were to be used, the benefits of both of these devices would be magnified so that unduly optimistic results would be obtained.

2. Stator circuit transients will be neglected, since their effect on the angular swing of machines has usually been found to be very small.

3. The resistance component of the system impedance and the synchronous condenser stator resistance will be neglected.

With these three assumptions, the necessary performance equations for this system may be taken as a special case of those given in references 3 and 4. The synchronous-condenser torque equation is

$$M\frac{d^2}{dt^2}\delta = -T_e \tag{1}$$

where T_e = condenser total electrical torque.

The condenser total electrical torque is

$$T_e = T_s + T_d\frac{d}{dt}\delta \tag{2}$$

In this analysis T_d was assumed to be small and constant. The value assumed is pessimistic, since the actual damping torque coefficient is certainly very much greater than 0.2.

The synchronous component of electrical torque is

$$T_s = i_q e_q \tag{3}$$

The quadrature-axis and direct-axis components of synchronous-condenser armature current are given by the equations

$$i_q = \frac{e_q}{Z_{11}}\sin\alpha_{11} + \frac{e_2}{Z_{12}}\sin(\delta - \alpha_{12}) \tag{4}$$

$$i_d = \frac{e_q}{Z_{11}}\cos\alpha_{11} - \frac{e_2}{Z_{12}}\cos(\delta - \alpha_{12}) \tag{5}$$

The driving-point and transfer impedances are defined by the equations

$$Z_{11} = |z_{11}|,\ Z_{12} = |z_{12}|$$

$$z_{11} = R_{11} + jX_{11},\ z_{12} = R_{12} + jX_{12}$$

$$\alpha_{11} = 90^\circ - \tan^{-1}\frac{X_{11}}{R_{11}},\ \alpha_{12} = 90^\circ - \tan^{-1}\frac{X_{12}}{R_{12}}$$

In the present case

$$z_{11} = jx_q + \frac{jx_2(r_3 + jx_3)}{r_3 + j(x_2 + x_3)}$$

$$z_{12} = jx_2 + jx_q + \frac{(jx_2)(jx_q)}{r_3 + jx_3}$$

The condenser voltage e_q is given by

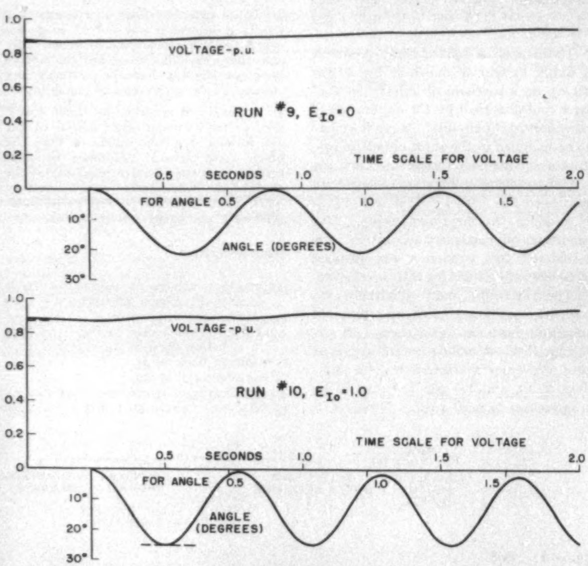

Fig. 2. Voltage dip and condenser swing produced by sudden application of arc-furnace load. See Fig. 1 for circuit

Case A: $x_2 = 0.25$, $x_3 = 0.5$, $r_3 = 0.5$

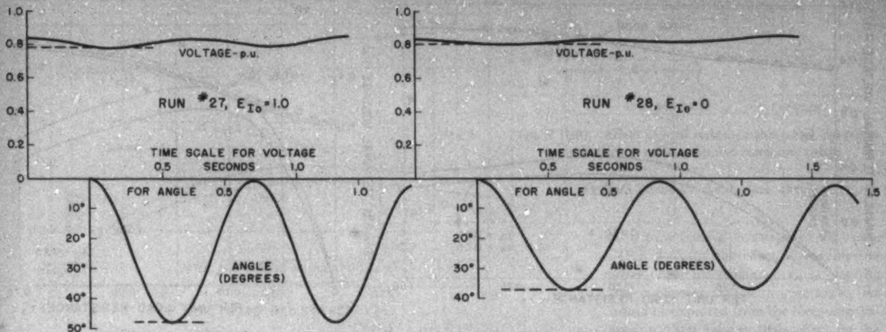

Fig. 3. Voltage dip and condenser swing produced by sudden application of arc-furnace load. See Fig. 1 for circuit

Case B: $x_2=0.5$, $x_3=0.5$, $r_3=0.5$

$$e_q=e_q'+i_d(x_q-x_d') \tag{6}$$

The condenser field flux is given by the field circuit equation

$$T_{d0}\frac{d}{dt}e_q'=E_I-e_I \tag{7}$$

The field current-resistance drop e_I is given by

$$e_I=e_q'+i_d(x_d-x_d') \tag{8}$$

The field applied voltage E_I is determined by the exciter and voltage regulator equations.

The assumed exciter equation is

$$T_e\frac{dE_I}{dt}=(E_I''-E_I) \tag{9}$$

where T_e=exciter field time constant=200 radians.

The exciter field voltage E_I'' is assumed to be limited by saturation so as to have the following values:

$$\text{for } E_I'<-2,\ E_I''=-2 \tag{10A}$$

$$\text{for } -2<E_I'<+4.5,\ E_I''=E_I' \tag{10B}$$

$$\text{for } E_I'>+4.5,\ E_I''=+4.5 \tag{10C}$$

where

$$E_I'=E_0'-\mu(e_t-e_0) \tag{11}$$

The magnitude of the condenser terminal voltage is

$$e_t=\sqrt{e_{dt}^2+e_{qt}^2} \tag{12}$$

where

$$e_{dt}=-i_qx_q \tag{13}$$

$$e_{qt}=e_q'-i_dx_d' \tag{14}$$

Initial Conditions

Before the application of the secondary short circuit it is necessary to calculate the initial values of e_q' and e_2. These values remain constant when the short circuit is applied, and are used to calculate the values of i_d, i_q, E_I'; E_I'', and E_I immediately following the short circuit.

Before the short circuit the current in the arc-furnace load is zero so e_q' and e_2 may be calculated as follows

$$i_d=\frac{E_I-e_t}{x_d}=\frac{E_I-1.0}{2-x_c} \tag{15}$$

$$e_2=e_t-x_2i_d=1.0-x_2i_d \tag{16}$$

$$e_{q0}'=e_t+x_d'i_d=1.0+x_d'i_d \tag{17}$$

After the short circuit has been applied, the required initial currents may be calculated from equations 4, 5, and 6 in the form

$$\left(1-\frac{x_q-x_d'}{Z_{11}}\cos\alpha_{11}\right)i_{d0}=\frac{e_{q0}'}{Z_{11}}\cos\alpha_{11}-\frac{e_2}{Z_{12}}\cos\alpha_{12} \tag{18}$$

$$i_{q0}=\frac{e_{q0}'+i_{d0}(x_q-x_d')}{Z_{11}}\sin\alpha_{11}-\frac{e_2}{Z_{12}}\sin\alpha_{12} \tag{19}$$

Other required initial conditions are

$$e_{dt0}=i_{q0}x_q \tag{20}$$

$$e_{qt0}=e_{q0}'-i_{d0}x_d' \tag{21}$$

$$e_{t0}=\sqrt{e_{dt0}^2+e_{qt0}^2} \tag{22}$$

$$e_{q0}=e_{q0}'+i_{d0}(x_q-x_d') \tag{23}$$

E_{I0} is unchanged by the short circuit (24)

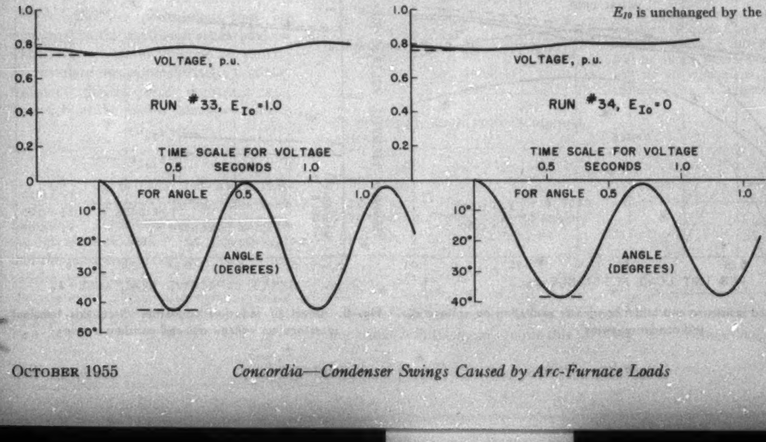

Fig. 4. Voltage dip and condenser swing produced by sudden application of arc-furnace load. See Fig. 1 for circuit

Case C: $x_2=0.25$, $x_3=0.25$, $r_3=0.25$

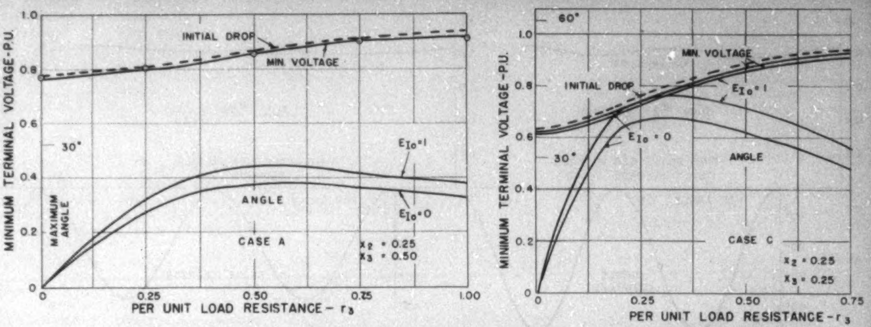

Fig. 5 (left) and Fig. 7 (right). Effect of load resistance and initial condenser excitation on voltage dip and condenser swing

$$e_{I0}=e_{q0}'+i_{d0}(x_d-x_d') \quad (25)$$

E_{I0}'' is given by equation 10 (26)

$$E_{I0}'=E_0'-\mu(e_{I0}-e_0) \quad (27)$$

Cases Studied

Three principal cases were studied:

Case	x_2	x_3	x_c
A	0.25	0.50	0.15
B	0.50	0.50	0.15
C	0.25	0.25	0.15

Cases A and B correspond to a condenser having a rating about equal to that of the arc furnace. Cases B and C are extreme in that the combined system and buffer reactance is 50 per cent on the arc-furnace base. In case C the condenser rating is about half that of the arc furnace. All values are in per unit on the condenser kilovolt-ampere base.

In addition, the capacitor reactance x_c was varied from zero to 30 per cent with the system conditions of case A. In the present case this is entirely equivalent to varying all of the condenser reactances by the same amount.

Results

For each case studied the condenser terminal voltage, rotor angle, and armature current were plotted by the differential analyzer. Selected examples showing the terminal voltage and rotor angle are shown in Figs. 2, 3, and 4. Ordinarily some other voltage in the power system, rather than the condenser terminal voltage itself, is of interest. However, in the present system the dip in any such voltage will be very nearly directly proportional to, although considerably smaller than, the dip in condenser terminal voltage. Thus the condenser terminal voltage dip e_t shows all the characteristics of the voltage dip of interest. Moreover, an estimate of the latter may be obtained simply by reducing the plotted dip in the ratio of the reactance between it and the infinite bus e_2 to the total system and buffer reactor reactance x_2. Fig. 3 illustrates very nearly the maximum effect of condenser swing on terminal voltage observed in all of the cases considered.

The armature current curves were obtained but have not been included in the paper. In no case was a large current oscillation produced by the swing. That is, the current oscillation was primarily only in the quadrature-axis component, which was never very great in comparison with the direct-axis component. Thus one would infer that there would be little effect of the swing on the voltage across a capacitor in series with the condenser armature.

The principal results obtained are summarized in Figs. 5, 6, and 7, where the minimum voltage and maximum angle are plotted as functions of the load resist-

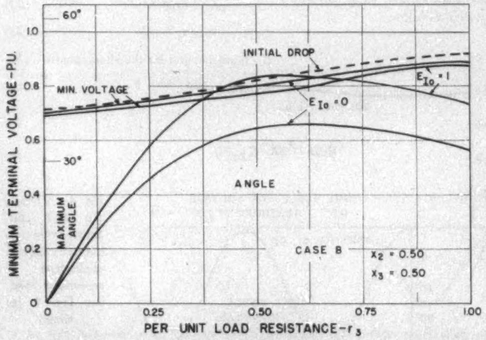

Fig. 6. Effect of load resistance and initial condenser excitation on voltage dip and condenser swing

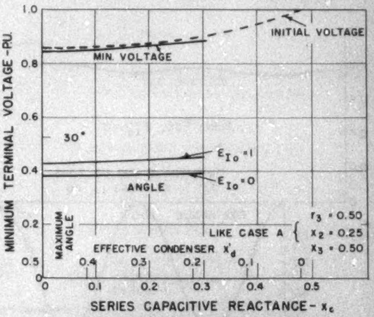

Fig. 8. Effect of reducing condenser direct-axis transient reactance on voltage dip and condenser swing

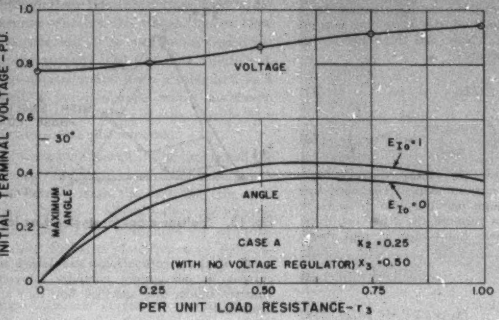

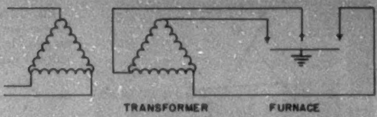

Fig. 9 (left). Effect of load resistance and initial condenser excitation on voltage dip and condenser swing

Fig. 10 (above). Arc-furnace circuit

ance r_3. It is seen that in all cases, in spite of any oscillations in voltage that may be produced by the condenser swing, the maximum dip occurs for zero load resistance (when there is no swing), and is only very slightly greater than the initial dip calculated using condenser direct-axis transient reactance. Also, the angular swings are in all cases moderate and there is no sign of instability.

It is of interest to record approximate values of transient power limit for the three cases studied. The transient power limit P_{max}' is very nearly the reciprocal of the transient transfer impedance z_{12}'. If resistance is neglected the transient transfer reactance x_{12}' is

$$x_{12}'=x_d'+x_2+\frac{x_d'x_2}{x_3}$$

Values of x_{12}' and P_{max}' for the three cases are:

Case	x_{12}'	P_{max}'
A	0.745	1.34
B	1.16	0.86
C	0.91	1.10

This maximum power limit may be compared to the maximum shock load to which the condenser may be subjected. To calculate this approximately, first the transient driving-point reactance x_{33}' viewed from the load is calculated, where

$$x_{33}'=x_3+\frac{x_d'x_2}{x_d'+x_2}$$

For case A, x_{33}' is 0.642; for case B, it is 0.699; and for case C, 0.392. The load resistance r_3 required to produce the maximum shock load P_s' is then $r_3=x_{33}'$ and the maximum shock load itself is approximately $(1/2x_{33}')$. The shock load on the condenser P_c' is, also very approximately, $x_2/(x_2+x_d')$ times the total shock load.

For the three cases:

Case	P_s'	P_c'	P_c'/P_{max}'
A	0.778	0.335	0.25
B	0.715	0.432	0.50
C	1.275	0.550	0.50

We have derived the values of the ratio of the actual shock load to the transient power limit in a roundabout way. Actually, it may be shown that under the stated assumptions this ratio is simply equal to the ratio of the system and buffer reactance x_2 to twice the load reactance x_3, and does not at all depend upon the condenser reactance.

$$\boxed{\frac{P_c'}{P_{max}'}=\frac{x_2}{2x_3}} \qquad (28)$$

From a somewhat different point of view, the maximum condenser swing to be expected can be calculated by considering that the steady-state load angle between the infinite bus and the condenser terminal voltage is given by the relation

$$P=\frac{1}{x_2}\sin\delta_s$$

The maximum steady-state power is

$$P=\frac{1}{2x_3}$$

Then the steady-state angle is approximately

$$\delta_s\cong\sin\delta_s=\frac{x_2}{2x_3}$$

and the maximum swing is approximately (in radians)

$$\boxed{\delta_{max}\cong 2\delta_s\cong\frac{x_2}{x_3}} \qquad (29)$$

Comparison with the figures shows this to be a conservative equation in all cases.

Fig. 8 shows the effect of varying the series capacitor reactance x_c, or varying the condenser transient reactance. As would be expected from the foregoing discussion, there is very little effect on the condenser swing.

Fig. 9 shows the maximum swing and initial voltage dip for the same case as Fig. 5, but with no voltage regulator. The minimum voltage was not plotted in Fig. 9 because without a voltage regulator it continually drops. Fig. 9 is included to show that the maximum swing is not appreciably affected by the voltage regulator.

These results indicate that the condenser swing is not very severe. It should be remembered, however, that the shock load may be applied not once but many times. If the application of load is synchronized with the condenser natural frequency, or with a subharmonic of it, the condenser can probably be thrown out of synchronism. This could presumably occur almost regardless of the values of the system parameters, but is unlikely because of the random nature of the load and of the considerable stability margin realized.

Appendix I. Single-Phase Short Circuits

All of the calculations reported in this paper have been based on a 3-phase short circuit. Actually, many of the disturbances will be single phase. In these cases there will be an equivalent 3-phase power disturbance, which in general will not corre-

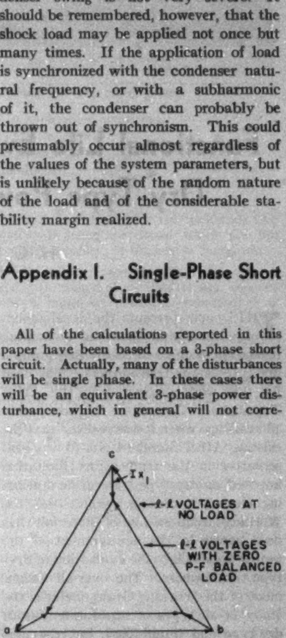

Fig. 11. Voltage drop for 3-phase load

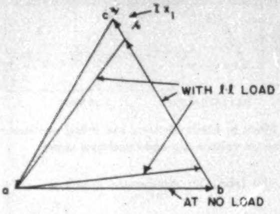

Fig. 12. Voltage drops for line-to-line load

spond exactly to the voltage disturbance in the phase most affected. It is therefore of interest to compare the magnitude of voltage change produced by 3-phase and single-phase currents of low power factor.

In Fig. 10 the furnace is supplied from a delta-connected transformer secondary. Thus there can be no ground current and thus no purely single-phase load in the wye-connected furnace.

On the basis of equal positive- and negative-phase-sequence reactances the following simple comparisons can be made by means of voltage diagrams.

Fig. 11, for a 3-phase load current I, shows that the reactive voltage drops are in phase with the line-to-neutral voltages. Each line drop is Ix_1 and the resultant voltage drop is also, from Fig. 11

$$\frac{1}{\sqrt{3}}(2Ix_1 \cos 30°) = Ix_1 \qquad (30)$$

Fig. 12 shows the voltage diagram for a line-to-line load of the same line current magnitude I. Now the three line-to-line voltage drops are

$$\Delta e_{bc} = \frac{2Ix_1}{\sqrt{3}} = 1.15Ix_1 \qquad (31)$$

$$\Delta e_{ab} = \Delta e_{ca} \cong \left(\frac{Ix_1 \cos 60°}{\sqrt{3}} = 0.29Ix_1\right) \qquad (32)$$

Fig. 13 shows the voltage diagram for a single-phase current load of the same line current through one line, which splits in two to return through the other two lines. Now the three line-to-line voltage drops are

$$\Delta e_{bc} = 0 \qquad (33)$$

$$\Delta e_{ab} = \Delta e_{ca} \cong \frac{1.5}{\sqrt{3}} Ix_1 \cos 30° = 0.75Ix_1 \qquad (34)$$

This comparison indicates that the line-to-line case would have a significant voltage drop only in one line-to-line voltage. Thus a reduced frequency of occurrence must be taken into account in evaluating the relative severity if it is assumed that the phases are loaded at random. The single-phase case is less severe on all counts. In regard to the line-to-line case, it is noted that, if transient reactance is used, $x_1 > x_2$, and the relative severity of the line-to-line case is further reduced. For example, if $x_2 = 0.8\ x_1$ (for the system as a whole), the voltage drop in terms of x_1 is reduced in the ratio $[(x_1+x_2)/2\ x_1] = 0.9$, and

$$\Delta e_{bc} = 0.9(1.15Ix_1) = 1.04Ix_1 \qquad (35)$$

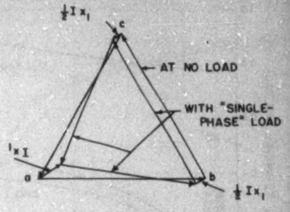

Fig. 13. Voltage drops for single-phase load

All of these comparisons are based on current, as one cannot compare kilovolt-amperes unless one specifies how they are measured.

References

1. Technical Problems Associated with the Application of a Capacitor in Series with a Synchronous Condenser, **R. L. Witzke, E. L. Michelson.** *AIEE Transactions*, vol. 70, pt. I, 1951, pp. 519–25.

2. The Application of a Series Capacitor to a Synchronous Condenser for Reducing Voltage Flicker, **P. M. Black, L. F. Lischer.** *Ibid.*, pp. 144–50.

3. Long Distance Power Transmission as Influenced by Excitation Systems, **C. Concordia, S. B. Crary, F. J. Maginniss.** *Ibid.*, vol. 65, 1946, pp. 974–87.

4. Power System Stability, Volume II (book), **S. B. Crary.** John Wiley and Sons, Inc., New York, N. Y., 1947, chap. 10.

Functional Life Evaluation of Group-2 Dry-Type Power Transformers

H. G. ZAMBELL
MEMBER AIEE

THIS paper presents the development of a functional means of evaluating insulation systems for ventilated group-2 dry-type power transformers. The need for this work originated in the AIEE Transformer Committee approximately 10 years ago when it was realized that the existing AIEE Standard No. *1*[1] was conservative in the temperature limitation imposed on dry-type transformers utilizing class-*B* insulation. Since 1947 the Working Group on Life of Materials[2] has been active in the development of the proper approach to life evaluation of dry-type transformers. The over-all assignment of the Working Group includes the study of all types of transformers, both dry-type and liquid-filled, but the program to date has been limited to ventilated dry-type power transformers. Reports[3,4] have been written on part of the work already performed.

The Working Group study has been aimed at establishing a philosophy of insulation system design based on the function served by each component of the system as distinct from the selection of insulating components based primarily on chemical composition. The desired end result of the work is the setting of standard temperature classifications for the insulation systems of transformers, and the development of model structures and associated test codes to be used in selecting proper system designs.[5] In this approach the chemical composition alone of the materials composing the insulation structure is not a limiting criterion. Instead the cyclic effects of temperature, humidity, and mechanical shock are considered with 60-cycle dielectric test voltage being applied between cycles to indicate the end point of the life of the insulation system under investigation.

For the group-2 dry-type transformer insulation system the life has been established[2,6] at 4 years' continuous operation at a temperature of 150 degrees centigrade (C). In order to accelerate the test program of simulated service conditions, considerably higher temperatures[7] are used and the humidity, mechanical shock, and dielectric test voltage applications are made severe. To prove a system, the life at each of three different elevated temperatures is obtained and the curve

---

Paper 55-452, recommended by the AIEE Transformers Committee and approved by the AIEE Committee on Technical Operations for presentation at the AIEE Summer General Meeting, Swampscott, Mass., June 27–July 1, 1955. Manuscript submitted March 28, 1955; made available for printing April 19, 1955.

H. G. Zambell is with the Allis-Chalmers Manufacturing Company, Pittsburgh, Pa.

The author expresses sincere thanks to W. C. Farneth, R. A. Ferguson, and C. M. Lane of the Pittsburgh Works of the Allis-Chalmers Manufacturing Company for their help in performing the test work and analyzing the results obtained.

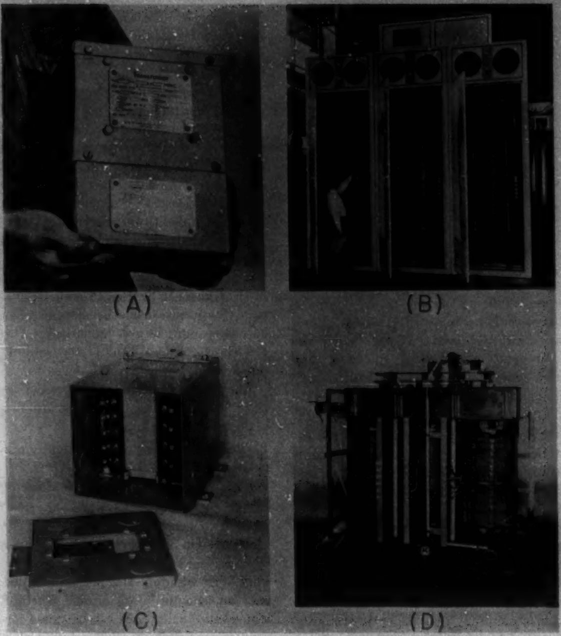

Fig. 1. Examples of 80 C rise ventilated dry-type transformers

A—1-kva single-phase 60-cycle Navy shipboard transformer
B—12,500-kva 3-phase unit substation transformer
C—5-kva single-phase distribution transformer
D—750-kva 3-phase load center transformer

through these points is extrapolated to determine whether the system has at least a 4-year life at a continuous operating temperature of 150 C. The validity of this approach has been established as a result of previous work[7] which has shown that insulation aging can be considered a chemical rate phenomenon.

Increasing interest in the functional life evaluation of dry-type transformers does not detract from the fact that the dry-type unit is a reliable piece of electric equipment as is evidenced by approximately 20 years of satisfactory field installation. Although the dry-type transformer is not used as widely as liquid-filled apparatus, nor applied in general to supply as large a load, it has proved to be equally capable of long usage under reasonably severe conditions. The Allis-Chalmers Manufacturing Company alone has manufactured over 3,500,000 kva of dry-type transformers ranging in size from midget single-phase 1-kva Navy shipboard units, Fig. 1(A), to giant 3-phase 12,500-kva power transformers, Fig. 1(B). Between these two extremes are the more familiar industrial single-phase dry-type unit, Fig. 1(C), and the typical 3-phase load center installation, Fig. 1(D).

In the early years of dry-type transformer design and operation, temperature standards were established on a minimum of laboratory data and field experience. The continued satisfactory operation of the older units attests to the wise decisions made by the designers and operators in the application of this relatively new piece of electric equipment. The early issues of AIEE Standard No. *1* specified insulating materials for electric apparatus on the basis of their chemical composition alone, i.e., whether they were organic or inorganic. A system of letter classifications, *O*, *A*, *B*, and *C*, was established for this purpose in the June 1940 issue of Standard No *1*.[1] The June 1947 issue of this Standard[8] recognized one segment of the increasing number of new insulating materials by including the addition of the temperature standard for class-*H* insulation. However, no changes were specified in any of the other insulation classifications. The February 1954 revision of AIEE Standard No. *1*[9] contains an addition to the class-*B* type of materials and recognizes the importance of the functional evaluation of insulation systems as is being investigated in both the transformer and rotating machinery[10] fields. Appendix I contains the relevant excerpts from each of the last three issues of Standard No. *1*. It is noteworthy that no changes have been made in the last 15 years in the temperature limitations imposed on the various insulation classes.

Although some attempt has been made in Standard No. *1* to differentiate between regions of higher temperature and lower temperature in the transformer itself, nevertheless the material class designations have become associated with transformers designed for a specific temperature limit. Consequently, there has been a pronounced tendency, e.g., to expect only class-*B*, -*H*, or -*C* materials in an 80 C average rise transformer even though a class-*A* material in a particular location might function better from an over-all transformer standpoint than any one of the other three higher temperature materials. In this example the transformer has been generally termed a class-*B* transformer. It has been recognized for some time that this method of classifying transformers, which restricts the use of materials to particular chemical compositions, is inadequate because:

1. It fails to recognize the numerous new materials being developed which are not readily classified as organic or inorganic.
2. It fails to recognize that the class-*B* and -*H* temperature limitations can be raised, based on published standards.[11]
3. It fails to take into account that materials of a lower temperature classification may be used satisfactorily in various parts of the insulation system of a transformer where the temperature is lower than the limiting hottest-spot temperature.

Since it was realized even in the early 1940's that dry-type transformer insulation should be selected on the basis of its function in the design, consideration was given to a revision of AIEE Standard No. *1* to take this into account. However, the Transformer Committee agreed that no change would be made until a co-operative laboratory investigation could be undertaken to determine what specific temperature limits should be established for dry-type transformers. The first standard values had been established as

Table I. Limits of Temperature Rise for Continuous Ratings[11]

Transformers and Reactors	Winding Temperature Rise by Resistance, C	Hottest-Spot Winding Temperature Rise, C
Oil-immersed	55	65
Dry-type: Group 1	55	65
Group 2	80	110
Group 3	150	180

105 C, 130 C, and 180 C hottest-spot temperatures for class-*A*, -*B*, and -*H* transformers respectively. It was recognized[12] that one or more of these temperatures could be increased, based on laboratory and field experience and taking into consideration improved materials and new types of materials as well as the functional approach.

The Working Group on Life of Materials, as a co-operative group of laboratories made up of material suppliers, transformer manufacturers, and transformer users, has been studying dry-type transformer insulation structures in an effort to establish more realistic temperature standards for dry-type transformers. In this work the main emphasis has been placed on a functional evaluation of the materials composing the insulation structure. This paper is primarily concerned with the present state of this work being performed by Allis-Chalmers, although some of the earlier findings are also reported as a part of the historical review. Some of the procedures used and the associated laboratory equipment are described in a certain amount of detail to enable those who plan to adopt the functional method to benefit from the Working Group's experience. Papers[2,13] by other members of the Working Group describe parallel investigations.

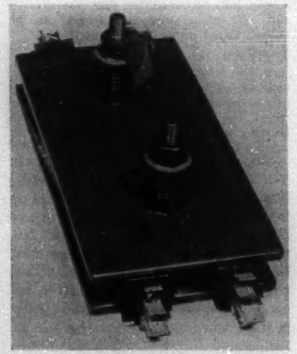

Fig. 2. Flat plate insulation aging assembly used in early investigations

It is not the intent of this paper to treat the classification[14] and characteristics[15,16] of insulating materials, nor to evaluate the chemical nature of thermal aging or the rate of insulation deterioration[7,17] as defined by existing "degree rules." Neither is it intended as a study of the physical properties[15,16] of materials as affected by humidity and mechanical shock. Instead, this paper is primarily concerned with the results so far obtained in developing a test code and a functional model which can be used to evaluate dry-type transformer insulation systems when specific conditions are prescribed. The references consider some of the subjects not covered by this paper.

The progress reported in the present activity of the Working Group falls into two main categories:

1. The development of a satisfactory test model and associated test code.
2. The evaluation of actual systems of insulation.

These two considerations are so closely interwoven in the program that they must be considered together throughout the work. In addition, the program is not only an attempt to determine whether temperature limitations can be raised for the various insulation classes but is also an effort to determine what particular insulation systems may be used under each standard temperature designation. As a part of the latter consideration, any materials may be used provided they function in the system in accordance with the requirements of standard test code specifications. This allows broad considerations of all newer materials which are difficult to classify by older methods.

Some of the results obtained by the Working Group have been incorporated in the latest National Electrical Manufacturers Association Standards for Transformers,[11] and are shown in Table I. This new Standard is a change to the new method of classifying transformers by temperature rather than by the materials used in the insulation system. The AIEE Transformer Committee has also approved this new method of classification.

Early Activities of Working Group

It was recognized early in the activities of the Working Group that the life evaluation of transformer insulation is a 3-step process, namely:

1. Material evaluation.
2. Functional model transformer investigation.
3. Transformer application.

This is a natural breakdown. Insulation system design requires first a consideration of the components of the insulation structure from a material standpoint, after which the particular functions of the materials are studied as to how they are actually shaped and used in the design. As a part of the latter investigation consideration is logically given to testing the material in a model in the laboratory before final incorporation in a production design. Although the Working Group's activities are confined to the establishment of the functional model concept and the associated test code, this does not mean that the material evaluation should be eliminated in considering the design of an insulation system. The material evaluation should always be present and in one sense constitutes a material screening procedure prior to functional model testing.

The original model considered for the evaluation of transformer insulation is shown in Fig. 2. This flat plate model consisted of bare straps of copper separated by layers of varnished glass cloth and clamped under a specified spring pressure between two steel plates. Aging was obtained by oven heat. Sixty-cycle dielectric breakdown tests and insulation resistance tests were performed at the end of each humidity cycle which occurred after each aging cycle.

Although a reasonable amount of laboratory work was done with the flat plate model, this construction was abandoned in May 1950 because low and erratic dielectric breakdown values were obtained. For example, the majority of the failures occurred at the ends, edges, or other pressure points in the samples. Furthermore, the use of this construction resulted principally in a material investigation rather than in a functional evaluation. The primary consideration was the phenol formaldehyde varnish used to impregnate the glass cloth. The only functional aspect was with relation to layer insulation, but even here the material was not shaped as it would be in a coil. Turn, major, and sectional insulations were not involved.

Fig. 3 (right). Mandrel insulation aging assembly used in early investigations

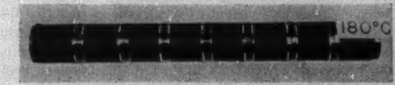

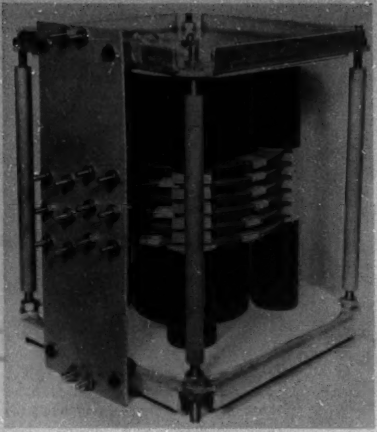

Fig. 4 (left). Functional test model for insulation aging study

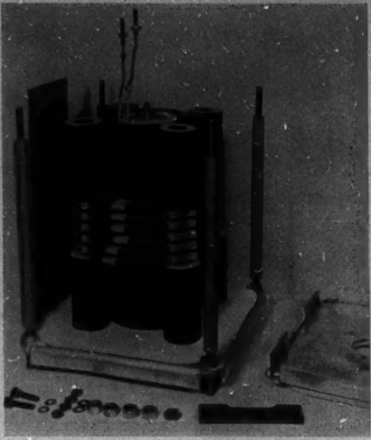

Fig. 5 (right). Functional test model for insulation aging study, top clamping plate removed

The second model considered was the mandrel type of model shown in Fig. 3. Again, this was not a true functional model since it was fundamentally adapted to an evaluation of layer insulation only. However, in view of other data having been reported[6] with this type of construction, it was decided to perform tests on class-*B* materials using this model. Actually, the Working Group had been doing some testing with the mandrel model prior to 1950.

Considerable testing was performed with the mandrel type of model using 50 per cent of the initial 60-cycle dielectric strength (dry) as the criterion of failure. Quinterra no. 1 sheet insulation impregnated with a phenol formaldehyde type of varnish was aged in ovens. Aging was performed at temperatures of 180 C, 200 C, and 250 C. Although somewhat different results were obtained from the various participating laboratories, the Working Group was able to recommend to the Transformer Committee that the class-*B* limiting hottest-spot temperature of 150 C, which was adopted by the AIEE Transformer Committee on October 21, 1948, should be continued. This recommendation was approved by the Transformer Committee on November 19, 1952, and has been adopted by the National Electrical Manufacturers Association,[11] but has not been incorporated into AIEE Standard No. *1*.

Introduction of Functional Approach

At the time the mandrel aging work was concluded in late 1952 considerable thought was given to a model which would be much more typical of actual transformer construction, and to an aging and test procedure more in line with the conditions imposed upon a transformer in the factory and in service. Examples of the early thinking[8] are:

1. A model employing individual and typical high-voltage (HV) and low-voltage (LV) windings, with representative major, sectional, layer, and turn insulations and with satisfactory mechanical clamping means.
2. A cyclic aging procedure in which the model would undergo periods of high temperature and periods of reduced temperature while at the same time experiencing percentage temperature gradients in its windings and insulation typical of those existing in transformers carrying load.
3. A series of environmental conditions to which the model should be exposed between heat-aging cycles. Consideration was given to humidification, mechanical shock, and test voltage applications.
4. The application of operating voltage during the heat-aging cycle, and a consideration of dirt accumulating on the model. The value of power factor tests was also treated.

The continued discussion of the functional approach lead to the conclusion on the part of the Working Group that a new model and an appropriate test code should be developed. A Subgroup of the working Group was appointed to perform the necessary work, including laboratory testing, to develop the model and the methods of aging and testing.

The first consideration of the Subgroup was with respect to the design of the model. The major factors were whether the model should be of the core-type construction or of the shell-type construction, and what particular voltage class should be used. It was quickly agreed that several models could be designed to represent the range in dry-type transformer design and construction. However, if the functional method were to be kept as simple as possible, at least in the beginning, it would be necessary to limit the construction to one particular type and for one particular voltage class. Consequently, the model shown in Fig. 4 was chosen. The construction represents either one leg of a core-type design, or the center leg of a shell-type unit. The electrical spacings were considered the minimum allowable values for apparatus of the 15-kv class.

The next consideration of the Subgroup was the nature of the heat-aging cycle and the effects of humidity and mechanical and dielectric stress. It was agreed that the model should not be aged in an oven or in a heat-controlled room, but instead should be heated by means of currents flowing in the two windings and so chosen as to duplicate transformer winding hot-test-spot temperatures and gradients and insulation temperatures. This, of course, is the whole criterion of the functional approach. The effect of humidity was considered necessary as a part of the over-all aging of the model. Consequently, the model was to be subjected to 90-per-cent relative humidity between heat-aging periods.

The method of application of mechanical shock or vibration to the model to simulate conditions existing during short-

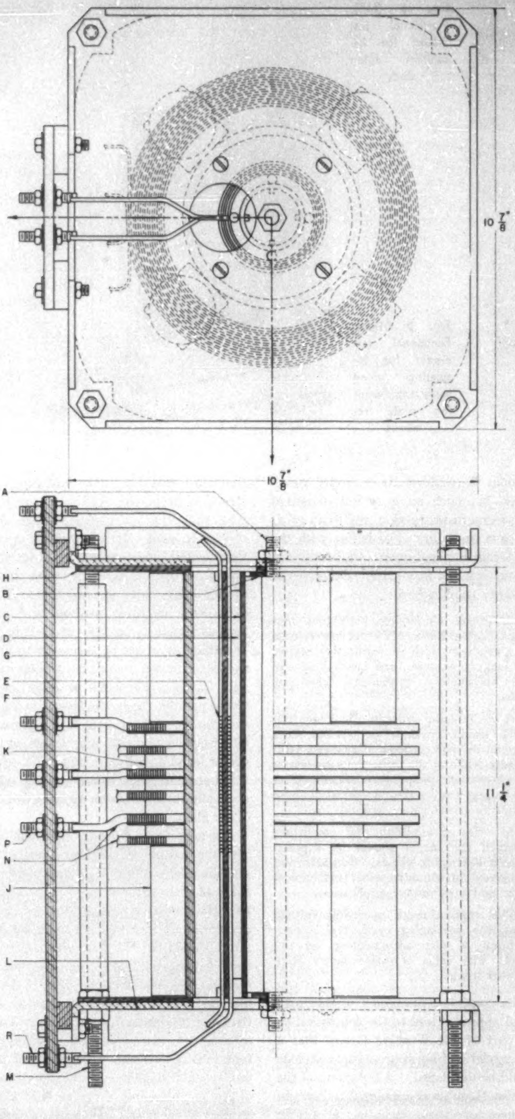

Fig. 6. Design of functional test model for insulation aging study

A—5/8-inch-diameter clamping rod
B—1 1/8-inch-diameter centering washer
C—1/8-inch LV barrier tube
D—1/4-inch duct
E—Two-layer LV winding
F—3/4-inch duct
G—1/4-inch HV barrier tube
H—1/8-inch yoke pad
J—HV coil support
K—3/8-inch-thick radial coil spacer
L—3/16-inch-thick aluminum end plate
M—3/8-inch-diameter clamping rod
N—HV winding section
P—HV terminal
R—LV terminal
Weight of model = 31 pounds

circuit test, shipment, or in actual operation proved to be extremely difficult to establish. There was no immediate information available on the severity of an applied shock or vibration. It was thought that either shock or vibration should be one of the conditions imposed on the model between heat-aging cycles since it seemed reasonable to believe that either of these would affect the life of the model. However, it was decided to postpone the actual specification of either shock or vibration until a complete study could be made. This has since been done and reported.[19]

The actual criterion of model failure was established as 60-cycle dielectric failure. Individual test voltages were selected to test the major, sectional, layer, and turn insulations before humidification between heat-aging cycles. All voltages were based on the major insulation test voltage being 75 per cent of the actual factory test voltage for the 15-kv class. The reduced test values were selected originally because at the time of each voltage application the model was more representative of a transformer having been in service for some period of time as contrasted to a new unit undergoing factory tests.

The remaining conditions to which the model could be subjected between heat-aging cycles were eliminated in an effort to simplify the procedure. This was especially true of the consideration of operating voltage at the time of heat aging. The control of the amount and kind of dirt which might be applied to the model also made this consideration impractical. Finally, power-factor testing was ruled out not only because of the time-consuming nature of all the tests but primarily because it was not at all clear what the results would mean with respect to the end point of the model.

The establishment of the original model and test code was followed by a consideration of the number of models which should be tested and the number of cycles which should constitute satisfactory performance or failure at a given aging temperature. It was agreed that a minimum of 30 models should be used in evaluating an insulation system if nothing at all is known about the strength of the system. Ac-

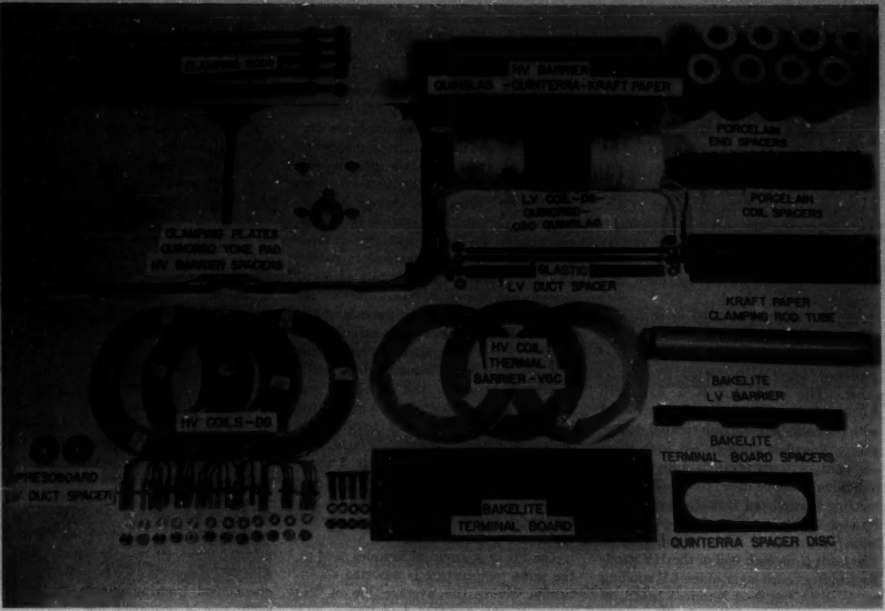
CLAMPING RODS
HV BARRIER
QUINGLAS -QUINTERRA-KRAFT PAPER
PORCELAIN
END SPACERS
PORCELAIN
COIL SPACERS
LV COIL-DG-
QUINORGO-
.030 QUINGLAS
CLAMPING PLATES
QUINORGO YOKE PAD
HV BARRIER SPACERS
GLASTIC
LV DUCT SPACER
KRAFT PAPER
CLAMPING ROD TUBE
HV COIL
THERMAL
BARRIER-VGC
BAKELITE
LV BARRIER
HV COILS-DG
BAKELITE
TERMINAL BOARD SPACERS
PRESSBOARD
LV DUCT SPACER
BAKELITE
TERMINAL BOARD
QUINTERRA SPACER DISC

Fig. 7. Component parts of functional test model. (Materials indicated were used in the final test program described in the text)

tually, in the work done to the present time, no such large number of models has been tested of any given design. Testing of a reasonable number, probably ten at a particular temperature, would be performed after a final test code was approved. The number of cycles to failure was established at between five and ten for a given aging temperature and heat-cycle duration. This range was picked specifically to insure obtaining the effect of cycling and to make it convenient to compare the performances of different systems of insulation.

After the completion of the first functional model design and the first test code, a series of tests was initiated in July 1953 to check the model design and the test code specifications. This work, which is described later in this paper in the sections entitled "Probing Tests" and "Final Tests," led to the design of the latest model construction shown in Figs. 4 through 7, and to the adoption of the latest test code.[3] The changes which were indicated as necessary following the probing tests have been incorporated in the latest test code specifications. In particular, it was found that in order to obtain failures in the model the dielectric test voltages had to be increased to the values corresponding to the 100-per-cent factory test voltage for 15-kv apparatus, and the dielectric tests had to be applied to the model in the humidified state. The following is a summary of the latest test code requirements.

1. Test cycle procedure
   a. Temperature aging.
   b. Dielectric test, dry, at ambient temperature.
   c. Mechanical shock. (The mechanical shock test is optional in the test code at the present time.)
   d. Humidification.
   e. Dielectric test under humid condition.
2. Sixty-cycle dielectric test procedure
   a. Major insulation from HV winding to ground and to LV winding, 31 kv rms for 1 minute.
   b. HV winding section-to-section insulation, 7 kv rms for 1 minute.
   c. HV winding turn insulation, 0.5 kv rms for 1 minute.
   d. LV winding layer insulation, 1.2 kv rms for 1 minute.

A more complete description of the test code is found in the section entitled "Functional Test Code."

Functional Test Model

The functional test model used in this investigation represented the combined thinking of the Subgroup as being typical of a 15-kv class of ventilated dry-type power transformers. The model is shown in Figs. 4 and 5, the design in Fig. 6, and the component parts in Fig. 7. The construction and materials shown, as described in this section, were used in the final test program described later in this paper under "Final Tests." The models used in the probing tests contained different materials and modified mechanical details which are described later in "Probing Tests." A description of the model construction follows.

The "core" consists of a 5/8-inch-diameter aluminum rod running axially through the center of the model. Around this rod is a 1/8-inch-thick Bakelite XX LV-to-ground barrier tube separated from the core rod by a 7/16-inch radial air duct, the spacing being maintained by two pressboard washer spacers. Four 1/4-inch-diameter glass polyester rods are used to space the LV winding from the LV-to-ground barrier tube.

The LV winding has two layers, 30 turns per layer, of no. 10 square wire with phenolic-base-varnish treated double-glass insulation. The insulation between layers consists of two thicknesses of 0.031-inch Quinglas. Each LV layer is packed out $3^{7}/_{8}$ inches on each end with two strips of 1/16-inch-thick Quinorgobord no. 1100. The LV–HV barrier tube is 1/4 inch thick and consists of 1/8-inch thick kraft paper with 1/32-inch-thick Quinterra type 5-2 and 0.031-inch Quinglas on each side. This tube is positioned by four 3/8-inch-diameter 3/8-inch-long brass spacers supported by each end plate.

The HV winding consists of three sections, each section being made up of a double-disk coil wound of two parallel copper conductors insulated from each other. The conductor is a flat strip 0.050-inch by 0.200-inch wire insulated with phenolic-base-varnish treated double glass. Porcelain spacers 3/8 inch thick are used between sections and between individual double-disk coils. The HV winding is insulated from each end plate by four 4-inch long porcelain spool insulators placed in line with the coil spacers. The leads from each coil of the HV winding and from each layer of the LV winding are brought out to a terminal board on one side of the model to facilitate performing the electrical tests.

The complete assembly is clamped by four 3/8-inch-diameter steel clamping rods between two $10^{7}/_{8}$-inch square aluminum end plates, each of which has placed against it a 1/8-inch-thick Quinorgobord yoke pad. The clamping rods are insulated with four 3/16-inch-thick kraft paper tubes. The assembly is thoroughly treated with a phenolic-base varnish.

A varnished glass-cloth washer, 0.010 inch thick, is placed below the top coil in each HV section. These washers act as thermal barriers by reducing the ventilation of the coils and therefore allow the proper temperature distribution to be reached. This construction was found necessary when, in some of the earlier tests, it was noted that the temperature gradients desired could not be reached.

The design of the model enables the following dielectric tests to be performed:

1. A major insulation test.
2. Two HV section-to-section tests.
3. Three HV turn-to-turn tests.
4. A LV layer-to-layer test.

Functional Test Code

A considerable number of changes have been made in the test code since it appeared in its first form. These changes are incorporated in the revision which is being released for trial use.[3] A brief summary of the more important provisions of the latest test code is outlined now.

The test code covers the recommended procedure to be followed in determining the operating temperature limits for dry-type power and distribution transformers. The primary aging factors are temperature and time. Since the tests are of an accelerated nature, the expected life at normal operating temperature is extrapolated from the life at test temperatures which are higher than normal to reduce the time of the test cycling to a practical limit. The life of a transformer is reduced when operated continuously at the maximum hottest-spot temperature limit. On the basis of experimental evidence and field experience this reduced life is taken as 4 years.[3,6] Each test is carried out simultaneously on a group of a number of identical samples sufficient to give the desired statistical accuracy. The life of a sample aged at one temperature is equal to the duration of temperature exposure during one test cycle multiplied by the number of cycles to failure, less 1/2 of 1 cycle.

The life of a group of samples aged at the same temperature is reported statistically, giving the average life of the group $\overline{X}$, the standard deviation σ, and the number of samples in the group N. The average life and the standard deviation are computed using the logarithm of life of individual samples. The word "failure" is construed to mean any form of dielectric flashover or breakdown of insulation which may occur on any of the specified electrical tests. The type of failure is reported.

Actual transformers are used where possible, but the use of models is permissible for larger transformers. The insulating system of the models must duplicate that of an actual transformer as closely as possible. All clearances can be no greater than in the actual transformer, and all materials used must be identical with those used in a transformer. The model must be so constructed as to allow a dielectric test on the various insulation components such as major insulation to ground, turn, section, and layer insulation.

The test procedure is a repeated test cycle consisting of the steps outlined in the section "Introduction of Functional Approach." All samples are given 60-cycle 1-minute hold dielectric proof tests at standard test voltages corresponding to the kilovolt class of the components of the model before any aging or cycling. These proof tests are applied at the same test point locations as the dielectric tests during the regular cycling procedure. Samples not passing the proof test are disqualified from further study in the evaluation of insulation life.

Exposure to elevated temperature is accomplished by circulating current through the windings, holding a constant hottest-spot test temperature. The aging

Fig. 8. Temperature aging test area

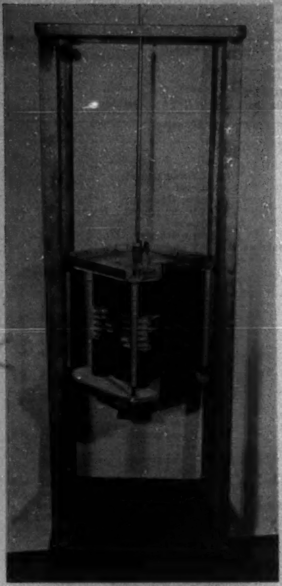

Fig. 9 (left). Mechanical shock test equipment

Fig. 10 (right). Humidity chamber

temperature and duration of each temperature aging cycle is so selected as to require 5 to 10 cycles to reach the average time to failure for a group of models. The temperature aging test area used in this investigation is shown in Fig. 8. The temperature aging equipment and the temperature aging procedure are outlined in Appendix II.

The 60-cycle 1-minute hold dielectric test values are either equal to the full 100-per-cent standard test values where such are available, or, when they are not available, correspond to the full level of insulation requirement. The tests are given in "Introduction of Functional Approach" in the order in which they are performed on the model.

A dielectric test between the LV winding and ground is not included in the test code, although it was considered. One reason for this is that there are practical difficulties in providing adequate clearances from the LV leads to ground on a model as small as the one used. In addition, the function of the LV insulation in a transformer is primarily that of a mechanical support. When this requirement is satisfied, electrical stresses on the LV winding insulation are quite low. Therefore, testing the LV winding insulation to ground dielectrically appears as an unwarranted expenditure of time and effort.

The mechanical shock test is optional since it has not yet been conclusively determined what direct effect, if any, this has on insulation life during aging. A shock test in excess of 100g acceleration has been tentatively recommended, using four shocks in succession per cycle. When used, this test is preceded and followed by mutual inductance measurements between the HV and LV windings to detect any possible physical displacement between them as an indication of deterioration of the supporting insulating material. This test is intended to simulate mechanical shocks which may occur during shipment and during short circuit. The mechanical shock test equipment used in this investigation is shown in Fig. 9. It is described in Appendix III.

Humidity exposure is of 24 hours' duration at approximately 90-per-cent relative humidity. The test temperature is maintained at a constant value within the range of 24 to 40 C. The measurement of dissipation factor of the insulation before and after humidification is optional since no satisfactory correlation between dissipation factor and dielectric failure has been determined as yet. The humidity chamber used in the tests performed is shown in Fig. 10. A description of this equipment and the procedure followed is given in Appendix IV.

Dielectric tests in the humid condition must be completed within 1/2 hour after removal of the samples from the humidity chamber. All dielectric failures are recorded along with the time in test cycles to produce this failure. Any sample whose insulation fails on any of the dielectric tests is disqualified from further dielectric tests for that particular mode of failure. However, this sample may continue to be used for determining the time to failure of a different insulating component.

The test code described in this section was used only in the final tests performed as described in the section on "Final Tests." The work performed in the probing tests followed somewhat different procedures as described in the section on "Probing Tests."

Functional Tests Performed

Since July 1953 a series of functional aging tests has been in progress with the following objectives:

1. To determine whether the test model specified to represent the insulation system of a 15-kv class of dry-type transformer was practical.
2. To verify experimentally the test procedure as outlined in the test code.
3. To recommend modifications in the model and test procedure if such were found necessary or desirable.

The Allis-Chalmers phase of this work was divided into two distinct categories, namely probing tests and final tests.

The probing tests represented the initial work with the functional model. Therefore the testing was somewhat random, although specific questions were investigated at each step. The work was divided into five separate test runs during which variations in model geometry, aging temperature, dielectric test voltage, mechanical shock, and degree of humidification were studied. These tests are described later and are summarized in Table II.

Upon completion of the probing tests in November 1954 a final test program was

Table II. Summary of Probing Test Procedure and Data

Test No.	Model No.	Aging Temperature C	Total Time Aged		Dielectric Test Voltages Kv				Mechanical Shock		Insulating Materials			Failures
			Cycles	Hours	HV to LV and Ground	HV Section	LV Layer	HV Turn	Times g	No. of Tests	HV Coil Spacer	End Spacer and Length in Inches	HV-LV Barrier	
I	1	260	6	576	23.5	5.25	0.9	0.2*	none	none	Bakelite	Bakelite, $2^7/_8$	Bakelite	none
I	2	260	6	576	23.5	5.25	0.9	0.2*	none	none				none
I	3	260	6	576	23.5	5.25	0.9	0.2*	none	none				none
II	4	260	4	384	31.0	7.0	1.2	0.8	≈30	1				HV-LV and ground, 3rd, wet HV turn, 4th, wet
II	5	260	4	384	31.0	7.0	1.2	0.8	≈30	1				HV-LV and ground, 3rd, wet . . HV turn, 4th, wet HV turn, 4th, dry
II	6	260	4	384	31.0	7.0	1.2	0.8	≈30	1				HV-LV and ground, 3rd, wet HV turn, 4th, dry
III	7	230	7	672	31.0	7.0	1.2	0.8	≈30	1				HV turn, 2nd, dry HV-LV and ground, 5th, wet
III	8	230	7	672	31.0	7.0	1.2	0.8	≈30	1				HV-LV and ground, 5th, dry . . HV turn, 7th, dry HV turn, 6th, wet . . . . HV turn, 7th, dry
III	9	230	7	672	31.0	7.0	1.2	0.8	≈30	1				HV-LV and ground, 4th, wet . . HV turn, 7th, dry LV layer, 5th, wet . . . . HV turn, 7th, dry
IV	10	210	10	960	31.0	7.0	1.2	0.8	≈30	1	porcelain	porcelain, 3	Bakelite	HV turn, 6th, wet . . . . HV turn, 10, dry HV-LV and ground, 10th, dry
IV	11	210	10	960	31.0	7.0	1.2	0.8	≈30	1				HV-LV and ground, 6th, wet† . . HV turn, 9th, dry HV-LV and ground, 7th, dry
IV	12	210	10	960	31.0	7.0	1.2	0.8	≈30	1				HV-LV and ground, 1st, wet† . . LV layer, 4th, wet HV turn, 1st, wet . . . . HV-LV and ground, 8th, dry HV turn, 2nd, wet
V	13	240	9	864	31.0	7.0	1.2	0.8	none	none				HV turn, 1st, wet . . . . HV-LV and ground, 5th, wet HV turn, 4th, wet . . . . HV turn, 9th, wet
V	14	240	9	864	31.0	7.0	1.2	0.8	none	none				HV-LV and ground, 3rd, wet
V	15	240	9	864	31.0	7.0	1.2	0.8	>100	4				HV-LV and ground, 3rd, wet LV layer, 4th, wet
V	16	240	9	864	31.0	7.0	1.2	0.8	>100	4				HV-LV and ground, 3rd, dry

* This voltage was applied while the models were in the humidity chamber.

† These were wet flashovers which occurred across the terminal board to the end plate and were due to inadequate geometry of the model as well as to inferior material used in the terminal boards. Therefore these results were not used in evaluating insulation life.

A 24-hour humidity exposure followed the mechanical shock test. For test I the relative humidity was below the required 90 per cent. For all other tests the relative humidity was 90 per cent at 28.5 C.

initiated at three aging temperatures in order to obtain a curve of life versus temperature for the model insulation system. By this time the probing tests had indicated that the functional model was satisfactory in most respects and that the test code could be used with some changes to represent the conditions to which a transformer could be subjected in the factory and the field. The program of final tests is also described later, and the procedure and results are summarized in Table III.

Probing Tests

Table III gives the probing test procedure and data. The models were tested in groups of three or four models each in accordance with the specifications of the earlier test codes. Five individual tests were performed as outlined.

TEST NO. I

The first models tested, models 1, 2, and 3, differed in construction from the latest model in that the distance from the windings to the end plate was only $2^7/_8$ inches instead of 4 inches, and Bakelite instead of porcelain was used for the HV coil spacers and the spacers between the HV winding and the end plates. The major differences between the test procedure used and the latest test code procedure summarized in the section entitled "Introduction of Functional Approach" were:

1. The dielectric tests were performed on the models in the dry state, with the exception of the HV turn test which was performed wet at the proof test voltage of 200 volts.
2. The remaining dielectric tests were performed at voltages corresponding to the 75-per-cent factory test voltage for the 15-kv class of apparatus.
3. No mechanical shock was applied.
4. The required 90-per-cent relative humidity was not reached. The humidity chamber described in Appendix IV was used in all tests except this first test.

This test was performed at an aging temperature of 260 C with 96 hours of aging per cycle. After 6 complete cycles or 576 total hours of aging, no dielectric failures were obtained even though in two of the models the HV-to-LV barrier tube was burned completely in half as is shown in Fig. 11. Since these burned-through sections had existed from the end of the third aging cycle and no failures had occurred, it was evident that the major insulation test voltage being used was insufficient to cause failure even with an air spacing alone.

Based on these results, and similar ones obtained by the other members of the Subgroup, the test code was made more severe as follows:

1. The test voltages were increased to correspond to the full 100-per-cent factory test voltage for 15-kv class apparatus.
2. The test voltages were specified to be applied to the model not only in the dry state immediately following temperature aging but also in a wet condition immediately after humidification.
3. A mechanical shock of approximately 30g in the dry state was specified.

Table III. Summary of Final Test Procedure and Data

Test No.	Model No.	Aging Temperature C	Total Time Aged: Cycles	Total Time Aged: Hours	Dielectric Test Voltages Kv: HV Turn	Dielectric Test Voltages Kv: LV Layer	Dielectric Test Voltages Kv: HV Section	Dielectric Test Voltages Kv: HV to LV and Ground	Mechanical Shock: Times g	Mechanical Shock: No. of Tests	Insulating Materials: HV Coil Spacer	Insulating Materials: End Spacer and Length in Inches	Insulating Materials: HV–LV Barrier	Failures
VI	17	220	4	280	0.5	1.2	7.0	31.0	> 100	4	porcelain	porcelain, 4	kraft paper	HV–LV and ground 2nd, dry
VI	18	220	5	350									Bakelite	HV–LV and ground, 3rd, dry
VI	19	220	5	350									Bakelite	LV layer, 3rd, wet LV layer, 4th, wet
VI	20	220	5	350									Bakelite	HV–LV and ground, 4th, wet
VI	21	220	5	350									Bakelite	HV turn, 5th, dry HV–LV and ground, 5th, wet
VI	22	250	4	86									Bakelite	HV turn, 1st, wet HV–LV and ground, 4th, wet
VI	23	250	4	86									Bakelite	HV–LV and ground, 4th, wet
VI	24	250	4	86									Bakelite	HV–LV and ground, 4th, dry
VI	25	250	4	86									Bakelite	HV–LV and ground, 3rd, dry
VI	26	280	4	32									Bakelite	HV turn, 3rd, dry HV–LV and ground, 2nd, wet
VI	27	280	4	32									Bakelite	HV–LV and ground, 3rd, wet
VI	28	280	4	32									Bakelite	HV turn, 3rd, dry HV–LV and ground, 2nd, wet
VI	29	280	4	32									Bakelite	HV–LV and ground, 3rd, wet
VII	30	220	8	768									laminated*	
VII	31	220	8	768									laminated*	
VII	32	220	8	768									laminated*	HV turn, 3rd, wet
VII	33	220	8	768									laminated*	LV layer, 8th, wet
VII	34	250	8	192									laminated*	HV turn, 2nd, dry
VII	35	250	8	192									laminated*	
VII	36	250	8	192									laminated*	LV layer, 8th, wet
VII	37	250	8	192									laminated*	
VII	38	280	8	64									laminated*	HV turn, 5th, dry
VII	39	280	8	64									laminated*	HV turn, 2nd, dry HV–LV and ground, 8th, wet
VII	40	280	8	64									laminated*	
VII	41	280	8	64									laminated*	HV–LV and ground, 8th, wet

* This barrier was 1/4 inch thick and consisted of 1/8-inch kraft paper with 1/32-inch Quinterra type 5-2 and 0.031-inch Quinglas on each side.

TEST NO. II

Models 4, 5, and 6 employed the same construction as models 1, 2, and 3. The only difference between the test procedure used and the latest test code procedure was the single application of a shock of approximately 30*g* instead of four applications of a shock in excess of 100*g*.

This test was performed at an aging temperature of 260 C with 96 hours of aging per cycle. A major insulation failure occurred in each of the three models after humidification following the third aging cycle, while HV turn failures occurred 1 cycle later. The HV-to-LV barrier tube was burned through on all models at the end of the third aging cycle.

This test showed that failures could be achieved as a result of the revisions made in the test code. However, either the aging temperature or the duration of aging was too severe since the 5-to-10-cycle criterion was not met. Consequently, a test at 230 C was suggested.

TEST NO. III

Models 7, 8, and 9 employed the same construction and followed the same test procedure as models 4, 5, and 6 except that an aging temperature of 230 C was used with 96 hours of aging per cycle.

Major insulation failures were obtained in the three models at the end of 4, 5, and 5 cycles; HV turn failures occurred at the end of 2, 6, and 7 cycles; and one LV layer failure was obtained at the end of the 5th cycle.

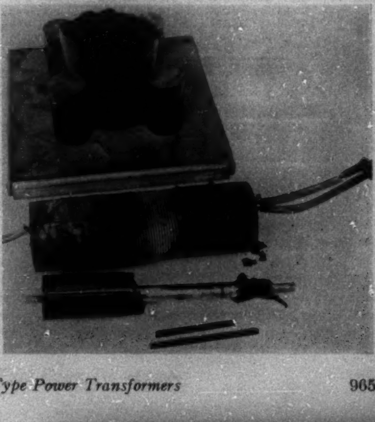

Fig. 11 (right). Results of extreme aging of functional test model, 576 hours at 260 C

This test showed that a reduction from 260 C to 230 C in aging temperature resulted in an increase in the number of cycles to failure from 3 to approximately 5. Therefore, an aging temperature of 210 C was suggested.

TEST NO. IV

Models 10, 11, and 12 differed from models 7, 8, and 9 only in that porcelain was used instead of Bakelite for the HV coil spacers and 3-inch-long porcelain was used instead of $2^{7}/_{8}$-inch-long Bakelite for the spacers between the HV winding and the end plates. The same test procedure was followed as was used with models 7, 8, and 9 except that the aging temperature was 210 C with 96 hours of aging per cycle.

Major insulation failures occurred in the three models at the end of 7, 8, and 10 cycles; HV turn failures were obtained at the end of 1, 2, 6, 9, and 10 cycles; and one LV failure occurred at the end of the 4th cycle.

This test proved conclusively that the trend indicated in the previous test, namely that a decrease in aging temperature results in longer model life, was true. With these results coupled with the results of the first two tests no additional work was done at the time in checking the aging temperature and the aging time per cycle. Instead, an investigation of the effect of mechanical shock was suggested.

TEST NO. V

Models 13, 14, 15, and 16 were identical in construction to models 10, 11, and 12. Models 13 and 14 received no mechanical shock, whereas models 15 and 16 were subjected to four shocks per cycle in excess of 100g. The aging temperature was 240 C with 96 hours of aging per cycle.

Models 13 and 14 experienced major insulation failures after 3 and 5 cycles, and HV turn failures after 1, 4, and 9 cycles; models 15 and 16 each experienced a major insulation failure after 3 cycles, while a LV layer failure occurred in model 15 after 4 cycles.

Obviously, no definite conclusion could be drawn from the results of this test even though the major insulation failures in the shocked models occurred earlier on the average than those in the unshocked models. However, it was decided by the Subgroup at the time (November 1954) that additional testing would be necessary with and without mechanical shock to determine the effect of shock before it was added to the test code. It is noteworthy in this test, though, that an increase in the aging temperature to 240 C resulted in all major insulation failures in 5 cycles or less.

SUMMARY OF PROBING TESTS

The results of the probing tests indicated the following:

1. Failures in the model could be achieved in the 5-to-10-cycle range if the proper aging temperature and aging time per cycle were chosen.
2. The effect of mechanical shock was not determined.
3. The HV turn dielectric test was too severe.
4. Insufficient spacing was specified between the HV winding and the end plates.

The last point is not apparent from the data in this paper. However, flashovers between the HV winding and the end plates were observed by all members of the Subgroup during some of the tests. When actual transformer design spacings were checked it was obvious that the model spacing was insufficient. Therefore, the 3-inch dimension was increased to 4 inches in the test code.

The numerous HV turn dielectric failures led to a check of the voltage distribution across the coils of a production dry-type power transformer during impulse test. This led to the conclusion that the 800-volt turn test was too severe. Consequently, a change was made in the test code to 500 volts.

Upon completion of the probing tests, the Working Group decided that sufficient testing had been performed to establish the model and the test code as satisfactory for trial use by industry. At that time, Allis-Chalmers initiated a series of tests to determine the life versus temperature characteristic of models aged at three temperatures in accordance with the latest test code.

Final Tests

During the probing tests the activities of the Subgroup were primarily concerned with the establishment of a functional model and a corresponding test code which could be used with confidence either in studying the proper operating temperatures for ventilated dry-type transformers or in investigating insulation systems for these units. Now that the model and test code had been shown to be representative, it remained to be proved that satisfactory and unsatisfactory insulation systems could be picked out by the tests.

The final test procedure and data are summarized in Table III. The models were tested in two groups of 13 and 12 models in accordance with the specifications of the latest test code as described in "Functional Test Code." Aging temperatures of 220 C, 250 C, and 280 C were used during each of the two tests performed. The aging times per cycle for these temperatures were 96 hours, 24 hours, and 8 hours respectively. These times were selected in an effort to achieve failures in the 5-to-10-cycle range, and

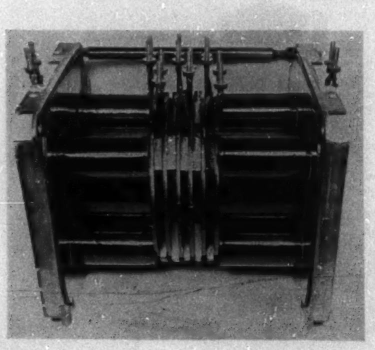

Fig. 12 (left). View of model aged during final tests at 280 C for 10 cycles, 80 hours of aging

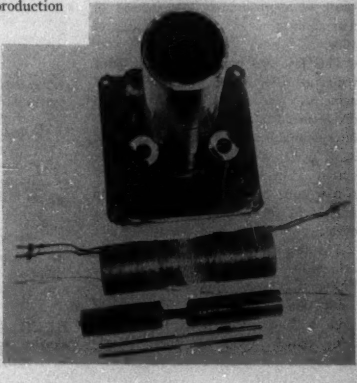

Fig. 13 (right). Components of model aged during final tests at 280 C for 10 cycles, 80 hours of aging

Table IV. Calculation of Life of Models Aged at 220 C During Final Tests

Model No.	Dielectric Test	Failure, Cycles	Total Time Aged		Statistical Life to Date		
			Hours	Cycles	Hours	Log of Hours	
30	HV–LV and ground	none	768	8	816	2.91169	
31	HV–LV and ground	none	768	8	816	2.91169	
32	HV–LV and ground	none	768	8	816	2.91169	
33	HV–LV and ground	none	768	8	816	2.91169	
	Average					2.91169	
	Average statistical life in hours (antilog of average log of hours)						816
30	HV turn	none	768	8	816	2.91169	
30	HV turn	none	768	8	816	2.91169	
30	HV turn	none	768	8	816	2.91169	
31	HV turn	none	768	8	816	2.91169	
31	HV turn	none	768	8	816	2.91169	
31	HV turn	none	768	8	816	2.91169	
32	HV turn	3rd, wet	288	3	240	2.38021	
32	HV turn	none	768	8	816	2.91169	
32	HV turn	none	768	8	816	2.91169	
33	HV turn	none	768	8	816	2.91169	
33	HV turn	none	768	8	816	2.91169	
33	HV turn	none	768	8	816	2.91169	
	Average					2.86740	
	Average statistical life in hours (antilog of average log of hours)						737
30	LV layer	none	768	8	816	2.91169	
31	LV layer	none	768	8	816	2.91169	
32	LV layer	none	768	8	816	2.91169	
33	LV layer	8th, wet	768	8	720	2.85733	
	Average					2.89810	
	Average statistical life in hours (antilog of average log of hours)						791
	Logarithmic average of all average data in hours						781

Table V. Calculation of Life of Models Aged at 250 C During Final Tests

Model No.	Dielectric Test	Failure, Cycles	Total Time Aged		Statistical Life to Date		
			Hours	Cycles	Hours	Log of Hours	
34	HV–LV and ground	none	192	8	204	2.30963	
35	HV–LV and ground	none	192	8	204	2.30963	
36	HV–LV and ground	none	192	8	204	2.30963	
37	HV–LV and ground	none	192	8	204	2.30963	
	Average					2.30963	
	Average statistical life in hours (antilog of average log of hours)						204
34	HV turn	2nd, dry	48	2	36	1.55630	
34	HV turn	none	192	8	204	2.30963	
34	HV turn	none	192	8	204	2.30963	
35	HV turn	none	192	8	204	2.30963	
35	HV turn	none	192	8	204	2.30963	
35	HV turn	none	192	8	204	2.30963	
36	HV turn	none	192	8	204	2.30963	
36	HV turn	none	192	8	204	2.30963	
36	HV turn	none	192	8	204	2.30963	
37	HV turn	none	192	8	204	2.30963	
37	HV turn	none	192	8	204	2.30963	
37	HV turn	none	192	8	204	2.30963	
	Average					2.24685	
	Average statistical life in hours (antilog of average log of hours)						177
34	LV layer	none	192	8	204	2.30963	
35	LV layer	none	192	8	204	2.30963	
36	LV layer	none	192	8	204	2.30963	
37	LV layer	8th, wet	192	8	180	2.25527	
	Average					2.29604	
	Average statistical life in hours (antilog of average log of hours)						198
	Logarithmic average of all average data in hours						192

were based on the experience obtained in the probing tests. Figs. 12 and 13 show the condition of a model and its components during the final tests at 280 C for 10 cycles.

TEST NO. VI

This test was designed to determine whether model 17, which incorporated a kraft-paper HV-to-LV barrier tube, treated with a casein glue, could be picked out by the test procedure as having an unsatisfactory insulation system for a group-2 dry-type transformer. This model was aged at 220 C for 96 hours per aging cycle. In addition, models 18 through 29, having what was considered a satisfactory insulation system, were aged in three groups of four models each, as outlined in Table III.

Model 17 was quickly selected by the test procedure as unsatisfactory. It experienced a major insulation failure in the dry state after only the second aging cycle. The kraft-paper tube was badly burned throughout its length, and in the vicinity of the winding hottest spots it had burned completely through.

Unexpectedly, models 18 through 29 also failed early in the cycling procedure. All except one of the 12 models failed the major insulation test after 2, 3, and 4 cycles, proving that the insulation system was unsatisfactory if the results of the probing tests could be taken as proof that the latest test code was representative. It was easily found that the insulation system itself was faulty. All 12 of the Bakelite HV-to-LV barrier tubes exhibited severe bulging at the inner surface of each tube with the result that bridging between the inside of the tube and the LV winding took place. The cause of the bulging was attributed to insufficient curing of the tubes by the supplier, with the result that the volatile matter still remaining in the tubes escaped during the early aging cycles and in so doing delaminated the inner surfaces of the tubes.

Although this circumstance ruined what set out to be an investigation expected to give a positive result, nevertheless the negative result again proved emphatically that the test code would pick out an unsatisfactory insulation system. A decision was immediately made to perform another test, only this time to use an improved barrier tube.

TEST NO. VII

Models 30 through 41 were aged in three groups of four models each, as shown in Table III. All models incorporated HV-to-LV barrier tubes constructed as follows:

One layer, 0.031-inch Quinglas.
Two layers, 0.015-inch Quinterra.
Six layers, 0.020-inch calendered kraft paper.
Two layers, 0.015-inch Quinterra.
One layer, 0.031-inch Quinglas.

Each layer was coated with an alkyd-type varnish. The tubes were finally treated with a phenolic-base varnish. These tubes, then, were made up of a combination of class-*A* and class-*B* materials.

Since this test was not started until the middle of January 1955, it was still in progress at the time this paper was submitted. However, as of the middle of March 1955, 8 cycles at each of the three aging temperatures were completed. Only two major insulation failures were obtained in the 12 models, these occurring after 8 cycles in two of the models aged at 280 C. HV turn failures occurred at only four test locations out of a possible

Table VI. Calculation of Life of Models Aged at 280 C During Final Tests

Model No.	Dielectric Test	Failure, Cycles	Total Time Aged Hours	Total Time Aged Cycles	Statistical Life to Date Hours	Statistical Life to Date Log of Hours	
38	HV–LV and ground	none	64	8	68	1.83251	
39	HV–LV and ground	8th, wet	64	8	60	1.77815	
40	HV–LV and ground	none	64	8	68	1.83251	
41	HV–LV and ground	8th, wet	64	8	60	1.77815	
Average						1.80533	
Average statistical life in hours (antilog of average log of hours)							64
38	HV turn	5th, dry	40	5	36	1.55630	
38	HV turn	none	64	8	68	1.83251	
38	HV turn	none	64	8	68	1.83251	
39	HV turn	2nd, dry	16	2	12	1.07918	
39	HV turn	none	64	8	68	1.83251	
39	HV turn	none	64	8	68	1.83251	
40	HV turn	none	64	8	68	1.83251	
40	HV turn	none	64	8	68	1.83251	
40	HV turn	none	64	8	68	1.83251	
41	HV turn	none	64	8	68	1.83251	
41	HV turn	none	64	8	68	1.83251	
41	HV turn	none	64	8	68	1.83251	
Average						1.74672	
Average statistical life in hours (antilog of average log of hours)							56
38	LV layer	none	64	8	68	1.83251	
39	LV layer	none	64	8	68	1.83251	
40	LV layer	none	64	8	68	1.83251	
41	LV layer	none	64	8	68	1.83251	
Average						1.83251	
Average statistical life in hours (antilog of average log of hours)							68
Logarithmic average of all average data in hours							62

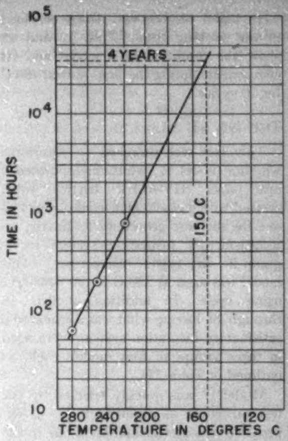

Fig. 14. Life versus temperature data obtained on final tests

36 (three for each of 12 models). These failures were experienced at the end of 2, 2, 3, and 5 cycles. Two LV layer failures, each at the end of 8 cycles, occurred out of a possible 12.

Although sufficient failures were not obtained to indicate the end of the test, the data for each of the aging temperatures, 220 C, 250 C, and 280 C, are treated statistically in Tables IV, V, and VI respectively. In these calculations, the life data for the individual insulation components (major, turn, layer) are averaged logarithmically. Where failures occurred the total number of cycles aged, less 1/2 cycle, is used; where no failures occurred the total number of cycles aged, plus 1/2 cycle, is used.

Since the life of each insulation component at each aging temperature was nearly the same, the over-all logarithmic average of the life of the models at each temperature was calculated. These three average values are plotted in Fig. 14 with a straight line drawn through them to give the life versus temperature characteristic of the insulation system tested. Although the test was not finished, extrapolation of the curve to the 150 C operating temperature for group-2 apparatus shows that the system already has a life equal to the 4-year criterion established in the test code. Actually, the characteristic could be made to show a life in excess of 4 years at 150 C if the life of the HV section insulation were included in each of the averages. It would have been proper to do this, but since no HV section failures had been experienced in any of the testing performed, it was decided not to include this component in the over-all calculation of life.

Summary of Final Tests

The results of the final tests support the conclusion reached at the completion of the probing tests, namely that the model is representative of tranformer construction and the test code is representative of transformer factory and field conditions. No difficulty was experienced in picking out satisfactory and unsatisfactory insulation systems. Also, the work proves that a satisfactory insulation system for group-2 dry-type power transformers can be shown statistically to have at least a 4-year life at a continuous operating temperature of 150 C when the method of test follows the specifications of the test code[3] being issued for trial use.

One point regarding the final tests is worthy of mention. After the spacing between the HV winding and end plates was increased from 3 inches to 4 inches following the probing tests, no flashovers were experienced in the final tests.

Conclusions

This paper has presented the development of a functional means of evaluating insulation systems for ventilated group-2 dry-type power transformers. The evolution of a representative test model and test code has been traced. Experimental data have been included to substantiate the conclusion that the functional method of evaluating dry-type transformer insulation systems is sound enough to be submitted to the transformer industry for trial use.

The other major purpose of this investigation, namely, to recommend modifications in the model and test procedure if such were found necessary or desirable, can be summarized as follows:

Transformer Model

No changes appear necessary in the latest model construction as a result of the work described in this paper. However, a word of caution is in order. Reasonable care should be exercised in winding and assembling the HV coils to insure against damage to the turn insulation which is under more than normal mechanical stress because of the small (7$^{3}/_{4}$-inch) coil diameter.

Temperature Aging

A modification in the aging temperatures and the aging time per cycle is necessary to insure that sufficient failures in the insulation components occur between 5 and 10 cycles. It appears that test no. VII will not have an end point within 10 cycles even though the life criterion of the test code has already been met after 8 cycles.

Mechanical Shock

This work presents no conclusive evidence that mechanical shock affects insulation system life, even after representative aging of the system. No changes in the mutual inductance measurements described in Appendix III were experienced in any of the testing. If a thorough study of the effects of mechanical shock does not prove conclusively that the system is affected by shock, this test should be eliminated from consideration as a possible test code specification in order to keep the procedure as simple as possible.

HUMIDIFICATION

No changes appear necessary in the specification of the applied degree of humidification. Experience has indicated that humidity is a necessary factor in the test procedure.

DIELECTRIC TESTS

The application of 100-per-cent factory test voltages to aged, completely wet insulation systems constitutes a very severe test considerably in excess of the conditions experienced normally in the factory or the field. That a system withstands these cyclic voltage applications and meets the established life criterion attests to the soundness of its design.

However, the HV turn failures experienced, while not statistically out of line, suggest that a study be made of the actual severity of the 500-volt test. There is reason to believe that a 200-volt test may be more representative of the maximum voltage existing across the turns during impulse test.

The lack of HV section dielectric failures could be expected since coil-to-coil and section-to-section clearances are primarily dictated by transformer cooling requirements. The order of dielectric tests as specified in the test code (major, HV section, HV turn, and LV layer) might be improved if it were changed to turn, section, layer, and major in order to avoid the possibility of the major insulation test affecting the results of the other three tests. The latter order was used in test no. VII, and while no conclusive results were obtained, the frequency of HV turn failures was reduced.

NUMBER OF SAMPLES TESTED

The number of models investigated in test no. VII did not satisfy the requirements of the test code since only four models were aged at each test temperature instead of the specified ten. However, if a total of 30 models (ten at each of three temperatures) were to be aged, the program would have to be a co-operative one with several laboratories assisting in the study in order to minimize the individual effort. Even if this were done it is debatable whether the results would differ materially from those obtained in this investigation.

In conclusion, the results of this investigation support the 150 C temperature specification of the National Electrical Manufacturers Association Standards for Transformers[11] and lead to the recommendation that AIEE Standard No. *1* recognize this same temperature for group-2 dry-type transformers.

Appendix I. Excerpts from AIEE Standard No. 1

The 1940 issue of Standard No. *1* contained the following descriptions of each insulation class:

"Class-*O* insulation consists of cotton, silk, paper, and similar organic materials when neither impregnated nor immersed in a liquid dielectric.

"Class-*A* insulation consists of: (1) cotton, silk, paper, and similar organic materials when either impregnated or immersed in a liquid dielectric; (2) molded and laminated materials with cellulose filler, phenolic resins and other resins of similar properties; (3) films and sheets of cellulose acetate and other cellulose derivatives of similar properties; and (4) varnishes (enamel) as applied to conductors.

"Class-*B* insulation consists of mica, asbestos, fiber glass and similar inorganic materials in built-up form with organic binding substances. A small proportion of class-*A* materials may be used for structural purposes only.

"Class-*C* insulation consists entirely of mica, porcelain, glass, quartz and similar inorganic materials."

The limiting hottest-spot temperatures were 90 C for class *O;* 105 C for class *A;* 130 C for class *B;* and no limit for class *C*.

The June 1947 issue included this description of class-*H* insulation: "Class-*H* insulation consists of (1) mica, asbestos, fiber glass and similar inorganic materials in built-up form with binding substances composed of silicone compounds, or materials with equivalent properties; (2) silicone compounds in rubbery or resinous forms, or materials with equivalent properties. A minute proportion of class-*A* materials may be had only where essential for structural purposes during manufacture." The hottest spot limiting temperature was set at 180 C.

The February 1954 issue included the addition of the word "organic" to the varnish description under class *A*, and incorporated the following sentences to the class-*B* description: "Fiber glass or asbestos magnet wire insulations are included in this temperature class. These may include supplementary organic materials, such as polyvinylacetal or polyamide films."

In addition, this revision of the Standard contained the following paragraph together with a discussion of the evaluation of insulation systems: "It is recognized that new synthetic insulating materials are continually being developed. These new materials cannot readily be classified on the basis of their chemical compositions. Their temperature limits should be evaluated by accelerated life tests, either as materials, or as components of complete insulation systems...."

Appendix II. Temperature Aging Equipment

The temperature aging test area is shown in Fig. 8. At the left of the models is a portion of the power supplies and meters used. Temperatures were controlled by means of thermocouple controllers and recorders connected to removable thermocouples in the models. The controllers maintained the specified hottest-spot temperatures within ±2 C. The HV and LV windings were supplied by separate power supplies which were adjusted to maintain equal HV and LV hottest-spot temperatures even though these temperatures were controlled by one thermocouple located in the HV winding. All conductors in each winding were connected in series.

Aluminum foil, 0.012 inch thick, was wrapped snugly around each model to maintain the temperature difference between the hottest spots of the windings and the hottest spot of the high-to-low barrier tube at less than 30 C as specified by the test code. In addition, the holes in the end plates, through which the LV leads pass, were closed with asbestos to minimize ventilation.

Appendix III. Mechanical Shock Equipment

The mechanical shock test equipment is shown in Fig. 9. This apparatus enabled the model to be dropped from a predetermined height onto a platform to obtain the acceleration required. The model was dropped upside down from the position in which it was aged to insure maximum stressing of the insulation subjected to the highest temperature. A round 3/8-inch-diameter rod was attached to the bottom center of the model and guided it during its fall. A cross pin inserted in the rod supported it and the attached model at a predetermined height above the platform. When the pin was removed the model dropped freely. A stiffening adapter was mounted on the end plate to prevent deformation of the end plate and to distribute the mechanical shock throughout the model structure. On the bottom of the adapter was mounted a brass pellet which was attached to the end plate with caulking compound. The drop height was adjusted to give a reduction in length of the pellet which would result in a shock in excess of 100*g*. A new pellet was used for each drop.

In order to detect any deformation or displacement of the coils from each other as a result of the shock, mutual inductance measurements were made each cycle before and after the shock application. As shown in Fig. 15, the two layers of the LV coil were connected in series and a current of 5 amperes was circulated. The top and bottom HV coils were connected in series opposition with each other and in series with a vacuum-tube voltmeter. Any dissymmetry in the windings was balanced out by the adjustment of the coarse, M_1,

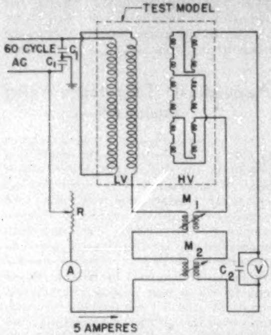

Fig. 15. **Mutual inductance measuring circuit used in checking effect of mechanical shock**

and the fine, M_1, mutual inductances. This permitted operating the voltmeter on a low scale. The mutual inductance before and after shock was then read directly. The apparatus was calibrated by introducing a controlled amount of displacement of one coil with respect to the other and measuring the resulting change in mutual inductance between them. Capacitors were placed across the power supply and across the vacuum-tube voltmeter to reduce disturbances in the measuring circuit.

Appendix IV. Humidity Chamber

The humidity chamber is shown in Fig. 10. It was built from 1/4-inch-thick clear plastic and measured 3 feet square by 2 feet high. It was capable of accommodating four models at one time. Water vapor was blown by fans into the chamber area from below the shelf to provide the humid atmosphere. The amount of water vapor was controlled by means of a wet bulb contact-making thermometer whose temperature difference between make and break was less than 0.01 C. A heat source consisting of two 500-watt lamps located below the shelf warmed the chamber. The temperature was controlled by means of a dry bulb thermometer. Each of the two fans used to recirculate the air between the upper and lower chambers had a capacity of 50 cubic feet per minute.

The humidity was maintained at 90 per cent with a dry bulb temperature of 29.5 C and a wet bulb temperature of 28.4 C. These temperatures were raised to 40.5 C and 39.5 C respectively during the high ambient temperatures accompanying warm weather.

Table VII. Temperature Distribution in Models Aged During Final Tests

Aging Temperature, C	Temperatures, C, for Each Thermocouple Location								
	1	2	3	4	5	6	7	8	9
220	185	197	220	185	185	216	220	209	218
250	211	227	250	210	210	246	250	235	249
280	236	254	280	235	235	275	280	266	277

Appendix V. Temperature Distribution in Model

The temperature distribution in the models undergoing aging was determined by means of monitoring models equipped with thermocouples. One monitoring model was used at each aging temperature. The thermocouples in this model were placed in the windings and on the barrier tubes. These thermocouples were located as shown in Fig. 16, which is a partial section of the model.

Thermocouples 3, 6, 7, and 8 were brazed to the coil conductors. Thermocouples 1, 2, 4, 5, and 9 were brazed to a piece of 1/2 by 1/2 by 0.005-inch copper. Thermocouples 1, 2, 4, and 5 were cemented to the barrier tube surfaces with an epoxy-type adhesive. Thermocouple 9, which was removable, was placed adjacent to thermocouple 7 over the same HV turn. It was wedged in place with a piece of silicone glass insulation. Thermocouples 6 and 8 were in the same radial position as thermocouple 7.

All thermocouples were located in accordance with the specifications of the test code. It had been established experimentally that the HV hottest-spot temperature occurred in the third coil from the top, one-third of the radial coil width from the innermost turn. In the LV winding and in the barrier tubes, the hot spot was found to occur on the level of the centerline between the second and third HV coils from the top.

The temperature distribution in the models aged during the final tests is shown in Table VII for the thermocouple locations in Fig. 16.

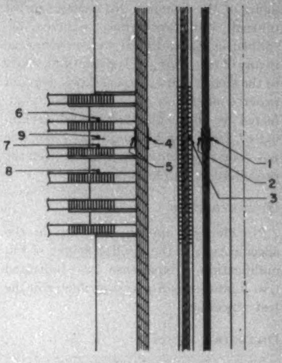

Fig. 16. **Location of thermocouples in model**

1—Inside LV barrier tube
2—Outside LV barrier tube
3—LV winding hottest spot
4—Inside HV barrier tube
5—Outside HV barrier tube
6—Second HV coil hottest spot
7—Third HV coil hottest spot (hottest spot of winding)
8—Fourth HV coil hottest spot
9—Removable thermocouple at hottest spot in third HV coil

References

1. General Principles Upon Which Temperature Limits Are Based in the Rating of Electrical Machinery. *AIEE Standard No. 1*, June 1940.

2. Proposed Test Code for Functional Temperature Endurance Tests of Ventilated Dry-Type Power and Distribution Transformers, **AIEE Committee Report.** *AIEE Transactions*, vol. 74, pt. III, Oct. 1955, pp. 971–77.

3. Temperature Classes for Dry-Type Power Transformers as Determined by Functional Tests, **Paul Narbut.** *Ibid.*, vol. 72, pt. III, Oct. 1953, pp. 917–23.

4. Functional Temperature Endurance Tests on a Silicone Glass Fiber Insulation System for Dry-Type Transformers, **M. L. Manning.** *Ibid.*, vol. 74, pt. III, Apr. 1955, pp. 91–100.

5. The Re-examination of Temperature Standards for Electrical Insulation, **Graham Lee Moses.** *Ibid.*, vol. 71, pt. III, Aug. 1952, pp. 681–85.

6. Aging Characteristics of Dry-Type Transformers at High Temperature, **H. C. Stewart, L. C. Whitman.** *Ibid.*, vol. 67, pt. II, 1948, pp. 1600–07.

7. Electrical Insulation Deterioration Treated as a Chemical Rate Phenomenon, **Thomas W. Dakin.** *Ibid.*, pt. I, pp. 113–22.

8. General Principles Upon Which Temperature Limits Are Based in the Rating of Electric Machines and Apparatus. *AIEE Standard No. 1*, June 1947.

9. General Principles Upon Which Temperature Limits Are Based in the Rating of Electric Machines and Other Equipment. *AIEE Standard No. 1*, Feb. 1954.

10. Test Code for Evaluation of Systems of Insulating Materials for Random-Wound Electric Machinery. *AIEE Standard No. 1C*, Jan. 1954.

11. Standards for Transformers. *NEMA Publication No. TR1-1954*, National Electrical Manufacturers Association, New York, N. Y., May 1954, par. TR1-2.012.

12. Low-Voltage, Air-Cooled Transformers Designed for 225 C Operation, **J. F. Dexter, M. L. Manning, H. P. Walker.** *Electrical World*, New York, N. Y., vol. 130, Aug. 14, 1948, pp. 97–169.

13. Functional Life Tests of Insulation Systems for Dry-Type Transformers, **Paul Narbut.** *AIEE Transactions*, vol. 74, pt. III, 1955 (*Paper 55-449*).

14. Temperature Classification of Insulating Materials, **K. N. Mathes.** *Report DF54SL 103*, General Electric Company, Schenectady, N. Y., June 10, 1954.

15. Symposium on Temperature Stability of Electrical Insulating Materials. *ASTM Special Technical Publication No. 161*, American Society for Testing Materials, Philadelphia, Pa., Aug. 1954.

16. Thermal Evaluation of Insulating Materials. *AIEE Special Publication S-61*, June 1954.

17. Principles for Temperature Classification of Insulating Materials by Functional Test, **K. N. Mathes.** *Ibid.*, pp. 8–11.

Proposed Test Code for Functional Temperature Endurance Tests of Ventilated Dry-Type Power and Distribution Transformers

AIEE COMMITTEE REPORT

FOR many years temperature limits for electric apparatus have been founded upon classification of insulating materials by broad general definitions based upon chemical composition.[1] Recently it has become apparent that this method no longer meets the needs of the industry and that a new approach is needed, based upon functional tests.[2–6]

The latest revision of AIEE Standard No. *1*[1] recognizes this need by the following statement: "The electrical insulation of equipment is made up of many different components, selected to withstand the widely different electrical, mechanical and thermal stresses occurring in different parts of the structure. To assure satisfactory service life, therefore, insulation specifications need to be supported by service experience or life tests, on the complete insulation system. Accelerated life tests are increasingly important as a means of evaluating the many new synthetic insulating materials that are available, thus shortening the period of service experience required before they can be used with confidence. It is desirable that life tests on materials be supplemented by tests on complete insulation system, representative of the different types of equipment. It is contemplated that, in the course of time, Institute Test Codes will be developed, giving procedures for such accelerated life tests, and other methods of evaluating insulating materials and systems."

Accordingly, this test code is intended to establish procedures for evaluating the insulating systems of ventilated dry-type power and distribution transformers. It is expected that codes covering other classes of transformers will be prepared from time to time as the lengthy but necessary study and trials are completed.

During the preparation of this code, members of the subgroup built and tested more than 50 transformer models in accordance with the recommended procedures. The results demonstrated that the procedures are workable, even though there were a few details on which further work will be necessary before final decisions can be made. The code therefore is offered for trial use in order to obtain wider distribution and to encourage discussion, criticism, and trial by others.

The object of this test code is to state a recommended procedure for determining operating temperature limits for ventilated dry-type power and distribution transformers to give a reasonable life expectancy under normal operating conditions. The subjects covered by this test code are: basic considerations, specifications for test samples, and the test procedure.

Basic Considerations

SECTION 1

The test covered by this test code is intended to give a direct evaluation of the composite insulation system of a dry-type transformer, tested as an integral unit.

SECTION 2

It is the intent of this test code to have each component of the composite structure operate and perform during the test under conditions which are as nearly as possible the same as its actual operating conditions in the transformer. Thus, it is intended that each of the components be evaluated in accordance with its actual function.

SECTION 3

The primary aging factors shall be temperature and time.

SECTION 4

Each test shall be carried out simultaneously on a group of a number of identical samples sufficient to give the desired statistical accuracy.

SECTION 5

The life of a sample, aged at one temperature, shall be equal to the duration of temperature exposure during one test cycle, multiplied by the number of cycles to failure, less one-half of one cycle. The life of a group of samples, aged at the same temperature, shall be reported statistically, giving the average life of the group $\bar{X}$, the standard deviation σ, and the number of samples in the group N. The average life and the standard deviation shall be computed using logarithm of life of individual samples.

A failure shall be construed to mean any form of dielectric breakdown of insulation or a dielectric flashover, which may occur on any of the specified electrical tests. The type of failure shall be reported.

SECTION 6

The life of a transformer is reduced when operated continuously at the maximum hot-spot temperature limit. On the basis of experimental evidence and field experience this reduced life will be taken as 4 years.[6,7]

SECTION 7

Tests specified in this test code are of an accelerated nature. Hence, extrapolation of the life obtained at the test temperature is required to obtain the temperature limit for normal life expectancy. This extrapolation may be carried out by one of the three alternate methods. The accuracy of this extrapolation is increased by making one of the test temperatures approach, as close as practical, the permissible operating temperature.

Method 1

This method shall be used when the least amount of information is available regarding the life of the insulating materials involved, or the life-temperature dependence. At least three groups of samples shall be tested at three (or more) different temperatures, differing, preferably, by not less than 10 per cent of the maximum test temperature, and the life for each group shall be determined. The three points, life versus temperature, shall

---

Paper 55-435, recommended by the AIEE Transformers Committee and approved by the AIEE Committee on Technical Operations for presentation at the AIEE Summer General Meeting, Swampscott, Mass., June 27–July 1, 1955. Manuscript submitted March 25, 1955; made available for printing April 6, 1955.

Personnel of the Working Group on Life of Materials: J L. Cantwell, *Chairman*, C. E. Arntzen, F. M. Clark, T. W. Dakin, J. F. Dexter, B. E. Ely, W. E. Harrison, Jr., M. H. Langford, M. L. Manning, J. S. Parkinson, W. W. Satterlee, W. M. Terry, Jr., F. J. Vogel, T. R. Walters, C. P. Xenis, H. G. Zambell, and Paul Narbut.

Acknowledgment and thanks are extended to those who have so freely given their time and knowledge and have conducted experimental work on which this test code is based.

The major work of preparing the code and trying out its procedures was done by the Subgroup on Functional Tests for Dry-Type Transformers of the Working Group on Life of Materials, with personnel as follows: Paul Narbut, *Chairman*, M. L. Manning, T. R. Walters, H. G. Zambell, W. W. Satterlee, and J. L. Cantwell.

be plotted on suitable co-ordinate paper, and the plotted curve extrapolated to determine the temperature to give 4 years of life.

As a co-ordinate paper for this plot it is advantageous to use a special paper with a logarithmic ordinate scale, to represent time (life), and a reciprocal of absolute temperature to represent temperature. The plot of life versus aging temperature on this paper is likely to be a straight line, or nearly so.

Note: This method of extrapolation shall be applied only for failures occurring in the same part of the insulating system. Should failures occur in more than one part of the system, data for each mode of failure shall be treated separately from others to determine the average life at the test temperature. Likewise, the temperature limit shall be determined by extrapolation separately for each mode of failure, and the lowest value obtained shall be used as representing the temperature limit for the complete transformer.

Method 2

This method of extrapolation assumes a certain form of life-temperature dependence, which has been experimentally proved to exist for many practical insulating materials. Hence, compared to method 1, method 2 is more restricted. Where applicable, however, it permits simplification of tests, as it requires only two test temperatures. Two groups of samples shall be tested at two different temperatures differing by not less than 15 per cent of the maximum test temperature, and the life for each group determined.

The two points, time versus temperature, shall be plotted on the special co-ordinate paper described under method 1, and a straight-line extrapolation used to determine the temperature to give 4 years' life. As an alternate method of extrapolation, in place of the co-ordinate paper described, the following equation may be used

$$\theta_1 = \frac{\ln (t_2/t_3)}{\dfrac{\ln (t_1/t_3)}{\theta_2+273} - \dfrac{\ln (t_1/t_2)}{\theta_3+273}} - 273 \qquad \textbf{(7A)}$$

where

θ_1 = temperature limit, degrees centigrade (C), to give life expectancy t_1, as provided in section 6

t_2 = life obtained at test temperature θ_2, in same units as t_1

t_3 = life obtained at test temperature θ_3, in same units as t_1

ln = logarithm to the base ϵ

Note: The note given under method 1 applies also to method 2.

Method 3

This method is applicable when the aging rate factor in the life-temperature dependence for the materials involved is known. In this case only one group of samples need be tested, and their life at one temperature determined.

The preferred equation for extrapolation is

$$\theta_1 = \frac{b}{\ln \dfrac{t_1}{t_2} + \dfrac{b}{273+\theta_2}} - 273 \qquad \textbf{(7B)}$$

where

b = rate factor in the life-temperature dependence of the required properties for the materials involved

For phenolic-base resins, varnishes, and similar materials, a value of constant b = 11,500 may be used with good approximation. Table I is based on this value of b, and on t_1 = 4 years (1,460 days), and may be used as a guide.

This method is the most restricted of the three methods given. Where applicable, however, it serves to simplify the testing procedure since only one test temperature is required.

Table I. Operating Temperatures When Insulation Consists of Phenolic-Base Resins

Aging Temperature, C	Hottest-Spot Operating Temperature Limit, C				
	Accumulated Days of Aging, (Life of the Samples)				
	5	10	20	40	80
188		110	120	130	140
202	110	120	130	140	150
216	120	130	140	150	160
230	130	140	150	160	170
246	140	150	160	170	180
263	150	160	170	180	190

Specifications for Test Samples

Section 10

Test samples must conform to the following requirements:

1. Whenever possible, actual transformers shall be used. For small transformers this may be the simplest, most direct, and least expensive form of samples.
2. For larger transformers the use of test models is permissible.

Section 11

If test models of dry-type transformers are used for test purposes, these shall be constructed in accordance with the following principles:

1. The arrangement of the different components, such as coils, supporting insulating members, spacers, electric barriers, layer insulation, and turn insulation, should be an essential duplicate of the transformer construction. Specifically, the manner of bracing and supporting of the high- and low-voltage coils used in the transformer shall be duplicated in the model.
2. All of the insulating clearances such as air clearances from the windings to grounded parts and to other windings, thickness of insulating spacers, barriers, and layer insulation shall be no greater than in the transformer represented by the model. Smaller clearances shall be permissible, provided they are sufficient to prevent failures due solely to inadequate geometry in the model.
3. The materials used for the various components of the structure of the model shall be identical with those used in the transformer.
4. The electric components shall be so arranged as to permit a dielectric test on the various insulation components, such as major insulation to ground, turn, section, and layer insulation, where such are present.

Section 12

The recommended test model for core-form dry-type transformers, representing a typical 15-kv-class insulation structure, is shown in Fig. 1. Although dimensions are specified in this figure, it should be recognized that these can be modified to represent the regular practices of different manufacturers. The high-voltage coil of this model shall be wound of two parallel conductors to permit dielectric test of turn insulation. The leads from each pair of twin sections are to be brought out separately to permit a section-to-section dielectric test. The low-voltage coil shall be wound of two layers to permit a test of layer insulation.

Test Procedure

Section 20

The test procedure shall consist of subjecting the test samples to a repeated test cycle, consisting of the following parts in the order given:

1. Temperature aging period.
2. Dielectric test, dry, at ambient temperature.
3. Humidification.
4. Dielectric test under humid condition.

Prior to the exposure to an elevated temperature on the first test cycle, dielectric screening tests shall be made on all samples, as indicated in items 2, 3, and 4 of this section. Samples not passing this screening test shall not be included in the statistical evaluation of life.

Section 21

Exposure to the elevated temperature shall be done by means of an electric current circulated in the windings of the test sample.

The test temperature shall be maintained constant at the hottest spot within the sample. The hot-spot temperature of each of the windings shall be the same. At other points within the sample, deviation from this temperature is permissible, although such deviation shall be within limits of the temperature distribution in the actual transformer. For dry-type transformers, such as are represented by the model shown in Fig. 1, the temperature difference between the hot-spot winding temperature and the hot-spot barrier temperature shall not exceed 30 C.

Any suitable method can be used for monitoring of the temperature of the samples during the temperature exposure The following method is recommended:

1. One of the group of test samples shall be equipped with thermocouples, and shall be used for temperature monitoring purposes only. The number and location of the thermocouples shall be such as to give an accurate measurement of the hot-spot temperature and give an adequate knowledge of the temperature distribution within the sample to satisfy the conditions given in the second paragraph of this section.

For the transformer model, Fig. 1, it was established experimentally that the hot-spot winding temperature occurs in the third section from the top, and one-third of the radial section width from the innermost turn. In the low-voltage winding and in the barrier tube, the hot-spot occurs on the level of the centerline between the second and third sections from the top.

2. For heating purposes, corresponding electric elements of all samples (e.g., all of the high-voltage windings, and also all of the low-voltage windings) shall be connected in series, to have the same current circulated in the like elements. Also, the physical arrangement of the samples with respect to each other shall be such as to promote equality of temperature rise in all samples. Equality of the temperature rise in all the samples may be monitored by thermometers located in each, or in several samples, the relative position of the thermometers being the same for all samples.

The hot-spot test temperature, once established, shall be maintained within ±2 C. Temperature difference between individual test samples shall not exceed 2 C. A periodic record of the temperature shall be taken to determine the average temperature during the temperature exposure cycle.

The aging temperature and duration of each temperature cycle shall be so selected as to require 5 to 10 cycles to reach the average time to failure for a group of samples. When several groups of samples are tested at different temperatures, the duration of test cycles for different groups shall be so selected as to require approximately the same number of cycles

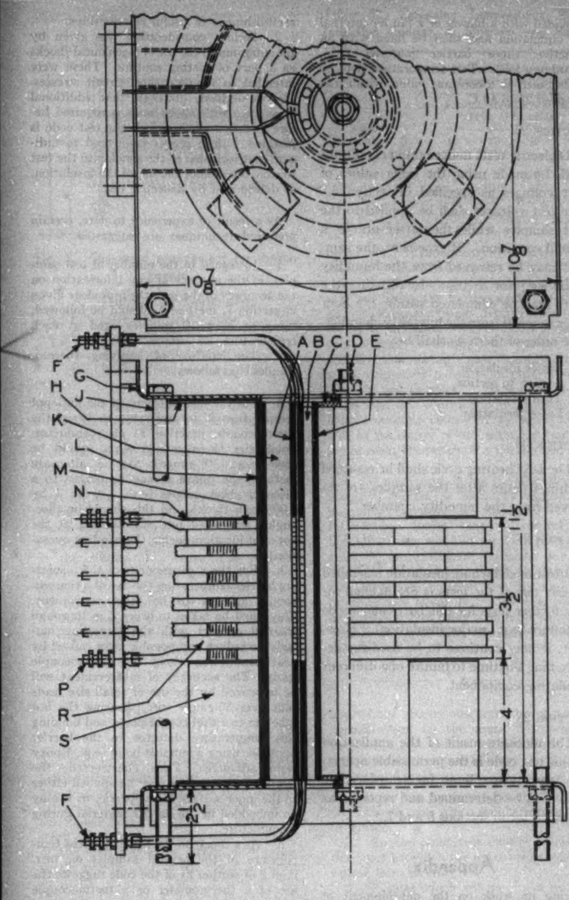

Fig. 1. Functional test model of a typical core-form dry-type transformer, 15-kv class

A. Two-layer low-voltage winding
B. 1/4-inch duct
C. $1^1/_2$-inch-diameter centering washers (2)
D. 5/8-inch-diameter clamping stud
E. 1/8-inch-thick insulating cylinder
F. Terminal connections, low voltage (4)
G. 1/8-inch-thick metal clamping plates (2)
H. 1/8-inch-thick insulation (2)
J. 3/8-inch-diameter clamping studs (4)
K. 5/8-inch duct
L. 1/4-inch-thick insulating cylinder
M. 1/2-inch duct
N. Insulating washers (2)
P. Terminal connections, high voltage (12)
R. 3/8-inch-thick radial spacers (20)
S. High-voltage coil supports, spaced 90 degrees (8)

Table II. Temperature Exposure Schedule

Duration of Temperature Exposure per Cycle, Days	Test Temperature for Operating Temperature Limits of Apparatus Groups 2 and 3 (Reference 8)	
	Group 2 (150 C)	Group 3 (220 C)
2 (48 hours)	246	325
4	230	308
8	216	292
16	202	276

to average failure. The heating-up time of the test samples at the beginning of the temperature cycle shall not exceed 5 hours. The temperature aging cycle shall commence when the required hot-spot temperature is established.

A suggested temperature exposure schedule is given in Table II. The temperature exposure shall be conducted in a room at normal ambient temperature in a relatively draft-free area, and the specimens shall be covered to exclude dirt.

Section 22

Dielectric tests on samples in a dry condition shall be made after allowing the test samples to be cooled off to the ambient room temperature. The allowable cooling time shall not exceed 4 hours.

The dielectric tests shall be equal to the full 100-per-cent standard test values where such are available. For the components for which no standard test is available, the test voltage shall be specified consistent with the industry's current practice, and shall correspond to the full level of insulation requirements.

Thus, for the 15-kv-class test model shown in Fig. 1, the kilovolt values for the dielectric test shall be as follows:

Major insulation from high-voltage winding to ground and to low-voltage winding, 31 kv rms for 1 minute.

High-voltage section to section, 7 kv rms for 1 minute.

High-voltage turn insulation, 0.5 kv rms for 1 minute.

Low-voltage winding layer insulation, 1.2-kv class, 1.2 kv rms per layer insulation for 1 minute.

Section 24

Exposure to high humidity shall be made under the following conditions:

1. Duration of humidity exposure shall be 24 hours.

2. For the humidity exposure the test samples shall be placed in a suitable enclosure in which humidity of approximately 90 per cent shall be maintained. To maintain this humidity, the bottom of the test chamber may be covered with a flat tray containing a saturated solution of ammonium dihydrogen phosphate ($NH_4.H_2PO_4$), or sodium sulfate, with undissolved excess of this salt present. The chamber shall be provided with a blower or a fan for internal air circulation and shall be lined with an effective vapor barrier material (e.g., aluminum foil). Test temperature shall be maintained at a constant value, within the range of 25 to 40 C.

Section 25

Dielectric tests under humid conditions shall be made using the same values of test voltages as specified in section 22. The test voltages shall be applied to the test samples while the latter are in a humid condition. If expedient, the samples may be removed from the humidity chamber prior to test. In this case the tests shall be completed within 1/2 hour after removal from the humidity chamber. The order of the tests shall be:

1. Major insulation.
2. Section to section.
3. Turn insulation.
4. Layer insulation.

Section 26

The next heating cycle shall be resumed within 4 hours after the samples are removed from the humidity chamber.

Section 27

A test model whose insulation has failed on any one of the tests is disqualified for any further tests for this particular mode of failure (e.g., major insulation). However, it may continue to be used for determining the time to failure of a different insulating component.

Section 28

The ultimate result of the application of this test code is the permissible operating temperature limit for transformers. This is to be determined and reported as provided for in sections 5 and 7.

Appendix

During its work on the development of the test code, the subgroup accumulated a considerable amount of experience. Also, it considered certain aspects of test procedure not included in the code. A summary of this information which is thought to be useful in the application of the code and in its further development is given here.

The use of the following test methods was considered and rejected, at least until further data and experience warrant their reconsideration:

1. Measurement of power factor of insulation under dry and humid conditions was considered. As a result of extensive measurements made on test models it was concluded that the present state of knowledge of the behavior of power factor with aging is not sufficient for its use as a criterion of failure of an insulating system. However, it was felt that accumulation of power-factor data is desirable as it may lead to the establishment of useful relationships.

2. Serious consideration was given by the subgroup to the use of mechanical shocks as a part of testing routine. These were intended to simulate short-circuit stresses. It was decided, however, that additional experience with shock tests is required before inclusion of these into the test code is justified. More recent tests tend to indicate that inclusion of the shock into the test routine does affect the life of the insulation, as determined by dielectric tests.

As a result of experience to date, certain preferred techniques are suggested.

1. In regard to the number of test samples, in the absence of any information on the accuracy of the test, the procedure given in section 7, method 1, should be followed, using at least 10 samples aged at each temperature, 30 samples total.

2. The method of applying thermocouples is as follows:

a. For the measurement of the hot-spot temperature it is preferable to braze the thermocouple junction to the conductor. Small size thermocouple wires should be used (e.g., 30 gauge). As an alternate method, the junction may be brazed to a piece of sheet copper (e.g., 1/2 by 1 by 0.005 inch thick), and this should be thoroughly imbedded into the winding at the hot-spot location during the winding operation.

b. For the measurement of the insulating barrier temperature the use of a thermocouple appears to be most convenient. Care must be taken to bring it in thorough thermal contact with the insulating material to reduce any possible error caused by heat conduction along the thermocouple leads. The accuracy of measurement will be improved by the use of small size leads (not over 30-gauge wire), brazing the hot junction to a thin copper plate, and bonding this temperature detector to the barrier material, using a suitable bond (e.g., Epoxy resin adhesive). Thus constructed, the temperature detector may be applied either to the inner surface of the barrier or it may be imbedded in the barrier material during manufacture.

c. As a check on the equality of the temperature of the several samples on test, item 2 of section 21 of the code suggests the use of a thermometer or a thermocouple located in several samples in an identical position. When testing 15-kv models, section 12, it was found that considerable care must be exercised in locating the thermocouple to obtain consistent and accurate results. An arrangement shown in Fig. 2 is suggested as a step in this direction. Copper strap *A* which contains the thermocouple, its dimensions, shape, and the exact location of the thermocouple junction must be carefully duplicated for all the thermocouples used in any one test. The same applies to the shape and size of the glass-fiber tape packing *B* which wedges the assembly between the sections of the model.

3. The second paragraph of section 21 provides for certain requirements in the temperature distribution within the sample. It was found in the tests on the 15-kv models that this requirement is not satisfied if the models are heated by electric current,

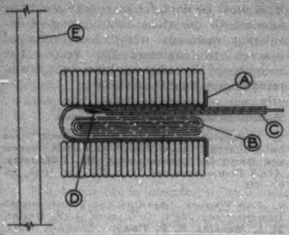

Fig. 2. Suggested arrangement for thermocouple

A. Thin, flexible copper strap
B. Glass-fiber tape packing
C. Thermocouple lead
D. Thermocouple junction
E. High-voltage barrier cylinder

in ambient air. Specifically, under these conditions the required barrier temperature is not attained.

It was found that enclosing the models individually in light aluminum foil enclosures remedies this situation. These aluminum enclosures serve a further purpose of thermally isolating the several models from each other, thus preventing the models at the ends of a row running cooler than those in the middle of a row. The preferred form of such an enclosure is a bell cover, made on a rectangular block form, open at the bottom but closed at the top, and extending down far enough to cover the flange of the bottom end plate. It should be of identical size and shape for all samples under test. It should cover the samples in a reasonably identical manner.

4. For the control of temperature of the samples during the heating cycle the use of an accurate electronic temperature controller is preferred. A reasonably accurate control may be obtained by the use of a sensitive thermostat (e.g., a Fenwall thermostat), heated by a coil connected in series with the test samples. It is to be understood that such control will not be necessary if an accurately controlled voltage is available as the source of the heating power and if the room temperature is maintained constant.

5. It was found during the tests than an accurate control of humidity during the humidity exposure is essential. It was furthermore found that to control the humidity using wet and dry bulb thermometers is quite difficult because, for the humidity specified in the code, the temperature difference between the dry and wet bulbs is only about 1 C. For this reason, humidity control using a suitable salt solution in a vapor-tight enclosure is recommended.

Table III. Operating Temperatures When Insulation Consists of Silicone-Type Resins

	Hottest-Spot Operating Temperature Limit, C			
	Accumulated Days of Aging (Life of Samples)			
Aging Temperature, C	10	20	40	80
278			210	220
293		210	220	230
309	210	220	230	
325	220	230		

Section 7 of the test code gives three methods of determining the permissible operating temperature of the transformers, based on the test data. It is suggested that Table I be used when the insulation consists of phenolic-base resins. It was deemed desirable to formulate a similar table for silicone-type resins. Table III is based on a conservative value of b in equation 7(B), as indicated by the available aging data for silicones.

References

1. General Principles Upon Which Temperature Limits Are Based in the Rating of Electric Machines and Other Equipment. *AIEE Standard No. 1*, Feb. 1954.

2. International Activities on Thermal Evaluation of Insulating Materials, L. J. Berberich. *AIEE Special Publication S-61*, June 1954, pp. 5–8.

3. Principles for Temperature Classification of Insulating Materials by Functional Test, K. N. Mathes. *Ibid.*, pp. 8–11.

4. General Problems Related to the Temperature Classification of Insulating Materials, H. F. Miller. *Ibid.*, pp. 12–13.

5. Temperature Classes for Dry-Type Transformers as Determined by Functional Tests, Paul Narbut. *AIEE Transactions*, vol. 72, pt. III, Oct. 1953, pp. 917–21.

6. The Re-examination of Temperature Standards for Electrical Insulation, Graham Lee Moses. *Ibid.*, vol. 71, pt. III, Aug. 1952, pp. 681–85.

7. Aging Characteristics of Dry-Type Transformer Insulation at High Temperature, H. C. Stewart, L. C. Whitman. *Ibid.*, vol. 67, pt. II, 1948, pp. 1600–07.

8. Standards for Transformers. *NEMA Publication No. TR1–1954*, National Electrical Manufacturers Association, New York, N. Y., May 1954, paragraph TR1–2.012.

◆

Discussion

A. M. Lockie (Westinghouse Electric Corporation, Sharon, Pa.): In evaluating any proposed functional test code, it seems essential that the basic philosophy of the functional test be kept in mind. The word "functional" implies that the results of the tests should be significantly related to the performance of the tested apparatus in actual service. Thus, it appears that functional testing, if it is to live up to its name, should have two objectives:

1. The evaluation of a new structure, to determine its rating or to compare its life expectany with that of service-proved structures.
2. The procurement of data which will permit determining the effect, on the life expectancy of the tested structure, of any anticipated loading; in other words, development of the basis of a guide for loading the apparatus.

These objectives are not incompatible, in that one series of tests, if properly dedesigned, will attain both. Indeed, the basic concept of functional testing requires that this should be the case.

The importance of the first objective is quite generally recognized. There is, however, evidence that in some cases the second may have been obscured by intensive concentration on the first. The requirements of a test code which will attain both objectives are noted as follows:

1. An aging procedure which incorporates, to the maximum practical extent, all of the stresses which will be encountered in service.
2. An end-point test closely related to the point at which the apparatus should be retired from service.
3. Results which will permit a realistic estimate of the effect on the life expectancy of any anticipated loading.

It is encouraging to note that the proposed code for dry-type power and distribution transformers meets these requirements quite well in its present form. There are some points which may require further examination, if the second objective is to be fully attained. For example, some form of mechanical shock to simulate the effect of fault currents would seem desirable. There is also evidence that some of the end-point test voltages were selected to ensure the obtaining of failures in a reasonable time, rather than to indicate unfitness for further service. The Appendix to the code, however, indicates that the working group is aware of these points and intends to study them further.

It appears that the working group has done an admirable job in developing a code which should lead to the attainment of both objectives of functional testing. It may well serve as a guide in the development of codes for other types of apparatus.

Graham Lee Moses (Westinghouse Electric Corporation, East Pittsburgh, Pa.): The Committee is to be congratulated on an excellent beginning in the creation of a test code for functionally evaluating dry-type transformers. The approach is realistic and rational. The thinking of this group parallels work now in progress in the Insulation Subcommittee and working groups of the Rotating Machinery Committee. The following comments are offered on the basis of our experience concerning points of differences as well as similarities.

An important stand has been taken on transformer insulation life as determined by these accelerated tests. Section 6 states: "It is to be realized that the life of a transformer is reduced when operated continuously at the maximum hot-spot temperature limit. On the basis of experimental evidence and held experience, this reduced life will be taken as 4 years." It appears from the subsequent text that this is a median or mean value. Perhaps it would be well to make this clear. Some specification of variability or confidence limits of the data would be appropriate.

The proposed test code offers three methods of interpreting and extrapolating data. Method 1 conforms quite closely to the method used by many investigators working with the life of insulation systems for electric machinery and approaches a preferred standard.

The description and limitations placed on test models in section 11 is handled well and makes clear that the models must have all of the essential insulation characteristics including space, clearances, and creepage distances, as well as insulation system and components.

The exposure of the windings to elevated temperatures by self-heating with electric current is, of course, desirable but has been found difficult to control in electric machinery models. We have found it difficult to reproduce the proper and consistent relations between hot-spot temperature and temperature of the various other components of the insulation system. The test code specifies very close control of the hot-spot test temperature within ±2 C, which appears to be a most difficult task. Certainly it is one which we are not ready to undertake on electric machinery models heated by current.

One of the most difficult and controversial problems has been the establishment of the end point of life criteria, especially where associated with dielectric overvoltage tests. It is interesting to note that the recommendations in the transformer test code are to use the full dielectric test value for a new winding on the major insulation. Thinking on rotating machinery overvoltage tests has been quite different, as some of the voltages now being used are only 20 per cent over the operating voltage.

Another difference between the proposed transformer test code and the rotating machinery test code now under consideration involves humidification. The transformer test code specifies 24 hours' humidification at 90 per cent relative humidity, whereas humidification on rotating machine insulation system is done at 100 per cent relative humidity with free moisture condensing on the insulation surfaces.

In the Appendix it is stated that insulation power factor has been considered as a criterion of failure of insulation, but is not being used because the knowledge of its behavior is not adequate. Our experience in aging insulation systems for rotating machinery has confirmed this and leads to the conclusion that the power factor between insulation systems is not significant especially with respect to dielectric strength. Changes in power factor of a single system may be of interest, if they can be interpreted in terms of physical changes; but the absolute power factor of insulation is of no great significance.

It is gratifying to observe the great strides that are being made in many divisions of the AIEE in working towards uniform methods of functional evaluation. Certainly the contributions of the AIEE committee on transformers are worthwhile and highly commendable.

M. L. Manning (Pennsylvania Transformer Company, Canonsburg, Pa.): Experience in presenting a paper on functional testing dealing with group 3 (220 C hottest spot permissible temperature) silicone-insulated dry-type transformers[1] indicates that additional background information about high-temperature materials and additional tests on models are desired.

Usage of high-temperature materials is becoming more complicated each day because of the influx of bonding resins having different curing temperatures. In striving to establish the validity of requirements that must be met by a test code, it is important to remember that one must remain practical in evaluating an insulation system. If application conditions dictate that 220 C continuous-temperature insulating materials in a transformer are required, similar materials should be evaluated in a test model at aging temperatures prescribed by the test code. Of importance in high-temperature materials, heat-cleaned glass fiber base material and high-temperature withstanding silicone resins and rubbers give better performance. Unless oil and sizing are removed from glass fibers, insufficient bond strength of the resin to the fibers exists and delamination will occur at high temperatures. This is highly important in an aging program in establishing failure points of a model.

Within the last decade, new groups of silicone materials have emerged from the laboratories. As with most bonding and impregnating resins, different formulations have been developed. Some resins have intermediate temperature-withstanding properties. Silicone impregnating resins having cure temperatures of approximately 150 C have been developed. Class *B* (phenolic resin-bonded glass fiber materials, for example) systems have been impregnated in this low-cure silicone resin varnish. Such insulation systems have different properties from those composed of heat-cleaned glass fiber high-temperature silicone resin-bonded materials. Hence, aging or failure points and toxicity differ.

Only the premium materials have been considered in all papers presented by the author.[2,3] Aging tests on such an insulation system as described in these papers help to establish background information for group 3 transformers.

In reviewing the temperature exposure schedule for group 3 transformers appearing in the eighth paragraph of section 21 of the test code, it is helpful to outline how the aging temperatures proposed originated. Aging tests on basic high-quality silicone resin and rubber-bonded heat-cleaned glass-fiber and asbestos materials indicate that after severe humidity and thermal cycling, failure may be expected near 325 C. These data may be found in the literature and by test experience. Also, substantiating data in models indicated that with reduced creepage distances over those used in transformers, flashover, not puncture, occurred on the barrier insulation after humidification at 350 C aging temperature of windings (325 C temperature of barrier insulation).[1]

At present, additional models having increased creepage distance to ground are being aged at 350 C to reach failure points by puncture. A subsequent paper will outline results.

Functional testing is gaining momentum in acceptance. But again we must emphasize the importance of co-operation by users and manufacturers of transformers. This must be done for success in obtaining answers to questions about aging of insulating materials which have been of concern to engineers for years. The members of the subgroup have kept this in mind in preparing the test code.

REFERENCES

1. FUNCTIONAL TEMPERATURE ENDURANCE TESTS ON A SILICONE GLASS FIBER INSULATION SYSTEM FOR DRY-TYPE TRANSFORMERS, **M. L. Manning.** *AIEE Transactions*, vol. 74, p. III, Apr. 1955, pp. 91–100.

2. LOW-VOLTAGE, AIR-COOLED TRANSFORMERS DESIGNED FOR 225°C OPERATION, **J. F. Dexter, M. L. Manning, H. P. Walker.** *Electrical World*, New York, N.Y., Aug. 14, 1948.

3. THE APPLICATION OF CLASS H-INSULATION TO TRANSFORMERS. **Melvin L. Manning.** *AIEE Transactions*, vol. 70, pt. II, 1951, pp. 1427–38.

J. L. Cantwell: The discussions are appreciated, and their suggestions will be given full consideration by the working group before publication of the code in final form.

It should be clearly understood that the writer, in discussing the comments, is not speaking for the working group but is expressing his own opinions.

Mr. Lockie is to be complimented on his clear statement of the two objectives which any functional test code should have. It is true that the second objective may in some cases be obscured by intensive concentration on the first. Nevertheless, it is believed that data obtained by the procedures of this code could be used for the attainment of both objectives.

Mr. Moses calls attention to the points of difference and similarity in comparison with the codes being prepared by the Rotating Machinery Committee.

The code includes three alternate methods of extrapolation. The intent is to permit a progressive simplification of the tests as more and more data are accumulated on a particular class of systems. It is hoped that the requirements of the code may eventually be reduced to method 3 alone; i.e., a system may be considered to have met the requirements if it withstands a specified number of cycles at one specified elevated temperature, based on the desired operating temperature. This, however, will require more knowledge than we have now.

It is true that the proper control of temperatures is perhaps the most difficult part of the recommended procedures. However, self-heating by electric current was considered the only suitable method for reproducing the substantial temperature differentials which are characteristic of these systems in service. Heating to a uniform temperature in an oven would be much simpler but could not be considered a functional test of such systems. On the other hand, oven heating is entirely adequate for the "motorette" tests of AIEE Standard No. 1C[1] as the rotating-machine systems which they represent have relatively minor temperature differentials. Further experience is needed to determine whether the proposed tolerances on temperature are realistic.

Differences in dielectric overvoltage tests and in humidity exposure are to be expected in codes for different types of apparatus, considering the fact that the test conditions are supposed to represent as nearly as possible the actual operating conditions, but on an accelerated basis. Under usual operating conditions, transformers are expected to withstand considerably more severe overvoltages than are rotating machines. On the other hand, rotating machines, small motors in particular, may often be installed and operated in damp locations which would be entirely unsuitable for ventilated transformers. These differences are, and should be, recognized in the two codes.

The 4-year life is intended to be a mean value. I agree that this should be made clear and that the inclusion of a specification on confidence limits would be desirable. It expected that this will be done before final publication.

Mr. Manning's paper, reference 1 of his discussion was omitted from one list of references in the code only because the list was limited to those considered necessary to document certain statements at the start of the paper and in section 6. The list is in no sense a complete bibliography of the subject.

The background information given by Mr. Manning on the behavior of various high-temperature insulations is interesting. I agree that additional information and further tests on models are desirable and am pleased to learn that Mr. Manning is continuing his efforts along those lines.

This code is the product of a considerable expenditure of time and effort by members of the working group and their associates. It is to be hoped therefore that others will study it, criticize it, and above all, use it, and also that data obtained by others will be made available to the working group so that the code may be revised where necessary to increase its usefulness to the industry.

REFERENCE

1. TEST CODE FOR THE EVALUATION OF SYSTEMS OF INSULATING MATERIALS FOR RANDOM-WOUND ELECTRIC MACHINERY. *AIEE Standard No. 1C*, Jan. 1954.

Functional-Life Expectancy Tests for Liquid-Filled Distribution Transformers

A. M. LOCKIE
MEMBER AIEE

Synopsis: The objectives of this paper are twofold: first, to show the need for functional life-test procedures for distribution transformers, which will permit determination of the relative life expectancy of different designs on a given load cycle and of one design on various load cycles; and second, to propose test and analytical procedures which appear to fulfill this need.

Life Expectancy and Functional Testing

SINCE transformers constitute a major portion of the capital equipment of most utilities, it is desirable that they be utilized to the maximum extent consistent with adequate service life.[1] While the cost of losses and restrictions on voltage regulation will sometimes limit loading of transformers, there are many instances where this is not the case. Furthermore, in investigating the economics of both design and application of transformers it is necessary to determine the extent to which loading could be increased if these limitations were removed.

Probably the best-known and most widely used information concerning the relationship of life expectancy and loading is that contained in the "Guide for Loading."[2] This document has been valuable in stimulating more economic utilization of transformers, but is limited in usefulness in several ways:

1. The underlying aging data are based on the effect of temperature on the tensile strength of cellulose in oil. Consequently they have limited significance for structures containing other materials. Furthermore, there is now some evidence that tensile strength is not an adequate measure of insulation quality in all applications.

2. It is assumed that a given amount of temperature exposure has the same effect on the life expectancy of all transformers. This makes no allowance for the skill of the manufacturer in using materials or in designing for minimum stresses in the insulation.

3. The arbitrarily selected end point of life [approximately 80 per cent (%) of the initial tensile strength] has no correlation with the ability of the transformer to continue in service.

Thus the present Guide for Loading does not provide means for evaluating the relative life expectancy of various insulation structures, nor is it easy to interpret in terms of the probable actual life in service of a given structure. Furthermore, both field experience and laboratory tests on complete transformers suggest that the indicated life expectancies are unduly conservative, at least in respect to distribution transformers.[3] These conditions indicate the need for an improved method of evaluating life expectancy. Before attempting to develop such a method, however, it will be helpful to review the factors which determine life.

FACTORS AFFECTING LIFE EXPECTANCY

Not all of the factors affecting life expectancy are known, nor are all of the mechanisms of failure clearly understood. In general, however, the following will be significant:

1. Materials used. Of predominant importance are the initial thermal, electrical, and mechanical properties of the various materials. It should be noted, however, that the relative importance of these properties depends on the function performed by the particular material.[4] Furthermore, various materials lose their initial properties at different rates, and the same material may lose various properties at different rates, during the aging process.[5]

2. Design stresses. These may be thermal, electrical, or mechanical in nature. Their relative importance will be determined not only by the nature and amount of material used but also by the skill of the designer in keeping stresses to a minimum commensurate with economical use of the materials.

3. Duty. This includes not only the normal load cycle on the apparatus but also such environmental factors as ambient temperature and exposure to abnormal currents and voltages.

4. Permissible deterioration. Deterioration to complete destruction of the apparatus will seldom be acceptable. The degree which can be tolerated will be determined largely by safety and service-continuity requirements and by the probability of incidence of abnormal operating conditions.

It seems probable that the best means of evaluating all of these factors is by the process which has come to be known as functional testing. Essentially, functional testing involves operating complete structures or models, under accelerated aging conditions which are more or less representative of actual service, until failure occurs on an end-point test which is presumed to indicate unfitness for further service. This form of testing does permit comparison of the life expectancy of various structures and may also permit a forecast of the service life expectancy of a given structure.

Paper 55-520, recommended by the AIEE Transformers Committee and approved by the AIEE Committee on Technical Operations for presentation at the AIEE Summer General Meeting, Swampscott, Mass., June 27–July 1, 1955. Manuscript submitted March 29, 1955; made available for printing May 11, 1955.

A. M. LOCKIE is with the Westinghouse Electric Corporation, Sharon, Pa.

REQUIREMENTS OF A FUNCTIONAL LIFE-EXPECTANCY TEST

The ideal test would consist of exposing a large number of full-scale samples of the design in question to the expected service in the field until failure occurs. This procedure would be prohibitively expensive, and so time-consuming that the results would be of little practical use when the tests were finally complete. Consequently, practical considerations dictate a certain sacrifice in accuracy by the use of a relatively small number of samples and a duty cycle sufficiently severe to insure deterioration to a selected level in a reasonably short length of time. In order to be significant, however, the test should evaluate the materials involved as they are used in the design in question. The duty cycle, although intensified to accelerate deterioration, should otherwise reproduce conditions likely to be encountered in normal service, and bear some definite relation to name-plate rating. The selected end point of deterioration should indicate the probability that the design could continue in normal service but would fail under moderate abnormal conditions. Finally, the procedure should be such that, by varying a readily measurable parameter, data may be obtained which will make it possible to interpret the results obtained by test, in terms of load cycles which may be encountered in the field.

The following proposals appear to meet these requirements reasonably well. It is expected that there will be differences of opinion regarding details, and the proposals are not made with the intent of formulating a test code. Rather, they are presented as a point of departure for discussion, out of which an acceptable code may evolve.

Basic Life-Expectancy Test

1. END-POINT TEST

1.0 A transformer shall be considered to have reached the nominal end point of its service life when it fails to withstand the following tests:

a. Short circuit at 15 times rated current for 2 seconds.

b. Impulse test per Table 11.030 of reference 6.

c. Dielectric and induced potential tests per reference 6, modified to have voltages reduced to 65% of those specified, as recommended in paragraph 22.140 of reference 7 for periodic field tests.

1.1 These tests shall be made in the sequence listed in 1.0. Failure to withstand any of these tests shall render it unnecessary to perform the remaining tests.

1.2 Transformers equipped with integral protective devices shall be tested with these devices as normally installed and calibrated, which may limit the magnitude or duration of the test currents or voltages.

2. AGING CYCLE

2.0 For accelerated aging, the daily loading shall be (at 30 degrees centigrade ambient):

a. 300% of name-plate kilovolt-amperes for 1 hour, followed by

b. 150% of name-plate kilovolt-amperes for 6 hours, followed by

c. no load for 17 hours.

During the entire cycle, the test units shall be excited at approximately rated voltage.

2.1 The loading specified in 2.0 shall be repeated for 4 consecutive days. On the following day, the loading shall be 300% for 1 hour, followed by 150% for 3 hours, followed by the end-point test of section 1. This 5-day loading shall constitute 1 aging cycle.

2.2 If the ambient temperature differs from 30 degrees centigrade by more than ±2 degrees centigrade, the loading specified in 2.0 and 2.1 shall be increased or decreased as specified in paragraph 32.015 of reference 2.

2.3 In transformers with integral overload protection, the protective device shall be recalibrated or inactivated, if necessary, to permit loading as specified in 2.0 and 2.1.

2.4 The aging cycle shall be repeated until failure occurs on the end-point test of section 1.

3. NORMAL LIFE EXPECTANCY

3.1 To obtain the maximum benefit from such tests, it would be desirable to set a minimum number of aging cycles which a given structure must endure before failing to withstand the end-point test of 1.0 in order to be classified as having "normal" life expectancy. Because of the meager information presently relating accelerated life tests of apparatus with actual service life, it is not practical to set such a limit at this time. Nevertheless, tests made in accordance with this procedure, on structures which have given satisfactory service in the field, will provide a bench mark for the evaluation of new structures. It will then be reasonable to predict that a new structure which endures an equal or greater number of aging cycles will have at least an equal life expectancy as the service-proven structure. After the accumulation of sufficient experience with such testing, the minimum number of aging cycles which must be endured to insure satisfactory life expectancy can be determined.

4. NATURE AND NUMBER OF TEST SPECIMENS

4.1 Since it is the purpose of these tests to evaluate the probable endurance of the tested structures in the field, the samples shall be complete structures, and shall be subjected to normal manufacturing processes in so far as is practical.

4.2 Because the tests involve complete apparatus, and a major portion of each specimen will be destroyed in the course of the tests, the number of specimens should be the minimum required to give significant results. Specifically, no less than four samples of a given structure shall be tested, and the endurance claimed for the tested structure shall be that of the unit which first fails to withstand the end-point tests.

5. TYPE TESTING

5.1 When two structures are so nearly alike that the difference may reasonably be expected to have no significant effect on their relative life expectancy, no useful purpose would be served by testing both. Consequently, the tests specified in this paper shall be considered as "type" tests, in that one set of tests shall suffice for a number of designs which are, in so far as life expectancy is concerned, duplicates. Specifically, for a given construction, i.e., coil grouping, electric connection, insulation system (including treatment, if any) and method of coil bracing, it shall not be necessary to test any structure if tests have been made on a unit of the same construction with equal or greater thermal, electrical, and mechanical stresses.

5.2 A manufacturer of a number of different ratings of the same construction, as defined in 5.1, may elect to determine a minimum life expectancy for the different ratings by building and testing sample transformers of this construction, in which the thermal, electrical, and mechanical stresses equal or exceed those in any of the different ratings.

COMMENTS

This procedure was established to comply, as far as seems practical, with the requirements set forth in the preceding section. It is recognized that other load cycles than that specified may prove to be satisfactory. In particular, it may be that it is impractical to specify the same initial load for distribution transformers of all sizes. These, however, are typical of the details which must be agreed upon by the appropriate standardizing bodies in the event that these principles become the basis of a standard procedure.

The selection of a degree of deterioration as the end point of useful life is of necessity, somewhat arbitrary. It is recognized that a level which would be realistic for one application would not necessarily be so for another. It might be argued that the end point of life on a given load cycle should be the point at which the tested structure is no longer capable of sustaining that cycle. This might be logical for an application in which the transformer is never subjected to short-circuit stresses or to overvoltage from lightning or switching. Ordinarily, however, a transformer will be exposed to such abnormal conditions on occasion. Hence, it seems reasonable to incorporate some abnormal currents and voltages in the life-expectancy test and to consider failure to withstand them as the end point of useful life. Limitation of such abnormal currents and voltages by integral protective devices seems logical in that those devices presumably will be present and effective in the field.

It should be noted that there is no mention of winding temperatures in the procedure. Probably the present form of temperature rating must be retained until such time as suitable "normal" life expectancies, as mentioned in 3.1, are established. Subsequently, however, manufacturers should be free to select the most economical combination of temperatures and materials to insure the specified life expectancy, has been suggested by other writers.[8]

Aging-Rate Curves

Tests made on a given structure in accordance with the procedure just described give a measure of its life expectancy on the particular load cycle used in those tests. Comparison of the results of such tests on two different structures will also give some indication as to which of the two will have greater life expectancy on other load cycles. They will not, however, provide data for computing the life expectancy of the tested structure on other load cycles. This problem would be greatly simplified if there were some definite relationship between load and rate of aging. Unfortunately, such a relationship does not exist except for steady-state loads. Hence, in comparing the aging produced by different load cycles, it is necessary to consider the corresponding temperature cycles.

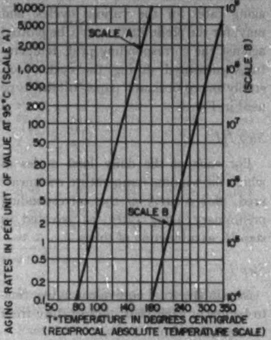

Fig. 1. Aging rates based on reduction in tensile strength of manila paper in oil

This is most conveniently done by means of "aging-rate" curves. An example of a sample calculation of an aging-rate curve is given in Appendix I. Aging-rate curves show, as a function of temperature, the speed with which the insulation reaches the selected end point of its life, relative to this speed at some reference temperature. For example, Fig. 1 shows that the tensile strength of manila paper in oil reaches any selected degree of deterioration 200 times as fast at 140 degrees centigrade as it does at 95 degrees centigrade, the reference temperature for that curve.[8]

Thus, as a preliminary to determining the life expectancy of a given insulation structure on a particular load cycle, an aging-rate curve must be established for the structure. Before setting forth a procedure for doing this, however, it is in order to review the relationship of load, temperature, and life.

RELATIONSHIP OF TEMPERATURE AND LIFE

In modern transformers, the most significant deterioration resulting from use is the progressive impairment of the mechanical and electrical properties of the insulation structure. As indicated earlier, the factors which affect this impairment are numerous, and vary in different structures. For a given structure, however, certain premises may be stated on which the subsequent procedures are based:

1. Deterioration of the electrical and mechanical properties of insulation is the result of irreversible chemical reactions.[9]

2. The velocity of these reactions, here termed the aging rate, is a function of temperature.

3. In consequence of 1 and 2, the total deterioration, here referred to as aging, is a function of temperature and time of exposure.

4. Failure occurs when some property of some particular part of the structure, here called the weakest spot, deteriorates to a level such that it can no longer support the applied electrical or mechanical stresses.

RELATIONSHIP OF TEMPERATURE AND LOAD

It is customary to base aging calculations on the temperature of the hottest spot. Actually, however, the temperature which directly affects life expectancy is that of the weakest spot, as defined in the foregoing. If the insulation structure were composed entirely of the same material and, further, if the stresses at all points were identical, then failure most probably would occur at the hottest spot in the windings. Since neither of these conditions is likely to occur in practice, it is quite possible, that failure may occur at some other point, whose temperature will be difficult, if not impossible, to measure or to calculate. In such cases, it will be impractical to establish a direct relationship between the actual temperature at the weakest spot and the load which produces it, and it will be necessary to resort to an indirect relationship.

The average copper temperature corresponding to any load and ambient temperature may be measured or calculated much more readily than may the hottest-spot temperature, and for that reason would be preferable to use as a measure of aging rates if its use did not result in significant error. Whether or not such will be the case in evaluating a given design will depend on whether the temperature at the weakest spot is closer to hottest spot or to average temperature, and also on the magnitude and rapidity of the load changes during the loading cycle. Probably, for the present, hottest-spot temperatures should be used, but the possibility of using average copper temperatures in the future should be given serious consideration where experiment shows that the weakest spot is remote from the hottest spot.

DETERMINATION OF AGING RATES

The following steps outline a procedure for obtaining the relative aging rates of an insulation structure as a function of the equivalent steady-state temperature producing the aging. It is applicable regardless of whether hottest-spot or average temperatures are used, with appropriate differences in wording. In order to accelerate the aging to a practical extent, high copper temperatures are required. For liquid-immersed apparatus, however, it is not practical to maintain such temperatures continuously, because the resulting liquid temperatures would become dangerously high. Consequently, it is necessary to resort to cyclic loading, as was done in the basic life-expectancy test.

Step I

For each point on the curve, test one or more samples of the structure to failure, following the procedure outlined in the basic life-expectancy test except using an appropriate value of load for the initial hour of the daily load cycle. One of the selected values of initial load should be that prescribed in the basic life-expectancy test. (It is suggested that a total of at least eight samples be used, and that of these two be tested at 250% initial load, two at 275%, two at 300%, and two at 325%.) The copper temperature should be measured or computed throughout at least 1 daily cycle for each different initial load.

Step II

Select a preliminary aging-rate curve which may be expected to be a rough approximation of the curve to be determined. This might be a curve which was previously established for a similar structure, or one obtained by testing the effect of aging on one of the major components of the insulating system (as, e.g., the curve shown in Fig. 1). If none of these appears to be appropriate, a preliminary curve may be obtained by computing the reciprocal of the ratio of the measured life expectancy, on each load cycle used in these tests, to the life expectancy found on the basic life-expectancy test cycle. These reciprocal ratios are the relative aging rates for the various cycles, and may, for the preliminary curve, be plotted against the corresponding peak temperatures measured during the cycle, preferably on co-ordinate paper of the type used in Fig. 1.

Step III

For each of the daily load cycles in which the winding temperature was measured, plot a curve of the corresponding preliminary aging rates, as selected in step II, as a function of time.

Step IV

Obtain the total equivalent aging time to failure at each peak temperature from the equation

$$t_e = \frac{AN}{a_p}$$

where

A = area under the curve of aging rates for the load cycle producing a particular peak temperature

N = number of such cycles to failure

a_p = aging rate corresponding to the peak temperature

The origin of this equation was given in an earlier paper.[3] Note that the product AN is the total aging to failure. When the final aging-rate curve has been established, this product should be the same for each load cycle used in the tests. This criterion is useful in showing the degree of accuracy of the curve-plotting and calculations.

Step V

Compute the reciprocal of the ratio of the total equivalent aging time to failure, for each different load cycle, to the total equivalent time to failure on the basic life-test cycle. This will give a new approximation of the effective aging rate for the cycle, and may be plotted against the corresponding values of peak temperature to obtain a new approximation of the aging-rate curve for the structure. Whether it is an accurate approximation will depend largely on the reliability of the underlying test data and the accuracy of the curve-plotting and reading used in the computations. It would be desirable to repeat steps III, IV, and V, using, instead of the preliminary aging rates, those obtained in step V. This will furnish data for still another aging-rate curve. The closeness with which this curve reproduces the preceding approximation will indicate whether further approximations are desirable.

CONVERSION TO ANOTHER REFERENCE TEMPERATURE

Steps I through V result in a curve such that the aging rate is unity at the peak temperature on the basic life-expectancy cycle. This temperature has no particular significance, and there may be occasions when it is desirable to have an aging-rate curve based on some other reference temperature. This may be obtained by dividing the rates, on the existing curve, by the rate, on the existing curve, corresponding to the new reference temperature, as shown in Appendix II.

COMMENTS

The recommended cyclic loading will be more severe than steady-state operation, since it introduces strains due to expansion and contraction, but is, in that respect, more representative of operation in the field. The peak temperatures existing for short times during the cyclic loading may affect the time to failure by introducing failure mechanisms which would not occur at lower temperatures. Any inaccuracy introduced thereby should be conservative, however, and is a hazard common to all accelerated-aging tests.

The suggested method of successive approximation may seem laborious, but no alternative technique is apparent. It is probable that, in view of the other uncertainties inherent in all aging tests and calculations, only one approximation of the curve is justifiable. It may be desirable to compute one or two points on the second approximation curve, to indicate the amount of change which would result by further approximation.

The minimum number of samples specified may lead to statistically inaccurate

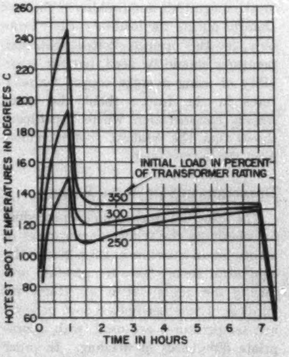

Fig. 2. Hottest-spot temperatures in typical transformer on aging-rate tests. Ambient temperature 20 degrees centigrade

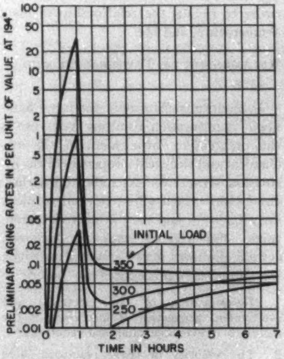

Fig. 3. Preliminary aging rates corresponding to temperatures shown in Fig. 2

Table I. Sample Determination of Aging-Rate Curve

Initial Load, % of Rating	350	325	300	275	250
Peak hottest-spot temperature (Fig. 2*), degrees centigrade	245	218	194	172	151
Aging cycles to failure (assumed)	2	16	80	500	2,000
Load cycles to failure = N	10	80	400	2500	10,000
Preliminary aging rates	40	5	1	0.16	0.04
Area under preliminary aging-rate curve (Fig. 3*) = A	7.56	1.31	0.254	0.065	0.0264
Total aging to failure = AN = equivalent time at 194 degrees	75.6	101	111	162	260
Preliminary rate at peak temperature = a_p	34	5.6	1	0.175	0.032
Equivalent time at peak temperature = $t_e = AN/a_p$	2.22	18.0	111	925	8,100
First approximation of aging rate at peak temperature (t_e on 300% cycle, divided by t_e on given cycle)	50	6.1	1	0.12	0.014
New A, from curves of approximation rates, like those of Fig. 3	8.02	1.07	0.201	0.032	0.0078
New AN	80	87	80	78	76
New a_p (from first approximation curve on Fig. 4)	50	6.2	0.95	0.125	0.016
New t_e	1.78	14.1	84	625	4,760
Second approximation of aging rate	47.2	5.95	1	0.134	0.018

* In Figs. 2 and 3, curves for 275 and 325% load are omitted for clarity.

results and render extrapolation of the curve beyond the range of the test data unreliable. Whether or not additional samples are desirable may be judged by the spread of points at the same temperature and the smoothness of the final curve.

Solution of Loading Problems

Having determined the basic life-expectancy and the aging-rate curve for a given structure, solution of the various loading problems becomes quite easy. A few examples will serve to indicate the general procedures:

Case I

To determine the life expectancy on any given load cycle:

1. Plot a curve of the copper temperatures developed by the given load cycle as a function of time. These temperatures may be calculated from the thermal characteristics of the structure in question.[10] They are preferably obtained by measurements made under load, after repeating the load cycle a sufficient number of times so that the temperature variation on successive cycles is duplicated.

2. Plot the aging rates at these temperatures as a function of time.

3. Determine the area under this aging-rate-time curve and divide by the time of the load cycle to obtain the equivalent (average) aging rate for the cycle.

4. In similar fashion, determine the equivalent aging rate of the basic life-expectancy cycle.

5. Multiply the life expectancy of the structure, on the load cycle used in the basic life-expectancy test, by the ratio of the equivalent aging rate obtained in item 4 to that obtained in item 3. The result will be the life expectancy of this structure on the new load cycle.

Case II

To determine the steady load which will produce the same aging as a given cycle in the same elapsed time:

1. Determine the equivalent aging rate for the given cycle, as in case I.

2. From the aging-rate curve, obtain the equivalent steady temperature.

3. Find the steady load which will produce this temperature.

Case III

To determine the duration of a specific steady load equivalent to a given load cycle:

1. Same as for case II.

2. From the aging-rate curve, obtain the aging rate at the temperature corresponding to continuous operation at the specified load.

3. Multiply the duration of the cyclic loading by the ratio of the aging rate at the cyclic load to the aging rate at the continuous load.

Case IV

To determine the cumulative aging effect of a number of different load cycles:

1. Select a reference continuous loading (preferably one resulting in a temperature within the range shown in the aging-rate curve).

2. Following the procedure of case III, determine the duration of the reference loading equivalent to each of the given load cycles.

3. Add the resulting durations to obtain the cumulative effect.

Summary

Heavier loading of distribution transformers offers substantial operating economies, but it seems unwise to increase loading substantially without a realistic appraisal of its probable effect on life expectancy. Similarly, the development of new insulating systems offers substantial potential economies, but the extent of these economies cannot be learned until the relative life expectancy of the new systems, as incorporated in the complete apparatus, is determined.

These and similar problems appear to require a standard method of rating the apparatus in terms of life expectancy, and also a means of interpreting this rating in terms of anticipated load cycles in the field. Standardized procedures along the line of those suggested here seem to offer practical means of attaining both objectives.

Appendix I. Sample Calculations of Aging-Rate Curve

The following numerical example may help to clarify the proposed procedure for obtaining an aging-rate curve. It is assumed that the transformer tested has the thermal characteristics used in the illustrative examples of Appendixes I and II of reference 2. Since the time constant for the hottest-spot rise over top-oil temperature is not given there, it is assumed here to have an average value of $7^1/_2$ minutes for the load range involved. It is further assumed that tests have been made as described in the main text, at 350%, 325%, 300%, 275%, and 250% of rating, developing the hottest-spot temperatures shown in Fig. 2, and resulting in failure on the proposed end-point test after 2, 16, 80, 500, and 2,000 aging cycles respectively.

The calculations and results are summarized in Table I. The "preliminary aging rates" were obtained by the last method mentioned in the text, namely, by dividing the number of cycles to failure, with 300% initial load, by the number of cycles to failure at each initial load, and plotting the resulting ratios as a function of the corresponding peak temperatures. For example, the rate at 350% initial load is 400/10 = 40, as is plotted at 245 degrees centigrade, in Fig. 4.

As might be expected, the points do not fall on a straight line. The exact shape of the curve drawn through them is not extremely important, however, as the subsequent operations will rectify errors in drawing it. The first approximation aging rates fall on a fairly straight line, as shown in Fig. 4. The second approximations do not differ greatly from the first,

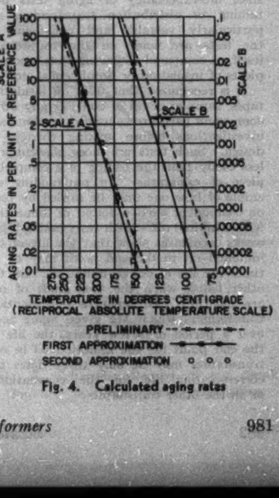

Fig. 4. Calculated aging rates

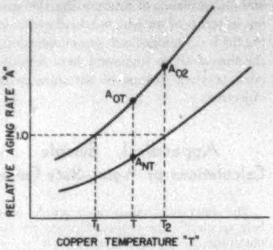

Fig. 5. Conversion of aging rates from one reference temperature to another

but indicate a change in the slope of the line which would be significant in extrapolation. While the latter points are shown on Fig. 4, the line is not shown, to avoid confusion. The small change shows that, although the total aging *AN* on the various cycles is not quite the same, further approximation could not be justified in this case.

The assumed number of load cycles to failure were not selected at random. They were obtained by assuming that the aging-rate curve of Fig. 1 is applicable, computing the relative aging per load cycle corresponding to the temperature cycles of Fig. 2, and selecting the number of cycles to failure in inverse proportion to the computed aging per cycle. Thus, an indication of the accuracy of the various computations in the example will be how well the "second approximation" compares with the curve of Fig. 1.

Extrapolation of the second approximation line indicates an aging rate of about 0.00003 at 95 degrees. Hence, to convert the computed aging rates to the same reference temperature as those of Fig. 1, they should be divided by 0.00003. If this is done, a close agreement is obtained.

Appendix II. Conversion of Aging Rate Curve from One Reference Temperature to Another

The validity of the procedure described in the text is readily demonstrated by reference to Fig. 5, where

A_{OT} = aging rate at any copper temperature T, relative to aging rate at original reference temperature T_1
A_{NT} = aging rate at copper temperature T, relative to aging rate at new reference temperature T_2
A_{O2} = value of A_{OT} at temperature T_2
L_T, L_{T_1}, L_{T_2} = life expectancy at T, T_1, and T_2 respectively

By definition

$$A_{OT}=\frac{L_{T_1}}{L_T},\ A_{NT}=\frac{L_{T_2}}{L_T},\ A_{O2}=\frac{L_{T_1}}{L_{T_2}}$$

Hence

$$\frac{A_{NT}}{A_{OT}}=\frac{L_{T_2}}{L_T}\,\frac{L_T}{L_{T_1}}=\frac{L_{T_2}}{L_{T_1}}=\frac{1}{A_{O2}}$$

and

$$A_{NT}=A_{OT}\,\frac{1}{A_{O2}}$$

References

1. Economical Utilization of Electric Power Equipment, **Herman Halperin.** *AIEE Transactions*, vol. 72, pt. III, Apr. 1953, pp. 203–20.

2. Guide for Loading Oil-Immersed Distribution and Power Transformers. *ASA Standard No. C57.32-1948*, and Appendixes, American Standards Association, New York, N. Y., 1948.

3. Life Expectancy of Oil-Immersed Insulation Structures, **W. A. Sumner, G. M. Stein, A. M. Lockie.** *AIEE Transactions*, vol. 72, pt. III, Oct. 1953, pp. 924–30.

4. The Re-examination of Temperature Standards for Electrical Insulation, **Graham Lee Moses.** *Ibid.*, vol. 71, pt. III, Aug. 1952, pp. 681–85.

5. Thermal Aging Properties of Cellulose Insulating Materials, **G. Malmlöw.** *ACTA Polytechnica*, Stockholm, Sweden, Electrical Engineering Series, vol. 2, 1948.

6. General Requirements for Transformers, Regulators, and Reactors. *ASA Standard No. C57.11-1948*, American Standards Association, New York, N. Y., 1948.

7. Test Code for Distribution, Power, and Regulating Transformers. *ASA Standard No. C57.22-1948*, *Ibid.*

8. The Functional Evaluation of Insulation for Small Dry-Type Transformers Used in Electronic Equipment, **R. L. Hamilton, H. B. Harms.** *AIEE Transactions*, vol. 73, pt. III-A, June 1954, pp. 605–10.

9. Electrical Insulation Deterioration Treated as a Chemical Rate Phenomenon, **Thomas W. Dakin.** *Ibid.*, vol. 67, pt. I, 1948, pp. 113–22.

10. Simplified Graphical Method of Computing Thermal Transients, **P. Narbutovskih.** *Ibid.*, vol. 66, 1947, pp. 78–83.

◆

Discussion

Herman Halperin (Commonwealth Edison Company, Chicago, Ill.): The paper indicates that considerable thought based on a wide background has been applied to this problem. I agree with the author's principle as to the samples to be tested, since life-expectancy or aging tests pertaining to distribution transformers are particularly valuable and convincing if the tests are made on the transformer itself, as compared to having tests made on pieces of insulation or simple coils, etc.

It is recognized that tests on insulating tapes, samples of oil or coils, or any other component parts are valuable in preliminary investigations before making changes in design. Such tests are more efficient and less costly than the testing of a completed piece of apparatus. An outstanding example of how one may be misled by tests on component parts is found in connection with inhibited oil. Such tests taking a few weeks or months show that the life of the inhibited oil to the end point may be 15 times the life of conventional oil. On the other hand, when the two kinds of oils are put into two separate but identical transformers which are given aging tests over a period of a few years, the life to the end point for the inhibited oil in one transformer may be only three times the corresponding life for the conventional oil in the other transformer.

In tests on transformers the life, as Mr. Lockie indicates, may be longer at a given loading than the tests on tapes in oil would indicate. I agree that the American Standards Association guide on loading transformers seems conservative.

Obviously, correlating data are needed between the results of life-expectancy or accelerating aging tests and the life in service for given load cycle, and temperature cycle. This takes time, but I think that our experience in Chicago over the past 30 years with accelerated aging tests on various cables has shown that such data may be obtained without an excessive amount of trouble.

Referring to the details of Mr. Lockie's test procedure, comments are as follows:

1. It seems desirable to have the test made on more than one transformer of a given type and design. The author proposes four transformers, which seems adequate.

2. The author's proposal to have loads such as 300 per cent (%) and 350% of name-plate rating for the first hour of heating with resulting temperature of around 200 and 250 degrees centigrade (C) do not seem desirable. First, exposure of the insulation to temperatures of 200 degrees or more for a matter of several minutes or more may introduce aging phenomena considerably different than those which apply for the insulation at service temperatures. Second, it becomes quite a problem to evaluate the heating that occurs during a sharp rise and decline in temperature, in view of all the assumptions involved. It seems desirable to follow Mr. Lockie's apparent point of getting the temperature of the winding conductor up to the high value quickly. According to Fig. 3, the use of an initial load of about 250% of name plate takes care of this requirement.

3. In connection with this load cycle, perhaps the final temperature after each application of heating current should be as high as 140 to 150 C. This would mean that after the initial high-load current for an hour or so, the final load current should be somewhat over Mr. Lockie's proposal of 150%.

4. To shorten the over-all time in weeks for a test, I would suggest that the load cycle consist of 17 hours of heating and 7 hours of cooling, instead of 7 hours of heating and 17 hours of cooling. This might result in the application of the current starting at, say, four in the afternoon.

5. As to the frequency of the application of end-point tests, I am not sure whether that should be applied every 5 days or every 10 days of testing.

6. During the end-point tests themselves, the proposal to have the short-circuit test at 15 times rated current at 2 seconds seems reasonable, as does the dielectric tests at 65% of the factory test voltage.

7. It is not clear why 100% of the

impulse test voltage for new transformers is proposed in the end-point tests. This calls for no reduction in the factory test for new transformers in contrast to the reductions proposed for the short-circuit and dielectric tests. Test data obtained by others show that there is a cumulative effect of repeated impulse tests which amounted to 20% in one case for 200 shots. On the other hand, we hope that the transformer in service will have about the same impulse strength as has been demonstrated in factory tests on new transformers. For these reasons, an offhand suggestion is that the impulse test should be 90% of the requirement for new transformers.

8. Various test data have indicated that the impulse strength of insulations varies considerably with temperature. This applies to some extent for 60-cycle dielectric strength. The implication of item 2.1 in the section "Aging Cycle," is that the end-point tests could be made immediately after the removal of the heating current, while the transformer is quite warm. On the other hand, this point is not covered definitely and so the one tester might make the test after the transformers have cooled down 2 or 3 hours. The factory tests for new transformers have been made while the transformer is at room temperature. They would be more convincing if they were made at elevated temperature, but this is not economically feasible in most cases. I would suggest that the test be made at a time of cooling that would correspond to the condition where the hottest-spot temperature is about 95 C.

9. I would be much interested in seeing further data on the point that average insulation temperatures should be given more emphasis than hottest-spot temperatures in connection with these tests.

I hope that Mr. Lockie's fine paper will accelerate the making of life-expectancy tests such as those he describes, and it would be fine if industry were to agree on the details of such tests.

M. F. Beavers (General Electric Company, Pittsfield, Mass.): The author presents an interesting proposal for evaluating the life of a complete transformer. The method proposed requires making certain assumptions as do all accelerated tests but they seem well founded in the light of present-day knowledge of insulation deterioration. Although, as the author recognizes, there may be many different opinions concerning the details of such an accelerated test, this study adds another milestone to the highway of progress in understanding and evaluating insulation life; the general procedure outlined in this paper will be useful no matter what agreement is reached as to the form of the test piece or to the order or magnitude of the loading cycles.

The author points out that the ideal test would involve a large number of complete transformers exposed to the expected field service until failure occurs. "This procedure would," he points out, "be prohibitively expensive and so time-consuming that the results would be of little practical use when the tests were finally complete. Consequently, practical considerations dictate a certain sacrifice in accuracy by the use of a relatively small number of samples and a duty cycle sufficiently severe to insure deterioration to a selected level in a reasonably short length of time."

A glance at the data given in Table I of the paper shows that approximately 2 to 2,000 aging cycles may be required to establish an aging rate curve for the transformer insulation structure under consideration. Since each aging cycle requires 1 week, this means 2 to 2,000 weeks or up to approximately 40 years.

It is clearly stated in the paper that the number of aging cycles to failure are "assumed" values which were based on the aging-rate curve of Fig. 1. This establishes a fine and consistent set of data for purposes of illustrating the procedure for establishing an aging-rate curve for a specific insulation structure. However, it is very unlikely that an actual insulation structure will perform in such a well-trained manner as the example given in the table. More likely than not, the data will be quite variable because of the nonuniformity of strains, stresses, varnish impregnation, bonding strength of adhesive-coated surfaces, etc. Furthermore, some of these factors are likely to change in characteristics with time, possibly because of such things as leaching action of the liquid on some of the materials and poor to fair compatibility of certain solids and the liquid. These and many other variables are, no doubt, some of the reasons why the American Standards Association loading guide assumes a conservative position in making recommendations on loading based on insulation deterioration alone.

In the General Electric Company three types of tests are used in evaluating insulation aging for liquid-filled distribution transformers: 1. tests on insulation components such as turn and layer insulation, 2. short-time overloads on assembled transformers, and 3. long-time full-load tests on assembled transformers.

The first type of test is used to compare the characteristics of one type of insulation against another. Since the turn and layer insulations are exposed directly to the hot-spot temperature of the conductor, the life of the transformer is very closely associated with the life of these two components. Therefore, considerable weight should be given to the mechanical and dielectric strength of these components.

This test is conducted by two different arrangements depending upon the nature of the insulation and size of conductor employed. When evaluating the turn insulation for rectangular wire, one arrangement is to place two strands of wire adjacent to each other in a test fixture such as is illustrated in Figs. 6 and 7. The strands are held together under a predetermined and constant pressure which allows for expansion of the conductor or for change in the dimensions of the turn insulation. Current is circulated through the strands to produce the desired temperature, which is continuously observed by means of a resistance bridge. Temperature up to 250 C can be obtained. The test jig is immersed in oil which can be maintained at any temperature from room temperature to 100 C. Sixty-cycle or impulse voltage is applied between strands. The voltage level may be held constant during the aging tests to determine the life to some percentage of initial strength, or it may be increased at any desired rate to determine the breakdown after a given exposure and while at the test temperature.

The second arrangement for this test, which may be used for evaluating layer insulation and turn insulation on either round or rectangular wire, is a coil consisting of several concentric layers of conductor wound around an insulating cylinder. Each layer consists of several turns of multiple strands electrically isolated from each other, and the layers are separated by the layer insulation under consideration. By means of a suitable arrangement of switches, the two strands of each coil can be opened or connected in series with the currents in each strand opposing, thus reducing the inductance of the coils so that the a-c and d-c resistances determined by the current and voltage readings are practically identical. When the coil circuit is open the strands may be given dielectric tests, such as 60-cycle, impulse, insulation resistance, power factor, etc., as desired.

The coil is placed in a tank of oil, thus

Fig. 6. Turn insulation test fixture

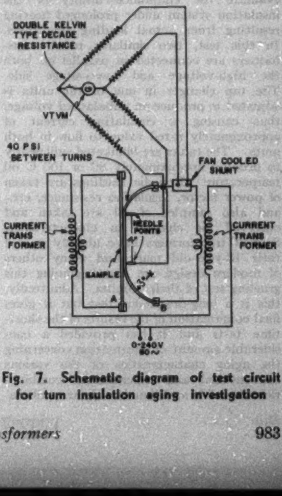

Fig. 7. Schematic diagram of test circuit for turn insulation aging investigation

simulating a small-scale model of a transformer with the desired insulation system. By means of a suitable, variable voltage source the coil current may be adjusted to any constant value or varied with time to produce a load-cycle effect. Several coils can be placed in series to obtain additional data for statistical evaluation of the results.

These model units have the advantage of being small in size, inexpensive, readily duplicated in construction, and they permit a more direct comparison between various insulation systems because of the similarity of the mechanical structure in all cases. Because of the simplicity of this coil and tank arrangement, it offers the possibility of representing the "model" liquid-filled test unit for class-*A* insulation evaluation studies similar to the studies under consideration in the dry-type transformer field.

The second type of test is used to check the over-all performance on a full-scale transformer under overload conditions. This test is similar to the cyclic test suggested by the author except that overloads of successively increasing severity but decreasing duration are applied on consecutive days until failure occurs. During the remainder of each 24-hour period, the transformer is left on excitation. By testing transformers having insulation systems which have been proved in actual service to give satisfactory performance, a bench mark for accelerated overload tests on full-scale transformers is established.

These two types of tests are basically short-time high-temperature accelerated aging tests which permit studies of the relative merits of various insulations and which also provide data for estimating insulation life at normal temperature by extrapolation. This procedure unquestionably provides useful information on life expectancy but there is always the possibility that certain reactions may take place at the higher temperature levels which do not occur at the normal temperature level, thus giving a prediction which may be seriously in error.

To reduce to a minimum the possibility of error, the third type of test is used to evaluate the endurance ability of the insulation system under prolonged heating resulting from actual loading conditions. In this test, two similarly rated transformers are connected in parallel on both the high-voltage and low-voltage side. The tap changer in one of the units is adjusted to produce an unbalanced voltage, thus causing a circulating current of approximately rated value to flow in both units. The tanks are blanketed sufficiently to produce approximately 80 or 100 C oil temperature. Periodic readings are taken of power factor, insulation resistance, etc., and also samples of oil are taken and observed for changes in characteristics. Several transformers have already passed their 18-year-old mark and many others of modern design are just beginning this grueling test of their stamina. Admittedly, this is a long-drawn-out test but it gives final confirmation of the results of the short-time tests and it has provided a considerable amount of information concerning the aging characteristics of the various conventional and experimental combinations of solids and liquids. Some combinations have shown excellent performance while others have been rejected on the basis of poor compatibility under prolonged heating conditions.

Before any agreement can be reached on a test code for evaluating transformer life, it is essential that some provision also be made to recognize the general aging effects on the materials due to prolonged heating. It is quite conceivable that a transformer having certain varnishes, adhesives, or synthetic materials would give a good account of itself under short-time high-temperature conditions. However, it is also possible that one or more of these materials might be slightly incompatible with the oil or other liquid in the transformer so that, in a matter of months or even years, the bonding characteristics or the dielectric quality of the components of the unit, as well as the liquid itself, may be adversely affected by the continuous exposure to normal operating temperature. Therefore some form of reasonably long-time test would appear necessary in any well-integrated life-expectancy evaluation program for liquid-filled transformers.

F. J. Vogel (Allis Chalmers Manufacturing Company, Milwaukee, Wis.): It was only a question of time before the life expectancy of oil-immersed transformers would be brought up. Power transformers as well as distribution transformers are involved. The various points which must be considered have probably for the most part been noted. It is natural that some of these would be questioned.

For example, should not the short-circuit test be the same as for new equipment? Also, I believe that the dielectric and induced tests should be the same as for new equipment. I have seen much old equipment returned, and when tested no apparent reduction in test strength was obtained.

Whether the aging tests will lead to the end points within a reasonable time would have to be determined by test. Hence, the proposal as made is one for tests to determine both the aging cycles and normal life expectancy.

The paper states that not only the hottest spot but the weakest spot must be given consideration. This is contrary to the present practice as described in the Standard,[1] which considers only the hottest spot.

The tests made by Satterlee[2] on small model power transformers are an effort in the same direction as Mr. Lockie's. It is desirable to work along these lines, as no doubt the solution of actual life problems and loading problems can be obtained only in this way.

REFERENCES

1. GENERAL PRINCIPLES UPON WHICH TEMPERATURE LIMITS ARE BASED IN THE RATING OF ELECTRIC MACHINES AND OTHER EQUIPMENT. *AIEE Standard No. 1*, 1954.

2. CONTROLLED TEMPERATURE AND INSULATION PROTECTION IN THE OPERATION OF POWER TRANSFORMERS, **W. W. Satterlee.** *AIEE Transactions*, vol. 71, pt. III, Jan. 1952, pp. 372–76.

C. F. Mitchell (Commonwealth Edison Company, Chicago, Ill.): The test program described should ultimately be of great value to the industry. Transformers have been rated in terms of temperature rise over ambient and for many years low ambient temperatures prevailing at the time of winter peak have been considered a basis for capability ratings far above name plate. Although the rate of mechanical and electrical deterioration of insulation as a function of temperature is reasonably well known, its correlation with failure rates has been but partially explored.

The functional test proposed by the author recognizes the daily cyclic range of temperatures to which transformers are exposed in service. It exaggerates the daily cyclic variation, but of necessity it cannot duplicate seasonal variations. There is little need for precise duplication of actual duty cycles since they must be greatly exaggerated in functional testing to secure results within practical time limits. The effect of actual loading on loss of life could, in my opinion, be made the subject of more study by utility operators. Such a procedure has already been outlined.[1]

The change to summer peak loading as a result of air conditioning is simplifying the problem of establishing and applying load capability ratings since the ambient temperature at the time of maximum load is always known to also be the maximum. In Commonwealth Edison Company we are conducting field tests on actual installations to determine the duration of exposure of insulation to various temperatures throughout the year. It is hoped that our results may be correlated with those of the author. Although in the long run planned economic loading of transformers must be based on actual life experience, the result of accelerated functional life testing will be exceedingly valuable in establishing aging rate curves.

Mr. Lockie suggests that eventually manufacturers should be free to select the most economical combination of temperatures and materials to ensure a specified life expectancy. Since operating people cannot hope to be able to control loading except within broad limits, it is difficult to see how such ratings would be used. Some criterion of transformer life is certainly needed other than the allowable rise of 55 C in order to plan most economical loading. For example, size obsolescence will dictate higher loadings on small sizes. Contingency loadings on networks and emergency conditions will require evaluation of life lost under extreme temperatures.

The author's efforts to establish a more realistic basis for loading policy are very much to be commended, and we look forward to the results of his testing. For functional life testing to be of the most value to the industry there must eventually be an agreement reached as to standardization of methods.

REFERENCE

1. LOAD LIMITS DETERMINED FOR DISTRIBUTION TRANSFORMERS, **Shelley Perry.** *Electrical World*, New York, N. Y., vol. 122, no. 18, Oct. 28, 1944, p. 86.

A. M. Lockie: It is encouraging to have discussion by representatives of both users and manufacturers of transformers, and to note that no serious fault is found with the principal thesis: that there is need for a test procedure which will furnish a basic measure of life expectancy and establish a guide for loading, and that these objectives may be attained by suitable cyclic loading tests.

Differences of opinion regarding the most desirable loading cycle were inevitable. It is impractical to present, here, all of the reasoning which led to the selection of the cycles proposed in the paper. Mr. Halperin's fear that very high peak temperatures may introduce abnormal failure mechanisms is shared by Mr. Beavers, and the possibility is acknowledged in the paper. This is a hazard common to all forms of accelerated aging, and we are faced with a choice between high temperatures, which may introduce complications, and long test times, which are objectionable. The 250% maximum initial load which Mr. Halperin prefers would, as indicated in Fig. 3, reduce the peak aging rate by a factor of 1/1,000, as compared to 350% load. Even with the increased heating time and heavier sustained load which he proposes, the reduced initial load would result in substantially increased duration of the tests. Further, increasing the magnitude of the sustained load seems undesirable, since it would result in oil temperatures well over 100 C. Perhaps experience may show that the typical aging rate curve for this type of apparatus has a greater slope than that of the hypothetical curve in Fig. 3. If such is the case, a practical degree of acceleration in aging may be possible without attaining temperatures over 200 C.

The difference of opinion on the end-point test, as expressed by Mr. Halperin and Mr. Vogel, is most interesting and important. Mr. Vogel's attitude is consistent with the provisions of the proposed test code for transformers.[1] It implies that the useful life of a transformer is over when it fails to pass the standard tests required for a new unit. It also implies that the reduced-level tests, now specified in the American Standard Association "Test Code for Distribution, Power and Regulating Transformers" (see reference 7 of the paper) for periodic testing of apparatus in the field, are inadequate to detect the end of life. The proposals in the paper were made after discussion with several transformer users, and are based on two assumptions:

1. That some deterioration below the quality level indicated by the tests on new equipment should be permissible, since the stresses represented by these tests are seldom encountered in the field.
2. That even though such stresses may be encountered occasionally the probability of these occasions is so small, in a large number of transformers, that some risk of failure is justifiable.

In my opinion the selection of the end-point test levels is one of many features of the proposed form of testing which must of necessity be somewhat arbitrary. However, if the testing is to be truly functional, it should represent the consensus of transformer users as a means of indicating, realistically, the end point of useful life.

As Mr. Beavers quite reasonably points out, test periods extending for several years are hardly compatible with the objectives of accelerated aging tests. The long-duration points were included in Table I, perhaps unwisely, simply to round out the illustration of the operations involved in establishing an aging-rate curve. In this early stage in functional testing, as Mr. Vogel suggests, it is difficult to forecast the duration of such tests, and a certain amount of exploratory testing will be necessary to arrive at loads which will keep the testing time within acceptable limits.

The accuracy of Mr. Beavers' prophecy that test results will be highly variable because of the numerous factors he enumerates, will be known only after a significant amount of testing has been completed. It would seem, however, that if functional testing serves no other purpose than to reveal the actual importance of these factors, it will be well worth while. Some discrepancy in test results is inevitable but if, as experience thus far suggests, the indicated minimum life expectancy is very much in excess of that indicated by the existing loading guides, it will be of considerable importance to those concerned with economical operation of apparatus. The ultimate value of the proposed procedures will, as Mr. Mitchell states, be indicated by the correlation of test results with field experience.

Mr. Beavers' description of the test procedures used by the General Electric Company is most interesting. Tests on insulation samples and partial assemblies, such as those he identifies as the first type, certainly are valuable in classifying materials as a guide to designers in their application. However, as pointed out in the paper and in Mr. Halperin's discussion, such tests have but limited significance with regard to the life expectancy of complete apparatus.

Tests of the second type are, indeed, similar in nature to those proposed in the paper, but the variable load cycle Mr. Beavers employs makes the establishment of an aging-rate curve much more difficult. However, the variable cycle would be quite satisfactory if, as is implied, the tests are intended solely to compare the thermal endurance of two structures, and not to establish a guide for loading.

The third type of test is said to be a final confirmation of the results of the accelerated tests, by operation under actual loading conditions. If, by actual loading conditions, Mr. Beavers means loading as experienced in the field, the procedure described seems questionable, since it does not include the effects of thermal expansion as encountered in normal loading, nor does it appear to include the effects of short circuits, impulse voltages, or power-frequency overvoltages. If a check on long-term compatibility of materials is necessary, it would seem more logical to use cyclic loading and end-point tests, in the manner described in the paper, employing an initial load of such magnitude that failure will not occur for the desired number of years.

It is regretted that space does not permit analysis of the other thought-provoking points brought out in the various discussions. Many of them are highly significant, and merit careful consideration before the establishment of a standard, functional-test procedure.

REFERENCE

1. PROPOSED TEST CODE FOR FUNCTIONAL ENDURANCE TESTS OF VENTILATED DRY-TYPE POWER AND DISTRIBUTION TRANSFORMERS, AIEE Committee Report. *AIEE Transactions*, vol. 74, pt. III, Oct. 1955, pp. 971–77.

A Power Class Recloser for Higher Speed Clearing of Distribution Circuits

E. J. FIELD
MEMBER AIEE

D. L. LEATHERBERRY
NONMEMBER AIEE

THE desirability of high-speed clearing of distribution circuits has long been recognized. In 1941 Matthews[1] focused attention on power arc-over damage on overhead distribution lines and the subject has presented itself at intervals since then. Havourd[2] recently added to the knowledge in this field and identified overhead conductor burndown as one of the major problems confronting the distribution engineer today. These reports direct attention to the need for higher speed interrupting devices. To minimize circuit disturbance when transient faults occur, higher speed reclosing after the first interruption is also important.[3]

Automatic circuit reclosers are becoming almost universally accepted and offer what is becoming recognized as the best solution to the problem of rapid circuit interruption. Their primary function to protect distribution circuits against transient faults is aided by high-speed circuit clearing ability that is inherently faster than conventional circuit breakers. However, even though all reclosers include in their normal operating sequence at least one first opening operation that is usually labeled "instantaneous," there is room for further improvement in order to provide even better protection for distribution circuits.

"Instantaneous" is a relative term that in practice has not been attained in ideal form. Industry standards[4] define instantaneous in this manner: "Instantaneous is a qualifying term indicating that no delay is purposely introduced in the action of the recloser." The significant phrase "no delay is purposely introduced" focuses attention on design limitations and a delay inherent in accelerating and moving the contact separating structures that result in a finite time lapse from the moment that the fault is initiated to the moment that circuit interruption is accomplished. Under the definition of instantaneous, some reclosers require as much as 48 cycles to clear the circuit of low-magnitude fault currents.

In the heavy-duty power class field, a recloser has been available with circuit clearing speed between the limits of $1^1/_2$ cycles and 3 cycles, but only up to a nominal application voltage of 7.2 kv. This operating speed has been improved still further and is now made applicable up to and including the 15.5-kv maximum design voltage for a 14.4-kv nominal voltage circuit.

Objectives

An evaluation of the problem of developing a power class recloser capable of higher speed clearing of circuits up to 14.4 kv nominal recognized that the most rapid possible acceleration of moving contacts was mandatory. The designer established certain objectives that included 1 cycle total elapsed time from initiation of the fault condition to circuit interruption, interrupting ability covering the entire range from minimum pickup current to maximum fault handling ability prescribed by standards for future design,[5] continuous current ratings between the limits of 100 and 280 amperes inclusive, an increase in low-current sensitivity for low-voltage, high-power-factor circuits, simplification of structure, and extension of the number of interruptions possible before requiring servicing. Believing that the most benefit could be realized from higher speed clearing by following it with a faster reclosure, higher speed reclosing was added to the objectives. It was also planned to incorporate a higher basic insulation level, safety lockout, and improved mechanical features in the tank and bushing structure.

Related Problems

Practical realization of the foregoing objectives entailed the development of an entirely new type of interrupter that would implement rapid contact separation and permit 1/2-cycle arcing with minimum arc energy. The total elapsed time of 1 cycle from the initiation of the fault introduced a need for extra rapid acceleration of the moving contact structure. This acceleration and its resulting high velocity leads directly to the problem of decelerating the moving mass and bringing it to rest at the end of the contact moving stroke. These requirements dictate maximum accelerating force at the start of contact separation, maximum velocity during contact separation, minimum driving force at the end of the stroke, minimum mass of the moving structure, and minimum velocity at the end of the contact separating motion. Obviously, some of these requirements are in conflict with one another. In addition to the design compromises usually necessary, ingenious design concepts were required to meet the stipulated conditions.

It may be considered that any interrupting device has for a given circuit condition some minimum contact separation below which circuit interruption cannot be accomplished. An ideal concept would be an interrupter that in the true sense of "instantaneous" separates its contacts only slightly more than the minimum distance required for circuit interruption. This should yield 1/2 cycle or less of arcing with minimum arc energy, because the separation necessary to obtain interruption has been instantly obtained and arc resistance has been held to a minimum by holding the contact separation to a minimum. A practical approach to this ideal interrupter introduces numerous related problems.

If too great a value is erroneously assigned to the magnitude of the minimum contact separation, the resulting arc energy will appreciably exceed the minimum amount possible. The high accelerating force stipulated and a need to keep the operating coil voltage drop to a minimum are conflicting requirements necessitating detailed analysis to obtain the most efficient electromagnetic system. Driving energy must approach zero towards the end of the stroke. Finally, the kinetic energy possessed by a high-velocity moving system poses a problem in the selection of materials and proportioning of components to withstand deceleration.

Approach to the Problem

Of the two basic types of automatic reclosers, one utilizes a series pilot coil or relay and a separate operating coil normally not energized. The other type has one coil serving the dual function of relay and operating coil and may separate the

---

Paper 55-510, recommended by the AIEE Switchgear Committee and approved by the AIEE Committee on Technical Operations for presentation at the AIEE Summer General Meeting, Swampscott, Mass., June 27–July 1, 1955. Manuscript submitted March 30, 1955; made available for printing May 6, 1955.

E. J. Field and D. L. Leatherberry are with the R&IE Equipment Division of I-T-E Circuit Breaker Company, Greensburg, Pa.

The authors acknowledge the contribution of A. C. Bates of their company to the analysis and solution of the problem described in the section entitled "Hydraulic Decelerator."

main contacts either by electromagnetic force or by tripping a latch and allowing a power spring to operate. The pilot coil type adapts itself to the most rapid separation of contacts, hence it was selected for the new recloser.

While it was not definitely known that a single contact interrupter was capable of handling the wide range of voltages and currents contemplated, it was believed that a single contact construction should be adopted. The reasons were that such construction lends itself to minimum moving mass and should theoretically deliver minimum arc energy. The compact construction that should be inherent with a single contact offers less drag when moved in a liquid medium and therefore results in appreciably less hydraulic friction. A single contact has the further advantage of economical maintenance because only one contact requires replacement. Single contact interrupters previously employed in reclosers were limited either in magnitude of normal frequency recovery voltage that they could interrupt or in the magnitude of the maximum fault current that they could handle. It was believed, however, that a new approach to this problem could result in an interrupter with more than adequate fault current handling ability and higher normal frequency recovery voltage capability.

Design Concepts

INTERRUPTER UNIT

Knowing that a fraction of a gram of insulating oil is converted into gas and carbon by each kilowatt-second of arc energy, an estimate of the arc energy generated for the maximum severity of fault condition anticipated leads to a conclusion that only a few cubic centimeters of oil will be involved in a given interruption. Theoretically then, only these few cubic centimeters of oil will be required in the apparatus if all of it can be effectively employed. This thought stimulated a study for a simple and practical means of introducing a small volume of oil to the arc and resulted in the development of what is termed an "oil column interrupter."

Basically, the oil column interrupter is a column of oil bounded by the inside walls of a hollow moving contact. The complete structure is illustrated in Fig. 1. In operation, the contact moves off of the stationary column of oil, progressively exposing cool clean oil to the area of the moving contact on which the resulting arc terminates. In conjunction with an interrupting pressure chamber and radial vents for rapid and effective diffusion of the arc products, the oil column was found to provide a highly effective single contact interrupter. Tests proved it to be more than capable of handling the fault currents and recovery voltages encountered in any application being considered.

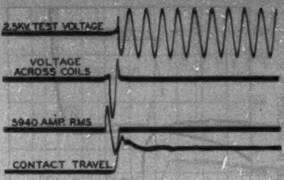

Fig. 2. Oscillogram revealing contact speed of early model

ELECTROMAGNETIC STRUCTURE

Early testing disclosed that, at currents approaching maximum rated fault capacity, effective circuit interruption was usually accompanied by spectacular evidences of the energy involved with the high-velocity moving contact structure. Oscillograms like the one in Fig. 2 disclosed that the high velocity caused the moving contact to approach the end of its stroke almost simultaneously with the occurrence of the first current zero. Consequently, the electromagnetic system remained energized, continuing the acceleration of the moving mass almost to the end of the stroke. A terrific impact was the natural result. Persistence of the driving force throughout the contact separating stroke and the kinetic energy inherent in a rapidly moving mass were damaging. Analysis of each oscillogram from a series of tests permitted determining the maximum velocity attained by the

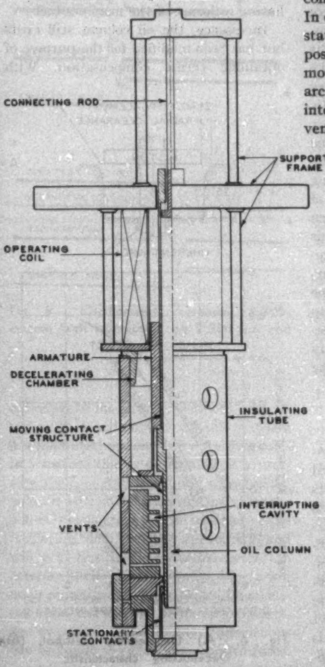

Fig. 1 (left). Section view of interrupter and electromagnetic structure

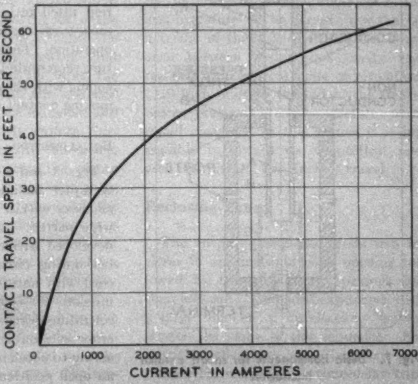

Fig. 3 (right). Relationship between maximum moving contact velocity and fault current magnitude

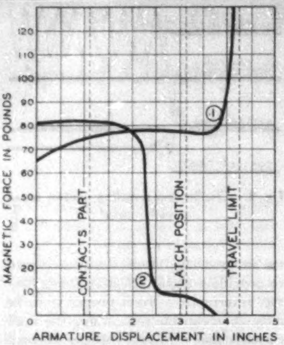

Fig. 4. Electromagnetic force displacement curves showing the conventional characteristic and the special characteristic resulting from a design study

moving contact for each of a wide range of currents.

A plot of these points resulted in the curve of Fig. 3. The velocity attained at high current values was ample evidence that the amount of energy at the end of the stroke must be reduced but without seriously affecting the initial acceleration. Three avenues of approach were: reduction of the mass, reduction of the electromagnetic force during the last portion of the stroke, and refinement of the existing decelerating dashpot in order to make it more effective.

The original electromagnetic system was conventional in that it consisted of an armature moving within a solenoid winding encased in magnetic material that provided a complete magnetic circuit. A force displacement analysis disclosed a characteristic identified as curve 1 in Fig. 4. The shape of this curve includes a magnetic force moving towards infinity at the end of the stroke, which, of course, aggravates the condition observed in tests. The electromagnetic system was redesigned to operate strictly on leakage flux, discarding the return magnetic path. Proper proportioning of the armature permitted a sharp cutoff in magnetic force at a designated point. The location of this cutoff point could be predetermined and set at any desired point of contact separation. It was also found possible to establish a secondary plateau or residual force following the cutoff point that would assure travel to latch when fault currents of low magnitude operated the recloser.

The newly developed magnetic force displacement curve is shown as curve 2, Fig. 4. This new characteristic provides an even greater initial accelerating force for the same number of ampere turns, while cancelling almost completely the magnetic force otherwise existing for the last part of the stroke. A secondary benefit accruing from the unique magnetic system is that the increased efficiency permits fewer coil turns for the same minimum operating current. Since the voltage developed across the operating coil is proportional to the number of turns, the maximum current for a given induced voltage was increased. This permits increasing the interrupting capacity rating of the lower continuous current rated reclosers, i.e., those with the most turns required for minimum pickup operation. The described magnetic structure represented a major forward step in coping with the problem of energy in the moving contact structure.

EQUALIZATION

Figs. 1 and 5 disclose that the new interrupter included an essentially closed chamber within which the main contacts were parted. Appreciable pressure was developed within the interrupting chamber during circuit interruption. In accord with natural laws governing transmission of hydraulic pressure, an accelerating force was imposed upon the cross-sectional area of the moving contact acting to accelerate the contacts towards an open position. At fault currents approaching maximum rated capacity, the pressure-generated accelerating force attained a very significant magnitude and augmented the electromagnetic force also acting to accelerate the moving contact towards an open position. These two co-operating forces, in conjunction with an impulse shock of appreciable magnitude that accompanied a 1/2-cycle interruption, complicated the problem of proportioning the mechanical design of the recloser to practical dimensions. Realizing that some means of compensating for or cancelling out the hydraulic accelerating force must be found, the structure schematically illustrated in Fig. 5 was devised.

With further reference to Fig. 5, section *B* represents the interrupting chamber that houses stationary contacts *G* and the main moving contact *H*. Outside of the interrupting chamber, the conducting member *C* that forms an extension of the moving contact is enlarged to form a secondary chamber within which a plunger *E* is inserted. Plunger *E* is stationary, being attached to the main framing member *F* by means of a connecting rod. Lateral ports *D* admit fresh oil to recharge the conductor cavity following reclosure of the main contacts.

In essence, the oil column still exists but has been modified for the purpose of obtaining thrust compensation. With

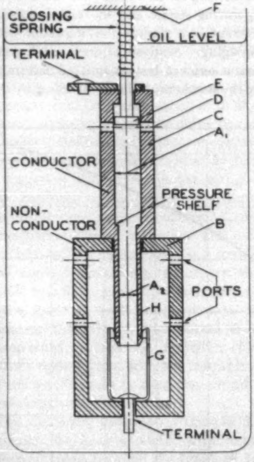

Fig. 5. Basic components for an oil column interrupter

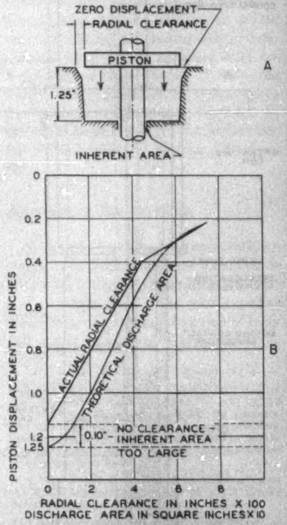

Fig. 6. (A) Decelerating dashpot. (B) Decelerating characteristic

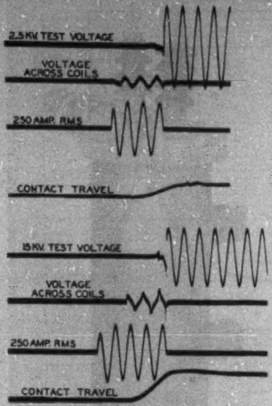

Fig. 7. Oscillograms comparing 250-ampere fault interruption on 2,500-volt and 15,000-volt circuits

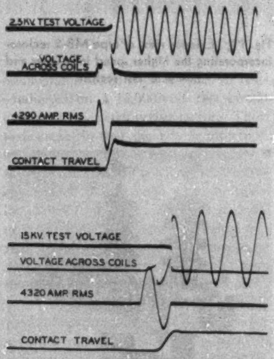

Fig. 8. Oscillograms comparing 4,300-ampere fault interruption on 2,500-volt and 15,000-volt circuits

reference to the internal bore of the moving contact and contact extension, there is a diametral discontinuity which results in a surface that is designated as a pressure shelf. Any hydraulic pressure developed within the interrupting chamber will be transmitted by the medium of the insulating fluid through the cavity and will act vertically downward upon the pressure shelf. This downward force will be in opposition to the upward force acting upon the end of the moving contact, and by proper proportioning of dimensions can be made to cancel the upward force. Different operating conditions may require either a net upward force or a net downward force. In the latter case, the scheme described offers a neat solution because both the upward electromagnetic force and the cancelling downward hydraulic force increase with increasing fault current.

Hydraulic Decelerator

The two previous sections have described a novel means of reducing the magnitude of both the kinetic energy of the moving system and the driving force during the latter part of the opening stroke. There must, of course, be some residual energy, otherwise the moving contact can not be depended upon to reach a latch open position.

The remaining problem is that of decelerating the moving contact and bringing it to rest in the latched position. The two means that have been introduced to minimize the energy existing towards the end of the stroke bring this problem of deceleration within the bounds of a simple hydraulic dashpot.

To obtain optimum benefit from a decelerating dashpot, the problem was approached on an analytic basis, utilizing dimensional constants that were dictated by space considerations. Previous tests had established the moving contact velocity that must be dealt with. Analysis of the travel record on a large number of oscillograms permitted plotting of the curve, already referred to and shown in Fig. 3. From the known constants and an assumed peak hydraulic pressure the remaining variables were calculated. Fig. 6(A) shows in simplified form the physical structure of the decelerating dashpot, also visible in Fig. 1. It is simply a shallow cavity with tapered walls into which a piston (the flange on the bottom end of the armature) must enter at the end of the stroke. It was necessary to establish the radial clearance between piston and cavity wall at each point of the taper, the clearance being such that the assigned peak pressure would not be exceeded and deceleration would be fairly uniform during passage of the piston into the cavity. The annular space between the piston and the cavity wall was considered as an orifice and the problem solved on the basis of ascertaining the theoretical area that this orifice should have at each point of piston displacement, measuring from the entry point. The area was then converted to terms of radial clearance.

Fig. 6(B) shows graphically both the total theoretical area and the radial clearance plotted as abscissa against an ordinate scale representing piston displacement from the point of entry. It is to be noted that some inherent port area always exists as necessitated by clearance between moving and stationary parts and by the necessary conventional slot in the iron armature. The curves show that as a result of the inherent area the clearance between piston and cavity wall reached a theoretical value of zero about 1/10 inch prior to the end of the stroke. Since practical reasons dictate some radial clearance in this region, it is impossible to obtain the theoretical port area for this last 1/10 inch of travel.

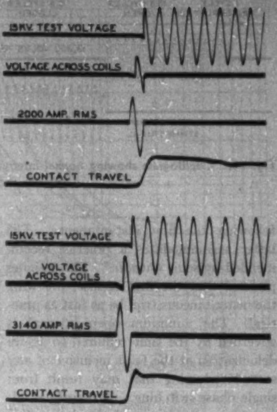

Fig. 9. One-cycle circuit interruption on 15,000-volt circuit for 2,000 amperes and 3,140 amperes

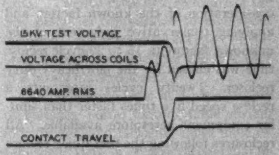

Fig. 10. 6,640 amperes interrupted on 15,000 volts at $4\frac{1}{2}$-per-cent power factor and maximum possible rate of rise of recovery voltage

Reclosing Time

The operating sequence of the new recloser is one instantaneous opening followed by two time-delay openings and then lockout. Extended experience with a large number of installations demonstrates the value of this sequence. For special applications, an adjustment permits either one or three time-delay trips

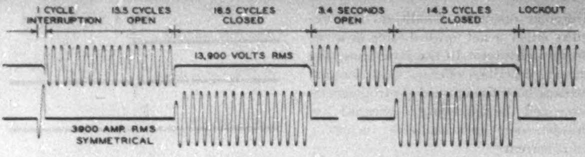

Fig. 11. Oscillogram showing normal interrupting and reclosing sequence to lockout, 4,000 amperes and 13,800 volts

following the first instantaneous. The latter accommodates a practice recommended by some authors.[6] The designer planned that the first reclose, following the instantaneous trip, be as fast as practical. The minimum open interval is governed by the time required to assure deionization at the fault inclusive of any secondary arcing that may result from single-phase switching. Wallace[3] has advanced reasons for a reclosing interval as short as 10 cycles for a light-duty interrupter. The device being discussed here must handle 100,000 kva of fault energy as determined on a 3-phase basis. In consideration of the known factors and applying conservative judgment of the unknown factors, a 15 to 20-cycle reclose time was chosen for the new heavy-duty recloser. Twenty cycles represents a reclose speed five times faster than similar equipment heretofore available. All reclosures following the first quick reclose have a fixed interval of 5 seconds.

Testing

After having developed a new type of interrupter and working out the solutions described in the foregoing for coping with the acceleration and velocity of the moving contact structure of a high-speed interrupter, it was necessary to verify performance effectiveness for the operating conditions anticipated in service. For this purpose, hundreds of tests were conducted under a wide variety of conditions. Tests were conducted at several different normal frequency recovery voltages ranging from 2,500 volts to 15,000 volts inclusive. Fault currents included a wide range of power factors ($4^1/_2$ per cent to 100 per cent) and varied in magnitude from 175 per cent of the continuous current-carrying rating of the apparatus to 20 per cent in excess of the maximum rated fault handling capacity. In addition to verifying interrupting ability and observing interrupting speed for these widely varied conditions, tests were conducted to determine the ability of the apparatus to quickly re-energize the circuit and still be capable of an immediate second interruption in the event that the fault was a persistent one.

An interesting fact disclosed by test oscillograms is that for the interrupter devised the interrupting time appears insensitive to service voltage changes between the limits of 2,500 volts and 15,000 volts. Since the apparatus is intended for application between the limits of 2.1 kv and 15.5 kv, tests above the latter value were not conducted and the upper limit of the insensitivity to voltage change has not been established. For example, Fig. 7 shows two oscillograms at essentially the same low-magnitude fault current for two different voltages, namely 2,500 volts and 15,000 volts. Similarly, the two oscillograms in Fig. 8 show interruption of 4,300 amperes of fault current on 2,500- and 15,000-volt circuits. This characteristic may be attributed to the extremely high speed of contact separation.

Fig. 9 shows oscillograms of 2,000 amperes and 3,140 amperes interrupted on a 15-kv circuit and illustrates tht the first instantaneous trip accomplishes 1-cycle interruption at these magnitudes. Fig. 10, showing 6,600 amperes, is one of the

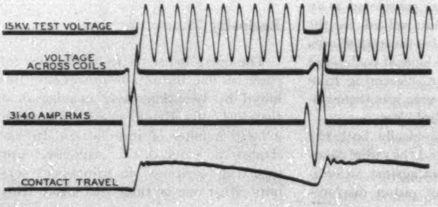

Fig. 12 (left). Oscillogram of two successive interruptions separated by 11 cycles

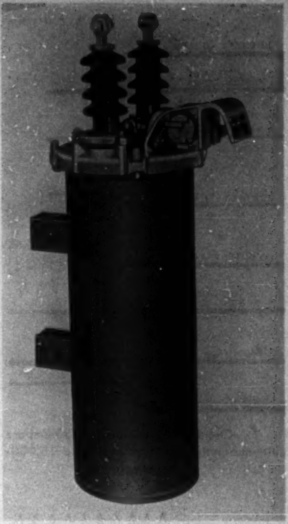

Fig. 13. Exterior view of type MB-2 recloser incorporating the higher speed interrupter and 20-cycle first reclose

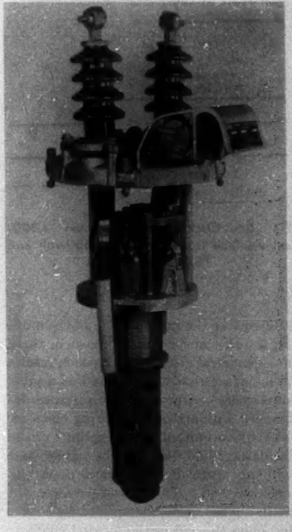

Fig. 14. The unit bushing, lid, and mechanism assembly

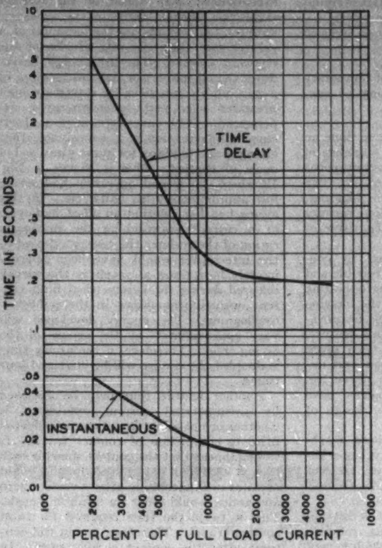

Fig. 15 (left). Recloser-fuse co-ordination band utilizing the new instantaneous curve

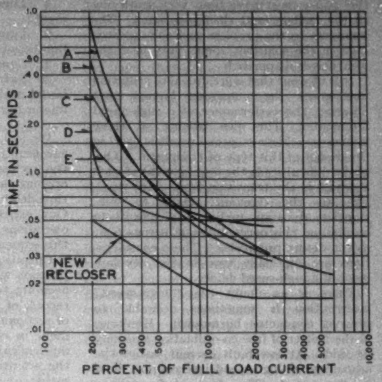

Fig. 16 (right). Comparison of new instantaneous curve with other known "instantaneous" or "fast" recloser time curves

oscillograms taken from a series of tests conducted on a 15,000-volt test circuit having $4^1/_2$-per-cent power factor. These tests establish that the 1-cycle interrupting ability extends at least to a value 20 per cent in excess of the rated interrupting capacity at this voltage. Rated capacity is 4,000 amperes rms symmetrical or 5,600 amperes rms asymmetrical current, based upon a circuit reactance to resistance ratio equal to 8. For the tests illustrated by Fig. 10, maximum severity was imposed upon the interrupter by adjusting synchronous switching for symmetrical current to obtain the absolute maximum rate of rise of recovery voltage.

Fig. 11 illustrates an interruption sequence to lockout under typical service conditions utilizing the standard operating sequence on a 13,800-volt circuit experiencing 4,000 amperes of fault current.

In order to test the ability of the new design to handle two successive interruptions separated by as little as 15 cycles of time, tests at reclosing intervals as short as 7 cycles were conducted. The oscillogram of Fig. 12 demonstrates 11-cycle reclosing performance on a 15,000-volt circuit with 3,140 amperes of fault current. Since practical reasons precluded an exhaustive study of 10-cycle reclosing, it was decided to have the quick reclose fall within a range of 15 to 20 cycles. This decision allows a comfortable safety margin and, as pointed out in a foregoing section, introduces a new and significant performance level to the user.

Summary

Special design considerations must be taken into account to provide unusually high contact acceleration and to cope with the moving structure velocity inherent in a 1-cycle interrupter. An external view and a view of the internal mechanism of a recloser incorporating these considerations are shown in Figs. 13 and 14 respectively.

The new design provides a full power class recloser for distribution circuits that offers both higher speed circuit interruption and higher speed reclosing. It provides these speed advantages together with continuous current-carrying capacity up to 280 amperes and with the maximum interrupting capability suggested for future design by industry standards.

The higher speed interrupting ability increases the ratio between time-delay opening and the first "instantaneous" opening to as high as 100 to 1 compared with older values of 20 to 1. Fig. 15 discloses the wide band available for good recloser-fuse co-ordination. The instantaneous time curve is believed to represent the fastest circuit interruption available in other than a fuse and is shown in comparison with other fast or instantaneous recloser curves in Fig. 16. It is a close approach to the ideal concept of a true instantaneous circuit interrupter.

A higher speed first reclose following higher speed circuit interruption offers optimum protection for distribution circuits. Twenty-cycle first reclosure of the new design is comparable to high-speed reclosing of transmission-type circuit breakers and is adopted for the first time in a power class recloser.

Comprehensive tests at a wide variety of voltages, power factors, fault current magnitudes, and reclosing times have established that a conservative margin exists between maximun performance ability and operating requirements for the rated values of this apparatus.

References

1. Power Arc-Over on Overhead Distribution Lines and Newly Developed Equipment for Protection Against Conductor Burndown From that Cause, **G. A. Matthews.** *AIEE Transactions*, vol. 60, 1941, pp. 596–604.

2. Burn-Down of Overhead Conductors, **R. M. Havourd.** *Electrical Light and Power*, Chicago, Ill., Oct. 1954, pp. 109–12.

3. An Improved Automatic Circuit Recloser, **J. M. Wallace.** *AIEE Transactions*, vol. 66, 1947, pp. 255–63.

4. Automatic Circuit Reclosers for A-C Distribution Systems. *AIEE Standard No. 50*, Jan. 1953.

5. Automatic Circuit Reclosers. *Publication No. SG13-1952*, National Electrical Manufacturers Association, New York, N. Y., Feb. 1952.

6. Time Delay Cuts Recloser Operations, Improves Coordination, **A. W. Edwards, R. J. Lawrence, P. E. Thornberry.** *Electric Light and Power*, Chicago, Ill., Aug. 1952, pp. 114–18

◆

Discussion

William J. Weinfurt (Line Material Company, South Milwaukee, Wis.): The development of the recloser as described in this paper must have been very gratifying to the authors and their associates. The approach to the problem and the methods used in the solutions comes very near the ideal classical approach.

It is obvious that a great deal of attention was given the numerous factors that influence the performance of a high-speed interrupter. The nice balance of these factors to achieve a special result is basic in the design of this type of equipment. One of the difficulties in the development of such a design is the transition from static analysis to the dynamic. Data to substantiate dynamic analysis are difficult to obtain and this necessitates numerous tests as the design progresses. These considerations are especially true in the development of a high-speed device.

There is no doubt that "high-speed" interruption is sometimes desirable to prevent conductor burn-down. However, in the matter of fuse co-ordination this may be said: At low fault current values the advantage of high-speed interruption must be discounted. The slope of fuse time-current curves is so much greater than the slope of instantaneous curves of the high-speed recloser that actually the area uncovered for broader co-ordination is not usable. Actually, there has been a recloser available for several years having an instantaneous time-current characteristic comparable, at high current values, in speed of interruption to the authors' design. It also has a nominal voltage rating of 14.4 kv, heavy-duty class.

The efficacy of using higher speed reclosing may be open to some consideration. Experience based on a large volume of recorded data indicates that there may be 1/3 the fuse blowing on co-ordinated fused branch lines when a more conventional interval of reclosing with two fast and two time-delayed interruptions is used. The cumulative heating effect on fuses must be more carefully considered with fast reclosing since it becomes a more important factor.

The authors are to be complimented on the excellent presentation. They have exploited an area of performance for reclosers that has merit as well as shortcomings.

G. D. Stevens and **A. C. Fagerlund** (Consumers Power Company, Jackson, Mich.): The authors are to be complimented on a very good presentation and a very thorough analysis of the problems inherent in the design of a power class recloser.

Consumers Power Company recognized the need for power class reclosers as early as 1946 and, at present, there are 1,500 single-pole units installed on substation distribution circuit exits operating from 4,800 volts up to and including 14,400 volts with the majority on circuits operating at 4,800/8,320 volts wye grounded. Ampere ratings of these reclosers are 100, 140, 200, and 280 amperes, depending upon the capacity of the substation transformer banks and the number of circuits.

The 8 years of experience with circuit reclosers has proved them to be a reliable and economical device for circuit protection with greatly improved service continuity. As a result of their use, the following benefits have been obtained.

1. Lower investment in substation equipment.
2. Lower operating costs due to reduced number of service calls.
3. Lower maintenance cost.
4. Extremely fast clearing of temporary faults and considerable lessening of conductor burn-downs.

We feel that the designers have done an excellent job on the operating sequence of the recloser in having one instantaneous opening and reclosing followed by two time-delay openings and then lock-out. Our experience with substation recloser operations has demonstrated the value of this sequence.

Operation counters employed in conjunction with reclosers must be reliable and accurate to permit studying the operating records of the reclosers against the blowing of sectionalizing fuses for possible improvement in circuit protection. This feature, mechanical in nature, has not been given the attention it should have had and unsatisfactory operating records have resulted. We assume the designers have considered this problem in the design of the recloser.

The fine record which has been established by reclosers of the 15-kv class immediately sets up a challenge to the designers to develop a single-pole recloser which can be used at higher voltages.

The growth of load and load density in the suburban and rural areas requires larger capacity substations for which it may be necessary to use power reclosers of ampere ratings and interrupting capacities higher than available at present. On the Consumers Power Company System, these substations are generally served at 46 kv. To insure better service, it would be desirable to operate the 46-kv lines closed in loop operation. Where the current rating and interrupting ability of a circuit breaker is not required or the cost is not justified, it is believed the use of a single-pole recloser of proper ampere and voltage rating could be the answer to this need.

K. L. Niebauer (Westinghouse Electric Corporation, East Pittsburgh, Pa.): The authors have described an interesting approach to the problem of high-speed circuit interruption. They are using extremely high contact speeds for interrupting the circuit with a minimum fault current time. In general practice contact speeds are maintained at reasonably low values while the interrupter design is used to effect interruption of the circuit with short arcing time.

The high-speed contacts introduce some problems that I do not feel were sufficiently explained in the paper. In Fig. 8 the contact separation was initiated after approximately 3/4 cycle of symmetrical fault current and the contacts reached the full open position just after the second current zero. I feel that the story would be more complete if an oscillogram of a totally asymmetrical fault current were shown. I cannot entirely agree that the symmetrical current interruption is the most difficult to handle. It has been my experience that the energy released in the interrupter is of major importance, especially where high-speed contact separation is involved. The exceptionally high speed of the contact separation should build up the dielectric strength between the parting contacts at a greater rate than the rate of rise of the recovery voltage. The arc energy breaks down the oil into a gas and this creation of a gas bubble can develop extremely high pressures when very much energy is experienced. With an asymmetrical fault current interruption it is conceivable that arcing could endure for more than a 1/4 cycle of current. This is shown in Fig. 12 where the second operation had arcing for approximately a half-cycle. If this arcing had been during an offset half-cycle at a current approaching the maximum rating of the recloser the energy released in the interrupter would have been approximately four times as much as the energy released during the symmetrical fault current operation as shown in the published oscillograms. The energy developed will vary approximately as the square of the arcing time. Therefore, if the arcing time is doubled the energy will be increased four times.

Another feature that may be disclosed by asymmetrical current operations is whether or not all interruptions are effected prior to completion of contact travel. It would appear that the contact speed is such that at high fault currents an opening could occur at or immediately after a current zero and arcing would occur for a full half-cycle. This is twice the time required for total contact travel. Therefore, arcing will continue after the contact is fully open. In this case interruption will have to occur with no new oil coming in contact with the arc. It would be interesting for the authors to discuss the result of such an operation.

The authors did not mention the recloser's ability to interrupt load current and transformer magnetizing current when used as a manual sectionalizing device. With the apparent length of the contact stroke it is assumed that the recloser operates quite satisfactorily in these cases. Reclosers are frequently used for line sectionalizing and must possess the ability to interrupt load currents, as well as low-power-factor energizing currents.

E. J. Field: In discounting the advantage of high-speed interruption at low-magnitude fault currents, Mr. Weinfurt seems to say, in effect, that low-magnitude fault currents are good for a system. In contrast, we consider that the ultimate objective is to have ciruit interruption and reclosure so rapid that both are accomplished in zero time, which is the same as having no faults at all. It is doubtful that any one would dispute the advantage of a truly faultless system.

Curve *B* of Fig. 16 is the published "fault" curve of the only recloser we know to be "available for several years." It is clearly slower than the subject of this paper, particularly in the range of currents representing the bulk of all fault currents.

It should be noted that the extra fast reclosure reported in this paper applies only to the first reclose following the instantaneous trip. This combination best serves the recloser's primary function which is to clear the circuit of transient faults with minimum disturbance. Subsequent reclosures are 5 seconds nominal for the purpose both of neutralizing an otherwise cumulative heating effect on fuses and for permitting an adequate open interval to clear semipermanent faults. This operating sequence is the conventional one used on the majority of all single-phase power class reclosers presently in service.

The comments of Mr. Stevens and Mr. Fagerlund are predicated upon their observations of what is believed to be the largest known general application of power class reclosers. This broad application with its multiple benefits results directly from application of reclosers as feeder breakers on a multiplicity of small substations, an idea worked out in detail and pioneered on the Consumers Power Company System. The comment on operation counters focuses attention on the ever-present need for supplementing sound and basic engineering concepts with careful attention to the detail design of co-operating components.

The theoretical concepts relating to current offset and arc energy expressed by Mr. Niebauer establish his familiarity in this field. Therefore he will probably recognize that the theoretical conditions he prescribes will not be encountered by the recloser because a totally asymmetrical fault current will not occur under even the worst conditions prescribed by industry standards for this equipment. Furthermore, the subject of this paper possesses an inherent characteristic that compensates for severe asymmetry. This is the fact that contact separation cannot start until after voltage appears across the coils. Coil voltage, in turn, cannot develop until after the first current zero, which obviously is at the termination of the severe offset current wave. Therefore the extension of the time base normally introduced by an asymmetrical loop does not occur during separation of the contacts. This coil voltage and contact travel relationship may be verified by reference to Figs. 2, 7, 8, 9, and 12.

From Fig. 3 and a knowledge of the contact separation it may be determined that contact velocity is appreciably less than Mr. Niebauer's surmise of total contact travel in 1/4 cycle. It must also be noted that Fig. 3 defines the contact speed prior to the adoption of measures discussed in the paper that reduced the travel speed of the final product. Another point mentioned but not enlarged upon in the paper is that some prototype tests did permit a current zero after the end of contact travel. Interruption was obtained in all such instances. This is because the contribution of the coil column to interruption, considered as a percentage of all contributing factors, is greatest at low fault currents (slow speed) and short contact separation. However this discussion is only of academic interest because the design adopted is timed to obtain interruption prior to the end of contact travel. The oil column is particularly effective for interrupting load current and magnetizing current. The assumption concerning this point is entirely correct.

We appreciate the interest shown and the challenging discussions presented, and thank the discussers for their participation.

Forecasting the Demand for Electricity

R. G. HOOKE
FELLOW AIEE

Purpose

WITH EVERY addition to the plant of an electric utility system there is presupposed, either consciously or unconsciously, some estimate of future loads, even if it be no more than a forecast that the enterprise will continue in business. If the addition is the result of careful study and planning, such study and plan must necessarily be based on a specific forecast of future requirements. In spite of the great importance of these forecasts, very little discussion of them has taken place in the industry and there appear to be great differences in the methods employed, ranging from the simplest extrapolations of past loads, to numerous rather complex techniques aimed at improved results. The purpose of this paper is to present a summary of the procedure used by one company in determining the future loads on the basis of which its plant facilities are designed.

Scope

The paper will deal with load forecasts looking from 6 months to as much as 10 years or even more into the future. These are the forecasts required by system planning engineers in making studies of alternative methods of system expansion. They are also the forecasts which determined whether or not the facilities necessary to carry loads are available today. However, the current load forecasts required for purposes of day-to-day system operation and heavily dependent on temperatures or weather conditions, will not be considered.

Summary

The method described consists of forecasting sales by classes of service for a time interval of either a year or a month, 10 years in the future. A secular trend is then drawn from present data to the forecast condition 10 years hence. Next, an estimate is made of expected deviations from trend, especially in the near-term years. By summing up the estimates of sales and adding losses and certain other adjustments, a forecast of total output is made. Expected peak demands, which are the ultimate objective of forecasts used in system planning, are obtained by a process of correlating peaks with consumption and system output.

Two Fundamentals

Anyone who has studied economic or stock market or business forecasting will undoubtedly accept the following as axioms: 1. there is no one certain method of forecasting, and 2. no individual is completely clairvoyant.

The first of these statements leads to the conclusion that in making a forecast every available approach should be brought to bear on the problem. Tentative answers should be arrived at by as many means as may be feasible. The final forecast should be undergirded by reasonable forecasts for as many related elements as can be isolated and separately studied. A forecast of peak kilowatts must be intelligently related to a forecast of total output; a forecast of output must be reasonably related to forecasts of sales. Sales forecasts must be broken down into forecasts of logically attainable residential, commercial, and industrial consumption, and so on. These again must be related to population trends, territorial changes, and other factors. If all of the parts which make up any whole can be analyzed and prognosticated separately, an integration of them, in which the parts together constitute one, or perhaps several, closed circles, is likely to be more accurate than a direct estimate of the whole.

It is possible to forecast peak demands

Paper 55-530, recommended by the AIEE Systems Engineering Committee and approved by the AIEE Committee on Technical Operations for presentation at the AIEE Summer General Meeting, Swampscott, Mass., June 27–July 1, 1955. Manuscript submitted March 25, 1955; made available for printing May 9, 1955.

R. G. Hooke is with the Public Service Electric and Gas Company, Newark, N. J.

The procedures described in this paper are not the work of any one individual; credit must be given all members of the Load Development Committee-Electric, of Public Service Electric and Gas Company, Newark, N. J., and to its staff.

by merely extrapolating the past history of peaks. However, system peak is the aggregate of the peak contributions of the several classes of service plus associated losses. Hence, an ideal approach would be to estimate peak by summation of class contributions but this would involve the forecasting and integration of class demands and losses. Most utilities do not at present have enough information to follow such a procedure completely, but they can approach it by reasoning and speculating about class sales, in kilowatt-hours (kw-hr), quantities related to the parts rather than to the whole; then, having forecast these parts, integrating them by various methods to produce an estimate of the whole. This is a helpful procedure since there may be differing trends in the contributions of the various classes of service to the combined peak which such a study may disclose. A case in point is sales to a local transportation company, once important in establishing peak demands, now negligible. In another instance, a very important change in month of occurrence of annual peak is forecast on the basis of studies of class loads.

A corollary of this proposition would state that mathematical methods of extrapolating known data are tools which may be an aid to judgment but must not be substituted for it. A perfect mathematical fit for past data may be very helpful for a short-range view of the future but may lead to absurd results if applied for the long range. Application of mathematical procedures therefore, either to the components of the data or to the whole, is only one of the possible ways of evaluating the future and should be employed with caution and appreciation of its limitations.

The second axiom suggests that group effort may be superior to individual performance. Hence there may be advantage in having forecasts handled by a forecasting committee. On such a committee numerous points of view can be brought to bear. There should be representatives from the operating departments closest to the phenomenon of growing, shifting loads and who are on the firing line when shortages of capacity occur; there should be representatives from the sales departments who sense the public pulse and know the sales promotion plans and problems; and finally there should be representatives from financing or management groups whose business acumen is invaluable and whose acceptance of the forecasts is essential. In setting up such a committee, however, it is important that the individuals be named as committee members in their own right and not as departmental representatives. As individuals they will submit their own ideas, argue and discuss results, and compromise findings to arrive at a committee viewpoint. Only by accident would this be an average of the viewpoints of the various departments. Frequently two individuals from the same department will hold drastically differing views. Experience since 1923, covering both the departmental and the individual-member approaches, has shown that the former leads to averaging of departmental forecasts and post mortem comparisons, while the latter promotes free discussion in which many conflicting views are reconciled through exchanges of opinion and sharing of results of research.

Basic Statistics

The basic statistics upon which any forecast of the future must rest are the historical records of the past. These must in some manner be extrapolated and modified in the light of what is known or expected as to the future. Fortunately most utilities, unlike an enterprise starting out in a new industry or with a new product, have reasonably adequate records of the past, i.e., records of past sales, past outputs, past system peak demands, and other pertinent material.

Since the system peak, in which planners are primarily interested, usually has a fairly definite seasonal pattern, it is clear that in so far as use is a determinant of peak, sales for the month or months when the peak may be expected to occur are of greater interest than sales for other months or for the year as a whole. For the purpose of this paper, it is assumed that a December annual peak is the historical experience; forecasts of December sales are, therefore, of particular interest. (In many areas the seasonal pattern appears likely to change in the near future, because of increasing summer air-conditioning load.)

There are, however, important benefits to be obtained from using annual sales and also from using sales for all months of the year. Forecasts of annual sales, based on past annual data, tend to eliminate accidental variations such as may occur for 1 month, if only 1 month in each year (as December) is the basis for the forecast. For near-term forecasts, monthly sales corrected for seasonal variation and meter-reading intervals may be used. This provides 12 points per year as a springboard from which to forecast the trend, rather than only one point per year, and thus tends to average out unavoidable accidental variations.

In most forecasting, it is advantageous to be able to use, interchangeably, data for the full year, data for 1 month in which the peak is likely to occur and data for each of the 12 months of the year taken individually. Seasonal factors and ratios should be computed so that statistics for any 1 month can readily be compared with statistics for any other month or for the full year. For some purposes

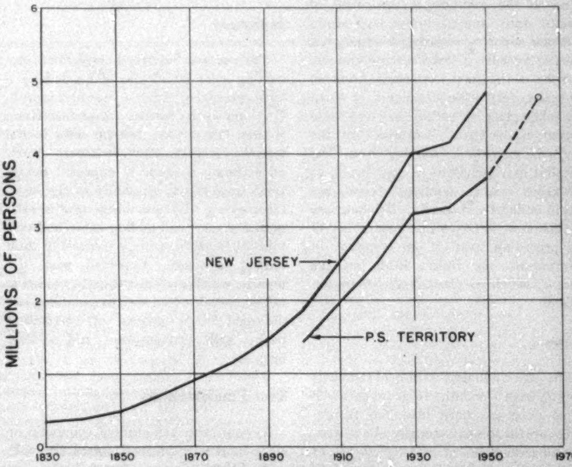

Fig. 1. Population growth.

December figures appear preferable, for others annual information seems better and in still others complete monthly statistics are preferable.

Remote-Point Philosophy

Most humans, when thinking of the future in terms of a projection of the historical past, are greatly influenced by the immediate present. It follows that the first step in every forecast may well be to consider, without undue concern for today, what a remote tomorrow may bring. "Remote" may mean 5 or 10 or 20 years hence; for the purpose of this paper, it is a period 10 years in the future.

Now, in the spring of 1955, with all 1954 data available, the question is, what will industrial or residential sales be in 1964? Clearly, in answering this question the important factor is not what the sales were in the last 2 or 3 months of 1954, or in all of 1954, but what has been happening to the sales for the last 10 or 20 years and, very important, what new influences are likely to appear in the next 10 years. In this speculation, many factors can be weighed and perhaps evaluated in hypothetical terms. There is opportunity for thorough discussion and for reconciliation of views. Some compromises, of course, are inevitable, as group agreement is evolved on what 1964 may logically have in store for electric utilities.

The Secular Trend

One of the dictionary definitions of "secular" is "existing or continuing through ages or centuries." When one attempts to establish the secular trend for a mass of data in a time series, one may be confident enough of the centuries (or years) in the central portions of the curve, but one can never tell whether or not the line is correctly drawn when it approaches the ends of the time scale; hence, the use of a remote-point forecast. It fixes the 10-year-off spot on the secular trend curve, i.e., on a smooth curve fitted to the historical data and extended into the future. It is recognized, of course, that for any particular year the actual statistics may, and probably will, depart from such a trend line, since this line theoretically represents conditions as likely to be exceeded as not. However, for the far future it is not possible to estimate such deviations and the secular trend is the logical objective toward which system development should be projected.

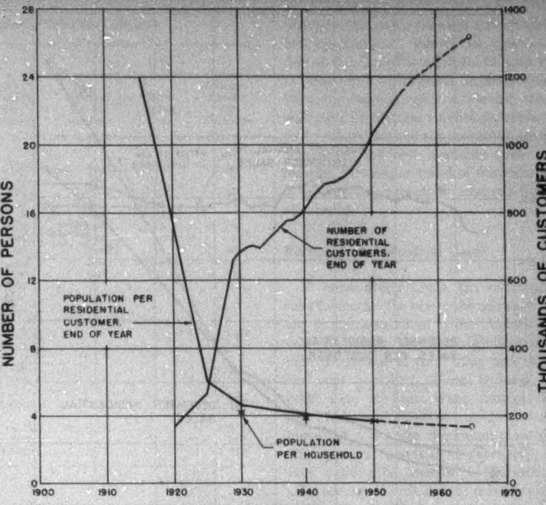

Fig. 2. Residential customer forecast

The trend line may be straight, or it may be a suitable curve; mathematical definition of it is usually feasible if wanted. If it is mathematically defined, fitting it to the historical data may also be mathematical, usually by the method of least squares, and it may then be mathematically extrapolated. Such a procedure is often employed as one, but only one, of the tools used in establishing the remote-point forecast.

Alternatively, however, the trend may be both fitted and prognosticated through the remote point by judgment and observation only and no mathematical equations for it ever established. The great advantage of the nonmathematical procedure lies in the opportunity it offers for the application of judgment as to the future. It is the preferred practice in most unstable situations.

Forecast of Residential Sales

Use of Population Forecasts

Population, of course, is one of the statistics most readily available for the long past and, by comparison with other quantities dealt with in this paper, it is one of the most accurately forecastable into the future. Any study depends heavily on the work of population experts. By analyzing and reconciling the conflicting views of such students of the subject and modifying their results to apply specifically to the utility's territory, a forecast of future population in the area served is derived; see Fig. 1.

The population per residential customer may be calculated from the company's records and forecast into the future, nothing that it is likely to approach a value related to size of household. An estimate of the number of residential customers can then be obtained by division and checked by a direct extention of available historical data; see Fig. 2. By forecasting consumption per customer, an estimate of total residential sales is obtainable; see Fig. 3.

Use of semilog paper in studying such statistics is often helpful, since on such paper a straight line represents a compound percentage increase. The results plotted in Fig. 3 may be checked as to reasonableness by this method. This is done in Fig. 4, which shows that the present forecast of 1964 residential use predicts a decreasing percentage increase, on the average, over the 10-year period.

Consumption Per Customer

Such a decreasing rate of growth appears acceptable after examination of the forecast of number of customers, related to population and not now subject to logarithmic increase, and after analysis of expected future use per customer; see curve *A*, Fig. 3. This latter is the most important element in the forecast of residential sales. One method of studying it has been called a "synthetic approach."

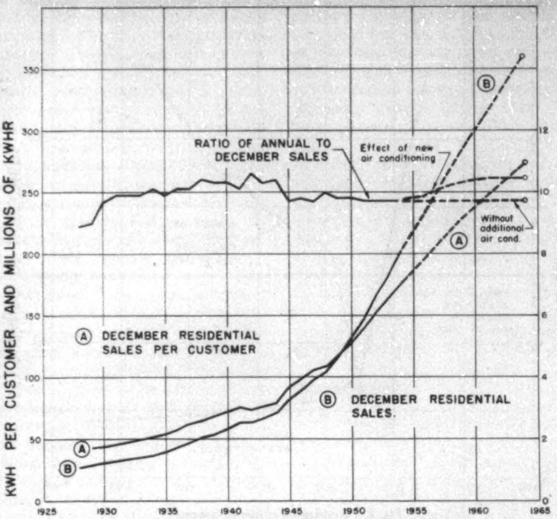

Fig. 3. **Forecast of residential sales, per customer and December total**

The forecaster is concerned with expected increasing use of various appliances or devices, usually the most recent introductions. Among the more important such items today are television sets, ranges, water heaters, and the numerous "weather makers" for drying, humidifying, heating, or cooling. It is necessary to study the probable increased "saturation" of the territory with these devices and the expected average use of each. There may, statistically, be more than 100 per cent (%) saturation of some appliances as there is today with radio sets, most homes having more than one.

Table I shows the results of a recent discussion of conflicting views on this problem. It is considered that this is an area in which load research can be most profitable if increased accuracy in residential forecasts becomes important, for at present much of the basic information required for this tabulation is of a low order of accuracy.

RECONCILIATIONS

It will be noted that Table I is set up on an annual-use basis, whereas the curves of Figs. 2, 3, and 4 are for the month of December of each year only. Several steps at the bottom of Table I reconcile the two, utilizing a ratio of December to annual forecast from a graph in Fig. 3. In practice, most of the information is forecast both ways and in many cases each component and each total is forecast independently. All of these elements must then be reconciled so that the same estimate is obtained by any appropriate combination of steps. It is surprising how frequently this procedure will disclose incompatible prognostications and result in important shifting of preliminary views.

All of the initial effort and discussion is devoted to the establishment of a reasonable expectation for residential sales at a time 10 years hence; 1964 in the details given. The intermediate years are bridged. This future point itself is considered to be only tentative until all of the work of any forecast is completed. Thus full freedom is allowed for the introduction of new information or opinion at any time. For instance, it may be that studies of commercial or industrial sales will bring to light some reason for reconsideration of previously accepted parts of the forecast.

SECULAR TREND AND DEVIATIONS

With the remote point relatively fixed (usually after establishing also the corresponding remote points for commercial and industrial sales) the next step is to construct a trend line from the present to the forecast future. Residential sales almost never deviate importantly from a smooth growth; the charts show such deviations only during the years of the Great Depression and the period of war curtailment. There is currently some slight indication of a postwar, abnormally accelerated growth, attributable perhaps to television. These are the influences to be considered in the construction of a trend line. Usually they do not present important difficulties in the case of residential sales. In long-range forecasting it is always assumed that for any period more than a year or two in the future residential sales will be on the secular trend. Deviations are likely to be insignificant and are almost certainly unpredictable.

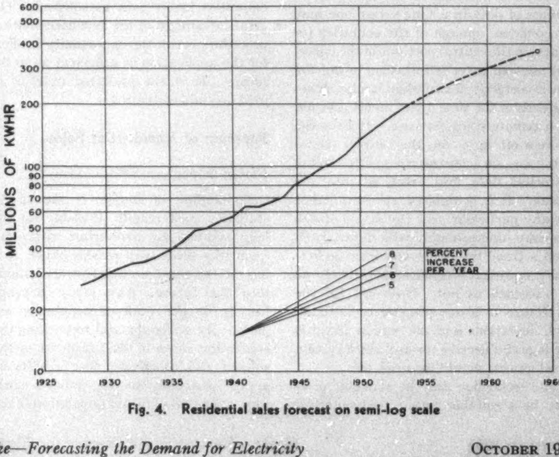

Fig. 4. **Residential sales forecast on semi-log scale**

Table I. Synthetic Forecast of Residential Sales Per Customer

Appliance	1954 Average Kw-Hr per Unit	1954 Saturation, %	1954 Average Kw-Hr per Customer	1964 Average Kw-Hr per Unit	1964 Saturation, %	1964 Average Kw-Hr per Customer
Television						
First set per customer	220	100	220	300*	100	300
Second set per customer	200	0	0	200	25	50
Range	1,200	4	48	1,200	10	120
Water heater	3,600	1.1	40	3,600	4	144
Dryer	660	0.6	4	600	1	6
Electric house heating	10,000	0	0	10,000	0.5	50
Deep freezer	680	6	41	750	10	75
Room cooler	400	6	24	400	50	200
Attic fans	260	6	16	250	10	25
Furnace fans	255	10	26	350	25	87
All other			1,307			1,800
Annual total per customer, kw-hr			1,726			2,857
Less more than proportionate room cooler growth, kw-hr			0			163†
Annual total per customer excluding more than proportionate room-cooler growth, kw-hr			1,726			2,694
Average number of customers			1,119,000			1,300,000‡
Annual sales excluding more than proportionate room-cooler growth, millions of kw-hr			1,930			3,500
Ratio: annual sales to December sales, excluding more than proportionate room-cooler growth			9.7			9.7§
December sales, millions of kw-hr			200			360
Total annual sales, millions of kw-hr			1,930			3,710

* Includes color TV.

† 200 − 24(2,857 − 200)/(1,726 − 24 × 24) = 163.

‡ Obtained from a chart similar to Fig. 2 except based on average number of customers throughout the year.

§ From Fig. 3; this ratio would be 10.3 if room-cooler adjustment were not made.

Forecast of Commercial Sales

The forecasting of commercial sales is very similar to that of residential sales. The work is done both with December data and with annual figures; also sometimes with monthly sales. These last are particularly useful when forecasting is for only a year or two in advance.

The relationship of commercial sales to population is weighed and expected new uses for electricity in commercial establishments are studied. Of course, summer air-conditioning is one of the most important of such uses. Both built-up forecasts and direct projections are employed, one is checked against the other and results are discussed at length in committee meetings. The final forecast for the 10-year-off point is also checked by relating it to the corresponding residential sales estimate on the theory that there should be a reasonable correlation between the two; see Fig. 5.

In determining a trend line for commercial sales, the deviations experienced are wider than is the case with residential sales. Evidently commercial sales are somewhat influenced by fluctuations in business conditions; much more so than residential sales. This adds to the difficulty of locating a satisfactory secular trend.

A procedure for recording applications for large blocks of power for commercial purposes is very helpful in studies of near-term commercial sales deviations from trend. The sales department maintains complete records of expected new demands of large commercial customers. Each month the ones which are cut in are deducted and any new ones added. This may provide a basis for explaining erratic variations and it establishes a known pool or backlog of applications for power. The size of this backlog depends on the current relationship between cut-ins and new applications. Hence, an examination of this record is a helpful indication of near-term commercial expectations. Such information, plus a careful consideration of business conditions, applied to the recent past and the probable future, constitutes the best available guide in locating the secular trend of commercial sales, and any expected variations from that trend.

Forecast of Industrial Sales

In most utility areas, the industrial sales forecast is the key to the accuracy of any prognostication of loads. Industrial sales are almost certain to constitute a high percentage of total sales and they are very variable. When business is good, sales are up. When business is poor, industrial sales may go to a very low point. If a new aluminum plant or blast furnace locates in the territory, a very substantial increase in industrial sales occurs; if such a plant moves away the loss may be a high percentage of total industrial sales. Such factors are almost completely unpredictable, and require special treatment. They exert a major influence on the accuracy of the over-all forecast. Hence, a very large part of the time in making any estimate is devoted to examination of industrial prospects.

VARIOUS APPROACHES USED

Among the various methods of making estimates of industrial sales for a remote future year, based on studies of the components or factors which will produce those sales, may be listed the following:

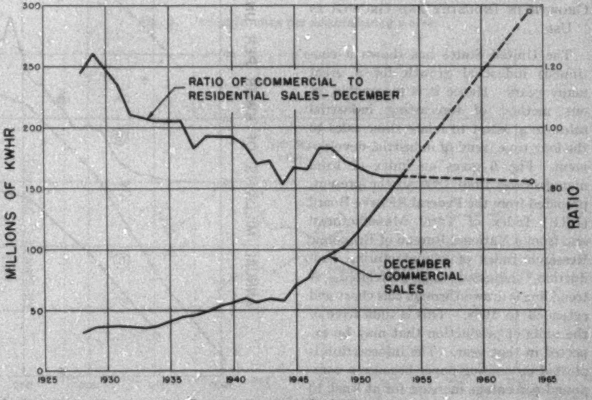

Fig. 5. Commercial sales forecast

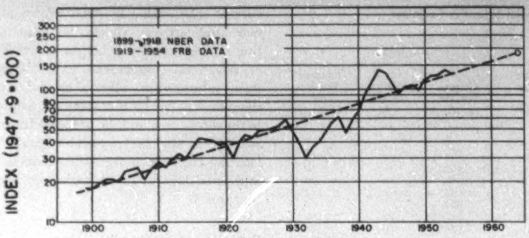

Fig. 6. Index of total manufactures

Table II. Index of Manufactures

Calculated From Value Added by Manufactures (U. S. Census of Manufactures) Compared with FRB Index of Toal Manufactures (1935–39 = 100)

Representative Years	Computed from Census of Manufactures	F.R.B. Index
1919	87	72
1925	93	90
1929	113	110
1935	86	87
1939	113	109
1947	212	194
1949	202	183

1. To forecast the growth in industry and the growth in use of electricity, per unit of growth in industry.
2. To forecast the growth in number of industrial workers and the growth in consumption of electricity per worker.
3. To forecast the monthly hours use by industry of its noncoincident billed demand for electricity and the growth in that noncoincident billed demand.
4. To separate industrial sales into different components depending on size of customer's business or on nature of use, and study separately the growth or decline of each of these elements in the local industrial economy, examining the relationship of each to the total industrial use.

It is proposed to discuss briefly each of these four approaches to a long-range industrial forecast. As will be recognized, they are applicable to such sales as a class, but not necessarily useful to forecast the future of any one customer. Any single user representing an important percentage of total industrial sales should be separately examined.

GROWTH IN INDUSTRY AND GROWTH IN USE

The United States has shown a continuous industrial growth for a great many years. Hence it is reasonable, as one method of forecasting industrial sales, to attempt to relate these sales to the long-time trend of industrial development. Fig. 6 gives an index of total manufactures from 1899 to the present, prepared from the Federal Reserve Board (FRB) Index of Total Manufactures[1] and from a National Bureau of Economic Research Index of Manufacturing Production,[2] adjusted and correlated. A trend line is drawn through this chart and extended to 1964. This is indicative of the units of production that may be expected in that year. The information is plotted on semilog paper because a compound percentage increase for at least 10 years into the future appears justified by the very long period of historical growth to which a percentage increase seems to apply.

Of course this information is based on the United States as a whole. Before using it for any particular territory, a detailed study is necessary to ascertain that that area has varied in its manufacturing output approximately as has the nation. If the territory is highly diversified, this is likely to be true. Such a check can be made through studies of the value added by manufactures, taken from the Census of Manufactures[3] and available by counties. The actual steps in one such correlation were the following.

1. Assume that the dollar value of production in the particular territory (Public Service Electric and Gas Company) increases as that of the state (New Jersey) since: 1. the value added by manufactures in 24 cities (Public Service Electric and Gas Company territory) was nearly a

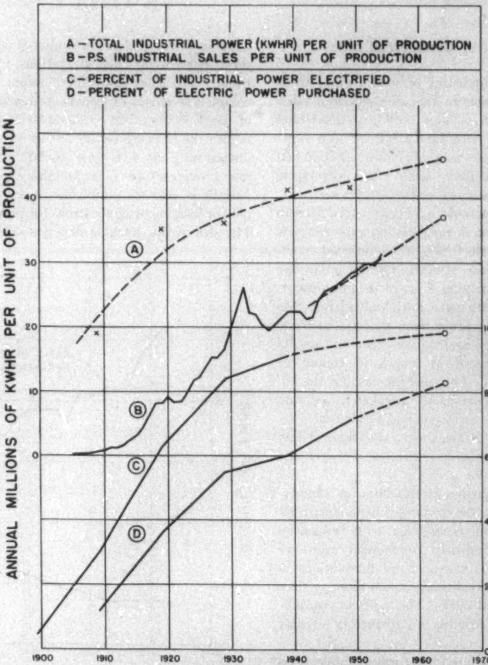

Fig. 7. Industrial sales per unit of production

constant 70% of that of New Jersey for the period 1899 to 1919, and 2. the value added by manufactures in 11 counties (Public Service Electric and Gas Company territory) was nearly a constant 90% of that of New Jersey for the period 1919 to 1947.

2. Assume that the dollar value of production in the state increases as that of the United States from the period 1899 to 1947, since the value added by manufactures in New Jersey was nearly a constant 5.6% of that of the United States for the same period.

3. Correct the value added by manufactures for the United States to a constant dollar base using the Consumers' Price Index[4] issued by the U. S. Bureau of Labor Statistics and transform into an index. This compares well with the FRB Index as shown in Table II. (The recent shift in the base of the FRB Index does not, presumably, invalidate this correlation.)

By dividing the utility's industrial sales by the index of production shown in Fig. 6, a quantity "kilowatt-hours sold per unit of production" is obtained. This is plotted in Fig. 7, curve *B*. Obviously, if this curve and the index are both extended to 1964, their product will give an industrial sales forecast for that year; see procedure 1 in the following forecast.

ANNUAL INDUSTRIAL SALES FOR 1964 AS FORECAST BY FIVE PROCEDURES

Procedure 1. Growth in Manufactures and Sales Per Unit

1. Index of total manufactures, Fig. 6, 180
2. Industrial sales per unit of production, Fig. 7, 37,000,000 kw-hr
3. Total industrial sales, item 1×item 2, 6,670,000,000 kw-hr

Procedure 2. Growth in Manufactures and Total Power Per Unit

1. Index of total manufactures, Fig. 6, 180
2. Total industrial power per unit of production, Fig. 7, 46,000,000 kw-hr
3. Per cent of power electrified, Fig. 7, 98
4. Per cent of electric power purchased, Fig. 7, 82
5. Total industrial sales, item 1×item 2× item 3×item 4, 6,670,000,000 kw-hr

Procedure 3. Growth in Workers and Sales Per Worker

1. Number of manufacturing workers, Fig. 8, 860,000
2. Industrial sales per worker, Fig. 8, 7,750 kw-hr
3. Total industrial sales, item 1×item 2, 6,670,000,000 kw-hr

Procedure 4. Hours Use of Billed Demand

1. Noncoincident billed demand, Fig. 9, 1,590 megawatt (mw)
2. Hours' use per month, Fig. 9, 350
3. Total industrial sales, item 1×item 2× 12, 6,670,000,000 kw-hr

Procedure 5. Large Customer Component

1. Number of customers with demand of 500 kw or more, Fig. 10, 670
2. Average sales to these customers, Fig. 10, 8,450,000 kw-hr
3. Per cent of total industrial sales, Fig. 10, 85
4. Total industrial sales, item 1×item 2÷ item 3, 6,670,000,000 kw-hr

NOTE: The ratio of annual to December industrial sales since 1950 has been 11.78, 11.65, 11.25, 11.32 and 11.55. This ratio is forecast as 11.5 for 1964. Hence December industrial sales are forecast as 6,670,000,000/11.5=580,000,000 kw-hr.

A corollary of this method is helpful. The industrial sales of a utility in its territory today probably represent practically all of the purchased industrial power. But this is not the total industrial power produced and it is a relatively recent development. Over the long term, power has been of at least three kinds, steam, hydraulic, and electric, and any of the three may have been either purchased or owner-produced. Is it possible to relate industrial sales of electricity to census data on total power produced in the area, of all kinds, over a long period of years, and what would be the relationship between this total power and the index of production (total manufactures) already discussed and forecast?

To refer again to New Jersey, statistics obtained from the U. S. Census of Manufactures[3] show that in the period 1899–1939 the percentage of total industrial power supplied by electricity increased from 5% to 91%; See Fig. 7, curve *C*. From U. S. Census,[3] Federal Power Commission[5] and Edison Electric Institute[6] data it is found that electric power pur-

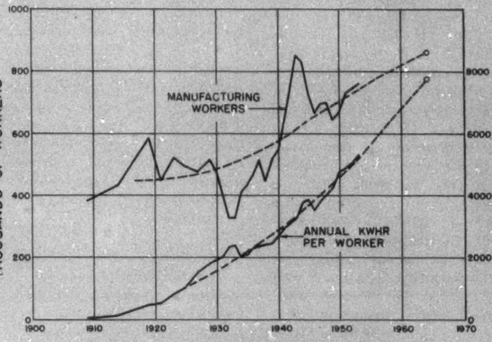

Fig. 8. Industrial sales per manufacturing worker

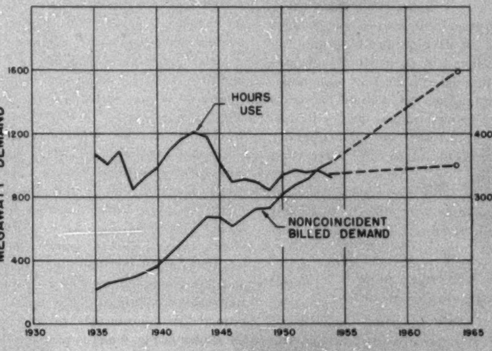

Fig. 9. Industrial demand and hours use

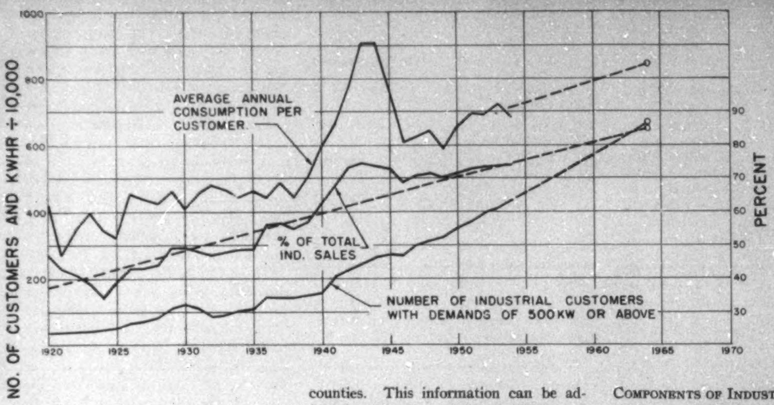

Fig. 10. Large customer industrial sales

chased from utilities in New Jersey, expressed as a percentage of total industrial power supplied by electricity, increased from 12% in 1909 to 71% in 1949; see Fig. 7, curve *D*. If the per cent of industrial power electrified is multiplied by the per cent of electric power purchased, the result will be the per cent of all industrial power purchased as electricity. If industrial sales in the utilities' territory are divided by the per cent of all industrial power purchased, the result will be the total power used in the territory, electric and otherwise, purchased or owner-generated. Dividing this by the index of production already discussed, Fig. 6, results in the quantity, total power used in the territory per point of index, or per unit of manufacturing production.

This quantity is also plotted in Fig. 7, curve *A*. It shows currently only a very moderate rate of growth, most logically forecast as a straight line. Forecasting this factor and the various percentages discussed, all of which must be asymptotic to something less than 100%, provides another method of indicating total industrial consumption at a time 10 years hence. This method may be described as "units of production times total power per unit times per cent of total power sold by utilities." It provides another set of figures to check the reasonableness of forecasts obtained by other methods and is shown in the foregoing forecast as procedure 2.

Growth of Number of Workers and Consumption Per Worker

From U. S. Department of Labor[7] statistics it is possible to ascertain the number of manufacturing workers by counties. This information can be adjusted to a given utility territory and forecast directly, or a probably better estimate may be obtained by a study of the age and sex pattern of the population and a projection of those elements or factors which will establish the number of workers in the future. Fig. 8 shows a forecast of manufacturing workers and a related estimate of industrial sales per worker. This is included as procedure 3 in the foregoing forecast. It is also feasible to study the number of hours worked per week, i.e., the average work week, and from this, and the number of workers, to forecast man-hours, and industrial sales per man-hour.

Hours' Use of Billed Demand

A totally different approach to the problem of forecasting industrial sales may be had by extending into the future the ratio, monthly industrial kilowatt-hour sales divided by the sum of the noncoincident demands billed to all industrial customers. This ratio is called "hours' use of billed demand," since it gives the average hours' use of the aggregate of all industrial customer demands in any month. It is very sensitive to industrial conditions at any particular time is and often used as a form of business index. If normal industrial conditions are assumed, as is customary for a remote future date, then a smooth line through the average of available data for this ratio is an interesting and fairly firm forecasting agent. Multiplied by a forecast of total noncoincident billed demand, which is relatively unaffected by business booms and depressions, a direct forecast of industrial sales is obtained. The hours' use ratio and the noncoincident billed demand are shown in Fig. 9 and in procedure 4 of the foregoing forecast.

Components of Industrial Sales

Many companies classify industrial sales into different codes. It is often possible to determine whether an industry is growing, static, or declining in the territory and for the various codes or classes employment records can be obtained and forecast. Consumption of electricity can be correlated with such information and forecast on an industry-by-industry basis. In the 1920's the electric trolley system was an important element in the sales of many companies. The use of power for this purpose, however, has steadily declined in most areas until now it is negligible. By a study based on industrial classifications, this fact could probably have been divined and allowance made for it in the forecasts, long before it occurred. At present in New Jersey the pharmaceutical and chemical industries are very strong and growing rapidly. On the other hand, the leather business and jewelry manufacturing, which were once large, are declining. In the textile industry there is a definite trend toward new plants in the South and the abandonment of older mills in the North.

Some 75% of the industrial sales of Public Service Electric and Gas Company are to customers with maximum-billed demands of 500 kw or more. These customers constitute only about 6.2% of the total number of industrial users and it has been found helpful to study their sales and demands separately on the hypothesis that they are representative of the entire industrial group. Since they are relatively few in number (about 400 in 1954), it is possible through sales contacts to bring to bear in such studies some direct knowledge of their individual prospects. It is found that the number of customers in a category of this size is increasing, that their consumption per customer is gaining, their aggregate demand is rising, and other similarly interesting growth factors are evident. Forecasts of their remote future and of their relationship to the total industrial classification are regularly made; see Fig. 10 and procedure 5 of the foregoing forecast. If desired, some of the methods already described may be applied to this numerically small group.

SUMMARY OF INDUSTRIAL FORECASTS

Five procedures for arriving at a remote-future forecast of industrial sales are summarized and reconciled in the foregoing forecast, and the final result is plotted in Figs. 11 (arithmetic) and 12 (semilog). While these procedures are not all entirely independent of each other, the various components, extended into the future, do produce a reasonably convincing body of data undergirding the final forecast. Wide error appears unlikely, assuming that there will be no major war or depression in the 10-year period. While such extraordinary disturbances may occur, to presume one or the other and establish its timing and magnitude as a basis on which to plan the development of a utility system would be to speculate with the welfare of the community. A thoroughgoing reorientation of all prognostications becomes a necessity if extraordinary changes in basic assumptions occur.

ESTABLISHING THE TREND

The virtue of having studied first the long-range future is apparent when one undertakes to establish a secular trend for industrial sales. By definition the remote point is a point expected to lie on the long-term trend. Also by definition, the secular trend is expected approximately to bisect the fluctuations of the actual data, i.e., plotted on arithmetic paper the areas above and below the line should be approximately equal given a long enough time period. Thus much of the difficulty of locating this line is eliminated. It may be fitted to the known data mathematically and extended arbitrarily to the remote point, or the entire process may be one of visual judgment only. Incidentally, it is, of course, possible that the location of the remote point itself may be influenced by mathematical extensions.

The forecast of a remote point also provides a bench mark or guide which is helpful in the current-term location of the secular trend. Factual data for this period too are unknown; it is not possible now to state whether the future will show that present industrial consumption is substantially above, only a little above, or perhaps below its secular trend. But acceptance of the distant point limits the present location possibilities.

An interesting example of this dilemma occurred a few years ago when most business indexes recorded conditions as far above normal. Such indexes are, in simplest terms, merely ratios of actual conditions either to a secular trend (if the index excludes growth) or to an average of conditions for certain chosen years, if the index includes growth as does the FRB Index of Manufactures;[1] see Fig. 6. Recently, these indexes have been recalculated on various revised assumptions of

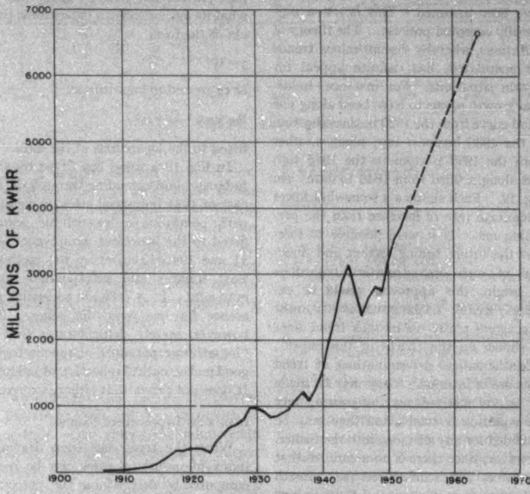

Fig. 11. Annual industrial sales

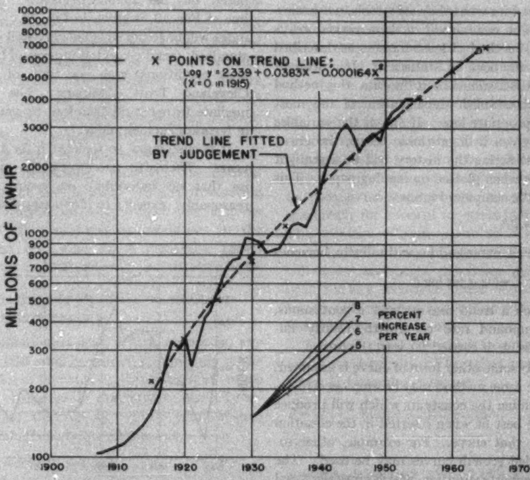

Fig. 12. Annual industrial sales and trends

trend line or base period and what they portrayed as indicating boom times when being experienced, are now confidently shown to have been only a little above normal.

COMMENT ON TRENDING

Throughout this discussion smooth, continuous trend lines and extrapolations have been assumed. This is not a universally accepted premise. The theory of mutations, whereby discontinuous trends are postulated, has definite appeal for certain situations. For instance, industrial growth seems to have been along one trend curve from the 1920 business bottom to the 1930 business top, along another from the 1932 bottom to the 1945 top, and along a third from 1946 to date; see Fig. 12. Each shows a a somewhat lower percentage rate of increase than the preceding one. If it were possible to forecast the future timing, extent and direction of such discontinuities, regardless of origin, this approach would be extremely useful. Lacking that ability, most forecasters prefer continuous trend lines as shown on the charts in this paper.

Mathematical determinations of trend lines are of interest. They may be made by several methods and, of course, once the equation is established they may be extended for any distance into the future. However, since there is no assurance that the forces which influenced past growth will continue unabated and that no new factors will be introduced, these mathematical prognostications must be recognized for what they are: tools, not brains.

The commonest of these procedures is the method of least squares as described in any book on statistics.[9] If a straight line is assumed to fit the data, this method will establish the equation of the most appropriate line. If one of the variables is given in logarithmic terms, the curve best fitting the history will be a straight line when plotted on semilog paper. This is the compound interest curve

$$Y=ab^x$$

which, expressed logarithmically, becomes

$$\log Y=\log a+x\log b$$

Such a trend line assumes a continuous, compound rate of growth, clearly impossible if carried far into the future.

If some other form of curve is assumed, the same method may be employed to determine the constants which will produce the best fit when inserted in the equation for that curve. For example, other so-called growth curves may be used. The Gompertz equation, which gives the usual S-curve of growth in the form

$$y=b_0b_1^{e^{Bx}}$$

is very frequently employed in such studies. However, in a recent publication by the National Industrial Conference Board,[8] while applied to many industries, this Gompertz equation was discarded for the electric utility industry because it "did not seem to answer the purpose particularly well." This study used what its author called a logarithmic parabola of the form

$$y=10^{a+bx+cx^2}$$

or expressed in logarithms

$$\log y=a+bx+cx^2$$

fitted to the logarithms of the data.

In Fig. 12 a trend line fitted by visual judgment and extending through the forecast of 1964 industrial sales, is compared with points on a logarithmic parabola fitted to the historical data (years 1920–41 and 1946–50 only) by the method of least squares and extrapolated mathematically. It is difficult to justify preference for one over the other. This, however, merely demonstrates that the "logarithmic parabola" happens to be a good mathematical reflection of judgment. It does not prove that either is correct.

INDEX OF INDUSTRIAL SALES

When the trend has been drawn, an index of industrial sales can be readily computed by determining the percentage deviation from the trend of each point on the curve of actual sales. Such an index, based on the nonmathematical trend line of Fig. 12, is given in Fig. 13. This index will be found to agree very well with standard, trend-corrected indexes of business conditions such as that of the Cleveland Trust Company. The immediate future may therefore be gauged in terms of such an index.

It is customary to forecast it for a few years. Thereafter, accepting the premise that no individual or group can reasonably expect to forecast distant booms or depressions, an index of 100 may be assumed. Fig. 13 shows the range through which this index has moved in the past and affords a basis for estimating quantitative variations. Before arriving at this forecast, careful study should, of course, be made of the views expressed by government and private economists, business men and others. A weighing of these and a study of the current economic situation is necessary. This is inevitably a nonmathematical process. It is a matter of research, and of appraisal of the economic scene, and is one of the most important elements in the near-term portion of any forecast. Once established, it is a simple matter to interpret such an index in terms of industrial sales.

A word of caution is perhaps pertinent at this point. In efforts to crystallize a near-term estimate considerable reliance is sometimes placed on detailed surveys of the plans of industrial customers. Such information may appear very complete and comprehensive and may be carefully tabulated and analyzed. Experience has demonstrated, however, that most industrial customers are overoptimistic. It costs them nothing to indicate an expectancy of large loads and it may insure, they think, that there will be plenty of power. Consequently, they are likely to overestimate heavily.

THE VERY LARGE CUSTOMER

There is a place, however, for a few carefully evaluated individual appraisals. With the tremendous increase in the use of electric energy for certain industrial processes, as in the chemical or metallurgical fields, it is not uncommon for a utility to include among its customers a very few whose requirements constitute such a large proportion of the total industrial sales that changes in their individual programs may seriously distort any forecast. These changes, of course, may at times be contrary to prevailing business trends.

Such a new customer, just coming on,

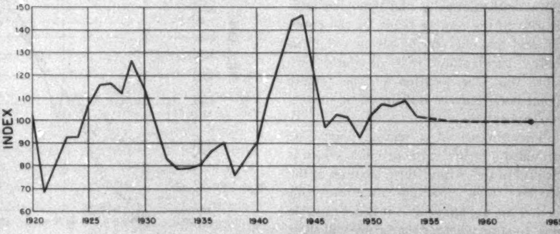

Fig. 13. Index of annual industrial sales

may cause the statistics to record a major business upturn even though excluding this new load the index of industrial sales may be in a depressed period. If included for several years in either a mathematical or visual determination of trend, this increment of sales may cause an unjustified forecast of accelerated growth.

Clearly there is a point in size beyond which individual customers cannot merely be added into the existing industrial group and forgotten. They must, instead, be treated as a separate sales class (such as residential or commercial), their future studied carefully, forecast individually, and added to all other forecasts to obtain an estimate of total sales. The index of industrial sales, Fig. 13, and other statistical components of the forecast must be calculated exclusive of these disturbances to group trends. Such treatment has been found necessary for a customer forecast to represent about 5% of total industrial sales.

Forecast of System Peak

LOSSES AND ADJUSTMENTS

With the major classes of sales, residential, commercial, industrial, and perhaps one or two large individual customers forecast into the future, remote points established, trends determined, and the intermediate values agreed upon, total output is obtained by adding certain minor items such as street lighting, company-use, and auxiliary requirements in generating stations, and a reasonable allowance for losses.

With losses there are also included adjustments which correct for calendar variations and for changes in meter-reading schedules. This is not an important factor if annual kilowatt-hours are under study. However, when the forecaster is concerned with December sales or with any other single month, it may be important, since, with continuous meter-reading schedules, it takes account of the fact that sales reported for any month cover consumption which occurred through part of that month and part of the preceding month, whereas output is for the calendar month only.

On an annual basis, total losses expressed as a percentage of total energy accounted for, have decreased substantially. Thirty years ago they often ran over 20%; currently, figures as low as 10% are not uncommon. After all adjustments and additions, the final estimate of output may again be checked for reasonableness by a direct projection of output data which goes back for many years.

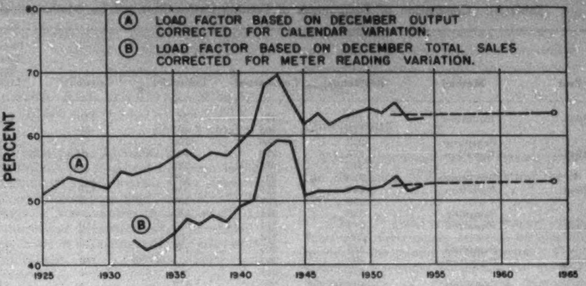

Fig. 14. Load factors

Only a forecast of load factor is now required to arrive at an estimate of the system peak. Forecasting load factor, however, is not easy. This ratio has wide and frequent variations, some undoubtedly due to variation in business conditions, others to accidental factors influencing the peak. Several approaches to this step seem justified.

FORECAST OF PEAK BY USE OF LOAD FACTOR

Two different load factors are plotted in Fig. 14. Both are for the month of December. One shows the relationship between peak and total monthly output corrected for calendar variation, the other between peak and total sales. Railway loads have been excluded in the second curve because of a rapidly declining trend, entirely contrary to the trend of all other components. This so-called sales load factor is lower because of the effect of losses and adjustments. There is some correlation between these load factors and the business cycle. The highest load factors tend to accompany great business activity; conversely the lowest load factors often are associated with low business conditions. However, the correlation at best is poor. In any forecasting of load factor, some weight may be given to expected business conditions in the near term, but on a qualitative rather than a mathematically quantitative basis.

FORECAST OF PEAK BASED ON CLASS CONTRIBUTIONS

Since the peak which occurs in any month must be related in some way to the sales of kilowatt-hours to different classes of customers in that month, one may assume that in any given year, system peak P can be represented as

$$P_1=k+dR_1+eC_1+fI_1$$

and for some other year

$$P_t=k+dR_t+eC_t+fI_t$$

where

P = monthly peak
R = monthly residential sales
C = monthly commercial sales
I = monthly industrial sales, all for the same month
k = an addition constant to be obtained from solution
d, e, f = multiplication constants to be obtained from solution

With the use of data for P, R, C, and I for an adequate number of years (at least 10), values for the constants k, d, e, and f which statistically most nearly fit the conditions can be determined by the method of least squares; see, for instance, reference 9. As a test of the data used in such a computation, coefficients of correlation or determination should be computed. The historical data, the equation obtained, and the future data to which they may be applied must all be logical and consistent. For example, months in which unusual contributions to peak occurred should be eliminated, the coefficients of the equation should be reasonable, and none should be negative. If helpful, other terms may be introduced, such as one reflecting some change related to passage of time or one to provide specifically for losses or for street lighting. The problem, of course, is to discover an equation with a set of constants which will most accurately determine system peak for any month in terms of various known or forecast components of kilowatt-hours for the same month.

Two such equations which have proved useful for forecasting December peak in terms of December sales are

$$P=110+2.408R+3.200C+2.157I, \qquad (1)$$

and

$$P=98.5-5.249T+2.559R+3.140C+2.525I. \qquad (2)$$

Table III. Comparison of Components of Evening Peaks Obtained by Mathematical Equations and by Sampling Process, Mw

Year	Method	Residential	Commercial	Industrial	"Constant"	Company Use and Street Lighting	Transport	Summation = Indicated Peak	Actual Peak
1939	Equation 1	132	171	262	110		29	704	718
	2	141	168	307	56		29	701	
	Sampling	253	186	230		44	35	748	
1947	Equation 1	225	278	495	110		18	1,126	1,122
	2	240	273	580	14		18	1,125	
	Sampling	329	230	430		95	22	1,106	
1948	Equation 1	242	299	510	110		6	1,167	1,168
	2	258	294	597	9		6	1,164	
	Sampling	339	274	437		100	7	1,157	
1949	Equation 1	274	324	512	110		5	1,225	1,211
	2	292	318	600	4		5	1,219	
	Sampling	373	265	453		102	5	1,198	
1950	Equation 1	307	355	625	110		4	1,401	1,417
	2	326	348	731	−2		4	1,407	
	Sampling	461	269	579		112	4	1,425	
1951	Equation 1	347	394	635	110		4	1,490	1,493
	2	368	386	743	−7		4	1,494	
	Sampling	460	340	572		122	4	1,498	
1952	Equation 1	382	426	722	110		2	1,642	1,612
	2	406	418	846	−12		2	1,660	
	Sampling	513	398	609		123	2	1,645	
1953	Equation 1	413	461	689	110		2	1,675	1,713
	2	439	452	807	−18		2	1,682	
	Sampling	556	421	575		142	2	1,696	
1954	Equation 1	467	519	737	110		2	1,835	1,850
	2	496	509	862	−23		2	1,846	
	Sampling	(not yet available)							

where P is in megawatts and all sales figures in millions of kw-hr adjusted for average December meter-reading interval, with the addition in equation 2 of a factor T representing time, i.e., the number of elapsed years since 1931 when the series on which the equation is based began.

Applying December sales data in these equations gives excellent approximations of system peaks less certain known contributions. Over the past 24 years, excluding the 3 war years, the maximum error in any forecast peak, assuming the sales estimates to be correct, would have been less than 3%, and the average error less than 1%.

Unfortunately, for a variety of reasons, some obscure, it has not so far been found feasible to determine the actual contributions to peak of various classes of sales by use of such equations. By sampling processes, it is possible to make fairly rigorous determinations of demands of various classes of service for 24 hours during heavy-load days. These curves when added together with appropriate losses included, must, of course, produce the load curve for the total system. If adjusted to peak-day conditions, they must add up to the system peak.

Table III shows a comparison of peak contributions actually obtained by studies of load samples and of the "peak contributions" obtained by equations 1 and 2. Although both processes add up very closely to the total system peak, only the sampling processes can be used to determine the actual contributions of classes. This is because only the sampling process provides curves of loads versus time, which can be added up to give system demands at various times of the day. These are the curves which must be used to study the effects of war-time, or year-round daylight saving or additional second-shift operation of industry, or other changing conditions. It is possible also to use such data, augmented by simultaneous day and evening readings of demands of all industrial and many large commercial customers (all of those having recording demand meters) to arrive at rough estimates of the peak contribution of each customer class, per million kw-hr of sales. This approach has been em-

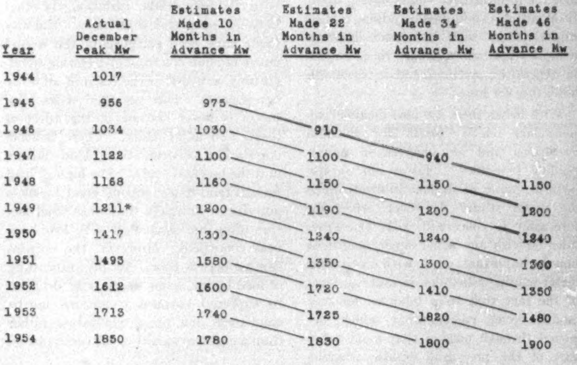

Year	Actual December Peak Mw	Estimates Made 10 Months in Advance Mw	Estimates Made 22 Months in Advance Mw	Estimates Made 34 Months in Advance Mw	Estimates Made 46 Months in Advance Mw
1944	1017				
1945	956	975			
1946	1034	1030	910		
1947	1122	1100	1100	940	
1948	1168	1160	1150	1150	1150
1949	1211*	1200	1190	1200	1200
1950	1417	1300	1240	1240	1240
1951	1493	1580	1350	1300	1360
1952	1612	1600	1720	1410	1350
1953	1713	1740	1725	1820	1480
1954	1850	1780	1830	1800	1900

*A peak of 1230 Mw occurred in this year on November 29.

Fig. 15. Comparison of actual system peak with forecasts. Diagonal lines connect forecasts made at same date. For example, in February 1945, after December 1944 peak of 1,017 mw, it was forecast that peak in December 1945, 10 months later, would be 975 mw; in December 1946, 22 months later, 910 mw; in 1947, 940 mw, and in 1948, nearly 4 years later, 1,150 mw. This was a forecast that war would end in 1945, and would be followed by business recession, with full recovery by 1948. One year later it was clear that recovery was already on way. In February 1950, Korean war and rearmament program were not foreseen and all forecasts made then, 1,300, 1,350, 1,410 and 1,480, were low. In 1951, under influence of "cold-war" hysteria, estimates for next 3 years, until 1954, were high

ployed in some national forecasting but must be discounted because of unpredictable variations which occur from year to year.

A final forecast of December 1964, peak is shown in the following forecast, which is based on the December sales estimates developed in this paper for that year. It includes also certain miscellaneous, relatively noncontroversial estimates, the most important being 152,000,000 kw-hr for losses and adjustments, and 90,000,000 kw-hr for station auxiliary use. If the sales forecasts are correct, these other estimates are unlikely to be seriously in error. Four different forecasts of peak result from the 2-load factor approaches and equations 1 and 2. The final prognostication is shown as an average of these, rounded to the nearest 100,000 kw.

Forecast of December Peak, 1964

Estimate of residential sales, December 1964, Fig 3, 360,000,000 kw-hr

Estimate of commercial sales, December 1964, Fig. 5, 295,000,000

Estimate of industrial sales, December 1964; see "Annual Industrial Sales for 1964 as Forecast by Five Procedures," 580,000,000

Total sales, 1,235,000,000

Estimate of street lighting, company use, auxiliaries, and losses and adjustments for December 1964, 263,000,000

Estimate of gross output, 1,498,000,000 kw-hr

Estimated peak, based on sales load factor forecast of 53

$$\frac{1{,}235{,}000{,}000+14{,}000{,}000\text{ (street lighting)}\times0.985\text{ (meter reading adjustment)}}{24\times31\times0.53}=3{,}120{,}000\text{ kw}$$

Estimated peak, based on output load factor forecast of 64

$$\frac{1{,}498{,}000{,}000}{24\times31\times0.64}\times0.991\text{ (calendar adjustment)}=3{,}120{,}000\text{ kw}$$

Estimated peak, based on equation 1

$$P=110+30/30.88\quad(2.408\times360+3.200\times295+2.157\times580)=3{,}080{,}000\text{ kw}$$

Estimated peak, based on equation 2

$$P+98.5-5.249(1964-1931)+30/30.88\,(2.559\times360+3.140\times295+2.525\times580)=3{,}140{,}000\text{ kw}$$

Forecast peak, 3,100,000 kw

In the last two equations the factor 30/30.88 adjusts all sales forecasts from a historical average meter-reading interval of 30.88 days to a convenient interval of 30 days, since these equations were developed on the basis of adjusting reported sales to their equivalent on a 30-day meter-reading interval.

This forecast assumes that peak loads will continue to occur in December. With 50% saturation of room coolers contributing to residential sales in summer as estimated, the summer peaks will be approximately equal to the winter peaks by 1964. Long before this date, the valley in the annual load curve, so important for maintenance work, is expected to be no more.

Results

The most important forecasts are those made from 1 to 3 or 4 years ahead. To the extent that these are correct, warning is given of probable needs for additions to plant. In Fig. 15 actual loads are compared with estimates made 10, 22, 34, and 46 months in advance. The information starts with 1945, when present methods were partially applied for the first time. Two failures are apparent. One of these occurred in 1946 when the widely heralded post-war industrial slump did not materialize. The other reflects inability to foresee the Korean episode and to evaluate the effect of the subsequent rearming program; estimates for 1950 and beyond, made before June of that year, were low, and the first estimate prepared after June 1950, was high. These results emphasize the unwisdom of forecasting major depressions and the impracticability of forecasting military action, but they also exhibit a reasonably satisfactory score except for such occurrences.

Conclusions

Two conclusions can be drawn from this discussion of load forecasting methods:

1. There is every reason to expect very substantial increases in demands for electric service in the coming 10-year period. Conservative forecasts, buttressed by various combinations of extrapolated historical statistics, justify this conclusion.

2. In nearer-term forecasts, from 1 to 4 years ahead, acceptable accuracy is also attainable, but 1. it is not wise to attempt to forecast a depression (the one attempt was a failure), and 2. the results of a shift to a war economy, which may occur at any time, are not likely to be foreseen.

References

1. Index of Total Manufactures. *Federal Reserve Bulletin*, Federal Reserve System, Washington, D. C.

2. Index of Manufacturing Production, Historical Statistics of the United States, 1789–1945. National Bureau of Economic Research, U. S. Bureau of the Census, Washington, D. C., 1949.

3. Census of Manufactures, U. S. Bureau of the Census, Washington, D. C., 1899–1947.

4. Consumers' Price Index, Monthly Labor Review, U. S. Bureau of Labor Statistics, Washington, D. C.

5. Electric Power Requirements of Industrial Establishments, 1939–1942 (Actual) 1943–1944 (Estimated); Industrial Electric Power 1939–1946; Production of Electric Energy and Capacity of Generating Plants, 1947–1950. Federal Power Commission, Washington, D. C.

6. Statistical Bulletin. Edison Electric Institute, New York, N. Y., 1939–1949.

7. New Jersey Manufacturing Workers. The Handbook of Basic Economic Statistics, Economic Statistics Bureau, Washington, D. C.

8. Growth Patterns in Industry. *Studies on Business Economics, No. 32*, Feb. 1952, National Industrial Conference Board, New York, N. Y.

9. Statistical Method (book), F. C. Mills. Henry Holt and Company, New York, N. Y., 1938, Chap. VII.

◆

Discussion

J. W. Reinhard (Department of Water and Power, Los Angeles, Calif.): The author is to be congratulated on his comprehensive paper. The methods and the information used to develop the estimates in New Jersey are similar for the most part to those used in Los Angeles, and this is reassuring to us in our efforts to predict the future.

In addition to kilowatt-hours, we develop kilowatt demands for load classifications that assist in recommending size and location of future substations, and these demands when adjusted for diversity factors and line losses indicate the required generation. The power system of Los Angeles has for the past 30 years made use of a land use survey to develop kilowatt demands for long-range planning of electrical load requirements. It is believed that this long-range planning has reduced early obsolescence of equipment and has contributed to the development over the years of the most efficient electrical system. I believe it worth while to mention that the curves developed for population and electrical requirements for the service area of the Public Service Electric and Gas Company could not readily be used for other parts of the country unless the character of area development was identical. Even though the premise for developing the information is the same, in the interpretation of results the general character of the area must be considered.

The paper contains many fundamental concepts of value to the planning engineer. I agree that industrial customers are overly optimistic in planning loads, many of which never materialize. Also, nonferrous metal plants and other large individual loads cannot readily be forecast but must be considered as individual special case.

The growth of air-conditioning loads throughout the country may present additional problems because of the probability that this load will have a very low diversity as compared with other major electrical appliances. It is possible during high-temperature weather for nearly all units to be on at the same time. In many areas home air conditioning in the next few years may become as commonly used as television is today, thereby creating a summer system peak where a winter peak exists today.

B. M. Carothers (Union Electric Company of Missouri, St. Louis, Mo.): The problem of load forecasting is receiving much attention. It is unique in that no really formalized or rigorous solution will ever be possible. Treatment of possibilities, and especially limitations of the mathematics is quite pertinent. It would be easy to lose sight of the limited significance to be attached to agreement of historical data or future forecast with any mathematical curve. This is well demonstrated by extensions of limited segments only, of past curves, in which the resulting wide discrepancies may be noted.

An element of discouragement arises in considering the subject matter. History has shown that military action and economic readjustments have a marked effect on loads. Even though forecast of time and magnitude of such events is not possible, they are almost certain to develop. On recognizing this condition any forecast of extended duration has a highly questionable degree of accuracy.

The concept of an envelope forecast has appeal. With one curve produced by optimistic personnel or with the use of optimistic factors, and another on the pessimistic side, the included area has considerable probability of circumscribing loads to be experienced. Planning based on such a forecast could then be made sufficiently flexible in times of construction to make some allowance for the vagaries of fate. Is such an approach utilized by the author?

Short-term forecasts are quite important and the considerable confidence is placed in their accuracy. Certainly, long term extensions are important if for no other reason than their use in checking against immediate planning.

K. M. Smith (Commonwealth Edison Company, Chicago, Ill.): This highly readable paper is of interest because it contributes something of value from experience. We subscribe in theory and practice to the statement about forecasting committees and their composition, and the following comments are offered from the point of view of a member of such a committee.

Because the job of forecasting breaks down into a process of applying judgment to the extension of known facts, it is agreed that this judgment can be better applied to the development of a series of load components than to the system total. However, the degree to which an analysis of these components can justifiably be carried is debatable. It is certainly necessary to note principal divergent trends such as that of the local transportation requirement mentioned. It is also obviously important to estimate the degree to which a company or community will share in total national business by identifying any major movement of industry or commerce to or away from a local area. Beyond this, the trends of the various indexes, such as horsepower per worker or rate of residential construction, may be so closely related to the level of national economic activity that it is difficult to escape the conclusion that the real job is one of forecasting such economic activity, and in terms of the total system load.

Table IV. Estimated Average Error, Per Cent

	For 10 Months	For 22 Months	For 34 Months	For 46 Months
From Fig. 15	2.7	4.5	7.0	9.8
Commonwealth Edison	2.2	3.8	5.1	7.2

Some people think that extensive analyses of components and the applications of various indexes and equations give a comforting feeling of activity and provide an excellent basis for discussion without actually contributing substantially to the accuracy of the over-all estimate. Others take the position that because of the economic importance of load estimates, almost any degree of refinement is useful and justifiable. In our company, we take the middle ground. Although we recognize the convenience and necessity of dealing with load components, we do so to a lesser degree of analysis than is suggested in the paper. Because of this and other differences in method, it may be of interest to compare results. Fortunately, data are available for such a comparison on the basis of Fig. 15, which shows estimates over a period of 10 years, varying from a forecasting time of 10 months to 46 months in advance of actual loads.

Omitting in both cases the 1945 estimate of postwar conditions with which we both had bad luck in certain respects, the comparison in terms of average error is shown in Table IV. The general level of error is the same in both series and both show the expected trend of greater error for the longer estimating periods, and to about the same degree. It would be interesting if similar data on estimating errors could be collected from other companies.

C. W. Watchorn (Pennsylvania Power and Light Company, Philadelphia, Pa.): The paper is most stimulating and a valuable contribution to the literature. It provides a basis for discussion for determining the capacity to be provided at some future time, rather than the preparation of an estimate as to what the load itself may actually be at that time. The load itself is secondary and really only a means to an end rather than the end itself. Actually, as stated in the paper, future loads are subject to many uncertainties, preventing close comparisons between estimated and actual loads. Such uncertainties, though within fairly definite limits, are similar to those related to the amount of capacity that may actually be available at a specified future time because of the effect of forced outages.

Thus, as with the problem of availability of capacity, the question of loads for which capacity is to be provided is likewise a probability problem[1,2] in which successful estimates of future loads depends on how much the actual trend deviates from the estimated trend, along with the extent to which the standard deviation of the actual loads from such actual trend differs from that estimated. This is in contrast with comparisons as shown by Fig. 15, where it is understood that the estimates are for loads treated as though they are expected to occur as certainties, even though subject to future revisions. Failures are scored when the actual loads deviate materially from those estimated and, presumably, success is scored when the comparisons are relatively close. This seems to be classing bad luck as failure and good luck as success.

In connection with the approach suggested here, it is desired to suggest that a curve similar to that in Fig. 12 but for the total of the load treated in the paper, together with its trend line and its corresponding percentage standard deviation would be most interesting. Further, a discussion is desired of the basis for what appears to be the belief of the author that correlations of various load components to various indexes and projections thereof are preferable to projections of the loads themselves in the first place, without their being correlated with prognostications by others of the future behavior of such indexes.

REFERENCES

1. ELEMENTS OF SYSTEM CAPACITY REQUIREMENTS, C. W. Watchorn. *AIEE Transactions*, vol. 70, pt. II, 1951, pp. 1163–85.

2. POWER AND ENERGY PRODUCTION, C. W. Watchorn. *Ibid.*, vol. 73, pt. III-B, Aug. 1954, pp. 901–08.

F. M. Kenney and **V. E. Hill** (Duquesne Light Company, Pittsburgh, Pa.): The paper represents a thorough and sincere attempt to place forecasting on as sound a basis as possible. It appears to represent many man hours of investigation and analysis, and it would be interesting to know how many individuals devote all or part of their time to this activity. Do the committee members of the author's company devote a large proportion of their time to the subject of forecasting?

In view of the large amounts in funds at stake in providing for additional generation and system expansion, certainly probable future loads should be determined as accurately as possible to prevent funds being spent ahead of time unjustifiably.

It would be interesting to know what the fitted compound percentage growth for the author's company has been over the years and how close the forecast estimate of 3,100,000 kw for 1964 would come to a projection of past growth.

To refer to the make-up of the forecasting committee, is not the planning section or department represented, or does such a group come under the operating departments? We particularly liked the comment that the individuals on the forecasting committee act as committee members in their own right and not as departmental representatives.

In reference to the procedure used for forecasting the residential sales, we use very much the same methods. However, the author shows a decreasing percentage in future years while we are still adhering to a constant percentage increase. We wonder if part of the difference might not be because the author's company is an electric and gas company, and therefore might not be promoting the use of some electric appliances, notably ranges, dryers and water heaters, as strongly as an all-electric company. We were in a similar position some years ago but are now completely separated from the gas company, and we hope that a wider use of the three appliances named will keep our residential consumption up.

Referring to the synthetic approach for forecasting residential sales per customer as illustrated on Table I, this procedure, though commonly used, seems open to question. The attempts to evaluate rather accurately the consumption of nine so-called large-use appliances totaling about 400 kw-hrs and then lumping the remainder of the consumption of 1,300 kw-hrs in one figure is somewhat inconsistent. Furthermore, appliance saturation figures are subject to inaccurate interpretation, and we wonder if the use of 100% saturation for television sets, per residential customer, is strictly correct in a procedure attempting to synthesize the total consumption of the average residential customer. One common method is to divide the estimated number of television sets by the number of residential customers but, for example, there are many sets in a given apartment building which has only one meter and, in this case at least, the apartment building unit is not even considered a residential customer. This criticism is of the procedure and not of the author, who agrees that the basic information is "of a low order of accuracy."

Since the total residential load has been increasing rather uniformly, would not simple projection of this growth be about as accurate as an attempt to break it down to increases from growth in population, increased usage per customer, etc?

The comment pertaining to the forecast of industrial sales, to the effect that this is the key to the accuracy of any prognostication, is certainly true for the Duquesne Light Company. Accurate forecasting for the residential and commercial load is lost in the variations experienced in the industrial sales, depending upon business conditions and upon addition (or loss) of large loads. In many cases, it is not possible to rely on the customer's estimate of his future requirements and we certainly agree that most customers tend to be over-optimistic. Errors of this sort, for a few large customers, can jeopardize the whole forecast.

In the section "Establishing the Trend," the author gives the impression that recent revisions of business activity indexes to a 1947–49 average base resulted from a false measure of general business given on the old base. He specifically mentions the FRB Index of Manufactures, which apparently is the Index of Industrial Production. The only adjustment made in this index is that of a seasonal nature and it has not been expressed as a percentage of a secular trend. The index, accordingly, compared today's business with that of the former base, which was 1939, and it naturally registered approximately 100 points more than it does on the new base, 1947–49. If this index is treated further to a secular trend adjustment, the resulting index is very little different on the new or the old base.

With reference to the section "Index of Industrial Sales," wherein the author states that an index of industrial sales agrees well with standard trend corrected indexes, we also have developed an industrial kilowatt-hour sales index which we find agrees fairly well with FRB and the University of Pittsburgh (local) industrial activity indexes.

The analysis of industrial sales for 1964, as described in the section "Annual Industrial Sales for 1964 as Forecast by Five Procedures," is somewhat perplexing. It is not understood how five methods give exactly the same forecast of industrial sales, even assuming, as the author points out, that there is some overlapping of the use of the same statistics among the different methods.

In reference to Fig. 15, the method of showing forecasts for various periods of time in advance and their connection with the date of making this forecast is most interesting and unique. The author and his company are to be commended for having the courage to present these data, which certainly enhance the value of the paper.

R. G. Hooke: The comments and discussion are much appreciated. It is interesting to note that in Los Angeles, the forecasters have developed a basis for estimating future peak demand for various components of the load and methods of combining these to produce area requirements. This is a delicate procedure, presumably based on a sampling of customer demands. Of course, land-use surveys and forecasts are a valuable basic element in any estimate of future developments. Los Angeles is to be congratulated on the thoroughness with which it has made such surveys at, it is understood, regular 5-year intervals.

Mr. Carothers asks the frequently raised question concerning a band or envelope forecast. In many situations this seems to be an acceptable procedure. The top or the bottom of the band may be used, depending on one's judgment, or perhaps on what one wishes to prove. Any expenditure for system expansion must be based on a load forecast. Differences of opinion on this forecast may be eliminated by agreement to accept an estimate which, in the judgment of a forecasting committee, is as likely to be exceeded as not. Allowance for uncertainties may then be made by providing adequate reserve over and above the forecast. The concept of an envelope is another means to the same end.

It is to be regretted that Mr. Smith did not contribute more information in his discussion, which shows the excellent record of the Commonwealth Edison Company's forecasting committee. Many estimators would be interested in a detailed exposition of the methods used to achieve the results shown in Table IV comparing errors in forecasting on a percentage basis. Such analyses are frequently made to compare errors in forecasting various load areas, or parts of the system, with each other and with the total system. Almost invariably it is found that the errors are related to two factors: the magnitude of the load being forecast and the amount of industrial load in the area. The larger the load, and the lower the proportion of industrial use it contains, the less the percentage error in the forecast. After all, the forecast is in effect an estimate of a difference between recent load and the load in some future year. The larger the load is, the larger the numerical error of the forecast is likely to be, but the percentage error will almost certainly decrease with size. This is to be expected because unanticipated or accidental occurrences are likely to cause much more important deviations, proportionately, in small loads than in large ones. The vital influence of the industrial component of the load has been discussed in the paper.

As Mr. Smith says, the basic problem is one of forecasting the national economy. But why in terms of the total system load? It seems clear that the effect of a business change on residential sales will be quite different from its effect on industrial sales, and this is important in forecasting peak loads. As to the desirable extent of breakdowns of past data into various pertinent components, there may be some question about the "comforting feeling" Mr. Smith alludes to. Occasionally, study of components produces discomfort for an individual whose ideas of the whole cannot be reconciled with his views of the parts. Also, study of components seems to be a very fruitful method of arousing discussion and effective group thinking in a forecasting committee; it is a major tool with which to examine nonconforming views.

Mr. Watchorn, recognizing that forecasting is an inexact science, offers the suggestion that new facilities should be installed on the basis of the probability of there being inadequate capacity to meet the demand. One element in the study of this probability would apparently be the probable deviation of the load from a forecast mathematical trend line. Another element, of course, would be the probability of various combinations of facility outages. This is a more sophisticated view of the problem than is usual. However, if all of the outage rates of system elements were adequately known and if computer time were available, it would still remain necessary to forecast the trend line of the load. The extension of this trend line should not be merely a mathematical process. Various rational methods of making, checking, and rechecking this forecast should be employed. How the need for addition of facilities is established, once this forecast is accepted, is another problem. Use of the percentage standard deviation of the load estimate from actual and of the probability of facility outages, both as determined by past experience, is entirely proper if one wishes to approach the final objective by Mr. Watchorn's procedure. However, it is laborious, and is considered by some a less justified use of time than is the study of the components, such as population changes or trends of industrial indicators, to which the forecast must be related and which some discussers seem to disparage.

In reply to Mr. Kenney and Mr. Hill, the members of the Load Development Committee of Public Service Electric and Gas Company spend only a very insignificant part of their time on load forecasting; on the average, probably not more than half a day each month. There are other individuals, however, who spend all their time on various analyses of loads, and some of this is directly related to load forecasting. It is estimated very roughly that for the Company as a whole there is about the equivalent of the full time of one and one-half men devoted to the forecasting of future loads.

There is no compound percentage rate of growth which fits either the past or the forecast future trend lines of the company's loads. A growth of 5.7% compounded annually from 1925 will arrive at the load which was experienced in 1954 but will not produce a trend line which fits the points of the intervening years. Similarly, a compound growth of 5.8% from 1954 will produce the current forecast for 1959 but a compound growth of 4.8% from 1954 will produce the most recent forecast for 1975. The rate to produce the forecast of 3,100,000 kw given in the paper for 1964 can, of course, be calculated.

System planning work is located in the Operating Department and is represented by two members including the chairman of the Load Development Committee.

A decreasing percentage growth in future years must be a characteristic of any sales in any company, if the forecast is extended far enough into the future.[1] It is quite possible that this is an earlier characteristic of a company promoting the sale of both electricity and gas.

A number of questions are raised concerning the forecast of residential sales per customer illustrated in Table I. As pointed out, the information available on which to base this type of analysis is sparing at best. However, it offers a useful basis for discussion, and it is surprising how often various individuals working independently will arrive at comparable forecast totals even though the several elements may differ substantially. The per-cent saturation as used in this table may be defined as the number of appliance units, television sets, or room coolers, etc., in the service area divided by the number of residential meters. Clearly it may be in excess of 100%.

The FRB Index of Manufacture mentioned in the paper is not the Index of Industrial Production. The two differ in that the latter includes certain mining and other enterprises, not pertinent to New Jersey's economy. This index was formerly based on the average 1935–39 as 100%; recently it was changed to 1947–49 as 100%. Neither the old nor the new index has been corrected for trend. Whether or not such correction would appear to change the level of business activity would depend on how the trend line was established; either result is possible. But the change from the old to the new 100% base did eliminate the false evidence of a major business boom.

As to the five methods of arriving at a forecast, they have been adjusted to produce the same answer. The important question is whether or not such adjustments can be made without resulting in unacceptable forecasts of some of the components. This is the point of the whole process of basing a forecast on a multiplicity of methods as independent of each other as possible.

Reference

1. Electric Power Futures, D. K. Blake. *Electric Light and Power*, Chicago, Ill., Aug. 20, 1954, p. 106.

An Approach to the Definition of Excitation System Response

T. J. BLISS
ASSOCIATE MEMBER AIEE

As THE electric power industry has grown in scope and complexity since its inception, so have the excitation systems used for a-c machine terminal voltage control. Available today are a number of different methods by which any deviation in the terminal voltage of a synchronous machine may be detected and corrected. These vary from the conventional rotating exciter with a direct-acting rheostatic regulator to the rectifier-type exciter with an electronic regulator. Because of the diversity of these systems, it is becoming increasingly desirable that the over-all excitation system performance be defined in some consistent manner. Presently available definitions cover the transient performance of certain rotating exciters alone but provide no means of taking into account the behavior of the other components of the excitation system. Nor, under present definitions, is it possible to estimate how much the transient behavior of an a-c machine may be improved by use of a given voltage-regulated excitation system as compared to a manually regulated system. Thus it appears that a definition of excitation system transient performance should be formulated which will take into account the effects of all elements of the excitation system regardless of their type or individual characteristics and which will be of assistance in evaluating the a-c machine performance under transient conditions.

It is the purpose of this paper to bring to the attention of the industry the need for such a definition, the requirements which it should meet, and the fundamental problems involved in formulating it, and to present a suggested definition.

The Excitation System

As defined by the proposed revision to the American Standards Association (ASA) Standard *C-42*,[1] the excitation system is "the source of field current for the excitation of a principal electric machine, including means for its control." Thus an excitation system may consist of no more than an exciter and a means for the operator to adjust the exciter terminal voltage manually. In the majority of modern installations, however, a regulator is used to perform this adjustment and so make the excitation system automatically regulated.

Fig. 1 shows the functional operation of the automatically regulated excitation system. As indicated, measuring equipment at the a-c machine terminals receives intelligence as to the voltage and current conditions there and delivers a signal proportional to the quantity regulated. This signal is received by the error detection device which determines if the regulated quantity is at the desired level and, if not, a signal is transmitted to the power amplifier indicating the degree and direction of error. The power amplifier which supplies the excitation required by the synchronous machine receives power from a supply, which may be the shaft in the case of a rotating exciter or an auxiliary a-c bus in the case of a rectifier-type exciter. Regardless of the type, the exciter behaves as an amplifier since it varies its output in response to the error signal and so attempts to change the excitation in the direction to reduce the error signal to zero. To prevent excessive overshooting of the voltage during transients or instability of the excitation system, a means of damping is also usually provided, which modifies the error signal as some function of the power amplifier output voltage.

The purpose of the preceding review of automatically regulated excitation systems has been to emphasize the fact that such a system is inherently a closed regulating loop. The behavior of this loop, composed of the measuring equipment, the error detection device, the power amplifier, and the a-c machine, is dependent

---

Paper 55-459, recommended by the AIEE Power Generation Committee and approved by the AIEE Committee on Technical Operations for presentation at the AIEE Summer General Meeting, Swampscott, Mass., June 27–July 1, 1955. Manuscript submitted March 30, 1955; made available for printing April 20, 1955.

T. J. Bliss is with the Westinghouse Electric Corporation, East Pittsburgh, Pa.

on the characteristics of every one of these components and cannot be defined without considering all of them.

Functions of Excitation Systems

To appraise the need for a definition of excitation system response correctly it is not only necessary to understand the composition of the system but also to consider its functions. To this end, it is submitted that automatically regulated excitation systems are applied in order to accomplish one or more of the following basic functions:

1. To maintain the voltage at the a-c machine terminals or at some other point in the power system at a relatively constant value with only slow or gradual load changes for long periods of time without attention from an operator.
2. To restore the voltage quickly at the regulated point following a sudden disturbance within the power system.
3. To permit stable operation of the a-c machine at low values of excitation near, or in, what is known as the dynamic stability zone.

Essentially, items 1 and 2 are concerned with steady-state and transient conditions respectively. Under the latter, the disturbance creating the transient could be a system fault, loss of field on a neighboring a-c machine, sudden application of a heavy load, or load rejection by the a-c machine. These power system disturbances and the minimizing effect provided by the excitation systems are briefly discussed in the following paragraphs.

Automatically regulated excitation systems have long been recognized as being of assistance in increasing the transient stability limit of a-c machines. Thus, the use of automatically regulated excitation systems make possible carrying a heavier load on the a-c machine without increasing the danger of transient instability. However, it is pertinent to note here that with modern high-speed relays and circuit breakers which limit faults to short duration, the gain in the transient stability limit obtained by a high-speed excitation system as compared to that with a slower one is relatively slight.[2,3] On the other hand, for less severe faults which may be cleared more slowly the speed with which the excitation system attempts to restore voltage becomes more critical.

Although the loss of excitation to an a-c machine may occur but rarely, a serious condition may result when one machine does lose its field and is not tripped off immediately. A heavy reactive load is then thrown on the remaining machines of the power system causing lower voltages and the possibility that system instability may result. The action of the excitation systems of the remaining machines in attempting to restore the voltage may then be the deciding factor in preventing a major system outage as a result of instability.

Fig. 1. Functional diagram of an automatically regulated excitation system

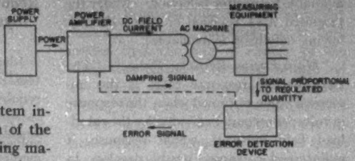

The sudden application, removal, or variation of a heavy load on a machine also results in a voltage disturbance at the machine terminals, the magnitude and duration of which are functions of the rapidity with which the excitation system can respond to the disturbance for a given a-c machine. The voltage drop resulting from the sudden application of loads has been studied in the past based on the use of rotating exciters with direct-acting rheostatic and indirect-acting exciter-rheostatic voltage regulators. Excellent data are available from this study which show the effect of varying the excitation system and a-c machine constants.[4,5]

Another type of disturbance, load rejection, is important in hydrogenerator applications where the runaway of the machine following loss of load may cause severe overvoltages. In these applications, the excitation system is relied on to reduce the excitation quickly and so limit the magnitude and duration of the overvoltage.

While features are frequently incorporated in the excitation system controls to obtain special characteristics such as the desired division of reactive load between parallel machines, these are considered to be of secondary importance as compared with the functions discussed in the foregoing material.

Evaluation of Excitation System Performance

Inasmuch as it is possible to specify the major functional requirements of the automatically controlled excitation system, it is only logical that some consistent method should be available by which the ability of a given excitation system to meet these requirements can be measured and expressed quantitatively.

With regard to the first objective of maintaining relatively constant voltage at the regulated point under normal operating conditions with only slow changes in the real and reactive load on the machine, there now exist proposed definitions undergoing final consideration by ASA for acceptance as American Standards which appear entirely satisfactory as definitive of the excitation system performance. These are as follows:

"Band of Regulated Voltage." "Band of regulated voltage is the band or zone, expressed in per cent of the rated value of the regulated voltage, within which the excitation system will hold the regulated voltage of an electric machine during steady or gradually changing conditions over a specified range of load."

"Nominal Band of Regulated Voltage." "Nominal band of regulated voltage is the band of regulated voltage for a load range between any load requiring no load field voltage and any load requiring rated load field voltage. Any compensating means used to produce a deliberate change in regulated voltage shall be inoperative when determining the nominal band of regulated voltage."

Certainly a purchaser's specification of a nominal band of regulated voltage of x per cent will indicate clearly to the vendor of the excitation system what is expected of it. Equally so will the vendor's guarantee of such performance signify to the purchaser what he may expect of the equipment.

With regard to the other major functional requirements of excitation systems designated as items 2 and 3 in the preceding section, the industry does not at present have any such helpful definitions. To correct this with respect to item 2, the ability of an excitation system in responding to transient disturbances in the power system, it is hoped that suitable definitions of excitation system response and excitation system response ratio may be formulated and accepted. Further definitions will be required to express the ability of the excitation system with regard to item 3, maintenance of stable operation of the a-c machine in the dynamic stability zone, but these are outside the scope of this paper and are not considered here.

Need for Definition of Excitation System Response

To clarify further the need for definitions of over-all excitation system performance, it is pertinent to review those available for exciter behavior. Under the proposed ASA revision of *C42*,[1] the following definition is available:

"*Main Exciter Response Ratio.*" "The main exciter response ratio is the numerical value obtained when the response in volts per second, is divided by the rated-load field voltage; which response, if maintained constant, would develop, in one-half second, the same excitation voltage-time area as obtained by an actual exciter. Note: the response is determined with no load on the exciter, with the exciter voltage initially equal to the rated load field voltage, and then suddenly establishing circuit conditions which would be used to obtain nominal exciter ceiling voltage. For a rotating exciter, response should be determined at rated speed. This definition does not apply to main exciters having one or more series fields, except a light differential series field or to electronic exciters."

This definition is in essence the same as the present ASA definition[1] for "nominal exciter response" which it will replace if accepted. The latter is in common use in the industry, and, for example, the AIEE-American Society of Mechanical Engineers Standard Specification and Data for Generators[6] requires that the nominal exciter response be not less than 0.5 in equipments which are built to these specifications.

The definition of exciter response ratio is useful in that it does permit quantitative specification and evaluation of the exciter performance under the prescribed test. However, knowledge of this quantity does not give an accurate picture of what may be expected of the over-all excitation system of which the exciter is only a part. Long-time delays in the voltage regulator could conceivably reduce the effectiveness of an exciter with a high response ratio to less than that achieved by an exciter with a lower response ratio assisted by a short-time-delay regulator.

Furthermore, the definition of exciter response ratio is inapplicable to many devices used to furnish excitation as noted in the definition itself. Or, in some cases, it may be possible to so interpret the definition as to permit making a response ratio test of a rotating exciter with field connections or sources of energy quite different from those which will exist when the excitation system is complete. These thoughts can only lead to the conclusion that definitions concerning the over-all transient response of excitation systems should be available that would apply regardless of the type of components in the system.

Requirements of an Excitation System Response Definition

Ideally, a definition for excitation system response should meet the following requirements:

1. It should be applicable to any automatic voltage-regulated excitation system regardless of the type or design of the individual components thereof.
2. It should permit a quantitative determination of the defined characteristic by test in the shop and in the field.
3. The defined characteristic in its quantitative form should be useful either directly or with mathematical manipulation in determining the degree with which the system fulfills its functional requirement of restoring the regulated voltage quickly following a sudden power system disturbance.
4. The defined characteristic should be such that knowledge of certain measurable characteristics of each of the components comprising the system would permit calculating the defined system characteristic through a uniform procedure acceptable to the industry.

Of these ideal requirements, the first two are self-explanatory, but discussion of the last two is in order. To illustrate the third requirement, assume an excitation system to have a response (or response ratio) of x. Certainly, it would be extremely desirable in, say, a transient stability problem, if one could conclude that the transient stability of the a-c machine using this excitation system would be x, or some function of x, times as great as with the same machine under constant excitation, all other conditions being the same. In view of the many factors entering the stability problem, this ideal may be beyond realization. However, as attempts are made to formulate the definition, every effort should be made to come up with one of recognizable significance in estimating the transient performance of the a-c machine to which the excitation system is applied.

The fourth ideal requirement is necessary for two reasons. First, a definition meeting the first and third requirements may not be compatible with the second, i.e., shop or field test to determine the defined characteristic may be impractical. In this case, an accepted procedure for the calculation of the quantity is required. Second, the components of an excitation system may be obtained individually from more than one manufacturer. A factory co-ordinated installation is then impossible, and a method of calculation is required to predict the over-all system behavior.

In any event, the requirements of an excitation system response definition as given here are ideals. The extent to which any definition may fulfill them remains to be determined.

Problems in Formulating the Definition

Having set down the ideal requirements of the definition, the practical problems involved in meeting them must be investigated. First, of all, as pointed out in the initial discussion of the automatically regulated excitation system, the a-c machine is a component within the closed control loop. As the excitation system endeavors to raise or lower the terminal voltage of the a-c machine, the flux linkages of the field must be changed. Due to the relatively long-time constant of the field, these flux linkages can change but slowly and so the a-c machine introduces the major time delay in the regulating loop. This delay cannot be ignored in determining the transient performance of the over-all excitation system. From this, it is concluded that the test to determine the excitation system response must be one in which the machine itself is included.

Two or more difficulties arise from this conclusion. For one, this virtually precludes making the test in the manufacturer's shop since it is only very rarely that an a-c machine is set up for test complete with the excitation system which it will have upon ultimate installation in the field. A possible solution to this problem is to substitute for the a-c machine a simulator circuit. Such a circuit might be a low power device which would produce an alternating voltage output proportional to the exciter terminal voltage (or a saturation characteristic might be added as well) under steady-state conditions and which would introduce a time delay in response to transient conditions of the same magnitude as that of the actual a-c machine. Such a circuit has been developed and used by the company with which the author is associated principally in testing the stability of various excitation systems. This device has proved very successful, but being designed for rotating exciters without series fields, it does not draw a significant load from the exciter. Therefore, it is not suitable for use with rotating exciters with series fields or with electronic exciters. The obvious solution to this is the use of a simulator capable of drawing a load current equal to the exciter rating. Unfortunately, exciters for large modern machines have ratings passing the 1,000-kw mark, and similar ratings for the simulator might well render it completely impractical.

A second problem caused by the presence of the a-c machine in the closed regulating loop of the excitation system is the fact that the time delay introduced by the a-c machine is a function of the impedance of the power system to which the machine is connected. With the a-c machine open-circuited (or operating into a system of infinite impedance), the delay introduced in the regulating loop by the machine has a time constant equal to the direct-axis transient open-circuit time constant T_{d0}' of the machine. Under the condition of a 3-phase fault at the machine terminals (operation into a system of zero impedance), the delay has a time constant equal to the direct-axis transient short-circuit time constant T_d'. These two time constants define the upper and lower limits respectively, but, depending on the power system impedance as measured from the machine terminals, the time constant may have any intermediate value. In many machines this time constant may thus vary from 8 seconds down to 1 second. It becomes apparent from this consideration that the excitation system response definition must specify a "standard" impedance for the power system into which the a-c machine is assumed to be operating for purposes of the test.

Either of the two limiting values of power system impedance (infinite or zero) appear as possible values to use for the test. However, with the infinite value, the time constant is then a maximum, and while the excitation system is most difficult to stabilize under this condition, the delay introduced by the machine is far from the value which is effective under actual transient conditions when the machine is connected to a power system. Favoring the use of the open-circuit condition for the excitation system response is the fact that a field test is quite practical.

Objections can be raised against the use of zero system impedance as obtained by a 3-phase fault at the machine terminals for the test as well. For one thing, the effective machine time constant is then unrealistically low since 3-phase faults at the terminals of an a-c machine rarely occur in practice. In addition, zero terminal voltage results in negligible saturation of the a-c machine, and account could not be taken of the saturation effects which may be of significance under more practical transient conditions. Another objection lies in the fact that the 3-phase fault condition results in a fixed zero voltage input to the measuring equipment in the regulating loop. A constant error signal is then delivered by the error detection device. Thus a response test, either actual or calculated, conducted by applying a 3-phase fault to the machine terminals in effect opens the regulating loop and tells little of the behavior of the loop under more normal conditions.

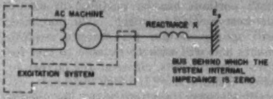

Fig. 2. Circuit to be used in making proposed measurement of excitation system response

From the foregoing, use of a specified power system impedance appears necessary. Such an impedance should result in a value of time delay in the machine typical of that under common operating conditions. This requirement, an outgrowth of the ideal requirement stated in the preceding section that the excitation system response definition be significant in terms of the transient performance to be expected, may well cause field testing as well as shop testing to become impractical. The ideal requirement that the excitation system response be calculable by an accepted procedure then becomes a very realistic necessity.

Many more problems remain in formulating the definition in addition to those discussed here. Rather than dwell on them in detail, a suggested definition of excitation system response is provided in the remaining portion of the paper.

Suggested Excitation System Response Definition

Based on the foregoing discussion, the following suggested definition is submitted:

Excitation System Response. The excitation system response is the rate of increase or decrease of the direct-axis transient internal voltage of the associated a-c machine connected through a specified constant reactance to a power system of zero internal impedance when the voltage of that power system is suddenly raised or lowered. The response may be expressed in volts per second or by a value obtained by dividing the volts per second by some designated voltage.

Fig. 2 shows the indicated circuit arrangement under which the rate of change of internal voltage is to be determined. The transient condition under which the response is determined is initiated by a sudden change in the voltage e_s of the power system bus to simulate a transient condition of some type in the power system.[1]

This definition, of course, fails to fulfill all of the ideal requirements previously listed. Practical shop or field testing becomes ruled out. However, it is submitted that the rate of change of the direct-axis transient internal voltage e_d' is of fundamental importance in determining how the transient performance of an a-c machine is affected by its excitation system. Selection of a proper value for the reactance between the machine and the "infinite" bus permits obtaining a time delay within the a-c machine of a magnitude comparable to that effective under realistic operating conditions. Modern calculating techniques permit calculation of response under this definition providing the characteristics of the components of the excitation system are adequately defined.

Based on such a definition of excitation system response, it should then become practical to define a specific procedure resulting in a quantity to be known as the excitation system response ratio. The various conditions which must be specified for this include the initial real and reactive load on the a-c machine, the initial value of the a-c machine terminal voltage, the value of the reactance, and the magnitude and direction of the sudden change in the system voltage.

Conclusions

The need for a definition describing the transient response of the complete excitation system has been discussed and amplified. Because of the presence of the a-c machine within the closed regulating loop of the excitation system, it is evident that the excitation system response definition must take into account the a-c machine. Ideally, the excitation system response definition should result in a quantity of real significance in estimating the transient performance of the machine with which the excitation system is used. Unfortunately, the importance of this requirement may render actual testing of the response impractical and necessitate the adoption of a specified mathematical approach in obtaining the response. A proposed definition of excitation system response has been offered.

References

1. AMERICAN STANDARD DEFINITIONS OF ELECTRICAL TERMS. *ASA C-42*, published by *AIEE*, 1941.

2. EXCITATION PROBLEMS IN HYDROELECTRIC GENERATORS SUPPLYING LONG TRANSMISSION LINES, C. L. Killgore. *AIEE Transactions*, vol. 66, 1947, pp. 1277–84.

3. POWER SYSTEM STABILITY, VOLUME II (book), S. B. Crary. John Wiley and Sons, Inc., New York, N. Y., 1947.

4. REGULATION OF A-C GENERATORS WITH SUDDENLY APPLIED LOADS, E. L. Harder, R. C.

Cheek. *AIEE Transactions (Electrical Engineering)*, vol. 63, June 1944, pp. 310–18.

5. REGULATION OF A-C GENERATORS WITH SUDDENLY APPLIED LOADS—PART II, E. L. Harder, R. C. Cheek, J. M. Clayton. *Ibid.*, vol. 69, pt. II, 1950, pp. 395–406.

6. STANDARD SPECIFICATION DATA FOR GENERATORS FOR LARGE 3,600-RPM 3-PHASE 60-CYCLE CONDENSING STEAM TURBINE-GENERATORS. *AIEE Standard No. 602*, Jan. 15, 1953.

◆

Discussion

S. M. Denton and **J. V. Baptist** (Bureau of Reclamation, Denver, Colo.): Mr. Bliss has done an excellent job in outlining the growth, background, and present requirements of excitation systems. His ideal requirements for excitation system response form a sound basis upon which to explore a system whereby a realistic approach to actual procedures may be established.

Mr. Bliss has apparently approached this problem from the manufacturer's viewpoint on the assumption that the designer can build into a given electric power system a complete generating unit including the a-c machine and all elements of the d-c excitation system. It is, of course, true that an automatically regulated excitation system is a part of a closed-loop system, and that all parts of the loop must be considered in evaluating the performance characteristics. However, we question whether this fact necessarily establishes that the definition of excitation system response must include part or all of the characteristics of the principal electric machine to which the excitation system is applied. Further, his proposed definition does not include all of the main machine part of the loop, but rather includes only that part of the loop which would be useful in certain types of problems. Mr. Bliss points out that one of the difficulties arising from the inclusion of the a-c machine in the definition of excitation system response is the preclusion of making tests in the manufacturer's shop. Similarly, Mr. Bliss states that adequate factory tests cannot be made on a portion of the excitation system loop omitting the a-c machine because the test procedure could not be set up to cover the various conditions of excitation requirements for rotating exciters with series fields or with electronic exciters. We can see that factory tests simulating exact operating conditions would be difficult, but believe that a method can be developed for measuring a typical speed of response for a portion of the closed control loop which does not include the a-c machine. With this known performance and other machine and system information available, calculations could then be made to cover any particular operating condition requirement designated.

After the generator characteristics have been selected for the particular system to which it will be connected, there is little that can be done to change the time constants of the principal a-c machine. Having selected the main machine characteristics, the purchaser will then select an excitation and voltage-regulating system best to meet the requirements. While these two are interrelated, the final selection of both portions can be modified to obtain the best over-all approach. The purchaser will specify certain performance requirements and will wish to be able to test for these requirements, either at the factory or after installation. It then becomes exceedingly important that a test for excitation system response requirements be established for that portion of the system external to the principal a-c machine.

If the characteristics of each component of the entire loop were known and mathematically expressed, it should be theoretically possible to calculate the response at any point in the loop to a given change in any other part of the loop. Practically, then, the choice of the portion of the loop to be included in the definition of excitation system response should be determined by the compromise which best fits the ideal requirements.

Therefore, we suggest for consideration that the point in the loop chosen to be the end point for definition of excitation system response be the open-circuit voltage of the exciter armature or equivalent device. This could be expressed on a volts per second basis, but it appears that a better basis would be an expression of the voltage rise as the time constant of the idealized exponential voltage rise curve. This quantity could be readily measured in the shop or field by open-circuit test methods. Additional constants and data would, of course, be required to calculate the actual response at the exciter output terminals under loaded conditions.

P. L. Dandeno and **K. R. McClymont** (Hydro-Electric Power Commission of Ontario, Toronto, Ont., Canada): Mr. Bliss is to be commended for his original approach to a definition of excitation system response. We suggest that one other basic function of an automatically regulated excitation system, not mentioned by the author, is: to permit stable operation of an a-c machine when supplying a capacitive load such as a long transmission line open-circuited at the receiving end.

The effect of excitation system response on transient stability limits is evaluated in reference 3 of the paper by assuming that: 1. the exciter voltage increases at a rate given by the ASA definition of nominal exciter response,[1] and 2. this response becomes effective at 0.05 second after fault initiation. On this basis it is concluded, in reference 3 of the paper, that normal rates of exciter response from 0.5 to 1.0 per unit are adequate in general for generators from a stability standpoint.

Tests we have made on several modern excitation systems for large hydraulic generators indicate that in general the overall response of modern excitation systems will be slightly less, and in some cases very much less, than that which would be obtained by the assumptions given in the discussion.

There are, of course, exceptions to the general rule that rates of exciter response from 0.5 to 1.0 per unit are adequate. Ontario Hydro is making a study to determine the effect of excitation system response on a 960-megavolt-ampere hydraulic station consisting of 1,660-megavolt-ampere units. It appears from the results obtained thus far that the system is transiently stable for exciter responses in the order of 1.5 per unit, but unstable for the usually specified response of 1.0. While we have not yet obtained final figures on the increased transient limits resulting from this faster response, it appears that the figure will be significant in this instance, since the transient stability of this system is critical.

High speed of response is also generally desirable on large synchronous-synchronous frequency changers serving as ties between large systems.

It is our belief that the speed of excitation system response considered adequate will be based in general upon the contribution of the excitation system to transient stability, and it is most important that a definition of excitation system response should define a quantity which can be used in transient stability studies.

We agree with the author that the a-c machine must be considered in determining the behavior of the excitation system. It is our belief that the major reason for the inclusion of the a-c machine in the regulating loop is because its characteristics will influence the stabilizing signals which are required for a given regulating system.

Adjustments to the stabilizing circuits of an excitation system are usually made with the generator on open-circuit, and it would not normally be necessary for the manufacturer to know the system impedance in order for him to determine the required stabilizing adjustments.

Thus, while we agree that the a-c machine requires consideration, we do not believe that it follows that it is necessary to use the rate of change of direct-axis transient internal voltage as the criterion of excitation system response. Several disadvantages of this choice are mentioned in the paper. On the other hand, the choice of the rate of change of exciter voltage as the criterion has the following advantages.

1. It is almost entirely unaffected by the system to which the generator is connected.
2. It can be measured.
3. A great deal of literature exists evaluating the effect of rate of change of exciter voltage on transient stability problems.
4. Knowing the rate of change exciter voltage, standard methods exist for evaluating performance for any connection.

The author has stressed both the desirability and the difficulty of shop testing an excitation system. In this respect, it would appear that the problem is similar to many other engineering problems. For example, a manufacturer is required to guarantee the thermal rating of his generators, although he cannot ordinarily de-

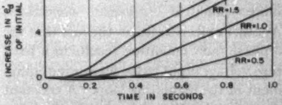

Fig. 3. Variation of e_d' during test proposed for excitation system response definition

termine the thermal rating by shop test; nonetheless, his prediction of the thermal rating will usually be very close to the actual thermal rating as determined by field test.

A definition of excitation system response must be carefully selected in order to arrive at a definition of maximum usefulness which will encourage continuing improvements in excitation systems.

REFERENCES

1. See reference 1 of the paper, definitions, *10.95, 440* and *10.95, 450*.

R. W. Ferguson (Westinghouse Electric Corporation, East Pittsburgh, Pa.): Mr. Bliss has clearly outlined the difficulties encountered in selecting a suitable basis for defining excitation system response and has, quite properly, emphasized the need for a "system" rather than a "component" approach to the problem. The suggested definition includes all the components of the system by using as a basis a theoretical test consisting of measuring the change in the direct axis transient internal voltage (called e_d' in this discussion) of a machine connected to an infinite bus through an external reactance (X_e) when the infinite bus voltage is suddenly changed.

In order to illustrate the relationship between the conventional definition of exciter response ratio and the proposed definition, a study was made using an analogue of the system shown in Fig. 2 of the paper. The specific conditions used for the study were as follows:

1. Initial generator loading—rated power at 0.85 power factor.
2. Initial terminal voltage—1.0 per unit.
3. External reactance (X_e)—0.30 per unit based on the 0.5 pound per square inch gauge hydrogen pressure rating of generator.
4. Change in infinite bus voltage, e_s—lowered 10 per cent.

These four conditions define the necessary parameters to specify completely the test in the proposed definition. Using a 3,600-rpm turbine-generator with typical constants and a magnetic amplifier regulator and excitation system, the curves shown in Fig. 3 were obtained for exciter response ratios of 0.5, 1.0, 1.5, and 2.0. While a plot of e_d' versus time would give a more correct indication of the relatively small effect of increasing the exciter response ratio, the curves of Fig. 3 were plotted in terms of per cent increase in e_d' in order to show clearly the variation in the shape of the curve caused by changing response ratio.

These studies show a definite correlation between change in e_d' and response ratio of the exciter. It should be noted that for a response ratio of 0.5 e_d' actually decreases a fraction of a per cent before starting to increase above the initial value at 0.4 second. The maximum increase in e_d' in 1 second was only approximately 8 per cent for the response ratio of 2. The diminishing effect of exciter response ratio illustrated by the curves is due to the ability of the higher response ratio exciters rapidly to restore the terminal voltage to rated conditions. The ultimate change in e_d' for the specific test was approximately 10.5 per cent. This value reflects the change in infinite system bus voltage and the readjustment of the internal angle of the machine to allow rated output of the generator under the new condition.

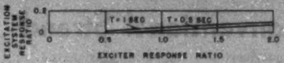

Fig. 4. Relationship between proposed definition of excitation system response ratio and exciter response ratio (T = time interval in seconds used as a basis for proposed definition)

The correlation of the proposed definition of excitation system response with exciter response ratio requires the precise formulation of a definition of excitation system response ratio. For the purposes of this discussion a definition analogous to the present definition of exciter response ratio was used. The excitation system response ratio was defined as the slope of a line in per unit per second having the same area over an interval of time (T) as the actual curve of e_d for the test previously described over the same interval of time. One per unit was set equal to the initial value of e_d'.

Since the rate of change of e_d' is much slower than the change in exciter voltage it is reasonable to consider the use of a longer time interval than the 0.5-second interval used in the definition of exciter response ratio. For the specific definition used in this discussion the values of excitation system response ratio using time intervals (T) of 0.5 and 1.0 second are shown as a function of exciter response ratio in Fig. 4. Since the two quantities have similar definitions the same scale has been used for both quantities to emphasize the difference between system response as measured by the variation of e_d' and exciter response. These curves also serve to justify the usual assumption of constant voltage behind transient reactance (system response = 0) in transient stability studies.

In order to evaluate the effect of a variation of e_d' similar to that shown in Fig. 3 on transient stability, a calculation of the transient stability power limit for the system shown in Fig. 2 of the paper was made using the following assumptions:

1. Unity power factor initial loading with rated generator terminal voltage.
2. Three-phase vault at terminals of the generator for 6 cycles.
3. X_e before fault, 0.3 per unit; after fault, 0.5 per unit.

Based on these assumptions the transient stability power limit was calculated for a constant voltage behind transient reactance (corresponding roughly to an exciter response of 0.5) and for a voltage behind transient reactance increasing linearly with time at the rate of 0.1 per unit per second (slightly in excess of the system response for an exciter response ratio of 2.0). The higher system response increased the transient stability power limit less than 2 per cent. This again confirms the relatively minor effect of excitation system response on the transient stability limit for typical turbine-generators. The higher external reactances and slightly different machine constants found in hydroelectric systems would result in a somewhat greater increase in transient stability limit as system response is increased.

The studies reported in this discussion show that there is a definite correlation between the proposed definition of excitation system response and the presently defined exciter response. Furthermore, by indicating the effect of the excitation system on the direct axis voltage behind transient reactance, the proposed definition is particularly useful in evaluating the performance of the synchronous machine during a system transient disturbance.

T. J. Bliss: I wish to thank each of those who presented discussions for their thought-provoking contributions. Mr. Ferguson's data are of particular help in demonstrating the behavior of the direct axis transient internal voltage under the proposed definition of excitation system response. His further demonstration of the point that the excitation system has a relatively minor effect on the transient stability of typical turbine-generators is well taken. In this connection, it is interesting to note the rather different conclusions arrived at by Mr. Dandeno and Mr. McClymont from tests on a hydroelectric system involving rather long transmission circuits.

All of the discussers have suggested that the definition be formulated about the behavior of the exciter terminal voltage; the former discussers suggest it be under load and the latter, under no load. In either case, calculations must be carried out involving the a-c machine time constants and saturation characteristics to determine the behavior of either the internal or terminal voltage of the a-c machine.

These latter quantities are of the ones of most direct significance in any type of power system transient calculation. Admittedly, with different system conditions the external impedance will be different than the value used in the response test as will be the voltage change of the infinite bus. However, if test definitions are formulated about the exciter terminal voltage, the same holds true, i.e., some particular error signal must be designated as the standard signal to be given the voltage regulator to make the exciter voltage change and this error signal would not be the same in most practical cases. For these reasons, it is doubtful if any test can be formulated which is of direct use in solving a power system transient problem for conditions other than those under which the test is made or calculated. Thus calculations involving the behavior within the regulating loop will continue to be necessary in solving problems involving power system transients where the refinement of including excitation system behavior is needed.

The need for definition of over-all excitation system response remains, however, and it appears that the quantity about which the definition should be written is that which the excitation system controls—the direct axis transient internal voltage.

A-C Resistance of Conventional Strand Power Cables in Nonmetallic Duct and in Iron Conduit

R. W. BURRELL
MEMBER AIEE

M. MORRIS
ASSOCIATE MEMBER AIEE

IN RECENT years the a-c resistance of pipe-cable systems has been the subject of a number of studies.[1–3] Based on a comprehensive study of actual pipe-cable systems, an AIEE Committee Report[3] presented working equations for the evaluation of loss components in pipe-cable systems with segmental conductors. The committee report established a rational approach, generally accepted by the industry, for evaluating the a-c resistance of segmental cables in steel pipe, thereby facilitating the determination of ampacity (current-carrying capability) of such systems.

A comparable study of the a-c resistance of power cables with conventional strand conductors is lacking. Published reports on the a-c resistance of 3-conductor and single-conductor cables of this type are limited. Salter, Shanklin, and Wiseman[4] investigated the a-c resistance of 3-conductor lead-covered cables from 350,000-circular-mil (CM) to 750,000-CM size. Brieger[5] reported on the a-c resistance of network mains cables of 4/0 and 500,000-CM size, including leaded and nonleaded types.

Based on reference 4, the Insulated Power Cable Engineers Association (IPCEA)[6] has published tabulations of a-c/d-c resistance ratio values for power cables with copper conductors for certain specified conditions of installation. The IPCEA values were established in connection with standard ampacity tables and in general are suitably conservative for the purpose intended. The tables do not, however, cover all of the conditions of installation which may be found in the general application of utility and industrial power cable systems. For example, the case of three single-conductor lead-sheathed cables installed in one duct and operated with sheaths short-circuited is not covered above the 250,000-CM size.

In utility studies of comparative plans and requirements, cases arise in which it is desired to evaluate, e.g., the difference in a-c resistance—and ampacity—between one size of three single-conductor lead-covered cables per duct, with sheaths short-circuited, and a smaller size of cables operated with sheaths open-circuited (jacketed cables).

In Table I are shown comparative values of a-c/d-c resistance ratios as listed in reference 6 and as calculated for various installations of 5-kv rubber or 15-kv paper-insulated 500,000-CM cables using equations given in the paper. It will be noted that, for the conditions of installation stated, the values quoted by IPCEA are reasonably satisfactory for average ampacity calculations.

It is frequently desirable, in making comprehensive evaluations, to determine not only the total a-c resistance or losses, but also the disposition of these losses among conductor, sheath, and metallic conduit, where present. A need exists for a comprehensive study of losses in power cable systems, similar to those made for pipe-cable systems,[2,3] which will present working equations for the determination of a-c resistance components for various conditions of cable construction and cable installation. Increasing interest in the use of aluminum conductor and/or aluminum sheath also points to the need for the development of such working equations adaptable to various construction materials.

Purpose and Scope

This paper presents an analysis of the 60-cycle a-c resistance of power cables with conventional strand copper or aluminum conductors, together with appropriate equations, either theoretical or empirical, which will permit calculation of component a-c losses for specific conditions of construction and/or installation. The effect of combinations of the following variables is included:

Construction: 3-conductor and 1-conductor.
Type of conductor: noncompact and compact.
Conductor material: copper and aluminum.
Sheath: lead or aluminum (open-circuited or short-circuited) and nonmetallic.
Conduit: nonmetallic (or in air) and magnetic.

With limited exception, the equations presented in the paper are not original with the authors but are based, generally, on already well-known expressions from the references cited. The equations for conductor loss are developed from published test data for leaded and nonleaded conventional strand power cables with copper conductors, applying accepted equations for sheath losses and solving for unknown constants in terms of best fit. The published data for single-conductor cable systems are limited. In the absence of published data for cables with aluminum conductors and/or aluminum sheaths, it is assumed that comparable effects are obtained as with conventional constructions. It is realized that the results indicated for these constructions may require modification in the light of test data which may become available.

It is hoped that additional test data for power cable systems will be forthcoming in the near future. In the meantime, it is the purpose of this paper to gather together expressions which, in so far as can presently be determined, are applicable for the common types of power cable systems.

Table I. A-C/D-C Resistance Ratios for 500,000-CM Cables With Copper Conductors

Type of Cable	Type of Stranding	Type of Sheath	Type of Duct or Conduit	A-C/D-C Resistance Ratio*	
				Calculated	Reference 6
3-conductor	compact sector	lead	nonmetallic	1.06	1.13
3-conductor	compact sector	lead	magnetic	1.12	1.13
3-conductor	standard concentric	nonmetallic	nonmetallic	1.05	1.06†
3-conductor	standard concentric	nonmetallic	magnetic	1.11	1.13
1-conductor‡	standard concentric	lead	nonmetallic	1.10	not applicable§
1-conductor‡	standard concentric	lead	magnetic	1.24	not applicable§
1-conductor	standard concentric	nonmetallic	nonmetallic	1.03	1.06†
1-conductor	standard concentric	nonmetallic	magnetic	1.10	1.13

* For operation at 75 degrees centigrade.
† IPCEA value, 1.13×0.94=1.06.
‡ Three per duct, sheaths short-circuited.
§ IPCEA Table not applicable above 250,000 CM.

Paper 55-468, recommended by the AIEE Insulated Conductors Committee and approved by the AIEE Committee on Technical Operations for presentation at the AIEE Summer General Meeting, Swampscott, Mass., June 27–July 1, 1955. Manuscript submitted March 28, 1955; made available for printing May 4, 1955.

R. W. BURRELL and M. MORRIS are with the Consolidated Edison Company of New York, Inc., New York, N. Y.

List of Symbols

A = factor in sheath proximity equation, $1/(1+0.00757\ R_s^2)$
B = factor in sheath proximity equation, $1/(1+0.0303\ R_s^2)$
c = mean sheath radius, inches
CI = conductor area, circular inches (= thousand CM per 1,000)
d = conductor diameter, inches
D = spacing between adjacent conductors, inches (equations 12, 23–26)
k = conductor transverse resistance factor applying to conductor proximity loss
K = conductor transverse resistance factor applying to conductor total loss
p = inside diameter of pipe, inches
R_{ac} = mean a-c resistance of conductors, per phase, microhms per foot
R_{dc} = d-c resistance of conductors, per phase, microhms per foot
R_s = d-c resistance of metallic sheath, microhms per foot
ΔR = incremental resistance due to extra a-c losses with conductor in magnetic conduit, microhms per foot
$\Delta R'$ = incremental resistance due to extra a-c losses with conductor in nonmetallic duct, microhms per foot
ΔR_c = conductor increment of resistance due to skin and proximity effects, microhms per foot
ΔR_p = incremental resistance due to pipe loss, microhms per foot
ΔR_s = incremental resistance due to total sheath loss, microhms per foot
ΔR_{sc} = incremental resistance due to sheath circulating current loss, microhms per foot
ΔR_{sp} = incremental resistance due to sheath proximity effect (eddy-current) loss, microhms per foot
s = distance between conductor center and cable center of 3-conductor cables, inches
S = spacing between adjacent conductors, inches
S' = geometric mean spacing between conductors, inches
X_s = reactance of cable sheath, microhms per foot
x = argument for Bessel function, used in determining conductor loss
Y_1 = conductor proximity effect
Y_0 = conductor skin effect
Y_c, Y_s = ratio of incremental resistance to d-c resistance of conductor
$\alpha = d/S$
μ = permeability
ρ = pipe resistivity, microhm-centimeters

Component Losses

In general, the component losses which exist in power cable systems under specific conditions are treated along the lines presented in reference 3. The component losses which contribute to the total a-c resistance are evaluated in terms of incremental resistances which add to the conductor d-c resistance to make up the total a-c resistance. The conductor d-c resistance is taken at the operating temperature. Equations given for resistance increments are converted to a-c/d-c ratios by dividing through by R_{dc}.

The loss categories considered are as follows:

1. Extra conductor loss (or resistance component): loss due to conductor skin and proximity effects. Designated by $\Delta R_c'$ in nonmetallic duct and by ΔR_c in iron conduit.

2. Sheath loss: loss due to circulating currents and/or eddy currents in metallic sheaths. Designated by ΔR_{sc} and ΔR_{sp} respectively.

3. Iron loss: loss due mainly to eddy currents and to a lesser extent due to hysteresis effect in the iron. Designated by ΔR_p.

A discussion of the nature of skin and proximity effect in cable conductors is given in references 1, 2, and 3 and in many standard references.

The loss due to circulating currents in single-conductor cables with short-circuited metallic sheaths is similar in nature to the shield-assembly loss of pipe-type cables.[2,3] However, as the resistance of lead or aluminum sheaths is ordinarily appreciably lower than the resistance of pipe-cable shield assemblies, the magnitude of this component is appreciably greater in the case of single-conductor metallic-sheathed power cables of similar conductor size.

In the case of single-conductor cables with open-circuited metallic sheaths (closely spaced) or 3-conductor cables with metallic sheaths, proximity effects (eddy-current losses) must be considered in the larger size cables. This effect is similar to the shield-assembly proximity loss in pipe cables.[3] For pipe-cable systems, the shield-assembly proximity effect generally can be neglected. However, for the type of power cables treated here, the sheath proximity effect is significant in magnitude.

The loss in iron conduit is similar to the pipe loss in pipe-cable systems and may be calculated using the equations given in reference 3, slightly modified on the basis of test results which indicate that losses in iron conduit are somewhat less than losses in steel pipe.

Extra Conductor Loss

In studying proximity effect in conductors, Arnold[7] reports that except for very large conductor sizes at close spacings the conductor proximity effect is practically the same for flat spacing as for triangular spacing. That is, for the more common sizes of power cables, up to 1,000,000 CM the conductor proximity effect depends essentially only on the actual spacing between adjacent conductors and not on the conductor arrangement. This treatment differs from that used in reference 3, where for the larger pipe-cable sizes the extra conductor loss was calculated, for cable in the cradled arrangement, on the basis of the geometric mean spacing. Experimental evidence appears to substantiate Arnold's treatment, and this treatment has been followed.

Table II. Values of K and x

Cable Construction	K	x
3-conductor, standard concentric	1.00	$6.8/\sqrt{R_{dc}}$
3-conductor, compact round	1.25	$6.1/\sqrt{R_{dc}}$
3-conductor, compact sector	1.20	$6.2/\sqrt{R_{dc}}$
1-conductor, standard concentric	1.17	$6.3/\sqrt{R_{dc}}$
1-conductor, compact round	1.35	$5.8/\sqrt{R_{dc}}$
1-conductor, compact segmental	2.5*	$4.3/\sqrt{R_{dc}}$

* From reference 3, for comparison.

Arnold has developed equations for conductor proximity effect in both single-phase[8] and 3-phase[9] operation. It is noted that the proximity effect is dependent on a factor k, the "transverse resistance ratio factor," which is affected by many construction factors, such as impregnation, tightness of conductor stranding, degree of oxidation of conductor strands, etc. Reference 3 gives cogent reasons why, for practical purposes, it is desirable to combine conductor skin and proximity effects. This may be evaluated in terms of a single argument

$$x = 6.80/\sqrt{KR_{dc}} \qquad (1)$$

In equation 1, K is kept in the denominator rather than in the numerator to differentiate from Arnold's k which applies only to conductor proximity effect. On the basis of test data, the value of K for compact segmental cables is reported in reference 3 to have a value of 2.5. Similarly, for various types of nonsegmental cable, where test data are available, corresponding values of x and K have been determined by obtaining the best fit between total measured and total calculated resistance values using the equations developed herein. The derived values of K are given in Table II.

It is shown in reference 3 that the extra conductor loss for compact segmental cables may be calculated using the simplified expression

$$\Delta R_c' = (1/\sqrt{R_{dc}} - 0.13)(1+4\alpha^2) \text{ microhms per foot} \qquad (2)$$

This expression may be written as

$$\Delta R_c' = x^2 R_{dc}[(x/79.5) - 0.0070](1+4\alpha^2) \text{ microhms per foot} \qquad (3)$$

where

$$x = 6.80/\sqrt{KR_{dc}}$$

Table III. Equations for Conductor Loss

Construction	Extra Conductor Resistance in Air. $\Delta R_c'$, Microhms per Foot	Equation No.
3-conductor, standard concentric	$(3.95/\sqrt{R_{dc}}-0.325)(1+4\alpha^2)$	(4)
3-conductor, compact round	$(2.82/\sqrt{R_{dc}}-0.260)(1+4\alpha^2)$	(5)
3-conductor, compact sector	$(3.01/\sqrt{R_{dc}}-0.271)(1+4\alpha^2)$	(6)
1-conductor, standard concentric	$(3.12/\sqrt{R_{dc}}-0.278)(1+4\alpha^2)$	(7)
1-conductor, compact round	$(2.52/\sqrt{R_{dc}}-0.241)(1+4\alpha^2)$	(8)
1-conductor, compact segmental	$(1\quad/\sqrt{R_{dc}}-0.13)(1+4\alpha^2)$	(9)

Equation 3 appears applicable for values of x to about 2.25. If the values of x from Table II are substituted in equation 3, the resulting equations for conductor loss are given in Table III. In the absence of test data on aluminum conductors which would allow determination of the proper value of K, it is assumed that the same value of K can be used as for the corresponding type of copper conductor. The expressions given in Table III are applicable for cables in air or in nonmetallic ducts.

Extra Conductor Loss for Installation in Magnetic Conduit

Studies reported in reference 3 indicated that in steel pipe the extra conductor loss is increased over the corresponding value in air by a multiplying factor K_c which may be taken as 1.7 for single-conductor cables in triangular formation and 2.0 for cradled formation. Accordingly, it appears reasonable to employ the multiplying factor of 1.7 in equations 4, 5, and 6 for 3-conductor cables in magnetic conduit and a multiplying factor of 2.0 in equations 7, 8, and 9 for single-conductor cables in magnetic conduit. It is assumed that these multiplying factors may be applied for iron conduit as well as steel pipe.

Sheath Loss

SHEATH CIRCULATING CURRENT LOSS

For single-conductor metallic-sheathed cables operated with sheaths short-circuited, the extra resistance component due to sheath circulating current loss may be calculated using the conventional equation

$$\Delta R_{sc}'=X_s^2R_s/(R_s^2+X_s^2) \text{ microhms per foot} \quad (10)$$

where

$$X_s=52.9 \log_{10} S'/c \text{ microhms per foot}$$

For lead-sheathed cables, where the value of R_s is appreciably larger than the value of X_s, equation 10 can be simplified further, as is customary, to the form

$$\Delta R_{sc}'=X_s^2/R_s \text{ microhms per foot} \quad (11)$$

Where the three single-conductor cables are installed in the same duct, it is assumed that the cradled configuration is representative so that in calculating X_s we may take

$$S'=1.26D(\sqrt{1-(D/p-D)^2})^{1/3} \text{ inches} \quad (12)$$

For lead-sheathed cables up to 1,000-000 CM, the mean value of X_s is 21.8 for the cradled configuration. Substituting this value in equation 11, the following simplified expression was obtained

$$\Delta R_{sc}' \text{ (cradled)} =475/R_s \text{ microhms per foot} \quad (13)$$

In reference 3 the sheath circulating current loss in magnetic pipe is found to be about 2.0 times the value in air. A multiplying factor of 2.0 appears to be consistent with the data of reference 5 for lead-sheathed cables and is assumed to hold for the power cable systems treated in this paper.

SHEATH PROXOMITY EFFECT (EDDY-CURRENT LOSS)

Eddy-current loss in cable sheaths has been studied by a number of investigators.[10-13] For comparable cases, essentially similar expressions are given:

A. Three-Conductor Cables

Equations for sheath proximity effect of 3-conductor cables given in references 10 and 11 may be developed in the form

$$\Delta R_{sp}'=3R_s[A(s/c)^2+B(s/c)^4] \text{ microhms per foot} \quad (14)$$

where

$$A=1/(1+0.00757R_s^2)$$

$$B=1/(1+0.0303R_s^2)$$

For lead-sheathed cables of relatively high resistance, equation 14 can be simplified to the form

$$\Delta R_{sp}'=\frac{396}{R_s}(s/c)^2+\frac{99}{R_s}(s/c)^4 \text{ microhms per foot} \quad (15)$$

Equation 15 is frequently given in the form of the first term only. As s/c on the average has a value of about 0.50, the second term in equation 15 has a value of approximately 1/16th of the first term and therefore may be neglected without seriously affecting the answer. A simple and sufficiently accurate expression for the sheath proximity effect of 3-conductor lead-covered cables can be written as

$$\Delta R_{sp}'=105/R_s \text{ microhms per foot} \quad (16)$$

Although no test data are available for 3-conductor cables in steel pipe or iron conduit, it is arbitrarily assumed that a multiplying factor of 1.7 may be used with equations 14, 15, and 16 to determine the sheath proximity loss ΔR_{sp} for 3-conductor cables in iron pipe.

B. Single-Conductor Cables

The sheath proximity effect of single-conductor metallic-sheathed cable varies widely with cable arrangement.[10-13] In considering the installation of three single-conductor cables per duct, the following general equations are of interest:

Equilateral triangle (applicable for triplex cables)

$$\Delta R_{sp}'=R_s[3(c/S)^2A+5/4(c/S)^4B] \text{ microhms per foot} \quad (17)$$

Flat

outer cables $$\Delta R_{sp}'=R_s[3/2(c/S)^2A+3/2(c/S)^4B] \text{ microhms per foot} \quad (18)$$

middle cables $$\Delta R_{sp}'=R_s[6(c/S)^2A+2(c/S)^4B] \text{ microhms per foot} \quad (19)$$

It is indicated in reference 14 that for the condition of rectangular spacing the proximity loss of both outer and middle cables is intermediate between the corresponding value for equilateral triangular arrangement and that for flat spacing. With three cables installed in one duct, actual arrangement is random. It will be noted that the average proximity loss is essentially the same for all three cable arrangements, and it would appear applicable to use equation 17 as a reasonable approximation of the average proximity loss for the case of three single-conductor cables per duct.

For single-conductor power cables with lead sheaths, equation 17 can be simplified, in terms of average loss, to the form

$$\Delta R_{sp}'=\frac{396}{R_s}(c/S)^2+\frac{99}{R_s}(c/S)^4 \text{ microhms per foot} \quad (20)$$

As in the case of 3-conductor cables, the second term can be neglected without serious error. For the usual case of single-conductor cables, the average value of c/s is 0.47, and the second term therefore is about 1/18th of the first term. A single, applicable expression can be taken in the form

$$\Delta R_{sp}' = \frac{420}{R_s}(c/S)^2 \text{ microhms per foot} \qquad (21)$$

or, approximately

$$\Delta R_{sp}' = 90/R_s \text{ microhms per foot} \qquad (22)$$

Comparison of equations 22 and 13 indicates that the ratio of sheath eddy-current losses to sheath circulating current losses is about 90/475, or approximately 20 per cent, so that the sheath eddy-current loss, while relatively smaller, nevertheless is not always negligible.

For cables with short-circuited sheaths, especially in the case of aluminum sheaths, the total sheath loss probably is less than the sum of values obtained using the equations given for circulating current loss component and eddy-current loss component as the local sheath current would tend to be reduced somewhat by the reaction effect of the circulating current. Use of the equations as given tends then to produce a conservative result. The degree of "shielding effect" produced by the circulating current is not determinable from existing test data. For lead-sheathed cables of moderate size, the effect probably is light, but for larger size cables with aluminum sheaths this factor needs further investigation, especially for the case of installation in magnetic conduit.

For cables in iron conduit or steel pipe present test data indicate a multiplying factor of 2.0 to be used with the equations for sheath loss in air or in nonmetallic duct.

Iron Loss

Rational equations for the calculation of the eddy-current and hysteresis losses in steel pipe are given in reference 3. Although no comprehensive measurements were made for iron conduit, data given in reference 1 indicate lower losses in iron conduit than in steel pipe. In a discussion of reference 3 by Morris, it is shown that the pipe loss is inversely proportional to the square root of the product of resistivity and permeability. Data from various sources give the values shown in Table IV for the resistivity and permeability of iron conduit and steel pipe. It is indicated, therefore, that the losses in iron pipe are lower than the losses in steel pipe in the ratio of 0.0112/0.0135 = 0.8(±). If the assumption is made that losses in iron conduit are 80 per cent of the losses calculated by the equations for pipe loss given in reference 3, satisfactory agreement is obtained between total measured and calculated values.

Table IV. Values for Resistivity and Permeability

Material	Resistivity ρ, Microhm-Centimeters	Permeability μ (H = 1)	$1/\sqrt{\rho\mu}$
Iron conduit	13.2	600	0.0112
Steel pipe	14.6	375	0.0135

Table V. Summary of Working Equation

	Incremental Resistance Component, Microhms per Foot	Equation No.	Multiplier in Magnetic Conduit
Conductor Loss:			
3-conductor, noncompact round	$\Delta R_c' = [3.95/\sqrt{R_{dc}} - 0.325](1+4\alpha^2)$	4	1.7
3-conductor compact round	$\Delta R_c' = [2.82/\sqrt{R_{dc}} - 0.260](1+4\alpha^2)$	5	1.7
3-conductor, compact sector	$\Delta R_c' = [3.01/\sqrt{R_{dc}} - 0.271](1+4\alpha^2)$	6	1.7
1-conductor, noncompact round	$\Delta R_c' = [3.12/\sqrt{R_{dc}} - 0.278](1+4\alpha^2)$	7	2.0
1-conductor, compact round	$\Delta R_c' = [2.52/\sqrt{R_{dc}} - 0.241](1+4\alpha^2)$	8	2.0
1-conductor, compact segmental	$\Delta R_c' = [1\quad/\sqrt{R_{dc}} - 0.130](1+4\alpha^2)$	9	2.0
Sheath Circulating Current Loss:			
1-conductor, metallic-sheathed	$\Delta R_{sc}' = \mathbf{X}_s^2\mathbf{R}_s/(\mathbf{R}_s^2+\mathbf{X}_s^2)$	10	2.0
1-conductor, lead-covered	$\Delta R_{sc}' = 475/\mathbf{R}_s$	13	2.0
Sheath Proximity Loss:			
3-conductor, metallic-sheathed	$\Delta R_{sp}' = 3\mathbf{R}_s\left[(s/c)^2\left(\frac{1}{1+0.00757\mathbf{R}_s^2}\right) + (s/c)^4\left(\frac{1}{1+0.0303R_s^2}\right)\right]$	14	1.7
3-conductor, lead-covered	$\Delta R_{sp}' = 105/R_s$	16	1.7
1-conductor, metallic-sheathed	$\Delta R_{sp}' = R_s\left[3(c/S)^2\left(\frac{1}{1+0.00757R_s^2}\right) + 5/4(c/S)^4\left(\frac{1}{1+0.0303R_s^2}\right)\right]$	17	2.0
2-conductor, lead-covered	$\Delta R_{sp}' = 90/R_s$	22	2.0
Iron Loss:			
3-conductor, steel pipe	$\Delta R_p = 0.89D - 0.115p$	25	
3-conductor, iron pipe	$\Delta R_p = 0.71D - 0.092p$	26	
1-conductor, steel pipe	$\Delta R_p = 0.34D + 0.175p$	23	
1-conductor, iron pipe	$\Delta R_p = 0.27D + 0.140p$	24	
Total A-C Resistance in Nonmetallic Duct:			
$R_{ac} = R_{dc} + \Delta R_c' + \ldots$			
$R_{ac}/R_{dc} = 1 + y_c' + \ldots$	where $y_c' = \Delta R_c'/R_{dc}$		

Single-Conductor Cables

Three single-conductor cables in pipe or conduit are assumed to be in the cradled arrangement so that the iron loss may be calculated by the following equations

For steel pipe

$$\Delta R_p = 0.34D + 0.175p \text{ microhms per foot} \qquad (23)$$

For iron conduit

$$\Delta R_p = 0.27D + 0.140p \text{ microhms per foot} \qquad (24)$$

Data for pipe losses given in references 2 and 3 were obtained with three single-conductor metallic-sheathed cables in pipe. Similar data for 3-conductor metallic-sheathed cables in iron conduit or pipe are not available. It is assumed, however, that the equation given in reference 3 for segmental cables in close triangular arrangement will give results that are conservative. On this basis, the following equations are taken as applicable:

For steel pipe

$$\Delta R_p = 0.89D - 0.115p \text{ microhms per foot} \qquad (25)$$

For iron conduit

$$\Delta R_p = 0.71D - 0.092p \text{ microhms per foot} \qquad (26)$$

Summary of Recommended Working Equations

A summary of the working equations which appear applicable for calculating the incremental resistance components of various types of power cable systems is given in Table V. These equations produce reasonably correct total a-c resistance values for conventional strand power cable systems with copper conductors and with nonmetallic or lead sheaths. In the absence of published data for power cables employing aluminum as a conductor or sheath material, the appropriate equations listed in Table V can be used. These are subject to such modification as future published test data may indicate to be desirable.

The values of a-c resistance calculated using the equations listed in Table V apply for the temperature of R_{dc} used. These are converted to the corresponding values of a-c/d-c resistance ratio by divid-

Table VI. Calculated A-C/D-C Resistance Ratios for Power Cables Operation at 60 Cycles, 75 Degrees Centigrade

		Type of Sheath										
		Nonmetallic		Lead						Aluminum-Polyethylene Jacket		
		1-Conductor, 5 Kv, Rubber		1-Conductor, 5 Kv, Rubber		1-Conductor, Paper-Insulated Standard Concentric			3-Conductor, 15 Kv, Paper-Insulated Compact Sector	1-Conductor, 5 Kv, Rubber Standard Concentric	1-Conductor, 15 Kv, Paper, Standard Concentric	3-Conductor, 15 Kv, Paper, Compact Sector
Conductor	Size, Thousand CM	Standard Concentric	Compact Round	Standard Concentric	Compact Round	0.6 Kv	15 Kv	27 Kv				
					In Nonmetallic Duct							
Copper	250	1.01	1.00	1.03	1.02	1.03	1.03	1.03	1.02		1.12	1.06
	500	1.03	1.02	1.10	1.08	1.10	1.10	1.11	1.06		1.30	1.16
	750	1.07	1.05	1.18	1.15	1.19	1.20	1.21	1.13		1.55	1.31
	1,000	1.12	1.09	1.31	1.25	1.30	1.32	1.34	1.22		1.84	1.48
Aluminum	250	1.00		1.02			1.02		1.01	1.08	1.07	1.03
	500	1.01		1.05			1.05		1.03	1.18	1.18	1.09
	750	1.03		1.10			1.10		1.07	1.34	1.34	1.17
	1,000	1.05		1.17			1.17		1.11	1.51	1.51	1.27
					In Iron Conduit							
Copper	250	1.03	1.02	1.07	1.07	1.07	1.08	1.09	1.04		1.27	1.10
	500	1.10	1.08	1.23	1.20	1.22	1.24	1.26	1.12		1.65	1.29
	750	1.19	1.16	1.44	1.37	1.43	1.45	1.48	1.25		2.21	1.55
	1,000	1.33	1.27	1.72	1.58	1.68	1.72	1.77	1.41		2.83	1.86
Aluminum	250	1.01		1.04			1.04		1.02	1.17	1.16	1.05
	500	1.05		1.13			1.12		1.06	1.38	1.38	1.16
	750	1.10		1.24			1.24		1.13	1.72	1.71	1.31
	1,000	1.16		1.40			1.39		1.21	2.07	2.07	1.48

ing through by the appropriate value of R_{dc}.

Representative Values of Calculated A-C/D-C Resistance Ratio for Power Cable Systems

Representative values of calculated a-c/d-c resistance ratio, based on the working equations given in Table V, are shown in Table VI for a number of types of power cable systems ranging in conductor size from 250,000 CM to 1,000,000 CM. The values are calculated for an operating temperature of 75 degrees centigrade. Values for conductor size below 250,000 CM can be extrapolated with sufficient accuracy. The 1,000,000-CM conductor size generally represents the upper limit for 3-phase power cable systems installed in one duct or conduit.

The values of a-c/d-c resistance ratio shown in Table VI are affected, of course, by dimensional variations. For the cases calculated, the cable build-up is in general accordance with Association of Edison Illuminating Companies-IPCEA specifications. For the systems with aluminum sheaths and polyethylene protective jackets, thickness of the sheath and covering is based on Table II of reference 14.

Discussion of Loss Components and Calculated A-C/D-C Resistance Ratios

The relative magnitude of the component losses in typical constructions of conventional strand power cable systems and also typical systems employing aluminum as a conductor and/or sheath material are shown in Figs. 1 through 4 for the condition of installation in nonmetallic duct and in Figs. 5 through 8 for the condition of installation in iron conduit.

Conductor Losses

In a discussion of reference 1, E. E. Hutchings gives a relatively simple expression for the proximity loss of three conductors in close triangular formation in air, namely

$$Y_1 = 1.5\alpha^2 Y_0 \qquad (27)$$

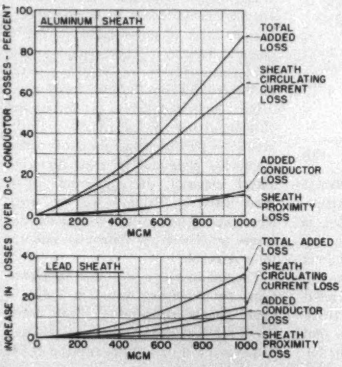

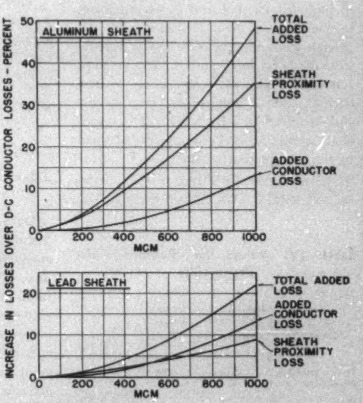

Fig. 1 (left) and Fig. 2 (right). Calculated losses of 15-kv lead-sheathed and aluminum-sheathed cables with copper conductors in nonmetallic duct or in air

Fig. 1 for single-conductor cables

Fig. 2 for 3-conductor cables

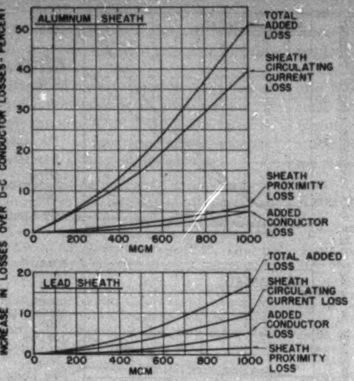

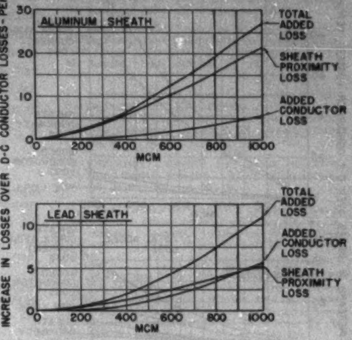

Fig. 3 (left) and Fig 4 (right). Calculated losses of 15-kv lead-sheathed and aluminum-sheathed cables with aluminum conductors in nonmetallic duct or in air

Fig. 3 for single-conductor cables

Fig. 4 for 3-conductor cables

In the notation of this paper

$$Y_1 = Y_c' - Y_0 \qquad (28)$$

Subtracting out standard values of Y_0 from the total conductor loss ratio Y_c', obtained using the equations given in Table V, the resultant values of conductor "proximity effect" were studied in relation to equation 27. The study indicated a constant, in equation 27, of approximately 2.3 for both 3-conductor cable systems, data from reference 4 (impregnated strands) and 1-conductor cable systems, data from reference 5 (dry strands).

Analysis of these resultant conductor proximity effects, using Arnold's 3-phase proximity loss equation,[9] indicated a value of k of approximately 0.73± for both the 3-conductor and single-conductor cable systems studied. The results for the 3-conductor cables are reasonably consistent with Arnold's indicated value of 0.75 for impregnated strand. However, he indicates a value of k for dry strand cables of 0.45 to 0.55. The available test data of reference 5 are not consistent with Arnold. Inconsistencies such as this have been noted previously. See, e.g., reference 3, Table II.

Obviously much work remains to be done on the subject of conductor losses in power cable systems. Relations with aluminum conductors may well be quite different than with copper conductors. Within the limits of present published data for copper conductor cables, the values of total conductor loss calculated for the systems listed in Table VI, indicate that, for cables with conductors closely spaced in air or in nonmetallic duct, the following simple relations may be used:

For 1-conductor noncompact conductors and for 3-conductor compact-sector conductors

$$Y_c' = 2.0\ Y_0 \qquad (29)$$

For 1-conductor compact conductors

$$Y_c' = 1.4\,Y_0 \qquad (30)$$

Values of Y_0 can be found in standard references. Simple approximations for copper and aluminum conductors, applicable for conductor sizes up to 1,000,000 CM at 75 degrees centigrade, are as follows:

For copper

$$Y_0 = 0.064(CI)^2 \qquad (31)$$

For aluminum

$$Y_0 = 0.0245(CI)^2 \qquad (32)$$

Equations 29 through 32 can be used as an approximation of the total conductor loss without serious effect on the total a-c/d-c resistance ratios shown in Table VI.

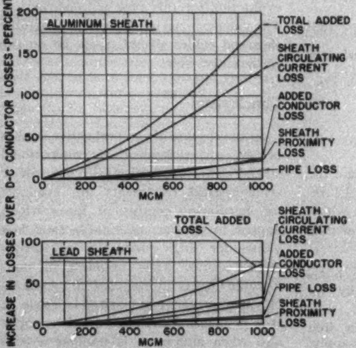

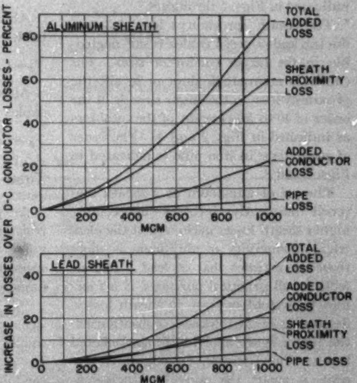

Fig. 5 (left) and Fig. 6 (right). Calculated losses of 15-kv lead-sheathed and aluminum-sheathed cable with copper conductors in iron conduit

Fig. 5 for single-conductor cables

Fig. 6 for 3-conductor cables

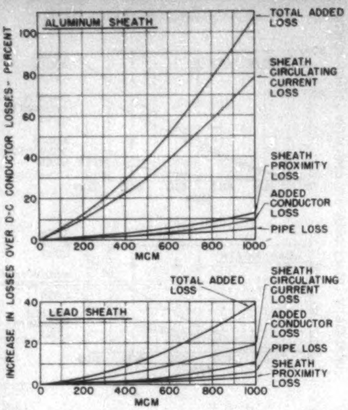

Fig. 7 (left) and Fig. 8 (right). Calculated losses of 15-kv lead-sheathed and aluminum-sheathed cables with aluminum conductors in iron conduit

Fig. 7 for single-conductor cables

Fig. 8 for 3-conductor cables

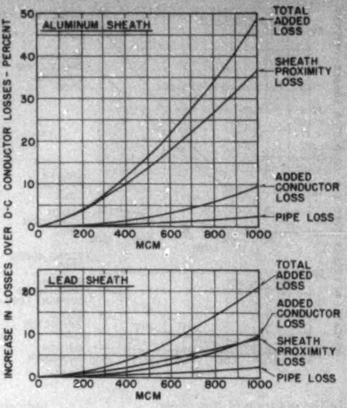

Sheath Losses

The values of a-c/d-c resistance ratio listed in Table VI are calculated, for single-conductor cable systems, on the basis of short-circuited cable sheaths, which is the usual condition of installation in utility and industrial power cable systems. In the larger conductor sizes, with lead-covered cables, the sheath circulating current loss becomes appreciable. If it is assumed that the total sheath loss is correctly given by the sum of the circulating current component and the proximity (eddy-current) component, the total sheath loss for single-conductor lead-covered cables is approximately twice the sheath loss of the same sized 3-conductor cable, in nonmetallic duct as indicated in Figs. 1 through 4, and somewhat more than twice as large in iron conduit as indicated in Figs. 5 through 8.

The sheath (proximity) loss of 3-conductor lead-covered cables is not negligible in the larger conductor sizes. For cables in nonmetallic duct or in air, the proximity loss, in the larger sizes, is of the order of 40 to 50 per cent of the total loss as indicated in Figs. 2 and 4. The order of magnitude in iron pipe is indicated in Figs. 6 and 8.

The use of aluminum as a sheath material inherently involves appreciably higher sheath losses inasmuch as the electrical conducivity of aluminum is more than seven times that of lead. The effect, for all practical purposes, is a fourfold to fivefold increase in sheath losses, depending on the thickness of sheath used, the higher figure applying to nonjacketed types. The increase, in regard to per cent, is about the same for single-conductor and 3-conductor cables. These effects are illustrated in Figs. 1 through 8.

Iron Loss

For the cable systems calculated, the effect of variations in cable dimensions served to change the iron loss only slightly with relatively negligible effect on the total a-c/d-c resistance ratio. For purposes of rough approximation, the following expressions give the value of iron loss, in the cases calculated, with less than 1-per-cent effect on the total loss ratio.

Copper conductors: 1-conductor cables

$$Y_p = CI/12 \tag{33}$$

Copper conductors: 3 conductor cables

$$Y_p = CI/28 \tag{34}$$

Aluminum conductors: 1-conductor cables

$$Y_p = CI/20 \tag{35}$$

Aluminum conductors: 3-conductor cables

$$Y_p = CI/50 \tag{36}$$

Total A-C/D-C Ratios

As previously indicated, the a-c/d-c resistances ratios listed in Table VI involve three major premises for which substantiating data are not available, namely:

1. That for calculating conductor losses the same K factors apply equally for copper and aluminum conductors.
2. That for obtaining values in iron conduit the same multiplying factors apply, for conductor loss, for either copper or aluminum conductor and, for sheath loss, for either lead or aluminum sheath.
3. That all calculated losses are directly additive.

Considerable further research is necessary to indicate proper treatment with regard to these points.

The usual equations given for sheath proximity loss are by no means rigid. Assumptions are made in the development of these equations as to uniformity of current density in the conductor cross section and the effect of sheath thickness. When the proximity effect in the conductors is large, the equations possibly overestimate the sheath loss as the resultant external magnetic field is reduced by the crowding of the currents towards each other. Arnold[9] has introduced empirical correction factors for lead-sheathed cables but test data on aluminum-sheathed cables are required to allow accurate evaluation for this type of construction. The values shown in Table VI for metallic sheathed cables should, then, be on the conservative side.

Conclusions

In the absence of comprehensive studies of the a-c resistance of conventional strand power cable systems, empirical or semiempirical treatments are available for calculating component losses which appear to produce reasonable total loss values for single-conductor and 3-conductor cables when installed in nonmetallic duct or in iron conduit. Applicable equations are summarized in Table V. It is assumed that these equations apply also when aluminum is used as a conductor material and/or as a sheath material although it is recognized that further experimental data may indicate the need for modification.

Based on the procedure given, values of a-c/d-c resistance ratio for a number of typical power cable systems are listed in Table VI. A few general remarks are made with respect to these ratios:

1. The extra a-c resistance component of lead-covered power cables installed in nonmetallic duct approximately equals the value for similar-type nonmetallic sheathed cables installed in iron conduit. This is consistent with the treatment in reference 6.

2. The extra a-c resistance component of aluminum conductor cables is approximately half the value for the similar size of copper conductor cables of similar type and covering.

3. For cables with aluminum sheaths, of the thickness assumed, the extra a-c resistance component is from 2 to $2^1/_2$ times the value for the same size and type of lead-covered cable.

No attempt is made to discuss the economics of application of aluminum as a sheath material. For duct installations, in the larger cable sizes, the indicated sheath losses are appreciably higher, as already stated, even for 3-conductor cables. Considerably more research is needed not only to establish accurate values for aluminum-sheathed cables but also to check the validity of procedures such as are given in Table V. In the meantime a consistent procedure is given which permits comparative evaluations of a-c resistance of various constructions.

References

1. A-C Resistance of Large Size Conductors in Steel Pipe or Conduit, **R. J. Wiseman.** *AIEE Transactions*, vol. 67, pt. II, 1948, pp. 1745–58.

2. A-C Resistance of Segmental Cables in Steel Pipe, **L. Meyerhoff, G. S. Eager, Jr.** *Ibid.*, vol. 68, pt. II, 1949, pp. 816–34.

3. A-C Resistance of Pipe-Cable Systems With Segmental Conductors, **AIEE Committee Report.** *Ibid.*, vol. 71, pt. III, Jan. 1952, pp. 393–414.

4. Resistance and Reactance of 3-Conductor Cables, **E. H. Salter, G. B. Shanklin, R. J. Wiseman.** *AIEE Transactions (Electrical Engineering)*, vol. 53, Dec. 1934, pp. 1581–89.

5. Impedance of 3-Phase Secondary Mains on Non-metallic and Iron Conduits, **L. Brieger.** *Bulletin*, Edison Electric Institute, New York, N. Y., Feb. 1938, pp. 61–66.

6. Current Carrying Capacity of Impregnated Paper, Rubber and Varnished Cambric Insulated Cables. *Publication No. P-29-226*, Insulated Power Cable Engineers Association, Montclair, N. J., 1st ed., Dec. 1943.

7. Proximity Effect in Solid and Hollow Round Conductors, **Dr. A. H. M. Arnold.** *Journal*, Institution of Electrical Engineers, London, England, vol. 88, pt. II, 1941, pp. 349–59.

8. Eddy-Current Losses in Single-Conductor Paper-Insulated Lead-Covered Unarmoured Cables of a Single-Phase System, **Dr. A. H. M. Arnold.** *Ibid.*, vol. 89, pt. II, no. 12, Dec. 1942, p. 636.

9. Eddy-Current Losses in Multi-Core Paper-Insulated Lead-Covered Cables, Armoured and Unarmoured, Carrying Balanced 3-Phase Current, **Dr. A. H. M. Arnold.** *Ibid.*, vol. 88, pt. II, no. 1, Feb. 1941, pp. 52–63.

10. Proximity Effect in Cable Sheaths, **Gerbert Bristol Dwight.** *AIEE Transactions*, vol. 50, Sept. 1931, pp. 993–98.

11. The Theory of Sheath Losses in Single-Conductor Lead-Covered Cables, **Dr. A. H. M. Arnold.** *Journal*, Institution of Electrical Engineers, London, England, vol. 67, 1929, pp. 69–96.

12. A Critical Study of a Three-Phase System of Unarmoured Single-Conductor Cables from the Standpoint of the Power Losses, Line Constants and Interference with Communication Circuits, **E. B. Wedmore, P. D. Morgan, S. Whitehead.** *Ibid.*, pp. 359–434.

13. Sheath Currents, Sheath Losses, Induced Sheath Voltages and Apparent Conductor Impedances of Metal Sheathed Cables Carrying Alternating Current, **K. W. Miller.** *Thesis*, University of Illinois, Urbana, Ill., 1929.

14. Aluminum Sheathed Power Cable, **W. A. Del Mar, E. J. Merrell.** *AIEE Transactions*, vol. 74, pt. III, June 1955, pp. 292–304.

15. Eddy-Currents in Thin Circular Cylinders, **F. W. Carter.** *Proceedings*, Philosophical Society, Cambridge, England, vol. 23, 1927, pp. 901–06.

◆

Discussion

George S. Haralampu (New England Power Service Company, Boston, Mass.): The authors are to be congratulated for the work they have done in compiling into one paper working equations for the calculation of the a-c resistance of 3-conductor and single-conductor cables. The little test data that are known support these equations, and if some day extensive test data are made available the equations may need a slight modification as the authors have stated.

It is satisfying to see that the R_{ac}/R_{dc} ratios, tabulated in Table V of the paper, agree fairly well with ratios obtained using the equations listed in the following. Although the authors have not mentioned the extra losses due to the shielding and binding tapes, the increase in the cable resistance due to these losses when three conductors are in a single conduit is of such a magnitude that they could very well be neglected.

The R_{ac}/R_{dc} ratio will vary for the same size conductor for different thicknesses of sheath (which will affect the sheath losses) and for different thicknesses of insulation (which will affect proximity effect and sheath losses). Since this is not shown in Table V of the paper, I assume the values given are average values. The working equations listed in Table IV take this variation into consideration.

The following is a tabulation of equations derived from the references listed and which are different from those used by the authors, to obtain the a-c resistance of 3-conductor round or noncompact sector copper cables in a nometallic duct.

SKIN EFFECT

$$X = 0.02768\sqrt{\frac{\mu f}{R_{dc}}}$$

The ratio R'/R_{dc} can be obtained from Table VII of this discussion.

$$\Delta R_{se} = R_{dc}\left(\frac{R'}{R_{dc}} - 1\right) \text{ ohms/1,000 feet}$$

PROXIMITY EFFECT

For noncompact sector conductors:

$$S = \frac{2\sqrt{K} + 4.5(C + 0.005)}{2.155} \text{ inches}$$

For compact sector conductors:

$$S = \frac{1.85\sqrt{K} + 4.44(C + 0.005)}{2.155} \text{ inches}$$

$$f_p = 6\left[\frac{GMR}{S}\right]^2\left(\frac{R'}{R_{dc}} - 1\right)$$

$$\Delta R_p = f_p(R_{dc}) \text{ ohms/1,000 feet}$$

SHEATH LOSSES

For round or sectored conductors:

$$r_i = \frac{2.155S + 2t}{2} \text{ inches}$$

$$r_o = r_i + t' \text{ inches}$$

$$r_{sh} = \frac{K'}{(r_o + r_i)(r_o - r_i)5.28} \text{ ohms/1,000 feet}$$

$$S_1 = \frac{1}{\sqrt{3}}(d + 2C) \text{ inches}$$

$$\Delta R_{sh} = \frac{8,370\,(S_1)^2 \times 10^{-6}}{r_{sh}(r_o + r_i)^2} \text{ ohms/1,000 feet}$$

SHIELDING TAPE LOSS

$$r_s = \frac{\rho' \times 10^{-3}}{8 r_m' t''} \text{ ohms/1,000 feet}$$

Table VII

(Reference 1)

X	R'/Rdc	X	R'/Rdc	X	R'/Rdc	X	R'/Rdc
0.0	1.00000	1.2	1.01071	2.4	1.15207	3.6	1.52879
0.1	1.00000	1.3	1.01470	2.5	1.17538	3.7	1.56587
0.2	1.00001	1.4	1.01969	2.6	1.20056	3.8	1.60314
0.3	1.00004	1.5	1.02582	2.7	1.22753	3.9	1.64501
0.4	1.00013	1.6	1.03323	2.8	1.25620	4.0	1.67787
0.5	1.00032	1.7	1.04205	2.9	1.28644	4.1	1.71516
0.6	1.00067	1.8	1.05240	3.0	1.31809	4.2	1.75233
0.7	1.00124	1.9	1.06440	3.1	1.35102	4.3	1.78933
0.8	1.00212	2.0	1.07816	3.2	1.38504	4.4	1.82614
0.9	1.00340	2.1	1.09375	3.3	1.41999	4.5	1.86275
1.0	1.00519	2.2	1.11126	3.4	1.45570		
1.1	1.00758	2.3	1.13069	3.5	1.49202		

$$X_m=0.0529\ \frac{f}{60}\log_{10}\frac{2S}{r_o'+r_i'}\ \text{ohms/1,000 feet}$$

Since r_o' is approximately equal to r_i' then, for tangent triangular spacing,

$S=2r_o'$ or $2r_i'$

and the mutual reactance equation becomes

$$X_m=0.0529\ \frac{f}{60}\log_{10}\frac{2(2r_i')}{2r_i'}\ \text{and, for 60 cycles,}$$

$$X_m=0.0529\log 2=0.0159\ \text{ohms/1,000 feet}$$

$$\Delta R_s=\frac{X_m^2 r_s}{X_m^2+r_s^2}\ \text{ohms/1,000 feet}$$

Since X_m^2 is very small, the foregoing equation simplifies to

$$\Delta R_s=\frac{X_m^2}{r_s}=\frac{254.0\times10^{-6}}{r_s}\ \text{ohms/1,000 feet}$$

METALLIC BINDING TAPE

The method for finding the increase in resistance due to binding tape loss is the same as outlined for the sheath losses, except for the change in the resistivity constants and radii.

$$r_b=\frac{K'}{(r_o''+r_i'')(r_o''-r_i'')}$$

$(r_o''-r_i'')$ = thickness of binding tape (0.004 inch may be used if actual thickness is not known)

$$\Delta R_b=\frac{8{,}370(S_1)^2\times10^{-6}}{r_b(r_o''+r_i'')^2}\ \text{ohms/1,000 feet}$$

The a-c resistance of a 3-conductor cable is, therefore:

$$R_{ac}=R_{dc}+\Delta R_{se}+\Delta R_p+\Delta R_{sh}+\Delta R_s\ \text{(if any)}+\Delta R_b\ \text{(if any) ohms/1,000 feet}$$

In Table VIII the R_{ac}/R_{dc} ratios obtained with the method are compared with the R_{ac}/R_{dc} ratios listed in Table V.

Table VIII

Size MCM	R_{ac}/R_{dc} Burrell and Morris Paper	R_{ac}/R_{dc} Discusser's Equations
250	1.02	1.019 – 1.033*
500	1.06	1.06 – 1.081*
750	1.13	1.13 – 1.14 *
1,000	1.22	1.22

* The variations of the R_{ac}/R_{dc} are due to different sheath thickness and different insulation thickness used for the same size conductors.

NOMENCLATURE

ΔR_{se} = increase in resistance due to skin effect in ohms per 1,000 feet
ΔR_p = increase in resistance due to proximity effect in ohms per 1,000 feet
ΔR_{sh} = increase in resistance due to sheath losses in ohms per 1,000 feet
ΔR_s = increase in resistance due to shield losses in ohms per 1,000 feet
ΔR_b = increase in resistance due to binding losses in ohms per 1,000 feet
R_{ac} = a-c resistance of cable in ohms per phase per 1,000 feet
R_{dc} = d-c resistance of cable in ohms per phase per 1,000 feet
$R'=R_{dc}+\Delta R_{se}$
r_{sh} = sheath resistance in ohms per 1,000 feet
r_s = shielding-tape resistance in ohms per 1,000 feet
r_b = binding-tape resistance in ohms per 1,000 feet
r_o = outside radius of sheath in inches
r_i = inside radius of sheath in inches
r_o' = outside radius of shield in inches
r_i' = inside radius of shield in inches
r_o'' = outside radius of binding tape in inches
r_i'' = inside radius of binding tape in inches
r_m' = mean radius of shielding tape in inches
C = conductor insulation thickness in inches
d = diameter of conductor in inches
f = frequency
f_p = proximity effect factor
GMR = geometric mean radius of conductor in inches
K = area of conductor in CM$\times10^{-6}$
K' = resistivity constant for binding tape or sheath
= 0.067 for copper
= 0.200 for lead
= 0.167 for steel
S = phase to phase spacing of conductors in inches
S_1 = distance between conductor center and sheath center for 3-conductor cables made up of round conductors. For sector conductors, d (diameter of conductor) should be 82–86 per cent of diameter of a round conductor having the same area (84 per cent is used as a compromise)
t = thickness of belt or of binding tape for H type, in inches (use $2t=0.025$ inches for conductor with binding tape where actual measurement is not known. This includes the paper intercolated with the tape)
t' = thickness of sheath in inches
t'' = thickness of shield in inches (use 0.004 inch if actual measurement is not known)
X = a parameter
X_m = mutual reactance between conductor and shield in ohms/1,000 feet
μ = permeability of the conductor
= 1.0 for copper
ρ' = resistivity of shield in ohms per circular-mil-foot
= 50 ohms per circular-mil-foot for copper

REFERENCES

1. Anaconda General Catalog, sect. 16, p. 18.

2. CIRCUIT ANALYSIS OF A.C. POWER SYSTEMS, Edith Clarke. John Wiley and Sons, Inc., New York, N. Y., vol. II, chapter on cables, pp. 48–85.

3. Westinghouse Transmission and Distribution Reference (4th edition), chapter on cables.

4. THE EFFECT OF GROUNDING METALLIC SHIELDING AND SHEATHS ON INSULATED POWER CABLES, R. C. Waldron. *Electrical World*, New York, N. Y., Sept. 30–Nov. 25, 1944.

5. General Cable Catalog, sect. 20, pp. 7–13.

L. Meyerhoff (General Cable Corporation, Bayonne, N. J.): The authors are to be commended on their thorough analysis of existing loss data and their extension of these results rationally to practical cases for which data are lacking. Unfortunately, in some cases it is necessary to extrapolate far beyond the scope of the original data with consequent uncertainty as to the applicability of the equations developed. This is recognized by the authors, but some elaboration may be in order.

In connection with sheath circulating current loss, it is stated that for certain cases on which data are available the sheath circulating current loss with the cables in iron pipe is 2.0 times the value in air. The authors also point out that for lead-sheathed cables other data point to the validity of the same multiplying factor. They then go on to assume that the factor may be used for other systems treated in the paper. Where the sheath resistance is not greatly different from those for which data are available the factor of 2.0 is likely to be sufficiently accurate. However, where the sheath resistance is of much lower order, as, for example, in the case of aluminum sheath, the factor of 2.0 may be quite out of line. The same comment applies to the factors of 1.7 and 2.0 relating to sheath proximity effect.

The limitations of the proposed equations, as here pointed out, are recognized by the authors in their statement that: "It is assumed that these equations apply also when aluminum is used as a conductor material and/or a sheath material although it is recognized that further experimental data may indicate the need for modification." It is this discusser's opinion that further data may indicate very substantial modification for the case of aluminum sheath and that actual incremental losses with aluminum sheath may turn out to be materially lower than indicated in some of the curves given in the paper. In the absence of actual data, however, the curves given are probably quite conservative and are not likely to lead to too high estimates of current-carrying capacity.

R. J. Wiseman (Okonite Company, Passaic, N. J.): The paper by Burrell and Morris is very timely. As the authors state, there is lacking a considerable amount of information on the subject. The paper by Salter, Shanklin, and Wiseman in 1934 (see reference 4 of the paper) might be considered the pioneer in the United States in obtaining proper data for 3-conductor lead-sheathed cables. This paper came about because of observations made by W. H. Cole of the Boston Edison Company in the early 1920's when he made some power loss tests and found that the losses were much higher than calculated values. This resulted in an elaborate investigation by several cable manufacturers and Electrical Testing Laboratories which was reported in the aforementioned paper. Later, IPCEA, while interested in the current-carrying capacity of cables in conduit, had Electrical Testing Laboratories conduct an elaborate study of the subject, having unshielded cables, resulting in two papers, one dealing with the a-c resistance (reference 1 of the paper under discussion) and the other the reactances of cables in conduit.[1] Unfortunately the number of various types of cables was very meager so we need additional data. Under these conditions, all we can do is to use the data available. This is what the authors have done, but in addition, they have broadened out to cover the various cable designs that may be encountered.

I am very glad that this paper has been prepared as it summarizes the various formulas for computing the effective a-c resistance for single- and 3-conductor cables, having lead and aluminum sheaths drawn into ducts and also in conduit. However, we must keep in mind that the formulas are empirical in nature, and in time, might have to be modified after further test data have become available.

It may be of interest to report that about a year ago we had occasion to test a 3-conductor, 500,000-CM 11-kv cable having an aluminum sheath. After making an a-c resistance test, the aluminum sheath was removed and replaced by a lead sheath and retested. The a-c resistance ratio for both sheaths was calculated, using the standard formula. We also just computed the ratio, using the formulas in the paper. The following table shows the results for each case for a conductor temperature of 82.8 C:

	Actual by Test	Calculated by	
		Standard	Burrell-Morris
Aluminum sheath	1.194	1.196	1.209
Lead sheath	1.091	1.071	1.068

We consider the comparison good between the actual value by test and both calculated values, and as it is much easier to use the Burrell-Morris method, it is our intention to do so.

REFERENCE

1. REACTANCE OF LARGE CABLES IN STEEL PIPE OR CONDUIT, William A. Del Mar. *AIEE Transactions*, vol. 67, pt. II, 1948, pp. 1409–15.

R. W. Burrell and **M. Morris:** We appreciate the comments made by the several discussers and are gratified that no serious disagreement is indicated in connection with the simplified method presented for the calculation of the a-c resistance of 3-conductor and single-conductor power cables when operating in air or in nonmetallic ducts.

We agree with Mr. Haralampu that the effect of the extra losses due to the shielding and binding tapes can readily be neglected for conventional designs and we therefore purposely omitted detailed formulas for inclusion of these effects. If it is desired to check the magnitude of these extra losses, equation 13, while overestimating the value of this component, nevertheless indicates that for the usual range of shield and binder tape resistance values, the influence is negligible. The formulas given by Mr. Haralampu should be helpful to those persons who wish to explore these losses in further detail.

It is true, as Mr. Haralampu states, that the over-all a-c/d-c resistance ratios will vary, for the same size conductor, for different insulation and sheath thicknesses. While not shown for 3-conductor cables in Table V, the effect of these variations is shown for single-conductor cable systems with lead sheaths. All of the values listed in Table V are calculated on the basis of appropriate Association of Edison Illuminating Companies or IPCEA standard insulation and sheath thicknesses except for the aluminum-sheathed, jacketed type cables which are in accordance with the sheath and jacket dimensions quoted in reference 14 of the paper.

Mr. Haralampu follows the conventional practice of calculating the conductor skin effect and proximity effect separately. Our views on this procedure are already given in the paper. The formula he lists for skin effect is standard. The formula quoted for proximity effect is essentially the same as equation 27 referred to in the paper. Our comments regarding this equation are already given in the paper.

In his Table VIII, Mr. Haralampu shows the effect of insulation thickness and sheath thickness in producing a limited range of variation in values of R_{ac}/R_{dc}.[*] The effect of these variations in calculating current-carrying capability of power cable circuits generally would be negligible.

Mr. Meyerhoff is justified in warning us that the "in pipe" multiplying factors found suitable for segmental cables may not apply directly for sheath losses in aluminum-sheathed cables. Mr. Meyerhoff indicates his belief that for aluminum-sheathed cables the demagnetizing effect of the relatively large sheath currents may serve to reduce materially the incremental losses quoted by us. It is to be hoped that clarification of this point by test data will be forthcoming in the near future.

Dr. Wiseman's comments are appreciated, particularly with respect to the test data reported on aluminum-sheathed cable. It is important that more data of this type be published in the near future in order that the validity of procedures applicable to the calculation of impedances and "ampacities" of power cables constructed with conventional materials be verified, or proper modifications indicated, for use with cables with aluminum conductors and/or sheaths.

Freezing Oil-Type Pipe Cables

EDWIN J. MERRELL
MEMBER AIEE

EARLY oil-type pipe cable installations usually were equipped throughout with semistop joints for maintenance purposes, the understanding being that freezing with dry ice (frozen carbon dioxide) could be employed at intermediate points. The need for the complex semistop joint as compared to the simpler normal joint became less and less apparent, as time in service built a comparatively enviable record of reliability for this class of cable. This has been particularly true in most parts of the United States where ample supplies of dry ice for freezing are readily available. Therefore, the recent growth in the number of pipe cable installations has witnessed a very marked reduction in the application of semistop joints on all designs of pipe cable, and in turn an increasing reliance upon the freezing technique as a primary tool in maintenance and rerouting work.[1]

Several experimental freeze runs were made in this connection on pipe cable at the Phelps Dodge Habirshaw Laboratory. In this paper various aspects of the technique are covered, as well as studies of the critical length of the freeze in relation to pipe diameter and to rate of flow of pipe oil, freeze strength, the effect of feeding a purge of dry gas adjacent to the drained side of a freeze, the time to attain a freeze with dry ice and acetone or the noninflammable methylene chloride, and with dry ice alone, and the effect upon the cable dielectric of freezing and thawing under high static head pressure, both in the case of unsheathed cable and with the polyethylene-sheathed compression cable.

Test Criteria

The first criterion is that the freeze procedure must not have a deleterious effect on system components.

A single pipe oil, namely Suniso no. 6, was employed on all test runs. It is characterized by a cold-set temperature of −25 degrees centigrade (C) and a hard-freeze temperature of −50 C. At −25 C it possesses a firm grease-like consistency, becoming progressively firmer at lower temperatures until converting to a hard, rosin-like material at −50 C. On warming, the plastic state develops again at about −45 C.

Based upon these characteristic temperatures, system oil has been taken to be in a condition of soft freeze between −25 and −49 C, and in a hard freeze at −50 C and below. This is a more or less pessimistic interpretation, since the usual pipe cable impregnants are more viscous than Suniso no. 6 and are characterized by a hard-freeze temperature of a different

---

Paper 55-446, recommended by the AIEE Insulated Conductors Committee and approved by the AIEE Committee on Technical Operations for presentation at the AIEE Summer General Meeting, Swampscott, Mass., June 27–July 1, 1955. Manuscript submitted March 29, 1955; made available for printing April 13, 1955.

EDWIN J. MERRELL is with the Phelps Dodge Copper Products Corporation, Yonkers, N. Y.

Fig. 1. Freeze setup including pipe, accumulators, and portable pumping plant

Fig. 2. Insulated freezing chamber consisting of two insulated 4-foot units side by side

order, approximately −40 C. Therefore, the holding properties of a hard freeze may be achieved on new cable under static conditions with the conductor at −40 to 45 C, and the pipe oil at −50 C. However, a degree of mixing in the case of cable designs with taped moisture seals is inevitable, so that the effective system freeze temperature for these types after service may not be significantly different from that of the pipe oil, particularly under dynamic conditions.

A related criterion is that a hard freeze has been deemed accomplished when it can withstand a hydrostatic head of 100 pounds per square inch (psi) gauge (250 feet of oil). It has been considered secure upon withstanding 300 psi gauge for 24 hours.

Two conditions of pipe oil flow have been assumed for study: static or zero flow, and a flow of 0.1 gallon per minute to represent dynamic conditions. Thus, the latter flow rate is typical of the oil demand of a line 1 day after having been shut down while under full load. In other words, this flow rate can exist in the manhole lengths adjacent to the pumping plant, whereas at the opposite end of the same line the flow is virtually zero. Likewise, it will be essentially zero on a short line or an unloaded line. It can of course be somewhat greater than 0.1 gallon per minute for very long lines and larger pipe sizes. A fairly accurate determination of typical rates of pipe oil

Table I. Summary of Pipe Cable Freezing Data Obtained on 3-Conductor H.O. Cable in 6-Inch Pipe

Freeze Material	End Point	Hours to Attain End Point (1)				Approximate Pipe Temperature in C 1 Foot Outside Freeze at Time of Attaining End Point				Amount of Material Consumed			
		4-Foot Freeze		8-Foot Freeze		4-Foot Freeze		8-Foot Freeze		Gallons of Liquid Heat-Transfer Medium		50-Pound Blocks of Dry Ice (3)	
		Static	Dynamic (2)	Static	Dynamic (2)	Static	Dynamic (2)	Static	Dynamic (2)	4-Foot Freeze	8-Foot Freeze	4-Foot Freeze	8-Foot Freeze
Dry ice and acetone or methylene chloride	Soft freeze in pipe oil (4)	2	4	2	3	2	5	13	6	Initial 6. Makeup less than 3 per 24 hours	Initial 12. Makeup less than 3 per 24 hours	Initial 7. Makeup 8 per 24 hours on static and 12 on dynamic	Initial 14. Makeup 16 per 24 hours on static and 24 on dynamic
	Soft freeze in conductor oil (4)	3	6	3	4	− 4	4	6	4				
	Hard freeze in pipe oil (5) (6)	5	? (7)	5	8	−16	? (7)	− 7	4				
	Hard freeze in conductor oil (5)	22 (8)	? (7)	6	10	−19	? (7)	−11	−2				
Dry ice alone	Soft freeze in pipe oil	5	? (7)	5	8	3		7	17	None	None	Initial 7. Makeup 5 per 24 hours on static and 7 on dynamic	Initial 14. Makeup 10 per 24 hours on static and 14 on dynamic
	Hard freeze in conductor oil	22 (8)		12	29	−10		− 5	12				

(1) Assuming an ambient of +25 C, a soft freeze of system oil at −25 C, and a hard freeze at −50 C.

(2) Pipe oil moving at the rate of 6 gallons per hour (0.1 gallon per minute) and under a pressure of 100 psi gauge as freeze is being accomplished. This is a typical maximum oil demand on a long line during the second day after being taken out of service.

(3) Original shipping weight is 50 pounds per cake, but loss is considerable in open storage over a 24-hour period. Consumption would be less than tabulated if each day's shipment were stored in an insulated box.

(4) A soft-freeze in oil is a plastic (grease-like) state and will hold a few psi. For example, when the skid wire temperature fell to −25 C, the pipe oil was presumed to have attained this state, etc.

(5) A hard freeze in oil is a rigid (rosin-like) state and will hold at least 300 psi gauge indefinitely.

(6) A system with polyethylene-sheathed compression cable will sustain the 300 psi loading of a hard freeze directly after the pipe oil has attained a hard freeze.

(7) Probably not attainable with ambients over +10 C.

(8) The 4-foot chamber just about attains a hard static freeze according to the conditions assumed. However, see the section on "Test Criteria" for other associated factors.

Table II. 4-Foot Static Freeze With Dry Ice and Acetone

6-Inch Pipe, Suniso No. 6, Three 1-Conductor 2,000,000-CM 315-Mil Wall, H.O. Cable, 1/16 by 3/16 Skid Wires, Conductors Tied in Close Triangle

Time, Hours	Pipe Oil Pressure, Psi		Temperature, C, Thermocouples Soldered Into Top Conductor												
	High Side	Low Side	−7′*	−5′	−2′	−1′	C/L†	1′	2′	3′	4′	5′	8′	18′	28′
0	25	25	16	16	16	16	16	16	16	15	15	15	15	14	14
1	25	25	16	16	11	9	8	9	11	14	15	15	15	13	14
2	25	25	14	12	−10	−15	−16	−14	−6	4	9	13	16	15	15
3	25	20	13	11	−21	−27	−28	−24	15	−4	5	11	16	16	16
5	25	10	9	−9	−32	−38	−39	−35	−25	−13	−3	6	18	18	19
8	25	0	3	−14	−40	−44	−45	−42	−32	−20	−8	3	17	19	19
10	25	0	0	−16	−42	−47	−47	−43	−35	−24	−13	−3	14	18	19
22	25	0	−10	−22	−45	−49	−49	−46	−40	−30	−19	−12	7	11	11
29	100	0	−8	−22	−45	−49	−49	−46	−39	−28	−18	−8	11	15	15
47	200	0	−12	−24	−46	−50	−50	−48	−41	−32	−22	−14	3	10	11
71	300	0	−9	−22	−45	−48	−48	−46	−39	−29	−19	−10	9	15	16
97	300	0	−3	−17	−42	−47	−47	−43	−36	−25	−15	−3	13	18	18

	Oil Triangle			Bottom Conductors West	Bottom Conductors East	Temperature, C, on Skids of Top Conductor						
	−2′	1′	3′	−2′	−2′	−2′	−1′	1′	3′	5′	8′	28′
0	15	16	16	16	16	16	17	17	15	15	15	14
1	−13	14	12	−11	−11	3	0	−14	13	15	15	14
2	−30	−31	2	−30	−31	−20	−26	−28	3	13	15	15
3	−37	−38	−6	−36	−37	−28	−35	−37	−4	12	18	18
5	−44	−45	−14	−42	−43	−39	−45	−47	−13	9	18	20
8	−48	−49	−19	−45	−46	−45	−49	−51	−20	5	17	20
10	−50	−50	−22	−48	−49	−47	−52	−56	−24	0	14	19
22	−52	−52	−28	−40	−51	−50	−54	−60	−31	−10	5	10
29	−52	−52	−27	−49	−51	−49	−53	−58	−29	−5	12	16
47	−53	−53	−30	−50	−52	−50	−54	−54	−32	−12	3	11
71	−52	−52	−27	−49	−50	−49	−53	−50	−30	−5	10	16
97	−49	−50	−23	−47	−49	−46	−51	−42	−25	0	13	18

	Trough	Ambient	Temperature, C, on Top of Pipe									
			−2′	−1′	1′	2′	3′	4′	5′	8′	18′‡	28′
0	14	16	16	22	23	19	17	17	17	17	14	14
1	−67	19	−63	−65	−65	−43	8	16	16	17	13	16
2	−67	21	−64	−65	−65	−48	−2	12	15	17	18	17
3	−66	22	−64	−65	−65	−50	−7	10	16	23	17	23
5	−66	22	−64	−65	−65	−52	−14	4	13	19	16	20
8	−66	21	−65	−66	−66	−53	−20	−2	10	19	16	21
10	−66	21	−65	−66	−66	−54	−24	−6	6	15	13	16
22	−66	15	−65	−65	−65	−54	−29	−15	0	12	7	12
29	−66	21	−66	−66	−66	−54	−26	−11	4	17	13	17
47	−66	18	−64	−66	−66	−55	−30	−16	−4	10	8	12
71	−66	20	−65	−66	−66	−54	−27	−12	−3	16	14	17
97	−65	22	−63	−65	−65	−52	−23	−6	6	17	18	20

* ′ stands for feet.

† C/L stands for centerline.

‡ Affected by freeze on thermocouple manifold.

flow may be made by means of the techniques described in another paper.[2]

Test Setup

The tests were made on 80-foot lengths of bare 6-inch and 8-inch steel pipe set in air with two 4-foot-long insulated freezing troughs in the middle. Hydrostatic head was supplied by an accumulator or by a single ladder portable pumping plant, and the latter was used on dynamic runs to circulate pipe oil at a constant rate, monitored by a flowmeter. For some of the tests, the setup was outdoors. Fig. 1 and 2 show the indoor arrangement.

The freeze troughs were set side by side. They were fabricated from sheet steel and cleared the pipe by 4 inches on each side, making it possible to charge the dry ice in large pieces, which helps to conserve it. Insulation consisted of a sandwich of 1 inch of Johns Manville Aircell with a layer of 5-mil aluminum foil inside and outside. This insulation also was wrapped around the pipe for 3 feet at either end of the troughs. It was quite effective, virtually completely preventing external condensation on the troughs.

Four cable constructions were employed in the series of tests: three 1-conductor 2,000,000-circular-mil (CM) compact copper segmental H.O. (taped moisture seal) cables with 315-mil wall; the same cable core in the extruded polyethylene-sheathed compression cable construction; three 1-conductor 500,000-CM compact copper H.O. cables with 650-mil wall; and three 1-conductor 2,000,000-CM compact copper H.O. cables with 505-mil wall. The cables were tied in close triangle formation for all runs.

Detailed locations of the thermocouples employed on the various runs are given in the tables. Briefly, thermocouples were soldered to the top conductor of the group, to the skid wires, in the triangular oil space surrounded by the three cables, along the pipe, and hung in the freeze trough and in the ambient air. Thermocouples, connected to points inside the pipe, were brought out through a manifold equipped with a freeze chamber which afforded a simple but effective seal.

To ascertain any possible supplementary support which the frictional grip of cable in the pipe might afford a freeze, a 1,000-pound dynamometer was secured to the cables at one end of the test setup through an adjustable linkage with a low-

Table III. 4-Foot Dynamic Freeze With Dry Ice and Acetone

Test Setup Same as in Table II

Time, Hours	Pipe Oil Pressure, Psi		Oil Flow Gallons per Hour	Temperature, C, on Thermocouples Soldered Into Top Conductor												
	High Side	Low Side		−7′*	−5′	−2′	−1′	C/L†	1′	2′	3′	4′	5′	8′	18′	28′
0	99	98	6	28	28	27	28	28	28	28	28	28	28	28	28	28
2	100	100	6	24	20	8	4	5	10	16	22	26	28	30	29	32
4	100	99	6	17	11	−13	−17	−18	−12	0	14	22	27	32	32	35
6	99	98	6	14	7	−20	−26	−25	−19	−5	10	21	27	34	34	37
8	102	100	6	12	5	−23	−28	−28	−21	−8	9	20	27	34	36	38
14	103	101	6	4	−3	−27	−34	−33	−27	−14	5	14	22	30	32	34
24	99	94	5	0	−7	−29	−33	−33	−27	−15	0	8	15	23	25	27
32	99	97	4	4	−4	−28	−33	−33	−26	−13	2	14	22	31	33	35
48	100	94	2	−3	−11	−33	−36	−36	−30	−19	−4	8	15	24	26	29
62	100	85	0	−6	−15	−35	−39	−37	−33	−22	−8	6	15	26	29	30
70	15	−8′	0	0	−16	−42	−46	−46	−42	−33	−20	−8	4	19	25	26

Time, Hours	Oil Triangle			Bottom Conductors		Temperature, C, on Skids of Top Conductor						
	−2′	1′	3′	West −2′	East −2′	−2′	−1′	1′	3′	5′	8′	28′
0	28	28	28	28	27	28	28	35	28	28	28	28
2	−19	−17	19	−21	−22	5	−6	−17	23	29	30	33
4	−32	−31	12	−32	−34	−17	−21	−35	19	30	33	36
6	−37	−35	9	−36	−38	−22	−29	−40	16	30	35	37
8	−38	−37	8	−37	−39	−25	−32	−43	15	30	35	39
14	−42	−39	4	−42	−43	−30	−37	−45	10	24	29	34
24	−42	−40	0	−41	−42	−32	−36	−45	5	19	23	28
32	−41	−39	2	−40	−41	−32	−36	−46	8	26	31	35
48	−43	−43	−4	−43	−43	−36	−39	−48	2	19	25	29
62	−46	−44	−8	−45	−46	−39	−42	−52	−4	19	27	30
70	−49	−49	−18	−46	−48	−45	−51	−52	−21	6	20	26

Time, Hours	Trough	Ambient	Temperature, C, on Top of Pipe									
			−2′	−1′	1′	2′	3′	4′	5′	8′	18′‡	28′
0	23	31	28	31	31	29	29	30	30	30	26	30
2	−66	34	−63	−65	−65	−36	20	29	31	31	28	33
4	−66	38	−63	−65	−65	−39	18	28	32	36	31	36
6	−66	37	−64	−65	−65	−40	17	29	33	37	33	37
8	−66	35	−64	−66	−66	−40	16	28	32	35	33	37
14	−67	30	−64	−66	−66	−43	11	24	28	31	29	34
24	−65	27	−62	−64	−64	−42	5	19	23	26	24	28
32	−65	31	−62	−65	−65	−42	9	23	28	33	31	35
48	−65	32	−64	−64	−64	−45	4	18	24	29	25	31
62	−66	28	−65	−66	−66	−48	−3	16	22	28	26	30
70	−65	27	−61	−65	−65	−51	−18	2	13	23	23	25

Footnotes are the same as for Table II.

friction 0-ring seal. The "at-rest" loading on the dynamometer was adjusted to 40 pounds.

Method of Test

Tests were run on an around-the-clock basis until steady state resulted. Directly following the initial check of all thermocouples under ambient conditions, the troughs were filled with cracked dry ice. Thereafter, measurements were made at hourly intervals, and the troughs charged with additional dry ice and liquid heat-transfer medium as necessary. Two liquid heat-transfer mediums were utilized separately, acetone and methylene chloride, and runs also were made with dry ice alone. Pressure was applied at one end of the pipeline, so that progress of a freeze also was indicated by a fall in the reading of the gauge on the low side.

On the dynamic runs, the portable pumping plant sustained a supply of pipe oil at 100 psi gauge, and the flow was controlled at 0.1 gallon per minute (6 gallons per hour) by manual operation of a needle valve on the down side. This valve would be just cracked at the start of a dynamic run; then, as the run proceeded, the valve was opened gradually to sustain a uniform flow at the desired 0.1 gallon per minute.

Test Results

An illustrative summary of test results on several 6-inch pipe runs is given in Table I. End point results obtained with only dry ice, i.e., without a liquid heat-transfer medium, are included for comparison with runs employing acetone together with dry ice. The summarized data have been adjusted to compensate for the various ambient temperatures under which the different runs were made.

Fig. 3 is a bar graph showing the state of progress on four typical dry ice and acetone freezes with cable in 6-inch pipe versus time at three pertinent locations: the steel pipe, the brass skid wires on the top conductor of the group in triangular formation, and in the copper strand of this top conductor.

Tables II through V are abbreviated records of typical runs with dry ice and acetone. Virtually identical results were obtained with the noninflammable methylene chloride as the liquid heat-transfer medium.

Table VI is the record of the breakdown of a freeze on the 2,000,000-CM H.O. cable under 300 psi gauge hydrostatic head. It starts as the steady state of an 8-foot freeze, with one 4-foot trough being dissipated at a time. The temperature pattern follows the procedure, and it is to be noted that once a hard freeze has been accomplished it is not lost easily. Thus, the remaining 4-foot freeze retained equilibrium until within 2 to 3 hours of breakthrough; the breakthrough occurred in the pipe oil, not in the insulation or at the conductor, as evidenced by the temperature record during the last 3 hours. Very little dry ice remained in the trough at this time, but the acetone level had been kept up, providing

Table IV. 8-Foot Static Freeze With Dry Ice and Acetone

Test Setup Same as in Table II

Time, Hours	Pipe Oil Pressure, Psi		Temperature, C, on Thermocouples Soldered Into Top Conductor												
	High Side	Low Side	−5′*	−3′	C/L†	1′	2′	3′	4′	5′	6′	7′	10′	20′	30′
0	25	25	28	28	28	28	27	27	27	26	27	28	29	29	29
1	25	24	23	16	16	16	16	16	20	24	26	27	30	30	30
2	26	18	10	− 6	−11	−11	− 8	− 3	5	13	17	23	29	29	30
3	18	0	− 1	−23	−29	−28	−25	−20	−12	5	15	21	28	28	29
5	23	0	−17	−40	−47	−46	−43	−35	−24	− 9	1	10	21	25	25
6	20	0	−22	−44	−52	−50	−46	−41	−29	−15	− 3	7	19	23	24
23	100	0	−32	−51	−58	−57	−54	−48	−39	−26	−13	0	18	21	25
34	200	0	−34	−52	−58	−57	−54	−49	−40	−28	−16	− 5	13	19	21
45	300	0	−33	−51	−57	−57	−54	−49	−39	−28	−14	− 2	17	21	22
54	300	0	−30	−50	−57	−56	−52	−47	−38	−25	−12	− 1	17	22	23

Time, Hours	Oil Triangle			Bottom Conductors		Temperature, C, on Skids of Top Conductor						
	C/L	3′	5′	West C/L	East C/L	C/L	1′	3′	5′	7′	10′	30′
0	27	26	26	27	27	28	28	26	27	28	30	30
1	−11	− 6	21	−15	−12	7	7	− 9	23	28	31	31
2	−31	−28	10	−37	−35	−19	−20	−29	11	25	28	29
3	−45	−35	3	−49	−46	−37	−35	−45	5	21	27	29
5	−55	−45	−10	−55	−55	−52	−50	−47	− 8	12	22	24
6	−57	−48	−14	−56	−57	−55	−54	−51	−14	9	20	23
23	−61	−53	−24	−60	−60	−60	−59	−56	−26	6	21	25
34	−61	−53	−26	−60	−60	−60	−59	−55	−28	− 2	14	21
45	−61	−53	−25	−61	−61	−61	−59	−60	−27	3	18	22
54	−59	−51	−23	−59	−59	−58	−57	−55	−25	0	18	22

Time, Hours	Trough	Ambient	Temperature, C, on Top of Pipe								
			C/L	1′	3′	4′	5′	6′	7′	10′	20′‡	30′
0	26	26	28	27	27	27	28	28	29	35	33	34
1	−65	25	−63	−64	−64	−42	17	22	29	33	32	33
2	−63	22	−62	−65	−65	−46	10	21	23	25	24	26
3	−65	22	−65	−65	−65	−50	3	17	21	24	23	25
5	−65	21	−65	−65	−65	−52	−11	7	15	21	22	22
6	−65	21	−65	−66	−66	−53	−15	4	12	20	21	21
23	−65	29	−66	−66	−66	−55	−24	− 3	12	25	19	26
34	−65	19	−65	−65	−65	−55	−27	−10	5	17	18	20
45	−65	26	−65	−65	−65	−55	−24	− 5	10	24	18	23
54	−64	22	−64	−65	−65	−52	−23	− 5	9	21	19	22

Footnotes are the same as for Table II.

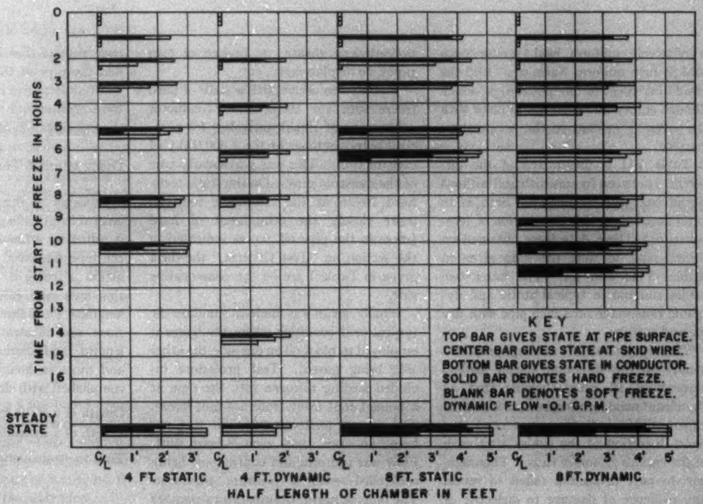

Fig. 3. Bar graph of pipe cable freeze formation with dry ice and acetone versus time, in a 6-inch pipe

Table V. 8-Foot Dynamic Freeze With Dry Ice and Acetone

Test Setup Same as in Table II

Time, Hours	Pipe Oil Pressure, Psi		Oil Flow Gallons per Hour	Temperature, C, on Thermocouples Soldered Into Top Conductor												
	High Side	Low Side		−5′*	−3′	C/L†	1′	2′	3′	4′	5′	6′	7′	10′	20′	30′
0	100	100	6	23	23	23	23	24	24	24	23	23	23	24	23	25
1	100	100	6	16	11	13	13	14	15	18	22	23	25	24	23	25
2	100	100	6	2	−7	−7	−8	−5	2	9	17	20	23	25	24	26
3	100	96	6	−9	−23	−23	−23	−19	−11	−1	11	18	21	25	25	28
4	102	97	6	−15	−32	−34	−31	−27	−19	−7	7	16	21	25	26	30
6	100	93	6	−23	−40	−44	−42	−38	−28	−15	3	15	20	27	29	32
8	100	84	6	−25	−44	−49	−46	−41	−32	−18	−1	13	20	28	31	34
9	105	66	6	−27	−44	−49	−46	−41	−33	−18	−2	9	17	26	29	31
10	106	0	0	−30	−47	−52	−49	−45	−37	−23	−7	7	11	27	30	32
11	300	0	0	−32	−50	−54	−52	−48	−40	−28	−12	2	12	25	29	31
24	300	0	0	−32	−50	−55	−53	−49	−42	−30	−15	2	10	24	28	30

Time, Hours	Oil Triangle			Bottom Conductors		Temperature, C, on Skids of Top Conductor					
	C/L	3′	5′	West C/L	East C/L	C/L	1′	3′	5′	7′	10′	30′
0	18	18	20	21	23	23	23	23	23	25	23	24
1	−15	−9	20	−21	−18	9	8	−10	22	24	24	25
2	−32	−21	13	−40	−38	−9	−15	−22	17	23	25	26
3	−42	−30	8	−48	−47	−25	−27	−27	13	23	26	28
4	−48	−35	7	−52	−50	−35	−34	−34	12	23	27	30
6	−54	−40	0	−57	−55	−46	−44	−42	10	25	29	33
8	−56	−43	−2	−58	−57	−50	−47	−44	8	24	29	34
9	−57	−44	−3	−58	−58	−51	−49	−46	4	23	29	33
10	−58	−46	−8	−59	−58	−55	−53	−52	−5	18	27	32
11	−60	−48	11	−60	−59	−58	−55	−56	−11	14	25	30
24	−60	−49	−13	−60	−59	−58	−56	−58	−13	13	24	30

Time, Hours	Trough	Ambient	Temperature, C, on Top of Pipe									
			C/L	1′	3′	4′	5′	6′	7′	10′	20′‡	30′
0	25	25	23	23	24	24	25	26	28	21	25	25
1	−68	28	−65	−65	−65	−17	18	25	25	26	22	26
2	−67	30	−64	−65	−64	−22	13	24	26	28	22	26
3	−67	31	−65	−65	−65	−24	12	22	26	29	25	29
4	−67	33	−65	−65	−65	−28	12	23	27	30	26	31
6	−66	34	−66	−65	−65	−29	10	23	27	30	29	33
8	−66	30	−66	−66	−66	−31	9	22	26	30	29	33
9	−66	29	−66	−66	−66	−31	5	19	25	29	28	31
10	−66	28	−66	−66	−66	−32	−5	15	21	27	26	29
11	−66	27	−66	−66	−66	−34	−10	10	18	25	25	28
24	−66	26	−66	−66	−66	−43	−12	8	17	25	24	28

Footnotes are the same as for Table II.

a relatively uniform heat-transfer path and in turn uniform warm-up. And the insulating effect of the first trough, which though empty had been left in place with its cover, is evident in the temperature pattern.

Table VII is illustrative of the differences between freezes with and without liquid heat-transfer medium, both as to attainment time and distribution of temperature. These data were obtained on 8-inch pipe, as were the data given in Tables VIII and IX. The latter two tables summarize typical static and dynamic runs made on 8-inch pipe with dry ice and acetone.

The dynamometer reading remained steady on the 40-pound at-rest reading throughout all runs, showing that no significant axial forces were at work on the cables. This indication was confirmed upon dissection of the cables after each of the various groups of runs. Thorough, part-by-part inspection failed to reveal any evidence of damage to dielectric or polyethylene sheath, no broken or torn tapes, no displacement, etc.

The time to accomplish a state of hard freeze with the 500,000-CM conductor cable was not significantly less for practical purposes than for the 2,000,000-CM construction. This was particularly true of the dynamic runs. On the static tests, hard freeze at the conductor followed more closely the attainment of hard freeze in the pipe oil, so, as indicated in the section on "Test Criteria," the data given in Table I are on the conservative side.

Finally, a run was made to simulate the typical field condition where the freeze is employed to block oil on one side, the other side being gassed. Test procedure included feeding nitrogen into the pipe at a point 1 foot away from a 4-foot freeze. The rate of feed was 25 cubic feet per hour, i.e., one tank each 8-hour shift. Flow was uniform and continuous, being controlled with a pressure regulator. The only significant temperature changes were rises of 8 to 10 C on the skid wires and the pipe at the foot of the gas feed. The temperatures in the body of the freeze were normal and unchanged throughout the test duration of 100 hours.

Discussion of Test Results

Analysis of the data shows that the critical length of a pipe cable freeze trough is primarily a function of the area within the pipe diameter, and that the time to attain a freeze is controlled directly by this area and inversely by the trough length. The following approximate equations are illustrative of this analysis, lengths and diameters being in inches and times in hours, the freeze being accomplished with dry ice and acetone

Length of a static freeze $L_s = D^2$ (1)

Length of a dynamic freeze $L_d = 1.7D^2$ (2)

Time to attain a static freeze $T_s = 1{,}200 \left(\frac{D}{L}\right)^2$ (3)

Table VI. Converting an 8-Foot Static Freeze With Dry Ice and Acetone to a 4-Foot Freeze, Then Melting Latter Under 300 Psi Hydrostatic Head

Test Setup Same as in Table II

Time, Hours	Pipe Oil Pressure, Psi		Temperature, C, on Thermocouples Soldered Into Top Conductor												
	High Side	Low Side	−5′*	−3′	C/L†	1′	2′	3′	4′	5′	6′	7′	10′	20′	30′
0	300	0	−35	−53	−59	−58	−58	−50	−41	−28	−16	−5	14	21	22
8	300	0	−26	−42	−55	−56	−54	−49	−40	−25	−12	0	20	25	27
24	300	0	−11	−28	−48	−50	−50	−46	−38	−26	−14	−3	16	23	24
48	300	0	−1	−17	−42	−47	−47	−44	−36	−24	−12	2	17	24	24
56	300	0	5	−13	−40	−45	−46	−43	−33	−20	−7	6	23	28	30
72	300	0	2	−15	−41	−45	−46	−42	−34	−23	−11	0	18	24	25
75	300	0	3	−15	−41	−46	−46	−42	−35	−22	−9	3	19	25	26
78	300	0	5	−14	−40	−45	−45	−42	−34	−21	−8	6	23	28	30
79	300	2	7	−12	−38	−42	−42	−39	−30	−19	−6	7	23	29	31
79½	300	50	7	−12	−36	−41	−41	−37	−30	−18	−5	7	24	20	31

	Oil Triangle			Bottom Conductors		Temperature, C, on Skids of Top Conductor						
	C/L	3′	5′	West C/L	East C/L	C/L	1′	3′	5′	7′	10′	30′
0	−63	−55	−26	−62	−62	−62	−60	−61	−29	−1	16	22
8	−59	−54	−24	−57	−58	−57	−59	−62	−26	−6	21	28
24	−54	−51	−24	−51	−52	−51	−54	−58	−26	2	17	23
48	−49	−50	−22	−46	−48	−45	−51	−61	−24	3	17	24
56	−48	−49	−19	−45	−46	−45	−50	−57	−21	10	25	30
73	−47	−49	−21	−45	−47	−43	−50	−57	−23	5	19	25
75	−48	−49	−20	−45	−47	−44	−50	−52	−22	7	21	26
78	−45	−47	−19	−43	−45	−43	−50	−44	−21	10	25	31
79	−40	−42	−17	−38	−40	−39	−46	−36	−20	11	25	31
79½	−38	−40	−15	−36	−38	−38	−43	−36	−19	12	26	32

	Trough	Ambient	Temperature, C, on Top of Pipe									
			C/L	1′	3′	4′	5′	6′	7′	10′	20′‡	30′
0	−67	23	−67	−67	−67	−55	−25	−7	8	22	20	24
8	−68	32	−66	−68	−68	−54	−22	0	14	26	26	29
24	−66	25	−64	−66	−66	−53	−23	−5	10	23	21	25
48	−66	25	−59	−65	−65	−51	−22	−4	10	23	23	26
56	−66	37	−64	−65	−65	−51	−17	6	17	29	28	31
73	−65	27	−62	−64	−66	−51	−20	−2	13	25	23	27
75	−66	30	−63	−65	−66	−52	−19	2	15	26	24	28
78	−57	35	−48	−57	−57	−43	−17	6	17	30	28	32
79	−58	35	−40	−49	−48	−35	−13	8	18	30	28	28
79½	−59	37	−35	−37	−35	−29	−10	9	19	31	29	34

Footnotes are the same as for Table II.

Time to attain a dynamic freeze

$$T_d = 2{,}000 \left(\frac{D}{L_d}\right)^2 \qquad (4)$$

where

D = over-all diameter of pipe, inches

L_d = length of freeze trough necessary to attain a hard freeze in reasonable time under dynamic conditions 1 day after a pipe cable is removed from service under load and with a 25 C ambient, inches

L_s = length of freeze trough necessary to assure a hard freeze under static conditions and with a 25 C ambient, inches

T_d = time to attain a freeze under dynamic conditions with a 25 C ambient, hours

T_s = time to attain a freeze under static conditions with a 25 C ambient, hours

Equations 1 through 4 are based upon the need to attain −50 C at the conductor to assure a hard freeze. This temperature is determined by the characteristic hard freezing temperature of Suniso no. 6. On the other hand, the extruded poly-

Table VII. Comparison of Conductor Temperatures in 8-Foot Static Freezes With and Without Liquid Heat-Transfer Medium

8-Inch Pipe, Suniso No. 6, Three 1-Conductor 2,000,000-CM 505-Mil Wall, H.O. Cable
1/16 by 3/16 Skid Wires, Conductors Tied in Close Triangle

Time, Hours	Temperature, C, on Thermocouples Soldered Into Top Conductor								Trough	Ambient
	C/L†	1′*	2′	3′	4′	5′	7′	10′		
With Dry Ice and Acetone										
0	21	21	21	21	21	21	21	21	22	22
2	3	3	3	4	9	14	18	21	−65	21
4	−24	−24	−23	−19	−11	−2	11	19	−65	23
6	−37	−37	−34	−29	−19	−8	4	15	−65	18
8	−47	−47	−44	−39	−28	−16	0	9	−65	21
10	−51	−51	−49	−43	−33	−20	−2	10	−65	19
15	−56	−55	−53	−48	−38	−26	−8	9	−65	20
20	−56	−56	−54	−49	−40	−28	−10	8	−65	18
24	−56	−56	−54	−49	−40	−29	−10	7	−65	20
With Dry Ice Only										
0	25	25	25	25	25	25	25	25	25	25
2	12	11	12	13	16	19	22	24	−64	18
4	−3	−2	−1	1	6	11	17	21	−65	19
6	−15	−14	−12	−8	−1	7	15	23	−65	23
8	−25	−25	−22	−16	−8	1	13	21	−65	24
10	−32	−31	−28	−23	−12	−4	12	19	−65	24
15	−41	−39	−36	−29	−18	−7	8	17	−65	22
20	−44	−44	−40	−34	−24	−13	5	16	−65	24
24	−46	−46	−43	−37	−26	−14	5	16	−65	24

Footnotes are the same as for Table II.

Table VIII. 8-Foot Static Freeze With Dry Ice and Acetone

Test Setup Same as in Table VII

Time, Hours	Pipe Oil Pressure, Psi		Temperature, C, on Thermocouples Soldered Into Top Conductor										
	High Side	Low Side	−5′*	−3′	C/L†	1′	2′	3′	4′	5′	7′	10′	15′
0	100	100	22	21	21	21	21	21	21	21	21	21	21
2	100	100	13	5	3	3	3	4	9	14	18	21	22
4	100	100	− 3	−18	−24	−24	−23	−19	−11	− 2	11	19	22
6	100	99	− 7	−29	−37	−37	−34	−29	−19	− 8	4	15	21
8	100	90	−20	−40	−47	−47	−44	−39	−28	−16	0	9	22
10	300	0	−25	−44	−51	−51	−49	−43	−33	−20	− 2	10	20
15	300	0	−30	−49	−56	−55	−53	−48	−38	−26	− 8	9	20
20	300	0	−32	−49	−56	−56	−54	−49	−40	−28	−10	8	20
24	300	0	−32	−49	−56	−56	−54	−49	−40	−29	−10	7	19
48	300	0	−32	−49	−56	−56	−54	−49	−40	−29	−10	7	20

	Oil Triangle		Bottom Conductors		Temperature, C, on Skids of Top Conductor			
			West	East				
	C/L	5′	C/L	C/L	C/L	1′	3′	10′
0	21	22	21	22	22	21	21	22
2	−23	−10	−27	−25	− 5	− 5	− 7	22
4	−42	−23	−45	−45	−28	−30	−29	20
6	−47	−27	−50	−50	−40	−41	−39	15
8	−54	−34	−55	−55	−49	−51	−49	13
10	−56	−37	−56	−56	−53	−54	−52	12
15	−59	−43	−59	−58	−57	−58	−57	12
20	−60	−43	−60	−59	−58	−59	−57	10
24	−59	−42	−58	−58	−57	−58	−56	8
48	−59	−42	−58	−58	−57	−59	−57	9

	Trough	Ambient	Temperature, C, on Top of Pipe									
			C/L	1′	3′	4′	5′	6′	7′	10′	20′	30′
0	22	22	22	22	22	22	22	22	22	22	22	22
2	−65	21	−64	−64	−64	−35	12	19	21	22	22	22
4	−66	23	−65	−65	−65	−40	5	15	18	22	23	23
6	−66	18	−65	−65	−65	−40	0	10	14	19	20	21
8	−66	21	−65	−65	−65	−44	− 3	9	10	20	23	23
10	−66	19	−66	−66	−66	−45	− 5	7	13	18	21	21
15	−66	19	−66	−66	−66	−47	−10	5	12	18	21	21
20	−66	18	−66	−66	−66	−48	−13	3	10	17	21	20
24	−66	19	−66	−66	−66	−47	−13	0	8	16	19	19
48	−66	24	−66	−66	−66	−47	−12	3	12	18	23	23

Footnotes are the same as for Table II.

ethylene sheath of the compression cable prevents migration of pipe oil into the cable dielectric, and since the usual pipe-type cable impregnants are characterized by a freeze temperature of about −40 C, hard freezing of this design of pipe cable may be obtained more readily, particularly under dynamic conditions.

Dry ice consumption is of the order of 100 pounds per foot of freeze per 24 hours under static conditions, and about double this amount under dynamic conditions. These figures include allowance for loss in storage; this loss is greatly dependent upon ambient, conditions of storage, etc.

Design of Freeze Trough

Fig. 4 shows a freeze trough, suitably sealed to permit the use of acetone or other liquid heat-transfer medium with the dry ice refrigerant. While a freeze may be attained without a liquid medium, it is actually easier to service the combination type of freeze which is also more efficient. Therefore, the combination freeze is to be preferred over a dry or

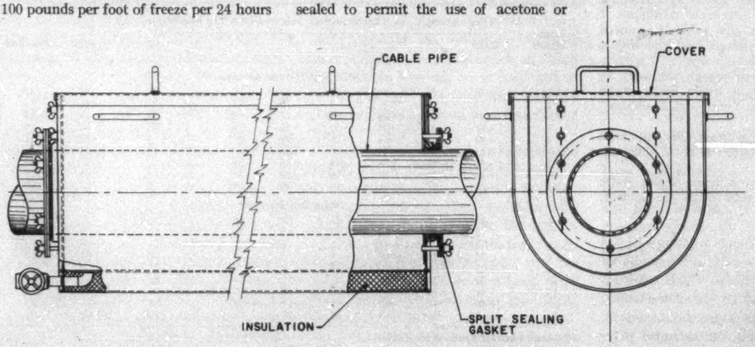

Fig. 4. Sheet metal freezing trough

Table IX. 8-Foot Dynamic Freeze With Dry Ice and Acetone

Test Setup Same as in Table VII

Time, Hours	Pipe Oil Pressure, Psi High Side	Pipe Oil Pressure, Psi Low Side	Oil Flow Gallons per Hour	Temperature, C, on Thermocouples Soldered Into Top Conductor −5′*	−3′	C/L†	1′	2′	3′	4′	5′	7′	10′	15′
0	100	100	6	20	20	20	20	20	20	20	20	20	20	20
2	100	100	6	9	7	0	1	3	8	13	17	19	21	21
4	100	100	6	− 6	−14	−20	−18	−12	− 5	3	10	18	20	22
6	100	100	6	−15	−25	−30	−28	−23	−13	− 3	6	16	18	23
8	100	100	6	−20	−33	−38	−35	−30	−19	− 6	3	15	17	24
10	100	100	6	−24	−38	−43	−40	−33	−23	−10	3	15	17	24
15	100	100	6	−25	−42	−46	−44	−37	−26	−14	0	13	14	21
20	100	100	6	−30	−44	−49	−46	−40	−30	−17	− 4	12	14	20
24	100	100	6	−30	−44	−51	−47	−41	−31	−18	− 5	12	12	18
30	100	100	6	−30	−45	−50	−47	−41	−31	−18	− 4	13	13	22

Time, Hours	Oil Triangle C/L	Oil Triangle 5′	Bottom Conductors West C/L	Bottom Conductors East C/L	Temperature, C, on Skids of Top Conductor C/L	1′	3′	10′
0	20	20	20	20	20	20	20	20
2	−20	− 6	−25	−24	− 2	− 4	− 3	21
4	−38	−18	−43	−43	−23	−25	−21	20
6	−46	−24	−49	−49	−35	−35	−33	20
8	−50	−27	−52	−52	−41	−41	−39	19
10	−53	−30	−54	−54	−46	−46	−43	19
15	−53	−31	−54	−54	−49	−50	−46	15
20	−56	−35	−57	−57	−52	−53	−50	15
24	−56	−35	−56	−56	−52	−53	−50	14
30	−56	−36	−56	−56	−52	−53	−50	16

Time, Hours	Trough	Ambient	Temperature, C, on Top of Pipe C/L	1′	3′	4′	5′	6′	7′	10′	20′	30′
0	20	20	20	20	20	20	20	20	19	19	19	18
2	−65	23	−62	−62	−63	−26	11	18	22	22	22	22
4	−65	24	−62	−62	−63	−30	7	16	20	23	23	23
6	−65	25	−64	−64	−64	−34	6	15	20	22	23	24
8	−65	22	−64	−64	−64	−35	5	14	19	22	23	23
10	−65	21	−64	−64	−64	−37	4	15	19	22	23	23
15	−65	18	−63	−64	−64	−38	0	10	15	19	20	20
20	−65	16	−64	−64	−64	−40	0	10	14	18	18	18
24	−65	19	−64	−64	−64	−40	− 2	8	13	17	18	18
30	−65	23	−64	−64	−64	−39	0	10	15	20	22	22

Footnotes are the same as for Table II.

plain dry ice freeze. With a leakproof freeze trough, minimum temperatures may be sustained with less than 20 per cent fill of dry ice, provided the pipe is kept covered with liquid heat-transfer medium. Care, of course, must be exercised in handling all materials employed in a freeze. The use of face shields by personnel associated with the operation is prudent.

Conclusions

1. Repeated dry ice freezes under hydrostatic heads as high as 300 psi have no deleterious effect on pipe cable components.
2. A freeze may be melted under a hydrostatic head of 300 psi with no deleterious effect on cable dielectric or the polyethylene jacket of compression cable.
3. When a hard freeze has been established, the pipe oil may be drained from one side, and a dry gas feed of 25 cubic feet per hour may be established 1 foot from the freeze on the drained side, without a significant effect on the temperature distribution in the freeze.
4. Freeze length is primarily a function of the cross-sectional area within the overall pipe diameter, conductor size being a minor factor.
5. Freeze length under dynamic conditions, such as shortly after a line has been shut down while under load, may have to be twice as long as under static conditions in order to attain a hard freeze in comparable time.
6. Time to attain a freeze is a function of both the pipe size and the trough length.
7. Requisite freeze length, whether under static or dynamic conditions, virtually dictates the location of this operation outside the manhole.
8. Dry ice alone is effective in holding a pipe cable freeze, but it takes somewhat longer to produce a freeze without the liquid transfer medium.

References

1. FREEZING PIPE CABLE PERMITS NEW SUBSTATION CUT-OVER, G. N. DeCowsky, R. A. Horenburger. *Electric Light and Power*, Chicago, Ill., vol. 32, sect. II, Sept. 1954, pp. 77–80.

2. OIL FLOW AND PRESSURE CALCULATIONS FOR PIPE-TYPE CABLE SYSTEMS, AIEE Committee Report. *AIEE Transactions*, vol. 74, pt. III, Apr. 1955, pp. 251–61.

◆

Discussion

John C. Parker (Memphis Light, Gas and Water Division, Memphis, Tenn.): The author is to be congratulated for presenting this timely paper containing interesting test data.

The paper indicates that semistop joints are not necessary in oil-type pipe cable systems because of the excellent service record of this cable and the use of the oil freezing technique in maintaining it. Although, the service record of the 18 miles of 115-kv oil-type pipe cable in Memphis is perfect and the oil in the pipe cable has been frozen a number of times without any difficulty, we believe that it is advantageous to use only the semistop type of joints. These joints permit:

1. Filling each section of the pipe line with oil immediately after cable installation.
2. Provisions to limit oil flow in case of a break or hole in the pipe line.
3. Rapid isolation of a section of pipe line in case of trouble.
4. Isolation of a section of pipe line so that static freezes can be made in a minimum time with a minimum pressure differential across them.

The oil flow rate of 0.1 gallon per minute used for the dynamic tests described in the paper appears to be greater than will usually be encountered in the field. For three circuits consisting of 40,065 feet of pipe cable, with three round single-conductor cables each having a diameter of 1.7 inches under a 0.1- by 0.2-inch D armor wire in a pipe with a $5^{1}/_{16}$-inch inside diameter, filled with Suniso no. 6 oil which was de-energized when the average copper temperature by resistance was 64.8 C, the average pipe temperature was 38.5 C and the average ambient earth temperature was 17.2 C; the measured rate of oil flow into the pipe line at one end with the other end closed was

Hours After De-energizing	Oil Flow Gallons Per Minute
1	2.04
6	0.34
12	0.16
24	0.07
48	0.01

Two types of freezes were selected for tests described in the paper, i.e., a soft freeze that will withstand a few pounds pressure and a hard freeze that will withstand at least 300 psi gauge indefinitely. Unfortunately, there is no indication of just how much more than 300 psi gauge the hard freeze would withstand. It is difficult to understand why a freeze to withstand 300 psi gauge (750 feet of oil) would ever be required on any oil-type pipe cable system. In the field when oil must be frozen in pipe cable, the oil pressure can safely be reduced to the minimum value that will insure a positive pressure in the pipe line and terminals. In case of a pipe cable circuit where the high point is 100 feet above the point to be frozen, 45 psi gauge would be adequate. Therefore, it appears that in the maintenance of oil-type pipe cable, freezes should rarely be required to withstand more than 45 psi gauge. Reducing pressure of a pipe cable circuit to the practical minimum will reduce the time required for a satisfactory freeze. Furthermore, it would appear that upon thawing a freeze, the greater the pressure differential across the freeze the greater the possibility of damage to the cable.

A typical static freeze of oil in the pipe cable described, at an ambient temperature of 15 C using a trough 20 inches long, required less than 6 hours. After freezing for 6 hours, a valve in the oil by-pass was opened on one side of the freeze with a pressure of 17 psi gauge on the other side and there was no oil flow. The actual freezing time is not known. Three-hundred pounds of dry ice was required to make this freeze and to maintain it for an additional 6 hours. Less than 2 hours was required to obtain a hard static freeze in a 2-inch oil by-pass pipe of a semistop joint with a trough 4 inches long. To freeze a 2-inch plug valve with its center line 13.5 inches from the center line of the $5^{9}/_{16}$-inch pipe containing cable required less than 3 hours. For this freeze the trough was 36 inches long and covered the $5^{9}/_{16}$-inch pipe, the 2-inch plug valve, and the 2-inch connecting pipe. These freezes were all made with dry ice and acetone in uninsulated troughs.

It is stated in the paper that, "Pressure was applied at one end of the pipe line so that progress of a freeze also was indicated by a fall in the reading of the gauge on the low side." It would be helpful if the author would include the data thus obtained in his closure.

M. H. McGrath (General Cable Corporation, Perth Amboy, N. J.): In the tests conducted by the author the oil employed was one having a "cold-set" temperature of −25 C and presumably a viscosity of approximately 800 Saybolt universal seconds (SUS) at 100 F. While this oil has been used as the filling medium on most of the high-pressure oil-filled pipe-type installations now in service in the United States, it would be of interest to know whether the author has given consideration to the problem which might be involved with filling oils of material lower pour points and viscosities. At the present time extensive use is being made in the United States, on self-contained low-pressure oil-filled cable installations, of an oil having a pour point of approximately −40 C and a viscosity of approximately 100 SUS at 100 F. Use of the latter oil for pipe-type installations would reduce transient pressures and permit longer feeds from a single oil-pressure-control station or alternately in some cases might permit the use of smaller diameter pipe and a reduced volume of filling oil and, in addition, maintenance of reserve supplies of a type of oil suitable for use on either type of system. Naturally, it would be essential to insure that it would be practical to carry out a freezing operation. However, it does not seem that this matter would present too serious a problem. In addition to an increase in the length of freeze, one could obtain for the duration of a freeze the advantage of a heavy filling oil by tapping the line pipe at opposite ends of the freeze location and by introducing a slug of heavy oil into the freeze region; the introduction of the heavy oil at one end of the freeze being made at a rate to compensate for the removal of the light filling oil at the opposite end. On removal of the freeze the slug of heavy oil could be removed in a similar manner.

R. J. Wiseman (Okonite Company, Passaic, N. J.): The paper by Dr. Merrell is quite interesting as it reports factors which influence the time it takes to freeze a pipe, the distance along the pipe influenced by the freezing, and the effect of heat in the conductors, on the time of freezing because of current flowing through the pipe.

This subject had to be considered by The Okonie Company in the early 1940's when the question arose as to if it were possible to isolate a section of a pipe to repair it if a leak occurred in the pipe or in case of a cable failure, after locating the fault, isolate the pipe at this point so as to repair the cable. Also, the question arose as to whether in the freezing we might injure the insulation. As we expected to furnish various pipe and cable sizes, it was decided to make tests to note the time it took to freeze a pipe. The criterion for satisfactory freezing was that with a full 200-psi pressure on one side of the freeze and atmospheric pressure on the other side, no oil should leak through the freeze as indicated by no loss of pressure on the high side.

Table X

Pipe Size OD, Inches	Length of Trough, Feet	Time to Freeze, Hours
$3^{1}/_{2}$	2	1
$5^{9}/_{16}$	$2^{1}/_{2}$	2
7	5	$4^{1}/_{2}$
$8^{5}/_{8}$	7	8

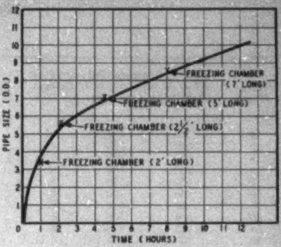

Fig. 5. Freezing time in pipe size

Cable area, 40
Type of oil, Suniso no. 6, 700-second
Freezing medium, acetone and dry ice
Temperature of freezing medium, 114 F.

It was known that a small size of pipe had a smaller area for oil than a large pipe, therefore it would take less time to freeze a small pipe. Also, it was obvious that it was desirable to have a longer freezing section for a larger size pipe. Several pipe sizes were set up with freezing troughs assembled around them and the cable size was such that the three conductors occupied approximately 60 per cent of the area of the pipe. The freezing medium used was dry ice and acetone.

Table X gives the time it took to freeze a pipe with the length of trough used. Obviously, there is something wrong with the formula.

The data shown can be plotted with pipe size against time to freeze, as shown in Fig. 5. Also, the plot will give an approximation of what size of trough and the freezing time for other pipe sizes. For example, a $6^{5}/_{8}$-inch pipe would take about 4 hours with a trough 4 feet long. It pays to be on the conservative side in the length of the trough, and allowance of another extra foot is worthwhile. Note the very short time for the small pipe sizes. Although the time of 8 hours for the $8^{5}/_{8}$-inch pipe seems long, actually today this time would be decreased because of the desire to use smaller pipe sizes for a given cable size which results in a much higher cable occupancy and lesser amount of oil.

Dr. Merrell suggests formulas for determining the length of a trough for freezing and also the time to freeze. Equation 1 of the paper for length of trough seems fairly accurate, but it is well to be on the conservative side. I am puzzled about equation 3 for time to attain a freeze. If

Table XI

Pipe Size, OD, Inches	Time to Freeze, Hours	Okonite Tests, Hours
3.5	98	1
5.63	38	2
7	24.5	4.6
8.63	16.1	8

the equation for L_s, the length of freeze, is substituted in equation 3 we obtain:

$$T_s=1{,}200\left(\frac{D}{D^2}\right)^2=\frac{1{,}200}{D^2}$$

that is, the time is indirectly proportional to the square of the diameter of the pipe, and the longer the time the smaller the pipe size. This results in the time periods shown in Table XI for several pipe sizes.

The tests shown in the table made by Okonite on a pipe assembly with no heat on the conductors. Question arose as to the possibility of freezing the pipe with the conductors carrying load and also what effect would it have on the power factor of the insulation. An assembly was made of three 1,250,000-CM conductors with a 0.300-inch wall of insulation installed in a 7-inch outside diameter (OD) steel pipe. The pipe length was 30 feet with a 5-foot freezing chamber in the center of the run. The three conductors were connected in series and the ends of the series set up were terminated in potheads to which power could be supplied for heating. This setup was more severe than the normal operation, in that there was extra heating in the pipe itself because of the single-phase current.

A test made with no heating on the cables showed the pipe to be frozen to −65 C after $4^3/_4$ hours and the curve of temperature versus time was flattening out.

During this freezing test a power factor test was made at 20 and 100 volts per mil. At room temperature (+30 C) they showed a value of 0.55 per cent; at (−37 C), 0.50 per cent; at (−50 C), 0.55 per cent; and at (−65 C), 0.64 per cent. After the test was completed, the power factor at room temperature came back to the original value.

The next test was with a 700-ampere load on the conductors. The temperature on the pipe at the start was 70 C. After 3 hours there was an indication that the temperature time curve would flatten out at −35 C which was not low enough to freeze the oil solid. The current was then dropped to 420 amperes (60 per cent of 700 amperes). In this case the pipe temperature dropped to −50 C and still not low enough to freeze the oil solid. Finally, a new run was made with a 350-ampere load (50 per cent of 700 amperes) and after $5^1/_2$ hours a temperature of −63 C was reached which was good, but after 11 hours the temperature reached −65 C and the oil was frozen solid enough for most practical purposes of leak location. The pressure drop test made at the end of the half-load freezing test showed that the pressure dropped from 200 psi to 120 psi in 1 hour and 10 minutes. As stated, these tests were made with single-phase current and, therefore, were more severe than for a 3-phase current of the same value. We feel certain that it is possible to freeze the oil in a pipe solid with half-load on the conductors because, with the knowledge gained, we would recommend a longer freezing chamber.

We hope that this information, in addition to that in Dr. Merrell's paper, will give assurance that pipe freezing can be done successfully, provided that the proper size of trough is used and that time is taken to achieve freezing. By reducing the pressure on the line to, say, 100 psi, it is possible to take care of any grades that may exist along the circuit.

Edwin J. Merrell: The discussers have raised a number of pertinent points for consideration. Mr. McGrath's question with reference to employing a pipe oil of viscosity lower than that of Suniso no. 6, namely, 700 to 800 Saybolt seconds at 100 F, is particularly apropos, because of the hydraulic aspect of pipe cable. Unfortunately, Suniso no. 6 is about as low a viscosity oil as is available, which combines low enough pour point for temperate locations with ability to be hard frozen by dry ice. The 100-100 oils, used in oil-filled cable, are free flowing at dry ice temperatures, so that improvision in accordance with Mr. McGrath's suggestion would have to be resorted to in order to achieve a freeze. With tape-sealed cable designs, that is, noncompression, dilution of the cable impregnant by the thin pipe oil no doubt would be sufficient to require its being flushed out of the dielectric and conductor by the injected viscous oil, as a prerequisite to obtaining a freezing point co-ordinated with the characteristic freeze temperature of dry ice and acetone. Attainment of the necessary degree of flushing probably would require treatment of a relatively long section of pipe, so as to produce the radial pressure necessary to drive the viscous oil down the labyrinth path to the conductor.

Mr. Parker has submitted valuable field observations of oil demand, and it is quite probable that the rate of 0.1 gallon per minute of the dynamic tests described in the paper is greater than usually will be encountered in field work. However, Mr. Parker's example covers a 500,000-CM conductor at only 65 C in a 5-inch pipe. A 2,000,000-CM conductor in an 8-inch pipe operating continuously at maximum copper temperature would exhibit a very much greater flow 24 hours after shutdown, both because of the larger volumes and because of the higher earth resistance due to drying which in turn would lengthen cooling time. A calculation, according to reference 2 of the paper, shows that for a 10-mile length of 138-kv cable in 8-inch pipe, an oil demand of 0.44 gallon per minute may be anticipated 24 hours after shutdown while under full load.

The 300-psi withstand figure was selected for various reasons, such as to demonstrate a margin of safety when freezing under full operating pressure, preparatory to a cutover, when freezing at the bottom of a hilly run, a line with a difference in elevation, end to end, of some 500 feet being currently under consideration, etc.

The static freeze data given by Mr. Parker correlate with that given in the paper. Reference to Table II shows that this test started with a conductor temperature of 16 C, which is virtually identical with Mr. Parker's 15, and developed a conductor temperature of −38 1 foot from the end of the freeze chamber in 5 hours. As stated in the paper under "Test Criteria," it is possible to achieve a freeze of comparatively high strength at a temperature of this order, if the cable impregnant has not been thinned with pipe oil. It takes a great deal longer to attain the −50 C, taken as assuring a full strength freeze.

The pressure drop data are given in the second and third columns of each table of the paper.

Dr. Wiseman's data are quite informative and include additional assurance of the efficacy of the freezing technique for oil-type pipe cable. Moreover, despite a seeming difference between Dr. Wiseman's observations and those given in the paper, a more detailed analysis shows that there is relatively close agreement in results, particularly close when the number of variables involved is considered. For example, it is possible that the characteristic freeze temperature of Dr. Wiseman's cable oil is somewhat different from that which was employed in the tests covered by this paper.

Dr. Wiseman's data were obtained on new cable under static conditions, which would enable attainment of a high-strength freeze condition with pipe oil at −50 C, but with the more viscous cable impregnant in the conductor at only −40 C, assuming oils identical in the two series of tests. This possibility is mentioned in the paper under "Test Criteria," and Tables II and VIII of the paper show that the time to reach −40 C for 6-inch ($6^5/_8$ OD) and 8-inch ($8^5/_8$ OD) pipe, with 4-foot and 8-foot troughs respectively, is 5 to 6 hours. Fig. 5 indicates 4 hours with a 5-foot trough on the $6^5/_8$ pipe and 8 hours with a 7-foot trough on the $8^5/_8$ size. This is a reasonable correlation, and the times apply so long as the cable oil is not diluted with the less viscous pipe oil.

However, when admixture of pipe oil with cable oil is assumed, which was the pessimistic view taken in the paper and reflected by the empirical formulas, then Tables II and VIII show that the time to attain the necessary −50 C at the conductor is at least 5 times that to reach −40 C in the case of the 6-inch pipe and about $1^1/_2$ times for the 8-inch size. Extrapolating the line through these two points to 3.5 inches results in a factor of at least 10, that is, it will take about 10 times as long to reduce the conductor temperature in a 3.5-inch OD pipe to −50 C as to −40 C with the usual or proportional length of freeze trough. Assuming a 2-foot trough, such as Dr. Wiseman employs for this size pipe, equation 3 gives the time to attain a −50 C freeze as 25 hours. Applying the factor of 10 reduces the 25 hours to 2.5 hours to attain −40 C, which, all things considered, is not too bad a correlation with his reported 1 hour. The variance can be accounted for by differences in initial temperature and copper size.

In this connection, Dr. Wiseman states in his discussion that the conductors in his tests occupied 60 per cent of the pipe area, whereas Fig. 5 indicates they occupied 40 per cent.

Summarizing, the discussers have highlighted the time advantage when attaining a freeze, if the oil in the cable dielectric and conductor can be brought to a hard-freeze at −40 C. Newly impregnated cable under static conditions satisfies this circumstance. However, when through load cycle the impregnant in the cable dielectric becomes diluted with pipe oil, which is characterized by a freeze temperature of −50 C or lower, a lower temperature must be reached before securing a hard freeze. Under dynamic conditions, the characteristically lower freeze temperature of the pipe oil must be attained throughout the cable structure, except of course for the continuously sheathed compression cable, as described in the paper under "Discussion of Test Results."

Economics of Higher Primary and Secondary Voltages for Commercial Areas

R. F. LAWRENCE
MEMBER AIEE

D. N. REPS
ASSOCIATE MEMBER AIEE

THE increasing use of higher secondary voltages in commercial areas continues to focus attention on various secondary voltages that are feasible from both engineering and economic standpoints. Previous studies[1–4] concentrated on economic comparisons of secondary-network systems designed on the basis of "second contingency," which means that, with two primary feeders and their associated network transformers out of service, continuity of supply to the load is maintained. This basis of system design is the exception rather than the rule for the majority of a-c secondary networks in this country. Both statistical surveys and theoretical studies[7,8] indicate that, for networks of medium and small size compared with the largest existing systems, "first-contingency" design provides for a reliable and economical system. A study was therefore conducted to determine the comparative cost of systems operating at a nominal secondary voltage of 265/460 volts, with 120/208-volt networks, basing system design at both voltages on first-contingency primary-feeder outage. This design results in a network system capable of supplying the load in the event of the loss of one primary feeder and its associated network units.

The previous studies showed favorable savings through the use of the higher secondary voltage. It was expected that single-contingency design would show a similar savings. However, another aspect of the system design, namely the use of higher primary-feeder voltages, also required investigation. Consequently, the studies for first-contingency design were extended to include this factor. Previous studies of second-contingency designs were made for systems supplied by eight primary feeders, and feeder cost was included for laterals only, on the basis that each network transformer would require 300 feet of lateral. The studies described herein include generalized costs for all primary-feeder circuits. These primary-feeder circuits include express feeders from the bulk power source to the network area, the main primary feeders, and the laterals. The studies show how the number of feeders supplying a network area affect costs for the two secondary voltages considered, as well as for three different primary-feeder voltages.

Premises of Study and Variables Investigated

The fundamental premises applying for the analyses made in these studies are the following: the distribution system supplies "congested" commercial areas as normally encountered in any large metropolitan area; the distribution system is completely underground; all equipment and installation costs are included for network transformers, network protectors, vaults, secondary mains and secondary ducts, primary-feeder circuits, and primary ducts. Secondary service, secondary manholes, and metering costs were not included in the study on the basis that the cost of these items is common to any system under consideration. All of the utility consumers are served at secondary voltage.

The per-unit (pu) costs used in this paper are based on installed equipment and construction costs which are representative average values. 1 pu is the installed cost of a 500-kva 13-kv 208-volt network transformer and protector in a vault. Relative cost per kilovolt-ampere (kva) is defined where used in the paper.

The results of the studies are divided into five major categories, which are discussed in more detailed as the results for each are presented in the paper:

1. Effect of secondary voltage upon secondary-network costs for uniformly distributed loads.
2. Economics of higher primary-feeder voltages, showing comparative costs of three primary-feeder voltages to serve a network load at either 208 volts or 460 volts.
3. Spot-network costs for different transformer ratings at 460 and 208 volts.
4. Mutual support of adjacent spot networks, and effect of the secondary voltage upon ability to transfer load economically.
5. Comparison of conventional network system and the spot-network/radial system for the two secondary voltages.

Effect of Primary Supply on Method of Analysis

A procedure was previously established to determine optimized costs of a conventional 120/208-volt or 265/460-volt network. Some alterations are required when two additional parameters are introduced. These parameters are the number of primary feeders serving the area and the voltage of the primary feeders. Consider the plan of analysis whereby a fixed area of 1 square mile is studied. One procedure was to determine system costs as a function of the load density in this fixed area. An example best illustrates the difficulties encountered in the use of this analysis when the effect on costs of the number and voltage of the primary feeders is included.

For example, consider a primary-feeder voltage of 4.16 kv. For a 5-feeder network, and an allowable load of 2,000 kva per feeder, the maximum network load that can be carried is 4×2,000 = 8,000 kva, for first-contingency design. As-

Paper 55-481, recommended by the AIEE Transmission and Distribution Committee and approved by the AIEE Committee on Technical Operations for presentation at the AIEE Summer General Meeting, Swampscott, Mass., June 27–July 1, 1955. Manuscript submitted March 30, 1955; made available for printing May 11, 1955.

R. F. LAWRENCE and D. N. REPS are with the Westinghouse Electric Corporation, East Pittsburgh, Pa.

suming a fixed area of 1 square mile (in the center of a much larger area assumed to have network coverage), the load density is 8,000 kva per square mile. If for the same condition, the number of primary feeders is increased to ten, the total network load is 9×2,000=18,000 kva, which is also 18,000 kva per square mile. The total load and load density may be increased by increasing the number of feeders above ten. However, one of the premises of this study is that it is impractical to consider more than ten feeders for first-contingency design. It is assumed that, for networks requiring more than ten feeders, second contingency, i.e., the simultaneous outages of two primary feeders, should be the basis of design.

As an alternate to increasing the number of feeders above ten, the area may be divided into two 1/2-square-mile areas. For this assumption, the total load in the 1-square-mile area could be doubled, and would be 36,000 kva, which is also 36,000 kva per square mile load density. However, it would then be practical to consider the total area as being supplied by two independent networks, each of 1/2-square-mile area with 18,000 kva of load, and each served by 10 feeders. Similarly extending the analysis by dividing the area into four units, the total load for each area supplied by ten feeders would be 18,000 kva, and the load density becomes 72,000 kva per square mile. If the foregoing example is outlined for a higher primary-feeder voltage, the same principles hold true, except that the permissible loading of a primary feeder is approximately proportional to the voltage.

Network-Transformer Application Factor

From the foregoing example, it is seen that the total network load and the area served, as well as load density, are interrelated variables. Fixing any two of these factors establishes the third. Because variable area must be considered, the premises for system design were chosen slightly different from those that are used in a fixed-area analysis. These premises lead to the transformer application factors that are used to determine transformer capacity for a given set of conditions, namely: load density; network load; secondary voltage; number of primary feeders; and primary-feeder voltage. A description of how these transformer application factors were determined is given in Appendix I. The transformer application factors are variable, depending upon the number of primary feeders and the ratio of the secondary main impedance to network-transformer impedance. A premise in the use of these factors to obtain a system design is that the network transformers will not be overloaded during first-contingency primary-feeder outage. Actually the application factor is the ratio of network-transformer capacity to network load and represents quite closely the average ratio usually attainable in practice.

In actual practice, transformer overloading, nonuniformity of load distribution, and "fringe effect" occur. Fringe effect is the term used to describe the above-average loading during first contingency of transformers on the periphery of the network area. Network design using the application factors derived in Appendix I can take into account transformer overloading, nonuniformity of load distribution, and fringe effect, to any degree desired. Having stipulated normal per-cent loading of network transformers with all primary feeders in service, the basis of design using these application factors permits the determination of network-transformer loading under first contingency.

Relative Costs Excluding Primary Supply

The relative cost of serving a uniform peak load density of 10 to 240 megavolt-amperes per square mile by a conventional network at 208 and 460 volts is shown in Fig. 1. The results are for first-contingency design. The costs for primary feeders are not included in these results. A 5-feeder network was considered in this analysis. In these results, load density alone is a suitable parameter because primary-feeder costs are not included and no limitation on primary-feeder capacity exists. However, the number of primary feeders influences the cost because the choice of the number of feeders affects many other factors in secondary-network system design. While the number of feeders affects total cost, the relative cost of 208-volt and 460-volt systems is practically the same for a different number of primary feeders, when considering the same number of feeders for either system. The spot-network/radial system costs shown in Fig. 1 are discussed later.

The curves of Fig. 1 for five feeders, first contingency, show similar comparative cost relationships as the curves for eight feeders, second contingency. For systems serving the same load, area, first-contingency design results in a lower cost system than second contingency, because less primary-feeder and network-transformer capacity is required in the first-contingency system. Relative cost of 208- and 460-volt networks are about the same for either first- or second-contingency design.

Relative Costs Including Primary Supply

Studies were made of serving a uniform peak load density with a conventional network including the cost of primary feeders. The following factors were considered as variables:

1. 460-volt secondary voltage compared to 208-volt secondary voltage.
2. Primary-feeder voltage of 4, 13, and 34 kv.
3. Primary-feeder distance including express feeders from the bulk power source to the edge of the network area.
4. Number of primary feeders.
5. Load density.
6. Total network load served.

Optimized secondary-network costs were obtained for both 208- and 460-volt networks for different numbers of primary feeders, including costs of mains and laterals but excluding the costs of express primary feeders. An available bulk power source for supplying the primary feeders was assumed to be located at distances of 0.1, 1, and 5 miles from the periphery of the network area. Express feeder costs were obtained and combined with the cost of the system within the network area. Three primary-feeder voltages of 4, 13, and 34 kv were considered. The size of the network systems costed on this basis was a function of primary-feeder voltage and number of feeders. The results of the studies are shown in Fig. 2.

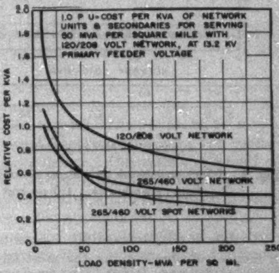

Fig. 1. Effect of secondary voltage on the cost of general and spot-network/radial systems. Primary-feeder costs are not included

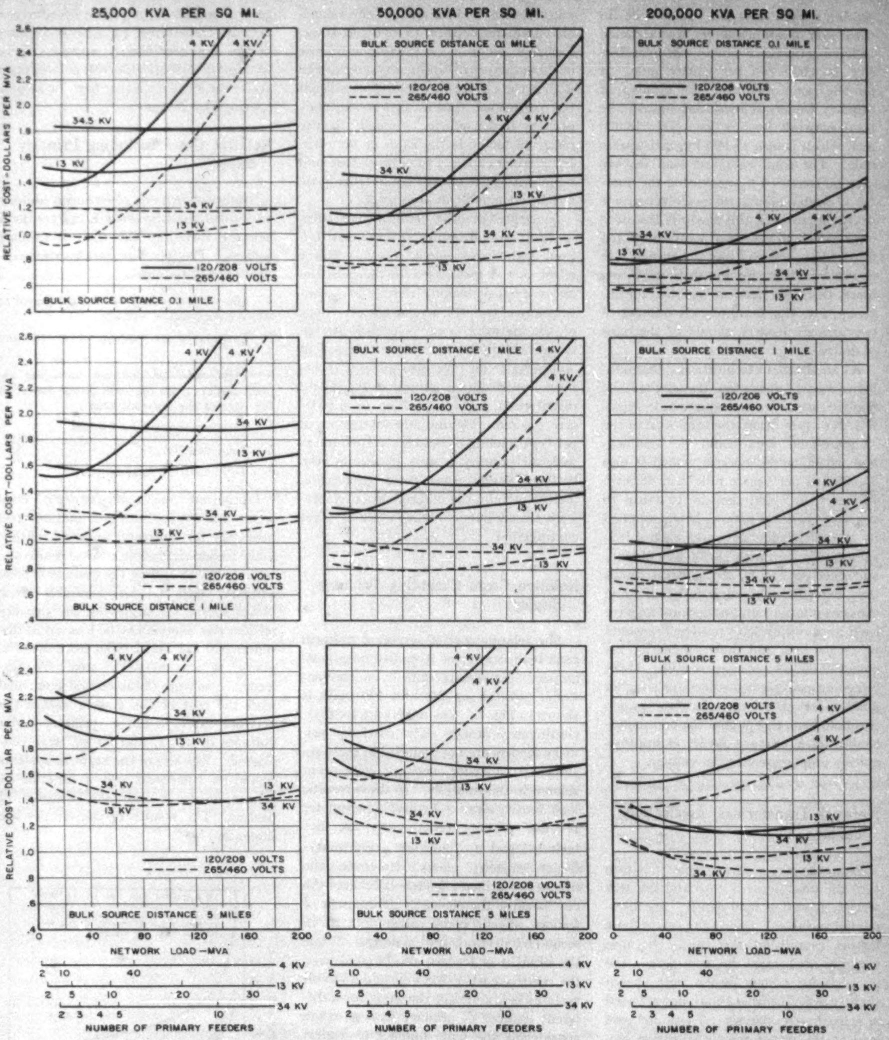

Fig. 2. Effect on network system cost of load density, network load, primary-feeder voltage secondary voltage, and distance of bulk power source from network area. 1.0 pu cost is the same as that of Fig. 1. Maximum number of primary feeders per network is ten

A study of the curves of Fig. 2 permits a number of observations, the most important of which are summarized here. It is uneconomical to serve either a 208- or 460-volt secondary network with a primary-feeder voltage of 4 kv for practically any load density unless the network load is small and a bulk power source is at the edge of the network area. A primary-feeder voltage of 13 kv is in general an economic voltage for serving a wide range of load densities and network loads, particularly if this voltage is available at a bulk power source near to the edge of the area. A primary-feeder voltage above 13 kv is economical for serving either a 208- or 460-volt secondary network, particularly where the bulk power

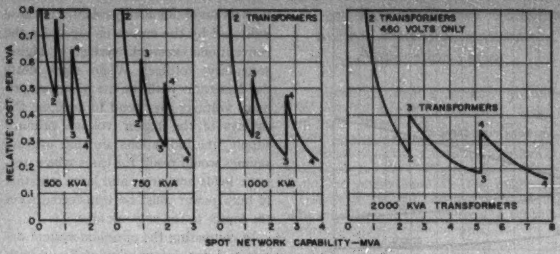

Fig. 3. Spot-network cost for different transformer ratings at 460 volts and 208 volts

source is an appreciable distance from the edge of the network area and long express feeders are required. The combination of a higher secondary voltage and a higher primary-feeder voltage becomes increasingly favorable as load density, network load, and distance of the bulk power source from the edge of the network area become greater.

The curves of Fig. 2 are generalized results which show trends, and do not necessarily provide exact values for application to a particular case. For example, it was assumed in the studies that a bulk power source was available. Consequently savings that might result due to the elimination of a transformation from transmission or subtransmission voltage to primary-feeder voltage are not apparent. The results of Fig. 2 indicate trends which show that a particular case should be studied carefully and should include consideration of both higher secondary and primary voltages.

Relative Costs of Isolated Spot Networks

Studies were made for serving concentrated loads with spot networks designed on a first-contingency basis. Fig. 3 shows the cost to serve a spot load with 500, 750, and 1,000 transformers at either 208 or 460 volts, 13-kv primary voltage. Costs for 2,000-kva transformers apply only for 460 volts. The minimum points of these curves are plotted in Fig. 4 to show comparison of spot-network costs at 208 volts and 460 volts. Spot loads in the order of 3,000 kva or higher can be more economically served at the higher secondary voltage. A smaller magnitude of spot load can be served economically at the higher secondary voltage, with first contingency as a design basis, compared to second-contingency design. These results do not include costs of primary feeders, although for a particular case the comparison can be made easily, including primary-feeder costs, knowing the specific conditions.

Mutual Support of Adjacent Multitransformer Installations

In practice, an a-c secondary network has both single- and multiple-transformer installations at various locations on the secondary grid. The locations of the multitransformer installations are dictated by the heavy spot load requirements. The spot networks thus formed are essentially self-sufficient, neither contributing much power to the network nor receiving much power from it in the event of a primary-feeder outage.

It is extremely difficult to obtain generalized information on power transfer via secondary ties between multitransformer installations. So many variables are involved that generalized results could not be confidently applied to specific cases. One special case considered in this study is that of two multitransformer spot-network installations connected to each other by a secondary tie, but otherwise isolated from the rest of the secondary mains system that would serve the surrounding areas. The cost per kva of serving the total load of both these spot networks is least when they, and their respective loads, are separated by zero distance. Cost evaluation of serving the loads of two such spot networks by either increasing the secondary-tie capacity between them, or adding more transformer capacity at each spot, is described in Appendix IV. The analysis is based on first contingency.

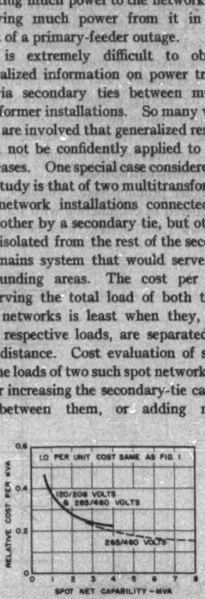

Fig. 4. Minimum-cost spot networks obtained from Fig. 3

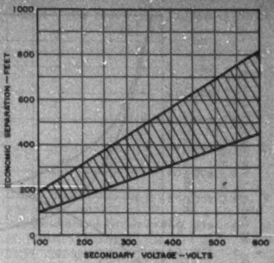

Fig. 5. Economics of interconnected spot networks

In considering the economics of tieing together spot networks with secondaries, there is a maximum separation beyond which it is not economical to add more secondary-tie capacity in an attempt to increase the firm capability of the two installations combined. This distance is variable with the size and number of transformers comprising the spot networks and with the secondary voltage. On the basis of first-contingency outage, i.e., one transformer out of service at one of the spot networks, it was found that the general zone of economic separation is 180 to 320 feet at 208 volts, and 360 to 640 feet at 460 volts. These results are illustrated in Fig. 5, which shows the effect of secondary voltage on the ability of adjacent spot networks to transfer load through a secondary tie between them. Power can be economically transferred a greater distance at the higher secondary voltage, but the economic separation is less for first-contingency design than for second-contingency design.

Spot-Network/Radial Distribution at 460 Volts

A system pattern utilizing large, multitransformer spot networks, with capability to reach for load at the higher secondary voltage, was studied for first-contingency design. This system is defined as a spot-network/radial system, and the procedure for its cost determination is discussed in Appendix IV.

In the economic study of the spot-network/radial system, several different patterns for radial secondaries and variable load densities were considered to find the optimized lowest-cost system conforming to this type of design. These

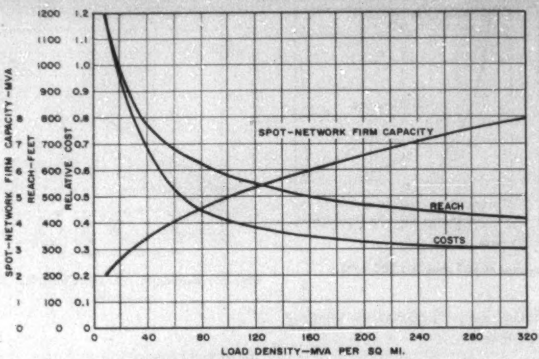

Fig. 6. Results of spot-network/radial system economic studies

resulting costs of the 460-volt spot-network/radial system are shown in Fig. 6. These costs are replotted in Fig. 1, where they are compared with the 208-volt and 460-volt general network system costs. These combined results for both the conventional and spot-network/radial systems shown in Fig. 1 show cost savings for higher secondary voltage, and first-contingency design, comparable to the results of studies based on second contingency.

The relative costs of Fig. 1 do not include primary-feeder supply. However, for conventional networks, the number of interlaced primary feeders affects the network-transformer application factor, and consequently system cost. As previously stated, the conventional network costs of Fig. 1 are based on five interlaced primary feeders. In the spot-network/radial system, the transformer application factor is not dependent on the number of primary feeders interlaced in the network area. Hence the relative positions of the cost curves of Fig. 1 will be affected somewhat by varying the assumed number of interlaced feeders serving the conventional networks.

In general, for conventional networks, an increase in the number of interlaced feeders reduces transformer application factor, with resultant lowered cost for transformers and secondaries. However, when the cost for the additional primary feeders is included, the cost savings in network transformer and secondaries is cancelled out by the higher primary system costs. This effect is illustrated in Fig. 2, where the cost of primary supply to the network is included.

Recognition of the fact that the 5-feeder network-transformer application factor used to obtain the conventional network system costs of Fig. 1 is typical of a large number of existing systems permits the conclusion that the savings for the spot-network/radial system as shown in Fig. 1 are conservative. In actual practice, a greater savings would be realized in the spot-network/radial system because of the almost universal existence of some concentrated loads in all network areas. The concentrated loads served directly by spot networks require less secondaries, and consequently the cost for serving a more realistically distributed load in an area of given density would be less than that shown for the spot networks of Fig. 1, which serve uniformly distributed load.

Higher primary-feeder voltages, when considered in conjunction with the spot-network/radial system, may be expected to show favorable savings similar to those indicated by the curves of Fig. 2 for the conventional network system of higher secondary voltage. While some costs not forseeable with the use of higher primary voltages may tend to decrease the savings of the higher voltage primary supply, the indications are that over-all savings would result for cases where network loads are large, and large amounts of bulk power must be transferred from the source to the network area.

In comparing the optimum system design and cost information of Fig. 6 with comparable information obtained from previous studies[1] of the spot-network/radial system based on second-contingency design, several effects can be noted. At a given load density, the spot-network firm capacity for optimum cost is less for designs based on first contingency. Thus at a given load density, a larger number of spot networks, each serving a smaller area, are more economical when the spot-network/radial system design is based on first rather than second contingency. The economic reach distance is somewhat less for first-contingency design.

Conclusions

1. In comparing the engineering and economic aspects of the alternative secondary voltages of 208 volts and 460 volts including the cost of primary supply to the network, network load as well as load density are important factors influencing comparative system designs and costs.

2. A primary-feeder voltage of 13 kv is generally economical to serve a network area having either 208 or 460 volts secondary voltage. The combination of a secondary voltage of 460 volts and a primary-feeder voltage above 13 kv becomes in-

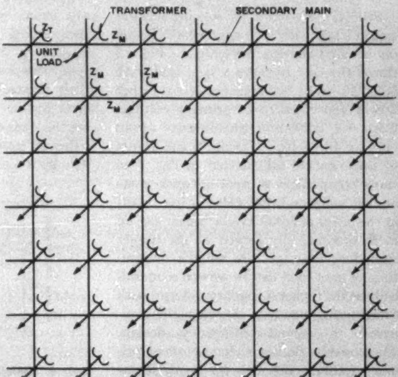

Fig. 7. Network used for study to obtain network-transformer application factors

Table I. Some Primary-Feeder Arrays

			Two-Feeder Array			
1	2	1	2	1	2	1
2	1	2	1	2	1	2
1	2	1	2	1	2	1
2	1	2	1	2	1	2
1	2	1	2	1	2	1
2	1	2	1	2	1	2
1	2	1	2	1	2	1
			Three-Feeder Array			
1	2	3	1	2	3	1
2	3	1	2	3	1	2
3	1	2	3	1	2	3
1	2	3	1	2	3	1
2	3	1	2	3	1	2
3	1	2	3	1	2	3
1	2	3	1	2	3	1
			Five-Feeder Array			
1	2	3	4	5	1	2
3	4	5	1	2	3	4
5	1	2	3	4	5	1
2	3	4	5	1	2	3
4	5	1	2	3	4	5
1	2	3	4	5	1	2
3	4	5	1	2	3	4
			Ten-Feeder Array			
1	2	3	4	5	6	7
8	9	10	1	2	3	4
5	6	7	8	9	10	1
2	3	4	5	6	7	8
9	10	1	2	3	4	5
6	7	8	9	10	1	2
3	4	5	6	7	8	9

creasingly favorable as load density, network load, and distance of the bulk power source from the periphery of the network become greater.

3. Spot loads in the order of 3,000 kva or higher can be more economically served at the higher secondary voltage. A smaller magnitude of spot load can be served economically with a spot network of first-contingency design, compared with a spot network of second-contingency design.

4. The maximum distance for economical transfer of power between interconnected spot networks is lower for first-contingency than for second-contingency design. The economic maximum separation for interconnected first-contingency spot networks is 180 to 320 feet at 208 volts, and 360 to 640 feet at 460 volts. For greater separation distances at both respective voltages, incremental firm capability of spot networks can be more economically obtained through the addition of transformer capacity at spot networks rather than through the addition of heavier secondary ties.

5. The spot-network/radial system is generally more economical than the general network for load densities of approximately 50,000 kva per square mile and higher. First-contingency design does not change the economics of spot-network/radial distribution appreciably from second-contingency design.

6. The combination of a higher primary-feeder voltage and the 460-volt spot-network/radial system can be expected to show savings greater than those indicated for higher-voltage primary supply to a 460-volt general network. To serve a large network area, the use of a fewer number of larger-size transformers arranged in multiple-unit spot networks results in fewer locations to which primary supply must be brought, and hence a reduction in total mileage of primary-feeder circuit.

Appendix I. General Network System Network-Transformer Application Factor

Application factor is defined as the ratio of installed network-transformer capacity to load. This factor is an extremely important parameter of network cost, since the total capacity of network transformers required to serve a given load will be directly proportional to the application factor. As defined herein, this factor can be considered as the reciprocal of the more commonly used ratio of peak load to installed transformer capacity, where the peak load is the design load for the network. The method employed for obtaining the application factors used in this study is as follows:

Consider a conventional hypothetical network system serving equal loads. Let these loads be represented by one unit of load at each junction of the secondary grid, which in turn is assumed to consist of square meshes making up a square-shaped network. Network transformers of a given rating are located with one at each junction. Each network transformer has an impedance Z_T, and the impedance of each section of secondary is Z_M. Such a system, with six meshes, or seven transformers, in both directions is shown in Fig. 7. Any given number of primary feeders (up to 49, i.e., one for each transformer) can serve such a system. Some possible primary-feeder arrays are given in Table I.

In these arrays, each number identifies the particular feeder serving the network unit located at that position in the system of Fig. 7. Note that the interlacing of two, three, five, or ten primary feeders in each array is such that when one feeder to the network is out of service the increased loading on the network units served by the remaining feeders is distributed as equally as possible.

Table II. Five-Feeder Array Omitting Feeder No. 1

	2	3	4	5		2
3	4	5		2	3	4
4		2	3	4	5	
2	3	4	5		2	3
4	5		2	3	4	5
	2	3	4	5		2
3	4	5		2	3	4

The application factor is based on the loss of one primary feeder. Thus the factor is a function of the following: the number of primary feeders; Z_M and Z_T, or the more commonly used term Z_M/Z_T; and the extent to which load is not uniformly distributed among the network units remaining in service when one primary feeder, out of the total number being considered, is out of service. To investigate the relationship between these factors, the system of Fig. 7 was set up on a d-c calculating board, and the loadings of network transformers throughout the system were tabulated for the condition of one feeder out of service, as the number of primary feeders and Z_M/Z_T were varied.

As an example of the procedure for conducting this study, consider the 5-feeder array. Removal of feeder no. 1 from service leaves the array of in-service feeders shown in Table II.

In setting up the 5-feeder, 49-transformer, 49-load system on the calculating board, the following conditions were satisfied:

1. All loads draw 1 pu current, both before and after a feeder outage.
2. All sections of secondary main have equal impedance.

From observing the primary-feeder array with feeder no. 1 out of service shown in Table II, it will be noted that the unsymmetrical pattern of locations for the

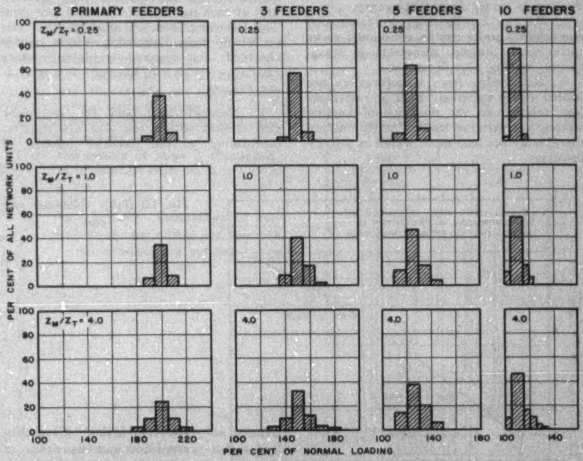

Fig. 8. Statistical distribution of network-transformer loadings under first contingency

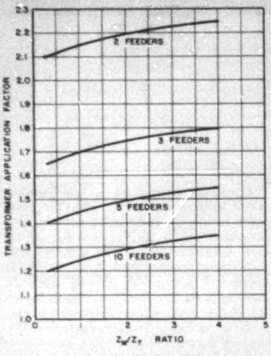

Fig. 9. Network-transformer application factors used as basis for economic studies

transformers served from the feeder out of service will result in unequal loading of the transformers remaining in service. The distribution curves of Fig. 8 represent the results of this statistical survey of transformer loadings under first contingency, i.e., with one feeder out of service.

In Fig. 8, the per cent of all the network units in the system that are loaded within the per-cent load intervals indicated are shown for two, three, five, or ten feeders, and for values of Z_M/Z_T of 0.25, 1.0, and 4.0. Study of these network-transformer-loading distribution curves under first contingency verifies several important effects:

1. As the number of feeders to the network increases, the dispersion or "spread" in transformer per-cent loading diminishes under first contingency.

2. As the Z_M/Z_T ratio decreases, and the network units can be considered to be more nearly bussed, dispersion in transformer loading also decreases.

3. Relatively few transformers are loaded either extremely high or extremely low, relative to the majority of loading values, but extreme loading conditions are more numerous and more severe as Z_M/Z_T increases.

The philosophy of secondary-network system design is that all load is to be served without service interruption, or undue damage to the system, under the contingency of one primary feeder out of service. But since a primary-feeder outage is a random occurrence which may involve any one of the feeders to the network, sufficient network-transformer capacity must be provided so that even the extremely loaded transformers of Fig. 7 are not loaded beyond some maximum allowable loading under first contingency. Thus the maximum per-cent loadings in the loading distribution "histograms" of Fig. 8 permit determination of the application factor required to keep network transformers from being loaded to more than a given value, in a system having a specified Z_M/Z_T ratio and number of primary feeders. Specification of normal loading (i.e., loading before a feeder outage) determines the kva represented by the per-cent loading values in Fig. 8.

Fig. 9 is a composite family of curves obtained from Fig. 8, and shows the transformer application factor versus Z_M/Z_T for different values of feeders to the network. This figure is the basis for determining the amount of network-transformer capacity required to serve a given amount of load in a system having a stipulated number of feeders and Z_M/Z_T ratio.

In the cost study to be discussed in Appendix II, network transformers are installed on the basis that the transformers which carry the heaviest load during a first contingency are loaded to their rated capacity.

Appendix II. General Network Cost Determination Without Primary Feeder Costs

The general network is considered to be the system employing a single network unit at each junction of the secondary grid. The following premises establish the basis on which general network system cost is obtained, for systems employing either 120/208 volts or 265/460 volts as a secondary voltage:

1. Network area and the secondary gird meshes within the area are squares, conforming to the assumed pattern of streets.

2. Load is assumed to be uniformly distributed along all streets.

3. Single network transformers of equal rating are located at every secondary mains junction in the system. Installed costs of network units are shown in Fig. 10.

4. Secondary mains are always multiple-conductor per phase, having a current-carrying capacity of 55 per cent of network-transformer rated amperes at secondary voltage. Secondary mains cost is shown in Fig. 11.

5. Only first contingency is considered. Hence the network-transformer application factors derived in Appendix I and shown in Fig. 9 are applicable.

6. Primary-feeder voltages considered are 4.16 kv, 13.2 kv, and 34.5 kv. Allowable maximum loadings per feeder at these voltages are 2,000, 6,000, and 15,000 kva respectively. Cost determination of primary feeders is discussed in Appendix III.

7. A maximum of ten primary feeders may be interlaced in any network area. Network areas containing a load in excess of the capability of ten primary feeders are served by two or more independent network systems.

The costing of 120/208-volt and 265/460-volt general networks is carried out in two major steps. In the first step, covered by this Appendix, costs of hypothetical networks are obtained, excluding primary-feeder costs. In the second part of the analysis, which is covered in Appendix III, the network load and area are determined by the number of primary feeders and the primary-feeder voltage. However, these two parts of the analysis cannot be completely divorced from each other, because the transformer application factor will depend on an assumed number of interlaced primary feeders, as depicted in Fig. 9. Hence, in obtaining the cost of networks excluding the primary feeders, either 2, 3, 5 . . . or 10 feeders were considered in order to provide a suitable application factor for obtaining the size of network transformer spaced at a given distance, in an area of given density.

At any load density, the optimum-cost system was obtained for 120/208-volt and 265/460-volt systems. The optimum-cost system is defined as the minimum-cost system capable of supplying the entire network load under the following conditions:

1. No network transformer is to carry more than its rated kva when one primary feeder is out of service.

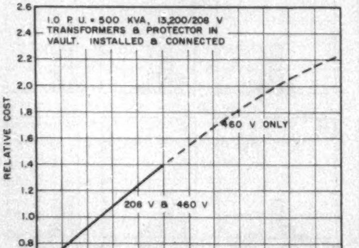

Fig. 10 (left). Network unit cost

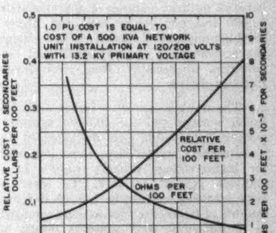

Fig. 11 (right). Secondary mains cost and impedance, as a function of current-carrying capacity

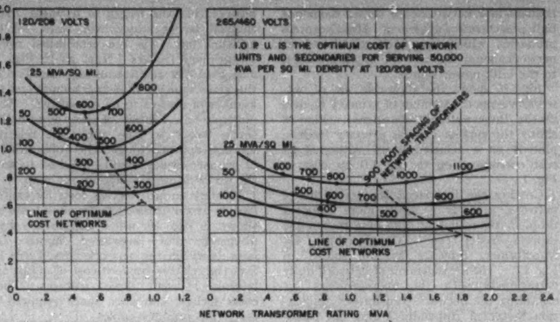

Fig. 12. **Procedure for optimizing general network system costs for 120/208- and 265/460-volt systems. Dotted curves define optimum-cost systems**

2. No secondary main is to carry more than its rated current at any time.

At each of several stipulated loads densities, network-transformer size (and hence corresponding spacing) was varied over a range sufficiently wide to give the combination of transformer size and spacing resulting in a minimum-cost combination of these two system components at that load density. Transformer size was not limited to standard ratings, but rather was allowed to assume the exact size required for optimum system cost. Transformer costs for sizes lying between standard sizes was obtained by interpolation between cost of standard-size units. The following specific steps comprise this analytical method:

1. Consider one of the two secondary voltages, e.g., 120/208 volts.
2. Choose a load density, e.g., 25,000 kva per square mile.
3. For the load density in step 2, choose a transformer spacing, e.g., 500 feet. Knowing the load density and the transformer spacing, the loading of the transformer, when all feeders are in service, is explicitly determined by obtaining the product of the square-mile area allocated to one transformer and the load density.
4. Assume a number of interlaced primary feeders, e.g, five. With the aid of Fig. 9, select a network-transformer size and secondary mains capacity such that the application factor and ratio Z_M/Z_T are compatible according to Fig. 9. Choice of transformer rating determines both Z_T in ohms, and also Z_M (from 500-foot spacing and 55-per-cent rule) which may be read in ohms from Fig. 11. For network-transformer impedance, 5 per cent and 10 per cent were the values used for 208-volt and 460-volt units respectively.
5. Sum the dollars cost for a network transformer, and secondary mains reaching half the spacing distance in four directions from the transformer. Divide this sum by the transformer loading. This gives the dollars per kva cost of a system conforming to the following values cited as examples in the previous steps: 120/208 volts secondary voltage; 25,000 kva per square-mile density; 500-foot spacing of network units; and five interlaced primary feeders.
6. Repeat steps 3 to 5 for another spacing of transformers, say 600 feet; then for several more spacings.
7. Repeat steps 3 to 6 for another load density, say 50,000 kva per square mile; then for several more densities.
8. Repeat steps 2 to 7 for 265/460 volts secondary voltage.

From the results of steps 1 through 8, the curves of relative cost per kva versus network-transformer rating of Fig. 12 are obtained. For each secondary voltage, calculations based on the foregoing procedure give a curve, at each density considered, with a minimum cost corresponding to the optimum combination of transformer size and spacing. The minimum-cost system at each density is then connected by the dotted lines shown, giving the costs of optimum general networks as a function of load density. The network-transformer rating and spacing giving minimum cost is plotted versus load density in Fig. 13. Optimum costs versus load density are replotted from Fig. 12 and appear in Fig. 1. In plotting relative costs, the 1.0 pu cost is taken as the dollars per kva cost of network-transformer installations and secondaries, to serve 50,000-kva-per-square-mile load density with the optimum-cost 120/208-volt system with 13.2-kv primary voltage.

Results of studies based on transformer application factors for other assumed numbers of interlaced primary feeders, e.g., two, three, and ten feeders, show that relative costs correspond very closely to those shown in Fig. 1, provided that the 1.0 pu cost is always considered to be the cost of the 120/208-volt system serving 50 megavolt-amperes per square mile, and supplied by the specific number of interlaced primary feeders considered.

Appendix III. Primary Feeder Costs

The primary-feeder circuits serving a secondary-network system can be considered as two components: the express feeders carried from the bulk power source to the periphery of the network area; and the feeders interlaced within the network area itself. Primary feeders within the network area may in turn be classified into two components: mains and laterals.

The first step in arriving at a method for costing primary feeders is to obtain a relationship between the length of primary-feeder circuit serving a network and the design parameters of the network system. Length of circuit is the final objective of

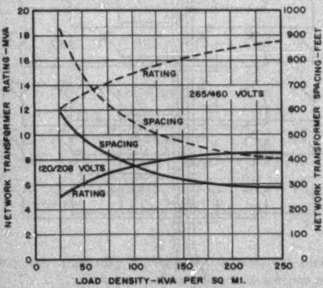

Fig. 13 (left). **Comparison of network-transformer ratings and spacings in optimum-cost systems**

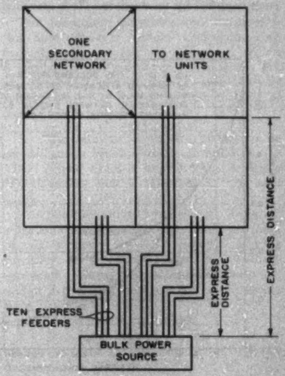

Fig. 14 (right). **Showing the assumed location of bulk power source and method of serving networks with express primary feeders**

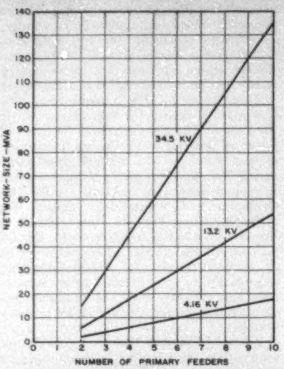

Fig. 15. Effect of number of primary feeders and primary-feeder voltage on network size

such an analysis since it can be assumed that feeder cost is directly related to the length of circuit. Differentiation between installed cost per foot of express feeders, mains within the network area, and laterals is necessary, however, in order to make costs more realistic.

The variables determining primary-feeder cost are:

1. Distance of bulk power source from the network.
2. Number of feeders.
3. Feeder voltage.
4. Area of network.
5. Number of network units within the network area.

Express feeder length is determined on the basis shown in Fig. 14. Note that where the network area load is too large to be served by the maximum allowable number of ten primary feeders at the desired voltage, two or more networks are formed, each served by the appropriate number of feeders required to carry the load, under first contingency. Fig. 14 shows a specific case of four separate network areas, each supplied by ten feeders. It is assumed that all four networks are served from one bulk power source as shown. Hence express primaries which serve the farthestmost networks must traverse the systems closest to the bulk power source.

Fig. 15 shows the allowable size of networks versus the number of primary feeders at the three voltages considered. Fig. 16 shows the cost of express primary feeders, plotted on a relative basis, with 1.0 pu cost corresponding to the 1.0 pu cost of Fig. 1.

Costing the interlaced feeders within a network area is a much more complex problem than that of obtaining reasonable express feeder costs. Consider the 49-transformer, 5-feeder system shown in Fig. 17. The arrangement of network units corresponds with the arrangements for obtaining the network-transformer application factor in Appendix I and the transformer and secondary costs in Appendix II. Five main feeders are considered to be carried fully across the network area. Laterals are carried perpendicular to the feeder mains, and serve the network units so as to give the interlacing pattern indicated by the feeder designations appearing alongside each network unit.

Using primary-feeder patterns similar to that of Fig. 17 as the basis for a mathematical derivation, total length in miles of primary-feeder circuit in a network area can be expressed as a function of the following three variables: network area in square miles; number of feeders; number of network units in the area. The results of such a study are given in Fig. 18, where the relative total mileage of interlaced primary-feeder circuits (mains plus laterals) in a network system is plotted versus the number of network units in the system, with one curve for each number of feeders. An interesting feature of these curves is that they are normalized so that a hypothetical, 1-feeder system is used as the reference for determining primary circuit length. This permits very simple calculation of primary length in the following manner:

Given a map of the array of network units to be served by interlaced primary feeders, find the length of a single, hypothetical feeder which will reach all the network units via the established routes for primary feeders. Next go to Fig. 18, and read the relative-mileage number for the given number of network units and the number of feeders to be considered. Then multiply the length of the hypothetical single feeder by the applicable relative-mileage number to get the total mileage of primary-feeder circuits required to serve the array of units shown on the map.

Primary circuit relative costs for express feeders at the three voltages considered are shown in Fig. 16, which has already been discussed. For interlaced mains and laterals within the network area, Table III lists the relative per-foot cost of mains and laterals at the three voltages. These costs include the duct space required to carry the primary cables.

In Fig. 13, resulting from the study described in Appendix II, it is seen that optimum-cost network systems at 120/208 volts and 265/460 volts do not utilize the same sizes of network unit. The higher-voltage system can utilize larger-size transformers, and consequently can serve the same load area with a fewer number of units. Fig. 13 shows that at 265/460 volts network transformers in an optimum-cost combination of transformers and secondaries may be spaced approximately $1^1/_2$ times the spacing required in the 120/208-volt system serving the same load area. The reduction in primary-feeder circuit length that can be realized because of fewer transformers for the higher secondary voltage is illustrated in Fig. 19, which depicts a 3-feeder system serving the same load area at either 120/208 volts or 265/460 volts. In costing the primary feeders for systems at either secondary voltage, this effect is automatically taken into account with the use of Fig. 18.

The analytical tools developed in the foregoing are used to determine the allowable size of 120/208-volt or 265/460-volt networks supplied by either 4.16-kv, 13.2-kv, or 34.5-kv primary feeders. Different distances of the bulk power source from the periphery of the network area are also

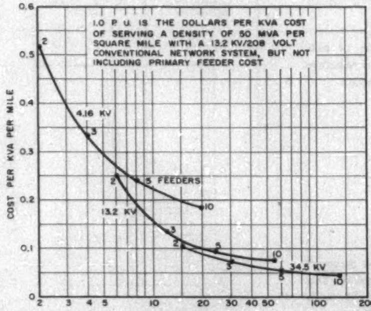

Fig. 16 (left). Express primary-feeder costs

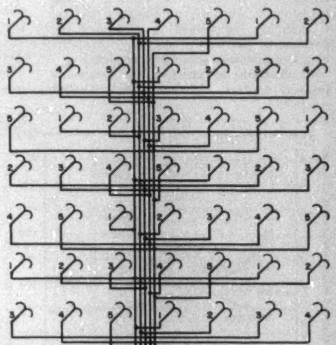

Fig. 17 (right). Showing the assumed interlacing pattern of primary feeders for obtaining primary-feeder costs

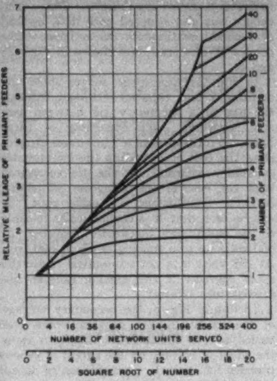

Fig. 18. Curves describing relationship between parameters affecting primary-feeder cost

considered, and system costs including primary feeders are computed for three different load densities and presented in curve form in Fig. 2.

Appendix IV. Spot-Network Radial System Cost Determination

The spot-network/radial system is made up of a number of spot networks that are designed to be independent of each other in supplying their respective loads. Each spot network, with the secondaries carried from it, resembles the system pattern pictured in Fig. 20. Secondary voltage is 265/460 volts. Fig. 20 shows a 4-transformer spot network, but in general two or more transformers may be considered. Each network unit in the spot network is supplied by a different primary feeder.

Table III. PU* Cost of Primary-Feeder Circuits for 1,000 Feet of 3-Conductor Cable

	4.16 Kv	13.2 Kv	34.5 Kv
Main feeder	0.333	0.444	0.667
Lateral	0.222	0.333	0.444

* Refer to Fig. 1.

Fig. 20 shows what is defined as a $1^1/_2$ block reach for 265/460-volt secondaries. Wherever the secondaries form a grid, it is assumed that junctions of the grid can be made only at street corners.

In determining the requirements for 265/460-volt secondary mains capability, distribution of load is based on Fig. 21, where the locations of equal-size loads within one square block are shown. Contiguous square blocks have loads placed similarly. In many instances it is possible to serve two or more services from the same tap-off point, where loads on both sides of the street are served from the same point on the secondary.

Each of the individual loads shown in Fig. 21 is assumed to be an integral multiple, or fraction, of 312 kva. At 265/460 volts three-phase, eight no. 4/0 copper conductors per phase can carry 390 amperes, which at this voltage is equivalent to 312 kva. Thus from the standpoint of design based on thermal capability, secondaries in the spot-network system are installed for a given pattern of loads and mains simply by using the number of conductors per phase required for carrying the amperes in that section of mains. In no case is the thermal capability of secondary conductors exceeded. Wherever required, additional conductors per phase, over and above thermal requirements, are added so that the voltage drop from the spot-network 265/460-volt bus to the farthest load does not exceed 5 per cent.

As in the general network system, permissible loading of network transformers is based on first contingency. Under first contingency, the network transformers remaining in service are loaded to 130 per cent of name-plate rating.

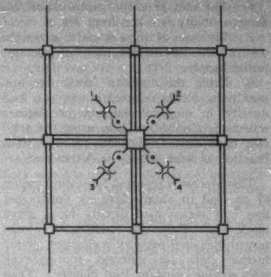

Fig. 20. Simplified layout of spot-network/radial system for $1^1/_2$-block reach for uniform density service

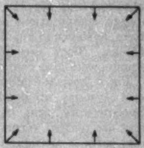

Fig. 21. Location of loads for spot - network/radial system

In obtaining the cost of the spot-network system, a system design optimizing procedure was employed. Based on the assumed system arrangement shown in Fig. 20, and the assumed load distribution of Fig. 21, the cost of such a system to serve a very large area of a given load density depends on the following considerations:

1. Spot-network load: Since load density is specified, the spot-network load fixes the size of the area served by one spot network.
2. City block size: The size of the blocks considered will affect the routing and capacity of secondaries to serve the load contained within the spot-network service area.
3. Primary-feeder voltage: Network unit installed cost is affected by primary-feeder voltage.

The foregoing considerations enter into the spot-network system cost-optimizing procedure in the following manner, which is similar to that employed in Appendix III of reference 1, except that in this analysis system design is based on first instead of second contingency.

1. The number of square blocks to be served and a block size are selected.
2. A load which is some integral multiple of 312/8=39 kva is selected for the unit loads.
3. The secondary mains are designed with sufficient conductors per phase installed in all sections so that current-carrying capacity of secondary mains is nowhere exceeded. Extra conductors per phase are added if required, to keep per-cent voltage drop to 5 per cent.
4. These mains are costed.
5. The load served is determined by multiplying the pu load by 12 and by the number of blocks.

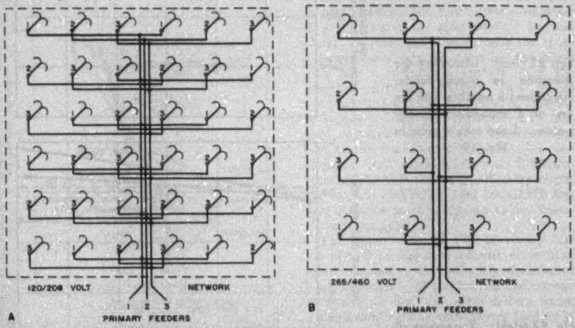

Fig. 19. Illustrating the reduction in primary-feeder circuit length possible with the use of larger-size network units in a higher secondary-voltage system

6. The cost of a spot network of this firm capability is taken from Fig. 4.

7. The sum of steps 4 and 6 gives the cost of the installation without primary-feeder supply.

8. Using the assumed block size and number of blocks selected in step 1 a load density in megavolt-amperes per square mile is determined. Then, using the total cost from step 7, the cost per kva as a function of load density is determined.

This process is repeated for several values of pu load to obtain data for dollars per kva cost versus load density for a given block size. Next, the number of blocks served by a spot network is changed, giving further data for different spot-network sizes serving constant load density. Then the block size is changed and another set of calculations made.

In the cost calculations just outlined, spot-network installed costs were obtained from Fig. 4. Secondary mains costs were obtained from Fig. 11. The results of these design computations are plotted in curve form, as shown in Fig. 22 for 700-foot square blocks. Block sizes of 300 and 500 feet square were also considered.

Fig. 6 shows the information for optimum-cost systems obtained from this study. Spot-network firm capacity, reach, and cost are plotted versus load density. The cost curve is reproduced in Fig. 1.

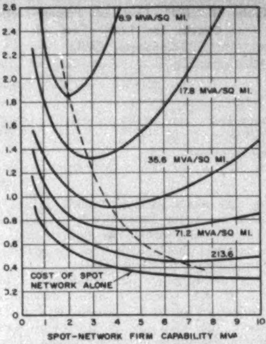

Fig. 22. Procedure for optimizing spot-network/radial system costs. Dashed curve connects minimum-cost points. 1.0 pu cost same as Fig. 1. 700-foot square blocks. Evenly distributed load. First contingency. 5-per-cent regulation

Primary-Feeder Supply to Spot Networks

In Appendix III it was demonstrated, with the aid of Fig. 19, how the permissible use of larger-size network transformers with a higher secondary voltage results in a reduction in circuit length of primary feeders, and hence a reduction in primary-feeder cost. A further reduction in primary-feeder circuit cost is possible in the 265/460-volt spot-network/radial system.

Fig. 23 shows the load area of Fig. 19 served by a 3-feeder spot-network system. This study has shown that in general the optimum network transformer size for use in spot networks is larger than the optimum size for use in the general network. Therefore the 16 network units of Fig. 19(B) are replaced with four 3-transformer spot networks for the purpose of illustrating this effect. The total length of primary-feeder circuit is less for the spot-network system of Fig. 23 than for the general 460-volt network system of Fig. 19(B).

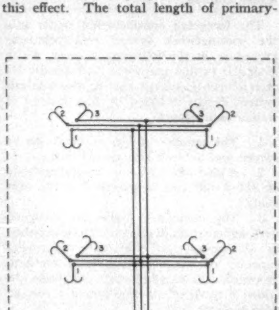

Fig. 23 (left). Illustrating the reduction in primary-feeder circuit length possible with the use of a spot-network/radial system. Load area is same as Fig. 19

Mutual Support of Multitransformer Installations

In Appendix II of reference 1 a method is presented for obtaining the optimum design and minimum cost for two spot networks some distance apart, which are tied together with secondaries through which some power may be transferred. The use of such a secondary tie results in a firm capability for the two spots combined, which is greater than the sum of their individual firm capabilities. This procedure was also adopted with first, instead of second, contingency as a basis. The results of this study are shown in Figs. 24 and 5.

In Fig. 24 the upper curves show the additional firm capacity attained through the use of a secondary tie between two spot networks, each consisting of three 500-kva transformers. The lower curves show the cost of providing the incremental capability afforded by the tie compared with the cost of providing an additional 500-kva transformer at each spot. It can be seen that it is economically feasible to tie such spot networks together at 460 volts up to a spacing of about 500 feet. At 208 volts it is not economical to tie the spots together if the spacing exceeds approximately 225 feet.

To obtain Fig. 5, the secondary voltage of the interconnected spot networks was varied over a considerable range, to show the effect of voltage on the extent of power transfer for such an arrangement of interconnected spot networks. Comparison of these results with those obtained for second-contingency design shows that the separation distance for economical power transfer is less for first-contingency design than for second-contingency design.

References

1. Economics of Various Secondary Voltages for Commercial Areas, T. C. Duncan, J. P. Neubauer, J. M. Comly, R. F. Lawrence, Miles Maxwell. *AIEE Special Publication S-66*, Sept. 1954, pp. 7–20.

2. A New Approach to the Problem of Higher Distribution Voltages, A. M. deBellis, S. B. Griscom. *Ibid.*, pp. 3–6.

3. Distribution Equipment Used on 265/460-Volt Networks and Its Operating Features

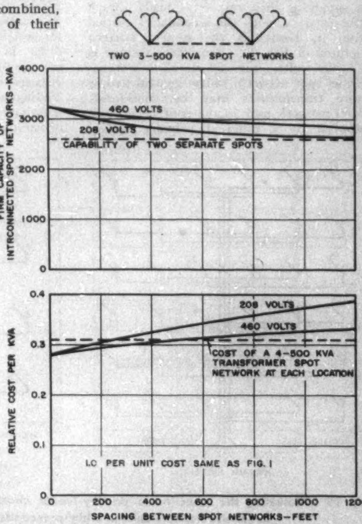

Fig. 24 (right). Economics of spot networks interconnected by secondary tie cables

L. Brieger, C. P. Xenis, A. J. Bisson, J. DeLellis. *Ibid.*, pp. 20–26.

4. Service Voltage Spread and Its Effect on Utilization Equipment, H. G. Barnett, R. F. Lawrence. *Ibid.*, pp. 51–56.

5. Secondary Network Equipment for 250- to 600-Volt Systems, R. L. Schwab, E. W. Stohr. *Ibid.*, pp. 26–31.

6. The Relative Feasibility of 460-Volt or 208-Volt Service in Commercial Buildings, H. G. Barnett, R. A. Zimmerman, H. E. Lokay. *Ibid.*, pp. 37–44.

7. The Probability of Coincident Primary-Feeder Outages in Secondary Networks, David N. Reps. *AIEE Transactions*, vol. 73, pt. III, Dec. 1954, pp. 1467–78.

8. Coincident-Outage Probability in Secondary-Network Vaults, David N. Reps. *Ibid.*, vol. 74, pt. III, Aug. 1955, pp. 580–86.

◆

Discussion

F. C. Van Wormer (General Electric Company, Schenectady, N. Y.): The authors' paper re-emphasizes the well-known inadequacy of 4 kv as a primary feed to a secondary network system. If a 265/460-volt network in high load per block areas is supplied by 13 kv feeders, only three or four 2,000-kva units may be carried per circuit under the usual feeder loading. This puts the 13-kv feeder supplying a 265/460-volt network about in the same position as a 4-kv feeder supplying a 120/208-volt network from the viewpoint of excessive number of feeders and duct line congestion. The authors have rendered a service in showing that the general rule, "when a distribution voltage level is raised it also raises the level of the economic voltage to supply the system, provided there is sufficient load to warrant raising the distribution voltage level," also applies to the secondary network system.

Fig. 1 of the paper shows considerable economic advantage in favor of a spot-network/radial system over the conventional network system for load densities above 50 megavolt-amperes (mva) per square mile.

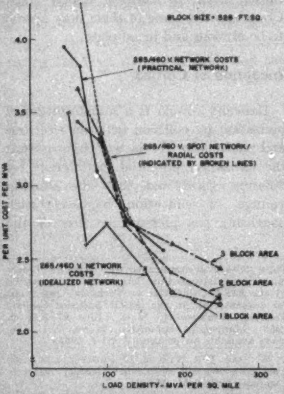

Fig. 25. Cost comparison of conventional network and spot-network/radial systems for a constant block size

In the conventional network system, the transformers are loaded to only 100-per-cent rating under single-contingency operation (Appendix II of the paper). In the spot-network/radial system, the transformers are loaded to 130 per cent under single-contingency operation (Appendix IV). Also, in the optimizing process used, the block size decreases as the load density is increased. Therefore, we do not feel that the two systems are compared on an equal and realistic basis in Fig. 1.

In a practical case the city block size stays fixed as the load density increases. In Fig. 25 we have compared the pu cost per mva of the spot-network/radial system with the conventional network system for 528-foot square blocks (0.01 square mile per block) as a function of the load density. Per-unit costs and allowable secondary cable loadings were used from reference 1 of the paper. In both systems transformer loading of 125 per cent rating under single contingency was allowed. Standard available transformer sizes were used. Secondary cables were selected on the basis of integral multiples of sets of eight no. 4/0 (American Wire Gauge) cables per duct.

Fig. 25 shows the cost per mva of the spot-network/radial system covering one, two, and three square blocks as a function of load density. The points plotted are at load densities such that the transformers at the spot are loaded to 125 per cent rating when one feeder is out of service.

Fig. 25 also shows the cost per mva of a practical conventional network system as a function of load density. Allowing 125-per-cent loading under single-contingency operation, a transformer application factor of 1.13 for a 5-feeder network was obtained from Fig. 9 of the paper for 10-per-cent impedance transformers and integral sets of eight no. 4/0 (American Wire Gauge) cables per duct sized on the 55-per-cent rule. The points plotted are at load densities such that the remaining transformers are loaded to a maximum of 125-per-cent rating when one feeder is out of service.

Fig. 25 shows that for a fixed block size of 528 feet there is no appreciable difference in cost between the two systems between 80 and 180 mva per square mile. Beyond about 180 mva per square mile the spot-network/radial system covering one block area has a definite advantage over the practical network system. This points out the true and valid use of a spot network to supply a large concentrated load. The spot network has already absorbed the cost of the transformer to be lost on contingency and each additional 2,000-kva transformer that can be justified by reaching out and picking up load adds 2,500 kva firm capacity to the spots up to five transformers per spot.

The lower curve of Fig. 25 shows cost per mva of an idealized 5-feeder network of infinite extent with uniformly distributed load, having 1/3 of the load at the corners according to Fig. 21. This system under a single-contingency transformer loading of 125-per-cent rating has a transformer application factor of 1.00 and requires secondary mains rated at 41.7 per cent of transformer rating. This idealized network system is the lowest in cost up to a load density of 200 mva per square mile, or more generally a load per block of 2,000 kva which requires a 2,000-kva transformer at each corner. For higher loads per block the spot-network/radial system has economic advantages.

When the spot-network/radial system and the conventional network system are compared on the realistic basis of a fixed block size, the radial system is not generally favorable until load densities in the order of 180 mva per square mile are encountered. The fact of large spot loads being the predominate load of the future serves to prevent network supplied distributed loads from reaching levels beyond the capabilities of one transformer per block. As in the past, the spot network will continue to be the logical method of supplying large building loads.

R. F. Lawrence and **D. N. Reps:** Mr. Van Wormer raises several interesting points for discussion. In all cases of network design regardless of primary and secondary voltage, economical network size, and number of primary feeders is a function of the variables which are related graphically in Fig. 2 of the paper. Although economic network-transformer sizes are larger for the 265/460-volt system, Fig. 2 shows, along the abscissa labeled "number of primary feeders," that a fewer number of feeders can supply a 265/460-volt network of any size, and at any density, at lower cost than a 120/208-volt network supplied with a necessarily larger number of 4-kv feeders.

The "general rule" might well be further generalized by shortening it to read: "When a distribution voltage level is raised, it also raises the level of the economic voltage to supply the system." The authors interpret "distribution voltage" to include secondary voltage. Studies of higher secondary and primary voltage for much lower densities than found in commercial areas further support this fact.

With regard to our approach to secondary-network system design and cost optimization, two specific points are mentioned in the discussion: city-block size, and network-transformer loading. It is stated that a more equitable basis of comparison between the 265/460-volt general network and the 265/460-volt spot-network/radial systems would result if the same, constant block size were assumed for both systems, and for all load densities. Also, it is stated that a network-transformer application factor of 125 per cent for first-contingency loading should be used for both systems.

The objective of our cost analysis is, in all cases, to optimize network-transformer and secondary-mains sizes to give the minimum-cost system for serving load having the given distribution and density. This objective was carried out for all system types and voltages. Varying the block size was necessary in order to obtain minimum "bench-mark" costs for the general-network and spot-network systems. It is interesting to note the relatively small effect block size has on general network cost, as shown in Fig. 12 of the paper, where the 265/460-volt system cost as a function of transformer rating is quite flat over a wide range of block sizes. For the spot-network/radial system operating at 265/460 volts, realistic load distribution found in practice (compared to uniformly distributed load assumed in the study) would reduce the cost of this system, because the location of spot networks to supply large spot loads nearby to those loads—a logical procedure for system development—would reduce investment in radial secondaries below that required for the system as costed in the study.

With regard to network-transformer application factor, the first sentence of Appendix I of the paper defines this term as the reciprocal of the familiar ratio of load to installed network-transformer capacity. Consequently, the application factor of 1.13 in the discussion, for the general network design, is equivalent to a ratio of peak load to installed network-transformer capacity of $1/1.13=0.89$. The ratios used in the paper are a function of number of feeders and Z_M/Z_T ratio, and for a 5-feeder system comparable to the one Mr. Van Wormer has used, are, from Fig. 9, between 0.72 and 0.64. These application factors are more realistic, based on the average for this ratio, obtainable from the reported ratios for the network systems for 40 cities, appearing in the most recent "A-C Secondary-Network Operations Report" of the Edison Electric Institute.[1] The average ratio for these 40 systems is 0.64.

Therefore, in comparative economic studies, the ratio of peak load to transformer capacity must be lower for the general distributed network than for the spot-network/radial system. Referring to Fig. 8 of the paper, for first contingency, the average loading of transformers in a conventional network may correspond to the loading for spot networks, but the dispersion of first-contingency loadings for transformers located singly is such that many may be loaded considerably above average with one feeder out of service. Moreover, in the general network, since any one of the feeders serving the network can be out of service, loadings within the highest per cent loading interval are not restricted to particular transformers. In general, any network transformer may be loaded to a value well above average under first contingency and since the conventional network must be designed to prevent any network transformer from being loaded to a value greater than the specified maximum, all transformers must be installed on the basis described in the paper.

In the single-primary-source spot-network/radial system, on the other hand the transformers remaining in service at any spot under first contingency are equally loaded. These loadings are entirely predictable because of the gathering power of the spot network.

For the foregoing reasons, the transformer application factor applied to spot-network/radial systems in our study is lower than that used for the conventional network with distributed network units. These reasons apply equally well to the systems Mr. Van Wormer has studied, although advantage was not taken of these inherent benefits of the spot-network/radial system in obtaining comparative costs. These factors will result in an increase of the conventional network-system costs of Fig. 25, and would show the spot-network system more favorable.

Reference

1. A-C Network Operations, 1950–1952. Report of Transmission and Distribution Committee, Edison Electric Institute, New York, N. Y., 1954.

Corona Studies—In Relation to Insulation

T. W. LIAO
MEMBER AIEE

J. R. NYE
ASSOCIATE MEMBER AIEE

H. H. BRUSTLE
ASSOCIATE MEMBER AIEE

J. G. ANDERSON
MEMBER AIEE

Review of Corona Studies

CORONA has been known and studied for a long time. It became of practical interest when it was recognized as a form of loss in high-voltage power transmission over half a century ago.[1] Hence the electric strength of air was studied[2,3] to determine the laws of corona inception and the phenomenon of brush discharges was studied[4,5] so as to understand the physics of corona. Soon the corona phenomenon was related to sparks in gases, and extensive work was done on this subject.[6–8] Several groups then studied other aspects of corona and breakdown and much data were produced. The results are too numerous to mention and are best summarized in several books[9–13] which also contain many references on specific subjects.

However, little attention has been paid to corona in liquids until recently,[14,15] although its importance was recognized long ago.[16] Solid insulation used in conjunction with either gases or liquids further complicated the corona phenomenon. Since composite insulation is commonly used in electric apparatus, such as cables, alternators, and capacitors, considerable attention has been given to this subject. As a result, much information of both a basic and a practical nature has been obtained throughout the past years.[17–20]

Although there have been literally many hundreds of publications on the subject of corona, there are relatively few papers on the methods of corona measurement. Some of the relevant publications have been referred to in several recent papers.[21–23] The reason for the limited literature is perhaps because on the one hand the detection of corona in simple capacitive test pieces is too simple to be repetitively reported, while on the other hand the measurement and interpretation of corona in composite insulation structures is so complicated and uncertain that individual scattered results are not conclusive and therefore not published.

In engineering work, corona measurements are made on insulation or insulating structures for two purposes. The first is to determine the corona-starting voltage of the structure, since such information is pertinent to the design of corona-free apparatus. The second is to determine the presence and extent of damage to insulation when it is subjected to overvoltages. Such information is valuable in the evaluation of insulation deterioration caused by high-potential testing or surges. There would be no need of damage studies if corona-free operation could always be insured.

Since corona inception and insulation damage are of practical importance, some of the factors that control the levels of inception and the degree of damage are reported. The data presented in this paper are mainly for the purpose of illustrating the basic underlying principles rather than to furnish design data. Consequently, some of them may appear to be obvious and incomplete.

Inception of Corona

Basically corona is a manifestation of ionization by collision between electrons and molecules. It is well known that the ionization potential is different for different gases and that the starting voltage of ionization increases with increasing gas pressure because of the

---

Paper 55-437, recommended by the AIEE Transmission and Distribution Committee and approved by the AIEE Committee on Technical Operations for presentation at the AIEE Summer General Meeting, Swampscott, Mass., June 27–July 1, 1955. Manuscript submitted March 22, 1955; made available for printing April 7, 1955.

T. W. Liao, J. R. Nye, H. H. Brustle, and J. G. Anderson are all with the General Electric Company, Pittsfield, Mass.

The authors acknowledge the direction and encouragement of J. H. Hagenguth, R. T. Walters, J. R. Meador, and M. E. Scoville, and also the assistance of their many associates in obtaining the data reported in this paper.

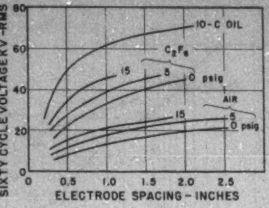

Fig. 1 (left). Comparison of corona-starting levels of a rod-to-plane gap in several insulating media and at various pressures

Fig. 3 (right). Comparison of 60-cycle and impulse corona-starting levels of a 1/2-inch-diameter sphere-to-plane gap

A—In air, for both 60-cycle and impulse levels
B—In oil, 60-cycle level
C—In oil, impulse level

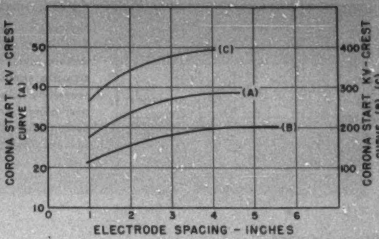

shorter mean-free-path between molecules. Roughly for the same reason corona inception or starting levels are higher in liquids. These influencing factors are illustrated in Fig. 1 by comparing the corona-starting levels in several insulating media at various gas pressures. Ionization in liquids is generally so intense that, except for highly divergent fields, once it starts it usually results in a complete breakdown of the gap unless arrested by a solid insulating barrier. This is also true in some cases for gases at high pressures, low spacings, or in fairly uniform electric fields.

Of the many other factors that influence the inception of corona, electrode configuration is one of the most evident. For example, it is commonly known that a sharper or smaller electrode gives a higher voltage gradient per unit applied voltage and, therefore, its corona-starting level is lower than that of a smoother or larger electrode. This can be demonstrated by an experiment conducted on three 3/4-inch-diameter rod-to-plane gaps in oil. The ends of the rods were hemispherical, flat with 1/8-inch radius edge, or flat with a sharp edge. As would be expected, the hemispherical rod, producing the least divergent field, had the highest corona-starting voltage and the sharp-edge electrode had the lowest. The ratios of the 60-cycle corona-starting levels for the three rods were 1.8, 1.5, and 1.0 respectively.

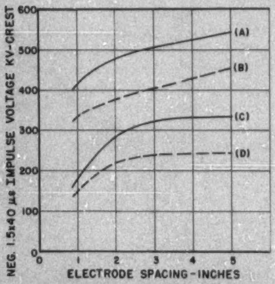

Fig. 2. Comparison of corona-starting levels of a sphere gap (A) and a rod gap (C) with sphere-to-plane (B) and rod-to-plane (D) gaps in 10-C oil

It is not always recognized, however, that the corona-starting voltage for a given electrode-to-plane configuration is lower than for a symmetrical configuration of the given electrode at the same spacing. That this is true is shown in Fig. 2. Here the impulse corona-starting levels of a sphere gap and a rod gap are compared with those levels for a sphere-to-plane and rod-to-plane configuration respectively. When the electrostatic fields of the two types of gaps are considered, it becomes apparent that the corona-starting level of the electrode-to-plane gap should be lower because the voltage gradient at the electrode is higher.

Voltage wave shape and frequency are other factors commonly spoken of as influencing the inception of corona. Yet when it is considered that the formative time of corona is only of the order of 1 microsecond or less, it is evident that the corona-starting level should be independent of the form of voltage as long as its duration is longer than microseconds. In many cases this is true, of course, as illustrated by curve *A* of Fig. 3 which shows that the corona-starting levels of both 60-cycle and 1.5x 40-microsecond impulse waves are the same for a 1/2-inch sphere-to-plane gap in air. This has also been found to be true for certain types of dry-type capacitors[20] for which the corona-starting level is independent of frequency from 60 cycles to 500,000 cycles at least.

However, there are conditions under which frequency and voltage wave shape have a decided effect upon corona inception. For example, if the 1/2-inch sphere-to-plane gap mentioned previously is tested in an oil medium, the 60-cycle corona inception is found to be considerably lower than the impulse corona inception. This effect is illustrated in curves *B* and *C* of Fig. 3 and is presumably explained by precorona space charge which has sufficient time to form on the slowly varying 60-cycle wave but not on the short-duration impulse wave. The assumption that the low 60-cycle corona inception is due to space charge can be speculated from another observation. It was noticed during the oscillographic study of 60-cycle corona in this gap that corona occurred at a lower voltage in the positive half-cycle than in the negative half-cycle. This implied that there must have been an excess of one polarity charge resulting in an additional field surrounding the sphere, so that the resultant field during the positive half-cycle was higher than that during the negative half-cycle.

One other well-known but important factor which influences the inception of corona is the placing of solid insulation in a gaseous or liquid gap. As predicted by classical field theory, the solid insulation, having a higher dielectric constant than that of gases and most liquids, produces a more intense electric field in the surrounding medium. This results in a corona-starting level lower than that for the corresponding all-gas or all-liquid case. Obviously, the higher the dielectric constant, the more pronounced is this effect.

Table I. Reduction of Corona-Starting Voltage of Insulation After 1-Minute Corona Exposure at Approximately $2^1/_2$ Times the Corona-Starting Voltage

	Corona-Starting Voltage, Kv Rms		
Sample	Initial	Immediately After Corona Exposure	Per-Cent Reduction
Paper	21.0	12.5	40.4
Paper	18.0	13.5	30.5
Paper	23.0	15.0	34.7
Paper	21.0	15.0	28.5
Mylar	21.0	12.0	42.9
Mylar	23.0	10.0	56.5
Mylar	22.0	12.0	45.4

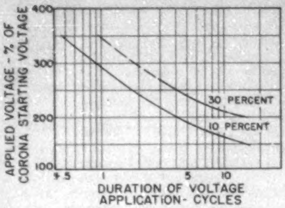

Fig. 4 (left). Per-cent reduction in corona-starting levels of capacitor samples caused by various overvoltages and durations of voltage application

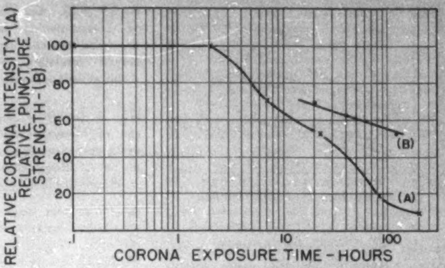

Fig. 6. Corona exposure time versus relative corona intensity (curve A) and relative puncture strength (curve B)

Corona Damage

In good design, corona can be avoided at both operating and test levels; however, there are frequent cases where corona damage is of interest to developmental engineers. Corona damage to solid insulation manifests itself in various ways. The more obvious indications are the physical surface eruption produced by electronic and ionic bombardment, and the charring of organic insulations resulting from the heat produced by the recombination processes. In many cases there are also long-range chemical effects brought about by the formation of acid-producing compounds.

There are also electrical manifestations of corona damage. For example, a reduction in corona-starting level frequently results from subjecting an insulating structure to voltages above its corona level. Table I shows such a reduction for a number of samples of oil-impregnated paper and Mylar (Dupont trade name) insulation tested between square-edged electrodes. These samples were subjected to a 1-minute voltage application at about $2^{1}/_{2}$ times the corona-starting voltage. The reduction in corona-starting voltage ranged from about 30 to 60 per cent.

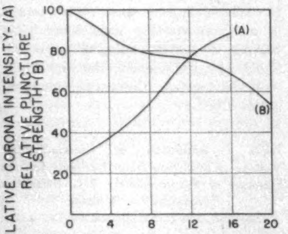

Fig. 5. Growth of corona intensity with time and corresponding reduction of puncture strength of damaged pressboard in oil

A—Pressboard between a 1/4-inch-diameter spherical electrode and a large grounded sphere

B—Puncture strength of damaged pressboard tested with a pair of $1^{3}/_{4}$-inch disk electrodes

To produce a given reduction in corona-starting level of a specific test arrangement, higher overvoltages are generally necessary for shorter durations of corona exposure. This can be illustrated by the capacitor data of Fig. 4 in that a 10-per-cent reduction of the 60-cycle corona-starting level requires a 150-per-cent overvoltage for 15 cycles whereas a 350-per-cent overvoltage is required for a 1/2-cycle wave.

Changes in corona intensity also are often an indication of damage. The changes, however, might be in either direction depending entirely upon the test conditions. For instance, the intensity of corona in oil-solid structures generally increases with the corona exposure time, even in a few minutes, as illustrated by curve *A* of Fig. 5. The increase in intensity is probably due to the continuous gas generation and surface damage caused by the corona impinging on the cellulose insulation. On the other hand, the intensity of corona in a small air gap adjacent to a sheet of silicone-treated glass cloth did not increase after many hours of corona bombardment. Actually, a substantial decrease was noted in some cases, as seen in Fig. 6. This decrease must be related to a change in the surface condition of the insulation during the time of corona exposure.

The most drastic effect produced by corona damage, of course, is a reduction in dielectric strength. The effect is especially pronounced when the corona intensity is high. Curve *B* of Fig. 5 shows a 50-per-cent strength reduction of pressboard after a 20-minute corona exposure. The extent of damage prior to breakdown is shown in Fig. 7. Severe fiber eruption is seen in the central light-color region while the dark pattern is the extended surface trackings. A reduction of dielectric strength was also noted for the glass cloth previously described, as shown in curve *B* of Fig. 6. In that case, however, the damage was probably of a microscopic or a chemical nature since no physical eruption of the surface was observed.

The foregoing is only a limited discussion of the subject of corona damage. Other measurements such as power factor and capacitance of insulation structures, which are in many cases related to corona damage, might also be used as a criterion of the inception of insulation damage.

Corona Measurements

Since ionization is always associated with emission of light, thermal expansion, and redistribution of charges in the electric circuits, corona can be detected visually, aurally, or by means of electrical

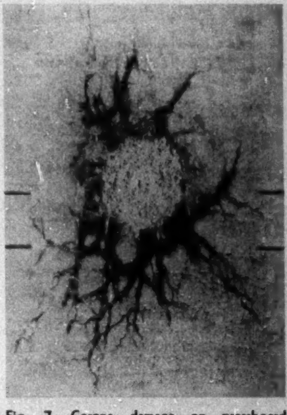

Fig. 7. Corona damage on pressboard causing a 50-per-cent reduction of dielectric strength

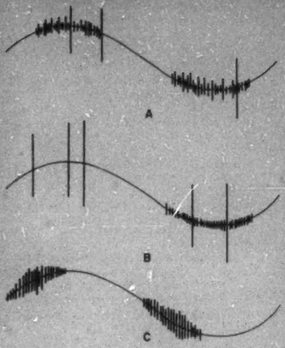

Fig. 8. Typical corona patterns on cathode-ray oscilloscope

A—Void and oil (large pulses) corona
B—Small diameter lead corona in air and oil (large pulses) corona
C—Corona in capacitor samples

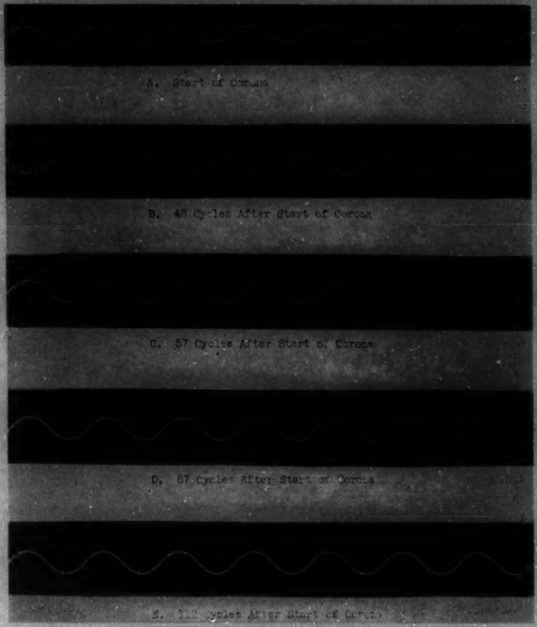

Fig. 9. Continuous time record of oscilloscopic indications of corona impinging on a pressboard barrier in a rod-to-plane gap in oil

measurements. However, when the corona is confined and cannot be viewed or heard or when quantitative data are desired, then the electrical method is the only means of corona measurement.

It has been known that corona pulse detection using oscilloscopic techniques offers several advantages over some other electrical methods such as meter measurements. By proper interpretation of corona pulses and patterns on the oscillograph screen it is possible in some cases to differentiate corona occurrences in different media[23] and to predict corona damage to insulation.[24] However, this usually requires an experienced operator who can identify with assurance the various types of corona occurring in a test sample as well as those occurring externally, whereas an inexperienced one might be in doubt. For instance, corona occurring in an oil-solid composite insulation with some air voids trapped in the solid might appear in the following manner and sequence. As the voltage applied to the sample is increased, a band of relatively low magnitude void corona pulses usually sets in at a lower voltage level than the relatively high intensity oil corona. The magnitude of the void corona, being confined, does not increase very much with subsequent increase in the applied voltage whereas the oil corona pulses, in general, increase very rapidly with voltage. On the other hand, the number of oil corona pulses does not increase as rapidly as the number of void corona pulses and they are much more random in phase relation with the applied voltage as shown in Fig. 8(A). These oil corona pulses are often confused with positive polarity streamers emanating in air from some part of the high-voltage test circuit, except the latter invariably occur at the crest of the applied voltage wave.

In another case, when small wire is used as connecting leads in the detection of oil corona in structures of the very-high-voltage class,[23] the corona pattern is somewhat different than that in the previous case. As the applied voltage is increased, a band of relatively low magnitude lead corona again sets in at a lower voltage level than the oil corona, but is very definitely confined only in the negative half-cycle of the applied wave. Like void corona, this type of corona increases very slowly with increasing voltage, even as high as several hundred kilovolts. Thus, when oil corona starts in the sample the corona pattern might look like that shown in Fig. 8(B). It is this familiar pattern that makes corona detection feasible at such high test voltages without an elaborate corona-free setup.[23]

Another familiar pattern is often found in the detection of corona in liquid-impregnated capacitors. Because of the heavy space charges produced at the edge of the foil electrodes during corona in each half-cycle, the corona generally extends from approximately the voltage zero to the voltage peak of the next half-cycle. This pattern is shown in Fig. 8(C). The intensity of this type of corona increases rapidly with a slight increase of voltage, thus giving another means of identification.

The patterns just described are those observed using a repetitive sweep on the oscilloscope. In those cases where a sequential distribution of corona pulses from cycle to cycle is of interest, a continuous time record of the phenomenon is necessary. Such a record, shown in Fig. 9, reveals the gradual increase of the number of corona pulses as voltage is continuously increased on a rod-to-plane gap with a barrier present. Although

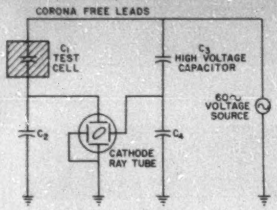

Fig. 10. Special high-voltage capacitance bridge for measuring space charge in oil

intermittent corona pulses are clearly shown in the early part of this record, they would appear quite continuous on a repetitive sweep. Interesting also is the fact that the first pulse occurs at the voltage peak, but successive pulses occur randomly over the cycle, even at voltage zero. Thus, this oscillographic method indicates that each corona pulse left sufficient postcorona space charge in the oil gap and on the barrier to modify seriously the formation of subsequent discharges.

In some cases, an oscillographic technique can also be used to study the formation of precorona space charge in liquids under high stress. Space charge in a dielectric between two plates is indicated by a change in capacitance or, in the case of the continuous separation of charge, by a flow of charge of low magnitude in the external circuit. This charge cannot be detected by a conventional pulse-type corona detector. However, with a special type of high-voltage capacitance bridge, as shown in Fig. 10, space charge production at rates as low as 100 micromicrocoulombs per second can be easily observed. This corresponds to currents of 10^{-10} ampere.

The bridge consists of three capacitance arms with all appreciable leakages either minimized or guarded out, and a fourth test cell arm having various electrodes immersed in oil. The very high leakage resistance cannot bleed off precorona space charge as fast as it is formed, permitting both rapid and slowly varying space charge measurements to be made. The rapid variation appears as distortion of the Lissajous figure on the oscilloscope, whereas slow, continuous production of charge causes the figure to drift on the screen due to the charging of capacitor C_1.

In one particular set of tests the test cell was fitted with a point-to-plane gap and filled with transformer oil. An application of high voltage resulted in the formation of a Lissajous figure on the cathode-ray tube screen as shown in trace 1 of Fig. 11(A). The area enclosed by this trace was proportional to the power loss in the test cell, the other arm of the bridge being practically lossfree. As the applied voltage was increased to about 7 kv, the figure began to drift slowly downward on the screen, indicating the steady formation of positive polarity space charge in the cell. As breakdown was approached, the figure began to open up drastically (trace 3), indicating a pronounced increase of power loss as well as space charge formation just prior to breakdown.

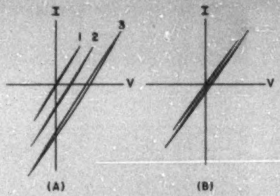

Fig. 11. Lissajous figures showing various amounts of space charge and power loss in oil under different test conditions

A—Point-to-plane gap
B—Rogowski (uniform-field) gap

When the point-to-plane electrode assembly was replaced with two uniform field Rogowski electrodes, this space charge effect appeared to be of either polarity and greatly reduced in magnitude, as shown in Fig. 11(B). In many cases, no space charge formation could be observed prior to breakdown, and no drastic increase in power loss below breakdown ever occurred. Hence, one would conclude that space charge formation may well be of most importance to the breakdown process in the nonuniform field case. Quantitative data on this phenomenon must await further study.

Summary

Many of the essential problems of corona inception and insulation damage have been discussed. The effects of materials, electrode configuration, space charge, and other factors have been shown to be of great importance. In practice, the complexity of these factors and their interactions necessitate further research work for some time to come, but, by a concerted approach, the fundamental laws are being determined.

References

1. High Voltage Power Transmission, C. F. Scott. *AIEE Proceedings*, vol. 15, 1898, p. 531.

2. Electric Strength of Air, J. B. Whitehead. *Ibid.*, vol. 29, 1910, pp. 1059–87.

3. The Law of Corona and Dielectric Strength of Air—II, F. W. Peek, Jr., *Ibid.*, vol. 31, Jan.–June 1912, pp. 1085–1126.

4. Brush Discharge, E. H. Cook. *Philosophical Magazine*, London, England, vol. 47, 1899, pp. 40–57.

5. Point Discharges, E. Warburg. *Annalen der Physik*, Leipzig, Germany, vol. 2.2, 1900, pp. 295–316.

6. The Theory of the Glow Discharge from Wires, J. S. Townsend. *Electrician*, London, England, vol. 71, 1913, pp. 348–50.

7. Corona and Spark Discharge in Gases, J. D. Stephenson. *Journal*, Institution of Electrical Engineers, London, England, vol. 73, 1933, pp. 69–83.

8. Transition from Corona Discharge to Spark in Non-Uniform Field, M. Suzuki. *Journal*, Institution of Electrical Engineers of Japan, Tokyo, Japan, vol. 56, 1936, pp. 755–60.

9. Elektrische Gasentladungen (book), A. Von Engel, M. Steenbeck. Julius Springer, Berlin, Germany, 1934.

10. Fundamental Processes of Electrical Discharge in Gases (book), L. B. Loeb. John Wiley and Sons, Inc., New York, N. Y., 1939.

11. Electrons in Gases (book), J. S. Townsend. Hutchinson, 1948.

12. Electrical Breakdown of Gases (book), J. M. Meek, J. D. Craggs. Oxford University Press, London, England, 1953.

13. Elektrische Funkenspannungen (book), M. O. Jorgensen. E. Munksgaard, Copenhagen, Denmark, 1943.

14. Effect of Corona Discharge on Liquid Dielectrics, Joseph Sticher, D. E. F. Thomas. *AIEE Transactions*, vol. 58, 1939, pp. 709–22.

15. Impulse Ionization and Breakdown in Liquid Dielectrics, G. M. L. Sommerman, C. J. Butte, E. L. C. Larson. *Ibid.*, vol. 73, pt. II, May 1954, pp. 147–55.

16. Laws of Corona and Spark-over in Oil, F. W. Peek, Jr. *General Electric Review*, Schenectady, N. Y., vol. 18, 1915, pp. 821–27.

17. Ionization Phenomenon in Cable Dielectrics, L. Henstschel. *Elektrische Betrieb*, Halle, Germany, vol. 23, 1925, pp. 292–94.

18. Corona Discharge on Alternators, R. H. Parsons. *Electrical Times*, London, England, vol. 87, 1935, p. 460.

19. The Effect of Corona on Solid Insulating Materials, A. M. Thomas. *Journal*, Institution of Electrical Engineers, London, England, vol. 91, pt. II, 1944, pp. 549–62.

20. Physical Concepts of Corona in Capacitors, J. R. Nye, W. R. Wilson. *AIEE Transactions*, vol. 72, pt. III, Aug. 1953, pp. 781–87.

21. Development of Corona Measurements and Their Relation to the Dielectric Strength of Capacitors, R. J. Hopkins, T. R. Walters, M. E. Scoville. *Ibid.*, vol. 70, pt. II, 1951, pp. 1643–51.

22. Detection et Etude de l'Ionization dans les Dielectriques Industriels, M. F. Viale. *Revue d'Electricite de Mecanique*, Paris, France, vol. 96, 1954, pp. 28–40.

23. Detection of Corona in Oil at Very High Voltages, T. W. Liao, J. S. Kresge. *AIEE Transactions*, vol. 73, pt. III-B, Dec. 1954, pp. 1389–95.

24. Impulse Corona—Detection, Measurement of Intensity, and Damage Produced, J. H. Hagenguth, T. W. Liao. *Ibid.*, vol. 71, pt. III, Jan. 1952, pp. 461–65.

◆

Discussion

E. H. Coxe (Ethyl Corporation, Baton Rouge, La.): At our company we have had an experience which illustrates some of the things the paper points out about corona.

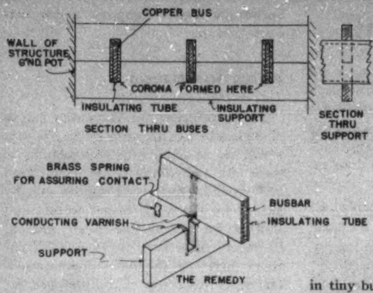

Fig. 12. Corona elimination on 13.8-kv switchgear bus supports

We operate 13.8-kv indoor metal-clad switchgear, the busses of which are supported as shown in Fig. 12. We found that corona was forming in the air gaps between the slots in the supporting members and the tubes which surround the bus conductors. This corona discharge could be heard, and it could be seen when the bus room was darkened. It was found, in some places, to have eaten halfway through the bus insulating tubes.

As the manufacturer reported no similar trouble at other locations, he pointed out that it was probably due to lowered breakdown voltage of air at our location because of high humidity and air contaminants. His recommendation was that we dry and purify the air. This would have been impossibly expensive so it was necessary to find another method of suppressing the corona.

Obviously, if there is no voltage across the air gap, there can be no corona. We eliminated the voltage by coating both surfaces with a conducting paint and connecting these coated surfaces together with a metal spring clip. The result was no more corona, even when we applied twice normal voltage to the busses. Somewhat to our surprise we were awarded a patent on this new application of a previously well-known principle.

T. W. Dakin (Westinghouse Electric Corporation, East Pittsburgh, Pa.): This paper describes some of the nature of corona and its effect on insulation much of which is in confirmation with the experience and published work of this discusser and his colleagues.[1,2] (Further valuable references in this field can be found in the bibliography of reference 1.) It is not made clear in the paper that the observed corona in mineral oil is largely influenced by the amount of the degassing of the electrodes following immersion. If the data reported by the authors were obtained with electrodes which were not degassed following immersion, the observed corona was merely a discharge in tiny bubbles at the surface. It then can be considered as air corona with the electric field increased by the higher dielectric constant of the oil in series with the bubbles.

In a recent conference paper I described a mechanism whereby the corona discharges in tiny bubbles in oil produces decomposition of the oil to gas (mostly hydrogen) which causes the bubble to grow and the corona to increase in magnitude. The increasing corona with time shown by Fig. 9 of the paper is in agreement with this mechanism. In my conference paper, it was also suggested that, in the absence of initial gas bubbles, electron field emission at points caused formation of gas so that tiny bubbles develop in time.

REFERENCES

1. Effect of Electric Discharges on the Breakdown of Solid Insulation, T. W. Dakin, H. M. Philofsky, W. C. Divens. *AIEE Transactions*, vol. 73, pt. I, May 1954, pp. 155–62.

2. Impulse Dielectric Strength Characteristics of Liquid-Impregnated Pressboard, T. W. Dakin, C. N. Works. *Ibid.*, vol. 71, pt. I, Nov. 1952, pp. 321–25.

F. S. Oliver (Doble Engineering Company, Belmont, Mass.): The authors, by exploring corona effects in oil and composite insulations, have added to the knowledge of the art in this field. However, there are a few cases where further amplification would be helpful.

One of these occurs when the authors state that in good design corona can be avoided at both operating and test levels. This is not always feasible, and furthermore is not always necessary. Field tests on a great many large high-voltage mica-insulated generators have shown that corona is always present at the operating voltage. At the present time it does not appear economically feasible to construct a corona-free generator. The important consideration is whether the corona present is producing insulation damage which may eventually result in failure. A well-designed generator thus is one in which the corona does not produce insulation damage. On the other hand, with rubber and other composite materials it is necessary to have practically no corona if insulation damage is to be avoided.

The authors have shown that in some cases relative corona intensity may decrease with continued application of voltage even though the breakdown strength has decreased. We have noted in similar instances a corresponding increase in power factor and would like to ask the authors if they have had similar experience.

We would also like to ask if the authors have investigated to see if the lowering of the corona starting voltage by an application of overpotential still persists after a "rest" period at zero potential or even at normal voltage.

T. W. Liao, J. R. Nye, H. H. Brustle and **J. G. Anderson:** Mr. Coxe's discussion has brought out a practical solution to a practical problem. Such application, although it is based on a previously well-known principle, is just what we hope to see more of to enrich the applied technology on the subject of corona.

Dr. Dakin has brought out an interesting and delicate question on the mechanism of initial discharges in oil. The degassing process following immersion is a sure way of eliminating tiny bubbles at the electrode surface. It is, however, much more complicated than using deaerated oil or merely depending on a long immersion time. Although all should accomplish the same end, there is still a possibility that bubbles would form in the presence of some nuclei in oil under electrical stress. This is also recognized by Dr. Dakin and has been the basic assumption of the gaseous theory of liquid breakdown.

In the test given in the paper, the electrode was kept in oil throughout the test and no degassing process was used. Corona started at about 50 kv (rms) or approximately at a maximum surface gradient of 400 kv (rms)per inch. It is felt that if bubbles were present, corona would have started at a lower applied voltage. Actually, corona was visible in the oil space between the electrode and the pressboard. However, it could originate from bubbles developed due to field emission as suggested by the discusser. In the experiment no attempt was made to measure the field emission current.

We agree with Mr. Oliver that for certain apparatus which is not liquid filled and with cellulose insulation it is not economically feasible at present to have a corona-free design. The point is well taken.

We have frequently measured power factor along with corona measurements. In general, power factor increases with the applied voltage above corona inception. However, in most cases the corona intensity also increases with it. In the case of silicone glass cloth where the corona intensity decreased with a continuous application of voltage, the power factor went up, confirming the observation made by Mr. Oliver. However, in a similar test with another silicone-treated material, the power factor decreased with decreasing corona intensity.

The lowering of corona starting voltage by an application of overpotential may or may not persist after a "rest" period. For instance, when corona trackings are found, a rest period usually does not help. On the other hand, when corona produces minute gas bubbles in an oil-impregnated insulation, a rest period of an hour or so would restore the corona starting voltage to its original value. In such cases, a rest period at a reduced voltage is frequently more effective than at zero voltage, since a light agitation of oil under stress often helps to drive the gas bubbles back to the oil.

ORACLE Computes Line Constants With Tensors

R. BRUCE SHIPLEY
MEMBER AIEE

MARTIN HOCHDORF
ASSOCIATE MEMBER AIEE

MARJORIE WATSON
NONMEMBER AIEE

EXPANSION of the Atomic Energy Commission installations at Oak Ridge and other power requirements in the region necessitated the construction of Tennessee Valley Authority's 1,440,000-kw Kingston Steam Plant. A very large part of this capacity will be transmitted to the Atomic Energy Commission project over six parallel 161-kv transmission lines, each approximately 10 miles long. For physical and economical reasons, the lines are on the same right of way. It was not practical to construct the lines electrically symmetrical nor physically identical in length because of line terminations. Two types of construction were used, single circuit with two ground wires for 8 miles and double circuit with one ground wire per circuit for 2 miles. A seventh line with two ground wires is on the same right of way for 3 miles of the single-circuit section, but this line has no common terminal with the other six lines.

The major technical problems that arose in the analysis of these circuits were: Would electrical and physical dissymmetry cause sufficient power current unbalance among the conductors to reduce appreciably their total current-carrying capacity? If so, could this be corrected by changing the phasing on the individual circuits? Could a zero-sequence equivalent circuit be derived to permit accurate application, settings, and analysis of ground relays?

The Oak Ridge National Laboratory agreed to provide time on its high-speed digital computer, the ORACLE, to solve this problem, because the Atomic Energy Commission is interested in the operation of these lines. Since computer time is at a premium, it was decided to determine equivalent circuits that might be used on a network analyzer. These equivalent circuits are:

1. A circuit that represents the 18 power conductors for the six parallel lines. The three conductors for the seventh line are ignored because a circuit including them would require a prohibitive number of mutual transformers. The derived equivalent circuit has 19 terminals and requires no mutual transformers. One terminal is common to all conductors. Thus, balanced 3-phase voltages of the proper magnitude can be applied to the equivalent circuit and the relative distribution of currents determined. This circuit has the same form as the equivalent circuit in Fig. 7(B) and is not shown.
2. A zero-sequence equivalent circuit of the seven lines with independent terminals for use on the a-c network analyzer. This circuit is shown in detail.
3. A zero-sequence equivalent circuit of the six parallel lines with a common terminal that can be used on a d-c network analyzer. This circuit is also shown in detail.

The basic data for the problem are the impedances derived from the physical design of the lines. The self-impedance for each conductor and each ground wire and the mutual impedances between them were computed. These data consist of 1,681 complex numbers and are too voluminous to be included here. Fig. 1 shows how the single-circuit section is arranged. Fig. 2 shows the double-circuit section.

Tensor analysis[1] was chosen as the method of approach because it offers an excellent method for interchanging data between a digital computer and a network analyzer.

Matrix Arrangement

The impedances for the entire length of the conductors are arranged in a matrix which has as many rows and columns as there are individual power conductors and ground wires. One matrix can be formed for the single-circuit section and another for the double-circuit section. However, these two matrices are combined here to facilitate computation. The rows from top to bottom are assigned successively to the impedances of the conductors, one row for each power conductor and one for each ground wire. The columns from left to right are similarly assigned and in the same order. There are 41 rows and 41 columns in the matrix.

The row established for one conductor intersects the column for the same conductor in the element which is its self-impedance. Each diagonal element represents the self-impedance of one conductor. The self-impedance with earth return of *A* phase of the line that has no common terminal is the upper left element of the matrix. The self-impedance with earth return of *B* phase of this line is placed in the second diagonal element position, etc., until the first 21 diagonal positions are assigned to the self-impedances of the power conductors. While a different arrangement can be used, this order of assignment of power conductors facilitates interpretation of results.

No mutual impedance exists between the ground wires of the single-circuit section and the ground wires of the double-circuit section. The self-impedances of the ground wires in each group are consecutive diagonal elements. This arrangement reduces computing time. The self-impedance of each ground wire with earth return is placed in the matrix just as is that of a power conductor.

All nondiagonal elements of the matrix are mutual impedances. The row for one conductor intersects the column for another in the element which is the mutual impedance of these two conductors.

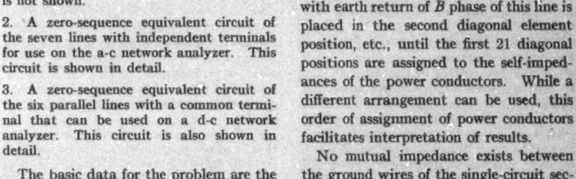

Fig. 1. Single-circuit section, seven parallel lines

Paper 55-478, recommended by the AIEE Transmission and Distribution Committee and approved by the AIEE Committee on Technical Operations for presentation at the AIEE Summer General Meeting, Swampscott, Mass., June 27–July 1, 1955. Manuscript submitted March 28, 1955; made available for printing May 12, 1955.

R. Bruce Shipley, Martin Hochdorf, and Marjorie Watson are with the Tennessee Valley Authority, Chattanooga, Tenn.

The computation was done at the Oak Ridge National Laboratory, which is operated by Carbide and Carbon Chemicals Company, a division of Union Carbide and Carbon Corporation. The authors wish to express their appreciation to Dr. R. A. Charpie, Assistant Director of Research of the Laboratory, for accepting the problem for solution on the ORACLE; to Dr. A. S. Householder, Chief of the Mathematics Panel, under whose direction and with whose encouragement the work was performed; to other members of the Panel for their active interest; and, particularly, to Miss M. R. Arnette for enthusiastically contributing her skill and computing knowledge to complete the problem.

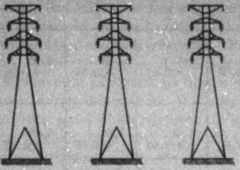

Fig. 2. Double-circuit section, six parallel lines

There are two such intersections. Since the mutual impedances are bilateral, the values are the same in the two positions. Each mutual impedance is calculated using a common earth return and as if only the two conductors exist. All of the elements of the matrix are complex numbers, some of which are zero.

Matrix Operations

When the last 20 rows and 20 columns, corresponding to the ground wires, are eliminated by Kron's method,[2] the resulting 21 by 21 matrix will then contain the self- and mutual impedances of the power conductors as modified by the ground wires. A set of 21 power conductors with these new design constants would perform in exactly the same manner as the original group of power conductors and ground wires. Thus, a major simplification is effected.

There are variations of the method used for eliminating rows and columns of a matrix. One method is to partition the original matrix into four parts, which separate the power conductors, the ground wires, and the mutual impedances between power conductors and ground wires. This partitioning is shown in Fig. 3 with the parts of the matrix labeled. Then the desired result can be accomplished by performing the following operations

$$Z = Z_1 - Z_2 Z_4^{-1} Z_3 \qquad (1)$$

This method requires taking the inverse of a 20 by 20 matrix whose elements are complex numbers. Due to the limited storage capacity available on the ORACLE, the matrix was partitioned further as shown in Fig. 4.

Since Z_4 is in diagonal form when compounded as shown in Fig. 4, the following matrix operations were performed by the computer

$$Z = Z_1 - DG^{-1}H - AF^{-1}B \qquad (2)$$

This procedure made it possible to invert a 14 by 14 matrix and a 6 by 6 matrix with complex elements rather than the larger 20 by 20 matrix.

The matrix Z may be used in a number of ways to obtain different results. It can be operated upon by Kron's sequence tensor[3] to yield all of the symmetrical component impedances of the circuits and any mutual impedance that exists between the sequence networks. However, only the zero-sequence equivalent circuit was obtained, because the mutual impedances between the sequence networks are small and because they cannot be used conveniently on an a-c network analyzer.

21 by 21 Z_1 Self and mutual impedances of power conductors.	21 by 20 Z_2 Mutual impedances between power conductors and ground wires.
20 by 21 Z_3 Mutual impedances between power conductors and ground wires.	20 by 20 Z_4 Self and mutual impedances of ground wires.

Fig. 3. Partitioning of impedance matrix

Equivalent Circuits

A connection tensor is required to transform Z into the zero-sequence impedance tensor from which an equivalent circuit is determined. This connection tensor is formed by considering the three conductors of each power circuit paralleled at one end and grounded at the other. Since seven circuits are involved,

21 by 21 Z_1	21 by 14 A	21 by 6 D
14 by 21 B	14 by 14 F	14 by 6 0
6 by 21 H	6 by 14 0	6 by 6 G

Fig. 4 (left). Final partitioning of impedance matrix

Z_1 = self- and mutual impedances of power conductors
A = mutual impedances between power conductors and ground wires in single-circuit section
D = mutual impedances between power conductors and ground wires in double-circuit section
B = mutual impedances between ground wires in single-circuit section and power conductors
F = self- and mutual impedances of ground wires in single-circuit section
H = mutual impedances between ground wires in double-circuit section and power conductors
G = self- and mutual impedances of ground wires in double-circuit section
0 = no mutual impedance between ground wire groups

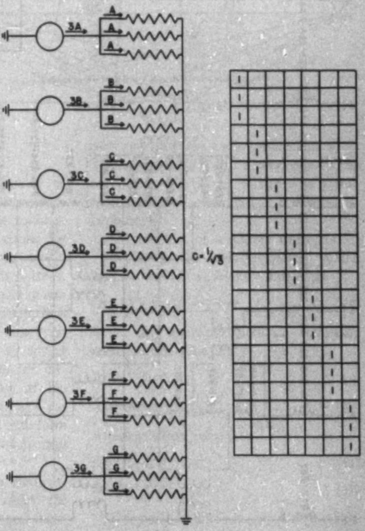

Fig. 5 (right). Transformation tensor

seven independent variable currents are assigned. The currents in the three phases of any one power circuit are assumed to be the same in magnitude and angle. The power circuits and the transformation tensor *C* are shown in Fig. 5. The operation

$$C_t Z C = Z'' \tag{3}$$

determines a 7 by 7 matrix containing the zero-sequence self- and mutual impedances for each of the seven lines.

The numerical results are shown in Fig. 6(A) where the main diagonal elements are zero-sequence self-impedances of the circuits and the nondiagonal elements are mutual impedances between them. Fig. 6(B) shows the derived zero-sequence equivalent circuit for use on the a-c network analyzer. This form retains independent terminals for each power circuit, and all impedances are positive for these circuits.

A zero-sequence equivalent circuit that does not require mutual transformers is derived in the following manner for the six power circuits which terminate on a

Line	1	2	3	4	5	6	7
1	2.30 +j6.94	1.78 +j2.05	1.64 +j1.29	1.52 +j0.90	1.41 +j0.67	1.32 +j0.54	1.25 +j0.49
2	1.78 +j2.05	7.01 +j19.69	5.65 +j7.66	5.23 +j4.66	4.91 +j3.50	4.51 +j2.66	4.24 +j2.38
3	1.64 +j1.29	5.65 +j7.66	7.22 +j19.03	5.64 +j6.43	5.27 +j4.36	4.82 +j3.15	4.50 +j2.71
[Z"] = 4	1.52 +j0.90	5.23 +j4.66	5.64 +j6.43	7.17 +j18.43	5.68 +j6.90	5.19 +j4.33	4.81 +j3.53
5	1.41 +j0.67	4.91 +j3.50	5.27 +j4.36	5.68 +j6.90	7.15 +j18.39	5.53 +j6.38	5.10 +j4.68
6	1.32 +j0.54	4.51 +j2.66	4.82 +j3.15	5.19 +j4.33	5.53 +j6.38	6.97 +j18.50	5.40 +j7.52
7	1.25 +j0.49	4.24 +j2.38	4.50 +j2.71	4.81 +j3.53	5.10 +j4.68	5.40 +j7.52	6.66 +j19.21

Fig. 6(A) (above). Zero-sequence impedance tensor for seven parallel lines

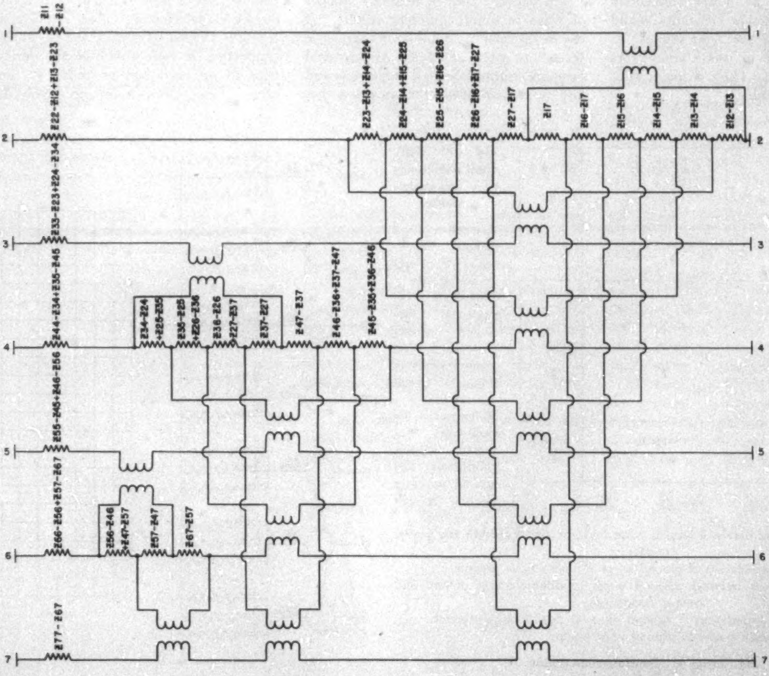
1
2
3
4
5
6
7
Z11-Z12
Z22-Z12+Z13-Z23
Z33-Z23+Z24-Z34
Z44-Z34+Z35-Z45
Z55-Z45+Z46-Z56
Z66-Z56+Z57-Z67
Z77-Z67
Z23-Z13+Z14-Z24
Z24-Z14+Z15-Z25
Z25-Z15+Z16-Z26
Z26-Z16+Z17-Z27
Z27-Z17
Z17
Z16-Z17
Z15-Z16
Z14-Z15
Z13-Z14
Z12-Z13
Z34-Z24+Z25-Z35
Z35-Z25+Z26-Z36
Z36-Z26+Z27-Z37
Z37-Z27
Z47-Z37
Z46-Z36+Z37-Z47
Z45-Z35+Z36-Z46
Z56-Z46+Z47-Z57
Z57-Z47
Z67-Z57

Fig. 6(B) (left). Zero-sequence equivalent circuit for seven parallel lines with independent terminals

common bus. The first row and column of Z'' is omitted and the inverse of the remaining 6 by 6 matrix is computed. Fig. 7(A) shows the inverse of the matrix. The equivalent circuit for six lines is determined from this inverse. It has seven terminals, six of which represent the line terminals and the seventh represents the common terminal. The admittance between any line terminal and the common terminal is equal to the sum of the admittances in a particular row of the inverse matrix. The admittance between any pair of line terminals is equal to the negative of the mutual admittance between these lines. The corresponding impedances are shown on the equivalent circuit in Fig. 7(B). If no significant negative resistances appear in the equivalent circuit, it may be used on the a-c network analyzer. If the power factors of the circuit impedances are similar, the equivalent circuit may be used on the d-c network analyzer. This equivalent circuit ignores the zero-sequence current in the line not terminating on the common bus.

Either of the equivalent circuits can be set up on the a-c network analyzer, from which the self- and mutual-impedances of the circuit can be read. The equivalent circuit in Fig. 6(B) is readily verified by tracing through the connections to obtain the correct self-impedance between the terminals of each line and the mutual impedances between pairs of lines.

[Y] =

Line	1	2	3	4	5	6
1	0.0097 -j0.0590	-0.0008 +j0.0227	0.0009 +j0.0075	0.0008 +j0.0045	0.0008 +j0.0032	0.0009 +j0.0033
2	-0.0008 +j0.0227	0.0100 -j0.0658	-0.0005 +j0.0167	0.0008 +j0.0062	0.0007 +j0.0036	0.0007 +j0.0032
3	0.0009 +j0.0075	-0.0005 +j0.0167	0.0100 -j0.0677	-0.0011 +j0.0199	0.0008 +j0.0063	0.0008 +j0.0046
4	0.0008 +j0.0045	0.0008 +j0.0062	-0.0011 +j0.0199	0.0100 -j0.0680	-0.0005 +j0.0171	0.0009 +j0.0077
5	0.0008 +j0.0032	0.0007 +j0.0036	0.0008 +j0.0063	-0.0005 +j0.0171	0.0103 -j0.0679	-0.0009 +j0.0234
6	0.0009 +j0.0033	0.0007 +j0.0032	0.0008 +j0.0046	0.0009 +j0.0077	-0.0009 +j0.0234	0.0097 -j0.0609

Fig. 7(A) (above). Inverse of zero-sequence impedance tensor with first row and column ignored. Lines are renumbered from 1 to 6

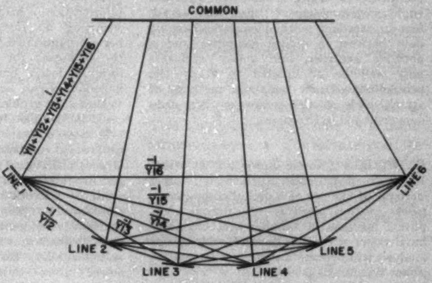

Fig. 7(B) (right). Zero-sequence equivalent circuit for six parallel lines with a common terminal. The impedances not labeled are determined in a manner similar to those shown

Computer Operations

In order to use existing subroutines for the ORACLE, the form of the matrix was changed to contain only real numbers. This representation may be derived from Ohm's law for an a-c circuit

$$(r+jx)(i+ji')=e+je' \tag{4}$$

The primed quantities are quadrature components. Equating real and imaginary terms

$$ri-xi'=e \tag{5}$$

$$xi+ri'=e' \tag{6}$$

These relations are expressed in matrix algebra by

$$\begin{bmatrix} r & -x \\ x & r \end{bmatrix}\begin{bmatrix} i \\ i' \end{bmatrix}=\begin{bmatrix} e \\ e' \end{bmatrix} \tag{7}$$

Each complex element, $r+jx$, in the matrix can be replaced by a matrix with two rows and two columns,[4] namely

$$\begin{bmatrix} r & -x \\ x & r \end{bmatrix}$$

An m by n matrix with complex elements becomes a $(2m)$ by $(2n)$ matrix with real elements. The results of operations on matrices in this form maintain the complex conjugate pattern, which provides an excellent check for computer accuracy. The computer can be programmed to check for this pattern.

The form described in the foregoing was used for the major part of the calculations performed on the ORACLE. However, a different scheme was used to invert the 18 by 18 matrix with complex elements. This was done because of the ORACLE's present limited storage capacity of 1,024 numbers. In real form this matrix would have required storage for 1,296 numbers.

Any matrix Z with complex elements can be expressed $Z=R+jX$, where the matrices R and X contain only real numbers and have the same dimensions as Z. The inverse of Z can be expressed in the form $Z^{-1}=Y=G-jB$, where G is a matrix of conductances and B is one of susceptances.

The product of a matrix times its inverse equals the identity matrix, which may be written as $I+j0$. Therefore

$$(R+jX)(G-jB)=I+j0 \tag{8}$$

From this multiplication the following relations are obtained

$$RG+XB=I \tag{9}$$

$$XG-RB=0 \tag{10}$$

whose solution gives

$$G=(R+XR^{-1}X)^{-1} \tag{11}$$

$$B=R^{-1}XG \tag{12}$$

This method made it possible to obtain

the real and imaginary parts of the inverse of the complex 18 by 18 matrix by performing two inversions, three multiplications, and one addition of real matrices. The necessity for inverting a 36 by 36 matrix was thereby avoided.

Since the entire problem was done intermittently over a considerable period of time, the over-all time required for its completion cannot be stated. The following machine times are representative. Inversion of an 18 by 18 matrix with real numbers required 12 minutes, that of a 6 by 6 matrix with complex elements (12 by 12 real), 7 minutes. Multiplication resulting in a 42 by 42 real matrix took approximately 1/2 hour while the time for multiplying two 18 by 18 real matrices required 5 minutes. All of these machine times are dominated by the time required for punching the results on paper tape. When, as is planned, magnetic tape output is made available on the ORACLE, the output time will be greatly reduced.

Conclusions

1. The combination of tensor analysis and a high-speed electronic digital computer provides an exact and practical method for the solution of difficult power circuit problems.

2. A zero-sequence equivalent circuit derived by this method permits accurate application, settings, and analysis for ground relaying.

3. The method presented is applicable for any number of circuits, irrespective of physical arrangement.

4. This method eliminates errors which would be introduced if simplifying assumptions were made to solve such a problem.

5. The zero-sequence equivalent circuits are obtained in a form that can be used on network analyzers.

6. Similar problems can be formulated by power engineers and sent to a computing center for actual solution, thereby avoiding an enormous amount of routine calculation.

References

1. TENSOR ANALYSIS OF NETWORKS (book), Gabriel Kron. John Wiley and Sons, Inc., New York, N. Y., 1939.

2. *Ibid.*, Chap. X.

3. *Ibid.*, Chap. XIII.

4. *Ibid.*, Chap. XXI.

◆

Discussion

Y. H. Ku (University of Pennsylvania, Philadelphia, Pa.): I should like to congratulate the authors for demonstrating the usefulness of C_tZC in solving important engineering problems. Tensor analysis offers an excellent method for interchanging data between a digital computer and a network analyzer, and young engineers may well be encouraged to study the possibilities of new tools and methods of attack such as the tensor method ably demonstrated in this paper.

G. W. Bills (North American Aviation, Inc., Downey, Calif.): Here is a fine example of the use of a digital computer in power system analysis. As digital computers increase in number and engineers have easier access to them, Kron's tensor analysis will become a more familar tool to power system engineers.

My curiosity was aroused by the statement, "Tensor analysis was chosen as the method of approach because it offers an excellent method for interchanging data between a digital computer and a network analyzer." Does this refer to the ease with which transformations can be made from one reference frame to another more suitable for analysis by an a-c network analyzer?

For transmission-line problems involving so many mutual impedances with the possibility of negative resistances appearing in the equivalents to be placed on an a-c network analyzer, it is possible that direct solutions of the entire problem could be more readily obtained on a digital computer than on a combination of computer and analyzer. At the Bonneville Power Administration, a load flow analysis technique requiring no inversion of matrices has been programmed for studies including up to 50 busses for the *IBM 650;* transformers, loads, line changing and mutual impedances can be accurately represented so that such problems as those in the paper could be completely solved digitally.

It now appears that digital computers can easily compete with a-c network analyzers with regard to power system problem and any group contemplating the purchase of an a-c network analyzer should carefully consider the possibility of obtaining a medium-priced general-purpose digital computer instead.

Incidentally, was there any noticeable power current unbalance among the conductors? At the Bonneville Power Administration we have never been able to observe an appreciable unbalance for such circuits.

R. B. Shipley, M. Hochdorf, and M. Watson: The authors wish to thank Mr. Ku and Mr. Bills for their favorable comments.

The statement which is quoted by Mr. Bills refers to 1. the method for formulating network problems on a digital computer, and 2. the fact that at different stages of the solution interchanges of data between an a-c network analyzer and a digital computer are possible (provided there are no negative resistances).

It is certainly possible to solve the complete problem on a digital computer. However, in this case the time available on the computer was limited. Consequently, the computer was used only for results that could not be ontained from our a-c network analyzer. The requirement of a large number of mutual transformers made it impossible to represent the individual power conductors and ground wires on the network analyzer. Also, as Mr. Bills expected, negative resistances did appear in the admittance matrix which necessitated the use of a computer to obtain power current division.

The currents did not divide equally between corresponding phases of the separate power circuits. The maximum difference was approximately 10 per cent and no attempt was made to balance these currents by rephasing the circuits. This difference has been verified by meter readings since the circuits have gone into service.

Another interesting aspect of current division is shown by paralleling all the conductors of the six circuits at both ends and applying a voltage across them. The largest current unbalance between phases of any circuit was then 20 per cent. This indicates the degree of coupling between the symmetrical component networks.

Functional Life Tests of Insulation Systems for Dry-Type Transformers

PAUL NARBUT
MEMBER AIEE

A SURVEY of recent literature indicates that the functional approach to the testing of apparatus is well entrenched in contemporaneous thinking.[1] In particular, it has made ever-increasing inroads into the evaluation of temperature endurance of insulating materials and insulation structure of electric apparatus.[2]

This paper deals with the experimental application of functional test principles to the evaluation of temperature endurance of dry-type power transformers. The object of the tests described here was not to test any specific design of dry-type transformer, but rather to give a trial run to a test procedure which was under consideration as a test code by a Subgroup of the AIEE Working Group on Life of Materials. Tests reported here were made at the Transformer Division of the Westinghouse Electric Corporation. Similar tests, although covering somewhat different aspects of the subject, were made by three other co-operating laboratories: those of Allis-Chalmers Manufacturing Company, General Electric Company, and Pennsylvania Transformer Company.[3] The results of the several years of joint effort and experience were incorporated in a proposed test code in an AIEE committee report.[4]

Basic considerations underlying the proposed functional test code were stated previously.[4,5] For convenience they are repeated here briefly.

1. Functional tests, as applied to apparatus, must evaluate its complete insulation structure as an integral unit.

2. Temperature and time are recognized as the major controlling factors. Experience to date indicates that other factors may be of some, although secondary, importance. When these are clearly identified, their inclusion in the test procedure is justifiable.

3. Criteria of failure shall represent, as nearly as possible, the ability of the transformer to render service under all normal service conditions. The word "normal" should refer to all service conditions that may be expected, such as overvoltages, overloads, short circuits, etc., pertaining to normal service.

4. The test procedure must be reasonably short, simple, and should be capable of giving reproducible results.

Evolution of Test Code for Dry-Type Power Transformers

In its present form the proposed test code[4] has the following provisions:

1. The test samples should preferably be complete apparatus taken from the production line. When complete apparatus is too large and expensive the use of models is permissible. These latter shall be essential duplicates of the prototype transformer in regard to electrical clearances, method of construction, and the materials used.

2. The test procedure provides for accelerated aging by exposure of the test samples to fixed elevated temperatures for a predetermined time. In a cyclic pattern temperature exposures are followed by 90 to 95-per-cent (%) humidity exposure and dielectric tests in humid condition. The aging temperature and the duration of temperature exposure per cycle are determined by the requirement that the time to failure should be between five and ten test cycles.

3. Dielectric test voltage shall be 100% test values, as applied to new transformers.

4. A test sample is considered as having failed if dielectric breakdown or flashover occurs on dielectric tests. If models are used as test samples this breakdown shall be of such a nature as not to be traceable to inadequate clearances in the model.

5. The ultimate result of application of the test code is a quantitative expression of the temperature-life endurance of the transformer. The presently proposed formulation of the code provides that this be expressed as a single value of the hottest-spot temperature to result in a mean life of the test samples equal to 4 years. Since the duration of the test, carried out at higher temperatures, is expected to be much shorter than this period of time, extrapolation of the test values of the mean life (e.g., days to failure) versus temperature is required.

These provisions will now be considered in greater detail.

Provision 1—The Test Sample

This provision remained substantially without change since it was formulated in the first version of the test code. As a part of this provision, the test code included a specific design for a test model to represent the 15-kv class of dry-type power transformers (Fig. 1, reference 5). This model was changed slightly by way of increasing the end clearances, and the clearances from the high-voltage (HV) winding to the corner posts, as these were found inadequate in the original design.

Provision 2—The Test Procedure

Originally, the test procedure required a short drying-off period of the test sample after humidity exposure and before applying the dielectric tests. This is in agreement with manufacturers' recommendations that ventilated dry-type transformers, after idle periods under humid atmospheric conditions, should be subjected to a drying-off operation before being energized. However, this provision met with some objections from the members of the Working Group on the ground that this recommendation frequently cannot be followed. Furthermore, tests on models built with class-*B* insulation under this provision resulted in no dielectric failures of insulation (either major, turn, or layer) even after a severe physical deterioration due to temperature exposure. This also proved to be true with transformers in service. For these reasons the requirement was changed to its present form. In this form, functionally, it probably represents the most severe conditions encountered by this apparatus in service.

Provision 3—Dielectric Test Voltage

Originally, the dielectric test voltages required in the test code were specified at 75% of the test voltages for new apparatus. This is in agreement with American Standards Association recommendations for dielectric acceptance tests on transformers prior to service.[6] Upon a more mature consideration of the matter by the Subgroup in the light of the functional requirements, and in view of the absence of failures in the trial tests made under the provision of the 75% dielectric test voltage, the use of the full 100% test values was adopted.

Provision 4—Definition of Failure

This requires no comment.

Provision 5—Extrapolation of the Life Versus Temperature Data Obtained in Test

Admittedly, 4-year life expectancy

Paper 55-449, recommended by the AIEE Transformers Committee and approved by the AIEE Committee on Technical Operations for presentation at the AIEE Summer General Meeting, Swampscott, Mass., June 27–July 1, 1955. Manuscript submitted March 29, 1955; made available for printing April 15, 1955.

Paul Narbut is with the Westinghouse Electric Corporation, Sharon, Pa.

The author is grateful for the assistance of his associates, G. A. Monito and J. A. Robinson, in carrying out these tests.

under continuous maximum load and ambient condition stipulated in the code has an element of arbitrary judgment in it. Adoption of this value was prompted by the need of such a bench mark in order to enable the test code to serve its ultimate objective, namely to provide a workable tool to determine the permissible hottest-spot operating temperature rise for this apparatus. Some justification for this 4-year bench mark was given in reference 5. Further justification for it may be found in the service record of ventilated dry-type transformers which covers a period of 20 years. It has been pointed out, and it may be true, that the establishment of such a bench mark is outside of the scope of this test code, and that it should be a function of another standardizing group of the AIEE. However, the need for the definite bench mark in the form of a normal life expectancy under the maximum test conditions cannot be denied if the functional test code is to serve its avowed ultimate purpose.

In regard to the method of extrapolation of the test data to the normal life expectancy point (e.g., 4 years' life) the test code provides that this extrapolation be carried out where possible on the basis of the Arrhenius chemical reaction rate law[7]

$$t = A\epsilon^{\frac{b}{T}} \tag{1}$$

where

t = mean life of samples at temperature T degrees absolute
ϵ = base of natural logarithms
b = a constant, depending largely on the nature of insulating materials
A = a constant, depending on materials and the method of testing (insulation end point)

Since equation 1 involves two constants, A and b, two sets of values of t and T will define the relationship completely. Thus when the total number of samples is divided into two groups and each group is tested at a temperature different from the other, two sets of values (t_1, T_1) and (t_2, T_2) will be obtained. Since these two points define the values of the two constants, any third pair of values (t_0, T_0) may be readily calculated by solving three simultaneous equations

$$t_1 = A\epsilon^{\frac{b}{T_1}}$$

$$t_2 = A\epsilon^{\frac{b}{T_2}}$$

$$t_0 = A\epsilon^{\frac{b}{T_0}}$$

Solving these for the extrapolated temperature T_0, corresponding to a desired life, such as 4 years (t_0 = 1,460 days), there results

$$T_0 = \frac{\ln(t_1/t_2)}{\frac{\ln(t_0/t_2)}{T_1} - \frac{\ln(t_0/t_1)}{T_2}} \tag{2}$$

Equation 2 (which is the same as equation 7(A) in the code) may be used for extrapolation. However, a simpler graphical method of extrapolation is made possible by co-ordinate paper currently coming into common use on which equation 1 plots as a straight line.[7]

Present formulation of the test code considers two other cases of extrapolation of the test data, namely, when the value of b is known or may be assumed (e.g., b is closely equal to 11,500 for phenolics), and another more general case, when even the Arrhenius law (equation 1) may not be safely assumed (method 1, section 7 of the Code). In this latter case several test points may be required (t versus T), and extrapolation, in general, cannot be safely carried out too far. However, three points will show whether or not the Arrhenius law is obeyed. Hence, method 1 of the test code provides for the use of three groups of samples, aged at three different temperatures. In all cases, extrapolation must be based on the life data for the same component of the composite insulation structure.

In its work on the development of the test code the Subgroup considered other environmental conditions in addition to thermal aging and humidity. Among these were the following factors.

1. *Vibration.* When present, vibration is a recognized environmental factor affecting the life of insulation. This factor was considered by the Subgroup, and some experimental work was done in an attempt to evaluate it. This phase of the test work is being reported by one of the other co-operating laboratories.

2. *Short-Circuit Mechanical Forces.* This factor has been given serious consideration since it was realized that one of the essential functions of insulation is mechanical support. It was conceivable that the failure of the insulation structure would result from mechanical rather than dielectric weakening. Since short circuits produce mechanical forces of a shock nature, a simple technique of shock application by dropping was developed for application on the 15-kv dry-type transformer models.

It was realized that the effect of shock may be twofold: it may produce a mechanical displacement due to the weakened support of the coils, or it may weaken the dielectric strength of the insulation system. The latter phase of the shock tests is reported in this paper.

At the time of the last revision of the test code the Subgroup was of the opinion that the shock tests should not be included in the test code routine pending further and more exhaustive study. Some of the test results reported here were obtained subsequent to this decision.

3. *Change in Power Factor With Aging.* This factor was also given serious consideration by the Subgroup. Measurement of power factor was included in many tests made by the co-operating laboratories; those made by the Westinghouse Transformer Division are reported in this paper. The results of these and other tests prompted the Subgroup not to include power-factor variation as a criterion of failure, pending further study.

Tests—Group 1

All tests reported here were made on 15-kv dry-type transformer models, built substantially in accordance with section 12 and Fig. 1 of the proposed test code,[4] using class-B materials. Two groups of tests were made. The first group was made during the summer of 1953, using four models, one of which was equipped with thermocouples for temperature monitoring. Only a brief account of this group of tests will be given here. The tests were of an exploratory nature. The object of the tests was to give a trial run to the procedure and to the criteria of failure specified in the first version of the test code. The latter included a drying-off period after the humidity exposure, and the use of 75% of test voltage applied to new transformers. The 100% test voltages were: major insulation, 31 kv; section to section, 7 kv; low-voltage (LV) layer insulation, 1.2 kv; and HV turn-to-turn insulation, 800 volts; all voltages rms, applied for 1 minute. Mechanical shock or vibration tests were not included.

The results of this first group of tests are briefly summarized:

1. With adequate instrumentation, the method of temperature and humidity control given in the code was found workable. Experience gained in these tests and in those run by the other co-operating laboratories led to the formulation of the Appendix to the test code.

2. It was found that when the models were heated by electric current and were freely exposed to room air, the high-low barrier temperature did not attain a value representative of actual transformers, as provided for in the test code. This difficulty was overcome by enclosing the models individually in a wrap of aluminum foil. This accomplished two objectives. First, it produced a more uniform temperature distribution in each model, closely representing that obtained in actual trans-

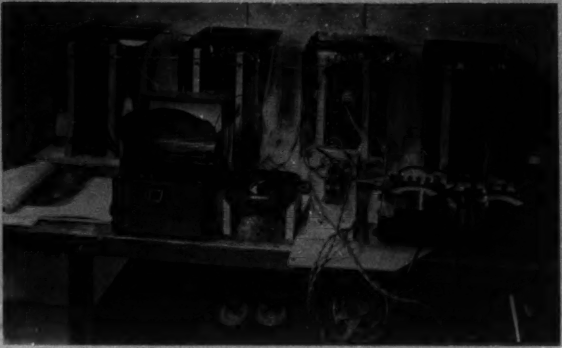

Fig. 1. Four models on heating cycle

formers. Second, it thermally isolated from each other the several models which were simultaneously on test, thus promoting the equality of temperatures of the different models. Fig. 1 shows the four models on test. The procedure of wrapping the models in aluminum foil was found satisfactory and was used on all subsequent tests. However, for future tests it is suggested that rectangular bell covers, closed tight at the top and open at the bottom, may be preferable from the point of view of convenience and consistency of results.

3. There were no failures under the conditions of these tests even after a severe deterioration of insulation caused by temperature exposure.

Results of these tests, and those by the other co-operating laboratories, served as a basis for revisions of the test code procedure, bringing it to its present form.

Tests—Group 2

The second group of tests was made following the provisions of the revised test code. The test voltages used were 100% values as indicated in the foregoing. In agreement with the broader scope of these tests, the procedure included a shock test on some of the models. The objectives of these tests were:

1. To test the provisions of the revised code.
2. To determine if the shock test is capable of detecting mechanical weakening of insulation.
3. To determine if mechanical shock will promote the dielectric failure of aged insulation.
4. To obtain further data on the variation of power factor to see if this could be used as a criterion of failure.
5. To determine if the test code procedure is adequate to detect differences in the materials used in the models.

Accordingly, eight 15-kv class models were built per Fig. 1 of the test code,[4] some of them with slight modifications, as follows: Models 4, 5, 6, 7, and 8 of identical design, per Fig. 1 of the test code, with class-*B* materials, tested as one group, using model 8 for temperature monitoring only. Models 11, 12, and 13 of design identical with Fig. 1 of the test code except with a high-low barrier made of different material. Model 13 was used for temperature monitoring only.

Electrical clearances were identical in all eight models. The test procedure used in testing models 6 and 7 was that given in the present edition of the code. The test procedure used for models 4, 5, 11, and 12 was also the same except that shock tests were included. In all cases power-factor measurements were made during each test cycle, as follows:

1. HV coil to LV and ground.
2. LV coil to HV and ground.
3. Turn to turn, HV winding (between two strands, all sections in parallel).
4. Layer to layer, LV winding.

The shock test, per test cycle, consisted of dropping the models four times from a height of 20 inches on a steel disk mounted on a concrete floor slab, using a brass pellet at the point of impact to give a controlled cushioning of the shock. The sequence of the test cycle, including the shock test, was as follows:

1. Temperature exposure, 3 days at 260 degrees centigrade hot spot. This temperature is intentionally higher than that suggested in the test code for group-2 apparatus because of the limitation in the time available for tests. The expected average time to failure for group-2 transformers was about 2 test cycles.
2. Cooling, followed by shock test, where applicable.
3. Dielectric tests at 100% test voltage in dry conditions.
4. Humidity exposure at 90 to 95% relative humidity for 24 hours. At the beginning of this series of tests, humidity was not controlled with desirable accuracy and was at times allowed to exceed these limits. It is suspected that this factor accounts for the dispersion in the power-factor measurements, and, possibly, is responsible for some of the earlier dielectric failures. The situation was corrected by the use of a humidity enclosure made of material impervious to water vapor, with an open tray of saturated solution of sodium sulphate covering the bottom surface, and a motor-driven air circulator.

Table I. Representative Record of Temperature During Aging Period

Temperature in Degrees Centigrade Duration of Heat Exposure is 3 Drops per Cycle

Heat Cycle Number	Thermocouples							
	HV	HVB	LV	4	5	6	7	8
1	261	254	263					
2	258	243	252	248	232	239	230	232
3	260	246	260	260	243	228	221	232
4	257	243	257	240	221	239	232	229
5	258	244	260	228	224	233		238
6	262	243	262	243	243	235	235	242
7	257	239	255	(discontinued)		243	246	236

Models 4, 5, 6, 7, and 8 heated simultaneously

Heat Cycle Number	Thermocouples						
	HV	HVB	LV	LVB	11	12	13
1	260	225	252	235	234	223	
2	260	221	250	234	248	232	
3	260	224	252	234	243	228	228
4	260	221	250	232	224	211	225
5	255	216	250	232	243	239	239
6	264	224	260	243	243	235	250

Models 11, 12, and 13 heated simultaneously

HV: HV coil, hottest spot.
LV: LV coil, hottest spot.
HVB: High-low barrier, hottest spot.
LVB: LV coil winding tube, hottest spot.
4 to 13: Temperature monitor thermocouple inserted between second and third sections from top of HV coil in models 4 to 13 respectively.

Table II. Power Factor, Per Cent, in Humid Condition

Cycle	High to Low and Ground	Low to High and Ground	LV Layer to Layer	HV Turn to Turn, All Sections in Parallel
Model No. 4				
Prelim.*	30	31.6	18.5	22.1
1	4.0	16.5	13.8	7.7
2	9.2	17.5	>60	32.8
3	8.7	19.5	>60	>60
4	4.5	10.6	>60	42.8
5	7.4	12.7	>60	>60
Test discontinued				
Model No. 5				
Prelim †	15.8	24.8	15.5	17.7
1	7.0	17.3	30	8.9
2	8.3	18.2	>60	30.4
3	11.8	23.0	>60	39.0
4	4.8	14.0	>60	30.4
5	6.8	16.2	>60	>60
Test discontinued				
Model No. 6				
Prelim.*	16.2	26.5	22	13.1
1				
2	9.4	22.2	>60	30.0
3	8.6	19.0	>60	37.4
4	4.1	11.5	45.8	30.3
5	6.2	13.0	>60	32.5
6	5.1	11.2	>60	28.8
7	5.75	12.8	>60	30.3
Model No. 7				
Prelim.*	18.7	28	19	13.4
1	6.5	21	12.6	6.4
2	9.4	18.4	19.4	>60
3	9.7	18	>60	>60
4	2.82	12.7	>60	30
5	4.9	11.4	>60	27.4
6	4.5	10.6	>60	31.3
7	4.7	11.8	>60	30.75
Model No. 11				
Prelim.	21.8	32.4	12.1	3.6
Prelim.‡	>60	>60	27.5	30.0
1	17.7	25.3	14.8	9.1
2	61.2	43.6	>60	>60
3	11.0	30.5	>60	>60
4	6.1	18.0	>60	>60
5	8.2	26.0	>60	>60
Test is continued				
Model No. 12				
Prelim.	15.8	28.5	13	4.6
1	21	31	14.5	10.4
2	4.6	24.8	28.4	>60
3	15.2	34.4	45.5	>60
4	5.4	15.1	>60	>60
5	4.2	14.2	>60	>60
Test is continued				

* Measured after 3 days at high humidity.
† Measured after 2 days at high humidity.
‡ Measured after 6 days at high humidity.

Table III. Record of Failures on Dielectric Tests

Temperatures in Degrees Centigrade Duration of Heat Exposure is 3 Days per Cycle

Major Insulation Test, 31 Kv RMS

Model	Shock	Failed	Life
4	yes	after 5th heat cycle, in dry condition	$4^{1}/_{2}$ cycles
5	yes	after 5th heat cycle, in dry condition	$4^{1}/_{2}$ cycles
6	no	withstood 7 cycles. Test is continued	>7 cycles
7	no	withstood 7 cycles. Test is continued	>7 cycles
11	yes	withstood 6 cycles. Test is continued	>6 cycles
12	yes	withstood 6 cycles. Test is continued	>6 cycles

Turn Insulation Test, 800 Volts RMS

Model	Shock	Top Two Sections	Middle Two Sections	Bottom Two Sections	Life
4	yes	after 3rd humidity	no failure, 6 cycles	after 4th humidity	$2^{1}/_{2}$ cycles
5	yes	after 5th, dry	after 5th, dry	no failure, 6 cycles	$4^{1}/_{2}$ cycles
6	no	no failure, 7 cycles	no failure, 7 cycles	no failure, 7 cycles	>7 cycles
7	no	after 2nd humidity	no failure, 7 cycles	no failure, 7 cycles	$1^{1}/_{2}$ cycles
11	yes	after 2nd humidity	after 2nd humidity	after 3rd humidity	$1^{1}/_{2}$ cycles
12	yes	after 2nd, dry	after 2nd humidity	after 5th, dry	$1^{1}/_{2}$ cycles

This arrangement automatically maintained a constant humidity of about 93% at room temperature, as indicated by the wet and dry bulb thermometers.

5. Dielectric tests in humid conditions, made immediately after removing each model from the humidity chamber, in the following order: major insulation, 31 kv rms; section to section, 7 kv rms; turn insulation, 800 volts rms; and layer insulation, 1,200 volts rms.

6. Power-factor and capacitance measurements, using a General Radio bridge, which had a limit of 60% on power factor. All dielectric tests and measurements were completed within 20 minutes after removal of each model from the humidity chamber.

This test cycle was repeated in the same order. Prior to the first heating cycle, a complete schedule of tests was given to each model in unaged condition. The results of all tests are given in Tables I, II, and III.

Table I gives representative values of the temperatures recorded during the heating periods. Table II gives variation of power factor of various components with aging. Commenting on this table, there seems to be no significant change in the power factor at the time of failure. In view of this it does not appear possible to use power-factor measurement as a criterion of failure. Nevertheless, in the writer's opinion, further study of the power-factor variation with aging is desirable, particularly under more accurately controlled humidity conditions, and using a larger number of samples to obtain better statistical representation.

Table III gives a record of failures on dielectric tests. The following comments may be made on the data given in this table:

1. There were no failures of the LV layer insulation nor of the section-to-section insulation for the 7 cycles of tests.

2. The average life of the major insulation is shown by these tests to be longer than the life of the turn insulation. Since the requirements for the major insulation test (31 kv rms for 1 minute) are fixed by the industry standard, while those for the turn insulation (800 volts rms, 1 minute) are a matter of judgment, the question naturally arises whether or not this estimated requirement is realistic, particularly when it is remembered that the normal operating voltage on the turn insulation is under 30 volts rms. Pending further study of this question, and based on a revised estimate of the surge voltage requirements for turn insulation, the AIEE Working Group on Life of Materials adopted a revision of the test voltage required for the turn insulation, 500 instead of 800 volts rms.

3. Comparing the test results on models 4 and 5 subjected to mechanical shock, and identical models 6 and 7 not subjected to the shock, it appears that the application of shock shortens the life of the insulation. Thus, on major insulation, the shocked models 4 and 5 failed both in the 5th test cycle, whereas models 6 and 7 continue beyond the 7th cycle. Similarly, on turn insulation, there is evidence of reduced insulation life on models subjected to mechanical shock. It appears premature as yet to recommend inclusion of the shock tests as a part of the test code primarily because of the difficulty of specifying what the shock requirements should be.

It must be pointed out that the severity of the shock impact used in these tests was quite great, and was measured in terms of several hundred *g*. At the end of 5 test cycles, models subjected to shock had several of the porcelain radial spacers cracked or broken, although they did not show any other signs of mechanical weakness.

4. Although the tests on models 11 and 12 have not yet been carried far enough to have failures of the major insulation, the results up to date show a distinctly different life performance of major insulation barriers used in these models as compared to those used in models 4 and 5. Both pairs of models were subjected to the same test routine, including the mechanical shocks. Yet models 11 and 12 continued in their 7th cycle, while models 4 and 5 had failed during their 5th cycle. Considering the consistency of the test results, this difference appears to be significant.

Summary

1. Tests were made to determine the practicability of the test procedure and of the provisions of the proposed test code. These tests, along with other tests made by the co-operating laboratories, formed the basis of the code.

2. The results show that the test procedure given in the test code is practical.

3. Observed life of the test samples (15-kv class models, class-*B* insulating materials) agreed with the expected life of group-2 apparatus well within the limits of the accuracy of tests.

4. Based on the test data available to date, the test procedure given in the code appears capable of clear differentiation between insulation structures built of different materials.

5. Tests show that mechanical shock may be an important factor in determining the life of dry-type transformers.

6. To establish this test code as an industry standard, additional tests are required on a sufficiently large number of samples to permit statistical analysis of the data. The tests should include at least ten samples aged at each of three different temperatures. The results of these tests must be correlated with available field experience.

References

1. THE PHILOSOPHY OF SIMULATED TESTING, **S. A. Gordon.** *ASTM Bulletin*, American Society for Testing Materials, Philadelphia, Pa., Oct. 1953, p. 27.

2. FUNCTIONAL EVALUATION OF MOTOR INSULATION SYSTEMS, **G. A. Cypher, R. Harrington.** *AIEE Transactions*, vol. 71, pt. III, Jan. 1952, pp. 251–53.

3. FUNCTIONAL TEMPERATURE ENDURANCE TESTS ON A SILICONE GLASS FIBER INSULATION SYSTEM FOR DRY-TYPE TRANSFORMERS, **M. L. Manning.** *Ibid.*, vol. 74, pt. III, Apr. 1955, pp. 91–100.

4. PROPOSED TEST CODE FOR FUNCTIONAL TEMPERATURE ENDURANCE TESTS OF VENTILATED DRY-TYPE POWER AND DISTRIBUTION TRANSFORMERS, **AIEE Committee Report.** *Ibid.* Oct. 1955, pp. 971–77.

5. TEMPERATURE CLASSES FOR DRY-TYPE POWER TRANSFORMERS AS DETERMINED BY FUNCTIONAL TESTS, **Paul Narbut.** *Ibid.*, vol. 72, pt. III, Oct. 1953, pp. 917–23.

6. DISTRIBUTION, POWER, and REGULATING TRANSFORMERS. *ASA C57.22–1948*, American Standards Association, New York, N. Y., 1948.

7. ELECTRICAL INSULATION DETERIORATION TREATED AS A CHEMICAL RATE PHENOMENON, **Thomas W. Dakin.** *AIEE Transactions*, vol. 67, pt. I, 1948, pp. 113–22.

◆

Discussion

H. B. Harms (General Electric Company, Fort Wayne, Ind.): Dr. Narbut's paper is a well-documented and worthwhile contribution to the record of a struggle to evolve a useful insulation test code for ventilated dry-type power transformers. It is very evident that it is intended that this test code will have been written with a firm background of experience.

There are four items mentioned in the paper and the references that we would like to re-emphasize:

1. So far, experience seems to have been centered about one transformer model and voltage class. There is no doubt that some or all of this experience can be used for other models. None the less, it must be expected that certain time delaying and discouraging technical difficulties will be encountered with them. Testing insulation systems by the use of models is not at all straightforward and must be done with much thought and care.

2. It is important to use an adequate number of test samples to predict insulation behavior with confidence. We feel Dr. Narbut was justified in making the conclusions he did, however, from the data he obtained from his limited sampling.

3. Test aging temperatures used in the paper and recommended in the test code seem to be unusually high. It is appreciated that these would be necessary if the Arrhenius law were strictly followed. But it is known that certain insulations have critical temperatures above which they deteriorate instantaneously and, in general, factors that influence degradation at high temperature are different from those influencing degradation at low temperatures. Preoccupation with getting data quickly can lead to a condition of dangerous extrapolation or interpretation.

The paper makes no mention of the insulating materials used in the models. Since the application is intended to be National Electrical Manufacturers Association Group 2, it must be assumed that they contained a substantial amount of organic binding substances which at 260 C must have been quickly dissipated. If the inorganic part of the insulation was mica, asbestos, fiberglass, or combinations of these, then at 260 C they should not have deteriorated other than to have become fragile to mechanical forces (because of the disappearance of the organic binders). They should have maintained their original electrical characteristics. It is deduced from this that the primary cause of failure was not electrical, but, instead, was due to a mechanical displacement, water absorption (in the case of failures after humidity), etc., and really had nothing at all to do with chemical changes in the insulation. In service these forces result from short-circuit conditions, thermal stresses, and from lightning and switching surges. A large percentage of transformer failures are attributable to these. So, in this case, extrapolation would appear to be "dangerously" conservative.

Without the benefit of a binder, which would be present indefinitely at the 150 C normal operating temperature, the transformer models probably failed prematurely. If this reasoning is correct then it seems logical that 100% test voltages would have to be used as recommended in the test code to get failures in a reasonable length of testing time. After the organic binders have been burned away it makes no difference what aging temperature is used. A more realistic representation of the test data would be a plot of aging time versus number of times vibrated, shocked, or some other controllable mechanical variable. Inorganic materials have indefinite endurance in the temperature ranges covered by the test code. Although in general they have a lower dielectric breakdown strength at the higher temperatures, this phenomenon is not a function of time.

4. To get any sensible idea of transformer life, the test voltages should bear some resemblance to the ones encountered in service. For designs in the 15-kv class, lightning and switching surges may well be the major factors; for electronic transformers, for another example, "working voltages" are normally well enough known to be used as base points. Once these "service" voltages are determined, it would seem logical to obtain test cycle voltages by scaling up all the basic voltages pretty much in the same proportion. To do otherwise (e.g., arbitrarily adjusting the turn insulation test voltage from 800 to 500 volts according to the recommendation of the AIEE Working Group on Life of Materials) would penalize a balanced design that planned to withstand them all for approximately the same length of time. To do otherwise also indicates a tendency to adjust test voltages to vindicate a specific design by failing components simultaneously.

Whether the test cycle voltages are applied by 60-cycle HV equipment, by surge tester, or by overvoltage induce methods, it would appear proper to base them all on the operating conditions (or industry standards that are supposed to represent these conditions) just as the designer bases his calculations on these conditions.

Paul Narbut: I am taking this opportunity to submit additional information on the results of the second series of tests, which

Table IV. Record of Failures (Additional Information)

Aging at 260 C Hottest Spot, 3 Days Per Heat Cycle

Major Insulation Test, 31 Kv RMS

Model Numbers	Model Material	Shock	Condition When Failed	Life, Cycles
4	P	Yes	Dry	$4^1/_2$
5	P	Yes	Dry	$4^1/_2$
6	P	No	Dry	$8^1/_2$
7	P	No	Humid	$7^1/_2$
11	Q	Yes	Dry	$9^1/_2$
12	Q	Yes	Dry	$9^1/_2$

Turn Insulation Test, 800 Volts RMS

Model	Shock	Number of Cycles to Failure and Condition When Failed: Top Section	Middle Section	Bottom Section	Life, Cycles
4	Yes	3, humid	6, no failure	4, humid	$2^1/_2$
5	Yes	5, dry	5, dry	6, no failure	$4^1/_2$
6	No	9, humid	9, humid	9, dry	$8^1/_2$
7	No	2, humid	9, humid	9, humid	$1^1/_2$
11	Yes	2, humid	2, humid	3, humid	$1^1/_2$
12	Yes	2, dry	2, humid	5, dry	$1^1/_2$

were not completed at the time of the writing of the paper, but which now are completed. The results of these tests are summarized in Table IV.

The top section of Table I gives the life of the models at the test temperature as determined by failure of the major insulation. The bottom section represents the life as determined by the failure of the turn insulation. There were no failures of the layer insulation, nor of the section insulation. Thus, according to Mr. Harms, the design was not balanced. No serious consideration was given, however, to the possibility of making the tests on these components more severe, since they appeared adequate in the light of the functional test requirements.

Examinations of the first part of the table leads one to the following conclusions, which may be somewhat tempered by the recognition that only very few samples were tested under identical conditions.

1. Inclusion of a mechanical shock resulted in a shorter life of the samples.
2. Use of different materials for the high-low insulating barrier resulted in a markedly different life of the samples. For Mr. Harm's information, the material used for the barrier tube of models 4 to 7, inclusive, was paper-phenolic laminate. That used in models 11 and 12 was glass cloth bonded with polyester-type resin. In reporting the test results, no emphasis was placed on the actual materials used in the construction of the test samples. This was partly because the primary object of the test was the Test Code itself and not a specific insulation system.

Commenting on Mr. Harm's remarks, I wish to take a mild issue with the statement that "testing of insulation systems by the use of models is not at all straightforward, and must be done with much thought and care." To be sure, it would be very desirable to develop a reliable and significant test of insulation systems that would be both "straightforward," and would require only little "thought and care." Anyone who knows of such a bonanza should speak out. In my opinion, the most straightforward sample for a functional test is a complete unit of apparatus from production line, which seems to be entirely feasible for small transformers, but not so for large power units. The next best is a model. It does require thought to specify it correctly. However, the tests made to date indicate that the use of models is promising. Of course, we should be careful not to close the door for a better approach, if such is proposed.

The idea that the failure of insulation may be due to mechanical weakening rather than electrical is entirely valid. The Subgroup made an effort to use mechanical failure of insulation as the end point. However, so far this venture was not crowned with success, as reported in this and related papers. Regardless of the foregoing, the mechanical weakening of the insulation must be a result of the chemical changes caused by thermal aging, if it is to be used as an end point of insulation life. Hence, it should be related to the duration and degree of temperature exposure, rather than to the number of mechanical shock or vibrations, as suggested by Mr. Harms.

In regard to the test voltage, Mr. Harms apparently does not realize that in power transformers 500-volt RMS test for turn insulation is some 30 times its normal operating voltage, whereas 31 kv for major insulation is only twice the operating voltage. The 500-volt test is specified to insure that the insulation has adequate strength to meet surge voltage conditions. Since there is no industry standard for the turn insulation test, its value is based on the best appraisal of service conditions. The 500-volt value may yet be changed if an adequate evidence justifying such a change is submitted.

Regarding other of Mr. Harm's remarks, I feel that they are adequately dealt with in the paper and in the Test Code itself, and therefore, require no further comments. This is particularly so because I feel that there is no basic difference between Mr. Harm's and my point of view on the basic philosophy of functional tests.

Flux Measurements in Magnetic Air Circuit Breaker Interrupters

W. A. CARTER
ASSOCIATE MEMBER AIEE

IN RECENT years the increase in severity of the interrupting duty imposed on magnetic air circuit breakers has emphasized the usefulness of exact knowledge of magnetic phenomena during interruption.

This paper is concerned in particular with the transient magnetic field associated with the blowout structures employed in magnetic air interrupters whose voltage ratings are in excess of 2,300 volts.

A study was made to develop means for precise flux measurement and oscillographic recording of field strength, saturation effects, flux distribution, and phase angle. It was essential that each oscillogram contain an instantaneous record of the magnetic field excited in response to an associated transient short-circuit current. A basic objective was to provide direct-reading traces requiring no further graphical or mathematical analysis.

The importance of instantaneous current and field records will be recognized by circuit-breaker designers as a key to the problem of isolating the magnetic field variable to achieve optimum interrupter performance. To the user of metal-clad switchgear, the procedure of this study may be of interest particularly if, as in the past, the application of power air circuit breakers is extended to higher ratings and consequent heavier duty. There may be assurance to the user of new structures that successful tests and reliable performance are both foreseeable because of accurate knowledge with which design problems are approached.

Herein is a description of the recording means together with data derived through transient measurement of the field associated with several experimental structures built during the development of a 7.2- to 13.8-kv circuit breaker.

Background

A basic process of arc extinction in present practice requires the development of high arc resistance as an effect of cooling and elongation within the interrupter.[1] To achieve efficient interruption, the designer must utilize the arc-movement caused by the interaction of two magnetic fields: the field surrounding the arc current filament and the associated field in which the arc is drawn. Direction and velocity of the arc movement are resultants of the four fundamental characteristics of the associated field already named: strength, saturation, distribution, and phase angle.

Principles of Measurement and Recording

A conventional method of acquiring data for these essential characteristics employs a calibrated search coil, the output voltage of which must be integrated either electrically or graphically to yield a field in accordance with the expression

---

Paper 55-460, recommended by the AIEE Switchgear Committee and approved by the AIEE Committee on Technical Operations for presentation at the AIEE Summer General Meeting, Swampscott, Mass., June 27–July 1, 1955. Manuscript submitted March 28, 1955; made available for printing April 20, 1955.

W. A. CARTER is with the I-T-E Circuit Breaker Company, Philadelphia, Pa.

$$\phi = -\frac{10^8}{N}\int_0^t e\,dt + C$$

where

ϕ = flux, maxwells
e = induced voltage per turn
N = number of turns linking the entire flux
t = time, seconds
C = constant of integration

This method, although generally reliable, entails considerable manipulation to ascertain proper calibrations and to interpret data.

Unique properties of the element bismuth provide two other methods applicable for transient measurements. They are reported as the Gauss effect and the Hall effect.[2,3] The use of bismuth avoids the time-consuming integration inherent with search-coil procedures, since output voltage need only be amplified to provide sufficient power to drive the galvanometer in the magnetic oscillograph.

The Gauss effect depends on the proportional change in resistance of a unit length of bismuth when the length is placed in a varying magnetic field. However, because of bismuth's high temperature coefficient of resistance, use of the Gauss effect requires that special provisions for temperature change compensation be incorporated.[4]

The Hall effect depends on the development of a slight potential difference between the surfaces of a bismuth strip containing a current when placed in a magnetic field, the lines of which are perpendicular to its plane. This potential difference, which is generally proportional to the magnitude of the transient field, except at low density values, is fed into a bridge circuit driven by a 2,000-cycle-per-second voltage source. The detected output voltage, when properly amplified, appears on a magnetic oscillogram as an amplitude-modulated wave, the envelope of which is representative of the magnetic field under investigation.

The Hall effect was selected for this study because fluxmeters employing this effect with necessary bismuth probes, temperature-compensated bridges and amplifiers were commercially available. Slight modification of commercial instruments makes them applicable for transient measurement. The components of the system are identified in the equipment diagram, Fig. 1.

Measurement Accuracy

Prior to measuring transient fields excited by various experimental blowout structures, the reliability of selected equipment was carefully appraised. The appraisal consisted of measuring and recording the transient magnetic field excited by a specially designed double Helmholtz coil, the field of which is calculable to a theoretical accuracy of ±0.1 per cent.[5,6] From a practical standpoint, the measurement system proved to contain a maximum error of ±5 per cent and a maximum phase shift of not over 5 degrees. This is shown in Fig. 2 on the following page.

Apparatus and Test Procedure

The test procedure consists of placing the probe in the air gap of a given structure and passing currents of short-circuit magnitude through the exciting coil or coils. An oscillogram is taken, simultaneously recording coil current and the magnetic field at a point in the air gap. Figs. 3, 4, and 5 indicate typical oscillograms. From these, each one of which is taken at the same relative spatial point in different structures, flux magnitude, phase angle between flux and exciting current and quantitative effects due to saturation of portions of the magnetic circuit may be determined. The synchronizing switch, shown in Fig. 1, is employed to control the degree of offset of the exciting currents in order that identical fields may be recorded by repetitive tests at different locations within the structure for the purpose of obtaining data describing field distribution throughout the interrupter.

Various forms of magnetic circuits were devised and tested. The results obtained are reported here.

Field Characteristics

The field strength characteristic is read directly from the envelope of the flux curve. The force per unit length of arc is a function of both magnitude of current and field intensity in the air gap. Arc travel through the chute is restricted and retarded by the interrupter plate material, spacing, chute vents, presence of static gases occupying the space through which the arc must travel, pressures due to thermal expansion of gases, etc. It is evident that sufficient force must be created to move both the arc and the ionized gas products of arcing through the arcing chamber irrespective of the foregoing restrictions.

The saturation characteristic is important in relation to field strength since the force per unit length of arc is reduced approximately to a direct proportionality with the arc current, once saturation has been reached.

As may be seen in Fig. 6, the magnetic field in the air gap, Fig. 1, undergoes saturation because of a saturated condition existing in the core and related parts of the structure. Bearing this point in mind, it is evident that adding turns to the blowout coil or coils lowers the value of exciting current required to produce the maximum field value. This condition is useful in obtaining optimum interrupting performance on currents within the normal continuous current rating of a circuit breaker, while additionally protecting the breaker from failure due to excessive blowout forces experienced during periods of maximum interrupting duty.

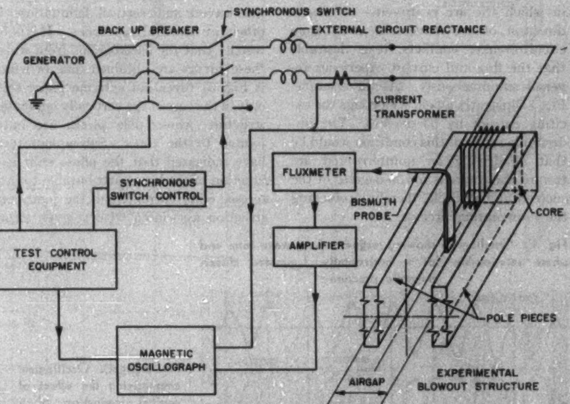

Fig. 1. Equipment diagram for flux measurement

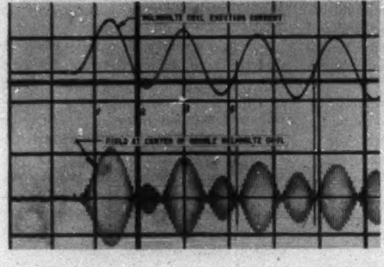

Fig. 2. Oscillogram used in the determination of instrumentation reliability

Timing Line No.	Peak Amperes	Theoretical Field,* Gausses	Measured Field, Gausses	Error, Per Cent†
1	67.2	374	380	+1.6
2	14.6	81	79	−2.8
3	88.5	493	511	+3.7
4	35.9	200	207	+3.5

* The theoretical field density $B = 5.56\, I_{pk}$ gausses.

† The theoretical field was used as a standard in calculating the per cent error.

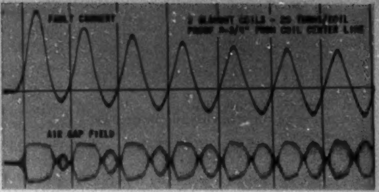

Fig. 4 (right). Oscillogram showing rapid saturation and slight degree of phase shift present in a horizontally laminated closed blowout structure

The number of additional turns is limited because the action of arc transfer, which energizes blowout coils, is impeded by an increase in reactive voltage drop.

The distribution of flux has been a difficult design factor particularly for large arc chutes used in higher voltage magnetic air circuit breakers. Uniform distribution is desirable in assuring that no portion of a chute be subjected to a disproportionate share of the effects of arc voltage.

The phase angle between the flux and the arc current determines the direction in which the arc is driven. To assure direction of arc movement away from circuit-breaker contacts, it is desirable that the flux and current experience reversal simultaneously. As an example, Fig. 5 illustrates a field which lags the exciting current by 53 degrees. The undesirable result of this condition would be that of driving an uninterrupted arc toward the contacts for 53 degrees of the succeeding half-cycle, thereby prolonging the interrupting process.

Comparative Field Characteristics

Of many structures tested, the characteristics of four are reviewed to identify certain interesting magnetic effects of construction differences. The four structures, illustrated diagrammatically as A, B, C, and D in Fig. 7, are comparable in that each assembly fits an interrupter whose arc runners are the same distance apart, the air gap width is the same, and all cores are of silicon transformer steel of equal cross-sectional area. Exciting ampere-turns are of the same order of magnitude. The structures have physical differences, the most important of which is the plane of lamination.

The distribution and field strength characteristics of the four structures are shown by the curves of Fig. 7. Fields are presented as per-unit quantities to allow direct comparisons. The dashed portions of the curves represent projected field symmetry.

The two curves derived for structure A emphasize the field effect of horizontally interleaved and vertical laminations in otherwise identical assemblies. It is noteworthy that the oscillograms from which these curves are obtained (one of which is Fig. 5) reveal an extreme phase shift only in the case of the vertically laminated structure whose pole pieces are butt-jointed to the cores. Subsequent tests have indicated that the phase shift is a function of the losses attributable to hysteresis, eddy current, and the joint construction associated with a given structure.[7] The phase angle is large in a vertically laminated structure, as would be expected, principally because of high losses incurred from eddy currents. Lines of flux entering and leaving the pole pieces perpendicularly have associated eddy currents whose paths are uninterrupted by laminating surfaces.

Two horizontally laminated structures, A and B, are identical except that B is divided into two halves and A is solidly closed. The advantages of the closed magnetic structure A are increased average magnetic strength and elimination of steep droop in the vicinity of the space between the halves of structure B.

Structure C, also horizontally laminated, is of single-coil, open-end design. As expected, leakage losses from the open end have the effect of substantially reducing field strength, in this case of the order of 50 per cent. Field distribution in the area of the arc runners is much less uniform than that of comparable structure A.

The curve for structure D shows the effects of vertical lamination, space between structure halves, and an increase in effective pole piece area. In the oscillograms, from which this curve is obtained a 50-degree phase shift appears, attributable to vertical lamination. The space between structure halves and the increase in effective pole piece area are responsible for nonuniform distribution near the arc runners and a reduction in field strength to 25 per cent as compared with the curve for structure A.

Conclusions

By application of established engineering principles and use of existing equip-

Fig. 3. Oscillogram showing magnetic field wave form and phase relationship for a horizontally laminated closed magnetic structure

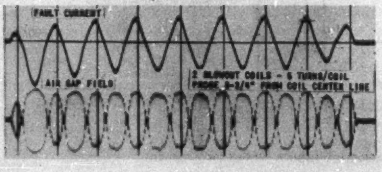

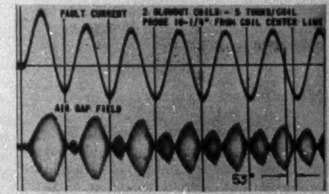

Fig. 5 (right). Oscillogram emphasizing the effect of vertical lamination of a closed structure on the flux wave form and shift

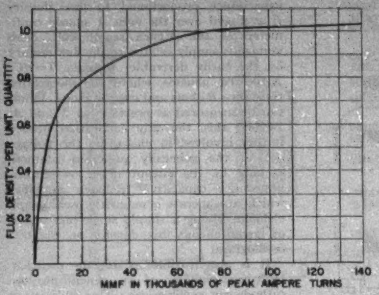

Fig. 6. Typical saturation curve for a point midway between arc runners

Breaker voltage rating: 15 kv
Material: silicon transformer steel
Laminations: horizontal
Turns per coil, 5

ment, somewhat modified, a means has been developed for isolating the magnetic field variable as a guide for design of reliable arc-extinguishing assemblies in magnetic air circuit breakers. Actual records of transient fields can be produced which require no further mathematical or graphical treatment to be useful in determining with reasonable certainty the magnitude and approximate phase angle to be expected of a field associated with a given design. Though discussed in connection with heavy-duty interrupters, the method can apply to investigations of magnetic fields for other apparatus.

Structure A, of Fig. 7, which in these test results exhibits generally high field strength and quite uniform distribution, is incorporated in the interrupter design of the 7.2 to 13.8-kv magnetic air circuit breakers for which the study was undertaken. A cross section of the breaker element, Fig. 8, shows the arrangement of the double-coil, closed magnetic circuit.

The actual structure incorporated in the circuit breaker is shown in Fig. 9 as arranged for high-current excitation during test runs. The bismuth probe is inverted to show the method of support and the protective plastic cover.

References

1. The Geometry of Arc Interruption, **B. W. Boehne.** *AIEE Transactions*, vol. 60, 1941, pp. 524-32.

2. Magnetic Phenomenon, **Alvin B. Kaufman.** *Radio-Electronic Engineering*, Chicago, Ill., Nov. 1951, pp. 41-43.

3. An AC-DC Gaussmeter, **Alvin B. Kaufman.** *Instruments*, Pittsburgh, Pa., vol. 26, Sept. 1953, pp. 1360-61.

4. Use of Bismuth-Bridge Magnetic Fluxmeter for A-C Fields, **G. S. Smith.** *AIEE Transactions*, vol. 58, Feb. 1939, pp. 52-55.

5. Absolute Measurements in Elasticity and Magnetism (book), **Andrew Grey.** The MacMillan Company, New York, N. Y., 1890, vol. 2, pt. II, chap. VI, pp. 245-59.

6. Standard Handbook for Electrical Engineers (book), edited by **A. E. Knowlton.** McGraw-Hill Book Company, New York, N. Y., 9th ed., sect. III, para. 328.

7. Characteristics of Overlapping Joints in Magnetic Circuits, **T. D. Gordy, H. L. Garbarino.** *AIEE Transactions*, vol. 71, pt. III, Jan. 1952, pp. 386-92.

◆

Discussion

T. E. Browne, Jr. (Westinghouse Electric Corporation, East Pittsburgh, Pa.): The effectiveness and economy of present-day magnetic air circuit breakers is the result of long and painstaking development. This paper illustrates one type of study which has served as a valuable tool to Westinghouse designers during the past 12 years. As shown by Mr. Carter, instantaneous flux records correlated with exciting current give invaluable insight into the effects of changes in such design factors as the shape, type of lamination, and riveting of the field pole pieces, number and arrangement of field winding turns, and so on. These studies must be correlated, of course, with a continuing program of laboratory testing

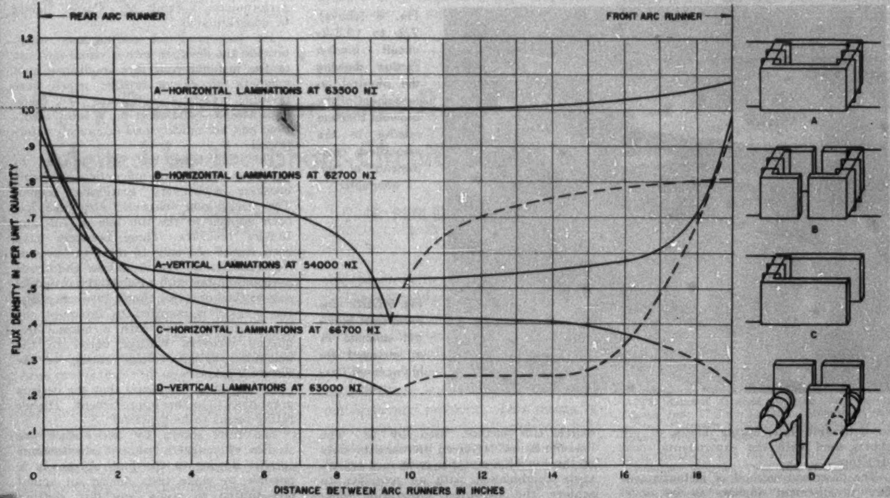

Fig. 7. Comparative magnetic field distribution in silicon transformer iron blowout structures for 15-kv breakers

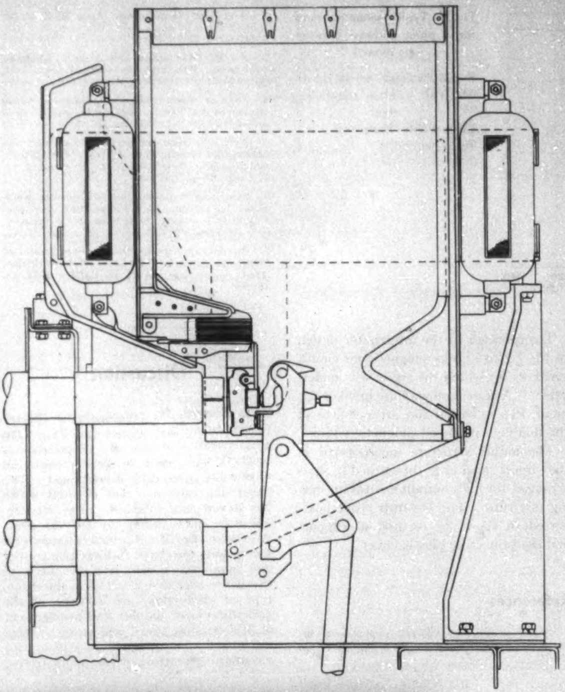

Fig. 8 (above). 7.2- to 13.8-kv circuit - breaker section showing the physical arrangement of the blowout structure relative to the associated components of the interrupter

Fig. 9 (left). Experimental blowout structure A as arranged for high-current excitation

to determine interrupting limits of arc chutes used with the experimental field structures.

The described method of instantaneous flux measurement appears to be novel but not preferable to the "conventional" search coil method used by us. The "manipulation" referred to consists only of the use of a suitable resistance-capacitance combination with an amplifier to achieve the indicated integration electrically, producing a voltage e_c across the capacitance proportional to flux density B averaged over the area A square centimeters of the N-turn search coil. This voltage is simply related to the flux density by the easily derivable formula $B = RC/NA \times 10^8 e_c$ gausses, where the integrating resistance R ohms and capacitance C farads can be measured as precisely as N and A. Beyond this, the only calibration needed is that involved in measuring the voltage e_c. In the generally preferred method, e_c may be the output of a low-output-impedance capacitive feedback amplifier which can operate a magnetic oscillograph element, giving a simple single-line record of instantaneous flux density on the test oscillogram.

It is also feasible to use the ordinary built-in amplifier of a general-purpose cathode-ray oscillograph. One interesting form of display with the cathode-ray oscillograph yields a cyclogram with flux density on one axis and exciting current magnitude on the co-ordinate axis. This gives a clear display of both distortion and phase shift of the flux with respect to the current. With a 2-beam scope, the flux and current waveforms can easily be compared on a common time axis.

Studies such as these were used in developing the 500,000-kva 15-kv magnetic air breaker described in a 1946 paper[1] from which Fig. 1 is here reproduced (see Fig. 10).

REFERENCE

1. SIZE REDUCTION AND RATING EXTENSION OF MAGNETIC AIR CIRCUIT BREAKERS UP TO 500,000 KVA, 15 KV, R. C. Dickinson, Russell Frink. *AIEE Transactions*, vol. 65, 1946, pp. 220–23.

J. D. Wood (I-T-E Circuit Breaker Company, Philadelphia, Pa.): In producing a switchgear paper that adds materially to the basic knowledge of circuit breaker performance, I think Mr. Carter should be congratulated.

He has produced oscillograms which provide the designer with a visual measure of the instantaneous flux conditions in a magnetic air circuit breaker which were invisible. These oscillograms are made with simple equipment in a very short time and are quickly and accurately interpreted.

This knowledge has been applied to improved designs of magnetic air circuit breakers with very gratifying results. The closed-loop magnetic structure has been applied to the full line of 7.2- and 13.8-kv breakers. These breakers have been tested not only to meet the present requirements of the American Standards Association, but also to meet the proposed new method of rating circuit breakers where the breaker is required to interrupt the symmetrical current with a normal frequency recovery voltage equal to the maximum design voltage rating of the circuit breaker.

Further studies indicate that the designs are subject to further improvement. Higher rating seems to be practical.

The tests shown by the author are studies of magnets without short-circuit current flowing in the interrupter. Is it possible to make tests during an actual interruption to study any flux shifting that might occur?

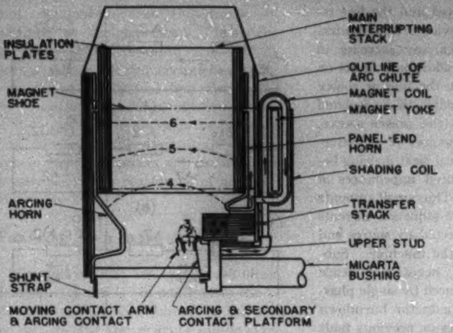

Fig. 10. Magnetic "de-ion" arc chute: 500,000 kva, 15 kv

It would be interesting to know what data are available as to the relation of flux density and the interrupting ability of an arc chute.

W. A. Carter: Mr. Browne is to be thanked for his discussion of the Bismuth method of transient magnetic field measurement. We cannot concur with his opinion of our method versus the search coil method to which he refers. It is not a question of the search coil versus the Bismuth wafer as a means of sensing magnetic flux but rather a question of direct measurement of flux density in absolute magnitude against the measurement of a derived flux density obtained by the integration of an induced voltage. The induced voltage is itself a true measurement. Its integral, however, is obtained in an artificial circuit and it is with this circuit that the greatest problems and disadvantages arise.

Electrical integration results in the loss of the zero value which is of the greatest importance in determining absolute magnitudes of magnetic fields responding from transient short-circuit currents which must be sustained and interrupted by a circuit breaker.

Another important disadvantage of the search coil–integrator combination is that no static calibration can be made and directly serve to measure transient dynamic phenomena. The Bismuth instrument is, however, calibrated directly by the field of a precalibrated permanent magnet, insuring maximum accuracy of measurements.

Finally, there are no simple integrating circuits available which are free from phase shift, distortion, and drift, particularly at power system frequencies.[1] Having no integrator, the Bismuth method does not have to cope with problems resulting from frequency limitations.

Physically, a sensing probe containing a Bismuth wafer is much smaller than a corresponding search coil thereby making possible the investigation of fields associated with smaller air gaps.

It is apparent then that the search coil method enjoys no real advantage over the employment of Bismuth either in ease of use, ability to measure d-c fields, dependability of data, or simplicity of test equipment.

One further comment which I would like to make is in regard to the method of test described by Mr. Browne. The employment of a cathode-ray oscillograph implies the study of a field produced by a structure which is in a state of either low-current or steady-state excitation or both. Experience has shown that only investigation of fields excited by values of magnetomotive force well in excess of that required to saturate the steel in the structure can supply the designer with information, the validity of which can be substantiated by extensive interruption tests in the laboratory.

The complimentary discussion by J. D. Wood is greatly appreciated by the author. The Bismuth method has been employed in transient flux measurement during actual interruptions of an arc with moderately successful results. The procedure followed was to place the probe in the space between the outside of the chute shell and the inside of the magnetic structure. Further work in this direction is currently being undertaken.

As part of a developmental program designed to determine the relationships existing between such variables as arc plate shape, spacing, thickness, and material, blowout structure size and position, and interrupting capacity, it is felt that the subject of the relation existing between the flux density and interrupting ability of a given chute will be included as a part of the subject matter of a future paper.

Reference

1. Elements of D-C Analog Computers, Granino A. Korn. *Electronics*, New York, N. Y., Apr. 1948, pp. 122–27.

Relay Protection for Lines Being Sleet-Melted by the Short-Circuit Method

J. C. HOGAN
MEMBER AIEE

C. G. PEBLER
ASSOCIATE MEMBER AIEE

SLEET formation on transmission lines was recognized as a serious operating problem as early as 1916 and shortly thereafter methods were devised to melt sleet.[1] In recent years various ways have been presented[2–5] for connecting lines and power sources to obtain the current necessary for sleet melting. Forced loading, phase shifting, and short circuiting are utilized extensively for this purpose.

Problems of relay protection during sleet melting were not specifically presented in former papers. The purpose of this paper is to present the particular problem of protection under such conditions and to propose a means of detecting faults on lines being sleet-melted by the short-circuit method.

The short-circuiting method which is used in many instances presents a difficult relaying problem. This means of sleet melting consists of applying a 3-phase-to-ground short circuit at one end of the line so that the resultant line current will be large enough to melt sleet. The source of power may be an isolated generator with step-up transformer which may be adjusted to supply the proper current. Some lines because of their particular length may lend themselves to sleet melting by direct connection to a station bus. Under these conditions the normal line relays cannot generally be set to give adequate fault protection.

Unique Problem of Line Relaying

The normal protective relaying equipment is usually located at the power source end of the line when the short-

---

Paper 55-469, recommended by the AIEE Relays Committee and approved by the AIEE Committee on Technical Operations for presentation at the AIEE Summer General Meeting, Swampscott, Mass., June 27–July 1, 1955. Manuscript submitted February 8, 1955; made available for printing May 11, 1955.

J. C. Hogan is with the University of Missouri, Columbia, Mo., but was with Commonwealth Associates, Inc., when this paper was prepared. C. G. Pebler is with Commonwealth Associates, Inc., Jackson, Mich.

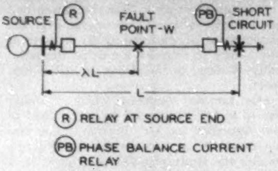

Fig. 1. Schematic diagram of faulted sleet-melted line and system

circuit method of sleet melting is employed. This protective equipment may consist of distance relays, pilot-wire relays, carrier current relays based on the directional- or phase-comparison principle, or overcurrent relays. Since the line already has a 3-phase-to-ground short circuit at its far end, the normal phase relays at the source end must either be removed from service and be replaced by other relays or their settings must be changed to make them less sensitive. Ground relays can normally be left in service.

In the case of distance relays the second- and third-zone elements must be blocked from tripping and the first zone must be set short of the end of the line. In some instances of extremely low voltage zone 1 may also have to be removed from service. If the normal line protection consists of pilot-wire relays they may be left in service when the intentional short circuit is applied outside of their zone of protection.

Directional-comparison carrier relays must be removed from service even though the intentional short circuit falls outside of their zone of protection because the line would automatically trip by second- and third-zone elements upon time delay if these elements were set to cover the entire length of line short-circuited for sleet melting. Phase-comparison carrier relays may be left in service if the intentional short circuit is outside of their zone of protection. This, however, would be objectionable since the transmitter nearest the intentionally faulted end would be keyed continuously.

Overcurrent relays, if utilized, must be set a safe margin above the sleet-melting current. In every case a certain portion of the line is unprotected. It will be shown that the percentage of the line upon which faults can be detected by overcurrent relays is dependent upon the type of fault, system impedance, and the relays applied.

During sleet-melting operations the lines and equipment are usually operating at or near their thermal capacities so that the sleet will be melted and the line returned to normal service in the shortest possible time. Hence any increase in line currents due to additional faults on the line may damage the line or source equipment. For example, if an isolated generator is used as the power source, there is a certain amount of negative-sequence current during sleet melting because of the unbalanced impedances of the line conductors. Thus small amounts of additional negative-sequence currents due to faults not detected by source end relays may damage the machine. Substantial amounts of negative-sequence currents may be produced by single phasing resulting from conductor burndown because of poor splices or previous fault damage and by phase-to-phase faults incurred by bouncing conductors accompanying ice unloading. It is imperative to remove any unintentional faults as soon as possible.

Proposed Method of Solution

Since relays at the source end cannot detect faults over the entire length of line, the proposed method of relaying which follows provides optimum protection for unsymmetrical faults. This method utilizes relays at the short-circuited end of the line which, together with the source end relays, provides complete protection for unsymmetrical line faults. The source end protection may consist of phase overcurrent relays, ground relay, and a negative-sequence overcurrent relay. In addition to the circuit breaker at the source end another circuit breaker is required between the line terminal and the 3-phase-to-ground short circuit at the far end of the line. The normal line breaker can serve this function. This breaker is equipped with a phase balance relay. Unsymmetrical faults which cannot be detected by the source end relays cause unbalanced line currents at the short-circuited end of the line. This unbalance is sufficient to initiate operation of a phase balance relay located at the short-circuited end. Operation of this relay opens the short-circuited end circuit breaker, thus removing the intentional 3-phase-to-ground short circuit. Since the fault is no longer obscured by the 3-phase-to-ground short circuit, the source end relays will operate to clear the fault. The arrangement used is shown in Fig. 1. It is to be noted, however, that unintentional 3-phase faults on the lines will not be seen by the far end relays and clearing for these faults must be initiated by the source end relays. Since the source end relays must be set a safe margin above the sleet-melting current, 3-phase faults can be detected over all but a small percentage of the line as shown later.

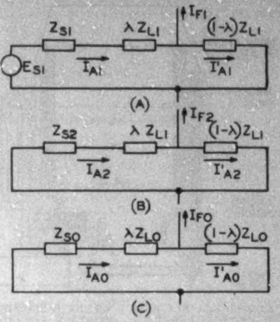

Fig. 2. Sequence network of system during fault:

A—Positive
B—Negative
C—Zero

It is proposed that, in the instance where several lines are connected in series for sleet melting, the relays at the sectionalizing points between extreme terminals be removed from service.

Faults on Lines During Sleet Melting

If a fault occurs during sleet melting on a line of length L at a distance l from the source, the symmetrical component networks[6] are as shown in Fig. 2. The circuit parameters are defined as follows:

Z_{S1}, Z_{S2}, Z_{S0} = sequence impedances of the source
Z_{L1}, Z_{L2}, and Z_{L0} = sequence impedances of the complete line of length L
$\lambda = l/L$ = ratio of line length from source to fault compared to total line length L
I_{A1}', I_{A2}', and I_{A0}' = sequence currents at the source end of line. The prefault sleet-melting current is taken as the base per-unit (pu) current

The positive- and negative-sequence impedances of the line are assumed to be equal ($Z_{L1} = Z_{L2}$). If instantaneous relaying is to be applied, calculations of currents are based on subtransient reactances of any machines involved; however, if slow-speed relaying is used, calculations are based on synchronous reactances of the machines. When an isolated generator is used as the source with slow-speed relaying, the positive- and negative-sequence source impedances are not equal. However, if a large system is used as a source of power, it will be composed of lines and transformers with equal positive-

and negative-sequence impedances in addition to the generators. Thus the generator sequence impedances will be only a part of the sequence networks involved and the system equivalent positive-sequence impedance will be approximately the same as its negative-sequence impedance. In the discussion to follow synchronous reactances will be used for positive-sequence reactances of any machines involved.

Faults as Seen From the Source

Considering first the case of a 3-phase fault at location W, in addition to the 3-phase-to-ground short circuit at the end of the line, the line currents will be symmetrical. Since the prefault sleet-melting current is equal to 1 pu the generated voltage of the equivalent source is given by

$$E_{S1}=Z_{S1}+Z_{L1} \text{ pu} \qquad (1)$$

Since the parameter Z_{S1} is made up of subtransient reactances for applications involving instantaneous relays, a correction factor must be applied to equation 1 and all other expressions for voltage or current used in this paper when instantaneous relaying is used. This correction factor is the ratio of $Z_{S1}+Z_{L1}$ (using synchronous reactances) to $Z_{S1}+Z_{L1}$ (using subtransient reactances). Thus, returning to the case of slow-speed relaying, the expression for the line current becomes

$$I_a=I_{a1}=\frac{Z_{S1}+Z_{L1}}{Z_{S1}+\lambda Z_{L1}} \qquad (2)$$

The total line current is thus a function of the location of point W at which the fault occurs. Since only positive-sequence currents are involved, the fault is best detected by overcurrent or impedance relays. These must be set for a safe margin higher than the sleet-melting current. Suppose, e.g., the overcurrent relays are set for a pickup of 1.2 times sleet-melting current. For this condition equation 2 becomes

$$I_a=1.2=\frac{Z_{S1}+Z_{L1}}{Z_{S1}+\lambda Z_{L1}} \text{ pu} \qquad (3)$$

or

$$\lambda=\frac{Z_{L1}-0.2Z_{S1}}{1.2Z_{L1}} \qquad (4)$$

Thus the overcurrent relay will protect for faults out to a point given by λ in equation 4. For values of λ greater than this value the overcurrent relays provide no protection. This zone of protection is dependent on the relative values of Z_{S1} and Z_{L1}. Thus the smaller the ratio of Z_{L1} to Z_{S1} becomes, faults occurring on a greater percentage of the line will go undetected. For the foregoing relay setting of 20 per cent above sleet-melting current and Z_{L1} approximately equal to Z_{S1}, the relays will detect faults on the 67 per cent of the line nearest the source. Faults occurring beyond that point will not be detected.

Table I. Sequence Currents at Source End and at Short-Circuited End of Line

	Double-Line-to-Ground Fault	Line-to-Line Fault	Line-to-Ground Fault
I_{a1}	$\dfrac{Z_{S1}+Z_{L1}}{Z_{S1}+\lambda Z_{L1}+\dfrac{(1-\lambda)Z_{L1}}{\left(1+\dfrac{1}{\gamma_2}+\dfrac{(Z_{L1})}{(Z_{L0})}\dfrac{1}{\gamma_0}\right)}}$	$\dfrac{Z_{S1}+Z_{L1}}{Z_{S1}+\lambda Z_{L1}+\dfrac{(1-\lambda)Z_{L1}}{\left(1+\dfrac{1}{\gamma_2}\right)}}$	$\dfrac{\left(1+\gamma_2+\dfrac{(Z_{L0})}{(Z_{L1})}\gamma_0\right)}{\left(\gamma_1+\gamma_2+\dfrac{(Z_{L0})}{(Z_{L1})}\gamma_0\right)}$
I_{a2}	$-\dfrac{(1-\lambda)Z_{L1}}{(Z_{S2}+\lambda Z_{L1})\left(1+\dfrac{1}{\gamma_2}+\dfrac{(Z_{L1})}{(Z_{L0})}\dfrac{1}{\gamma_0}\right)}I_{a1}$	$-\dfrac{(1-\lambda)Z_{L1}}{(Z_{S2}+\lambda Z_{L1})\left(1+\dfrac{1}{\gamma_2}\right)}I_{a1}$	$\dfrac{\dfrac{(1-\lambda)Z_{L1}}{Z_{S2}+Z_{L1}}}{\left(\gamma_1+\gamma_2+\dfrac{(Z_{L0})}{(Z_{L1})}\gamma_0\right)}$
I_{a0}	$-\dfrac{(1-\lambda)Z_{L1}}{(Z_{S0}+\lambda Z_{L0})\left(1+\dfrac{1}{\gamma_2}+\dfrac{(Z_{L1})}{(Z_{L0})}\dfrac{1}{\gamma_0}\right)}I_{a1}$	0	$\dfrac{\dfrac{(1-\lambda)Z_{L0}}{(Z_{S0}+Z_{L0})}}{\left(\gamma_1+\gamma_2+\dfrac{(Z_{L0})}{(Z_{L1})}\gamma_0\right)}$
I_{a1}'	$\dfrac{1}{\left(1+\dfrac{1}{\gamma_2}+\dfrac{(Z_{L1})}{(Z_{L0})}\dfrac{1}{\gamma_0}\right)}I_{a1}$	$\dfrac{1}{\left(1+\dfrac{1}{\gamma_2}\right)}I_{a1}$	$\dfrac{\gamma_2+\dfrac{(Z_{L0})}{(Z_{L1})}\gamma_0}{\left(\gamma_1+\gamma_2+\dfrac{(Z_{L0})}{(Z_{L1})}\gamma_0\right)}$
I_{a2}'	I_{a1}'	I_{a1}'	$-\dfrac{\gamma_2}{\left(\gamma_1+\gamma_2+\dfrac{(Z_{L0})}{(Z_{L1})}\gamma_0\right)}$
I_{a0}'	$\dfrac{(Z_{L1})}{(Z_{L0})}I_{a1}'$	0	$-\dfrac{\gamma_0}{\left(\gamma_1+\gamma_2+\dfrac{(Z_{L0})}{(Z_{L1})}\gamma_0\right)}$

Note: γ_1, γ_2, and γ_0 are as given in equations 6, 7, and 8 respectively.

In a similar manner the sequence currents can be determined for unsymmetrical faults and the response of relays sensitive to negative-sequence currents, ground currents, and unbalanced phase currents can be predicted; see Appendix I. The sequence currents at the source end and at the short-circuited end of the line are given in Table I.

These equations for the sequence currents can be used to determine the zone of protection afforded by different relays at the source end. For example, overcurrent relays at the source end set for 1.2 pu current will pick up if λ=0.59 for a line-to-line fault, i.e., only when the fault is in the nearest 59 per cent of the line. Such calculations will show in every case that the relays at the source end are not capable of detecting all the faults.

For complete protection of line and source equipment it becomes necessary to use some additional scheme for fault detection. Examination of the currents at the short-circuited end of the line will lead to the method proposed for detecting faults anywhere on the line.

Faults as Seen From the Short Circuited End

Referring again to Table I and calculating the line currents at the short-circuited end for unsymmetrical faults, these will be found unbalanced even though the faults are near the short-circuited end. This unbalance can be used for fault detection.

For a line-to-line fault the ratio of maximum to minimum phase currents at the short-circuited end will be 2 regardless of line and source impedances. For a line-to-line-to-ground fault this ratio will be greater than 2. Standard phase unbalance relays applied at the short-circuited end will detect these faults occurring anywhere along the line.

A line-to-ground fault on the short-circuited line will also cause unbalanced line currents at the short-circuited end. From the relations given in Table I it is seen the I_{a2}' and I_{a0}' do not approach 0 as λ approaches 1. The ratio of maximum to minimum line current for this case cannot be expressed as a simple ratio in terms of circuit parameters.

The example given in Appendix II illustrates the method of solution for a line-to-ground fault on the line. The curves of line currents versus point of fault can be used to determine the ratio of maximum to minimum current to be used to verify the operation of the phase balance current relays for this type of fault.

Summary

The following statements regarding protection of lines during sleet melting by the short-circuit method may thus be made:

1. Certain types of protective relays at the source end must be removed from service before sleet melting by the short-circuit method.
2. Source end relays left in service will only detect faults occurring on a portion of the line.
3. Small unbalances or overcurrents which cannot be detected by the source end relays may damage the lines or other equipment because they are already operating at or near their thermal capacity.
4. The method proposed using phase balance current relays at the short-circuited end of the line in addition to the source end relays can detect unsymmetrical faults occurring on any part of the line.
5. The proposed arrangement of relaying provides generator protection within the limits prescribed by the short-circuit section of *ASA-C50*.[7]

Appendix I. Determining Sequence Currents and Predicting Relay Response

Considering the unsymmetrical faults (line to line, line to ground, and double line to ground) relays sensitive to negative-sequence currents, ground currents, or unbalance between phase currents may be applied in addition to the overcurrent relay. Connecting positive-, negative-, and zero-sequence networks in parallel gives the equivalent circuit for a double-line-to-ground fault at point *W*. Solving for I_{a1} yields

$$I_{a1}=\cfrac{E_{S1}}{Z_{S1}+\lambda Z_{L1}+\cfrac{1}{\cfrac{1}{(1-\lambda)Z_{L1}}+\cfrac{Z_{S2}+Z_{L1}}{(1-\lambda)(Z_{L1})(Z_{S2}+\lambda Z_{L1})}+\cfrac{Z_{S0}+Z_{L0}}{(1-\lambda)Z_{L0}(Z_{S0}+\lambda Z_{L0})}}} \tag{5}$$

Let

$$\gamma_1=\frac{Z_{S1}+\lambda Z_{L1}}{Z_{S1}+Z_{L1}} \tag{6}$$

$$\gamma_2=\frac{Z_{S2}+\lambda Z_{L1}}{Z_{S2}+Z_{L1}} \tag{7}$$

$$\gamma_0=\frac{Z_{S0}+\lambda Z_{L0}}{Z_{S0}+Z_{L0}} \tag{8}$$

Substituting equations 1, 7, and 8 into equation 5 gives the positive-sequence current at the source end. Thus

$$I_{a1}=\cfrac{Z_{S1}+Z_{L1}}{Z_{S1}+\lambda Z_{L1}+\cfrac{(1-\lambda)Z_{L1}}{\left(1+\frac{1}{\gamma_2}+\frac{(Z_{L1})1}{(Z_{L0})\gamma_0}\right)}} \tag{9}$$

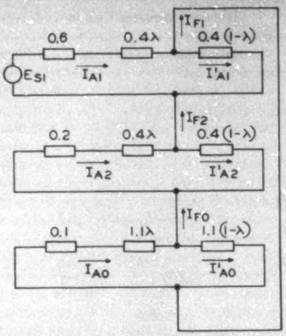

Fig. 3. Connection of sequence network for example

Also

$$I_{a2}=-\frac{E_{S1}-I_{a1}(Z_{S1}+\lambda Z_{L1})}{Z_{S2}+\lambda Z_{L1}} \tag{10}$$

or substituting equations 1 and 9 into equation 10 gives

$$I_{a2}=-\frac{(1-\lambda)Z_{L1}}{(Z_{S2}-\lambda Z_{L1})\left(1+\frac{1}{\gamma_2}+\frac{(Z_{L1})}{(Z_{L0})}\frac{1}{\gamma_0}\right)} \tag{11}$$

Similarly

$$I_{a0}=-\frac{(1-\lambda)Z_{L1}}{(Z_{S0}+\lambda Z_{L0})\left(1+\frac{1}{\gamma_2}+\frac{(Z_{L1})}{(Z_{L0})}\frac{1}{\gamma_0}\right)} \tag{12}$$

The foregoing sequence currents at the source end are given in Table I. Source end sequence currents are also given for the line-to-line and line-to-ground faults in this table. In all three of the fault conditions discussed it is noted that

$$\lim_{\lambda\to 1} I_{a1}=1 \tag{13}$$

$$\lim_{\lambda\to 1} I_{a2}=0 \tag{14}$$

$$\lim_{\lambda\to 1} I_{a0}=0 \tag{15}$$

For faults occurring near the faulted end of the line the current unbalance at the source end becomes small and the faults become impossible to detect with source end relays.

These equations for the sequence currents can be used to determine the zone of protection afforded by different types of relays at the source end. Consider, e.g., a line-to-line fault with $Z_{L1}=Z_{S1}=Z_{S2}$ and overcurrent relays at the source end set at 1.2 pu current. For this condition equation 7 yields the following relationship

$$\gamma_2=\frac{1+\lambda}{2} \tag{16}$$

$$I_{a1}=\cfrac{2}{1+\lambda+\cfrac{(1-\lambda)}{\left(1+\frac{2}{1+\lambda}\right)}} \tag{17}$$

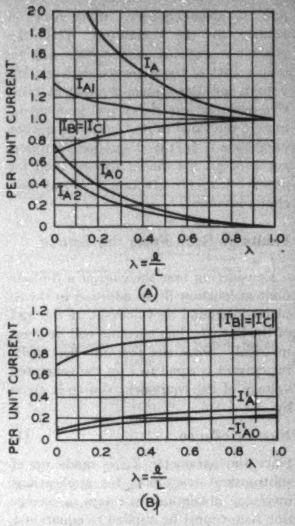

Fig. 4. Variation of line and sequence currents with fault location:

A—Source end
B—Short-circuited end

Simplifying

$$I_{a1}=\frac{3+\lambda}{2(1+\lambda)} \tag{18}$$

Also

$$I_{a2}=-\frac{(1-\lambda)}{(1+\lambda)\left(1+\frac{2}{1+\lambda}\right)}\frac{(3+\lambda)}{2(1+\lambda)} \tag{19}$$

or

$$I_{a2}=-\frac{(1-\lambda)}{2(1+\lambda)} \tag{20}$$

Using equations 18 and 20 to obtain the line currents yields

$$I_{a2}=I_{a1}+I_{a2}=1.0 \tag{21}$$

$$I_b=a^2I_{a1}+aI_{a2}=\frac{3a^2+a^2\lambda-a+a\lambda}{2(1+\lambda)} \tag{22}$$

$$I_c=aI_{a1}+a^2I_{a2}=\frac{3a+a\lambda-a^2+a^2\lambda}{2(1+\lambda)} \tag{23}$$

Solving for the magnitude of I_b and I_c gives

$$|I_b|=|I_c|=\frac{\sqrt{13+2\lambda+\lambda^2}}{2(1+\lambda)} \tag{24}$$

To determine the zone of protection substitute $|I_b|=|I_c|=1.2$ into equation 24. This gives

$$1.2=\frac{\sqrt{13+2\lambda+\lambda^2}}{2(4+\lambda)} \tag{25}$$

Solving equation 25 gives $\lambda=0.59$. Thus any line-to-line faults occurring on the 41 per cent of the line nearest the 3-phase-to-ground short circuit will not be detected. The zone of protection can also be established for line-to-ground and double-line-to-ground faults by the use of the relations given in Table I. In all cases the relays at the source end are not capable of detecting faults at all points along the line.

The double-line-to-ground fault conditions as seen by the source end relays were derived in equations 5 through 12. It is now necessary to determine the effects of the fault upon the currents at the short-circuited end of the line. Solving first for the sequence components of the currents at the short-circuited end gives

$$I_{a1}'=\frac{E_{S1}-I_{a1}(Z_{S1}+\lambda Z_{L1})}{(1-\lambda)Z_{L1}} \tag{26}$$

Substituting equations 1 and 9 into equation 26 gives

$$I_{a1}'=\frac{Z_{S1}+\lambda Z_{L1}+\dfrac{(1-\lambda)Z_{L1}}{\left(1+\dfrac{1}{\gamma_2}+\dfrac{(Z_{L1})}{(Z_{L0})}\dfrac{1}{\gamma_0}\right)}-(Z_{S1}+\lambda Z_{L1})}{(1-\lambda)Z_{L1}}I_{a1}$$

or

$$I_{a1}'=\frac{1}{\left(1+\dfrac{1}{\gamma_2}+\dfrac{(Z_{L1})}{(Z_{L0})}\dfrac{1}{\gamma_0}\right)}I_{a1} \tag{27}$$

Similarly

$$I_{a2}'=I_{a1}' \tag{28}$$

$$I_{a0}'=\frac{(Z_{L1})}{(Z_{L0})}I_a' \tag{29}$$

For faults near the short-circuited end the foregoing currents remain unbalanced. This unbalance may thus be used for fault detection.

Solving now for the line currents gives

$$I_a'=I_{a1}'+I_{a1}'+\frac{(Z_{L1})}{(Z_{L0})}I_{a1}'$$

$$I_b'=a^2I_{a1}'+aI_{a1}'+\frac{(Z_{L1})}{(Z_{L0})}I_{a1}'$$

$$I_c'=aI_{a1}'+a^2I_{a1}'+\frac{(Z_{L1})}{(Z_{L0})}I_{a1}'$$

or

$$I_a'=\left(2+\frac{Z_{L1}}{Z_{L0}}\right)I_{a1} \tag{30}$$

$$I_b'=I_c'=\left(-1+\frac{Z_{L1}}{Z_{L0}}\right)I_{a1} \tag{31}$$

Taking the ratio of maximum to minimum line current gives

$$\frac{|I_a'|}{|I_b'|}=\frac{2+\dfrac{Z_{L1}}{Z_{L0}}}{1-\dfrac{Z_{L1}}{Z_{L0}}} \tag{32}$$

Since the ratio of Z_{L1} to Z_{L0} is less than 1, equation 32 may be expressed as

$$\frac{|I_a'|}{|I_b'|}>2 \tag{33}$$

Thus standard phase unbalance relays applied at the short-circuited end will detect double-line-to-ground faults occurring anywhere along the line.

For a line-to-line fault the ratio of maximum to minimum line current becomes

$$\frac{|I_a'|}{|I_b'|}=2 \tag{34}$$

Thus, regardless of the line and source impedances or the point at which the fault occurs, the maximum line current at the short-circuited end is twice the minimum line current assuring operation of phase unbalance relays at the short-circuited end.

Appendix II. Method of Solving Line-to-Ground Fault

Since the ratio of maximum to minimum line currents at the short-circuited end cannot be given in a simple expression for a line-to-ground fault, an example will be given showing the method of solution. For the purpose of simplifying the example, the resistances have been neglected. The following reactances are used:

$X_{S1}=0.6$ pu	$X_{L1}=0.4$ pu
$X_{S2}=0.2$ pu	$X_{L2}=0.4$ pu
$X_{S0}=0.1$ pu	$X_{L0}=1.1$ pu

The equivalent circuit is given in Fig. 3. Substituting sequence impedances into equations 6, 7, and 8 yields

$$\gamma_1=\frac{0.6+0.4\lambda}{1.0} \tag{35}$$

$$\gamma_2=\frac{0.2+0.4\lambda}{0.6} \tag{36}$$

$$\gamma_0=\frac{0.1+1.1\lambda}{1.2} \tag{37}$$

Substituting these values into the expressions given in Table I for the sequence currents for a line-to-ground fault gives

$$I_{a1}=\frac{0.75+1.53\lambda}{0.558+1.722\lambda} \tag{38}$$

$$I_{a2}=\frac{0.32(1-\lambda)}{(0.558+1.722\lambda)} \tag{39}$$

$$I_{a0}=\frac{0.44(1-\lambda)}{(0.558+1.722\lambda)} \tag{40}$$

$$I_{a1}'=\frac{0.27+1.53\lambda}{0.558+1.722\lambda} \tag{41}$$

$$I_{a2}'=-\frac{0.16+0.32\lambda}{0.558+1.722\lambda} \tag{42}$$

$$I_{a0}'=-\frac{0.04+0.44\lambda}{0.558+1.722\lambda} \tag{43}$$

Solving for line currents gives

$$I_a=\frac{1.51+0.77\lambda}{0.558+1.722\lambda} \tag{44}$$

$$|I_b|=|I_c|=\frac{\sqrt{0.148+1.392\lambda+3.658\lambda^2}}{0.558+1.722\lambda} \tag{45}$$

$$I_a'=\frac{0.07+0.77\lambda}{0.558+1.722\lambda} \tag{46}$$

$$|I_b'|=|I_c'|=|I_b|=|I_c| \tag{47}$$

Curves showing variation in currents as a function of the point at which the fault occurs are given in Fig. 4. From Fig. 4(A) it can readily be seen that ground faults occurring in approximately the last 20 per cent of the line will not be detected from the source end. The ground current is almost zero so that ground relays are inoperative and the conductor current is insufficient to operate overcurrent relays which are set for a pickup of about 120 per cent of the current required for sleet melting.

Fig. 4(B), however, shows the phase current at the short-circuited end to be of sufficient magnitude and unbalance to operate a phase balance current relay for unintentional line-to-ground faults anywhere on the line. This then provides a means of tripping the short-circuited end breaker which, when opened, changes the nature of the unintentional fault so that it can be detected and cleared from the source end.

References

1. Sleet and Ice Troubles on Transmission Lines in New England, C. R. Oliver. *AIEE Transactions*, vol. 44, 1925, pp. 574–79.

2. Forty-Two Years' Experience Combating Sleet Accumulations, A. N. Shealy, K. L. Althouse, R. N. Youtz. *Ibid.*, vol. 71, pt. III, Aug. 1952, pp. 621–28.

3. Sleet Melting on the American Gas and Electric System, S. C. Bartlett, C. A. Imburgia, G. H. McDaniel. *Ibid.*, pp. 704–09.

4. Sleet-Melting Practices—Niagara Mohawk System, H. B. Smith, W. D. Wilder. *Ibid.*, pp. 631–34.

5. Sleet-Thawing Practices of the New England Electric System, C. P. Corey, H. R. Selfridge, H. R. Tomlinson. *Ibid.*, pp. 649–57.

6. Circuit Analysis of A-C Power Systems (book), Edith Clarke. John Wiley and Sons, Inc., New York, N. Y., vol. 1, 1943.

7. Rotating Electric Machinery. *ASA Standard No. C50*, American Standards Association, New York, N. Y., Mar. 1943.

Discussion appears on page 1072

Discussion

G. W. Hampe (Commonwealth Edison Company, Chicago, Ill.): The removal of faults on lines which are being de-iced is important for the reasons given in the paper, plus the following:

1. A fault arc might be blown over into another line on the same right of way.
2. Zero phase sequence current may be induced into other lines on the same right of way.
3. Fault current superposed on melting current may cause annealing of conductors or other damage.

Actually, faults on lines which are being de-iced are surprisingly rare, probably for the following reasons:

1. The melting periods are usually short.
2. The high currents cause the conductors to repel each other magnetically.

On our 138-kv system at least, there has been only one known case of conductors swinging together while de-icing. It is of course possible for an iced static wire to break and fall into conductors. Also, occasionally, conductors jump up when de-iced to contact a static wire.

The Commonwealth Edison Company practices glaze prevention and removal by the following methods:

1. Glaze prevention by forced loading (mostly at 138 kv). Except for changing sensitivity taps on one phase-comparison relay scheme previous to the ice season, there is no special relaying.
2. Ice removal from subtransmission or distribution lines mostly at 34.5 kv, by phase-shift methods. Normal relaying is kept in service as much as practical, but many distance relays are made inoperative. Transfer bus overcurrent relays operating on high-ratio current transformers with a selector switch are quite common. At smaller substations or distribution centers, there may be no relaying. In recent installations, ratio selectors are applied so that the normal line relays can be kept in service at reduced sensitivity, and the ground relays kept at normal sensitivity.
3. Ice removal from short links of high-voltage (138- or 69-kv) lines by short-circuiting and tying to 34.5- or 12-kv busses. Special overcurrent relays may be used to supplement the relays on the transformers supplying the melting current.
4. Short-circuiting (grounding) 138-kv lines for melting from source voltages which are approximately normal. The so-called melting system usually includes several transmission links and may include transformers. The normal relays are thermally inadequate where full melting current flows and some line current transformers must be shunted for the thermal reasons also. Special phase overcurrent and ground relays are used at one station, and by the addition of auxiliary current transformers on some lines, at one transmission substation. Where several lines in parallel supply the melting line, normal relaying can usually be retained on the paralleled lines.

The most specialized ice melt protection is a set of undervoltage relays on the bus at a transmission substation. These take one of three settings by a selector switch under operator control. The trip circuit is connected to all circuit breakers on the melting system bus. In Commonwealth Edison Company practice, the lines under melt are not usually grounded through a circuit breaker. Hence, it is not practical to apply relays at the grounded end. If the situation can be considered sufficiently critical, the use of relays to detect unbalanced currents or voltages offers another approach to the problem, and we are indebted to the authors for the suggestion.

H. R. Tomlinson (New England Electric System, Boston, Mass.): The authors have presented an excellent analysis of the problems encountered in providing protection for equipment during sleet-melting operations.

One question which might arise in the minds of some readers is the extent to which special relaying equipment can be justified. That is, by an insurance analogy, is the premium cost excessive for the probability of the hazards? In the last 25 years of sleet-thawing operations by the New England Electric System, there is not a single case on record whereby overload relays at the sources were required to clear an unintentional fault on a line being thawed. This might be an unfair amount of good fortune. On the other hand, there are several features about these operations which are conducive to such a record.

1. Generally, the voltage applied at the source end of a short-circuited line is considerably less than the normal operating voltage. This practically precludes the probability of insulation failure during sleet melting.
2. When the thawing current is provided by an isolated generator or transformer, the short-circuit current availability to an unintentional fault might be insufficient to burn off the conductors. This practically precludes the probability of a permanent fault resulting by a jump contact during ice unloading.
3. During sleet melting, the normal hazards to line operation, such as lightning, wind, etc., do not prevail. Also, the time factor is low for an involvement in an unusual hazard.

Another factor to consider in determining the need for special protection is the amount of operating supervision which is assigned to sleet-melting operations. The general practice by the New England Electric System is to call in off-duty operators who devote their time exclusively to operating and supervising the sleet-melting procedure. These special operators are charged with the responsibility of constant supervision and to make immediate correction if any condition arises which might endanger equipment. The installation of a complete protective system will not obviate the need for special operators; however, the need for special operators does obviate a requirement for a greater degree of protection.

The authors state that during sleet-melting operations, lines and equipment are usually operated at their thermal capacities. If equipment is isolated to supply the thawing current, it is not necessarily true that such equipment will be operated at thermal capabilities. Unless the equipment capability exactly matches the thawing load, some thermal reserve is available for unbalanced line currents and for negative sequence currents in generator rotors.

The authors have presented a solution for cases requiring complete protection.

J. C. Hogan and **C. G. Pebler**: The discussions have presented many interesting points of view relative to the techniques used for sleet prevention and sleet melting.

Mr. Hampe's scheme utilizing undervoltage relays connected to the bus potential transformers at a subtransmission substation with a selector switch controlled by the operator to provide one of three settings for ice-melt protection is very intriguing. It would be interesting to know the details of the application and the degree of protection which is afforded.

The need for complete line protection during sleet melting has been questioned by both discussers. It is true that individual cases utilizing the short-circuit method may not require this degree of protection. The application covered by the paper, however, came about through the use of one or two generators which are isolated from the system and used to provide a variable voltage supply to control the magnitude of the sleet-melting current. This presents a most hazardous condition since the generators may be operating near their full load current rating and any unbalance is confined to these machines.

Where generators are isolated there is a need for greater protection against possible unbalanced condition. The "American Standard for Rotating Electrical Machinery" (*ASA C50*), establishes generator load unbalance ability for a time of less than 30 seconds. No definite information is available on this ability for extended periods of time but the capability to withstand unbalanced loading will probably vary with machine design. It is certain that the magnitude of negative sequence current which a generator can withstand for any period of time decreases with the loading. Operating near full load therefore increases the possibility of damage caused by unbalance.

The statement by Mr. Tomlinson that "when the thawing current is provided by an isolated generator or transformer the short-circuit current availability to an unintentional fault might be insufficient to burn off the conductors" presupposes that no permanent faults or arcing contacts will be encountered. Experience shows, however, that the heavy loading during sleet melting may cause a poor line connection to overheat and fail which otherwise would be undetected. Furthermore, sudden unloading of one conductor may cause a rebound and result in physical contact between the phases. This may lead to arcing faults which should be quickly removed to prevent further conductor damage.

Automatic fault protection versus operator judgment and speed of fault removal also affects the plan of protection to be applied. Many companies prefer to relieve their operators of making decisions in situations of this nature.

The authors wish to thank the discussers for their contributions.

Testing of D-C Interrupters on A-C Test Circuits

K. CHEN
STUDENT MEMBER AIEE

E. W. BOEHNE
FELLOW AIEE

WITH the expansion of modern electric power systems, large a-c testing plants have been constructed with appropriate facilities for testing large a-c interrupters. Meanwhile d-c interrupters of higher interrupting capacity are being built to meet the needs of growing d-c systems. The testing of the new d-c interrupters would normally call for the installation of new large d-c testing plants if the conventional methods of testing d-c interrupters were used. The great expense of building high-capacity d-c testing plants can be saved if some appropriate method can be found to test large d-c interrupters on the existing a-c test circuits, provided the test results thus obtained are as informative as those obtained from the conventional d-c tests. It is the purpose of this paper to make such a proposal.

Criteria of Simulation of D-C Tests on A-C Circuits

The purpose of testing interrupters is twofold: to establish proper ratings and to obtain definite knowledge of the performance of the tested interrupters. If these purposes can be fulfilled by conducting the tests on a-c circuits, the simulation of d-c and a-c tests is justified.

The phenomena of current interruption have been analyzed[1] and quantitative performance criteria have been established for both a-c and d-c interrupters.[2-4] These analyses are characterized by the presentation of exact expressions for the arc energy released as a function of the arc voltage developed by the interrupter. This quantitative knowledge for both a-c and d-c circuits forms the necessary bridge which makes possible the accurate testing of d-c interrupters on a-c circuits provided, of course, that arc current and recovery voltage criteria are maintained, all in their proper time relationships.

It follows that an a-c test on a d-c interrupter which (1) releases a controlled and known amount of energy, (2) maintains the proper instantaneous voltage across the interrupter following interruption, (3) achieves the maximum arc current within the interrupter, and (4) accomplishes these criteria within a known and specified arcing time can be considered the equivalent of d-c performance. If a-c tests can be conducted under these specifications, d-c interrupters can be expected to demonstrate the same physical characteristics of external flame, contact burning, and audible report as experienced on the d-c test, thus giving supporting physical evidence that the circuit breaker has been adequately tested.

Control of A-C Test Circuit

The accomplishment of the foregoing equivalent performance of a d-c interrupter can only be realized in an a-c power testing laboratory equipped with modern, accurately timed controls. Testing is obviously performed on a single-phase circuit. Axiomatically, the four interrelated conditions just described which are necessary to produce the equivalent of d-c performance from an a-c test circuit require a minimum of four variables which can be accurately controlled in the testing laboratory. It follows that, with the availability of four controllable variables, equations can be set up whose solution will dictate the required conditions for equivalence. A theoretical analysis is presented which shows one method by which this equivalence can be approached.

ONE METHOD FOR EQUIVALENCE

Magnitude of A-C Test Voltage. The alternator voltage is controlled principally by its field current. With various alternator coil arrangements, a further variation of generator voltage can be attained. Test voltages higher or lower than the rated alternator voltage are obtained by transformers. Usually the secondary of such transformers consists of several coils which can be arranged in a multitude of combinations so that various voltages are available with full testing capacity. Voltage is further modulated by the test frequency employed.

Magnitude of A-C Short-Circuit Current. This is controlled by series reactors inserted in the test circuit as well as by the alternator voltage and is independent of frequency.

Angle of A-C Voltage at Fault Initiation. This is controlled by means of a synchronous switch which can initiate the short-circuit current at any desired angle on the a-c test voltage curve.[5] This is an important feature in the control of arc energy.

Frequency. The frequency is controlled by adjusting the speed of the alternator drive and is the most important controllable variable to achieve the equivalence discussed in this paper.

Additional control of the a-c test circuit may be obtained by inserting a shunt inductance, a series resistance, or a shunt resistance in the test circuit. It is not necessary to introduce an additional parameter in the test circuit in order to simulate d-c tests on a-c circuits. However, that there are certain merits in such a procedure will be shown in a later section.

A casual inspection of the d-c circuit-breaker performance in relation to the preceding controllable variables will show that breaker speed and the arc voltage wave shape and magnitude will also enter the picture in the final analysis. The former can be mitigated by providing a controllable interval between the initiation of the current and the tripping of the d-c breaker and in this way further controlling the angle and instantaneous current at the time of contact parting. The nature of the arc voltage enters the problem in a predominate manner and is a necessary item in determining the proper combination of circuit variable, previously outlined, in order to achieve test equivalence. The nature of arc voltage, however, can only be obtained by test. As a result, preliminary testing must be carried out to determine this inherent characteristic before converging on the final test settings to demonstrate the breaker rating.

CONCLUSIONS

Before proceeding with the graphical and quantitative analysis and proof of the equivalence, the following conclusions may be drawn for the benefit of the reader in an administrative capacity.

Paper 55-508, recommended by the AIEE Switchgear Committee and approved by the AIEE Committee on Technical Operations for presentation at the AIEE Summer General Meeting, Swampscott, Mass., June 27–July 1, 1955. Manuscript submitted March 30, 1955; made available for printing May 3, 1955.

K. CHEN is with Westinghouse Electric Corporation, Pittsburgh, Pa., and E. W. BOEHNE is with the Massachusetts Institute of Technology, Cambridge, Mass.

Portions of the paper are from an MS Thesis in Electrical Engineering submitted by K. Chen to the Massachusetts Institute of Technology.

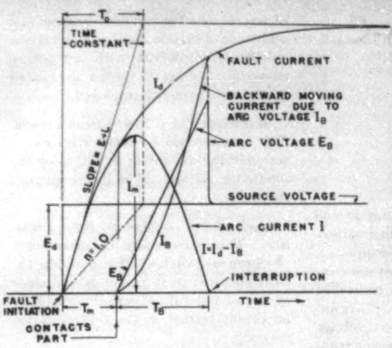

Fig. 1 (left). A typical d-c interruption produced by a breaker which opens T_m seconds after fault initiation and produces a linearly rising arc voltage which results in interruption after T_B seconds of arcing. This performance is simulated on an a-c circuit as shown in Fig. 2

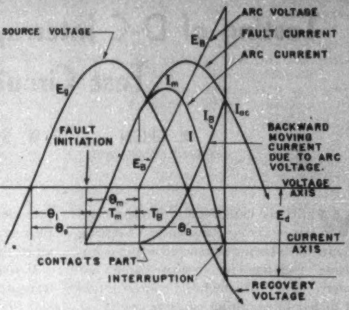

Fig. 2. The a-c simulation of the d-c performance shown in Fig. 1. Here the same arc voltage acts in an a-c circuit to produce the same peak arc current, arc energy, and arcing time as in the d-c case shown. The development of this simulated performance on an accurate quantitative basis is the aim of this paper

1. D-c circuit interrupters (fuses or circuit breakers) can be adequately tested on modern a-c laboratory circuits where the generator frequency is controllable and where a single-phase synchronous switch is available. (Stations having no frequency control can make tests at the proper generator speed during the normal deceleration of the machine.)

2. It is believed that such tests would give all the necessary oscillographic evidence of meeting the essential criteria of d-c performance as well as the outward visible performance of equivalent d-c interruption.

3. Total quantitative arc energy relations for d-c and a-c breakers are embodied in this paper and equated to assist the formulation of a-c equivalent circuits for the laboratory testing of d-c interrupters. This is approached by using novel methods of circuit synthesis which include the energy criterion as one of the most important ingredients of the specification. Peak current and recovery voltage criteria were also matched by developing an original method of approach which can be applied to a wide range of breaker requirements.

4. Arc energy equations all show that the symmetrical short-circuit kilovolt-amperes are the dimensional energy base which are modulated by the arc energy coefficient *k*. This is expressed in dimensionless relations capable of being converted to curve and table form.

5. The limited space in this paper did not allow the consideration of additional available means of circuit control which would enhance and refine the technique described here. These consist essentially of shunt parameters across the circuit-breaker bushings and/or employing pre-tripping techniques.[4]

6. The arc energy equations contained here are applicable to all types of a-c and d-c interrupters and offer an unusual opportunity to study the design factors which influence the energy liberated in circuit breakers and fuses.[2,3,6]

7. The student of the subject who pursues the techniques suggested here will unquestionably improve the procedures outlined in this paper by laboratory application. The pursuit of these efforts should aid in predetermining circuit-breaker performance and in particular verify the extent to which the predictions of this analysis with respect to a-c and d-c equivalence are confirmed by actual breaker tests.

8. The symmetrical short-circuit megavolt-amperes (mva) should be retained in the circuit-breaker standard as the energy base of all liberated energy within the breaker as described by the energy coefficient *k*.

Graphical Picture

Before proceeding with a quantitative analysis of the equivalence through formal equations, a pictorial understanding of the problem will be presented here. In this way the physics of the problem will become better understood and, at the same time, the reader can become acquainted with the nomenclature used throughout the paper.

The short circuit which develops in a d-c system is shown in Fig. 1 and assumes a linear system inductance and resistance. The current I_d rises in a typical exponential manner and would reach a maximum value (E_d/R) determined by the system resistance if not arrested by the promptness of the modern d-c breaker. At a time T_m the breaker contacts part and the arc which develops gives rise to a rapidly increasing arc voltage E_B which will be assumed to rise linearly at N volts per second. As previously demonstrated,[3] this arc voltage can be correctly considered to develop its own current I_B, which would oppose the d-c short-circuit current I_d. The net current I is the difference between these two currents and comes to zero after an arcing interval of T_B seconds. Accompanying the fall of current to zero,* the arc voltage turns and falls to the system voltage E_d which appears across the breaker following interruption. The energy W released by the breaker is the integration of the wattage E_BI over the arcing interval T_B.

The essential criteria to be duplicated in the a-c test circuit are:

1. The peak arc current I_m; see Fig. 1.
2. The proper recovery voltage across the circuit breaker just following current zero, namely E_d.
3. The same total arc energy release W.
4. To accomplish items 1 through 3 in about the same total arcing time T_B.

These results are reproduced in the a-c test circuit shown in Fig. 2. Here the a-c circuit is closed 64.5 degrees following the normal voltage zero in a 28-cycle test circuit, producing a current which rises at the same general rate as in the d-c case. The d-c breaker responds in its customary manner (since it has not been told that it is now functioning in an a-c circuit), parts its contacts in the same interval T_M, and produces the same linearly rising arc voltage E_B. The circuit is so chosen that the same peak current I_m results; interruption takes place in about the same over-all time; the arc energy produced is exactly the same as in the d-c case; and the recovery voltage which appears across the breaker following interruption is in-

---

* Oscillographic records show that in the region of current zero the arc current tapers off to a small leakage current which is maintained by the system voltage. This prevents any oscillatory phenomena at interruption and explains why arc voltage and current seek proportionality just prior to the so-called interruption.

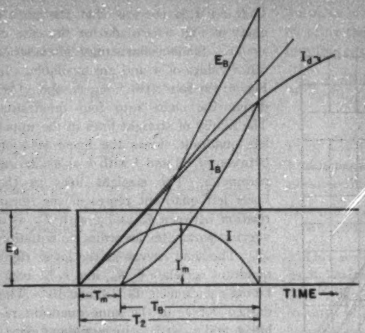

Fig. 3. The interruption of a low-voltage d-c fault by a fast circuit breaker. This performance is simulated in a low-frequency a-c circuit as shown in Fig. 4

Fig. 4 (right). The a-c simulation of the d-c performance shown in Fig. 3. Here the d-c performance is whittled out of a low-frequency a-c circuit producing quantitatively correct performance. The recovery voltage keeps the same polarity relationship as in the d-c case

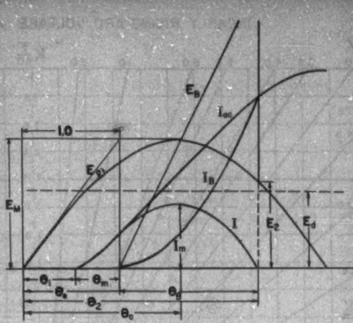

stantaneously the same in magnitude (although opposite in polarity) as in the d-c case, namely E_d. The breaker has accordingly experienced what might be considered an authentic d-c interruption if the sudden reversal of voltage polarity from arc voltage extinction value to the instantaneous recovery voltage value in the arc wave can be shown to be of no great consequence.

The duplication of all the foregoing essential requirements by empirical methods would be time consuming, expensive, and possibly destructive to the test sample. Instead, by predetermining the nature of the arc voltage characteristic of the d-c breaker, it is then possible to proceed to duplicate all the essential performance criteria by computing the a-c test frequency, voltage, reactance, and closing angle in advance of the test. Such a procedure of circuit synthesis is outlined in the remainder of this paper and further elaborated in reference 4. Figs. 3 and 4 outline a separate solution which is also practical for high-speed d-c breakers of moderate voltage, and which maintain the recovery voltage polarity the same as is the case for normal d-c interruption.

Determination of Controlled Variables in A-C Test Circuit

Linearly Rising Arc Voltage

The purpose of this section is to show how the controlled variables in the a-c test circuit may be determined mathematically or graphically to bring about the equivalence of a-c and d-c tests according to the criteria established previously. In a d-c test, the voltage across the interrupter following the extinction of the arc is simply the d-c system voltage E_d. The maximum arc current is given by the following equation which is developed in Appendix II.

$$I_m=\frac{E_d}{R}[(1-m\epsilon^{-T_m/T_0})+n(\ln\ m+1-m)] \qquad (1)$$

where

$$m=\frac{n}{n+\epsilon^{-T_m/T_0}} \qquad (2)$$

The total arc energy released by the interrupter is given by the following equation which was developed in a previous paper[3]

$$W=2(139)T_m k_n \times \text{mva watt-hours} \qquad (3)$$

where the dimensionless arc energy function k_n is

$$k_n=\frac{nT_0}{T_m}\left[\frac{q^2}{2}\left(1+n-\frac{2}{3}nq\right)+[\epsilon^{-q}(q+1)-1](\epsilon^{-T_m/T_0}+n)\right] \text{ watts per volt-ampere} \qquad (4)$$

$$q=T_B/T_0 \qquad (5)$$

$$n=\frac{1-\epsilon^{-(T_m/T_0+q)}}{\epsilon^{-q}+q-1} \qquad (6)$$

The plotting of k_n versus T_0/T_m for various values of n is shown in Fig. 5.

If the same interrupter functions in an a-c circuit, the performance may be completely described by the following equations

$$W=\left(\frac{2E_g I_{sc} J}{2\pi f}\right) \qquad (7)$$

$$J=n\left[\frac{1}{2}\theta_B{}^2\left(\cos\theta_1-\frac{1}{4}n\theta_B{}^2\right)-(\theta_B\sin\theta_2+\cos\theta_2-\cos\theta_e)\right] \qquad (8)$$

$$E_2=\sqrt{2}E_g\sin\theta_2 \qquad (9)$$

$$I_m=\sqrt{2}I_{sc}\left(\cos\theta_1-\cos\theta_0-\frac{1}{2}\frac{\sin^2\theta_0}{n}\right) \qquad (10)$$

$$\theta_B=\left(\frac{2(\cos\theta_1-\cos\theta_2)}{n}\right) \qquad (11)$$

$$n=\left(\frac{\sin\ \theta_0}{\theta_0-\theta_e}\right) \qquad (12)$$

$$\theta_B=\theta_2-\theta_e \qquad (13)$$

$$E_g=I_{sc}2\pi fL \qquad (14)$$

$$\theta_m=2\pi fT_m \qquad (15)$$

$$\theta_e=\theta_1+\theta_m \qquad (16)$$

$$N=\sqrt{2}E_g(2\pi f)n \qquad (17)$$

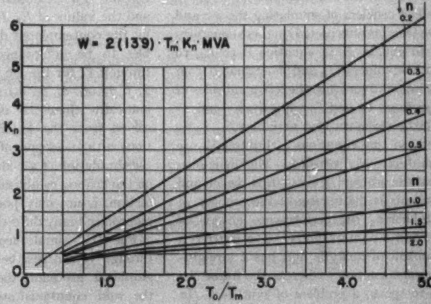

Fig. 5. The relationship between the linearly rising arc voltage slope n and the energy coefficient K_n in the determination of the arc energy released in a d-c circuit breaker. The source of these relations is given in equation form in this paper

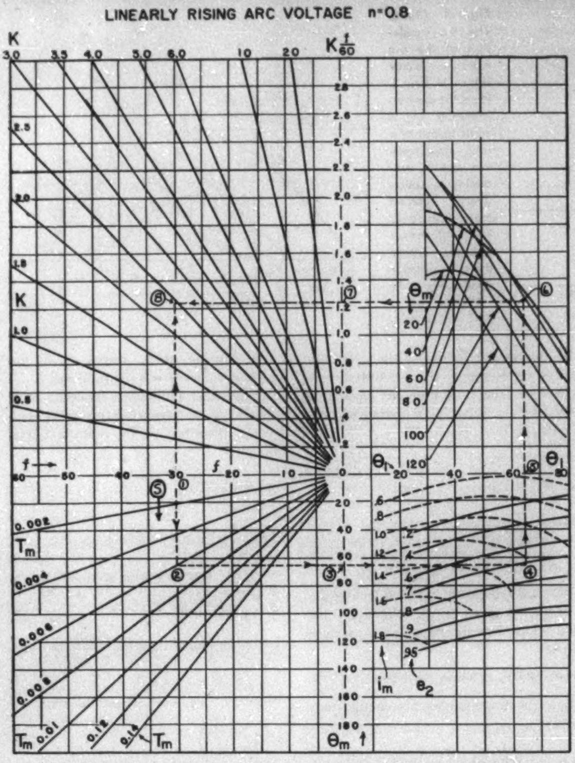

Fig. 6. A typical master chart for the determination of the a-c frequency, voltage, current, and closing angle to be used in the a-c simulation of the desired d-c performance

Most of these 11 simultaneous equations are derived in Appendix I. The balance are simple relations by definitions and need no further explanation.

The problem of simulating the a-c and d-c tests, as interpreted by these equations is to equate E_2 in equation 9 to E_d, to put the values of I_m and W evaluated from equations 1 and 3 to the left-hand sides of equations 10 and 7 respectively, and to whittle the controlled variables E_g, L, θ_1, and f so that equations 7 through 17 are simultaneously satisfied. Thus it is seen that the problem of simulating the a-c and d-c tests is the reverse of the problem of establishing the performance criteria of a-c and d-c interrupters. The latter is a problem of analysis and has a straightforward solution; whereas the former is, so to speak, a problem of synthesis. In general, synthesis problems have no unique solutions and sometimes may have no solutions. In the present case, with E_B and T_m estimated by the designer, and the values of E_2, I_m, and W dictated by the contemplated d-c test, the variables to be determined in equations 7 through 17 for the a-c test are E_g, I_{sc}, n, J, f, θ_B, θ_1, θ_s, θ_2, θ_0, L, and θ_m. Axiomatically these 12 unknowns can be solved from the 11 simultaneous equations with one degree of freedom. Hence the simulation of a-c and d-c tests, based on the criteria established in the previous section, is not only possible but may be realized in many different ways.

The 11 simultaneous equations 7 through 17 can best be solved through a graphical procedure because several of the said equations are transcendental. It is for this purpose that the master chart of Fig. 6 is made for the case of $n=0.8$. Similar charts may be made for other values of n and are available. In Fig. 6, the four axes f, θ_m, θ_1, and $kf/60$ divide the chart into four quadrants. The family of straight lines in the upper left quadrant shows the linear relation between $kf/60$ and f with k as a varying parameter. The straight lines in the lower left quadrant represent the linear relation between θ_m and f with T_m as a varying parameter according to equation 15. The solid curves in the lower right quadrant correlate θ_1, θ_m, and e_2 by combining equations 9, 11, 13, and 16. The dashed curves in the same quadrant relate θ_1 and θ_m with i_m by combining equations 10, 12, and 16. In the upper right quadrant the arc energy function $kf/60$ is related to θ_1 and θ_m by making use of equations 7, 8, 11, and 13 to plot the curves. Note that equation 17 is implied by the condition $n=0.8$ for the chart. Thus the master chart in Fig. 6 graphically represents the set of 11 simultaneous equations except equation 14, which will be used later to determine L after a trial-and-error solution for I_{sc} is obtained through the use of the chart. This point will be clarified in the following example.

For illustration, consider a d-c circuit breaker designed to have an opening time $T_m=0.006$ second and an arc voltage which rises linearly with a rate of $N=420{,}000$ volts per second. A d-c test is contemplated for testing the performance of the circuit breaker in clearing a short-circuit fault on a 2,000-volt d-c line with a resistance of 0.04 ohm and an inductance of 0.40 millihenry. In other words, the time constant T_0 of the d-c circuit is 0.010 second. The expected maximum

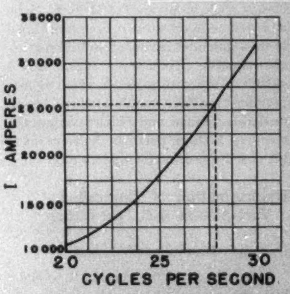

Fig. 7. A typical auxiliary curve determined from graphically computed data obtained by the multiple use of Fig. 6 and used to fix the a-c frequency necessary to produce the desired peak arc current in the simulated test

arc current I_m and arc energy W in this d-c test can be determined by carrying out the following calculation

$$n=\left(\frac{NT_0}{E_d}\right)=\frac{420{,}000}{2{,}000}\times 0.01=2.1 \text{ per unit} \tag{18}$$

$$\frac{T_0}{T_m}=\left(\frac{0.01}{0.006}\right)=1.667 \tag{19}$$

From n and T_0/T_m, k_n may be determined to be 0.523; see Fig. 5. Hence, from equation 3

$$\begin{aligned} W&=2(139)T_m k_n\times\text{mva}\\ &=2(139)(0.006)(0.523)\times\frac{(2{,}000)^2}{0.04}\times 10^{-6}\\ &=87.3 \text{ watt-hours} \end{aligned} \tag{20}$$

From equations 2 and 1

$$m=\left(\frac{n}{n+\epsilon^{-T_m/T_0}}\right)=\left(\frac{2.1}{2.1+\epsilon^{-0.6}}\right)=0.793 \tag{21}$$

$$I_m=\frac{2{,}000}{0.04}\,[(1-0.793\epsilon^{-0.6})+2.1(\ln 0.793+1-0.793)]=25{,}600 \text{ amperes} \tag{22}$$

The values of $E_d=2{,}000$ volts, $I_m=25{,}600$ amperes, and $W=87.3$ watt-hours are then inserted into equations 7 through 17. As there is one degree of freedom in solving the simultaneous equations, an arbitrary choice of $n=0.8$ is made. A trial-and-error procedure is then used to solve the simultaneous equations with the aid of the master chart in Fig. 6. First, a frequency, say, $f=30$ cycles per second is assumed. Then, from equation 17

$$\sqrt{2}E_g=\left(\frac{N}{2\pi f n}\right)=\frac{420{,}000}{2\pi\times 30\times 0.8}=2{,}785 \text{ volts} \tag{23}$$

hence

$$e_2=\left(\frac{E_2}{\sqrt{2}E_g}\right)=\frac{2{,}000}{2{,}785}=0.717 \tag{24}$$

Then, starting from point 1 in Fig. 6, one may trace the chart vertically and horizontally in a counterclockwise direction to point 2 as indicated by the arrows in Fig. 6. Point 2 is determined by the information of $T_m=0.006$. Going horizontally from point 2, $\theta_m=65$ degrees is read at point 3. Point 4 is determined by virtue of the information that $e_2=0.717$ given by equation 24. This gives $\theta_1=65$ degrees at point 5. Using the value of θ_m read at point 3, one may determine points 6 and 7 by going vertically from point 5 and then horizontally from point 6 to point 7. Point 8 is the horizontal projection of point 7 and vertical projection of point 1. At point 8, $k=2.48$ watt-hours per mva is read. Since

$$W=kE_g I_{sc}\times 10^{-6} \tag{25}$$

the value of I_{sc} may be calculated by substituting the values of k just determined into this equation

$$\sqrt{2}I_{sc}=\left(\frac{2W\times 10^6}{k\sqrt{2}E_g}\right)=\frac{2\times 87.3\times 10^6}{2.48\times 2{,}785}\ 25{,}250 \text{ amperes} \tag{26}$$

Point 4 in Fig. 6 also indicates that $i_m=1.26$, from which the maximum arc current may be computed

$$\begin{aligned} I_m&=\sqrt{2}I_{sc}i_m\\ &=25{,}250\times 1.26=31{,}800 \text{ amperes} \end{aligned} \tag{27}$$

This is not the desired value for I_m as indicated by equation 22 which was 25,600 amperes. However, a curve of I_m versus f in Fig. 7 may be produced by repeating the same procedure of tracing the chart a number of times. It is found from Fig. 7 that $f=28$ cycles per second produces the desired current $I_m=25{,}600$ amperes and is therefore the correct test frequency to be used.

It follows that

$$\sqrt{2}E_g=2{,}985 \text{ volts, } \theta_1=64.5 \text{ degrees, and } \sqrt{2}I_{sc}=21{,}000 \text{ amperes}$$

Finally the inductance to be inserted in the test circuit is given by equation 14

$$L=\left(\frac{\sqrt{2}E_g}{2\pi f\sqrt{2}I_{sc}}\right)=\left(\frac{2{,}985}{2\pi\times 28\times 21{,}000}\right)=0.808\times 10^{-3} \text{ henrys} \tag{28}$$

In summary the controls on the a-c test circuit should be set as follows:

Test voltage = 2,110 volts (rms)
Test frequency = 28 cycles per second
Test circuit inductance = 0.808 millihenry
Fault initiation angle = 64.5 electrical degrees

Figs. 1 and 2 compare the d-c and a-c tests and show the voltage and current wave forms in proper scales based quantitatively on the example just given.

Rectangular Arc Voltage

Similar equations may be derived and charts drawn for the case of rectangular or flat top arc voltage.[4] Only the equations will be given now.

The maximum arc current and the total arc energy released in a d-c test are given by the following equations derived in a previous paper[3]

$$I_m=I_{dc}\,(1-\epsilon^{-T_m/T_0}) \tag{29}$$

$$W=T_0E_BI_{dc}\left(i_m+e_c\ln\frac{e_c}{e_c+i_m}\right) \tag{30}$$

where

$$e_c=\frac{E_B-E_d}{E_d} \tag{31}$$

The equations describing the a-c test were derived in two other papers[1,2]

$$W=\frac{2E_gI_{sc}e_BQ}{2\pi f} \tag{32}$$

$$Q=\frac{1}{2}\theta_B(\cos\theta_1+\cos\theta_2)+(\sin\theta_e-\sin\theta_2) \tag{33}$$

$$E_2=\sqrt{2}E_g\sin\theta_2 \tag{34}$$

$$\begin{aligned} I_m&=\sqrt{2}I_{sc}\,(\cos\theta_1-\cos\theta_e) \text{ if } e_B>1\\ &=\sqrt{2}I_{sc}[(\cos\theta_1-\sqrt{1-e_B^2})-\\ &\qquad e_B(\sin^{-1}e_B-\theta_e)] \text{ if } e_B<1 \end{aligned} \tag{35}$$

$$e_B=\left(\frac{\cos\theta_1-\cos\theta_2}{\theta_B}\right) \tag{36}$$

$$\theta_B=\theta_2-\theta_e \tag{37}$$

$$E_g=I_{sc}2\pi fL \tag{38}$$

$$\theta_m=2\pi fT_m \tag{39}$$

$$\theta_e=\theta_1+\theta_m \tag{40}$$

$$E_B=\sqrt{2}E_ge_B \tag{41}$$

The interested reader who wants to use the related charts is referred to reference 4 from which the material of this paper is excerpted.

Nomenclature

The nomenclature used and described here is consistent, as far as possible, with the published work in this area referred to in the references. The per-unit (pu) system is used whenever possible to enable the application of this work to any circuit interrupter on a quantitative basis. Lower-case letters are used to denote voltages and currents in pu of the peak values of the system whenever possible. Capital letters are used to represent the actual magnitude of currents, voltage and the parameters. For example, where E_M is the crest value of the alternating voltage E_g and E_B is the arc voltage in volts then $e_B=E_B/E_M$ and is the pu arc voltage expressed as a ratio which is dimensionless.

The rates of rise of voltage and current are also expressed in terms of the system in which it occurs. The pu slope of the a-c source voltage at time of voltage zero is taken as unity. This slope has the magnitude $E_m\omega$ volts per second. In the d-c system the unit of slope of voltage is the direct voltage E_d divided by the time constant of the circuit T_0, which is L/R. The actual rates of rise of voltage in volts per second are termed N while the pu rates of rise are labeled n. Hence the pu rate of rise of the linearly rising arc voltage of the d-c circuit breaker is

$$n=\frac{N}{\left(\dfrac{E_d}{T_0}\right)}=\left(\frac{NT_0}{E_d}\right)=\left(\frac{NL}{E_dR}\right)$$

E_g = rms a-c test voltage, volts
E_M = maximum value of alternating voltage, used as base for pu voltages in a-c system
E_B = arc voltage, volts
E_d = d-c test voltage, volts; unit voltage base for d-c tests
E_2 = voltage across the interrupter following interruption, volts
e = voltage for system used, pu
e_B = arc voltage, pu
e_c = pu arc voltage in excess of d-c test voltage $= e_B - 1$
e_2 = pu voltage across the interrupter following interruption
f = frequency of test voltage
I = net instantaneous current, amperes
I_d = d-c short-circuit current uninfluenced by the breaker, amperes
I_{d0} = maximum d-c short-circuit current, amperes. Unit current base for direct currents $= (E_d/R)$
I_{sc} = rms symmetrical a-c short-circuit current, amperes
I_M = peak value of symmetrical a-c short-circuit current, amperes. Used as unit base for alternating currents
I_m = maximum instantaneous arc current, amperes
I_B = backward moving current due to the arc voltage, amperes
i = pu current
i_B = pu backward moving current due to the arc voltage
i_m = pu maximum instantaneous arc current
I_{sc} = a-c short-circuit current uninfluenced by the breaker
J = integral of the wattage coefficient curve over the arcing period for the linearly rising arc voltage case. A dimensionless trigonometric function
k = arc energy coefficient for a-c tests, watt-hours per mva
k_n = dimensionless arc energy function for d-c tests, watt-hours per mva-seconds
L = circuit inductance, henrys
m = a defined function of n, T_m, and T_0
N = slope of the linearly rising arc voltage, volts per second
n = pu slope of the linearly rising arc voltage
Q = arc-current-time area over the arcing period for the rectangular arc voltage case
q = arcing time in pu of the time constant of the d-c test circuit
R = resistance, ohms
r = pu resistance
T_B = arcing time, seconds
T_m = circuit-breaker opening or fuse melting time, seconds*
T_0 = time constant of the d-c test circuit, seconds
T = period of a-c circuit
T_1 = fault initiation time after last voltage zero, seconds
T_2 = time when interruption takes place following last voltage zero prior to fault initiation, seconds
t = time, seconds
W = arc energy, watt-hours
ϵ = Naperian logarithm base (2.718...)
θ = electrical angle, radians
θ_B = arcing time, radians
θ_e = angle at which the arc voltage is introduced measured from last voltage zero. Includes θ_1, radians
θ_m = circuit-breaker opening* or fuse melting angle, radians
θ_0 = angle at which the maximum instantaneous arc current occurs, radians
θ_1 = fault initiation angle from last voltage zero, radians
θ_2 = angle at which the interruption takes place measured from same voltage zero as θ_1, radians
π = ratio of circumference to diameter of a circle (3.14159...)
ω = angular frequency $= 2\pi f$

By these definitions several simple and important relations result which will make the definitions clearer and enhance their application

$$e_B = \frac{E_B}{E_d} \text{ for d-c case} \tag{42}$$

$$e_B = \frac{E_B}{E_M} \text{ for a-c case} \tag{43}$$

$$i = \frac{I}{I_M} \text{ for a-c case} \tag{44}$$

$$i = \frac{I}{I_{d0}} \text{ for d-c case} \tag{45}$$

$$E_M = \sqrt{2}E_g \tag{45A}$$

$$E_B = Nt = \left(\frac{nE_d}{T_0}\right)t \text{ for linearly rising arc voltage} \tag{46}$$

$$I_{d0} = \frac{E_d}{R} \tag{46A}$$

$$I_M = \sqrt{2}I_{sc} = \sqrt{2}\left(\frac{E_g}{\omega L}\right) \tag{47}$$

$$i_B = \frac{I_B}{I_M} \text{ for a-c case} \tag{48}$$

$$i_B = \frac{I_B}{I_{d0}} = \frac{I_B R}{E_d} \text{ for d-c case} \tag{49}$$

$$i_m = \frac{I_m}{I_M} \text{ for a-c case} \tag{50}$$

$$i_m = \frac{I_m}{I_{d0}} \text{ for d-c case} \tag{51}$$

$$\text{mva} = E_g I_{sc} \times 10^{-6} = \text{single-phase symmetrical mva for a-c case} \tag{52}$$

$$\text{mva} = E_d I_{d0} \times 10^{-6} \text{ for d-c case} \tag{53}$$

$W = k \times \text{mva}$ = arc energy in watt hours per loop of current

$$q = \frac{T_B}{T_0} \tag{54}$$

$$n = \frac{NT_0}{E_d} \text{ (d-c case)} = \left(\frac{1 - \epsilon^{-Tm/T_0}\epsilon^{-q}}{\epsilon^{-q} + q - 1}\right) \tag{55}$$

$$n = \frac{N}{E_m \omega} = \left(\frac{NT}{E_m 2\pi}\right) \text{ (a-c case)} \tag{56}$$

$$\theta_2 = (\theta_e + \theta_B) \tag{57}$$

$$\theta_e = (\theta_1 + \theta_m) \tag{58}$$

$$T_0 = \frac{L}{R} \tag{59}$$

$$T = \frac{2\pi}{\omega} \tag{60}$$

$$T_2 = (T_m + T_B) \tag{61}$$

Appendix I. Derivation of Equations for Performance in A-C Circuits of Interrupters Having Linearly Rising Arc Voltages

The equations derived in this appendix are based on the assumptions that the a-c circuit is purely inductive and that the arc is interrupted without reignition at the first current zero after the interrupter functions.

Voltage After Interruption

Referring to Fig. 2, the linearly rising arc voltage e_B may be written

$$e_B = n(\theta - \theta_e), \text{ for } \theta \geqq \theta_e \tag{62}$$

where n is the pu slope of e_B. The base slope of voltage is that of the alternating voltage E_g at $\theta = 0$ or $E_m\omega$. Since the circuit is purely inductive, the backward moving current i_B in pu is the time integral of the arc voltage e_B, or

$$i_B = \frac{1}{2}n(\theta - \theta_e)^2 \text{ for } \theta \geqq \theta_e \tag{63}$$

Interruption of arc current takes place at θ_2, where i_B cancels the forward moving current; i.e.

$$\frac{1}{2}n(\theta_2 - \theta_e)^2 = \cos\theta_1 - \cos\theta_2 \tag{64}$$

Hence the arcing angle is

$$\theta_B = (\theta_2 - \theta_e) = \sqrt{\frac{2(\cos\theta_1 - \cos\theta_2)}{n}} \tag{65}$$

This equation shows that θ_2 is a function of θ_1 and n, and so governs the voltage across the interrupter after the arc interruption since

$$e_2 = \sin\theta_2 \tag{66}$$

The true magnitude of E_2 is equal to the pu e_2 multiplied by E_m.

Arc Energy

The arc energy released by the interrupter is directly proportional to the integral

$$J = \int e_B i(d\theta) = \int e_B(I_{sc} - i_B)d\theta \text{ for the arcing period}$$

$$J = \int_0^{\theta_2 - \theta_1} n\theta\left(\cos\theta_1 - \cos(\theta_e + \theta) - \frac{1}{2}n\theta^2\right)d\theta$$

$$J = n\left[\frac{1}{2}\theta_B^2\left(\cos\theta_1 - \frac{1}{4}n\theta_B^2\right) - (\theta_B\sin\theta_2 + \cos\theta_2 - \cos\theta_e)\right] \tag{67}$$

---

[*] T_m and θ_m in circuit-breaker testing are quite flexible and alter considerably if pretripping is employed. In d-c breakers where the opening time is quite important to performance, T_m can be determined by the breaker provided the initial rate of rise of current is properly simulated and practical relay or breaker trip latches are employed and tested as part of the breaker design.

The arc energy in watt-seconds is

$$W=\left(\frac{2E_gI_mJ}{2\pi f}\right) \qquad (68)$$

If k = arc energy in watt-hours per mva of the a-c system capacity, then

$$k=\left(\frac{2\times J\times 10^6}{2\pi f\,3{,}600}\right)=K_2\frac{J}{f}\text{ watt-hours per mva per loop} \qquad (69)$$

from which (for curve construction) the following is used

$$k\frac{f}{60}=\left(\frac{2J\times 10^6}{2\pi\times 60\times 3{,}600}\right)=1.474\,J\text{ watt-hours per mva} \qquad (70)$$

The relation 1.474 J describes the factor k for the 60-cycle case.

Maximum Arc Current

The arc current reaches its maximum value at θ_0 where the arc voltage e_B is equal to the test voltage E_g. Hence θ_0 is given by the equation

$$n(\theta_0-\theta_e)=\sin\theta_0 \qquad (71)$$

The solution of θ_0 encounters a transcendental equation. Best results are hence achieved by plotting a simple family of curves relating n, θ_e, and θ_0 from which θ_0 can be readily determined for use in equation for the peak value of arc current

$$i_m=\int_{\theta_1}^{\theta_0}\sin\theta d\theta-\frac{1}{2}\sin\theta_0(\theta_0-\theta_e)$$

$$i_m=\cos\theta_1-\cos\theta_0-\frac{1}{2}\left(\frac{\sin^2\theta_0}{n}\right) \qquad (72)$$

Appendix II. Derivation of Maximum Current Equation for Interrupters Having Linearly Rising Arc Voltage in a D-C Circuit

The pu backward moving current caused by the linearly rising arc voltage in a d-c circuit having a time constant T_0 may be shown to be[3,4]

$$i_B=\left(\frac{t}{T_0}-1+\epsilon^{-t/T_0}\right)n \qquad (73)$$

The total pu arc current is the difference between the forward and the backward moving currents and is given by equation 74

$$i=(1-\epsilon^{-(t+Tm)/T_0}]-n\left(\frac{t}{T_0}-1+\epsilon^{-t/T_0}\right) \qquad (74)$$

Note: $t=0$ here when the contacts part and the arc voltage is introduced.

By setting (di/dt) to zero, the time at which the arc current reaches its peak may be determined. This time is found to be

$$t=-T_0\ln\left(\frac{n}{n+\epsilon^{-Tm/T_0}}\right) \qquad (75)$$

Substituting equation 75 into equation 74 gives the maximum arc current in pu, namely

$$i_m=(1-m\epsilon^{-Tm/T_0})+n(\ln m+1-m) \qquad (76)$$

where

$$m=\frac{n}{n+\epsilon^{-Tm/T_0}} \qquad (77)$$

References

1. The Geometry of Arc Interruption, E. W. Boehne. *AIEE Transactions*, vol. 60, 1941, pp. 524–32.
2. Performance Criteria for Current-Limiting Power Fuses—I, II, C. L. Schuck, E. W. Boehne. *Ibid.*, vol. 65, 1946, pp. 1028–48, disc. pp. 1191–94.
3. Performance Criteria of D-C Interrupters, E. W. Boehne, M. J. Jang. *Ibid.*, vol. 66, 1947, pp. 1172–80.
4. Testing of D-C Interrupters on A-C Test Circuits, K. Chen. *M. S. Thesis*, Massachusetts, Institute of Technology, Cambridge, Mass., 1951.
5. High-Capacity Circuit-Breaker Testing Station, J. B. MacNeill, W. B. Batten. *AIEE Transactions (Electrical Engineering)*, vol. 61, Feb. 1942, pp. 49–56.
6. Electric Fuses (book), H. W. Baxter. Edward Arnold, London, England, 1950.

◆

Discussion

Russell Frink (Westinghouse Electric Corporation, East Pittsburgh, Pa.): To the designer of d-c circuit breakers the problem of providing adequate d-c tests is very real. The rapid growth of the electrochemical-chemical industry has created a demand for breakers of higher and higher interrupting capacity, but d-c testing facilities are not available and not economically justified. The authors are to be commended for their excellent analysis of the problem and development of methods for testing d-c interrupters on a-c circuits.

However, as with many involved technical analyses, it is very easy to become so engrossed with mathematics as to lose sight of the fundamentals. To illustrate this, at any given instant during the interruption of the circuit, the rate of change of current is proportional to the circuit voltage minus the sum of the arc voltage and the IR drop. When these two quantities are equal, the rate of change is zero and the current has reached its maximum value. However, in Fig. 3, the crest of the current I is shown considerably later than the point at which E_B is equal to E_d.

Also, it would seem that the first testing method presented is too complicated to be of practical use. Because of design and tooling costs, any new breaker developed must be aimed at a wide range of applications and must be tested under varying conditions. In outlining procedure, the authors state that the arc voltage characteristic is estimated by the designer. However, in preparing this discussion, a large number of oscillograms for three different types of d-c breakers were studied and the conclusion reached that the arc voltage characteristic varies with test conditions. To illustrate this, Fig. 8, shows two successive oscillograms of the arc voltage generated by a particular interrupter with two different rates of current rise. All other conditions remained the same, and the voltage and time scales are the same. From this it appears that another criterion must be added to the four listed in the paper, and that is rate of current rise. It has also been found that other test conditions can cause the arc voltage characteristic to vary, and one arc chute may display approximately linear, rectangular, or trapezoidal arc voltage depending on conditions. Accordingly, it seems that in order to determine what arc voltage characteristic to use for a given set of conditions, tests must be made under those conditions and the technique would revert to a process of cut and try.

On the other hand, the test method shown in Figs. 3 and 4 is a method which we have used for several years and gives a very close approximation of actual d-c conditions. Tests made at 8 cycles provide a test interval of 1/60 of a second with a voltage variation of less than 8 per cent from the maximum. Under these conditions, we have been able to make tests at approximately 1,400 volts with a rate of rise of almost 9,000,000 amperes per second. For higher rates of rise, the generators are run at a higher frequency, and transformers are used to reduce the test circuit reactance. However, under these conditions, the available period of substantially direct voltage is narrowed.

This method has proved a very useful tool in the development of d-c breakers and fused d-c circuits.

K. Chen and **E. W. Boehne**: The need for providing more accurate test facilities for d-c breakers has been confirmed by the discussion of Mr. Frink, and we are pleased to note that others have also found it possible to test d-c interrupters on a-c test circuits with considerable accuracy. As pointed out in the paper it is essential that "preliminary testing must be carried out to determine the nature of the arc voltage before converging on the final test settings to demonstrate the breaker rating."

Mr. Frink points out that the arc voltage is a function of the circuit conditions. This is certainly true and forms the foundation of the first three references of the paper and is axiomatic with the circuit breaker engineer. The determination of the nature of the arc voltage of the d-c interrupter (unless established from previous test data and experience) must be determined for the particular test circuit conditions in order to enter the equations and charts presented in our paper. Since the nature of the arc voltage is the most important single characteristic of a d-c interrupter, it is usually found that the characteristics are tabulated in table and curve form for a variety of circuits and as modulated by the geometry and materials of the interrupter.

It follows that the circuit breaker engineer in attempting to establish and demon-

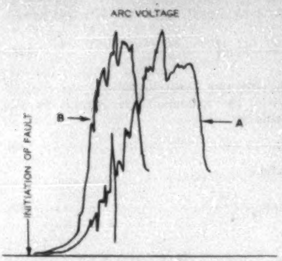

Fig. 8. Superimposed oscillograms showing variation in arc voltage characteristic with rate of rise of current

A—2,200,000 amperes per second
B—3,700,000 amperes per second

strate the rating of a particular d-c interrupter on an a-c circuit in as short a testing time as possible, will proceed in the a-c test laboratory and be aided by a set of charts (Fig. 6 is a sample) prepared in advance, which will clearly guide his decisions of frequency, voltage, impedance, and time of fault initiation so as accurately to establish performance criteria for the d-c circuit breaker over a wide range of applications. The advantages in so proceeding are

1. The release of energy can be controlled in such a manner as gradually to approach the predetermined maximum, for the particular arc voltage encountered, without destroying the breaker (as is possible) in the process of a random search.

2. The goals can be fully achieved in an over-all shorter testing time.

3. When witnessed by the customer the tests can be shown to produce all the essential performance criteria in the d-c circuit including the arc energy to be released in the d-c application.

4. Because of item 3 the influence of grounded metal parts, housings, overhead clearances can be demonstrated in the test cell.

The fact that the d-c breaker frequently meets its most difficult job in circuits of low rates of rise of current (highly inductive) can be demonstrated.

Mr. Frink objects to the inaccuracies of the sketched currents and voltages in Fig. 3, pointing out that the arc current must peak as the arc voltage crosses the system voltage. We apologize for our poor sketching but hasten to point out that all the equations and concepts of the paper are based upon the accepted fundamentals of Ohm's and Kirchoff's law and that the mathematics presented support the fundamentals instead of "losing sight of them." It should be further pointed out that the principles of superposition are used freely throughout the paper (and in references 1–3) in spite of the fact that the arc resistance is nonlinear in all circuit breakers. These demonstrations have required the revision of the "previously considered fundamental" that the application of superposition was limited strictly to linear circuits. Several well-known fundamental electrical engineering texts now leave the door slightly ajar on this point since 1947.

The approach used in the paper inherently considers and applies the correct rate of rise of current. This is indicated by the fact that peak currents are met within the proper over-all arcing time. The rate of rise of current determines the current at contact parting and is satisfied within the relations presented.

Reference

1. *Discussion* by **Harry Sohon** of reference 3 of the paper.

Current Loci of Salient-Pole Synchronous Motors: An Extension of Blondel Theory

JOHN F. H. DOUGLAS
FELLOW AIEE

A SYNCHRONOUS motor has two sets of current loci: the constant output and the excitation loci. For non-salient-pole motors these loci are circles, according to Blondel.[1] While used occasionally for salient-pole motors, they are regarded as approximate. Some of the proofs for the constant output loci are sufficiently general to demonstrate that they are exact for all synchronous motors. Previous use of Blondel's circular excitation loci led to results at variance with test and theoretically in error, because of another discovery of Blondel, the 2-reaction theory.[2,3] A search has failed to disclose any reconciliation of the discoveries of Blondel or an exact geometrical definition of the excitation loci.

This paper is based on the following assumptions of Doherty and Nickle[4] and Douglas.[5]

1. Reactance has two chief values, direct and quadrature, called X_d and X_q.

2. Both vary with the field current but their ratio K is nearly constant.

3. The ratio K may be found by graphical analysis or experiment and is 1.3 to 2.0.

When pole shoes are concentric with the armature surface K is in the range 1.3 to 1.8. When the air gap is shaped to give a close approximation to a sine wave of flux density the ratio K is nearly 2.0.

Summary of Results

This paper shows that the excitation loci for salient-pole motors are epitrochoids. They may be found by taking the sum of four phasors shown in Fig. 1 and giving the locus HK and in the working range the circle HJ. They are useful in predicting power factor. In Fig. 1 the circle HL is the circle usually used.

The following definitions briefly summarize the rules for drawing the four phasors forming the epitrochoid: difference of potential line to neutral V, internal induced voltage E_0, armature resistance to alternating current, per phase r, angle from V to pole axis δ. The following symbols are used for brevity:

$$I'=(V/X_D),\ E'=(E_0/V) \quad (1)$$

$$R=(r/X_D),\ \alpha=(KR) \quad (2)$$

Thus in Fig. 1 take the sum of the four currents I_1,I_2,I_3, and I_4 given in polar coordinates by equations 3 through 6

$$I_1=I'\alpha\underline{/0^\circ} \quad (3)$$

$$I_2=(0.5)(K+1)(I')\underline{/-90^\circ} \quad (4)$$

$$I_3=(E'I')\underline{/90^\circ+\alpha-\delta} \quad (5)$$

$$I_4=(0.5)(K-1)(I')\underline{/90^\circ-2\delta} \quad (6)$$

The circle HJ and the epitrochoid HK can be distinguished in the working range only on a large-scale drawing. The closest circle has its center at the point E. If distance BE is termed I_6, BE is found to make an angle (2α) with the vertical and has a length given by equation 7.

$$I_5=(I_3I_4)/[I_3+(3.45)(I_4)] \quad (7)$$

Paper 55-507, recommended by the AIEE Rotating Machinery Committee and approved by the AIEE Committee on Technical Operations for presentation at the AIEE Summer General Meeting, Swampscott, Mass., June 27–July 1, 1955. Manuscript submitted June 10, 1954; made available for printing May 5, 1955.

John F. H. Douglas is with Marquette University, Milwaukee, Wis.

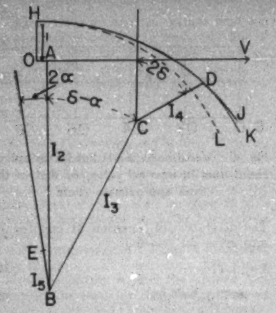

Fig. 1. Excitation locus of salient-pole motor. Epitrochoid HJ is better than Blondel's locus HL. Locus HJ is found as the sum of four currents I_1 to I_4 defined by equations 3 through 6

If the resistance r is negligible the current I_1 is zero and the angle α is zero, and the phasor I_5 is vertical. It is believed that it may be neglected in the largest motors, but may not in the smaller.

This paper demonstrates the correctness of equation 7 in two ways: by an example and by applying the theory of errors. It was verified by large-scale drawings. Equations 3 through 6 can be transformed into accepted basic relations for salient-pole motors.

Properties of Epitrochoid Current Locus of Salient-Pole Synchronous Motor

An epitrochoid is a curve generated by one circle rolling over another. In the particular case when the tracing point is on the circumference of the rolling circle, the curve is an epicycloid. In the case when the fixed and the rolling circle have equal radii, and the center of the rolling circle moves through the angle δ, the rolling circle moves through the angle (2δ). In Fig. 1, the epitrochoid HK is generated if the radii of the fixed and rolling circles are equal and each equal to half of the value in equation 4.

The axis of an epitrochoid is its line of symmetry; it is determined as the line on which I_3 and I_4 are in phase. It is in the position where δ is minus α. The angle Δ is defined as the angle between I_3 and the axis of the epitrochoid. The angle Δ is equal to δ plus α.

In Fig. 1 the dashed line is the circle computed by Blondel's rules. The approximate circle defined by equation 7 is so close to the epitrochoid that only a large-scale drawing will reveal it.

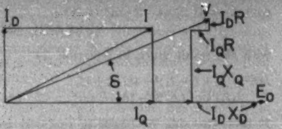

Fig. 2. Basic phasor diagram for salient-pole motor. V is line voltage, E_0 the induced voltage, I the current. Subscripts mark components, D for direct and Q for quadrature. Angle δ is the power angle

Basic Phasor Diagram and Equations for Salient-Pole Synchronous Motors

This diagram, shown in Fig. 2, is defined as one in which the pole axis is horizontal. The components of current and of IR and IX drop are shown. This diagram is termed basic, since the proof of the epitrochoid is based upon it. The equations applying to Fig. 2 are

$$E_0=V\cos\delta-I_QR+I_DX_D \tag{8}$$

$$V\sin(\delta)=I_QX_Q+I_DR \tag{9}$$

These equations are expressed more simply if equations 1 and 2 are used, and if the relation defining K as the ratio of X_D to X_Q is used. Thus the equations become

$$E'I'=I'\cos\delta-I_QR+I_D \tag{10}$$

$$I'\sin\delta=I_Q/K+I_DR \tag{11}$$

To solve equations 10 and 11 simultaneously and accurately, terms in R must be considered terms in R^2 may be neglected. When thus solved for I_D and I_Q, the result is

$$(I_Q/I')=(KR)\cos\delta+K\sin(\delta)-(KR)E' \tag{12}$$

$$(I_D/I')=(KR)\sin\delta-\cos(\delta)+E' \tag{13}$$

Points of novelty are believed to be their compact and simple form and their adaptability for use inpolar, co-ordinates.

The proof of equations 3 through 6 is based on the basic equations 12 and 13 by changing equations 3 through 6 into a form that can be compared with 12 and 13. This will be done in the next section of this paper.

Proof That the Epitrochoid Meets the Requirements of the Basic Equations

The current taken by a motor is represented by the sum of equations 3 through 6. The first step is the rotation of the current phasor counterclockwise by the angle δ so that V is as shown in Fig. 2. This is done by adding δ to the several angles. Thus

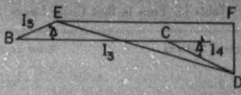

Fig. 3. Geometrical construction used to find the radius of best circle locus. Angle Δ taken from axis of epitrochoid

$$I/I'=KR\underline{/\delta}+0.5(K+1)\underline{/\delta-90^\circ}+E'\underline{/90^\circ+\alpha}+0.5(K-1)\underline{/90^\circ-\delta} \tag{14}$$

Calling the cosine of α unity and equating the sine of α to the angle, and changing equation 14 into rectangular co-ordinates is the next step in the proof. In rectangular co-ordinates, and with E_0 as the axis

$$I/I'=(KR)(\cos\delta+j\sin\delta)+0.5(K+1)\times(\sin\delta-j\cos\delta)-KRE'+jE'+\left(\frac{K-1}{2}\right)(\sin\delta+j\cos\delta)=(KR\cos\delta+K\sin\delta-KRE')+j(KR\sin\delta-\cos\delta+E') \tag{15}$$

This is identical with the basic equations demonstrating the epitrochoid by comparison.

Proof That the Epitrochoid Locus of a Salient-Pole Motor May Be Replaced by a Circle

In Fig. 1 the current locus HK is very close to a circle. It must not be confused with the approximate circle of Blondel shown dashed as HL. The problem may be restated thus: If the phasor I_5 is made equal to

$$I_5=(I_3I_4)/[I_3+(4-h)I_4] \tag{16}$$

then it must be shown that the error is small if $h=0.55$, and also that it is the least possible error. The working range is taken from zero to a power angle of 0.8 radian. The proof is simpler if Fig. 1 is drawn with I_3 as a reference, as shown in Fig. 3. In Fig. 3

$$DE^2=(EF)^2+(FD)^2=[I_3+(I_4-I_5)\cos\Delta]^2+(I_4+I_5)^2\sin^2\Delta \tag{17}$$

The steps between equations 17 and 18 are given in the Appendix.

$$DE^2=(I_3+I_4-I_5)^2+(I_5I_3+4I_5I_4-I_3I_4)\Delta^2-I_4I_5\Delta^4 \tag{18}$$

To secure a very small error the radius must be close to $(I_3+I_4-I_5)$ and the two remaining terms in equation 18 must balance as closely as possible. Two proofs will be given. In this section assume that $h=0.55$ and compute the error for a particular case. Consider the case where I_4 is 0.5 and I_3 is 1.2.

Table I. Error in Best Circle Locus

Angle Δ, Radians	Error in DE^2
0.200	+0.0019
0.400	+0.0059
0.600	+0.0059
0.800	−0.0079

By equation 16 the current I_5 assumes the form in equation 19 and DE^2 takes the form in equation 20

$$I_5=(1.2)(0.5)/(1.2+3.45(0.5))=0.204 \quad (19)$$

$$DE^2=1.496^2+0.053\Delta^2-0.102\Delta^4 \quad (20)$$

Table I shows that the error in DE^2 is small. The maximum error in DE is (1/6 per cent); the mean square error is much less.

The error function is plotted in Fig. 4. The dashed line at the level $DE^2=1.496^2+0.003$ gives an even smaller mean square error than is indicated by the table. The conclusion is that in the working range there is an approximate circle locus much better than the Blondel approximate circle and very close to the theoretically exact epitrochoid. The proof that h has the best value of 0.55 is in the Appendix.

One question of interest is whether resistance can be neglected. It is believed that in the smaller motors it cannot be neglected where accurate results are desired. For a particular case of I_3 or 1.2, a K of 2, and a δ of 45 degrees, the error in the power-factor angle was computed as 1 degree for each per cent of resistance.

Appendix. Detailed Mathematical Steps

The steps between equations 17 and 18 are as follows. On expanding equation 17 equation 21 is obtained

$$DE^2=I_3^2+2I_3(I_4-I_5)\cos\Delta+(I_4-I_5)^2\times\cos^2\Delta+(I_4+I_5)^2\sin^2\Delta=I_3^2+I_4^2+I_5^2+2I_3(I_4-I_5)\cos\Delta-2I_4I_5(\cos^2\Delta-\sin^2\Delta) \quad (21)$$

The next step involves the use of the trigonometric identities in equations 22 and 23

$$\cos\Delta=1-2\sin^2(\Delta/2) \quad (22)$$

$$\cos^2\Delta-\sin^2\Delta=1-8\sin^2(\Delta/2)+8\sin^4(\Delta/2) \quad (23)$$

with the result given in equation 24

$$DE^2=(I_3+I_4-I_5)^2+4(I_3I_5+4I_4I_5-I_3I_4)\sin^2(\Delta/2)-16I_4I_5\sin^4(\Delta/2) \quad (24)$$

If now the sine of (Δ/2) is replaced by (Δ/2), equation 18 is obtained.

Next the proof that in equation 16 the value of h should be 0.55 is given. The first step is to put equation 16 in 18 with the result given in equation 25

$$DE^2=(I_3+I_4-I_5)^2+(I_4I_5)(h\Delta^2-\Delta^4) \quad (25)$$

The second step is one of preparation for the application of the method of least squares. Here the maximum value of Δ is called Δ_m having the value 0.8; the ratio of Δ to Δ_m is called Z. The constant K gives a term required by least squares and aids in getting the most probable radius of the circle. When this notation is used, equation 25 takes the form given in equation 236

$$DE^2=(I_3+I_4-I_5)^2+(I_4I_5)\Delta_m^4(K')+I_4I_5\Delta_m^4[-K'+(h/\Delta_m^2)Z^2-Z^4] \quad (26)$$

The last bracket may be termed the error function and may be more compactly written as

$$e=(-K'+PZ^2-Z^4) \quad (27)$$

where the constants K and P are to be determined so that the error is a minimum.

The first principle in least squares is that the error is at least when the average error is zero. Thus

$$\int_0^1 e\,dZ=0=(-K'+(P/3)-0.2) \quad (28)$$

When equation 28 is used to eliminate K' from equation 27 it becomes

$$e=0.2-(P/3)+PZ^2-Z^4 \quad (29)$$

The second rule in the theory of least squares requires that the square of e be found, its average value be found, and then this value be differentiated for a minimum. The value of e^2 is given by equation 30

$$e^2=(0.2-P/3)^2+2P(0.2-P/3)Z^2+P^2Z^4-(2P)(0.2-P/3)Z^4-2PZ^6+Z^8 \quad (30)$$

The average squared error is given by equation 31

$$\int_0^1 e^2dZ=(0.2-P/3)^2+(2P/3)(0.2-P/3)+P^2/5-(2P/5)(0.2-P/3)-2P/7+(1/9)=(16/225)-(16/105)P+(4/45)P^2 \quad (31)$$

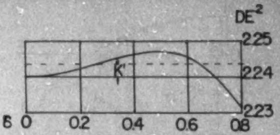

Fig. 4. Variation in the radius DE of epitrochoid from its nominal value, or that of the best approximate circle

The derivative of equation 31 equated to zero gives the relations

$$P=(6/7) \quad (32)$$

$$h=(6/7)\Delta_m^2=0.55 \quad (33)$$

$$K'=(2/7)-0.2=0.086 \quad (34)$$

$$DE^2=(I_4+I_3-I_5)^2+0.41I_4I_5\times\left(\frac{6P}{7}Z^2-Z^4-0.086\right) \quad (35)$$

The mean square error in DE^2 is found by putting equation 32 in 31 and taking the square root with the result

$$DE^2=(I_3+I_4-I_5)^2+0.035(I_4I_5)\pm 0.31(I_4I_5) \quad (36)$$

Expressed as a percentage error, the probable error in the radius DE is

$$\text{Error}=1.6\left(\frac{I_4I_5}{(I_3+I_4-I_5)^2}\right) \quad (37)$$

For the case chosen previously as an illustrative example the probable error is

$$\text{Error}\ (1.6)(0.204)(0.5)/(1.496)^2=0.073 \text{ per cent} \quad (38)$$

Thus it is established by the theory of probabilities that in the working range the epitrochoid may be accurately approximated by a circle.

References

1. MOTEURS SYNCHRONES A COURANT ALTERNATIF, A. Blondel. *L'Industries Electrique*, Feb. 1895.

2. THE SALIENT POLE SYNCHRONOUS MACHINES, A. Blondel. *Ibid.*, 1899, p. 481.

3. A. Blondel. *Transactions*, International Congress, St. Louis, Mo., 1904, pp. 620 and 635.

4. SYNCHRONOUS MACHINES. I—AN EXTENSION OF BLONDEL'S TWO-REACTION THEORY, E. R. Doherty, C. A. Nickle. *AIEE Transactions*, vol. 45, June 1926, pp. 912–47.

5. TRANSVERSE REACTION IN SYNCHRONOUS MACHINES, J. F. H. Douglas. *Ibid.*, vol. 46, Feb. 1927, pp. 30–38.

◆

Discussion

L. T. Rosenberg (Allis-Chalmers Manufacturing Company, Milwaukee, Wis.): The paper represents an important step toward understanding the behavior of synchronous machines. Recent progress in synchronous-machine sizes and construction has shown that errors considered small today may assume importance in the machines of tomorrow.

It is stated in the paper that X_q and X_d vary with field current and obviously these are not the unsaturated synchronous reactances defined in the AIEE Standards. Since X_d appears in all four components of the excitation locus of Fig. 1 it would be wise to use some additional symbol or subscript such as X_{ds} to indicate that saturation must be taken into account. The author also states that the phasor diagram of Fig. 2 "is termed basic, since the proof of the epitrochoid is based upon it." To anyone not familiar with Dr. Douglas' many fine contributions to the literature on electric machines, this might be inadequate justification. However, Fig. 2 has additional claims to the term basic, since it has formed the basis of many synchronous machine papers for over 25 years. In fact, a similar phasor diagram was published by Dr. Douglas as early as 1927; see reference 5.

I should like to ask the author whether the analysis is sufficiently broad so that it can be applied to the limiting cases of 1. a nonsalient pole machine, and 2. a salient pole reluctance-type synchronous motor.

G. F. Tracy (University of Toronto, Toronto, Ont., Canada): The author states that K, in integral-horsepower motors, ranges from 1.3 to 2.0. An examination of the design data of 10 motors ranging in size from 200 horsepower to 2,250 horsepower corroborated these figures by showing for K a minimum value of 1.26 and a maximum value of 1.89.

If the excitation is zero, the current I_3 is zero and the locus of the total current is determined only by I_4. This is the case in certain types of clock motors. Synchronizing torque in such motors is dependent on a value of K considerably greater than unity.

It is interesting to observe that for a cylindrical-rotor machine the factor K in equations 3 through 6 becomes unity (since X_d is equal to X_q); the current I_4 disappears, and the expression for the total current is

$$I=\frac{rV}{X_d^2}\underline{/0}+\frac{V}{X_d}\underline{/-90}+\frac{E_0}{X_d}\underline{/90-(\delta-\alpha)}\cdot$$

This is approximately the same as the expression usually used in the circle diagram of a cylindrical-rotor machine, the approximation being due to neglecting r^2 and assuming X_d equal in magnitude to the synchronous impedance.

John F. H. Douglas: In general, the points made by the discussers are well taken. The two limiting cases are of interest, namely, the smooth-core cylindrical rotor, and the reluctance torque motor. If the internal construction is isotropic, the phasor I_4 is missing and reluctance torque is zero. If the motor has no excitation the phasor I_3 is missing. The degree of anisotropy may be measured by the factor K. It may be shown mathematically that the largest value of K that may be expected is 2, which is confirmed by Prof. Tracy's data. The questions asked by Mr. Rosenberg are answered by Prof. Tracy.

A Method for Studying Circuit Transient Recovery Voltage Characteristics of Electric Power Systems

W. C. KOTHEIMER
ASSOCIATE MEMBER AIEE

AN IMPORTANT factor which is considered by circuit-breaker engineers is the time function of the potential across the contacts of a circuit breaker immediately after current interruption; this is defined as the circuit transient recovery voltage.[1] In the past two decades much has been published on the determination of recovery voltage characteristics of power systems by analytical methods.[2–5] These methods become quite complex when more than very simple circuits are considered; consequently, the experimental approach to the problem becomes more practical, and several experimental methods have been developed for making such measurements directly.[6,7] One of these, the current injection method utilizes the principle of injecting into the de-energized circuit recurrent low-voltage current surges having essentially a constant, positive, current-time derivative starting at zero current, and recording the transient voltage response of the circuit on a cathode-ray oscillograph.

The method described in this paper differs from the current injection method in that the recovery phenomenon is initiated by the discontinuation in a vacuum rectifier of a negative current-time derivative at zero current. The resulting current wave form is more nearly analogous to that occurring in an actual current interruption in a circuit breaker. The circuit under test is better isolated from the current supply after the start of the recovery voltage phenomenon, and the equipment required is simpler than that used previously. It is portable and can be assembled quickly.

Basic Circuit and Theory of Operation

A similarity exists between the manner in which a half-wave rectifier supplying a load ceases to conduct at current zero and the arcing current interruption which takes place in a power circuit breaker. In both instances the circuit interruption takes place at current zero, neglecting any postarc conduction in the circuit breaker. The similarity of this action is shown in Fig. 1, which compares the circuits and wave forms.

The American Standards Association standards[1] define the transient recovery voltage as the voltage appearing across the terminals of a current interrupting device upon interruption of the current. The circuit transient recovery voltage is defined as the transient recovery voltage characterizing the circuit and obtained with 100-per-cent normal frequency recovery voltage, a symmetrical current, and no modifying effect of the circuit breaker. The rectifier wave forms shown in Fig. 1(B) approach the conditions defined for the circuit transient recovery voltage very closely. Because of the nature of its operation the rectifier cannot force interruption of the circuit at any other time but current zero and has extremely little conduction after current zero. The transient recovery voltage obtained in a half-wave rectifier circuit qualifies therefore as the circuit transient recovery voltage.

This principle is applied to the study of circuit transient recovery characteristics of a de-energized system by connecting a low-voltage half-wave rectified current source in place of the circuit breaker as shown in Fig. 2. The cathode-ray recording equipment is connected to the same points, and the wave forms recorded will be as shown in Fig. 1(B) for E_{2-3}, the voltage across the rectifier load circuit. When the rectifier ceases to conduct, the voltage across its load circuit is not zero and must return to zero in a manner characterizing the transient recovery voltage characteristics of the circuit. The significant difference between the recovery characteristics as measured in this manner and the actual circuit transient recovery voltage measured directly across the circuit-breaker

---

Paper 55-476, recommended by the AIEE Transmission and Distribution Committee and approved by the AIEE Committee on Technical Operations for presentation at the AIEE Summer General Meeting, Swampscott, Mass., June 27–July 1, 1955. Manuscript submitted March 29, 1955; made available for printing May 11, 1955.

W. C. KOTHEIMER is with the General Electric Company, Philadelphia, Pa.

The author wishes to acknowledge the contributions of J. H. Drake, J. B. Conner, and A. Klopfenstein of the Southern California Edison Company, and of W. F. Skeats of the General Electric Company.

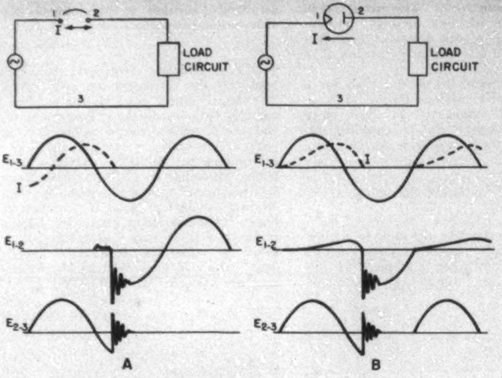

Fig. 1. Similarity of current interruption in a power circuit breaker (A) and in a half-wave rectifier (B)

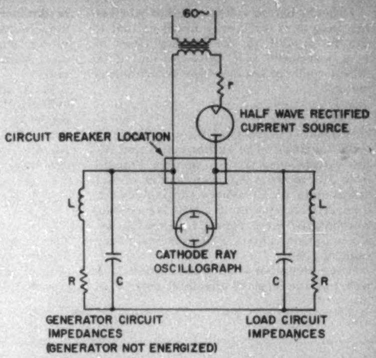
60~
r
HALF WAVE RECTIFIED CURRENT SOURCE
CIRCUIT BREAKER LOCATION
L
L
CATHODE RAY OSCILLOGRAPH
R
C
C
R
GENERATOR CIRCUIT IMPEDANCES (GENERATOR NOT ENERGIZED)
LOAD CIRCUIT IMPEDANCES

Fig. 2. Connection of half-wave interruption equipment to study transient recovery voltage characteristics in a typical power system installation

terminals is the absence of the normal frequency (60-cycle) recovery voltage. However, this is of little consequence because the change in the normal frequency voltage during the short interval in which the transient takes place is very small and can usually be neglected. Also, if desired, it can be added readily because it is known. The reason for recording the voltage across the rectifier load circuit instead of directly across the rectifier which interrupts the current is to eliminate the unwanted transient characteristics of the low-voltage external current supply.

A brief mathematical analysis of the operation of the rectifier will help to clarify the wave forms shown in Fig. 1(B). Consider the simple circuit shown in Fig. 3. It consists of a low-voltage a-c source, a vacuum diode rectifier, and a reactive load. At the time when the voltage E_{1-3} swings negative, assuming that the previous transient voltages have died out so that E_{2-3} is zero, E_{1-2} also will be negative and the diode will start to conduct. When this happens the load circuit will be subjected to the applied 60-cycle a-c potential. The 60-cycle shunt capacitive reactance of most power system circuits is very much larger than the inductive reactance of the busses, transformers, and generators and may be neglected in writing the following differential equation describing the current and voltage relations in the rectifier load circuit after the rectifier starts to conduct

$$(l+L)\frac{di}{dt}+i(R+r)=E_m \sin \omega t \tag{1}$$

The solution of equation 1 for the current in the load is

$$i=\frac{E_m}{Z}\sin(\omega t+\lambda-\theta)-\frac{E_m}{Z}[\sin(\lambda-\theta)]\epsilon^{-\left(\frac{R+r}{L+l}\right)t} \tag{2}$$

The angle λ designates the phase angle of the generator voltage when the rectifier starts to conduct. For the conditions of no initial voltage across the load λ is zero. The angle θ is the phase angle of the total circuit and includes the effect of the internal resistance of the rectifier, the series current control resistor, and the internal reactance of the supply source. The current in the load while the rectifier is conducting is therefore

$$i=\frac{E_m}{Z}\sin(\omega t-\theta)+\frac{E_m}{Z}(\sin\theta)\epsilon^{-\left(\frac{R+r}{L+l}\right)t} \tag{3}$$

where

$$\theta=\tan^{-1}\frac{\omega(L+l)}{R+r}$$

$$Z=\sqrt{(R+r)^2+\omega^2(L+l)^2}$$

The voltage across the load is given by

$$E_{2-3}=iR+L\frac{di}{dt} \tag{4}$$

or

$$E_{2-3}=E_m\left(\frac{R}{Z}\sin(\omega t-\theta)+\frac{\omega L}{Z}\cos(\omega t-\theta)+\frac{Rl-rL}{Z(L+l)}(\sin\theta)\epsilon^{-\left(\frac{R+r}{L+l}\right)t}\right) \tag{5}$$

Now the rectifier ceases to conduct again when the current attempts to reverse. The phase angle ωt of the supply voltage at this time is designated as ϕ and is related to the circuit parameters by the following equation

$$\frac{\sin\phi}{\cos\phi-\epsilon^{-\left(\frac{R+r}{\omega L+\omega l}\right)\phi}}=\tan\theta \tag{6}$$

In any inductive circuit ϕ has a value between π and 2π so that the rectifier conducts for appreciably more than a half-cycle. When current interruption occurs, the voltage across the load circuit is not zero but returns to zero by a time function which is determined by the load circuit parameters including the stray capacitance. To obtain a quantitative evaluation of the recovery voltage characteristic produced in this manner, the displacement on the oscillogram of the voltage wave E_{2-3} just prior to zero is taken as the crest value of the actual line voltage. If the horizontal sweep of the oscilloscope is calibrated, the initial rate of rise of the recovery voltage can be calculated easily.

In the foregoing analysis the resistance r was assumed to include the series resistor and also the internal resistance of the

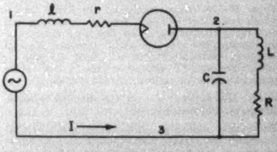

Fig. 3. Simplified circuit showing significant parameters

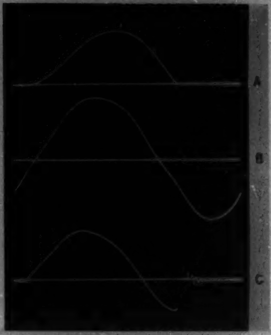

Fig. 4. Cathode-ray oscillogram showing the current and voltage wave forms of Fig. 3

A—Current wave form
B—Supply voltage, E_{1-3}
C—Voltage across the load circuit, E_{2-3}

rectifier. The latter was assumed to have a constant value; however, this is not strictly true for it is a well-known fact that the internal resistance of a conducting vacuum diode increases rapidly near current zero. In this circuit it is important that the current wave form for a short interval before current zero resemble closely a portion of a sine wave near zero. If the nonlinearity of the rectifier is not minimized, it can cause distortion of the current wave form with the result that errors will be introduced in the recovery characteristic if the circuit has more than one natural frequency of oscillation. The effect of this nonlinearity upon the operation of the circuit is to cause the voltage across the load to decrease slightly just prior to current zero. This effect can be detected in the oscillogram in Fig. 4 where it causes a slight curvature of the voltage trace just before the start of the transient oscillation. It can be minimized by making the series resistor much larger than the internal resistance of the rectifier and by using several rectifiers in parallel.

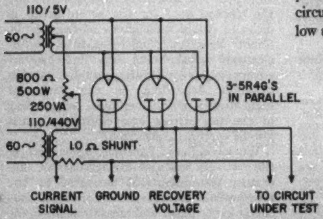

Fig. 5 (left). Schematic diagram of equipment for studying circuit transient recovery voltage characteristics

Equipment for Practical Applications

A schematic diagram of the equipment which was used to study recovery voltages is shown in Fig. 5. The rectifier consists of three type-*5R4G* vacuum rectifiers in parallel. A series resistor minimizes the effect of rectifier nonlinearity and provides for adjustment of the current supplied by a small 110/440-volt lighting transformer. The cathode-ray oscilloscope is connected directly across the rectifier load circuit. For most circuits the 60-cycle impedance of the load is so low that the voltage developed across it by this method is very small and must be amplified in the oscilloscope to produce sufficient deflection on the screen. The frequency response of the oscilloscope amplifier must therefore be sufficiently wide to record the recovery voltage without introducing distortion.

The transient recovery voltage phenomenon occurs in a very short interval after the rectifier stops conducting. Because this phenomenon is the only portion of the voltage wave form which is of interest, the cathode-ray oscilloscope horizontal sweep should therefore be synchronized and adjusted to expand this portion of the wave form sufficiently to display the recovery characteristic to advantage. When properly adjusted and synchronized, the recurrent transient recovery voltage pattern will appear stationary on the screen and can be photographed easily.

A means for measuring the average load current should be incorporated in the circuit to facilitate setting the current level within the rating of the rectifier tube. This can be either a d-c ammeter or a calibrated shunt and a d-c voltmeter as shown in Fig. 5. The shunt has the added advantage of providing a means for observing the current wave shape during conduction in order to check the rectifier linearity. With the equipment just described an average load current of 1.5 amperes d-c can be used without damage to the rectifiers. At this current level and with an oscilloscope sensitivity of approximately 48 millivolts per inch, it is possible to record the recovery voltages of circuits having a 60-cycle reactance as low as 0.01 ohm.

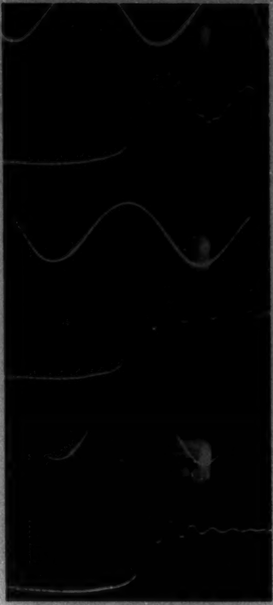

Fig. 6. Cathode-ray oscillograms of recovery characteristics obtained by the half-wave interruption method on three different test circuits at the General Electric Switchgear Development Laboratory

Results of Laboratory and Field Tests

The electrical characteristics of most power generation and distribution circuits usually are such that the damping is below critical, causing the circuit transient recovery voltage to be oscillatory in nature. A series of test circuits having such oscilla-

Table I. Comparison of Laboratory Tests for Characteristics of Single-Frequency Oscillatory Circuits

	Resonant Frequency		Test Circuit Q	
Test Circuit No.	By Direct Measurements, Cycles per Second	From Recovery Characteristics, Cycles per Second	By Direct Measurements	From Recovery Characteristics
1	12,400	12,600	3.03	3.07
2	10,100	9,900	3.84	3.80
3	4,970	4,940	7.40	7.60
4	6,270	6,350	2.46	2.48
5	3,150	3,180	4.72	4.78
6	4,500	4,370	1.73	1.77
7	2,230	2,180	3.37	3.40
8	1,120	1,080	3.38	3.40
9	16,100	15,500	10.1	10.6

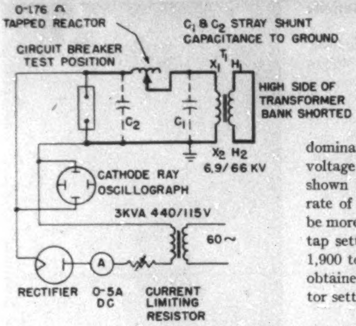

Fig. 7. Schematic diagram of half-wave interruption equipment and a typical test circuit at the Center Substation of the Southern California Edison Company

tory characteristics were set up in the laboratory and oscillograms were made of their recovery voltage characteristics using the circuit of Fig. 5. The resonant frequency and the Q of each test circuit were measured with standard laboratory instruments and the results compared to the values determined from the recovery voltage characteristics. Table I shows this comparison. The close agreement of these data attests to the validity of the half-wave interruption method for determining circuit recovery voltage characteristics.

To evaluate further the performance of this equipment, it was used to measure the recovery characteristics of several test circuit arrangements at the Switchgear Development Laboratory of the General Electric Company in Philadelphia. An oscillogram of one of these tests is shown in Fig. 6. The results obtained compared favorably with the known recovery voltage characteristics of these circuits. The circuits contained a large alternator, a tapped reactor, and the associated bus equipment. The additional sine wave on the records is a calibration voltage from a high-frequency oscillator.

In the summer of 1954 at the suggestion of W. F. Skeats, J. H. Drake of the Southern California Edison Company used the low-voltage half-wave interruption technique described in this paper to study circuit transient recovery voltage in a circuit breaker test installation at the Center Substation of the Southern California Edison Company. A schematic circuit of this installation is shown in Fig. 7. The apparatus tested consisted of two 66/6.9-kv transformer banks having ratings of 1,500 and 30,000 kva. A current-limiting reactor having a maximum reactance tap of 1.76 ohms was connected in the secondary circuit. Predominantly single-frequency recovery voltage characteristics were obtained as shown in Figs. 8 and 9. The recovery rate of the 1,500-kva bank was found to be more or less independent of the reactor tap settings whereas a variation of from 1,900 to 2,800 volts per microsecond was obtained for maximum to minimum reactor settings with the 30,000-kva bank.

Conclusions

The method for studying recovery voltages by using a half-wave vacuum rectifier to simulate repetitive interruption of the circuit produces recovery voltage phenomena which qualify as the circuit transient recovery voltages as defined by the American Standards Association standards. Results of laboratory and field tests have shown that the method is readily applicable to power system circuit configurations and yields results which are in good agreement with those obtained by other methods. The equipment required is simple, inexpensive, and readily available. Tests are conducted at a relatively low voltage and current level so that circuit changes such as reactor or transformer tap changes can be made with safety and dispatch. The method requires that the test circuit contain a complete d-c path; however, this limitation does not restrict seriously the scope of its application.

References

1. Alternating-Current Power Circuit Breakers. *ASA Standard No. C3.74*, American Standards Association, New York, N. Y., Dec. 1953, p. 7.

2. Circuit Breaker Recovery Voltages, Magnitudes and Rates of Rise, **Robert H. Park, Wilfred F. Skeats.** *AIEE Transactions*, vol. 50, Mar. 1931, pp. 204–39.

3. The Determination of Circuit Recovery Rates, **E. W. Boehne.** *AIEE Transactions (Electrical Engineering)*, vol. 54, May 1935, pp. 530–39.

4. Practical Calculation of Circuit Transient Recovery Voltages, **J. A. Adams, W. F. Skeats, R. C. Van Sickle, T. G. A. Sillers.** *Ibid.*, vol. 61, Nov. 1942, pp. 771–79.

5. Transient Recovery-Voltage Characteristics of Electric-Power Systems, **H. P. St. Clair, J. A. Adams.** *Ibid.*, Sept., pp. 666–69.

6. Recurrent Surge Oscillographs and Their Application to Short Time Transient Phenomena, **K. J. R. Wilkinson.** *Journal*, Institution of Electrical Engineers, London, England, vol. 83, 1938, pp. 663–72.

7. The Recovery-Voltage Analyzer for Determination of Circuit Recovery Characteristics, **G. W. Dunlap.** *AIEE Transactions (Electrical Engineering)*, vol. 60, Nov. 1941, pp. 958–62.

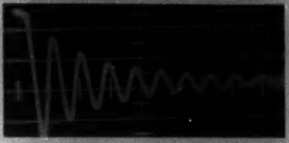

Fig. 8. Recovery characteristics of the test circuits at the Center Substation of the Southern California Edison Company. Reactor tap = 1.76 ohms, transformer = 500 kva, 66,000/6,900 volts. Time base calibration = 50 microseconds per division. Recovery voltage rate = 760 volts per microsecond

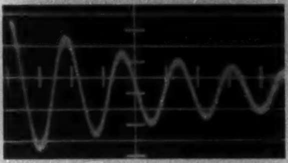

Fig. 9. Recovery characteristics of the test circuits at the Center Substation of the Southern California Edison Company. Reactor tap = 1.76 ohms, transformer = 10,000 kva, 66,000/6,900 volts. Time base calibration = 10 microseconds per division. Recovery voltage rate = 1,900 volts per microsecond

Discussion

D. J. Lemens (Line Material Company, South Milwaukee, Wis.): This is a comparatively simple method of determining circuit transient recovery voltage which should prove useful in the design, test, and application of a-c circuit interrupting devices.

In laboratory studies with a circuit similar to that shown on the schematic diagram of Fig. 5, we have found that in most cases a single rectifier is sufficient. Parallel rectifiers are necessary only when the test circuit impedance is of such a low value that insufficient voltages develop across the test circuit for satisfactory deflection of the cathode-ray oscilloscope. Parallel rectifiers, because of interelectrode capacitance, tend to modify the recovery voltage of test circuits.

While the equipment is simple and easily assembled, considerable care must be exercised in the selection of components and the method used for the actual setup in order to obtain satisfactory measurements. Shunt capacitance due to leads and interelectrode capacitances will influence recovery voltage measurements by varying amounts, depending on the particular high-current circuit studied. Grounding of the test circuit and equipment must also be carefully considered.

We have found excellent agreement in the recovery voltages of high-current laboratory test circuits as measured by the interrupted current wave method disclosed in the paper and measurements made

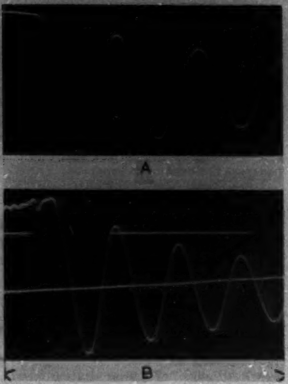

Fig. 10. Single-frequency recovery voltage obtained on a 5.2-kv circuit with a short-circuit current of 5,000 amperes

during actual circuit interruption. The cathode-ray oscillograms of Fig. 10 show the single-frequency recovery voltage obtained on a 5.2-kv circuit having a short-circuit current of 5,000 amperes. Oscillogram *A* was made with the interrupted current wave circuit while oscillogram *B* was made during an actual circuit interruption.

The oscillograms of Fig. 11 show the multiple frequency recovery voltage obtained on a 7.8 kv-circuit with a 6,000-ampere short-circuit current. Here again oscillogram *A* was made with the interrupted wave circuit. Oscillogram *B* was obtained during an actual short-circuit interruption by a fuse cutout.

The frequencies of the recovery voltage transients of oscillograms *A* and *B* of both Fig. 10 and 11 are the same. Differences apparent in the oscillograms are caused by slight variations in the time base of the measurements by the interrupted current wave method from the time base on measurements during actual circuit interruptions.

The interrupted current wave method is a useful tool for test laboratories where knowledge of circuit transient recovery voltage is rapidly becoming necessary. Calculation of circuit transient characteristics is extremely complex and at best is only an approximation because of the assumptions necessary in regard to the distributed capacitance and inductance of generators, reactors, busses, etc. With this method transient circuit behavior can be readily determined in both the laboratory and the field.

W. C. Kotheimer: Mr. Lemens' interesting discussion of the half-wave interruption method for measuring transient recovery voltages brings out some precautions concerning the effects of rectifier shunt capacitance and grounding of the test circuit not brought out in the paper. The oscillograms shown, comparing recovery voltages recorded during fault current interruptions and those obtained by the half-wave interruption method speak for the validity of the method.

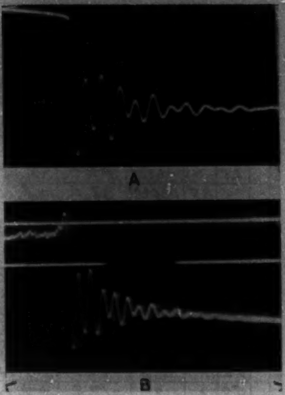

Fig. 11. Multiple-frequency recovery voltage obtained on a 7.8-kv circuit with a short-circuit current of 6,000 amperes

In regard to the use of parallel rectifiers, the increased current is not the only advantage obtained. It also reduces the effect of the nonlinearity of the internal resistance of the rectifier near current zero, which can cause errors in the recovery voltage produced if the test circuit has multiple-frequency characteristic. The large resistor in series with the rectifier also helps greatly in reducing this effect.

A Rational Method for the Step-by-Step Calculations in Power System Transient Stability Studies

E. O. NORINDER
NONMEMBER AIEE

IN STUDIES of the transient stability of power systems with a network analyzer the step-by-step method is generally used. Here, a special method for the step-by-step calculations is described. These calculations, based on the ordinary step-by-step equation, are matched to ordinary office calculators. The method has shown itself to be fast and reliable in extensive investigations of the transient stability of the Swedish power system.

Differential Equation for Motion of Group of Power Stations

The differential equation for an average load angle of a group of power stations that moves in a mutually synchronous manner is deduced as a function of the electric power delivered from the group. Obviously, the equation also applies to a single synchronous machine. The mechanical torques from the prime movers are assumed to be constant.

The following quantities are introduced:

t = time, seconds
f_0 = normal frequency, cycles per second of the power system
$f(t)$ = momentary frequency, cycles per second of the power station group
$\varphi(t)$ = an average load angle in electrical degrees of rotors of the power station group with respect to a reference axis rotating at normal speed
W_0 = kinetic energy of the power station group, megajoules at undisturbed operation
$P(t)$ = electric power, megawatts from the power station group
P_m = mechanical power, megawatts to the power station group from its prime movers at undisturbed operation

At an arbitrary time the frequency of the power station group will be

$$f(t)=f_0+\frac{1}{360}\frac{d\varphi(t)}{dt} \qquad (1)$$

There is for every period of time mechanical energy from the prime movers = electrical energy + increment in kinetic energy + energy dissipated as losses.

Paper 55-479, recommended by the AIEE Transmission and Distribution Committee and approved by the AIEE Committee on Technical Operations for presentation at the AIEE Summer General Meeting, Swampscott, Mass., June 27–July 1, 1955. Manuscript submitted November 15, 1954; made available for printing May 11, 1955.

E. O. Norinder is with the Swedish State Power Board, Stockholm, Sweden.

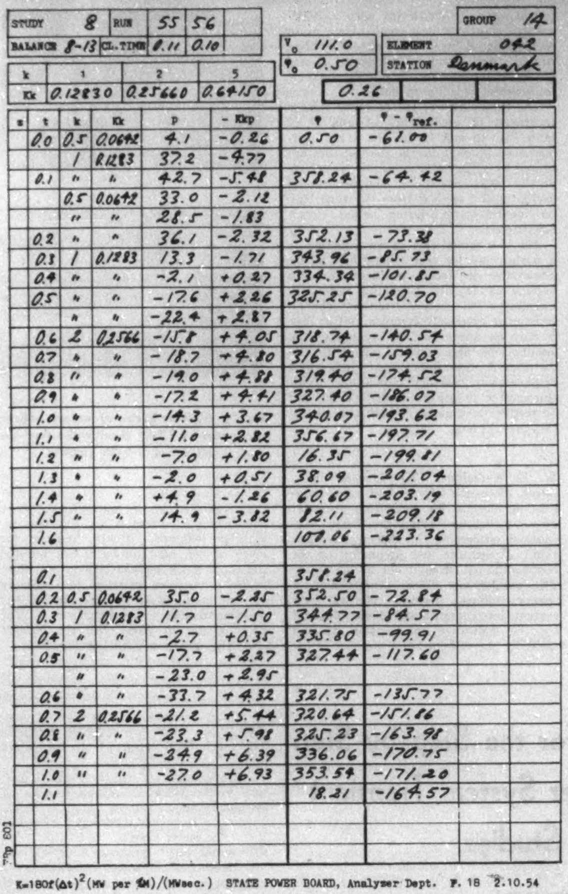

STUDY 8	RUN	55	56		
BALANCE 8-13	CL. TIME	0.11	0.10		

k	1	2	5
Kk	0.12830	0.25660	0.64150

V_0 111.0
φ_0 0.50

GROUP 14
ELEMENT 042
STATION Danmark

0.26		

s	t	k	Kk	p	- Kkp	φ	φ - φref.		
	0.0	0.5	0.0642	4.1	-0.26	0.50	-61.00		
		1	0.1283	37.2	-4.77				
	0.1	"	"	42.7	-5.48	358.24	-64.42		
		0.5	0.0642	33.0	-2.12				
		"	"	28.5	-1.83				
	0.2	"	"	36.1	-2.32	352.13	-73.38		
	0.3	1	0.1283	13.3	-1.71	343.96	-85.73		
	0.4	"	"	-2.1	+0.27	334.34	-101.85		
	0.5	"	"	-17.6	+2.26	325.25	-120.70		
		"	"	-22.4	+2.87				
	0.6	2	0.2566	-15.8	+4.05	318.74	-140.54		
	0.7	"	"	-18.7	+4.80	316.54	-159.03		
	0.8	"	"	-19.0	+4.88	319.40	-174.52		
	0.9	"	"	-17.2	+4.41	327.40	-186.07		
	1.0	"	"	-14.3	+3.67	340.07	-193.62		
	1.1	"	"	-11.0	+2.82	356.67	-197.71		
	1.2	"	"	-7.0	+1.80	16.35	-199.81		
	1.3	"	"	-2.0	+0.51	38.09	-201.04		
	1.4	"	"	+4.9	-1.26	60.60	-203.19		
	1.5	"	"	14.9	-3.82	82.11	-209.18		
	1.6					108.06	-223.36		
	0.1					358.24			
	0.2	0.5	0.0642	35.0	-2.25	352.50	-72.84		
	0.3	1	0.1283	11.7	-1.50	344.77	-84.57		
	0.4	"	"	-2.7	+0.35	335.80	-99.91		
	0.5	"	"	-17.7	+2.27	327.44	-117.60		
		"	"	-23.0	+2.95				
	0.6	"	"	-33.7	+4.32	321.75	-135.77		
	0.7	2	0.2566	-21.2	+5.44	320.64	-151.86		
	0.8	"	"	-23.3	+5.98	325.23	-163.98		
	0.9	"	"	-24.9	+6.39	336.06	-170.75		
	1.0	"	"	-27.0	+6.93	353.54	-171.20		
	1.1					18.21	-164.57		

Tp 801

K=180f(Δt)^2(MW per %M)/(MWsec.) STATE POWER BOARD, Analyser Dept. F. 18 2.10.54

Fig. 1. Step-by-step calculation form. Changes in network conditions for first run on form shown in Table I. Adding-machine tapes with calculations to obtain load angles for t=0.1, 0.2, and 0.3 second shown in Figs. 2, 3, and 4

Table I. Changes in Network Conditions in First Stability Run on Form, Fig. 1

Time, Seconds	Change in Network Condition
0.00	Three-phase short circuit near sending end of important 380-kv line
0.11	Faulted line disconnected at sending end
0.14	Faulted line disconnected at receiving end
0.54	Line reclosed at both ends with fault cleared

If the losses are neglected or the mechanical power for losses corrected, the following is obtained for the time dt

$$\frac{f(t)}{f_0}P_m dt = P(t)dt + W_0 \frac{d\left(\frac{f(t)}{f_0}\right)^2}{dt}dt \qquad (2)$$

When a disturbance occurs $d\varphi(t)/360dt$ can be neglected in relation to f_0 as long as the synchronism between the station groups is not completely lost. Accordingly, after performing the derivation, the following swing equation is obtained

$$\frac{d^2\varphi(t)}{dt^2} = \frac{180f_0}{W_0}(-P(t)+P_m) \qquad (3)$$

Step-by-Step Equation

The ordinary step-by-step equation is deduced according to the general principles in Appendix XII of reference 1. It is assumed that the power system is in a suitable way represented in a network analyzer. Regarding the representation in network analyzers of power systems for studies of the transient stability, the reader is referred to references 2 and 3.

In addition to those previously mentioned the following quantities are introduced:

Δt = step-interval, seconds
φ_n = load angle of power station group, electrical degrees at the time $t=n\Delta t$
$(\text{mva})_A$ = power in megavolt-amperes in the real system corresponding to 1 per cent power in the analyzer system
K = acceleration constant for power in analyzer per cent from power station group
p = scale reading on analyzer wattmeter when electric power is measured from station group
k_p = scale factor of analyzer wattmeter for converting scale reading to per-cent analyzer power
p_{-0} = scale reading on analyzer wattmeter when electric power from station group is measured at undisturbed operating conditions

The load angle φ_{n+1} of the station group at the time $t=(n+1)\Delta t$ can be calculated with satisfactory accuracy from φ_n and the value of $d\varphi(t)/dt$ in the middle of the time interval $n\Delta t<t<(n+1)\Delta t$, if the steps Δt are not made too long. From this follows the equation

$$\varphi_{n+1} = \varphi_n + \left(\frac{d\varphi(t)}{dt}\right)\Delta t \qquad (4)$$

where $t=(n+0.5)\Delta t$.

According to the same principle the following is obtained for the foregoing interval

$$\varphi_n = \varphi_{n-1} + \left(\frac{d\varphi(t)}{dt}\right)\Delta t \qquad (5)$$

where $t=(n-0.5)\Delta t$.

From equations 4 and 5 and through the integration of the swing equation 3, the following is obtained

$$\varphi_{n+1} = 2\varphi_n - \varphi_{n-1} + \frac{180f_0\Delta t}{W_0} \times \int_{(n-0.5)\Delta t}^{(n+0.5)\Delta t}(-P(t)+P_m)dt \qquad (6)$$

The acceleration constant K is introduced according to the relation

Table II. Adding-Machine Calculations of Load Angle φ_1 for $t=1\Delta t$ with No Changes in Network Configuration During $0<t<0.5\Delta t$

Operation No.	Rule	Counterpart in Equation 10, etc.
1–1	Print register-emptying sum	empty-register check
1–2	Print station-group no.	facilitates possible later check of printed tape
1–3	Add $(-Kkp)$ valid during $0<t<0.5\Delta t$ five times	$+5(-Kkp)$ during $0<t<0.5\Delta t$
1–4	Add prime mover increment five times	$+5Kk_{p-0}p_{-0}$
1–5	Print register-emptying sum	$5(-Kkp)$ during $0<t<0.5\Delta t$ $+5Kk_{p-0}p_{-0}$
1–6	Print register-emptying sum	empty-register check
1–7	Add result of operation 1-5 with last figure discarded*	$+0.5(-Kkp)$ during $0<t<0.5\Delta t$ $+0.5Kk_{p-0}p_{-0}$
1–8	Add initial load angle (φ_0)	$+\varphi_0$
1–9	Print nonemptying sum†	φ_1
1–10	Subtract load angle $(\varphi_{1\,\mathrm{ref}})$ or $(\varphi_{1\,\mathrm{ref}}+360.00)$ of reference station group‡	$-\varphi_{1\mathrm{ref}}$
1–11	Print register-emptying sum	$\varphi_1-\varphi_{1\,\mathrm{ref}}$
1–12	Note in first empty row of form the result of operation 1–9 in φ column and result of operation 1–11 in $\varphi-\varphi_{\mathrm{ref}}$ column. Calculate next station group	

* Raise last retained figure if discarded figure is higher than four.

† If result of operation 1–9 is not between 0.00 and 360.00, add or subtract 360.00 to get φ_1 between 0.00 and 360.00. Repeat operation 1–9. For setting analyzer, load angles are wanted between 0 and 360 degrees.

‡ If reference station group is calculated, add 360.00. In operation 1–12, note result of operations 1–9 and 1–11 on a blotting paper, besides noting load angle in the form. Values on blotting paper used in the calculations of following station groups.

Table III. Adding-Machine Calculations of Load Angle φ_{n+1} for $t=(n+1)\Delta t$ with Change in Network Configuration During $(n-0.5)\Delta t<t<(n+0.5)\Delta t$

Operation No.	Rule	Counterpart in Equation 8, etc.
2–1	Print register-emptying sum	empty-register check
2–2	Print station-group no.	facilitates possible later check of printed tape
2–3	Add each $(-Kkp)$ valid during $(n-0.5)\Delta t<t<(n+0.5)\Delta t$ a number of times equal to the number of tenths of a step-interval Δt that $(-Kkp)$ is valid during $(n-0.5)\Delta t<t<(n+0.5)\Delta t$	$+10(-Kkp)$ time average during $(n-0.5)\Delta t<t<(n+0.5)\Delta t$
2–4	Print register-emptying sum	$10(-Kkp)$ time average during $(n-0.5)\Delta t<t<(n+0.5)\Delta t$
2–5	Print register-emptying sum	empty-register check
2–6	Add result of operation 2–4 with last figure discarded*	$+(-Kkp)$ time average during $(n-0.5)\Delta t<t<(n+0.5)\Delta t$
2–7	Add last load angle (φ_n) in φ-column of form two times	$+2\varphi_n$
2–8	Subtract load angle (φ_{n-1}) next to last in φ column of form	$-\varphi_{n-1}$
2–9	Add prime mover increment	$+Kk_{p-0}p_{-0}$
2–10	Print nonemptying sum†	φ_{n+1}
2–11	Subtract load angle $(\varphi_{n+1\,\mathrm{ref}})$ or $(\varphi_{n+1\,\mathrm{ref}}+360.00)$ of reference station group‡	$-\varphi_{n+1\,\mathrm{ref}}$
2–12	Print register-emptying sum	$\varphi_{n+1}-\varphi_{n+1\,\mathrm{ref}}$
2–13	Note in first empty row of form, result of operation 2–10 in φ column and result of operation 2–12 in $\varphi-\varphi_{\mathrm{ref}}$ column. Calculate next station group	

* Raise last retained figure if discarded figure is higher than four.

† If result of operation 2–10 is not between 0.00 and 360.00, add or subtract 360.00 to get φ_{n+1} between 0.00 and 360.00. Repeat operation 2–10. For setting the analyzer the load angles are wanted between 0 and 360 degrees.

‡ If reference station group is calculated, add 360.00. In operation 2–13, note result of operations 2–10 and 2–12 on a blotting paper besides noting load angle in the form. Values on blotting paper used in calculations of following station groups.

$$K=\frac{180f_0(\Delta t)^2(\mathrm{mva})_A}{W_0} \qquad (7)$$

For evaluating the integral in equation 6 its time average during $(n-0.5)\Delta t<t<(n+0.5)\Delta t$ is taken, then equation 7 and the relation between scale reading and analyzer power is introduced. It is observed that $k_{p-0}p_{-0}$ $(\mathrm{mva})_A$ corresponds to P_m. The step-by-step equation is arrived at as follows

$$(-Kk_pp) \text{ time average during } (n-0.5)\Delta t<t<(n+0.5)\Delta t+2\varphi_n-\varphi_{n-1}+Kk_{p-0}p_{-0}=\varphi_{n+1} \qquad (8)$$

The fourth term of the left member of equation 8 occurs, when constant prime mover torques are assumed with the same value in the calculation of every step of the load angle of the power station group in question. The fourth term represents the load angle increment due to the prime movers. Because of that

$$Kk_{p-0}p_{-0}=\text{prime mover increment} \qquad (9)$$

It is assumed that the fault enters the power system at $t=0$. For $t<0$ the load angle φ is constant and $(-Kk_pp)$ equal to $-Kk_{p-0}p_{-0}$. When no changes in the network configuration occur during $0<t<0.5\Delta t$, by putting $n=0$ in equation 8, the following simplified relation for the load angle φ_1 for $t=1\Delta t$ is obtained

$$0.5(-Kk_pp) \text{ during } 0<t<0.5\Delta t+0.5Kk_{p-0}p_{-0}+\varphi_0=\varphi_1 \qquad (10)$$

Practical Accomplishment of Calculations

It is assumed that the power system is reproduced in a network analyzer and that the analyzer is in balance for the operating conditions before a fault enters into the power system. Further, it is assumed that in the analyzer the power from the different groups of stations can be determined when their load angles are known.

A calculation form, with the notations from two stability runs entered, is shown in Fig. 1. The calculations are explained in connection with the first stability run on the form. They are similar for the different station groups and because of this they are described for the group in the form only.

Initial Data for Stability Run

For each station group, the head of a form according to Fig. 1 is filled in, as will be explained in connection with the station group in the form of the figure.

In the stability run the following is valid

$f_0=50$ cycles per second
$(\mathrm{mva})_A=4$ mva per per-cent analyzer power (11)
$\Delta t=0.10$ second

For the station group in Fig. 1 the following is valid

$W_0=2{,}806$ megajoules
$\varphi_0=0.50$-degree = load angle for normal operating conditions (12)

According to equation 7 and the foregoing data the following is obtained for the station group

$$K=\frac{180\times 50\times 0.1^2}{2{,}806}=0.12830 \qquad (13)$$

For $k=1$, 2, and 5, $K\cdot k$ is entered in the form head. (In the actual analyzer k is always 1, 2, or 5 multiplied by a power of 10.)

For the stability run the changes in network conditions are shown in Table I.

Computation of Load Angle φ_1 for $t=1\Delta t$

With the load angles set to normal op-

Operation number in Table 1.	Print on tape.	Color of print. (Black=pos.) (Red =neg.)
1-1	xc	
1-2	14 #	Black
	4.77 -	Red
	4.77 -	"
1-3	4.77 -	"
	4.77 -	"
	4.77 -	"
——	26	Black
	26	"
1-4	26	"
	26	"
	26	"
1-5	22.55 xc	Red
1-6	xc	
1-7	2.26 -	"
1-8	50	Black
1-9	1.76 □c	Red
Note 2.	360.00	Black
1-9	358.24 □	"
1-10	422.66 -	Red
1-11	64.42 xc	"

Fig. 2. Adding-machine tape with calculation of load angle φ_1 for t=0.1 second of first stability run on form in Fig. 1

Operation number in Table 2.	Print on tape.	Color of print. (Black=pos.) (Red =neg.)
2-1	xc	
2-2	14 #	Black
	5.48 -	Red
	5.48 -	"
	5.48 -	"
	5.48 -	"
	5.48 -	"
2-3	5.48 -	"
	2.12 -	"
	2.12 -	"
	2.12 -	"
	1.83 -	"
2-4	41.07 xc	"
2-5	xc	
2-6	4.11 -	"
2-7	358.24	Black
	358.24	"
2-8	50 -	Red
2-9	26	Black
2-10	712.13 □	"
Note 2.	360.00 -	Red
2-10	352.13 □	Black
2-11	425.51 -	Red
2-12	73.38 xc	"

Fig. 3. Adding-machine tape with calculation of load angle φ_2 for t= 0.2 second of first stability run on form in Fig. 1. According to changes in network conditions indicated in Table I, faulted line is connected in both ends during 6/10 of the interval 0.05<t<0.15 second. During 3/10 of interval, faulted line is disconnected in sending end. During 1/10 of interval, faulted line is disconnected in both ends. With the load angles set to t=0.1 second, the three (−Kkp) values entered in the form for t=0.1 second have been calculated from measurements with network set according to conditions indicated. Consequently, (−Kkp) values are added six, three, and one times respectively in operation 2–3

Operation number in Table 3.	Print on tape.	Color of print. (Black=pos.) (Red =neg.)
3-1	xc	
3-2	14 #	Black
3-3	2.32 -	Red
	352.13	Black
3-4	352.13	"
3-5	358.24 -	Red
3-6	26	Black
3-7	343.96 □	"
3-8	429.69 -	Red
3-9	85.73 xc	"

Fig. 4. Adding-machine tape with calculation of load angle φ_3 for t=0.3 second of first stability run on form in Fig. 1

erating conditions, the power from each station group is measured without the fault applied and with the fault applied. The scale constant *k* and scale reading *p* are entered in the *k* and *p* columns of the form as they are read. From the form head *Kk* is found and entered with 4 decimals in the *Kk* column of the form. Then *Kk* and *p* are multiplied by an automatic multiplying machine. As *Kk* is entered with 4 decimals and *p* with 1 decimal, the result is always *Kkp* with 5 decimals in the resulting register of the multiplying machine. The result is entered with 2 decimals and shifted sign in the $-Kkp$ column of the form. The prime mover increment is equal to *Kkp* calculated from the measurements for normal operating conditions. Because of that the first value in the $-Kkp$ column is entered with shifted sign in the thick-lined rectangle in the right-hand part of the form head.

For the station group in Fig. 1 and normal operating conditions $p=4.1$ per cent is read on the wattmeter scale of the analyzer with scale constant $k=0.5$. From the form head, $Kk=0.64150$ is found for $k=5$. As $k=0.5$ is valid for the meas-

Table IV. Adding-Machine Calculations of Load Angle φ_{n+1} for $t=(n+1)\Delta t$ with No Changes in Network Configuration During $(n-0.5)\Delta t<t<(n+0.5)\Delta t$

Operation No.	Rule	Counterpart in Equation 8, etc.
3–1	Print register-empyting sum	empty-register check
3–2	Print station-group no.	facilitates possible later check of printed tape
3–3	Add $(-Kkp)$ for $t=n\Delta t$	$(-Kkp)$ time average during $(n-0.5)\Delta t<t<(n+0.5)\Delta t$
3–4	Add last load angle (φ_n) in φ column of form two times	$+2\varphi_n$
3–5	Subtract load angle (φ_{n-1}) next to last in φ column of form	$-\varphi_{n-1}$
3–6	Add prime mover increment	$+Kk_{p-0}p_{-0}$
3–7	Print nonemptying sum*	φ_{n+1}
3–8	Subtract load angle $(\varphi_{n+1\,ref})$ or $(\varphi_{n+1\,ref}+360.00)$ of reference station group†	$-\varphi_{n+1\,ref}$
3–9	Print register-emptying sum	$\varphi_{n+1}-\varphi_{n+1\,ref}$
3–10	Note result of operation 3–7 in φ column and result of operation 3–9 in $\varphi-\varphi_{ref}$ column of form. Calculate next station group	

* If result of operation 3–7 is not between 0.00 and 360.00, add or subtract 360.00 to get φ_{n+1} between 0.00 and 360.00. Repeat operation 3–7. For setting analyzer, load angles are wanted between 0 and 360 degrees.

† If reference station group is calculated, add 360.00. In operation 3–10, note result of operations 3–7 and 3–9 on a blotting paper besides noting load angle in form. Values on blotting paper used in calculations of following station groups.

ured value, $0.1\times0.64150=0.0642$ is entered in the Kk column of the form. With the fault applied $p=37.2$ per cent with scale constant $k=1$ is found. From the head of the form the corresponding $Kk=0.1283$ is found. Through the multiplications -0.26 and -4.77 result in the $-Kkp$ column of the form. According to the rules mentioned the prime mover increment is 0.26, and this value is entered in the thick-lined rectangle in the right-hand part of the form head.

To make clearer the swings of the station groups it is desired to determine the load angles in relation to a certain large group of stations. This is called the reference station group and the load angle of this station group is called the reference angle. The reference station group is always measured and calculated first. From calculations similar to those to be described, for the load angle at $t=0.1$ of the reference station group, $\varphi_{1\,ref}=62.66$. In addition to noting this angle in the form of the reference station group, $\varphi_{1\,ref}$ and $(\varphi_{1\,ref}+360)$ are noted on a blotting paper to be used in the calculations of the following station groups.

The load angle φ_1 is calculated from equation 10 by a printing adding machine according to the rules of Table II. The adding-machine tape for the station group of the reproduced form is shown in Fig. 2.

Computation of Load Angle φ_{n+1}

Computation of the load angle φ_{n+1} for $t=(n+1)\Delta t$ when changes in network configuration occur during $(n-0.5)\Delta t<t<(n+0.5)\Delta t$ is as follows. The load angles corresponding to $t=n\Delta t$ have been calculated and are set in the analyzer. The load angles for $t=(n+1)\Delta t$ are obtained from equation 8. For each station group the power p is measured for each network configuration valid during $(n-0.5)\Delta t<t<(n+0.5)\Delta t$ and with the corresponding k and Kk entered on the form in the order in which the network configurations are valid. The $(-Kkp)$ values are calculated by the multiplying machine exactly as described. The time average of $(-Kkp)$ during $(n-0.5)\Delta t<t<(n+0.5)\Delta t$ and equation 8 are calculated by the adding machine according to the rules of Table III. The adding-machine tape for the calculation of the load angle φ_2 for the station group of the reproduced form is shown in Fig. 3. In this case three different network configurations are used for the measurements according to the changes in network configuration indicated in Table I.

Computation of the load angle φ_{n+1} for $t=(n+1)\Delta t$ when no changes in network configuration occur during $(n-0.5)\Delta t<t<(n+0.5)\Delta t$ is as follows. The load angles and network configuration corresponding to $t=n\Delta t$ are set in the analyzer. The new load angles are obtained from equation 8. For each station group the power p is measured and with the corresponding k and Kk entered in the form. The $(-Kkp)$ values are calculated as described. For each station group, the $(-Kkp)$ value is equal to the first term of equation 8. The adding-machine calculations to obtain a new load angle are described in Table IV. They are similar to the latter part of the calculations described in the previous paragraph.

Advantages of the Method

1. The calculations are matched to standard office calculators and made in a time-saving and systematic manner.

2. A printed tape is obtained for the more complicated calculations. The tape can easily be checked and kept as a verification of the calculations.

3. Notations during the stability run are reduced to a minimum.

With one man making measurements and multiplications and one man operating the adding machine, complete stability runs on a 16-machine system have been made in less than 3 hours.

References

1. SYSTEM STABILITY AS A DESIGN PROBLEM, R. H. Park, E. H. Bancker. *AIEE Transactions*, vol. 48, Jan. 1929, pp. 170–94.

2. POWER SYSTEM STABILITY (book), S. B. Crary. John Wiley & Sons, Inc., New York, N. Y., vol. I, 1945; vol. II, 1947.

3. POWER SYSTEM STABILITY (book), E. W. Kimbark. John Wiley & Sons, Inc., New York, N. Y., vol. I, 1948.

◆

Discussion

E. L. Harder (Westinghouse Electric Corporation, East Pittsburgh, Pa.): A comparison of the calculation method proposed in the Norinder paper with that generally used in step-by-step studies today is shown in Fig. 5. The left column under the figure shows the usual calculations. First the power P_n is read, subtracted from your initial power, the acceleration calculated, the change in velocity, and the new velocity which will apply for the interval under consideration. Based on this velocity, the change in angle is calculated and then the angle at the end of the interval. This requires a subtraction, two multiplications, an addition, a further multiplication, and an addition. Further, the initial power and the several steps must be recorded in the table as indicated by the symbol R. This makes a total of 13 operations. In contrast, the proposed method requires reading the machine power P_n and multiplying it by a constant $k\Delta t$. Then proceed directly to calculate the new machine angle by the formula shown in which $k\Delta tP_0$ is constant throughout the calculations, whereas ϕ_n and ϕ_{n-1} are the two previous values of the angle. The addition of $2\phi_n$ is charged as a single addition though it requires adding ϕ_n twice. This partially compensates for the fact that the additions in the right-hand column are single-address additions whereas those in the left column are two additions. The total operations by the new method are seven. The first two multiplication steps in the left-hand method could be combined, reducing the operations from 13 to 11. However, they are generally kept separate to facilitate changing Δt frequently. This is less necessary in the right-hand method for the following reason.

If several system conditions exist during one time interval, this does not necessitate changing Δt. For example, suppose the fault is on up until 0.11 second at which the first breaker clears and the second

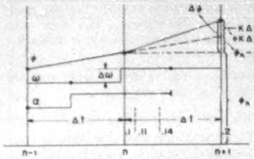

Fig. 5. Calculation of machine angle at n+1

R	P_n	R	P_n
−	P_0-P_n.		
R		X	$K\Delta tP_n$
X	$\alpha_n=K(P_0-P_n)$		
R		R	$\phi_{n+1}=-K\Delta tP_n$
X	$\Delta\omega=\alpha_n\Delta t$		
R		+	$+K\Delta tP_0$
+	$\omega_{n+.5}=\omega_{n-.5}+\Delta\omega$		
R		+	$+2\phi_n$
X	$\Delta\phi=\omega_{n+.5}\Delta t$		
R		−	$-\phi_{n-1}$
+	$\phi_{n+1}=\phi_n+\Delta\phi$		
R		R	
13		7	

breaker clears at 0.14 second. Instead of considering the acceleration constant from 0.05 second to 0.15 second, three power values are read at 0.1 second corresponding to these three conditions. The first one is considered to be affected for 0.6 of the interval, the second one 0.3 of the interval, and the third one 0.1 of the interval. These are readily added in by an adding machine by punching the first value six times, the second value three times, and the third value once, and then shifting the decimal place. Thus, a composite term $-k\Delta tP_n$ provides for the correct acceleration from time = 0.05 to time = 0.15. The other three terms in the expression are not affected by this acceleration.

The formula for the angle in the right-hand column of Fig. 5 is actually identical to that used in the left-hand column as can easily be proved. Referring to the figure, the last two terms of the formula give the previous angle plus the increment which would have occurred had the velocity not changed whereas the first two terms give the angle increments due to the velocity increment caused by the acceleration from the middle of the preceding interval to the middle of the interval under consideration. This makes it possible to eliminate any explicit consideration of velocity.

The Westinghouse network calculators with which the author is familiar, are direct reading in power and so would not require two of the columns shown in Fig. 1 of the paper. Also, we do not generally use the last column but plot the angles directly.

However, we do find it necessary to change time intervals fairly frequently for another reason. Whenever time intervals used result in an angle change of any machine during the interval of more than 20 degrees, accuracy requires that we go back and change to a smaller time interval. For this reason, our operating group feels that the time interval column must be carried and also a column to show the times at which various switching operations are performed so that this part of the calculation will be clear. Considerable time is saved by using as large intervals as possible, consistent with this limitation, even though it does require changing the interval size from time to time.

When several people are available at the calculator and a multimachine problem is being run, the results can be obtained more quickly and checked completely by dividing the work among the several people. It would not be feasible to provide each one with a desk calculator and adding machine. For example, in an 18-machine problem, three generating stations might be assigned to each of six people. They can then run the swing curve faster and completely check it by rotating the calculation sheets to the next person faster than this could be done by the method described in the paper. However, it is quite possible that even though the desk calculator and adding machine are not used in this case, some gain will be possible by utilizing a form which incorporates the method described in the paper having fewer calculation steps. The paper does not go into the procedure for changing time steps and this will be somewhat more complicated than is used now. Due to this, certainly not all of the gain indicated in Fig. 5 can be realized per step, but the total number of steps will be less if the time intervals are kept as large as possible.

Our conclusions at the moment are that it will be well worth companies who own their own boards and operate such studies with one or two persons to look into this method of using an adding machine and desk calculator to speed up their work. On large studies where several persons are available and waiting for the results to decide on subsequent studies, the work can be done faster by several persons rather than by two persons using the calculators. However, some gain may be obtained from the new form and from the proposed method for making changes within an interval.

The author is to be congratulated on this novel approach to the problem.

Y. H. Ku (Moore School of Electrical Engineering, University of Pennsylvania, Philadelphia, Pa.): I would like to congratulate the author for giving this rational for the step-by-step calculations and for reducing the usual 13 steps to 7 steps as commented on by Dr. E. L. Harder during his excellent presentation.

C. C. Young (General Electric Company, Schenectady, N. Y.): There is a continuous search for rapid, accurate methods for analyzing the transient stability of power systems. Mr. Norinder is presenting a mechanized method involving a tape adding machine for making the additions and subtractions involved during a step-by-step solution. The multiplying of (KK_pP) for each machine still must be done separately using some other device. The necessity of making this multiplication separately seems to be the major drawback to this method. The author's company recognized this problem some time back and evolved a swing curve calculator.[1] This device not only makes the multiplication automatically but makes the "prime mover increment" subtraction as well. Thus only two simple algebraic additions for each machine are necessary to determine a new angle setting at each point. In the analysis of large power systems, our experience has been that with a total of four people (a reader, plus three recorders and calculators) by the time the last machine's power is read, the new angles on the first machines have been calculated and are ready to be set. Thus the time is utilized to its maximum efficiency. Even with fewer people, a swing curve can be made rapidly and accurately.

Concerning the speed with which the author indicates stability runs can be made using his method, his statement is difficult to evaluate. The time to make a "complete" stability run is a nebulous thing since it is an undefinable quantity which is a function of the time intervals used and the behavior of the system. If the author could give some better measure such as the time required to calculate each point for all 16 machines, and a better evaluation of the method can be made.

REFERENCE

1. SWING CURVE CALCULATOR MAKES BETTER STABILITY STUDIES FASTER, W. G. Heffron, F. S. Rothe. *Electrical World*, New York, N. Y., Apr. 11, 1955.

E. O. Norinder: In reply to Mr. Young's question, in a 16-machine system the active powers are measured and the new angles calculated as described, the new angles set, and the setting checked in 15 minutes when two men make the stability run.

A New 500-Megavolt-Ampere Air Magnetic Circuit Breaker of Simplified Design

M. J. REILLY
ASSOCIATE MEMBER AIEE

D. E. WESTON
MEMBER AIEE

THE air magnetic power circuit breaker is a relatively new development in the field of circuit protection. Although the principles involved have been well known for many years, power circuit breakers which have been made with the use of this knowledge did not become commercially available until comparatively recently. Since then they have become almost universally accepted and now enjoy a very prominent position among the various types of circuit breakers.

Magnetic circuit breakers find their greatest use on electric circuits of 13.8 kv and below, and provide interrupting capacities up to 500 megavolt-amperes (mva). There is little doubt, however, that these limits will be extended in the near future, particularly as regards interrupting capacity.

The air magnetic power circuit breaker has played an important role in making possible modern, completely enclosed metal-clad switchgear with all its advantages of safety, convenience, low cost, ease of installation, pleasing appearance, and simple, inexpensive maintenance. When used with metal-clad switchgear the magnetic circuit breaker is in the form of unit which can be easily removed from the cubicle for inspection or maintenance, or to substitute a spare unit. The accessibility of all parts of the magnetic circuit breaker makes it particularly suited to a program of maintenance with a minimum of time out of service.

The magnetic circuit breaker is widely used in utilities, both in the generation of electric power and its transmission and, in industry, for feeder protection and for control in heavy manufacturing. They are used both indoors and outdoors and are well adapted as replacement units for obsolete and under-capacity breakers.

In modern industry, where profits are so closely associated with the ability to produce continuously without interruption, electric outages, for whatever reason are often intolerable. The ability to produce electricity, as well as the use of it, must be safeguarded at all times. The power circuit breaker, by its simplicity and design for ease of maintenance, can contribute heavily to the uninterrupted generation and use of electricity. Inasmuch as the modern circuit breaker is so widely applied in many and varied industrial requirements, and considering the costliness of power outages and the expense of time consuming maintenance, it is important that a design program for such a circuit breaker includes as one of its primary requirements that of functional and mechanical simplicity. Considerations such as these were an important factor in the design and development of the new 500-mva air magnetic circuit breaker, Fig. 1, to be described.

Functional Requirements

An air magnetic circuit breaker consists of three principal parts: the interrupting device; the contact structure; and the operating and control mechanism. Each of these parts performs an important function in itself and, when properly co-ordinated, all can contribute to a simple, trouble-free design.

Performance Requirements

The magnetic air circuit breaker performs the duty of interrupting the electric circuit in a unique manner. Because interruption must be accomplished under the condition of the relatively low dielectric strength of air at atmospheric pressure, the breaker must immediately gain and then maintain a controlling influence over the electric circuit being interrupted. Evidence of this controlling influence by the magnetic air circuit breaker is to be found in the relatively high arc voltage that is imposed during interruption. The effect of this high arc voltage is to reduce the dielectric stress across the breaker contacts to the equivalent of the differential between it and the system voltage.

This high arc voltage is achieved by so constricting, elongating, and cooling the arc that its effective resistance is increased at an extremely high rate. When the value of the arc resistance is made large with respect to the inductance of the external circuit, it brings the short-circuit current more nearly in phase with the system voltage and, at the same time, substantially reduces the magnitude of the short-circuit current.

CIRCUIT DURING INTERRUPTION

Fig. 2 geometrically illustrates the changes that occur during a normal high-current interruption. Two current loops of a symmetrical short-circuit current are shown, and the circuit breaker contacts have been considered as parting at a current zero. In the first loop the arc voltage e_a is shown to have a uniform but low value (5 per cent of E_m). Although this small arc voltage has had some effect in reducing the magnitude and shifting the phase of the short-circuit current, the circuit breaker is not yet prepared to interrupt the circuit. The second loop, however, shows the control that the circuit breaker is now imposing on the circuit. The arc resistance has increased rapidly so that a high arc voltage is produced (65 per cent of E_m). As a result the short-circuit current has been reduced to 30 per cent of its original value, and has been made to shift from 90-degree displacement to nearly 0 degree with respect to the system voltage. The effect of this controlling influence is to extinguish the arc successfully, because at the point of interruption only a small voltage differential is impressed upon the air gap between the circuit-breaker contacts. A relatively smaller voltage stress is placed on the air gap, and a longer time is gained to permit the air gap to build up its dielectric strength before the occurrence of a normal system voltage peak.

Without the controlling influence of the arc voltage, current zero would always occur at substantially a system voltage peak, and the full value of E_m would be impressed across the circuit-breaker contact gap. Even if the gap were capable of withstanding the value of E_m, the voltage, in going from zero to E_m, would oscillate about the E_m point, thus actually impressing nearly $2E_m$ on the circuit breaker.

Therefore, in overcoming the natural low insulation recovery strength of atmospheric air, the air magnetic circuit breaker becomes a high arc voltage device

---

Paper 55-509, recommended by the AIEE Switchgear Committee and approved by the AIEE Committee on Technical Operations for presentation at the AIEE Summer General Meeting, Swampscott, Mass., June 27–July 1, 1955. Manuscript submitted March 30, 1955; made available for printing May 23, 1955.

M. J. REILLY and D. E. WESTON are with the Allis-Chalmers Manufacturing Company, Boston, Mass.

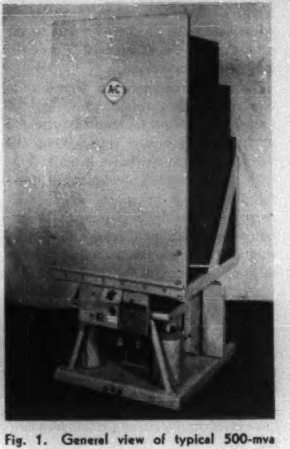

Fig. 1. General view of typical 500-mva 13.8-kv air magnetic circuit breaker

which develops its voltage drop by inserting a controlling resistance into the circuit. This resistance acts as a phâse-shifting device to bring current and voltage zeros more nearly together at the time of circuit interruption, and is used during the burning cycle of the arc as a means of maintaining the arc energy at a uniformly low level. Inserting this resistance in the circuit before arc interruption automatically provides a damping resistance for controlling the rate of rise and amplitude factor of the natural-frequency recovery voltage characteristics of the systems to which it is applied.

The Interrupting Device

The design of an interrupting device, as dictated by performance requirements, must center around those characteristics which will help to increase the resistance of the arc as rapidly as possible. Simplicity of design as an aid to easy maintenance and long uninterrupted service is an important consideration. In the 500-mva air magnetic circuit breaker being described, all of these conditions have been taken into account and provided for.

Fig. 3 is a general view of the circuit breaker with some of the enclosures removed to show the contact arrangement. Fig. 4 shows the interrupting device in more detail and shows its arrangement in relation to the contact structure. Full advantage has been taken of the natural thermal effect of the heated arc products to rise in a vertical direction by placing the interrupting device above the circuit-breaker contacts. In like manner, the location of the interrupting device takes advantage of the blowout effect of the contact and bushing configuration.

The Barrier Stack

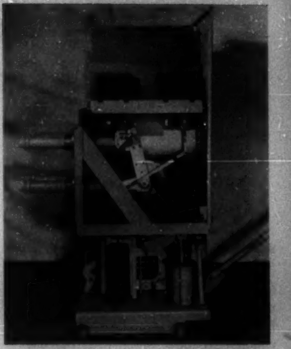

Fig. 3. Side view of a 500-mva 13.8-kv air magnetic circuit breaker with barriers removed to show contacts and magnetic blowout structure

The barrier stack is the heart of the interrupting device. It is here that the greatest influence can be brought to bear on the arc during circuit interruption. The barrier stack is composed of a series of refractory plates of high zircon content. The plates have a porous surface which present a very large cooling area to the arc. Reducing the temperature of the arc is an important part of the over-all attempt to increase its resistance and thereby produce the required high arc voltage. The plates of the barrier stack have slots in the lower end which vary in depth and location in such a manner that, when arranged in a spaced relationship, the only path available to the arc is a long, tortuous one which greatly elongates the arc and contributes another factor to the increase of its resistance. The slots in the barrier stack plates gradually narrow down and then disappear altogether, thus constricting the arc in its upward travel and reducing its diameter as still another means of building up arc resistance. It is thus possible to have in one simple part all of the basic requirements for successful arc interruption. However, to bring the barrier stack into full play, the arc must be made to move more efficiently than thermal effects natural blowout alone can provide. It is here that the magnetic blowout structure comes into effect.

Magnetic Blowout

In the *MC-500* circuit breaker, the magnetic blowout structure consists of a blowout coil and pole pieces at each end of the barrier stack. The physical arrangement of components permits this simplified blowout structure. The blowout coils are introduced into the current path during the opening of the circuit breaker at the time the arc transfers to the arc runners. At this time a magnetic field is produced which forcibly propels the arc upward and into the barrier stack. The blowout structure, like the barrier stack, is simple in design, contains no moving or wearing parts, and is easily accessible.

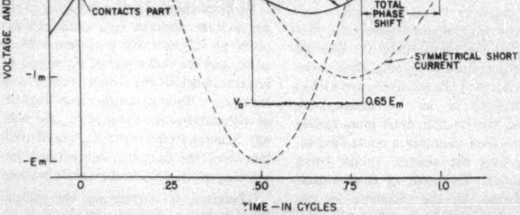

Fig. 2. Geometry of 2-loop interruption showing effect of arc voltage on magnitude and phase of short-circuit current

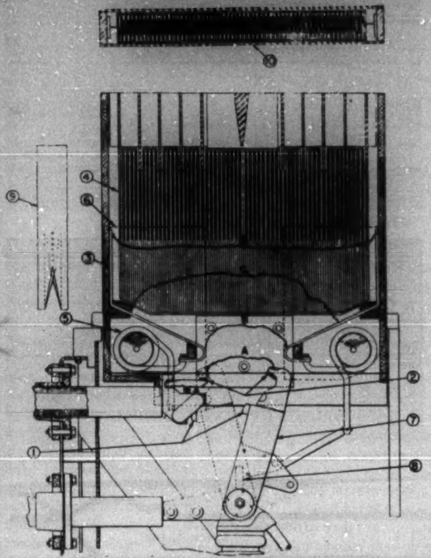

Fig. 4. Cross-section diagrams of a 500-mva circuit breaker. Lines A, B, C, and D indicate successive stages of arc position

1—Main contacts
2—Arcing contacts
3—Arc runners
4—Barrier stack
5—Blowout coils
6—Pole extensions
7—Moving contact arm
8—Puffer tube
9—End view of barrier stack
10—Plan view section of barrier stack at top of plate slots

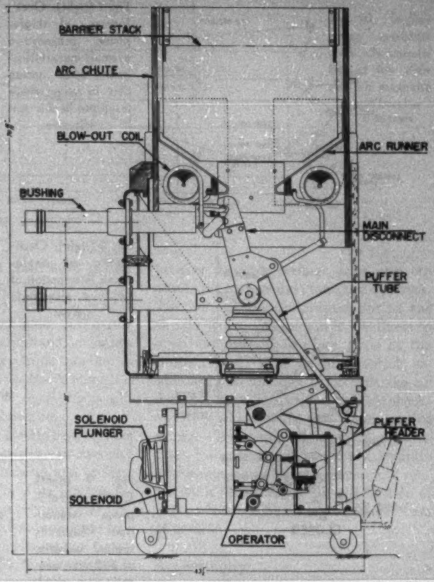

Fig. 5. Detail side view of a 500-mva circuit breaker showing physical arrangement of component parts

Interruption of Small Currents

While the magnetic field produced by the passage of large currents during arcing provides ample propelling force to the arc, at low currents, such as encountered in the interruption of magnetizing currents and small load currents, the magnetic field has little effect. Although successful interruptions would be obtained, the time required to extinguish the arc would be considerably longer than at higher currents. Consequently, the design of the *MC-500* circuit breaker includes a puffer, the function of which is to provide the means of rapidly moving the arc into the barrier stack when the magnetic field is not strong enough to do so. Here too, simplicity was one of the principal design objectives. The result is a puffer having no additional moving parts. The circuit-breaker opening springs are used, by means of a piston and cylinder assembly, to provide the source of air needed during the opening stroke. The air is led through a series of rigid, fixed tubes to the hinge point of the movable contact arms where a fixed nozzle directs the air in a predetermined direction into the arcing area, thus aiding the arc to move into the barrier stack. Although very little air is required and pressures are not significant, the puffer enables the *MC-500* circuit breaker to reduce the arcing time at low currents by at least 500 per cent.

Contact Structure

While the barrier stack and magnetic structure work to bring about successful arc interruption, the contact structure also plays an important role in making the arc move rapidly into the interrupting zone. As shown in Fig. 4, the *MC-500* circuit breaker has two principal sets of contacts. These are the main current-carrying contacts and the arcing contacts. The main contacts take no part in circuit interruption, but enable the circuit breaker to fulfill its other prime function of carrying load currents continuously for long periods of time without overheating or deteriorating. The main contacts are silver plated for good conductivity and must not be subjected to arcing to preserve their current-carrying ability. The stationary part of the main contact consists of a number of spring-loaded fingers, providing a series of independent contact points against the solid face of the moving main contact. Each stationary finger has two contact surfaces, a "make" and "break" surface and a current-carrying surface. During circuit-breaker operation, the stationary contact finger moves its contact point in such a way so that the important current-carrying point never takes part in circuit making or circuit opening. Fig. 4 shows the physical arrangement of the component parts.

The arcing contacts protect the main

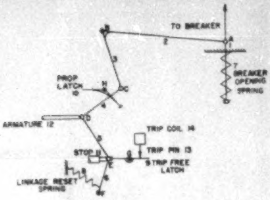
TO BREAKER
A
B
1
2
3
7
BREAKER
OPENING
SPRING
PROP
LATCH
10
H
C
4
ARMATURE 12
D
TRIP COIL 14
5
STOP 11
G
TRIP PIN 13
E
9 TRIP FREE
LATCH
8
LINKAGE RESET
SPRING
6
F

OPEN

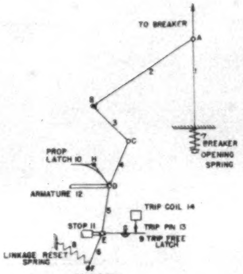
TO BREAKER
A
1
2
B
3
C
7
BREAKER
OPENING
SPRING
PROP
LATCH 10
H
4
D
ARMATURE 12
TRIP COIL 14
5
STOP 11
G
TRIP PIN 13
9 TRIP FREE
LATCH
E
8
LINKAGE RESET
SPRING
6
F

CLOSED

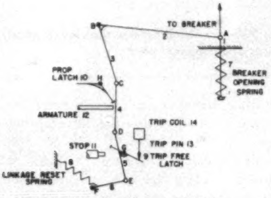
B
TO BREAKER
A
2
1
3
7
BREAKER
OPENING
SPRING
PROP
LATCH 10
H
C
ARMATURE 12
4
D
TRIP COIL 14
STOP 11
G
TRIP PIN 13
9 TRIP FREE
LATCH
5
LINKAGE RESET
SPRING
8
6
E

TRIP FREE

Fig. 6. Schematic diagram of solenoid-operated circuit-breaker mechanism

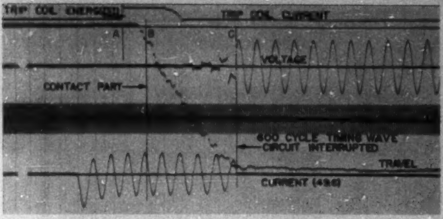

Fig. 7 (right). Oscillogram of single-phase interruption of small current illustrating short arcing time in range where magnetic field is not effective

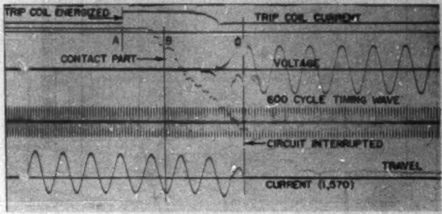

Fig. 8 (right). Oscillogram of single-phase interruption of full-load magnitude current

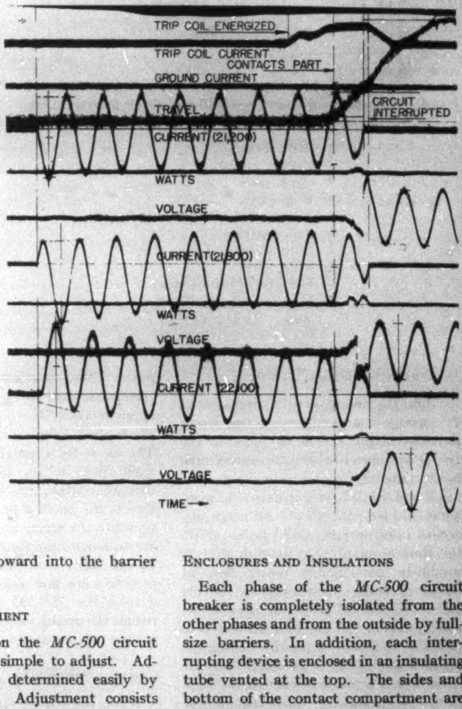

Fig. 9 (right). Oscillogram of 3-phase interruption illustrating typical behavior of 500-mva magnetic circuit breaker in range of rated short-circuit current

contacts by being the first parts to touch in closing and the last to part in opening. They assume the wear and deterioration imposed by arcing in repeated operations of the circuit breaker. The contact surfaces are clad with a tungsten arc-resisting alloy which reduces erosion caused by arcing while, at the same time, limiting the emission of metallic particles into the arc which would tend to reduce its resistance. A feature of the arcing contact structure is the blow-on effect produced by the shape of the contacts. Before contact part, the mechanical forces produced by the current flow tend to force the arcing contacts together to prevent premature opening. After contact part, these same mechanical forces act on the arc to move it upward into the barrier stack.

CONTACT ADJUSTMENT

The contacts on the *MC-500* circuit breaker are very simple to adjust. Adjustments can be determined easily by visual inspection. Adjustment consists only of setting main contact pressure and arcing contact lead.

ENCLOSURES AND INSULATIONS

Each phase of the *MC-500* circuit breaker is completely isolated from the other phases and from the outside by full-size barriers. In addition, each interrupting device is enclosed in an insulating tube vented at the top. The sides and bottom of the contact compartment are also insulated with full-size barriers. Bushings are of high dielectric strength

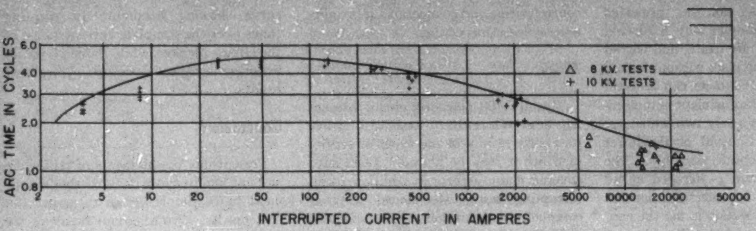

Fig. 10. Single-phase performance characteristics of the 500-mva air magnetic circuit breaker

paper phenolic and have a foil layer at the flange location to reduce voltage stress. Flanges are cemented to the bushing tubes by a process which has proved highly satisfactory by long usage and many tests. Principal insulating members are of flame-retardant material which will not sustain combustion in case of fire. A high-strength porcelain insulator is used as a support for the movable contact arms of the circuit breaker. Operating links between the disconnects and the mechanism are fiber glass reinforced polyester material and have high impact and mechanical strength as well as superior insulation properties. A steel panel on the front of the circuit breaker completely isolates the high-voltage parts when installed in metal-clad switchgear. The panel is hinged in such a manner as to provide proper electrical clearances when the circuit breaker is in service and yet permit it to be stored in the disconnected position without any increase in space requirements, which results in substantial economies in floor area; see Fig. 5 for side view of the 500-mva circuit breaker.

Mechanical Requirements

The mechanical operation of the circuit breaker cannot be overlooked when reliability and simplicity are being considered. While the device must function properly in handling a short-circuit current, this is only one of its duties, and usually an infrequent one. The normal day-to-day use of the circuit breaker involves the mechanical parts which must be rugged and well designed to provide long life when used with the high speeds and fast accelerations necessary in circuit-breaker service.

The closing power for the *MC-500* magnetic circuit breaker is provided by a solenoid operating mechanism of unusually simple design. The solenoid armature acts directly on the closing linkage, which consists of only four separate links. Fig. 6 shows the schematic arrangement of the solenoid operator linkage in the open, closed, and trip-free positions. Point *E* is a temporarily fixed point, held by the trip latch. A tripping impulse will release point *E* at any time the circuit breaker is required to open, permitting link 6 to rotate and links 4 and 5 to move downward. Thus the circuit breaker is always mechanically trip-free in any position irrespective of the operating condition of the solenoid armature.

Needle bearings are used in many places in the operating mechanism to increase the speed of the mechanism and to simplify maintenance. Only one latch is required in the tripping mechanism because the design of the latch load was kept to a minimum, thereby eliminating the necessity of the more complicated and critical series latch arrangements. The trip coil acts directly on the trip latch which again promotes simplicity and reliability by doing away with linkages. The main operating crank 3 operating the circuit-breaker movable contact arms also operates the springs used for opening power. The springs are compressed during the closing stroke and remain in readiness to open the movable contact arms at the proper speed. The opening spring assemblies also function to provide the air used by the puffers, and to provide shock-absorber action at the end of the opening stroke. By combining all of these functions into one simple assembly, maintenance requirements are lessened and simplicity is furthered by the elimination of parts which might otherwise be a source of trouble.

Accessibility

The *MC-500* magnetic circuit breaker is arranged for utmost accessibility of parts. One man can handle any part of the circuit breaker easily and without special

Table I. Representative Test Data for Type MC-500 13.8-Kv 500,000-Kva RUPTAIR Circuit Breaker. Three-Phase Tests, 50 Cycles

Test No.	System Voltage, Kv	Short-Circuit Current Phase			Interrupting Time			3-Phase, Kva
Open tests								
9099C	11	1,980	2,030	1,920	2.60	2.45	1.85	36,400
9190C	11	5,700	5,600	6,000	2.35	2.65	2.50	108,000
9362C	12.7	21,200	21,800	22,100	2.00	3.40	3.40	562,000
9364C	11	15,600	25,000	23,600	2.00	3.95	3.95	423,500
Close-open operation of close-open—3-minute close-open—3-minute close-open								
9298A	11	21,400	20,100	18,100	2.30	2.70	2.60	336,000
9298B	11	18,000	23,600	23,100	2.15	2.50	2.35	342,000
9298C	11	22,700	19,300	27,000	2.05	2.40	2.30	348,000

Table II. Representative Test Data for Type MC-500 13.8-Kv 500,000-Kva RUPTAIR Circuit Breaker. Single-Phase Tests, 60 Cycles

Test No.	Voltage to Neutral, Kv	Short-Circuit Current, Amperes	Arcing Time, Cycles	Interrupting Time, Cycles	Equivalent 3-Phase, Kva
197–138.1	10.4	3.68		3.75	89
197–125.2	10.4	8.45		4.5	202
197–112.1	10.4	26.4		5	630
197–124.2	10.4	49.6		6.5	1,190
197–129.2	10.4	125		6	2,950
197–143.1	10.4	422		5.5	10,100
197–145.2	9.7	1,570		4.0	37,500
197–146.1	10.1	1,760		4	42,000
530711–05	8.35	10,400	1.4	2.8	248,000
530427–19	8.0	20,500	0.8	2.2	490,000
530610–02	7.70	24,300	0.83	2.16	580,000
530610–01	7.60	24,400	1.10	2.41	583,000

devices. Contacts can be inspected easily without removing any hardware, since the barriers, arc chute, and barrier stack are fitted into place without fastening devices. The contacts can be completely exposed for adjustment or replacement after removing only two screws per phase to permit removal of the lower part of the arc chute assembly. The operating mechanism is exposed at all times, although it is protected from dirt and injury by its location under the contact structure housing. Auxiliary devices such as relay, closing rectifier, and auxiliary switches are all readily accessible on the lower part of the circuit breaker. Primary bushing disconnect fingers are of the multiple finger type, and are attached to the circuit breaker for ease of inspection.

The *MC-500* circuit breaker is equipped with wheels and casters of large diameter to permit efficient insertion or removal in the cubicle and to asure easy portability over rough floors. Wheels are far enough apart to provide stability. Rugged interlocks insure that the circuit breaker will not be placed in the wrong cubicle. All control wiring and connections are readily accessible for inspection.

Tests

The *MC-500* magnetic circuit breaker has been exhaustively tested to prove its ability in any of the types of service in which it may be placed. Tests have covered many aspects in addition to interrupting tests. Mechanical tests of complete circuit breakers and components dielectric tests, closing tests, and capacitor-switching tests were among those made. Interrupting tests were made under many conditions and included 3-phase interruptions as well as single-phase tests at various duty cycles. Fig. 7, 8, and 9 show three typical oscillograms from the interrupting tests. These illustrate the performance of the *MC-500* breaker at low currents (50 amperes), load magnitude currents (1,570 amperes), and short-circuit currents (22,000 amperes). The oscillograms show that the basic requirements for interruption in an air magnetic device have been well met. Fig. 10 presents in more comprehensive form a curve showing maximum interrupting times over the complete current range of the circuit breaker, while Tables I and II list other pertinent data from typical test results.

Conclusion

Present-day requirements of reliability and low maintenance demand that equipment be of simple design to assure the best results. Power circuit breakers are no exception, and are expected to perform their required duties in a safe and efficient manner and at a low cost to the user. A new 500-mva air magnetic circuit breaker for use at 13.8 kv has been designed with these objectives in mind. Careful attention to detail has resulted in a circuit breaker which, while complying with all performance requirements, has also exhibited, to a marked degree, a simplicity which will provide its users with long, low-cost, and trouble-free service. It may well serve as the pattern by which other ratings of air magnetic circuit breakers may be designed to the benefit of all industry.

◆

Discussion

G. D. Wood (I-T-E Circuit Breaker Company, Pittsburgh, Pa.): I would like to discuss the paper from the point of view of circuit breaker testing.

From the voltages used, at least some of the testing would appear to have been done in Europe. I have something in common with the authors in that I have also tested circuit breakers of this same rating abroad and have had to cope with the various procedures commonly used abroad which differ from the practices in the United States.

One of the differences is that the standard voltages used abroad are different from ours and the test generators are designed to agree with these operating voltages. The operating voltages jump from 10–11 kv to 20–22 kv and therefore the test generators are wound for 11 and 22 kv.

To test an American 13.8-kv breaker with a maximum design voltage of 15 kv requires some adjustment of the test circuit to obtain the desired voltages and currents. The authors and I used different solutions to the problem with quite different test results.

The voltage at which interrupting tests are made is extremely important. Designers have found that, if tests are made at the maximum design voltage, no difficulties are found at the required lower voltages. In fact at half voltage, we have found that the megavolt-ampere limit of the breaker is increased some 15 to 20 per cent. It seems impractical to make tests to demonstrate a rating at any voltage less than the maximum design voltage.

Fig. 11 shows the available voltages of two of the test stations abroad. Since the 3-phase tests reported are nearly all at 11 kv, it would appear that the connections (*a*) for Station 1 or connection (*c*) for Station 2 may have been used. There is one circuit opening test that was reported at 12.7 kv which may have been connection (*d*) of Station 1 or overexcitation of connection (*c*) of Station 1. The voltages reported would appear to be open-circuit voltage of the machine and the normal frequency recovery voltage would be somewhat less, and no doubt would be well within the 15 per cent permitted by the Test Code but there might be some question of it being within the 4 to 5 per cent experienced on some systems.

In contrast with the procedure, our tests used connection (*c*) of Station 1 and any voltage up to 22 kv was available. To obtain the desired voltage to test a 13.8-kv breaker, the machines were excited to 16 kv or above. It was found necessary to use two machines in parallel to keep the recovery voltage up to the desired value. With this connection, tests were made having normal frequency recovery voltages up to 15 kv as required by the breaker rating and above the 14.5 kv required by the maximum voltage of a 13.2-kv system.

Single-pole tests are not required by the standards except where the 3-phase tests are considered inadequate. If single-phase tests are made, two methods are provided in the Test Code.

The first is for grounded faults of effectively grounded system. For this test, 57 per cent of line-to-line voltage is used. The megavolt-amperes of the single-pole tests are multiplied by 3 to obtain the 3-phase equivalent, as used in the paper.

The second method is to be used for ungrounded faults on either grounded or ungrounded systems, or for grounded faults on an ungrounded system. For this condition, single-pole tests are to be made at 87 per cent of line-to-line voltage and full rated current. The megavolt-amperes or a single-pole test is then multiplied by 2 and not 3 for the equivalent 3-phase megavolt-amperes (see *C37.9-2.6.1.2b*). Where 3-phase tests are inadequate, this is the test that would be needed to demonstrate the breaker rating. These tests would require a voltage of 13 kv and full current corresponding to 15 kv or 19.4 kiloamperes. This is quite different than the 8-kv tests shown in the paper.

Fig. 12 shows the relation of the voltages used in the tests reported in the paper to the system voltages and to the breaker rating, both 3 phase and single phase. In view of the large discrepancy between the test voltages and both the system requirements and the breaker rating, the question arises as to the suitability of these tests to demonstrate that the breaker meets the Test Code requirements for the rating that has been assigned, or is usable on circuits where this breaker is usually applied.

There also seems to be a discrepancy between the current values shown in the table and the currents used to calculate the megavolt-amperes shown in the table. Perhaps the authors will explain this discrepancy and its point on the oscillogram.

The single-opening test (*9362-C*) or 11-kv close-open—3-minute close-open—is not equivalent to the American close-open—15-second close-open delay. The 3-minute delay between tests is less severe than the American 15-second delay.

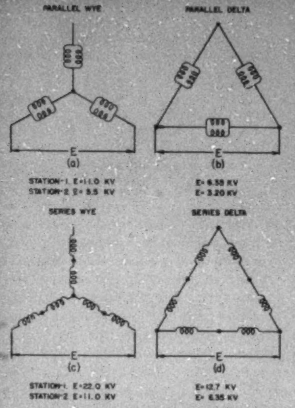

Fig. 11. Available voltages of two European test stations' generator connections

The many deficiencies in the tests reported naturally raise various other questions which would otherwise be taken for granted. Some of these are as follows:

1. Where the tests made with the circuit breaker in the structure in which it is used so as to duplicate ground clearances?
2. Which side of the breaker was connected to the source to represent the worst condition in service?

At this rating, it is possible to make tests abroad in stations having different voltage ratings from ours, and by proper use of the facilities to secure the proper voltages, currents, and power factors required to demonstrate the circuit breaker rating. It is also possible to make tests on the American duty cycle of close-open—15-second close-open.

Russell Frink (Westinghouse Electric Corporation, East Pittsburgh, Pa.): We at Westinghouse have studied this paper with considerable interest, since we described a 500-mva 13.8-kv magnetic air circuit breaker before the Institute in January 1946, almost 10 years ago. In general, we are in agreement with the authors concerning the merits of breakers of this type for the ratings in which they can be built, and wish to congratulate the authors on their selection of horizontal drawout construction. There are several items in this paper which would be interesting to discuss, but these comments will be limited to one, and that is rating.

The authors state that this new breaker is rated at 500 mva, 13.8 kv, and that the breaker has been exhaustively tested, and they list representative test data. We do not believe that these data substantiate the rating assigned. Assigning a rating to a circuit breaker implies that the rating is determined by existing standards, and, in this case, the accepted standards are ASA *C37.4* through *C37.12*. The data presented are at variance with the standards on three points: the test voltage, the duty cycle, and the determination of the kilovolt-amperes.

The voltage ratings for indoor oilless power circuit breakers are listed in Table II of Standard *37.6-1953*. For the subject breaker, they are as follows: rated kv, 13.8; maximum design kv, 15.0; and minimum kv for rated interrupting mva, 11.5. Standard *9-2.6.1.1a* states: "For direct testing, the circuit voltage immediately before the test shall be equal to the maximum design voltage rating of the circuit breaker." Interpreting the term "system voltage" which appears in the paper to mean the voltage of the system on which the test is made, or the voltage immediately before test, no tests are listed even at the rated voltage of the breaker, not to say maximum design kilovolts. We have run volt-ampere curves on a number of magnetic interrupters, and they are not constant kilovolt-ampere devices; they are only fitted into standards which are based on constant kilovolt-amperes.

On a typical interrupter it was found that a reduction in the test voltage of approximately 30 per cent increased the maximum current-interrupting capacity by approximately 300 per cent. We therefore question that tests at 11.0 and 12.7 kv demonstrate the ability of a breaker to operate with a system voltage of 15 kv. We recognize that the standards permit a 15-per-cent tolerance in recovery voltage, but this is not a tolerance in test voltage. We also observe that test *9362C*, the oscillogram of which is reproduced in Fig. 9, shows approximately $12^{1}/_{2}$-per-cent a-c decrement during the test, which would indicate that the restored voltage on this test would be approximately $87^{1}/_{2}$ per cent of the initial test voltage.

As to the duty cycle to be used to establish rating, this is covered by ASA Standards *4-6.5* and *4-6.18*. These standards state that a standard interrupting rating shall be based on the standard operating duty cycle which shall be two unit close-open operations with a 15-second interval between operations. Standard *9-2.6.1.1c* states that standard operating duty tests are made at both minimum voltage and maximum design voltage.

The method for figuring kilovolt-amperes is covered in Standards *4-6.11*, *4-6.11.1*, *4-6.13*, and *9-2.6.1.2b*. Reduced to a few words, 3-phase kilovolt-amperes equal to the test voltage times the maximum current in any phase times 1.732; and for single-phase tests is equal to twice the test voltage times the interrupted current. Using these formulas, test *9298C* calculates 515,000 kva. No other tests listed are as much as 500,000 kva.

We realize that many other tests have probably been made and that undoubtedly tests have been made or will be made which substantiate the rating of the breaker. Our only point is that the test data displayed do not substantiate this rating according to American Standards.

M. J. Reilly and **D. E. Weston**: The discussers have commented on the table of representative test data given in the paper. The table, as presented, presents only representative data of a very large number of development and proof tests performed in three laboratories over a period of several years. It does not attempt to define or cover all the conditions necessary to show complete proof of the ability of the device.

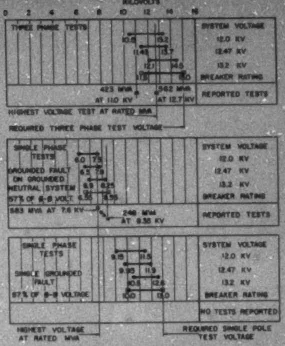

Fig. 12. Relation of voltages used in reported tests to system voltage and breaker rating, both 3 phase and single phase

Such a table would be prohibitive for this type of presentation.

Mr. Wood has indicated from his reading of the test data, that at least some of these tests were performed in foreign laboratories. The laboratories at K.E.M.A. in Arnhem, Holland, and the laboratories at General Electric Company, Ltd., in Birmingham, England, were used for both development and proof testing. This added inconvenience and expense was judged necessary for this breaker in recognition of the fact that a device of this type is, to a certain degree, voltage sensitive and tests must be made where capacity is available at maximum design voltage.

Table I of the paper shows data taken directly from certified test sheets of one of the European laboratories. The column of 3-phase kilovolt-amperes is, therefore, given as a summation of the single-phase–symmetrical kilovolt-amperes values in accordance with the symmetrical system of rating. This table can be supplemented with a column giving kilovolt-amperes ratings in accordance with ASA *C37.4* as follows:

	Symmetrical 3-Phase Kva	3-Phase Kva per ASA
9099C	36,400	38,600
9190C	108,000	104,000
9362C	562,000	574,000
9364C	423,500	476,000
9298A	336,000	408,000
9298B	342,000	450,000
9298C	348,000	515,000

The megavolt-ampere rating according to ASA *C37.4* gives, in each case, a larger figure than the symmetrical rating as presented.

The two figures of kilovolt-amperes in the foregoing are arrived at as follows (test *9362C* as an example):

Symmetrical 3-Phase Kva

Phase recovery voltage × a-c component of phase current

Phase *A* $8.63 \times 21.2 = 183$
Phase *B* $8.70 \times 21.6 = 188$
Phase *C* $8.85 \times 21.6 = 191$

562 mva 3 phase

ASA *37.4*

Phase volts × $\sqrt{3}$ × phase current $\sqrt{3}$
$8\ 85 \times 3 \times 21.6\sqrt{3} = 574$ mva 3 phase

The column in the table listed as system voltage lists the test circuit setting for normal excitation. Referring again to test *9362C*, the actual recovery voltage for this test was $8.85\times\sqrt{3}$ or 15.4 kv, a bit over the maximum design voltage required by ASA Standards.

The figures given in Table I of representative test data, based on the certified test reports, are quite conservative as compared to the figures as determined by the ASA.

Mr. Wood's other two questions can be covered by the statement that all proof tests on this breaker were performed in the enclosure as used in standard production. Tests throughout the complete current range were made with both the stationary contact on the source side, moving blade grounded, and with the moving blade on the source side, the stationary contacts grounded. Full investigations of severity of interrupting duty as a function of symmetry of current, point on wave of contact part, and all other factors recognized as influencing interrupting performance, were satisfied by test proof.

The breaker not only represents a large simplication in design, but also a completely proved device functionally in its simplicity.

Microwave System Parameters for Reliable Communications

A. ALVIRA
NONMEMBER AIEE

I. T. CORBELL
ASSOCIATE MEMBER AIEE

LOWEST cost designs which meet specified reliability and signal-to-noise (S/N) requirements are primary objectives of the microwave system planner. This paper provides signposts which guide the designer along the most direct route to his objective. Nomograms and charts are provided which eliminate complicated and laborious computations. Application of the nomograms is illustrated by designing a typical multiple-path microwave system.

Analysis of data obtained from operating microwave systems provides a sound basis for predicting performance of future systems. Some of the factors which affect performance are propagation, initial system design, equipment, and maintenance. Since the selection of equipment and quality of maintenance are controlled by the user, system design and propagation are primary considerations in this paper.

Pioneer Systems Provide Data for Designing New Systems

Results of analyzing propagation data from 25 microwave paths are shown in Fig. 1. The paths were all over 20 miles in length and were located over various types of terrain. Paths near the Gulf of Mexico, in the Midwest, and in eastern mountain areas are included. The operating frequency was near 2,000 megacycles for most paths. In all cases path fades fall within the boundary curves in Fig. 1. The fading boundary curves tend to deviate from the Rayleigh distribution in the deep-fade region. By carefully observing the distribution of data within the boundaries, the solid curve of Fig. 1 was established as a good average. An empirical equation which fits the average curve was derived and is shown in Fig. 1.

An average value for the variation with path length is combined with the equation in Fig. 1 to give the empirical equation for the path margin shown in Fig. 2. For easier design application, a nomographic solution of the empirical equation for margin is given in Fig. 2. Experience has shown that, during the worst month, the total fading time observed on systems with more than four or five paths agrees closely with that predicted by Fig. 2.

Microwave Beams Bend Downward

The average attenuation of an unobstructed microwave beam through the atmosphere is practically equal to the theoretical free-space attenuation. Free-space attenuation between isotropic antennas is given in Fig. 3.

In the tropospheric region where microwave beams travel, the temperature pressure, and water vapor content of the atmosphere normally decrease with height. This causes the atmospheric refractive index to vary with height. A beam traveling through a medium with a varying refractive index is curved. Various studies have shown that under average atmospheric conditions the variation in refractive index with height results in a downward curvature of microwave beams. This curvature is about one-quarter of the earth's curvature. Rather than draw the beam as a curve, an accepted convention is to draw it as a straight line, and to compensate by assuming that the earth has an effective radius of 4/3 true earth radius. A profile of the terrain and microwave beam between two stations is used to determine height of towers required for beam clearance over intervening obstructions. The task of plotting path profiles is simplified by using curved graph paper. This graph paper and a typical profile are shown in Fig. 4.

Because path profiles are sometimes plotted on rectangular co-ordinate paper, a correction to 4/3 earth conditions is given in Fig. 5. The actual beam clearance shown on rectangular co-ordinate paper is reduced by the amount shown in Fig. 5. If path profiles are drawn to true-earth scale, the actual beam clearance on a 4/3 earth basis is greater by the number of feet shown in Fig. 6.

Path Obstructions Attenuate Signal

The effect of path clearance on received microwave energy is a function of the terrain, the antenna height, and the type of obstruction. The signal strength increases and decreases as the clearance is increased above line of sight. These phenomena are shown in the region above zero clearance in Fig. 7 for reflection from knife-edge, average terrain, and smooth terrain surfaces. All curves shown in Fig. 7 intersect at theoretical free space loss [zero decibels (db)] and 0.6 (60 per cent) of first Fresnel zone path clearance. The geometry of Fresnel zones is discussed in reference 1. Experience has shown that 0.6 Fresnel zone path clearance is a good design objective.

Six-tenth Fresnel zone path clearance is a function of the signal frequency, path length, and location of the obstruction. A nomographic solution for required clearance is given in Fig. 8. The general derivation and geometry of the problem are discussed in reference 2. For 0.6 Fresnel zone path clearance, the microwave beam must clear all obstructions by the number of feet shown in Fig. 8.

Received signal strength decreases as the clearance is reduced below 0.6 Fresnel

---

Paper 55-516, recommended by the AIEE Carrier Current Committee and approved by the AIEE Committee on Technical Operations for presentation at the AIEE Summer General Meeting Swampscott, Mass., June 27–July 1, 1955. Manuscript submitted March 28, 1955; made available for printing May 9, 1955.

A. Alvira and I. T. Corbell are with the General Electric Company, Syracuse, N. Y.

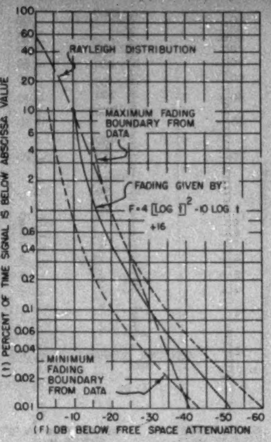

Fig. 1. Distribution of fading data obtained from 25 microwave paths. Paths were all over 20 miles in length

zone as shown in Fig. 7. Diffraction loss is a function of terrain and type of obstruction. An average value which is used as a design objective is shown in Fig. 9.

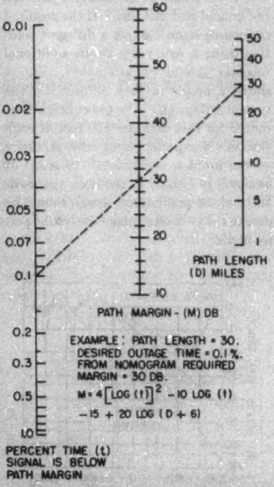

Fig. 2. Nomogram of predicted path outage time as a function of path margin and length. Nomogram applies to paths with 0.6 Fresnel zone clearance during the worst fading month

All Paths Require Fading Margin

Types of fading most prevalent at microwave frequencies are classed as multipath and upward bending. Multipath fading is caused by reflected energy which arrives at the receiver out of phase with the direct beam. The interfering energy may be reflected by discontinuities in the troposphere or from the ground. Abnormal atmospheric variations cause the microwave beam to bend upward from its normal path. The depth of the fade depends upon the amount of path clearance reduction and terrain, as shown in Fig. 7. Each of these types of fading has been described extensively in previous papers.[3,4]

Multipath fading is probable on paths located over highly reflective terrain such as water and swamps. This fading is usually rapid and affects space-separated antennas differently. Although path-fading margin reduces the likelihood of circuit interruption, consideration should be given to space-diversity receivers on overwater paths. Upward bending usually causes longer periods of low signal strength, and separated antennas are affected alike. Adequate path margin or increased path clearance reduce the likelihood of circuit interruptions from upward bending fades.

Path margin values in the nomogram in Fig. 2 are based upon average performance observed on paths affected by all prevalent types of fading. These values are recommended as design objectives for paths with 0.6 Fresnel zone clearance.

Low-clearance paths are more susceptible to upward bending fades than paths with 0.6 Fresnel zone clearance. If a path is designed with less than 0.6 Fresnel zone clearance, an additional fading margin should be added to that obtained from Fig. 2. The amount of extra margin is a function of terrain and climatic condition. If the path is located over average terrain (not water), the value of extra margin shown in Fig. 10 should be adequate for the worst fading month.

User Requirements Establish System Objectives

An example illustrating the design of a typical system provides a convenient method for showing the application of the nomograms derived in the previous sections. The procedure for calculating performance of a system is shown in Tables I through III. The objectives of the system are rightfully established by the user. These objectives specify the type and number of voice or telegraph circuits required between various locations in the system, and the reliability and S/N of each circuit.

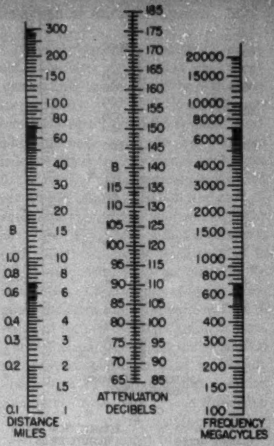

Fig. 3. Nomogram for free-space loss between isotropic antennas. B scales are used for distances less than one mile

The location and types of channels may be conveniently recorded on a channel diagram similar to the example shown in Fig. 11. Initially the channel diagram will not show repeater stations such as station *B* in Fig. 11. Repeater stations are located by the path survey.

Since no method of communication is perfect, the user should determine the reliability required in the system. Some of the factors affecting reliability are quality of maintenance, equipment failures, power interruptions, and signal fading.

Outage time resulting from inadequate maintenance, equipment failures, and power interruptions can be reduced after installation; however, outages caused by fading are difficult to reduce after installation. The path margin required to meet system requirements is most eco-

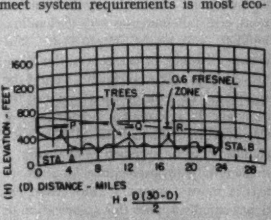

Fig. 4. Typical path profile plotted on 4/3 earth radius paper

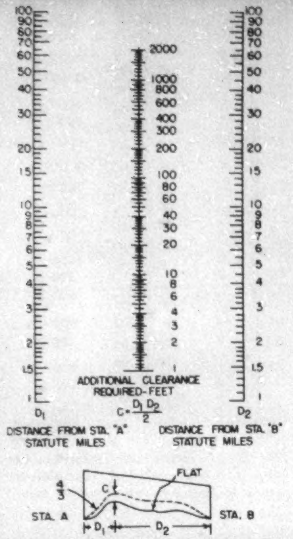
ADDITIONAL CLEARANCE REQUIRED-FEET
$C = \frac{D_1 D_2}{2}$
D_1
DISTANCE FROM STA. "A" STATUTE MILES
D_2
DISTANCE FROM STA. "B" STATUTE MILES
FLAT
4/3
C
STA. A
STA. B
D_1
D_2

Fig. 5. Nomogram for converting profile data plotted on rectangular co-ordinate paper to 4/3 earth radius values

nomically designed into the system before installation.

Equipment degradation is not included in the nomogram in Fig. 2. Equipment degradation is a function of initial system design, and the quality and frequency of routine maintenance checks. Microwave equipment can be maintained so that average performance agrees with manufacturer's specifications. An extra path margin for equipment degradation reduces the maintenance effort required to meet user system requirements. Margin for equipment degradation is not included in this design example.

The application of the system, or the preference of the user, establishes the specified S/N including crosstalk on each channel. In frequency-division systems, crosstalk increases with the loading, number, and length of channels. The channel loading, or per cent of the channels in use simultaneously, should be specified. In time-division systems the crosstalk is essentially independent of these factors. Though the S/N of each channel may be specified individually, a single minimum specification for all channels is more common. The system designer usually applies this specification to the longest channel in the system. A design based upon the longest channel automatically satisfies the requirements of shorter channels.

Excessive S/N requirements increase costs, especially in long systems. A typical value of 50 db *FIA* weighted[6] is assigned to all channels of Fig. 11. Because the actual noise level in watts is required for later calculations, the S/N ratio is converted to the equivalent noise power in watts. The normal signal level is 0 db referred to 1 milliwatt (dbm); see Fig. 12. The minimum usable channel S/N establishes the point where all lower S/N values are considered circuit interruptions. This point is often called threshold. Because the definition of threshold varies with different types of equipment, it should be specified by the user. A typical value for minimum usable S/N is 35 db. The allowable per-cent time below minimum usable S/N is 0.5 per cent (approximately 7 minutes per day) for this example. A convenient form for recording these requirements and subsequent calculations is shown in Tables I through IV.

Terrain Topography Establishes Need for Repeater Stations

Preliminary path profiles may now be constructed for each path. Because the usefulness of these profiles depends upon the accuracy of the data plotted, large scale maps of 1 or 2 miles to the inch with contour intervals not exceeding 20 feet should be used. A typical path profile is shown in Fig. 4 for path *A* to *B* of the example system.

As the profiles are plotted, some paths may be obviously impossible because of intervening obstructions several hundred feet high. These paths are immediately discarded, and alternate locations should be chosen if possible. If the locations are fixed, an additional repeater station may be required. If the obstruction is near one end of a short path, a passive-reflector repeater may be the answer.

Because contour maps do not show trees or man-made objects, their heights should be estimated for the highest points on each profile, such as *P*, *Q*, and *R* in Fig. 4. If a prior knowledge of the area is possessed, it should be used for the estimate; otherwise, 75 feet is usually a safe guess for wooded areas.

Fig. 8 is used to determine the required clearance over the highest points in each profile. The required clearance values above the height of the trees or other obstruction are plotted as shown at *P*, *Q*, and *R* in Fig. 4. Tentative tower heights may be estimated by drawing a line on the path profile which just clears the 0.6 Fresnel zone points, as shown in Fig. 4. The tower height is the distance between the ground and this line. If the required towers are over 350 feet a different solution using a new route or an additional repeater should be attempted. Fig. 4 shows a profile of path *A* to *B* for the system in Fig. 11. The tower heights required for this path are 250 feet at each station. Before checking the accuracy of the profiles, accessibility to sites, or availability of land at the sites, the feasibility of the preliminary design should be checked by determining the path performance.

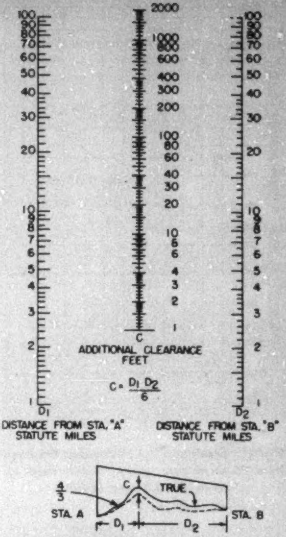
ADDITIONAL CLEARANCE FEET
$C = \frac{D_1 D_2}{6}$
D_1
DISTANCE FROM STA. "A" STATUTE MILES
D_2
DISTANCE FROM STA. "B" STATUTE MILES
4/3
C
TRUE
STA. A
STA. B
D_1
D_2

Fig. 6. Nomogram for converting path profile data plotted on true-earth paper to 4/3 earth radius values

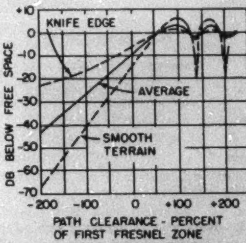

Fig. 7. Typical effect of path clearance on received signal strength

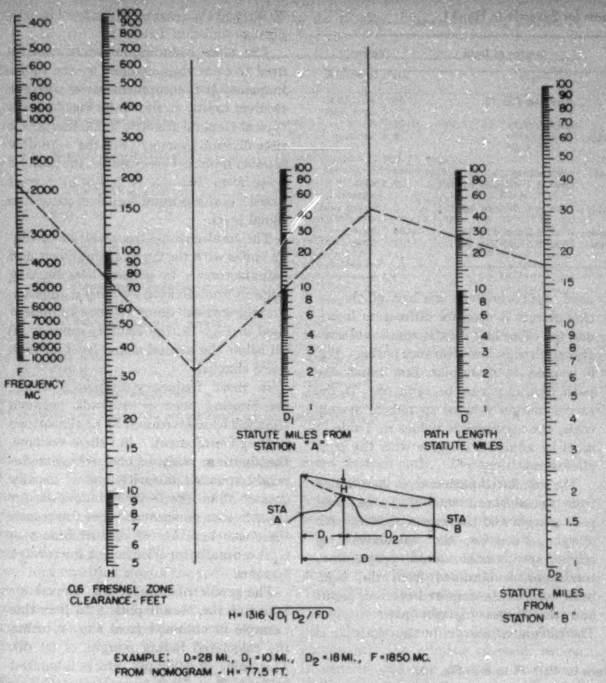
F
FREQUENCY MC
400
500
600
700
800
900
1000
1500
2000
3000
4000
5000
6000
7000
8000
9000
10000
H
0.6 FRESNEL ZONE CLEARANCE - FEET
1000
900
800
700
600
500
400
300
200
150
100
90
80
70
60
50
40
30
20
15
10
9
8
7
6
5
D1
STATUTE MILES FROM STATION "A"
D
PATH LENGTH STATUTE MILES
D2
STATUTE MILES FROM STATION "B"
STA A
STA B
H
D1
D2
D
H = 1316 √(D1 D2 / FD)
EXAMPLE: D=28 MI., D1=10 MI., D2=18 MI., F=1850 MC.
FROM NOMOGRAM - H=77.5 FT.

Fig. 8. Nomogram for 0.6 Fresnel zone path clearance

Allowable Path Noise and Fade Margin

The system requirements established by the user are used for path design objectives. The main-line part of the system usually contains at least one channel which reaches from one end of the system to the other. If the specified S/N ratio and reliability for this channel are achieved, specifications for all shorter channels usually are met.

Path design objectives are established by assuming that the allowable channel noise and outage time caused by fading on the longest channel are equally divided between all paths. These values are shown in Table I, for the typical example of Fig. 11, as "Average noise per path" and "Average allowable time below minimum usable S/N." If the system contains spur links or junctions, such as shown at station *D* in Fig. 11, the longest channel from the terminal of the spur link should be used to determine average spur path requirements. The spur paths are then designed to meet the requirements of the longest channel.

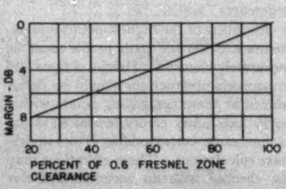

Fig. 9. Prediction of average diffraction loss for low-clearance paths

The receiver input level required to meet the specified average noise level per path may be obtained from an equipment characteristic curve, such as Fig. 13. Likewise the receiver input for minimum usable S/N may be obtained from Fig. 13. These values are tabulated in Table I, and are −88 db referred to 1 watt (dbw) and −108 dbw respectively for the time-division equipment used in this example.

Selection of Antenna System

Path performance calculations determine the size of antennas and transmission lines, and how well the path meets specifications. Calculations must be performed for each path in the system. Both allowable noise per path and required fade margin determine signal level input to the receiver under normal propagation conditions. Figs. 2 and 10 are used to determine the required fading margin for the path. Fig. 2 shows that the 24-mile path shown in Fig. 4 requires 27.5-db path margin for 0.125-per-cent outage time. Since the path has adequate clearance, the extra fading margin in Fig. 10 required for low-clearance paths is zero. The receiver input signal under normal propagation conditions must be 27.5 db above the level required to meet specified minimum usable S/N (−108 dbw from Table I). Thus, a receiver input level of −80.5 dbw is required to meet the outage time specifications. Since the −80.5-dbw level required to provide the necessary path margin is greater than the −88-dbw level required to meet the specified S/N, −80.5 dbw is used as the path design objective. These values are tabulated in Table II, and establish the power level required at the receiver.

Gains and losses include fixed free-space attenuation, estimated diffraction losses, transmitter power, duplexer filter, and coupling losses. The values are tabulated in Table II for the present example. The algebraic sum of the fixed gains and losses (−121 dbw) provide a power level as shown in Table II. The difference between this level (−121 dbw) and the required receiver input level (−80.5 dbw) is the required antenna system gain of the path (40.5 db).

For the required antenna system gain of 40.5-db 6-foot parabolic antennas are chosen as a first guess. The two antennas located at each end of the path provide a total gain of 56 db, as shown in Table II. This leaves 15.5 db for transmission line losses. The length of transmission line re-

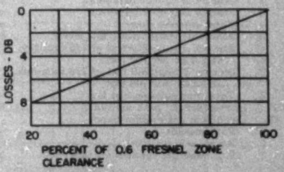

Fig. 10. Prediction of additional fading margin required for typical low-clearance 2,000-megacycle paths

Table I. System Requirements for Example in Fig. 11

Item	Characteristic	Source of Data	Value
A	User channel requirements		
1	Average S/N per channel	user and Fig. 12	50 db = 10×10^{-9} watt
2	Minimum usable S/N per channel	user	35 db
3	Allowable per-cent time below minimum usable S/N per channel	user	0.5 per cent
B	Average requirements per path		
1	Number of paths common to specified channel	path survey	4
2	Average allowable noise per path	item A.1 divided by B.1	2.5×10^{-9} watt
3	Average allowable time below minimum usable S/N per path	item A.3 divided by B.1	0.125 per cent
4	Average receiver input level per path, S/N basis	item B.2 and Fig. 13	−88 dbw
5	Average receiver input level per path for minimum S/N	item A.2 and Fig. 13	−108 dbw

quired is obtained from the path profile plus an additionallength required between the tower base and the microwave equipment. For the example in Table II, 260 feet are required at each station. Since a 7/8-inch transmission line has a loss of approximately 2.5 db per 100 feet, it is chosen for a first trial. The total loss of both transmission lines is 13 db, as shown in Table II.

The positive difference of 2.5 db between actual and allowable transmission line loss for this example represents the excess path margin. This excess margin may be used to decrease cost by using higher loss transmission lines, lower gain antennas, or shorter towers. If the excess is only 2 or 3 db, the design usually is not altered. If shorter towers are used, approximately one-half of the excess margin is used for diffraction losses, and the other half for the additional margin required in low-clearance paths. Fig. 9 is used to determine how much the path clearance can be reduced. If the excess margin is used to reduce system costs, the appropriate values in Table II must be adjusted to agree with the path alterations.

The calculated path margin is obtained from the algebraic sum of the required path margin and the excess (deficit) path margin. Likewise, the calculated receiver input, under normal propagation conditions, is obtained from the algebraic sum of the required receiver input and the excess (deficit) path margin. The calculated margin in this example is 30 db, and the receiver input level is −78 dbw, as shown in Table II.

Table II. Performance Calculations for Path A to B in Fig. 11

Item	Characteristic	Source of Data	Value
C	Receiver input level		
1	Path length	path survey	24 miles
2	Required path margin for 0.6 Fresnel zone clearance	Fig. 2 using item B.3 from Table I and C.1	27.5 db
3	Additional path margin for low-clearance paths	Fig. 10 and the path profile in Fig. 4	0 db
4	Total required path margin	sum of C.2 and C.3	27.5 db
5	Required receiver input to meet outage time requirements	algebraic sum of B.5 from Table I and C.4	− 80.5 dbw
6	Required receiver input to meet user specifications	highest power level in B.4, Table I, and C.5	− 80.5 dbw
D	Fixed losses and gains		
1	Transmitter power	equipment manufacturer	+ 13 dbw
2	Coupling and filter losses between equipment and antenna system at both stations	equipment manufacturer	− 4 db
3	Free-space loss	Fig. 3 using C.1	−130 db
4	Diffraction loss for low-clearance path	Fig. 9 and path profile in Fig. 4	0 db
5	Total fixed losses and gains	algebraic sum of D.1 through D.4	−121 dbw
E	Antenna system gain		
1	Required gain	difference between C.6 and D.5	40.5 db
2	Station *A* (6-foot parabola)	antenna manufacturer	28 db
3	Station *B* (6-foot parabola)	antenna manufacturer	28 db
4	Total antenna gain	sum of E.2 and E.3	56 db
3	Allowable transmission line losses	difference between E.1 and E.4	15.5 db
6	Station *A* loss (260 feet of 7/8-inch line at 2.5 db per 100 feet)	transmission line manufacturer	6.5 db
7	Station *B* loss (260 feet of 7/8-inch line at 2.5 db per 100 feet)	transmission line manufacturer	6.5 db
8	Total transmission line loss	sum of E.6 and E.7	13 db
F	Excess (deficit) path margin	E.5 minus E.8	+ 2.5 db
G	Calculated path performance		
1	Path margin	sum of F and C.4	30 db
2	Receiver input level	sum of F and C.6	− 78 dbw
3	R-F noise per channel for this path	Fig. 13 using G.2	0.13×10^{-9} watt
4	Outage time caused by fading for this path	Fig. 2 using C.1 and G.1*	0.085 per cent

* If additional path margin for a low-clearance path is shown in item C.3, subtract this value from G.1 for use in Fig. 2.

The noise including crosstalk contributed to each voice channel by the radio-frequency (r-f) equipment varies with the receiver input, as shown in Fig. 13 for a typical General Electric 2,000-megacycle time division system. For the −78-dbw receiver input in this example, the path r-f noise from Fig. 13 is 0.13×10^{-9} watt based upon a normal signal of zero-dbm signal level.

The total channel noise shown in Fig. 13 varies with the type of equipment and manufacturer. In general, the limiting noise in time-division systems is random. For the typical time-division equipment used in Fig. 13, the limiting noise is 70 db below the normal signal level on each voice channel.

In most frequency-division systems, the limiting noise is crosstalk between channels which is caused by nonlinearities in the r-f equipment. For these systems, the limiting value of channel noise depends upon r-f linearity and is usually greater than the −70 dbm shown for time-division equipment.[5] For this reason the channel quality of time-division systems is usually superior in long microwave systems.

The predicted outage time caused by fading on the 24-mile path *A* to *B* in this example is obtained from Fig. 2, using the calculated fading margin of 30 db. This value of 0.085 per cent is tabulated in Table II.

Site Selection and Path Survey

Before continuing further with system calculations, the actual sites for each station should be selected. Some important considerations of a good site are accessibility, availability of power, and cost of site property.

Information on each of these factors may be obtained by visiting the sites tentatively selected from the map survey. Investigation may show that other sites in surrounding areas are superior to those chosen from maps. The procedure for selecting sites is covered thoroughly in references 7 and 8.

Elevation of the highest points and antenna sites on the path profile must be accurately checked. Height of trees and man-made obstructions should be determined at these controlling points within ±10 feet. Any errors in the elevation values cause corresponding errors in system calculations. These elevations may be checked with an accurate altimeter against available bench marks. Regular surveying instruments may be used, but

Table III. Channel Performance Calculations for the Dispatch Channel Between Stations A and E in Fig. 11

Item	Characteristic	Source of Data	Value
H	Multiplex noise		
1	Noise per modulation	equipment manufacturer and Fig. 12	−65 dbm into 600 ohms = 0.3×10^{-9} watt
2	Number of modulations	channel diagram in Fig. 11 (number of parties on channel minus 1)	1
3	Total multiplex noise	item H-1 times H-2	0.3×10^{-9} watt
I	R-f equipment noise and cross-talk		
1	Path A to B	path calculations, item G.3 in Table II	0.13×10^{-9} watt
2	Path B to C	path calculations*	0.2×10^{-9} watt
3	Path C to D	path calculations*	0.5×10^{-9} watt
4	Path D to E	path calculations*	1.0×10^{-9} watt
5	Total r-f noise	sum of I.1 through I.4	1.83×10^{-9} watt
J	Total channel noise including crosstalk	sum of H.3 and I.5	2.13×10^{-9} watt
K	Channel S/N	Fig. 12 using item J	57 db
L	Predicted channel outage time caused by fading during worst month		
1	Path A to B	path calculations, item G.4 in Table II	0.085 per cent
2	Path B to C	path calculations*	0.100 per cent
3	Path C to D	path calculations*	0.130 per cent
4	Path D to E	path calculations*	0.150 per cent
5	Total channel outage time	Sum of items L.1 through L.4	0.465 per cent

* Calculations for these paths are performed by the method shown in Table II.

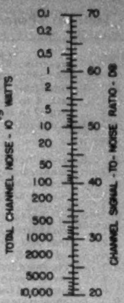

Fig. 12. Nomogram for conversion of S/N to equivalent noise power in watts. Normal signal level is 0 dbm

the cost will be fairly high in most cases. Points at least 100 feet on either side of the path should be checked. If the path passes near any structure or peak, the area and elevations should be scrutinized carefully. Adequate clearance must be provided on either side of the path as well as under it. After the path surveys are completed, path performance calculations must be revised to agree with the actual data.

Final Calculation of S/N and Fading Time

Using the corrected path performance calculations, the predicted S/N and fading outage time for each channel in the system may be calculated. Total channel noise including crosstalk consists of noise introduced by each multiplex modulation and demodulation, and of the noise and crosstalk introduced by r-f equipment on each path. The multiplex noise per modulation is constant for the particular type of equipment used and represents the noise measured with the multiplex and demultiplex equipment connected back to back. It is shown as 65 dbm or 0.3×10^{-9} watt for the example in Table III. This value is multiplied by the number of modulations on the channel. For frequency-division multiplex equipment, the number of modulations is usually one per system. For time-division equipment, the number of modulations per channel is equal to the number of active parties on the channel minus one. For this example, using time-division equipment, the number of modulations is one for the dispatch channel between station *A* and *E* in Fig. 11, but four for the party channel between the same stations.

R-f equipment noise including crosstalk for each channel is determined by adding the contribution of each r-f path common to the channel. The noise of path *A* to *B* was calculated in Table I, that noise for other paths in this example in Table III.

Total channel noise is obtained from the sum of the multiplex and r-f equipment noise, as shown in Table III. The resulting channel S/N is obtained by converting this noise to db using Fig. 12.

Total outage time caused by fading predicted for each channel is obtained by adding the predicted outages for all r-f paths common to the channel, as shown in Table III. The value for path *A* to *B* was calculated in Table II. The outage values for the other paths in this example are shown in Table III.

The same process may be repeated for each channel in the system if desired. Since the performance of shorter channels will be superior to longer channels, calculations for a single long channel are often adequate to predict system performance. A comparison between the total predicted path outage time and channel S/N and the user requirements will indicate if adjustments are needed. For this example the predicted path outage time is 0.465 per cent versus an allowable outage time of 0.5 per cent. The predicted channel S/N is 57 db versus a required value of 50 db. Thus, the user's requirements are satisfied.

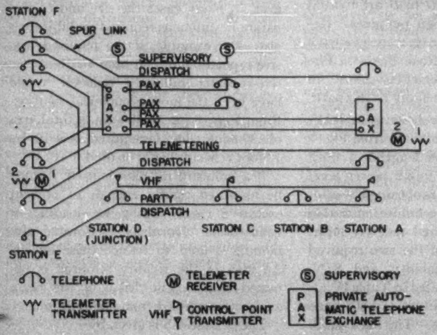

Fig. 11 (left). Typical microwave communication channel diagram

Fig. 13 (right). Typical time-division microwave equipment performance characteristics for a single r-f path. Normal channel level is 0 dbm, and noise includes crosstalk with all channels fully modulated

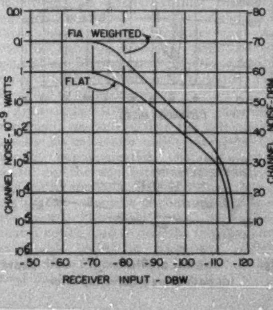

Table IV. Performance Calculation for Path Shown in Fig. 14 Using a Passive Repeater

Item	Characteristic	Source of Data	Value
M	Path length		
1	Path *A* to *D*	path profile, Fig. 14	1.0 mile
2	Path *D* to *B*	path profile, Fig. 14	8.5 miles
N	Path margin	Fig. 2 using distance equal to sum of M.1 and M.2 and allowable outage time from B.3 in Table I	21 db
P	Receiver input level		
1	To meet outage time requirement	Algebraic sum of B.5 from Table I and N	− 87 dbw
2	To meet S/N requirement	B.4, Table I	− 88 dbw
3	Required	larger level of P-1 and P.2	− 87 dbw
Q	Fixed path losses and gains		
1	Transmitter power	equipment manufacturer	+ 13 dbw
2	Filter and coupling losses at station *A* and *B*	equipment manufacturer	− 4 db
3	Free-space loss, path *A* to *D*	Fig. 3 using distance in M.1	−103 db
4	Free-space loss, path *D* to *B*	Fig. 3 using distance in M.2	−119 db
5	Total fixed loss and gain	Algebraic sum of Q.1 through Q.4	−213 dbw
R	Antenna system gain		
1	Total required gain	Difference between P.3 and Q.5	126 db
2	Station *A* (10-foot parabola)	antenna manufacturer	+ 33 db
3	Station *B* (10-foot parabola)	antenna manufacturer	+ 33 db
4	Total antenna gain	sum of R.2 and R.3	66 db
5	Station *A* transmission line loss (85 feet of 7/8-inch line at 2.5 db per 100 feet)	transmission line manufacturer	− 2.1 db
6	Station *B* transmission line loss (85 feet of 7/8-inch line at 2.5 db per 100 feet)	transmission line manufacturer	− 2.1 db
7	Total transmission line loss	sum of R.5 and R.6	− 4.2 db
8	Total antenna system gain	sum of R.4 and R.7	+ 61.8 db
S	Passive repeater gain		
1	Required gain	difference between R.1 and R.8	64.2 db
2	Gain using two 10-foot parabolas*	antenna manufacturer	66 db
T	Excess (deficit) path margin	S.2 minus S.1	+ 1.8 db
U	Calculation of path performance		
1	Path margin	sum of T and N	22.8 db
2	Receiver input level	sum of P.3 and T	− 85.2 dbw
3	R-f noise and crosstalk level for this path	Fig. 13 using U.2	1.2×10^{-9} watt
4	Outage time for this path	Fig. 2 using U.1	0.1 per cent

* If a billboard reflector is used, the area is determined from Fig. 15 to provide the gain in S.1. Item T will then be zero.

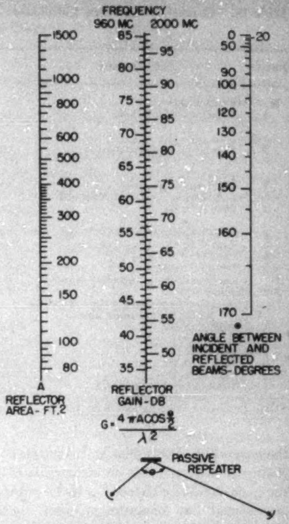

Fig. 15. Nomogram for size of billboard-type passive repeater in 2,000- and 960-megacycle systems

Passive Repeaters Bounce Signal Around Obstructions

If an obstruction which blocks a microwave signal is near one end of a short path, a passive repeater may be the most economical solution. The passive repeater may consist of two parabolic antennas connected back to back, or of a single billboard flat reflector. In either case, a portion of the microwave beam is intercepted and retransmitted to the next station. The following example for a 2,000-megacycle system illustrates the principles involved.

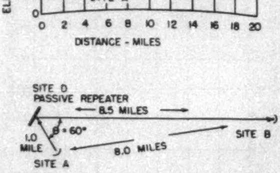

Fig. 14. Typical profile on 4/3 earth paper for path using passive repeater

Two sites *A* and *B* are located 8.0 miles apart, as shown in Fig. 14. The path profile shows that an obstruction at *C* prevents a line-of-sight path with practical antenna heights. A study of surrounding terrain shows that site *D* provides adequate clearance to both sites *A* and *B*. Therefore, a passive repeater at *D* is a possible solution to the problem.

Paths *A* to *D* and *D* to *B* are treated as two paths for design purposes. Required 0.6 Fresnel zone clearance for each path is determined from Fig. 8. The same system requirements shown in Table I are assumed to apply to this path.

The path lengths are shown in Table IV. The path margin is obtained from Fig. 2 using the sum of the lengths of both paths. The receiver input power level to provide this margin is obtained by adding the margin to the minimum usable receiver level. Required receiver input is the greatest level of the two required to meet system reliability and S/N. These values are tabulated in Table IV.

Total path losses consist of both fixed and variable quantities. The fixed quantities are tabulated in Table IV. The difference between the sum of the fixed quantities and the required receiver input represents the combined gain required of the passive repeater and the antenna systems at sites *A* and *B*.

For this example, 10-foot parabolic antennas and 7/8-inch transmission lines are selected at sites *A* and *B* for the first trial. This gives a total antenna system gain of 61.8 db. The gain required of the passive repeater becomes 64.2 db. In this case two 10-foot parabolic antennas at site *D* will be very satisfactory. However, in many cases the size and cost of parabolic antennas required prohibit their use. For example, if the required passive-repeater gain had been 75 db, a passive-repeater billboard reflector would have been the most economical solution. From Fig. 15 for 75-db gain, a total area of 120 square feet is required, or a 10- by 12-foot reflector could be used.

If a billboard reflector is used, it must be mounted rigidly enough to prevent excessive losses during ice loading or windstorms. Normally, perforated aluminum is used to reduce these effects. An idea of the rigidity required is obtained from a knowledge of the beam angles transmitted from the reflector.

The beamwidth is given by

$$\phi = \frac{58.7\lambda}{L} \qquad (1)$$

where

ϕ = the beamwidth, degrees
λ = the wavelength, feet
L = length of a side of the reflector, feet

The horizontal dimension is used for horizontal beamwidth, and the vertical dimension is used for vertical beamwidth. After a suitable antenna system has been chosen at the passive repeater, the path calculations are performed in a normal manner, as shown in Table IV.

Conclusions

1. A statistical study of fading data from operating systems provides a sound base for predicting operation of microwave systems. The method presented for predicting fading time has given good results on a monthly basis with systems with at least four or five well-designed paths.

2. Specification of user requirements is a prerequisite to good microwave system design. The user must specify the quality, reliability, and application of the communication channels.

3. Calculation of microwave system performance is simplified by using nomograms and charts. Also, a tabular form similar to the tables presented guides the designer to the most economical choice of system components to satisfy user requirements.

4. Even though 0.6 Fresnel zone path clearance is a good design objective, lesser clearances are not ruled out in all cases. For example, if the path margin exceeds that necessary to meet user requirements, the use of lower towers will often result in a lower cost system which still meets specifications.

References

1. RADIO WAVE PROPAGATION, **C. R. Burrows, S. S. Atwood.** Academic Press, New York, N. Y., 1949, pp. 78–80.

2. U.H.F. RADIO-RELAY SYSTEM ENGINEERING, **J. J. Egli.** *Proceedings*, Institute of Radio Engineers, New York, N. Y., vol. 41, Jan. 1953, pp. 115–24.

3. SELECTIVE FADING OF MICROWAVES, **A. B. Crawford, W. C. Jakes, Jr.** *The Bell System Technical Journal*, New York, N. Y., vol. XXXI, no. 1, Jan. 1952, pp. 68–90.

4. A STATISTICAL STUDY OF SELECTIVE FADING OF SUPER-HIGH FREQUENCY RADIO SIGNAL, **R. L. Kaylor.** *Ibid.*, vol. XXXII, no. 5, Sept. 1953, pp. 1187–1202.

5. VARISTOR MODULATORS FOR CARRIER SYSTEMS, **R. S. Caruthers.** *AIEE Transactions*, vol. 73, pt. I, Sept. 1954, pp. 291–98.

6. A NEW ULTRAHIGH-FREQUENCY MULTIBAND MILITARY RADIO RELAY SYSTEM, **John G. Nordahl.** *Ibid.*, Nov. 1954, pp. 526–31.

7. MICROWAVE SITE SELECTION IN UNDEVELOPED COUNTRY, **R. D. Pynn.** *Transactions*, Institute of Radio Engineers, New York, N. Y., Professional Group on Communications Systems, vol. C52, July 1954, pp. 9–15.

8. MICROWAVE REPEATER SITE PLANNING AND DEVELOPMENT, **R. D. Chapman.** *Ibid.*, pp. 16–32.

9. TROPOSPHERIC PROPAGATION: A SELECTED GUIDE TO THE LITERATURE. *Proceedings*, Institute of Radio Engineers, New York, N. Y., Committee on Wave Propagation, vol. 41, May 1953, pp. 588–94.

Discussion

G. E. Farmer (Tennessee Valley Authority, Chattanooga, Tenn.): The authors are to be commended for adding appreciably to the all too meager supply of data on microwave.

As a technical question only, we note that no loss for reradiation from the antennas is included in the calculations in Table IV. Is this loss negligible?

The second point is a minor one, but we question the necessity of setting a 1.0-mile channel specifically at 0.6 Fresnel, as indicated under item 7 in Table IV.

Marshall L. Ribe (Signal Corps Engineering Laboratories, Fort Monmouth, N. J.): This is a logical and easily understandable procedure for engineering microwave radio relay systems, and should be of assistance to the inexperienced. Figs. 1 and 2 are particularly helpful in enabling the designer to make an intelligent decision on the transmission margin he should provide. Similar information concerning the distribution of fade durations would be an additional help, since the user may find a few long fades more acceptable or less so than many short ones, depending upon his requirements.

The conclusions of the short discussion concerning the relative merits of time and frequency division multiplex systems are not universally agreed upon. A time division system, to maintain a 70-db signal to interchannel crosstalk ratio, must possess a high degree of timing stability, and requires a generous bandwidth. The interchannel crosstalk generated in pulse-phase modulated and pulse amplitude-modulated systems is often intelligible, and hence requires a greater degree of suppression than in single side-band suppressed carrier, frequency division multiplexed systems, for the same subscriber approval. As future time division systems are designed with more attention to conservative spectrum occupancy, the interchannel crosstalk advantage mentioned will likely disappear. Frequency division systems give adequate performance, as evidenced by their present extensive use.

The significance of Fig. 7, and the recommendation for use of 0.6 first Fresnel zone clearance will perhaps be clearer if it is explained that the path loss varies over and under the free-space value with increasing clearance, and that the 0.6 value is that where free-space loss is first attained as clearance is increased. The dangers of path clearances greatly in excess of the 0.6 clearance value should be pointed out, especially where multipath transmission is a possibility. The seriousness of this type of fading is difficult to overemphasize in the climates and over the terrains where it is prevalent. An amplified discussion of the conditions under which it may be expected, and the siting and diversity expedients which may alleviate it would be helpful.

The definition of "threshold" in the section "User Requirements Establish System Objectives" is not a universally accepted one. The threshold of a receiver is often considered to be the minimum signal level at which the modulation gain of the particular system is retained. Systems may be designed to give the desired signal-to-noise preformance at different levels with respect to threshold. Evidently the maximum fade which can be tolerated before a system becomes inoperable is one which barely misses piercing the system threshold and, depending upon the desires of the customer, only very infrequent and short-duration fades to threshold may be tolerable.

Irving D. Perry (Public Service Electric and Gas Company, Newark, N. J.): The authors are to be congratulated on providing data to survey the performance of microwave equipment for proposed installations.

When microwave channels are used for communication, telemetering or voice short-duration fade-outs can be tolerated. However, when microwave channels are used for line relaying where carrier current is not satisfactory, fade-outs cannot be tolerated. The Public Service Electric and Gas Company and Philadelphia Electric Company have jointly used a 3-mile long microwave channel for line relaying for a 132-kv line and remote-trip for transformer banks which are directly connected to line. Monitoring signals are continuously transmitted in both directions. During 4 years' operation, we have never had a complete fade-out.

The use of storage batteries, static changers and static line voltage regulators for plate and filament power supply will eliminate rotating equipment and provide a reliable power supply where continuous operation is essential as required for line relaying.

A. Alvira and **I. T. Corbell**: The authors appreciate the many helpful comments submitted. In answer to Mr. Farmer's question regarding reflector reradiation losses, our experience indicates that the metallic losses in well-built reflectors are negligible. With regard to his question concerning low-clearance short paths, Fig. 9 applies to all path lengths.

As to Mr. Ribe's question regarding threshold, we believe that the user should specify his minimum usable signal for the various communication channels, determined by the application of the channel, and not by the capabilities of the microwave equipment. Because of constant misuse of the word "threshold," we recommend that it not be used to describe the minimum acceptable signal in microwave system design. For this reason, threshold is not used Tables I through IV.

The Calculation of the Complete Time/Current Characteristics of Cartridge Fuses With Single Wire Element

A. E. GUILE
NONMEMBER AIEE

Synopsis: A review is given of previous attempts to solve the thermal equations for a filled fuse with single wire element lying along the axis of the cartridge. A new solution is then developed, which is based upon analysis applied by Grünberg[1] to high-voltage cables. This solution is used to calculate prearcing times, and is checked experimentally for four copper wires of different diameters and for one silver wire. For currents above about 1.4 times minimum fusing current, the error in the calculated prearcing time at a given current for all these wires does not exceed 25 per cent (%), and is generally much less, throughout the whole range. A comparison with other methods of predicting time/current characteristics shows the present solution to be superior.

Minimum fusing currents for silver and copper wires can be calculated within about 5% of the true value. An allowance for the effect of oxidation of copper is given for this purpose. The prearcing time below which heat loss from the element is negligible can be calculated accurately, and is shown to be a function of element cross section. The effect of varying filler parameters on time/current characteristics is shown, and the thermal conductivity of quartz powder is discussed.

Introduction

THERE are several simple methods of calculating a time/current characteristic, such as assuming Newton's law of cooling to apply, or using one of several empirical equations. These enable certain trends to be predicted, or facilitate an attempt to fit a curve to a few test results. However, Newton's law of cooling does not apply to any great range of cartridge fuse operation, and the fact that a characteristic obtained from an empirical equation may fit certain test results has no physical meaning.

Läpple[2] remarks that "it must always be borne in mind that the only real way of progressing in the engineering problem of designing fuses, with time/current characteristics well-suited to their different kinds of application, is to study the mathematics of the problem." He says that "the treatment of the problem by these empirical equations is only useful, so far as no better basis is available to help in considering the quantitative influence of the elements of design, and in planning and elaborating experiments."

The calculation of the time/current characteristic of a fuse is essentially a thermal problem: the fuse element or some part of it has to be raised to melting temperature by the current flowing in the element. The solution of the thermal equations where there is heat loss from the element requires certain assumptions to be made as to modes of heat flow and boundary conditions, and also requires that the geometry of the fuse shall be fairly simple.

In this paper consideration has been limited to the case of a single wire embedded in powder contained in a cylindrical cartridge, with the wire lying along the axis of the cylinder. Even with this simple configuration the solution which is obtained here involves making assumptions, and previous methods of solution are discussed and their limitations shown. In most commercial types of fuses the configuration precludes direct analysis. However, it is of interest to mention that cases such as a single strip element of rectangular cross section and of wires or strips wound helically are now being studied. The method used in these cases is based upon the analysis given in this paper and the results are promising. The present paper therefore describes initial stages of an investigation which is aimed at aiding the design of fuses and the planning and reduction of costly testing.

The Mechanism of the Prearcing Period

A mechanism for the prearcing period has been described by Carne.[3] At high current densities where melting starts at the element surface, the prearcing time is made up of three parts:

1. The time to heat the wire to its melting temperature in the solid state.
2. The time to provide some part of the latent heat of fusion of the element.
3. The time for the element to break up into globules.

Carne[4] showed that time 3 is a function of the current at the start of arcing, but that it is very much smaller than time 1. Time 2 is only the very small time lag between the outside surface of the wire reaching melting temperature and sufficient energy being supplied to melt a finite thickness of metal at the surface. Tests show that time 1 is often as much as 95% of the prearcing time. Since the latent heat of fusion of an element is usually about one-sixth to one-third of the heat necessary to bring it to melting temperature,[3] it follows that the whole latent heat of the element does not have to be supplied.

Hence in the region of the greatest currents where the prearcing times are small they are chiefly determined by the time taken for the element to reach melting temperature. At currents below the critical value, the prearcing times are greater, and again the time to heat the wire to melting temperature is predominant.

The Thermal Equations

I = constant direct current through the element flowing after time $t=0$
A_1 = cross-sectional area of wire
m_1 and m_2 = density of wire and filler
c_1 and c_2 = specific heat of wire and filler
k_1 and k_2 = thermal conductivity of wire and filler
θ_1 and θ_2 = temperature rise above ambient of wire and filler
J = Joule's equivalent
z = axial co-ordinate
r_1 = radius of wire
r_2 = inner radius of cartridge
$2L$ = length of element
ρ_0 = resistivity of wire at ambient temperature
ρ = resistivity of wire at temperature rise θ_1, given by $\rho=\rho_0(1+\alpha\theta_1)$

Then for the cartridge fuse considered here, the heat conduction equation is

$$A_1c_1m_1\frac{\partial\theta_1}{\partial t}=k_1A_1\frac{\partial^2\theta_1}{\partial z^2}+\frac{I^2\rho}{JA_1}-Q_1 \qquad (1)$$

where Q_1, the heat flow per unit time per unit length from the wire to the filler, is given by

$$Q_1=-2\pi r_1k_2\left(\frac{\partial\theta_2}{\partial r}\right)_{r=r_1}$$

and may be determined from

Paper 55-514, recommended by the AIEE Switchgear Committee and approved by the AIEE Committee on Technical Operations for presentation at the AIEE Summer General Meeting, Swampscott, Mass., June 27–July 1, 1955. Manuscript submitted December 14, 1954; made available for printing May 9, 1955.

A. E. Guile is with Queen Mary College, London University, London, England.

The author would like to acknowledge the advice and encouragement given by Professor W. J. John of Queen Mary College, University of London.

The subject matter of this paper forms part of a thesis presented for the Ph.D. degree at London University.

$$m_2c_2\frac{\partial\theta_2}{\partial t}=k_2\left(\frac{\partial^2\theta_2}{\partial z^2}+\frac{\partial^2\theta_2}{\partial r^2}+\frac{1}{r}\frac{\partial\theta_2}{\partial r}\right) \tag{2}$$

with conditions

1. $r_1 \leqq r \leqq r_2$
2. $t=0$, $\theta_1=\theta_2=0$ for all r and z $(-L<z<+L)$
3. $z=\pm L$, $\theta_1=\theta_2=0$ for all r and t

Condition 2 limits consideration to the case where the fuse is not preloaded before the fault occurs. The effect of preloading on the prearcing time and other characteristics has been investigated.[5] Condition 3 is a reasonable assumption since the end terminals are usually of sufficient mass for the temperature rise not to exceed about 5% of melting temperature, and this maximum rise only occurs near minimum fusing current.

The Special Case of No Heat Loss From the Element

In the region where the current is sufficiently high for the loss of heat from the element to be neglected, then

$$\int_0^t \frac{I^2}{A_1^2}dt=\frac{I^2t}{A_1^2}=\frac{c_1m_1J}{\rho_0\alpha}\log_e(1+\alpha\theta_1) \tag{3}$$

This integral is sometimes called the current-heat integral[6] and has a constant value for a given material whatever the size of element.

Tests by Van Liempt and De Vriend[7] showed that for prearcing times of the order of 0.1 second, heat loss from very fine wires can be neglected, and Boehne[8] suggested a corresponding time of 0.02 second.

Previous Methods of Solving the Thermal Equations

No complete solution to equations 1 and 2 with the boundary conditions appropriate to the fuse appears to exist. A number of solutions have been put forward over a period of years, in which various assumptions and approximations have been made.

All methods involve the assumption that wire and filler specific heats, densities, and thermal conductivities remain constant at some average value. This is reasonable since their variation over the melting temperature range is only of the order of 20%, whereas the wire resistivity varies by some 500%.

Ikeda and Yoneta[9] gave a solution where the heat loss from the wire surface was defined by Newton's law of cooling instead of by equation 2, but any solution involving this assumption is necessarily very restricted in its application.

Wintergerst[10] gave a solution to the case where there was assumed to be no loss of heat to the filler, i.e., $Q_1=0$ in equation 1, and where the wire resistivity was assumed to remain constant at some average value throughout the heating. This solution has no application to the determination of time/current characteristics since the radial heat loss will always exceed the axial loss at any point near the center of the element.[11]

Equations 1 and 2 were solved by Schubert[12] by making the following assumptions, in addition to the boundary conditions given in the section on "The Thermal Equations":

1. Axial flow of heat in wire and filler neglected; i.e., wire considered to be infinitely long.
2. Temperature rise at outer boundary of filler considered to be zero; i.e., filler considered to extend to infinity.
3. Resistivity of wire assumed to be a constant average value; i.e., ρ_{av} replaces $\rho_0(1+\alpha\theta_1)$

The temperature rise of a wire for times greater than $t=\frac{r_1^2m_2c_2}{k_2}$ given as

$$\theta_1=\frac{I^2\rho_{av}}{4\pi^2r_1^2k_2J}\log_e\left(\frac{2.25\,k_2t}{m_2c_2r_1^2}\right) \tag{4}$$

For shorter times the characteristic given by equation 4 has to be allowed to merge into the straight line given for the case of no heat loss by equation 3 when plotted on log/log paper. In this range, therefore, the calculated time will be less than the actual prearcing time by the amount of the breakup time.

An electrical analogue was constructed[11] which used the similarity between thermal and electrical quantities to represent the thermal conditions in the fuse under both transient and steady-state conditions. The analogue was designed to obtain temperature distributions, which is made possible by the fact that both radial and axial heat flow are simulated, whereas analytical solutions involve neglecting one or the other of these modes. Assumptions 1 and 2 made by Schubert are eliminated in the analogue but assumption 3 remains.

The analogue is inherently more accurate for the determination of temperature distributions than for prearcing times, so that it will not be considered as a method of obtaining time/current characteristics, although after analysis of its sources of errors it can compare favorably with some analytical solutions. It is used, however, to check the validity of certain assumptions made in obtaining the present solution; see the Appendix for further discussion.

Newton's law of cooling cannot apply to transient thermal conditions in a cartridge fuse so that its range is very limited, and tests have shown that this simple approximation applies more to wires in free air.[3]

An empirical equation put forward by Prince and Williams[13] is

$$t=\frac{K}{I^2-I_{\min}^2} \tag{5}$$

where

$I_{\min}$ = minimum fusing current
K = square of current that melts wire in 1 second with no heat loss

This establishes the shape of what is sometimes called the "square characteristic." It is merely an expression for a curve which joins two known points of the curve, viz: $(t=\infty, I=I_{\min})$ and $(I^2t=K, I>>I_{\min})$.

Another empirical equation is Johann's[14]

$$(I-I_{\min})^2t=a+bt^{1/3} \tag{6}$$

The last term does take some account of heat storage in the immediate neighborhood of the element, and since the equation has two constants a and b it can represent a whole family of curves.

The Present Solution Based Upon Grünberg's Analysis for Cables

It is desirable that a solution to equations 1 and 2 should be obtained where

1. The solution is continuous over the whole range.
2. The assumptions are as few and as reasonable as possible.
3. The form is convenient for use in engineering practice.

The method of analysis used by Grünberg[1] in the case of high-voltage cables is suitable for a fuse with circular section element centrally located in a filled cartridge.

Fuse Carrying Direct Current

The fuse considered is one where a circular section element is surrounded by granular filling powder and enclosed in a ceramic cartridge. It is assumed that the length/diameter ratio of the fuse is great enough for the temperature rise at the mid-point of the element not to be affected by axial flow of heat along the element or within the filler. This assumption is discussed in the Appendix.

Equation 1 then becomes

$$A_1c_1m_1\frac{\partial\theta_1}{\partial t}=\frac{I^2\rho}{JA_1}-Q_1 \tag{7}$$

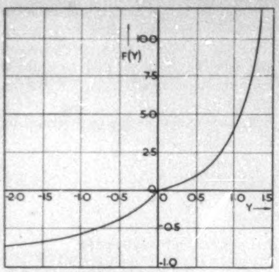

Fig. 1. The function $F(y)=\epsilon^{Y^2}(1+\text{erf}y)-1$

and equation 2 becomes

$$m_2c_2\frac{\partial\theta_2}{\partial t}=k_2\left(\frac{\partial^2\theta_2}{\partial r^2}+\frac{1}{r}\frac{\partial\theta_2}{\partial r}\right) \tag{8}$$

$$Q_1=-2\pi r_1k_2\left(\frac{\partial\theta_2}{\partial r}\right)_{r=r_1} \tag{9}$$

Except for very low overcurrents no appreciable quantity of heat will reach the outer boundary of the filler during the time when the wire is being heated to its melting temperature, so that the cartridge can be ignored and the filler considered to extend to infinity. See the Appendix.

This gives the boundary condition

$$(\theta_2)_{r=\alpha}=0 \tag{10}$$

At the wire surface

$$\theta_1=(\theta_2)_{r=r_1} \tag{11}$$

The fuse is considered to be initially unloaded and at ambient temperature, i.e.

$$(\theta_1)_{t=0}=(\theta_2)_{t=0}=0 \tag{12}$$

It was shown by Grünberg and Sontz[15] that from equations 8, 10, 11, and 12 θ_2 can be expressed in the form

$$\theta_2=\sqrt{\frac{r_1}{r}}f(r-r_1,t)=\sqrt{\frac{r_1}{r}}f \tag{13}$$

with sufficient accuracy for practical requirements. When this approximation is made in the fuse application the thermal conductivity of the filler k_2 must be replaced by a value k_2^1. The relationship between k_2 and k_2^1 is determined later.

The function $f(r-r_1,t)=f(x,t)$ is given by

$$m_2c_2\frac{\partial f}{\partial t}=k_2^1\frac{\partial^2 f}{\partial x^2} \tag{14}$$

and defined by the limits

$$(f)_{x=0}=\theta_1 \tag{15}$$

$$(f)_{x=\alpha}=0$$

and initial condition

$$(f)_{t=0}=0 \qquad (15)$$

The method of Laplace transformation is used with the notation

$$\bar{F}=\int_0^\alpha \epsilon^{-pt}F(t)dt$$

Then

$$\bar{Q}_1=-2\pi r_1k_2\left(\frac{\partial\bar{\theta}_2}{\partial r}\right)_{r=r_1} \tag{16}$$

$$(\bar{\theta}_1)=(\bar{\theta}_2)_{r=r_1}=(\bar{f})_{r=r_1} \tag{17}$$

$$(\bar{f})_{x=\alpha}=0$$

$$\bar{\theta}_2=\sqrt{\frac{r_1}{r}}\bar{f}(r-r_1) \tag{18}$$

$$\frac{d^2\bar{f}}{dx^2}=a_2^2pf \tag{19}$$

where $a_2^2=(c_2m_2)/k_2^1$.

Table I. Quartz Filling Powder, Sample 1

% Weight	Grain Size	
20	− 36	+ 60
57	− 60	+ 90
20	− 90	+100
3	−100	+150

The resistivity of the wire is considered to vary linearly with temperature, i.e.

$$\rho=\rho_0(1+\alpha\theta_1)$$

so that

$$A_1c_1m_1p\bar{\theta}_1=\frac{I^2\rho_0}{JA_1p}+\frac{I^2\rho_0\alpha\bar{\theta}_1}{JA_1}-\bar{Q}_1 \tag{20}$$

From equations 17 and 19

$$\bar{f}=B\epsilon^{-a_2x\sqrt{p}} \tag{21}$$

where $B=\bar{\theta}_1$ from equation 17 so that

$$\bar{\theta}_2=\bar{\theta}_1\sqrt{\frac{r_1}{r}}\epsilon^{-a_2(r-r_1)\sqrt{p}} \tag{22}$$

and from equation 16

$$\bar{Q}_1=2\pi r_1k_2^1\bar{\theta}_1\left(a_2\sqrt{p}+\frac{1}{2r_1}\right)$$

and from equation 20

$$\bar{\theta}_1=\frac{I^2\rho_0}{JA_1^2m_1c_1p(p+2m\sqrt{p}-n)} \tag{23}$$

where

$$m=\frac{\pi r_1k_2^1a_2}{A_1c_1m_1}$$

$$n=\frac{\dfrac{I^2\rho_0\alpha}{JA_1}-\pi k_2^1}{A_1c_1m_1}$$

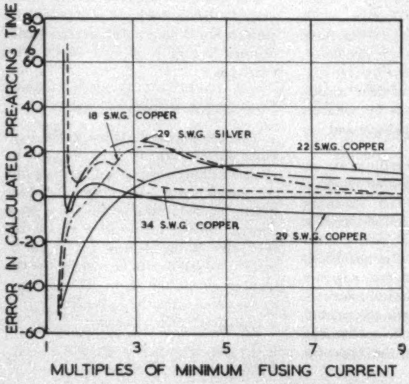

Fig. 2 (left). The accuracy of the present method of calculating prearcing times

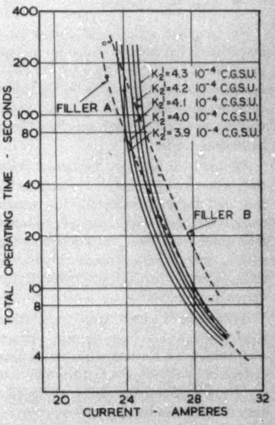

Fig. 3 (right). Comparison of test and calculated time/current characteristics of 29 S.W.G. copper wire

—— Calculated characteristic

– – – Test characteristic

Filler A—mixed grain size quartz, sample 1, density 1.62

Filler B—mixed grain size quartz, sample 1, density 1.70

It may be shown that, following the method used by Grünberg, the inverse transformation of equation 23 can be made giving

$$\theta_1=\frac{I^2\rho_0}{2JA_1^2c_1m_1\sqrt{m^2+n}}\times \left(\frac{1}{z_1}F(z_1\sqrt{t})-\frac{1}{z_2}F(z_2\sqrt{t})\right) \quad (24)$$

where

$$z_1=-m+\sqrt{m^2+n}$$

$$z_2=-m-\sqrt{m^2+n}$$

$$F(y)=\epsilon^{y^2}(1+erfy)-1$$

$$erfy=\frac{2}{\sqrt{\pi}}\int_0^y \epsilon^{-\phi^2}d\phi$$

Equation 24 enables the wire temperature and time to be related for any given current; in particular the time for a given current to bring the element center to melting temperature may be found.

The function $F(y)$ is plotted against y in Fig. 1, over a range which covers that normally required in the fuse application.

FUSE CARRYING ALTERNATING CURRENT

If the wire resistivity is assumed to remain at a constant average value, then it is possible to solve the thermal equations when the current is a function of time. A solution has been obtained by the author for the case where the current is given by $i=Im \sin \omega t$. However, it is only necessary to consider the d-c solution in practice for the following reasons:

1. The form of the solution for a current of even the simple form $i=Im \sin \omega t$ is not suitable for a number of calculations.

2. In practice the form of the short-circuit current is initially much more complex than a pure sine wave.

3. The heating effect is given by $\int_0^t i^2Rdt$ and if $i=Im \sin \omega t$, then

$$\int_0 i^2Rdt=\frac{Im^2R}{2}\left(t-\frac{\sin 2\omega t}{2\omega}\right)$$

i.e., the heating effect of a sinusoidal current does not differ from that of its rms value if $t>>1/(2\omega)$. Hence for times greater than about 1 cycle the effect is that of direct current and equation 24 applies. It is shown later (in Table VII) that for times less than 1 cycle the heat loss from the element is negligible for all practical wire sizes, and the exact form of the current wave can then be taken into account in calculating the time from the current heat integral (equation 3).

Equation 24 is therefore sufficient to calculate the time/current characteristics where there is heat flow from a single wire element carrying direct or alternating current.

Table II. 29 S.W.G. Silver in Sample 1 Quartz Filler of Density 1.62

Current, RMS Amperes	RMS Current, / Minimum Fusing Current	Prearcing Time on Test, Seconds	Prearcing Time Calculated From Equation 24, Seconds	% Error of Calculated Time
250	11.2	0.0086	0.0093	+ 8.1
180	8.15	0.0171	0.0183	+ 7.0
120	5.35	0.043	0.048	+11.6
90	4.0	0.077	0.093	+20.5
70	3.13	0.138	0.173	+25.3
50	2.23	0.375	0.45	+20.0
40	1.79	0.88	0.96	+ 9.0
30	1.34	5.5	4.8	−13.0
28	1.25	20.0	9.9	−50.0
25	1.13	250	135	−46.0

Table III. 34 S.W.G. Copper in Sample 1 Quartz Filler of Density 1.62

Current, RMS Amperes	RMS Current, / Minimum Fusing Current	Prearcing Time on Test, Seconds	Prearcing Time Calculated From Equation 24, Seconds	% Error of Calculated Time
150	13.5	0.0081	0.0080	+ 1.5
70	6.3	0.043	0.044	+ 2.5
55	4.95	0.075	0.078	+ 4.0
45	4.05	0.125	0.13	+ 4.0
35	3.15	0.236	0.253	+ 7.2
30	2.7	0.37	0.415	+ 11.2
25	2.25	0.67	0.78	+ 16.3
22	1.98	1.22	1.38	+ 11.3
20	1.8	2.3	2.4	+ 4.3
19	1.71	4.1	4.35	+ 6.1
17	1.53	18.5	20	+ 8.1
16.5	1.49	24.5	102	+315

Table IV. 29 S.W.G. Copper in Sample 1 Quartz Filler of Density 1.62

Current, RMS Amperes	RMS Current, / Minimum Fusing Current	Prearcing Time on Test, Seconds	Prearcing Time Calculated From Equation 24, Seconds	% Error of Calculated Time
250	14.0	0.0155	0.0142	− 8.4
225	12.65	0.019	0.0178	− 6.3
200	11.25	0.024	0.023	− 4.2
175	9.34	0.0330	0.0305	− 7.6
150	8.42	0.045	0.0425	− 5.5
125	7.03	0.069	0.065	− 5.8
100	5.62	0.112	0.105	− 6.2
70	3.93	0.253	0.25	− 1.2
60	3.37	0.37	0.37	0
50	2.81	0.61	0.62	+ 1.6
45	2.53	0.825	0.865	+ 4.8
40	2.25	1.22	1.28	+ 4.9
35	1.97	2.08	2.21	+ 6.2
31	1.74	4.0	4.15	+ 3.8
30	1.69	5.1	5.2	+ 2.0
28	1.57	9.8	9.3	− 5.1
26	1.46	25.8	25.0	− 3.1
25	1.405	45	63	+47

Table V. 22 S.W.G. Copper in Sample 1 Quartz Filler of Density 1.62

Current, RMS Amperes	RMS Current, / Minimum Fusing Current	Prearcing Time on Test, Seconds	Prearcing Time Calculated From Equation 24, Seconds	% Error of Calculated Time
540	12.4	0.055	0.0555	+ 1.0
350	8.06	0.122	0.138	+13.0
250	5.76	0.253	0.29	+14.5
200	4.62	0.43	0.49	+14.0
170	3.92	0.64	0.72	+12.5
150	3.46	0.89	0.97	+ 9.1
130	3.0	1.31	1.37	+ 4.6
115	2.66	1.93	1.95	+ 1.5
100	2.31	3.2	3.0	− 6.8
90	2.08	4.8	4.1	−14.6
80	1.85	8.1	6.3	−22.2
70	1.61	16.0	11.0	−30.5
60	1.38	49	28	−42.4
56	1.29	115	51	−55.5

Table VI. 18 S.W.G. Copper in Sample 1 Quartz Filler of Density 1.62

Current, RMS Amperes	RMS Current, / Minimum Fusing Current	Prearcing Time on Test, Seconds	Prearcing Time Calculated From Equation 24, Seconds	% Error of Calculated Time
1,000	11.6	0.136	0.136	0
900	10.4	0.168	0.17	+ 1.2
750	8.7	0.243	0.25	+ 3.0
600	6.95	0.38	0.40	+ 5.2
450	5.22	0.67	0.75	+12.0
350	4.05	1.12	1.35	+21.5
300	3.48	1.55	1.9	+22.7
250	2.9	2.47	3.0	+21.5
200	2.32	3.0	5.4	+ 8.0
180	2.09	7.0	7.2	+ 3.0
160	1.85	10.8	10.45	− 3.5
140	1.62	18.0	16.5	− 8.3
120	1.39	40	31	−22.5
110	1.27	120	49	−59

Table VII. Current Above Which Heat Loss May Be Neglected

Wire S.W.G.	Wire Material	Current on Test for No Heat Loss	Current Calculated for No Heat Loss From Equation 28	Prearcing Time on Test for No Heat Loss, Seconds
34	copper	55	56.5	0.084
29	copper	85	83.5	0.15
22	copper	190	174	0.48
18	copper	300	294	1.5
29	silver	90	85	0.078

COMPARISON OF CALCULATED TIME/CURRENT CHARACTERISTICS WITH EXPERIMENTAL RESULTS

Time/current characteristics of prearcing time plotted against rms current in the prearcing period were obtained experimentally for copper wires of four different diameters and for one silver wire. The filler used was quartz powder of mixed grain size, see Table I, in a porcelain cartridge 14 centimeters long and 3.5 centimeters internal diameter. The filler was compacted to a density of 1.62.

The times calculated from equation 24 are compared with prearcing times obtained on test in Tables II through VI, and the percentage errors of the calculated time are plotted in Fig. 2. In order to make these calculations it is necessary to determine the value of k_2^1. Fig. 3 shows that, for sample 1 filler with density 1.62, $k_2^1=4.2\ 10^{-4}$ centimeter-gram-second units and this value was used in equation 24. Fig. 2 shows that using this value of k_2^1 in the calculations for all the wires tested, prearcing times are given which are within 25% of the test values for any current from short circuit to below twice minimum fusing current.

PRESENT SOLUTION APPLIED TO THE CASE OF NO HEAT LOSS FROM THE ELEMENT

In the case of a very heavy current where no heat is lost from the element, equation 3 holds and this may be rewritten

$$\theta_1=\frac{1}{\alpha}\left(\epsilon^{\frac{\rho_0\alpha I^2t}{A_1^2C_1m_1J}}-1\right) \tag{25}$$

Consider equation 24 as the current increases

$$\text{Limit }(n)_{I\to\infty}=\frac{I^2\rho_0\alpha}{JC_1A_1^2m_1}$$

$$\text{Limit}\left(\frac{z_1}{z_2}\right)_{I\to\infty}=\pm\sqrt{n}$$

then equation 24 becomes

$$\theta_1=\frac{I^2\rho_0}{2JA_1^2c_1m_1\sqrt{n}}\left\{\frac{1}{\sqrt{n}}[\epsilon^{nt}(1+erf\sqrt{nt})-1]+\frac{1}{\sqrt{n}}[\epsilon^{nt}[1+erf(-\sqrt{nt})]-1\right]\right\}$$

$$\theta_1=\frac{1}{\alpha}\left(\epsilon^{\frac{\rho_0\alpha I^2t}{A_1^2C_1m_1J}}-1\right)$$

Hence in the limit, equation 24 becomes equal to equation 25 and therefore yields the correct solution for no heat loss.

REGION WHERE THE ASSUMPTION OF NO HEAT LOSS IS VALID

From the previous section it can be seen that the conditions for no heat loss are

$$n=\frac{I^2\rho_0\alpha}{Jc_1A_1^2m_1}$$

$$\frac{z_1}{z_2}=\pm\sqrt{n}$$

There are therefore two conditions for no heat loss

Table VIII. Minimum Fusing Currents

Material	S.W.G.	Minimum Fusing Current, Amperes: Test	Calculation	Calculation Corrected for Oxidation
Copper	34	11.1	16.2	10.9
Copper	29	17.8	24	18.7
Copper	22	44.0	49.3	44
Copper	18	85.5	85.3	80.2
Silver	29	22.5	24	

$$I^2>>\frac{\pi k_2^1JA_1}{\rho_0\alpha} \tag{26}$$

$$I^2>>\frac{\pi k_2^1JA_1}{\rho_0\alpha}\,\frac{c_2m_2}{c_1m_1} \tag{27}$$

The ratio $(c_2m_2)/(c_1m_1)$ has the value of 0.28 for copper and quartz and of 0.42 for silver and quartz; hence only inequality 26 need be considered since this also embraces 27 for normal fuse materials.

The point at which heat loss becomes negligible is shown by the time/current characteristic plotted on log/log paper becoming the linear of slope −2, since I^2t = a constant in this region.

The currents at which the characteristic departs from linearity for the fuses tested are shown in Table VII, together with the currents calculated from inequality 26 by putting

$$I^2=\frac{10\pi k_2^1JA_1}{\rho_0\alpha} \tag{28}$$

It can be seen from Table VII that the current above which heat loss can be neglected may be calculated accurately from equation 28, and that the corresponding prearcing time varies very considerably with fuse element section. This latter variation may be seen from equation 28 by putting $(I^2t)/(A_1^2)$ = a constant where heat loss is negligible. This shows that the limiting value of prearcing time is proportional to the wire cross-sectional area.

CALCULATION OF MINIMUM FUSING CURRENTS OF COPPER AND SILVER WIRES

The steady-state temperature rise may be calculated from equation 24: If

I_{min} = minimum fusing current
θ_m = the temperature rise above ambient at melting

then in equation 24 as $I\to I_{min}$ with $t\to\alpha$ it may be seen from Fig. 1 that $F(z_1\sqrt{t})\to -1$ and $F(z_2\sqrt{t})\to -1$ so that equation 24 becomes

$$\theta_1=\frac{I^2\rho_0}{\pi k_2^1JA_1-I^2\rho_0\alpha} \tag{29}$$

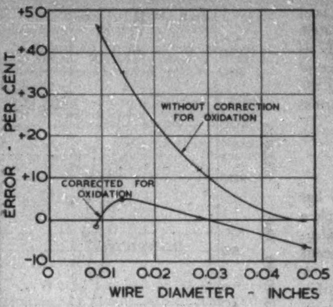

Fig. 4 (left). Variation of error in calculation of minimum fusing current with wire diameter for copper wires

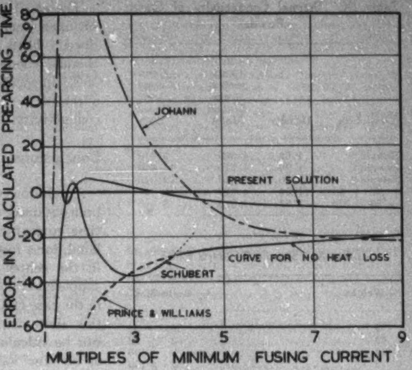

Fig. 5 (right). Comparison of present solution for obtaining prearcing times with other methods. 29 S.W.G. copper wire in quartz filler

Hence

$$I_{\min}=\sqrt{\frac{\pi k_2{}^1 J A_1 \theta_m}{\rho_0(1+\alpha\theta_m)}} \tag{30}$$

Values of minimum fusing current calculated from equation 30, together with those obtained on test, are shown in Table VIII. Fig. 4 shows that minimum fusing currents calculated from equation 30 are in considerable error for very small copper wires, but that the error falls as the diameter is increased. The error is due mainly to oxidation of the element which causes a reduction in the effective area of cross section. This is illustrated by the fact that the calculated minimum fusing current for 29 S.W.G. copper has an error of 35% whereas that for 29 S.W.G. silver is within 6% of the true value. As the diameter increases the effect of the oxide skin becomes proportionally less and the error falls.

It if is assumed that an oxide layer is formed, the depth of which is independent of wire diameter, then a very simple correction can be made: viz., that of reduced area A_1 in equation 30. When 18 S.W.G. and 34 S.W.G. copper wires had been heated for some hours at a current just below minimum fusing value, the oxide layer was allowed to flake away, and micrometer measurements showed reductions in area of 20% and 50% respectively. If it is assumed that an oxide layer of radial depth 0.0015 inch is formed irrespective of wire diameter then reductions in area of 13% and 55% would result for these two wires.

On the assumption that, for the wires tested, heating at or just below minimum fusing current for some hours causes an oxide layer 0.0015 inch deep, a new calculation can be made from equation 30. Table VIII and Fig. 4 shows that the calculated value of minimum fusing current is then within about 5% of the correct value.

RELATION BETWEEN MINIMUM FUSING CURRENT AND CURRENT ABOVE WHICH HEAT LOSS CAN BE NEGLECTED

If I_N = minimum current at which there is no heat loss from the element, then equations 28 and 30 show that

$$\frac{I_N}{I_{\min}}=\sqrt{\frac{10(1+\alpha\theta_m)}{\alpha\theta_m}}$$

$\frac{I_N}{I_{\min}}=3.52$ for silver

$\frac{I_N}{I_{\min}}=3.49$ for copper

Hence for copper and silver elements of any diameter, heat loss from the element may be neglected at a current 3.5 times minimum fusing current. This ratio applies to calculated values, so that for small diameter wires the calculated value of minimum fusing current should be modified to allow for oxidation in the way shown.

Comparison With Other Methods of Predicting Time/Current Characteristics

The times for 29 S.W.G. copper wire to reach melting temperature for various currents, obtained by some of the methods outlined earlier, are compared in accuracy with the present solution (equation 24) in Fig. 5. In this comparison the following points emerge.

Since the curve given by the present solution becomes asymptotic to the no heat loss solution fairly slowly and gives times somewhat greater than it, this makes some allowance for the break-up time and gives less error than Schubert's analytical solution. In the longer time range the present solution gives better agreement with test, due mainly to the assumption of a constant average resistivity having been avoided. For short times the solution given by the Prince and Williams equation ("square characteristic") agrees with Schubert since both assume no heat loss, but at longer times it shows even greater errors than this solution. Fig. 5 shows that Johann's method does not produce a better result than the square characteristic.

Effect of Filler Parameters on Time/Current Characteristics

At short fusing times where the heat lost through the filler is small, the thermal conductivity of the filler has no effect upon the characteristic. Fig. 3 shows how very considerably the characteristic is influenced by even small changes in thermal conductivity, in the region where there is appreciable heat loss. The parameter varied in Fig. 3 is not the thermal conductivity k_2 but is $k_2{}^1$.

RELATION BETWEEN K_2 AND $K_2{}^1$

Consider a wire heated in filler under steady-state conditions: Then

$$k_2=\frac{w\log_e\left(\frac{r}{r_1}\right)}{(\theta_1-\theta_r)2\pi Jl} \tag{31}$$

where

w = power loss in wire
θ_r = temperature rise at any radius r
l = wire length

Equation 29, which represents exactly the same condition, may be rewritten as

$$k_2{}^1=\frac{w}{\pi J\theta_1 l} \tag{32}$$

From equations 31 and 32

Table IX. Thermal Conductivity of Quartz Powder

Grain Size	Density	k_2^1 Centimeter-Gram-Second Units	k_2 Centimeter Gram-Second Units
Sample 1	1.62	4.210^{-4}	9.910^{-4}
Sample 1	1.70	4.710^{-4}	11.310^{-4}
Sample 2	1.70	5.010^{-4}	12.010^{-4}
− 36 + 52	1.59	4.510^{-4}	10.410^{-4}
−150 +200	1.53	4.010^{-4}	8.610^{-4}

Table X. Sample 2 Quartz Filler

% Weight	Grain Size
9	− 36 + 52
69	− 52 + 72
19.5	− 72 +100
2.5	−100 +150

Table XI. 18 S.W.G. Copper

I, Amperes, Length/Diameter	Time to Reach Melting Temperature, Seconds			
	∞	2.8	2.33	1.86
130	240	1,100	2,600	
140	100	240	480	
160	25.2	32.4	46.8	294
180	12	14	15.4	21.3
200	6.4	6.8	7.4	8.6
250	2.54	2.54	2.54	2.54

$$k_2 = \frac{\theta_1 \log_e\left(\frac{r}{r_1}\right)}{2(\theta_1-\theta_r)} k_2^1 \qquad (33)$$

The value of k_2^1 can be found by test (e.g., from Fig. 3), and then from equation 33 the thermal conductivity k_2, which is a mean effective value including the effects of radiation, convection, and conduction, may be found. Conversely if values of thermal conductivity are known for filling media, then the reverse process enables the effect on the time/current characteristic to be calculated when a change in filler is made. Some typical values of k_2 and k_2^1 obtained from time/current characteristics are shown in Table IX.

Figs. 3 and 6 show changes in time/current characteristic with density and with grain size. In the tests with varied grain size the filler was fully compacted and its density was found to change from 1.50 for −200 grain size to 1.59 for −36+52.

In the case of sample 2 powder, the sieve analysis of which is shown in Table X, a check showed that the value of thermal conductivity obtained in this way agreed very closely with that obtained by the standard method using parallel hot and cold plates with thermocouples.

The effect of variation of specific heat of filler may similarly be calculated. Specific heats do not vary as widely as thermal conductivities and a change of 100% in specific heat has only about the effect of a change of 40% in thermal conductivity.

Conclusions

A solution to thermal equations has been obtained, which enables the complete time/current characteristic to be calculated, for a fuse with single wire element in the center of a filled cartridge. A simple allowance is required for oxidation in the case of a copper element, and with this allowance minimum fusing current can be calculated to within about 5% of its true value. The solution shows that the current above which heat loss from the element can be neglected is a function of element cross section and can be calculated accurately. This current bears a constant ratio of 3.5 to the minimum fusing current.

This solution has been compared with solutions previously given, and is shown to be more complete than any of these. Since the solution holds throughout the whole time range, it allows examination to be made of the effect of filler parameters on the time/current characteristic.

Appendix. Examination by Analogue of Validity of Assumptions Made in Obtaining the Present Solution

Validity of Neglecting Axial Heat Loss

In this investigation the analogue was arranged to simulate a fuse of constant cartridge diameter but of varying length. The times for the element center to reach melting temperature as the ratio of element length to the cartridge outside diameter was varied were recorded for two wires. Where the ratio is infinity there is no axial heat flow. These times (in seconds) are shown in Table XI for the larger wire.

It can be seen that, even for wires as large as 18 S.W.G. wire, the effect of axial heat flow is not great. It is only at currents below twice minimum fusing current that the melting time is affected. If the length/diameter ratio is 2.8, as in all the fuses tested, then for currents as low as 1.5 times minimum fusing current the assumption of no axial heat loss reduces the melting time by no more than about 15%. Fig. 2 shows that there is in fact a tendency with the larger wires (22 and 18 S.W.G.) for the calculated time to be increasingly less than the prearcing time as the current falls below twice minimum fusing current. In the case of the smaller wires, the effect of oxidation predominates, and the error in calculated time is positive.

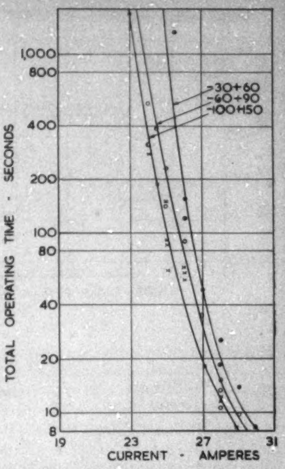

Fig. 6. Time/current characteristics with varied filler grain size. 29 S.W.G. silver in quartz powder

- ● −30 +60 grain size
- ○ −60 +90 grain size
- × −100 +150 grain size

Validity of Assuming Zero Temperature Rise at Outer Boundary of Filling Powder

The maximum temperature rise at the outer boundary of the filler over the whole current range was found to be about 100 degrees centigrade and this occurred only very close to minimum fusing current.

References

1. Short-Circuit Heating of High Voltage Cables, G. Grünberg. *Journal of Physics*, Moscow, USSR, vol. 4, 1941, pp. 463–72.

2. Electric Fuses—A Critical Review (book), H. Läpple. Butterworths Scientific Publications, London, England, 1952.

3. A Mechanism for the Fuse Pre-Arcing Period, E. B. Carne. *AIEE Transactions*, vol. 72, pt. III, Aug. 1953, pp. 593–99.

4. Phenomena Determining the Break-up of Fusible Elements, E. B. Carne. *Ph.D Thesis*, Queen Mary College, London University, London, England, 1952.

5. The Effects of Pre-loading on Fuse Performance, A. E. Guile. *Proceedings*, Institution of Electrical Engineers, London, England, vol. 102, pt. A, 1955, pp. 37–44.

6. The High-Rupturing-Capacity Cartridge Fuse, With Special Reference to Short-Circuit Performance, J. W. Gibson. *Journal*, Institution of Electrical Engineers, London, England, vol. 88, 1941, pp. 2–24.

7. The Melting Time of Fuse Wires, Van Liempt, De Vriend. *Zeitschrift fuer Physik*, Berlin, Germany, vol. 98, 1935, pp. 133–40.

8. Performance Criteria for Current-Limit

ing Power Fuses—II, E. W. Boehne. *AIEE Transactions*, vol. 65, 1946, pp. 1034–44.

9. Mathematical Investigation of Fusing, **Ikeda, Yoneta.** *Engineering Memoirs*, Hokkaido University, Sappora, Japan, vol. 2, 1930, pp. 147–59.

10. On the Melting Time of Fuses, **E. Wintergerst.** *Zeitschrift fuer angewandte Physik*, Berlin, Germany, vol. 2, 1950, pp. 167–74.

11. An Analysis of an Analogue Solution Applied to the Heat Conduction Problem in a Cartridge Fuse, **A. E. Guile, E. B. Carne.** *AIEE Transactions*, vol. 72, pt. I, 1953 (Jan. 1954 section), pp. 861–68.

12. On a Solution of the Heat Conduction Equation Which Enters into the Theory of Electrical Fuses, **G. U. Schubert.** *Zeitschrift fuer angewandte Physik*, Berlin, Germany, vol. 2, 1950, pp. 171–79.

13. The Current-Limiting Power Fuse, **D. C. Prince, E. A. Williams, Jr.** *AIEE Transactions (Electrical Engineering)*, vol. 58, Jan. 1939, pp. 11–18.

14. Formula for Current/Time Characteristics of Fuses and Their Application for Determining the Characteristics, **H. Johann.** *Elektrotechnische Zeitschrift*, Wuppertal-Eberfeld, Germany, vol. 58, 1937, pp. 684–86.

15. Calculation of Short-Circuit Heating of High Voltage Cables, **G. Grünberg, M. Sontz.** *Journal of Physics*, Moscow, USSR, pp. 97–112.

16. The Theory of the Low Voltage High Breaking Capacity Fuses, **R. Freiberger.** *Revue Generale de l'Electricite*, Paris, France, vol. 45, 1939, pp. 407–14.

Discussion

J. C. Lebens (Bussmann Manufacturing Company, St. Louis, Mo.): The author should be complimented on an excellent treatment of an extremely complex subject. Even though consideration was limited to the simple case of a single wire embedded in powder contained in a cylindrical cartridge, with the wire lying along the axis of the cylinder, the solution obtained by the author involves making assumptions.

As pointed out by the author the configuration of most commercial types of fuses precludes direct analysis so the paper is of academic interest only. This interest is enhanced by an excellent bibliography of foreign material, not usually available to the United States engineer.

I am sure that all fuse designers at some time have attempted to set up the equations so that the rating and time-current characteristics of a low-voltage fuse can be calculated without running tests. Unless the problem is simplified until it no longer is of commercial value the equations become so complicated that it takes longer to calculate than to prepare and test physical samples. Perhaps the modern computer laboratories now available could speed up the computations.

Even so, after the calculations are complete, it still is necessary to apply a correction factor to bring the calculated values in step with the experimental data. Unfortunately the author has limited his tests to copper and silver wire of relatively small cross-sectional area so that he does not establish if the same correction factor will apply over the entire range or if a series of factors are required.

Hence the amount of testing required to establish the validity of the equations prevents them from becoming practical, useful tools for the fuse designer. However, the author states that cases such as a single strip element of rectangular cross section and of wires or strips wound helically are now being studied using the method based upon the analysis given in the paper and the results are promising.

It will be interesting to see if from this beginning it may be possible to extend the method so that commercial fuses can be analyzed.

J. W. Gibson (Electric Transmission Ltd., Stoke-on-Trent, England). It has been suggested on the basis of rather limited experimental evidence that the current heat integral increases somewhat if the current density in the element reaches very high values. This was thought to be caused by a greater proportion of the latent heat of fusion having to be supplied before arcing commences.

If this is correct, the effect will be to change the slope of the time/current characteristic at very short times from 2 to somewhat less than 2 and so, by acting in a way contrary to that of heat loss from the element, apparently to reduce the value of current above which heat loss is negligible.

Will the author please give his views?

A. E. Guile: Mr. Leben's remarks are interesting and quite rightly indicate the difficulties in applying calculations to commercial types of fuses. Where a fuse, such as one with a single strip element of uniform rectangular section, has a characteristic similar to that of the simple fuse considered here, then the characteristic can be predicted. However, when such elements are used in commercial fuses, considerable changes in the characteristics appear; e.g., the change in slope from −2 to 1 to −3.5 to 1 reported recently for multiple strips with holes.[1] Each type of fuse needs considerable testing, and calculations of this kind may be of practical use only if the tests show a characteristic, similar over at least some range, to those considered here, so that further testing may be reduced with the aid of predicted values.

Reference

1. Ribbon Elements for High-Voltage Current-Limiting Fuses, **A. H. Powell, C. L. Schuck.** *AIEE Transactions*, vol. 74, pt. III, Aug. 1955, pp. 635–43.

Surge Attenuation in Power Cables

W. W. VALENTINE
MEMBER AIEE

J. K. DILLARD
MEMBER AIEE

J. M. CLAYTON
ASSOCIATE MEMBER AIEE

IN THIS paper surge attenuation data on power cables are presented which were obtained from field tests on selected cables of several voltage classes and constructions. Included in the paper are several examples illustrating how the data can be applied to the analytical solution of simple surge protection problems.

Because of the trend toward the use of underground circuits in urban areas, the problem of surge protection of equipment connected to overhead lines through cables is assuming increasing importance. In many applications, the short-time impulse characteristic of insulation may result in substantial economies through the use of reduced insulation or a fewer number of lightning arresters. In some cases, lightning arresters can be omitted altogether at the transformer end of the cable,[1] in which cases direct cable entrances to the transformers are possible, leading to additional savings through the elimination of transformer bushings.

Anacom studies[2,3,4] have been helpful in determining the most economical application of lightning arresters consistent with the insulation levels of protected equipment on both overhead and cable circuits. Full advantage cannot be taken of all the economic possibilities inherent in the higher short-time impulse strength of insulation, however, unless accurate data are available on all the factors which influence the magnitude and shape of surge voltages impressed on the protected apparatus. Two factors which appreciably affect the magnitude and duration of surge voltages at the receiving end of a cable are the surge impedance and surge attenuation properties of the cable.

Paper 55-558, recommended by the AIEE Protective Devices Committee and approved by the AIEE Committee on Technical Operations for presentation at the AIEE Summer General Meeting, Swampscott, Mass., June 27–July 1, 1955. Manuscript submitted March 30, 1955; made available for printing May 26, 1955.

W. W. Valentine is with the Potomac Electric Power Company, Washington, D. C., and J. K. Dillard and J. M. Clayton are with the Westinghouse Electric Corporation, East Pittsburgh, Pa.

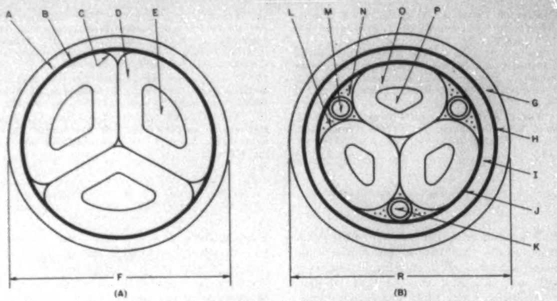

Fig. 1. Cross-section view of cables tested. Letters are identified in Tables I and II

A—Types 1 and 2, 15-kv cable
B—Type 3, 40-kv cable, and type 4, 69-kv cable

Cable surge impedances can be calculated with fair accuracy. Unfortunately, only limited data[5,6] are available on the attenuation of traveling waves on cable circuits. For this reason, the reduction of surge voltages caused by attenuation has been neglected in Anacom studies involving cable circuits, except for the attenuation inherent in the computer elements. The purpose of the test program described in this paper was to obtain these data on a number of representative cable circuits.

Cables on the Potomac Electric Power Company system were made available for testing at intervals over the past 2 years as it was feasible to take the circuits out of service. The tests were made with a synchronograph, a low-voltage repetitive-surge generator which has been described in the literature.[5]

Scope of Tests

The primary purpose of the tests was to obtain fundamental attenuation data on cables of various voltage classes and lengths for the range of lightning wave shapes normally encountered in practice. Measurements were made on 15-, 40-, and 69-kv cables ranging in length from 2,000 to slightly over 32,000 feet. Cross-section views of the various type of cables are shown in Fig. 1. The physical constants of the cables identified by the letters in Fig. 1 are summarized in Tables I and II. Also the lengths of the cables tested are given in the tables.

Attenuation and distortion measurements were made for a wide range of lightning wave shapes with fronts ranging from less than 1 to over 8 microseconds (ms), and wave tails ranging from 10 to 120 ms. In addition to the attenuation measurements, the surge impedance and propagation velocity were determined for all the cables tested.

Table I. Physical Characteristics of Type-H 15-Kv Cables

Symbol*	Type 1, 15 Kv	Type 2, 15 Kv
A	$^9/_{64}$-inch lead sheath	$^9/_{64}$-inch lead sheath
B	0.004-inch bronze or steel binder	0.004-inch bronze or steel binder
C	0.003-inch perforated copper tape	0.003-inch perforated copper tape
D	$^{13}/_{64}$-inch paper	$^{13}/_{64}$ inch paper
E	500,000-circular-mil stranded sector copper	350,000-circular-mil stranded sector copper
F	$2^5/_8$-inch diameter	$2^{13}/_{16}$-inch diameter
Lengths tested, feet	1,998	10,366
	6,310	
	11,736	
	17,162	
	23,472	

* Identified in Fig. 1(A).

Test Equipment and Procedures

Since the measurements were made on installed cables, it was not practical or economical to use a full-scale high-voltage surge generator in the tests. The measurements were made with the synchronograph,[5] which is a repetitive-surge generator and synchronized receiver for studying lightning problems in the field. The generator produces simulated lightning surges over a wide range of wave shapes, having magnitudes in the range of 50 to 400 volts. Since surges are applied repetitively, at the rate of one per cycle of the supply frequency, transient phenomena in the system under investigation appear as stationary waves when observed with an oscillograph.

In all cases the attenuation measurements were made on cables without taps. This was necessary since reflections from taps would alter the voltage in the cable under test, and it would not be possible to distinguish attenuation effects from the effects of reflections from the taps.

Cable surge impedances were determined by two methods: 1. The surge was applied to the cable through a resistor used to represent the cable surge impedance. The value of the resistor was adjusted until the voltage across the resistor equaled the voltage across the cable. When the voltage divides equally between the resistor and cable, the resistor equals the cable surge impedance. 2. The surge impedance determined by the first method was checked by measuring the receiving-end voltage with the receiving end open-circuited and also terminated with its surge impedance. If the terminating resistor is the true surge impedance, the voltages for open-circuit and terminated conditions have a ratio of 2 to 1. The

Table II. Physical Characteristics of Gas-Filled Low-Pressure 40-Kv Cable and Medium-Pressure 69-Kv Cable

Symbol*	Type 3, 40 Kv	Type 4, 69 Kv
G	neoprene jacket†	neoprene jacket†
H	none	two 0.008-inch asbestos neoprene tapes, one 0.012-inch half-lapped neoprene, two 0.005-inch bronze tapes butted and staggered
I	0.141-inch Habirloy "A" alloy lead sheath	0.125-inch lead sheath
J	0.005-inch bronze binder tape over 0.012-inch paper belt	0.005-inch bronze binder tape over 0.012-inch paper belt
K	0.350-inch outside diameter by 0.030-inch wall copper tube	0.350-inch outside diameter by 0.030-inch wall copper tube
L	0.003-inch perforated copper tape	0.003-inch perforated copper tape
M	two helical steel gas channels 0.370-inch outside diameter of strip 0.250-inch by 0.025-inch	two helical gas channels 0.410-inch outside diameter of strip 0.250-inch by 0.027-inch
N	paper filler	paper filler
O	0.350-inch paper with two aluminum-backed paper tapes	0.400-inch paper including copper shield
P	450,000-circular mil compact sector copper	600,000 - circular mil compact sector copper
R	3.55-inch diameter	4.1-inch diameter
Lengths tested, feet	2,061	17,590
	3,024	32,654
	5,359	

* Identified in Fig. 1(B).
† Neoprene jacket: one 0.0015-inch acetate tape, 10-per-cent lap; three 0.030-inch neoprene-faced tapes with fabric face inside applied close butt with staggered joints; one 0.030-inch neoprene-faced tape applied fabric outside with butt joints staggered; one 0.015-inch neoprene-skim coated tape, fabric side out with 10-per-cent lap; and wax finish.

Fig. 2. Oscillograph and synchronograph set up for measuring attenuation with surges applied at pothead of 40-kv cable shown on right

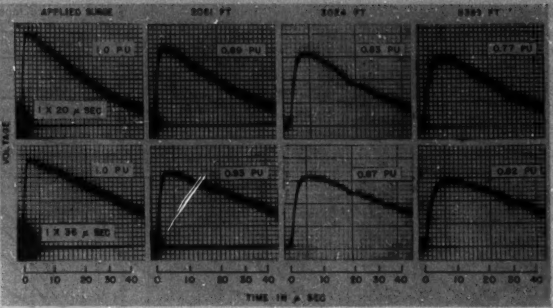

Fig. 3. Typical oscillograms showing attenuation and distortion of 40-kv cable for the indicated wave shapes and cable lengths with crest magnitudes in per unit shown on the oscillograms

values of surge impedances determined by the two methods were in good agreement. The velocity of propagation was determined by applying the surge to an open-ended cable and measuring the time until the reflected wave returns.

In many cases attenuation measurements were made with open-circuit and also surge-impedance terminations. The measurements by both methods were in good agreement indicating that the value used for the surge impedance was correct. However, only the results obtained with the surge-impedance termination are reported in this paper. This method is preferred since complete wave detail of the surges at both ends of the cable can be determined, as the wave shapes are not influenced by reflections in the cable.

The synchronograph set up for making measurements on a 40-kv cable is shown in Fig. 2. A similar oscillograph and synchronized sweep are used for recording receiving-end voltages simultaneously with the applied surge. Some typical oscillograms showing attenuation and distortion in 40-kv cables are shown in Fig. 3. Similar oscillograms were recorded with fast sweeps to provide more accurate details on wave fronts.

Results of Tests

The electrical characteristics of the cables on which the studies were made are summarized in Table III. Surge impedances and propagation velocities were measured directly as described previously. From these quantities the permittivity, inductance, and capacitance were calculated by the following equations[7]

$$V_{\text{cable}}=\frac{V_{\text{light}}}{\sqrt{k}}$$

$$V_{\text{cable}}=\frac{1}{\sqrt{LC}}$$

$$Z=\sqrt{\frac{L}{C}}$$

where

V_{cable} = propagation velocity in cable
V_{light} = propagation velocity of light
k = permittivity or dielectric constant of cable insulation
L = inductance of cable
C = capacitance of cable
Z = surge impedance of cable

With the measured quantities and the known propagation velocity of light, the other quantities can be calculated.

The results of the attenuation and distortion measurements are presented in curve form in Figs. 4 and 5. This method seems to be the most condensed form of presenting the data since it is not practical to give the results in oscillographic form. In analyzing the oscillograms, the crest magnitude, time to 90 per cent of crest, time to crest, and time to have value were read. In plotting the curves of Figs. 4 and 5 which describe the wave front, the time to 90-per-cent crest has been used and not the time to the actual crest. This was done for a number of reasons. In lightning-arrester application problems, the rate of rise on the wave front is of prime importance. The time to 90-per-cent crest is more descriptive of the rate of rise on the wave front than the time to crest. This is particularly true on fronts longer than 2 or 3 ms where there is appreciable rounding off near the crest. In some cases, the time to crest is more than twice the time to 90 per cent of crest. Obviously the time to crest in such cases is not descriptive of the average rate of rise on the wave front. Also the crest of the wave is not a well-defined point and selecting it is largely a matter of judgment; whereas, the time to 90-per-cent crest is a definite point on the wave.

An analysis of the oscillograms showed that the time to half value of the applied surge had a very significant effect on attenuation. Small variations in the front did not affect attenuation appreciably. Attenuation was essentially unchanged when the tail was held constant and the time to 90-per-cent crest varied from 0.6 to 1.2 ms. However, waves with fronts of the order of 3 to 4 ms to 90-per-cent crest have less attenuation than waves having 1-ms fronts. It is believed the reason for this is that, with a long front, the tail is sustained at a higher voltage for a longer time, and this has the same effect as increasing the wave tail.

The curves of Figs. 4 and 5 give attenuation for the range of wave tails used in the tests. Straight-line interpolation is suggested for determining attenuation for wave tails not specifically covered by the curves, and also where theti me to 90-per-cent crest is between 1 and 4 ms.

Table III. Electrical Characteristics of Cables Tested

Type No.	Voltage Class, Kv	Surge Impedance, Ohms	Propagation Velocity, Feet per Ms	Inductance L,* Microhenrys per Foot	Capacitance C,* Micromicrofarads per Foot	Permittivity k,* (Dielectric Constant)
1	15	18	520	0.035	107	3.6
2	15	23	520	0.044	84	3.6
3	40	25	450	0.056	89	4.8
4	69	26	530	0.049	73	3.4

*Since the accuracy of the measured values are within 5 per cent, the calculated values are within 10 per cent.

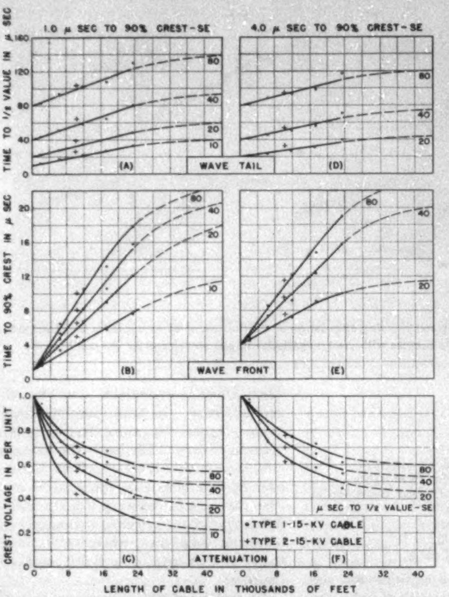

Fig. 4. Curves showing attenuation and distortion in 15-kv cables

A and D—Time to half value
B and E—Time to 90-per-cent crest
C and F—Attenuation

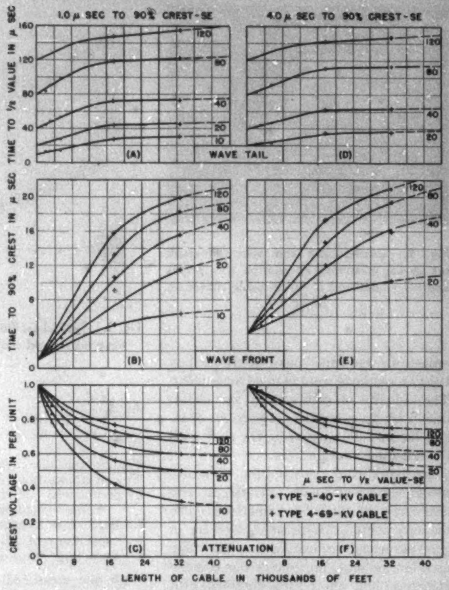

Fig. 5. Curves showing attenuation and distortion in 40- and 69-kv cables

A and D—Time to half value
B and E—Time to 90-per-cent crest
C and F—Attenuation

Comparing Figs. 4 and 5 indicates more attenuation for the 15-kv cables than for the higher voltage cables. Attenuation is caused primarily by the shunt resistance of the insulating material between conductor and sheath and by the series resistance of the conductor and sheath. Comparing cables having the same conductor size and sheath cross-section area, the variation in attenuation should depend upon the difference in shunt resistance. Assuming the same insulating material, shunt resistance increases with thickness of insulation. This increase in shunt resistance should reduce the shunt losses and, therefore, result in higher voltage cables having less attenuation.

From Fig. 5 it will be noted that a single family of curves has been drawn for the 40- and 69-kv cables, although the lengths tested did not overlap and provide direct evidence that both cables have attenuation of the same order of magnitude. However, the points appear to fall on a smooth curve having the same general shape as the curves of Fig. 4 which are plotted for the same type of cable with different lengths.

All measurements were made with applied surges of the order of 100 to 200 volts. Some limited tests[6] which have been made indicate attenuation in cables is essentially linear with voltage magnitude and does not change appreciably for voltages in the range of actual lightning surges. If the dielectric losses in the cable insulating material are nonlinear with voltage, it is believed that higher losses should be expected at the higher voltages. Therefore, attenuation determined by the low-voltage measurements should be on the conservative side as compared with high-voltage surge attenuation.

Application of Data

The attenuation data can be used in a number of ways in the application of lightning arresters on cable-connected equipment. One application is to take attenuation into account in the conventional traveling-wave calculation.[7] The method which is suggested for doing this is illustrated by the following example.

Example 1—Complete Traveling-Wave Analyses

Complete traveling-wave analyses, including the effect of surge attenuation, can be made graphically through the use of curves given in the paper. As an illustrative example of the procedure, consider a 40-kv 5,359-foot cable of 25-ohm surge impedance connected to an overhead line of 450-ohm surge impedance. The velocity of propagation of the surge in this cable is 450 feet per ms, so that 12 ms are required for a surge to travel from one end of the cable to the other. Data taken in the field on such a cable are available for comparison with the calculated volt-time curves.

When an incoming surge E_t encounters the line-cable junction, a surge

$$E=\frac{2Z_C}{Z_L+Z_C}E_t=0.105E_t$$

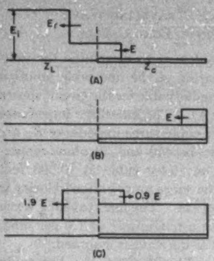

Fig. 6 (above). Traveling-wave analysis where surge encounters mismatch in impedances

A—Reflected and forward waves at mismatch

B—Voltage doubles at open end

C—Reflected and forward waves at mismatch

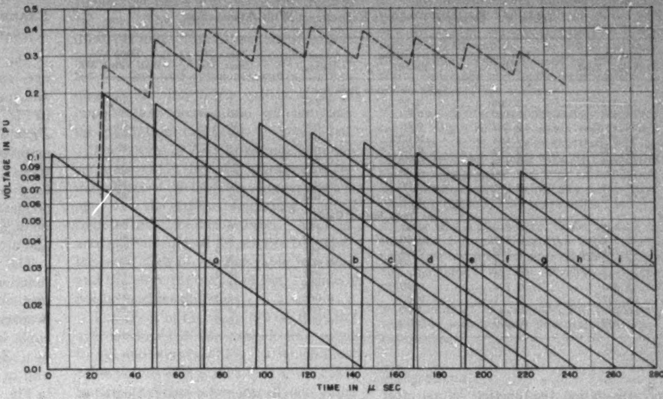

Fig. 7 (above right). Traveling-wave calculation neglecting attenuation and distortion. Line traveling-wave voltage is 1.0 per unit

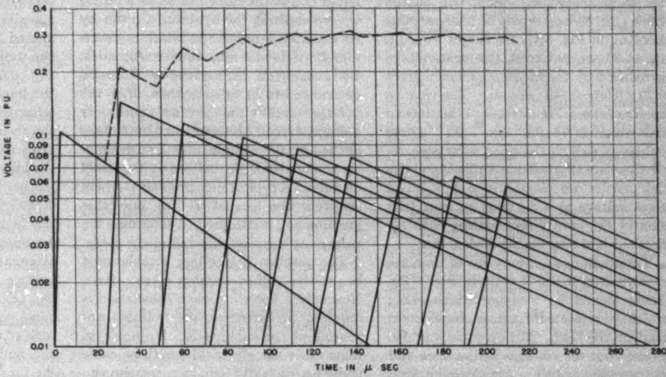

Fig. 8 (right). Traveling-wave calculation with attenuation and distortion considered

is transmitted down the cable, as shown in Fig.6(A), where Z_L and Z_C are the line and cable surge impedances respectively. At the open end of the cable, the surge E doubles and returns to the cable-line junction. When it strikes the junction, a second surge equal to

$$\frac{(Z_L-Z_C)}{(Z_L+Z_C)}E=0.9E$$

is reflected and it travels down the cable adding to the voltage left by the surge E, as shown in Fig. 6(C). The phenomenon repeats until a steady state is reached. Fig. 6 is drawn for a square-front wave with a very long tail, but only details of the picture are changed by considering other wave shapes; i.e., each surge which meets the open end of the cable doubles, and each surge which strikes the junction adds 1.9 times the surge magnitude to the potential already at that point.

Neglecting attenuation and distortion for a moment, suppose a surge coming in on the overhead line has a front which rises to 1.0 per-unit voltage in 3 ms and an exponential tail which falls to half value in 45 ms. When this surge encounters the line-cable junction, its crest magnitude is reduced to 0.105 per unit and, on semilogarithmic paper, it has the shape given by curve *a* of Fig. 7. After 24 ms, the reflection from the open end returns to the junction and jumps to 1.9 × 0.105 = 0.20 per unit, given by curve *b* of Fig. 7. Total potential at the junction is then the sum of the two curves. The reflected wave, 0.9 × 0.105 = 0.0945 per unit, travels down and back in another 24 ms, jumping to 1.9 × 0.0945 = 0.179 per unit at the junction, as given by curve *c*. Crest magnitudes of successive reflections are tabulated in Table IV, and those at the junction are plotted in Fig. 7. The total potential as a function of time (the sum of the curves) is shown by the dashed line.

To include the effects of attenuation and distortion, the curves of Fig. 5 based on the field data are used. If there were

Table IV. Example 1—Surge Reflections, No Attenuation

E	Open End, 2E	Junction, 1.9E	Reflection, 0.9E
0.105 (*a*)*	0.210	0.200 (*b*)	0.0945
0.0945	0.189	0.179 (*c*)	0.0850
0.0850	0.170	0.161 (*d*)	0.0765
0.0765	0.153	0.145 (*e*)	0.0688
0.0688	0.138	0.131 (*f*)	0.0620
0.0620	0.124	0.117 (*g*)	0.0557
0.0557	0.112	0.106 (*h*)	0.0502
0.0502	0.100	0.095 (*i*)	0.0452
0.0452	0.090	0.086 (*j*)	0.0407

* Letters in parentheses indicate curves on Fig. 7.

Table V. Example 1—Surge Reflections, With Attenuation

Distance Traveled, Feet	Junction, 1.9E	Attenuation Factor	Adjusted Voltage	Time to Crest, Ms	Time to Half Value Ms
		At Line-Cable Junction			
10,718	0.200	0.73	0.146	7.0	70
21,436	0.180	0.64	0.115	12.6	80
32,154	0.162	0.61	0.099	16.0	84
42,872	0.146	0.60	0.087	17.6	85
53,590	0.131	0.60	0.078	18.0	85
64,308	0.118	0.60	0.071	18.0	85
75,026	0.106	0.60	0.063	18.0	85
85,744	0.096	0.60	0.057	18.0	85
96,462	0.086	0.60	0.051	18.0	85
		At Open End of Cable			
5,359	0.210	0.82	0.172	3.8	60
16,077	0.189	0.68	0.128	9.4	80
26,795	0.170	0.62	0.105	14.0	82
37,513	0.153	0.60	0.092	16.6	84
48,231	0.138	0.60	0.083	18.0	85
58,949	0.124	0.60	0.074	18.0	85
69,667	0.111	0.60	0.066	18.0	85
80,385	0.100	0.60	0.060	18.0	85
91,103	0.090	0.60	0.054	18.0	85

no attenuation, the junction voltage after the surge makes one round trip on the cable (10,718 feet) would be 0.20 per unit. Looking in Fig. 5(C) for surges with 1.0 ms to 90-per-cent crest, the crest voltage is reduced by the factor 0.73 which gives $0.73\times0.20=0.146$ per unit. The time to crest is 7.0 ms, Fig. 5(B), and the time to half value is 70 ms, Fig. 5(A). These values as well as those for successive reflections are tabulated in Table V and the new curves are plotted in Fig. 8. The total voltage as a function of time (the sum of the curves representing each reflection) is shown by the dashed line.

Total voltages as functions of time are replotted on a linear scale in Fig. 9(B). These should be compared with 9(A), which is replotted from an oscillogram made in the field. The example was also worked out for voltages at the open end of the cable, and these are plotted in Fig. 10(B) which should be compared with the replotted oscillogram of Fig. 10(A).

In example 1, lightning arresters have not been considered in the calculations. However, the effect of arresters located at either end of the cable can be determined by representing the lightning arrester by its equivalent resistance, which is determined by its volt-ampere characteristics. For example, if the arrester resistance is determined to be 10 ohms then, after the voltage reaches the arrester spark-over voltage, the cable is terminated in 10 ohms at the arrester location, and the traveling-wave analysis is carried out in the usual manner. A typical such problem is where arresters are located at the line-cable junction and it is desired to determine the voltage at the receiving end of the cable.

The problem of how long a cable must be to be self-protecting often arises. Normally a traveling-wave calculation is required to determine the voltages appearing at the cable ends. However, in some cases the electrical length of cable may be sufficiently long in comparison to the wave tail so that reflections in the cable do not increase the initial cable voltage. A typical such case is illustrated by the following example.

EXAMPLE 2—TRAVELING-WAVE ANALYSIS OF LONG CABLES

The problem is to determine the voltages appearing at the line-cable junction and open end of cable for the circuit shown in Fig. 11(A). The line surge impedance Z_L and the cable surge impedance Z_C are assumed to be 450 and 30 ohms respectively. The 15-kv cable is 10,000 feet long and the surge propagation velocity is 500 feet per ms. The line traveling wave voltage has a magnitude of 1.0 per unit, and a 1.0x20-ms wave is assumed.

The initial voltage at the line-cable junction is $(2Z_C/Z_L+Z_C)1.0=0.125$ per unit. A voltage wave of this magnitude propagates to the open-circuit end of the cable, is reflected, and results in a voltage of $(2Z_L/Z_L+Z_C)0.125\times0.46=0.108$ per unit at the line-cable junction, as shown in Fig. 11(A). The factor 0.46 is the attenuation factor from Fig. 4(C) corresponding to a 1.0x20 wave which has propagated 20,000 feet. The wave shape of the reflected wave is determine from Fig. 4(A) and (B). The total voltage at the line-cable junction is the sum of the reflected wave and the initial voltage, as shown in Fig. 11(A). Subsequent reflections do not increase the voltage above the initial value of 0.125 per unit.

The initial receiving-end voltage is $0.125\times2.0\times0.58=0.146$ per unit, where the factor 2.0 accounts for the voltage doubling at the open end, and 0.58 is the attenuation factor for 10,000 feet. The voltage resulting from the first reflection is $(Z_L-Z_C/Z_L+Z_C)0.073\times2.0\times0.66=0.084$ per unit, where 0.073 is the magnitude of the wave reflected from the open end, and 0.66 is the attenuation factor for the surge that travels from the open end to the line-cable junction and back to the open end. From Fig. 4(C) the attenuation factors for 10,000 and 30,000 feet are 0.58 and 0.38 respectively. Therefore,

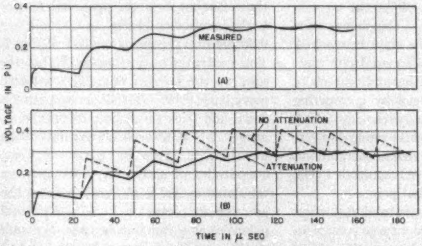

Fig. 9. **Voltage at line-cable junction in per unit of line traveling-wave voltage**

A—Replot of voltage measured in the field
B—Calculated voltages with and without attenuation

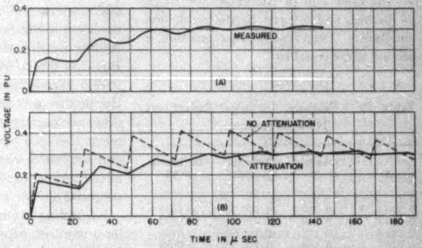

Fig. 10. **Voltage at open end of cable in per unit of line traveling-wave voltage**

A—Replot of voltage measured in the field
B—Calculated voltages with and without attenuation

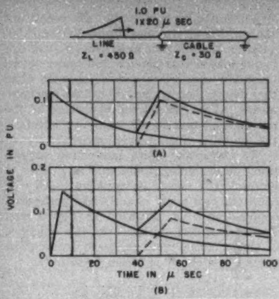

Fig. 11. Traveling-wave calculation for case where reflections in cable do not increase voltage above initial value

A—Calculated voltage at line-cable junction
B—Calculated voltage at open end of cable

the attenuation factor for the 20,000 feet is 0.38/0.58 or 0.66. The calculated receiving-end voltage using the wave shapes determined from Fig. 4 is shown in Fig. 11(B).

For the constants used in example 2, reflections do not increase the voltage at the cable ends, and, therefore, it is a simple calculation to determine the voltage at the cable ends. Similar calculations which have been made for a large number of cases are summarized in Fig. 12. The curves are plotted to show the maximum permissible wave tail as a function of cable length for the condition that reflections in the cable do not increase the initial voltage at the line-cable junction. For example, from Fig. 12(B), the maximum permissible wave tail for a 15-kv 10,000-foot cable is 20 ms, if the front is 1.0 ms. The receiving-end voltage is 0.146 per unit. In all cases the voltage is 0.125 per unit at the line-cable junction for the line and cable constants used in example 2. For other values of surge impedance or propagation velocity, similar calculations can be made, as outlined.

The curves of Fig. 12 assume that the surge current in the cable is limited by the magnitude of the line traveling-wave voltage; i.e., the stroke-terminating point is remote from the cable pothead. A special analysis[1] is required for strokes terminating very close to the line-cable junction, and therefore the curves of Fig. 12 should not be used for this case.

The effect of the wave tail on the voltage developed in the cable is illustrated by the oscillograms of Fig. 13, which show cable voltages for a 3024-foot 40-kv cable having a 25-ohm surge impedance. The line surge impedance is 450 ohms. When the line traveling-wave voltage has a 14-ms tail, the cable voltage is 0.19 per unit of the line voltage. With a 120-ms tail, the cable voltage is 0.70 per unit. This illustrates the influence of the wave tail on the cable voltage. Increasing the cable length or decreasing the wave tail tends to reduce the magnitude of the voltage developed in the cable.

Conclusions

The following conclusions are based on the surge attenuation measurements made on four types of cables.

1. The wave tail of the applied surge has a significant effect on surge attenuation, and the wave front has a minor effect.

2. The measurements indicated less attenuation on the higher voltage cables (40 and 69 kv) as compared with the lower voltage 15-kv cables. The lower attenuation is believed to be caused by the higher shunt resistance and lower series resistance of the high-voltage cables.

3. The difference in attenuation measured on two types of 15-kv cable was not appreciable. It is believed the data can be applied to other similar type of cables and that in many cases the type of cable will not influence attenuation any more than changing the incoming wave tail a few ms.

4. For the case where cable voltage is increased by reflections, the cable length and wave tail have an appreciable effect on the maximum voltage developed in the cable.

5. A method is presented for taking attenuation into account in a traveling-wave calculation.

References

1. Direct Stroke Protection of High-Voltage Switching Stations and Transformers, S. B. Griscom, J. K. Dillard, A. R. Hileman. *AIEE Transactions*, vol. 74, pt. III, June 1955, pp. 354–68.

2. Surge Protection of Cable-Connected Equipment, R. L. Witzke, T. J. Bliss. *Ibid.*, vol. 69, pt. I, 1950, pp. 527–42.

3. Co-ordination of Lightning Arrester Location with Transformer Insulation Level, R. L. Witzke, T. J. Bliss. *Ibid.*, pt. II, 1950, pp. 964–75.

4. Surge Protection of Transformers Based on New Lightning-Arrester Characteristics, J. K. Dillard, T. J. Bliss. *Ibid.*, vol. 73, pt. III-B, Oct. 1954, pp. 1305–11.

5. Lightning Problems Solved With the Synchronograph, E. L. Harder, J. M. Clayton. *Ibid.*, vol. 72, pt. III, June 1953, pp. 375–83.

6. Field Investigation on the Surge Performance of a Large Unit-Connected Steam Turbine Generator, H. R. Armstrong, S. B. Howard, I. B. Johnson. *Ibid.*, vol. 71, pt. III, 1952, pp. 1023–29.

7. Electrical Transmission and Distribution Reference Book (book). Westinghouse Electric Corporation, Pittsburgh, Pa., 4th ed., 1950, chap. 15.

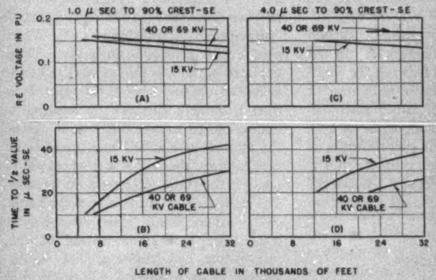

Fig. 12. Curves showing maximum permissible wave tails and corresponding receiving-end voltages so that initial cable voltage is not increased by reflections. Voltage at line-cable junction is 0.125 per unit of line traveling-wave voltage. Calculations based on $Z_L = 450$ ohms, $Z_C = 30$ ohms, and propagation velocity = 500 feet per ms

A and C—Receiving-end voltage in per unit of line traveling-wave voltage
B and D—Maximum permissible wave tail of surge applied at sending end

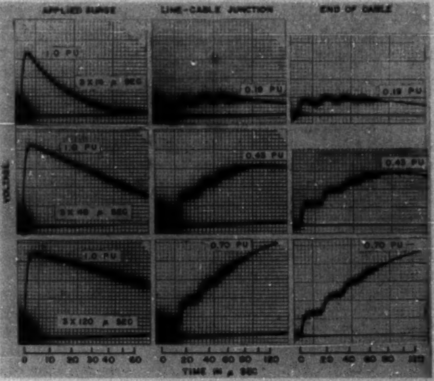

Fig. 13. Oscillograms showing effect of wave tail on magnitude of voltage developed in a cable

Discussion

R. W. Atkinson (retired, General Cable Corporation, Bayonne, N. J.): Certain conditions may increase considerably the attenuation over that found in the tests here reported. For instance, the power factor of the insulation, except for cables of the oil filled type, may increase considerably at stresses occasioned by lightning impulses.

The amount and effect of these ionization losses cannot be measured by the method used by the authors. However, measurements can be made of the extra attenuation caused by the metal shielding tapes now so commonly used to prevent ionization in the insulation. These tapes may be so wound that the steep wave front impulse currents will follow the helical path of the shielding tape. This will multiply the ohmic loss and thus increase the attenuation. It is possible to design the cable construction so as to magnify these losses and, thus, the attenuation. Since the authors do not refer to shielding it is presumable that their data apply to unshielded cable and that, for shielded cables, the attenuation will be greater than for the cables used.

W. W. Valentine, J. K. Dillard, and J. M. Clayton: The authors wish to thank Mr. Atkinson for his comments. He points out that with high-voltage surges the cable insulation has a higher power factor, and this is one reason that attenuation under actual lightning conditions can be greater than that determined by the low-voltage measurements. Thus, in taking advantage of the reported attenuation in applying arresters, the application will be conservative.

Mr. Atkinson offers interesting suggestions on designing metal shielding tapes to increase the surge attenuation. All the cables in this series of tests had perforated copper tapes as indicated in Fig. 1 and Tables I and II. Therefore, the influence of the shielding tape on surge attenuation cannot be determined from these tests.

Control of Electrostatic Voltage Distribution in Power Transformer Design

SAUL BENNON
MEMBER AIEE

R. J. COSSAART
NONMEMBER AIEE

ONE OF the problems involved in power transformer design is the control of the electrostatic voltage distribution produced by surge voltages applied to the line terminals. For waves with a relatively steep front this initial electrostatic distribution is to a large extent determined by the capacitance network formed between the winding elements, the core and the tank structure. This paper describes the wide range of control of this distribution achieved in interleaved shell form windings by the proper application of static plates.

General Capacitance Network

As a considerable part of the recent literature[1,2] concerning electrostatic distribution has related to the core form type of winding, it may be of value to compare the capacitance network of the interleaved shell form-fit transformer with that of the conventional core form transformer. Fig. 1(A) indicates the equivalent network of a 2-winding interleaved shell transformer, while Fig. 1(B) represents the corresponding network for a core form unit. Enough of the networks is shown to establish the pattern of the capacitances involved.

An examination of the two types of network reveals that both have a set of coil-to-coil capacitances C_H and C_L in series in the high- and low-voltage windings respectively. Also, both have distributed winding to ground capacitances C_{HG} and C_{LG}. However, there is a distinct difference in the winding-to-winding capacitance C_{HL} in the two networks. In the case of the interleaved network the winding-to-winding capacitance is lumped at the winding terminals rather than distributed along the winding as in the core type of network. This concentration of the mutual capacitance coupling at the ends of windings or groups simplifies the control of electrostatic surge transfer by the use of static plates.

Static Plate Construction

The construction of static plates built by the company with which the authors are associated is illustrated by the partially cutaway sketch in Fig. 2. It consists of a sheet of metal foil sandwiched between two sheets of pressboard. The sheets of pressboard termed washers are cut to the general contour of the actual coils of the winding. The foil contains a gap to avoid forming a short-circuited turn. Connection to the foil layer is made by means of the pigtail shown. The internal and external edges are protected by pressboard channels. Spacer blocks are glued to the pressboard washers to form oil ducts on either side of the static plate.

A static plate for the high-voltage line coil of a 450 basic impulse insulation level winding of a 90,000-kva transformer is shown in Fig. 3. Fig. 4 shows a static plate assembled with a high-voltage winding group.

Control of Distribution Within Windings

The original purpose behind the application of static plates was to control the initial voltage distribution within a transformer winding due to surges reaching its line terminal. Their use for this purpose dates back to the early years of "surge-proof" transformers.[3,4] When used in this manner a single static plate is placed parallel to the line coil and connected to the first turn of the coil. It is then extremely effective in securing a uniform surge voltage distribution across the face of the line coil, and therefore in turn between the coils of the whole winding. If the static plate were not present the voltage distribution across the turns of the line coil would be determined by a capacitance network consisting of the turn-to-turn and turn-to-ground capacitances. This, in general, will result in a much poorer voltage distribution.

While retaining the static plate for the purpose just outlined, the design engineer today applies the static plate for a variety of other purposes when required. Two of the more important applications of the static plate will be discussed in the succeeding paragraphs.

Paper 55-521, recommended by the AIEE Transformers Committee and approved by the AIEE Committee on Technical Operations for presentation at the AIEE Summer General Meeting, Swampscott, Mass., June 27–July 1, 1955. Manuscript submitted March 25, 1955; made available for printing May 13, 1955.

Saul Bennon and R. J. Cossaart are with the Westinghouse Electric Corporation, Sharon, Pa.

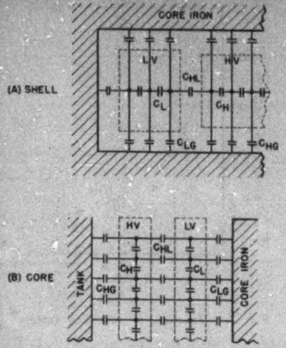

Fig. 1. Equivalent capacitance networks

Control of Surge Transfer Between Windings

Since surge voltages can be transferred electrostatically between transformer windings it is frequently desirable to isolate the lower voltage windings from effects due to surges applied to the high-voltage line terminal. Since the mutual coupling is concentrated at the ends of the winding, this isolation can be accomplished rather simply. The low-voltage line coil can be placed opposite the high-voltage line static plate and provided with its own static plate. An arrangement of this type is shown in Fig. 5 for one phase of a double-wye transformer with a delta tertiary. Under the conditions shown the low-voltage line group and the tertiary group adjacent to it are effectively shielded by the low-voltage line static plate. Of course, in this case the low-voltage static plate simultaneously fulfills its other purpose of distributing any surges applied to the low voltage across the line coil and the remainder of the group. If the high-voltage winding had been delta, corresponding shielding could be achieved by providing an additional static plate at the neutral end of the low-voltage winding.

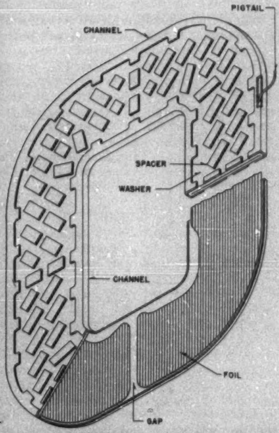

Fig. 2. Partial cutaway sketch of static plate

The shielding effect of a static plate used in this manner is a result of the effective grounding of the low-voltage terminal through the surge impedance R of the connected low-voltage line. It is entirely independent of the decrease in voltage at points due to the voltage divider effect inherent in a capacitance network. Fig. 6(A) represents the effective circuit seen by a surge applied to the high-voltage line terminal. To the right there is the capacitance network to ground of the high-voltage winding. This network determines the initial voltage distribution in the high-voltage winding itself. The circuit to the left of the high-voltage line determines the surge transfer between windings. The capacitance network beyond C_{HL} is represented by a box which contains the various coil-to-coil, coil-to-ground, and winding-to-winding capacitances of the low- and tertiary voltage windings. Considering only the portion of the circuit involved in electrostatic surge transfer and representing the low- and tertiary voltage capacitance network by a single capacitance C_G to ground, there results the simple circuit of Fig. 6(B). Point H represents the high-voltage line and its static plate, and point L represents the low-voltage line and its static plate. Any effect produced at L will be produced proportionately at all other points of the capacitance network, which can be considered as a capacitance voltage divider. It is therefore necessary only to determine the effect of the surge impedance R at point L.

In the Appendix it is shown that when a uniformly rising surge front is applied to the high-voltage terminal the voltage E_L attained at L when a voltage E_H is reached at H after time T, is given by

$$E_L = K_C S(x) E_H$$

where

$$K_C = \frac{C_{HL}}{C_G + C_{HL}}$$

$$S(x) = \frac{1-\epsilon^{-x}}{x}$$

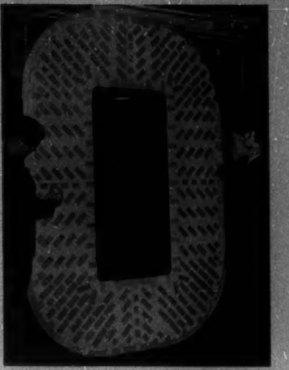

Fig. 3. Static plate for 450-basic impulse insulation winding of 90,000-kva power transformer

$$x = \frac{T}{R(C_G + C_{HL})}$$

The factor K_C represents the reduction in voltage at L due to the capacitance divider effect of the capacitance network. The factor $S(x)$ is the shielding factor and is a function of the ratio of the time to crest T of the applied wave to the time constant $R(C_G+C_{HL})$ of the resistance capacitance network. This shielding factor is plotted in Fig. 7 for values of x in the range occurring in power transformers.

Just as a rapidly rising front produces a positive crest at L, a rapidly decreasing tail will produce a negative crest at L. It is therefore necessary to consider the effective shielding to the decrease in voltage after the crest has been reached. If, after the wave applied at H has increased uniformly to E_H in time T, it is uniformly decreased to zero in the additional time T' the voltage E_L after time $T+T'$ can be expressed as

$$E_L(T+T') = -K_C S(x, x') E_H$$

where

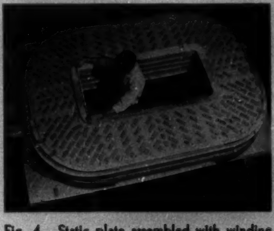

Fig. 4. Static plate assembled with winding group

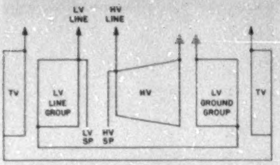

Fig. 5. Winding grouping of a double-wye-delta transformer

$$S(x,\, x') = S(x') - S(x)\epsilon^{-x'}$$

$$x' = \frac{T'}{R(C_G + C_{HL})}$$

The factor $S(x,x')$ is the effective shielding factor for the tail of the wave applied to the high-voltage terminal. The extreme case, that of instantaneous chopping, corresponds to $x'=0$. This yields

$$S(x,\, x')_{x'=0} = 1 - S(x)$$

which is also plotted in Fig. 7.

For the special case where $R=0$, such as would occur if a static plate were connected to a solidly grounded neutral, both shielding factors are zero corresponding to complete isolation.

These shielding factors have been evaluated under the assumption of a pure capacitance network and are therefore most accurate for very short wave fronts or impulses. However, the most severe electrostatic stresses are produced by surges of this type.

Control of Initial Distribution of Multigroup Windings

Under normal conditions the initial distribution within shell form windings is fairly uniform. This is because of the small number of large surface area coils used within the windings, with its resulting low ratio of ground capacitance to series capacitance. Under certain special conditions small portions of a winding may be separated from the main body of the same winding. For example, in Fig. 8(A) there is shown an arrangement of windings in which the first two coils of the high-voltage winding are separated from the body of the high-voltage wye-winding by a portion of the low-voltage delta winding. In this special arrangement there exist, as shown in Fig. 8(A), two fairly large capacitances to ground, C_{1G} and C_{2G}, on either side of the series connection S. These capacitances tend to lower the initial per-cent voltage at point S when surges are applied to the high-voltage line terminal. Since coils 1 and 2 represent a small portion of the total high-voltage winding, the point S in the final voltage distribution will tend to approach line voltage. It is therefore desirable to raise the initial voltage of S and thus avoid the initial voltage distortion as well as the subsequent winding oscillation. Since, again, the capacitances C_{1G} and C_{2G} are concentrated at the ends of the winding groups, they can be counteracted by properly located static plates as indicated in Fig. 8(B). The static plate at X is connected to the high-voltage line terminal and it tends to raise the initial electrostatic potential of coil 2 and the series connection S. The static plate at Y redistributes this rise in potential of the series connection over the face of the first and subsequent coils of the body of the high-voltage winding.

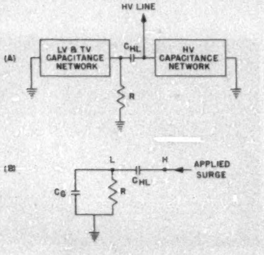

Fig. 6. Simplified networks for double-wye-delta transformer

Summary

Proper application of static plates in the interleaved shell form-fit transformer gives the designer a large measure of control over initial electrostatic voltage distributions. This control can be exercised over electrostatic surge transfer between the windings as well as electrostatic distributions within individual windings. The concentration of mutual capacitance coupling at the ends of windings or winding groups in the interleaved shell construction greatly facilitates the control of surge transfer between windings by means of static plates.

Appendix. Derivation of Equations

Using the Heaviside notation, the operational form $E_L'(p)$ of the voltage appearing at L in Fig. 6(B) due to a rectangular wave of amplitude E_H applied at H can be written[6]

$$E_L'(p) = \frac{pRC_{HL}}{pR(C_G + C_{HL}) + 1} E_H 1$$

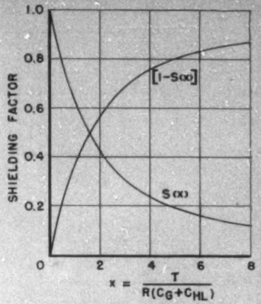

Fig. 7. Variation of shielding factors

The solution of this is

$$E_L'(t) = E_H\left(\frac{C_{HL}}{C_G + C_{HL}}\right)\epsilon^{-\frac{t}{R(C_G+C_{HL})}}$$

The voltage $A(t)$ at L for unit voltage at H is

$$A(t) = \left(\frac{C_{HL}}{C_G + C_{HL}}\right)\epsilon^{-\frac{t}{R(C_G+C_{HL})}}$$

The voltage $E_L(t)$ at L due to a voltage $e_H = E_H t/T$ applied at H can be evaluated by the superposition theorem

$$E_L(t) = e_H(0)A(t) + \int_0^t A(t-\lambda)e_H'(\lambda)d\lambda$$

$$E_L(t) = \frac{E_H}{T}\left(\frac{C_{HL}}{C_G + C_{HL}}\right)\epsilon^{-\frac{t}{R(C_G+C_{HL})}} \times \int_0^t \epsilon^{\frac{\lambda}{R(C_G+C_{HL})}} d\lambda$$

$$E_L(t) = E_H\left(\frac{C_{HL}}{C_G + C_{HL}}\right)\frac{R(C_G + C_{HL})}{T} \times \left(1 - \epsilon^{-\frac{t}{R(C_G+C_{HL})}}\right)$$

When the point H reaches a value of E_H after time T the value of E_L will be

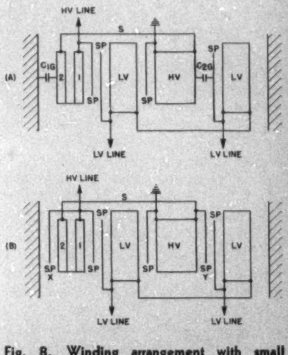

Fig. 8. Winding arrangement with small portion separated from body of winding

$$E_L=E_L(T)=E\left(\frac{C_{HL}}{C_G+C_{HL}}\right)\times\left(\frac{1-\epsilon^{-\frac{T}{R(C_G+C_{HL})}}}{\frac{T}{R(C_G+C_{HL})}}\right)$$

This can be written as

$$E_L=E_HK_CS(x)$$

where

$$K_C=\frac{C_{HL}}{C_G+C_{HL}}$$

$$S(x)=\frac{1-\epsilon^{-x}}{x}$$

$$x=\frac{T}{R(C_G+C_{HL})}$$

If after reaching the crest value E_H the applied wave were to decrease uniformly to zero in the additional time T', the resulting value of E_L for $T<t<T+T'$ would be by superposition

$$E_L(t)=E_HK_C\left(\frac{1-\epsilon^{-\frac{t}{R(C_G+C_{HL})}}}{x}-\frac{1-\epsilon^{-\frac{(t-T)}{R(C_G+C_{HL})}}}{x}-\frac{1-\epsilon^{-\frac{(t-T)}{R(C_G+C_{HL})}}}{\frac{T'}{R(C_G+C_{HL})}}\right)$$

Simplifying and defining x' as

$$x'=\frac{T'}{R(C_G+C_{HL})}$$

$$E_L(t)=E_HK_C\times\left(\frac{\epsilon^{-\frac{t-T}{R(C_G+C_{HL})}}-\epsilon^{-\frac{t}{R(C_G+C_{HL})}}}{x}-\frac{1-\epsilon^{-\frac{t-T}{R(C_G+C_{HL})}}}{x'}\right)$$

For $t=T+T'$ this reduces to

$$E_L(T+T')=E_HK_C\left(\frac{\epsilon^{-x'}(1-\epsilon^{-x})}{x}-\frac{1-\epsilon^{-x'}}{x'}\right)$$

or, with the use of the previously defined function $S(x)$

$$E_L(T+T')=-E_HK_C[S(x')-S(x)\epsilon^{-x'}]$$

References

1. Improved Core Form Transformer Winding, E. J. Grimmer, W. L. Teague. *AIEE Transactions*, vol. 70, pt. I, 1951, pp. 962–67.

2. Electrostatic Voltage Distribution and Transfer in 3-Winding Transformers, P. A. Abetti. *AIEE Transactions*, vol. 73, pt. III-B, Dec. 1954, pp. 1407–16.

3. Surge-Proof Transformers, H. V. Putman. *AIEE Transactions*, vol. 51, Sept. 1932, pp. 579–600.

4. Effect of Transient Voltages on Power Transformer Design, K. K. Palueff. *AIEE Transactions*, vol. 48, July 1929, pp. 681–706.

5. Operational Circuit Analysis (book), V. Bush. John Wiley & Sons, Inc., New York, N. Y., 1937.

◆

Discussion

P. A. Abetti (General Electric Company, Pittsfield, Mass.):

Electrostatic and Initial Voltage Distribution

The authors apparently use the terms "electrostatic voltage distribution" and "initial voltage distribution" without differentiation. It will be well therefore to clarify the theoretical and practical difference between the two, by defining both terms unequivocally.

The electrostatic distribution in a transformer is defined as the distribution which is determined exclusively by the electrostatic field, that is, only by the capacitances of the transformer structure. As is well known, transformers comprise self-inductances, mutual inductances, resistances, and conductances, in addition to capacitances. Therefore, rigorously speaking, the electrostatic distribution cannot be measured in a transformer. An electrostatic distribution very similar to it can be measured, however, on a network of lumped capacitors, such as the capacitance board of an electromagnetic model,[1] or on a network of lumped resistors, such as the d-c board which has been used for 20 years in Pittsfield.

The initial voltage distribution is defined as the voltage distribution measured on an actual transformer, or on an electromagnetic model, at very short times after the application of a steep-fronted impulse voltage. Since the term "short time" is open to different interpretations, it will be useful to explain how this distribution is measured in practice. A steep-fronted wave is applied to the line end of a transformer winding, Fig. 9, $x = 100$ per cent (%) and oscillograms of voltage versus time are taken at various points along the impulsed winding or other windings. For instance, assume that an oscillogram was recorded at the mid-point of the impulsed winding, Fig. 9, $x = 50\%$. We now pick out a time t_0, less than the time τ_f at which the applied wave reaches crest, and measure the applied voltage at that time AB, Fig. 9, and the voltage at $x = 50\%$, AC, Fig. 1, at the same time. The ratio of the segments AC/AB is defined as the initial distribution measured at the time t_0. It is necessary to specify the time t_0 of measurement since both theory and experience show that the value of the ratio AC/AB depends upon the time of measurement.

If for simplicity we consider only applied waves with linear fronts of length τ_F, it can be shown that the difference between the electrostatic and the initial distribution 1. does not depend upon the length of the front of the applied wave, 2. increases with the time t_0 ($t_0 \leqq \tau_F$) of measurement, and 3. increases with the fundamental frequency of oscillation of the winding on which the measurement is made.

It is clear therefore that the electrostatic and the initial voltage distributions would rigorously coincide only if measurements were made at $t_0 = 0$, which is impossible in practice. The choice of the finite time of measurement t_0 is the result of a compromise. In fact, to approach as closely as possible the electrostatic distribution, the time t_0 should be as small as possible. However, if t_0 is small the segments AB and AC are short, and they cannot be scaled accurately on the film because the thickness of the trace is constant. Therefore the segments AB and AC should be as long as possible, which would require steep fronts and large values of t_0. It also follows that shorter times t_0 should be used for low-voltage windings than for high-voltage windings. It can be concluded that the choice of the time of measurement t_0 is best left to the judgment of the specialists in measurements with the transient analyzer. It may be added that in long-time scale models[3] extremely short equivalent fronts can be obtained and times t_0 of the order of 1/100 of a microsecond. Also in long-time scale models greater accuracy in scaling the film is obtained by accurate amplification of the measured voltages, so that the oscillograms cover the whole screen.

Calculation of Effective Capacitance

Considering now Fig. 6 it is evident that the shielding factor controlled by the static plate refers to the initial and not to the electrostatic voltage distribution, which rigorously corresponds to an infinitely steep front or to $R = \infty$. For the electrostatic distribution the shielding factor is always $S'(x) = 1$. To compute the shielding factor for the initial distribution it is necessary to know the values of the capacitances C_{HL} and C_G indicated in Fig. 6. While the computation of the first from the design data presents no difficulties, the second is actually an effective capacitance, for which the authors do not give any method of computation. Since C_G enters into the factor K_C in the equation for the voltage E_L at the low-voltage terminals, it is very important to compute C_G accurately, and this will be attempted here. Considering for simplicity a 2-winding transformer, we will assume at first that the low-voltage winding is uniform and comprises an infinite number of coils. This second assumption is evidently incorrect, since there are only a few coils in the low-voltage groups, and will be removed later. For an infinitely large number of coils, if C_L is the total series capacitance between coils and C_{LG} the total capacitance to ground, the electrostatic voltage distribution in the low-voltage winding is

$$E_L(x)=K_C\frac{\sinh \alpha x}{\sinh \alpha} \tag{1}$$

where

$$\alpha=\sqrt{C_{LG}/C_L} \tag{2}$$

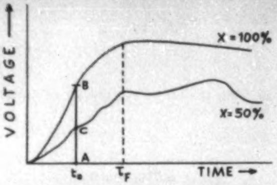

Fig. 9. Voltages versus time measured at the line end, (x = 100%), and at mid-point, x = 50%, of a transformer winding

and x is the distance from the low-voltage neutral end. The well-known saw-tooth pattern due to the turn-to-turn capacitances, which may increase the voltages between coils, but which has little effect on the effective capacitance, is ignored here.

The effective capacitance is defined as the capacitance of a single capacitor which will store the same energy as the low-voltage capacitance network, if the voltage $E_L(0)$ is applied to it. The energy stored in the low-voltage capacitance network is

$$W=\frac{1}{2}C_{LG}\int_0^1 E^2_L(x)dx+\frac{1}{2}C_L\int_0^1\left[\frac{dE(x)}{dx}\right]^2dx \tag{3}$$

which yields

$$W=\frac{1}{2}\frac{K_C^2}{\sinh^2\alpha}\left[\frac{C_{LG}}{2\alpha}(\sinh\alpha\cosh\alpha-\alpha)+\frac{\alpha^2C_L}{2\alpha}(\sinh\alpha\cosh\alpha+\alpha)\right] \tag{4}$$

or, substituting equation 2

$$W=\frac{1}{2}K_C^2\frac{C_{LG}}{\alpha}\operatorname{cotanh}\alpha \tag{5}$$

so that

$$C_{eff}=\frac{C_{LG}}{\alpha}\operatorname{cotanh}\alpha=\alpha C_L\operatorname{cotanh}\alpha=\sqrt{C_{LG}C_L}\operatorname{cotanh}\alpha \tag{6}$$

For $\alpha>3$, cotanh α can be assumed equal to unity and the familiar equation[3] for C_{eff} is obtained.

Since the energy stored must be equal to the energy delivered, and the applied voltage is the same, the current flowing into C_{eff} must be the same as the current flowing into the low-voltage capacitance network. This yields

$$C_{eff}=\frac{C_L}{E_L(0)}\left.\frac{dE_L(x)}{dx}\right|_{x=0}=\alpha C_L\operatorname{cotanh}\alpha \tag{7}$$

This second method will be used to determine the effective capacitance when the number N of low-voltage coils is small. It can be shown[4] that the voltage at the mth coil ($0\leqq m\leqq N$) is given by

$$E_L(m)=K_C\frac{\sinh\alpha'\frac{m}{N}}{\sinh\alpha'} \tag{8}$$

with

$$\alpha'=2N\sinh^{-1}\frac{\alpha}{2N} \tag{9}$$

The effective capacitance is then

$$C_{eff}=N\frac{C_L}{E_L(N)}[E_L(N)-E_L(N-1)]=NC_L\left(1-\frac{\sinh\alpha'\frac{N-1}{N}}{\sinh\alpha'}\right) \tag{10}$$

which yields

$$C_{eff}=NC_L\left[1-\cosh\frac{\alpha'}{N}-\operatorname{cotanh}\alpha'\sinh\frac{\alpha'}{N}\right] \tag{11}$$

It is easily verified that equation 9 for $N=\infty$ takes as limiting value

$$\lim_{N\to\infty}\alpha'=\alpha \tag{12}$$

and consequently the limit of equation 11 for $N=\infty$ is, recalling equation 2,

$$\lim_{N\to\infty}C_{eff}=NC_L\frac{\alpha'}{N}\operatorname{cotanh}\alpha'=\frac{C_{LG}}{\alpha}\operatorname{cotanh}\alpha=\alpha C_L\operatorname{cotanh}\alpha \tag{13}$$

in agreement with equations 6 and 7.

References

1. Transformer Models for the Determination of Transient Voltages, P. A. Abetti. *AIEE Transactions*, vol. 72, pt. III, June 1953, pp. 468–80.

2. Long-Time-Scale Models of Transformers for the Determination of Transient Voltages, P. A. Abetti, H. B. Belck. *AIEE Transactions*, vol. 73, pt. IIIA, Apr. 1954, pp. 345–53.

3. Abnormal Voltages Within Transformers, L. F. Blume, A. Boyajian. *AIEE Transactions*, vol. 38, pt. I, 1919, pp. 577–614.

4. *Discussion* by P. A. Abetti of Voltage Divider for Measuring Impulse Voltages on Transmission Lines, S. B. Griscom, B. L. Lloyd, A. R. Hileman. *AIEE Transactions*, vol. 73, pt. IIIA, Apr. 1954, pp. 235–37.

Saul Bennon, R. J. Cossaart: Mr. Abetti has raised two pertinent questions relating to surge voltage analysis. The first is the distinction between "electrostatic" and "initial" voltage distributions. The term "electrostatic distribution" refers to the distribution produced in the equivalent capacitance network of the transformer by a sheer fronted rectangular wave. It is admittedly a theoretical concept for two reasons. First, the capacitance network cannot be entirely divorced from the actual conducting elements of the windings and, second, it is impossible to generate a sheer front wave, that is, one rising to crest in zero time. The term "initial distribution" has, on the other hand, been used rather loosely in the past to refer to either the electrostatic distribution mentioned or the actual distribution at very short times after the application of steep-fronted surges. The reason for this ambiguity lies in the origin of the term "initial distribution." Historically, it stems from the analytical methods developed for the study of surge oscillations in transformer windings. In the standing-wave method the winding response is analyzed in terms of an initial distribution and a final distribution of voltage within a winding. The difference between these distributions results in the harmonic components of oscillation. In this method of approach the initial distribution has generally been calculated from the capacitance network assuming a theoretical sheer-front wave.

If the term "initial distribution" is restricted to refer only to the actual distribution existing at short times following the application of surge voltage, as suggested by Mr. Abetti, there will be differences, between the two distributions. Mr. Abetti has covered these very thoroughly in his discussion. In actual design practice, however, the use of the electrostatic network and a theoretical sheer-front wave to estimate the actual voltages at short times represents a conservative approach. This is true because, as pointed out in the paper, the maximum crest surges which appear at transformer terminals in service will usually have the steepest fronts, and also the actual distribution will usually, be less than that calculated in this manner.

The second point raised by Mr. Abetti is the method used to evaluate C_G in the shielding factor equation. This was not covered in the paper because it was somewhat beyond its intended scope. Nevertheless, it represents an actual design problem and therefore merits consideration. In the interleaved shell form-fit construction the number of coils in any one low-voltage group will be relatively small. It will generally vary from two to six coils. Since each pair of coils determines one series capacitance the number of series capacitance elements will vary from one to three. For example, in Fig. 1(A) two series capacitances are shown which corresponds to a 4-coil low-voltage group. Because of the small number of capacitances involved, the simplest approach is usually direct network reduction. For the most part this merely involves a sequence of series and parallel combinations of capacitance elements. For cases where larger numbers of coils are involved the equations presented by Mr. Abetti could be used to advantage in evaluating the effective capacitance.

Lightning Protection in a 24-Kv Station—Field and Laboratory Studies

H. R. ARMSTRONG
MEMBER AIEE

R. W. FERGUSON
ASSOCIATE MEMBER AIEE

A. R. HILEMAN
ASSOCIATE MEMBER AIEE

THE results of synchronograph field tests and Anacom laboratory studies on a 24-kv multiline bus are presented. Previous studies[1-4] on higher voltage stations indicated the influence of multiple lines on the surge voltage at the bus and the connected transformer. Extrapolation of these data to lower voltage systems seemed questionable, however, because of material differences in the station circuit constants. This study extends the station surge performance data down to the 24-kv level and provides additional verification of the miniature system method by means of synchronograph field tests.

The results of the study are discussed in three parts:

1. Anacom study for shielded lines.
2. Anacom study for unshielded lines.
3. Comparison of Anacom and synchronograph results.

Station Layout

The investigation was confined to one multiline bus of a large 24-kv multibus station. In Fig. 1 the major dimensions are shown for the 9-line bus with supplying transformer. The connected lines are open wire on wood poles and are assumed to be, for the purpose of the problem, either shielded or unshielded. On this effectively grounded 24-kv system it is possible to use 20-kv lightning arresters with 150-kv basic-impulse-insulation-level (BIL) transformer insulation. At voltages 100 kv and above, the ratio of the transformer BIL to arrester discharge voltage at 5,000 amperes discharge current is usually of the order of about 1.6, as compared to a ratio of greater than 2 for the 24-kv system. In terms of the simple 1-line arrester-transformer case, the larger ratio tends to permit a greater separation distance between the arrester and the transformer. However, as the system voltage decreases, the ratio of the transformer BIL to the rate of rise of the incoming surge voltage increases, which tends to permit a smaller separation distance. The combination of these two factors causes a decrease in the allowable transformer-to-arrester separation distance as the system voltage decreases.[5,6,7] For the case of the compact bus with multiple lines, the modification of the incoming surge by the bus and any possible arrester spark-over add an additional significant factor. The net result is a shift in importance of the application factors when considering lightning protection of stations in the subtransmission voltage range

Wave Shape and Magnitude of Incoming Surge

The degree of lightning protection required for adequate protection of station equipment is dependent on whether or not the connected overhead lines are adequately shielded. Low-voltage stations frequently have unshielded connected lines. However, shielding of low-voltage circuits is becoming increasingly prevalent in the industry and therefore both situations are analyzed.

STATION WITH SHIELDED OVERHEAD LINES

Lightning surges which can be hazardous to electric equipment can originate in two ways:

1. Backflash—strokes terminating on the line-shielding system and possessing sufficient magnitude to cause a flashover of the line insulation.
2. Sideflash or shielding failure—strokes terminating directly on the phase conductor.

Induced voltages on the phase conductor, resulting from strokes terminating on the overhead ground wire but possessing insufficient current to cause flashover of the line insulation, produce surge voltages within the station which are of much lower severity than the aforementioned two types of waves.[4] Therefore, this case of induced or coupled voltages will not be considered in the formulation of lightning protection.

The afore-mentioned two types of strokes can terminate anywhere along the incoming line or within the station. Because the station is well shielded and the grounding resistance is very low, it is assumed that there is practically no possibility of a sideflash or shielding failure within the station. It is recognized that strokes terminating immediately adjacent to the station are more hazardous to station equipment than strokes which terminated distant from the station. However, the probability of occurrence of a sideflash or backflash within 1 mile of the station on a well-shielded line with low pole-grounding resistance is so low that it is uneconomical and unrealistic to provide protection based on this condition if maximum protection is to be attained at minimum cost.[4] Therefore, the following discussion is based on strokes terminating 1 mile or more from the station.

Traveling voltage waves arriving at the station entrance over 1 mile of line can be classified into two general types: long-tail waves and short-tail waves. The long-tail waves result from a sideflash where the stroke current is insufficient to cause flashover to the pole down lead. Short-tail waves result either from a backflash or from a sideflash where the stroke current is sufficient to cause flashover to the pole down lead. These two types of waves and their probability of occurrence will be discussed to determine the proper wave shape and magnitude of the incoming surge voltage.

Long-tail waves

Sideflashes seldom occur on a well shielded system, but when they do there usually will be a flashover to the pole down lead which diverts the surge current to ground. This results in a wave chopped at a time as determined by the time-lag curve of the line insulation. The insulation of the line, here considered, consists of wood and post-type insulators whose time-lag curve is assumed to be the same as given in reference 8. Recent high-voltage surge tests on transmission lines[9] showed that chopped waves will attenuate more rapidly than full waves. Chopped waves upon reaching the station over 1 mile of line will closely approximate the wave shape and magnitude of a surge resulting from a backflash. Therefore, sideflashes which possess sufficient current to cause flashover to the pole ground will be considered along with backflashes.

The magnitude of the full wave caused by a side flash is limited to the full-wave insulation strength of the line insulation or 750 kv. Assuming the stroke current wave shape to be 4x40 microseconds (ms),[8] the voltage on the conductor will have

---

Paper 55-556, recommended by the AIEE Protective Devices Committee and approved by the AIEE Committee on Technical Operations for presentation at the AIEE Summer General Meeting, Swampscott, Mass., June 27–July 1, 1955. Manuscript submitted March 30, 1955; made available for printing May 12, 1955.

H. R. ARMSTRONG is with The Detroit Edison Company, Detroit, Mich., and R. W. FERGUSON and A. R. HILEMAN are with the Westinghouse Electric Corporation, East Pittsburgh, Pa.

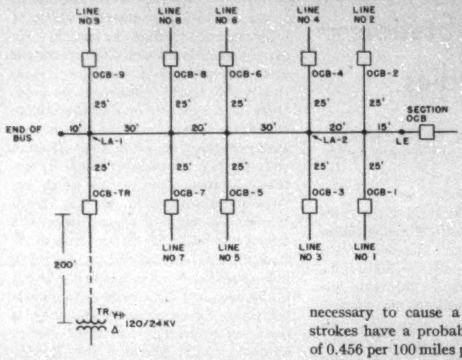

Fig. 1. Single-line diagram of 24-kv station showing circuit feet between junctions

the same shape. The stroke current necessary to raise the conductor to the BIL of the line is 3,700 amperes, based on a 400-ohm line. The lower limit of voltage on the phase conductor, below which it is inconceivable that damage to station apparatus could result, is set somewhat arbitrarily at 100 kv which requires a stroke current of 500 amperes.

Lightning strokes in the 500- to 3,700-ampere range are found from the probability curve to make up 20 per cent of the total strokes.[8] Because the isokeraunic level (IKL) is 35 thunderstorm days per years in the area where this system is located, stroke incidence is expected to be about 117 strokes per 100 miles of transmission line per year.[8] Since shielding failures on well-shielded lines occur for only 0.1 per cent of all the strokes to the transmission line, the probability of obtaining a full or long-tail wave on a phase conductor is 0.023 per 100 miles per year or once in 4,350 years for any 1 mile of line.

Short-tail waves

For the line here considered, a stroke current of 145,000 amperes or more is necessary to cause a backflash. These strokes have a probability of occurrence of 0.456 per 100 miles per year for an IKL of 35.[8] To this should be added the probability for the case of a sideflash where the stroke current is 3,700 amperes or greater so as to produce chopped waves on the phase conductor. These strokes have a probability of occurrence of 0.094 per 100 miles per year. Adding these two values, the total probability of obtaining short-tail waves is 0.550 per 100 miles per year or once in 182 years for any 1 mile of line.

It is apparent that the probability of obtaining a short-tail wave is about 22 times as great as for the full or long-tail waves. Because of this fact, and because the probability of obtaining a full wave is small, it was decided to base this study of lightning protection for stations with shielded overhead lines on the case of a short-tail surge arriving at the station entrance.[1,2,3]

The characteristics of the incoming surge were based on the case of a backflash, the probability of occurrence being higher for this phenomena. Other assumptions which influence the selection of the wave shape used were:

1. Pole-grounding resistance, 10 ohms.
2. Span length, 200 feet.
3. Insulation strength of the wood and post-type insulators, 750 kv, wet.
4. Stroke current wave shape, 4x40 ms.
5. Coupling factor between the ground wire and phase conductor, 23 per cent.

The incoming wave shape and magnitude are based on a stroke current of 160,000 amperes which results in flashover to the phase conductor but is just insufficient to cause a second flashover at an adjacent pole.[8,10] The voltage on the phase conductor is composed of two components: the coupled voltage of 276 kv which is placed on the phase conductor before flashover and the much higher component which appears after the ground-wire voltage backflashes to the phase conductor and applies the pole-top or ground-wire potential of 1,200 kv to the phase conductor. The wave shape of the pole-top potential was obtained from oscillograms from the Anacom study used to estimate lightning performance of distribution lines.[8] As the voltage wave travels along the line, it will be reduced in magnitude and changed in shape by two phenomena: decrease in ground-wire current and corona. Generally, the ground-wire voltage will be essentially zero within two span lengths of the struck point. Based on mathematical analysis, the coupled voltage on the phase conductor before flashover vanishes and the phase conductor voltage after flashover is reduced by approximately 20 per cent when the ground wire voltage vanishes.[10] Attenuation and distortion of the wave caused by corona can be evaluated from recent high-voltage tests.[9] The phase conductor voltage which has been reduced only by the decrease in ground-wire current is shown by the solid line of Fig. 2. Assuming a negative polarity wave, the dotted line is the voltage which enters the station after traveling 1 mile, as evaluated by use of attenuation and distortion data of a 0.927-inch conductor.[9] Therefore, based on a surge originating from a stroke of 160,000 am-

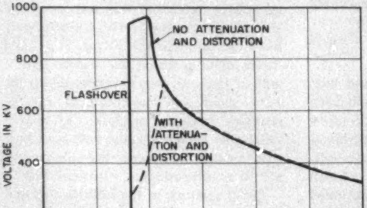

Fig. 2 (left). Attenuation and distortion of surge voltage caused by corona[9]

Fig. 3 (right). Discharge characteristics of a 20-kv line-type lightning arrester subjected to a 5,000-ampere 10x20-ms current wave with test data from analogue indicated

– Actual characteristics
0 Test points from analogue

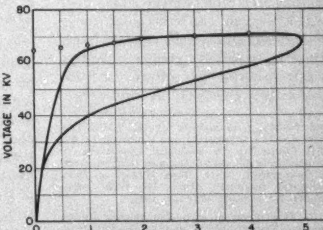

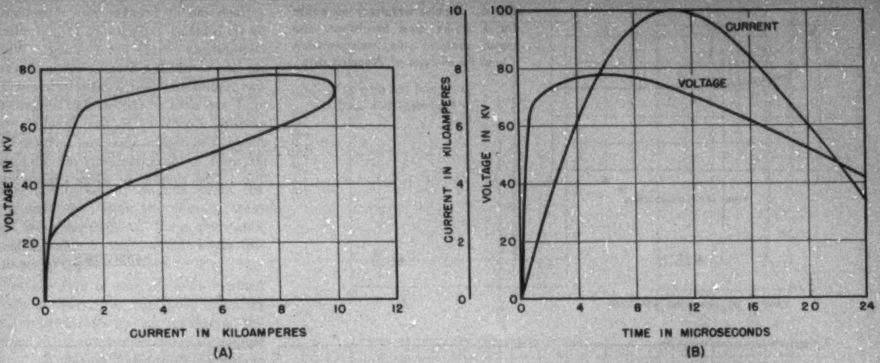

Fig. 4. Discharge characteristics of a 20-kv line-type lightning arrester for a 10,000-ampere 10x20-ms discharge current

A—Volt-ampere characteristic B—Discharge current and voltage

peres at a point 1 mile from the station, a 700-kv surge having a wave shape of approximately 1.5x8 will arrive at the station.

Station with Unshielded Overhead Lines

For the case of a station with unshielded incoming lines, the current discharges through the surge impedance of the lines. Therefore, relatively low-current magnitudes are required to produce high surge voltages. This is in contrast to the high currents necessary to produce backflash in the case previously considered for a station with shielded overhead lines where the current discharges through the down lead and grounding impedance which is relatively low. Because the probability of occurrence of low-current magnitude strokes is high, protection of station equipment is based on a stroke terminating immediately adjacent to the station.

The most severe voltages at the station are produced when the line does not flash to ground and most of the surge current is discharged by the lightning arrester at the station. Thus, the characteristics of lightning-arrester discharge currents can be used as a guide in selecting a suitable surge current magnitude and wave shape. The largest arrester discharge current measured in field investigations on a 25-kv system was 10,000 amperes and the highest rate of rise of arrester discharge current was between 5,000 and 5,500 amperes per ms.[11] In another study of discharge currents in distribution arresters[12] in which the system voltages ranged from 120 to 24,000 volts, the maximum arrester discharge current recorded was estimated to be about 25,000 amperes. However, only 5 per cent of the records exceeded 10,000 amperes. Field investigations on arresters in substations[13] which were largely composed of voltage classes from 22 to 44 kv show a maximum arrester discharge current of 10,000 amperes. The maximum front of the discharge current for currents above 5,000 amperes is 1.5 ms and the average front is about 3.0 ms.

From these field investigations, the decision was made to base the formulation of lightning protection for the 24-kv station with unshielded lines on a stroke current of 10,000 amperes crest having a rate of rise of 4,000 amperes per ms terminating immediately adjacent to the station. These assumptions are consistent with the previous published paper by R. L. Witzke and T. J. Bliss[14] which has received general acceptance in the industry. This paper should be consulted for a more complete discussion of the justification of the assumptions.

Anacom Study

Techniques used in handling power system problems on the Anacom have been given in detail in previous literature.[1,2,5,14] Briefly, the principle is to set up the circuit in miniature on the computer, using an appropriate time base and an impedance multiplier. A low-voltage surge is then applied repetitively to the computer circuit and the resultant voltages are measured by an oscillograph.

One phase of the 24-kv station, shown in Fig. 1, was set up on the Anacom. The distributed constants of the bus structure were represented by pi-sections whose inductance and capacitance were determined from the surge impedance and velocity of surge propagation, 400 ohms and 1,000 feet per ms respectively. Lengths of bus from 10 to 25 feet were represented by single pi-sections and capacitances of bus support insulators, obtained from field measurements, were included in the Anacom circuit.

Table I. Assumed Spark-Over Voltages for 20-Kv Line-Type Lightning Arresters

Voltage Rate of Rise,* Kv per ms	Spark-Over Voltage, Kv
250 or below	83
250 to 400	90
400 to 500	95

* Standard test voltage rate of rise is 167 kv per ms which gives a spark-over voltage of 83 kv.

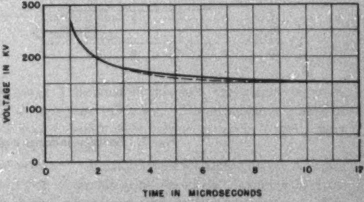

Fig. 5. Impulse withstand curve for 23-kv bushings showing representation used for analysis of Anacom data

— Actual curve
- - - Representation used

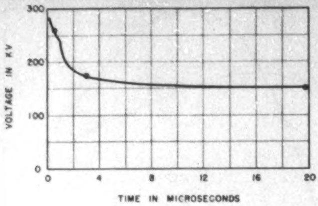

Fig. 6. Impulse withstand test points for a 25-kv class transformer and curve showing the representation used for analysis of Anacom data

0 Actual test points
– Representation used

Each circuit breaker was represented by its bushing capacitance of 300 micromicrofarads (mmf) per bushing. When the line to which a breaker was connected was assumed opened, a capacitance of 300 mmf was used as the breaker equivalent circuit. Likewise, if the breaker was closed, the capacitance was increased to 600 mmf, or the capacitance of both bushings. The equivalent surge capacitance

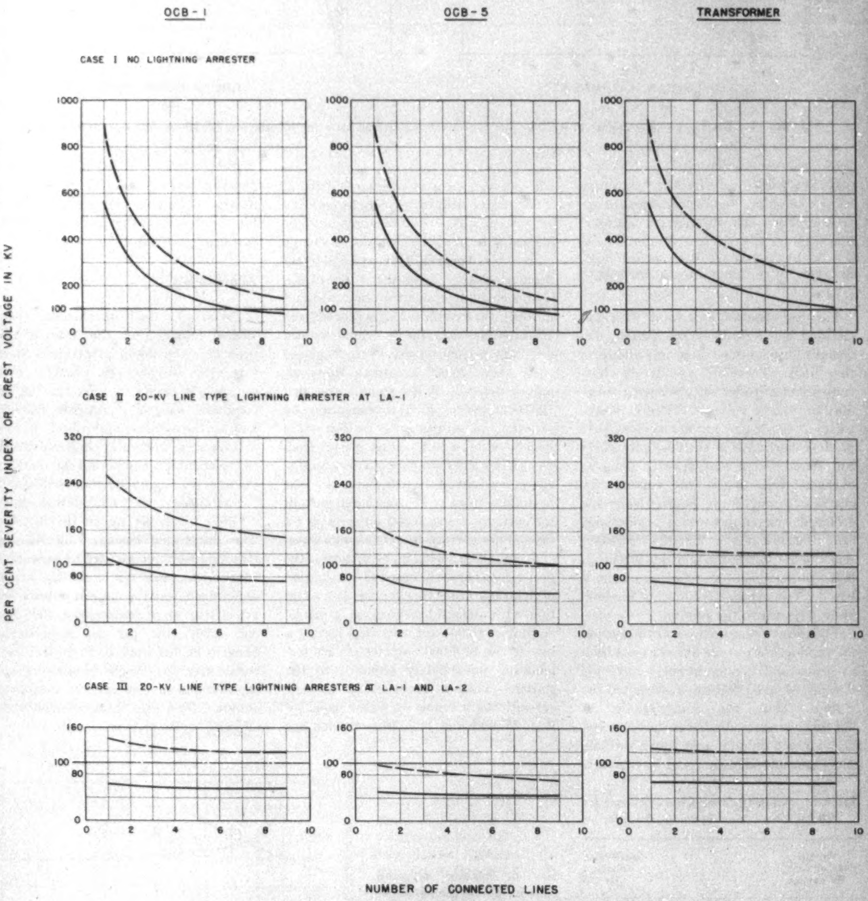

Fig. 7. Severity indexes and crest voltages for stations with shielded overhead lines

—— Severity index
- - - - Crest voltage

of the transformer was estimated to be about 2,000 mmf. This value will vary with the form of transformer construction; in general the shell form have a higher value than the core form. However, this value of capacitance is fairly representative. Since transmission lines connected to the bus were assumed to be so long that reflections from the far end would not return in time to affect the surge voltages within the station, these lines were represented by a resistance equal in value to the 400-ohm surge impedance of the line.

For the case of stations with shielded overhead lines, the lightning arresters were represented by an analogue described in previous papers on protection of extra-high-voltage stations.[1,2] Discharge characteristics of the analogue and of a 20-kv line-type lightning arrester subjected to a 5,000-ampere 10x20 ms current surge are compared in Fig. 3.

For the case of stations with unshielded overhead lines, the lightning-arrester discharge voltage was held constant at 78 kv, a value corresponding to a 10,000-ampere discharge current. Assuming a constant stroke current of 10,000 amperes, the amount of current discharged by the arrester will vary with the number of connected lines. This varies from approximately 8,000 to 10,000 amperes for nine lines and one line connected respectively. Also when two arresters are in service, the first arrester that the surge meets will discharge the larger current. However, the surge can initially arrive at either arrester depending on the line from which the surge is assumed to originate. Considering these factors, it was decided to hold a constant arrester discharge voltage of 78 kv, which is the same as assuming a constant discharge current of 10,000 amperes through all arresters. This will lead to conservative results.

Since the lower part of the lightning-arrester volt-ampere curve could not be obtained with either of the analogues used, voltages at the arrester locations were held higher on the tail of the surge by the analogue than would be the case in practice. This is especially true in case of stations with unshielded lines and should be taken into account when evaluating the severity of surge voltages at equipment terminals. Fig. 4 shows the discharge characteristics of the 20-kv line-type lightning arrester for a 10,000-ampere 10x20 ms discharge current. The analogue held a constant voltage of 78 kv; however, actually, because of the discharge characteristics, the voltage at 24 ms is reduced to 54 per cent of its crest value.

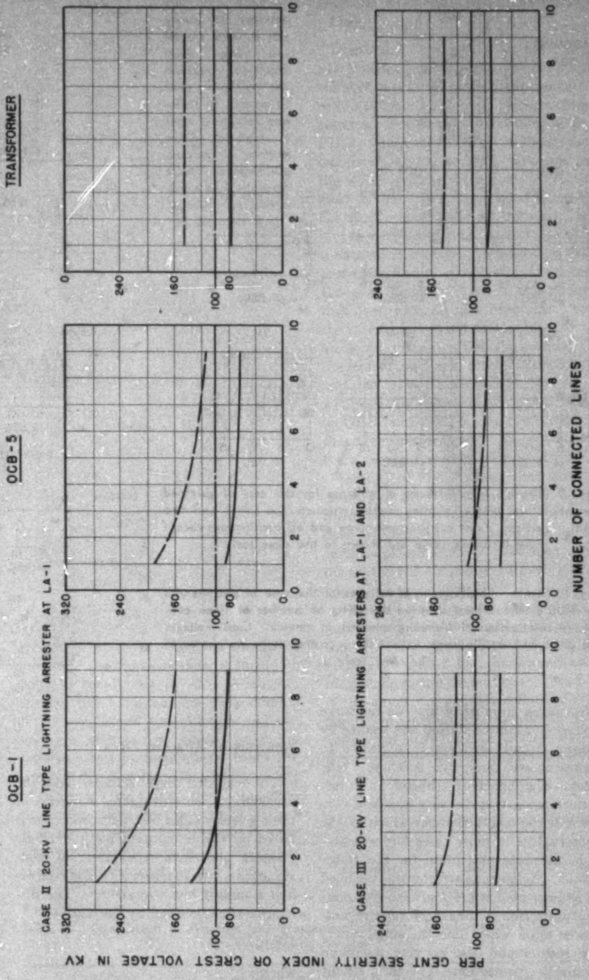

Fig. 8. Severity indexes and crest voltages for stations with unshielded overhead lines

—— Severity index
---- Crest voltage

The rate of rise of voltage at lightning-arrester locations (*LA-1* and *LA-2* of Fig. 1) varies with the number of connected lines. For example, with only one line connected the rate of rise of voltage at *LA-1* was approximately 500 kv per ms for stations with unshielded lines. Because of this fact, the spark-over voltage will vary. Therefore three values of spark-over voltage given in Table I were used.

Voltages were measured on the Anacom circuit at all the circuit breakers, arrester locations, and at the transformer. The

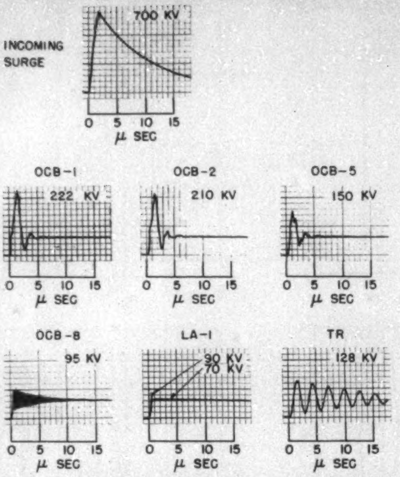

Fig. 9 (above). Oscillograms of voltages for the case of shielded overhead lines with a lightning arrester connected at LA-1 and two lines in service. Crest voltages are given and all oscillograms except the incoming surge are shown to the same scale

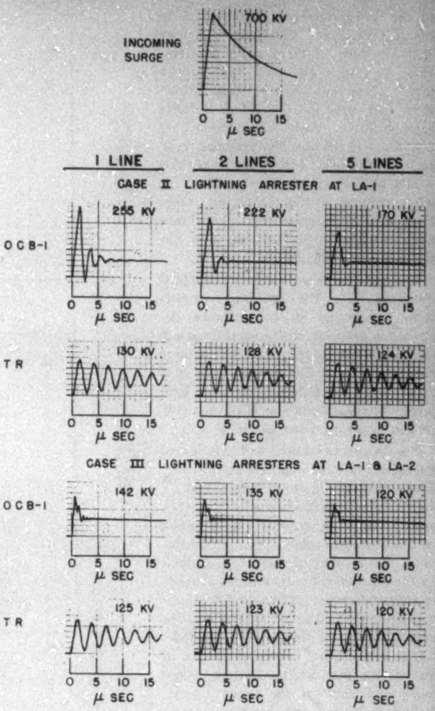

Fig. 10 (right). Oscillograms of voltages for the case of stations with shielded overhead lines showing the effect of number of lines connected and number of lightning arresters in service. Crest voltages are given and oscillograms except the incoming surge are shown to the same scale

effect of the number of lines on the surge voltages within the station was studied by closing circuit breakers in sequence to represent two, three, five, seven, and nine lines. The lightning arrester to transformer separation distance was held constant at 200 feet, a distance which will be conservative in most cases but will provide adequate protection for the transformer. A lightning arrester was assumed to be connected at *LA-1* so as to give positive protection to the transformer regardless of upon which line the surge enters the station and also to give maximun available protection to the circuit breakers. Lightning surges were applied to line no. 1 through a resistance of 400 ohms, equal to the surge impedance of the line. This line was selected because surges entering the station on this line result in highest voltages at breaker positions remote from the arrester location *LA-1*. For a small number of lines connected, the voltages at *OCB-1* will rise to high crest values. Therefore an additional arrester was placed at *LA-2*, and the effect of the number of lines connected to the station was again studied.

Analysis of Anacom Data

The recorded surge voltages from the oscillograms were evaluated in terms of their severity index.[1,2] This procedure is based on the integration method of expressing the disruptive effect of nonstandard waves in terms of that of equivalent standard test waves.[5,14,15] The disruptive effect is given by the relation[16]

$$\text{DE} = \int e^{K_2} dt$$

where

e = the surge voltage as a function of time
K_2 = a constant

Per-cent severity index (SI) is the ratio, expressed in per cent, of the crest voltage of the surge under consideration to the crest voltage of a surge of the same shape which will just stress the insulation to the impulse-withstand curve. Or, to put it another way, per-cent SI of a surge of any odd shape is the ratio, expressed in per cent, of the crest voltage of a reference wave having the same disruptive effect as the odd wave to the crest voltage of the same reference wave which will just stress the insulation to its impulse-withstand curve.

In this study, consideration was given to the disruptive effect of surges on the transformer insulation, and on the circuit-breaker insulation. SI of surges on the circuit-breaker insulation are expressed in terms of the external portion of the 23-kv bushing having an impulse-withstand curve as shown in Fig. 5. Any wave which will stress the bushing to this curve has a SI of 100 per cent; for example, both a 338-kv $1^1/_2$x40-ms wave chopped at 1.5 ms and a 235-kv $1^1/_2$x40-ms wave chopped at 10 ms have SI of 100 per cent. Equating the expressions for disruptive effect of these two waves, the constant K_2 comes out to be 6.3 for the 23-kv circuit breaker. SI of surges on the transformer were expressed in terms of the standard impulse-withstand tests for the 150-kv BIL transformer. Therefore, either a 175-kv $1^1/_2$x40-ms wave chopped at 3 ms or a 150-kv $1^1/_2$x40-ms full wave

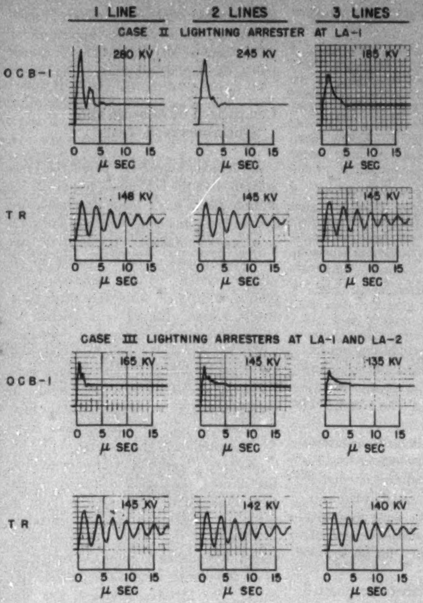

Fig. 11. Oscillograms of voltages for the case of stations with unshielded overhead lines showing the effect of number of lines connected and number of lightning arresters in service. Crest voltages are given and all oscillograms are shown to the same scale

have SI of 100 per cent on the transformer insulation. Based on these two standard test waves, the constant K_2 is 9.1 for the transformer insulation. The impulse-withstand curve for the transformer is shown in Fig. 6. The curve was plotted from calculated values of SI and therefore passes through the chopped-wave and full-wave test points, protection being co-ordinated on these two points.

Discussion of Anacom Results

Surge voltages were photographically recorded at all of the breakers and at the transformer. However, the maximum voltage within the station occurs at *OCB-1*. Therefore, only voltages at three locations were analyzed: at the transformer, at *OCB-1*, and at *OCB-5*. Voltages at *OCB-5* were analyzed to give visual evidence that surge voltages at breaker positions physically closer to the lightning-arrester positions have lower crest voltages and SI.

SI and crest voltages obtained from oscillograms taken on Anacom are shown by the curves of Figs. 7 and 8. Any SI higher than 100 per cent cannot be tolerated, and arrester locations which result in such voltages at the transformer or at circuit breakers should be avoided. At the same time, it should be kept in mind that SI of 100 indicate surges which have the same disruptive effect as withstand test voltages and not voltages which will cause insulation failures. If a protective level below the withstand test voltage is desired, results of this study are still applicable but then protection must be based on a SI less than 100 per cent. For example, in some conservative applications all SI higher than 90 per cent might be ruled out.

Stations with Shielded Overhead Lines

Low-voltage systems with their high BIL woodpole lines permit higher surge voltages in per unit of the equipment BIL within the station than do higher voltage systems. For example, the ratio of line BIL to equipment BIL for a 230-kv system is about 1.6 or 1.7[4]; however, for the 24-kv system, here considered, the ratio is 5.0. In a previous paper on lightning protection in a 120-kv station,[8] it was concluded that, with three lines connected, the station is inherently self-protecting and no arresters are required. However from Fig. 7, case I, it is noticed that even with all nine lines connected, the transformer is not protected when no arrester is present within the station. If the transformer were placed immediately adjacent to the transformer breaker *OCB-TR*, then, by reason of the curves of SI for *OCB-1* and *OCB-5*, case I, it is evident that the transformer will be protected if there are eight or more connected lines.

Case II of Fig. 7 shows that with an arrester at *LA-1* only, the station equipment will be protected if two or more lines are connected. If an additional arrester is placed at *LA-2*, then the station apparatus will be protected even if only one line is connected.

Typical oscillograms of voltages at various positions within the station are shown in Fig. 9. It is noted that the voltage at *OCB-1* has the highest crest magnitude within the station. The effect of the number of connected lines and the number of arresters in service on the surge voltages at *OCB-1* and at the transformer is portrayed by the oscillograms shown in Fig. 10.

Stations with Unshielded Overhead Lines

Stations with unshielded overhead

Table II. Comparison of Anacom and Synchronograph Tests, Transformer at OCB-TR, No Lightning Arrester

No. of Lines Connected	Voltage Measured	Magnitude, Kv		Front, ms*		Tail, ms	
		Anacom	Synchronograph	Anacom	Synchronograph	Anacom	Synchronograph
1	Incoming surge	700	700	1.4	1.4	13.0	13.4
	Line entrance	960	965	5.0	4.9	24.0	22.0
	Transformer	960	965	4.3	4.5	23.0	20.0
	End of bus	960	965	4.3	4.0	23.0	20.0
2	Incoming surge	700	700	1.4	1.3	12.5	11.7
	Line entrance	600	600	3.7	3.8	18.3	16.5
	Transformer	600	580	2.9	2.7	17.6	14.4
	End of bus	600	590	2.9	2.6	17.6	15.0
4	Incoming surge	700	700	1.4	1.3	12.5	12.4
	Line entrance	360	350	2.7	3.2	14.5	14.0
	Transformer	360	350	2.0	1.9	13.8	13.8
	End of bus	360	350	2.0	1.9	14.0	14.0

* Front is arbitrarily defined as time to 90-per-cent crest.

Table III. Comparison of Anacom and Synchronograph Tests, Transformer at OCB-TR, 20-Kv Line-Type Lightning Arrester at Line Entrance

No. of Lines Connected	Voltage Measured	Magnitude, Kv		Front, ms*		Tail, ms		Period of Oscillation, ms	
		Anacom	Synchronograph	Anacom	Synchronograph	Anacom	Synchronograph	Anacom	Synchronograph
1	Incoming surge	425	425	1.4	1.4	14.1	12.6		
	Line entrance	67	68	0.7	0.6				
	Transformer	130	130	0.8	0.6			3.2	3.1
	End of bus	130	130	0.8	0.8			3.2	2.9
2	Incoming surge	425	400	1.4	1.4	14.2	12.6		
	Line entrance	68	68	0.7	0.7				
	Transformer	125	125	0.9	0.8			3.2	3.2
	End of bus	125	120	0.9	0.9			3.2	2.9
4	Incoming surge	370	325	1.4	1.4	13.0	12.7		
	Line entrance	68	67	0.6	0.6				
	Transformer	110	105	1.0	0.8			3.2	3.2
	End of bus	115	110	1.0	0.9			3.2	3.0

* Front is arbitrarily defined as time to 90-per-cent crest.

lines should have lightning arresters within the station regardless of the number of lines which are connected. For lines of 1,000-kv BIL, voltages of three or more times the equipment BIL are possible even with all nine lines connected.

For only one arrester applied at *LA-1*, the curves of Fig. 8, case II, show that four or more connected lines are necessary to protect adequately the station apparatus. This is in contrast to the case of stations with shielded overhead lines where, with one arrester at *LA-1*, two or or more connected lines should be in service to assure adequate lightning protection. If arresters are placed at *LA-1* and *LA-2* then the station equipment is protected regardless of the number of lines in service.

The data shown in Fig. 8 for stations with unshielded lines also can be used for the case of a shielding failure immediately adjacent to the station on shielded overhead lines. These data show that with two arresters in service adequate lightning protection can be secured for all station equipment.

The effect of the number of connected lines and the number of arresters in service on the surge voltages appearing at *OCB-1* and at the transformer is shown by the oscillogram sequence of Fig. 11.

Comparison of Anacom and Synchronograph Tests

A previous paper[3] compared the tests performed in the field on an actual 120-kv station with a study made on a miniature system in the analogue computer and good results were obtained. To verify further the assumptions made in setting up an electric system on the Anacom, synchronograph[16] field tests were made on a 24-kv station. Surges were applied at the section breaker through a resistance equal in value to the surge impedance of the transmission line, and voltages were measured at the line entrance *LE*, at the transformer *TR*, and at the end of the bus, as shown by Fig. 1. The distance from the transformer to the bus was varied by connecting a length of conductor to give the desired separation distance. Tests were made both with and without a lightning arrester at the line entrance position and the circuit breakers were closed in sequence to show the reduction in surge voltages caused by multiple circuits. The arrester analogue was the same as used in previous studies[16] and consisted of a battery and diodes in series.

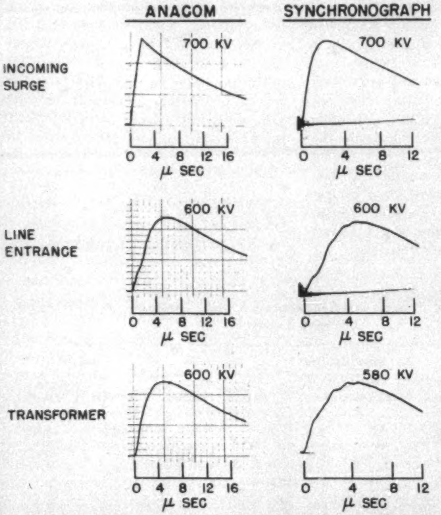

Fig. 12. Comparison of oscillograms of voltages from the Anacom and synchronograph studies for two lines connected and no lightning arrester. Transformer is located at OCB-TR. Crest voltages are given. Oscillograms are not to same scale

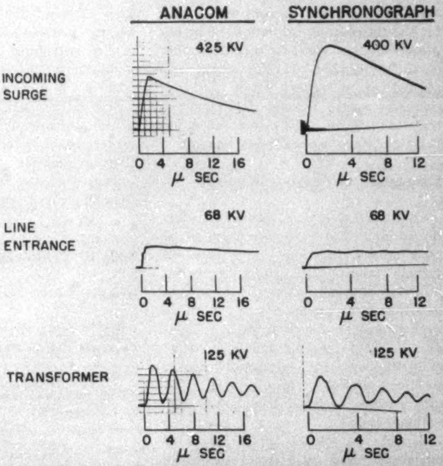

Fig. 13. Comparison of oscillograms of voltages from the Anacom and synchronograph studies for two lines connected and a 20-kv lightning arrester at line entrance position. Transformer is located at OCB-TR. Crest voltages are given. Oscillograms are not to same scale

Duplicate circuit conditions were set up on the Anacom to obtain comparative data. Only two cases of synchronograph data are given here, this being sufficient to show the good agreement between the results obtained. The cases selected for correlation were for a 1.4x13-ms incoming surge wave shape with the transformer immediately adjacent to the breaker *OCB-TR*. Both cases of with and without a lightning arrester at the line entrance position were studied.

Surge voltages obtained from synchronograph tests are compared with those from the Anacom study in Tables II and III. Figs. 12 and 13 show the oscillograms for the case of two connected lines. In comparing the oscillograms, it should be noted that the voltage and time scales from the synchronograph and Anacom oscillograms are not the same.

Both the tables and the figures show that the miniature system used in the Anacom gave results that agree closely with the synchronograph field tests. It is concluded that when the dimensions and circuit constants of a station are accurately known, the results obtained from miniature system studies can be used with confidence in lightning protection problems.

The primary use of the synchronograph is to test apparatus and systems under field conditions. However, it is possible through the use of carefully constructed circuit elements to set up a miniature system on a unity time and impedance base and apply the synchronograph surge generator to this circuit to obtain surge voltage distribution throughout the system. After initially comparing the results on the miniature, unity base system with actual synchronograph test made on the existing system, the miniature system can be changed or expanded to study projected stations and the results obtained can be used with assurance in lightning-arrester application problems. This method of miniature system studies by use of the synchronograph has been used successfully by the Detroit Edison Company.

Conclusions

1. Although low-voltage stations are compact and have high values of capacitance to ground, the high BIL of modern wood-pole lines permits high surge voltages to enter the station.

2. The ratio of the line BIL to the equipment BIL is much higher in low-voltage systems than in higher voltage systems. Therefore, with no lightning arrester in the station, the resultant surge voltages in per unit of the equipment BIL at equipment terminals are much higher in low-voltage stations.

3. Connected lines cannot sufficiently reduce the surge voltages within the station so that the station is inherently self-protecting without lightning arresters. Even with all nine lines connected, for the case of stations with shielded lines, the surge voltage at the transformer is more severe than the insulation strength of the 150-kv BIL transformer.

4. For stations with shielded overhead lines and with only one 20-kv line-type lightning arrester at *LA-1*, two or more connected lines are necessary to afford adequate protection to the station equipment.

5. For stations with unshielded overhead lines and with only one 20-kv arrester at *LA-1*, four or more lines are necessary to provide protection for the station apparatus.

6. With two arresters in the station at *LA-1* and *LA-2*, the station is adequately protected regardless of the number of connected lines.

7. From this and previous comparisons of field and miniature system studies made on stations covering a range of voltage levels, it is concluded that, when the dimensions and circuit constants of the station are accurately known, the results of miniature system studies of circuit surge performance can be used with confidence in formulating the required degree of lightning protection.

References

1. Lightning Protection in Extra-High Voltage Stations—Analysis, Anacom Study, and Results, I. W. Gross, T. J. Bliss, J. K. Dillard. *AIEE Transactions*, vol. 71, pt. III, 1952, pp. 482–92.

2. Lightning Protection in Extra-High-Voltage Station—Influence of Multiple Circuits, I. W. Gross, L. B. LeVesconte, J. K. Dillard. *Ibid.*, vol. 72, Oct. 1953, pp. 882–90.

3. Lightning Protection in a 120-Kv Station—Field and Laboratory Studies, J. K. Dillard, H. R. Armstrong, A. R. Hileman. *Ibid.*, vol. 73, pt. III-B, 1954, pp. 1143–52.

4. Direct Stroke Protection of High-Voltage Switching Stations and Transformers, S. B. Griscom, J. K. Dillard, A. R. Hileman. *Ibid.*, vol. 74, pt. III, June 1955, pp. 354–68.

5. Co-ordination of Lightning-Arrester Location With Transformer Insulation Level, R. L. Witzke, T. J. Bliss. *Ibid.*, vol. 69, pt. II, 1950, pp. 964–75.

6. Evaluation of Lightning-Arrester Lead Length and Separation in Co-ordinated Protection of Apparatus Against Lightning, T. J. Carpenter, I. B. Johnson, L. E. Saline. *Ibid.*, pp. 933–44.

7. Surge Protection of Transformers Based on New Lightning-Arrester Characteristics, J. K. Dillard, T. J. Bliss. *Ibid.*, vol. 73, pt. III-B, Oct. 1954, pp. 1305–11.

8. A Method of Estimating Lightning Performance of Distribution Lines, J. M. Clayton, A. R. Hileman. *Ibid.*, Aug., pp. 933–45.

9. High-Voltage Impulse Tests on Transmission Lines, C. F. Wagner, I. W. Gross, B. L. Lloyd. *Ibid.*, pt. III-B, Apr. 1954, pp. 196–210.

10. *Discussion* by C. F. Wagner of Proposed Basic Impulse Insulation Levels for High-Voltage Systems, J. E. Clem, J. R. Meador, W. J. Ridge, A. H. Powell. *Ibid.*, vol. 69, pt. II, 1950, pp. 961–62.

11. Lightning Investigations on the 25-Kv System of the West Penn Power Company, William C. Bowen, Edward Beck. *Ibid.*, vol. 66, 1947, pp. 831–37.

12. Discharge Currents in Distribution Arresters—II, K. B. McEachron, W. A. McMorris. *Ibid.*, vol. 57, June 1938, pp. 307–14.

13. Field Research on Lightning-Arrester Discharges, G. D. McCann, Edward Beck. *Ibid.*, vol. 66, 1947, pp. 625–30.

14. Surge Protection of Cable-Connected Equipment, R. L. Witzke, T. J. Bliss. *Ibid.*, vol. 69, pt. I, 1950, pp. 527–42.

15. Evaluation of the Integration Method for Analysis of Nonstandard Surge Voltages, Andrew R. Jones. *Ibid.*, vol. 73, pt. III-B, Aug. 1954, pp. 984–90.

16. Lightning Problems Solved With the Synchronograph, E. L. Harder, J. M. Clayton. *Ibid.*, vol. 72, pt. III, June 1953, pp. 375–83.

◆

Discussion

W. F. Griffard (Commonwealth Associates, Inc., Jackson, Mich.): It is gratifying to know that studies are being conducted on existing installations to substantiate the accuracy and adaptability of synchronograph and Anacom studies. Certainly industry is in need of a means of readily determining the effects of transient overvoltages on a given installation for the purpose of procuring the most economically justifiable protection.

With this objective in mind, it is reasonable to assume that information on protective devices other than lightning arresters might be sought during the course of such a study. Specifically, was any data obtained on this installation using line entrance gaps for protection of remote equipment with lightning arresters mounted adjacent to the power transformer?

We have used a protective combination of lightning arresters adjacent to transformers and line entrance gaps on each line exit quite successfully for a considerable number of years. Our record would indicate that these secondary protective devices have their place in providing backup protection for the outlying station equipment and should be given consideration when station protection is engineered.

Conclusion 6 states "With two arresters in the station at *LA-1* and *LA-2*, the station is adequately protected regardless of the number of connected lines." For lines which are temporarily disconnected by means of open switches or breakers, however, adequate protection may not be afforded if those lines are subjected to surges. Such operating conditions occur and should not be overlooked in applying surge protection. The use of line entrance gaps on each circuit exit will assure a degree of protection under such conditions.

H. R. Armstrong, R. W. Ferguson, and **A. R. Hileman:** The authors wish to thank Mr. Griffard for his excellent points. Specifically, no data were obtained using line entrance gaps and lightning arresters mounted adjacent to the power transformer. However, the voltage magnitude which appears at *OCB-1* and *OCB-5* can be obtained from Figs. 7 and 8.

For the case where a line is energized and the circuit breaker closed, the location and number of arresters within the station should be based on protection of all station equipment. If the arresters are located so as not to give adequate protection to the closed circuit breaker, additional arresters should be used or the existing arresters relocated so as to give complete over-all protection. The use of gaps in this case can cause an outage on the system.

For the other normal case of de-energized line and an open circuit breaker at the station, rod gaps are unnecessary on Westinghouse oil circuit breakers. For a surge arriving at the open breaker, the impulse strength is co-ordinate so that flashover will occur across the breaker bushing before it will occur across the open contacts. Because the line is de-energized, this flashover to ground will not result in an outage and the breaker bushing will not be damaged.

For some operating conditions the circuit breaker may be open but the line energized from the other end. This type of condition, although not normal for the majority of lines, may be the usual operating condition on a specific line. For this case, a surge arriving at the open breaker and flashing over to ground will constitute a fault on the system. The fault current across the breaker bushing can damage the bushing depending on the time duration and magnitude of the fault current. In deciding what adequate protection should be, the probability of this case occurring should be investigated. If this is a normal condition of operation or if this fault on the system is highly undesirable, then it is prudent to apply lightning arresters on the line side of the breaker. However, if this condition has a low probability of occurrence, many companies provide neither rod gaps nor lightning arresters on the line side of the breaker. An intermediate condition may exist so that rod gaps on the breaker bushing can be economically justified. The rod gaps will allow fault current to flow but will provide some protection for the breaker bushing.

A Computer for Economic Scheduling and Control of Power Systems

C. D. MORRILL
NONMEMBER AIEE

J. A. BLAKE
NONMEMBER AIEE

AS ELECTRIC power systems become larger, the problem of obtaining optimum economic operation becomes more difficult. One reason is the increased importance of considering transmission losses in the allocation of generation. Another is because of the inability of systems engineers to keep pace with changes in the many factors affecting operating costs. As a result, a number of methods of automatic and semiautomatic computing have been tried. In 1949, George, Page, and Ward[1] suggested the use of a network analyzer to obtain station-loading schedules. Recently, a refinement of this method permitting some operational flexibility was described by Early, Phillips, and Shreve.[2] Imbugia, Kirchmayer, and Stagg[3] have described an incremental slide rule and a means for calculating penalty factors based on transmission losses. Harder[4] has suggested a computer for solving the co-ordination equations. The use of digital computers in obtaining loading schedules has been described in papers by Travers, Harker, Long, and Harder[5] and by Kirchmayer, Habermann, and Thomas.[6]

A difficulty with some of these methods is the amount of labor and time involved in obtaining new solutions when changes occur in fuel costs, station incremental heat rates, or the transmission system. With most of these methods, the solutions must be monitored so that, as each of the station incremental cost curves approaches a break point, the stored data (the slopes and intercepts of the curves of the station incremental costs) may be changed.

Principles of incremental loading, co-ordination of incremental losses with incremental production costs, derivation of loss equations, and benefits of economic scheduling are covered elsewhere.[5–10]

This paper describes an economic dispatch computer employing circuits and techniques used in electronic differential analyzers.[11–13] The computer seeks to overcome the deficiencies of some of the current computing methods, to obtain a computing accuracy limited only by the accuracy of the input data, and to retain the maximum freedom, flexibility, and operating ease inherent in analogue computers of the electronic differential-analyzer type. The paper also describes the use of the computer in the automatic control of a power system, suggests ways of using the computer to determine the incremental cost of power delivered to neighboring systems, the optimum utilization of hydro power, and other economic-dynamic relationships, and discusses the principal advantages of the method.

Application to Scheduling and Control

It is felt that an understanding of the use of the computer in the economic allocation of generation will be obtained through a description of the operating procedure. An artist's conception of a representative installation for a large power system is shown in Fig. 1. Each of the station simulators is contained in one of the two cabinets. A prototype station simulator, which was used in the study covered in Appendix III, is shown in Fig. 2. To plot a set of dispatch curves, the following procedure is used.

The plug-in boxes containing the loss coefficients and the incremental heat-rate data for each generating unit are inserted into the station simulator. The switches on the front of each station simulator are set according to the availability or nonavailability of each of the generating units at that station. Station low-limit controls (not shown) are set according to the requirements for local area protection. If required, the station high-limit controls are set. The cost of fuel is stored by means of the fuel-cost dial.

At the console, Fig. 1, the dispatcher fixes, with the controls in the two rows near the bottom of the control panel, the values and directions of tie-line powers to be used in the calculations. The variables to be recorded on the plotter, at the left side of the console, and appropriate recording scale factors are selected by means of the group of four knobs near the center of the control panel. The switch at the lower right-hand corner of the panel is then turned to "Raise" or "Lower" and the recorder automatically plots, say, station 1 generation as a function of total generation. In the same way λ the incremental cost of received power, may be plotted as a function of total generation. It might prove useful to plot station or generating unit incremental heat-rate curves as a function of generation. Other plots displaying useful information in

---

Paper 55-528, recommended by the AIEE System Engineering Committee and approved by the AIEE Committee on Technical Operations for presentation at the AIEE Summer General Meeting, Swampscott, Mass., June 27–July 1, 1955. Manuscript submitted February 4, 1955; made available for printing May 11, 1955.

C. D. MORRILL and J. A. BLAKE are with the Goodyear Aircraft Corporation, Akron, Ohio.

The authors are indebted to the many individuals cited in the references for the development of the basic information on economic operation of power systems. They are particularly grateful to R. H. Travers and D. F. Shook of the Ohio Edison Company, who several years ago suggested the use of operational analogue-computer circuits for the solution of power-system economic problems, and who have supplied many valuable suggestions during the development of the computer.

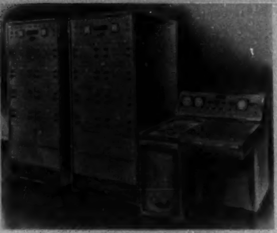

Fig. 1. Artist's conception of a representative economic dispatch computer for large power system

graphical form could, of course, be obtained.

If the console control is turned from "Plot" to "Dispatch," predicted tie-line powers and nonconforming loads may be replaced by actual powers and loads. The most economic dispatch may be obtained in one of two ways.

In the first dispatch method, operation is completely manual. The metered values of tie-line powers are set on the console controls. The "Raise-Lower" switch is operated until the total computed system generation, as read on one of the meters above the plotter, is equal to the metered total system generation. As its selector switch is rotated, the other meter indicates the generation required from each station.

The second dispatch method is completely automatic but requires that an additional slide wire be ganged to the total generation, system deviation, and tie-line recorders. Circuits in the console compute the total required system generation and automatically increase or decrease the total computed value accordingly; see Fig. 3 and Appendix I. As before, the meter indicates λ and total and individual station generations.

When the computer is used in the manner described, its outputs, voltages representing P_1, P_2, etc., may be used to control station regulating-point setters or similar portions of existing load-control equipment for automatic and continuous system control. The method used to compute these outputs is described in Appendix I.

Other Applications

Travers et al.[8] have shown how the incremental cost or worth of "sale" or "purchase" power may be

$$\frac{dC_t}{dP_t}=\lambda\left[1-2\sum_m B_{mt}P_m\right]-2\lambda B_{tt}P_t \qquad (1)$$

where

$\frac{dC_t}{dP_t}$ = incremental cost of power at a tie point, dollars per megawatt-hour (\$/mwhr)

λ = incremental cost of received power, \$/mwhr

B_{mt} = transmission loss coefficient of the tie point with respect to the power generated at station m, mw^{-1}

P_m = power generated at station m, mw

P_t = tie-line power, positive for purchased power, mw

Since all the terms on the right-hand side of equation 1 are either constants stored in the computer or variables generated by the computer, the computer readily calculates the incremental cost of tie-line power. The calculated value is displayed on a meter and can be automatically plotted as a function of tie-line and total system generations

A use of the computer not fully explored is the study of the economic operation of systems with hydroelectric generating stations. Electronic differential analyzers have already demonstrated their usefulness in flood-control problems.[14] It seems probable that at least the short-range economic allocation of hydro power[15–17] may be determined by means of the computer. A curve follower of the type described by Vance and Haas[18] may be used to generate an input signal proportional to predicted system load as a function of time. Each of the hydro stations, including the transmission loss of each, may be simulated by a unit almost identical to the steam plate simulators. By use of the method of Chandler, Dandeno, Glimn, and Kirchmayer,[15] the fuel-cost dial of each hydro station may be adjusted until the daily load requirements, as generated by the curve follower, and the total daily usage requirements at each hydro station have been met. The

Fig. 2. Prototype station simulator and can containing loss coefficients

water evaluation figures obtained from this study may be left on the fuel-cost dials and system dispatch curves plotted.

Other uses of the computer, such as the determination of the incremental cost of transmitting power through a system, will be apparent to those familiar with economic scheduling problems.

Advantages

The primary advantages of this computational method result from its inherent flexibility. The addition of a station to a system requires only the addition of a single plug-in station simulator to the computer and a change of resistances in the plug-in cans that store the transmission loss coefficients. An addition of or modification to generating units at a station is handled in the same way as a change in loss coefficients; that is, by changing resistors in plug-in cans. Changes that may occur more often, a change in fuel cost, equipment outages, or station high or low limits, are provided for by front-panel controls.

The accuracy of this method substantially exceeds the accuracy of the data. The resistors representing the important transmission loss coefficients, the poten-

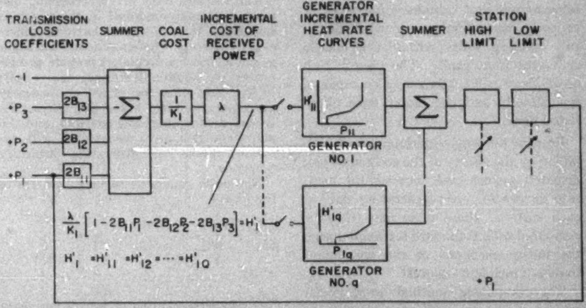
TRANSMISSION LOSS COEFFICIENTS
SUMMER
COAL COST
INCREMENTAL COST OF RECEIVED POWER
GENERATOR INCREMENTAL HEAT RATE CURVES
SUMMER
STATION
HIGH LIMIT
LOW LIMIT
-1
+P3
+P2
+P1
2B13
2B12
2B11
-Σ
1/K1
λ
H'11
P11
GENERATOR NO. 1
Σ
λ/K1 [1 - 2B11P1 - 2B12P2 - 2B13P3] = H'1
H'1 = H'11 = H'12 = ··· = H'1Q
H'1q
P1q
GENERATOR NO. q
+P1

Fig. 3. Block diagram showing method of solving co-ordination equations

tiometers representing fuel costs and incremental costs of received power, and the method of presenting the relationship between incremental heat-rate and unit generation are accurate to better than 1 per cent; if the accuracy of the data warrants it, component accuracies to 0.1 per cent or better may be obtained. Overall computing accuracy is virtually independent of the size of the system.

Computing speed greatly exceeds requirements; with a new value of λ set into the computer, all the individual plant generations are computed in less than 0.001 second. In practice, the computing speed is reduced so that the plotter can record solutions accurately. Because incremental production costs are represented throughout their entire range, no computer adjustments are required during a solution. Complete generation schedules can be produced at a rate of about two or three stations per minute. When the computer is used for automatic control, its speed is purposely reduced even further

The circuits used have demonstrated a very high degree of reliability over years of development, refinement, and field use. All the vacuum-tube computing circuits are used with an extremely large percentage of negative feedback. Furthermore, a stabilization system, described in Appendix II, is used to correct automatically and continuously changes due to the normal aging of vacuum tubes and other circuit components.

The computer is quite easy to maintain. Suppose, for example, that with the outputs of the computer fed to automatic load control or telemetering equipment, a vacuum tube deteriorates to a point where it should be replaced. The stabilization and alarm circuit, Appendix 2, indicates an alarm, takes the computer off control, shows in which cabinet the fault has occurred, which station simulator within that cabinet is not working properly, and, finally, which of the 3-tube plug-in units within the station simulator is at fault. The plug-in unit or all three of its tubes may be replaced immediately and the faulty tube eliminated later.

Routine preventive maintenance is simplified by the ability of the console to plot dispatch curves and incremental heat-rate curves for each generating unit at each station; these plots may then be compared with a standard set taken during the initial checkout of the equipment to detect incipient failures.

The computing method used is described in Appendix I. In addition to analogue computational methods give in references already cited, high and low limits and incremental heat-rate data are simulated by biased diode circuits similar to those described in a paper by Morrill and Baum.[19]

Appendix II provides information on the stabilization and alarm system. Appendix III shows the results of using the computer to obtain dispatch curves for a three-station system.

Conclusions

This paper has described a method of computing economic dispatching information by combining data on fuel costs, incremental heat rates, incremental transmission losses, and station limits with data on system loads and tie-line power requirements. Its use should enable those responsible for economic operation of power systems to take advantage of new data more quickly. Brief use of the computer has shown the importance, in terms of annual operating costs, of obtaining the best possible station and tie-line incremental cost data. The use of a flexible high-speed computer to obtain dispatch sheets and to make other economic studies should enable many of those engaged in the seemingly endless calculations required to keep up with system changes to spend more time in improving the accuracy of the input data, particularly fuel costs, incremental maintenance costs, and incremental heat rates.

The principal advantage of the method described is the ease with which changes may be made to the computer to correspond to station and system changes. Other advantages are accuracy, speed, reliability, automatic error detection, and ease of maintenance.

Appendix I. Method

The method used in the economic dispatch computer described in this paper is essentially that of most electronic differential analyzers, wherein resistors and high-gain d-c feedback amplifiers provide precise means of summing, scaling, etc. Scale factors that must be varied conveniently are represented by linear potentiometers. Biased diodes, precision resistors, and d-c amplifiers provide a convenient and accurate means of generating arbitrary functions.

The basic equations to be solved are of the form

$$\frac{dF_{cn}}{dP_n}+\frac{\lambda\partial P_L}{\partial P_n}=\lambda \qquad (2)$$

where

$\frac{dF_{cn}}{dP_n}$ = incremental cost of generation, plant n, \$/mwhr

λ = incremental cost of received power \$/mwhr

$\frac{\partial P_L}{\partial P_n}$ = incremental transmission losses attributable to plant n, mw/mw

Since this equation is both implicit and nonlinear and since there will normally be a large number of such equations to be solved simultaneously, solution by ordinary means is extremely difficult.

If

$$\frac{\partial P_L}{\partial P_n}=2\sum_m B_{nm}P_m \qquad (3)$$

and if

$$\frac{dF_{cn}}{dP_n}=K_n\frac{dH_n}{dP_n} \qquad (4)$$

where

K_n = fuel cost of station n, \$/1,000 Btu

$\frac{dH_n}{dP_n}$ = incremental heat rate, plant n, 1,000 Btu/mw-hr

then

$$\frac{dH_n}{dP_n}=\frac{\lambda}{K_n}\left(1-2\sum_m B_{nm}P_m\right) \qquad (5)$$

Since, for most economical loading of individual generating units within a station, the incremental heat rates of each generating unit must be equal to the station incremental heat rate

$$\frac{dH_n}{dP_n}=H_n'=H_{n1}'=H_{n2}'=H_{nq}'=\frac{\lambda}{K_n}\left[1-2\sum_m B_{nm}P_m\right] \qquad (6)$$

where

H_{nq}' = incremental heat rate, generating unit q, plant n, 1,000 Btu/mw-hr

A method of solving this equation for P_n is shown in Fig. 4; this block diagram represents one of a number of station simulators.

It is customary in using electronic differential analyzers to assume that the answers, in this case, P_1, P_2, ..., P_n, ..., are available. From the left side of Fig. 4, the term within the brackets on the right-hand side of equation 6 is developed from a unit voltage and voltages representing the individual station generations. The resultant sum is divided by K_1 represented by a potentiometer, and multiplied by λ through a potentiometer having a shaft common with an identical potentiometer in each of the station simulators. The voltage resulting from these last two operations represents the incremental heat rate, H_1', for the station according to equation 5; it is applied to a set of electronic function generators each relating generating unit power to its incremental heat rate. Depending on which generators are connected and on the functions stored, a voltage is produced representing the station power for a particular value of λ. This voltage and the voltages developed by the other

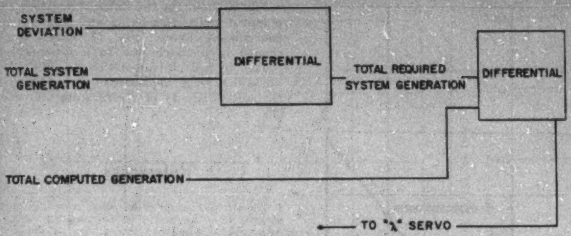

Fig. 4. Solution of control equation

station simulators are connected to the input terminals (left side of Fig. 4).

The control of the computer is accomplished in a manner indicated by the block diagram, Fig. 3; with this circuit, λ automatically increases or decreases until the total computed generation is equal to the total required generation.

Appendix II. Stabilization and Alarm

Before the error correction and alarm circuit, one of which is installed in each cabinet, is discussed, it might be desirable to review a basic operation in electronic differential analyzers. Fig. 5 shows a circuit using three resistors and a d-c amplifier to sum two voltages. The three most important requirements of an amplifier used in this way are as follows:

1. The gain of the amplifier is so great that no appreciable error is introduced by assuming that it is infinite; normal gains of such amplifiers are 100,000 to 200,000 compared with net gains, with feedback, of about 0.1 to 10.

2. Current into the amplifier (input-tube grid current) is so small that no appreciable error is introduced by assuming that it is zero; normal input currents are about 5×10^{-11} amperes compared with normal signal currents of about 10^{-4} amperes.

3. The voltage at the input to the amplifier required to reduce the output voltage to zero (sometimes called zero drift) is so small that no appreciable error is introduced by assuming that it is zero; normal zero drift with stabilization is about 200 microvolts compared with nominal signal voltages of about 50 volts.

Other characteristics of the amplifier are that its output must be capable of going both positive and negative if problem variables may be of either sign; and that the incremental gain of the amplifier must be negative so that a resistor connected between output and input provides negative feedback. With these characteristics, for all finite output voltages, the voltage at the summing point is zero, 1 and 3; and all the current that flows through input resistors flows through the feedback resistor, 2. The current that flows through R_1 due to e_1 is e_1/R_1; the current through R_2 is e_2/R_2. The current flowing through R_0 is the sum of these two so that the voltage across R_0 is proportional to the sum of the input voltages. But, since the end of R_0 that is connected to the input terminal of the amplifier (summing point) is at zero voltage (ground), the voltage measured between the amplifier output terminal and ground is also proportional to the sum of the two input voltages.

There is no difficulty in maintaining large amplifier gain, item 1, and low input current, item 2; however, because of the aging of vacuum tubes and other circuit components, there may be some amplifier drift, item 3.

Fig. 6 shows a simplified schematic diagram of a circuit that will maintain the amplifier input terminal very nearly zero for all normal variations in component characteristics; furthermore, if the circuit is unable to maintain the required condition, it flashes an alarm.

The average value of the error at the summing point is sampled by a commutator approximately three times per second. The sampled value, which might be, say, 100 microvolts, is amplified by about 50,000. The amplified signal is applied to a second section of the commutator for detection and, after filtering, is used to change the amplifier bias to bring the summing-point voltage to zero. If, for any reason, the voltage at the summing point is large enough, perhaps one or two millivolts, the amplified error will be large

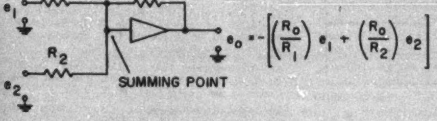

Fig. 5. Computer method of summing two voltages

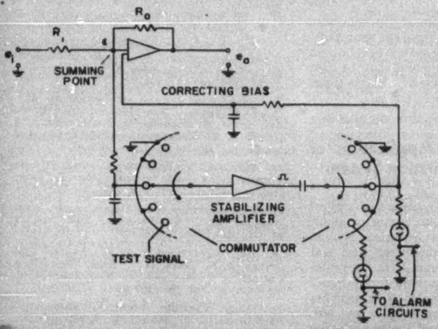

Fig. 6. Simplified schematic of error correction and alarm circuit

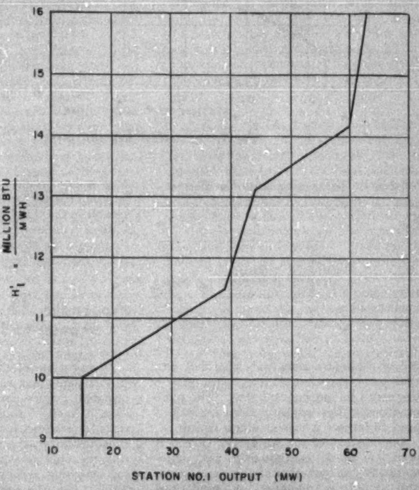

Fig. 7. Incremental heat rate, plant 1

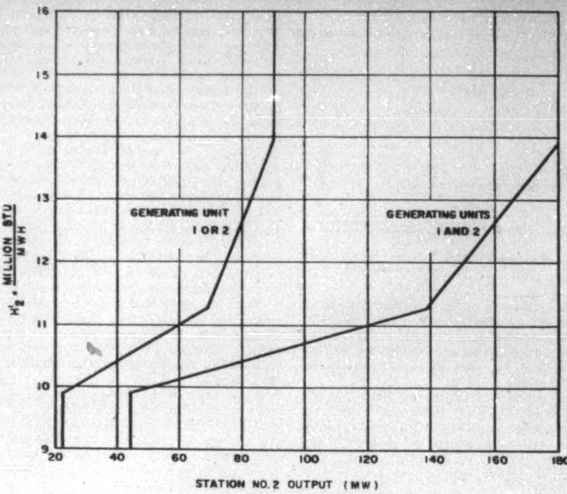

Fig. 8. Incremental heat rate, plant 2

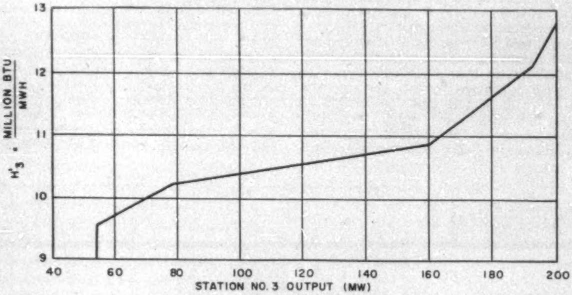

Fig. 9. Incremental heat rate, plant 3

Table I. Transmission Loss Coefficients

B_{nm}	1	2	3
1	0.000589		
2	0.000104	0.000460	
3	−0.000108	0.000241	0.000245

1. Units are, mw^{-1}.
2. The matrix is symmetrical, i.e., $B_{12} = B_{21}$.

enough to light a neon bulb identified with that particular channel and, thus, with a particular computing amplifier. The pulse produced at the output of the neon bulb is used to initiate a master alarm circuit.

One channel of the stabilizing system is used to check continuously and automatically the operation of the commutator and stabilizing amplifier. A small test signal of about three millivolts is applied to a spare channel and, if the amplified output fails to flash a separate neon bulb, trouble in the stabilizing system is indicated. Loss of pulses in this channel may be used to operate the alarm system. In this sense, the computing system is fail-safe.

Appendix III. Application of Computer to 3-Station System

A prototype of the computer described in this paper was used to obtain economic dispatch curves for a 3-station system. Figs. 7, 8, and 9 show the incremental heat rates for stations 1, 2, and 3; in the prototype computer, the simulator for station 2 was the only one provided with switches for switching generating units in and out. Table I lists the values of the transmission loss coefficients used in this study.

Fig. 10 shows the two different dispatches obtained when considering and neglecting transmission losses. Fig. 11 shows the change in dispatch due to a 5-per-cent change in fuel cost at station 2. Fig. 12 shows the change in dispatch by considering the nonavailability of a generating unit at station 2.

References

1. Co-ordination of Fuel Cost and Transmission Loss by the Use of the Network Analyzer to Determine Plant Loading Schedules, **E. E. George, H. W. Page, J. B. Ward.** *AIEE Transactions*, vol. 68, pt. II, 1949, pp. 1152–63.

2. An Incremental Cost of Power-Delivered Computer, **E. D. Early, W. E. Phillips, W. T. Shreve.** *Ibid.*, vol. 74, pt. III, June 1955, pp. 529–35.

3. A Transmission Loss Penalty Factor Computer, **C. A. Imburgia, L. K. Kirchmayer, G. W. Stagg.** *Ibid.*, vol. 73, pt. III-A, June 1954, pp. 567–71.

4. Economics Load Dispatching, **E. L. Harder.** *Westinghouse Engineer*, Pittsburgh, Pa., vol. 14, 1954, pp. 194–200.

5. Loss Evaluation—Part III. Economic Dispatch Studies of Steam-Electric Generating Systems, **R. H. Travers, D. C. Harker, R. W. Long, E. L. Harder.** *AIEE Transactions*, vol. 73, pt. III-B, Oct. 1954, pp. 1091–1104.

6. Automatic Digital Computer Applied to Generation Scheduling, **A. F. Glimn, L. K. Kirchmayer, R. Habermann, Jr., R. W. Thomas.** *Ibid.*, pp. 1267–75.

7. Economic Loading of Steam Power Plants and Electric Systems (book), **M. J. Steinberg, J. H. Smith.** McGraw-Hill Book Company, Inc., New York, N. Y., 1935.

8. Transmission Losses and Economic Loading of Power Systems, **L. K. Kirchmayer, G. H. McDaniel.** *General Electric Review*, Schenectady, N. Y., Oct. 1951, pp. 39–46.

9. Loss Formulas Made Easy, **A. F. Glimn, R. Habermann, L. K. Kirchmayer, G. W. Stagg.** *AIEE Transactions*, vol. 72, pt. III, Aug. 1953, pp. 730–37.

10. Loss Evaluation—Part II. Current- and Power-Form Loss Formulas, **E. L. Harder, R. W. Ferguson, W. E. Jacobs, D. C. Harker.** *Ibid.*, vol. 73, pt. III, June 1954, pp. 716–31.

11. Electronic Analog Computers (book), **G. A. Korn, T. M. Korn.** McGraw-Hill Book Company, Inc., New York, N. Y., 1952.

12. Analog Methods in Computation and Simulation (book), **W. W. Soroka.** *Ibid.*, 1954.

13. Application of Electronic Differential Analyzers to Engineering Problems, **C. A. Meneley, C. D. Morrill.** *Proceedings*, Institute of Radio Engineers, New York, N. Y., vol. 41, 1953, pp. 1487–96.

14. GEDA Application to Flood-Control and Water Distribution Problems. *Engineering Report GER-6053*, Goodyear Aircraft Corporation, Akron, Ohio, May 4, 1954.

15. Short-Range Economic Operation of a Combined Thermal and Hydroelectric Power System, **W. G. Chandler, P. L. Dandeno, A. F. Glimn, L. K. Kirchmayer.** *AIEE Transactions*, vol. 72, pt. III, Oct. 1953, pp. 1057–65.

16. Short-Range Load Allocational Hydro-Thermal Electric System, **John J. Carey.** *Ibid.*, vol. 73, pt. III-B, Oct. 1954, pp. 1105–12.

17. Co-ordination of Hydro and Steam Generation, **C. W. Watchorn.** *Ibid.*, vol. 74, pt. III, Apr. 1955, pp. 142–50.

18. An Input-Output Unit for Analog Computers, **P. R. Vance, D. L. Haas.** *Proceedings*, Institute of Radio Engineers, New York, N. Y., vol. 41, Oct. 1953, pp. 1483–86.

19. Diode Limiters Simulate Mechanical Phenomena, **C. D. Morrill, R. V. Baum.** *Electronics*, New York, N. Y., vol. 25, Nov. 1952, pp. 122–26.

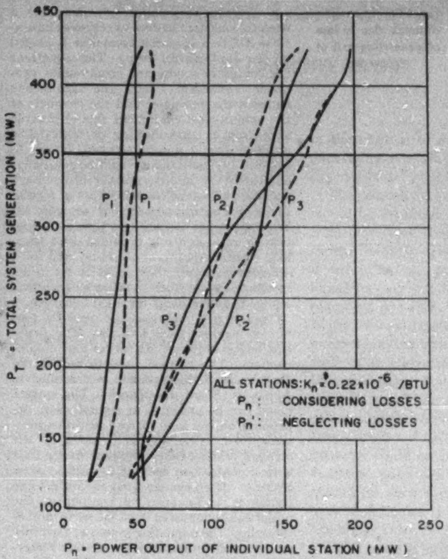

Fig. 10. Difference in dispatch when transmission losses are considered or ignored

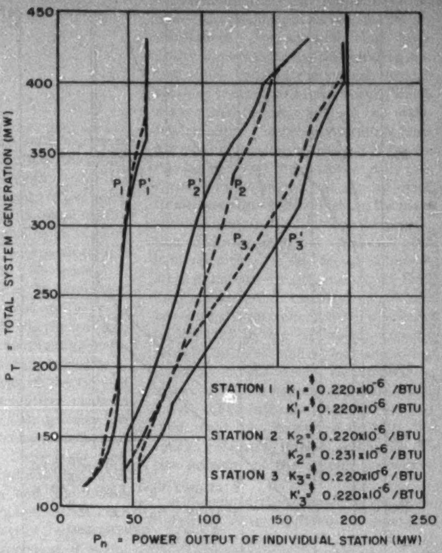

Fig. 11. Change in dispatch resulting from a 5-per-cent change in fuel cost at plant 2

Discussion

R. H. Travers (Ohio Edison Company, Akron, Ohio): The paper is particularly interesting in describing many standard components and computing circuits previously developed and proved for applications in other fields of industry and reassembled and applied to this special problem confronting the power industry.

The mathematics involved in this power-dispatching problem is familiar to computer people from other applications and the scope of the power system tends to introduce many variable parameters which makes automatic computer solutions of the resultant equations very desirable.

In this application the problem of handling generating station incremental cost data has been solved in a direct manner. Provision is made for representing each individual generating unit's incremental heat rate function independently. They by use of "off-on" switches the incremental heat rate cards corresponding to the units actually in operation at any one time are turned "on" and the computer automatically determines the correct cost-megawatt relationship needed for solving the coordination equations for economic dispatch. The indicating lights associated with these cards make a convenient annunciator panel for quickly determining which generators are being included in the solution.

The fuel cost multiplier dial for each generating station can also be used for representing limitations due to high cooling water temperature and deterioration in boiler or turbine efficiencies.

From discussions with the authors since the paper was written it is understood that each individual generating unit incremental heat rate card can be equipped with "high-" and "low-" megawatt limit setters. This provides means for determining more accurately correct dispatches with equipment liimitations such as mill outages, etc.

The equipment as described in the paper is complete and self-contained for those who merely wish to plot out a set of dispatch curves for particular generating conditions and then hand these curves to their dispatchers and let them operate accordingly.

For those who wish to feed in tie-line powers automatically from slide wires and keep up to date on dispatch at all times by recognizing all of the variable parameters, it is necessary to provide a group of meters to read simultaneously all of the voltages representing generating station outputs.

In the ultimate application where the computer actually assumes control and automatically sets the regulating points for each station in the user's load control equipment, careful study must be given to the over-all system so as to provide: 1. adequate protection against excessive rate of response of generations, 2. adequate protection against tube failures, 3. metering for monitoring the equipment to be certain of correct operation, and 4. provisions for keeping the power system control in operation at times when the computer is out of service for maintenance, or for solving cost of power at tie-line points for economy interchange transactions, etc. In many load control systems in use today these features can easily be incorporated with the addition of relatively few standard devices which are readily available from the manufacturers of load control equipment. The authors are to be commended for familiarizing themselves with this power system problem.

L. M. Haupt, Jr. (Agricultural and Mechanical College of Texas, College Station, Tex.): The need for a computer in the load dispatcher's office to solve the "loss equations" for economic dispatch is ably summarized. The loss equations at present in use are of similar form, although the coefficients may be different depending upon the approximations and assumptions made. The solution for any given set of equations is the same regardless of how they are solved or the type of computer used. In other words, each set of equations has a unique solution.

Any computer used should give a solution with an accuracy in line with the accuracy of the data from which the loss equations were obtained after the possible errors due to approximations and assumptions have been taken into account. Although desirable, there is actually no need for greater accuracy.

Analogue computers, whether electronic or not, are adaptable to the solution of these loss equations. They may be designed with the required accuracy. The solutions are easy to interpret. The computations are

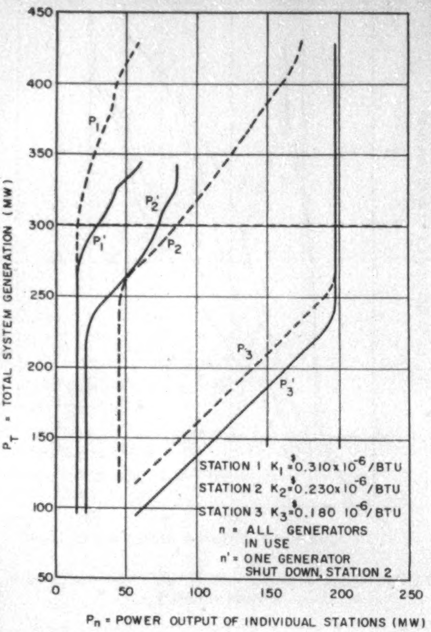

Fig. 12. Change in dispatch due to loss of generating unit at plant 2

fast and reliable. It should be possible to design such a computer, especially one of the electronic differential-analyser type, that will take care of nonlinear characteristics or parameters, etc., and to design one that will give automatic dispatch. Apparently the one described is such a computer. The added feature of plotting various characteristics should be valuable. With the development of computers that satisfactorily solve dispatch equations, more study can be given to developing equations that do not include as many approximations and assumptions.

C. D. Morrill and **J. A. Blake**: The discussions are gratefully acknowledged. As Mr. Travers pointed out, each station simulator can be equipped with high-and low-megawatt-limit setters for each of the cards representing incremental heat rates for individual generating units within a station. Later discussions with Mr. Travers have shown that, although this feature eliminates the requirement for separate high- and low-limit setters for the station simulators, it does not eliminate the desirability of such controls. It is desirable to have a station low-limit setter for area protection that operates independently of the particular generating units available within a station. Thus, when a generating unit is taken out of service, and the corresponding push-button switch on the station simulator is opened, it is not necessary for the dispatcher to readjust the controls representing the lower limits of individual generators. The same argument applies to the need for separate station high-limit controls. If, because of a transformer outage, the station high limit is less than the sum of the individual generator high limits, the computer must recognize this condition independently of the generating units in service.

Travers, in his discussion, also cited a need to consider the rate of response limitations before a dispatch computer is placed in the load-control loop. The equations the computer solves are steady-state economic equations. Thus, the transducers between the computer and the channels of the load-control equipment should provide smoothing or rate limiting or both. The problem should not be serious; failure to provide any smoothing would be somewhat equivalent to an overzealous dispatcher's assistant who kept changing base or regulation point settings every few seconds. It has occurred to the authors that participation or ratio controls provided with some load-control equipment could be used for a different purpose; they could be set in accordance with each station's economic ability to follow short-term load changes.

Travers also mentions the need for protection against tube failures. The problem has two parts: detection and disconnection. The method used to handle the first phase of this problem is described in Appendix II of the paper. The second phase can be provided in several ways, depending on the kind of load-control equipment used. One way is to open up the channel of raise-lower impulses in common with a contact on each of the other alarm circuits. If servos are used to connect the computer to load-control equipment, the power can be removed from the servo motors "freezing" the regulating points at their last values. Electronic versions of this "freezing" operation are also possible. These last methods also permit taking the computer out of the control loop for service or routine preventive maintenance, or for use by the engineers in certain system economic studies.

The authors have discussed the utility of this computer with engineers in a number of power companies throughout the country. As a result, several changes have been made and optional alternatives provided. A digital voltmeter has been substituted for the meters to decrease the probability of reading errors.

Variable resistors may be substituted for fixed resistors so that *B* constant may be changed on fairly short notice. Switching between two or more sets of *B* constants for on-peak or off-peak operation can also be provided.

In the last paragraph of Professor Haupt's discussion is a statement of what, to the authors, is one of the most important contributions made by computers. It seems likely that, if engineers and operating personnel can be relieved of some of the routine but necessary requirements of their jobs, long-range benefits through better planning and the development of improved data and methods should greatly exceed those of the more obvious direct savings.

Automatic Load Shedding

AIEE COMMITTEE REPORT

IN RECENT years, there have been numerous system disturbances resulting in serious load interruptions. Although there were several causes, the result was the loss of generating capacity to the system or to a portion thereof. The excess of system load relative to the remaining system generation caused a drop in frequency and voltage, in turn resulting in loss of station auxiliaries.[1] This led to a further loss of generating capacity, and ultimately to a major system shutdown.

Some of the interruptions were caused by slow removal of system faults, causing system instability. Such trouble could have been avoided by the use of adequate protective equipment, including fast primary relaying, backup protection, adequate circuit breakers properly maintained, and in some cases high-speed reclosing.

Some other major load interruptions occurred in spite of high-speed fault clearing. When a particular system, or a component part thereof, does not have sufficient reserve generation (either generating units or transmission connections), separation may cause distress regardless of the speed of fault clearing.[2] Load shedding may then be mandatory. It is likely that such situations will become more serious with the increase in size of generating units and with a tendency to give preferential consideration in the scheduling of load to the newer and larger units.

Some interruptions may not have involved system faults at all, but in any case, if the excess load had been promptly removed, the system would have carried the remaining load, permitting more prompt restoration of service to the entire load.

Although some of the following discussion undoubtedly encroaches on the territory of the System Operations Subcommittee of the AIEE Committee on System Engineering, such discussion is believed to be essential to consideration of the devices used for load shedding.

Need for Automatic Load Shedding

The need for automatic load shedding depends on whether or not dispatchers and operators can act fast enough in an emergency. The required speed of response of the operator is largely a function of the amount of excess load relative to generation or, more accurately, the resulting rate of decay of frequency.

The greatest rate of change of frequency would be expected when a small system with more load than generation loses its tie to a larger system. A typical example is an industrial plant with generation equal to only one-half of its total load, operating in parallel with a utility. Loss of the tie would result in 100 per cent (%) overload on the industrial plant's generators. Fig. 1 (extracted from reference 3) indicates that regardless of the type of machine or of the assumptions made in calculating the curves, a dangerously low frequency is reached much sooner than an operator could react. There is no question that automatic load shedding is required for such a case, and that a fast-operating device is required, at least for the higher rates of change of frequency.

With a large utility system, it is improbable that the excess of load over generation, due to tie-line opening, would ever be greater than perhaps 33%, in which case it might be argued that there would be time enough for manual load shedding. However, for a severe overload, it is doubtful that manual load shedding would be fast enough to save the system. Fig. 2 is an example of frequency and voltage conditions during an actual disturbance. About half of the system was shut down, and the entire system might easily have been lost. Had adequate measures been taken after a few seconds, there would have been no loss of generation or load. However, the first effective manual measures occurred 140 seconds after the start of the disturbance.

To Split or Not to Split

System splitting may in some cases be as necessary as load shedding and, in certain special cases, may actually replace load shedding.

System splitting is obviously necessary in the case of the small industrial operating in parallel with the utility. Regardless of the industrial load relative to the industrial generation, the latter can easily be overloaded if a disturbance on the utility system leaves some utility load tied to the industrial system. Hence, it is essential to split the industrial system from the utility.

System splitting can substantially replace load shedding in certain special circumstances. For example, one large utility has a remote hydrogenerating station which supplies the system through two long transmission lines, both of which are required to carry the load, and maintain stability. Instability resulting from a tripout of one line is detected at the receiving end, and the system is split (via carrier-current control) at several other locations so that the load left on the main system substantially matches the generation of the main system. Similarly, the load remaining on the separated hydro station matches its generation. If both lines are lost, then load shedding would be required; but this condition would not be detected by the out-of-step tripping relay in the lines. Therefore, some other detecting means would be required to achieve the same system separation. Following the disturbance, the load that was shed could then be picked up from the remote generating station, and finally the two portions of the system resynchronized.

Although in the example of the small industrial, system splitting was essential, and in the example of the large utility it was advantageous, system splitting will be disadvantageous in many cases for the following reasons:

1. There may be no proper location for a split. Load shedding must then be used to maintain the system intact.
2. It may be difficult to determine the proper location to split, either in the planning stage, or by automatic devices in actual operation.
3. An incorrect split may accentuate the disturbance rather than relieve it.

Reasons 2 and 3 may make automatic splitting impractical on large interconnections where automatic dispatching leaves different areas short of local generation at different hours.

Need for a Questionnaire

Since there is little published information on load shedding,[3,4] the Committee decided upon a questionnaire to determine such unknowns as the following:

Paper 55-615, recommended by the AIEE Relays Committee and approved by the AIEE Committee on Technical Operations for presentation at the AIEE Pacific General Meeting, Butte, Mont., August 15–17, 1955. Manuscript submitted June 14, 1955; made available for printing June 23, 1955.

The personnel of the Working Group on Devices for Control of Load Shedding and System Separation of the AIEE Committee on Relays are: A. J. McConnell, *chairman*, L. L. Brandow, A. W. Adams, M. A. Bostwick, F. P. Brightman, M. D. Ewing, F. S. Fehr, L. L. Fountain, R. A. Larner, W. E. Marter, H. P. Sleeper, G. B. Steeb, and Frank von Roeschlaub.

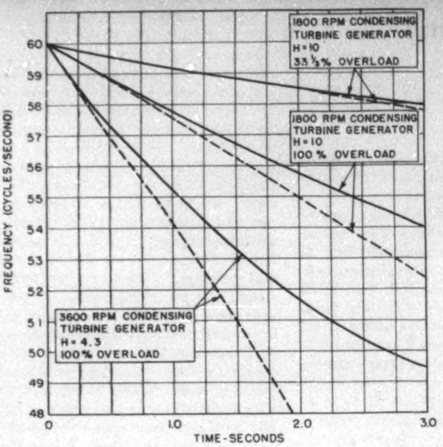

Fig. 1. Frequency-time characteristics of turbine generators resulting from overload

H—Inertia constant
Dashed lines—Resistance load
Solid lines—2% reduction of total kw load for each 1% frequency drop

1. Is there a predominant philosophy with respect to load shedding?

2. Is load shedding generally necessary? Is its use increasing? Is its use decreasing? Why is it not used?

3. What are the devices or combinations of devices that are used for load shedding?

4. If underfrequency relays are used, how are they used?

5. Is system splitting commonly used? What devices are used?

6. Are available devices satisfactory? If not, why not?

Seventy-nine questionnaires were distributed, of which 52 (66%) were returned answered.

Summary of Questionnaire

I. Do you use any automatic load-shedding means on your system?, 20 yes; 32 no

- A. To relieve system-wide overload?, 8 yes
- B. To drop load on an overloaded portion of the system after an inadvertent separation?, 12 yes
- C. To cause a separation:
  - 1. Within your system, between predetermined load areas, when one area becomes overloaded and net power is flowing out of it?, 2 yes
  - 2. At interconnections with other systems, if your system is overloaded and furnishing power to the interconnected system?, 6 yes
- D. Other (please explain), 4 answers

Typical answers: "Drop one of the customer's furnaces if he thermally overloads ties." "Drop load to keep transmission network intact."

II. What primary detecting devices do you use for load shedding?

- A. Frequency relays, 16
- B. Rate-of-change-of-frequency ("inertia")[8] relays, 1
- C. Power relays, 5
- D. Area load totalizer, 1
- E. Combinations of primary devices, 3 (A and C); 1 (B and C); 1 (A and D)
- F. Other? Others included an undervoltage-underfrequency combination, directional overcurrent, undervoltage, induction-disc frequency relays modified to close on undervoltage, and thermal relays, 4 answers

III. If frequency relays are used for load shedding, are they used:

- A. To remove a single block of load at a certain frequency, with no intentional time delay?, 5 yes
- B. Same as A but with time delay?, 7 yes
- C. To shed smaller blocks of load successively at different frequencies?, 5 yes
- D. To shed smaller blocks of load at the same frequency but at successively longer times?, 3 yes
- E. Combinations of C and D?, 2 yes
- F. Other? "Underfrequency time-delay tripping is blocked by voltage relay." Other comments involved manual load shedding, 5 answers

IV. If you use system-separating means, what primary detecting devices are used? In this question, system separation should be primarily for load shedding, or for attempting to match load with generation.

- A. Overpower?, 1 yes
- B. Underfrequency?, 6 yes
- C. Power directional in combination with underfrequency?, 4 yes
- D. Out-of-step-tripping relay?, 3 yes
- E. Other? Others included line protective relays, undervoltage-underfrequency combination and voltage-controlled overcurrent relay with long time delay, 4 answers

V. Do the devices of IV:

- A. Separate at the location of the detecting device?, 13 yes
- B. Separate at a distance by remote control?, 1 yes

VI. If you have used load shedding in the past, and have abandoned it, please state why?, 9 answers

"No longer needed" (various reasons), 6
"Load dropping at unattended station caused longer outage than necessary," 1
"Unreliable relay operation," 1
"Other members of interconnection do not perform load shedding," 1

VII. If you now use load shedding, do you plan to:

- A. Extend its use?, 7 yes; 6 no
- B. Abandon it?, 2 yes; 5 no

"Due to system growth, and obsolescence of small power plants." "Present trend toward unattended stations is making present method inadequate."

VIII. If you do not now use load-shedding devices:

- A. Do you plan to install them in the future?, 5 yes; 20 no

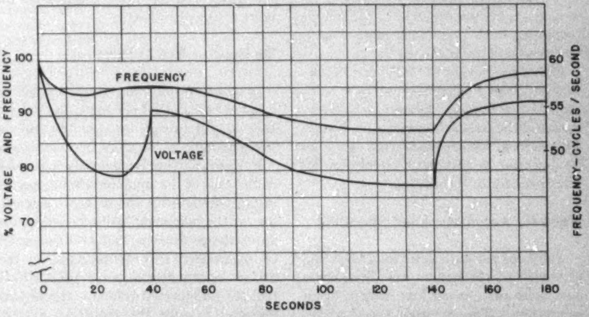

Fig. 2. Voltage and frequency versus time during an actual major system disturbance

1. If yes, for what purposes?
"To relieve system-wide overload," "To drop load on an overloaded portion of the system after an inadvertent separation," "Maintenance of system voltage," "To meet N.W. Power Pool arrangements and prevent system break-up."
2. With what devices?
6 answered frequency relays; 1, inertia relay; 1, undervoltage and 1, out-of-step tripping.

B. If you have considered automatic load shedding and have concluded not to use it, please give reasons, 13 answers

Typical answers: "Manual load shedding considered adequate." "Other members of interconnection do not use it." "Unnecessary load shedding detrimental to service." "Not required." "Too hot to handle policy-wise." "We are still living right and carrying a large rabbit's foot."

IX. If you use any load-shedding or system-separating means which you believe to be unique, please describe briefly, 2 answers

"A power relay contact in series with a low-frequency contact on a frequency recorder (never did work—probably too slow)." "When small industrial generation is required to separate from the utility with which it normally is paralleled, we use a scheme which is superior to the frequency relay in my opinion. This scheme consists of an induction-type voltage relay connected in a nul voltage circuit which is a balance between the customer's bus voltage and an independent source from the utility. The independent utility source may not always be available, but where the scheme can be used, it has many advantages:

1. The scheme is fast as it operates on the first swing.
2. Setting is simple (relay can be set to operate for loss of either source or only for out-of-step voltage).
3. Scheme is reliable as it only has to differentiate between zero voltage and a voltage (depending on the setting) which is normally just above the voltage due to loss of one source."

X. In your opinion, are available devices sufficient for your needs with respect to load shedding, system splitting, and combinations of the two?, 25 yes; 7 no

"Devices are available, but too expensive."

XI. If your answer to Question X was "No," please state wherein you believe available devices are insufficient for your needs, 10 comments

"Not sufficiently accurate," 2
"Too difficult to calibrate," 1
"Too slow in operation," 1
"A field for a dependable device which will promptly recognize trouble and initiate action without waiting for substantial frequency drops," 5
"Not sufficiently dependable," 1

Committee Notes on Questionnaire

Because of the wide variety of answers received, it is difficult to establish general patterns. However, the results appear to indicate that closely knit utilities, which operate principally in the larger metropolitan areas, have developed little need for load shedding as yet. Most of the need has occurred where the transmission networks are extensive, especially when there is the danger of losing a sizable remote generating source.

Apparently, there will be a modest increase in the use of load shedding, since those planning its initial use (five) outnumber those planning to abandon it (one).

Underfrequency relays, used alone, outnumbered all other devices, 16 out of 20 so reporting. Also, when used in combination with another device, underfrequency relays are the most common. However, there appears to be a need for a fast, dependable rate-of-change-of-frequency relay, 5 so reporting.

One deterring factor in the use of automatic load shedding is the unattended station, because of the delay in re-establishing customer service. However, one utility has reported the use of a frequency relay to reconnect the load when the frequency has returned substantially to normal. Load should be restored in this manner on a staggered basis to avoid pumping.

Another deterring factor is that all members of an interconnected system must use load shedding if the purpose is to keep the entire interconnected system intact. Load shedding on a small system is of no use if that system can be subjected to a portion of the load of a giant neighbor. In fact, one small utility abandoned load shedding for this reason. Apparently, the small utility had an agreement with its larger neighbor that the former would not open the interconnection during low-frequency and power-out conditions.

Conclusions

Most systems have not yet needed automatic load shedding. However, its use is gradually increasing and is usually instituted after the first serious disturbance resulting in excess load compared to generation.

A serious disturbance is likely to result in a rate of decay of frequency too rapid for manual corrective measures to be successful. This is especially true when a small system with more load than generation loses its tie to a larger system. The rate of frequency decay may also be too fast for induction-disk frequency relays.

System splitting, in conjunction with load shedding, may be essential, desirable or disadvantageous, depending upon the type of system involved and upon the specific reasons for the system trouble.

The frequency relay is the most widely used device for load shedding, although a fast, dependable rate-of-change-of-frequency relay would at least partially replace the underfrequency relay.

References

1. The Effect of Frequency Reduction on Plant Capacity and on System Operation, **H. A. Bauman, G. R. Hahn, C. N. Metcalf.** *AIEE Transactions*, vol. 73-B, Feb. 1955, pp. 1632–37.

2. The Effect of Frequency and Voltage, **Richard Holgate.** *Ibid.*, pp. 1637–46.

3. Application and Test of Frequency Relays for Load Shedding, **L. L. Fountain, J. L. Blackburn.** *Ibid.*, pp. 1660–64.

4. Load Shedding by Underfrequency Relays, **J. S. Braddock.** *Electric Light and Power*, Chicago, Ill., Oct. 1953, pp. 117–18.

5. Inertia Relay "Anticipates" to Facilitate Reclosure, **J. T. Logan, J. H. Miles.** *Electrical World*, New York, N. Y., Apr. 6, 1940, pp. 69–72.

◆

Discussion

James T. Logan (Engineering Specialist, St. Petersburg, Fla.): To one who has been closely associated with problems involving high-speed switching for the past two decades, the need for reliable frequency-responsive control devices is genuinely appreciated. While pioneering the practice of high-speed circuit reclosure in the early 1930's, load shedding presented a major problem in connection with co-ordinating the operations of industrial plant by-product generating facilities with the utilities' supplemental power sources. In such operations it is necessary, upon failure of the utilities' power source, to drop sufficient load in the plant to prevent "swamping" the local generating equipment. This requires high-speed switching; otherwise the local generators will be shut down, interrupting the entire plant operation. Similar problems on utilities' systems were encountered where the loss of a major interconnection or power source to fringe load areas left local generating units badly overloaded.

To meet these emergencies, it was necessary to develop a rate-of-frequency change-responsive device known as an "inertia" relay. The response of this relay proved to be fast enough to avoid shutting down local generating equipment, by tripping a tie breaker between an essential bus to which the generators and essential feeders are connected and a nonessential bus with lesser important loads left connected to the supplemental power source. This high-speed tripping of the bus tie breaker not only left loads within capacity connected to the generating units, but also permitted application of high-speed reclosure to the supplemental

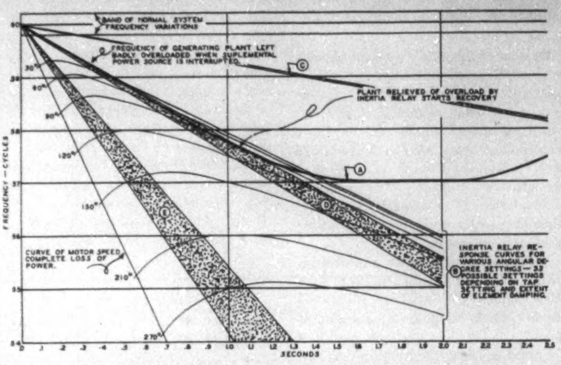

Fig. 3. **Operating characteristics of inertia relay showing response to system frequency variations**

A—Frequency-time curve for load area where automatic load shedding was successfully applied

B—Typical response curves of inertia relay

C—Calculated time-frequency characteristic envelope of 1,800-rpm condensing turbine generator: H = 10, $33^{1}/_{3}\%$ overload

D—Calculated time-frequency characteristic envelope of 1,800-rpm condensing turbine generator: H = 10, 100% overload

E—Calculated time-frequency characteristic envelope of 3,600-rpm condensing turbine generator: H = 4.3, 100% overload

power source breaker (breaker reclosure without intentional delay), thereby preventing an interruption to the feeders connected to the nonessential bus. Thus, the inertia relay, because of its reliable high-speed response, permitted loss of the supplemental power source from transient causes without interrupting service supplied from either the essential or nonessential busses.

Included in Fig. 3 are a few of the characteristic response curves of the inertia relay. Superimposed on these curves are the envelopes of the time-frequency characteristics of turbine generators resulting from overloads. These envelopes are reproductions of Fig. 1 in the paper. Judging from the replies to the questionnaire sent out by the committee, the inertia relay is relatively unknown, even though there are many such relays performing well in service.

In regard to the paper, it appears that a major reason for the future application of automatic load shedding and/or system splitting is overlooked: the declining ratio between system or area loads and the size of generating units being installed today. It is not infrequent for some utilities to install generators with a capacity of from 25 to 40% of the system or area demand. In such instances, it is uneconomical to operate sufficient spinning reserve, even if available, to protect against the loss of such units. The net result is that loss of so large a unit overloads interconnections or other supplemental power sources to the extent that they are tripped out, leaving the area or system deficient in generating capacity. In such emergencies it may be necessary to curtail load in a matter of cycles, rather than seconds, to prevent widespread and prolonged service failures to the entire area.

Where large interconnected systems are involved, the loss of generation will not result in an appreciable change in frequency unless the load area involved becomes isolated due to loss of overloaded tie lines. Even in such cases, load shedding is essential only if the rate-of-frequency decay is such as to indicate that the frequency will not become stable at some subnormal level, say 58 or 59 cycles. A case of trouble of this type has been described.[1] For troubles of this nature, flat-frequency relays would be at a distinct disadvantage since, in the case referred to, it required 18 minutes to restore normal frequency—but without interruption. Of the 15 inertia relays subjected to this disturbance, only one operated and that correctly, due to an out-of-step condition.

The inertia relay is an anticipatory device since it responds to the rate-of-frequency change only. If the rate-of-frequency decay is sufficient to indicate loss of a power plant within a few seconds, unless relieved of overload, the relay can be set to respond to this impending shutdown within 1/4 to 1 second. On the other hand, if the rate-of-frequency decay is slow enough to indicate that automatic switching is unnecessary, the relay will not respond.

In reference to Fig. 3, if a system or load area should become deficient in generating capacity to the extent that the rate-of-frequency decay is along the heavy line marked *A*, the inertia relay would close contact in 0.45 second if set on the 30-degree tap. For a 90-degree setting, the relay would respond in 0.90 second. If, however, the rate-of-frequency is more gradual, indicating that self-recovery is possible, the relay would not respond. Also, for this particular decay, the relay would not respond for the 120-degree or any higher setting.

It should be noted that the relay characteristics are well suited for two of the three rates of frequency decay shown by the turbine generator curves in Fig. 1. By changing the inertia element dampening, the relay could be made to respond to the 1,800-rpm H-10 $33^{1}/_{3}\%$ overload curve; however, I predict there will be much controversy over automatic load shedding for this relatively slow rate-of-frequency decay.

The foregoing discussion is not intended as a promotional "plug" for the inertia relay, but merely to point out that there is now available a device with characteristics almost ideally suited for load-shedding purposes, but one which is relatively unknown.

REFERENCE

1. Discussion by J. T. Logan of "A NEW FREQUENCY RELAY FOR POWER-SYSTEM APPLICATIONS, H. J. Carlin, J. L. Blackburn. *AIEE Transactions*, vol. 63, 1944, p. 1421.

A. J. McConnell (Project Committee Chairman): Mr. Logan points out that the committee report did not stress the importance of the increasing use of generating units which are large with respect to the total system generation. This is certainly an important factor, since the loss of such a unit would result in a greater rate of decay of frequency than would the loss of a smaller unit.

In addition to its obvious advantage during a rapid rate of change of frequency, the inertia relay would appear to be advantageous whenever a slow frequency decay results in a minimum frequency from which the system can recover. The inertia relay would avoid unnecessary load shedding, whereas the underfrequency relay might shed load when not necessary. On the other hand, the inertia relay might permit a slow reduction of frequency to a dangerous level. Perhaps a combination of two relays, one operating on rate of change of frequency and one operating at a low frequency, such as 56 cycles per second, might provide the ideal combination. Of course, a single relay, combining those features, would be even more acceptable.

Bureau of Reclamation 230-Kv Transmission Lines in North Dakota

THOMAS M. AUSTIN
MEMBER AIEE

Synopsis: A double-circuit 230-kv transmission line from the Garrison Dam power plant to Bismarck, N. Dak., and a single-circuit 230-kv transmission line from Bismarck to Jamestown, N. Dak., were recently constructed by the Bureau of Reclamation as a part of the proposed ultimate system to transmit power from the Federal power plants on the Missouri River to wholesale customers in the Missouri River Basin. The lines are designed for National Electrical Safety Code heavy-loading conditions with additional vertical strength in the crossarms to support the conductors with $1^1/_2$-inch radial thickness of ice. The conductors used on both circuits of the Garrison-Bismarck line are 795,000-circular-mil (CM) steel-reinforced aluminum cable (ACSR), *26 Al/7 st.* The conductors on the Bismarck-Jamestown line are 954,000-CM ACSR, *54 Al/7 st.* Two 1/2-inch high-strength-grade 7-wire class-*A* galvanized steel-strand overhead ground wires are used for the full length of each line. The design features of these transmission lines are typical of Bureau of Reclamation lines constructed since 1946.

THE Garrison-to-Bismarck and the Bismarck-to-Jamestown 230-kv transmission lines in North Dakota are a portion of the network of transmission lines being constructed by the Bureau of Reclamation to distribute federally generated power to wholesale consumers within the Missouri River Basin. The Garrison-to-Bismarck line is a double-circuit line forming a portion of the main circuits interconnecting the power plants being constructed on the Missouri River by the Corps of Engineers, Department of the U. S. Army. The lines are being extended from Bismarck down the Missouri River to Fort Randall, S. Dak., and Sioux City, Iowa. Power plants are now under construction at the Garrison, Fort Randall, and Gavins Point dams. Future power plants are planned for construction at Oahe and Big Bend. The Bismarck-to-Jamestown 230-kv line extends eastward from Bismarck, N. Dak., and forms a portion of a system planned to supply power to wholesale customers in eastern North Dakota and western Minnesota. The location of these transmission lines is shown in Fig. 1.

Studies of the power system on the Bureau's a-c network analyzer showed that the circuits between Garrison Dam and Bismarck should be capable of carrying a peak load of 300,000 kw and that a peak load of 225,000 would need to be transmitted from Bismarck to Jamestown. After a study of these requirements, the desired reliability of service and the costs of single- and double-circuit lines, it was decided to construct a 230-kv double-circuit steel tower line from Garrison to Bismarck with six 795,000-CM ACSR conductors and two 1/2-inch galvanized steel overhead ground wires. It was decided that one 230-kv single-circuit steel tower line with three 954,000-CM ACSR conductors and two 1/2-inch galvanized steel overhead ground wires should be adequate for the Bismarck-to-Jamestown line.

The Garrison-Bismarck transmission line consists of 60.0 miles of double-circuit line plus two single-circuit lines, each 2.66 miles long. The single-circuit lines extend from the switchyard at the Garrison Dam power plant across the face of the dam to a point on the east side of the Missouri River where the two single-circuit lines come to a single-double circuit tower and continue as a double-circuit line to the Bismarck Substation near Bismarck, N. Dak. Single-circuit towers are used adjacent to the Washburn Substation on both sides, and adjacent to the Bismarck Substation to aid in changing the conductors from vertical to horizontal configuration. A typical double-circuit suspension-type tower is shown in Fig. 2. The Bismarck-Jamestown transmission line is a single-circuit steel-tower line, 98.3 miles long, extending from the Bismarck Substation, near Bismarck, to the Jamestown Substation near Jamestown, N. Dak. A typical single-circuit suspension-type tower is shown in Fig. 3. These lines are now in service transmitting power at 115,000 volts. They are scheduled for conversion to 230,000-volt operation as soon as the power plant at Garrison Dam is ready in 1955. The design features of these transmission lines are typical of Bureau of Reclamation lines constructed since 1946.

Summary of Electrical and General Design Data

Voltage: 230 kv.

Length of line: Garrison-to-Bismarck, 62.66 miles; Bismarck-to-Jamestown, 98.30 miles.

Types of structure: Garrison-to-Bismarck, double-circuit steel towers; Bismarck-to-Jamestown, single-circuit steel towers.

Design loading: National Electrical Safety Code[1] heavy-loading; vertical load due to $1^1/_2$-inch radial thickness of ice.

Ruling span: Garrison-to-Bismarck, 1,050 feet; Bismarck-to-Jamestown, 1,150 feet.

Insulators: Standard 10-inch diameter by $5^3/_4$ inch spacing, 15,000 pounds; suspension, single string, 16 units; dead end, double string, 17 units per string; critical positive impulse flashover voltage for $1^1/_2$x40-microsecond wave for 16 insulators, 1,425 kv.

Conductors: Line, Garrison-to-Bismarck, six 795,000-CM ACSR, *26 Al/7 st;* ultimate strength, 31,200 pounds; Bismarck-to-Jamestown, three 954,000-CM ACSR, *54 Al/7 st;* ultimate strength, 34,200 pounds; overhead ground wires, two 1/2 inch 7-wire high-strength-grade class *A* galvanized steel; ultimate strength, 18,800 pounds.

Maximum tension at full load conditions: Double circuit line conductors, 12,000 pounds; single circuit line conductors, 12,000 pounds.

Allowable reduced static tension in conductor caused by suspension insulator swing into ruling span with broken conductor in an adjacent span: Double circuit, 8,500 pounds; single circuit, 8,500 pounds.

Overhead ground wires: Double circuit, 7,000 pounds; single circuit, 7,000 pounds. No reduction in static tension in overhead ground wires is permissible because of short length of overhead ground wire suspension link.

Final tension at 60° F, no wind: Double circuit line conductors, 5,500 pounds; single circuit line conductors, 5,600 pounds.

Overhead ground wires: Double circuit: 2,520 pounds; single circuit, 2,750 pounds.

Final wire sag, no wind, at ruling span: Double circuit line conductors at 60 degrees Fahrenheit (F), 27.8 feet; at 120 F, 31.5 feet; single circuit line conductors at 60 F, 36.6 feet; at 120 F, 40.4 feet.

Overhead ground wires: Double circuit, at 60 F, 25.3 feet; at 120 F, 28.4 feet; single circuit, at 60 F, 31.3 feet; at 120 F, 33.9 feet.

Line clearance to structures: As shown in Fig. 4.

Paper 55-622, recommended by the AIEE Transmission and Distribution Committee and approved by the AIEE Committee on Technical Operations for presentation at the AIEE Pacific General Meeting, Butte, Mont., August 15–17, 1955. Manuscript submitted October 28, 1954; made available for printing June 23, 1955.

THOMAS M. AUSTIN is with the Bureau of Reclamation, Denver, Colo.

The author wishes to express his appreciation to many of his associates, especially K. T. Deutsch and R. S. Dorcas, for their work in the development of the designs presented in this paper.

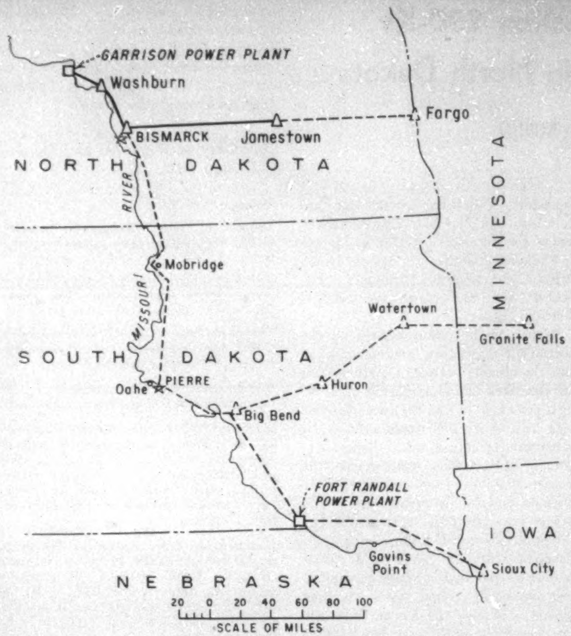

Fig. 1. Bureau of Reclamation 230-kv system in the Missouri River Basin

Wire spacing at structures: As shown in Fig. 4.

Mid-span separation, conductor to overhead ground wire at 60 F at ruling span: Double circuit, 26.8 feet; single circuit, 30.0 feet.

Assumed tower footing resistance, 15 ohms.

Isokeraunic level, 30.

Probable outages per year due to lightning: Double circuit, 0.3 per circuit; single circuit, 0.5.

Conductor clearance above ground at 60 F: Uncultivated land, 31 feet; cultivated land, 33 feet; railroads, 41 feet.

Galloping conductor ellipses, see Fig. 5.

Lightning Protection

The lines are shielded for their entire length by two 1/2-inch 7-wire high-strength-grade class-*A* galvanized-steel strands, located to give a protective angle at the structure of 20 degrees or less for the outside conductors. The overhead ground wires are grounded at each structure through the suspension clamp or dead-end fitting, the tower steel body and 5/8-inch by 10-foot copperweld ground rods. One ground rod is driven under each of the four tower footings and attached to the stub angle or the tower leg by soft copper wire.

Loading Conditions

A study of weather conditions in the central part of North Dakota indicated that the following conditions had been encountered.

Icing conditions: Ice of 1/2 to 3/4 inches radial thickness covering eight times during the 19 years previous to 1949; $1^{1}/_{2}$-inch radial thickness of ice once during the 19 years.
Wind velocities: During icing conditions, from 0 to 40 miles per hour with gusts up to 65 miles per hour. The higher velocities are not likely to occur under extreme icing conditions.
During nonicing conditions, 0 to 60 miles per hour with gusts to 90 miles per hour.
Temperature range: minus 30 F to plus 95 F.

Local utilities in the area have designed their lines for National Electrical Safety Code heavy-loading conditions with occasional additional storm guying. Therefore it was decided to design these lines for National Electrical Safety Code heavy-loading conditions except that the vertical design load on the steel towers was increased to support the conductors and overhead ground wires with $1^{1}/_{2}$-inch radial thickness of ice and 4-pounds-per-square-foot wind pressure at 0 F with all wires intact and a safety factor of 1.25 based on the yield point of the steel. The permissible side swing of the conductors is determined with a 70-mile-per-hour 7.6-pound-per-square-foot wind on the bare conductors.

Galloping Conductors

The conductors on the Garrison-Bismarck-Jamestown 230-kv lines are relatively heavy and the spans are long. Under these conditions, according to articles Davison[2,3] and others,[4] it is safe to assume that the amplitude of galloping will not exceed approximately one-half the maximum conductor sag. Half-sag ellipses for these lines are shown in Fig. 5. There is ample clearance for the half-sag ellipses. Conductor and overhead ground wire spacing was determined primarily by the clearance to structure requirements and the mid-span separation required between conductors and overhead ground wire for lightning protection and switching surge requirements. On the double-circuit towers, the center crossarms are extended 8 feet on each side to prevent contacts between conductors because of jumping when ice falls off one conductor, or from other causes.

Conductor and Overhead Ground Wire Tensions

Using the chosen conductors, designs for maximum loaded tensions of 12,000 pounds in each conductor resulted in economical construction. This maximum tension results in normal unloaded conductor tensions of 5,500 to 5,600 pounds at 60 F, which is low enough to promote long life of the conductors but still high enough to limit the sag to values which permit the use of 1,050-foot ruling span for the double-circuit line and 1,150-foot ruling span for the single-circuit line with towers of reasonable heights. Increased tension would increase the weight of the towers required, even though less tower height would be necessary, for approximately the same span lengths. Maximum overhead ground wire tensions of 7,000 pounds were chosen, resulting in normal tensions of only 2,500 to 2,750 pounds at 60 F; thus decreasing the probability of failure due to vibration fatigue.

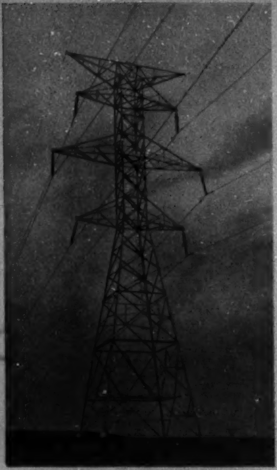

Fig. 2. Double-circuit suspension-type tower Garrison-Bismarck 230-kv transmission line

Corona Losses and Radio Interference

The corona losses are somewhat less than 1.0 kw per 3-phase mile, now considered an acceptable loss for lines of this voltage. The corona losses were calculated by the method of Carroll and Rockwell.[5] The average elevation of the lines is 2,000 feet above sea level. The calculated 3-phase fair weather corona loss per mile is 0.8 kw per circuit for the double-circuit line and 0.6 kw for the single-circuit line. The minimum conductor diameter on these lines is approximately 1.1 inches; therefore radio interference from the lines is not expected to be objectionable.[6]

Insulation and Clearances

Because lightning arresters are not used at transmission line structures, and because lightning strokes occurring on the line at some distance from a substation will be considerably attenuated before reaching the substation where lightning arresters are installed, it is desired to have the impulse insulation level higher for the transmission line than for the substation equipment. The wet flashover voltage of the insulation should be high enough to withstand switching surges. Test results with recommended safety factors applied indicate that standard insulators will withstand switching surge voltages of approximately 70 per cent of the impulse flashover value.[7] This is still somewhat higher than the rated 60-cycle wet flashover value. On the suspension-type structures and at dead ends with jumper support insulators, the insulation from phase to ground consists of 16 standard 10- by 5$^{3}/_{4}$-inch, 15,000-pound insulator disks. At dead ends without jumper support insulators, the phase-to-ground insulation is 17 standard insulator units. The average elevation of the lines from Garrison to Bismarck to Jamestown is approximately 2,000 feet above sea level. The relative air density at 2,000 feet is 0.93. The estimated lightning performance wa scalculated by the AIEE Committee method.[8] The isokeraunic level in North Dakota is approximately 30 storm days per year. For design purposes the footing resistance was assumed to be 15 ohms though actual measurements of footing resistances average somewhat less. The maximum permissible stroke current before flashover at the structure is as follows:

Double-circuit 1,050-foot spans, 160,000 amperes
Single-circuit 1,150-foot spans, 160,000 amperes

The maximum permissible stroke current before flashover at mid-span is as follows:

Double-circuit 1,050-foot spans, 26.8-foot mid-span separation, 140,000 amperes
Single-circuit 1,150-foot spans, 30.0-foot mid-span separation, 135,000 amperes

The estimated lightning outages per year are 0.3 per circuit on the double-circuit line and 0.5 on the single-circuit line. These values indicate that good performance should be obtained from the lines and that there is relatively good co-ordination between the mid-span clearance and the structure insulation.

The insulating value of insulators is directly proportional to the relative air density. The critical positive flashover value for 16 insulator units is 1,425 kv for a 1$^{1}/_{2}$x40-microsecond wave. Therefore the switching surge insulation is 1,425(0.70) (0.93) = 928 kv. The normal peak line to neutral voltage is 187.5 kv for a 230-kv (rms) line. The switching surge insulation is therefore 4.95 times the normal voltage. Maximum switching surges are not expected to exceed three times normal voltage.

A careful study of conductor side swing and clearances was conducted for these lines. It was decided that switching surge insulation should be maintained at the maximum expected wind and side swing; therefore all structures were located to maintain a minimum clearance of 5 feet 6 inches from the conductor to the tower steel at 7.6 pounds per square foot wind pressure on the bare conductors. The minimum expected insulation value of a 5-foot 6-inch air gap is 1,025 kv, which exceeds the switching surge insulation value of the 16-unit insulator string. At 5-foot 6-inch clearance, the side swing on the *DSH*-type tower is 40.3 degrees, and on the *SH*-type tower, 38.2 degrees. Experience has shown that the maximum winds and lightning are not likely to occur simultaneously. At approximately a 30-degree conductor side swing, the clearance from the conductor to tower steel is 7 feet 6 inches, the impulse insulation of which co-ordinates well with that of 16 insulators for lightning strokes.

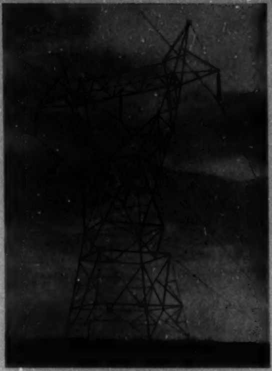

Fig. 3. Single-circuit suspension-type tower Bismarck-Jamestown 230-kv transmission line

Transpositions

To maintain balanced conditions on the three phases of each circuit between Garrison and Bismarck and thus to insure proper relay operation, it was decided that one transposition barrel, and two transpositions, should be installed. The Washburn Substation is located about one-third of the distance from Garrison to Bismarck, therefore we decided that one transposition would be made at Washburn within the substation, and one transposition of the rolling type on *DTRH*-type towers would be located midway between Washburn and Bismarck. To maintain a better balance between circuits, opposite phasing is used on corresponding sections of the two circuits, e.g., *ABC* from top to bottom on one circuit and *CBA* from top to bottom on the other circuit. On the Bismarck-Jamestown line it was decided to install only one transposition, as this line is being extended to Fargo, N. Dak.

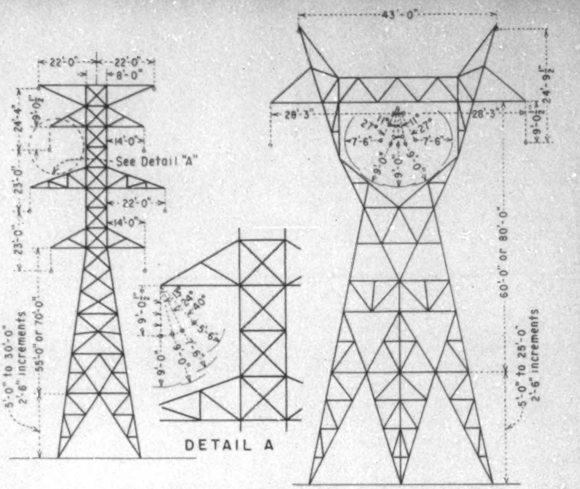

Fig. 4. Steel-tower outlines and clearance diagrams

Vibration Dampers and Armor Rods

Because of the importance of these lines and experience with vibration failures on the overhead ground wires of 115-kv lines in the Missouri River Basin, it was decided to use preformed galvanized steel armor rods at all suspension points on the overhead ground wires, and tapered aluminum armor rods at all suspension points on the ACSR conductors. In addition, Stockbridge type vibration dampers are installed at both ends of all spans of the conductor and overhead ground wires. On the overhead ground wires, the first vibration damper adjacent to the suspension clamps was located 3.1 feet from the center of the clamp to place it beyond the end of the preformed armor rods. If the second damper should be required, it will be 2.5 feet from the first.

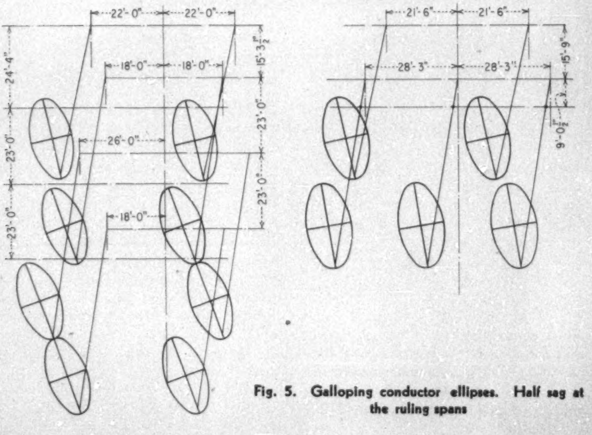

Fig. 5. Galloping conductor ellipses. Half sag at the ruling spans

Nonmagnetic Suspension Clamps

At the relatively high currents expected to be carried on these lines, the losses in standard forged steel or malleable iron suspension clamps on the conductors are an appreciable amount. For example, at an average current of only 235 amperes, the loss in a standard ferrous suspension clamp for 795,000-CM ACSR is 14 watts, whereas the loss in a good nonmagnetic clamp is about 1 watt at the same current. At 4 mils per kilowatt-hour the annual value of the excess loss in each ferrous clamp will be $0.4555. At higher currents, the differences in losses become much greater. The extra cost for aluminum alloy clamps was $2 each (bid by the construction contractor); therefore, it was considered well worth while to use nonmagnetic suspension clamps.

Structure Design

Design criteria as listed in the following were set up for the Garrison-Bismarck and Bismarck-Jamestown steel towers:

STEEL TOWERS

Procurement specification drawings and text for both lines were prepared on the basis of inviting bids on the bidder's own designs. Limitations and requirements were shown or stated to cover the following points for the several types of towers:

1. Body heights, range and increment of leg extensions, type of extension framing (tension or compression), location of horizontal frames, typical cable attachment details, and provisions for climbing and bird protection.
2. Minimum phase spacing, ground wire separation and cone of protection, and conductor clearances to steel.
3. Wind, wire, and special loadings, with criteria for application.
4. Permissible unit stresses, column formulas, inductance-reactance limitations. Unit stresses are shown in terms of basic yield point, with the invitation to employ high-strength steels wherever advantageous.
5. Provisions for full-scale tower tests before production-line fabrication.

For the Garrison-Bismarck (double-circuit) line only, because of the urgency in getting the line under construction, it was necessary to carry actual design of the structures to a point sufficient to permit earlier procurement of stub angles under separate contract.

The design loads were established consistent with the steel-tower data shown in the summary of steel-tower design requirements to follow. Longitudinal components of conductor tension for suspension towers under broken-wire assump-

Table I. Garrison-Bismarck Steel-Tower Design Requirements

Tower Type	Line Angle Range, Degrees	Maximum Single-Span Length, Feet	Maximum Sum of Adjacent Spans at 0 Degrees Line Angle, Feet	Maximum Sum of Adjacent Spans at Maximum Line Angle, Feet	Maximum Distance Between Conductor Low Points, Feet	Maximum Distance Between Overhead Ground Wire Low Points, Feet	Maximum Uplift at Each Conductor or Overhead Ground Wire, Pounds
DSH	0 to 3	1,600	3,200	2,100	1,600	2,000	1,500
DSAH	3 to 15	1,800	3,600	2,100	2,000	2,500	1,500
*DSAH-1**	0 to 3	1,800	3,600	2,100	2,000	2,500	1,500
DTH	0 to 30	2,000	4,000	2,100	2,500	3,000	1,500
DTRH†	0	1,600	3,200		1,600	2,000	1,500

* Same as *DSAH*, except with symmetrical crossarms.

† Same as *DSH*, except only two crossarms on one side and one on the other, for use as a transposition tower.

Table II. Bismarck-Jamestown Steel-Tower Design Requirements

Tower Type	Line Angle Range, Degrees	Maximum Single-Span Length, Feet	Maximum Sum of Adjacent Spans at 0 Degrees Line Angle, Feet	Maximum Sum of Adjacent Spans at Maximum Line Angle, Feet	Maximum Distance Between Conductor Low Points, Feet	Maximum Distance Between Overhead Ground Wire Low Points, Feet	Maximum Uplift at Each Conductor or Overhead Ground Wire, Pounds
SH	0 to 3	1,600	3,200	2,300	1,600	2,000	1,500
SAH	3 to 15	1,800	3,600	2,300	2,000	2,500	1,500
*SAH-1**	0 to 3	1,800	3,600	2,300	2,000	2,500	1,500
TH	0 to 30	2,000	4,000	2,300	2,500	3,000	1,500
DTRH†	0	1,600	3,200		1,600	2,000	1,500

* Same as *SAH* except for symmetrical crossarms.

† Transposition towers same as on double circuit line.

tions are based on the statically reduced values. Basic over-all factors of safety (based on yield point of steel used) are as follows:

Double circuit, all types 1.5.
Single circuit, type *SH* 1.25; other types 1.5.

Wherever required to assure meeting any more critical loading combinations and varying safety factors specified by the National Electrical Safety Code, loads were adjusted upward or a separate and independent load schedule was shown. Also, an independent load schedule was established on all towers for the intact condition (no broken wires) with $1^1/_2$ inches of ice, 4-pound wind, and zero degrees temperature, for a factor of safety of 1.25.

The towers furnished under the supply contract, designed and approved on the foregoing basis, successfully passed full-scale tests with very few minor changes in member sizes or details.

TOWER FOOTINGS

A study of foundation conditions and the nature of soils found along these lines led to the adoption of three basic types of footings, all employing stub angles embedded in concrete.

1. Auger type, undercut, or belled at the bottom, with concrete placed directly in excavation and cap-formed above grade. Designs of this type were provided for *DSH, DTRH, DTRH-1, SH, SAH,* and *SAH-1* towers for use wherever feasible.

2. Pad type with undercut, in hand excavation, with pad concrete placed directly in excavation and a formed stem poured above the pad. Designs of this type were provided for all towers, for use in tight soils either as an alternative to the auger type where foundation loading exceeded the capacity of any reasonably proportioned auger type.

3. Pad type without undercut, in machine excavation with formed pad and stem. Designs of this type were provided for all towers, for use wherever the nature of soil encountered precluded the use of types 1 or 2.

All of these types were designed to resist the most critical combination of thrust or uplift with accompanying shears imposed by the supported tower under its design loading, with a safety factor at least equivalent to that of the tower.

Summary of Steel-Tower Design Requirements

Garrison-to-Bismarck double-circuit line: Safety factor, 1.5 based on the yield point of the steel; unbalanced loading assumptions equivalent to the following broken conductors at reduced static tension.

Structure type: *DSH* for line angles 0 to 3 degrees, two conductors or two overhead ground wires or any one conductor and one overhead ground wire, all on the same face; *DSAH* for line angles over 3 to 15 degrees inclusive, any combination of three wires, all on the same face; *DTH* for all dead ends and line angles over 15 to 30 degrees inclusive, all conductors and overhead ground wires on the same face.

For further data on the Garrison-to-Bismarck line see Table I.

Bismarck-to-Jamestown single-circuit line: Safety factors: for *SH*-type towers, 1.25 based on the yield point of the steel; for all other types, 1.5 based on the yield point of the steel.

Unbalanced loading assumptions equivalent to the following broken conductors at reduced static tension.

Structure type: *SH* for line angles 0 to 3 degrees, one conductor or one overhead ground wire; *SAH* for line angles over 3 to 15 degrees inclusive, two conductors or two overhead ground wires or any one conductor and one overhead ground wire, all on the same face; *TH* for all dead ends and line angles over 15 to 30 degrees inclusive, all conductors and overhead ground wires on the same face.

For further data on the Bismarck-to-Jamestown line see Table II.

References

1. NATIONAL ELECTRICAL SAFETY CODE. National Fire Protection Association, Boston, Mass., fifth edition.

2. DANCING CONDUCTORS, A. E. Davison. *AIEE Transactions*, vol. 49, Oct. 1930, pp. 1444–49.

3. DESIGN FOR MINIMIZED TRANSMISSION WIRE CONTACTS, A. E. Davison. *Bulletin*, Hydro-Electric Power Commission of Ontario, Toronto, Ontario, Canada, vol. 29, Jan. 1942, pp. 16–23.

4. GALLOPING CONDUCTORS AND A METHOD FOR STUDYING THEM, E. L. Tornquist, C. Becker. *AIEE Transactions*, vol. 66, 1947, pp. 1154–61.

5. EMPIRICAL METHOD OF CALCULATING CORONA LOSS FROM HIGH-VOLTAGE TRANSMISSION LINES, Joseph S. Carroll, Mabel MacFerran Rockwell. *AIEE Transactions (Electrical Engineering)*, vol. 56, May 1937, pp. 558–65.

6. INVESTIGATION OF RADIO NOISE AS IT PERTAINS TO THE DESIGN OF HIGH-VOLTAGE TRANSMISSION LINES, H. L. Rorden, R. S. Gens. *AIEE Transactions*, vol. 71, pt. III, Jan. 1952, pp. 466–81.

7. ELECTRICAL CLEARANCES FOR TRANSMISSION-LINE DESIGN AT THE HIGHER VOLTAGES, P. L. Bellaschi. *AIEE Transactions*, vol. 73, pt. III, 1954, pp. 1192–1200.

8. A METHOD OF ESTIMATING LIGHTNING PERFORMANCE OF TRANSMISSION LINES, AIEE Committee Report. *AIEE Transactions*, vol. 69, pt. II, 1950, pp. 1187–96.

Impulse Tests on Low-Voltage Windings of Distribution Transformers

J. E. HOLCOMB
MEMBER AIEE

FOR impulse testing of transformers the American Standards Association specifies a $1\frac{1}{2}$x40-microsecond wave.[1] Many distribution transformers have low-voltage windings rated 600 volts or less. These windings have very few turns and therefore very low impedance to impulse voltage waves. For this reason an excessively large impulse generator would be required to apply a $1\frac{1}{2}$x40 microsecond wave from terminal to terminal of the winding. Even if an impulse generator of sufficient capacity were available, the application of a $1\frac{1}{2}$x 40-microsecond wave to the low-voltage winding would in many cases induce excessively high voltages in the high-voltage winding.

For these reasons the American Standards Association permits the test to be made by connecting the low-voltage terminals together and applying the impulse from terminals to ground. This tests the insulation to ground but not the internal insulation of the winding. For a quality control test to do a thorough job it must include a test which will stress the turn and layer insulation in the low-voltage coil. Such a test has been included on a production basis in the quality control test since 1952.

A comparison of the ratios of the impulse crest voltages to the 60-cycle rms operating voltages for oil-filled distribution transformers is shown in Table I, which shows that the highest ratios (of basic impulse level to rms voltage) occur in the lowest voltage ratings. It follows that if a low-voltage winding is subjected to an impulse voltage with a crest value equal to the corresponding basic impulse insulation level (BIL) and if an electromagnetically induced voltage equal to this value multiplied by the turn ratio should appear across the high-voltage winding, the latter winding would be subjected to a voltage far in excess of its BIL.

The problem of protecting the high-voltage windings during impulse tests on low-voltage windings is a serious one. The terminal voltages can be controlled by the use of external impedances or even by short-circuiting the winding; but voltages between parts of the winding cannot always be controlled in this manner. In fact, in some cases the internal voltage gradients may actually be increased when the winding is loaded by an impedance. Unfortunately, it is not always possible to predict what these voltage gradients will be for a particular transformer without an expensive and time-consuming investigation. There is the added disadvantage that on many transformers a short-circuited winding will drastically reduce fault detection sensitivity, and the test should not be simplified at the expense of this sensitivity.

The same comparison of the ratios of the impulse crest voltages to the 60-cycle rms operating voltages show that an impulse test on the high-voltage winding will induce only very small voltages in the low-voltage winding and will not adequately test the latter winding. For these reasons a completely reliable quality control impulse test must include a test designed primarily to test the transformer low-voltage windings.

Field Investigation Results and Transient Considerations

Other investigators[2,3] have shown that a large percentage of the lightning surges which arrive at transformers in service do so by way of the low-voltage lines. This emphasizes the desirability of a searching test on the low-voltage winding because in service it is almost as likely to be subjected to lightning surges as the high-voltage winding.

These investigators[3] have shown that when lightning strikes in the vicinity of a transformer in service, the ground potential is raised and the lightning currents flow outward on every possible path. If the midtap of the transformer low-voltage winding is connected to ground the surge currents will then flow outward through the two halves of the low-voltage winding so that the effect of these two currents might be expected to cancel out, leaving no net electromagnetic effect. In an actual transformer the two halves of the low-voltage winding cannot occupy identical locations; so there is never a perfect current balance or flux cancellation. In fact, the voltage induced in the high-voltage winding by this surge current has been found to be similar to that induced by a short-tailed impulse wave applied between terminals of the low-voltage winding.

Almost all consumer equipment (rated 600 volts or less) has an insulation level which will not withstand impulse voltages of 25 kv for periods exceeding 1 or 2 microseconds. Such equipment can be expected to flash over when impulse waves of longer duration are applied even if the voltage is considerably lower than 25 kv. Because of this and because the secondary conductors between the distribution transformer and the consumers' premises are usually short, seldom exceeding 1,000 feet in length, it is unlikely that in service surges of 25-kv magnitude exceeding 1 or 2 microseconds in length will be applied to distribution transformer low-voltage windings.

The practice of applying short-tailed impulse waves between terminals of the low-voltage windings of distribution transformers on a production basis was started in 1952.[4] Since that time, many thousands of transformers have been tested and put into service. The very small number of customer complaints on transformers which have been tested in this manner indicate that a test of this type is very effective in eliminating faulty transformers, and that transformers that will withstand such a test will successfully withstand surges which might be expected in service.

Transient Behavior of Distribution Transformers

A previous paper[5] states that when a rectangular traveling wave is applied to the high-voltage winding of a power transformer, the voltages within the transformer windings consist of four components:

Table I. Comparison of Ratios

Typical 60-Cycle Operating Voltage, RMS	Typical Impulse BIL, Kv Crest	Ratio of BIL to Operating Voltage
240	30	125
480	30	62.5
2,400	60	25
4,800	75	15.6
7,200	95	13.2
13,200	95	7.2

Paper 55-27, recommended by the AIEE Transformers Committee and approved by the AIEE Committee on Technical Operations for presentation at the AIEE Pacific General Meeting, Butte, Mont., August 15–17, 1955. Manuscript submitted October 19, 1954; made available for printing June 23, 1955.

J. E. Holcomb is with the General Electric Company, Pittsfield, Mass.

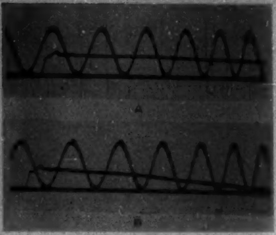

Fig. 1. Voltage induced on 7,200-volt winding of 10-kva 7,200 120/240-volt transformer when 0.5x1.5-microsecond wave is applied to 120-volt winding. Frequency of timing wave 50 kc per second, giving period of 20 microseconds

A—With no fault B—With 1-turn fault

1. A voltage transmitted electrostatically to the low-voltage winding, depending on the relations of distributed capacitances of the low-voltage to the high-voltage winding and ground, and independent of the turn ratios.

2. A free oscillation in the high-voltage winding, consisting of a number of space harmonics, and which, through the electromagnetic and electrostatic fields, induces a corresponding forced oscillation in the low-voltage winding.

3. A free oscillation in the low-voltage winding, depending on the distributed constants of the winding.

4. A unidirectional voltage surge transmitted to the low-voltage winding by electromagnetic induction which is very nearly directly proportional to the turn ratio and is independent of the distributed capacitance. It is a simple function of the short-circuit inductance of the transformer and of the surge impedances of external circuits.

The same principles apply when the impulse voltage is applied to the low-voltage windings of distribution transformers. However, the voltage transmitted by the capacitance relationship from the low-voltage to the high-voltage winding is negligible. Also, because of the few turns in the low-voltage windings, the oscillations in this winding are negligible. The free oscillations in the high-voltage windings are of considerable importance since they affect the internal stresses in this winding. It is well known that the front of the induced wave is sloped off by the leakage reactance between transformer windings. Because of the relatively slow rate of rise of this induced wave, its peak value may be controlled by shortening the length of the tail of the applied wave. Thus, by applying the proper wave shape to the low-voltage winding, the magnitude of the voltage wave induced in the high-voltage winding can be controlled even though the peak voltage of the applied wave is held at the level required by the American Standards Association. This provides an effective means of testing transformers because the insulation in all the windings can be properly stressed. However, because the applied voltage wave is short the usual fault detection methods may not be applicable.

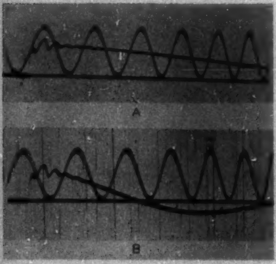

Fig. 2. Voltage induced on 2,400-volt winding of 10-kva 2,400 120/240-volt transformer. Same conditions and frequency as in Fig. 1

A—With no fault B—With 1-turn fault

Fault Detection by Induced Voltage Wave Method

About 1940, considerable work was done experimentally to develop impulse test equipment which would apply impulses to the low-voltage windings of small pole-type distribution transformers. Testing circuits were used which would apply the proper crest voltages to the low-voltage winding and, by controlling the length of the applied wave, induce the proper voltage on the high-voltage winding. The induced voltage wave, viewed by means of a cathode-ray oscillograph, was used for the purpose of detecting failures.

Because early data indicated the importance of a searching test on the transformer low-voltage windings, this test is included in the quality control impulse testing of distribution transformers.[4] As in the previous test, the induced voltage wave is observed by means of the cathode-ray oscillograph, and thousands of tests have shown that it is a very sensitive and very reliable method of detecting failures.

To show the sensitivity of this method of fault detection, simulated faults were made by wrapping one turn of insulated wire around the outer transformer winding. This turn is loosely coupled to both high-voltage and low-voltage windings. Because of the loose coupling, the fault is harder to detect than a 1-turn fault buried in either winding. Many tests have been made to verify this statement. Consequently the changes in wave shape shown in the oscillograms are somewhat smaller than would be the case when the smallest failure occurs in the transformer itself. The turn faults referred to in the succeeding paragraphs refer to these simulated turn faults.

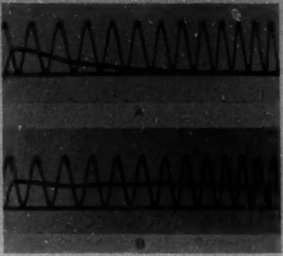

Fig. 3. Voltage across an impedance in the neutral of a 10-kva 7,200 120/240-volt transformer when a 1 1/2x40-microsecond wave is applied to the 7,200-volt winding. For frequency of timing wave see Fig. 1

A—With no fault B—With 1-turn fault

The reader is referred to the oscillogram in Fig. 1(A), in which is shown the voltage wave induced on the high-voltage winding of a transformer rated 10-kva 7,200 120/240 volts when a 0.5x1.5-microsecond wave is applied to the low-voltage winding. Fig. 1(B) shows this induced voltage wave when there is a 1-turn fault in the transformer. In like

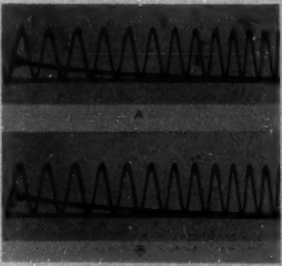

Fig. 4. Voltage induced on the 120-volt winding of a 10-kva 7,200 120/240-volt transformer when a 1 1/2x40-microsecond wave is applied to the 7,200-volt winding. For frequency of timing wave see Fig. 1

A—With no fault B—With 1-turn fault

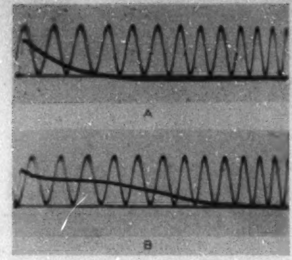

Fig. 5. Voltage across an impedance in the neutral of a 10-kva 2,400 120/240-volt transformer when a $1^{1}/_{2}$x40-microsecond wave is applied to the 2,400-volt winding. For frequency of timing wave see Fig. 1

A—With no fault B—With 1-turn fault

manner Fig. 2(A) shows the voltage wave induced on the high-voltage winding of a transformer rated 10-kva 2,400 120/240 volts when a 0.5x1.5-microsecond wave is applied to its low-voltage winding. Fig. 2(B) shows this induced voltage wave when there is a 1-turn fault in the transformer. A comparison of Fig. 1(B) with Fig. 1(A) and of Fig. 2(B) with Fig. 2(A) will illustrate the sensitivity of this method of fault detection when tests of this type are made on small distribution transformers.

Comparison of Fault Detection Methods When Testing High-Voltage Windings

In 1944 the method of observing the voltage induced on a winding other than the one under test was studied and compared to several other methods of fault detection.[6] It was found to be fairly sensitive in detecting distribution transformer faults when a $1^{1}/_{2}$x40-microsecond impulse was applied to the high-voltage winding and the voltage induced on the low-voltage winding was observed by means of the cathode-ray oscillograph. However, the neutral impedance method of failure detection proved to be far more sensitive for this application and consequently has been used almost exclusively.

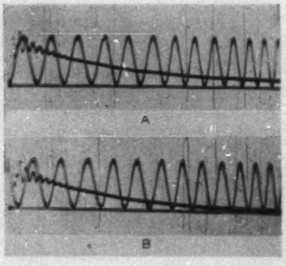

Fig. 6. Voltage induced on the 120-volt winding of a 10-kva 2,400 12/0240-volt transformer when a $1^{1}/_{2}$x40-microsecond wave is applied to the 2,400-volt winding. For frequency of timing wave see Fig. 1

A—With no fault B—With 1-turn fault

The relative sensitivities of the two methods are illustrated by Figs. 3 through 6 inclusive. Fig. 3(A) is the voltage wave across an impedance between the ground and the neutral of a transformer rated 10-kva 7,200 120/240 volts when a $1^{1}/_{2}$x40-microsecond wave is applied to the high-voltage winding. Fig. 3(B) shows this voltage wave when there is a 1-turn fault in the transformer. Fig. 4(A) shows the voltage wave induced on the low-voltage winding of this transformer when a $1^{1}/_{2}$x40-microsecond wave is applied to the high-voltage winding and Fig. 4(B) shows the same voltage wave when there is a 1-turn fault in the transformer.

Fig. 5(A) is the voltage wave across an impedance between ground and the neutral of a transformer rated 10-kva 2,400 120/240 volts when a $1^{1}/_{2}$x40-microsecond wave is applied to the high-voltage winding. Fig. 5(B) shows this voltage wave when there is a 1-turn fault in the transformer. Fig. 6(A) shows the voltage wave induced on the low-voltage winding of this transformer when a $1^{1}/_{2}$x40-microsecond wave is applied to the high-voltage winding and Fig. 6(B) shows the same wave when there is a 1-turn fault in the transformer. A comparison of these oscillograms will show that the neutral impedance method of fault detection is the more sensitive of the two methods.

Impulse Testing of Low-Voltage Windings of Large High-Voltage Distribution Transformers

Another important group of distribution transformers comprises those used to step down subtransmission voltages to distribution voltages. Many of these are single-phase transformers, usually 100 to 500 kva with 22- to 66-kv primaries and 2.4- to 15-kv secondaries. In testing the secondary windings of these transformers many of the same problems are encountered as in testing the smaller pole-type transformers. However, the physical spacings between windings are much greater because of the insulation requirements, and the induced voltage waves on the high-voltage windings are not nearly so sensitive to faults as is the case for the small low-voltage transformers. Consequently, it may be desirable to use other fault detection methods when testing this type of transformer.

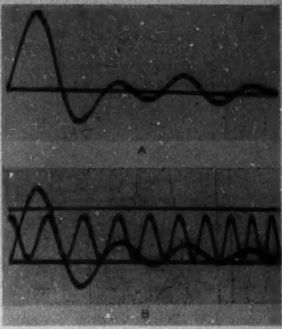

Fig. 7. Voltage across an impedance in the neutral of a 333-kva 67,000 to 7,200-volt transformer when a 1.5x27-microsecond wave is applied to the 7,200-volt winding

A—With no fault. Timing wave is omitted but sweeping speed is same as that in B
B—With 1-turn fault. Frequency of timing wave 10 kc, giving a period of 100 microseconds

Waves of fairly long duration can be applied to the low-voltage winding of this type of transformer without overstressing the high-voltage winding, even with its terminals isolated, and it is possible to use the neutral impedance method of fault detection. For this type of transformer, the oscillograms of Fig. 7 and 8 compare

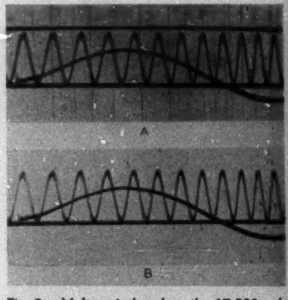

Fig. 8. Voltage induced on the 67,000-volt winding of a 333-kva 67,000 to 7,200-volt transformer with no fault when 1.5x27-microsecond wave is applied to 7,200-volt winding. For frequency of timing wave see Fig. 1

A—With no fault B—With 1-turn fault

the relative sensitivities of the neutral impedance and induced wave method of fault detection.

Fig. 7(A) is the voltage wave across an impedance between ground and the neutral of a transformer rated 333-kva 67,000 7,200 volts when a 1.5x27-microsecond wave is applied to the low-voltage winding. Fig. 7(B) shows this same voltage wave when there is a 1-turn fault in the transformer. Fig. 8(A) is the voltage wave induced on the high-voltage winding of this transformer when the 1.5x27-microsecond wave is applied to the low-voltage winding. Fig. 8(B) is the induced voltage wave when there is a 1-turn fault in the transformer. In this case the induced voltage wave changes very little when failure occurs, and it is doubtful if a 1-turn failure could be detected with the use of this method. The voltage wave across the neutral impedance clearly shows that failure has occurred. This indicates that, when it is possible to apply a voltage wave of this duration, the neutral impedance method of fault detection is the preferable method. It may still be the preferable method when waves of shorter duration are used, but further investigation is required to determine the minimum wave length permitting its use.

Conclusions

1. In impulse testing of many ratings of distribution transformers having relatively high turn ratios, the standard $1^{1}/_{2}$x40-microsecond wave cannot be applied between terminals of the low-voltage winding because excessive voltages would be induced in the high-voltage winding.

2. The magnitude of the voltage induced in the high-voltage winding can be held within limits by reducing the duration of the voltage wave applied to the low-voltage winding. Therefore, the use of voltage waves of shorter duration than $1^{1}/_{2}$x40 microseconds is recommended as an effective means for impulse testing the low-voltage windings of such transformers.

3. A voltage wave of short duration applied to the low-voltage windings of distribution transformers is an effective test for eliminating defective transformers.

4. A voltage wave of 1 or 2 microseconds duration is representative of the higher voltage surges applied to the transformer low-voltage winding terminals in service.

5. When short-duration voltage waves are applied to the low-voltage winding, observation of the voltage wave shape induced in the high-voltage winding provides a very sensitive method of detecting faults in transformers with high-voltage ratings of 15 kv and under.

6. For transformers with high-voltage ratings above 15 kv, further investigation is required to determine whether the induced voltage detection method will have sufficient sensitivity or whether other methods, such as the neutral current or the applied voltage methods, should be used.

References

1. Distribution, Power, and Regulating Transformers. *ASA C57.22-1948*, American Standards Association, New York, N. Y., 1948, paragraph 22.115.

2. Lightning Investigation on a Rural Distribution System, **D. D. MacCarthy, D. A. Stann, D. R. Edge, W. C. McKinley.** *AIEE Transactions*, vol. 68, pt. I, 1949, pp. 428–38.

3. Voltage Stresses in Distribution Transformers Due to Lightning Currents in Low-Voltage Circuits, **K. D. Beardsley, W. A. McMorris, H. C. Stewart.** *AIEE Transactions*, vol. 67, pt. II, 1948, pp. 1632–35.

4. The Production Impulse Testing of Distribution Transformers, **E. D. Treanor, H. C. Stewart, J. E. Holcomb.** *AIEE Transactions*, vol. 71, pt. III, Oct. 1952, pp. 808–13.

5. Effect of Transient Voltages on Power Transformer Design-IV, **K. K. Palueff, J. H. Hagenguth.** *AIEE Transactions*, vol. 51, Sept. 1932, p. 601.

6. Impulse-Failure-Detection Methods as Applied to Distribution Transformers, **H. C. Stewart, J. E. Holcomb.** *AIEE Transactions (Electrical Engineering)*, vol. 64, 1945, pp. 640–44.

◆

Discussion

F. J. Vogel (Allis-Chalmers Manufacturing Company, Milwaukee, Wis.): The paper calls attention to several difficulties in impulse testing both low-voltage windings and windings of low inductance. In such cases, use of a reasonably sized surge generator results in a very short wave tail. Recognition of this fact permits various options, such as using a resistance to ground at the grounded terminal or short-circuiting the winding under test. The use of tests with short tails seemed to be deprecated.

Actually, as pointed out by the paper, short-tailed waves do provide an adequate test. It is felt that these statements apply equally well to power transformers, and that a limiting capacitance of the surge generator would be desirable since currents similar to those in service would be obtained. A 0.1-microfarad capacitance was suggested.

As stated, short-circuiting the windings cannot be always done safely, and this method does not provide an adequate test. Connecting a series resistance also reduces the value of current neutral tests. Current neutral tests are as satisfactory with the shorter tail tests and are more realistic.

The induced-voltage-test discussions in the paper are very interesting. In the case of high-voltage potential transformers, current neutral measurements were very small, because of the exceeding high impedance, even with partial failures, and the current transmitted at the start of the impulse, because of capacitance, was extremely large. Hence current neutral measurements did not seem very satisfactory. When the voltage induced in the low-voltage windings was measured, it was found that the capacitance current was reduced and that faults were located more successfully than with current neutral measurements. Voltage oscillograms were not always very sensitive. Thus, for some types of transformers induced impulse tests appear desirable.

W. L. Teague and **L. B. Rademacher** (Westinghouse Electric Corporation, Sharon, Pa.): The use of voltage waves of very short duration such as $1/2\times1^{1}/_{2}$ microseconds for impulse-testing low-voltage windings of distribution transformers may place a reasonably severe stress across the winding. However, with the mid-point grounded, and with the short duration of the surge, the insulation from coil-to-ground is stressed very little. It is true that when the standard $1^{1}/_{2}\times40$-microsecond wave is impressed across the low-voltage winding an exceedingly high voltage may be induced in the high-voltage winding and a large source of energy would be required to sustain the 40-microsecond tail. These facts have been recognized in the American Standards Association (ASA) Standards, and two alternate methods are provided for testing such low-impedance windings.

Method 1. One method permitted by ASA Standards is to apply the surge to both ends of the winding simultaneously. This method of test for low-impedance distribution transformer windings gives an excellent stress to the winding-to-ground insulation but a rather poor stress across the winding. This small stress across the winding results because the relatively low impedance and high through capacitance of the winding tends to keep all the parts of the winding at the same potential. With a higher impedance and lower through capacitance, a greater voltage stress would be placed across the winding. Fig. 9–11.

Fig. 9 demonstrates how these characteristics of the low-voltage winding tend to bring the X_2 bushing of the 240-volt winding of a 15-kva distribution transformer to the same potential as the X_1 and X_3 bushings which were surged simultaneously. The upper trace on the oscillogram is the applied wave while the lower trace is the voltage measured at the X_2 bushing. The difference between the two races is the voltage applied across one half of the winding. After the crest is reached, the X_2 bushing is at the same potential as the applied surge which thus gives the excellent stress to ground. In this example, about 10 per cent of the applied surge was across one half of the winding, and the full stress of the applied surge was placed on the winding-to-ground insulation.

In Figs. 10 and 11, the effect of more turns in the winding is shown. The relatively smooth trace is the surge applied to the ends of a 2,400-volt winding. The oscillating trace is the potential at the mid-point of the winding. In this case 50 per cent of the applied surge was across one half of the winding. As in Fig. 9, the complete winding was given an excellent test to ground. It should be noted that the mid-point of the winding oscillates to 120 per cent of the applied wave. With other winding characteristics for this method of test the mid-point might oscillate higher. These facts must be recognized and provision made for the over-

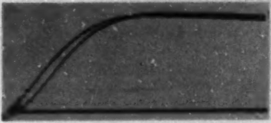

Fig. 9. Surge applied to both ends of 240-volt winding. Timing sweep 15 microseconds

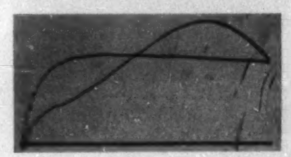

Fig. 10. Surge applied to both ends of 2,400-volt winding. Timing sweep 15 microseconds

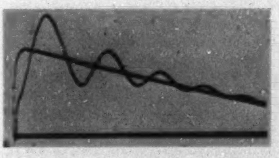

Fig. 11. Surge applied to both ends of 2,400-volt winding. Timing sweep 50 microseconds

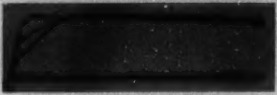

Fig. 12. Surge applied to one end of 240-volt winding. Other end grounded through 200 ohms. Timing sweep 15 microseconds

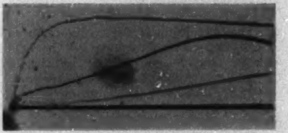

Fig. 13. Surge applied to one end of 2,400-volt winding. Other end grounded through 200 ohms. Timing sweep 15 microseconds

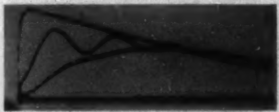

Fig. 14. Surge applied to one end of 2,400-volt winding. Other end grounded through 200 ohms. Timing sweep 50 microseconds

voltages. Fig. 11 is for the same condition as Fig. 10, except for the timing sweep used. The longer sweep was used for Fig. 11 to demonstrate how the oscillations are damped and the mid-point of the winding approaches the applied wave.

Method 2. The other method permitted by ASA Standards is to apply the surge to one end of the winding with the other end grounded through a resistor not to exceed 500 ohms. This method gives an excellent test to the winding-to-ground insulation and a good test to the insulation across the winding. The oscillograms in Fig. 12 show how the voltage is distributed across the winding and resistance. The upper trace is the voltage applied to the X_1 bushing of the 15-kva distribution transformer. The middle trace is the voltage at the X_2 bushing, and the lower trace is the voltage at the X_3 bushing which is grounded through 200 ohms. Approximately 60 per cent of the applied voltage is distributed across the winding for a short duration and then all the winding is stressed to ground to the approximate magnitude of the applied surge.

The effect of more turns in the winding is demonstrated in Figs. 13 and 14 which are for a 2,400-volt winding of a distribution transformer. In this case, the stress across the winding is greater and is applied for a longer time. In Fig. 13, the upper trace is the applied wave while the middle and lower trace are the mid-point of the winding X_2 and the end X grounded through 200 ohms, respectively. Initially, 95 per cent of the voltage is applied across the total winding and 70 per cent is applied between the line end and the mid-point of the winding. Fig. 14 is the same as Fig. 13, except with a longer sweep. It shows how the complete surge stress is applied to the winding-to-ground insulation.

To detect faults developed during the two methods discussed the usual procedure as described in the ASA Standards will apply. Since the first method of test places the emphasis on stressing the insulation to ground, the voltage oscillograms would be preferred. In the second method of testing, either or both voltage and current oscillograms may be used.

In this paper the author has described another method of testing the low-voltage winding of distribution transformers. To stress the internal insulation of the winding, a compromise on the duration of the voltage and also the stress to ground at the mid-point of the winding is made. The first ASA method discussed emphasizes the test to ground, but makes some compromise on the stresses across the winding. A good test to ground is likewise made with the second method while a much better test is given to insulation across the winding. Impulse testing is complicated, and for each particular use the testing techniques should be thoroughly understood for best results.

J. E. Holcomb: The interest shown by the discussers is greatly appreciated. Both discussions help to emphasize the fact that the impulse testing of transformers is extremely complicated and that a thorough understanding of the testing technique is necessary. While it is relatively easy to develop and use testing methods for use with a particular transformer design, it becomes increasingly difficult as the variety of transformers to be tested increases.

Test records for the production-line impulse test indicate that almost half of the larger kilovolt-ampere sizes of distribution transformers that are rejected fail because of defects in the low-voltage windings. On the other hand, for the smaller sizes less than 15 per cent of the rejections are due to defects in the low-voltage coils. These data apply only to layer-wound distribution transformers and cannot be extended to apply to power transformers, since, for thermal and mechanical reasons, the core construction is entirely different. The author has had no experience in the use of short-tailed impulse waves in testing power transformers and cannot comment.

Development work indicates that the impulse generator circuit used to produce the proper applied voltage wave shape may seriously alter the sensitivity of the induced wave method of fault detection. Specifically, if the shunt resistance used to control the length of the tail of the applied wave is too low, this sensitivity is drastically reduced. This can be overcome by varying the impulse generator capacity but may be hard to achieve in practice if a large variety of transformers are to be tested. Therefore, the method may find its most useful application in production-line impulse testing where the equipment is set up to test a large number of transformers within a limited rating range.

As Mr. Teague and Mr. Rademacher point out, the impulse voltage waves of short duration applied to one low-voltage terminal of the transformer with the mid-point grounded stresses the insulation between coil and ground very little. However, in service most of these transformers are connected with the mid-point connected to ground and consequently the stresses this winding will be subjected to are similar to those described in the paper. Furthermore, a high-potential test of 10 kv is applied between these low-voltage coils and ground during low-frequency tests.

The short-tailed impulse test was selected because it was felt that the coil would be stressed as severely as possible without flashover of the bushing. It should be pointed out that the test voltage is applied to the X_3 bushing with the X_2 bushing grounded. A voltage equal in magnitude but of opposite polarity is induced on the X_1 terminal, so that the total voltage across the coil is twice that applied to the X_3 terminal. In this way a voltage of 50 kv can be applied across the low-voltage coil after the transformer is assembled without flashing over the low-voltage bushings.

One of the most important parts of any test is fault-detection sensitivity. The major objection to both of the methods described by Mr. Teague and Mr. Rademacher is the questionable fault-detection sensitivity. It may be possible to detect some faults of small magnitude by careful comparison of voltage and current oscillograms when these testing methods are used but development work indicates that fault detection sensitivity is rather poor. Consequently, these methods cannot be readiy applied to pole-type transformers which are produced in large quantities. However, for larger sizes of transformers, which do not normally operate with the low-voltage mid-point grounded, these methods should be considered.

Power Autotransformer Current Interruption with an Air-Break Disconnect Switch

M. W. ANDERSON
MEMBER AIEE

THIS paper covers the preliminary investigation, field testing, and analysis of results incident to interruption of both exciting and paralleled load currents to a bank of power autotransformers by an air-break disconnecting switch. The interruptions were made on the high-voltage side of a bank consisting of three single-phase units, wye-connected, with solid grounding. The bank is triple rated, 90/120/150 mva at 220/115.5 kv. A delta-connected 13.2-kv tertiary winding is provided for neutral stabilization and harmonic suppression. The air-break disconnecting switch is rated 1,200 amperes at 196/230 kv, it is a triple-pole, single-throw, gang-operated switch without arcing horns. The paper is based upon performance of equipment of Seattle Lighting Department.

The basic design of the high-voltage bus consists of three sections, one of which is shown in Fig. 1. A fourth section is also provided, without the autotransformer bank, and with a single bus tie oil circuit breaker connecting the main and transfer busses. Space has been provided for bank high-voltage breakers, which have not been installed because the low bus loading would permit the deenergizing of any one bus section without disrupting service.

Owing to changes in the grid of the Northwest Power Pool, the bus loading was scheduled to increase by the addition of a large block of interchange power. This power would enter near one end of the bus and flow by displacement nearly the full length of the station. This flow would make the continuity of the bus essential; no longer could a bus section be taken out for clearance of a bank. Multiple connection to the transfer bus was out of the question, because protective relaying would then be solely dependent upon backup from distance stations, and could involve major system disruption in case of a fault.

The problem was to isolate the autotransformer bank from its bus section without disturbing the power flow through that section. It must be accomplished without endangering equipment and personnel and, if possible, with the existing disconnecting switches.

Preliminary Investigation

The first solution would appear to be the direct action of opening the disconnect switches to the banks. If a parallel path is available, one path may be interrupted and the load transferred to the alternate path. The difficulty of interruption will depend upon the impedance to the increased load and upon the impedance of the path being interrupted. Each path has a bank of autotransformers in series with it, and because of the impedance of the bank, there is a voltage drop and phase shift proportional to the current through the bank. If one bank is isolated on the high-voltage side, a voltage will appear across the disconnecting means equal to the sum of effects due to this impedance and the transient arc restrike during interruption.

The effect of voltage drop through the bank may be partially compensated for by adjustment of the secondary taps of the bank to be isolated. By lowering the taps, the ratio of transformation, primary to secondary, is increased and the bank will drop the flow of reactive power. This, in turn, will step up to a higher voltage the primary electromotive force when the bank is disconnected. However, the disconnect voltage will still be proportional to station loading because of the phase shift through the banks. Preliminary calculation indicated a value of 3,880 volts for this electromotive force, with a current of 90 amperes in each primary before interruption. This current is the lowest normal daily load and it occurs in the early morning hours.

Although the voltage due to transformer impedance was subject to rigid calculation, there remained the analysis of transient effects due to arcing at the time of interruption. An examination of the literature was made for information concerning arc behavior and switch performance. Strom[1] quotes a value of 34 volts per inch of contact separation on currents over 68.5 amperes. Slepian,[2] in an earlier paper, assigns a value of 50 volts rms per centimeter for interruption of arcs under 1,000 amperes. A very complete report by Andrews, Janes and Andersson[3] gives the data from a series of tests of horn gap switches under a variety of conditions. Unfortunately, the voltage levels were much lower than those under consideration. An extrapolation of their data confirmed the opinion that interruption of parallel load current might be possible. No information was found to indicate the amount of erosion which might be expected on arcing surfaces due to the currents involved. Although arcing horns could be expected to protect the switch parts, their use seemed inadvisable because of restricted overhead clearances and the possibility of extended arc activity.

It was then determined to investigate the possibility of interrupting the magnetizing current. These banks of autotransformers have a very low exciting current, averaging 1.73 amperes at rated line to line voltage, 220 kv. A survey of air-switch practice by an AIEE group[4] indicated that at least one utility was successful with interruptions of exciting current to an 83,000-kva bank of transformers at 220 kv, by means of an air-break switch. The current was about 3 amperes, but no other details of the operation were available.

The reignition voltage for this operation is very great, reaching an instantaneous value of 179.5 kv in $^1/_4$ cycle after voltage zero. Complicating the operation is the fact that the current lags the voltage by 78.9 degrees. This puts the voltage crest at (90 − 78.9) or 11.1 degrees after current zero. On a 60-cycle basis, this interval is about 514 microseconds. However, the greatest deionization and dielectric recovery value is concentrated in the first microseconds,[2] after which the increase in dielectric strength is an exponential function with an ever-decreasing rate of rise.

Paper 55-623, recommended by the AIEE Transmission and Distribution Committee and approved by the AIEE Committee on Technical Operations for presentation at the AIEE Pacific General Meeting, Butte, Mont., August 15–17, 1955. Manuscript submitted April 25, 1955; made available for printing July 12, 1955.

M. W. ANDERSON is with the Lighting Department, City of Seattle, Seattle, Wash.

The author wishes to express his indebtedness to Everett J. Harrington, test and research engineer of the Bonneville Power Administration, for his help in preparing for these tests and interpreting the results; and also to thank Prof. F. R. Bergseth of the University of Washington for his assistance and guidance leading to the solution of voltage recording problems in the tests.

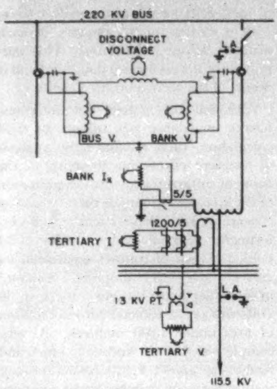

Fig. 1. Bus section arrangement

Preliminary Tests

Since there were few references to the conditions found in this problem, the next step seemed to be physical experimentation to determine the limits of safe operating procedure. Owing to the configuration of the system, it was possible to set up an isolated power circuit for the tests. Power would be furnished by a 67,000-kva hydrogenerator and transmitted over an isolated line to the bank of autotransformers under test. Control of the impressed voltage could be maintained from 50 to 250 kv, without disturbing normal system operation. After conducting exciting current tests, the bus tie could be closed, and the bank paralleled with the remainder of the station for parallel load current tests.

Because of the ease with which the voltage could be controlled, it was decided to start the exciting current tests at 50 kv and proceed upwards by 25-kv steps to a point where arcing was dangerous or switch spacings insufficient to put out the arc. For opening parallel load currents, arrangements were made to shift the 115-kv network to get tests at 0, 50 and 90 amperes on the primary side of the bank. These tests would be conducted with the 220-kv bus in the normal operating condition, except that one bus tie breaker would be left open so that a single bus tie breaker could be used as backup for the test.

A standard 6-element oscillograph was used, three elements of which recorded the voltage across the disconnect switch and three elements the currents at the time of interruption. For obtaining the voltage traces, adapters were fitted to the capacitance taps of the 220-kv bushings of both the autotransformer and the bus tie oil circuit breaker. These taps were loaded with capacitors to give equal voltages and the two connections per phase fed to the control grids of an electronic voltage amplifier. The output of this amplifier was then used to drive the oscillograph galvanometer.

The final setup of equipment was completed and exciting current interruptions were made at 50, 75, 100, 150, 200, 215, 230, and 242 kv. Owing to the surprisingly low arc activity, the 220-kv bus was restored to normal, fully connected to the system, and an interruption was made at 230 kv, the bus voltage at that hour.

The results of these first tests were very gratifying. The arcs observed were uniformly thin and blue, with little thermal energy. The arc from the interruption at 242 kv, shown in Fig. 2, was about 5 feet in length, well within the capabilities of the switch to open. The arc obtained from opening the exciting current to the bank from the fully closed bus was even less, being slightly more than 2 feet in length. Apparently the capacitance of the isolated line caused the extended arc in the earlier tests.

Following these tests of exciting current interruptions, two banks of autotransformers were paralleled on both primary and secondary sides, with the common secondary isolated from load. The disconnect switch was then opened and no visible arc seen.

The loading on the secondary bus was then adjusted to give a current of 50 amperes in the primary of each of the two banks in parallel. The interruption that followed gave evidence of being beyond the safe operating range of the switch. While the arc length was relatively short, it was extremely bright and of large diameter. No examination of the switch was made after this test.

The final test was made with all three banks in parallel. The primary current was about 100 amperes, but was reduced to 90 amperes when the taps of the bank to be de-energized were lowered to give unity power factor flow. The interruption was then made, as shown in Fig. 3, and was very similar to the previous test, except that a few sparks of hot metal were visible on the fixed or jaw end of the switch. Because of the intense heat of the arcs and the probability of disconnect switch damage, the tests were discontinued. Both bus sections adjacent to the switch were grounded and an examination of the disconnect made.

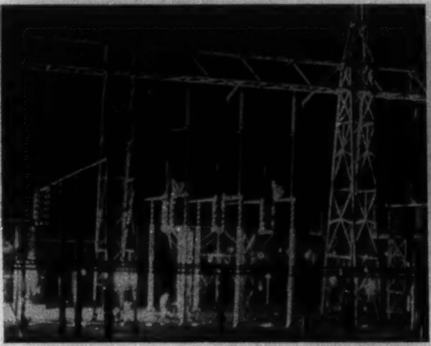

Fig. 2. Exciting current interruption at 242 kv, isolated test system

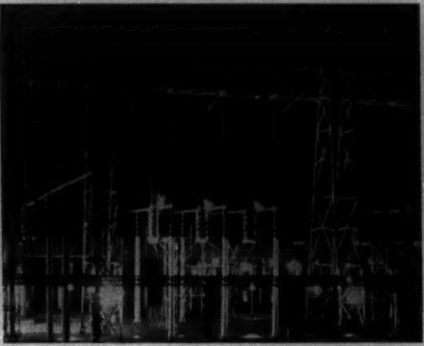

Fig. 3. Paralleled load current interruption at 90 amperes

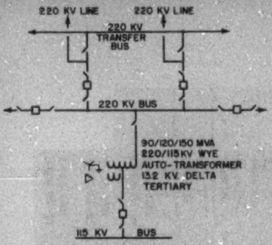

Fig. 4. Instrumentation for final test; one phase only shown

In the examination, smoke stains were found on the jaws and over the outer half of the blades. The only apparent damage incurred was a few small pits on the outer jaw surfaces. The silver contacts of both jaws and blades seemed unharmed in any way. Apparently there was no pitting on the blades because the arc at interruption followed down the blades toward the hinge, a phenomenon common to all the tests.

Final Tests

The preliminary tests had indicated that the interruption of the autotransformer bank exciting currents was a safe operation, but several records were needed as proof of the physical phenomena observed. To obtain these records, the final tests were organized.

The instrumentation is shown for one phase in Fig. 4. To obtain accurate records of any overvoltage condition, traces were taken of both bus and autotransformer primary phase-to-ground voltages, as well as of the difference between them. Traces were also taken of the three tertiary voltages, the exciting currents and the circulating current within the delta tertiary.

Since trouble had been experienced with the electronic voltage amplifiers used in the preliminary tests, it was decided to attempt a different approach to the problem of voltage recording. The 220-kv bushings are equipped with a capacitance tap for voltage measurements. However, these taps have an open-circuit voltage of 3,600 volts, and this voltage collapses to zero with a current drain of only 13.5 milliamperes. They are a source of low-current high-voltage energy. The galvanometers of the magnetic oscillograph, on the other hand, require a small voltage and relatively high current.

The difficulty is overcome by the use of a small, high-turn ratio, radio-type transformer, which is paralleled with sufficient capacity to burden the tap to a voltage which will give the desired current for deflection of the galvanometer. Tests on a similar device indicated good ratio and phase-angle characteristics up to 10 kc in frequency. The transformers used for the final tests had a ratio of 34 to 1 and were checked for frequencies from 20 to 2,000 cycles per second.

For recording the small values of exciting current, 5/5 ampere wound-type 5-kv current transformers were inserted in the neutral ends of the autotransformer windings. This required the removal of the power neutral bus, and to protect these current transformers from inrush currents they were paralleled with unfused 5-kv hook-stick operated switches. These switches were kept closed at all times except during each test. The tertiary current was measured by three current transformers operated series primary, parallel secondary, to give an ultimate ratio of 400/5 amperes.

On the day of the test, equipment was assembled and all clearances obtained. Weather conditions were adverse, it was cold and windy with showers of mixed rain and snow. Because no difficulties had been experienced during the preliminary tests with interruptions of exciting current to the bank from the closed bus, all of the final tests were made in this manner without recourse to an isolated system. Arc activity and the duty on the disconnect switch appeared to be much less with this method of operation.

In all, six interruptions were made. The test weather was variable, the first, third, fourth, and sixth tests were made with a moderate breeze blowing and light mixed rain and snow falling. The second test was made during a squall, with wind velocity estimated at 40 to 45 miles per hour and heavy snow falling. The fifth test was made in calm, with neither rain nor snow falling.

The arc activity was much less than that associated with the preliminary tests. The maximum contact separation was a little more than 2 feet before final interruption. Fig. 5 shows a typical interruption. Figs. 6, 7, and 8 are the oscillograms of tests 1, 2, and 3. The fourth, fifth, and sixth test oscillograms are not shown; they are essentially reproductions of the first test.

On the second and third tests, restrikes followed by inrush currents occurred. Apparently, the arcs were blown out or otherwise extinguished for a fraction of a cycle, followed by restrikes on two phases and the inrush currents. The greatest magnitude of these currents was 8 amperes peak value on the second test, which cannot be considered objectionable, although fully offset from the axis. On the third test, the restrike occurred on the phase formerly extinguished. In this case, phase 1 was nearly at crest when the restrike occurred, and phase 3 followed. But with phases 1 and 3 conducting, phase 2 was energized through circulating current in the tertiary delta and there was not sufficient reignition voltage across the disconnect switch to start the arc.

Verified in these tests was the fact that excitation for one phase was being carried by circulating current within the delta tertiary. The current traces for the delta show the characteristic third harmonic wave, but upon interruption of one phase, there is added a fundamental component.

It will be noted that while 2-phase currents and ground can carry the bank 3-phase excitation by means of a circulating current within the delta tertiary, one phase alone cannot do so. With a single-phase quantity on the delta tertiary, the

Fig. 5. Typical exciting current interruption from the bus, 226 kv

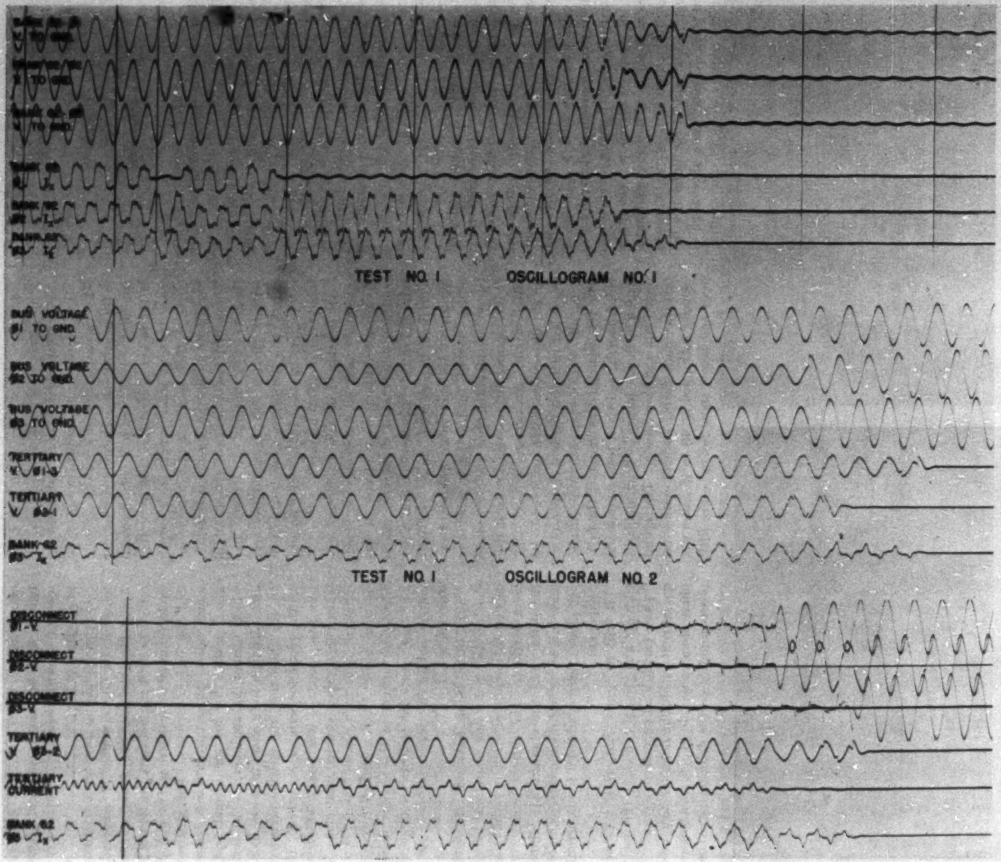

Fig. 6. First test

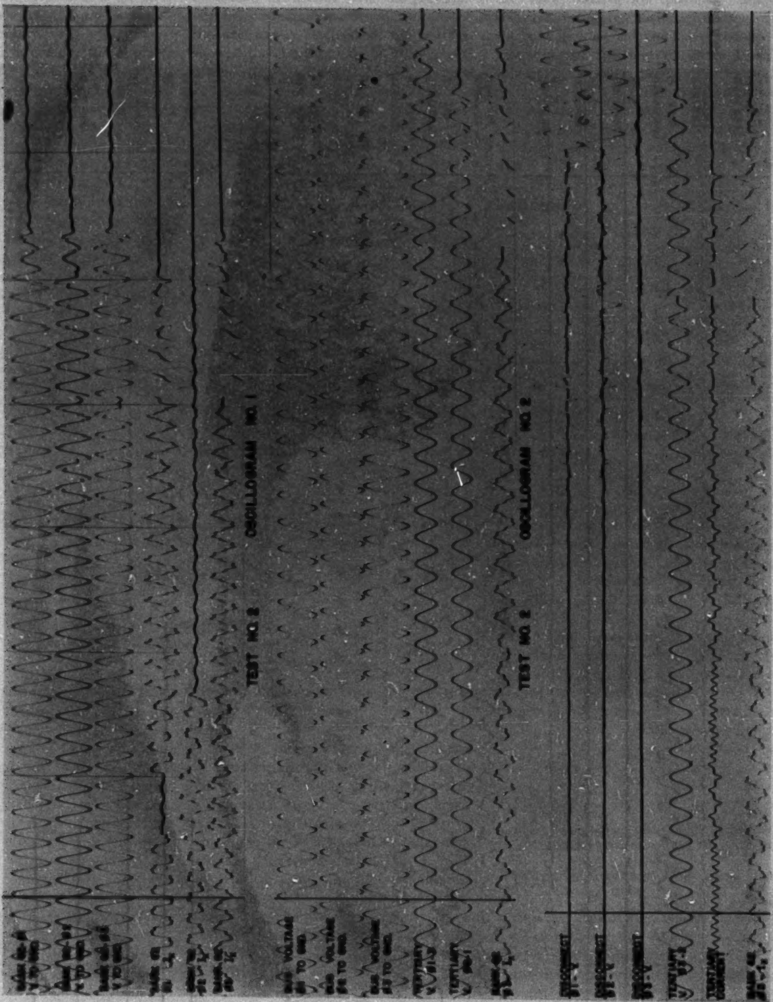

Fig. 7. Second test

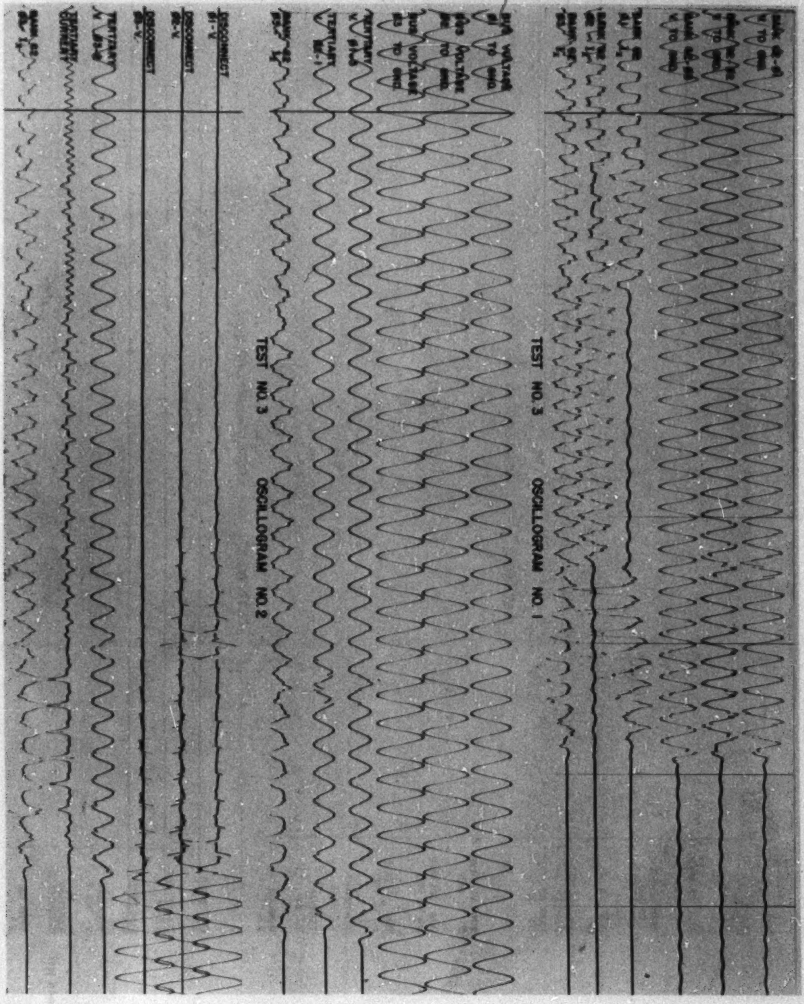

Fig. 8. Third test

effective exciting impedance of the bank becomes twice the normal phase-exciting impedance, and the remaining current drops to half its previous value. This is verified by the oscillograms, as is the fact that all three bank voltages are part of a single-phase quantity.

The impedance necessary to suppress the arc in the first phase to be extinguished was much smaller than had been anticipated. These disconnect switches have blades which rotate about their longtitudinal axes to relieve the pressure of the fixed jaws against the flattened ends of the blades. The clearance at the time that the blades are fully rotated, before the lift out of the jaws is begun, is about $^1/_2$ inch if the blades are perfectly centered in the jaw openings, which is usually not the case in the rather loose alignment of this type of switch. However, this small gap was sufficient to cause the loss of current to one phase, until the blade rubbed the jaws during withdrawal. Thus a short-phase interruption is visible during the beginning of each test.

The voltage across the switch was taken as the difference between bus and transformer 220-kv bushing potentials. As the switch opened, each voltage cycle continued to increase over the previous one before reignition took place. After the arc was re-established, the voltage showed the characteristic high-frequency components of arc drop in free air. These voltages appeared to be inversely proportional to frequency, ranging from 16 kv rms at 900 cycles per second to 4 kv rms at 4,000 cycles. There were no overvoltage conditions of any kind observed, the sine wave encompassing entirely the voltages observed. The average time of interruption of all tests was less than 31 cycles on a 60-cycle-per-second basis.

Conclusions

There is no hazard to equipment and personnel from the interruption of autotransformer exciting currents by an air-break disconnect switch, from a stable voltage source, on the equipment tested. While relatively few interruptions were made, the variety of conditions incident to the tests failed to reveal any abnormal or injurious conditions. It must be remembered that two circumstances make the easy interruption possible; first, the delta-connected tertiary winding of the bank and, second, the low-impedance grounding of the neutral. Since these two conditions are a prerequisite to successful operation of the power autotransformer bank, it is probable that these results are applicable to similar equipment similarly arranged resulting in a great saving in substation design.

References

1. LONG 60-CYCLE ARCS IN AIR, A. P. Strom. *AIEE Transactions (Electrical Engineering)*, vol. 65, Mar. 1946, pp. 113–18.

2. EXTINCTION OF A LONG A-C ARC, J. Slepian. *AIEE Transactions*, vol. 49, Apr. 1930, pp. 421–30.

3. INTERRUPTING ABILITY OF HORN-GAP SWITCHES, F. E. Andrews, L. R. Janes, M. A. Andersson. *AIEE Transactions*, vol. 69, pt. II, 1950, pp. 1016–27.

4. REPORT ON TRANSFORMER MAGNETIZING CURRENT AND ITS EFFECT ON RELAYING CURRENT AND AIR SWITCH OPERATION, AIEE Committee Report. *AIEE Transactions*, vol. 70, pt. II, 1951, pp. 1733–40.

Power-Line Carrier Coupling—An Analysis

M. G. BIENHOFF
ASSOCIATE MEMBER AIEE

IN THE development of the power-line carrier art in this country, attention has usually been focused on the carrier frequency itself, with the hope that the side bands would take care of themselves. This approach has been fairly successful. Nevertheless, the attempt to apply carrier-current communications in greater and greater quantity and over greater distances with concurrent demand for better quality and reliability has led to a number of application problems; and in the last few years, with the commercial development of the aperiodic coupler[1] and Moynihan's study of the effects of trapping with high-Q traps,[2] increased attention has been given to the side bands which, after all, carry the intelligence.

Since the rate at which information can be transmitted over any communication system is proportional to the bandwidth, a systematic study of power-line carrier coupling, viewed as a problem of transmitting a frequency band of maximum width, rather than one or two discrete frequencies, should be of some interest to power-system communications engineers. Results will be presented in a perfectly general way, so that they can be applied to older traps and capacitors as well as to new ones.

Bandwidth

A circuit having a frequency response limited only at the high end by prescribed shunt capacities and series inductances, usually the unavoidable parasitic elements, can be used at frequencies higher than its natural cutoff frequency by resonating each frequency-limiting branch with a suitable reactive element; but this process cuts off the response at lower frequencies so that the bandwidth, in cycles, is not changed. It is also theoretically possible, by using more complicated resonating networks, to break the passband into a number of sections which can be individually located as desired anywhere in the frequency spectrum. The fundamental restriction can be written as follows

$$\sum_i(\omega_{ui}-\omega_{li})=\omega_0 \qquad (1)$$

where

ω_{ui}, ω_{li} = the upper and lower limit frequencies respectively of the various bands

ω_0 = the cutoff frequency of the network in its natural state

This is called the conservation-of-bandwidth principle.[3] As expressed here, however, the principle is rigorously established only when the treatment is subject to certain restrictions. The resonating networks must be 2-terminal networks of pure reactances and all frequency-limiting elements must be resonated the same way. If all restrictions on treatment are abandoned, the principle is not disintegrated, it is just elasticized. Series and shunt peaking

---

Paper 55-698, recommended by the AIEE Carrier Current Committee and approved by the AIEE Committee on Technical Operations for presentation at the AIEE Fall General Meeting, Chicago, Ill., October 3–7, 1955. Manuscript submitted March 14, 1955; made available for printing August 22, 1955.

M. G. BIENHOFF, recently with the U. S. Bureau of Reclamation, Phoenix, Ariz., is now with the U. S. Army, Corps of Engineers, Los Angeles District, Los Angeles, Calif.

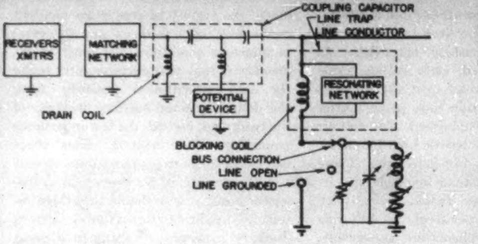

Fig. 1 (left). Carrier engineer's view of transmission line phase terminal

networks, for example, are used in video amplifiers to square up the corners of the passband, thus extending the useful frequency range. Gain and bandwidth can be traded one for the other, as in stagger tuning to increase bandwidth, and the use of loosely coupled air-core transformers to increase gain at radio frequencies. Dissipative elements can be added to increase bandwidth at the expense of increased losses.

Unfortunately, in coupling carrier frequency energy to high-voltage power lines, the frequency response is limited by series capacity and shunt inductance, Fig. 1, and the aforementioned principles, which have been well established for many years, do not apply directly. Here the limitation is an economic one. The shunt inductance and series capacitance can easily be increased by putting traps in series and capacitors in parallel, but this is expensive, and so are traps and capacitors designed with higher than usual inductance and capacitance.

To see how the bandwidth is limited for a system with specified series capacities and shunt inductances, write, say, the loop equations for the network using Laplace transform theory with p as the complex frequency variable. The variable terms in these equations will all be of one of these forms: $K_a i$, $K_b pi$, or $K_c i/p$, where the K_a's represent resistances, the K_b's represent inductances, the K_c's represent reciprocal capacities, and the i's are current.

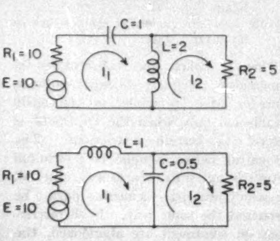

Fig. 2. Example of transformation used to establish bandwidth principle

Let the equations be transformed by putting $p=1/q$. The typical terms become $K_a i$, $K_b i/q$, and $K_c qi$. If $q=\rho+j\phi$ is then regarded as the complex frequency variable, the new equations will represent a network of the same configuration, but now the K_b's (and corresponding branches) are reciprocal capacities and the K_c's are inductances. In other words, in going from the p-plane to the q-plane, all capacitors in the original network have been changed to inductors, and vice versa. Since the equations in the q-plane represent a network limited, then, by shunt capacities and series inductances, the principle of conservation of bandwidth can be applied as expressed in equation 1

$$\sum_i (\phi_{ui}-\phi_{li})=\phi_0 \tag{2}$$

One can now transform the equations and network back to the p-plane ($p=\sigma+j\omega$), taking the foregoing property along; and, noting that points on the ϕ-axis in the q-plane are the negative reciprocals of corresponding points on the ω-axis in the p-plane, obtain the following from equation 2

$$\sum_i \left(\frac{1}{\omega_{li}}-\frac{1}{\omega_{ui}}\right)=-\frac{1}{\omega_0} \tag{3}$$

Since the sum in equation 2 was taken over the positive real-frequency axis in the q-plane, equation 3 will apply to the negative real-frequency axis in the p-plane. Because of the symmetry of the positive and negative real-frequency axes, however, for the positive ω-axis

$$\sum_i \left(\frac{1}{\omega_{li}}-\frac{1}{\omega_{ui}}\right)=\frac{1}{\omega_0} \tag{4}$$

This is the principle of conservation of bandwidth for networks limited by series capacities and shunt inductances. As in the previous case, the principle is found to be flexible to a certain extent if fussy restrictions are avoided. It might be well to point out, however, that existing 2-frequency tuning panels and line traps do nothing to increase the bandwidth. They just break it up into two chunks.

If all the bandwidth is taken in a single band, equation 4 can be reduced to the following form

$$B=\frac{1}{2\pi}(\omega_u-\omega_l)=\frac{\omega_m^2}{2\pi\omega_0} \tag{5}$$

where

B = the bandwidth, cycles per second

$\omega_m=\sqrt{\omega_u\omega_l}$ = the band mean frequency

In a network limited in frequency response by certain prescribed shunt inductances and series capacities, the bandwidth is proportional to the square of the band mean frequency.

This principle can also be established independently in a manner analogous to that used by Bode to establish the well-known bandwidth principle for networks limited by shunt capacities and series inductances.[3] The method outlined in the foregoing, while perhaps the more difficult to follow, serves to emphasize the comparison between the two types of networks and indicates that the extensive empirical knowledge about bandwidth which has been accumulated for networks limited by shunt capacities and series inductance can be adapted for application to the much less common networks exemplified by the problem of power-line carrier coupling. A numerical example illustrating the foregoing development is given here for a typical network having series capacity and shunt inductance; see the upper circuit of Fig. 2. No units are assigned to the various quantities; the transformation does not have a complete physical interpretation and the process must be regarded as a mathematical manipulation.

The loop equations for the upper circuit of Fig. 2 are

$$10I_1+\int I_1 dt+2\frac{dI_1}{dt}-2\frac{dI_2}{dt}=10$$

$$5I_2+2\frac{dI_2}{dt}-2\frac{dI_1}{dt}=0$$

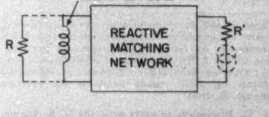

Fig. 3. Suggested circuit for developing resonating networks for blocking coil

The Laplace transformation puts these equations in terms of the complex frequency variable p

$$\left(10+\frac{1}{p}+2p\right)I_1-2pI_2=10$$

$$(5+2p)I_2-2pI_1=0$$

Now transforming with $p=1/q$

$$\left(10+q+\frac{2}{q}\right)I_1-\frac{2}{q}I_2=10$$

$$\left(5+\frac{2}{q}\right)I_2-\frac{2}{q}I_1=0$$

By inspection it can be seen that these are the equations of the lower circuit of Fig. 2, a circuit having shunt capacity and series inductance.

Solving for I_2

$$I_2=\frac{10}{5+\left(\frac{5q}{2}+1\right)(10+q)}$$

Confining attention to the real-frequency axis in the q-plane $(q=\rho+j\phi)$

$$I_2=\frac{10}{15-\frac{5}{2}\phi^2+26j\phi}$$

At $\phi=0.61$, the response is down 3 decibels. Applying the principle of conservation of bandwidth for this network

$$\sum_i(\phi_{ui}-\phi_{li})=\phi_0=0.61$$

Now to find the bandwidth law for the upper circuit of Fig. 2, simply transform back to the p-plane $(p=\sigma+j\omega)$

$$\sum_i\left(\frac{1}{\omega_{li}}-\frac{1}{\omega_{ui}}\right)=0.61$$

This equation can be applied on either the positive or the negative real-frequency axis.

The frequency ω_0 in equations 3, 4, and 5 is the cutoff frequency of the network in its untreated high-pass condition. Although the time-honored 3-decibel figure was used in the example, the foregoing principles will apply for any arbitrary method of determining ω_0, as long as the same method is used in determining the ω_u's and ω_l's. The rest of this article will be concerned with elementary networks containing only one frequency-limiting reactor, either a shunt inductor or a series capacitor; in each case ω_0 will be defined as the frequency at which the reactance of the frequency-limiting element equals a resistance not differing greatly from the input or output impedance of the network. If this resistance is 500 ohms, for example, ω_0 for a 0.002-microfarad capacitor would be 10^6 radians per second (160 kc). For a 0.25-millihenry coil, ω_0 would be 2×10^6 radians per second (320 kc). The value of B determined from equation 5 using this definition of ω_0 will be called the nominal bandwidth and the corresponding limit frequencies will be called the nominal band limits.

Line Traps

If it were not for the switching behind the trap, Fig. 1, the blocking coil and coupling capacitor could be considered as a single network and matching and tuning networks could be determined accordingly. (The term "blocking coil" will be used to refer to the line trap minus its resonating network.) But even though the line is connected to the bus at least 99 per cent of the time, the bus impedance itself will change as other lines and transformers are switched. Transformers will appear on the bus as capacitors, provided they are physically close to the bus (close in comparison with a quarter-wave length at carrier frequencies), but line impedances will probably vary widely. Trap reactance has commonly been relied on to block transmission of carrier to the bus, but it is quite likely that the trap reactance will series-resonate with the bus reactance at certain frequencies in the passband, causing great attenuation, and Moynihan has suggested, after studying the problem, that the Q of traps be reduced to increase the resistance component of the trap impedance.[2]

Therefore, the trap should be resonated so that the resistive component of its impedance will be as high as possible over the passband, with no reliance whatever placed on the reactive component. One method of attacking this problem is to use the following artifice. Imagine the blocking coil removed from the line, Fig. 3, shunt it with a resistor R, and attempt to construct a network of pure reactances which will match this combination, considered as a load, over as wide a band as possible to a generator whose internal impedance is purely resistive and adjustable to any value R'. An estimate of the band over which it may be possible to do this can be obtained immediately from equation 5. In this case ω_0 is taken as the frequency at which the coil reactance equals the resistance R.

$$B_N=\frac{\omega_m^2}{2\pi\omega_0}=2\pi f_m^2\frac{L}{R} \tag{6}$$

where

B_N = the nominal bandwidth
L = the blocking coil inductance
$f_m=\omega_m/2\pi$ = the band mean frequency, cycles per second

Assuming that the required network has been constructed, connect to it instead of a generator just the matching resistor R', and then return to the connection between resistor R and the blocking coil. Since only reactive elements have been crossed, it will be found that the resistor R is also matched to the network over the same band. Resistor R can be removed. The blocking coil and the network will now show a constant resistance R over the band B_N.

Of course it is only possible to do this approximately, although the error can probably be reduced as much as desired by using more complex reactive networks. Fig. 4 shows a blocking coil with a 2-stage resonating network and some of the impedance curves which can be obtained. These and other curves in this paper are presented as functions of the frequency function u so that they can be used for all values of ω_0 and ω_m. The function u has the following properties: It has the value zero for the band mean frequency and the values -1 and $+1$ for the lower and upper limit frequencies respectively of the nominal band B_N; it has the values $-u_1$ and $+u_1$ for the limit frequencies of any other band of width B_Nu_1 with the same mean frequency ω_m. The curves of Fig. 4 show the impedance only in the lower portion of the band. The resistive and reactive components of the impedance of this and other networks which will be presented are even and odd functions respectively of the function u, so that the values on the other side of the band can be determined from symmetry.

The expression for the impedance of the network of Fig. 4 is

$$\frac{Z}{R_2}=\frac{1-ju(1-k+k^2u^2)}{1+(1-2k)u^2+k^2u^4} \tag{7}$$

where

Z = the impedance of the entire network
$u=\frac{\omega_0}{\omega_m}\left(\frac{\omega}{\omega_m}-\frac{\omega_m}{\omega}\right)$
$\omega_0=R_2/L_1$
$k=L_1/(R_2^2C_2)$
$\omega_m^2=1/L_1C_1=1/L_2C_2$

If $k=0$, then $L_2=1/C_2=0$; the resonating network reduces to a single stage and the circuit is that of the conventional single-frequency trap. The resistor R_2 is usually not physically present, however, and R_2 in the equivalent circuit will represent the loss components of the coil and capacitor. It is about 10,000 ohms for the traps in common use. The nominal bandwidth for this resistance, assuming a blocking-coil inductance of 250 microhenrys, is

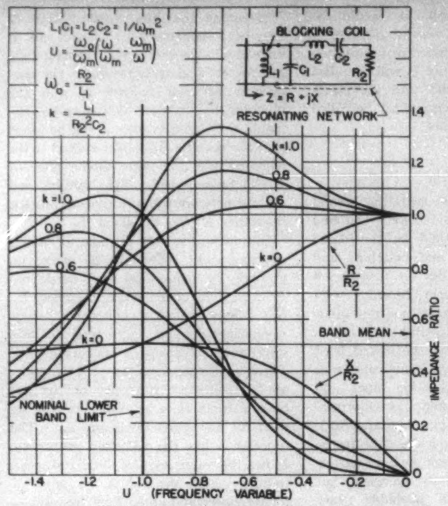

Fig. 4. Circuit and universal impedance curves for line trap with 2-stage resonating network

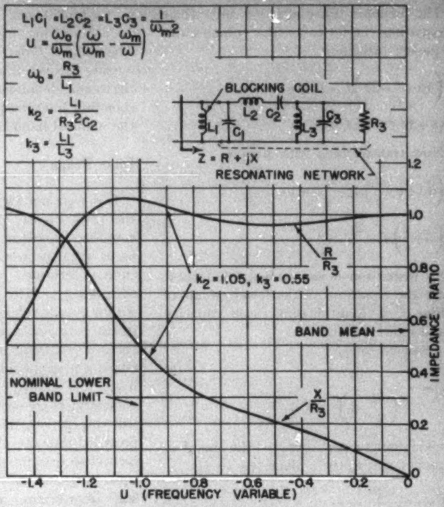

Fig. 5. Circuit and universal impedance curves for line trap with 3-stage resonating network

only 1,500 cycles at 100 kc, so Fig. 4 shows only a little over one-third of the lower half of a 6-kc band. It can be shown that the resistance of the single-frequency trap at the band-limit frequencies increases as R_2 is decreased until the nominal band, as defined in equation 6, equals the actual band, after which it decreases. The best value of R_2 for the conventional single-frequency trap, then, can be obtained from equation 6 by putting B_N equal to the actual bandwidth. The resistance of the trap at the band limits is, from Fig. 4, half of the value of R_2 so determined. By adding the second stage with $k=1$ to the resonating network, the minimum resistance of the trap in the same band is doubled. Or, if the widest possible band should be of interest, the addition of a second stage to the resonating network will double the frequency band over which a specified minimum resistance can be maintained.

By adding a third stage to the resonating network, still greater control of the characteristics of the trap is obtained. The curve shown in Fig. 5 was selected for constant resistance and increased bandwidth. With parameters as shown, the band over which the trap can maintain a specified minimum resistance is increased another 18 per cent. Probably other values of the parameters would give somewhat greater bandwidth at the expense of greater variation in resistance. The equation for the trap with a 3-stage resonating network is

$$\frac{Z}{R_3} = \frac{1 - ju(A + Bu^2 + k_2^2k_3^2u^4)}{1 + Cu^2 + Du^4 + k_2^2k_3^2u^6} \qquad (8)$$

where

$u = \frac{\omega_0}{\omega_m}\left(\frac{\omega}{\omega_m} - \frac{\omega_m}{\omega}\right)$
$\omega_0 = R_3/L_1$
$A = 1 + k_3 - k_2$
$B = k_2(k_2 - k_3^2 - 2k_3)$
$C = 1 + 2k_3 + k_3^2 - 2k_2$
$D = k_2^2 - 2k_2k_3 - 2k_2k_3^2$
$k_2 = L_1/(R_3^2C_2)$
$k_3 = L_1/L_3$
$\omega_m^2 = 1/(L_1C_1) = 1/(L_2C_2) = 1/(L_3C_3)$

Coupling Capacitor

The matching networks to be presented here for the coupling capacitor are analogous to the networks shown for the blocking coil. The terminating resistor may represent the output impedance of the final radio-frequency power amplifier. It is assumed that this can be adjusted to any desired value with a suitable output transformer. The drain coil and the potential-device network will be ignored. They have high impedances and do not have a very great effect on the network at carrier frequencies.

There is not as much flexibility in designing the coupling capacitor network as in the trap network. This is because an attempt is made either to match the capacitor network to the line and the trap impedances in parallel at the transmitting end, or to match the line to the trap and capacitor networks in parallel at the receiving end; in resonating the trap there was no need to match anything. Where the bandwidth of the trap is inversely proportional to resistance, the bandwidth of the capacitor network is directly proportional to its matching resistance.

Fig. 6 shows the circuit and impedance curves for the capacitor with a 2-stage matching network. The circuit is essentially the same as that given recently by Krings and Woodworth.[4] The equation is

$$\frac{Z}{R_2} = \frac{1 + ju(1 - k + k^2u^2)}{1 + k^2u^2} \qquad (9)$$

where

$u = \frac{\omega_0}{\omega_m}\left(\frac{\omega}{\omega_m} - \frac{\omega_m}{\omega}\right)$
$\omega_0 = 1/(R_2C_1)$
$k = R_2^2C_1/L_2$
$\omega_m^2 = 1/(L_1C_1) = 1/(L_2C_2)$

The conventional single-frequency line tuner ($C_2 = 1/L_2 = 0$) is obtained by again putting $k=0$, and the impedance curves for this network are also shown in Fig. 6.

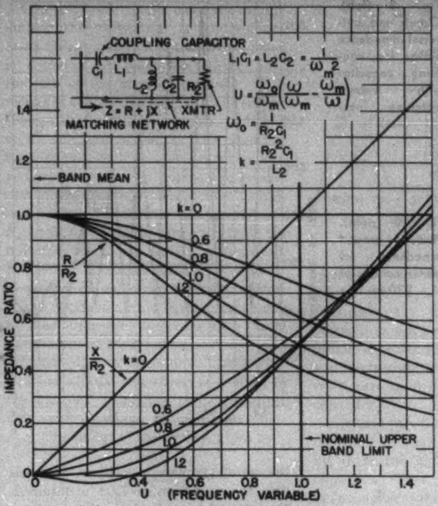

Fig. 6. Circuit and universal impedance curves for coupling capacitor with 2-stage matching network

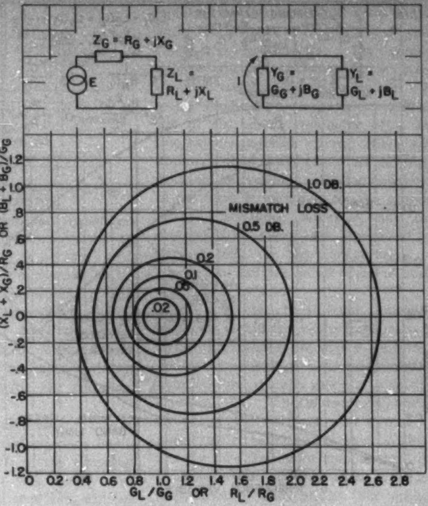

Fig. 7. Mismatch loss curves

Assuming that the desired bandwidth B and the resistance R_N to be approximated with the capacitor network (whose actual impedance is Z in the foregoing equation) are known, the nominal bandwidth B_N based on R_N can be calculated. If B is less than 0.4 B_N, as it may well be on lower voltage lines, conventional single-frequency tuning with $R_N = R_2$ may as well be used. If B is greater than 0.4 B_N, assume for the moment that $R_2 = R_N$, in which case the nominal bandwidth B_{N2} determined with reference to resistor R_2 is equal to B_N. Plot the point $u = B/B_{N2} = B/B_N$ on the line $R/R_2 = 1$. This value of u represents the actual band limits when $R_2 = R_N$. Connect this point to the origin with a straight line. For any other value of R_2, the actual band limits will correspond to the value of u at the point of intersection of this line with the horizontal line $R/R_2 = R_N/R_2$. The reason for the change is that the scale of u changes with a change in R_2 and R_2 has to be adjusted to obtain the best match. Now to select the best 2-stage matching network try various values of R_N/R_2, selecting for each a value of k which will give the most uniform mismatch loss over the actual band with limits determined by the diagonal line. Since the reactive mismatch is always at its worst at the band limit, it is best to select a k which will give a good resistance match at this point. At the band mean, the mismatch will be purely resistive. If $B = B_N$, for example, the diagonal line is at 45 degrees and $R_N/R_2 = 0.74$, $k = 0.8$ will give about a 35-per-cent resistance mismatch at the band mean and about a 40-per-cent reactance mismatch at the actual band limit.

Mismatch loss curves are of some help in obtaining a uniform mismatch loss over the desired band. A set of curves is shown in Fig. 7. The expression for the mismatch loss in decibels is

$$10 \log_{10}\left[1+\frac{(R_G-R_L)^2+(X_G+X_L)^2}{4R_LR_G}\right] \quad (10)$$

where

$R_G + jX_G$ = the generator impedance
$R_L + jX_L$ = the load impedance

For mismatch loss less than 1 decibel, the following approximation gives the loss within 5 per cent

$$1.1\,\frac{(R_G-R_L)^2+(X_G+X_L)^2}{R_LR_G} \quad (11)$$

$$=1.1\,\frac{\left(1-\dfrac{R_L}{R_G}\right)^2+\left(\dfrac{X_G+X_L}{R_G}\right)^2}{\dfrac{R_L}{R_G}}$$

Because the capacitor circuit of Fig. 6 and the trap circuit of Fig. 4 are mutually inverse networks, the curves of Fig. 4 can be read as admittance curves for the capacitor circuit of Fig. 6. Values of u and k determined with reference to the capacitor circuit apply directly to the curves of Fig. 4, the curves being read as GR_2 and BR_2 where $1/Z = G + jB$. Similarly, the curves of Fig. 6 can be read as admittance curves for the trap circuit of Fig. 4.

Two sets of curves for the 3-stage capacitor network are shown in Fig. 8. For these curves u and ω_0 have been based on R_N rather than R_3, so that the value of u corresponding to actual band limits does not change as R_3 is changed. The parameters $k_2 = 0.6$, $k_3 = 0.6$, and $\alpha = 1.4$ were selected to give approximately constant mismatch loss over a band 1.3 times the nominal band. Within this band the mismatch loss stays within the limits of 0.12 to 0.16 decibels. The parameter values $k_2 = 0.9$, $k_3 = 0.65$, and $\alpha = 1.2$ were selected to give approximately constant mismatch loss over a band 0.9 times the nominal band. Within this band the mismatch loss is about 0.04 decibel. Wider bandwidths can undoubtedly be obtained with increased but not excessive variation in mismatch loss.

The equation for the 3-stage capacitor network is

$$\frac{Z}{R_N}=\frac{\alpha+ju(A+Bu^2+k_2^2k_3^2u^4)}{1+Cu^2+k_2^2k_3^2u^4} \quad (12)$$

where

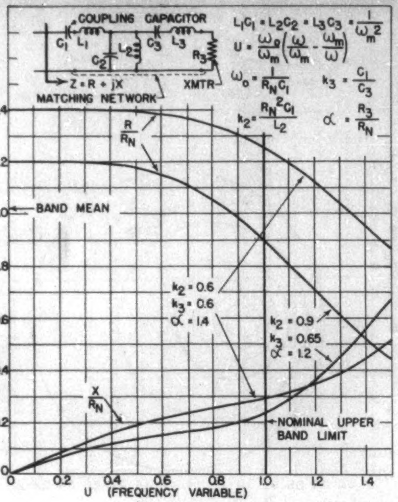

Fig. 8 (left). Circuit and universal impedance curves for coupling capacitor with 3-stage matching network

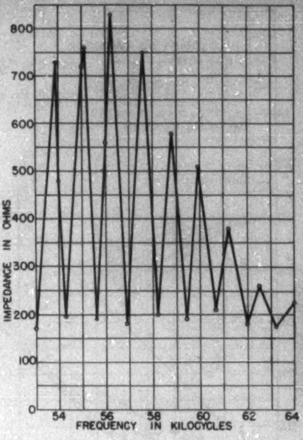

Fig. 10 (right). Phase-to- ground impedance of center conductor of a 230-kv line

R_N = the resistance to be approximated

$u = \frac{\omega_0}{\omega_m}\left(\frac{\omega}{\omega_m} - \frac{\omega_m}{\omega}\right)$
$\omega_0 = 1/(R_N C_1)$
$A = 1 + k_3 - \alpha^2 k_2$
$B = -k_2(k_3^2 + 2k_3 - \alpha^2 k_2)$
$C = k_2(\alpha^2 k_2 - 2k_3)$
$k_2 = R_N^2 C_1/L_2$
$k_3 = C_1/C_3$
$\alpha = R_3/R_N$
$\omega_m^2 = 1/(L_1C_1) = 1/(L_2C_2) = 1/(L_3C_3)$

If ω_m is put at infinity in the circuit of Fig. 8, then $L_1 = C_2 = L_3 = 0$, and the circuit becomes that of the aperiodic coupler introduced in this country a few years ago. It is unlikely that the parameters have the same values but, otherwise, the curves would apply. However, positive values of u now correspond to negative frequencies, so the only curves of practical interest are those obtained by symmetry for negative u. The nominal lower band limit is, of course, the cutoff frequency ω_0.

It is probably quite practical to match coupling capacitors to a band-pass characteristic by using the drain coil for first-stage tuning, as shown in Fig. 9. The analysis is difficult, however, and the symmetry is lost.

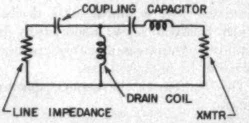

Fig. 9. Coupling capacitor with 2-stage matching network using drain coil for first stage

Application

It is believed that the problem of matching a power transmission line at carrier frequencies has not been completely understood. Fig. 10 shows the impedance to ground over a portion of the carrier-current spectrum of the center conductor of a flat 230-kv steel-tower transmission line, with 795,000-circular-mil steel-reinforced aluminum-cable conductors on 28-foot 10-inch spacing and overhead ground wires all the way. The conductor was shunted at the local end with a 2-frequency trap and a 0.001-microfarad coupling capacitor with tuning circuits grounded out, as shown in Fig. 11. The capacitor then shows a low admittance in comparison with the line over most of the carrier spectrum and the trap shunting effect is negligible at and near its resonant frequencies of 57 and 135 kc. The most striking feature shown in the curve is the wide periodic variation in the impedance. Because the variations are regular, it seems logical to assume that they are caused by reflections from a discontinuity in the line a distance L from the local terminal. The distance to the discontinuity in number of wave lengths is $n = L/\lambda$, where λ is the wave length at a given frequency and, with the use of $\lambda f = v$ the velocity of propagation, the expression $n = Lf/v$ is obtained. Now the velocity of propagation on open-wire lines is high and constant, hence

$$\frac{dn}{df} = \frac{L}{v} \tag{13}$$

From the graph it is seen that n is changing by one-fourth wave length every 640 cycles. Assuming a velocity of 98 per cent of the speed of light

$$L = v\frac{dn}{df} = 71 \text{ miles}$$

Since the line is 69.9 miles long, it is clear that the reflections come from the remote terminal. Yet the other end of the line was terminated, not in a short or open circuit but in a line trap, capacitor, and tuning unit tuned in the conventional manner to 57 and 135 kc.

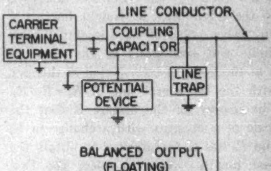

Fig. 11. Test circuit used to obtain curve in Fig. 10

Conventional tuning methods usually employ the transmitter or an oscillator as an energy source and the tuning panel is adjusted for maximum current into the line at the carrier frequency. This results in a perfect match with the energy source at the carrier frequency, but it is not the best match for the band nor does it ever result in a characteristic impedance termination unless the remote end of the line has already been terminated in the line characteristic impedance Z_k or is far enough away so that the reflected wave is greatly attenuated. Neither of the latter conditions is likely to prevail on a powert ransmission line.

The problem can be seen more clearly by examining the impedance of a transmission line which is not characteristically terminated, as a function of frequency. This impedance will travel in a circle in the complex impedance plane enclosing, but never passing through the point Z_k. The radius of the circle is given by

$$R=\frac{|Z_k|}{\sinh\left(2\alpha L+\log_e\left|\frac{Z_0+Z_k}{Z_0-Z_k}\right|\right)} \qquad (14)$$

where

αL = the attenuation of the line, nepers
Z_0 = the terminating impedance

The center of the circle has the same angle as Z_k and amplitude $\sqrt{(|Z_k|^2+R^2)}$. The line impedance will travel once around the circle each time the line length changes by a half wave length. The impedance of the line of Fig. 10 will travel around the circle five times in a 6-kc band. The best compromise match is the conjugate of Z_k, and for this condition, in fact, mismatch loss is the same for all points on the circle. By matching to the line impedance at a single frequency, one matches only to some point on the circumference, and this side will be a rather poor match for points on the other side of the circle.

To obtain a high-quality carrier channel, then, it will be necessary to find the characteristic impedance of the line and determine the desired characteristics of the terminating networks by calculation. At the receiving end, the trap and capacitor networks in parallel should approximate the line characteristic impedance. Of course, the impedance of the trap circuit varies with switching and it will be necessary to assume some compromise value. At the sending end the capacitor network should match the line and the trap circuit in parallel. If transmission alternates in direction, as with the present single-frequency carrier equipment, a reasonable compromise is to adjust the capacitor networks to approximate the line characteristic impedance at both ends. It is possible to obtain a better match for both the line and the transmitter in this case by adding resistance in series with the coupling capacitor.

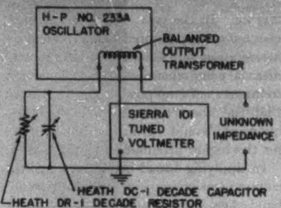
H-P NO. 233A OSCILLATOR
BALANCED OUTPUT TRANSFORMER
SIERRA 101 TUNED VOLTMETER
UNKNOWN IMPEDANCE
HEATH DC-1 DECADE CAPACITOR
HEATH DR-1 DECADE RESISTOR

Fig. 12. Bridge circuit for impedance measurements

Checks on the adjustment of the capacitor network should be made looking in at the high side of the coupling capacitor. This point will usually not be accessible; the network can still be checked, however, by substituting for the coupling capacitor a dummy with the same capacity. It may prove desirable to add a dummy drain coil too.

Traps have always been a problem. Since the present designs use variable taps connected on the inside of the blocking coil for the fine adjustment, to retune a trap it is not only necessary to take the line out of service but usually a line crew and winch truck must be called out also to lower the trap to the ground. There is no apparent reason why the elements of the resonating network should not be housed in a small container which could either be inserted in the blocking coil or attached directly to the line conductors with a hotstick. The adjustment of the resonating network could then be changed by removing it from the line and connecting it to a dummy blocking coil.

Knowledge of the characteristic impedance is necessary for engineering high-quality broad-band channels. Since the attenuation of power lines at carrier frequencies is very low, the characteristic impedance will be a nearly pure resistance determined by line geometry. Equations for the impedance of low-loss lines in air have been developed from field theory[5]

$$R_p=276\log_{10}(d/r) \qquad (15)$$

$$R_c=138\log_{10}(d/r) \qquad (16)$$

The first equation applies to 2-wire lines where r is the conductor radius, and d is the separation. The second equation applies to coaxial lines and d and r are the radii of the outer and inner conductors respectively. The former will probably be fairly accurate for phase-to-phase coupling of carrier current. It seems likely that the phase-to-ground use of the center conductor of a flat line with overhead ground wires will approach the coaxial case. At any rate it should be possible to develop equations of the form $K\log_{10}(d/r)$ for the characteristic impedance, where K and the method of finding an equivalent d depend only on the configuration of conductors and are independent of scale and conductor size.

In applying broad-band coupling methods, it will frequently be necessary to measure complex impedance. A bridge for measurements at carrier-current frequencies has recently become available commercially. The homemade bridge circuit of Fig. 12 will also appeal to many carrier people, since most of them already own the major components. It is necessary to determine the complex impedance by calculation. The author has found that the output transformer on the Hewlett-Packard oscillator has a very good balance for measurements at the impedance levels ordinarily encountered in carrier work. At any rate, the transformer balance can always be checked by balancing the bridge, reversing connections to the two outside legs of the transformer, and rebalancing. The circuit as shown is used for measuring impedances with negative phase angle. For impedances with positive phase angle, the capacitance decade is placed in parallel with the unknown.

Networks similar to those developed in the foregoing can probably be applied to improve the passband characteristics of 2-frequency tuning panels and traps where difficulties in paralleling receivers and transmitters make it necessary to take the bandwidth in two sections. The analysis is difficult, however, and the problem is left to those who have the opportunity to attack it experimentally.

Conclusions

The design and construction of high-quality broad-band carrier channels will cost more in time, effort, and investment than the systems in use in this country at present. Even so, power-line carrier will continue to be a most attractive communication method for the electric power industry, especially where long distances make the alternatives of microwave or physical telephone lines a very expensive proposition.

The power system communications engineer designing a broad-band carrier channel will probably wish for blocking coils of somewhat higher inductance than the present coils (about 250 microhenrys), especially if he attempts to keep trap resistance two or three times the line impedance. But if he cannot have them at reasonable cost, he will do without, perhaps sacrificing bandwidth or quality, sometimes putting two traps in series, or adding a second capacitor behind the trap. The second capacitor, if resonated to show a low impedance over the band, will reduce the variations of impedance caused by switching and permit resonating the trap to a lower resistance and a broader band. Perhaps the best expedient, however, is to go to higher frequencies. A 250-microhenry trap with a 3-stage resonating network can maintain 1,000 ohms over an 18-kc band at 100 kc, or over a 74-kc band at 200 kc. In the past, the lower frequencies have been favored because of lower attenuation but Cheek and Moynihan,[6] after a comprehensive study of carrier-frequency noise on power lines, concluded that the lower noise levels at high frequencies would probably compensate for the higher attenuation in most cases.

In applying broad-band coupling, the communications engineer will want broad-band class-A final radio-frequency power amplifiers for the sending end of his channel so that he can combine the outputs of his older transmitters without worrying about the effects of mutual loading. He will also want modulator panels for translating the frequency of wide bands at by-passes, so that he can apply amplification without causing singing. And when broad-band power amplifiers and frequency translators are available, he will wish to consider, the single-side-band multiplexing systems brought to a high state of development over a period of many years in the telephone industry.

References

1. A Broad-Band Coupling Unit for Power-Line Carrier with Associated Potential Device, **John A. Doremus, Robert P. Crow, William H. Freeman.** *AIEE Transactions*, vol. 71, pt. III, Oct. 1952, pp. 870–87.

2. Application of Line Traps to Power-Line Carrier Systems, **J. D. Moynihan.** *Ibid.*, Dec. 1952, pp. 1058–62.

3. Network Analysis and Feedback Amplifier Design (book), **Hendrik W. Bode.** D. V. Van Nostrand Company, Inc., New York, N. Y., 1945, pp. 211–14.

4. Analysis of Losses in Power-Line Carrier Coupling Circuits, **F. C. Krings, J. L. Woodworth.** *AIEE Transactions*, vol. 73, pt. III, Oct. 1954, pp 1213–18.

5. Principles of Electricity and Electromagnetism (book), **Gaylord P. Harnwell.** McGraw-Hill Book Company, Inc., New York, N. Y., 1949, pp. 521–22.

6. A Study of Carrier Frequency Noise on Power Lines: Part II. Results of Field Measurements, **R. C. Cheek, J. D. Moynihan.** *AIEE Transactions*, vol. 70, pt. II, 1951, pp. 1325–34.

Apparatus Noise Measurement

R. J. WELLS
NONMEMBER AIEE

ALMOST all noise measurement techniques and test codes used for measuring the noise of electrical equipment are based on the 1950 American Standard Association test code for apparatus noise measurement.[1] This is now considered obsolete, and is being revised to conform to latest techniques by the ASA writing group *Z24-W-25*. The new code will undoubtedly have a great impact on noise measurement procedures used with electrical apparatus. Since the code will not be in print for a year or two, it is hoped that the information presented in this paper will serve as a guide in the measurement of apparatus noise in the interim before such publication. It should aid particularly in the current emphasis of the concept of total sound power.

The main tasks set by the subcommittee are:

1. Procedures for the measurement of total radiated acoustic power.

2. Procedures for the measurement of sound pressure level at specified locations.

To date, most of the work of this group has been concerned with the measurement of total acoustic power, the primary subject of this paper. Only objective measurements are being standardized, though subjective criteria are being studied by other exploratory groups. Also, a separate exploratory group is studying the problem of noise measurements which are hampered by the presence of high-velocity air streams.

Sound Power Measurement

Most test codes have been concerned only with the measurement of sound pressure levels at specified locations. Such data are usually inadequate and seldom offer a fair means of comparison of the noise of different types of machines. It is much like giving the voltage output of a generator without specifying the load or the available power. Also, slight modifications in a machine may change the sound pressure level at one point by several decibels without appreciably affecting the total radiated power. A sound power specification is a much more fundamental quantity than a sound pressure level. Actually, at distances somewhat removed from a machine, the sound level in a given room is almost solely dependent on the sound power output. Also, once the sound power is known, it is possible to compute the sound pressure level, within engineering accuracy, at any specified location in a given enclosure.

There are several methods of sound power measurement under consideration. However, at the outset it should be pointed out that any such measurement should at least be made in octave bandwidths. Almost all sound criteria in current use are based on octave-band analyses rather than mere weighted network levels. In certain cases, it may be necessary to employ even more narrow bands.

FREE FIELD MEASUREMENTS

A space integration of the total sound power radiated into a free field is perhaps the most basic approach to sound power measurement. This may be accomplished by means of a point-by-point survey of the sound pressure over the surface of a hypothetical sphere, or hemisphere, surrounding the device under test. The radius of such a sphere, and the locations of the various microphone positions, are of some importance though they are not highly critical since the same acoustic power must pass through all concentric spheres. In general, however, the radius chosen should be such as to avoid the near sound field, where reactive conditions exist, and the microphone positions should be spaced as uniformly as possible

---

Paper 55-725, recommended by the AIEE Rotating Machinery Committee and approved by the AIEE Committee on Technical Operations for presentation at the AIEE Fall General Meeting, Chicago, Ill., October 3–7, 1955. Manuscript submitted June 6, 1955; made available for printing August 15, 1955.

R. J. Wells is with the General Electric Company, Schenectady, N. Y.

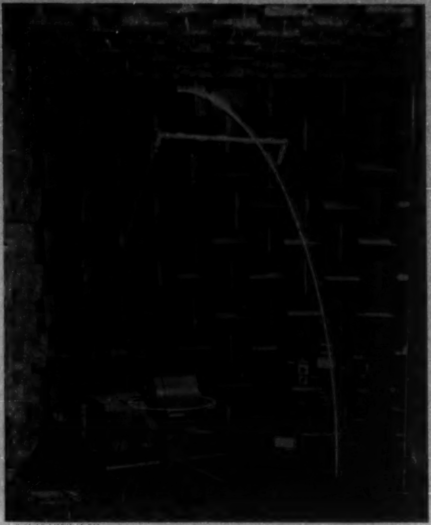

Fig. 1. Automatic equipment for the free-field integration of total sound power in use in the General Electric anechoic room in Schenectady

over the surface of the test sphere. With regard to the first condition, a radius equal to twice the maximum dimension of the machine, or not less than 3 feet, is considered as about a minimum. The point arrays indicated in reference 6 have been suggested by the General Radio Company to meet the second objective. The number of points chosen depends upon the directivity of the source. For the higher octave bands if accuracy is desired, it is advisable to use the 20-point array. In many cases a certain degree of symmetry may be present. If desired, such symmetry may be utilized to minimize the number of measurement positions required.

Acoustic directivity increases markedly at the higher frequencies. Hence, a large number of microphone positions may be required to obtain an accurate average for a band of 4,800 to 9,600 cycles per second (cps). Perhaps it would be best not to specify fixed locations as standard microphone positions, but rather to set down rules from which optimum positions may be chosen for different types of machines. In fact, one of the basic advantages of the sound power approach to noise specification is the test flexibility in this respect. Actually, fixed discrete microphone positions are not required, and the use of automatic rotating devices may be preferable. In one such equipment which tests at General Electric have indicated to be satisfactory, the noise source is rotated on a turntable while the microphone travels along a 90-degree arc about an axis perpendicular to the turntable axis. As a result, the microphone effectively traverses a spiral path about the noise source. To weight the output signal in proportion to the incremental zone of the test sphere, a cosine potentiometer may be employed. An alternative possibility is the use of a cosine drive on the traveling microphone. The microphone signal is, of course, fed to an integrating or averaging circuit and then to a meter.

Regardless of what microphone positions are used, the objective is simply to obtain an average sound pressure level over the chosen test surface. Better still, assuming sound intensity to be proportional to the square of the sound pressure—as it should be in a free field—the average intensity may be obtained with automatic equipment by squaring the signal before averaging it. Given the average sound intensity, the total radiated sound power, in watts, may be obtained simply by multiplying the intensity by the area of the test surface.

To summarize, the following relations are obtained

$$\text{sound pressure level} = L_p = 20 \log_{10} \frac{p}{0.0002}$$

in decibels referred to 0.0002 microbars (1)

where

p = rms sound pressure, microbars

$$\text{sound intensity} = I = \frac{p^2}{\rho c} 10^{-7} \text{ watts per centimeter}^2 \quad (2)$$

assuming spherical wave, where

ρ = density of medium (air), centimeter-gram-second units

c = velocity of sound in medium, centimeter-gram-second units

If I represents the average sound intensity over an area S, centimeter², then the total power radiated through this surface is

$$W = IS \text{ watts} \quad (3)$$

For purposes of calculation, it is often convenient to express sound power as a level. The reference base of 10^{-13} watts appears to be most common, though it has not been standardized to date. With this reference level

$$\text{sound power level} = L_w = 10 \log_{10} \frac{W}{10^{-13}} \quad (4)$$

in decibels referred to 10^{-13} watts. These relations may be combined in the form

$$L_w = \bar{L}_p + 10 \log S - 0.5 \quad (5)$$

where S is now expressed in square feet, and $\bar{L}_p$ represents the average sound pressure level, preferably the rms average level for greatest accuracy.

If preferred, equation 5 may be written in terms of W, the total sound power in watts, as

$$10 \log_{10} W = \bar{L}_p + 10 \log S - 130.5 \quad (6)$$

REVERBERANT FIELD MEASUREMENTS

An alternative approach to sound power measurements involves the use of a reverberation room. In a large reverberant enclosure, the sound pressure level due to a given sound source is essentially independent of position. Thus, for any particular reverberant room, the average sound level is determined solely by the acoustic power of the sound source. Hence, assuming that the room is properly calibrated, the sound power being developed by an apparatus may theoretically be obtained from a single sound level measurement. In practice, the sound is never perfectly diffused, so the use of the average sound level for several locations is preferable.[2,3]

Again, with the reference base of 10^{-13} watts, the sound power level may be determined from the average sound pressure level by means of the relation

$$L_w = \bar{L}_p + 10 \log R - 6.5 \quad (7)$$

where R is a constant dependent only upon the absorptive properties of the room. In terms of watts, equation 7 takes the form

$$10 \log_{10} W = L_p + 10 \log R - 136.5 \tag{8}$$

The constant R may be computed from the theoretical relation

$$R = \frac{a}{1-\bar{a}} \tag{9}$$

where

$a = \bar{a}A$ = total absorption in room, sabines.
A = total surface area of room, square feet.
$\bar{a}$ = average absorption coefficient of room surfaces.

A measurement of the reverberation time of the room will suffice to determine, $\bar{a}$ and a from

$$T = \frac{0.049\ V}{-A \ln(1-\bar{a})} = \frac{0.049\ V}{\bar{a}A} = \frac{0.049\ V}{a} \tag{10}$$

where

T = reverberation time = time required for a 60-decibel drop in sound level, seconds.
V = volume of room, cubic feet.

In the opinion of the writer, however, a superior method is to make use of a standard source of known sound power output. This procedure requires but a minimum of equipment and eliminates what otherwise appears to be a source of systematic error, namely, the existence of increased sound levels near the walls and corners of the room.[4] The known sound power source may be a standard machine, the sound power of which has been accurately determined by a free-field integration procedure, or from a test in a calibrated reverberation room such as the Riverbank room or the Bureau of Standards room. An alternative sound source is a loudspeaker of high acoustic impedance driven by octave bands of a monitored electrical noise signal. In either case, the standard source is sounded in the room to be calibrated and the difference between the average sound pressure level and the known sound power level is determined by octave bands.

The accuracy of sound power measurements in a reverberation room is in general limited by the degree of sound diffusion within the room and by the constancy of its calibration. The degree of diffusion is a function of the room dimensions and absorption, and the character of the noise itself. For low frequencies a large room is required. The minimum frequency for which a reasonable state of diffusion exists in a rectangular room may be estimated[6] from

$$f_{\min} = \frac{10^4/\sqrt{V}}{\sqrt{\Delta f + \frac{4}{T}}} \tag{11}$$

where Δf is the bandwidth of the noise in cycles per second, or in the case of a very wide-band noise, it may be taken as the bandwidth of the sound analyzer being used. Moreover, the room dimensions should be approximately but not exactly equal. Thus, for work with pure tones down to a frequency of about 120 cps dimensions of 20 by 25 by 30 feet might be chosen. As might be deduced from equation 11, broad-band noise will tend to be more uniformly diffused than pure tones. Hence, where strong, pure tones are present, it may be necessary to use quite a few measurement points in order to obtain a good space average. This may be accomplished by moving the microphone along a circular arc through the room, and using electronic equipment to obtain an integrated average level.[2] An alternative procedure has been used at the National Bureau of Standards. This involves the placement of nine microphones in a random pattern in the middle of the room, the outputs of the microphones all being connected in series parallel. Rotating or fixed vanes, or diffusers, may also be employed to improve the response of a reverberation room. Usually a large rotating vane with a fixed microphone position will have an effect like one with a fixed vane and a rotating or multiple microphone system.

The constancy of the room calibration is, of course, dependent upon the constancy of the contents of the room. For this reason, few, if any, people should be permitted within the room during tests. However, an additional source of error is the fact that, at the higher frequencies, a considerable portion of the total absorption in a rather live room is due to molecular absorption in the air itself. Since such absorption varies with the atmospheric conditions, and if high accuracy is required above about 2,000 cps, care should be taken to maintain constant conditions of temperature and humidity.

SEMI-REVERBERANT FIELD MEASUREMENTS

High quality free-field or reverberation rooms are rather expensive test facilities. Many people interested in noise are therefore forced to make their measurements in factory or laboratory areas where the walls, etc., are neither acoustically dead nor completely reflecting. In such an enclosure the sound level does not follow the inverse square law, 6-decibel drop per doubling of distance, in the neighborhood of the microphone positions, as it should in a free-field. Neither is the sound level essentially independent of location as it should be in a truly random or reverberant field. However, since measurements must often be made under such conditions, an outline of a procedure by which the data may be obtained in as accurate a way as possible has been suggested.

The recommended procedure is as follows. First, microphone positions that would be satisfactory in a free field are chosen. Then the noise of one machine is measured by two methods:

1. In the test room.
2. In a free field, perhaps outdoors on a calm, quiet day, with the machine suspended or mounted as it would be in the test room. No reflecting surface, other than the ground should be within 100 feet. The microphone positions should duplicate those used in the test room.

The room coefficient R should then be computed for each octave band from

$$R = \frac{4S}{\text{Antilog}_{10}\left(\frac{L_{pt} - L_{p0}}{10}\right) - 1} \tag{12}$$

where

S = area of surface defined by the microphone positions, square feet.
$\bar{L}_{pt}$ = average sound pressure level in test room under calibration.
$\bar{L}_{p0}$ = average sound pressure level in free field.

If desired, this one machine may now be set aside as a standard noise and later used to evaluate other rooms, in which event, the octave-band free-field sound power spectrum should be computed from

$$L_w = \bar{L}_p + 10 \log_{10} S - 0.5 \tag{13}$$

The sound power level of any machine under test in a room calibrated as indicated may now be determined from

$$L_w = \bar{L}_{pt} - 10 \log_{10}\left\{\frac{1}{S} + \frac{4}{R}\right\} - 0.5 \tag{14}$$

decibels referred to 10^{-13} watts. This must be computed for each octave band, and the powers in the various bands should be added to obtain the over-all sound power level.

The method outlined has the advantage of requiring no tests and no decisions regarding the state of the sound field within the test chamber. The initial presumption was that the room is neither a free field nor a truly reverberant room. However, if the room is actually free-field, to a distance corresponding to the microphone positions, then the values for R, as computed from equation 12, will be infinite. Equation 14 then reduces to the free-field equation 5. Conversely, if the room is highly reverberant

$$\frac{4}{R} >> \frac{1}{S} \tag{15}$$

so equation 14 reduces to equation 7. Thus, the free-field and reverberant-field methods are seen to be but special cases of the more general method applicable to semireverberant rooms. In general, however, measurements made in semireverberant sound fields are less accurate than those made under either of the other two conditions. One of the primary reasons for this is local effects at some of the microphone positions caused by reflections from nearby walls and other machines. Such errors may be minimized by using as open a test area as possible.

Presentation of Data and Criteria

Sound power data are probably best presented as a sound power level octave-band spectrum. However, to provide a basis of comparison with previous sound pressure level measurements and standards, the data may also be presented as computed free-field average levels at a specified distance. If the machine normally rests on a hard floor, this computation may be made from the hemispherical radiation relation

$$\bar{L}_p = L_w - 20 \log_{10} r - 7.5 \qquad (16)$$

where r is the specified distance in feet. For a freely suspended machine or a small hand-held device the spherical radiation relation

$$\bar{L}_p = L_w - 20 \log_{10} r - 10.5 \qquad (17)$$

should be employed.

Sound control criteria are usually specified in terms of octave-band sound pressure levels at the location of interest. However, as previously mentioned, once the sound power spectrum is known, the average sound pressure spectrum at a given radius from the machine may be computed for any enclosure with known acoustical properties. Equation 14, solved for $\bar{L}_{pi}$, may be used for this purpose. Once this computation is made, the acceptability of the machine noise may be ascertained by comparison with suitable tolerance criteria. Such criteria may be based on deafness risk,[6,7] speech interference,[6,7] sound level ranks,[6–8] loudness,[9–11] etc. It is also possible to express criteria directly in terms of the sound power delivered to the area in question.[12]

References

1. Test Code for Apparatus Noise Measurement. *ASA Z24.7-1950.* American Standards Association, New York, N. Y., 1950.

2. Measurement of Sound Power, R. J. Wells, G. N. Sawyer. *Noise Control*, New York, N. Y., vol. 1, 1954, Mar. 1955, p. 59.

3. Direct Measurement of the Efficiency of Loudspeakers by Use of a Reverberant Room, H. C. Hardy, H. H. Hill, L. G. Ramer. *Proceedings*, National Electronics Conference, Chicago, Ill., vol. 8, Jan. 953, pp. 99–107.

4. Interference Patterns in Reverberant Sound Fields, R. V. Waterhouse. *Noise Control*, New York, N. Y., vol. 27, Mar. 1955, pp. 247–58.

5. Vibration and Sound (book), P. M. Morse, McGraw-Hill Book Company, Inc., New York. N. Y., second edition, 1948, p. 420.

6. Handbook of Noise Measurement, Arnold P. G. Peterson, Leo L. Bernaek. General Radio Company, New York, N. Y., 1954.

7. Handbook of Acoustic Noise Control, Wright Air Development Center, Wright Patterson Air Force, Ohio, vol. 2, "Noise and Man," 1952.

8. A Community's Reaction to Noise: Can it Be Forecast? K. N. Stevens, W. A. Rosenblith, R. H. Bolt. *Noise Control*, vol. 1, Jan. 1955, pp. 63–71.

9. Instruments and Techniques for Measurement and Evaluation of Industrial Noise, D. Calloway. *Proceedings*, Annual National Noise Abatement Symposium, National Noise Abatement Council, New York, N. Y., Oct. 1951, vol. 2.

10. A Loudness Chart for Octave-Band Data on Complex Sounds, F. Mintz, F. G. Tyzzer. *Noise Control*, vol. 24, New York, N. Y., Jan. 1952, pp. 80–82.

11. We Can Reduce Truck Noise, L. C. Kibbee. *Proceedings*, Annual National Noise Abatement Symposium; National Noise Abatement Council, New York, N. Y., Oct. 1953, vol. 4.

12. Noise Reduction of Machinery and Vehicles, R. O. Fehr, R. J. Wells. *Noise Control*, vol. 1, Jan. 1955, pp. 30–39.

The Application of a New Nontracking Butyl to High-Voltage Instrument Transformers

R. A. PFUNTNER
MEMBER AIEE

R. S. NORMAN
NONMEMBER AIEE

B. W. WILTERDINK
ASSOCIATE MEMBER AIEE

Synopsis: A new nontracking butyl insulation which will not carbonize even under severe surface contamination has been applied to 15,000-volt outdoor instrument current transformers, and makes practical still higher voltage outdoor butyl designs. The discovery of a novel principle[1] to overcome the susceptibility of organic materials to carbonization and tracking and the application of this principle to butyl rubber have enabled this major advance to be made.

For many years outdoor instrument transformers as well as most other outdoor electric apparatus have employed metal casings, porcelain bushings, and appropriate gasketing means to prevent loss or contamination of the insulating media. The desire to provide a more trouble-free construction requiring greatly reduced maintenance has led to the use, in recent years, of 1-piece homogeneous insulation systems which combine the functions of insulating and casing in one material such as molded butyl or cast epoxide resin.[2,3]

The application of molded butyl for low- and medium-voltage instrument transformer insulation has advanced steadily since 1948.[2,4–6] More than 150,000 molded butyl transformers are now in service on electrical utility systems all over the country. These include indoor transformers at 600 to 15,000 volts and outdoor transformers at 600 to 5,000 volts.

European manufacturers have been very active in the development of cast epoxide resin transformers for higher voltages, but the application has been limited to indoor service. The addition of porcelain skirts to cast resin bushings and transformers has been found necessary to withstand severe outdoor weathering conditions.[3]

Above 5,000 volts the outdoor use of organic insulators has not been practicable where the atmospheric contamination is excessively severe. In atmospheres containing salt fog and/or dust and industrial contaminants, conducting deposits are formed on the surface of the exposed insulation material. Leakage currents result which produce surface arcing with localized temperatures as high as 2,000 to 3,000 degrees

---

Paper 55-715, recommended by the AIEE Transformer Committee and approved by the AIEE Committee on Technical Operations for presentation at the AIEE Fall General Meeting, Chicago, Ill., October 3–7, 1955. Manuscript submitted June 6, 1955; made available for printing July 29, 1955.

R. A. Pfuntner, R. S. Norman, and B. W. Wilterdink are with the General Electric Company, West Lynn, Mass.

Acknowledgement and appreciation are expressed to A. A. Kessel, M. W. Albright, A. C. Bluestein, C. F. Gurnham, and many others who contributed to this development.

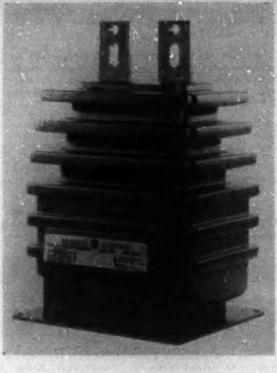

Fig. 1. Hy-Bute/60 current transformer for 15,000-volt outdoor applications

centigrade. Repeated arcing breaks down the organic components of the insulation to form a carbonaceous residue. As there is insufficient oxygen available for effective oxidation, the carbon accumulates and forms as a conducting path. When the arcing conditions are severe, even porcelain bushings will crack and chip from thermal shock and will no longer be able to serve as insulators.

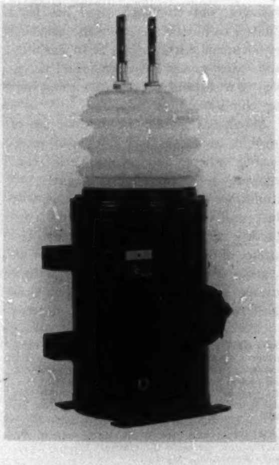

Fig. 2. Conventional 15,000-volt outdoor current transformer utilizing metal case and porcelain bushing

New Outdoor Material—Hy-Bute/60

The development of a nontracking butyl insulation based on the application of the internal oxidation mechanism has been successfully accomplished.[1] This mechanism, which is activated by high temperatures, is built into the butyl rubber. It is believed that the oxidation mechanism takes place concurrently with any breakdown of the organic components from the localized arcing so that no free carbon is formed.

This material as applied to instrument transformers has been designated as Hy-Bute/60. It retains the outstanding electrical, physical, and chemical properties of conventional butyl[4,5]: resistance to ozone and corona, tearing and abrasion, acids and alkalies as well as high dielectric strength and excellent heat-aging properties. In addition to its nontracking characteristics, Hy-Bute/60 is superior to conventional butyl with respect to thermal conductivity and is self-extinguishing by the American Society for Testing Materials *D635-44*, flammability test.[7]

15,000-Volt Outdoor Transformers

Instrument current transformers utilizing Hy-Bute/60 have been designed and built for 15,000-volt outdoor application, Fig. 1. The molded butyl construction results in a transformer substantially smaller and lighter than previous conventional designs such as shown in Fig. 2. In addition, it eliminates the hazard of porcelain breakage and the necessity of periodic maintenance to prevent corrosion.

The complete adequacy of Hy-Bute/60 for this service has been established by extensive laboratory and field testing on 5,000-volt transformers. Included are highly accelerated surface creepage tests in salt-fog chambers and at severe seacoast locations. Similar tests are under way on 15,000-volt designs, with preliminary results after several hundred hours indicating equivalent outstanding performance. The following is a detailed description of these test procedures as well as the results obtained to date on the 5,000-volt designs.

Accelerated Laboratory Tests

Laboratory equipment for testing these transformers under extremely accelerated conditions consists of a vented stainless-steel chamber, Fig. 3, continuously supplied with a dense fog of 10-per-cent NaCl and 1.2 per cent MgCl (both salts have approximately four times the concentration normally found in sea water). The MgCl contributes to the severity of the test by caking the salts on the transformer surface. The sample transformers can be energized continuously at any desired test voltage. Table I shows the results of tests in the laboratory salt-fog chamber on 5,000- and 15,000-volt porcelain bushings, 5,000-volt outdoor current transformers insulated with conventional butyl, and similar transformers insulated with Hy-Bute/60.

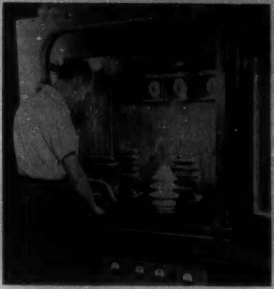

Fig. 3. Laboratory salt-fog chamber for accelerated creepage tests

All samples were tested at 5,000 volts including the 15,000-volt porcelain bushings. Figs. 4 through 7 show typical samples after exposure to this test. The cracking, chipping, and ultimate failure of the porcelain bushings (49 hours for the 5,000-volt bushings and 432 hours for the 15,000-volt bushings) emphasize the severity of the test. The conventional butyl failed in 107 hours by the expected tracking mechanism while the Hy-Bute/60 showed no signs of tracking after 1,400 hours.

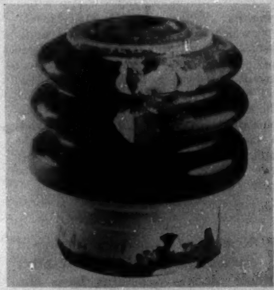

Fig. 4. Conventional 5,000-volt porcelain bushing after 49 hours at 5,000 volts in laboratory salt-fog test

Table I. 5,000-Volt Salt-Fog Tests

	No. Tested	Hours on Test	Results
Porcelain bushings			
5,000-volt design	3	less than 80	cracked and chipped
15,000-volt design	3	less than 500	cracked and chipped
5,000-volt current transformer			
Conventional butyl	6	less than 110	carbonized track and failures
Hy-Bute/60	7	over 1,200	no tracking

Table II. Atmospheric Conditions at Test Locations

Location of Test	Company	Atmospheric Condition
San Francisco, Calif.	Pacific Gas and Electric	salt fog
Los Angeles, Calif.	Southern California Edison	salt fog
Philadelphia, Pa.	General Electric service shop	industrial smoke
Denver, Colo.	General Electric service shop	high altitude
Seattle, Wash.	General Electric service shop	heavy rain
Houston, Tex.	General Electric service shop	humid, high temperature
Miami, Fla.	Florida Power and Light	humid, high temperature
El Paso, Tex.	El Paso Electric Company	dry, high temperature
Fairmont, W. Va.	Monongahela Power Company	industrial smoke
Minneapolis, Minn.	General Electric service shop	snow, low temperature
Lynn, Mass.	General Electric plant	rain, snow, industrial smoke

Table III. 5,000-Volt Service Tests at San Francisco

5,000-Volt Current Transformers	No. Tested	Hours on Test	Results
Standard butyl	6	1,100 to 2,600	failure by carbonized track
Hy-Bute/60	6	8,000	no damage (test still in progress)

OUTDOOR SERVICE TESTS ON COMPLETE TRANSFORMERS

Since 1952 several electrical utilities have been co-operating with the General Electric Company in a program of critical evaluation of various types of atmospheres found throughout the country. The test locations shown in Table II were selected as being typical of areas in which transformers may be used. Six butyl transformers were installed and operated at each location without any cleaning or other normal maintenance.

The conclusions drawn from this study were that the atmospheric conditions most conducive to creepage attack were those involving salt fog and spray. Very severe conditions of this sort exist in certain areas on the West Coast, such that precautions in the design and maintenance of all outdoor electric apparatus used in these locations are necessary.[8–11] Adequate insulator performance is maintained by the use of oversize bushings and regular cleaning programs. The initial West Coast installation in the test program was within 100 yards of the ocean at the Rodondo steam plant of the Southern California Edison Company. Further investigation disclosed an even more severe condition at the Pacific Gas and Electric test area at Seal Rock, San Francisco. This installation is located in a ravine open to the ocean so that the prevailing westerly winds funnel the salt fog and spray into the test area; see Fig. 8.

Table III shows the results to date of the San Francisco tests on 5,000-volt outdoor transformers identical to those tested in the laboratory. Tests were operated at 5,000 volts both in the laboratory and at San Francisco. Conventional butyl-insulated transformers at Seal Rock showed visible creepage damage in less than 100 hours. Ultimate failure was by surface tracking in 1,100 to 2,600 hours as compared to 40 to 110 hours in the accelerated laboratory test chamber. Hy-Bute/60-insulated transformers show no damage of any kind after 8,000 hours. This test is still in progress and additional Hy-Bute/60 tests have been established in other areas.

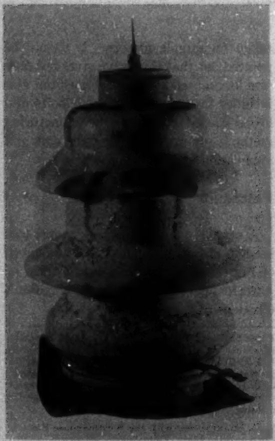

Fig. 5. Conventional 15,000-volt porcelain bushing after 432 hours at 5,000 volts in laboratory salt-fog test

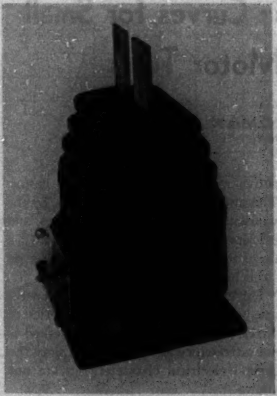

Fig. 6. Conventional butyl 5,000-volt current transformer after 107 hours at 5,000 volts in laboratory salt-fog test

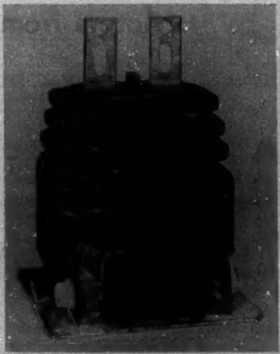

Fig. 7. Hy-Bute/60 5,000-volt current transformer after 1,400 hours at 5,000 volts in laboratory salt-fog test

Fig. 8. Pacific Gas and Electric test area at Seal Rock, San Francisco

HIGH-CURRENT ARC-OVER TESTS

Under certain conditions, outdoor electric insulators are subjected to high-current power arc overs. These arc overs may be initiated by excessive localized sparking in contaminated atmospheres or, more frequently, by high-voltage line surges resulting from lightning strokes.[9] The damage is occasionally serious enough to necessitate replacement of the insulator before service can be restored.

Arc-over tests were conducted with currents ranging from 5,000 to 75,000 crest amperes on both Hy-Bute/60 transformers and porcelain bushings arranged to have equivalent flashover distances. Fig. 9 shows the results of these tests. No carbonization was observed on any of the Hy-Bute/60 samples, and laboratory tests detected no effect on the electrical characteristics of the insulation. The only damage was a very slight surface erosion. At 10 to 20,000 amperes, the glaze on the porcelain bushings was partially destroyed and the skirts were cracked and chipped.

Conclusion

The successful development of nontracking Hy-Bute/60 has made possible the construction of butyl-molded instrument transformers for outdoor applications at 15 kv and above under the most severe atmospheric conditions. The elimination of metallic casings, porcelain bushings, and gasket seals effects a substantial reduction in size and weight and reduces maintenance to a negligible factor.

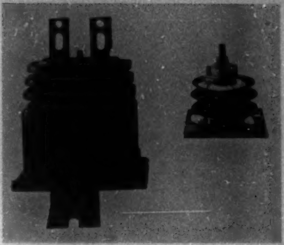

Fig. 9. Porcelain bushing and Hy-Bute/60 transformer after arc-over tests at 21,000 crest amperes

References

1. NONTRACKING ORGANIC INSULATIONS, **R. S. Norman, R. A. Pfuntner, A. A. Kessel.** *AIEE Transactions*, vol. 74, pt. III, 1955 (*Paper 55-699*).

2. REVOLUTIONARY ADVANCE IN INSTRUMENT TRANSFORMER DESIGN, **I. F. Kinnard.** *General Electric Review*, Schenectady, N. Y., vol. 52, no. 6, June 1949, pp. 15–19.

3. INSTRUMENT TRANSFORMERS WITH SYNTHETIC RESIN INSULATION, **Alfred Imhof.** CIGRE, Paris, France, 1954.

4. A NEW DRY TYPE INSULATION FOR INSTRUMENT TRANSFORMERS, **R. A. Pfuntner, R. E. Franck, F. R. D'Entremont.** *AIEE Transactions*, vol. 69, pt. I, pp. 453–58.

5. EVALUATION OF BUTYL INSULATION FOR OUTDOOR INSTRUMENT TRANSFORMERS, **J. A. McDonnell, H. E. Crabtree.** *AIEE Transactions*, vol. 70, pt. II, 1951, pp. 2021–25.

6. INSULATING INSTRUMENT TRANSFORMERS—A CONTINUING CHALLENGE, **R. S. Norman.** *General Electric Review*, Schenectady, N. Y., vol. 57, no. 4, July 1954, pp. 42–54.

7. *ASTM-D635-44*, American Society for Testing Materials, Philadelphia, Pa.

8. TESTS AND DEVELOPMENTS IN CONNECTION WITH HOT-LINE INSULATOR WASHING, **G. Leslie Hill.** *AIEE Transactions*, vol. 66, 1947, pp. 1203–16.

9. FLASHOVERS OF SUSPENSION INSULATORS DUE TO CONTAMINATION, **H. A. Adler, W. H. Wickham, M. S. Oldacre.** *AIEE Transactions*, vol. 67, pt. II, 1948, pp. 1680–85.

10. PERFORMANCE OF DUST-CONTAMINATED INSULATORS IN FOG, **Bradley Cozzens, T. M. Blakeslee.** *Ibid.*, pp. 1686–92.

11. INSULATOR SURFACE CONTAMINATION, **H. A. Frey.** *Ibid.*, pp. 1420–25.

Developing Iron Loss Curves for Small Motors from Motor Tests

V. C. SHANEMAN
ASSOCIATE MEMBER AIEE

A METHOD is outlined for obtaining motor iron loss curves in watts per cubic inch versus maximum flux density from induction motor tests. The curve is a valuable design tool for predicting motor performance.

Discussion

During the past decade, the designer of small motors has been constantly on the alert for ways and means of reducing the labor and material cost of his product. A direct approach to the problem of reducing material cost is to reduce the volume of the active magnetic material in the motor. This approach is limited, of course, by the ventilation system, noise limitations, and efficiency requirements. Consequently, a trend to less expensive grades of electric steels has resulted.

For existing designs, a change in steel can be made on the basis of a series of direct comparison tests. This method is not satisfactory for a new design since the general electrical characteristics are not known.

The basic problem confronting the designer is to develop a method of obtaining a motor iron loss curve from test data taken on sample motors. It should be pointed out that this curve gives not only iron loss caused by the steel itself but also includes losses in the through bolts and losses caused by various manufacturing methods such as riveting of the core and application of frame.

Procedure

A sample 4-pole split-phase motor was used to obtain the motor iron loss curve of Fig. 1. This curve is in the form of watts loss per cubic inch versus maximum flux density.

Paper **55-728**, recommended by the AIEE Rotating Machinery Committee and approved by the AIEE Committee on Technical Operations for presentation at the AIEE Fall General Meeting, Chicago, Ill, October 3–7, 1955. Manuscript submitted June 8, 1955; made available for printing August 26, 1955.

V. C. SHANEMAN is with the Westinghouse Electric Corporation, Lima, Ohio.

The author wishes to express his gratitude to L. W. Buchanan, Westinghouse Electric Corporation, Lima, Ohio, for his suggestions and guidance in the preparation of this paper.

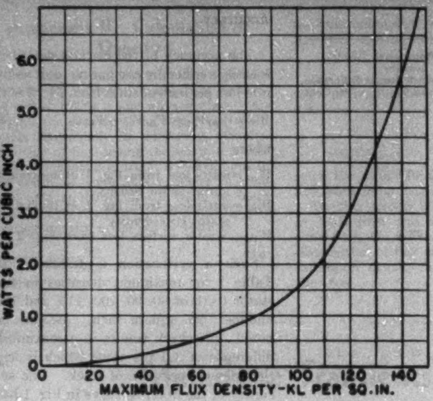

Fig. 1. Motor iron loss

To obtain the desired iron loss curve, only full-load and locked saturation tests are required. From these tests, a separation of losses can be made by the method outlined by Veinott[1] for as many values of line voltage as desired. The usual procedure for taking a full-load saturation test is to vary the terminal voltage from approximately 127 to 73 per cent of rated voltage while holding rated frequency, torque, and full-load temperature. For the purpose of this paper, however, the range of voltage variation should be extended as far as motor limitations will permit to cover the widest possible range of flux density. The flux density in each part of the circuit is, of course, a function of the line voltage and can be calculated from punching constants.

The purpose of the separation of losses is to obtain total motor iron loss as a function of maximum stator tooth density. At this point, it is convenient to convert total motor iron loss to iron loss per inch of core length by dividing the total motor iron loss by the length of the core in the test motor; see Fig. 2. This curve is a valuable design aid in this form, but is valid only for motors with the same stator and rotor punching, the same number of poles, and the same air gap as in the test motor.

To obtain a general iron loss curve from the aforementioned curve, it is necessary to separate the rotor surface loss from the total motor iron loss. Many small motor designers prefer the method developed by Johns from work by Spooner and Kincaid[2] for calculating rotor surface loss; see Appendix I. A rotor surface loss curve calculated by this method is shown in Fig. 2. A coefficient of 2.3 was assumed for the steel used in the test motor. This assumption may be subject to question; however, it is a function of the grade of steel being used and is an empirical quantity based upon considerable experience in working with various grades of steel. Since standard small motor design procedures consider total motor iron loss to consist of only stator tooth loss, stator iron loss, and rotor surface loss, total stator iron loss per inch of stack is represented by the difference between the ordinates of the two curves in Fig. 2. This difference has been plotted as Fig. 3.

The remaining problem is to convert this curve of total stator iron loss per inch of stack length into a general curve of watts per cubic inch versus maximum flux density. The following were drawn from the test motor stator punching dimensions

$$B_{sc}=0.872B_{st} \tag{1}$$

$$V_{sc}=2.35\ V_{st} \tag{2}$$

where

B_{sc}, B_{st} = maximum flux densities in the stator core and stator teeth respectively

V_{sc}, V_{st} = volumes of iron in the stator core and stator teeth respectively

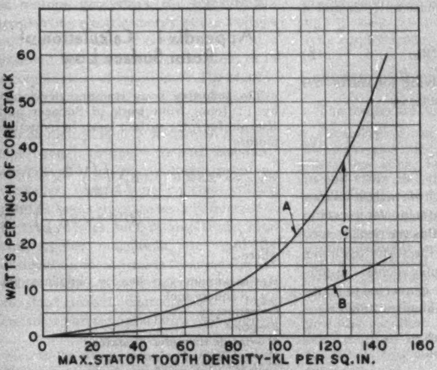

Fig. 2. Loss curves

A—Total motor iron loss
B—Rotor surface loss
C—Stator iron loss

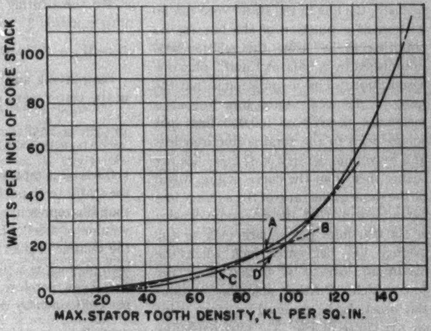

Fig. 3. Difference between ordinates of curves of Fig. 2

A—Stator iron loss
B—Stator iron loss as $f(B_{st}^2)$
C—Stator iron loss as $f(B_{st}^3)$
D—Stator iron loss as $f(B_{st}^4)$

Table I. Accuracy Check of Method

	Density, Kilolines per Inch^2	Watts Loss per Inch^3	Iron Volume, Inch^3	Watts Loss per Inch	Total Iron Loss for 1-Inch Stack from Fig. 2	Difference, Per Cent
Stator teeth	80	0.90	2.86	2.57		
Stator core	69.8	0.67	6.706	4.49		
Rotor				4.0		
Total iron loss				11.06	10.6	4.3
Stator teeth	90	1.16	2.86	3.32		
Stator core	78.5	0.85	6.706	5.70		
Rotor				5.2		
Total iron loss				14.22	13.6	4.6
Stator teeth	100	1.55	2.86	4.43		
Stator core	87.2	1.09	6.706	7.31		
Rotor				6.6		
Total iron loss				18.34	17.9	2.5
Stator teeth	110	2.12	2.86	6.06		
Stator core	96.0	1.39	6.706	9.32		
Rotor				8.2		
Total iron loss				23.58	23.3	1.2
Stator teeth	120	3.05	2.86	8.72		
Stator core	104.8	1.79	6.706	12.00		
Rotor				10.1		
Total iron loss				30.82	30.5	1.0

Total stator iron loss per inch of stack can be written simply as

$$W_s = W_{st} + W_{sc} \tag{3}$$

where W_{st} and W_{sc} are watts loss in the stator teeth and stator core respectively per inch of stack.

Since the stator iron loss curve was plotted as a function of maximum stator tooth density, it is obvious that the loss represented by every point on the curve is made up of the sum of the average loss in the stator teeth at the maximum density indicated and the average loss in the stator core at 87.2 per cent of this maximum density; see Appendix II. Consequently, the loss in the stator core can be written as a function of the loss in the stator teeth by using the relationships established by equations 1 and 2 plus one assumption. This assumption is that the ratio of the total stator iron loss at a maximum density of 100,000 lines per square inch to the total stator iron loss at a maximum density of 87,200 lines per square inch from the curve of Fig. 3 will be the same as the ratio of the average loss per cubic inch when the maximum density is 100,000 lines per square inch to the average loss per cubic inch when the maximum density is 87,200 lines per square inch. Further, a similar relationship must also be assumed for every point on the curve of Fig. 3. This reasoning permits one to write that, in general

$$W_{sc} = \frac{V_{sc}}{V_{st}}\left(\frac{B_{sc}}{B_{st}}\right)^n W_{st} \tag{4}$$

The exponent n in this equation is a variable. For practical purposes, however, n can be assumed to be a constant for a particular range of the curve and can be evaluated as accurately as desired. The author found that curve A in Fig. 3 could be approximated fairly accurately by assuming the iron loss to be a function of B_{st}^2, B_{st}^3, and B_{st}^4 in the ranges indicated in the following

$B_{st}^2(n=2)$ for $0 \leqq B_{st} \leqq 85{,}000$ lines per square inch

$B_{st}^3(n=3)$ for $85{,}000 < B_{st} \leqq 115{,}000$ lines per square inch

$B_{st}^4(n=4)$ for $115{,}000 < B_{st} \leqq 150{,}000$ lines per square inch

By substituting equations 1, 2, and 4 into equation 3

$$W_s = W_{st} + 2.35(0.872)^n W_{st} \tag{5}$$

Simplifying and solving for watts loss in the stator teeth results in

$$W_{st} = \frac{W_s}{1 + 2.35(0.872)^n} \tag{6}$$

Since W_{st} represents the watts loss in the stator teeth per inch of stack, it follows that W_{st} represents watts loss for a specific volume of steel. In this particular case, the volume of steel in the stator teeth per inch of stack is 2.86 cubic inches. Equation 6 can therefore be converted to watts per cubic inch by dividing by 2.86, or

$$\text{watts loss per cubic inch} = \frac{W_s}{2.86[1 + 2.35(0.872)^n]} \tag{7}$$

This is the equation used to convert curve A in Fig. 3 to the general form of watts per cubic inch; see Fig. 1.

Accuracy

The accuracy of the method described is easily verified by comparing total motor iron loss per inch of stack from Fig. 2 with

$$W_T = W_{Bt} V_{st} + W_{Bc} V_{sc} + W_{\text{Rotor}} \tag{8}$$

where

W_{Bt} = watts loss from Fig. 1 at maximum stator tooth density
W_{Bc} = watts loss from Fig. 1 at maximum stator core density
W_{Rotor} = rotor surface loss from Fig. 2

Such a verification is tabulated in Table I for maximum densities in the stator teeth of 80, 90, 100, 110, and 120 kilolines per square inch. As can be noted, this check results in a maximum difference of 4.6 per cent, which is less than 1 watt per inch of stack. The accuracy of the iron loss curve in Fig. 1 has also been verified by comparing the calculated motor core loss with tested motor core loss with equally satisfactory results on production motors of two frame sizes.

Conclusions

It is recommended that this method be used in place of the Epstein test to obtain a general motor iron loss curve because of the excellent results obtained plus the fact that an experience factor must be applied to the Epstein test data to obtain an equivalent curve. The experience factor is needed to account for losses in the frame, rivets, and through bolts. For general motor design, however, a saturation curve for induction motors must be obtained by some other method such as the Epstein test.

Appendix I. Calculation of Rotor Surface Loss

The following is an equation developed by F. Johns from work of Spooner and Kincaid for rotor surface losses in induction motors

$$W_{\text{Rotor}} = {}^{*}2.3 \times 10^{-8} \times B_g^{2.3}\left(\frac{f}{p}\right)^{1.55} \times (D')^{2.05}\sqrt{S_p}\left(\frac{e}{\Delta}\right)^{1.22} W$$

where

B_g = maximum gap density, kilolines per square inch
f = frequency
p = poles
D' = inside diameter of stator
S_p = number of primary slots
e = stator slot opening
Δ = single air gap (mechanical)
W = width of stack

---

* This is an empirical quantity which varies with the type of steel used. Its normal range is from 0.9 to 2.6.

Appendix II. Calculation of Density

The flux at any point in the core and teeth of an induction motor may be considered to follow a sine wave in time. Although the density along any given tooth varies sinusoidally in time only, the distribution of flux among the teeth of a pole varies sinusoidally from a maximum in the tooth or teeth at the center of each pole to a minimum in the tooth or teeth midway between poles. Consequently, the average density in the stator teeth is

$$\text{average } B_{st} = \frac{\Phi_m}{A_{st}} \qquad (9)$$

where

Φ_m = maximum flux per pole
A_{st} = the area of iron normal to the flux path in the stator teeth per pole

The maximum density in the stator teeth is obtained by dividing equation 9 by 0.637, or

$$B_{st} = \frac{\Phi_m}{0.637 A_{st}} \qquad (10)$$

since the ratio of the average value of a sine wave to its maximum value is 0.637.

The flux density in the stator core varies in both time and space because of the time variation of flux and the sinusoidal distribution of flux among the teeth. The maximum density in the stator core is, therefore,

$$B_{sc} = \frac{\Phi_m}{A_{sc}} \qquad (11)$$

where A_{sc} is twice the stator core area obtained from the product of radial depth below slot in the stator and the stator stack length.

References

1. Segregation of Losses in Single-Phase Induction Motors, C. G. Veinott. *AIEE Transactions (Electrical Engineering)*, vol. 54, Dec. 1935, pp. 1302–06.

2. No-Load Induction Motor Core Losses, T. Spooner, C. W. Kincaid. *Ibid.*, vol. 48, Apr. 1929, pp. 645–55.

Metadyne Transients

K. A. FEGLEY
ASSOCIATE MEMBER AIEE

THE NAME metadyne has been given by Pestarini[1] to a whole class of d-c machines. As defined by Pestarini, "A metadyne is a machine provided with an armature, having a commutator upon which bear at least three brushes per cycle of the machine, commutation being independent of the main winding of the stator or any eventual magnetic member acting upon the armature." An ordinary d-c shunt, series, or compound motor or generator would not be a metadyne since it has only two brushes per 360 electrical degrees or cycle.

Metadynes may be designed to operate as motors, generators, d-c transformers (converting electric energy at one voltage and current value to electric energy at a different voltage and current value) or in a combination of functions. The steady-state characteristics of metadynes are described by Pestarini.[1]

The definition of a metadyne is inclusive enough to apply to both constant-current and constant-voltage machines. However, control-type constant-voltage rotating generators are usually referred to by trade names, such as amplidyne, rototrol, regulex, magnavolt, etc., and the designation metadyne is reserved for machines with a constant-current or nearly constant-current characteristic. These constant-current machines have cross-fields, two fields lying 90 electrical degrees from one another. Cross-field machines were described by Rosenberg[2] as early as 1904. Riaz[3] has analyzed the transient response of the simple metadyne generator under the assumption of no saturation and negligible eddy-current effects. His stability analysis also neglects the effect of the main field winding.

It is the purpose of the present paper to analyze the transient behavior of the 4-brush constant-speed metadyne generator. The analysis presented includes consideration of eddy currents and saturation. The effects of parameter changes and winding additions are determined, making the analysis applicable to many metadyne connections.

Summary of Results

The results are discussed in six parts:

1. Stability of the metadyne generator: Metadyne generator instability may occur. Stable operation, however, is easily obtained. The effect of machine parameters on stability is examined.

2. Method of damping: The two methods of damping suggested by Pestarini,[1] resistance damping and series-winding damping, are examined. In addition, a new method of metadyne generator damping is presented. This new method permits rapid adjustment of the damping for each new load condition. It is also superior to other methods in that it has no effect on the steady-state operation of the metadyne generator.

3. Speed of response: The speed of response of the metadyne generator is very rapid when compared to the response of either a separately excited d-c generator or an amplidyne. The amplidyne has three circuits, each with its own time constant. The effective time constant for the complete amplidyne is always larger than the largest circuit time constant. The effective time constant of a metadyne generator can be much shorter than the time constant of any of the circuits in the metadyne. The effect of circuit resistance and inductance on the speed of response of the metadyne generator is determined.

4. Effect of eddy currents: Short-circuited stator windings are used to represent eddy-current paths. In a metadyne generator that has all the iron in the magnetic circuit laminated, eddy currents have only a small effect on the transient response. When not minimized by laminating the iron, eddy currents may be important and their damping effect may be beneficial.

5. Influence of additional windings: The simple metadyne generator has a single separately excited stator winding. Other independently excited stator windings may be added to the simple metadyne generator to modify the steady-state operation. The effect of these additional windings on the transient response of the metadyne generator is examined.

6. Effect of saturation: The peak transient flux in a stable metadyne generator may be many times as large as the steady-state flux. Transient saturation, therefore, may be an important consideration even though steady-state saturation does not occur. The effect of parameter changes on the amount of transient saturation is examined. The influence of transient saturation on metadyne generator response is discussed.

Many of the results were obtained from a differential analyzer study of the metadyne generator, compared with experimental data, and were found to give a good check.

Comparison of Several Machines

To understand the operating characteristics of the metadyne generator, it is helpful to compare the metadyne with other d-c machine connections. Fig. 1(A) shows a separately excited d-c generator. A change in the input voltage will cause a

---

Paper 55-108, recommended by the AIEE Rotating Machinery Committee and approved by the AIEE Committee on Technical Operations for presentation at the AIEE Fall General Meeting, Chicago, Ill., October 3–7. Manuscript submitted October 13, 1954; made available for printing July 18, 1955.

K. A. Fegley is with the University of Pennsylvania, Philadelphia, Pa.

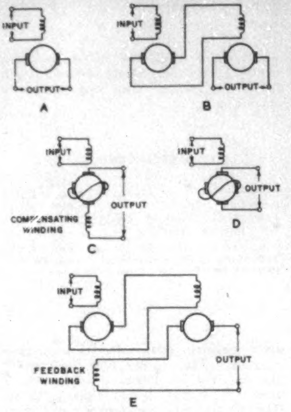

Fig. 1. Comparison of some commutator machines

A—D-c generator
B—Two d-c generators in cascade
C—Amplidyne
D—Metadyne generator
E—Two d-c machines in cascade with negative feedback

corresponding change in the voltage induced in the armature circuit. When a large power gain is required, two d-c generators may be connected in cascade as shown in Fig. 1(B).

The amplidyne of Fig. 1(C) gives two stages of power amplification without using two separate machines. The flux set up by the excitation current in the stator field winding produces a rotational electromotive force (emf) in the armature winding. One pair of armature brushes is short-circuited and carries armature current. The armature reaction flux caused by the current in the short-circuited path lies 90 electrical degrees from the field flux. It will therefore produce a maximum rotational emf between a pair of brushes placed 90 electrical degrees from the short-circuited brushes. The second pair of brushes carry load current. A stator compensating winding also carries load current. The magnetomotive force (mmf) of the compensating winding is equal in magnitude and opposite in direction to the mmf caused by the load current in the armature winding. The output voltage of the amplidyne is proportional to the input voltage.

The metadyne generator of Fig. 1(D) is identical to the amplidyne except for the elimination of the compensating winding. In this case the load current armature reaction mmf opposes the excitation current mmf and the output current is proportional to the input voltage. Large changes in the load resistance have little effect on the load current.

The metadyne generator is equivalent to two d-c generators in cascade with negative feedback from the output of the second generator to the input of the first. This arrangement is shown in Fig. 1(E).

Nomenclature

D = determinant of the impedance matrix
i = instantaneous current
i = current matrix
K = speed-voltage coefficient. For example, the speed-voltage induced in the d winding due to i_q amperes in the q winding is $K_q i_q$ volts
L = self-inductance or leakage inductance when the subscript λ is added
M = mutual inductance between the two windings designated by the subscripts
N = metadyne speed; also effective number of winding turns
p = the operator d/dt
R = resistance
t = time
T = a time constant
v = a voltage matrix
V = direct voltage
Y = admittance matrix
Z = impedance matrix
ϕ = flux

Subscripts

even numbers = direct-axis stator windings
odd numbers = quadrature-axis stator windings
1 = fictitious winding for eddy currents or an independently excited or short-circuited stator winding
2 = main excitation winding
3 = amplifying winding connected in series with the q winding and producing a mmf in the same direction as the mmf of the q winding
4 = damping winding connected in series with the q winding and lying in the direct axis
5 = damping winding connected in series with the d winding and lying in the quadrature axis
6 = fictitious winding for eddy currents or an independently excited or short-circuited stator winding
8 = amplifying winding connected in series with the d winding and producing a mmf in the same direction as the mmf of the d winding
d = direct-axis armature (rotor) winding or direct-axis magnetic circuit
g = fictitious winding for eddy currents in the load. The field winding of a d-c machine with a solid iron frame was used for some experimental work. The eddy-currents in the load are important in this case
λ = a leakage inductance
n = load circuit
q = quadrature-axis armature winding or quadrature-axis magnetic circuit
α = total direct-axis armature winding circuit. This subscript is used to denote total quantities in the circuit that includes the d winding, e.g., if the d, 5, and 8 windings only are connected in series, $R_\alpha = R_d + R_5 + R_8$
β = total quadrature-axis armature winding circuit. This subscript is used to denote total quantities in the circuit that includes the q winding, e.g., if the q, 3 and 4 windings only are connected in series, $R_\beta = R_q + R_3 + R_4$

Metadyne Equations

The metadyne generator studied on the differential analyzer is shown in Fig. 2. For the assumptions of constant metadyne speed and no saturation, the metadyne equations for the circuit of Fig. 2 are

$$\begin{aligned} v_2 &= (R_2 + pL_2)i_2 + pM_{26}i_6 - p(M_{28} + M_{2d})i_\alpha - pM_{24}i_\beta \\ 0 &= pM_{26}i_2 + (R_6 + pL_6)i_6 - p(M_{68} + M_{6d})i_\alpha - pM_{64}i_\beta \\ 0 &= -p(M_{28} + M_{2d})i_2 - p(M_{68} + M_{6d})i_6 + (R_\alpha + K_5 + pL_\alpha)i_\alpha - (K_3 + K_q - pM_{\alpha\beta})i_\beta - (K_1 + pM_{15})i_1 - pM_{ng}i_g \end{aligned} \quad (1)$$

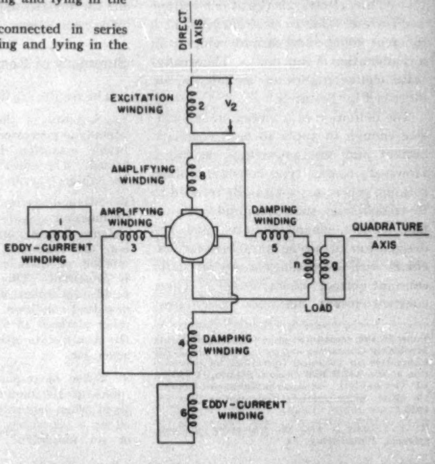

Fig. 2. The metadyne generator studied on the differential analyzer

$$0=-(K_2+pM_{24})i_2-(K_6+pM_{46})i_6+(K_d+K_\beta+pM_{\alpha\beta})i_\alpha+(R_\beta+K_4+pL_\beta)i_\beta+p(M_{1q}+M_{13})i_1$$

$$0=-pM_{1d}i_\alpha+p(M_{1q}+M_{13})i_\beta+(R_1+pL_1)i_1$$

$$0=-pM_{ng}i_\alpha+(R_g+pL_g)i_g$$

where

$$\begin{aligned}
R_\alpha&=R_3+R_5+R_d+R_n\\
R_\beta&=R_3+R_4+R_q\\
L_\alpha&=L_3+L_5+L_d+L_n+2M_{3d} \qquad (2)\\
L_\beta&=L_3+L_4+L_q+2M_{3q}\\
M_{\alpha\beta}&=M_{43}+M_{4d}-M_{3q}-M_{35}
\end{aligned}$$

Equation 1 can be written by inspection. The metadyne equations can also be written in the matrix form

$$v=Zi \qquad (3)$$

where

$$Z=\begin{array}{c|c|c|c|c|c|c|}
 & 2 & 6 & \alpha & \beta & 1 & g\\
\hline
2 & R_2+pL_2 & pM_{26} & -p(M_{23}+M_{2d}) & -pM_{24} & & \\
6 & pM_{26} & R_6+pL_6 & -p(M_{63}+M_{6d}) & -pM_{46} & & \\
\alpha & -p(M_{23}+M_{2d}) & -p(M_{63}+M_{6d}) & R_\alpha+K_5+pL_\alpha & -(K_3+K_q-pM_{\alpha\beta}) & -(K_1+pM_{1d}) & -pM_{ng}\\
\beta & -(K_2+pM_{24}) & -K_6-pM_{46} & K_d+K_\beta+pM_{\alpha\beta} & R_\beta+K_4+pL_\beta & p(M_{1q}+M_{13}) & \\
1 & & & -pM_{1d} & p(M_{1q}+M_{13}) & R_1+pL_1 & \\
g & & & -pM_{ng} & & & R_g+pL_g\\
\hline
\end{array} \qquad (4)$$

The impedance matrix Z can be conveniently obtained from Kron's[4] "primitive machine" and a "connection" matrix, or it can be written by inspection.

The currents in the several circuits of the metadyne are given by the matrix equation

$$i=Yv \qquad (5)$$

where the admittance matrix Y is the inverse of Z.

In Appendix I the metadyne equations are given as prepared for the differential analyzer. They are written in integral form and the assumption of no saturation is removed.

Stability of the Metadyne Generator

The stability of the metadyne generator can be investigated by applying Routh's[5] stability criterion to the determinant of the impedance matrix. The labor involved in applying Routh's criterion increases sharply as the order of the determinant increases. The criterion is applied to the simple metadyne generator with a single main field winding and no other independently excited stator windings. The presence of amplifying and damping windings does not change the order of the determinant and does not greatly increase the labor of applying the criterion. The addition of independently excited stator windings or eddy-current paths, however, does increase the order of the determinant.

The impedance matrix Z for the simple metadyne generator is

$$Z=\begin{array}{c|c|c|c|}
 & 2 & \alpha & \beta\\
\hline
2 & R_2+pL_2 & -pM_{2\alpha} & \\
\alpha & -pM_{2\alpha} & R_\alpha+pL_\alpha & -K_\beta\\
\beta & -K_2 & K_\alpha & R_\beta+pL_\beta\\
\hline
\end{array} \qquad (6)$$

The subscripts α and β refer to the circuits that include the d and q windings respectively. The impedance matrix of equation 6 is applicable to metadyne generators both with and without amplifying windings, damping windings and/or a load impedance.

The determinant of the impedance matrix is

$$\begin{aligned}
D=\;&p^3(L_2L_\alpha L_\beta-M_{2\alpha}^2L_\beta)+p^2(L_2L_\alpha L_\beta+\\
&L_2L_\beta R_\alpha+L_\alpha L_\beta R_2-M_{2\alpha}^2R_\beta)+\\
&p(R_2R_\alpha L_\beta+R_2R_\beta L_\alpha+R_\alpha R_\beta L_2+ \qquad (7)\\
&K_\alpha K_\beta L_2-M_{2\alpha}K_2K_\beta)+K_\alpha K_\beta R_2+\\
&R_\alpha R_\beta R_2=ap^3+bp^2+cp+d
\end{aligned}$$

Routh's criterion applied to this cubic equation leads to the following requirements for stability:

1. The determinant coefficients a, b, c, and d must all be different from zero and have the same sign.
2. $\gamma=(bc-ad)/b$ must be different from zero and have the same sign as the determinant coefficients a, b, c, and d.

Since a, b, c, and d are always positive for the simple metadyne generator, it is only necessary to investigate the γ term.

The metadyne generator is on the threshold of instability when γ is zero. Inserting the machine parameters into the equation for γ and equating γ to zero results in

$$\begin{aligned}
&[L_2L_\beta R_\alpha+L_\alpha L_\beta R_2+(L_2L_\alpha-M_{2\alpha}^2)R_\beta]\times\\
&\quad(R_2R_\alpha L_\beta+R_2R_\beta L_\alpha+R_\alpha R_\beta L_2+\\
&\quad K_\alpha K_\beta L_2-M_{2\alpha}K_2K_\beta)-L_\beta(L_2L_\alpha-\\
&\qquad M_{2\alpha}^2)(K_\alpha K_\beta R_2+R_\alpha R_\beta R_2)=0 \qquad (8)
\end{aligned}$$

If there is perfect coupling between the d and 2 windings in the simple metadyne generator with no auxiliary windings, the machine is completely stable. With perfect coupling, $(L_2L_\alpha-M_{2\alpha}^2)$ is equal to zero. The only other term with a negative sign in equation 8 is $M_{2\alpha}K_2K_\beta$ and it is never greater than $K_\alpha K_\beta L_2$. If there is perfect coupling, the left-hand side of equation 8 can then never become zero and sustained oscillations will not occur.

The assumption of perfect coupling is not realistic and oscillations may occur in the metadyne generator. Shifting the brushes from the neutral position and/or the addition of a stimulating winding (a winding that, with respect to a given closed circuit, sets up a flux due to the brush current flowing through it, and so induces a rotational emf in the given circuit in the same direction as the brush current) may also cause oscillations.

Fig. 3 shows the relationship between the field circuit resistance and the load circuit resistance required to give stable operation, other machine parameters being constant and preassigned. All other parameters being constant, the minimum load circuit resistance required for stability increases and then decreases as the field circuit resistance is increased. For usual values of field resistance, the minimum load circuit resistance required for stability, increases for an increase in the load circuit inductance or the short-circuited quadrature-axis armature circuit inductance.

For very large values of field circuit resistance, there is little danger of instability since the required minimum load circuit resistance is small. An unstable metadyne generator can also be made stable by increasing the resistance of the short-circuited quadrature-axis armature circuit, decreasing the speed of the driving machine or adding damping windings. Fig. 4 shows the effect of the speed of the driving machine on the minimum resistance necessary for stability.

Methods of Damping

Three possible methods for damping the metadyne generator are:

1. Series-winding damping: a stator winding in the direct-axis carrying quadrature-axis armature current (direct-axis damping) or a stator winding in the quadrature-axis carrying direct-axis armature current (quadrature-axis damping).
2. Resistance damping: resistance in either the short-circuited quadrature-axis armature circuit or in the load circuit.

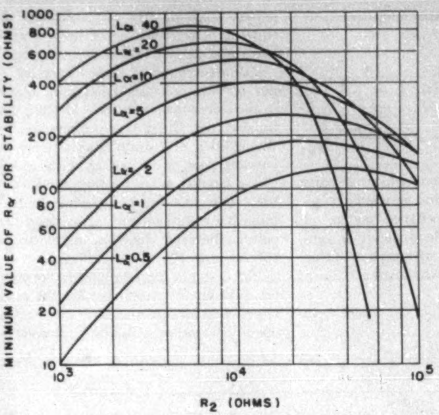

Fig. 3. Minimum resistance in direct-axis circuit for stability as a function of the excitation circuit resistance. The fixed parameters are

$K_2 = 5{,}000$ volts per ampere
$K_d = K_q = 100$ volts per ampere
$L_2 = 250$ henrys
$M_{2d} = 4.5$ henrys
$R_q = 1.0$ ohm
$L_d = L_q = 0.1$ henry

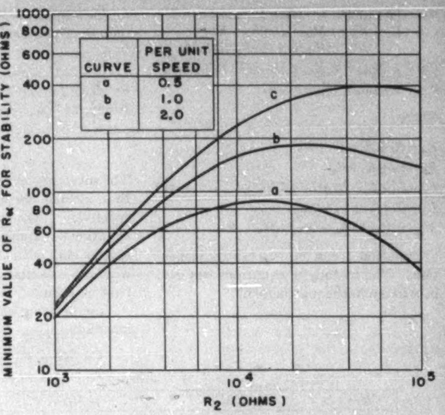

Fig. 4. Minimum resistance in direct-axis circuit for stability as a function of the excitation circuit resistance. For curve b, the parameters given for Fig. 3 apply. $L_d = 1.0$ henry

3. Short-circuited stator winding damping: a short-circuited stator winding in the direct-axis.

Series-Winding Damping

Either direct-axis damping or quadrature-axis damping will reduce the transient peaks of the load current. Whether direct-axis or quadrature-axis damping is better is therefore dependent on other considerations.

Figs. 5, 6, and 7 show the effect of series-winding damping on the steady-state mmf in both axes; the damping is expressed in per cent, where 100-per-cent damping corresponds to a damping winding with the same number of effective turns the armature winding in the same axis.

With a constant voltage applied to the excitation winding, direct-axis damping decreases the steady-state mmf in both axes, while quadrature-axis damping decreases the steady-state mmf in the quadrature axis and increases the mmf in the direct axis.

If the steady-state load current is to remain the same after the addition of series-winding damping, the excitation voltage V_2 must be increased. With constant load current, direct-axis damping does not affect the steady-state mmf in either axis; while quadrature-axis damping has no effect on the steady-state mmf in the quadrature axis but does cause an increased steady-state mmf in the direct axis. Because of the relatively small steady-state mmf in the direct axis however, the effect of damping on this mmf need not be an important consideration.

The ratio of the steady-state mmf in the quadrature axis to the mmf in the direct axis is normally considerably greater than unity. Fig. 7 shows the dependence of this ratio on direct-axis resistance and quadrature-axis damping. Direct-axis damping has no effect on this ratio.

Since the quadrature-axis mmf is greater than the direct-axis mmf, care must be exercised to avoid saturation in the quadrature axis. Damping windings take space on the stator structure and leave that space unavailable for iron. To avoid reducing the iron cross section in the quadrature axis, the damping winding may be placed in the direct axis. It is not necessary, however, that the pole arc for a direct-axis pole and a quadrature-axis pole be the same. The ratio of the direct-axis pole arc to the quadrature-axis pole arc may be chosen after deciding where to place the damping winding.

Fig. 8 shows the effect of series-winding damping on the quadrature-axis armature current and the direct-axis armature current; see Appendix II for numerical data relating to differential analyzer runs.

With direct-axis damping, the direct-axis armature current and the quadrature-axis armature current decrease slightly and in the same ratio for a constant excitation voltage. If the load current is held constant by increasing the excitation voltage, the quadrature-axis current will also be restored to its original value. With quadrature-axis damping the direct-axis armature current is decreased and the quadrature-axis armature current increased. Holding the load current constant by increasing the excitation current results in a larger quadrature-axis armature current and larger losses.

The choice between direct-axis damping and quadrature-axis damping depends upon the particular application. For a majority of cases, direct-axis damping will probably be the best choice.

Resistance Damping

The additional loss introduced with resistance damping is the principle disadvantage of this type of damping. Metadyne generators usually operate with a low load voltage and a high load current. The addition of resistance to the load circuit is therefore particularly undesirable. The addition of resistance to the load circuit also increases the current in the quadrature-axis armature circuit and causes additional loss in the circuit. This increase in quadrature-axis armature current was also noted for quadrature

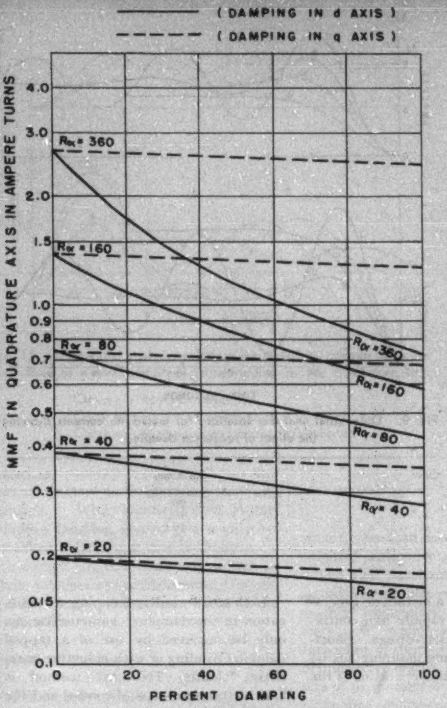

Fig. 5. Effect of series-winding damping on the quadrature-axis mmf. The curves are based on the following parameters

K_2 = 5,000 volts per ampere
K_d = K_d = 100 volts per ampere
R_2 = 5,000 ohms
V_2 = 100 volts
R_β = 10 ohms

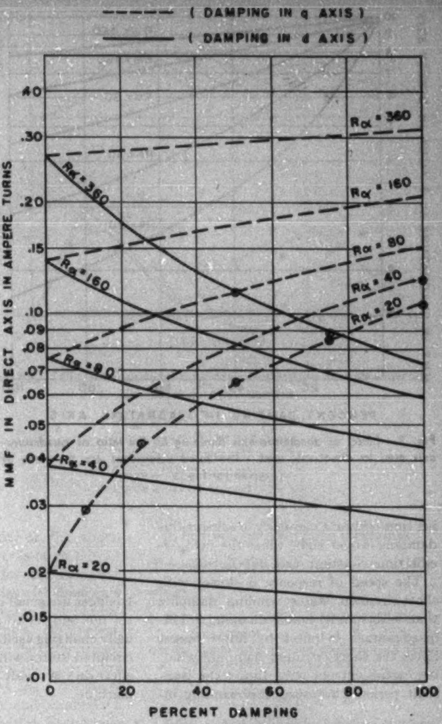

Fig. 6. Effect of series-winding damping on the direct-axis mmf. The fixed parameters are the same as for Fig. 5

axis series-winding damping. In that case, the increased current did not cause an increase in the quadrature-axis mmf or flux. With resistance damping, however, the quadrature-axis mmf and flux increase as the damping resistance in the load circuit is increased.

Damping resistance in the quadrature-axis armature circuit does not cause an increase in the quadrature-axis mmf or flux and the losses caused by this damping resistance are usually lower than with load circuit resistance damping. These lower losses are because of the lower current in the quadrature-axis armature circuit. In Fig. 9 the effect of resistance damping on the quadrature- and direct-axis armature currents can be noted.

Resistance damping in either circuit has an adverse effect on the speed of response of the metadyne. Resistance damping causes a decrease in the natural frequency of the oscillatory component of the underdamped transient current and an increase in the time constant of the overdamped current. Series-winding damping, on the other hand, causes an increase in the natural frequency of oscillation. A comparison of Figs. 8 and 9 shows the time constant to be better with series-winding damping than with resistance damping.

Short-Circuited Stator Winding Damping

The addition of a short-circuited stator winding with a time constant longer than the time constants of the other metadyne generator circuits (load circuit, source circuit, and short-circuited armature circuit) increases the damping of the transient currents. If the short-circuited stator winding is placed in the quadrature axis, it also increases the peak value of the transient current in the quadrature-axis armature winding. With a short-circuited stator winding in the direct axis (excitation axis), however, the damping effect is obtained without an increase in the peak transient current in either armature circuit. A short-circuited stator winding in the direct axis is therefore useful as a damping winding.

The effect of a short-circuited stator winding in either axis is shown in Figs. 10 and 11. The transient currents for curves *c* in Fig. 10 are almost critically damped. The short-circuited stator wind-

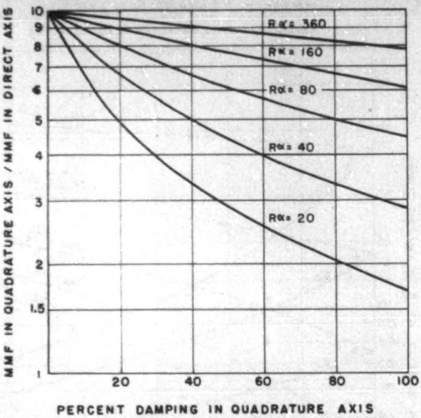

Fig. 7. Effect of quadrature-axis damping on the ratio of quadrature-axis mmf to direct-axis mmf. The fixed parameters are the same as given for Fig. 5

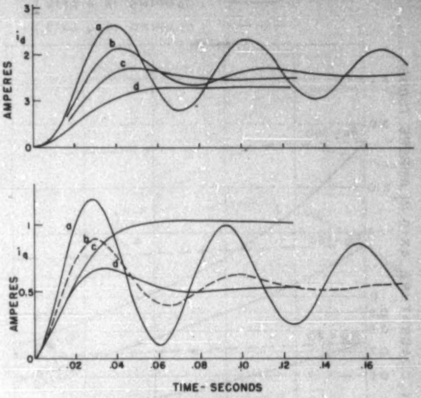

Fig. 9. Differential analyzer solutions for metadyne currents showing the effect of resistance damping

Curve	Rα, Ohms	Rβ, Ohms
a	20	4
b	20	10
c	20	20
d	45	20

ing time constant necessary to achieve this damping is over eight times the field circuit time constant and $T_2>T_\alpha>T_\beta$.

The speed of response is slower with short-circuited stator winding damping than with series-winding damping. This disadvantage is offset by lower losses. Since the short-circuited damping winding carries current only during the transient period, the losses this winding introduces are small in a metadyne generator not subject to a rapidly and continually changing excitation voltage. Short-circuited stator-winding damping has no effect on the steady-state operation of the machine.

With series-winding damping, a modification in the damping characteristic can only be achieved by use of a tapped damping winding or with inductive or resistive shunts. The first method is limited to a few steps of control and the

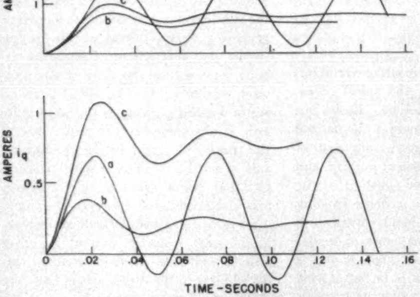

Fig. 8. Differential analyzer solutions for metadyne currents showing the effect of series-winding damping

Curve a—No damping
Curve b—Direct-axis damping
Curve c—Quadrature-axis damping

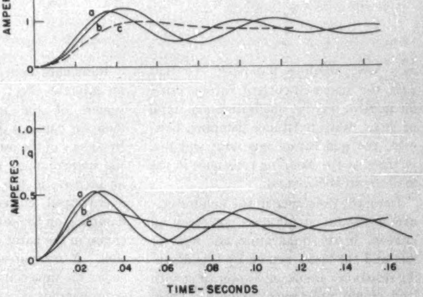

Fig. 10. Differential analyzer solutions for metadyne currents showing the effect of a short-circuited stator winding in the direct axis

Curve a—No stator winding
Curve b—Winding time constant, 0.04 second
Curve c—Winding time constant, 6.35 seconds

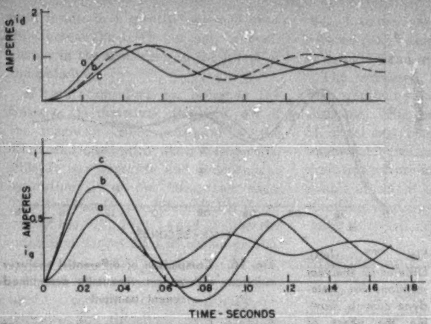

Fig. 11. Differential analyzer solutions for metadyne currents showing the effect of a short-circuited stator winding in the quadrature axis

Curve a—No stator winding
Curve b—Winding time constant, 0.02 second
Curve c—Winding time constant, 0.04 second

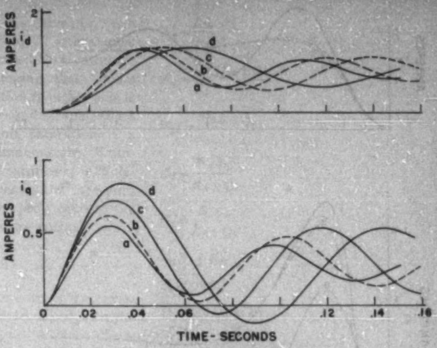

Fig. 12. Differential analyzer solutions for metadyne currents showing the effect of eddy currents

Eddy-current paths time constant
Curve a—0.005 second
Curve b—0.01 second
Curve c—0.02 second
Curve d—0.04 second

second method is cumbersome and expensive. With short-circuited stator winding damping, control can readily be achieved by adding a variable resistor to the circuit. A trial-and-error process is then satisfactory to determine the required amount of resistance for a given application.

Speed of Response

The negative feedback inherent in the metadyne generator results in very quick response at the expense of power gain. The time constant for the entire metadyne may be smaller than any or all of the time constants of the several circuits. Such rapid response cannot be obtained from d-c generators or amplidynes.

The speed of response of a normal separately excited d-c generator is limited by the field circuit time constant or the armature circuit time constant, whichever is larger. An amplidyne with perfect compensation is limited in speed of response by the time constant of the field circuit, the load circuit, or the short-circuited path, whichever is largest.

The time constant for the complete metadyne generator varies with changes in machine parameters, load circuit parameters, and source circuit parameters. Inspection of the roots of the determinant of impedance matrix, equation 7, for many sets of parameters shows the dependence of the time constant on circuit parameters.

Equation 7 can be written in the nondimensional form

$$s^3+2\delta_c s^2+s+h=0 \tag{9}$$

where

$s=p/\omega_n$

$\delta c=\dfrac{1}{2\omega_n}\dfrac{b}{a}$

$h=\dfrac{1}{\omega_n^3}\dfrac{d}{a}$

$\omega_n=\sqrt{\dfrac{c}{a}}$

Table I. Effect of Parameter Changes

Parameter Change, Holding All Other Parameters Constant	Change in Damping Coefficient δ	Change in Undamped Natural Frequency $\omega_n\omega_r$	Change in Natural Frequency $(\omega_n\omega_r)(1-\delta^2)^{1/2}$
Increase speed of drive motor	decrease	increase	increase
Increase R_α	increase	increase	decrease
Increase R_β	increase	decrease	decrease
Increase R_3	decrease	increase	increase
Increase L_α	irregular	decrease	decrease
Increase L_β	decrease	decrease	irregular
Increase L_3	decrease	increase	increase
Increase R_α and L_α, L_α/R_α constant	increase	decrease	decrease
Increase R_β and L_β, L_β/R_β constant	increase	decrease	decrease
Increase R_3 and L_3, L_3/R_3 constant	decrease	increase	increase

In factored form equation 9 becomes

$$(s^2+2\delta\omega_r s+\omega_r^2)(s+\sigma\omega_r) \tag{10}$$

where

δ = the damping coefficient of the oscillatory component
σ = the apparent damping coefficient of the nonoscillatory component
ω_r = the undamped natural frequency of the oscillatory component

With δ_c and h known, δ and σ can be read directly from the cubic chart developed by Y. J. Liu.[8] The nondimensional undamped natural frequency ω_r and the dimensional undamped natural frequency $\omega_n\omega_r$ can be calculated from the equations

$$\omega_r=\left(\frac{h}{\sigma}\right)^{1/3} \text{ and } \omega_n\omega_r=\omega_n\left(\frac{h}{\sigma}\right)^{1/3} \tag{11}$$

Table I indicates the effect on the damping ratio δ, the undamped natural frequency $\omega_n\omega_r$ and the damped natural frequency $\omega_n\omega_r\sqrt{1-\delta^2}$ of various parameter changes. As is illustrated by Fig. 3, the effect of an increase in a parameter value may be dependent on the absolute value of a parameter. Table I is based on the following base parameters values; the range of parameter variation is indicated in parentheses.

K_δ = 50 volts per ampere (50 to 200)
K_q = 50 volts per ampere (50 to 200)
K_3 = 2,500 volts per ampere (2,500 to 10,000)
R_α = 19.5 ohms (10 to 200)
R_β = 10 ohms (1.0 to 10)
R_3 = 1,000 ohms (1,000 to 5,000)

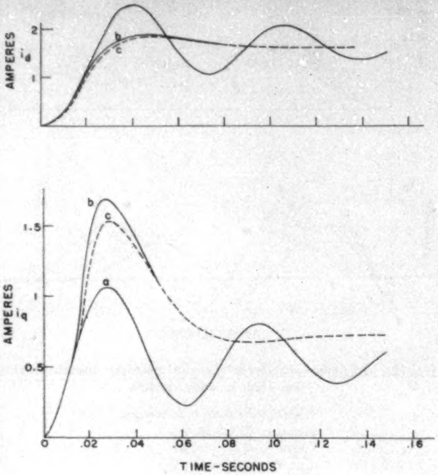

Fig. 13 (left). Differential analyzer solutions for metadyne currents showing the effect of saturation

Curve a—No saturation

Curve b—Saturation in quadrature axis

Curve c—Saturation in both axes

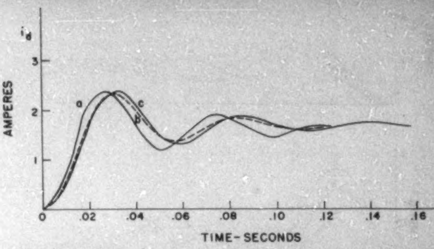

Fig. 16. Comparison of differential analyzer solutions with an experimentally determined current transient

Curve a—Experimentally determined transient

Curve b—Differential analyzer solution with eddy currents neglected

Curve c—Differential analyzer solution with eddy-current effects included

$L_\alpha=1.0$ henrys (0.1 to 2.0)
$L_\beta=0.1$ henrys (0.1 to 2.0)
$L_2=250$ henrys (250 to 1,000)
$M_{2d}=4.5$ henrys (4.5 to 4.75)

Effect of Eddy Currents

Two short-circuited stator windings, one in the direct axis and one in the quadrature axis, can be used to represent the eddy-current paths in the iron of metadynes and other rotating machines if all the iron in the magnetic circuit is laminated. The time constant of these fictitious windings is chosen to be the same as the time constant for the eddy-current paths.

Eddy currents in a metadyne generator that has all of the iron structure laminated have little effect on the transsient behavior. Adequate lamination yields a time constant for the fictitious eddy-current winding that is small compared to the time constants of the real windings.

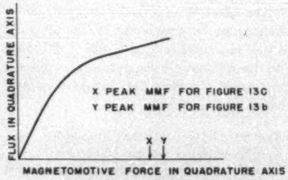

Fig. 14. Quadrature-axis saturation curve used for Fig. 13b and c

Although the effect of the eddy currents is relatively slight in the metadyne generator, it may be an undesirable effect in that it delays the response of the load current to changes in the excitation current. Fig. 12 shows the quadrature-axis armature current and the direct-axis armature current (load current) in the metadyne generator for several eddy-current path time constants. The period of the damped oscillations in both axes is increased when an increase is made in the time constant for the eddy-current paths. The damping of the transient components is practically constant for the range of time constants used for Fig. 12. Larger eddy-current path time constants do cause increased damping of the transient currents.

Influence of Additional Windings

The simple metadyne generator has a single separately excited stator winding. Other metadyne generator configurations use additional independently excited stator windings. These additional stator windings make possible a wide variety of steady-state characteristics for the metadyne generator.

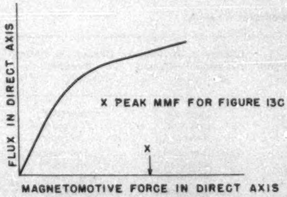

Fig. 15. Direct-axis saturation curve used for Fig. 13c

Eddy currents have the same effect on the transient behavior of the metadyne as a pair of short-circuited or independently excited stator windings with the corresponding time constant. As discussed earlier, the effect of eddy currents on the transient behavior is small since the time constant for the eddy-current paths is small. Additional independently excited stator windings, however, are likely to have time constants comparable to the time constant of the main field winding and the time constants of the armature circuits. Independently excited stator windings with these larger time constants have more than a negligible effect on the transient behavior. The additional stator windings may lie in one axis only. If the additional stator windings do lie in both axes, it is unlikely that they will have equal time constant. Figs. 10 and 11, referred to previously, show the effect of a short-circuited or independently excited stator winding in one axis only.

Effect of Saturation

In normal design, the flux density in the frame of a metadyne is lower than in any other part of the magnetic circuit. An increase in the circuit mmf to greater than normal value will cause saturation first in the armature teeth. Further increases in the circuit mmf will cause the stator poles and armature core to saturate. Thus a large increase in the circuit mmf results in a greatly increased mmf drop across the teeth but only a small change in the mmf drop in the frame of the metadyne.

If saturation does not occur in the frame of the metadyne, the only part of the magnetic circuit common to the direct and quadrature axes, it is permissible to use separate and independent saturation curves for these two axes. This was done for the differential analyzer runs of Fig. 13. Figs. 14 and 15 show the saturation curves used in obtaining Fig. 13.

Steady-state saturation in machines used for control purposes is usually undesirable and therefore these machines are designed to operate at low flux densities. In underdamped machines the transient flux densities may become much larger than the steady-state flux densities. This is especially true of the direct-axis flux density where the steady-state mmf is small. For example, for curve *c* of Fig. 10, the peak flux in the direct axis is almost ten times as large as the steady-state direct-axis flux and for curve *a* of Fig. 9, the peak direct-axis flux is over 50 times as large as the steady-state flux in the direct axis. The ratio of the peak quadrature-axis flux to the steady-state quadrature-axis flux is approximately 2 for both of the cases just cited.

The following changes (holding other machine parameters and the excitation voltage constant) increase the peak flux in the direct axis in an underdamped system: 1. increasing R_α; 2. increasing R_β; 3. decreasing the speed of the drive motor; 4. removing amplifying windings in the direct axis; 5. removing amplifying windings in the quadrature axis; 6. removing the series damping winding in the quadrature axis; 7. decreasing R_1; 8. increasing R_6; and 9. increasing L_α.

The peak flux in the quadrature axis is increased in an underdamped system by the following changes (holding other machine parameters and the excitation voltage constant): 1. increasing R_α; 2. decreasing R_β; 3. decreasing the speed of the drive motor; 4. increasing R_1; 5. increasing R_6; and 6. increasing L_α.

Transient but not steady-state saturation in the direct axis, obtained by decreasing the iron cross section in the direct axis, causes: 1. a reduced peak value of i_2; 2. a reduced peak value of i_d; 3. a reduced peak value of i_q; 4. a reduced peak value of ϕ_d; 5. a reduced peak value of ϕ_q; and 6. an increased time constant.

The corresponding transient quadrature-axis saturation causes: 1. a reduced peak value of i_2; 2. a reduced peak value of i_d; 3. an increased peak value of i_q; 4. a reduced peak value of ϕ_q; 5. little change in ϕ_d; and 6. an increased time constant.

The increased damping that occurs with transient saturation in either axis is desirable. The only undesirable effect of direct-axis transient saturation is a somewhat increased time constant. Transient quadrature-axis saturation is undesirable in that it increases the time constant and increases the peak value of the quadrature-axis armature current.

Experimental Check

Metadyne generator current transients were experimentally determined with the aid of an oscillograph. A close check was obtained between experimentally determined transients and differential analyzer solutions. Fig. 16 shows a comparison of the load current transient determined experimentally and by use of the differential analyzer. This figure also shows that the effect of eddy currents is negligible in this case.

Appendix I. Metadyne Equations in Integral Form

Equations 1 for the metadyne generator can be written in integral form and modified to allow the inclusion of magnetic circuit saturation. Equations 12 give the modified equations in integral form. These equations can readily be shown to correspond to equations 1 by differentiating each equation with respect to time and inserting the definitions of equations 13 and 14.

$$i_2=\frac{V_2t}{R_2}-\int i_2dt-W_2\phi_d$$

$$i_6=-A_6\int i_6dt-W_6\phi_d$$

$$i_1=-A_1\int i_1dt-W_1\phi_q$$

$$\begin{aligned}i_d=&-A_d\int i_ddt+G_d\int\phi_qdt+A_{1d}\int i_1dt+\\&A_{gd}\int i_gdt+W_d\phi_d+W_{5d}\phi_d+B_{gd}i_g\end{aligned}\tag{12}$$

$$\begin{aligned}i_q=&-A_q\int i_qdt+G_q\int\phi_ddt+A_{2q}\int i_2dt+\\&A_{6q}\int i_6dt-A_{8q}\int i_ddt+W_{4q}\phi_d-W_q\phi_q\end{aligned}$$

$$i_g=-A_g\int i_gdt+\frac{M_{ng}}{L_g}i_d$$

ϕ_d and ϕ_q are functions f of the total mmf in the direct and quadrature axis respectively, so that

$$\phi_d=f(N_2i_2+N_6i_6-N_8i_d-N_di_d-N_4i_q)\tag{13}$$

$$\phi_q=f(N_1i_1+N_3i_q+N_qi_q-N_5i_d)$$

also

$$A_1=\frac{L_{2\lambda}}{R_2}\frac{R_1}{L_{1\lambda}}$$

$$A_6=\frac{L_{2\lambda}}{R_2}\frac{R_6}{L_{6\lambda}}$$

$$A_d=\frac{L_{2\lambda}}{R_2}\frac{R_\alpha+Q_5}{L_{\alpha\lambda}}$$

$$A_g=\frac{L_{2\lambda}}{R_2}\frac{R_g}{L_g}$$

$$A_q=\frac{L_{2\lambda}}{R_2}\frac{R_\beta+Q_4}{L_{\beta\lambda}}$$

$$B_{gd}=\frac{M_{ng}}{L_{\alpha\lambda}}$$

$$G_d=\frac{S_qA_\alpha}{R_\alpha+Q_5}$$

$$G_q=\frac{S_dA_\beta}{R_\beta+Q_4}$$

$$S_dN_d=K_d$$

$$S_qN_q=K_q$$

$$(S_dN_2+Q_2)=K_2$$

$$(S_dN_4+Q_4)=K_4$$

$$(S_dN_6+Q_6)=K_6$$

$$(S_dN_8+Q_8)=K_8$$

$$(S_qN_1+Q_1)=K_1\tag{14}$$

$$(S_qN_3+Q_3)=K_3$$

$$(S_qN_5+Q_5)=K_5$$

$$(L_{2\lambda}+N_2^2)=L_2$$

$$(L_{4\lambda}+N_4^2)=L_4$$

$$(L_{6\lambda}+N_6^2)=L_6$$

$$(L_{d\lambda}+N_d^2)=L_d$$

$$L_{\alpha\lambda}=(L_{8\lambda}+L_{5\lambda}+L_{d\lambda}+L_{n\lambda})$$

$$L_{\beta\lambda}=(L_{3\lambda}+L_{4\lambda}+L_{q\lambda})$$

$$t=\frac{\text{real time, seconds}}{L_2/R_2}$$

$$W_1=\frac{N_1}{L_{1\lambda}}$$

$$W_2=\frac{N_2}{L_{2\lambda}}$$

$$W_6=\frac{N_6}{L_{6\lambda}}$$

$$W_d=\frac{N_8+N_d}{L_{\alpha\lambda}}$$

$$W_q=\frac{N_3+N_q}{L_{\beta\lambda}}$$

$$W_{4q}=\frac{N_4}{L_{\beta\lambda}}$$

$$W_{5d}=\frac{N_5}{L_{\alpha\lambda}}$$

Appendix II. Numerical Data for the Test Machine and Differential Analyzer Runs

All experimental work was done on an amplidyne rated at 115 volts, 3.25 amperes and 3,450 rpm. The machine was driven at a constant speed of 3,600 rpm. The parameters of the test machine for the differential analyzer and experimental runs

Table II. Parameters for Test Machine, Per-Unit Basis

Fig.	K_d	K_q	K_1	K_2	K_4	L_α	L_β	L_1	L_2	L_4	L_g	L_n	R_α	R_β	R_1	R_2	R_4	Saturation* d	Saturation* q	Damping† d	Damping† q	N
8*a*	1	1	1	1	1	1	1	1	1	1	1	1	0.95	1	1	2	1					1
8*b*	1	1	1	1	1	1	1	1	1	1	1	1	0.95	1	1	2	1			*x*		1
8*c*	1	1	1	1	1	1	1	1	1	1	1	1	0.95	1	1	2	1				*x*	1
9*a*	1	1	1	1	1	1	1	1	1	1	1	1	1.0	0.645	1	1	1					1
9*b*	1	1	1	1	1	1	1	1	1	1	1	1	1.0	1.61	1	1	1					1
9*c*	1	1	1	1	1	1	1	1	1	1	1	1	1.0	3.22	1	1	1					1
9*d*	1	1	1	1	1	1	1	1	1	1	1	1	0.225	3.22	1	1	1					1
10*a*	1	1		1		1	1		1		1	1	0.95	1		1						1
10*b*	1	1		1	1	1	1		1	1	1	1	0.95	1		1	1/16					1
10*c*	1	1		1	1	1	1		1	1	1	1	0.95	1		1	0.004					1
11*a*	1	1		1		1	1		1		1	1	0.95	1		1						1
11*b*	1	1	1	1		1	1	1	1		1	1	0.95	1	1/8	1						1
11*c*	1	1	1	1		1	1	1	1		1	1	0.95	1	1/16	1						1
12*a*	1	1	1	1	1	1	1	1	1	1	1	1	0.95	1	1/2	1	1/2					1
12*b*	1	1	1	1	1	1	1	1	1	1	1	1	0.95	1	1/4	1	1/4					1
12*c*	1	1	1	1	1	1	1	1	1	1	1	1	0.95	1	1/8	1	1/8					1
12*d*	1	1	1	1	1	1	1	1	1	1	1	1	0.95	1	1/16	1	1/16					1
13*a*	1	1	1	1	1	1	1	1	1	1	1	1	0.95	1	1	1	1					1
13*b*	1	1	1	1	1	1	1	1	1	1	1	1	0.95	1	1	1	1		*a*			1
13*c*	1	1	1	1	1	1	1	1	1	1	1	1	0.95	1	1	1	1	*b*	*a*			1
16*a*, 16*b*	1	1	1	1		0.632	1		1		1	1	0.95	0.125		1						1
16*c*	1	1	1	1	1	0.632	1	1	1	1	1	1	0.95	0.125	1	1	1					1

* Saturation in the *d* or *q* axis is indicated by the letters *a* and *b* which refer to Figs. 14 and 15 respectively.

† Series damping windings with $^{3}/_{16}$ as many effective turns as the armature winding in the *d* or *q* axis are indicated by *x*.

shown in the figures are given on a per-unit basis in Table II. The base values are

$K_d = 59.0$ volts per ampere

$K_q = 51.0$ volts per ampere

$K_1 = 22.4$ volts per ampere $= 0.95K_q\sqrt{L_1/L_q}$

$K_2 = 2{,}250$ volts per ampere

$K_4 = 23.2$ volts per ampere $= 0.95K_d\sqrt{L_4/L_d}$

$L_d = 0.155$ henry

$L_q = 1.05$ henrys

$L_n = 0.233$ henry

$L_g = 0.130$ henry

$L_\alpha = 0.393$ henry

$L_\beta = 0.130$ henry

$L_1 = 0.025$ henry

$L_2 = 220$ henrys

$L_4 = 0.025$ henry

$R_\alpha = 20.0$ ohms

$R_\beta = 6.20$ ohms

$R_1 = 10.0$ ohms

$R_2 = 2{,}910$ ohms

$R_4 = 10.0$ ohms

$R_g = 10.0$ ohms

metadyne speed $= N = 3{,}600$ rpm

The mutual inductance terms are calculated from the equations

$M_{1q} = 0.95\sqrt{L_1L_q}$ henry

$M_{24} = 0.95\sqrt{L_2L_4}$ henry

$M_{2d} = 0.95\sqrt{L_2L_d}$

$M_{4d} = 0.95\sqrt{L_4L_d}$ henry

$M_{gn} = 0.95\sqrt{L_gL_n}$ henry

References

1. Metadyne Statics (book), J. M. Pestarini. John Wiley and Sons, Inc., New York, N. Y., 1952.

2. The 50th Anniversary of the Cross-Field Dynamo, Emanuel Rosenberg. *Electrical Engineering*, vol. 73, March 1954, pp. 203–08.

3. Transient Analysis of the Metadyne Generator, M. Riaz. *AIEE Transactions*, vol. 72, pt. III, 1953, pp. 52–62.

4. The Application of Tensors to the Analysis of Rotating Electrical Machinery (book), Gabriel Kron. *General Electric Review*, Schenectady, N. Y., 1938.

5. Advanced Part of the Dynamics of a System of Rigid Bodies, Vol. II, (book), E. J. Routh. MacMillan and Company, London, England, 1930.

6. Servomechanisms—Charts for Verifying Their Stability and for Finding the Roots of Their Third and Fourth Degree Characteristic Equations, Y. J. Liu. Massachusetts Institute of Technology, Cambridge, Mass., 1941.

Sonance Design of Large Induction Motors

R. L. WALL
ASSOCIATE MEMBER AIEE

MOTOR noise must be reduced to ever lower levels to meet the new demands of motor users, in line with the public's desire for quieter environments. The increasing awareness of noise is largely caused by the progressive mechanization of present-day living where intimate contact with noise-producing machines is inevitable, and by the emphasis in recent years on the psyiological and psychological effects of noise on people.

At present, there is no reasonable sound level that can be set which will ensure that, if the noise produced by a motor is below this level, it will be satisfactorily quiet in all applications. Acceptable sound levels and characteristics must be determined for each type of application and, in some cases, for individual motors. For determining the acceptable noise levels there is a need for a meaningful, standard method of evaluating motor noise. This is a basic problem, as fundamental and important as the reduction of motor noise itself.

Sources of Noise in Motors

The physical factors that make an induction motor a machine for converting electric energy into mechanical energy also make it a machine for converting this energy into acoustical energy. The problem of sonance design is to reduce the acoustical efficiency of these machines so that they will produce less noise. Induction motor noise may be classified in three main groups:

1. Magnetic noise.
2. Mechanical noise.
3. Aerodynamic noise.

All three kinds of noise are generally produced by any motor, and any one kind may be predominant depending upon the type of motor.

Magnetic noise is produced by mechanical vibration of the motor frame or components, where the vibromotive force is supplied by the magnetic fields of the motor. The noise produced by the slot harmonics is generally the most objectionable magnetic noise, since this has a relatively high frequency. It is caused by radial motions of the stator in nodal patterns of four, six, or more nodes. The frequencies and pole structures of the most bothersome force waves in large motors can be calculated from the following equations[1]

Frequency of force wave, cycles per second (cps)	Number of nodes in force wave	
$\left(\frac{R(1-s)}{P}-2\right)f$	$(2R-2S-4P)$	(1)
$\left(\frac{R(1-s)}{P}\right)f$	$2(R-S)$	(2)
$\left(\frac{R(1-s)}{P}+2\right)f$	$(2R-2S+4P)$	(3)

where

R = number of rotor slots
S = number of stator slots
P = number of pairs of poles in motor winding
s = slip
f = power line frequency, cps

$$s=\frac{N_s-N}{N_s}$$

where

$$N_s=\frac{60f}{P}$$

N = actual rotor speed, revolutions per minute

By knowing the frequencies and number of poles of these forces and the vibratory characteristics of the stator and frame, it is generally possible to avoid the coincidence of a forcing frequency and an objectionable resonance. Noise from this source can be controlled by present-day design methods and is not a serious problem in large induction motors.

Mechanical noise in induction motors is caused by rotor unbalance, bearings, and the effects of mechanical fits and tolerances. Noise produced by mechanical vibration resulting from the forces produced by an unbalanced rotor can be minimized by careful rotor balancing and generally is not a major problem.

Bearings are sometimes a source of noise, especially where ball or roller bearings are used. The bearings themselves do not radiate much noise but the forces produced by the bearings act on the bearing housings and endshields and cause them to vibrate and so to produce noise. In most cases, this is not forced vibration but resonant vibration that is impact-excited. Some of the factors that affect ball-bearing noise are lubrication, cleanliness of the bearing, surface finish of the balls and races, radial and axial clearances, the fits between the inner race and shaft and the outer race and housing, and alignment.

Mechanical tolerances and fits do not cause noise directly unless they are such that rattles are produced. They do affect magnetic noise if they produce an unsymmetrical air gap or tilt the rotor with respect to the stator, or if the rotor or stator are out of round. They also affect mechanical noise by causing misalignments.

Like magnetic noise, mechanical noise can be minimized by good design and manufacturing techniques. Also, like magnetic noise it usually is not a serious problem in large motors.

Aerodynamic noise is often the predominant noise produced by large induction motors. This is a broad classification that includes fan noise, air-flow noise, and the noise produced by the siren action of radial rotor and stator ducts.

Fans produce a broad-band type of noise that is not objectionable unless high intensities are involved. It is possible to have predominant individual frequencies that occur at the fundamental fan blade frequency, and/or its harmonics. This usually occurs when an improper fan is used for the job or when the fan runs too close to irregular, stationary objects.

Numerous tests on motors have shown that, where fan noise is predominant, the sound energy produced varies approximately as the fifth power of the peripheral velocity of the fan blade tips. All types of fans of the same capacity do not make the same amount of noise, but the fans on a high-speed motor can produce objectionable sound levels even when optimum designs are used.

To reduce the noise produced by motors where fan noise is predominant, the most desirable course to follow is reduction of the noise at the fan itself. To an extent this can be accomplished by the design and selection of the fan to do a particular job. The design of the fan is often af-

---

Paper 55-724, recommended by the AIEE Rotating Machinery Committee and approved by the AIEE Committee on Technical Operations for presentation at the AIEE Fall General Meeting, Chicago, Ill., October 3-7, 1955. Manuscript submitted June 7, 1955; made available for printing July 22, 1955.

R. L. WALL is with the General Electric Company, Schenectady, N. Y.

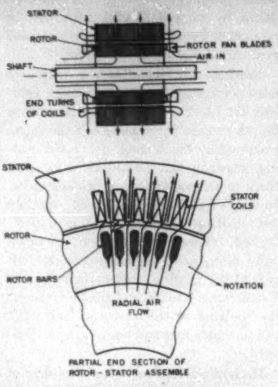

Fig. 1. Sketch showing source of duct noise. Air flows through radial rotor and stator ducts that causes siren effect

fected by other considerations, and the net result may be that the fans still produce too much noise, and it is impracticable to reduce further the noise at the fan itself.

In motors having radial ducts in the rotor and stator for ventilation, the predominant noise is often that produced by the siren action of these ducts. This noise is more objectionable than fan noise in that it is a pure-tone high-frequency noise. Fig. 1 shows how this noise is produced. The air flowing in the stator ducts is periodically turned on and off by the passing of rotor ducts and bars. This gives rise to a noise at a frequency of the number of rotor bars times the running speed in revolutions per second. To reduce this noise the siren has to be made as inefficient as possible but, at the same time, there are certain air-flow requirements to be maintained.

In spite of good design practices, if nothing additional is done to reduce the aerodynamic noise, objectionable noise may be produced by large motors. It is then necessary to employ other means of reducing this noise to satisfactory levels. One such method is the use of dissipative-type mufflers. These mufflers are constructed in such a way that the air entering and leaving the motor must make a series of 90-degree and/or 180-degree bends. This duct work may be lined with sound-absorbing material and can be effectively used to reduce aerodynamic noise.

As an example, the effectiveness of acoustic treatment of the air intakes and exhausts of a 4-pole open dripproof motor of several thousand horsepower will be considered. The predominant noise produced by this motor without the acoustic treatment was duct noise. The rotor of this machine produces a pure tone noise at about 2,300 cps. The average over-all sound pressure level (SPL) of the noise produced by the motor without the mufflers was 98 decibels (db) re 0.0002 dynes per centimeter^2 at a distance of 5 feet from the motor. By definition

$$SPL = 20 \log_{10} \frac{P_1}{P_0}$$

where

P_1 = the sound pressure in question
P_0 = a standard reference pressure of 0.0002 dyne per centimeter^2

The average level produced by the motor with the mufflers was 86 db under the same conditions. Although significant, these numbers alone do not adequately describe the noise produced by the motor with and without the mufflers. The octave band frequency analyses, Table I, show the distribution of the sound energy over the frequency spectrum for the two conditions and also the difference between the two conditions.

Table I. Octave Band Frequency Analyses

Octave Bands, Cps	1. Motor Without Mufflers	2. Motor With Mufflers	Difference Between 1 and 2
	Over-all SPL, Decibels		
	98 re 0.0002 Dynes per Centimeter^2	86	12
	Distribution of Sound Energy, Db		
20 to 75	81	77	4
75 to 150	86	81	5
150 to 300	88	80	8
300 to 600	85	70	15
600 to 1,200	87	68	19
1,200 to 2,400	94	76	18
2,400 to 4,800	91	73	18
4,800 to 9,600	84	62	22

For these tests the motor was running at no load on rated line voltage and frequency, and the measurements were made in essentially free field conditions. The reduction of 18 db or more obtained for all frequencies above 600 cps was eminently satisfactory.

These data are useful, but are not the complete story on the noise-producing characteristics of the motor. They represent the noise the motor would produce under a given set of conditions. It must be recognized that the noise this motor will actually produce may vary considerably, depending on its acoustic environment. It is therefore desirable to rate the noise produced by the motor on a sound power basis because the sound power produced is essentially unaffected

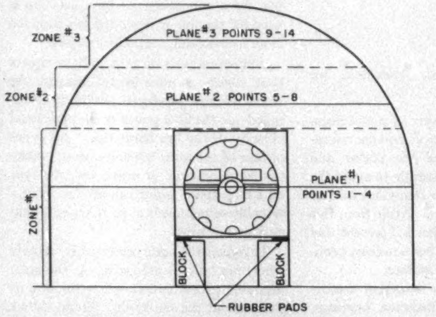

Fig. 2. Location of microphone positions for noise measurements on motor without mufflers

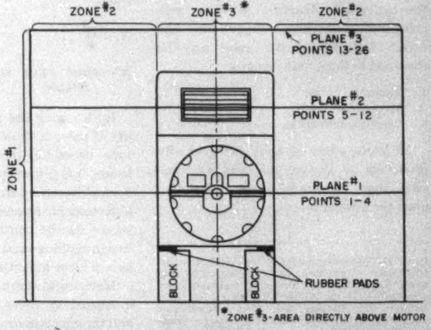

Fig. 3. Location of microphone positions for noise measurements on motor with mufflers

by environment, whereas the SPL is environment-sensitive. The sound power produced determines the latent ability of a motor to produce noise. Through the use of sound power data the distance factor usually associated with noise measurements is eliminated, and these data can be used to predict the noise that will be produced under a variety of conditions. Sound power data also provide a better means of comparing the noise produced by motors of various sizes and shapes.

In this motor the dissipative mufflers are contained in a removable cover. To evaluate the effectiveness of the noise-reducing treatment, the over-all sound power level (PWL), and octave power levels of the noise produced by the motor with and without the cover were determined. The difference in the physical size and shape of the motor with and without the cover was such that two different measurement procedures were necessary. Figs. 2 and 3 show the arrangement of the measuring points for each test.

In the test without the cover, 14 measuring points were used, all of which were located 9 feet from the geometrical center of the motor. The points lie on a hypothetical hemisphere that completely encloses the motor. The points are arranged in three planes, and the average over-all and octave levels at each plane were used to compute the power levels in its corresponding zone. The power levels in each zone were combined to obtain the total power levels. PWL is computed using

$$PWL = SPL + 10 \log_{10} S - 0.5$$

where

PWL = sound power level, db re 10^{-13} watt
SPL = the average sound pressure level, db re 0.0002 dyne per centimeter^2
S = the area of the enclosing area, feet^2

By definition,

$$PWL = 10 \log_{10} \frac{W_1}{W_0}$$

where

W_1 = the sound power of the sound source in question, watts
W_0 = the standard reference power of 10^{-13} watt

For the test with the cover, 26 measuring points were used and located as shown in Fig. 3. Because of practical limitations it was not possible to maintain the hemispherical relationship used in the test on the motor without the cover. The over-all and octave power levels were determined using the previously described procedure. Table II shows the sound power data of the noise produced by the motor with and without the mufflers.

Table II. Sound Power Data

Sound Power in Octaves, Cps	1. Motor Without Mufflers	2. Motor With Mufflers	Difference Between 1 and 2
	Total Sound Power, Watts		
	0.293	0.033	0.260
	Distribution of Sound Power, Watts		
20 to 75	0.011	0.005	0.006
75 to 150	0.022	0.013	0.009
150 to 300	0.033	0.009	0.024
300 to 600	0.016	0.001	0.015
600 to 1,200	0.023	0.001	0.022
1,200 to 2,400	0.112	0.004	0.108
2,400 to 4,800	0.066	0.002	0.064
4,800 to 9,600	0.010	0.000	0.010

PWL or sound power, watts, can be calculated from the equation

$$PWL = 10 \log \frac{W}{10^{-13}} \text{ watt}$$

or

$$PWL = 10 \log W + 130$$

where W is the sound power in watts of the noise source in question. The total PWL without mufflers is 10 log 0.293+130 = 124.7 or 125 db; the total PWL with mufflers is 10 log 0.033+130 = 115 db.

A comparison of the sound power data is perhaps more indicative of the differences between the two conditions than are SPL data. For instance, the total sound power in the 1,200 to 2,400-cps octave band that contains the duct noise frequency was reduced from 0.112 to 0.004 watt or by a factor of 28. This corresponds to a reduction of 14 db re 10^{-13} watt. The average SPL of this octave was reduced 18 db re 0.0002 dyne per centimeter^2. From the equation for computing PWL using SPL it would be expected for the db PWL to be reduced by the same amount. However, the 10 log S term of the equation was not the same for both conditions. For the tests with the muffler it was larger; nor was the sound energy distribution in space the same, hence the difference is accounted for. A difference such as this is significant when comparing the noise output of various machines or determining noise reduction. If only SPL were used, this difference would go unnoticed. The motor shown in Fig. 4 is typical of the size and type that receive extensive acoustic treatment.

Noise Measurement Standards

It is generally conceded that the basic reason for making noise measurements is to obtain information that will allow to predict people's response to the noise in a certain location, under certain conditions.

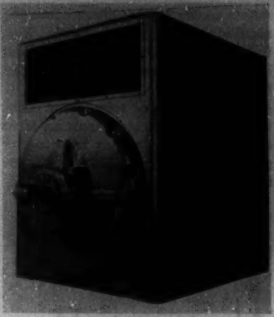

Fig. 4. Typical size and type of motor in which dissipative mufflers are used to reduce aerodynamic noise

For this reason, it is important that noise measurements made in accordance with standard codes should furnish information that can be used to make these predictions.

It should be remembered that the data obtained from standard tests do not necessarily indicate the acceptability of the noise. These data merely furnish part of the information required to determine whether or not a motor will meet certain noise requirements. The present noise measurement standards call for the measurement of over-all SPL at several points located at various positions around the machine and at a certain distance from the machine. The noise produced by rotating machines is complex in nature and is composed of many frequencies. Even to begin to evaluate this type of noise, it is necessary to determine, the distribution of the sound energy over the audible frequency spectrum. For most work, octave band analyses provide a sufficiently detailed picture of the frequency distribution. These data are required to use the noise evaluation criteria.

The inclusion of octave band measurements in the present standards is perhaps the most important immediate need. Going further into the problem, another need can be seen. That is the need for the rating of machine noise by the machine's latent ability to produce noise and not the noise produced under a given set of conditions. The sound power, as a function of frequency, produced by a machine is a true rating of the machine's noise-producing ability. The sound power produced for constant operating conditions is essentially independent of acoustic environment, and it is not necessary to specify at what distance from the machine the noise was measured. With these data, the noise that will be produced in a variety of acoustic environments can be predicted.

The importance of noise control is obvious, and noise measurements are often an important part of any noise-control problem. The advantages of the latest noise-measurement techniques and noise-evaluation criteria, as described in this article, make desirable the inclusion of such practices in standard noise measurement codes.

References

1. THE NATURE OF POLYPHASE INDUCTION MACHINES, P. L. Alger. John Wiley and Sons, Inc., New York, N. Y., 1951.

2. ACOUSTICS, Leo L. Beranek. McGraw-Hill Book Company, Inc., New York, N. Y., 1954.

3. HANDBOOK OF ACOUSTIC NOISE CONTROL, VOLUME I. *WADC Technical Report 52-204*, Wright Air Development Center, Dayton, Ohio.

4. HANDBOOK OF NOISE MEASUREMENT, A. P. G. Peterson, Leo L. Beranek. General Radio Company, 1954.

5. ACOUSTIC MEASUREMENTS, L. L. Beranek. John Wiley and Sons, Inc., New York, N. Y., 1949.

6. AMERICAN STANDARD ACOUSTICAL TERMINOLOGY. *ASA Z24.1-1951*, American Standards Association, New York, N. Y., 1951.

Aluminum in Heavy Current Conductors

WILLIAM DEANS
FELLOW AIEE

IN ORDER that a conductor material may be considered in the design of heavy current busses, its characteristics, both mechanical and electrical, must be known. Useful data on tubes of both copper and aluminum are given in Table I. Even though the conductivity of aluminum is lower than that of copper, the disadvantage is not in proportion. Lower conductivity results in a better skin effect ratio, so that in an aluminum conductor the cross section is used more effectively. Aluminum and copper conductors should be designed so that they will not be called upon to run at total temperatures above 100 degrees centigrade (C) continuously. Temperatures above this value may result in annealing. Joints of aluminum conductors require more careful attention than those of other materials, but with a joint properly designed completely satisfactory performance may be expected.

Data for Round Tubular Conductors

In Appendix I data are given on round tubes. The perimeter is of interest in estimating the dissipation of heat. Section modulus is useful in estimating fiber stress under mechanical load and the self geometric mean distance (self GMD) is of interest when inductance and reactance are of concern. All these are independent of the material of the conductor; each is a function of dimensions only. Table I includes weight and resistance data for aluminum and also for copper. While present interest is especially in aluminum, data on copper may be of use for comparison. Resistance data for aluminum tubes are given at 70 C and at 85 C. The 70 C data are for use where it is felt that advantage cannot be taken of the extra allowable temperature rise for silvered contact surfaces or the equivalent. Data for 85 C are for use where advantage is taken of this extra allowable temperature rise. The choice of 85 C rather than 90 C, allowable under certain AIEE rules, is based on the author's strong feeling that 85 C is as close as dangerous temperature should be approached. This will be discussed later.

A-C Resistance of Tubes

Data in Table I are for copper of 98-per-cent conductivity and for aluminum of the electrical conductor (EC) grade of 61-per-cent conductivity. For rough calculation, the resistance data may be converted to a new conductivity, as for instance, 57 per cent, by direct ratio; however, such a conversion will result in but an approximate value for the a-c resistance. In general, a-c resistance computed for the new conductivity on this direct ratio basis will probably be higher than the actual resistance at the new conductivity. The ratio R_{ac}/R_{dc} is a function of the resistivity of the material. Corresponding to a higher value of resistivity is a better distribution of the current over the cross section, so that conductor cross section is more effectively used. Hence the a-c resistance of a conductor is not directly proportional to the resistivity of the material.

When the a-c resistance data in Table I are plotted in the form of curves, it is noted that for a given outside diameter of tube, as the thickness of the tube is increased, the a-c resistance first decreases very rapidly, reaches a minimum, and then for greater thicknesses actually increases. The a-c resistance of a solid rod is higher than that of a tube of the same outside diameter over a wide range of tube thickness. There is a thickness for which the a-c resistance of a tube of particular outside diameter is a minimum. For both copper and aluminum, thicknesses for which a-c resistances per foot of tube reach minima are the same, regardless of outside diameters. For copper this optimum thickness is 0.5 inch, and for EC aluminum it is 0.7 inch approximately. In commercial design, the thickness of the tube would probably be held to a value somewhat less than these optimum values, because the curves are flat in the neighborhood of the optimum values. For copper, one would think roughly of 0.4 inch as the maximum to be considered and for aluminum, about 0.55 inch. Because of the better skin effect ratio of aluminum, the cross section of the aluminum conductor is used more effectively, and it is sometimes possible to design for a conductor of aluminum with the same outside diameter as one of copper, both with the same resistance per foot.

Maximum Safe Temperature

A length of conductor in a heavy current bus must function in a dual capacity. Obviously, it has to be a satisfactory conductor, and when there is a fault on the circuit, forces act on the conductor and the conductor must function as a structural member. Particularly with

---

Paper 55-261, recommended by the AIEE Switchgear Committee and approved by the AIEE Committee on Technical Operations for presentation at the AIEE Electrical Utilization of Aluminum Conference, Pittsburgh, Pa., March 15–17, 1955. Manuscript submitted December 15, 1954; made available for printing April 20, 1955.

WILLIAM DEANS is with the I-T-E Circuit Breaker Company, Philadelphia, Pa.

Table I. Properties of Bus Conductors—Round Tubes

				Copper							Aluminum						
					At 20 C			At 85 C				At 70 C			At 85 C		
					R_{dc}	R_{ac}		R_{dc}	R_{ac}			R_{dc}	R_{ac}		R_{dc}	R_{ac}	
Thickness, Inches	Cross Section, Square Inches	Section Modulus, Inches³	Self GMD, Inches	Weight, Pounds per Foot	Microhms per Foot	Microhms per Foot	R_{ac}/R_{dc}	Microhms per Foot	Microhms per Foot	R_{ac}/R_{dc}	Weight, Pounds per Foot	Microhms per Foot	Microhms per Foot	R_{ac}/R_{dc}	Microhms per Foot	Microhms per Foot	R_{ac}/R_{dc}
D, 3.5; Perimeter 11.00 Inches																	
0.10	1.07	0.88	1.72	4.14	7.71	7.78	1.01	9.67	9.69	1.00							
0.15	1.58	1.27	1.70	6.12	5.21	5.24	1.01	6.55	6.57	1.01	1.85	10.17	10.20	1.01	10.69	10.72	1.01
0.20	2.07	1.62	1.69	8.03	3.97	4.02	1.01	4.98	5.03	1.01	2.43	7.75	7.79	1.01	8.14	8.18	1.01
0.25	2.55	1.94	1.67	9.89	3.23	3.31	1.03	4.05	4.12	1.02	2.99	6.29	6.35	1.01	6.61	6.67	1.01
0.30	3.02	2.23	1.65	11.69	2.73	2.86	1.05	3.43	3.54	1.03	3.54	5.33	5.40	1.02	5.59	5.67	1.02
0.35	3.46	2.49	1.64	13.42	2.38	2.58	1.09	2.98	3.15	1.06	4.06	4.64	4.75	1.03	4.87	4.97	1.02
0.40	3.90	2.72	1.62	15.10	2.11	2.40	1.14	2.65	2.89	1.09	4.57	4.12	4.28	1.04	4.33	4.49	1.04
0.45	3.11	2.93	1.61	16.71	1.91	2.31	1.21	2.40	2.73	1.14	5.05	3.73	3.95	1.06	3.91	4.12	1.06
0.50	4.71	3.11	1.59	18.26	1.75	2.29	1.31	2.19	2.65	1.21	5.52	3.41	3.70	1.09	3.58	3.86	1.08
0.55	5.10	3.28	1.58	19.75	1.62	2.20	1.42	2.03	2.64	1.30	5.97	3.15	3.54	1.13	3.31	3.70	1.12
0.60	5.47	3.42	1.56	21.18	1.51	2.32	1.54	1.89	2.60	1.38	6.41	2.94	3.44	1.17	3.09	3.57	1.16
0.65	5.82	3.55	1.55	22.55	1.42	2.34	1.66	1.78	2.60	1.47	6.82	2.76	3.38	1.23	2.90	3.49	1.20
0.70	6.16	3.66	1.54	23.86	1.34	2.37	1.77	1.68	2.63	1.57	7.22	2.61	3.35	1.29	2.74	3.46	1.26
0.80	6.79	3.84	1.51								7.95	2.37	3.35	1.42	2.49	3.44	1.39
0.90	7.35	3.98	1.49								8.62	2.19	3.38	1.55	2.30	3.48	1.52
D, 4.0; Perimeter 12.57 Inches																	
0.10	1.23	1.17	1.97	4.75	6.72	6.73	1.00	8.44	8.45	1.00							
0.15	1.81	1.68	1.95	7.03	4.54	4.56	1.01	5.70	5.72	1.01	2.13	8.85	8.88	1.01	9.30	9.33	1.01
0.20	2.39	2.16	1.94	9.25	3.45	3.49	1.01	4.33	4.37	1.01	2.80	6.73	6.76	1.01	7.07	7.10	1.01
0.25	2.95	2.60	1.92	11.41	2.80	2.86	1.03	3.51	3.57	1.02	3.45	5.45	5.50	1.01	5.73	5.78	1.01
0.30	3.49	3.00	1.90	13.51	2.36	2.48	1.05	2.96	3.06	1.03	4.09	4.61	4.68	1.02	4.84	4.91	1.02
0.35	4.01	3.37	1.89	15.55	2.05	2.24	1.09	2.58	2.72	1.06	4.70	4.00	4.10	1.03	4.20	4.30	1.03
0.40	4.52	3.71	1.87	17.53	1.82	2.08	1.14	2.29	2.50	1.09	5.30	3.55	3.69	1.04	3.73	3.86	1.04
0.45	5.02	4.02	1.86	19.45	1.64	2.00	1.22	2.06	2.35	1.14	5.88	3.20	3.40	1.06	3.36	3.55	1.06
0.50	5.50	4.29	1.84	21.31	1.50	1.98	1.32	1.88	2.28	1.22	6.44	2.92	3.18	1.09	3.07	3.32	1.08
0.55	5.96	4.55	1.83	23.10	1.38	1.98	1.43	1.73	2.26	1.30	6.99	2.70	3.04	1.13	2.83	3.17	1.12
0.60	6.41	4.77	1.81	24.83	1.29	1.99	1.55	1.61	2.24	1.39	7.51	2.51	2.95	1.18	2.63	3.06	1.16
0.65	6.84	4.98	1.80	26.51	1.20	2.02	1.67	1.51	2.24	1.48	8.02	2.35	2.90	1.24	2.47	2.99	1.21
0.70	7.26	5.16	1.78	28.12	1.14	2.04	1.80	1.42	2.26	1.59	8.51	2.21	2.88	1.30	2.33	2.96	1.28
0.80	8.04	5.47	1.76								9.43	2.00	2.87	1.45	2.10	2.96	1.41
0.90	8.77	5.71	1.73								10.27	1.83	2.91	1.59	1.93	2.99	1.55
D, 4.5; Perimeter 14.14 Inches																	
0.10	1.38	1.49	2.22	5.36	5.96	5.97	1.00	7.48	7.49	1.00							
0.15	2.05	2.16	2.20	7.94	4.02	4.04	1.01	5.04	5.06	1.01	2.40	7.84	7.86	1.01	8.23	8.26	1.01
0.20	2.70	2.78	2.18	10.47	3.05	3.13	1.01	3.83	3.86	1.01	3.17	5.95	5.98	1.01	6.25	6.28	1.01
0.25	3.34	3.36	2.17	12.94	2.47	2.53	1.03	3.10	3.15	1.02	3.91	4.81	4.86	1.01	5.06	5.10	1.01
0.30	3.96	3.90	2.15	15.34	2.08	2.16	1.05	2.61	2.70	1.03	4.63	4.06	4.12	1.02	4.26	4.32	1.02
0.35	4.56	4.40	2.14	17.68	1.80	1.96	1.09	2.27	2.39	1.06	5.35	3.52	3.61	1.03	3.70	3.78	1.03
0.40	5.15	4.86	2.12	19.97	1.60	1.83	1.15	2.01	2.19	1.10	6.04	3.12	3.24	1.04	3.28	3.40	1.04
0.45	5.73	5.28	2.11	22.19	1.44	1.77	1.23	1.81	2.07	1.15	6.71	2.81	2.98	1.06	2.95	3.11	1.06
0.50	6.28	5.67	2.09	24.35	1.31	1.76	1.33	1.65	2.01	1.22	7.37	2.56	2.79	1.09	2.69	2.91	1.09
0.55	6.83	6.03	2.07	26.45	1.21	1.74	1.44	1.52	1.98	1.31	8.00	2.35	2.66	1.13	2.47	2.78	1.12
0.60	7.35	6.36	2.06	28.49	1.12	1.75	1.56	1.41	1.97	1.40	8.62	2.19	2.58	1.18	2.30	2.67	1.16
0.65	7.86	6.66	2.05	30.46	1.05	1.76	1.68	1.32	1.97	1.50	9.21	2.04	2.55	1.24	2.15	2.62	1.22
0.70	8.36	6.93	2.03	32.38	0.99	1.78	1.81	1.24	1.98	1.60	9.80	1.92	2.52	1.31	2.02	2.60	1.29
0.80	9.30	7.40	2.00								10.90	1.73	2.51	1.46	1.82	2.58	1.42
0.90	10.18	7.79	1.98								11.93	1.58	2.55	1.62	1.66	2.62	1.58
D, 5.0; Perimeter 15.71 Inches																	
0.10	1.54	1.85	2.47	5.97	5.35	5.36	1.01	6.72	6.73	1.01							
0.15	2.29	2.69	2.45	8.86	3.60	3.62	1.01	4.52	4.54	1.01	2.68	7.03	7.05	1.01	7.38	7.40	1.01
0.20	3.02	3.48	2.43	11.69	2.73	2.76	1.02	3.43	3.46	1.01	3.54	5.33	5.35	1.01	5.59	5.62	1.01
0.25	3.73	4.22	2.42	14.46	2.21	2.26	1.03	2.84	2.88	1.02	4.37	4.31	4.34	1.01	4.52	4.56	1.01
0.30	4.43	4.91	2.40	17.17	1.86	1.95	1.05	2.33	2.41	1.03	5.19	3.63	3.68	1.02	3.81	3.87	1.02
0.35	5.11	5.56	2.39	19.81	1.61	1.76	1.10	2.02	2.14	1.06	5.99	3.14	3.22	1.03	3.30	3.38	1.03
0.40	5.78	6.16	2.37	22.40	1.42	1.64	1.15	1.79	1.96	1.10	6.78	2.78	2.89	1.04	2.92	3.03	1.04
0.45	6.43	6.72	2.35	24.93	1.28	1.59	1.24	1.61	1.84	1.15	7.54	2.50	2.66	1.06	2.62	2.77	1.06
0.50	7.07	7.24	2.34	27.39	1.17	1.56	1.34	1.46	1.79	1.23	8.29	2.27	2.48	1.09	2.39	2.59	1.09
0.55	7.69	7.73	2.32	29.80	1.07	1.55	1.45	1.35	1.77	1.32	9.01	2.09	2.37	1.13	2.20	2.47	1.13
0.60	8.29	8.18	2.31	32.14	0.99	1.56	1.57	1.25	1.75	1.41	9.72	1.94	2.29	1.18	2.04	2.37	1.17
0.65	8.88	8.59	2.30	34.42	0.93	1.58	1.70	1.16	1.75	1.51	10.41	1.81	2.26	1.25	1.90	2.33	1.23
0.70	9.46	8.97	2.28	36.64	0.87	1.59	1.83	1.09	1.76	1.61	11.08	1.70	2.24	1.32	1.79	2.31	1.29
0.80	10.56	9.65	2.25								12.37	1.52	2.23	1.47	1.60	2.29	1.44
0.90	11.59	10.21	2.23								13.59	1.38	2.26	1.63	1.46	2.32	1.60
D, 5.5; Perimeter 17.28 Inches																	
0.10	1.70	2.25	2.72	6.57	4.85	4.87	1.01	6.09	6.10	1.01							
0.15	2.52	3.28	2.70	9.77	3.27	3.29	1.01	4.10	4.12	1.01	2.96	6.37	6.39	1.01	6.69	6.71	1.01
0.20	3.33	4.26	2.69	12.91	2.47	2.50	1.02	3.10	3.13	1.01	3.90	4.82	4.85	1.01	5.07	5.09	1.01
0.25	4.12	5.18	2.67	15.98	2.00	2.05	1.03	2.51	2.55	1.02	4.83	3.90	3.93	1.01	4.09	4.13	1.01
0.30	4.90	6.04	2.65	18.99	1.68	1.77	1.05	2.11	2.18	1.03	5.74	3.28	3.33	1.02	3.44	3.49	1.02
0.35	5.66	6.86	2.64	21.94	1.45	1.58	1.09	1.83	1.93	1.06	6.64	2.84	2.91	1.03	2.98	3.05	1.03
0.40	6.41	7.62	2.62	24.84	1.29	1.47	1.15	1.61	1.77	1.10	7.51	2.51	2.61	1.04	2.63	2.73	1.04
0.45	7.14	8.34	2.61	27.67	1.15	1.42	1.23	1.45	1.66	1.15	8.37	2.25	2.39	1.06	2.36	2.50	1.06
0.50	7.85	9.01	2.59	30.43	1.05	1.39	1.32	1.32	1.62	1.23	9.21	2.05	2.24	1.10	2.15	2.33	1.09
0.55	8.55	9.64	2.57	33.14	0.96	1.39	1.45	1.21	1.60	1.32	10.02	1.88	2.13	1.14	1.97	2.22	1.13
0.60	9.24	10.23	2.56	35.79	0.89	1.40	1.58	1.12	1.58	1.42	10.83	1.74	2.06	1.19	1.83	2.14	1.17
0.65	9.90	10.78	2.54	38.38	0.83	1.41	1.70	1.04	1.58	1.51	11.61	1.62	2.03	1.25	1.70	2.09	1.23
0.70	10.55	11.29	2.53	40.90	0.78	1.44	1.84	0.98	1.59	1.62	12.37	1.52	2.02	1.33	1.60	2.08	1.30
0.80	11.81	12.21	2.50								13.85	1.36	2.01	1.48	1.43	2.06	1.45
0.90	13.00	12.99	2.47								15.24	1.24	2.04	1.65	1.30	2.09	1.61

Table I Continued

				Copper							Aluminum						
					At 20 C			At 85 C				At 70 C			At 85 C		
Thickness, Inches	Cross Section, Square Inches	Section Modulus, Inches^3	Self GMD, Inches	Weight, Pounds per Foot	R_{dc} Microhms per Foot	R_{ac} Microhms per Foot	R_{ac}/R_{dc}	R_{dc} Microhms per Foot	R_{ac} Microhms per Foot	R_{ac}/R_{dc}	Weight, Pounds per Foot	R_{dc} Microhms per Foot	R_{ac} Microhms per Foot	R_{ac}/R_{dc}	R_{dc} Microhms per Foot	R_{ac} Microhms per Foot	R_{ac}/R_{dc}
D, 6.0; Perimeter 18.85 Inches																	
0.10	1.85	2.69	2.97	7.18	4.44	4.45	1.01	5.58	5.59	1.01							
0.15	2.76	3.93	2.95	10.68	2.99	3.01	1.01	3.75	3.76	1.01	3.23	5.83	5.84	1.01	6.12	6.14	1.01
0.20	3.64	5.11	2.94	14.12	2.26	2.29	1.02	2.84	2.86	1.01	4.27	4.41	4.43	1.01	4.63	4.65	1.01
0.25	4.52	6.23	2.92	17.50	1.82	1.87	1.03	2.29	2.33	1.02	5.29	3.56	3.59	1.01	3.74	3.77	1.01
0.30	5.37	7.29	2.90	20.82	1.53	1.61	1.05	1.92	1.99	1.03	6.30	2.99	3.04	1.02	3.14	3.19	1.02
0.35	6.21	8.30	2.89	24.07	1.33	1.44	1.09	1.66	1.76	1.06	7.28	2.59	2.65	1.03	2.72	2.78	1.03
0.40	7.04	9.24	2.87	27.27	1.17	1.34	1.15	1.47	1.61	1.10	8.25	2.28	2.38	1.04	2.40	2.49	1.04
0.45	7.85	10.14	2.85	30.40	1.05	1.30	1.23	1.32	1.51	1.15	9.20	2.05	2.18	1.07	2.15	2.28	1.06
0.50	8.64	10.98	2.84	33.48	0.95	1.27	1.33	1.20	1.47	1.23	10.13	1.86	2.04	1.10	1.95	2.12	1.09
0.55	9.42	11.77	2.82	36.49	0.88	1.27	1.46	1.10	1.45	1.33	11.04	1.71	1.94	1.14	1.79	2.02	1.13
0.60	10.18	12.52	2.81	39.44	0.81	1.28	1.58	1.02	1.44	1.42	11.93	1.58	1.87	1.19	1.66	1.94	1.17
0.65	10.93	13.22	2.79	42.33	0.75	1.29	1.72	0.95	1.44	1.52	12.81	1.47	1.85	1.26	1.55	1.90	1.23
0.70	11.66	13.88	2.78	45.17	0.71	1.31	1.85	0.89	1.45	1.63	13.66	1.38	1.84	1.33	1.45	1.89	1.31
0.80	13.07	15.07	2.75								15.32	1.23	1.83	1.49	1.29	1.88	1.45
0.90	14.42	16.11	2.72								16.90	1.11	1.85	1.66	1.17	1.90	1.62
D, 6.5; Perimeter 20.42 Inches																	
0.10	2.02	3.17	3.22	7.79	4.09	4.11	1.01	5.14	5.16	1.01							
0.15	2.99	4.64	3.20	11.60	2.75	2.77	1.01	3.45	3.47	1.01	3.51	5.37	5.38	1.01	5.64	5.66	1.01
0.20	3.96	6.05	3.19	15.34	2.08	2.11	1.01	2.61	2.63	1.01	4.64	4.06	4.08	1.01	4.26	4.28	1.01
0.25	4.91	7.39	3.17	19.02	1.68	1.72	1.03	2.11	2.14	1.02	5.75	3.27	3.30	1.01	3.44	3.47	1.01
0.30	5.84	8.66	3.15	22.64	1.41	1.48	1.05	1.77	1.83	1.03	6.85	2.75	2.79	1.02	2.89	2.93	1.02
0.35	6.76	9.87	3.14	26.20	1.22	1.33	1.09	1.53	1.62	1.06	7.93	2.38	2.44	1.03	2.50	2.55	1.02
0.40	7.67	11.02	3.12	29.70	1.07	1.23	1.15	1.35	1.48	1.10	8.98	2.10	2.18	1.04	2.20	2.29	1.04
0.45	8.55	12.11	3.10	33.14	0.96	1.19	1.24	1.21	1.39	1.15	10.02	1.88	2.00	1.07	1.97	2.09	1.06
0.50	9.43	13.14	3.09	36.52	0.87	1.14	1.30	1.10	1.35	1.23	11.05	1.71	1.87	1.10	1.79	1.95	1.09
0.55	10.28	14.12	3.07	39.84	0.80	1.17	1.46	1.01	1.34	1.33	12.05	1.56	1.78	1.14	1.64	1.85	1.13
0.60	11.12	15.04	3.06	43.10	0.74	1.18	1.59	0.93	1.33	1.43	13.03	1.45	1.72	1.19	1.52	1.78	1.17
0.65	11.95	15.92	3.04	46.29	0.69	1.19	1.72	0.87	1.32	1.53	14.00	1.35	1.69	1.26	1.41	1.75	1.24
0.70	12.75	16.74	3.03	49.43	0.65	1.20	1.86	0.81	1.33	1.64	14.95	1.26	1.68	1.34	1.32	1.73	1.31
0.80	14.33	18.25	3.00								16.79	1.12	1.67	1.49	1.18	1.72	1.46
0.90	15.83	19.59	2.97								18.56	1.02	1.70	1.67	1.07	1.74	1.63
D, 7.0; Perimeter 21.99 Inches																	
0.10	2.17	3.69	3.47	8.40	3.80	3.81	1.01	4.77	4.78	1.01							
0.15	3.23	5.41	3.45	12.51	2.55	2.57	1.01	3.20	3.22	1.01	3.78	4.98	4.99	1.01	5.23	5.24	1.01
0.20	4.27	7.06	3.44	16.56	1.93	1.95	1.01	2.42	2.44	1.01	5.01	3.76	3.78	1.01	3.95	3.97	1.01
0.25	5.30	8.64	3.42	20.54	1.55	1.59	1.03	1.95	1.98	1.02	6.21	3.03	3.06	1.01	3.18	3.21	1.01
0.30	6.32	10.14	3.40	24.47	1.30	1.37	1.05	1.64	1.69	1.03	7.40	2.54	2.59	1.02	2.67	2.71	1.02
0.35	7.31	11.58	3.39	28.33	1.13	1.23	1.09	1.41	1.50	1.06	8.57	2.20	2.25	1.03	2.31	2.36	1.03
0.40	8.29	12.95	3.37	32.14	0.99	1.14	1.15	1.25	1.37	1.10	9.72	1.94	2.02	1.04	2.04	2.11	1.04
0.45	9.26	14.26	3.35	35.88	0.89	1.09	1.23	1.12	1.28	1.15	10.85	1.74	1.85	1.07	1.82	1.93	1.06
0.50	10.21	15.50	3.34	39.56	0.81	1.08	1.34	1.01	1.25	1.24	11.97	1.57	1.73	1.10	1.65	1.80	1.09
0.55	11.15	16.68	3.32	43.19	0.74	1.08	1.46	0.93	1.23	1.33	13.06	1.44	1.64	1.14	1.51	1.71	1.13
0.60	12.06	17.80	3.31	46.75	0.68	1.09	1.60	0.86	1.22	1.43	14.14	1.33	1.59	1.19	1.40	1.64	1.18
0.65	12.97	18.87	3.29	50.25	0.64	1.10	1.74	0.80	1.22	1.53	15.20	1.24	1.57	1.26	1.30	1.61	1.24
0.70	13.86	19.88	3.28	53.69	0.60	1.11	1.87	0.75	1.23	1.65	16.24	1.16	1.55	1.34	1.22	1.60	1.31
0.80	15.58	21.75	3.25								18.26	1.03	1.55	1.50	1.08	1.59	1.47
0.90	17.25	23.42	3.21								20.22	0.93	1.56	1.68	0.98	1.61	1.64
D, 7.5; Perimeter 23.56 Inches																	
0.10	2.33	4.24	3.71	9.01	3.54	3.55	1.01	4.45	4.46	1.01							
0.15	3.46	6.24	3.70	13.42	2.38	2.39	1.01	2.98	3.00	1.01	4.06	4.64	4.65	1.01	4.87	4.89	1.01
0.20	4.59	8.15	3.69	17.78	1.80	1.82	1.01	2.25	2.27	1.01	5.38	3.50	3.52	1.01	3.68	3.70	1.01
0.25	5.69	9.99	3.67	22.07	1.45	1.49	1.03	1.82	1.85	1.02	6.67	2.82	2.85	1.01	2.96	2.99	1.01
0.30	6.79	11.75	3.65	26.30	1.21	1.28	1.05	1.52	1.58	1.04	7.95	2.37	2.41	1.02	2.49	2.52	1.02
0.35	7.86	13.43	3.63	30.47	1.05	1.14	1.09	1.32	1.39	1.06	9.21	2.04	2.10	1.03	2.15	2.20	1.03
0.40	8.92	15.04	3.62	34.57	0.92	1.06	1.15	1.16	1.27	1.10	10.46	1.80	1.88	1.04	1.89	1.97	1.04
0.45	9.97	16.58	3.60	38.62	0.83	1.03	1.24	1.04	1.20	1.15	11.68	1.61	1.72	1.07	1.69	1.79	1.06
0.50	11.00	18.05	3.59	42.63	0.75	1.00	1.33	0.94	1.16	1.24	12.89	1.46	1.60	1.10	1.53	1.67	1.09
0.55	12.01	19.46	3.57	46.54	0.69	1.01	1.47	0.86	1.15	1.33	14.08	1.34	1.52	1.14	1.41	1.59	1.13
0.60	13.01	20.80	3.56	50.40	0.63	1.01	1.60	0.80	1.14	1.43	15.24	1.24	1.47	1.19	1.30	1.52	1.18
0.65	13.99	22.08	3.54	54.21	0.59	1.03	1.74	0.74	1.14	1.54	16.40	1.15	1.45	1.27	1.21	1.50	1.24
0.70	14.95	23.29	3.53	57.95	0.55	1.04	1.88	0.69	1.14	1.65	17.53	1.08	1.44	1.34	1.13	1.48	1.31
0.80	16.84	25.56	3.49								19.74	0.95	1.44	1.51	1.00	1.47	1.47
0.90	18.66	27.60	3.46								21.87	0.86	1.45	1.69	0.91	1.49	1.65
D, 8.0; Perimeter 25.13 Inches																	
0.10	2.48	4.84	3.97	9.62	3.32	3.33	1.01	4.16	4.18	1.01							
0.15	3.70	7.13	3.95	14.33	2.23	2.24	1.01	2.79	2.81	1.01	4.34	4.34	4.36	1.01	4.56	4.58	1.01
0.20	4.90	9.32	3.93	18.99	1.68	1.70	1.01	2.11	2.13	1.01	5.74	3.28	3.29	1.01	3.44	3.46	1.01
0.25	6.09	11.44	3.92	23.59	1.35	1.39	1.03	1.70	1.73	1.02	7.13	2.64	2.66	1.01	2.77	2.80	1.01
0.30	7.26	13.47	3.90	28.12	1.14	1.19	1.05	1.43	1.47	1.03	8.51	2.21	2.25	1.02	2.33	2.36	1.02
0.35	8.41	15.42	3.88	32.59	0.98	1.07	1.09	1.23	1.30	1.06	9.86	1.91	1.96	1.03	2.01	2.05	1.03
0.40	9.55	17.29	3.87	37.01	0.86	0.98	1.15	1.08	1.19	1.10	11.19	1.68	1.75	1.04	1.77	1.84	1.04
0.45	10.67	19.08	3.85	41.36	0.77	0.95	1.24	0.97	1.12	1.15	12.51	1.51	1.60	1.07	1.58	1.67	1.06
0.50	11.78	20.80	3.84	45.65	0.70	0.94	1.35	0.88	1.09	1.24	13.81	1.36	1.50	1.10	1.43	1.56	1.09
0.55	12.87	22.45	3.82	49.88	0.64	0.94	1.48	0.80	1.07	1.33	15.09	1.25	1.42	1.14	1.31	1.48	1.13
0.60	13.95	24.03	3.81	54.05	0.59	0.95	1.60	0.74	1.06	1.44	16.35	1.15	1.37	1.19	1.21	1.42	1.18
0.65	15.01	25.54	3.79	58.16	0.55	0.96	1.74	0.69	1.06	1.54	17.69	1.07	1.36	1.27	1.13	1.40	1.24
0.70	16.05	26.98	3.77	62.21	0.51	0.96	1.88	0.65	1.07	1.66	18.82	1.00	1.35	1.35	1.05	1.38	1.32
0.80	18.10	29.68	3.74								21.21	0.89	1.34	1.51	0.93	1.37	1.47
0.90	20.07	32.13	3.71								23.53	0.80	1.36	1.69	0.84	1.39	1.66

Table I Continued

Thickness, Inches	Cross Section, Square Inches	Section Modulus, Inches^3	Self GMD, Inches	Copper							Aluminum						
				Weight, Pounds per Foot	At 20 C			At 85 C			Weight, Pounds per Foot	At 70 C			At 85 C		
					R_{dc} Microhms per Foot	R_{ac} Microhms per Foot	R_{ac}/R_{dc}	R_{dc} Microhms per Foot	R_{ac} Microhms per Foot	R_{ac}/R_{dc}		R_{dc} Microhms per Foot	R_{ac} Microhms per Foot	R_{ac}/R_{dc}	R_{dc} Microhms per Foot	R_{ac} Microhms per Foot	R_{ac}/R_{dc}
D, 8.5; Perimeter 26.70 Inches																	
0.10	2.64	5.48	4.21	10.23	3.14	3.15	1.01	3.95	3.96	1.01							
0.15	3.94	8.07	4.20	15.25	2.09	2.11	1.01	2.63	2.64	1.01	4.61	4.08	4.09	1.01	4.29	4.30	1.01
0.20	5.22	10.57	4.19	20.21	1.58	1.60	1.01	1.98	2.00	1.01	6.11	3.08	3.10	1.01	3.24	3.25	1.01
0.25	6.48	12.98	4.17	25.11	1.27	1.31	1.03	1.60	1.62	1.02	7.60	2.48	2.50	1.01	2.60	2.63	1.01
0.30	7.73	15.30	4.15	29.95	1.07	1.13	1.05	1.34	1.38	1.03	9.06	2.08	2.11	1.02	2.18	2.22	1.02
0.35	8.96	17.54	4.13	34.73	0.92	1.01	1.09	1.15	1.22	1.06	10.50	1.79	1.84	1.03	1.88	1.93	1.03
0.40	10.18	19.69	4.12	39.45	0.81	0.93	1.15	1.02	1.12	1.10	11.93	1.58	1.65	1.04	1.66	1.72	1.04
0.45	11.38	21.76	4.10	44.10	0.72	0.90	1.25	0.91	1.05	1.15	13.34	1.41	1.50	1.07	1.48	1.57	1.06
0.50	12.57	23.75	4.09	48.69	0.66	0.87	1.33	0.82	1.02	1.24	14.73	1.28	1.40	1.10	1.34	1.46	1.09
0.55	13.74	25.66	4.07	53.23	0.60	0.88	1.47	0.75	1.01	1.33	16.10	1.17	1.33	1.14	1.23	1.39	1.13
0.60	14.89	27.49	4.06	57.70	0.55	0.90	1.61	0.70	1.00	1.44	17.45	1.08	1.29	1.20	1.18	1.33	1.18
0.65	16.03	29.25	4.04	62.12	0.51	0.90	1.75	0.65	1.00	1.54	18.79	1.00	1.27	1.27	1.05	1.31	1.25
0.70	17.15	30.94	4.02	66.47	0.48	0.91	1.89	0.60	1.01	1.66	20.10	0.94	1.26	1.35	0.98	1.30	1.32
0.80	19.33	34.11	3.99								22.65	0.83	1.26	1.51	0.87	1.29	1.48
0.90	21.49	37.02	3.96								25.19	0.75	1.27	1.70	0.79	1.30	1.66
D, 9.0; Perimeter 28.27 Inches																	
0.10	2.80	6.15	4.47	10.84	2.94	2.95	1.01	3.70	3.71	1.01							
0.15	4.17	9.08	4.45	16.16	1.97	1.99	1.01	2.48	2.49	1.01	4.89	3.85	3.86	1.01	4.05	4.06	1.01
0.20	5.53	11.90	4.43	21.43	1.49	1.51	1.01	1.87	1.89	1.01	6.48	2.91	2.92	1.01	3.05	3.07	1.01
0.25	6.87	14.63	4.42	26.63	1.20	1.23	1.03	1.51	1.53	1.02	8.05	2.34	2.36	1.01	2.46	2.48	1.01
0.30	8.20	17.26	4.40	31.78	1.00	1.05	1.05	1.26	1.30	1.03	9.61	1.96	1.99	1.02	2.06	2.09	1.02
0.35	9.51	19.80	4.38	36.86	0.87	0.94	1.09	1.09	1.15	1.06	11.15	1.69	1.73	1.03	1.77	1.82	1.03
0.40	10.81	22.25	4.37	41.88	0.76	0.88	1.15	0.96	1.05	1.10	12.67	1.49	1.55	1.04	1.56	1.62	1.04
0.45	12.09	24.61	4.35	46.84	0.68	0.84	1.24	0.86	0.99	1.15	14.17	1.33	1.42	1.07	1.40	1.48	1.06
0.50	13.35	26.89	4.34	51.74	0.62	0.83	1.35	0.78	0.96	1.24	15.65	1.20	1.32	1.10	1.26	1.38	1.09
0.55	14.60	29.08	4.32	56.58	0.56	0.83	1.47	0.71	0.95	1.33	17.11	1.10	1.26	1.14	1.16	1.31	1.13
0.60	15.83	31.19	4.30	61.36	0.52	0.83	1.60	0.65	0.94	1.44	18.56	1.02	1.21	1.20	1.07	1.26	1.18
0.65	17.05	33.22	4.29	66.07	0.48	0.84	1.75	0.61	0.94	1.55	19.98	0.94	1.20	1.27	0.99	1.23	1.25
0.70	18.25	35.18	4.27	70.73	0.45	0.85	1.89	0.57	0.95	1.67	21.71	0.88	1.19	1.35	0.93	1.22	1.32
0.80	20.61	38.86	4.24								24.15	0.78	1.18	1.52	0.82	1.21	1.48
0.90	22.90	42.26	4.21								26.84	0.70	1.20	1.70	0.74	1.23	1.67
D, 9.5; Perimeter 29.85 Inches																	
0.10	2.95	6.87	4.72	11.44	2.79	2.80	1.01	3.50	3.51	1.01							
0.15	4.41	10.14	4.70	17.07	1.87	1.88	1.01	2.35	2.36	1.01	5.16	3.65	3.66	1.01	3.83	3.84	1.01
0.20	5.84	13.31	4.68	22.64	1.41	1.43	1.01	1.77	1.79	1.01	6.85	2.75	2.76	1.01	2.89	2.90	1.01
0.25	7.27	16.37	4.67	28.15	1.13	1.16	1.03	1.42	1.45	1.02	8.51	2.21	2.23	1.01	2.32	2.34	1.01
0.30	8.67	19.33	4.65	33.60	0.95	1.00	1.05	1.19	1.23	1.03	10.16	1.85	1.88	1.02	1.95	1.98	1.02
0.35	10.06	22.20	4.64	38.99	0.82	0.89	1.09	1.03	1.09	1.06	11.79	1.60	1.64	1.03	1.68	1.72	1.03
0.40	11.44	24.97	4.62	44.31	0.72	0.83	1.15	0.91	0.99	1.10	13.40	1.41	1.47	1.04	1.48	1.53	1.04
0.45	12.80	27.64	4.60	49.58	0.64	0.80	1.24	0.81	0.93	1.15	14.99	1.26	1.34	1.07	1.32	1.40	1.06
0.50	14.14	30.23	4.59	54.78	0.58	0.79	1.35	0.73	0.91	1.24	16.57	1.14	1.25	1.10	1.19	1.30	1.09
0.55	15.46	32.72	4.57	59.92	0.53	0.78	1.47	0.67	0.89	1.34	18.12	1.04	1.19	1.14	1.09	1.23	1.13
0.60	16.78	35.13	4.55	65.01	0.49	0.79	1.61	0.62	0.89	1.44	19.66	0.96	1.15	1.20	1.01	1.19	1.18
0.65	18.07	37.45	4.54	70.03	0.46	0.80	1.76	0.57	0.89	1.55	21.18	0.89	1.13	1.27	0.93	1.16	1.25
0.70	19.35	39.69	4.52	74.99	0.43	0.80	1.89	0.54	0.89	1.67	22.68	0.83	1.12	1.35	0.87	1.15	1.32
0.80	21.79	43.76	4.49								25.53	0.74	1.12	1.52	0.78	1.15	1.48
0.90	24.32	47.85	4.46								28.50	0.66	1.13	1.71	0.69	1.16	1.67
D, 10.0; Perimeter 31.42 Inches																	
0.10	3.11	7.62	4.97	12.05	2.65	2.66	1.01	3.32	3.33	1.01							
0.15	4.64	11.26	4.95	17.99	1.77	1.78	1.01	2.23	2.24	1.01	5.44	3.46	3.47	1.01	3.64	3.65	1.01
0.20	6.16	14.79	4.94	23.86	1.34	1.35	1.01	1.68	1.70	1.01	7.22	2.61	2.62	1.01	2.74	2.75	1.01
0.25	7.66	18.21	4.92	29.67	1.08	1.10	1.02	1.35	1.37	1.02	8.97	2.10	2.12	1.01	2.20	2.22	1.01
0.30	9.14	21.53	4.90	35.43	0.90	0.95	1.05	1.13	1.17	1.03	10.71	1.76	1.79	1.02	1.85	1.87	1.02
0.35	10.61	24.74	4.89	41.12	0.78	0.85	1.09	0.98	1.03	1.06	12.44	1.51	1.55	1.03	1.59	1.63	1.03
0.40	12.06	27.84	4.87	46.75	0.68	0.79	1.15	0.86	0.94	1.10	14.14	1.33	1.39	1.04	1.40	1.45	1.04
0.45	13.50	30.85	4.85	52.32	0.61	0.76	1.24	0.77	0.88	1.15	15.82	1.19	1.27	1.07	1.25	1.33	1.06
0.50	14.92	33.76	4.84	57.83	0.55	0.75	1.35	0.69	0.86	1.24	17.49	1.08	1.18	1.10	1.13	1.23	1.09
0.55	16.33	36.58	4.82	63.27	0.51	0.74	1.48	0.63	0.85	1.34	19.14	0.98	1.12	1.14	1.03	1.17	1.13
0.60	17.72	39.30	4.80	68.66	0.47	0.75	1.61	0.58	0.84	1.44	20.77	0.91	1.09	1.20	0.95	1.12	1.18
0.65	19.09	41.93	4.79	73.99	0.43	0.76	1.76	0.54	0.84	1.55	22.38	0.84	1.07	1.27	0.88	1.10	1.25
0.70	20.45	44.47	4.77	79.25	0.40	0.76	1.90	0.51	0.85	1.68	23.97	0.79	1.06	1.36	0.83	1.09	1.32
0.80	23.12	49.30	4.74								27.10	0.70	1.06	1.52	0.73	1.09	1.49
0.90	25.73	53.79	4.71								30.16	0.63	1.07	1.71	0.66	1.10	1.67
D, 10.5; Perimeter 32.99 Inches																	
0.10	3.27	8.41	5.22	12.66	2.52	2.53	1.01	3.16	3.17	1.01							
0.15	4.88	12.44	5.20	18.90	1.69	1.70	1.01	2.12	2.13	1.01	5.72	3.29	3.30	1.01	3.46	3.47	1.01
0.20	6.47	16.35	5.19	25.08	1.27	1.29	1.01	1.60	1.61	1.01	7.59	2.48	2.49	1.01	2.61	2.62	1.01
0.25	8.05	20.15	5.17	31.19	1.02	1.05	1.03	1.29	1.31	1.02	9.43	2.00	2.01	1.01	2.10	2.12	1.01
0.30	9.61	23.83	5.15	37.25	0.87	0.90	1.05	1.08	1.11	1.03	11.27	1.67	1.70	1.02	1.76	1.78	1.02
0.35	11.16	27.41	5.14	43.25	0.74	0.81	1.09	0.93	0.98	1.06	13.08	1.44	1.48	1.03	1.51	1.55	1.03
0.40	12.69	30.87	5.12	49.18	0.65	0.75	1.16	0.82	0.90	1.10	14.88	1.27	1.32	1.04	1.33	1.38	1.04
0.45	14.21	34.24	5.10	55.06	0.58	0.72	1.25	0.73	0.84	1.16	16.65	1.13	1.21	1.07	1.19	1.26	1.06
0.50	15.71	37.49	5.09	60.87	0.53	0.71	1.36	0.66	0.82	1.24	18.41	1.02	1.12	1.10	1.08	1.17	1.09
0.55	17.19	40.65	5.07	66.62	0.48	0.71	1.48	0.60	0.81	1.34	20.15	0.94	1.07	1.14	0.98	1.11	1.13
0.60	18.66	43.71	5.06	72.31	0.44	0.71	1.61	0.56	0.80	1.44	21.87	0.86	1.03	1.20	0.91	1.07	1.18
0.65	20.11	46.67	5.04	77.94	0.41	0.72	1.77	0.52	0.80	1.55	23.57	0.80	1.02	1.27	0.84	1.05	1.25
0.70	21.55	49.53	5.02	83.51	0.38	0.73	1.91	0.48	0.80	1.68	25.26	0.75	1.01	1.36	0.78	1.04	1.33
0.80	24.38	54.99	4.99								28.57	0.66	1.01	1.53	0.69	1.03	1.49
0.90	27.14	60.08	4.96								31.81	0.59	1.02	1.72	0.62	1.04	1.68

Table I Continued

				Copper							Aluminum						
					At 20 C			At 85 C				At 70 C			At 85 C		
Thickness, Inches	Cross Section, Square Inches	Section, Modulus, Inches³	Self GMD, Inches	Weight, Pounds per Foot	R_{dc} Microhms per Foot	R_{ac} Microhms per Foot	R_{ac}/R_{dc}	R_{dc} Microhms per Foot	R_{ac} Microhms per Foot	R_{ac}/R_{dc}	Weight Pounds per Foot	R_{dc} Microhms per Foot	R_{ac} Microhms per Foot	R_{ac}/R_{dc}	R_{dc} Microhms per Foot	R_{ac} Microhms per Foot	R_{ac}/R_{dc}
D, 11.0; Perimeter 34.56 Inches																	
0.10	3.42	9.25	5.46	13.27	2.40	2.41	1.01	3.02	3.03	1.01							
0.15	5.11	13.68	5.45	19.81	1.61	1.62	1.01	2.02	2.03	1.01	5.99	3.14	3.15	1.01	3.30	3.31	1.01
0.20	6.79	17.99	5.43	26.30	1.21	1.23	1.01	1.52	1.54	1.01	7.95	2.37	2.38	1.01	2.49	2.50	1.01
0.25	8.44	22.19	5.42	32.72	0.98	1.00	1.03	1.23	1.25	1.02	9.90	1.90	1.92	1.01	2.00	2.02	1.01
0.30	10.00	26.26	5.40	39.08	0.82	0.86	1.05	1.03	1.06	1.03	11.82	1.59	1.62	1.02	1.67	1.70	1.02
0.35	11.71	30.22	5.39	45.38	0.71	0.77	1.09	0.88	0.94	1.06	13.72	1.37	1.41	1.03	1.44	1.48	1.03
0.40	13.32	34.06	5.38	51.62	0.62	0.71	1.15	0.78	0.85	1.10	15.61	1.21	1.26	1.04	1.27	1.32	1.04
0.45	14.92	37.80	5.35	57.79	0.55	0.69	1.24	0.69	0.80	1.16	17.48	1.08	1.15	1.07	1.13	1.20	1.06
0.50	16.49	41.42	5.34	63.91	0.50	0.68	1.35	0.63	0.78	1.24	19.33	0.97	1.07	1.10	1.02	1.12	1.09
0.55	18.06	44.94	5.32	69.97	0.46	0.68	1.48	0.57	0.77	1.34	21.16	0.89	1.02	1.14	0.94	1.06	1.13
0.60	19.60	48.55	5.31	75.96	0.42	0.68	1.62	0.53	0.76	1.45	22.98	0.82	0.98	1.20	0.86	1.02	1.18
0.65	21.14	51.66	5.29	81.90	0.39	0.69	1.77	0.49	0.76	1.55	24.77	0.76	0.97	1.28	0.80	1.00	1.25
0.70	22.65	54.87	5.27	87.77	0.36	0.70	1.92	0.46	0.77	1.68	26.55	0.71	0.96	1.36	0.75	0.99	1.33
0.80	25.64	60.99	5.24								30.05	0.63	0.96	1.53	0.66	0.98	1.49
0.90	28.56	66.73	5.21								33.47	0.56	0.97	1.72	0.59	0.99	1.68
D, 11.5; Perimeter 36.13 Inches																	
0.10	3.58	10.12	5.72	13.88	2.30	2.31	1.01	2.89	2.90	1.01							
0.15	5.35	14.98	5.70	20.73	1.54	1.55	1.01	1.93	1.94	1.01	6.27	3.00	3.01	1.01	3.15	3.16	1.01
0.20	7.10	19.72	5.68	27.51	1.16	1.18	1.01	1.46	1.47	1.01	8.32	2.26	2.27	1.01	2.38	2.39	1.01
0.25	8.84	24.32	5.67	34.24	0.93	0.96	1.03	1.17	1.19	1.02	10.36	1.82	1.84	1.01	1.91	1.93	1.01
0.30	10.56	28.81	5.65	40.90	0.78	0.82	1.05	0.98	1.01	1.03	12.37	1.52	1.55	1.02	1.60	1.62	1.02
0.35	12.26	33.17	5.64	47.51	0.67	0.74	1.10	0.84	0.90	1.06	14.37	1.31	1.35	1.03	1.38	1.41	1.03
0.40	13.95	37.41	5.62	54.05	0.59	0.68	1.16	0.74	0.82	1.10	16.35	1.15	1.20	1.04	1.21	1.26	1.04
0.45	15.62	41.53	5.60	60.54	0.53	0.66	1.25	0.66	0.76	1.16	18.31	1.03	1.10	1.07	1.08	1.15	1.06
0.50	17.28	45.54	5.59	66.95	0.48	0.65	1.36	0.60	0.74	1.24	20.25	0.93	1.02	1.10	0.98	1.07	1.10
0.55	18.92	49.44	5.57	73.32	0.44	0.64	1.48	0.55	0.73	1.34	22.17	0.85	0.97	1.14	0.89	1.01	1.13
0.60	20.55	53.23	5.55	79.62	0.40	0.65	1.62	0.50	0.73	1.45	24.08	0.78	0.94	1.20	0.82	0.97	1.18
0.65	22.16	56.91	5.54	85.85	0.37	0.66	1.78	0.47	0.73	1.56	25.97	0.73	0.93	1.28	0.76	0.95	1.25
0.70	23.75	60.48	5.52	92.03	0.35	0.66	1.91	0.44	0.73	1.68	27.84	0.68	0.92	1.36	0.71	0.94	1.33
0.80	26.89	67.31	5.49								31.52	0.60	0.92	1.53	0.63	0.94	1.49
0.90	29.97	73.73	5.46								35.13	0.54	0.93	1.73	0.56	0.95	1.69
D, 12.0; Perimeter 37.70 Inches																	
0.10	3.74	11.03	5.96	14.49	2.20	2.21	1.01	2.76	2.77	1.01							
0.15	5.58	16.34	5.95	21.64	1.48	1.49	1.01	1.85	1.86	1.01	6.54	2.88	2.89	1.01	3.02	3.03	1.01
0.20	7.41	21.51	5.94	28.73	1.11	1.13	1.01	1.39	1.41	1.01	8.69	2.17	2.18	1.01	2.28	2.29	1.01
0.25	9.23	26.56	5.92	35.76	0.89	0.92	1.03	1.12	1.14	1.02	10.82	1.74	1.76	1.01	1.83	1.85	1.01
0.30	11.03	31.47	5.90	42.73	0.75	0.78	1.05	0.94	0.97	1.03	12.92	1.46	1.48	1.02	1.53	1.56	1.02
0.35	12.81	36.25	5.88	49.64	0.64	0.70	1.09	0.81	0.85	1.06	15.01	1.25	1.29	1.03	1.32	1.35	1.03
0.40	14.58	40.91	5.87	56.49	0.57	0.65	1.15	0.71	0.78	1.10	17.08	1.10	1.15	1.04	1.16	1.20	1.04
0.45	16.33	45.23	5.85	63.28	0.51	0.63	1.24	0.64	0.74	1.16	19.14	0.98	1.05	1.07	1.03	1.10	1.06
0.50	18.06	49.90	5.84	70.00	0.46	0.62	1.35	0.57	0.70	1.23	21.17	0.89	0.98	1.10	0.94	1.02	1.09
0.55	19.78	54.16	5.82	76.66	0.42	0.62	1.48	0.52	0.70	1.33	23.19	0.81	0.93	1.15	0.85	0.97	1.13
0.60	21.49	58.34	5.81	83.27	0.38	0.62	1.62	0.48	0.69	1.44	25.19	0.75	0.90	1.20	0.79	0.93	1.18
0.65	23.18	62.41	5.79	89.81	0.36	0.63	1.76	0.45	0.70	1.56	27.16	0.69	0.89	1.28	0.73	0.91	1.25
0.70	24.85	66.36	5.77	96.29	0.33	0.64	1.92	0.42	0.70	1.68	29.12	0.65	0.88	1.36	0.68	0.90	1.33
0.80	28.15	73.94	5.74								32.99	0.57	0.87	1.53	0.60	0.90	1.50
0.90	31.38	81.09	5.71								36.78	0.51	0.89	1.73	0.54	0.91	1.69
D, 12.5; Perimeter 39.27 Inches																	
0.10	3.90	11.98	6.22	15.10	2.11	2.12	1.01	2.65	2.66	1.01							
0.15	5.82	17.76	6.20	22.55	1.42	1.43	1.01	1.78	1.79	1.01	6.82	2.76	2.77	1.01	2.90	2.91	1.01
0.20	7.73	23.39	6.18	29.95	1.07	1.08	1.01	1.34	1.35	1.01	9.06	2.08	2.09	1.01	2.18	2.19	1.01
0.25	9.62	28.89	6.17	37.28	0.86	0.88	1.03	1.08	1.09	1.02	11.28	1.67	1.69	1.01	1.75	1.77	1.01
0.30	11.50	34.25	6.15	44.56	0.72	0.75	1.05	0.90	0.93	1.04	13.48	1.40	1.42	1.02	1.47	1.49	1.02
0.35	13.36	39.48	6.14	51.77	0.62	0.67	1.09	0.77	0.82	1.06	15.66	1.20	1.24	1.03	1.26	1.30	1.03
0.40	15.21	44.57	6.12	58.92	0.54	0.62	1.15	0.68	0.75	1.10	17.83	1.06	1.10	1.04	1.11	1.15	1.04
0.45	17.04	49.54	6.10	66.01	0.48	0.60	1.24	0.61	0.70	1.16	19.97	0.94	1.01	1.07	0.99	1.05	1.06
0.50	18.85	54.38	6.09	73.04	0.44	0.59	1.35	0.55	0.67	1.23	22.09	0.85	0.94	1.10	0.90	0.98	1.09
0.55	20.65	59.10	6.07	80.01	0.40	0.59	1.48	0.50	0.67	1.33	24.20	0.78	0.89	1.15	0.82	0.93	1.13
0.60	22.43	63.69	6.06	86.92	0.37	0.59	1.62	0.46	0.66	1.44	26.29	0.72	0.86	1.20	0.75	0.89	1.18
0.65	24.20	68.16	6.05	93.77	0.34	0.60	1.77	0.43	0.67	1.56	28.36	0.66	0.85	1.28	0.70	0.87	1.25
0.70	25.95	72.52	6.02	100.56	0.32	0.61	1.92	0.40	0.67	1.68	30.41	0.62	0.84	1.36	0.65	0.86	1.33
0.80	29.41	80.88	5.99								34.46	0.55	0.84	1.53	0.57	0.86	1.50
0.90	32.80	88.80	5.96								38.44	0.49	0.85	1.73	0.52	0.87	1.69
D, 13.0; Perimeter 40.84 Inches																	
0.10	4.05	12.97	6.46	15.70	2.03	2.03	1.00	2.55	2.56	1.01							
0.15	6.06	19.23	6.45	23.46	1.36	1.37	1.01	1.71	1.72	1.01	7.10	2.65	2.66	1.01	2.79	2.80	1.01
0.20	8.04	25.35	6.43	31.16	1.02	1.04	1.01	1.29	1.30	1.01	9.43	2.00	2.01	1.01	2.10	2.11	1.01
0.25	10.01	31.32	6.42	38.80	0.82	0.85	1.03	1.03	1.05	1.02	11.74	1.61	1.62	1.01	1.69	1.70	1.01
0.30	11.97	37.15	6.40	46.38	0.69	0.72	1.05	0.86	0.89	1.03	14.03	1.34	1.36	1.02	1.41	1.43	1.02
0.35	13.91	42.84	6.39	53.90	0.59	0.65	1.09	0.74	0.79	1.06	16.30	1.16	1.19	1.03	1.21	1.24	1.03
0.40	15.83	48.39	6.37	61.36	0.52	0.60	1.16	0.65	0.72	1.10	18.56	1.02	1.06	1.05	1.07	1.11	1.04
0.45	17.74	53.81	6.35	68.75	0.46	0.58	1.25	0.58	0.67	1.16	20.79	0.91	0.97	1.07	0.95	1.01	1.06
0.50	19.64	59.09	6.34	76.09	0.42	0.57	1.36	0.53	0.65	1.23	23.01	0.82	0.90	1.10	0.86	0.94	1.09
0.55	21.51	64.25	6.32	83.36	0.38	0.57	1.49	0.48	0.64	1.33	25.21	0.75	0.85	1.15	0.79	0.89	1.13
0.60	23.37	69.28	6.30	90.57	0.35	0.57	1.63	0.44	0.64	1.44	27.39	0.69	0.83	1.20	0.72	0.85	1.19
0.65	25.22	74.18	6.29	97.72	0.33	0.58	1.76	0.41	0.64	1.56	29.56	0.64	0.81	1.28	0.67	0.84	1.25
0.70	27.05	78.95	6.27	104.82	0.31	0.59	1.93	0.38	0.65	1.69	31.70	0.60	0.81	1.36	0.63	0.83	1.33
0.80	30.66	88.14	6.24								35.94	0.53	0.81	1.54	0.55	0.83	1.50
0.90	34.21	96.86	6.21								40.10	0.47	0.82	1.74	0.49	0.84	1.69

Table I Continued

				Copper							Aluminum						
					At 20 C			At 85 C				At 70 C			At 85 C		
Thickness, Inches	Cross Section, Square Inches	Section, Modulus, Inches³	Self GMD, Inches	Weight, Pounds per Foot	R_{dc} Microhms per Foot	R_{ac} Microhms per Foot	R_{ac}/R_{dc}	R_{dc} Microhms per Foot	R_{ac} Microhms per Foot	R_{ac}/R_{dc}	Weight Pounds per Foot	R_{dc} Microhms per Foot	R_{ac} Microhms per Foot	R_{ac}/R_{dc}	R_{dc} Microhms per Foot	R_{ac} Microhms per Foot	R_{ac}/R_{dc}
D, 13.5; Perimeter 42.41 Inches																	
0.10	4.21	14.03	6.72	16.31	1.96	1.97	1.01	2.46	2.46	1.00							
0.15	6.29	20.77	6.70	24.38	1.31	1.32	1.01	1.64	1.65	1.01	7.37	2.55	2.56	1.01	2.68	2.69	1.01
0.20	8.36	27.38	6.69	32.38	0.99	1.00	1.01	1.24	1.25	1.01	9.79	1.92	1.93	1.01	2.02	2.03	1.01
0.25	10.41	33.85	6.67	40.33	0.79	0.81	1.03	0.99	1.01	1.02	12.20	1.54	1.56	1.01	1.62	1.64	1.01
0.30	12.44	40.16	6.65	48.21	0.66	0.70	1.05	0.83	0.86	1.04	14.58	1.29	1.31	1.02	1.36	1.38	1.02
0.35	14.46	46.34	6.63	56.03	0.57	0.62	1.10	0.72	0.76	1.06	16.95	1.11	1.14	1.03	1.17	1.20	1.03
0.40	16.46	52.36	6.62	63.79	0.50	0.58	1.16	0.63	0.69	1.10	19.29	0.98	1.02	1.05	1.03	1.07	1.04
0.45	18.45	58.25	6.60	71.49	0.45	0.56	1.25	0.56	0.65	1.16	21.62	0.87	0.93	1.07	0.92	0.97	1.06
0.50	20.42	64.00	6.59	79.13	0.40	0.55	1.36	0.51	0.62	1.23	23.93	0.79	0.87	1.10	0.83	0.90	1.09
0.55	22.38	69.62	6.57	86.71	0.37	0.55	1.49	0.46	0.62	1.33	26.22	0.72	0.82	1.15	0.76	0.85	1.13
0.60	24.32	75.10	6.55	94.22	0.34	0.55	1.63	0.43	0.61	1.44	28.50	0.66	0.79	1.20	0.70	0.82	1.18
0.65	26.24	80.44	6.54	101.68	0.32	0.56	1.78	0.40	0.62	1.56	30.75	0.61	0.78	1.28	0.64	0.81	1.25
0.70	28.15	85.66	6.52	109.08	0.29	0.57	1.93	0.37	0.62	1.69	32.99	0.57	0.78	1.36	0.60	0.80	1.33
0.80	31.92	95.71	6.49								37.41	0.50	0.77	1.54	0.53	0.79	1.50
0.90	35.63	105.27	6.46								41.75	0.45	0.78	1.74	0.47	0.80	1.70
D, 14.0; Perimeter 43.98 Inches																	
0.10	4.37	15.07	6.97	16.92	1.89	1.90	1.01	2.37	2.37	1.00							
0.15	6.53	22.36	6.96	25.29	1.26	1.27	1.01	1.58	1.59	1.01	7.65	2.46	2.47	1.01	2.59	2.60	1.01
0.20	8.67	29.49	6.94	33.60	0.95	0.96	1.01	1.19	1.20	1.01	10.16	1.85	1.86	1.01	1.95	1.96	1.01
0.25	10.80	36.47	6.92	41.85	0.76	0.78	1.03	0.96	0.98	1.02	12.66	1.49	1.50	1.01	1.56	1.58	1.01
0.30	12.91	43.30	6.90	50.03	0.64	0.67	1.05	0.80	0.83	1.04	15.13	1.24	1.26	1.02	1.31	1.33	1.02
0.35	15.01	49.97	6.89	58.16	0.55	0.60	1.10	0.69	0.73	1.06	17.59	1.07	1.10	1.03	1.12	1.15	1.03
0.40	17.09	56.50	6.87	66.22	0.48	0.56	1.16	0.61	0.67	1.10	20.03	0.94	0.98	1.05	0.99	1.03	1.04
0.45	19.16	62.87	6.85	74.23	0.43	0.54	1.25	0.54	0.63	1.16	22.45	0.84	0.90	1.07	0.88	0.94	1.06
0.50	21.21	69.11	6.84	82.17	0.39	0.53	1.36	0.49	0.60	1.23	24.85	0.76	0.83	1.10	0.80	0.87	1.09
0.55	23.24	75.20	6.82	90.06	0.36	0.53	1.49	0.45	0.59	1.33	27.24	0.69	0.79	1.15	0.73	0.82	1.14
0.60	25.26	81.15	6.80	97.88	0.33	0.53	1.63	0.41	0.59	1.44	29.60	0.64	0.76	1.20	0.67	0.79	1.18
0.65	27.26	86.97	6.79	105.64	0.30	0.54	1.78	0.38	0.59	1.56	31.95	0.59	0.75	1.28	0.62	0.78	1.25
0.70	29.25	92.64	6.77	113.34	0.28	0.55	1.94	0.35	0.60	1.69	34.28	0.55	0.75	1.36	0.58	0.77	1.33
0.80	33.18	103.60	6.74								38.88	0.49	0.75	1.54	0.51	0.76	1.50
0.90	37.04	114.04	6.71								43.41	0.44	0.76	1.74	0.46	0.77	1.70
D, 14.5; Perimeter 45.55 Inches																	
0.10	4.52	16.18	7.22	17.53	1.82	1.82	1.00	2.28	2.29	1.01							
0.15	6.76	24.46	7.20	26.20	1.22	1.23	1.01	1.53	1.54	1.01	7.93	2.38	2.39	1.01	2.50	2.50	1.00
0.20	8.99	31.68	7.18	34.82	0.92	0.93	1.01	1.15	1.16	1.01	10.53	1.79	1.80	1.01	1.88	1.89	1.01
0.25	11.19	39.20	7.17	43.37	0.74	0.76	1.03	0.92	0.94	1.02	13.12	1.44	1.45	1.01	1.51	1.52	1.01
0.30	13.38	46.55	7.16	51.86	0.62	0.65	1.05	0.77	0.80	1.04	15.69	1.20	1.22	1.02	1.26	1.28	1.02
0.35	15.56	53.74	7.14	60.29	0.53	0.58	1.10	0.67	0.70	1.06	18.24	1.03	1.06	1.03	1.09	1.11	1.03
0.40	17.72	60.78	7.12	68.66	0.47	0.54	1.16	0.58	0.65	1.10	20.77	0.91	0.95	1.05	0.95	0.99	1.04
0.45	19.86	67.67	7.11	76.97	0.42	0.52	1.25	0.52	0.60	1.16	23.28	0.81	0.86	1.07	0.85	0.90	1.06
0.50	21.99	74.41	7.09	85.22	0.38	0.51	1.36	0.47	0.58	1.23	25.77	0.73	0.81	1.10	0.77	0.84	1.09
0.55	24.11	81.00	7.07	93.40	0.34	0.51	1.49	0.43	0.57	1.33	28.25	0.67	0.76	1.15	0.70	0.79	1.14
0.60	26.20	87.44	7.06	101.53	0.32	0.51	1.63	0.40	0.57	1.44	30.71	0.62	0.74	1.20	0.65	0.76	1.18
0.65	28.28	93.74	7.04	109.59	0.29	0.52	1.79	0.37	0.57	1.57	33.15	0.57	0.73	1.28	0.60	0.75	1.25
0.70	30.35	99.90	7.02	117.60	0.27	0.53	1.94	0.34	0.58	1.69	35.57	0.53	0.72	1.37	0.56	0.74	1.33
0.80	34.43	111.80	6.98								40.35	0.47	0.72	1.54	0.49	0.74	1.50
0.90	38.45	123.16	6.96								45.07	0.42	0.73	1.74	0.44	0.75	1.70

respect to its functioning as a structural member, maximum temperature of operation is of importance. Investigation shows that 100 C (the temperature of boiling water) is to be regarded as the maximum temperature at which the conductor material should be allowed to run continuously, and this applies to copper and to aluminum. When exposed continuously for a long time to temperatures very little above 100 C, copper and aluminum may become completely annealed. Indeed, annealing may occur if the conductor is run for very long times at even lower temperatures. An actual temperature of 90 C is allowable under certain AIEE rules. It is the author's preference to limit the temperature for conductors used in heavy current busses to 85 C. It might be argued that coincidence of maximum load and maximum ambient is rare, but it may be pointed out that heavy current busses are often used as generator leads. They are expected to be used at close to rating day in and day out, so that in such applications it is quite probable that because the loading is high continuously the ambient may be very high at the same time and for long periods.

The aluminum companies have developed an aluminum alloy of the heat treatable type which certainly is better mechanically than the EC grade of aluminum, and may be at least the equal of usual copper. This alloy has a conductivity in the neighborhood of 57 per cent, but the difference in conductivity between this 57 per cent and the 61 per cent for EC aluminum is not especially alarming in view of arguments outlined previously. This alloy sounds attractive, because a higher unit stress is allowable, and data so far available indicate that it will maintain its mechanical characteristics satisfactorily when continuously at temperatures somewhat above 100 C. For similar reasons, the silver bearing coppers are also interesting.

Joints

Somewhere in a bus, joints are necessary between lengths of conductors. Welding techniques successfully applied to aluminum open possibilities for treating these joints. By these welding processes it is possible to make a very satisfactory flexible connector by welding aluminum laminations endwise to a solid piece, the latter to be used for connection to the main conductor. In such a connector, effective use of all laminations is provided without the handicap of high resistances between laminations possible in other forms. The terminal members of such connectors may be connected to the lengths of conductors either by bolting or by welding. Where welding is possible in the field, both ends of these connectors may be welded, one to one length of conductor and the other end to the next length. Or, where it is not, one end of each connector may be welded in the factory to one end of one conductor, and the other end may be bolted to the next length of conductor in the field.

Proper attention is necessary to bolted joints in general, but with EC aluminum a bolted joint must receive special attention. For a satisfactory bolted joint, pressure over the area of contact between the two conductor members must be held as high as possible continuously, and if, in addition, the joint can be made airtight so that the atmosphere will be absolutely excluded, a thoroughly satisfactory joint may be expected. No discussion will be attempted regarding silvered versus nonsilvered surfaces, nor the use of compounds, but some discussion seems to be in order regarding the maintenance of satisfactory unit pressure at the contact surfaces. The unit pressure must be maintained satisfactorily, even with variations in dimensions of the conductor material, due perhaps to temperature changes. This indicates that the bolt should be so applied as not to have a fixed distance between the faces of its head and nut. One way to accomplish the desired result is to use Belleville washers with bolts. When such washers are used, it is necessary to use a bolt of larger size than would be used for a rigid bolt and washer connection. The resistance of a joint varies inversely and approximately hyperbolically with the unit pressure. For equal resistances of contacts, unit pressures must be equal. When a simple bolt and rigid washer are used, the area of contact of the contacting surfaces is annular in shape, of a diameter about equal to the effective diameter of the head of the bolt. A bolt can produce a certain force, and that bolt force, divided by the annular area, gives the unit pressure. When a Belleville washer is used, the effective area of contact between the members is again annular and of a diameter approximately equal to the diameter of the Belleville washer. This area of contact is higher than the area of contact for a simple bolt and rigid washer. Therefore, to get the same unit pressure, a larger bolt is necessary.

For slow changes in current magnitude, conductor material and bolts follow approximately the same temperature versus time curve, and if there is not too great a difference in coefficients of linear expansion, the pressure will not change substantially. However, on rapid changes of loading and, particularly, a rapid change corresponding to the heavy current of a short circuit, the conductor material itself is heated rapidly by the high current, and it takes time for heat to be transmitted to the bolt. With a simple bolt, there would result a very high unit pressure which is likely to produce permanent deformation of the conductor material due to cold flow. Then, when the joint cools, the conductor material shrinks but the bolt does not, and a loose joint may be the result. With the Belleville washer or its equivalent, it is possible for the conductor material to increase in thickness and to decrease. These changes in thickness simply deform the Belleville washers more or less, so that more nearly constant unit pressure may be expected.

Housings

As material for the housing of a high current bus, whether segregated, nonsegregated, or isolated phase type, aluminum seems to be ideal. It has a relatively high conductivity and is light in weight. Its high conductivity minimizes the I^2R of the currents induced in the housing of proper thickness, and therefore minimizes the temperature rise. This is important because the temperature of the housing measures the height of the thermal dam over which the heat must flow on its way from the conductor to surroundings.

Appendix I. Data For Round Tubes

Table I contains data regarding round tubular conductors of outside diameters from 3.5 to 14.5 inches, and thicknesses in 0.05-inch increments. Copper and aluminum are covered. The data were computed; tests on samples confirmed the computations. The data include:

1. Pertinent to conductor dimensions:
   a. Outside diameter and perimeter.
   b. Thickness.
   c. Cross section.
   d. Self GMD.
2. Pertinent to copper:
   a. Weight per foot.
   b. R_{dc}, R_{ac}, and R_{ac}/R_{dc} at 20 C.
   c. R_{dc}, R_{ac}, and R_{ac}/R_{dc} at 85 C.
3. Pertinent to aluminum:
   a. Weight per foot.
   b. R_{dc}, R_{ac}, and R_{ac}/R_{dc} at 70 C.
   c. R_{dc}, R_{ac}, and R_{ac}/R_{dc} at 85 C.

In Table I R_{ac} and R_{ac}/R_{dc} are for 60 cycles per second.

Discussion

K. T. Ashdown, Nathan Swerdlow (General Electric Company, Philadelphia, Pa.): The information given in Mr. Deans' paper on the a-c resistance and other data on round tubes, both copper and aluminum, is very interesting and helpful to the industry.

In the closure of his paper, Mr. Deans questions the advisability of silver plating aluminum conductors at selected points. He states that because the silver did not cover the entire surface of the aluminum, there was a danger of corrosion setting in at the edge of the silver plate.

In a 1952 paper[1] presented at New Orleans and another[2] at New York in 1953, data were given to show the effectiveness of the silver-plating system developed by the company with which the authors are associated. The danger of corrosion at the edge of the silver plating is eliminated by the proper plating procedure. Such a procedure insures that the zinc strike extends well beyond the edge of the silver plate. This together with a coating of zinc-chromate-bearing grease applied to the entire silvered area, precludes the possibility of any corrosive action between the silver and the aluminum. Fig. 1 shows the results of silver-plated aluminum samples prepared as described and exposed to 100-per-cent humidity for 1,000 hours. These samples showed no evidence of corrosion. Thus, laboratory results together with our field experience have proved that there need be no hesitancy in applying silver plate to only those portions of an aluminum conductor where a joint is to be made.

With regard to the merits of silver plating vs. nonsilver plating, refer to the closure of our paper, "The Use of Aluminum in the Construction of High-Capacity Busses."

Another point raised by Mr. Deans was the use of Belleville washers. Mr. Deans incorrectly stated that in a paper[1] by one of the authors it was implied that joints made with Belleville washers were inferior to those made without these washers. Table IV of reference 2 together with Table I of the closure to that paper shows the results of cycling tests. The point that is emphasized by these tables is that there is no improvement in performance of the silver-plated joint when Belleville washers are used instead of flat washers with lock washers. An important point to remember with respect to changes in pressure on silver-plated surfaces is that the silver-plated joint is less sensitive to pressure changes

Fig. 1. Silver-plated aluminum bus bar after 1,000 hours of exposure to 100-per-cent humidity. A portion of the protective covering has been removed to show excellent condition of bar. Arrow points to edge of silver-plated surface

than unplated joints especially in aluminum conductors. Thus, pressure changes associated with temperature cycling of silver-plated aluminum joints have relatively small effect on the contact resistance of the joint.

Mr. Deans is also concerned over operating aluminum conductors at temperatures over 85 C. In a paper[3] by G. W. Stickley and C. O. Smith of the Aluminum Company of America, there is given a series of curves (Figs. 8 and 10) which show the strength of conductor grades of aluminum at various temperatures. A study of the curves together with the authors' conclusion no. 10 show that the tensile strength of the aluminum at "slightly elevated" temperatures (100 C) has little, if any, harmful effect upon its tensile strength. This fact is further minimized by the safety factor which is used in the proper application of these conductors. Furthermore, the type of nonsilvered connections for aluminum conductors of heavy current buses as advocated by Mr. Deans automatically limits the total operating temperature of these conductors to 70 C in accordance with Industry Standards (American Standards Association, AIEE, National Electrical Manufacturers Association). With the data presented in Reference 3 and if silver-plated connections are used, aluminum conductors can be applied on the basis of 90 C operating temperature as set forth by Industry Standards.

REFERENCES

1. Application of Aluminum Channel Conductors for Station Bus, E. J. Casey, Nathan Swerdlow. *AIEE Transactions*, vol. 71, pt. III, December 1952, pp. 1004–09.

2. Performance of Electrical Joints Utilizing New Silver Coating on Aluminum Conductors, T. J. Connor, W. R. Wilson. *AIEE Transactions*, vol. 72, pt. III, August 1953, pp. 702–12.

3. Mechanical Properties of Aluminum Electrical Bus, G. W. Stickley, C. O. Smith. *Electrical Engineering*, vol. 73, August 1954, pp. 706–11.

C. P. Xenis (Consolidated Edison Company of New York, Inc., New York, N. Y.): I would like to supplement and confirm some of the points Mr. Deans has made concerning bolted connection equipment with Belleville washers. Mr. Deans referred to a symposium in New Orleans where I presented the results of extensive tests on bolts in which we found excellent support for the statement that Belleville washers seem to make the difference between success and failure.

I was exposed to the same comments Mr. Deans has made, that one author produced some test results showing that the Belleville washers were catastrophic and gave him terrible results; so there was a contradictory presentation there. Of course, there was no time to analyze his work. In the meantime, we have used thousands of these connections with Belleville washers and we have 2 to 4 years of experience.

I had a survey made of those connections and had them checked, and they are all just as good as they were the day they were put in. The contact resistances are extremely low, and the results are excellent.

Mr. Deans gave an excellent explanation as to why Belleville washers do a good job. I would like to add one more technical detail to that, at least one of the explanations I had why the results are so good. That is, if you refer to history a little bit, around 1938 or 1939, they used a lot of aluminum in Germany and there are a large number of articles which were written on that subject.

The Germans were aware of creep, therefore in order to provide the cushioning effect they were looking for, they used coil springs on their connections, not the Belleville type, but a regular coil spring of rather large size.

The idea was to limit the amount of exerted pressure in order to limit the amount of creep. Most of those joints were not successful. The reason was that the springs were so strong and of such length that creep did occur and the spring followed it. But there was such a tremendous amount of follow-up that creep continued and the spring kept pressing with the result that there was a tremendous amount of creep until unbalanced conditions were reached.

It is for that reason that some people were suspicious of springs in making aluminum connections, but the Belleville washer, in addition to spreading the pressure evenly, as Mr. Deans very clearly explained, does another thing: When you apply the Belleville washer, and let us say you flatten it or practically flatten it, you are exerting the maximum pressure. Let us assume that there is a slight amount of creep. The Belleville washer will tend to open up slightly and appreciably reduce the pressure. In other words, if you develop any creep, you automatically reduce the pressure until you reach a pressure which is perfectly correct to maintain good contact and not cause any further creep. It is an automatic adjustment, and we know that if you have the right pressure you can avoid further creep. That, I think, is one of the explanations for the excellent performance with Belleville washers.

Our experience is based also on steel bolts, and I am saying this without extensive tests, that even if we were to use aluminum bolts I still would want to use Belleville washers with them.

R. R. Cope (Aluminum Company of America, New Kensington, Pa.): I simply thought it would be worthwhile to point out some of Alcoa's thinking with respect to the high-strength aluminum bus conductor to which Mr. Deans referred.

We actually think in terms of two products. We are producing what we call our no. *2 EC* bus conductor in a *T-6* temper and in a *T-8* temper. It is a magnesium-silicide-type alloy and in the *T-6* temper, we can guarantee 55-per-cent conductivity; in the *T-8* temper where we get somewhat higher strength, we can guarantee 57-per-cent conductivity. Now, the method used for producing the number *2 EC T-8* is different from simply extruding the no. *2 EC T-6* and for that reason, the 57-per-cent conductivity alloy takes a premium price.

I think what is eventually going to happen is that most builders of a distribution bus conductor, for instance, are going to buy the 55-per-cent conductivity alloy, having the best economic combinations of high strength and high conductivity.

It will be that some will want a conductivity between 55 per cent, which is available, and 61 per cent, with the *EC* grade. I think those people who will need that higher conductivity will simply pay the higher price and purchase that commodity.

G. E. Heberlein (I-T-E Circuit Breaker Company, Philadelphia, Pa.): There was some mention made of the use of aluminum bolts for creating pressure in making electric connections in aluminum assemblies.

I want to caution some people by an experience that I had where I learned something that I will not forget too easily. A number of years ago we were building some outdoor structures of aluminum for one of the power companies. The power company requested that we use aluminum bolts to avoid possible corrosion.

And I, not reluctantly at all, thought that was a good idea. After agreeing, we went back to the plant and made up some assemblies, and since we used 1/2-inch aluminum bolts, and 1/2-inch galvanized steel bolts in our structures and in our joints, we thought we ought to do a little bit of testing on the 1/2-inch aluminum bolts by comparision.

In bolting together, as I remember it, either 3/8- or 1/2-inch conductor with aluminum bolts (these figures are rather vague now, but they will indicate somewhat the proportion of what I am trying to bring out in this discussion) we used a galvanized bolt with a yield on the order of 35,000 pounds per square inch, and without lubrication. We tightened them with a torque wrench, as I believe, on the order of 60 foot-pounds. We had high-strength aluminum bolts by comparison that had the same yield point.

I found that we would twist those off at 35 foot-pounds, so even though we were presumably tightening the joint and elongating the bolt as a spring at a much lower tension, the bolts were failing.

Then, I realized what the difficulty was. In a bolt which is used in combined torsion and tension, as the aluminum bolt was, its lack of elongation in torsion did not permit the compressive loading or the extending of the bolt that is equivalent to the galvanized steel bolt and even though the aluminum bolts were as strong, they could not be used.

We tried lubrication. I do not recall whether we used no-oxide, graphite, or something else, but we found that effect still prevalent, so I had to go back and ask the power company if we could use galvanized bolts and they agreed.

C. J. Hartman (Commonwealth Associates, Jackson, Mich.): In his use of Belleville washers, what does Mr. Deans think about the use of a flat washer in connection with the Belleville washer in order to be sure to distribute the load?

William Deans: Mr. Xenis was good enough to discuss the paper, and I think the only comment I could make is to thank him, and amen.

I am glad to know we could have some conductivities between 55 and 61 per cent, though to me that is not very important. Whether it is 55 or 57, I do not care too much. The a-c resistance is not proportional to the resistivities of the materials, but it has to do with the distribution of the current over the cross sectional area, and resistivity is not too important so long as we know what it is going to be. Then we can design.

I do not think there is anything I can add to Mr. Heberlein's discussion.

With respect to Mr. Hartman's comment, I would not like to use a flat washer with a Belleville washer. I hope somebody from the Navy is present because this remark will be pertinent to those inspectors.

If you have two overlapping parts of bars and you bolt those together, please do not ever expect that your area of contact is obtained by multiplying the width by the length of that overlap. It is not.

The area of contact is that which is produced by the compression effect of the bolts. It is annular in shape, and is the area as affected by the bolts. You get very little pressure in the regions between bolts.

If you use a flat washer in combination with a Belleville washer, you will have the advantage of the Belleville washer, but there is the disadvantage that you increase the area of contact by the flat washer and therefore, in order to get the same unit pressure as you would without the flat washer, you will have to use a larger bolt.

If you want to use simply a single big bolt, then it might be possible to consider a flat washer in combination with a Belleville washer.

Mr. Xenis' discussion prompts me to make a comment here and that is, do not put a Belleville washer on some existing bolt combination and then expect successful results. A joint is a matter of design and that design includes the bolt and the characteristics of the Belleville washer in proper balance with due respect to the necessary unit pressure. You want to get unit pressure as high as possible to minimize the resistance of the joint, and limit it so as to prevent creep.

This is not with respect to Mr. Hartman's discussion and maybe I am anticipating something which should be a comment on Mr. Swerdlow's paper, but the discussion by K. T. Ashdown and Nathan Swerdlow introduces the subject of what you do to the surfaces which you bring into contact. I avoided it in the paper, but I cannot help remarking here that I do not believe silver plating is necessary, and in fact, I believe that you are introducing an element of danger when you do put silver on the surface. I am talking of aluminum.

There is a tendency to analyze aluminum on the basis of our experience with copper. Let us be courageous and look at aluminum as a new material which has its peculiar characteristics and let us treat it separately from copper. Let us not tie our minds to copper except within a restricted field because you can not predict the reactions of an American by analyzing the reactions of a fellow in the South Pacific, and it is the same thing with aluminum and copper. Let us think of aluminum as aluminum.

My main objection to silver on aluminum, and please understand I am talking about high-current busses where we have intermittently placed areas of silver plating, is that you are leaving yourself open to trouble from corrosion, because of the high difference in potential between aluminum and silver. Also, it is necessary that the silver be quite carefully deposited on the aluminum in order that you may have a successful silver plating.

I stress that I am talking about intermittently placed silver. Where aluminum is applied in switchgear or in bus ways, and you silver plate the whole surface, you have practically eliminated danger from corrosion because all you are exposing to the atmosphere is silver.

Right now, there are many (four or five) compounds which have been developed and found highly successful.

The Aluminum Company of America has developed a special kind of compound. Burndy has developed another special kind of compound, and if you do not like the special ones, you can use the common greases like No-Ox-Id, Grade *A* Special, the California Oil people's compound, or even plain vaseline.

The compounds are open to one objection, and that is that the surfaces so treated may collect dust on the way to the job; therefore, preparation should be done on the job.

In the paper, it is stressed that conductor temperature should be limited to well under 100 C. It is perhaps not clear that this is necessary where one wants to use physical characteristics that might suffer from exposure to temperature. Of course, if one designs to physical characteristics of the annealed state, conductor temperature is relatively unimportant.

Experiences With the Use of Aluminum in Windings for Dry-Type Power Transformers

E. W. TIPTON
MEMBER AIEE

IN 1951 the supply of copper was critically short and the demand for transformers and other electric machinery using large amounts of copper was high. More transformers were needed than could be built with the copper allotted for that purpose. As a result, it was only natural that designers had a strong incentive to look for a substitute for copper. The only real possibility was, and is, aluminum. In contrast to reports of dwindling high-grade copper-ore supplies, aluminum ore is plentiful and the production facilities for aluminum were greatly expanded during the war. The effect of the relative cost of aluminum and copper was such that even before the postwar shortage of copper, designers had been investigating the use of aluminum for electrical conductors.

Reasons for Application to Dry-Type Transformers

So far as transformers are concerned, dry-type power transformers offered certain advantages in the use of aluminum windings. The lower conductivity of aluminum results in larger coils and a bigger core. In a liquid-filled transformer it may call for more insulation, more oil, and a larger and more expensive tank. The case of a dry-type transformer is of a simple light-weight construction and its size is frequently determined by the size of steel-clad switchgear with which dry-type power-center transformers are co-ordinated in appearance. A somewhat larger core-and-coil structure does not add greatly to the cost of the case. Dry-type power transformers use class *B* insulation and a minimum of solid insulating materials. The principal insulator is air. Consequently, a small increase in the size of the core and coils only slightly increases the cost of insulation. One other consideration is that dry-type transformers are installed indoors. This eliminates one of the more serious problems in the use of aluminum windings because in such applications there are no aluminum-to-aluminum or aluminum-to-copper connections which are subjected to the moisture of outdoor weather.

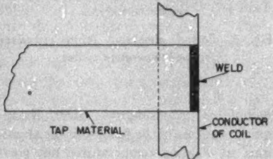

METHOD OF WELDING TAP TO CONDUCTOR

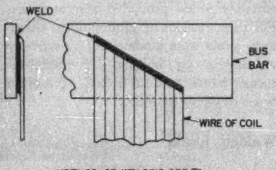

METHOD OF WELDING MULTI-STRAND COIL LEAD TO BUS BAR

Fig. 1. Welded aluminum joints

Basis of Design

As a result of these considerations, it was decided to build a number of dry-type power transformers with aluminum windings which would release an amount of copper for other types of transformers. In all a total of over 100 transformers in ratings from 225 to 3,000 kva were built with aluminum windings. The complete conducting circuit from terminal to terminal in both high- and low-voltage windings was made of aluminum. This construction eliminated all copper-to-aluminum joints except those from the transformer terminals to the customer's leads. No attempt was made to determine performance levels which would result in the most economical design with aluminum. All the transformers were designed to meet the guarantees of no-load loss, full-load loss, and impedance which applied to transformers of the same rating when wound with copper.

Electrical Properties—Effect on Design

The principal electrical property affecting the use of aluminum is its conductivity which is only 61 per cent of that for a copper conductor of the same cross section. Keeping the winding resistance per unit length the same as a copper conductor requires a wire 28 per cent greater in diameter and 64 per cent greater in cross-section area. Table I shows other relations based on an aluminum conductor of the same resistance per unit length. Since the actual design of the transformer was on the basis of equal losses the cross-sectional area of the aluminum conductors averaged 1.68 times the area of its copper equivalent. The use of a larger conductor results in more space being required for the winding. This, in turn, gives a longer average length of turn. Also, the larger winding requires a larger opening in the iron which lengthens the mean turn of the iron circuit. To compensate, a larger iron section must be used to keep the iron loss the same as in the copper-wound transformer and this still further increases the length of the winding. To compensate for these factors a larger aluminum wire than the

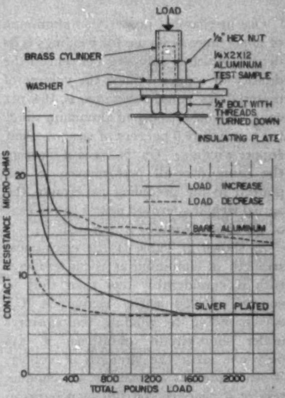

Fig. 2. Contact resistance as a function of pressure with aluminum bars

---

Paper 55-686, recommended by the AIEE Transformers Committee and approved by the AIEE Committee on Technical Operations for presentation at the AIEE Fall General Meeting, Chicago, Ill., October 3-7, 1955. Manuscript submitted February 10, 1955; made available for printing July 19, 1955.

E. W. Tipton is with the Westinghouse Electric Corporation, Sharon, Pa.

Acknowledgment is made to F. W. Benke, who carried out the test program on bolted joints.

Table I. Comparison of Aluminum and Copper Conductors Having Equal Resistance Per Unit Length

	Copper	Aluminum
Resistance	1.00	1.00
Diameter	1.00	1.28
Cross-section area	1.00	1.64
Volume	1.00	1.64
Weight	1.00	0.495
Watts per pound I^2 R	1.00	2.02
Ampere per square inch of section	1.00	0.61
Watts per square inch of surface	1.00	0.78

theoretical size of wire must be used.

Mechanical Properties—Effect on Design

One mechanical property of aluminum of importance in its use for windings is its density which is only 30.2 per cent of the density of copper. Since the volume of material for equal resistance is 164 per cent one would expect an aluminum winding to weigh 49.5 per cent of an equivalent copper winding. On the basis of meeting the same over-all performance as explained in the preceding paragraph, the actual weight averaged nearly 54 per cent of the copper winding it replaced.

As shown in Table II the mechanical strength of aluminum at room temperature is considerably less than that of copper. At 250 degrees centigrade (C), corresponding to winding temperatures under short-circuit conditions, it has only one sixth the strength of copper. When loaded as a beam as are conductors in a pancake coil the span between supports can be only 40 per cent as great for equal strength. However, in a design with equal resistance per unit length, the aluminum conductor has a diameter 28 per cent greater and a section modulus 2.13 times as great. In such a winding the span between spacers can be 85 per cent of the span used in copper windings. For transformers of the size being discussed, up to 3,000 kva, the tensile strength of aluminum is not a serious handicap. In very large transformers where the repulsion between inner and outer windings on short circuit becomes high the tensile strength might become a problem.

Other mechanical properties of importance are corrosion resistance and melting point. These properties have a controlling effect on the problem of joining aluminum conductors which will be discussed in a later paragraph.

Thermal Properties—Effect on Design

The thermal conductivity of aluminum, like its electrical conductivity, is less than that of copper, being about 59 per cent. This is not an important factor in transformer design since the thermal drop in the winding material is a negligible part of the winding-temperature rise. On the basis of equal loss for unit length of conductor the aluminum winding has an advantage because the wattage per square inch of surface is only 78 per cent as great as in a copper winding.

Comparison of Aluminum and Copper-Wound Transformers

Table III gives a comparison between 100 transformers built with aluminum conductors and 100 copper-wound transformers of similar ratings. Some of the ratios vary slightly with kilovolt-amperes but the figures given are the average for all units. In weight, the aluminum-wound transformers are 3 per cent heavier in active material with 22 per cent more steel and 46 per cent less conductor weight. They are also somewhat larger in dimensions, being 7.6 per cent higher and approximately 9 per cent greater in each floor space dimension.

Table II. Mechanical Strength of Aluminum and Copper

	Aluminum		Copper	
	Hard	Annealed	Hard	Annealed
Tensile strength (psi) 25 C	27,000	12,000	50,000	34,000
Tensile strength (psi) 250 C		4,000		24,000
Yield strength (psi) 25 C*	24,000	4,000	45,000	11,000
Elongation per cent in 2 inches	15	45	6	45

* 0.2 per cent offset.

Joints—General

One of the serious problems in the manufacture of aluminum windings is that of making joints. Copper conductors can be easily and quickly resistance-brazed without fluxes to make a good noncorrosive joint having low resistance and good mechanical strength. For aluminum, because of its lower melting point of 650 C compared with 1,074 C for copper, there is no comparable brazing method. Also, because of the rapidity with which aluminum oxidizes in air an acid flux is required which is difficult to remove after brazing. Aluminum can be joined to aluminum using inert-arc gas-welding techniques. Considerable skill is required because of the fluidity of the aluminum at welding temperatures but good joints result. Permanent joints between aluminum and copper are difficult to make and are subject to severe electrolytic corrosion unless protected from moisture. For these reasons all aluminum-to-aluminum joints were made either by inert-arc welding or by bolting. Aluminum-to-copper joints were all bolted. No other types of joints were used.

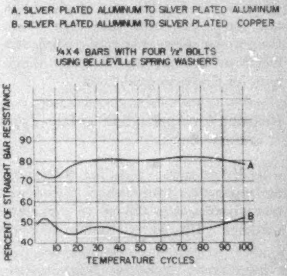

Fig. 3. Bolted aluminum joints resistance versus temperature cycles

Welded Joints

Conductors used in the aluminum windings were rectangular and averaged from 1/16 to 1/8 inch thick and 5/16 to

Table III. Comparison of Aluminum and Copper Transformers, Averages of 100 Dry-Type Ratings from 300 to 3,000 Kva

Ratio of Aluminum to Copper Design

Factor	Ratio
Active material in winding. Weight	0.537
Electrical steel. Weight	1.220
Total active material. Weight	1.032
Iron cross section	1.110
Area of opening in core	1.210
Induction in core	0.936
No-load loss. Tested	1.060
Load loss. Tested	0.990
Stray loss in per cent of I^2R loss	1.110
Watts per pound in winding. Tested	1.930
Amperes per square inch of conductor section	0.598
Coil diameter	1.090
Height over core	1.076

7/16 inch wide. Splices were made by butt-welding using inert-arc welding techniques with argon gas. A number of samples 4 inches long including such a butt weld averaged only 1.6 per cent greater resistance than samples of equal length without a welded joint. A number of techniques were worked out for welded-aluminum joints. Two of these are shown in Fig. 1. To weld taps into disk-type pancake-coil windings the conductor of the coil was notched out for a space equal to the tap width and the tap was extended across the coil conductor until its end was even with the inner edge of this notch. The weld which holds the two together then occupies the space of the notch and requires no space between coil sections. When welding multistrand coil leads to bus bars the coil lead was cut at an angle to increase the length of the weld. Except at the tips of the strands a separation was maintained between the coil lead and the bus bar. The end of each strand was then welded to the bus bar. The separation helped to prevent the conductor strands from overheating when the bus bar was brought up to welding temperature. Although these joints were slow to make and more costly than resistance brazes as used in copper winding, good joints were obtained and no difficulty was experienced with them.

Bolted Joints

To determine the best bolting pressures to use in bolted joints tests were made with two lengths of aluminum bars 1/4 by 2 inches bolted with a 1/2-inch bolt. Threads on the bolt were cut off and a measured load was applied in a testing machine. The contact resistance was then measured as a function of the bolt tension. Resistance decreased rapidly with increasing loads up to a total of about 1,600 pounds but as the load was released the resistance increased at a much slower rate. Tests were made with bare aluminum bars and also with silver-plated bars with results as shown in Fig. 2. Based on these tests it was decided to silver-plate all contact surfaces for bolted joints whether of aluminum or copper.

Aluminum will cold-flow under rather moderate stresses and it was feared that under conditions of temperature cycling the contact pressure in bolted joints might be decreased. To protect against this effect Belleville spring washers were used on all bolts. A special washer was designed to give a load of 1,800 pounds with a deflection of 0.011 inch. Since the thermal expansion of a 1-inch-thick joint of aluminum with a 200-C temperature rise is less than 0.01 this was felt to be adequate.

Fig. 4. Core and coils aluminum-wound dry-type transformers rated 500 kva, 3 phase, 60 cycles

To test various types of bolted joints temperature-cycling tests were made. The results for silver-plated aluminum to aluminum and silver-plated aluminum to silver-plated copper using Belleville washers are shown in Fig. 3. The sample joints were between 1/4 by 4-inch bars with a 4-inch overlap and using four 1/2-inch bolts on $1^3/_4$-inch centers. The temperature cycle consisted of raising the joints to the specified temperature by circulating current and then allowing the joints to return to ambient temperature. The aluminum-to-aluminum joint had 50 cycles with a joint temperature of 109 C and 50 with a joint temperature of 142 C. The aluminum-to-copper temperature, because of the lower resistance, had 50 cycles with a joint temperature of 86 C and 50 cycles to a joint temperature of 104 C.

Resistance measurements were made from points 4 inches either way from the center of the joint using needle-point contacts. Contact resistance was taken as the measured resistance minus the resistance calculated for the two bars when butt-welded at the joint. Per cent of straight bar resistance is the contact resistance in per cent of the resistance of a bar having the same section as one bar and a length equal to the overlap. For copper to aluminum, half the length is assumed to be copper and half aluminum. In both types of joint the joint resistance was less than an equal length of bar without a joint and did not materially increase after 100 temperature cycles. Torque required to remove the bolts after the test did not decrease below the value at the start.

Table IV. Cost Ratio of Aluminum-Wound to Copper-Wound 750-Kva 3-Phase 60-Cycle 4,160-to-480/277-Volt 4-Wire Dry-Type Transformers

Transformer Part	Item	Weight Ratio	Cost Ratio	Per Cent of Total Difference in Cost
Coils	Conductor material (strap)	0.64	1.76	65.5
	All material including strap		1.61	67.9
	Labor		1.20	6.8
	Total coil cost		1.52	74.7
Core and core parts	Core and core parts	1.16	1.13	16.8
General assembly	Materials		0.81	−2.7
	Labor		1.79	11.2
	Total		1.30	8.5
Core and coil assembly complete			1.33	100.0

Cost Data

While the manufacturing and design problems were satisfactorily solved the aluminum-wound transformer did not prove economical. An analysis of the cost ratios is shown in Table IV. Cost of the core-and-coil structure proved to be 33 per cent higher than cost of the equivalent copper-wound transformer. Two-thirds of the cost difference was due to the cost of the glass-insulated aluminum strap which, at the time, cost 2.76 times as much per pound as copper. Most of this additional cost was in the drawing and covering of the wire since the aluminum wire bar costs were only 1.13 times as great as copper costs. To make the use of aluminum economical, it would be necessary for aluminum fabricators to find means to reduce the wire-processing costs.

Eighteen per cent of the excess cost of the aluminum transformer was in the coil winding and general-assembly labor costs. Most of this was due to the increased cost of inert-arc welding the coil taps, leads, and bars. This represents another place where more work is needed to develop lower cost and quicker methods for joining aluminum. Another 17 per cent of the increased cost results from the longer mean turn and greater weight of the core. Since this cost is less than proportional to the increase in weight it offers little chance for future cost reduction.

Conclusions

1. The technical problems incident to the successful design and manufacture of small and moderate-sized dry-type transformers were successfully solved.

2. Over 100 transformers up to 3,000 kv in size were built in a time of copper shortage releasing a considerable quantity of copper for other transformers.

3. These transformers have been in service from 3 to 4 years with no difficulty of any kind.

4. Cost of an aluminum-wound transformer was one third higher than the equivalent copper one. In the period since these units were built the processing cost of aluminum conductors has been reduced but not enough to make it economical at the present time.

5. More work is needed on methods of joining aluminum to speed up the manufacturing processes and to reduce the joining costs.

Design and Evaluation of Butyl-Rubber-Insulated Power Cable

J. C. CARROLL
ASSOCIATE MEMBER AIEE

A. R. LEE
ASSOCIATE MEMBER AIEE

R. B. McKINLEY
ASSOCIATE MEMBER AIEE

THE significant discovery in 1937 by Sparks and Thomas[1,2] that isobutylene could be copolymerized with small quantities of diolefins (such as isoprene) to give products which could be vulcanized[3] culminated in research efforts to produce a synthetic rubber with controlled unsaturation. Polyisobutylene itself is completely saturated in the chemical sense, and is therefore highly resistant to the degrading effects of oxygen, ozone, sunlight, heat aging, etc. Unfortunately, however, the complete saturation existing in this polymer renders it incapable of crosslinking or vulcanization. Therefore, efforts to utilize the attractive properties of this material as a cable insulation were necessarily confined to mechanical mixtures, or dispersions, with vulcanizable elastomers, notably natural rubber.[4] The copolymerization of isobutylene with isoprene, to yield a product with unsaturation introduced in controlled amounts, made available an elastomer incorporating the excellent resistance of isobutylene to degrading effects, and permitting vulcanization, or crosslinking, through the unsaturated bond of the isoprene unit. The number of isoprene units in the butyl rubber molecule is sufficient for vulcanization purposes with little or no excess remaining as active sites after vulcanization to permit attack by oxygen, ozone, etc.

Intensive research from 1940 to 1943 by the authors' associates led to the development of practical butyl rubber-insulating compounds capable of vulcanization in conventional equipment. At that time, production of this new polymer was limited to pilot plant runs, and the first commercial application of butyl rubber-insulated cable in any appreciable quantity did not take place until 1944., Prior to this development, the best high-voltage compounds utilized natural rubber, which requires complete protection against ozone generated by corona. This protection is effected by thoroughly dispersing the rubber in a vegetable oil derivative, or "factice," which coats the rubber particles and protects these highly unsaturated molecules from attack by oxygen, ozone, and ultraviolet light. These oil-base insulations, when carefully formulated and processed, have given excellent service within their limits of operating temperatures and environment. However, as with all materials, such limitations do exist and thus is generated the constant search for materials with improved inherent properties.

Aging and Ozone Tests

The early evaluations of butyl rubber compounds confirmed the theoretical excellence of the new "tailor-made" copolymer as being strongly resistant to the attacks of the environmental enemies of natural rubber, or other unsaturated elastomers such as *GR-S*. It was apparent that here was an ozone- and heat-resistant insulation that so far exceeded the best known oil-base rubbers that it was necessary to devise new and more stringent methods of test in order to define properly its characteristics.

The superior heat and ozone resistance of butyl rubber to oil-based compound is shown by Table I, which compares the physical properties of cable insulations before and after accelerated aging tests. Further comparison of the ability of butyl insulation to resist heat aging is shown in Fig. 1. Cable samples wrapped on a mandrel and subjected to 300 degrees Fahrenheit (F) in an air oven show embrittlement of oil-base insulation after 25 hours, while butyl rubber insulation remains flexible after 96 hours' exposure.

The excellent ozone resistance of butyl rubber is recognized in the fact that while oil-base insulations are tested for 3 hours at an ozone concentration of 0.015 per cent (%) maximum by volume,[5] the ozone resisting butyl rubber insulation is tested for 3 hours at an ozone concentration of 0.030% maximum by volume.[6] Further evidence is provided by the result of a test on a sample of No. 6 American Wire Gauge (AWG) solid conductor insulated with 10/64-inch thickness of

---

Paper 55-668, recommended by the AIEE Insulated Conductors Committee and approved by the AIEE Committee on Technical Operations for presentation at the AIEE Fall General Meeting, Chicago, Ill., October 3-7, 1955. Manuscript submitted June 3, 1955; made available for printing July 18, 1955.

J. C. Carroll, A. R. Lee, and R. B. McKinley are with the General Electric Company, Bridgeport, Conn.

The authors acknowledge gratefully the excellent assistance and encouragement of L. E. Howard, C. O. Hull, B. J. Mulvey, C. H. Seaberg, and especially J. B. Felter and his associates, whose careful testing supplied the data for this paper.

Table I. Physical Properties

	Typical Butyl Insulation Values	Typical Oil-Base Insulation Values
Original		
Tensile strength, psi	800	750
Elongation, %	500	450
After 7 Days in Air Oven		
Tensile strength, psi	600, 100 C	600, 80 C
Elongation, %	400, 100 C	125, 80 C
After Oxygen Pressure Test		
Tensile strength, psi	600 } 168 hours at 80 C	600 } 48 hours at 70 C
Elongation, %	400 } 168 hours at 80 C	125 } 48 hours at 70 C
Air Pressure Heat Test, 20-hours, 80 pounds, 127 C		
Tensile strength, psi	600	350
Elongation, %	400	100
Ozone Resistance		
0.03% by volume	24 hours, tests discontinued after 24 hours	Less than 1 hour

butyl rubber, which was wrapped around a mandrel four times the insulated diameter of the cable, and exposed to an ozone concentration of 0.2% by volume. The sample had not failed after 24 hours' exposure to this test.

Ozone resistance in itself does not necessarily indicate a corresponding ability to resist the effects of corona discharge. The ability of butyl rubber insulations to resist corona is shown by U-bend tests in which samples of insulated cable are bent in a U shape around a mandrel having a diameter four times that of the sample, and placed with the bottom of the U in contact with a grounded metal plate. A potential equal to 100 volts per mil of insulation is applied between the conductor and the metal plate. Samples of butyl rubber-insulated cable have withstood this test without failure for periods in excess of 100 hours.

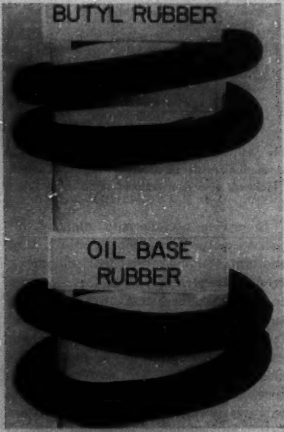

Fig. 1. Comparative heat resistance of rubber insulations at 300 F, butyl at 96 hours and oil base at 25 hours

In addition to its inherent ability to withstand oxidation, ozone, corona, and heat, butyl rubber exhibits a high degree of resistance to sunlight and weathering. Samples subjected to outdoor exposure in an atmosphere combining moderately corrosive industrial elements and salt air, show no evidence of sunchecking, or surface cracking, after a period of 7 years.

Extended Temperature Tests

Although a great number of data were available on short-time high-temperature and accelerated-aging tests, it was felt necessary to determine the stability of the butyl insulation after long-time overloads. Accordingly, in 1946, these tests were started with the use of current loading of the conductors to raise the temperature of the insulation. The cable tested consisted of no. 6 AWG stranded copper-insulated with 16/64-inch thickness of butyl rubber covered with a copper shielding tape, and placed in open air. One length operated continuously at a copper temperature of 85 C and another at 121 C. These load tests were continued for over 5 years.

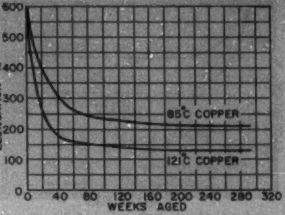

Fig. 2. Effect of long-time load test on elongation of no. 6 AWG, 16/64-inch butyl rubber insulation, shielded

Physical tests of the insulation for both tensile strength and elongation were taken at periodic intervals as well as dielectric power factor measurements at both room and operating temperatures at a voltage stress of 10 kv. Figs. 2 through 4, illustrating the results of these tests, are very significant and have substantiated the theoretical stability of this insulation at elevated temperatures, as well as the reliability of the accelerated tests. It will be observed from Fig. 2 that the elongation at both 85 and 121 C copper temperature becomes lower at a gradually decreasing rate until the end of approximately 40 weeks, after which time there is little change in the material. It will be noted that at the end of 293 weeks or $5^1/_2$ years, at 85 C the elongation was 220%, and at 121 C, 115%. Fig. 3 shows the tensile strength change at both 85 and 121 C copper temperature and again it will be observed that the tensile strength lessens during the first 40 weeks and then reaches practical stability. The per cent of original tensile strength at 85 C is 67% at the end of the $5^1/_2$-year period and is 37% of the original at 121 C copper temperature. This outstanding performance is unlike other types of rubber

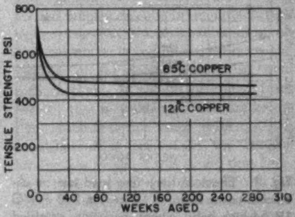

Fig. 3. Effect of long-time load test on tensile strength, no. 6 AWG 16/64-inch butyl rubber insulation, shielded

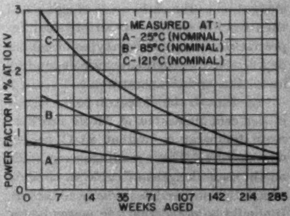

Fig. 4. Effect of long-time load test on dielectric power factor at 10-kv, no. 6 AWG 16/64-inch butyl rubber insulation, shielded

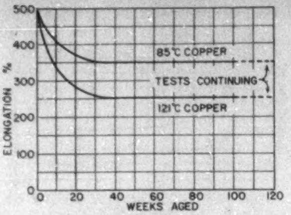

Fig. 5. Effect of long-time load test on elongation on no. 2/0 AWG 19/64-inch butyl rubber insulation, shielded

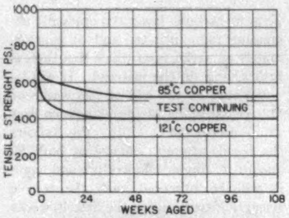

Fig. 6. Effect of long-time load test on tensile strength, no. 2/0 AWG 19/64-inch butyl rubber insulation, shielded

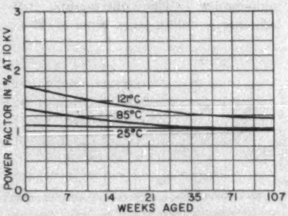

Fig. 7. Effect of long-time load test on dielectric power factor at 10-kv, no. 2/0 AWG 19/64-inch butyl rubber insulation, shielded

in that butyl insulation has a relatively high depreciation in tensile strength and elongation in the early cycle of aging and then reaches equilibrium in physical depreciation, whereas other types of rubber depreciate at a progressive rate depending upon time and temperatures.

Fig. 4 shows the dielectric power factor in per cent measured at 10 kv, both at room temperature and at 85 C copper temperature. These readings were made on the same lengths of cable as that on which the physical tests were observed. It should be noted that the power factor has continued to decrease slightly over this period at the elevated temperature. The same trend is shown on the length which operated at 121 C over the same length of time.

To confirm these results on later production of cable manufactured by more modern methods, duplicate tests were made using no. 2/0 AWG conductor, insulated with 19/64-inch butyl rubber and shielded over-all. These tests have been running for a period of 2 years and the observed results are shown in Figs. 5 through 7. Fig. 5 illustrates the depreciation in elongation, and here again the initial decrease takes place during the first 36 weeks, at which time the elongation remains practically stable at both 85 and 121 C copper temperature. The elongation at the end of the period at 85 and 121 C is 350% and 260% respectively. Fig. 6 shows the depreciation in tensile strength and the same trend is observed as in Fig. 3 on the previous test. Once again, in Fig. 7 is shown the phenomenal record of the power factor at 85 C starting at 1.33% and after 105 weeks remaining stable at 1.01%. Likewise at 121 C the original power factor is 1.7% and after the same period of time, decreases to 1.21%.

These observations have been further confirmed by field experience in numerous conditions of overloading, either because of deliberate overcurrents or high ambients or mutual heating. In one case, a no. 4/0 AWG 15-kv cable was subjected to daily loads of 400 amperes with peaks of 490 amperes for a period of several months. Although the normal rating is 235 amperes, this cable continued to operate satisfactorily. When removed for replacement with the proper size, it was found to have suffered practically no deterioration and was placed in service on other circuits. Another case involving 5-kv cable crowded together in a buried wooden trough created maximum temperatures of well over 100 C for a period of 3 years, so that the neoprene covering was completely embrittled. Yet the butyl rubber retained an elongation of 340% and a tensile strength of 510 pounds per square inch (psi).

Moisture Absorption

In any rubberlike insulation, a very important characteristic is the ability to withstand long immersion in water. This can be measured in several ways. For routine production work, short-time gravimetric and electrical tests have been devised and specified by industry standards. For laboratory investigations such as this, long-time immersion over a period of months or even years is of great help in evaluating the moisture resistance of the material.

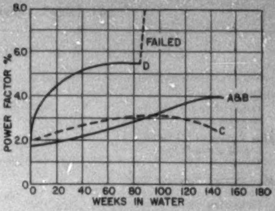

Fig. 8. Effect of long-time immersion on dielectric power factor at 80 volts per mil of butyl rubber insulation and oil-base rubber

A—19/64 butyl rubber at 70 C
B—10/64 butyl rubber at 50 C
C—4/64 butyl rubber at 50 C
D—4/64 oil-base rubber at 50 C[8]

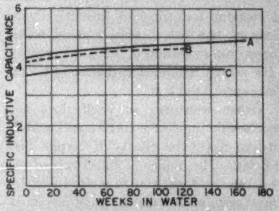

Fig. 9. Effect of long-time immersion on SIC of butyl rubber insulation. Thickness and temperatures same as in Fig. 8

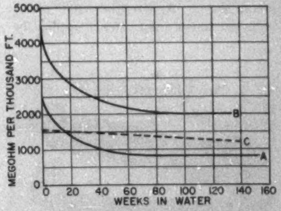

Fig. 10. Effect of long-time immersion on insulation resistance of butyl rubber insulation. Thickness and temperatures same as in Fig. 8

In service, a cable may often be subject to water immersion, in which cases the water temperature will seldom exceed a temperature of 25 C. However, to accelerate these tests, water temperatures of 50 or 70 C were chosen. The test procedure consists of immersing samples of insulated cable in water baths, closely controlling the water temperature, and periodically measuring the insulation power factor, dielectric constant (SIC), and insulation resistance. Similar data on other materials were reported by McKinley and Seaberg[7] and by DeBaene and Anderson.[8]

Table II. Corona Measurements on Butyl Rubber-Insulated Cable

Test Voltage, Kv	Ionization Intensities, Micromicrocoulombs, Cable No. 1	2	3	4	5	6
6						
7				90		
8	60					
9		60	300			
11		150	600	300		
14	300	300				60
16					20	300
17						300
18					100	
20						300
23					500	

Construction of cables: all no. *1/0* AWG. 19/64-inch butyl rubber, copper-shielding tape; over-all, 15-kv rating. Cable nos. 1 and 2: cement on conductor, cable tape over insulation; nos. 3 and 4: semiconducting tape on conductor, cable tape over insulation; nos. 5 and 6: semiconducting tape on conductor and over insulation.

The following data apply to three samples reported:

Sample	Conductor Size	Wall	Test Temperature, C
A	no. *2* AWG	19/64 inch	70
B	no. *2/0* AWG	10/64 inch	50
C	no. *6* AWG	4/64 inch	50

The immersion tests were continued for varying periods up to 155 weeks. Figs. 8 and 9 show the power factor and SIC during test. Fig. 8 also shows, for comparison, data on oil-base rubber brand *G* taken from DeBaene and Anderson,[9] who selected brand *G* as the most stable oil-base rubber reported.

On all samples, measurements were made at 40 and 80 volts per mil. However, for simplicity, only the 80-volt-per-mil values are shown. Fig. 10 shows the insulation resistance values obtained.

Corona Detection and Control

Although it has been shown that butyl rubber is outstanding in ozone resistance, experience demonstrates that to provide additional factors of safety, it is necessary to guard thoroughly all types of rubber against internal ionization. All voids must be eliminated at the surface of the conductor and throughout the insulation wall. The earlier attempt to eliminate such defects centered around complete bonding of the insulation to the conductor and filling of the strand interstices. Also, a greater number of strands were utilized in order to provide a smoother surface and promote better bonding. Nevertheless, many unexplained service failures occurred shortly after being energized, even though the cables had successfully passed all required factory high-voltage tests and dielectric measurements. It became apparent that more sensitive methods were required to weed out the small but important defects, and to serve as better guides for manufacturing techniques.

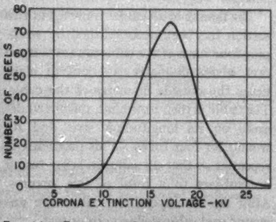

Fig. 11. Frequency distribution of ionization levels on 15-kv butyl-rubber-insulated cables for 1954

Over a period of years, many investigators had worked on more sensitive ionization detectors than the then usually accepted change in the dielectric power factor with voltage.[9] This apparatus had been used experimentally on design determinations of capacitors, bushings, current transformers, and cable samples. However, no practical application was made for quality control of cable until about 1948. Graham, Duffy, and Foster[10] described a practical filter circuit which would eliminate extraneous noise, and which would detect the voltage at which internal ionization first appeared and the level at which it would be extinguished.

The introduction of such detectors opened up new fields in the cable art and provided a tool whereby the designer could easily check the merit of insulations and various cable assemblies. For example, Table II shows ionization data on three types of cable assemblies, utilizing various methods of shielding, both internal and external to the insulation. It is readily apparent that constructions 5 and 6, utilizing semiconducting tape both for strand shielding and for application to the outer surface of the insulation, result in much higher corona extinction voltages than the other constructions. It should also be noted that the constructions 3 and 4, without the semiconducting tape applied to the outer surface of the insulation, have corona extinction voltages at approximately operating potentials, and indicate strong discharge between the insulation and the shielding tape. The energy of the discharge probably indicates to some degree the relative characteristics of the void spaces. However, many more data would be needed to confirm this, and it is minor in this case compared to the importance of the corona extinction voltage. It was from these and a mass of similar data that it was concluded necessary to utilize semiconducting surfaces at the conductor above 2 kv, and the semiconducting material over the insulation on all shielded cables of 10 kv and over.

Fig. 12. Enlarged section of cable insulation showing small particle which caused low ionization level

The technique of measuring corona level on full-reel lengths has been utilized as a quality control criterion since 1949. It was necessary to increase the rating of the equipment to 240 kva at 60 kv in order to handle long lengths of medium-voltage cable. Fig. 11 is a distribution curve of corona levels on full-reel lengths of 15-kv cable for the year 1954. This method has proved to be a very sensitive and valuable tool to aid in determining needed improvements in manufacturing techniques. With practice in reading the instruments, it is possible to estimate the location of the defect within the cable construction. It should be noted from Fig. 11 that a number of reels are below the established minimum value. Upon examination of several of the lengths having low levels, it was found that complete coverage was not obtained from the shielding tapes. In such cases, it is possible to correct the deficiency and proceed with the completion of the cable.

In one case, the instrument reading appeared to indicate a defect within the wall of the insulation on a no. *4* AWG 15-kv cable, 2,000 feet in length. The cable was cut in half and the portion with low reading was bisected again and again, until the defect was isolated into a 10-foot piece. The outer coverings were removed and probing devices utilized to obtain the location of the defect as closely as possible. These few inches were then sliced with a microtome until the defect was found. It was identified as a particle of undispersed filler, approximately 20 mils in diameter. Fig. 12 is an enlarged photograph of the particle embedded in the insulation, illustrating the remarkable sensitivity of this testing method.

Table III. Alternating Voltage Breakdown Tests on Butyl-Insulated Cable

Conductor Size, AWG	Insulation Thickness, Inches	Natural Logarithm (D/d)	Maximum Stress at 60-Cycle Breakdown		
			1 Minute	5 Minutes	24 Hours
2/0	10/64	0.557		412	318
2	10/64	0.72		469	344
4/0	10/64	0.448	612		
6	16/64	1.25	449	329, 318, 339, 462	364, four samples 288, two samples
			509	360 450, 491, 365, 407, 407, 365	
6	19/64	1.433		379	435
2	19/64	1.11	604	590	272
1/0	19/64	0.959	543 333 578		
2/0	19/64	0.883			342
B-strand					325, two samples
4	21/64	1.34			303
2/0	29/64	1.15	387		
2	39/64	1.645	505	316	

Electrical Evaluation

Evaluation of a material to be used as cable insulation must include complete electrical data. In the development of butyl as a solid dielectric insulation, many electrical tests have been made in the laboratories of the authors' company. These data, correlated with the physical and heat-aging data just described, result in thorough knowledge both of butyl itself as an insulating material and as used in full-scale cable designs. The data reported in the following sections have been obtained on representative cables of varying conductor sizes and thicknesses of insulation wall. All cables were manufactured in accordance with commercial practice and according to Insulated Power Cable Engineers Association standards.[11] The electrical tests are separated into three general categories: dielectric strength, ionization level (corona extinction voltage), and load cycle aging.

DIELECTRIC STRENGTH

Dielectric strength of butyl-insulated cables is reported for several different voltage conditions, described as follows.

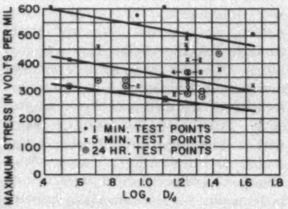

Fig. 13. Alternating voltage breakdown tests on butyl-rubber-insulated cable

ALTERNATING VOLTAGE, TIME

To study the effect of variation of conductor size and insulation thickness as they relate to the 60-cycle alternating voltage breakdown, a number of samples of butyl-insulated cables have been tested. Further, to establish the relationship of time to breakdown strength, various of these samples have been subjected to different times of voltage application. Table III details the cable description, the test times, and the value of breakdown voltage obtained in terms of maximum stress at the conductor surface. The authors believe that maximum stress at the conductor surface is the controlling stress in voltage breakdown of cables constructed with solid dielectrics, i.e., a homogenous wall of insulation.

It should be noted that the voltage breakdown tests are performed in the following manner. The 1-minute tests are conducted by uniformly raising the voltage, applied between conductor and grounded shield, at a rate to obtain breakdown in approximately 1 minute. In the case of the 5-minute and 24-hour tests, the test voltage applied is that specified by the Insulated Power Cable Engineers Association standard for factory alternating voltage test for 5 minutes, or 24 hours as the case may be. The voltage is then raised in increments of 20% over the preceding step for the applicable period of time until failure is obtained. Fig. 13 shows the correlation of these test results in relation to natural logarithm (*D/d*) which is the geometric factor of the cables. This method of evaluating the breakdown values results in a comprehensive picture of the relationship of breakdown voltage to the geometric relation of cable conductor size and insulation wall thickness. As would be expected, the breakdown voltage decreases as the ratio of insulation wall thickness to conductor diameter increases.

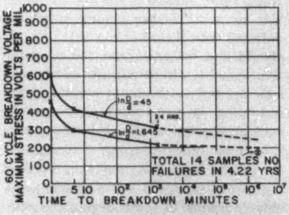

Fig. 14. Relation of alternating voltage breakdown of butyl-rubber-insulated cables with time

Fig. 14 demonstrates the relation of time to 60-cycle alternating voltage of butyl-insulated cable. The solid part of the curve is derived from Fig. 13 for the limits of. geometric factor investigated. The dashed portion of each of the curves in Fig. 14 represents the range of times not fully investigated. However, this portion of the curve is supported by the evidence of a test on a total of 14 samples of butyl-insulated cables. These 14 cables have a geometric factor of 1.25 (no. *6* AWG stranded copper conductors with 16/64-inch butyl insulation), and have been subjected to a continuous voltage of 20-kv conductor to ground for 4.22 years without failure. As shown by Fig. 14, this voltage results in a maximum stress of 168 volts per mil. This continuous voltage stress compares with a stress of 58.7 volts per mil if the cable were operated at its rated voltage.

ALTERNATING VOLTAGE AFTER FLEXURE

Since all cables are subject to flexure, or bending, during reeling in factory and unreeling and installation in the field, it is necessary to consider the effect of such flexure on the dielectric strength. Tests have been made on butyl-insulated cables both from a long-time and a 24-hour standpoint.

The flexing of all cables reported in this section has been accomplished by wrapping four turns of the cable around a mandrel whose diameter is equal to eight times the outside diameter of the cable. The cable is then unwound, rolled 180 degrees on its longitudinal axis and rewound for four turns. This procedure is repeated so that all samples being tested are subject to a total of five flexures. After the last cycle, the cables are unwound and subjected to voltage test.

It will be observed, Fig. 14, that a total of 14 samples of no. *6* AWG 16/64-inch

Table IV. No. 2/0 AWG, B-Strand 19/64-Inch Butyl-Rubber-Shielded Cables Voltage Breakdown 24-Hour Step-Up Test at Room Temperature, Initial Voltage 20 Kv, 20% Increment Every 24 Hours

Sample Nos.	Condition	Ionization Level, Kv B	Ionization Level, Kv A	Hours at Each Voltage Step 20.0 Kv	24.0 Kv	28.8 Kv	34.6 Kv	41.5 Kv	49.8 Kv	59.7 Kv	71.6 Kv
1	N-F	16.3		24.0	24.0	24.0	72.0	24.0	24.0	24.0	0.5*
2	F	12.3	13.2	24.0	24.0	24.0	72.0	24.0	22.1*		
3	N-F	16.7		24.0	24.0	24.0	72.0	24.0	24.0	24.0	0.5*
4	F	12.0	14.3	24.0	24.0	24.0	72.0	24.0	24.0	1.0*	
5	N-F	13.1		24.0	24.0	24.0	72.0	24.0	24.0	24.0	1.2*
6	F	15.1	14.2	24.0	24.0	24.0	72.0	24.0	24.0	24.0	1.3*
7	N-F	15.3		24.0	24.0	24.0	72.0	24.0	24.0	21.7*	
8	F	12.0	12.6	24.0	24.0	24.0	72.0	24.0	24.0	1.2*	
9	N-F	14.8		24.0	24.0	24.0	72.0	24.0	24.0	5.0*	
10	F	15.3	18.2	24.0	24.0	24.0	72.0	24.0	24.0	0.1*	
11	N-F	15.2		24.0	24.0	24.0	72.0	24.0	24.0	12.5*	
12	F	15.3	15.3	24.0	24.0	24.0	72.0	24.0	24.0	24.0	0.9*

* Failure at this time and voltage.
F = samples flexed five times over mandrel diameter eight times that of cable diameter.
N-F = not flexed.
B = ionization level before flexing.
A = ionization level after flexing.

butyl-insulated cable were subject to voltage for 4.22 years. Of these, seven were subjected to the flexing procedure described and seven were merely unwound from their shipping reels. All samples were formed into U's with a diameter of 4 feet and hung in the bent position for the duration of the test. As has been observed in the previous paragraphs, no failures were experienced in any of the 14 samples.

Table IV gives the results of 24-hour voltage breakdown tests on cables subjected to and not subjected to the flexure procedure. The cables are no. *2/0* AWG class-*B*[11] strand with 19/64-inch butyl insulation. Semiconducting fabric tapes are used over the conductor and the insulation. A copper shielding tape is applied over the outer semiconducting tape. The results of this test show no significant difference in voltage breakdown due to the flexure procedure. They also correlate well with the 24-hour breakdown curve established in Fig. 13.

Table V. Air Oven and Oxygen Bomb Tests Alternating Voltage Breakdown After Aging

Oven Temperature	Time for Aging for Kv Breakdown at Room Temperature 1 Week	2 Weeks	3 Weeks	4 Weeks
Air Oven Test: Unaged Breakdown, 23 Kv				
70 C	27	27	28	24
90 C	23	28	27	26
121 C	22	26	26	26
Oxygen Bomb Test, 300 psi: Unaged Breakdown, 23 Kv				
Bomb Temperature				
80 C	24	28	25	23

Table VI. Air Pressure Heat Test (80 PSI) Alternating Voltage Breakdown After Aging

Test Temperature	Time for Aging for Kv Breakdown at Room Temperature 6 Hours	12 Hours	18 Hours	24 Hours	30 Hours
70 C	28	26	26	29	28
90 C	27	21	23	26	27
121 C	22	23	28	24.5	28

Unaged breakdown, 23 kv.

ALTERNATING VOLTAGE AFTER AGING

Some insulations have a serious deterioration in short-time alternating voltage breakdown strength with time of aging. To investigate this property, a series of 1-minute breakdown tests were run on samples of butyl-insulated cables subjected to three types of accelerated aging at various temperatures and with varying times.

Tables V and VI contain the results of 1-minute alternating voltage breakdown tests made on samples of no. *14* AWG solid-copper conductor insulated with 3/64-inch butyl rubber. The data obtained show that, within experimental limits, butyl-insulated cables are not affected by accelerated aging over a wide variety of time, temperature, and aging conditions.

IMPULSE STRENGTH, 1½x40-MICROSECOND WAVE

Fig. 15 plots the results of many of the impulse breakdown tests obtained on butyl-insulated cables. The impulse wave used in all tests has been of 1½x40-microsecond duration according to AIEE standards for impulse testing procedures. This chart shows the relationship of impulse breakdown to the thickness of insulation of the butyl-insulated cables tested. For comparison, the AIEE basic insulation levels for electrical equipment are shown in relation to the insulation thickness for the standard grounded neutral cables. Most of the cables tested ranged in conductor size from no. *6* to no. *2/0* AWG with class-*C*[11] stranding. Three tests are reported for no. *2/0* AWG 15-kv cables with class-*B* stranding. The dotted curve included in Fig. 15 is the average breakdown value for ordinary grades of rubber-insulated cable as reported by Halperin and Shanklin.[13]

The results of these tests indicate that properly designed and manufactured butyl-insulated cables have inherent impulse strength compatible with basic-impulse-insulation-level requirements up to the 35-kv level. Further, variation in conductor size and stranding does not appear to affect this relation to an appreciable degree.

IONIZATION LEVEL

Determination of ionization level, or corona extinction voltage, to be described, of cables has proved invaluable from a design and manufacturing standpoint. However, if the theory that this type of test is sound and valid in proper design and manufacture of high-voltage rubber-insulated cable, it should also obtain after a cable has been subjected to operating conditions, including flexing and thermal expansion of the various components of the cable.

Therefore, tests have been made to investigate the ability of properly designed high-voltage butyl-insulated cables

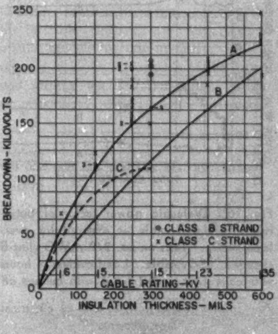

Fig 15. Impulse voltage breakdown of, curve A, butyl-rubber-insulated cable compared to BIL, curve B, and impulse breakdown of ordinary rubber, curve C[13]

Table VII. Effect of Thermal Cycles on Ionization Level

Conductor Temperature, C	No. of Cycles at Indicated Temperature	Total Elapsed Cycles	Ionization Level, Kv*
25	0	0	12.0
43	15	15	13.0
82	15	30	14.1
90	11	41	15.1
100	15	56	
110	11	67	
120	15	82	
130	11	93	12.3

* Measured at room temperature after cycles indicated.

Cable: Single conductor no. *2/0* AWG, class-*B* strand copper conductors, semiconducting fabric tape, 19/64-inch butyl rubber insulation, semiconducting fabric tape, lapped copper shielding tape and 6/64-inch jacket.

Temperature cycles: Four hours with current on and 2 hours with current off, repeated continuously.

to retain acceptable ionization level after flexing as described previously, after conductor-heating cycles from room temperature to elevated temperatures, and after tests involving continuously applied overvoltage in conjunction with conductor-heating cycles. The cables used in these tests are of the design utilizing semiconducting fabric tapes over the conductor and the insulation.

The cables described in Table IV have been subjected to ionization level test before and after flexure. Table IV contains the values obtained. This shows that despite the severe bending to which half of these samples were subjected, the ionization level is the same in properly designed butyl-insulated cables whether or not they are subjected to conditions of bending encountered in the field.

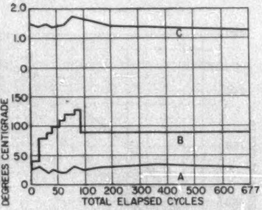

Fig. 16. Dielectric power factor of butyl-rubber-insulated cable as affected by overload cycles. Tests on no. 2/0 AWG class-B stranded, 15-kv cable. Load cycles: 4 hours with current on and 2 hours with current off

A—Copper temperature at time of electrical measurements

B—Maximum copper temperature during load cycles

C—Power factor measured at room temperature and 40 volts per mil

The effect of temperature cycles on ionization level is shown in Table VII. The cables involved in this test are no. *2/0* AWG, class-*B* stranding, copper conductor, semiconducting tape over the conductor, 19/64-inch butyl insulation with semiconducting and copper-shielding tapes applied immediately over the insulation. A 6/64-inch-thick jacket is applied over-all. These cables have been subjected to temperature cycles as shown in Table VII by circulating current in the conductor. A total of six samples are included in this test. The average ionization level of all samples is shown in Tables V and VI, at the end of each new temperature condition. The levels are measured at room temperature rather than at the elevated temperature, more clearly to demonstrate the effect of thermal expansion. If the ionization level were to be taken at the elevated temperature, the insulation would be at its expanded volume for that particular temperature and would be exerting a considerable pressure on both the strand and insulation shielding. Upon subsequent cooling, voids in the construction can form if the design is improper and it will be evidenced by low ionization level. It is thus important that ionization levels be determined after the cables have cooled.

The results of this test, Table VII, demonstrate the ability of properly designed butyl-insulated cables to retain their ionization level after severe temperature cycles; also that with proper conductor shielding, class-*B* stranding is entirely satisfactory for this class of cable.

Load Cycle Aging Tests

Butyl rubber has been shown by analysis of its chemistry, long-time continuous heat-aging tests, and many accelerated aging tests to have remarkable stability against high-temperature aging. However, this property does not assure in itself that a butyl-insulated cable will operate satisfactorily under conditions of varying temperature conditions such as are encountered in actual service conditions. Very few, if any, power circuits operate with load factors of 100% and the majority operate at around 50% to 60% load factor.

Two tests are included to show the effect of heating (or load) cycles on cables with relatively heavy walls of butyl rubber insulation. The cables tested had walls of 19/64 inch and 29/64 inch which are equivalent to circuit ratings of 15 and 25 kv respectively. These heavier walls were chosen because the volumetric expansion of the insulation is more critical with these larger, higher voltage cables.

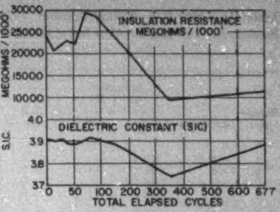

Fig. 17. Dielectric constant and insulation resistance measurements under same conditions as in Fig. 16

Load Cycle to High Temperatures

A total of six samples of butyl-insulated cables were subjected to heat cycling by means of circulating low-voltage current through the conductors. The cables are no. *2/0* AWG class-*B* strand rating 15-kv grounded neutral and are described in detail in Table VII. The load cycle consists of heating for 4 hours to the desired temperature and then cooling for 2 hours.

Figs. 16 and 17 give the average results for the six samples of no. *2/0* AWG 15-kv cables after 677 cycles. Of particular interest is the fact that these cables were subjected to a series of temperature cycles in 10 C steps up to 130 C for a total of 93 cycles and then were subjected to an additional 584 cycles at 90 C. The results of this show complete stability of all electrical characteristics for the duration of the test.

The data shown by Figs. 16 and 17 are of particular importance from the standpoint of demonstrating the ability of properly designed butyl-insulated cables to withstand the temperatures that might be encountered under emergency overload and short-circuit conditions in service. Based on these and other tests, the authors are rating butyl-insulated cables as manufactured by their company at the following temperatures for emergency operation:

Cable Rating, Volts	Normal Continuous Operating, C	Emergency Operating Temperature for 100 Hours per Year, C
0 to 600	90	125
601 to 8,000	85	115
8,000 to 15,000	85	105

Load Cycle Aging with Overvoltage

Overvoltage load cycle aging tests on cables have been established by long usage as being the ultimate in proving out the design and insulation characteristics, since

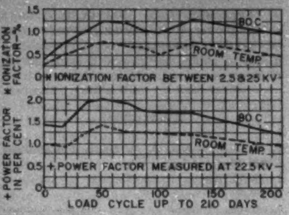

Fig. 18. Overvoltage load cycle tests. Average results of five samples of no. 2/0 AWG 29/64-inch butyl rubber-insulated cable. Continuous voltage of 21.6-kv conductor to ground. Conductor loading to 80 C, 4 hours on and 4 hours off

they most closely approach service conditions. As in any testing, it is necessary to provide some acceleration of test conditions to provide results in a reasonable length of time. This section of the paper will give results obtained on no. *2/0* AWG 25-kv grounded neutral cables insulated with 29/64 inch of butyl rubber, operating under temperature cycles to 80 C and with continuous voltage of 21.6-kv conductor to ground. The voltage is equal to 150% of cable rating and to a 3-phase circuit voltage of 37.4 kv.

The purpose of the test is to provide data on heavier walls of butyl insulation such as would be used at 25 and 35 kv. The data also provides confirmation of the excellent operating record of butyl-insulated cables at 15 kv and under.

Before load cycling, samples of this cable were subjected to 21.6-kv voltage continuously for a total of 327 days. At this time, current loading through the conductor was commenced. These cycles were 4 hours current on to a temperature of 80 C and then current off for 4 hours. Fig. 18 shows the results of 210 days of load cycling as measured by power factor at 22.5 kv and by ionization factor. Ionization factor is the difference between the power factor measured at 2.5 kv and 25-kv test voltage.

Results show stability of both power factor and ionization factor after 210 days of testing. The slight increase in power factor at the start of the test may be attributed to some additional crosslinking of insulation molecules during the application of temperature and voltage. After this crosslinkage is completed, the power factor of the insulation returns to the original value.

Fig. 19 shows the relation of test voltage to insulation power factor at both room and 80 C conductor temperatures and at the start and completion of the load cycling test. Table VIII gives a summary of the results of Fig. 18 and shows the minimum and maximum values of power factor for the five samples reported. It is also of interest to note that these samples showed no corona at 26 kv (limit of laboratory test equipment) at the start of the test and also showed none at 26 kv after completion of the 210 days of load cycling.

Operating Experience

In the 10 years from 1944 to 1955, a total of 13,500,000 conductor feet of butyl rubber-insulated power cable was produced by the company with which the authors are associated. This ranges in conductor size up to and including 1,500,000 circular mils, and in voltage rating up to and including 15-kv ungrounded neutral. Fig. 20 shows that this represents 10,270 mile-years of operation. Although the early service experience was relatively unsatisfactory because of unforeseen difficulties in applying the new material, and which resulted in numerous replacements, the program of better shielding and corona level testing, coupled with improved manufacturing techniques, has resulted in a service record which is excellent. Included in the total produced since 1949 is 2,800,000 feet of 15-kv cable which has operated with only one service failure attributable to a manufacturing defect.

Table VIII. Load Cycle Aging Test of Butyl-Insulated Cables With Continuous Overvoltage

Days on Test	Power Factor at 22.5 Kv					
	Room Temperature			80 C Temperature		
	Minimum	Average	Maximum	Minimum	Average	Maximum
0	0.97	1.00	1.01	1.31	1.37	1.45
52	1.27	1.37	1.72	1.70	2.02	2.72
122	1.10	1.16	1.50	1.39	1.65	2.36
210	0.77	0.92	1.21	0.89	1.22	1.88

Cable: Single-conductor, no. *2/0* AWG semiconducting tape, 29/64-inch butyl rubber semiconducting tape, copper shielding tape, 6/64-inch neoprene jacket.

Continuous voltage: 21.6 kv to ground.

Temperature cycles: Four hours with current on to 80 C and 4 hours with current off to room temperature.

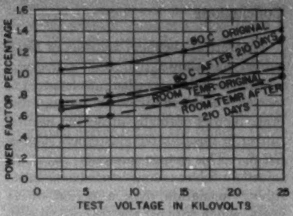

Fig. 19. Overvoltage load cycle aging test. Relation of insulation power factor and voltage. Same conditions as in Fig. 18

Therefore, although this insulation is relatively new in comparison with the older types of natural rubber and oil-base compounds, it seems apparent that its inherent characteristics, as well as the widespread utilization to date, will make it even more attractive to power cable users in the future. As stated at the start the prewar rubber compounds have enjoyed an enviable record of service. However, it is doubtful that they have been called upon to operate up to full capacity for a very large percentage of their life. Certainly they have not been subjected to the types of overloads cited in this paper. Yet it is well known from annual statistics that the kilowatt-hour output per kw of installed capacity has been steadily increasing for the last 20 years. It is therefore a safe assumption that a great many cables in the past have operated at full capacity only a small percentage of the time that they will be fully loaded in the future. This means that for a given maximum allowable copper temperature, the over-all average temperature will be considerably higher than it was 20 or 30 years ago. If this average is in the order of 10 C, it is probable that the life of cables utilizing the older types of insulation will be cut in half. The increased loads and overloads of the future will require such "tailor-made" insulations as butyl rubber.

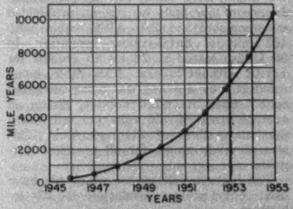

Fig. 20. Record of cumulative service of butyl rubber-insulated cable by one manufacturer

Conclusions

Theoretical chemical analysis of butyl rubber has shown that it is a material which provides excellent resistance to oxygen, ozone, sunlight, heat aging, and other factors normally attacking natural rubber or unsaturated elastomers such as *GR-S.* This paper presents data obtained on cables manufactured with butyl rubber insulation over a period of 11 years, which support the theoretical conclusion as to the excellence of this material when used as a high-voltage solid dielectric. From these data, it is concluded that:

1. Butyl-rubber-insulated cables have exceptional resistance to the effects of oxygen and ozone.

2. Butyl-rubber-insulated cables show no evidence of sunchecking or surface weathering after long-time exposure to moderately corrosive industrial atmospheres.

3. Extended temperature tests, up to $5^{1}/_{2}$ years, and numerous accelerating aging tests prove the ability of butyl-rubber-insulated cables to withstand heat aging. These data permit the service operation of the cables up to 90 C conductor temperature at 600 volts, and 85 C conductor temperature for voltages from 601 to 15,000 volts, with the assurance of long economic life. These as well as load cycle aging tests demonstrate the ability of the cables to operate up to 125 C conductor temperatures (depending on voltage rating) for emergency loading conditions for periods of 100 hours per year.

4. Butyl-rubber-insulated cables have exceptional resistance to moisture absorption at elevated temperatures.

5. Assured absence of internal ionization in cable constructions is essential, particularly at higher voltages. Use of corona extinction voltage-detecting equipment results in improved cable design and provides assurance of freedom from internal ionization when it is used as a quality control procedure.

6. Dielectric strength of butyl-rubber-insulated cable is more than adequate for all service conditions.

   The impulse strength is greater than that required by AIEE basic insulation levels for circuits in which these cables are used. Since switching surges are very seldom encountered of magnitude of more than five to seven times normal voltage, Fig. 14 shows that butyl-insulated cables have switching surge strengths in excess of those normally expected.

   Flexing tests show that bending of properly designed butyl cables does not affect their dielectric strength.

   Dielectric strength is not affected by temperature aging.

7. Butyl-rubber-insulated cables designed with proper types of conductor and insulation shielding retain their ionization levels after bending and temperature cycles.

8. Load cycle testing, with and without overvoltage, demonstrates the ability of butyl-rubber-insulated cables to retain their excellent thermal and electrical properties under conditions of thermal expansion.

9. Experience from 1944 to 1955 on a total of over 10,000 conductor-mile years of service operation of butyl-rubber-insulated cables has provided confirmation of laboratory evaluations.

References

1. **R. M. Thomas, D. C. Field.** *United States Patent no. 2,273,158*, 1939.

2. **W. J. Sparks, R. M. Thomas.** *United States Patent no. 2,356,128*, 1939.

3. **Butyl Rubber—A New Hydro Carbon Product, R. M. Thomas, I. E. Lightbrown, W. J. Sparks, P. K. Frolich, E. V. Murphree.** *Industrial and Engineering Chemistry*, Easton, Pa., vol. 32, 1940, p. 1283.

4. **W. H. Smyers.** *United States Patent no. 2,226,590*, 1937.

5. *ASTM Specification D574-54T.* American Society for Testing Materials, Philadelphia, Pa.

6. *ASTM Specification D1352-54T, Ibid.*

7. **Moisture Versus Rubber Insulation, R. B. McKinley, C. H. Seaberg.** *General Electric Review*, Schenectady, N. Y., vol. 55, 1952, p. 56.

8. **Moisture Studies on Ozone-Resisting and Type RH-RW Rubber Insulations, E. C. DeBaene, C. A. Anderson.** *AIEE Transactions*, vol. 73, pt. III-B, 1954 (Feb. 1955 section), pp. 1746–54.

9. **A Method for Detecting the Ionization Point on Electrical Apparatus, G. E. Quinn.** *AIEE Transactions (Electrical Engineering)*, vol. 59, Dec. 1940, pp. 680–82.

10. **The Measurement and Investigation of Ionization Level of Rubber Insulated Cables, R. C. Graham, E. K. Duffy, W. P. Foster.** *AIEE Transactions*, vol. 67, pt. II, 1948, pp. 1107–17.

11. **General Specifications for Wire and Cable with Rubber Insulation.** *IPCEA S-19-81*, Insulated Power Cable Engineers Association, Montclair, N. J., 1951.

12. **Impulse Strength of Insulated-Power-Cable Circuits, Herman Halperin, G. B. Shanklin.** *AIEE Transactions*, vol. 63, 1944, pp. 90–97.

◆

Discussion

William A. Del Mar (Phelps Dodge Copper Products Corporation, Habirshaw Wire and Cable Division, Yonkers, N. Y.): Some 7 years ago my company gave up the manufacture of oil-base insulation and changed to butyl rubber which seemed destined to supplant the older type because of the superior properties brought out in the paper. The electric strength was not as high as we would have liked, but it was ample. In one of our tests we ran an unshielded neoprene-sheathed 2/0 AWG cable with 160 mils of butyl-rubber insulation, in 30 C tap water at 25 kv to ground for 1 year without failure. This cable, being rated at 5 kv 3 phase, was being subjected to 8.7 times its rated voltage, giving an average stress of 156 volts per mil and a maximum stress of 211 volts/mil. This was certainly ample for all practical purposes.

The highest voltage for which we have used butyl-rubber insulation is 22 kv 3 phase.

The authors have alluded to their shielding practice and appear to begin external shielding at 10 kv. While the greater part of our output of 5-kv cable is unshielded, because so demanded by customers, it is significant that, in the last few years, both the quantity and the proportion of shielded cable has been steadily increasing. The reasons are probably safety to personnel, fewer faults from lightning, and from concentrations of charging current discharging to ground, and ease of locating faults by bridge methods.

Our preferred type of shielding is semiconducting tape covered with copper drain wires. The tape has conspicuously printed on it instructions to remove at joints and terminals.

R. C. Graham (Rome Cable Corporation, Rome, N. Y.): This paper is particularly commendable in that the authors have attempted to relate actual service experiences in addition to an analysis of a very complete series of laboratory tests. However, some clarification regarding experience with butyl might be added. The authors refer to first commercial application in 1944, but we believe this must have been very limited since only a few hundred pounds of butyl were legally available for wire and cable applications at that time. In fact, this material continued in relatively short supply and underwent many technical changes so that it has been only within the last 5 years that the compounds described have been available and produced.

The authors indicate that oil-base insulations "have given excellent service." Perhaps a few words about this service record would be appropriate inasmuch as it extends over a period greater than 50 years. This type of insulation has proved that it is satisfactory on signal, control, and power cables—either in the air or underground. In fact, most of our larger utilities and railroads specify such a material today. The authors present no evidence to substantiate why such an excellent record has been obtained. The data presented on butyl insulation are so overwhelming that by inference, the oil-base insulation has few qualifying characteristics. If test data do not reflect experience, then which should be questioned—the experience or the tests?

It is certainly a commendation and perhaps it is coincidence, but the authors of this paper as well as of the other two papers on butyl insulation,[1–2] have selected oil-base compound for their comparisons. It would be interesting if the comparison were made against other compounds such as a high-rubber-content heat-resistant rubber "submarine" compound, which, of course, would probably not be recommended for high-voltage applications, but by all of the reported tests (except ozone or corona resistance) would also show more favorable results than oil-base insulation.

In so far as ozone resistance is concerned, we believe that all authors have been guilty of a testing error which could lead to erroneous conclusions. The authors report ozone tests on 5,000-volt insulation wall thicknesses with no further coverings. I think that these authors will agree that most of the cable used today in this voltage class utilizes a neoprene jacket directly over and adherent to the underlying insulation. Industry specifications are quite clear that the ozone test on such a cable must be conducted with the jacket in place (due to possible damage of underlying insulation if removed) so that the test really discloses the ozone resistance of the neoprene jacket on the finished cable as it is used. It would, therefore, appear that a properly ozone-resistant sheath would be the important design factor and would be little affected by the ozone resistance of the underlying insulation, either oil-base or butyl.

The test data reported in the three papers on oil-base compounds indicate some reasonable uniformity, but the divergency of the results on the butyl compounds as reported are rather large by comparison. For example, original tensile strength values vary from 670 to 1,275 pounds per square inch, elongations from 400 to 720%, depreciation in aged elongation (7 days in 121 C oven) from 48 to 95.5% of the original. Similar divergency is noted in dielectric strength results where the various authors do not seem in unanimous agreement, particularly in so far as comparison with oil-base insulation is concerned.

Perhaps this indicates that there is an appreciable difference between different butyl compounds which should be recognized. As one manufacturer of butyl-insulated cable, we are aware that uniformity of butyl rubber itself is still one of the important requirements to any assessment of its properties. Long experience has proved that careful control is necessary to manufacture satisfactorily the oil-base insulation which does not readily lend itself to ordinary and conventional methods. With this background, the uniformity and performance of oil-base compounds are unexcelled as tested in all the years of growth of the electrical industry in the United States and abroad.

In regards to the superiority of butyl compounds on heavy overloads, I presented a paper[3] as part of an AIEE Insulated Conductor Committee report wherein both ozone-resistant insulations (butyl and oil-base) had the same limiter maximum design temperature at 220 C whereas conventional *RW-RH* rubber compound had a design temperature of 265 C. These temperatures were agreed upon from the combined test data submitted by several cable manufacturers.

Regarding the continuous operating temperature of 85 C for butyl insulation, do the authors recommend a more heat-resistant neoprene jacket than that now used on oil-base-insulated cables rated at 70 C?

I have also been involved in tests and use of butyl insulation and must agree with all authors that this material should also provide an excellent high-voltage cable insulation for somewhat higher continuous operating temperatures than now generally used. Experience alone will prove the validity of the tests.

References

1. Some Performance Characteristics of High-Voltage, Rubber Insulated Cables, S. J. Rosch. *AIEE Transactions*, vol. 74, pt. III, Dec. 1955, pp. 1217–23.

2. Modern High-Voltage Rubber-Insulations, W. H. Couch, G. H. Hunt, N. D. Kenney, P. H. Ware. *Ibid.* (*Paper 55–693*).

3. Overload Classifications for Secondary Network Cables, R. C. Graham. *Ibid.*, Oct. 1955, pp. 916–19.

G. S. Eager, Jr. (General Cable Corporation, Bayonne, N. J.): It is important to realize, as is the case with oil-base rubber, butyl rubber can be compounded in many ways to give great variations in properties. A high-grade butyl compound should give the best compromise of electrical, physical, aging, corona, and moisture resistant properties. In analyzing this paper, we are led to believe that the authors are presenting data on a particular compound; and if they are, this compound appears to have many desirable properties required for a high-voltage rubber-insulated power cable. However, very little data are given on the electrical moisture resistance and no data are given on the mechanical moisture absorption; and as will be indicated later, the a-c breakdown is quite low. Our company has evaluated commercial samples of butyl cables made by many manufacturers and have found many to have over-all high quality, but some to have serious failings in one or more respects. For example, one manufacturers cable (no. *1* AWG, 22/64-inch insulation thickness) failed at the test potential of 40 volts per mil after only 180 days' immersion in tap water at 50 C. The mechanical moisture absorption was 100.5 milligrams per square inch when tested 7 days in water at 70 C. Samples from some other manufacturers, however, had excellent mechanical and electrical moisture resistance. Another sample (350,000-circular-mil, 10/64-inch insulation thickness) had an a-c breakdown less than 180 volts per mil average stress at 60 cycles per second, which is very low.

The a-c breakdown data presented in Table III indicate relatively low values for high-voltage rubber insulation. The data presented under 5 minutes presumably were obtained as specified by the Insulated Power Cable Engineers Association (IPCEA) Standard *S-19-81* (but modified to start at factory test voltage in place of twice factory a-c test voltage). When the IPCEA procedure is strictly followed, the minimum average voltage stress at breakdown is expected to exceed approximately 180 volts per mil (twice routine factory a-c test voltage). If the maximum stress values of Table III are translated to average values, they are much lower and in some cases fail by a large degree to exceed the minimum expected value of 180 volts per mil. Take, for example, the no. *2* AWG conductor having a wall thickness of 39/64 inch, the average value of voltage stress is only 125 volts per mil; also the no. *6* AWG conductor having a wall thickness of 16/64 inch, the average stress is only 145 volts/mil. The starting voltage equal to factory routine in place of twice factory routine alternating voltage accounts only to a small degree for the low values. (Note Fig. 14 of the paper which indicates that for times between 5 and 15 to 25 minutes the breakdown values do not differ greatly.) Our experience with butyl insulation of our own manufacture has been that regular production cables have an average a-c breakdown strength greatly exceeding the expected 180 volts per mil value.

The impulse voltage breakdown values presented in Fig. 15 are somewhat misleading. Our experience has been that the impulse strength of natural-rubber oil-base compounds is much higher than that indicated by curve *C* of Fig. 15. The relatively low values given by curve *C* perhaps can be explained by the fact that these data were taken from cables manufactured in the early 1940's and considerable improvement has been made in the last 15 years. With reference to impulse voltage breakdown, our experience with butyl insulation has been that it considerably exceeds the values given in curves *B* and *C* of Fig. 15.

J. C. Carroll, A. R. Lee, and R. B. McKinley: Mr. Del Mar has commented on the dielectric strength of butyl-rubber-insulated power cables and has given some data. The authors certainly agree with Mr. Del Mar's conclusion to the effect that the dielectric strength of butyl-rubber-insulated power cables when properly designed and manufactured is more than adequate to meet all conditions of service. In regard to Mr. Del Mar's comment concerning the use of external shielding, the authors believe Mr. Del Mar has misunderstood one portion of the paper. In the section of the paper under the subject "Corona Detection and Control" it is pointed out that the use of semiconducting material over the insulation is mandatory at voltages of 10 kv and above. This does not mean that insulation shielding is not used below this value. It is the practice of the authors' company to supply metallic shielding on cables rated above 5 kv, and a great deal of cable in the 5-kv class is also supplied with shielding. In many instances, even below the 10-kv level, semiconducting tapes are used between the insulation and the metallic shield.

Mr. Graham has raised several interesting questions and comments. In reference to the experience obtained by the authors on field service of butyl-insulated power cables it should be noted from Fig. 20 that millions of feet of this type of cable were supplied prior to 1950. Changes have been made during the entire history outlined in the paper since this is the only way that technological progress can be made. In regard to the question as to why the oil-base insulations have attained such an excellent service record, we feel, as stated in the paper, that it is doubtful that these cables have been called upon to operate to full capacity for a very large percentage of their life. The authors cannot agree with Mr. Graham that ozone-resistance tests on butyl-rubber-insulated power cables without external coverings is a testing error since the ozone-resisting qualities of rubber insulations must be an important factor in consideration of its characteristics. There are many designs of cable for high-voltage operation that must be assured of inherent ozone resistance of the insulation itself. In the case of shielded cables with or without an external jacket it is important that ozone resistance be built into the insulation in case of accidental damage or corrosion of the shield. Even in the case of cables which have an adherent neoprene jacket directly over the insulation it is important that ozone resistance be built in as a secondary defense if the neoprene fails due to ozone cracking. In respect to Mr. Graham's comment on the divergence of results reported in the various papers on this subject, we can only point out that he has answered his own question, inasmuch as it is known that varying results can be obtained depending upon the design of the insulation and also the cable itself. In the work that the authors' company has done a balanced compound has been obtained that will give excellent service under all conditions. The authors believe that a properly compounded neoprene jacket is satisfactory for use with butyl-rubber-insulated power cables rated at 85 C.

The comment by Mr. Graham concerning the performance of butyl-rubber insulation on secondary network cables should be clarified. The overload temperature ratings given in this paper apply to long-time overloading up to 100 hours per year, which is allowed throughout the life of the cable and without materially effecting the life of the cable. The limit for operating temperature on secondary networks is intended for short-time (4 hours) operation and it is acknowledged that such cables will be damaged since the criterion for setting these temperatures is visual damage in the insulation. These two temperature ratings cannot, therefore, be considered on the same basis.

Mr. Eager has raised a question as to the moisture resistance of the butyl-insulated cable both from a mechanical and electrical standpoint. Figures 8, 9, and 10 of the paper give electrical data under conditions of long-time immersion in water and were included because the authors felt that long-time test data would be of more interest to users than the short-time 2-week test normally used by the industry for production control. Many short-time tests have been made by the authors' company but lack of space in a paper of such length ruled against the inclusion of these data as well as mechanical moisture-absorption results. It should be noted, however, that butyl-rubber-insulated power cables now being manufactured by the authors' company consistently run less than 0.010 gram per square inch as determined by the gravimetric method of moisture resistance. In regard to Mr. Eager's comments on the two cables which showed test failures at an average stress below 180 volts per mil, we have the following comments: We plead guilty to an error in the case of the no. *2* AWG conductor with a wall thickness of 39/64-inch. In checking back on the records we find that a value was picked from the wrong column of figures, that no such test was ever made on this cable, and the value should not have been included. In respect to the no. *6* conductor with a wall thickness of 16/64-inch it might be noted that this was a sample of a very early design that did not include semiconducting material at the conductor surface and at the insulation surface. It should be noted, however, that the omission of these two points on the curve will not affect the shape of the curve nor will it in any way detract from the conclusion that butyl-rubber-insulated power cables have more than sufficient dielectric strength for all conditions of service. In regard to Mr. Eager's comment on the impulse voltage breakdown values of Fig. 15, it should again be pointed out that curve *C* was reproduced from the Halperin-Shanklin paper for ordinary grades of rubber insulation. The referenced paper does include data on oil-base insulations indicating their average breakdown under impulse conditions to be somewhat higher than for ordinary grades of rubber. However, the test data available and presented in that paper showed such a spread of results that the minimum breakdown of oil-base insulations was not significantly different to allow higher withstand values of impulse strength to be set up. Curve *A* of this paper for butyl-rubber-insulated power cables is also well in excess of both curves *B* and *C* and may be considered as a minimum breakdown curve for this type of cable.

REFERENCE

1. See reference 12 of the paper.

Equivalent Circuit for the Concatenation of Induction Motors

Y. H. KU
FELLOW AIEE

THE equivalent circuit of an induction motor under steady-state operation is well known.[1] Let $F=f/f_0$=ratio of actual to normal frequency. The equivalent circuit is shown in Fig. 1 which is a simplified diagram of Fig. 1 in reference 2.

In Fig. 1 are the following terms:

$n=1-s$=ratio of actual to synchronous speed
R_s+jX_s=impedance of stator windings
R_r+jX_r=impedance of rotor windings
X_m=magnetizing reactance
I_s=stator current
I_r=rotor current
V=voltage source

The steady-state relation between the voltage of the source and the stator current of the motor is

$$\frac{V}{F}=I_s\left[\frac{R_s}{F}+jX_s+\frac{1}{\dfrac{1}{jX_m}+\dfrac{F-n}{R_r+j(F-n)X_r}}\right] \tag{1}$$

As discussed in reference 2, equation 1 also applies to transient conditions, if the per-unit line frequency F is replaced by $-jp$, where p is the time differential operator $d/\omega dt$, where $\omega=2\pi f_0$ and time is measured in electrical radians instead of in seconds.

The equivalent circuit that is applicable to transient conditions is shown in Fig. 2. Notice that for $f=f_0$ at synchronous speed, $F=1$ and $F-n=1-n=s$ in Fig. 1. For steady-state operation, $-jp$ in Fig. 2 is also equal to 1, and $-jp-n=s$, the slip. Here the differential operator p operates on the stator current which is of fundamental frequency in the steady state. In terms of Laplace transforms

$$V(p)=Z(p)I_s(p) \tag{2}$$

where $V(p)$ and $I_s(p)$ are the Laplace transforms of the voltage source and the stator current, and

$$Z(p)=R_s+pX_s+\frac{pX_m[R_r+(p-jn)X_r]}{R_r+(p-jn)(X_r+X_m)} \tag{3}$$

It will be shown that by suitably modi-

Paper 55-675, recommended by the AIEE Rotating Machinery Committee and approved by the AIEE Committee on Technical Operations for presentation at the AIEE Fall General Meeting, Chicago, Ill., October 3-7, 1955. Manuscript submitted January 31, 1955; made available for printing July 18, 1955.

V. H. Ku is with the Moore School of Electrical Engineering, University of Pennsylvania, Philadelphia, Pa.

All the oscillographic records were taken on a Westinghouse 9-element oscillograph at Tsing Hua University, Peiping, China.

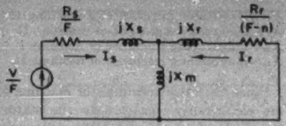

Fig. 1. Equivalent circuit of induction motor

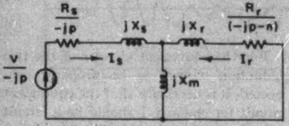

Fig. 2. Equivalent circuit applicable to transient conditions

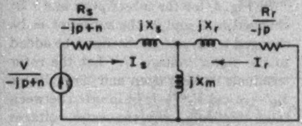

Fig. 3. Modified equivalent circuit

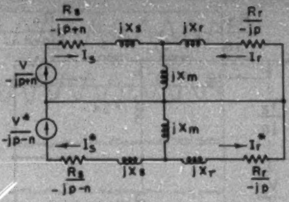

Fig. 5. Positive-sequence and negative-sequence equivalent circuits referring to the rotor

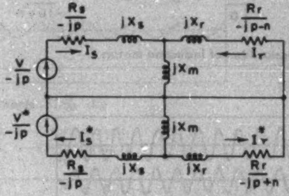

Fig. 6. Positive-sequence and negative-sequence equivalent circuits referring to the stator, for transient conditions

fying the equivalent circuit shown in Fig. 2 and combining two equivalent circuits for the two induction motors in concatenation, an equivalent circuit for the system of two machines can be obtained. The behavior of the two machines can then be studied from the final equivalent circuit. An actual example will be given showing the check between experimental and calculated results of transient currents and transient power.

Equivalent Circuit Referring to Rotor

If the stator current is referred to the rotor, the equivalent circuit that is applicable to transient conditions can be obtained by substituting $-jp$ for $F-n$ or $-ip+n$ for F in Fig. 1. The modified equivalent circuit is shown in Fig. 3. For steady-state operation, the stator current viewed from the rotor as a reference frame will appear to have the same frequency as the rotor current, which is of slip frequency. Hence $-jp$ in Fig. 3 corresponds to s and $-jp+n$ corresponds to $s+n=1$, which values check with $F=1$ and $F-n=s$ in Fig. 1.

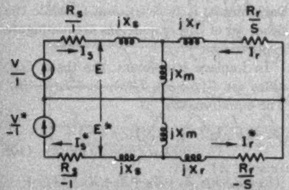

Fig. 4. Positive-sequence and negative-sequence equivalent circuits for steady-state operation

If $V(p+jn)$ and $I_s(p+jn)$ represent the Laplace transforms of $V\epsilon^{-jnt}$ and $I_s\epsilon^{-jnt}$ respectively, the operational or transform equations for the induction motor are

$$[R_s+(p+jn)(X_s+X_m)]I_s(p+jn)+(p+jn)X_mI_r(p)=V(p+jn) \quad (4)$$

$$[R_r+p(X_r+X_m)]I_r(p)+pX_mI_s(p+jn)=0 \quad (5)$$

Solving $I_r(p)$, the Laplace transform of I_r, from equation 5 and substituting in equation 4, there is

$$V(p+jn)=Z(p+jn)I_s(p+jn) \quad (6)$$

where

$$Z(p+jn)=R_s+(p+jn)(X_s+X_m)-\frac{p(p+jn)X_m^2}{R_r+p(X_r+X_m)} \quad (7)$$

Notice that the expression given in equation 7 is either obtained by substituting $-jp+n$ for F in equation 1 or obtained by substituting $(p+jn)$ for p in equation 3. In fact, equation 6 is directly obtainable from equation 2 by Heaviside's "shifting formula" or by "complex translation" in Laplace transforms.

It may be pointed out here that $Z(p)$ given by equation 3 represents the positive-sequence operational impedance of the induction machine,[3] and a conjugate expression (with respect to p) represents the negative-sequence operational impedance of the induction machine.

In Fig. 4, both positive-sequence and negative-sequence equivalent circuits are shown for steady-state operation. Similarly, Fig. 5 shows both sequence equivalent circuits referring to the rotor and Fig. 6 shows both sequence circuits referring to the stator, for transient conditions.

Concatenation of Induction Motors

The diagram of connections for concatenation of two polyphase induction motors is shown in Fig. 7. The rotor terminals of machine I are electrically connected to the stator terminals of machine II. The two rotors are mechanically coupled and are running at the same speed.

Let

i_1 = stator current of machine I
i_2 = rotor current of machine I
i_3 = stator current of machine II
i_4 = rotor current of machine II
V_1 = voltage at stator terminals of machine I
V_2 = voltage at rotor terminals of machine I
V_3 = voltage at stator terminals of machine II
R_1+jX_1 = stator impedance of machine I
R_2+jX_2 = rotor impedance of machine I

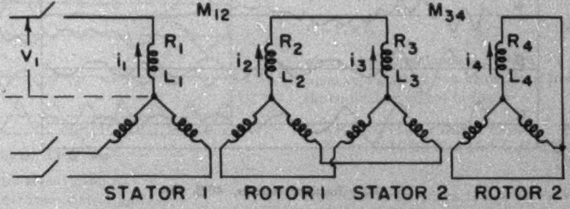

Fig. 7. Diagram of connections for concatenation of induction motors

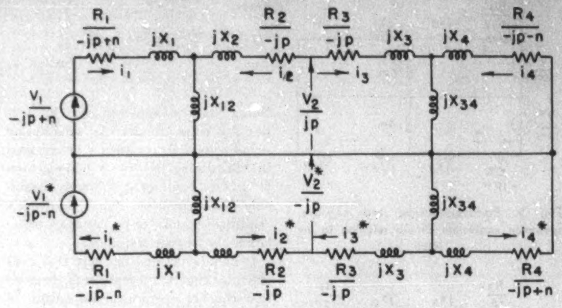

Fig. 8. Equivalent circuit for concatenation of induction motors

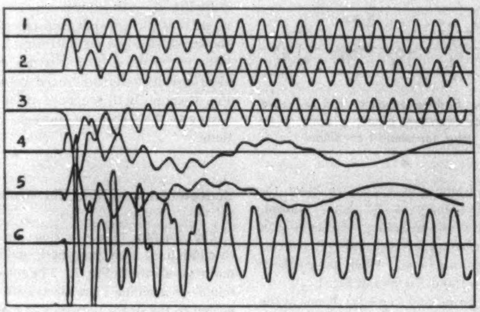

Fig. 9. Transient currents, 10% slip

1—Line voltage V
2, 3—Stator current i_1
4, 5—Rotor current i_2
6—Rotor current i_4

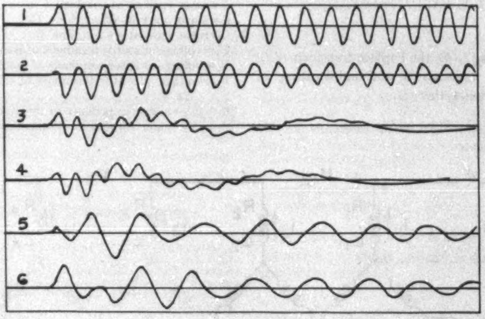

Fig. 10. Transient currents, 40% slip

1—Line voltage V
2—Stator current i_1
3, 4—Rotor current i_4
5, 6—Rotor current i_2

R_3+jX_3 = stator impedance of machine II
R_4+jX_4 = rotor impedance of machine II
X_{12} = magnetizing reactance of machine I
X_{34} = magnetizing reactance of machine II

Since the rotor terminals of machine I are electrically connected to the stator terminals of machine II, the following relations exist

$$i_2=-i_3 \qquad (8)$$

$$V_2=V_3 \qquad (9)$$

For the equivalent circuits of the two induction motors to be properly connected, it is necessary that the equivalent circuit for machine I should be a circuit referring to its rotor as in Fig. 5, and that the equivalent circuit for machine II should be a circuit referring to its stator as in Fig. 6.

In Fig. 5, let the subscripts s and r be changed to 1 and 2, the subscript m be changed to 12, and a subscript 1 be added to the stator voltage V. Let the rotor terminals be kept open and the voltages $V_2/-jp$ and $V_2^*/-jp$ be inserted between these terminals, as in the stator voltages shown in Fig. 6.

In Fig. 6, let the subscripts s and r be changed to 3 and 4, the subscript m be changed to 34 and a subscript 3 be added to the stator voltage V and its conjugate V^*.

According to the relations given in equations 8 and 9, the right end terminals of Fig. 5 (i.e., the rotor terminals of machine I) with inserted voltages $V_2/-jp$ and $V_2^*/-jp$ are then connected to the left end terminals of Fig. 6 (i.e., the stator terminals of machine II) with terminal voltages $V_3/-jp$ and $V_3^*/-jp$. The interconnection of these two equivalent circuits for the two induction motors in concatenation results in a single equivalent circuit as shown in Fig. 8.

In Fig. 8, it is seen that $i_2=-i_3$ and $V_2=V_3$.

A total of six operational or transform equations can be written by inspection of the equivalent circuit. For balanced operation, one set of three loop equations are sufficient to solve for the three variables i_1, i_2 $(=-i_3)$, and i_4, while the other set of three equations are conjugate expressions.

In Laplace transforms, the three variables are $I_1(p+jn)$, $I_2(p)$, and $I_4(p-jn)$. The equations are

$$[R_1+(p+jn)(X_1+X_{12})]I_1(p+jn)+(p+jn)X_{12}I_2(p)=V_1(p+jn) \qquad (10)$$

$$[(R_2+R_3)+p(X_2+X_{12}+X_3+X_{34})]I_2(p)+pX_{12}I_1(p+jn)-pX_{34}I_4(p-jn)=0 \qquad (11)$$

$$[R_4+(p-jn)(X_4+X_{34})]I_4(p-jn)-(p-jn)X_{34}I_2(p)=0 \qquad (12)$$

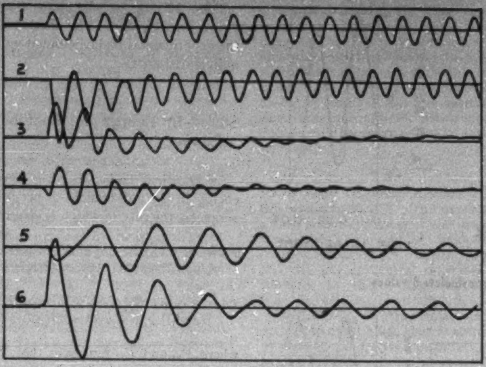

Fig. 11. Transient currents 53% slip

1—Line voltage V
2—Stator current i_1
3, 4—Rotor current i_3
5, 6—Rotor current i_4

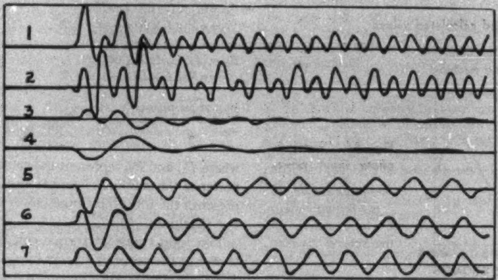

Fig. 12. Transient power, 53% slip

1—Power from i_{1a} and V_{ab}
2—Power from i_{1c} and V_{bc}
3—Rotor current i_4
4—Rotor current i_3
5—Stator current i_{1a}
6—Stator current i_{1c}
7—Line voltage V_{ab}

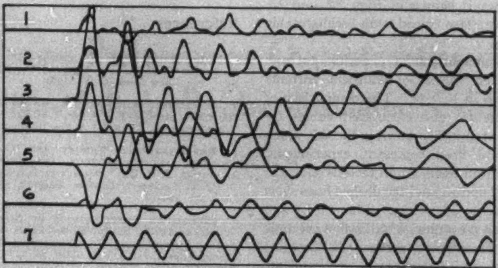

Fig. 13. Transient power, 53% slip

1—Power from i_{2c} and V_{2bc}
2—Power from i_{2a} and V_{2ab}
3—Rotor current i_4
4—Rotor current i_{2c}
5—Rotor current i_{2a}
6—Stator current i_{1a}
7—Line voltage V

Note the inverse transforms of $I_1(p+jn)$, $I_3(p)$ and $I_4(p-jn)$ are i_1e^{-jnt}, i_3 and i_4e^{jnt} respectively.

By solving equations 10, 11, and 12 simultaneously by operational calculus or Laplace transforms, the transient currents in the stator and rotor windings of the two machines can be obtained for different operating speeds.

Transient Power

It is well known that the equivalent circuit shown in Fig. 1 or Fig. 4 gives relations of power and torque under steady-state operation. The steady-state input power to the stator is given by the product of V and I_s (both magnitudes) times the cosine between the phasors $\bar{V}$ and $\bar{I}_s$. This relation is sometimes expressed as the dot product of $\bar{V}$ (or $\bar{V}_1$) and $\bar{I}_s$(or $\bar{I}_1$). The power received by the rotor, according to the equivalent circuit given in Fig. 4, is $I_r^2(R_r/s)$. Subtracting the rotor resistance losses $I_r^2R_r$, the available power that is convertible into mechanical power is $I_r^2(1-s)(R_r/s)$. Now the per-unit torque is equal to the per-unit power divided by per-unit actual speed. Hence the per-unit torque is numerically equal to $I_r^2(R_r/s)$. Similarly, subtracting the stator resistance losses $I_s^2R_s$ the available power that is transferable across the air gap can be given as the dot product of E (Fig. 4) and $\bar{I}_s$, where $\bar{E}$ is equal to $\bar{V}-I_sR_s$.

The equivalent circuit given in Fig. 8 gives also the correct relations of power under transient operation. The input power to the first machine can be expressed as

$$P_1 = V_1 \times I_1 \tag{13}$$

where V_1 and I_1 represent the instantaneous voltage and current expressions which consist of sinusoids and damped sinusoids in general cases. A factor of 3/2 should be added to the right-hand side of equation to get 3-phase power, since the maximum values of voltage and current waves are used.

The input power to the second machine is

$$P_2 = V_2 \times I_2 \tag{14}$$

where the instantaneous voltage V_2 is equal to V_3, which can be obtained from the equivalent circuit in Fig. 8.

$$\begin{aligned} V_2 = V_3 &= [R_2+(X_2+X_{12})p]I_2+X_{12}p(I_1\angle -nt) \\ &= [R_3+(X_3+X_{34})p]I_3+X_{34}p(I_4\angle nt) \end{aligned} \tag{15}$$

Note that in equations 14 and 15 V_2, V_3, I_1, I_2, I_3 and I_4 all consist of sinusoids and damped sinusoids, $I_1\angle -nt$ denotes that

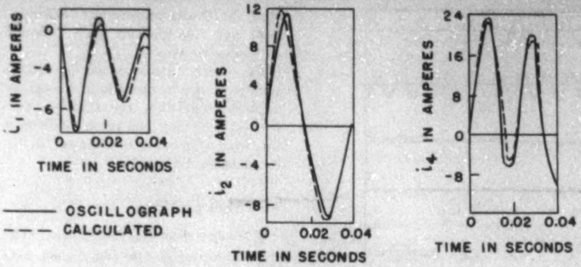

Fig. 14. Comparison of experimental and calculated values

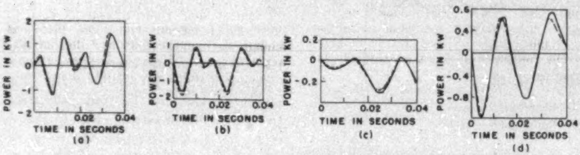

Fig. 15. Comparison of experimental and calculated values

A, B—Input power to the first machine
C, D—Input power to the second machine

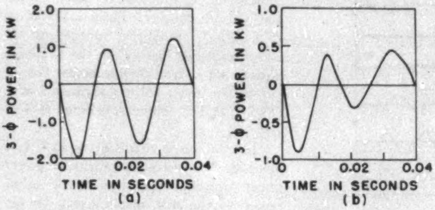

Fig. 16. Total 3-phase input power

A—Input power to the first machine
B—Input power to the second machine

the different components of I_1 are referred to the rotor of machine I, $I_4\underline{/nt}$ denotes that the different components of I_4 are referred to the stator of machine II, and p is the time differential operator.

Experimental Check

Two identical induction motors were used in the actual experiments. The constants are

$R_1 = R_3 = 1.141$ ohms

$R_2 = R_4 = 0.437$ ohm

$X_{12} = X_{34} = 45.8$ ohms

$X_1 = X_3 = 97.3$ ohms

$X_2 = X_4 = 22.9$ ohms

$\omega = 314$

The transient currents in the stator and rotor windings are shown in Figs. 9, 10, and 11 for 10 per cent (%) slip, 40% slip and 53% slip, respectively. The figures are traced from the oscillographic records taken some time ago. In each case, curve 1 represents the line voltage. The transient power input to the first and second machines is shown in Figs. 12 and 13, which are also traced from oscillographic records.

The comparison of experimental and calculated values for transient currents is shown in Fig. 14. The comparison of experimental and calculated values for transient power is shown in Fig. 15, where the solid lines represent experimental values from oscillograph records shown in Figs. 12 and 13, and the dashed lines show the calculated values. Fig. 15(A) and (B) show power input to the first machine by the 2-wattmeter method; (C) and (D) show power input to the second machine.

Fig. 16 shows the total 3-phase power input to the first machine and the second machine; (A) the input power to the first machine, and (B) the input power to the second machine.

Figs. 12 to 16 all show transient power for 53% slip. The check between the experimental and calculated values is quite satisfactory.

Stored-Up Energy and Rotational Power

In transient cases, there is stored-up energy in the inductances or per-unit reactances, the rate of which is given by

$$P_{1s} = (X_1 + X_{12})[I_1(pI_1)] + (X_2 + X_{12}) \times [I_2(pI_2)] + p[(X_{12} \cos nt)(I_1 \times I_2)] \quad (16)$$

$$P_{2s} = (X_3 + X_{34})[I_3(pI_3)] + (X_4 + X_{34}) \times [I_4(pI_4)] + p[(X_{34} \cos nt)(I_3 \times I_4)] \quad (17)$$

where P_{1s} and P_{2s} represent the rates of stored-up energy in the inductances of machines I and II.

The transient power that contributes to the rotational energy is given by

$$P_{1r} = (I_1 \times I_2)(pX_{12} \cos nt) = nX_{12}(I_1 \times I_2)\underline{/-nt-\pi/2} \quad (18)$$

$$P_{2r} = (I_3 \times I_4)(pX_{34} \cos nt) = nX_{34}(I_3 \times I_4)\underline{/-nt-\pi/2} \quad (19)$$

$$P_r = P_{1r} + P_{2r} = n[X_{12}(I_1 \times I_2) + X_{34}(I_3 \times I_4)]\underline{/-nt-\pi/2} \quad (20)$$

where P_{1r} and P_{2r} represent the rotational power of the machines I and II and P_r represents the total rotational power of the two machines.

The total transient torque can be obtained in the per-unit system by dividing P_r in equation 20 by the per-unit actual speed $n = 1 - s$. For further discussion about the rate of stored-up energy and rotational power, refer to the Appendix of reference 4, part 5, and Appendix III of reference 4.

References

1. The Nature of Polyphase Induction Machines (book), P. L. Alger. John Wiley & Sons, Inc., New York, N. Y., 1951.

2. Switching Transients in Wound Rotor Induction Motors, P. L. Alger, Y. H. Ku. *AIEE Transactions*, vol. 73, pt. III-A, Feb. 1954, pp. 19–27.

3. Revolving-Field Theory and General Analysis of Synchronous and Induction Machines, Y. H. Ku. *Proceedings*, Institution of Electrical Engineers, London, England, vol. 99, 1952, pp. 410–27.

4. Studies on Concatenation of Induction Machines, IV, Y. H. Ku, T. S. Chu, S. S. Sun. *Science Reports*, Tsing Hua University, Peiping, China, series A, vol. 4, Sept. 1940, pp. 233–42.

5. Transient Analysis of Rotating Machines and Stationary Networks by Means of Rotating Reference Frames, Y. H. Ku. *AIEE Transactions*, vol. 70, pt. I, 1951, pp. 943–57.

6. Equivalent Circuits of Electric Machinery (book), G. Kron. John Wiley & Sons, Inc., New York, N. Y., 1951.

Discussion

T. J. Higgins (University of Wisconsin, Madison, Wis.): The paper both comprises an interesting use of Laplace transform theory for determination of the transient responses in two concatenated induction motors and an evidence of the usefulness of equivalent circuits for study of the transient performance of rotating machines.

The curves of Fig. 14 encompass a gratifying agreement between measured values of current response (by oscillograph) and calculated values (presumably, from the time expressions obtained by inverting the transforms of the currents as obtained from solutions of equations 10, 11, and 12 and substitution of the given numerical values in these time expressions). Again, the curves of Figs. 15 and 16 evidence very good agreement between measured values of power and corresponding values calculated from the instantaneous values of current and voltage.

These excellent agreements between corresponding measured and calculated values of current and power attest the correctness of the theory set out in the paper.

In conclusion, it may be of interest to note that the theory enabling calculation of power and energy flow by Laplace transform procedures has been advanced recently by the discusser.[1]

REFERENCE

1. LAPLACE TRANSFORM DETERMINATION OF ENERGY-FLOW IN TRANSIENT CIRCUIT ANALYSIS, T. J. Higgins, K. O. King. *Proceedings*, 1955 National Electronics Conference, Chicago, Ill. vol. 11, 1955.

Edward Erdelyi (Syracuse University, Syracuse, N. Y.): The author has shown in a masterly fashion how to develop the positive and negative sequence equivalent circuit for the transient performance of two concatenated induction motors from the simple steady-state equivalent circuit of the induction motor. The powerful method is also applicable to the calculation of other transient phenomena of induction motors.

The advantage of the method becomes apparent by comparing Fig. 7 and Fig. 8 of the paper. A conventional transient analysis based on Fig. 7 would involve a system of nine differential equations, the solution of which would demand considerable computational work. The author's method based on Fig. 8 involves only the solution of six simultaneous equations, which can be reduced easily to two systems of three equations each.

P. L. Alger (General Electric Company, Schenectady, N. Y.): The paper provides a very useful extension of the usual equivalent circuit theory of induction machines, to include both transient phenomena and the use of several machines and/or windings in series. The transformation from one machine or winding to any other, while keeping all the equations on the normal 60-cycle basis, that is accomplished by dividing the resistances and the voltages by the frequency ratio, is particularly interesting.

These methods apply equally well in the calculation of the effects of the air-gap field harmonics, which are especially important in part-winding starting.

It is my opinion that the use of induction machines with two or more distinct windings will grow, so that the theory given in this paper should be increasingly useful in the years ahead.

Y. H. Ku: I appreciate very much the valuable comments of Professors Higgins and Erdelyi and the important suggestion of Mr. Alger that "the theory given in this paper should be increasingly useful in the years ahead."

For a 3-phase induction machine, the differential equations are

$$R_s i_{sA} + L_s p i_{sA} + Mp\left[i_{rA}\cos nt + i_{rB}\cos\left(nt+\frac{2\pi}{3}\right) + i_{rC}\cos\left(nt-\frac{2\pi}{3}\right)\right] = v_{sA} \quad (21)$$

$$R_r i_{rA} + L_r p i_{rA} + Mp\left[i_{sA}\cos nt + i_{sB}\cos\left(nt-\frac{2\pi}{3}\right) + i_{sC}\cos\left(nt+\frac{2\pi}{3}\right)\right] = v_{rA} \quad (22)$$

where $p = d/dt$, the subscripts A, B, and C denote the voltages and currents in phases A, B, and C. In the per-unit system, L_s corresponds to $(x_s + x_m)$, L corresponds to $(x_r + x_m)$, and M corresponds to x_m in equations 4 and 5.

By means of symmetrical components, as pointed out by Professor Erdelyi, the foregoing set of equations is transformed to

$$R_s i_{s1} + L_s p i_{s1} + Mp(i_{r1}e^{-jnt}) = v_{s1} \quad (23)$$

$$R_r i_{r1} + L_r p i_{r1} + Mp(i_{s1}e^{-jnt}) = v_{r1} \quad (24)$$

where the subscript 1 denotes the positive-sequence component of voltage or current. It may be mentioned that there are four more equations like equations 21 and 22 for the stator and rotor phases B and C. Similarly, there are two more equations similar to equations 23 and 24 for the negative-sequence components. The positive and negative sequence sets of equations are conjugate to each other.

Taking the Laplace transforms term by term and assuming the system initially quiescent, equations 23 and 24 give

$$(R_s + L_s s)I_{s1}(s) + MsI_{r1}(s-jn) = V_{s1}(s) \quad (25)$$

$$(R_r + L_r s)I_{r1}(s) + MsI_{s1}(p+jn) = V_{r1}(s) \quad (26)$$

where $I_{s1}(s)$, $I_{s1}(s)$, $V_{r1}(s)$, and $V_{s1}(s)$ are the Laplace transforms of $i_{s1}(t)$, $i_{r1}(t)$, $v_{s1}(t)$, and $v_{r1}(t)$ respectively, and s represents the complex variable. (In the paper, p is used instead of s.) By the theorem of complex translation (which corresponds to Heaviside's shifting formula), equation 25 gives

$$[R_s + (s+jn)L_s]I_{s1}(s+jn) + M(s+jn)\times I_{r1}(s) = V_{s1}(s+jn) \quad (27)$$

which corresponds to equation 4 of the paper, while equation 26 corresponds to equation 5 of the paper. Dividing both sides of equation 27 by $-js+n$ and both sides of equation 26 by $-js$, the positive-sequence equivalent circuit is obtained as shown in Fig. 5.

Some Performance Characteristics of High-Voltage Rubber-Insulated Cables

S. J. ROSCH
ASSOCIATE MEMBER AIEE

THE past decade has seen a definite trend towards the use of nonmetallic-sheathed cables for service voltages from 2 to 15 kv. For insulation, such cables have been furnished with various types of rubber and rubberlike compounds as well as thermoplastic such as polyethylene. For nonmetallic sheathing, the most prevalent materials have been various compounds of neoprene. Occasionally, jackets have been made with acrylonitrile rubber but more recently, such coverings have been made of polyvinyl chloride (PVC), high-molecular-weight polyethylene, or a flame-retarding type of polyethylene.

Since the quantities of such cables purchased annually have reached many millions of feet and since the voltage limitation at which such cables are suitable has been discussed by some[1] as 35 kv and projected by others[2] as 66 or even 132 kv, it was felt that basic information of some of the performance character-

---

Paper 55-678, recommended by the AIEE Insulated Conductors Committee and approved by the AIEE Committee on Technical Operations for presentation at the AIEE Fall General Meeting, Chicago, Ill., October 3-7, 1955. Manuscript submitted March 8, 1955; made available for printing July 19, 1955.

S. J. ROSCH is with the Anaconda Wire and Cable Company, Hastings-on-Hudson, N. Y.

The author wishes to express his appreciation to his associates for having given of their time and comments in a review of this paper.

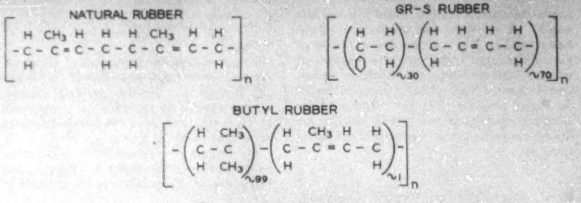

Fig. 1. Molecular structure

istics of the insulations used would be of interest. Accordingly, an investigation was carried out on the performance of a group of 5-kv cables representing the products of five different manufacturers. Subsequently, 15-kv cables of the same manufacturers were obtained to determine impulse dielectric strength. In the present paper, only high-voltage cables in which the insulation is of rubber or rubberlike compositions and the outer covering is neoprene are discussed.

Nature of Cables Investigated

In the case of the 5-kv cables, each length was a nonshielded single-conductor no. 8 American Wire Gauge cable rated at 5 kv for installation directly in the soil, aerially, or in underground ducts. Three are insulated with butyl rubber compounds and will, for the purpose herein, be referred to as *A*, *B*, and *C*. The other two are insulated with oil-base rubber compositions and will be referred to as *D* and *E*.

The 15-kv cables are from the same manufacturers and presumably insulated with the same compounds. All are metallically shielded 4/0 American Wire Gauge, except for length *A* which is 350,000 circular mils. In purchasing the various cables, care was taken that they were representative of commercial types having the foremost reputation for quality in their respective fields. Cable *E* could only be obtained with 25/64-inch insulation whereas all the others had standard industry thickness of 19/64-inch for 15-kv grounded neutral service.

Oil-Base Rubber Versus Butyl Compounds

Some discussion is necessary to explain the reasons why oil-base and butyl rubber insulations are being offered as insulation for high-voltage rubber-insulated cables.

Natural rubber, and the same is true for *GR-S* rubbers, have what is known chemically as double bonds, as shown in Fig. 1. It is the latter feature which makes natural and *GR-S* rubber capable of being readily vulcanizable, a feature which is also known chemically as the presence of "unsaturation." It is this very feature which makes these rubbers poor in resistance to attack by at least two chemical agents such as ozone and oxygen.

Natural rubber and *GR-S* rubber compounds can be given a high degree of resistance to the effects of contact with oxygen through blending with suitable chemicals known as antioxidants, but the latter have little effect on vulnerability to attack by ozone. Ozone resistance can only be imparted to such compounds by blending them with substantial quantities of vulcanized vegetable oils also known as factice, or similar materials. This has the effect of reducing the nerve of the rubber or bringing the latter into a state of relaxation. This also has the effect of substantially reducing the tensile properties of such compounds but does impart a degree of ozone resistance not inherent in the original rubber composition prior to blending with different types of factice.

Butyl rubber, on the other hand, contains few double bonds. It is a specially tailored polymer based on polyisobutylene (PIB) also known as Vistanex, which is thermoplastic and not vulcanizable, to which has been added from 1.0- to 2.5-per-cent unsaturation or just enough to enable compounds made from this polymer capable of being vulcanized. It is the presence of only this very small degree of unsaturation which accounts for the high degree of resistance to oxidation and ozone found in butyl rubber compounds. However, this same feature makes it much more difficult to vulcanize such compounds through use of the types of ingredients generally employed with natural or synthetic rubber compounds. This means that great care must be exercised in selecting the compounding and vulcanizing ingredients for "curing" butyl rubber insulating compounds, particularly from the point of view of their possibly contributing additional double bonds to the compound. For example, the accidental addition of 1 per cent of natural rubber or certain synthetic rubbers to a butyl rubber compound would adversely affect the proper vulcanization and some of the performance characteristics of that butyl rubber compound.

Ozone Resistance—Its Importance

It is today almost universal that all rubber and rubberlike insulations intended for operation at over 2 kv must possess at least a minimum amount of ozone resistance. This is because with any conductor carrying high-voltage alternating current, the air adjacent to the

Table I. Details of Initial Physical Properties and Per-Cent Retention of Original Elongation after Various Aging Periods

Nature of Data	Cables					
	A	B	C	D	E	A'*
Initial						
Tensile, pounds per square inch	1,275	760	670	790	810	1,135
Elongation, per cent	720	530	490	520	340	670
Recovery, inches	3/8	1/4	3/16	1/8	3/16	5/16
200-per-cent modulus, pounds	285	485	320	420	570	285
Air pressure heat test at 260 degrees Fahrenheit (F) and 80-pound pressure with retention of original elongation, per cent						
After 20 hours	96.5	73.5	92.0	29.0	57.5	98.5
After 40 hours	100.0	57.5	79.5	7.5	38.5	104.5
After 80 hours	93.0	53.0	77.5	0	14.5	99.5
80 C (176 F) oxygen bomb at 300-pound pressure with retention of original elongation, per cent						
After 7 days (168 hours)	96.0	81.0	104.0	40.0	84.0	88.0
After 14 days (336 hours)	88.5	72.0	98.0	3.9	72.0	89.0
After 28 days (672 hours)	88.5	53.0	73.5	0	44.0	86.0
121 C (250 F) air oven, atmospheric pressure with retention of original elongation, per cent						
After 7 days (168 hours)	95.5	56.5	68.5	21.0	8.8	102.0
After 14 days (336 hours)	93.5	49.0	61.5	0	7.3	100.0
After 28 days (672 hours)	83.0	41.5	54.5	0	0	92.0

* A' represents a single conductor 4/0 with 19/64-inch wall of butyl rubber insulation, metallic shielding tape, neoprene outer jacket for operation at 15 kv grounded neutral, produced by manufacturer A. This applies also to Table II.

insulation may be broken down by the intensity of the surrounding electric field. This electrical breakdown, or ionization of the surrounding air, converts the oxygen in the latter to ozone O_3. Unless rubber or rubberlike insulation has been fortified artificially, or has such fortification inherently, ozone attacks such compounds at the points of double bond, the attack being in the form of surface cracks which continue to deepen and result in well-known ozone cracking.

Ozone resistance is a function of ozone concentration in the air immediately adjacent to the insulation and degree of bending or stretching of the insulation. Increasing either of these conditions increases the vulnerability to ozone attack.

Other Essential Properties

Besides adequate ozone resistance, other essential properties contributing to a reliable high-voltage rubber-insulated cable may be summarized as follows:

1. Good initial physical properties.
2. A high degree of retention of physical properties, particularly elongation, after subjection to a series of accelerated aging conditions.
3. Adequate insulation resistance at operating temperature, both in air and in water.
4. Electrical stability in water and air as evidenced by low power factor and specific inductive capacitance with the least amount of variation over a range of temperatures and electric stresses.
5. Additional evidence of stability in water by means of low mechanical moisture absorption.
6. Adequate 60-cycle dielectric strength.
7. Adequate impulse dielectric strength.
8. High, maximum permissible operating temperature to provide highest current-carrying capacity ratings.

There is no single property which will of itself ensure reliable operation of a given type of cable. A proper balance of all of these properties is required. The remainder of the paper deports the extent these properties are evidenced by these cables when subjected to a series of test conditions.

Discussion of Test Results

1. PHYSICAL PROPERTIES BEFORE AND AFTER ACCELERATED AGING

Examination of the data in Table I indicates:

(a) Both butyl and oil-base insulations have adequate initial physical properties, particularly elongation, the most important physical characteristic essential in rubber and rubber-like insulating compounds.

(b) After accelerated-aging tests, butyl insulations as a class appear to retain their physical properties to a greater degree than oil-base types.

(c) The greater resistance to the effects of heat and oxidation is an indication that butyl cables may be rated at higher maximum permissible temperatures for continuous operation as well as for emergency overloads than oil-base types. This means that butyl cables may have higher current-carrying capacity ratings.

Note: At the time this investigation was started, only one make of 15-kv cable was available, namely, that obtained from manufacturer *A* a year prior to the investigation. It is for that reason that only tests on this cable, designated as *A'*, were possible to include in Tables I and II. The four remaining makes of higher voltage cables were recently obtained and the only tests that could be reported are the impulse dielectric strength tests given in Tables VIII and IX.

2. EFFECT OF WATER AND TEMPERATURE ON SPECIFIC INDUCTIVE CAPACITANCE AND POWER FACTOR

Examination of the data in Table II indicates:

(a) Only 1 month of immersion in water at elevated temperatures such as 70 degrees centigrade (C) is more than sufficient to bring out the superior electrical stability of butyl insulated cables in contrast with the oil-base types. The difference becomes much more pronounced when the data are examined after a similar period of immersion in water at 80 C.

There may be some who question the need for conducting tests in water at as high a temperature as 80 C. Careful reflection will reveal that there are considerable quantities of high-voltage rubber-insulated cables, shielded and nonshielded, furnished with nonmetallic sheathing. The primary function of such sheaths is to provide the underlying insulation with the necessary protection against mechanical damage and a variety of environmental influences that may adversely affect the life of the insulation. Where contact with water is anticipated, it becomes important to make certain that the type of insulation used possesses the maximum degree of inherent moisture resistance possible to attain because moisture will eventually penetrate the nonmetallic sheathing, particularly if the latter is of neoprene composition. It is also known that industry standards prescribe the following operating temperatures for these two classes of insulation:

Operating Voltage, Kv	Maximum Safe Continuous Operating Temperature, C	
	Oil-Base	Butyl
0 to 8	75	80*
8.1 and over	70	80*

* A number of manufacturers of butyl-rubber-insulated cables have already increased this value to 85 C.

Therefore, the oil-base cables must be capable, at least in the 0- to 8-kv range, to operate in water at temperatures up to 75 C. On the other hand, the butyl rubber cables must have excellent moisture resistance at least up to 80 C.

(b) Temperature, duration of immersion, and voltage stress have a pronounced effect on the specific inductive capacity and power factor of the insulations under test. The product of these two properties is directly proportional to dielectric loss. It is well known that high dielectric loss adds to cumulative heating and, if the latter is excessive, this will affect the ultimate temperature rating for continuous operation. Therefore, it is interesting to note that even after 28 days in water at 80 C and with a stress of 80 volts per mil, which is approximately five times the average operating stress to ground of the 5-kv cables (dielectric loss varies as the square of the voltage), butyl rubber cables appear to be considerably less affected than oil-base types.

(c) Even in 70 C water after 28 days' immersion, the power factor of the oil-base insulations is many times that of the butyls, at least ten times higher for cable *D*, and four times higher for cable *E*. Of the oil-base insulations tested, cable *E* possesses a definitely greater degree of stability over cable *D*.

3. RESISTANCE TO OZONE CRACKING

The ozone concentrations used in this series of tests were slightly higher than those generally required by the industry standards for these respective classes of material. The standard ozone concentrations are: 0.010 to 0.015 per cent by volume for oil-base rubber insulations; and 0.025 to 0.030 per cent by volume for butyl rubber insulations.

From the data in Table III it can readily be seen that, as a class, butyl rubber insulations possess an overwhelmingly superior resistance to ozone than the oil-base rubber insulations. With increasing use of high-voltage rubber-insulated nonmetallic-sheathed cables and the need for a good ozone-resistant insulation, the growing trend towards butyl-rubber-insulated cables for such service is readily understandable.

4. EFFECT OF WATER AND TEMPERATURE ON INSULATION RESISTANCE

From Table IV it can readily be seen:

(a) As a class, butyl rubber insulation possesses very much higher insulation resistance than oil-base rubber insulations.

(b) Many observers including the author have questioned the value of high insulation resistance as a means of judging the quality of a power cable. Without arguing the merits of this subject, all agree that stability of insulation resistance may be an important criterion of insulation quality. For cables intended for operation with nonmetallic sheathing, stability of insulation resistance in water at a given temperature does appear

Table II. Effect of Water and Temperature on Power Factor and Specific Inductive Capacitance at Two Voltage Stresses, Volts per Mil

Nature of Tests	A 40	A 80	B 40	B 80	C 40	C 80	D 40	D 80	E 40	E 80	A′ 40
Specific inductive capacitance											
In water at 50 C, after 1 day	3.87	3.90	3.71	3.72	3.89	3.90	3.90	4.01	4.11	4.11	3.68
In water at 50 C, after 14 days	3.85	3.86	3.77	3.78	3.94	3.97	4.23	4.24	4.21	4.18	3.67
In water at 50 C, after 28 days	3.85	3.86	3.82	3.83	3.90	4.04	4.28	4.29	4.27	4.27	3.67
In water at 70 C, after 1 day	3.76	3.77	3.65	3.65	3.97	4.00	4.02	4.02	4.18	4.09	3.62
In water at 70 C, after 14 days	3.78	3.80	3.85	3.89	4.13	4.17	4.40	4.42	4.35	4.36	3.66
In water at 70 C, after 28 days	3.80	3.81	4.02	4.06	4.17	4.25	6.39	6.74	5.17	5.17	3.68
In water at 80 C, after 1 day	3.72	3.73	3.87	3.87	3.94	3.98	4.11	4.12	4.29	4.26	3.65
In water at 80 C, after 14 days	3.74	3.80	4.20	4.27	4.19	4.23	7.66	9.21	5.17	5.41	3.71
In water at 80 C, after 28 days	3.85	3.86	4.29	4.36	4.38	4.41	8.78	11.13	6.45	6.60	3.72
Power factor, per cent											
In water at 50 C, after 1 day	1.46	2.10	0.42	0.85	0.46	1.14	2.35	2.78	1.93	2.37	0.91
In water at 50 C, after 14 days	1.35	1.80	0.93	1.25	1.05	1.64	2.28	2 .70	1.89	2.24	0.87
In water at 50 C, after 28 days	1.09	1.42	1.23	1.56	1.24	1.78	2.48	2.74	2.17	2.42	0.81
In water at 70 C, after 1 day	1.52	1.82	1.35	1.60	1.52	2.08	3.96	4.28	3.92	4.32	1.25
In water at 70 C, after 14 days	1.05	1.55	2.34	2.85	2.45	3.10	10.97	11.85	7.43	7.59	1.17
In water at 70 C, after 28 days	0.99	1.52	2.80	3.76	2.48	3.14	37.2	40.2	11.95	12.15	1.05
In water at 80 C, after 1 day	2.01	2.47	1.94	2.35	2.15	2.77	5.90	6.4	7.2	7.55	1.66
In water at 80 C, after 14 days	1.59	1.97	4.40	5.45	4.35	4.90	47.9	58.3	18.4	20.8	1.40
In water at 80 C, after 28 days	1.41	1.80	4.28	5.79	3.56	4.02	48.6	61.6	23.6	25.4	1.11

to be a desirable characteristic regardless of basic initial quantitative values.

Butyl-rubber-insulated cables are definitely superior in this regard to the oil-base-insulated cables.

(c) Insulation resistance varies inversely with temperature. This is the case with each of the 5 cables under test. However, the value of insulation resistance of 0.5 megohm–1,000 feet for cable *D* after only 28 days in water at 70 C, a temperature considerably less than the 75 C permitted for operation of such cables in dry or wet locations in the 0- to 8-kv voltage range, would hardly be considered conducive to good operating performance in extremely wet locations.

5. MECHANICAL MOISTURE ABSORPTION

The resistance of rubber and rubber-like compounds to immersion in water and the best means of expressing this property have long been subjects of considerable technical discussions. It has been argued that, since these are electric insulations, the best method is to determine the degree of retained electrical properties after a given period of immersion in water at some elevated temperature. Another school of technologists feels that it is of equal importance to determine the mechanical moisture absorption of the insulation gravimetrically, i.e., to measure the actual amount of water absorbed after a given period of immersion in water at some elevated temperature such as 70 C, expressing such effect in terms of milligrams per square inch of insulating surface exposed to water.

Both of these viewpoints were considered during the present investigation and the results obtained lead to the following observations:

(a) The measurements in Table II were designed to determine the degree of electrical stability with prolonged immersions in water at various temperatures. As pointed out in the section entitled "Effect of Water and Temperature on Specific Inductive Capacitance and Power Factor," there is no question but that the greatest degree of such electrical stability was exhibited by the butyl-rubber-insulated cables.

(b) Examination of Table V also reveals that the butyl rubber insulations absorb considerably less water than oil-base insulations when tested under standard conditions employed in such test, namely, in distilled water at 70 C.

(c) Since butyl-rubber-insulated cables may be called upon to operate at temperatures of up to 85 C, it was decided to conduct also the gravimetric test at 90 C. Table V confirms the fact that, even under these conditions, butyl rubber insulations are decidedly much more stable than oil-base insulations.

(d) Regardless of the merits of the two methods of moisture-absorption testing, and which possesses the greatest significance in determining insulation stability, it would certainly seem reasonable to conclude that the class of insulation which

Table III. Resistance to Ozone Cracking at Various Ozone Concentrations

Nature of Test	A	B	C	D	E
Insulated Power Cable Engineers Association and American Society for Testing Materials ozone test procedure					
Hours to failure at 0.020-per-cent concentration	168+	168+	168+	1³/₄	³/₄
Hours to failure at 0.034-per-cent concentration	168+	168+	168+	2	1¹/₂

Table IV. Effect of Water and Temperature on Insulation Resistance

Nature of Test	Insulation Resistance, Megohms–1,000 Feet A	B	C	D	E
In water at 50 C, after 1 day	2,480			99	74
In water at 50 C, after 14 days	7,640	7,250	14,500	50	63
In water at 50 C, after 28 days	16,600	7,750	4,880	44	65
In water at 70 C, after 1 day	784	2,885	1,670	10	5.8
In water at 70 C, after 14 days	2,760	1,660	825	2.5	5.2
In water at 70 C, after 28 days	2,920	1,743	873	0.5	4.1
In water at 80 C, after 1 day	395	943	806	3.9	2.4
In water at 80 C, after 14 days	1,017	225	140	0.4	3.3
In water at 80 C, after 28 days	1,523	287	182	0.35	1.7

Table V. Moisture Absorption, Gravimetric Method

Nature of Test	Moisture Absorbed, Milligrams per Square Inch of Exposed Surface A	B	C	D	E
After 7 days in distilled water					
At 70 C	12.2	10.7	14.1	90	35.6
At 90 C	14.3	8.2	8.5	too high to measure	95.0

Table VI. 60-Cycle Dielectric Strength of 5-Kv Cables, Kilovolts at Room Temperature

A	B	C	D	E
51.8	47.5	43.2	47.5	79.7

excels under both types of test should possess the greater degree of stability from an electrical and physical point of view as far as operation under moist conditions is concerned.

6. 60-CYCLE DIELECTRIC STRENGTH ROOM TEMPERATURE

Examination of the data in Table VI indicates:

(a) The average of such tests on two samples of each of the five makes of cable gives the oil-base types some superiority over the butyl rubber types.

(b) However, it should be noted that it is hardly reasonable, in the case of the oil-base compounds, to average two such dissimilar results as 47.5 kv and 79.7 kv in order to arrive at an average dielectric strength value of 63.6 kv as representative of the oil-base cables compared to an over-all average for the three butyl rubber cables of 47.5 kv.

(c) If the values of 47.5 kv obtained for the oil-base cable of manufacturer *D* are compared to the over-all average or even the individual average values obtained for each of *A*, *B*, and *C* respectively, there appears to be no inherently higher dielectric strength (determined at room temperature) for manufacturer *D*'s oil-base cable than for any of the three butyl rubber cables. However, if the comparison is made between the butyl cables and the oil-base cable of manufacturer *E*, there is no question that the latter possesses greater dielectric strength under these conditions of testing.

Note: Since these are nonshielded cables having the jacket in intimate contact with the underlying insulation, and since the total thickness of insulation and jacket in the dielectric field to ground (the jacket in some cases may contribute to the dielectric strength values obtained under these comparatively short-time tests) varied with the different 5-kv samples, it was thought advisable to include the over-all diameters at this time. These are: for *A*, 0.53 inch; for *B*, 0.59 inch; for *C* and *D*, 0.60 inch; and for *E*, 0.56 inch.

Table VII. 60-Cycle Dielectric Strength of 5-Kv Cables at 90 C

Cable Designation	Sample No.	Breakdown	
		Kv	Time
A	1	60.0	3 minutes 41 seconds
	2	50.4	4 minutes 55 seconds
B	1	50.4	1 minute 45 seconds
	2	50.4	0 minutes 33 seconds
C	1	37.0	instantaneous
	2	35.0	0 minutes 18 seconds
D	1	35.0	1 minute 51 seconds
	2	50.4	2 minutes 14 seconds
E	1	60.0	0 minutes 3 seconds
	2	60.0	0 minutes 40 seconds

Test Schedules
35.0 kv, 5 minutes
42.0 kv, 5 minutes
50.4 kv, 5 minutes
60.0 kv, 5 minutes

(d) If, for the sake of speculation, it is assumed that the thickness of insulation and neoprene jacket may be considered as contributing to the dielectric strength obtained, and if it is recalled that the conductor in all of these 5-kv cables was no. 8 American Wire Gauge with a nominal diameter of 0.129 inch, then the average breakdown strength of each of these lengths, in volts per mil, becomes: for *A*, 259; for *B*, 206; for *C*, 184; for *D*, 202; and for *E*, 370. Viewed in this manner, oil-base cable *E* has considerably higher dielectric strength than any of the butyl cables, but the same can certainly not be claimed for oil-base cable *D*.

(e) Both classes of cable have adequate dielectric strength under this type of test.

7. 60-CYCLE DIELECTRIC STRENGTH AFTER SAMPLES MAINTAINED AT 90 C FOR 24 HOURS

Examination of Table VII indicates:

(a) At an elevated temperature of 90 C maintained for 24 hours, there seems to be very little superiority in dielectric strength for either butyl or oil-base rubber-insulated cable.

(b) It is interesting to note that the considerable gap between the room-temperature, dielectric-strength values of oil-base compounds *D* and *E* has been narrowed considerably, with cable *E* showing only slightly superior results.

(c) Both classes of cable possess adequate dielectric strength under this type of test.

8. IMPULSE DIELECTRIC STRENGTH TESTS

These were the only tests conducted outside the laboratories of the company with which the author is associated. These are also the only tests conducted on samples of the five makes of 15-kv cables. Examination of Tables VIII and IX indicates:

(a) Whereas, in the 5-kv group, one oil-base cable possesses higher impulse strength, there seems to be little difference in the values obtained for the 15-kv cables.

(b) Comparing the values obtained with those recommended,[3] it can readily be seen that both classes of cable have adequate impulse strength.

Table VIII. Impulse Dielectric Strength of 5- and 15-Kv Cables, Room Temperature, Standard $1^1/_2$x40-Microsecond Wave

Type of Cable	Impulse Breakdown, Kv, for Different Cable Designations					
	A	B	C	D	E	Minimum Recommended[3]
5 kv	145	158	122	155	208	85
15 kv	322	243	205	278	349*	95

* Cable *E* had 25/64-inch wall of insulation. All other 15-kv cables had 19/64-inch insulation.

Conclusions

This investigation is being continued. The data presented herein should be considered as a progress report from which certain definite conclusions of importance may be drawn, chief of which are:

1. It has been shown that butyl rubber cables possess greater resistance to oxidation and ozone, and greater electrical stability in water at elevated temperatures and voltage stresses.

2. Although on the various dielectric strength tests at least one oil-base cable appears to be superior to the butyl cables, there is no question but that the latter have more than adequate dielectric strength to meet the various service conditions encountered.

3. From the point of view of desirable characteristics, not in any one particular property but in an over-all balance of adequate essential properties as outlined in the paper, the butyl rubber cables tested appear to have the advantage over the oil-base cables considered in this investigation.

4. Although only one commercial length of each make of cable was tested, the data obtained do possess significance as regards some of the characteristic performance properties of the two classes of cable insulations, since they were conducted on cables having the foremost reputation in their respective fields.

5. Butyl rubber cables are able to transmit greater quantities of power with lower dielectric losses not only under normal conditions of operation but also under periodic emergency overload conditions.

Table IX. Impulse Dielectric Strength of 5- and 15-Kv Cables, Room Temperature, Standard $1^1/_2$x40-Microsecond Wave

Type of Cable	Impulse Breakdown for Different Cable Designations, Volts per Mil										
	A		B		C		D		E		Minimum Recommended[3]
	Average	Maximum	Average	Maximum	Average	Maximum	Average	Maximum	Average	Maximum	Average
5 kv	725	1,590	678	1,610	519	1,230	659	1,565	967	2,190	546
15 kv	1,084	1,470	818	1,200	690	1,010	936	1,370	893*	1,455*	319

* Cable *E* had 25/64-inch wall of insulation. All other 15-kv cables had 19/64-inch insulation.

References

1. W. L. Immer. *Electrical West*, New York, N. Y., June 1954, p. 132.

2. Underground Cable: Design and Development, L. G. Brazier. *The Electrical Journal*, London, England, Aug. 20, 1954, p. 563.

3. Impulse Strength of Insulated-Power-Cable Circuits, H. Halperin, G. B. Shanklin. *AIEE Transactions*, vol. 63, 1944, pp. 1190–97.

4. High Voltage-High Temperature Rubber Insulation, W. H. Couch, W. K. Freeman. Second Annual Signal Corps Symposium, Dec. 1953.

5. The Electrical Properties of Butyl Rubber, I. C. Eaton, A. V. Roberts, E. E. Sheldon. American Chemical Society, Atlantic City, N. J., Apr. 1946.

6. Type ABP High-Voltage Insulation, L. F. Hickernell. T & D Committee, Edison Electric Institute, New York, N. Y., Oct. 1946.

7. Butyl Rubber-Manufacture and Research, R. M. Thomas. *India Rubber World*, New York, N. Y., May 1954, p. 203.

8. Applications of Butyl Rubber: Present and Future, W. H. Peterson. *Ibid.*, June 1954, p. 366.

9. High Voltage Cables for Industrial Power Distribution, R. C. Waldron. PIEA-PESA Conference, 1954.

10. Lead vs. Nonmetallic-Sheathed Underground Cables, S. J. Rosch. Pacific Coast Electrical Association, March 1952.

11. Butyl Rubber Compounding for Insulations, E. W. Schwartz. Third Annual Signal Corps Symposium, Dec. 1954.

12. Butyl Insulation, W. C. Smith. *Ibid.*, Dec. 1954.

13. Butyl Rubber Engineering Data, E. N. Cunningham, L. B. Turner. Stanco Distributors, New York, N. Y., Nov. 1945.

◆

Discussion

Philip J. Croft (Canada Wire and Cable Company Limited, Toronto, Ont., Canada): This paper is an extremely timely and important contribution on a subject which hitherto has not sufficiently engaged the attention of the technical writers, and its author is to be congratulated on an interesting presentation.

Mr. Rosch is further to be complimented for dealing to a certain extent with the underlying chemistry of the types of rubber-like materials with which he is dealing, in interest of clearing up the all-too-common confusion between "corona" and "ozone," and of demonstrating the basic reasons why some types of material are more ozone-resistant than others.

The test results which he has displayed do not quite clearly indicate whether they were made on only one length of each type of cable, but if this is so, the astonishing superiority of length *A* might almost suggest that this particular length could have been what horticulturists refer to as a "sport." Even apart from the special qualities of this length *A*, there does appear to be a somewhat confusing variation of properties, between lengths insulated with the same type of compound. It would be interesting to see a similar comparison based on a larger number of samples, and preferably displaying both butyl-based and oil-factice-based insulations by each manufacturer.

Nevertheless, an undoubted superiority of the butyl-based insulations, especially in the matter of insulation resistance and dielectric power factor, is clearly demonstrated in the paper, and now that the early processing difficulties have been largely solved by most manufacturers, we shall doubtless continue to see cables insulated with butyl-rubber compounds applied at higher voltages and operated at temperatures approaching those associated with paper cable.

I feel, however, that it would be wrong to permit persistence of the impression, already current in some quarters, that all troubles encountered with rubber-insulated cables on medium-high-voltage circuits have been due to shortcomings in the types of insulation hitherto available, and that butyl-based compounds would be a panacea-for-all-ills in this regard.

Oil-based rubber insulation has been a most useful material for many years, affording a relatively high degree of ozone-resistance compared with other types such as the various "code" rubbers.

In Canada, where such troubles as have been experienced with high-voltage rubber insulations appear to have closely paralleled those encountered in the United States, it has become evident that the great majority of cases of trouble, especially where ozone-cracking has been involved, has been due to an insufficient understanding of the proper function of insulation shielding and the inadvised use of unshielded cables. There have, for example, been many cases of the application of unshielded rubber cables at 5,000 volts or higher, in locations where conductive contamination could not fail to accumulate, with the familiar result of static discharge, sparking, and burning.

There also have been instances, at 13,000 volts and thereabouts, in which shielded single-conductor rubber cables have been used as aerial jumpers on full-voltage insulators, with the shield left floating, ungrounded, to carry its induced charge, with what results you may imagine. It is recognized that recommendations with regard to shielding practices are given by the Insulated Power Cable Engineers Association, and the inclusion of these in our Canadian Code is at present under consideration.

It would be a pity if a valuable new material should have its fine qualities obscured by the same sort of misapplication as may in many cases have shadowed the true worth of other materials.

E. B. Curdts (James G. Biddle Company, Philadelphia, Pa.): As Mr. Rosch says, in discussing the effects of water and temperature on insulation resistance, the value of insulation resistance as a means of judging the quality of a power cable insulation may be open to question. However, a practical and simple field measurement method of determining the condition of installed cable is certainly of interest to operating people.

Since insulation resistance measurements are commonly used for this purpose it is highly desirable to have some understanding of what causes the changes in measured values which may occur in the butyl compounds as compared to the oil-based compounds.

I am, therefore, naturally interested in Table IV in the paper which indicates for some of the butyl samples an increase in insulation resistance of over six times after 28 days' submersion at constant temperature. Before accepting these values as indicating some unusual property of the particular compound involved, which may later be encountered in service, I would like to ask Mr. Rosch if they might be due to some heat-aging process because of the newness of the particular samples used. If this is the case then the test data as given in Table IV covering the effects of water and temperature on insulation resistance may not be realistic from an operating point of view.

According to Fig. 10 in the paper Carroll, Lee and McKinley,[1] water immersion almost immediately reduces the insulation resistance in butyl-insulated cable. Furthermore, their Fig. 17 indicates some sort of heat-aging effect, whatever the mechanism may be.

I would appreciate it greatly if Mr. Rosch would comment on this relatively unimportant aspect of the paper.

Reference

1. Design and Evaluation of Butyl-Rubber-Insulated Power Cable, J. C. Carroll, A. R. Lee, R. B. McKinley. *AIEE Transactions*, vol. 74, pt. III, Dec. 1955, pp. 1204–12.

S. J. Rosch: The author is indebted to Mr. Croft for the information given in his discussion. It was the author's intent, in presenting this paper, to make available some of the characteristic properties of high-voltage cables insulated with the types of "rubber" compounds available today. It would have been preferable to obtain more than one length of each make of cable, and to have included tests on all of these lengths. However, experience indicates that unless the additional lengths of each make of cable differed in some basic design feature from each other, that the only benefit to be derived from such additional testing would be to secure further knowledge regarding the longitudinal uniformity of the respective makes of cable. The author feels that the large number of tests conducted on each length, tests which in some cases were continued for considerably longer periods than reported at the time the paper was written, are representative of the performance characteristics of these respective makes of cable. It is hoped that data of similar nature will be made available by other observers.

Regarding Mr. Croft's comments on the results obtained on length *A*, the author wishes to refer him to a re-examination of the data on length *A′*, obtained a year earlier than length *A*, and differing from the latter in size of conductor and thickness of insulation. The results obtained on *A′* do follow the typical pattern exhibited by length *A* and would indicate that the data obtained with *A* are not unusual but rather typical of this particular make of butyl-rubber insulation.

As to the variations in test results obtained with different makes of butyl-rubber insulations, reference to the molecular structure of natural GR-S and butyl rubber indicates quite clearly that the available amount of unsaturation is a maximum with natural rubber but an absolute minimum with butyl. It is the amount of unsaturation which accounts for the ability to vulcanize a compound. The extremely small amount of unsaturation in butyl makes it much more difficult, although far from impossible, to "cure" butyl-rubber compounds properly. The variations in data reported for makes *A*, *B*, and *C*, and referred to by Mr. Croft, are undoubtedly due to different vulcanization systems used by each of these manufacturers. However, the characteristic data reported for lengths *A*, *B*, and *C* do reflect a typical behavior pattern as a class of insulating material. No such typical behavior pattern could be deduced from a study of similar data reported for the oil-base insulations *D* and *E*.

Mr. Croft is correct in his contention that butyl-rubber insulation is not to be considered as a panacea for all cable ills. His illustration of what may occur through the use of nonshielded nonmetallic-sheathed rubber-insulated cable at 5 kv is very much to the point. Nor can one overlook the difficulties that may be encountered with a shielded cable if the shield is not properly terminated and grounded. Oil-base rubber insulations have given a good account of themselves in high-voltage service involving temperatures not exceeding 70 to 75 C. Today's trend, however, seems to point to the need for higher operating temperatures both for normal as well as emergency use, either in dry or wet locations, and the data in the paper do indicate that butyl-rubber insulations meet these requirements, and are capable of operation at conductor temperatures of 85 C.

As previously stated, there is no single criterion of cable quality. Each of the various properties play their part in assuring the ultimate consumer that the particular cable design has the potential possibility of yielding satisfactory operating performance under the type of operating conditions on his system. The data in the present progress report indicate that butyl-rubber insulations possess more than adequate essentials when subjected to each of the criteria studied in the present phase of this investigation.

As regards the comments by Mr. Curdts regarding some of the insulation resistance values obtained on length *A*, the author would point out that this phenomenon of improved insulation resistance with prolonged immersion in water at a given temperature is not unusual. Such behavior is largely a function of the type of filler ingredients rather than a "heat-aging" process as inferred by Mr. Curdts. Reference to Table IV will show that this phenomenon occurs not only at 80 C but at 50 C as well. For a material that is vulcanized for several hours at temperatures higher than 150 C and which, from Table I, shows only moderate aging when subjected to 121 C for 28 days, one can hardly attribute much heat-aging in 28 days at only 50 C. The author frankly has no clear-cut explanation to account for the improvement in insulation resistance exhibited by length *A* other than the data obtained are as reported. It is our understanding that others who have made tests on conductors insulated with a somewhat similar compound have obtained the same results.

Transformer Temperatures on Short Circuit

W. C. SEALEY
FELLOW AIEE

WHEN transformers carry short-circuit current, the temperature of the copper and its surrounding insulation increases rapidly. After the short circuit is removed the temperature decreases to the temperature of the cooling medium. During the time the temperature of the insulation is higher than normal, the loss of life in the insulation occurs at a greater than normal rate. Since the rate of temperature decrease is on the average much slower than the rate of temperature increase, the loss of life during the cooling-off period is much greater than during the heating period. In general, the American Standards Association standards[1] call for transformers to withstand heating of 25 times the normal current for 2 seconds, or slightly less heating for lower currents.

Typical Transformers

For most power transformers and distribution transformers other factors such as desired efficiency, heat dissipation, etc., limit the watts per pound of the copper to a sufficiently low value so that heating on short circuit is not a design limitation. However, there are important instances where these factors do not require sufficient copper area for short circuits and, in such cases, the heating on short circuit becomes a design limitation. Typical of such cases are the following:

1. Tertiary windings having reduced capacity.
2. Auto transformers having increased rating or increased capacity on the reduced range taps. Typical of this example are most step regulators.
3. Windings where the guaranteed short-circuit current is more than 25 times the normal current.
4. Windings where the short-circuit time at 25 times the normal current is greater than 2 seconds.

Practically all such transformer windings are low-voltage windings with a relatively small amount of conductor insulation.

Typical Winding Characteristics

For the purpose of comparison and analysis, the following characteristics represent the most usual values for transformer windings discussed in this paper.

1. Ten-per-cent eddy-current loss at 95 degrees centigrade (C).
2. Temperature gradient for the hot-spot copper to the adjacent oil at 10 watts per pound of copper loss of between 10 and 25 C. The value of 25 C is representative of the gradients in many of the reduced-capacity tertiary windings as they have been made in the past. Some windings have had gradients higher than this figure. The value of 10 C is representative of a value which will probably have some use in the future if the proposed equation is adopted and also of some windings which have been made in the past. The space between the curves covers representative windings without including extreme cases on either side.

Values slightly different than these could be selected for examining the proposed method and comparable results obtained without affecting the conclusions drawn.

Calculation Methods

The present American Standards Association standards[1] call for calculation based on all heat stored in the copper and do not introduce the heat-dissipating capacity of the winding as a parameter in the determination of the current density. This method is satisfactory for transformer windings having a continuous capacity of at least 4 per cent of the short-circuit rating. However, for windings which do not have a continuous rating, this method does not adequately

---

Paper 55-714, recommended by the AIEE Transformers Committee and approved by the AIEE Committee on Technical Operations for presentation at the AIEE Fall General Meeting, Chicago, Ill., October 3–7, 1955. Manuscript submitted May 31, 1955; made available for printing July 21, 1955.

W. C. Sealey is with the Allis-Chalmers Manufacturing Company, Milwaukee, Wis.

specify design requirements for service conditions. One solution would be to specify a maximum temperature gradient between the copper and the cooling medium for such transformers based on, e.g., 4 per cent of short-circuit current being carried continuously.

A recent proposal which is in the process of being incorporated in the standards, perhaps with some modification, is to calculate the temperature rise based on heat being absorbed in the conductor insulation in addition to the copper and to introduce as a parameter the rate of heat dissipation during the cooling part of the cycle. This recent proposal requires an increase in the copper cross section for many cases covering oil-insulated transformer windings with continuous ratings where the current density in the copper is a design limitation. For windings not having continuous ratings, the new proposals require provision for heat dissipation which is desirable and was their intention. The present method imposes no requirements for heat dissipation but is based solely on the thermal capacity of the copper.

There has been no evidence that, for apparatus having continuous ratings, an increase in the copper cross section is necessary. In fact, because of better relaying, the average duration of short circuits is less and, if anything, a reduction in the copper cross section rather than an increase is in order. Before the new proposals are actually incorporated in the standards, it seems desirable to investigate the proposed method to determine the reasons for the inconsistency and what can be done to take care of it.

Present Standards

The present standards for oil-insulated transformers are based on all heat being absorbed in the copper with an initial temperature of 95 C and a final temperature not to exceed 250 C, see reference 1, section 12.051.

The present standard equation for determining the ultimate temperature may be simplified to.[1, 2]

$$\text{final temperature} = T_0 + 2nt\left((1+nt)\times(T_0+234.5)+\frac{309.2e}{1+nt}\right) \qquad (1)$$

where

T_0 = initial temperature
t = time of short circuit, seconds
e = per-unit eddy-current loss at 75 C
$n = 0.9\times10^{-6}$ (I^2R watts per pound at 75 C)

Proposed Method of Calculation

The equation proposed for the calculation of the temperature rise of oil-insulated transformers is

$$\text{final temperature} = \theta_t = 95 + 329.5m(1+e_s+0.6m) \qquad (2)$$

$$m = \frac{Wt}{309.5\left(174+0.045T_a+110\dfrac{A_i}{A_c}\right)} \qquad (3)$$

where

e_s = per-unit eddy-current loss at starting temperature
W = watts per pound, I^2R loss at 75 C on short circuit
T_a = average of initial and final temperatures
A_i = cross section of insulation
A_c = cross-section area of copper

To determine the permissable temperature rise, a time factor f is calculated using the equation

$$f = \frac{178.3+110\dfrac{A_i}{A_c}}{W_1}G \qquad (4)$$

where

W_1 = the total watts per pound at 95 C corresponding to normal load on the transformer
G = the temperature difference between hottest copper and average oil with normal load on the transformer

A table of temperature limits corresponding to values of the time factor f has been set up in the proposal, see Table 12.052. These values for class-*A* insulation are shown by curves *A* and *B* of Fig. 1. Curve *A* is for oil-immersed insulation and curve *B* for dry-type insulation.

Calculations by Present Method

Essentially, the calculations of values of allowable watts per pound of copper for comparison purposes consist of substituting the typical values and an assumed watts per pound in the equations given to determine the final temperature. If this temperature is above or below the established safe limit, recalculation using a higher or a lower value of watts per pound is performed. This process is repeated and a curve of watts per pound versus final temperature is plotted until a final temperature equal to the safe temperature is obtained, e.g.

$$\text{final temperature} = T_0 + 2nt\left((1+nt)\times(T_0+234.5)+\frac{309.2e}{1+nt}\right)$$

where

$T_0 = 95$ for oil-immersed transformers
$t = 2$ for a 2-second short circuit

$$e = \frac{(234.5+95)^2}{(234.5+75)}20.10 = 0.113$$

Assume I^2R watts per pound at 95 C = 10,800

$$n = 0.9\times10^{-6}\frac{(234.5+75)}{(234.5+95)}10,800 = 0.0915$$

$$\text{final temperature} = 95 + 4\times0.0915\left((1+0.0915\times2)329.5+\frac{309.2\times0.113}{1+0.0915\times2}\right)$$

Final temperature = 248.5.
Standard allowable temperature = 250.
Total watts per pound including 10-per-cent eddy current equals 10,800 + 10 per cent = 11,880.

A value of 11,900 watts per pound is plotted as the ordinate of line *A* in Fig. 2. This value represents present practice and will be compared with the permissable watts per pound as calculated by the proposed equation and proposed sliding scale of temperature limits.

Calculations by Proposed Method

Calculations by the proposed method follow a similar pattern using equations 2 and 3 to determine the temperature reached for assumed values of watts per pound. These values are plotted as curves *A*, *B*, *C*, *D*, *E*, and *F* in Fig. 3. Equation 4 and curve *A* of Fig. 1 give the safe temperature for each value of A_i/A_c and true gradients of 10 and 25 C at 10 watts per pound of copper. (The gradient used in the proposed equation is 10 degrees greater in each case using the conventional hot-spot allowance of 10 C.) These values are plotted on the corresponding curves *A* to *F* as curves *H* and *J* for 10 and 25 C respectively. The watts per pound determined in this manner for 10 and 25 C gradient for various ratios of A_i/A_c are plotted as curves *B* and *C* respectively in Fig. 1. These curves are plotted with ratio A_i/A_c as abscissa.

Calculations

An examination of the kind of wire and insulation used for these low-voltage windings will help determine the limits of ratio A_i/A_c which apply to these practical transformer windings.

Most oil-immersed transformers where the short-circuit heating is a design limitation are low-voltage windings with a relatively small amount of conductor insulation. The widths of the individual

Table 12.052. Short-Circuit Temperature Limits for Transformers

Oil-Immersed Transformers, Class-A Insulation, 95 C Hot-Spot		Dry-Type Transformers, Class-A Insulation, 105 C Hot-Spot	
Temperature Limit	Time Factor, f	Temperature Limit	Time Factor, f
265	63	270	326
260	93	260	616
255	138	250	1,159
250	204	245	1,588
245	301	240	2,175
240	443	235	2,974
235	652	230	4,064
230	956	225	5,546
225	1,399	220	7,652
		215	10,303

strands used are generally between 0.250 and 0.500 inch. The thickness of the insulation may vary from zero for bare wire and practically zero for enameled wire to a 0.020-inch increase in conductor dimension.

The curves of Fig. 4 have been plotted to show the values of the ratio of insulation cross-section area to copper cross-section area, (i.e., the ratio A_i/A_c) for the typical wires which are used for such low-voltage windings. An examination of these curves shows that the ratio A_i/A_c is considerably less than 0.2 for most of the wire being used and in many cases below 0.1.

Because the heat generated in the copper must travel through the thicknesses of insulation to heat the conductor insulation, there probably should be some limit on the thickness of insulation used for the heating calculations. An examination of the curves of Fig. 2 would indicate that a limitation of 0.5 on the value of A_i/A_c would be reasonable. As these curves show, one way to increase the allowable watts per pound of the copper is to use more conductor insulation. Since the thermal drop through the insulation is small compared to the drop from the surface of the insulation to the oil, this is in accordance with the facts. However, there is a limit to which this is effective in reducing the short-circuit duty and provision can easily be made by limiting the maximum value of A_i/A_c to something like 0.5 or other selected value.

Comparison of Curves

A comparison of curve *A* with curves *B* and *C* of Fig. 2, shows that practically all of the common sizes of conductors require either greater copper cross section or an increased thickness of insulation compared to the present standard to meet the proposed short circuit requirements. The natural question is: What evidence is there that an increase in the quantity of material is really needed for windings having a considerable continuous rating? The first place to look is the service record; there no indication is found that more material is needed. Evidently there is disagreement between the results obtained by calculation and in service.

It is known that in deriving the proposed method there was a large element of judgement in selecting the numerical values. There was a wide range of choice possible for several factors. An examination of these factors where judgement was involved might help in removing the discrepancy. These factors include the following.

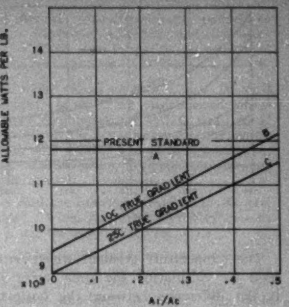

Fig. 2. Comparison of watts per pound allowed by present proposal with the present standards

1. The method of calculating the gradient used for calculating the time factor *f*.
2. The degree rule used for establishing the temperature variation corresponding to the time factor.
3. The permissable loss of life on short circuit combined with the probability of the severity of the short circuits to which the transformer would be subjected during its life.

The selection of the exact values in these cases is admittedly difficult. However, the best check on the values selected is a comparison of results with the results obtained from service experience. When these disagree, a re-examination of the decisions made is in order.

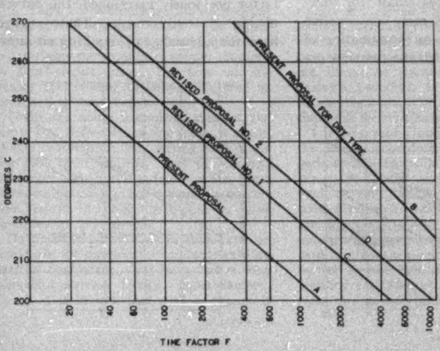

Fig. 1. Proposed temperature limits on short circuit for class-A insulation

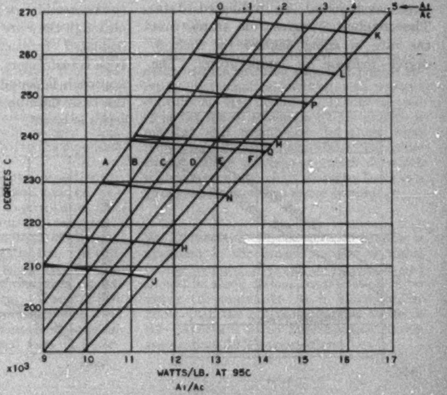

Fig. 3. Actual temperature and permissable temperature curves for oil-insulated transformers

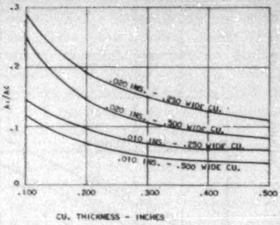

Fig. 4 (left). Variation of A_i/A_c with wire and insulation size

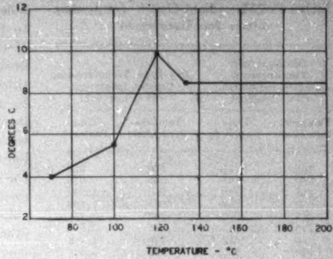

Fig. 6 (right). Temperature rise necessary to double rate of deterioration at 50 per cent of total life

The temperature gradient which was used for calculating the time factor *f* is the difference between the hottest copper and the average oil. This is more conservative than using the temperature difference between the hottest copper and the adjacent oil but it has little physical significance. The true gradient represents the physical phenomenon of heat dissipation more closely and it can be determined more accurately.

It is difficult to justify this extra hidden margin in the light of the final results. It would be advantageous to eliminate this extra margin and use for *G* in the equation for *f* either the difference between the hottest copper and the hottest oil or alternatively the difference between the average copper and the average oil. Besides eliminating a hidden margin, this has the advantage of having the equations more closely represent the actual physical conditions and is a step toward avoiding putting more material in the windings than was formerly used.

In calculating the values of safe temperatures corresponding to the values of time factor *f*, various degree rules were used based on published data. The common 8-degree rule states that the rate of aging doubles for each 8-degree increase in temperature. The values listed show the increments in temperature which were used as values for the rate to double.

For class-*A* oil: 3–4–5–6–7–8–8–8, etc.
For class-*A* dry: 6–7–8–9–10–10–10, etc.

Physically, it might be expected that the aging rate on a short-time basis would be very similar for the dry-type and oil-immersed materials at the elevated temperatures. This assumption would result in higher allowable temperatures in Fig. 1 for the oil-immersed insulation than for the dry-type insulation. The assumption which was made of equal life at the starting temperatures results in higher allowable temperatures for dry-type than for oil-immersed insulation. The difference in allowable temperatures of 45 C seems difficult to believe.

If it is assumed that the dry-type temperatures are safe, why shouldn't they be used for oil-immersed apparatus also? The result would be curves *E* and *F* of Fig. 5. These curves probably depart too much from past experience to be readily acceptable at this time although they are probably safer for oil-insulated transformers than for dry-type transformers. A more conservative approach is found in an examination of the basic data on which the temperature series is based.

Several different curves representing different aging conditions are shown in reference 3. The conditions for the 50-per-cent curve of Fig. 7 of this reference replotted in Fig. 6 herein probably represent average conditions. This shows variations of degrees for doubling of 5 to 10 degrees from 95 to 120 C and a value of 8.5 degrees above 130 C. The 8-degree rule is slightly more conservative than this curve, and represents a 15 C increase in allowable temperatures above those shown by line *A* of Fig. 1. Curves *B* and *C* of Fig. 7 are drawn to represent the 8-degree rule. These curves are derived on the same basis as the curves of Fig. 2, except choosing different data for the aging curve and the gradient calculations. Even they will require more material in the winding than the present standard in some cases, but the difference is much smaller. It does not permit the further reduction in material that should be permitted by better relaying.

If the allowable temperatures of curves *B* and *C* of Fig. 7 were increased by 10 C based on a re-evaluation of the third factor previously mentioned, the curves of Fig. 8 would result. These curves have the advantage of requiring no more

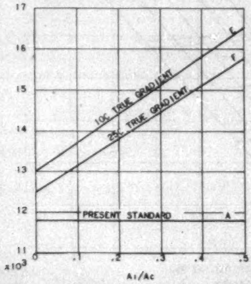

Fig. 5. Comparison of watts per pound allowed using dry-type class-A temperature limits with the present standards

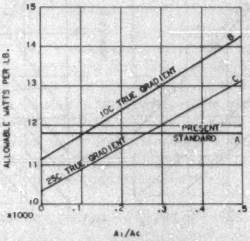

Fig. 7. Comparison of watts per pound allowed by revised proposal no. 1 with the present standards

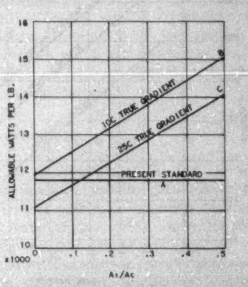

Fig. 8. Comparison of watts per pound allowed by revised proposal no. 2 with the present standards

material than the present standards in a greater number of cases. Viewed in the light of the permissible temperatures allowed for dry-type transformers and because of the fact that the present limits are too low and bare and insulated conductors in accordance with curve A are in common use, the curves of Fig. 8 should receive serious consideration for the standards.

It seems unrealistic to require more material in apparatus, on the basis of theoretical calculations where the assumptions contain a large factor of judgement, when all the evidence points to a decrease. A re-examination of the assumptions, as just outlined, gives more consistent results, based on equally tenable assumptions.

Accordingly, the following conclusions are reached:

Conclusions

It is recommended that the following proposals be incorporated in the standards when the new method of temperature calculation is incorporated for oil-immersed equipment:

1. The thermal time factor should be based on the true gradient between hot-spot copper and the adjacent oil.

2. Some limitation (a maximum value of A_t/A_c of 0.5 is suggested) should be placed on the maximum ratio of A_t/A_c for calculation.

3. The allowable temperature limits on short circuit should be increased by from 15 to 25 C for oil-immersed equipment.

It is recommended that the following changes be made in the proposed standards before they are adopted:

1. Change the paragraph on the calculation on the time factor f in the proposed standards by substituting the word "top" for "average" in the calculation of θ so that θ is the steady-state hot-spot temperature rise at continuous current rating above top oil temperature for oil-immersed equipment. The paragraph will then read:

12.052 THERMAL LIMIT OF TRANSFORMERS FOR SHORT-CIRCUIT CONDITIONS

a. The temperature, as calculated by methods given in 12.053, of the conductor material in the windings of transformers under the short-circuit conditions specified in 12.050 shall not exceed the limiting values given in Table 12.052 for the respective time factors f given in the table.

b. The time factor shall be calculated as follows:

$$= \frac{C\theta}{W} \tag{12.052}$$

where

f = time factor, seconds
θ = steady-state hot-spot temperature rise at continuous current rating: 1. above top oil temperature for oil-immersed transformer equipment; 2. above ambient air temperature for dry-type transformer equipment
W = watts per pound of conductor material at the temperature corresponding to Q temperature rise and standard ambient conditions
C = thermal capacitance per pound of conductor material, and its associated turn insulation, as calculated by equation 12.053b.

c. The values of both C and W shall be taken at 95 C for oil-immersed transformer equipment; at 105 C and 150 C respectively for dry-type transformer equipment with class-A and class-B insulation; and at 180 C for dry-type transformers with class-H insulation.

2. Add the following sentence to the test code: "When the value of A_t/A_c exceeds 0.5, use the value of 0.5 for A_t/A_c."

3. Increase the temperatures in column 1 corresponding to the time factor f in the table for oil-immersed transformers in the proposed standards by 25 C. The table will then appear as shown in Table 12.052.

References

1. AMERICAN STANDARDS FOR TRANSFORMERS, REGULATORS AND REACTORS. *ASA C57-12*, American Standards Association, New York, N. Y., 1949.

2. SHORT TIME HEATING OF TRANSFORMERS, W. C. Sealey. *Allis-Chalmers Electrical Review*, Milwaukee, Wis., vol. VI, no. 1, March 1941, pp. 24–25.

3. FACTORS AFFECTING THE MECHANICAL DETERIORATION OF CELLULOSE INSULATION, F. M. Clark. *AIEE Transactions (Electrical Engineering)*, vol. 61, Oct. 1942, pp. 742–49.

4. SHORT-TIME THERMAL AND MECHANICAL LIMITS FOR TRANSFORMERS AND REACTORS, J. E. Clem. *AIEE Transactions*, vol. 72, pt. III, June 1953, pp. 432–45.

5. INCREASED CURRENT RATINGS FOR STEP REGULATORS, William C. Sealey. *AIEE Transactions*, vol. 74, pt. III, Aug. 1955, pp. 737–41.

6. LOADING TRANSFORMERS BY TEMPERATURE, V. M. Montsinger. *Ibid.*, vol. 49, Apr. 1930, pp. 776–90.

7. EFFECT OF OVERLOADS ON TRANSFORMER LIFE, L. C. Nichols. *Ibid.*, vol. 53, 1934, pp. 1616–21.

◆

Discussion

F. J. Vogel (Allis-Chalmers Manufacturing Company, Milwaukee, Wis.): The paper really discusses changes already proposed to determine the amount of copper required for short-circuit duty. The new rule increases the amount of copper required as compared to the old rule.

There are many arguments against the new rule. Before discussing these, it would be well to state that the thinking back of the new rule regarding the effect of adjacent insulation and that the deterioration takes place during the cooling is basically correct even though the methods to care for these variables are not rigorous.

On the other hand, it is rare that a change is made in the standards that makes existing lines of equipment, that have had a long successful service record, unsatisfactory. Unless it is known that such a change is mandatory, by unsuccessful service records, making such a change would seem to be adding unnecessary cost to satisfactory equipment. Even where such changes seemed mandatory in the past, there are many examples of where its application has been deferred or made inapplicable to existing lines. As another alternate to Mr. Sealey's proposal, I would suggest that such a clause might be added to the proposed change in the standards.

I have a more fundamental objection to the whole procedure. There are no experimental data available to prove any of it. When the old rule was proposed, tests were made on coils and the condition of the material after such tests investigated. In this age, functional testing is being used for the opposite purpose, to see if materials can be used at higher temperatures. Would it not be well to defer this new proposal until tests justified the change? There is a proposal right now to use functional tests to determine the life of distribution transformers. Evidently we do not know all about such structures or their capabilities.

The acceptance of the new rule by many demonstrates the easy way that people accept a mathematical solution even without considering the premises. I believe that even the life of materials by themselves is not too well established, let alone what happens to them in assemblies. The practice of setting up elaborate methods which may not take care of all variables leads to a wrong impression and is not justified.

W. C. Sealey: Mr. Vogel's discussion is pertinent to the general subject of transformer temperatures on short circuit and should be given serious consideration in revising the standards It is heartening to know that the recommendations made in the paper are under consideration in the appropriate AIEE committees.

Efficiency of Grounding Grids with Nonuniform Soil

J. ZABORSZKY
MEMBER AIEE

STUDIES devoted to predetermination of ground resistance on the basis of geometric dimensions and ground resistivity generally assume that the resistivity of the soil is uniform.[1] While this assumption is frequently justified in view of the usually meager knowledge of the actual ground resistivity distribution and the mathematical difficulties caused by any nonuniformity of the ground resistivity, it also can be misleading under certain conditions.

A case in point is a ground electrode site which contains a shallow but moist top-soil layer of fairly good conductivity overlaying poorly conducting rock. On such a site grounding grids situated in the soil layer would normally be used.

Highly refined techniques[2–4] have been developed for calculating the ground resistance of grounding grids in uniform soil. An attempt to apply these to nonuniform soil can be unsatisfactory, however, since conditions change markedly if the nonuniformity is substantial.

The study of a special type of grounding grid is developed here for nonuniform conditions with the expectation of obtaining at least approximately quantitative indications of what might be expected on grids of more conventional design.

Nomenclature

H=depth of upper soil layer, meters
R=radius of conductor ring, meters
R_i=radius of conductor ring number i from the center of the grid starting with R_1
d=diameter of the conductor forming the ring, meters
λ=electric conductivity, mhos per meter
λ_1=electric conductivity of the top layer of ground, mhos per meter
λ_2=electric conductivity of the bottom layer of ground, mhos per meter
μ=dimensionless factor derived from conductivities in equation 15
b_{rs}=general distance defined in Fig. 6, meters
c=distance defined in Fig. 5, meters
c_{rs}=general distance defined in Fig. 6, meters
r=self-ground resistance, ohms
$r_m, r_{12}, r_{23} \ldots$=mutual ground resistances ohms
r_0=ground resistance of a single ring in uniform soil, ohms
r_μ=increment of ground resistance caused by higher resistivity bottom layer of soil, ohms
r_c=resistance correction term, equation 5, ohms
r_{gr}=ground resistance of grid, ohms
p=distance defined in Fig. 5, meters
I=total ground current, amperes
i=current density in soil, amperes per meter square
$i_1, i_2 \ldots$=dimensionless current ratios; see equation 24
G=potential gradient in soil, volts per meter
V=absolute potential, volts
$K(k)$=complete elliptic integral of the first kind
k, k_{rs}=moduli of complete elliptic integral of first kind, see equations 13 and 17
x, y, z=rectangular co-ordinates, Figs. 5 and 6
x, ϕ, z=cylindrical co-ordinates, Fig. 5

The Type of Grid Studied

The type of grid selected for mathematical expediency consists of concentric rings of round thin conductor buried in the uniform top-soil layer which is assumed to overlay a higher resistivity but also uniform rock layer.

Conventional grounding grids usually consist of a rectangular mesh, characterized by a uniform average density of conductor (feet of conductor per square feet of area). To make the information obtained here approximately applicable to such conventional grids, uniform average density of conductor material will also be maintained throughout the proposed concentric grid. This can be achieved by selecting the successive radii, starting with R_1 of the smallest ring so that

$$R_i+1=1/2(R_1+\sqrt{R_1^2+4R_i^2}) \qquad (1)$$

Such selection produces a constant ratio of the conductor length in each ring to the annular area of which it is the outer boundary.

Before discussing the full grid it seems desirable to record some results relating to one element of the grid, i.e., one-ring electrode in nonuniform soil.

Single-Ring Electrode

Mathematical expressions for the ground resistance of a single ring-shape electrode buried in a soil layer of uniform thickness and conductivity overlaying a homogeneous rock body of a different conductivity are derived in Appendix II.

From equation 21, the ground resistance of a ring-shaped electrode buried in soil of uniform λ_1 conductivity ($\mu = 0$) is

$$r_0=\frac{0.580}{\lambda_1 R}\log\frac{16R}{d}+\frac{0.505}{\lambda_1 b_{01}}K(k_{01})\text{ ohms} \qquad (2)$$

Thus the increase (or decrease) of ground resistance contributed by the underlying layer of different conductivity is from equation 22

$$r_\mu=\frac{0.505}{\lambda_1}\sum_{r=1}^{\infty}\sum_{s=1}^{4}\frac{\mu^r}{b_{rs}}K(k_{rs})\text{ ohms} \qquad (3)$$

Consequently, the total ground resistance for two differing soil layers is

$$r=r_0+r_\mu=r_0\left(1+\frac{r_\mu}{r_0}\right) \qquad (4)$$

Based on these relations, Fig. 1 shows the variation of the ground resistance of a single ring buried either in uniform soil (ratio of conductivities $\lambda_2/\lambda_2=1$) or in nonuniform soil ($\lambda_2/\lambda_1\neq 1$) plotted against the ratio of ring radius R to the depth of the top layer H. It has been assumed for the computation of these curves that the ring is buried halfway through the depth of the top layer (values for any depth of burial can be obtained from equations 2 through 4), so H for the uniform conductivity case represents twice the depth of burial. A constant ratio of the conductor diameter d to depth of top layer H, $d/H=1/100$, was assumed for plotting Fig. 1. As can easily be observed from equations 2 and 4, a deviation in the d/H ratio can be taken into consideration by adding

$$r_c=\frac{0.580}{\lambda_1 R}\log\frac{10^{-2}}{d/H} \qquad (5)$$

to values read from Fig. 1. These corrections are shown in Fig. 2. These two illustrations, Figs. 1 and 2, then can be used directly for estimating ground resistances of single-ring electrodes in nonuniform ground. It may be observed from these two illustrations that the presence of a high-resistivity lower soil layer raises the ground resistance very substantially, indeed; if the difference in soil conductivities λ_1 and λ_2 is large enough, the actual ground resistance may be many times that calculated on the basis of the conductivity of the top layer and on the assumption of uniform conductivity throughout.

Paper **55-713**, recommended by the AIEE Transmission and Distribution Committee and approved by the AIEE Committee on Technical Operations for presentation at the AIEE Fall General Meeting, Chicago, Ill., October 3–7, 1955. Manuscript submitted May 31, 1955; made available for printing August 17, 1955.

J. Zaborszky is with the Washington University, St. Louis, Mo.

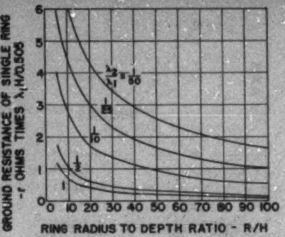

Fig. 1. Ground resistance of single ring of radius R buried at depth $h_1 = H/2$ in top layer of soil of depth H. λ_1 and λ_2 are respective conductivities of top and bottom layers of soil. Ratio of conductor diameter to depth $d/H = 1/100$. Ordinate scale multiplied by $0.505/\lambda_1 H$ gives ohms

In the extreme case, when the conductivity of the underlying rock becomes zero, the ground resistance of the ring becomes infinitely large. It also may be observed from Fig. 1 and 2 that an increase of the radius of the ring effectively reduces the ground resistance while the use of a larger diameter conductor is much less effective.

Efficiency of the Grid

When several concentric rings are connected to form a single grounding grid, the distribution of the ground current between the individual rings and the ground resistance of the entire grid can be calculated by the use of self- and mutual resistances which are derived in Appendixes II and III. Figs. 3 and 4 are based on these results.

Shown in Fig. 3 is the variation of the total ground resistance of a grid of the studied type with the conductivity ratio λ_2/λ_1 of the two layers in the soil. The ground resistance is expressed in per cent of the ground resistance that would be obtained if all the conductor length in the grid were used in one single-ring electrode of appropriate diameter. It can be observed from this diagram that the ground resistance of the grid will be about twice as large for the grid studied here and, interestingly, the extent of the nonuniformity of the conductivities has only limited effect on this ratio. In other words, the conductor length is much more efficiently used in one single ring than in the grid.

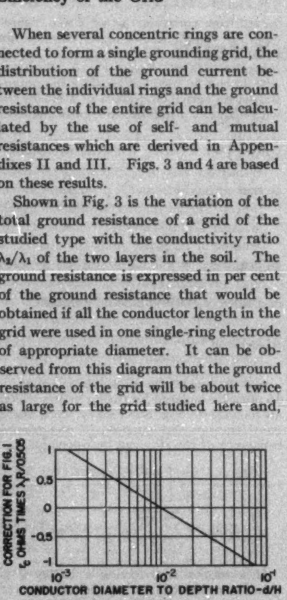

Fig. 2. Additive correction to Fig. 1 for diameter ratios $d/H \neq 1/100$

Shown in Fig. 4 is the variation of the current discharged from one unit length of conductor as function of the distance from the center of the grid. It may be observed that this current density, which is a measure of the efficiency of the individual sections within the grid, takes on a high value only on the periphery of the grid and drops rapidly toward the center of the grid, even if the difference in the conductivities is relatively moderate such as $\lambda_2/\lambda_1 = 1/2$.

Conclusions

The foregoing discussions show conclusively that even relatively moderate vertical variations of the ground resistivity have extensive effects on the efficiency and ground resistance of grounding grids. Such variations should be a major consideration in predetermining ground resistances and the results of this paper are believed to give some aid toward that end.

It may be seen that an underlying higher resistivity layer in the soil renders the inner portion of grounding grids increasingly ineffective, with increasing nonuniformity of soil conductivities. It is more economical to use the conductor material spread out on as large a periphery as feasible rather than use it to form a grid with a smaller periphery; the periphery rather than the area of the grounding electrode determines the ground resistance.

While the numerical results expressed in the equations and illustrations apply strictly only for the special type of grid that was studied, it is expected that they give good approximations also for square mash grids using the same conductor length and diameter if the area is not very elongated. Also while only such cases were studied here where the conductivity of the lower layer in the soil is smaller than the conductivity of the top layer, the equations which were derived apply equally for the reverse situation.

It is not very unusual to encounter grounding sites with two layers of markedly different conductivities although the conductivity within the individual layer would also be more or less nonuniform in actual sites. Such inner variations are not considered here. Not considered are also inductive effects accompanying the ground resistance.

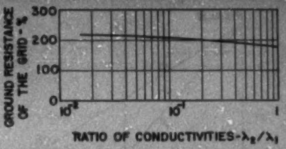

Fig. 3. Ground resistance of grid in per cent of ground resistance of single ring using the same length and diameter conductor as the grid. Ratio of outside grid radius to depth of top layer is 55, its ratio to conductor diameter is 5,000; four rings with radii as specified in equation 1; grid buried to half depth of top layer of soil. λ_1 and λ_2 are respective conductivities of top and bottom layers of soil

Appendix I. Electric Potential of Ring Buried Deep in Uniform Soil

If a point source of current I amperes is buried in uniform material of conductivity λ mhos per meter, then across the surface of a sphere with radius ρ meters and the point source as its center the current density will be

$$i = \frac{I}{4\pi\rho^2} \text{ amperes per square meter} \tag{6}$$

and so the voltage gradient perpendicular to the sphere will be

$$G = \frac{I}{4\pi\lambda\rho^2} \text{ volts per meter} \tag{7}$$

Taking the potential at infinity as zero, the potential at distance ρ from the point source is

$$V = \frac{I}{4\pi\lambda\rho} \tag{8}$$

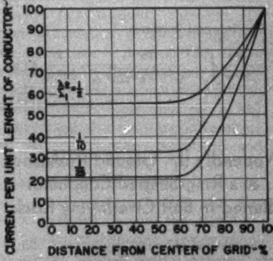

Fig. 4. Current discharge into ground per unit length of conductor as a function of the distance from center of grid. Distance expressed in per cent of outside radius of grid; current density expressed in per cent of its value at the periphery. Same system as in Fig. 3

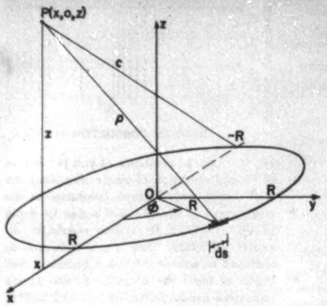

Fig. 5 (left). Geometry and co-ordinate system for one single-ring electrode in uniform soil

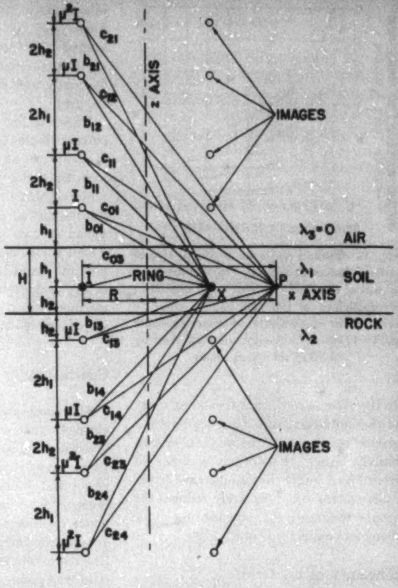

Fig. 6 (right). Ring buried in soil layer of conductivity λ_1 over uniform body of conductivity λ_2 and images

Fig. 5 shows the centerline (ellipse) of a conducting ring. If this ring, which will be first considered of infinitesimal thickness, discharges into the uniform material that surrounds it I amperes current, then a $ds = R d\phi$ meter long section of it discharges

$$dI = \frac{I}{2\pi} d\phi \text{ amperes} \tag{9}$$

According to equation 8, this dI current produces at point $P(x, 0, z)$ a potential of

$$dV = \frac{dI}{4\pi\lambda\rho} \text{ volts} \tag{10}$$

The entire ring produces at that point a potential of

$$V = \frac{1}{4\pi\lambda} \frac{I}{2\pi} \int_0^{2\pi} \frac{d\phi}{\rho} \text{ volts} \tag{11}$$

where

$$\rho = \sqrt{(x - R\cos\phi)^2 + R^2 \sin^2\phi + z^2} \tag{12}$$

With the substitution[6]

$$\cos\phi = 2\sin^2\alpha - 1$$

and

$$k^2 = \frac{4Rx}{c^2} = \frac{4Rx}{(R+x)^2 + z^2} = 1 - \frac{(x-R)^2 + z^2}{(x+R)^2 + z^2} \tag{13}$$

The integral becomes

$$V = \frac{I}{2\pi^2\lambda c} \int_0^{\pi/2} \frac{d\alpha}{\sqrt{1 - k^2 \sin^2\alpha}} = \frac{I}{2\pi^2\lambda c} K(k) \tag{14}$$

Appendix II. Ground Resistance of a Ring-Shaped Conductor Buried in Soil Overlaying Rock

The method of images can be used. Since both boundary planes between the three materials produce images, there results a 2-way infinite sequence of images, some of which are indicated in Fig. 6. If both air and rock have zero conductivity, $\lambda_2 = \lambda_3 = 0$, all of these images discharge into the uniform medium of conductivity λ_1 a current equal to the actual ground current of the ring. The ground resistance of the ring (the ratio of its potential to the current it discharges) in this image system equals its true ground resistance under the actual conditions.

If $\lambda_2 \neq 0$, a modification of this method is possible, similar to the modification used in electrostatic theory for different dielectrics. In this process, whenever an image is taken on the boundary between soil and rock, the current of the image reduces in a ratio

$$\mu = \frac{\lambda_1 - \lambda_2}{\lambda_1 + \lambda_2} \tag{15}$$

Thus the images are not carrying equal currents now; rather the currents are varying, as shown in Fig. 6. The whole space still has λ_1 conductivity and the ground resistance of the ring for this idealized combination still yields its true ground resistance for actual conditions.

The potential caused by the ring and all its images at point P in Fig. 6 will be the sum of the potentials caused at point P by the ring and its individual images. So with equation 14

$$V(x) = \frac{I}{2\pi^2\lambda_1} \left[\frac{1}{c_{01}} K(k_{01}) + \frac{1}{c_{03}} K(k_{03}) + \sum_{r=1}^{\infty} \sum_{s=1}^{4} \mu^r \frac{1}{c_{rs}} K(k_{rs}) \right] \tag{16}$$

where c_{rs} is defined in Fig. 6 and

$$k_{rs} = \frac{2\sqrt{Rx}}{c_{rs}} \tag{17}$$

Since $(x-R)^2 + z^2 = \text{constant}$ is the equation of a circle in the $x-z$ plane with its center at $x = R$ on the x axis, it can be observed from equation 13 that k and, consequently, V will be essentially constant on slender toroids, the centerline of which coincides with the ring in Fig. 5. So equation 14 can be used to calculate the potential on an actual ring made of a conductor with diameter d if $d \ll R$ and, consequently

$$\left(R - \frac{d}{2}\right) \leq x \leq \left(R + \frac{d}{2}\right),\ z \ll R,\ R + x \cong 2R$$

so that

$$c_{03} \cong 2R \tag{18}$$

$$k_{03} \cong \sqrt{1 - \left(\frac{d}{4R}\right)^2} \tag{19}$$

and since $(d/4R)^2$ is a small number

$$K(k_{03}) \cong \ln \frac{16R}{d} \tag{20}$$

For the images the c_{rs} values in equation 15 must be replaced by the b_{rs} values which are defined in Fig. 6. Finally, with these considerations and equation 16, the ground resistance of the ring can be calculated as

$$r = \frac{V(R)}{I} = \frac{1}{2\pi^2\lambda_1} \left[\frac{2.3}{2R} \log \frac{(16R)}{d} + \frac{1}{b_{01}} K(k_{01}) + \sum_{r=1}^{\infty} \sum_{r=1}^{4} \mu^r \frac{1}{b_{rs}} K(k_{rs}) \right] \tag{21}$$

If a second ring having a radius x is situated concentrically in the same plane with the ring of radius R, a mutual resistance of these two is defined from equation 16 by

$$r_m=\frac{V(x)}{I}=\frac{1}{2\pi^2\lambda_1}\left[\frac{1}{c_{01}}K(k_{01})+\frac{1}{c_{03}}K(k_{03})+\sum_{r=1}^{\infty}\sum_{s=1}^{4}\mu^r\frac{1}{c_{rs}}K(k_{rs})\right] \quad (22)$$

Note that the mutual resistance will be the same on the basis of equation 22 and the geometry of Fig. 6 in either direction between the two rings, which is of course as it should be.

Appendix III. Current Distribution on Grid

For a grid consisting of concentric ring electrodes in one plane, the common voltage V of the grid can be calculated as

$$\begin{aligned}V&=I_1r_1+I_2r_{12}+I_3r_{13}+I_4r_{14}\\V&=I_1r_{12}+I_2r_2+I_3r_{23}+I_4r_{24}\\V&=I_1r_{13}+I_2r_{23}+I_3r_3+I_4r_{34}\\V&=I_1r_{14}+I_2r_{24}+I_3r_{34}+I_4r_4\end{aligned} \quad (23)$$

These equations are simple applications of the superposition principle stating that the voltage of each ring is jointly produced by its own ground current and the ground current of the other rings. Self-resistances r_1, r_2, r_3, and r_4 are defined by equation 21; mutual resistances r_{12}, r_{13}, $r_{14}\ldots r_{34}$ are defined in equation 22. I_1, I_2, I_3, and I_4 are the ground currents of the various rings.

Introducing the dimensionless ratios

$$i_1=\frac{I_1}{I_1}=1,\ i_2=\frac{I_2}{I_1},\ i_3=\frac{I_3}{I_1},\ i_4=\frac{I_4}{I_1} \quad (24)$$

and subtracting successively the individual equations of equation 23 from the first of these equations

$$\begin{aligned}0&=(r_1-r_{12})+i_2(r_{12}-r_2)+i_3(r_{13}-r_{23})+i_4(r_{14}-r_{24})\\0&=(r_1-r_{13})+i_2(r_{12}-r_{23})+i_3(r_{13}-r_3)+i_4(r_{14}-r_{34})\\0&=(r_1-r_{14})+i_2(r_{12}-r_{24})+i_3(r_{13}-r_{34})+i_4(r_{14}-r_4)\end{aligned} \quad (25)$$

Simultaneous solutions of equation 25 then yield the ratios i_2, i_3, and i_4. With this, the relative current distribution is known. If the total ground current of the grid $I=I_1+I_2+I_3+I_4$ is known, then

$$I_1=\frac{I}{1+i_2+i_3+i_4} \quad (26)$$

and

$$I_2=I_1i_2 \quad I_3=I_1i_3 \quad I_4=I_1i_4 \quad (27)$$

Now any equation of equation 23 yields V and so the resulting ground resistance of the grid is

$$r_{gr}=\frac{V}{I}\ \text{ohms} \quad (28)$$

Generalization for more than four rings is obvious.

References

1. DESIGN CHARTS FOR DETERMINING OPTIMUM GROUND-ROD DIMENSIONS, J. Zaborszky, Joseph W. Rittenhouse. *AIEE Transactions*, vol. 72, pt. III, Aug. 1953, pp. 810–17.

2. GROUNDING GRIDS FOR HIGH-VOLTAGE STATIONS, E. T. B. Gross, B. V. Chitnis, L. J. Stratton. *Ibid.*, pp. 799–810.

3. ANALYTICAL EXPRESSIONS FOR THE RESISTANCE OF GROUNDING SYSTEMS, S. J. Schwartz. *AIEE Transactions*, vol. 73, pt. III-B, Aug. 1954, pp. 1011–16.

4. GROUNDING GRIDS FOR HIGH-VOLTAGE STATIONS. II—RESISTANCE OF LARGE RECTANGULAR PLATES, Eric T. B. Gross, Richard B. Wise. *Ibid.*, vol. 74, pt. III, Oct. 1955, pp. 801–09.

5. POTENTIALFELDER DER ELECTROTECHNIK, F. Ollendorf. J. Springer, Berlin, Germany, 1932.

Future Application Needs of Carrier Pilot Relaying

T. A. CRAMER
ASSOCIATE MEMBER AIEE

F. C. KRINGS
MEMBER AIEE

THE electrical industry has exhibited an expansion rate characterized by the doubling of kilowatt-hour output every 10 or 11 years. This geometric rate of growth has, in turn, required a similar increase in the use of carrier for all types of communication functions; however, this paper is mainly concerned with the future needs for carrier pilot-relaying channels.

Other types of communication media, such as microwave, will undoubtedly play a part in the expansion of pilot-relaying channels. However, carrier will continue to provide an overwhelming majority of these relaying channels because carrier is the best over-all answer to the combined need for speed, reliability, economy, and simplicity.

The carrier-relaying installations, which presently number about 3,000, may increase to double the present number as the electrical industry expands in the next decade. If frequencies for these additional relaying channels are to be obtained as well as frequencies for the future carrier channels for transferred trip, supervisory control, telemetering, and dispatching communication, then something must be done now about the impending frequency-congestion problem. In fact, some areas are already experiencing serious frequency congestion.

Maximum Utilization of the Carrier Spectrum

Because of the special nature of the carrier-relaying application, there are a number of practical steps that can be taken to achieve maximum utilization of the carrier spectrum. One of these is the frequent repeating of the same frequency throughout the power transmission system. Usually the same frequency can be reused on nonadjacent line sections. This practice makes maximum use of the impedance of the two line traps tuned to the same frequency and of the isolation obtained by the intervening line section, as shown in Fig. 1. The repeating of existing frequencies has already helped to solve congestion in some areas, and this practice should be expanded.

Another important step is to use a receiver sensitivity adequate for the particular application but not greater than necessary. The large majority of the transmission lines are of relatively low attenuation and, of course, a relay channel is always fully trapped; therefore, the carrier attenuation of an average line may be less than 10 decibels (db). Thus, the sensitivity setting need only be sufficiently above line attenuation to give an adequate margin (approximately 10 db) for the changes in attenuation resulting from adverse weather conditions and other causes. Increasing the sensitivity beyond the requirements of the application is equivalent to wasting the frequency spectrum because this would require an increased spacing between channels to avoid interference.

The third and most important step is to use carrier equipment with characteristics which will permit the closest possible frequency spacing. The important equipment characteristics are: selectivity or bandwidth of the receiver, frequency stability, and reduction in harmonic output.

Paper 55-695, recommended by the AIEE Carrier Current Committee and approved by the AIEE Committee on Technical Operations for presentation at the AIEE Fall General Meeting, Chicago, Ill., October 3–7, 1955. Manuscript submitted June 7, 1955; made available for printing July 25, 1955.

T. A. CRAMER is with the General Electric Company, Syracuse, N. Y., and F. C. KRINGS is with the General Electric Company, Schenectady, N. Y.

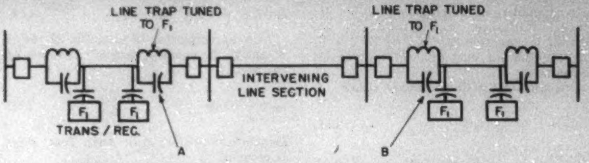

Fig. 1. The frequency of a relay channel f_1 is reused on nonadjacent line sections. The line traps A and B tuned to f_1 and intervening line section help provide isolation

Selectivity is the characteristic used to define the ability of the receiver to reject an unwanted signal. Therefore, the greater the selectivity, the closer the channels can be spaced and thus the frequency spectrum is used to a maximum. However, there is a limit to the amount of selectivity that can be used since the tuned circuits giving the desired characteristic also cause a delay in the build-up and decay time of the received relaying signal as well as causing a phase shift.[1]

New Carrier-Relay Equipment Characteristics

The new carrier-relay equipment described has been designed to fulfill all of these basic requirements. To obtain the minimum possible spacing between carrier-relaying channels, the selectivity of the new receiver has been increased to the maximum value which can be employed without increasing the over-all relaying time; i.e., the time between the keying of the transmitter and the build-up of current in the remote receiver relay is sufficiently short so that directional-comparison relays of the electromechanical type can be used without requiring additional relaying time. The selectivity characteristic is shown in Fig. 2 and has the same bandwidth for any frequency from 30 to 200 kc. This improvement is made possible by the use of filter techniques instead of the simple tuned circuits that have been used in previous designs.

The large increase in selectivity obtained with this new design will enable two or three relay channels to occupy the space formerly taken by one channel. Spacings closer than 5 kc can be used under the more severe application conditions; i.e., even when the range of the channel is to be 40 db (sensitivity setting is to be 40 db) and the channels are closely coupled together. In the more normal application, 1 to 3 kc will be ample spacing for the relaying function. Thus, the task of finding new carrier frequencies has been made relatively easy.

Direct crystal control of the new transmitter is used for maximum frequency stability. A carefully designed filter is included in the transmitter output circuit to attenuate all harmonics that fall in the 30-to 200-kc band by more than 50 db, and an even greater attenuation for harmonics above this band. The transmitter filter has a sufficiently low insertion loss so that 10 watts of carrier power is delivered at the output terminal.

The new design uses the techniques and practices that have been highly successful in preceding equipments. Long-life or preaged tubes are conservatively used and will give the 1- to 2-year average life expected of equipment for this type of service. Transistors were considered for this design but power transistors are still somewhat in the development state, and it was decided to obtain further experience before placing them in an equipment already having a remarkable reliability record. The new equipment is illustrated in Fig. 3.

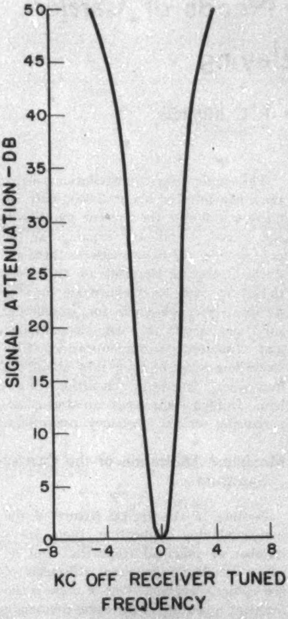

Fig. 2. Typical receiver filter selectivity characteristic

Voice-Communication Facilities of the New Equipment

This new design for minimum channel spacing is based upon a new philosophy with regard to the emergency or test telephone communication feature. With the advent of carrier pilot relaying more than 20 years ago, everyone recognized the desirability of having voice communication between the terminals for original adjustments and subsequent testing of the channel. In some cases, the relay channel was depended upon for regular system communication with the result that the necessity for transmitting good voice quality became the criterion for channel bandwidth and channel spacings rather than the relaying function. Investigation has revealed that carrier and relay engineers recognize that the test communication may well be eliminated in favor of maximum selectivity, resulting in the maximum number of carrier-relay channels in the available spectrum. A better arrangement is to group the relaying frequencies closely together and thus clear a space in the spectrum for a high-grade party-line carrier-telephone channel.

In this design, therefore, provision has been made for voice communication only during the adjustment period by a portable plug-in voice unit consisting of a modulator and voice receiver. This is illustrated in Fig. 4.

This voice unit is completely transistorized and utilizes small-size components to improve its portability. The reliability and the standardization of transistors have progressed sufficiently to allow their conservative application to this incidental voice feature. Transistors for this purpose contribute to the small-size and low-power absorption features that are desirable but in no way present a hazard to the relaying function.

The bandwidth of the relay receiver filter is much too narrow for communication; however, by using only a portion of this filter, sufficient bandwidth is obtained for voice communication without affecting the selectivity of the relaying function. The control circuits are arranged so that a power output of approximately 1 watt is used for communication, but with

Fig. 3. Typical directional-comparison relaying assembly in a 72-inch swing-rack cabinet

the protective relays having full preference over the channel at all times. The protective relays can either increase the transmitter power instantly to 10 watts or turn the carrier off, as required. Thus, provision for communication facilities for maintenance or adjustment has been provided without sacrificing the requirement of maximum selectivity and, consequently, minimum permissible spacing.

The Spacing of Existing Relay Channels

The minimum permissible spacing between any two channels is dependent upon the characteristics of the channel equipment having the lesser degree of selectivity. Therefore, the spacing between existing relay channels and a channel using the new design of equipment would be determined by the selectivity characteristic of the existing channel equipment. This may mean that some of the older outmoded equipment which uses too much of the frequency spectrum should be replaced; however, the more recent equipments are adequate in all respects except for their selectivity.

Recognizing the need for improved selectivity for equipments already installed, a filter has been designed that will give the required selectivity characteristic when added to these existing equipments. The filter, when mounted on a chassis, is called a selective amplifier. The amplification is necessary to make up the loss through the filter. The selective amplifier, illustrated in Fig. 5, can be applied to many equipments now in service.

Conclusions

The number of carrier-relaying installations may double in the next decade. This tremendous expansion in relaying channels along with the expected expansion in other types of carrier applications will cause serious frequency congestion unless the following steps are taken now to achieve maximum utilization of the carrier spectrum. The important steps are:

1. The use of carrier-relaying equipment with maximum permissible selectivity, such as the equipment described in this paper.
2. The use of sensitivity settings that are no greater than necessary for the application.
3. The reuse of the frequencies of relay channel on other nonadjacent line sections of the transmission system.

Reference

1. THE RELATION BETWEEN BANDWIDTH AND SPEED OF RESPONSE IN POWER SYSTEM CONTROL CHANNELS, J. S. Smith. AIEE *Transactions*, vol. 71, pt. III, Dec. 1952, pp. 1047-51.

Discussion

S. C. Bartlett (American Gas and Electric Service Corporation, New York, N. Y.): We find the paper most interesting and we very definitely agree with the basic premises leading to this study and development of an improved carrier relay set. At first sight it might appear that carrier-current relaying, at least the power directional type, in requiring simply an "off-on" function of the carrier, could be handled in a very narrow portion of the spectrum. On the other hand, we find, particularly as we go toward higher line voltage and power, the time available for the transmission of the carrier signal—especially the change from "on" to "off"—narrows down to a fraction of a millisecond. This rate of change, in turn, requires substantial bandwidth and the ideal set must be a compromise between the telemetering-type equipment and voice-channel equipment. The authors' solution to obtain the required bandwidth with the closest possible spacing from adjacent channels through the use of band-pass filters is excellent. We wish the paper might have shown by curves or other means the relation between rate of change and selectivity as we know it with conventional circuits, and again, the relation by using the band-pass filters.

As far as crystal control is concerned, we have used it for years for carrier-current telephone, telemetering, and more recently for transfer trip, and certainly have no resistance to its application for relaying. We assume that in the interest of attaining the required rate of change the crystal oscillator will run continuously. This is not objectionable except that the local receiver, being on the same frequency, must be protected by adequate shielding.

We further agree with a modulator as used with the pilot relay set should be restricted primarily to the purposes of channel testing, for emergency communication, and as such, it could be a very elementary device capable of providing only bare intelligibility.

The work of the authors is to be commended, not only in the preparation of this paper, but particularly in the concept and development of the equipment itself.

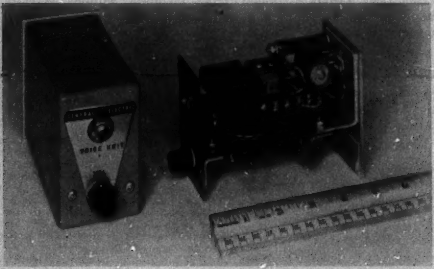

Fig. 4 (left). Plug-in voice unit combining voice modulator and voice receiver, shown with cover removed

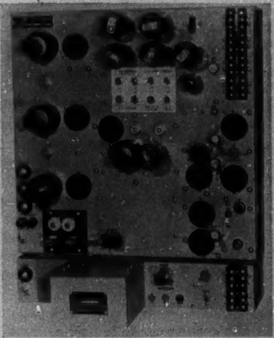

Fig. 5 (right). Selective amplifier unit added to a superseded model of directional - comparison relaying assembly

J. G. Carter (Westinghouse Electric Corporation, Baltimore, Md.): The authors have shown a number of methods in which better use can be made of the frequency spectrum, not only by using up-to-date equipment, but by applying it more carefully.

I would like to suggest one further method, that of using the spectrum between 200 and 400 kc. A discontinuous function like relaying will offer negligible interference to other services in this range, all of which are coastal communication and therefore unlikely to be interfered with by radiation from power lines in any case.

The authors state that "in the more normal application 1 kc to 3 kc will be ample spacing for the relaying function." However, close examination of the curve in Fig. 2 indicates that the receiver filter attenuates a signal 1 kc off center by about 8 db.

Assuming that the receiver requires a 10-db signal/noise ratio to give an adequate margin for reliable operation, it would seem that an undesired signal 1 kc away would need to be 2 db below the level of the desired signal.

Now if we consider two relay channels on adjacent line sections, each transmitter receiver will only be separated by a line trap from the bus. A single-frequency line trap under the most favorable conditions has a resonant resistance of 9,000 ohms at average frequency, and the trap for the next section, tuned 1 kc off, would have a resistance of about 4,000 ohms. Beyond this is, say, a 500-ohm line, so the maximum attenuation between sections due to the traps is 28 db. However, this is seldom if ever realized because the signal couples to the other two phases which are untrapped, and then back to the original phase, so that the effective attenuation of the traps might be only 10 db and it would be unsafe to count on more than this.

The undesired signal from the adjacent section thus will be only 10 db down from full transmitter output, and the desired signal must be 2 db above this. Therefore the attenuation of the line section is limited to 8 db under the worst conditions of weather, switching, etc., for reliable operation. I would question whether so low an attenuation could be considered a "normal" application.

George W. Fox (Union Electric Company of Missouri, St. Louis, Mo.): The authors seem to have done an excellent job in defining the problem that confronts all large users of carrier and at the same time have offered several solutions.

Our system has, for some time now, felt the squeeze of less and less carrier channel spectrum space availability for typical carrier use such as relaying, voice, telemetering, and supervisory. This problem has become even more acute when large power systems, having a considerable amount of power-line carrier, interconnect with other large utilities for pool operation. The communication engineer then not only has to worry about his own carrier needs, but also when planning new channels or rearrangement of channels in his system he must now consider what interference may be produced with his interconnected neighbors.

The lack of carrier spectrum space already has, or will shortly, force many utilities to go to more expensive means for handling various intelligences required for relaying, telemetering, load control, etc. One such medium is microwave. We do not feel that the ultrahigh- and superhigh-frequency arts have yet progressed to the point where relaying channels can be indiscriminately placed on microwave when other forms of communication (principally carrier) exist. We do not wish to imply that microwave cannot, or should not, be used for relaying applications. However, for the long-haul systems, we still prefer carrier—even to the extent of taking an existing voice channel off of carrier and putting it on microwave in order to gain spectrum space for carrier relaying channels. It is definitely believed, as was pointed out in this paper, that increasing receiver selectivity, hence decreasing bandwidth, thereby allowing closer "carrier stacking," is a step in the right direction. Of course, one must pay careful attention to carrier design details to see that over-all relaying time is not increased. Some consideration must also be given to receiver sensitivity. Crystal-controlled transmitters with attendant receiver stability are necessary when one starts stacking carrier with minimum guard bands.

This paper echoes thinking which we have had for years. We never have sanctioned the dual use of relay carrier channels for both relaying and voice functions. We have always felt that relay channels should be kept clean as possible and should be designed as such; namely, for relay functions and not for high-quality voice (with its requirement for greater bandwidth). Almost invariably other voice channels such as carrier, microwave, etc. are available to service personnel over the same routes as the relay carrier. We have always purchased carrier with the voice feature added merely as a convenience to our communication and relay testers. The voice-channel quality does not necessarily have to be high for such purposes and the usage is held to a minimum.

This paper mentions repeating carrier frequencies at different points in the system. We have never followed such a practice and feel that such should be avoided if at all possible. We have found it virtually impossible completely to trap carrier signals and therefore feel that one lays himself open to possible embarrassment should it be found that false relay operations are attributable to other carrier signals. Thus far we have been able to stagger frequencies relying on sharp receiver selectivity.

T. A. Cramer and F. C. Krings: We are glad to receive Mr. Bartlett's comments, particularly those regarding the telephone use of the channel. The crystal oscillator does operate continuously in order to avoid the starting time delay and since this is not a high-gain receiver the shielding problem is not difficult.

Mr. Carter mentions the use of the 200- to 400-kc band as a suitable place for protective relaying and this equipment is designed so that it can easily be extended into that band by changing crystals and filters, but we feel that a word of warning should be given since this band still is used for airway beacons. Any utility contemplating the use of frequencies above 200 kc should assure themselves that they will not cause interference to some local installation. Regarding the remainder of his discussion, if conditions were as he has stated then, I would agree that spacings of 1 to 3 kc would not be possible in a normal installation. Our field experience has shown that today the impedance looking from the line into the bus is not 500 ohms as assumed, but more like 100 ohms or even 50 ohms. With this low bus impedance it can readily be seen how frequencies can be repeated on alternate line sections and in some cases on the opposite side of the same bus. This has actually been done in practice and it is for this reason that we always advise that the minimum frequency spacing be determined by field test rather than by office calculation.

Mr. Fox's comments are very clear and helpful, and we would like to comment on his statements regarding the repeating of carrier frequencies. This practice has been used successfully for years by several utilities, and when properly done represents no hazard to correct carrier relaying. It appears that Mr. Fox is fortunate in his system since he can eventually repeat some of his relaying frequencies and thus obtain more channels without actually using any additional carrier spectrum space.

Economic Selection of Auxiliary Drive Motors in Power Plants

E. T. B. GROSS
FELLOW AIEE

V. F. BOBROWICZ
ASSOCIATE MEMBER AIEE

DRIVE motors for auxiliaries in steam power plants are generally selected by means of simple time-tested methods. It is wise to review these application methods from time to time to effect additional economies. The existence of relatively large margins between design requirements of auxiliaries and the nominal ratings of their drive motors suggests a study of the necessity of these margins.[1] It was decided to review the auxiliaries in a typical modern power plant to determine what margins actually existed after the power plant was in operation. This required obtaining typical data at the power plant, including the actual motor outputs for various generator loads.

On this basis it was possible to determine whether the drive motors installed were the most favorable alternatives available. The analyst is here at an obvious advantage in comparison with the designer since the actual requirements of the auxiliaries are known and any uncertainties in the design figures can be eliminated.

Descriptive Information on the Specific Power Plant

The steam power plant studied was built within the last 3 years. The specific unit went into operation in mid-year of 1953. The generator output is normally 75 megawatts (mw) throughout most of each operating day though the name-plate rating of the unit is 60 mw.

The auxiliaries under consideration were those driven by motors operating at 2,300 volts. The motors are listed in Table I, and more detailed information is given in Tables II and III. The induction motors have squirrel-cage rotors, standard dripproof covers and class-*A* insulation. In many cases a modified class-*A* insulation, specifically for power plant use, was installed. These motors have service factors of 1.15. Any synchronous motors are provided with motor-generator sets as exciters and operated at unity power factor (pf). The enclosure used is such that no service factor is allowed.

While there are two boiler feed pumps available for the unit, only one is motor driven. Each is designed to supply the full demand and the motor-driven pump is normally in use. Further discussions of the power plant and its auxiliaries are contained in later sections.

Design Requirements of the Auxiliaries

When a new unit for a power plant is in its design stages, engineers representing various manufacturers and the utility are involved in the selection and application of equipment. When the pumps, fans, and coal mills are contracted, arrangements are made to select the drive motors by one of two methods. The manufacturers may provide the design engineer with the characteristics of the auxiliaries referred to the motor side of the coupling. On the basis of this information, the design engineer makes the choice of drive motor for the specific application. Another method involves purchasing the auxiliary and its drive motor as one complete unit. In this way, the pump, fan, or coal mill manufacturer negotiates directly with motor vendors for the drive motor and furnishes his product along with its motor as a package unit. In some of these cases, motor and auxiliary will be manufactured by divisions of the same company. Most of the installed drive motors for the auxiliaries in the plant under study were selected by the latter of the two methods.

These design requirements were compared with the nominal and maximum ratings of the drive motors installed and the margins in the motors were computed. The results of this comparison are presented in Table IV.

The maximum available horsepower (hp) is the rating of the motor times its service factor. Since all the induction motors have either class-*A* insulation (or class-*A* insulation for power-house use) and dripproof covers, all service factors are 1.15. Class-*A* insulation is good for a total temperature of 105 degrees centigrade (C) without charring or unduly shortening its life. This total temperature is based on a 40 C ambient temperature, a 40 C temperature rise for an open or dripproof motor, a 15 C rise for hot spots, and 10 C to permit the service factor.

It can be seen from Table IV that the maximum hp which the motor can deliver continuously without injurious temperature rise is from 25.0 per cent to 58.6 per cent greater than the maximum design brake hp input into the coupling of the auxiliary. The design brake hp requirements contain additional margins because of the mechanical design of the auxiliary. These margins on the mechanical side are common. In designing fans, for instance, certain conditions which can be maintained on test are seldom, if ever, duplicated in an actual installation. It is practically impossible for the manufacturer to test a fan under actual service conditions. The connections made to a fan may influence its performance to such a degree that it would be unwise for the mechanical engineer to select a fan without large tolerances.

Large margins are also common in the boiler feed pumps. (These pumps are usually driven by the largest motors in the power plant.) Gaffert[2] states that a customary margin above the maximum boiler output may be about 20 per cent. The maximum design requirements on boiler feed pumps are for capacities corresponding to 120 per cent and even 125 per cent of the normal full-load boiler rating.

Whether the mechanical design margins actually exist can only be determined after the power plant is in operation. If they are present, the margins between maximum drive motor loads and drive motor ratings will be even greater than the margins indicated in Table IV.

The generator ordinarily operates at an output of either 30 or 75 mw and only a few hours each week at 45 and 60 mw. The total number of operating hours per week at each of the levels of unit output are listed in Table V.

More specifically, the unit is scheduled to operate Monday through Friday with a daytime load of 75 megawatts and a

---

Paper 55-681, recommended by the AIEE Power Generation Committee and approved by the AIEE Committee on Technical Operations for presentation at the AIEE Fall General Meeting, Chicago, Ill., October 3–7, 1955. Manuscript submitted June 6, 1955; made available for printing July 19, 1955.

E. T. B. GROSS and V. F. BOBROWICZ are with the Illinois Institute of Technology, Chicago, Ill.

The authors wish to acknowledge the help received in discussions with design engineers of consulting engineering firms and with application engineers of various manufacturers. The authors are very grateful to the operating engineers of the modern power plant referred to in this investigation; this study could not have been possible without their co-operation in supplying important data from the records. Thanks are due to Dr. G. J. Matchett, Professor of Economics at Illinois Institute of Technology, for his contributions in various informal discussions.

Table I. Motors Considered

Auxiliaries	No. of Drive Motors	Type of Motor	No. of Poles	Rated Hp of Installed Motors
Boiler feed pumps	1	induction	2	2,000
Induced draft fans	2	induction	6	600
Forced draft fans	2	induction	6	350
Coal mills, pulverizers, and exhausters	3	induction	8	350
Circulating water pumps*	2	induction	12	250
Condensate pumps	2	induction	6	200
Service water pumps*	3	induction	4	200
Ash-sluice pumps	2	induction	4	125
Soot-blower air compressors	2	synchronous	22	400

* Indicated motors are vertically mounted.

Table II. Name-Plate Data of Installed Motors

Auxiliary Driven by Motor	Rating, Hp	Full-Load Speed, Rpm	Full-Load Current, Amperes	Insulation Class
Boiler feed pump	2,000	3,570	425	*A*
Induced draft fans	600	1,180	132	*A*
Forced draft fans	350	1,185	78	*A*
Coal mills, pulverizers, and exhausters	350	880	85	*A*
Circulating water pumps	250	585	60	*A*
Condensate pumps	200	1,170	46.5	*A*
Service water pumps	200	1,770	45.3	*A**
Ash-sluice pumps	125	1,775	29	*A**
Soot-blower air compressors	400	327	80.3	*A*

* Class-*A* insulation, Power-House type.

Table III. Characteristics of the Installed Motor

Auxiliary Driven by Motor	Locked Rotor Torque, Per Cent of Full-Load Running Torque	Break-down Torque, Per Cent of Full-Load Running Torque	Locked Rotor Current, Per Cent of Full-Load Current	Efficiency at Fraction of Rating, Per Cent			Pf at Fraction of Rating		
				1/2	3/4	4/4	1/2	3/4	4/4
Boiler feed pump	75	200	550	94.1	95.2	95.6	0.890	0.910	0.920
Induced draft fans	100	200	550	91.5	93.2	93.5	0.848	0.893	0.908
Forced draft fans	100	200	650	90.8	92.5	92.8	0.810	0.855	0.885
Coal mills, pulverizers, and exhausters*	200			90.6	92.4	92.6	0.796	0.847	0.887
Circulating water pumps	90	200	575	90.2	91.4	91.4	0.732	0.820	0.860
Condensate pumps	100	200	650	88.5	91.1	91.8	0.850	0.885	0.890
Service water pumps	100	200	613	90	92	92	0.820	0.880	0.900
Ash-sluice pumps	110	200	600	88	90.5	91	0.800	0.870	0.890
Soot-blower air compressors	40		325	92.8	93.7	94.0	†	†	†

* Characteristics not available, estimates are shown.

† Normally at unity pf.

night load of 30 megawatts. Between 6:30 and 7:00 a.m., the load is increased from 30 mw to 75 mw. In the evening the load is decreased to 30 megawatts between 11:00 and 11:30 p.m. On Saturday, the schedule is similar to the weekday schedule except that the load is not increased to 75 mw until between 7:30 and 8:00 a.m. The Sunday schedule is to increase the load from 30 to 45 mw at about 7:00 a.m. The load remains at an average of 45 mw throughout the day, except for a peak period at 75 mw which occurs between the hours of 6:00 and 9:00 p.m.

Current taken by each motor at each of the preceding levels of unit load was metered. Motor currents corresponding to a test condition of 80 mw were also obtained. These data are presented in Table VI.

In most cases, the currents tabulated for the fans were read before the loads on the two motors had time to equalize. As the unit is brought to a new level of output, the fans may not pick up equal shares of load. This period of unbalance may even last for a few minutes after the unit has reached its new level of output. This accounts for the difference in current taken between the fan motors. This difference is especially noticeable between the two motors driving the ininduced draft fans.

The currents taken by the fan motors at 80 mw are shown in Table VI as being less than the current at 100 per cent of unit output. This is because of favorable atmospheric conditions on the day the tests were made at 80 mw. The fan currents at 75 mw are for adverse barometric pressure conditions. Hp output and current of a fan motor vary directly as the absolute temperature, and inversely as the absolute pressure.[3]

The load on the induced draft fan drive motors is also influenced by the temperature of the oil in the fluid coupling and by the relative cleanliness of the mechanical precipitators. One factor affecting the load on the forced draft fans is air recirculation. The quantity of recirculated air is greater at lower loads. During the test, the quantity of recirculated air was reduced as the load on the boiler came up to where the generator output was 80 mw.

Some of the auxiliaries are shown as OFF in Table VI. These are the auxiliaries which either do not normally operate at certain levels of generator load or are stand-by units. Coal mill no. 1 is off below 55 mw because of an undesirable low feeder speed. This mill is in use at all outputs above 55 mw. River water conditions dictate whether or not two circulating water pumps are needed. Generally, during the summer months, both pumps are in operation because of the warmer temperature of the water. The ash-sluice pump and soot-blower air compressor are operated intermittently each day. The total time the ash-sluice pump is operating amounts to about 3 hours each day. The soot-blower air compressor works for about 5 hours each day.

Actual Output of the Drive Motors

From the currents in Table VI and the efficiency and pf characteristics of Table III the motor output was computed using.

$$(hp_{\text{out}})_j = \frac{\sqrt{3}EI_j(pf)_j(eff)_j}{745.7} \qquad (1)$$

where

$(hp_{\text{out}})_j$ = the motor output corresponding to the jth level of unit output, hp
I_j = the current taken by the motor corresponding to the jth level of unit output, taken from Table IV
E = the line voltage, assumed 2,300 volts at the motor terminals
$(pf)_j$ = the pf of the motor at an output of $(hp_{\text{out}})_j$
$(eff)_j$ = the efficiency of the motor at an output of $(hp_{\text{out}})_j$

The voltage was assumed at 2,300 volts on the terminals of the motor. The bus voltage at the plant is normally 2,350 volts and may be as high as 2,380 volts

Table IV. Margins Above Maximum Design Requirements Provided by Installed Motors

Auxiliaries	Maximum Design Brake Hp Requirements	Hp of Installed Motor	Margin of Nominal Hp Above Design Brake Hp, Per Cent	Maximum Hp Available, Including Service Factor	Margin of Maximum Hp Above Design Brake Hp, Per Cent
Boiler feed pumps	1,750	2,000	14.3	2,300	31.4
Induced draft fans	540	600	11.1	690	28.7
Forced draft fans	322	350	8.7	402	25.0
Coal mills	310	350	12.9	402	29.6
Circulating water pumps	199	250	25.6	287	44.2
Condensate pumps	156	200	28.2	230	47.5
Service water pumps	145	200	38.0	230	58.6
Ash-sluice pumps	113.5	125	10.1	144	26.6
Soot-blower air compressors	388	400	3.0		

Table V. Total Number of Operating Hours Per Week at Each Level of Unit Output

Unit Output, Mw	Output, Per Cent of 75 Mw	Number of Hours per Week
30	40	51.75
45	60	8
60	80	9.5
75	100	98.75

during time of light loads. The assumption of 2,300 volts is justifiable considering the accuracy of the current readings and the voltage drop in the cables to the motors.

The efficiencies and pf were determined by linear interpolation of the characteristics in Table III. The fan motor outputs were below one half of rated load at times of light generator outputs. The forced draft-fan drive motor output was as low as 30 per cent of motor rating at a generator output of 30 mw. The output of the drive motor on the induced draft fan was only 17.5 per cent of its rating at 30 mw. Since the characteristics in Table III included efficiencies and pf for loads above 50 per cent of motor rating, it was necessary to assume efficiencies and pf for all motor outputs below one half of name-plate rating. These assumed values were read from induction motor circle diagrams.

Complete data on the drive motors for the mills, pulverizers, and exhausters were not available and efficiencies and pf had to be assumed. The drive motors are National Electrical Manufacturers Association (NEMA) design *C*, but the pf and efficiencies tabulated by manufacturers do not include these motors.

The efficiencies and pf which were assumed are those corresponding to a design-*B* motor and are probably higher than the actual efficiencies and pf. This assumption leads to calculated motor outputs which may be larger than they actually are. However, this assumption is conservative and the error introduced is negligible.

The drive motor outputs as computed from equation 1 are given in Table VII. For purposes of comparison, the hp ratings of the motors and the maximum design brake hp requirements are retabulated. It should be noted from Table VII that none of the motors deliver their name-plate rating; only in one case, that of induced draft fan no. 2, is the load on the drive motor greater than the maximum design brake hp. This is because of a transient unbalance of load between the two fans, as discussed earlier.

The results presented in Table VII confirm preliminary estimates of margins between load requirements and drive motor ratings. Not only do the margins listed in Table IV exist but they are in reality even larger because of the margins incorporated into the mechanical design of the auxiliaries. It is now appropriate to reconsider the choices of drive motors for these auxiliaries.

Method of Economic Analysis

Basis of Comparison

A comparison is made between the installed motors and the various alternative motors on the basis of difference of present worths of future expenditures. The alternative motors are called challengers and the installed motors defenders. This terminology is that used in equipment replacement studies and modified to suit the need herein.

The advantage of the challenger over the defender expressed in terms of present worth (PW) is

PW of challenger's advantage =

$$[(UAC)_D-(UAC)_{ch}]\,\frac{(1+i)^n-1}{i(1+i)^n} \qquad (2)$$

where

$(UAC)_D$ = the uniform annual cost (UAC) equivalent of all expenditures attributable to the defender over its primary service life

$(UAC)_{ch}$ = the UAC equivalent of the challenger over its primary service life

$\frac{(1+i)^n-1}{i(1+i)^n}$ = the PW factor for converting a UAC series to its present equivalent[8]

The interest rate i will be discussed later. It can be seen from equation 2 that the PW will be compared over the same number of years n for all alternatives. This will be done regardless of what may be later assumed for the lives of the alternatives.

The first term of equation 2, $[(UAC)_D-(UAC)_{ch}]$, is the UAC advantage of the challenger over the defender. Cost advantages are being used to simplify calculations and to eliminate computation of complete total expenditures. The challenger's advantage, or defender's inferiority, is comprised of two major parts. The first is a capital recovery cost advantage and the second is an advantage of annual equivalent operating expenditures. For any motor, the annual

Table VI. Comparison of Motor Name-Plate Current with Actual Current Taken

Auxiliary Driven by Motor	Rated Current, Amperes	Current* Taken Corresponding to Unit Output of 40 Per Cent	60 Per Cent	80 Per Cent	100 Per Cent	106.5 Per Cent
Boiler feed pump	425	230	250	285	345	360
Induced draft fan no. 1	132	48	56	71	115	120
Induced draft fan no. 2	132	43	57	75	124	107
Forced draft fan no. 1	78	36	40	48	66	58
Forced draft fan no. 2	78	37	40	47	63	56
Coal mill pulverizer and exhauster no. 1	85	off	off	60	64	63
Coal mill pulverizer and exhauster no. 2	85	58	59	58	63	61
Coal mill pulverizer and exhauster no. 3	85	56	58	58	60	63
Circulating water pump no. 1	60	43	45	45	44	44
Circulating water pump no. 2	60	off	off	off	off	off
Condensate pump no. 1	46.5	26	27	28	31	33
Condensate pump no. 2	46.5	off	off	off	off	off
Service water pump no. 1	45.3	30	30	30	30	30
Service water pump no. 2	45.3	off	off	off	off	off
Service water pump no. 3	45.3	off	off	off	off	off
Ash-sluice pump no. 1	29	20			20	
Ash-sluice pump no. 2	29	off	off	off	off	
Soot-blower air compressor no. 1	80.3	65			65	
Soot-blower air compressor no. 2	80.3	off	off	off	off	

* In amperes.

cost of capital recovery which includes depreciation and interest is

$$\text{capital recovery} = (C-S)\frac{i(1+i)^N}{(1+i)^N-1} + Si \qquad (3)$$

where

C = the initial cost of the motor including shipping, testing, and installation costs

S = the salvage value of the motor at the end of its primary service life

$\frac{i(1+i)^N}{(1+i)^N-1}$ = the capital recovery factor

N = the primary service life of the motor and will be defined later

The annual equivalent of operating costs and other expenditures attributable to the motor are given by

$$\text{annual expenditures} = Q+M+T \qquad (4)$$

where

Q = annual incremental costs of power consumed by the motor, and will be discussed later

M = uniform annual equivalent of maintenance costs, including routine maintenance, bearing replacements, and coil revarnishings

T = annual charges for state taxes, local taxes, and insurance

Combining the annual cost of capital recovery as given in equation 3, with the uniform annual equivalent of operating and other costs, as given in equation 4, the UAC equivalent of all expenditures attributable to any motor is defined as

$$(UAC) = (C-S)\frac{i(1+i)^N}{(1+i)^N-1} + Si+Q+M+T \qquad (5)$$

INITIAL COSTS AND SALVAGE VALUES

The price of the motor to the utility was computed from catalogues using appropriate discounts. The prices of the defenders were acquired from the operating utility and converted to present day prices in order to have all prices referred to the same date. The prices did not include moving the motor into its place in the plant. Costs of connecting and testing also were not included.

An average range of installation and testing costs is from 2 to 5 per cent of the motor price depending on size of the motor and its location in the power plant. In this study, 3 per cent of the motor price was assumed.

Salvage values of the motors upon termination of their service lives are a function of motor weight if junk values are assumed. A figure of $70 per ton was the best junk price which could be received for the types of motors considered in this study under current conditions.

The rate of return used in economic studies should not be less than the cost of capital to the company, whatever may be the source of investment funds available to it. Also, this rate of return should not be less than the rate that could be otained if the funds were to be invested elsewhere with similar risk and similar tax status. Another factor that may be considered is the rate currently being earned by the company on its capital investment.

In the case of privately owned power companies, the fair rate of return which is allowed by the respective Commerce Commission is the rate of return which should be used in investment studies. The fair rate of return set by the various state Commerce Commissions has ranged between 5.8 per cent and 7.0 per cent, depending upon the size of the corporation and the ease with which the management can borrow capital. While the operating utility of the specific power plant studied is not the largest, it is among the most progressive in its region and should be able to acquire capital at a comparatively low cost. With this in mind, 5.8 per cent is chosen as the rate of return to use in economic studies for this utility.

Income tax is commonly included in utility investment studies as a fixed charge. In this study, however, income tax will be included in the interest rate i. Use of 5.8 per cent as the rate of return on investment after taxes was justified. Modification of the rate of return after taxes permits the of an interest rate which includes the effect of the income tax. Since the income tax rate is 52 per cent, the interest rate is

$$i = \frac{5.8 \text{ per cent}}{1-0.52} = 12.083 \text{ per cent} \qquad (6)$$

as used in this study: it can also be referred to as the rate of return before income taxes. To ease computation, 12 per cent was actually used.

A further assumption is that income will remain constant regardless of the alternative chosen. As long as the choice of drive motor for any auxiliary does not limit the unit output, which it should not, revenue will remain constant. However, if the investment in motor A is less than the investment in motor B, the net income will be larger if motor A is installed. It is this small difference in net income which will be neglected as a simplifying assumption.

ESTIMATING MOTOR LIFE

Matchett[6] states that the proper life to use in economic studies is the period of time during which the asset will be in operation for the major purpose for which it was originally acquired. This period of time does not include the number of years that the asset may be utilized in either a downgraded or a stand-by capacity. Terborgh, in his "Dynamic Equipment Policy,"[15] refers to this as the primary service life of the asset, i.e., the period prior to its first replacement. In this study, this period is the same as the total life span of the motor. This is true because of the assumption that the motor is scrapped at the termination of its primary service life.

As an additional assumption, obsolescence, either of the steam power plant or of any of the drive motors, may be neglected. This greatly simplifies the analysis since only physical deterioration need be considered as affecting the primary service life. Primary service life, as it is used throughout this study, can now be defined as the number of years the motor will operate continuously before a major failure occurs.

Motor manufacturers provided some characteristics of the motors which would relate primary service life to some other variable quantity. It appears that the variable quantity affecting primary service life is the internal temperature of the motor. Life and temperature are related by a logarithmic function. It was decided to use the most optimistic of various rules in determining the primary service life of the motors, and the resulting curves for class-A and class-B insulations are shown in Fig. 1.

The ordinate of the curve is expressed in terms of maximum load expressed as multiple of rating instead of in temperature. The relation is obvious since, for a motor with class-A insulation, a 10 C temperature rise above rated load is permitted to allow for a 15-per-cent service factor. The total temperature rise to the maximum rating of a class-A motor is 50 C.[7] This same motor with class-B insulation is permitted a total rise of 80 C. Since the losses above full load vary primarily as the square of the current, a maximum rating for the class-B motor in the same ambient could now be assumed. It is this rating which corresponds to the 1.15-per-unit rating of the motor with class-A insulation.

It was assumed that no motor would have a primary service life of more than 40 years. In the analysis to follow, while motors will be applied to deliver more output than their name-plate rating, the maximum ratings, Fig. 1, assumed in the foregoing will not be exceeded.

Table VII. Comparison of Motor Rating and Maximum Design Requirements of Auxiliary with Actual Hp Outputs of Motors

Auxiliary Driven by Motor	Rated Hp	Maximum Design Brake Hp	Hp Output Corresponding to Unit Output of 40 Per Cent	60 Per Cent	80 Per Cent	100 Per Cent	106.5 Per Cent
Boiler feed pump	2,000	1,750	1,031	1,128	1,301	1,602	1,675
Induced draft fan no. 1	600	540	125	162	282	516	540
Induced draft fan no. 2	600	540	105	169	313	559	478
Forced draft fan no. 1	350	322	105	131	191	281	241
Forced draft fan no. 2	350	322	111	131	187	267	231
Mill, pulverizer, and exhauster no. 1	350	310	off	off	252	273	268
Mill, pulverizer, and exhauster no. 2	350	310	241	246	241	268	257
Mill, pulverizer, and exhauster no. 3	350	310	231	241	241	252	268
Circulating water pump no. 1	250	199	165	176	176	170	170
Circulating water pump no. 2	250	199	off	off	off	off	off
Condensate pump no. 1	200	156	105	110	115	130	140
Condensate pump no. 2	200	156	off	off	off	off	off
Service water pump no. 1	200	145	124	124	124	124	124
Service water pump no. 2	200	145	off	off	off	off	off
Service water pump no. 3	200	145	off	off	off	off	off
Ash-sluice pump no. 1	125	113.5	80			80	
Ash-sluice pump no. 2	125	113.5	off	off	off	off	
Soot-blower air compressor no. 1	400	388	326			326	
Soot-blower air compressor no. 2	400	388	off	off	off	off	

Costs of Power Consumed

The annual costs of power consumed by the drive motor Q is given by

$$Q=\sum_{j}\frac{(hp_{\text{out}})_j 0.7457}{(eff)_j}(a_j)(h_j) \qquad (7)$$

where

j = the level of unit output
$(hp_{\text{out}})_j$ = the motor output corresponding to the jth level of unit output and is obtained from Table VII
$(eff)_j$ = the motor efficiency at the jth level of unit output
a_j = the incremental cost of power to operate the motor at jth level of unit output
h_j = the number of hours per year that the unit operates at the jth level of output

The incremental cost of power at various levels of output a includes incremental fuel costs and incremental plant maintenance costs; see Table VIII. Operating costs other than fuel and plant maintenance are constant regardless of alternative choice and are, therefore, omitted.

The number of hours per week at various levels of generator load are given in Table V. The power plant is in operation all year except for 3 to 4 weeks during the annual shutdown for maintenance. Hours per year h_j at each level of output are obtained by multiplying the hours per week from Table V by 49 weeks. It is assumed that the generator output cycle will remain identical to that discussed in the foregoing for the period of time encompassed by this study.

Table VIII. Incremental Cost of Power Consumed by Station Auxiliaries

Increment of Gross Generation, Per Cent of 75 Mw	Incremental Costs (Fuel and Incremental Maintenance), Mills per Net Kilowatt-Hour
40 to 60	2.21
60 to 80	2.26
80 to 100	2.36

A simplification will be incorporated into the computation of operating costs. Instead of using equation 7 to arrive at total operating expenditure, the challengers' annual advantages, equation 8, will be calculated. This advantage, or net saving, can be expressed as

$$Q_D-Q_{Ch}=0.7457\sum_{j}(hp_{\text{out}})_j(a_j)(h_j)\times\left(\frac{1}{(eff)_{Dj}}-\frac{1}{(eff)_{Chj}}\right) \qquad (8)$$

where

$(eff)_{Dj}$ = the defender's efficiency at the jth level of unit output
$(eff)_{Chj}$ = the challenger's efficiency at the jth level of unit output

It was assumed that for a given frame size and nominal hp rating, the motor efficiency and pf characteristics will not be influenced by the choice of insulation class. Efficiencies above nominal ratings were estimated on the basis of the motor circle diagram.

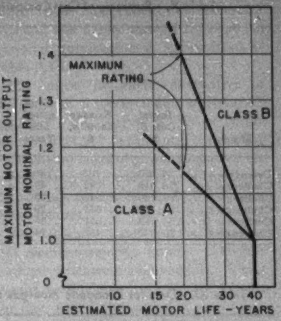

Fig. 1. Estimated life of class-A and class-B motors

Maintenance Costs, Taxes, and Insurance

Equation 4 includes a term M, which is the annual equivalent of maintenance costs directly attributable to the motor; it includes the annual equivalent of the costs of bearing replacement and coil revarnishings. This equivalent annual maintenance cost is

$$M=C_{BR}\left(\frac{1}{(1+i)^{a_1}}+\frac{1}{(1+i)^{a_2}}+\ldots+\frac{1}{(1+i)^{a_n}}\right)\frac{i(1+i)^N}{(1+i)^N-1}+C_{CV}\left(\frac{1}{(1+i)^{b_1}}+\frac{1}{(1+i)^{b_2}}+\ldots+\frac{1}{(1+i)^{b_n}}\right)\frac{i(1+i)^N}{(1+i)^N-1}+M^R \qquad (9)$$

where

C_{BR} = the cost of each bearing replacement
C_{CV} = the cost of each coil revarnishing
M_R = the routine annual maintenance cost attributable to motor
a_n = the year during which the nth bearing replacement occurs
b_n = the year during which the nth coil revarnishing occurs
$\frac{1}{(1+i)^n}$ = a PW factor to convert a future expenditure to its present equivalent
$\frac{i(1+i)^N}{(1+i)^N-1}$ = the capital recovery factor

Table IX. Data for Economic Analysis of Boiler Feed Pump Drive Motor

Motor	Nominal Hp Rating	NEMA Design Class	Insulation Class	Efficiency at Fraction of Rating, Per Cent 1/2	3/4	Full	Price of Motor, $	Motor Weight, Pounds
Defender	2,000	*B*	*A*	94.1	95.2	95.6	31,555	2,100
Challenger *A*	1,750	*B*	*A*	94.0	95.1	95.5	27,203	1,835*
Challenger *B*	1,750	*B*	*B*	94.0	95.1	95.5	29,243	1,835*
Challenger *C*	1,500	*B*	*A*	93.9	95.0	95.4	23,068	1,575*
Challenger *D*	1,500	*B*	*B*	93.9	95.0	95.4	24,798	1,575*
Challenger *E*	1,250	*B*	*B*	93.8	94.9	95.3	20,354	1,310*

* Estimated.

Table X. Summary of Cost Comparison for the Boiler Feed Pump Drive Motor

Motor	Initial Cost C, $	Salvage Value S, $	Estimated Life Years	Capital Recovery Costs, Equation 3, $	Power Costs, (Challenger's Advantage), Equation 8, $	Maintenance Costs, Equation 10, $	Taxes and Insurance, Equation 11, $	PW of Challenger's Advantage, Equation 2, $
Defender	32,501	735	40	3,941		195	560	
Challenger *A*	28,018	642	40	3,398	50	168	490	5,482
Challenger *B*	30,120	642	40	3,641	50	181	527	3,184
Challenger *C*	23,760	551	29	2,959	35	142	416	9,098
Challenger *D*	25,542	551	35	3,168	35	153	447	7,130
Challenger *E*	20,965	459	24	2,689	−56	126	367	11,506

Table XI. Data for Economic Analysis of Circulating Water Pump Drive Motors

Motor	Nominal Rating, Hp	NEMA Design Class	Insulation Class	Efficiency at Fraction of Rating, Per Cent			Price of Motor, $	Motor Weight, Pounds
				1/2	3/4	4/4		
Defender	250	*B*	*A*	90.2	91.4	91.4	6,133	5,000
Challenger *A*	200	*B*	*A*	89	90.5	90.5	5,452	4,500*
Challenger *B*	200	*B*	*B*	89	90.5	90.5	6,483	4,500*
Challenger *C*	150	*B*	*B*	89.5	90.5	90.5	5,584	4,000*

* Estimated.

Table XII. Summary of Cost Comparison for Each Circulating Water Pump Drive Motor

Motor	Initial Cost C, $	Salvage Value, $	Estimated Life, Years	Capital Recovery Costs, Equation 3, $	Power Costs, (Challenger's Advantage), Equation 8, $	Maintenance Costs, Equation 10, $	Taxes and Insurance, Equation 11, $	PW of Challenger's Advantage, Equation 2, $
Defender	6,317	175	40	765		38	111	
Challenger *A*	5,615	158	40	681	−17	34	98	1,191
Challenger *B*	6,677	158	40	809	−17	40	117	−141
Challenger *C*	5,751	140	30	713	−17	34	101	784

Table XIII. Data for Economic Analysis of Condensate Pump Drive Motors

Motor	Nominal Rating, Hp	NEMA Design Class	Insulation Class	Efficiency at Fraction of Rating, Per Cent			Price of Motor, $	Motor Weight, Pounds
				1/2	3/4	4/4		
Defender	200	*B*	*A*	88.5	91.1	91.8	2,591	2,500
Challenger *A*	150	*B*	*A*	90	91.5	91.5	2,182	2,075*
Challenger *B*	150	*B*	*B*	90	91.5	91.5	2,727	2,075*
Challenger *C*	125	*B*	*A*	90	91.5	91.5	1,951	1,550
Challenger *D*	125	*B*	*B*	90	91.5	91.5	2,439	1,550
Challenger *E*	100	*B*	*B*	89	91	92	1,889	1,500*

* Estimated.

defined earlier and is used to convert the present equivalent to a UAC series over the service life of the motor

The cost of a bearing replacement or a coil revarnishing including labor and materials is about 5 per cent of the initial cost of the motor. These capital expenditures for maintenance occur 6 to 10 years apart. Again, it was decided to use the most optimistic figures.

The routine annual maintenance is a small percentage of initial cost and, to some extent, is included in the incremental power costs in Table VIII. Since many of the items in equation 9 are approximations, equivalent annual motor maintenance costs were determined by multiplying the initial cost of the motor by a fixed percentage.

Solving equation 9 with the preceding approximations, the equivalent annual motor maintenance cost is

$$M = 0.6 \text{ per cent (initial cost of motor)} \quad (10)$$

State and local taxes and insurance costs can also be expressed as a fixed percentage of the initial motor cost. The annual expenditure for taxes and insurance is

$$T = 1.75 \text{ per cent (initial cost of motor)} \quad (11)$$

The insurance costs included in equation 11 comprise 0.07 per cent of the initial cost of the motor.

The necessary assumptions have been made and a method has been outlined for comparing alternative motors to the installed motor. The next step is now to choose the alternatives and compare them on an economic basis.

Review of Installed Drive Motors

MOTORS DRIVING THE MAJOR PUMPS

The boiler feed pump is driven by a 2,000-hp motor through an hydraulic coupling. The maximum design brake hp requirement was 1,750 hp. Under typical operating conditions, the motor outputs at 40, 60, 80, and 100 per cent of generator load were 1,031, 1,128, 1,301, and 1,602 hp respectively; see Table VII.

In choosing the challengers for this motor, the characteristics of the load were matched to the motor. The centrifugal boiler feed pump has a low inertia and requires low breakaway torque. Since the motor drives the pump through a hydraulic coupling, the motor normally starts unloaded and is accelerated to speed with little load. The acceleration of the pump and the speed of the pump are controlled by the oil pressure in the hydraulic coupling. The starting duty on the pump is not critical, hence voltage drop on starting may be neglected.

The challengers chosen are listed in Table IX. Three of the challengers, the 1,500-hp motors and the 1,250-hp motor, will be operating at times above their nominal ratings. However, the motors will be below the maximum ratings indicated in Fig. 1, even at a generator output of 80 mw.

Table X summarizes the economic comparison between the defender and challengers on the basis of PW of the challengers' UAC advantage over a 25-year period. Challenger *E* is at a net disadvantage relative to the defender on annual cost of power consumed but, in spite of this, it is the most efficient alternative from an over-all economic standpoint. Since challenger *E* operates above its nominal rating a major part of the time, its efficiency is lower than the defender's, hence the higher cost of power consumed.

It can be seen from Table X that

challenger *E* could be replaced after 24 years and still show a saving relative to the defender. Also, it should be noted that the PW of any challenger's advantage over the defender's is approximately equal to the difference between their initial costs, irrespective of the life estimate.

The cost comparison of the drive motors for the boiler feed pump reveals that all the challengers chosen would have shown a net savings over the installed motor. This comparison also shows that, for the challengers chosen, the estimated life and the annual cost of power consumed did not affect the analysis appreciably.

The circulating water pump is a low-head and high-capacity pump. The torque required at full speed and zero capacity is greater than the torque required at full load. If the pump discharge valve were opened as the motor is energized, the load would be reduced and would permit the use of normal starting torque motors. If the discharge valve were closed during starting, it would be necessary to use a motor which could drive the pump under this condition.

The pump is mounted vertically. Gaffert[2] indicates that vertical circulating water pumps have been applied in recently built power stations since increasing capital costs have required consideration of a means to decrease building volume and floor space. Circulating water pumps are usually designed for slow-speed operation. The installed pumps operate at 585 rpm.

Table XI lists the challengers chosen for the circulating water pump. Challenger *C* will require an open discharge valve on starting since it is a normal-starting torque motor. The maximum design brake hp is 199 hp. A summary of the economic comparison of these challengers to the defender appears in Table XII.

The most favorable of the alternatives is challenger *A*, which is a 200-hp class-*A*-insulated normal-starting torque motor. The defender is a 250-hp class-*A*-insulated normal-starting torque motor. The PW of the next 25-year savings is $1,191 for each motor or $2,382 for the two drive motors required for the circulating water pumps. According to the life estimates made, there should be no difference in service life between the defender and challenger *A*.

All three challengers listed in Table XII are at a disadvantage relative to the defender on cost of power consumed because of the lower over-all efficiency of all the challengers caused by differences in motor design. Motors of 250 hp and larger are of a generally different design than those below 200 hp. It may be possible to effect further economies by applying all motors of ratings below 250 hp at lower voltages.

Challenger *B* in Table XII is at a net disadvantage relative to the defender. Again, as with the boiler feed motor, the relations between challengers and defender PW are similar to the relations between motor initial costs. For the circulating water pump motors this is not so pronounced as it is for the boiler feed pump motor because of the lower intial cost of the smaller motor. The estimate of motor life and power cost advantage has a larger effect on the smaller motors.

The condensate pumps, or hot-well pumps, are used to remove the condensate from the main condenser and deliver it to the feed-water system. This pump is a medium-head and medium-capacity pump with a low breakaway torque. The choice of challengers is indicated in Table XIII. The defender is a 200-hp normal-starting torque motor with a full-load speed of 1,170 rpm. The challengers are all normal-starting torque motors.

The maximum design brake hp was 156 hp. At 75 mw, the motor output was 130 hp. The maximum motor output was 140 hp at a generator load of 80 mw. In making estimates of motor life, 130 hp is used as the maximum normal output.

Table XIV gives the results of an economic comparison between the installed drive motor for the condensate pump and five challengers. The most favorable alternative is challenger *C*, a 125-hp motor with class-*A* insulation. The PW of the savings over the next 25 years is $910 per motor, $1,820 for the two motors required. Since these motors are smaller and lower priced than the motors analyzed in the foregoing a greater effect of life estimate and power costs is noted.

Vertical mounting is also used for the service water pumps. Characteristic curves of these pumps were not available. However, the characteristic curves of a service water pump will look very much the same as those for a typical boiler feed pump. This pump is generally a medium-head and medium-capacity pump and is used to provide service water for various miscellaneous requirements. Since it can be expected to have a low breakaway torque, normal-starting torque motors may be applied. Table XV lists the challengers chosen.

The defender is a 200-hp motor with a 1,770 rpm. The maximum design brake hp requirement was 145 hp. Load on the motor was independent of generator load and was a maximum of 124 hp. An economic comparison is summarized in Table XVI.

The most favorable alternative is challenger *E*, a 100-hp motor with class-*B* insulation, which gives a PW of future savings of $1,262 per motor. Neglecting the fact that costs of power consumed are applicable to only one motor of the three, the savings realizable are $3,786 for the three motors.

The ash-sluice pump is a medium-head and medium-capacity pump. Complete characteristics were not available. These pumps operate only for a total of 3 hours per day, hence, the saving in power consumed by operating at a higher efficiency with an alternative motor is negligible. Generally, ash-sluice pumps are high-pressure clear-water pumps which furnish the power to operate the entire ash-sluice system.

Table XVII lists the challengers. The maximum design requirement is 113.5 brake hp. Maximum motor output under normal conditions is 80 hp. The defender is a normal-starting torque motor rated at 125 hp and 1,775 rpm.

The economic analysis is summarized in Table XVIII. Challenger *C*, a 75-hp motor with class-*A* insulation, is the most favorable alternative with a net amount of $541 per motor as the PW of the savings in capital recovery and maintenance costs for the next 25 years. The saving is $1,082 for both ash-sluice-pump motors.

MOTORS DRIVING THE DRAFT FANS, COAL MILLS, AND AIR COMPRESSORS

The induced draft fan is powered by an induction motor with normal-starting torque through an hydraulic coupling. Although the fan has a high inertia, the acceleration of the drive motor is not influenced because of the coupling. Upon starting, the motor is brought up to speed with little or no load. From then on, the speed of the fan and its acceleration are controlled by the hydraulic coupling. The maximum design requirement is 540 brake hp. The motor output was as high as 559 hp during brief periods of load unbalance between the fans. Challengers for the installed induced draft fan motor are listed in Table XIX. The defender is a 600-hp motor with a full-load speed of 1,180 rpm.

In Table XX are summarized the comparison between alternatives on the basis of PW of the next 25-year saving. Because of the efficiency characteristics of the motors, a disadvantage was noted in the cost of power consumed at large loads by the challengers. However, the saving

Table XIV. Summary of Cost Comparison for Each Condensate Pump Drive Motor

Motor	Initial Cost C, $	Salvage Values, $	Estimated Life, Years	Capital Recovery Costs, Equation 3, $	Power Costs, (Challenger's Advantage), Equation 8, $	Maintenance Costs, Equation 10, $	Taxes and Insurance, Equation 11, $	PW of Challenger's Advantage, Equation 2, $
Defender	2,669	88	40	324		16	46	
Challenger *A*	2,247	73	40	273	25	13	39	679
Challenger *B*	2,809	73	40	341	25	16	49	39
Challenger *C*	2,010	54	33	248	25	12	35	910
Challenger *D*	2,512	54	37	306	25	15	44	361
Challenger *E*	1,946	52	23	252	24	12	34	840

Table XV. Data for Economic Analysis of Service Water Pump Drive Motors

Motor	Nominal Rating, Hp	NEMA Design Class	Insulation Class	Efficiency at Fraction of Rating, Per Cent 1/2	3/4	4/4	Price of Motor, $	Motor Weight, Pounds
Defender	200	*B*	*A*	90	92	92	3,680	2,450
Challenger *A*	150	*B*	*A*	90	91.5	92	3,236	2,050*
Challenger *B*	150	*B*	*B*	90	91.5	92	3,814	2,050*
Challenger *C*	125	*B*	*A*	91.5	92	92	2,768	1,550
Challenger *D*	125	*B*	*B*	91.5	92	92	3,080	1,550
Challenger *E*	100	*B*	*B*	91	91.5	91.5	2,538	1,550

* Estimated.

Table XVI. Summary of Cost Comparison for Each Service Water Pump Drive Motor

Motor	Initial Cost C, $	Salvage Value S, $	Estimated Life, Years	Capital Recovery Costs, Equation 3, $	Power Costs, (Challenger's Advantage), Equation 8, $	Maintenance Costs, Equation 10, $	Taxes and Insurance, Equation 11, $	PW of Challenger's Advantage, Equation 2, $
Defender	3,791	86	40	460		23	66	
Challenger *A*	3,333	72	40	405	9	20	58	588
Challenger *B*	3,929	72	40	477	9	24	69	−94
Challenger *C*	2,851	53	40	346	8	17	50	1,131
Challenger *D*	3,173	53	40	385	8	19	56	760
Challenger *E*	2,614	53	26	331	5	16	46	1,262

Table XVII. Data for Economic Analysis of Ash-Sluice Pump Drive Motors

Motor	Nominal Rating, Hp	NEMA Design Class	Insulation Class	Efficiency at Fraction of Rating, Per Cent 1/2	3/4	4/4	Price of Motor, $	Motor Weight, Pounds
Defender	125	*B*	*A*	88	90.5	91	1,584	1,550
Challenger *A*	100	*B*	*A*	88	90.5	91	1,363	1,550*
Challenger *B*	100	*B*	*B*	88	90.5	91	1,608	1,550*
Challenger *C*	75	*B*	*A*	88	90	90.5	1,122	1,250*
Challenger *D*	75	*B*	*B*	88	90	90.5	1,367	1,250*
Challenger *E*	60	*B*	*B*	88	90	90.5	1,149	1,000*

* Estimated.

realized at light loads by the smaller motors compensated for the loss at large loads, resulting in a net advantage in cost of power consumed by each challenger.

The most favorable choice of drive motor for the induced fans is challenger *A*, a 500-hp motor with class *A*-insulation. If the life estimates are accurate, these motors will have to be replaced after 23 years but a saving of $832 per motor could still be realized. This amounts to approximately $1,664 for the two motors driving the induced draft fans.

The forced draft fans are directly coupled to their drive motors. Normal-starting torque motors have sufficient torque to break the fans away from rest, but it is suggested that the accelerating capability of the drive motor be checked against the moment of inertia of its load to insure that the motor is capable of accelerating the fan without overheating. Since the drive motors are not required to start the fans more than a few times each year, some overheating may be tolerated.

Challengers for the analysis of the forced draft fan drive motor are listed in Table XXI. The maximum design requirement is 322 brake hp. From Table VII, the maximum motor output is 281 hp. The installed motor is rated at 350 hp and has a speed of 1,185 rpm. A cost comparison appears in Table XXII. The most favorable alternative is challenger *C*, a 250-hp motor with class-*A* insulation. As for the induced draft fans' drive motors the efficiency characteristics are such that a major saving in power consumed is realized at light loads with a smaller motor. The present worth of challenger *C*'s advantage over the next 25 years is $1,209. Considering both fans, the saving becomes $2,418 by taking advantage of the margin provided by the service factor.

Complete data on either the coal mills or their drive motors were not available. Each mill has a capacity of 17 tons per hour. The mill manufacturer specifies a 350-hp motor for the type of bowl mill installed at the power plant. Such pulverizer requires a high-starting torque motor, but the mill has a low effective inertia at the motor shaft. The installed motor is a NEMA design *C* high-starting torque motor and is rated at 350 hp with a speed of 880 rpm. The maximum motor output, as determined from actual load data at the power plant, was 273 hp.

Since motor characteristics were not available, efficiencies were estimated using the characteristics of normal-starting torque motors. Exact torque requirements of the mills could not be acquired, hence the economic comparison of possible drive motor alternatives is of value only as an indication of potential saving. Table XXIII lists possible alternatives and Table XXIV summarizes the analysis. If the load characteristics were such as to permit application of a 300-hp motor, a saving of $494 for each motor could be realized. This is a saving of $1,482 for all three motors. However, if the starting requirements of the mill were such as to permit application of a 250-hp motor, the saving would be $1,327, or $3,981 for all three motors. The potential saving is sufficient to warrant further investigation.

Table XVIII. Summary of Cost Comparison for Each Ash-Sluice Pump Drive Motor

Motor	Initial Cost C, $	Salvage Value S, $	Estimated Life, Years	Capital Recovery Costs, Equation 3, $	Power Costs, (Challenger's Advantage), Equation 8, $	Maintenance Costs, Equation 10, $	Taxes and Insurance, Equation 11, $	PW of Challenger's Advantage, Equation 2, $
Defender	1,632	54	40	198		10	29	
Challenger *A*	1,404	53	40	170	0	8	25	267
Challenger *B*	1,656	53	40	201	0	10	29	−24
Challenger *C*	1,156	44	29	144	0	6	18	541
Challenger *D*	1,406	44	35	174	0	8	25	236
Challenger *E*	1,183	35	23	153	0	7	21	440

Table XIX. Data for Economic Analysis of Induced Draft Fan Drive Motors

Motor	Nominal Rating, Hp	NEMA Design Class	Insulation Class	Efficiency at Fraction of Rating, Per Cent			Price of Motor, $	Motor Weight, Pounds
				1/2	3/4	4/4		
Defender	600	*B*	*A*	91.5	93.2	93.5	6,780	5,725
Challenger *A*	500	*B*	*A*	91.3	93	93.3	5,832	5,400
Challenger *B*	500	*B*	*B*	91.3	93	93.3	7,290	5,400
Challenger *C*	450	*B*	*B*	91.1	92.8	93.1	6,720	5,185

The only synchronous motors considered in this study were those driving the soot-blower air compressors. In the economic comparison, only the motors were reviewed. While the exciter size is indicated in Table XXV, the saving realized by using a smaller exciter was not included in the challengers' advantages.

Table XXV lists the possible alternatives, and Table XXVI summarizes the economic analysis of the drive motors for the soot-blower air compressors. The maximum design requirement was 388 brake hp and the actual maximum motor output was 326 hp. The installed motor is rated at 400 hp and has a speed of 327 rpm. Since the soot-blower air compressor operates for only 5 hours each day, the net difference between alternatives in the cost of power consumed is negligible. Challenger *C* is the most favorable alternative. It is a 300-hp synchronous motor with class-*A* insulation. The saving is $706 for each motor, $1,412 for the two motors.

A summary of the total saving which could have been realized appears in Table XXVII. The approximate saving, expressed in terms of the PW of the equivalent annual costs during the next 25 years, totals $27,500.

Torque Characteristics

The economic study has been based on consideration of the thermal characteristics of the motors. It is realized that the torque requirements may sometimes be the determining factor in motor selection. The reduction in name-plate rating of the motor carries with it corresponding reductions in locked rotor torque and breakdown torque. Since stations are designed on the basis of certain assumed low-voltage conditions, it is important that these be rechecked to be sure that, during system trouble or bus transfer, the motors will not stall or fail to start. For example, the 2,000-hp boiler feed pump motor originally chosen has a breakdown torque of 200 per cent of this name-plate rating. With the suggested motor rating of 1,250 hp, the value would become 150 per cent of the brake hp requirements of 1,675 hp. The voltage dip that could be tolerated would fall from 30 to 17 per cent. To obtain increased torque in the lower name-plate rating motor would add to the cost. In the case of pulverizer mills, the locked rotor torque might be considered as the deciding factor.

Summary and Conclusions

Margins existing between design requirements of the major auxiliaries in a specific power plant and the ratings of their drive motors were investigated. Actual operating data obtained after this power plant was in operation showed that the maximum design figures of brake hp required by the auxiliaries are in general larger than the maximum requirements under typical operating conditions. An economic analysis was made to determine whether the installed drive motors in the specific power plant were the most favorable alternatives available. The saving realizable by application of economically efficient motors was tabulated. The entire study required many simplifying assumptions; however, certain general conclusions may be stated:

1. The use of conservative or rule-of-thumb methods in the application of drive motors for the auxiliaries in a steam power plant may lead to uneconomically large margins between the maximum design requirements of the auxiliaries and the drive motor ratings.

2. The maximum design brake hp of the pumps and fans includes some margin above the expected full-load requirements. This may lead to large differences between motor output and motor ratings after the power plant is in operation.

3. By applying smaller motors and by taking advantage of the service factors available, certain economies may be effected. These savings are realizable because of the lower initial cost of the motor and appear to be independent of assumed motor life. Also, in many cases, the saving in cost of power consumed by the motor may be significant if a smaller motor could be operated at a higher percentage of its rating and, hence, at a higher efficiency.

4. Use of an insulation class which permits a greater maximum thermal rating on a specific motor may be advantageous in some applications. This is especially true where the starting torque required by the load is low in comparison to full-load torque, such as for a centrifugal boiler feed pump.

5. The potential saving which may be realized will in most cases justify a detailed analysis of the drive motors to be applied.

6. The economies may be realized at no apparent decrease in reliability of the power plant, although operating a motor at a higher per cent of rated load or at occasional overloads may shorten its useful service life.

7. In any motor application study, it is necessary to know the characteristics of the load in detail to avoid possible duplication of margins.

8. Higher over-all plant efficiency will be the final result of detailed analyses of drive motor applications.

Comparison Between Design and Analysis

As pointed out, the designer is at a disadvantage in comparison with the analyst because the designer cannot know what the actual requirements will be. However, since the necessary design margins are considered and included by the mechanical designer in the selection of all auxiliary equipment, such as fans, pumps, and mills, it is highly desirable to

Table XX. Summary of Cost Comparison for Each Induced Draft Fan Drive Motor

Motor	Initial Cost C, $	Salvage Value S, $	Estimated Life, Years	Capital Recovery Costs, Equation 3, $	Power Costs, (Challenger's Advantage), Equation 8, $	Maintenance Costs, Equation 10, $	Taxes and Insurance, Equation 11, $	PW of Challenger's Advantage, Equation 2, $
Defender	6,993	200	40	839		42	122	
Challenger *A*	6,007	189	23	777	21	36	105	832
Challenger *B*	7,508	189	32	925	21	45	131	−605
Challenger *C*	6,922	181	25	881	43	42	121	16

Table XXI. Data for Economic Analysis of Forced Draft Fan Drive Motors

Motor	Nominal Rating, Hp	NEMA Design Class	Insulation Class	Efficiency at Fraction of Rating, Per Cent 1/2	3/4	4/4	Price of Motor, $	Motor Weight, Pounds
Defender	350	*B*	*A*	90.8	92.5	92.8	4,439	3,800
Challenger *A*	300	*B*	*A*	90.6	92.3	92.6	3,960	3,100
Challenger *B*	300	*B*	*B*	90.6	92.3	92.6	4,950	3,100
Challenger *C*	250	*B*	*A*	90.4	92.1	92.4	3,492	3,100
Challenger *D*	250	*B*	*B*	90.4	92.1	92.4	4,367	3,100

Table XXII. Summary of Cost Comparison for Each Forced Draft Fan Drive Motor

Motor	Initial Cost C, $	Salvage Value S, $	Estimated Life, Years	Capital Recovery Costs, Equation 3, $	Power Costs, (Challenger's Advantage), Equation 8, $	Maintenance Costs, Equation 10, $	Taxes and Insurance, Equation 11, $	PW of Challenger's Advantage, Equation 2, $
Defender	4,572	133	40	554		27	80	
Challenger *A*	4,079	109	40	496	9	24	71	620
Challenger *B*	5,099	109	40	619	9	31	89	−541
Challenger *C*	3,597	109	26	456	34	22	63	1,208
Challenger *D*	4,498	109	34	551	34	27	79	298

Table XXIII. Data for Economic Analysis of Coal Mill Drive Motors

Motor	Nominal Rating, Hp	NEMA Design Class	Insulation Class	Efficiency at Fraction of Rating, Per Cent* 1/2	3/4	4/4	Price of Motor, $	Motor Weight, Pounds
Defender	350	*C*	*A*	90.6	92.4	92.4	5,682	4,750
Challenger *A*	300	*C*	*A*	90.4	92.2	92.4	5,131	3,800
Challenger *B*	300	*C*	*B*	90.4	92.2	92.4	6,180	3,800
Challenger *C*	250	*C*	*A*	90.1	91.9	92.1	4,403	3,350
Challenger *D*	250	*C*	*B*	90.1	91.9	92.1	5,362	3,350

* Estimated.

select the motors as economically as is feasible, and with as little additional margins as well; it is clear that the motors should neither be too large nor too small. The designers must consider a reasonable margin to make certain that no one piece of equipment ever forms a bottleneck. For example, particular conditions in a plant may suggest the selection of a larger coal mill to handle a certain quality of coal which would be under emergency conditions. Under such circumstances, the motor must be designed for the maximum requirements established by the enlarged rating of the coal mill using the lowest possible quality of coal.

As indicated in Table XXVII, the results of the analysis show that it would have been possible to save $27,500 by closer selection of the auxiliary drive motors. This gap between the designer, who looks into the future, and the analyst, who knows what he got, demonstrates the margins which the designer considered justifiable, and at least a part of this gap is produced by realistic margins based on variables which are difficult to predict. On the other hand, smaller motors mean further savings in other auxiliary equipment, as, for example, cables, switchgear, and station transformers.

References

1. *Discussion* of reference 8, Eric T. B. Gross. P. 1665.

2. Steam Power Stations, G. A. Gaffert. McGraw-Hill Book Company, Inc., New York, N. Y., 4th ed., 1952.

3. Steam Power Plants, Phillip J. Potter. The Ronald Press Company, New York, N. Y., 1949.

4. Electrical Engineering Economics, D. J. Bolton. Chapman and Hall Ltd., London, England, vol. 1, 3rd ed., 1950, vol. 2, 2nd ed., 1951.

5. Principles of Engineering Economy, Eugene L. Grant. The Ronald Press Company, New York, N. Y., 1950.

6. Economic Factors Affecting Selection and Replacement of Power Plant Equipment, Gerald J. Matchett. *Proceedings*, American Power Conference, Illinois Institute of Technology, Chicago, Ill., vol. 16, 1954, pp. 258–63.

7. Motors and Generators. *NEMA Standards Publication No. MGI*, National Electrical Manufacturer's Association, New York, N. Y., March 1955.

8. Effect of Reduced Voltage and/or Frequency Upon Steam Plant Auxiliaries, O. D. Butler, C. J. Swenson. *AIEE Transactions*, vol. 73, pt. III-B, 1954 (Feb. 1955 section), pp. 1628–32.

9. Tables of Useful Lives of Depreciable Property. *Bulletin F, IRS Publication no. 173*, Internal Revenue Service, United States Treasury Department, Washington, D. C., 1942.

10. Standard Handbook for Electrical Engineers, Archer E. Knowlton. McGraw-Hill Book Company, Inc., New York, N. Y., 8th ed., 1949, sections 7 and 10.

11. Combustion Engineering, Otto de Lorenzi. Combustion Engineering Inc., New York, N. Y., 1953.

12. Lincoln's Industrial-Commercial Electrical Reference, E. S. Lincoln. The Electrical Modernization Bureau, Inc., New York, N. Y., section on Motors and Generators, 2nd ed., 1952.

13. Mapi Replacement Manual. Machinery and Allied Products Institute, Chicago, Ill., 1950.

14. Fundamentals of Alternating Current Machines, A. Pen-Tung Sah. McGraw-Hill Book Company, Inc., New York, 1946.

15. Dynamic Equipment Policy, George Terborgh. *Ibid.*, 1949.

16. Company Procedural Manual on Equipment Analysis. William Kelly and Company, Chicago, Ill., 1951.

17. Economics of Major Auxiliary Drive Motors in Steam Power Plants, V. F. Bobrowicz. *M. S. Thesis*, Illinois Institute of Technology, Chicago, Ill., 1955.

◆

Discussion

Frank V. Smith (Sargent and Lundy, Chicago, Ill.): The authors have made an interesting contribution to the economic study of power-plant auxiliary motors and it should be helpful to others who wish to analyze this matter in detail.

Table XXIV. Summary of Cost Comparison for Each Coal Mill Drive Motor

Motor	Initial Cost C, $	Salvage Value S, $	Estimated Life, Years	Capital Recovery Costs, Equation 3, $	Power Costs, (Challenger's Advantage), Equation 8, $	Maintenance Costs, Equation 10, $	Taxes and Insurance, Equation 11, $	PW of Challenger's Advantage, Equation 2, $
Defender	5,852	166	40	710		35	102	
Challenger *A*	5,182	133	40	659	− 4	31	90	494
Challenger *B*	6,365	133	40	772	− 4	38	111	−611
Challenger *C*	4,536	117	31	562	−10	27	79	1,327
Challenger *D*	5,522	117	36	670	−10	33	96	298

Table XXV. Data for Economic Analysis of Soot-Blower Air Compressor Drive Motors

Motor	Nominal Rating, Hp	Maximum Exciter Rating, Kw	Insulation Class*	Efficiency at Fraction of Rating, Per Cent			Price of Motor, $†	Motor Weight, Pounds
				1/2	3/4	4/4		
Defender	400	5.0	*A*	92.8	93.7	94.0	5,679	5,800
Challenger *A*	350	4.5	*A*	92.4	93.4	93.7	5,277	4,500
Challenger *B*	350	4.5	*B*	92.4	93.4	93.7	7,704	4,500
Challenger *C*	300	3.7	*A*	92.0	93.1	93.4	4,896	4,180
Challenger D	300	3.7	*B*	92.0	93.1	93.4	7,148	4,180
Challenger *E*	250	3.1	*B*	91.4	92.6	93.0	6,547	3,735

* Same insulation for stator and rotor.

† Excluding exciter.

Table XXVI. Summary of Cost Comparison for Each Soot-Blower Air Compressor Drive Motor

Motor	Initial Cost C, $	Salvage Value S, $	Estimated Life, Years	Capital Recovery Costs, Equation 3, $	Power Costs, (Challenger's Advantage), Equation 8, $	Maintenance Costs, Equation 10, $	Taxes and Insurance, Equation 11, $	PW of Challenger's Advantage, Equation 2, $
Defender	5,850	203	40	708		35	102	
Challenger *A*	5,435	158	40	660	−1	33	95	440
Challenger *B*	7,936	158	40	962	−1	48	138	−2,383
Challenger *C*	5,043	146	27	635	−2	30	88	706
Challenger *D*	7,433	146	34	911	−2	45	130	−1,908
Challenger *E*	6,743	131	23	889	−7	40	118	−1,639

Table XXVII. Summary of Total Savings Which Could Have Been Realized

Auxiliary Driven by Motor	Installed Motor Rating, Hp	Most Favorable Alternative			Number of Motors	Approximate Total Saving, $
		Rating, Hp	Insulation Class	Saving per Motor, $		
Boiler feed pump	2,000	1,250	*B*	11,506	1	11,506
Induced draft fans	600	500	*A*	832	2	1,664
Forced draft fans	350	250	*A*	1,209	2	2,418
Coal mills, pulverizers, and exhausters	350	300	*A*	494	3	1,482
Circulating water pumps	250	200	*A*	1,191	2	2,382
Condensate pumps	200	125	*A*	910	2	1,820
Service water pumps	200	100	*B*	1,262	3	3,786
Ash-sluice pumps	125	75	*A*	541	2	1,082
Soot-blower air compressors	400	300	*A*	706	2	1,412
Total for all auxiliaries					19	27,552

They have worked out the economics of tailoring the motors closely to the actual load experienced in the operation of a station at rated load and fully realize that at the time that the station was being designed it would not be practical or perhaps desirable to use the motors that they have suggested, but nevertheless, it is interesting to see the savings that could be obtained. Some comments might be made on the particular problem that faces the designer in making these selections.

Most electrical designers feel that they should maintain some margin in the motor rating above the brake horsepower calculated by the mechanical engineer for the equipment. It may be that the mechanical engineer has included a sufficient margin in his assumptions and the electrical engineer should be quite familiar with the details of his calculations. However, we should sympathize with the mechanical engineer. He does not have an easy task. His assumptions as to head and friction loss in pipes and ducts can be reasonably correct for a specific condition although he has to realize that friction loss will no doubt increase with age (it is to be noted that the readings given in the paper were taken when the plant was relatively new), but his major problem is to know the total station output for which he should really design. By various devices, an output can be obtained which is considerably more than the name-plate rating. A typical unit might have a name-plate rating of 60,000 kw and guaranteed capability of 75,000 kw at $3^{1}/_{2}$-inch vacuum with five feed water heaters. If the vacuum is improved to $1^{1}/_{2}$ inches, the capacity goes to 78,000 kw. If the top heater is taken out of service, it will go to 81,000 kw. The manufacturers may well provide a flow margin above guarantee of some 5 per cent and if this were realized, the output would be 85,000 kw. If the boiler and turbine were overpressured, the figure could be raised even higher. To what degree is the mechanical engineer justified in designing the whole auxiliary system for this maximum rating? This is a matter of judgment and probability, but it must be realized that the operator will be very unhappy if he discovers that the only reason he cannot get more output from the turbine is because of a limitation in one of the auxiliaries.

One item not mentioned is the practice of many utilities of designing for operation at reduced voltage and frequency which results in oversize equipment as far as normal load is concerned.

Another item not referred to is the ambient temperature. All calculations have been based on the assumption that this is the standard value of 40 C. For certain motors, it may well be that a higher ambient can be experienced and this factor must be taken into account.

A comment might be made on Fig. 1 of the paper. This is a useful way of presenting the situation and the views of the manufacturers will be interesting. The ordinate scale should be clarified by stating that the motor nominal rating is at 40 C. Class *A* insulation is good for a total temperature of 105 C and class *B* for 130 C, or 25 C more. It is general practice to regard class *B* insulation as good for an observed temperature rise of 20 C more than class *A* with the same life. It would therefore appear that the class *B* motor could be operated at 60 C rise and should have normal life with a motor output of $\sqrt{\frac{60}{40}}=1.22$ times the motor nominal rating at 40 C. The figure corresponding to a class *A* motor with 50 C would be $\sqrt{\frac{70}{50}}=1.32$ with a life reduction of one half. Factors other than insulation might require some reduction of these figures.

It would be helpful to have some statistical data on the actual life of motors in service. We believe it will be found that many motors applied quite conservatively have had to be rewound long before the 40 years suggested. Dirt and dust entering the windings of open motors are no doubt a factor. This is why open motors have a service factor while enclosed motors do not.

The matter of using class *B* insulation on high-speed motors is partly a peculiarity of the pricing system. For a large 3,600-rpm motor such as a boiler feed pump, the increase in price for changing from class *A* to class *B* insulation is $7^1/_2$ per cent while the increased horsepower obtained would seem to be about 22 per cent. This applies only to certain speeds and sizes; for others, the increase in price is as much or more than the increase in horsepower. The reason this procedure is not followed more often is perhaps because the operators do not like to have a motor with a name-plate rating below the normal operating output of the motor. It is difficult to explain to the plant personnel that it is proper to operate this particular motor frequently above its rating; also, as the authors point out, the locked rotor and breakdown torque are functions of the name-plate rating and these, of course, are reduced correspondingly. If the manufacturer were asked to put a name plate on the motor giving the higher rating with 60 C rise, the price would be increased.

E. T. B. Gross and V. F. Bobrowicz: We sincerely appreciate Mr. Smith's discussion. His comments on the problems confronting a power-plant mechanical design engineer, together with his clarification of the pricing system of class *B* insulated motors, provide a valuable supplement to the paper. We fully agree that the mechanical design engineer must add many margins and that the electrical design engineer must accept them, but we maintain that additional margins on the electrical side should be kept to a meager minimum.

It may be pointed out that even though improperly designed auxiliaries may limit unit output in case of unit overload or operation at reduced frequency and voltage, the drive motors will hardly ever limit output of the unit under these conditions. The motors may become overloaded temporarily and some shortening of life result therefrom.

Since the output of fans and centrifugal pumps decreases rapidly with decreases in speed (brought about by reduced voltage supplied to induction motors, or by reduced frequency) only the selection of oversized pumps and fans will prevent them from becoming bottlenecks; however, even when such equipment of larger than nominal rating is selected, the motor ratings need not be matched with the increased nominal rating of the driven equipment, but only such motors selected which are appropriate for maximum unit load at rated frequency and voltage.

It appears that the manufacturers of pumps and fans are now seriously considering the economic advantages of class *B* and class *H* insulated motors. Recently published material refers to matching the load by using class *H* (silicone) insulation. In one example, the following data are given: "Silicone insulated motors give a service factor ranging up to 50 per cent compared with 15 per cent for class *A*. This extra service factor of 50 per cent makes possible the installation of class *H* motors rated at normal load requirements and yet meeting initial or intermittent overloads, or loads that can not be matched with standard frame sizes. In one pumping application, intermittent loads range up to 9.2 hp though the normal load is 5 hp. Instead of using a 10-hp class-*A* motor, as would be the old practice, a 5-hp silicone class-*H* motor may be used. This means, in addition to less capital investment, better power factor and higher efficiency because smaller silicone-insulated motors operate nearer full load more of the time than larger motors rated to meet maximum overloads."

Our choice of a 40-year normal motor life may seem optimistic. "There is really no reason why modern motors should not last this long" was the opinion of an application engineer of one large motor manufacturer with whom we discussed this problem some time ago. However, had we chosen a figure of less than 40 years, the results of our analysis would have led to similar conclusions.

The curve of motor life suggested by Mr. Smith is probably more realistic than the one of Fig. 1. However, Mr. Smith's curve would make class *B* insulated motors appear the more favorable since the motor could now be operated at a maximum load of 1.22 per unit without any loss of life.

Ten Part-Winding Arrangements in Sample 4-Pole Induction Motor

J. J. COURTIN
MEMBER AIEE

Synopsis: Using a 75-horsepower 4-pole 3-phase motor on which design and test data has previously been published,[1] and without dividing the winding into segments smaller than its natural phase belts, it was determined that there are 10 possible different arrangements for half of the winding, each of which would be suitable for making the necessary connections to a part-winding starter composed of two line starters and a timing relay. To determine which of these arrangements would produce the more favorable characteristics of torque, line currents, and noise, tests were conducted on each and the results are presented. The winding pitch was then raised to a higher percentage than normally used and the effects of this variation on the test data and on some of the motor magnetomotive force waves are also given.

THE test a-c motor is a National Electric Manufacturers Association design-*C* frame-445 440-volt 3-phase 60-cycle 1,770-rpm 75-horsepower induction motor having a double-cage aluminum rotor and a conventional polyphase stator winding. There are 60 partially closed stator slots and 50 rotor slots. The complete winding is connected parallel-star and has five turns in each coil. The original pitch was 1 to 12 or 73.3-per-cent chording.[1] Because the rating is one frequently used in part-winding starting applications, this study was considered of special value and interest.

In the polyphase winding each phase appears in proper sequence the same number of times as there are poles in the winding. In this 3-phase 4-pole winding there are 12 phase belts, each phase appearing four times, and each belt being made up of five coils in series. Part-winding starting generally employs one half of the belts of each phase at start or two each of the *A*, *B*, and *C* groups in the case of the 4-pole motor. It can be seen quite readily that there is a choice of ten different half-winding arrangements about the periphery of the 4-pole stator depending on the selection of phase belts to be connected. In the application of motors with part-winding starters a number of these arrangements have been used, sometimes with unsatisfactory results in regard to torque and noise characteristics. This study was made to obtain pertinent test experience on each half-winding arrangement in one motor having good accelerating torque with normal accelerating noise on full-winding line starting and with well-established machine constants and known performance.

Paper 55-732, recommended by the AIEE Rotating Machinery Committee and approved by the AIEE Committee on Technical Operations for presentation at the AIEE Fall General Meeting, Chicago, Ill., October 3–7, 1955. Manuscript submitted July 5, 1955; made available for printing August 24, 1955.

J. J. Courtin is with the Westinghouse Electric Corporation, Buffalo, N. Y.

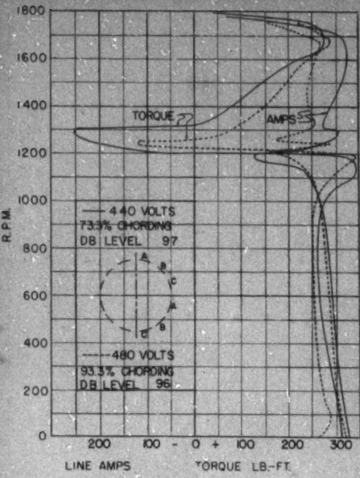

Fig. 1 (left). Adjacent poles connected

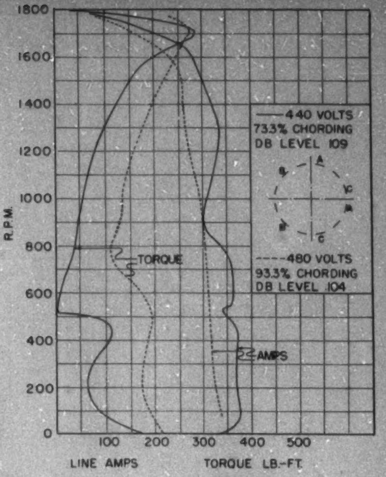

Fig. 3 (right). Adjacent poles except phase-B groups opposite

Test Procedure

The procedure followed was to remove the winding connection cables only, leaving the original winding intact. One cable was then connected to each side of each phase belt, identified, and brought directly to the outside of the motor. There were then a total of 24 cables permitting any desired connection arrangement of the 12 groups. At rated 440 volts and 60 cycles, with the relative polarity of each phase belt maintained the same as in the full winding, speed-torque curves were taken by dynamometer in the usual manner covering each of the 10 half-winding arrangements.

The solid line curves of Figs. 1 through 10 represent the tested torque and line current characteristics on the original winding which had a coil pitch of 1 and 12 or 73.3-per-cent chording. The 12 groups are represented in each figure in a circular manner descriptive of their distribution around the stator; each section line in the circumference representing the five top-coil sides of a phase belt. The letters *A*, *B*, and *C* on the circles indicate the phase belts included in the connection tested. Sections not lettered indicate the omitted phase belts in each case.

The noise level readings shown in Figs. 1 through 10 are the maximum decibel

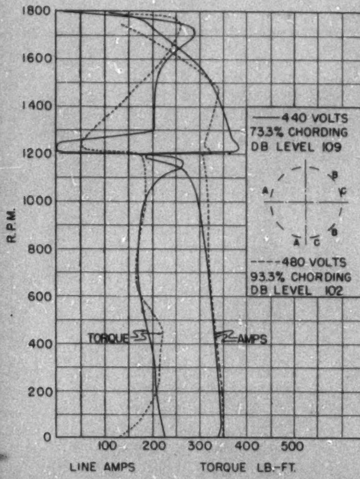

Fig. 2 (left). Adjacent poles except phase-A groups opposite

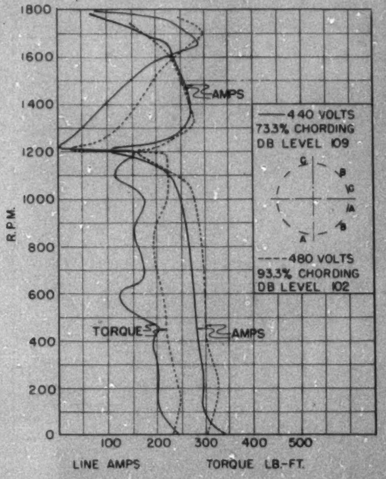

Fig. 4 (right). Adjacent poles except end groups

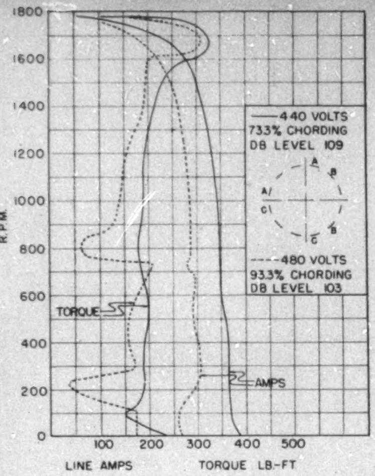

Fig. 5 (left). Alternate pairs of groups connected

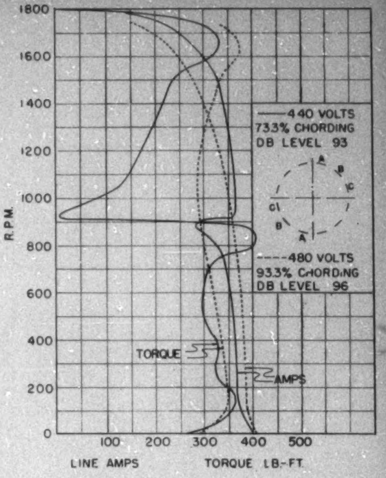

Fig. 7 (right). Alternate poles connected

values recorded for a free acceleration from standstill in each case. The sound level meter was located at a 3-foot distance from the front of the motor which was coupled to the dynamometer. Total inertia of the rotating elements was 66 pound-feet squared of which 19 pound-feet squared was the motor rotor alone. Average room level was 74 decibels for the solid line curves and 81 decibels when the dotted line curves were run. No corrections were made for room level. The American Standards Association sound reference level applies.[2]

To test the effects of increasing the winding pitch it was necessary to rewind the stator completely. This was done in such a way as to employ the same number of turns per coil and the same conductor sizes as in the original winding. The winding pitch was raised from 1 and 12 or 73.3-per-cent chording to 1 and 15 or 93.3-per-cent chording. This change increased the length of the end turns and the weight of copper used from 73 to 84 pounds for the complete winding. The higher winding pitch raised the fundamental chording factor 9 per cent and, consequently, the applied voltage was raised a corresponding percentage from 440 to 480 volts for comparative testing. The flux per pole was thereby of the same magnitude for both windings.

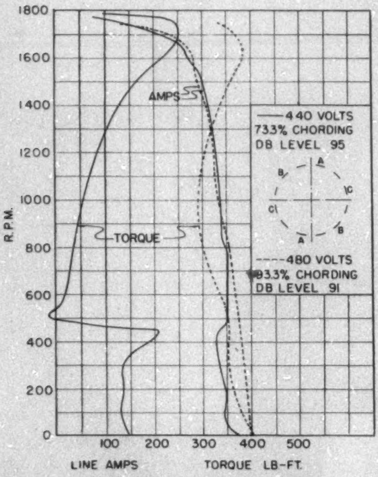

Fig. 6 (left). Alternate groups connected

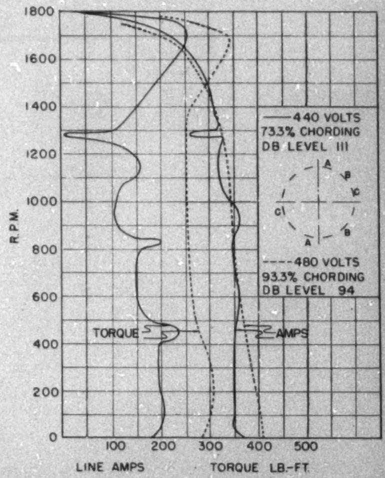

Fig. 8 (right). Alternate poles except one phase-B group

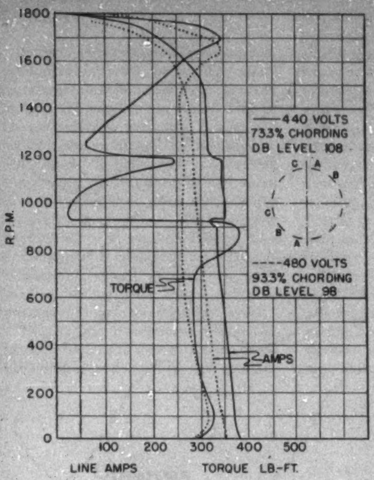

Fig. 9 (left). Alternate poles except one phase-C group

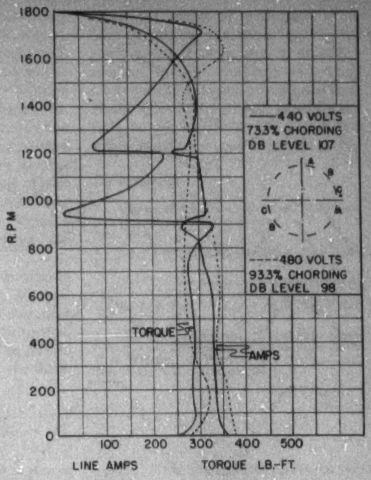

Fig. 10 (right). Alternate poles except one phase-A group

Evaluation

Because of the differences in applied voltage, it is considered that a comparison of power requirements for starting for the various arrangements could be more properly made on the basis of kilovolt-amperes than on line current and Table I was made accordingly. With the original winding with 73.3-per-cent chording, connection 5, Fig. 5, was the only arrangement capable of accelerating to full running speed on half the winding. The maximum kilovolt-ampere value to reach full speed is then the locked rotor value for half the winding. For those arrangements where subsynchronous cusps occur in the torque curve, it would be necessary to energize the complete winding to attain full speed. The maximum kilovolt-ampere values in these instances are taken from the full-winding current curves, Fig. 11, at the revolutions per minute corresponding to the cusp on half-winding.

Table I. Comparison of Starting Power Demand

	Locked Rotor Kilovolt-Amperes per Horsepower		Maximum Value Kilovolt-Amperes per Horsepower, 0 to 1,800 Rpm	
	Pitch		Pitch	
Figs.	1 to 12	1 to 15	1 to 12	1 to 15
1	3.17	3.54	4.57	4.37
2	3.40	3.87	4.57	4.37
3	3.40	3.84	5.24	4.78
4	3.50	3.33	4.57	4.37
5	3.96	3.00	3.96	5.21
6	3.76	4.42	5.24	4.42
7	4.06	4.49	4.93	4.49
8	3.81	4.51	4.57	4.51
9	3.91	3.94	4.93	3.94
10	3.71	4.21	4.93	4.21
11	5.71	5.55	5.71	5.55

Connections 6, 7, 8, 9, and 10 for the 93.3-per-cent chorded winding have, what are considered, good torque curves for part winding. However, as anticipated by a recent paper on part winding torques,[3] the starting power required is greater than for the lower pitch part winding because of the increased number of energized slots and the corresponding decrease in the stator slot reactance.

It is interesting to note that, while the acceleration noise level decreased in all cases with the higher winding pitch, the torque curve improved only where the magnetomotive force wave shape for the part winding was improved. In Fig. 12, the *A* waves show little difference

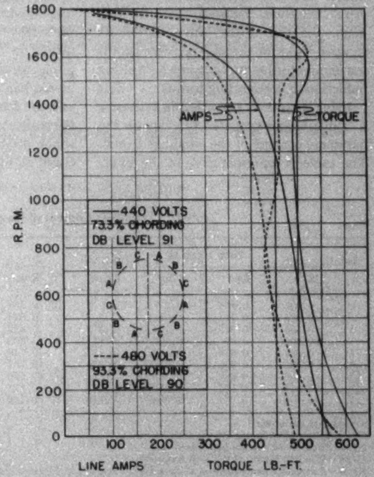

Fig. 11. Full winding, all groups connected

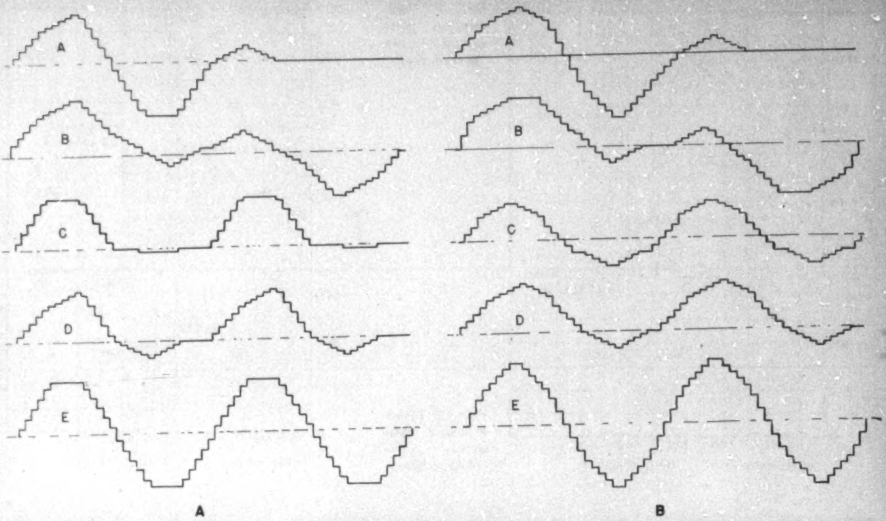

Fig. 12 (A). Magnetomotive force plots, 1 to 12 pitch. (B). Magnetomotive force plots 1 to 15 pitch

A—Half-winding adjacent poles; see Fig. 1
B—Half-winding alternate pairs of groups; see Fig. 5
C—Half-winding alternate groups; see Fig. 6
D—Half-winding alternate poles; see Fig. 7
E—Full winding; see Fig. 11

in general shape and the torque curves of connection 1 both show the presence of a strong 6-pole field with cusping at 1,200 rpm. Wave *B* shows accentuation of flat spots with the increased chording and, consequently, the connection-5 torque curve became undesirable. Waves *C* and *D* both show reduction of flat spots and improved symmetry with the higher winding pitch and great improvement in torque curves for connections 6 and 7 were, therefore, realized. Full-winding magnetomotive force wave *E* shows sharper peaks for the 93.3-per-cent chording and its torque curve shows a resulting reduction in accelerating torque.

Using a method suggested in reference 4, Table II was prepared to evaluate the harmonic content of the windings tested. The table is representative of the alternate group and alternate pole arrangements; see Figs. 6 and 7. It shows the presence of even harmonics of large magnitude in the short-chorded 1- and 12-pitch arrangements. The second harmonic has an amplitude of 35.3 per cent and the fourth harmonic 12.1 per cent of the main wave. It is the second harmonic which produces the cusp in the solid line curve of Fig. 7 and the fourth harmonics which causes the cusp in Fig. 6. With the winding pitch of 1 and 15, the amplitudes of the second and fourth harmonics are reduced to 9.06 and 4.54 per cent of the fundamental. At the same time the odd harmonics, except for the seventh, were increased, the most important being the fifth harmonic from 2.28 to 3.64 per cent.

Other than the reduced accelerating torque, the performance of the motor on full winding indicated little effect of the higher order of odd harmonics accompanying the unusually high winding pitch. Comparative performance features at rated 75-horsepower loading are as given in Table III. The lowered value of minimum accelerating torque for the full winding would be of small consequence if the motor were applied with a part-winding starter.

Table II. Harmonic Content of Flux Wave

	Pitch 1 and 12				Pitch 1 and 15			
n	Kdn	Kpn	Kdpn	Ampl	Kdn	Kpn	Kdpn	Ampl
1	0.957	0.914	0.875	100	0.957	0.995	0.953	100
2	0.833	0.743	0.618	35.3	0.833	0.208	0.173	9.06
4	0.425	−0.995	−0.423	12.1	0.425	−0.407	−0.173	4.54
5	0.200	−0.50	−0.100	2.28	0.200	0.866	0.173	3.64
7	−0.149	0.978	−0.146	2.38	−0.149	−0.743	0.111	1.67
8	−0.232	0.208	−0.048	0.068	−0.232	−0.755	0.175	2.30
10	−0.200	−0.866	0.173	1.97	−0.200	0.866	−0.173	1.81
11	−0.111	0.105	0.012	0.013	−0.111	−0.407	0.045	0.43
13	0.102	0.669	0.068	0.059	0.102	0.174	0.018	0.145

n = order of harmonic.
Kdn = Distribution factor for the *n*-th harmonic.
Kpn = Pitch factor for the *n*-th harmonic.
Kdpn = Winding factor of the *n*-th harmonic.
Ampl = Amplitude percentage of main wave.

Table III. Comparative Performance—Full Winding

	Winding Pitch 1 and 12	Winding Pitch 1 and 15
Voltage	440	480
Starting torque, pound-feet	622	590
Pullout torque, pound-feet	528	524
Minimum torque, pound-feet	480	426
Full load torque, pound-feet	222	222
Full load amperes	92.6	85.0
Full load efficiency, per cent	92.4	92.6
Full load power factor, per cent	85.8	85.4
Full load, rpm	1770	1771
No load amperes	26.4	24.7
Locked rotor amperes	563	500

Conclusion

In the applications of squirrel cage induction motors with part-winding starting, the greatest disadvantage appears to be that the acceleration sound level on the part winding connection is often too high for the locality of the installation. The sample 75-horsepower ball-bearing motor when running alone at full speed has a 74-decibel level. For a full-winding line-start acceleration, the measured sound level of 91 decibels coupled to a dynamometer is considered a normal and satisfactory value. Of the ten part-winding arrangements tested only one was found to have a comparable level.

This was the arrangement in which alternate phase belts were connected in the half-winding and in which the chording was 93.3 per cent of the pole pitch, test curves of which are shown in Fig. 6. To the ear this full voltage acceleration was in no way objectionable and would be considered satisfactory for any location where equipment of this size would be installed. The speed-versus-torque and current curves for this arrangement show that the motor will attain running speed at a current demand of 78 per cent of that required for a full-winding line start. This is comparable to results obtained with an 80-per-cent voltage resistor-type starter.

While the maximum power demand to reach running speed for the adjacent pole arrangement, Fig. 1, is higher than for the alternate phase belt connection, the former arrangement has the advantage of drawing the lowest power increment and might be preferable where power company regulations require that starting current increments be limited to specified values. However, the sound levels for the adjacent pole arrangement would be too high for many locations and such an application should be avoided where sound level is an important factor.

References

1. REPORT ON DOUBLE-CAGE ROTOR SYMPOSIUM, J. J. Courtin. *AIEE Transactions*, vol. 72, pt. III, Aug. 1953, pp. 657–62.

2. American Standards Association, New York, N. Y.

3. SPEED-TORQUE CALCULATIONS FOR INDUCTION MOTORS WITH PART WINDINGS, P. L. Alger, Y. H. Ku, C. H. T. Pan. *Ibid.*, vol. 73, pt. III-A. Apr. 1954, pp. 151–60.

4. ELECTRIC MACHINERY, VOLUME II—ALTERNATING CURRENT MACHINES, M. Liwschitz-Garik, C. C. Whipple. D. Van Nostrand Company, Inc., New York, N. Y., 1946, pp. 128–36.

◆

Discussion

P. L. Alger (General Electric Company, Schenectady, N. Y.): Mr. Courtin's paper contributes a great deal to our knowledge of part-winding starting of polyphase motors. However, this subject is a very extensive one, and there is a great deal more yet to be done before the problems can all be resolved.

Suppose we consider a 4-pole 3-phase winding only, and limit ourselves to part windings in which the normal phase belts of the winding are kept intact. If we use only half of the windings on the first step of the starting cycle, there are 16 different ways in which the six active phase belts can be arranged, as shown in Table IV. Three pairs of these—numbers *2* and *6*, *5* and *7*, and *12* and *14*—have exactly the same magnetomotive force distribution, so that there are only 13 possible half windings with different magnetomotive force patterns.

All the adjacent pole patterns produce large 2-pole and 6-pole fields. Since these differ by only one pair of poles from the fundamental 4-pole field, they produce large unbalanced shaft forces, and, therefore, are likely to produce a good deal of noise and vibration during starting. The amount of this noise will vary widely with the size of motor, the type of load, and the installed conditions, so that adjacent pole windings have decided limitations. On the other hand, the adjacent pole patterns group the adjacent windings together, and, therefore, have generally lower locked rotor currents.

The alternate pole patterns produce large 8-pole and 16-pole fields, which maintain balanced shaft forces and give relatively quiet acceleration, except in cases of special slot numbers and core dimensions that permit resonant frequency vibrations. The per unit values of these different harmonic fields for each of the 13 windings are shown in Table IV, with the most important field in each case underlined. Inspection of the table shows that 10 out of the 13 windings have such large forward harmonic fields that the torque will normally go to zero or below if the winding has the usual pitch of about 73 per cent. The remaining three windings—numbers *10*, *11*, and *12*—are hybrids, containing both adjacent and alternate pole groups. They have no large forward revolving fields, but they have both odd and even harmonics, so that their performance is not good, as illustrated by Fig. 8 of the paper, which applies to winding *11*. Winding *13* is free of large forward fields, and, therefore, looks very attractive, but it has a very large backward 2-pole field, which makes the locked rotor torque low, and may even cause the motor to start backward on the first step.

Comparison of the ten torque curves given in the paper with their harmonic fields shown in the table indicates a good agreement in every case between the theory and test. It is interesting to note that windings *5* and *7*, which have identical magnetomotive force patterns, were both tested, as shown in Figs. 9 and 10 of the paper. While the two test curves are very similar, their shapes are not identical, indicating the difficulty in getting accurate test torque curve data by the usual dynamometer test method.

I agree with Mr. Courtin's conclusion that the only way to get adequate torque, to bring the motor to full speed on the first step, and also to get low noise with a half winding, is to use an extra long winding pitch, such as 93 per cent. As the author points out, this lowers the half-winding reactance, and makes the locked rotor current on the first step approximately 80 per cent of full load value.

In view of these limitations, it is my opinion that with half-winding starting, it is essential to close the second contactor within 2 or 3 seconds after the first one, so that the full winding of the motor is used in acceleration. If this is done, the torque and noise on the first step become unimportant, and there is, therefore, little need to use a motor of special design. For

Table IV. Characteristics of the 16 Possible Half Windings of a 3-Phase 4-Pole Motor

Winding		Principal Forward Fields With 0.733 Pitch (4-pole mmf = 1)						Torque Curve Shown in Fig.	Comments	
No.	Pattern	2P	6P	8P	10P	14P	16P	No.	Noisy	Torque Dip
1	6------	0.396	*0.656*	0	0.052	0.083	0	1	Yes	Extreme
2	5---1---	0.281	*0.465*	0.236	0.074	0.058	0.162		Yes	Large
3	4-1----1-	0.290	*0.482*	0	0.052	0.226	0	4	Yes	Large
4	4-1-1----	0.251	*0.416*	0.236	0	0.195	0.162		Yes	Large
5	4---2---	0.145	0.241	*0.408*	0.052	0.113	0	10	Yes	Large
6	3-3-----	0.281	*0.465*	0.236	0.074	0.058	0.162		Yes	Large
7	3--3----	0.145	0.241	0.408	0.052	0.113	0	9	Yes	Large
8	3---3---	0	0	*0.472*	0	0	0.163	7	No	Large
9	3-2---1--	0.205	*0.340*	0	0.116	0.159	0	2	Yes	Large
10	3-1---2--	0.145	0.241	0.236	0.104	0.113	0.162		Yes	Moderate
11	3-1-1---	0.145	0.241	0.236	0.052	0.113	0.326	8	Yes	Moderate
12	3--1-1-1--	0.075	0.124	0.236	0.074	0.218	0.162		Yes	Moderate
13*	2--2--2--	0	0	0	0.156	0	0	5	Yes	Moderate
14	2---2-1-1-	0.075	0.124	0.236	0.074	0.218	0.162		Yes	Moderate
15	2-1-1--1-1-	0.106	0.177	0	0.052	*0.307*	0	3	Yes	Severe
16	1-1-1-1-1-1-	0	0	0	0	0	*0.486*	6	No	Severe

* Has large backward 2-pole field, giving low locked rotor torque.

this reason, and because it is desirable to have the current on the first step not more than 65 per cent of full value, the use of a long-pitch winding does not appear attractive. Summing up, if the phase belts are kept intact, and only half of them are used on the first step, standard motors should be satisfactory in most cases, but the result obtained will be only increment starting, with the full locked rotor current reached on the second step, and not true part-winding starting.

However, it is quite feasible to use 2/3 of the phase belts instead of only half on the first step, and with this arrangement it is possible to get reasonably good accelerating torque and low noise, with only 65 per cent current, on the first step, so that in this way true part-winding starting is possible. This alternative method of starting is described in a paper by Miss Agacinsky and the discusser.[1]

REFERENCE

1. A NEW METHOD FOR PART-WINDING STARTING OF POLYPHASE MOTORS, **P. L. Alger, Lorraine M. Agacinsky.** *AIEE Transactions*, vol. 75, pt. III, 1956 (*Paper no. 55-846*).

D. C. Martin and **R. F. Horrell** (Electric Machinery Manufacturing Company, Minneapolis, Minn.): The paper presents considerable practical information on a current problem. The results confirm our experience that it is essential to know the shape and harmonic content of the magnetomotive force wave. The effect of the amount of chording cannot be neglected. The author has presented the data on all available connections and indicates the effect of chording on the magnetomotive force wave and on noise. The connection used in Fig. 5 has been discussed at some length.[1] We have found good torque characteristics with normal chording, but poor characteristics near full pitch. On a few motors connected per Fig. 3, tests indicated that the torque would be reduced in accordance with the pitch, i.e., our tests at 61.1 per cent chording fell between the 73.3 and 93.3 per cent curves shown in Fig. 5, and our tests at 61.1 per cent chording fell below the 73.3 per cent curve of Fig. 5. It would be interesting to see the results of a similar study on 6- and 8-pole machines, since more varied connections can be made.

In larger motors, it is necessary to use chording to a greater degree to obtain the desired motor performance, hence the most desirable chording for part-winding functions may be undesirable with respect to other more important considerations. This brings the use of part-winding back to the basic problem: What is the desired end result? Three possible end results may be considered:

1. Use as increment start. Here the connection of Fig. 1 with any chording would probably be best, since the motor would accelerate to about 1,200 rpm and require the lowest kilovolt-amperes initially before transferring to full winding.

2. Use to accelerate a low WK^2, unloaded auxiliary. The connection of Fig. 5 with normal chording would be best provided the time of acceleration is not too great.

3. Noise. If noise is of prime consideration then the connection of Fig. 6 with near full pitch would suffice. Noise is relatively unimportant if of short duration, such as the 2 to 5 seconds required for transfer to full winding.

It would be interesting to know if there was any auxiliary equipment used in conjunction with the dynamometer when obtaining the speed-torque-current curves. Since test points were not indicated on the curves, it is possible some means employing an oscillograph was used.

We have naturally experienced rapid and excessive heating even on partial voltage when taking speed-torque points with a dynamometer. This would naturally be of more concern on larger motors such as our company manufactures. How was this factor of heating handled during test?

REFERENCE

1. PART-WINDING STARTING OF SQUIRREL-CAGE MOTORS, **Marvin Brown.** *Electrical Manufacturing*, New York, N. Y., Jan. 1954, pp. 108–13.

J. J. Courtin. To illustrate the great variations in starting characteristics depending on the relative positioning of the energized phase groups was a main purpose in preparing this paper. Mr. Alger's study shows that there are additional half-winding arrangements possibilities for 4 pole, 3 phase, that were not considered and gives a "character analysis" of each. His efforts are greatly appreciated by the author.

In taking the experimental data reported in the paper, the noise levels for the nonsymmetrical group arrangements were very objectionable and of such a magnitude that they could not be recommended even for momentary connection. Of the symmetrical half windings with normal chording the adjacent-pole (Fig. 1), alternate-group (Fig. 6), or the alternate-pole (Fig. 7) arrangement would be suitable for noise for most industrial applications. Of these the adjacent-pole pattern is preferred by the writer since it has the lowest initial current, has accelerating torque to 2/3 of running speed, and is generally observed to be quiter than the alternate-pole pattern. The noise is highest when the motor is operating at the speed of a subsynchronous cups in the half-winding torque curve. For best starting action the timing relay for the second contactor should be adjusted on each installation to operate just before the rate of motor acceleration noticeably decreases. This connects the line to the full winding before the motor reaches the cups speed and where this is near 2/3 of full speed, provides a smooth, continuous acceleration. Also, the magnitude of the current increment for closing the second half of the winding is diminished when it occurs at the higher speed. However, where the magnitude of the unbalanced shaft forces becomes a mechanical consideration to be reckoned with as in large 8-pole motors, the alternate group arrangement would be preferred, since the forces would be more evenly balanced and the starting power increment lower than for the alternate pole pattern. As Mr. Alger has stated, it is desirable to have the current on the first step not more than 65 per cent of full value. However, the alternate-pole half winding always has an initial current greater than 70% of full value whereas the adjacent-pole winding always has initial currents within the 65 per cent value for normally chorded motors.

The use of 2/3 of the phase belts in a part winding is certainly worthy of consideration, since it opens additional versatility in applying standard motors. The disadvantage that must be weighed is the great unbalance in the line currents which makes up the average 65 per cent current on the first step. Also, the 2/3 winding scheme does not permit using standard 3-phase line-starters which is the economic advantage of the half winding start.

The discussion of Mr. Martin and Mr. Horrell indicates experiences which concur with that of the writer and confirm the readings taken on the sample motor. However, their confidence in recommending the use of the alternate pair connection of Fig. 5 for low inertia acceleration is not entirely shared for the general case. In particular, the noise level for bringing the sample motor to full speed would be objectionable for many locations. With this exception the organization of data and conclusions drawn are considered an improvement on the paper and are greatly appreciated.

Torque curves for the ten arrangements were taken in the normal manner by dynamometer, recording points at various speeds. The test curves were then traced exactly as originally drawn but on the prepared form as illustrated. Individual points were not transferred. Since heating was not too great a factor in this relatively small motor, no extraordinary methods were needed to control heating other than to run the motor frequency at no load to keep the temperature within safe limits. All curves were taken at full voltage.

Report on the Operation of Switched Capacitors

AIEE COMMITTEE REPORT

THIS report is limited to the discussion of capacitor switching as used on electric transmission and distribution systems for the improvement of system conditions. The report covers only shunt capacitor applications and is formulated to provide a resumé of the existing literature and known experience and thereby constitutes a relatively short report containing the pertinent factors to be considered in such applications.

Previous reports have covered the performance, operation, and maintenance of shunt capacitors.[1,2] These reports contained little information about capacitor switching. It was reported at that time that only 35 per cent of all capacitors installed were regularly switched. Approximately half of these, about 17 per cent, were switched automatically, the other half were switched manually. There is considerable literature published on capacitors.[3,4] Reliable estimates at the end of the year 1954 indicate that about 45 per cent of all shunt capacitor installations are fixed, 25 per cent are switched manually, and 30 per cent are switched by automatic control devices. The trend seems definitely towards more switched banks in general and more automatically switched banks in particular.

Capacitors can be connected directly to any distribution or transmission circuit of any voltage. Switched capacitors have been installed over the range of 208 volts through and including 115,000 volts. There are many specific reasons for using switched capacitors and there are also many switching control arrangements to obtain the desired results.

Reasons for Switching Capacitors

The fundamental reason for switching capacitors is to improve system performance. Some of the following specific reasons for switching are:

1. *Variable Kilovar Demand.* A variable kilovar (kvar) demand can result from several types of load. Furnaces, large industrial plants, air-conditioning and refrigeration equipment, or pumping installations can place large, fluctuating reactive demands on the system. Also, the I^2X requirements of the system itself vary with the system loading. Switched capacitors installed at the load and on the lines can supply the reactive kvar. The switched capacitors may be located on the customer's premises or on the utility system's lines. The capacitors can be switched directly with the load or separately by means of suitable switchgear and control devices.

2. *Voltage Regulation.* Voltage regulation of a system may require the use of a large capacitor installation at peak load compared to the reactive demand of the off-peak load. This, either by itself or in conjunction with the system voltage changes between on peak and off peak, may result in excessive voltage during off-peak periods. Excessive voltage, besides being generally undesirable, may cause wave-form distortion owing to transformer overexcitation, causing objectionable harmonics to flow in the line. Switching permits the use of capacitors as large as needed during peak load periods without the objection of excessive boost in light load voltages. Switched capacitors may also be co-ordinated with voltage regulators to obtain voltage ranges not practical to obtain with regulators alone.

3. *Avoidance of Excessive Leading Generator Power Factor.* In cases where the capacitive kvar connected to the system are of sufficient capacity to correct the light load power factor at the generator terminals to unity or leading, it may be necessary to switch the capacitors to prevent abnormally low excitation. Capacitors reduce the excitation required on the generators to maintain the voltage level. The system stability margin is reduced with lower generator excitation.[3]

4. *Reduction of I^2R and I^2X Losses.* It may be necessary to switch capacitors in accordance with load kvar requirements to minimize I^2R and I^2X losses in the line such as would result from lagging or leading current in the line.

5. *Provision for Emergency Voltage Boost.* Capacitors can be switched to provide an emergency voltage boost. Special situations may arise where temporary relief is required at some location, and time is not available to engineer and install additional circuits to supply the load. The installation of switched capacitors may provide relief until permanent corrective measures can be taken. Capacitors can also be switched in special circuits to operate them at overvoltage for short periods to obtain added kvar for motor starting, system stability, or extreme voltage or power-factor improvement. This may also be the case after a prolonged outage.

6. *Maximum Utilization of Power Equipment.* The maximum utilization of the capacity of power equipment may require switching on of capacitors during heavy load to reduce current loadings by improving the power factor. The use of capacitors might also augment the range of, or eliminate the need for, a voltage regulator or regulating transformer.

7. *Control of Reactive Current Flow.* Capacitors strategically located and switched make possible greater utilization of all parts of the systems by controlling the flow of reactive current and maintaining the voltage level.

There are undoubtedly many other reasons for switching capacitors. It is the intent here to point out the possibilities without reference to any economic justification. The economics of such applications may vary widely for different systems.

Switching Means

Capacitor switching equipment usually consists of circuit breakers or switches such as are used for fault and/or load interruption on transmission and distribution circuits. Some of the common types and the applications in which they are used are described in the following.

INDOOR BREAKERS

Metal-enclosed capacitor equipments or housings on circuits 15 kv or below often use indoor air or oil circuit breakers. These equipments house the circuit breaker in a separate compartment to protect it from the weather and to provide safety to operating personnel. In some cases modification of the interrupting chambers of these breakers is necessary to insure proper switching of the capacitive load by controlling prestrikes when energizing and/or restrikes when interrupting. Air breakers usually do not require modification. When a circuit breaker is purchased for capacitor switching, the manufacturer should be advised so that he can make modifications to the breaker, if necessary, for its contemplated duty.

OUTDOOR BREAKERS

On large outdoor banks, outdoor oil circuit breakers are usually used. Some modifications are usually necessary on these as are in the indoor oil breakers used in metal enclosed capacitor installations. Compressed air circuit breakers are suitable for capacitor switching, generally without modifications.

Paper 55-710, recommended by the AIEE Transmission and Distribution Committee and approved by the AIEE Committee on Technical Operations for presentation at the AIEE Fall General Meeting, Chicago, Ill., October 3-7, 1955; Manuscript submitted June 6, 1955; made available for printing August 2, 1955.

The personnel of the AIEE Capacitor Subcommittee are: B. H. Schultz, *chairman*, R. M. Butler, W. C. Fowler, K. B. Hapgood, and L. T. Williams.

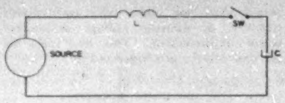

Fig. 1. A simplified capacitor switching circuit for a single bank

OIL SWITCHES

On pole-mounted switched capacitor banks, small single-phase or 3-phase oil switches are often used. These switches are generally solenoid or motor-operated and do not have fault-interrupting ability. Fault protection for the whole bank must be provided by group-fusing in each phase.

Capacitor oil switches are also often used for fairly large capacitor banks in substations. Fault protection then is usually provided by a backup circuit breaker. The modern trend in capacitor switching is more and more toward the use of these capacitor oil switches because they are specially designed for capacitor switching and because of the economics involved.

LOAD BREAK SWITCHES

Another device sometimes employed for capacitor switching is the load interrupter switch. This device, like the oil switch, does not provide fault protection. Load interrupter switches are usually derated for capacitor switching and have a limited number of operations before the interrupting device must be changed. Switching of capacitor banks with load interrupter switches may be either manual or automatic. Generally, load interrupters are not suitable for switching parallel capacitor banks.

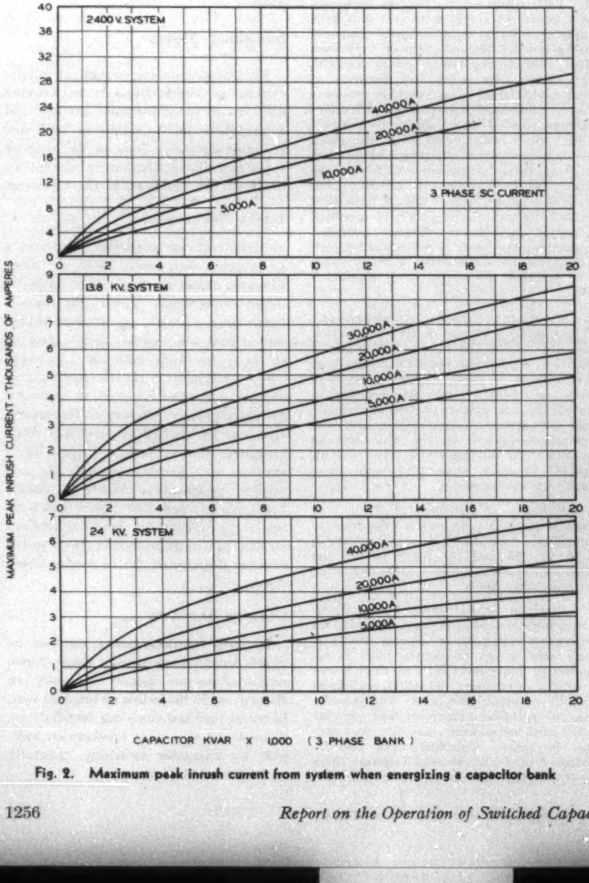

Fig. 2. Maximum peak inrush current from system when energizing a capacitor bank

Problems of Capacitor Switching

The switching of capacitor circuits presents problems not encountered in the usual load-switching application. This fact was recognized from experience obtained in switching moderately long high-voltage cables and long high-voltage transmission lines. These observations were made before capacitor bank installations had become large enough to create this problem in capacitor switching.

INRUSH TRANSIENTS—SINGLE BANKS

Inrush Currents

When a capacitor bank is energized, a comparatively large inrush current can flow into the bank. At the moment of circuit closing, the completely uncharged capacitor represents a short circuit to the system and the inrush current to the capacitor bank is limited only by the impedance of the circuit supplying the bank.

Fig. 1 represents a typical circuit with one capacitor bank. The inductance L represents the line, transformer, and source inductance of the system. The maximum inrush current occurs when the circuit is closed at voltage peak. This current can be calculated by using the following equation.

$$I_{\max}=I_0\left(1+\sqrt{\frac{\text{short-circuit kva}}{\text{capacitor kvar}}}\right)$$

where I_0 = crest value of the steady-state current.

The foregoing equation applies to single-phase and 3-phase banks, delta and wye. It assumes that the capacitor was not charged when energized. If the bank is fully charged and opposite in phase to the source voltage, the inrush current is twice the value obtained by the equation.

The inrush currents for single banks (no parallel bank) usually range from 5 to 15 times the normal capacitor current. This may or may not be harmful to the switches, depending on the number of switching operations per day, week, or month. Highly repetitive rates require special consideration either because of extra maintenance of breaker contacts or the necessity for special contacts or derating factors.

The curves in Fig. 2 show the maximum peak inrush current for several system voltages and short-circuit currents as a function of the capacitor kvar. The peak current is the sum of the fundamental (60-cycle) current crest plus the transient current crest. No allowance is made for decay of the transient current, therefore the values shown are slightly high but on the safe side.

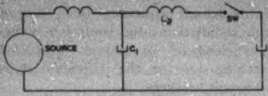

Fig. 3. A simplified capacitor switching circuit for parallel banks

Inrush Frequency

The inrush transient current frequency is the natural frequency of the circuit

$$\text{inrush frequency } f=f_0\sqrt{\frac{\text{short-circuit kva}}{\text{capacitor kvar}}}$$

where f_0 is the power frequency.

Transient Capacitor Voltages

If the capacitors initially are uncharged, the maximum transient capacitor voltage can theoretically be twice the steady-state capacitor voltage. If the capacitors initially are charged to the same potential and the same polarity as the closing-in voltage, there will be no transient overvoltages. If the capacitors initially are charged to the same potential but opposite polarity as the closing-in voltage, the maximum transient capacitor voltage can theoretically be nearly three times the steady-state capacitor voltage. Maximum practical values for transient overvoltages, however, are 1.8 times for an uncharged bank and 2.7 times for a bank charged at opposite polarity.

INRUSH TRANSIENTS—PARALLEL BANKS

Inrush Currents

When two or more steps of a bank are switched independently, i.e., when an adjacent bank is already energized, a very high inrush current can occur. An equivalent circuit for this condition is shown in Fig. 3.

Nearly all of the inrush current is supplied by the charged capacitor bank C_1 and is limited only by the small inductance L_2 in and between the banks. The maximum inrush current into capacitor bank C_2 occurs when the switch is closed at voltage peak. It can be calculated approximately by the following equation.

$$\text{maximum peak inrush current} = \sqrt{2}\, E\sqrt{\frac{C_t}{L_2}}$$

where

L_2 = the circuit inductance between banks, henrys

C_t = the total capacitance (two capacitances in series) of the circuit, farads

$$C_t=\frac{1}{\dfrac{1}{C_1}+\dfrac{1}{C_2}}$$

Again, this equation for inrush current assumes that the capacitor C_2 was not charged when energized. If the bank being energized is fully charged and at opposite polarity to the source voltage, the inrush current is twice the value obtained by the equation.

Resistance also has an effect in limiting the inrush current but is not nearly as effective as reactance. If the resistance is neglected, the calculated current will be slightly high and, therefore, on the safe side.

Field experience indicates that the magnitude of the peak inrush current for parallel banks usually is between 20 and 250 times the steady-state capacitor current. The transient inrush current usually decays to an insignificant value in less than 0.016 second (1 cycle).

Even with very large banks of capacitors, the energizing currents are usually below the rated momentary current of the circuit breakers. Although the circuit breakers are built to withstand the contact-burning and mechanical stresses produced by an occasional closing of the breaker against a short circuit, frequent closing operations with high inrush currents can cause rapid contact deterioration. The mechanical shock and stresses produced by the extremely high rate of rise of the current is also a very severe problem.

Inrush Frequency

The frequency of the inrush current depends on the C_t and L_2 circuit values

$$\text{inrush frequency in cycles per second} = \frac{1}{2\pi\sqrt{C_t L_2}}$$

Transient Capacitor Voltages

While the transient capacitor voltages obtained when switching parallel capacitor banks are theoretically the same as those obtained when energizing a single bank, experience has shown that a parallel bank will cause substantially lower transient voltages than those that may be experienced in switching a single bank.[5]

CAPACITOR FUSING

The capacitor bank fuses, either group fuses and/or individual fuses must be selected so that they will withstand the maximum inrush currents associated with such switching operations.

CURRENT-LIMITING REACTORS

Often it is necessary or desirable to limit the capacitor bank inrush current. One means for providing this function is the installation of an inrush-current-limiting reactor in each phase. The desired reactance of such equipment may easily be calculated by the following equation

$$L_a=\left[L\left(\frac{I_1}{I_2}\right)^2-1\right]$$

where

L_a = inductance to be added

I_1 = maximum actual inrush current between banks

I_2 = maximum desired inrush current between the two banks

L = actual inductance between two banks causing inrush current I_1

DE-ENERGIZING CAPACITOR CIRCUITS

Restrikes

The opening of a capacitive circuit presents additional problems. The initial voltage across the switch contacts following the breaking of a capacitive circuit is practically zero since the capacitor on the load side of the switch holds the same instantaneous voltage as existed on the supply line at the instant of break. This condition permits any switch to interrupt the circuit quite easily at an early current zero value. However, 1/2 cycle later the voltage across the switch contacts is twice the crest value of the fundamental since the capacitor has retained a charge equal to crest of one polarity while the supply voltage has changed to crest of the opposite polarity. This condition is illustrated in Fig. 4. If the contacts of the switching device have opened sufficiently to withstand this double voltage without restriking, the circuit is successfully cleared.

In some types of switching equipment the travel of the movable contact may not be fast enough to insure sufficient dielectric strength across the open contacts after 1/2 cycle. The circuit will then restrike with the following possible occurrences: Since the capacitor is at crest voltage of one polarity and the supply circuit at crest voltage of the opposite polarity, the capacitor voltage will reverse and change to the polarity of the source. However, the capacitor voltage will overshoot by an amount equal to its attempted change of voltage. This will result in a total voltage (transient plus steady-state) of nearly three times its previous steady-state voltage. At the first current zero the circuit may again be interrupted and, in this worst case, three times normal crest voltage will remain on the capacitor. These conditions are shown in Fig. 5. One-half cycle later, four times the fundamental crest voltage will appear across the breaker

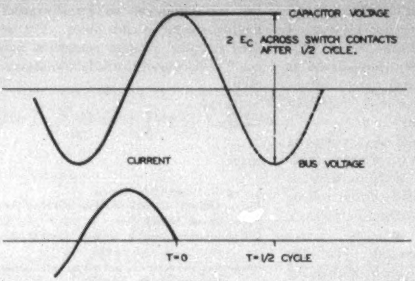

Fig. 4. Opening a simple capacitor circuit as shown in Fig. 1. Voltage across switch contacts at moment of break is zero, but 1/2 cycle later value is twice the crest value

contacts. If by this time the contacts have not separated far enough to prevent it, another restrike may occur with the possible result of still higher voltages at the capacitor following current zero.

The foregoing values apply to a bank of capacitors with its neutral solidly tied to the supply neutral. More severe overvoltages across the circuit-breaker contacts may occur when switching off a wye-connected bank with floating neutral.

On the occurrence of restrikes in the case of parallel switched banks, high oscillatory currents may result caused by the low impedance of the circuit between banks. This substantially increases the loss of material from the breaker or switch contacts and thus increases the maintenance costs of the interrupting device.

In practice, the interruption of capacitor circuits can be handled by most modern, standard circuit breakers without the occurrence of abnormally high voltages, even with the capacitors connected in floating wye. However, it is recommended that the capacitor manufacturer or the switchgear representative be consulted regarding breaker applications in connection with capacitors. This is especially true for exceptionally large or high-voltage banks.

Switching Duty

Switched capacitors should not be energized repeatedly in rapid sequence unless provisions are made to discharge the bank rapidly so that, on the next reenergizing operation, the inrush current will not exceed the permissible current limitations of any equipment in the circuit. If a capacitor is switched off and then switched on again when the full charge remains on the capacitor, the inrush current can be double the value of the uncharged condition. The total voltage at the capacitor can then reach a maximum of nearly three times the peak voltage. Highly repetitive switching operations may therefore require special consideration.

In general, intelligence relays should have sufficient bandwidth and time delay to avoid unnecessary switching operations. It is common practice to provide longer time delay, in some cases, to permit the capacitor control to ride through fluctuations of the intelligence signal which would otherwise cause unnecessary and even undesirable capacitor switching operations.

Multistep switched capacitor banks usually involve smaller bandwidth settings of the response relays to obtain close regulation of voltage or power factor. This fact often necessitates the use of longer time delays to avoid unnecessary switching operations caused by fluctuations of small duration.

Multistep capacitor banks generally are controlled by one master relay and a multistep control device. Usually the steps of the capacitor are switched on and off in a definite sequence. In the case of large installations, the control is sometimes designed to provide equalized switching duty on the individual steps and circuit breakers.

SWITCHING AT LOW AMBIENT TEMPERATURES

Consideration should be given to the ambient temperature range at locations where capacitors may be energized while they are at a temperature below a permissible value. Usually capacitors can be energized at ambient temperatures as low as −18 degrees centigrade with very little risk of damage to the capacitor. Low temperature capacitors, however, may be chosen which can be energized at temperatures as low as −40 degrees centigrade.

Intelligence Used to Control Capacitor Banks

The selection of a method for controlling switched capacitors should be based upon the benefits desired from the capacitors. Any of the following intelligences may be used.

VOLTAGE

Voltage is a commonly used signal for controlling capacitor switching. A contact-making voltmeter having suitable characteristics is used to initiate the switching operation. In addition to the voltage-sensitive element, a time delay

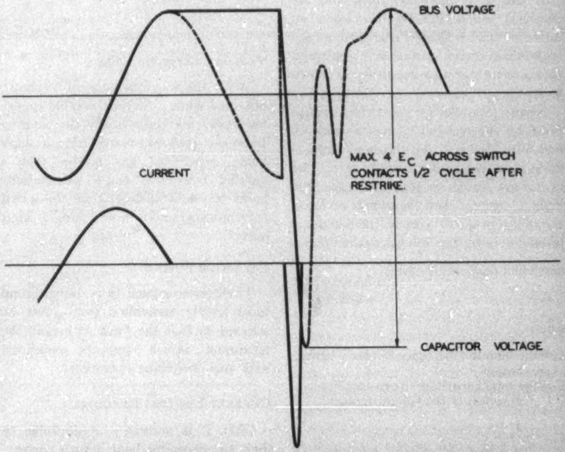
BUS VOLTAGE
MAX. 4 E_C ACROSS SWITCH CONTACTS 1/2 CYCLE AFTER RESTRIKE.
CURRENT
CAPACITOR VOLTAGE

Fig. 5. Opening a simple capacitor circuit showing maximum effect of one restrike

may be incorporated into the control circuit to prevent excessive operation of the switching equipment. Make of the "raise" contact of the device will switch the capacitor bank on and make of the "lower" contact will switch the bank off (through the time delay). The spread between the raise and lower contacts is called the bandwidth. The fundamental consideration for selecting the bandwidth is that it always be larger than the voltage change produced by one switched capacitor step. If this rule is not followed, repetitive switching or pumping will occur. The wider the bandwidth, the fewer will be the switching operations and the larger will be the variations in the voltage. Practical experience shows that a bandwidth of 1.5 times the expected voltage rise is a satisfactory value.

A convenient equation for calculating the voltage rise for one capacitor step is as follows

$$\text{per-cent voltage rise} = \frac{\text{3-phase kvar of capacitor step} \times 100}{\text{system symmetrical short-circuit kva}}$$

This equation assumes that the calculations of short-circuit kva have been based upon the reactance only of the system.

TIME

Time is often used as intelligence for switching capacitors to the extent that a regular time cycle can fit in the curve of total reactive load. Provisions to change the cycle on selected days of the week are available (omitting devices). Such fixed schedules cannot take into account unusual conditions that may be encountered, however. This prevents its ability to provide all the possible benefits of switched capacitors. Switching errors or unusual load conditions might result in excessive voltage if only time control is used. To eliminate this danger, a wide bandwidth voltage relay is sometimes used to override the time switch and to avoid excess boost in voltage (voltage override).

If it is desired to operate at two different voltages, a time switch can be used to short-circuit out a resistor inserted in series with the voltage relay. When the resistor is in the circuit, the voltage relay senses a lower voltage and the control therefore regulates the bus voltage higher and vice versa.

CURRENT

Current control is often employed for use on regulated circuits where voltage is not a satisfactory signal for capacitor switching and where load variations do not cause inconsistent changes in the load power factor. The current transformer which feeds the sensing device (contact-making ammeter) should be connected on the load side of the capacitor bank so that the current to the bank is not measured. This arrangement requires a separate control for each bank, i.e., a multistep current-initiated switching arrangement requires a control for each step. Each bank then is switched on when a given current is exceeded and switched off when the current falls below that basically same value.

CURRENT-COMPENSATED VOLTAGE

On some systems, voltage alone may not be a satisfactory reference for switching capacitors because of close proximity of the regulators. When the current is high and the voltage is also high, a voltage control would tend to switch off the capacitors. This would be exactly contrary to what is desired. The solution to this problem is to change the calibration of the voltage relay as a function of current. Control devices are available for effecting this compensation.

KVAR

A kvar control is best suited when it is desired to keep the kvar supply on a given line within certain limits to reduce system losses and voltage drop and to release generating and transmission capacity. The kvar supplied to the bus can be measured and, upon reaching a given value, the capacitors are switched to keep the kvar supplied through the line within prescribed limits. This type of control is similar to a voltage control except that a kvar relay is used instead of a voltage-sensitive relay. The setting of the kvar relay requires a rather careful study of loads and the load power-factor ranges to determine the system requirements.

POWER FACTOR

Power-factor control is not a very satisfactory means for controlling switched capacitors because this method would cause pumping at light load and low power factor unless desensitizing auxiliaries are used. The same end result can usually be obtained more satisfactorily with kvar or current control.

TEMPERATURE

Temperature-actuated controls are being used experimentally to switch capacitors at points where air-conditioning and refrigeration are a large part of the reactive load. The simplicity of such controls is, of course, a desirable feature but, at the same time they are limited in their use.

A modification being tried to obtain more desirable characteristics is a temperature-modified voltage control. In this control the calibration of a voltage relay is changed as a function of the ambient temperature.

LINE-DROP COMPENSATION

If it is important to keep the voltage constant (within the limits of the bandwidth) at some point remote from the capacitor installation, line-drop compensation can be applied to the control equipment for switching the capacitors. By this method the voltage at the bus (capacitor location) is raised to compensate for the line drop in the same manner as line-drop compensation is applied on voltage regulators. The secondary current from the current transformer in the load circuit is passed through a resistor and the voltage across this resistor is subtracted from the secondary voltage of a potential transformer. In this way a fairly constant voltage can be obtained at any given point on the feeders when the load power factor is reasonably constant.

CO-ORDINATION OF SWITCHED CAPACITORS WITH REGULATORS

Current, time, or kvar are the proper types of intelligence to be used to switch capacitors on voltage-regulated feeders. Voltage-controlled capacitors may be applied at the end of a regulated feeder circuit provided line-drop compensation is not used, or only the resistance settings of the compensator are used.

When capacitors and regulators are used on the same bus, the capacitor voltage step should be as large as practical in the interest of economy and to keep the number of switching operations to a minimum. A voltage step of about half of the voltage range of the regulator is desirable unless this results in a temporary voltage change that cannot be tolerated. The control voltage for the capacitor should be supplied from a point head of the regulator. If one or more capacitor banks are located near a regulator and the limit switches of the regulator can be used, this offers a simple, inexpensive means of controlling the capacitors and there is no problem of co-ordination. This method of control assumes that the voltage is the only intelligence to be considered.

References

1. Report of a Survey on the Performance of Shunt Capacitors, **AIEE Committee Report.** *AIEE Transactions*, vol. 68, pt. II, 1949, pp. 1200–07.

2. Report on the Operation and Maintenance of Shunt Capacitors, **AIEE Committee Report.** *Ibid.*, pp. 1208–18.

3. Bibliography on Power Capacitor 1925–1950. *AIEE Special Publication S-43*, Jan. 1952.

4. Bibliography on Power Capacitor 1950–1952, **AIEE Committee Report.** *AIEE Transactions*, vol. 72, pt. III, Dec. 1953, pp. 1336–39.

5. Switching Capacitive Kilovolt-Amperes With Power Circuit Breakers, **N. E. Dillow, I. B. Johnson, N. R. Schultz, A. E. Were.** *AIEE Transactions*, vol. 71, pt. III, 1952, pp. 188–200.

6. Automatic Capacitor Control for Industrial Plant, **L. Stone.** *Electrical World*, New York, N. Y., vol. 94, Sept. 21, 1929, pp. 574–75.

7. Controlling Power Factor Automatically, **A. Smith.** *Power*, New York, N. Y., vol. 73, Apr. 21, 1931, pp. 632–34.

8. Condenser Control; Hand or Automatic. *Electrical World*, New York, N. Y., vol. 104, Oct. 13, 1934, p. 646.

9. Switching Large H. V. Static Condensers, **H. Grunewald.** *V. D. E. Fachberichte*, Berlin, Germany, 1935, pp. 25–28.

10. Why not Switch Capacitors With the Load? **J. W. Butler, E. B. Pope.** *General Electric Review*, Schenectady, N. Y., vol. 41, Aug. 1938, pp. 366–69.

11. Automatically Controls Shunt Capacitors, **R. V. Sanford.** *Electrical World*, New York, N. Y., vol. 112, July 5, 1939, p. 200.

12. Capacitors Switched by Automatic Unit, **R. V. Sanford.** *Electrical West*, New York, N. Y., vol. 83, Oct. 1939, pp. 40–41.

13. Automatic Control of Plant Capacitors. *Electrical World*, New York, N. Y., vol. 112, Dec. 2, 1939, pp. 92, 94.

14. Analysis of Factors Which Influence the Application, Operation, and Design of Shunt Capacitor Equipments Switched in Large Banks, **J. W. Butler.** *AIEE Transactions*, vol. 59, 1940, pp. 795–800.

15. Automatic Switching Multiplies Capacitor Effectiveness, **W. H. Cuttino, J. E. Hobson.** *Electric Light and Power*, Chicago, Ill., vol. 18, Oct. 1940, pp. 40–43.

16. Double Saving by Switching Capacitors, **F. P. Gilpin, S. H. Pollock.** *Ibid.*, vol. 20, Sept. 1942, pp. 38–41.

17. Tests and Analysis of Circuit-Breaker Performance When Switching Large Capacitor Banks, **T. W Schroeder, E. W. Boehne, J. W. Butler.** *AIEE Transactions (Electrical Engineering)*, vol. 61, Nov. 1942, pp. 821–31.

18. Switching of Parallel Connected Condensers, **S. A. Stigant, A. J. Good.** *Beama Journal*, London, England, vol. 50, July 1943, pp. 222–27; vol. 50, Aug. 1943, pp. 252–53.

19. Automatic Control Switches Capacitors, **R. E. Marbury.** *Electrical World*, New York, N. Y., vol. 121, May 27, 1944, p. 1986.

20. Automatic Control and Switching Equipment for Capacitor Banks and Its Application, **T. W. Schroeder, W. C. Bloomquist.** *AIEE Transactions (Electrical Engineering)*, vol. 63, Sept. 1944, pp. 649–54.

21. Extending the Use of Shunt Capacitors by Means of Automatic Switching, **W. H. Cuttino.** *AIEE Transactions (Electrical Engineering)*, vol. 63, Sept. 1944, pp. 674–78.

22. Capacitor Problem; Switch Control. *Power Plant Engineering*, Chicago, Ill., vol. 48, Sept. 1944, p. 109; vol. 48, Nov. 1944, pp. 104–08.

23. When and How to Switch Capacitors Automatically, **W. H. Cuttino.** *Factory Management and Maintenance*, New York, N. Y., vol. 103, July 1945, pp. 148–52.

24. Automatic Switching of Shunt Capacitors, **W. H. Cuttino.** *Petroleum Engineer*, Dallas, Tex., vol. 16, Aug. 1945, pp. 145–46.

25. Selection and Application of Automatic Control for Capacitors, I-III, **W. C. Bloomquist, T. W. Schroeder.** *General Electric Review*. Schenectady, N. Y., vol. 48, Oct. 1945, pp. 7–11; vol. 48, Dec. 1945, pp. 22–31; and vol. 49, March 1946, pp. 37–41.

26. Switched Capacitors Retrieve Line Loading Capacity, **R. O. Loomis, E. J. Archbold.** *Electrical World*, New York, N. Y., vol. 125, Apr. 27, 1946, pp. 46–48.

27. Automatic Switching Schemes for Capacitors, **W. H. Cuttino.** *Power Plant Engineering*, Chicago, Ill., vol. 51, June 1947, pp. 101–03; also in *AIEE Transactions*, vol. 66, 1947, pp. 311–14.

28. Power Factor Correction Controlled by Time Clocks, **R. H. Heidirch.** *Factory Management and Maintenance*, New York, N. Y., vol. 105, July 1947, pp. 111–13.

29. Capacitors Switched by Bus Tie Breaker, **A. A. Straub.** *Electrical World*, New York, N. Y., vol. 128, Aug. 29, 1947, pp. 45–46.

30. Selection of Control Equipment for Automatic Switching of Capacitors, **W. C. Bloomquist.** *Ibid.*, Nov. 22, 1947, pp. 88–91.

31. Switched Capacitors Back Bus Regulation, **F. M. Reed.** *Ibid.*, Dec. 6, 1947, p. 89.

32. Automatic Control of Static Condensers, **J. W. Fawcett.** *Electrical Review*, London, England, vol. 103, Aug. 31, 1948, p. 347.

33. Pole-Mounted Automatically Switched Capacitors Prove Economical, **C. F. Myers.** *Electric Light and Power*, Chicago, Ill., vol. 26, Sept. 1948, pp. 64–66.

34. Switched Capacitors Control Voltage and Improve System Loading, **N. N. Smeloff, O. Ramsaur.** *Electrical World*, New York, N. Y., vol. 130, Dec. 4, 1948, pp. 85–87.

35. Switching of Distribution Capacitors by Manual and Automatic Means, **R. J. Hopkins, N. R. Schultz.** *General Electric Review*, Schenectady, N. Y., vol. 54, Apr. 1951.

36. Capacitor Switching Benefits Whole System Investment, **N. N. Smeloff, O. Ramsaur.** *Electrical World* New York, N. Y., vol. 137, May 19, 1952, pp. 161–3.

37. Capacitor Switching Phenomena, **R. C. Van Sickle, J. Zaborsky.** *AIEE Transactions*, vol. 70, pt. I, 1951, pp. 151–59.

38. Switching of Large Shunt Capacitor Banks for 15-Kv Service by Compressed Air Circuit Breakers, **B. P. Baker.** *AIEE Transactions*, vol. 70, pt. II, 1951, pp. 1697–1703.

39. Oil Switch and Voltage Control Give Low Cost Capacitor Switching, **W. R. Smith, D. R. Stemler, W. H. Cuttino.** *Electrical World*, New York, N. Y., vol. 135, Jan. 1951, pp. 57–60.

40. Switching High-Voltage Shunt Capacitor Banks, **A. W. Funkhouser, R. C. Van Sickle, D. F. Shankle.** *AIEE Transactions*, vol. 70, pt. I, 1951, pp. 129–37.

41. Control of Switched Capacitors, **R. L. Tremaine, W. H. Cuttino.** *Westinghouse Engineer*, East Pittsburgh, Pa., vol. 12, March 1952, pp. 72–77.

42. What Control Is Best for Switched Capacitors? **R. L. Tremaine, W. H. Cuttino.** *Electrical World*, New York, N. Y., vol. 137, June 16, 1952, pp. 120–22.

43. Automatic Capacitors Increase Circuit Capacity, **A. W. Edwards, H. Brooks.** *Ibid.*, April 7, 1952, p. 146.

44. Bus Regulation Plus Capacitors Takes Care of System Voltage, **D. R. Pattison, F. M. Reed.** *Ibid.*, May 19, 1952, pp. 147–9.

45. Oil Circuit Breaker for Switching 115-Kv Shunt Capacitors, **W. N. Leeds, J. H. Pehrson, C. F. Cromer.** *AIEE Transactions*, vol. 72, pt. III, Oct. 1953, pp. 1066–72.

46. Shunt Capacitors in Large Transmission Networks, **E. C. Starr, E. J. Harrington.** *Ibid.*, Dec. 1953, pp. 1129–37.

47. Westinghouse Electrical Transmission and Distribution Reference Book. Westinghouse Electric Corporation, Pittsburgh, Pa., 1950.

◆

Discussion

H. E. Smith and **J. E. Rembusch** (Commonwealth Edison Company, Chicago, Ill.): The committee has done an excellent and a thorough job in covering basic factors involved in capacitor switching.

However, we believe that there are three other methods of controlling switched capacitors which might deserve some mention and on which we would like to comment. The first of these is the so called "voltage divider" method of switching which seems to us might offer considerable economic value as a means of switching large blocks of capacitors needed purely for system control.

Another method of control is one on which a rather appreciable amount of development work has been done, that is, remote control of individual capacitor banks or groups of banks by means of an audio signal sent out by a radio transmitter. For this purpose it is generally proposed to utilize the present radio equipment available for dispatching line crews. Success has been achieved in developing such a control, but permission from the Federal Communications Commission to operate a pilot model has, for the time being, been denied.

A third method of capacitor control under investigation is the possibility of using telephone company circuits.

We have at substations, etc., on our system, some 203,000 kva of power-factor correction equipment consisting of rotating machines and capacitors which can be manually controlled. The balance of our Power-Factor corrective equipment consists of 521,000 kva of capacitors on distribution feeders, of which 323,000 kva are permanently connected and 198,000 are switched. It is obvious that some selective means of switching capacitors on a local and a system basis would be useful if it can be accomplished economically. However, since this is not readily accomplished, we have, with the exception of some isolated cases, relied on time switch control of capacitors in the Chicago area for the following reasons and in the following manner.

1. Most of our large generators have automatic voltage control which permits the system to operate at slightly leading Power-Factor and maintain proper voltage levels. Our major substations also have voltage-regulating equipment to maintain fairly constant levels on our subtransmission system.

We prefer to locate our switched capacitors out on the distribution feeders in order to gain the maximum voltage improvement and the maximum loss reduction throughout our entire system. Our 4-kv and 12-kv feeders are all regulated and, with the exception of a small percentage, they are short; hence the voltage variation on the feeder from the first customer to the last is not great enough to enable us to use voltage as the initiating means to switch capacitors.

2. We are unable to use current or kilover control for capacitors on our feeders as many of our medium-size industrial customers close down at 4 p.m. This of course means that capacitors installed on these feeders would not be in service at the time of the evening peak.

3. We run both winter and summer peak loads and thus we are not able to use temperature as an initiating means for capacitors since they would then be out of service in the winter months.

Our time switches (Sunday excepted) are set to bring all the capacitors on the system between 6:30 a.m. and 8:00 a.m. and to disconnect the capacitors between 10:00 p.m. and 1:00 a.m. We have a limited amount of capacitors time-switched on and off of the system on Saturday to care for industrial needs of the system. Using time switches in the manner outlined guarantees that we will be able to bring all switched capacitors into service at the time of our system generating peak which, of course, always comes on a weekday.

When we first started using time-switch-controlled capacitors we adjusted them in advance of a holiday so that the capacitors would not switch on during the holiday. However, we have discontinued this practice, and there is a possibility that we may partially discontinue the Sunday omission as during the recent hot summer we ran a peak load on a residental substation and on several feeders on a Sunday evening.

C. M. Lytle (Kansas City Power and Light Company, Kansas City, Mo.): This is a well-prepared report on methods of controlling switched capacitors and on the troubles that may be expected and means of mitigating the troubles. It is a timely report because as systems become larger they use higher voltages for both transmission and distribution lines. These higher voltage lines each add more fixed charging current which in turn means that a larger proportion of the capacitors installed must be switched.

About the only thing that can be added is a record of my company's installations in the summer of 1955 when we had a peak load of 577 megawatts at 90 per cent power factor.

	Kvar	Per Cent
Fixed units	69,585	36.5
Time clock	72,240	38.0
Current control	19,980	10.5
Thermostat	11,280	6.0
Supervisory (manual)	17,100	9.0
Total	190,185	100.0

B. H. Schultz (Chairman, AIEE Capacitor Subcommittee): The committee report did not include information on the switching methods cited by Mr. Smith and Mr. Rembusch as there has been little published information or experience to date on these switching methods. The AIEE Capacitor Subcommittee will welcome papers on these switching or control methods as soon as anyone has operating experience or economic comparisons to make.

Design Principles of Flux-Switch Alternators

S. E. RAUCH
NONMEMBER AIEE

L. J. JOHNSON
ASSOCIATE MEMBER AIEE

Synopsis: The general problem of the design of a peak-power minimum-volume high-frequency alternator which employs the flux-switch principle is discussed. Included in this paper are analyses of general configuration, generated voltage and frequency, magnetic circuit, generator losses, and materials. A design procedure which employs the use of a set of empirically derived constants which determine various mechanical and electrical parameters is presented. The design charts can be used for flux-switch alternators ranging in power from 100 to 5,000 watts and for shaft speeds from 10,000 to 50,000 rpm. A sample design based on the use of the design charts is developed for a 50,000-rpm 3-kw 250-volt single-phase flux-switch alternator with permanent magnet excitation.

THERE have arisen a series of applications in air-borne equipment which have placed a premium upon miniaturization of the power component and which in addition demand large peak powers in the range of 100 watts to 10 kw for relatively short-duty cycles without cooling. Auxiliary power supplies for missile guidance systems provide an excellent illustration of the special need to which the present discussion is directed. The desired design features which are sought for these power supplies include minimum weight and volume, high peak power for short-duty cycles, high-quality regulation for controlled shaft speed, and improved efficiency ratings over standard rotary equipment.

The flux-switch alternator, which falls in the general class of high-frequency inductor alternators,[1-5] has shown the important property of successful application in missile systems. The flux-switch method develops an armature flux linkage which varies between equal positive and negative magnitudes. This is in contrast to the pulsating unidirectional flux change that occurs in the more conventional inductor alternator. The design discussion is directed towards a permanent magnet-excited alternator because of the low excitation losses involved and the capability of maintaining good regulation. It is possible of course to replace the permanent magnets with appropriate field windings without altering the basic performance.

Simplified Example of Flux-Switch Principle

To illustrate the mechanism of a flux-switch alternator, a simple example is presented in Fig. 1(A) and (B). For convenience in discussion the rotor is shown as a 2-salient-pole stack of laminations on a shaft. The stator consists of a pair of permanent magnets, a dual set of laminated yokes, and a pair of stator windings. The flux paths in Fig. 1(A), which are shown by arrows, indicate a flux direction from left to right in both windings. When the rotor has moved 180 electrical degrees, as in Fig. 1(B), the flux linkage through the coils has been reversed in direction but has the same magnitude as in Fig. 1(A).

It can be seen that for each revolution of the rotor a complete reversal of flux is obtained, and 4 cycles of the output voltage occur. The salient poles of the stator operate in the conventional pulsating-flux manner.

An advantage of the flux-switch design can be demonstrated as follows. The induced voltage in the stator winding for a given frequency is proportional to the number of turns and the total flux change.

Paper 55-730, recommended by the AIEE Rotating Machinery Committee and approved by the AIEE Committee on Technical Operations for presentation at the AIEE Fall General Meeting, Chicago, Ill., October 3–7, 1955. Manuscript submitted October 20, 1954; made available for printing July 21, 1955.

S. E. Rauch is with the University of California, Santa Barbara, Calif., and L. J. Johnson is with the Hufford Machine Works, Los Angeles, Calif.

The authors wish to acknowledge the contributions of Dr. William McLean and his associates at the Naval Ordnance Test Station, Inyokern, California, to the original development of miniature flux-switch alternators in air-borne equipment.

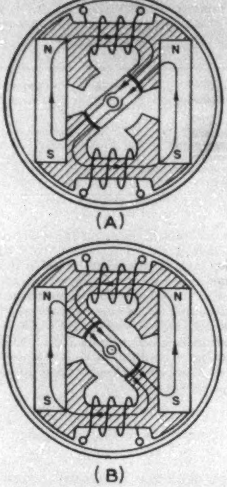

Fig. 1. Simple flux-switch alternator schematic illustrating the flux-switch principle

For a given working flux density, the flux switch produces twice the flux density change as that produced by unidirectional pulsating flux methods. Since power output is proportional to the square of the voltage, it follows that for the volume operating in a flux-switch operation four times the power can be obtained, assuming all other factors are equal. From the foregoing observations it can be seen that the working cross section of the stator yoke can be reduced by a factor of two for complete flux reversal; therefore the volume of copper for stator windings can be increased. As a consequence, the power lost in such a unit can be reduced effectively. The resulting increase in duty cycle when peak power is required is a significant advantage for applications in the missile field. For the benefit of large power-generator designers, it may be noted that peak powers can be obtained from alternators described in this paper without a resulting destructive mechanical or electrical damage to the rotary equipment.

General Design Considerations

The engineering design techniques developed for piloted aircraft have proved very successful in supplying power equipment having the characteristics of continuous duty and long life. These power units, which were designed especially for the general commercial and military piloted aircraft, observed the primary requisite of conservation of weight. Volume and efficiency were placed secondary to the weight reduction. In pilotless aircraft, such as guided missiles, volume is the critical factor for both the generator equipment and fuel and, consequently, new design concepts must be considered for the development of these specialized auxiliary power systems. In this paper design considerations are discussed which include general configuration, generated voltage and frequency, analysis of magnetic circuit, the division and extent of generator losses, and, finally, the selection of materials to approach optimum performance.

CONFIGURATION

Since the flux-switch principle employs magnetic material in the most effective manner, i.e., the flux is driven both positive and negative within saturation limits, configurations which provide flux-switch operation can yield higher performance per unit volume. For the purpose of providing an approximate constant reluctance path for the d-c magnetic field, it is desirable that the rotor poles exceed the stator poles. A stator pole will be defined as a salient magnetic path which at some position of the rotor provides a low reluctance path for the rotor flux. As a varying reluctance tends to cause flux variations in the main field, which in turn produce eddy-current losses and demagnetizing forces to the d-c field, a constant reluctance design is a necessity for optimum performance.

For both simplicity of construction and the obtaining of flux switching, it is convenient to have the number of stator poles equal to an integer multiple of the number of d-c magnetic poles. Fig. 2 is a typical example illustrating such a combination. If p_s is the total number of stator poles, p_r is the total number of rotor poles, n the shaft speed in revolutions per minute (rpm), and f is the frequency of the voltage induced in the stator coils in cycles per second (cps), then it follows that the output frequency and shaft speed for alternators in the class represented by Fig. 2 are related by

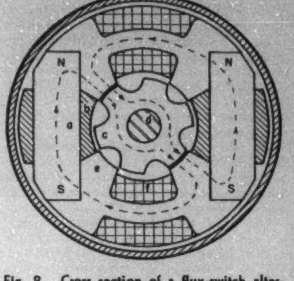

Fig. 2. Cross section of a flux-switch alternator having four stator and six rotor poles

a—Permanent magnets
b—Magnet shielding
c—Rotor laminations
d—Nonmagnetic shaft
e—Stator laminations
f—Windings

$$(\text{cps}) = p_r \frac{n(\text{rpm})}{60} \qquad (1)$$

Table I provides several possible combinations of stator and rotor poles which conveniently provide flux-switch operation as well as an approximate constant reluctance to the main d-c field. The three shaft speeds shown are representative speeds for the direct-driven high-frequency alternators. Fig. 2 represents a flux-switch alternator for which $p_r=6$, and $p_s=4$, as shown in Table I, second entry.

In the case of permanent magnet excitation, simplicity of assembly as well as mechanical ruggedness are obtained by the use of a single pair of magnets. Magnets with shaped fields, as shown in Fig. 2, are effective in space utilization and increased available magnetic energy per magnet volume. If further increase in frequency is desired, it is preferable to in-

Table I. Typical Constants for Rotor Poles, Stator Poles, and Frequency in a Flux-Switch Alternator

Rotor Poles P_r	Stator Poles P_s	Cycles per Revolution	Cps		
			12,000 rpm	24,000 rpm	48,000 rpm
5	4	5	1,000	2,000	4,000
6	4	6	1,200	2,400	4,800
7	4	7	1,400	2,800	5,600
9	4 or 8	9	1,800	3,600	7,200
10	4 or 8	10	2,000	4,000	8,000
11	4 or 8	11	2,200	4,400	8,800
13	4, 8, or 12	13	2,600	5,200	10,400

crease the number of salient poles of the stator rather than the number of d-c magnet poles. The single pair of magnets should be accompanied by magnetic shielding to obtain the highest output for the magnetic material volume. Such shielding is indicated in Fig. 2 by the cross section labelled *b*.

The general category of generators discussed operates with shaft speeds ranging from 10,000 to 50,000 rpm. As a consequence, the mechanical problems associated with the rotor assembly such as balancing and alignment require special attention. Since it is desirable to employ relatively small air gaps for peak power, any whip or resonant condition in the rotor must studiously be avoided. Shaft resonances below maximum speeds can be tolerated in some more standard rotary power units however, for the machines discussed the lower speed resonances can be destructive. For the aforementioned reasons a mechanical design of the rotor must include precision bearings, rigid rotor shaft assemblies, and a careful dynamic balancing of the complete rotor assembly over the total range of shaft speed. In addition, the magnetic circuit alignment must not create mechanical resonance within the rotor speed range.

When using permanent magnets for field excitation, the manufacturing process is simplified by performing all machinery and assembly operations with the magnets nonmagnetized. This procedure eliminates the trapping of magnetic particles such as chips and metallic dust inside the closed assembly. As a consequence the scoring of stator and rotor assemblies, the fouling of bearings, etc., can be avoided with reasonable shop practices. The mechanical arrangement of the magnetic material must be such that the permanent magnets can be easily magnetized after complete assembly of the unit. The twin magnet field structure, such as shown in Fig. 2, labelled *a*, provides a convenient system which meets the foregoing considerations.

GENERATED VOLTAGE AND FREQUENCY

The generated voltage is directly related to the number of rotor poles p_r, the shaft speed n in rpm, the total change of flux linkages ϕ in the flux-switch section of the stator, and the number of turns N in series in a winding. The frequency in cps is determined by the previously given equation 1.

The generated voltage E_g in volts per winding is given by

$$E_g=\frac{Np_rn\phi f_v10^{-8}}{60} \qquad (2)$$

where f_v is a form factor whose magnitude is determined by the voltage wave shape and the selection of average or rms units.

The most favorable winding geometry for the minimizing of copper resistance and winding reactance is the placing of the windings around the stator yoke, as shown in Fig. 2, labelled *f*. The resulting production problem requires either a winding of the stator before assembly or the use of special winding techniques. The windings could be placed around the stator poles as a winding convenience; however, this latter practice yields a lower power and efficiency rating because of the longer length per turn and poorer winding space factor.

The reactive and real components of power delivered by the generator are independent of the number of turns in the winding but are directly dependent upon the mean length of winding turn, the volume of copper used, and the magnetic circuit configuration. The inductive reactance of the generator is determined in a major part by the configuration of the soft-iron laminated portion of the magnetic circuit and, to a much less degree, by the permanent magnet section. A good design of the soft-iron yoke can yield a low internal inductance; e.g., a typical 1-kw flux switch generator can have an internal inductance of approximately 0.0024 henry when rated at 120 volts, 2,000 cps.

The design should endeavor to minimize the harmonic content of the generated voltage wave form to reduce internal losses, such as hysteresis and eddy currents, which increase rapidly with increasing frequencies. Furthermore, if capacitance correction is used, the harmonic components of the voltage are lost as wasted power and give rise to additional heat losses. The magnitudes of the generated harmonics can be controlled by the characteristics designed into the varying reluctance path of the magnetic circuit.

MAGNETIC CIRCUIT ANALYSIS

In generators of small volume which are to be designed for large peak outputs, it is important to use permanent magnet material which has the dual characteristics of large energy products and nearly rectangular demagnetization curves. In addition, the permanent magnetic must retain sufficient stored energy to maintain the magnetic flux at an approximate constant level for all positions of the rotor.

The problem of stabilization of the permanent magnets when they are subjected to the demagnetization influences of both air gaps and alternating magnetomotive forces can be considered as follows. The fundamental equation for the magnetic circuit shown in Fig. 2 is

$$F_m=\mathbf{H}_is_i+\mathbf{H}_gs_g\pm\Delta F \qquad (3)$$

$$\Delta F=0.4\pi(N_ai_a-N_si_s)$$

where

F_m = the magnetomotive force supplied by the magnet, gilberts

H = the magnetizing force, oersteds

s = the distance, centimeters

Subscripts i, g = the soft-iron and air-gap lengths respectively

ΔF = the alternating magnetomotive force caused by the armature current and compensating current in the magnetic shield

N, i = the number of turns and current respectively, amperes

Subscripts a, s = armature and shield respectively

Magnet shielding can be used effectively to minimize the magnitude of ΔF. This type of shielding consists basically of short-circuit turns with very small resistance placed around the magnet in a manner such that, when the magnet flux tends to change, a current flows which opposes that change. As a result, ΔF can be reduced to only a small percentage of the total armature reaction when the proper design of the magnetic shielding is used.

Fig. 3 represents the general schematic for the operating characteristic of the permanent magnet field used in the alternators. The point P_g is determined by the intersection of the equivalent negative air-gap line and the curve of flux ϕ versus magnetic potential rise in the magnet, which defines the average operating condition of flux ϕ_0 and magnetomotive force F_{g0}. When the demagnetizing force $-\Delta F$ is applied to the circuit, the operating point is lowered to P_1 on the curve. The alternating influence of $\pm\Delta F$ leads to the cyclical variation on the minor hysteresis loop P_1P_2. The average flux ϕ is reduced from ϕ_0 to ϕ_1; however, a stable magnet is obtained for further demagnetizing forces not exceeding ΔF in magnitude. It is to be noted that the larger the demagnetizing force, the more the average total flux in the air gap is reduced. The minor hysteresis loop P_3P_4, with an average total flux ϕ_2, indicates the operation of the magnetic circuit for a maximum demagnetizing force, such as the case when no magnet shielding is employed.

The foregoing discussion indicates that the length and cross-sectional area of the magnet will be larger in magnitude than the dimensions defined by the air-gap condition alone. In general, the use of a longer length and smaller cross-sectional area than that indicated by the maximum energy product produces a magnet which has a safety tolerance for unexpected short-circuit conditions, such as might be

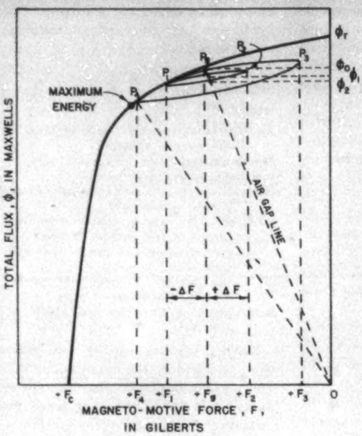

Fig. 3 (left). Typical flux ϕ versus magnetomotive force F for a permanent magnet

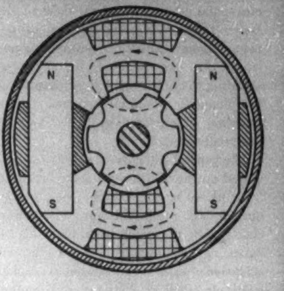

Fig. 4 (right). Low-reluctance path for the flux-switch alternator of Fig. 2

represented by the operating characteristic P_3P_4.

The inductance L_w of an armature winding is determined by the number of turns N in series in a single winding and the magnetic circuit configuration. The role of the various parameters which contribute to the value of the inductance L_w in henrys of a single winding is as follows

$$L_w = \frac{0.4\pi N^2 \times 10^{-8}}{R} \tag{4}$$

where R is the effective reluctance of the magnetic path. In Fig. 2, the reluctance for each path is the sum of the reluctances through the soft iron, air gaps, and permanent magnets, i.e.

$$R = \frac{s_i}{\mu_i A_i} + \frac{s_g}{\mu_g A_g} + \frac{s_m}{\mu_m A_m} \tag{5}$$

where

s, μ, A = the length, centimeters, the instantaneous permeability, and cross-section area, centimeters^2

Subscripts i, g, m = iron, air gaps, and permanent magnet, respectively

For the path shown in Fig. 2, the reluctance of the permanent magnet path is an order of magnitude greater than the combined soft-iron and air-gap reluctance. It could be concluded that the permanent magnet reluctance is the major contributor to the effective inductance. Such is not the case, however, because there exists a much lower reluctance parallel circuit, as indicated in Fig. 4. It can be seen in Fig. 4 that a closed magnetic path exists which does not include the permanent magnet. Thus, the effective inductance per stator winding is determined to a first approximation by equation 6

$$L_w = \frac{0.4\pi N^2 \times 10^{-8}}{\left(\frac{s_i}{\mu_i A_i} + \frac{s_g}{A_g}\right)} \tag{6}$$

where the magnitudes of the parameters are to be evaluated for a magnetic path shown in Fig. 4. For all normal operating conditions, the air-gap contribution to reluctance is the major controlling factor of a generator winding inductance.

At high frequencies, even though the value of the total inductance L_w is small, the inductive reactance of the generator will limit the power output and yield poor voltage regulation. It therefore becomes necessary to use capacitance correction for the obtaining of peak power and acceptable voltage regulation. When capacitance correction is used, the peak power output is limited by winding resistance and saturation of the iron sections of the path shown in Fig. 4.

An optimum permanent magnet structure can be designed for high-frequency alternators of the type described herein which will produce good voltage regulation and large peak power ratings when capacitance correction is employed.

Generator Losses

Mechanical losses in high power to weight ratio generators of the type discussed herein are relatively small because of the reduction in diameters of the rotating parts and the use of precision bearings. Precision bearings yield low frictional losses, and small rotor diameters considerably reduce the importance of windage. As a consequence, mechanical losses play a very minor role in determining the over-all efficiency of the generator.

The division of electrical losses is somewhat unconventional from the point of view of low-frequency power generation. The usual design procedure allows an equal distribution of losses between copper and core; however, in high-frequency applications the core losses must become the major consideration. In many earlier high-frequency designs, such as in audio-frequency transformers, the core loss was kept low by working the iron at very low flux densities. Such a practice leads to excessive weight and volume in the magnetic structure. Although the iron losses increase approximately as the square of the working flux density, it is to be noted further that the power output per unit volume of core also increases in the same manner. As the design objective includes the minimizing of over-all volume, it becomes apparent that high losses per unit volume of core material can be employed to an advantage. The resulting reduction of core volume offers the further advantage of reduced copper losses because the length of turn of the copper winding will be decreased and the corresponding resistance decreased proportionally. As a result the major heating is caused by the iron losses. This avoids the usual problems of hot spots in the windings and is considered to be an added premium in design. In contrast to the equal division of losses, conventional designs leading towards minimum volume should have iron-to-copper-loss ratios of the order of 4 to 1.

Table II. Specifications for a Sample Flux-Switch Alternator

Rated output, kw	3
Rated shaft speed, rpm	50,000
Rated voltage, rms	250, single phase
Rated frequency, cps	5,000
Power factor	unity
Minimum over-all efficiency, per cent	80
Duty cycle	continuous with cooling
Regulation, per cent	25, maximum

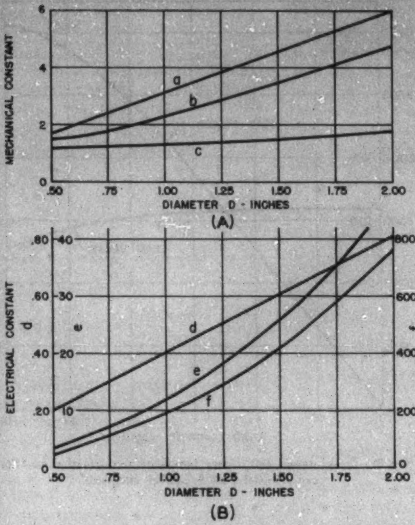

Fig. 5(A). Relationship of mechanical design constants to diameter D of rotor for a shaft speed of 10,000 rpm. (B). Relationship of electrical design constants to diameter D of rotor for a shaft speed of 10,000 rpm

a—Minimum allowable air-gap clearance between rotor and stator, $\text{inches}\times10^{-3}$
b—Over-all generator diameter, inches
c—Minimum length to be added to rotor working length, inches
d—Generated volts per turn per rotor length l
e—Core loss, watts, per rotor length l
f—Maximum power output, watts, per rotor length l

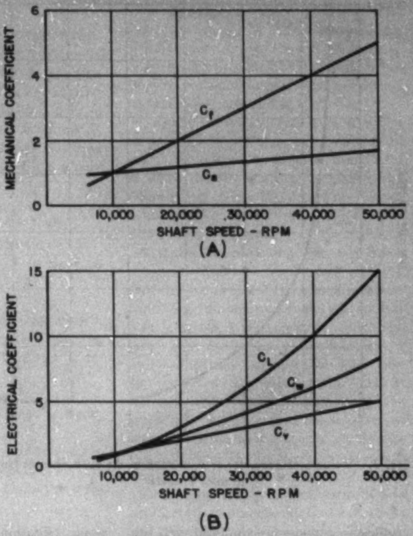

Fig. 6(A). Relationship of mechanical coefficients as a function of shaft speed. (B). Relationship of electrical coefficients as a function of shaft speed

C_a—Air-gap factor
C_f—Frequency factor
C_L—Core loss per rotor length factor
C_v—Generated volts per turn per rotor length factor
C_w—Maximum power output per rotor length factor

Sample Design

Consider the design of a flux-switch alternator having the characteristics as shown in Table II. The general configuration, as shown in Fig. 2, is to be followed. Since an important objective of the design is to minimize the volume of the generator, it will be necessary to select core materials with low core loss and high flux densities. Materials such as monimax or sinamax have very favorable properties of low core loss and high flux densities; however, these materials are relatively expensive and would be ruled out in most cases for the sake of economy. A good substitute is oriented steels such as Armco oriented *T-S*. Although it has a higher core loss factor, it can be worked at flux densities which are of the order of 20 per cent greater than that permitted with monimax or sinamax, which leads to a higher volt-ampere rating per pound.

Alnico V is to be used as the permanent magnet material since it has the largest energy product per unit volume and weight of the various available permanent magnet materials. The shape of the **B-H** characteristic of Alnico V offers the additional advantage of a good voltage regulation characteristic.

Design Charts

The electrical design procedure will employ the use of a set of empirically derived design constants involving the various parameters, as shown in the charts of Figs. 5 through 7. The information presented in these charts was obtained empirically from the design of flux-switch alternators ranging in power from 100 watts to 5 kw for speed variations from 10,000 to 50,000 rpm. The efficiencies for generators in this category have proved to be in the 80-to 90-per-cent range.[2]

Figs. 5(A) and (B) relate the diameter *D* to certain design constants of the magnetic material in the rotor section for a basic shaft speed of 10,000 rpm. Fig. 5(A) is a plot of the minimum allowable air-gap clearance between rotor and stator, the over-all generator diameter, and the minimum length to be added to the length *l* of the magnetic section of the rotor with the diameter *D*. In Fig. 5(B) there is shown the relationships of the diameter *D* to the electric parameters, including generated volts per turn per length *l*, core loss in watts per length *l*, and the maximum power output in watts per length *l*. Figs. 6(A) and (B) provide coefficients which extend the constants of Fig. 5 to include the shaft speed range from 10,000 to 50,000 rpm. Fig. 6(A) presents the relationships of shaft speed to the mechanical constsnts C_a and C_f, which are air-gap and frequency coefficients respectively and defined such that C_a and C_f are unity at the base speed of 10,000 rpm. Similar information is shown for the electric coefficients C_L, C_v, C_w in Fig. 6(B), where C_L, C_v, and C_w are the

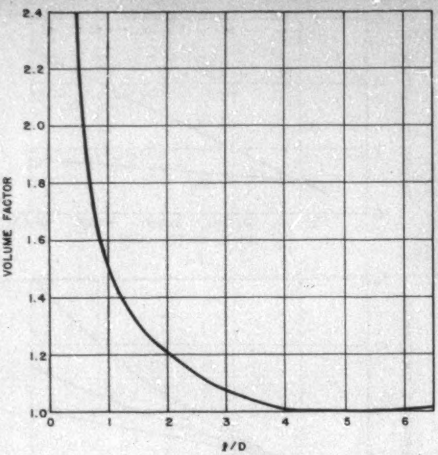

Fig. 7. Volume of generator as a function of the ratio of rotor length to rotor diameter

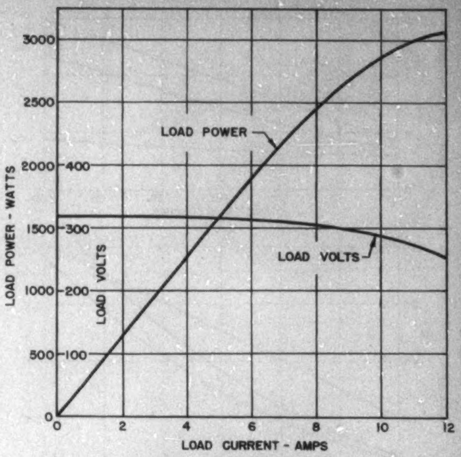

Fig. 8. Power output and voltage regulation versus load current for experimental 3-kw flux-switch alternator

coefficients for core loss, induced volts per turn per l, and maximum power output of watts per l respectively.

The first step in the design procedure involves the selection of the rotor diameter D. Fig. 5(B), curve f, relates maximum power output per working length l to the diameter D at 10,000 rpm. Fig. 6(B) defines the magnitude of the increase in power rating at 50,000 rpm, i.e., $C_w=8.3$. Thus, 8.3 times the maximum power out put per l at 10,000 rpm will yield the maximum power output per l at 50,000 rpm. For an $l=1$ inch, the power output factor at 10,000 rpm is given by 3,000/8.3=360 watts per inch. From curve f, Fig. 5(B) it is concluded that $D=1.38$ inches.

As the major design objective is to minimize the total volume of the generator, it is important to determine the relative volume in comparison to minimum volume of any choice of the l/D ratio which yields the given power rating. Fig. 7 presents the relationship of volume to l/D for generators in the abovementioned power range. It can be seen that the choice of an $l/D=1/1.38=0.7$ is not a desirable choice since the volume-increase coefficient is approximately 1.8 times the minimum volume. For this reason a new choice of D is in order. The curve of Fig. 7 indicates that a ratio of $l/D=4.3$ yields the minimum volume for generators of this power range. A further consideration which affects the final choice of an operating l/D is mechanical stability. A long slender rotor is subject to whip and harmonic vibrations which cannot be controlled at the higher shaft speed rating of 50,000 rpm; therefore, a reasonable restriction of l/D not to exceed 1.5 shall be observed for the problem under consideration. The resulting increase in volume over the minimum does not exceed 30 per cent and is considered a reasonable sacrifice in volume for mechanical stability. With the foregoing conditions imposed, the final diameter of the magnetic section of the rotor is determined as follows. The equivalent output power that would be needed at 10,000 rpm is 3,000/8.3=360 watts. With the use of the data shown in curve f, Fig. 5(B), it can be concluded that the rotor size which can deliver 360 watts at 10,000 rpm or 3 kw at 50,000 rpm, and which also satisfies the simultaneous relationship of $D=2/3\ l$, can be found to be $D=1.125$ inches and $l=1.7$ inches.

It is possible now to estimate the magnitudes of certain design constant limitations from Fig. 5 and 6 which determine the final electrical characteristics of the unit at 50,000 rpm.

ROTOR

To conform with the general configuration of Fig. 2, the rotor will have six salient poles equally spaced. The pole pitch will be $(\pi D)/6=(\pi 1)125/6=0.590$ inch. For the best design the rotor slots should span one half of the pole pitch plus a minimum of three times the air-gap length. Fig. 5(A), curve a, recommends a minimum rotor clearance of $1/2\ s_g=0.0035\ C_a$. For a shaft speed of 50,000 rpm, the factor $C_a=1.66$, as shown in Fig. 6(A). It follows that

$$\text{rotor pole span}=\frac{\pi D}{12}-\frac{3}{2}s_gC_a=\frac{(\pi 1)125}{12}-3\times 0.0035\times 1.66=0.295-0.018=0.277\text{ inch}$$

$$\text{area of pole face}=\text{pole span}\times l=0.277\times 1.7=0.47\text{ inch}^2$$

STATOR

The stator contains only four poles spaced equally around the rotor; therefore

$$\text{pole pitch}=\frac{\pi D}{4}=\frac{(\pi 1)125}{4}=0.885\text{ inch}$$

The stator pole span shall be made equal to the rotor pole span; and therefore:

Stator pole span $=0.277$ inch.
Area of stator pole at air gap = stator pole span $\times l=0.277\times 1.7=0.47$ inch^2.

Generated Voltage and Flux

The configuration, as shown in Fig. 2, has been found experimentally to produce approximate sinusoids when zero load is applied. As total harmonic distortion does not exceed 10 per cent, the alternating flux calculations shall be based upon sinusoidal wave form. From Fig. 5(B), curve c, and Fig. 6(B), coefficient c_v, the induced voltage per turn of the stator winding at no load can be estimated as follows

induced volts per turn = (volts per turn per inch at 10,000 rpm)(C_v for 50,000 rpm)l = $0.455\times5\times1.7=3.97$ volts per turn

From the basic equation relating sinusoidal voltage E_{rms} induced in a coil, i.e.

$$\phi=\frac{E_{rms}10^8}{4.44Nf}$$

where

ϕ = total flux, maxwells
N = number of turns in coil which the flux links
f = the frequency, cps

$$\text{no-load peak flux } \phi=\frac{3.97\times10^8}{4.44\times5{,}000}=1.79\times10^4 \text{ maxwells}$$

If no capacitance correction were used, the no-load flux would be the maximum peak flux in the stator yoke; however, with a capacitance correction the total peak flux can be considerably larger than the no-load peak flux. It is necessary, therefore, to estimate the effective internal inductance of the stator windings. A series connection of the two stator windings will be used. The number of turns $2N$ in series on the stator will be the desired no-load voltage divided by the volts per turn as previously calculated. With the design objective set for a maximum 25-per-cent increase of no-load over full-load voltage, the no-load voltage becomes 313 volts and the resulting number of turns $2N$ in series is given by

$$2N=\frac{313}{3.97}=80 \text{ turns}$$

INDUCTANCE

To estimate the effective inductance L of the generator, it is assumed that the effective inductance is evaluated for the position of the rotor where the area of flux path for each stator to rotor pole is equal, such as shown in Fig. 4. It is estimated that the a-c permeability of the laminations at 5,000 cycles is approximately 500. For the present example, the mean length around the magnetic loop as shown in Fig. 5 is 2.5 inches. The air-gap length is 0.012×2.54 centimeters, and the air-gap cross section is $1/2\times0.47\times6.45$ centimeters^2, yielding an air-gap reluctance of 0.020. The reluctance of the iron path is $(2.5\times2.54)/(0.47\times6.45\times500)=0.004$. The total reluctance is estimated to be 0.024. The total effective inductance of the generator is given by 2 L_w, where L_w is defined by equation 4

$$L=2\left(\frac{1.256\times40^2}{0.024}\right)\times10^{-8}=1.7 \text{ millihenrys}$$

MAXIMUM REACTIVE FLUX

The inductive reactance is $2\pi fL$ ohms, or 53 ohms. The full-load current is $3{,}000/250=12$ amperes. The reactive voltage, which is the maximum induced voltage in the windings, is $53\times12=636$ volts when the capacitance reactance is used for power-factor correction. The maximum value of the reactive flux occurs at full load and is given by

$$\text{maximum reactive flux}=\frac{636\times10^8}{4.44\times80\times5{,}000}=3.65\times10^4 \text{ maxwells}$$

STATOR YOKE

With the use of a working peak density of 14,000 gausses in the stator yoke, the cross section of the stator yoke can be determined as follows

$$\text{stator yoke area}=\frac{36{,}500}{14{,}000}=2.6 \text{ centimeters}^2$$

The effective stack length, with a stacking factor of 0.9, has a value of $1.7\times2.54\times0.9=3.88$ centimeters. The stator yoke depth is given by

$$\text{stator yoke depth}=\frac{2.6}{3.88}\times\frac{1}{2.54}=0.26 \text{ inch}$$

CORE LOSS

Fig. 5(B), curve *e*, describes the core loss typical for this type of generator. For a $D=1.125$ inches and a shaft speed of 10,000 rpm, there occurs a 15-watt-per-inch loss. The core loss for 50,000 rpm with an $l=1.7$ inches is evaluated to be

$$\text{core loss}=15\times1.7\times C_w=15\times1.7\times8.3=210 \text{ watts}$$

As a check on the foregoing core-loss prediction, it is possible to estimate the lamination weight of the rotor and stator and to compare the watts per pound loss with commercially published values. The average path cross section is equal approximately to the yoke cross section, which is $0.26\times1.7\times0.9=0.4$ inch^2. With an average length of 2.5 inches, a total volume of laminations is $2\times0.4\times2.5=2.0$ inch^3. The weight is given as approximately 2.0 inch$^3\times0.3$ pounds per inch$^3=0.6$ pounds. The watts per pound loss is $210/0.6=350$ watts per pound, which is in agreement with published estimates.

COPPER LOSS

The length of turn per winding is approximately 4.5 inches. The total length of windings is $80\times4.5=360$ inches = 30 feet. In accordance with the previous quotation of having a core-to-copper-loss ratio of 4, the maximum copper loss shall be set at 50 watts; therefore, the maximum allowable resistance is $50/144=0.35$ ohm. In lieu of the copper temperature of 100 degrees centigrade and the increase in resistance because of skin effect, a no. 18 wire is found to meet the maximum resistance requirement of 0.35 ohm.

The copper cross section of a single turn is 1,624 circular mils, or 0.0013 inch.^{2} To obtain the cross-sectional area in which the winding is to be placed, the following procedure is used. The over-all diameter taken from curve *b*, Fig. 5(A), is 2.65 inches. Subtract from the value of 2.65 inches the rotor diameter, two times the yoke thickness, and two times the sheet thickness of 1/16 inch to obtain 0.88 inch. There remains a radial distance of 0.44 inch per winding stack. Since the area varies as the square of the radius, a radial thickness between the shell case and outer stator yoke of 0.2 inch is selected. The winding span along the stator yoke is 0.75 inch. The total cross-section area for the 40 turns of no. 18 wire is 0.15 inch^2. The total copper cross section is $0.0013\times40=0.052$ inch^2. The area to copper cross-section ratio of 3 is satisfactory to accommodate the 40 turns and the additional necessary insulation materials.

PERMANENT MAGNETS

To evaluate the approximate individual demagnetizing effects that arise under full-load operation of the alternator, it is first necessary to appraise the leakage factors in the circuit. From the many empirical methods developed for determining leakage and fringing, the technique described in reference 6 has been selected for use in the following manner.

Let F and f be defined such that

$$F\mathbf{B}_gA_g=\mathbf{B}_mA_m$$

$$f\mathbf{B}_gs_g=\mathbf{H}_ms_m$$

where the constants F and f are functions of the geometry of the magnetic circuit. The value of f varies over a small range, usually from 1.2 to 1.5, with a value of $f=1.35$, typical for most permanent magnet circuits. The leakage constant F usually varies from 2.0 to 10. It is shown in reference 6 that for the circuit of Fig. 3 a value of $F=2.3$ is predicted.

The individual demagnetizing effects in the magnetic circuit arising in the operation of the alternator are indicated in equation 3. The loss resulting from the effective air gap of the circuit is

$$H_gs_g=\frac{2.3\times17{,}900\times0.012\times2.54}{1.35\times0.235\times6.45}=610 \text{ gilberts}$$

For a minimum average permeability of 500 specified for the iron path at the peak reactive voltage, the peak loss in magnetomotive force in the iron for an average path length of 2.5 inches and cross section of 2.6 centimeters² is

$$H_4 s_4 = \frac{36{,}500 \times 2.5 \times 2.54}{2.6 \times 500} = 180 \text{ gilberts}$$

To present a conservative estimate of the effectiveness of the magnet shielding, it is assumed that a maximum residual of 20 per cent of the total armature reaction remains uncompensated by the magnetomotive force of the magnet shielding. As a result a possible maximum value for ΔF is

$$\Delta F = 0.08\pi(N_a i_a) = 110 \text{ gilberts}$$

The magnetomotive force of the magnet under full-load operation must be able to withstand a maximum demagnetizing force of

$$F_4 = 610 + 180 + 110 = 900 \text{ gilberts}$$

Since most applications of the alternator require that the magnets be not derated by temporary short-circuit currents, the magnets should be stabilized in their completed circuit to withstand a total demagnetization force of a short-circuit current at rated speed. The magnitude of ΔF will not be doubled because of the current-limiting characteristic of the design of the alternator; a maximum demagnetizing force of $F_4 = 1{,}000$ gilberts shall be considered possible.

Alnico V has a **B-H** characteristic such that the demagnetizing force $\mathbf{H}_m$ should not exceed 475 oersteds; thus

$$\mathbf{H}_m s_m > 1{,}000$$

$$s_m > \frac{1{,}000}{475} = 2.1 \text{ centimeters} = 0.83 \text{ inch}$$

The average flux density of Alnico V is approximately 11,000 gausses when operated on a minor hysteresis loop which has the maximum demagnetizing condition near the maximum energy point. The cross-sectional area of the magnet is given by

$$A_m = \frac{2.3 \times 17{,}900}{11{,}000} = 3.74 \text{ centimeters}^2$$

For a working rotor length of $l = 1.7$ inches, the cross-section dimensions of the magnet become 1.7 inches by 0.34 inch.

Experimental Evaluation

With the use of the magnitudes of the various parameters calculated in the foregoing sample design method, a flux-switch alternator was constructed for the purpose of evaluating the accuracy of the design procedure. The voltage and power performance of the unit are shown in Fig. 8. The full-load voltage of 250 volts at rated load of 3,000 watts was achieved within the specified voltage-regulation requirement.

The over-all efficiency of the alternator was measured carefully at 88 per cent at full load. This would indicate a total loss of 360 watts in the unit. The sample design estimated a 210-watt core loss and a 50-watt copper loss in the winding. In addition there occurred a copper loss in the magnet shielding and mechanical losses. The magnet shielding consisted of one turn of copper with approximately the same cross section as the copper in a single winding, i.e., 0.052 inch². The total power dissipated in the single turn did not exceed 5 watts; therefore there occurred approximately a 100-watt dissipation in mechanical losses. The alternator had a total weight of 42 ounces, with an over-all length of 3 inches and a diameter of 2.65 inches.

Conclusions

A design procedure for flux-switch alternators is presented in this paper. The design charts which form the basis of the method were developed empirically from previous experimental data for flux-switch alternators in the 100- to 5,000-watt range. Emphasis has been directed towards the design of high-frequency power units which maximize the output per volume.

The results of the sample design for a 3-kw alternator, which are verified experimentally, indicate that the observance of the principles outlined herein can assist in obtaining the design of flux-switch alternators having the characteristics of peak power with minimum volume.

References

1. A 24,000-RPM ALTERNATOR FOR AIRCRAFT, **T. J. Martin.** *Electrical Engineering*, vol. 68, March 1949, p. 243.

2. HIGH-FREQUENCY ALTERNATORS, **S. E. Rauch, L. J. Johnson.** *Ibid.*, vol. 73, Aug. 1954, pp. 735-37.

3. DESIGN OF PERMANENT-MAGNET ALTERNATORS, **R. M. Saunders, R. H. Weakley.** *Ibid.*, vol. 70, Nov. 1951, p. 991.

4. THE THEORY OF THE INDUCTOR ALTERNATOR, **J. H. Walker.** *Journal*, Institution of Electrical Engineers, London, England, vol. 89, 1942, p. 227.

5. HIGH FREQUENCY ALTERNATORS, **J. H. Walker.** *Ibid.*, vol. 93, 1946, pt. 2, pp. 67-80

6 PERMANENT MAGNET DESIGN, **Earl M. Underhill.** *Electronics*, New York, N. Y., Dec. 1943, p. 126.

◆

Discussion

Robert M. Saunders (University of California, Berkeley, Calif.): In this fine paper the authors do indicate (albeit somewhat obscurely) the necessity of maintaining a constant reluctance magnetic circuit as far as the permanent magnets are concerned. Since I consider this point extremely important, I will take this opportunity of re-emphasizing it.

Concerning the problem of having the permanent magnets subjected to high-frequency magnetomotive forces, I should like to inquire if the magnet shields really are performing a necessary function. It is well known that the incremental permeability of Alnico V is very low. In fact one may think of Alnico V as a constant flux source under many conditions. If the permeability of the magnets is very low, then the leakage paths assume a more significant role as paths for the armature reaction flux. At the outset I would be inclined to say that the magnet shielding coils were quite unnecessary. The answers to two questions might serve to clarify this issue: (1) Did the authors compare units built with and without the shielding coils? (2) Was the 5-watt dissipation in the shielding coil an experimentally observed value or a calculated one?

S. E. Rauch and **L. J. Johnson**: The authors wish to thank Mr. Saunders for his interesting and valuable questions concerning the effectiveness of magnet shielding in the types of alternators described in this paper. In answer to his first question, it is possible to state definitely on the basis of comparative experimental tests that magnet shielding is necessary in order to prevent destructive demagnetization during short-circuit conditions. In addition, the load characteristics are improved approximately 30 per cent for regulation under rated loads. A change of reluctance in the armature circuit and armature reaction have comparable demagnetizing effects on permanent magnets. Magnet shielding as presented in the paper is very effective in reducing the transient or cyclical demagnetizing forces. Mr. Saunders' remark on the requirement of constant reluctance in the magnetic circuit is equivalent to a statement that all demagnetizing forces on a permanent magnet must be held constant for optimum power to volume ratios. In other words, peak demagnetizing forces must be equalized by magnet shielding.

The 5-watt description in the magnet shielding loop was a calculated value based upon previous experimental data.

Predetermination of Sound Pressure Levels of Magnetic Noise of Polyphase Induction Motors

E. ERDELYI
MEMBER AIEE

Synopsis: This paper gives a general procedure for calculating in decibels the slot frequency sound pressure level produced by a polyphase induction motor operating at any arbitrary speed and load. To do this, it is necessary, first, to calculate the frequencies, pole numbers, and magnitudes of the important air-gap magnetic fields; second, to calculate from these the frequencies and magnitudes of those air-gap force waves with relatively few nodes that are most likely to produce noise; third, to calculate the stiffness and resonant frequencies of the core and frame structure for vibrations of low numbers of nodes; fourth, from all these, to calculate the radial deflections of the stator core and frame that are due to the significant slot frequency force waves; and, fifth, to calculate the decibel level of sound pressure at any point in space that is caused by the calculated deflection of the frame. After outlining the procedure required for these five steps in some detail, the paper gives the numerical results of calculations and the corresponding test sound levels for a particular 4-pole, 30-horsepower polyphase induction motor of open-frame construction. Calculations and tests were made for six operating conditions with different loads, voltages, and line frequencies. The calculated values for the six conditions were 86, 88, 91, 75, 62, and 82 decibels respectively, and the corresponding test values were 88, 90, 94, 74, 64, and 85, showing excellent agreement.

ELECTRICAL engineers have known for decades that polyphase induction motors of all sizes produce and radiate unpleasant noise. Many efforts of a practical nature have been made to reduce the noise level in induction motors of all sizes. From the viewpoint of users of medium-sized induction motors of more than one pole pair, it is the magnetic noise that is felt to be the most troublesome factor.

Early research in the magnetic noise of induction motors was closely linked with investigations of other effects of higher harmonic magnetic flux density waves in the air gap. Even until recently the recommendation for low magnetic noise level induction motors was intimately related to slot combinations. Krondl,[1,2] Hildebrand,[3] Kron,[4] and Morrill[5] have discussed in great detail the question of slot combinations, and the calculation of the mode, frequency, and magnitude of the radial force waves responsible for the vibration and noise of induction motor frames. Using these "rules," designers found that the concept of most opportune slot numbers is practicable only for a definite type of motor and they became aware that the noise problem was not a simple, electromagnetic one, but also one of engineering mechanics and acoustics.

Alger,[6,7] who was the first to provide a simplified, comprehensive treatment embracing all phases of the problem, was also the originator of the concept of "sonance design." According to him, the induction motor as regards its mechanical vibrations can be represented as a simple inextensional ring, and he analyzed the motor's natural behavior on this basis. To analyze its acoustic behavior Alger chose to represent the motor by an infinitely long vibrating cylinder. He provided the designer with formulas and curves of sound intensities of the noise radiated from the induction motor. Simultaneously, Jordan in Germany provided a simplified solution.[8,9] His assumptions regarding the vibrational aspect of the motor is approximated by a radiating sphere, and Gauss's theorem is used to determine the sound power level at a distance from the motor.

In the method as presented by Alger it is assumed that the "stiffening" effect of the frame can be neglected. Although this assumption was necessary at the start of an investigation of all phases of the magnetic noise, it cannot be justified in the noise analysis of medium-sized induction motors for the following reasons.

It is the aim of every designer to mismatch the frequencies and modes of the forces creating the vibrations, and the natural frequencies of the induction motor's structure. However, the natural frequencies of an induction motor differ considerably from those of the stator core alone. In addition, the stator core has but one natural frequency in each mode, while the more complicated structure of the induction motor may have three or more important natural frequencies in each mode. (The term "mode" denotes the number of complete periods of a sinusoidally distributed quantity along the periphery of the stator bore.) This can be observed clearly from Fig. 1. The dashed curve illustrates the dynamic deflections of a stator core represented by a single ring. The deflection amplitudes increase gradually with the frequency of the force wave until resonance is reached. Beyond the resonant frequency the amplitudes attenuate continuously with the increase of frequency. The full curve represents the same plot of a structure consisting of two rings connected by radial ribs and mounted on a support which approximates the actual motor structure more closely. After the first resonance the amplitude attenuates, but suddenly increases again, to reach several new resonances at different points of the frequency range.

This, however, is not the only objection to the single-ring theory. It can be verified that the sound waves radiated by the stator core are strongly attenuated by the outer ring. It becomes obvious that the major part of the magnetic noise is caused by the vibration of the frame.

It will be the purpose of this paper to develop further the method as initiated by Alger, by avoiding many simplifications necessitated in the original treatment. The analysis involves three disciplines of physical science, and is consequently discussed in three different sections.

Symbols and Notations

ELECTRICAL QUANTITIES

B_σ, B_ρ = amplitude of the σth or ρth flux density harmonic

Paper 55-726, recommended by the AIEE Rotating Machinery Committee and approved by the AIEE Committee on Technical Operations for presentation at the AIEE Fall General Meeting, Chicago, Ill., October 3-7, 1955. Manuscript submitted June 6, 1955; made available for printing July 22, 1955.

E. ERDELYI is with Syracuse University, Syracuse, N. Y.

The contents of the paper are an excerpt from a dissertation submitted in partial fulfillment of the requirements for the degree of doctor of philosophy in the University of Michigan. The author wishes to express his sincere gratitude to P. L. Alger, consulting engineer, for guidance and assistance during every phase of the investigation. Thanks are also due to the Medium Induction Motor Department of the General Electric Company for sponsoring the work. Acknowledgments are further due to Dr. G. Horvay and Dr. R. Plunkett, both of the General Electric Company, for their valuable suggestions. The help of Dr. F. S. Beckman and J. F. Terlato, of the International Business Machines Corporation, who programmed the final calculations for the electric data-processing machine, is also gratefully acknowledged.

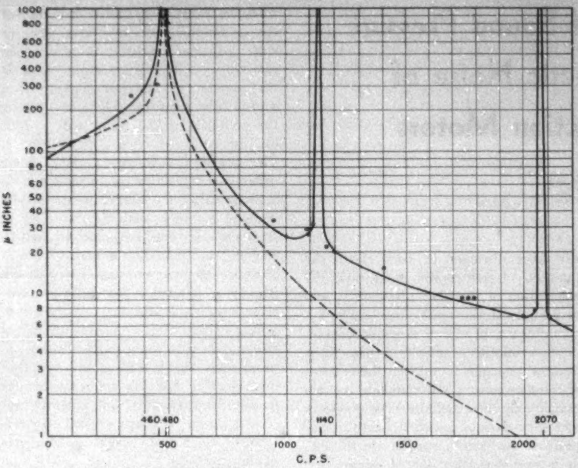

Fig. 1. Comparison of dynamic behavior of single ring with that of induction motor structure

b = constant defined by equation 10(A)

$b(x_1, t)$ = ordinate of radial flux density distribution at x, at time t

c_1, c_2, c_{1s}, c_{2s} = integer constants

f = frequency

g = length of air gap

k_c = Carter coefficient

m_r = order of mode of radial force waves

p = number of pole pairs

$\mathcal{P}$ = permeance function

Q_1 = number of stator slots

Q_2 = number of rotor slots

q = number of slots per pole per phase

s_{10} = width of stator slot opening

t = time

x_1 = position of a point in air gap ($x_1 = 0$ at center of reference phase)

β = a function of (s_{10}/g)

ϵ = eccentricity of air gap

η_1, η_2 = coefficient in permeance function

μ_0 = permeability of free space

Π = amplitude of force wave

ρ = order of rotor harmonic referred to a double pole pitch, as fundamental period

$\rho' = p\rho$ order of rotor harmonic referred to air gap circumference as fundamental period

σ = order of stator harmonic referred to a double pole pitch as fundamental period

σ' = order of stator harmonic referred to air gap circumference as fundamental period

τ = pole pitch

τ_t = tooth pitch

ω = circular frequency $(2\pi f)$

ω_f = frequency of force wave

ENGINEERING MECHANICS QUANTITIES

A_i = amplitude of sinusoidally varying quantity

A_m, a_m, B_m, b_m = Fourier expansion coefficients

b = subscript denoting bending

D = rigidity factor

E = Young's modulus

$E' = E/(1-\sigma^2)$

I = moment of inertia

i = subscript denoting inner ring

K_r = constant to replace summation

k_{ij} = coefficient of potential energy

l = length

m = order of mode

m_{ij} = coefficient of kinetic energy

Q = generalized force

q = generalized co-ordinate

r = subscript denoting principal mode

T = kinetic energy

U, u = radial displacement of outer and inner ring

V = potential energy

W, w = tangential displacement of outer and inner ring

W^e = work of external force

y = normalized eigenvector component

μ = mass per radian

ψ = phase angle or rotation of cross section

σ = Poisson's ratio

ω = frequency of force wave

ω_r = natural frequency of rth principal mode

ACOUSTIC QUANTITIES

c = sound velocity

$H_m^{(1)}$ = Hankel function of order m

$[H_m^{(1)}]'$ = derivative of Hankel function of order m

h = separation constant

I = sound pressure integral

k = constant

p = pressure

p_0 = static pressure

q = velocity

Z_n = circular cylinder function

z = co-ordinate

ρ_0 = density

ω = circular frequency

Electromagnetic Force Waves in Air Gap

The noise of electromagnetic origin appears at different frequencies depending on the nature of the driving forces. The double-frequency noise is excited by the main air-gap field. These 120-cycles-per-second (cps) radial forces are unavoidable as the induction motor could not function without the main flux. The effect is generally harmless in smaller or medium-sized induction motors and produces a humming sound. For large 2-pole motors, where the radial force wave due to the fundamental flux is a second-mode force wave, the vibration and noise caused by these forces may become vigorous.

The troublesome magnetic noise can be traced mainly to radial forces which occur when the air-gap flux density distribution contains two harmonic fluxes with pole pairs differing by a small integer. The higher harmonic flux density distributions are inherent in the limitations of induction motor-winding arrangements, and could be avoided only if the number of phases and the number of slots per phase could be substantially increased. The amplitude of these so-called space harmonics, which create the radial forces, depend on the armature current. The nonuniform permeance of the air gap caused by the open or semiopen slots of the stator creates the so-called permeance harmonics. The order and frequency distribution of these are the same as those caused by the slot harmonic flux distribution waves. However, the magnitude depends mainly on the supply voltage and is independent of the load current.

The rotating fundamental and higher harmonic flux density distributions will cause a continuous change of the energy density in the air gap. As a consequence radial rotating force waves occur which modulate the average attraction between the stator and rotor. The mechanical response to these force waves is a forced vibration of the induction motor structure which creates the noise.

To bring the treatment into a manageable mathematical form it is necessary to make simplifying assumptions, i.e., the magnetic induction in the air gap is assumed proportional to the magnetomotive potential difference radially across the air gap. Symmetrical, balanced, 3-phase, integral slot, double-layer windings are assumed for the stator, and closed slots, nonskewed squirrel-cage windings for the rotor.

The calculation of the force wave due

to the main air-gap flux density is given in detail in references 6 and 7. The calculation of the mode, amplitude, and frequency of the radial force waves caused by the interaction of higher harmonic flux density distributions is given in reference 10, and has previously been given by Alger,[7] Krondl[1,3] Morrill,[5] and others, without considering the influence of the permeance harmonic. This could, in the past, be justified because most of the writers were interested only in the mode and frequency of the force wave, as they did not compute the vibrational response of the motor. In an analysis intended to calculate the dynamical response of the induction motor, the cumulative influence of the permeance harmonics and the increase in the magnitude of the force waves by combinations of the flux density harmonics, other than slot harmonics, cannot be neglected.

From consideration of the magnetic energy in the air gap it can be shown that the radial force per unit area is

$$\Pi(x_1, t) = (1/2)(1/\mu_0)b^2(x_1, t) \text{ newtons per meter}^2 \quad (1)$$

where $b(x_1, t)$ is the resultant magnetic induction in the air gap. Assuming that all magnetic lines cross the air gap radially, and assuming an unsaturated machine, the magnetic induction in the air gap can be expressed as

$$b(x_1, t) = b_1(x_1, t) + b_2(x_1, t) \quad (2)$$

In this equation, $b_1(x_1, t)$ is the resultant of magnetic induction due to the currents in the stator, and can be expressed as

$$b_1(x_1, t) = \sum_\sigma B_\sigma \sin[\omega t - (\sigma' \pi x_1/p\tau)] \quad (3)$$

and $b_2(x_1, t)$ the magnetic induction in the air gap due to the rotor currents

$$b_2(x_1, t) = \sum_\rho \sin[\omega_\rho t - (\rho' \pi x_1/p\tau)] \quad (4)$$

The order of the stator harmonic σ satisfies the equation

$$\sigma' = p(3c_1 + 1) \quad (5)$$

and the order of the rotor harmonics satisfies the equation

$$\rho' = c_2 Q_2 + \sigma' \quad (6)$$

where c_1 and c_2 are any integers, positive or negative, including zero.

The so-called slot harmonics, i.e., those caused by the distribution of each phase belt in a small number of slots, are responsible for the major part of the magnetic noise. They obey the conditions.

$$\sigma_s' = c_{1s} Q_1 + p \text{ and } \rho_{s2}' = c_{2s} Q_2 + p \quad (7)$$

where c_{1s} and c_{2s} are constants, and may be any positive or negative integer except zero. A negative expression for σ' or ρ' denotes that the direction of rotation of the corresponding flux density wave opposes the direction of the main flux density distribution.

To obtain the resultant for the flux density distribution of a slot harmonic order it becomes necessary to add the magnitude of the corresponding permeance harmonic to equation 3.

The consideration of the air-gap permeance variation can be simply treated by using a suggestion of Weber[11] and Heller.[12] The permeance of a slotted armature can be expressed approximately by the average value and the first two harmonics as

$$\mathcal{P}(x) = [1 + 2\eta_1 \cos(Q_1 \pi x_1/p\tau) - 2\eta_2 \cos(2Q_1 \pi x/p\tau)](\mu_0/gk_c) \quad (8)$$

where

$$\eta_1 = \beta \binom{2b}{b-1} \Big/ \left[2^{2b-1} - \beta \binom{2b}{b}\right] \quad (9)$$

and

$$\eta_2 = \beta \binom{2b}{b-2} \Big/ \left[2^{2b-1} - \beta \binom{2b}{b}\right] \quad (10)$$

In these equations

$$b = (\tau_t/s_{10}) - 1 \quad (10A)$$

and β is a function of the ratio of the slot opening width to air-gap length, originally established by Carter. Fig. 6.11 of reference 2 reproduces this curve.

The foregoing expressions for η_1 and η_2 are strictly true only for integral values of b. For nonintegral values of b an approximation can be found by interpolation.

The first two permeance harmonics may be found by dividing the amplitude of the fundamental flux distribution by k_c, and multiplying it by η_1 and η_2 respectively. When combining slot and permeance harmonics of the same order, it is important to remember that the slot harmonics are produced by the primary current, while the magnetizing current is responsible for the permeance harmonics. These two are out of phase by an angle $(\theta_1 - \theta_m)$ and must be combined vectorially. The vectorial combination depends further on the number of slots per pole per phase, i.e., on q. For even values of q the positively rotating first slot harmonic and the positively rotating permeance harmonic add, while the negatively rotating slot harmonic and the associated negatively rotating permeance harmonic subtract. For odd values of q the positively rotating waves subtract, and the negatively rotating waves add.

Introducing the expressions thus obtained for the flux density waves into equation 1, and after trigonometric transformations, the following components of the resulting force can be recognized as:

1. Constant forces uniformly distributed over the whole armature circumference.
2. Double-frequency force waves.
3. Nonpulsating and nonrotating force waves distributed sinusoidally.
4. Product terms.

$$B_{\sigma'} B_{\rho'} \cos\left\{(\omega \pm \omega_{\rho'})t - [(\sigma' \pm \rho')(\pi x_1/p\tau)]\right\} \quad (11)$$

A careful analysis shows the force waves under categories 1, 2, and 3 to be unimportant from a noise production viewpoint, with the exception of the 120-cps force wave due to the fundamental flux density wave in 2-pole motors. The force waves in category 4 will most frequently become responsible for strong noise-producing force waves if the expression

$$\sigma' \pm \rho' = m_v \quad (12)$$

has a low integral value.

The mode of the forced vibration of the induction motor frame will depend largely on quantity m_v of the force wave. If $m_v = 0$, a uniform force distribution pulsating with frequency $\omega_1 - \omega_{\rho'}$ will result. The case $m_v = 1$ represents the well-known 1-sided pull. The resultant 1-sided force revolves around the air gap with an angular velocity $\omega_1 \pm \omega_{\rho'}$. This occurrence has been extensively treated in the literature. Case $m_v = 2$ will arise if there are two flux distribution waves with pole pairs differing by two in the air gap. The sinusoidally distributed force wave will have two complete periods around the air gap. This force wave tends to deform the stator core periodically in the shape of an ellipse. The vibrations of the stator core are transferred by the elastic system to the outer frame. The vibration amplitudes in this mode may become significant and a high-intensity noise occur. On account of its rigidity the deformations of the rotor in this mode are insignificant with the exception of the case where the frequency of the force wave coincides with the critical frequency of the rotor.

The conditions for m_v larger than two, but still a small number, are similar to the second-mode deformation. The tendency now will be to deform the stator into the shape of a polygon which rotates. The flexural rigidity of the stator increases rapidly with the order of the mode, and as a consequence the dynamic

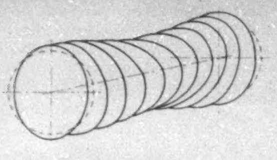

Fig. 2. Shift of force waves created by slot harmonics

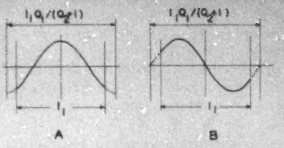

Fig. 3. Force distribution along generatrix in skewed bar rotors

deflections will rapidly decrease with increased mode orders. In medium induction motors it will suffice to consider force waves up to the fourth mode only. Higher modes may become significant in cases where the natural frequency of the induction motor in that mode coincides or is near to the force wave frequency in the same mode.

From the vast number of force waves caused by the interference of the flux density waves in the air gap, the low-mode force waves resulting from the interaction of one stator and one rotor slot harmonic are the most frequent and dangerous ones from the viewpoint of noise production. The amplitude of these may be increased by some other flux combination as shown in the Appendix.

The frequency of the radial force waves is of utmost importance and can be calculated from equation 11. Considering the harmonics to be the result of the respective fundamental currents, the frequency of force waves due to interaction of two flux density waves rotating in the same direction is found to be

$$\omega_f = [(\rho'/p)-1](1-s)\omega \tag{13}$$

and for those due to interaction of two flux density waves rotating in opposite direction

$$\omega_f = \{2+[(\rho'/p)-1](1-s)\}\omega \tag{14}$$

Again the interaction of flux waves of the first slot harmonic order are most bothersome and their mode order and frequency are as follows:

1. Positively rotating first-order stator slot harmonic interacting with positively rotating first-order rotor slot harmonic

$$m_{v(+,+)} = (Q_1+p)-(Q_2+p) = Q_1-Q_2;$$
$$\omega_{(+,+)} = (Q_2/p)(1-s)\omega$$

2. Negatively rotating first-order stator slot harmonic with positively rotating first-order rotor slot harmonic

$$m_{v(-,+)} = (Q_1+p)+(Q_2+p) = -Q_1+Q_2+2p;$$
$$\omega_{(-,+)} = [2+(Q_2/p)(1-s)]\omega$$

3. Positively rotating first-order stator slot harmonic with negatively rotating first-order rotor slot harmonic

$$m_{v(+,-)} = (Q_1+p)+(-Q_2+p) = Q_1-Q_2+2p;$$
$$\omega_{(+,-)} = [2-(Q_2/p)(1-s)]\omega$$

4. Negatively rotating first-order stator slot harmonic with negatively rotating first-order rotor slot harmonic

$$m_{v(-,-)} = (-Q_1+p)-(-Q_2+p)$$
$$= -Q_1+Q_2;\ \omega_{(-,-)} = (Q_2/p)(1-s)\omega$$

The mode of the force waves created by the interaction of higher slot harmonics can be calculated for those of the ξ the order to be

$$\xi(Q_1-Q_2);\ \xi(Q_1-Q_2)+2p;\ \text{and}\ \xi(-Q_1+Q_2)+2p$$

The amplitude of the force waves can be shown to be

$$\Pi = (1/2)(10^7/4\pi)B_\sigma' B_\rho' \text{ newtons per meter}^2 \tag{15}$$

or

$$\Pi = 55.6\, B_\rho' B_\sigma', \text{ pounds per square inch} \tag{16}$$

INFLUENCE OF MAGNETIC SATURATION, SKEW, AND AIR-GAP ECCENTRICITY

The simplifying assumptions which lead to the equation for the calculation of the force waves are seldom satisfied. Nonideal conditions encountered in practice may change the amplitude of the force waves and be responsible for new force waves. The effect of magnetic saturation in iron will depend on the stator phase connections. In a wye-connected induction motor primary, no triple harmonic current can flow, and the flux distribution wave will be flattopped. This may introduce third and fifth harmonic positively rotating flux density waves of the same speed as the fundamental. In a delta-connected motor, the magnetizing currents may contain third and higher harmonic components which will create pulsating and rotating flux distribution waves of fundamental pole pitch of third and five times normal frequency respectively. The pulsating flux distribution wave of three times normal frequency can be resolved into two waves rotating in opposite directions. In addition, the saturation of the tooth tips of the stator slot harmonics and of the rotor slot bridges will effectively increase the amplitude of the permeance harmonics.

INFLUENCE OF SKEWING

Skewing has two different effects on the flux distribution and consequently on the force waves. The force waves created by the interaction of flux distribution waves caused by fundamental currents are not reduced by skewing. The force wave itself appears twisted to the left and to the right along the rotor axes, as shown in Fig. 2, i.e., the force distribution which has been uniform along a generatrix of the rotor will vary for skewed bar rotors. The effect of skewing can be analyzed by resolving the force waves into two component waves, as shown in Fig. 3. The first component represents a cosine-shaped force distribution along a generatrix with the period $l_1Q_1/(Q_2+1)$, and an amplitude at the mid-point of the stator. This wave is in time phase with the skewed force wave. The second com-

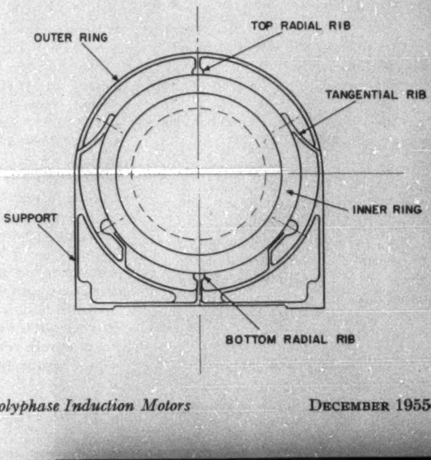

Fig. 4. Simplified cross section of induction motor

ponent has a sine-shaped force distribution along the length of the stator. The origin of the sine wave is in the middle of the core, has the same period as the first component, but is displaced by $\pi/2$ radians on the armature periphery. The force waves caused by higher harmonic rotor currents may be considerably reduced by skewing, because of the increased differential leakage of the squirrel-cage rotor to higher harmonics.

INFLUENCE OF AIR-GAP ECCENTRICITY

The air gap of an eccentric rotor can be approximately expressed as

$$g(x_1)=g+\epsilon\cos(x_1\pi/p\tau) \tag{17}$$

where x_1 is measured from the point where the air gap is largest. In approximation, the air-gap permeance will vary as a reciprocal of $g(x_1)$ which can be resolved in series

$$1/g(x_1)=(1/g)[a_0+a_1\cos(\pi x_1/p\tau)+a_2\cos(2\pi x_1/p\tau)+\ldots+a_v\cos(v\pi x_1/p\tau)+\ldots] \tag{18}$$

Multiplying the fundamental air-gap induction by the expression in the square bracket, two sets of flux density waves of the order $(\sigma'+v)$ and $(\sigma'-v)$ will appear. Because v may have a value of 1, flux density waves that differ only by 1 will appear. As a consequence, the phenomenon of the 1-sided pull will occur, and other new force waves will be created. If the rotor shaft is not in the same line with the axis of the rotor, the radial length of the variable air gap will become a function of the rotor speed. It will then be necessary to replace in equations 17 and 18 $(\pi x_1/p\tau)$ by $(\pi x_1/p\tau)-\omega_r t$, where ω_r is the angular velocity of the rotor.

Dynamic Response of Motor Frame to Electromagnetic Force Waves

The solution to the vibrational behavior of an induction motor, which is a continuous system, leads to a set of partial differential equations. The complexity of an induction motor structure makes it necessary to establish these from Lagrange's equations of motion. The necessary expression for the elastic and kinetic energies will be found by the application of the principle of Rayleigh and Ritz. The cross section of an induction motor is shown in Fig. 4.

The stator structures of induction motors may differ greatly in design, but they all consist of cylindrical rings, radial and tangential ribs, and supports. To make the problem susceptible to a numerical solution it is essential to define the structural relations of the elements which determine the dynamic behavior of the system as a whole. It will be necessary to make assumptions based upon empirical observations, such as the effect of damping and related matters, as follows:

1. All displacements are extremely small compared with the dimensions of the system.
2. All vibrations take place in planes perpendicular to the axis of the motor.
3. The stator core made up of steel laminations will be considered as a homogenous body.
4. The cross section determining the rigidities of the stator core extends radially from the bottom of the stator slot to the outer diameter of the punchings, and the stator teeth and windings add only to the mass.
5. The outer ring will be considered a complete cylinder. The local effects of plate and free edges of ventilating openings will be ignored since they can be treated separately as secondary effects.
6. The mass of the ribs, supports, and other components of the frame's casting will be supposed to be uniformly distributed when calculating the kinetic energy of the ring.
7. The end shields will be ignored. It has been experimentally determined that the effect of the end shields on the mode shapes and frequencies of the main system is negligible.
8. The motor will be analyzed as if it were a free body in space. Measurements show that the natural frequencies and modes are almost the same whether the motor is bolted to the base or supported on rubber blocks. The experiments of Plunkett[13] have proved that a normal base has negligible effective mass compared to that of the motor, as frequencies are over 500 cps.
9. Experimental evidence indicates that elastic damping can be considered negligible if the system be not at, or very near to, a resonance.

With the use of a system of generalized co-ordinance, Lagrange's equation of motion can be written as

$$(d/dt)(\partial T/\partial\dot{q}_j)-(\partial T/\partial q_j)+(\partial V/q_j)=0 \tag{19}$$

To apply the theory of small oscillations, the equation can be simplified to

$$m_i\ddot{q}_i+\sum_j k_{ij}q_j=0 \tag{20}$$

This equation represents a system of n differential equations of the same type as the one encountered in the theory of electric circuits. The solution can be attempted by setting

$$q_i=A_i\sin(\omega t+\psi) \tag{21}$$

$$\ddot{q}_i=-\omega^2A_i\sin(\omega t+\psi) \tag{22}$$

If these values of q_i and $\ddot{q}_i$ are substituted into the system of equations defined by equation 20, simultaneous equations will result. Lest the system have only a trivial solution, its determinant of the coefficients must vanish. The determinant will have n roots in ω^2, the so-called eigenvalues, from which the resonant frequencies can be calculated.

When these eigenvalues are introduced into the system of equations given by equation 20, solutions for the coefficients A_i can be obtained. The n eigenvalues will yield n such solutions, each representing a so-called principal mode of vibration. The A_i quantities are called eigenvectors, and there will be altogether n eigenvectors, each with n components. Each eigenvector determines an orthogonal principal mode of oscillation, which is purely harmonic, i.e., all particles move with the same frequency and phase. The magnitude of the eigenvector components are not independent and are determined only so far as their ratio is concerned. It is of advantage to choose the value in such a way as to make

$$\sum(A_i^{(r)})^2=1 \tag{23}$$

which is called the normalizing condition, and to express the eigenvectors as

$$y_i^{(r)}=A_i^{(r)}/[\sum(A_i^{(r)})^2]^{1/2} \tag{24}$$

The steady-state dynamic deflections caused by the vibratory forces can also be found by applying Lagrange's equation in the form

$$m_i\ddot{q}_i+\sum_j q_jk_{ij}=Q_i\sin(\omega t+\psi) \tag{25}$$

where Q_i is a so-called generalized force. It is very difficult to solve such a system of equations, but the deflection can be easily computed by using the principle that the maximum potential energy in the vibrating system is of the same magnitude as the maximum kinetic energy. In reference 10 it is shown that the static deflection in the rth mode is

$$q_{is}^{(r)}=\frac{\sum Q_jA_j^{(r)}A_i^{(r)}}{\omega_r^2\sum m_j[A_j^{(r)}]^2} \tag{26}$$

and the dynamic deflection is

$$q_i^{(r)}=\sum_{r=1}^{r=n}q_{is}^{(r)}\frac{\omega_r^2}{\omega_r^2-\omega^2} \tag{27}$$

On applying the Rayleigh-Ritz method, assumptions are made for the deflection curves, usually expressing it as a Fourier series, with undetermined coefficients. These coefficients are used as generalized co-ordinates. Next the kinetic and elastic energies are expressed as functions of the co-ordinates, and then introduced into Lagrange's equation of motion. The coefficients of this system of equations will

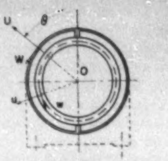

Fig. 5 (left). System of co-ordinates for vibrating stator

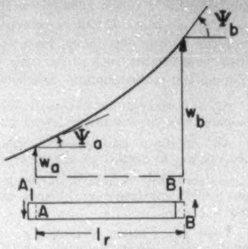

Fig. 6. Deformations of radial rib

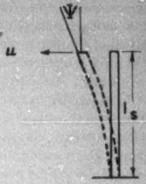

Fig. 7 (right). Deformations of supports

yield the characteristic determinant whose nonvanishing solutions can then be established. Theoretically the deflection equations should have an infinite number of terms and the determinant would become of infinite order. In practical problems it becomes a necessity to consider finite rather than infinite determinants by assuming as negligible the higher orders of members representing the deflection curves.

Energies of Components of Induction Motors

The outer frame and the inner core will be considered as cylindrical shells, as explained in the assumptions. In reference 10 it is shown that, when considering these components as inextensive, the potential energy of bending can be expressed as

$$V_b=(D/2r_0^3)\int_0^{2\pi}[(d^2u/d\theta^2)-u]^2d\theta \qquad (28)$$

where

$$D=(EI)/(1-\sigma^2) \qquad (29)$$

The meaning of the symbols is given in Fig. 5. The kinetic energy of the core or frame can be calculated to be

$$T=(\mu/2)\int_0^{2\pi}(u^2+w^2)d\theta \qquad (30)$$

Elastic Energy of Radial Ribs

Ribs are subjected to extensional and bending deflections during vibration. Based on notations of Fig. 6, the extensional energy can be calculated to be

$$V_e=(1/2l_r)E_rA_r(u_a-u_b)^2 \qquad (31)$$

and the energy of bending deflections as

$$\begin{aligned}V_b=6(D_r/l_r^3)(w_b-w_a)^2-\\ 6(D_r/l_r^2)(w_b-w_a)(\psi_a+\psi_b)-\\ 2(D_r/l_r)(\psi_a^2+\psi_b^2+\psi_a\psi_b)\end{aligned}$$

The elastic energy of the tangential ribs is extremely small, and to simplify the analysis may be neglected.

Elastic Energy of Supports

Based on Fig. 7, the elastic energy can be expressed

$$V_b=[D_s/l_s][(6u^2/l_s^2)-(6u\psi/l_s)+2\psi^2] \qquad (32)$$

On the basis of actual solutions of the dynamic equations of the system, it was found that the consideration of extensional energies of the outer and inner rings change the results of the analysis of the lower mode vibrations by a negligible amount. However, this cannot be ignored in either very small or medium 2-pole induction motors.

The radial displacement of the outer ring, Fig. 5, in the most general case, can be represented by

$$U=\sum_m(A_m\cos m\theta+B_m\sin m\theta) \qquad (33)$$

and correspondingly for the radial displacement of the inner ring, the expansion will be chosen as

$$u=\sum_m(a_m\cos m\theta+b_m\sin m\theta) \qquad (34)$$

The values of *m* are chosen 2, 3... After preliminary calculations, it is seen that six terms in each Fourier series represent the deflection functions with a sufficient approximation for practical purposes.

To satisfy the conditions of deformations of the inner core and outer frame without extensions, it is necessary to choose the tangential displacement of the outer rings as

$$W=\sum_m(1/m)(B_m\cos m\theta-A_m\sin m\theta) \qquad (35)$$

and for the inner ring

$$w=\sum_m(1/m)(b_m\cos m\theta-a_m\sin m\theta) \qquad (36)$$

The coefficients of all the deflection curve expansions are time-dependent functions of sinusoidal form.

Introducing the radial and tangential deflection expressions into the energy expressions 28, 29, 30, 31 and 32, Lagrange's equations can be written with the use of the Fourier coefficients as generalized co-ordinates

When evaluating the bending energies, no-product terms containing a generalized co-ordinate of odd subscript, multiplied by one of even subscript. This fortunate situation simplifies the numerical work. The 24-by-24 determinant reduces to two 12-by-12 determinants. The limitations of space precludes writing out all the 144 members of each determinant.

The task of finding the eigenvalues and eigenvectors of the two determinants involves great computational difficulties but can nowadays be solved with advanced digital electronic computers in a fraction of an hour. The numerical work, the results of which are given in the Appendix, have been carried out on the electric data-processing machine of the International Business Machines Company.

The results of a typical vibrational analysis are represented in Fig. 8 for the second-mode vibrations of the experimental motor. The difference between the single-ring theory and the more complete analysis becomes clear. A single uniform ring is symmetrical about any diameter. For this reason there will be two vibrations of the same frequency associated with each mode. The designation of one is arbitrary, and the other will be displaced by a quarter-wave length. Since the real motor is made up of two such rings, interconnected with ribs and mounted on a support, there will be four frequencies associated with each mode. Fig. 8(A) shows the mode at which the sinusoidal distribution of the deflection has the amplitude of the top radial rib, and is called a cosine mode. Two points on the same radial line, each belonging to one ring, are both moving outward at the same instant. This mode of vibration is referred to as an in-tact mode. In Fig. 8(B) the amplitude of the displacement distribution is again at the top rib. However, the point of the outer ring is moving outward, while at the same instant the corresponding point on the same radial line of the inner ring is moving inward. The type of vibration is referred to as a counter-tact mode. In Fig. 8(C), the zero amplitude of the sine wave displacement coincides with the top rib. This motion is designated a sine

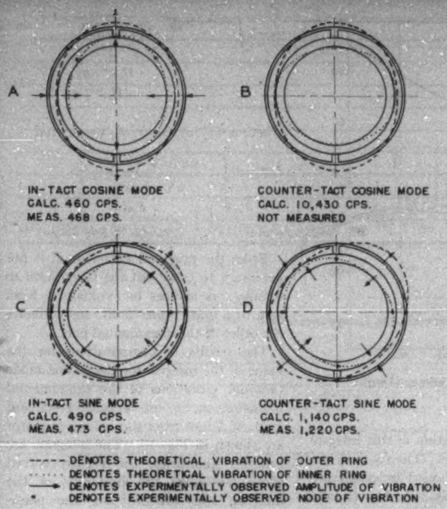
A
B
C
D
IN-TACT COSINE MODE
CALC. 460 CPS.
MEAS. 468 CPS.
COUNTER-TACT COSINE MODE
CALC. 10,430 CPS.
NOT MEASURED
IN-TACT SINE MODE
CALC. 490 CPS.
MEAS. 473 CPS.
COUNTER-TACT SINE MODE
CALC. 1,140 CPS.
MEAS. 1,220 CPS.
----- DENOTES THEORETICAL VIBRATION OF OUTER RING
...... DENOTES THEORETICAL VIBRATION OF INNER RING
→ DENOTES EXPERIMENTALLY OBSERVED AMPLITUDE OF VIBRATION
• DENOTES EXPERIMENTALLY OBSERVED NODE OF VIBRATION

Fig. 8 (left). Calculated and measured second mode vibrations of induction motor

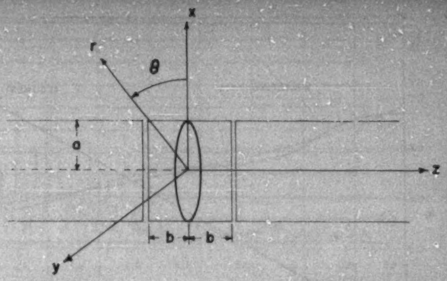

Fig. 9 (above). System of co-ordinates for vibrating cylinder

mode, as the two points of the rings on the same radial line move outward at the same instant, and it is an in-tact sine mode. Fig. 8(D) represents the corresponding counter-tact sine mode. The complete modes of vibration contain also harmonic components which complicate the shape of the displacement along the directrix of the vibrating cylinder.

The forced response, i.e., the steady-state deflections of the outer frame can be readily found by using the natural frequencies and the eigenvectors of the complete system. It is of advantage to find first the vibration amplitude caused by a single-mode single-frequency force wave. With the aid of the principle of superposition, any picture of complete vibration can be constructed.

It will be necessary first to resolve the rotating force wave given by the general equation

$$P(\theta, t)=P_{m_\nu}\cos(\omega t-m_\nu\theta) \tag{37}$$

into two component waves by carrying out the trigonometric operation

$$P(\theta, t)=P_{m_\nu}\cos\omega t\cos m_\nu\theta+P_{m_\nu}\sin\omega t\sin m_\nu\theta \tag{38}$$

This last equation represents two pulsating force distributions displaced by one quarter length along the armature circumference, and lagging by one quarter of a cycle. The elastic energy caused by static deflection as a result of the cosine force distribution can be found to be

$$W^{(\nu)}=(\pi/2)P_{m_\nu}a_{m_\nu} \tag{39}$$

and this must be equal to the kinetic energy. Equating these energies and carrying out the necessary substitutions, can show that the static deflection in rth principal mode will be

$$A_n^{(r)}=[P_{m_\nu}(\pi/2)y_{am_\nu}](y_{An}/K_r) \tag{40}$$

where

$$K_r=(\pi/2)\omega_r^2\sum[\psi_t(m^2-1)(y_{am}^2+y_{bm}^2)+\mu_0(m^2-1)(y_{Am}^2+y_{Bm}^2]/m^2 \tag{41}$$

The dynamic deflection can be given by

$$A_r^{(r)}=[P_{m_\nu}(\pi/2)y_{am}^{(r)}y_{An}^{(r)}\omega_r^2]/[K_r(\omega_r^2-\omega^2)] \tag{42}$$

With the use of this equation the deflection at the top rib due to the pulsating cosine wave can be calculated and, similarily, the same quantity caused by the pulsating sine component of the wave.

To find the magnitude of the total displacement of the outer ring at the top rib, it is necessary to add first the deflection produced by the rth principal modes and caused by the cosine component of the force wave. Then the deflections produced by the rth principal modes corresponding to the sine component of the force wave are summed separately. Finally, the two components are combined by the parallelogram law. The result will be

$$A_m=\left\{\left[\sum_{r=1}^{r=n}A_m^{(r)}\cos\right]^2+\left[\sum_{r=1}^{r=n}A_m^{(r)}\sin\right]^2\right\}^{1/2} \tag{43}$$

Sound Radiated by Vibrating Frame

Since virtually all modern sound detectors respond directly to variations in pressure, it is of interest to determine the sound pressure at a characteristic point near the induction motor. For this purpose the acoustic wave equation

$$\nabla^2 p=(1/c^2)(\partial^2 p/\partial t^2) \tag{44}$$

where

$$c^2=\gamma p_0/\rho \tag{45}$$

will be solved for the special case at hand.

The frame of an induction motor is by no means of a shape, that lends itself easily to this radiation and boundary value problem. It therefore becomes essential to make approximations without losing sight of their physical significance. The stator, as illustrated in Fig. 9, will be extended on both sides by semi-infinite cylinders, so that the vibrations of the stator will not be transmitted to the extensions. This artifice can be represented by an infinitely long cylinder vibrating in a belt only.

When the specified assumptions are made that the pressure variations will have the same frequency as the vibrations of the stator, the instantaneous pressure can be expressed as

$$p=p\exp(-j\omega t) \tag{46}$$

If equation 46 is introduced into equation 44, the wave equation may be written

$$(\nabla^2+k^2)p=0 \tag{47}$$

where

$$k^2=\omega^2/c^2 \tag{48}$$

The solution of the wave equation in cylindrical co-ordinates is

$$p=\sum_n\exp(jn\theta)[Z_n(r\sqrt{k^2-h^2})]\times\exp(jhz-j\omega t) \tag{49}$$

The constants in these solutions must be evaluated to satisfy the boundary conditions, i.e., the behavior of the sound pressure p, at the surface of the cylinder and at infinity.

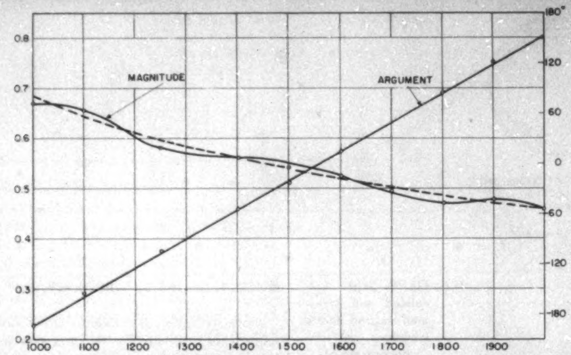

Fig. 10. Sound pressure integral for second mode vibrations of experimental motor

Amplitude and frequency of the vibrations of the cylindrical surface determine the velocity of the particles on the cylindrical surface when secondary reactions are neglected. The gradient of pressure and the time differential of velocity are correlated by Newton's second equation of motion. Hence

$$\rho(\partial q/\partial t)=\partial p/\partial r \qquad (50)$$

When each single-mode and single-frequency vibration are considered individually, the sound pressure on the cylindrical surface ($r=a$) must for all values of z, beween $+b$ and $-b$, satisfy the condition

$$(\partial p/\partial r)_{r=a}=jA_m\omega^2\rho \exp(jm\theta-j\omega t) \qquad (51)$$

and be zero for any other values of z on the cylindrical surface. Furthermore, Summerfeld's radiation conditions must be satisfied at infinity.

The solution of the wave equation is carried out in reference 10, where it is shown that

$$p(r,\theta,z,t)=(w^2\rho_0 A_m/\pi)\times \exp(jm\theta-j\omega t)I(m,b,r,z) \qquad (52)$$

where

$$I(m,b,r,z)=\int_{-\infty}^{+\infty}[\sin(hb)/hb]\exp(jhz)\times \frac{H_m^{(1)}(r\sqrt{k^2-h^2})}{[H_m^{(1)}]'(a\sqrt{k^2-h^2})} \qquad (53)$$

The value of the integral for $z=0$, i.e., at the middle of the vibrating belt is given by

$$I(m,b,r)_{z=0}=2\int_0^{\infty}[\sin(hb)/hb]\times \frac{H_m^{(1)}(r\sqrt{k^2-h^2})}{[H_m^{(1)}]'(a\sqrt{k^2-h^2})} \qquad (54)$$

The numerical solution of this integral causes some difficulty. The roots of the derivatives of the Hankel functions are not available and it is necessary to take recourse to a numerical integration. For this purpose it becomes advantageous to evaluate the integral in three parts as follows

$$I_1=2\int_0^{\delta}[\sin(hb)/hb]\times \frac{H_m^{(1)}(r\sqrt{k^2-h^2})}{[H_m^{(1)}]'(a\sqrt{k^2-h^2})}\,dh \qquad (55)$$

where $0<\delta<k$

$$I_2=2\int_0^{a\sqrt{k^2-\delta^2}}\frac{\sin(\alpha\sqrt{\eta^2-y^2})}{\alpha\sqrt{\eta^2-y^2}}\times \frac{H_m^{(1)}(\beta y)}{[H_m^{(1)}]'y}\,dy \qquad (56)$$

where $\alpha=(b/a)$, $\beta=(r/a)$, $\eta=ak$, and

$$I_3=-4\int_0^{\infty}\frac{\sin(\alpha\sqrt{\eta^2-x^2})}{\alpha\sqrt{\eta^2-x^2}}\times \frac{K_m(x)}{K_{m-1}(x)+K_{m+1}(x)}\,dx \qquad (57)$$

From the practical viewpoint it is not necessary to carry out the integration to infinity; it suffices to evaluate it from zero to a finite upper limit, and estimate the order of the unevaluated part.

The results of computations for the value of the integral for the second-mode (4-node) vibrations of the experimental induction motor for a point $\theta=0$, and $z=0$, at 1 foot from the induction motor are shown in Fig. 10. The integrals are complex quantities, the slightly waved curve represents the amplitude of the integral, the straight line the phase angle.

Results of theoretical calculations are given in dynes per square centimeter. It is now customary to specify the sound pressure level based on 0.0002 dyne per square centimeter as a standard reference sound pressure, and to express this quantity in terms of decibel units defined by

$$SPL=20\log_{10}(p/0.0002) \qquad (58)$$

Table I. Comparison of Calculated and Measured Resonant Frequencies of Experimental Motor

Mode	Description of Mode	Calculated CPS	Measured CPS	Error, Per Cent
Second	Counter-tact sine	1,140	1,220	−6.6
	In-tact cosine	460	468	−1.8
			482	−4.4
	In-tact sine	490	473	+3.6
Third	In-tact sine	1,225	1,240	−1.25
	In-tact cosine	1,170	1,080	+8.5
			1,156	+1.2
	Counter-tact sine	1,580	1,540	+2.5

Table II. Comparison of Calculated and Measured Sound Pressure Levels (SPL) of Experimental Motor

Motor Operation			Distance of Microphone from Stator, Feet	Description of Noise	Noise Frequency, CPS	Calculated SPL, Decibels*	Measured SPL, Decibels	Figure Containing Record	Error, Per Cent
Amperes	Volts	CPS							
40	440	60	1	main	1,716	85.9	87.8	10	−2.2
40	367	50	1	main	1,419	87.7	90.0	11	−2.6
40	294	40	1	main	1,121	90.8	94.0	12	−3.4
No load	440	60	1	main	1,735	74.8	74.0	13	+1.1
40	440	60	1	side	1,475	62.0	64.0	10	−3.1
40	440	60	2	main	1,716	82.1	84.5	14	−2.9

* Data taken from Table VI.

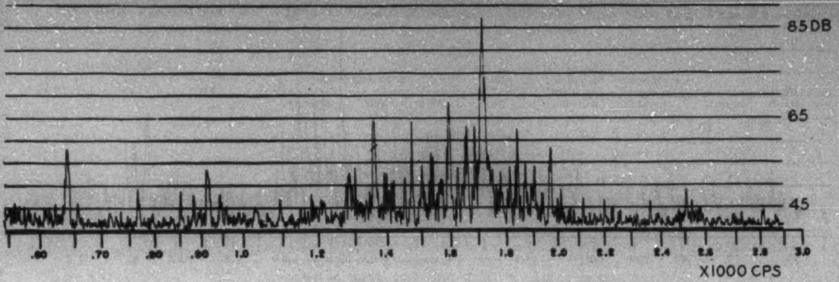

Fig. 11. Sound spectrum of experimental motor at 40 amperes, 440 volts, 60 cps

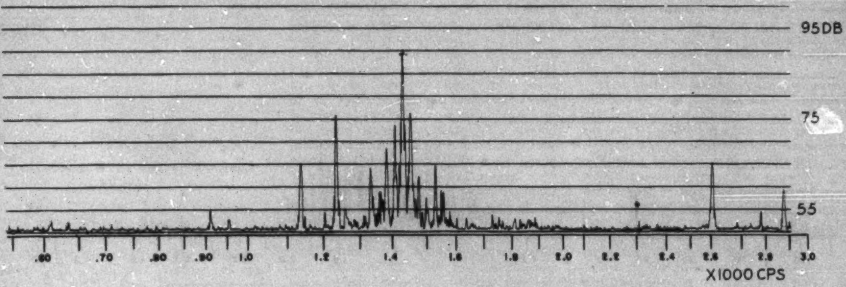

Fig. 12. Sound spectrum of experimental motor at 40 amperes, 369 volts, 50 cps

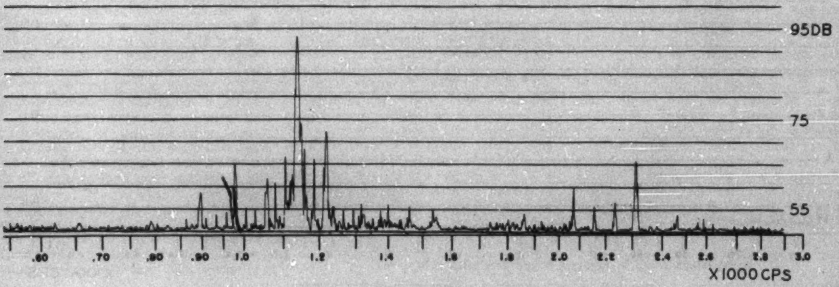

Fig. 13. Sound spectrum of experimental motor at 40 amperes, 293 volts, 40 cps

Conclusions

The method outlined in a general manner for the calculations of sound pressures of magnetic noise has been used in detailed computations in reference 10, and a review of the results is given in the Appendix.

A comparison of calculated and experimentally established resonant frequencies is given in Table I, while Table II records the calculated and measured sound pressure levels (SPL) of the experimental motor at different operating conditions. The records of the experimental sound spectra are given in Figs. 11 through 16.

A study of the results reveals good agreement between calculated and measured values. Considering the extreme complexity of the problem, the approximation and assumptions, together with the large number of numerical operations which had to be made, the agreement between theory and experiment is better than expected. It would, as a rule, be unreasonable to expect the theoretical results to approach sound measurements

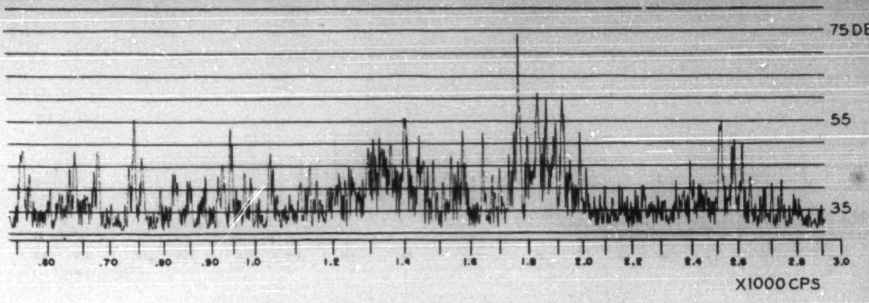

Fig. 14. Sound spectrum of experimental motor at no load, 440 volts, 60 cps

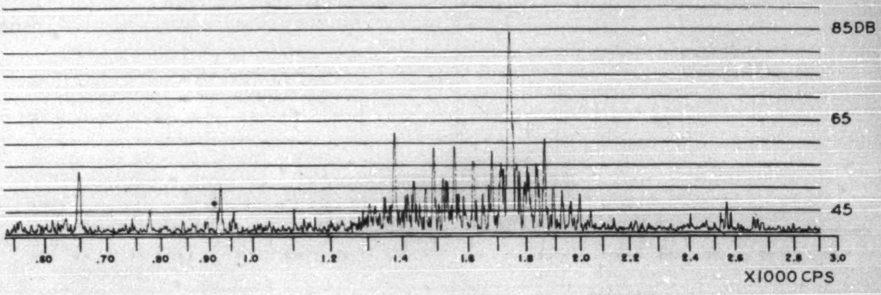

Fig. 15. Sound spectrum of experimental motor at 40 amperes, 440 volts, 60 cps. The microphone at this recording was 2 feet from motor

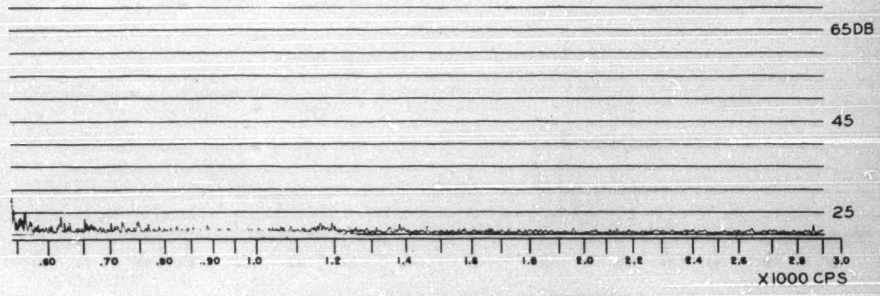

Fig. 16. Sound spectrum of ambient noise in anechoic room

by such a close margin. In view of the agreement between theoretical and test results, it can be concluded that a method has been established to calculate:

1. The natural behavior and forced response of stators of medium induction motors.

2. The sound pressure levels of the magnetic noise caused by electromagnetic forces in the air gap of induction motors.

It is only proper to stress the fact that while the analysis presented in this paper is of a general nature, solutions for specific designs of induction motors would have to be carried out separately for each class of design.

It is reasonable to question whether this tedious and complex method, involving the use of most advanced electronic digital computers, is practicable. Clearly the total study is a greater task than can be carried out by a single individual. However, it is possible to calculate and construct curves representing the dynamic deflections as a function of the frequency and mode order for a constant amplitude force wave in a manner

Table III. Force Waves Resulting from First-Order Slot Harmonics in Experimental Motor

Rotor Harmonics	Stator Harmonics −29	Stator Harmonics +31
−26	$m_\nu=6$ $f_f=27(1-s)f$	$m_\nu=10$ $f_f=2-27(1-s)$
+28	$m_\nu=2$ $f_f=2+27(1-s)f$	$m_\nu=6$ $f_f=27(1-s)f$

Table V. Summary of Calculated Deflections for Second-Mode Force Waves of Experimental Motor

Motor Operating Amperes	Motor Operating Volts	Motor Operating CPS	Noise Frequency, CPS	100-Pounds-per-Radian Deflection, μ Inches	Force Wave Pounds per Radian	Deflection, μ Inches	Deflection, μ Centimeters
40	440	60	1,716	9.23	84.5	7.8	19.6
40	367	50	1,419	14.4	84.5	12.17	30.7
40	294	40	1,121	28.2	84.5	23.9	60.5
No load	440	60	1,735	9.15	23.1	2.12	5.34
40	440	60	1,475	12.98	4.6	0.6	1.51

illustrated in Fig. 1. The solution of the integral for the calculation of the sound pressure level can also be plotted as a function of the noise frequency and mode for a characteristic point of the induction motor. The resonant frequencies which are of utmost importance can be tabulated. The only analytical work left for the designer would be the calculation of the force waves. The remaining task would then be the selection of the right information from prepared curves, and the calculation of the sound pressure level by simple slide rule operations.

Appendix. Data and Review of Calculations for Experimental Motor

The theory contained in the paper has been applied to an experimental motor of the following name plate data: 30 horsepower, 4-pole, 440 volts, 3-phase, 60 cps, 1,780 rpm, 38 amperes, temperature rise 40 degrees, frame *K-365*.

The most important design data of the motor are as follows: outer diameter of stator punchings 13.5 inches, diameter of stator bore 9 inches, outer diameter of rotor 8.952 inches, inner diameter of rotor 2.625 inches, length of stator 5.75 inches, number of stator slots 60, depth of stator slot 1.15 inches, average width of stator slot 0.3 inch, stator slot opening 0.125 inch, total number of conductors in stator 960, phase connection delta, coil pitch 1–12; number of cast aluminum non-skewed rotor bars 54, cross-sectional area of rotor bar 0.19 square inch, cross-sectional area of cast aluminum rotor end rings 1.50 square inch. The weight of the inner ring is 120 pounds; that of the cast-iron frame 95 pounds.

The modes and frequencies of the force waves caused by the interaction of the first-order slot harmonics are given in Table III. They are well in the audible range, and the amplitudes are of the same order of magnitude. But only the force wave resulting from the interference of the positively rotating 28th rotor harmonic acquires significance. A detailed calculation has shown that the second-mode (4-node) deflection amplitude as a response to a second-node sinusoidal force wave of 100 pounds-per-square-inch amplitude is of the order of 10 microinches for frequencies between 1,000 and 2,000 cps. A sixth-mode (12-node) force wave of the same amplitude would cause deflections of the order of 1/10 microinch in the same frequency range. The sound pressure caused by the vibration of the motor in the sixth and 10th mode would be well below the threshold of hearing.

A closer analysis of the higher harmonic flux density waves in the air gap of the experimental motor reveals the interesting fact that other harmonic flux density wave combinations will result in second-mode force waves of the same frequency as the second-mode force wave of the slot harmonic; see Table IV.

A detailed calculation will again show that only the first and the last force wave have amplitudes large enough to be considered.

The amplitude of the 29th stator slot harmonic flux density wave has been calculated to be 0.1415 weber per square meter. The amplitude of the associated permeance harmonic is 0.145, and the resultant of these two, 0.235 weber per square meter. The amplitude of the 28th rotor slot harmonic flux density wave is 0.158 weber per square meter. The amplitude of the force wave resulting from these two flux density harmonics is 55.4 pounds per radian. This force wave is of the second mode (4-node) and its frequency 1,716 cps. The amplitude of the second-harmonic flux density wave caused by the current and induced in the rotor by the 29th stator flux density harmonic is 0.027 weber per square meter. The magnitude of the force wave due to the interference of these last two flux density waves is 29.2 pounds per radian. It is again a 4-node wave of 1,716 cps. The two calculated force waves are 2.7 degrees apart and the amplitude of the resultant wave is 84.5 pounds per radian.

At no load, the fundamental rotor current will become negligible and with it the 28th slot harmonic flux density wave. Consequently, at no load the first component of the previously calculated force wave can be entirely ignored. The amplitude of the second harmonic rotor flux density wave will be 0.0214 weber per square meter, and the amplitude of the 2-mode (4-node) force wave 23.1 pounds per radian. The frequency of this wave is 1,735 cps. The amplitude of another 2-mode force wave caused by the interaction of the 31st stator slot harmonic and the 32nd rotor harmonic have been calculated to be 4.6 pounds per radian at 1,475 cps, when the motor was operating at 60 cps and at full load. Computations have also been carried out for the motor operating at full load with the supply frequency reduced to 50 and 40 cps respectively.

The results of the rather lengthy calculations to find the resonant frequencies in different modes are given in Table I. The eigenvectors pertaining to these resonances are given on pages 189–92 of reference 10. A typical deflection curve, calculated for a 2-mode (4-node) 100-pounds-per-radian amplitude force wave between 1,000 and 2,000 cps, is given in Fig. 1. Table V reproduces the calculated deflections for second-mode force waves of

Table IV. Second-Mode Force Waves in the Experimental Motor of Frequency $2-27(1-s)f$

Interfering Flux Waves Stator, σ	Interfering Flux Waves Rotor, ρ	Rotor Harmonic Induced by Stator Harmonic	Remarks
−29	28	1	significant
−23	22	− 5	
−17	16	−11	
−11	10	−17	
− 5	4	−23	
1	−2	−29	significant

Table VI. Calculated Sound Pressures of Experimental Motor

Motor Operating Amperes	Motor Operating Volts	Motor Operating CPS	Noise Frequency, CPS	Deflection, Centimeters, 10^{-6}*	I†	Equation‡	10^{+6}	10^4§	$\log_{10}$	RMS, SPL, Decibels
40	440	60	1,716	19.6	0.492		116.0	1.98	4.296	85.9
40	367	50	1,419	30.7	0.560		79.0	2.43	4.385	87.7
40	294	40	1,121	60.5	0.650	17.8	49.6	3.47	4.540	90.8
No load	440	60	1,475	5.34	0.485		118.9	0.55	4.738	74.8
40	440	60	1,735	1.51	0.545		86.0	0.126	3.100	62.0
40	440	60	1,716	19.6	0.315		116.0	1.28	4.107	82.1

* Identical with last column of Table V.

† Column 4 values taken from Fig. 10.

‡ $b\rho/\pi\ 2(0.0002)=(13.2\times1.21\times10^{-8}\times5\times10^{3}/\pi\ 2)=17.8$.

§ Product of columns 5, 6, 7, and 8.

Value of r is 51.5 centimeters in all rows except the last where $r=82.0$ centimeters.

the experimental motor. The sound pressures have been calculated in accordance with the theory, with the use of the following data: $c=34,400$ centimeters per second; $\rho_0=0.00121$ gram per cubic centimeter, i.e., values at 20 degrees centigrade and 760-millimeter mercury pressure have been used. The final calculation of the sound pressure is given in Table VI.

References

1. THE PARASITIC FORCES IN INDUCTION MOTORS M. Krondl. *Bulletin Oerlikon*, London, England, vol. 24, 1931, p. 654; vol. 25, 1931, p. 665.

2. NOISE OF ELECTRICAL MACHINERY, M. Krondl. CIGRE, Paris, France 1939.

3. QUIET INDUCTION MOTORS, L. E. Hildebrand. *AIEE Transactions*, vol. 49, July 1930, pp. 848–56.

4. INDUCTION MOTOR SLOT COMBINATIONS, Gabriel Kron. *Ibid.*, vol. 50, June 1931, pp. 757–68.

5. HARMONIC THEORY OF NOISE IN INDUCTION MOTORS, Wayne J. Morrill. *AIEE Transactions (Electrical Engineering)*, vol. 59, Aug. 1940, pp. 474–80.

6. THE NATURE OF POLYPHASE INDUCTION MACHINES (book), P. L. Alger. John Wiley & Sons, Inc., New York, N. Y., 1951.

7. THE MAGNETIC NOISE OF POLYPHASE INDUCTION MOTORS, P. L. Alger. *AIEE Transactions*, vol. 73, pt. III-A, Apr. 1954, pp. 118–25.

8. THE LOW NOISE ELECTRIC MOTOR (book), H. Jordan. W. Girrardet, Essen, Germany (in German), 1950.

9. APPROXIMATE CALCULATION OF THE NOISE PRODUCED BY SQUIRREL-CAGE MOTORS, H. Jordan. *The Engineers' Digest*, New York, N. Y., vol. 10, 1949, p. 222.

10. PREDETERMINATION OF THE SOUND PRESSURE LEVELS OF MAGNETIC NOISE IN MEDIUM INDUCTION MOTORS, E. Erdelyi. Doctoral dissertation, University Microfilms, Ann Arbor, Mich., 1955. See also bibliography.

11. THE SLOTTING FACTOR IN ELECTRICAL MACHINERY, E. Weber. *Elektrotechnische Zeitschrift*, Berlin, Germany (in German), vol. 32, 1928, p. 858.

12. ADDITIONAL TORQUES OF SQUIRREL-CAGE MOTORS AT STARTING, F. Heller. *Archiv fuer Elektrotechnik*, Springer-Verlag, Berlin, Germany, vol. 29, 1935, p. 173.

13. MEASUREMENT OF MOBILITY, R. Plunkett. *Journal of Applied Mechanics*, New York, N. Y., vol. 21, 1954, p. 250.

◆

Discussion

R. F. Horrell (Electric Machinery Manufacturing Company, Minneapolis, Minn.): I agree with the ideas presented by this paper, and feel it applies more aptly to the smaller or National Electrical Manufacturers Association frame-size motors which have realitively shallow frames in comparison to the depth of core back of the stator slot. In this case the stator core may approach the rigidity of the frame. On larger machines, the reverse may be true and I would like to ask if the author has observed or considered any cases where the core vibrated within and independently of the frame? In this case the model points would be at the ribs, and the frame can be considered dead since it does not respond to the core vibrations. I feel sure that other manufacturers have experienced this condition at some time the same as we have, although it is not a common occurrence.

E. Erdelyi: The author wishes to express his thanks to Mr. Horrell for his discussion. Mr. Horrell was right in pointing out that the analysis of the paper is applicable to medium-size induction motors only, as emphasized in reference 4.

In large induction motors with a considerable number of pole pairs, the frame is generally stiffer than the stator core. An independent vibration of the core with nodes at the ribs may occur if the frequency of the driving force happens to approach the natural frequency of the single ring alone. The analytical treatment of this case can be carried out by the method given in the paper, and very little computational work would be required as the elastic equations of the single inextensional ring are quite simple.

Characteristics of Single-Conductor Electric Cable at High Frequency

J. T. SABOL
ASSOCIATE MEMBER AIEE

IN MOST electrical applications, some means of transmitting the electric energy from the source to the point of usage is necessary. High-frequency induction-heating applications are no exception, but they present a more complex transmission problem because of the phenomenon of skin and proximity effects, which substantially limit current-carrying capacities of bus bars, coaxial cables, or single-conductor cables used. This paper deals exclusively with the characteristics of single-conductor cables transmitting power at frequencies of 10,000, 3,000, and 1,000 cycles. Tabulations have been made of physical characteristics of the cables used in both the calculations and the tests in addition to resistance and reactance values per unit (pu) length at 10,000, 3,000, and 1,000 cycles. Current-carrying capacities of various diameter cables and for different arrangements at these same frequencies are tabulated. Calculations are based on the established equations given which apply to higher and lower frequencies than those used. Multipliers shown on the tables for correcting the values of cables in conduit and of ambient temperature other than 30 degrees centigrade (C) are the same as apply for 60-cycle frequency.

Resistance and Reactance Calculations

The a-c resistance and portion of reactance associated with flux lines in copper pu length of isolated solid round conductors are

$$R_e=\frac{\rho}{\pi A_0^2}KA_0\frac{M_0\left(\frac{KA_0}{2}\right)}{M_1\left(\frac{KA_0}{2}\right)}\text{Cos}\left(\theta_0-\theta_1+\frac{3\pi}{4}\right) \tag{1}$$

$$X_e=\frac{\rho}{\pi A_0^2}KA_0\frac{M_0\left(\frac{KA_0}{2}\right)}{M_1\left(\frac{KA_0}{2}\right)}\text{Sin}\left(\theta_0-\theta_1+\frac{3\pi}{4}\right) \tag{2}$$

where

ρ = resistivity
A_0 = diameter of copper

$K=2\pi\sqrt{\frac{2f}{\rho}}=\frac{\sqrt{2}}{d}$

$M_0, M_1, \theta_0, \theta_1$ = Bessel functions[1]
f = frequency, cycles per second

d = reference depth $=\frac{1}{2\pi}\sqrt{\frac{\rho}{f}}$
(absolute-ohm-centimeter system)

$d=3,160\sqrt{\frac{\rho}{f}}$ (ohm-inch system)

Rearranging these equations and multiplying by two to obtain values pu length of run (go and return) results in:

$$R_e=0.898\frac{\rho}{A_0d}\frac{M_0}{M_1}\frac{\left(\frac{1}{\sqrt{2}}\frac{A_0}{d}\right)}{\left(\frac{1}{\sqrt{2}}\frac{A_0}{d}\right)}\times \text{Cos}\left(\frac{3\pi}{4}-(\theta_1-\theta_0)\right) \tag{3}$$

Paper 55-679, recommended by the AIEE Insulated Conductors Committee and approved by the AIEE Committee on Technical Operations for presentation at the AIEE Fall General Meeting, Chicago, Ill., October 3–7, 1955. Manuscript submitted June 11, 1952; made available for printing July 17, 1955.

J. T. SABOL is with the Ohio Crankshaft Company, Cleveland, Ohio.

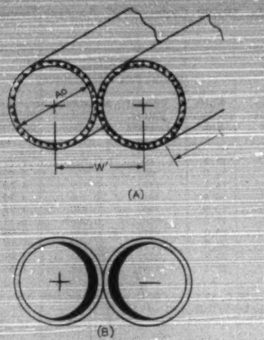

Fig. 1. Two cables, side by side

$$X_e=0.898\frac{\rho}{A_0 d}\frac{M_0}{M_1}\frac{\left(\frac{1}{\sqrt{2}}\frac{A_0}{d}\right)}{\left(\frac{1}{\sqrt{2}}\frac{A_0}{d}\right)}\times \operatorname{Sin}\left(\frac{3\pi}{4}-(\theta_1-\theta_0)\right) \quad (4)$$

$$X_e=R_e \operatorname{Tan}\left(\frac{3\pi}{4}-(\theta_1-\theta_0)\right) \quad (5)$$

Since these equations apply to isolated conductors, correction for the proximity effect inherent to transmission lines must be included in resistance and internal reactance calculations. This correction factor is

$$\frac{1}{\sqrt{1-\left(\frac{A_0}{W'}\right)^2}} \quad (6)$$

where W' is the distance between centers of conductors.

Therefore, the corrected resistance and reactance pu length of cable side by side is

$$R=0.898\frac{\rho}{A_0 d}\frac{M_0}{M_1}\frac{\left(\frac{1}{\sqrt{2}}\frac{A_0}{d}\right)}{\left(\frac{1}{\sqrt{2}}\frac{A_0}{d}\right)}\times \operatorname{Cos}\left(\frac{3\pi}{4}-(\theta_1-\theta_0)\right)\frac{1}{\sqrt{1-\left(\frac{A_0}{W'}\right)^2}} \quad (7)$$

$$X=R \operatorname{Tan}\left(\frac{3\pi}{4}-(\theta_1-\theta_0)\right) \quad (8)$$

Equation 8 gives the reactance pu length of run as a result of flux within the conductor. For external reactance, the following equation applies

$$X_e=8\pi f 2.54\times 10^{-9} \operatorname{Cosh}^{-1}\frac{W'}{A_0} \text{ ohm/inch} \quad (9)$$

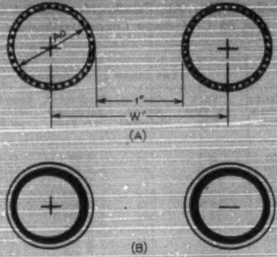

Fig. 2. Two cables, 1-inch spacing

When applying these equations to stranded conductors, a problem of the nonhomogeneous cross section of the stranded conductor arises. In the calculations herein, it is assumed that the resistivity of the stranded conductor is equal to the resistivity of the copper multiplied by the ratio of the cross-sectional area occupied by the stranded conductor to the actual cross-sectional area of the copper.

These are established equations for resistance and reactance and include both skin and proximity effects of conductors carrying alternating currents. These effects, though nominal at 60-cycle frequency, are appreciable enough to cause a reduction as great as 40 per cent in current-carrying capacity when conducting a 10,000-cycle current. Approximate distribution of current in the copper conductor is shown in Figs. 1(B) through 3(B) and represents combined skin and proximity effects. The uniform current distribution shown in Fig. 4 is for an isolated conductor in free air. For solid copper at 85 C, the reference depth d is 0.029 inch for 10 kc, 0.052 inch for 3 kc, and 0.092 inch for 1 kc. It is evident from these distributions of current that a multiplicity of cables arranged with similar polarities opposite will utilize a greater portion of the copper and thus approach uniform circumferential distribution. With such arrangement for a given cable temperature, the radiation of I^2R loss per cable is reduced, consequently reducing current-carrying capacity. The effect of radiation influence between conductors is appreciable for spacings of 2 inches or less horizontally and 4 inches or less vertically with a 2-cable arrangement.

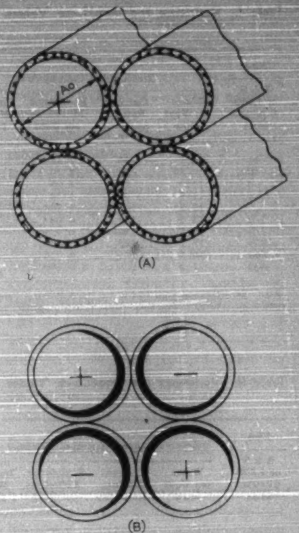

Fig. 3. Four cables, similar polarities opposite

Calculated values of resistance and impedance using the foregoing equations are given in Tables I, II, and III. Curves plotted in Fig. 5 provide a visual comparison of 10,000-cycle, 1,000-cycle, and d-c resistance of cables investigated. Current-carrying capacity and watts per foot of run are also given in Tables I, II, and III. Physical characteristics of extraflexible cables used in the calculations and standard stranded cables are given in Tables IV and V. These calculations are based on assuming a copper temperature of 85 C, and a copper

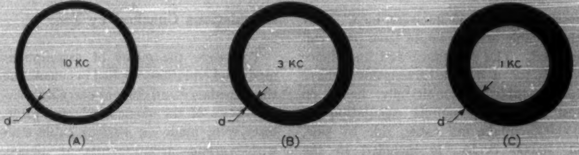

Fig. 4. Current distribution of isolated conductor in free air

Table I. Resistance and Impedance Values. Cables in Free Air, Extraflexible, Stranded Cable, 10,000 Cycles, 30 C Ambient Temperature, 85 C Maximum Copper Temperature

Size	Two Cables Side by Side				Two Cables 1-Inch Spacing				Four Cables Similar Polarities Opposite			
B & S or 1,000 Circular Mils	Watts per Foot Run	Current Rating, Amperes	Resistance, Milliohms per Foot	Impedance, Milliohms per Foot	Watts per Foot Run	Current Rating, Amperes	Resistance, Milliohms per Foot	Impedance, Milliohms per Foot	Watts per Foot Run	Current Rating, Amperes	Resistance, Milliohms per Foot	Impedance, Milliohms per Foot
14	8.1	33	7.44	16.50	8.1	34	6.90	29.80	13.4	60	3.72	8.25
10	8.75	53	3.10	13.30	9.0	56	2.85	25.30	14.0	95	1.55	6.65
6	11.0	76	1.93	11.95	11.6	82	1.71	22.13	14.5	137	0.772	4.78
4	11.8	91	1.42	10.50	12.0	100	1.205	20.00	15.2	164	0.568	4.20
2	12.3	100	1.23	10.05	12.8	113	1.000	17.40	15.9	180	0.490	4.02
1/0	13.5	117	0.99	8.29	15.0	139	0.775	15.91	17.3	210	0.395	3.31
4/0	15.3	145	0.725	7.64	16.6	176	0.533	14.10	20.0	262	0.290	3.06
250	17.2	162	0.655	7.57	18.6	194	0.495	13.70	22.2	292	0.262	3.03
350	19.5	184	0.575	6.71	20.4	222	0.415	12.67	25.3	332	0.230	2.69
500	21.2	208	0.480	6.41	22.7	258	0.340	11.83	27.1	375	0.192	2.56

Note: Multiply ampere rating by the following values for rating at other than 30 C ambient: For ambients of 20 C, 40 C, and 50 C, multiply by 1.08, 0.90, and 0.79 respectively. For two cables in nonmagnetic conduit, multiply current values by 0.73. This note also applies to Tables II and III.

Table II. Resistance and Impedance Values. Cables in Free Air, Extraflexible, Stranded Cable, 3,000 Cycles, 30 C Ambient Temperature, 85 C Maximum Copper Temperature

Size	Two Cables Side by Side				Two Cables 1-Inch Spacing				Four Cables Similar Polarities Opposite			
B & S or 1,000 Circular Mils	Watts per Foot Run	Current Rating, Amperes	Resistance, Milliohms per Foot	Impedance, Milliohms per Foot	Watts per Foot Run	Current Rating, Amperes	Resistance, Milliohms per Foot	Impedance, Milliohms per Foot	Watts per Foot Run	Current Rating, Amperes	Resistance Milliohms per Foot	Impedance, Milliohms per Foot
14	7.9	33	7.25	8.06	7.9	34	6.86	11.3	11.3	56	3.62	4.03
10	8.5	56	2.70	4.82	8.6	59	2.46	8.06	12.2	95	1.35	2.41
6	11.6	96	1.26	3.94	12.0	105	1.10	6.85	14.8	172	0.504	1.58
4	11.9	117	0.87	3.54	12.2	129	0.735	6.30	15.6	212	0.348	1.41
2	12.0	130	0.71	3.10	12.7	148	0.580	5.40	15.7	235	0.284	1.24
1/0	13.8	158	0.552	2.72	14.6	185	0.426	4.94	18.0	285	0.221	1.09
4/0	15.2	187	0.434	2.40	16.1	224	0.320	4.40	19.8	338	0.173	0.96
250	17.2	211	0.384	2.38	18.9	255	0.291	4.30	22.5	382	0.154	0.95
350	18.2	236	0.325	2.17	20.4	296	0.233	3.90	23.5	425	0.130	0.87
500	20.8	278	0.270	2.04	22.5	340	0.195	3.60	27.0	500	0.108	0.82

Table III. Resistance and Impedance Values. Cables in Free Air, Extraflexible, Stranded Cable, 1,000 Cycles, 30 C Ambient Temperature, 85 C Maximum Copper Temperature

Size	Two Cables Side by Side				Two Cables, 1-Inch Spacing				Four Cables, Similar Polarities Opposite			
B & S or 1,000 Circular Mils	Watts per Foot Run	Current Rating, Amperes	Resistance, Milliohms per Foot	Impedance, Milliohms per Foot	Watts per Foot Run	Current Rating, Amperes	Resistance, Milliohms per Foot	Impedance, Milliohms per Foot	Watts per Foot Run	Current Rating, Amperes	Resistance, Milliohms per Foot	Impedance, Milliohms per Foot
14	8.0	34	6.90	7.0	8.0	34	6.82	7.57	11.6	58	3.45	3.5
10	8.7	59	2.50	2.82	8.7	60	2.40	3.50	12.5	100	1.25	1.41
6	11.6	98	1.21	1.76	12.2	107	1.06	2.52	14.8	176	0.484	0.704
4	11.3	123	0.75	1.37	12.4	140	0.630	2.18	14.9	224	0.30	0.548
2	11.5	151	0.507	1.17	12.6	175	0.410	1.88	15.0	272	0.203	0.468
1/0	13.6	197	0.350	1.025	13.1	234	0.270	1.71	17.8	355	0.140	0.410
4/0	15.2	240	0.265	0.915	16.7	296	0.190	1.52	20.0	433	0.106	0.366
250	16.9	270	0.234	0.890	19.0	328	0.176	1.47	22.1	487	0.093	0.356
350	18.9	305	0.203	0.816	20.3	372	0.147	1.35	24.6	550	0.081	0.326
500	20.6	358	0.160	0.752	24.6	463	0.115	1.25	26.6	645	0.064	0.301

resistivity of 0.855 microhm-inch. Only the 2-cable arrangements have been calculated. The resistance and impedance values for a 4-cable arrangement have been established empirically, based on test results. A sample calculation for 350,000-circular-mil cable, side by side, at 10,000 cycles, is included in the Appendix.

Calculations Checked by Test

To prove the effect of assumptions made and equations applied in calculating the impedance and current-carrying characteristics of the single-conductor cable, tests were made on various cable sizes with various arrangements at 10,000, 3,000, and 1,000 cycles. In all cases, it was found that the experimental results did not deviate more than 10 per cent from the calculated values. Fig. 6 shows the arrangement of equipment used: a motor generator *M-G* supplying the high-frequency power, generator output metered by a voltmeter *V1*, a wattmeter *W1*, a varmeter *R1*, and an ammeter *A1*. Capacitance *C* is added to

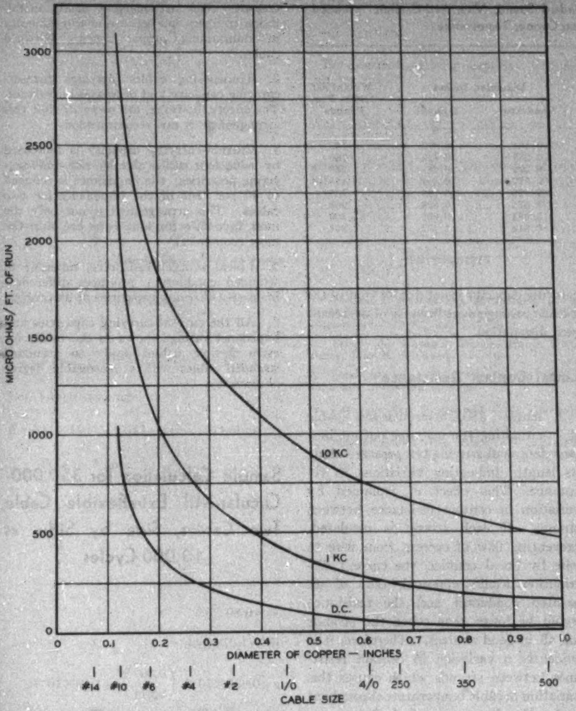

Fig. 5. Curves of resistance versus cable size, two cables side by side for 10 kc, 1 kc, and direct current

balance the machine as close to unity as possible for accurate power readings. Two 26-foot lengths of cable are connected to bus stud outlet *B*, and friction tape *E* is used at 1-foot intervals to maintain proximity; transite supports hold cables in air and a positive electric connection *G* short-circuits cables on the generator. Cable current and voltage are metered by Ammeter *A2* and voltmeter *V2*. Only the 24-foot length of cable from *V2* to *G* is used in applying test results, thereby eliminating the 2-foot loop caused by the insertion of current transformer *CT2*. Thermocouple wires *T1*, *T2*, and *T3* are brazed on one cable at positions shown to determine location of maximum temperature rise.

Simultaneous readings of meters are taken from which impedance *Z* is computed. The power metered at *W1* includes not only the I^2R loss of the cable but also capacitor, bus, and stray losses. A test was made using copper tubing and the I^2R loss measured calorimetrically to check the value used for stray losses. Precautions are taken to eliminate external factors from affecting results, such as maintaining still air, accuracy of meters, good thermocouple wire contact, and using the same potentiometer for recording temperatures *T1*, *T2*, and *T3* during test.

Table IV. Characteristics of Electric Cable. Extraflexible, Varnished-Cambric Insulation Glyptal-Treated Braid Cover, 85 C Maximum Copper Temperature

Size	Conductor					
B&S or Closest 1,000 Circular Mils	No. of Strands	Size of Strands	Insulated Thickness in 64ths	Diameter, Inches Conductor	Diameter, Inches Over-All	Weight per 1,000 Feet, Pounds
14	19	27	2	0.071	0.185	24
10	27	24	3	0.121	0.265	65
6	61	24	4	0.181	0.370	156
4	125	24	4	0.261	0.455	268
2	175	24	5	0.360	0.585	361
0	275	24	5	0.460	0.685	532
0000	550	24	5	0.613	0.855	976
250	650	24	6	0.673	0.945	1,190
350	925	24	6	0.799	1.070	1,642
500	1,325	24	7	0.970	1.275	2,345

Current Carrying Capacity

The maximum current which a cable can safely carry is determined by the maximum allowable temperature for that cable. All current values herein listed are based on an ambient temperature of 30 C and a maximum temperature rise of 55 C. Since current-carrying capacity depends on the maximum allowable temperature of the copper, the ability of a unit length of cable run to dissipate the power adsorbed I^2R, establishes these values. Cable arrangement, spacing, contact resistance and positioning determine copper temperature for a given current. For the 2-cable arrangement, the current-carrying capacity is calculated by using the watts pu length, which result in a temperature rise of 55 C in ambient of 30 C, as established by previous 60-cycle tests. The calculated high-frequency resistance values as tabulated are used in this current determination.

Arrangements

The resistance is lower and current-carrying capacity is higher for the two-cable arrangements with the outside of the cables spaced 1 inch apart than with the cables side by side. The increase in current-carrying capacity is somewhat greater than the square root of the reduction of resistance because for a given temperature the cables spaced 1 inch apart dissipate higher power. It was found that the majority of decrease of resistance and increase of heat dissipation caused by spacing occurs within a spacing of about 1 inch, and any further

Table V. Characteristics of Electric Cable. Standard Strand, Varnished-Cambric Insulated Single Braided, 85 C Maximum Copper Temperature

Size	Conductor					
B&S or Closest 1,000 Circular Mils	No. of Strands	Diameter of Each Strand, Inches	Insulated Thickness in 64ths	Diameter, Inches Conductor	Diameter, Inches Over-All	Weight per 1,000 Feet Pounds
6	7	0.0612	4	0.184	0.373	130
4	7	0.0772	4	0.232	0.422	180
2	7	0.0974	4	0.292	0.482	265
0	19	0.0745	5	0.373	0.594	415
0000	19	0.1055	5	0.528	0.749	765
250	37	0.0822	6	0.575	0.828	908
350	37	0.0973	6	0.681	0.955	1,260
500	37	0.1162	6	0.814	1.172	1,866

increase in spacing results in little effect. Therefore, in the tabulations, a 1-inch spacing has been chosen.

A test was made to find the effect of transposing the cables as shown in Fig. 7. This test was made using 250,000-circular-mil cable, and it was found that the current-carrying capacity is increased 4.5 per cent and the impedance value is decreased 9 per cent by transposing 13 times in a 26-foot run. This arrangement was not given further test because of the extremely small advantage gained by transposing.

The current-carrying capacity and impedance values for the 4-cable arrangement, Fig. 3, are established by test. Comparing the 2-cable and 4-cable arrangements it was found that the individual ratios of current-carrying capacity, resistance, and impedance are approximately the same for different sized cables. These ratios are as follows:

Current for four cables = 1.8 currents for two cables.
Resistance for four cables = 0.4 resistance for two cables.
Impedance for four cables = 0.4 impedance for two cables.

With the 4-cable arrangement, the individual resistance of each cable is reduced because of more uniform current distribution. However, the current-carrying capacity is not double that of the 2-cable arrangement because of decreased heat dissipation.

Lineal Contact Resistance

A single 350,000-circular-mil cable short-circuiting the machine output in a large loop had varying temperature along its length, indicating variations in resistance. This effect is explained by variation in contact resistance between strands. If each strand is insulated, preventing flow of current from wire to wire by lineal contact, the current distribution would approach that of an isolated conductor and the resistance would be lower than when the strands are all in good contact. Therefore, it is evidently a variation in contact resistance between strands which causes this variation in cable temperature throughout its length.

Conclusions

1. It is obvious from the current and impedance values given in the tables that standard stranded cables can be used efficiently to transmit high-frequency power over relatively long distances.

2. Current-carrying capacity of conductors is increased by spacing throughout the length of run; the impedance is also increased. Such arrangement makes installation cumbersome because of the difficulty in maintaining proper spacing between cables.

3. Transposing cables increases current-carrying capacity and decreases impedance. The effects, however, are so small that this arrangement is not recommended.

4. Current-carrying capacity is increased by using four cables side by side and staggering polarities; the impedance is reduced to 40 per cent of the impedance for two cables. This arrangement is not only the most favorable for long runs but also the most economical.

5. Lineal contact resistance, inherent to stranded conductors, produces differences in current-carrying capacities of like cables.

6. All the current-carrying capacities and impedance ratings shown in the tables for extra flexible cables apply to standard stranded cables with a reasonable degree of accuracy.

Sample Calculation for 350,000-Circular-Mil Extraflexible Cable Two Cables, Side by Side, at 10,000 Cycles

$$A_0 = 0.80$$

$$W' = 1.070 \text{ inch}$$

$$\rho = 0.855 \times 10^{-6} \left(\frac{0.80}{0.611}\right)^2 = 1.46 \times 10^{-6}$$

$$A_s = 10^{-3}\sqrt{373{,}300} = 0.611 \text{ (conversion: actual circular mils to diameter)}$$

$$d = 3{,}160\sqrt{\frac{\rho}{f}} = 0.0382$$

$$\text{proximity factor} = \frac{1}{\sqrt{1-\left(\frac{A_0}{W'}\right)^2}} = 1.505$$

$$\frac{A_0}{\sqrt{2}d} = 14.8$$

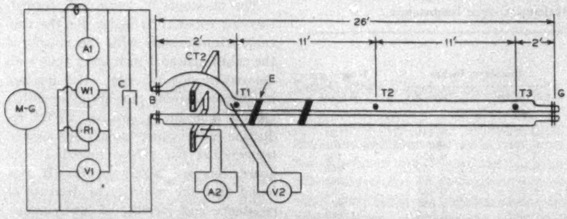

Fig. 6. Arrangement of test equipment used in determining current-carrying capacity and impedance values

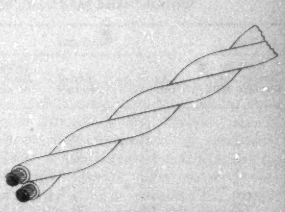

Fig. 7. Two cables, transposed

$$R=0.898\left(\frac{\rho}{A_0 d}\right)\frac{M_0\left(\frac{A_0}{\sqrt{2}d}\right)}{M_1\left(\frac{A_0}{\sqrt{2}d}\right)}\times$$

$$\text{Cos}\left(\frac{3\pi}{4}-(\theta_1-\theta_0)\right)\frac{1}{\sqrt{1-\left(\frac{A_0}{W'}\right)^2}}$$

$$=517\times 10^{-6}\times 1.02\times 0.7246\times 1.505=574\times 10^{-6}\text{ ohm}$$

$$X=R\text{ Tan}\left(\frac{3\pi}{4}-(\theta_1-\theta_0)\right)=574\times 10^{-6}\text{ Tan }43.56=550\times 10^{-6}\text{ ohm}$$

$$X_0=8\pi f\times 2.54\times 10^{-9}\text{ Cosh}^{-1}\frac{W'}{A_0}\times 12=6{,}132\times 10^{-6}\text{ ohm}$$

$$Z=\sqrt{R^2+(X+X_0)^2}=6{,}710\times 10^{-6}\text{ ohm}$$

For 1-inch spacing

$$R=381\times 10^{-6}\times 1.088=415\times 10^{-6}\text{ ohm}$$

$$X=400\times 10^{-6}\text{ ohm}$$

$$X_0=0.01226\text{ ohm}$$

$$Z=0.01267\text{ ohm}$$

For current-carrying capacity (10 kc, side by side)

$$\text{Watts}=I^2R\text{ to }I=\sqrt{\frac{W}{R}}=195\text{ amperes}$$

where $W=22.1$ for 350,000-circular-mil cable (cable isolated). For two cables side by side $=195\times 0.92=184$.

References

1. Bessel Functions for Engineers, N. W. McLachlan. Oxford University Press, London, England, pp. 140–41, and 182–83.

2. Fields and Waves in Modern Radio, Simon Ramo, John R. Whinnery. P. 332.

3. *Catalogue No. GEA-3754*, General Electric Company, Schenectady, N. Y.

4. *Catalogue No. 37*, General Cable Company, Sec. 15, p. 6.

5. Specifications for Soft or Annealed Copper Wire. *AIEE Standard* No. 61, Dec. 16, 1927.

Discussion

T. J. Higgins (University of Wisconsin, Madison, Wis.): An exhaustive account of the theory and data available for the design of bus systems is encompassed in a paper by the discusser.[1] I have kept this account up-to-date through maintenance of a file on the subsequently published literature and presentation of this latter in a conference paper, as part II of the foregoing paper, at the 1954 AIEE Fall General Meeting. However, he does not find therein information on the resistance and reactance of stranded conductors as used for in-plant distribution which is equivalent to that in Mr. Sabol's excellent paper. In consequence, he believes Mr. Sabol's formulation of design equations for the resistance and reactance of stranded cables, subsequent experimental investigation of their accuracy, and careful investigation of other influential design factors such as current-carrying capacity and desirable geometric arrangement comprise a valuable contribution in the field of in-plant power distribution at induction-heating frequencies.

Reference

1. The Design of Bus-Bar Industrial Systems: An Epitomization of Available Data, T. J. Higgins. *AIEE Transactions*, vol. 64, 1945, pp. 385–400; disc. pp. 486–88.

Digital Calculation of Network Impedances

A. F. GLIMN
MEMBER AIEE

R. HABERMANN, JR.
ASSOCIATE MEMBER AIEE

J. M. HENDERSON
ASSOCIATE MEMBER AIEE

L. K. KIRCHMAYER
MEMBER AIEE

THE operation of an electrical network may be defined by means of driving point and transfer impedances. According to the American Standard Association definition,[1] the driving point impedance at any pair of terminals of a network is the ratio of an applied potential difference to the resultant current at these terminals, all terminals being terminated in any specified manner. Similarly, the transfer impedance between any two pairs of terminals of a network is the ratio of a potential difference applied at one pair of terminals to the resultant current at the other pair of terminals, all terminals being terminated in any specified manner.

Driving point and transfer impedances as a circuit analysis technique have been widely used in such electrical utility engineering problems as load flow, short circuit, regulation, stability, and transmission loss studies. In stability studies, the driving point and transfer impedances are measured with all other terminals being short circuited.[2] In other studies, the driving point and transfer impedances are measured with all other terminals open and are then designated as self- and mutual impedances.

The self- and mutual resistances of the transmission system are used in several methods of calculating transmission loss formulas,[3,4] and are usually obtained by measurements on the network analyzer and then transcribed to punched cards for calculations undertaken by an automatic digital computer.

This paper describes several digital methods of calculating self- and mutual impedances that have been successfully programmed for an automatic digital computer. These new methods offer several distinct advantages over previous analogue methods:

1. Greater accuracy.
2. Lower cost.

Paper 55-680, recommended by the AIEE System Engineering Committee and approved by the AIEE Committee on Technical Operations for presentation at the AIEE Fall General Meeting, Chicago, Ill., October 3–7, 1955. Manuscript submitted June 7, 1955; made available for printing July 19, 1955.

A. F. Glimn, R. Habermann, Jr., J. M. Henderson, and L. K. Kirchmayer are with the General Electric Company, Schenectady, N. Y.

The authors wish to thank Miss Arlene Schwartz for her invaluable assistance in the preparation of the digital computer programs.

3. Very small set-up time as general programming decks are available.

4. Elimination of necessity of transcribing network analyzer results to punched cards and associated time and possibility of error when these self- and mutual impedances are required for digital circuit studies.

The techniques described may be applied to the determination of driving point and transfer impedances for cases in which the terminals are terminated in any other specified manner.

The high-speed internally programmed digital computer applied to electrical network problems provides the utility engineer with a new tool for obtaining more economical and accurate network solutions.

Network Analyzer Measurement of Self- and Mutual Impedances

Consider the schematic circuit representation of a power system as shown in Fig. 1, in which a given bus is selected as the reference bus. The circuit performance is defined by the following equation

$$\mathbf{E}_{\text{bus}} = \mathbf{Z}_{\text{bus}}\mathbf{I}_{\text{bus}} \tag{1}$$

The self- and mutual impedances ($\mathbf{Z}_{\text{bus}}$) which relate all bus voltages and bus currents are desired.

The following procedure is used to determine the network self- and mutual impedances of the transmission system by means of a network analyzer; see Fig. 2:

1. Remove from ground all line-charging capacitors, synchronous condensers, loads, and generators.
2. Ground the reference bus.
3. Impress a known current at a given bus and read the resulting voltages at all busses.

The mutual impedance between the energized bus and each of the other busses in the network is given by the ratio of the voltage at each of these busses to the impressed current. The self-impedance of the energized bus is, of course, equal to the voltage at that bus divided by the impressed current.

This procedure is repeated with currents impressed, in turn, at each of the busses in the network. In this way a complete set of network self- and mutual impedances is obtained.

Description of Digital Methods

Three methods of computing network self- and mutual impedances by means of an automatic digital computer have been programmed by the authors. The procedure used in each of the methods is described in the following, and is illustrated by application to the simple system in Fig. 3.

Method I: Matrix Analysis of Power System Network

This method is an application of Kron's method of analysis of stationary networks.[8] The first step in its application is the specification of the network branch impedance matrix. This is a diagonal matrix and relates branch voltages to branch current flow as shown in the following:

$$\mathbf{E}_{\text{branch}} = \mathbf{Z}_{\text{branch}}\mathbf{I}_{\text{branch}} \tag{2}$$

The branch impedance matrix for the system of Fig. 3 is

$$\mathbf{Z}_{\text{branch}} = \begin{array}{c|ccccccccc} \text{branch} \backslash \text{branch} & \text{b1} & \text{b2} & \text{b3} & \text{b4} & \text{b5} & \text{b6} & \text{b7} & \text{b8} & \text{b9} \\ \hline \text{b1} & 0.042+j0.126 & & & & & & & & \\ \text{b2} & & 0.004+j0.0365 & & & & & & & \\ \text{b3} & & & 0.006+j0.140 & & & & & & \\ \text{b4} & & & & 0.028+j0.084 & & & & & \\ \text{b5} & & & & & 0.004+j0.1215 & & & & \\ \text{b6} & & & & & & 0.004+j0.0365 & & & \\ \text{b7} & & & & & & & 0.028+j0.084 & & \\ \text{b8} & & & & & & & & 0.028+j0.084 & \\ \text{b9} & & & & & & & & & 0.056+j0.168 \end{array} \tag{3}$$

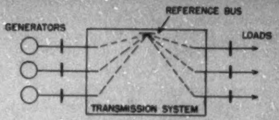

Fig. 1. Schematic representation of network

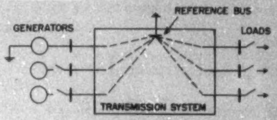

Fig. 2. Method of measurement of self- and mutual impedances

As can be seen, the branch impedances are the line and transformer impedances of the network. The axis numbers are the numbers assigned to the elements in Fig. 3.

In method I the configuration of the network is defined by means of a transformation matrix $\mathbf{C}_t$. This matrix relates the voltage at each bus (with respect to an arbitrary reference) to the voltage across each of the branch elements. It also relates the voltage acting around each loop in the network to the branch voltages. Thus

$$\mathbf{E}_{\text{bus, loop}} = \mathbf{C}_t\mathbf{E}_{\text{branch}} \tag{4}$$

The assumed positive direction of current flow is indicated by the arrow along the branch as shown in Fig. 3. That loop currents and branch currents thread common elements in the same direction is an allowance for method II and not required for this method. The $\mathbf{C}_t$ used to relate bus voltages and loop voltages to the branch voltages for the system of Fig. 3 is

bus or loop	b1	b2	b3	b4	b5	b6	b7	b8	b9
B1	−1		1.09						−1
B2		−1				−1			
B3									
B4			1.09				1	1	
$\mathbf{C}_t$ = B6						−1			
B7			1.09					1	
B8			1.09						
B10			1.09						−1
L1	1			1			1	1	1
L2		1	1.01869		1	1	0.93458	0.93458	

(5)

Here the reference was assumed as bus 3.

Specification of the transformation matrix $\mathbf{C}_t$ is the equivalent of drawing up a network analyzer plugging diagram of the network. The electrical location of each bus with respect to the reference is defined, as well as the composition of each loop in the system. For example, the voltage at bus 1 with respect to bus 3 is equal to the voltage in branch 3 multiplied by the turns ratio of transformer 2 minus the voltages in branches 9 and 1. Also, the matrix $\mathbf{C}_t$ indicates that loop 1 is composed of branches 1, 4, 7, 8, and 9; while loop 2 is made up of branches 2, 3, 5, 6, 7, and 8. The effects of off-nominal turns ratios are also represented. The voltage acting around loop 2 as viewed looking upward from bus 3 is equal to the voltages in branches 6, 2, and 5 plus the voltages in 7 and 8 multiplied by the turns ratio of transformer 1 plus the voltage in branch 3 multiplied by the product of the turns ratios of transformers 1 and 2.

The concept of invariant transformation as developed by Kron is briefly reviewed here in order to introduce the next step. Consider a given circuit in which the voltages, impedances, and currents are

$$\mathbf{E}_{\text{old}} = \mathbf{Z}_{\text{old}}\mathbf{I}_{\text{old}} \tag{6}$$

If it is possible to relate this set of voltages to a new set of voltages $\mathbf{E}_{\text{new}}$ such that

$$\mathbf{E}_{\text{new}} = \mathbf{C}_t{}^*\mathbf{E}_{\text{old}} \tag{7}$$

then, for the impedances to be transformed such that the total input power is invariant, the following relations must be satisfied

$$\mathbf{I}_{\text{old}} = \mathbf{C}\mathbf{I}_{\text{new}} \tag{8}$$

$$\mathbf{Z}_{\text{new}} = \mathbf{C}_t{}^*\mathbf{Z}_{\text{old}}\mathbf{C} \tag{9}$$

where $\mathbf{C}$ is obtained by interchanging the rows of columns of $\mathbf{C}_t$, and $\mathbf{C}_t{}^*$ is obtained by conjugating the elements of $\mathbf{C}_t$. In the methods of this paper, $\mathbf{C}_t$ is equal to $\mathbf{C}_t{}^*$ since all the elements of the matrix $\mathbf{C}_t$ are real numbers. Also

$$\mathbf{E}_{\text{new}} = \mathbf{Z}_{\text{new}}\mathbf{I}_{\text{new}} \tag{10}$$

From the relations given in equations 4, 7, 8, 9, and 10, the following may be written

$$\mathbf{I}_{\text{branch}} = \mathbf{C}\mathbf{I}_{\text{bus, loop}} \tag{11}$$

$$\mathbf{Z}_{\text{bus, loop}} = \mathbf{C}\mathbf{Z}_{\text{branch}}\mathbf{C} \tag{12}$$

Also

$$\mathbf{E}_{\text{bus, loop}} = \mathbf{Z}_{\text{bus, loop}}\mathbf{I}_{\text{bus, loop}} \tag{13}$$

By interchanging rows and columns, the matrix $\mathbf{C}$ is obtained from $\mathbf{C}_t$ which is given by equation 5. Thus

branch \ bus or loop	B1	B2	B3	B4	B6	B7	B8	B10	L1	L2
b1	−1								1	1
b2		−1								1.01869
b3	1.09			1.09		1.09	1.09	1.09		
b4									1	1
$\mathbf{C}$ = b5										1
b6		−1			−1					0.93458
b7				1					1	0.93458
b8				1		1			1	
b9	−1							−1	1	

(14)

Performing the operations indicated in equation (12) yields

$\mathbf{C}_t\mathbf{Z}_{\text{branch}}\mathbf{C} = \mathbf{Z}_{\text{bus, loop}} =$

bus or loop \ bus or loop	B1	B2	B3	B4	B6	B7	B8	B10	L1	L2
B1	0.10513 +j0.46033	0	0	0.00713 +j0.16633	0	0.00713 +j0.16633	0.00713 +j0 16633	0.06313 +j0.33433	−0.09800 −j0.29400	0.00666 +j0.15545
B2	0	0.00800 +j0.07300	0	0	0.00400 +j0.03650	0	0	0	0	−0.00800 −j0.07300
B3	0	0	0	0	0	0	0	0	0	
B4	0.00713 +j0.16633	0	0	0.06313 +j0.33433	0	0.03513 +j0.25033	0.00713 +j0.16633	0.00713 +j0.16633	0.05600 +j0.16800	0.05900 +j0.31246
B6	0	0.00400 +j0.03650	0	0	0.00400 +j0.03650	0	0	0	0	−0.00400 −j0.03650
B7	0.00713 +j0.16633	0	0	0.03513 +j0.25033	0	0.03513 +j0.25033	0.00713 +j0.16633	0.00713 +j0.16633	0.02800 +j0.08400	+0.03283 +j0.23395
B8	0.00713 +j0.16633	0	0	0.00713 +j0.16633	0	0.00713 +j0.16633	0.00713 +j0.16633	0.00713 +j0.16633	0	0.00666 +j0.15545
B10	0.06313 +j0.33433	0	0	0.00713 +j0.16633	0	0.00713 +j0.16633	0.00713 +j0.16633	0.06313 +j0.33433	−0.05600 −j0.16800	0.00666 +j0.15545
L1	−0.09800 −j0.29400	0	0	0.05600 +j0.16800	0	0.02800 +j0.08400	0	−0.05600 −j0.16800	0.18200 +j0.54600	0.05234 +j0.15701
L2	0.00666 +j0.15545	−0.00800 −j0.07300	0	0 05900 +j0.31246	−0.00400 −j0.03650	0.03283 +j0.23395	0.00666 +j0.15545	0.00666 +j0.15545	0.05234 +j0.15701	0.06714 +j0.48652

(15)

Since the voltages acting around each loop in the network are zero, the loop currents may be eliminated as variables. The impedance matrix $\mathbf{Z}_{\text{bus, loop}}$ may be compounded as follows

$$\boxed{\begin{array}{c} \mathbf{E}_{\text{bus}} \\ \hline \mathbf{E}_{\text{loop}} \end{array}} = \boxed{\begin{array}{c|c} \mathbf{Z}_1 & \mathbf{Z}_2 \\ \hline \mathbf{Z}_3 & \mathbf{Z}_4 \end{array}} \times \boxed{\begin{array}{c} \mathbf{I}_{\text{bus}} \\ \hline \mathbf{I}_{\text{loop}} \end{array}} \tag{16}$$

Then, since $\mathbf{E}_{\text{loop}}$ equals zero

$$\mathbf{E}_{\text{loop}} = 0 = \mathbf{Z}_3\mathbf{I}_{\text{bus}} + \mathbf{Z}_4\mathbf{I}_{\text{loop}}$$

and

$$\mathbf{Z}_4{}'_{\text{loop}} = -\mathbf{Z}\mathbf{I}_{\text{bus}}$$

By multiplying through by the inverse of $\mathbf{Z}_4$ the following is obtained

$$\mathbf{I}_{\text{loop}} = -\mathbf{Z}_4{}^{-1}\mathbf{Z}_3\mathbf{I}_{\text{bus}} \tag{17}$$

By substituting equation 17 into 16 the following is obtained

$$\mathbf{E}_{\text{bus}} = [\mathbf{Z}_1 - \mathbf{Z}_2(\mathbf{Z}_4)^{-1}\mathbf{Z}_3]\mathbf{I}_{\text{bus}} \tag{18}$$

$$= \mathbf{Z}_{\text{bus}}\mathbf{I}_{\text{bus}} \tag{19}$$

Thus

$$\mathbf{Z}_{\text{bus}} = \mathbf{Z}_1 - \mathbf{Z}_2(\mathbf{Z}_4)^{-1}\mathbf{Z}_3 \tag{20}$$

By inspection of equations 15 and 16, the network loop impedance ($\mathbf{Z}_4$) is given by

$$\mathbf{Z}_4 = \begin{array}{c} \\ \text{L1} \\ \text{L2} \end{array} \begin{array}{c|c} \text{L1} & \text{L2} \\ \hline 0.18200+j0.54600 & 0.05234+j0.15701 \\ \hline 0.05234+j0.15701 & 0.06714+j0.48652 \end{array} \tag{21}$$

The network loop admittance matrix may be obtained[5] by inverting Z_4. Thus

$$\mathbf{Z}_4{}^{-1} = \begin{array}{c} \\ \text{L1} \\ \text{L2} \end{array} \begin{array}{c|c} \text{L1} & \text{L2} \\ \hline 0.57125-j1.83313 & -0.07582+j0.64257 \\ \hline -0.07582+j0.64257 & 0.26372-j2.23457 \end{array} \tag{22}$$

By performing the operations indicated by equation 20, the following matrix of self- and mutual impedances is obtained

$$\mathbf{Z}_{\text{bus}} = \begin{array}{c|c|c|c|c|c|c|c|c} & \text{B1} & \text{B2} & \text{B3} & \text{B4} & \text{B6} & \text{B7} & \text{B8} & \text{B10} \\ \hline \text{B1} & 0.02986+j0.17162 & 0.00542+j0.03970 & 0 & 0.01003+j0.11333 & 0.00271+j0.01985 & 0.00564+j0.09748 & 0.00123+j0.08164 & 0.01759+j0.13305 \\ \hline \text{B2} & & 0.00678+j0.06093 & 0 & 0.00672+j0.04370 & 0.00339+j0.03046 & 0.00380+j0.03470 & 0.00089+j0.02569 & 0.00348+j0.03370 \\ \hline \text{B3} & & & 0 & 0 & 0 & 0 & 0 & 0 \\ \hline \text{B4} & & & & 0.01318+j0.12485 & 0.00336+j0.02185 & 0.00611+j0.09892 & -0.00095+j0.07299 & 0.00533+j0.09605 \\ \hline \text{B6} & & & & & 0.00369+j0.03348 & 0.00190+j0.01735 & 0.00044+j0.01285 & 0.00173+j0.01685 \\ \hline \text{B7} & & & & & & 0.01904+j0.13768 & 0.00396+j0.09244 & 0.00492+j0.09533 \\ \hline \text{B8} & & & & & & & 0.00886+j0.11189 & 0.00450+j0.09460 \\ \hline \text{B10} & & & & & & & & 0.03597+j0.18857 \end{array} \tag{23}$$

This matrix is symmetrical.

METHOD II: SELF- AND MUTUAL IMPEDANCES FROM IMPRESSED CURRENTS

The network analyzer procedure of sequentially impressieg current at each bus in the network and reading the voltage distribution can be simulated digitally by calculating the voltage distribution for an assumed impressed current. The steps in the digital computation are indicated as

1. With the reference bus grounded, impress a current $1+j0$ at a generator or load bus in the network.

2. Assume a current flow through the network from the energized bus to the reference.

3. Compute in each branch the voltage resulting from the assumed flows in step 2.

4. Compute the voltage acting through each loop by summing the branch voltage in the loop. Include the effects of off-nominal transfer ratios.

5. Compute the balancing currents required to make the summation of the voltages around each loop equal to zero.

6. Superimpose the balancing flows determined in step 5 on the assumed flows of step 1.

7. Determine the branch voltages due to the exact flows determined in step 6

8. In terms of the branch voltages of step 7 determine the voltage at each bus in the network with respect to the reference.

The voltages determined in step 8 are numerically equal to the open-circuit impedances since the impressed current was equal to $1+j0$. In a manner similar to network analyzer procedure, the complete set of impedances may be determined by repeating steps 1 through 8 with currents impressed in turn at each of the network busses.

PREPARATION OF PROBLEM FOR DIGITAL SOLUTION BY METHOD II

In method II the network is defined in terms of loops and tracks. A procedural requirement of the method is that loop currents threading a common branch do so in the same direction. Positive direction of flow in radial branches is assumed directed into the loop network. The current directions indicated in Fig. 3 have been chosen to satisfy these conventions.

To define the geometry or configuration of a network, it is necessary, in addition to outlining the composition of the various loops in the network, to describe how the various lines and busses are connected. In this method, the connection pattern is defined in terms of tracks. The tracks specify the sequence in which the network branches and busses appear along a path which originates at the reference and threads the network in a negative direction (against the arbitrarily chosen direction of positive flow) to a radial bus or to a junction beyond which the lines and busses appear in another track. The network is completely "tracked" when every bus in the network appears in a track. From the foregoing, it is apparent that the network tracks may be used to relate bus voltages throughout the network to the reference.

A number of authors have used the loop-track concept in solving network

Table I. Tracks Selected for the System of Fig. 1

Track 1, B-b	Track 2, B-b
9-3	9-3
8-2-	8-2-
7-8	7-8
4-7	4-7
1-4	5-1-
10-1	2-5
8-9	6-2
	3-6

problems by digital means.[6,7] The tracks used in the digital determination of the open-circuit self- and mutual impedances of the simple system considered in this paper are shown in Table I. The particular notational scheme used for this study is that an element in the track is specified by $B-b\pm$ where B is the bus at the input end of branch b, shown plus for lines and minus for transformers. For example, track 1 is indicated by a dashed-line path drawn in Fig. 4.

ASSUMED FLOWS AND RESULTING VOLTAGE DROPS DUE TO IMPRESSED CURRENTS

As pointed out in the statement of method II, it is necessary to assume a distribution of flow in the network due to impressing current at a given bus. The only requirement on the assumed flow distribution is that there be continuity of flow, i.e., the current entering a junction equals that leaving the junction. From this and from the previous discussion of tracks, it is seen that the assumed flow between the energized bus and the reference may be assumed through the line elements in the track between the energized bus and the reference. Of course, where off-nominal transformer ratios exist in the track, their effect must be considered in determining the assumed flow in the elements between the transformer and the reference bus. The assumed branch flows resulting from impressing a current of $1+j0$ at bus 1 are shown in Table II as I_{branch}. The branch voltages due to these current flows are shown as E_{branch} and are given by

$$\mathbf{E}_{branch}=\mathbf{Z}_{branch}\mathbf{I}_{branch} \qquad (2)$$

LOOP VOLTAGES DROPS AND BALANCING FLOWS

In this method of analysis the branch current distribution resulting from current impressed at a given bus may be considered to have two components: 1. arbitrarily assumed distribution of current, and 2 a set of balancing currents which circulate in the network loops. The balancing currents produce voltages in the network loops which nullify those produced by the assumed currents. Thus, the superposition of the balancing flows on the assumed flows results in the correct distribution of flow in which each of the fundamental electric circuit relationships are satisfied, i.e.: 1. the summation of currents into a junction is zero, and 2. the summation of branch voltages around each loop is zero.

The relationship between the set of loop-balancing currents and the set of loop voltages resulting from an assumed distribution of flow is

$$\mathbf{I}_{loop}=-\mathbf{Y}_{loop}\mathbf{E}_{loop} \qquad (24)$$

Here $\mathbf{Y}_{loop}$ is the loop admittance matrix, equation 22, and is equal to the inverse of the loop impedance matrix, equation 21. The loop impedance matrix $\mathbf{Z}_4$ may be obtained directly by the operation $\mathbf{C}_t'\mathbf{Z}_{branch}\mathbf{C}'$ where $\mathbf{C}_t'$ is defined by

$$\mathbf{E}_{loop}=\mathbf{C}_t'\mathbf{E}_{branch} \qquad (25)$$

In a network in which there are no off-nominal transformer ratios, the net voltage acting around each loop is obtained by merely summing the branch voltages around the loop. However, when off-nominal ratios are present, the net loop voltage is computed in terms of the branch voltages as viewed from an arbitrary reference point in the loop. Similarly, in a loop with no transformers, the circulating current has the same value in each branch in the loop. Where transformers are encountered, the circulating current is expressed in terms of that value existing at the reference point in the loop.

For the system of Fig. 3 the loop voltages E_{L1} and E_{L2} are related to the branch voltages E_{b1}, $E_{b2}-E_{b9}$ by the transformation matrix $\mathbf{C}_t'$ which is shown as

$$\mathbf{C}_t'=\begin{array}{c|c|c|c|c|c|c|c|c|c|}
 & b1 & b2 & b3 & b4 & b5 & b6 & b7 & b8 & b9 \\
L1 & 1 & & & 1 & & & 1 & 1 & 1 \\
L2 & & 1 & 1.01869 & & 1 & 1 & 0.93458 & 0.93458 & \\
\end{array} \qquad (26)$$

This matrix is, of course, identical to the submatrix used in method I to relate loop and branch voltages. This is evident from an inspection of equation 5.

The voltages in loops 1 and 2 resulting from the assumed flow distribution for current impressed at bus 1 are calculated from equation 25. Thus

$$\mathbf{E}_{loop}=\begin{array}{c|c|}
L1 & 0.08400+j0.25200 \\
L2 & 0.05900+j0.31246 \\
\end{array} \qquad (27)$$

For example

$$\begin{aligned}E_{L1}&=E_{b1}+E_{b4}+E_{b7}+E_{b8}\\
&=0+(0.02800+j0.08400)+(0.02800+\\
&\qquad j0.08400)+(0.02800+j0.08400)\\
&=0\,08400+j0.25200\end{aligned}$$

Matrixes 22 and 27 can now be used in equation 24 to determine the loop balancing currents

$$\mathbf{I}_{loop}=\begin{array}{c|c|}
L1 & -0.30468-j0.00419 \\
L2 & -0.54547+j0.01457 \\
\end{array} \qquad (28)$$

BRANCH FLOWS FROM LOOP FLOWS

The balancing currents flowing in the individual branches of the network are related to the loop-circulating currents by

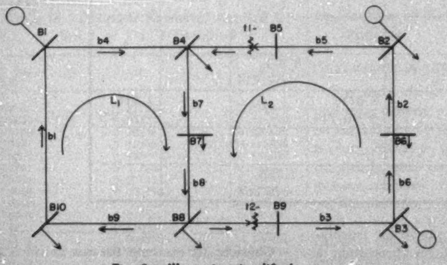

Fig. 3. Illustrative simplified system

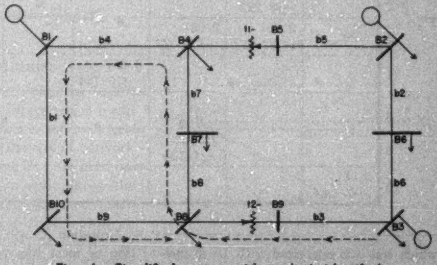

Fig. 4. Simplified system with track 1 identified

the matrix **C**′. This is the transpose of the transformation matrix $\mathbf{C}_t'$ which in turn relates loop voltages to branch voltages. The **C**′ matrix of method II is identical to the submatrix in method I which relates branch and loop currents.

Branch balancing currents obtained by

$$\mathbf{I}_{\text{bal}}=\mathbf{C}'\mathbf{I}_{\text{loop}} \tag{29}$$

for impressed current of $1+j0$ at bus 1 are given in Table II as I_{bal}. The exact branch currents (the balancing currents superimposed on the assumed flows) are also shown in Table II as

$$\mathbf{I}_{\text{total}}=\mathbf{I}_{\text{bal}}+\mathbf{I}_{\text{branch}} \tag{30}$$

BRANCH VOLTAGE DROPS AND BUS VOLTAGES

As indicated in step 7 in the statement of method II, branch voltages due to the exact current distribution must be computed. These voltages, of course, are related to the current flows by the branch impedances. Thus

$$\mathbf{E}_{\text{branch}}=\mathbf{Z}_{\text{branch}}\mathbf{I}_{\text{total}} \tag{31}$$

The branch voltages resulting from unit current impressed at bus 1 are shown in Table II.

The voltages at each network bus are then determined with respect to the reference bus by summing the branch voltages in each track away from the reference. Voltages determined in this fashion are the open-circuit impedances between the energized bus and the other network busses. The form of this calculation is indicated by Table III for the case in which bus 1 is energized with $1+j0$ current.

METHOD III—AN ITERATIVE SOLUTION FOR BUS VOLTAGES

Both the methods previously described are direct methods in that the answer produced are accurate within the precision carried in the problem solution. Iterative problem solutions, using repetitive calculations, are frequently superior for digital-computer application. The application of iterative means to the problem of impedance calculations consists of successively improving an assumed set of bus voltages until satisfaction of Kirchoff's laws has been achieved within the precision desired in the problem solution.

In the ultimate solution, the sum of all currents entering a bus p (node) must equal zero; see Fig. 5. Thus

$$\sum_q Y^{pq}(E_q-E_p)=0$$

where

Y^{pq} = admittance between bus p and bus q
E_q = voltage at bus q
E_p = voltage at bus p

Then

$$\Big(\sum_q Y^{pq}\Big)E_p=\sum_q Y^{pq}E_q$$

and

$$E_p=\frac{\sum_q Y^{pq}E_q}{\sum_q Y^{pq}} \tag{32}$$

The admittance matrix $\mathbf{Y}^{pq}$, for the system of Fig. 3 is as follows:

$$\mathbf{Y}^{pq}=\begin{array}{c|cccccccccc} p\diagdown q & 1 & 2 & 3 & 4 & 5 & 6 & 7 & 8 & 9 & 10\\ \hline 1 & & & & 3.571-j10.714 & & & & & & 2.381-j7.143\\ 2 & & & & & 0.271-j8.222 & 2.967-27.077 & & & & \\ 3 & & & & & & 2.967-j27.077 & & & 0.306-j7.130 & \\ 4 & 3.571-j10.714 & & & & & & 3.571-j10.714 & & & \\ 5 & & 0.271-j8.222 & & & & & & & & \\ 6 & & 2.967-j27.077 & 2.967-j27.077 & & & & & & & \\ 7 & & & & 3.571-j10.714 & & & & 3.571-j10.714 & & \\ 8 & & & & & & & 3.571-j10.714 & & & 1.786-j5.357\\ 9 & & & 0.306-j7.130 & & & & & & & \\ 10 & 2.381-j7.143 & & & & & & & 1.786-j5.357 & & \end{array} \tag{33}$$

Equation 32 will apply to the calculation of most bus voltages throughout a system; however, when off-nominal turns-ratio transformers occur in the system, Fig. 6, the effect of the off-nominal turns-ratio upon the current flowing into bus p must be taken into account. In this case

$$\sum_q Y^{pq}(E_q-E_p)+(1+k)_{pl}\times\sum_m Y^{lm}(E_m-E_l)=0$$

whence

$$E_p=\frac{\sum_q Y^{pq}E_q+(1+k)_{pl}\sum_m Y^{lm}(E_m-E_l)}{\sum_q Y^{pq}} \tag{34}$$

The transformer requires that

$$E_l=(1+k)_{pl}E_p \tag{35}$$

In the application of this method to the computer, one (driving point) bus voltage is set equal to $1+j0$, the reference bus voltage is set equal to $0+j0$, and an initial voltage distribution assumed. The computer is then required to recognize which of the equations 32, 34, or 35 should be used for each bus, and perform the indicated calculation. When all voltages have been calculated, the calculation is repeated with the use of the improved set of voltages to calculate a further improved set. When the desired convergence has been achieved, the input current to the system is calculated and the self- and mutual impedances determined. The actual computer program includes the use of an "accelerating factor" to speed the convergence of the voltages to final values

Consider, for example, the case in which bus 1 is energized with a voltage of $1+j0$.

Table II. Branch Flows and Voltages Due to Impressing 1+j0 at Bus 1

Branch	I_{branch}	E_{branch}	I_{bal}	I_{total}	$Z_{branch}\ I_{total}$
1	0	0	−0.30468−j0.00419	−0.30468−j0.00419	−0.01227−j0.03857
2	0	0	−0.54547+j0.01457	0.54547+j0.01457	−0.00271−j0.01986
3	1.09+j0	0.00654+j0.15260	−0.55566+j0.01484	0.53434+j0.01484	+0.00113+j0.07490
4	1+j0	0.02800+j0.08400	−0.30468−j0.00419	0.69532−j0.00419	+0.01982+j0.05839
5	0	0	−0.54547+j0.01457	−0.54547+j0.01457	−0.00395−j0.06621
6	0	0	−0.54547+j0.01457	0.54547+j0.01457	−0.00271−j0.01986
7	1+j0	0.02800+j0.08400	−0.81447+j0.00942	0.18553+j0.00942	+0.00440+j0.01585
8	1+j0	0.02800+j0.08400	−0.81447+j0.00942	0.18553+j0.00942	+0.00440+j0.01585
9	0	0	−0.30468−j0.00419	−0.30468−j0.00419	−0.01636−j0.05142

The first assumed values of voltages at all busses are tabulated in Table IV under iteration no. 0. In the calculation of any given voltage, the improved value of all other voltages is used. The voltages are determined in the order of the listing of the busses in Table IV.

As a typical step, consider the calculation of E_4. In general

$$E_4 = \frac{Y^{4-1}E_1 + Y^{4-7}E_7 - (1+k)_{4-8}Y^{5-2}(E_5 - E_2)}{Y^{4-1} + Y^{4-7}} \tag{36}$$

The values of E_2 and E_5 for the first iteration are zero, as shown in Table IV. The first iteration for E_4 is then

$$E_4 = \frac{(3.571-j10.714)(1+j0)+(3.571-j10.714)(0)-(0.93458)(0.271-j8.222)(0-0)}{3.571-j10.714+3.571-j10.714} \tag{37}$$

$$=0.5+j0$$

An appropriate accelerating function is

$$E = 1.3(E_{new} - E_{old}) + E_{old}$$

Therefore

$$E_4 = 1.3(0.5-0)+0 = 0.65+j0$$

The values for the first iteration for the remaining bus voltages are shown in Table IV under iteration 1.

The second iteration for E_4 using the appropriate values of other voltages from Table IV is given by

$$E_4 = \frac{(3.571-j10.714)(1+j0+0.42250+j0)-0.93458(0.271-j8.222)\times(0.60747-0.18294+j0.01071)}{7.142-j21.428}$$

(Note that the best-known values of other voltages are used: E_5 and E_7 from the first iteration, but E_2 from the second iteration).

$$E_4 = \frac{(4.88993-j11.98125)(7.142+j21.428)}{510.1673}$$

$$=0.57169+j0.03766$$

Use

$$E_4 = 1.3(0.57169+j0.03766-0.65-j0)+0.65+j0$$
$$=0.54820+j0.04896 \tag{38}$$

Table V gives the results of the iterations for the case in which bus 2 is energized with a voltage of 1+j0 and the initial values for the voltages on all other busses equal to the final values as shown in Table IV.

When a converged set of voltages has been calculated for a given bus energized at 1+j0 voltage, the input current at the energized bus can be calculated from a relation of the form

$$I^n = \sum_q Y^{nq}(1-E_q) + \sum_m (1+k)_{nl} Y^{lm}(E_l - E_m) \tag{39}$$

With input current and all bus voltages known, the self- and mutual impedances are obtained by dividing the bus voltages by the impressed current.

Table III. Computer Results of Method II, Bus 1 of Fig. 3 Energized

Bb	R	X
0903	0.001133	0.074898
0802−	0.001235	0.081639
0708	0.005641	0.097489
0407	0.010047	0.113339
0104	0.029866	0.171630
1001	0.017595	0.133067
0809	0.001234	0.081648
0903	0.001133	0.074898
0802−	0.001235	0.081639
0708	0.005641	0.097489
0407	0.010047	0.113339
0501−	0.009390	0.105924
0205	0.005441	0.039710
0602	0.002728	0.019859
0306	0.000015	0.000008

Application of Automatic Digital Computer

GENERALITY OF THE METHOD

The methods set forth thus far in the paper are general procedures which could be carried out by slide rule on small networks. However, for the size of network frequently encountered in utility transmission systems, the magnitude of the calculating effort would, of course, make such an approach impractical. Thus, in the past these impedances have generally been obtained by network analyzer measurements. The digital methods set forth in this paper are appropriate for stored-program digital computers.

A stored-program computer is one in which a large internal data storage is present where both the instructions and the constants used in a particular problem may be read in initially and called up for action with very little delay. These computers are generally referred to as medium and large-sized units as compared to the simple multiplier now used in many punched-card installations for financial calculations.

COMPUTER USED IN DEVELOPMENT

The specific computer used by the authors in the development of these methods was the International Business Machines type-650 magnetic drum data-processing machine. The type-650 is characterized by the fact that its main data storage is a magnetic drum rotating at a speed of 12,000 rpm, on which are arranged storage positions for 2,000 10-decimal digit numbers with their sign. The average time in which a number may be obtained from the drum is 2.4 milliseconds. The approximate operating times are, in milliseconds: for multiplication, 12.5; for division, 16.5; and for addition, 3.5 milliseconds.

The communication with the computer is in terms of standard punched cards with the input reading at a rate of 200 cards

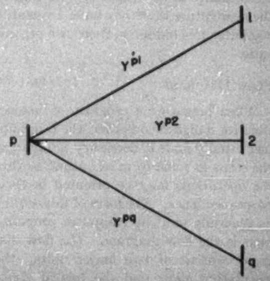

Fig. 5. Notation for nodal circuit analysis

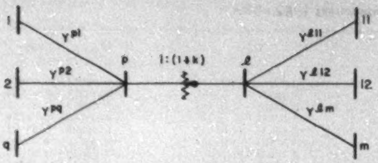

Fig. 6 (above). Nodal circuit analysis with off-nominal turns-ratio transformers

Fig. 7 (right). General Electric Analytical Engineering Section type-650 computer installation

per minute and the output punching at the rate of 100 cards per minute. The instructions for this computer are of the single-datum address form. The 10-digit instruction word is composed of a 2-digit operation instruction (add, subtract, divide, multiply, shift), a 4-digit indication of the location in memory where the data are stored, (data address), and a 4-digit indication of where in memory the next instruction will be found. The *650* computer installation of the General Electric Analytical Engineering Section is shown in Fig. 7.

For example, the computer instructions for the operation (a), $(b)=c$ would be written as follows; see Table VI:

$a=12345.67891$ at address 1001
$b=023.4567891$ at address 1002
$c=289589.9649$ to be sent to 1003

This type of computer is so balanced that it is of approximately equal value for financial computations involving large volumes of input-output data as well as engineering computations which are generally characterized by a moderate amount of data and a fairly long calculating sequence. It has been indicated that many of the proposed installations are going to be in electrical utility companies. Thus, many utility engineers will find in the near future that they have a versatile computer tool hidden in their own organization.

FLOW DIAGRAMS

When preparing a program of instructions for a digital computer, the programmer usually finds it necessary to organize the steps in some form of outline so that the operations may be oriented in their proper sequence. The form of this outline as generally used by computer programmers is the flow diagram. The flow diagram consists of two major units: the calculating steps and the logical steps. The calculating sequence, consisting of many steps, may be represented by a single box on a flow diagram. A logical step is one in which there is a choice involved. In a digital computer, all choices are reduced to taking alternative instructions on negative values of certain numbers or by taking alternate instructions on zero values of certain numbers. A flow diagram is thus made up by connecting the arithmetic steps with logic steps with lines to indicate the sequence of operations.

Figs. 8, 9, and 10 show flow diagrams for methods I, II, and III, described earlier. These flow diagrams indicate only the major steps, and what appears to be a simple arithmetic box may, in turn, itself be represented by a detailed flow diagram, which it would usually be

Table IV. Results of Method III Iterations, Bus 1 Energized

	Iteration Number						
Bus	0	1	2	3	7	8	Final
1	$1+j0$	$1+j0$	$1+j0$	$1+j0$	$1+j0$	$1+j0$	$1+j0$
2	0	$0+j0$	0.18294 $-j0.01071$	0.21909 $+j0.00310$	0.22819 $+j0.00862$	0.22832 $+j0.00812$	0.22980 $+j0.00834$
3	0	0	0	0	0	0	0
4	0	0.65 $+j0$	0.54819 $+j0.04894$	0.65969 $+j0.02483$	0.64391 $+j0.05506$	0.65490 $+j0.05227$	0.65082 $+j0.05473$
5	0	0.60747 $+j0$	0.51232 $+j0.04573$	0.61653 $+j0.02320$	0.60178 $+j0.05145$	0.61205 $+j0.04885$	0.60824 $+j0.05114$
6	0	$0+j0$	0.11889 $-j0.00695$	0.10673 $+j0.00408$	0.11484 $+j0.00382$	0.11394 $+j0.00411$	0.11488 $+j0.00415$
7	0	0.42250 $+j0$	0.46755 $+j0.03179$	0.64173 $+j0.05469$	0.55687 $+j0.06173$	0.55901 $+j0.06395$	0.55681 $+j0.06400$
8	0	0.36615 $+j0$	0.54340 $+j0.07400$	0.47295 $+j0.07921$	0.46216 $+j0.07462$	0.46418 $+j0.07281$	0.46289 $+j0.07331$
9	0	0.33591 $+j0$	0.49853 $+j0.06788$	0.43389 $+j0.07266$	0.42399 $+j0.06845$	0.42588 $+j0.06678$	0.42466 $+j0.06725$
10	0	0.94685 $+j0$	0.76154 $+j0.04121$	0.77789 $+j0.03174$	0.76760 $+j0.03279$	0.77118 $+j0.03071$	0.76982 $+j0.03142$

Table V. Results of Method III Iterations, Bus 2 Energized

	Iteration Number						
Bus	0	1	2	3	7	8	Final
1	$1+j0$	0.60794 $+j0.05902$	0.64081 $+j0.00539$	0.65642 $-j0.00255$	0.65270 $-j0.01613$	0.65565 $-j0.01766$	0.65343 $-j0.01635$
2	0.22980 $+j0.00834$	$1+j0$	$1+j0$	$1+j0$	$1+j0$	$1+j0$	$1+j0$
3	0	0	0	0	0	0	0
4	0.65082 $+j0.05473$	0.72156 $-j0.00752$	0.73092 $-j0.01698$	0.74746 $-j0.02536$	0.72318 $-j0.03121$	0.71808 $-j0.02818$	0.72067 $-j0.03025$
5	0.60824 $+j0.05114$	0.67435 $-j0.00702$	0.68310 $-j0.01586$	0.69856 $-j0.02370$	0.67586 $+j0.02916$	0.67110 $-j0.02633$	0.67352 $-j0.02827$
6	0.11488 $+j0.00415$	0.61553 $-j0.00124$	0.46534 $+j0.00037$	0.51039 $+j0.00000$	0.50008 $+j0.00000$	0.49997 $+j0.00000$	0.50000 $+j0.00000$
7	0.55681 $+j0.06400$	0.60284 $+j0.02355$	0.62101 $+j0.00676$	0.54441 $+j0.02394$	0.56570 $+j0.00371$	0.56867 $-j0.00037$	0.56933 $+j0.00093$
8	0.46289 $+j0.07331$	0.50274 $+j0.03827$	0.37673 $+j0.06534$	0.41569 $+j0.03024$	0.41792 $+j0.02934$	0.41803 $+j0.03243$	0.41809 $+j0.03184$
9	0.42466 $+j0.06725$	0.46122 $+j0.03511$	0.34562 $+j0.05994$	0.38136 $+j0.02774$	0.38341 $+j0.02691$	0.38351 $+j0.02975$	0.38356 $+j0.02921$
10	0.76982 $+j0.03142$	0.50074 $+j0.05573$	0.53569 $+j0.02367$	0.55851 $+j0.00783$	0.55268 $+j0.00353$	0.55414 $+j0.00388$	0.55256 $+j0.00432$

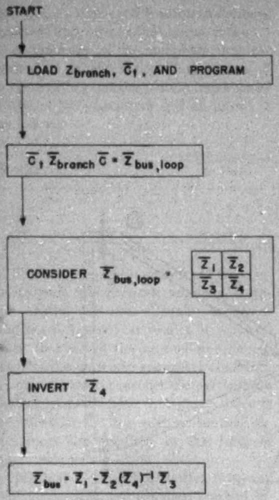
START
LOAD Z_{branch}, $\overline{C}_t$, AND PROGRAM
$\overline{C}_t\,\overline{Z}_{branch}\,\overline{C} = \overline{Z}_{bus,loop}$
CONSIDER $\overline{Z}_{bus,loop} = \begin{array}{|c|c|}\hline \overline{Z}_1 & \overline{Z}_2 \\ \hline \overline{Z}_3 & \overline{Z}_4 \\ \hline\end{array}$
INVERT $\overline{Z}_4$
$\overline{Z}_{bus} = \overline{Z}_1 - \overline{Z}_2(\overline{Z}_4)^{-1}\,\overline{Z}_3$

Fig. 8. Computer flow diagram for method I

necessary to develop before the detailed coding could proceed.

For example, consider the flow diagram of method II as shown in Fig. 9. The first major step consists of loading into machine memory the branch impedances, the connection matrix $\mathbf{C}_t'$, and the program for determining $\mathbf{Y}_{loop}$. Then, the calculation of the matrixes $\mathbf{Z}_{loop}$ and its inverse $\mathbf{Y}_{loop}$ is performed. Next, the generator index m is set equal to 1 and the remainder of the program and remaining data required are loaded. The foregoing has consisted of preparation for the main calculation which is to be repeated for each generator. This main calculation consists of initializing various voltages and currents by setting them equal to zero, and then performing the arithmetic necessary to develop the set of bus voltages throughout the system. With the arithmetic performed and the answers punched out, a test is made to see if this calculation has been performed for the last generator or if more similar calculations remain to be done. If more calculations remain, the index m is increased by 1 and another pass through the main calculating loop is made. Eventually, m becomes equal to M, the total number of generators; and the calculation is complete.

Table VI. Computer Instructions

Location of Instruction	Instruction			Description
	Operation	Data Address	Next Instruction Address	
0500	60	1001	0501	Reset add a
0501	19	1002	0502	Multiply by b
0502	31	0008	0503	Shift right 8 and round
0503	20	1003	0504	Store result c

Study With Large System

The power system of Fig. 11 was used as an example in order to assist in judging the merits of the various approaches described. This system consists of 30 busses,

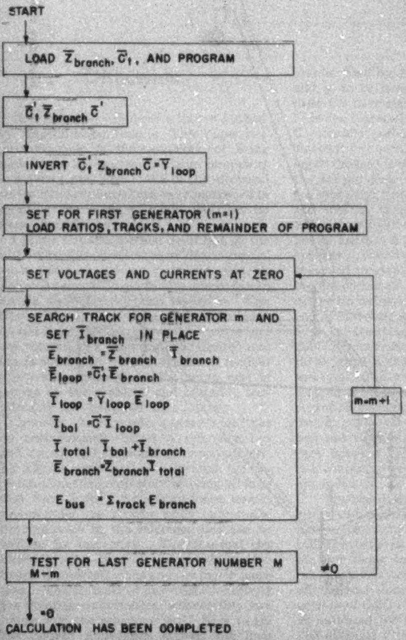
START
LOAD $\overline{Z}_{branch}$, $\overline{C}_t$, AND PROGRAM
$\overline{C}_t'\,\overline{Z}_{branch}\,\overline{C}'$
INVERT $\overline{C}_t'\,Z_{branch}\,\overline{C} = \overline{Y}_{loop}$
SET FOR FIRST GENERATOR (m=1)
LOAD RATIOS, TRACKS, AND REMAINDER OF PROGRAM
SET VOLTAGES AND CURRENTS AT ZERO
SEARCH TRACK FOR GENERATOR m AND SET $\overline{I}_{branch}$ IN PLACE
$\overline{E}_{branch} = \overline{Z}_{branch}\;\overline{I}_{branch}$
$\overline{E}_{loop} = \overline{C}_t'\,\overline{E}_{branch}$
$\overline{I}_{loop} = \overline{Y}_{loop}\,\overline{E}_{loop}$
$\overline{I}_{bal} = \overline{C}'\,\overline{I}_{loop}$
$\overline{I}_{total}\;\;\overline{I}_{bal} + \overline{I}_{branch}$
$\overline{E}_{branch} = \overline{Z}_{branch}\overline{I}_{total}$
$E_{bus} = \Sigma_{track}\,E_{branch}$
m=m+1
TEST FOR LAST GENERATOR NUMBER M
M−m
≠0
=0
CALCULATION HAS BEEN COMPLETED

Fig. 9. Computer flow diagram for method II

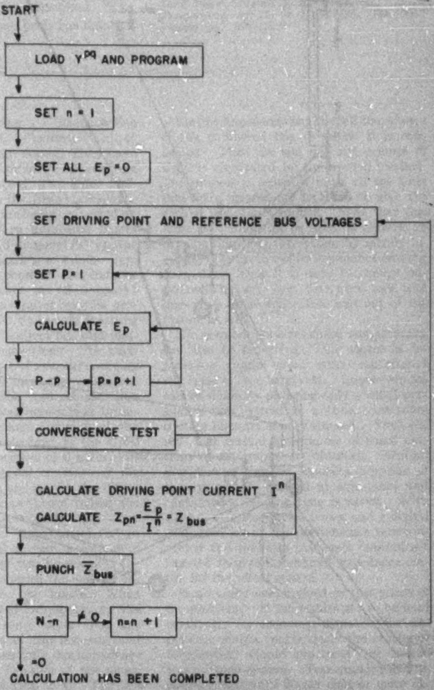
START
LOAD Y^{pq} AND PROGRAM
SET n = 1
SET ALL $E_p = 0$
SET DRIVING POINT AND REFERENCE BUS VOLTAGES
SET p = 1
CALCULATE E_p
P−p
p = p+1
CONVERGENCE TEST
CALCULATE DRIVING POINT CURRENT I^n
CALCULATE $Z_{pn} = \dfrac{E_p}{I^n} = Z_{bus}$
PUNCH $\overline{Z}_{bus}$
N−n
≠0
n=n+1
=0
CALCULATION HAS BEEN COMPLETED

Fig. 10. Computer flow diagram for method III

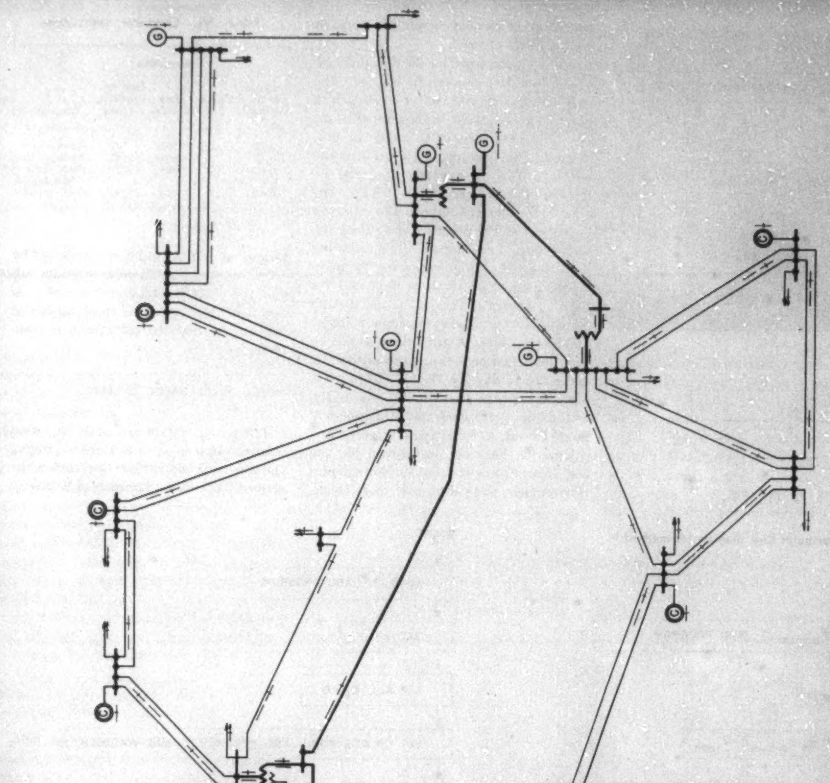

Fig. 11. Illustrative system study

38 lines, 14 loops, and 5 autotransformers representing off-nominal turns ratios.

A summary of the computer time required to obtain the self-impedances of all generators and the mutual impedances between the generators and all busses is as follows:

Method	Computer Time in Hours
I	4
II	1
III	2

The time to obtain and record these results from the network analyzer is approximately 4 hours. Usually, in obtaining network analyzer results, it is necessary to average the mutual impedances to obtain a perfectly symmetrical matrix.

The digital approaches are particularly advantageous when: 1. high accuracy is required, and 2. the self and mutual impedances are required in the form of punched cards.

Method I requires a shorter program, but more data storage than method II. It is thought that it will, in general, be easier to prepare the problem for solution by method I than by method II. These two programs are prepared for a maximum of 15 loops and 60 lines but may be extended by using cards as temporary storage. Methods I and II require the inversion of a matrix in size equal to the number of loops and, consequently, they are both limited in this respect. For a system with a very large number of busses, the calculating time for method I becomes prohibitvely long because of the matrix operations required by equation 20. For all three methods, the computing times become more nearly equal for smaller systems.

The preparation of the problem for solution will be the simplest by method III. Also, method III is much less limited with respect to size of network that can be handled in the *650* than methods I and II.

Conclusions

Three methods of obtaining self- and mutual impedances suitable for use in high-speed internally programmed digital computers have been described. The application of these methods has resulted in more economical calculation of transmission loss equations. These methods are also suitable for determination of other forms of driving point and transfer impedances. It is thought that electric utility engineers will continue to find many other problems for which automatic digital computers will provide more accurate and economical solutions.

References

1. American Standard Definitions of Electrical Terms, *ASA C42-1941*, American Standards Association, New York, N. Y., 1941.

2. Power System Stability (book), S. B. Crary. John Wiley and Sons, Inc., New York, N. Y., vols. I and II, 1945.

3. Analysis of Total and Incremental Losses in Transmission Systems, L. K. Kirchmayer, G. W. Stagg. *AIEE Transactions*, vol. 70, pt. II, 1951, pp. 1197–1205.

4. Loss Formulas Made Easy, A. F. Glimn, R. Habermann, Jr., L. K. Kirchmayer, G. W. Stagg. *AIEE Transactions*, vol. 72, pt. III, Aug. 1953, pp. 730–37.

5. Tensor Analysis of Networks (book), G. Kron. John Wiley and Sons, Inc., New York, N. Y., 1939.

6. Digital Load Flow Studies, L. A. Dunstan. *AIEE Transactions*, vol. 73, pt. III-A, Aug. 1954. pp. 825–832.

7. Automatic Digital Computer Solution of Load Flow Studies, J. M. Henderson. *AIEE Transactions*, vol. 73, pt. III-B, 1954 (Feb. 1955 section), pp. 1696–1702.

Discussion

R. Bruce Shipley (Tennessee Valley Authority, Chattanooga, Tenn.): This paper is a good example of the advancement being made in the application of digital computers to network problems. We of the electrical utility industry have been very backward in adopting the methods made available by Kron about 20 years ago.

I prefer the first method described by the authors because it seems more direct and because I have had some experience with it. The slowness of this method is surely due to matrix multiplication and inversion. Can this be improved by using other techniques? Would it be faster to eliminate one row and one column at a time until the desired matrix is obtained? A modification of method I providing more flexibility, more ease in setting up the problem, and probably considerably less computer time follows.

Consider, for example, a system that has no transformers. Select a reference bus and number all other busses consecutively. By Kron's mesh method determine the impedance matrix completely ignoring all lines that form loops. This impedance matrix representing the system when only radial lines connect to the reference bus can be written by inspection. The diagonal elements are the sums of the impedances between the reference bus and the bus in question. The mutuals (if any exist) are simply the common impedances between any two busses and the reference bus. Now to get the desired impedance matrix, the lines that were ignored are inserted one at a time. This is done by forming a **C** for each line that is to be inserted. Fortunately all of these **C**'s have the same form. They have *l*'s in the diagonal. The last column of the **C** contains off-diagonal *l*'s. The "off-diagonal *l*'s" occur in the rows corresponding to the busses that are being connected by the subject line. When numbered busses are connected, two "off-diagonal *l*'s" appear and one of them carries a minus sign. When the subject line connects the reference bus to another bus, only one off-diagonal *l* appears. Thus the computer may be programmed to give $\mathbf{C}_t\mathbf{ZC}$ by merely inserting the impedance of the subject line and indicating its terminal connections. The engineer is thereby relieved of ever determining a **C** or inserting it into the computer. $\mathbf{C}_t\mathbf{ZC}$ has one more row and column than the original **Z** that was determined by inspection. The rows and columns of the original **Z** remain unchanged in the $\mathbf{C}_t\mathbf{ZC}$ operation since this portion of **C** is the unit matrix. The off-diagonal elements of the new row and column are merely the difference between two impedances (when the line connects two numbered busses) which are indicated by the "off-diagonal *l*'s" in **C**. The new diagonal element is the sum of self-impedances of the two busses plus the line impedance minus twice the mutual impedance between the two busses. When the line being inserted terminates on the reference bus and some other bus, the off-diagonal elements of the last row and column of $\mathbf{C}_t\mathbf{ZC}$ contain only one impedance as indicated by the location of the single "off-diagonal *l*" appearing in **C**. The last diagonal element of $\mathbf{C}_t\mathbf{ZC}$ contains the sum of the line impedance and the self-impedance of the numbered bus to which it is connected. Then the last row and column of $\mathbf{C}_t\mathbf{ZC}$ is eliminated by the normal method. The process is repeated until all the lines that were ignored are included to give the desired impedance matrix. Note that this same procedure can be used to remove an existing line from the system by merely inserting the negative of its impedance into the computer. Thus it is eady to change impedances of any lines that were used and lines may be switched into and out of the system at will.

A-c network analyzer speed and accuracy can also be improved. One source of inaccuracy results from stray capacitance currents in the analyzer. Improvements can be made by plugging only a small portion of the system at a time. Interconnecting lines are simply ignored. Thus the self- and mutual impedances of small portions of the system are obtained. Mutual impedances between separate portions of the system are ignored at this point and considerable reading time is saved. With the use of a connection tensor and a digital computer, all of the portions are interconnected and the lines that were omitted are inserted to give the desired impedance matrix for the whole system.

Is accuracy overstressed in this phase of the problem? If the results are to be used eventually for economic dispatch, the impedance matrix (particularly the resistance component) should represent the actual transmission system. Transmission-line resistance may vary 20 per cent or more depending upon the ambient temperature and the line current. The importance of accuracy is further deemphasized if the usual *B* constant assumptions are introduced. If *B* constants must be used, they should be derived so that *PB* gives the correct value for the partial derivative. *B* constants derived for the purpose of making *PBP* check the transmission losses can introduce appreciable error in the *PB* product.

H. W. Hale and **J. B. Ward** (Purdue University, Lafayette, Ind.): This paper makes a significant contribution to the art of transmission system analysis. At present, there is a definite need for the accuracy of digital methods in the calculation of network impedances for use in loss equations. While published results[1] have demonstrated a close correlation between the losses determined by summing RI^2 over all lines and those determined by the application of loss equations, there have been no means of allocating the observed discrepancy to specific factors.

The discussers have long been of the opinion that the inaccuracies involved in the measurement of the network impedances may cause substantial error in the loss equation coefficients. The use of digital methods in the computation of the impedances will eliminate this source of error and should result in improved loss equations. In addition, with this source of unknown error removed, it should be possible to make a thorough evaluation of the inaccuracies resulting from various assumptions and approximations.

We wish to raise a point concerning the methods used in the present paper. It appears that the three methods are based on the condition that the reference bus voltage is zero. In effect this approach determines the network impedances for the specific case of the neutral terminals of the autotransformers being connected to the reference bus. This is not a true representation of actual system conditions. Kron[1] has shown that, provided certain conditions are met, such a representation is proper; however, the limitations of such an equivalent should be recognized in order for it to be used intelligently.

It is deemed likely that, as digital methods are developed for treating an increasing number of transmission system problems, the digital calculation of network impedances will become increasingly important. The authors are to be commended for their timely contribution to this phase of network analysis.

REFERENCES

1. See reference 3 of the paper.
2. TENSORIAL ANALYSIS OF INTEGRATED TRANSMISSION SYSTEMS—PART II, Gabriel Kron. *AIEE Transactions*, vol. 71, pt. III, 1952, pp. 505–12.

E. E. George (Ebasco Services, Inc., New York, N. Y.): This paper contains much information that is interesting and useful. The table comparing the three methods of impedance calculation is of especial value.

It is difficult for the average engineer to understand these methods unless he works them out long-hand for a small system. This presupposes familiarity with matrix multiplication, a subject neglected in many recent books on engineering mathematics and in our usual engineering handbooks.

There are several minor details of the paper which might confuse the inexperienced reader. Under method I, two chains of loop voltages are included in the transformation matrix, but the basic principle (independent meshes) involved in their selection is nowhere explained.

Equations 12 and 20 would be easier to follow if the order of multiplication and the order of forming rows and columns in multiplying the matrices were designated by arrows or otherwise. There are conventional standards for these things, but how do you find them when you need them?

The authors are to be commended for spelling out some of the subscripts for various quantities. This makes the paper much easier to read because it lessens the number of symbols which have to be kept in mind.

Equation 16 is a conventional abbreviation for a large compound matrix but it would help to explain that $\mathbf{Z}_1$ represents the bus terms, $\mathbf{Z}_4$ the loop terms, $\mathbf{Z}_3$ the loop to bus mutuals, etc.

The derivation of the accelerating function is evident after the final iteration, but how does one proceed to find this function when working the problem for the first time? The accelerating function is needed because the solution, like most admittance methods, is very slow to converge. If voltages instead of currents are required, it seems that very few iterations would be needed because most voltages on a power system are close to 100 per cent, but line currents can have any value. Mathematicians favor the admittance method because it is easier to modify the network for transmission-line changes, but there appear to be other ways of taking care of this problem when working with the impedance method.

It might be interesting to know how methods I, II, and III would compare in time if a *701* or similar large computer were available for matrix inversion, using the *650* computer for the balance of the work. Method I appears to be the most direct for typical conditions.

Tsai H. Lee (The Detroit Edison Company, Detroit, Mich.): The digital computer has made mathematics an attractive and practical tool in power system analysis. The authors have provided an excellent demonstration as to what can be done when mathematical rigor is combined with the digital computer to analyze a classical network problem. It is time for power system engineers to examine critically many of the traditional problems solved by slide-rule and a-c network analyzers. Some of the problems known to be under investigation by various companies interested in applying digital computers to system engineering include:

1. Network impedance calculations.
2. Short-circuit calculations.
3. Load flow studies.
4. Stability studies.
5. Loss studies.
6. Microwave relaying.
7. Preparation of impedance data from equipment punched-card file.
8. Parameter study in bundle conductor design.

The author's statement that the digital method provides greater accuracy is really an understatement. We have found that in cases where the resistance is required in network impedance calculations, the results from the a-c network analyzer are far from satisfactory. For example, the resistance is required in the leakage impedance matrix for the loss formula, and in the determination of system X/R ratios for circuit breaker applications. The inherent limitations of the a-c network analyzer in angle measurements and the fact that most system impedances have angles around 60–80 degrees led us to use the digital method for the leakage impedance matrix in our 1954 loss study.

The method we used was essentially "Method II, Using Impressed Currents." A leakage matrix impedance was developed for the 120-kv system containing 12 loops and about 50 elements. Since we did not have the IBM *650* at that time, we used the UDEC at Wayne University for matrix inversion, and the IBM *604* for the other calculations. The symmetry of the leakage impedance matrix provided a convenient check on the results. The UDEC-*604* procedure is quite satisfactory, although rather time-consuming.

At present we are converting this into a *650* program which is capable of handling systems up to 26 loops. This larger system is possible by making the matrix inversion a separate *650* run. Further savings in *650* storage can be achieved by storing only the upper half of the symmetric matrix. The program makes use of a "complex arithmetic interpretive routine" which makes the *650* behave as if it were a complex arithmetic computer. Programming network problems is very simple using this method.

Matrix inversion generally has limitations other than available computer storage, e.g., round-off errors and the number of useful digits in the inverse. Most power-system loop impedance matrices have large diagonal elements which make them better-behaved than matrices from many other physical systems. It would be appreciated if the authors can tell of their experiences in inverting power system matrices, especially the higher order ones.

A. F. Glimn, R. Habermann, Jr., J. M. Henderson, and **L. K. Kirchmayer:** Several interesting points have been raised by the discussers.

Mr. Shipley has proposed a method somewhat parallel to method I but probably a great deal shorter in calculation time. The method of closing a radial network, ("tree"), one loop at a time looks promising. With no experience with the method, we would expect a favorable computer time comparison with method II.

Our concern with accuracy deserves a few words of explanation. We define error or inaccuracy as the difference between actual and observed or calculated value of a quantity; a mistake as an error due to misunderstanding or inadventure; and a blunder as an error resulting from ignorance or carelessness.

Automatic digital computation reduces the opportunities for mistakes and blunders to which such mass data handling as the determination of network impedances is subject. In addition, the accidental and systematic errors peculiar to analogue computation do not appear in digital calculation. Accidental errors arise from such sources as imperfection of the observer's senses, the effects of voltage fluctuations, heat, etc., upon the instruments, or other unavoidable causes. Systematic errors result from such causes as the observer's bias in reading the instrument and instrument calibration. The numerical process errors of truncation and round-off error, such as exist in digital computation, are negligibly small.

The foregoing indicates that much of the error heretofore met in impedance determination is reducible. We believe such reduction should be made since it is economically justified.

As suggested by Mr. Shipley, we also have found interconnection procedures useful for systems too large for the network analyzer or for a digital program. We have used similar procedures for the interconnection of loss formulas.[1]

We agree with Dr. Hale and Dr. Ward that the elimination of network impedance measurement error should result in improved loss equations. Regarding their statement that grounding the reference bus in the determination of the network impedances is not a true representation of actual system conditions, we have the following comments:

Kron has shown[3] that a tensor equation properly representing system performance is

$$\mathbf{E}_j - \mathbf{t}_j{}^* E_R = \mathbf{Z}_{jk}\mathbf{I}^k + (\lambda_j - \lambda_j{}^*) Z_{aa} I^n \qquad (40)$$

$$E_R = -Z_{aa} I^n$$

where Z_{jk} are the network impedances described in the subject paper, and

E_R = reference bus voltage

I^n = current supplied to the system when the reference generator is energized and all other loads and generators are disconnected. This current is the sum of the autotransformer neutral currents for this condition and is due to off-nominal turn ratios in the network loops

$Z_{aa} = -\dfrac{E_R}{I^n}$ = the self-impedance between the junction of the autotransformer neutrals and the reference bus

t_j = the ratio of current flowing in the short-circuited reference generator to the current flowing in generator j when network impedances are determined as described in the paper

$\lambda_j = 1 - t_j$

Where off-nominal turn ratios are such that the expression $(\lambda_j - \lambda_j{}^*)$ is not negligible, equation 40 is necessary completely to specify network performance.

The t_j and λ_j are easily calculated from the impedances determined in the paper since the impedances are, in fact, the voltage distribution when $1+j0$ current is impressed at generator j. Furthermore, all line currents are readily available in method II so that t_j may be determined by taking the ratio of the current in the reference generator and that in generator j.

Mr. George has raised the point that some principle for the selection of the independent meshes should be explained. It is our practice to inspect the loop transformation matrix to see that each element in the network appears at least once in the matrix unless such element is radial. From a count of the number of busses and elements in the network, we determine the number of loops required, and we use the matrix in a generic check to be sure that the sum of the currents entering each bus is zero. It can be shown[3] that for a single network,

$$\mu = \text{number of independent meshes} = \gamma - \alpha + 1 \qquad (41)$$

where

α = the number of junctions in the network and γ is the number of elements (impedances plus ratio transformers) in the network

Our choice of the accelerating function is mainly the result of experience in a great many iterative solutions of digital studies. As pointed out by Mr. George, method III is extremely slow to converge unless some accelerating means is used.

The use of a "complex arithmetic interpretive routine," as suggested by Mr. Lee, does indeed make programming of a study such as network impedance determination very simple. It must be remembered, however, that the price of such simple programming is extra computer operating time

Our experience in inverting power system matrices is simply that we have had no trouble—yet; we have performed such studies on five systems, each less than 15 loops. Our inversion program, and, in fact, all programs indicated in the paper, are written in fixed decimal point arithmetic. However, a floating point inversion program is available if our present procedure fails on a particular system.

The authors wish, of course, to thank the discussers for their comments and suggestions. We anticipate, along with the discussers, that digital computers will becom of increasing value to power system engineers.

REFERENCES

1. ANALYSIS OF LOSSES IN LOOP-INTERCONNECTED SYSTEMS, A. F. Glimn, L. K. Kirchmayer, G. W. Stagg. *AIEE Transactions*, vol. 72, pt. III, Oct 1953, pp. 944–53.

2. See reference 2 of H. W. Hale and J. B. Ward discussion of the paper.

3. TENSOR ANALYSIS OF NETWORKS (book), Gabriel Kron. John Wiley and Sons, Inc., New York, N. Y., 1939.

A New High-Capacity Anode Air Circuit Breaker

S. A. BOTTONARI
MEMBER AIEE

J. H. SPROW
ASSOCIATE MEMBER AIEE

THE past 15 years have seen a great increase in the installed capacity of mercury-arc rectifiers for transportation, industrial, and electrochemical applications. The trend toward higher d-c operating voltages, higher unit rectifier ratings, and larger grouping of units, particularly in electrochemical services, has imposed increasing duty on rectifier switching equipment.[1] To meet these present and future demands, and also to incorporate improvements indicated by the industry's past experience, a new anode circuit breaker has been developed.

Anode circuit breakers are used in each anode circuit of a mercury-arc rectifier unit for automatically isolating an anode which conducts current in the reverse direction, a condition ordinarily called arc back or sometimes backfire. The use of anode breakers for clearing arc backs minimizes momentary circuit disturbances, and reduces the stresses on associated equipment by quickly clearing the fault. Without the use of anode breakers, an entire rectifier unit must be tripped out of service by the opening breakers on both the d-c and a-c sides to permit the faulted rectifier anode to recover. The anode circuit breaker, by interrupting the circuit between the transformer and the anode, in effect opens both sides at once and no other switching operation is required to interrupt the arc back.

On normal load, the anode breaker carries pulsating unidirectional current. When an arc back occurs, current flows in the reverse direction to normal and substantially the transformer winding is subjected to a short circuit. If other units are in parallel with the arcing-back unit, their d-c output is also fed into the arc back, and this also passes through the corresponding pole of the anode breaker.

Paper 55-722, recommended by the AIEE Switchgear Committee and approved by the AIEE Committee on Technical Operations for presentation at the AIEE Fall General Meeting, Chicago, Ill., October 3-7, 1955. Manuscript submitted June 7, 1955; made available for printing July 22, 1955.

S. A. BOTTONARI and J. H. SPROW are with the Westinghouse Electric Corporation, East Pittsburgh, Pa.

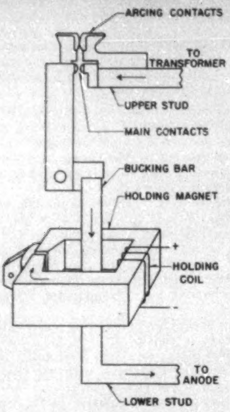

Fig. 1. Diagram of circuit-breaker operation

Thus, in effect, the anode breaker in interrupting an arc-back must open an a-c fault having a high d-c component, so that the total fault current does not naturally pass through zero as in an ordinary a-c fault. This condition requires that the interrupter of an anode breaker must be designed and built similar to a d-c breaker. This means that, in the present state of the art, it must develop sufficient arc resistance to reduce the current to zero, i.e., a higher arc voltage as compared to the requirement in a-c arc interruption.

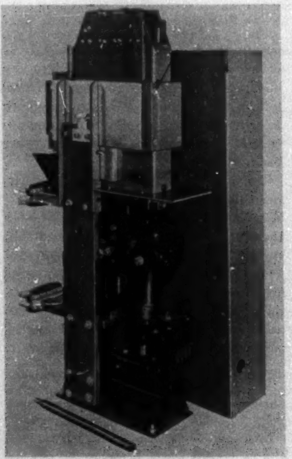

Fig. 2. Single-pole assembly

Because of the high magnitude of arc-back currents in present systems, anode breakers are of the high-speed type,[2] which means substantially that, for arc backs occurring at the normal point of transition from conduction to nonconduction, the duration of the arc-back current must be limited to one loop of current; i.e., it must be forced to zero after having reached its first crest.

Since the arc-back current is reverse to normal load current, the anode circuit breaker must inherently be a reverse current-tripping breaker. To achieve reverse current tripping, anode breakers generally employ a polarized holding magnet. When current flows in the normal direction, it sets up a magnetic flux aiding the holding magnet flux. A reversal of this current decreases the total flux, thus tripping the breaker. This is illustrated in Fig. 1.

In the development of this new type of anode breaker, certain design objectives were suggested by operating experience with preceding designs. The following features appear to be the most important:

1. Reliability of operation.
2. High-speed opening.
3. Mechanical and electrical simplicity.
4. Ease of inspection and maintenance.
5. Minimum number of parts.

In this list of prominent requirements the interrupting speed has been a subject of much discussion. There has been no small amount of opinion indicating that speed in an anode circuit breaker is of paramount importance. The authors hold that, while speed is of great importance, other duties are required of the anode breaker in actual service which are, so far as the designer is concerned, opposed to simple speed of interruption considered alone.

For one thing, the anode breaker pole must carry continuous loads of over 2,000 amperes and may approach 3,000 amperes in the near future. The amperes in this case are rms amperes of pulsating unidirectional current and not the simple direct current.[3] This current consequently causes more heating for equal numerical values than pure direct current and the corresponding design problem is more severe. The over-all problem imposes practical limits to the reduction in weight of the movable current-carrying parts such as the movable contact members.

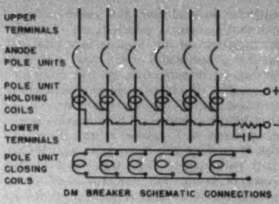

Fig. 3. Schematic diagram of 6-pole assembly

In anode circuit-breaker applications, nearly every interruption involves clearing a fault which would result in a maximum short-circuit current of a system. In addition, continuous processes do not permit convenient access to the equipment for servicing except at planned intervals. Both of these circumstances require that a circuit breaker operate with a minimum of attention during production periods. Although it is obviously impossible to build a breaker that will interrupt an indefinitely large number of faults without maintenance, the realistic design practice should be to make the over-all structure sufficiently durable so that inspection and maintenance is not required after each arc-back opening. This again forces the designer to incorporate more weight in high-speed movable parts than would be required if speed alone were the paramount criterion of performance.

Pole-Unit Construction

The anode circuit breaker under discussion is unique in that the assembly is made up of six identical pole units, Fig. 2, each of which is an independently operating unit. There is no mechanical tie between poles, and the only electrical tie is through

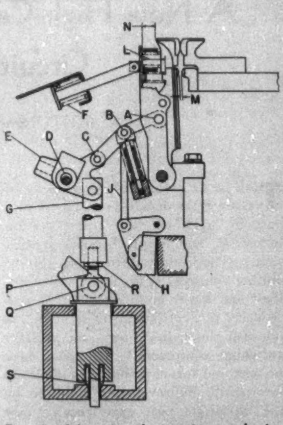

Fig. 4. Schematic of operating mechanism

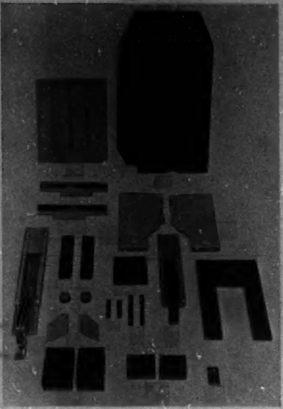

Fig. 5. Unassembled parts of arc chamber

control circuits. This completely eliminates all critical mechanical adjustments between the separate poles and, thereby, further reduces maintenance. The arrangement is shown schematically in Fig. 3.

Because of the random nature of anode faults, the breaker ordinarily remains closed for long periods of time, and then may trip and be reclosed several times before the system returns to stable conditions. Reliable tripping is obtained through the use of noncorrosive materials and adequate opening forces. Proper closing is somewhat more difficult to achieve because accumulations of foreign particles on the holding magnet surfaces may cause failure of the breaker to hold in. This difficulty is reduced by having the magnet holding surface in a vertical plane and by designing the magnet so that the holding magnetic flux can be increased sufficiently during the closing operation to hold the breaker during the closing impact. With an intentional series air gap in the holding magnet circuit, the effect of an increase in the armature air gap resulting from foreign particles will not cause the pole unit to fall open from a moderate decrease of holding force. Because of the vertical holding magnet surfaces, any dirt that does collect may be removed easily as the surfaces are readily accessible for cleaning and inspection.

The individual pole unit is closed quickly by means of a d-c solenoid. To obtain fast closing without excessive shock, the springs and linkage systems have been designed to match the force curve of the closing solenoid. The use of a solenoid on each pole unit not only provides desirable fast-closing action but entirely eliminates the necessity of making mechanical adjustments required when one closing device operates a 6-pole assembly.

High opening speed is essential in anode circuit-breakers to limit the magnitude of fault current which has a rapid rate of rise. To obtain high opening speed, the moving contact arm and toggle linkage must be carefully designed for minimum weight. The main contact fingers are made from a copper section to obtain maximum strength and heat dissipation and yet be as light as possible in weight. The moving toggle linkage is made of high-strength alloy to reduce the weight of moving parts. The moving contact current is conducted through a hinge joint instead of shunts because of simplicity, durability, small space requirements, and low weight.

Noncritical contact adjustment has been achieved without sacrificing speed of operation since there is a gap of 1/8 inch between the main contacts before the arcing contacts part. This also results in improved transfer of current from the main contacts to the arcing tips with only insignificant pitting of the main contact surfaces.

Fig. 4 shows the general construction of the contact-operating linkage. This shows the moving contact arm in the position where the arcing contact tips are just touching. The closing and opening linkage is comprised of pin *B*, Fig. 4, and the links on either side. Although pin *B* does not go over center, the toggle cannot collapse as long as the armature *H* is held by the magnetic attraction of the holding magnet. If the armature is released, pin *B* will move upward which causes its toggle to collapse and the moving contact arm will be pulled open by the spring *F*. Pin *C* remains nearly stationary until the contact arm is open, then it is moved upward by the retrieving spring *S* in the closing magnet.

The closing toggle is comprised of pin *C*, Fig. 4, and the links on either side. In this toggle, pin *C* moves over center, but it is prevented from moving further by the compressive force present in the pull rod *G* when the closing solenoid plunger hits the bottom of the closing magnet. This toggle can be closed or opened manually by inserting a maintenance handle *E* and raising or lowering the handle. If the armature is not held, the toggle nearest the moving contact arm will collapse and the breaker will open. The breaker can also be tripped with or without load current by simply de-energizing the holding coil circuit.

Fig. 6. Six-pole draw-out assembly

Arc-Chute Construction

The arc-interrupting element is of the magnetic "De-ion"[4] type especially modified for the development of high arc voltage and the interruption of high currents. It consists essentially of a U-shaped blowout magnet with a single blowout coil combined with a suitable arc chute. The arc chamber, enclosed in an insulating jacket, is located between the blowout magnet pole faces.

Fig. 2 shows the assembled blowout magnet and arc chute. Fig. 5 shows the unassembled parts of the arc chute. The deionizing element consists of spaced plates of fired refractory zircon porcelain cemented into a compact unit, similar to the ceramic arc chutes which have been used so successfully in a-c power circuit breakers. No asbestos composition is used where the arc will be exposed to it. The complete interrupter thus has high heat-shock resistance, low moisture absorption, and high dielectric strength. This results in an ability to withstand numerous arc interruptions with a low rate of deterioration.

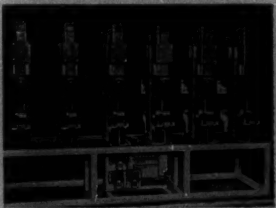

Fig. 7. Six-pole frame-mounted assembly

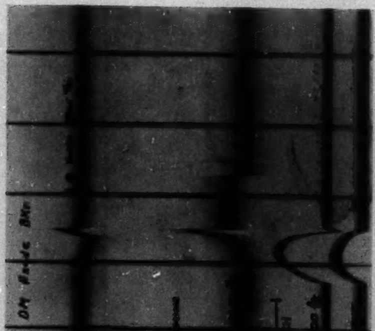

Fig. 8 Oscillogram of 750-volt d-c 6,000-kw test

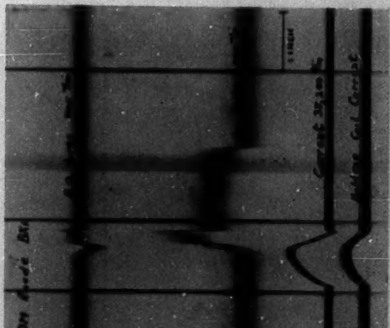

Fig. 9. Oscillogram of 1,500-volt d-c 6,000-kw test

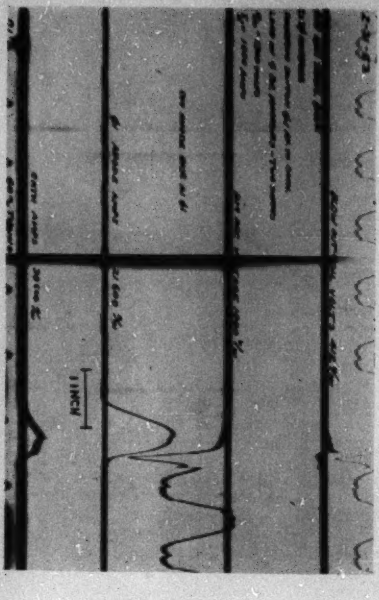

Fig. 10. Oscillogram of 1,300-volt d-c test with 4,000-kva rectifier feeding a 5,900-kw generator

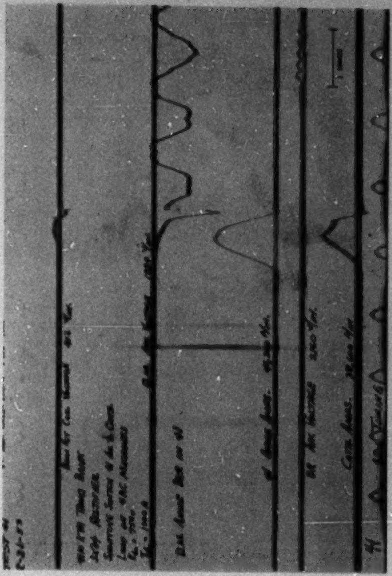

Fig. 11. Oscillogram of 750-volt d-c rectifier test

Table I. Results of Tests

Test	No. of 72,000-Ampere Potlines	Peak Current, Amperes	Time to Peak Current, Milli-seconds	Time to Extinction, Milli-seconds
1*	1	59,000	8.4	13.9
2*	1	60,000	9.3	13.9
3	1	48,000	8.8	12.5
4*	2	63,000	8.4	14.6
5*	2	62,000	8.4	13.9
6*	2	61,000	8.8	13.4
7*	2	61,000	8.4	13.9
8	1	44,000	4.6	12.1
9	1	34,000	4.6	12.1
10	1	52,000	7.9	13.4
11†	2	46,000	15.8	20.4
12	2	23,000	3.2	13.4

* Transition interruptions.

† Anode short-circuiting switch closed at 180 degrees after transition causing delay in anode circuit-breaker opening.

Application and Ratings

Referring to Figs. 6 and 7, the pole unit shown in Fig. 2 can be arranged in 6-pole assemblies for either draw-out or stationary mounting. These circuit breakers can be used in systems with ratings up to 1,000 volts d-c and 3,000 rms anode amperes. Each pole unit has an interrupting rating of 75,000 amperes.[3]

Tests

During the development of this anode circuit breaker, many laboratory tests of its interrupting performance were made. Direct-current tests were made on a machine combination of 6,000 kw total at 750 and 1,500 volts. Fig. 8 shows an oscillogram of the interruption of a full short circuit on this system at 750 volts. Final current would have been 80,000 amperes, but the breaker limited the current to 43,000 amperes in 7.5 milliseconds. Total interrupting time was 13 milliseconds. Fig. 9 shows a similar test at 1,500 volts on a system the final short-circuit current of which would have reached 40,000 amperes.

Simulated arc-back tests were made in the laboratory on a 4,000-kva 6-phase double-wye-connected rectifier in parallel with the 5,200-kw generator combination at 1,300-volt d-c output.

Arc backs were simulated by using a quick-make switch to short circuit the anode to which the breaker under test was connected. A total of 38 interruptions, resulting in eight tests of transition from conduction to nonconduction, were made. The transition openings resulted in 24,000- to 25,000-ampere crest anode currents. Peak inverse voltage, i.e., maximum open-circuit voltage across the breaker under test was approximately 2,500 volts. Fig. 10 shows a typical oscillogram made of a transition test on this setup.

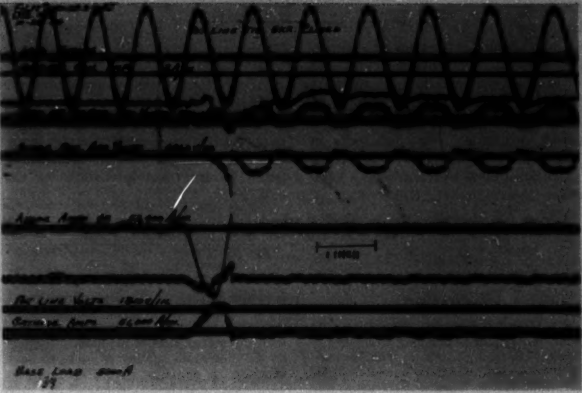

Fig. 12. Oscillogram of test on 650-volt d-c 145,000-ampere potline

Twelve tests were also made with the pole unit in one phase of a 6-phase rectifier which had an output of 750 volts d-c. Four of these interruptions occurred at transition which resulted in a crest anode current of 42,500 amperes and a peak inverse voltage of 1,150 volts. A typical oscillogram is shown in Fig. 11.

In addition to the laboratory interrupting tests, field tests were made on two of the largest potline supplies in this country. In one typical series of tests, a total of 24 simulated arc-back interruptions were made. Table I shows a representative group of 12 consecutive tests, part of which were on a single 72,000-ampere potline supply at a 650-volt d-c output and part of which were on two of the 72,000-ampere supplies connected in parallel. No maintenance, such as readjustment or replacement of parts, was required during the total of 24 arc-back interruptions tests. At the conclusion of the tests, the circuit breaker was still in satisfactory condition for continued service, both for carrying-current and arc-back interruptions. Table I shows

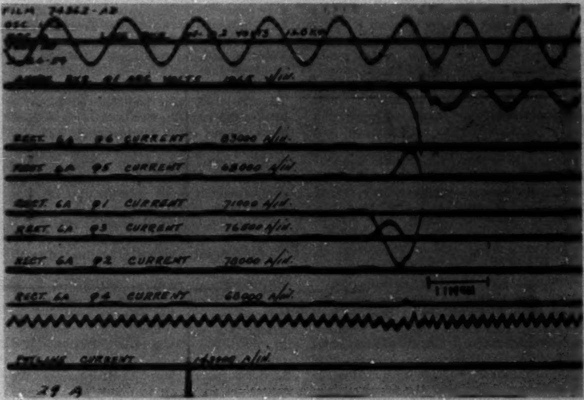

Fig. 13. Oscillogram of test on 850-volt d-c 125,000-ampere potline

the results of these tests, in six of which the simulated arc back occurred at transition which results in the maximum current to be interrupted. Arc-back current did not exceed 61,000 amperes and the total interrupting time did not exceed 14.6 milliseconds on the transition tests. A typical oscillogram can be seen in Fig. 12.

Additional tests were made on a large potline operating at 850 volts. A typical oscillogram of this test is shown in Fig. 13. During these tests, the breaker showed excellent performance with respect to consistency of operation, contact life, and stability of adjustments. This new design anode circuit breaker not only meets higher voltage and current requirements but also incorporates many operating and performance features of great interest and advantage to the industry.

References

1. FIELD TESTS OF A 100-MEGAWATT RECTIFIER INSTALLATION, J. K. Dillard, John Kiefer, C. S. Hague. *AIEE Transactions*, vol. 74, pt. I, May 1955, pp. 245–55.

2. LARGE AIR CIRCUIT BREAKER STANDARDS. *NEMA SG-3*, National Electrical Manufacturers Association, New York, N. Y.

3. POOL CATHODE MERCURY-ARC POWER CONVERTERS. *ASA C34.1-1949*, American Standards Association, New York, N. Y., 1949.

4. MAGNETIC "DE-ION" AIR BREAKER FOR 2,000–5,000 VOLTS, L. R. Ludwig, R. H. Nau. *AIEE Transactions (Electrical Engineering)*, vol. 59, Sept. 1940, pp. 518–22.

◆

Discussion

Robert N. Wagner (Aluminum Company of America, Pittsburgh, Pa.): The authors are to be congratulated on a well-written, clear and concise paper. But more important, the authors and their company are to be commended on the development of a completely new engineered piece of apparatus in a field where there has not been a wide choice of good devices.

The Aluminum Company of America has had one of these circuit breakers installed in one of their plants on a trial basis for about 1 year. While I have not seen the breaker personally, the engineers at the plant advise that the unit is well designed, simple, rugged, and apparently will have low maintenance. It has withstood many artificial and natural arc backs without requiring repair or replacement of parts. It is quiet in operation.

In the early model there were some details concerning auxiliary switches and linkages that showed up weaknesses and need improvement.

I have studied a large number of oscillograms of operations of the breaker. It seems that the average breaker time to peak current is about 10 per cent longer than what has been considered the optimum in the industry to date. This means 10 per cent higher peak current.

Apparently the breaker blowout features are so constructed that the arc is extinguished very rapidly after current peak. This is verified by the fact that most oscillograms show an overswing of the trace at zero. Undoubtedly this accounts for the fact that the voltage developed across the breaker is 30 to 50 per cent higher than previous experience.

Both of these characteristics are nominal in value, and it would be very difficult quantitatively to evaluate their effect on the life of the breaker or the other electric components of the circuit.

L. L. Baird (General Electric Company, Philadelphia, Pa.): The authors have pointed out that high opening speed is important in an anode circuit breaker but have wisely considered the other requirements of an anode air circuit breaker such as reliability and adequate service life. How well these factors have been evaluated and combined determines the worth of the design, and the contribution to the art.

The authors state that this anode breaker is unique in that six identical pole units are used, each of which is an independently operating unit. It is not entirely consistent with the stated aims of mechanical simplicity and minimum number of parts to have provided six separate closing mechanisms. The separate mechanisms have been used to "eliminate all critical mechanical adjustments between separate poles," but from the diagrams presented each pole has been provided with a mechanical adjustment which would not appear to be any less critical than if a mechanical tie was used between poles with a single closing mechanism.

In an anode breaker, it is desirable to have a combination of opening speed and interrupter action which will limit the crest value of the current loop as much as possible to reduce magnetic stresses on other circuit components. The oscillograms presented do not indicate sufficient arc voltage significantly to decrease the initial current peak. On circuits with higher rates of rise there would be even less limiting of the crest value.

In Figs. 10 and 11, the cathode current shows a sharp decrease at the time of peak anode current. Is this caused by the d-c machine circuit breakers opening? Whatever the cause, the anode breaker has been assisted in clearing the circuit.

Fig. 12 shows backup breaker arc volts. It appears that this breaker opened simultaneously with the anode breaker pole. Where is this breaker in the test circuit? Does it aid the interruption of the test breaker?

The oscillogram in Fig. 13 is interesting. The arc back was initiated on phase 1, but by the time the arc back is cleared, all other phases cease conducting. Were the other breaker poles tripped open by the rapidly decreasing forward current? Such action is undesirable for essential service applications in which only the phase having the arc back should be de-energized. Opening of the other breaker poles would also have aided the test pole to clear the circuit.

In the paper, under the heading of tests, no data have been presented to substantiate the continuous current rating of 3,000 amperes. What standard of heating performance was used in assigning this current rating?

S. A. Bottonari and **J. H. Sprow**: We appreciate and wish to thank Mr. Wagner and Mr. Baird for their interest and the comments that have been submitted.

Replying to Mr. Wagner's discussion, we wish to state the following.

1. The design of the auxiliary switch linkage has been changed to correct the mechanical difficulty that has been encountered.

2. Mr. Wagner points out that the average time to peak current is about 10 per cent longer than that considered optimum in the industry to date. This occurs because the contact lead or the gap between the main contacts when the arc tips part is about 50 per cent greater than in the previous designs. The following advantages are obtained:

(*a*). The adjustment of the contact lead is very much less critical.

(*b*). Maintenance is reduced and longer main contact life and adjustment results.

(*c*). Main contact surfaces are maintained in good condition for conducting of normal load current.

(*d*). Transfer of current from main contacts to the arc contacts during tripping operation of faults is improved.

(We feel that these advantages more than offset the 10 per cent increase in peak current.)

3. The development of arc voltage accounts for rate of decay of current, so consequently, this accounts for the higher arc voltages noted by Mr. Wagner. Fundamentally, high arc voltages are necessarily related to fast interruptions of direct currents.

In reply to Mr. Baird's discussion, many items were necessarily omitted for the sake of brevity, and we have the following comments on his questions:

1. The number of different parts used in a 6-pole installation of the new breaker is much smaller than the number of parts for a comparable integrated 6-pole breaker. Also, due to the simplicity of the closing solenoid, the total number of all parts is probably comparable with the number of parts for a motor-operated 6-pole breaker; at the same time, the use of crossbars, gear trains, motors, etc., has been eliminated. This also means a reduced inventory of variety for the user.

2. On the new breaker, provision has been made to adjust the main and stationary contacts of each pole, compared with the same adjustments on each pole of a 6-pole breaker. One additional adjustment on each solendoid, completely independent of other poles, should then be compared with the several related adjustments usually required with a motor mechanism. Our contention is that adjustments on the new

breaker are not so critical as those on single-panel 6-pole assemblies, which lends to greater simplicity as far as the user is concerned.

3. Speed has been considered from the standpoint of operational advantages as outlined in the comments given on Mr. Wagner's discussion. Further, the breaker has been tested for performance on the basis of systems limited to rates of rise of 10 million amperes per second.

4. In Fig. 10 and 11, the sharp cathode current drop is not due to any backup breaker action. This is a natural reduction of current that occurs when a single anode breaker-pole arcs back, and the remaining five poles do not arc back. A more complete treatise on this condition was given in a paper by Dillard and Baldwin.[1]

5. In Fig. 12, the illustration is not sufficiently clear to show that the backup breaker did not trip open until 4/7 of a cycle later. The trace which has been interpreted as arc-volts is actually a trace of the holding coil current, with the zero line given. The film actually shows the start of the anode cathode voltage across the backup breaker about 200 degrees after fault extinction. The backup breaker was in series with the breaker under test.

6. In Fig. 13, it will be noted that phases *3* and *5* of the same phase group as phase *1* have contributed all the fault current possible for this test. The purpose of the test was to check the interrupting ability of the anode breaker. All six phases were timed to trip intentionally for this test, but in actual practice only pole units conducting reverse current will trip out, as substantiated in many other tests with this and previous designs.

7. With regard to temperature rating of the breaker at 3,000 amperes, tests indicate that when the breaker is in an enclosure such as a cubicle, the maximum temperature rise is approximately 50 degrees. This is within the standard limits of 15 degrees above ambient permitted for an enclosure plus 50 degrees rise as permitted for class *A* insulation.[2]

References

1. Rectifier Arc-Back Study on the Analogue Computer, J. K. Dillard, C. J. Baldwin, Jr. *AIEE Transactions*, vol. 73, pt. I, July 1954, pp. 198–208.
2. See reference 2 of the paper, pt. II, p. 1.

Measurement of Resistance of Energized A-C Motor Windings

K. J. WALDSCHMIDT
ASSOCIATE MEMBER AIEE

A METHOD has recently been presented which allows the resistance of a-c windings to be measured while the circuit is energized.[1] The method to be described herein, although not as universally applicable as the previously described method, achieves the same end without the use of special equipment.

Discussion

One of the most widely used methods of determining the temperature rise of electric machinery operated at constant load is to measure the resistance of the windings after thermal equilibrium has been reached. The average temperature of the windings can then be calculated from the change in resistance over the measured ambient temperature value.

The conventional method of obtaining the hot resistance is to operate the motor at a constant load sufficiently long to establish thermal equilibrium, then de-energize the windings and measure the resistance. In many instances this method is entirely satisfactory, but it does have inherent disadvantages which may prove unsatisfactory for certain applications. These disadvantages are:

1. To determine when thermal equilibrium has been established, either the motor must be disassembled prior to testing and thermocouples inserted, or the test must be run an excessive period of time to be sure that the windings have leveled out thermally.
2. The rate of cooling of the windings is maximum immediately upon de-energization. A period of time elapses after de-energization before the resistance can be measured and the value obtained is therefore somewhat less than the value at shutdown. It is common practice to record a series of resistance readings at known time intervals after de-energization and extrapolate back to time of de-energization. This is not entirely accurate, especially if considerable time elapses before the first reading is obtained.
3. In certain continuous tests it may be necessary to obtain the resistance periodically without disrupting the test by stopping the motor.

Method

In order to use a Wheatstone bridge to measure the resistance of energized a-c windings, two conditions regarding the connection of the bridge must be fulfilled. First, the two points where the bridge is to be connected must be at very nearly the same alternating potential so that the bridge will not be damaged and, second, the incoming power lines must be at the same direct (bridge) potential so that the source resistance does not shunt the circuit being measured.

The circuit shown in Fig. 1 fulfills these two requirements. The motor and choke coil windings being balanced (or very nearly), the incoming power lines will be at the same direct potential and, consequently, the source resistance will not affect the resistance being measured. It should be pointed out that a center tap of the winding under test is necessary to apply this circuit; however, the great majority of present-day motors are of dual voltage and a center tap is therefore readily available on the high-voltage connection. For the choke coil it is quite convenient to use the secondary of a dual-voltage transformer or another single-phase motor of approximately equal rating. Fig. 2 shows the circuit used for 3-phase resistance measurement. Again, it is necessary to have a winding center tap available.

Interpretation of Bridge Reading

Examination of Figs. 1 and 2 shows the reading obtained on the bridge to be a series-parallel combination of the motor and choke coil windings. To convert the bridge reading to the desired line-to-line motor winding resistance, it is necessary to make certain assumptions which result in a negligibly small error.

Referring to Fig. 1, it is assumed that the resistance of M_1 is equal to that of M_2, and, likewise, C_1 is equal to C_2; in actual motors there is apt to be a small difference in resistance between these windings. It is therefore assumed that no bridge current flows into the source, i.e., both incoming power lines are at the same direct (bridge) potential. A discussion of the error introduced by this assumption is found in the Appendix.

Paper 55-731, recommended by the AIEE Rotating Machinery Committee and approved by the AIEE Committee on Technical Operations for presentation at the AIEE Fall General Meeting, Chicago, Ill., October 3–7, 1955. Manuscript submitted June 17, 1955; made available for printing August 15, 1955.

K. J. Waldschmidt is with the A. O. Smith Corporation, Milwaukee, Wis.

The author wishes to acknowledge the help of L. Makous, A. O. Smith Corporation, in conjunction with whom these circuits were developed.

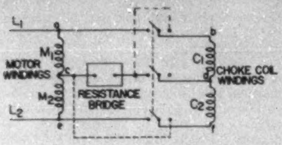

Fig. 1. Circuit for measurement of resistance of energized single-phase windings

In Fig. 1, denoting the resistance of each portion of the winding under test by M, that of each portion of the choke coil by C, and the bridge reading by R, the line-to-line winding resistance is

$$2M = 4(R - C/2)$$

If lead and switch resistances are not negligible, the equation will have to be modified slightly. Lumping the lead resistance between points a and b with C_1, between e and f with C_2, and considering these as new choke coil resistances C', the line-to-line winding resistance is

$$2M = 4[R - (R_B + C'/2)]$$

where R_B is the lead resistance associated with the bridge between points c and d.

For Fig. 2 the line-to-line winding resistance is given by

$$2M = 6R - 2C$$

where M, R, and C have the same connotation as for the single-phase case. If the lead resistance is not negligible, it is necessary to make a slight circuit change to keep the circuit balanced. Denoting the lead resistance between points a and b, c and d, and e and f (all assumed equal) by R_L, insertion of a resistance 3/2 R_L between points h and K results, for the line-to-line winding resistance, in

$$2M = 6(R - R_B) - 2(C + 2R_L)$$

where R_B again is the lead resistance associated with the bridge between points g and h. As for the single-phase case, it is assumed that all the windings are balanced. The error introduced by not inserting a resistance 3/2 R_L between points h and K (for the case of the lead resistance being significant) was not calculated.

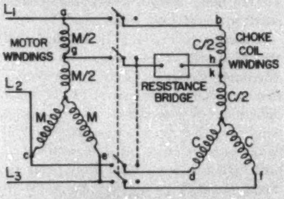

Fig. 2. Circuit for measurement of resistance of energized 3-phase windings

Procedure

Although the procedure to be followed in applying this circuit is more or less self-evident, there are a few items it may be well to point out.

1. With regard to associated equipment, the resistance of the choke coil should not be greater than the winding under test so that a fair degree of sensitivity is obtained.
2. Before connecting the bridge into the circuit, the voltage across that portion of the circuit into which the bridge is inserted should be measured. If more than a few volts appears, it may be short-circuited by an electrolytic motor-starting capacitor having a few hundred microfarads of capacity.
3. When not actually taking a reading, the choke coil should be disconnected from the circuit by means of the switch indicated to prevent the windings from heating. Following a reading, the resistance of the choke coil should be measured, the dotted portions of Figs. 1 and 2 being used for this purpose, and the value obtained should be used in calculating the resistance of the winding under test. The temperature rise of the choke coil will be very low if it is energized only while taking resistance measurements. Hence, the rate of cooling of the choke coil will be low enough to obtain accurate resistance values after shutdown.

Fig. 3 shows a comparison of temperature rise versus time by thermocouple and resistance for a 1-horsepower 220/440-volt totally enclosed motor. The choke coil used in obtaining these data was another motor of equal rating. As expected, the rise by resistance is somewhat higher than by thermocouple.

Conclusions

The method given is a practical means of obtaining the resistance of energized a-c windings without a need for special equipment. But it is only applicable to windings having a center tap available.

Appendix. Discussion of Error

For convenience in calculating, approximate equations were given for obtaining the test winding resistance from the bridge reading. These equations were approximate only if unbalanced resistances appeared in the circuit, i.e., if no unbalance exists, the equations are exact.

When unbalance exists, an exact solution of the circuits is virtually impossible since it requires a knowledge of the source resistances and of any other loads paralleling the test winding. Furthermore, assuming source resistances known, an exact analysis leads to at least a cubic equation in the unknown winding resistance.

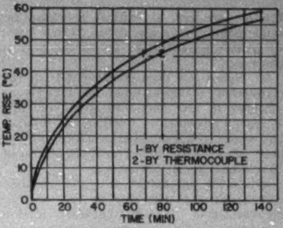

Fig. 3. Temperature rise versus time by resistance and thermocouple, 1-horsepower 1,800-rpm 3-phase totally enclosed induction motor

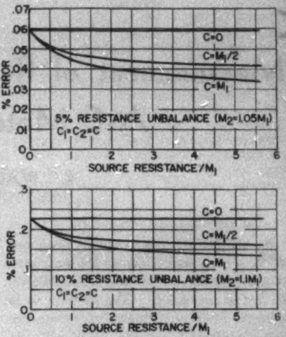

Fig. 4. Error resulting from use of approximate equations for calculating winding resistance

Using the approximate equations, error resulting from unbalance varies with the ratio of source resistance to winding resistance, and choke coil resistance to winding resistance, and, of course, with the degree of unbalance. For the single-phase case, Fig. 4 gives the error resulting from both 5 and 10-per-cent winding resistance unbalance plotted as functions of both source and choke coil resistance. The maximum error with 10-per-cent unbalance is only 0.23 per cent; for 5-per-cent unbalance the maximum error is 0.06 per cent.

The error was calculated in the following manner. Values of M_1 and M_2 were assumed, with M_2 first 5 per cent and then 10 per cent greater than M_1. Values of C and the source resistance were assumed, and an exact calculation was made to determine the resistance, looking into the circuit from the bridge terminals. With this bridge reading, the value of the line-to-line winding resistance was calculated using the approximate equation and comparing it with the original assumed value. An 8-place desk calculator was used in carrying out the computations. In view of the small error introduced by the approximations in the single-phase case, a similar calculation for the 3-phase condition was not made.

Reference

1. A Circuit for Measuring the Resistance of Energized A-C Winding, R. E. Seely. *AIEE Transactions*, vol. 74, pt. I, May 1955, pp. 214–18.

Discussion

R. E. Seely (General Electric Company, Fort Wayne, Ind.): Mr Waldschmidt is to be congratulated for developing a new simple means of measuring the resistance of energized dual-voltage a-c windings. The circuit which Mr. Waldschmidt uses seems quite novel to me since it does not require the use of capacitors to isolate the flow of the d-c bridge current as did the circuit which I described in a recent paper.[1] The fact that the capacitors are not needed in Mr. Waldschmidt's circuit should mean that the bridge in his circuit should not be effected by switching surges in the line supplying the energized winding. I would appreciate the author's comments on this.

In his paper, Mr. Waldschmidt only makes reference to tests on a 1-hp 230/440-volt motor. I would appreciate information on the range of motor sizes which have been tested using his circuit.

No doubt this circuit is normally used to measure resistance of motor windings when the motor is running under load. I was wondering if it had ever been used to get winding resistance when a motor was stalled and, if so, whether there are any particular problems in getting satisfactory readings.

I also wonder whether Mr. Waldschmidt has ever considered making the circuit of Fig. 2 such that the bottom two choke coils are connected in parallel when checking their resistance. If this were done then the bridge would read *C* and not 3/2 *C*.

REFERENCE

1. See reference 1 of the paper.

T. J. Higgins (University of Wisconsin, Madison, Wis.): This paper describes a rather unique mode of measurement of resistance of the windings of a-c motors while energized. The data of Fig. 3 evidence a particular merit of this method, as compared with thermocouple measurement. Those who have occasion to desire knowledge of the resistance of windings under load operation should find the method described in this paper a very useful one, when applicable.

K. J. Waldschmidt: I appreciate the comments of the discussers. In regard to Mr. Seely's question regarding switching surges, very little disturbance of the bridge galvanometer has been noted due to line-voltage surges. This is undoubtedly due to the symmetry of the circuit into which the bridge is connected. Mr. Seely's inference that the capacitors used in the circuit described by him[1] are responsible for galvanometer disturbance is open to question. Line-voltage fluctuations due to switching are a relatively high-frequency phenomena which should be effectively short-circuited by the series capacitors. It would seem more reasonable that the bucking transformer presents a different ratio of transformation for the high-frequency surges than for the fundamental line frequency, and therefore the surges are not entirely "bucked out." The circuit described by Mr. Seely was set up and galvanometer disturbance due to switching surges noted. It was found that with moderate line-voltage fluctuation, the galvanometer disturbance was noticeable but not overly annoying. However, when the series capacitors were by-passed (in which case the source resistance would be measured in parallel with the load resistance), the disturbance of the galvanometer became quite violent. It is appreciated that the bridge setting in the latter case was such that the same voltage difference would cause a higher disturbance than in the former case; the conclusion may be drawn, however, that something other than the capacitors is responsible for the disturbance.

In regard to motor sizes tested, the circuit has been used almost exclusively on fractional-horsepower sizes. For large integral motors, it would probably be necessary to use a Kelvin bridge. The circuit has not been used to measure resistance with the motor locked, although there should not be any particular problems when used for this purpose. I did not have available a dial-type bridge, and felt the change in resistance under locked conditions would be too rapid to follow with a decade-box-type bridge. With a decade-box-type bridge, a value of resistance could be preset and readings taken when this value was attained. A word of caution is perhaps in order here if the circuit is to be used on locked single-phase motors. In most cases it will be found that the auxiliary winding is paralleled with one half of the main winding, and the combination in series with the other half of the main winding on the high-voltage connection. The center-tap will not then be at a potential mid-way between the line potential, and damage to the bridge might possibly result if connected in.

REFERENCE

1. See reference 1 of the paper.

Insulation Characteristics of Wood and Suspension Insulators in Series

J. M. CLAYTON
ASSOCIATE MEMBER AIEE

D. F. SHANKLE
MEMBER AIEE

IN THE design and selection of transmission-line insulation, consideration must be given to three types of voltage which can appear across the insulation. These are lightning surges, switching surges, and normal operating voltage. With wood-pole structures, where the insulation may consist of a combination of porcelain insulators with wood in series, the insulators and wood should be proportioned to give the most suitable design as determined by line performance and economic considerations. Therefore, line design requires a knowledge of the insulation characteristics of different combinations for the various applied voltages. Since insulation strength is influenced by weather, the characteristics should be known under both wet and dry conditions.

A large volume of data has been published on the insulation characteristics of various combinations of porcelain insulators and wood. However, the range of combinations that may be under consideration in designing wood-pole structures for operation at 230 kv has not been completely covered. The performance of porcelain insulators under impulse and 60-cycle voltages is presented in the literature for wet and dry conditions.[1,2] Also, the impulse and 60-cycle characteristics of both wet and dry wood are published.[3,4,5] Data are available on the impulse characteristics of wood and porcelain combinations under wet and dry conditions, with the range of combinations being covered more completely for dry conditions.[5] A recent paper presents the impulse strength under wet conditions of wood and suspension-insulator combinations typical of 230-kv construction and below.[6] The characteristics of wood and porcelain insulators, when subjected to switching surges either alone or in series combination, have been investigated only to a very limited degree.[7] Insulation strength under wet conditions is particularly lacking, and further data would be of value in the design of transmission lines. This paper presents the results of impulse, switching-surge, and 60-

---

Paper 55-712, recommended by the AIEE Transmission and Distribution Committee and approved by the AIEE Committee on Technical Operations for presentation at the AIEE Fall General Meeting, Chicago, Ill., October 3-7, 1955. Manuscript submitted June 8, 1955; made available for printing August 2, 1955.

J. M. CLAYTON and D. F. SHANKLE are with the Westinghouse Electric Corporation, East Pittsburgh, Pa.

The authors wish to acknowledge the assistance of W. A. Schulz, Public Service Company of Indiana, Inc., and L. B. LeVesconte, Sargent and Lundy Engineers, in planning the test program. Their studies of 230-kv wood-pole designs emphasized the need for further data on the insulation characteristics of these structures. The pole-top structure and suspension insulators used in the tests were furnished by the Public Service Company of Indiana, Inc.

Table I. Combinations of Insulators and Wood

No. of Suspension Insulators, 10-Inch Diameter, $5^3/_4$-Inch Spacing	Wood in Series,* Feet	Nominal System Voltage, Kv
4	0	69
4	4	69
8	7	115
10	0	115 to 138
10	13	138 to 161
12	9	161 to 230
12	13	230
14	0	230
14	13	230

cycle flashover tests made of various combinations of standard suspension insulators in series with a large spar crossarm, thereby supplementing the previously published data.

Tests were made with the number of insulators ranging from 4 to 14, and the length of wood ranging from 0 to 13 feet. This range of values is characteristic of insulation levels of lines ranging from 69 to 230 kv. Tests were made on nine wood and porcelain combinations, with the results presented so that the insulation strength added by the wood can be determined for other combinations not specifically covered by the tests. Insulation characteristics were determined for both wet and dry conditions.

Scope of Tests

The primary objectives of the tests were to extend the impulse data on wood and porcelain combinations, and to determine the switching surge strength of wood. Also it was desirable to complete the series of tests by obtaining 60-cycle flashover data. To accomplish this, tests were made to determine the impulse, switching surge, and 60-cycle flashover characteristics under wet and dry conditions on various combinations of insulators and wood; see Table I.

The nominal system voltage corresponding to the various combinations is shown in the right column. For 69 and 115 kv, the number of insulators and length of wood are representative of typical constructions in these voltage classes. The combination of 10 insulators and 13 feet of wood is not representative of any voltage class; however, by interpolation the data on this combination can be used on lines in the 138- to 161-kv class. Several combinations representative of 230-kv construction were studied.

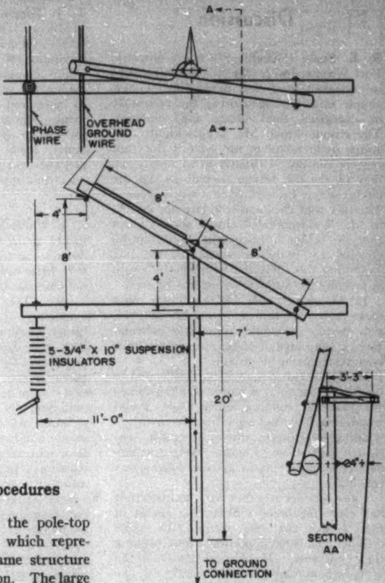

Fig. 1. One side of 230-kv H-frame structure used in tests. Details of ground wire down lead shown in section AA

Test Equipment and Procedures

All tests were made on the pole-top structure shown in Fig. 1, which represents one side of an H-frame structure typical of 230-kv construction. The large spar crossarm and pole are cresoted seasoned yellow pine. The diameter of the crossarm ranges from 8 to $8^3/_4$ inches, and the short section of pole included in the flashover path is $9^1/_2$ inches in diameter. None of the structure members was changed in the course of the tests.

The maximum length of crossarm that could be included in the flashover path is 11 feet, the distance from the insulator-suspension point to the pole. Two additional feet of wood was placed in the flashover path by including the 2 feet of pole just above the crossarm. This was possible since the overhead ground wire down lead was mounted away from the pole as indicated in section *AA* of Fig. 1. Shorter lengths of wood were obtained by placing wire bands short-circuited to ground around the crossarm at the desired distance from the insulator string. The length of the insulator string was changed by adding or removing insulators, and not by short-circuiting part of the insulators in a string. All tests were made using the same group of standard suspension insulators having a diameter of 10 inches and spacing of $5^3/_4$ inches.

A 3/4-inch-diameter copper tube, 10 feet long, was placed on the insulator string to simulate the presence of the line conductor. Also a 1/2-inch rod, 10 feet long, was placed in the position normally occupied by the ground wire. With the simulated conductor and ground wire, the field distortion and voltage distribution across the insulation should closely approximate that of an actual line. Details of the pole-top test structure and of the simulated conductors are shown in Fig. 2.

In the wet tests, standard rain was applied by the rain maker shown in Fig. 2(F). Standard rain is water having a resistance of 7,000 ohms per cubic inch applied at the rate of 0.2 inch per minute. Before starting a series of wet tests, the test sample was throughly wet and checks were made to determine when the flashover voltage had dropped to the wet value. These tests showed the voltage dropped to the wet value within 2 to 3 minutes after the application of rain, and then leveled off without further appreciable change. For the dry tests, the moisture content of the wood was much the same as would be expected on an actual line, since the test specimen remained outside until brought into the laboratory for testing.

IMPULSE TESTS

All impulse tests were made using standard $1^1/_2$x40-microsecond waves of positive polarity. This polarity was used since positive surges applied to the

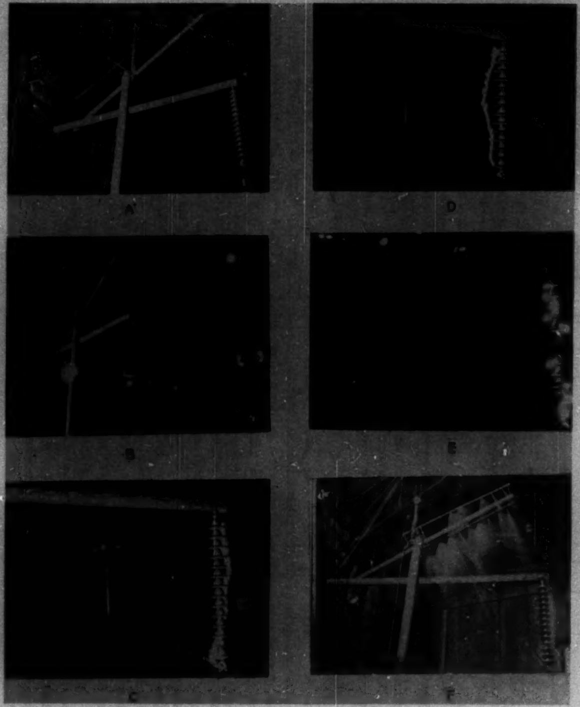

Fig. 2. Pole-top structure and typical flashovers

A—Half of H-frame structure with 14 insulators
B—Corona discharge prior to 60-cycle flashover
C—60-cycle flashover of 14 insulators
D—Switching-surge flashover of 14 insulators
E—Impulse flashover of 12 insulators plus 9 feet of wood
F—Impulse flashover of 14 insulators under wet conditions

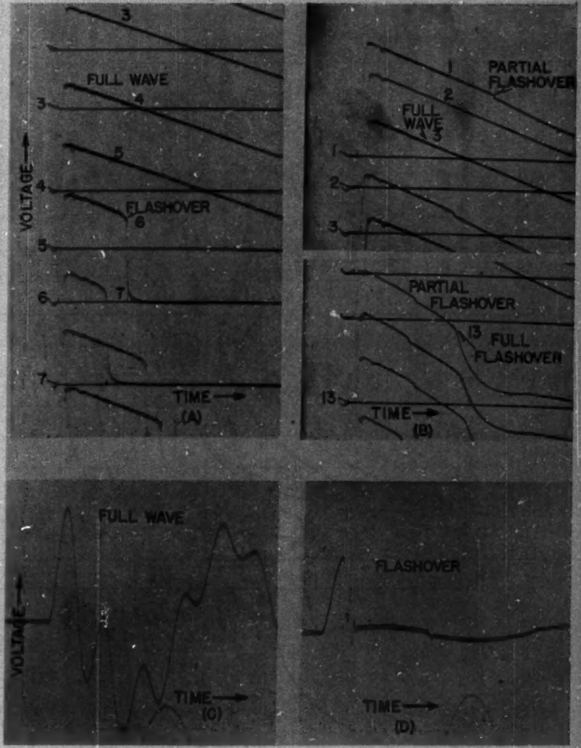

Fig. 3. Typical oscillograms of $1^1/_2$x40-microsecond waves and switching surges

A—$1^1/_2$x40-microsecond wave applied to 10 insulators
B—$1^1/_2$x40-microsecond wave applied to 8 insulators plus 7 feet of wood
C—Switching surge applied to four insulators plus 4 feet of wood
D—Switching surge applied to 10 insulators plus 13 feet of wood

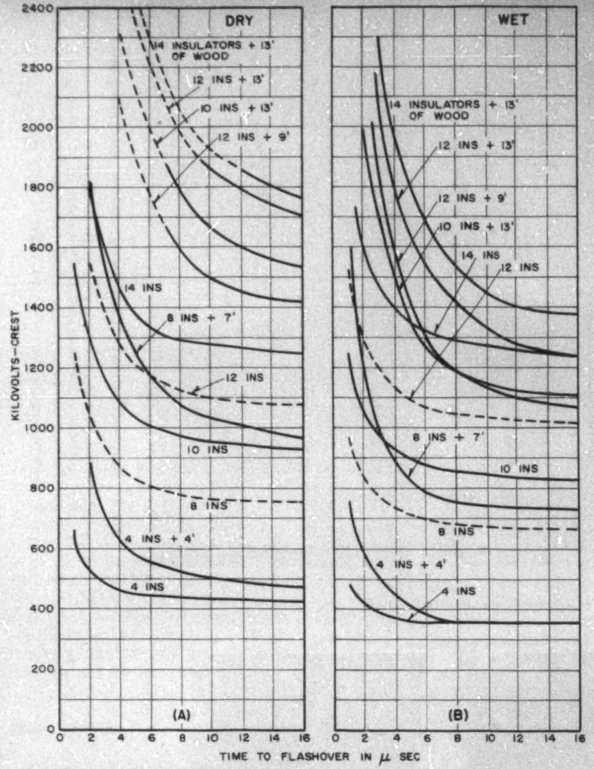

Fig. 4. Summary of impulse tests based on positive 1 1/2x40-microsecond waves

A—Dry, corrected to standard conditions, pressure = 29.92-inch mercury, temperature = 77 degrees Fahrenheit and humidity = 0.6085-inch mercury

B—Wet, standard rain, water with a resistance of 7,000 ohms per cubic inch applied at the rate of 0.2 inch per minute

simulated line conductor correspond in polarity to a natural lightning stroke of negative polarity terminating on the overhead ground wire, i.e., in both cases the line conductor is positive with respect to ground. The tests were based on lightning strokes of negative polarity, since approximately 90 per cent are negative. Some typical oscillograms of the test waves are shown in Fig. 3(A) and (B).

SWITCHING SURGE TESTS

Switching surges were simulated in the laboratory by the energizing transient which results when two 500-kv transformers connected in cascade are energized at the crest of the applied voltage wave. The transient voltage obtained by this method has a frequency of 300 cycles per second and rises to first crest in 1,700 microseconds. The transformers were energized by a switching scheme synchronized with the 60-cycle voltage and, therefore, produced a uniform switching transient each time. The switching surges were recorded by a magnetic oscillograph using a capacitance coupling device and a d-c amplifier with an integrating circuit. Some typical oscillograms are shown in Fig 3(C) and (D).

60-CYCLE TESTS

The 60-cycle flashover voltage was determined by the usual laboratory technique of gradually increasing the applied voltage with a stepless regulator until flashover occurs, and measuring the voltage at time of flashover. The procedure is repeated five times and the average value is taken as the flashover voltage.

Results of Tests

The results of the impulse, switching surge, and 60-cycle tests are presented and discussed separately.

IMPULSE TESTS

The complete results of the impulse tests are summarized by the volt-time curves of Fig. 4, which were obtained by plotting the crest magnitude of the applied surge against the time to flashover. In the dry tests on the combinations having high insulation levels, the magnitude of the applied voltage was not high enough to obtain the short times to flashover. Therefore, the extrapolated values have been indicated by dashed lines on the upper four curves of Fig. 4(A). For each combination tested, curves are given for the insulators with wood in series and for the same number of insulators alone. Therefore, the insulation strength added by the wood is indicated by comparing the two sets of curves. The relative impulse strength under dry and wet conditions is shown by comparing the curves of Fig. 4(A) with those of Fig. 4(B).

The results of tests on insulators alone are summarized by the time-lag curves of Fig. 5, which are plotted directly from the volt-time curves of Fig. 4. The curves are based on flashover tests on strings of 4, 10, and 14 insulators only, which are the only lengths tested without wood in series. The volt-time curves of Fig. 4 for 8 and 12 insulators are plotted from the time-lag curves of Fig. 5. The volt-time curves for 8 and 12 insulators are needed in Fig. 4 so that the insulation strength added by wood in combination with 8 or 12 insulators can be determined.

In general the curves of Fig. 5(A) are in excellent agreement with the published time-lag curves[1,2] for standard suspension insulators, which are based on much more extensive tests. For most points, the two sets of curves do not differ by more than 2 to 3 per cent; however, the 6- and 8-microsecond curves differ by as much as 5 to 6 per cent in some cases. The curves of Fig. 5 are not intended to replace previously published data,[1,2] or other data that may be available on dry suspension

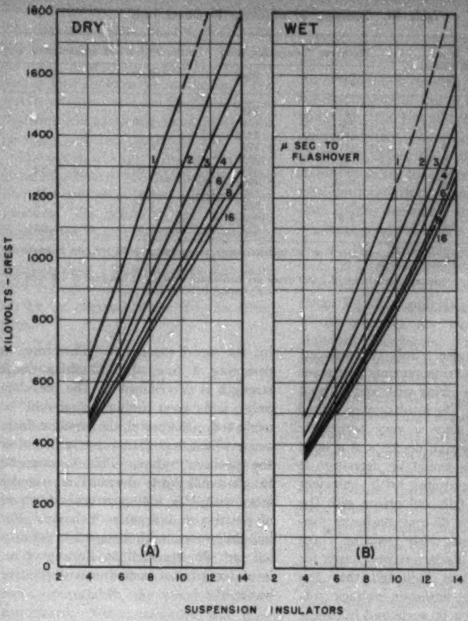

Fig. 5 (left). Time-lag curves of standard suspension insulators having a diameter of 10 inches and 5³/₄-inch spacing

A—Dry, corrected to standard conditions
B—Wet, based on standard rain

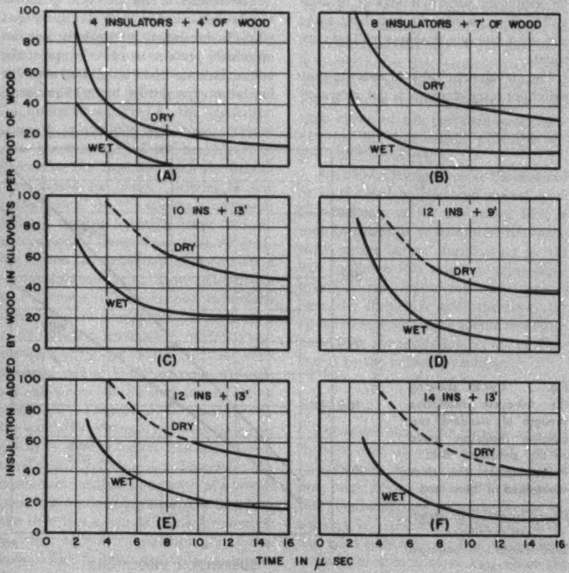

Fig. 6 (below). Insulation strength added by wood in kilovolts per foot of wood

Dry—Corrected to standard conditions
Wet—Based on standard rain

insulators. Their purpose is to present the results of these tests, and to compare the insulation strength of insulators alone under wet and dry conditions.

Comparing the curves of Fig. 5(A) and (B) indicates that standard rain has appreciable effect on the impulse strength of insulators alone. These results caused some concern and were checked very carefully since in the past it has been assumed that the impulse strength of porcelain was relatively unaffected by rain. The possibility was investigated that in the wet tests some of the insulators may have been punctured, resulting in a lower flashover value. However, the subsequent 60-cycle wet tests were in good agreement with the published data,[1,2] indicating the insulators were in good condition during the wet impulse tests. Also the shape and grouping of the wet time-lag curves, Fig. 5(B), are different from the dry curves of Fig. 5(A). This suggests that the flashover phenomenon has been influenced by the rain. If the effect of a punctured insulator is a constant error, then it will not change the shape and grouping of the time-lag curves. Although the wet tests on insulators alone are limited to strings of 4, 10, and 14 insulators, indications are that rain has appreciable effect on the impulse strength of porcelain, and this problem should be investigated further.

The results of other tests reported in the literature[3] indicate that rain has appreciable effect on the impulse strength of electric equipment. Several hundred tests were made on breakers, switches, all types of insulators, bushings, and current and voltage transformers using positive and negative waves. In these tests the wet withstand values for about one third of the tests are below the dry values by about 10 per cent or more.

The curves of Fig. 6 present the insulation strength added by wood as a function of time in kilovolts per foot of wood. They were obtained from the curves of Fig. 4 by subtracting the insulation of the insulators from the total insulation strength of the wood-porcelain combination, and dividing by the number of feet of wood. Inspection of the curves indicates that the insulation strength added per foot of wood is influenced by the number of insulators and also by the length of the wood. However, this influence is not so critical as to preclude the possibility of using the data for insulator-wood combinations not specifically covered by the tests. For example, in the wet tests for the combinations of four insulators plus 4 feet of wood and eight insulators plus 7 feet of wood, the wood adds 20 and 22

Table II. Summary of Switching Surge Tests

No. of Insulators	Wood in Series, Feet	Flashover Voltage, Pu*	
		Dry	Wet
4	0	+1.00†	+1.00† −0.95
4	4	+1.04 −0.92	+1.00 −0.95
10	0	+1.00† −0.98	+1.00† −0.93
10	13	+1.04 −0.94	+0.98 −0.92
14	0	+1.00† −0.93	+1.00† −0.98
14	13	+0.96	+0.94 −1.00

Positive and negative signs indicate polarity of switching surge.

* 1.0 pu is the positive flashover voltage of insulators alone.

† Reference values taken as 1.0 pu.

Table III. Summary of 60-Cycle Flashover Tests

No. of Insulators	Wood in Series, Feet	Flashover Voltage, Kv, Rms		Ratio, With Wood to Insulators Only	
		Dry*	Wet†	Dry*	Wet†
4	0	282	188		
4	4	283	177	1.00	0.94
8	0	495‡	335‡		
8	7	491	370	0.99	1.10
10	0	582	401		
10	13	591	461	1.01	1.15
12	0	715‡	480‡		
12	9	692	527	0.97	1.10
12	13	727	553	1.02	1.15
14	0	818	605		
14	13	822	624	1.00	1.03

* Corrected to standard conditions, pressure is 29.92-inch mercury, temperature is 77 degrees Fahrenheit, and humidity is 0.6085-inch mercury.

† Standard rain, water having a resistance of 7,000 ohms per cubic inch applied at the rate of 0.2 inch per minute.

‡ From previously published data.[1,2]

kv per foot respectively at 4 microseconds; see Fig. 6(A) and (B). In the higher insulation levels, Fig. 6(C) to (F), wet wood adds 43 to 50 kv per foot at 4 microseconds. In using the data, it is suggested that the curves be used which most nearly approximate the number of insulators and length of wood under consideration.

The typical impulse oscillograms of Fig. 3 will be discussed briefly. In the wet and dry tests with wood in the flashover path, a partial flashover was observed in many cases; i.e., the insulators only flashed over, apparently without breakdown of the wood insulation. A partial flashover could not be distinguished from full flashover by a visual observation since full flashover is not always accompanied by external arcing across the wood. However, the partial flashover was indicated by a small step in the oscillogram, as shown in Fig. 3(B). When full flashover does occur over a porcelain and wood combination, the voltage does not immediately drop to zero as it does in the case of insulators alone, as indicated in Fig. 3(A). In the case of wood insulation the sustained voltage is caused by the resistance of the wood, which is high as compared with the resistance of an arc across an insulator string. The volt-time curves of Fig. 4 are based on the time to full flashover, with the partial flashovers being disregarded.

SWITCHING SURGE TESTS

The results of the switching surge tests, summarized in Table II, have been presented in per-unit (pu) values. In each case the positive flashover value of the insulators alone is taken at 1.0 pu, and this is compared with the flashover voltage of the same number of insulators with wood in series. Only the cases are presented where measurements were made on the insulator string with and without wood in series. The results are presented in pu values, since a very accurately calibrated measuring device and a large number of tests would be necessary to determine magnitudes with sufficient accuracy for a fair comparison with the impulse and crest 60-cycle flashover voltages. In general, only two or three switching surge flashovers were made for each case. These indicated that the switching surge flashover voltage was between the crest 60-cycle and full-wave impulse values. Therefore, in designing for switching surges, it should be conservative to assume the switching surge and crest 60-cycle flashover voltages are equal.

The pu values in Table II indicate that switching surge strength is not increased by the wood insulation. Therefore, in designing a line, the switching surge strength is determined by the porcelain only, and wood insulation should be neglected. In general, the negative flashover voltage was 2 to 7 per cent below the positive values. This is opposite to what has been observed in impulse tests with $1^{1}/_{2}$ x 40-microsecond waves of positive and negative polarity. For impulse waves, higher negative polarity voltages are required to flash over an insulator string, as compared with positive waves.[1,2]

60-CYCLE TESTS

The results of the 60-cycle flashover tests summarized in Table III show that 60-cycle insulation strength is not increased by wood. However, some of the values indicate that wood increases the insulation strength by 10 to 15 per cent.

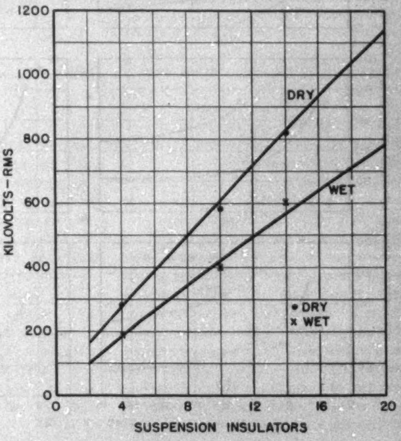

Fig. 7. Curves showing the 60-cycle insulation strength of standard suspension insulators based on the published data.[1,2] Points indicate the values obtained in these tests

Dry—Corrected to standard conditions

Wet—Based on standard rain

These apparent increases are probably due to limitations in the measuring accuracy and variations in the flashover values of the insulators, and do not represent a true increase in insulation. The results of these tests are further evidence that 60-cycle insulation strength must be based on porcelain insulators only.

The curves of Fig. 7 are a reproduction of data published[1,2] on the 60-cycle insulation strength of standard suspension insulators. The points on the curves, indicating the values obtained in this series of tests, are in good agreement with the previous data. This indicates that flashover voltage was not influenced appreciably by the presence of the H-frame structure.

Application of Data

The results of these tests have shown that switching-surge and 60-cycle insulation strengths are not increased by wood. Therefore, in designing for these voltages, the required number of insulators should be determined from the published literature,[1,2] or other data that may be available for the specific insulators should be used. Since wood increases the impulse insulation strength of wood-pole structures appreciably, the wood should be considered. Some examples will illustrate the use of the data for determining the impulse strength of wood structures.

In designing a wood-pole structure, a common problem that arises is the determination of the impulse insulation strength of the structure, which is needed in estimating line lightning performance. As indicated in Fig. 4, the insulation strength is variable with time. Therefore, the first part of the problem is to determine the time on which the insulation should be based. Studies of line performance[9] on the analogue computer using a typical lightning wave (4 x 40 microseconds) have shown that the voltage across the insulation is essentially a chopped wave in most cases. The effects of the tower inductance and reflections from adjacent towers are to produce a short duration wave which is closely approximated by a standard $1^{1}/_{2}$ x 40 wave chopped in 2 to 4 microseconds, depending upon span length and tower footing resistance. Therefore, in reference 9, the insulation strength has been based on the 2- to 4-microsecond time-lag curves; see Table I, reference 9. Therefore, the equivalent insulation strength of a wood-porcelain combination should be based on the time lags given in Table I, reference 9, when estimating lightning performance. This is illustrated by an example.

EXAMPLE 1

Determine the equivalent insulation for wet conditions of a shielded 230-kv line where insulation consists of 12 suspension insulators and 10 feet of wood. Since the spans are 1,000 feet and the footing resistance 10 ohms, the insulation strength should be based on 4 microseconds, as indicated in Table I, reference 9. In this example it is assumed that the available data on the insulators indicate that the 4-microsecond strength is 1,300 kv for wet conditions. From Fig. 6(D), the wood adds 50 kv per foot or a total of 500 kv. Therefore, the total insulation is 1,800 kv. From Fig. 6 of reference 9, 1,800 kv at 4 microseconds are equivalent to 17 standard insulators; the estimating method is based on standard insulators. Therefore, in using the line performance estimating curves,[9] 17 insulators should be used in entering the curves.

Another typical problem is co-ordination of the porcelain-wood insulation with the parallel air gap. It may be desirable to co-ordinate the two paths so that flashover always occurs through the air gap, thereby preventing flashover across the wood insulation. Or it may be desirable for the two paths to have equal insulation. If it is desirable for the paths to have equal insulation, then the comparison should be based on the time-lag values in Table I, reference 9. If it is desirable for the air gap to flashover always, then a range of time lags should be investigated to make sure that the air-gap insulation is always below the porcelain-wood combination. The data in the curves of Fig. 6 can be used for plotting the volt-time curve of the porcelain-wood combination for comparison with the air-gap volt-time curve.

The 230-kv line in example 1 is assumed to be shielded by overhead ground wire. For the case of an unshielded line, it may be desirable to determine the maximum stroke current terminating on the line conductor that does not cause flashover. In this case a full wave appears over the insulation and, therefore, the 16-microsecond strength should be used in estimating line insulation, as will be illustrated by the following example.

EXAMPLE 2

Determine the stroke current required to flash over an unshielded line having 12 insulators and 9 feet of wood. The line surge impedance is 400 ohms, and the 16-microsecond strength of the insulators is 1,110 kv. From Fig. 6(D), wet wood adds 5 kv per foot at 16 microseconds, or a total of 45 kv. Since the line surge impedance is 200 ohms looking in two directions, the current required to cause flashover is 1,155/200 or 5,775 amperes. The stroke-current probability curve indicates that about 85 per cent of the strokes to transmission lines exceed this value.[9]

In applying the data obtained in these tests, it should be recognized that all impulse tests were made on a single sample of wood and do not apply to all types of wood. In general, the data will be most applicable to large spar crossarms similar to the type used in the test. Some similar tests on small spar and plank crossarms, indicate a higher insulation strength than reported herein.

Conclusions

The conclusions based on the results of these tests may be summarized as follows:

1. Wood insulation increases the impulse strength of wood and porcelain combinations appreciably. The insulation strength added by the wood depends on the length of wood, number of insulators in series, the time-lag curve considered, and whether the conditions are wet or dry.

2. Limited tests made on insulators alone indicate that standard rain reduces the impulse strength of insulators. These tests indicate that the effect of rain on insulators should be studied further.

3. Wood insulation under wet or dry conditions does not increase the switching surge or 60-cycle strength of wood and porcelain combinations. Therefore, switching surge and 60-cycle insulation must be based on the porcelain insulators only.

References

1. FLASHOVER CHARACTERISTICS OF INSULATION, P. H. McAuley. *Electric Journal*, East Pittsburgh, Pa., July 1938.

2. ELECTRICAL TRANSMISSION AND DISTRIBUTION REFERENCE BOOK (book). Westinghouse Electric Corporation, Pittsburgh, Pa., 4th ed., chap. 18, 1950.

3. LIGHTNING AND 60-CYCLE POWER TESTS ON WOOD-POLE LINE INSULATION, P. L. Bellaschi. *AIEE Transactions*, vol. 66, 1947, pp. 838–47.

4. LIGHTNING STRENGTH OF WOOD IN POWER TRANSMISSION STRUCTURES, Philip Sporn, J. T. Lusignan, Jr. *AIEE Transactions* (*Electrical Engineering*), vol. 57, Feb. 1938, pp. 91–101.

5. WHAT WOOD MAY ADD TO PRIMARY INSULATION FOR WITHSTANDING LIGHTNING, J. T. Lusignan, Jr., C. J. Miller, Jr. *Ibid.*, vol. 59, Sept. 1940, pp. 534–40.

6. 230-KV WOOD-POLE TRANSMISSION-LINE DESIGN, J. J. Trainor, L. B. LeVesconte. *Ibid.*, vol. 73, pt. III-A, June, 1954, pp. 522–28.

7. DIELECTRIC STRENGTH OF STATION AND LINE INSULATION TO SWITCHING SURGES, P. L. Bellaschi, L. B. Rademacher. *Ibid.*, vol. 65, 1946, pp. 1047–54.

8. THE INFLUENCE OF RAIN ON VOLTAGE TESTS, M. Bockman. *CIGRE*, Paris, France, 1954.

9. A METHOD OF ESTIMATING LIGHTNING PERFORMANCE OF TRANSMISSION LINES, AIEE Committee Report. *AIEE Transactions*, vol. 69, pt. II, 1950, pp. 1187–95.

Discussion

Brent Ottinger (Consumers Power Company, Jackson, Mich.): To design a well-balanced structure with the flashover distance to ground co-ordinated with insulator impulse strength, the engineer must be able to predict the impulse insulation added by wood in series with porcelain.

This papern presents, in usable form, additional data on insulation strength expected for lengths of wood characteristics of higher voltage wood-pole transmission lines.

Since the impulse insulation added by wood depends upon internal moisture, it would be of interest to know if a specimen of the crossarm was tested for per cent moisture for dry and wet conditions.

Some advantages are gained with the use of double plank crossarms. What results might have been expected under similar test conditions if the specimen had been double-plank fir crossarms?

W. H. Knutz (Northern Indiana Public Service Company, Hammond, Ind.) Acceptance of the results of this paper would call for greatly increasing the lengths of wood paths, additions of more porcelain, or some combination of both, on transmission lines of moderate voltage. Experience indicates that this increase of insulation is not warranted.

The flashover values of wet wood added to porcelain, as stated in the paper, are based on 0.2 inch of rain per minute. This is 12 inches per hour—a deluge experienced in few sections of the world. Then too, lightning would be called on to strike during this downpour and further strike a line. The cost of many coincidences is prohibitive.

In 16 years' experience in 1,632 year-miles of shielded and grounded wood-pole transmission lines, purposely set out to observe, we have had 0.9 outages per 100 circuit-miles per year. The wood insulation in these lines was calculated to have 70 per cent of the impulse insulation value of wood with 15-per-cent moisture content.

H. A. Cornelius (Commonwealth Edison Company, Chicago, Ill.): This paper shows that "standard rain" in the laboratory reduces the wet impulse voltage withstand level for porcelain insulators about 10 per cent below the dry impulse voltage withstand level. Since the AIEE standard for "rain" is water having a resistivity of 7,000 ohms per cubic inch, it is obvious that the impulse voltage withstand level of dirty and wet insulators in the field will be lower than in the laboratory. Surface contamination may produce low-resistivity water, with increases in surface leakage currents and lowered sparkover values.

Have the authors made any tests to determine the effects of lower resistivity "rains?" Also, were all the tests made on the same wood members, or on different wood members to avoid any cumulative effect on a particular wood member from applying repeated impulse test voltages?

F. E. Andrews and **R. W. Caswell** (Commonwealth Edison Company, Chicago, Ill.): One of the important facts brought out by this paper is the reduction in impulse strength of porcelain insulators under wet conditions. It is noted that in the examples, which are for wet conditions, the authors have used insulator flashover values from the AIEE Committee Report.[1] These impulse flashover values for porcelain are on the basis that the wet and dry values are the same. It is therefore of interest to consider how the use of these new data, showing reduction in impulse flashover when the porcelain is wet, will affect such calculations. A comparison of the expected tripout rate developed by each method under wet conditions has been made.

1. 69-kv wood-pole line with static wire using five $5^{3}/_{4}$- by 10-inch suspension insulators in series with 4 feet of wood arm. Span length 200 feet.

2. 138-kv wood-pole H-frame line with static wires using eight $5^{3}/_{4}$- by 10-inch suspension insulators in series with 7 feet of wood. Span length 600 feet.

3. 230-kv wood-pole H-frame line with static wire using twelve $5^{3}/_{4}$- by 10-inch suspension insulators in series with 10 feet of wood. Span length 1,000.

In each case the calculations were made for structure ground resistances of 10, 20, and 50 ohms; isokeraunic level was 45.

As may be expected, the lower flashover value for porcelain under wet conditions increases the estimated tripout rate. However, for the lines considered with a 10-ohm ground resistance, the resultant rate after the increase is less than one per 100 miles per year. With a resistance of 20 ohms the increase is from just about one per 100 miles per year to about 1.5. However, with 50 ohms resistance the tripout rate increases from the range of from three to five depending on line characteristics to the range of four to eight per 100 miles per year. It will be recognized that the change in tripout rate due to lower flashover value of porcelain will be materially affected by what percentage of the total insulation the porcelain represents. From this it appears that where an appreciable amount of wood is used in series with porcelain to provide the impulse insulation and the ground resistance is reasonably low, the use of the lower impulse insulation value for porcelain under wet conditions will not make any significant increase in the tripout rate.

Reference is made to Fig. 3(B) covering partial flashover and the statement that full flashover of wood is not always accompanied by external arcing across the wood. Some connection with the fact that wood has an arc quenching ability as far as 60-cycle flashovers are concerned may exist. Would the authors care to elaborate further?

The tests covered in this paper refer to suspension-type insulators in series with wood members and show that wet impulse flashover of the suspension insulators is less than the dry value. Similar data covering pin-type insulators normally used on 34.5-kv to 69-kv lines would be of value.

REFERENCE

1. See reference 9 of the paper.

J. M. Clayton and **D. F. Shankle**: We wish to thank the discussers for their comments.

With reference to Mr. Ottinger's question, no measurements to determine per-cent moisture were made for dry or wet conditions. However, in the dry tests the moisture content should be typical of that found in actual service since the specimen was stored outdoors preceding the laboratory tests. In the wet tests the specimen was thoroughly wet and checks were made to determine that the flashover voltage had dropped to the wet value before starting a series of tests. However, the depth of moisture penetration was not determined.

As to the insulation characteristics of double-plank fir crossarms, the results of impulse tests on large spar and plank crossarms has been reported.[1] In general, the impulse strength at 4 microseconds of the plant crossarm is about twice that of the large spar crossarm. At 16 microseconds it is approximately five times the strength of the spar crossarm. The impulse strength of a double-plank crossarm may be somewhat less than the single plank tested, depending upon the cross-section areas.

With regard to Mr. Knutz's comments on the results of the tests, these impulse values for large-spar crossarms are in good agreement with similar tests.[1] Other tests on a plank crossarm indicate that it has much higher insulation strength than a spar crossarm.

The tests were made using standard rain of 0.2 inch per minute since this is the usual laboratory procedure, and also the results can be compared with other published data obtained under similar conditions. No tests were made to determine the effect of rate of rainfall on the insulation strength of wood and porcelain.

In reply to Mr. Cornelius' question on the effect of contamination and low-resistivity water no tests were made for these factors.

With reference to the cumulative effect from repeated application of impulse voltages, all tests were made on the same wood members. However, cumulative effects on the wood appear to be negligible since the insulation strength of the wood did not change much for various combinations tested.

Messrs. Andrews and Caswell raise a question concerning the arc-quenching ability of wood with regard to 60-cycle current. In the impulse tests where the time to flashover was of the order of 6 to 16 microseconds, very little external arcing across the wood was observed. For shorter times to flashover some arcing across the wood was visible, but seldom over the full length of the wood. The exception to this is that in the wet tests full length arcs over the wood were observed. In the switching surge and 60-cycle flashover tests very little arcing over the wood was observed.

The fact that the insulation breaks down without external arcing over the wood indicates that the current flows through the wood and not over its surface. It is logical to assume that the flow of current through the wood generates deionizing gases that tend to quench the 60-cycle power follow current. The generation of these gases may depend on the nature of the impulse flashover. In the case of a short time to flashover occurring in a few microseconds where the flashover path is over the surface of the wood, there may be a tendency for the 60-cycle current to follow the same path. In the situation there would be little or no deionizing gases generated in the wood. Whereas if the impulse flashover is through wood, the 60-cycle current should follow the same path and expell gases which may extinguish the follow current. Thus the nature of the impulse flashover may have significant effect on the ability of the wood to interrupt 60-cycle power follow current.

REFERENCE

1. See reference 6 of the paper.

Sequence Impedances of Symmetrical 3-Phase Transformer Connections

B. A. COGBILL
FELLOW AIEE

DURING the past 40 years or so, a large amount of material on the circuit theory of transformer impedance characteristics has been published in the form of specific technical articles and as parts of articles and books of broader scope. This material covers a number of aspects of the subject including circuit theory of multicircuit transformers,[1–4] equivalent circuits,[5–11] analyses in terms of symmetrical components,[12,13] method of making calculations,[3] and tests. Although a large part of the published material relates to 3-phase transformer connections, practically all of the fundamental circuit theory is developed from a single-phase point of view. From such development certain basic concepts have emerged which have been carried over, more or less logically, to the 3-phase problem.

In the general application of the method of symmetrical components to the solution of 3-phase problems, 3-phase circuits are resolved into three single-phase circuits, one for each of the sequences, positive, negative, and zero. These so-called sequence circuits can be expressed in a number of forms such as diagrammatic equivalent circuits, physical equivalent circuits, and mathematical equations which relate the various voltages, currents, and impedances; the choice of form depends upon how they are to be used. But regardless of their form, the sequence circuits of 3-phase transformer connections are usually derived by making full use of concepts which have been developed on a single-phase basis. Such procedure has been found to yield correct results in all of the more common cases such as connections which have only two sets of terminals and multicircuit connections which consist of simple wye and delta circuits only. Therefore there is a strong temptation to generalize by assuming that the procedure is applicable to all 3-phase transformer connections. To make such an assumption, however, is a mistake and can lead to incorrect results because the concept that all mutual impedances are bilateral which allows the single-phase problem to be greatly and beautifully simplified is not completely applicable to the derivation of the sequence circuits of all 3-phase transformer connections. Apparently this fact and, more important, its implications which are exposed in this paper are not generally recognized.

That the existence of this situation has at least been suspected by others is unquestionable. Rather vague hints that all is not as it should be appear in a number of places in the published literature; one article[2] is devoted to a discussion of the effects of "these strange phenomena" on the theory of 3-circuit transformers. Furthermore it is inconceivable that published equivalent circuits of some particular 3-phase transformer connections could have been developed and used without their peculiarities having been questioned. Yet, apparently, no thorough investigation has been presented.

This paper presents such an investigation. The paper consists of a theoretical analysis of the sequence impedance characteristics of symmetrical 3-phase transformer connections in general which, in effect, is a development of circuit theory for the sequence circuits.

This analysis is conducted on the basis of impedances as viewed from the external terminals of the transformer connections, starting with self- and mutual impedances and carried through to usable expressions which completely define the impedance characteristics for the three sequences. The general analysis includes all possible symmetrical 3-phase transformer connections. The derived mathematical expressions can be converted to equivalent circuits; however, in some cases the equivalent circuits may consist of other than simple impedance elements. In Appendix I a method of determining from test that part of the mutual impedances which prevents their being reciprocal is given. The sequence voltage equations are converted to equations in terms of $\alpha\ \beta 0$ components in Appendix II. Some illustrative examples are given in Appendix III.

Nomenclature

E_{Ah}, E_{Bh}, E_{Ch} = per-unit (pu) voltage from neutral terminal to A, B, and C terminals respectively of the h terminal set based on magnitude of rated no-load line-to-neutral voltage

I_{Ak}, I_{Bk}, I_{Ck} = pu current flowing into terminals A, B, and C respectively of the k terminal set based on the voltage base used for E_{Ak} and an arbitrary volt-ampere base which is common for all impedances and currents

Z_{AhAh} = pu self-impedance of circuit from line terminal Ah to neutral terminal Nh based on an arbitrary volt-ampere base, which is common for all impedances and currents, and the voltage base used for E_{Ah}

Z_{AhBk} = pu mutual impedance between circuits Ah to Nh and Bk to Nk based on same volt-ampere base as Z_{AhAh} and voltage bases corresponding to E_{Ah} and E_{Ak}

$\underset{1}{E_h}$, $\underset{2}{E_h}$, $\underset{0}{E_h}$ = positive-, negative-, and zero-sequence components of E_{Ah}

$\underset{1}{I_k}$, $\underset{2}{I_k}$, $\underset{0}{I_k}$ = positive-, negative-, and zero-sequence components of I_{Ak}

φ_h, φ_k = angles through which the positive-sequence components of no-load voltages at terminal sets h and k respectively must be rotated to bring them in phase with an arbitrary reference voltage

$\underset{1}{E_h}' = \underset{1}{E_h} \exp j\varphi_h$

$\underset{2}{E_h}' = \underset{2}{E_h} \exp(-j\varphi_h)$

$\underset{1}{I_k}' = \underset{1}{I_k} \exp j\varphi_k$

$\underset{2}{I_k}' = \underset{2}{I_k} \exp(-j\varphi_k)$

$\underset{1}{Z_{hk}}$ = pu mutual impedance which reflects the influence of current $\underset{1}{I_k}'$ on the voltage $\underset{1}{E_h}'$

$\underset{1}{Z_{kh}}$ = pu mutual impedance which reflects the influence of current $\underset{1}{I_h}'$ on the voltage $\underset{1}{E_k}'$

$\underset{1}{Z_{hh}}$ = pu self-impedance which reflects the influence of current $\underset{1}{I_h}'$ on the voltage $\underset{1}{E_h}'$

$\underset{1}{Z_{h-k}}$ = pu positive-sequence series-opposition (short-circuit) impedance between terminal sets h and k

$\underset{1}{Z_{1(hk)}}$ = pu positive-sequence branch mutual impedance between terminal sets h and k with terminal set no. 1 as reference

$\underset{1}{Z_{1(hh)}}$ = pu positive-sequence branch self-impedance at any terminal set h with terminal set no. 1 as reference

$\underset{2}{Z_{hk}}$, $\underset{2}{Z_{kh}}$, $\underset{2}{Z_{hh}}$, $\underset{2}{Z_{h-k}}$, $\underset{2}{Z_{1(hk)}}$, $\underset{2}{Z_{1(hh)}}$ = same as the foregoing except for negative sequence

$\underset{0}{Z_{hk}}$, $\underset{0}{Z_{kh}}$, $\underset{0}{Z_{hh}}$, $\underset{0}{Z_{h-k}}$ = same as the foregoing

---

Paper 55-671, recommended by the AIEE Transformers Committee and approved by the AIEE Committee on Technical Operations for presentation at the AIEE Fall General Meeting, Chicago, Ill., October 3–7, 1955. Manuscript submitted May 31, 1955; made available for printing July 18, 1955.

B. A. COGBILL is with the General Electric Company, Pittsfield, Mass.

The author gratefully acknowledges the many helpful comments and suggestions made by A. N. Garin and the valuable criticisms of L. Rabins.

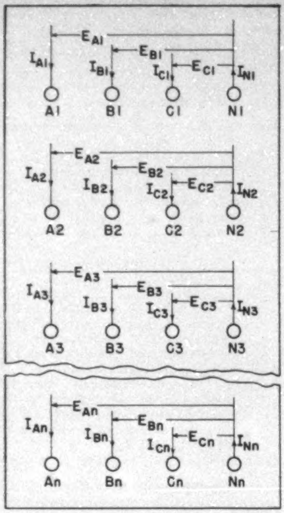

Fig. 1. Terminals of multicircuit 3-phase transformer connections

except for zero sequence

$$Z_{hk}'=\frac{1}{2}[(2Z_{AhAk}-Z_{AhBk}-Z_{AhCk})\cos(\varphi_h-\varphi_k)+\sqrt{3}(Z_{AhBk}-Z_{AhCk})\sin(\varphi_h-\varphi_k)]$$

$$Z_{hk}''=\frac{1}{2}[(2Z_{AhAk}-Z_{AhBk}-Z_{AhCk})\sin(\varphi_h-\varphi_k)-\sqrt{3}(Z_{AhBk}-Z_{AhCk})\cos(\varphi_h-\varphi_k)]$$

$$Z_{1(hk)}'=\frac{1}{2}(\underset{1}{Z_{1-h}}+\underset{1}{Z_{1-k}}-\underset{1}{Z_{h-k}})$$

$$Z_{1(hk)}''=Z_{hk}''-Z_{h1}''-Z_{1k}''$$

Self- and Mutual Impedances

SINGLE-PHASE BASIS

The definitions of self- and mutual impedances as applied to transformer connections are the same as those for any static linear network:

"The self-impedance at any pair of terminals of a network is the ratio of an applied potential difference to the resultant current at these terminals, all other terminals being open."[14] "The mutual impedance between any two pairs of terminals of a network is the ratio of the open-circuit potential difference between either pair of terminals to the current at the other pair of terminals, all other terminals being open."[14]

Thus the self-impedance at any pair of terminals of a transformer is simply the self-impedance of the winding connected between the two terminals; and the mutual impedance between any two pairs of terminals is simply the mutual impedance between the windings associated with the two pairs of terminals. Although these definitions are on a single-phase basis, they apply for all transformer connections including 3-phase connections. It should be noted that the definition of mutual impedance implies that the roles of the two pairs of terminals can be interchanged without affecting the results. In other words, mutual impedances of static linear networks are bilateral or reciprocal.

SEQUENCE BASIS

From the definitions of self- and mutual impedances on a single-phase basis definitions on a sequence basis could be deduced, thus:

1. The positive-sequence self-impedance at any terminal set of a 3-phase transformer connection is the ratio of an applied positive-sequence potential difference (on a line-to-neutral basis) to the resultant positive-sequence current at this terminal set, all other terminal sets being open. Negative- and zero-sequence self-impedances could be defined in a similar manner.

2. The positive-sequence mutual impedance between any two terminal sets of a 3-phase transformer connection is the ratio of the open-circuit positive-sequence potential difference (on a line-to-neutral basis) at either terminal set to the positive-sequence current at the other terminal set, all other terminal sets being open. Negative- and zero-sequence mutual impedances could be defined in a similar manner.

These definitions may be satisfactory as such, but they do not reveal the relations between impedances on a single-phase basis and those on a sequence basis; nor do they even suggest that the characteristics of the impedances on one basis might differ from those on the other. Actually, the foregoing definitions of positive- and negative-sequence mutual impedances are not strictly correct in that they imply reciprocity in all cases. Therefore, to investigate thoroughly the concepts of sequence self- and mutual impedances, explicit algebraic expressions in terms of ordinary self- and mutual impedances are derived in the following analysis:

Fig. 1 shows diagrammatically the terminals of a 3-phase multicircuit transformer connection having n terminal sets, each of which consists of three line terminals and a neutral terminal. The diagram is intended to give no hint of the winding circuits associated with the various terminal sets. The coil connections may consist of any number of delta circuits, wye circuits, phase interconnections, autotransformer connections, series connections, parallel connections, coupling circuits, and combinations of these. (Using the definition of Garin and Paluev,[3] "The term phase interconnection will be used to describe circuits in which the electrical and magnetic phases to not coincide." In other words, each electrical phase is not restricted to a single magnetic phase. Examples of this type of circuit are zigzag, extended delta, inscribed delta, and various phase-shift connections.) In fact, the core (or cores) and coils may be constructed, arranged, and connected in any conceivable manner provided:

The connection possesses 3-phase symmetry, defined as follows:

A system of impedances possesses 3-phase symmetry if positive-sequence current through the system or any part thereof produces only positive-sequence potential differences between any two points of the system, negative-sequence current produces only negative-sequence potential differences, and zero-sequence current produces only zero-sequence potential differences.

It is assumed that, if the coils associated with any terminal set are connected so that a physical neutral point exists, as in the case of a wye circuit, then this neutral point is connected to the neutral terminal through zero impedance. If, as in the case of a delta circuit, no physical neutral point exists, the neutral terminal is assumed to be isolated from the coils as far as electrical connections are concerned; however, if necessary for visualization of line-to-neutral voltages, the neutral terminal may be assumed to be symmetrically connected to the coils through extremely high impedances.

For steady-state conditions of currents which vary sinusoidally with time at a single constant frequency, the voltages from line terminals to neutral terminal of any terminal set h can be expressed in complex-quantity notation as functions of line currents and self- and mutual impedances, thus

$$E_{Ah}=\sum_{k=1}^{n}(Z_{AhAk}I_{Ak}+Z_{AhBk}I_{Bk}+Z_{AhCk}I_{Ck}) \quad (1)$$

$$E_{Bh}=\sum_{k=1}^{n}(Z_{BhAk}I_{Ak}+Z_{BhBk}I_{Bk}+Z_{BhCk}I_{Ck}) \quad (2)$$

$$E_{Ch}=\sum_{k=1}^{n}(Z_{ChAk}I_{Ak}+Z_{ChBk}I_{Bk}+Z_{ChCk}I_{Ck}) \quad (3)$$

in which all currents, voltages, and impedances are in pu based on a common volt-ampere base and voltage bases are related to one another in the same manner as corresponding positive-sequence rated no-load voltages.

The various impedances in equations 1, 2, and 3 are for line-to-neutral circuits. Thus, e.g., Z_{AhAk} is the mutual impedance between the two circuits Ah to Nh and Ak to Nk; if $k=h$, $Z_{AhAk}=Z_{AhAh}$ is the self-impedance of the circuit Ah to Nh. All mutual impedances are reciprocal, i.e.

$Z_{AhBk}=Z_{BkAh}$, etc.

Using standard equations given in any text on symmetrical components[12] all currents of equations 1, 2, and 3 are replaced by their symmetrical components and the symmetrical components of voltages are found to be

$$\begin{aligned}\underset{1}{E_h}=\frac{1}{3}\sum_{k=1}^{n}\{&[(Z_{AhAk}+Z_{BhBk}+Z_{ChCk})+\\&a^2(Z_{AhBk}+Z_{BhCk}+Z_{ChAk})+\\&a(Z_{AhCk}+Z_{BhAk}+Z_{ChBk})]\underset{1}{I_k}+\\&[(Z_{AhAk}+Z_{BhCk}+Z_{ChBk})+\\&a^2(Z_{AhCk}+Z_{BhBk}+Z_{ChAk})+\\&a(Z_{AhBk}+Z_{BhAk}+Z_{ChCk})]\underset{2}{I_k}+\\&[(Z_{AhAk}+Z_{AhBk}+Z_{AhCk})+\\&a^2(Z_{ChAk}+Z_{ChBk}+Z_{ChCk})+\\&a(Z_{BhAk}+Z_{BhBk}+Z_{BhCk})]\underset{0}{I_k}\}\end{aligned}\tag{4}$$

$$\begin{aligned}\underset{2}{E_h}=\frac{1}{3}\sum_{k=1}^{n}\{&[(Z_{AhAk}+Z_{BhCk}+Z_{ChBk})+\\&a(Z_{AhCk}+Z_{BhBk}+Z_{ChAk})+\\&a^2(Z_{AhBk}+Z_{BhAk}+Z_{ChCk})]\underset{1}{I_k}+\\&[(Z_{AhAk}+Z_{BhBk}+Z_{ChCk})+\\&a(Z_{AhBk}+Z_{BhCk}+Z_{ChAk})+\\&a^2(Z_{AhCk}+Z_{BhAk}+Z_{ChBk})]\underset{2}{I_k}+\\&[(Z_{AhAk}+Z_{AhBk}+Z_{AhCk})+\\&a(Z_{ChAk}+Z_{ChBk}+Z_{ChCk})+\\&a^2(Z_{BhAk}+Z_{BhBk}+Z_{BhCk})]\underset{0}{I_k}\}\end{aligned}\tag{5}$$

$$\begin{aligned}\underset{0}{E_h}=\frac{1}{3}\sum_{k=1}^{n}\{&[(Z_{AhAk}+Z_{BhAk}+Z_{ChAk})+\\&a^2(Z_{AhBk}+Z_{BhBk}+Z_{ChBk})+\\&a(Z_{AhCk}+Z_{BhCk}+Z_{ChCk})]\underset{1}{I_k}+\\&[(Z_{AhAk}+Z_{BhAk}+Z_{ChAk})+\\&a(Z_{AhBk}+Z_{BhBk}+Z_{ChBk})+\\&a^2(Z_{AhCk}+Z_{BhCk}+Z_{ChCk})]\underset{2}{I_k}+\\&[(Z_{AhAk}+Z_{BhBk}+Z_{ChCk})+\\&(Z_{AhBk}+Z_{BhCk}+Z_{ChAk})+\\&(Z_{AhCk}+Z_{BhAk}+Z_{ChBk})]\underset{0}{I_k}\}\end{aligned}\tag{6}$$

in which a is the usual operator used in analyses by the method of symmetrical components, i.e.

$$a=\exp j\frac{2\pi}{3}=-\frac{1}{2}+j\frac{\sqrt{3}}{2}$$

Positive-, negative-, and zero-sequence components of voltage are denoted by $\underset{1}{E}$, $\underset{2}{E}$, and $\underset{0}{E}$ respectively. Similar notation is used for currents and impedances. To simplify notation, identification of the reference phase is omitted from the subscripts of symmetrical components of voltages and currents, it being understood that in all cases the reference is phase A. Thus, for example, $\underset{1}{E_h}$ is used instead of the usual notation which would be $\underset{1}{E_{Ah}}$.

Three-phase symmetry has been assumed. It follows from the definition of such symmetry that the coefficients of $\underset{2}{I_k}$ and $\underset{0}{I_k}$ in equation 4, the coefficients of $\underset{1}{I_k}$ and $\underset{0}{I_k}$ in equation 5, and the coefficients of $\underset{1}{I_k}$ and $\underset{2}{I_k}$ in equation 6 must each be equal to zero. Equating these coefficients to zero and solving the resulting six equations yields

$$Z_{AhAk}=Z_{BhBk}=Z_{ChCk}\tag{7}$$

$$Z_{AhBk}=Z_{BhCk}=Z_{ChAk}\tag{8}$$

$$Z_{AhCk}=Z_{BhAk}=Z_{ChBk}\tag{9}$$

Equations 7, 8, and 9 are the sole criteria of 3-phase symmetry of multicircuit transformer connections. It will be noticed that in each of these equations the phase identification subscripts appear in cyclic order, which is exactly as would be expected for symmetry.

It should be pointed out that 3-phase symmetry does not require that

$$Z_{AhAk}=Z_{AhBk}$$

$$Z_{AhAk}=Z_{AhCk}$$

or

$$Z_{AhBk}=Z_{AhCk}$$

Therefore, these relations cannot be taken for granted. Consequently, for the sake of generality, it will be assumed that

$$\left.\begin{aligned}Z_{AhAk}\neq Z_{AhBk}\\Z_{AhAk}\neq Z_{AhCk}\\Z_{AhBk}\neq Z_{AhCk}\end{aligned}\right\}\tag{10}$$

Substitutions of equations 7, 8, and 9 in equations 4, 5, and 6 yield

$$\underset{1}{E_h}=\sum_{k=1}^{n}(Z_{AhAk}+a^2Z_{AhBk}+aZ_{AhCk})\underset{1}{I_k}\tag{11}$$

$$\underset{2}{E_h}=\sum_{k=1}^{n}(Z_{AhAk}+aZ_{AhBk}+a^2Z_{AhCk})\underset{2}{I_k}\tag{12}$$

$$\underset{0}{E_h}=\sum_{k=1}^{n}(Z_{AhAk}+Z_{AhBk}+Z_{AhCk})\underset{0}{I_k}\tag{13}$$

In general the positive-sequence components of no-load voltages, taken simultaneously at the various sets of terminals will not be in phase with one another. This also applies to the negative-sequence components; this is the result of either arbitrary designation of corresponding phases of the various terminal sets or differences in coil connections associated with the various terminal sets or a combination of the two. It is desirable to eliminate the effects of this condition to simplify the analysis. Therefore, let

$$\underset{1}{E_h}'=\underset{1}{E_h}\exp j\varphi_h\tag{14}$$

$$\underset{1}{I_k}'=\underset{1}{I_k}\exp j\varphi_k \text{ or } \underset{1}{I_k}=\underset{1}{I_k}'\exp(-j\varphi_k)\tag{15}$$

$$\underset{2}{E_h}'=\underset{2}{E_h}\exp(-j\varphi_h)\tag{16}$$

$$\underset{2}{I_k}'=\underset{2}{I_k}\exp(-j\varphi_k) \text{ or } \underset{2}{I_k}=\underset{2}{I_k}'\exp j\varphi_k\tag{17}$$

This is exactly the same type of rotation and is used for the same purpose as that used for wye-delta transformer connections in terms of symmetrical components, i.e., positive-sequence components of voltage and current experience a phase rotation of 90 degrees in one direction because of the wye-delta transformation while negative-sequence quantities experience the same angular rotation, but in the opposite direction. The angle may be 30 degrees instead of 90 degrees depending upon the convention used in designating corresponding phases of the wye and delta terminal sets.

Substitutions of equations 15 and 17 in equations 11 and 12 respectively followed by substitutions of the resulting equations in equations 14 and 16 respectively yield.

$$\underset{1}{E_h}'=\sum_{k=1}^{n}\underset{1}{Z_{hk}}\underset{1}{I_k}'\tag{18}$$

$$\underset{2}{E_h}'=\sum_{k=1}^{n}\underset{2}{Z_{hk}}\underset{2}{I_k}'\tag{19}$$

in which

$$\underset{1}{Z_{hk}}=(Z_{AhAk}+a^2Z_{AhBk}+aZ_{AhCk})\exp j(\varphi_h-\varphi_k)\tag{20}$$

$$\underset{2}{Z_{hk}}=(Z_{AhAk}+aZ_{AhBk}+a^2Z_{AhCk})\exp j(\varphi_k-\varphi_h)\tag{21}$$

Equations 20 and 21 can be expanded respectively to

$$\underset{1}{Z_{hk}}=Z_{hk}'+jZ_{hk}''\tag{22}$$

$$\underset{2}{Z_{hk}}=Z_{hk}'-jZ_{hk}''\tag{23}$$

in which

$$Z_{hk}'=\frac{1}{2}[(2Z_{AhAk}-Z_{AhBk}-Z_{AhCk})\cos(\varphi_h-\varphi_k)+\sqrt{3}(Z_{AhBk}-Z_{AhCk})\sin(\varphi_h-\varphi_k)]\tag{24}$$

$$Z_{hk}''=\frac{1}{2}[(2Z_{AhAk}-Z_{AhBk}-Z_{AhCk})$$

$$\sin(\varphi_h-\varphi_k)-\sqrt{3}(Z_{AhBk}-Z_{AhCk})\cos(\varphi_h-\varphi_k)] \quad (25)$$

The positive-sequence self-impedance at any terminal set h can be obtained from equation 22 by letting $k=h$, thus

$$\underset{1}{Z}_{hh}=\frac{1}{2}[(2Z_{AhAh}-Z_{AhBh}-Z_{AhCh})-j\sqrt{3}(Z_{AhBh}-Z_{AhCh})]$$

From equation 9 and because of the fact that actual mutual impedances are reciprocal

$$Z_{AhCh}=Z_{AhBh}$$

Therefore, the positive-sequence self-impedance at any terminal set h becomes

$$\underset{1}{Z}_{hh}=Z_{AhAh}-Z_{AhBh} \quad (26)$$

Similarly from equation 23, the negative-sequence self-impedance at any terminal set h can be found to be

$$\underset{2}{Z}_{hh}=Z_{AhAh}-Z_{AhBh} \quad (27)$$

From equation 13, the zero-sequence self-impedance at any terminal set h can be found to be

$$\underset{0}{Z}_{hh}=Z_{AhAh}+2Z_{AhBh} \quad (28)$$

A discussion of the significance of equations equivalent to equations 26, 27, and 28, in practically the same form, has been presented by Garin[15] and will not be repeated here. By interchanging the positions of the h and k subscripts in equations 24 and 25 and utilizing equations 7, 8, and 9, it will be seen that

$$Z_{kh}'=Z_{hk}' \quad (29)$$

$$Z_{kh}''=-Z_{hk}'' \quad (30)$$

Therefore interchange of positions of subscripts in equations 22 and 23 results in

$$\underset{1}{Z}_{kh}=Z_{hk}'-jZ_{hk}'' \quad (31)$$

$$\underset{2}{Z}_{kh}=Z_{hk}'+jZ_{hk}'' \quad (32)$$

Equations 22 and 23 are expressions for the positive- and negative-sequence mutual impedances between any two terminal sets h and k, h being the terminal set at which the voltage is measured and k being the terminal set at which the current is measured. Equations 31 and 32 are expressions for the positive- and negative-sequence mutual impedances between the same two terminal sets but with their roles reversed, k being the terminal set at which the voltage is measured and h being the terminal set at which the current is measured. A glance at these four equations reveals some rather interesting facts:

1. The positive-sequence mutual impedances are, in general, nonreciprocal. Moreover, they are nonreciprocal in a very definite manner. If actual mutual impedances are pure inductive reactances, as usually assumed in transformer-impedance circuit theory, then the positive-sequence mutual impedances between any two terminal sets are the negative conjugates of one another.

2. The same is true of the negative-sequence mutual impedances.

3. The positive-sequence mutual impedance from one terminal set to another terminal set is equal to the negative-sequence mutual impedance taken in reverse order. In other words

$$\underset{1}{Z}_{hk}=\underset{2}{Z}_{kh} \text{ and } \underset{1}{Z}_{kh}=\underset{2}{Z}_{hk}$$

From equation 13, the zero-sequence mutual impedance is

$$\underset{0}{Z}_{hk}=Z_{AhAk}+Z_{AkBk}+Z_{AhCk} \quad (33)$$

Interchanging the positions of the h and k subscripts in equation 33, and application of equations 8 and 9 results in

$$\underset{0}{Z}_{hk}=\underset{0}{Z}_{kh} \quad (34)$$

Therefore, the zero-sequence mutual impedances between terminal sets are, unlike the positive- and negative-sequence mutual impedances, always reciprocal.

Series-Opposition Impedances

SINGLE-PHASE BASIS

For practical reasons, the impedance characteristics of transformers are usually expressed in terms of series-opposition impedances (generally referred to as short-circuit or leakage impedances) instead of self- and mutual impedances. On a single-phase basis, the pu series-opposition impedance between any two windings r and s on the same magnetic circuit is given by the well-known expression

$$Z_{r-s}=Z_{rr}+Z_{ss}-2Z_{rs}$$

where

Z_{rr}, Z_{ss} = the pu self-impedances of the r and s windings respectively
Z_{rs} = the pu mutual impedance between the two windings

The derivation of this expression is based on the assumption that the sum of the pu currents in the two windings is zero, i.e.

$$I_r+I_s=0$$

SEQUENCE BASIS

Similarly, the positive-sequence series-opposition impedance between any two terminal sets h and k is the impedance which would be measured if the currents at the two terminal sets were forced to meet the relation

$$\underset{1}{I}_h'+\underset{1}{I}_k'=0 \quad (35)$$

It is, of course, assumed that no other terminal sets are carrying current.

For negative and zero sequence, the forced relations are

$$\underset{2}{I}_h'+\underset{2}{I}_k'=0 \quad (36)$$

$$\underset{0}{I}_h+\underset{0}{I}_k=0 \quad (37)$$

Utilizing equations 18 and 35, the positive-sequence series-opposition impedance between terminal sets is found to be

$$\underset{1}{Z}_{h-k}=(\underset{1}{E}_h'-\underset{1}{E}_k')/\underset{1}{I}_h'=\underset{1}{Z}_{hh}+\underset{1}{Z}_{kk}-\underset{1}{Z}_{hk}-\underset{1}{Z}_{kh} \quad (38)$$

Similarly, from equations 19 and 36 the negative-sequence series-opposition impedance can be found to be

$$\underset{2}{Z}_{h-k}=\underset{2}{Z}_{hh}+\underset{2}{Z}_{kk}-\underset{2}{Z}_{hk}-\underset{2}{Z}_{kh} \quad (39)$$

From equations 13, 28, 33, 34, and 37, the zero-sequence series-opposition impedance between terminal sets h and k can be determined

$$\underset{0}{Z}_{h-k}=\underset{0}{Z}_{hh}+\underset{0}{Z}_{kk}-2\underset{0}{Z}_{hk} \quad (40)$$

It will be noticed that equation 40 is of the same form as that of the series-opposition impedance between windings on a single-phase basis whereas equations 38 and 39 are of slightly different form. The difference, of course, is because the positive- and negative-sequence mutual impedances are not necessarily reciprocal.

Substitutions of equations 22 and 31 in equation 38, and substitutions of equations 23 and 32 in equation 39 yield

$$\underset{1}{Z}_{h-k}=\underset{1}{Z}_{hh}+\underset{1}{Z}_{kk}-2Z_{hk}' \quad (41)$$

$$\underset{2}{Z}_{h-k}=\underset{2}{Z}_{hh}+\underset{2}{Z}_{kk}-2Z_{hk}' \quad (42)$$

But from equations 26 and 27

$$\underset{1}{Z}_{hh}=\underset{2}{Z}_{hh}$$

$$\underset{1}{Z}_{kk}=\underset{2}{Z}_{kk}$$

Therefore

$$\underset{1}{Z}_{h-k}=\underset{2}{Z}_{h-k} \quad (43)$$

Equation 43 states that the positive- and negative-sequence series-opposition impedances between any two terminal sets are equal, as would be expected.

Also there is nothing unusual about equations 41 and 42. When self- and mutual impedances were combined to obtain these expressions, the *j* terms, which prevent the mutual impedances from being reciprocal, disappeared. Therefore, the nonreciprocal feature of positive- and negative-sequence mutual impedances does not appear in the expressions for positive- and negative-sequence series-opposition impedances between any two terminal sets. It might be concluded from this that the nonreciprocal feature has no practical effect on the impedance characteristics of 3-phase transformer connections because these characteristics are usually expressed in terms of series-opposition impedances, which appear to be free of the effects. Related to such reasoning, there is a popular misconception that the impedance characteristics, with the possible exception of zero sequence, of 3-phase transformer connections can be completely expressed in terms of series-opposition impedances between all possible pairs of terminal sets. That such reasoning is, in general, unsound is revealed by continuing the analysis to obtain sequence branch impedances.

Branch Impedances

SINGLE-PHASE BASIS

The usual procedure in developing the circuit theory of multicircuit transformers on a single-phase basis is to assume that all windings are carrying current and that the sum of the pu currents in the various windings on the single magnetic circuit is zero. In other words, magnetizing current is neglected, which is justifiable in case of single-phase transformers having a closed magnetic circuit of high-permeability material. This assumption having been made, the number of independent winding currents is reduced to one less than the number of windings involved; and expressions for voltages across individual windings as functions of winding currents and transformer impedances alone become meaningless. Continuation of the analysis from this point usually leads to a system of transformer voltage equations[4] or an equivalent system of current equations.[16] In either case, the number of independent voltages and currents is one less than the number of windings involved. The system of voltage equations is of the form

$$E_r - E_1 = \sum_{s=2}^{n} Z_{1(rs)} I_s,\ r = 2, 3, \ldots, n$$

where *n* is the number of windings involved, and winding no. 1 is designated as the reference winding. The impedances $Z_{1(rs)}$ are referred to as branch impedances and each consists of three series-opposition impedances, thus

$$Z_{1(rs)} = \frac{1}{2}(Z_{1-r} + Z_{1-s} - Z_{r-s})$$

If there are only three windings, 1, *r* and *s*, $Z_{1(rs)}$ is that branch of the 3-terminal star equivalent network which connects to the no. 1 terminal; hence the logic of the name branch impedance and the subscript notation.

The transformer voltage equations (or current equations) are the ultimate mathematical expressions which define the impedance characteristics of the transformer. They are the equations which the equivalent circuit must satisfy if such is used to represent the transformer impedance characteristics.

SEQUENCE BASIS

To obtain the voltage equations on a sequence basis and the sequence branch impedances which they yield, the general analysis is continued.

Equation 18 can be partially expanded to

$$\underset{1}{E}_h{}' = \underset{1}{Z}_{h1} \underset{1}{I}_1{}' + \sum_{k=2}^{n} \underset{1}{Z}_{hk} \underset{1}{I}_k{}' \qquad (44)$$

Making the assumption that magnetizing current is negligible, which is justifiable in the case of positive sequence

$$\sum_{k=1}^{n} \underset{1}{I}_k{}' = 0$$

from which

$$\underset{1}{I}_1{}' = -\sum_{k=2}^{n} \underset{1}{I}_k{}' \qquad (45)$$

Substitution of equation 45 in equation 44 yields

$$\underset{1}{E}_h{}' = \sum_{k=2}^{n} (\underset{1}{Z}_{hk} - \underset{1}{Z}_{h1}) \underset{1}{I}_k{}' \qquad (46)$$

The positive-sequence component of voltage at terminal set no. 1, which is arbitrarily chosen as the reference terminal set, is from equation 46

$$\underset{1}{E}_1{}' = \sum_{k=2}^{n} (\underset{1}{Z}_{1k} - \underset{1}{Z}_{11}) \underset{1}{I}_k{}' \qquad (47)$$

Subtracting equation 47 from 46 to obtain the difference between the positive-sequence component of voltage at any terminal set *h* and the reference terminal set

$$\underset{1}{E}_{h1}{}' = \underset{1}{E}_h{}' - \underset{1}{E}_1{}' = \sum_{k=2}^{n} \underset{1}{Z}_{1(hk)} \underset{1}{I}_k{}',$$
$$h = 2, 3, 4, \ldots n \qquad (48)$$

in which

$$\underset{1}{Z}_{1(hk)} = \underset{1}{Z}_{hk} + \underset{1}{Z}_{11} - \underset{1}{Z}_{h1} - \underset{1}{Z}_{1k} \qquad (49)$$

The system of positive-sequence transformer voltage equations is given in equation 48; and the positive-sequence branch impedance between any two terminal sets *h* and *k* with terminal set no. 1 as reference is given in equation 49. It should be noted that positions of subscripts of the branch impedance have significance. Within the subscript parenthesis, *h* represents the terminal set between which and terminal set no. 1 voltage is measured and *k* represents the terminal set at which current is measured.

Utilizing the general equation 22, equation 49 becomes

$$\underset{1}{Z}_{1(hk)} = (Z_{hk}{}' + Z_{11}{}' - Z_{h1}{}' - Z_{1k}{}') +$$
$$j(Z_{hk}{}'' - Z_{h1}{}'' - Z_{1k}{}'') \qquad (50)$$

There are only three impedances in the *j* term of equation 50 because from equations 25 and 8,

$$Z_{11}{}'' = 0$$

By use of the general equation 41, equation 50 can be reduced to

$$\underset{1}{Z}_{1(hk)} = Z_{1(hk)}{}' + jZ_{1(hk)}{}'' \qquad (51)$$

in which

$$Z_{1(hk)}{}' = (\underset{1}{Z}_{1-h} + \underset{1}{Z}_{1-k} - \underset{1}{Z}_{h-k})/2 \qquad (52)$$

$$Z_{1(hk)}{}'' = Z_{hk}{}'' - Z_{h1}{}'' - Z_{1k}{}'' \qquad (53)$$

Later $Z_{1(hk)}{}''$ will be expressed in terms of winding-to-winding series-opposition impedances. By referring to equations 29, 30, and 41, it can be seen that interchanging the positions of the subscripts *h* and *k* in equation 51 results in

$$\underset{1}{Z}_{1(kh)} = Z_{1(hk)}{}' - jZ_{1(hk)}{}'' \qquad (54)$$

Equation 48 gives the difference between the positive-sequence component of the voltage at any terminal set and that at the reference terminal set as the sum of $(n-1)$ terms. One of the terms is the product of the terminal set's own positive-sequence component of current and a branch impedance, whereas each of the other terms is the product of some other terminal set's positive-sequence component of current and a branch impedance. Thus, in each of equations 48, there is one branch impedance $\underset{1}{Z}_{1(hh)}$ which resembles a self-impedance, so it will be referred to as a branch self-impedance. The remaining $(n-2)$ impedances, $\underset{1}{Z}_{1(hk)}$ for $k=2$ to n and $k \neq h$, resemble mutual impedances, so they will be referred to as the branch mutual impedances.

Table I. Phase-Shift Angles and Impedance Relations for Combinations of Simple Wye and Delta Connections

Connection	$(\varphi_h-\varphi_k)$, Degrees	Impedance Relations
Wye to wye or delta to delta	0 or 180	$Z_{AhBk}=Z_{AhCk}$
Wye to delta	30 or 210	$Z_{AhAk}=-Z_{AhCk}$ and $Z_{AhBk}=0$
Wye to wye or delta to delta	60 or 240	$Z_{AhAk}=Z_{AhBk}$
Wye to delta	90 or 270	$Z_{AhBk}=-Z_{AhCk}$ and $Z_{AhAk}=0$
Wye to wye or delta to delta	120 or 300	$Z_{AhAk}=Z_{AhCk}$
Wye to delta	150 or 330	$Z_{AhAk}=-Z_{AhBk}$ and $Z_{AhCk}=0$

Upon letting $k=h$ and utilizing equations 8, 9, 25, and 38, equation 51 yields

$$\underset{1}{Z_{1(hh)}}=\underset{1}{Z_{1-h}} \qquad (55)$$

This is the positive-sequence branch self-impedance which appears in equation 48 and is simply the positive-sequence series-opposition impedance between the h and the reference terminal sets.

The positive-sequence branch mutual impedance between terminal sets h and k with terminal set no. 1 as reference is given by equation 51, while that between terminal sets k and h (order reversed) is given by equation 54.

The negative-sequence equations which correspond to equations 48, 51, 54, and 55 can be found to be

$$\underset{2}{E_h'}-\underset{2}{E_1'}=\sum_{k=2}^{n}\underset{2}{Z_{1(hk)}}\underset{2}{I_k'} \qquad (56)$$

$$\underset{2}{Z_{1(hk)}}=Z_{1(hk)}'-jZ_{1(hk)}'' \qquad (57)$$

$$\underset{2}{Z_{1(kh)}}=Z_{1(hk)}'+jZ_{1(hk)}'' \qquad (58)$$

$$\underset{2}{Z_{1(hh)}}=\underset{2}{Z_{1-h}} \qquad (59)$$

The assumption that the sum of pu terminal currents is zero, which was made in the positive- and negative-sequence cases, is not generally applicable in the analysis of zero-sequence characteristics, especially in cases of 3-phase 3-legged core-type construction; and, most certainly, regardless of type of core or cores, the sum of the zero-sequence components of terminal currents cannot be assumed to be zero if any circuits, such as a delta connection, are involved which provide a path for circulating zero-sequence current. Therefore, the approach to zero-sequence branch impedances must be made without this assumption.

Substitution of equation 33 in equation 13 yields

$$\underset{0}{E_h}=\sum_{k=1}^{n}\underset{0}{Z_{hk}}\underset{0}{I_k} \qquad (60)$$

but from equation 40

$$\underset{0}{Z_{hk}}=\frac{1}{2}(\underset{0}{Z_{hh}}+\underset{0}{Z_{kk}}-\underset{0}{Z_{h-k}}) \qquad (61)$$

Although $\underset{0}{Z_{hk}}$ is the zero-sequence mutual impedance between terminal sets h and k, it will also be referred to as the zero-sequence branch impedance between the two terminal sets to make equation 60 as nearly as possible consistent with equations 48 and 56. It should be noted that there is no reference terminal set in case of zero sequence because the assumption that $\Sigma I=0$ has not been made.

It has already been shown that the zero-sequence mutual impedances between terminal sets are always reciprocal. This fact is not altered by referring to them as zero-sequence branch impedances.

Significance of General Equations

The branch mutual impedances given by equations 51, 54, 57, and 58 are very similar to the sequence mutual impedances given by equations 22, 23, 31, and 32 in that they exhibit the same type of nonreciprocal characteristics which have been pointed out with respect to the latter. However the statement regarding negative conjugates does not apply because, in general, $Z_{1(hk)}'$ has both real and imaginary components.

Since there are $(n-1)$ equations 48 and since each contains $(n-1)$ impedance terms, there are $(n-1)^2$ impedances involved of which $(n-1)$ are branch self-impedances and the remaining (n^2-3n+2) are branch mutual impedances. In the most general case, none of the mutual impedances is reciprocal; therefore, the necessary and sufficient number of independent impedances required to define the positive-sequence impedance characteristics of a 3-phase transformer having n terminal sets is $(n-1)$.^{2}

Depending upon the way in which the windings are arranged and connected, some or all of the branch mutual impedances may be reciprocal, so the number of independent impedances is less than $(n-1)^2$ in a large majority of cases.

If there are no phase interconnections, the possible winding connections are limited to those which, in effect, are equivalent to simple wye and delta circuits. In such cases, possible values of the angle $(\varphi_h-\varphi_k)$ are limited to those which can be obtained with the various combinations of simple wye and delta connections; and for each possible angle, it can be shown that certain definite relations exist between the mutual impedances Z_{AhAk}, Z_{AhBk}, and Z_{AhCk}. A list of the possible angles and associated relations between mutual impedances is given in Table I.

Substitution of any one of these combinations of angle and impedance relations in equation 25 reduces Z_{hk}'' to zero. Therefore if there are no phase interconnections $Z_{1(hk)}''$, equation 53, reduces to zero, which makes all branch mutual impedances reciprocal. Hence, the number of independent branch mutual impedances is reduced to $(n^2-3n+2)/2$, and the total number of independent branch impedances, self plus mutual, is $n(n-1)/2$. In some cases which involve phase interconnections, reciprocity of branch mutual impedances can be obtained by arranging the windings on the magnetic phases in a manner which results in $Z_{1(hk)}''=0$. This is illustrated in example 1 of Appendix III.

The system of equations 48 defines the positive-sequence impedance characteristics of the transformer based on the assumption that magnetizing currents can be neglected. It, with equation 45, gives all of the information needed for construction of the n-terminal positive-sequence equivalent circuit of a transformer having n terminal sets, except the phase shifts which were eliminated by equations 14 and 15. If necessary for a particular analysis, these phase shifts can be injected by proper rotation of positive-sequence quantities before combining with the other sequences to obtain actual line quantities. Such procedure is no different from the usual 90-degree rotation of positive-sequence quantities required in analyses which include delta-wye transformations. Although all of the necessary information is contained in equations 45 and 48, in some cases it may not be possible to construct an equivalent network made up of simple elements because of the nonreciprocal feature which some of the mutual branch impedances may possess.

The only difference between positive- and negative-sequence branch mutual impedances is the difference in algebraic sign before the j term. Otherwise all of the foregoing discussion with respect to positive sequence also applies to the negative sequence.

The system of equations 60 completely defines the zero-sequence impedance characteristics of the transformer as viewed from the terminals. It contains n^2 impedances of which n are self-impedances and $n(n-1)$ are mutual impedances. Since all of the mutual impedances are reciprocal, the number of independent mutual impedances is $n(n-1)/2$ and the total number of independent impedances required to define the zero-sequence impedance characteristics is $n+n(n-1)/2=n(n+1)/2$.

In circuits which have no physical neutral point and which are not connected to other circuits, no zero-sequence current can flow. Thus, the number of terms in each of equations 60 may be less than n and the number of independent impedances required to define the zero-sequences impedance, as it is viewed from the terminals, may be less than $n(n+1)/2$.

The system of equations 60 gives all of the information necessary for construction of the zero-sequence equivalent circuit of a transformer having n terminal sets. The branch self-impedances which appear therein may be pure zero-sequence magnetizing impedances or a combination of series-opposition impedances between windings and magnetizing impedances. An example of the former is the zero-sequence self-impedance of a simple wye circuit in the absence of any circuit such as a delta connection, which allows zero-sequence current to circulate. Examples of the latter are a wye circuit in the presence of a delta circuit, and a zigzag connection. Some zero-sequence self-impedances may be infinite for practical purposes, such as in the case of a delta-connected circuit.

Determining Branch Impedances

The positive-sequence branch self-impedance as given by equation 55 is simply the series-opposition impedance between the h and reference terminal sets. A convenient method of determining the series-opposition impedance between terminal sets in terms of winding-to-winding series-opposition impedances, after details of windings and connections are known, has been presented by Garin and Paluev.[3] The series-opposition impedance between any two terminal sets can also be obtained by a direct short-circuit test.

The positive-sequence branch mutual impedance give by equation 51 consists of the sum of two terms. The first term contains three series-opposition impedances, each of which can be determined by either calculation or test as explained in the preceding paragraph. The second term $j\underset{1}{Z}_{1(hk)}''$ is somewhat more elusive; however, it also can be determined either by calculation or by test.

After details of windings and connections are known, it is possible to obtain an expression for $\underset{1}{Z}_{1(hk)}''$ as a function of winding-to-winding series-opposition impedances by a number of methods, all of which involve consideration of the h, k, and reference terminal sets simultaneously. A comparatively simple method based on conservation of phasor power,[3] which gives all of the required terminal-set-to-terminal-set series-opposition impedances in addition to $\underset{1}{Z}_{1(hk)}''$, may be shown as follows:

Assume that only the h, k, and reference terminal sets are carrying current, then from equation 48

$$\underset{1}{E}_{h1}'=\underset{1}{Z}_{1(hh)}\underset{1}{I}_h'+\underset{1}{Z}_{1(hk)}\underset{1}{I}_k' \tag{62}$$

$$\underset{1}{E}_{k1}'=\underset{1}{Z}_{1(kh)}\underset{1}{I}_h'+\underset{1}{Z}_{1(kk)}\underset{1}{I}_k' \tag{63}$$

The total phasor power input per electric phase is

$$P+jQ=\underset{1}{E}_{h1}'\underset{1}{I^*}_h'+\underset{1}{E}_{k1}'\underset{1}{I^*}_k'=\underset{1}{Z}_{1(hh)}\underset{1}{I}_h'\underset{1}{I^*}_h'+\underset{1}{Z}_{1(hk)}\underset{1}{I}_k'\underset{1}{I^*}_h'+\underset{1}{Z}_{1(kh)}\underset{1}{I}_h'\underset{1}{I^*}_k'+\underset{1}{Z}_{1(kk)}\underset{1}{I}_k'\underset{1}{I^*}_k' \tag{64}$$

Assume

$$\underset{1}{I}_h'=M$$

$$\underset{1}{I}_k'=Ne^{j\theta}$$

in which M and N are real quantities. Substitutions of these expressions in equation 64 yield

$$P+jQ=\underset{1}{Z}_{1(hh)}M^2+\underset{1}{Z}_{1(kk)}N^2+[\underset{1}{Z}_{1(hk)}+\underset{1}{Z}_{1(kh)}]MN\cos\theta+j[\underset{1}{Z}_{1(hk)}-\underset{1}{Z}_{1(kh)}]MN\sin\theta \tag{65}$$

Substitutions of equations 51, 54, and 55 in equation 65 yield

$$P+jQ=\underset{1}{Z}_{1-h}M^2+\underset{1}{Z}_{1-k}N^2+(\underset{1}{Z}_{1-h}+\underset{1}{Z}_{1-k}-\underset{1}{Z}_{h-k})MN\cos\theta-2\underset{1}{Z}_{1(hk)}''MN\sin\theta \tag{66}$$

After the details of windings and connections are known, the phasor power loss per magnetic phase for the same assumed conditions can be found by the method presented by Garin and Paluev[3] to be

$$P+jQ=M^2f_1(Z)+N^2f_2(Z)+MN\cos\theta[f_3(Z)]+MN\sin\theta[f_4(Z)] \tag{67}$$

in which Z represents winding-to-winding series-opposition impedances.

Based on conservation of phasor power, the total (net) input per electric phase must be equal to the total loss per magnetic phase. Also, since M, N, and θ are arbitrary and independent of one another, corresponding coefficients in equations 66 and 67 can be equated thus

$$\underset{1}{Z}_{1-h}=f_1(Z) \tag{68}$$

$$\underset{1}{Z}_{1-k}=f_2(Z) \tag{69}$$

$$\underset{1}{Z}_{1-h}+\underset{1}{Z}_{1-k}-\underset{1}{Z}_{h-k}=f_3(Z)$$

$$2\underset{1}{Z}_{1(hk)}''=-f_4(Z)$$

From these equations, the following can be found

$$\underset{1}{Z}_{h-k}=f_1(Z)+f_2(Z)-f_3(Z) \tag{70}$$

$$\underset{1}{Z}_{1(hk)}''=-\frac{1}{2}f_4(Z) \tag{71}$$

Use of this method of obtaining the positive-sequence branch impedances in terms of winding-to-winding series-opposition impedances is illustrated in example 1 of Appendix III.

As stated previously, the first term of the positive-sequence branch mutual impedance can be obtained by making three short-circuit tests. The second term can be obtained indirectly from tests in the following manner.

It is shown in Appendix I that

$$\underset{1}{Z}_{1(hk)}''=\pm\sqrt{\underset{1}{Z}_{h-k}(\underset{1}{Z}_{1-h//k}'-\underset{1}{Z}_{1-h//k})} \tag{72}$$

in which $\underset{1}{Z}_{h-k}$ is the series-opposition impedance between the h and k terminal sets. Its value can be obtained from a short-circuit test between the two terminal sets.

$\underset{1}{Z}_{1-h//k}'$ is the apparent series-opposition impedance from the reference terminal set to the h and k terminal sets in parallel, on a pu basis. It can be calculated from the values of $\underset{1}{Z}_{h-k}$, $\underset{1}{Z}_{1-h}$, and $\underset{1}{Z}_{1-k}$ which in turn can be determined from short-circuit tests between terminal sets as indicated by the subscripts. Thus

$$\underset{1}{Z}_{1-h//k}'=\frac{2(\underset{1}{Z}_{h-k}\underset{1}{Z}_{1-h}+\underset{1}{Z}_{h-k}\underset{1}{Z}_{1-k}+\underset{1}{Z}_{1-h}\underset{1}{Z}_{1-k})-(\underset{1}{Z}_{1-h}^2+\underset{1}{Z}_{1-k}^2+\underset{1}{Z}_{h-k}^2)}{4\underset{1}{Z}_{h-k}}$$

$\underset{1}{Z}_{1-h//k}$ is the actual series-opposition impedance from the reference terminal set to the h and k terminal sets in parallel. It can be obtained from a direct short-circuit test made by applying power to the reference terminal set with both the h and k terminal sets short-circuited.

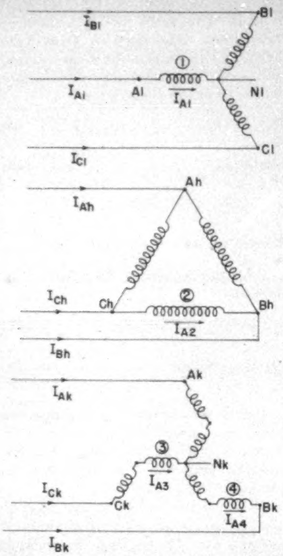

Fig. 2. The wye-delta-zigzag transformer connection

Number of Tests Required

Based on the previous discussion, the total number of independent impedances required to specify the positive-sequence impedance characteristics of a transformer having n terminal sets is, in general, $(n-1)^2$. Therefore, $(n-1)^2$ tests are required to obtain these impedances, assuming that only one impedance is obtained from each test. The $(n-1)^2$ tests can be as follows:

1. Short-circuit tests between all possible pairs of terminal sets. This is a total of $n(n-1)/2$ tests.
2. Short-circuit tests between the reference terminal set and all possible combinations of two other terminal sets short-circuited simultaneously. This is a total of $(n-1)(n-2)/2$ tests.

The sum of tests no. 1 and tests no. 2 is $(n-1)^2$.

It is theoretically possible to obtain the necessary information from tests other than those outlined in the foregoing. For instance, during a short-circuit test from one terminal set to another terminal set, voltages at the inactive terminal sets can be measured. If the values (both magnitude and phase angle) can be determined with sufficient accuracy, the tests outlined under 2 can be avoided; however, this hardly seems practical with commercial test equipment.

The choice of plus or minus sign in equation 72 can be determined from calculation based on details of design or by tests of the type mentioned in the preceding paragraph but of a qualitative nature only.

In general, the total number of impedances required to specify the zero-sequence impedance characteristics has been shown to be $n(n+1)/2$; therefore, this number of zero-sequence tests is required. They can be:

1. Impedance tests at each terminal set with all other terminal sets open. This is a total of n tests.
2. Impedance tests between all possible pairs of terminal sets. This is a total of $n(n-1)/2$ tests.

The sum of tests no. 1 and tests no. 2 is $n(n+1)/2$.

Conclusions

The theoretical analysis presented herein leads to the following conclusions:

1. In general, the necessary and sufficient number of independent impedances required for specification of the positive- or negative-sequence impedance characteristics of a symmetrical 3-phase transformer connection is $(n-1)^2$, in which n is the number of terminal sets.
2. In the absence of phase interconnections, the number of independent impedances given in conclusion no. 1 is reduced to $n(n-1)/2$.
3. In general, the necessary and sufficient number of independent impedances required for specification of the zero-sequence impedance characteristics of a symmetrical 3-phase transformer connection is $n(n+1)/2$, in which n is the number of terminal sets.
4. In general, simple short-circuit tests between all possible pairs of terminal sets will not give sufficient information for specification of the positive- or negative-sequence impedance characteristics of a multicircuit transformer connection.
5. Some positive- and negative-sequence mutual impedances between terminal sets can be nonreciprocal if phase-interconnected windings are involved.
6. Some of the positive- and negative-sequence branch mutual impedances which appear in the transformer voltage equations and which are used in constructing equivalent circuits of multicircuit transformers can be nonreciprocal if phase interconnections are involved.
7. All zero-sequence mutual impedances are always reciprocal.
8. Although in some cases it may not be possible to express the positive- and negative-sequence impedance characteristics completely in terms of series-opposition impedances between terminal sets, it is always possible to express them in terms of series-opposition impedances between windings.
9. The effects of nonreciprocal mutual impedances are particularly serious in cases of parallel operation of multicircuit transformers which are not identical and which contain phase interconnections; see example 2, Appendix III.
10. In Appendix II the general equations in terms of symmetrical components are converted to equations in terms of $\alpha\beta0$[13] components. A comparison of the two sets of equations reveals:

    a. In terms of symmetrical components there are no mutual impedances between quantities of different sequences; but within both positive- and negative-sequence expressions there are nonreciprocal mutual impedances.
    b. In terms of $\alpha\beta0$ components there are mutual impedances between α and β quantities but no nonreciprocal mutual impedances are involved.

Therefore, from the point of view of equivalent circuit representation $\alpha\beta0$ components have an advantage because by their use it is possible to represent the mutual impedances in conventional equivalent circuits made up of simple elements.

Appendix I. Determination of $Z_{1(hk)''}$ from Test

Referring to equation 48, if a series-opposition test is applied between the reference terminal set and the h and k terminal sets in parallel, the following equations result

$$\underset{1}{E}_{h1}{}'=\underset{1}{Z}_{1(hh)}\underset{1}{I}_h{}'+\underset{1}{Z}_{1(hk)}\underset{1}{I}_k{}' \tag{73}$$

$$\underset{1}{E}_{k1}{}'=\underset{1}{Z}_{1(kh)}\underset{1}{I}_h{}'+\underset{1}{Z}_{1(kk)}\underset{1}{I}_k{}' \tag{74}$$

$$\underset{1}{E}_{h1}{}'=\underset{1}{E}_{k1}{}' \tag{75}$$

From which it can be found that

$$[\underset{1}{Z}_{1(hh)}-\underset{1}{Z}_{1(kh)}]\underset{1}{I}_h{}'=[\underset{1}{Z}_{1(kk)}-\underset{1}{Z}_{1(hk)}]\underset{1}{I}_k{}'$$

which can be rearranged to obtain

$$\underset{1}{I}_h{}'=\frac{[\underset{1}{Z}_{1(kk)}-\underset{1}{Z}_{1(hk)}](\underset{1}{I}_h{}'+\underset{1}{I}_k{}')}{\underset{1}{Z}_{1(hh)}+\underset{1}{Z}_{1(kk)}-\underset{1}{Z}_{1(hk)}-\underset{1}{Z}_{1(kh)}} \tag{76}$$

and

$$\underset{1}{I}_k{}'=\frac{[\underset{1}{Z}_{1(hh)}-\underset{1}{Z}_{1(kh)}](\underset{1}{I}_h{}'+\underset{1}{I}_k{}')}{\underset{1}{Z}_{1(hh)}+\underset{1}{Z}_{1(kk)}-\underset{1}{Z}_{1(hk)}-\underset{1}{Z}_{1(kh)}} \tag{77}$$

Substitutions of equations 76 and 77 in equations 73 and 74 yield

$$\underset{1}{E}_{h1}{}'=\underset{1}{E}_{k1}{}'$$

$$=\frac{[\underset{1}{Z_{1(hh)}}\underset{1}{Z_{1(kk)}}-\underset{1}{Z_{1(hk)}}\underset{1}{Z_{1(kh)}}](\underset{1}{I_h'}+\underset{1}{I_k'})}{\underset{1}{Z_{1(hh)}}+\underset{1}{Z_{1(kk)}}-\underset{1}{Z_{1(hk)}}-\underset{1}{Z_{1(kh)}}} \quad (78)$$

Dividing equation 78 by $(I_h'+I_k')$ to obtain the desired series-opposition impedance

$$\underset{1}{Z_{1-h//k}}=\frac{\underset{1}{E_{h1}'}=\underset{1}{E_{k1}'}}{\underset{1}{I_h'}+\underset{1}{I_k'}}$$

$$=\frac{\underset{1}{Z_{1(hh)}}\underset{1}{Z_{1(kk)}}-\underset{1}{Z_{1(hk)}}\underset{1}{Z_{1(kh)}}}{\underset{1}{Z_{1(hh)}}+\underset{1}{Z_{1(kk)}}-\underset{1}{Z_{1(hk)}}-\underset{1}{Z_{1(kh)}}} \quad (79)$$

Substitutions of equations 51, 54, and 55 in equation 79 yield

$$\underset{1}{Z_{1-h//k}}=\underset{1}{Z_{1-h//k}'}-\frac{[Z_{1(hk)}'']^2}{\underset{1}{Z_{h-k}}} \quad (80)$$

in which

$$\underset{1}{Z_{1-h//k}'}=\frac{2(\underset{1}{Z_{1-h}}\underset{1}{Z_{1-k}}+\underset{1}{Z_{1-h}}\underset{1}{Z_{h-k}}+\underset{1}{Z_{1-k}}\underset{1}{Z_{h-k}})-(\underset{1}{Z_{1-h}}^2+\underset{1}{Z_{1-k}}^2+\underset{1}{Z_{h-k}}^2)}{4\underset{1}{Z_{h-k}}}$$

Solving equation 80 for $Z_{1(hk)}''$

$$Z_{1(hk)}''=\pm\sqrt{\underset{1}{Z_{h-k}}(\underset{1}{Z_{1-h//k}'}-\underset{1}{Z_{1-h//k}})} \quad (81)$$

Appendix II. Conversion to $\alpha\beta 0$ Components[12]

If the positive- and negative-sequence currents which appear in equations 48 and 56 are expressed in terms of α and β components, these equations become

$$\underset{1}{E_{h1}'}=\frac{1}{2}\sum_{k=2}^{n}\underset{1}{Z_{1(hk)}}(I_{\alpha k}'+jI_{\beta k}') \quad (82)$$

$$\underset{2}{E_{h1}'}=\frac{1}{2}\sum_{k=2}^{n}\underset{2}{Z_{1(hk)}}(I_{\alpha k}'-jI_{\beta k}') \quad (83)$$

Solving equations 82 and 83 for the α and β components of voltage

$$E_{\alpha h1}'=\frac{1}{2}\sum_{k=2}^{n}[(\underset{1}{Z_{1(hk)}}+\underset{2}{Z_{1(hk)}})I_{\alpha k}'+j(\underset{1}{Z_{1(hk)}}-\underset{2}{Z_{1(hk)}})I_{\beta k}'] \quad (84)$$

$$E_{\beta h1}'=\frac{1}{2}\sum_{k=2}^{n}[(\underset{1}{Z_{1(hk)}}+\underset{2}{Z_{1(hk)}})I_{\beta k}'-j(\underset{1}{Z_{1(hk)}}-\underset{2}{Z_{1(hk)}})I_{\alpha k}'] \quad (85)$$

Substituting equations 51 and 57 in equations 84 and 85

$$E_{\alpha h1}'=\sum_{k=2}^{n}\left[\frac{1}{2}(\underset{1}{Z_{1-h}}+\underset{1}{Z_{1-k}}-\underset{1}{Z_{h-k}})I_{\alpha k}'-Z_{1(hk)}''I_{\beta k}'\right] \quad (86)$$

$$E_{\beta h1}'=\sum_{k=2}^{n}\left[\frac{1}{2}(\underset{1}{Z_{1-h}}+\underset{1}{Z_{1-k}}-\underset{1}{Z_{h-k}})I_{\beta k}'+Z_{1(hk)}''I_{\alpha k}'\right] \quad (87)$$

Equations 86 and 87 do not contain any nonreciprocal mutual impedances; but they do contain mutual impedances between α and β quantities as long as $Z_{1(hk)}''\neq 0$.

Appendix III. Examples

Example 1

The classic example of a multicircuit transformer having phase interconnections is the wye-delta-zigzag connection in which the zig and zag windings have the same number of turns. Such a connection is shown in Fig. 2. The terminals of the wye circuit have been chosen as the reference terminal set; the terminals of the delta circuit are designated as h and those of the zigzag circuit are designated as k. The windings per magnetic phase are identified by numbers 1, 2, 3, and 4, as in Fig. 2.

From equation 48

$$\underset{1}{E_{h1}'}=\underset{1}{Z_{1(hh)}}\underset{1}{I_h'}+\underset{1}{Z_{1(hk)}}\underset{1}{I_k'} \quad (88)$$

$$\underset{1}{E_{k1}'}=\underset{1}{Z_{1(kh)}}\underset{1}{I_h'}+\underset{1}{Z_{1(kk)}}\underset{1}{I_k'} \quad (89)$$

From equation 55

$$\underset{1}{Z_{1(hh)}}=\underset{1}{Z_{1-h}} \quad (90)$$

$$\underset{1}{Z_{1(kk)}}=\underset{1}{Z_{1-k}} \quad (91)$$

and from equations 51 and 54

$$\underset{1}{Z_{1(hk)}}=\frac{1}{2}(\underset{1}{Z_{1-h}}+\underset{1}{Z_{1-k}}-\underset{1}{Z_{h-k}})+jZ_{1(hk)}'' \quad (92)$$

$$\underset{1}{Z_{1(kh)}}=\frac{1}{2}(\underset{1}{Z_{1-h}}+\underset{1}{Z_{1-k}}-\underset{1}{Z_{h-k}})-jZ_{1(hk)}'' \quad (93)$$

Utilizing the method presented by Garin and Paluev[8] or any other convenient method, the various terminal-set-to-terminal-set series-opposition impedances can be expressed in terms of winding-to-winding series-opposition impedances

$$\underset{1}{Z_{1-h}}=Z_{1-2} \quad (94)$$

$$\underset{1}{Z_{1-k}}=\frac{1}{2}Z_{1-3}+\frac{1}{2}Z_{1-4}-\frac{1}{6}Z_{3-4} \quad (95)$$

$$\underset{1}{Z_{h-k}}=\frac{1}{2}Z_{2-3}+\frac{1}{2}Z_{2-4}-\frac{1}{6}Z_{3-4} \quad (96)$$

All that remains to be done is to get an expression for $Z_{1(hk)}''$ in terms of winding-to-winding series-opposition impedances. This is accomplished by use of the method described in the section entitled "Determining Branch Impedances."

Referring to Fig. 2 and using the no-load voltage at terminal $A1$ as the reference

$\varphi_h=\varphi_k=90°$

From equation 15

$$\underset{1}{I_h}=-j\underset{1}{I_h'} \quad (97)$$

$$\underset{1}{I_k}=-j\underset{1}{I_k'} \quad (98)$$

Letting $\underset{1}{I_h'}=M$ and $I_k'=N\epsilon^{j\theta}$, equations 97 and 98 become

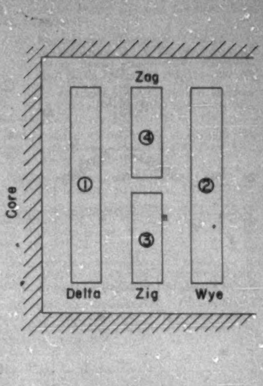

Fig. 3. Symmetrical arrangement of wye, delta, and zigzag windings which results in $Z_{1(hk)}''=0$

$$\underset{1}{I_h}=-jM \quad (99)$$

$$\underset{1}{I_k}=-jN\epsilon^{j\theta} \quad (100)$$

Using these as the pu input currents at the h and k terminal sets, the pu currents in the windings of magnetic phase A can be found to be

$$I_{A1}=-M-N\epsilon^{j\theta} \qquad I_{A3}=-\frac{ja}{\sqrt{3}}N\epsilon^{j\theta}$$

$$I_{A2}=M \qquad I_{A4}=\frac{ja^2}{\sqrt{3}}N\epsilon^{j\theta}$$

Using the method of Garin and Paluev,[8] the pu phasor power loss per magnetic phase is

$$P+jQ=M^2Z_{1-2}+N^2\left(\frac{1}{2}Z_{1-3}+\frac{1}{2}Z_{1-4}-\frac{1}{6}Z_{3-4}\right)+MN\cos\theta\left(Z_{1-2}+\frac{1}{2}Z_{1-3}+\frac{1}{2}Z_{1-4}-\frac{1}{2}Z_{2-3}-\frac{1}{2}Z_{2-4}\right)+MN\sin\theta\left(\frac{1}{2\sqrt{3}}(Z_{1-4}+Z_{2-3}-Z_{1-3}-Z_{2-4})\right)$$

Thus from equations 68 through 71

$$\underset{1}{Z_{1-h}}=Z_{1-2} \quad (101)$$

$$\underset{1}{Z_{1-k}}=\frac{1}{2}Z_{1-3}+\frac{1}{2}Z_{1-4}-\frac{1}{6}Z_{3-4} \quad (102)$$

$$\underset{1}{Z_{h-k}}=\frac{1}{2}Z_{2-3}+\frac{1}{2}Z_{2-4}-\frac{1}{6}Z_{3-4} \quad (103)$$

$$Z_{1(hk)}''=\frac{1}{4\sqrt{3}}(Z_{1-3}+Z_{2-4}-Z_{1-4}-Z_{2-3}) \quad (104)$$

Equations 101, 102, and 103 are the same as 94, 95, and 96 and serve as a check.

After substituting the appropriate subsequent equations in equations 88 and 89, the following are obtained

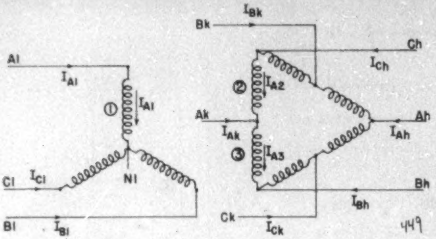

449

Fig. 4. The wye-delta - inscribed delta transformer connection

$$\underset{1}{E_{h1}}'=Z_{1-2}\underset{1}{I_h}'+\left[\frac{1}{4}(2Z_{1-2}+Z_{1-3}+Z_{1-4}-Z_{2-3}-Z_{2-4})+j\frac{1}{4\sqrt{3}}(Z_{1-3}+Z_{2-4}-Z_{2-3}-Z_{1-4})\right]\underset{1}{I_k}' \quad (105)$$

$$\underset{1}{E_{k1}}'=\left[\frac{1}{4}(2Z_{1-2}+Z_{1-3}+Z_{1-4}-Z_{2-3}-Z_{2-4})-j\frac{1}{4\sqrt{3}}(Z_{1-3}+Z_{2-4}-Z_{2-3}-Z_{1-4})\right]\underset{1}{I_h}'+\left(\frac{1}{2}Z_{1-3}+\frac{1}{2}Z_{1-4}-\frac{1}{6}Z_{3-4}\right)\underset{1}{I_k}' \quad (106)$$

Equations 105 and 106 specify the positive-sequence impedance characteristics of the transformer in terms of winding-to-winding series-opposition impedances. It should be noted that the coefficient of $\underset{1}{I_k}'$ in equation 105 is not the same as the coefficient of $\underset{1}{I_h}'$ in equation 106 in that the algebraic sign before the j term is plus in one case and minus in the other. Therefore, unless $Z_{1-3}+Z_{2-4}-Z_{2-3}-Z_{1-4}=0$, it is not possible to represent the positive-sequence impedance characteristics of the transformer by an equivalent circuit made up of practical elements. If $Z_{1-3}+Z_{2-4}-Z_{2-3}-Z_{1-4}$ can be reduced to zero by physical symmetry of coils on each magnetic phase or otherwise, the mutual branch impedances will be reciprocal and a conventional 3-terminal either star or mesh equivalent circuit can be used. Fig. 3 shows a symmetrical arrangement of the coils which accomplish this.

Example 2

Continuing from example 1, assume that the windings on each magnetic phase are physically arranged so that the pu impedances (only reactive components for sake of simplicity) on an arbitrary volt-ampere base are

$Z_{1-2}=j0.24$ $\qquad$ $Z_{2-3}=j0.05$

$Z_{1-3}=j0.18$ $\qquad$ $Z_{2-4}=j0.12$

$Z_{1-4}=j0.10$ $\qquad$ $Z_{3-4}=j0.06$

Equations 105 and 106 become

$$\underset{1}{E_{h1}}'=j0.2400\underset{1}{I_h}'+(j0.1475-0.0217)\underset{1}{I_k}' \quad (107)$$

$$\underset{1}{E_{k1}}'=(j0.1475+0.0217)\underset{1}{I_h}'+j0.1300\underset{1}{I_k}' \quad (108)$$

If a second transformer were exactly the same as the first except for a change of connections which interchanged the roles of windings 3 and 4, the no-load voltage phasor diagram and the three positive-sequence impedances between pairs of terminal sets would be exactly the same as those of the first transformer. Therefore, it might be concluded that the two units should operate perfectly in parallel. That such is not the case is demonstrated as follows:

Using subscripts R and S to distinguish quantities of the two transformers, equations 107 and 108 become

$$\underset{1}{E_{h1R}}'=j0.2400\underset{1}{I_{hR}}'+(j0.1475-0.0217)\underset{1}{I_{kR}}' \quad (109)$$

$$\underset{1}{E_{k1R}}'=(j0.1475+0.0217)\underset{1}{I_{hR}}'+j0.1300\underset{1}{I_{kR}}' \quad (110)$$

and the corresponding equations for the second transformer are

$$\underset{1}{E_{h1S}}'=j0.2400\underset{1}{I_{hS}}'+(j0.1475+0.0217)\underset{1}{I_{kS}}' \quad (111)$$

$$\underset{1}{E_{k1S}}'=(j0.1475-0.0217)\underset{1}{I_{hS}}'+j0.1300\underset{1}{I_{kS}}' \quad (112)$$

Because the two units are paralleled at all three terminal sets

$$\underset{1}{E_{h1R}}'=\underset{1}{E_{h1S}}' \text{ and } \underset{1}{E_{k1R}}'=\underset{1}{E_{k1S}}' \quad (113)$$

Substitutions of equations 109, through 112 in equations 113 and solving the resulting equations for the various I's yield

$$\underset{1}{I_{hR}}'=(0.500-j0.170)\underset{1}{I_H}'-j0.149\underset{1}{I_K}' \quad (114)$$

$$\underset{1}{I_{kR}}'=j0.276\underset{1}{I_H}'+(0.500+j0.170)\underset{1}{I_K}' \quad (115)$$

$$\underset{1}{I_{hS}}'=(0.500+j0.170)\underset{1}{I_H}'+j0.149\underset{1}{I_K}' \quad (116)$$

$$\underset{1}{I_{kS}}'=-j0.276\underset{1}{I_H}'+(0.500-j0.170)\underset{1}{I_K}' \quad (117)$$

where

$\underset{1}{I_H}'=\underset{1}{I_{hR}}'+\underset{1}{I_{hS}}'$ = combined h current of two units in parallel

$\underset{1}{I_K}'=\underset{1}{I_{kR}}'+\underset{1}{I_{kS}}'$ = combined k current of two units in parallel

If the combined currents at the h and k terminal sets are

$\underset{1}{I_H}'=0.00+j0.50$ $\qquad$ $\underset{1}{I_K}'=0.80-j0.60$

currents at individual terminal sets are

$\underset{1}{I_{1R}}'=-0.3596+j0.0332$ $\qquad$ $|\underset{1}{I_{1R}}'|=0.3611$

$\underset{1}{I_{hR}}'=-0.0044+j0.1308$ $\qquad$ $|\underset{1}{I_{hR}}'|=0.1309$

$\underset{1}{I_{kR}}'=0.3640-j0.1640$ $\qquad$ $|\underset{1}{I_{kR}}'|=0.3993$

$\underset{1}{I_{1S}}'=0.4404+j0.0668$ $\qquad$ $|\underset{1}{I_{1S}}'|=0.4454$

$\underset{1}{I_{hS}}'=0.0044+j0.3692$ $\qquad$ $|\underset{1}{I_{hS}}'|=0.3692$

$\underset{1}{I_{kS}}'=0.4360-j0.4360$ $\qquad$ $|\underset{1}{I_{kS}}'|=0.6166$

The current at the various terminal sets expressed in pu of currents corresponding to perfect parallel operation are

$\underset{1}{I_{1R}}'=0.897$ $\qquad$ $\underset{1}{I_{1S}}'=1.104$

$\underset{1}{I_{hR}}'=0.523$ $\qquad$ $\underset{1}{I_{hS}}'=1.477$

$\underset{1}{I_{kR}}'=0.799$ $\qquad$ $\underset{1}{I_{kS}}'=1.233$

It is easily seen that this is a far from satisfactory division of currents.

Example 3

Shown in Fig. 4 is a wye-delta connection with a third set of terminals taken from the mid-points of the delta windings. The terminals of the wye circuit have been arbitrarily chosen as the reference terminal set; the terminals taken from the apexes of the delta are designated h and those taken from the mid-points are designated k. The windings per magnetic phase are identified by numbers 1, 2, and 3 as indicated in the figure.

Utilizing the method employed in example 1, the following are obtained from equation 48:

$$\underset{1}{E_{h1}}'=\underset{1}{Z_{1-h}}I_h'+(Z_{1(hk)}'+j\underset{1}{Z_{1(hk)}}'')\underset{1}{I_k}' \quad (118)$$

$$\underset{1}{E_{k1}}'=(\underset{1}{Z_{1(hk)}}'-jZ_{1(hk)}'')\underset{1}{I_h}'+Z_{1-k}\underset{1}{I_k}' \quad (119)$$

in which

$\underset{1}{Z_{1-h}}=(2Z_{1-2}+2Z_{1-3}-Z_{2-3})/4$

$Z_{1-k}=(Z_{1-2}+Z_{1-3}+Z_{2-3})/2$

$Z_{1(hk)}'=(2Z_{1-2}+2Z_{1-3}-Z_{2-3})/4$

$Z_{1(hk)}''=\frac{\sqrt{3}}{4}(Z_{1-3}-Z_{1-2})$

The negative sequence equations corresponding to equations 118 and 119 can be found from equation 56 to be

$$\underset{2}{E_{h1}}'=\underset{1}{Z_{1-h}}\underset{2}{I_h}'+(Z_{1(hk)}'-jZ_{1(hk)}'')\underset{2}{I_k}' \quad (120)$$

$$\underset{2}{E_{k1}}'=(Z_{1(hk)}'+jZ_{1(hk)}'')\underset{2}{I_h}+\underset{1}{Z_{1-k}}\underset{2}{I_k}' \quad (121)$$

It is not possible to represent equations 118 and 119 by a conventional equivalent network made up of practical elements unless $Z_{1-2}=Z_{1-3}$. The same is true with respect to equations 120 and 121.

Using equations 86 and 87 of Appendix II, the voltage equations can be expressed in terms of α and β components, thus

$$E_{\alpha h1}'=\underset{1}{Z_{1-h}}I_{\alpha h}'+Z_{1(hk)}'I_{\alpha k}'-Z_{1(hk)}''I_{\beta k}' \quad (122)$$

$$E_{\alpha k1}'=Z_{1(hk)}'I_{\alpha h}'+Z_{1(hk)}''I_{\beta h}'+\underset{1}{Z_{1-k}}I_{\alpha k}' \quad (123)$$

$$E_{\beta h1}' = \underset{1}{Z}_{1-h} I_{\beta h}' + Z_{1(hk)}' I_{\beta k}' + Z_{1(hk)}'' I_{\alpha k}' \tag{124}$$

$$E_{\beta k1}' = Z_{1(hk)}' I_{\beta h}' - Z_{1(hk)}'' I_{\alpha h}' + \underset{1}{Z}_{1-k} I_{\beta k}' \tag{125}$$

The interconnected α and β equivalent networks which represent equations 122 through 125 can be constructed with practical elements, but there will be bilateral mutual impedances between α and β quantities.

References

1. Theory of Three-Circuit Transformers, A. Boyajian, *AIEE Transactions*, vol. 43, 1924, pp. 508–28.
2. Progress in Three-Circuit Theory, A. Boyajian. *Ibid.*, vol. 52, Sept.–Dec. 1933, pp. 914–17.
3. Transformer Circuit Impedance Calculations, A. N. Garin, K. K. Paluev. *Ibid.* (*Electrical Engineering*), vol. 55, June 1936, pp. 717–30.
4. Alternating Current Machinery (book), L. V. Bewley. The Macmillan Co., New York, N. Y., 1949.
5. Equivalent Circuits, F. M. Starr. *AIEE Transactions*, vol. 51, June 1932, pp. 287–98.
6. An Equivalent Circuit for the Four-Winding Transformer, F. M. Starr. *General Electric Review*, Schenectady, N. Y., March 1933, p. 150.
7. A Useful Equivalent Circuit for a Five-Winding Transformer, L. C. Aicher, Jr. *AIEE Transactions* (*Electrical Engineering*), vol. 62, Feb. 1943, pp. 66–70.
8. Some Practical Equivalent Circuits for Multi-Circuit Transformers, David Morris. *Proceedings*, Institution of Electrical Engineers, London, England, vol. 98, pt. II, Apr. 1951, p. 256.
9. Equivalent Circuit for the Multi-Winding Transformer, E. Uhlmann. *Journal*, Allmanna Svenska Elektriska Aktiebologet, London, England, vol. 24, 1951, pp. 17–22.
10. Multi-Winding Transformers, R. Willheim. *Electrical Times*, London, England, June 14, 1951, pp. 991–94.
11. The Equivalent Circuit of the Multi-Winding Transformer, R. Willheim. *Research and Engineering* (book), ed. by W. Petersen. Julius Springer, Berlin, Germany, 1930, pp. 280–90.
12. Circuit Analysis of A-C Power System (book), Edith Clarke. John Wiley and Sons, Inc., New York, N. Y., vol. 1, 1943, vol. 2, 1950.
13. Symmetrical Components (book), C. F. Wagner, R. D. Evans. McGraw-Hill Book Co., Inc., New York, N. Y., 1933.
14. American Standard Definitions of Electrical Terms (book). AIEE, Aug. 1941.
15. Zero-Phase-Sequence Characteristics of Transformers, A. N. Garin. *General Electric Review*, Schenectady, N. Y., vol. 43, 1940, pp. 131–36, and 174–79.
16. Transformer Engineering (book), L. F. Blume, A. Boyajian, G. Camilli, V. M. Montsinger. John Wiley and Sons, Inc., New York, N. Y., 1951.
17. Method of Symmetrical Co-ordinates Applied to the Solution of Polyphase Networks, C. L. Fortescue, *AIEE Transactions*, vol. 37, 1918, pp. 1027–40.

Principles and Practices of Modern System Planning

A. P. FUGILL
FELLOW AIEE

IN THE electric power industry, planning for the future has always been an integral part of the responsibility for being prepared to carry ever-increasing loads. In the early days, the art of planning for system development may have been more intuitive than precise, but the foundations for present-day concepts were being well laid. The influence of proper planning on a company's earnings gradually became more fully recognized so that in the last few years there has been a widespread effort throughout the industry to make it more effective. As improved technologies made system planning more of a science and less of an art, attention was turned to improvements in organizational pattern. It is now generally recognized that planning in its broadest sense has an important place in the electric power industry distinct from design engineering and operation. System planning is thus defined by the AIEE System Planning Subcommittee of the Committee on System Engineering: "System planning is the preparation of a rational program for the development of an electric power system, so that it can evolve in an orderly and economic manner. It includes forecasting and analyzing loads, rationalizing standards of service, anticipating trends in equipment design and co-ordinating the various elements of the system into a well-designed whole; it is particularly concerned with plans for changes and additions to generation, transmission, substations, and distribution facilities. It is not concerned with the problems of day-to-day operation or design except to the extent that these problems affect future system development. Briefly, electric system planning is the process of determining when, what facilities should be provided where in order to assure adequate electric service at minimum average annual cost to the community." In the modern concept of the term, the activities of the planning engineer affect not only the engineering and operating departments but also the construction, commercial, and financial departments, and are certainly of vital interest to management.

Two basic patterns for a planning organization seem to have evolved. Since both have their advantages and disadvantages, the actual organization in most companies is a combination of the two. In one pattern the organization is functional, with a separate planning department usually reporting directly to a high level officer in the company, given overall responsibility for planning throughout the system but with no design engineering or operating responsibilities. In the other pattern, perhaps the more traditional one, the organization is regional, with planning functions combined with design engineering or/and operating functions for each part of the complete system; for instance, one group may have responsibility for generation, another for transmission, and another for distribution.

In The Detroit Edison Company, the planning organization more closely approximates the second basic pattern. The Planning and Project Engineering Department carries the major responsibility for planning for system development but also is responsible for basic design and other engineering. Within this department, the regional pattern is followed, with different groups responsible for the component parts of the system. In addition, many other departments and also top management, have a distinct part in the planning activities. To provide the necessary co-ordination with this type of organization, the committee idea is used. These committees, composed of representatives from all interested departments, generally function as advisory or study groups with authority to make recommendations but with the responsibility for action left with the line organization.

To show how such an organization functions, three steps which are fundamental to all system planning are discussed in the following:

1. Prediction of the total system load and its distribution throughout the territory served.

Paper 55-673, recommended by the AIEE System Engineering Committee and approved by the AIEE Committee on Technical Operations for presentation at the AIEE Fall General Meeting, Chicago, Ill., October 3–7, 1955. Manuscript submitted June 2, 1955; made available for printing July 18, 1955.

A. P. Fugill is with The Detroit Edison Company, Detroit, Mich.

a. For short-term planning, 5 years or less.

b. For long-range planning, 5 to 25 years.

2. Determination of the standard of service to be maintained.

3. Development of the most economical system to meet these requirements.

Short-Term Total Load Prediction

The prediction of the total system load is especially important because it determines to a large extent when the money for system expansion will be spent and is an important factor in how much money is to be spent. The amount of generation needed can be determined directly from the total load to be carried. Much has been published in the technical press about load prediction. Techniques have been presented for processing known facts of past history on system loads, integrating that information with known future plans for residential, commercial, and industrial expansion, and taking into account the best thinking on business, economics, and political trends for the future. The value of such work should not be underestimated. The Detroit Edison Company takes advantage of all the technical help it can get. In the last analysis, however, the company depends on the judgment and experience of men in the organization who have lived with this problem for many years. A Load Study Committee under the chairmanship of the manager of engineering has the responsibility to carry on a continuous study of the Company's probable future electric system load growth. Its membership consists of representatives of the engineering, operating, commercial, and financial departments and its findings are reported to a vice president. This committee prepares a load growth curve for the electric system which, with top management approval, forms the basis for all system development. For short-term load prediction, this curve has proved quite accurate, and, when conditions change suddenly, the committee can make the necessary corrections immediately.

Short-Term Load Distribution Prediction

This committee does not attempt to determine the distribution of load throughout the franchise area. This is left to the engineering and operating departments, with whatever assistance they need from other interested departments. Until a few years ago, it was generally sufficient to extrapolate historical load growth curves by areas and introduce corrections for known variations caused by the expansion plans of industrial customers. The residential and commercial load pattern, which was dependent upon the increased use by existing customers and the addition of new customers resulting from a series of well-distributed small-scale building operations, could be predicted with sufficient accuracy. All that has changed in the past few years. The decentralization trend in industry, the growth of mass residential housing, and the fast expansion of suburban shopping centers have changed the land-use picture rapidly. A decision by one large customer sometimes with very little advance warning, can cause a large load to develop in an entirely unexpected location. Gradually, a pattern is beginning to evolve, however, and, by keeping in close contact with local industry, realtors, and commercial customers about their future plans, it is now possible to prepare for most eventualities. The location of railroads and the availability of water and sewage facilities provide a valuable clue to the direction in which future expansion is likely to take place. Since the timing is the most difficult factor to predict, it is still necessary to reschedule proposed construction rather more frequently than is desirable. In any event, future system plans must be made flexible, subject to change as developments take place. It no longer safe to assume that a particular area will not require a major supply source just because its present character is rural or suburban.

Long-Range Prediction

Most companies, however, feel that they must have as definite plans as possible for much longer periods; certainly 10 years and probably 20 to 30 years. In many cases, conditions 20 years hence may have a vital effect on the construction program of the next few years. Take the trend toward higher voltages in transmission, subtransmision, or distribution as an example. It is generally believed that some day voltages higher than the present ones will be used in all these areas. In most cases, the time for starting these higher voltage systems, however, depends on the rate of load growth over the next 20 years or perhaps the load which will exist 25 or 30 years from now. Quite frequently it is desirable, in order to obtain the most economical over-all plan, to convert the system several years earlier than is actually necessary from the operation standpoint.

The degree of accuracy obtained for 5-year predictions cannot be expected when predicting conditions 25 years hence. To obtain a sufficient degree of accuracy, different methods are needed and many approaches have been tried. The Detroit Edison Company has used many of the conventional methods. The system load curve has merely been extrapolated at different rates of increase, introducing the effect of a possible recession or slowdown in growth. The historical curves of percentage of total load by areas have been used and extended with modifications based on a knowledge of special trends in particular areas. The problem has been approached by an analysis of the known trends in each of the different classes of load—residential, commercial, and industrial. But it is recognized that changes in the character of the different areas, in the social habits of people, and in business activity are important influences which can only be approximated in any analysis.

In this long-range planning for both total load and load distribution, therefore, The Detroit Edison Company is thankful that in 1947 the Detroit Metropolitan Area Regional Planning Commission was established. Its purpose was to try to determine and perhaps influence a pattern of growth for the whole metropolitan area, to set up a land-use pattern, and to predict probable population shifts, movement of industry, and employment requirements. It was hoped that such information would permit more intelligent planning for all utilities—gas, water, sewer, electricity, and transportation—and improved placement of industry, real estate developments, and recreation facilities. At the same time, it might tend to rejuvenate blighted areas and prevent the further deterioration of other areas. The whole effort was a cooperative one between private industry and the public authorities with equal representation from both groups, It has proved a very successful endeavor, and the benefit of this work is just now beginning to show in the planning efforts.

Among other valuable data, this commission has made available estimates of the growth of population and manufacturing employment in the metropolitan area. Although this does not cover the entire service territory, it does cover the area where the bulk of the load exists. In compiling these data, the commission has divided the total territory covered into areas, each area being as homogeneous in character as possible. Using the years 1950 and 1970, the population and the manufacturing employees in each area were estimated. Since this information was far more authoritative than any similar data The Detroit Edison Company could compile, it was decided to use this in predicting a load for 1970. Although this work was originally done to estimate future revenue and was concerned with kilowatt-hours more than with kilowatts, it was relatively simple to convert it to the peak load basis needed for system development planning. These estimates were made for both an optimistic and pessimistic economic outlook. In the former case, a continuous period of prosperity was assumed. For the latter case, a 5-year slowdown was introduced with a load increase based on a study of experience in the last depression.

For each area the residential, commercial, industrial, and miscellaneous loads were estimated separately, using the population and manufacturing employment figures for each area. For the residential load, the ratio of population to customers was assumed to decrease slightly, and the use per customer was assumed to increase at the same rate per year which has existed since 1948, about 6 per cent per year.

For commercial loads, the number of customers was estimated by using the present ratio of residential to commercial customers in each area and reducing the ratio slightly because of the trend toward super markets and integrated shopping centers. The use per customer was assumed to increase at 6 per cent per year, the same rate as has existed since 1940.

It was more difficult to predict the industrial load growth from the number of manufacturing employees because of the wide variation of use per employee in the various types of industry. For the United States as a whole, for instance, in 1947 the kilowatt-hours used annually per employee for several industries were as follows:

Chemical, 42,000
Petroleum, 38,000
Primary metals, 23,000
Machinery, 4,800
Automobile, 8,400

Hence, if the increased number of employees was caused by the chemical industry, the increase in load per employee would be far greater than if it were caused by an automobile factory. Since 1939, the load per employee has increased 4.8 per cent per year for the whole United States but only 1.5 per cent per year in The Detroit Edison Company's territory. This is probably because of the rapid growth, nation wide, in the aluminum and electrochemical industries, while Detroit's growth has been largely in the machinery and automotive industry. For instance, in the United States 24 per cent of all manufacturing employees are in these low-use industries, while in Detroit the figure is 64 per cent. Excluding the chemical, iron and steel, and fabricated metals group, the figure for the United States is 2.7-per-cent increase per year, which is the value that was used unless a more definite knowledge of the industry pattern in the area was available.

By summing up for all areas, a total load for the system was obtained. This figure was checked for reasonableness by several methods and seemed to stand the tests. The maximum figure for 1970, by the way, turned out to be just about three times the peak load in 1952, which was the time base used in the study, a tripling of load in 18 years.

Determination of Standard of Service

In determining the standard of service to give the customers, again a committee works in co-operation with the line organization. Since the broad question of service is far too comprehensive to be covered here, only one phase of the subject—the continuity of service—will be considered. Although all electric power companies are particularly conscious of any interruption of service to a customer, it is not economically feasible, perhaps not even possible, to provide perfect service. Over the years, what is considered the proper balance between cost and probability of outage throughout the system has been developed. That balance is not a constant, however, and it must be constantly borne in mind that continuous service is becoming increasingly important to all customers. Each year more residential and farm customers as well as small commercial customers are using more electricity and are so dependent upon continuity of electric service that even short outages may cause them real hardship and financial loss.

For many industrial and large commercial customers, the change in conditions is even more radical because of decentralization and automation. Many of these customers have been used to multiple underground feeds with a low interruption rate. When they move to a less concentrated load area, they are not prepared to accept the somewhat greater interruption rate resulting from overhead feeds. Furthermore, with the growth of automation in many industrial processes, the situation is aggravated. In many cases, it is no longer only a question of a complete interruption of service. As some of this equipment is now designed, a voltage dip causes a complete interruption of the process because of the characteristics of the automatic control. It is desirable to reduce the number of voltage dips to a reasonable minimum, but there must also be a recognition on the part of the designer of the automatic equipment and the user of their responsibility to make the equipment less sensitive to transient change in voltage.

Although a practice has been made of continuously reviewing customer service, the management has come to the conclusion that this function should be strengthened by the establishment of a Service Study Committee. This committee, under a chairman reporting directly to the manager of engineering, is composed of high-level representatives of the engineering, operating, commercial, and financial departments. Their assigned duty is to study service requirements, analyze service defects, correlate programs for the maintenance and improvement of the quality of service, and to make recommendations on specific programs to be undertaken for general improvement in service by the system. Although this committee has been very active for several months, it is still too early to report on what has been accomplished except that results to date have been very promising.

Design for System Development

The third step in system planning, the design of the system itself, is closely associated with engineering design and system operation. It is distinctly a job for engineers with a high degree of competence as technical specialists and as system planners with a broad outlook.

There is no need to discuss the detailed techniques which are used in this phase of system development. Load division and voltage regulation studies, stability studies, and fault studies are part of the daily routine of engineers in this work. Without any disparagement of the value of this work or the technical ability required, it is not particularly difficult to design an electric system to meet a given set of specifications. The real problem is to determine the most economical system to meet these requirements.

There are always several methods to accomplish the desired result, not all equally good but all entirely adequate. Either intuitively or by a formal study, these plans must be measured against the expense to determine which one will give the over-all lowest cost relative to the benefits derived. This economic comparison of alternative plans is becoming such a complicated procedure that some companies are creating specialists who spend all their time in this field of engineering economics as differentiated from the broader field of economics as it affects the company's financial position and rate structure.

In The Detroit Edison Company this work of design for system development is done largely in the engineering departments, with assistance as required from the operating and construction departments. To provide over-all co-ordination and make available the experience and judgment in the various departments, a System Development Committee has recently been reorganized under a chairman reporting directly to the manager of engineering. This committee consists of supervisory heads in the departments most concerned with system development. Their function is to review plans for major system development prepared by the line organization and to make recommendations to management concerning those plans which affect broad company policies. This committee is very useful to the planning activities.

Machine Computation in Engineering

A brief discussion of the impact of large scale computing machines on the practice of engineering may be in order, particularly as it affects system planning. It is part of the engineering responsibility to reduce the cost of producing electricity to a minimum consistent with the quality of service it is desired to maintain. Some of this reduction can be obtained from refinements in the design of the overall system and its component parts. Much of this reduction in the future, however, must come from more precision in system planning. Some way must be found to tailor the construction more closely to actual needs, to predict more accurately just when each facility will be needed, and how large it should be for greatest economy. In other words, by more accurate knowledge, it should be possible to reduce safely the margin in facilities which has to be included to take care of the limitations in the predictions.

In many cases it is known how to obtain this more accurate knowledge, but the volume of computation and data processing needed make it uneconomical or even impossible to obtain. For instance, all load prediction has its roots in the historical record of past loads. But to obtain all the data on total load and load distribution in the form desired is a recording and analyzing job which requires far too much man power and costs too much; therefore approximations have to be made. Again, in evaluating the effect of different emergencies on customer service, more statistical data could be procured and more precise methods for using the techniques of outage probability could be developed if it were not for the fact that the amount of calculation and data handling is out of reason. As further examples, in making economic studies of alternative plans, in evaluating system losses, in combining system losses with power plant efficiencies, or in making any of the analytical studies necessary in designing a system, the mere weight of computation is often overwhelming. So approximations are made and enough margin is introduced to cover those approximations. This additional margin costs money.

The increasing availability of large scale analogue and digital computers seem to offer a way out of this morass of computation and data processing. The network analyzer, which is widely used in system study work, went a long way toward simplifying the solution of the problem of system performance. Without such equipment, few would have been able to design as economical systems as are now in use. Of course, the systems would still have been adequate, but it would have been necessary to provide more margin in the equipment. Also, occasionally, a transmission line might have been installed in the wrong place or a cable added which did not carry its fair share of the load.

And now the large scale digital computer seems to be developing into an even more useful tool. The Detroit Edison Company is perhaps more fortunate than many other electric power companies, having had available for several years card-programmed computing machines which have been calculating customers' bills and employee payrolls. Now the company has a far more powerful computer. Two university computation laboratories are available with a competent consulting staff and large-scale computing machines. For several years therefore these machines have been applied to engineering problems with encouraging success. Real progress is expected in the next few years. The industry, particularly in the engineering field, is just on the threshold of the application of large-scale machine computation to the solution of the problem. The work to date, however, shows that the availability of such a tool will completely change the ideas on many of the problems where the necessity for making extensive calculations or processing large quantities of data has made approximations necessary. With the greater accuracy obtainable, really significant dollar savings can be made by reducing the margin for ignorance now in use in planning for system development.

Development of Personnel

One other situation relative to system planning deserves consideration. It is recognized by those close to system planning activities, that the personnel engaged in this development work needs specialized training. That need is growing more important with each passing year. For the most part, the people who are now in system planning have grown up with the job and gradually acquired the necessary skills. The problem ahead is to fill the ranks with younger men, perhaps those right out of college. With the engineering field as broad as it is today, the educational institutions do well to give the graduate engineer a good basic understanding of the principles of engineering. They can hardly be expected to train him in the specialized field in which he may find himself after graduation. There are a few courses available in some universities, particularly in the graduate area, under the general classifications of system engineering which cover the technical side of system planning, i.e., the methods for making studies of system performance. Similar information is available in scattered form in text books and company-sponsored courses. But there seem to be no co-ordinated programs to develop an engineer with the conventional bachelor's degree into a planning engineer with specialized knowledge. About all that can be done is to start him working in this field with the hope that he will acquire the necessary knowledge as he works.

If this function of adequate system planning as it seems to be developing for the future is to be performed, this problem of providing some organized educational and training programs should be considered. These programs should include, in addition to the courses referred to as system engineering, such subjects as the application of modern computers, the use of sampling techniques, probability methods and statistical analysis, and the basic principles of economics and accounting. It is possible that this responsibility could be shouldered by the educational institutions, preferably in the graduate area, with the co-operation of the industry. In any case, it is up to the electric power industry where such trained personnel is needed, to make that need known and initiate action to get such programs started.

Discussion

R. G. Hooke (Public Service Electric and Gas Company Newark, N. J.): It is a tradition of the publishing industry, I believe, that an author who writes what his readers enjoy reading is likely to find favor. Perhaps that is why some of us in Public Service Electric and Gas Company have thoroughly enjoyed Mr. Fugill's well-organized and thoughtful presentation of the ways of modern system planning. We subscribe without qualifications to his "three steps which are fundamental to all system planning."

Our first co-ordinated effort at load forecasting was made in 1923 when an interdepartmental committee was organized for this purpose. Although there have been the inevitable changes of personnel and important modifications of procedure over the years, our present Load Development Committee still establishes the first fundamental parameter for system planning; the load to be planned for this year, next year, and 10 years hence.

In the early 1940's with the advent of unit substations and the trend toward more or less promiscuous tapping of our subtransmission system to supply what were then wartime emergency loads, we began to set down certain rules in accordance with which we were satisfied to plan the system. In the dozen years since that time, these rules have become formalized into what we call our "Planning Standards." These are largely empirical statements of the facility outages to be designed for and the service to be rendered under both normal and emergency conditions. Service, of course, is defined by the two factors, voltage and continuity. We find that definite establishment of standards for these factors greatly simplifies system planning work. There is never any argument about expansion schemes which fail to meet our service standards. Such proposals are simply not offered and the time necessary to convince their advocates that they are inadequate is saved.

Mr. Fugill's third fundamental involves economic analyses. We started an approach based on annual carrying charges not long after the organization of our Load Development Committee. At that time we were impressed by the conception that it is not capital expenditure which counts, but the annual costs necessary to provide the service by one or another of the various alternative means. Perhaps one reason for this was the fact that our planning organization was (and is) a part of the operating department where the emphasis tends to be on annual expenses rather than on capital costs.

More recently we have found the expression "minimum present worth of all future revenue requirements" very helpful in our thinking about economic problems. It seems to tie in better with the terminology familiar to management from financial statements, since "revenue requirements" clearly means the money necessary to pay all costs, both of operation and of capital recovery. The phrase, however, does not imply that revenue may never exceed requirements or must be limited in any way. Some use the term "fixed charges" to mean capital recovery only, i.e., return on capital plus depreciation; others include taxes and insurance in their definition; while a third group considered operation and maintenance also as a part of "fixed charges," no matter whether expressed as a percentage of fixed costs or directly estimated in annual dollars. Similar confusion surrounds the words "annual costs" and "annual expenses." But when we speak of the revenue requirements of each of several plans, there is never any confusion; we are including all of the costs and we are stating the facts in trenchant terms from the standpoint of those to whom our findings are addressed. A plan which minimized the present worth of all future revenue required to service it is clearly the economic choice, to be discarded only if some other proposal has advantages justifying added requirements for revenue. Incidentally, this descriptive terminology also helps to avoid use of erroneous procedures in economic studies and is particularly effective in certain specific situations, for instance in justifying the replacement of an under-reading customer's meter.

Mr. Fugill emphasizes very effectively the fact that closer and closer planning is a major source of those savings necessary to permit utilities continued operation with rate increases far less than proportionate to the increases in costs of practically all other things we buy. This was the principal argument justifying purchase by Public Service of the initial portion of its a-c network analyzer in 1937. We are impressed and we would like to compliment the Detroit Edison Company on its progressive policies in applying digital computers to engineering and planning problems. It appears to us that in this area utilities may be at the threshold of a major advance in techniques. Mr. Fugill speaks of his use of these computers in somewhat general terms. Perhaps it would be possible for him to recite some specific problems to which they are currently being applied. We have used an International Business Machines (IBM) type 604 recently for the development of depreciation annuity tables and per-cent–condition factors for various lives and dispersion patterns. We are also considering the use of computers not only to handle intricate engineering problems, but also to aid in analyzing our load forecasts, applying diversities and producing final figures of kilowatt and kilovar loads for network analyzer application. We should be interested to know more about the most recent problems on which they have been found helpful in Detroit.

The over-all results of system planning are very difficult to measure. Of course, they appear in the safely narrowing margins of reserve. While this is not a welcome process for the operating supervisor, it is surely one of the objectives to be striven for from the point of view of the economic welfare of the community, provided always that it is accompanied by improving service continuity and voltage regulation.

Fig. 1 shows that on the Public Service system, even without correcting for the declining purchasing power of our dollar, there has been a substantial downward trend in gross dollars of fixed plant investment per kilowatt of system peak demand. All of the improvement, of course, cannot be credited to system planning, but surely a substantial amount of it rests on more accurate load forecasting, recognition of acceptable minimum planning standards, and properly conceived economic comparisons of alternative projects. Again we think Mr. Fugill is to be congratulated for the organization and clarity of his paper.

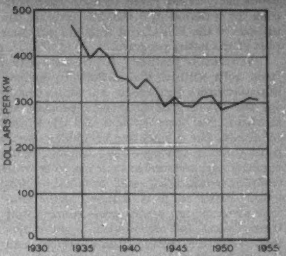

Fig. 1. Dollars invested in electric plant per kilowatt of system annual peak load (not corrected for inflation)

A. J. Wood (General Electric Company, Schenectady N. Y.): The purpose of this discussion is to point out our experience in the advanced education of power system engineers. Mr. Fugill's excellent paper discusses the requirements and functions of a power system planning engineer and points out that system planners must have a large fund of knowledge both in the technical and in the economic aspects of engineering which may be acquired through experience and formalized educational programs.

In 1949, the company with which the discusser is associated, after requests by utility executives and engineers for assistance in establishing their own training programs, offered to the electrical utility industry an intra-industry educational program, the Power Systems Engineering Course (PSEC).[1] This course, a specialized technical training program, is an outgrowth of 25 years' experience in educational courses given for the training of power system application engineers of the discusser's company. It was offered to the industry as a whole when it was recognized that a co-operative educational program was an economic answer to the necessity for an effective, organized training course for power system engineers.

The PSEC is an integrated program consisting of (1) formal classroom lectures, (2) informal seminar sessions, (3) inspection trips to various electric equipment manufacturing facilites, and (4) an engineering work assignment program. The formal classroom lecture series consists of four basic technical courses in power system analysis, power system protective relaying, surge phenomena, and advanced circuit analysis and operational methods. These courses are augmented by classes in electrical utility engineering practices, transmission losses and the economic operation of power systems, and a supervised course in the solution of power systems engineering problems. These seven courses, each running for a period of 8 months, provide the nucleus of the PSEC, but they are only one part of the entire program.

The series of seminars, led by authorities from both utilities and electric equipment manufacturers, provides an opportunity for the PSEC participants to gain an insight into the power system as a whole and to discuss the application of modern computers, both analogue and digital, with engineers experienced in their use in solving complex engineering and economic problems. Broad subjects included in the seminar program are power generation, power transmission and distribution, power system protection, power system control, and the application of computers and analyzers to system problems. Further insight into system engineering is provided by inspection trips to the electric equipment manufacturing facilities located close at hand.

One of the most important experiences of the PSEC student is the engineering work assignment program which enables the utility engineer to study problems of his own system. These assignments are under the guidance of engineers experienced in the various special fields of power system application engineering and provide a further opportunity for the utility engineer to gain the broad-gauge experience which is required by system planning.

As of 1955, 124 engineers have completed the course. These engineers represent enrollment from 37 domestic utilities, 9 foreign utilities, 6 consulting engineering firms, and 2 universities, as well as engineers from the company with which the discusser is associated. In addition to the direct participants, the graduates have assisted in setting up similar courses taught in graduate schools and as company courses in several locations throughout the United States. It is estimated that the total number of engineers who have participated in these courses, directly and indirectly, is in the neighborhood of three to four times the number who have participated directly in the PSEC.

Mr. Fugill points out that the electrical utility industry must examine carefully the problem of providing organized educational and training programs. With this we agree. Furthermore, we believe that the type of program represented by the PSEC, an intra-industry training program, given with the co-operation of the electrical utility companies, engineering colleges and universities, and electric equipment manufacturers is a major step in the proper and economical training of power systems engineers.

REFERENCE

1. THE POWER SYSTEMS ENGINEERING COURSE, L. E. Saline. *General Electric Review*, Schenectady, N. Y., vol. 54, no. 9, 1951, pp. 18–21.

A. P. Fugill: In Mr. Hooke's discussion he raised two points which will be covered in this closure. The expression "minimum present worth of all future revenue requirements" which the Public Service Electric and Gas Company is using in economic comparisons, warrants considerable attention. It may state what is actually meant more accurately than some expressions used by others for the same purpose. It may also appeal to those in the financial phase of the business. It does, however, have the disadvantage of being in a language strange to the everage engineer. Like so many expressions used in economic comparison studies, its meaning would have to be clearly defined before it would be generally accepted by many in the industry.

Mr. Hooke suggests that mention be made of specific problems where digital computers are currently being used. Typical engineering problems now being solved by The Detroit Edison Company on the IBM Type *650* EDPM are:

1. Optimum power plant load scheduling incorporating the effect of transmission losses.
2. Computation of interchange billing for economy power transfer between interconnected systems.
3. Calculation of optimum turbine heat balance cycles for turbine design and plant operation.
4. Determination of pipe stresses for steam piping layout.
5. Calculation of total losses by summation of individual branch losses in a system network to determine optimum locations for capacitors.
6. Determination of fault currents in a complex system network. This problem is still in the early stages of development.
7. Preparation of general subroutines useful in the treatment of matrices and other mathematical solutions needed in system network manipulation.

In Mr. Wood's discussion, he has given a good description of the effort the General Electric Company is making to fill the void in training facilities for system planning engineers. Our company has taken advantage of this course several times and found it most valuable. There are also a few other sources of training for system engineering available in different cities. Still more of this type of organized education is desirable, since these courses can accomodate only a relatively few engineers. These courses, however, concentrate on the technical side of power system engineering. There is also a need for greater availability of training in the other subjects mentioned in the paper, which are necessary to develop a well-rounded planning engineer.

The author wishes to thank these discussers for the interest they have shown in this paper and for the effort they have spent in preparing their discussions.

General Study of Area Supply Methods

J. A. CASAZZA
ASSOCIATE MEMBER AIEE

J. R. RANKIN
ASSOCIATE MEMBER AIEE

ELECTRIC power systems usually have four superimposed voltage levels as follows:

1. Utilization level.
2. Distribution level.
3. Subtransmission level.
4. Transmission level.

Each of these levels may be visualized as a web covering the area of the system. The webs decrease in density from the utilization level to the transmission level.

Experience has shown that a major element in power system costs is that of the connections between these levels. In this analysis the connections between the distribution and utilization levels are called distribution transformers, the connections between subtransmission and distribution levels are called substations and the connections between transmission and subtransmission levels are called switching stations. These connections essentially consist of step-down transformers with the necessary switching and protective apparatus. The function of these step-down transformers, is to allow the higher-voltage web to supply power to the lower-voltage web. Because of its greater density the lower-voltage web makes the power available to a larger portion of the area.

The utilization, distribution, and subtransmission webs are usually split into separate sections of parts, the utilization web sometimes having several thousand times as many parts as the distribution web, the distribution web having up to several hundred times as many parts as the subtransmission web, and the subtransmission web having up to 20 or 30 parts. The transmission web is usually not split. Each part of a web is often supplied from the next higher voltage web through step-down transformers at a single location, i.e., each step-down transformer installation supplies a radial load. On occasion, two or more parts of a web are combined to form one part which is supplied by step-down transformers at different locations. Such combinations are as follows:

Paper 55-669, recommended by the AIEE System Engineering Committee and approved by the AIEE Committee on Technical Operations for presentation at the AIEE Fall General Meeting, Chicago, Ill., October 3–7, 1955. Manuscript submitted June 7, 1955; made available for printing July 18, 1955.

J. A. CASAZZA is with the Public Service Electric & Gas Company, Newark, N. J., and J. R. RANKIN is with Rutgers University, New Brunswick, N. J.

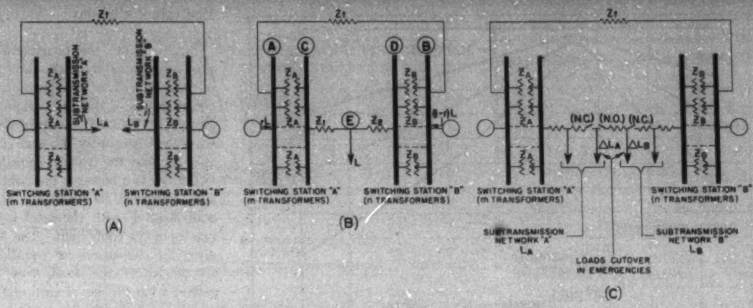
Z1
Z1
Z1
ZA
ZB
SUBTRANSMISSION NETWORK "A"
SUBTRANSMISSION NETWORK "B"
LA
LB
SWITCHING STATION "A" (m TRANSFORMERS)
SWITCHING STATION "B" (n TRANSFORMERS)
(A)
A
C
D
B
rL
(1-r)L
E
L
(B)
(N.C.)
(N.O.)
(N.C.)
ΔLA
ΔLB
SUBTRANSMISSION NETWORK "A" LA
LOADS CUTOVER IN EMERGENCIES
SUBTRANSMISSION NETWORK "B" LB
(C)

Fig. 1. Equivalent circuits

A—Radial networks B—Integrated networks C—Normally separate networks with emergency cutovers

1. Banked secondaries on distribution transformers.
2. Secondary networks.
3. Primary networks supplied by two or more substations.
4. Subtransmission networks supplied by two or more switching stations.

On other occasions, normally open ties are established between two parts of a web. Load is transferred from one part to the other in the event of an outage of a step-down transformer supplying either part. Examples of such emergency cutovers are

1. Secondary cutovers in the event of distribution transformer outages.
2. Primary cutovers to another substation in the event of substation transformer outages.
3. Subtransmission network cutovers to another switching station in the event of the occurrence of switching station transformer outages.

To summarize, the three general methods of supplying distribution and subtransmission networks are the following:

1. Supplying one network radially from each step-down transformer location.
2. Integrating the separate networks so that they effectively become one large network supplied from several step-down transformer locations.
3. The same as item 1, except providing normally open ties between networks to make possible cutovers from one network to the other under outage or emergency conditions.

The supply method chosen should result in the minimum over-all cost. The cost will depend on the effect of each method on the supply system, the step-down transformers, and the subtransmission or distribution networks. The factors that should be considered are the following:

1. Service reliability.
2. Thermal and voltage conditions, both normal and emergency.
3. Short-circuit duties.
4. Relaying and protection difficulties.

Scope

This analysis has been limited to studies of the supply to the subtransmission. However, it is felt that the methods used are applicable to investigations of the supply to other voltage levels.

In general, the most costly element in the supply to subtransmission networks is the switching station. This is especially true of systems in developed areas where the existing transmission and subtransmission webs provide relatively complete area coverage, and load increases are supplied by interpolating new switching stations and increasing the capacity of existing switching stations. On this type of system an increasing proportion of the cost of supplying subtransmission will be invested in switching stations in the future. Since it has been prepared for such a system, this analysis has been mainly confined to determining the effect on the load that can be supplied of: 1. the supply method, and 2. the number and sizes of the step-down transformers at each switching station. It has been limited to cases where only two switching station locations are involved.

A detailed investigation of the effect of transmission system conditions and subtransmission network conditions on the load that can be supplied is also included for the case when the subtransmission networks are integrated.

General Approach

As is usual in most practical engineering problems, this type of analysis involves a vast number of variables. To arrive at some conclusions, the approach consists of selecting typical values for most of the variables, changing the variables one at a time to determine their relative importance, and drawing conclusions based on the most important variables.

This analysis uses the per-unit (pu) system. Although it was actually made on a 100-mva base, the pu results are applicable to any other base provided the pu ratings and impedances are correct. The use of the pu system makes the results useful in investigations of the best supply method for all load sizes at any voltage level.

Assumptions

To simplify the analysis, the following assumptions have been made:

1. All loads have the same power factor and are coincident; losses are considered part of the loads.
2. All impedances have the same phase angle.
3. All high-tension and low-tension busses in the step-down transformer stations are solidly closed.
4. Thermal conditions on the step-down transformers limit the amount of load that can be supplied.
5. Facilities adequate to supply the load with any one step-down transformer out of service are provided.
6. All the transformers at a step-down transformer station have the same impedance and rating.

Assumptions 1 and 2 do not cause ap-

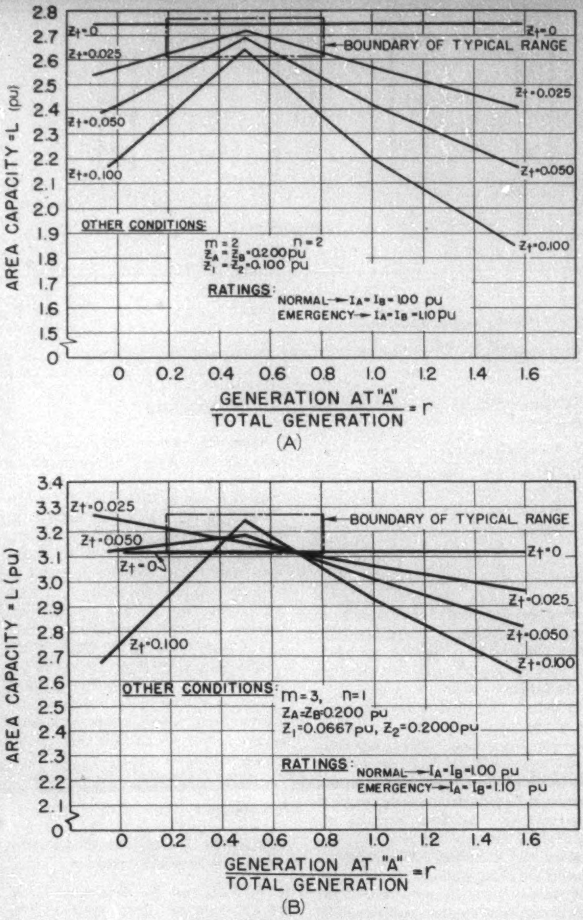

Fig. 2. Effect of bulk supply system

preciable error.[1] Short-circuit duties would require bus section reactors in many cases, contrary to assumption 3. However, the usual arrangement of these reactors results in transformer loadings substantially the same as those resulting from assumption 3. Since voltage conditions sometimes limit the amount of load that can be carried, assumption 4 is not always correct. However, in such cases proper use of reactive sources in the load area will make assumption 4 reasonable. Assumption 5 is reasonable when spare transformers are provided at each location and the total number of transformers is small. The spare transformers limit the duration of an outage to a short period, thus making the probability of an overlapping outage very small and relatively independent of the total number of transformers. Assumption 6 is based on conventional practices.

Equivalent Circuits

Fig. 1 shows the equivalent circuits used in the analysis of the three methods of supply. The transmission system equivalent is of the type originally suggested by Ward.[2] It consists of an equivalent generator at each transmission bus and the transfer impedance between the two busses. The subtransmission equivalent shown in Fig. 1(B) is an equivalent Y with the total load being one leg of the equivalent. The Appendix gives the derivations of equations used to determine the load that can be carried with the use of each of the three supply methods for the conditions investigated.

Importance of Variables

Radial Subtransmission Networks

With radial subtransmission networks, the area capacity depends only on the number and sizes of the transformers at each supply location as described in the Appendix.

Integrated Subtransmission Networks

With the integration of subtransmission networks, the firm capacity depends upon the following factors, as shown in the second section of the Appendix, and in Fig. 1(B).

Transformers: number (m, n); size (I_A, I_B); impedance (Z_A, Z_B).

Equivalent subtransmission impedances (Z_1, Z_2)

Supply system transfer impedance (Z_t)

Proportion of equivalent generation at each high-tension bus (r, $1-r$)

Figs. 2(A) and 2(B) show the effect of the bulk supply system, i.e., r and Z_t, on the area capacity. Increases in Z_t have little effect, provided the equivalent generation is balanced. Changes in the balance of equivalent generation have little effect when Z_t is small. Consequently, the supply system has little effect on the area capacity if either the transfer impedance is small or the equivalent generation is balanced. One or both of these conditions usually exist on the Public Service Electric and Gas Company (PSEG) system.

Figs. 3(A) and 3(B) show the effect of the subtransmission system, i.e., Z_1 and Z_2. The area capacity depends on both the ratio of Z_1 to Z_2 and the sum of Z_1 and Z_2. The more important factor is the ratio of Z_1 to Z_2. For the conditions shown in Figs. 3(A) and 3(B), the maxi-

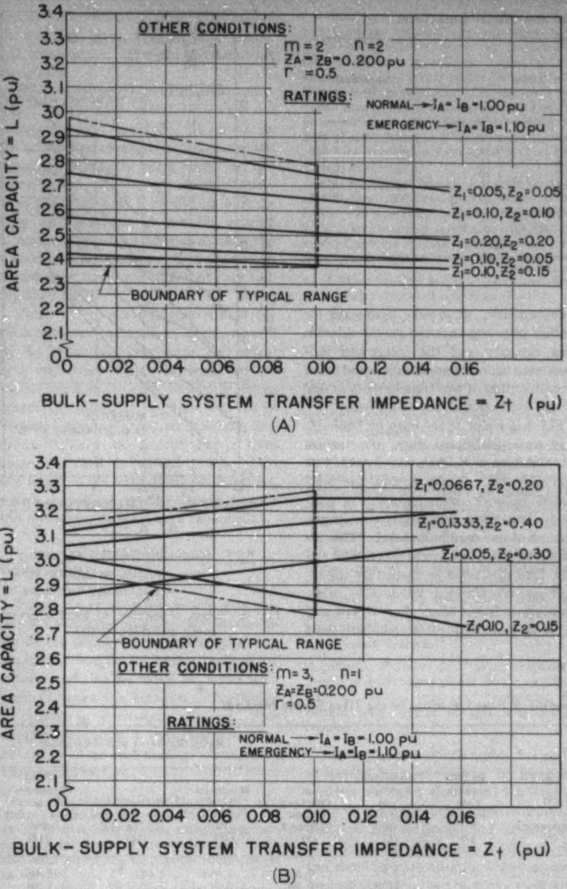

Fig. 3. Effect of subtransmission system

mum area capacity occurs when the ratio of Z_1 to Z_2 is equal to the ratio of n to m and the total of Z_1 and Z_2 is a minimum. This relationship between the ratios of Z_1 to Z_2 and of n to m is the result of having transformers of the same size at both switching stations. Although it has not been proved, it is believed that the maximum integrated network area capacity will occur when the ratio of Z_1 to Z_2 is approximately the same as the ratio of Z_A/m to Z_B/n when the two switching stations have transformers of different sizes. A comparison of the curve for $Z_1=0.10$ and $Z_2=0.10$ with the curve for $Z_1=0.10$ and $Z_2=0.15$ in Fig. 3(A) and a comparison of the curve for $Z_1=0.0667$ and $Z_2=0.20$ with the curve for $Z_1=0.10$ and $Z_2=0.15$ in Fig. 3(B) shows how sensitive the area capacity is to subtransmission conditions.

This explains the large changes in area capacity that have occurred in actual cases when a large spot load or a new subtransmission circuit is added. Consequently, the effect on the area capacity of all subtransmission changes and additions must be carefully studied. If this is not done, a subtransmission addition that increases the subtransmission capacity may decrease the firm switching station capacity.

Radial Networks with Emergency Cutovers

The area capacity for separate subtransmission networks with emergency cutovers depends only on the sizes of the transformers and the amount of load that can be transferred in emergencies.

Assumptions Concerning Variables

To compare the three basic supply methods the following assumptions were made concerning integrated subtransmission networks:

$$Z_t=0$$

$$Z_1=\frac{Z_A}{m}$$

$$Z_2=\frac{Z_B}{n}$$

These assumptions were based on an investigation of the values of Z_t, Z_1, and Z_2 on the PSEG system and the results shown in Figs. 2(A), 2(B), 3(A), and 3(B), which indicate that they will give a relatively high value for the area capacity. Table I compares the actual values of these factors with the theoretical values resulting from the assumptions.

Results

Table II compares the area capacities for the three supply methods for various assumed numbers and sizes of transformers at the two supply locations.

Column 9 of Table II shows the increased capacity of integrated networks as compared with radial networks. These benefits become a smaller proportion of the area capacity as the area capacity increases.

The maximum capacity possible from the use of emergency cutovers is indicated. In general, emergency cutovers make possible a maximum area capacity greater than the integrated network capacity by about the same amount that the integrated network capacity is greater than the radial network capacity.

The transferable loads increase the radial network area capacity by the total amount of transferable load, provided the transferable load is divided so that normal transformer ratings are not exceeded. Table II shows each source normally supplying one-half the total transferable load, which results in outage conditions becoming critical and which makes pos-

Table I. Comparison of Theoretical and Actual Impedances

Area	Approximate Equivalent Transformer Representation, A/B	Actual Z_t	Actual Z_1	Actual Z_2	Theoretical* Z_1	Theoretical* Z_2
1	2-75's/3-55's	0.06	0.09	0.10	0.063	0.067
2	4-55's/1-55	0.01	0.03	0.15	0.050	0.200
3	2-75's/2-55's	0.03	0.08	0.11	0.063	0.100
4	2-55's/2-55's	0.03	0.13	0.20	0.100	0.100
5	3-55's/1-55	0.09	0.06	0.50	0.067	0.200
6	1-55 /3-55's	0.07	0.24	0.20	0.200	0.067

* Based on $Z_1 = \frac{Z_A}{m}$; $Z_2 = \frac{Z_B}{n}$

The typical impedance for a 55-mva (name-plate) transformer bank is 0.200 per unit at 100 mva, and for a 75-mva (name-plate) transformer bank 0.125 per unit at 100 mva.

sible the maximum benefits of the emergency cutovers. Table II also shows that the maximum area capacity occurs when the total transferable load is equal to the emergency rating of the smallest transformer bank supplying the load. Consequently, the optimum transferable load becomes a smaller proportion of the total load as the area capacity increases. This makes the maximum benefits of emergency cutovers seem more feasible as loads increase.

The difference between the integrated network area capacity and the radial network area capacity, as shown in column 9 of Table II, is also the amount of transferable load that is required with radial networks to equal the integrated network area capacity. It is very significant for system planning that the radial network area capacity and the integrated network area capacity are almost equal, with a combination of two transformers at one supply location and four at the other.

Fig. 4 is a plot of the data in Table II, plus some additional data, for various combinations of banks normally rated at 1.00 per unit. It shows that the integrated network area capacity is relatively low when there are two transformers at one supply location. This results from the excessive proportion of the total load that must be carried by the remaining transformer when the other transformer is out of service. Fig. 4 and Table II show that a 3/1 combination of

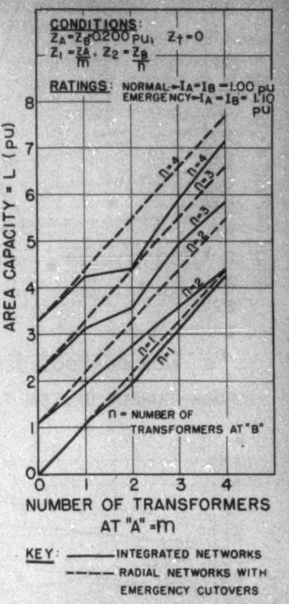

Fig. 4. Effect of number of transformers at each switching station

Table II. Comparison of Area Capacities for the Three Supply Methods

Source A: No. of Transformers, m (1)	Source A: Ratings,* PU Normal (2)	Source A: Ratings,* PU Emergency (3)	Source B: No. of Transformers, n (4)	Source B: Ratings,* PU Normal (5)	Source B: Ratings,* PU Emergency (6)	Radial Network Area Capacity, PU (7)	Integrated Network Area Capacity, PU (8)	Δ Column 8 Minus Column 7 (9)	Radial Networks with Emergency Load Cutovers: Maximum Area Capacity, PU (10)	Radial Networks with Emergency Load Cutovers: Normal Load on Each Source, L_A/L_B, PU (11)	Radial Networks with Emergency Load Cutovers: Total Transferable Load† $(\Delta L_A + \Delta L_B)$, PU (12)
2	1.00	1.10	2	1.00	1.10	2.20	2.75	0.55	3.30	1.65/1.65	1.10
2	1.00	1.10	2	1.55	1.75	2.85	3.39	0.54	3.95	1.65/2.30	1.10
2	1.55	1.75	2	1.55	1.75	3.50	4.39	0.89	5.25	2.625/2.625	1.75
3	1.00	1.10	1	1.00	1.10	2.20‡	3.12	0.92	3.30	2.75/0.55	1.10
3	1.55	1.75	1	1.00	1.10	3.50‡	4.41	0.91	4.60	4.05/0.55	1.10
3	1.55	1.75	1	1.55	1.75	3.50‡	4.96	1.46	5.25	4.375/0.875	1.75
3	1.00	1.10	2	1.00	1.10	3.30	3.58	0.28	4.40	2.75/1.65	1.10
3	1.00	1.10	2	1.55	1.75	3.95	4.22	0.27	5.05	2.75/2.30	1.10
3	1.55	1.75	2	1.00	1.10	4.60	5.06	0.46	5.70	4.05/1.65	1.10
3	1.55	1.75	2	1.55	1.75	5.25	5.69	0.44	7.00	4.375/2.625	1.75
3	1.00	1.10	3	1.00	1.10	4.40	4.96	0.56	5.50	2.75/2.75	1.10
3	1.00	1.10	3	1.55	1.75	5.70	6.24	0.54	6.80	2.75/4.05	1.10
3	1.55	1.75	3	1.55	1.75	7.00	7.91	0.91	8.75	4.375/4.375	1.75
4	1.00	1.10	1	1.00	1.10	3.30‡	4.26	0.96	4.40	3.85/0.55	1.10
4	1.00	1.10	2	1.00	1.10	4.40	4.40	0	5.50	3.85/1.65	1.10
4	1.00	1.10	2	1.55	1.75	5.05	5.03	−0.02	6.15	3.85/2.30	1.10
4	1.55	1.75	2	1.00	1.10	6.35	6.39	0.04	7.45	5.80/1.65	1.10
4	1.55	1.75	2	1.55	1.75	7.00	7.01	0.01	8.75	6.125/2.625	1.75
4	1.00	1.10	3	1.00	1.10	5.50	5.87	0.37	6.60	3.85/2.75	1.10
4	1.00	1.10	3	1.55	1.75	6.80	7.15	0.35	7.90	3.85/4.05	1.10
4	1.55	1.75	3	1.00	1.10	7.45	8.08	0.63	8.55	5.80/2.75	1.10
4	1.55	1.75	3	1.55	1.75	8.75	9.32	0.57	10.50	6.125/4.375	1.75
4	1.00	1.10	4	1.00	1.10	6.60	7.15	0.55	7.70	3.85/3.85	1.10
4	1.00	1.10	4	1.55	1.75	8.55	9.07	0.52	9.65	3.85/5.80	1.10
4	1.55	1.75	4	1.55	1.75	10.50	11.38	0.88	12.25	6.125/6.125	1.75

* Typical winter ratings of 55 mva (name-plate) 132/26-kv transformer bank are: normal, 100 mva, emergency, 110 mva. Typical winter ratings of 75 mva (name-plate) 132/26-kv transformer bank are: normal, 155 mva, emergency, 175 mva.

† One-half of total should be transferable in each direction to keep amount of load transferred for any one emergency to a minimum.

‡ Cases are not realistic, since the load supplied by the source with one transformer would be interrupted until the load is transferred.

supply transformers makes better use of the available transformer capacity than a 2/2 combination when the networks are integrated.

Fig. 4 also shows the area capacities which result with radial networks and emergency load cutovers. It illustrates the relative advantages of this method of supply, particularly when there are two transformers at one switching station. This indicates that it would be particularly advantageous to convert existing integrated networks to radial networks with emergency cutovers when the second transformer bank is installed at a switching station.

Table III shows a comparison of the theoretical area capacities, as determined by the methods of this report, and actual area capacities for several areas on the PSEG system. The relatively close agreement indicates the results given in Table II are applicable to practical conditions. They are slightly higher than those obtained in actual areas. This is a result of the simplifying assumptions, which were intentionally slanted to give the maximum possible area capacities.

Conclusions

Based on the results of this analysis, which considered only the thermal capacity of the supply transformers, the best supply method for the heavy loads of the future seems to be radial networks with normally open ties between the networks to provide for emergency cutovers. This supply method will have the following effects on some of the other elements in the over-all picture:

1. Subtransmission facilities must be adequate for the loads that are cut over in the event of switching station transformer outage, and for outage of subtransmission facilities with all switching station transformers in service.

This should not require any more subtransmission than is required with integrated networks if approximately one-half the transferable load is normally supplied by each of the two switching stations. This load can also be transferred in the event of subtransmission outages. In certain cases, less subtransmission may be required than with integrated networks since the proper amount of transferable load will make possible the maximum use of spare subtransmission capacity under either switching station transformer outage or subtransmission outage conditions.

2. Loadings in excess of conventional emergency ratings may result on both subtransmission and supply transformers during the period between the occurrence of a supply transformer outage and the execution of the required load cutover. Since this period will be of short duration, these loadings should not become a limitation.

3. Additional emergency-switched capacitors may be required to maintain adequate voltage when loads are transferred from one source to another. Based on an 85 per cent (%) power factor for the transferable load, preliminary investigations indicate that required total megavars of emergency-switched capacitors will be 15% to 25% of the total mva of transferable load to limit the emergency voltage to 95% of the normal minimum.

This should not become a serious requirement since the transferable load power factor will generally be much higher than 85%. Any required capacitors may also be useful for other system and local area outages.

4. Circuit-breaker duties will be lower than those with integrated networks.

5. Relaying and protection costs will be reduced, since relay co-ordination will be simplified.

6. Service reliability will not be decreased, since the extent of major disasters will be confined to one switching station and interarea relief will be at least as great as with integrated networks. The transferable loads will be dually supplied, since they can be supplied from two different sources, thus insuring a high degree of service reliability. However, these loads must be transferred without interruption. This involves taking a calculated risk in the short period that these loads are tied to both sources. Breaker-interrupting duties may be in excess of ratings, and relays may not operate properly if another fault occurs during this period. However, this risk is very small, and of the type often taken in the day-to-day operation of the present system.

7. Phase shifters and other expensive means of controlling power flow sometimes required with integrated networks for certain bulk system outages will not be required.

Although considerable additional study of specific cases is required, the foregoing analysis indicates that from the over-all point of view the heavy subtransmission loads of the future should be supplied radially by each switching station; facilities should be provided for the emergency load cutovers required to make maximum use of switching station transformer and subtransmission line capacity under outage conditions.

Table III. Comparison of Theoretical and Actual Area Capacities for Integrated Networks

Area	Approximate Equivalent Transformer Representation, A/B	Winter Area Capacity,* Mva	
		Actual	Theoretical†
1	2-75's/3-55's	405	422
2	4-55's/1-55	375‡	426
3	2-75's/2-55's	325	339
4	2-55's/2-55's	260	275
5	3-55's/1-55	305	312
6	1-55 /3-55's	275	312

* Based on thermal limitations.

† Based on approximate equivalent transformer representation, and results tabulated in Table II.

‡ Capacity is below normal due to high voltage bus being operated open at switching station *A*.

Appendix. Method for Determining Area Capacity

Nomenclature

I_A = mva rating of each transformer at switching station *A*

I_B = mva rating of each transformer at switching station *B*

L = total load that can be supplied in the area, i.e., area capacity

L_A = total load normally supplied by switching station *A*

L_B = total load normally supplied by switching station *B*

m = number of transformers at switching station *A*

n = number of transformers at switching station *B*

r = proportion of load supplied by equivalent generator at bus *A*

$(1-r)$ = proportion of load supplied by equivalent generator at bus *B*

Z_t = transfer impedance between high-tension busses of the two switching stations

Z_A = impedance of each transformer at switching station *A*

Z_B = impedance of each transformer at switching station *B*

Z_1 = equivalent impedance from low-tension bus at switching station *A* to equivalent load point, as shown in Fig. 1(B)

Z_2 = equivalent impedance from low-tension bus at switching station *B* to equivalent load point, as shown in Fig. 1(B)

Because of the simplifying assumptions, the analysis can be made on an algebraic basis, with mva treated as current.

Radial Subtransmission Networks

Referring to Fig. 1(A), L_A was calculated with the use of normal ratings for the transformers and all transformers in service at switching station *A*. L_A was also calculated with the use of emergency ratings for the transformers with one transformer out of service. The lower of the two values is the load that can be carried at switching station *A*. L_B was similarly calculated.

The area capacity L is the sum of the loads that can be carried at the two switching stations.

Integrated Subtransmission Networks

Referring to Fig. 1(B), assuming the transformers at switching station *A* limiting and letting V_{AE} be the voltage drop from bus *A* to bus *E*

$$V_{AE}=mI_A\left(\frac{Z_A}{m}+Z_1\right) \tag{1}$$

$$V_{AE}=(rL-mI_A)Z_t+(L-mI_A)\left(\frac{Z_B}{n}+Z_2\right) \tag{2}$$

Equating 1 and 2, and solving for L

$$L=\frac{mI_A\left[\frac{Z_A}{m}+Z_1+\frac{Z_B}{n}+Z_2+Z_t\right]}{\frac{Z_B}{n}+Z_2+rZ_t} \qquad (3)$$

Now, assuming side B transformers limiting

$$V_{BE}=nI_B\left(\frac{Z_B}{n}+Z_2\right) \qquad (4)$$

$$V_{BE}=[(1-r)L-nI_B]Z_t+(L-nI_B)\times \left(\frac{Z_A}{m}+Z_1\right) \qquad (5)$$

Equating 4 and 5 and solving for L

$$L=\frac{nI_B\left[\frac{Z_A}{m}+Z_1+\frac{Z_B}{n}+Z_2+Z_t\right]}{\frac{Z_A}{m}+Z_1+(1-r)Z_t\Big]} \qquad (6)$$

To determine the area capacity, i.e., the total load which may be carried, L was calculated for the following six conditions:

1. All transformers in service and side A limiting.
2. All transformers in service and side B limiting.
3. One transformer out of service at side A and side A transformers limiting. (Equation 3 was solved with m replaced by $m-1$.)
4. One transformer out of service at side A and side B transformers limiting. (Equation 6 was solved with m replaced by $m-1$.)
5. One transformer out of service at side B and side A transformers limiting. (Equation 3 was solved with n replaced by $n-1$.)
6. One transformer out of service at side B and side B transformers limiting. (Equation 6 was solved with n replaced by $n-1$.)

Normal transformer ratings were used in determining L for the cases where all transformers are in service. Emergency transformer ratings were used in determining L for the cases where one transformer was out of service. The minimum value of L calculated was defined as the area capacity for the supply condition being investigated.

Radial Subtransmission Networks with Emergency Load Cutovers

Referring to Fig. 1(C), L_A and L_B were calculated using normal ratings for the transformers with all transformers in service. L_A and L_B were also calculated using of emergency ratings for the transformers with the largest transformer bank (at either A or B) out of serivce. The maximum area capacity is the smaller of the foregoing two totals.

The total transferable load, $\Delta L_A+\Delta L_B$, is the difference between this area capacity and the radial network area capacity, determined as indicated above, and is equal to the emergency rating of the smallest transformer bank. To limit the amount of load to be transferred for any one emergency, ΔL_A was assumed equal to ΔL_B. The normal load on source A is the sum of ΔL_A and the emergency ratings of the transformers at A with one transformer bank out of service. The normal load on source B is the sum of ΔL_B and the emergency ratings of the transformers at B with one transformer bank out of service.

Calculations

The calculations for integrated networks were first done in longhand and then checked using an *IBM 604* calculator. The longhand calculations required approximately 15 man-days while the calculation on the International Business Machine equipment required less than 2 man-days' preparation time and less than 15 minutes' machine time.

References

1. THE COORDINATED USE OF A-C AND D-C NETWORK ANALYZERS, J. A. Casazza, W. S. Ku. *Proceedings*, American Power Conference, Illinois Institute of Technology, Chicago, Ill., vol. 16, 1954, pp. 448–52.

2. EQUIVALENT CIRCUITS FOR POWER-FLOW STUDIES, J. B. Ward. *AIEE Transactions*, vol. 68, pt. I, 1949, pp. 373–82.

◆

Discussion

J. M. Henderson (General Electric Company, Schenectady, N. Y.): This paper provides an excellent appraisal of the several methods of electric power supply to subtransmission load areas. The analysis is sound and it is difficult to take exception to the conclusions drawn by the authors. They have demonstrated that where area capacity is limited by the thermal capacity of the supply transformers, and where suitable subtransmission substation tie circuits are already available, the radial supply scheme with provision for emergency throwover of transferable load is preferable. That is, they show that this method of supply permits maximum use of transformer capacity, while the capacity obtainable with an integrated network is less because of the unequal or unproportionate load division between supply transformers during emergency operation with one transformer out of service. Further advantages cited by the authors for the radial emergency cutover method of supply over the integrated network are reduced short-circuit duties as well as reduced complexity of system relaying.

These advantages are obtained at the expense of the additional switching required to switch the transferable load from one source station to another. In addition, in some instances this transfer pattern may involve additional subtransmission circuit investment. It might be of interest, therefore, if the authors would comment on these points and, if possible, provide some evaluation of their over-all significance.

It should also be emphasized that the margins favoring the radial-emergency cutover and integrated network methods of supply over the straight radial method are dependent to a considerable extent on the ratio of the transformer emergency and normal ratings. For example, with the supply system consisting of two stations each containing four transformers, and with transformer emergency capability 33% higher than normal, the straight radial method would permit maximum use of available transformer capacity with one unit out of service. The foregoing may be thought of as a special case in which the required transferable load is zero.

As the authors point out, there is usually little justification for normally closed interarea subtransmission ties, as bulk-power transfers between areas should be handled at the higher voltage transmission level. In addition, such normally closed subtransmission ties can sometimes become drastically overloaded during transmission emergency conditions.

In conclusion, the authors are to be complimented for this excellent analysis of a major problem now confronting many utility planning engineers.

K. M. Smith and **A. H. Getty** (Commonwealth Edison Company, Chicago, Ill.): The authors are to be congratulated on their contribution to a basic area of system planning. Using the method presented in the paper, it is possible to calculate the approximate area capacity of alternate methods of supply. The method described for calculating the area capacity of an integrated network has several practical limitations however, and will not replace the calculating board for specific areas.

The results of studies for the future development of our subtransmission system agree generally with the conclusion of this paper: that high-density loads can best be supplied from radial substations. We have used emergency load transfers with success on both distribution and subtransmission systems. However, integrated subtransmission networks have also been economically applied in areas of light or medium load density.

The relative area capacity calculated for the three methods of supply will be considerably influenced by the ratio of normal to emergency thermal capability used for the transformers. For example, with one type of transformer widely used on our system, the emergency capability of three transformers is approximately equal to the normal capability of four transformers. Using these ratings, the area capacity of a substation with four transformers of equal size is limited by normal load capability and could not be increased either by emergency load transfers or by integrated network connections. This is considerably different from the results presented in the paper. With the emergency transformer rating only about 10% higher than the normal rating as used by the authors, there is considerable advantage in using emergency load transfers between substations of four transformers each.

The statement was made that the emergency loadings which will result before the execution of the required load transfer should not be a limitation. The validity of this statement is also dependent upon the specific thermal ratings used. With two transformers of equal size at each substation and the load conditions that were assumed in the paper, the short-time emergency load on a transformer would be 50% more than its emergency rating. This is considerably above the short-time (30-minute) ratings that have been developed for our system. If lower short-time ratings are used, the relative advantage of radial substations with emergency load transfers will not be as great as indicated in the paper, particularly for substations with two transformers each.

While mention was made of several advantages of radial operation with emergency load transfers to supply heavy loads, it should not be inferred that this method will be most economical at all load densities. Assuming that loss of a transformer should not cause an interruption of service to customers, any radial method of supply inherently requires an initial installation of two or more transformers. We have economically used single transformers supported by integrated network ties as the initial substation installation to supply the subtransmission system in outlying areas.

J. A. Casazza and **J. R. Rankin:** The discussions have raised a number of pertinent points. Mr. Henderson has pointed out that advantages of radial networks with emergency cutovers are obtained at the expense of additional switching and subtransmission facilities. This is true. At present Public Service plans to transfer substations with loads up to about 5,000 kva. A transfer of several substations with a total load of 15,000 kva is planned in one area. The spare subtransmission capacity required for subtransmission outages in the network to which the loads are transferred has been found adequate for such cutovers. The switching is accomplished by motor-operated disconnects actuated by loss of voltage. The transfer to the alternate supply is made by interrupting the normal supply, by opening the circuit breaker at its source end. This, however, involves a momentary load interruption. No momentary interruptions are desired in transferring the larger blocks of load indicated in this paper. Specific investigation of methods of accomplishing this are in progress in two areas. It is hoped that additional switching facilities will be minimized by using substations with a low average loading per existing line terminal as the transferable loads. Additional subtransmission requirements should be kept to a minimum if about one half the transferable load is normally supplied by each switching station. If this is done, normal conditions should not require more subtransmission. The difference between normal and emergency subtransmission ratings can be utilized when outages require the transfer of load.

Both Mr. Henderson and Messrs. Smith and Getty have pointed out that the differentials between the various supply methods are very dependent upon the ratio of normal to emergency ratings used for the transformers. This is true and indicates the possibility that some consideration should be given to the supply method in determining transformer ratings. The ratings used in this paper were based on conventional rating practices for the sizes and types of transformers involved.

Messrs. Smith and Getty have correctly pointed out that the relative advantages of radial networks with emergency cutovers will be less than indicated if the short-time loading conditions become critical. The time required to make the necessary load transfers, the loss of transformer life that is acceptable, and acceptable short-time subtransmission loadings will determine the extent of this limitation.

Mr. Henderson has stated that there is little justification for normally closed interarea subtransmission ties. Messrs. Smith and Getty, however, have indicated that integrated networks are preferable with lighter loads, particularly since this makes possible the use of only one transformer bank when establishing a new switching station. We agree with Messrs. Smith and Getty and did not intend to imply that radial networks with emergency cutovers is the best supply method for all load densities. Our paper attempted to determine the best supply method for the heavier loads of the future. At present, integrated networks predominate on the Public Service system.

Mr. Henderson also stated that interarea subtransmission ties can become drastically overloaded during bulk-system outages. This has not been a problem on our system in the past, since spare subtransmission capacity required for subtransmission outages has been adequate for the loads superimposed on subtransmission during bulk-system outages. Recent a-c network analyzer studies have indicated the possibility that this may become a problem as transmission system loads increase.

The discussions have helped to clarify the paper and are much appreciated.

Equivalent Circuits for Single-Phase Motors

G. R. SLEMON
MEMBER AIEE

IN THIS paper equivalent circuits suitable for use with network analyzers are developed for a number of types of single-phase motors. The approach used allows the equivalent circuits to have the following features:

1. Most elements in the equivalent circuit correspond directly to sections of the magnetic circuit of the machine, allowing the physical picture of the machine to be retained in its equivalent circuit.
2. Individual adjustments are provided in the circuit for each leakage reactance, mutual reactance, winding resistance, for turns-ratio, and for speed.
3. The terminals of the equivalent circuit represent the actual terminals of the machine. This allows the circuit to be interconnected directly to other machines or supply networks.
4. Direct measurements can be made of input current and voltage, mechanical power output, and torque as a function of speed.
5. The principal effects of magnetic saturation, iron losses, and space harmonics can be included where required.

Equivalent circuits for individual types of single-phase motors have been developed by many authors and general methods of developing these circuits have been described by Kron.[1] In almost all of these approaches to the problem an attempt has been made to produce a circuit containing only resistance, inductance and capacitance elements, and voltage sources such as are available on network analyzers designed for power system studies. To do this, symmetrical component, cross-field and phase-shift transformations have often been used with the result that much of the physical significance of the circuit is lost. Derived rather than actual voltages are applied, capacitors and sometimes negative resistors are required, and much of the opportunity to include saturation effects is lost.

It is shown herein that the primary limitation of conventional network analyzers in handling these circuits can be removed by the addition of a simple electronic varible-ratio transformer of voltage ratio 1 to *jn*. Other limitations such

---

Paper 55-684, recommended by the AIEE Rotating Machinery Committee and approved by the AIEE Committee on Technical Operations for presentation at the AIEE Fall General Meeting, Chicago, Ill., October 3–7, 1955. Manuscript submitted January 31, 1955; made available for printing July 19, 1955.

G. R. Slemon is with the University of Toronto, Toronto, Ont., Canada.

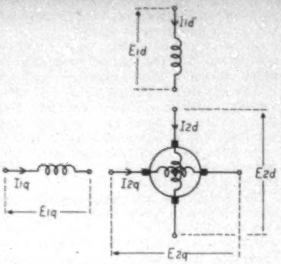

Fig. 1. Equivalent coils of a general cross-field machine

as the residual resistance of inductors will still remain. To overcome these, the possibility of using the transformer-analogue type of network analyzer[2] for machine design problems is discussed.

Equivalent Circuit of a General Cross-Field Machine

Equivalent circuits for most types of single-phase motor can be derived by applying appropriate constraints to the equivalent circuit of a general cross-field machine which has a salient-pole stator and a round rotor. Fig. 1 shows the arrangement of the equivalent coils of such a machine, the direct- and quadrature-axis stator coils having effective turns N_d and N_q respectively. The effective number of turns is the actual number of turns multiplied by the appropriate fundamental-frequency winding factor. It is assumed that the effects of harmonics can be neglected in the initial development of the equivalent circuit and can be added later by superposition, if necessary. The rotor is considered to be commutated in its direct and quadrature axes and may be replaced for purposes of analysis by two coils each having N_d effective turns.

The equivalent circuits in this paper are developed by a method described in an earlier paper[3] which related to transformers and polyphase machines. It is shown in Appendix I that the form of the electric equivalent circuit of an electromagnetic machine is basically the dual of the form of its magnetic circuit; reluctances in the magnetic circuit are replaced by inversely proportional inductances in the electric circuit.

The first step in analyzing the machine is the reduction of its magnetic field to a magnetic circuit of lumped magnetic reluctances each of which represents the reluctance offered to a mutual or leakage flux. This reduction is outside the scope of this paper but it should be noted that all simplifying assumptions are introduced at this stage. At standstill, the machine of Fig. 1 may be considered as two 2-winding transformers which are mutually independent except that direct- and quadrature-axis fluxes exist simultaneously in parts of the magnetic field and may thus produce some intersaturation effects. Neglecting this factor for the moment, independent magnetic circuits may be produced for the two axes, as shown in Fig. 2. S_{md} and S_{mq} are the reluctances to the main mutual fluxes ϕ_{md} and ϕ_{mq}. S_{1d} and S_{1q} are the reluctances to the stator leakage fluxes and S_2 is the rotor leakage reluctance which will normally but not necessarily be the same for both axes.

The equivalent electric circuits of Fig. 3 are dual in form to the corresponding circuits of Fig. 2 and may be derived by a simple topological method.[3] Reluctances have been replaced by inductive reactances of value

$$X=\omega\frac{N_d^2}{S}$$

and mesh fluxes have been replaced by nodal voltages

$$V=j\omega N_d\phi$$

All quantities in the electric circuits have been referred to the number of turns N_d in the direct-axis stator winding. When actual terminal quantities are required, these can be obtained by attaching ideal transformers with appropriate turns-ratios. To complete the equivalent circuits at standstill, the winding resistances may be added as part of the electric circuits attached to the machine terminals.

Effects of Rotation

Voltages are produced in the fictitious rotor coils because of two effects. Transformer voltages are induced just as if the coils were stationary. These voltages V_{md} and V_{mq} are already included in the circuits of Fig. 3. In addition, rotational voltages are produced in the coils of each axis due to rotation through the net flux of the other axis. These rotational voltages may be introduced by the use of appropriate ideal transformers.

Let the angular velocity of the rotor be n ω electric radians per second. The net fluxes denoted ϕ_{2d} and ϕ_{2q} linking the direct- and quadrature-axis rotor coils are the vector differences of the mutual fluxes ϕ_{md} and ϕ_{mq} and their respective rotor leakage fluxes. The rotational voltage injected into the quadrature-axis circuit is given by

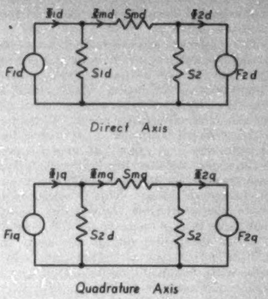

Fig. 2. Magnetic circuits of a cross-field machine

$$V_{rq}=-n\omega N_d\phi_{2d}$$

But in the electric circuit

$$V_{2d}=j\omega N_d\phi_{2d}$$

Therefore the voltage injected into the quadrature axis may be obtained as

$$V_{rq}=jnV_{2d}$$

Similarly the voltage injected into the direct axis is

$$V_{rd}=jnV_{2q}$$

In the equivalent circuit the injection of these voltages is accomplished by special unilateral variable-ratio transformers having voltage ratios of 1 to jn and 1 to $-jn$, and current ratios of 0 to 1. Fig. 4 shows the complete equivalent circuit of a general 2-axis machine with all stator and rotor terminals brought out. An additional bilateral transformer of ratio N_q to N_d is required to obtain the actual voltage and current at the quadrature-axis stator-terminals. The rotor terminals are those which would be available if the machine were ideally commutated in its direct and quadrature axes. Thus, the circuit fulfills the requirement that it be directly connectable to external electric circuitry.

If the direct and quadrature-axis fluxes are not sinusoidally distributed, the equations for the rotational voltages may not be quantitatively correct. The rotational voltages will however still be proportional to the net rotor fluxes. This additional effect can be included by introducing into the voltage ratios of transformers T_1 and T_2, factors relating the effective rotational fluxes to the actual fluxes.

The mechanical power output and torque for the machine at any value of speed may be found by direct measurements on the equivalent circuit using a double-element wattmeter. Mechanical power output is given by

P = real part of $(I_{2d}V_{rd}^{*}+I_{2q}V_{rq}^{*})$

The torque may be found as

$$T=\frac{P}{n\omega p}$$

where p is the number of pole pairs

But since this expression becomes indeterminate at standstill, an alternative direct measurement of torque is preferable

$$T=\frac{1}{\omega p}\,[\text{imaginary part of }(I_{2q}V_{2d}^{*}-I_{2d}V_{2q}^{*})]$$

The conventional equivalent circuit of a single-phase induction motor with no voltage applied to its quadrature-axis stator winding is developed from that of Fig. 4 in Appendix II.

Provision for Saturation and Iron Losses

The method of developing equivalent circuits described earlier associates each inductive reactance in the electric circuit with a magnetic reluctance in the machine. If the value of this reluctance is dependent on the flux established in it, a similar relationship will exist between the corresponding inductive reactance and the voltage across it. A first and usually sufficient approximation to the effect of magnetic saturation may be obtained by assuming that each reactance in the equivalent circuit is either constant or dependent on only one flux component. For example, it might be assumed that in the circuit of Fig. 4 all reactances are constant except the magnetizing reactances X_{md} and X_{mq}. Curves can be drawn for X_{md} and X_{mq} as functions of the voltages V_{md} and V_{mq} respectively. Then for each setting of the equivalent circuit the reactance are adjusted until the reactance and voltage measured in the analyzer correspond to a point on the corresponding curve.[4] Leakage reactances which are proportional to their leakage fluxes may be treated in a similar manner.

Where the reluctance of a magnetic member is dependent on the sum of a leakage and mutual flux, this member should be represented as a separate inductive reactance in the electric equivalent circuit, with a voltage proportional to the vector sum of the fluxes across it. The basic assumptions on saturation are therefore made by the designer in the process of reducing the magnetic field of a machine to a magnetic circuit. In general, the complexity of the circuit for an adequate representation will increase as the degree of saturation is increased. But an increase in the number of elements in the analyzer representation does not increase the time for obtaining results disproportionately. An additional saturation effect arises from the simultaneous existence of direct and quadrature components of flux. For example, the reactance X_{mq} in Fig. 4 may depend not only on the quadrature-axis mutual flux represented by the voltage V_{mq} but also on the direct-axis flux V_{md} acting across its magnetic path. This intersaturation effect is complicated by its dependence on the magnitudes of V_{md} and V_{mq} and also on the angle between them. Preliminary studies have shown the effect to be most pronounced when the voltages are in phase and almost negligible for the usual operating condition when they are approximately in quadrature. Further work is in progress to determine the practical methods of approximating this and other secondary saturation effects to sufficient accuracy.

All inductive reactances in the equivalent circuit which represent the reluctances of iron paths will have associated with them some iron losses. Where these losses are of sufficient importance to the characteristics being measured, they may be represented by resistances shunting the appropriate inductive reactances. These resistances may be found from computed values of loss or, alternatively, from the use of the complex permeability of iron.[3]

Split-Phase Motors

In split-phase or resistance-start motors the resistance-to-reactance ratio of the quadrature-axis stator circuit is made greater than that of the direct-axis stator circuit to produce a phase shift between the axis fluxes and, therefore, a starting torque. The squirrel-cage rotor may be represented by making the two voltages E_{2d} and E_{2q} in Fig. 4 equal to zero. Fig. 5 shows an equivalent circuit of this type of motor. Both stator windings are supplied from a common line voltage E_1 and the line current I_1. Direct measurements may be made of torque/speed, line-current/speed, winding-current/speed and also of the effects of varying resistances, reactances, and the turns-ratio.

Capacitor Motors

In capacitor motors the required phase shift between the direct- and quadrature-axis fluxes is produced by introducing a capacitor of reactance X_c into the quadrature-axis stator circuit, as shown in Fig. 5. In taking a torque/speed curve for this machine, the capacitive/reactance can be adjusted to the value appropriate to the starting-speed or running-speed range under consideration. The equivalent circuit is particularly convenient since the capacitor voltage can be measured directly. The most advantageous use of standard capacitors can be studied by adjusting various circuit parameters.

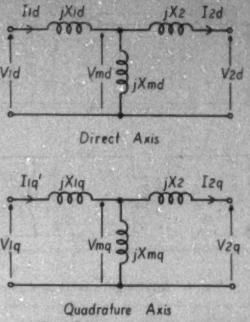

Fig. 3. Equivalent electric circuits of a cross-field machine at standstill

Shaded-Pole Motors

The shaded-pole motor is constructed with one winding encompassing the complete pole, while a second short-circuited winding encompasses only part of the pole. The windings are concentrated but the air gap is relatively uniform. The cross-field approach may be used in the analysis of this motor by considering it as a general 2-axis machine with its direct-axis stator coil and one quadrature-axis coil connected in series to the supply, while a second quadrature-axis coil is short-circuited. If only fundamental fluxes were considered, an equivalent circuit could be obtained by applying appropriate restrictions and additions to the general circuit of Fig. 4. Large space harmonics are, however, produced by the concentrated windings and their effects must be included to obtain an adequate circuit. Separate equivalent circuits can be drawn for each of the space harmonics. Since all harmonic circuits are excited from the same line current, the composite equivalent circuit consists of all the harmonic component circuits connected in series in both direct and quadrature axes at the air gap.[5] In the equivalent circuit shown in Fig. 6, the fundamental-frequency and third-harmonic circuits only are shown. The effects of higher harmonics might be included but these can usually be added as minor corrections calculated from the

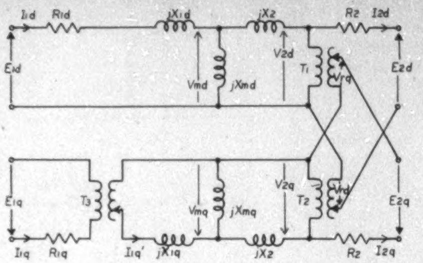

Fig. 4. Equivalent circuit of a general cross-field motor

Transformer	Voltage Ratio	Current Ratio
T_1	1 to $+jn$	0 to 1
T_2	1 to $-jn$	0 to 1
T_3	N_q to N_d	N_d to N_q

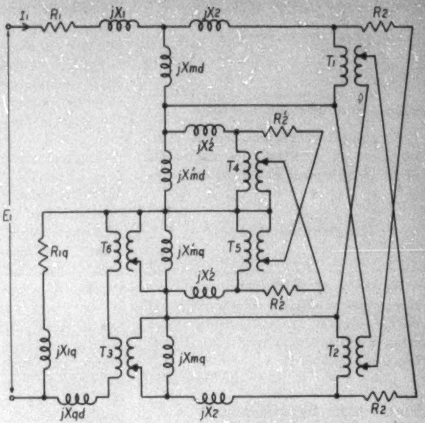

Fig. 6. Equivalent circuit of shaded-pole motor

Transformer	Voltage Ratio	Current Ratio
T_1	1 to $+jn$	0 to 1
T_2	1 to $-jn$	0 to 1
T_3	N_q to N_d	N_d to N_q
T_4	1 to $+j3n$	0 to 1
T_5	1 to $-j3n$	0 to 1
T_6	N_q to N_d'	N_d^1 to N_q

currents obtained with this limited circuit.[5] In Fig. 6, R_1 and X_1 are the resistance and leakage reactance of the main winding, R_{1q} and X_{1q} are the resistance and leakage reactance of the shaded-pole winding, and X_{qd} is the mutual leakage reactance of the main and shaded-pole windings. All primed parameters refer to the third-harmonic portion of the circuit and are referred to the effective direct-axis turns N_d. The effects of stator winding factors, frequency, and rotor skewing are included in evaluating these parameters. N_q^1 is the effective number of quadrature-axis turns producing third-harmonic space flux.

The torque is the sum of the fundamental frequency and the harmonic components and can be measured in each portion of the circuit as described previously. Harmonic torques are negative over a considerable portion of the speed range.

Double Squirrel-Cage Motors

The method of developing equivalent circuits may easily be extended to include motors with double or multiple rotor windings. Each rotor winding requires a set of unilateral variable-ratio transformers to inject its required rotational voltages. A magnetic circuit for a machine with double rotor winding might be developed on the assumptions that: 1. each stator and rotor winding has a separate leakage flux, 2. the three windings share a common mutual flux, and 3. additional leakage flux links both rotor windings. When developed into its electric equivalent form using the principle of duality, the circuit of Fig. 7 is obtained. R_2 and R_3 are the equivalent resistances and X_2 and X_3 are the self-leakage reactances of the two rotor windings. X_{23} is the mutual leakage reactance between the two rotor windings.

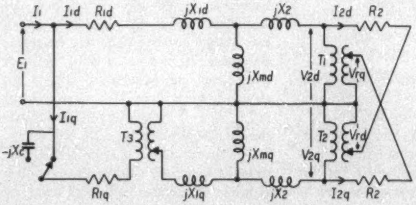

Fig. 5. Equivalent circuit of split-phase motor and capacitor motor. Transformer ratios given in Fig. 4

A more exact set of assumptions as to flux paths may be necessary, especially if one rotor winding is deeply imbedded. An additional flux path linking the stator and the outer rotor winding can be included without difficulty, but the form of the equivalent circuit should be redeveloped from first principles. The stator terminals in Fig. 7 have been left open to allow for any of the systems of stator supply such as capacitor, split-phase, and 2-phase systems.

Single-Phase Commutator Motors

The introduction of a rotor commutator with brushes in the direct and quadrature axes allows the terminals of the fictitious direct- and quadrature-axis coils to be brought out. It is then possible to supply these rotor coils from external circuits or to introduce a short circuit in one rotor axis only. Alternatively, brushes may be placed on the rotor in an axis other than the direct and quadrature axis. In this way a fixed relationship is established between the direct- and quadrature-axis currents.

The equivalent circuit of an elementary commutator machine with brushes in the direct and quadrature axes is shown in

Fig. 8. This circuit differs from that of Fig. 4 because of the following factors. A set of brushes in one axis continuously short-circuits the rotor turns undergoing commutation through the brush resistances, thus producing the effect of a short-circuited coil in the other axis. This effect is included by considering the rotor to consist of four fictitious coils, two of which are short-circuited by the brushes while the remaining two act as an ideally commutated rotor. R_3 and X_3 are the resistance and reactance of the circuits of the equivalent short-circuited coils, and X_{23} is the mutual reactance between the main and short-circuited rotor coils on any one axis. Additional bilateral transformers have been added to the circuits of the main rotor coils to include the turns-ratio between the number of effective direct-axis turns N_d on which the rotor reactances are based and the effective number of turns in each rotor axis N_{rd} and N_{rq}.

The circuit of Fig. 8 places no restrictions on the rotor and stator connections. Equivalent circuits for most types of commutator motors can be obtained by applying the appropriate constraints and by simplifying the arrangement wherever possible.

Series Motors

The winding arrangement and equivalent circuit for a directly compensated series motor are shown in Fig. 9. In this machine brushes are introduced in the quadrature axis only. This quadrature-axis rotor circuit and the two stator circuits are all connected in series to the supply. The terminals of the voltages E_{3q} and E_{3d} in Fig. 8 are left open-circuited by the absence of a direct-axis set of brushes. Their associated circuitry may therefore be omitted. The voltage E_{2d} is replaced by a short circuit. Reactances through which no current flows have also been omitted.

If full compensation is obtained in the quadrature axis ($N_q = N_{rq}$), the circuit of Fig. 9 can be further simplified by omitting the shunt reactance X_{mq}, transferring the elements R_3, X_{23} X_{23}, and X_1, across T_5 and eliminating T_3 and T_5. The voltage ratio of T_2 would then have to be 1 to $-jn(N_q/N_d)$.

A circuit for an inductively compensated series motor may be obtained by a minor alteration of the circuit of Fig. 9. The quadrature-axis stator coil is short-circuited through its resistance R_{1q} and reactance X_{1q}. The transformer T_3 is eliminated and the supply voltage is applied to the direct-axis stator winding and the quadrature-axis rotor winding in series.

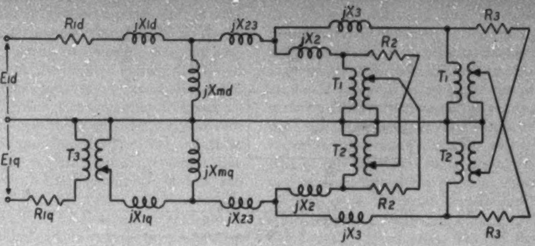

Fig. 7. Equivalent circuit of motor with double squirrel-cage rotor. Transformer ratios given in Fig. 4

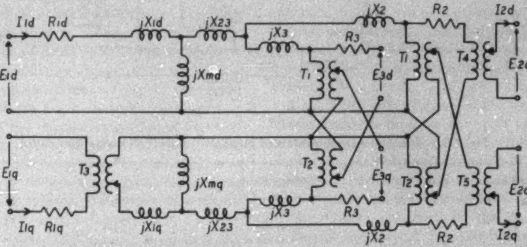

Fig. 8. General equivalent circuit of a single-phase commutator machine

Transformer	Voltage Ratio	Current Ratio
T_1	1 to $+jn$	0 to 1
T_2	1 to $-jn$	0 to 1
T_3	N_q to N_d	N_d to N_q
T_4	N_d to N_{rd}	N_{rd} to N_d
T_5	N_d to N_{rq}	N_{rq} to N_d

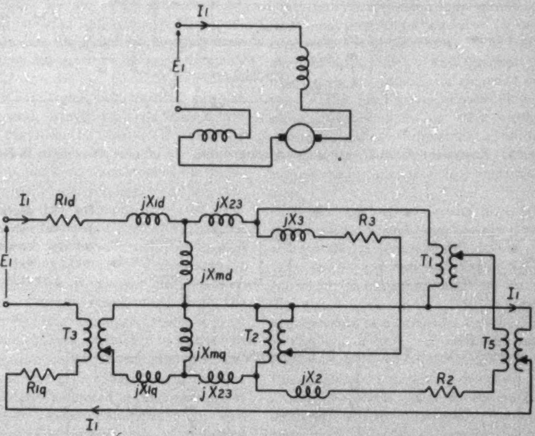

Fig. 9. Winding arrangement and equivalent circuit of a compensated series motor. Transformer ratios given in Fig. 8

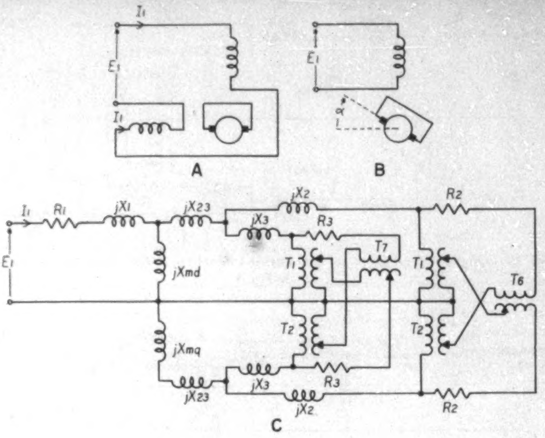

Fig. 10. Winding arrangements and equivalent circuit of a repulsion motor

Transformer	Voltage Ratio	Current Ratio
T_1	1 to $+jn$	0 to 1
T_2	1 to $-jn$	0 to 1
T_6	1 to $-\tan\alpha$	$-\tan\alpha$ to 1
T_7	1 to $\cot\alpha$	$\cot\alpha$ to 1

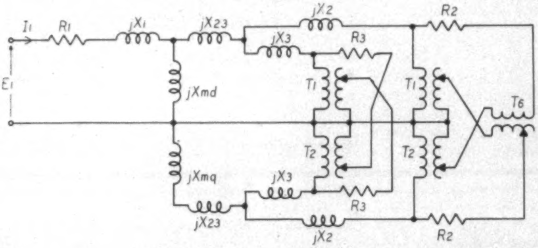

Fig. 11. Equivalent circuit of repulsion-induction motor. Transformer ratios given in Fig. 10

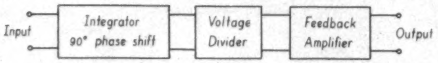

Fig. 12. Block diagram of unilateral voltage transformer with voltage ratio 1 to ±jn

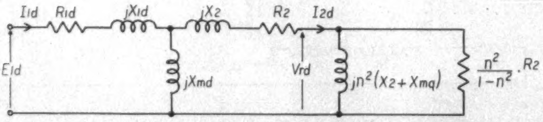

Fig. 13. Conventional equivalent circuit for a single-phase induction motor

Repulsion Motors

Two approaches may be used in the development of an equivalent circuit for a repulsion motor. In the first, the brushes are considered to be in the quadrature axis. The direct- and quadrature-axis stator coils are connected in series to the supply, as shown in Fig. 10(A). If the stator has only a single winding of N effective turns at α degrees from the direct axis, it may be replaced by equivalent stator windings of $N \cos\alpha$ and $N \sin\alpha$ turns in the direct and quadrature axes respectively. This replacement is, however, valid only if the stator has magnetic symmetry about these axes. If not, the second approach described later should be used. An equivalent circuit for the repulsion machine of Fig. 10(A) may be developed by altering the connections to the circuit of Fig. 9. The transformer T_5 is replaced by a short circuit and the supply is connected to the direct- and quadrature-axis stator coils in series. For a machine with a single stator winding, the resistances R_{1d} and R_{1q} and the reactances X_{1d} and X_{1q} may be combined to represent the resistance and leakage reactance of the single winding. Bilateral transformers of ratios $\cos\alpha$ to 1 and $\sin\alpha$ to 1 may be added at the direct- and quadrature-axis air gaps and the effect of altering the brush angle may be observed by adjusting the ratios of these transformers. Torque is measured in the previously described manner.

If the stator has a single winding and is magnetically salient, it is preferable to consider the axis of the stator winding as the direct axis. The short-circuiting brushes on the commutator are then at an angle α to the quadrature axis, as shown in Fig. 10(B). Suppose the current in this short-circuited rotor circuit is I_r. The equivalent currents in the direct rotor axes will then be determined:

$$I_{2d} = I_r \sin\alpha$$

and

$$I_{2q} = I_r \cos\alpha$$

The voltage in the rotor axes will be constrained by the relationship

$$V_{2d} \sin\alpha + V_{2q} \cos\alpha = 0$$

These relationships can be represented in the equivalent circuit by a pair of bilateral transformers of ratios 1 to $\sin\alpha$ and 1 to $\cos\alpha$ in series interconnecting the direct and quadrature rotor axes. These two transformers can be replaced by a single transformer of ratio 1 to $-\tan\alpha$, as shown in the equivalent circuit of Fig. 10(C), if the actual brush current is not required.

The effect of the coils short-circuited by the rotor brushes will be felt in both axes and will depend on the brush angle α. The voltages E_{3d} and E_{3q} will, therefore, be linked by a bilateral transformer of ratio 1 to cot α, since brushes at angle α produce the effect of a set of short-circuited brushes on the commutated turns at an angle $(\alpha+90)$.

The torque is determined from the sum of the four power measurements associated with the output voltages of the four nonbilateral transformers and their associated currents. Over certain ranges of speed, the effect of the coils short-circuited under the brushes may be neglected, thus simplifying the operation of the model circuit.

THE REPULSION-INDUCTION MOTOR

The repulsion-induction motor has two rotor windings. The outer winding is commutated as in a repulsion motor while the inner winding is a squirrel cage. An equivalent circuit for this motor can easily be derived from the general circuits of Figs. 4 and 8. The circuit shown in Fig. 11 has been simplified by neglecting the effect of the coils short-circuited under the brushes. This effect can, however, be included by introducing a third rotor winding with an appropriate set of self- and mutual-leakage reactances. In Fig. 11, R_2 and X_2 are the equivalent resistance and leakage reactances of the outer commutated windings, R_3 and X_3 are the resistance and leakage reactance of the inner squirrel-cage winding, and X_{23} is the mutual leakage reactance between these two windings.

Network Analyzers for Use With Equivalent Circuits

The equivalent circuits developed in this paper have been arranged specifically for use with network analyzers rather than as an aid to calculation. Both conventional and transformer-analogue network analyzers may be used. While the former is probably of greatest interest because of its general availability, the latter has a number of advantages for this type of work.

Most conventional network analyzers are equipped with resistances, inductive reactances, and variable-ratio bilateral transformers and these constitute the main part of the equivalent circuit elements. The only addition required is the unilateral voltage transformer having a ±90-degree phase shift and a variable ratio. This transformer can be produced as shown in the block diagram of Fig. 12 by the use of: 1. a Miller integrator circuit which produces a phase shift of very nearly 90 degrees which can be corrected to 90 degrees in following coupling networks; 2. a calibrated voltage divider on which the speed ratio n can be set; and 3. an amplifier with sufficient feedback to obtain linearity of amplification and very low output impedance. Four of these units are required for the representation of most of the commutator motors and for double squirrel-cage induction motors but two units are sufficient for split-phase, capacitor, and series motors. More than four units might be required if harmonic effects were included in certain circuits.

A number of difficulties are frequently encountered in using the elements of conventional network analyzers to represent machine circuits. These circuits require a number of pure inductive reactances to represent the several paths of the mutual and leakage fluxes. Only in the stator circuits is there a series resistance in which the residual resistance of practical inductors can be absorbed. Significant errors can occur over certain regions of speed because of the unavoidable presence of these residual resistances in conjunction with rotor reactances.

A similar and more serious difficulty occurs because of the requirement for ideal variable-ratio transformers. Practical transformers will have both resistance and leakage reactance which cannot always be included as part of the required circuit. The values of the resistance and reactance will also change with changes in ratio, making it necessary to readjust certain elements for each ratio setting. In addition, there are errors introduced by the magnetizing impedance of the transformers but these can be largely eliminated by the use of electronic compensators.[3] At the loss of some generality, certain of these transformers can be eliminated. For example, the transformer T_3 in Fig. 5 can be removed if a separate source of voltage of value $N_d(E_1/N_q)$ is made available for excitation of the quadrature-axis stator winding. The line current must then be found by vector addition of the direct-axis current I_{1d} and the quadrature-axis current multiplied by the appropriate turns-ratio. Unfortunately, each operation of this sort made to compromise the equivalent circuit with the limitations of the analyzer results in some loss of simplicity or facility of operation.

The disadvantages encountered in the conventional type of analyzer are almost completely eliminated in the transformer-analogue network analyzer.[3] In this analyzer all voltage/current relationships are represented by variable-ratio voltage transformers, the ratios being equal to the per-unit resistance and reactance. The only currents flowing in the analyzer are those caused by the residual magnetizing currents of the transformers and these are made negligible by adequate compensation. Positive and negative values of pure resistance and pure reactance are independently available. The universal unit of this analyzer can be arranged as two separate impedance units or voltage sources, or as a circuit transformer on which complex voltage and current ratios can be set independently. The unilateral transformers required for these equivalent circuits can thus be provided by setting the current ratio at zero. The measurement system of this analyzer is similar in operation to that of conventional types; voltages and currents are indicated in rectangular or polar form and both active and reactive power measurements are available.

A small network analyzer of the transformer-analogue type consisting of eight universal units and a measurement system would be sufficient for the circuits of the split-phase, capacitor, and series motors, while 14 universal units would handle any of the circuits presented in this paper. The same units could be used for polyphase induction and commutator machine analysis.[3] Provision might be made in such a special-purpose analyzer for ganging of the various speed settings and for double-element wattmeters to allow direct measurement of total torque.

Conclusion

A method has been described whereby equivalent circuits suitable for special network analyzers can be developed for most types of single-phase motors. The equivalent circuits preserve the physical significance of the impedance elements and also of the machine terminals allowing direct measurements of most desired quantities and easy adjustment of parameters. The effects of magnetic saturation can be included to a close approximation.

Typical equivalent circuits have been developed for several types of single-phase motor. The structure and complexity of these circuits can be varied to suit the established computations used by an individual designer or to fulfill the special requirements of a particular design.

The use of both conventional transformer-analogue network analyzers with these equivalent circuits is described. It is suggested that small special-purpose analyzers of the transformer-analogue type would provide an economical and accurate tool for the solution of problems in motor analysis and design.

Appendix I. Derivation of Electric Equivalent Circuit from a Magnetic Circuit

Any magnetic circuit may be represented mathematically by the mesh-flux matrix equation

$$[F]=[S][\phi] \tag{1}$$

where

$[F]$ = the magnetomotive forces in the meshes
$[S]$ = the self- and mutual reluctances of the meshes
$[\phi]$ = the mesh fluxes

Two substitutions are necessary to transform the relationships of equation 1 to its electrical form. Let

$$[F]=N[I] \tag{2}$$

where

N = a reference number of turns in the equivalent coils linking the magnetic circuit
$[I]$ = the currents in those coils

If the fluxes $[\phi]$ vary sinusoidally there will be induced in the N turns of the linking coils the voltages

$$[V]=j\omega N[\phi] \tag{3}$$

Substituting equations 2 and 3 into equation 1 gives

$$N[I]=S\frac{[V]}{j\omega N}$$

or

$$[I]=\frac{[S]}{j\omega N^2}[V] \tag{4}$$

Equation 4 is a set of nodal-voltage equations in which the currents injected at the nodes $[I]$ are related to the voltages between nodes $[V]$ by negative or inductive susceptances. The value of each inductance is given by

$$L=N^2/S \tag{5}$$

Since mesh and nodal equations are duals of each other, the circuits represented by equations 1 and 4 will be dual in form and their elements will be related by the number of turns and the angular frequency. The electric circuit may be drawn from examination of equation 4 or by a topological technique which is demonstrated in reference 2.

Appendix II. Derivation of the Equivalent Circuit of a Single-Phase Induction Motor

For a single-phase induction motor with squirrel-cage rotor, the rotor voltages E_{2d} and E_{2q} in Fig. 4 will be zero and the quadrature-axis stator winding will be left open-circuited. The conventional equivalent circuit for this machine[6] is shown in Fig. 13. It is seen that the quadrature-axis portion of the circuit and the rotational transformers are reduced to a single admittance linking the voltage V_{2d} and the current I_{2d}.

In Fig. 4, let $X_2+X_{mq}=X$. Then

$$V_{2q}=+jnV_{2d}\left(\frac{jX}{R_2+jX}\right) \tag{6}$$

also

$$V_{rd}=-jnV_{2q}$$

Substituting equation 6 gives

$$V_{rd}=\left(\frac{jn^2X}{R_2+jX}\right)V_{2d} \tag{7}$$

The direct-axis rotor current is found by substituting V_{2d} from equation 7 into

$$\begin{aligned} I_{2d}&=(V_{2d}-V_{rd})/R_2\\ &=\left(\frac{R_2+jX}{jn^2X}-1\right)\frac{V_{rd}}{R_2}\\ &=\left(\frac{R_2+j(1-n^2)X}{jn^2XR_2}\right)V_{rd} \end{aligned}$$

Separating the real and imaginary components of the admittance gives

$$I_{2d}=\left(\frac{1-n^2}{n^2R_2}-j\frac{1}{n^2X}\right)V_{rd} \tag{8}$$

Thus the relationship between V_{rd} and I_{2d} is represented by a resistance $n^2R_2/(1-n^2)$ in parallel with an inductive reactance n^2X, as shown in Fig. 13. It should be noted that the physical identity of the magnetizing reactance X_{mq} has been lost and with it the possibility of assessing and including the quadrature-axis saturation effect.

References

1. Equivalent Circuits of Electric Machinery (book), G. Kron. John Wiley and Sons, Inc., New York, N. Y., 1951.

2. Transformer-Analogue Network Analysers, M. W. Humphrey Davies, G. R. Slemon. *Proceedings*, Institution of Electrical Engineers, London, England, vol. 100, pt. II, 1953, pp. 469–86.

3. Equivalent Circuits for Transformers and Machines Including Non-Linear Effects, G. R. Slemon. *Ibid.*, pt. IV, pp. 129–43.

4. A Method of Approximate Steady-State Analysis for Non-Linear Networks, G. R. Slemon. *Ibid.*, pt. I, pp. 275–87.

5. Equivalent Circuits and Their Application in Designing Shaded-Pole Motors, S. S. L. Chang. *AIEE Transactions*, vol. 70, pt. I, 1951, pp. 690–99.

6. Theory of Alternating-Current Machinery (book), A. S. Langsdorf. McGraw-Hill Book Co., Inc., New York, N. Y., 1937, p. 668.

◆

Discussion

P. L. Alger (General Electric Company, Schenectady, N. Y.): There is a growing appreciation of the use of equivalent circuits to represent electric machines, and the use of analyzers or digital computers to calculate the performance of complete systems formed by combining such circuits. This paper, therefore, is of especial interest, and represents an important contribution to the subject.

I wish, however, that the author had made use of the revolving-field-theory circuits instead of the cross-field theory, since it appears to me that the cross-field theory has a vital defect. This defect arises from the well-known fact that the secondary resistance R_2 of a squirrel-cage motor increases with the rotor frequency, so that its value at double line frequency may be two or more times its value at slip frequency. This "skin effect" must be allowed for in the circuit, if the calculated results are to be of practical use in the study of single-phase motor performance. It is my understanding that there is no way to account for this change of resistance with frequency using the cross-field theory. This theory looks at the rotor circuits from the primary side and, therefore, considers all the rotor currents as having line frequency throughout. For this reason, I have chosen to use the revolving-field theory in all my own work on electric machines, and have found it eminently satisfactory from the two view points of ready understanding and accurate numerical results.

Edward Bretch (Century Electric Company, St. Louis, Mo.): While this paper does not state specifically that the equivalent circuits shown therein apply to squirrel-cage motors, the implication is that they are intended to represent squirrel-cage motors.

The application of the equivalent circuits, disclosed in this paper, to motors of the type indicated by Fig. 1 is not questioned but the validity of the assumption that a commutated rotor is the equivalent squirrel-cage rotor is questionable.

With a rotor having commutated short circuits, they are stationary with respect to the stator while, with the squirrel cage, they are stationary with respect to the rotor. A single commutated short circuit at the proper angle with respect to the stator produces a speed-torque characteristic similar to the d-c series motor while a single rotor short circuit, fixed with respect to the rotor, produces a torque that brings the rotor to a neutral position where it locks.

In order to approximate the squirrel-cage action, the four points of brush contact on the commutator (Fig. 1) must be permanently short-circuited so that the short circuits are fixed with respect to the rotor. A commutator in the rotor introduces what Professor Bewley calls "substitution of circuits,"[1] which action is not present in the squirrel-cage rotor.

If Fig. 1 does not correctly represent the single-phase squirrel-cage motor, it follows that the equivalent circuits shown therein are not suitable for single-phase squirrel-cage motors.

Reference

1. Flux Linkages and Electromagnetic Induction, L. V. Bewley. The Macmillan Co., New York, N. Y., chap. III, p. 12.

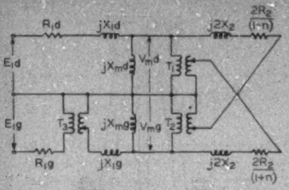

Fig. 14. Equivalent circuit for squirrel-cage motor with cross-field to revolving field transformation at the air gap

Transformer	Voltage Ratio	Current Ratio
T_1, T_2	1 to j	$-j$ to 1
T_3	N_q to N_d	N_d to N_q

G. R. Slemon: Mr. Alger's observation that there is no known way to take into account the effect of frequency on the rotor resistance with the cross-field theory is correct. The rotating-field theory provides the best approach to the analysis of the rotor of a squirrel-cage machine. On the other hand there is a good case for preserving the cross-field approach to the stator analysis because it corresponds to the physical arrangement of the windings and allows direct connection and measurement. These two seemingly conflicting points of view can be combined into the single equivalent circuit shown in Fig. 14. The cross-field theory is used for the stator portion of the circuit including the magnetizing reactances X_{md} and X_{mq}. The stator may be connected for split-phase, capacitor, or 2-phase operation. The air-gap voltages on the two axes V_{md} and V_{mq} may then be resolved into this symmetrical component form

$$\begin{bmatrix} V_1 \\ V_2 \end{bmatrix} = \frac{1}{\sqrt{2}} \begin{bmatrix} 1 & -j \\ 1 & j \end{bmatrix} \times \begin{bmatrix} V_{md} \\ V_{mq} \end{bmatrix}$$

The $\sqrt{2}$ factor is included in the transformation to make it power invariant. Multiplying the second of the foregoing equation through by $(-j)$ results in

$$\begin{bmatrix} V_1 \\ -j\ V_2 \end{bmatrix} = \frac{1}{\sqrt{2}} \begin{bmatrix} 1 & -j \\ -j & 1 \end{bmatrix} \times \begin{bmatrix} V_{md} \\ V_{mq} \end{bmatrix}$$

This symmetrical transformation matrix can be realized in the equivalent circuit by a symmetrical connection of two bilateral phase-shift transformers each having a voltage ratio 1 to j. The voltages obtained are $\sqrt{2}$ times the required symmetrical component voltages V_1 and V_2. The positive- and negative-sequence rotor impedances are therefore multiplied by 2 to maintain power invariance. The resulting circuit allows individual adjustment of the positive- and negative-sequence rotor resistances and therefore combines the advantages of the cross-field and rotating-field theories.

The cross-field to rotating-field transformation may also be used at the air gap of motors with multiple squirrel-cage rotor windings. In commutator machines the rotor does not have radial symmetry and the rotating field concepts are not so readily applied. It may however be possible to use a symmetrical-component transformation from stator to rotor and a second transformation back from symmetrical component to cross-field form between the rotor winding and the brush terminals.

In reply to Mr. Bretch, the circuits of Figs. 5, 6, and 7 apply specifically to squirrel-cage machines. The essential concept in applying the cross-field theory to the rotor is the replacement of the rotating squirrel-cage rotor winding by two sinusoidally distributed fixed windings in space quadrature. These windings produce the same magnetomotive force as the actual rotor winding, have the same induced or transformer voltages as the actual winding, and also have applied to them the generated voltage which would result from their rotation through the flux of the other axis of the machine. For equivalence it is necessary only that the rotor impedance be chosen to make the lumped short circuits in the two axes of the cross-field model have the same effect as a distributed short circuit in the actual rotor.

Research on the Electric Breakdown of Fully Impregnated Paper Insulation for High-Voltage Cables

P. GAZZANA PRIAROGGIA
NONMEMBER AIEE

G. PALANDRI
NONMEMBER AIEE

Synopsis: Research on the dielectric strength of high-voltage cables can be very conveniently carried out on "models." Either plate or cylindrical capacitors can be used for this purpose. This paper reports the results of many tests both at power frequency and at impulse, which have the purpose of investigating the separate and combined influence of a series of different factors affecting the dielectric strength of a fully impregnated paper insulation as used in high-voltage cables.

The main factors investigated are the following:

Paper impermeability.
Paper density.
Paper thickness.
Oil viscosity.
Oil pressure.
Electrode surface shape.
Electrode surface nature.
Butt-space thickness.
Butt-space position with respect to electrodes.
Butt-space relative position.

The paper ends with a comparison of results obtained on models and on actual oil-filled cables, which show a good agreement if certain assumptions are taken into consideration.

WHEN research is carried out in any field, numerous governing factors, all acting simultaneously, come into play and make the task of the research investigator a difficult one. It remains with the investigator to try to isolate these various factors, to evaluate their partial effects, and finally to superpose and combine them in a deliberate manner in order to obtain an understanding of their interdependence and correlation.

As oil-impregnated paper dielectrics of the type used in high-voltage cables are the sole subject matter of this paper, discussion is confined to one particular element of those which come into play in the manufacture of the complex structure represented by a high-voltage cable. Moreover, of this particular element an even more specific aspect is analyzed, i.e., the dielectric breakdown strength at both power frequency and impulse.

Even with the scope of the investigation reduced to within this very much confined boundary, the number of variable factors still remaining is so large that it becomes necessary to revert to the analytical process just mentioned, which is basic to all types of scientific research. Thus the problem resolves itself into one of determining the experimental method to be employed in a study of the dielectric

Paper 55-692, recommended by the AIEE Insulated Conductors Committee and approved by the AIEE Committee on Technical Operations for presentation at the AIEE Fall General Meeting, Chicago, Ill., October 3-7, 1955. Manuscript submitted June 7, 1955; made available for printing August 8, 1955.

P. GAZZANA PRIAROGGIA and G. PALANDRI are with Pirelli S.p.A., Milan, Italy.

The tests referred to are part of the research work carried out during the past 8 years by the Research Laboratories of Pirelli S.p.A. at Bicocca, Milan, Italy. The authors are grateful to Dr. L. Emanueli for his suggestions, encouragement and helpful discussion. They also wish to thank many members of the Pirelli Research Laboratories for their co-operation. The permission of the Pirelli S.p.A. to publish this paper is also greatly appreciated.

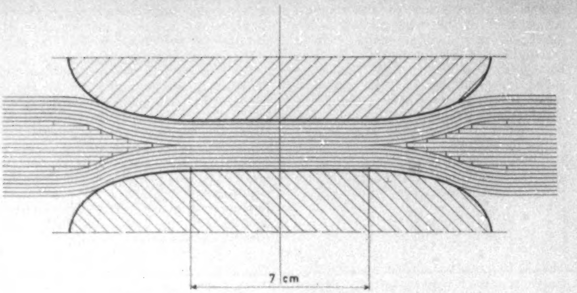

Fig. 1. Schematic representation of plate capacitor

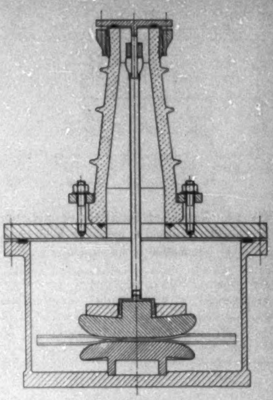

Fig. 2. Complete test assembly of plate capacitor

strength of an insulant composed of oil-impregnated paper such as is used in high-voltage cables.

It will be evident that, with the aforementioned analytical approach a specimen of finished cable will not be a suitable sample for experimentation. It will be necessary to employ samples in which the only variables present, of the many to be found in a finished cable, will be those which influence dielectric strength, all or nearly all others being excluded.

This is the reason that fundamental research on cable dielectrics must be directed to experimentation on models. While the work must, of course, be supplemented and accompanied by tests carried out on full-scale cables, it does provide a fundamental step which is extremely useful and its importance cannot be overstressed.

However, success in the use of models is contingent upon the skill of the research investigator in choosing the most appropriate model, i. e., one which enables a particular variable to be isolated and studied in the most significant manner. The widespread lack of confidence in results of research work carried out by means of models is often due to a failure to recognize that this method of research requires much experience and skill. Thus, unsatisfactory results attributed to the use of the model method are often due rather to choice of a model incapable of bringing out the influence of the variables under investigation.

Test Models

Among the variables found in a finished cable there is a very important one: flexure and bending of the dielectric, which must be eliminated in the initial study inasmuch as its presence can mask the basic dielectric phenomena. Of course, flexure and bending will have to be given thorough consideration after a full investigation of the influence of those factors involving only true dielectric phenomena.

As a first requirement the models must therefore have adequate mechanical rigidity. As a consequence they must be capacitors either in plate or cylindrical form.

It should be mentioned that experimentation on capacitors for the purpose of studying cable dielectrics differs from that for studying high-voltage capacitors.

The fundamental problem of a high-voltage capacitor in fact is a dielectric problem at the edges of its metal foils, whereas the fundamental problem of a high-voltage cable insulated with oil-impregnated paper is mainly a dielectric problem of the butt-spaces between the edges of the paper tapes with which the cable is wound. The latter problem does not exist in high-voltage capacitors because the dielectric is normally made up of paper sheets having approximately the same dimensions as the metal foils.

The statement that the fundamental problem of a cable from the point of view of the dielectric strength is one of the butt-spaces does not mean that other important matters affecting dielectric strength itself can be disregarded, such as the problem of the nature of paper and oil, as will be shown later. Problems of this kind may in part be treated independently of the main problem. However, the problem of the butt-spaces in a stratified dielectric is the one most characteristic of cable insulation. It follows that models suitable for experiments on cable dielectrics should not involve "edge" or "end" problems.

While the following paragraphs will cover the matter in detail, it should be mentioned here that experimentation on plate capacitors is not always equivalent to experimentation on cylindrical capacitors. Very often it is not easy or even possible to represent in a plane field factors which can be studied in a cylindrical field. On the contrary, it may be difficult to isolate certain factors in a cylindrical capacitor, whereas this can be readily accomplished by use of a plate capacitor. Of course as the plate capacitor is the simplest to construct, it will be convenient to revert to it whenever it will suffice for the proposed task.

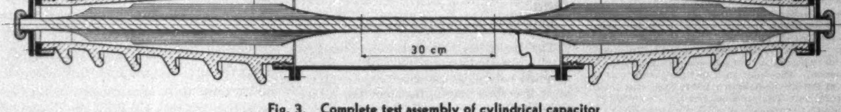

Fig. 3. Complete test assembly of cylindrical capacitor

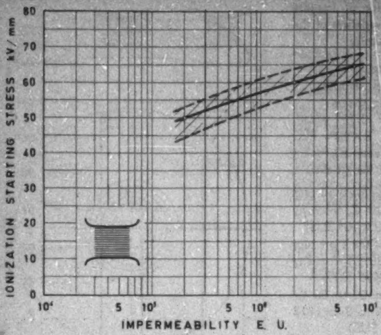

Fig. 4. Ionization starting stress as a function of paper impermeability

Capacitor: plate
Electrodes: steel, smooth
Sample: 12 plain paper sheets
Paper: density 0.75 g/cm³, sheet thickness 0.08 mm (3 mils)
Oil: mineral, thin
Pressure: atmospheric
Temperature: 20 C

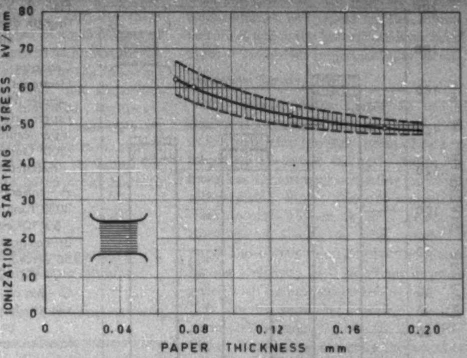

Fig. 6. Ionization starting stress as a function of paper sheet thickness

Sample: variable number of paper sheets to form a total thickness of 1 mm (40 mils)
Paper: density 0.75 g/cm³ impermeability 2×10^6 EU (300 to 800 Gurley seconds for paper of from 3- to 8-mil thickness)
For other data see Fig. 4

Plate Capacitor as Test Model

The plate capacitor as used in the tests described later in the paper is made as follows: The plates consist of two circular flared electrodes usually made of steel with plane circular surfaces facing each other and having a diameter of 7 centimeters (2³/₄ inches). These surfaces can be made purposely smooth or corrugated as desired, as will be described later.

The dielectric interposed between the electrodes consists of a certain number of circular paper disks having a diameter of 35 cm (14 inches), with or without perforations according to the particular case to be considered. These paper disks are divided into two groups, usually of the same thickness, externally spaced by means of a set of coaxial paper rings having different internal diameters, so that each group must adhere to the adjacent electrode shaping itself against its flared surface for a short distance; see Fig. 1.

In this way the components of the electric stress which necessarily exist near the edges and which are parallel to the plane surface of the electrodes, are prevented from causing "edge punctures."

The capacitor is then introduced into a cylindrical container which is closed by means of a vacuum- and pressure-tight cover equipped with a high-voltage bushing; see Fig. 2. The technique of preparation, i.e., drying and impregnation, is described in Appendix I.

The plate capacitor is suitable for investigating practically all the problems of dielectric strength in high-voltage cables with the exception of those which specifically involve the helical symmetry of the cable dielectric. Moreover, it is suited to investigate certain factors which cannot be completely isolated in a cylindrical capacitor, (because the butt-spaces, or oil gaps, cannot be totally eliminated). These factors are:

1. Paper impermeability.
2. Paper density.
3. Paper thickness (in itself and not as an indirect cause of oil gap thickness).
4. Nature of the impregnating oil (in so far as it fills the pores of the paper and not the butt-spaces of the stratified dielectric).

Cylindrical Capacitor as Test Model

The cylindrical capacitor is the closest simulation of cable, the ultimate objective of this research. As employed in the experiments, it is made as follows: The inner electrode is a metal rod 2 meters (6 feet 7 inches) long, the surface of which can be smooth or covered by a helically wound layer of copper wires (to reproduce the surface of a stranded conductor) or wound with conductive tapes.

Around this inner electrode insulated paper tapes of the desired characteristics are helically wound in order to build up a certain dielectric thickness. The outer electrode is obtained by means of a helically wound metal tape.

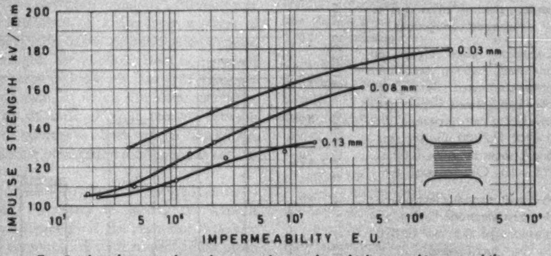

Fig. 5. Impulse strength as a function of paper sheet thickness and impermeability

Sample: variable number of paper sheets to form a thickness of 1 mm (40 mils)
Paper: sheet thickness 0.03 mm (1 mil), density 0.7 to 0.85 g/cm³, sheet thickness 0.08 mm (3 mils), density 0.75 g/cm³, sheet thickness 0.13 mm (5 mils), density 0.75 g/cm³
For other data see Fig. 4

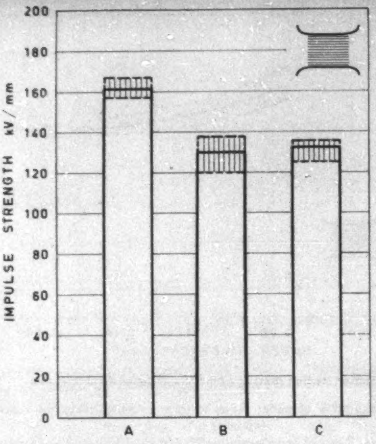

Fig. 7. Variation of impulse strength due to variation of the oil viscosity

Capacitor: plate
Electrodes: steel, smooth
Sample: 12 plain sheets
Paper: density 0.75 g/cm^3, impermeability 2×10^6 EU (300 Gurley seconds); sheet thickness 0.08 mm (3 mils)

A—compound of thick oil plus 30% rosin at 20 C, viscosity 5×10^4 cst (23×10^4 SUS)
B—compound of thick oil plus 30% rosin at 85 C, viscosity 150 cst, (695 SUS)
C—thin oil from 20 to 85 C, viscosity from 25 to 3 cst (118 to 36 SUS)
Pressure: atmospheric

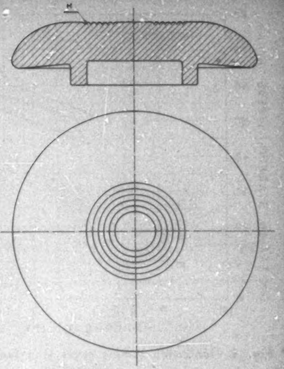

Fig. 8 (right). Schematic representation of a corrugated electrode. R = radius of curvature of the corrugations

The influence of the capacitor edge effect is eliminated by building up two impregnated paper "stress cones" at the ends of the rod with a technique very similar to that used in high-voltage cable sealing ends. The effective length of the cylindrical capacitor to which the full testing voltage is applied is thus reduced to 30 cm (1 foot) only.

The capacitor is then introduced inside a steel pipe terminating with a porcelain insulator on each end; see Fig. 3. The ends of the inner electrode are attached by soldering to the top flanges of the porcelain insulators, whereas the outer armor is electrically connected to the steel pipe. The technique of preparation is described in Appendix II.

The cylindrical capacitor, because of the much more laborious preparation involved, is normally used either for investigations which cannot be carried out successfully on plate capacitors, as already mentioned, or as an over-all check on a series of results obtained on plate capacitors before drawing practical conclusions applicable to cables.

In the main portion of the paper results of tests on cylindrical capacitors are not discussed in any particular detail. However reference to them is made near the end of the paper in establishing a comparison between tests on cylindrical and plate capacitors.

Dielectric Strength Tests

As the title indicates, this paper is limited to the discussion of a particular class of dielectrics, i.e., those made of paper sheets fully impregnated with insulating oil or compound. Moreover, with but few exceptions, only wood pulp paper impregnated with thin mineral oil, having a viscosity of 25 centistokes (cst), i.e., 118 Saybolt universal seconds (SUS), at 20 degrees centigrade (C), is considered. Therefore dielectrics not fully impregnated with oil, i.e., those with gaseous inclusions, are excluded.

It is not intended to deal here with all possible conditions which may affect the dielectric strength. Only certain phenomena will be illustrated and discussed which seem worth recording either for their novelty or because they bring out new aspects of already known phenomena. The tests to be considered follow.

Power Frequency (50-Cycle) Ionization Test

The power frequency (50-cycle) ionization test commonly refers to the test consisting in measuring the voltage, by means of a discharge detector, at which the insulation failure starts. This denomination seems not quite correct because the phenomenon appears to be somewhat different from simple ionization, such as, for instance, the ionization of gas.

It is in fact believed that in a first stage a true "cracking" of the insulating oil under electric stress takes place, whereas the gaseous ionization appears in a second stage after the oil has cracked and the gas phase replaces the liquid phase.

The detection of this ionization stage is effected by well-known methods$^{1-3}$ by observing on the screen of a cathode-ray

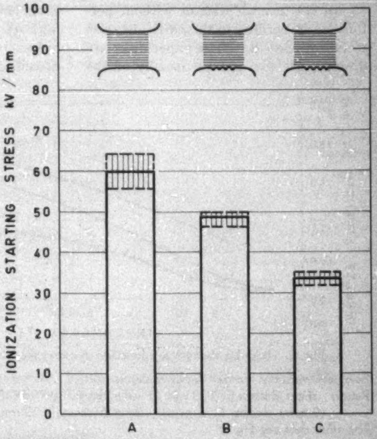

Fig. 9. Variation of ionization starting stress due to electrode corrugations

Capacitor: plate. Electrodes: one steel, smooth; the other brass, corrugated. Sample: 12 plain paper sheets. Paper: density 0.75 g/cm^3; impermeability 2×10^6 EU(300 Gurley seconds); sheet thickness 0.08 mm (3 mils). Oil: mineral, thin

A—steel smooth electrodes
B—brass electrode having corrugations of 0.5 mm (0.020-inch) radius
C—brass electrode having corrugations of 1 mm (0.040-inch) radius
Pressure: atmospheric
Temperature: 20 C

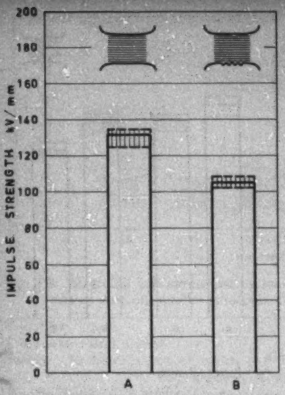

Fig. 10. Variation of impulse strength due to electrode corrugations

Capacitor: plate
Electrodes: one steel, smooth; the other brass, corrugated
Sample: 12 plain paper sheets
Paper: See Fig. 7
Oil: mineral, thin
A—steel electrodes, smooth
B—brass electrode having corrugations of 1 mm (0.04-inch) radius

Pressure: atmospheric Temperature: 20 C

oscillograph the appearance of small higher frequency oscillations superposed on the power frequency (50 cycles) coinciding with the peaks of the wave.

The ionization test is carried out starting from a voltage about 30 per cent (%) below the anticipated ionization inception voltage and increasing the applied stress by steps of 2 kv per millimeter (mm), 50.8 volts per mil, every 10 minutes.

Impulse Tests

The European Standard 1/50 wave test is employed. Starting from a stress of about 30% below the anticipated impulse strength, the applied stress is increased by steps of 5 kv per mm (127 volts per mil) each, applying five shots per step, with an interval of 15 seconds between two successive shots, up to breakdown which is observed on a cathode-ray oscillograph.

In tests on plate capacitors it is obviously necessary to specify the applied polarities only if the capacitor dielectric is asymmetrical with respect to its mean plane.

In the tests to be described the polarity was not reversed during the test. It can be stated, however, that reversal of polarity has very little bearing on fully impregnated paper dielectrics. Also, for these dielectrics the number of applied shots at each step is of no practical importance.

In all figures reported in the following sections, average value and dispersion range are generally indicated. By dispersion range a range of approximately six times the standard deviation is meant. It should be noted that in all figures the average values are based on at least 10 different tests.

Test Results on Plate Capacitors Made with Plain Paper Sheets

INFLUENCE OF PAPER IMPERMEABILITY

The common concept of impermeability is often erroneous. The influence of "impermeability", i.e., air resistance is often confused with the influence of "density", i.e., specific gravity. The reason is that it is found to be very difficult or even impossible to isolate completely the influence of variations of impermeability from other factors. Probably this is because it is practically impossible to alter the impermeability of the paper without introducing at the same time important variations in the physical structure of the paper sheets (fiber length, hydrocellulose content, density, etc.). As a consequence, it is difficult to obtain numerical data of the dielectric strength as a function of the impermeability alone.

The paper density is here expressed in grams per cubic centimeter (g/cm^3) and is obtained as a ratio between the weight per unit surface (grams per centimeter squared (g/cm^2)) and the thickness in cm of the paper sheet.

The impermeability is here measured in practical units, or Emanueli Units (EU)[4] (EU$=10^8$ absolute units).

In the following are reported test results obtained on papers in the manufacture of which the best efforts have been made to isolate the impermeability factor.

Ionization Starting Stress

The impermeability factor, to which enormous importance has been attributed in the past from the standpoint of power frequency dielectric strength, seems to have less importance according to more recent tests. Fig. 4 refers to ionization tests on plate capacitors, of a dielectric thickness of 1 mm (40 mils), made of paper sheets 0.08 mm (3 mils) thick, and having a density of 0.75 g/cm^3 impregnated with thin mineral oil.

It can be seen that varying the impermeability from 2×10^5 to 2×10^6EU (40 to 300 Gurley seconds) the average value of the ionization starting stress varies from 50 to 60 kv per mm (1,270 to 1,520 volts per mil). The figure does not show the variation of ionization starting stress from 0 to 10^5 EU (0 to 20 Gurley seconds).* This is of the order of 10%.

Impulse Strength

The behavior on impulse is not very different. Considering, for instance, the same type of paper as in ionization starting stress, if the impermeability is varied from 2×10^5 to 2×10^6 EU (40 to 300 Gurley seconds) the impulse strength varies from 105 to 132 kv per mm (2,670 to 3,350 volts per mil); see Fig. 5. The impulse strength shows very little variation from 0 to 10^5 EU (0 to 20 Gurley seconds).

Fig. 11. Variation of ionization starting stress due to oil pressure

Capacitor: plate
Electrodes: steel, smooth
Sample: 12 plain sheets
Paper: See Fig. 7

A_1—compound thick oil plus 30% rosin, viscosity 5×10^4 cst, (23×10^4 SUS) at 20 C, pressure 14 atm (200 psi)
B_1—Same compound as in A_1, pressure atmospheric
A_2—Thin mineral oil, pressure 14 atm (200 psi)
B_2—Same oil as in A_2, pressure atmospheric

Temperature: 20 C

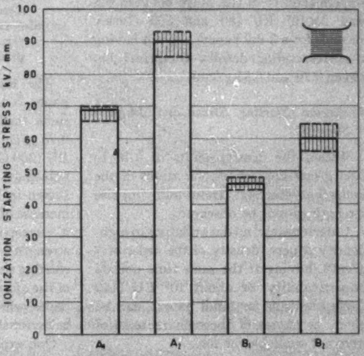

---

* The air resistance values expressed in Gurley seconds inserted in parentheses besides the EU are not to be considered as strictly equivalent. The Gurley seconds values reported have not been measured directly on the paper used for the tests but obtained from a graph plotted with values of impermeability against air resistance for papers of different qualities, impermeability and thickness tested both with the Emanueli porosity tester and the Gurley densimeter.

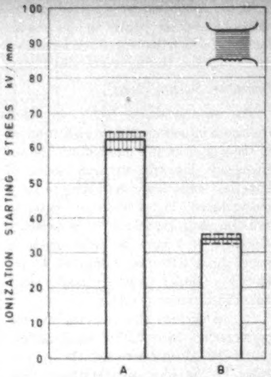

Fig. 12. Variation of ionization starting stress due to oil pressure with corrugated electrodes

Capacitor: plate
Electrodes: one steel, smooth; the other brass, having corrugations of 1 mm (0.040 inch) radius
Sample: 12 plain paper sheets
Paper: See Fig. 7
Oil: mineral, thin
A—pressure: 14 atm (200 psi)
B—pressure: atmospheric
Temperature: 20 C

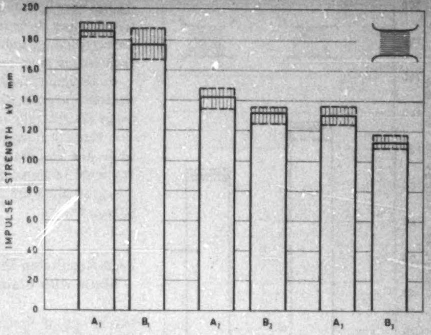

Fig. 13 (right). Variation of impulse strength due to oil pressure

Capacitor: plate
Electrodes: steel, smooth
Sample: variable number of paper sheets to form a total thickness of 1 mm (40 mils)
Oil: mineral, thin
Temperature: 20 C
A_1—Paper: density 0.9 g/cm³; impermeability 200×10⁶ EU (10,000 Gurley seconds); sheet thickness 0.03 mm (1 mil); pressure 14 atm (200 psi)
B_1—Paper: same as in A_1; pressure: atmospheric
A_2—Paper: density 0.75 g/cm³; impermeability 2×10⁶ EU (300 Gurley seconds); sheet thickness 0.08 mm (3 mils); pressure 14 atm (200 psi)
B_2—Paper: same as in A_2 Pressure: atmospheric
A_3—Paper: density 0.75 g/cm³; impermeability 1×10⁶ EU (300 Gurley seconds), sheet thickness 0.13 mm (5 mils); pressure 14 atm (200 psi)
B_3—Paper: same as in A_3 Pressure: atmospheric

Influence of Paper Density

The influence of paper density is a factor even more difficult to isolate and particularly difficult to separate from the impermeability because a certain value of impermeability can be obtained practically only if the density is maintained within very close limits.

For instance, it is difficult if not almost impossible to obtain papers having an impermeability in the range between 0.5 and 2×10⁶ EU (80 and 300 Gurley seconds for a 3-mil paper) and not having a corresponding density comprised between 0.70 and 0.85 g/cm³.

Ionization Starting Stress and Impulse Strength

Within the density limits of 0.70 to 0.85 g/cm³ appreciable variations of the ionization starting stress and impulse strength cannot be observed.

Unfortunately, no data relating to high-density papers (density of the order of 1 g/cm³), having at the same time normal impermeability, or about 10⁶ EU (140 Gurley seconds for 3-mil paper), can be given, as papers of these characteristics were not available for test.

Emphasis is placed on the practical impossibility of separating the impermeability factor from the density factor; however, it is still useful to mention test results on papers having very high density and at the same time very high impermeability. Reference is made to papers normally known as extradense or supercalendered, widely used in some countries.

A paper of this kind, having sheet thickness of 0.07 mm (2.75-mil), density of 1.1 g/cm³ and impermeability of 2×10⁷ EU (3,500 Gurley seconds) impregnated with thin mineral oil, has given the following test results on plate capacitors of a dielectric thickness of 1 mm (40 mils).

Ionization starting stress: average value 51 kv per mm (1,300 volts per mil); dispersion range 10%.
Impulse strength: average value 160 kv per mm (4,060 volts per mil); dispersion range 5%.

The higher impulse strength of this paper compared with one of about the same thickness but having a density of 0.75 g/cm³ and impermeability of 2×10⁶ EU (300 Gurley seconds) is in fairly good agreement with the general behavior shown in Fig. 5., according to which an increase of the impermeability determines a corresponding increase of the impulse strength. On the contrary, the ionization starting stress is decidedly lower than that of the aforementioned type of low-density paper, which is not in agreement with the behavior shown in Fig. 4.

One explanation of this which has led to much debate is based on the consideration that the higher the density the higher the dielectric constant of the paper, and consequently the higher the stress applied to the oil films between paper sheets. Another explanation, however, could be that the paper mill treatment, necessary to produce extradense paper, greatly affects the paper sheet structure and perhaps also the surface "activity" of the cellulose; see the next section, regarding tests on plate capacitors made with partly perforated sheets.

Influence of Paper Sheet Thickness

In this section the influence of paper sheet thickness per se will be treated and any part it may play as a determining factor of butt-space thickness will be ignored.

Ionization Starting Stress

Fig. 6 deals with the variation of the ionization starting stress as a function of paper sheet thickness for papers having a density of 0.75 g/cm³ and impermeability of 2×10⁶ EU (300 and 800 Gurley seconds for 3- and 8-mil paper respectively), impregnated with thin mineral oil.

For an increase of the sheet thickness from 0.08 to 0.2 mm (3 mils and 8 mils), the average value of the ionization starting stress decreases from 60 to 49 kv per mm (1,520 to 1,250 volts per mil).

Impulse Strength

In Fig. 5 the influence of sheet thickness is also shown. To take, for instance, into consideration papers of a density of 0.75 g/cm³ and impermeability of 2×10⁶ EU

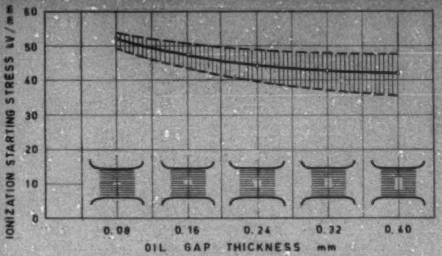

Fig. 14. Single oil gap surrounded by insulating paper. Ionization starting stress of capacitor as function of oil gap thickness

Capacitor: plate
Electrodes: steel, smooth
Sample: 12 paper sheets of which one to five are perforated in corresponding points
Paper: density 0.75 g/cm^3; impermeability 2×10^6 EU (300 Gurley seconds); sheet thickness 0.08 mm (3 mils)
Oil: mineral, thin Pressure: atmospheric Temperature: 20 C

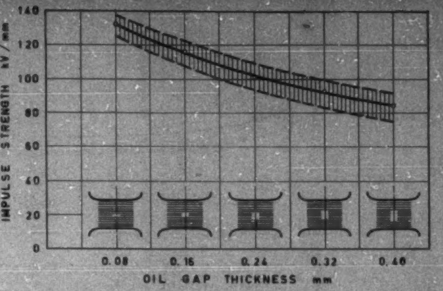

Fig. 16 Single oil gap surrounded by insulating paper. Impulse strength of the capacitor as a function of oil gap thickness

Sample: 12 paper sheets of which one to five are perforated in corresponding points
For other data see Fig. 14

(300 and 600 Gurley seconds for 3- and 5-mil paper respectively), it can be seen that for an increase of sheet thickness from 0.08 to 0.13 mm (3 to 5 mils), the impulse strength decreases from 132 down to 120 kv per mm (from 3,350 down to 3,050 volts per mil).

It may be interesting to give a tentative explanation of the phenomenon of decrease of the dielectric strength with increase in sheet thickness. It is useful to start from the consideration that this phenomenon practically ceases to exist, when considering impulse strength, if multi-ply paper sheets are used instead of paper sheets composed of a single ply as with those generally considered here.

A probability type of explanation could be assumed taking into account the fact that the probability of alignment of defects of different paper sheets is correspondingly less, as the sheets comprised in a certain dielectric thickness become more numerous. This hypothesis, however, does not hold as the law of decrease of dielectric strength for single-ply paper, as a function of sheet thickness, is still valid if, instead of the total dielectric thickness, the number of sheets under test is kept constant.

A more reliable hypothesis could perhaps be founded on the consideration that the phenomenon under discussion is simply a phenomenon of decay of the dielectric qualities of the paper when increasing the sheet thickness. The reason for this is uncertain; it can, however, be observed that the structure of the paper sheet (e.g., orientation of fibers) varies a great deal when the sheet thickness is varied.

INFLUENCE OF VISCOSITY OF IMPREGNATING OIL

Viscosity is another of those factors which are difficult to isolate. Variations of viscosity always involve variations of chemical structure or at least variations of length of the molecular chains.

The phenomena, however, to which the results given hereunder apply, seem to be controlled only by variation of viscosity, even if other variables are present.

Ionization Starting Stress

The influence of viscosity in this regard is not at all clear as the surprising result is obtained that the ionization starting stress decreases when the viscosity is increased. Considering, in fact, the usual cable paper having a density of 0.75 g/cm^3, impermeability of 2×10^6 EU (300

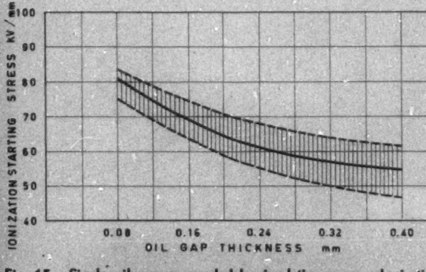

Fig. 15. Single oil gap surrounded by insulating paper. Ionization starting stress of oil as function of oil gap thickness

Oil: mineral, thin Pressure: atmospheric Temperature: 20 C

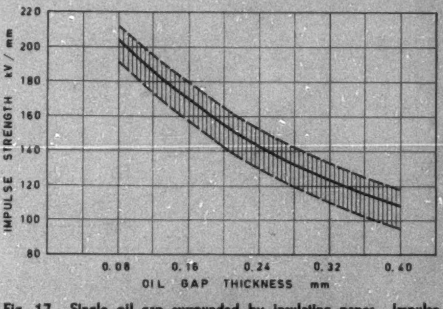

Fig. 17. Single oil gap surrounded by insulating paper. Impulse strength of oil as a function of oil gap thickness

Oil: mineral, thin Pressure: atmospheric Temperature: 20 C

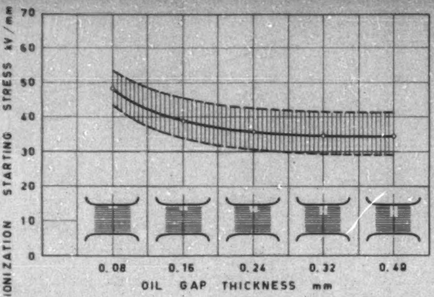

Fig. 18. Single oil gap adjacent to metal electrode. Ionization starting stress of the capacitor as a function of oil gap thickness

Sample: 12 paper sheets of which 1 to 5 perforated sheets adjacent to electrode

For other data see Fig. 14

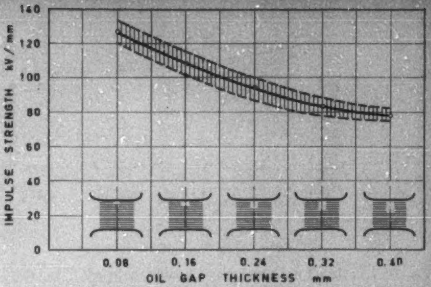

Fig. 20. Single oil gap adjacent to metal electrode. Impulse strength of capacitor as a function of oil gap thickness

For all other data see Fig. 18

Gurley seconds), sheet thickness of 0.08 mm (3 mils), the ionization starting stress decreases from 60 kv per mm (1,520 volts per mil) when thin mineral oil (viscosity 25 cst (118 SUS) at 20 C) is used, to 47 kv per mm (1,190 volts per mil) for a compound made of thick mineral oil plus 30% rosin (viscosity 5×10⁴ cst (23×10⁴ SUS) at 20 C).

This result, which is obtained also with other thick oils or compounds, is difficult to explain; it could be perhaps related to surface effects which are at present receiving attention in the research work of the authors' company, to be described in the next section.

Impulse Strength

Here the influence of viscosity is definitely opposite to that found at power frequency. To consider the same type of paper as that just described, the impulse strength varies from 132 kv per mm (3,350 volts per mil) corresponding to thin mineral oil, to 161 kv per mm (4,090 volts per mil) corresponding to a compound of thick cable oil plus 30% rosin.

To confirm the view that this effect is to be attributed only to increase of viscosity, it was found that heating the compound just mentioned to 85 C, viscosity 150 cst (695 SUS) the impulse strength of the capacitor is reduced to 130 kv per mm (3,300 volts per mil). These phenomena are clearly represented by Fig. 7.

INFLUENCE OF SHAPE OF ELECTRODE SURFACE

Reference is made here to the influence exercised by the surface of stranded conductors. The effect of stranding is simulated by engraving in the flat surface of one of the electrodes a set of circular corrugations, the profile of which has a radius of curvature either of 0.5 or 1 mm (0.02 or 0.04 inch); see Fig. 8.

Ionization Starting Stress

The results are summarized in Fig. 9. To take into consideration capacitors of 1 mm (40-mil) insulation thickness made of the usual cable paper having a density of 0.75 g/cm³, impermeability of 2×10⁶ EU (300 Gurley seconds), sheet thickness of 0.08 mm (3 mils), impregnated with thin oil, it can be seen that the ionization starting stress from 60 kv per mm (1,520 volts per mil) for plain electrodes decreases to 48 kv per mm (1,220 volts per mil) for electrodes having corrugations with a radius of curvature of 0.5 mm (0.02 inch) and to 34 kv per mm (863 volts per mil) for electrodes having corrugations with a radius of curvature of 1 mm (0.04 inch).

The result is interesting and unexpected because the well-known equations by Levi-Civita, as well as more recent calculations relating the electrostatic field of oil-filled cables,[6] show that the smaller

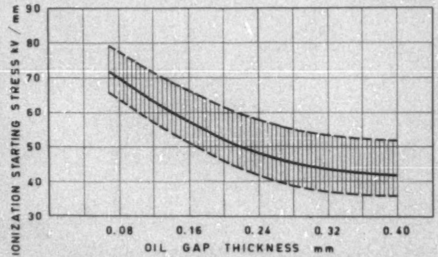

Fig. 19. Single oil gap adjacent to metal electrode. Ionization starting stress of the oil as a function of oil gap thickness

Oil: mineral, thin Pressure: atmospheric Temperature: 20 C

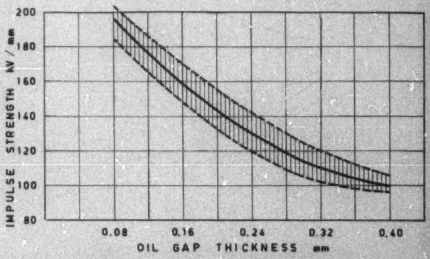

Fig. 21. Single oil gap adjacent to metal electrode. Impulse strength of oil as a function of oil gap thickness

Oil: mineral, thin Pressure: atmospheric Temperature: 20 C

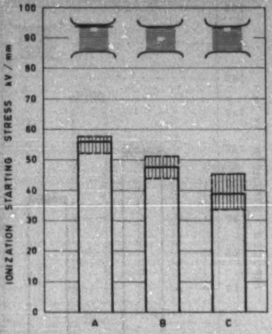

Fig. 22. Single oil gap. Variation of ionization starting stress of capacitor due to nature of surfaces adjacent to oil gap

Capacitor: plate Electrodes: steel smooth
Sample: 10 plain sheets plus two adjacent sheets perforated in corresponding points
Paper: See Fig. 14 Oil: See Fig. 14

A—oil gap adjacent to electrode covered with sheet of carbon black paper
B—oil gap surrounded by insulating paper
C—oil gap adjacent to bare metal electrode

the radius of curvature of the corrugations, the higher (even if only slightly higher) the maximum stress on the paper insulation, i.e., exactly the opposite to what would be expected from the results.

An explanation of this could be that the maximum stress in the paper insulation is of less importance than the thickness of the oil gaps adjacent to the electrode, which are correspondingly smaller when the radius of curvature of the corrugations is decreased. It is known, in fact, that the smaller the gap the higher the dielectric strength of the oil; see also the next section, concerning tests on plate capacitors made with partly perforated sheets.

Impulse Strength

If only one of the electrodes is corrugated, the influence of the polarity applied to this electrode cannot a priori be disregarded. It is found, however, that there is little, if any, effect of polarity.

Fig. 10 refers to the same type of paper as that in Fig. 9. It is shown that the impulse strength decreases from 132 kv per mm (3,350 volts per mil) for plain electrodes, to 105 kv per mm (2,670 volts per mil), for electrodes having corrugations with a radius of curvature of 1 mm (0.04 inch). The diagram does not show the difference between results obtained with a radius of curvature of 0.5 mm (0.02 inch) and those obtained with a radius of 1 mm (0.04 inch), as it is very little (of the order of 5%), certainly much smaller than that observed at power frequency (40%). This behavior is difficult to explain.

INFLUENCE OF STATIC PRESSURE OF OIL

The influence of the oil pressure cannot be investigated independently of other factors such as those already examined (paper thickness and impermeability, oil viscosity, electrode shape, etc.). Following are results obtained in some particular cases.

Ionization Starting Stress

Fig. 11 shows that for an increase of static pressure of 14 atmospheres (atm) (200 pounds per square inch (psi)) starting from atmospheric pressure, the ionization starting stress increases from 60 to 90 kv per mm (1,520 to 2,290 volts per mil) if thin mineral oil is used, whereas it increases from 47 to 69 kv per mm (1,190 to 1,750 volts per mil), for a compound of thick mineral oil plus 30% rosin. In both cases an increase of 50% can be observed.

The paper used for these tests is the usual cable paper having a density of 0.75 g/cm^3, impermeability 2×10^6 EU (300 Gurley seconds) and sheet thickness of 0.08 mm (3 mils).

If instead of plain electrodes a corrugated electrode is used with a radius of curvature of the corrugations of 1 mm (0.04 inch), the same increase of static pressure of 14 atm (200 psi) causes an increase of ionization starting stress from 34 to 62 kv per mm (864 to 1,570 volts per mil), if thin oil is employed; see Fig. 12. In this case the increase is more than 80%.

The influence of pressure could be explained as an increase of the cracking voltage of the oil not very different from the increase of the cracking temperature in the thermal cracking due to pressure. The relative increase of the cracking voltage seems to be higher when large oil gaps (free space between paper sheets and corrugations) are present.

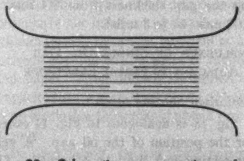

Fig. 23. Schematic representation of a testing sample to investigate the influence of butt-spaces

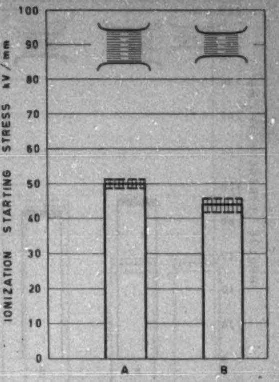

Fig. 24 Influence of butt-spaces. Variation of ionization starting stress of capacitor due to variation of sheet thickness

Sample: perforated sheets interleaved with plain paper sheets to make an insulation thickness of about 1 mm (40 mils), with plain sheets adjacent to electrodes
Paper: density 0.75 g/cm^3 impermeability 2×10^6 EU (300 and 600 Gurley seconds for 3- and 5-mil paper respectively)

A—paper sheet thickness 0.08 mm (3 mils)
B—paper sheet thickness 0.13 mm (5 mils)

For other data see Fig. 14

Impulse Strength

The influence of the static pressure at impulse is not so great as at power frequency; it is, however, not to be disregarded completely.

Fig. 13 compares the increases of impulse strength due to an increase of pressure of 14 atm (200 psi) for three different types of paper impregnated with thin cable oil. For instance, it can be seen that the usual cable paper, having a density of 0.75 g/cm^3, impermeability of 2×10^6 EU (300 Gurley seconds) and sheet thickness of 0.08 mm (3 mils), shows an increase of the impulse strength from 132 to 142 kv per mm (3,350 to 3,610 volts per mil), i.e., about 8%.

Tests on Plate Capacitors Made with Partly Perforated Sheets: Influence of Oil Gaps in Stratified Dielectric

The test on plate capacitors to be described and the influence of oil gaps in a stratified dielectric form the most interesting and pertinent portion of this research study on cable dielectrics. As will

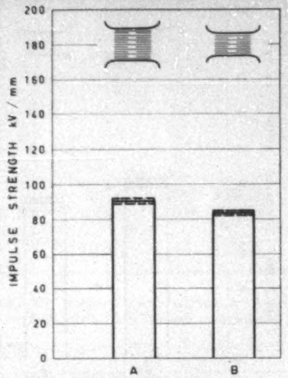

Fig. 25. Influence of butt-spaces. Variation of the impulse strength of the capacitor due to the sheet thickness

Sample: perforated sheets interleaved with plain paper sheets to make an insulation thickness of about 1 mm (40 mils) with plain sheets adjacent to electrodes

Paper: density 0.75 g/cm^3 impermeability 2×10^6 EU (300 and 600 Gurley seconds for 3- and 5-mil paper respectively)

A—paper sheet thickness 0.08 mm (3 mils)
B—paper sheet thickness 0.13 mm (5 mils)

For other data see Fig. 14

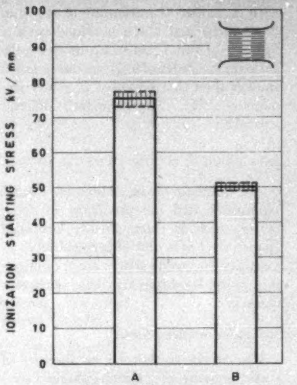

Fig. 26. Influence of butt-spaces. Variation of ionization starting stress of the capacitor due to variation of oil pressure

Capacitor: plate
Electrodes: steel, smooth
Sample: plain paper sheets interleaved with perforated sheets, with plain sheets adjacent to metal electrodes, to make an insulation thickness of about 1 mm (40 mils)
Paper: density 0.75 g/cm^3 impermeability 2×10^6 EU (300 Gurley seconds), sheet thickness 0.08 mm (3 mils)
Oil: mineral, thin

A—pressure: 14 atm (200 psi)
B—pressure: atmospheric

Temperature: 20 C

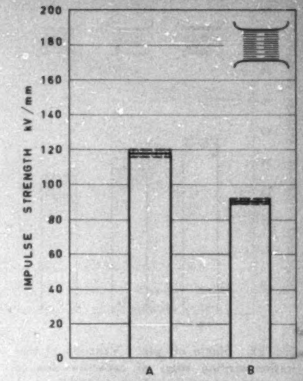

Fig. 27. Influence of butt-spaces. Variation of impulse strength of capacitor due to the variation of oil pressure

For all data see Fig. 26

be illustrated, the distinction between the case of an oil gap adjacent to an electrode and that of an oil gap separated from the electrodes by paper sheets, i.e., surrounded by insulating paper, is of fundamental importance.

Influence of Single Oil Gap Surrounded by Insulating Paper

For the sake of simplicity, capacitors made with only one type of paper are taken into consideration, for instance, with the usual cable paper having a density of 0.75 g/cm^3, impermeability of 2×10^6 EU (300 Gurley seconds) and sheet thickness of 0.08 mm (3 mils), impregnated with thin oil.

The investigation is carried out as a function of a variable oil gap thickness on capacitors made of 12 paper sheets. The variable gap thickness is obtained by perforating from 1 to 5 adjacent sheets on aligned points.

Ionization Starting Stress

Fig. 14 shows the variation of the ionization inception stress of the capacitor as a function of the oil gap thickness. It may be interesting to deduce from Fig. 14 the stress on the oil gap corresponding to ionization inception. This is shown by Fig. 15 which is based on an assumed ratio of about 1.6 between the dielectric constant of the impregnated paper and that of the thin oil.

It can be seen that a 50% increase of the ionization starting stress of the oil is obtained when varying the gap from 0.4 to 0.08 mm (15 to 3 mils).

Impulse Strength

Fig. 16 corresponds to Fig. 14, whereas Fig. 17 corresponds to Fig. 15. Fig. 17 shows that an 80% increase of the impulse strength of the oil is obtained on decreasing the gap thickness from 0.4 mm to 0.08 mm (15 to 3 mils).

Influence of Single Oil Gap Adjacent to Metal Electrode

Ionization Starting Stress

Fig. 18 is analogous to Fig. 14 except for the position of the oil gap. A very interesting fact may be observed. The average curve of Fig. 18 is everywhere lower than the corresponding curve of Fig. 14. The difference between the two curves is small for small gap thickness: 5% for a gap of 0.08 mm (3 mils) and increases for larger gaps: 20% for a gap of 0.4 mm (15 mils).

Fig. 19 shows the calculated values of the stress on the oil gap corresponding to the ionization inception: the increase of ionization starting stress is about 65% for a decrease of gap thickness from 0.4 to 0.08 mm (15 to 3 mils).

Impulse Strength

Fig. 20 is analogous to Fig. 16 except for the position of the oil gap. The tests have been carried out applying a negative polarity to the electrode adjacent to the gap. However, check tests indicate that the difference in results obtained with the opposite polarity is practically negligible. Also, in this case it may be observed that the average curve of Fig. 20 is everywhere lower than the corresponding one of Fig. 16. Therefore both at power frequency and at impulse the electric strength is definitely lower when the oil gap is adjacent to a metal electrode.

In a similar way to what has been found at power frequency, it may be observed that the difference between the average curve of Fig. 20 and that of Fig. 16 is small for small gaps: 5% for a 0.08-mm gap (3 mils) and increases correspondingly for larger gaps: 10% for a 0.4-mm gap (15 mils).

Fig. 21 shows the calculated values of stress on the oil gap corresponding to the breakdown voltages. It can be seen that

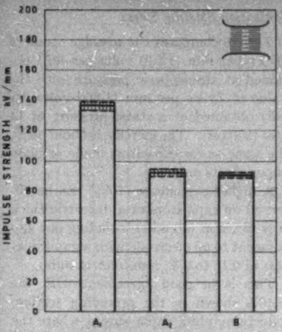

Fig. 28. Influence of butt-spaces. Variation of impulse strength of the capacitor due to variation of oil viscosity

Capacitor: plate
Electrodes: steel, smooth
Sample: See Fig. 26
Paper: See Fig. 26

A_1—compound thick oil plus 30% rosin at 20 C, viscosity 5×10^4 cst, (23×10^4 SUS)
A_2—compound thick oil plus 30% rosin at 85 C, viscosity 150 cst, (695 SUS)
B—thin mineral oil from 20 to 85 C, viscosity from 25 to 3 cst, (118 to 36 SUS)

Pressure: atmospheric

the increase of the oil impulse strength, when the gap thickness is decreased from 0.4 to 0.08 mm (15 to 3 mils), is still about 95%.

From these results a very important conclusion may be reached, i.e., that the nature of the surface (dielectric or metallic) in contact with an oil gap has a fundamental bearing on the dielectric strength of the oil gap. This point will be discussed again in the following section.

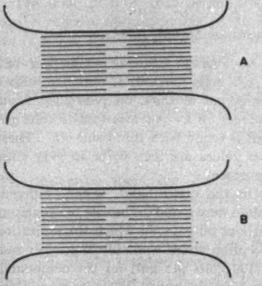

Fig. 29.

A—Schematic representation of test sample to investigate influence of 50-to-50 registration
B—Schematic representation of test sample to investigate influence of 30-to-70 registration

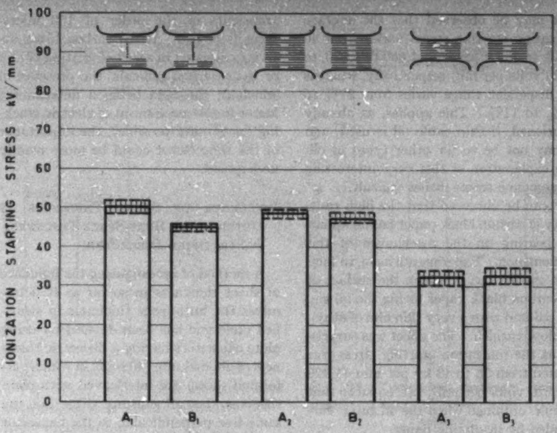

Fig. 30. Influence of paper tapes registration. Variation of ionization starting stress of the capacitor due to paper type and registration

Capacitor: plate
Electrodes: steel, smooth
Sample: perforated paper sheets interleaved with single (or double) plain sheets to make insulation thickness of about 1 mm (40 mils), with perforated sheets adjacent to electrodes
Oil: mineral, thin
Pressure: atmospheric
Temperature: 20 C

A_1, A_2, A_3: registration represented 30-to-70
B_1, B_2, B_3: registration represented: 50-to-50
A_1, B_1—Paper: density 0.9 g/cm³; impermeability 200×10^6 EU (10,000 Gurley seconds); sheet thickness 0.03 mm (1 mil)
A_2, B_2—Paper: density 0.75 g/cm³; impermeability 2×10^6 EU (300 Gurley seconds); sheet thickness 0.08 mm (3 mils)
A_3, B_3—Paper: density 0.75 g/cm³; impermeability 1×10^6 EU (300 Gurley seconds); sheet thickness 0.13 mm (5 mils)

A consequence of practical importance with regard to cables is that the lack of adherence between insulating paper and conductor is a more serious defect than the lack of adherence between paper layers in the dielectric. This is specially true for impulse tests.

Influence of Single Oil Gap Adjacent to Electrode Screened with Carbon Black Paper

The very important subject of the influence of surfaces on the dielectric strength is here again treated to consider particularly the influence of an oil gap of 0.16-mm (6-mil) thickness, adjacent to an electrode covered with a sheet of carbon black paper. Attention will be limited to a capacitor impregnated with thin oil having an insulation thickness of about 1 mm (40 mils).

The designation "carbon black paper" is not quite sufficient to identify clearly the type of paper meant here, as not all papers containing carbon black dispersed in the cellulose pulp show identical behavior in this respect. Only carbon black papers such as those used for many years for screening cable conductors are to be taken into consideration.

Ionization Starting Stress

It is found that the average ionization inception stress is 56 kv per mm (1,420 volts per mil).

It may be interesting to compare on the same diagram, see Fig. 22, the ionization starting stresses of three plate capacitors having the same dielectric thickness of 1 mm (40 mils), including an oil gap of the same thickness: about 0.16 mm (6 mils) but in three different conditions:

1. Oil gap adjacent to a metal (steel) electrode.
2. Oil gap surrounded by insulating paper.
3. Oil gap adjacent to an electrode covered with carbon black paper.

It may be observed that the average ionization starting stress varies from 40 to 48, to 56 kv per mm (1,000 to 1,220, to 1,420 volts per mil) respectively, whereas the dispersion range varies from 27% to 14%, to 11%. This applies, as already mentioned, if thin cable oil is used, and it may not be so for other types of oil. The explanation of this very interesting phenomenon seems rather difficult.

It can be observed that the high resistivity of carbon black paper has no apparent bearing on the mechanism of this phenomenon. Experiments have, in fact, been carried out in which the surface of the carbon black paper facing the oil gap was painted with a very thin film of ethylcellulose varnish. The effect was surprising as the ionization starting stress was lowered from 56 to 48 kv per mm (1,420 to 1,220 volts per mil), i.e., equal to that which is obtained when the oil gap is surrounded by insulating paper.

In other words, the dielectric strength of the oil gap seems to be very closely dependent on the surface activity of the carbon black and not on its ohmic resistivity.

In a similar way the decrease of ionization starting stress from 48 to 40 kv per mm (1,220 to 1,000 volts per mil) when changing from an oil gap surrounded by insulating paper to an oil gap adjacent to a metal electrode, could be attributed to a particular effect of the metallic surface, which is perhaps simply a lack of activity with respect to that of the cellulose or of the carbon black. Research to explore into the mechanism of this action is still in progress and promises hope of a conclusion in the not too distant future.

A practical consequence affecting the manufacture of oil-filled cables is that the carbon black paper, apart from chemical considerations which are beyond the scope of this research, exercises a much more important action than its simple function of electrostatic screening of the cable conductor. In other words, the use of carbon black paper counteracts the effect of a lack of adherence between the insulating paper and the conductor surface by providing a significant increase in the ionization starting stress of the interposed oil gap.

Surprising behavior is shown by the carbon black paper in impulse tests. It is found here, in fact, a very slight difference (5% at most) of impulse strength between the case of oil gap adjacent to a metal electrode and that of gap adjacent to carbon black paper.

The activity of the carbon black seems therefore closely associated to the time factor and is practically nonexistent for transients of the order of 100 microseconds or less. If the carbon black activity consisted in a sort of fixation of ions or hydrocarbon radicals, the presence of which in the field being a determining factor in the mechanism of electric cracking (as is quite possible), the importance of the time factor could be more readily understood.

Influence of Sheet Thickness as Determining Butt-Space Thickness in Stratified Dielectric

A method of investigating the influence of sheet thickness in so far as it determines the butt-space thickness in stratified dielectric has been devised by using plate capacitors having a dielectric thickness of about 1 mm (40 mils) in which perforated sheets are interleaved with plain sheets so that all gaps are aligned on the same line perpendicular to the capacitor plates. Gaps adjacent to the electrodes are avoided for fear that the electrode factor could partly mask the sheet thickness factor; see Fig. 23. In other words, the influence of the gap thickness when several gaps in series are present is investigated.

Ionization Starting Stress

Fig. 24 shows the behavior of capacitors made with paper of two different sheet thicknesses, 0.08 and 0.13 mm (3 and 5 mils) respectively. Both papers have a density of 0.75 g/cm^3 and impermeability of 2×10^6 EU (300 and 600 Gurley seconds for 3 and 5 mil paper respectively) and are impregnated with the usual thin oil. The average ionization inception stress varies from 50 kv per mm (1,270 volts per mil) for the smaller thickness to 44 kv per mm (1,120 volts per mil) for the larger one.

Impulse Strength

Fig. 25 is analogous to Fig. 24. The average impulse strength is 90 kv per mm (2,290 volts per mil) for a sheet thickness of 0.08 mm (3 mils) and 81.5 kv per mm (2,070 volts per mil) for that of 0.13 mm (5 mils).

Influence of Static Pressure

The influence of pressure when gaps are involved can of course be investigated in a variety of different cases. Attention is limited to the same type of capacitor as referred to in the preceding section and to a paper having a density of 0.75 g/cm^3, impermeability 2×10^6 EU (300 Gurley seconds), sheet thickness of 0.08 mm (3 mils) impregnated with thin oil.

Ionization Starting Stress

Fig. 26 compares the average value of 50 kv per mm (1,270 volts per mil) obtained at atmospheric pressure with the value of 73 kv per mm (1,860 volts per mil) obtained at a static pressure of 14 atm (200 psi). The increase is about 50%, the same as for capacitors made of plain paper sheets only.

A higher percentage (70%) can be observed on capacitors of a dielectric thick ness of 1 mm (40 mils) including one gap adjacent to an electrode with a gap thickness of 0.16 to 0.32 mm (6 to 12 mils).

This is in good agreement with the results shown in the preceding section, concerning plain paper sheets, where the greater effect of pressure is evident when a large oil gap thickness is present. It seems therefore that it is chiefly the "free" oil that is affected by an increase in pressure.

Impulse Strength

The influence of pressure on impulse strength is much greater on capacitors including oil gaps. Fig. 27 shows the increase from the value of 90 kv per mm (2,290 volts per mil) obtained at atmospheric pressure to that of 118 kv per mm (3,000 volts per mil) obtained at 14 atm (200 psi). The increase is of 31%, whereas in capacitors without gaps it was found that there was an increase of only 8%.

Influence of Oil Viscosity

The previously noted influence of oil viscosity requires further consideration at this point. The same type of capacitors and same type of paper are employed as in the test discussed in the preceding section.

Ionization Starting Stress

An average value of 47 kv per mm (1,190 volts per mil) is obtained with a compound of thick oil plus 30% rosin, whereas 50 kv per mm (1,270 volts per mil) is found with thin cable oil. These two values are seen to be in very close agreement.

On the other hand, widely different values were found in the case of capacitors without oil gaps, in which the ionization inception stress was still 47 kv per mm (1,190 volts per mil) for the compound, but 60 kv per mm (1,520 volts per mil) for the thin oil. In other words, when the thickness of the free oil gap is increased, the results observed with thin oil become very close to those obtained with thick compounds.

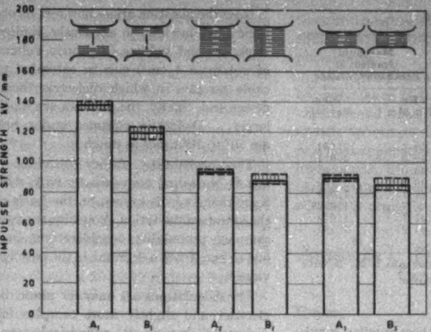

Fig. 31. Influence of paper tapes registration. Variation of impulse strength of capacitor due to paper type and registration. For all data see Fig. 30

Impulse Strength

Also in the case of a dielectric including oil gaps, the enormous influence of oil viscosity is confirmed. Starting from a strength of 90 kv per mm (2,290 volts per mil) for a viscosity of 25 cst (118 SUS) (thin oil at 20 C), a value of 138 kv per mm (3,500 volts per mil) is found when the viscosity is raised to values of the order of 5×10^4 cst (23×10^4 SUS) (compound of thick mineral oil plus 30% rosin at 20 C).

An almost equal value is found if a compound of thick mineral oil plus 32% polybutylene is employed, viscosity 10^4 cst (4.6×10^4 SUS) at 20 C.

If, however, the tests are carried out at a temperature of 85 C, at which the viscosity of rosin compound is 150 cst (695 SUS) and that of the polybutylene compound is 100 cst (460 SUS), in both cases a value of 92 kv per mm (2,330 volts per mil) is obtained, which is practically identical to that for the thin oil.

The conclusion is that below a viscosity value of approximately 10^3 to 10^2 cst (4,600 to 460 SUS) no practical variation of impulse strength is observed. Not even if the viscosity is as low as 1 to 3 cst (32 SUS), thin cable oil at 85 C, does the impulse strength value decrease below 90 kv per mm (2,290 volts per mil). Fig. 28 shows some of these results.

INFLUENCE OF RELATIVE POSITION OF BUTT-SPACES WITHIN STRATIFIED DIELECTRIC

The purpose of this section is to deal with a particular problem in cable taping, that of investigating the effect of a 30-to-70 registration of the tapes as compared with a 50-to-50 registration. These two different overlay patterns can be well simulated with plate capacitors in which oil gaps have been aligned in two different ways.

Fig. 29(A), where gaps are alternated with single plain sheets, simulates a 50-to-50 registration.

Fig. 29(B), where gaps are alternated with pairs of plain sheets, represents a 30-to-70 registration. In both cases gaps adjacent to the electrodes are now included to bring the condition of the capacitor dielectric nearer to that of a cable dielectric.

Limiting the investigation to capacitors of 1 mm (40-mil) insulation thickness, impregnated with thin oil, three different types of paper are considered which may be of particular interest for practical applications:

1. Density 0.8 g/cm³, sheet thickness 0.03 mm (1 mil), impermeability 2×10^6 EU (40 Gurley seconds).
2. Density 0.75 g/cm³, sheet thickness 0.08 mm (3 mils), impermeability 2×10^6 EU (300 Gurley seconds).
3. Density 0.75 g/cm³, sheet thickness 0.13 mm (5 mils), impermeability 10^6 EU (300 Gurley seconds).

Ionization Starting Stress

Power frequency test results are summarized by Fig. 30. The advantage of a 30-to-70 registration as compared with a 50-to-50 registration is greatest (about 10%) for the thinnest paper: 0.03 mm (1 mil); it is only 3% for the 0.08-mm (3-mil) paper; and is practically nil for the 0.13-mm (5-mil) paper.

Impulse Strength

Fig. 31 corresponds to Fig. 30. Here the advantage of a 30-to-70 registration as compared to a 50-to-50 one is more noticeable than at power frequency: 15% for the 0.03-mm (1-mil) paper; 7% for the 0.08-mm (3-mil) paper; and 6% for the 0.13-mm (5-mil) paper.

An explanation of the results of this section is not easy to arrive at. It is inter-

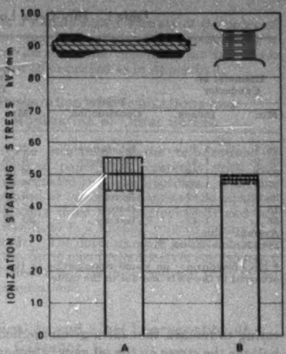

Fig. 32. Comparison between ionization starting stresses of plate and cylindrical capacitors

A—Capacitor: cylindrical
Electrode: inner, brass, smooth, 28 mm ϕ (1.10 inch); outer, tinned copper tape
Sample: 20 mm (0.800 inch) wide paper tapes; tapes lapped in the same direction; registration: 30-to-70; butt-space width: 2 mm (0.080 inch); total insulation thickness: 1.5 mm (0.060 inch)

B—Capacitor: plate
Electrode: steel, smooth
Sample: perforated sheets interleaved with pairs of plain sheets, with perforated sheets adjacent to electrodes, to make insulation thickness of about 1 mm (40 mils)

Paper: density 0.75 g/cm³; impermeability 2×10^6 EU (300 Gurley seconds); sheet thickness 0.08 mm (3 mils)
Oil: mineral, thin
Pressure: atmospheric
Temperature: 20 C

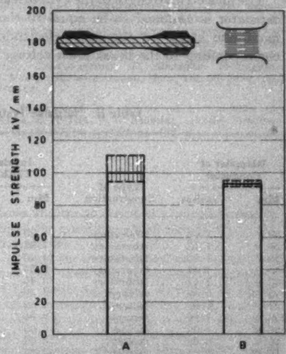

Fig. 33. Comparison between impulse strengths of plate and cylindrical capacitors

A—See Fig. 32
B—See Fig. 32

Table I. Fifty-Cycle Long-Time Test, 4-Hour Steps

Diameter of Conductor		Type of Construction	Insulation Thickness		Breakdown Voltage, Kv	Maximum Gradient at Breakdown Voltage	
Mm	Inches		Mm	Inches		Kv Per Mm	Volts Per Mil
28.7	1.13	laboratory	1.40	0.055	64	48.5	1,230
35.9	1.41	laboratory	3.50	0.138	135	42.0	1,070
27.6	1.08	factory	6.00	0.236	230	46.0	1,170
27.5	1.08	factory	6.10	0.240	230	46.5	1,180
28.2	1.11	factory	5.90	0.232	210	42.7	1,090
16.5	0.65	factory	13.50	0.532	325	41.7	1,060*
36.1	1.42	factory	20.50	0.808	575	42.1	1,070
Average value						44.21	1,120
Standard deviation, %						5.72	

* No breakdown: on visual examination of the sample after the test the puncture was found to have occurred in the ends and not in the cable.

esting to remark that for a given applied voltage the stress on the oil gaps is higher for a 30-to-70 than for a 50-to-50 registration while the gap thickness is obviously the same. The explanation therefore cannot be found in stressing but should be looked for in the "barrier" phenomena, of which, however, very little is yet known.

Comparison Between Results Obtained on Plate and Cylindrical Capacitors

The comparison between results obtained on plate and cylindrical capacitors will be limited to a typical case, i.e., to check the results obtained in the preceding section, particularly considering capacitors made with 0.08 mm (3-mil) thick paper reproducing a 30-to-70 registration. The inner electrode of the cylindrical capacitor used for these tests is a smooth rod having a diameter of 28 mm (1.10 inch).

The dielectric strength of the cylindrical capacitor is assumed to be equal to the maximum stress on the inner electrode corresponding to the breakdown voltage. (By "breakdown" either impulse breakdown or ionization inception is meant.) Figs. 32 and 33 refer to power frequency and impulse testing respectively.

The average values obtained on cylindrical capacitors are in good agreement with those on plate capacitors. The former are a little higher but the dispersion range is also larger, which is easily understandable if the much less precise construction of cylindrical capacitors (hand-lapped insulation) as compared to plate capacitors is taken into account.

Considerations Relating to Practical Applications to Cables

In the preceding section the good agreement between results on plate and cylindrical capacitors was purposely shown. The cylindrical capacitor insulated with helically wound tapes, as already mentioned, is the model which most nearly simulates the cable dielectric, therefore the agreement mentioned makes it possible to extend logically to cables the knowledge acquired through plate capacitor tests.

Now the question arises how results obtained on models of extremely limited thickness and volume (dielectric volume of not even 4 cm^3) can be extended to cable samples in which dielectric thicknesses and, chiefly, the volumes are much larger. (Dielectric volumes under test are 10^3 to 10^4 times as much.)

The probability theory provides a means of dealing conveniently with such a problem.[9] As is known on the basis of the standard deviation shown by tests on samples, probability considerations lead one to anticipate a decrease in the average values.

The calculations are easy for plane dielectrics and slightly more complex for dielectrics having a cylindrical symmetry; if, however, dielectrics of the type considered in this paper are taken into account the situation becomes much simpler.

In fact if, for instance, Figs 24 and 25 are examined, and more particularly the results observed on the 0.08 mm (3-mil) paper it can be seen that the dispersion range is very small, the standard deviation being less than 1%. The theoretical decay, as a consequence, is also very small: it is a few per cent only for an increase of volume of 10^4 times, and can be disregarded in practice.

Now, the theoretical decay will coincide with the actual decay only if the cable insulation is perfectly made as that of a capacitor model.

It is here that the factor which, as pointed out at the beginning of this article, was purposely neglected, i.e., the "bending" of the cable dielectric comes into play.

It is found that the mechanical defects of the insulation due to a deficiency in flexibility of the cable are among the most important reasons of disagreement between results on cables and results on models. It can also be added that the agreement (or disagreement) between the two is a realiable index of the insulation quality.

It is useful to give in Tables I and II some results of dielectric strength at power frequency and at impulse obtained on samples which include both laboratory-made cylindrical capacitors having an insulation thickness of 1.5 mm (60 mils), and factory-made cables having a dielectric thickness up to 24 mm (950 mils).

The dielectric strength results at power frequency (50 cycles) given in Table I are breakdown values obtained in long-times tests: 4-hour steps of 2 kv per mm (51 volts per mil) each. A very close agreement between the values just men-

Table II. Impulse Tests 1/50-Microsecond Wave

Diameter of Conductor		Type of Construction	Insulation Thickness		Breakdown Voltage, Kv	Maximum Gradient at Breakdown Voltage	
Mm	Inches		Mm	Inches		Kv Per Mm	Volts Per Mil
28.7	1.13	laboratory	1.30	0.051	−112.5	−92.5	−2,350
28.8	1.13	laboratory	1.35	0.053	−125.0	−96.8	−2,460
28.7	1.13	laboratory	1.40	0.055	+137.5	+104.0	+2,640
35.9	1.41	laboratory	3.35	0.132	−300.0	−98.3	−2,500
35.8	1.41	laboratory	3.40	0.134	+300.0	+98.8	+2,510
10.95	0.43	factory	5.50	0.216	+365.0	+96.2	+2,440
27.7	1.09	factory	6.00	0.236	+450.0	+90.5	+2,300
28.0	1.10	factory	6.00	0.236	−475.0	−95.0	−2,110
27.8	1.09	factory	6.00	0.236	+450.0	+90.0	+2,290
16.5	0.65	factory	13.00	0.512	±730.0	±93.7	±2,380*
16.4	0.65	factory	13.25	0.522	+750.0	+95.2	+2,420
27.8	1.09	factory	23.50	0.925	±1350.0	±98.5	±2,500*
28.0	1.10	factory	23.60	0.929	−1300.0	−95.5	−2,430
28.5	1.12	factory	24.50	0.965	±1350.0	±94.8	±2,410*
Average value						95.7	2,430
Standard deviation, %						3.64	

* See footnote of Table I.

tioned and ionization starting stresses has, however, been checked on capacitors.

The conductors have been screened purposely with a helically wound conductive tape both in the case of laboratory models and in that of cables, in order to make their dielectric conditions equal.

The insulating paper with which the conductors of both laboratory models and cables have been lapped, is the same wood pulp paper having a density of 0.75 g/cm^3, impermeability of 2×10^6 EU (300 Gurley seconds), thickness of 0.08 mm (3 mils), cut into tapes 20 mm (0.8 inch) wide, lapped with a 30-to-70 registration and 1 to 2 mm (0.04 to 0.08 inch) wide butt-spaces.

As may be seen, the agreement between all the recorded dielectric strengths, is very good provided the maximum stresses on the inner conductors corresponding to the breakdown voltages are used as the basis of comparison.

This agreement, it must be repeated, is based on the assumption that perfectly made and fully impregnated dielectrics are under consideration, characterized by the further fact that in tests carried out on models the dispersion of results is extremely small.

Conclusion

The present paper is intended to show a few dielectric phenomena which seem to be either of scientific interest in themselves or of interest in the application relative to high-voltage cables, particularly of the oil-filled type.

The most interesting phenomena from a purely scientific standpoint are perhaps those relating to the influence of surface activity on the dielectric strength, while for the applications to the cables the analysis of the behavior of the butt-spaces is of more immediate practical use.

What has been illustrated is far from being a completed research on these very interesting subjects; above all, much work still must be done to bring a decisive contribution to the explanation of these phenomena.

Throughout this article the opportunity has been taken to touch on the subject of experimental analysis carried out by models to obtain information useful in practical applications and to indicate the high degree of confidence that can be placed in this extremely profitable method when it is properly employed.

Appendix I. Preparation of Plate Capacitor

Drying

The container and the electrodes are accurately washed with light gasoline before introducing between them the paper sample made as indicated in the section "Plate Capacitor as Test Model."

The container is then closed by means of a vacuum-tight cover and then placed in a thermostatic stove where it is dried for 24 hours at a temperature of 100 to 110 C under a vacuum of about 0.02 to 0.05 mm Hg.

The residual pressure after drying, with pump closed for 1 hour, does not exceed the value of 0.05 to 0.1 mm Hg.

Impregnation

Before impregnation, which is carried out at atmospheric pressure, the oil is degasified at 80 C in a degasifier which operates under a vacuum of about 0.03 to 0.05 mm Hg. When the impregnation is over, vacuum is broken by means of dry nitrogen. The containers, closed in order to protect them from the atmosphere, are then left to cool down in the ambient.

Appendix II. Preparation of Cylindrical Capacitor

Drying and Impregnation of Capacitor Dielectric

The inner electrode, accurately washed with light gasoline, is hand lapped with insulating paper tapes, then dried in a vacuum tight tank at a temperature of 100 C for 24 hours with a vacuum of the order of 0.1 mm Hg applied. The impregnation is carried out under vacuum in the same tank with oil degasified as in Appendix I.

Preparation of Terminations and Application of Outer Screen

The insulation of the terminations is made of paper rolls separately dried and impregnated as in the preceding. They are applied by hand on the ends of the capacitor (already dried and impregnated) and are chamfered in a suitable way by means of a knife. The outer screen is finally wound on the central part (cylindrical) of the capacitor dielectric and on the chamfered parts of the terminations.

Sealing and Final Impregnation of Capacitor

The cylindrical capacitor prepared as described is placed inside the steel pipe terminated with porcelain insulators, described in the section "Cylindrical Capacitor as Test Model."

Vacuum of the order of 0.1 mm Hg is applied for 15 hours at ambient temperature. Then the final impregnation with degasified oil is carried out.

References

1. Measurement of Discharge in Dielectrics, A. N. Arman, A. T. Starr. *Journal*, Institution of Electrical Engineers, London, England, vol. 79, 1936, pp. 67–79.

2. The Detection of Initial Failure in High-Voltage Insulation, J. B. Whitehead, M. R. Shaw, Jr. *AIEE Transactions* (*Electrical Engineering*), vol. 60, June 1941, pp. 267–272.

3. The Measurement and Investigation of Ionization Level of Rubber Insulated Cables, R. C. Graham, E. K. Duffy, W. P. Foster. *Ibid.*, vol. 67, pt. II, 1948, pp. 1107–17.

4. The Emanueli Porosity Tester, L. Emanueli. *Paper Trade Journal*, New York, N. Y., Sept. 8, 1927.

5. Applicazioni di calcolo numerico approssimato alla determinazione del campo elettrostatico nel dielettrico di un cavo unipolare in olio fluido, (Determination of the Electrostatic Field of a Single Core Oil Filled Cable by means of Approximate Numerical Calculation), P. Gazzana Priaroggia. *L'Energia Elettrica*, Milan, Italy, vol. 26, 1949, pp. 701–17.

6. Insulation Breakdown as a Function of Area, L. R. Hill, P. L. Schmidt. *AIEE Transactions*, vol. 67, pt. I, 1948, pp. 442–46.

◆

Discussion

Bror Hansson (Aktiebolaget Liljeholmens Kabelfabrik, Stockholm, Sweden): When reading a paper on the dielectric strength of oil-impregnated paper, one is always fascinated by the curious fact that a combination of just two components, the paper and the oil, can give material for new investigation and such splendid new papers as that under discussion, many decades after it was discovered that there is no better insulator than impregnated paper.

The greatest value of their paper seems to me to be that the authors have carefully defined the test specimens and conditions and given numerical values for the results. Unfortunately many papers written by others earlier and covering related subjects (adjacent variations in the paper, the oil, the electrodes or the types of stresses imposed on the samples) cannot as to their numerical values be directly compared with the results of this paper. Oil, paper, treatment, sample size, etc., are not necessarily the same today as they were 10, 20, or 30 years ago, and we lack a common denominator for comparing the results.

Would it not be a worthy project for the AIEE Committee on Insulated Conductors to carry on this research on a still broader basis and try to arrive at a complete answer to all the questions we all should like to ask the authors.

Would the authors allow us to accept, for instance, their test specimens as standard, if the same paper and oil could be distributed to many laboratories each of which undertook to investigate a small section of the problem? Table III shows that it is a tremendously wide problem which could hardly be covered completely by one laboratory.

It would perhaps not be necessary to investigate all the possible combinations ($3\times3\times6\times3\times5\times3\times3\times3\times3\times3\times9\times5\times6\times4\times4\times4\times2=32{,}099{,}036{,}400$) but a

Table III. Some Variables in Testing

Variable	Least No. of Qualities Which Should Be Tested	Remarks
Paper density	3	Dense paper should give better short-time strengths but is more difficult to impregnate (with thick oil) and gives higher losses, and thus lower long-time a-c strength.
Paper air resistance	3	
Paper thickness	6	Thin paper gives higher strength but is costly and mechanically weak. Is the long-time a-c strength really higher for thin paper?
Oil viscosity	3	Thin oil for a-c capacitors and oil-filled cables Thick oil for d-c and impulse capacitors and for mass-impregnated cables.
Electrode distance	5	High- and low-voltage cables, capacitors.
Electrode material	3	Al, Cu, Sn, Pb
Electrode shape	3	
Carbon paper	3	Inside, outside, in between
Carbon paper thickness	3	For instance 0.02, 0.05, 0.1 mm
Paper+oil+gas	3	Air, nitrogen, freon etc.
Oil pockets (voids)	9	3 diameters, 3 thicknesses
Temperature	5	−20, 0, +30, +60, +90, +120 C
Pressure	6	$^1/_3$, 1, 3, 6, 15 atmospheres. Some combinations of insulating material give a straight line, others an asymptotic "strength versus pressure" curve for some kinds of stresses.
Direct current	4	Instantaneous, 1-hour, 10-, and 1,000-hour strengths.
Alternating current 50 p/s	4	Instantaneous, 1-hour, 10-, and 1,000-hour strengths.
Alternating current 1,000 p/s	4	Instantaneous, 1-hour, 10- and 1,000-hour strengths.
Impulses	2	$^1/_{50}$, chopped, etc.

study committee would certainly find more variables of interest to investigate and as more than one test would be needed to give a sure average for each combination it seems obvious that the question, "What is the dielectric strength of impregnated paper?" has so many answers that some co-ordinated research would be welcome. Would the Insulated Conductor Committee be willing to sponsor such co-ordination? There are certainly many laboratories who would be willing to co-operate.

The d-c strength is not only of interest for d-c cables and capacitors. Ordinary a-c cables are stressed by direct current from restriking in circuit breakers and, moreover, the behavior of the insulation under d-c stress is of great theoretical interest.

Theoretically, the d-c stresses should (due to higher insulation resistance) plant themselves mostly in the cellulose component when the a-c stresses should (due to lower specific inductance capacitance) occur in the oil component. When, however, the dielectric strength of one component for some reason is very high or very low (for instance, the oil due to a high- or a low-oil pressure) the breakdown may occur anywhere.

It should perhaps be remarked that in the Table III, no regard has been taken of the chemical composition of the oil or the paper.

N. Klein (Israel Institute of Technology, Haifa, Israel): This interesting paper has the merit of systematically investigating breakdown properties of oil-impregnated paper insulation. Many of the results indicate that the dielectric strength is primarily affected by the size and location of the butt spaces. Some impulse test measurements of this investigation however do not seem to comply with this view. Thus, when a single 0.08-mm-thick oil gap is surrounded by insulating paper the impulse strength according to Fig. 16 is about 132 kv/mm; the same impulse strength is recorded in Fig. 5 for the case that there is no gap in the insulation. Similar equality is found when the gap is 0.13 mm thick and only when there are many butt spaces in series does the impulse strength decrease (see Fig. 25). It is noticed also that when a gap occurs next to a steel electrode the impulse strength does not decrease strongly for thinner, 0.08-mm gaps and extrapolation leads to the question as to whether the presence of even smaller gaps at an electrode at all influences the impulse breakdown stress. Did the authors carry out such experiments with 0.03-mm papers! These test results might suggest that impulse breakdown processes do not always start in or due to butt spaces. This view is partly supported also by the observations that when a gap is next to an electrode impulse, results with opposite polarity do not differ and that carbon black paper with a gap adjacent to it hardly influences the impulse breakdown strength. One possibility for the explanation of the behavior in the cases quoted might be that breakdown is initiated in oil spaces occurring at the electrode due to paper surface unevenness.

The introductory experiments on gapless insulations by which the influence of density, impermeability, and paper thickness are investigated might permit also partial interpretation of the results in terms of unevenness of paper surface. Experiments with gaps adjacent to a steel electrode are important. Did the authors carry them out also with electrodes made of other metals, and especially with customary conductor metals as copper and aluminum?

Influence of electrode corrugations seems to be involved due possibly to opposing effects of decrease of stress and increase of oil space with corrugation radius and this might perhaps be the reason for the seeming inconsistencies of the measurements.

Carbon black is a strongly absorptive material. Do the authors think that the considerable increase in ionization stress, when a gap is adjacent to carbon black papers, might be due to the absorption of impurities of the gap by the carbon black!

Many of the results indicate the importance of the time factor in impulse tests, as, e.g., increase of impulse strength with paper density, viscosity, pressure, etc. It is thought that more light might be thrown on the influence of these and other parameters by carrying out impulse tests not only with customary wave shapes, but rectangular waves of varying duration.

Finally, it would be interesting to know how the sample thickness and the parallelity of electrode surfaces were checked in the experiments; and also whether oil spaces between spacer disks and insulation proper did not influence ionization starting stress measurements.

These investigations contribute to knowledge on the involved subject of breakdown in oil-impregnated paper insulation and stimulate further research, and the authors are to be commended for their great effort.

Kenneth S. Wyatt (Phelps Dodge Copper Products Corporation, Yonkers, N. Y.): It is now nearly 5 years since I became aware of these researches, and each year I saw them develop. They have been exceedingly carefully carried out in a scientific manner, and I am glad to see this account of them. However, this paper covers only a small part of the ground, and I had hoped that the scope would have been broader. Perhaps this can be explored in subsequent papers.

The agreement between the results on flat-plate capacitors and actual cables once again demonstrates the usefulness of the maximum stress theory. This is especially true and easy to discern, where the breakdown results are not masked by a number of uncontrolled variables. For example, in cables made 20 years ago or more, the taping was irregular in overlay and variable in looseness, registrations were serious, upon bending before impregnation the tapes slipped in bunches leaving preferential impregnating paths at intervals so that drying was often irregular, the insulation structure was loose and full of creases and pockets of high-loss rosin compound. Under such conditions it was practically impossible to see the clear working of the maximum stress principle. Even today we find cable insulations, e.g., polyethylene, which are nonhomogeneous to a high degree and breakdown is so irregular that the maximum stress principle is entirely masked. Where these variables are not fully controlled, it suffices to use average stress rather than maximum stress as a basis for specifications.

While we had long known the advantage of carbon black paper in giving an equipotential surface to the conductor, we had suspected that there was an advantage beyond this, and that it was due to the damping effect of the high-resistance paper on high-frequency components which are nearly always present in a high-voltage setup. This can be seen on an oscillograph. The authors brush this explanation aside, saying that the effect is the same over a wide range of conductivity of the carbon black paper. We shall be glad to see the results of further investigations in this field.

The extension of the authors' results on flat paper capacitors to actual cables which have to flex is only very lightly touched upon Take the matter of overlay of the tapes, for example. While a 50-50 overlay may give fair results on a rigid model, it would be suicidal in a commercial cable which has to be capable of being bent, and a 70-30 overlay is not much better. Extensive work with wafers, some of which was published in 1938,[1] demonstrated how the paper folds up and forms creases in the butt spaces of such a structure when the cable is wound and unwound on a reel. After this has happened the breakdown is much lower. This we have known for a long time. Even a 25-75 overlay is unsatisfactory because the "step" leakage path becomes too short when opened up at a bend.

In extending these results to actual working cables there are a great many variables to be considered and brought under control, otherwise the most perfect mechanical structure of the insulation will not last long under conditions of flexing, and then we are back where we started. In order to slip without permanent displacement, the tightness of winding must be correct, the smoothness of the paper must be considered, and if the tightness is to be uniform and of a correct value after drying, the moisture content of the paper and its uniformity, the shrinkage characteristics of the paper, all must be controlled.

The researches described, when supplemented by further work to make their application to working cables sure beyond doubt, will make it possible to reduce insulation wall thicknesses and to work with a lower factor of safety, especially at the higher voltages. The paper is thus of great importance beyond the fact that it is an example of research precisely carried out with unusual attention to control of the many variables.

REFERENCE

1. MECHANICAL UNIFORMITY OF PAPER-INSULATED CABLES, K. S. Wyatt, D. L. Smart, J. M. Reynar. *AIEE Transactions (Electrical Engineering)*, vol. 57, Mar. 1938, pp. 141-54.

L. Meyerhoff (General Cable Corporation, Bayonne, N. J.): The authors deserve high commendation for the very able conception, planning, and execution of a timely investigation. Of particular value is the new tool which they have made available for the study of power frequency breakdown strength by means of nondestructive ionization level determination. They have apparently satisfactorily demonstrated by their tests that for low-pressure oil-filled cable the 50-cycle breakdown strength is very closely related to the ionization level, the two types of tests apparently producing essentially the same values. The authors are careful to point out that this correlation between ionization level and breakdown strength does not necessarily apply to other types of cable. Indeed, it does not appear likely that such a correlation can exist if the insulation is not completely saturated or if the oil is of substantially higher viscosity than is true for low-pressure oil-filled cables. However, exploration of the value of the ionization level method for other types of cable would be highly desirable.

The data given are in the main quite consistent with one another. However, certain discrepancies are here noted. Fig. 16 shows impulse strength as a function of oil gap thicknesses from 0.08 to 0.40 mm, the gaps being surrounded by insulating paper. Fig. 20 shows the same relationship where the gaps are adjacent to a metal electrode. If these curves are extrapolated to zero oil gap thickness, the breakdown value obtained is about 150 kv/mm in each case. However, from Fig. 5 the breakdown value for corresponding paper with no gap (0.8-mm paper of 2 by 10^8 EU impermeability) is only 13 kv/mm. This compares further with a value of 132 kv/mm for 0.08-mm oil gap for the conditions in Fig. 16 and 127 kv/mm for those in Fig. 20. Can the authors offer any explanation for this seeming discrepancy? Is it possibly a measure of the reproducibility of the method? If the latter is the correct explanation, can any significance be attached to the difference between the results in Fig. 16 and 20?

There appears also to be some inconsistency between the data shown in Fig. 18 and 30. According to Fig. 18 the ionization starting stress with a 0.08-mm gap adjacent to an electrode is 48 kv/mm. From Fig. 30, *A2* and *B2*, which involve the same kind of paper, the ionization starting stresses are respectively 49 and 47 kv/mm with a 0.08-mm gap at each electrode and additional gaps (three in *A2* and five in *B2*) in the body of the insulation. The stresses given are average stresses, but the controlling stresses are, of course, those in the oil gaps. On the basis of a ratio of 1.6 between the dielectric constant of saturated paper and that of oil, the stresses in the oil gaps are, respectively, 73, 64, and 57 kv/mm. A somewhat similar discrepancy appears between the data in Fig. 14 and those in Fig. 26(B). According to Fig. 14 the average ionization starting stress with a 0.08-mm gap in the body of the insulation is 52 kv/mm, whereas with six such gaps in Fig. 26(B) the ionization starting stress is 50 kv/mm. The corresponding stresses in the oil gaps are 80 and 63 kv/mm, respectively. Can the authors offer an explanation for these seeming inconsistencies aside from reproducibility?

The noting of these discrepancies is not intended to minimize the very great value of the paper as a whole. It does emphasize, however, what the authors themselves indicate, that although they have unquestionably made a good start, much additional work still remains to be done.

The data bring out many important and valuable points. One example may suffice. The gain in dielectric strength, as measured by ionization starting stress, resulting from conductor shielding is well illustrated by the data. Thus, with a corrugated electrode, corresponding to an unshielded conductor, the ionization starting stress, according to Figure 12(B), is only 33 kv/mm even with no gap in the insulation. On the other hand, with a smooth electrode, according to Fig. 18, the value is 48 kv/mm with a gap next to the electrode and is presumably higher with no gap. Fig. 22 shows a substantial further gain by using a carbon black shield. The authors point out that the impulse strength of their samples is not greatly affected by the use of carbon black paper. This is in line with data which we have obtained on cables, showing that conductor shielding mainly serves to improve uniformity of impulse breakdown values but does not affect materially the maximum values obtained.

R. W. Atkinson (General Cable Corporation, Bayonne, N. J.): This paper is an exceedingly fine contribution to the subject. The conception and carrying out of the research and the reporting of the immense amount of data deserve very great praise. This careful reporting allows the reader independently to agree with very many of the conclusions and, on the other hand, to substitute, in some cases, his own analysis for that of the authors.

I would like to outline the many ways in which I support their conclusions substantially or completely, but I believe it will be more useful to discuss some ways in which I would substitute a different analysis. I would single out for favorable comment the authors' suggested explanation of the first stages of ionization of the oil as a chemical action comparable to "cracking" by heat. That seems to be a far better explanation of the effect of pressure upon ionization and breakdown than any suggested explanation of which I have previous knowledge. It seems to fit all of the observations, those of the authors as well as any other pertinent observations that I recall.

Again, I would agree with the authors' analysis of the ionization and subsequent failure at power frequency of their test capacitors and cables as being a function of the oil spaces and the stresses therein. Their data and analysis are powerful substantiation of that. For impulse voltage, however, I do not accept that explanation. I believe the primary determinant of impulse strength is the performance of the impregnated tapes, not that of the oil spaces. There are other factors which play a secondary role although by no means an insignificant one. Indeed, where the paper has very low density and impermeability, these secondary effects become more important and may even become dominant. I find that most of their impulse test data are very well correlated on the assumption that the dielectric strength of their capacitors is primarily the sum of the strength of the total number of unperforated tapes in series, together with a relatively small contribution by each oil film. This remains generally true whether the various oil gaps resulting from tape perforations are scattered through the thickness or are grouped together either in the middle of the insulation wall or adjacent to one of the electrodes. Thus, the behavior of a sample having a number of oil gaps in series with a number of tapes is as though the oil films contributed relatively little to the breakdown of the remaining insulation wall in the brief period of the impulse. This may be considered in considerable detail for the particular type of paper on which so many tests are reported, namely paper 0.8 mm (3 mils) in thickness and of 300 seconds Gurley impermeability. The results of the various impulse tests on this paper saturated in one type of low-viscosity oil and made at atmospheric pressure, are assembled in Table IV. Calculated values of unit strength of the paper are shown first on the assumption that the oil spaces contribute nothing to the dielectric strength of the sample and then on the basis that each gap, regardless of its thickness, contributes 40% as much as one layer of paper. It will be seen that, in the test groups where there is only one gap of varying thickness, either method gives good correlation. In the tests in which there are varying numbers of gaps of constant thickness, a better correlation is given by the assumption that each oil space contributes a constant amount. This brings all values into good agreement.

Table IV. Data from Authors' Figures, as Noted, and Discusser's Calculations Therefrom

Details of Test Sample				From Figs. 10 & 16			From Figs. 10 & 20			From Figs. 27 & 28			From Figs. 31-A2 31-B2		
1	2	3	4	A	B	C	A	B	C	A	B	C	A	B	C
0	12	1.00	1.00	132	132	132	132	132	132						
1	11	0.92	0.95	132	143	139	128	139	135						
2	10	0.83	0.87	116	140	133	108	133	124						
3	9	0.75	0.79	102	139	129	92	122	116						
4	8	0.67	0.70	92	138	131	84	126	120						
5	8	0.61	0.77										92	149	120
5	7	0.58	0.62	84	145	135	79	136	127						
6	7	0.54	0.72							90	166	125			
7	6	0.46	0.68										89	192	130

Column 1—Number of oil gaps.
Column 2—Number of paper tapes (not perforated).
Column 3—Proportion of total sample thickness occupied by paper tape.
Column 4—Same as (3) but adding 40% of one paper tape for each oil gap.

For each group of three columns applying to the different figures,
Column A is the impulse strength in kv per mm from the figure.
Column B is the (A) value divided by the value shown in column 3. This is the apparent tape strength if the entire contribution of the oil is neglected.
Column C is the (A) value divided by value in column 4. This is the apparent strength of each tape on assumption that each oil gap has a strength equal to 40% of that of one tape, regardless of position or thickness of gap.

From the theoretical standpoint one may picture the oil gap as ionizing at a potential well below the breakdown voltage of the sample and, thereby, building up a space charge on the face of the boundary tape. This theory allows an analysis of what should happen in detail to modify the general theory I have stated. There should be some voltage across the oil gaps, making the total voltage across the specimen somewhat greater than the combined voltage across the tapes. The total voltage across a given total oil thickness should be greater if this is divided into a number of thin layers spaced at intervals than if concentrated in a single thick film. It is not expected that the formation of these space charges will be entirely without other effect upon the adjacent tape than the formation of a quiescent layer of charge on its surface. It is to be expected that the ions, striking the surface of the tape at some velocity, will penetrate to some depth below the surface, resulting in an effective thinning of the wall of tape and corresponding reduction of its effective strength. This last effect will be greater for porous paper than for that which is less permeable and will be greater for thick oil films than for thin. The reduction of strength of the tape by the process described and the contribution of the oil gap to the over-all voltage are, it will be noted, in opposite directions.

On the basis of this process, paper of low density and high permeability will have low strength because of being a poor barrier compared with impermeable paper. This is because the paper that is permeable to air flow will also be relatively permeable to the energetic ions received from the oil films between tapes or from tiny oil spaces within the tapes. Moreover, the permeable tapes will be especially susceptible to penetration by the more rapidly moving ions stemming from thick oil films.

In addition to the data assembled in Table I, the authors show the effect on impulse strength of the paper impermeability and of oil viscosity, also of hydrostatic pressure. The effect of paper impermeability furnishes a rather critical way of distinguishing between the correlation of the data by their method and by the foregoing method. Were the stress in the oil film the significant parameter, the impermeable paper, being also more dense (grams per centimeter cube) and thus of higher dielectric constant, should give lower strength than the permeable paper, as is the case at 50 cycles. But, on the assumption that the strength lies primarily in the paper, it is natural that the higher strength should lie, as it does, in the more dense paper. Also, Fig. 31, (A) and (B), together with Fig. 5, give some basis for studying the effect of oil gaps in series with very impermeable paper. The respective values of 138 kv and of 120 kv with oil gaps in Fig. 31 may be compared with the value for the same paper of 178 kv in Fig. 5. If, for both of the paper groupings in Fig. 31, we assume the 1-mil gap has a strength equal to 38% of that of the 1-mil high-density paper, we obtain complete co-ordination with the strength shown in the test of Fig. 5 without gaps. Thus, here the 1-mil gap has approximately the same proportion of the strength of the 1-mil high-strength paper as have the various thicker gaps in terms of the 3-mil lower density paper. This makes the 1-mil oil gap to have roughly one half the strength of those 3 mils and above. The comparison, here, with the 3-mil lower density paper, is not very direct, but seems quite consistent with the theory indicated herein.

The effects on impulse strength of oil viscosity and of hydrostatic strength are reasonably explained either on the basis of the authors' analysis or of that given in the foregoing. It is to be noted that, in our own work, with cables, we have found no significant increase of dielectric strength either with increasing viscosity or with increasing hydrostatic pressure. This is not inconsistent with the authors' findings inasmuch as our data were determined with paper of high density and impermeability where it seems quite reasonable that viscosity and pressure effects on impulse strength should vanish.

As I have stated, the authors' analysis explains very well the power frequency performance of the test samples. Thus, this analysis shows directly why, at power frequency, paper of low density (grams per centimeter cube) has higher strength than with dense paper, because of its lower dielectric constant and the corresponding lower stress in the oil films at the same over-all average stress. This is entirely in line with data by J. B. Whitehead on cylindrical capacitors or cable models and also with Whitehead's analysis.

The authors point out that, at 50 cycles, the use of an oil of very high viscosity results in a reduction of dielectric strength, contrasting with the increase obtained with impulse voltage. It seems to me that, with the very high viscosity used, there may be lack of complete impregnation at room temperature. This can be true because of shrinkage of the oil during cooling even though the impregnation were complete at high temperature. At 50 cycles this would result in ionization and low strength whereas, under the foregoing analysis, the impulse strength would not suffer as a result of the presence of these small voids. On the other hand, there would result the full gain due to the high viscosity and less free movement of ions.

A further word is required to apply the analysis to the case of thick insulation as on a high-voltage cable. With the 1-mm (40-mil) wall used in these test samples, it appears that the whole insulation wall must act as a unit and fail only when the total strength of the entire thickness has been exceeded. Since, in a thick wall, there can be significant lateral spreading of the ions produced in each oil gap, it would seem likely that when the total strength of some finite thickness considerably less than the total wall has been reached that portion will fail with the releasing of a sufficient energy to puncture adjacent layers with the consequent avalanche successively penetrating the entire wall even though the sum of the strengths of all the layers might exceed the applied voltage.

A most interesting practical conclusion comes from these discussions. It appears that, at the power frequency, the stress at breakdown shown by the authors for cable is generally somewhat greater than customarily found for similar commercial cables in the United States. On the other hand, the values for impulse strength are lower than encountered here. This ties in perfectly with the authors' test data and their analysis for power frequency and the foregoing analysis for impulse. With the lower dielectric constant obtained from the relatively low density paper used in Europe, the stress in the oil gaps is lower than with the high density used here. Accordingly, the power frequency strength should be greater. On the other hand, under impulse, this is not consequential since the strength is determined by the paper. Consequently, the higher strength on impulse which is obtained in the United States is to be expected. Perhaps the authors may adopt the American practice of using a portion of high-density low-porosity paper near the conductor. This should increase the impulse strength with little sacrifice of that at power frequency. Perhaps, also these data and discussions may lead United States practice to the use of lower density paper in the outer layers with no loss of impulse strength but some increase in the 60-cycle strength.

I cannot close without again expressing to these authors and to their long-time associate and mentor, Luigi Emanueli, appreciation of the value and importance of the contribution they have made.

William A. Del Mar (Phelps Dodge Copper Products Corporation, Yonkers, N. Y.): A paper on cables from the engineers of the Pirelli Company is an event of importance to the Institute, particularly as it may be assumed to have been sponsored by such a distinguished authority as Luigi Emanueli.

The work on flat capacitors is remarkable in inception, in the accuracy with which it was carried out, and the clearness with which it is presented. It affords neat proofs of facts which we have known in much less definite ways.

I have little to comment upon and nothing to criticize in relation to this part of the paper.

It is unfortunate that the authors did not attempt further to differentiate between impermeability and specific gravity in relation to electric strength, a subject treated by P. Cloke and K. K. Khandelwal.[1] These authors tell of testing papers of equal specific gravities but different impermeabilities and finding an increasing electric strength with increasing impermeability, thus proving the importance of high air resistance, as measured by a Gurley densimeter regardless of specific gravity, as a means of obtaining high electric strength.

I do not understand why the authors are surprised to find that their test results on simulated stranded conductors do not agree with the Levi-Civita formula[2,3] as this formula is based on a dielectric, like rubber, which fills the strand valleys and not on one like paper which bridges tangentially across the valleys, as shown in K. S. Wyatt's wafers.[4]

Under "Viscosity" the authors find that the 50-cycle ionization starting stress is lower with viscous oil than with thin oil. This is not consistent either with our observations of electric strength or with theory as a higher ionization starting stress should be obtained with viscous oil due to the greater ion immobility imposed by the high viscosity. On the other hand, the authors employed rosin to thicken their oil, thereby radically adding to the polar content, and this fact no doubt explains their particular test results.

At impulse voltages the expected effect is observed, the viscous oil being superior to the thin oil, for with the short duration of the stress the large polar elements in the rosin do not respond because of their inertia.

The explanation of the lower ionization stress in air gaps at the electrode surface as compared with air gaps surrounded by paper, either insulating or semiconducting, probably lies in the comparatively low voltage of ion emission from metals. We are here concerned with the work function of the metal.

It is of interest to note that carbon black paper does not appreciably increase impulse strength. This is, of course, apart from its shielding effect on stranded conductors.

Figs. 26 and 27 are of interest in connection with high-pressure oil-filled cable, which has come into use in Europe for very-high-voltage cables, such as the 425-kv cables in Sweden. Fig. 26 shows a 50% increase in ionization inception voltage from atmospheric pressure to 200 psi, but Fig. 27 shows only 31% improvement in impulse strength.

The use of gap thickness down to 3 mils is shown to have little influence, a circumstance which led to the development of cables with paper less than 1 mil thick, by means of which the deficiency in impulse strength was more than overcome.[5,6]

Neither Appendix I nor Fig. 2 shows any means to measure the thickness of the dielectric after drying and impregnating. We find, in such devices, a reduction of about 9%, using a pressure of 1.67 psi (0.118 kilogram per square centimeter). It would be interesting to know how this was done.

My particular interest in this paper is its bearing on a question which is now being studied by the AIEE Committee on Insulated Conductors, namely, "Is there any constant stress at breakdown in a cylindrical dielectric?"

Among Europeans the mere asking of such a question is little short of heresy, it being assumed almost as a matter of doctrine that the answer to that question is: "Yes; the stress at the surface of the inner conductor, usually designated as the maximum stress, is a constant at breakdown for a given dielectric."

Due to this almost religiously held belief, there is a tendency in many European publications not to analyze test data very critically, especially if they tend superficially to confirm the maximum stress theory.

In the United States that state of mind does not exist, and designs are based on average stress, with reservations on minimum conductor sizes, as indicated by the uniform insulation thicknesses recommended in Association of Edison Illuminating Companies (AEIC) specifications, for practically all conductor sizes, both in relation to 60 cycles and impulse.

The use of sector designs with no suggestion to change the insulation thickness and the use of the same insulation thickness for round conductors in 3-conductor cables as in the much larger diameter hollow-core conductors are other cases in point.

P. H. Hoover's paper showing that the maximum stress near breakdown is not at the conductor surface may have assisted in leaving this question open.[7]

The authors must, therefore, recognize that in bringing their data to the United States, they are exposing themselves to considerable questioning; for, if cables should be designed on the basis of uniform maximum stress, to obtain equal safety factors, the AEIC specifications for oil-filled cables, and possibly other AEIC specifications, would have to be rewritten to conform with this theory. As it now stands, the specification for oil-filled cable says that the designs are based on the assumption that the impulse strength of the insulation is at least 1,300 volts per mil average stress.

My view is that maximum stress is not the sole criterion on which to base uniform safety factor of oil-filled cables but is one of three criteria, the others being the average stress and the minimum stress, a view which I owe, in large measure, to Louis Domenach. However, this is not necessarily final, and I await the result of studies being made by the Insulated Conductors Committee of the Institute.

Table II is a very impressive piece of evidence in favor of the maximum stress theory as applied to impulse strength of oil-filled cables, as the standard deviation of 3.64 inches is remarkably low, especially when compared with the standard deviation for average stress, which is about 20%. It is made clear in the paper that results such as these are obtained only on perfectly impregnated cable and presumably on perfect mechanical construction. I would like to know how the authors ascertained that these particular cables, selected, no doubt, from a great many made by the Pirelli Company, were accepted as perfect specimens.

Stress is laid on the difference between flexed and unflexed samples. The laboratory-made samples were unflexed. Were the factory-made cables also unflexed? If so, they were hardly "factory-made" as factory processes involve flexing. If flexed, why do they fall in line so neatly with the unflexed laboratory-made samples?

An argument against the maximum stress theory has been certain data which tended to show that cables with small conductors had a higher breakdown voltage than cables with large conductors, the insulation thicknesses being such as to give equal maximum stresses with a given applied voltage. Neither Table I nor Table II affords any light on this point.

Fifty-cycle breakdown stresses may depend so much on dielectric loss heating and the rate of rise of voltage, such as the 4-hour steps used in these tests, that it is unsafe to generalize very much on the data presented.

The following questions involving the comparison of data on flat capacitors with data on cables arose upon reading this paper.

1. All the flat capacitors are 1 mm (40 mils) thick. It is well known that the electric strength (volts per mil) of any sheet insulation is a function of the thickness up to a certain critical thickness above which it is uniform. This, we have found, is also true of the ionization inception voltage. Are the authors sure that the 1-mm thickness they use in their capacitor tests is above this critical thickness? If 1 mm is not above the critical thickness, comparison with cylindrical capacitors with thicker insulation may give results which are entirely fortuitous. Some preliminary tests we have made on flat samples without oil gaps throw on the adequacy of 1-mm samples.

2. Comparing the 50-cycle data on flat capacitors with the data on cables, the voltage inception of ionization of the former is compared with the actual breakdown of the latter. Is this a fair comparison? In preliminary tests we have made, the actual breakdown voltage (voltage rising 1 kv every 2 minutes), runs at least 10% higher than the ionization inception point. Should not the ionization inception have been measured for the cables in order to make the comparison significant?

3. The comparison of flat capacitors and the laboratory-made capacitors, as given in Fig. 32, may be invalidated by the fact that in the latter the ratio of maximum stress to average stress is 1.05, which is too close to distinguish between the two stresses.

In such a cylindrical capacitor, where the insulation is thin compared to the conductor size, the stress on the oil in the gap spaces is nearly uniform throughout the thickness of insulation and oil ionization occurs throughout the cable. These capacitors are similar, in this respect, to those used by Dr. J. B. Whitehead, in which high breakdown was obtained with paper of low density because its lower dielectric constant had the effect of throwing a low stress on the oil.[8] Where, however, the insulation is comparatively thick, as in an actual high-voltage cable, ionization may ionize and possibly impair the inner layers of oil, while the surrounding layers of un-ionized insulation will resist breakdown better, the higher the impermeability of the paper.

REFERENCES

1. The Variation at Constant Density of the Dielectric Breakdown of Paper with Air Resistance, **Paul Cloke, Krishna K. Khandelwal.** *AIEE Transactions*, vol. 71, pt. I, Nov. 1952, pp. 309–14.

2. **E. Jona.** *Transactions*, International Electrical Conference, St. Louis, Mo., vol. 2, 1904, pp. 550–70.

3. **Levi-Civita.** *Rendiconti*, Circolo Matematico di Palermo, Palermo, Italy, vol. 20–1, 1905, p. 172.

4. See reference 1 of discussion by **Kenneth S. Wyatt.**

5. **L. Domenach.** Paper *217*, CIGRE, Paris, France, 1954.

6. **J. Oudin, H. Thévenon.** *Revue Générale de l'Électricite*, Paris, France, vol. 62, 1953, p. 584.

7. The Mechanism of Breakdown of Dielectrics, **P. L. Hoover.** *AIEE Transactions*, vol. 45, June 1926, pp. 983–97.

8. The Dielectric Strength and Life of Impregnated-Paper Insulation—IV, **J. B. Whitehead, J. M. Kopper.** *AIEE Transactions*, vol. 64, Apr. 1945, pp. 171–77.

L. I. Komives (The Detroit Edison Company, Detroit, Mich.): This is one of the most interesting and valuable papers which we have had the opportunity to discuss for quite some time. The tests described attack the problem of what makes a high-voltage cable work at its very inception. It confirms a number of ideas which cable engineers considered to be true; it raises questions concerning some ideas which were considered valid; and it throws light in the directions toward which other similar tests may be conducted. I certainly hope that some of the problems opened up will be investigated by either the authors or others, including the role of surface effects which will also influence the bending of the cable, the influence of higher viscosity compounds with a flatter viscosity range, as well as others.

The following observations apply to particular parts of the paper:

1. The use of the 3-mil (0.08-mm)-thick tape was a fortunate choice. At least I feel that almost every manufacturer of good high-voltage cable has sufficiently well-developed machinery and processes to enable the manufacturer the use of paper of this thickness. Paper thickness less than 3 mils presents problems which have not been solved by many as yet. I agree with the authors' conclusion that thickness of tape has a decided influence on the behavior of the cable in service, its dielectric strength, a-c or impulse, etc.

2. We heartily agree with the conclusions drawn by the authors concerning impulse tests in general that the number of shots have no particular importance when evaluating impulse strength of the cable. This dogmatic statement may be made for plate capacitors without any and for typical cable insulation comprised of several layers with butt spaces with very few reservations. It is our experience that it probably has a considerable influence on the impulse strength of joints or terminals.

3. It was very interesting to note that the impermeability factor seems to have less importance from the standpoint of power-frequency dielectric strength than was thought before. If we use impermeability and density interchangeably, this has been confirmed to my satisfaction in tests reported in a 1942 paper.[1] The effect of the density of the paper on impulse strength is another matter and our interpretation of Fig. 5 puts more weight on density than the authors seem to feel it is entitled to. This is a very important consideration because it means that one cannot have both good results on a-c life tests and high impulse strength, at least not with insulating materials now available. In any compromise, it is more important to retain good characteristics under a-c potential than high impulse strength as the judicious application of lightning arresters or other protecting devices could control surge voltage.

4. With reference to the influence of the viscosity of the impregnating oil on the ionization starting stress, the results obtained by the authors were not as surprising to us as it seems to have been to them. We do know that ionization starting stress is greatly influenced by the viscosity of the compound and by pressure, the higher the pressure the less the influence. We do agree with the authors, however, that surface effects discussed in this part of the paper should receive more attention in cable research work than it has in the past. This will help not only in understanding dielectric phenomena connected with it, but also such mechanical phenomena as papers sliding on each other when the cable is bent, etc. It was interesting to note the authors' findings concerning the influence of viscosity on impulse strength. Perhaps this could be carried further and the effect of heating on a compound having a viscosity of 3,000 Saybolt universal seconds (SUS) (about 700 cst) at 100 C could be determined, which may show higher impulse strength at 85 C than the capacitors impregnated with a very low viscosity compound.

5. We were very interested in the findings concerning the influence of the shape of the electrode surface on ionization starting stress and on impulse strength. In the United States strand-shielding has been used for a longer time and in lower voltage cables than in Europe, and this has been a constant source of discussion between European and American cable engineers. We feel that the authors substantiated the American view that electrodes having corrugations result in lower ionization starting stress and impulse strength than electrodes with smooth surface. The 25–30% given under "Impulse Strength" confirms Detroit figures reported in 1941.[2] We are glad to see that at least some European cable engineers are coming around to our views on this matter.

It was interesting to see that a static pressure of 14 atm (200 psi) increased the ionization starting stress by as much as 80% with thin oils. We are wondering what this would be with much more viscous oils.

6. Perhaps the most interesting findings in the paper concern the influence of oil gap adjacent to a metal electrode, an electrode screened with carbon black paper and surrounded by insulating paper. Fig. 22, which by the way is not correctly described in the paper, confirms what could be best described as an instinctive feeling which this reviewer had for a long time. We have always felt that a carbon black paper strand-shielding results in a more favorable electrode surface than any other construction in a high-voltage cable because the carbon black paper is physically and mechanically closet to the insulating papers. We are sorry to see that an oil gap adjacent to an aluminized paper (favorite construction both in Europe and in the United States) has not been included in the tests tabulated in Fig. 22. We do not believe that it would have the same effect as a carbon black paper; it might have the effect (see Fig. 22-(B)) as the oil gap surrounded by insulating papers.

It is interesting to theorize on the effect of surface activity of the carbon black paper on the dielectric strength of the oil gap. We hope to see more on this subject; perhaps the American cable manufacturer who has been partial to this construction will also make the necessary additional tests.

7. We have followed the description of the effect of the paper sheet thickness on the butt space thickness in the stratified dielectric with much interest as this will have a great influence on the finished cable insulation. The cable engineer with sufficient experience who has had the opportunity to dissect cable samples subjected to impulse strength could, we think, predict the impulse strength of a given cable insulation by knowing the type of papers used and by dissecting a sample chosen at random. We believe that the lining up of butt spaces in the cable insulation has a decided influence on its impulse strength. In a well-made cable this phenomenon is under better control than in a cable produced on a lesser quality paper-taping machine.

8. We would like to point out that Tables I and II affirm the theory that maximum stress is a better measure of dielectric strength than the average stress.

REFERENCES

1. 120-Kv High-Pressure Gas-Filled Cable, **I. T. Faucett, L. I. Komives, H. W. Collins, R. W. Atkinson.** *AIEE Transactions*, vol. 61, Sept. 1942, pp. 658–65; disc. pp. 1021–38.

2. Impulse Strength as a Measure of Cable Quality, **L. I. Komives.** *AIEE Transactions*, vol. 60, Oct. 1941, pp. 929–34; disc. pp. 1339–44.

P. Gazzana Priaroggia and **G. Palandri:** The authors wish to thank first of all M. H. McGrath for the excellent presentation of their paper which so much contributed to its encouraging reception.

The authors also wish to thank all the distinguished American cable engineers and those of other countries who took part in the discussions and were so kind as to express such favorable comments on their research work.

These discussions have been of the greatest to the authors who will try herewith to reply in detail to all questions and remarks.

In reply to Mr. Hansson, the authors agree in general with his views. Mr. Hansson's proposal for co-operation between several laboratories in a research program on paper capacitors designed to serve as cable dielectric models is very interesting and deserves encouragement. Perhaps this proposal could be sponsored by a CIGRE Study Committee.

In reply to Mr. Klein's discussion and with respect to his point concerning the seeming inconsistencies between Fig. 5 and Fig. 16, the authors would refer to their replies to Mr. Meyerhoff and Mr. Atkinson. The points raised by Mr. Klein deserve careful consideration. Experiments with gaps adjacent to metal electrodes were only carried out with steel electrodes.

It is quite possible that the surface effect of carbon black paper in increasing the ionization starting stress is due to absorption of ions by the carbon black.

The sample thickness was very carefully checked by means of a micrometer gauge, a differential reading being made with and without the sample between the electrodes.

The parallelism of the electrode surfaces was automatically obtained by means of a centering device (not shown in the drawings) which guaranteed the alignment of the axes of the two electrodes.

The oil spaces between spacer disks and insulation were extremely small because spacers were made with very thin paper disks so that the thickness of the oil spaces could be negligible as compared to the thickness of the oil gaps being investigated. Moreover, the foregoing oil spaces are located in a region of the specimen in which the electric stress is definitely lower than in the central part of the sample having a diameter of 7 cm.

In reply to Mr. Wyatt, the matter of 50/50 overlay as compared to a 70/30 overlay was given only as an example of the application of experimental work on aligned gaps and was not intended to be a basis for practical cable taping. However, it is interesting to note that Mr. Wyatt considers "suicidal" not only a commercial cable having a 50/50 overlay, but also one having a 30/70 overlay because he says that he has demonstrated that such a cable forms creases in the butt-spaces when it is wound and unwound. The authors can assure Mr. Wyatt that, though inadvisable for several reasons, it is now possible to make commercial cables having a 50/50 overlay which shows no wrinkling whatsoever after numerous bends. This result became possible after the introduction of new theories of cable taping which enable the taping technique to be based on a true scientific foundation.

In reply to Mr. Meyerhoff's very valuable discussion, his remark that the curves of Fig. 16 and Fig. 20 if extrapolated to zero oil gap thickness give a breakdown value of 150 kv/mm instead of 132 kv/mm as shown in Fig. 5 is quite logical. However the difference is not at all due to lack of "reproducibility."

It has in fact been found that in the case of Fig. 16 the presence of an oil gap up to 0.08 mm, in a 1-mm-thick capacitor, does not seem to impair the impulse strength at all. For a gap thickness of 0.08 mm, about 50% of the time the breakdown paths are found outside the oil gap. This does not happen with gaps greater than 0.08 mm. The mechanism of the barrier phenomena certainly comes into play but its exact effect is not quite clear.

On the contrary, in the case of Fig. 20 it has been found that an oil gap up to 0.08 mm definitely impairs, even though only slightly, the impulse strength of the sample. It is also interesting to note that in this case (gap adjacent to one electrode and an oil gap thickness of 0.08 mm) 90% of the time the breakdown paths are in the gap.

In all these tests the reproducibility is excellent and the authors attach considerable theoretical significance to the difference between the curves of Fig. 16 and 20. Of course it must be understood that the type of paper greatly influences the relationships shown on all of the afore-mentioned curves, therefore reproducibility can be assured only if the physical properties of the paper employed remains constant. The quality *per se* of the paper, however, does not alter the general nature of the phenomena described.

Mr. Meyerhoff's remark on the seeming inconsistencies between Fig. 18 and Fig. 30 and between Fig. 14 and Fig. 26 is also very reasonable. However, in these cases the authors can again offer full assurance of good reproducibility. Whereas in the case of a single oil gap the stress in the oil, calculated according to an elementary electrostatic distribution, seems to be the determining factor for ionization inception; on the contrary, in the case of oil gaps in series the observed phenomena cannot be explained by simple electrostatic considerations. The authors again regret not to be able to offer a sound scientific explanation for this case but will try to offer an hypothesis.

If the dielectric losses in each gap due to the movement of charged particles were so high on approaching ionization inception as to alter appreciably the electrostatic stress distribution between oil and paper it could perhaps be understood why the apparent stress at ionization inception on the oil (based on elementary electrostatic considerations) is lower when several gaps in series are present.

This consideration of course might greatly affect the significance of the curves of Fig. 15 and Fig. 19 which are calculated from Fig. 14 and Fig. 18 according to simple electrostatic assumptions. The conclusion might be, also having in mind Mr. Atkinson's discussion, that both at impulse and 50 cycles the breakdown mechanism is very complicated and cannot be explained simply on the assumption of electrostatic distribution independent of barrier or other phenomena or conversely.

In reply to Mr. Atkinson, the authors in their account of the impulse tests did not actually attempt to propose an explanation of the results obtained on the basis of oil stresses alone. The only hint given by the authors for this point of view is in Fig. 17 and 21 which represent curves of the stress in the oil gaps calculated in correspondence with the breakdown voltages at impulse. The authors agreee on several points with Mr. Atkinson's interesting analysis of their impulse results. However, the deviations from his analysis are so many and important that in preparing a paper the authors did not feel inclined to state that the primary determinant of impulse strength is the performance of the impregnated tapes. Mr. Atkinson himself states that there are other factors which play a role which is by no means insignificant.

Even in the 50-cycle results there are facts which cannot be explained by considerations based only on the stresses in the oil. For this reason curves 15 and 19 were given but without proposing a definite theory based on oil stresses. In their reply to Mr. Meyerhoff the authors have discussed some discrepancies which arise when an analysis based on oil stresses only is considered.

Mr. Atkinson's calculations based on the assumption that each oil gap, regardless of its thickness, contributes 40% as much as one layer of paper, though showing good correlation with the various results, seem to us to be too empirical and we would be rather reluctant to accept them as they stand.

The authors do not share entirely the point of view that an oil gap ionizes on impulse at a potential well below the breakdown voltage of the sample. For instance, the impulse strength of the oil calculated in Fig. 21 for a gap thickness of 0.4 mm (namely 100 kv/mm) is identical to that which can be obtained directly on a gap of the same spacing between 10-mm-diameter spheres. Also, the results of Fig. 27 support, in the authors' opinion, the influence of the impulse ionization level of the oil on the breakdown voltage of the capacitor.

The authors have also speculated as to whether the lower ionization inception value found by using an oil of higher viscosity may have been due to imperfect impregnation caused by shrinkage, but have no evidence to support it. In any event many experiments seem to show that incomplete impregnation, if present, is not the major factor.

In this regard the authors would like to report an experiment which seems to ascribe greater importance to viscosity than to other factors in relation to ionization inception.

The authors have repeated the tests of Figs. 14 and 18, but using an oil of higher viscosity [5,000 cst at 20 C (22,700 S.U.S.)] instead of thin oil.

While the curve of Fig. 14 remained practically unaltered, the values of curve 18 were lowered considerably. In fact, curve 18 for the viscous oil started from 37 kv/mm for a 0.08-mm gap and decreased to 25 kv/mm for a gap of 0.4 mm. If incomplete impregnation were the only reason for the decrease of ionization inception values of Fig. 18 when a more viscous oil is employed, it would not explain why the curve of Fig. 14 remained substantially unaltered. These phenomena are not simple and require further investigation.

Mr. Del Mar's discussion was extremely valuable to the authors. In reply, the authors believe that Fig. 4 and Fig. 5 give adequate evidence of the effect of impermeability in increasing the dielectric strength, both at 50 cycles and at impulse, for papers of approximately equal specific gravity. As for specific gravity the authors did not conceal their opinion that specific gravity, if it could be isolated as a factor, would act in an opposite direction from impermeability in all cases.

The reference to Levi-Civita formulas was perhaps not clear enough in its meaning. A complete mathematical calculation of stresses taking into account the paper bridges across the strand valleys has been carried out in reference 5 which Mr. Del Mar seems to have neglected. However, if stresses in the paper only are considered, these calculations give results which do not differ materially from those obtainable with the Levi-Civita formulas applied to a uniform dielectric filling the strand valleys.

The authors' intention was to point out that on 50-cycle tests the stress in the paper is of secondary importance in capacitors with corrugated electrodes. Also, the stress in the oil in the strand valleys is of little importance. Instead the main factor is the thickness of the free oil between the paper and the corrugated electrodes. This thickness is comparatively larger the greater the diameter of the elementary strands.

The authors have found in many cases decreasing ionization inception stress with increasing oil viscosity also with pure mineral oil. This applies particularly to capacitors with oil gaps adjacent to an electrode. In this regard the authors would refer to their reply to Mr. Atkinson.

The authors appreciate that the foregoing findings are in conflict with current theories of 50-cycle breakdown.

The authors believe they have emphasized sufficiently in the paper the fact that they are dealing with fully impregnated paper dielectrics and therefore it is difficult to understand why Mr. Del Mar speaks of air gaps.

The thickness of the dielectric was measured by means of differential readings taken with a very accurate micrometer gauge always with the same pressure (0.3 kg/cm^2) applied to the upper electrode. A centering device to avoid decentering of electrodes was also employed.

Readings were taken: (1) before inserting the paper dielectric between the electrodes (of course before drying), (2) after drying and impregnating, (3) after breakdown, (4) finally after removal of the paper sample.

The authors can assure Mr. Del Mar that every step has been taken, or at least they think so, to avoid errors in the measurement of either mechanical or electrical quantities.

Mr. Del Mar has raised once more the question of "maximum" versus "average" stress. The authors believe that the matter will be clarified if the basic science aspect of the problem is considered separately from the engineering design aspect of the problem.

The problem from a basic science aspect would read: "Is there any constant stress at breakdown in a cylindrical dielectric?" The authors' answer is: "Yes, there is a constant stress at breakdown, namely the maximum stress, with no exceptions, for any inslulation thickness or conductor diameter under the following conditions: (1) If the dielectric is uniformly stratified paper fully impregnated with thin oil, screened both in side and outside with a perfectly uniform screen, i.e. stranding effects being absent. (2) If thermal instability effects are absent. (3) If by breakdown the inception of the insulation failure is meant, obtained by raising the voltage slowly."

The authors have no doubt about this and can supply much experimental data in addition to the data given in the paper.

The problem from an engineering design aspect would be: "Are oil-filled cables to be designed according to the criterion of maximum stress only?" The authors' answer is "No" and never have the authors stated otherwise. There are several reasons for this answer, including: (1) The attainment of an absolutely uniform dielectric wall is a much more difficult technological problem for large conductors than for small conductors. (2) The same consideration applies to 3-core cables as compared to single-core cables. Uniformity of the dielectric is undoubtedly more difficult to obtain in the case of 3-core cables. (3) Nonuniformity in the application of the outer screen on the dielectric and inaccurate workmanship in jointing are of much greater importance when the thickness of the dielectric is small compared to the conductor diameter than when the opposite is the case. It is here that a design criterion based on the "minimum stress" comes into play.

Therefore if a cable engineer is to design a cable to have a uniform safety factor, he will have to consider how the different technological factors come into play in relation to the perfection of his manufacturing facilities and jointing capabilities. Of course any improvement of cable technology and of jointing technique will be a step towards the adoption of a unique value of maximum stress as design criterion for all cables.

Mr. Del Mar wants to know how the authors determined whether the test cables were perfect enough for the purpose. The authors used two criteria: consistency of results and inspection of taping after breakdown. The authors can assure Mr. Del Mar that they did not have to make any special or careful selection of cable samples for the tests. The standard of manufacture, after the introduction of the new theories of taping in recent years, has so improved results that such selection proved unnecessary.

All tests on factory-made cables were made on bent cables. The consistency of results obtained on these cables and the laboratory-made unflexed samples demonstrates that the new taping criteria referred to has made it possible to manufacture cables which retain their original characteristics even after repeated flexing.

The breakdown stress at 50 cycles can of course be altered by dielectic loss heating. However, the authors can assure Mr. Del Mar that with a basic power factor of 0.0020, such as is now obtainable on oil-filled cables manufactured in Italy and other European countries, it is easy to verify that no important thermal effect can take place in high-voltage tests.

The authors have ample evidence to show that a 1-mm thickness is located in the uniform flat portion of the curve relating dielectric strength to thickness.

The authors also have at hand evidence on oil-filled insulation showing that the actual breakdown does not exceed by more than about 10% the ionization inception point. Once a specimen starts to ionize, it is only a matter of time before it breaks down.

The authors would be grateful to Mr. Del Mar if he could suggest a method of measuring the ionization inception level in a 220-kv oil-filled cable in which the ionization inception point would presumably occur at about 550 kv rms.

As far as the authors are aware the highest voltage, for which an ionization electronic detector is presently available, is 150 kv.

The comparison between flat and cylindrical capacitors was not made to verify the maximum stress theory but to demonstrate that the preparation technique was sufficiently good to give comparable and consistent results in both cases.

The contention that surrounding layers of unionized insulation are better able to resist breakdown the higher the impermeability of the paper, can hold only for very short time tests (rapid voltage rise) but not for tests based on 4-hour steps such as used by the authors.

In reply to Mr. Komives' very interesting discussion, his view that the number of shots probably has considerable influence on the impulse strength of joints or terminals is not entirely shared by the authors. In a large number of impulse tests made on oil-filled cable accessories the authors have found no evidence of "fatigue effects" being present on impulse in paper dielectrics of any type provided the latter are fully impregnated (i.e. include no air bubbles) with thin cable oil. When "fatigue effects" occur they are, in the authors' experience, always associated with the presence of free gas.

The authors would like to explain more clearly than perhaps was stated in the paper, that impermeability and specific gravity, while being inseparably associated, produce, in their opinion, directly opposite effects.

High impermeability, in the authors' findings, improves the "barrier" action and always results in higher strength both at 50 cycles and impulse. Theoretically, specific gravity alone should not affect the barrier action but should always result in a lower strength both at 50 cycles and impulse because of the higher dielectric constant involved and consequent higher stress on the oil.

However, in papers having both high impermeability and high density, the effect of permeability is predominant on impulse probably because on impulse the oil stress is not so important as at 50 cycles, as pointed out in Mr. Atkinson's discussion.

The authors would be interested in having the details of the experiments which have led Mr. Komives to the conclusion that an increase in the viscosity of the impregnating oil causes a decrease of the ionization inception level. These data should provide further independent substantiation of the authors' findings.

As for the influence of viscosity on impulse strength the authors have stated that for viscosities lower than approximately 10^3 to 10^2 cst (4,600 to 460 SUS) no practical decrease of impulse strength is observed. Therefore only if the compound mentioned by Mr. Komives has a viscosity higher than 10^3 cst (4,600 SUS) at 85 C will it show a higher impulse strength at this temperature than that shown for capacitors impregnated with rosin compound. If the compound is Oronite 32, the viscosity at 85C would be approximately 6,500 SUS and therefore the impulse strength would be sensibly higher.

The increase of ionization inception stress due to a static pressure of 14 atm (200 psi) is of the order of 40 to 45% at 20 C for a plate capacitor of the type of Fig. 11 made of unperforated sheets impregnated with a compound of thick mineral oil plus 30% rosin (viscosity 5.10^4 cst (23.10^4 SUS) at 20 C).

The same applies for a compound of mineral oil plus 32% polybutylene (viscosity 10^4 cst (4.10^4 SUS) at 20 C).

We can confirm Mr. Komives' feeling that a gap adjacent to an aluminized paper tape has theoretically the same effect as an oil gap surrounded by insulating paper. However, this is true only in theory because in practice a screen made with aluminized paper is likely to have butt-spaces with uncovered aluminium surfaces which will greatly reduce the advantage of this type of screen.

The authors would also like to comment on certain questions put to Mr. McGrath at the Fall General Meeting but which have not been submitted in writing.

The lengths of cable which were subjected to tests were not specially made but were taken from normal production. These lengths, prior to testing, were bent several times about a 6-foot-diameter drum.

The oil pressure used in making tests on factory lengths was only a little above atmospheric (of the order of 0.5 kg/cm²).

The procedure used in the impregnation of the plate capacitors was to bring the degassed oil into the container, while maintaining vacuum in the latter, and when the container was full, to the level of the top of the bushing, to break the vacuum with dry nitrogen.

Where the authors speak of tests carried out at atmospheric pressure they mean that no pressure was applied to the oil after the container was full except that corresponding to the oil head in the bushing (about 45 cm of oil).

The absorption of nitrogen by the oil of the container was certainly negligibly small in the very short time required for impulse or ionization testing. Tests made by keeping the container under oil pressure by means of a reservoir set at a pressure slightly above atmospheric gave practically the same results as those obtained with the container protected simply by an inert atmosphere.

The method of preparation of cylindrical capacitors is very similar to that of making a cable pothead or joint. Certainly it would be preferable if only one impregnation process were to be utilized. However, it is difficult to obtain satisfactory chamfering on unimpregnated paper tubes.

Furthermore the authors were able to ascertain by test that the 2-stage impregnation was excellent and as good as one carried out in a single stage.

With regard to the statement made concerning impulse tests in the section of the paper in "Dielectric Strength Tests" that in "these dielectrics" the number of applied shots is of no practical importance, the authors mean any type of paper dielectric fully impregnated with thin cable oil.

This applies to both capacitors and cables of any thickness of insulation whatsoever, the only requirement being that no free air or gas be present in the dielectric.

Single-Phase Induction Motor Noise Due to Dissymmetry Harmonics

D. F. MUSTER
NONMEMBER AIEE

G. L. WOLFERT
ASSOCIATE MEMBER AIEE

IN THE natural development of induction motor design, various theories have been proposed to account for the noise produced by the motors under various load conditions. The primary aim of the earlier theories is to explain the presence of certain discrete frequency components found in the noise spectra of particular motors.[1,2,3] More recently, an attempt has been made to extend the theory to include predetermination of noise levels.[4] Here additional frequency components are accounted for which can be attributed to mechanical and electromagnetic dissymmetries.

What is usually considered within the scope of these earlier theories will be defined herein as the "first-order motor-noise problem." This includes proper selection of such items as a rotor-stator slot combination, winding distribution, amount of skew, open or closed slots, etc., so that the noise level expected from a specific motor design will be as low as possible. It is assumed in these theories that the permeability of the rotor and stator iron is infinite (no saturation exists), the stator voltage and current are sinusoidal, and the air gap is uniform around the periphery of the motor. A motor designed in accordance with these theories should produce a minimum of magnetic noise with components at only 120 cycles per second (cps) and the frequencies of the basic slot permeance harmonics. If the response of the major motor parts is minimized at these frequencies, then there should be essentially no magnetic noise.

Since motors still produce noise—much of which cannot be accounted for by theory—there is a large area of the over-all problem still remaining which is the so-called "residual" problem. It is convenient to lump within its scope such items as the effect of dissymmetries (mechanical and electromagnetic), nonlinearities (e.g., caused by saturation), nonuniformities, and the inevitable clearances and tolerances incident to the mass production of motors. It is this area of the over-all problem which has been studied.

Before the results of this investigation are discussed, it is pertinent to make certain general statements concerning the origin and transmission of air-borne noise from fractional horsepower motors, or from any mechanical device. Any detectable noise must originate with a force which causes a part to vibrate. Then, either the vibrating part or another to which the motion is transmitted serves as a radiator. Thus, from origin to detection, any noise follows this sequence: force, vibrator, transmission path radiator. If the magnitude of the forces or the transfer of energy between any two points of this sequence is changed, there is a corresponding change in the noise produced.

In this paper, only a study of the forces which produce noise in single-phase induction motors is discussed, in particular, dissymmetry harmonic forces and the parameters which govern them. The remaining items in the sequence are considered secondary factors which, under circumstances favorable to them, can govern the noise-producing potential of a motor.

Nomenclature

P_m = number of poles in radial magnetic force wave
f_m = frequency of radial magnetic force wave
S_r = number of rotor slots
S_s = number of stator slots
a = positive integer determined by harmonic content of stator winding distribution
p, q = order of rotor and stator dissymmetry, respectively
b = positive integer determined by harmonic content of stator current
k, l = positive integers
P = pairs of stator poles in motor
f = line frequency
$\omega = 2\pi f$
s = slip $\left(=\frac{n_s-n}{n_s}\right)$
n_s = synchronous speed $(=f/P)$
n = actual speed $(=(1-s)n_s)$
$\mathcal{P}$ = permeance intensity
$\mathcal{P}_r^k$ = amplitude of kth harmonic of permeance variation caused by rotor slots
$\mathcal{P}_s^l$ = amplitude of lth harmonic of permeance variation caused by stator slots
$\overline{\mathcal{P}}_r^p$ = amplitude of pth harmonic of permeance variation caused by rotor dissymmetry

---

Paper 55-729, recommended by the AIEE Rotating Machinery Committee and approved by the AIEE Committee on Technical Operations for presentation at the AIEE Fall General Meeting, Chicago, Ill., October 3–7, 1955. Manuscript submitted June 23, 1955; made available for printing August 1, 1955.

D. F. MUSTER is with the General Electric Company, Schenectady, N. Y., and G. L. WOLFERT is with the General Electric Company, Fort Wayne, Ind.

Table I. Pole Structures and Frequencies of Force Waves for Various Rotor Slot Combinations

No. of Rotor Slots	Pole Structure (k = l = 1)	Synchronous Speed Force Frequencies, Cps
41	2,10,18	1,110,1,230,1,350
42	4,12,20	1,140,1,260,1,380
43	6,14,22	1,170,1,290,1,410
44	8,16,24	1,200,1,320,1,440

$\bar{\mathcal{P}}_s^q$ = amplitude of qth harmonic of permeance variation caused by stator dissymmetry
$\mathcal{P}_T$ = air-gap permeance intensity
α = angular space co-ordinate
i = current
$\mathfrak{F}$ = magnetomotive force
$\mathfrak{R}$ = reluctance
$\mathfrak{R}_T$ = total reluctance
$\mathfrak{R}_S$, $\mathfrak{R}_R$ = reluctance between the stator and rotor surfaces and the mid-surfaces, respectively
φ = flux density

Present Method of Selecting Slot Combinations for Minimum Noise

An important part of the first-order problem is the proper selection of a rotor-stator slot combination for minimum magnetic noise due to the basic slot permeance harmonic forces. After Kron,[1] the pole structures P_m (nodal pattern of force wave, i.e., a radial force wave with n nodes has n poles) and frequencies f_m

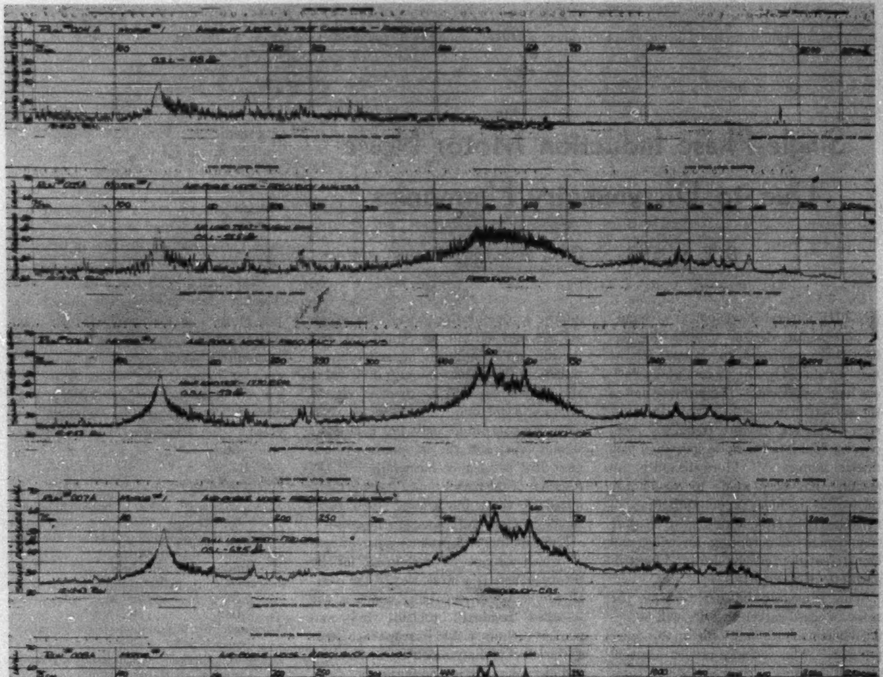

Fig. 1. Typical noise spectra of a type-I 1/2-horsepower motor

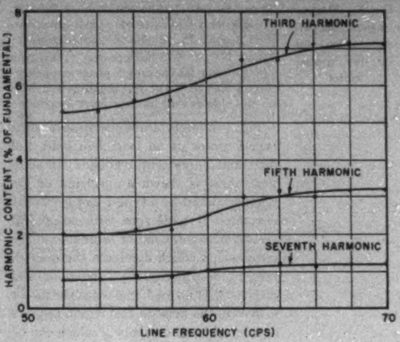

Fig. 2. Harmonic content of stator current at various line frequencies

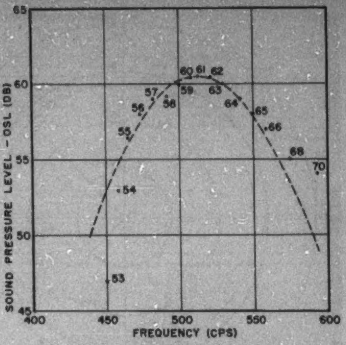

Fig. 3. Dissymmetry peak components for various line frequencies

which characterize these forces are given by

$$P_m = 2(kS_r - lS_s)\overset{+}{\underset{-}{o}}4aP \tag{1}$$

$$f_m = \frac{S_r f}{P}(1-s)\overset{+}{\underset{-}{o}}2bf \tag{2}$$

The symbol o indicates that the term which follows should be added, omitted, and subtracted to obtain all possible combinations, i.e., there are nine force waves characterized by P_m and f_m from equations 1 and 2 for fixed values of k, S_r, S_s etc.

In general, the first rotor resonance (a 2-node mode) and the 4-node circumferential mode of the stator shell are the major causes of noise in most small, single-phase induction motors. In a few motors, higher stator shell resonances (usually no higher than the 6- or 8-node mode) may be excited, or low-order line frequency harmonics from torque pulsations may appear at the motor mountings. As a general rule, slot combinations are chosen to give harmonic force waves with pole structures and frequencies which are different from these important resonances.

For fixed values of the parameters k, l, S_r, . . ., equations 1 and 2 represent a group of nine radial force waves produced by intermodulation of the harmonic components in the expressions which represent the space and time distribution of the air-gap permeance.

As an example, consider a 4-pole motor with the following characteristics: 36 stator slots, a 2-node rotor resonance at 600 cps, and a 4-node stator shell resonance at 1,400 cps.

Within the framework of the first-order theories, it is desired to determine from the noise viewpoint the optimum number of rotor slots. For these theories, no saturation, no stator current harmonics, and a sinusoidal winding distribution are assumed. This implies then that, in equation 1, $a = b = 1$. The pole structures and frequencies of the basic slot permeance harmonic forces for various numbers of rotor slots are given in Table I.

From Table I it can be seen that 41- and 42-slot rotors cause harmonic force waves with two and four poles respectively which are potential noise sources. In particular, the 4-pole force waves from the 42-slot rotor might well excite the 4-node resonance of the stator shell. The 43-slot rotor is a better choice, but the 44-slot rotor is probably best since the force waves it produces by interaction with the stator slots have pole structures which do not match the frequency or nodal pattern of the resonant modes of the stator shell. In practice, 36-slot stator, 4-pole motors are built with 40-, 44-, 48-, 52-, and 56-slot rotors for quiet operation.

Effect of Dissymmetries on Noise

If it can be assumed that the first-order noise problem has been solved satisfactorily, then, except for small components at the frequencies of the basic slot harmonic forces, there should be virtually no magnetic noise peaks in the noise spectrum of the motor. However, the assumptions upon which the solution of the first-order problem is based are violated in practice. Rotor castings are some-

Table II. Summary of Force Waves

Source	P_m,* Poles	F_m,* Cps
A. Basic rotor and stator slot harmonics	$2(kS_r-lS_s)\overset{+}{\underset{-}{o}}4aP$	$kS_r(1-s)\frac{f}{P}\overset{+}{\underset{-}{o}}2bf$
	$4(kS_r-lS_s)\overset{+}{\underset{-}{o}}4aP$	$2kS_r(1-s)\frac{f}{P}\overset{+}{\underset{-}{o}}2bf$
B. Intermodulation, basic slot and rotor dissymmetry harmonics	$2(kS_r-lS_s)(\pm)2p4\overset{+}{\underset{-}{o}}aP$	$[kS_r(\pm)p](1-s)\frac{f}{P}\overset{+}{\underset{-}{o}}2bf$
C. Intermodulation, basic slot and stator dissymmetry harmonics	$2(kS_r-lS_s)\overset{+}{\underset{-}{o}}2q\pm4aP$	$\left[kS_r(1-s)\frac{f}{P}\right]\overset{+}{\underset{-}{o}}2bf$
D. Intermodulation, basic slot, rotor, and stator dissymmetry harmonics	$2(kS_r-lS_s)\pm2q(\pm)2p\overset{+}{\underset{-}{o}}4aP$	$[kS_r(\pm)p](1-s)\frac{f}{P}\overset{+}{\underset{-}{o}}2bf$
E. Rotor dissymmetry harmonics	$2p\overset{+}{\underset{-}{o}}4aP$	$p(1-s)\frac{f}{P}\overset{+}{\underset{-}{o}}2bf$
F. Stator dissymmetry harmonics	$2q\overset{+}{\underset{-}{o}}4aP$	$\overset{+}{\underset{-}{o}}2bf$
G. Intermodulation, rotor and stator dissymmetry harmonics	$2p\pm2q\overset{+}{\underset{-}{o}}4aP$	$p(1-s)\frac{f}{P}\overset{+}{\underset{-}{o}}2bf$

* $(a, b) = (1, 2, 3, \ldots)$; a and b assume positive integral values determined by the respective harmonic content of the expressions for the space distribution ν of the pole winding and the time-dependent function of the stator current i. For example, if $i = I_1 \cos \omega t + I_3 \cos 3\omega t + I_5 \cos 5\omega t$, then $b = 1, 2, 3, 4$, and 5.

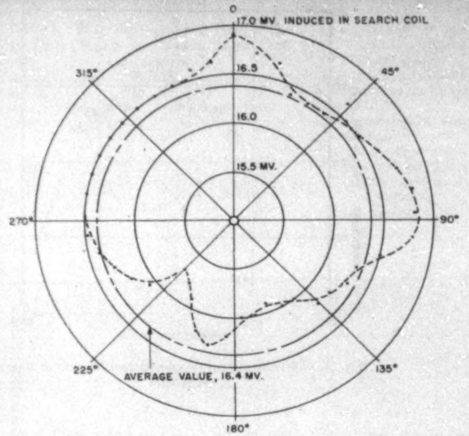

Fig. 4. Electromagnetic dissymmetry of the rotor for the special motor

times porous, the rotor periphery may be eccentric with respect to the journals, the stator bore may be noncircular or offset with respect to the motor bearings, etc. The presence of any or all of these dissymmetries is reflected in the noise spectrum of the motor.

In general, it is felt that the restrictive assumptions of the first-order theories are frequently misleading in that a major portion of the noise produced by induction motors can be traced to their violation. For this reason then, the assumptions are dropped which imply that mechanical parts are concentric and uniform and that electrical and magnetic characteristics can be described as being sinusoidal, uniform, and unsaturated. The permeance approach used by Kron[1] is extended to include the effects of various forms of electrical and mechanical dissymmetries upon radial force waves in the air gap of a single-phase induction motor. (The discussion specifically excludes the interaction which produces force waves with time-varying amplitude which are the cause of slip noise, the low-frequency pulsing noise frequently associated with induction motors.)

The details of this analysis are given in Appendix I, with a summary of the more important noise sources (i.e., those forces which have a small number of poles) which are produced by intermodulation. These are all included in the following expressions

$$P_m = (\mathring{\pm})2(kS_r - lS_s)\mathring{\pm}2q(\mathring{\pm})2p\mathring{\pm}4aP \qquad (3)$$

$$f_m = (\mathring{\pm})\frac{S_r f}{P}(1-s)(\mathring{\pm})\frac{pf}{P}(1-s)\mathring{\pm}2bf \qquad (4)$$

The symbol ($\mathring{\pm}$) indicates that this term must be used with the same sign in the pole structure expression as in the frequency expression, i.e., $+k$, in the pole structure term is associated with the $+k$ term in frequency expression. Equations 3 and 4 characterize (for fixed values of k, and l, . . .) radial force waves with 81 pole structures at 27 frequency values. It is possible that waves of the same pole structure and frequency values will result which will reduce the total number of different waves. For a more detailed explanation of p and q, a and b, see Appendix II. For a more complete expansion of equations 3 and 4, see Table II.

An examination of the terms in equation 3 discloses that a stator dissymmetry can add a new pole structure at an existing force frequency, but can add no new force frequency. A rotor dissymmetry, on the other hand, will add additional force frequencies as well as new pole structures.

Rotor and stator slot permeance harmonics cause force frequencies no closer than 120 cps apart, but rotor dissymmetry harmonics add new force frequencies which at synchronous speed are 60 cps apart in a 2-pole motor, 30 cps apart in a 4-pole motor, 20 cps apart in a 6-pole motor, etc.

Application of the Theory of Dissymmetry Harmonic Force Waves

The tests described in this paper were conducted on two types of single-phase induction motors with the following general characteristics:

Type I: A 1/2-horsepower, 1,725-rpm 115/230-volt 60-cps single-phase capacitor-start 4-pole, 36- to 44-slot combination.

Type II: 1 1/2-horsepower, 1,650-rpm 115/230-volt 60-cps single-phase capacitor-start 4-pole 36- to 44-slot combination with no end shields and having sleeve bearings.

Fig. 1 shows typical noise spectra for a type-I motor at no load, half load, full load, and 30-per-cent overload. In addition, there is shown a spectrum of the noise produced by a type-I motor when it is rotated at 1,725 rpm, with no applied voltage across the motor terminals. The components which dominate the over-all noise of these motors are between 350 and 800 cps. At no load, and when the motor is driven, the noise in this region appears as a broad-band component which can be attributed to the flow of cooling air in the motor. As load is applied to the motor, discrete peaks appear in this frequency range at frequencies of 480 and 600 cycles and at about 510 cps.

The dominant series of peaks between 480 and 600 cps, which can be seen in the spectra of Fig. 1, are caused by an interaction between the broad-band cooling-air noise and the motion of the rotor as it vibrates in its first bending mode. The dynamic natural frequency of the rotor in its first bending mode occurs at about 515 cps. (A distinction is made between the two natural frequencies of a rotor-bearing assembly, one measured when the rotor is at rest and a second measured when the rotor is turning at a given speed. The first is called a "static," the second, a "dynamic" natural frequency of the rotor.) Since only the forces which excite the rotor resonance are of concern here the mechanism by which the interaction is accomplished will not be discussed.

In a series of tests the line frequency of the voltage applied to the motor was varied from 50 to 70 cps. The observed stator current contains strong third and fifth harmonics of the line frequency. The configuration of the rotor and stator are such that their profiles are not circular nor does the geometric center of the stator bore and of the periphery of the rotor coincide with the center rotation of the bearings. At line frequency of 60 cps an harmonic analysis of the stator current shows a third harmonic of 6.3 per cent of the fundamental stator current and a fifth harmonic of 2.5 per cent. The analysis for other line frequencies are shown in Fig. 2. Profiles of the stator bores disclose that in all cases the stators are free from any first-order dissymmetry. With respect to their own bearings, the rotors exhibit a strong first-order dissymmetry (eccentricity) and much smaller higher order dissymmetries.

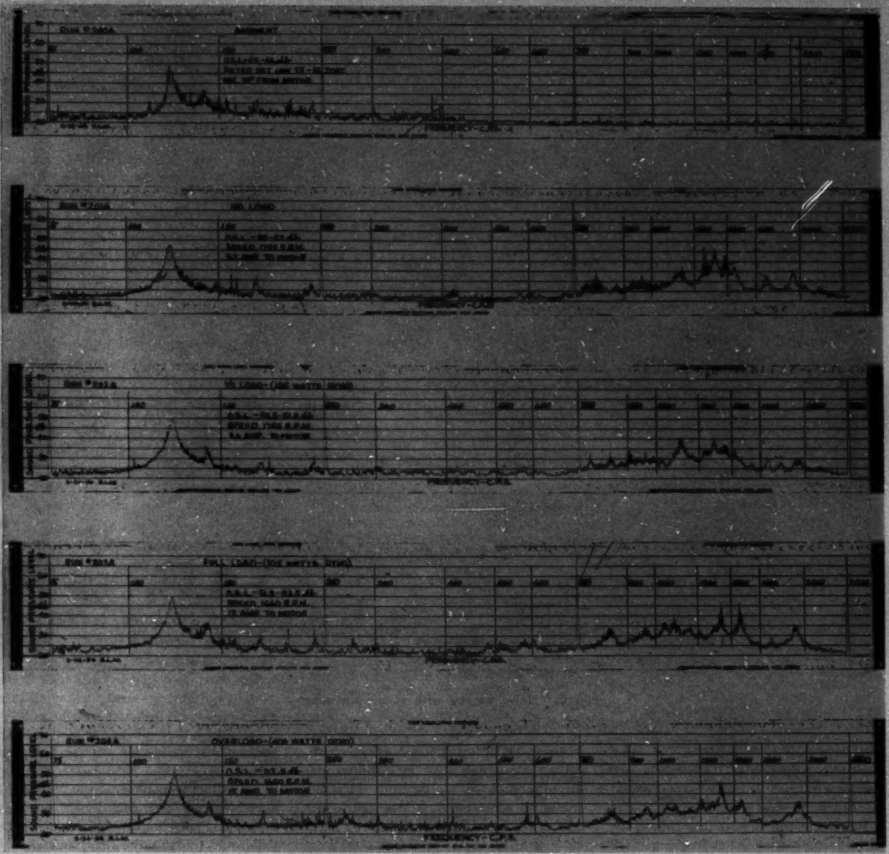

Fig. 5. Noise spectra with no stator dissymmetry

EXAMPLE OF 2-POLE FORCE WAVE

If the theory developed in Appendix I is applied, which takes into account both rotor and stator dissymmetries and stator current harmonics, it is found that for this particular type of motor there is a 2-pole dissymmetry force at $[8f+30(1-s)]$ cps; see item *E*, Table II.

The peak noise component at about 510 cps, shown in Fig. 1, is caused by an interaction between the rotor at or near its dynamic resonance and the flow of cooling air. It could be expected that, if the rotor is driven at a frequency off its resonance and the stator current harmonics are constant, the peak values observed in the noise spectra will follow the dashed line in Fig. 3. This line represents the amplitudes at and near this resonance of the rotor if the Q of the system were equal to eight. The actual peaks for the various line frequencies occur at the points shown in Fig. 3; this indicates that the exciting forces are not constant over the entire range of frequencies.

If it is assumed that the stator current contains third and fifth harmonics, then it has been shown that the magnitude of the dissymmetry forces is proportional to the square of the expression for the stator current. This gives rise to force waves of various frequencies; in particular, at the frequency which is of interest, to a force wave with magnitude governed by the product of the separate magnitudes of the third and fifth harmonics of the stator current.

Let the stator current be given by

$$i = I_1 \cos \omega t + I_3 \cos 3\omega t + I_5 \cos 5\omega t \qquad (5)$$

then the magnitude of the frequency term of interest is proportional to the product I_3I_5; see equation 14, et seq. From Fig. 2 it can be seen that at

54 cps, $I_3I_5 \sim 2\times5.25 = 10.5$
60 cps, $\sim 2.5\times6.2 = 15.5$
70 cps, $\sim 3.2\times7.1 = 22.7$

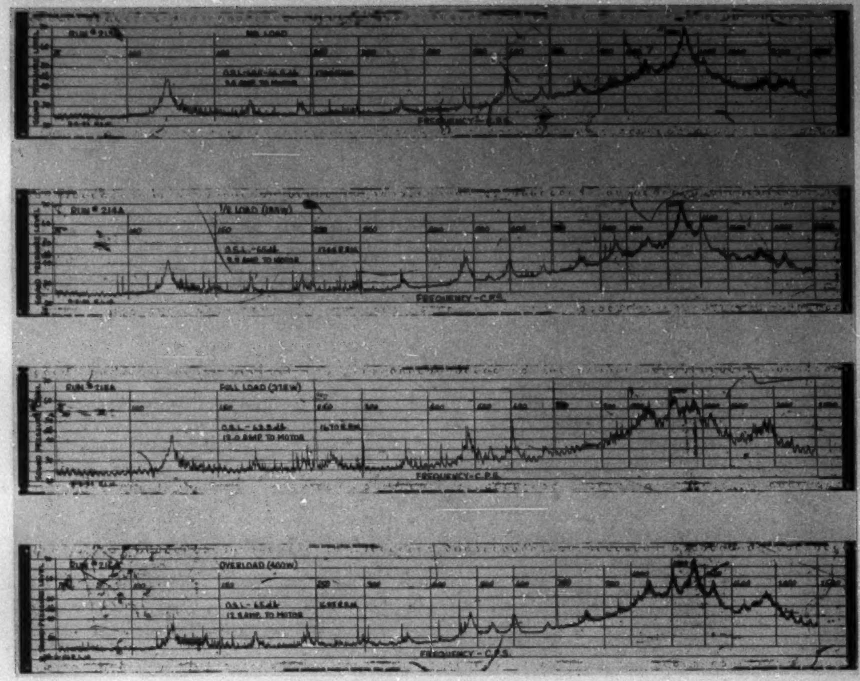

Fig. 6. Noise spectra with stator dissymmetry

The force ratio 10.5/15.5=0.677 is equivalent to a reduction of 3.4 decibels, and the force ratio 22.7/15.5=1.462 is equivalent to an increase of 3.3 decibels.

It is interesting to note then that, if the plotted values at these line frequencies are changed accordingly, the new points fall near or on the symmetrical curve, indicating that there is a direct relationship between the force and the response and, more important, that the magnitude of the low-order harmonics is reflected directly in the magnitude of the force waves which result. Thus, in the type-I motors, as the percentage of third and fifth harmonic in the stator current increases, the noise which results increases correspondingly. In this particular case, a 2-node bending mode of the rotor is excited by the 2-pole radial force wave at the same frequency, resulting in a corresponding single-frequency peak in the motor noise.

Example of 4-Pole Force Wave

The type-II motor is constructed carefully so that the rotor and stator possess virtually no inherent, low-order mechanical dissymmetries. At the optimum relative position of stator and rotor the combined eccentricity is less than 6 per cent of the mean air-gap distance. (Mean air gap distance is defined as the radial distance between the center of rotation of the rotor-bearing center and the geometric center of the stator bore.) A strong first-order stator dissymmetry (eccentricity) equivalent to 67 per cent of the mean air-gap distance can be achieved by displacing the center of rotation of the rotor with respect to the geometric center of the stator bore.

In addition, the rotor for the type-II motor has inherent electromagnetic dissymmetries which are not apparent from its outward appearance. The combined maximum variation in the rotor profile and runout is less than 1.5 per cent of the mean air gap. Nevertheless, there is a maximum variation of 8 per cent in the voltage induced in a search coil as the rotor rotates past it. This effect can be caused by air holes in the aluminum rotor bars or by variations in the bridging depth.

An harmonic analysis of the plot of induced voltage as a function of position shown in Fig. 4 indicates first-, second,-third- and fourth-order dissymmetries of 1.8, 0.6, 0.2, and 1.0 per cent respectively with negligible higher order harmonic variations. Thus, in the type-II motor there are appreciable inherent first- and fourth-order rotor dissymmetries which can cause a first-order stator dissymmetry.

The noise spectra of the motor operated under various load conditions is shown in Fig. 5 for essentially no stator dissymmetry (less than 6 per cent of the mean air gap), and in Fig. 6 for a strong first-order stator dissymmetry (an eccentricity equivalent to 67 per cent of the mean air gap). Two features of these spectra are particularly significant: the lack of components in the range from 480 to 600 cps and the components of large magnitude near 1,200 cps which are associated with large values of eccentricity.

Effects at Rotor Resonance

The dynamic natural frequency of the rotor-bearing assembly in the type-II motor is about 900 cps. As a consequence, the dissymmetry forces at $[8f+30(1-s)]$ which are present in this motor just as they are in the type-I motor cannot excite the first bending mode of the rotor and, correspondingly, there are no single-frequency components in the region from 480 to 600 cps. In both Figs. 5 and 6 the components at other frequencies dominate the over-all noise of the motor, although measurable peaks appear in the spectra of Fig. 6.

Effects at Stator Resonance

It is more interesting to observe the behavior of the dominant peaks at about 1,170, 1,290, and 1,410 cps, particularly, at no-load and full-load conditions. For a 36- to 44-slot combination, the magnetic forces caused by permeance harmonics occur at 1,200, 1,320, and 1,440 cps (no load) with pole structures of 8, 16, and 24 poles, Table I, but the presence of a first-order rotor dissymmetry produces new 6-14-, and 22-pole forces at 1,170, 1,290, and 1,410 cps in this motor. The 4-node (elliptical) stator shell resonance occurs at 1,180 cps and cannot be excited by the permeance harmonics because of the mismatch between their nodal patterns and that of the stator shell resonance. In practice this is difficult to realize completely since high-order harmonics from other sources can produce by intermodulation low-magnitude four-pole forces near the frequency of the stator shell resonance.

In terms of the parameters of equations 3 and 4, the special motor is characterized by: $S_r=44$, $S_s=36$, $p=1$, $q=0$, (for 6-per-cent eccentricity), $q=1$ (for 67-per-cent eccentricity), $a=1$, $b=1$, $P=2$, $f=60$, $s=0$ (for no load), and $s=0.083$ (for full load). The indices k and l can assume any positive integral value, but assume that $k=l=1$, i.e., consider only the basic slot harmonics. If these values are applied to equations 3 and 4, the pole structures and frequencies given in Tables III and IV are obtained.

It can be seen that none of the force waves given in Table III have a nodal pattern which matches that of the 4-node stator shell resonance, although the frequencies of all of them occur near 1,180 cps. In the spectra of Fig. 5 no significant components are seen in the range from 1,000 to 1,500 cps.

At maximum eccentricity new force waves are produced by intermodulation as shown in Table IV. Among these waves there is the triplet characterized by:

$P_m=4$, $f_m=1{,}170$, 1,290, and 1,410 cps at no load

$P_m=4$, $f_m=1{,}062$, 1,183, and 1,303 cps at full load

Correspondingly it can be seen that the spectra of Fig. 6 include significant components at these frequencies. Thus, in both cases, the theory accounts for the principal noise spectrum characteristics.

It can be concluded then that the presence of electrical, electromagnetic, and mechanical dissymmetries (separately or in combination) produces a new set of magnetic force waves in addition to those predicted by Kron.[1] If these waves are of appropriate nodal pattern and frequency, they will excite resonances of either the rotor or stator.

Appendix I. A Method of Analysis for Determining Radial Force Frequencies in Single-Phase Induction Motors

The method of analysis outlined herein yields the characteristics of radial force waves produced by intermodulation between air-gap permeance variations caused by rotor and stator slots, and rotor and stator dissymmetries, winding distribution harmonics, and stator current harmonics.

Let $\mathcal{P}_0$ denote the average permeance intensity between the surfaces of stator or rotor and a cylindrical surface midway between them. With reference to the stator, the permeance intensity $\mathcal{P}_R$ between the rotor and mid-surfaces is given by

$$\mathcal{P}_R=\mathcal{P}_0+\sum_{k=1}^{\infty}\mathcal{P}_r{}^k\cos kS_r(\alpha-2\pi nt)+\sum_{p=1}^{\infty}\overline{\mathcal{P}}_r{}^p\cos p(\alpha-2\pi nt) \tag{6}$$

Similarly, the permeance intensity $\mathcal{P}_S$ between the stator and mid-surfaces is given by

$$\mathcal{P}_S=\mathcal{P}_0+\sum_{l=1}^{\infty}\mathcal{P}_s{}^l\cos lS_s\alpha+\sum_{q=1}^{\infty}\overline{\mathcal{P}}_s{}^q\cos q\alpha \tag{7}$$

Permeance is the reciprocal of reluctance $\mathcal{R}$ and

$$\mathcal{R}_T=\mathcal{R}_S+\mathcal{R}_R \tag{8}$$

Table III. Important Magnetic Force Waves in Special Motor for Minimum Eccentricity (q=0)

Loads	P_m, Poles	F_m, Cps
No load	6, 14, 22	1,170, 1,290, 1,410
	8, 16, 24	1,200, 1,320, 1,440
	10, 18, 26	1,230, 1,350, 1,470
Full load	6, 14, 22	1,063, 1,183, 1,303
	8, 16, 24	1,090, 1,210, 1,330
	10, 18, 26	1,117, 1,237, 1,357

Equation 8 yields

$$\mathcal{P}_T=\frac{\mathcal{P}_S\mathcal{P}_R}{\mathcal{P}_S+\mathcal{P}_R} \tag{9}$$

From equations 6 and 7 in equation 9

$$\mathcal{P}_T=\frac{1}{\mathcal{P}_S+\mathcal{P}_R}\Big[\mathcal{P}_0{}^2+\mathcal{P}_0\sum_k\mathcal{P}_r{}^k\cos kS_r(\alpha-2\pi nt)+\mathcal{P}_0\sum_l\mathcal{P}_s{}^l\cos lS_s\alpha+\mathcal{P}_0\sum_p\overline{\mathcal{P}}_r{}^p\cos p(\alpha-2\pi nt)+\mathcal{P}_0\sum_q\overline{\mathcal{P}}_s{}^q\cos q\alpha+\sum_k\sum_l\mathcal{P}_r{}^k\mathcal{P}_s{}^l\times\cos kS_r(\alpha-2\pi nt)\cos lS_s\alpha+\sum_l\sum_p\mathcal{P}_s{}^l\overline{\mathcal{P}}_r{}^p\cos lS_s\alpha\cos p(\alpha-2\pi nt)+\sum_k\sum_q\mathcal{P}_r{}^k\overline{\mathcal{P}}_s{}^q\cos kS_r(\alpha-2\pi nt)\cos q\alpha+\sum_p\sum_q\overline{\mathcal{P}}_r{}^p\overline{\mathcal{P}}_s{}^q\times\cos p(\alpha-2\pi nt)\cos q\alpha\Big] \tag{10}$$

which can be reduced to

$$\mathcal{P}_T=\mathcal{P}_a\Big\{\mathcal{P}_0+\sum_k\mathcal{P}_r{}^k\cos kS_r(\alpha-2\pi nt)+\sum_l\mathcal{P}_s{}^l\cos lS_s\alpha+\sum_p\overline{\mathcal{P}}_r{}^p\cos p(\alpha-2\pi nt)+\sum_q\overline{\mathcal{P}}_s{}^q\cos q\alpha+\sum_k\sum_l\frac{\mathcal{P}_r{}^k\mathcal{P}_s{}^l}{2\mathcal{P}_0}\{\cos[(kS_r+lS_s)\alpha-2\pi kS_rnt]+\cos[(kS_r-lS_s)\alpha-2\pi kS_rnt]\}+\sum_l\sum_p\frac{\mathcal{P}_s{}^l\overline{\mathcal{P}}_r{}^p}{2\mathcal{P}_0}\times\{\cos[(p+lS_s)\alpha-2\pi pnt]+\cos[(p-lS_s)\alpha-2\pi pnt]\}+\sum_k\sum_q\frac{\mathcal{P}_r{}^k\overline{\mathcal{P}}_s{}^q}{2\mathcal{P}_0}\{\cos[(kS_r+q)\alpha-$$

Table IV. Important Magnetic Force Waves in Special Motor for Maximum Eccentricity (q=1)

Loads	P_m, Poles	F_m, Cps
No load	4, 6, 8, 12, 14, 16, 20, 22, 24	1,170, 1,290, 1,410
	6, 8, 10, 14, 16, 18, 22, 24, 26	1,200, 1,320, 1,440
	8, 10, 12, 16, 18, 20, 24, 26, 28	1,230, 1,350, 1,470
Full load	4, 6, 8, 12, 14, 16, 20, 22, 24	1,063, 1,183, 1,303
	6, 8, 10, 14, 16, 18, 22, 24, 26	1,090, 1,210, 1,330
	8, 10, 12, 16, 18, 20, 24, 26, 28	1,117, 1,237, 1,357

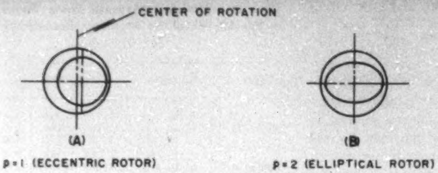

Fig. 7. Low-order rotor dissymmetry

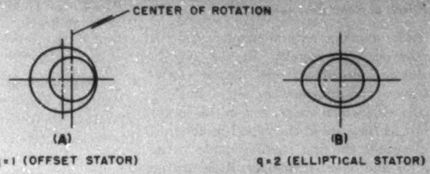

Fig. 8. Low-order stator dissymmetry

$$2\pi kS_rnt]+\cos[(kS_r-q)\alpha-2\pi kS_rnt]\}+\sum_p\sum_q\frac{\bar{\mathcal{P}}_r{}^p\bar{\mathcal{P}}_s{}^q}{2\mathcal{P}_0}\times\Big\{\cos[(p+q)\alpha-2\pi pnt]+\cos[(p-q)\alpha-2\pi pnt]\}\Big\} \quad (11)$$

where

$$\mathcal{P}_a=\frac{\mathcal{P}_0}{\mathcal{P}_S+\mathcal{P}_R}$$

The stator winding distribution ν (referred to the same α co-ordinate base) is characterized by the expression

$$\nu=\sum_{u=1,3,5\ldots}^{\infty}\nu_u\cos uP\alpha \quad (12)$$

Further, the stator current, as a function of time, can be given in the form

$$i=\sum_{v=1,3,5\ldots}^{\infty}I_v\cos v\omega t \quad (13)$$

By equations 12 and 13, the magnetomotive force $\mathfrak{F}(=i\nu)$ becomes

$$\mathfrak{F}=\sum_u\sum_v\frac{\nu_uI_v}{2}[\cos(uP\alpha+v\omega t)+\cos(uP\alpha-v\omega t)] \quad (14)$$

The flux density φ is given by

$$\varphi=\mathcal{P}_T\mathfrak{F} \quad (15)$$

The expression for the radial force in the air gap as a function of space and time is obtained by using equations 11 and 14 in equation 15 and squaring. The result of this computation is summarized in Table II for all potential noise-producing force waves in the air gap of single-phase induction motors.

Appendix II. Significance of p and q

Let p denote the order of dissymmetry which causes a variation in the maximum value of flux with respect to the rotor. This variation revolves with the rotor or at some multiple of the rotor speed and can be caused only by a mechanical or electrical dissymmetry of the rotor. Rotor dissymmetries of first and second orders are shown in Fig. 7.

The letter q denotes a dissymmetry which causes a change in the maximum value of flux with respect to the stator. This variation does not revolve with the rotor but is stationary in space, and is thus considered a stator dissymmetry. Stator dissymmetries of first and second orders are shown in Fig. 8.

References

1. Induction Motor Slot Combinations, G. Kron. *AIEE Transactions*, vol. 50, June 1931, pp. 757–68.

2. Harmonic Theory of Noise in Induction Motors, Wayne J. Morrill. *AIEE Transactions (Electrical Engineering)*, vol. 59, Aug. 1940, pp. 474–80.

3. Cause and Elimination of Noise in Small Motors, W. R. Appleman. *Ibid.*, vol. 56, Nov. 1937, pp. 1359–67.

4. Predetermination of the Sound Pressure Levels of Magnetic Noise of Polyphase Induction Motors, E. Erdelyi. *Doctoral Dissertation*, University Microfilms, Ann Arbor, Mich., 1955.

5. The Nature of Polyphase Induction Machines, P. L. Alger. John Wiley and Sons, Inc., New York, N. Y., 1951, chap. 9.

◆

Discussion

Edward Erdelyi (Syracuse University, Syracuse, N. Y.): The paper is a very interesting and timely analysis, as the answer to the noise question of single-phase induction is becoming very urgent. In the not too distant past, single-phase motors of the type described by the authors have been used in large appliances such as washing machines and refrigerators. The motors in these were mounted in the lower part of the apparatus and shielded by constructional components. Furthermore, the compressors, pumps, and other equipment associated with these apparatus have masked the noise of the driving motor. This is not so in present-time room-type air conditioners. A considerable amount of engineering work was expended to design lower noise level components and the noise of the motor is not masked any more. The noise reduction caused by dissymmetries becomes important.

In most publications, the question of dissymmetries have been noted and methods suggested as to how to find the forcewaves caused by these. The detailed analytical work has not been previously carried out with the thoroughness of this paper. It will be, therefore, a welcome addition to reference sources.

The analysis may also become useful in the quality control of mass production methods. Tools wear out and this introduces dissymmetries in the product which, as shown, create additional magnetic noise. Careful analysis of the frequency spectrum of sample motors may indicate which of the tools should be replaced to improve the quality of the product.

J. L. Oldenkamp (General Electric Company, Fort Wayne, Ind.): The authors have provided a valuable tool for reducing motor noise by considering the dissymetries which exist as well as the air-gap permeance. This paper represents a major contribution to the art of the design of single-phase motors. An appreciable noise reduction in several motor lines has been effected by using the criteria given in this paper.

P. L. Alger (General Electric Company, Schenectady, N. Y.): This paper constitutes a marked advance in the theory of magnetic noise of rotating machines. In a transformer, the magnetic noise is chiefly due to magnetostriction, and its calculation is therefore, a highly empirical matter. In an induction motor, the magnetic noise is nearly all due to radial forces acting across the air gap, and, therefore, it should be readily calculable, as demonstrated by Dr. Erdelyi. However, as the authors of this paper show, the noise actually produced is largely due to resonant frequency vibrations of the motor core and/or the shaft. Hence, as in all resonant frequency phenomena, the importance of very small forces at the critical frequencies is greatly magnified, and the actual magnitude of the noise is largely dependent on the damping, or Q factor, of the motor structure.

Now that the authors have so well and thoroughly explained the nature and effects of the numerous air-gap dissymmetries in small motors, the next step will be to develop a quantitative theory, calibrated by test data. I look forward to rapid progress in this field in the near future. It seems reasonable to expect that further work will enable the over-all magnetic noise levels of these small motors to be predicted and controlled with much greater accuracy than seemed possible only a short time ago.

Reference

1. Predetermination of Sound Pressure Levels of Magnetic Noise of Polyphase Induction Motors, E. Erdelyi. *AIEE Transactions*, vol. 74, pt. III, 1955.

Double-Energy Conversion in an Air Gap—A Novel Asynchronous Frequency Changer

W. LA PIERRE
MEMBER AIEE

J. Y. LOUIS
STUDENT MEMBER AIEE

IN VIEW of the growing demand for power in modest amounts in the 400- to 900-cycle range, it seems timely to report the results of a study recently completed on a novel type of induction frequency changer. This machine, in which two energy conversions occur simultaneously in the air gap, is of interest in a number of ways. It encourages a review of the method of energy conversion by induction from the polyphase rotating field, and it raises unanswered questions concerning magnetization and core losses. In the machine studied, a 4-pole stator winding was used to drive the rotor at the usual speed of 1,750 to 1,790 rpm, depending on the load. A 6-pole winding on the same stator, when excited by capacitors, generated a polyphase voltage of higher frequency in the range of 85 to 90 cycles, also depending on the load. Two rotating fields were thus set up in the air gap; a 4-pole 60-cycle field revolving at 1,800 rpm and a 6-pole field revolving somewhat slower than the rotor. The analysis proceeds in the usual way starting from the 60-cycle terminals and the customary single-frequency equivalent circuit can be used. The 6-pole winding, operating at negative slip, has an output frequency that yields the power flow out of the rotor which is required by the load. The study was addressed to two questions: first, can the machine be analyzed by the usual method and, second, what modifications occur in the magnetizing current and the stator core loss as a consequence of the joint use of the iron by two rotating fields?

The machine used in the study is a 4-speed 110-volt 5-horsepower 60-cycle machine in which the two stator windings occupy the same slots. The windings have half-pitch coils and the phase groups are reconnectable to form consequent 8- and 12-pole arrangements. The stator has 72 slots. This was originally an experimental machine which was used in the development of the large multispeed motors employed for ship propulsion 35 years ago. It has ample iron. Frequently changer operation has been studied by various students in the laboratory over a period of 5 years.

Nomenclature

r_1 = primary resistance per phase to neutral of motor winding
x_1 = primary leakage reactance per phase to neutral of motor winding
v = primary impressed voltage per phase to neutral of motor winding
r_2 = rotor resistance per phase to neutral, referred to the motor primary winding
x_2 = rotor leakage reactance per phase to neutral, referred to the motor primary winding
g = primary exciting conductance per phase, representing the core loss current of the motor winding, mhos
b = primary exciting susceptance per phase, representing the magnetizing current of the motor winding, mhos
s = slip of the rotor with respect to the motor synchronous speed
r = equivalent power-conversion resistance of the motor, ohms
p = power converted by the motor, watts per phase
$Fr+W$ = friction and windage loss, watts per phase
P = power input via the rotor of the generator, watts per phase
$-R$ = equivalent power-converting resistance of the generator per phase to neutral, referred to the generator stator winding, ohms
R_2 = rotor resistance per phase to neutral, referred to the generator stator winding, ohms
X_2 = rotor leakage reactance per phase to neutral, referred to the generator stator winding, ohms
R_1 = generator stator resistance per phase to neutral, ohms
X_1 = generator stator leakage reactance per phase to neutral, ohms
I = generator output current per terminal, amperes
G = primary exciting conductance per phase, representing the core loss current of the generator winding, mhos
B = primary exciting susceptance per phase, representing the magnetizing current of the generator stator winding, mhos
f_0 = output frequency of the generator winding, cycles per second (cps)
f = supply frequency, cps
$F=f\left(\frac{\text{number of poles in generator winding}}{\text{number of poles in motor winding}}\right)$
S = slip of the rotor with respect to the generator rotating air-gap flux
V = output voltage of the generator winding, phase to neutral, volts

Analysis

It would seem from a cursory view that two windings on the same stator would be electromagnetically coupled as in the transformer. Such coupling exists coil by coil, but, as shown in Fig. 1, the net coupling over a complete phase is zero. In the machine tested, no transformer voltage could be detected at the stator terminals with low-impedance portable voltmeters.

The equivalent circuits of the machine are shown in Fig. 2. These are simplified by placing the magnetizing branch at the machine terminals, a modification which has the advantage of shortening the algebraic descriptions with very little accompanying loss of accuracy over the normal load range. A motor slip is assumed. This determines the motor equivalent impedance and permits the computation of power converted to mechanical form, referring to Fig. 2

$$r=r_2\left(\frac{1-s}{s}\right)$$

$$p=\frac{v^2r_2\left(\frac{1-s}{s}\right)}{\left(r_1+\frac{r_2}{s}\right)^2+(x+x_2)^2}$$

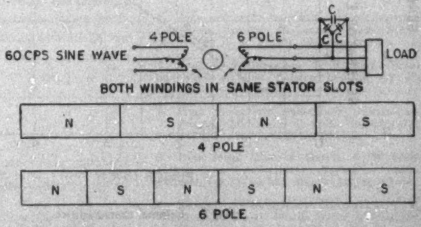

Fig. 1. Overlay of winding phase groups to show electromagnetic uncoupling

---

Paper 55-676, recommended by the AIEE Rotating Machinery Committee and approved by the AIEE Committee on Technical Operations for presentation at the AIEE Fall General Meeting, Chicago, Ill., October 3–7, 1955. Manuscript submitted March 7, 1955; made available for printing July 18, 1955.

W. LA PIERRE and J. Y. LOUIS are with Columbia University, New York, N. Y.

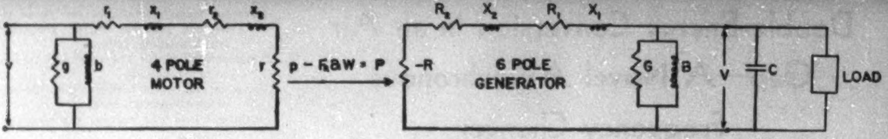

Fig. 2. Equivalent circuit

$$P=p-(Fr+W)$$

The power converted by motor action p less the mechanical losses is the power reconverted to electrical form in the 6-pole winding. At a given generator terminal voltage V the required equivalent power-converting resistance R is specified by the amount of power converted by generator action P

$$R=\frac{1}{2}\left\{2(R_1+R_2)+\frac{V^2}{P}+\sqrt{\left[2(R_1+R_2)+\frac{V^2}{P}\right]^2-4[(R_1+R_2)^2+(X_1+X_2)^2]}\right\}$$

$$S=\left|\frac{R_2}{-R+R_2}\right|$$

$$f_0=F\left(\frac{1-s}{1+S}\right)$$

The generator slip required can thus be calculated and, from this, the output frequency. The voltage at which the machine will operate depends on the reactive volt-ampere balance, i.e., upon the amount of capacity used and upon the reactive volt-ampere demands of the induction generator and load.[1–6]

The computed output frequencies at various loads check closely with test values as may be seen in Table I. The calculated frequency is based upon the known input motor power, motor voltage, motor slip, and generator voltage at each test point. The discrepancy at high overload is caused in part, at least, by poor experimental data.

Several operating parameters of the machine plotted against power output are shown in Fig. 3. The machine is noisier under double-frequency operation than when running as a motor. The output voltage wave shape is sinusoidal but the exciting current on the 6-pole side contains nonsynchronous harmonic components.

Table I. Comparison of Calculated and Experimental Results

Three-Phase Power Output, Kilowatts	Frequency, Cps	
	Calculated	Experimental
0.64	88.8	89.0
2.14	87.8	87.9
3.00	86.6	86.7
3.85	85.6	85.7
4.60	71.8	74.6

Magnetization and Core Loss

One of the most interesting parts of the study was the investigation of the magnetic behavior of the stator iron under the combined influence of two fields having different numbers of poles and rotating at slightly different speeds. To obtain controlled conditions, the rotor was driven at synchronous speed while the two stator windings were supplied respectively with synchronized 90- and 60-cycle voltages. The magnetization characteristics of the machine were surveyed by varying the two applied voltages in a systematic manner. It was found that additional magnetizing current was required by each winding when the other was excited. The total core loss in the stator was increased by the simultaneous

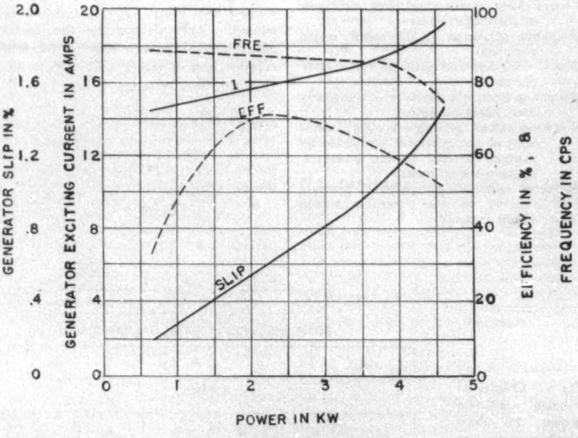

Fig. 3. External characteristics

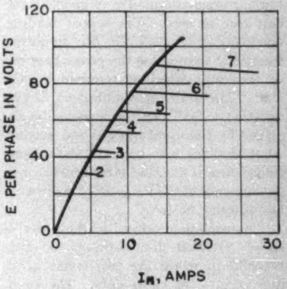

Fig. 4. Magnetizing current, 4-pole winding at 60 cps

2—60 volts, line to line
3—80 volts, line to line
4—100 volts, line to line
5—120 volts, line to line
6—140 volts, line to line
7—165 volts, line to line

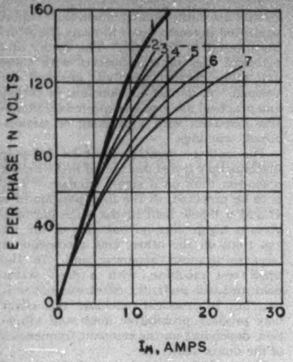

Fig. 5 (left). Magnetizing current, 6-pole winding at 90 cps

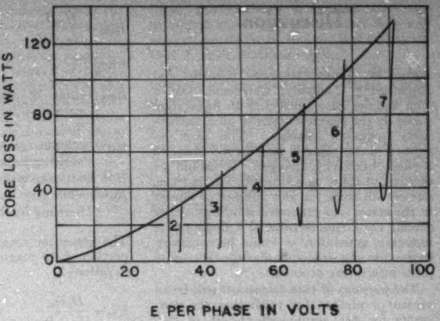

Fig. 6 (right). Core loss supplied by the 4-pole winding

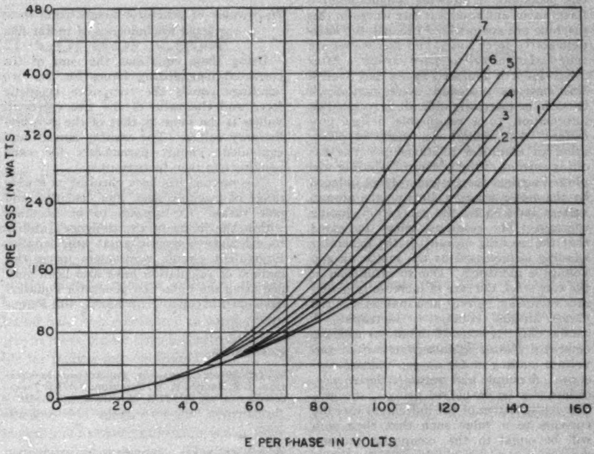

Fig. 7. Core loss supplied by the 6-pole winding

action of two rotating air-gap fluxes but, in all cases, the 4-pole core loss decreased as the 6-pole flux was increased and the 6-pole winding supplied the majority of the core loss.

The results of this part of the study are shown in Figs. 4 through 7. Fig. 4 shows the magnetizing current required by the 4-pole 60-cycle winding. The heavy curve is the ordinary saturation characteristic. The horizontal curves show the magnetizing current needed, as the 6-pole winding was also excited with various 90-cycle voltages. The 4-pole terminal voltage was held constant while the 6-pole 90-cycle voltage was varied from zero to about 130 volts per phase. The numbers on the curves refer to the different runs; see Fig. 4. Fig. 5 shows the family of experimentally determined 6-pole 90-cycle saturation curves. Figs. 6 and 7 show the 4- and 6-pole core losses. The 4-pole core losses decrease as the 6-pole winding is excited to higher voltages. Total core losses increase in all cases when both windings are excited simultaneously. Core loss power under asynchronous frequency changer operation, however, passes from the 60-cycle terminals to the rotor and across the air gap again before it is absorbed by the iron. This result was not expected and is not explained.

Conclusion

Computations of machine performance can be made with confidence using equivalent leakage impedance figures obtained by blocked rotor tests. The leakage reactance is proportional to the frequency. It is necessary to use proper magnetizing current and core loss, which are quite different from the normal, single-winding values.

It would be interesting to see how windings with higher pole ratio would perform, although there seems to be no reason to suppose that higher output frequency would not be readily available. Rotor overheating caused by the presence of the two currents seems to be no problem. The rotor resistance should be low to reduce the frequency drop as much as possible.

References

1. Capacitive Excitation for Induction Generators, E. D. Basset, F. M. Potter. *AIEE Transactions (Electrical Engineering)*, vol. 54, May 1935, pp. 540–44.

2. Self-Excitation of Induction Motors, C. F. Wagner. *Ibid.*, vol. 58, Feb. 1939, pp. 47–51.

3. Self-Excitation of Induction Motors with Series Capacitors, C. F. Wagner. *AIEE Transactions*, vol. 60, 1941, p. 1241.

4. Induction Generator Theory and Application, J. E. Barkle, R. W. Ferguson. *AIEE Transactions*, vol. 73, pt. III, Feb. 1954, pp. 12–19.

5. A Self-Excited Induction Generator with Regulated Voltage, McConnell. *AIEE Transactions*, vol. 73, pt. I, Nov. 1954, pp. 288–95.

6. Frequency Changers, T. H. Carr. *Power and Works Engineer*, London, England, vol. 46, Dec. 1951, pp. 407–11.

7. High Speed By Frequency Conversion, B. Pringle. *Machinery*, London, England, vol. 80, no. 2047, Feb. 7, 1952, pp. 234–35.

8. High Speed Electric Drives, G. W. Stubbings. *Power and Works Engineer*, London, England, vol. 39, no. 453, March 1944, pp. 63–64.

9. Single-Unit Frequency Converters, L. E. Hildebrand. *General Electric Review*, Schenectady, N. Y., vol. 38, no. 5, May 1935, pp. 226–29.

Discussion

Byron M. Jones (Reliance Electric and Engineering Company, Cleveland, Ohio): The authors have presented an interesting paper on the characteristics of an asynchronous frequency changer. The case described in the paper is that for a 3-phase to 3-phase frequency changer. It should be obvious to those versed in the art that this device will work for any number of phases in the motor and generator windings. Predicting the characteristics of a single-phase induction generator, as would be necessary in the case of a single-phase output, presents some interesting problems.

The purpose of this discussion will be to present a method for predicting the constants for the equivalent circuit of this machine, and hence the exciting current. The problems involved in following a rigorous procedure of drawing magnetomotive force waves and resultant flux waves in this machine are complicated because the magnetomotive force waves and flux waves are time variant as well as space variant. After some study, it appeared to me that even if this rigorous procedure were performed, it would be extremely difficult to reduce this information to a reasonable design procedure. An attempt was made to determine an empirical relationship. The exciting current of the generator winding was plotted against the air-gap voltage induced by the motor winding, holding the air-gap voltage induced by the generator winding constant. The resultant curve indicated that the exciting current in the generator winding is increased as the motor air-gap voltage is increased. Due to saturation of the core steel, the rate of increase in generator excitation current also increases as the motor air-gap voltage is increased. A similar effect is noted if the motor exciting current is plotted against generator air-gap voltage holding motor air-gap voltage constant. A simple and accurate design procedure can be developed using a straight-line extrapolation of the individual exciting currents to a value such that their sum will be equal to the composite exciting current.

Briefly, this is the procedure. The magnetic path of the machine for each winding is divided into five parts: the stator core, the stator teeth, the air gap, the rotor teeth, and the rotor core. The effective areas and lengths of these sections are computed. The flux density in each of these portions is computed for each windingly individually. The composite flux density in each portion is obtained by adding the value of flux density induced by the motor winding to the value of flux density induced by the generator winding. The magnetizing force for each portion of the magnetic circuit can be obtained from standard *B-H* curves for the motor flux, the generator flux, and the composite flux. It will be noted that in all cases the composite magnetizing force is greater than or equal to the sum of the motor magnetizing force and the generator magnetizing force. The composite magnetizing force must be supplied in part by each winding. The motor magnetizing force, for each portion of the magnetic circuit, is computed as shown in the following:

$$H_{ma}=\frac{H_mH_c}{H_m+H_g}$$

where

H_{ma} = value of motor magnetizing force corrected for influence of generator flux

H_m = preliminary value of motor magnetizing force

H_c = composite magnetizing force

H_g = preliminary value of generator magnetizing force

The generator magnetizing force for each portion of the magnetic circuit is computed as follows:

$$H_{ga}=\frac{H_gH_c}{H_m+H_g}$$

where

H_{ga} = value of generator magnetizing force corrected for influence of motor flux

Using these equations the sum of the corrected magnetizing forces for the two windings equals the composite magnetic force and the ratio of the two corrected values is the same as that of the two preliminary values. The exciting current and equivalent circuit parameters for each winding can then be computed.

This method has been checked on a wide range of machine sizes, flux densities, and pole ratios. It appears to be accurate within the limits of the designer's ability to calculate magnetic areas and lengths. Equivalent circuit parameters using this method of calculation have also been verified using the induction generator equation developed in a paper by Barkle and Ferguson.[1]

REFERENCE

1. INDUCTION GENERATOR THEORY AND APPLICATION, **J. E. Barkle, R. W. Ferguson.** *AIEE Transactions*, vol. 73, pt. III-A, Feb. 1954, pp. 12–19.

P. L. Alger (General Electric Company, Schenectady, N. Y.): The induction motor with two or more distinct windings is a long-known, but little understood, variety of electric machine that deserves more consideration by teachers as well as by practicing engineers. Besides the frequency changer described by the authors, motors designed for part-winding starting, multispeed motors, concatenated motors, and various other schemes for motor speed control use multiwinding machines. Papers presented in recent years indicate the growing interest in this field. The theory and practical uses of transformers with three and more distinct windings are well developed. A similar development of theory and practical use is to be expected for induction machines with additional, or sectionalized, windings.

The authors mention thatt he 4/6-pole machine they tested was noisier in 2-winding operation than on a single winding. This is to be expected, as the superposition of a 4- and a 6-pole field in the same machine gives a higher flux on one side of the air gap than on the other, and a consequent large unbalanced magnetic pull. In the small test machine, with a deep stator yoke and stiff shaft, the effect was not serious, but in practical machines this effect may produce prohibitive noise and vibration, depending on the resonant frequencies of the motor shaft, etc.

The noninductive relation of the 4- and 6-pole windings is lost if either winding is arranged with as many circuits as poles. This, and the need for maintaining balanced shaft forces, poses severe limitations on the design of these multiwinding machines.

The shift of the core loss supply from the 4-pole to the 6-pole winding as the 6-pole voltage is increased may be explained by the fact that a considerable portion of the core loss, due to the tooth frequency losses, is supplied by the motor torque, and not by transformer action. The tooth frequency losses may be considered as "magnetic friction" due to the air-gap flux passing over the "roughness" of the rotor and stator slot openings. Also, the torque developed by the motor, to overcome the windage as well as the bearing and magnetic friction losses, is supplied only in part by the rotor slip-frequency currents. Besides this normal induction motor torque proportional to the slip, there is a small synchronous torque due to the hysteresis loss in the rotor, just as in a true hysteresis motor.

If the rotor of an induction machine has no bars and, therefore, no rotor currents, there is still a rotor loss and, therefore, an air-gap torque, due to the core loss in the rotor. As such a motor passes through synchronous speed, its (hysteresis) torque reverses abruptly, just as in a true synchronous motor.

In an actual motor with rotor bars, the fraction of the no-load loss torque supplied by the hysteresis effect will vary with the flux. When the 6-pole winding was excited with 90 cycles, and the 4-pole winding was excited with synchronized 60 cycles, the torques per rpm of slip are propor-

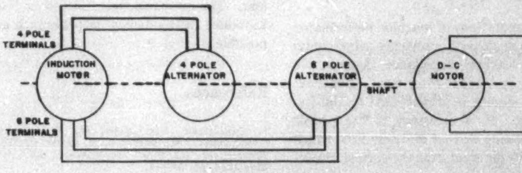

Fig. 8. Test for core losses

tional to the squares of the respective voltages.

Evidently, for the test machine, the 6-pole winding produced more of the loss torque than the 4-pole winding, and its proportion increased when the 6-pole flux increased.

W. LaPierre and J. Y. Louis: We are grateful for the clarifications offered by Mr. Alger and Mr. Jones. The composite flux used by Mr. Jones in design calculations is the peak flux occasioned when the two separate magnetomotive forces add directly. The sum $H_{ms} + H_{gs} = H_s$ by definition. The composition magnetomotive force is obtained from *B-H* curves using the sums of the individual motor and generator flux densities in the various parts of the machine including the return paths as well as the path of maximum in phase flux density it is presumed. In our tests we noticed a slight tendency for the 90-cycle voltage to be modulated at slip frequency at no load. The magnetizing currents, however, were more steady. From this evidence it is clear that the simplified computation suggested does not account for all the factors but it is gratifying that it yields practical results.

The drastic shift of core losses from the low-pole of the high-pole winding under completely synchronized test conditions might not be wholly explained by the rotor hysteresis effect. The test for core losses was made as shown in Fig. 8. The core losses so obtained were then used in power-balance computations for asynchronous frequency changer operation with the results shown in the paper.

Aluminum-Sheathed Control Cable

E. E. McILVEEN
ASSOCIATE MEMBER AIEE

WITH AN increasing supply of aluminum and a fluctuating supply of the classical underground cable-sheathing material for electrically insulated conductors, namely, lead, it is natural for the various segments of the electrical industry, whether engineering, purchasing, or management, to be interested in the development of aluminum-sheathed cables.[1,2] This discussion transcends this aspect, however, for its primary concern is how aluminum can be used to advantage as a control cable sheath in a system that requires no additional armor and is in sharp contrast to the familiar conduit installation. Engineering with aluminum was never more meaningful than when exploiting the physical properties of this light metal for cable sheathing. This particular paper is limited to control cables for generating plant and substation and for industrial and commercial applications.

The aluminum-sheathed control cable need be considered unique only in respect to the sheath material, but the gain in mechanical ruggedness over the ordinary lead-covered or nonmetallic-finished cables is so pronounced that it is clear there is no need to protect it with conduit or additional armor. To illustrate this and other attributes quantitatively, it would be well to select a specific type of cable. If the choice falls on a relatively new high-temperature insulation of the silicone rubber family[3] it would serve a dual purpose, for this class of insulation has been considered in some quarters as more tender than hitherto acceptable for pulling into conduits.

To digress for a moment, it might be noted that to make steam plants more efficient for electric-power generation, engineers have been increasing boiler temperatures and pressures. This trend has reached the point where auxiliary equipment in the immediate area must be able to operate at ambients considerably above those formerly used. Not only has this created a need for a practical high-temperature electric system, but has also increased the extent and importance of this system because of the necessity of elaborate controls. In addition to power plants and prime movers, many industrial manufacturing processes are also concerned with these high ambients as well as process vapors. Not only have the usual rubber insulations deteriorated in this service, but conduit systems have a propensity for collecting moisture and deleterious chemicals, and this has aggravated the situation. The silicone rubber-insulated aluminum-sheathed cable provides a practical solution to this problem.

Cable Construction

The constructional components of this specific type of multiple-conductor cable as illustrated in Fig. 1 may be summarized:

Conductor, sizes 18 through 6 American Wire Gauge (AWG) with class-*B* stranding and lead alloy-coated copper.

Insulation, 600-volt wall of Okotherm 200, a silicone gum rubber base insulation conservatively rated for continuous operation at 150 and up to 200 degrees centigrade (C) under certain conditions.

Covering, single color-coded glass braid with heat-resisting lacquer finish on each conductor.

Core Assembly, up to 61 conductors depending on their size, cabled with heat-resisting fillers where needed, and a layer of asbestos tape.

Sheath, wall of 99.6 per cent (%) pure, seamless aluminum; see Table I. Corrosion protective coverings are furnished where required.

Length, present production facilities permit this cable to be furnished in 500-foot lengths.

Sheathing Particulars

There are three distinct methods of applying aluminum sheaths now in commercial use in Europe,[1] namely, direct extrusion, welding of formed strip, and tube draw-down or sinking method. For the control cable described herein, the latter method of tube-sinking was selected because: 1. it is a relatively simple operation and does not require a large capital investment, 2. it is applicable to other than high-temperature insulations, for example, the thermoplastics such as polyethylene and polyvinyl-chloride, and 3. it is possible through proper selection of tube size to control the sheath physicals and thereby approach the 1/4-hard temper that experience has shown to be most satisfactory for this end use.

Paper 55-691, recommended by the AIEE Insulated Conductors Committee and approved by the AIEE Committee on Technical Operations for presentation at the AIEE Fall General Meeting, Chicago, Ill., October 3-7, 1955. Manuscript submitted March 22, 1955; made available for printing August 26, 1955.

E. E. McILVEEN is with The Okonite Company, Passaic, N. J.

By limiting the maximum length of finished control cable to 500 feet, it permits the use of selected seamless tubing which has been extruded from a single billet, thereby eliminating stop marks that can be sources of weakness. This imposes no real hardships with such cables because they are seldom used in longer lengths. In some cases remnant ends may be more numerous than with 3,000-foot lengths, for example, but this condition is preferable to having these longer lengths with questionable welds. In time, the quality of these tube welds will undoubtedly improve.

Much has been published on the tube-sinking method of sheathing, so it is unnecessary to go into it further other than to note the following basic steps:

1. Stretch the tube out in a straight line.
2. Thread in the pulling line.
3. Pull in the cable core.
4. Draw down or sink the tube on to the core.

In the cold working of the aluminum by the sheathing operation, the tensile strength increases proportionally with the percentage of reduction in cross section while the elongation decreases, although not in direct proportion. Typical physicals are 14,200 pounds-per-square-inch breaking strength with elongation of 13% in 2 inches. Dimensionally, since the wall thickness is for all practical purposes constant, with only a 1-mil gain observed on a 35-mil wall, the length must increase in inverse proportion to the reduction int he tube diameter. The relationship is

$$L''(D''-t'')t''=L'(D'-t')t'$$

where L=length, D=over-all diameter in inches, and t=wall thickness in inches.

The matter of sheath wall thickness can be rationalized on the sole basis of bending performance during handling, since aluminum's greater hardness, higher tensile strength, and lighter weight than lead reduces the possibility of damage during installation. Acccordingly, Table I was originally established on the basis of 66% of the recognized lead-sheath walls for rubber-insulated conductors, and was then modified from information gained on experimental cables. If the wall thickness is plotted against maximum core size, the result is a straight line except at the lower end. Experience has shown that with normal installation practices, no buckling or deformation of the sheaths occurs with these wall thicknesses.

Cable Characteristics

With the type defined, it is now possible to examine the behavior of particular sizes in comparative mechanical, electrical, and thermal tests designed to established their characteristics in relation to recognized wiring systems.[4] These include electric metallic tubing (EMT) with type-*T* wire installed therein, interlock-armored cable, nonmetallic-sheathed cable designated as type *NM*, and others as may be noted in the data presentations. Incidentally, aluminum sheaths are a new development, and hence no reference to them will be found in the current National Electrical Code.[4]

Mechanical Tests

The resistance of the completed cable to mechanical abuse can be studied through simulated impact and crush tests. By use of a Frankfort Arsenal impact machine with a 27.5-pound weight falling a distance of 7 inches, the data presented in Table II were developed. The head on the weight contacting the cable had a 1/2-inch radius cross section. The endurance limit given in Table II in terms of impact cycles was considered reached when a ground developed as indicated by a 6-volt buzzer signal.

The crush test was performed by means of a 12,000-pound Southwark Universal hydraulic testing machine[5] by which an increasing compressive force was applied to the cable specimen through a flat $2^3/_8$-inch diameter plate. The point at which the specimen was reduced to one-half its original diameter was noted as was that at which a buzzer signal indicated a ground. The data showing compressive force in pounds versus distance between plates are summarized in Table III, having been previously plotted in detail in Fig. 2.

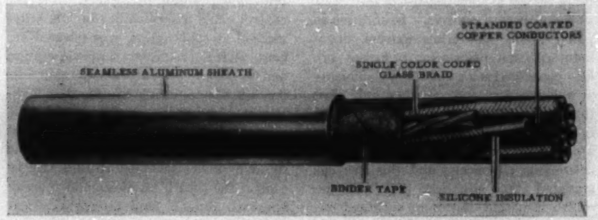
STRANDED COATED COPPER CONDUCTORS
SEAMLESS ALUMINUM SHEATH
SINGLE COLOR CODED GLASS BRAID
BINDER TAPE
SILICONE INSULATION

Fig. 1. Multiconductor silicone rubber-insulated aluminum-sheathed cable

Discussion of Mechanical Tests

The impact test results presented in Table II show that the aluminum-sheathed control cable, as represented by 3-conductor no. 14 AWG specimens, is more resistant to repeated impact than similar sized interlock-armored cables of either steel, bronze or aluminum, and nonmetallic-finished cables, as well as EMT with type-*T* installed therein. As would be expected, the standard heavy-wall rigid steel conduit is more resistant to repeated impact. The results of each test run are shown separately, and the wide variations are due primarily to the variations in the geometric arrangement of the conductors with respect to the U-shaped head on the weight.

While the 3-conductor no. 4 AWG experimental specimens are not in the category of control cable, test results on them are included to show the relative strength of the seamless aluminum sheath versus a typical bronze interlocked armor finish in the larger sizes. The experimental cores were identical; and analysis of the results, with respect to the anticipated point at which electric grounds should develop, indicated that some redesign of the core components was desirable regardless of the type of outer covering. On a comparative basis, the seamless aluminum sheath again showed some advantage.

The crush test data, summarized in Table III, were plotted in Fig. 2 before the values for the table were picked off. Many tests were run, and the accuracy was much greater than could be claimed for the impact test. In successive specimens, it was not infrequent for the points to be identical. Study of curves 1 and 3 in Fig. 2 will show that with identical cores, the seamless aluminum and copper sheaths have virtually the same shape, and that they practically coincide. Using as a criterion the compressive force required to squeeze the specimens to one-half their original over-all diameter, it will be noted that in the 3-conductor no. 14 size, the seamless aluminum-sheathed cable is superior to the interlock-armored cable, the nonmetallic-covered cable, and EMT. In ultimate compressive strength, as indicated by the buzzer signal, this same relationship also held true. Unfor-

Table I. Thickness for Drawn-Down Aluminum Sheaths

Core Diameter, Inches	Sheath Thickness, Nominal, Mils
0.240 to 0.400	35
0.401 to 0.740	45
0.741 to 1.050	55
1.051 to 1.300	65
1.301 to 1.560	75
1.561 to 1.820	85
1.821 to 2.060	95
2.061 to 2.300	105
2.301 to 2.550	115
2.551 to 2.800	125

Table II. Impact Test Results

Diameter, Inches	Description	Test Series	No. of Blows to Cause Failure			
			Test 1	Test 2	Test 3	Average
0.465	3-cdr* no. 14, $^3/_{64}$-inch silicone rubber 35-mil aluminum sheath	(a)	20	35	23	
		(b)	35	20	24	26.1
0.525	3-cdr no. 14, $^3/_{64}$-inch rubber-type-*R* interlocked steel armor	(a)	20	18	10	
		(b)	13	18	20	16.5
0.645	2-cdr no. 14, $^3/_{64}$-inch PVC† type-*T*, nylon-interlocked steel armor	(a)	12	10	16	
		(b)	10	13	16	12.8
0.525	2-cdr no. 14, $^3/_{64}$-inch type-*R* interlocked aluminum armor	(a)	19	2	20	
		(b)	15	4	9	11.5
0.425	3-cdr no. 14 with ground wire, $^3/_{64}$-inch PVC type-*NM*, braid finish		21	13	22	18.7
0.700	Four 1-cdr no. 14, $^3/_{64}$-inch PVC type-*T* in $^1/_2$-inch electrical metallic tubing		26	14	22	20.7
0.840	Four 1-cdr no. 14, $^3/_{64}$-inch PVC type-*T* in rigid metal conduit		227			227.0
0.610	7-cdr no. 14 (7*x*), $^3/_{64}$-inch butyl rubber 42-mil aluminum sheath		48	49	38	45.0
0.930	3-cdr no. 4, 600-volt experimental, 54-mil aluminum sheath	(c)	177	145	161	161.0
1.100	3-cdr no. 4, 600-volt experimental, interlocked bronze armor		106	103		104.0

* cdr = conductor. This also applied to Tables III through VIII.

† PVC = polyvinyl chloride. This also applies to Tables III through VIII.

(a), First series of tests.

(b), Second series of tests (as checks).

(c), Conductors in flat configuration at center of impact area.

tunately, no bronze interlock-armored cable was available for direct comparison with specimen no. 6.

By way of rationalizing the impact and compression resistance of these various cables or wiring systems, it may be noted that, within limits, a compact solid core with a snug-fitting and substantial metallic sheath is inherently stronger than relatively loose-fitting metallic coverings of a similar strength over cores with little or no supporting fillers. This is true whether these metallic coverings are interlock-armor or the thin-wall EMT. The heavy-wall rigid conduit is obviously beyond the limits. To explain further, the circle has the smallest possible circumference for a given area or cross section, and when a compressive force is applied to a compact solid core with a snug-fitting metallic sheath, this sheath must stretch as the specimen is squeezed out of round; the tensile strength of the sheath is a major factor in its resistance to compression, and hence the shape of the curves 1, 3, and 6 in Fig. 2. On the other hand, the empty aluminum tube, curve 7, and the interlock-armored cables and EMT were not filled solid, and collapse of the shell-like walls was accomplished by a relatively minor bending force. It is obvious that an easily stretched metal like lead would not suffice, and that a hardened aluminum sheath is desired where it is both a moisture barrier and armor.

ELECTRICAL TESTS

A study of the dielectric strength of the completed cable after various degrees of bending, and at elevated temperatures, is desirable to assess its ability to withstand the rigors of installation and service. Accordingly, the 3-conductor no. 14 silicone-rubber aluminum-sheathed cable was bent and tested as detailed in Table IV. Neither severe bending nor elevated temperatures made any significant change in its excellent dielectric strength level.

To demonstrate the inherent moisture resistance of the insulation, a 10-foot length of the 3-conductor no. 14 silicone rubber core, without its sheath, was immersed in 20 C water and its insulation resistance was determined periodically. After 2 weeks it was still above 50,000 megohms. It follows that end seals are not mandatory, nor is there need for this aluminum-sheathed system to be vapor-tight if a moisture-resisting insulation is used on the core conductors.

THERMAL TESTS

Ampacity

While it is unlikely that control circuits would regularly carry loads of 25 or 30 amperes, or be installed within the walls of a typical wood frame building, nevertheless the 3-conductor no. 14 Okotherm-insulated aluminum-sheathed cable might be called upon to fulfill this function.

Table III. Crush Test Results

Type No.	Description of Specimens	Average Pressure, Pounds	Average Distance Between Plates, Inches
1	3-cdr no. 14, $^3/_{64}$-inch silicone rubber, 35-mil aluminum sheath	0	0.465
		4,000	0.270
		8,000 (a)*	0.230
		11,000 (b)†	0.190
2	3-cdr no. 14, $^3/_{64}$-inch rubber type-*R*, interlocked steel armor	0	0.525
		4,000	0.280
		4,500 (a)	0.260
		5,500 (b)	0.245
3	3-cdr no. 14, $^3/_{64}$-inch silicone rubber, 35-mil copper sheath	0	0.485
		4,000	0.265
		6,500 (a)	0.240
		12,000	0.200
4	3-cdr no. 14, with ground wire, $^3/_{64}$-inch PVC, type-*NM*, braid finish	0	0.425
		2,700 (a)	0.215
		4,000	0.190
		6,250 (b)	0.145
5	Four 1-cdr no. 14, $^3/_{64}$-inch PVC type-*T* in $^1/_2$-inch electrical metallic tubing	0	0.700
		2,400 (a)	0.350
		4,000	0.250
		6,925 (b)	0.180
6	3-cdr no. 4, 600-volt experimental, 54-mil aluminum sheath	0	0.930
		4,000	0.605
		8,000 (b)	0.525
		10,000	0.495
7	Empty aluminum tube, 35-mil wall	0	0.475
		500	0.260
		1,000	0.140
		1,500	0.120
		2,000	0.100
		3,000	0.090
		4,000	0.080

* (a) = Specimen crushed to half original diameter at this load.

† (b) = Buzzer sounded indicating short circuit to ground.

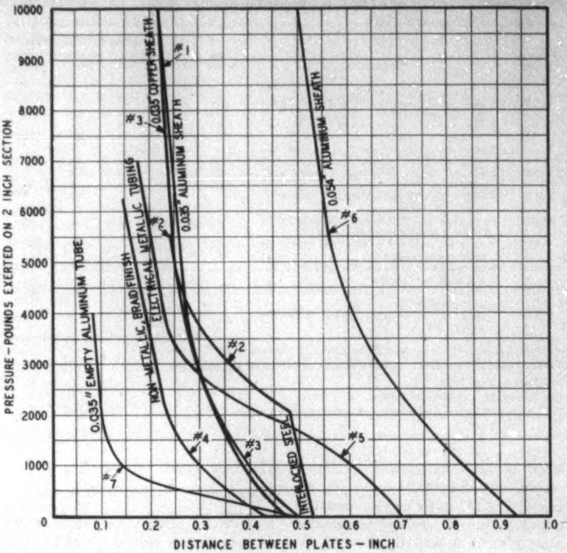

Fig. 2. Crush test

Hence, current loading tests were made as a check on its performance under these conditions. An 11-foot by 15-foot by 5-inch wooden test panel was constructed in accordance with the Underwriters' Laboratories, Inc., standard setup[6] without extra heat insulation in the panel, and the cable was installed therein. The results are shown in Table V. It is obvious the cable can easily handle the maximum load recognized in the National Electrical Code[4] for a no. 14 AWG cable, as well as appreciable overloads, without damage to the cable or supporting structures.

Arcing

The effects of continued arcing due to faults between a conductor and the sheath would be of interest only if unusually high fault current could flow through a critical high impedance. Since it is of concern to the Underwriters' Laboratories,[6] tests were made in comparison with other types as have been detailed in Table VI.

The setup for the arcing tests involved a series circuit with heavy-duty variac, a 30-ampere fuse, and an 800-foot coil of no. 12 AWG insulated wire for the 125-volt test and a 585-foot coil of no. 12 AWG for the 220-volt test. About 25 amperes were caused to flow from the conductor to the sheath across a critical gap through an arc initiated by short-circuiting the conductor to the sheath with a 1/2-inch carbon rod. The potential required to initiate this was 125 volts in the first group and 220 in the second group. It was difficult to control and was not self-perpetuating unless the metal had been artificially heated to its fusing temperature. The correlation with service conditions is open to discussion.

The results of the arcing test are shown in Table IV. Molten metal was produced in all cases and there were no significant differences. If propitious circumstances existed, the seamless-sheathed aluminum and copper construction would, however, be less likely to initiate a continuous arcing fault because of their inherently low ground path resistance. Once started however, the better insulating qualities of their dielectric would be favorable to long arcing.

Table IV. Dielectric Strength Test

Three-Cdr No. 14 AWG, 2/64-Inch Silicone Rubber, Aluminum Sheath

Specimen Condition	At 20 C	At 150 C
Straight section	24.0 kv	23.0 kv
Coiled around diameter = 6×outside diameter	26.0 kv	24.0 kv
Coiled around diameter = 3×outside diameter	23.2 kv	No test

Table V. Current Loading Test

Three-Cdr No. 14 AWG

Conductor Connection, No. in Series	Amperes per Cdr	Panel Ambient, C	Temperature Rise, C	
			Conductor	Sheath
2	25	35.3	35.4	29.2
2	31	40.0	47.5	42.6
3	20.5	39.3	34.2	27.0
3	25	43.0	47.0	41.5
3	37	53.5	116.5	92.0

Table VI. Arcing Tests

Initiation Potential, Volts	Description of Specimen, No. 14 AWG	Duration of Arc, Seconds (Sec)	Remarks; Distances in Inches
125	2-cdr type-*R*, interlocked aluminum armor	6 sec; re-established itself in 3 sec	arc easily initiated, 3/4 inch of armor burned away
125	2-cdr type-*T*, interlocked steel armor	15 sec with insulation burning 30 sec	arch intermittent, 3/8 inch of armor burned away
125	3-cdr type-*R*, interlocked steel armor	16 sec with insulation burning 30 sec	conductors short-circuited and fused, armor damaged for 1 1/2 inches
125	3-cdr 2/64-inch silicone rubber, 35-mil aluminum sheath	2 sec with core burning 5 sec	arc hard to initiate, 1/4 inch of sheath damaged, cdrs fused
220	2-cdr type-*R*, interlocked aluminum armor	40 sec with insulation burning 70 sec	arc extinguished when short-circuited to armor which damaged for 2 inches
220	2-cdr type-*T* interlocked steel armor	15 sec with insulation burning 10 sec	arc extinguished when short-circuited to armor which damaged for 1/2 inch
220	3-cdr type-*R*, interlocked steel armor	12 sec with insulation burning 50 sec	arc extinguished when short-circuited to armor which damaged for 1 inch
220	3-cdr 2/64-inch silicone rubber, 35-mil aluminum sheath	60 sec with flame blown out	gases blew out arc after 60 seconds in two tests; in 3rd was self sustaining until cdr fused
220	3-cdr MI	60 sec, and then shut off	arc was self-sustaining and test shut off due to short sample

Table VII. Flame Test

Description of Specimen, No. 14	Time to Failure	Contribution to Flame	Remarks
3-cdr with ground wire, *NM* braid finish	2 min., 12 sec.	intense and flame extended 10 inches above cable	braid charred and cdrs bare over 4-inch area
2-cdr type-*R* with interlocked aluminum armor	1 min., 55 sec.	some due evolved gases	core burned out, armor weak but intact
2-cdr type-*T* with interlocked steel armor	1 min., 10 sec.	none, but smoking	armor became cherry red in 1 minute; core burned out
3-cdr $^{3}/_{64}$ inch silicone rubber, 35 mil aluminum sheath	none in 2 hours	some between 2 minutes and 12 minutes	inert except for 10 minutes when gas escaped through small melted opening, insulating silica formed
3-cdr $^{3}/_{64}$ inch silicone rubber, 35 mil copper sheath	none in 2 hours	none	sheath surface oxidized over entire sample

Flame Test

Since these cables might be subjected to an open flame in the event of a fire, it would be desirable to ascertain their behavior under such conditions from the standpoint of: 1. contribution to the flame, and 2. circuit integrity. Accordingly, specimens were subjected to the flame of a Meeker gas burner at a position about 2 inches from the burner tip. This burner produces a flame temperature of about 1,000 C and can melt the aluminum in this test. A potential of 110 volts was impressed between the conductors and sheath, and a $7^{1}/_{2}$-watt lamp was inserted in series with the circuit to indicate the development of a ground to be considered the failure point.

The results of the flame test are summarized in Table VII. The *NM* and interlocked armor types all failed electrically within a few minutes, whereas the seamless aluminum as well as the copper-sheathed silicone rubber-insulated specimens would have lasted indefinitely. Since the aluminum has a lower melting point than the copper, 657 versus 1,083 C, and a greater resistance to heat flow, it is not surprising that the sheath wall was ultimately breached in a fine crack by melting after 2 minutes, but even after 2 hours of intense heating to cherry red, the circuit was still good electrically and the sheath damage was confined to a $1^{1}/_{2}$-inch section. In the course of this heating, the silicone rubber insulation was reduced to a nonconducting silica which maintains the insulation level and continuing service until permanent repairs can be effected.

Cable Utilization

The data exhibited in Tables II through VII quantitatively establish some significant characteristics upon which the utilization of aluminum-sheathed control cables can be based. Appropriate comments have been presented with each test. It now remains to show how these seamless, aluminum-sheathed cables can be used to advantage.

ELIMINATES CONDUITS

Since the primary mechanical, electrical, and thermal properties of this cable are equal to or better than that offered by EMT systems, interlocked-armored cable, and nonmetallic-sheathed cable, it follows that the aluminum-sheathed cable described could be used safely in any installations normally made with these methods of wiring. For example, this would include exposed and concealed work in dry locations, as well as where exposed to the weather, or to liquids, chemicals, vapors, or fumes which were not injurious to unprotected aluminum. Where exposed to destructive corrosive conditions, this aluminum-sheathed cable should be protected by coatings or coverings suitable for these conditions.

This means that aluminum-sheathed cables can be installed in place of conduit or other types of systems in many applications. Thus, the frequent problem of trying to get a clear line for rigid conduit through a maze of existing pipes can be solved by forming the aluminum-sheathed cable to the most accessible route, as illustrated in Fig. 3. The cable can be formed easily with standard bending tools to a radius of six times its outside diameter (OD), which is in line with normal bends in conduit installations. Bending tools or devices are recommended to prevent the possibility of occasional unsightly localized bends. This construction may be fastened in place with galvanized iron or aluminum pipe clamps at intervals of approximately 6 feet.

Fig. 3. Aluminum-sheathed cables easily installed around pipes, heat exchanges, and other obstructions. Regular conduit clamps provide all necessary support for these circuits

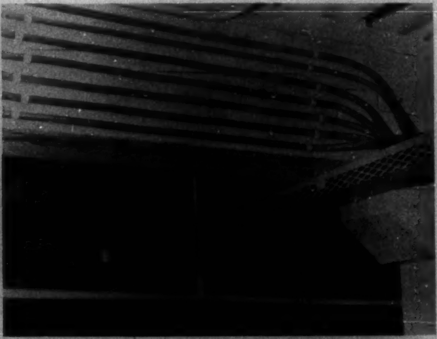

Fig. 4. The flexibility of aluminum-sheathed cables demonstrated by twisting right-angle turns made when leaving cable tray. Ease of installation by use of cable clamps or trays also shown

Table VIII. Silicone-Rubber-Insulated Aluminum-Sheathed Cable, 0–600 Volts

No. of Cdrs	No. 18 AWG, 7×0.0152 In., 2/64 In.		No. 16 AWG, 7×0.0192 In., 2/64 In.		No. 14 AWG, 7×0.0242 In., 2/64 In.		No. 12 AWG, 7×0.0305 In., 2/64 In.		No. 10 AWG, 7×0.0385 In., 3/64 In.		No. 8 AWG, 7×0.0486 In., 4/64 In.		No. 6 AWG, 7×0.0612 In., 4/64 In.	
	OD	Lbs/M′*	OD	Lbs/M′	OD	Lbs/M′	OD	Lbs/M′	OD	Lbs/M′	OD	Lbs/M′	OD	Lbs/M′
1									0.330	92	0.390	132	0.430	173
2	0.380	85	0.400	97	0.430	115	0.470	139	0.615	234	0.735	327	0.810	418
3	0.400	96	0.425	113	0.455	138	0.495	182	0.650	302	0.785	434	0.885	601
4	0.430	112	0.455	133	0.490	171	0.550	233	0.710	351	0.855	524	0.935	724
5	0.460	130	0.490	158	0.545	216	0.595	270	0.765	419	0.950	652	1.050	879
6	0.500	143	0.550	187	0.595	234	0.655	301	0.850	497	1.050	792	1.165	1,036
7	0.500	150	0.550	199	0.595	252	0.655	323	0.850	541	1.050	842	1.165	1,148
10	0.640	238	0.690	288	0.750	363	0.825	466						
19	0.765	355	0.825	444	0.920	614	1.015	805						
37	1.040	662	1.125	834	1.255	1,149	1.385	1,514						
61	1.315	1,073	1.425	1,356	1.580	1,739	1.750	2,446						

* Pounds per thousand feet.

SMALL DIAMETER

Aluminum-sheathed cables have a relatively small over-all diameter, and a very compact and neat arrangement can be achieved where multiple runs are involved. This is an obvious asset since the great increase in instrumentation in modern power plants has placed a premium on space behind the panel boards and in the areas radiating from the control centers. Where many parallel circuits are involved, tray installations are accomplished easily, as shown in Fig. 4. A comparison of the ODs in Table VIII with those of other wiring methods will be of some interest to designing engineers.

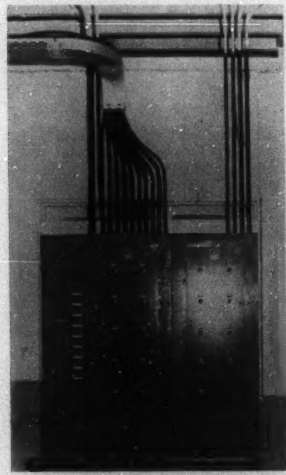

Fig. 5. Aluminum-sheathed cables with neoprene protective coverings

HEAT AND FLAME RESISTANCE

Conventional nonmetallic sheaths are limited in their ability to protect the relatively new classes of high-temperature insulations because they tend to harden and crack with time or otherwise deteriorate. Whether it is a butyl insulation rated at 90 C or a silicone rubber compound rated at temperatures up to 200 C, an aluminum sheath will provide both mechanical protection and a liquid or vapor barrier. Cables of this type are finding use around generating plants in close proximity to boilers.

Where greater resistance to fire or a reduction in the fire hazard involved with nonmetallic-sheathed cables or interlock-armored cables is required, aluminum-sheathed cables are available. Where circuit integrity, even in event of a fire, is desirable, a properly designed silicone rubber type of insulated, aluminum-sheathed cable should be considered. Such cables will not exude flammable compound.

IMPERVIOUS SHEATH

Since the sheath is a continuous aluminum tube it is impervious to liquids, vapors, and gases and thereby provides complete protection to the insulation against attack by agents such as gasoline, benzine, kerosene, toluene, crude petroleum, natural gases, coal-tar derivatives and liquids, as well as other solvents or swelling agents.

CORROSION RESISTANCE

The sheath discussed in this paper is made of *EC* grade, 99.6% pure aluminum. Relative to the other aluminum alloys in commercial use, it is in a preferred position from the standpoint of corrosion resistance. A complete discussion of the performance of aluminum in various corrosive environments is beyond the scope of this paper, but ample data are available. It should be kept in mind, however, that variations in local conditions make it difficult to predict with accuracy the life of a given metal, and if possible the performance should be checked against actual experience in the location under consideration.

These aluminum sheaths are especially resistant to atmospheric corrosion in dry locations, as well as to many outdoor industrial exposures. For example, aluminum conduit was used exclusively in a new ammonium-nitrate plant. In another case it has performed well in a sulfur-

Fig. 6. For dry indoor locations, easy connections to fuse boxes made with regular armored cable connectors

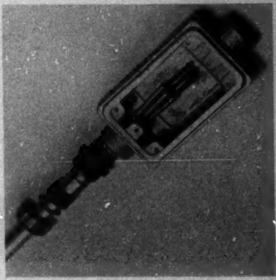

Fig. 7. Conduit outlet box showing method of assembling components

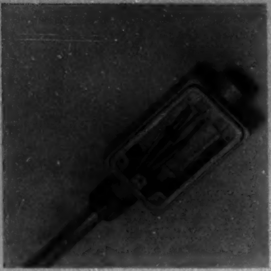

Fig. 8. Conduit outlet box with silicone rubber watertight seal allowing normal, easy terminations or splices

contaminated atmosphere. A good performance record has been established in the petroleum and petro-chemical industry since it has excellent resistance to corrosive attack by petroleum, its products and fractions. It has done well in the pulp and paper industry,[7] and many others. Hollingsworth and Raine[1] claim that the degree of surface attack which can occur in some outdoor industrial atmospheres will be directly proportional to the amount of soot and electrolyte collected on the metal.

Investigations by Hollingsworth and Raine in England, where considerable aluminum-sheathed cable is in use, have shown that when aluminum is embedded in Portland cement which has a pH value over 11.0, some pitting corrosion occurs during setting, but it is unlikely to be serious, and that thereafter it virtually ceases. When embedded in plaster, the effect is less than with cement. They warn, however, not to install it in contact with damp whitewashed walls or touching absorbent mediums, such as permanently damp paper or wood. In such cases it should be mounted so that there will be an air space between it and these surfaces. The object is to avoid wall surface electrolytes and local points of contact which have differences in oxygen concentration, either or both being capable of producing active corrosion cells.

In general, corrosive action on aluminum may occur where strong chlorides or alkalies are encountered, and with some vapors such as from hydrochloric acid or chlorine. In these cases protective coatings or coverings are recommended as shown in Fig. 5. It is well recognized that aluminum should not be placed in direct contact with copper, bronze, or brass in wet locations. In contrast, the effects of contact with zinc, iron, tin, or cadmium are negligible and clamps employing these metals may be used in many exposed locations.

Before leaving this discussion on corrosion, it may be noted that a seamless tubing is less likely to be affected by corrosion than is a helically applied armor where the corrosive media can collect in the crevices between the laps.

Easily Terminated

The silicone-rubber-insulated aluminum-sheathed high-temperature cable can be terminated easily by clamping in junction boxes, just as armored cable now is handled, Fig. 6, or by screwing into conduit boxes through the use of a box connector especially designed for the purpose; see Figs. 7 and 8. It is not a complicated or costly fitting, however, and can be applied easily; see Fig. 9. Since the insulation is moisture-resisting, end seals are not required to preserve the insulation level of the system. In short, this cable can be terminated in the same way as any other conventional rubber-insulated control cable.

Fig. 9. Simple terminations to motors and control apparatus easily made with aluminum-sheathed cables

As shown in Fig. 10, the aluminum sheath can be removed easily by means of a circular tube cutter used to score the surface lightly, and a helical tube cutter, used to generate a light helical score, after which the aluminum may be peeled back with a pair of long-nose pliers. Thus the sheath may be removed to expose the single-conductor lengths needed to fan out to the terminal blocks or to train along the cabinet frame to various locations, sometimes a distance of as much as 4 or 5 feet.

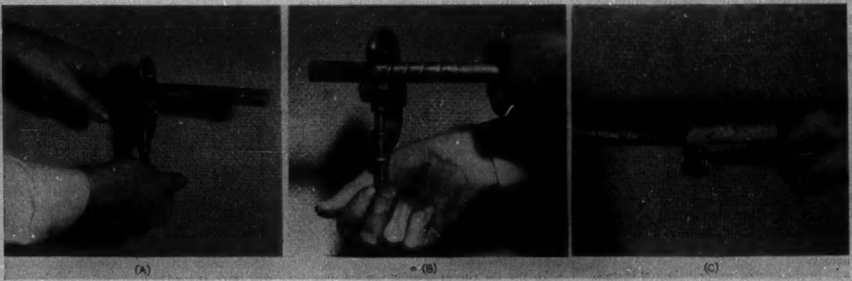

Fig. 10. Removing seamless aluminum sheath

A—Step 1: Score it lightly with circular tube cutter
B—Step 2: Use helical tube cutter from circular score up to cable end, being certain not to cut through sheath
C—Step 3: Peel off with pliers as shown

Service Background

While some sporadic experimental work with aluminum-sheathed cables had been achieved both in this country and abroad by the early 1940's, it remained for a worldwide shortage of lead to become the incentive that brought about a commercially practical method of sheathing in 1948. Since that date, several thousands of miles of cable sheathed by the drawing-down method have been produced in England. The physical properties of the metal are now being recognized as an advantage for both power and control cables.

After some preliminary work in early 1949 at New Kensington, Pa., a 26-pair no. 22 AWG latex-insulated cable core was sheathed by successive operations involving first a tube reduction and then a tube sinking. This is basically the method now employed in making the cables described, except that the tube is supplied now in long lengths by the primary aluminum producers for the cable makers, who then pull in the core and effect the drawing-down or sinking.

The 26-pair aluminum-sheathed telephone cable was installed at Alcoa Point Comfort, Tex., plant in 1950, and recent inspection has shown no deterioration. Some of this cable had a corrosion-protective covering for underground conduit and aerial use. The aerial section, incidentally, was attached to a messenger by a spinner. The unprotected aluminum-sheathed cable was exposed to both inside and outside atmospheres. The cable was spliced by using a 99.90% aluminum sleeve which was longer and somewhat smaller in diameter than ordinarily found where lead sleeves are used on conventional telephone cables. A lead-tin wiping solder was used and the only essential difference between this and the standard procedures for splicing lead sheath cables was the fluxing.

Since 1950, aluminum-sheathed silicone-insulated cables have been finding increasing applications in generating stations, glass plants, food-processing plants, drying kilns, foundries, and industrial plants in general. To cite one case history, some 3-conductor no. 14 and 6-conductor no. 14 cable with neoprene-protective covering was installed where, due to the presence of large quantities of brine, the atmosphere was quite corrosive. The estimated job cost, even with the protective covering, was slightly under a steel conduit job with type *TW* wire, and the actual cost was even less, which proved that no installation difficulties developed. Aluminum - sheathed cables of all types have been in commercial production in Canada since about 1952, and some power cables have been installed in this country.[2]

Summary

Drawn-down aluminum can be used as a control cable sheath that needs no additional armor. Its hardness, tensile strength, and inherent rigidity are characteristics which make it a superior means of protecting relatively small insulated conductors in contrast to the protection offered by conventional interlocked armor. In tests it appears to have an advantage even over electrical metallic tubing. Silicone-rubber-insulated aluminum-sheathed cables have unique heat resistance and flame resistance and provide a safe wiring system for high-ambient service.

Drawn-down aluminum sheaths can be applied over almost any insulation, and they could gain utilization for both exposed and enclosed work in dry locations, as well as where exposed to the weather, to liquids, chemicals, vapors, or fumes which are not injurious to unprotected aluminum. Where exposed to destructive corrosive conditions the sheaths should be protected by coatings or coverings suitable for these conditions. It is a truly impervious sheath which obviously excludes deleterious liquids or vapors from the insulation. Aluminum-sheathed cables with conventional cores can be installed easily, do not require seals, and are economically attractive in the over-all installation cost.

Conclusion

A control cable with snugly fitting aluminum sheath can withstand impact blows and crushing pressure better than a similar cable with either braid, lead sheath, or interlocked armor of either steel or aluminum. A compact solid core with a snug-fitting metallic sheath is stronger inherently than a loose-fitting, partially filled covering of similar material since it does not fail by bending as it collapses, but rather by stretching in tension. Drawn-down aluminum sheaths present a means of obtaining an improved, low-cost wiring system. Aluminum-sheathed cable should find wide application in generating stations, oil refineries, chemical plants, paper mills, steel mills, and industrial and commercial establishments in general.

References

1. Aluminum-Sheathed Cables, **P. M. Hollingsworth, P. A. Raine.** *Proceedings*, Institution of Electrical Engineers, London, England, vol. 101, pt. II, no. 84, Dec. 1954, pp. 603–28.

2. Aluminum-Sheathed Power Cable, **W. A. Del Mar, E. J. Merrell.** *AIEE Transactions*, vol. 74, pt. III, June 1955, pp. 292–304.

3. Silicone Insulated Cable Practice, **H. T. Armitt.** Signal Corps Engineering Symposium, Asbury Park, N. J., Dec. 1953.

4. National Electrical Code. National Fire Protection Association, Boston, Mass.; 1953 edition, chap. 3.

5. Universal Hydraulic Testing Machine. *Electrical World*, New York, N. Y., vol. 123, no. 9, Mar. 3, 1945, p. 150.

6. Fact Finding. *Report No. 20589*, Underwriters' Laboratories, Inc., New York, N. Y., Jan. 15, 1951, pp. 42, 49.

7. Proceedings of the Conference on the Electrical Utilization of Aluminum. *AIEE Special Publication T-72*, "Corrosion of Aluminum as Used for Cable Armor in Paper Mills," **B. J. Mulvey, J. F. Quinlan.** Mar. 1955, pp. 127–30.

◆

Discussion

Robert E. Wilson (Consultant, Richmond, Calif.): We are completing the design and presently making the take-off for the entire branch light and power wiring for a new factory.

As in the case of our first limited installation (Figs. 4, 5, and 9) we chose this cable, protected with neoprene and cable tape, due to the corrosive nature of the product handled; namely, sauerkraut. The plant in which we made the first installation a year ago reports absolutely no trouble.

One thing which we have found in connection with this type of cable (another make, using copper for the sheath), is that when installed with solid metallic glands for waterproofing the entry into a box, and subject to vibration, the sheath will fatigue and crack at the gland.

In the Okotherm installation we used a rubber-bushed compression fitting wil small brass grounding prongs for the connection to boxes. The resiliency of the rubber evidently prevents fatigue in the sheath at that point, which results in a satisfactory installation.

A. R. Lee and **E. L. Crandall** (General Electric Company, Bridgeport, Conn.): The author is to be congratulated on a well-prepared and worth-while contribution to the art of cable design. There is no doubt that an integral aluminum sheath as covering for cables with many types of insulations will offer the advantages outlined by the author. The company with which the discussers are associated has done a considerable amount of basic development in aluminum-sheathed cables using the draw-down method. As a result of this work we would like to state that, in general, our conclusions

Fig. 11. Inside of aluminum tube showing air bubble encountered in press stop area (magnification 3x)

agree very well with those of the author. However, we would like to add a few comments.

First, it is noted that the author states the lengths of cable that can be produced by the draw-down method are limited to 500 feet, and he indicates that this limit is set because of the use of selected seamless tubing which has been extruded from a single billet. It should be pointed out, we believe, that the limits of lengths may be either longer or shorter than the 500 feet indicated in the paper depending on the diameter of sheath to be obtained, its associated wall thickness, and length of tubing available from suppliers.

For many applications of control and power cable, longer lengths than can be currently provided by single billet tubing are desirable. However, at the present time there may be precautions necessary in using multiple billet tubing. For example, Fig. 11 shows a blister, due to the entrapment of air in the press stop area, encountered in a length of tubing produced by the multiple billet method. It should be noted that this blister occurred on the inside of the tube where it would be difficult, if not impossible, to detect. In Fig. 12, using, a magnification of 25X, it will be noted that this blister destroyed effectively about one half the wal thickness of the finished tube. This problem of flaws or other defects in the stop mark area, of course, are very similar to those experienced in the wire and cable industry in the production of lead sheaths some 30 years ago.

It is felt, however, that aluminum sheathing may be applied by the draw-down method from tubes extruded by the multiple billet process provided the characteristics of the metal in the press stop and weld area can be improved by proper extrusion and foundry practice to the point where it is the equivalent of the metal produced by the single billet extrusion. It is hoped that the producers of aluminum tube will give consideration to the problem, and will work to the end of producing multiple billet extrusions free from such defects.

We note that the author shows mechanical tests—impact, crush, and compression—and compares the strength of an aluminum-sheathed cable with cables having an interlocked armor. We note that the cable constructions utilizing interlocked armor did not have fillers. We would, therefore, expect a somewhat lesser resistance to crush and impact when compared with aluminum-sheathed cables, which have a fully filled construction and an asbestos binder tape which acts as a cushion. We would expect results obtained on interlocked armor having a fully filled core to be considerably greater than that indicated in the paper. Further, the author does not tell us the thickness of strip used in the interlocked armor constructions, but we would assume these to be 20-mil-thick strip for the steel and 25 mils for the aluminum according to normal commercial practice. This is compared with the 35-mil-thick aluminum sheath and again we would expect the results to come a good deal closer together if the constructions had the same thickness of metal.

It is further noted that the paper indicates that aluminum-sheathed cables may be installed with a radius of six times the cable outside diameter with proper bending tools. We believe that a word of caution should be inserted to indicate that this does not apply to pulling such cables around sheaves or corners having radii six times the cable outside diameter. It is well established that such bending will cause buckling of the aluminum sheath. Further, it should be noted that the minimum bending radius, using bending tools, will still be determined by the allowable bending radius of the insulation used in the cable construction.

As a minor point of correction, we note that the paper states that *EC* grade aluminum is 99.6% pure, whereas the standard specifications normally list this material as being 99.45% minimum aluminum. However, it is noted that *EC* grade aluminum obtained at this time commercially will usually analyze about 99.6%.

As a point of further interest, we have produced a silicone-rubber-insulated cable very much similar in construction to that described in the paper. The electrical characteristics of our cable, over the range of conditions investigated, agree very well with the results described in this paper.

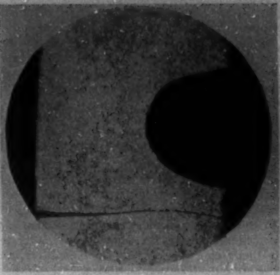

Fig. 12. Longitudinal cut through air bubble of Fig. 11, showing approximate 50-per-cent reduction in tube wall thickness (magnification 25x)

Philip J. Croft (Canada Wire and Cable Company Limited, Toronto, Ont., Canada): The author is to be complimented on a worthy addition to the growing volume of useful literature on the subject of aluminum-sheathed cables.

Although the title of the paper indicates its preoccupation with cables for control circuits, its content deals also with power-wiring auxiliary circuits involving high ambient temperatures, in which the particular advantages of a silicone-rubber in-

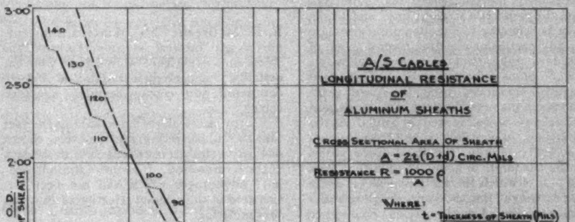

Fig. 13. Plot of longitudinal sheath resistance against cable diameter

sulant are also significant. There does not appear to be any essential connection between the use of silicone-rubber insulation on the one hand, and of aluminum sheating on the other, but a combination of the two, in high-temperature moist applications, is impressive.

In Canada, there is a valuable volume of experience with aluminum-sheathed cables of all kinds, including control cables and auxiliary circuit wiring cables. In our country, where such cables are used by utilities in locations such as central power stations and substations which are not open to the general public, they are not usually considered within the purview of the Code authorities. When the same cables are used in industrial plants, however, they must be of types approved in accordance with our Code, which is entirely similar to the National Electric Code in the United States. As a result, the manufacturers have put forward for approval numerous types of aluminum-sheathed cable, commencing with the *RH*-rubber-insulated type in greatest demand, but now including several asbestos-insulated types, for operation up to 200 C conductor temperature (about as hot as one would wish to operate a copper wire). Silicone-rubber cables have been manufactured and will be submitted for Canadian Code approval in due course. The advantage of this nonhygroscopic rubber-like insulation, as compared to asbestos, is especially significant at joints and terminations of the mechanical type which are popular in such applications.

With regard to the aluminum sheathing itself, it is interesting to note that the tests for mechanical strength, etc., reported by the author, follow along the same lines as those conducted by the laboratories of the Canadian Standards Association, upon which Code approval was granted. The test results are entirely similar.

The author states that "if the sheath thickness is plotted against maximum core size, the result is a straight line" and I take it he is referring to the maximum core size for any particular selection from a group of standard tube sizes. In my company's method of manufacture, a series of standard extruded-aluminum tube sizes are used, varying in diameter in steps of 1/4 inch, and in thickness-of-wall in steps of 5 mils. As the variations in possible core diameter are practically infinite, the draw-down varies within the limits of about 15 to 30%. Thus the plot of which the author speaks is not a single straight line, but an ascending staircase consisting of short portions of a number of straight lines.

Conversely, the plot of longitudinal sheath resistance against cable diameter is a descending staircase consisting of short portions of a number of curves, each one of which is a hyperbola. Such a curve, with values corresponding to our standard production, is shown in Fig. 13.

This matter of sheath resistance is assuming a good deal of importance with us. As the Canadian Electrical Code permits the use of the sheath for the grounding of noncurrent-carrying parts, our inspection authorities are showing great interest in this characteristic.

S. J. Rosch (Anaconda Wire and Cable Company, Hastings-on-Hudson, N. Y.): The author has presented an interesting case for a type of cable construction that has considerable merit in meeting the demands for a type of insulated cable intended for operation under ambient conditions higher than normal. I would, however, take strong exception to his statement that the aluminum-sheathed Okotherm cable may be used at temperatures up to 200 C. No data have been advanced to indicate that this construction would be suitable for use even at 150 or over 100 C for continuous operation.

At a technical session of the AIEE 1955 Winter General Meeting, in discussing the paper on *MI* cable which employs a copper instead of an aluminum sheath, we criticized the authors for advocating a 200 C temperature for the *MI* cable because it is our feeling that copper may not be operated continuously at temperatures in excess of 150 C. I would therefore suggest that the author revise the maximum operating temperature of his aluminum-sheathed cables to a temperature not exceeding 125 C but preferably 110 C in order to avoid future complications, particularly at points of connection where insurance of an adequate ground continuity may be highly essential.

E. E. McIlveen: Mr. Wilson's comments are of real interest as they represent the views and experience of someone who has actually engineered installations of both aluminum and copper seamless sheathed cables.

We are particularly interested in the fact that the rubber bushing in the fitting shown in Fig. 7 helps prevent fatigue in the sheath at the termination. It is one of those "windfall" advantages which had not been anticipated in the original selection of this particular fitting.

With reference to the length limitation, we actually said that by limiting the maximum length to 500 feet, it permits the use of tubing which has been extruded from a single billet. Messrs. Lee and Crandall are quite right, the actual length of this tubing may be more or less than 500 feet depending on the volume of aluminum required for a given wall thickness and diameter. We perhaps indulged in an oversimplification, the main object of which was to indicate the available cable lengths was on the order of 500 feet, not 1,000 feet or more.

The two microphotographs, Figs. 11 and 12, are very much to the point, and serve to illustrate the current problem involved with welds which are mandatory with tubing produced from multiple billets. No doubt, advances in the technology of aluminum extrusions will eventually solve this problem. These microphotographs are a real contribution to the paper.

Mr. Croft's discussion contributes additional information on this relatively new subject, and shows the versatility of the aluminum sheath as a protective covering for many types of insulated conductors. It is of importance that such systems have gained acceptance in Canada. Mr. Croft's curve of sheath resistances (Fig. 13) is thought provoking in that it highlights the possibilities of low-resistance grounding, and use as a current-carrying medium. This latter application would, however, invoke careful design of the terminal fittings.

Mr. Rosch questioned the use of either aluminum or copper at 200 C. It was not intended that these silicone-rubber-insulated aluminum-sheathed cables should be rated at 200 C for general use, but rather for particular applications, for example, in foundries where replacements of ordinary rubber is frequent. It is of interest, however, that Russell[1] has conclusively shown that with both 40-mil and 32-mil wires, the aluminum showed no significant oxidation at 260 for 286 days whereas bare copper exhibited pronounced oxide peeling from the surface. Oxidation was shown to be not an important factor for either metal at 150 C. In view of the conductors being generally made of copper in these control cables, it is probable that unless they are protected by a metallic coating, the limiting temperature might well be 150 C for continuous rating with a silicone-rubber insulation. Other insulations with lower ratings would, of course, confer their ratings on aluminum-sheathed cables of which they become a part.

REFERENCE

1. EFFECT OF HEATING AT 300 AND 500 F ON PROPERTIES OF ALUMINUM AND COPPER WIRE, A. S. Russell. *Wire and Wire Products*, New York, N. Y., Mar. 1952, pp. 255–56.

Modern High-Voltage Rubber Insulation

W. H. COUCH
NONMEMBER AIEE

G. H. HUNT
NONMEMBER AIEE

N. D. KENNEY
MEMBER AIEE

P. H. WARE
MEMBER AIEE

RUBBER-INSULATED cables, especially in the voltage range of 2 to 35 kv, are being increasingly utilized in the expansion of the electrical industry. It is anticipated that the output for class-I systems in the United States will be approximately 900 billion kilowatt-hours in 1963. Such a load will require efficient design of the electrical, mechanical, and thermal characteristics of the rubber power cables in both industrial and utility circuits. Furthermore, the cable designers and the operating engineers must have a knowledge of modern rubber insulations and their properties under various service conditions.

Because of the technological advancements in rubber compounds, there are available (high-voltage) insulations which are far different from the "India rubber," which insulated the Sommering and Schilling cable installed in 1811 across the Isar River near Munich.

One of the earliest rubber-insulating compounds developed in this country was the so-called oil-base type. Cables insulated with natural-rubber oil-base compounds were installed for communication and other low-voltage services in the 1860's. There is no standard definition of an oil-base compound; however, in general, it contains various vulcanized vegetable oils, bitumens, reclaimed rubbers, and either natural or (*GR-S*) synthetic rubbers. Of course, these compounds also contain other chemicals for vulcanization, resistance to oxidation, and other desired properties.

Although oil-base rubber power cables have been and are being installed for many types of service, cable engineers for years have recognized the need of a rubber insulation with operating characteristics which were not attainable with that type of rubber compound.

The development of synthetic rubbers in recent years has provided a material which, when properly used in a rubber compound, results in an insulation having greater resistance to deterioration from heat, aging, ozone, and moisture than was previously available. This synthetic rubber is butyl which was developed in this country in 1937 as a result of research by R. W. Thomas and W. J. Sparks of the Standard Oil Company of New Jersey. Butyl rubber is described by the chemist as a hydrocarbon with a much lower degree of unsaturation than either natural rubber or *GR-S* synthetic rubber. Since the tendency to oxidize and deteriorate from ozone decreases with the lowering of the unsaturation, the saturated bonds of butyl permits the compounding of a rubber insulation having better aging properties, greater resistance to heat, and lower susceptibility to ozone than is possible with other rubber-insulating compounds. The moisture-resistant properties have also been improved.

Since the commercial production of butyl in March 1943, there has been an increasing quantity of butyl-rubber power cables installed under various service conditions such as aerial, submarine, direct burial in the earth, in conduits, and in ducts.

The purpose of the paper is to present the characteristics and the effects of environments and service conditions upon modern rubber insulations for power cables. Only natural and synthetic oil-base and butyl-rubber compounds are considered.

Cable Construction and Service Conditions

CABLE CONSTRUCTION

Although the purpose of this paper is to present the characteristics of oil-base and butyl-rubber compounds, it is necessary to consider the various types of cable constructions in which these insulations are used. Rubber-insulated power cables in this country for operation in the voltage range of 2 to 35 kv have in general the following basic design features:

Conductor:
Copper or aluminum; solid (usually not used over 5 kv and for sizes larger than 8 American Wire Gauge); class-*B* stranding (Insulated Power Cable Engineers Association (IPCEA) or American Society for Testing Materials (ASTM)); class-*C* stranding (IPCEA or ASTM).

Conductor coating:
Tin, lead, or lead alloy coating (aluminum, no coating).

Strand shielding:
Conducting material is applied over the surface of the conductor and vulcanized, or firmly bonded, to the inner surface of the insulation.

Insulation:
Ozone-resistant rubber compounds.

Tape:
When a metallic shield is recommended, it is spiralled over a rubber tape and/or a paper tape or a semiconducting layer. Nonshielded cables may have a braid or a rubber tape over the insulation. Single-conductor nonshielded cables are manufactured with a rubber (neoprene) jacket directly over the insulation.

Shielding tape:
When shielding[1] is required, in general a metallic non-magnetic tape of suitable width and at least 0.0025 inch thick is spiralled over the insulated (taped) conductor. Although most metallic shields are of tinned copper, Monel, stainless steel, bronze, and aluminum metals are used. (5-kv single-conductor cables with semiconducting rubber jackets are in service.)

Multiconductor cable:
Individual conductors are cabled together and interstices filled with suitable materials to make a round and compact unit. A cable tape is often used to bind the conductors together.

Protective coverings:
Modern rubber-insulated cables have various types of protective coverings such as lead, fibrous materials, flat metallic tapes, and round wire metallic armor. Except for submarine services, most rubber cables are protected by a neoprene jacket. Other types of thermosetting materials (natural, Buna- and butyl-rubber compounds) and thermoplastics (polyvinyl chloride, polyethylene) are also used for nonmetallic sheaths.

The cable design, especially the type of covering, depends upon the service conditions. Each installation should be considered separately in order to choose the rubber cable best suited for the service. A detailed discussion of cable constructions is not within the scope of this paper.

SERVICE CONDITIONS

In evaluating rubber insulations, it is necessary to have a knowledge of the environmental conditions and the deteriorating accelerating conditions in which the materials may operate. Obviously, it is not possible to list all of them; however, there are certain ones which are common to many installations such as those listed in Table I. Evaluating a cable insulation involves recognizing first the value of various characteristics needed for the

---

Paper 55-693, recommended by the AIEE Insulated Conductors Committee and approved by the AIEE Committee on Technical Operations for presentation at the AIEE Fall General Meeting, Chicago, Ill., October 3–7, 1955. Manuscript submitted June 9, 1955; made available for printing August 24, 1955.

W. H. COUCH, G. H. HUNT, N. D. KENNEY, and P. H. WARE are with the Simplex Wire & Cable Company, Cambridge, Mass.

service and, secondly, the hazards or deteriorating influences present in the service conditions and their effects thereon.

There has been a trend in this country, since the 1920's, to use nonmetallic rubber cables, i.e., to use cables protected by other than a continuous metallic sheath, such as lead. The only true barrier to many outside environments is a metal sheath. As examples, water and air diffuse through thermosetting and thermoplastic jackets and, of course, fibrous coverings, armor wires, and metallic tapes are poor barriers to such action. It is for this reason that all nonmetallic cables are subjected to two nearly universal environments, namely, oxygen and water.

Another possible service environment to which high-voltage rubber may be exposed is ozone. Insulated conductors operating at a high voltage, unless perfectly shielded electrically, may be exposed to ozone at the surface of the insulation because of the ionization of the air in the electric field. It has been proved in both the laboratories and in field installations that such an action may cause cutting of rubber, which results in cable failure caused by a decrease in the dielectric strength. Since it is not possible to perfectly shield electrically, the insulation, the effect of ozone upon the rubber must be considered in the evaluating studies.

Rubber insulations, like other organic materials, are affected by heat. Power cables, unlike control and communication cables, operate at temperatures usually at least 20 degrees centigrade (C) above ambient temperature because of the heat generated by the current in the conductors and the dielectric loss. The rate of deterioration from oxidation and moisture increases with an increase in temperature. In other words, the service life of a rubber-insulated cable depends not only upon the direct effect of such environments as air, water, ozone, etc., but upon the acceleration of their effect caused by the influence of heat.

Table I. Cable Service Environments and Deteriorating Accelerating Conditions for Nonmetallic Sheathed Cables

Service Environments	Source
Oxygen	air free oxygen in water
Water	surrounding medium for submarine service wet ducts and manholes ground water condensation rain snow
Ozone	corona discharges in cable electrical discharges external to cable
Deteriorating Accelerating Conditions	
Temperature	heat from currents and/or ambient conditions
Electrical stress	impressed or induced voltage

No matter how well-compounded a rubber insulation may be, to have a prolonged physical life under many types of service conditions, it is of no value unless it has the proper dielectric strength. Not only must the a-c dielectric strength be considered but the d-c and the impulse strength of the insulation should be evaluated.

It is not possible, within the limitations of a single paper to report and evaluate the effect of all types of service conditions to which a high-voltage rubber cable insulation may be subjected. For this reason only the most prevalent environments and accelerating factors are considered, namely: air (oxygen), water, ozone, heat, and voltage.

Obviously, it is not feasible to expose rubber insulations to these conditions for 20 to 40 years to determine their properties. As in the development of other equipment used by the electrical industry, accelerated tests are utilized by the cable research engineers in developing new products. Over a period of nearly 40 years, accelerated aging tests have proved of value in predicting the aging properties of rubber compounds. The value of carefully controlled accelerated tests has been great and has produced in a reasonably short time surprisingly accurate information on long-time actual performance.

Comparative Properties of Oil-Base and Butyl-Rubber Insulations

Aging and Heat-Resistant Characteristics

Before discussing the stability of high-voltage oil-base and butyl-rubber compounds it must be first recognized that the common reference to a "rubber insulation," is technically incorrect. Rubber insulations do not consist of 100-percent natural or synthetic rubber. Various materials are compounded with the rubber to obtain vulcanization and desirable characteristics. As an example, oil-base rubber compounds, as previously mentioned, may contain vulcanized vegetable oils, bitumens, reclaimed rubbers, and a small percentage of either natural or (*GR-S*) synthetic rubbers. Similarly, butyl-rubber compounds consist of several ingredients. Obviously there is a variation in both the ingredients and the percentages thereof in the rubber compounds of various manufacturers. It is for this reason that all data and information relative to the properties of oil-base and butyl-base rubber compounds given in this paper should not be considered as being catholic but indicative.

The deterioration of rubber compounds with age is generally considered to result from the combined action of oxygen and heat, plus, of course, the influence of other environmental factors which may be present, such as microbial life, moisture light, and ozone. Rubber chemists have introduced certain substances called antioxidants which retard the attack of oxygen on rubber. Over the years these materials have extended the useful life of rubber compounds manyfold. However these materials have been largely selected, on the basis of empirical tests which showed one material to be superior to others. Ordinary shelf-aging or service-aging is far too slow for this purpose, so that it has been necessary to devise certain so-called accelerated aging tests to determine which materials would give improved aging qualities.

The first of the accelerated aging tests was the air-oven aging test developed by W. C. Geer in 1916. This consists essentially of blowing a current of air at an elevated temperature past the specimens under test. Experience extending back nearly 40 years indicates that this test has been extremely valuable in selecting better age-resisting compounds.

Originally, these tests were carried out at 122 degrees Fahrenheit (F) (50 C) to 158 F (70 C) but, as compounds were improved, service demands became more severe so that the test temperature was gradually raised to accelerate the effect of the increased severity of service. For example, when copper operating temperatures were 122 F (50 C), a test temperature of 158 F (70 C) offered a certain amount of acceleration. With copper operating temperatures increasing to 185 F (85 C) it is apparent that the test temperature needs to be raised to higher values to offer any measure of the suitability of the insulations for service at that temperature.

The air-oven test is a measure of the effect of heat and oxidation on rubber compounds. However, there is the possibility that the use of high temperature may overemphasise the effect of heat without sufficiently accelerating the role of oxidation in the process. For this reason the oxygen-pressure aging (so-called oxygen bomb) test was brought out by Bierer and Davis in 1924. In this, test rubber-compound specimens are

Table II. Standard Accelerated Aging Tests for High-Voltage Insulation, 4 Stranded, 0.156-Inch Wall

Tests	Natural Rubber Oil Base	GR-S Base	Butyl
Tensile Strength, Pounds per Square Inch, Unaged	750	850	850
Per cent of unaged tensile strength			
Air-pressure heat test, 20 hours, 260 F, 80 pounds per square inch	65	105	98
Oxygen-pressure heat test, 7 days, 176 F, 300 pounds per square inch	60	125	95
Air-oven heat test, 7 days, 250 F	105	145	99
Elongation, Per Cent, Unaged	500	350	500
Per cent of unaged elongation			
Air-pressure heat test, 20 hours, 260 F, 80 pounds per square inch	20	55	68
Oxygen-pressure heat test, 7 days, 176 F, 300 pounds per square inch	25	70	65
Air-oven heat test, 7 days, 250 F	15	20	48

Table III. Prolonged Exposure to Accelerated Aging High-Voltage Insulations, 14 Solid, 0.047-Inch Wall

Tests	Natural Rubber Oil Base	GR-S Oil Base	Butyl
Per Cent of Unaged Tensile Strength			
Air-pressure heat test, 80 hours, 260 F, 80 pounds per square inch	0	60	94
Oxygen-pressure heat test, 1 year, 176 F, 300 pounds per square inch	0	0	90
Air-oven test, 1 year, 250 F	0	0	45
Per Cent of Unaged Elongation			
Air-pressure heat test, 80 hours, 260 F, 80 pounds per square inch	0	10	62
Oxygen-pressure heat test, 1 year, 176 F, 300 pounds per square inch	0	0	38
Air-oven test, 1 year, 250 F	0	0	25

Fig. 1. Effect of air-pressure heat aging on high-voltage insulations

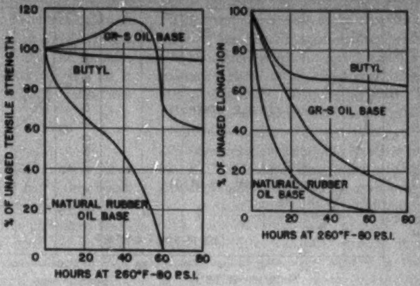

Fig. 2. Effect of oxygen-pressure aging on high-voltage insulations

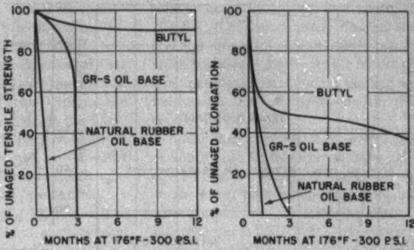

aged in oxygen under a pressure of 300 pounds per square inch for various times usually at a temperature of 158 F (70 C) or 176 F (80 C). This test is primarily for determining the relative resistance to atmospheric oxygen (aging quality) of rubber stocks which are not expected to be exposed in service to abnormal heat or other unusually severe aging temperatures. A test at 176 F (80 C) in the oxygen bomb is approximately twice as fast in predicting time to a given deterioration as a test at 158 F (70 C). The oxygen bomb test can be used, therefore, to check on the prediction of the air-oven test. It is not inconceivable that a compound might show excellent relative life at a high temperature and yet not have unusually good normal temperature aging which is thought to depend more upon the effect of oxygen unaccompanied by excessive heating. However, if a compound shows good resistance to deterioration in both a high-temperature (121 C) air-oven test and in the oxygen bomb test, it seems reasonably certain that it will have good aging qualities in service.

As a further attempt to predict the behavior of rubber compounds in severe conditions of heat and oxidation, the U.S. Rubber Company in the late 1920's developed the air-pressure heat test which consists of aging rubber specimens in air at 80-pound-per-square-inch pressure and at 260 F (126 C), usually for a period of 20 hours. Although designed particularly as a means for evaluating truck inner tubes which operate at high temperatures and pressures, this test has proved useful in developing compounds for use in unusually severe service conditions where excessive heat and oxidation are likely to be deteriorating factors.

It should be pointed out that no one nor all of these tests combined can give an actual service life prediction in terms of years, since service conditions vary widely. These tests are of comparative value, however, in predicting which compounds are likely to have a superior

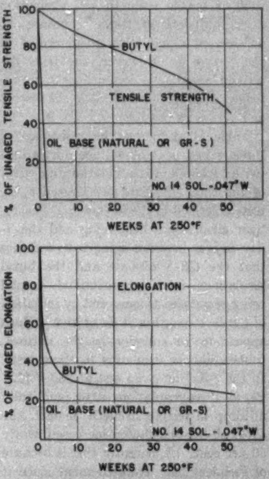

Fig. 3. Effect of air-oven aging at 250 F (121 C) on ozone-resisting insulation

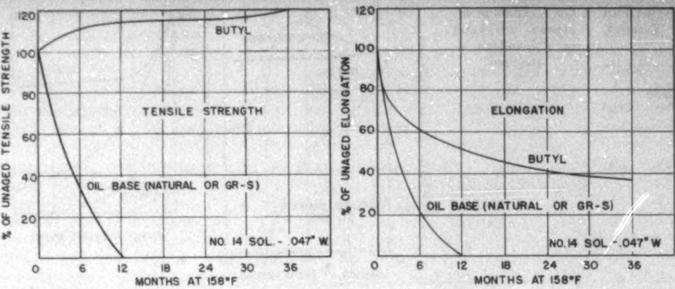

Fig. 4. Effect of air-oven aging at 158 F (70 C)

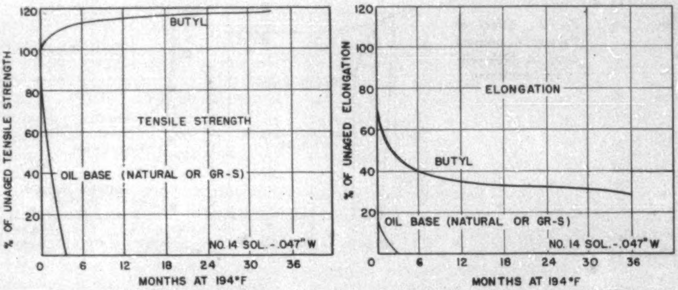

Fig. 5. Effect of air-oven aging at 194 F (90 C)

life expectancy. For specification purposes it is usually stated that a compound shall not suffer more than a specified percentage loss in certain physical properties such as tensile strength and elongation after a relatively brief exposure to accelerated aging tests as described in the foregoing. However, the tests described herein have been deliberately prolonged in an attempt to make the testing as rigorous as possible.

Table II compares the resistance of three types of high-voltage insulations (with 5-kv walls) to the deteriorating effect of the three standard accelerated aging tests described in the foregoing. The 20-hour air-pressure heat-aging and the 7-day oxygen-pressure aging tests indicate that the *GR-S* oil-base and the butyl insulations have approximately equal aging properties as measured by retention of tensile strength and elongation. Both appear to be superior to the natural-rubber oil-base insulation in these tests. In the 7-day air-oven test at 250 F (121 C), all three insulations show practically no drop in tensile strength, in fact, the *GR-S* oil-base insulation increased nearly 50 per cent. Apparently this is because of incipient heat embrittlement since it will be noticed that the retention of elongation for this compound on this test is only 20 per cent as compared with 48 per cent for the butyl compound.

Not only do the relative short-time accelerating tests indicate the better physical stability of the butyl-rubber compound as compared to either type of oil base but the comparison is confirmed by the data obtained from prolonged, accelerated aging tests.

Prolonged exposure to the same test environment has been made by using a smaller conductor size (no. 14 solid) and with a thinner wall (0.047 inch) of insulation to emphasize any differences in aging properties of the three insulations. The longer tests and the thinner walls clearly show the longer life expectancy of butyl high-voltage insulation when exposed to higher than usual temperatures. See Tabel III and Figs. 1 through 3.

The butyl-rubber compound still retains good physical properties after 80 hours of air-pressure aging at 260 F (126 C), 1 year of oxygen-pressure aging at 176 F (80 C), or 1 year of air-oven aging at 250 F (121 C). In contrast, the natural-rubber oil-base insulation has no elongation after 80 hours of air-pressure aging, 1 month of oxygen-pressure aging, or 1 month of air-oven aging at 250 F (121 C). The *GR-S* oil-base insulation, although somewhat better, still shows almost complete loss of physical properties after relatively short aging periods in each of the three tests.

Butyl-rubber samples show excellent retention of physical properties even after 3 years in air at either 158 F (70 C) or 194 F (90 C). The oil-base compound properties are so poor physically that they can no longer be tested after approximately 1 year in air at 158 F (70 C), 3 months in air at 194 F (90 C), or 1 week in air at 250 F (121 C), see Figs. 3 through 5. Although there were differences noted in the tensile and elongation values of the *GR-S* oil-base and natural-rubber oil-base insulations reported in Figs. 3 through 5, they were so small that for

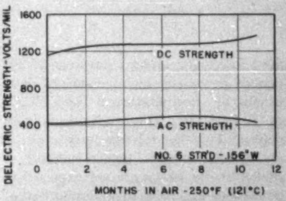

Fig. 6. Effect of air-oven aging at 250 F (121 C) on dielectric strength of butyl insulation

Table IV. Effect of Heat on Butyl

Exposure Temperature = 464 F (240 C)
Time of Exposure = 30 Minutes
Environment = Air
Thickness of Insulation = 0.063 Inch

Tests	Per Cent of Original Values after Exposure
Tensile strength	75
Elongation	60
A-c dielectric strength	85
D-c dielectric strength	95

simplicity a single curve was used to represent both types. Even natural-rubber heat-resisting insulations will, in general, be mechanically and, thus, electrically worthless after 2 years in air at 158 F (70 C), 6 months in air at 194 F (90 C), or 3 weeks in air at 250 F (121 C).

Although even 1 week at 250 F (121 C) causes severe physical deterioration to the oil-base compounds, much longer periods of air-oven aging at 250 F (121 C) appear to have surprisingly little effect upon many of the properties of the new high-voltage high-temperature insulations. For example, after 11 months in air at 250 F (121 C), the butyl compound showed no decrease in either a-c or d-c dielectric strength, Fig. 6, no cracking after 10 hours' exposure to 0.2-per-cent ozone by volume (15 times specified industry required concentration, Table IX), no cutting after 50 hours at a stress of 100 volts per mil a-c in the vertical U test, and unimpaired electrical stability in water at 158 F (70 C), Table V. The effect of the severe heat, which an insulation might be subjected to under short-circuit conditions, upon the physical properties of the two types of rubber compounds can be seen in Fig. 7.

Samples of 5-kv (0.156-inch wall) natural oil-base, *GR-S* oil-base and butyl-rubber-insulated conductors were subjected to 450 F (232 C) for 15 minutes. A study of Fig. 7 shows the severe deterioration of both oil-base samples, but no visual effect of heat upon the butyl compound. To accentuate its heat-resisting characteristics, a butyl-insulated (0.063-inch wall) conductor was exposed to a temperature of 464 F (240 C) for 30 minutes, see Table IV. Even after this exposure, the sample retained approximately 75 per cent of its original tensile strength and 60 per cent of its original elongation. The a-c dielectric strength average approximately 85 per cent of the original value and the d-c dielectric strength depreciated only 5 per cent. In an investigation of impulse characteristics, a no. 6 stranded conductor with a 0.156-inch wall (5 kv) of butyl-rubber insulation was heated for 20 months at 250 F (121 C). At the end of this period, the impulse strength was 1,200 volts per mil for a 1.5x40 wave. The original value was 1,000 volts per mil.

MOISTURE RESISTANCE

Properly compounded butyl-rubber high-voltage insulation has a low-water absorption and shows good retention of physical properties after prolonged soaking in water at either 158 F (70 C) or at 194 F (90 C). This can be seen in Figs. 8 through 10. In each case it will be noticed that the values for this type of insulation indicate substantial superiority of stability over the typical oil-base insulations, included for comparison.

As a rule, it has been experienced that natural or accelerated aging impairs the ozone resistance of oil-base high-voltage insulation. Similarly, old, or even air-oven or oxygen-bomb-aged samples of oil-base insulations as well as the older types of rubber submarine cable insulation will usually show substantially higher water absorption and poorer electrical stability in water than new, unaged samples.

This does not appear to be true with butyl-rubber high-voltage high-temperature insulation which has good moisture resistance, excellent electrical properties, and good corona resistance as well as good physical properties, even after accelerated aging. Fig. 11 shows the 1,000-cycle electrical stability in water at 158 F (70 C) for a butyl high-voltage insulation before and after air-oven aging for 1 week at 250 F (121 C). Although both samples show low increases in capacitance after 6 months' soaking, it is apparent that the aged sample is the better. Electrical stability values in water are not shown for the oil-base insulation after 7 days' air-oven aging at 250 F (121 C), since after this test the physical properties are too poor to permit much handling. However, the results on the unaged sample show its marked inferiority to the butyl compound in this type of test.

Much longer periods of air-oven aging at 250 F (121 C) have surprisingly little effect upon the water-resisting properties of the butyl high-voltage high-temperature insulations. For example, after 11 months in air at 250 F (121 C), butyl high-voltage insulation shows unimpaired

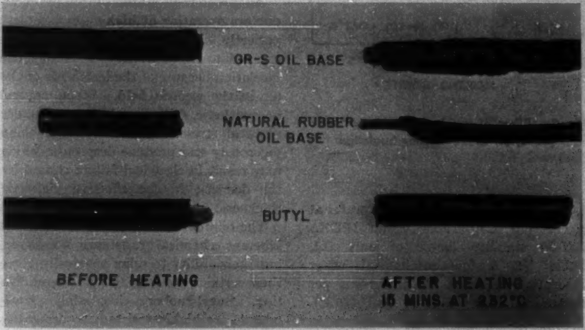

Fig. 7. Effect of high-temperature heating on ozone-resisting insulation

Table V. Effect of Air-Oven Aging at 250 F (121 C) on the Electrical Stability of Butyl in Water at 158 F, Wire No. 6 Stranded, 0.156-Inch Wall*

Tests	Power Factor, Per Cent			Dielectric Constant, 1-Day Soak	Change in Capacity, Per Cent	
	1-Day Soak	8-Day Soak	29-Day Soak		8-Day Soak	29-Day Soak
Before air-oven aging	0.8	1.0	1.9	3.70	1.5	6.0
Air-oven-aged at 250 F (121 C)						
4 months	0.8	1.2	1.9	3.75	1.9	6.2
8 months	1.0	1.2	1.7	3.60	2.2	5.7
11 months	0.9	1.2	1.6	3.80	1.7	5.2

*Samples aged in air oven at 250 F then given electrical stability test in water at 158 F (1,000-cycle test).

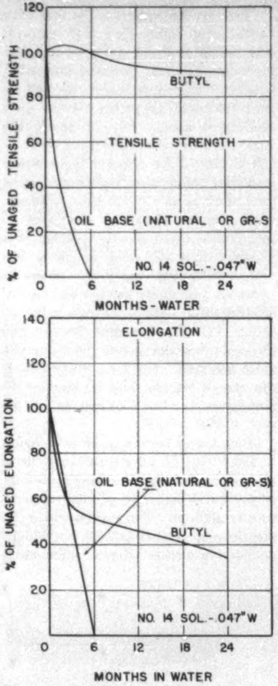

Fig. 8. Effect of soaking in water at 158 F (70 C) on ozone-resisting insulation

1,000-cycle electrical stability in water at 158 F (70 C), Table V, an IPCEA *EM-60* stability factor of only 0.1, Table VI, a low mechanical water absorption value of 12 milligrams per square inch after 7 days at 158 F (70 C), Table VII, and is unchanged in insulation resistance, Table VIII.

The outstanding stability of this type of insulation is shown by the fact that, in each case, butyl-rubber high-voltage insulation after 11 months in air at 250 F (121 C) meets the usual specification requirements for ozone resistance, mechanical water absorption, or electrical stability in water—tests which, as a rule, are only applicable to new, unaged samples of insulation. For aging of this severity no comparable data can be offered on oil-base insulations as they become worthless after only 1 week or so at 250 F (121 C), while these tests are after 11 months at 250 F (121 C).

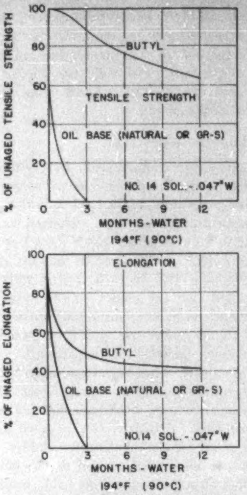

Fig. 9. Effect of soaking in water at 194 F (90 C) on ozone-resisting insulation

Ozone Resistance

As previously stated, insulated conductors operating at high voltage, unless perfectly shielded electrically, may be exposed to ozone at the surfaces of the insulation because of the ionization of the air in the electric field. When natural or synthetic (*GR-S*) rubbers are under physical stress, ozone can attack them vigorously and produce deep cuts, which may result in electrical failure caused by the decrease in the effective dielectric thickness.

The oil-base insulations do not possess inherent chemical resistance to ozone, but their ability to relax physically gives them certain resistance to ozone deterioration. Butyl-rubber insulating compounds are highly resistant to ozone because of the low unsaturation of butyl.

For several years there have been industry specifications for so-called ozone-resistant rubber insulations in which it is specified that the rubber insulation on a conductor shall not show any signs of cracking when bent around a specified diameter and exposed to an ozone concentration of 0.010 to 0.015 per cent for 3 hours. This test is for insulations when new.

Both oil-base and butyl-rubber high-voltage insulations meet this test when properly compounded. However, the ability to retain this resistance to ozone deterioration with age varies between the two types of insulations. An example of the resistance to ozone of the two rubber compounds can be seen by examining Fig. 12. Two samples of oil-base high-voltage rubber-insulated cables and a sample of cable insulated with butyl were subjected to the 0.015-per-cent ozone- and the 0.030-per-cent ozone-concentration tests. An interesting feature of these tests is that the samples were from cables approximately 3 years old. It will be noted that for both these tests the oil-base insulations have ozone cuts, whereas the butyl insulation was not affected. Three years before the tests under discussion were performed, the oil-base samples met the requirements of the 0.010 to 0.015-per cent ozone concentration after a 3-hour test. However, even when new, the oil-base insulations failed to pass a test of 3 hours without cracking in the ozone concentration of 0.03 per cent.

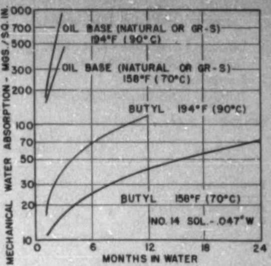

Fig. 10. Mechanical water absorption, ozone-resisting insulation

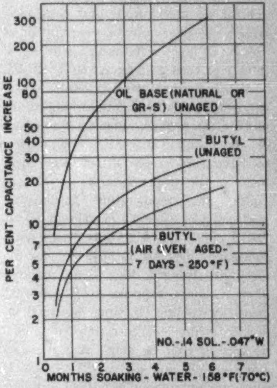

Fig. 11. Electrical stability in water, 1,000 cycles, 158 F (70 C), ozone-resistant insulation

Table VI. Effect of Air-Oven Aging at 250 F (121 C) on the Stability Factor of Butyl, Wire No. 6 Stranded, 0.156-Inch Wall*

Tests	Dielectric Constant, 1 Day	Change in Capacitance, Per Cent		Immersed in Water at 122 F (50 C) — Power Factor, Per Cent				Stability Factor	
				1 Day		14 Days			
		1 to 14 Days	7 to 14 Days	40 Volts per Mil	80 Volts per Mil	40 Volts per Mil	80 Volts per Mil	14 Days	14 to 1 Days
Before air-oven aging	3.71	1.4	0.5	1.0	1.3	1.2	1.5	0.3	0
Air-oven-aged at 250 F									
4 months	3.61	1.5	0.6	0.9	1.1	1.4	1.4	0	−0.2
8 months	3.65	1.4	0.6	0.9	1.0	1.1	1.2	0.1	0
11 months	3.63	1.5	0.8	1.0	1.2	1.2	1.3	0.1	−0.1
IPCEA limits on unaged insulation		10 maximum	3 maximum					1.0 maximum	0.5 maximum

*Stability factor per IPCEA method *EM-60* before and after air-oven aging at 250 F (121 C).

Table VII. Effect of Air-Oven Aging at 250 F (121 C) on the Mechanical Water Absorption of Butyl, Wire No. 6 Stranded, 0.156-Inch Wall

Tests	7 Days in Water at 158 F (70 C), Milligrams per Square Inch
Unaged	4.1
Air-oven-aged at 250 F (121 C)	
4 months	11.0
8 months	8.8
11 months	12.0

These data are very pertinent as they indicate that all so-called ozone-resistant rubber insulations do not retain this property as they age, whereas butyl retains this resistance. The stability of the butyl-rubber compounds in ozone is indicated by the data in Table IX. After 11 months in air at 250 F (121 C), butyl shows no cracking after a 10-hour exposure to the 0.2-per-cent ozone by volume (15 times industry required concentration). None of the oil-base insulations passed these tests since oil-base insulations become brittle after relatively short exposures to air at 250 F (121 C).

CORONA RESISTANCE

Butyl high-voltage insulation has good corona resistance as measured by the vertical U test and shows no cutting after a 70-hour exposure to 100 volts per mil a-c stress. *GR-S* oil-base insulation also withstands a similar vertical U test but, in general, natural-rubber oil-base high-voltage insulation fails in a relatively short time.

After 7 days of air-oven aging at 250 F (121 C), butyl high-voltage insulation still withstands a 70-hour exposure to the vertical U test without cracking, while *GR-S* oil-base fails within 0.5 hour.

Moreover, even after 11 months of air-oven aging at 250 F (121 C), butyl high-voltage insulation does not crack in the vertical U test with exposures of up to 70 hours; see Table X.

DIELECTRIC STRENGTH

Among the obvious requirements of a high-voltage cable insulation is one of proper dielectric strength. Based upon the thickness of insulation specified by the IPCEA and upon phase-to-phase 60-cycle alternating voltages of 5 to 15 kv, rubber-insulated cables are operated at an approximate average voltage stress of 30 volts per mil and at a maximum stress generally not over 60 volts per mil.

Although the dielectric strength of a short length of insulated cable may be 1.4 to 2.4 times that of a long length, it is a common practice to use short lengths (10 feet active) in determining the dielectric strength of various types of insulations. The data in this paper relative to dielectric strength should be considered as indicative and not specific. Dielectric strength values vary not only between various rubber compounds but between samples of the same insulation.

Table XI compares the short-length 60-cycle quick-rise and step-rise, d-c quick-rise, and impulse dielectric strengths of representative butyl- and oil-base-insulated no. 4 American Wire Gauge 15-kv (0.297-inch wall of insulation) cables.

Although the 60-cycle quick-rise dielectric strength tests indicated a higher value for the butyl insulation as compared to the oil-base rubber, the difference probably has no significance. Some investigators of the dielectric strength of rubber insulations have felt that the 60-cycle step-rise test is more searching than the older 60-cycle quick-rise method in seeking out imperfections, voids, and mechanical damages. It is claimed that the step-rise test allows time enough for the voltage stress to develop an intense discharge in any void that is present.

A few years ago data were published which reported the 60-cycle step-rise voltage dielectric strength of some butyl compounds as being inferior to the dielectric strength of oil-base (natural) compounds. This feature was attributed to butyl compounds either having inherently lower a-c dielectric strength or being so manufactured as to have voids or imperfections too small to detect. The a-c step-rise breakdown voltage curves in Fig. 13 indicate that the butyl- and oil-base (natural) rubber insulations have approximately the same dielectric strength. While the data show that for walls less than 250 mils the step-rise strength of butyl may be lower than that of an oil-base insulation, for heavier walls the step-rise strength is higher; however, the differences are small. The oil-base curve is from published data for the natural rubber type.[8] Sixty-cycle step-rise data for *GR-S* oil-base insulation are limited to those given in Table XI; however, there appears to be but little difference between either type of oil-base rubber compound and butyl,

Table VIII. Effect of Air-Oven Aging at 250 F (121 C) on the Insulation Resistance of Butyl Insulation; Wire No. 6 Stranded, 0.156-Inch Wall

Tests	Insulation Resistance Megohm Constant at 60 F (15.6 C), — 1,000 Feet
Unaged	100,000+
Air-oven-aged at 250 F (121 C)	
4 months	100,000+
8 months	100,000+
11 months	100,000+

Table IX. Effect of Air-Oven Aging at 250 F (121 C) on the Ozone Resistance of Butyl Insulation; Wire No. 6 Stranded, 0.156-Inch Wall

Test	Ozone Test,* Hours
Unaged	10+no cutting
250 F air-oven-aged	
4 months	10+no cutting
8 months	10+no cutting
11 months	10+no cutting

*Mandrel, 4 times outside diameter.
Ozone concentration, 0.2 per cent by volume.
Rest, none.

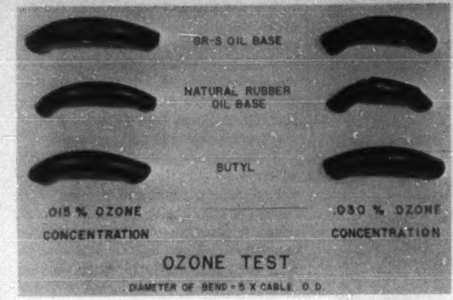
GR-S OIL BASE
NATURAL RUBBER OIL BASE
BUTYL
.015 % OZONE CONCENTRATION
.030 % OZONE CONCENTRATION
OZONE TEST
DIAMETER OF BEND = 5 X CABLE O.D.

Fig. 12 (left). Effect of two ozone concentrations on high-voltage insulations

Table X. Effect of Air-Oven Aging at 250 F (121 C) on Corona Resistance of High-Voltage Insulations; Wire No. 4 Stranded, 0.297-Inch Wall

Vertical U Test: Mandrel = 10 Times Outside Diameter; Stress = 100 Volts per Mil A-C; Rest = 5 Minutes

	Natural-Rubber Oil-Base Insulation, Hours	GR-S Oil-Base Insulation, Hours	Butyl Insulation, Hours
Unaged	0.5, outside cutting	70+, no cutting	70+, no cutting
Air-oven-aged at 250 F (121 C)			
7 days	unfit for test	0.5, outside cutting	70+, no cutting
11 months	unfit for test	unfit for test	70+, no cutting

Table XI. Dielectric Strength Tests; No. 4 American Wire Gauge 0.297-Inch Wall Insulation, 10-Foot Active Test Length

Type	Butyl	Oil-Base (Natural)	Oil-Base (GR-S)
60-cycle quick-rise breakdown, volts per mil*	370	300	300
60-cycle step-rise breakdown, volts per mil†	330	260	260
D-c quick-rise breakdown, volts per mil‡	1,100	820	1,200
Impulse 1.5x40-wave breakdown, volts per mil	800	720	680

*500 volts per second.
†60 kv held for 5 minutes, then voltage increased in 5-kv steps and held for 5 minutes.
‡700 volts per seconds.

although the average test value for the butyl insulation is slightly higher.

The impulse dielectric strength of the butyl compound is slightly higher than for the oil-base materials. Fig. 14 shows the impulse strength as a function of the thickness of insulation for butyl and oil-base rubber compounds. The values for butyl are the average of tests taken in the electrical laboratory, whereas the oil-base (natural) data are from published literature.[2] Test data reported herein give slightly higher impulse breakdown for the oil-base rubber compound with a 297-mil wall than is shown in the curve.

The d-c dielectric strength tests performed on No. 4 American Wire Gauge 15-kv (0.297-inch wall) cables reported herein indicated that the d-c dielectric strength of the natural-rubber oil-base insulation is less than for the *GR-S* oil-base and butyl compounds.

Effect of heat on the dielectric strength of the rubber insulations was discussed in the section entitled "Aging and Heat-Resistant Characteristics." After 30 minutes at 464 F (240 C), butyl test samples showed practically no decrease in dielectric strength, see Table V. This stability was also noted in a test whereby a no. 6 stranded conductor with a 0.156-inch wall (5 kv) of butyl was exposed for 20 months to 250 F (121 C) without any decrease in impulse strength.

After being exposed to 250 F (121 C) for approximately 11 months, samples of butyl insulation were measured for a-c and d-c dielectric strength, see Fig. 6. Again the dielectric strength remained relatively constant as compared to the unaged values at room temperature. Such a test could not be made on the oil-base samples because, as pointed out in the section entitled "Aging and Heat-Resistant Characteristics," the oil-base types show almost complete loss of physical properties after 1 week at 250 F (121 C).

It must be recognized that the dielectric strength values given in the report must be taken as being indicative rather than limiting. A variation between tests and various manufacturers' products should be expected.

LOAD-CYCLE TESTS

It is seldom that a power cable is operated at a constant temperature. Variable loads and changes in ambient temperatures cause conductor and insulation temperatures to fluctuate. Such a condition results in the expansion and the contraction of the conductors and insulation as well as in other cable components. There is also a variation in the oxidation rate of the insulation. In a study of high-voltage rubber insulations and cable constructions, several cables were given overload life tests. One 17-kv and three 22-kv single-conductor no. 2/0 stranded butyl-rubber shielded and neoprene-jacketed cables were tested by applying 32 kv to ground continuously, and by using a current (10 hours out of 24 daily) sufficient to raise the conductor temperature to about 239 F (115 C). After 334 daily (8,016 hours) load cycles, there were no insulation failures and the ionization level was still more than 25 per cent higher than the rated operating voltages to ground.

Similar tests have been made on single-conductor No. 2/0 butyl-insulated, shielded 19-kv grounded-neutral cable. When subjected to 26 kv (2.4 × normal a-c rating) and having conductor temperatures of 212 F (100 C) to 252 F (122 C), over 9,000 hours of cycling were required to produce a failure. The overload life of a varnished cambric cable with a conductor temperature of 212 F (100 C) is about 600 hours, which is very short in comparison with the performance of the butyl-rubber insulated cable.

Load-cycle tests were made on single-conductor no. 4 rubber-insulated shielded neoprene-jacketed 15-kv grounded cable. Both oil-base and butyl-type cables were involved in these tests. All samples on load cycles had approximately 25 feet of active length and were tested in air at room temperature. Twenty-six kv a-c was applied continuously across the insulation with current through the conductor 10 hours out of every 24 hours. The conductor temperature under load was approximately 176 F (80 C). The results of the tests are given in Table XII. The butyl-insulated cable was more resistant to failure

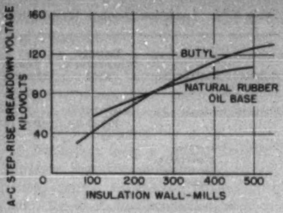

Fig. 13. Effect of wall thickness on a-c step-rise dielectric strength of high-voltage insulations

on this test than the oil-base cable. Under voltage only, and no current, all samples withstood 2,000 hours at 26 kv without failure. This is an indication that heat caused by current loading may be the contributing factor in the load test failure.

As noted in Table XII, some failures occurred under or near the terminations. This may be because of faulty test terminations; however, the same technique was followed on all cables and no faults under or near a stress cone occurred on the butyl sample. The authors believe that the load-cycling test data give another indication of the physical and electrical stability of butyl as a function of heat and aging.

Current-Carrying Capacities

As early as the 1890's studies were being made as to the allowable current ratings of insulated cables. Increasing industrial and utility loads make such a study even more important today. It is not within the scope of this paper to discuss all the factors upon which the current-carrying capacity of a cable depends. However, a fundamental requirement is that the insulation should not be heated above a determined safe operating temperature. The operating temperature of the insulation is a function of the rise of temperature above the ambient temperature due to the I^2R losses and, in some cases, the dielectric losses

The safe operating temperatures of rubber insulations depend upon their ability to resist deterioration under many service conditions. The effect of heat, aging, moisture, and ozone upon oil-base and butyl insulations has been previously discussed herein. Present properties of both types of rubber compounds permit higher conductor temperature operation than possible with some of the earlier types of rubbers. Operating conductor temperatures have increased to 75 C for oil-base compounds and to 85 C for butyl-rubber insulating compounds. There are 5- and 15-kv butyl-rubber insulated cables in operation at conductor temperatures of 90 C.

It is the exceptional resistance of the butyl-rubber insulation to deterioration from heat and aging which permits a conductor insulated with this material to be operated at higher temperatures than deemed advisable with other types of rubber compounds. Because of this characteristic, butyl-insulated cables carry more current per pound of conductor than possible with the older types of high-voltage rubber insulation. Table XIII gives the current-carrying capacity of three single-conductor 15-kv rubber-insulated cables in a duct bank with one cable per duct. The current rating for various sizes of conductors is given as a function of conductor temperatures namely, 75 C, 80 C, 85 C, and 90 C. The 80 C, 85 C. and 90 C ratings are restricted to the butyl insulations A comparison of these ratings as a ratio of the rating for a conductor temperature at 75 C is given in Fig. 15.

In comparing the current ratings of cables insulated with butyl and oil-base rubber, an interesting feature is observed. The decrease in permissible current loading due to an increase in the ambient temperature is less for the butyl than for the oil-base type. A study of the curves in Fig. 16 clearly proves this point. Assume that a butyl-insulated and an oil-base insulated cable are installed under identical conditions and are operating at an ambient temperature of 20 C. If the ambient temperature rises to 40 C, the current loading of the 75 C oil-base cable must be reduced to 80 per cent of the rating at 20 C, whereas it is necessary to reduce the rating of the 85 C butyl cable to only 84 per cent in order not to exceed the specified maximum permissible conductor temperature.

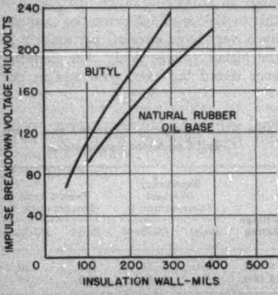

Fig. 14. Effect of wall thickness on impulse strength of high-voltage insulations

For many installations the proper size of conductors is based not only upon the normal system rating but upon the time and magnitude of emergency overloads and/or short circuits. Cable overload and short-circuit ratings depend upon the magnitude of the current, its duration, and the previously applied load, as well as the ability of the cable components to withstand higher than normal temperatures without serious damage.

There are so many variables involved in determining the conductor sizes for the various combinations of currents and times of application that it is not possible to give a comprehensive rating table or a discussion of the subject in this paper. However, there have been aging and heat characteristic studies made on rubber insulations which give data for suggesting emergency overloading and short circuit loading conductor temperatures. W. H. Couch and G. J. Crowdes[8] report insulation damage temperatures for several types of rubber insulations which are shown in Table XIV.

The damage temperatures are the temperatures at which it is felt that the insulation should not be operated for the specified time as excessive deterioration of the material may have occurred. Note that the damage temperatures for the oil-base compounds are not only lower than for the butyl but the time of exposure is only 10 to 15 minutes as compared to 30 minutes for the latter. These data and the data given in this paper indicate that a butyl-rubber compound can be operated at a higher emergency overload or short-circuit loading temperature than an oil-base compound. It should be recognized that not only must a factor of safety be used in establishing these ratings but the temperature must

Table XII. Load-Cycling Tests on Single-Conductor No. 2 Rubber-Shielded Neoprene-Jacketed 15-Kv Grounded-Neutral Cable

Impressed voltage = 26 Kv, A-C to Ground
Loading = 10 Hours Out of Every 24 Hours
Temperature = Approximately 80 C During Loading

	Oil-Base (GR-S)	Oil-Base (Natural)	Butyl
Time to Failure-hours	11* 29*	86† 3‡	760§

*Failed at end of stress cone.
†Failed in cable section 12 inches from end of cone under shield. Fault cut out at end of 76 hours and new stress cone made. Cable failed after 10 additional hours cn voltage. Second fault 1 inch from end of cone, same as first fault.
‡Failed in active section of cable.
§No failure, cable still on test.

Table XIII. Current-Carrying Capacity of Three Single-Conductor 15-Kv Rubber-Insulated Cables in a Duct Bank, One Cable per Duct, 100-Per-Cent Load Factor, 20 C Ambient Temperature

Size Conductor, American Wire Gauge or 1,000 Circular Mils	Current per Cable, Amperes: Oil-Base, Conductor Temperature 75 C	80 C	Butyl 85 C	90 C
2	170	176	182	187
1/0	221	229	236	243
3/0	288	298	308	317
250	356	369	381	392
350	427	442	457	470
500	521	540	557	574
750	655	679	701	722

not be so high that other cable parts, such as tapes, fillers, etc., be damaged. The conductor temperatures in Table XV are given as a guide to emergency overloading and short-circuit loading temperatures.

These ratings are probably conservative. Butyl-insulated cables are in service based upon conductor sizes designed on higher limiting conductor temperatures. When the size of a conductor is chosen on the basis of an overload or short circuit rating, a smaller size will be required for a butyl-insulated cable than for the oil-base type because of the butyl having better resistance to aging and heat.

DIELECTRIC CONSTANT, POWER FACTOR, AND INSULATION RESISTIVITY

Among the electrical properties of interest in a cable insulation are the dielectric constant, power factor, and the resistivity. The dielectric constant (specific inductive capacity) as a measure of the capacitance of the insulation must be considered from two points of view. First, a lower value of dielectric constant will result in lower charging current in the cable at operating voltage; under some circumstances the charging current may become an appreciable part of the current supplied to the cable. While this is not a limiting factor for the rubber-insulated cable class, it may enter in as an economic factor to some extent.

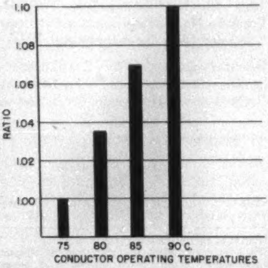

Fig. 15. Ratio of current rating at various conductor temperatures to rating for conductor temperature at 75 C

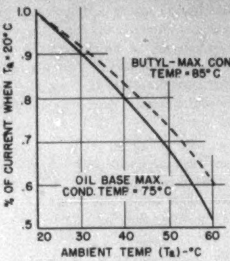

Fig. 16. Ambient temperature correction factors

The second consideration of dielectric constant must be made in connection with the insulation power factor; the product of these two quantities, known as the loss factor, is a measure of dielectric loss in the cable. With the application of rubber insulation to higher voltages, the dielectric loss may become sufficient to be considered for its effect on the cost of transmission, and low values of the loss factor are desirable.

Insulation resistivity is a quantity commonly measured with direct current. It can be used, in comparison with past history, as a measure of the condition of the cable, although the absolute magnitude of resistivity is not particularly significant as long as it does not become so low as to have an adverse effect on the a-c leakage or power factor.

Table XVI gives typical values of these three quantities as measured on samples of No. 4 American Wire Gauge stranded 15-kv shielded cable. The dielectric constant of the butyl-rubber samples averaged slightly less than those measured on on the natural rubber and *GR-S* types of oil-base insulation. However, a considerable difference in power factors was noted, with an average range of 1.5 per cent for butyl, 3.0 per cent for natural-rubber oil-base, and 6.5 per cent for the *GR-S* oil-base samples. The typical insulation resistivity megohm constant of the butyl-rubber insulation was measured as approximately four times that of the oil-base compounds.

Table XIV. Insulation Damage Temperatures

Rubber	Designation	Damage Temperatures, F(C)	Time, Minutes
Natural	oil-base	356 (180) to 392 (200)	10 to 15
GR-S	oil-base	392 (200)	15
Butyl	low water absorptive, heat- and ozone-resisting	464 (240)	30

Operation Experience

Over a considerable period of years, the use of rubber-insulated cable has expanded not only in volume but also in operating voltage and cable types. They are now rather commonly used for voltages up to 15 kv and, for special cases, as high as 35 kv. Constructions have expanded from the earlier simple ones of rubber and lead sheath or braid to those, for example, with shields and protective coverings of neoprene or thermoplastic jackets, stainless steel outer tapes, and many others.

Oil-base insulation has been by far the predominant insulation used for power cables in the past and has had a good record. The newer butyl-insulation rubber compounds because of the superior characteristics pointed out in this paper, have performed excellently in 8 years of operation. Furthermore, cables insulated with butyl insulation are in operation where overloading, high ambient temperatures, and economic loading would not support the oil-base materials.

In a period from December 1948 through April 1952, for example, there are company records showing that several million feet of cable were in service. Of this quantity 51 per cent were in the 0- to 600-volt class, 38 per cent were from 601 to 5,000 volts, and 11 per cent were in the 5,001- to 17,000-volt range. Extension of this to 1955 would increase the quantity by a very large amount, particularly in the higher voltage field. The performance record has been good and in line

Table XV. Emergency Overload and Short-Circuit Conductor Temperatures

Voltage Rating	Emergency Overload Temperature, C: Butyl	Oil-Base	Short-Circuit Temperature, C: Butyl	Oil-Base
5,000	105	85	150	120
15,000	95	80	135	110

Emergency ratings are for a total time of 100 hours in any one year.
Short circuits are for a duration of 5 seconds.

with predictions of the properties of the butyl insulation.

In two locations, where butyl-rubber-insulated cables have been connected to open-wire lines, there have been cable failures. However, whereas cables insulated with oil-base rubber and other types of insulation have a similar record, it appears that the problem is more basic with respect to system characteristics and basic-impulse-insulation-level ratings than to cable.

A classification of services condensed from the study of operating experience previously mentioned is shown in the Appendix.

Table XVI. Dielectric Constant, Power Factor, and Insulation Resistivity

	Insulation		
	Oil-Base		
	Natural	GR-S	Butyl
Dielectric constant, 60 cycles a-c	4.2	4.2	3.8
Power factor, per cent	2.0 to 4.0	6.0 to 7.0	1.0 to 2.0
Insulation resistivity, megohm constant — 1,000 feet at 60 F	30,000	40,000	150,000

Conclusions

There are two general types of high-voltage rubber insulations being used in this country for power cables in the range of 2 to 35 kv. These insulations are the older ozone-resistant type, commonly known as oil-base, and a newer type compounded with butyl, which is a synthetic rubber. Oil-base insulations usually contain various vulcanized vegetable oils, bitumens, reclaimed rubber, and either natural or (*GR-S*) synthetic rubbers. Butyl compounds contain butyl rubber which is a hydrocarbon of low unsaturation plus other compounding ingredients.

Cables insulated with either type have been installed under various service conditions such as aerial, submarine, direct burial in the earth, conduit, and in underground ducts. There is an increasing demand for butyl-insulated cables because of their high permissible operating temperatures, resistance to aging and heat, as well as to deterioration from ozone and moisture.

Numerous tests have been made in evaluating the physical, thermal, chemical, and electrical characteristics of oil-base and butyl-rubber-insulating compounds and their susceptibility to service environments. Based upon field experience and the tests and their interpretations as discussed in this paper, it is concluded that:

1. Butyl and oil-base rubber insulations differ in their properties. The butyl insulation has greater resistance than either natural or synthetic (*GR-S*) oil-base rubber compounds to:

    a. Aging and heat.
    b. Deterioration from moisture.
    c. Deterioration from ozone and corona.

2. The initial dielectric strength characteristics of the two types of high-voltage rubber insulation are approximately the same. There is an indication that the a-c dielectric strength of the butyl insulation is slightly greater than for the oil-base insulations. The d-c dielectric strength of the *GR-S* oil base and butyl rubbers is comparable; however, the natural-rubber oil base appears to have a lower value. The impulse strength of the butyl-rubber compound is slightly greater than for the oil-base insulations. Aging tests indicate a greater stability of dielectric strength with age for the butyl rubber as compared to that for the oil-base types.

3. The dielectric constant and power factor are lower and the insulation resistivity is higher for butyl-rubber insulation.

4. The excellent stability of physical, thermal, chemical, and electrical characteristics with age and heat permits butyl-insulated cables to be operated at higher temperatures for normal loads, emergency overloads, and short circuits.

Appendix. Classification of Services

General Types of Installations

1. In conduit and raceways:
   Dry and wet locations, and hot places.
2. Underground:
   a. In underground ducts for control, primary, and secondary distribution.
   b. For direct burial—power and control, and signal service.
3. Aerially:
   a. Tree wire.
   b. Self-supporting aerial cables—power, control and signal.
   c. Field spun aerial cables—power, control and signal.
4. Submarine:
   Nonleaded wire armored.

Classification of Users

1. Utilities.
2. Municipalities.
3. Railroads.
4. Paper mills.
5. Steel mills.
6. Coal mines.
7. Copper mines.
8. Oil refineries.
9. Chemical plants.
10. Aluminum plants.
11. Industrial plants and many others.

Geographical Range

1. South America.
2. Mexico.
3. Hawaii.
4. Alaska.
5. Continental U.S.A.—practically complete coverage:
   a. Florida to Maine.
   b. Texas to Washington.
   c. Massachusetts to California.

References

1. RECOMMENDED SHIELDING PRACTICES. *Standard S-19-81*, Insulated Power Cable Engineers Association.

2. HIGH-VOLTAGE RUBBER INSULATED SUBMARINE POWER CABLES, H. B. Slade. *Proceedings*, Institution of Electrical Engineers, London, England, PART II-A, SYMPOSIUM OF PAPERS ON INSULATING MATERIALS, March 1953.

3. HIGH-TEMPERATURE CLASSIFICATION OF RUBBER AND RUBBERLIKE INSULATION OF NETWORK CABLE BY OVEN-HEATING TESTS, W. H. Couch, G. J. Crowdes. *AIEE Transactions*, vol. 74, pt. III, Oct. 1955, pp. 930–38.

4. SYNTHETIC RUBBER, G. S. Whitby. John Wiley & Sons, Inc., New York, N. Y.

5. HIGH VOLTAGE—HIGH TEMPERATURE RUBBER INSULATION, W. H. Couch, W. K. Freeman. Second Annual Signal Corps Symposium, Dec. 1953.

6. MOISTURE STUDIES ON OZONE-RESISTING AND TYPE RH-RW RUBBER INSULATIONS, E. C. De Baene, C. A. Anderson. *Ibid.*, vol. 73, pt. III-B, 1954 (Feb. 1955 section), pp. 1746–54.

7. CHEMISTRY AND TECHNOLOGY OF RUBBER, Davis, Blake. Reinhold Publishing Corporation, New York, N. Y.

8. SCIENCE OF RUBBER, edited by D. K. Memmler. *Ibid*.

Discussion follows

Discussion

E. G. Driscoll (Phelps Dodge Copper Products Corporation, Yonkers, N. Y.): The authors of this paper are to be commended on an excellent presentation of a subject which can very well be controversial. It is readily apparent that a vast amount of testing has been done to achieve the graphical presentation which is self-explanatory in so far as the conclusions drawn.

However, there are certain elements regarding oil-base insulations which are difficult, if not impossible, to present graphically. First, is the realization that oil-base insulations differ not only among manufacturers, but also with any one manufacturer. The insulating properties are dependent on the vegetable oil used as the starting point, and the quality of this material varies always; it is a natural product and subject to the vagaries of nature. In applying it as insulation the most rigorous controls are needed not only to make a quality insulation, but also because any relaxation of controls produces scrap. Even when the process of insulation has been satisfactorily accomplished there are pitfalls to be avoided by more special handling. Oil-base insulations exhibit plastic tendencies which lead to easy deformation by heat or pressure, or both; they exhibit an unfortunately high degree of thermal expansion which must be cushioned if a metallic covering such as a shield is to be applied.

In the face of these inherent difficulties and weaknesses, innumerable quantities of cable have given excellent service and should reflect much credit on the cable manufacturers. However, when butyl rubber became available, it was soon apparent that better cable could be produced and, surprisingly, with even less rigidity of control achieve a greater degree of uniformity. This quality, along with superior ozone resistance, higher operating temperature, and a harder, less expansible product led my company to discontinue the use of oil base in 1948. Oil-base rubber was the best for high-voltage rubber for many decades, but it is now certainly in the realm of: "To be first is progress, to have been first is antiquity."

There is one omission in the authors' presentation having to do with shielding. In addition to tape shielding which has been standard for many years, there is also wire shielding, defined in the recent issue of American Society for Testing Materials *D1350–54T* as a layer of tin- or alloy-coated copper wire applied helically in intimate contact with a layer of semiconducting material directly over the insulation. This type of shield, according to our tests, enjoys a higher corona level than is found with tape shield and this fact is even more marked when compared with tape shield applied over nonsemiconducting material such as paper bedding tapes. The resistance of a wire shield is constant and is not plagued by contact resistance variations as with helically applied metal tape. A tape shield can be ruptured during manufacture especially when a thermosetting sheath is vulcanized over it and will cause loss to the manufacturer if it can be discovered or trouble for the user if it is not found before being put in service. The wire shield does not suffer this trouble because all of the wires cannot be broken in any one place at one time. Of advantage to the user is the fact that the wire shield can be used as is for a ground lead at splices and terminations.

W. H. Couch, G. H. Hunt, N. D. Kenney, and **P. H. Ware:** We thank Mr. Driscoll for his comments. They are pertinent and we are in quite close agreement with them.

One point which should be clarified is the subject of shielding. Mr. Driscoll has questioned the omission from this paper of mention of a particular type of shielding. Since we were primarily concerned with insulation in this paper, no attempt was made to cover different methods of shielding and only a passing notice was taken of the particular type of shielding used on some samples.

Contact Life of Voltage-Regulating Relays

C. W. SCHOENDUBE
ASSOCIATE MEMBER AIEE

R. L. ELLIOTT
NONMEMBER AIEE

FEEDER voltage regulators must operate for long periods without inspection or maintenance to provide economical voltage regulation. The expense of routine inspection may be reduced as the reliability of the components of the regulator is increased. In the past, inspection has been required most frequently for the contacts of the voltage-regulating relay. Occasional cleaning and dressing of these contacts is necessary to prevent sticking which will run the regulator to its limit position.

By adding contact-holding devices and arc suppressors to the step voltage regulator control discussed by Lennox,[1] electrical life of the voltage-regulating relay contacts in excess of 20 years is indicated.

Control Action

In this control, the time-out and return-to-neutral timer operations on either side of the voltage band are directly effected by the voltage-regulating relay contacts. No auxiliary relays are required. Closing and subsequent reopening of a pair of relay contacts result in respective forward and reverse operation of the timer at full rated power. With no contact-holding devices but with arc suppressors connected across the contact pairs, arcing is reduced to a level barely detectable to the naked eye.

Contact-holding devices had been employed on previous controls using the same voltage-regulating relay in different circuitry. Such devices were energized simultaneously with the actuation of auxiliary relays. They serve to increase contact pressure of the voltage-relay contacts and thereby reduce contact arcing. In the case of auxiliary relays, excessive frequency of operation or chatter is prevented.

The control under discussion appears to operate excellently without holding devices. Absence of auxiliary relays and the low contact duty imposed by the timer motor make such devices seem unnecessary. Measurements of radio and television interference levels which were markedly lower than previous controls support this conclusion.

Results of Field Test of Control

Service experience of 3 months was obtained on such a control, which will be referred to hereafter as control *A*. Examination of its voltage-relay contacts disclosed evidence of electrical erosion; a small spot about 1/64 inch in diameter was visible on each contact. These contacts are shown in Fig. 1. Note that the direction of material transfer is from the moving contacts, shown at the left of the figure, to the stationary contacts shown at the right. This results

---

Paper 55-718, recommended by the AIEE Relays Committee and approved by the AIEE Committee on Technical Operations for presentation at the AIEE Fall General Meeting, Chicago, Ill., October 3–7, 1955. Manuscript submitted March 30, 1955; made available for printing August 8, 1955.

C. W. SCHOENDUBE and R. L. ELLIOTT are with the General Electric Company, Pittsfield, Mass.

The authors wish to express their thanks to T. W. Hall for the design of the transient integrator used in this study.

in the formation of a crater on the moving contacts and in a peak on the stationary contacts. The stationary contacts in this instrument are located directly above the moving beam contacts. The hemispherical contacts are of platinum-iridium alloy.

Three aspects of the peak and crater formation merited further investigation:

1. Why did the formation occur in such short a period with such extremely low levels of visible arcing?
2. With the presence of contact wipe, could the combination of peak and crater produce mechanical locking of contacts?
3. Would a thermal condition be created which would eventually cause welding of the contacts and, if so, after what period of time?

Study of Contact Action and Arc Phenomena

The first step in obtaining answers to these questions was to excite the control *A* from a stabilized 60-cycle-per-second (cps) voltage supply and to bring a contact pair to the point of touching. It was felt that perhaps motions produced by system voltage fluctuations plus the natural 120-cps vibration might be the cause of the contact erosion. It should be pointed out that the moving beam of the voltage relay and its contacts are never stationary, regardless of the amount of damping provided. There is always some 120-cps vibration present on the beam. This is derived from the 60-cps excitation of the relay coil.

Since the contact motion and, hence, the expected region of arcing would be very small, it was necessary to excite the control from a well-stabilized voltage source to maintain the floating beam and its contact within the arcing region. An electronic voltage regulator was used to obtain this closely regulated source which, except for line surges, tends to maintain a ±0.01-volt bandwidth.

When the voltage relay was adjusted so that a pair of contacts were touching with a minimum of pressure, observation with a 10X magnifying lens answered the first of the questions. The observation revealed a tiny and apparently continuous arc between the contact pair. Measurements showed that it required a supply voltage change of about 0.35 volt to traverse the complete arcing band—from the point of initial contact to the point of contact closure at which no arcing was visible. The continuous arc persists for the initial 0.20 volt of this band and appears less and less frequently in the remainder of the band with the development of greater contact pressures. In the initial 0.1 volt of this band, slight fluctuations in the stabilized supply would cause movements which superimposed upon the self-generated 120-cps vibration of the relay would occasionally open the contact pair. These momentary openings were accompanied by discharges visible to the naked eye. Also, in this band, the timer performed as would be expected, operating first in one direction and then the other, without completing a timing cycle.

Fig. 2 shows two typical traces of the voltage across the contacts while in the arc of the "sizzle" band. Note the regions of oscillatory discharges. The frequency of these discharges is a function of the circuit parameters. Although physically not discernible in Fig. 2, the arc voltage peaks are actually two to six times greater than the peaks visible on this oscillogram. These spiked extensions of the visible peaks were observed on an oscilloscope. It is these spikes of voltage that trigger the transient recorder mentioned later.

Accelerated Life Tests

After the foregoing observations and measurements, a contact pair was set in the sizzle band by careful adjustment of the electronic regulator and a life test was made. After 1,900 hours of practically continuous sizzle, the contacts stuck together. Fig. 3 shows the contact pair with oxidation products removed. This reveals the typical peak and crater formation. The open-circuit voltage across the contacts is 130 volts. The timer current is 65 milliamperes.

Another type of control, control *B*, was available having a different balanced beam relay but similar control action. This second instrument had the stationary contacts located directly above and below the moving beam contacts, in turn fastened above and below the end of a cantilever spring suspension. The contacts were flat disks of platinum-ruthenium alloy.

The contacts of this relay were placed in the sizzle band and a life test was made. After 2,100 hours of nearly continuous sizzle, the contacts stuck. However, voltage surges or a light tap on the control panel would free the contacts. After 2,300 hours, the latter factors would no longer part the contact pair and the test was terminated. Fig. 4 is an oscillogram of the arc voltage across the contact pair. The open-circuit voltage across the contacts is 24 volts. The timer current is 85 milliamperes. Fig. 5 shows the contacts after the life test, again revealing the peak and crater formation. It is the authors' opinion that the peak on the stationary contact and the crater on the moving one will occur on this type of control regardless of the contact shapes, materials, or arrangements.

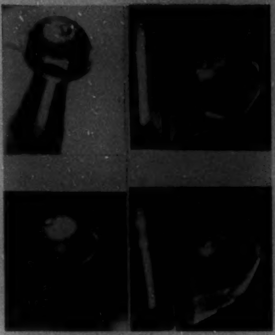

Fig. 1. Platinum-iridium contacts from voltage relay of control A. Moving contacts are at left and stationary contacts at right

Estimating Actual Operating Life

The Transient Integrator

There remained the problem of translating the accelerated life test data into estimated operating life. For this purpose, a transient integrator circuit was devised. Fig. 6 is a circuit diagram of the device. Briefly, it operates as follows: The contact arc voltage is impressed upon the control grid of a thyraton through a high pass filter which eliminates most of the frequency components of 60 cycles and below. An electric clock is connected to the plate circuit of the thyraton. In the absence of control grid voltage, only the negative half-cycles of the 60-cycle plate voltage appear on the clock motor, which is insufficient to operate it.

An adjustable d-c bias voltage is applied to the screen grid of the thyraton. A positive voltage pulse on the control grid exceeding a value determined by the screen bias will cause the tube to fire and supply one alternate positive half-cycle of the clock motor voltage, thus causing it to run. Hence, when sizzling occurs, a series of high-frequency pulses is applied to the control grid. Each positive pulse having a peak great enough to fire the tube will cause the clock to move slightly and record the proportional arcing time.

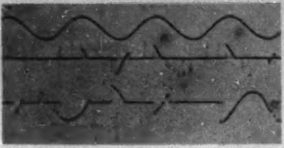

Fig. 2. Oscillogram showing portions of continuous traces of arc voltage across platinum-iridium contacts of voltage-regulating relay used in control A. Timing trace at top is 60 cycles per second

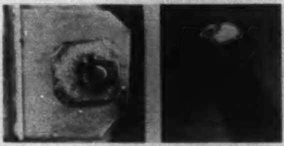

Fig. 3. Platinum-iridium voltage-relay contacts of control A after 1,900-hour continuous-sizzle life test

OPERATING LIFE

The operating life of control *A*, without the contact-holding effect, was estimated as follows:

1. The integrator was placed across the suppressor resistor located across a contact pair which was continuously sizzling. An average sizzling rate R_0 in clock hours per day was then established, which was known to give a contact life L_0 of 1,900 hours, if allowed to progress.
2. The control panel and integrator were placed on a single-phase regulator-regulating shop voltage. The relay was set for a ±1-volt band and the timer was set for 30-second delay. An average sizzling rate for the relay on the shop system R_x was established.
3. The estimated contact operating life on the shop system for the particular bandwidth and timer settings could then be calculated as

$$L_x = \frac{R_0}{R_x}\,\frac{L_0}{8{,}760}\ \text{years}$$

Substituting the test values

$$L_x = \frac{12}{0.46}\,\frac{1{,}900}{8{,}760} = 4^1/_3\ \text{years}$$

This seems to be a reasonable value judging from the erosion rate of the contacts tested in the field. It indicates that, on this system, the relay contacts of control *A* without holding effect must be inspected, cleaned, and polished, roughly every 3 or 4 years.

For a given voltage band and timer setting, little difference in contact life may be expected on feeders of different voltage characteristics. The regulator normally maintains the moving contacts within the voltage band. The moving contacts are equally likely to occupy any part of this band. When subject to a voltage which changes with load cycles, the expectancy is for the moving contacts to occupy each equal part of the band for equal periods of time. Hence, for a given band, the per cent of total time spent in the sizzle bands will be substantially the same on all feeders.

For control *B*, also without holding effect, and having the relay with flat platinum-ruthenium contacts located vertically in line, contact life may be obtained by direct ratio of the continuous sizzle lives, assuming only that the transient integrator recording rate ratio R_0/R_x remain the same; this is a valid assumption since the disturbing vibrations, the resulting transients, and the continuous sizzle contact life are very comparable.

Thus, after $2{,}100/1{,}900 \times 4^1/_3 = 4^3/_4$ years, light sticking of contacts could be expected which may be broken by line surges. Contacts should be cleaned and polished before this number of years.

Contact Holding and Its Effect on Contact Life

The maintenance interval indicated by the life test was unsatisfactory, and a method of increasing the interval was sought. The basic problem was that the stable balanced beam relay is a relatively slow-moving device, unable to develop the large force-displacement energies required to impart velocity closure to contacts. As a result, the contact-making forces are low, and small disturbances can cause contact sizzle.

The obvious solution was to insert contact-holding devices such as had been used on all previous models of voltage-regulating relays. Only a small amount was required. About 0.3 volt would, upon initial contact, move the contacts across 85 per cent of the measured sizzle band and, in so doing, develop higher contact forces. Holding devices in the form of coils located in the relay itself and excited by timer currents were provided. No great sacrifice is imposed upon the control by the use of such small holding effect. The regulator can still hold a voltage band of substantially less than ±1 volt.

Control *A* with the integrator was again placed on the regulator regulating the shop power. Results of this final test indicated an R_x value of 0.006 and, hence, an estimated life 75 times greater than was indicated on the same control without the holding device. This life is more than the expected life of the regulator.

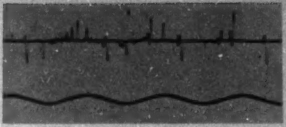

Fig. 4. Oscillogram showing part of a continuous trace of arc voltage across the platinum-ruthenium voltage-relay contacts shown in Fig. 5. Timing trace is 60 cycles per second

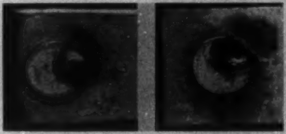

Fig. 5. Platinum-ruthenium voltage-regulating relay contacts of control B after 2,300-hour continuous-sizzle life test. Stationary contact is at left and moving contact at right

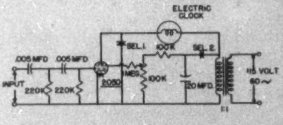

Fig. 6. Circuit diagram of transient integrator used in contact life study

Conclusion

Improvements of the control such as described herein, contribute materially to the goal of eliminating the control as a factor in regulator maintenance. The life of the voltage-regulating relay contacts has been greatly increased through use of contact holding without serious sacrifice in minimum band setting.

In the control with holding effect, only the voltage-regulating relay contacts would require maintenance. Hence, the increase in contact life represents a severalfold increase in control reliability which is reflected as lower operating cost for the regulator.

Reference

1. CONTROL FOR STEP VOLTAGE REGULATORS, T. C. Lennox *AIEE Transactions*, vol. 74, pt. III, Oct. 1955, pp. 900–03.

Discussion

O. J. Lindquist (Commonwealth Edison Company, Chicago, Ill.): The paper shows an excellent investigation of the contact life of voltage-regulating relays. The work of the authors will surely result in more reliability, less maintenance, and longer contact life for voltage-regulating relays.

Voltage regulation of substation busses is much used in Chicago. In some locations, equipment such as large welders and arc furnaces cause frequent voltage fluctuations of up to 1 per cent on the regulated bus. Therefore, we believe the holding effect should be adjustable so that where necessary the bandwidth and the holding effect can both be increased. Wattmeter charts, taken as described in the discussion of the paper by Mr. Lennox,[1] clearly showed cases where the voltage-regulating relays were too active, requiring that the holding effect be increased to avoid contact deterioration.

REFERENCE

1. CONTROLS FOR STEP VOLTAGE REGULATORS, T. C. Lennox. *AIEE Transactions*, vol. 74, pt. III, 1955, pp. 1407–09.

C. W. Schoendube: Mr. Lindquist in his discussion of Mr. Lennox's paper contributes a wattmeter and lamp circuit which serves as a useful tool in optimizing the performance of tap changer controls. Mr. Lindquist mentions that this circuit shows up cases of overactive voltage regulating relays. In connection with this subject, the following comments apply to the controls discussed in our paper.

1. With the voltage relay contacts in the sizzle band, and with no holding effect provided, the contacts are making and breaking close to 120 times per second. At this severe rate of cycling, better than 4 years are required to produce contact welding with the control on a shop system regulator.
2. Frequent interruptions of this severe cycling, such as produced by welder or furnace loads, only leads to less duty on the voltage relay contacts.
3. Adding holding effect practically eliminates the 120-cps duty from the picture.
4. The resulting duty, produced by frequent load fluctuations alone, should still result in contact life many times greater than that obtained for a relay without holding effect.

We believe that the benefits derived from an adjustable holding effect, considered desirable by Mr. Lindquist, should be marginal in the case of the subject control.

Two Large Electric Arc Furnaces—Electrical Characteristics and Corrective Equipment

S. W. LUTHER
MEMBER AIEE

J. D. GHESQUIERE
ASSOCIATE MEMBER AIEE

C. E. QUICK
ASSOCIATE MEMBER AIEE

ELECTRIC arc furnaces have presented power system engineers with major problems for a great many years. Beginning about 1910 with single-phase furnaces of a few hundred pounds of capacity and demands of a few hundred kilovolt-amperes (kva), the size has grown to 200 tons of capacity with demands exceeding 30,000 kva in 1955. Furnace transformer sizes have increased from a few hundred kva to 25,000/33,000 kva. Electrode voltages have increased from less than 100 volts to more than 500 volts. As the present trend indicates that electric arc furnaces are to assume a greater role in the steel industry, problems are on the increase. Much has been written concerning the nature of those encountered and the solutions employed.[1–9]

Electric arc furnaces are characterized by fluctuating loads, and the direct-arc type produces fluctuations so severe that some protective or corrective measures are essential in almost every case. Exceptions occur in those cases where the steel plant is located in an area where available short-circuit capacity is great enough to supply the arc furnace without undesirable flicker results.

The utility has an obligation to all of its customers, and the revenue from furnace loads must be balanced against the costs of corrective measures necessary to prevent disturbances to other customers. The increases in the size of furnaces and in the electrode voltages have resulted in increases in load fluctuations, both in magnitude and in rate of occurrence, especially in the cyclic flicker range, despite the increase in system sizes.

In this paper the electrical characteristics of two 25,000-kva 150- to 200-ton direct-arc furnaces with 510 volts between electrodes are described as well as the corrective measures installed to permit operation on the electric system of The Detroit Edison Company.

The Problem

A steel company in the Detroit area has an integrated steel plant for production of hot and cold rolled steel. Three-phase electric arc furnaces are utilized for production of the steel. Prior to the installation in August 1954 of the two 25,000-kva furnace transformers, this plant was equipped with one 13,333-kva, two 15,000-kva, and one 16,000-kva furnaces with maximum secondary voltage of 320 volts. These furnaces were supplied from a power-plant 120-kv bus having a short-circuit capacity of 2,000 megavolt-amperes (mva) at minimum generation. The 120- to 24-kv step-down station supplying these furnaces is located on utility property in the proximity of the steel plant, some 3 miles from the power plant. The 24-kv busses supplying the steel company are isolated from other loads; see Fig. 1.

The installation of two 24-foot-diameter 150- to 200-ton electric furnaces, each supplied by a 25,000-kva transformer (with additional water cooling, rating is increased to 33,000 kva) with a maximum secondary voltage of 510 volts, was proposed late in 1952. Based on the knowledge that the existing furnaces approaches the maximum size which could be supplied from the 120-kv bus at the power plant, modifications in the electric system, or corrective measures, were indicated. These changes were necessary to keep voltage flicker, especially in the cyclic range, to other customers within acceptable limits.[6,7] These flicker limits for The Detroit Edison Company are 0.5 volt for cyclic flicker and 1.0 volt for extremely frequent flicker on the power plant bus (120-volt base).

Paper 55-743, recommended by the AIEE System Engineering Committee and approved by the AIEE Committee on Technical Operations for presentation at the AIEE Fall General Meeting, Chicago, Ill., October 3–7, 1955. Manuscript submitted June 3, 1955; made available for printing July 26, 1955.

S. W. LUTHER, J. D. GHESQUIERE, and C. E. QUICK are with The Detroit Edison Company, Detroit, Mich.

The authors wish to express their appreciation to Prof. Tarboux, University of Michigan, and to T. H. Lee, The Detroit Edison Company, for their assistance. They made the stability studies of the system for various condenser-reactor combinations and confirmed studies of the transient performance of the system.

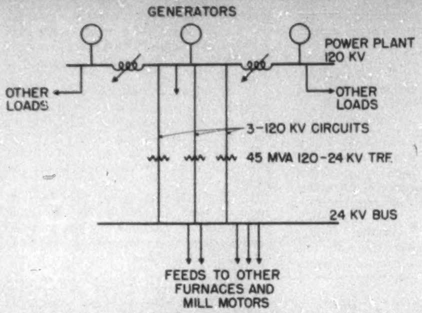
GENERATORS
POWER PLANT
120 KV
OTHER LOADS
OTHER LOADS
3-120 KV CIRCUITS
45 MVA 120-24 KV TRF.
24 KV BUS
FEEDS TO OTHER FURNACES AND MILL MOTORS

Fig. 1. One-line schematic diagram of system prior to alterations and increase of load

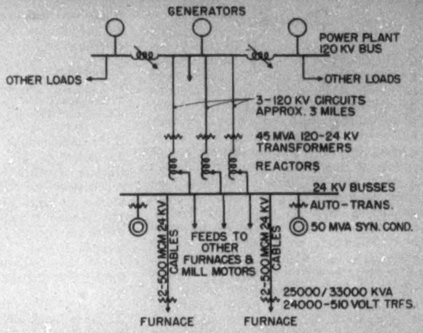
GENERATORS
POWER PLANT
120 KV BUS
OTHER LOADS
OTHER LOADS
3-120 KV CIRCUITS
APPROX. 3 MILES
45 MVA 120-24 KV
TRANSFORMERS
REACTORS
24 KV BUSSES
AUTO-TRANS.
50 MVA SYN. COND.
12-500 MCM 24 KV CABLES
FEEDS TO OTHER FURNACES & MILL MOTORS
12-500 MCM 24 KV CABLES
25000/33000 KVA
24000-510 VOLT TRFS.
FURNACE
FURNACE

Fig. 2. One-line schematic diagram of system including addition of condensers, reactors, and additional load

The extremely frequent rate flicker has been used as the flicker limitation in the application of arc furnaces by the industry for many years, and has general acceptance as indicated in published reports.[1,8] The cyclic flicker caused by arc furnaces has not been used as a limitation to the operation. A study of old records and data indicates cyclic flicker did exist but that the kva swings were of insufficient value to cause visible light flicker. The application of the first 16,000-kva installations on the company's system forced the consideration of cyclic flicker as a limitation. This condition was evident from the data of tests and from customer complaints.

The Approach

The determination of the method of supply required an accurate evaluation of the magnitude of the expected furnace load swings. Data were not available on 25,000-kva 510-volt installations. Complete tests were available on 16,000-kva 300-volt installations as well as on smaller sizes. Published data[1-9] were of considerable assistance. Preliminary transformer design data were obtained from the manufacturer of the 25,000-kva transformers.

Utilizing all data, experience, rules of thumb, calculations, and extrapolation of curves to include 25,000-kva transformers, the predicted values of load swings were estimated to be: 15,500 kva, single phase at 60 per-cent power factor at an extremely frequent rate, (rate of less than one per second), and 11,000 kva, single phase at 60 per-cent power factor at a cyclic rate.

Several methods of serving the load were considered. The limiting factor is the permissible flicker to other customers. As may be seen in Fig. 1, the power plant which serves the area including the steel mill has three operating busses tied together by regulating transformers. Generators are distributed over the busses as required for loading and operation. Any major change in bus arrangement would involve both economics and system operation. The three methods considered are described in the following:

1. One method of serving the load would be to isolate it from other power plant load. However, the amount of generation required for the heavy load swings is not consistent with basic load. Also, while the load factor of the steel plant load is relatively high, there are many and frequent periods when the load is practically zero. This type of load fluctuation is not consistent with efficient or even practical boiler and generator operation.

2. A second method would be the rearrangement of the power plant busses to increase the available short-circuit capacity and thereby absorb greater load swings. Such a rearrangement is unduly costly and restricts efficient system operation.

3. A third method would be to continue supplying the new furnace load from the system then utilized, and to install corrective measures at the 24-kv bus supplying the steel load. The installation of adequate reactive generation, utilizing synchronous condensers, near the load would shunt a sufficient portion of the furnace load swings from the remainder of the system.

Load considerations and system stability for the customer's mill motors dictated the use of three 120-kv feeds to the step-down station, three 120- to 24-kv transformers and operation with the 24-kv busses tied together. Calculations, based on this arrangement

Fig. 3. Three 12.5-mva single-phase reactors and a 45-mva transformer

Fig. 4 (above). 50/60-mva synchronous condenser

Fig. 5 (right). 24-foot-diameter hearth direct arc furnace

indicated that it would be necessary to provide 100-megavar low-reactance synchronous condensers on the 24-kv bus to reduce the cyclic flicker to the permissible limit on the 120-kv power plant bus. Since the 24- to 13.8-kv associated autotransformers would represent 3-per-cent reactance (100-kva base), approximately 100 mva of 12-per-cent transient reactance condensers (or 300-mva conventional condensers) were required. The installed cost of conventional 300-mva condensers would obviously be high, and space requirements and operating complexities also made this installation undesirable. Very limited information was available relative to cost, design, size, and characteristics of very-low-reactance machines. The use of series capacitors with standard condensers to reduce the reactance was considered, but was eliminated when costs and operations were analyzed.

The Solution

Decision was made to install relatively low-reactance machines and also to install reactors in series with the 120- to 24-kv transformers, thereby forcing the condensers to supply the required amount of the fluctuating load.

Stability studies were made using various combinations of condensers and reactors. These studies indicated that two 50-mva 45-per-cent reactance condensers with 75-mva reactors of 80-per-cent reactance would be unstable. Decision was finally made to install two 50-mva 30-per-cent transient-reactance condensers with 75-mva 50-per-cent reactors in the feeds. This combination is well within the safe margin of stability and was the most desirable combination when costs, delivery, performance, flexibility, and existing station installations were considered.

The Equipment

The final installation is shown in Fig. 2 and consists of the following major items:

1. A power-plant 120-kv bus with a short-circuit capacity of 2,000 mva at minimum generation.

2. Three 120-kv overhead lines from the power plant site to the 120- to 24-kv step-down station located in the vicinity of the steel plant. Each circuit is approximately $3^1/_2$ miles in length.

3. Three 120- to 24-kv 45-mva transformers; see Fig. 3.

4. Three reactors: three single-phase air-cooled air-core, outdoor, 12,500-kva 6,920-volts 1,800-ampere units per reactor with 35-, 40-, 45-, and 50-per-cent taps.

5. Three 24-kv busses connected in ring.

6. Two 48/64-mva 24- to 13.5-kv autotransformers with 2.87-per-cent impedance.

7. Two synchronous condensers; see Fig. 4.

50,000 kva at 1/2-pound hydrogen pressure.

60,000 kva at 15-pound hydrogen pressure.

Water-cooled heat exchangers utilizing cooling tower.

13,800 volts at 600 rpm.

Subtransient reactance, 17.5 per cent.

Transient reactance, 30 per cent.

Synchronous reactance, 91 per cent.

Rotor WR^2, 1,633,000 pounds-feet^2.

Electronic automatic field control, cross-compounded.

15 feet 1 inch by 40 feet 8 inches of floor space.

18 feet $3^3/_4$ inches high.

539,100 pounds approximate weight.

Mechanical equivalent of approximately an 80,000-kva condenser of standard reactance.

8. Furnace feeds: Two 500,000-circular-mil, 3-conductor 24-kv cables for each 25,000-kva furnace, each 6,000 feet long. There are four other furnaces and three mill feeds from the common 24-kv busses.

9. Electric furnaces; see Fig. 5: Two 150/200-ton 24-foot-diameter arc furnaces, each supplied by a 25,000/33,000-kva water-cooled 3-phase transformer with 4.0-per-cent impedance 510-volt tap. Voltage rating and taps are as follows: 24,000 primary, 510, 470, 390, 294, 270, and 156 secondary.

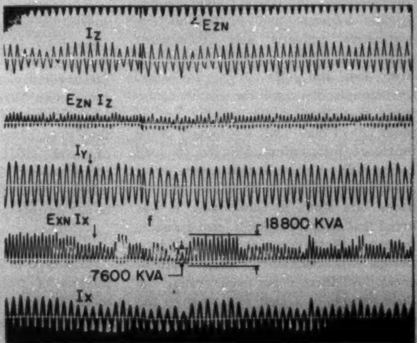

Fig. 6. Sample of cyclic flicker during operation on 510-volt tap

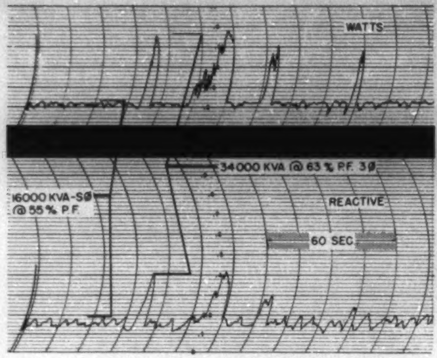

Fig. 7. Indication of single- and 3-phase furnace operation

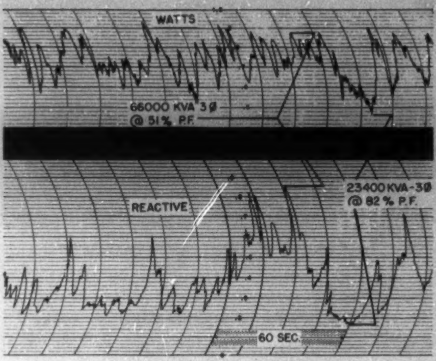

Fig. 8. Kilowatts and kilovars during gradual heavy load variations while operating on 510-volt tap

Operating Tests

The customer's installation of the furnaces was completed prior to the installation of the condensers. Previous calculations indicated that operation of the furnaces at a maximum secondary voltage of 390 volts would keep the voltage flicker within operating limits. The customer co-operated both in the limited operation and in all tests required. Tests made at the customer and at the 120-kv bus indicated operation at 390 volts was satisfactory pending the completion of the condenser installation.

Additional tests were made after all equipment was in service. Tests were made at the metering room adjacent to the furnace installation. The 24-kv metering transformers in the individual furnace feeds were used for current and potential measurements. Instruments and meters utilized were: integrating kilowatt-hour and kilovar-hour meters, graphic kilowatt and kilovar meters, voltmeters, ammeter, and a 6-element oscillograph which recorded 3-phase amperes, kva, and volts. A voltage-biased oscillograph was used for the measurement of voltage flicker at the power-plant 120-kv bus. Only a summary of the pertinent information relative to load swings will be given in this paper.

During previous tests on other furnaces, and again in these tests, it was noted that the operation of large furnaces produces three different types of load swings with resultant voltage disturbances. All three types occur during the early periods of a melt and prior to the period of stable operation. The load characteristics during the period of stable operation are not included herein. The three type of swings are described in the following.

Type 1 (Cyclic)

This type of load fluctuation has a magnitude of about 11,400 kva, single phase, at 60-per-cent power factor, with a duration of 4 to 12 cycles and occurs from four to six times per second. The fluctuations are present during the first 30 minutes of melting after a cold charge of metal. This frequency of variation results in a cyclic flicker of the frequency causing the greatest irritation to the eye[2]; see sample oscillogram, Fig. 6.

Note that the rapidly recurring single-phase fluctuations are superimposed on the longer duration 3-phase load swings. The variation in power factor is from a normal of 75 per cent to 60 per cent.

Type 2 (Extremely Frequent)

This type of load variation has greater magnitude and a lower rate of occurrence than type 1. These single-phase load swings of 19,000 kva at 60-per-cent power factor occur at random intervals but not more often than once a second. These load swings are most severe during the first 10 to 15 minutes after a cold charge of metal. This type is the usual single-phasing which has been accepted in the past as the limiting factor in application of arc furnaces; see Fig. 7.

Type 3

This type of load change is a gradual increase of 3-phase load from a normal value to twice normal. The increase occurs over a period of several seconds and lasts from 5 to 10 seconds before decreasing gradually to a normal value. This change was recorded while operating at 470 and 510 volts. The greatest variation of this type recorded was from 23,400 kva at 82-per-cent power factor to 66,000 kva at 51-per-cent power factor. This type of load swing need not be considered as a flicker problem but must be reckoned with for relaying and other operating problems, such as system ties, interconnections, and regulation equipment both on lines and generators; see Fig. 8.

Conclusions

It is worthy of note that the 15-minute billing demand with all six furnaces operating approximately equals the sum of the kva name-plate ratings of the furnace transformers. The tests confirm, within reasonable limits, the load swings predicted from calculations. While the single-phase swings at the extremely frequent rate were slightly higher than anticipated, the variation was not sufficient to be serious or critical. The cyclic swings were very close to the anticipated values. Oscillograph voltage measurements made at the power-plant 120-kv bus show a cyclic flicker of about 0.5 volt or 0.4 per cent. It appears that the condensers are doing the job.

References

1. Power Company Service to Arc Furnaces, L. W. Clark. *AIEE Transactions (Electrical Engineering)*, vol. 54, Nov. 1935, pp. 1173–78.

2. The Visual Perception and Tolerance of Flicker, Committee Report. Electrical Testing Laboratories, New York, N. Y., 1937.

3. Electric Metal—Melting Furnaces. *EEI Publication No. G4*, Edison Electric Institute, New York, N. Y., Jan. 1940.

4. ARC-FURNACE LOADS ON LONG TRANSMISSION LINES, T. G. LeClair. *AIEE Transactions (Electrical Engineering)*, vol. 59, Apr. 1940, pp. 234–39.

5. LARGE ELECTRIC-ARC FURNACES—PERFORMANCE AND POWER SUPPLY, B. M. Jones, C. M. Stearns. *Ibid.*, vol. 60, July 1941, pp. 763–69.

6. CONSIDERATIONS IN SUPPLYING ARC FURNACES, F. M. Starr, O. B. Falls. American Iron and Steel Institute, New York, N. Y., 1941, pp. 463–74.

7. LAMP FLICKER ON ELECTRIC POWER SYSTEM, S. B. Griscom. *Westinghouse Transmission and Distribution Reference Book*, Westinghouse Electric Corporation, Pittsburgh, Pa., 4th ed., 1950, pp. 719–40.

8. ELECTRIC ARC FURNACES AND EQUIPMENT PRODUCING HEAVY FLUCTUATIONS, PARTS I AND II, B. M. Jones. Edison Electric Institute, New York, N. Y., 1950.

9. THE APPLICATION OF A SERIES CAPACITOR TO A SYNCHRONOUS CONDENSER FOR REDUCING VOLTAGE FLICKER, P. M. Black, L. F. Lischer. *AIEE Transactions*, vol. 70, pt. I, 1951, pp. 144–50.

Discussion

J. G. Tarboux (University of Michigan, Ann Arbor, Mich.): The authors have presented an interesting paper on a most important installation. It is my intention to comment briefly on the small part of the early studies in which I was involved, namely, an investigation of the transient torque-angle stability of the various components.

Certain basic assumptions were made in order to simplify the work. These assumptions resulted in a slight simplification of the circuit diagram of Fig. 2 of the paper.

1. The generators were lumped into one equivalent machine and assumed to be isolated from the bulk power network.
2. The two synchronous condensers were also lumped into a single equivalent machine.
3. The furnace load was treated as a shunt impedance.
4. Similarly all mill motors were considered as one single synchronous machine operating at 100 per cent power factor.

From these assumptions the circuit was reduced to a 3-machine problem with one shunt impedance load, with three transmission circuits between the generating source and the 24-kv bus.

Several studies were made, but as an illustration of the results obtained I refer to only three as representative.

1. One of the three transmission-line circuits, including one transformer-reactor bank, switched out of service, with normal full load at the steel mill.
2. Two transmission-line circuits in operation with initial normal full load at the steel mill, with a sudden increase of furnace load by 20 mva at 50 per cent power factor.
3. A 3-phase sustained short circuit on one of the three transmission circuits between transformer secondary and reactor bank, with normal full load at the steel mill.

The results of these studies are shown in Figs. 9, 10, and 11. Three curves are shown, namely: mill motors behind the generating station; synchronous condensers behind the generating station; mill motors behind the synchronous condensers.

The general conclusions arrived from this study all indicate that, within the scope of the premises which were initially laid down, the system is stable. It is recognized that many elements influence the results obtained and conceivably more severe tests might be applied. Effects of voltage regulators at the generating station and at the condensers and the interconnection with the bulk power network would aid stability, so that the results obtained are considered somewhat on the pessimistic side.

H. Watson Tietze (Public Service Electric and Gas Company, Newark, N. J.): The authors are to be commended for this exceptional paper with its complete background data and actual operating results. It is a welcome addition to previous papers on the subject of power supply for arc furnaces.

The arc furnaces discussed have unusual characteristics and are of unusual size. Most utilities have had no experience in this field. On the other hand, recent studies on the economics of steel mill operation have indicated the definite future trend towards the use of electric arc furnaces in the manufacture of quality steel. Moreover, these studies show that for economical operation very large furnaces must be used.

The oscillographs included in the paper show the very pronounced effect which the operation of such furnaces can have upon a large portion of a company's transmission and distribution system. Particularly important is the finding that cyclic flicker is present. Utility engineers therefore must be particularly alert to the consequences, and make detailed studies if they are to protect the high quality of service being rendered to lighting customers.

The magnitude of the corrective measures necessary in this instance requires that emphasis be placed on two points:

1. Cost studies of electric furnace versus other methods of steel manufacture must include the installed value of measures to correct the inherent flicker.
2. There is the fullest need for complete and close co-operation of the three parties involved: the furnace manufacturer, the prospective operator, and the electrical utility supplying power to the project.

Charles W. Vokac (Whiting Corporation, Harvey, Ill.): The paper describes the load characteristics of two large arc furnaces, the resulting problems, and the corrective equipment necessary.

These furnaces are equipped with cable winch electrode drives operated by large reversing motors.

It is no longer necessary to reverse electrodes with reversing motors to control the load in arc furnaces. I wonder what the load characteristics of the furnaces would be if the electrodes were positioned, instead, by a balanced hydraulic electrode drive operated by relatively smaller nonreversing motors.

That system lends itself well to the higher speed, response, and compatible acceleration of the electrode necessary to cope properly with the rapidly changing conditions within the furnace. Certainly, a better response to these conditions, faster acceleration, and a higher terminal speed of the electrode reached quickly to correct the conditions, should result in a better load characteristic, fewer problems, and less corrective equipment required to make the furnace a better neighbor on the line.

Fortunately, these things mean more efficient operation to the subscriber too. Unfortunately, but perhaps not for long, such a hydraulic system had not as yet been applied to reversing such large electrodes. But it has been applied and is now being used on several furnaces with smaller electrodes and the comparative results are most interesting. On larger furnaces the difference should be even greater.

B. M. Jones and **C. M. Stearns** (Duquesne Light Company, Pittsburgh, Pa.): Our company has been supplying electric arc furnaces for steel melting since 1908, and we have always been searching for additional data on the most economical methods of supplying the larger and larger electric arc furnaces that are being built and marketed all the time.

We feel that The Detroit Edison Company has done more electrical testing of electric arc furnaces than any other utility company, although we also have done considerable testing, and we have been guided by their experience and their published information. Therefore, we are glad to have access to their data on these very large electric arc furnaces. Such complete data, backed by actual tests, will be very useful to power companies, steel companies, and furnace builders in this problem of melting steel electrically as a competitor for open-hearth steel melting.

A few years ago, we had a request for the installation of two furnaces of this same size on our system, and we recommended that synchronous condensers and buffer reactors be installed to reduce the voltage flicker to an acceptable value. We felt that the cost of the corrective equipment in place was about the same as the cost of the electric arc furnaces in place, and these extra costs (the synchronous condenser, etc.) on the steel company have delayed the decision to proceed with this installation. The paper confirms our calculations that the synchronous condenser had to be installed to reduce the flicker to a tolerable value on our system.

These large electric arc furnaces, either due to their size or very high electrode voltage, cause load swings of a much higher magnitude than we expected. Our extrapolated values of Detroit Edison data for smaller furnaces more or less indicate that the expected load swings would be only approximately one half of those actually encountered on these large furnaces in Detroit. This applies to the so-called extremely frequent load swings. See Table I.

From the data provided in this paper, electric systems would have to be very strong to be able to serve furnaces of this size without corrective equipment. Based upon the figures given herein, a system with 4,000,000-kva short-circuit duty at the point of connection would be required to serve these furnaces, using the extremely frequent load swings and the allowable volt-

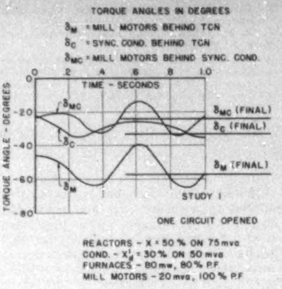

Fig. 9

age fluctuation of 1 volt set up by The Detroit Edison Company. Similarly, in order to serve the furnaces with cyclic loan swings and allowable voltage fluctuation of 0.5 volt set up by the company, a system with 5,700,000-kva short-circuit duty would be required. This just about definitely indicates that synchronous condensers would be required on almost everyone's system to be able to serve these furnaces. It is apparent from the foregoing that the cyclic load swings as encountered in these very large electric arc furnaces, rather than the extremely frequent swings, are the governing factor as far as system requirements to serve them are concerned.

If the very large load fluctuations, both cyclic and extremely frequent, of the large furnaces are the result of the very high electrode voltage, we wonder if this high electrode voltage is actually essential in furnaces of this size. Somebody must pay for the synchronous condenser and equipment and its installation, and therefore this must be reflected in the cost of producing steel from such large furnaces. Then the question arises: Do the reduced production costs per ton from these very large furnaces justify the carrying charges on the synchronous condenser investment necessary for such furnaces? Regardless of who pays for the synchronous condenser installation, the price at which the steel is produced by these furnaces must be reflected in the sale price of the steel, and hence if the utility company makes the investment, these carrying charges must be included in the rates charged the steel company for the power. Also, if the steel company makes the synchronous condenser investment, the carrying charges must also be reflected in the price at which it sells the steel produced by these electric arc furnaces.

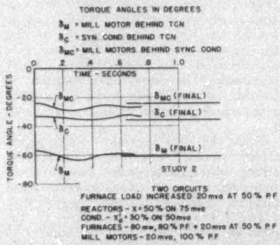

Fig. 10

In reference to Fig. 7, the figures shown are a little perplexing, and we feel that the authors could make this clearer. For example, if the lower figure of 16,000 kva is a 3-phase value, then the load swing between it and the higher 3-phase value of 34,000 kva is 18,000 kva at 69 per cent power factor. If the lower figure is actually single phase as shown, then the single-phase swing becomes less in going from a lower value to the higher 3-phase value.

The measured value of flicker at the generating station bus was given as 0.5 volt. Does this represent the operation of one large furnace, both large furnaces, or are all furnaces including the smaller ones considered? Clarification of this point would be helpful.

I think it would be well to include just where the voltage flicker curve of The Detroit Edison Company may be found.

Was the location of the 1-volt flicker, as The Detroit Edison Company standard, on the Trenton Channel 120-volt bus? If not, where was it?

It would be interesting to explain why the three 45,000-kva 120/24-kv transformers were installed for this steel-melting load before these last two large furnaces were installed, as 135,000 kva of stepdown transformer capacity appears large for the demand mentioned.

Do the 15-minute demands you quoted apply to the load of the six furnaces only, or to the entire mill load, including load other than the furnaces? This is also referred to in the first paragraph under Conclusions on page 5.

Does your experience prove that the cyclic figure is caused by the large furnaces as such, or by the large furnaces with higher secondary voltages? Or maybe the cyclic figure is inherent in all electric arc furnaces, and is of such a small value relative to the frequency swings in these smaller furnaces that it is no problem.

D. D. Clarke (Kansas City Power and Light Company, Kansas City, Mo.): A question of terminology with regard to the use of "single-phase kilovolt-amperes" arises as to whether this is used on the basis of the largest phase current or the equivalent 3-phase wattmeter reading on test.

Another question as to the use of the term "regulating transformer": Does this mean a load ratio control transformer or is it in effect a variable reactor? The diagram would indicate that it is used as a variable reactor.

The type of generator voltage regulators that are used on the generators may in our experience have some effect on the satisfactory results of a large arc furnace installation. It would be of interest to know whether the voltage regulators are of the forced field type.

A casual review of the equipment indicates that the installation in this case will be effective with more than one furnace bumping the system in coincidence. A discussion of this consideration would be of interest, especially as to a specific analysis of the test data that was reviewed during the study. With multiple arc furnace installations, the "extremely frequent" and the "cyclic" reactive swings of two or several furnaces most certainly must occasionally be coincident. A satisfactory application should consider the statistical probability of this on customer's usage.

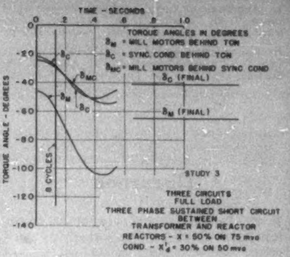

Fig. 11

S. W. Luther, J. D. Ghesquiere, and C. E. Quick: We appreciate the comments and discussions which have been presented. Dr. Tarboux's presentation covers an important aspect of the problem, and is self-explanatory. We are in full agreement with Mr. Tietze's points to be emphasized, particularly the co-operation of the parties involved.

Mr. Vokac asks what the load characteristics would be for hydraulically controlled electrodes. We, of course, have no experience whatever with hydraulic electrode controls, so can give no factual answer. However, if we assume a very fast rate of response for hydraulically controlled electrodes, it would appear that the large gradual swings might be considerably lessened, and the extremely frequent swings might be somewhat lessened. We do not believe that any control mechanism can be made to move these 24-inch by 18-feet electrodes fast enough appreciably to affect the cyclic flicker after it has started. A

Table I. Single-Phase Instantaneous Very Frequent Load Swings and Power Factors of the Swings for Various Size Electric Arc Furnaces

(Data from curves of L. W. Clark, The Detroit Edison Company)

Furnace Transformer N.P. Rating	Single-Phase Swing—Noncyclic	
	Kva	Power Factor Per Cent
2,000	2,300	.43
3,000	3,100	.46
4,000	3,800	.47
5,000	4,300	.50
6,000	5,000	.52
7,500	5,600	.55
10,000	6,500	.60
16,000	8,000	
25,000*	10,000†	.60

*Detroit Edison data from the paper.
†Corresponding noncyclic flicker is 11,400 kva at 60 per cent power factor occurring four to six times per second.

control which could anticipate the cyclic flicker and position the electrodes to prevent it would be required.

Mr. Jones and Mr. Stearns raise several very good questions. We will take them in order. Fig. 7 is the actual chart taken during an early portion of a melt. The chart shows the furnace operating single phase at 16,000 kva for about 50 seconds, then swinging to 34,000 kva, 3 phase over about a 5-second interval, back to 16,000 kva, single phase for 20–25 seconds then up to about 36,000 kva, 3 phase over a 10–20-second interval and abruptly back to 16,000 kva, single phase. Each change from single-phase to 3 phase and from 3 phase to single phase is a single phase swing.

The cyclic flicker of 0.5 volt (120-volt base) was measured on the generating station bus with a voltage biased Brush recorder. All six furnaces were operating at the time measurements were being made.

The voltage flicker curve used by our company is taken from a report on the visual perception and tolerance of flicker.[1] We use a nominal curve for absolute limit which represents a compromise between the borderlines of visibility and irritation. Since the absolute limit is reached infrequently, the normal value of cyclic flicker is well below the borderline of visibility. Approximately similar values are shown in the AIEE "Power Supply for Resistance Welding Machines."[2]

As stated under "The Problem," both the 0.5-volt limit for cyclic flicker and 1.0-volt limit for extremely frequent flicker are applied at the power plant bus for this particular problem.

The stepdown station serving the steel load is directly adjacent to a stepdown station serving other loads. One large transformer is used to provide emergency service to either the steel load or the other load. Prior to the installation of the two large furnaces this transformer was normally closed to the "other load" bus with throw-over to the steel bus. With the addition of the large furnaces this arrangement was reversed, providing normal service to the steel load.

The billing demand for the furnaces is separate from that of other steel mill load. The 15-minute billing demand of the six furnaces alone has continued to be approximately equal to the sum of the kilovolt-ampere name-plate ratings of the furnace transformers.

We have observed cyclic flicker on 12,000- and 16,000-kva furnaces, with single-phase load swings of approximately 3,000 kva, 10 to 12 times per second. During the tests on the 12,000- and 16,000-kva furnaces it was observed that increase in electrode voltage increased the cyclic load swing. Preliminary tests made on the 25,000-kva furnaces confirmed previous observations; when operating at the same electrode voltage as was used on the 16,000-kva furnaces the cyclic load swing was of the same magnitude; when operating at higher electrode voltages the cyclic load swing increased very considerably. It is perhaps worthy of note that the 25,000-kva furnaces operating at 310 volts have a load of 16,000 kva. It would seem that increase in electrode voltage rather than in size of furnace causes the increase in cyclic load swing.

REFERENCES

1. THE VISUAL PERCEPTION AND TOLERANCE OF FLICKER. Report for Project 10, Utilities Coordinated Research, Inc., 1937, Fig. 11.

2. POWER SUPPLY FOR RESISTANCE WELDING MACHINES. *AIEE Special Publication S45*, 1952, Fig. 26.

Controls for Step Voltage Regulators

T. C. LENNOX
ASSOCIATE MEMBER AIEE

Synopsis: A unique control circuit for step voltage regulators is described. An auxiliary relay with four pairs of contacts has been eliminated; this results in reduced maintenance and quiet operation. Full integrating time delay is obtained by means of a motor-driven time-delay relay operated directly by the contacts of the voltage-regulating relay. Sparking on the voltage-regulating relay contacts is reduced to a minimum.

The Problem

CONTROLS for step voltage regulators usually consist of a servo loop, as shown in Fig. 1. The time-delay relay is interposed between the voltage-regulating relay and the driving motor of the tap-changing mechanism.

Time delay may be applied in several different ways. It may be cumulative. In this case, each short-time voltage deviation will cause some movement of the timing device with no reset action until the timing cycle is complete and a tap change is made. The motor drive of the regulator may serve for this purpose if a sufficient gear ratio is provided between motor and tap changer. The separate time-delay relay is then omitted. The objection to this system is that, once the time delay is used up, a brief and self-correcting voltage error may cause an unnecessary tap change. A second tap change in the opposite direction will follow to restore normal voltage.

Alternatively, instantaneous reset may be used. In this case, a succession of momentary voltage changes may keep the relay from completing its cycle to correct a large error in the average voltage. As another alternative, free from either of these objections, the timing may be "integrating," running back and forth at the same speed, to sum up the time algebraically for correct and incorrect voltage. Thus, if the voltage is outside the acceptable band in one direction more than it is inside, the relay will ultimately time out and the voltage will be corrected. Two such integrating relays for raising and lowering of the voltage respectively may be combined in a single relay in which the timing-out action for raising becomes the timing-back movement for lower, and vice versa.

An integrating double-action timer of this type is shown in Fig. 2. The right-hand view shows the reversible synchronous motor and other electric components. The left view shows the timing dial. Around the dial are switches which are opened and closed by the dial movement. At the top, two switches are closed to energize the regulator motor at the end of a timing period. This period may be adjusted by screwing the timing pins into the holes adjacent to the required figures showing the time in seconds. At the bottom, two switches are mounted which close at the beginning of a timing operation to set up the runback circuit. This allows the dial to return to the starting position and gives the integrating action. The marked disk on the end of the motor shaft enables the motion of the relay to be observed when adjusting the control, the relatively slow movement of the dial being difficult to follow.

The rugged, reversible, synchronous motor is a desirable device to power such a relay; and the current and voltage required by its coils are well within the capacity of the voltage-regulating relay contacts. The chief problem presented is the need to run the motor in the reverse direction to return it to the starting position whenever the voltage-regulating relay is rebalanced with both contacts open. These motors have separate windings for clockwise and counterclockwise rotation. When one winding is in use, the other should be completely de-energized.

Paper 55-717, recommended by the AIEE Relays Committee and approved by the AIEE Committee on Technical Operations for presentation at the AIEE Fall General Meeting, Chicago, Ill., October 3–7, 1955. Manuscript submitted March 30, 1955; made available for printing July 20, 1955.

T. C. LENNOX is with the General Electric Company, Pittsfield, Mass.

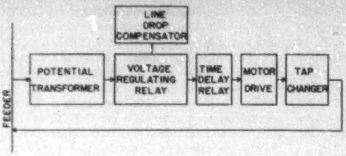

Fig. 1 (left). Control loop of step voltage regulator

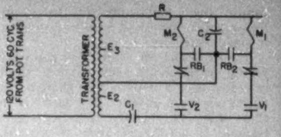

Fig. 3 (right). Internal connections of time-delay relay

In the past, an auxiliary relay has been used to reset the circuits so that the motor would be energized, through the run-back contact, to return the timing dial to its starting position whenever the voltage is corrected or returns to the band without correction. A relay so connected responds instantaneously to all voltage changes that go outside of the voltage band. This results in very frequent operation of the auxiliary relay. If the voltage is on the edge of the band, chatter of the auxiliary relay armature and contacts can result, unless substantial holding effect is provided in the voltage-regulating relay.

A superior arrangement may be obtained if the time-delay relay can be made to run in either direction as required without the help of an auxiliary relay. When the voltage-regulating relay closes a contact and starts the motor, a run-back contact immediately closes. Following this, the motor must run forward when the voltage-regulating relay contact is closed and reverse to run back when it is opened, this reversal being repeated as often as the voltage leaves and re-enters the band.

This action is difficult to arrange with a reversible, synchronous motor which requires full voltage on one coil and no voltage on the other for satisfactory operation. If full voltage is applied to one coil and a reduced voltage such as 50 per cent of normal is applied to the other, the motor may lock itself out and refuse to run at all.

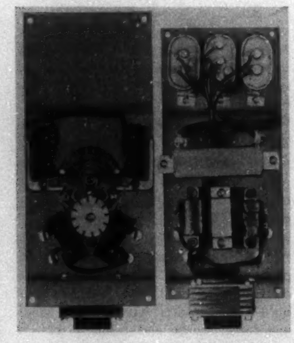

Fig. 2. Time-delay relay, front and back views

The Solution

The circuit for operating the motor is shown in Fig. 3. There are two capacitors C_1 and C_2, a resistor R, and a transformer with two secondary windings E_2 and E_3. In addition, there are the motor coils M_1 and M_2 and run-back switches RB_1 and RB_2. The voltage-regulating relay contacts are shown as V_1 and V_2. The output contacts of the relay which close at the end of the timing cycle are not shown. They would appear in the wiring diagram of the regulator motor drive. In addition to providing the relay action described in the foregoing, a desirable feature of this circuit is that the current in the voltage-regulating relay contacts and the recovery voltage across them are no more than are required to connect and disconnect the motor directly on a 110-volt line.

Fig. 4 shows the active elements of the circuit in the neutral position of the timer with the voltage-regulating relay in the balanced position, both motor coils being open-circuited. Capacitor C_2 is connected in series with resistor R across voltage E_3 from the transformer. The open-circuit voltage E_0 of both voltage-regulating relay contacts is the vectorial sum of transformer voltage E_2 and the capacitor voltage C_2 as shown by the voltage vectors.

Fig. 5 shows the active circuits and voltage vectors when a voltage-regulating relay contact V_1 has just closed. Capacitor C_1, coil M_1, and resistor R are connected in series across (E_2+E_3) from the transformer. The voltage on capacitor C_2 is the vectorial difference of E_3 and R. When the time-delay relay moves in response to voltage on M_1, run-back switch RB_1 is actuated and its normally open contact closes and stays closed throughout the timing cycle. This connects M_2 in parallel with C_2. For voltage M_1 to be the normal coil voltage, and for voltage C_2 and hence the voltage on coil M_2 to be zero under this condition, and for the conditions described later for run-back to be fulfilled, the following values are required for the various elements.

$$C_1=\frac{10^6}{2\pi fZ\sin\phi}\text{ microfarads (series resonance } M_1 \text{ and } C_1)$$

$$C_2=\frac{10^6\sin\phi}{2\pi fZ}\text{ microfarads (parallel resonance } M_2 \text{ and } C_2)$$

$$R=\frac{Z}{1-\cos\phi}\text{ ohms}$$

where Z ohms is the impedance of either M_1 or M_2 and $\cos\phi$ their power factor

$$E_2=E\cos\phi$$

$$E_3=\frac{E}{1-\cos\phi}$$

where E is the normal voltage required for the coils M_1 or M_2.

When the regulated voltage has been corrected and the voltage-regulating relay has been rebalanced with both contacts open, the active circuits and voltage vectors will be as shown in Fig. 6. The normally open contact of run-back switch RB_1 will be closed so that M_2 and C_2 will be in parallel and connected in series with R across E_3. The values given in the foregoing result in full voltage E across M_2 to run back to the neutral position of the timing dial and reopen RB_1. During this run-back period no voltage is applied to M_1 because its circuit is open. Thus, the required voltage conditions are fulfilled.

The switches RB_1 and RB_2 have both normally open and normally closed contacts. The latter are placed in series with the contacts of the voltage-regulating relay as shown in Fig. 3; otherwise, closure of a voltage-regulating relay contact for the same direction of motion as given by the run-back switch would connect capacitor C_1 across transformer circuit E_2. This action would be useless and might weld the voltage-regulating relay contact.

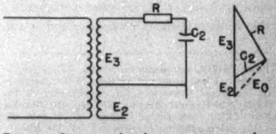

Fig. 4. Circuit and voltage vectors at relay neutral

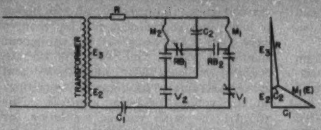

Fig. 5 (left). Circuit and voltage vectors during forward motion

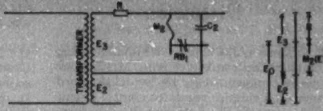

Fig. 6 (right). Circuit voltage vectors during runback

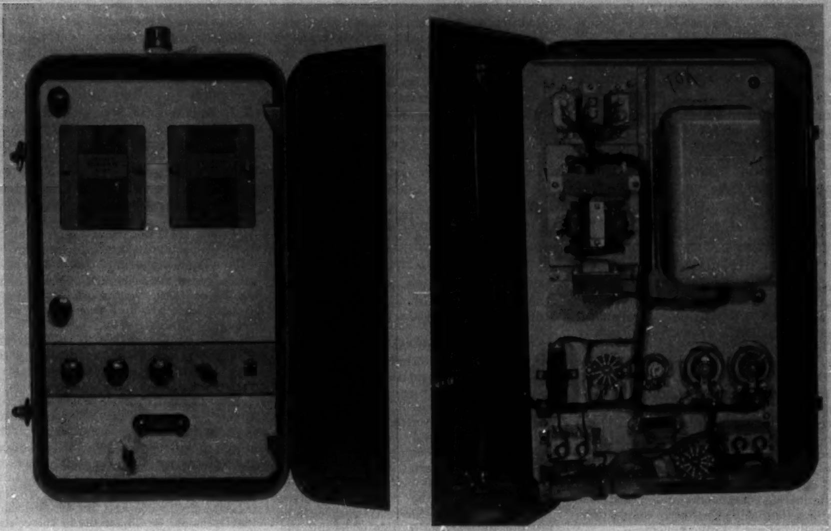

Fig. 7. Control panel for step voltage regulator

The open-circuit voltage across the contacts of the voltage-regulating relay will be E_0, as shown in Fig. 6, when in the run-back zone. This voltage, like that in Fig. 4, is more than the normal voltage E of the coils M_1 or M_2 but more nearly in phase with the coil current so that, in the network as constructed, the recovery voltage at current zero is never greater than it would be with the motor directly on the line at normal voltage. The low power factor of the motor, about 50 per cent, is favorable in obtaining this result. The current in the contacts of the voltage-regulating relay is the normal coil current for the motor.

The voltage applied to the relays is obtained from the potential transformer and represents the output voltage of the regulator. When the line-drop compensator is in use, this voltage will vary with changes in load and may rise to as much as 10 per cent or more above its normal value. On the other hand, provision is made to adjust the normal output voltage of the regulator over a considerable range. The result is that the relays must operate satisfactorily with voltages from 100 to 135 volts.

Voltage above its rating applied to the coils of the motor tends to saturate the iron of its magnetic circuit and to cause a disproportionately large increase in current. This will increase the severity of sparking on the contacts of the voltage-regulating relay. It will also result in a change in coil power factor, thus detuning the network. Low voltage, on the other hand, will reduce the current in the contacts and is unobjectionable unless carried to the point of insufficient motor torque. The 115-volt motor will run with ample torque at 70 volts or even less. The transformer in the network is wound with such ratio so as to give a motor voltage E varying from 80 to 108 with a circuit voltage of 100 to 135. This assures optimum performance of voltage-regulating relay contacts.

Fig. 7 shows the control panel for a regulator carrying the devices described Hand controls include a power circuit breaker, a selector switch, a test rheostat, a line-drop compensator, a reversing switch for the line-drop compensator, and potential test terminals.

Conclusion

The control as described is a marked improvement over previous controls. Elimination of an auxiliary relay results in eight less contacts to maintain. This relay was a source of noise and vibration, and its removal results in quiet operation of the control and in improved action of the voltage-regulating relay contacts. Spark suppression circuits and holding coils are added to the voltage-regulating relay to improve contact life.[1] The control is very easily adjusted, requiring remarkably little attention, and will operate for long periods with no cleaning, polishing, or replacement of contacts. It has been applied to single-phase step voltage regulators for about 1 year.

Reference

1. Contact Life of Voltage-Regulating Relays, C. W. Schoendube, R. L. Elliott. *AIEE Transactions*, vol. 74, pt. III, 1955, pp. 1398–1401.

Discussion

H. C. Brem (Allis-Chalmers Manufacturing Company, Milwaukee, Wis.): Mr. Lennox is to be commended for his straightforward paper on a simpler regulator control circuit which contains the following ideal features and components:

1. Elimination of auxiliary relay and contacts.
2. Integrator feature in the time delay with variable adjustments.
3. Decreased sparking on the voltage-regulating relay.

While the author stresses the uniqueness of the circuit, the simplicity by elimination is the highlight of the design. The simplicity of operation leads to a better understanding by those who operate the equipment. The remarks of his paper do not do justice to the extensive development necessary to arrive at such a design.

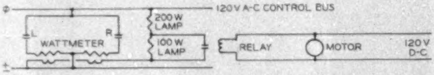

Fig. 8. A 2-element graphic wattmeter

The Allis-Chalmers Manufacturing Company has furnished, with great acceptance for over 22 years, a control which was initially designed to be as simple and as trouble-free as possible. It included a voltage integrator which eliminated the extraneous relays. Our original and fundamental design was not much different than that revealed by Mr. Lennox. His ideal control was evolved through a process of eliminating components that caused past trouble. The Allis-Chalmers control was originally designed without them.

The fact that two independent designs are almost identical, but many years apart in conception, gives a strong indication of the soundness of the basic principles involved. The Allis-Chalmers operating record of over two decades with the control has proved the control leads to long operating life and good service. Mr. Lennox can also expect such fine results as time goes on.

O. J. Lindquist (Commonwealth Edison Company, Chicago, Ill.): The device described by Mr. Lennox is clever and practical. It represents a definite improvement because the timing motor is directly actuated by the voltage-regulating relay rather than through an auxiliary relay. Hence the auxiliary relay is eliminated not only without sacrifice, but with over-all gains in reliability and maintenance. Because the contacts for the tap-changing drive motor are cam operated, the response to the voltage-regulating relay is certain and reliable.

Because equipment such as large welders and arc furnaces produce frequent voltage fluctuations of up to 1 per cent on the regulated bus, we believe the holding effect should be ajustable so that where necesary the bandwidth and the holding effect can both be increased.

It may be of interest to mention a system we use in Chicago to study the operation of step-type voltage-regulating equipment. It is especially useful where load-ratio-control transformers are operated in parallel. A 2-element graphic wattmeter is connected as shown in Fig. 8.

The current elements of the wattmeter are connected in series with a lamp load consisting of a 100-watt and a 200-watt lamp. Whenever the tap-changing drive motor is energized, the relay short-circuits out the 100-watt lamp, this increasing the current in the wattmeter coils. One potential element of the wattmeter is energized by closing of the "raise" contact of the voltage-regulating relay. In the same way, the other potential element is energized by the closing of the "lower" contact. Therefore, the wattmeter chart shows whenever the voltage-regulating relay called for higher or lower voltage and whenever tap changes were made. The tests with this equipment showed in general that several of the tap changes per day were unnecessary and could be eliminated by changing the settings on the voltage-regulating controls. This allowed the same voltage regulation for fewer tap changes, or better voltage regulation for the same number of tap changes. In cases where the charts showed that the voltage regulating relays were too active, the holding effect was increased to save contact deterioration.

T. C. Lennox: Mr. Brem's observations on the similarities between the control described in the paper and the Allis-Chalmers control are quite correct. However, the significant difference between them is that holding effect is provided for the voltage-regulating relay contacts in the control I have described. In a companion paper,[1] it is shown that the voltage relay contacts, without holding effect, experience practically continuous arcing when operating at the edges of the voltage bandwidth. Test results on these two almost identical controls indicate a 4- to 5-year contact maintenance interval. This interval is increased by an estimated 75 times by provision of a small contact holding effect. This increase in contact life represents a major increase in reliability and service.

Mr. Lindquist presents an interesting circuit for studying the action of controls on load ratio control transformers. This should prove a very useful tool in optimizing the performance of tap-changing equipment.

We wholeheartedly agree with Mr. Lindquist in using holding effect for voltage-regulating relay contacts but do not believe that it should be adjustable in the control described. Further discussion is included with the aforementioned paper.[1]

Reference

1. Contact Life of Voltage Regulating Relays, **C. W. Schoendube, R. L. Elliott.** *AIEE Transactions,* vol. 74, pt. III, Feb. 1955, pp. 1398–1401.

Rural Electric System Planning

J. H. RIXSE, JR.
MEMBER AIEE

THE importance of system planning has been recognized by the Rural Electrification Administration (REA) since its establishment as a lending agency in 1935. A plan of development for the purpose of serving rural consumers has consistently been a requirement for the lending of funds to rural electric systems. In the early days of the program, system-planning techniques were relatively simple, consisting essentially of load estimates for unserved areas and the requirements for rural lines to serve given sections of these areas. As the systems developed and experience was gained, the concept changed from one of planning for rural lines to that of planning for feeders and substation areas. In turn, planning techniques have advanced to the consideration of the distribution system as a whole and its economic co-ordination with generation and transmission facilities. In this evolutionary process the REA, in the role of a banker, has established the broad guidelines while the actual planning has been carried out by Administration's 1,076 electric borrowers and their engineers.

It is the purpose of this paper to discuss the broader aspects of rural electric system planning, which is predominantly distribution system planning, as currently seen by the REA. Particular attention is given to planning developments to date, future trends and needs, and the essential elements of system planning. Even though planning has been an integral part of the development and expansion of rural electric systems, phenomenal load forecasts clearly establish its continuing cornerstone importance, as all of the electrical utility industry is recognizing. This is sufficient cause for mutual examination, study, and benefit.

General

The background for this paper has been a continuous study and interest in all phases of planning with emphasis on utility system planning and, more particularly in recent years, rural electric system planning. The principles involved are the same regardless of application. The relative importance of elements, considerations, and practices of planning will vary however. In the electrical utility industry, system planning is quite different from community or industrial sales planning. The electrical utility industry has been putting considerable attention on planning bulk power transmission systems and generation facilities. Long-range planning of distribution systems has, until recent years, not received its proportionate share of attention considering that distribution facilities represent nearly one-half of electrical utility property investment. The development and expansion of the rural electric systems throughout the country during the past 20 years necessitated and, in turn, were made possible only by the application of planning principles.

The term "rural electric systems" as used herein refers primarily to those properties which have been financed by the REA. These systems serve approximately one-half of the consumers in rural America. They are relatively small. All are less than 20 years old. The weighted age of all facilities is approaching 10 years. There are 1,076 such systems operating 1,354,000 miles of line, serving 4,259,000 consumers. They borrowed about $3,000,000,000 from the Federal Government. 81 per cent of these funds are invested in the distribution plant. During the past 12 months, 23 per cent of the approximately $165,000,000 borrowed was for the purpose of increasing the capacity of existing facilities, exclusive of generation facilities, transmission lines, new substations, and new distribution lines.

Consulting engineers have been vitally interested in the planning, design, construction, and expansion of these rural electric systems because of professional interest and responsibility and because they represented a challenge. Manufacturers have been vitally interested because they provided new markets and need for new equipment and materials. The REA has been interested in and has constantly encouraged sound planning in the design, construction, and development of these rural electric systems because of the tremendous responsibility involved in the loans that have been made. It has recognized that this interest cannot rest with the initial line construction because, as the loads continue to increase, sound practical development based on well-developed current long-range engineering plans is necessary to safeguard adequately the taxpayers' interest. A tangible expression of this interest is expressed in references 1 and 2.

The planning that has gone into the rural electric systems has, as have the systems themselves, gone through an inevitable process of growth. The initial application of planning was to a concept of rural lines in restricted areas serving very light loads. Later planning principles were applied to the concept of feeders and substation areas. The years immediately following World War II, with the extensive expansion of all electrical utility systems of all types and the rapid growth of loads, all of which was shared by the rural electric systems, presaged the current applications of planning and the need for further attention, refinements, and better understanding in the years ahead. Rural electric system planning, although it has many of the characteristics of general electrical utility system planning, also has its own particular needs and adaptations. This is a characteristic of planning which is a general practice applied to specific cases.

System planning is applied to each individual rural electric system by the management and engineers of each system. The engineers, in some cases, are on the payroll of the system. In other cases, they are consulting engineers. In many instances management utilizes a combination of the two. A very important point at this stage, and one in which the REA is vitally interested, is that system planning engineering is separate and apart from construction and design engineering. The engineers working with these rural electric systems and the engineers on the REA staff recognize the need for improvement in the techniques applied.

The development of these rural electric systems was made possible by, and has in turn contributed to, many improvements in design, construction, equipment, and material. At the root of this, however, was planning. By looking ahead and developing plans on a long-range basis, many innovations and practices were found practical and economical and were applied to the benefit of the entire utility industry. These include the widespread use of long-span construction, high-strength conductors, single-bushing transformers, common primary secondary multigrounded neutral systems, standardization of pole top configurations, and automatic oil circuit reclosers, as well as the acceptance of 7.2/12.45 kv and 14.4/24.9 kv as standard distribution voltages.[3] Design techniques which were developed and applied include a uniform comprehensive voltage-regulation study, standardization of sectionalizing analysis, establishment of voltage standards, and criteria for line regulation.[4-7] In addition, a number of the consulting engineers have been continually developing for their own use refinements of techniques specifically applicable to the rural electric systems with which they are concerned.

Trend Data

The statistical trends of these rural electric systems are similar to that of the over-all electrical utility industry. They are quite similar to the trends for rural facilities of other utilities. Hence, although the following data apply only to the rural electric systems, parallels and correlations with other published data can be readily found.

Fig. 1 represents a nation-wide average of the saturation of farm electrification and, for these rural electric systems, the farm energy requirements from 1940 to 1975. With 95 per cent of all farms having central station service, one-half of which are served by these rural electric systems, the significant fact is the predicted continued rapid growth in energy usage.

Industry forecasts of energy consumption are shown in Table I. The REA and the Federal Power Commission estimates apply to rural loads.[8,9] The *Electrical World* estimate is industry-wide.[10] The correlation is close. The planning engineer with these figures before him has a definite challenge. Not only are design criteria involved but also the inevitable need for new and improved materials and equipment. The planning engineer assumes that energy usage and system demands will continue to grow even beyond these forecasts.

Paper 55-746, recommended by the AIEE System Engineering Committee and approved by the AIEE Committee on Technical Operations for presentation at the AIEE Fall General Meeting, Chicago, Ill., October 3-7, 1955. Manuscript submitted June 7, 1955; made available for printing July 27, 1955.

J. H. RIXSE, JR., is with the Rural Electrification Administration, Washington, D. C.

The author acknowledges the contributions from various consulting engineers and members of the Rural Electrification Administration staff. Particular acknowledgement is made of the personal participation, contribution, and support of R. G. Zook, J. E. O'Brien and E. A. Loetterle. Particular credits are given to L. B. Crann, R. W. Schlie, H. R. Smith, and W. L. Woehler to whose special studies reference was made in this paper.

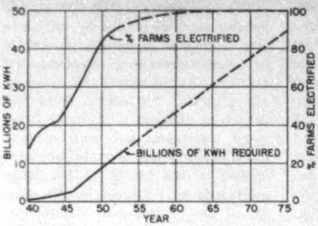

Fig. 1 (left). Farms electrified and energy usage

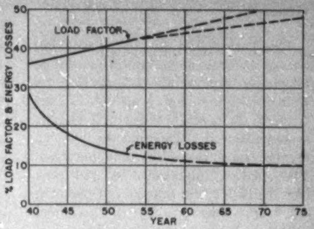

Fig. 3 (right). Load factor and energy loss trends

Table II illustrates the application of new techniques, materials, and equipment according to a well-developed system plan. It shows the trend on the rural electric systems in the use of 14.4/24.9-kv distribution. Although substantial, the use of this voltage has been and will continue to be very selective. Its use on rural electric systems has been primarily for areas of low consumer density, for areas requiring express feeders, and for situations wherein future uncertainties require continuance of distribution systems in lieu of transmission, pending the evolvement of a more definitive system requirement.

Fig. 2 shows a comparison of average load and consumer trends on the rural electric systems. One major significance of these data is the rapid increase in circuit loading. On these systems this has introduced problems of economical conductor selection, sectionalizing, regulation, load pickups, and operation. This trend clearly reflects the situation for the next several decades. There will be limited increase in the number of consumers coincident with the rapidly rising energy consumption. The long distances and the unusual exposures of the rural systems to the forces of nature will continue. This combination is one of the principal ingredients of the problem facing the engineer designing and planning the rural electric system of tomorrow.

Fig. 3 shows the rising trend of load factor and the decreasing trend of energy losses as the rural electric systems age and the loads increase. The load factor, for example, has increased from 36 per cent on these systems in 1940 to approximately 43 per cent in 1953. The average energy losses have decreased from 28.6 to 14.4 per cent. The latter is very significant for two reasons: reports to the Federal Power Commission by the utilities show a 1953 energy loss of 11.4 per cent; and, rural electric system distribution transformers, which account for over one-half of distribution system losses, average 0.85 per consumer, which is considerably higher than the national average.

Table I. 1954 Forecast of Energy Requirements

Surveyors	Energy Consumption Estimates
REA (rural)	doubling in 10 years—tripling by 1975
Federal Power Commission (rural)	330-per-cent increase by 1975
Electrical World (industry-wide)	tripling by 1970

Fig. 4 shows the general trend for all rural electric systems of loads in comparison with design capacity. Obviously the individual systems or individual portions of systems differ but, on the average, this represents the general condition. It clearly reflects the result of consistent planning in the past.

Elements Necessary for Rural Electric System Planning

The principles of planning are the same regardless of application. The interpretations or elements particularly applicable are influenced by the specific case in hand. How these would be stated would depend upon the judgment of the individual, the type of utility property under consideration, the specific nature of the utility service area, the position of the individual in the utility system, and the experience which he has had with system planning. For the case in hand, an enumeration of the elements follows:

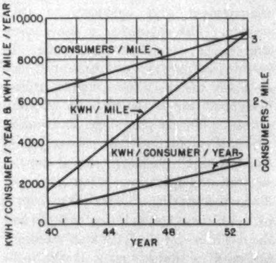

Fig. 2. Average load and consumer trends

1. Management recognition and support.
2. Competent engineering.
3. Adequate basic data.
4. Rigorous treatment of data and planning techniques.
5. A minimum of self-imposed restrictions.
6. Operation and maintenance practices.
7. Sound service standards.
8. Recognition of consumers' changing needs.
9. Practical planning criteria.
10. Alternative plans.
11. Differentiation between immediate construction plans and long-range engineering plans.
12. Positive use of planning results and review and extension of system plans.

The understanding and application of these elements are not the sole responsibility of the engineer. It is a joint engineering-management responsibility; however, management can and should look to the engineer for initiative, foresight, and stability in the engineering guidance he provides. Application and understanding of each element obviously must suit the individual characteristics of a given situation. That reflects the fundamental principle which all must recognize, namely, that system planning is a co-ordinated and tailored operation; it is not and cannot be standardized as can many of the technical mechanics of engineering. Only the techniques of planning can be standardized.

Table II. REA Systems Usage, 14.4/24.9-Kv Distribution

Year	Miles	Systems
May 1952	10,988	37
September 1954	27,907	72
June 1955	33,000	75

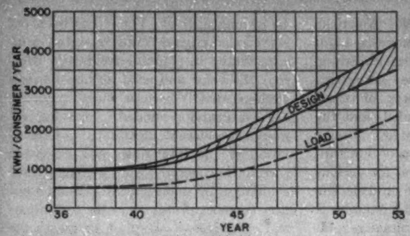

Fig. 4 (left). Comparison of average system load and design capacity

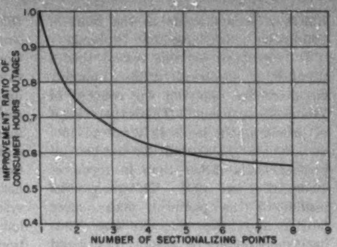

Fig. 6 (right). Comparison — service continuity improvement and circuit sectionalization

Assumed
Same number of consumers each section
Same type of sectionalizing devices.
Uniform system conditions. Equally spaced devices

Discussion of the Elements for Rural Electric System Planning

Management Recognition and Support

Long-range system engineering planning is a basic management necessity. Management recognition and support are also basic to productive system planning and practical application of its results. Sound system planning is insurance to management and inexpensive insurance at that. Its cost is low. For example, a $6,000-expenditure for an average rural electric system would represent approximately 2/10ths of 1 per cent of the present investment. At an amortization rate of 10 per cent, it would be paid for by a management decision, based on its conclusions, to delay a $60,000-capital improvement for just 1 year.

Competent Engineering

System planning requires engineers who have acquired or are capable of acquiring the special characteristics and abilities which this particular field demands. It is a specialty. It takes years for an engineer to develop a staff technically proficient in the design of a generating plant; the same is true in the field of system planning. Not only must the engineer be technically proficient but, to gain and hold the respect and support of management, he must be sensitive to the need for constant re-evaluation and for the application of new ideas and approaches. Long-range system engineering planning for distribution system engineers is a relatively new field in which competency, or proficiency, must be developed.

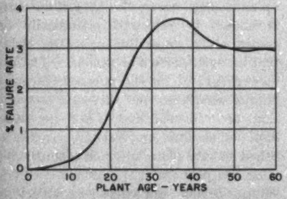

Fig. 5. Typical failure-rate curve for an average all-new electrical utility outside plant

Adequate Basic Data

This is of fundamental importance to the system planning engineer. The engineer must, at all times, be alert to appraising the adequacy of the data with which he is working and the methods by which they were derived. As an example, consider just one item of basic data, namely, load estimates. Load estimating is at the root of all utility planning, but the estimates must be recognized as such. Also, even though the total load on a system 10 years from today may be as now estimated, it does not mean that the pattern will develop similarly throughout the entire area. Hence, segregation of load estimates by geographical areas is as important as segregation by types of consumers.

Rigorous Treatment of Data and Planning Techniques

Planning by its very nature can easily lead into the abstract and extreme generalization. The experienced planning engineer, however, is rigorous in his treatment of data and in applying the techniques of his profession. His work is as rigorous as that of a structural engineer in designing the details of a 100,000-kva substation. The planning engineer develops techniques in which basic economic, statistical, mathematical, and engineering principles are observed. Treatment is orderly and complete. The results are reduced to definite understandable terms for use by management. Alternatives, advantages, disadvantages, and substantiating data are presented succinctly so that management can work constructively with the results.

A Minimum of Self-Imposed Restrictions

Distribution system planning must be realistic even though it deals with an uncertain future. It must be approached on a reasonable basis without built-in fears and self-imposed restrictions. Although the experience of the past and conditions of the present must be considered, they should not restrict provisions for meeting future needs. What appears to be an important obstacle today may be insignificant when the loads are three to six times today's loads. By the very process of restriction, future development may be stifled. Long-range system engineering planning requires freedom. Restraint is required, however, in the application and the management evaluation of the alternatives. No portion of a system plan should be accomplished

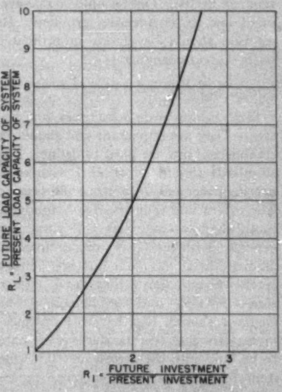

Fig. 7. Relationship of the ratio of future-to-present capacity with the ratio of future-to-present system investment

unless it is applicable in the light of conditions which have then evolved.

It is perhaps for this reason that a number of electrical utility planning engineers are applying the concept of "timeless expansion." This is the concept of providing for loads in terms of 150, 200, 300, 400, 500, and 600 per cent of present loads rather than in terms of 1959, 1970, and 1975. This makes the results of the planning study more flexible and adaptable. It also lends itself more readily to periodic review and adjustment. Such techniques, however, take the soundest of engineering judgment and rigorous treatment to maintain stability and practicality.

OPERATIONS AND MAINTENANCE PRACTICES

System planning must provide for and recognize operation and maintenance needs. Wherever possible, co-ordination should be achieved so as to avoid unnecessary maintenance where property is to be scheduled for replacement. Also, system changes should have as one objective the improvement of operation and maintenance activities.

With respect to the rural electric systems, this is of particular importance because many of the systems have not yet reached a stable maintenance need. Fig. 5 is a typical failure-rate curve for an "all new" outside electrical utility plant which is the basic condition of these rural electric systems. Their average weighted age is now approaching 10 years. It is noted from the curve that there is ahead a sharp increase in maintenance needs. This is both a management and an engineering problem. Its solution should be closely co-ordinated with system planning.

SOUND SERVICE STANDARDS

Service standards sometimes are elusive. They are important and should be established, but are hard to define. The standards should be applied with engineering judgment to each specific system. The extent and refinements of standards established in each case will vary. In general, however, they might include, among others, voltage regulation, voltage levels, flicker limitations, and outage time—planned and unplanned. The engineer should, together with management, arrive at the standards which are to be built into the future system. One item for the planning engineer in his periodic review of the long-range system plan is a check on actual conditions to assure conformance with and to seek improvements of service standards. In this connection, at the 1954 American Power Conference,[11] the Duquesne Light Company and the Commonwealth Edison Company presented some interesting information. The engineers of those companies have recommended, and the managements have adopted, specific standards of service in terms of interruption, by types of service and for various portions of the system. For rural electric systems financed by the REA, standards have been established for voltage regulation and voltage levels.[6,7]

RECOGNITION OF CONSUMERS' CHANGING NEEDS

The greatest variable that the distribution system planning engineer must consider is the consumers' needs. The change in rate of increase in energy usage, shifting of population, development of industry, and construction of highways all affect the consumers' demands and energy usages on the various portions of the distribution system. What may appear to be a relatively simple problem can in a matter of several years become rather complex. This should be recognized in the flexibility of plans recommended, which should include possible or probable alternatives. In anticipation of what might be normal changes in consumer needs, the engineer can go a long way toward handling this problem. Periodic or continuous reappraisal of system conditions as related to the long-range system plans also can effectually accommodate this element.

PRACTICAL PLANNING CRITERIA

Consideration of the elements so far clearly leads to one logical conclusion and it is engineering "in principle." There must be criteria. The criteria must be practical. They must consider the elements discussed herein. They must be sufficiently flexible so as to provide for future changes in the art of distribution system design. Very few criteria have been established for rural electric systems. This is a tremendous engineering challenge. Consulting engineers and the staff engineers of the REA are working on it. The best answers will come from experience, co-operation, and a free exchange of professional judgment through media such as the AIEE. Criteria applicable to each specific system must be established by the management-engineering team of that system.

ALTERNATIVE PLANS

Reference has been made heretofore to alternatives. The need for alternatives when dealing with the future would seem to be inescapable. Yet it has been observed that engineers unacquainted or inexperienced in planning frequently overlook the value and need for alternatives. Perhaps that is because many engineers are construction-minded. Planning requires considerable flexibility and recognition of the intangibles and provision therefor in concrete form for comparative evaluation by management. As an engineer becomes proficient in the techniques and objectives of planning, he grasps the significance of and the need for the application of alternatives. In turn management develops greater confidence in him.

DIFFERENTIATION BETWEEN IMMEDIATE CONSTRUCTION PLANS AND LONG-RANGE ENGINEERING PLANS

An electric system requires immediate construction plans upon which the financial, personnel, material, and operational needs of the next year or two can be based. These are very specific. They provide for immediate commitment. There are no alternatives. Sometimes this is construed to be system planning, but it is not. Long-range engineering planning goes beyond and provides for the unknowns of the future. An analogy would be a comparison of a staking engineer with the owner-supervising engineer of a consulting engineering firm. The staking engineer is concerned principally with specifics which are definite, easily seen, and not too difficult to accomplish. This is analogous to immediate construction plans. The responsibility of the owner-supervising engineer is broad. He is faced with a variety of tangible and intangible considerations, many of which are not engineering in nature and yet with which he must successfully cope. This is analogous to long-range engineering planning.

POSITIVE USE OF PLANNING RESULTS AND REVIEW AND EXTENSION OF SYSTEM PLANS

A system plan, the results of a long-range system engineering study, should be on the tables and desks of the manager and the engineer operating the system, where they can refer to it, use it, mark it up as changes occur, and keep it current. It should be reviewed periodically or continuously, depending upon the situation on each particular system. The review should be for the purpose of determining whether or not the basic assumptions are still valid and, if not, the basic data and assumptions should be re-established and the plans adjusted accordingly. A second purpose of the review is to develop specific immediate construction plans for incorporating the required facilities into the system.

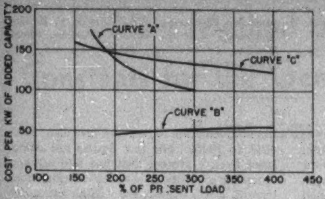

Fig. 8. Cost trends for increasing capacity

REA and Rural Electric System Planning

As stated previously, the REA is interested in the engineering phases of the rural electric systems it financed. That engineering interest is becoming more intensive, particularly with respect to planning, because of the banker's interest. The consulting engineers retained by and the engineers on the payroll of these rural electric systems, who are responsible for their specific systems, are being constantly encouraged to utilize more effectively long-range system engineering planning.[1,2] Meanwhile, the experience of these rural electric systems has shown the need for the development of general criteria and techniques which will enable the systems, engineers, and manufacturers to meet their future needs. The consulting engineers retained by a number of these rural electric systems have been directing their attention toward the techniques and criteria for planning applicable to their clients' systems under conditions three to six times the present load. This is commendable.

In the meantime, the staff of the REA is conducting studies toward the development of general system design criteria, equipment and material needs, and operation and maintenance techniques which will be required by all engineers and systems to meet the inevitable rural electric system loads many times those now being served. This is actually planning for system planning. The results will provide factors which permit better evaluation of conditions by the Administrator and specific techniques for use by engineers and management alike. Already some of these special planning studies being conducted by staff engineers of the REA have indicated tools which are expected to be of considerable benefit. They are quite preliminary and their application and limits are still being studied.

One of the studies concerned sectionalizing criteria. Fig. 6, which is one of the preliminary results, shows a probable relationship between consumer outage time and the number of sectionalizing points on a distribution circuit. The ordinate is in unit terms and would be applied to the "yardstick" established for each particular system by its own engineer and management. This curve provides tangible evidence and support of shorter circuits or, at least, a maximum optimum number of automatic sectionalizing devices. This is quite important when considering relative values for substations and feeder loading. This study with its mathematical derivations is continuing.

Fig. 7 shows a probable relationship of future-to-present system capacity with the ratio of future-to-present system investment. It, also, was developed by the staff engineers of the REA as part of a study analyzing the relationship of additional capital investment requirements for incremental increases in consumer usage. It assumes at any given time that the capacity and investment of a specific system are correlated and by the use of this simple curve the financial needs, as related to load growth, are indicated. An experimental application is being made to analyses of retail rate structures. It would appear that this curve, or some modification thereof, has a potential value with respect to long-range estimates and to general engineering and management checks on detailed alternative plans. In any event, these studies do show that the curve must be based upon the specific conditions expected for the system and type of intended application. Studies, mathematical analyses, and practical tests are continuing to determine the parameters of this technique as a system planning tool.

In Fig. 8, curves *A* and *B* represent data from theoretical studies made on actual systems to which arbitrary substantial load increases such as house heating were applied. Curve *C* represents the effect of applying the curve in Fig. 7 to a rural electric system. A number of conclusions can be drawn, mostly indicators of areas of further study. But one conclusion is positive, namely, generalization cannot be applied to a specific system unless all of the relevant factors therein are properly treated. Curve *A* represents a system for which financial requirements necessitated the keeping of facilities and capacity to an absolute minimum at every stage of its development. Thus, when subjected to a rapidly rising load, an inordinately large amount of capital improvement was necessary. The system represented by curve *B*, on the other hand, was one in which more consideration was given during the course of its development to maintaining flexibility of system capacity; thus, when subjected to a rapid rise of load, it was better able to accommodate the demand.

Conclusion

Planning has proved indispensable in the design, construction, and development of rural electric systems during the past 20 years. However, the tremendous loads forecast for the next 20 years increase the importance of system planning. As a matter of fact, it becomes one of the most fundamental requirements.

Planning, which must be recognized and supported by management and carried out by competent engineers, trained and experienced in the field, will assure the most economical and practical expenditure of funds, the anticipation and development of new materials and equipment, and, in general, will provide a sound basis for system operation, maintenance, and expansion. As the electrical utility industry is emphasizing system planning, so are the rural electric systems. The principal difference is that these 1,076 systems are relatively small, are primarily distribution systems, and have had little of the tremendous experience of the rest of the industry. Their weighted age is less than 10 years, and their engineering is usually provided by consulting engineers. They are distinctly rural and are faced with many special problems. Yet, through planning, the REA and these rural electric systems expect to meet the challenge in co-operation with all segments of the electrical utility industry.

References

1. ELECTRIC SYSTEM CAPACITY. *REA Bulletin 60-2*, Rural Electrification Administration, Washington, D. C., Sept. 18, 1953.

2. GUIDE FOR THE PREPARATION OF ENGINEERING SYSTEM STUDIES FOR ELECTRIC DISTRIBUTION BORROWERS. *REA Bulletin 60-3, Ibid.*, June 9, 1954.

3. RURAL DISTRIBUTION VOLTAGES, W. M. Edmunds, G. B. Roloson. *AIEE Transactions*, vol. 67, pt. II, 1948, pp. 1324–26.

4. PROCEDURE FOR MAKING VOLTAGE DROP STUDIES. *REA Bulletin 45-1*, Rural Electrification Administration, Washington, D. C., Feb. 20, 1953 (latest revision).

5. PROCEDURE FOR MAKING A SECTIONALIZING STUDY ON RURAL ELECTRIC SYSTEMS. *REA Bulletin 61-2, Ibid.*, June 1953 (latest revision).

6. VOLTAGE LEVELS ON RURAL DISTRIBUTION SYSTEMS. *REA Bulletin 169-4, Ibid.*, March 1952 (latest revision).

7. VOLTAGE REGULATOR APPLICATION ON RURAL DISTRIBUTION SYSTEMS. *REA Bulletin 169-27*, *Ibid.*, March 1954 (latest revision).

8. News Release, United States Department of Agriculture, Washington, D. C., May 21, 1954.

9. ESTIMATED POWER REQUIREMENTS OF THE U. S. FEDERAL POWER COMMISSION. Washington, D. C., June, 1954.

10. *Electrical World*, New York, N. Y., Sept. 20, 1954.

11. SERVICE CONTINUITY STANDARDS AID PLANNING AND OPERATION, W. J. Lyman, V. E. Hill. *Proceedings*, American Power Conference, Illinois Institute of Technology, Chicago, Ill., vol. XVI, 1954, pp. 409–16.

◆

Discussion

Harry Dewar (Patterson and Dewar, Decatur, Ga.): The paper is a good summary of the over-all aspects of engineering planning for the continued increase in electric load on rural electric distribution systems. In fact, we think it is the most comprehensive paper we have on this subject and appreciate that you have attempted to give freedom for the application of good engineering judgment to meet the ever-changing conditions accompanying load growth.

While there must be criteria for system planning, we can continue to recognize that today's criteria may not fit tomorrow's need. We must continue "open end" planning and be willing to abandon any self-imposed restrictions in looking at a new project if conditions and experience indicate them to be impractical. The procedure in the REA Bulletin *60-4* is good and we used this principle in selecting conductor sizes in 1937 on an REA project in Colorado built to carry heavy irrigation pump loads. However, to determine feeder conductivity on the basis of line-loss economics and regulation for a given load density without regard to continued growth beyond present estimates is a fallacy.

Based on past experience in numerous alternate designs and studies, we believe it is entirely possible that practical results in system planning for any particular system might be achieved over a period of years through substantially different approaches; for example, in decisions made with respect to the number of substations and associated transmission selected for any particular stage of a project development. This opinion is substantiated in some degree by the considerable variation in the choice of distribution and transmission voltage and substation practice between different public utilities operating with apparent good planning results in the same general area. In the end, the fact that the approach varies may give the better over-all answers to the whole industry.

In reviewing the system improvements on different projects and the corresponding system studies prepared several years earlier, we find that we hesitate to construct new feeders or rebuild existing feeders out the first few miles from wholesale power sources without using a conductor size within the range of the so-called maximum economical conductor for use on rural distribution. This often means a capital expenditure substantially above present needs or even the needs estimated for the life of the particular system study. Correspondingly, we often find it practical to continue use of existing feeders to loads above those estimated initially, and through delay, save in over-all cost and gain the chance to accumulate data that will aid to justify the largest practical capacity addition when this addition is needed.

A load density can be estimated for an individual circuit such that the circuit is designed and constructed with the maximum size of conductor in close to the power source practical for use on rural lines. From this maximum size out it is assumed that the conductivity is decreased in proportion to the economics for decrease in this total load distributed over the particular feeder. Present costs indicate that no. 2 through no. 2/0 conductivity generally is the largest economical range for conductors on rural electric distribution. As the new rural circuits are designed individually, based on a load density to give maximum conductivity, future load growth beyond the capacity of the feeder can be handled with construction of additional circuits, or by increase in below-maximum capacity of existing circuits, or by the addition of new wholesale power sources.

No pretense is made that any design is fool-proof and that future growth will not require limited rebuilding and in instances abandoned or reduced use of certain facilities. Generally, as loads increase, existing load centers are continued. The new load centers are established with respect to old sources at locations that require new heavy feeders and conversion of light line for comparatively short distances out across and supplying existing lines. Experience in the study of individual projects so designed in the past, with redesign of these projects made a few years later to supply continued load growth, indicates good flexibility in continued use of facilities from existing and new load centers, with possibly minimum overbuilding and minimum rebuilding.

W. J. Hauck (Rural Electrification Administration, Portland, Oreg.): While the paper covers a lot of ground, its keynote is that engineers must change their thinking from construction and design engineering to system planning engineering. This point cannot be given too much emphasis.

Table I reveals the REA as being more pessimistic than either the *Electrical World* or the Federal Power Commission. Yet its borrowers have the best and youngest potential of all. Sprinkler irrigation, air conditioning, and space heating are going to force rural loads up at an ever-accelerating rate for the next two decades. The three formulas from my paper, "System Improvement Planning," indicate the following average consumptions for rural users.

1955	1975	Multiple
567 kwh/mo.	2,654 kwh/mo.	4.67
310 kwh/mo.	1,267 kwh/mo.	4.09
341 kwh/mo.	1,243 kwh/mo.	3.64

The first figures were derived from the curve derived for average REA borrowers in the Northwest. (The curves for some predict much greater increases.) The second set of figures were calculated from the same average borrowers but were based on the rate of increase prevalent from 1941 to 1945. The last figures are calculated from a system that has had adverse operating conditions due to mountainous terrain, trees, storms, etc. High rates also have involved. Yet all these indicate that the loads will far more than triple by 1975.

To the section headed "A Minimum of Self-Imposed Restrictions" should be added the concept of planning for the saturated system. After all, 600 per cent of the present load on some systems is not very much and might be reached in a very short time.

R. W. Retherford (Chugach Electric Association, Anchorage, Alaska): I consider the paper excellent. Within my experience it has been apparent that the degree of flexibility in system plans is inversely proportional to the firmness of predictions for system usage. Present system planning in Alaska finds a unique requirement that heavily favors present designs which can easily meet problems of future growth. It is the present high cost of wholesale power. These costs range from a high of about five cents per kilowatt-hour to a low of about 12 mills per kilowatt-hour with the hydro coal and oil resources. In this great land these costs can only come down. Present high costs require planning for absolute minimum losses. This means that a feeder today economically loaded can carry increasing load as power costs go down. Losses rule today in Alaska economic designs. Perhaps voltage regulation will rule tomorrow.

John H. Rixse, Jr.: Mr. Dewar's general comments are appreciated. They indicate that the paper has accomplished its intended purpose, namely, to fill the gap in planning which exists and to which insufficient attention has been given. He speaks from a background of considerable experience as evidenced in the text by the type of planning problems with which he has coped. His testimony to the abandonment of "self-imposed" restrictions is a very healthy observation.

It is quite obvious that Mr. Hauck also speaks from a background of considerable interest and experience, with respect to planning. Particularly noteworthy is his observation that engineers must change their thinking as they move from "construction and design" to "planning." His reference to "the concept of planning for the saturated system" is quite intriguing, has merit, and should be investigated further, both from the standpoint of a general concept and of individual application.

Mr. Retherford's comments are an excellent illustration of how planning must suit the case in hand and yet maintain sound basic principles. His comments further emphasize the great dependence of successful planning upon the firmness of load predictions.

A New Method of Determining Constants for the General Transmission Loss Equation

E. D. EARLY
MEMBER AIEE

R. E. WATSON
ASSOCIATE MEMBER AIEE

IN A previous paper[1] the authors developed the following expanded form of the transmission loss equation, termed a general transmission loss equation

$$P_L=\sum_m\sum_n P_m B_{mn} P_n+\sum_n B_{n0}P_n+K_{L0} \quad (1)$$

and demonstrated that it was capable of accurately representing transmission losses for systems where substation loads vary at different rates with respect to total system load. The simplified form of the transmission loss equation, consisting of only the first term of equation 1, was shown to be applicable only to the special case where substation loads remained a constant fraction of total system load.

The method presented in reference 1 for determining constants for the general transmission-loss equation was based upon differences of bus-voltage phase angles between power supply sources and loads, as determined by a network-analyzer study of the system. The accuracy of this method was demonstrated by its application to a 3-source 4-load system having characteristics considered adverse to the phase-angle method.

The purpose of this paper is to present a theoretical derivation of the general transmission loss equation 1 and a method of determining its constants based upon system self- and mutual impedances and generator phase angles, load, and generator currents, as determined for two base cases by a network-analyzer study. The method takes into account both the real and imaginary components of generator and load currents. It is similar in derivation and determination of constants to methods previously presented by Kirchmayer and Stagg[2] and by Harder[3] for the simplified form of the loss equation and all assumptions applicable to the derivation of this equation are retained, except that the assumption that individual load currents remain a constant fraction of total load current is replaced by the assumption that the individual load currents are linear complex functions of the total load current, namely.

$$I_j=I_j^0+l_jI_{LT} \quad (2)$$

where

l_j = the complex rate of change of the jth load current with respect to the total load current I_{LT}

I_j^0 = the value of the jth load current when the phasor sum of all load currents becomes zero

Derivation of General Transmission Loss Equation

The derivation of the general transmission loss equation 1 is shown in Appendix I, where the equation constants are shown to have the following values

$$B_{mn}=(R_{mn}-R_{mk}l'^k-l'^jR_{jn}+R_{LL})K_{mn}+(R_{mk}l''^k-l''^jR_{jn})H_{mn} \quad (3)$$

$$B_{n0}=2L_0^k[(R_{nk}-l'^jR_{jk})K_{nk}-(l''^jR_{jk})H_{nk}] \quad (4)$$

$$K_{L0}=(I_0'^jI_0'^k+I_0''^jI_0''^k)R_{jk} \quad (5)$$

where

$$R_{LL}=(l'^jl'^k+l''^jl''^k)R_{jk} \quad (6)$$

$$l_j=l_j'+jl_j'' \quad (7)$$

$$I_j^0=I_j^{0\prime}+jI_j^{0\prime\prime} \quad (8)$$

$$K_{mn}=\frac{1}{V_mV_n}[(1+S_mS_n)\cos\theta_{mn}+(S_m-S_n)\sin\theta_{mn}] \quad (9)$$

$$H_{mn}=\frac{1}{V_mV_n}[(S_m-S_n)\cos\theta_{mn}-(1+S_mS_n)\sin\theta_{mn}] \quad (10)$$

$$K_{nk}=\frac{1}{V_nV_k}[(1+S_nS_k)\cos\theta_{nk}+(S_n-S_k)\sin\theta_{nk}] \quad (11)$$

$$H_{nk}=\frac{1}{V_nV_k}[(S_n-S_k)\cos\theta_{nk}-(1+S_nS_k)\sin\theta_{nk}] \quad (12)$$

$$S_m=\frac{Q_m}{P_m}$$

$$S_n=\frac{Q_n}{P_n}$$

$$S_k=\frac{Q_k}{P_k}$$

where

θ_{mn} = difference in the bus voltage phase angle between sources m and n

R_{mn}, R_{mk}, R_{jk} = the self- and mutual resistances between generators, between generators and loads, and between loads

Application of Method

The system selected for illustrating application of the method, shown in Fig. 1, is a 3-source 4-load loop system. It is the same system as that used in reference 1 to illustrate the application of the phase-angle method of determining constants for the general transmission-loss equation. A total of 15 cases representing typical distribution of power supply by sources for peak period, median, and valley period load conditions will be studied to test the accuracy of the method. The load distribution, in megavolts (mw), for three load periods is shown in Table I. It will be noted that each of the loads varies at a different rate, that they do not remain a constant fraction of the total system load, and that the difference in the ratio of the valley load to the peak load is representative of that normally found between substations serving different types of loads on a typical power system. The distribution of the change in total system loads by loads is as follows:

Load no. 1,	38.34 per cent
Load no. 2,	18.33 per cent
Load no. 3,	30.00 per cent
Load no. 4,	13.33 per cent
Total	100.00 per cent

Network-Analyzer Data

The system self- and mutual resistances between generators, between generators and loads, and between loads are measured as described in references 2 and 3. It should be noted that measurements between loads are not required for the simplified loss equation. The $R_{mn}-R_{jk}$ resistance matrix for Fig. 1's system:

	G_1 L_1	G_2 L_2	G_3 L_3	L_4
G_1 L_1	0.049628	0	0.015343	0.030842
G_2 L_2	0	0	0	0
G_3 L_3	0.015343	0	0.032485	0.025126
L_4	0.030842	0	0.025126	0.050802

Paper 55-720, recommended by the AIEE System Engineering Committee and approved by the AIEE Committee on Technical Operations for presentation at the AIEE Fall General Meeting, Chicago, Ill., October 3-7, 1955. Manuscript submitted June 6, 1955; made available for printing July 22, 1955.

E. D. EARLY is with the Southern Services, Inc., Birmingham, Ala., and R. E. WATSON is with the Leeds and Northrup Company, Philadelphia, Pa.

Data for two base cases are required, one for peak period loads and one for valley period loads. The cases selected as base cases (*A*-2 and *C*-5) represent minimum loss conditions. The load-flow diagrams for these cases are shown in Figs. 2 and 3. The following network-analyzer readings are required for each base case:

1. Record voltage magnitudes, mw, megavars (mvar), and angles for all generators and loads, including condensers, capacitors, and line-charging capacitors.
2. Record scalar value of all line currents.
3. Record such other readings as may be desired for checking purposes, such as line mw and mvar.

Selection of Q/P Ratios

The first and most important operation in computing the value of the loss equation constants is the selection of the proper *Q/P* ratios for each generator and each load. It has been shown by another author[3] that deducting that part of the reactive generation which does not vary with real power generated and including it as part of the load supplied from the same bus produces *Q/P* ratios for each generator which are reasonably constant over a wide range of generation. It is interesting to note that this operation also produces *Q/P* ratios for each load that are constant as the total system load varies between its maximum and minimum value.

The procedure of selecting *Q/P* ratios is to pick for each load a *Q/P* ratio requiring the transfer of such reactive power from the generator supplying the load bus as to give a generator *Q/P* ratio as nearly constant as possible for the peak period and valley period base cases. Other cases studied on the network analyzer should be used to check the *Q/P* ratios selected. Reactive power supplied by fixed or switched capacitors, synchronous condensers, and line-charging capacitors should be included with the load.

The procedure of determining the *Q/P* ratios for generator no. 1 and load no. 1 is shown in Table II. The *Q/P* ratios selected are as follows: for generators nos. 1, 2, and 3—1 −0.60, 2 −0.35, and −0.35 respectively; and for loads no. 1, 2, 3, and 4— −0.65, −0.40, −0.40, and −0.50 respectively.

Rate of Change of Load Currents

Having obtained an adjusted value of reactive power for the loads in selecting the *Q/P* ratios, the next step is the computation of the load currents for both the peak period and valley period base cases with respect to a common reference phasor, such as the bus voltage of the generator selected to be grounded in determining the system self- and mutual resistances. The relative rates of change of the load currents and value of each load current when the phasor sum of all load currents is zero can now be determined from the following relationships

$$I_j=(l_j'+jl_j'')(I_{L_T})+I_j^\circ \tag{13}$$

$$(l_j'+jl_j'')=\frac{(I_j)_{\text{peak}}-(I_j)_{\text{valley}}}{(I_{L_T})_{\text{peak}}-(I_{L_T})_{\text{valley}}} \tag{14}$$

to be as follows:

Load Currents	$l_j'+jl_j''$	$I_j^{\circ\prime}+I_j^{\circ\prime\prime}$
I_{L_1}	0.405056+*j*0.054634	−0.422376−*j*0.197961
I_{L_2}	0.174598−*j*0.021893	+0.254696−*j*0.007483
I_{L_3}	0.288310−*j*0.012578	+0.539382+*j*0.388973
I_{L_4}	0.132036−*j*0.020163	−0.371702−*j*0.183529
I_{L_T}	1.000000+*j*0.000000	0.000000+*j*0.00000

Determining Value of L$_K^0$

The data and equations are now available for computing the value of all constants except L_k°, the value of each load when the phasor sum of all load currents is zero, which is required for computation of the B_{n0} constants. The values of L_k° can be determined from the computed value of K_{L0}, the peak period and valley period values of L_k, and the total load using the following relationship

$$L_k^\circ=(L_k)_{\text{valley}}-\frac{(L_k)_{\text{peak}}-(L_k)_{\text{valley}}}{(L_T)_{\text{peak}}-(L_T)_{\text{valley}}}\times [(L_T)_{\text{valley}}-K_{L0}] \tag{15}$$

Empirical Determination of R$_{LL}$ and K$_{L0}$

R_{LL} can be computed from network-analyzer data using equation 6, and K_{L0} can be so computed from equation 5. However, in determining constants for the simplified loss equation, it was found desirable to determine R_{LL} (w' in another method) empirically[2,3] by setting the computed system loss equal to the I^2R loss for the base case, and it will probably be desirable to determine the value of R_{LL} and K_{L0} for the general loss equation empirically in a like manner, this being possible since there are two base cases. The procedure for doing this is as follows:

1. Compute value of B_{mn} constants in terms of R_{LL} by equation 3 using the average of the two values of K_{mn} and H_{mn} determined for the two base cases.
2. Determine values of L_k° in terms of K_{L0} by equation 15 and then compute value of B_{n0} constants in terms of K_{L0} by equation 4 using the average of the two values of K_{nk} and H_{nk} determined for the two base cases.
3. Set up equations for total system loss in terms of R_{LL} and K_{L0} for the two base cases, using equation 1, and set them equal to the I^2R losses for these cases.
4. Solve the two simultaneous equations so obtained for R_{LL} and K_{L0}.

The values of R_{LL} and K_{L0} obtained empirically by this procedure are

$R_{LL}=0.020631$

$K_{L0}=0.018735$

which when substituted into equations 3 and 4 give the constants for the general transmission loss equation shown in the following

$B_{11}=+0.017766$

$B_{12}=-0.010076$

$B_{13}=-0.014439$

$B_{10}=-0.032804$

$B_{21}=-0.010076$

$B_{22}=+0.023158$

$B_{23}=+0.001938$

$B_{20}=+0.027018$

$K_{L0}=+0.018735$

$B_{31}=-0.014439$

$B_{32}=+0.001938$

$B_{33}=+0.017196$

$B_{30}=+0.033247$

The values of R_{LL} and K_{L0} computed from equations 5 and 6 are not far different from those determined empirically, being

$R_{LL}=0.020621$

$K_{L0}=0.022804$

The agreement between empirically determined and computed values of R_{LL} and K_{L0} depends largely upon the generator and load *Q/P* ratios selected, the empirically determined values compensating for errors which are introduced by these ratios.

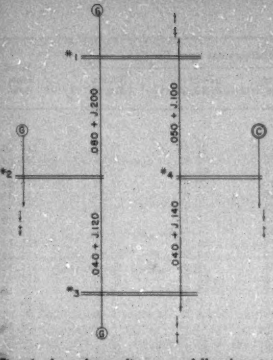
G
*1
.080 + J.200
.050 + J.100
G
C
*2
*4
.040 + J.120
.040 + J.140
*3
G

Fig. 1 Impedance diagram. All values in per unit on a 100-megavolt-ampere base. This applies also to Figs. 2 and 3

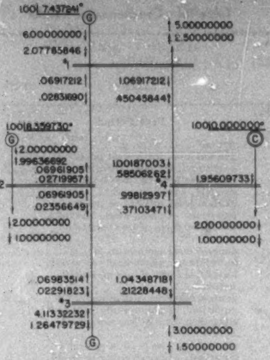
1.00|7.437241°
G
6.00000000
2.07785846
5.00000000
2.50000000
*1
.06917212
.02831690
1.06917212
.45045844
1.00|8.359730°
G
1.00|10.000000°
C
2.00000000
1.99636692
.06961905
.02719957
1.00187003
.58506262
*2
*4
1.95609733
.06961905
.02356649
.99812997
.37103471
2.00000000
1.00000000
2.00000000
1.00000000
.06983514
.02291823
1.04348718
.21228448
*3
4.11332232
1.26479729
G
3.00000000
1.50000000

Fig. 2. Base case A-2 load flow

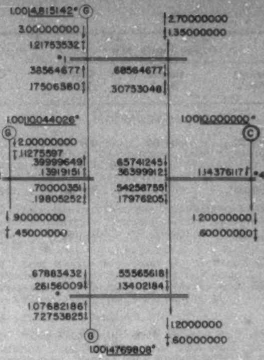
1.00|4.815142°
G
3.00000000
1.21753532
2.70000000
1.35000000
*1
.38564677
.17506580
.68564677
.30753048
1.00|10.044026°
G
1.00|10.000000°
C
2.00000000
1.11275597
.39999649
.13919151
.65741245
.36399912
1.14376117
*2
*4
.70000351
.19805252
.54258755
.17976205
.90000000
.45000000
1.20000000
.60000000
.67883432
.26156009
.55565618
.13402184
*
1.07682186
.72753825
G
1.00|4.769808°
1.2000000
.60000000

Fig. 3. Base case C-5 load flow

Comparison of Results

A comparison of incremental and total loss values given by the general loss equation 1, using the constants shown in the foregoing, which were determined in accordance with the method developed in this paper, with actual incremental and total loss values is shown in Table III. Incremental and total loss values given by the general loss equation using constants developed by the phase-angle method[1] and such values given by the simplified form of the loss equation[4] are also shown.

The incremental loss values given by the general loss equation using constants developed herein are in close agreement with the actual incremental loss values; they equal in accuracy results acquired with the use of constants obtained by the phase-angle method. But total system losses, while in acceptable agreement with I^2R losses, are somewhat less accurate than those obtained by the use of the phase-angle method. This indicates that the relationship between the B_{n0} and B_{mn} constants obtained by the method presented in this paper are not as good as those given by the phase-angle method; it has been previously pointed out that the B_{n0} constants have a greater effect upon total loss than upon incremental loss values.[1]

The incremental and total loss values given by the simplified form of the loss equation show that this form of the equation is not capable of representing adequately both incremental losses and total loss over a wide range of system conditions when the individual loads vary at different rates and do not remain a constant fraction of the total system load, the error in incremental loss values being of such magnitude as to affect materially the economy loading of power supply sources.

The cases shown in Table III represent peak period, median, and valley period loads with power supplied by each source covering the full range from minimum to maximum output. System I^2R losses range from a minimum of 0.9 per cent to a maximum of 11.6 per cent, and incremental loss values vary from −25 per cent to +35 per cent. The difference in bus-voltage phase angle between power supply sources runs as high as 45 degrees.

Conclusions

The method of computing constants for the general loss equation presented in this paper supplements the phase-angle method previously presented[1] and will be of particular value for application to line-type systems, systems where the range of reactance-resistance ratios are extreme, and systems having two transmission voltage levels, these being conditions under which the accuracy of the phase-angle method may be in question.

It may be found desirable to determine the general loss equation constants by both methods as a check on accuracy, since close agreement of the constants can be determined by the two completely different methods, which will prove the accuracy of the constants obtained.

Appendix I. Derivation of Loss Equation

With the use of the Einstein summation convention, whereby the occurrence in a product of the same letter as both a superscript and subscript index represents a summation over that index ($P^mB_{mn}P^n =$

Table I. Load Distribution

Load No.	Peak Period Load Mw	Median Load Mw	Valley Period Load Mw
1	500	385	270
2	200	145	90
3	300	210	120
4	200	160	120
Total	1,200	900	600

Table II. Determination of Generator and Load Q/P Ratios

	Case A-2 Peak Period	Case C-5 Valley Period
Generator no. 1	6.000+j2.078	3.000+j1.218
Reactive transferred to load	−j5.750	−j3.105
Net	6.000−j3.672	3.000−j1.887
Generator no. 1 Q/P ratio	−0.60	−0.60
Load no. 1	−5.000−j2.500	−2.700−j1.350
Reactive transferred from generator	+j5.750	+j3.105
Net	−5.000+j3.250	−2.700+j1.755
Load no. 1 Q/P ratio	−0.65	−0.65

Table III. Comparison of Results

Power Supply Mw					Incremental Loss Per Cent			
Source No. 1	Source No. 2	Source No. 3	Case No.	Loads	Source No. 1	Source No. 2	Source No. 3	Total Loss Mw
				Peak Period				
200.00	800.00	357.93	*A*-1	actual*	−25.76	37.41	16.36	157.93
				general loss equation method of paper†	−22.63	37.11	12.96	164.34
				general loss equation phase-angle method‡	−22.14	35.41	13.07	157.75
				simplified form of loss equation§	−20.00	40.81	17.32	174.24
600.00	200.00	411.33	*A*-2	actual*	2.29	1.37	0.72	11.33
				general loss equation method of paper†	2.13	1.47	0.92	11.32
				general loss equation phase-angle method‡	1.92	1.26	1.00	11.05
				simplified form of loss equation§	1.43	2.57	2.63	12.27
200.00	400.00	710.73	*A*-3	actual*	−25.76	21.74	23.71	110.73
				general loss equation method of paper†	−24.76	19.95	23.54	114.58
				general loss equation phase-angle method‡	−23.58	19.66	22.94	111.14
				simplified form of loss equation§	−21.75	23.73	27.93	124.96
629.18	400.00	200.00	*A*-4	actual*	5.69	9.08	−6.77	29.18
				general loss equation method of paper†	5.24	9.32	−6.42	28.98
				general loss equation phase-angle method‡	4.55	8.37	−5.90	26.78
				simplified form of loss equation§	4.06	10.19	−4.91	28.24
300.00	600.00	379.01	*A*-5	actual*	−15.57	24.48	10.49	79.01
				general loss equation method of paper†	−15.66	25.91	10.02	84.57
				general loss equation phase-angle method‡	−15.31	24.72	10.07	81.33
				simplified form of loss equation§	−13.87	28.75	13.47	90.97
400.00	200.00	634.64	*A*-6	actual*	−10.35	6.02	13.09	34.64
				general loss equation method of paper†	−11.43	6.36	14.38	37.68
				general loss equation phase-angle method‡	−10.79	6.45	13.95	36.64
				simplified form of loss equation§	−10.20	8.74	17.33	43.33
				Median				
200.00	400.00	348.44	*B*-1	actual*	−13.86	17.55	10.82	48.44
				general loss equation method of paper†	−14.30	18.55	11.08	51.88
				general loss equation phase-angle method‡	−13.71	17.86	10.77	50.07
				simplified form of loss equation§	−11.86	20.12	12.94	50.92
400.00	200.00	308.83	*B*-2	actual*	− 1.56	4.66	2.74	8.83
				general loss equation method of paper†	− 2.02	5.10	3.17	9.09
				general loss equation phase-angle method‡	− 1.92	4.84	3.01	9.03
				simplified form of loss equation§	− 1.30	5.49	3.85	8.83
327.39	400.00	200.00	*B*-3	actual*	− 4.62	14.05	1.84	27.39
				general loss equation method of paper†	− 5.48	15.41	2.30	29.37
				general loss equation phase-angle method‡	− 5.45	14.53	2.32	28.16
				simplified form of loss equation§	− 4.28	16.13	3.32	28.57
				Valley Period				
417.17	200.00	0.00	*C*-1	actual*	7.33	3.83	−7.93	17.17
				general loss equation method of paper†	7.51	3.56	−7.95	16.95
				general loss equation phase-angle method‡	7.05	2.96	−7.83	16.91
				simplified form of loss equation§	7.60	2.08	−9.39	17.93
0.00	200.00	469.51	*C*-2	actual*	−20.66	14.25	19.32	69.51
				general loss equation method of paper†	−20.87	13.78	20.25	73.68
				general loss equation phase-angle method‡	−19.56	13.80	19.29	69.90
				simplified form of loss equation§	−16.75	14.97	21.42	65.25
200.00	0.00	421.03	*C*-3	actual*	− 7.37	−0.26	10.89	21.03
				general loss equation method of paper†	− 8.33	0.30	12.03	22.57
				general loss equation phase-angle method‡	− 7.53	0.73	11.23	20.89
				simplified form of loss equation§	− 5.96	0.25	11.96	19.22
100.00	300.00	233.86	*C*-4	actual*	−11.96	14.51	9.20	33.86
				general loss equation method of paper†	−12.53	15.49	9.64	36.40
				general loss equation phase-angle method‡	−11.87	14.96	9.15	35.04
				simplified form of loss equation§	− 9.53	15.80	9.93	30.55
300.00	200.00	107.68	*C*-5	actual*	0.54	5.90	−1.09	7.68
				general loss equation method of paper†	0.24	6.33	−0.86	7.67
				general loss equation phase-angle method‡	0.24	5.88	−1.03	7.87
				simplified form of loss equation§	1.42	5.46	−1.74	6.65
100.00	400.00	143.00	*C*-6	actual*	−11.34	18.25	6.73	43.00
				general loss equation method of paper†	−11.92	19.77	6.91	46.52
				general loss equation phase-angle method‡	−11.44	18.89	6.59	44.82
				simplified form of loss equation§	− 9.02	20.04	7.17	40.70

* I^2R loss and actual incremental loss as determined by the $\Delta L/\Delta P$ method; see reference 1.

† Computed by equation 1, using the constants shown in the section entitled "Empirical Determination of R_{LL} and K_{Li}."

‡ Taken from Table IV, reference 1.

§ Taken from Table VIII, reference 4.

$\sum_m \sum_n P_m B_{mn} P_n$), real and reactive transmission losses may be expressed as follows

$$P_L'+jP_L''=I^{*m}Z_{mn}I^n+I^{*m}Z_{mk}I^k+I^{*j}Z_{jn}I^n+I^{*j}Z_{jk}I^k \quad (16)$$

where

superscripts m, n = power supply sources
j, k = loads
I^* = the conjugate form[5]

Let it be assumed that the load currents are linear complex functions of the total load current, given by the following expressions:

$$I_j^*=I_j^{*0}+l_j^*I_{LT}^* \quad (17A)$$

$$I_k=I_k^0+I_{LT}l_k \quad (17B)$$

Substituting equation 17 and the following relationships

$$I_{LT}=-\sum_n I_n \quad (18A)$$

$$I_{LT}^*=-\sum_m I_m^* \quad (18B)$$

$$l_k=l_k'+jl_k'' \quad (19A)$$

$$l_j^*=l_j'-jl_j'' \quad (19B)$$

into equation 16 gives

$$P_L'+jP_L''=I^{*m}I^n[Z_{mn}-Z_{mk}l'^k-l'^jZ_{jn}+(l'^jl'^k+l''^jl''^k)Z_{jk}]-jI^{*m}I^n(Z_{mk}l''^k-l''^jZ_{jn})+I^{*m}I_0^k(Z_{mk}-l'^jZ_{jk})+I_0^{*j}I^n(Z_{nj}-Z_{jk}l'^k)+jI^{*m}I_0^k(l''^jZ_{jk})-jI_0^{*j}I^n(Z_{jk}l''^k)+(I_0'^jI_0^k+I_0''^jI_0''^k)Z_{jk} \quad (20)$$

But

$$I_m^* I_n = \frac{P_m + jQ_m}{V_m} \frac{P_n - jQ_n}{V_n^*} \qquad (21)$$

and substituting the following relationships

$$\frac{Q_m}{P_m} = S_m \qquad \frac{Q_n}{P_n} = S_n$$

into equation 21, gives

$$\begin{aligned} I_m^* I_n = \frac{P_m P_n}{V_m V_n} [& (1 + S_m S_n) \cos(\theta_m - \theta_n) + \\ & (S_m - S_n) \sin(\theta_m - \theta_n) + \\ & j(S_m - S_n) \cos(\theta_m - \theta_n) - \\ & j(1 + S_m S_n) \sin(\theta_m - \theta_n)] \\ & = P^m P^n (K_{mn} + jH_{mn}) \end{aligned} \qquad (22)$$

Substituting equation 22 and similar relationships for $I_m^* I_k^\circ$ and $I_j^{*\circ} I_m$ into equation 20 and retaining only the real part gives the following expression for the real transmission loss

$$\begin{aligned} P_L' = P^m P^n [& (R_{mn} - R_{mk} l'^k - l'^j R_{jn} + \\ & R_{LL}) K_{mn} + (R_{mk} l''^k - l''^j R_{jn}) H_{mn}] + \\ & 2P^n L_0^k [(R_{nk} - l'^j R_{jk}) K_{nk} - \\ & (l''^j R_{jk}) H_{nk}] + K_{L0} \end{aligned} \qquad (23)$$

where

$$R_{LL} = (l'^j l'^k + l''^j l''^k) R_{jk} \qquad (24)$$

$$K_{L0} = I_0^{*j} R_{jk} I^k \qquad (25)$$

$$K_{mn} = \frac{1}{V_m V_n} [(1 + S_m S_n) \cos\theta_{mn} + (S_m - S_n) \sin\theta_{mn}] \qquad (26)$$

$$H_{mn} = \frac{1}{V_m V_n} [(S_m - S_n) \cos\theta_{mn} - (1 + S_m S_n) \sin\theta_{mn}] \qquad (27)$$

$$K_{nk} = \frac{1}{V_n V_k} [(1 + S_n S_k) \cos\theta_{nk} + (S_n - S_k (\sin\theta_{nk}] \qquad (28)$$

$$H_{nk} = \frac{1}{V_n V_k} [(S_n - S_k) \cos\theta_{nk} - (1 + S_n S_k) \sin\theta_{nk}] \qquad (29)$$

$$S_m = \frac{Q_m}{P_m} \qquad S_n = \frac{Q_n}{P_n} \qquad S_k = \frac{Q_k}{P_k}$$

References

1. A GENERAL TRANSMISSION LOSS EQUATION, E. D. Early, G. L. Smith, R. E. Watson. *AIEE Transactions*, vol. 74, pt. III, June 1955, pp. 510–20.

2. ANALYSIS OF TOTAL AND INCREMENTAL LOSSES IN TRANSMISSION SYSTEMS, L. K. Kirchmayer, G. W. Stagg. *Ibid.*, vol. 70, pt. II, 1951, pp. 1197–1205.

3. LOSS EVALUATION—PART II. CURRENT- AND POWER-FORM LOSS FORMULAS, E. L. Harder, R. W. Ferguson, W. E. Jacobs, D. C. Harker. *Ibid.*, vol. 73, pt. III-A, June 1954, pp. 716–31.

4. *Closure* of reference 1.

5. TENSORIAL ANALYSIS OF INTEGRATED TRANSMISSION SYSTEMS—PART I. THE SIX BASIC REFERENCE FRAMES, G. Kron. *AIEE Transactions*, vol. 70, pt. II, 1951, pp. 1239–48.

◆

Discussion

A. F. Glimn, L. K. Kirchmayer and **R. D. Wood** (General Electric Company, Schenectady, N. Y.): This interesting paper serves to stimulate several comments and questions.

The method of calculation of the B_{n0} coefficients in this paper requires the determination of the mutual resistances between all loads. For example, for a system of 100 loads, it would be required to determine approximately 5,000 mutual resistances. A method that we have used to determine the B_{n0} and the K_{L0} coefficients involving only a fraction of this work utilizes a combination of circuit theory and a least squares solution for w^1, B_{n0}, and K_{L0}. The accuracy of this formula has been found to be comparable to that described in the paper.

We would like to ask the authors what criteria they suggest or use in determining the accuracy requirements of a formula for the determination of incremental losses. Also, what per cent accuracy do the authors associate with the incremental production cost data on the Southern Company system?

One suggested method to determine the accuracy requirements of an incremental loss formula is to determine the effect of inaccuracies in incremental loss upon the increase in fuel consumption. We have made a comparative study for the system of the paper in order to measure loss formula inaccuracies in terms of money. Typical incremental cost data assumed for the three plants such that moderately heavy losses were obtained with schedules calculated from a knowledge of the incremental plant costs with transmission losses neglected. Schedules were calculated using the different loss formulas, and the differences in annual fuel cost evaluated. Assuming the savings to be obtained by the use of the loss formula of reference to be 100 per cent, the following table gives the percentage of the savings obtained by the other loss formulas.

Type of Formula		Per Cent of Savings Obtained
General Loss Formula	Phase angle method[1]	100.0
	Method of paper	100.0
	Glimm, Kirchmayer, Wood	100.0
Simplied[2] Loss Formula		99.3

Thus, it is seen for this particular system and the assumed incremental cost data that for all practical purposes the same fuel economy was obtained with either the general or simplified form of the loss formula.

REFERENCES

1. See reference 1 of the paper.
2. See reference 4 of the paper.

J. K. Dillard (Westinghouse Electric Corporation, Pittsburgh, Pa.): Mr. Early and Mr. Watson have produced a fine paper dealing with the evaluation of transmission losses. This paper goes a long way toward a completely general solution of the loss problem. They present an expanded or general form of the transmission loss formula as shown in equation 1 of the paper. The authors call the first term of the equation, which is widely used in loss studies, the simplified form of the formula. The most obvious objection to the general form is the enormous amount of additional computation required to solve for the constants.

In the example given in the paper to illustrate the application of the general formula each of the loads varies at a widely different rate. Table III shows that losses obtained using the general formula are in fairly good agreement with the I^2R or actual losses, whereas values obtained using the simplified form are not as good. The authors are cautioned not to expect the same improvement in dispatch.

In economy dispatch it is neither total nor losses nor incremental losses which are of prime importance, but rather the fuel costs (or production costs) to deliver a given load. Minimum fuel costs are obtained when every station in the system is operating at the bottom of a flat U-shaped curve where a change of generation in either direction will increase the delivered power cost. Since the slope of the operating curve of each station is nearly zero, small deviations from the optimum dispatch should not change the costs significantly.

To test the effect of small departures from the optimum dispatch, a study has been made on an actual system having a peak load of about 1,200 mw to determine the penalty which might be expected if a large nonconforming load were assumed to vary in proportion to the total system load.[1] The nonconforming load amounts to 75,000 kw at peak and may vary anywhere within the striped area of Fig. 4. If it were treated like other loads, the assumed variation would be a straight line through the origin. To obtain the maximum deviation from the system load pattern, the nonconforming load was represented by two horizontal lines, being high when the system load is low, and conversely. Such representation is an upper limit of nonconformity. The difference in fuel costs was calculated with the load first treated as conforming to the system load pattern and then as following the maximum nonconformity.[1] The system load cycle was assumed to be 736 mw for 30 per cent of the time, 945 mw for 30 per cent, and 1,224 mw for 40 per cent. It was found that the maximum penalty for dispatching the load as conforming would be $689 per year. The actual penalty would be less since the load will be closer to the system pattern most of the time.

It is desirable, of course, to obtain losses as accurately as possible within practical limits. In a number of studies on real systems, losses obtained using the simplified form of the loss formula check percentage-wise as well as the general form checks the example in the paper. If they did not, the formula would not be a very

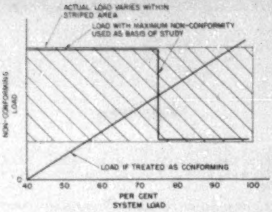

Fig. 4. Representation of a load for maximum nonconformity

good mathematical replica of the system. Our practice has been to examine the variation of each load critically. Those loads which deviate substantially from the system load pattern are treated as nonconforming loads. So far, we have not encountered a system where more than a few loads had to be represented this way. Incidentally, large loads which vary in random fashion, like the one shown in Fig. 4, should be dispatched as nonconforming regardless of the form of loss formula used.

In spite of the additional computation, a more general approach than is possible with the simplified formula has promise in some situations. There are extensive systems which can be divided into two, or more, large areas in which total area loads vary at different rates. This can turn out to be a complicated problem because the way area loads vary with each other changes, more often than not, with the seasons. In some cases, there is considerable variation from day to day as would be the case when cool weather results in dropping large summer air-conditioning loads in one area of the system. At the present time, the practical way to handle these situations is to use seasonal formulas, each one based on the best over-all representation of the system over a period of several months.

REFERENCE

1. LOSS EVALUATION—IV, ECONOMIC DISPATCH COMPUTERS PRINCIPLES AND APPLICATION, W. H. **Osterle**, **E. L. Harder**. *AIEE Transactions*, vol. 75, pt. III, 1956 (*Paper No. 56-163*).

W. R. Brownlee (Southern Services, Inc., Birmingham, Ala.): This paper provides needed contributions to the art of fuel-cost–transmission-loss co-ordination, especially in the following respects:

1. It demonstrates that a general loss equation may be derived in a manner similar to the numerous published methods of deriving simplified loss equations, but including the substantial influence of nonuniform load variations.
2. It provides rigorous values of total and incremental losses for comparison with the results of calculated constants.
3. It shows the feasibility, at least with the simple system illustrated, of calculating directly certain modifying terms, such as R_{LL} (similar to "w''") in reasonable agreement with empirical calculations using total losses.

The authors point out that, except for improvement of incorporating nonuniform load variations, the method is subject to the assumptions of previous methods outlined by Kirchmayer and Stagg[1] and by Harder.[2] Therefore, this method lacks certain vital advantages of the method derived previously by Early, Watson, and Smith,[3] which utilizes phase-angle functions[4] to determine a set of constants. I agree with the authors that the most critical operation in their latest method is the selection of the proper Q/P ratio for each generator and each load. The inference of the section, "Selection of Q/P Ratios," is that the amount of reactive power transferred from a generator to its local load should be such that resulting Q/P ratios for this generator will be the same for peak and valley loading, and that the Q/P ratio of the corresponding load should also be the same for the peak and valley conditions. However, calculations made in this manner, using the generation and load shown in Table II for the peak and valley cases, results in Q/P values of about 0.40 for both the generator and the load, compared with the authors' results of some $1^1/_2$ times this value. Since the higher values were used in the calculations, it appears that considerable weight must have been given to cases other than the two base cases. Other authors have not provided any more rational approach to the selection of Q/P ratios. Cahn[5] recommends using only zero or negative values for Q/P. Others have suggested deriving ratios by interchanging generation between units, the loads remaining constant. Obviously, this is in opposition to the general pattern of increasing generation to supply increases in system load. In view of these widespread mixtures of science and witchcraft, there is substantial doubt as to whether any method which involves such a selection of Q/P ratios is adequate for the primary determination of a set of constants for a typical power system.

One use indicated for this new method is the treatment of line-type systems. Constants for such a system may be derived by the method previously described by the authors,[3] with one minor modification. It has been shown[6] that the incremental losses from point *1* to point *3* in a network may be obtained through use of the incremental losses from point *1* to point *2* and from point *2* to point *3*. Consider a line-type system in which plant A is connected to plant B by a high-voltage low-resistance line, with plant B operating in a network of moderate voltage lines with a number of other plants. The incremental losses from each generator to the component system load may be obtained directly as has been outlined for all plants except plant A. The incremental loss of plant A to the system load is then calculated by computing the incremental loss of plant A to plant B, using the high X/R ratio and actual phase angle of the high-voltage line, and the incremental loss already developed from plant B to the load. This provides an accurate incremental loss from plant A to the load.

The authors have outlined a method for the empirical determination of quantities R_{LL} and K_{L0}. In view of the difficulty of selecting adequate Q/P ratios for both generators and loads, it may be desirable to calculate the B_{n0} values empirically. It appears that this might make it unnecessary to use the Q/P ratios for the loads. Do the authors feel this would be advantageous?

REFERENCES

1. See reference 2 of the paper.
2. See reference 3 of the paper.
3. See reference 1 of the paper.
4. CO-ORDINATION OF INCREMENTAL FUEL COSTS AND INCREMENTAL TRANSMISSION LOSSES BY FUNCTIONS OF VOLTAGE PHASE ANGLES, **W. R. Brownlee**. *AIEE Transactions*, vol. 73, pt. III-A, 1954, pp. 529–41.
5. THE DETERMINATION OF INCREMENTAL AND TOTAL LOSS FORMULAS FROM FUNCTIONS OF VOLTAGE PHASE ANGLES, **C. R. Cahn**. *Ibid.*, vol. 74, pt. III, 1955, pp. 161–76.
6. COORDINATION OF LOSSES IS VITAL, **W. R. Brownlee**. *Electrical World*, New York, N. Y., Apr. 18, 1955, pp. 109–11.

E. D. Early and **R. E. Watson:** We are gratified to note that the greater accuracy of the general transmission loss equation compared to the simplified form of the loss equation was not questioned by any of the discussers, critical comment being limited to the additional cost required to determine the constants for the general form of the equation and to the necessity of using the most accurate loss equation available.

Actually the additional work and cost required to determine the constants for the general transmission loss equation is negligible. The only additional network analyzer readings required are the self- and mutual impedances between loads not supplied from a generator bus, since all self- and mutual impedances between generator buses and mutual impedances between generator busses and load busses are required for determining the constants for the simplified loss equation.

A recent loss study of the Southern Company system, which covers 100,000 square miles and has a peak load of some 3,300 mw, was represented on the network analyzer by 23 generators and 47 loads of which 22 loads were fed from generator buses. A total of 850 readings of self- and mutual impedances were required for the simplified loss equation and only 326 additional readings of self- and mutual impedances between loads were required for the general transmission loss equation. The time required for the additional readings was less than 1 hour. For smaller systems the additional time required would be reduced proportionately. Fortunately, the extra readings required even for a large system are only a small fraction of the 5,000 additional readings suggested by Messrs. Glimn, Kirchmayer, and Wood.

We are unable to understand Mr. Dillard's reference to the "enormous amount of additional computation required to solve for the constants." For a 20-source system, the simplified loss equation has 210 constants. The general loss equation has the same 210 constants plus 21 additional constants. The 210 constants found in both equations are computed in a similar manner and the work required to compute the 21 additional constants is no greater per constant. The additional computation required is certainly less than 15 per cent. Mr. Dillard may have had in mind the additional computation required to determine the constants for the general loss equation by the phase angle method[1] which does require additional computation, although still within practical limits even for the largest system when the nonrigorous method presented in the closure of reference (1) is used and computations are made on an advanced-type digital computer.

It is true, as pointed out by Messrs. Glimn, Kirchmayer, and Wood, that the less accurate incremental loss values given by the simplified form of the loss equation may not materially affect the economic dispath for certain systems. It is equally true that for other systems there will be a substantial effect. Since the additional work and expense of determining constants for the general form of the loss equation is negligible, the fact that the greater accuracy of this equation may not be necessary for a particular system does not in our opinion justify the use of the less accurate simplified loss equation, which could not be used with confidence without determining the effect of its use upon the economy dispatch, which would also require determining constants for the general loss equation and comparing dispatches using the two loss equations for various system load conditions.

Mr. Dillard refers to a study made to determine the effect of treating a large nonconforming load as conforming and found the penalty to be only $689 a year. By using the general loss equation the characteristics of this load could have been taken into account regardless of when the peak occurred and a substantial part of the $689 annual loss avoided as well as the cost of the special study, provided the nonconforming load followed a consistent pattern.

Mr. Brownlee correctly points out that selection of the proper Q/P ratios is the outstanding weakness of the method presented in this paper for determining constants for the general transmission loss equation, as it is with the similar method used for determining constants for the simplied form of the loss equation. The assumption that Q/P ratios remain constant as well as other assumptions common both to the method presented in this paper and to the similar method used for the simplified form of the equation are either eliminated or relaxed in the phase angle method of determining constants for the general transmission loss equation previously presented.[1] For this reason many will want to use the phase angle method in spite of the additional cases required to be studied on the network analyzer and the additional computation required.

Mr. Brownlee's suggestion that it might be desirable to determine the value of the B_{n0} constants empirically appears to have considerable merit and deserves further study. For example, a zero Q/P ratio might be used for all generators by transforming all reactive power to the loads and then the necessity of determining Q/P ratios for loads avoided by determining the value of the B_{n0} constants empirically.

REFERENCE

1. See reference 1 of the paper.

Bibliography and Summary of Fault Location Methods

AIEE COMMITTEE REPORT

AMERICA'S electric power companies are justly proud of their records for continuity of service. These records have been maintained and improved in recent years in spite of rising maintenance costs and economics which dictate higher line loading. The demand for reliable service has led to the development of a number of methods of locating faults with a minimum of inconvenience to customers.

General-purpose procedures for locating faults are generally selected on the basis of speed and accuracy of the method, the cost, ruggedness, and bulk of the apparatus, equipment maintenance required, and what skills the operator must have. Where a choice of methods is available in a specific instance, the one used depends on several factors, principally on the length of circuit, kind of circuit (overhead or cable), and type of fault (sustained or temporary).

The purpose of this report is to present an extensive bibliography on fault location methods. In compiling the bibliography, the search of the literature was carried back to 1940; however, a few articles published prior to 1940 were uncovered and these are listed, too. Included with most of the references are one or two statements giving the gist of the content of the paper or article.

Brief summaries of the most common fault location methods are given in Tables I and II, which are intended chiefly as guides to the literature. They show some features of each method, some references to it in the bibliography approximate accuracy, and principal use.

Overhead Lines

Fault location methods applicable to overhead lines are listed in Table I. Some methods work only on de-energized lines, and, hence, can locate only sustained faults. More frequently encountered, however, are transient or temporary faults which clear after a few cycles and permit automatic or manual reclosure. Although no permanent outage results, such faults often cause damage to conductors or insulators. To locate and inspect damage caused by transient faults, the locator must operate automatically and make a record before the line circuit breaker trips. The table indicates whether the methods are used on energized or de-energized lines. All the methods listed are applicable to any voltage class, but some are economical only for high-voltage lines.

Underground Cables

Accuracy is most important in locating faults where buried or pipe-type cable systems are employed, because expensive excavation is necessary to reach the source of trouble. Often one method is used to find the approximate, and a more precise one for the exact fault location.

Table II lists methods used on cables. Since most cable faults are sustained, temporary fault locators are seldom used on cables. However, cable fault location methods must be adaptable to the nature of the fault. Faults can be classified as:

1. Low-resistance faults.
2. High-resistance faults.
   a. Reducible faults.
   b. Bumper faults.
   c. Water faults.
3. Open-circuit faults.

Reducible faults are those which can be burned or carbonized to a solid short circuit or a low-resistance fault. Carbonizing is accomplished through the application of a high voltage. Bumper faults are those which cannot be carbonized but which flash over and recover periodically with voltage applied. Water faults occur where cables are submerged and cannot be carbonized in all cases. Methods listed in the table for low-resistance faults can be applied to high-resistance faults after they are reduced.

The first step in cable fault location is identification of the class of fault. This is done by continuity tests, and special test sets are available for this purpose. The methods listed in Table II apply to all voltage classes; however, carbonizing is very difficult at voltages above 69 kv. The type of cable and location of cable are also factors which must be taken into consideration.

Paper 55-700, recommended by the AIEE Transmission and Distribution Committee and approved by the AIEE Committee on Technical Operations for presentation at the AIEE Fall General Meeting, Chicago, Ill., October 3-7, 1955. Manuscript submitted June 7, 1955; made available for printing July 26, 1955.

The personnel of the Working Group under the General Systems Committee are: J. K. Dillard, *chairman*, L. O. Barthold, R. S. Grumbach, and A. J. Schultz. Working Group of the General Systems Subcommittee: I. B. Johnson, *chairman*.

Table I. Summary of Fault Location Methods on Overhead Lines

Method of Location	Bibliography References	Probable Maximum Error, Per Cent of Line Length	Operates on Energized Lines	Operates on De-energized Lines
Annunciator Ammeter Ammeter targets at terminals of the faulted line give approximately the division of fault current from which fault location can be calculated	1	20	yes	no
Automatic Oscillograph Similar to above except current and voltage measurement are both utilized	1, 2, 28	10	yes	no
Fault-Generated Surge A surge, caused by sudden collapse of voltage at the fault, travels to the line's terminals and is reflected successively between the station bus and the fault impedance. Time of travel is measured electronically and converted to circuit miles	5, 9, 52, 60, 61, 113	1	yes	no
	87, 113	1	no	yes
Magnetic Link Similar to the automatic oscillograph method the except fault current and voltage are measured by the residual magnetism in an iron link	12	20	yes	no
Pulse Radar A short pulse is applied to the line, and the time of travel of the pulse to and from the fault is measured electronically. Time of travel is converted to circuit miles	39, 44, 50	1	no	yes
	3, 6, 7, 49	1	yes	yes
	8, 56, 59, 70, 113		general description	
Resonance A variable-frequency source is connected to the line. At regularly spaced intervals in frequency, the line exhibits a series resonance chacteristic. The spacing of these intervals is directly related to distances to the fault	11, 18, 51	2	no	yes
Tower Target Lightning currents in the tower leg releases a target visible to ground or air patrols	46	0	yes	no
Tracer An easily identified tracer signal is applied to the line which can be picked up by portable detection equipment. As the line is patroled, diminishing signal strength shows nearness to the fault	41, 58, 90	0	yes*	no

* Line is energized with fault still on; will not locate temporary faults.

Table II. Summary of Fault Location Methods on Underground Cables

Method of Location	Bibliography References	Approximate Accuracy, Per Cent	Locates Low-Resistance Faults	Locates High-Resistance Faults*	Locate Open Circuit
Agitation The existence of partial breaks is detected by a noise amplifier while the cable is agitated	80, 86, 100	†		†	
Bridge Impedance to the fault is measured of total cable impedance, giving distance to the fault of cable length, per cent	14, 16, 20, 27, 29, 30, 37, 42, 57, 71, 72, 73, 74, 80, 81, 99, 100, 101, 102, 105	0.5 to 1.0	yes	yes	no
	19, 20, 25, 33, 35, 52, 97, 108		yes	no	no
Charging Current A comparison of charging in open and normal conductors gives the approximate distance to the break	17, 35, 42, 80, 84, 100	approximate only	no	no	yes
Capacitor Discharge A capacitor is charged until it flashes over a series gap and discharges through the fault. A loud report results at the fault	14, 15, 20, 22, 27, 32, 35, 36, 37, 42, 43, 48, 50, 52, 55, 80, 99, 102	to nearest manhole	yes	yes	no
Fall in Potential Voltage drop to fault measured from each end of the cable	16, 72, 82, 107	10	yes	yes	no
Frequency Modulation The frequency of the signal applied to the cable increases linearly with time, repeating its scan periodically. The difference in frequency between the applied and reflected signals indicates distance to the fault	79	1 on telephone cable	yes		
Pulse Radar A short pulse is applied to the cable. The time of pulse travel is measured electronically and converted to circuit miles	3, 35, 45, 57, 79, 80, 99, 100, 104, 105, 111	various up to 1	yes	yes	yes
Resonance A variable frequency source is connected to the cable. At regularly spaced intervals in frequency the cable exhibits a series resonance characteristic. The spacing of these intervals is directly related to distance to the fault	80, 101	approximate	yes	no	yes
Sheath Drop A direct voltage is applied to the faulted conductor. The return current in the sheath is measured with test prods. The direction of flow reverses when the fault is passed	16, 35, 42, 80, 83, 99	nearest manhole	yes	yes‡	no
Tracer An easily identified signal, e.g., 60 cycles per second, is applied to the faulted conductor. Tracer signal strength indicates nearness to the fault	12, 13, 14, 20, 21, 26, 27, 29, 30, 34, 35, 38, 42, 47, 52, 53, 57, 80, 89, 91, 100, 101, 102, 105	various; some within several feet	yes	yes§	yes

* Without carbonizing. † Does not locate the point of severance. ‡ Bumper faults and open conductor water faults only. § Bumper faults only.

Bibliography

AIEE Publications

1. A Simple Method for Locating Ground Faults, **John I. Holbeck.** *Electrical Engineering*, vol. 63, no. 3, March, 1944, pp. 89–92.

A summary of some approximate location systems as well as the description and operating experience of an annunciator ammeter system.

2. Fault Location and Relay Performance Analysis by Automatic Oscillographs, **H. P. Dupois, W. E. Jacobs.** *AIEE Transactions (Electrical Engineering)*, vol. 65, June 1946, pp. 442–46.

Analysis of oscillograms of fault currents and voltages at one or more stations; it locates faults with an accuracy of ±10 per cent of line length. Curves of fault current and impedance versus line length are required for each line and for all combinations of operating conditions (breakers open, etc.).

3. Pulse Echo Measurements on Telephone and Television Facilities, **L. G. Abraham, A. W. Lebert, J. B. Maggio, J. T. Schott.** *AIEE Transactions*, vol. 66, 1947, pp. 541–48.

A 1-microsecond d-c pulse is applied to communication lines and the echo pattern is viewed on a cathode-ray oscillograph. The position of the echo on the sweep denotes location of fault while magnitude and polarity indicate the nature of the fault or discontinuity.

4. The "Linascope"—An Echo-Ranging-Type Fault Locator for High-Voltage Lines, **J. R. Leslie, K. H. Kidd.** *Ibid.*, vol. 67, pt. II, 1948, pp. 1162–67.

Methods are discussed which use: 1. a 24-microsecond 1/10- to 100-volt d-c pulse for locating sustained faults on a de-energized line; and 2. 24-microsecond 500-volt peak-to-peak 250-kc wave burst, capacitively coupled, for sustained and temporary faults on energized lines.

5. A Transmission Line Fault Locator Using Fault-Generated Surges, **R. F. Stevens, T. W. Stringfield.** *Ibid.*, pp. 1168–78.

Type *A* and *B* systems are discussed, the latter requiring a microwave channel. A special device couples to center phase of bus. Measurements are recorded photographically and are accurate to ±1 per cent of line length.

6. A Transient Fault Locator for High-Voltage Transmission Lines, **L. R. Spaulding, C. C. Diemond.** *Ibid.*, vol. 68, pt. II, 1949, pp. 1005–10.

Type *C* Bonneville Power Administration system uses a 10-kv 1-microsecond d-c pulse automatically coupled to the faulted phase 2 cycles after the fault. Results are recorded photographically.

7. The Linascope Transmission Line Fault Locator, **K. H. Kidd.** *Ibid.*, vol. 70, pt. II, 1951, pp. 1008–13.

A discussion of operating experience and improvements on the locator described in reference 4.

8. Traveling Wave Relations Applicable to Power-System Fault Locators, **L. J. Lewis.** *Ibid.*, pp. 1671–80.

A mathematical discussion of wave propagation and reflection including a method for predicting the nature of reflected waves for various line discontinuities.

9. Fault Location by Pulse Time Modulation, **R. W. Hughes, N. Weintraub.** *Electrical Engineering*, vol. 69, no. 11, Nov. 1950, pp. 1009–11.

A discussion of the Bonneville Power Administration type-*B* Fault Generated Surge system with emphasis on microwave equipment used.

10. Electronic Pulse-Type Fault Locator Experience, **R. L. Brinton.** *Electrical Engineering*, vol. 74, no. 4, Apr. 1955, pp. 282–84.

A general description of a radar type-fault locator and operating experience is given. Methods of coupling to line are described. Training and skill of personnel are covered.

U. S. Periodicals

11. A Method of Locating Faults on Overhead Transmission Lines by Means of High Frequency, **J. E. Allen, G. J. Gross.** *Bulletin*, Edison Electric Institute, New York, N. Y., vol. 3, no. 8, Aug. 1935, p. 309.

A variable-frequency source connected to the line exhibits resonance at periodic intervals in frequency. Spacing of resonance points shows distance to the fault.

12. Recent Developments in Cable Fault Locating, **James A. Vahey.** *Ibid.*, vol. 7, no. 3, March 1939, pp. 96–100.

A discussion of the "Lundin" fault locator and its application to various types of faults.

13. Tracer Impulses Locate Cable Faults, **P. L. Weir.** *Electrical World*, New York, N. Y., vol. 114, no. 2, July 13, 1940, pp. 57–58 (81–83).

Employs directional impulse tracing currents. Method accurately finds all types of faults on 13.2-kv network feeders without field calculations or disconnecting network transformers.

14. Locating Faults on Buried Cable, **R. K. Woodson.** *Ibid.*, no. 22, Nov. 30, 1940, pp. 42–43 (1608–09).

The author describes Lundin set, bridge, and capacitor discharge methods.

15. Use Capacitance Discharge to Locate Cable Faults, **W. D. Seal.** *Ibid.*, vol. 117, no. 12, March 21, 1942, pp. 84–85 (1006–07).

Noise produced by discharge of energy stored in the cable is used to locate fault to nearest manhole. High voltage is applied to cable by a constant-current transformer.

16. Locating Cable Faults in Pipe-Type SMD Cable, *Ibid.*, no. 26, June 27, 1942, p. 78, (2248).

Three methods are proposed for locating leaks and faults in 120-kv pipe-type gas-filled cable. These are: 1. bridge method; 2. sheath drop method; and 3. fall-in potential method.

17. Charging Locates Open Cable Faults, **F. E. Reeves.** *Ibid.*, vol. 118, no. 10, Sept. 5, 1942, pp. 81–82 (785–86).

A discussion of using charging current to locate open cable faults. Fault located within a few feet on a 5-mile cable and within 300 feet on an 11-mile cable.

18. Power Line Fault Locator, **W. H. Blankmeyer.** *Electronics*, New York, N. Y., Jan. 1944, pp. 168–70.

A brief description of a portable resonance-type locator similar to that described in reference 2.

19. Potentiometer Method to Locate Cable Faults, **H. G. Yarill.** *Electrical World*, New York, N. Y., vol. 121, no. 16, Apr. 15, 1944, pp. 120, 124 (1444, 1448).

A bridge method presented for use on large size cable (500,000 circular mils) of comparatively short length. Unique feature is a compensator to eliminate the effect of parasitic currents in cable sheath.

20. Fault Location on Non-Metallic Sheath Cables, **H. N. Ekvall.** *Ibid.*, Apr. 1, 1944, p. 82 (1246); April 29, 1944, p. 90 (1620); May 27, 1944, p. 108 (1990).

A brief resumé of various methods of fault location is given in three groups: Group I—electric pickup methods; group II—bridge methods for locating faults to ground; and group III—miscellaneous methods.

21. Interrupter Locates Submarine Cable Faults, **D. F. Tulloch.** *Ibid.*, vol. 122, no. 6, Aug. 5, 1944, p. 108.

A Lundin fault locator is used successfully to locate submarine cable faults.

22. Cable Field Testing and Fault Location, **W. D. Fenn, I. A. Gray.** *Ibid.*, no. 8, Aug. 19, 1944, pp. 97–99.

Methods of testing cables and locating faults are described. D-c and a-c cable testing is compared. Three specific examples are cited.

23. Location of Line Faults, **M. A. Honnel.** *Electronics*, New York, N. Y., Nov. 1944, p. 110.

A discussion of elementary pulse-reflection phenomenon as verified by laboratory and field tests.

24. Portable Cable Testing Outfit. *Electrical World*, New York, N. Y., vol. 122, no. 8, Aug. 19, 1944, pp. 113–14.

Construction details and circuit diagram are given for d-c cable tester used by authors of reference 22.

25. Nomograph Aids in Locating Cable Faults, **Richard Hoeller.** *Ibid.*, no. 24, Dec. 9, 1944, p. 130.

Nomograph to be used in conjunction with a Murray Loop.

26. R. F. Oscillator Aims Locating Cable Faults, **G. L. Danner.** *Ibid.*, vol. 123, no. 2, Jan. 20, 1945, p. 132.

A 550-kc oscillator modulated at 1,000 cycles was connected to one end of a faulted cable and a portable radio was used as a detector to locate fault.

27. Cable Test Program Uses Portable Kenotron Set, **J. C. Parker.** *Ibid.*, no. 5, Feb. 3, 1945, pp. 82–83.

Incipient cable faults are carbonized with a truck-mounted Kenotron set. Faults are located with a Murray loop or tracer signal. A-c and d-c testing are compared. Causes of faults are listed.

28. Fault Current-Distance Curves Help Locate Transmission Trouble, **C. S. Roadhouse, O. R. Hantla.** *Ibid.*, no. 13, March 31, 1945, pp. 60–61.

Automatic oscillograph recordings of transient and sustained faults are referred to precalculated charts to locate type and location of fault. Fault is located within 5 to 10 miles on a 270-mile line.

29. Cable Trouble Caused by Spilled Chemicals, **N. W. Thurston.** *Ibid.*, no. 17, Apr. 28, 1945, pp. 80–81.

Fault is located by using Lundin interrupter-type fault analyzer and Murray loop.

30. Practical Methods for Locating Faults in Non-Metallic Cables, **M. S. Gilbert.** *Ibid.*, no. 21, May 26, 1945, pp. 90–91.

Methods and equipment are described for identifying and locating various types of faults on unshielded underground cables. Techniques were developed at the Civil Aeronautics Experimental Station. Surge impulse and Wheatstone bridge are discussed.

31. Raised Voltage Improves Fault-Locating Set, **M. W. Ghen.** *Ibid.*, no. 25, June 23, 1945, pp. 95–96.

A voltage-doubler circuit is used to increase the voltage output of a Kenotron set from 10 kv to 25 kv. A greater percentage of high-resistance faults can now be carbonized.

32. Portable Bridge for High-R Cable Faults, **T. G. Hieronymus.** *Ibid.*, vol. 124, no. 11, Sept. 15, 1945, p. 107.

A 50-kv d-c slide-wire-bridge Murray loop is used to locate high-resistance cable faults which refuse to burn down to solid ground. Faults have been located within a cable section in a 10-mile circuit.

33. Cable Faults Located Quickly and Conveniently. *Ibid.*, no. 18, Nov. 10, 1945, p. 138.

A capacitor discharge impulse tester is used to locate over 200 cable faults.

34. Inductive Pickup for Fault Location, **G. L. Danner.** *Ibid.*, vol. 125, no. 7, Feb. 16, 1946, p. 130.

An iron core search coil and audio amplifier are used to pick up tracer signal to locate faults having a resistance less than 300 ohms. Circuit diagram for impulse generator and amplifier.

35. Cable Fault Location, **F. Buck, W. Upham.** *Bulletin*, Edison Electric Institute, New York, N. Y., vol. 14, no. 3, March 1946, pp. 85–86.

A summary of methods in use by 28 utilities. Most companies use several methods. No general preference is shown for any one method.

36. Condenser Pop Aerial Cable Fault, **Floyd W. Buck.** *Electrical World*, New York, N. Y., vol. 125, no. 21, May 25, 1946, p. 111.

A capacitor discharge surge impulse tester is used to locate faults on aerial cable. Cost is $340.00. Circuit diagram is shown.

37. Buried Cable Faults Located by Sonic Detector, **F. S. Benson, G. L. Hill, C. R. Machen.** *Ibid.*, vol. 125, no. 25, June 22, 1946, p. 82.

After approximate location with bridge measurement, the condenser discharge method finds exact location with the aid of an audio vibration detector.

38. Locates Faults in Street Lighting Circuits, **C. E. White.** *Ibid.*, vol. 126, no. 7, Aug. 17, 1946, p. 87.

A 6-volt d-c battery, hummer, and step-up transformer are used as a tracer signal source to supply a signal for an inductive coil pickup and audio amplifier to locate fault within 1 foot.

39. Improved Method of Transmission Line Fault Location. *Ibid.*, vol. 127, no. 11, March 15, 1947, pp. 130–32.

An electronic fault detector which operates on the radar principle locates faults within 0.1 mile.

40. Radar on New South Wales Railways, **A. H. Gray.** *Railway Signalling and Communications*, New York, N. Y., Apr. 1947, pp. 237–38.

41. Mobile Detector Locates Faults on Overhead Lines, **S. Freeman, Jr., H. Haas.** *Electrical World*, New York, N. Y., vol. 128, no. 7, Aug. 16, 1947, pp. 76–77.

A test capacitor, inserted in the faulted line, accentuates the 5th harmonic voltage on the line. The line is patrolled with a sensitive detector, then the fault is located. Applicable to short lines only.

42. Locating Faults in Underground Cables, **D. F. Tulloch.** *Ibid.*, no. 19, Nov. 8, 1947, pp. 109–11.

Common types of cable faults are described. In practice a Lundin set is used to classify each fault, after which an appropriate location system is applied.

43. Impulse Cable Fault Locator, **F. W. Buck.** *Ibid.*, no. 24, Dec. 20, 1947, pp. 82–84.

Construction details for fault locator described in reference 36.

44. Pulse Radar Used to Locate Faults, **G. G. Meudenhall.** *Ibid.*, vol. 130, no. 19, Nov. 6, 1948, p. 88.

A portable pulse-echo locator is described for use on de-energized lines. A positive transparency of normal reflection pattern helps to identify fault echoes.

45. Improved Surge-Reflection System Locates Cable Faults, **J. P. Lozes, Jr.** *Ibid.*, pp. 89–91.

A pulse-echo d-c system is discussed which can distinguish between fault reflections and normal discontinuities. Accuracy is limited to one or two blocks.

46. Visual Flashover Indicator, **H. L. Rorden.** *Ibid.*, vol. 132, no. 19, May 7, 1949, p. 71.

Lightning current in the tower leg is used to ignite a small gunpowder charge which releases the flashover target visible from the air.

47. Locating Grounds on 480-Volt, 3ϕ Delta Systems, **B. G. Forbes.** *Power Generation*, New York, N. Y., vol. 53, Sept. 1949, pp. 60–61.

Description of simple method of locating grounds in power plants with a low-range voltmeter of about 0 to 10- or 0 to 15-volt scale.

48. Test Unit for 15-Kv Cables Features Portability, **F. E. Reeves.** *Electric Light and Power*, Chicago, Ill., vol. 28, March 1950, p. 96.

A high-voltage Kenotron set for cable testing and fault location is described. The capacitor discharge impulse method is used for fault location.

49. Transient Fault Locator Proves Out in Operation, **L. R. Spaulding.** *Electrical World*, New York, N. Y., vol. 133, no. 25, June 19, 1950, p. 110.

A brief description of the Bonneville Power Administration type-*C* (pulse-echo) locator with comments on operating experience.

50. Fault Locator Use Discriminating Detector. *Ibid.*, vol. 134, no. 19, Nov. 6, 1950, p. 110.

A commercially manufactured capacitor discharge transmitter and detector for cables up to 26-kv are described.

51. Portable Fault Locator Proves Practicable, **T. J. Allen, C. C. Brickmore.** *Electric Light and Power*, Chicago, Ill., vol. 29, Sept. 1951, pp. 106–08, and 110.

Description of a portable resonance locator based on principle described in reference 2. A second method using d-c pulses at varying pulse rates is discussed.

52. Cable Fault Locating Practices in Philadelphia, **R. S. Diggs.** *Ibid.*, Oct. 1951, pp. 76–81, and 126.

Three methods are presented with comments on their applications:

1. A-c tracer method (60 cycles).
2. Thyratron tracer method (chopped direct current).
3. Impulse tracer (capacitor discharge method).

53. Locating Ground Faults in Buried Non-Metallic Cable, **Herschel Thomas.** *Electrical World*, New York, N. Y., vol. 137, no. 18, May 5, 1952, pp. 124–26.

A fixed and movable prod connected to an indicating meter pickup ground potential produced by a pulse generator. It is used for street lighting cable to locate fault within 1 or 2 feet.

54. Locate Cable Faults with Low-Cost Device, **C. W. Cornforth.** *Ibid.*, vol. 138, no. 4, July 28, 1952, p. 106.

A pocket compass and messenger rings are used to locate the faulted phase of a cable.

55. Fault Locator Weeds Out Incipient Cable Faults, **J. L. Redmond.** *Ibid.*, no. 26, Dec. 29, 1952, p. 88.

A capacitor discharge impulse-type fault locator is used to locate incipient cable faults.

56. Trouble Shooting in the Electronic Way, **R. L. Brinton.** *Electrical West*, New York, N. Y., March 1953, vol. 110, no. 3, p. 86.

57. Versatility Provided in Cable Fault Locating, **E. J. Steeve.** *Electrical World*, New York, N. Y., vol. 139, no. 18, May 4, 1953, p. 98.

Cable fault location facilitated by placing test equipment on a truck. The three methods of location used are radar, impulse fault locator, and Murray loop.

58. Thyratron Tube Locator Spots Overhead Grounds, **F. M. Hartz.** *Ibid.*, vol. 140, no. 10, Sept. 7, 1953, pp. 92–93.

Truck-mounted signal generator receives power from unfaulted phases and applies signal to faulted phase. The portable search coil and amplifier pickup signal by induction. Method locates 90 per cent of overhead ground faults.

59. Shoot Line Trouble With Radar, **J. L. Whysong, H. L. Garton, J. F. Bracker.** *Ibid.*, no. 20, Nov. 16, 1953, pp. 118–21.

Radar type of locator used to locate faults on overhead and underground transmission and distribution lines and on telephone and control cables is described. Detailed circuit diagram of equipment is included. Results are tabulated for various types of lines and faults.

60. Stages Faults by Electronic Master and Slave Units of New System That Locates Faults on Line Transmission Line. *Ibid.*, 141, no. 13, March 29, 1954, pp. 30–31.

Description and results of staged-fault locator tests. New equipment for locating faults on line transmission lines is described. Pulse sent out by fault is recorded at master and slave station.

61. Flashovers Located to the Exact Tower. *Electrical West*, New York, N. Y., vol. 112, no. 3, March 1954, pp. 70–71.

News item covering tests described in reference 60.

62. Fault Locator Tests, *Electrical World*, New York, N. Y., vol. 141, no. 17, Apr. 26, 1954, p. 48.

Extension of tests given by reference 60.

British Periodicals

63. The Electrical High Pressure Testing of Cables and the Localization of Faults, **J. Urmston.** *Journal*, Institution of Electrical Engineers, London, England, vol. 69, 1933, p. 983.

64. Methods for Locating Breaks in Cable Conductors, **J. H. Savage.** *Distribution of Electricity*, vol. 6, 1933, p. 1380.

65. Cable Fault Locating by Induction Methods, **W. Redmayne.** *Distribution of Electricity*, London, England, vol. 8, 1935, p. 1179.

66. Localizing Faults on Low Tension Distribution Cables, **G. W. Stubbings.** *Ibid.*, p. 1871.

67. Testing Cables with D-C Pressures and Localizing High Resistance Cable Faults, **C. Grover.** *Ibid.*, vol. 10, 1937, pp. 2326, 2335, and 2351.

68. Cable Fault Localization Sources of Error and Their Magnitude, **E. W. Golding.** *Electrical Times*, London, England, 1937, vol. 92, p. 103.

69. A New Method of Fault Location, **K. R. Green.** *Distribution of Electricity*, London, England, vol. 10, 1938, p. 2386.

70. Notes on Cable Fault Localization, **W. Redmayne.** *Ibid.*, vol. 11, 1938, p. 34.

71. Open Circuit Faults, **W. Woodiwiss.** *Electrical Review*, London, England, vol. 128, 1940–41, pp. 637–38.

Various types of faults and bridge methods are discussed.

72. Locating Cable Faults, **G. W. Stubbings.** *Ibid.*, vol. 129, Sept. 29, 1941, pp. 301–02.

Methods for locating 3-phase-to-ground faults are presented. Fall of potential and Werren methods is described.

73. The C. R. Indicator as a Detector, **J. G. Park.** *Electrical Times*, London, England, vol. 102, Sept. 17, 1942, pp. 400–02.

An arrangement is presented for using a cathode-ray tube as a null detector in an impedance bridge for cable fault location.

74. Fault Location on Low Resistance Feeders. *Ibid.*, Nov. 26, 1942, pp. 760–62.

A discussion of Murray loop test.

75. Spark Testing Cables, **J. H. Savage.** *Distribution of Electricity*, London, England, vol. 16, 1943, p. 101.

76. Locating Faults in Practice, **F. J. Batten.** *Mining, Electrical and Mechanical Engineer*, London, England, vol. 23, 1943, p. 101.

77. Cable Testing. *Electrical Review*, London, England, vol. 136, May 11, 1945, p. 674.

This is a review of reference 80.

78. Induction Methods of Cable Fault Localization, **W. Redmayne.** *Distribution of Electricity*, London, England, vol. 17, 1945, p. 353.

79. New Methods for Locating Cable Faults, Part III, **E. F. Roberts.** *Journal*, Institution of Electrical Engineers, London, England, vol. 93, pt. III, Nov. 1946, pp. 385–404.

A technical discussion of the pulse echo and frequency-modulation methods of fault location on coaxial communication cables.

80. Location of Faults in Low-Voltage Cables with Special Reference Factory Techniques, **J. H. Savage.** *Ibid.*, vol. 92, pt. II, pp. 580–93.

A comprehensive survey of cable fault location systems including a special sheath-drop method capable of finding faults of resistance up to 10 megohms.

81. Cable Testing with Wheatstone Bridge, **G. Alder.** *Technique*, Montreal, Canada, vol. 21, June 1946, pp. 435–46.

82. Submarine-Cable Fault, **M. Datta.** *Electrical Review*, London, England, vol. 139, Aug. 23, 1946, p. 303.

Three-phase-to-ground 1-phase open fault located by fall of potential method. Method necessitated stringing a temporary cable 800 yards across a river.

83. Sheath-Drop Method of Locating Cable Fault, **R. C. Yates.** *Electrical Engineer and Merchandiser*, Melbourne, Australia, vol. 23, Feb. 15, 1947, pp. 356–58.

84. Open-Circuit Cable Faults, **F. P. Meadows.** *Electrical Times*, London, England, vol. 111, May 8, 1947, pp. 525–26.

85. Fault Location on Transmission Lines. *Electrical Engineer and Merchandiser*, Melbourne, Australia, June 16, 1947, pp. 73–75.

86. Locating Partial Breaks in Multi-Core Jumper Cables. *Engineer*, London, England, vol. 184, Nov. 28, 1947, p. 515.

All cable conductors are connected in series. Agitation of the cable at the partial break produces an audible noise in detection equipment.

87. New Method for Location of Faults in Overhead Transmission Lines by Means of Impulse Tests, **S. Margonlis, P. Fournaries.** *Engineers Digest* (American edition), New York, N. Y., May–June, 1948, pp. 177–79, July, pp. 239–43.

Theoretical analysis of two location systems with the use of high-voltage d-c pulses of long duration. The spacing of successive reflections from the fault show distance of the fault from the monitoring stations.

88. Fault Location and Relay Protection, **E. W. Knapp, B. C. Ricks.** *Electrical News and Engineering*, Toronto, Canada, vol. 57, June 15, 1948, pp. 86–88, 100–01.

Residual flux in magnetic links gives a measure of fault current and voltage and, thereby, the distance to the fault. Accuracy is from 10 to 20 per cent.

89. Induction Cable Fault Locator. *Engineer*, London, England, vol. 186, July 16, 1948, p. 61.

1,000-cycles-per-second tracer method. A sensitive detector traces field pattern which changes abruptly at the fault.

90. Method for Detection of Sustained Earth Faults in Rural Overhead Lines Protected by Petersen Coils, **B. D. Zelikin.** Institution of Electrical Engineers, London, England, vol. 95, pt. II, Oct. 1948, pp. 617–19.

An electrostatic field measuring device detects abnormal field pattern when one conductor is grounded. By sectionalizing the line, the faulted section is isolated.

91. Cable Fault Locator, **F. E. Planer.** *Electrical Review*, London, England, vol. 145, July 8, 1949, pp. 57–78.

A brief description of a sensitive, highly directive receiver for 50-cycle tracer currents.

92. Cable Fault Localisation, **G. W. Stubbings.** *Electrical Times*, London, England, vol. 117, Jan. 5, 1950, pp. 13–14.

Werren's test is described. This is a bridge method used for detecting a double conductor-to-ground cable fault.

93. Cable Fault Locator, **F. E. Planer.** *Electric News and Engineering*, Toronto, Canada, vol. 60, Apr. 1951, pp. 112, 114–15.

94. Fault Location, **J. G. Boggis.** *Electrical Times*, London, England, vol. 120, Sept. 6, 1951, pp. 420–22.

A discussion of the fall of potential method in place of a Murray's loop for low-voltage cables. Method is advocated for short lengths only.

95. Fault Location on L. V. Mains, **L. T. Snow.** *Ibid.*, vol. 121, Jan. 10, 1952, pp. 63–66.

A discussion of the accuracy of bridge methods including the effect of connected loads.

96. Fault-Throwing Tests on 132 kv Grid System Under Normal Working Conditions, **W. Casson, F. H. Birch.** *Proceedings*, Institution of Electrical Engineers, London, England, vol. 97, pt. I, 1950, pp. 279–302.

Foreign Language Periodicals

97. Kabel-Fehlerortsbestimmung Mittels Einer Einzigen Messung, **L. Rozsas.** *Elektrotechnik und Maschinenbau*, Vienna, Austria, vol. 64, Nov.–Dec. 1947, pp. 180–81; see also *Engineer's Digest* (American edition), New York, N. Y., vol. 5, March-April 1948, p. 152.

A modified Murray bridge for use where auxiliary leads are required between ends of the faulted cable.

98. Einmessung von Fehlerorten an Starkstromleitungen Mittels Wanderwellen, **E. Huster.** *Elektrotechnik*, Berlin, Germany, vol. 1, Apr. 1948, pp. 2–6.

Fault location on high-voltage lines by means of impulse waves.

99. Localisation des Defauts dans les Cables Souterrains, **J. Bonnemain.** *Bulletin V.8*, Société Francaise des Electriciens, Paris, France, Aug.–Sept. 1948, pp. 387–91.

A discussion of methods used for various type of faults including water faults.

100. Recherche des Defauts dans les Cables Souterrains, **H. Aschere.** *Ibid.*, pp. 397–412.

The author discusses the general problem of locating faults in underground cables. The nature of the faults, methods for their detection and location, and examples of established cases are discussed.

101. Recherche des Defauts dans les Cables en Case Discontinuite et de Faible Isolement, **L. Dupuis.** *Ibid.*, pp. 417–8.

Three methods are given for rapid location of faults in this class.

102. Recherche des Defauts dans les Cables Souterrains, **M. Roger.** *Ibid.*, pp. 419–26.

The author discusses methods and apparatus to locate and detect faults on underground cables, particularly 12-kv network cables.

103. Application de la Methode du pont de Sauty au Reperage des Defauts sur les Cables de Grande Longueur, **H. Josse, R. Tellier.** *Ibid.*, pp. 427–29.

A method for obtaining correction factors for improved accuracy is given.

104. Application de la Methode des Impulsions a la Localisation des Defauts dans les Cables, **G. LeParquier.** *Ibid.*, pp. 434–38.

An accurate pulse-echo system is presented together with test data on cables up to 220 kv. The tests were also effective on 3-terminal cables.

105. Recherche des Defauts sur les Cables Basse-Tension, **C. Philippe.** *Ibid.*, pp. 439–50.

The location of faults on signal, telephone, and power networks for the railroads is discussed. The power network is made up of 3- or 4-conductor cables with impregnated paper insulation operated at a maximum of 500 volts.

106. Bewaehrte Messverfahren zur Fehlerortbestimmung in Starkstromkabelnetzen, **A. Bierhals.** *Elektrotechnik*, Berlin, Germany, vol. 3, no. 11, Nov. 1949, pp. 345–52.

Proved methods for locating faults in power cable systems, critical survey of published methods; for best accuracy in locating faults, exact cable length is usually required; since electrical methods of determining cable length are inaccurate, cable length should be measured when installed.

107. Fehlerortungen in Leitungsschleifen mit Alladrigem Erd.-bzw. Kurzschluss, **G. Scharsig.** *Elektrotechniker*, Wuppertal-Eberfeld, Germany, vol. 2, June 1950, pp. 167–68.

Fall-in potential method is used to locate multiple ground faults and phase-to-phase faults.

108. En Variant av Kjente Metoder til Bestemmelse av Feilsted pa Sterkstromkabler, **S. E. Nielson.** *Electro-Teknisk-Tidsskift*, Oslo, Norway, vol. 64, Jan. 15, 1951, pp. 24–27; see also English abstract in *Engineer's Digest*, London, England, vol. 12, July 1951, pp. 220–22.

A variation of Varley's method including methods for: 1. determining the condition of the cable at the fault; 2. a method for locating 3-phase faults without auxiliary leads, and 3. a method for locating ground faults on short cables of large cross sections.

109. La Localizacion des los Desperfectos en los Cables de Energia Electrica, **J. Zanier.** *Revista Electrotecnica*, Buenos Aires, Argentina, vol. 37, Oct. 1951, pp. 371–85.

Various methods of locating cable faults are described. Causes of cable faults are listed.

110. Fehlerortung an Starkstromkabeln mit Hochfrequenz, **H. Wechsung.** *Elektrizitaetswirtschart*, Berlin, Germany, vol. 51, no. 10, May 20, 1952, pp. 230–36.

Fault location in power cables with the use of a high-frequency detector.

111. Ervaringe Nopgedaan in het Amsterdamse Kabilnet met een Nieuw Apparaat voor het Uitmeten van Kabelfouten, **J. M. Faber.** *Ingenieur*, Hague, Holland, vol. 65, no. 15, April 10, 1953, pp. 67–70.

Radar type of fault locator used in Amsterdam network.

112. Committee Reports, Transmission Line Fault Locator Committee. *Journal*, Institution of Electrical Engineers of Japan, Tokyo, Japan, vol. 73, no. 733, 1953, p. 120.

113. Investigations and Practical Experiences of Transmission-Line-Fault Locators in Japan, **Tomiyama Fujitaka, Saba.** CIGRE, Paris, France, vol. III, 1954, paper 308.

A comprehensive summary of development and application of pulse-echo and Fault Generator Surge type of fault locators. Included are results of field tests.

Miscellaneous

114. Testing and Trouble Finding. Underground Systems Reference Book. National Electric Light Association, New York, N. Y., 1931, p. 223.

115. Fault Locating Methods Used on Underground Cable Systems. Edison Electric Institute, New York, N. Y., 1935.

116. Alternating-Current Bridge Methods (book), **B. Hague.** Pitman Publishing Corporation, New York, N. Y., 1946.

117. Fault Localizing and Testing (book), **F. C. Raphael, C. A. Grover.** *Ibid.*, New York, N. Y., 1946.

118. Transmission Line Locator, **W. G. Hoyle.** *Report PR A135*, National Research Council of Canada, Ottawa, Canada, Sept. 1946.

119. Location of Underground Cable Failures, **M. S. Gilbert.** *US CAA Technical Development Note No. 41*, Civic Aeronautics Administration, Washington, D. C., June 1946, p. 5.

120. Fault Location—Quarter Wave Length Resonance Method, **H. B. Slade.** *Minutes*, Edison Electric Institute, New York, N. Y., Appendix VII, 1948.

121. Cable Fault Location on the Philadelphia Electric Company System, **J. E. Johnson.** *Ibid.*, Appendix X.

◆

Discussion

E. B. Curdts (James G. Biddle Company, Philadelphia, Pa.): A few comments concerning this paper may be of interest to those dealing with the underground cable phase of this problem.

First, I would like to take mild exception to the subdivisions of the high-resistance fault classification, particularly the term "bumper faults." I am not sure how the use of the word "bumper" got started, or what the word is intended to convey. I have questioned a few public utilities people who are experienced in this field, and they say they have never heard of its use in this connection. In any event, it seems to be a slang word that does not have a place in an AIEE technical paper.

The flashover fault, which is a quite common type of high-resistance fault, is apparently the one defined in the paper as a so-called bumper fault. It involves a gap, paralleled by a high, fairly stable resistance. Such faults are sometimes difficult actually to carbonize, or recarbonize after the initial failure, but they are, nevertheless, reducible from a fault-locating point of view provided a voltage of sufficient magnitude and time duration is applied. The "water fault" as well as the dry flashover fault can be included in this category.

It seems to me that Table II, which attempts to classify in a rather vague way methods of location for underground cables in terms of accuracy of location and type of fault, is subject to considerable clarification and qualification to be of much use.

The Edison Electric Institute has scheduled publication of a new edition of the "Underground Systems Reference Book." In the volume will be found a chapter dealing with the fundamentals of the power-cable fault-locating problem, presented both from engineering and practical operating points of view. It extracts from reported experiences and the voluminous literature of the past, methods of location which have given consistent results, and discusses the advantages and limitations of the various methods in regular use today. I believe this book will provide the information necessary to evaluate practical and modern methods of power-cable fault location.

Electrical Utility Load Forecasting

W. WALLACE GODARD
NONMEMBER AIEE

RAPID growth in the last decade has made it essential for the electrical utility industry to develop better ways of anticipating future requirements. That is why there is so much interest in load forecasting. Planned action in this work is worth while, and in today's economy sound planning is essential to successful operations. An electrical utility is not as free as other industries to plan a certain capacity and determine that it will take on just so much and no more business. Its planning must take into account the aggregate coincident demands of its many customers. The customer best remembers those times when the utility company, for whatever reason, might not have been ready to serve his needs immediately.

At the hazard of oversimplifying, it is suggested that the secret of rendering more and better electrical service at competitive prices with reasonable profit is to predict and plan ahead and to be ready at all times to meet the power needs of the general public.

Essentials of a Good Plan

Those responsible for the operation of a business should realize that their plan of predicting future requirements must be well organized but not necessarily complex.

Good planning in the electrical utility business involves the three following essential features:

1. Evolving a single, controlling pattern of probable economic conditions.
2. Developing a schedule of business volumes, expressed in specific functional terms, as a basis for future operations.
3. Conditioning the organization to cope with problems which may arise with unforeseen departures from the approved pattern.

It has been suggested that this paper emphasize in detail the application of economic factors and the relationships of variables in predicting the various components of electric utility load. It will proceed along the lines of a specific estimate.

It is well to remember that the sales or marketing representatives are the "eyes and ears" upon which the business should rely rather heavily. Through them the temper of a local situation may be judged and many of the possibilities of the future evaluated. They and the rate engineers are often able to assist greatly in shaping and trending the several class factors.

No forecast is more accurate than its basic premise, including the correctness of the expressed relationships of the variables to be applied successively in the calculations. If the approved economic pattern and other underlying factors are realized and the anticipated relationships between elements hold closely, the forecast would prove to be good.

Each utility has a characteristic situation of its own. In an industrial area having good diversity, it is not strange that sales to large light and power customers should closely reflect variations in national economic indicators. Neither is it strange that the nation's materials and man power will flow more readily to such an area in support of programs for building plant and equipment. With increased industrial activity and building, an accelerated flow of materials and supplies for residential construction should be expected.

A utility company having relatively less large commercial and industrial business and more residential or rural would have a lower dependence on an industrial index in its estimating and would have even more reason to keep well informed on consumers' buying intentions.

Such fundamental principles will be applied in estimating the component classes of electric utility load. The estimate will be made for a typically industrial area covering a period of 5 years, from 1950 through 1954. This is long enough to span a 2- or 3-year construction period for the installation of generators or other principal facilities. In choosing this period, a comparison of estimated and actual loads, is allowed for as a test of the method of estimate.

The question is sometimes raised, "Where does the twilight zone between forecasting and projections start and stop?" Experience shows that in looking further ahead, it is necessary to depend increasingly on a sort of general projection. The twilight zone starts about 12 to 18 months from date of estimate and intensifies rapidly. Wherever practicable a plan of correlation tied to the economic pattern is the practical procedure in compensating for lack of specific foresight.

Since there was not time for extensive discussion of the economic pattern, and since 1954 was chosen to end the estimate period, the presently known values of selected economic functions will be used. This is the same as assuming that a developed pattern of the economy would be truly accurate. The deviations of estimated load from actual can then be regarded as a test of the method only.

In selecting economic indicators, factors were chosen which serve as common vocabulary pieces in the exchange of opinions with other forecasters. The following are typical and the last three are specifically used in the calculation of this estimate.

Paper 55-531, recommended by the AIEE System Engineering Committee and approved by the AIEE Committee on Technical Operations for presentation at the AIEE Summer General Meeting, Swampscott, Mass., June 27–July 1, 1955. Manuscript submitted April 4, 1955; made available for printing September 19, 1955.

W. WALLACE GODARD is with The Cleveland Electric Illuminating Company, Cleveland, Ohio.

This paper incorporates certain adaptations of information presented in 1952 by F. Warren Brooks of the Cleveland Electric Illuminating Company, gained in his rate study work. At the AIEE Fall General Meeting at New Orleans in 1952 he dealt with the philosophy of need and approach in forecasting. He has sponsored considerable further work in load forecasting and rate studies.

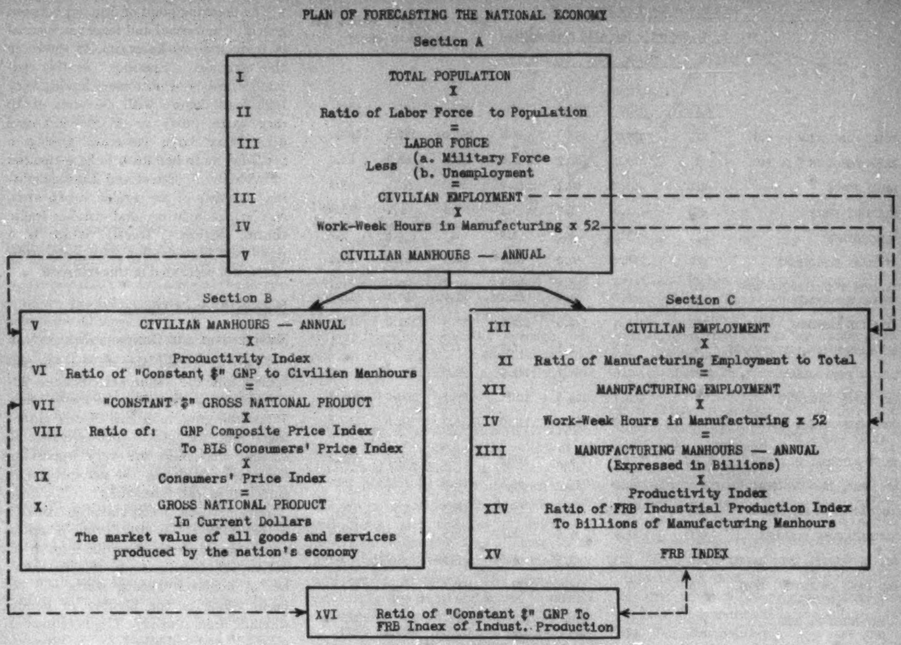
PLAN OF FORECASTING THE NATIONAL ECONOMY
Section A
I TOTAL POPULATION
X
II Ratio of Labor Force to Population
=
III LABOR FORCE
Less (a. Military Force
(b. Unemployment
=
III CIVILIAN EMPLOYMENT
X
IV Work-Week Hours in Manufacturing x 52
V CIVILIAN MANHOURS — ANNUAL
Section B
V CIVILIAN MANHOURS — ANNUAL
X
Productivity Index
VI Ratio of "Constant $" GNP to Civilian Manhours
=
VII "CONSTANT $" GROSS NATIONAL PRODUCT
X
VIII Ratio of: GNP Composite Price Index
To BLS Consumers' Price Index
X
IX Consumers' Price Index
=
X GROSS NATIONAL PRODUCT
In Current Dollars
The market value of all goods and services
produced by the nation's economy
Section C
III CIVILIAN EMPLOYMENT
X
XI Ratio of Manufacturing Employment to Total
=
XII MANUFACTURING EMPLOYMENT
X
IV Work-Week Hours in Manufacturing x 52
=
XIII MANUFACTURING MANHOURS — ANNUAL
(Expressed in Billions)
X
Productivity Index
XIV Ratio of FRB Industrial Production Index
To Billions of Manufacturing Manhours
XV FRB INDEX
XVI Ratio of "Constant $" GNP To
FRB Index of Indust. Production

Fig. 1. Plan of forecasting national economy

Economic Factors Specific to This Estimate

Factor	Explanatory
U. S. population	continental U. S.
U. S. nonfarm housing starts	no. of family dwelling units
Federal Reserve Board (FRB) Index of Industrial Production	physical production in per cent of 1947–49 average, after elimination of seasonal variations. On a per-day basis. (FRB)
Hours in work week, U. S., all manufacturing	Bureau of Labor Statistics (BLS) reports, average hours per employee-week

The selection of these and other factors can and should accommodate some plan for testing the consistency of proposed patterns or forecasts of the economy. Appendix I describes such a plan; see Fig. 1. Fig. 2 shows a comprehensive economic data sheet covering the period of this estimate. Specifically, Fig. 2 and Tables I through IV include these factors for all the years of 1947 through 1954.

General Procedure and Terminology

The procedure will be to estimate class loads separately and combine them on a coincident basis. Thus the annual service area maximum load will be estimated.

The kilowatt-hour (kw-hr) sales and load factor will be estimated for each class as a basis for calculating its contribution to the service area maximum. As a technical convenience, the load factors to be used will do more than the usual load factor. They will span from the "at-customer" sales to the "at-power-plant" contribution to the service area maximum. This involves the adaptation of special information on class loads. The terminology is not elaborate; it is indicated in the daily load chart in Fig. 3.

The maximum load of the service area, which is a daytime maximum, is obvious. The lower curve is typical of the residential and general commercial classes combined. It illustrates the occurrence of a class maximum at a different time from the service area maximum. It also illustrates the class contribution to the service area maximum.

The significance of the terms "at plant" and "at customer" may be seen easily from Fig. 4, a 1-line diagram which serves principally to fix the concept that system losses, as well as diverse timing of customer demands on the system, are essential to any such estimate of service area requirements.

Sales or Load Classes

The breakdown of the total sales or load will identify the following classes:

1.00 Residential: exclusive of commercially metered multifamily accounts.
2.00 General Commercial: 0 to 20 kilowatt demands, Commercial and Industrial including public authorities.
3.00 Residential plus General Commercial, as combined for estimating.
4.00 Large Commercial and Industrial: exclusive of Specifics, but including Public Authorities.
5.00 Specifics: very large customers estimated individually.
6.00 Street and Traffic Lighting.
7.00 Railroads and Railways.
8.00 Miscellaneous groups: relatively small.

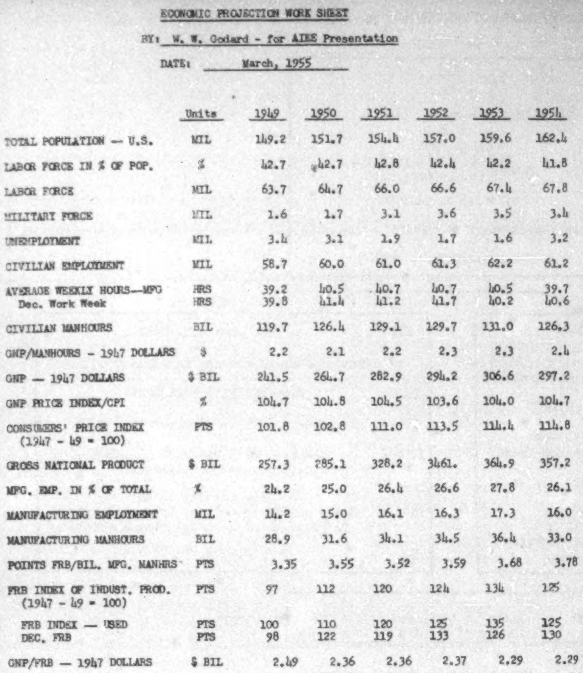

ECONOMIC PROJECTION WORK SHEET

BY: W. W. Godard - for AIEE Presentation

DATE: March, 1955

	Units	1949	1950	1951	1952	1953	1954
TOTAL POPULATION — U.S.	MIL	149.2	151.7	154.4	157.0	159.6	162.4
LABOR FORCE IN % OF POP.	%	42.7	42.7	42.8	42.4	42.2	41.8
LABOR FORCE	MIL	63.7	64.7	66.0	66.6	67.4	67.8
MILITARY FORCE	MIL	1.6	1.7	3.1	3.6	3.5	3.4
UNEMPLOYMENT	MIL	3.4	3.1	1.9	1.7	1.6	3.2
CIVILIAN EMPLOYMENT	MIL	58.7	60.0	61.0	61.3	62.2	61.2
AVERAGE WEEKLY HOURS—MFG	HRS	39.2	40.5	40.7	40.7	40.5	39.7
Dec. Work Week	HRS	39.8	41.4	41.2	41.7	40.2	40.6
CIVILIAN MANHOURS	BIL	119.7	126.4	129.1	129.7	131.0	126.3
GNP/MANHOURS - 1947 DOLLARS	$	2.2	2.1	2.2	2.3	2.3	2.4
GNP — 1947 DOLLARS	$ BIL	241.5	264.7	282.9	294.2	306.6	297.2
GNP PRICE INDEX/CPI	%	104.7	104.8	104.5	103.6	104.0	104.7
CONSUMERS' PRICE INDEX (1947 - 49 = 100)	PTS	101.8	102.8	111.0	113.5	114.4	114.8
GROSS NATIONAL PRODUCT	$ BIL	257.3	285.1	328.2	3461.	364.9	357.2
MFG. EMP. IN % OF TOTAL	%	24.2	25.0	26.4	26.6	27.8	26.1
MANUFACTURING EMPLOYMENT	MIL	14.2	15.0	16.1	16.3	17.3	16.0
MANUFACTURING MANHOURS	BIL	28.9	31.6	34.1	34.5	36.4	33.0
POINTS FRB/BIL. MFG. MANHRS	PTS	3.35	3.55	3.52	3.59	3.68	3.78
FRB INDEX OF INDUST. PROD. (1947 - 49 = 100)	PTS	97	112	120	124	134	125
FRB INDEX — USED	PTS	100	110	120	125	135	125
DEC. FRB	PTS	98	122	119	133	126	130
GNP/FRB — 1947 DOLLARS	$ BIL	2.49	2.36	2.36	2.37	2.29	2.29

Fig. 2. Economic data sheet

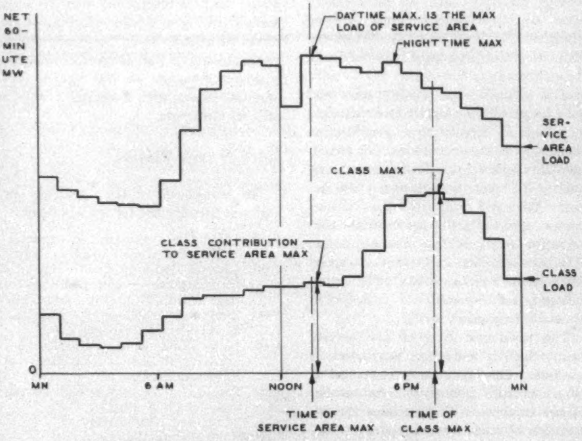

Fig. 3. Typical daily load and terminology

The breaking point of demand between general commercial and large commercial is frequently 20 kilowatts, as shown in this estimate. "Specifics," in this estimate, consists of customers having very high load factors with demands of 10 megawatts (mw) or more, and any other very large customer having a specially controlled load, to be estimated individually. "Street and Traffic Lighting" consists of all regular street, area, and bridge lighting, and various traffic control devices. "Rural," which is a significant classification with some utilities, is not separated in this estimate.

Estimates by Classes

RESIDENTIAL AND GENERAL COMMERCIAL

In these classes, the number of customers and the kw-hr per customer determine the total volume of kw-hr sales. While the gross additions of new customers and the gross disconnections of existing customers are very important for general planning, the net increase is sufficient in load forecasting.

National and local statistics usually make it necessary to devise practical adaptations in estimating the number of residential customers. In this the number of nonfarm housing starts will be used, which is the number of family dwelling units started. This is estimated monthly and published by the Bureau of Labor Statistics (BLS) for the country as a whole.

In the industrial area covered by this estimate there has been a marked similarity between net increase in residential customers and the mathematical product of national housing starts and the FRB Index. This is the basis for Fig. 5. Generally speaking, 1 per cent (%) of the FRB Index multiplied by 1% of the number of national housing starts has approximated the net increase in these customers. This refers to the basic increase, exclusive of acquisitions of established distribution service facilities and other similar changes.

A multiple correlation method might have been used to build an equation but by practical observation an acceptable equation for the net increase in customers has been evolved and applied throughout the period of estimate, as follows

$$n_x = \frac{(\text{FRB})}{(100)}\left(\frac{S_x+S_{(x-1)}}{2\times 100}\right)[1.1658-0.0324(x-1946)] \pm \text{unusual changes}$$

where

n = net increase in residential customers
S = U. S. nonfarm housing starts
x = year of the net increase
$(x-1)$ = previous year

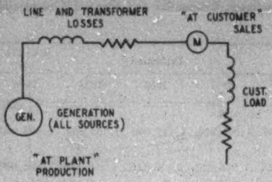

Fig. 4 (left). At-plant to at-customer terminology

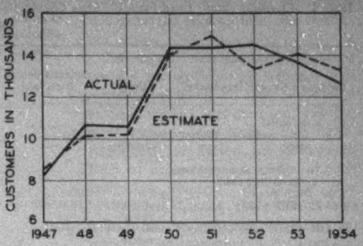

Fig. 6 (right). Residential customers: basic increase estimated and actual

The "unusual changes" would be transfers to or from other classes, changes in the extent of the service area, and would possibly involve some of the larger housing projects metered individually as residential service.

The application of this and similar equations requires continuous observation. However, it shows close correlation with actual up to the present time. Fig. 6 is a comparison of the calculated and actual basic net increase for 1947 through 1954. The maximum deviation was 8.8% in 1952 when the FRB Index was affected considerably by a 2-month, nationwide steel strike. No other deviation is as great as 5% and most of them are less than 2%.

Average use in the year is determined by predicting the annual increase and adding it to the previous year's average use. This kw-hr increase is determined with a degree of judgment based on previous experience and consultation with local marketing people. The promotion of major appliances and the probable attitude of consumers in the purchase of additional major electric appliances are pertinent factors.

The estimated customers, kw-hr increase in average use, and the other details are shown in Table I. The estimated total kw-hr sales to the class is the product of the average number of customers and the average use.

Characteristic of observations which can be made, it is interesting that force of habit and the convenience of electricity in the home assert themselves even through short recessions as graphically shown in Fig. 7. Average use is charted with disposable personal income. It is included expressly to show the continuing rise in residential average use, even in years when the income is marking time or slackening off for a year or so.

GENERAL COMMERCIAL

The general commercial class is handled in a manner similar to residential. Additional considerations are the changing state of business, the migration of customers to and from the large commercial group, and changes in marketing practices within the area. These make it more difficult to predict the customer and kw-hr increases. The commercial or marketing representatives' contacts with these customers, and a knowledge of the field conditions are important to the decision.

Based on opinions prevailing in 1949, the basic customer increase was projected at 800 per year and the annual increase in average use was set at 300 kw-hr. These increases vary considerably from year to year, and should be judged broadly. The actual basic customer increase in the 5-year period has been 820 per year, 20 more than the forecast. This is shown in Table I.

RESIDENTIAL AND GENERAL COMMERCIAL

Residential and general commercial classes are next combined into a single class for estimating the contribution to annual service area maximum. The class load factor varies with average use per customer. The relationship, as shown in Fig. 8, is almost linear. It should be remembered that this factor spans from the at-customer sales to the at-plant contribution to the service area maximum.

Knowing the kw-hr sales and the class load factor, it is easy to calculate the contribution of the combined class to the service area maximum based on the number of hours in the year. Detail calculations are shown in Table I. This can be designated as a class contribution calculated in advance. Since the period of this estimate is passed, contributions of this and other classes, also can be estimated ex post facto. The deviation of the advance calculation from the ex post facto estimate is a good test of the plan of estimating.

These deviations are shown for the residential and general commercial class in Table I. In per cent of actual, the residential deviations ranged from a low of −1.5% to a high of −5.1% in the period 1950 through 1953. Ex post facto estimates were not available for 1954 in time to be included. The estimate being 5.1% lower than actual in 1951 is apparently related to the "Korea" rush in the purchase of heavy appliances and other similar factors. There were two notable surges upward in retail sales in 1950.

LARGE COMMERCIAL AND INDUSTRIAL

In a comprehensive way, the large commercial and industrial class would also involve two component classes. There is a correlation class, and a few large customers who are estimated individually, the specifics class.

The correlation group has general characteristics closely related to variations in the national economy. This is the basis of the predictions of load factor and sales, through correlation with the FRB Index, which is one of the most fundamental factors in this plan. Through this load class alone it determines over 60% of the kw-hr requirements of

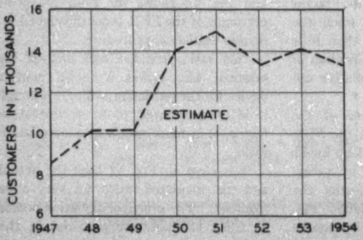

Fig. 5. Residential customers: basic increase estimated by equation

Table I. Electrical Utility Load Forecast, Class Contribution to Net 60-Minute Service Area Maximum, Residential and General Commercial Classes, Estimate 5Y150—AIEE

Reference No. and Description	Units	Estimate Source Reference	"Actual"			Estimated				
			1947	1948	1949	1950	1951	1952	1953	1954
1.00 Residential										
1.10 U.S. nonfarm housing starts	family dwelling units	BLS	849,000	931,600	1,025,100	1,396,000	1,091,300	1,127,000	1,103,800	1,220,200
1.11 Average of current and preceding years			759,750	890,300	978,350	1,210,550	1,243,650	1,109,150	1,115,400	1,162,000
1.20 FRB index	points	FRB	100	104	97	112	120	124	134	125
1.21 FRB ÷ 100	multiplying factor	1.20 ÷ "100"	1.00	1.04	0.97	1.12	1.20	1.24	1.34	1.25
1.22 Ratio modifying factor	multiplying factor	experience	1.08	1.14	1.11	1.04	1.00	0.97	0.94	0.91
1.23 Basic residential customer gain as a % of U.S. housing starts	per cent	$\frac{1.21\times 1.22}{100}$	1.08	1.19	1.08	1.16	1.20	1.20	1.26	1.14
1.30 Customers										
1.31 Basic increase	no.	1.11×1.23	8,206	10,618	10,557	14,000	14,900	13,300	14,100	13,200
1.32 Special increase	no.	*				1,400	8,600	750	1,350	500
1.33 Total increase	no.	1.31+1.33	8,206	10,618	10,557	15,400	23,500	14,050	15,450	13,700
1.34 December customers	no.	previous December+increase	332,494	343,112	353,669	369,050	392,550	406,600	422,050	435,750
1.40 Average customers	no.	$\frac{\text{December}+\text{previous December}}{2}$	328,712	338,432	348,887	361,360	380,800	399,575	414,325	428,900
1.50 Average use	kw-hr per customer	predicted	1,556	1,640	1,734	1,874	2,039	2,204	2,379	2,564
1.60 Kw-hr sales to class	millions	1.40×1.50	511.3	555.4	604.9	677.2	776.5	880.7	985.7	1,099.7
2.00 General commercial										
2.10 Customers										
2.11 Basic increase	no.	800 per year	1,156	1,151	993	800	800	800	800	800
2.12 Special increase	no.	*				+350	−5,600		−700	+250
2.13 Total increase	no.	2.11+2.12	1,156	1,151	993	1,150	−4,800	800	100	1,050
2.14 December customers	no.	previous December+increase	43,599	44,750	45,743	46,900	42,100	42,900	43,000	44,050
2.20 Average customers	no.	$\frac{\text{December}+\text{previous December}}{2}$	43,194	44,411	45,434	46,325	44,500	42,500	42,950	43,525
2.30 Average use	kw-hr per customer	predicted	6,169	6,496	6,658	6,960	7,260	7,560	7,860	8,160
2.40 Kw-hr sales to class	millions	2.20×2.40	266.4	288.4	302.4	322.4	323.1	321.3	337.6	355.2
3.00 Residential and general commercial composite class										
3.10 Average number of customers		1.40+2.20	371,906	382,843	394,321	407,685	425,300	442,075	457,275	472,425
3.20 Kw-hr sales	millions	1.60+2.40	777.7	843.8	907.3	999.6	1,099.6	1,202.0	1,323.3	1,454.9
3.30 Average use	kw-hr per customer	3.20÷3.10	2,091	2,204	2,301	2,452	2,585	2,719	2,894	3,080
3.40 Corresponding load factor of sales on class contribution to annual net 60-minute maximum service area load at power plants	%	graphic based on 3.30 and curve of load factor ×average use	53.8	54.4	55.0	55.8	56.6	57.2	57.8	58.5
3.50 Class contribution to annual net 60-minute maximum service area load at power plants	mw	(3.20÷3.40)÷ hours in year ÷1,000								
3.51 As calculated in advance	mw	(see above)				204	222	239	261	284
3.52 As estimated ex post facto	mw	special study	168	178	187	207	234	248	267	na†
3.53 Deviation of 3.51 over 3.52	mw	(3.51−3.52)				− 3	−12	− 9	− 6	na
	%	÷3.52×100				−1.5	−5.1	−3.6	−2.2	na

* Unusual increases such as acquisition of other electric systems or reclassification of customers.

† "Actual" is an ex post facto appraisal. This also applies to Tables II through V.

the service area, though it would be a much smaller part of operating revenues. The first objective in this class is to determine the load factor.

Usually the load factor will be lower when the level of industrial production is lower in the annual average than it is in the month of the annual service area maximum. The ratio of the annual FRB Index to the FRB Index in the month of December is used as a multiplying factor by which a basic load factor will be modified to allow for this tendency. Similarly, an increase in basic load factor might be expected in years when the annual FRB Index is higher than it is in December. A further modification of load factor is based on the relative use of electricity.

The similarity of variations of the kw-hr sales to this class and the FRB Index is evident in Fig. 9, in which kw-hr and the index are charted by years. Even when considered by months, the relationship is significantly reliable. Fig. 10 is included to show the FRB by months and Fig. 11 shows the ratio of kw-hr per point of the FRB Index developed by regular statistical procedure.

This ratio, trended and shaped for seasonal use, makes a useful control device for the particular utility. Though it is often referred to as a correlation factor, it is more precisely a correlation ratio.

It is clear in Fig. 12 that the actual and the calculated ratios run very close together. The principal deviation occurs at times of major irregularities in the

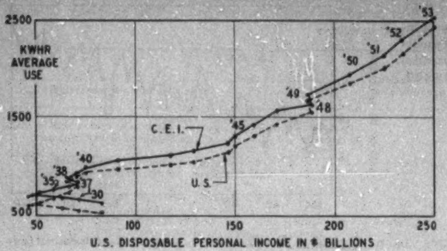

Fig. 7. Residential kw-hr per customer and U. S. disposable personal income

industrial world, as in the years 1949, 1950, and 1952.

Fig. 13 shows the deviation more clearly. These major deviations at times occurred because of coal or steel strikes, or other principal economic shifting. In a shift such as the deviation occurring late in 1950, for known causes, the correlation ratio can be trended back to normal over an assumed period of time, for use in estimates.

To return to the subject of load factor modification, the FRB correlation ratio is the key to the modification of class load factor for changes in the relative use of electricity by the class. The modifying factor is the quotient of the average of 12 monthly correlation ratios in the year and the December ratio, both expressed in kw-hr per point of the FRB Index.

Studies have also indicated an interesting tendency of the load factor of this large commercial and industrial correlation group to be the same when adjusted by ratio to a basic 42-hour work week, based on the actual work week reported for U. S. all manufacturing. With some give and take, the adjusted annual load factor, on a 42-hour basis, was 55%. The modifying factor to allow for relative application of the work force is the ratio of hours reported in the actual work week to the basic 42 hours per week.

The load factor of the class may now be calculated. It is the product of the basic 55% load factor and the three multiplying factors. They modify the basic 55% for variations in industrial production, in relative use of electricity, and in the application of the work force. Note that the 55% is a characteristic of this particular estimate. Kw-hr sales to the class is the product of the annual FRB Index and the average monthly correlation ratio multiplied by 12.

The class contribution to the annual service area maximum at power plants is calculated from the kw-hr sales and the estimated load factor. The contribution calculated in advance has been compared with the contribution as estimated ex post facto. Except for the year 1950, which under the impetus of the Korean developments made a sudden and full recovery from the 1949 recession, the deviation is quite acceptable. All of this class calculation is detailed in Table II. The other 6 years show an average deviation of 2%.

SPECIFICS

The specifics class consists of electrochemical loads of 10 mw or more, and any other load of 10 mw or more which is specially controlled. These were excluded from the total large commercial and industrial class to form the correlation group.

The probable maximum demands of the specifics are predicted by company representatives, based on their knowledge of the individual situations and consultations with the customers. The coincidence and loss factors are determined from an engineering knowledge of each individual situation. As in the case of the load factors, these factors also span from the customer maximum demand to the maximum of the company power plants. For definition, see Table III. The contribution to annual service area maximum is estimated for each customer as the product of the at-customer maximum and the corresponding coincidence-and-loss factor. The sum of the customer's contributions to the service area peak constitutes the contribution of the class. The details of calculation are shown in full in Table III.

The contribution as calculated in advance has been compared with the contribution as estimated ex post facto. This brings out the deviations which might be charged specifically to the method of estimating. In this estimate they are quite acceptable.

STREET AND TRAFFIC LIGHTING

Street and traffic lighting is shown in Table IV to have a very low contribution to the daytime peak. It is less than 0.5 mw in any month of this estimate.

RAILROADS AND RAILWAYS

Railroads and railways usually requires specific consideration by company representatives and the customers. The estimate, to be consistent, should take into account current opinions and past performance. The latter would be reflected in class deviations of previous estimates; see Table IV.

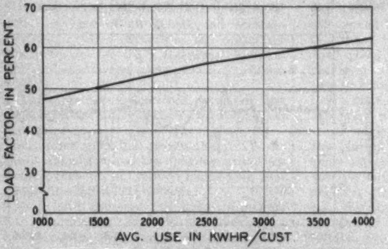

Fig. 8. Residential and general commercial (combined) load factor and average use

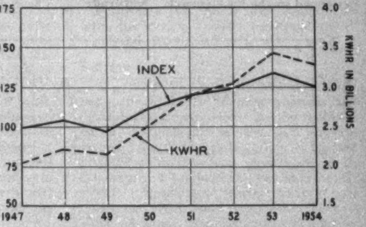

Fig. 9. FRB Index of Industrial Production and large commercial and industrial (exclusive of Specifics) kw-hr sales, by years

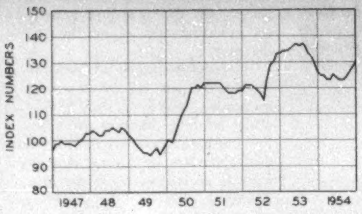

Fig. 10 (left). FRB Index of Industrial Production, by months; 1947–49 = 100

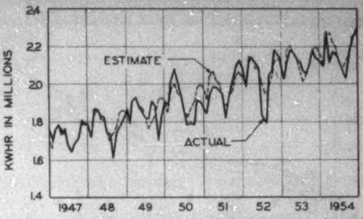

Fig. 12. Large commercial and industrial (exclusive of Specifics) correlation ratio, estimated and actual, by months. Kw-hr per point of FRB Index

MISCELLANEOUS

The other miscellaneous group, also in Table IV, includes special sales contracts and company use. An experience load factor and the total estimated kw-hr are the basis for calculating the class contribution to the annual service area maximum. It is a very small load in this estimate.

This completes the several classes. The estimated net 60-minute maximum load of the service area is the sum of the individual class contributions, as shown in Table V and Figure 14.

In the period of estimate, the maximum occurred in December with only one exception. The 1954 peak was in November, but was only 3 or 4 mw higher than the December peak.

Deviations Test

If a good job is done in setting up the economic pattern, the over-all test of this method is the deviation of the estimated service area maximum from the actual. The range of these deviations is shown in Table V. It ranges from +2 to +43 mw and from +0.2% to +4.3%. The 5-year average was 2.3%. Exclusive of the unusual Korea year, 1950, the average of the unadjusted deviations is 1.9%.

Weather is automatically incorporated in the class contributions, by this method, to the extent of typical weather experienced in the base period. Naturally, there were departures from typical weather at time of annual maximum loads and after adjustment for these, the range of deviations is from +11 to +27 mw. This is from +1.0% to +3.1%. Exclusive of the Korea year they would average 1.3%.

The deviations of estimate from actual are plotted in megawatts in Fig. 15 and in per cent in Fig. 16. The percentage deviations show good consistency. The solid line represents unadjusted deviations; the heavy, broken line deviations after actual loads were adjusted for abnormalities of weather; the lightweight line represents deviations after further adjustment for the deviation of individually estimated large customers. The weather-adjusted deviation averages 1.5%. Allowing for deviation of four individually estimated large customers, the arithmetic average of deviations is 1.3%.

Incremental Test

Whatever the method used in making such an estimate, it is well to make a practical check by some other approach. This is done regularly in the author's company, by a study of all large-commercial and industrial customers having a proved or prospective demand of 0.5 mw or more. Through appropriate contacts with them, their probable load changes during the first two years of the estimate period are determined. These are translated into probable class effect on the service area maximum and this is given a judgment comparison with the economic correlation estimate. For the details of this incremental plan, see Appendix II. Also, see the suggested references in Appendix III.

Conclusions

1. The economic correlation method of load forecasting, as applied in this estimate, automatically makes allowances for curtailments, displacements, and new loads not specifically known to company or customer representatives at time of estimate.

2. The use of popularly recognized economic indicators facilitates the exchange of opinions with other forecasters.

3. The FRB Index of Industrial Production and the BLS average weekly hours per employee for U. S. all manufacturing are most important factors in this method. They apply directly to a class of load which makes the major contribution to the annual daytime maximum load of the service area.

4. The method used in this estimate is flexible and reliable. It is relatively simple, and highly effective in predicting electrical-requirements of the service area.

5. The operation of this method of forecasting as a principal part of an electrical utility's regular planning, will condition the organization for better performance.

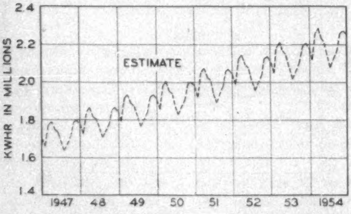

Fig. 11. Large commercial and industrial (exclusive of Specifics) correlation ratio, estimated kw-hr per point of FRB Index, by months

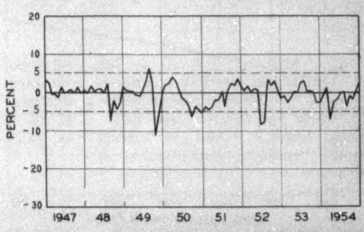

Fig. 13. Large commercial and industrial (exclusive of Specifics) correlation ratio deviation of actual from estimate. Kw-hr per point of FRB Index, per cent deviation of actual from estimate

Table II. Electrical Utility Load Forecast, Class Contribution to Net 60-Minute Service Area Maximum Large Commercial and Industrial, Exclusive of Specifics, Estimate 5Y150—AIEE

Reference No. and Description	Units	Estimate Source Reference	"Actual" 1947	"Actual" 1948	"Actual" 1949	Estimated 1950	Estimated 1951	Estimated 1952	Estimated 1953	Estimated 1954
4.00 Large commercial and industrial, exclusive of Specifics	20 kilowatt-demand or more									
4.10 Load factor on class contribution to annual net 60-minute maximum of service area		see 4.14 (c)								
4.11 Volume of industrial production—seasonally adjusted										
(a) FRB Index, December	points	predicted	103	102	98	122	110	133	126	130
(b) FRB Index, annual average	points	predicted	100	104	97	112	120	124	134	125
(c) Ratio of annual to December	multiplying factor	(b) ÷ (a)	0.971	1.020	0.990	0.918	1.008	0.932	1.063	0.962
4.12 Relative use of electricity Kw-hr per point of FRB										
(a) December	millions	predicted	1.790	1.878	1.911	1.981	2.047	2.115	2.182	2.249
(b) Annual average month of the year	millions		1.739	1.784	1.855	1.930	1.997	2.063	2.130	2.196
(c) Ratio of annual to December	multiplying factor	(b) ÷ (a)	0.972	0.950	0.971	0.974	0.976	0.975	0.976	0.976
4.13 Application of the work force Average hours in work week, U. S.										
(a) December, all manufacturing	hours	predicted	41.2	40.0	39.8	41.4	41.2	41.7	40.2	40.6
(b) Ratio to 42-hour basic	multiplying factor	(a) ÷ "42"	0981	0.952	0.948	0.986	0.918	0.993	0.957	0.967
4.14 Annual load factor of sales on class contribution to maximum of service area at power plants, December										
(a) Basic load factor of 42-hour work week	%	experience	55	55	55	55	55	55	55	55
(b) Composite adjusting factor 4.11 (c) × 4.12 (c) × 4.13 (b)	multiplying factor		0.926	0.922	0.911	0.882	0.965	0.902	0.993	0.980
(c) Estimated load factor	%	(a) × (b)	50.9	50.7	50.1	48.5	53.1	49.6	54.6	49.9
(d) Estimated ex post facto	%		48 1	50.5	49.2	49.8	51.2	49.1	53.4	
4.20 Kw-hr sales to class										
4.21 Calculated in advance	millions	4.11(b) × 4.12(b) × 12	2,086	2,226	2,159	2,594	2,876	3,070	3,425	3,294
4.22 Estimated ex post facto	millions		2,065	2,220	2,157	2,513	2,873	3,029	3,427	3,256
4.30 Class contribution to annual net 60-minute maximum load of the service area at power plants										
4.31 As calculated in advance $\frac{4.20}{4.14(c)\times\text{hours in year}\times\text{"1,000"}}$	mw	calculated	468	500	492	611	618	705	716	754
4.32 As estimated ex post facto	mw		490	500	500	576	640	703	732	na
4.33 Deviation of 4.31 over 4.32	mw	(4.31 − 4.32) ÷ 4.32 × 100	−32	0	−8	+35	−22	+2	−16	na
	%		−4.5	0	−1.6	+6.1	−3.4	+0.3	−2.2	na

Appendix I. Forecasting the National Economy

Businessmen have viewed the national economy with increasing interest and hopes for a better understanding of its operational aspects. Better knowledge of its factorial relationships should provide a basis for better opinions regarding the future.

The output of many large business units tends to vary with the physical output of the nation's factories and mines or with the dollar volume of all goods and services produced. These functions are popularly measured by the FRB Industrial Production Index and the gross national product (GNP).

This pamphlet describes some of the general relationships of these two indicators; also, their relationship to population, labor force, work week and productivity. While these relationships are mathematical in nature, they do not reduce forecasting to a simple mechanical operation.

It is still necessary to make numerous key assumptions. This is facilitated by a knowledge of past stages of the economy and trends of certain relationships, which, arranged in a logical array, furnish a positive means of testing one's own opinions and those expressed by others. It is a sort of circular or triangular pattern wherein the ends must meet; see Fig. 1 for a diagram of the plan, and Fig. 2 for a typical data sheet.

Forecasting Technique: Fig. 1

SECTION A

I. The starting point for forecasts of both GNP and the FRB Index is the total population of the United States. The differential between birth and death rates multiplied by the population in any given year gives the change in population for the year. Recently, the annual rate of gain has been about 2,000,000.

II. The percentage of population available as a work force varies, depending on which of certain factors are dominant in the current economic situation. Some of these factors are: the number of married women working, the number of persons in the armed forces, the population birth rate, the distribution of population, and the number of enforced retirements.

III. The product of the series I and II is the available work force. Subtracting estimated unemployment and the number in the military force gives total civilian employment.

IV. The BLS series on the average weekly hours of production workers in manufacturing is fairly representative of the work week in all sectors of the economy and is used here because it is historically consistent and readily available. A simple multiplication by 52 gives representative annual hours of work per employee.

V. The number of annual civilian man hours is derived from the product of annual hours per manufacturing worker times civilian employment.

I through V. These five components form the common basis for estimates of GNP and the FRB.

SECTION B

VI. GNP in "constant dollars" eliminates the influence of price changes and measures the variations in the nation's output of goods and services on a physical volume basis. The ratio of this "Constant $" GNP to civilian man hours is, in effect, a measure of productivity per man hour.

VII. Man-hours times output per man-hour gives total GNP in constant-value dollars. The data for the years 1929 to date were developed in a study by George Jaszi of the Department of Commerce.

VIII. Since the prices affecting the value of GNP are a mixture of wholesale

Table III. Electrical Utility Load Forecast, Class Contribution to Net 60-Min. Service Area Maximum, Specifics, Estimate 5Y150—AIEE

			"Actual"			Estimated				
Reference No. and Description	Units	Estimate Source Reference	1947	1948	1949	1950	1951	1952	1953	1954
5.00 Specifics: electrochemical loads of 10 mw or more and any other load of 10 mw or more which is specially controlled										
5.10 Estimated December 60-minute maximum at customer										
5.11 Customer *A*	mw	predicted by a company representative and the customer					36	36		
5.12 Customer *B*	mw					19	31	31	31	31
5.13 Customer *C*	mw		26	33	39	33	33	33	25	25
5.14 Combined	mw	sum	26	33	39	52	100	100	56	56
5.20 Corresponding coincidence and loss factor, customer maximum to customer contribution to maximum of service area*										
5.21 Customer *A*	multiplying factor	experience					0.969	0.969		
5.22 Customer *B*	multiplying factor	experience				0.969	0.969	0.969	0.969	0.969
5.23 Customer *C*	multiplying factor	experience	0.500	0.515	0.487	0.750	0.750	0.750	0.750	0.750
5.24 Combined	multiplying factor	5.34 ÷ 5.11	0.500	0.515	0.487	0.827	0.900	0.900	0.875	0.875
5.30 Contribution to annual net 60-minute maximum of the service area at power plants, as estimated in advance										
5.31 Customer *A*	mw	5.11×5.21					35	35		
5.32 Customer *B*	mw	5.12×5.22				18	30	30	30	30
5.33 Customer *C*	mw	5.13×5.23	13	17	19	25	25	25	19	19
5.34 Combined	mw	sum	13	17	19	43	90	90	49	49
5.40 Contribution, as estimated ex post facto										
5.41 Customer *A*	mw	special study					34	35		
5.42 Customer *B*	mw	special study				24	25	24	20	21
5.43 Customer *C*	mw	special study				19	32	23	26	31
5.44 Combined	mw	sum	13	17	19	43	91	82	46	51
5.45 Deviation of 5.34 over 5.44	mw	5.34 − 5.44				0	−1	+8	+3	−2
	%	5.34 − 5.44 ÷ 5.44×100				0	−1.1	+9.8	+6.5	−3.9

* Coincidence and loss factor expresses the at-plant equivalent contribution of the individual class or customer, in terms of their own maximum demands in the period.

Table IV. Electrical Utility Load Forecast, Class Contribution to Net 60-Min. Service Area Maximum, Street Lighting, Railways and Miscellaneous Classes, Estimate 5Y150—AIEE

			"Actual"			Estimated				
Reference No. and Description	Units	Estimate Source Reference	1947	1948	1949	1950	1951	1952	1953	1954
6.00 Street and traffic lighting										
Contribution to annual net 60-minute maximum of the service area at the power plants	mw	experience	0.3	0.3	0.3	0.4	0.4	0.4	0.4	0.4
7.00 Railroads and railways										
Contribution to annual net 60-minute maximum of service area at power plants	mw	predicted by a company representative and the customer	24	24	20	22	26	27	27	27
8.00 Miscellaneous group										
8.10 Kw-hr sales to										
public schools contract	millions	predicted								
emergency schedule	millions	predicted								
total	millions	sum	16.3	17.5	19.3	19.4	20.2	21.0	21.8	21.8
8.20 Kw-hr company use	millions	predicted	13.2	13.9	13.9	12.3	12.3	2.3	12.3	12.3
8.10+8.20 kw-hr	millions	sum	29.5	31.4	31.2	31.7	32.5	33.3	24.1	34.1
8.30 Load factor on contribution to maximum of the service area	%	experience and knowledge of loads	0.37	0.32	0.30	0.35	0.35	0.35	0.35	0.35
8.40 Contribution to annual net 60-minute maximum of the service area at the power plants $\frac{8.10+8.20}{8.30\times\text{hours in year}\times\text{"1000"}}$	mw	calculated	11	10	12	10	11	11	11	11

and retail, an index of the GNP average price factor is measured against a more common price indicator, the BLS Consumers' Price Index.

IX. The historical relationship of the BLS Consumers' Price Index to the GNP Composite Price Index multiplied by the Consumers' Price Index produces an overall conversion factor. This product times the constant $ GNP gives a current-dollar GNP.

X. GNP in current dollars is the market value of all goods and services produced.

SECTION C

XI. To develop a forecast of the FRB Index, the starting point under this plan is the ratio of manufacturing employment to total civilian employment. Since manufacturing employment is more volatile than other groups, this ratio varies primarily with the "ups and downs" of business.

XII. Multiplying the ratio from series XI by civilian employment from series III gives the volume of manufacturing employment.

XIII. Manufacturing employment multiplied by the average hours per week per production worker in manufacturing, from series IV, times 52 gives the annual volume of manufacturing man-hours. Note that this average hours per week is the second of the basic elements in section *A* to be used in developing the FRB Index. Since these same two elements were used in developing the GNP forecast, the whole

Table V. Electrical Utility Load Forecast, Annual Net 60-Minute Maximum Load of Service Area, Mw at Power Plants, Estimate 5Y150—AIEE

Item No.	Description	Estimate Source Reference	"Actual" 1947	"Actual" 1948	"Actual" 1949	Estimated 1950	Estimated 1951	Estimated 1952	Estimated 1953	Estimated 1954
1	Residential and general commercial	3.51				204	222	239	261	284
		3.52	168	178	187					
2	Large commercial and industrial excluding specifics	4.31				611	618	705	716	754
		4.32	490	500	500					
3	Specifics, large electrochemical, etc.	5.34				43	90	90	49	9
		5.44	13	17	19					
4	Street and traffic lighting	6.00				(Less than 0.5 mw)				
5	Railroads and railways	7.00	24	24	20	22	26	27	27	27
6	Miscellaneous group	8.40	11	10	12	10	11	11	11	11
7	Estimated net 60-minute maximum load	sum				890	967	1,072	1,064	1,125
8	Actual net 60-minute maximum load	records	706	729	738	853	965	1,051	1,054	1,082
9	Deviation of estimate from actual									
	Megawatts	(7−8)				+37	+2	+21	+10	+43
	Per cent	(9+8)×100				+4.3%	+0.2%	+2.0%	+0.9%	+4.0%
10	Deviation after allowance for abnormal weather	calculated								
	Megawatts					+27	+12	+11	+20	+13
	Per cent					+3.1%	+1.3%	+1.0%	+1.9%	+1.2%
11	Deviation after allowance for normal weather and for deviation of individually estimated large customers	calculated								
	Megawatts					+27	+18	−8	+3	+1
	Per cent					+3.1%	+1.9%	−0.7%	+0.3%	+0.1%

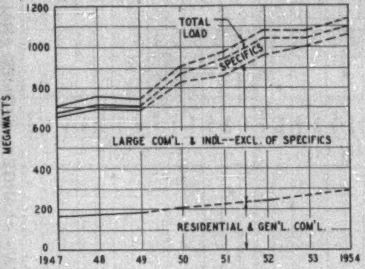

Fig. 14 (left). Total service area load by class contribution

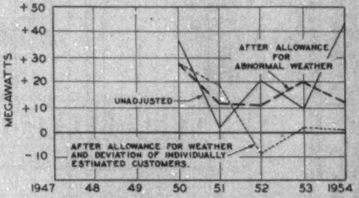

Fig. 15. Estimated annual service area net 60-minute maximum load, mw deviation of estimate from actual

procedure forces one to make a consistent basic pattern forecast.

XIV. The number of points of FRB Index per billion man-hours in manufacturing is an indicator of manufacturing productivity per man-hour.

XV. Multiplying man hour productivity ratio from series XIV by the number of man-hours gives the total number of points of the FRB Index, which is a measure of the physical output of the nation's factories and mines.

XVI. The ratio of "Constant $" GNP per point of FRB serves as a test check on the consistency of the FRB and GNP forecasts.

See Appendix III for the sources of the foregoing information.

Appendix II. Incremental Method of Electric Load Forecasting

The incremental method is another approach to load forecasting. Determining the expected "fundamental" changes in the load from the month of "base" load depends on a review of individual customers having proven or prospective demands larger than a stated minimum size, such as 0.5 mw or more.

December is generally chosen as the base month to eliminate the need of seasonal adjustments in estimating future annual peaks. The estimating of monthly peaks will entail the consideration of seasonal peaks.

The incremental impact of load changes can be estimated and the result applied in modification of the service area maximum of the base month, to estimate future annual peaks. It is assumed that the large commercial and industrial loads, of less than 0.5 mw, will vary in about the same proportion as the larger ones. The load of other classes can be transplanted from the correlation method of estimating. Thus, the total service area maximum can be estimated by this incremental method.

The method is as good as the opinions or the plans built into it. It will serve well for a year or two in advance—if due allowance is made for the changing character of industrial production in its effect on the coincident demand of the class. Refer to Figs. 17, 18, and 19.

Fig. 17 shows the face of a special envelope for individual large customers. It is posted and handed to the marketing or sales contact man as part of the regular estimate procedure, for his reference in judging past changes. The estimate form, Fig. 18, in this envelope is also available, showing past predictions. The record of maximum mw demand, power factor, mw billing demand, days in period billed, megawatt-hours billed, and load factor is helpful to the contact man

Fig. 16 (right). Estimated annual service area net 60-minute maximum load per cent deviation of estimate from actual

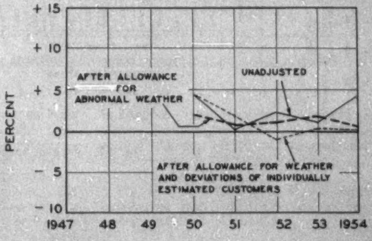

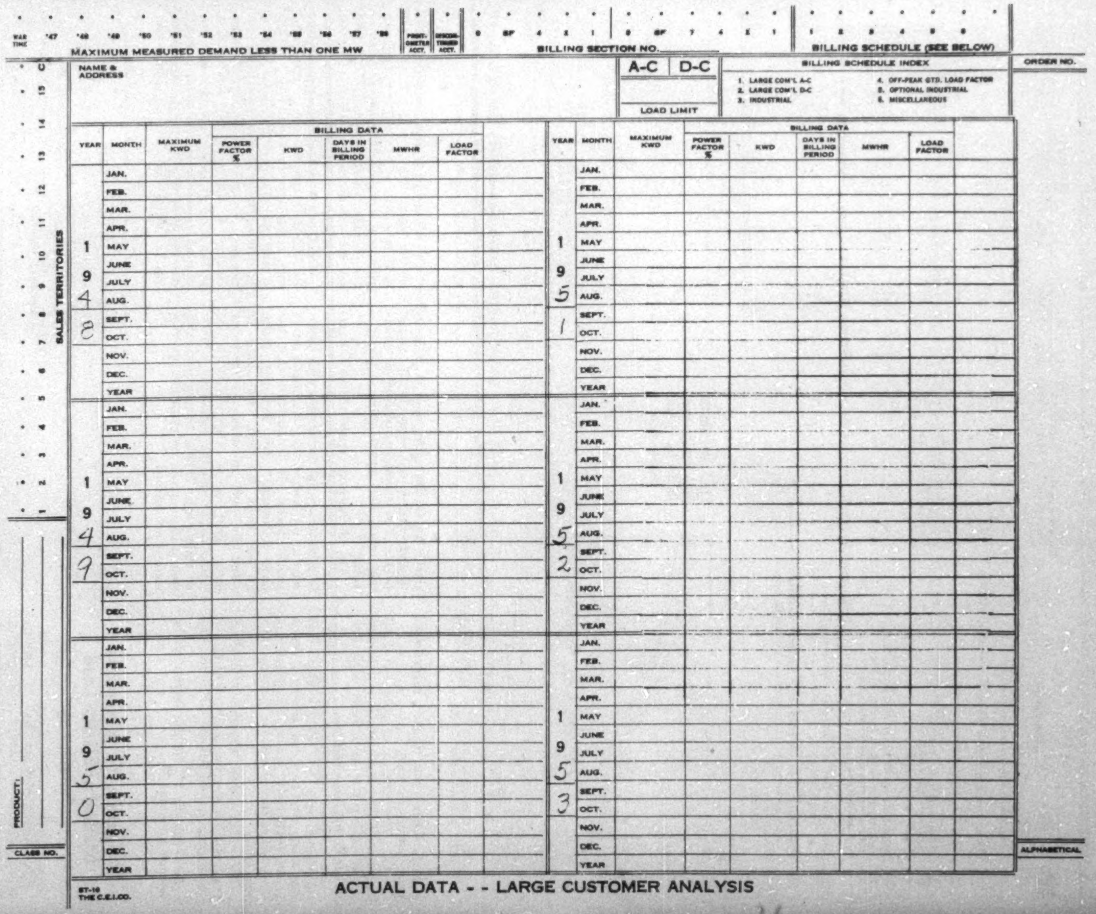

WAR TIME '47 '48 '49 '50 '51 '52 '53 '54 '55 '56 '57 '58 PRINT-OMETER ACCT. DISCON-TINUED ACCT. 8 8F 4 2 1 8 8F 7 4 2 1 1 2 3 4 5 6

MAXIMUM MEASURED DEMAND LESS THAN ONE MW

BILLING SECTION NO.______

BILLING SCHEDULE (SEE BELOW)

ORDER NO.

NAME & ADDRESS

A-C D-C

LOAD LIMIT

BILLING SCHEDULE INDEX

1. LARGE COM'L A-C
2. LARGE COM'L D-C
3. INDUSTRIAL
4. OFF-PEAK GTD. LOAD FACTOR
5. OPTIONAL INDUSTRIAL
6. MISCELLANEOUS

SALES TERRITORIES

C 15 14 13 12 11 10 9 8 7 6 5 4 3 2 1

PRODUCT:

CLASS NO.

ALPHABETICAL

YEAR	MONTH	MAXIMUM KWD	BILLING DATA					
			POWER FACTOR %	KWD	DAYS IN BILLING PERIOD	MWHR	LOAD FACTOR	
1948	JAN.							
	FEB.							
	MAR.							
	APR.							
	MAY							
	JUNE							
	JULY							
	AUG.							
	SEPT.							
	OCT.							
	NOV.							
	DEC.							
	YEAR							
1949	JAN.							
	FEB.							
	MAR.							
	APR.							
	MAY							
	JUNE							
	JULY							
	AUG.							
	SEPT.							
	OCT.							
	NOV.							
	DEC.							
	YEAR							
1950	JAN.							
	FEB.							
	MAR.							
	APR.							
	MAY							
	JUNE							
	JULY							
	AUG.							
	SEPT.							
	OCT.							
	NOV.							
	DEC.							
	YEAR							

YEAR	MONTH	MAXIMUM KWD	BILLING DATA					
			POWER FACTOR %	KWD	DAYS IN BILLING PERIOD	MWHR	LOAD FACTOR	
1951	JAN.							
	FEB.							
	MAR.							
	APR.							
	MAY							
	JUNE							
	JULY							
	AUG.							
	SEPT.							
	OCT.							
	NOV.							
	DEC.							
	YEAR							
1952	JAN.							
	FEB.							
	MAR.							
	APR.							
	MAY							
	JUNE							
	JULY							
	AUG.							
	SEPT.							
	OCT.							
	NOV.							
	DEC.							
	YEAR							
1953	JAN.							
	FEB.							
	MAR.							
	APR.							
	MAY							
	JUNE							
	JULY							
	AUG.							
	SEPT.							
	OCT.							
	NOV.							
	DEC.							
	YEAR							

ST-10
THE C.E.I.CO.

ACTUAL DATA - - LARGE CUSTOMER ANALYSIS

Fig. 17. Face of special envelope for individual large customers

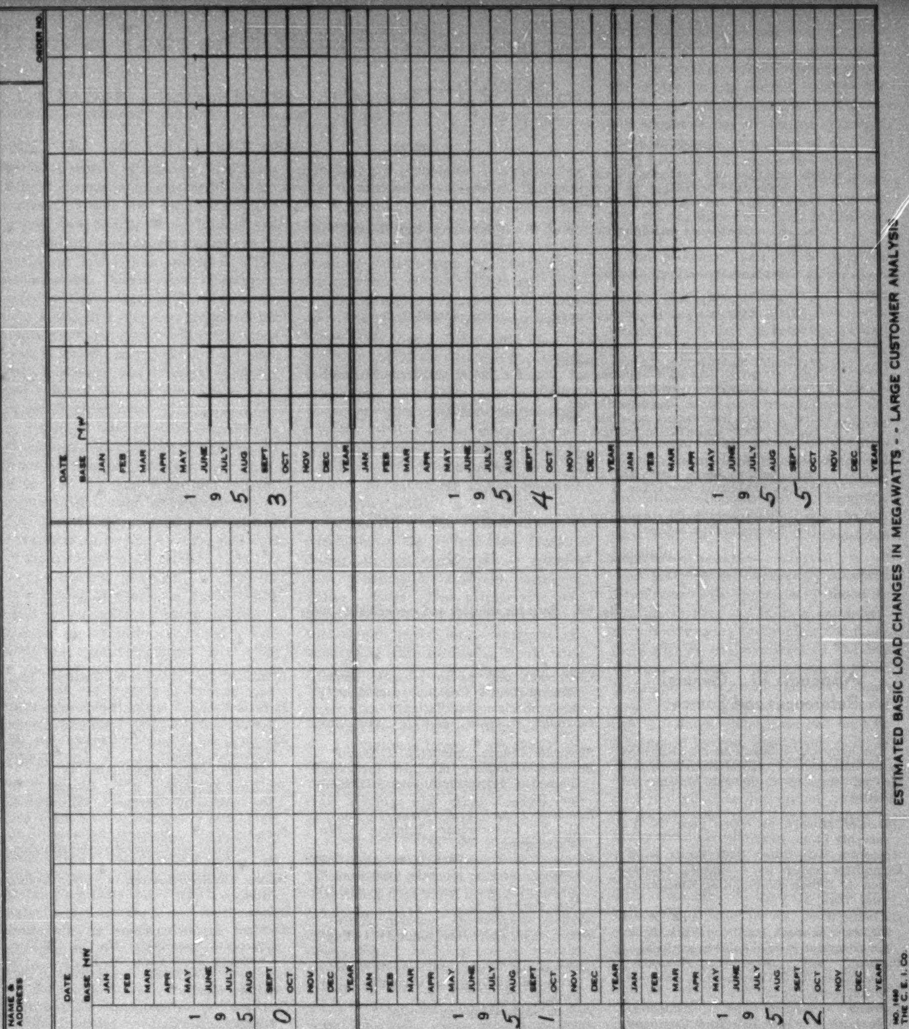

NAME & ADDRESS

ORDER NO.

1950
DATE
BASE MW
JAN FEB MAR APR MAY JUNE JULY AUG SEPT OCT NOV DEC YEAR

1951
JAN FEB MAR APR MAY JUNE JULY AUG SEPT OCT NOV DEC YEAR

1952
JAN FEB MAR APR MAY JUNE JULY AUG SEPT OCT NOV DEC YEAR

1953
DATE
BASE MW
JAN FEB MAR APR MAY JUNE JULY AUG SEPT OCT NOV DEC YEAR

1954
JAN FEB MAR APR MAY JUNE JULY AUG SEPT OCT NOV DEC YEAR

1955
JAN FEB MAR APR MAY JUNE JULY AUG SEPT OCT NOV DEC YEAR

ESTIMATED BASIC LOAD CHANGES IN MEGAWATTS - - LARGE CUSTOMER ANALYSIS

NO. 1680
THE C. E. I. Co.

Fig. 18. Form carried in large envelope of the named customer, Fig. 17, for recording anticipated changes in load of large customers

and in other departments. The margin descriptions provide for punch-outs for mechanical sorting. Product, sales territory, schedule name, load limit, etc., are part of this information. The form stock is white, heavy ledger bond. The custom-made envelopes are 10 by 12 inches, actual.

Fig. 18 shows the form for recording anticipated changes in the load of large customers. It is carried in the large envelope, Fig. 17, of the named customer. The base reference month and customer maximum for the month in question are recorded at the head of the column. The marketing or sales contact man fills in the predicted load changes for 2 or 3 years in advance. The previous predictions are always available for review. Only fundamental changes are to be reported, not seasonal changes. The stock is blue paper, 9 by 11 inches, actual.

Fig. 19 is the form used for the large commercial and industrial class of customers, exclusive of specifics.

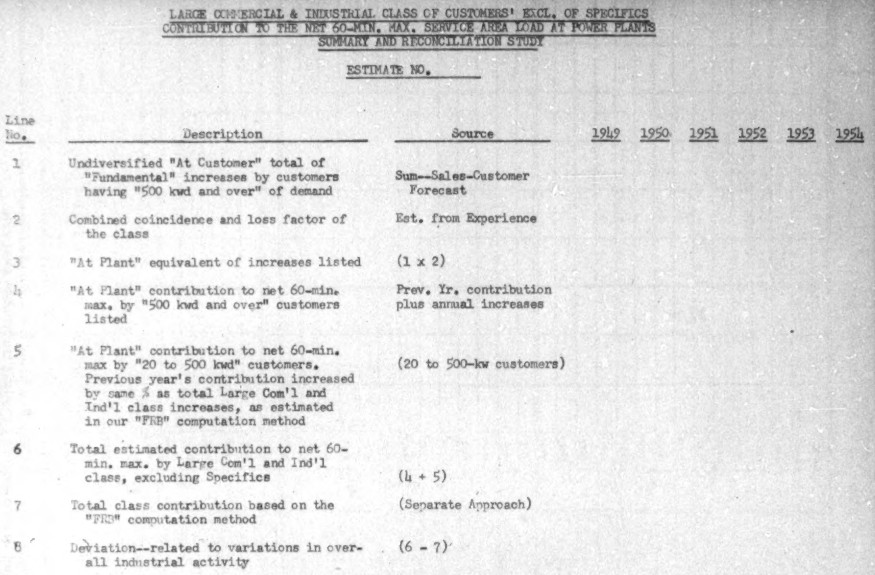

LARGE COMMERCIAL & INDUSTRIAL CLASS OF CUSTOMERS' EXCL. OF SPECIFICS
CONTRIBUTION TO THE NET 60-MIN. MAX. SERVICE AREA LOAD AT POWER PLANTS
SUMMARY AND RECONCILIATION STUDY

ESTIMATE NO. ______

Line No.	Description	Source	1949	1950	1951	1952	1953	1954
1	Undiversified "At Customer" total of "Fundamental" increases by customers having "500 kwd and over" of demand	Sum--Sales-Customer Forecast						
2	Combined coincidence and loss factor of the class	Est. from Experience						
3	"At Plant" equivalent of increases listed	(1 x 2)						
4	"At Plant" contribution to net 60-min. max. by "500 kwd and over" customers listed	Prev. Yr. contribution plus annual increases						
5	"At Plant" contribution to net 60-min. max by "20 to 500 kwd" customers. Previous year's contribution increased by same % as total Large Com'l and Ind'l class increases, as estimated in our "FRB" computation method	(20 to 500-kw customers)						
6	Total estimated contribution to net 60-min. max. by Large Com'l and Ind'l class, excluding Specifics	(4 + 5)						
7	Total class contribution based on the "FRB" computation method	(Separate Approach)						
8	Deviation--related to variations in overall industrial activity	(6 - 7)						

Fig. 19. Form for summary and reconciliation study

Appendix III. General References and Sources

The following publications are suggested as an indication of typical references, and are not intended to indicate preferential selections.

Advanced Management, New York, N. Y., monthly (June 1950).

American Statistician, New York, N. Y.

Committee reports (as available), Association of Edison Illuminating Companies, New York, N. Y.

Business Week, U. S. News and World Report, Newsweek, etc., New York, N. Y. (business and special reports sections).

Business and Economic Forecasting (pamphlet), U. S. Chamber of Commerce, Washington, D. C.

Business Forecasting (book), Frank D. Newbury, McGraw-Hill Book Company, New York, N. Y.

Business Outlook, pamphlet on Annual Forum—NIC Board.

Business Record, monthly, National Industrial Conference Board.

Business reviews issued by various banks.

Census of Manufactures, U. S. Bureau of Census, Washington, D. C.

Conference and forum releases, annual, General Electric Company, and Westinghouse Electric Corporation.

Controller Magazine, monthly, New York, N. Y.

Economic Almanac, annual, NIC Board.

Economic Indicators, monthly, President's Council of Economic Advisers, Washington, D. C.

Economic Report of the President, annual, U. S. Government Printing Office, Washington, D. C.

Edison Electric Institute, publications and releases, weekly, monthly, and annual; special committee reports (as available), New York, N. Y.

Electrical Engineering, monthly, AIEE.

Electric Light and Power, monthly, Chicago, Ill.

Electrical Merchandising, monthly, McGraw-Hill Publishing Company, New York, N. Y.

Various engineering handbooks.

Electrical World, weekly, (reports), McGraw-Hill Publishing Company, New York, N. Y.

Fortune Magazine, monthly, (Business Round-Up section).

FRB Bulletin, monthly, Federal Reserve Board, Washington, D. C.

FRB charts (book), quarterly, Federal Reserve Board, Washington, D. C.

Handbook for Forecasting, Prentice Hall Inc., New York, N. Y.

Harvard Business Review, bimonthly, Harvard University Press, Cambridge, Mass.

Reports of the President's Committee on the Economic Report, U. S. Government Printing Office, Washington, D. C.

Statistical Abstract of U. S., annual, U. S. Department of Commerce, Washington, D. C.

Survey of Current Business, monthly, U. S. Department of Commerce, Washington, D. C.

United Business Services, weekly, Boston, Mass.

Indexes

Abridged Reader's Guide to Periodical Literature, monthly, H. W. Wilson Company, New York, N. Y.

Industrial Arts Index, monthly, H. W. Wilson Company, New York, N. Y.

Catalogue of Government Publications, monthly, U. S. Government Printing Office, Washington, D. C.

Sources of Information for Appendix I

Items I, II, III, VII, and X—U. S. Department of Commerce.

Items IV and IX—U. S. Department of Labor, Bureau of Labor Statistics.

Other information—Federal Reserve System, Board of Governors, or derived.

Transfer Tests on Station Auxiliary Busses

L. E. BACKER
ASSOCIATE MEMBER AIEE

PAUL BARTH
ASSOCIATE MEMBER AIEE

R. A. HUSE
MEMBER AIEE

D. W. TAYLOR
FELLOW AIEE

THE transfer of station auxiliaries from one source to another by the interrupted source or dead throwover method has become more difficult of successful accomplishment as the size of generating units has increased. The accompanying larger size, 3,600-rpm motors, with their greater time constants, have lengthened the time required for residual voltage decay, while the more compact boilers and their fuel systems, with relatively less storage capacity, have reduced the time permissible for a successful throwover. This paper gives the results of tests on station auxiliaries during interrupted throwovers and points to possible means of effecting faster transfer and, at the same time, reducing the possibility of damage to the motors.

A characteristic auxiliary bus scheme in common use on unit systems, and used for the last eight units installed by Public Service Electric and Gas Company of New Jersey, is shown in Fig. 1. The auxiliary generator on many systems is replaced by a transformer connected directly to the generator leads. In starting or shutting down generating units, the auxiliaries are transferred between the two sources of auxiliary power, and this routine or normal transfer may be made either by paralleling, in which case there is no problem of interruption of the auxiliaries, or by the interrupted source method. An automatic transfer, however, made in case one source fails, must be by the interrupted source method, and many have elected to use this method for both the normal and automatic transfers. As the conditions under which an automatic transfer are made may be the most severe, and as a scheme which will be successful under these conditions will also suffice for the routine or normal transfer, the contents of this paper refer in general to the emergency conditions.

To inaugurate an automatic transfer, it is necessary to recognize that the normal source has failed or is about to fail. Any scheme used should, as far as possible eliminate the probability of a throwover due to temporary conditions that will be rectified before the auxiliaries are adversely affected. When a fault occurs on the auxiliary generator, or the auxiliary transformer, or their leads, the operation of the differential relays or other protective relays on this equipment is an indication that the source is lost. These same relays can be connected to trigger the throw-over. Under this condition, there is no difficulty in recognizing the failure of the source. There are other conditions necessitating a throwover that are not so easily recognized, and a period of time that may be called the recognition period must be allowed to determine if the condition warrants a transfer.

This period is from *A* to *B* in Fig. 2, which shows the voltage-time relations during an interrupted source transfer that is caused by a slowly decreasing source voltage. Low voltage due possibly to a prolonged system disturbance, that would persist long enough to adversely affect the auxiliaries, should cause a throwover. On the other hand, low voltage due to a faulted motor or transmission line that will be remedied quickly by protective devices, or the voltage drop due to starting a large motor, should not cause a throwover. This recognition time varies according to the protective relay settings and other reasons, but in general may be several seconds.

When low voltage has persisted until the triggering relay operates, the circuit breaker to the source in trouble is tripped. This time is designated by *B* on the curve. While the breaker to the new source may now be closed without intentional time delay, Fig. 2 is based on a transfer scheme that prohibits the closing of the breaker to the new source until the residual voltage has decayed to 25 per cent (%), so that there is no possibility of the inrush current damaging the motor windings.

The curve from *B* to *C* indicates the decay of the residual voltage during the transfer from one source to the other. This transfer time is sometimes referred to as dead time. With motors of 1,800 rpm and below, the residual voltage will probably reach 25% in 30 to 35 cycles. With the addition of a large 3,600-rpm motor connected to this same bus, the residual voltage may take from 60 cycles to 100 cycles to decay to the same value. At *C* the breaker to the new source closes, the motor inrush current reduces the new source voltage, and then as the motors accelerate the voltage recovers until the normal value is reached at *D*. The total time that the motors are subjected to low voltage is from *A* to *D*, and if this is too long, or the average voltage too low, the auxiliaries will cease to function properly.

The maximum permissible time for the interval *A* to *D* depends on the characteristics of the auxiliaries and varies with the particular unit; but with present-day boilers fired by pulverized coal, the mills and exhausters are the determining factor. As the mills and exhausters decelerate, they reach a speed where they no longer supply the proper ratio of air to fuel to support combustion. When this occurs, the mills and exhausters must be shut down immediately, for if the flame is extinguished and voltage is then restored to the motors, unignited fuel will be blown into the furnace, with the possibility of a disastrous explosion.

As yet there is no generally accepted direct sensing device to detect flame instability or even the point of extinction, so it is customary to monitor the flame indirectly by the condition of the bus voltage. An undervoltage relay is timed to shut off the fuel supply before the flame would be extinguished upon the total loss of voltage. This time can only be determined by test, and as this point of flame extinction varies somewhat with the load, air-fuel mixture, nozzle conditions, etc., the full test time cannot be relied on for the relay timing and a factor of safety should be allowed.

Four 110,000-kw units, one at Essex Generating Station and three at Sewaren Generating Station, were equipped with ball mills with separate motor-driven exhausters, and tests showed that the flame did not become unstable for at least 30 seconds after the mills and exhausters were tripped. Setting the loss of flame relay for 15 to 18 seconds permitted an ample factor of safety and adequate time for the three steps of the transfer. With a relay blocking the closure of the new source breaker until the residual voltage had dropped to 25%, dead times of 50 to 90 cycles were obtained, and the operation has been satisfactory. To test the action of a source refusing to pick up the auxiliary load, a bus was transferred to the auxiliary generator with the generator's regulator out of service; the generator's voltage was

---

Paper 55-92, recommended by the AIEE Power Generation Committee and approved by the AIEE Committee on Technical Operations for presentation at the AIEE Winter General Meeting, New York, N. Y., January 31–February 4, 1955. Manuscript submitted December 2, 1954; made available for printing April 20, 1955.

L. E. Backer, Paul Barth, R. A. Huse, and D. W. Taylor are with the Public Service Electric and Gas Company, Newark, N. J.

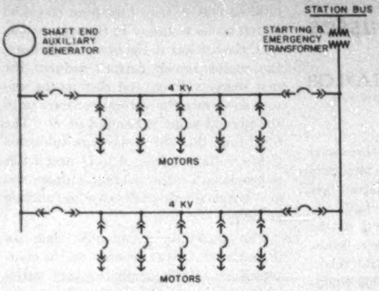
SHAFT END AUXILIARY GENERATOR
STATION BUS
STARTING & EMERGENCY TRANSFORMER
4 KV
MOTORS
4 KV
MOTORS

Fig. 1 (above). Typical 1-line diagram, 4-kv auxiliaries

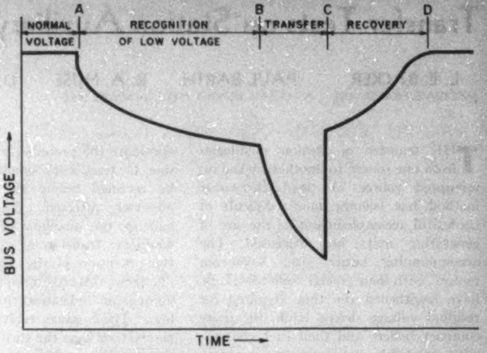

Fig. 2 (right). Voltage-time relations during transfer

allowed to decrease until the recognition relay operated and the bus was automatically transferred back to the transformer. This was accomplished without any noticeable effect on the operation of the main unit.

On the last two 145,000-kw units at Kearny Generating Station, the pulverizers were of the bowl type, and the exhausters were connected to the same motor as the pulverizer. They had relatively low inertia, and the flame became unstable in 10 seconds after the motor circuit breakers were tripped, which left insufficient time for the three steps of the transfer with a reasonable factor of safety. Also, the boiler water circulators and other auxiliaries on the units, while not as critical as the mills and exhausters, were approaching them in sensitivity to low voltage, and it seemed probable that as the size of units increased, greater difficulty might be encountered in effecting dead throwovers. It was therefore thought desirable to study the possibility of reducing the over-all time of the disturbance during transfer and, at the same time, limit the inrush current to reasonable values.

To study the factors affecting an interrupted transfer, a series of oscillograph tests was run on the two 145,000-kw units at Kearny Generating Station. While many of these tests are similar to those given in previous papers,[1] the Kearny tests are indicative of the results obtained with larger size motors.

Table I gives the auxiliary motor data for the 145,000-kw unit at Kearny Generating Station. The auxiliary supply data are as follows: For the auxiliary generator, 12,500 kva; 10,000 kw; 0.80 power factor; 4,160 volts; 1,735 amperes; 0.98 short-circuit ratio; $T_{d0}' = 4.85$ seconds; $T_d' = 0.52$ second; $T_a = 0.14$ second; $X_d = 128\%$; $X_{d(\text{sat.})}' = 13\%$; and $X_d'' = 10.2\%$. For the starting transformer: 9,000 kva, oil-immersed, self-cooled; 13,800-4,160 volts; impedance is 5.7% at 9,000 kva; and system impedance is 1.0% at 9,000 kva.

The voltage drop and current inrush that are occasioned by the starting of a 3,000-horsepower 3,600-rpm boiler feed pump motor together with its 600-horsepower 1,200-rpm condensate pump motor (both connected to the same breaker) are shown in Figs. 3 and 4. While the voltage drop is not excessive, these tests were made with normal bus voltage. As motors should be capable of starting with the bus voltage less than normal, a drop to 70% may occur under these conditions, particularly when started from the auxiliary generator. A recognition period of at least 2 to 3 seconds would be required if starting with 90% normal voltage was necessary.

The effect of variations in the dead time on the recovery time is shown in Fig. 5. For curve *A*, the new source breaker is closed when the residual voltage has dropped to 18%, for curve *B*, 40%; and for curve *C*, 72%. There was no intentional time delay for curve *C*, the interval between the opening of the one breaker and the closing of the other breaker being approximately 12 cycles. It is noticed that for curve *A* the voltage returns to 90% of normal in about 3.5 seconds; curve *B*, 2.4 seconds; and curve *A*, 0.4 second.

A further study of the decay of residual voltage is given in Fig. 6. The decay of residual voltage where only motors of 1,800 rpm or less are involved is shown in curve *A*. A voltage of 25% is reached in

Table I. Auxiliary Motor Data, 145,000-Kw Unit at Kearny

Motors	Boiler Feed Pump	Induced Draft Fan	Forced Draft Fan	Exciter	Condensate Pump	Circulating Pump	Mill and Exhauster	Gas Recirculating Fan	Boiler Recirculating Pump
No. of motors	2	2	2	1	2	2	4	2	2
Horsepower of each	3,000	1,500	1,500	675	600	350	350	250	350
Rpm	3,585	880	1,192	895	1,193	390	1,750	890	1,174
Volts	4,160	4,160	4,160	4,160	4,160	440	440	440	440
Amperes	370	195	187	88.5	75	480	411	304	401
Kva	2,670	1,410	1,350	640	540	366	314	232	306
Locked rotor amperes	2,100	1,075	1,030	950	425	3,000	2,950	1,550	2,160
Open-circuit time constant, seconds	4.45	0.544	1.90	1.20	2.10	0.219	0.35	1.06	0.60
Short-circuit time constant, seconds	0.220	0.028	0.09	0.0408	0.088	0.024	0.015	0.0367	0.0267
H, kw-seconds per kva	1.8	3.0	3.2	3.5	0.70	0.60	5.6	11.9	1.35
Motor kw at 145 mw	1,760	0	1,030	340	415	172	218	192	196

Note: The table does not include spare motors. Boiler normally pressurized, induced draft fan not used. Miscellaneous other load 880 kw or approximately 9% of total.

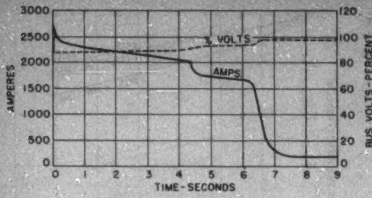

Fig. 3 (left). Start of 3,000-horsepower boiler feed pump and 600-horsepower condensate pump on unloaded starting transformer

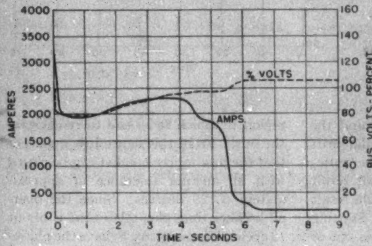

Fig. 4 (left). Start of 3,000-horsepower boiler feed pump and 600-horsepower condensate pump on auxiliary generator (1.7-mw initial load) with voltage regulator

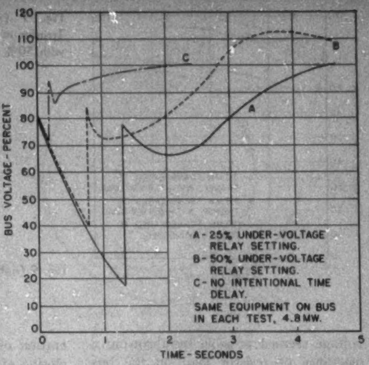

Fig. 5 (above). Transfer to auxiliary generator and recovery

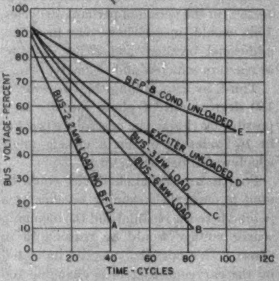

Fig. 6. Residual voltage decay during transfer

33 cycles. The boiler feed pump motor, with its condensate motor without any additional motors connected to the bus, results in curve *E*, where in 100 cycles the residual voltage is only down to 52%. Combining all the motors on a bus with a load of 3 megawatts (mw) results in curve *C*, where the 25% point is reached in 77 cycles. This same bus loaded to 6 mw, which is equivalent to approximately 150 mw on the main unit, results in the voltage decaying along curve *B* with the 25% point being reached in 65 cycles. As a matter of interest, inasmuch as separate motor-driven exciters are used, the exciter voltage decrement curve is shown by curve *D*. While it is usual to have at least two feedwater pumps in operation, at light loads only one may be in service, so a variation from curve *A* to curve *C* is possible under the normal range of operating conditions.

Fig. 7 shows the variation in the voltage recovery with different auxiliary loads. With an auxiliary load of 3.1 mw, the transfer from the auxiliary generator to the transformer results in curve *A*; with 5.3 mw, curve *B*; and with approximately full load of 11.7 mw (two busses), which corresponds to full load on the unit, the voltage recovery is shown by curve *C*. The voltage recovery in transferring from the transformer to the auxiliary generator is shown in Fig. 8. Inasmuch as there is no emergency or automatic transfer from the transformer to the auxiliary generator, only one-half of the auxiliary load, or one bus, would ever be transferred at one time. Curves *B* and *C* represent the full-load condition, the difference being that curve *B* is a transfer to an unloaded generator, while curve *C* is the transfer of one bus to the generator when the generator is already carrying the other bus with approximately the same load as the bus being transferred.

The deceleration of the motors during the period that they are without any source is given in Fig. 9. With the heavily loaded bus (6 mw) the frequency dropped 10% in 30 cycles and 16% in 60 cycles.

The angular displacement between the residual voltage of the decelerating motors and the initial source voltage is shown in Fig. 10. In the case of a heavily loaded bus (6 mw), the two voltages are 180 degrees apart in about 13 cycles and back in phase in 21 cycles. With the lightly loaded bus (3 mw) the voltages are 180 degrees out of phase in 20 cycles, and they are back in phase in 29 cycles. The slopes of the curves are quite similar after 200 degrees. A number of tests confirmed the fact that these two curves form the limits over the operating range of the main units. Calculations indicated that if the circuit breaker to the new source could be closed within ±90 degrees from the in-phase position, the inrush current would not exceed the locked rotor current at 110% impressed voltage. Tests made with a 10-cycle dead time resulted in inrush currents of 6,500 rms amperes at a phase angle of 60 degrees, 7,100 rms amperes at 90 degrees, and 13,700 rms amperes at 150 degrees. In the last case, the inrush current was about 40% greater than rated locked rotor current.

The most practical way of reducing the total time that the auxiliaries are subjected to less than normal voltage is to reduce the time of the dead period; several means were considered, four of which are discussed now.

First, it is evident from the deceleration curves of Fig. 10 that if the dead period could be reduced to about 3 cycles, the angular drift in that time would be negligible. To accomplish this, however, would mean either relying on electric interlocks and the assurance that the first source breaker would trip in all cases, or a mechanical tying of the two breakers together to form, in effect, a double-throw circuit breaker. The electric interlock was considered too risky, and combining the two mechanisms to form one breaker too impractical with conventional bus layouts.

Second, a quick reduction in residual

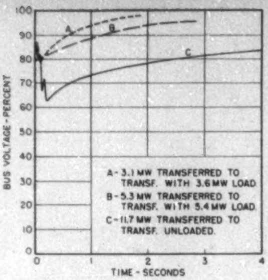

Fig. 7 (left). Voltage recovery. Transfer to starting power transformer with 50% undervoltage relay setting

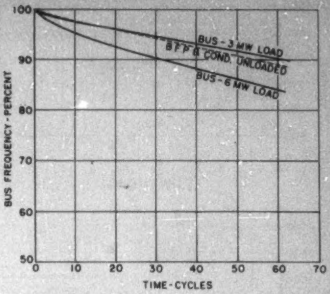

Fig. 9 (right). Bus frequency during transfer

voltage seemed possible by throwing a reactance or resistor load on the bus during the dead period. It is calculated that a limited short circuit could be designed to reduce the residual voltage to 25% in the period of perhaps 10 cycles. This would mean, however, installing additional breakers and either resistors or reactors, which would be costly.

Third, by establishing the two sources 180 degrees out of phase initially it is possible by closing the new source breaker in 16 cycles to obtain a closing angle which would be satisfactory.

Fourth, a phase-angle device could be used to close the incoming breaker at a point where the residual and the incoming source voltage would be reasonably in phase. The angular velocity indicated by the curves of Fig. 10 is changing too rapidly to permit the safe operation of an actuating device in the first 200 degrees. However, beyond this point the variation in angular velocity is greatly reduced and the use of such a device is feasible. Inasmuch as there is an interval of 10 cycles between the operation of the actuating device and the closing of the breaker, the angular drift during this period caused by the variation of auxiliary load should not result in a closure at an angle that would result in excessive inrush current. Starting with the two sources 180 degrees out of phase, and skipping the first in-phase point, it was thought possible that a relay could trigger the incoming breaker 10 cycles ahead of the second in-phase point. This delay would result in a dead period of 30 to 35 cycles, which has the additional advantage of increasing the leeway in the closing angle because the residual voltage has decayed to a lower value.

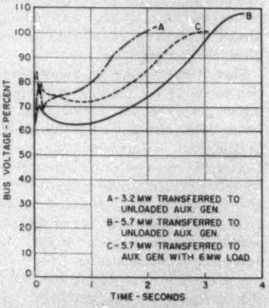

Fig. 8. Voltage recovery. Transfer to auxiliary generator with 50% undervoltage relay setting

The phasor diagram shown in Fig. 11 illustrates the relationship between a new source voltage E_t, residual bus voltage E_b, and equivalent motor voltage IX_m. In normal operation, the source reactance is approximately one-quarter of the total motor reactance based on locked rotor current values. From the diagram it is seen that, if the terminus of the residual bus voltage phasor lies on the arc or to the left of a circle drawn about 0 as its center and with a radius of 1.38 per-unit voltage, the motor inruch current will not exceed 110% of rated locked rotor current. It is recognized that this is only an approximate relationship since the residual voltage of individual motors does not necessarily coincide with the bus voltage, nor do their locked rotor currents vary linearly with applied voltage.

Fig. 12 is a polar representation of residual voltage, both as to magnitude and phase angle as a function of time. In this case, the bus is being transferred from the generator to the transformer. An arc with a radius of 1.38 per-unit voltage, Fig. 11, has been drawn with the terminal of the transformer voltage phasor as a center. The area to the left of this arc *AA'*, Fig. 12, represents the region in which it is safe to re-energize the bus. From this figure it is apparent that the new source breaker can be closed with an angular tolerance of approximately ±120 degrees. Since the overall breaker time plus relay time is about 12 cycles, it is necessary to have the phase-angle detection relay set to operate at a corresponding angle ahead of the incoming bus. For Kearny Generating Station, this angle has been established as 325 degrees.

Figs. 13 and 14, based on test data, show the performance which can be expected under the limits of light and heavy load operation, taking into account the shift in initial phase angle and the angular drift during the time of relay operation. These indicate that the angular deviations will not exceed 110 degrees. For light load operation, the reclosing angle is only 75 degrees ahead, whereas for heavy loads the angle is 110 degrees behind. This was done to minimize the inrush current since at light load the residual voltage is higher and the source impedance drop less.

In applying the foregoing to scheme 3 which has a 16-cycle dead period, closure of the new source circuit breaker

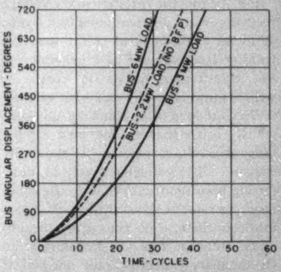

Fig. 10. Bus angular displacement during transfer

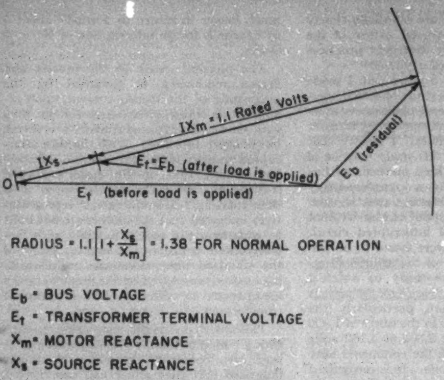
IXm = 1.1 Rated Volts
IXs
Et = Eb (after load is applied)
Eb (residual)
O
Et (before load is applied)
RADIUS = 1.1 [1 + Xs/Xm] = 1.38 FOR NORMAL OPERATION
Eb = BUS VOLTAGE
Et = TRANSFORMER TERMINAL VOLTAGE
Xm = MOTOR REACTANCE
Xs = SOURCE REACTANCE

Fig. 11. Relationship between source voltage, residual voltage, and equivalent motor voltage

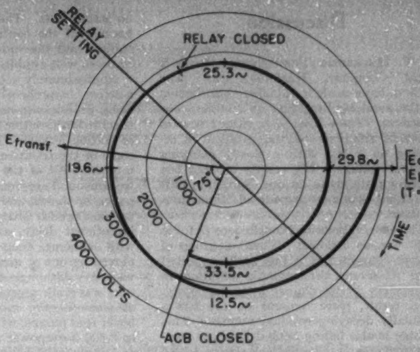
RELAY SETTING
RELAY CLOSED
25.3~
Etransf.
19.6~
29.8~
Egen
Ebus
(T=0)
75°
1000
2000
3000
4000 VOLTS
33.5~
12.5~
TIME
ACB CLOSED

Fig. 13. Transfer of 3 mw, light load on main generator

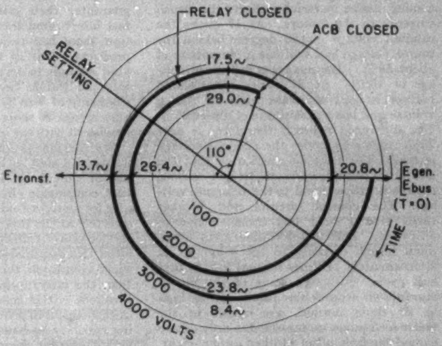
RELAY CLOSED
ACB CLOSED
RELAY SETTING
17.5~
29.0~
110°
13.7~
26.4~
20.8~
Etransf.
Egen.
Ebus
(T=0)
1000
2000
3000
4000 VOLTS
23.8~
8.4~
TIME

Fig. 14. Transfer of 6 mw, heavy load on main generator

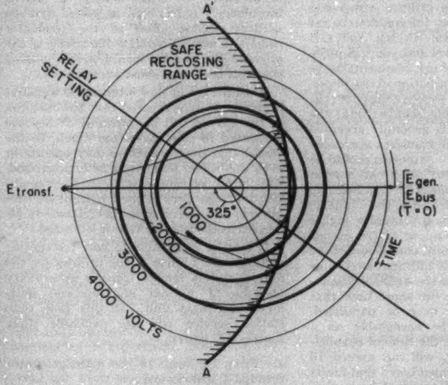
A'
SAFE RECLOSING RANGE
RELAY SETTING
Etransf.
Egen.
Ebus
(T=0)
325°
1000
2000
3000
4000 VOLTS
TIME
A

Fig. 12. Typical transfer indicating relay operation zones and safe reclosing range

would result in a satisfactory inrush current provided the two source voltages were initially within ±50 degrees. For all normal operating conditions, variations in angle between the sources are within the limits just given; however, in the case of a system split, it is possible for the angle to be greater. Under these extreme conditions, a lockout relay would be required to block reclosure, and reclosure would be made by a residual voltage relay set at 50%. Slightly higher inrush currents might be realized under these unusual conditions.

While scheme 3 is still under consideration, a trial installation of scheme 4 is proceeding. Various types of relays were considered, and the stock relay that was thought to be applicable was the Westinghouse type *H-3*. This relay, with voltage coils substituted for current coils, was tested in the laboratory and installed at Kearny Generating Station. An oscillograph test was run on a simulated throwover, but instead of the relay actually closing the breaker to the new source the relay energized a time trace on an oscillograph. The results of this test confirmed previous tests of phase-angle relay operation. The incoming breaker would have closed within 10 degrees of the incoming source. Additional relays are now being installed so that each of the two busses on one unit is equipped with two relays. The previous residual voltage relay that blocked the closing of the breakers to the new source has been reconnected in parallel with the contacts of this phase-angle relay and reset for 50% voltage instead of 25%. In case the phase-angle relay fails to close the breaker by the time the residual voltage has dropped to 50%, the voltage relay will operate.

It is believed that these tests on phase-angle displacement have indicated the practicability of closing in on the new source by means of a phase-angle relay or similar actuating device sufficiently close to the in-phase point so that a successful and relatively fast throwover can be obtained without damaging the motors.

Reference

1. Bus Transfer Tests on a 2,300-Volt Station Auxiliary System, A. A. Johnson, H. A Thompson. *AIEE Transactions*, vol. 69, pt. I, 1950, pp. 386-94.

Discussion

W. F. Mackenzie (Pennsylvania Power & Light Company, Hazleton, Pa.): The authors have made a valuable contribution to the available literature on auxiliary bus transfers. They have also offered several practical solutions to the problem of reclosing on a bus with a slowly decaying residual voltage. The results of dead bus transfer tests made on our Sunbury Unit 2 in April 1950 may provide additional useful data.

The observations and conclusions of these tests are as follows: When a group of motors connected to a bus is disconnected from its source, the magnetic conditions in the motors do not change instantaneously. As a result, there remains on the bus a gradually decaying residual voltage. This voltage is also falling behind in phase position with respect to its 60-cycle source. The magnitude and phase angle of this residual voltage at the time of closure to the incoming source materially affects the inrush currents to the motors. At 17 cycles the residual voltage is 180 degrees behind the source voltage and still has a magnitude of about 50%. This makes a difference voltage of 150%. At 27 cycles the residual voltage is back in phase with the source voltage and has a magnitude of about 25%. The difference voltage, therefore, is only 75%. After 38 cycles the residual voltage is zero. The tests also indicated that the maximum inrush currents to the various motors is proportional to the difference voltage. The control circuits and breaker times give a dead bus transfer time of 15 cycles. This transfer time gives maximum inrush currents to the 4-kv bus of approximately 14 times normal for the first half cycle. Although some of the inrush currents to a particular motor ran as high as 27 times normal, the inrush to the boiler feed pump motor was the only one to exceed the fully offset blocked rotor current. With the addition of a fixed time relay to increase the dead bus time to 27 cycles the macimum inrush current to the bus was practically halved. The inrush to the inindividual motors was reduced correspondingly. Although these transfer tests indicated the advantage of the longer transfer time, no additions have been made at Sunbury to insert additional time delay and at the present time all of the 4-kv busses still have a dead bus transfer time of 15 cycles. During the tests dead bus times as long as 60 cycles were attempted without adverse effects on plant operation.

All units at Sunbury have been using this nondelayed transfer initiated by the generator and transformer protective relays only, since the installation of the various units the number of transfers has been quite high since relay operation is usually checked when the units come off the line. To date we have experienced no motor difficulties resulting from excessive inrush currents.

J. Curtis Hoyt (Gilbert Associates, Inc., New York, N. Y.): This paper and the paper listed as reference 1 of this discussion present a valuable addition to the literature on this subject and are particularly complementary because the one paper is primarily theoretical and the other is primarily based on actual tests. They are especially timely because of the controversial nature of the subject and the widely divergent practices or large, well-established utilities.

Approximately 4 or 5 years ago, I made a rather comprehensive study of actual operating practices in several utilities with respect to both routine and emergency transfer of station auxiliary busses. I believe that some of the results of this study may be of interest. All of the three methods of bus transfer enumerated in a complementary paper by Lewis and Marsh,[1] that is, continuous circuit, interrupted circuit without intentional delay, and interrupted circuit with deliberate delay were found to be employed by one or more of the utilities interviewed. Although the study to which I refer was made several years ago, the ratings of some of the motors, particularly the boiler feed pumps, were in the range of 1,500 to 2,500 horsepower at 2,300 or 4,160 volts and therefore I believe the comments may be applicable at this time. It is recognized that motor manufacturers are reluctant to guarantee their products when used with fast interrupted transfers or to recommend that these fast transfers be used for their products. One of the utilities which was kind enough to furnish information to me was the Public Service Electric and Gas Company of New Jersey and you will probably recognize some of my comments to be consistent with the information in this paper.

For routine station service transfers, that is, when a unit is being brought onto the line or shut down, it is generally accepted that continuous circuit transfers are desirable for many reasons. Attention should be directed to the fact that when two station service power transformers are paralleled to effect this continuous transfer, the available short circuit on the bus is usually higher than the interrupting rating of the circuit breakers. It is generally considered to be uneconomical to provide sufficient interrupting capacity to handle the available short-circuit current during the short time that the two transformers may be paralleled. Although this may be acceptable as a calculated risk because the time of paralleling, in all probability, will not exceed 10 seconds, it should be remembered that faults such as in cables and terminal boxes frequently occur during switching operations. Also, the hazards of switching errors and their consequences are increased by paralleling procedures.

Available oscillographic records at the time of my study indicated that the residual voltage was 180 degrees out of phase with the source after 13 to 18 cycles following source interruption. This checks very closely with the 20 cycles mentioned in the paper. Therefore, with a fast interrupted transfer the current inrush is very high, generally 12 to 15 times normal current. There is at least one oscillogram available taken on a motor-driven exciter which shows a value as high as 19 times rated current. It should be pointed out, however, that these high inrushes exist only during the first half-cycle of re-energization, after which the current reduces rapidly to values consistent with normal motor accelerating current values and the system returns to normal in about 1 second. For a delayed interrupted transfer the initial inrush may be only about equal to normal starting current values but the system takes much longer to return to normal—about 3 to 4 seconds for an interruption of 50 to 60 cycles.

The physical shock to the motors and driven machinery is governed by the magnitude of the inrush current upon reapplication of the power source voltage, thus with the fast interrupted transfer it is severe but of short duration. With the slow interrupted transfer its magnitude and duration approximate that of the motor's normal starting characteristics at the speed it is then rotating. Manufacturers' representatives indicated that the motors are not built to withstand the shocks possible with fast interrupted transfers. However, some of the standard reduced-voltage motor-starting methods employed by the manufacturers incorporate, in effect, a fast interrupted transfer step.

This shock conceivably may cause damage over a period of time. The experience of at least two operating companies, however, indicated that they either had experienced no failures of their motors or they had not found any damage traceable to this cause. They had not been able to find any evidence of ill effects to either motors or driven machinery. It has been suggested that the natural cushion effect of the conductor insulation acts to mitigate the effects of the physical shock and it should be remembered that this is of very short duration.

With the use of slow interrupted transfers it should be remembered that the function of the motors will be impaired if they are permitted to slow down too much, to the extent that pressure relays may operate or even the burner flame may be extinguished. This latter, of course, is an extreme condition but regardless of the length of transfer interruption the system disturbance is increased as the transfer time is increased.

It may be interesting to note the specific method used by one of the utilities for the normal station service transfer upon every occasion of normal start-up and shut-down of a main unit. In this case, each station service bus has available three sources of power:

1. From the leads of the main generator through a transformer.

2. From a high-voltage bus through a transformer.

3. From a station service quick-start steam-turbine-driven auxiliary generator.

Three control switches are placed adjacent to each other, each to control one of these source breakers. The circuitry is so designed that regardless of whether one or more of these circuit breakers is closed when it is desired to close a circuit, the operation of its associated control switch to the "close" position will first trip any source breakers which are then closed, other than its associated breaker, and upon completion of interlocking circuits through normally closed auxiliary switches the closing circuit of the associated breaker is energized and the breaker closed. It is hardly conceivable that any faster means of interrupted transfer could be designed while still maintaining the safety provisions of interlocking, and yet this is one of the companies which reported that it was unable to find any evidence of damage in any motor or driven equipment traceable to fast interrupted transfers.

REFERENCE

1. TRANSFER OF STEAM-ELECTRIC GENERATING-STATION AUXILIARY BUSSES, D. G. Lewis, W. D. Marsh. *AIEE Transactions*, vol. 74, pt. III, June 1955, pp. 322–30.

J. H. Kinghorn (American Gas & Electric Service Corporation, New York, N. Y.): The authors have made a worth-while contribution to the literature on auxiliary bus transfer schemes. While they have made an intriguing case for scheme *4* it seems to the writer that they have passed too lightly over scheme *3*.

The principal objection to scheme *4* is the fact that it depends upon the positive action of a phase-angle measuring relay. For the case illustrated, where the incoming transformer is initially 180 degrees out of phase with the bus, it would appear that the relay is within its contact closing zone at the instant the source breaker opens and additional interlocking might be needed if closure is not to be initiated until the instant shown. Dependence on the relay and perhaps additional devices reduces to some degree the reliability of the scheme. This is apparently recognized by the authors in including an undervoltage relay should fail. It must be realized, however, that under such a condition the advantage of the shorter dead time has been lost.

On the other hand, scheme *3* could readily be applied to the case illustrated by simply providing the device initiating a transfer with multicontacts and permitting one to trip the normal supply while the other energizes the closing circuit of the emergency supply. If this causes the emergency supply to close too quickly a single auxiliary relay could be interposed to delay the action any amount desired. This scheme could probably not be so readily applied when the incoming transformer and bus are initially in phase if conditions of lightly and heavily loaded bus are both to be met. In this case a compromise might be made by using the scheme only for emergency transfer and assuming that this would not occur during light load conditions. If it is felt such an assumption is unjustified, the phase-angle device appears to offer a solution. Normal operation with bus and emergency source initially in phase is preferred by many people because it permits paralleling of sources as the method of transferring for all except emergency conditions.

Consideration needs also be given as to whether an undervoltage recognition scheme for initiating a transfer is of much practical value for the particular switching setup being used. It is necessary to determine what conditions can cause undervoltage, how they are detected, and whether the emergency source will be affected in the same way. As an example, a setup similar to Fig. 1 in the paper, but with the normal supply consisting of a transformer connected directly to the main generator leads in place of the auxiliary generator, is widely used. Undervoltage can occur on the auxiliary bus because of a fault in the main generating unit or its associated transformers, or because of loss of main generator excitation. In both cases primary protective relays should detect the trouble quickly and could initiate the transfer. It can occur because of some abnormal system condition which reduces the generator terminal voltage. In this

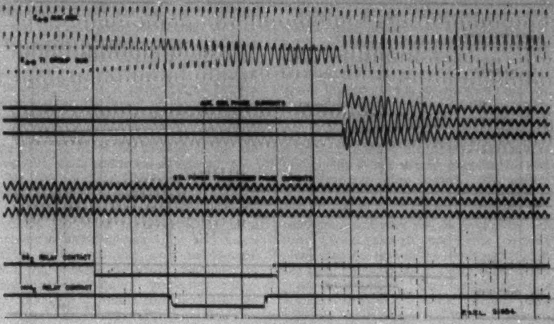

Fig. 15. No. 7 generator throwover test at light load. Test 7: transfer of 71 group bus to auxiliary generator

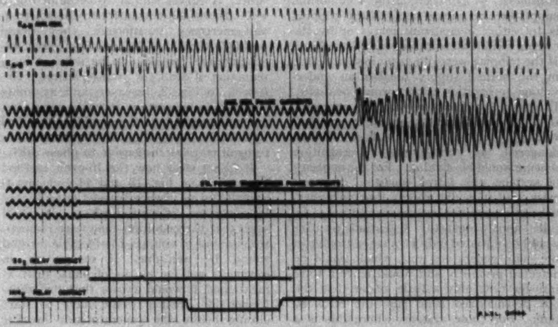

Fig. 16. No. 7 auxiliary generator throwover test at light load. Test 10: transfer of 71 group bus to auxiliary generator

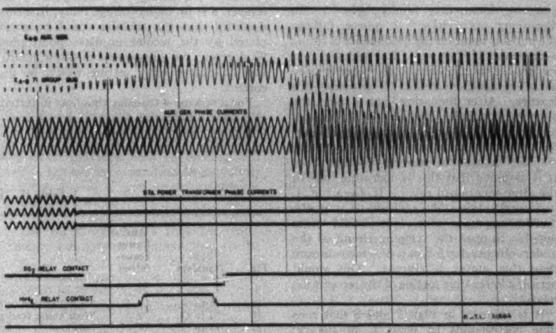

Fig. 17. No. 7 auxiliary generator throwover test at full load. Test 2: transfer of 71 group bus to auxiliary generator

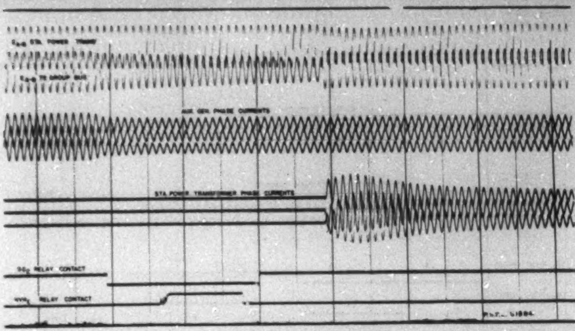

Fig. 18. No. 7 auxiliary generator throwover test at full load. Test 3: transfer of 72 group bus to station power transformer

case analysis may show that the emergency source will be similarly affected and transfer is useless. It can occur if the 4-kv normal supply breaker should trip. If this tripping is by either overcurrent relays or by the control switch no transfer would be desired. If the tripping were due to an insecure latch in the normal supply breaker an undervoltage recognition scheme would be useful. If system conditions require the generator to absorb reactive and so reduce its terminal voltage to a point where auxiliaries are endangered an undervoltage recognition scheme would be of value. For the majority of systems this latter condition does not exist, and it would appear that an undervoltage recognition system would never be called upon to operate. Essentially transfer would be initiated only because of trouble in the main generating unit, which would be detected promptly and would leave a total transfer time only a little longer than the bus de-energized time plus the recovery time. For those systems where this is a practical approach there should be little difficulty in obtaining a total transfer time well within the boiler limitations.

Arnold R. Kelly (Esso Research and Engineering Company, Linden, N. J.): In discussing recognition of source failure, the authors mention the desirability of riding over temporary failures. It is assumed that an inverse-time undervoltage relay is used as a recognition relay to provide this feature. After discussing Figs. 3 and 4, the authors conclude that 2 to 3 seconds recognition time would be required for starting under 90% voltage, to prevent initiating transfer because of starting voltage drop. It is assumed that this is operating time of the afore-mentioned relay. If, from Fig. 4, it normally takes $5^1/_2$ seconds to start the 3,000-horsepower motor, it would seem possible to open the tripping circuit of the undervoltage relay for, say, $6^1/_2$ seconds each time this motor is started. This would permit a lower time setting of the recognition relay.

It is assumed in Figs. 7 and 8 that zero time corresponds to point *C* of Fig. 2; also, that the 50% relay setting mentioned in the captions of Figs. 7 and 8 refers to the residual voltage just prior to zero time.

It is stated that the most practical way of reducing total time is by reducing "dead" time. If curves similar to those of Fig. 5 were drawn for a transfer to the starting-and-emergency transformer, they would probably show that the recovery (or reaccelerating) time would also be reduced by a reduction of dead (or transfer) time. Referring to Fig. 2, however, and assuming that it is in proportion, it would seem that an equal gain in total time could be obtained by reducing recognition time, perhaps by a recognition relay responsive to phase drift.

It is not clear how the 16-cycle method (scheme *3*) or Fig. 13 and 14 (scheme *4*) apply to an emergency transfer not initiated by generator differential relays. It would seem that if recognition time were required to sense loss of voltage, the 16-cycle method would be unusable. If recognition in scheme *4* was by means of phase drift as mentioned, it would appear that the transformer-side breaker would have to start closing before the generator-side breaker could open. Since this would preclude closing the former breaker through a *b* contact of the latter, it would appear that the difference between breaker tripping and closing times would have to be depended on to prevent paralleling. If recognition in scheme *4* is by undervoltage relay, it seems doubtful that the transfer could be completed by the second in-phase point plus 90 degrees; for subsequent in-phase points the 325-degree relay setting would be incorrect.

For a scheme *4* transfer that was initiated generator differential relays, it seems probable from the motor short-circuit time constants that "dead-time" voltage would be too low to actuate the phase-angle relay. In this case, transfer would be completed by means of the residual voltage relay.

From the foregoing, it would seem that the phase-angle relay is useful only for manually initiated "dead" transfers.

It is wondered why the residual voltage relay settings were raised from 25 to 50%. By the same reasoning as in Fig. 11, the maximum safe setting would be 38%. Conversely, if 50% is safe for the residual voltage relays, corresponding to $IXm = 1.2$, the arcs in Figs. 11–14 could be drawn at radius 1.5.

The authors are to be congratulated on the inspired use of polar representation in Figs. 12, 13, and 14. These diagrams present an exceptionally clear picture of the transient phenomena occurring during transfer.

S. B. Griscom (Westinghouse Electric Corporation, East Pittsburgh, Pa.): This paper is a most comprehensive and informative work on the subject of power house auxiliary transfer. The test data of Figs. 1 to 9 the of great value to the industry, since it is virtually impossible to calculate the resultant characteristics of the various combinations of motors and driven loads.

The curves of Fig. 6 and Fig. 10 are of particular interest. The data so given, analyzed by the procedure of Fig. 11, enable the safe reclosing range of Fig. 12 to be determined. One of the most interesting facts pointed up by the authors is that reclosing in a time of the order of 1/2 second is feasible, if the exact time of energizing the closing coil is varied slightly in accordance with phase angle. So doing permits the use of conventional switchgear while at the same time avoiding inrush currents exceeding the motor capabilities.

The use of alternate sources having a 180-degree displacement is novel and at first glance perhaps a little startling. However, when it is considered that the two sources cannot be paralleled anyway, there seems no fundamental reason why the two busses should not be set up 180 degrees apart.

On the basis of the data presented, the fourth scheme has considerable merit. This sort of problem has many intangibles and the operating record of a trial installation would be of great interest.

Paul Barth: At the time of the writing of the paper, we expressed our intention to make a complete, fast controlled angle-reclosing installation on one of the 145-mw units at Kearny Generating Station. This has been completed and tests have been conducted to verify anticipated results.

Table II. Results of Tests

Fig.	Bus Transfers	Aux. Power Transferred	Notes	Angle HV4* Closed Deg.	Angle ACB Closed, Deg.	Time of Transfer (Cycles)	Initial Peak Current†
15	71 to G	1.4	No boiler feed pump	68	85 before	35	0.48
16	71 to G	2.5	With boiler feed pump	75	80 before	38	0.23
17	71 to G	5.0	Full load	90	5 after	31	0.21
18	72 to T	5.7	Full load	92	0	$30^1/_2$	0.20

* Modified *HV3* Westinghouse relay was assigned *HV4* nomenclature in production.

† Ratio of initial peak current to the connected locked rotor peak asymmetrical.

Of 17 tests conducted, including extreme operating conditions, all results were consistent, satisfactory and as calculated.

The setting of the *HV4* relay is 38 degrees. From Table II the residual drifts from 30 degrees to 54 degrees during operation of the angle relay, depending on the rate of the residual voltage drift. The time of operation of the *HV4* relay beyond its setting is setting is slightly more than $1^{1}/_{2}$ cycles. Breaker closing times are consistent at 9.3 cycles.

D. W. Taylor: It is with considerable satisfaction that we have received these discussions with operating experiences, data, and problems.

The phase slip data from Sunbury Unit 2 given by Mr. Mackenzie and the phase slip data presented from Mr. Hoyt's investigation indicate consistency with our Kearny test data. Also, Mr. Mackenzie's and Mr. Hoyt's fast transfer results without controlled angle, 1/2 cycle, give inrush currents of the same magnitude as our test data. This resemblance would indicate sufficient similarity to conclude that the operating experiences of other utility companies are a comparative guide to these practices. Therefore a continued compilation of operating success as well as operating failures should be of considerable value as a future guide.

These discussers report they have found no cases of damage due to fast transfers. We know of the failure of a modern 2,000 horsepower motor during the last year. The company involved added a fixed time delay. We prefer not to take any chances on this point.

Mr. Hoyt aptly expresses the evaluation of the generally accepted continuous circuit transfer along with its advantages and disadvantages. We preferred to use the same interrupted source method for both the normal and emergency conditions.

Mr. Kinghorn expresses interest in scheme *3*. We agree that scheme *3* offers possibilities on a par with scheme *4*. We tried scheme *4* first as it appeared to be less dependent on the speed of closing of the circuit breaker and less critical to the rate of angular drift. On another installation late in 1955, where the breaker speeds are favorable, we intend to use scheme *3*.

Mr. Kelly and Mr. Kinghorn question the value of undervoltage as a source of relay information to initiate transfer. We too question the value of undervoltage as a measure of auxiliary instability and seek a better device, possibly even mechanical, that will reliably anticipate instability of performance. Primary protective relays are also used to initiate emergency transfer and the undervoltage relay is necessary to evaluate the recovery probability of the auxiliary generator under load and to detect field failure. However with a transformer instead of a house generator, we would use this same undervoltage relay to take care of a transfer necessitated by a system disturbance. In general we have our emergency source transformer connected to a different bus section than the main generator. There is a possibility, depending on the system connections, that a system disturbance would unduly lower the generator voltage, but would not so lower the voltage on the emergency transformer. So even though the main transformer was cut off its bus, the auxiliary load would be transferred to the emergency source, and the boiler would be purged, the water level maintained, and the boiler kept under control. In the case of cable feeds to industrial auxiliary power with the possibility of remote separation, then the phase drift relay mentioned by Mr. Kelly may be quite practical as a transfer initiator.

Referring to Mr. Kinghorn's comments that it would appear that an additional relay is necessary in scheme *4* to prevent the possible immediate closure of the new source breaker upon the opening of the normal source breaker, this is so but we do not use a time delay relay but a sequential arrangement of contacts with an auxiliary relay that serves the same purpose. Naturally any relay that is added is a possible hazard but this circuit is not overly complicated and the relays are fairly rugged. The undervoltage relay to initiate transfer was included mainly as a precaution to cover any conditions that were not discovered by our tests. Even though our tests covered many months, both in the laboratory and in the field, we could not possibly cover every operating condition. One such condition is a scrambled system. While normally there will only be a few degrees difference between any of our bus sections, our system has an occasion been split and we could not study nor predict the operation of the phase-angle relay if the emergency source was in no way connected to the generator.

Referring to Mr. Kelly's remarks, while it is possible to open the trip of the relay triggering the transfer during the starting period of a large motor and possibly lower the time setting of the recognition relay, this was not thought desirable. With a house generator there is a possibility that the voltage regulator will not function properly and the voltage of the generator will collapse as the motor is started. That is one of the occasions the throwover should function.

In closing, we are gratified that so many have shown such an interest in the topic and hope that as more tests are conducted, and more thought is given to the subject better schemes of fast transfer will result, as we believe the transfer problem will become more important as the size of generating units increase.

•

Two-Axis Method of Analyzing Electric Machines

K. Y. TANG
MEMBER AIEE

ROBERT L. COSGRIFF
ASSOCIATE MEMBER AIEE

FIG. 1(A) shows the basic 2-pole machine which will be analyzed. It consists of a stator with two windings displaced by an angle α. The two windings will be called the *A* and *B* windings and will have N_A and N_B turns. The conductors on the rotor are represented by the small circles.

The following assumptions will be made:

1. The air-gap flux distribution is sinusoidal.

2. The air gap is uniform.

3. The stator winding *B* may be divided into two quadrature windings as shown in Fig. 1(B) so that the B_x component will have $N_B \sin \alpha$ turns and the B_y component will have $N_B \cos \alpha$ turns. These two component windings with i_B flowing will give the same magnetomotive forces (mmf) along the *X* and *Y* axes as the original *B* winding in Fig. 1(A).

4. The rotor conductors may be represented by two groups of conductors, or the *X* and *Y* coils in Fig. 1(B), which are placed at space quadrature. Each of these two rotor coils will have N_R turns so that $N_R i_X$ will give the same rotor mmf along the *X* axis and $N_R i_Y$ will give the same rotor mmf along the *Y* axis as those produced by the actual rotor along the *X* and *Y* axes.

5. Saturation effect may be neglected.

6. Core loss may be neglected but it can be added at the input terminals.

By leaving the angle α between the windings *A* and *B* as a variable, various types of single-phase and polyphase machines may be analyzed. The positive senses of the different quantities are indicated in Fig. 1.

The purpose here is to obtain an equivalent circuit which may be applied to

---

Paper 55-276, recommended by the AIEE Rotating Machinery Committee and approved by the AIEE Committee on Technical Operations for presentation at the AIEE Middle Eastern District Meeting, Columbus, Ohio, May 4–6, 1955. Manuscript submitted January 31, 1955; made available for printing September 20, 1955.

K. Y. Tang and Robert L. Cosgriff are with Ohio State University, Columbus, Ohio.

This work was supported in part by a grant from the Ohio State University Committee for the Allocation of Research Foundation Grants in the aid of fundamental research. The writers wish to acknowledge the encouragement of Professor E. E. Dreese, Chairman of the Department of Electrical Engineering, and the co-operation of the Antenna Research Laboratory in the final preparation of the manuscript. Also, the authors are indebted to students for their helpful suggestions.

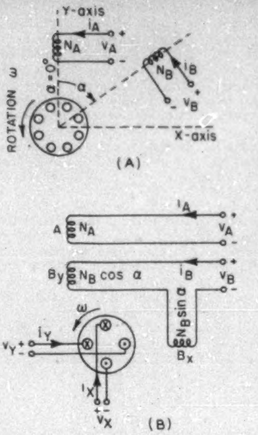

Fig. 1. A—Schematic diagram of basic machine. B—Modified diagram of basic machine

a-c machines. The equivalent circuit of each machine considered is obtained by the proper interconnections of the different parts of the derived network. The procedure is first to derive the four basic loop voltage equations for the four windings *A*, *B*, *X*, and *Y* in Fig. 1(B) and then from these equations to set up an equivalent circuit.

The balanced 2-phase induction motor, the capacitor motor, and the a-c tachometer will be considered to illustrate how the derived equivalent circuit may be modified (often simplified) to that of a specific machine. Also, it is felt desirable to indicate the relations between the new symbols and those commonly used in textbooks and technical papers.

Method of Analysis

The equivalent circuit will be derived from the four basic voltage drop equations for the four windings *A*, *B*, *X*, and *Y* in Fig. 1(B).

The voltage drop equation for each of the two stator windings *A* and *B* is of the form

$$v=Ri+\frac{d(N\phi)}{dt}=Ri+\frac{d(Li)}{dt} \tag{1}$$

where $(N\phi)=(Li)$ is the total flux linkages of each winding due to currents flowing in the different windings and $d(N\phi)/dt$ is the induced voltage drop.

The voltage drop equation for each of the two rotor windings *X* and *Y* is of the form

$$v=Ri+\frac{d(N\phi)}{dt}+v_s \tag{2}$$

where v_s is the speed voltage drop due to the rotor conductors cutting the air-gap flux, and is proportional to the rotor speed and the *X*-axis or *Y*-axis air-gap flux.

Thus, it is necessary to find the total flux linkages $(N\phi)=(Li)$ for each of the four windings and the *X*-axis and *Y*-axis air-gap fluxes which will give the two speed voltages in the two rotor windings.

Definition of Fluxes

To find the two air-gap fluxes which will give the two rotor speed voltages and also the total flux linkages $(N\phi)=(Li)$ which will give the induced or transformer voltage in each of the four windings, it is convenient to define the fluxes along the *X* and *Y* axes as indicated in Fig. 2.

The two stator coils and the two rotor coils will produce leakage fluxes and mutual fluxes, as defined in the following. The subscript *m* is used to designate mutual fluxes which cross the air gap and link all coils in either the *X* or the *Y* axis. For example, ϕ_{Am} is the mutual flux set up by i_A in coil *A* and links all the coils in the *Y* axis, and ϕ_{Xm} is the mutual flux set up by i_X in coil *X* and links all the coils in the *X* axis.

1. Fluxes in webers set up by i_A in coil *A*:

ϕ_A' = minimum leakage flux or portion of flux set up by i_A in coil *A*, which does not interlink with any other coil even when $\alpha=0$ degrees
ϕ_{Al} = portion of flux which does not cross the air gap but all of which interlinks with coil *B* when $\alpha=0$ degrees. This is a leakage flux when $\alpha=90$ degrees or when coil *B* is not used
ϕ_{Am} = mutual flux crossing air gap and linking *A*, B_y, and *Y*
Flux linking *A* and *Y* without linking B_y is assumed to be negligible

2. Fluxes in webers set up by i_B in coil *B*:

ϕ_B' = minimum leakage flux or portion of flux set up by i_B in coil *B* which does not interlink with any other coil even when $\alpha=0$ degrees. The *X*-component is $\phi_B' \sin \alpha$ and the *Y*-component is $\phi_B' \cos \alpha$
ϕ_{Bl} = portion of flux which does not cross the air gap but all of which interlinks with coil *A* when $\alpha=0$ degrees. The *X*-component is $\phi_{Bl} \sin \alpha$ and the *Y*-component is $\phi_{Bl} \cos \alpha$
ϕ_{Bm} = mutual flux crossing air gap and linking *B*, *Y*, and *A* when $\alpha=0$ degrees. The *X*-component is $\phi_{Bm} \sin \alpha$ and the *Y*-component is $\phi_{Bm} \cos \alpha$
Flux linking B_y and *Y* without linking *A* is assumed to be negligible

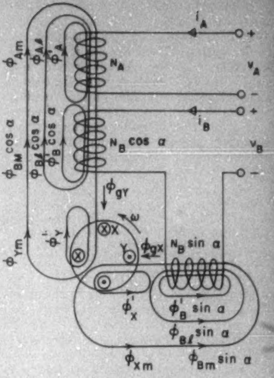

Fig. 2. Fluxes of modified basic machine

3. Fluxes in webers set up by i_X in coil *X*:

ϕ_X' = leakage flux linking coil *X*
ϕ_{Xm} = mutual flux crossing air gap and linking *X* and B_x. This is a leakage flux when $\alpha=0$ degrees or when coil *B* is not used

4. Fluxes in webers set up by i_Y in coil *Y*:

ϕ_Y' = leakage flux linking coil *Y*
ϕ_{Ym} = mutual flux crossing air gap and linking *Y*, *A*, and B_y
Flux linking *Y* and B_y without linking *A* is assumed to be negligible
Flux linking *Y* and *A* without linking B_y is assumed to be negligible

Following the viewpoint of Arnold, West, Puchstein, and Lloyd, it is assumed that the rotor *X* and *Y* conductors cut not only the mutual fluxes which cross the air gap but also the rotor leakage fluxes; that is, the air-gap fluxes include the rotor leakage fluxes ϕ_X' and ϕ_Y'. Letting ϕ_{gX} be the air-gap flux along the *X*-axis and ϕ_{gY} that along the *Y*-axis results in

$$\phi_{gX}=\phi_X'+\phi_{Xm}+\phi_{Bm} \sin \alpha \tag{3}$$

$$\phi_{gY}=\phi_Y'+\phi_{Ym}+\phi_{Bm} \cos \alpha+\phi_{Am} \tag{4}$$

Flux Linkages of Windings

To find the induced or transformer voltage drops $d(N\phi)/dt$ in equations 1 and 2, it is necessary to determine the total flux linkages $(N\phi)=(Li)$ in weber turns for each of the four windings. With the aid of Fig. 2, they are

$$(N\phi)_A=N_A(\phi_A'+\phi_{Al}+\phi_{Bl} \cos \alpha+\phi_{Am}+\phi_{Bm} \cos \alpha+\phi_{Ym}) \tag{5}$$

$$\begin{aligned}(N\phi)_B=N_B \cos \alpha(\phi_B' \cos \alpha+\phi_{Al}+{}&\\ \phi_{Bl} \cos \alpha+\phi_{Am}+\phi_{Bm} \cos \alpha+\phi_{Ym})+{}&\\ N_B \sin \alpha(\phi_B' \sin \alpha+\phi_{Bl} \sin \alpha+{}&\end{aligned}$$

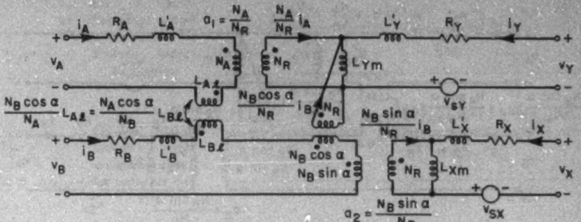

Fig. 3. Equivalent circuit with instantaneous values

$$\phi_{Bm} \sin \alpha + \phi_{Xm})$$

$$= N_B(\phi_B' + \phi_{Bl} + \phi_{Al} \cos \alpha + \phi_{Am} \cos \alpha + \phi_{Bm} \cos^2 \alpha + \phi_{Ym} \cos \alpha + \phi_{Bm} \sin^2 \alpha + \phi_{Xm} \sin \alpha) \quad (6)$$

$$(N\phi)_X = N_R(\phi_X' + \phi_{Xm} + \phi_{Bm} \sin \alpha) = N_R \phi_{gX} \quad (7)$$

$$(N\phi)_Y = N_R(\phi_Y' + \phi_{Ym} + \phi_{Bm} \cos \alpha + \phi_{Am}) = N_R \phi_{gY} \quad (8)$$

where N_R may be considered as the effective turns for either the rotor X coil or the rotor Y coil. In the case of a squirrel-cage rotor, it is not necessary to know N_R when the rotor values are expressed in the usual stator terms.

The Four Basic Equations in Terms of $(N\phi)$

The four basic equations are obtained by writing the voltage drop equations for the two stator windings A and B, and the two rotor windings X and Y, as indicated in equations 1 and 2. The derivation of these equations will now be considered.

With $(N\phi)_A$ and $(N\phi)_B$ in equations 5 and 6, the voltage drop equations for the stator windings A and B are

$$v_A = R_A i_A + N_A \frac{d}{dt}(\phi_A' + \phi_{Al} + \phi_{Bl} \cos \alpha + \phi_{Am} + \phi_{Bm} \cos \alpha + \phi_{Ym}) \quad (9)$$

$$v_B = R_B i_B + N_B \frac{d}{dt}(\phi_B' + \phi_{Bl} + \phi_{Al} \cos \alpha + \phi_{Am} \cos \alpha + \phi_{Bm} \cos^2 \alpha + \phi_{Ym} \cos \alpha + \phi_{Bm} \sin^2 \alpha + \phi_{Xm} \sin \alpha) \quad (10)$$

Using $(N\phi)_X$ and $(N\phi)_Y$ in equations 7 and 8, the voltage drop equations for the rotor windings X and Y are

$$v_X = R_X i_X + N_R \frac{d}{dt}[\phi_X' + \phi_{Xm} + \phi_{Bm} \sin \alpha] + v_{SX} \quad (11)$$

$$v_Y = R_Y i_Y + N_R \frac{d}{dt}[\phi_Y' + \phi_{Ym} + \phi_{Bm} \cos \alpha + \phi_{Am}] + v_{SY} \quad (12)$$

where

$$v_{SX} = +\omega N_R \phi_{gY} = \omega N_R(\phi_Y' + \phi_{Ym} + \phi_{Bm} \cos \alpha + \phi_{Am}) \quad (13)$$

$$v_{SY} = -\omega N_R \phi_{gX} = -\omega N_R(\phi_X' + \phi_{Xm} + \phi_{Bm} \sin \alpha) \quad (14)$$

$$\omega = \frac{2\pi \text{ rpm}}{60} \frac{2}{2} \text{ radians per second} \quad (15)$$

The speed voltages v_{SX} and v_{SY} (as in the case of the generated electromotive force of a d-c generator $E_g = K\phi n$) are proportional to the number of turns N_R, the air-gap flux ϕ_{gX} or ϕ_{gY}, and the speed ω. The signs in equations 13 and 14 are due to the choice of the positive senses of fluxes and voltages, the direction of rotation, and the consideration of these speed voltages as voltage drops.

The Four Basic Equations in Terms of (Li)

It is believed that the four basic equations and the derived equivalent circuit will have more meaning and perhaps more usefulness in the solution of problems if they are expressed in terms of (Li)'s instead of the $(N\phi)$'s. A reason for this belief is that the differential equation of a circuit contains terms of the form $L\,di/dt$ and the steady-state equation of a circuit contains factors of the form $X = \omega L$. The relations between the (Li)'s and the $(N\phi)$'s are given in the Appendix.

The four basic equations 9 through 12 may be expressed in terms of (Li) by making the proper substitution of (Li) for $(N\phi)$. Thus

$$v_A = R_A i_A + \frac{d}{dt}\left(L_A' i_A + L_{Al} i_A + \frac{N_A}{N_B} \times L_{Bl} i_B \cos \alpha + \frac{N_A^2}{N_R^2} L_{Ym} i_A + \frac{N_A N_B}{N_R^2} L_{Ym} i_B \cos \alpha + \frac{N_A}{N_R} L_{Ym} i_Y\right)$$

$$= R_A i_A + \left(L_A' + L_{Al} + \frac{N_A^2}{N_R^2} L_{Ym}\right) \frac{di_A}{dt} + \left(\frac{N_A \cos \alpha}{N_B} L_{Bl} + \frac{N_B N_A \cos \alpha}{N_R^2} L_{Ym}\right) \times \frac{di_B}{dt} + \frac{N_A}{N_R} L_{Ym} \frac{di_Y}{dt} \quad (16)$$

$$v_B = R_B i_B + \frac{d}{dt}\left(L_B' i_B + L_{Bl} i_B + \frac{N_B}{N_A} L_{Al} i_A \cos \alpha + \frac{N_B N_A}{N_R^2} L_{Ym} i_A \times \cos \alpha + \frac{N_B^2}{N_R^2} L_{Ym} i_B \cos^2 \alpha + \frac{N_B}{N_R} L_{Ym} i_Y \cos \alpha + \frac{N_B^2}{N_R^2} \times L_{Xm} i_B \sin^2 \alpha + \frac{N_B}{N_R} L_{Xm} i_X \sin \alpha\right)$$

$$= R_B i_B + (L_B' + L_{Bl}) \frac{di_B}{dt} + \frac{N_B \cos \alpha}{N_A} \times L_{Al} \frac{di_A}{dt} + \frac{N_B N_A \cos \alpha}{N_R^2} L_{Ym} \frac{di_A}{dt} + \frac{N_B^2 \cos^2 \alpha}{N_R^2} L_{Ym} \frac{di_B}{dt} + \frac{N_B \cos \alpha}{N_R} \times L_{Ym} \frac{di_Y}{dt} + \frac{N_B^2 \sin^2 \alpha}{N_R^2} L_{Xm} \frac{di_B}{dt} + \frac{N_B \sin \alpha}{N_R} L_{Xm} \frac{di_X}{dt} \quad (17)$$

$$v_X = R_X i_X + \frac{d}{dt}\left(L_X' i_X + L_{Xm} i_X + \frac{N_B}{N_R} L_{Xm} i_B \sin \alpha\right) + v_{SX} = R_X i_X + L_X' \frac{di_X}{dt} + L_{Xm}\left(\frac{di_X}{dt} + \frac{N_B \sin \alpha}{N_R} \frac{di_B}{dt}\right) + v_{SX} \quad (18)$$

$$v_Y = R_Y i_Y + \frac{d}{dt}\left(L_Y' i_Y + L_{Ym} i_Y + \frac{N_B}{N_R} L_{Ym} i_B \cos \alpha + \frac{N_A}{N_R} L_{Ym} i_A\right) + v_{SY}$$

$$= R_Y i_Y + L_Y' \frac{di_Y}{dt} + L_{Ym}\left(\frac{di_Y}{dt} + \frac{N_B \cos \alpha}{N_R} \frac{di_B}{dt} + \frac{N_A}{N_R} \frac{di_A}{dt}\right) + v_{SY} \quad (19)$$

$$v_{SX} = \omega\left[L_Y' i_Y + L_{Ym}\left(i_Y + \frac{N_B \cos \alpha}{N_R} i_B + \frac{N_A}{N_R} i_A\right)\right] \quad (20)$$

$$v_{SY} = -\omega\left[L_X' i_X + L_{Xm}\left(i_X + \frac{N_B \sin \alpha}{N_R} i_B\right)\right] \quad (21)$$

The new symbols will have a clearer meaning when these equations are applied to definite examples at the end of the paper. A better physical picture of the rotor constants and rotor currents will be obtained when these quantities are expressed in the more familiar terms as in the single-phase and polyphase induction motors.

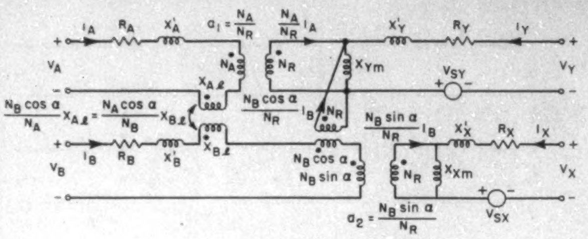
I_A
R_A
X_A'
$a_1 = \frac{N_A}{N_R}$
$\frac{N_A}{N_R} I_A$
X_Y'
R_Y
I_Y
+
V_A
N_A
N_R
X_{Ym}
V_Y
−
$X_{A\ell}$
V_{SY}
$\frac{N_B \cos\alpha}{N_A} X_{A\ell} = \frac{N_A \cos\alpha}{N_B} X_{B\ell}$
$\frac{N_B \cos\alpha}{N_R} I_B$
N_R
$\frac{N_B \sin\alpha}{N_R} I_B$
X_X'
R_X
I_X
$X_{B\ell}$
I_B
R_B
X_B'
V_B
$N_B \cos\alpha$
$N_B \sin\alpha$
N_R
X_{Xm}
V_X
V_{SX}
$a_2 = \frac{N_B \sin\alpha}{N_R}$

Fig. 4. Equivalent circuit with steady-state values

Equivalent Circuit

An equivalent circuit, as shown in Fig. 3, may be derived from equations 16 through 21; that is, the four Kirchhoff's emf equations for the circuits A, B, X, and Y will satisfy equations 16 through 21. The positive senses for the currents and the polarity markings for the voltages are indicated in the diagram. It should be emphasized that the frequency in every part of the equivalent circuit is the same.

Since equations 16 through 21 are expressed in terms of inductances and instantaneous values, these equations and the equivalent circuit in Fig. 3 may be used for transient study. In fact, the differential equations can be obtained directly from the equivalent circuit of the particular machine being considered. The transient solution of these differential equations can then be solved, if desired, by using differential analyzers.

Perhaps a brief remark concerning the rotor terminal voltages v_X and v_Y, in the case of a squirrel-cage rotor, should be made at this time. Since the rotor bars are short-circuited by the end rings, $v_X = 0$ and $v_Y = 0$. That is, these terminals are short-circuited.

Steady-State Equivalent Circuit

It must be remembered that the basic machine in Fig. 1(A) represents a 2-pole machine. This was done for simplicity and clearness.

When a single-phase or a polyphase motor is analyzed under steady-state operation, it is convenient to have a steady-state equivalent circuit, which will now be considered.

If a 2-pole a-c machine is operating under steady-state condition

$$\omega_0 = 2\pi f = \frac{2\pi(\text{synchronous rpm})}{60}\frac{P}{2}$$

electric radians per second

$$= \frac{2\pi(\text{syn rpm})}{60}\frac{2}{2}$$

electric radians per second

$$S = (1-\text{slip}) = \frac{\text{actual rpm}}{\text{syn rpm}}$$

$\omega = S\omega_0$ electric radians per second

$$X_A' = \omega_0 L_A'$$

$$X_{Al} = \omega_0 L_{Al}$$

$$X_B' = \omega_0 L_B'$$

$$X_{Bl} = \omega_0 L_{Bl}$$

$$X_X' = \omega_0 L_X'$$

$$X_{Xm} = \omega_0 L_{Xm}$$

$$X_Y' = \omega_0 L_Y'$$

$$X_{Ym} = \omega_0 L_{Ym}$$

Then the steady-state expressions for the equations 16 through 21 may be written

$$\dot{V}_A = [R_A + j(X_A' + X_{Al})]\dot{I}_A + j\frac{N_A \cos\alpha}{N_B} X_{Bl}\dot{I}_B + jX_{Ym}\frac{N_A}{N_R}\times \left[\frac{N_A}{N_R}\dot{I}_A + \frac{N_B \cos\alpha}{N_R}\dot{I}_B + \dot{I}_Y\right] \quad (22)$$

$$\dot{V}_B = [R_B + j(X_B' + X_{Bl})]\dot{I}_B + j\frac{N_B \cos\alpha}{N_A} X_{Al}\dot{I}_A + jX_{Ym}\frac{N_B \cos\alpha}{N_R}\times \left[\frac{N_A}{N_R}\dot{I}_A + \frac{N_B \cos\alpha}{N_R}\dot{I}_B + \dot{I}_Y\right] + jX_{Xm}\frac{N_B \sin\alpha}{N_R}\left[\frac{N_B \sin\alpha}{N_R}\dot{I}_B + \dot{I}_X\right] \quad (23)$$

$$\dot{V}_X = [R_X + jX_X']\dot{I}_X + jX_{Xm}\times \left[\dot{I}_X + \frac{N_B \sin\alpha}{N_R}\dot{I}_B\right] + \dot{V}_{SX} \quad (24)$$

$$\dot{V}_Y = [R_Y + jX_Y']\dot{I}_Y + jX_{Ym}\times \left[\dot{I}_Y + \frac{N_B \cos\alpha}{N_R}\dot{I}_B + \frac{N_A}{N_R}\dot{I}_A\right] + \dot{V}_{SY} \quad (25)$$

$$\dot{V}_{SX} = S\left[X_Y'\dot{I}_Y + X_{Ym}\times \left(\dot{I}_Y + \frac{N_B \cos\alpha}{N_R}\dot{I}_B + \frac{N_A}{N_R}\dot{I}_A\right)\right] \quad (26)$$

$$\dot{V}_{SY} = -S\left[X_X'\dot{I}_X + X_{Xm}\times \left(\dot{I}_X + \frac{N_B \sin\alpha}{N_R}\dot{I}_B\right)\right] \quad (27)$$

From Fig. 3 and equations 22 through 27, a steady-state equivalent circuit as indicated in Fig. 4 may be obtained for 2-pole a-c machines. It should be pointed out that the frequency is the same in every part of Fig. 4 and that the symbols in the X and Y circuits are in rotor terms. Since the equivalent circuits of single-phase and polyphase induction motors are usually expressed in stator terms, it may be advisable to express the rotor values in stator terms as indicated in Fig. 5. Some of the relations between the new symbols and the more familiar symbols used in textbooks and technical papers will now be considered.

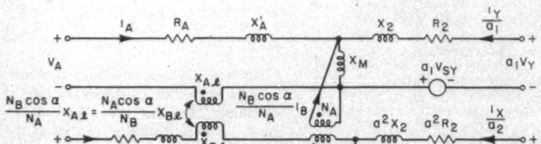
I_A
R_A
X_A'
X_2
R_2
$\frac{I_Y}{a_1}$
+
V_A
X_M
$a_1 V_{SY}$
$a_1 V_Y$
−
$X_{A\ell}$
$\frac{N_B \cos\alpha}{N_A} X_{A\ell} = \frac{N_A \cos\alpha}{N_B} X_{B\ell}$
$\frac{N_B \cos\alpha}{N_A} I_B$
N_A
$a^2 X_2$
$a^2 R_2$
$\frac{I_X}{a_2}$
$X_{B\ell}$
I_B
R_B
X_B'
V_B
$N_B \cos\alpha$
X_S
$a_2 V_{SX}$
$a_2 V_X$

Fig. 5. Equivalent circuit with rotor values in stator terms

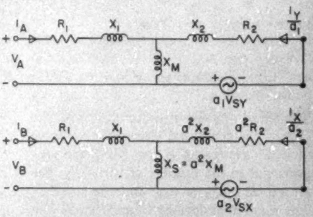
I_A
R_1
X_1
X_2
R_2
$\frac{I_Y}{a_1}$
V_A
X_M
$a_1 V_{SY}$
I_B
R_1
X_1
$a^2 X_2$
$a^2 R_2$
$\frac{I_X}{a_2}$
V_B
$X_S = a^2 X_M$
$a_2 V_{SX}$

Fig. 6. Steady-state equivalent circuit for 2-phase induction motor

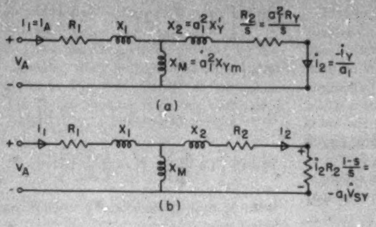
$I_1 = I_A$
R_1
X_1
$X_2 = a_1^2 X_Y'$
$\frac{R_2}{s} = \frac{a_1^2 R_Y}{s}$
V_A
$X_M = a_1^2 X_{Ym}$
$\dot{I}_2 = \frac{-\dot{I}_Y}{a_1}$
(a)
I_1
R_1
X_1
X_2
R_2
I_2
V_A
X_M
$\dot{I}_2 R_2 \frac{1-s}{s} = -a_1 \dot{V}_{SY}$
(b)

Fig. 7 (left). Per phase equivalent circuit for 2-phase induction motor

Fig. 9 (right). Steady-state equivalent circuit for capacitor motor

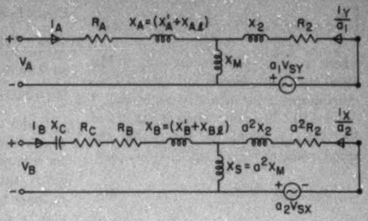

First, let

$$a_1 = \frac{N_A}{N_B}$$

$$a_2 = \frac{N_B \sin \alpha}{N_R}$$

$$a = \frac{a_2}{a_1} = \frac{N_B \sin \alpha}{N_A}$$

For a symmetrical rotor

$$R_X = R_Y$$

$$X_X' = X_Y'$$

and for a uniform air gap

$$L_{Xm} = L_{Ym}$$

$$X_{Xm} = X_{Ym}$$

Then, the rotor values in stator terms are:

1. To express the rotor Y values in stator A winding terms

$R_2 = a_1^2 R_Y =$ rotor resistance
$X_2 = a_1^2 X_Y' =$ rotor leakage reactance
$X_M = a_1^2 X_{Ym} = Y$-axis magnetizing reactance

2. To express the rotor X values in stator B winding terms

$$a_2^2 R_m = a_2^2 R_Y = \frac{a_2^2}{a_1^2} R_2 = a^2 R_2$$

$$a_2^2 X_X' = a_2^2 X_Y' = \frac{a_2^2}{a_1^2} X_2 = a^2 X_2$$

$X_S = a_2^2 X_{Xm} = X$-axis magnetizing reactance

$$= a_2^2 X_{Ym} = \frac{a_2^2}{a_1^2} X_M = a^2 X_M$$

When the rotor values are expressed in stator terms, the steady-state equivalent circuit of Fig. 4 becomes that given in Fig. 5. It should be noted that the turns ratio of the ideal transformer which couples the stator B winding to the magnetizing branch X_M of the stator A winding has been changed to $N_B \cos \alpha / N_A$.

To illustrate the use of the derived steady-state equivalent circuit in Fig. 5, the steady-state operation of the 2-phase induction motor, the capacitor motor, and the a-c tachometer will now be considered.

Steady-State Operation of 2-Phase Induction Motor

When a balanced 2-phase induction motor is operating under steady-state conditions, its usual equivalent circuit in stator terms may be derived from Fig. 5. The following relations obtain

$$\omega_0 = 2\pi f$$

$$\alpha = 90 \text{ degrees}$$

$$N = N_A = N_B$$

$$a_1 = \frac{N_A}{N_R} = \frac{N}{N_R}$$

$$a_2 = \frac{N_B \sin \alpha}{N_R} = a_1$$

$$a = \frac{a_2}{a_1} = 1$$

$$\dot{V}_B = j\dot{V}_A$$

$$\dot{I}_B = j\dot{I}_A$$

$$\dot{I}_X = j\dot{I}_Y$$

$$R_1 = R_A = R_B$$

$$X_1 = (X_A' + X_{Al}) = (X_B' + X_{Bl})$$

$$R_X = R_Y$$

$$X_X' = X_Y'$$

Since the air gap is uniform

$$L_{Xm} = L_{Ym}$$

$$X_{Xm} = X_{Ym}$$

and thus

$$X_M = X_S$$

For a squirrel-cage rotor, the rotor bars are short-circuited by the end rings and $V_X = 0$ and $V_Y = 0$; i.e., these terminals are short-circuited.

With these conditions, from Fig. 5 the steady-state equivalent circuit for a 2-phase induction motor is given in Fig. 6. Since $\dot{V}_B = j\dot{V}_A$, $\dot{I}_B = j\dot{I}_A$ and $\dot{I}_X = j\dot{I}_Y$, it remains to show that $\dot{V}_{SX} = j\dot{V}_{SY}$. This will now be considered.

The speed voltages, from equations 26 and 27 may be written

$$a_2^2 \dot{V}_{SX} = S[a_2^2 X_Y' \dot{I}_Y + a^2 X_{Ym}(\dot{I}_Y + a_1 \dot{I}_A)] \\ = S[X_2 \dot{I}_Y + X_M(\dot{I}_Y + a_1 \dot{I}_A)] \quad (28)$$

$$a_1^2 \dot{V}_{SY} = -S[a_1^2 X_X' \dot{I}_X + a_1^2 X_{Xm} \times (\dot{I}_X + a_2 \dot{I}_B)] = -S[X_2(j\dot{I}_Y) + X_M j(\dot{I}_Y + a_1 \dot{I}_A)] \quad (29)$$

or

$$\dot{V}_{SX} = j\dot{V}_{SY} \quad (30)$$

Thus, the phase A and phase B circuits in Fig. 6 are similar except for the 90-degree phase displacement between the corresponding voltages and corresponding currents.

Using the phase A circuit for the equivalent circuit on the per phase basis, the usual equivalent circuit for an induction motor will now be derived. The voltage drop equation for the rotor Y circuit is

$$(R_2 + jX_2)\frac{\dot{I}_Y}{a_1} + jX_M\left(\dot{I}_A + \frac{\dot{I}_Y}{a_1}\right) + a_1 \dot{V}_{SY} = 0 \quad (31)$$

The speed voltage $a_1 \dot{V}_{SY}$ may be written

$$a_1 \dot{V}_{SY} = -S[a_1 X_X' \dot{I}_X + a_1 X_{Xm}(\dot{I}_X + a_2 \dot{I}_B)] \\ = -S\left[a_1^2 X_X \frac{\dot{I}_X}{a_1} + a_1^2 X_{Xm}\left(\frac{\dot{I}_X}{a_1} + \dot{I}_B\right)\right] \\ = -S\left[X_2\left(j\frac{\dot{I}_Y}{a_1}\right) + X_M\left(j\frac{\dot{I}_Y}{a_1} + j\dot{I}_A\right)\right] \quad (32)$$

Letting $\dot{I}_1 = \dot{I}_A$ and $\dot{I}_2 = -\dot{I}_Y/a_1$ allows equation 31 to be written in the form of the following:

$$[R_2 + j(X_2 + X_M)(1-S)]\dot{I}_2 - jX_M(1-S)\dot{I}_1 = 0 \quad (33)$$

or

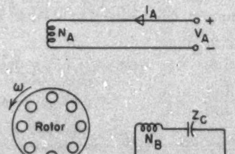

Fig. 8. Schematic diagram of capacitor motor

$$\left[\frac{R_2}{s}+j(X_2+X_M)\right]\dot{I}_2-jX_M\dot{I}_1=0 \qquad (34)$$

where $s = (1-S)$ is the slip. The usual equivalent circuit for a 2-phase induction motor is that indicated in Fig. 7 (A) or (B). By comparison of Fig. 6 and Fig. 7(B), it should be noted that the speed voltage

$$-a_1\dot{V}_{SY}=\dot{I}_2R_2\,\frac{(1-s)}{s} \qquad (35)$$

for a balanced 2-phase induction motor operating under steady-state condition is always in phase with $\dot{I}_2 = -\dot{I}_Y/a_1$.

It may be seen from Fig. 7(B) that the following can be determined on the per phase basis

$$\text{Input watts}=V_AI_1\cos(\dot{V}_A,\dot{I}_1)$$
$$=V_AI_A\cos(\dot{V}_A,\dot{I}_A) \qquad (36)$$

$$\text{Copper losses}=(I_1^2R_1+I_2^2R_2)$$
$$=(I_A^2R_A+I_Y^2R_Y) \qquad (37)$$

$$\text{Rotor output}=a_1V_{SY}I_2\cos(-\dot{V}_{SY},\dot{I}_2)$$
$$=V_{SY}I_Y\cos(\dot{V}_{SY},\dot{I}_Y) \qquad (38)$$

$$\text{Rotor output torque}=\frac{\text{rotor output watts}}{S}$$
$$\text{(syn watts)} \qquad (39A)$$

$$=7.04\,\frac{\text{rotor output watts}}{\text{actual rpm}}$$
$$\text{(pound-feet)} \qquad (39B)$$

Steady-State Operation of Capacitor Motor

Fig. 8 shows the schematic diagram of a capacitor motor. It is assumed that the two stator windings A and B are connected to a single-phase source so that $\dot{V}_A = \dot{V}_B = \dot{V}$. When this motor is operating under steady-state conditions, its equivalent circuit may be derived with the aid of Fig. 5. The following relations exist

$\omega_0=2\pi f$

$\alpha=90$ degrees

$a_1=\dfrac{N_A}{N_R}$

$a_2=\dfrac{N_B}{N_R}$

$a=\dfrac{a_2}{a_1}=\dfrac{N_B}{N_A}$

$\dot{V}_B=\dot{V}_A=\dot{V}$

$X_A=(X_A'+X_{Al})$

$X_B=(X_B'+X_{Bl})$

$R_X=R_Y$

$X_X'=X_Y'$

Since the air gap is uniform, then

$L_{Xm}=L_{Ym}$

$X_{Xm}=X_{Ym}$

and thus

$X_S=a^2X_M$

Under these conditions with the aid of Fig. 5, the steady-state equivalent circuit for a capacitor motor is given in Fig. 9. From equations 26 and 27, the following expressions for the speed voltages may also be derived.

$$a_2\dot{V}_{SX}=S\left[aX_2\frac{\dot{I}_Y}{a_1}+aX_M\left(\frac{\dot{I}_Y}{a_1}+\dot{I}_A\right)\right] \qquad (40)$$

$$a_1\dot{V}_{SY}=-S\left[aX_2\frac{\dot{I}_X}{a_2}+aX_M\times\right.$$
$$\left.\left(\frac{\dot{I}_X}{a_2}+\dot{I}_B\right)\right] \qquad (41)$$

The currents $\dot{I}_A$, $\dot{I}_B$, $\dot{I}_X$, $\dot{I}_Y$ may be found by writing the four loop voltage equations for the circuit in Fig. 9. For simplicity, let $\dot{Z}_A = R_A + jX_A$, $\dot{Z}_M = jX_M$, $\dot{Z}_2 = R_2 + jX_2$, $\dot{Z}_S = jX_S$, $\dot{Z}_B = R_B + jX_B$ and $\dot{Z}_C = R_C - jX_C$. Then

$$\dot{V}=(R_A+jX_A)\dot{I}_A+jX_M\left(\dot{I}_A+\frac{\dot{I}_Y}{a_1}\right)$$
$$=\dot{Z}_A\dot{I}_A+\dot{Z}_M\left(\dot{I}_A+\frac{\dot{I}_Y}{a_1}\right) \qquad (42)$$

$$0=(R_2+jX_2)\frac{\dot{I}_Y}{a_1}+jX_M\left(\dot{I}_A+\frac{\dot{I}_Y}{a_1}\right)+$$
$$a_1\dot{V}_{SY}=\dot{Z}_2\frac{\dot{I}_Y}{a_1}+\dot{Z}_M\left(\dot{I}_A+\frac{\dot{I}_Y}{a_1}\right)-$$
$$S\left[-j\frac{\dot{Z}_S}{a}\left(\frac{\dot{I}_X}{a_2}+\dot{I}_B\right)+aX_2\frac{\dot{I}_X}{a_2}\right] \qquad (43)$$

$$\dot{V}=[(R_B+jX_B)+(R_C-jX_C)]\dot{I}_B+$$
$$jX_S\left(\dot{I}_B+\frac{\dot{I}_X}{a_2}\right)=(\dot{Z}_B+\dot{Z}_C)\dot{I}_B+$$
$$\dot{Z}_S\left(\dot{I}_B+\frac{\dot{I}_X}{a_2}\right) \qquad (44)$$

$$0=a^2(R_2+jX_2)\,\frac{\dot{I}_X}{a_2}+jX_S\left(\dot{I}_B+\frac{\dot{I}_X}{a_2}\right)+$$
$$a_2\dot{V}_{SX}=a\dot{Z}_2\frac{\dot{I}_X}{a_2}+\frac{\dot{Z}_S}{a}\left(\dot{I}_B+\frac{\dot{I}_X}{a_2}\right)+$$
$$S\left[-j\dot{Z}_M\left(\dot{I}_A+\frac{\dot{I}_Y}{a_1}\right)+X_2\frac{\dot{I}_Y}{a_1}\right] \qquad (45)$$

Solving equations 42 through 45 simultaneously and following a similar procedure given by Puchstein and Lloyd.[1]

$$\dot{I}_A=\frac{\dot{C}_1\dot{B}_2-\dot{C}_2\dot{B}_1}{\dot{A}_1\dot{B}_2-\dot{A}_2\dot{B}_1} \qquad (46)$$

$$\dot{I}_B=\frac{\dot{A}_1\dot{C}_2-\dot{A}_2\dot{C}_1}{\dot{A}_1\dot{B}_2-\dot{A}_2\dot{B}_1} \qquad (47)$$

where

$$\dot{A}_1=S\left[j\dot{Z}_A-X_2\left(1+\frac{\dot{Z}_A}{\dot{Z}_M}\right)\right]$$

$$\dot{B}_1=-\left[a\dot{Z}_2+(\dot{Z}_B+\dot{Z}_C)\left(\frac{1}{a}+a\,\frac{\dot{Z}_2}{\dot{Z}_S}\right)\right]$$

$$\dot{C}_1=\dot{V}\left[S\left(j-\frac{X_2}{\dot{Z}_M}\right)+\left(\frac{1}{a}+a\,\frac{\dot{Z}_2}{\dot{Z}_S}\right)\right]$$

$$\dot{A}_2=\left[\dot{Z}_A\left(1+\frac{\dot{Z}_2}{\dot{Z}_M}\right)+\dot{Z}_2\right]$$

$$\dot{B}_2=S\left[-aX_2+(\dot{Z}_B+\dot{Z}_C)\left(\frac{j}{a}-a\frac{X_2}{\dot{Z}_S}\right)\right]$$

$$\dot{C}_2=\dot{V}\left[\left(1+\frac{\dot{Z}_2}{\dot{Z}_M}\right)+S\left(\frac{j}{a}-a\,\frac{X_2}{\dot{Z}_S}\right)\right]$$

With $\dot{I}_A$ and $\dot{I}_B$ determined, then from equations 42 and 44

$$\frac{\dot{I}_Y}{a_1}=\frac{\dot{V}}{\dot{Z}_M}-\left(1+\frac{\dot{Z}_A}{\dot{Z}_M}\right)\dot{I}_A \qquad (48)$$

$$\frac{\dot{I}_X}{a_2}=\frac{V}{\dot{Z}_S}-\left(\frac{\dot{Z}_S+\dot{Z}_B+\dot{Z}_C}{\dot{Z}_S}\right)\dot{I}_B \qquad (49)$$

With the aid of Fig. 9, the following relations may be obtained quite readily

$$\text{stator input}=VI_A\cos(\dot{V},\dot{I}_A)+VI_B\times$$
$$\cos(\dot{V},\dot{I}_B) \qquad (50)$$

$$\text{stator copper loss}=I_A^2R_A+I_B^2(R_B+R_C)$$
$$(51)$$

$$\text{rotor copper loss}=\left(\frac{I_Y}{a_1}\right)^2R_2+\left(\frac{I_X}{a_2}\right)^2a^2R_2$$
$$=I_Y^2R_Y+I_X^2R_X \qquad (52)$$

$$\text{rotor output}=a_1V_{SY}\left(\frac{I_Y}{a_1}\right)\cos(\dot{V}_{SY},I_Y)+$$
$$a_2V_{SX}\left(\frac{I_X}{a_2}\right)\cos(\dot{V}_{SX},\dot{I}_X) \qquad (53)$$

$$\text{torque}=\frac{\text{rotor output watts}}{S}\text{(syn watts)} \qquad (54)$$

A-C Tachometer

In some systems of automatic control, it is desirable to have a signal which is proportional to the angular velocity of a shaft. Quite often, it is convenient to have this signal in the form of an alternating voltage of constant frequency.

A small squirrel-cage induction motor with two windings spaced 90 degrees apart, such as that shown in Fig. 8 without Z_C, may be used. A suitable alternating voltage of constant amplitude and frequency is applied to winding A, which is sometimes referred to as the input winding. A voltage of the same frequency is then generated in winding B, also referred to as the output winding. This generated voltage of winding B is applied to the high-impedance grid circuit of a vacuum-tube amplifier and thus winding B can be considered as open-circuited so that $I_B = 0$.

Ideally, the magnitude of the signal voltage generated in winding B should be linearly proportional to the rotor speed, and the phase of this generated voltage should be fixed with respect to the applied voltage V_A.

The equivalent circuit for the a-c tachometer may be represented by that given in Fig. 9 (omitting R_C and X_C). The applied voltage is V_A and the desired voltage is V_B. With $I_B = 0$, then

$$\dot{V}_B = ja^2X_M\left(\frac{\dot{I}_X}{a_2}\right) \tag{55}$$

Equation 55 indicates that it is necessary only to determine $\dot{I}_X/a_2$, which may done by writing the 3-loop voltage equations in Fig. 9 and then solving them simultaneously. Thus

$$\dot{V}_A = \dot{Z}_A\dot{I}_A + jX_M\left(\dot{I}_A + \frac{\dot{I}_Y}{a_1}\right) = (\dot{Z}_A + jX_M)\dot{I}_A + jX_M\frac{\dot{I}_Y}{a_1} \tag{56}$$

$$0 = \dot{Z}_2\frac{\dot{I}_Y}{a_1} + jX_M\left(\dot{I}_A + \frac{\dot{I}_Y}{a_1}\right) + a_1\dot{V}_{SY} = jX_M\dot{I}_A + (\dot{Z}_2 + jX_M)\frac{\dot{I}_Y}{a_1} - S\left(aX_2 + \frac{X_S}{a}\right)\frac{\dot{I}_X}{a_2} \tag{57}$$

$$0 = a^2\dot{Z}_2\frac{\dot{I}_X}{a_2} + ja^2X_M\frac{\dot{I}_X}{a_2} + a_2\dot{V}_{SX} = SaX_M\dot{I}_A + Sa(X_2 + X_M)\frac{\dot{I}_Y}{a_1} + a^2(\dot{Z}_2 + jX_M)\frac{\dot{I}_X}{a_2} \tag{58}$$

when equations 56 through 58 are solved simultaneously

$$\frac{\dot{I}_X}{a_2} = \frac{-\dot{V}_ASX_MR_2}{a\{[\dot{Z}_A\dot{Z}_2^2 - X_M^2(\dot{Z}_A + \dot{Z}_2) + jX_M\dot{Z}_2 \times (2\dot{Z}_A + \dot{Z}_2) + S^2(X_2 + X_M)] \times [\dot{Z}_A(X_2 + X_M) + jX_2X_M]\}} \tag{59}$$

$$\dot{V}_B = \frac{-j\dot{V}_ASaX_M^2R_2}{[\dot{Z}_A\dot{Z}_2^2 - X_M^2(\dot{Z}_A + \dot{Z}_2) + jX_M\dot{Z}_2 \times (2\dot{Z}_A + \dot{Z}_2) + S^2(X_2 + X_M)] \times [\dot{Z}_A(X_2 + X_M) + jX_2X_M]} \tag{60}$$

Ideally, $\dot{V}_B$ should be equal to some constant times the rotor speed S. This means that the distortion S^2 term in the denominator of equation 60 should be eliminated by introducing special devices in the system.

Conclusions

An equivalent circuit, as shown in Fig. 3 has been derived which can be adapted to that of a particular machine. Since the resultant equivalent circuit involves resistances, inductances, and instantaneous values, differential equations may be written directly from the circuit for transient study.

Also, a steady-state equivalent circuit as shown in Fig. 4 or Fig. 5 has been derived for the steady-state operation of a particular machine.

An advantage of the equivalent circuit in Fig. 3, Fig. 4, or Fig. 5 is that it is not necessary to start from the beginning for the analysis of the different machines.

Appendix. Relations Between the (Li)'s and (Nφ)'s

If any two coils are in the same magnetic path so that the reluctances are equal, then the inductances are proportional to the square of the turns. Thus

$$\frac{L_{Am}}{N_A^2} = \frac{L_{Bm}}{N_B^2} = \frac{L_{Xm}}{N_R^2} = \frac{L_{Ym}}{N_R^2}$$

$$\frac{L_{Al}}{N_A^2} = \frac{L_{Bl}}{N_B^2}$$

and

$$N_A\phi_A' = L_A'i_A$$

$$N_A\phi_{Al} = L_{Al}i_A$$

$$N_A\phi_{Bl} = \frac{N_A}{N_B}L_{Bl}i_B$$

$$N_A\phi_{Am} = L_{Am}i_A = \frac{N_A^2}{N_R^2}L_{Ym}i_A$$

$$N_A\phi_{Bm} = \frac{N_A}{N_B}(N_B\phi_{Bm}) = \frac{N_A}{N_B}L_{Bm}i_B = \frac{N_AN_B}{N_R^2}L_{Ym}i_B$$

$$N_A\phi_{Ym} = \frac{N_A}{N_R}(N_R\phi_{Ym}) = \frac{N_A}{N_R}L_{Ym}i_Y$$

$$N_B\phi_B' = L_B'i_B$$

$$N_B\phi_{Bl} = L_{Bl}i_B$$

$$N_B\phi_{Al} = \frac{N_B}{N_A}L_{Al}i_A$$

$$N_B\phi_{Am} = \frac{N_B}{N_A}(N_A\phi_{Am}) = \frac{N_B}{N_A}L_{Am}i_A = \frac{N_BN_A}{N_R^2}L_{Ym}i_A$$

$$N_B\phi_{Bm} = L_{Bm}i_B = \frac{N_B^2}{N_R^2}L_{Ym}i_B = \frac{N_B^2}{N_R^2}L_{Xm}i_B$$

$$N_B\phi_{Ym} = \frac{N_B}{N_R}(N_R\phi_{Ym}) = \frac{N_B}{N_R}L_{Ym}i_Y$$

$$N_B\phi_{Xm} = \frac{N_B}{N_R}L_{Xm}i_X$$

$$N_R\phi_X' = L_X'i_X$$

$$N_R\phi_{Xm} = L_{Xm}i_X$$

$$N_R\phi_{Bm} = \frac{N_R}{N_B}L_{Bm}i_B = \frac{N_B}{N_R}L_{Xm}i_B = \frac{N_B}{N_R}L_{Ym}i_B$$

$$N_R\phi_Y' = L_Y'i_Y$$

$$N_R\phi_{Ym} = L_{Ym}i_Y$$

$$N_R\phi_{Am} = \frac{N_R}{N_A}(N_A\phi_{Am}) = \frac{N_R}{N_A}L_{Am}i_A = \frac{N_A}{N_R}L_{Ym}i_A$$

Reference

1. THE CROSS-FIELD THEORY OF THE CAPACITOR MOTOR, A. F. Puchstein, T. C. Lloyd. *AIEE Transactions (Electrical Engineering)*, vol. 60, Feb. 1941, pp. 58–62.

A New Method for Part-Winding Starting of Polyphase Motors

P. L. ALGER
FELLOW AIEE

LORRAINE M. AGACINSKY
APPLICATION PENDING

Synopsis: Part-winding or "step-starting" of polyphase induction motors for holding down the initial starting current inrush is on the increase. The conventional scheme provides two half-current starting contactors, each with three poles. The motors have dual-voltage 9-lead windings, arranged in two independent Y's, separately connected to the two contactors. The two contactors are closed in sequence with a few seconds' delay between, giving about 60 per cent (%) current on the first step. The delay must be very short, because the accelerating torque on half-winding is usually low, the motor may be noisy, and the rate of heating is high.

The paper describes a new method of part-winding starting, in which two half-current contactors are used also, the first to close having four poles, and the second only two. Preferably, a Y connection is used, and two-thirds of the winding, instead of only half, is connected on the first step, as in Fig. 1. This gives superior accelerating

---

Paper 55-846, recommended by the AIEE Rotating Machinery Committee and approved by the AIEE Committee on Technical Operations for presentation at the AIEE Conference on Application of Motors to Space Heating and Cooling Equipment, St. Louis, Mo., October 19–20, 1955. Manuscript submitted June 15, 1955; made available for printing September 26, 1955.

P. L. ALGER and LORRAINE M. AGACINSKY are with the General Electric Company, Schenectady, N. Y.

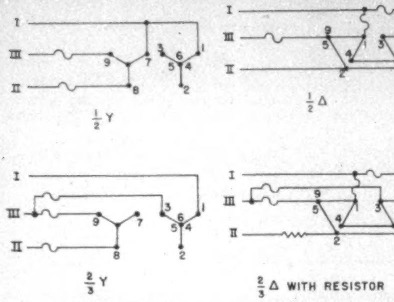

Fig. 1. Simplified diagrams of first-step connections. Preferred schemes for step-starting of polyphase motors

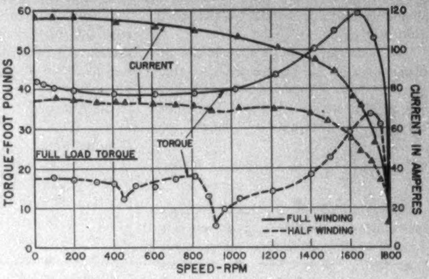

Fig. 3. Torque-current curves for standard 4-pole 7½ hp general-purpose-motor half-Y-connection leads on 7, 8, 9...

torque, with reduced noise, vibration, and heating. Or the same contactors may be used to start the motor on half-winding with delta as well as with Y connection. By providing five instead of four poles on the first contactor, a delta-connected motor can also be started on two-thirds winding, with superior accelerating performance.

This new control panel performs every function required for conventional half-winding starting, with either Y-connected or delta-connected motors. It also provides for two-thirds winding starting with superior accelerating torque. The method therefore overcomes the difficulties associated with usual part-winding starting, and appears to fill satisfactorily the long-standing need for a simple method of reduced-current starting for polyphase motors.

Purpose of Part-Winding Starting

To avoid severe dips in voltage, many power companies have adopted rules that limit the current inrush permitted in starting a motor. On 4-wire 220-volt systems the limit is often set at 400 amperes, corresponding to a 30-horsepower (hp) motor with full-voltage starting. However, the rules usually allow a much larger current to be drawn, provided the current is added in successive increments a few seconds apart. The idea is to give the voltage regulators time to return the voltage to normal after each step, and so to hold the voltage at all times above the desired minimum.

To comply with these rules, the custom has developed of connecting only half of a motor winding to the line at first, and closing the other half after a brief delay, controlled by an automatic timer. This part-winding or step-starting method allows much larger motors to be used than are permissible with full-winding starting, and costs less than other ways of meeting all the requirements. Thus, it is steadily becoming more popular.

In view of this trend, and the growing demand for large motors on low-voltage systems, especially for air conditioning, it is timely to analyze the need for step-starting more broadly, and to determine the best way of meeting it.

Requirements for Satisfactory Step-Starting

Besides the lower initial current inrush, step-starting gives a lower initial motor torque, and thus provides "soft starting," reducing the shocks on gears, couplings, and other parts of the equipment. This is an advantage in some applications. Also, it increases the time before the motor reaches full speed, allowing the oiling system of the driven equipment to become fully effective before maximum load is imposed on bearing surfaces.

To sum up, for fully satisfactory results, step-starting should:

1. Reduce the initial current inrush to about 60% of normal full-voltage starting current.
2. Bring the motor nearly to full speed in not more than about 5 seconds, before the timer closes the second half of the winding, so that the second current inrush will be very small. This requires that the minimum accelerating torque of the motor be 30% or more of full-load torque.
3. Be applicable to perfectly standard dual-voltage motors of all speeds (low-voltage connection only), whether Y-connected or delta-connected.
4. Accomplish these three results without overheating, without noise, and without undue mechanical stresses on the windings, all at a cost little greater than required for usual full-voltage full-winding starting.

Conventional Method of Step-Starting

The practice established over the past few years employs Y-connected motors with nine leads brought out for dual-voltage use. The control panel is provided with two half-current 3-pole contactors, two sets of half-current thermal overload relays, and an adjustable automatic timer. On the first step, the lines are closed on motor leads 7, 8, and 9, placing one half of the winding in circuit, in a symmetrical Y connection; see Fig. 2. With only half the coils active, the winding produces additional magnetic fields with synchronous speeds lower than the fundamental, causing one or more low torque points at about 25%, 40%, 50%, or 70% of full speed, depending on the

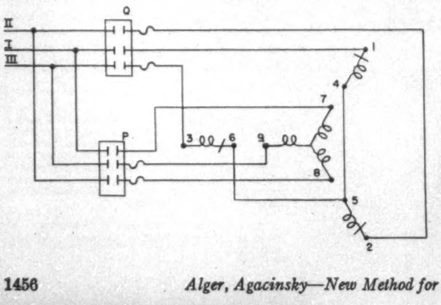

Fig. 2. Conventional part-winding connections for Y-connected motor, half-winding. Windings marked with diagonal line are idle on first step. This also applies to Figs. 5, 6, 8, 10, 11, and 13

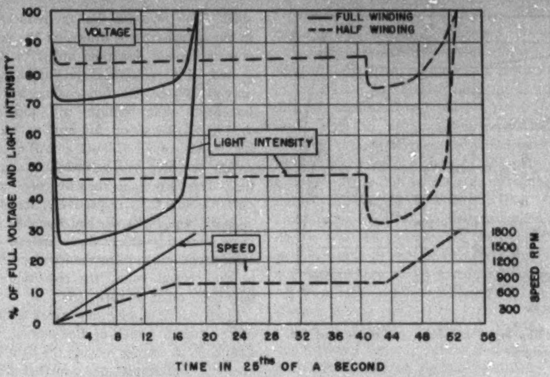

Fig. 4. Comparative voltage drop and corresponding light intensity in conventional part-winding starting, standard 4-pole 40-hp general-purpose motor

winding arrangement; see Fig. 3. Thus, the motor may not come to full speed in a reasonable time, or at all, on the first step.

As the 60% current is flowing in only half the total conductor area, the current density in the winding copper is 120% of that in normal full-voltage starting, and the rate of temperature rise is about 150% of normal. The winding will therefore reach its limiting temperature, and the relays will clear the motor from the line, in about two-thirds of the usual time, or perhaps 15 seconds, if the motor fails to accelerate within this time. To avoid this, and leave a liberal margin for the additional heating in acceleration after the full winding is closed in, it is desirable to set the timer for only 2 or 3 seconds' interval between the first and second steps. When this is done, the full winding will usually be closed while the motor is still at low speed, and the second inrush of current will bring the total to nearly the same value as with full-winding starting.

Fig. 4 shows the speed and applied voltage versus time for a typical Y-connected 40-hp motor of this type, when started without any connected load. The light intensity of a lamp connected from line to neutral on the supply voltage at the motor terminals is shown. In this case, the motor came to 40% speed on the first step with the half-Y connection in 0.64 second, remained there until the full winding was closed in after 1.08 seconds more, and then came to full speed in 0.4 second. When the motor was started on the full winding at full voltage, it came to speed in only 0.72 second. If the motor had been connected to a typical compressor load, the starting times would have been much longer. The maximum voltage drop was nearly the same in the two cases, without allowing for any recovery of the voltage between the first and second steps, as might have occurred on an actual power system with proper voltage regulators.

By choice of winding arrangement and other factors, the designer can vary the motor performance over a considerable range. For lowest initial current, and best locked-rotor torque, the active stator coils should be grouped on one side of the motor, and this arrangement is commonly used for motors intended to start on half-winding. However, this gives rise to an unbalanced force on the shaft, which will create noise and vibration during acceleration. This may be tolerable on many applications, especially for the smaller motors, but it is likely to give trouble when the shaft dimensions, the connected load, or the motor supports are such as to magnify or prolong the vibration. With this one-sided coil grouping, a torque dip is likely to occur at about 70% speed (for a 4-pole motor), making acceleration beyond this speed difficult with a loaded compressor. By giving the rotor a little higher resistance than normal, the low point in the torque curve can be raised at the expense of efficiency and heating under load.

By spacing the active coils symmetrically around the periphery, the air-gap forces can be kept in balance, and the vibration eliminated. But this tends to give a higher initial current, and introduces a torque dip at 25% or 50%; see Fig. 3. A higher rotor resistance, or a longer stator coil throw will again help to overcome the low torque, at the expense of higher losses, and/or higher initial current inrush. It is theoretically possible, for the first step, to select some active coils from each phase belt of the winding in such a way as to minimize the torque dips, but this is not a practical solution for standard motors. Whatever winding arrangement is used, the motor is likely to have a good deal more slot frequency noise during acceleration than when the full winding is connected.

For example, the presence of both 4-pole and 8-pole fields in the air gap at the same time, in a motor having a difference of 8 between stator and rotor slot numbers, produces a 4-node slot frequency force wave, whereas the 4-

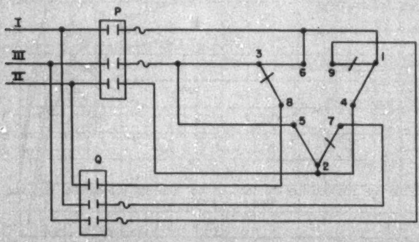

Fig. 5. Part-winding connections for delta-connected motor half-winding

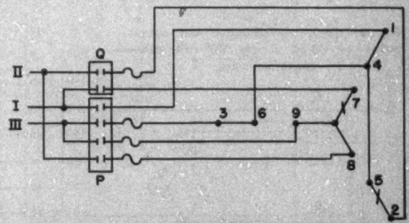

Fig. 6. Two-thirds winding connection for Y-connected motor

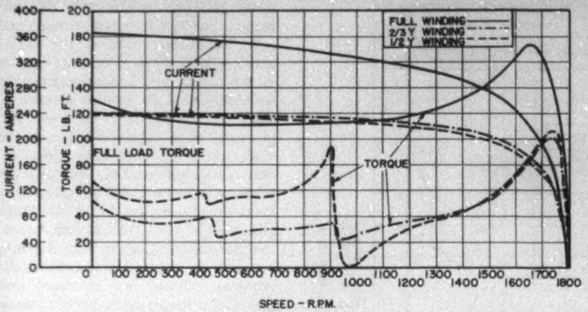

Fig. 7. Torque-current curves of Y-connected 25-hp motor with half-, two-thirds, and full-winding connection

pole field alone only creates an 8-node force wave. The 4-node wave produces some 16 times as great a deflection of the frame as an 8-node wave for the same magnetic flux density. Also, in the case of a 4-node force wave, the resonant frequency of the frame is likely to occur below the full speed of the motor, giving rise to a "shriek" as the motor accelerates through this point; whereas with an 8-node force wave, the resonant frequency is usually far above the running speed.

Everything considered, therefore, with the usual half-Y arrangement for step starting, it is proper to set the timer for only 2 or 3 seconds, and to expect the second step to occur with the motor at low speed, giving full locked-rotor current. In this way, the duration of abnormal heating, noise, and vibration is cut short. At first glance, from the viewpoint of the power company, there seems to be no objection to this practice, as the current inrush rules are fully complied with. From the viewpoint of the motor manufacturer and his customers, the practice has the advantages of minimizing the need for special motor designs, and lessening the risk of complaints about noise or vibration.

On close examination, however, the plan does not seem attractive. From the viewpoint of the power company, the reduction in voltage dip and in light flicker is very slight. To refer to Fig. 4, the dip in voltage was 25% on full-winding starting, and on half-winding starting 17% on the first step and 5% more on the second step. In the first case, the light intensity fell to 31.5% of normal for about 0.76 second, and then returned to normal. In the second case, the light fell to 46% for 1.6 seconds than fell to only 35%, and finally returned to normal in 0.44 second. Even if the system voltage does recover, due to regulator action, between the first and second starting steps, the net benefit from step-starting appears to be very small. One reason is that the reduction in the actual current drawn on the first starting step is less than might be expected. For example, if the line impedance is 25% of the full-winding motor impedance, the voltage will dip to $1/(1+0.25)=0.80$ on full-winding starting, and to $1.67/(1.67+0.25)=0.87$ on the first step with half-winding starting. The currents in the two cases will be 80% and 52% respectively, instead of 100% and 60%, as they would be if there were no voltage dip. Instead of the current inrush being reduced by 40% of the normal value, the reduction is only 28%, on an ampere basis.

Since the light intensity varies about as the fourth power of the voltage, a drop to 87% voltage reduces the light to about 57% of normal, and a further drop to 80% voltage reduces it to about 41%.

It is important to realize that the flicker caused by a sudden increase in the voltage is likely to be more objectionable than that caused by an equal drop in voltage, since a sudden increase in light intensity may be painful to the eyes, whereas a sudden decrease is not. With step-starting, the acceleration from low speed on the second starting step, and the voltage recovery, are likely to be rapid, so that the net result as far as light flicker is concerned may be almost as objectionable as with full-winding starting. Thus, the conventional scheme of part-winding starting offers only a small advantage at best, with respect to either voltage regulation or light flicker.

From the viewpoint of the motor manufacturer also, the conventional scheme appears unattractive on close examination. If the motor does not come to speed readily on the first step,

Fig. 8 (below). Two-thirds winding connection for delta-connected motor

Fig. 9 (right). Speed-torque and current curves of 40-hp 4-pole 220-volt delta-connected motor

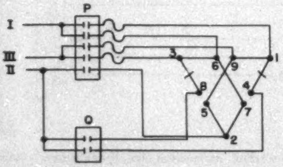

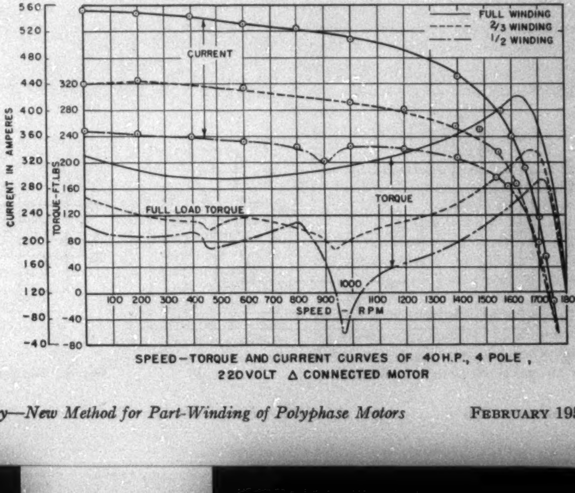

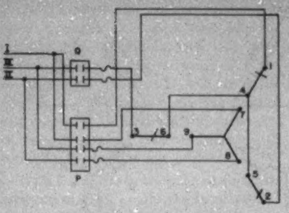

Fig. 10. Preferred half-winding Y connection with standard control panel

some operator or service man is likely to reset the timer to give it more time. If the thermal relays clear the motor from the line as a result of heating, the service man is likely to install higher current relay heaters. If the starting period is prolonged, the coil ends will be subjected to sustained vibration because of the high-current forces, and at the same time they will be overheated, so that they will be more flexible and less able to withstand the forces. Thus, regardless of any instructions provided by the manufacturer, motors with conventional step starting may be required to operate on a much more severe starting cycle than intended.

From the cost viewpoint, it is desirable to use two half-size contactors, since these will not cost very much more than the single full-size contactor used with full-winding starting. This is the reason that Y windings and not delta windings are used. As Fig. 5 indicates, if a delta winding is used with the conventional scheme of half-winding, each pole of the first contactor to close must carry the current in two of the motor leads, and those of the second contactor will carry the current only in one lead. Hence, the two contactors must have capacities of 76% and 29% of normal current respectively. Their cost will therefore be a good deal more than for the two 50% contactors required for Y windings.

As delta windings are preferable from a design viewpoint in many of the motors in the 20- to 300-hp size range, it is a distinct handicap to be limited to Y windings. This fact, and the need for taking care that the torque, noise, vibration, and heating shall all be reasonably satisfactory on the half-winding connection, make the inherent cost of the motor somewhat greater. The designer must choose whether to make all his motors in this way, and thus add to the cost of standard motors, or let motors for part-winding starting be special, and thus add further to their cost.

From this review, it appears that the conventional scheme of step-starting, with Y half-windings, does not adequately meet items 2, 3, or 4 in the section "Requirements for Satisfactory Step-Starting." While experience up to the present has been chiefly with 4-pole motors, it appears that the scheme will be more satisfactory for motors with larger numbers of poles, and will be least satisfactory for 2-pole motors.

New Method of Step-Starting

The limitations of the conventional method all stem from the use of only half the number of stator coils on the first step. A good way to overcome these is to use more than half the coils, which will give a better pattern of magnetomotive force distribution in the motor, and so raise the low points in the torque curve and reduce the noise and vibration.

One convenient way to secure the results is to connect two-thirds of the winding on the first step. The preferred scheme for a Y winding is that shown in Fig. 6. In this method, four of the motor leads are connected on the first step, two from each of the half-Y-windings. Then in each half-winding two phases are connected in series, as in a single-phase line-to-line connection. The effect is to utilize all of one phase, and half of each of the other two phases of the complete winding. Since the currents are constrained to flow through two adjacent phases in series, the effective reactance is $2/\sqrt{3}$ times the 3-phase reactance. Thus the average current drawn from the three lines is practically identical with that drawn in the conventional half-Y-connection. The unbalance between the currents is quite moderate. In a particular case, of a 25-hp 4-pole motor, the currents on the first step were 200, 210, and 310 amperes, averaging 240 amperes, as compared with 240 amperes on the usual half-Y-connection and 365 amperes on the full-winding connection.

Fig. 7 shows the torque and current curves of this motor with the three schemes. As appears from the curve, the marked torque dip that occurs on the half-winding connection is reduced to a trivial amount on the two-thirds connection. The minimum torque on two-thirds winding in this case is 32% of full load torque, and the motor comes up to speed promptly on the first step. The per cent of normal full-winding locked-rotor current (average value) varies a good deal with individual designs, but is nearly always between 60% and 70% and it differs very little from the current on half-winding start. The starting torque on two-thirds winding is a little

Fig. 11 (below). Preferred half-winding delta connection with standard control panel

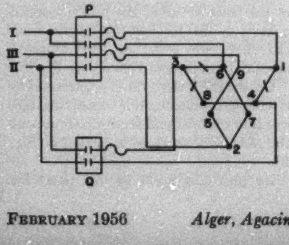

Fig. 12 (right). Torque-current curves of two-thirds delta-connected 40-hp motor with and without external resistance

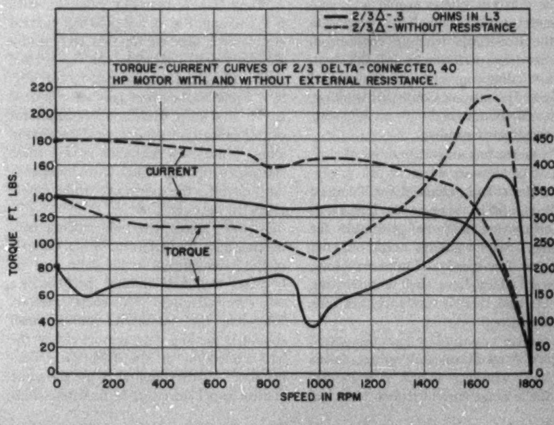

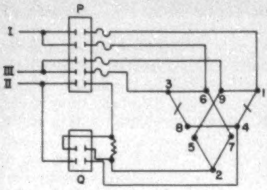

Fig. 13 (left). Two-thirds delta connection with one series resistor

Fig. 14 (right). Split-winding connections for Y connected and delta-connected 3-phase motors

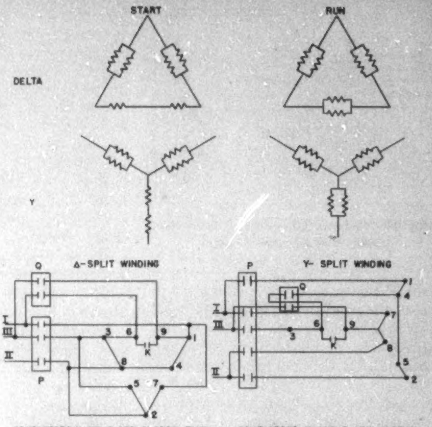

CONTACTORS K AND P ARE CLOSED, THEN K IS OPENED, AND Q IS CLOSED AFTER A SUITABLE DELAY.

THE POLES OF P CARRY 76% OF LOAD CURRENT, THOSE OF Q CARRY 29%.

CONTACTORS K AND P ARE CLOSED, THEN K IS OPENED, AND Q IS CLOSED AFTER A SUITABLE DELAY.

THE POLES OF P AND Q EACH CARRY 50% OF LOAD CURRENT

lower for the same current than on the half-winding, because of the small negative phase sequence torque due to the current unbalance, but this is more than made up in most cases by the reduced amount of harmonic torque dip. This two-thirds Y scheme gives a smooth torque curve and reasonably quiet starting on almost any standard dual-voltage motor, including the 2-pole motor.

For best performance, with the two-thirds connection, it is desirable to use an asymmetric alternate-pole grouping of the motor winding, i.e., the three line terminals of the motor should come from adjacent phase belts, *A*, −*B*, and *C*; and one of the motor circuits per phase should contain only north poles, and the other only south poles. This arrangement ensures balanced air-gap forces, whatever the current distribution, and it also ensures that the harmonic fields produced by the separate phases will partly offset each other. Experience has shown that this winding arrangement is preferable for standard general-purpose motors, for full-winding as well as part-winding starting. If a symmetric alternate-pole winding were used, with the line terminals coming from alternate phase belts, *A*, *C*, and *B*, the harmonics of the different phases would add, and the motor would usually fail to accelerate on the two-thirds winding connection. The starting performance of the two-thirds winding connection is usually good with an adjacent-pole symmetric winding, but is usually not good with an adjacent-pole asymmetric winding.

If a motor has an odd number of slots per pair of poles, an adjacent-pole grouping of the coils is required for balanced windings, and in this case the half-winding connection may be preferable for starting. Such windings occur only on small or low-speed induction motors, however, which have such low starting currents that there is rarely any need for reduced-current starting.

A similar two-thirds connection gives comparable results on dual-voltage, delta-connected windings, except that in this case the average current drawn from the line is about 15% more than for the half-delta-connection, and the torque is correspondingly greater also. This is true because with the delta connection there is no way to put two out-of-phase legs in series, as in the Y case. Fig. 8 shows the connections for the two-thirds delta scheme, and Fig. 9 the curves of a typical 40-hp motor with the three connections.

By adding extra poles to a standard contactor, the additional number of lead connections required for the two-thirds winding schemes can be provided for, without exceeding the half-current capacity used in the conventional half-winding Y scheme. For example, with a Y winding, Fig. 6, a 4-pole half-current contactor is used on the first step, and a similar 2-pole contactor for the second step. For a delta-connected motor, Fig. 8, a 5-pole half-current contactor is used for the first step, while a 2-pole contactor of this capacity is adequate for the second step. Since each contactor pole in these schemes supplies current to an independent circuit, the currents will divide properly between them.

In some cases, the half-winding connection may be preferred, either because of the lower current in the delta case, or because the half-winding performance may be adequate for some motors. Therefore the standard control panel should be arranged to permit either the half-connection or the two-thirds connection. To do this, and to use the same control panel for either Y or delta windings, both contactors should have 50% current capacity.

The standard panel will then use two contactors with four and two poles respectively, as shown in Figs. 6, 10, and 11. This fully provides for half-Y, two-thirds Y, and half-delta connections, but will not take care of the two-thirds delta connection. Therefore on half-delta the control should provide for closing the second contactor in about 3 seconds, since the motor cannot be relied upon to accelerate on the half-winding.

To provide for starting delta-connected motors on two-thirds winding, and to allow for the occasional use of three steps instead of two, one extra contactor pole is required. For a delta motor, this extra contactor pole will connect terminal 2 to line II, or for a Y motor it will connect terminal 7 to line I. Closing this extra contactor as a second step, after closing half the delta winding, or two-thirds the Y winding, on the first step will raise the current from about 0.6 to 0.8 of full value, with higher torque, quieter operation, and less heating. By connecting a resistor in series with one of the poles of either the first or second contactor, the torques and currents on the first two steps can be adjusted accurately to desired values; see Fig. 12.

On the third step, the 2-pole contactor is closed, connecting the remaining terminal to the line, and short-circuiting out the resistor, if used, as indicated in Fig. 13.

By providing space on the panel for

the addition of the resistor and/or the extra contactor pole when especially requested, the standard panel will have very wide application, covering all types of polyphase motor. It will then be feasible to adjust the starting torque and current to fit particular requirements, or to meet unusual field conditions, with a minimum of extra cost or delay.

With regard to heating, the two-thirds connection gives nearly the same rate of temperature rise on the first starting step as the half-winding in the delta case, but only two-thirds the rate of the half-Y-winding. For, the current per leg is practically the same per cent of normal in the half and two-thirds delta cases as in the conventional half-Y case, about 60% of normal full-voltage full-winding locked-rotor current. In the two-thirds Y case however, the current per leg is only 50% of normal locked-rotor current, and the rate of heating is the same as in a normal full-winding start. But the minimum torque in the case of either two-thirds Y or two-thirds delta is higher than in either half-winding case, so that the motor may be relied upon to bring the motor to full speed promptly on the first step. Thus, the timing of the second starting step is immaterial, and the second current inrush will be very small, if there is any increase in the current at all. Also the heating in a normal start will be much less than with the conventional half-winding method, and the risk of increasing the starting duty by a long setting of the timer is removed.

It is true that with the two-thirds winding connections, the currents are somewhat unbalanced. In a typical Y case, there are two low-current and one high-current values, varying 25% either way from the average. In the delta case, there are two high-current and one low-current values, varying from 10% to 15% from the average. Even in the conventional half-Y case, the currents are usually unbalanced about 5% each way from the average. These unbalances in current are of no importance whatever, for the negative phase sequence component of the currents is supplied by other near-by rotating machines on the system, because of their low negative phase sequence impedances; and the small voltage unbalance caused at the motor terminals will therefore be highly localized. The long-standing custom of using open-delta autotransformers, with unbalanced currents for reduced-voltage starting, confirms these views.

So far as light flicker is concerned, the light will probably decrease less when the voltage is unbalanced than when it is balanced. If all three phase voltages dip to 80%, the light goes down to $(0.80)^4 = 0.41$ of normal. But if one phase voltage dips only to 90% while the other two dip to 75%, giving the same average, the total light is $^1/_3\,[(0.90)^4+2\,(0.70)^4] = 0.45$ of normal. If the lighting near the motor is connected to only one phase, the motor leads can be connected so that this phase will have the highest voltage.

Other Possible Methods of Step-Starting

The autotransformer method of reduced-voltage starting is unattractive, because of the relatively high costs of the autotransformer and the two contactors required, and also because of the current surge that occurs when the motor is transferred to full voltage. A reconnection of the motor winding from Y start to delta run, as is often the procedure abroad, requires additional contactors, gives only one-third torque at start, and also gives a current surge on the final starting step, which conditions rule out this method.

Another way to use more than half the winding without excessive starting current is to connect the two halves of one of the phases in series on the first step, leaving the other two phases in normal parallel connection; see Fig. 14. This scheme has been described in an earlier paper.[1] It gives about half normal torque, and about 70% average current, with an excellent torque curve, complete freedom from noise and vibration, and reduced heating. Also, there is no current surge on the second step. Its disadvantage is that it requires a third (small) contactor, which must be accurately timed, and which therefore has a higher over-all cost. With a delta winding, if the extra contactor should fail to clear promptly before the full winding is closed in, the last step would produce a direct short circuit across the line terminals. With a Y winding, this cannot occur, as one leg of the winding is always in series with the extra contactor. The currents are widely unbalanced with this arrangement, and their average value, about 70% of full-winding current for Y windings and 80% for delta windings, is higher than desirable.

It appears therefore that this split-winding scheme does not meet all the requirements, and must be limited to special cases. It is particularly applicable to 2-pole motors with Y windings.

It is also possible to introduce series resistors, or reactors, in one or more of the motor lines, and to short-circuit these after the motor has reached full speed. For example, a resistor with an ohmic value 1.5 times the impedance per phase of a Y-connected winding, if put in series with one phase, will reduce the torque to half normal, and the average current to about 80% of normal. Or two resistors of 1.0 times the phase impedance placed in series with two of the motor leads, will reduce the torque to half normal and the average current to 75% of normal. With such a series impedance scheme, motor noise and vibration are less than in normal full-voltage starting, and the rate of heating will be less in the same proportion as the torque. However, two full-size starting contactors will be required, besides a timer and the resistors. Even though the second contactor, used to short-circuit the resistors, has low voltage across it, and does not have to carry any current during starting, it must carry the full operating current continuously, and it will therefore have a cost comparable to the normal full-winding contactor. Hence, the simple series impedance scheme is more costly than either of the part-winding schemes already described, and is therefore limited to special cases.

Advantages of New Method

Summing up, it appears that the conventional Y-connected half-winding method of step-starting, Fig. 2, does not adequately meet the requirements for step-starting, as it cannot be relied upon to bring the motor to full speed on the first step, it gives undue noise and (often) vibration during the initial starting period it is also likely to overheat in this period and it is not applicable to delta-connected motors.

On the other hand, it appears that the two-thirds winding method of step-starting meets all these requirements, is comparable with the conventional method in cost and in all other respects, and offers the opportunity to obtain still better performance at a very moderate increase in cost by using an auxiliary starting resistor and one more contactor pole.

Specifically, the proposed scheme of a standard control panel with two contactors of 50% current capacity, the one to close first having four poles and the second having two poles, together with a suitable timer, will provide the following features:

1. It will be suitable for the conventional half-winding starting of any Y-connected motor as commonly used, with about 60% average current on the first step; see Fig. 10. With this scheme, the motor may have

a dip in torque at some low speed, and therefore the timer should be set for less than 5 seconds.

2. It will be suitable for two-thirds winding starting on any standard Y-connected motor, Fig. 6, in which case the motor should come to speed on the first step without difficulty, and with less heating than for the half-winding. For this case, the timer setting can be 10 seconds or more, and is not in any way critical.

3. It will be suitable for starting any delta-connected motor on the half winding, giving the same current and starting performance as the half-Y-winding, see Fig. 11. For this case also, the timer should be set for less than 5 seconds.

4. By the addition of a separate single-pole contactor, or a fifth pole on the first contactor, and/or a single resistor, the control panel may be modified to provide for two-thirds starting on any Y-connected or delta-connected motor with smooth acceleration in either two or three steps, as preferred. In this case again, the timer setting is not critical, at least for the third step. By choosing the resistor properly, a close adjustment of the torque and current can be made to suit the requirements exactly. Also, for 3-step starting, by placing the resistor in series with the appropriate motor lead, the 2-current increments can be adjusted to preferred values.

5. Any dual-voltage motor with nine leads brought out may be started on part winding, with one or another of these connection schemes, whether the motor has two or more poles, is delta-connected or Y-connected, or special in any way.

References

1. Starting Characteristics and Control of Polyphase Squirrel-Cage Induction Motors, **H. M. Norman.** *AIEE Transactions*, vol. 45, 1926, p. 369.

2. Split-Winding Starting of 3-Phase Motors, **P. L. Alger, H. C. Ward, Jr., F. H. Wright.** *AIEE Transactions*, vol. 70, 1951, pt. I, p. 867.

3. The Nature of Polyphase Induction Machines (book), **P. L. Alger.** John Wiley & Sons, Inc., New York, N. Y., 1951.

4. Part-Winding Starting of Squirrel-Cage Motors, **Marvin Brown.** *Electrical Manufacturing*, New York, N. Y., vol. 53, 1954, p. 108.

◆

Discussion

C. P. Potter (Wagner Electric Corporation, St Louis, Mo.): This paper points out that the "conventional" method of part-winding starting polyphase motors has four disadvantages: (1) heating during starting; (2) noise during starting; (3) mechanical stresses during starting; (4) failure of the motor to reach full speed in a reasonable time, or at all.

While it is true that these disadvantages exist, I know of no instance where any of them have caused any difficulty with motors manufactured by the company with which I am affiliated and a great many such installations have been made. Heating, noise, and mechanical stresses have not been severe, and it makes no particular difference whether a motor reaches full speed on the first step or not. The initial current is approximately 60% of the locked rotor value and if the motor does not start the second step is 40% of the locked rotor value. If it comes up to speed, the current on the second step is reduced materially.

It seems to me that the principal disadvantage of the new method proposed by the paper is the unbalance of the locked rotor currents on the first step of the starter. When the three currents are 200, 210, and 310 amperes, respectively, it does not seem quite fair to say that since the average of these values is 240 amperes that this is just as good as the 240 amperes balanced current obtained with the usual half wye-connection. The paper states that "these unbalances in current are of no importance, whatever, for the negative phase sequence component of the currents is supplied by other nearby rotating machines on the system...and the small voltage unbalance...will therefore be highly localized." Locked rotor currents are of particular importance in localities where there are very few motors installed and of no importance whatever where there are many motors in the neighborhood. It is my opinion that the power companies may want to limit the amount of current unbalance in each installation and not depend on the balancing effect of other motors, which may, or may not, be present I do not like to use 4-pole and 5-pole contactors but that is a matter of personal prejudice.

I doubt the accuracy of the statement that the proposed scheme will be suitable for any wye-connected motor. I think that it is possible to build wye-connected motors which will run perfectly satisfactorily but cannot be started by any of these methods. It seems to me that in all cases where part-winding starting is used, approval should be obtained from the motor manufacturer in order to avoid misunderstanding and possible difficulty.

Mr. Alger and Miss Agacinsky deserve congratulations for presenting an excellent paper on such a practical subject.

J. J. Courtin (Westinghouse Electric Corporation, Buffalo, N. Y.): In applying motors with part-winding starters, the results obtained on the first step depend on the relative positioning of the active phase belts about the periphery of the stator. It has been shown that there are 13 different half-winding arrangements for a 4-pole 3-phase motor. All of these result in reduced line currents since the impedance for half a winding in an iron core is always greater than for the two halves in parallel. However, some of these arrangements, due to dissymmetry in the magnetomotive force pattern, can produce noise to an objectionable degree. Satisfactory results are obtained for most applications by using motors in which the half-winding arrangement and other design features are known to be suitable. In many cases this means a special motor. Some users have been discouraged from further applications after standard motors proved unsatisfactory on the conventional half-winding connection and then the only recourse was removal and modification of the motor.

The proposed control panel with its various connection possibilities as described in this paper seems to offer mainly some opportunity for making simple adjustments or modifications at the installation. For a star-connected motor the 1/2 wye and one or more 2/3 wye connections could be experimented with if need be and that one most suited to the application could be employed.

The 1/2 winding connection for a dual-voltage delta motor shown in Fig. 11 is of particular value since it permits use of half-size contactors whereas the top 3-pole contactor in the conventional arrangement of Fig. 5 must be sized for 76% of running line current. Probably a majority of standard dual-voltage 220/440-volt motors in the 40- to 125-hp range are delta-connected. Unlike the 1/2 wye, the 1/2 delta with the Fig. 11 connection permits rearranging the energized groups in several different patterns by exchanging the motor cables in the event that the original connection is not satisfactory. Therefore, the application of a standard dual-voltage motor on 1/2 delta could be approached with more confidence.

The author's explanation of the internal group positioning in the two 2/3 winding connections of the 25-hp wye and the 40-hp delta could be simplified. The 4-pole 3-phase motor has 12 phase groups. For the 1/2 winding in each case the arrangement was 3---3---, the numbers indicating the energized groups. For the 2/3 winding, at least two arrangements are possible in each case. These are 3 - 1 - 3 - 1 - and 4 - - 4 - -. The former has flat spots in the magnetomotive force wave and a cusp at half speed but would have lower values of current since a number of slots are not energized. The latter has a good magnetomotive force wave and torque available through the accelerating range and having no unenergized slots has higher values of current.

The 2/3 wye is actually an open-delta connection to the 3-phase lines in which the applied voltage on the coil groups is reduced $13^{1}/_{2}\%$. This accounts for the lower locked rotor torque than obtained with the 1/2 wye. The 2/3 delta has full voltage on the groups and, therefore, has higher locked rotor torque and currents than 1/2 the winding since more groups are active.

P. L. Alger and Lorraine M. Agacinsky: The purpose of the new 4/2-pole contactor panel is to give freedom to use any of several alternate part winding connections for starting, and especially to allow the use or either wye- or delta-connected motors. We agree that the conventional 1/2 winding wye scheme is perfectly adequate in many cases, and we expect that it will continue to be widely used, even with the new control panel. However, we believe that the 2/3 winding scheme is often preferable.

It is not easy to foresee the behavior of all possible winding arrangements, and it is, therefore, a good thing to be able to try out alternative schemes in the field, as the new panel allows. A change from 1/2 wye to 2/3 wye only requires interchanging a few leads on the new panel, and it is equally easy to shift the active phase belts to the most favorable combination for the particular motor.

Although Fig. 8 in the paper is described as a 2/3 delta winding, it is actually a 5/6 winding. For, in this figure, only one corner of one of the half-delta windings is left open, and each of the apparently idle legs carries half as much current as the other legs. This is true, because when voltage is applied across two corners of a delta, say across phase *A*, the current through the *B* and *C* phases in series will be half as great as the *A* phase current. Hence, in Fig. 8, the effective part of the winding is 4/6 plus 2/6 times 1/2, or 5/6.

A true 2/3 delta connection can be made by using ten leads for a dual-voltage motor, or six leads for a single-voltage motor, and either of these will give the same performance as the 2/3 wye winding. That is, with the true 2/3 delta connection, the average locked rotor current will be nearly identical with that for the 1/2 delta connection, but the motor will have superior accelerating torque, less noise, and less heating in most cases. In this way, the new control panel can be used without change to provide full-speed acceleration on the first step with about 65% current on either wye or delta motors. This is particularly useful for the larger motors that are preferably connected delta, and are often single-voltage machines.

It is important to note that the 2/3 connection is like a split-phase motor, as the phase angles of the currents in the two active legs are about 100 degrees apart, instead of the usual 120 degrees. With the recommended alternate pole, asymmetric connections, this has the effect of markedly reducing the dip in the torque curve at half speed. The dip is greater with an alternate-pole symmetric winding, however, so such a machine should be started on the 1/2 winding connection.

Mr. Potter has suggested that the line current unbalance on the 2/3 connection may be objectionable. We do not think so, for the reasons given in the paper. It should be remembered that the total light output of a bank of lamps on a 3-phase circuit is greater for a given average phase voltage when the voltages are unbalanced than when they are balanced. For, the light varies about at the fourth power of the voltage, so that the increase in light output from the lamps on the high-voltage phase is much greater than the decrease from those on the low voltage. If the lamps are all on one phase, it is only necessary to rotate the motor leads to bring the high voltage across the near by lamp circuit again to bring the flicker down to a smaller amount when the voltages are unbalanced than when they are balanced. There is no objection from the heating viewpoint, because the currents in the circuits of the motor winding, and series-connected relay heaters, are balanced on the 2/3 as well as on the 1/2 winding connection.

LATE DISCUSSIONS

The following discussions were received too late to be included with the papers.

Low-Voltage Network Current Limiters

Discussions of papers 55-443, 55-444, 55-434 55-445, 55-473, 55-432, 55-474, and 55-441, published in Power Apparatus and Systems, October 1955, pages 913–44.

R. L. Hicks (Toronto Hydro-Electric System, Toronto, Ont., Canada): With further regard to the recently published papers on limiters and their co-ordination with secondary and network cables, an account of experience in operating a network system without limiters may prove of interest.

This network system is operated by the Toronto Hydro-Electric System in Toronto, Canada. Although not large when compared with cities such as New York, it is not a small network. The present network demand is approximately 70,000 kva. It is expected that, in the very near future, network load will be greater than 100,000 kva.

The approach to network secondary in Toronto has been different than in the United States. Rather than use a rubber or paper cable and protect it with limiters to ensure fault clearing and thus decrease the danger of manhole fires and explosions, Toronto has tried to obtain a cable with better burn-off characteristics, and which inherently reduces the hazard of fire and explosion. The cable used is 500,000-circular-mil (MCM) single-conductor asbestos-insulated lead-covered cable. Three single-conductor cables are installed in one 4-inch duct to form a circuit, and a bare neutral is installed in a separate duct. This is a completely leaded system with wiped lead sleeve joints.

From the late 1930's, when the asbestos-insulated cable was first used, until the late 1940's, little data were obtained on fault clearing because there were relatively few faults. Experience showed, however, that this asbestos-insulated cable satisfactorily cleared whatever faults did occur. In the late 1940's construction of a subway was begun in Toronto, and, during its construction, considerable data on faults and fault clearing were obtained. Except under very abnormal conditions, fault clearing has been extremely satisfactory. One long length of secondary cable was roasted, but this was due to a primary fault and the failure of a network protector to open, rather than an initial secondary fault. The unit which failed to open was a new installation, and had only one tie circuit to the balance of the network completed when the fault occurred. The secondary fault current was large enough to roast this circuit over a period of time, but not large enough to blow the protector fuses. It is doubtful that there was enough current to blow limiters had they been installed.

Although limiters are not generally used in Toronto, a few have been installed to protect long radial runs from the network and to protect small lengths of old cable such as 500-MCM 3-conductor and 1,000-MCM single-conductor paper-insulated lead-covered cable which has been incorporated in the network. As far as I know, none of these limiters have ever blown.

Although asbestos-insulated lead-covered cable costs more on a footage basis than do other commonly used secondary cables, comparative studies have indicated that because of the cost of limiters and limiter accessories and the lower current rating of other types of cable, such a secondary system does not prove more expensive in the final analysis. We feel that the asbestos-insulated cable is particularly good for carrying heavy short-time overloads.

We realize at the same time that asbestos-insulated cable is not perfect, and that trouble was experienced when it was used in networks in the United States in the 1930's. I believe that the trouble at that time resulted from the violent reaction when water penetrated the cable. Fortunately, Toronto has a relatively dry underground system. There are occasional floods, but these have been neither frequent nor severe enough to warrant the purchase of submersible network equipment. In the original asbestos-insulated cable, the insulation was a matted mass of asbestos; the insulation in the asbestos-insulated cable now used in Toronto is made up of thin asbestos tapes wrapped around the conductor. Tests indicate that this taped asbestos cable has not the violent reaction to water that the older asbestos cable had.

In spite of satisfactory performance, we are still trying to obtain a better cable and are working with our supplies to reduce still further the amount of inflammable and potentially explosive material in the cable insulation and to reduce the adverse effects when the insulation is exposed to moisture.

At the same time, we are closely following development and experience in the types of network secondary discussed in the subject papers.

W. R. Bullard (Ebasco Services, Inc., New York, N. Y.): In none of these papers or discussions have I found more than mere passing mention of networks operating without the benefit of limiters to aid clearing of faults in secondary mains. Yet, data presented in an Edison Electric Institute report on a-c network operations for 1950–52[1] indicate that, at that time, 21 out of 57 companies reporting had neither limiters nor fuses in secondary mains to sectionalize the network itself. Although not shown in this report, it is well known that many companies which do use limiters or fuses for sectionalization do not apply them to the entire system but only to portions where it is considered that ability for self-clearing of faults is lacking or doubtful. Thus it is apparent that, at least as late a date as 1952, a very large segment of operating practice relied upon burning clear of secondary faults. Much of this no doubt reflects a preference for the simpler solidly connected system as compared to the complications introduced by the limiters plus the partial interruptions to service caused by their functioning. This situation leads me to comment briefly on the subject of self-clearing faults.

EARLY EXPERIMENTS WITH SELF-CLEARING FAULTS

In the early beginning of network development, simple short-circuit tests were made on several of these smaller systems to obtain information on self-clearing ability. These tests consisted of creating faults of various types in typical low-voltage mains cables connected directly to the network. The faults included nails or tools driven into the cables, use of copper wires bridging from sheath to a bared section of conductor, sheath peened over into contact with a bared section of conductor, and others. In these very early tests, the results were invariably the same; an arc would be formed, but would be extinguished very quickly and normal operating conditions would be restored except for a possible open conductor. In fact, the results created the impression that it was practically impossible to produce a sustained arcing fault. However, these tests were not designed to explore systematically and fully the entire range of short-circuit currents and conditions that might be encountered in networks as they existed then or would exist subsequently. The conditions were taken as encountered on the network installations in service at the time.

For an appreciable period of time the installation and operation of networks proceeded with satisfactory operating experience, including satisfactory clearing of faults without benefit of fuses or limiters. Then a sustained arcing fault occurred in one of the smaller systems. This led to repetition of some of the short-circuit tests on somewhat broader scale, and with a determination to produce experimentally, if possible, a sustained arcing fault so as to learn what conditions were necessary to cause it. As before, all faults of a casual nature cleared themselves very quickly, but a sustained arcing fault that gradually consumed a considerable length of cable finally was produced. This was done by binding together very solidly the bared ends of all four conductors of a circuit of single-conductor cables, and then energizing them from the network. This of course created a "dead" short circuit, and in a short time the cables became very hot. "Smoke" was emitted copiously and when one of the conductors finally acquired a gap in the short-circuit path, a sustained arc was created. The basic difference in conditions for a sustained arc from those of a self-clearing arc then were readily apparent. That is, a self-clearing arc is one in a cable having "fresh" volatilizable insulation, and the gases evolved quickly extinguish it. A sustained arc is one in a cable in which the insulation (more or less throughout its length) has been partially or wholly carbonized. In this case the action is much like that of a carbon arc lamp. Not only are the "blow-out" gases lacking but also the insulation has become more or less conducting, thus tending to re-establish the fault should the arc be extinguished.

Further investigation of the service failure that prompted this study revealed that the cable run involved and some other neighboring runs consisted of three lead-sheathed single-conductor cables in the same duct with a neutral of old "rope-lay" bare copper. The space occupied in the duct was high and mechnical damage had been caused at numerous places during installation by the jamming and pressing of the rope-lay neutral against the lead sheaths of the other cables. Thus there were numerous incipient failures, and it seemed probable that two or more faults had occurred closely together in time due to a triggering effect of the first one, thus prolonging the heating and producing the conditions necessary to create a sustained arc. Of course, a considerable number of sustained arcing faults have been encountered since that time but the few that I have had occasion to investigate have involved unusual or special conditions of one kind or another that contributed to producing the particularly tenacious kind of fault required to damage insulation badly before the fault develops into the purely arcing type.

LATER RESEARCH

Of course, since the very early short-circuit tests I have mentioned a great deal of research on burn-off characteristics has been conducted, culminating in the development of current limiters, and bringing us ultimately to the stage of refinement in design and application represented by this series of papers. Most of the more comprehensive burn-off experimentation was directed toward determining minimum values of current necessary to burn conductors in two when they were involved in absolutely "dead" (non-arcing) short circuit, and the results have been used to some extent as a criterion for design of solidly connected networks. Curiously enough, little attention has been paid by the industry in general to the basic nature of the self-clearing action that I have described and indeed for lack of published discussion of the matter it may be that it is not really understood by some operating companies.

THE SOLIDLY CONNECTED SYSTEM POINT OF VIEW

Without in the least wishing to minimize the importance and great merit of the work that has been done in developing and standardizing current limiters, I think it may be well to include in the record mention of some adverse considerations, from the point of view of those who operate solidly connected systems. They are

1. Installation costs are appreciable, especially where application of limiters to an old solidly connected system is involved.

2. Limiters involve operating complications, and require good application engineering to insure proper protection co-ordination. This may be difficult or burdensome for some of the smaller companies.

3. They cause partial service interruption when they function, and to some extent may represent a source of maintenance expense unless very carefully designed for dependable service over long periods under all conditions of operation.

4. As pointed out in some of the discussion, they are something less than 100 per cent effective in the over-all job of protection.

Casual fault conditions that will produce a completely solid short circuit are by no means common. In fact they are difficult to picture. In the case of very large conductors, mechanical factors and the preponderance of metal over insulation may play a part. Experience with which I am familiar indicated that sustained faults, at least in the smaller solidly connected networks, are very rare. This consideration, plus those given in the foregoing, no doubt are largely responsible for decision of some companies to continue solidly connected practice for network mains throughout, and the reluctance of others to adopt limiters for other than restricted portions of their systems.

REFERENCE

1. 1950–52 A-C NETWORK OPERATIONS REPORT Publication No. *54-5*, Edison Electric Institute New York, N. Y., 1954.

ERRATA

"Optimum Design of Induction Torque Motors and Servomotors" by Gerald Weiss; published in Power Apparatus and Systems, October 1955, pages 809-15.

As a result of a typographical error, equation 6 was incorrect as printed. This equation should read:

$$T/W=\frac{p}{4\pi f}y_{max}$$

"Report on the Operation of Switched Capacitors," an AIEE Committee Report; published in Power Apparatus and Systems, December 1955, pages 1255–60.

As a result of an error in the original manuscript, the equation appearing under the heading "Current-Limiting Reactors" (page 1257) was incorrect as printed. This equation should read:

$$L_a=L\left[\left(\frac{I_1}{I_2}\right)^2-1\right]$$